

Annual Cumulated Index

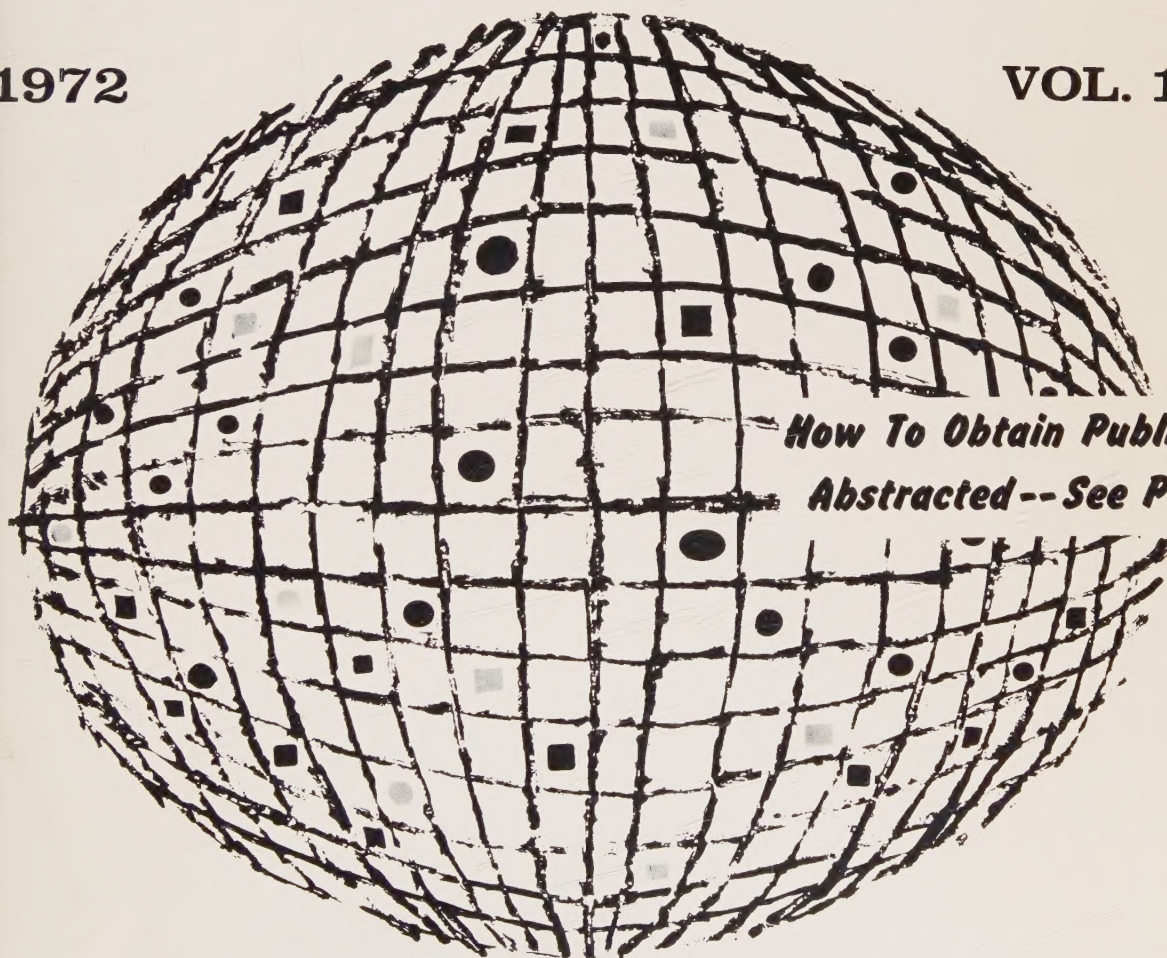
ACCESSION NOS. A72-10001 to A72-45794

INTERNATIONAL AEROSPACE ABSTRACTS

PART 2, SUBJECT INDEX, M - Z

1972

VOL. 12



*How To Obtain Publications
Abstracted -- See Page V*

PUBLISHED BY THE TECHNICAL INFORMATION SERVICE
AMERICAN INSTITUTE OF AERONAUTICS AND ASTRONAUTICS



Digitized by the Internet Archive
in 2023

L
50
57
p. 12
1972
Index
p. 2
N/c
sci

12
500
Isi
vol. 12
1972
Index
pt. 2
M-Z
N/c
sci

8 March 1973

INTERNATIONAL AEROSPACE ABSTRACTS

ANNUAL

CUMULATED

INDEX

PART 2

SUBJECT INDEX, M – Z

VOLUME 12

JANUARY – DECEMBER

1972

ACCESSION NUMBERS A72-10001 to A72-45794

INTERNATIONAL AEROSPACE ABSTRACTS is prepared and published semimonthly (except June and December, which have three issues) by the Technical Information Service, American Institute of Aeronautics and Astronautics, Inc., for the Institute and the National Aeronautics and Space Administration under Contract No. NASW-2422.

SUBSCRIPTION INFORMATION. Semimonthly issues: United States and Possessions, 1 year, \$110 postpaid; foreign countries, 1 year, \$125 postpaid. Cumulated index volumes: United States and Possessions, 1 year, \$75 postpaid; foreign countries, 1 year, \$90 postpaid.

EDITORIAL OFFICE: 750 Third Avenue, New York, N.Y. 10017. SUBSCRIPTION OFFICES: 750 Third Avenue, New York, N.Y. 10017; Third Avenue and Springtown Road, Alpha, N.J. 08865. Second-class postage paid at Phillipsburg, N.J. Copyright © 1972 by the American Institute of Aeronautics and Astronautics, Inc. (The indexes, however, may be reproduced for any bibliographic purpose.)
TELEPHONE: 212 TN 7-8300

TWX: 212 867-7265

STAFF, AIAA

Administrator—Technical Information Programs, Robert R. Dexter

STAFF, TECHNICAL INFORMATION SERVICE

Director, John J. Glennon

Associate Director—Administrative, Thomas J. Meskel

Associate Director—Technical, Irene W. Bogolubsky

Abstracts Editor, Nanu Davis

Index Editor, Angelica Mihalakos

Chief Librarian, Patricia M. Marshall

CONTENTS

PART 1

INTRODUCTION	iii
HOW TO OBTAIN PUBLICATIONS ABSTRACTED	iv
CROSS REFERENCES	iv
PERIODICALS SCANNED	v - xxv
SUBJECT INDEX, A - L	A1 - A1065A

PART 2

INTRODUCTION	iv
HOW TO OBTAIN PUBLICATIONS ABSTRACTED	v
CROSS REFERENCES	v
SUBJECT INDEX, M - Z	A1066 - A2171

PART 3

INTRODUCTION	iii
HOW TO OBTAIN PUBLICATIONS ABSTRACTED	iv
PERSONAL AUTHOR INDEX	B1 - B908
CONTRACT NUMBER INDEX	C1 - C33
MEETING PAPER & REPORT NUMBER INDEX	D1 - D14
ACCESSION NUMBER INDEX	E1 - E80

INTRODUCTION

INTERNATIONAL AEROSPACE ABSTRACTS (IAA) is an abstracting and indexing service covering the world's published literature in the field of aeronautics and space science and technology. IAA is issued semimonthly, on the 1st and 15th of each month.

Coverage of Published Literature

The following types of publications are covered in IAA:

- Periodicals (including government-sponsored journals) and books.
- Meeting papers and conference proceedings issued by professional societies and academic organizations.
- Translations of journals and journal articles.

Coverage of Reports ("Unpublished" Literature)

Abstracts and indexes of report literature are issued in SCIENTIFIC AND TECHNICAL AEROSPACE REPORTS (STAR), which is published by the Scientific and Technical Information Office, National Aeronautics and Space Administration.

By special arrangement between NASA and the American Institute of Aeronautics and Astronautics, IAA is issued in coordination with the twice-monthly schedule of STAR, which appears on the 8th and 23rd of each month.

IAA and STAR both utilize identical subject categories and indexes, which are described below.

Thus the two services provide comprehensive access to the national and international unclassified report and published literature of current significance to aerospace science and technology.

Arrangement of the Semimonthly Issues

IAA is arranged in two major sections:

- (1) Abstracts Section. This section contains complete bibliographic citations with informative abstracts as required, arranged by appropriate subject categories to facilitate scanning. The subject categories are numbered from 01 to 34, and the scope of each category is outlined in the Table of Contents and again at the beginning of each category in the Abstracts Section. Each entry is prefixed by the IAA accession number.
- (2) Index Section. Five indexes are contained in this section: Subject, Personal Author, Contract Number, Meeting Paper and Report Number, and Accession Number. Each index is prefaced by explanatory notes.

Cumulated Indexes

The Semiannual Cumulated Index is issued promptly at the end of the first six months and the Annual Cumulated Index is issued promptly at the end of the twelve-month period.

Each cumulated index contains the following sections: A—Subject Index, B—Personal Author Index, C—Contract Number Index, D—Meeting Paper and Report Number Index, and E—Accession Number Index.

Indexing Vocabulary

The Preliminary Edition of the NASA THESAURUS (December 1967) (NASA SP-7030) is the authority for the indexing vocabulary that appears in the subject indexes to STAR and IAA. The NASA Thesaurus should be consulted for a total picture of the current indexing vocabulary and associated cross-reference structure. Copies of the NASA Thesaurus may be obtained from the National Technical Information Service or the U.S. Government Printing Office at a price of \$8.50 for the three-volume set. A one-volume NASA THESAURUS ALPHABETICAL UPDATE (September 1971) of 623 pages is available from the National Technical Information Service (NTIS), Springfield, Va. 22151, for \$6.00.

Information regarding SCIENTIFIC AND TECHNICAL AEROSPACE REPORTS and the availability of INTERNATIONAL AEROSPACE ABSTRACTS to organizations having contractual arrangements with NASA may be obtained from the following address:

National Aeronautics and Space Administration
Scientific and Technical Information Office
Attention: Code KSI
Washington, D. C. 20546

Documents announced are available from the AIAA Technical Information Service as follows:

- Paper copies of accessions announced in IAA and STAR and of other documents in the TIS library are available at \$5.00 per document up to a maximum of 20 pages. The charge for each additional page is \$0.25.
- Microfiche of documents announced in IAA are available at the rate of \$1.00 per microfiche on demand. Documents available in this manner are identified by the symbol # following the accession number in the Abstracts Section and in the Meeting Paper and Report Number and the Accession Number Indexes.
- Minimum air-mail postage to foreign countries is \$1.00.
- A number of publications, because of their special characteristics, are available only for reference in the library.

**PLEASE REFER TO THE ACCESSION NUMBER
WHEN REQUESTING PUBLICATIONS**

**how
to
obtain
publications
abstracted**

Address all inquiries and requests to:

Technical Information Service
American Institute of Aeronautics
and Astronautics, Inc.
750 Third Avenue, New York, N. Y. 10017

Telephone: 212 TN-7-8300
TWX: 212 867-7265

CROSS REFERENCES

The subject index includes two types of cross references to aid the user of the index in locating the material being sought:

1. "USE" references (U) direct the user to alternate headings under which material on the subject will be found, for example

COLUMBIUM
U NIOBIUM

2. "NARROWER TERM" references (NT) refer the user to more specific headings in the same subject area, for example

LUMINESCENCE
NT ELECTROLUMINESCENCE

Either a Notation of Content or the actual title of the publication appears under each subject heading. They are listed under several subject headings which provide multiple access to the subject of each accession. The *IAA* accession number is located under and to the right of the NOC or the title. It is preceded by numbers identifying the issue and page of *International Aerospace Abstracts* where the accession is located.

To illustrate:

Issue Number	Page Number	Accession Number
14	p2146	A72-30920

M

M WINGS

U VARIABLE SWEEP WINGS

MACH CONES

Fast hyperbolic MHD flow past point source, considering geometry and disturbances singularities of MHD Mach cones

02 p0266 A72-12369

Holographic interferometry of Mach wave field generation by supersonic turbulent jet, noting visible conical wave front from core edge

13 p1898 A72-29580

Mach stem generation by colliding spherical pressure waves in spark ignited combustible gas, noting simultaneous deflagration wave characteristics

24 p3462 A72-45028

MACH INERTIA PRINCIPLE

Tensor-tensor theory of gravitation, introducing first effect of Mach principle

04 p0573 A72-14905

Earth velocity through microwave background, discussing absolute and relative motion, inertial frame and distant matter distribution and Mach principle

14 p2157 A72-30624

MACH NUMBER

Characteristic scale lengths of stationary ionic collisional shocks in Q device perpendicular to magnetic field, presenting shock thickness variation with Mach number and density

01 p0105 A72-10028

Modified implicit continuous fluid Eulerian technique for numerical solution of time dependent fluid flow for Mach numbers from zero to infinity

01 p0049 A72-10226

X-type pseudoshock at high Mach number compared with lambda-type pseudoshock, discussing loss at duct center by leading shock wave

01 p0050 A72-10397

Shock wave propagation from channel in free space for various Mach numbers, using method of characteristics

02 p0202 A72-11590

Real gas tailored shock tube Mach numbers by analytical method, investigating driver temperature effect

02 p0205 A72-12269

Performance similarity of supersonic axial compressors with gas mixtures of different thermodynamic properties, verifying validity of critical Mach number of rotation

[ONERA, TP NO. 966] 04 p0463 A72-15556

Heat pipe temperature gradient initial conditions for ideal gas model, introducing two phase Mach number for choking phenomena analysis

[AIAA PAPER 72-22] 05 p0749 A72-16913

Finite difference method for transonic airfoil design for wide range of angles of attack and Mach numbers

06 p0755 A72-17629

Surface friction coefficient dependence on Mach number and velocity gradients in adiabatic compressible laminar gas flow

08 p1107 A72-21311

Stable large amplitude high Mach number ion acoustic shocks in collisionless plasma, obtaining electron density as function of time

09 p1364 A72-23445

Mach number distribution along critical streamline in compressed layer in front of cylinder in supersonic flow

10 p1415 A72-23752

Two dimensional shock wave interaction with bends in rectangular duct, showing far wall Mach reflection

10 p1464 A72-23879

Rectangular skin panel vibration modes aerodynamic damping dependence on Mach number, dynamic pressure, mode shape and turbulent boundary layer thickness

[AIAA PAPER 72-402] 11 p1568 A72-25423

Impact probe displacement effects in supersonic turbulent boundary layer in terms of Mach number profiles

11 p1572 A72-26005

Numerical calculation of sonic flow around wing section with rounded leading edges, obtaining Mach number distribution, boundary characteristic shape and velocity field

12 p1751 A72-27181

Electrical conductivity of shock wave produced Xe plasma measured by probe, noting dependence on Mach number

15 p2284 A72-31583

Noise measurements during shock free and underexpanded operation modes of supersonic cold model jet at moderate exit Mach number

15 p2179 A72-32017

Transient flow induced in convergent-divergent nozzles by shock front impingement, investigating nozzle shape and Mach number effects on formation process of reflected shock

15 p2179 A72-32143

Precursor photoionization production of ionization onset point equivalent electron number densities, calculating phenomenon occurrence Mach number

15 p2281 A72-32407

Postfrontal ion acoustic shock turbulence as function of Mach number and electron/ion temperature ratio, using particle in cell technique

15 p2281 A72-32424

Study of circular arc airfoils with asymptotic critical Mach number. I

17 p2484 A72-34744

Influence of the angle of attack on the performance of high-deflection stator blades

17 p2484 A72-34889

Calculations of the turbulent boundary layer in supersonic nozzles.

17 p2485 A72-35237

Velocity distribution and Mach number in a supersonic molecular beam of plane symmetry

17 p2486 A72-35423

Performance and limitations of shock tubes with imploding detonation drivers.

21 p3128 A72-40767

On the conditions for the appearance of the Mach effect in the reflection of an oblique shock wave in supersonic flow

21 p3046 A72-41339

Reynolds number and drive power variation with Mach number, pressure and temperature in cryogenic wind tunnel

[AIAA PAPER 72-995] 21 p3040 A72-41581

Aerodynamic characteristics of bodies of revolution with large fineness ratios at Mach numbers ranging from 0.2 to 6.0

22 p3134 A72-42286

Flow equations for axisymmetric compressible conical flow in Busemann nozzle, noting numerical method for integral lines construction for given Mach number

22 p3134 A72-42288

Limit Mach number in a gas undergoing partial dissociation and single ionization

22 p3244 A72-42624

Frequency dependence of axially oscillated nozzles admittance real and imaginary parts for different Mach numbers, convergence angles and curvature radii, comparing theory and experiment

24 p3433 A72-45144

Mach reflection from overexpanded nozzle flows.

24 p3365 A72-45794

MACH-ZEHNDER INTERFEROMETERS

Double beam Mach-Zehnder interferometer, discussing optical element imperfection induced degradation elimination by Moire technique

07 p0985 A72-19406

Superheterodyne radiometers for millimeter and submillimeter waves, using Mach-Zehnder interferometer frequency mixer for parasitic signal suppression

08 p1440 A72-21265

Design of an inexpensive, 30 cm diameter, long path difference interferometer.

17 p2553 A72-34640

A unitized and portable holographic interferometer. [ASME PAPER 72-HT-10]

20 p2927 A72-39681

Interferometric method for measuring electro-optic coefficients in crystals.

21 p3095 A72-40138

MACHINE LEARNING

U LEARNING MACHINES

MACHINE LIFE

U SERVICE LIFE

MACHINE ORIENTED LANGUAGES

NT LANGUAGE PROGRAMMING

Linear and nonlinear material static and dynamic structural analysis using NASTRAN digital computer program with finite element approach
01 p0140 A72-10983

Language for description of onboard control system location and attitude control operations during spacecraft maneuvering
05 p0726 A72-16456

Interactive simulation language-8 for minicomputer and programming procedures for nonlinear differential equations solution, considering integration step size and computational accuracy and speeds
07 p0951 A72-20334

Abstract family of multistorage tape acceptors and associated languages, discussing wedge operation and applications
12 p1787 A72-27675

Machine oriented language for modular computer programming, discussing subprogram composition, conditional addresses and description table structure
19 p2769 A72-38089

Process computation systems, discussing translator programs for conversion of user programs into machine language
21 p3024 A72-41002

MACHINE RECOGNITION

U ARTIFICIAL INTELLIGENCE

MACHINE STORAGE

U COMPUTER STORAGE DEVICES

U CORE STORAGE

MACHINE TOOLS

NT BORING MACHINES

Multilead electrical spark discharge machining for mass production technology, noting carburetor slot cutting and data processing equipment applications
01 p0078 A72-11097

Book on electrochemical machining covering metallurgical effects, electrolytes, tool design, rotating surfaces and operating costs
06 p0821 A72-17819

Numerically controlled machine tools accuracy, discussing feed spindle and displacement/angle measuring system errors determination through angular step transducers and laser interferometer
07 p0955 A72-19684

Large automated tape placement machine tool design and construction for laying up aircraft structures from composite materials
08 p1177 A72-21690

Automatic riveting machine for fuel tight aircraft structures, describing process technique and machine design details and features
09 p1319 A72-22906

Computer controlled electron beam machine for microcircuit fabrication, using digital technique capable of working on complex patterns
10 p1459 A72-23956

Die-casting machine design trends, considering uses of elbow lever and hydraulic systems and programmed control
16 p2399 A72-34142

Numerical control component insertion for missile IC electronic module, tabulating producer-user survey data for designs usage and machine tools
17 p2532 A72-35923

Testing the impact accuracy of the NEK-8 HERF machine
18 p2695 A72-36274

Thermochemical techniques application to corrosion protection of metallic powders, mechanical parts and tools, describing chromizing, chromaluminizing, tantaluminizing and niobiumizing processes
[ONERA, TP NO. 1049] 19 p2817 A72-37769

Mandrel design for the filament winding process
19 p2808 A72-38168

Book - Aluminum brazing handbook
19 p2810 A72-38720

Investigation of the dependence of the smoothness of rectilinear motion in precision-equipment mechanisms on the form of the microrelief of contacting surfaces
24 p3403 A72-45325

MACHINE TRANSLATION

Computer programming for minimization of time required for retranslation with compilers, discussing finite state machine modeling with circulating page loose system
24 p3383 A72-45670

MACHINE-INDEPENDENT PROGRAMS

Computer programming languages, discussing system dependent and problem-oriented languages, ALGOL, FORTRAN and applicability ranges
17 p2523 A72-35444

MACHINERY

Analytical and graphical calculations of stress concentration coefficients and stress gradients in machine parts with recesses and finite depth cuts
01 p0144 A72-11377

Soviet book on structural shape effects of machine parts on durability, covering production, gear transmissions shafts, axles, threaded joints, etc
03 p0364 A72-13966

Optimal synthesis of multiparametric machine systems by LP search/determinate analog of random search/, applying to oscillatory models
06 p0821 A72-17726

Machine parts surface hardening and smoothing by vibrating hard alloy sphere impact at ultrasonic frequency
08 p1176 A72-21050

Machine metals fatigue life, creep theory and stress and strain kinetics in severe environments, formulating physical equations
08 p1246 A72-21805

Design information for machinery to incorporate welding positions and joints, fatigue mechanisms, loads, combined stresses and plate and cast materials properties
09 p1409 A72-23621

Oscillations excitation, proposing models for percussive rotational action machines operation and dog tooth clutches processes
13 p1954 A72-28386

Algorithm for optimal strategy in statistical plant control for machine parts production and assembly, discussing measuring equipment errors effects
13 p1965 A72-29168

Rotating machines self excited lateral vibration and instability avoidance and identification
[ASME PAPER 72-DE-21] 14 p2167 A72-30865

Vibrational diagnostics of operational conditions of machines for wear, design faults and efficiency evaluation
16 p2425 A72-33408

Book - Vibration and acoustic measurement handbook.
21 p3086 A72-41533

Energy balance equation for machine unit with rotating element, noting energy distribution in periodic and nonperiodic operation modes
22 p3181 A72-41857

Russian book - Dynamics and acoustics of machines.
22 p3182 A72-42126

Machine vibration diagnostics and damping, emphasizing filter lattice foundation structures, probability analysis and Bayes formula application
22 p3182 A72-42127

Viscoelastic and active vibration isolators for foundation isolation of polyharmonic vibrational effects of operating machines
22 p3182 A72-42131

Machine elements vibration parameters from dynamic model of planetary gears, noting energy spectrum, correlation and amplitude distribution functions
22 p3182 A72-42132

Material properties, metallurgy, production technology and operational factors effects on machinery structural strength
23 p3347 A72-43733

Conference on Fluid Machinery, 4th, Budapest, Hungary, September 11-16, 1972, Proceedings.
24 p3393 A72-45351

MACHINING

NT CHEMICAL MACHINING

NT ELECTROCHEMICAL MACHINING

NT MILLING [MACHINING]

NT SPARK MACHINING

NT ULTRASONIC MACHINING

Warpage control of large Al alloy forgings machining of jumbo jet components, using packing and storage methods
[SAE PAPER 710801] 01 p0074 A72-10280

Steel and Ti-Al-V alloy surface integrity during various machining methods, considering microstructures, residual stress profiles and fatigue characteristics
[SME PAPER IQ 71-237] 01 p0076 A72-10972

Se and Te additions effects on low carbon steels formability and machinability from metallurgical examination and workability tests
07 p0994 A72-19480

Hardenability and pearlite stage isothermal transformation properties of direct-quenching low Cr case-hardening steels, discussing Mn, Mo and Ni alloying effects on machinability
07 p0995 A72-19571

Electromechanical machining metal removal mechanism based on configurational localization model, relating wear processes to electron exchange and free energy margin decrease
07 p0996 A72-19989

Laser applications in industrial machining and welding, describing theory and operation of optically pumped ruby, glass-Nd, YAG-Nd, Ar and carbon dioxide lasers
07 p1007 A72-20224

Dimensional metal working by material erosion involving stereomechanical energy transmission to surface of nonrigid mechanical body
08 p1173 A72-21027

Metal working by plasma beam in turning machine, applying to high strength alloys
08 p1175 A72-21045

Industrial applications of lasers, considering programmable machining, distance measurement, computer memories, communication, night clubs, machine

shops, aircraft manufacture and tunnel boring machine alignment
08 p1182 A72-21207

German monograph on plasma arc machining and cutting of metallic materials on lathe as function of electric power and torch performance
09 p1317 A72-22327

Heat treatment and machining for distortion control of large Al alloy forgings for DC 10 aircraft
09 p1317 A72-22476

Materials processing with carbon dioxide lasers, noting cutting, welding and hole drilling applications
10 p1485 A72-23969

Electrical discharge machining of zirconium diboride, considering operations and tooling requirements
[AIAA PAPER 72-329] 11 p1637 A72-25365

Transitional microstructure of machined surface layer due to built-up edge disintegration
11 p1638 A72-25508

Hydroplasma metal removal for surface cleaning of heat resistant alloys, using electric contact plasma arc machine
11 p1641 A72-26673

Bending roller adjustment parameters for casing shaping in machining process
11 p1642 A72-26815

Commercially available laser systems applications to welding, drilling, scribing and other machining operations
11 p1652 A72-26984

Surface integrity machining practices application to jet engines production, noting cost reduction and process selection and quality control improvement
[ASM PAPER W 72-27,2] 12 p1862 A72-28163

Combined heat treatment and machining effects on Mg-Nd alloys structure and mechanical properties, noting strain hardening mechanism
14 p2125 A72-31042

Economics of material cutting and removal by plasma torches, presenting cutting rates as function of plate thickness for different materials
15 p2243 A72-31321

Electron beam welding, machining and drilling, discussing technical and economic factors
16 p2399 A72-33540

Precision laser system for micromachining applications, describing optical system
17 p2563 A72-35183

Laser machining of thin films. I - Irradiation characteristics of a focused Q-switched YAG laser beam.
18 p2695 A72-36518

Machining boron-epoxy composites.
19 p2809 A72-38386

Influence of deviations in the shape of the base surface on the precision of turbine blade machining operations
22 p3182 A72-41863

MACROCLIMATE

U CLIMATE

MACROMOLECULES

U MOLECULES

MACROSCOPIC EQUATIONS

Inhomogeneous microstructure elastoplastic medium, examining strain and work in plastic deformation
02 p0293 A72-12427

Wave equations for electromagnetic wave propagation in electron-ion-neutral particle magnetoplasma, using macroscopic approach
12 p1852 A72-27850

MACULAR VISION

U VISION

MAGELLANIC CLOUDS

Papers on Magellanic Clouds covering properties, observational and theoretical approaches, supernovae remnants, color-magnitude diagrams, globular clusters, etc
03 p0424 A72-13251

Stellar photometric observations in Magellanic Clouds, presenting photoelectric sequences in UVB system, interstellar reddening and extinction data
14 p2159 A72-30737

Spectrographic and photometric observations of supergiants and foreground stars, in the direction of the Large Magellanic Cloud.
19 p2858 A72-37855

Magellanic clouds structure and dynamics from optical and radio observations, discussing interconnecting magnetic field existence
19 p2865 A72-38481

A more accurate determination of the structural features of the instability strip of classical Cepheids from Gascoigne's photoelectric data in the Small Magellanic Cloud
21 p3113 A72-41757

Model atmosphere analysis of the A 31a-O supergiant HD 33579 in the Large Magellanic Cloud.
22 p3225 A72-42386

Observation of several X-ray sources in 1970 September.
22 p3219 A72-42554

Gamma radiation of Magellanic Clouds and metagalactic origin of cosmic rays.
23 p3328 A72-43264

- The analysis of the small Magellanic Cloud supergiant HD 7583. 23 p3336 A72-43555
- MAGIC TEES**
Coaxial and stripline wideband microwave hybrid junctions equivalent to magic Tees with improved electrical properties 05 p0636 A72-16344
- MAGMA**
Fractional crystallization and crustal contamination roles in origin of quaternary basaltic magmas from Black Rock Desert Region in Utah 06 p0810 A72-18515
Sr isotope data indication of Glass Mountain rhyolite lava as part of parent silicic magma 11 p1623 A72-26240
Crystallization experiments on Apollo 11 magmas of K and Rb-rich basalt, discussing plagioclase characteristics 11 p1723 A72-26523
Electron microprobe analysis of chromian spinels from Apollo 14 rocks indicating crystallization from high aluminum low iron magma 12 p1865 A72-27113
Morphology and petrography of volcanic ashes. 18 p2685 A72-36222
Mineralogy, petrology and chemistry of lunar rock 12039. 23 p3339 A72-44127
- MAGNESIUM**
NT MAGNESIUM ISOTOPES
Cation distribution observation over nonequivalent lattice sites in shocked orthopyroxene, noting Mg and Fe order-disorder 01 p0053 A72-10293
Impurity diffusion of Ag, Cd, In, Sn and Sb in magnesium single crystals, observing valence effect on activation energy 03 p0378 A72-14254
Molecular oxygen evolution Mn catalyst photoactivation as two-quantum process, discussing kinetic model computer simulation 04 p0484 A72-15740
Mg dispersion hardening techniques, exploring internal oxidation of alloys containing rare earths 07 p1011 A72-19481
Mg ion excitation by electron collision in solar chromosphere studies, calculating scattering cross sections 07 p1081 A72-20234
Electric pulse initiated pyrogen jet sputter igniter consisting of magnesium-fluorocarbon coated bridgwire and pellet enclosed in Mk 1 or 2 gilding metal cup 08 p1221 A72-20774
Visual and motion picture studies of ignition and burning characteristics of Mg particle clusters in flames of gas mixtures 09 p1411 A72-22886
Pressure effect on combustion rate of Mg particles in water vapors 09 p1411 A72-22887
Burning process of low boiling Mg particle moving in relation to gaseous oxidizer, assuming heat and mass transfer occurrence by diffusion-conduction mechanism 09 p1411 A72-22888
Ignition and incendiarity of laser irradiated single micron size Mg particles suspended in stoichiometric methane air mixture 10 p1564 A72-25140
Mg addition effect on high temperature mechanical properties of nickel-alumina alloy, studying particle coarsening mechanism changes 11 p1664 A72-26856
OSO-6 Mg X spectroheliogram data for corona electron density map construction during 7 March 1970 solar eclipse period 13 p2031 A72-29529
Mg filterheliogram comparison with Ca spectroheliogram, noting correlation coefficient between location and intensity of bright features on sun 13 p2045 A72-29708
Magnesium particle combustion in rarefied air during pressure changes, discussing combustion time decrease with pressure increase 14 p2170 A72-30236
Temperature dependent Mg and Fe hyperfine doublets in lunar olivine, indicating slow cooling crystallization 15 p2303 A72-31302
Singly ionized Ca and Mg electron impact broadened resonance lines from rapid scanning Fabry-Perot spectrometer measurements in shock tube generated high temperature plasma 15 p2282 A72-32643
Reaction rate and activation energy of low temperature oxidation of Mg particles in nitrous oxide 16 p2476 A72-32353
Mg ignition in nitrous oxide at 600-800 C, determining induction period as function of particle mass and gas stream temperature 16 p2476 A72-32354
Measurements of the limb darkening in the forbidden MgI line at 4571.1 Å. 17 p2608 A72-35078

- A compact grating spectroheliograph for the MgII resonance lines. 17 p2554 A72-35079
Balloon-borne UV spectrophotometer observation of Mg II resonance doublet at 2795 and 2802 Å in stellar spectra, comparing to Ca II line widths 20 p2965 A72-38907
Mg-Al powder mixtures sintering and coining, describing fabrication procedure, microstructure and mechanical properties 21 p3067 A72-40832
Broadening and shift of magnesium lines by van der Waals interaction with argon atoms and by microfields. 22 p3208 A72-42388
Fabrication and properties of graphite fiber reinforced magnesium. 22 p3193 A72-43035
- MAGNESIUM ALLOYS**
Al-Mg alloy under reverse bending fatigue in aqueous sodium chloride with constant load and potentiostatic control, determining anodic polarization effects on fatigue life 01 p0087 A72-11033
Extruded anodized AlMgSi alloy matrix precipitate surface defects, noting wood grain effect, segregated bands, microstructural stains and heterogeneous zones 01 p0077 A72-11042
Equilibrium state and microhardness of phase diagrams in Mg-rich region of Mg-Nd-Zn system 03 p0370 A72-13185
Grain size effect on age hardened Mg-Zn alloy yield and flow stress, using tensile test and electron and optical microscopy at various temperatures 03 p0374 A72-13716
Mg-Zn alloys precipitation hardening mechanism at various aging stages, considering yield strength increase due to interface dislocations 03 p0374 A72-13717
Magnesium alloys torsional vibration damping correlation with texture orientation resulting from fabrication method 03 p0375 A72-13930
Substructure of cast alloys based on Al-Mg system from electron diffraction microscopy 03 p0377 A72-14023
Portevin-Le Chatelier effect in Al-Mg single crystals during tensile tests, investigating strain rate influence on stress 03 p0378 A72-14257
Alloying, thermal and mechanical treatment effects on Mg alloys damping properties under elastic vibrations, showing test results consistency with materials microdeformation theory 05 p0671 A72-15987
Prolonged heatings effect on heat resistant magnesium alloys microstructure and mechanical properties 05 p0680 A72-17208
Accelerated fatigue limits for Al and Mg alloys from transverse bend test data 06 p0827 A72-17398
Interfacial dislocations and failure in tension of directionally solidified Al-Cu-Mg eutectic 07 p1016 A72-19937
Mg alloys compositions, melting points, mechanical properties and applications 09 p1327 A72-22479
Ignition delay time and combustion mechanism of Al-Mg alloys single particles in combustion products of oxidizer-fuel mixture 09 p1373 A72-22885
Extruded dispersion strengthened Mg-MgO alloys microstructure, discussing high temperature creep effect on dislocation structure changes 09 p1328 A72-22984
Microstructure and mechanical behavior of unidirectionally solidified magnesium-magnesium nickel eutectic composite over range of solidification rates 09 p1330 A72-23376
Metallographic study of denuded zones from diffusional flow in hydrided Mg superplastic alloy with Zn and Zr 09 p1331 A72-23383
German monograph on transition elements Cr, Mn and Zr influence on Al-Zn-Mg alloys stress corrosion covering electron microscope studies and loop-bending tests 10 p1493 A72-23769
X ray diffraction study of molten Mg-Cd alloy atomic structure, demonstrating existence of Mg-Cd compounds 10 p1497 A72-24678
Stress corrosion crack paths in Al-Zn-Mg alloys, showing normal coincidence with grain boundaries 11 p1652 A72-25289
Mn content effect on mechanical properties and corrosion fatigue and stress corrosion cracking resistance of Al-Mg casting alloys 11 p1658 A72-25850
Prolonged heating effect on heat resistant Mg alloys microstructure and mechanical properties 11 p1660 A72-26143

- Cavitation by creep of Mg alloys, using density measurements and metallurgical examinations 11 p1661 A72-26650
Electron microprobe analysis of solute segregation near grain boundaries in Al-Zn-Mg alloy after quenching and aging heat treatment 13 p1973 A72-28652
Al and AlMg single crystals static recovery and stacking fault energy at 77-500 K in plastic deformation, noting cross slip onset at 500 K 13 p1978 A72-29222
Commercial and laboratory Mg alloys for die and sand casting, high strength and extruding applications 14 p2113 A72-30269
Ultrasound damping in Mg and Al alloys by structural grains and dislocation oscillations during work hardening, recrystallization and oversaturated solid solution decay 14 p2122 A72-30957
Thermal and microstructural analysis of phase interactions in Mg alloys of Mg-Nd-Y system 14 p2124 A72-31028
Phase equilibrium of Mg base solid solutions of Mg-Li-Sn system at 200-500 C, analyzing microstructure, microhardness and electrical resistivity 14 p2124 A72-31029
Composition dependence of ultrasonic velocity in binary Mg base alloys measured by pulse method 14 p2143 A72-31030
Alloying effect on structural transformations and strain hardening during aging of two phase α - β Mg-Li-Zn alloys 14 p2124 A72-31031
Li addition effects on Mg mechanical properties temperature dependence and notch sensitivity of binary Mg-Li alloys 14 p2125 A72-31041
Combined heat treatment and machining effects on Mg-Nd alloys structure and mechanical properties, noting strain hardening mechanism 14 p2125 A72-31042
Volumetric analysis of Th, Zr and Li hydrides precipitation in Mg alloys, determining rate equation and activation energy 15 p2257 A72-32118
Solution kinetics of secondary phases in cast dendritic and nondendritic Mg-Zn and Mg-Zn-Zr alloys, using cylindrical and spherical diffusion models 15 p2257 A72-32119
Mg base alloys precipitation processes studied by electron microscopy, emphasizing Mn precipitation in Mg-Th alloy 16 p2405 A72-32998
Al-Cu-Mg alloys room temperature age hardening, determining effects of tension load up to plastic deformation from measurements of mechanical properties and electrical resistance [DFVLR-SONDDR-188] 16 p2408 A72-33674
Crack propagation in Al-Cu-Mg alloy sheet under vibratory bending loads, noting crack length to loading cycles number relationship 16 p2408 A72-33677
New observations of preprecipitation phenomena in Al-Mg and Al-Mg-Zn alloys 17 p2566 A72-34286
Effect of additions of Cu and Zr on stress corrosion cracking of Al-Mg alloys. 19 p2820 A72-38370
Internal stresses in a superplastic Mg alloy. 20 p2935 A72-39002
Correlation analysis techniques to characterize acoustic emission pulses from Mg alloys, obtaining time varying spectra 20 p2924 A72-39281
Effect of alloying on the decay of an aluminum-magnesium solid solution 20 p2942 A72-39823
Burning of particles of an aluminum-magnesium alloy 20 p2987 A72-40041
Mechanism of high temperature creep of aluminum-magnesium solid solution alloys. 21 p3069 A72-41299
Influence of the cycling frequency and directional anisotropy on the fatigue strength of AMg6BM aluminum-alloy sheet 21 p3070 A72-41356
Investigation of the drop forging process applied to magnesium alloys 22 p3183 A72-42816
Magnesium alloys containing rare-earth metals as materials with special physical properties 22 p3192 A72-42817
Deformable magnesium alloys with scandium and yttrium 22 p3192 A72-42820
Stability of Al₃Mg₂ particles against diffusive coagulation in aluminum-magnesium alloys 23 p3301 A72-43649
Ultrasonic treatment of the MA2-1 alloy during recrystallization 23 p3303 A72-44096
Alloying, thermal and mechanical treatment effects on Mg alloys damping properties under elastic vibra-

tions, showing test results consistency with materials microdeformation theory 24 p3415 A72-45729

MAGNESIUM COMPOUNDS

NT CHLOROPHYLLS

NT DOLOMITE [MINERAL]

NT ENSTATITE

NT FORSTERITE

NT MAGNESIUM FLUORIDES

NT MAGNESIUM OXIDES

NT TALC

Proton and fluorine nuclear magnetic spin-lattice relaxations due to internal rotations in magnesium fluorosilicate hexahydrate 04 p0564 A72-15636

Composition diagrams and properties of intermetallic compounds of magnesium in binary and ternary systems 15 p2252 A72-31196

MAGNESIUM FLUORIDES

Radiation damage in MgO, ZnO and magnesium fluoride, considering energy dependence and roles of radiolysis and elastic collisions 03 p0404 A72-14088

Heat resistance of magnesium, barium and calcium fluorides as solid lubricants in air, hydrogen and water vapor at 100-1100 C 06 p0836 A72-18433

MAGNESIUM ISOTOPES

Solar MgH isotopic abundance ratios and photospheric lines, correcting previous overestimation for sunspot spectra analyses 07 p1071 A72-19179

MAGNESIUM OXIDES

Radiation damage in MgO, ZnO and magnesium fluoride, considering energy dependence and roles of radiolysis and elastic collisions 03 p0404 A72-14088

Thermal conductivity of aluminum, beryllium and magnesium oxides lattices at high temperatures 06 p0828 A72-17615

Visual observations of wall in turbulent pipe flow, using suspending solid MgO particles 09 p1306 A72-22310

Extruded dispersion strengthened Mg-MgO alloys microstructure, discussing high temperature creep effect on dislocation structure changes 09 p1328 A72-22984

Computer algorithms for scattering functions of condensed aluminum or magnesium oxides in combustion products for various temperatures and particle sizes 11 p1747 A72-26966

Increased volume fraction effect on transverse rupture strength and fracture toughness of hot pressed and annealed composites of polycrystalline magnesium oxide 13 p1980 A72-29828

Dispersed particle shape effect on elastic behavior of magnesium oxide composites at low graphite concentrations 15 p2260 A72-31585

Polycrystalline aluminum and magnesium oxide ceramics fracture strength, considering plastic deformation and twinning role in crack nucleation 23 p3305 A72-43505

MAGNESYN [TRADEMARK]

U SERVOMOTORS

MAGNET COILS

Analysis of cryogenic suspensions for use in spacecraft 22 p3230 A72-42208

MAGNETIC ABSORPTION

U ELECTROMAGNETIC ABSORPTION

MAGNETIC AMPLIFIERS

Push-pull magnetic amplifier circuit operation as variable polarity dc source for electroplating applications 11 p1603 A72-25279

T equivalent circuit magnetic modulator system with split excitation windings on four separate cores magnetized by HF source, noting null drift due to hysteresis 11 p1603 A72-25281

Two stage magnetic operational amplifier transfer function, time constants and control stability conditions, using difference equation approach 11 p1605 A72-26466

MAGNETIC ANNULAR SHOCK TUBES

Current sheet velocity limitation in magnetically driven shock tube with plasma electrodes, examining wall ablation and friction and Hall current effects [AIAA PAPER 72-409] 11 p1695 A72-26160

MAGNETIC ANOMALIES

Geomagnetism, discussing world field distribution, secular variation, paleomagnetism, archaeomagnetism, origin, magnetic anomaly and earth electromagnetic induction 01 p0053 A72-10168

Gravity and magnetic anomalies interpretation in terms of buried spherical bodies, calculating bodies size and depth of burial 01 p0064 A72-11101

Spiral geometry and distribution of global geomagnetic anomalies, discussing ideal liquid motion between concentric spherical surfaces of earth sub-core and core radii 02 p0218 A72-11952

Papers on world geomagnetic survey 1957-1969 covering land, sea, airplane and polar-orbiting geophysical observatory satellite observations, magnetic anomalies and reference field 02 p0219 A72-12080

Geomagnetic storms and anomaly observation by Satellite 1964 83C telemetry data transmission to ground stations network 02 p0219 A72-12083

Ionospheric disturbance in American zone during IGY-IGC, showing latitudinal, annual and diurnal solar variations effects and regional geomagnetic anomaly 06 p0806 A72-17641

Auroral zone electron precipitation events before and at negative magnetic bays onset, presenting balloon recordings of bremsstrahlung X-rays intensity 06 p0808 A72-18092

D region positive ion and electron conductivities and densities measurement by parachute borne blunt probes during 1970-1971 winter anomaly 09 p1376 A72-22373

VLF phase changes due to particle precipitation into geomagnetic anomaly during solar proton events explained by exponential ionospheric models with effective reflecting height 11 p1599 A72-26765

Autocorrelation functions of anomalous magnetic field and earth crust structure of central portion of Arctic Ocean, using sliding energy spectrum method 13 p1946 A72-28589

Spiral geometry and distribution of global geomagnetic anomalies, discussing ideal liquid motion between concentric spherical surfaces of earth sub-core and core radii 13 p1949 A72-29264

Anomalous magnetic and gravitational field models autocorrelation function behavior dependence on circular cylindrical sources depth and spacing 14 p2101 A72-30647

Geomagnetic field multipoles effects on radiation belt particle motion for analysis of true anomalies 15 p2222 A72-31280

Theory of magnetically conjugate transport of cold plasma in the outer low-latitude ionosphere 17 p2548 A72-35218

Drift characteristics of the main eccentric geomagnetic dipole 18 p2689 A72-36872

Possibility of determining the secular variation of geomagnetic field components from the distribution of total-vector modulus variation 18 p2689 A72-36873

Diurnally varying neutral wind effects on lower F region ionization distribution, noting Appleton anomaly disappearance time 19 p2794 A72-38865

Identification of short polarity events by transforming marine magnetic profiles to the pole 20 p2917 A72-39476

ASW aircraft magnetic anomaly detection (MAD)/system range limitation due to residual maneuver noise, discussing real time compensation for geomagnetic gradient interference 22 p3177 A72-42322

Magnetic anomalies in New Guinea-New Zealand region from geomagnetic measurements with proton magnetometer, noting effects of andesite-basalt volcanic processes and nuclear precession signal 23 p3284 A72-43380

Autocorrelation functions of anomalous magnetic field and earth crust structure of central portion of Arctic Ocean, using sliding energy spectrum method 24 p3397 A72-45089

Critical-point anomalies in the electron-paramagnetic-resonance linewidth and in the zero-field relaxation time of antiferromagnets. 24 p3432 A72-45674

MAGNETIC CIRCUITS

Magnetostatic interactions of cylindrical magnetic domain propagation circuits in ferromagnetic overlay without in-plane fields [IEEE PAPER 2,1] 03 p0331 A72-13752

Variable flux reset ferroresonator voltage regulator with adjustable terminal characteristics using magnetic and thyristor circuits [IEEE PAPER 17,1] 03 p0311 A72-13770

Magnetic-transistor master oscillator with digital analog converter as programmer for needed output voltage frequency shifts 07 p0946 A72-19959

YIG-tuned microwave transistor oscillator design and performance, considering resonance phenomena and magnetic circuit effects on applications 08 p1139 A72-20985

Far field radiation pattern from magnetic line source covered with moving uniaxial or isotropic nondispersive dielectric or cold plasma sheaths 08 p1137 A72-21985

Magnetic integrated circuits design and fabrication problems involving branched and logic circuits and solid state structures controlled domains 10 p1448 A72-24279

Magnetic and transistorized magnetic digital-to-analog converters 17 p2529 A72-34768

Contactless relay circuits employing a branched-core magnetic modulator with second-harmonic output 19 p2771 A72-37302

MAGNETIC COILS

Plasma flow interaction with magnetic pulse field barrier from magnetic coil for short plasmoids formation 09 p1362 A72-23211

Trap magnetic system with coil generated field increasing towards periphery, showing radial dependence and acting ponderomotive forces 09 p1363 A72-23215

Superconducting coil design for magnetic suspension of supersonic wind tunnel balance 10 p1460 A72-24760

Electrical loss measurements in superconducting magnets at 60 Hz for Nb-Sn ribbon and Nb-Ti cable and multifilament coils 10 p1460 A72-24760

MAGNETIC COMPASSES

Magnetic compass use in instrument flight conditions, suggesting emergency procedures during aircraft system failures 15 p2238 A72-32212

MAGNETIC CONTROL

Interelectrode gap position control of discharge in coaxial gas heater with arc rotated by magnetic field 02 p0201 A72-12865

SAS-A satellite attitude control and determination systems, discussing momentum wheel development, nutation damper and magnetic torquing 03 p0442 A72-14398

Controlled thermonuclear fusion for space propulsion, discussing magnetic-confinement and laser-plasma fusion engines 04 p0556 A72-14889

Geomagnetic control over latitude variation of total electron content in equatorial ionosphere 04 p0515 A72-14931

Toroidal plasma column in Tokamak systems, discussing field inhomogeneity role in maintaining equilibrium with conducting casing, confirming magnetic field and transformer iron core 04 p0557 A72-15171

Steady state angular motion stability of passive magnetically stabilized satellites, using Liapunov method 05 p0726 A72-16464

Long term spin and misalignment in orbit of Azur satellite with passive magnetic attitude control system 05 p0727 A72-16466

AEROS satellite active magnetic attitude control system, describing magnetometer system, sun and IR earth sensors, spin stabilization and axis and spin rate control torque generation 05 p0727 A72-16473

Magnetic multipole confinement of magnetic field-free He and Ar plasmas in vacuum chamber, observing decay 06 p0854 A72-17505

Misalignment angle of Azur satellite orientation axis relative to geomagnetic field vector 06 p0892 A72-18145

Closed line magnetic confinement device filled with laser produced hydrogen plasma, discussing laser beam high speed numerical control for injected pellet interception [CLEA PAPER 12,1] 07 p1040 A72-19392

Optimal test conditions in magnetoscopic control by electrical system for subsurface defects detection, obtaining tangential magnetic field on carbon steel plates 07 p0991 A72-20421

Hydrogen plasma production, using linearly polarized microwaves with superimposed magnetic field 13 p2010 A72-28683

Variable magnetic baffle as control device for Kaufman electron bombardment ion thrusters with hollow cathode [AIAA PAPER 72-488] 13 p2027 A72-28949

Carrier wave behavior in n-type GaAs slab under crossed dc electric and magnetic fields, investigating traveling space charge amplifier magnetic control 14 p2143 A72-30941

Hybrid low power consumption magnetic/fluidic pulse shortener for fluid logic control circuits consisting of short cylindrical chamber with input and output port 16 p2350 A72-33179

Geomagnetic attitude control of an axisymmetric spinning satellite. 17 p2619 A72-34201

The magnetic control of the lower ionospheric absorption at lower latitudes. 17 p2546 A72-34697

- Pulsed IR laser for heating superdense plasma to high temperature, featuring inertial confinement by use of short duration energy and strong magnetic field
19 p2843 A72-38823
- High-resolution spectroscopy using magnetic-field-tuned semiconductor lasers.
20 p2933 A72-39561
- Pulsed metallic-plasma generators.
20 p2958 A72-39781
- Small oscillations of gravity gradient satellite in circular near-equatorial orbit, discussing operational efficiency of magnetic damping systems
22 p3230 A72-42223
- Compression of high current relativistic electron beams using converging magnetic fields.
23 p3315 A72-43525
- Optimal gyroresonator control in electric oscillating field by HF magnetic Lorentz force in terms of relativistic electron trajectory drifts
23 p3290 A72-44200
- Waves generated in the configuration of a magnetically confined and field-permeated axisymmetric jet.
23 p3322 A72-44307
- Theory of magnetically tunable band-pass filters
23 p3273 A72-44360
- Magnetic control of arc plasma and its application for welding.
24 p3406 A72-44777
- MAGNETIC CORES**
- Ferrite core memory for space flight devices, comparing 1 bit storage capacity power consumption with MOS cell
[DGLR PAPER 71-090] 02 p0196 A72-12734
- Computerized design algorithm for ferrite core memory system, considering cross-temperature effect under worst driving conditions
[IEEE PAPER 11, 8] 03 p0327 A72-13766
- Double shunt feedback controlled ferroresonant voltage regulator using magnetic component with simulated core saturation
[IEEE PAPER 17, 3] 03 p0311 A72-13772
- Polyphase signal generators, using reversed flux region propagation in saturable ring core controlled by switching transistors operation
[IEEE PAPER 17, 5] 03 p0322 A72-13773
- Supermagnetic magnetization and ac core loss temperature dependence under slow temperature cycling in vacuum, noting anomalous Barkhausen effect
04 p0564 A72-15718
- Reliable, economical and easily operated read-only magnetic core storage devices for control computers, discussing design features
10 p1445 A72-24639
- Modulation oscillations in ferromagnetic core-based LF signal generators and frequency doublers, deriving differential equations for converter operation and formulas for static characteristics
13 p1930 A72-29049
- Contactless relay circuits employing a branched-core magnetic modulator with second-harmonic output
19 p2771 A72-37302
- Self-excited parametric oscillations at the second harmonic in a parametric system with a triple-post ferromagnetic core
19 p2774 A72-38586
- MAGNETIC DIFFUSION**
- Magnetic diffusion into moving cylindrical incompressible plasma with radial divergence
10 p1521 A72-24413
- On the diffusion of the perturbing toroidal magnetic field from the core to the mantle.
21 p3048 A72-40501
- MAGNETIC DIPOLES**
- Electric quadrupole to magnetic dipole f-values for CO fourth positive and nitrogen Lyman-Birge-Hopfield systems, using curve of growth method
01 p0103 A72-10092
- Zero relative velocity surfaces in bounded circular three body problem in presence of magnetic dipole, deriving Jacobi integral
01 p0127 A72-10358
- Rotating solar magnetic dipole with 26 7/8 day period from polar geomagnetic and spacecraft interplanetary field observations
02 p0277 A72-11899
- Magnetosphere deformation by solar wind, comparing accuracy of free molecular flow and double dipole models
02 p0218 A72-11948
- Weak dipole magnetic field effect on oscillation frequencies of conducting gaseous polytrope stars, using variational equation
02 p0260 A72-12310
- Rotating dipole sector structure of interplanetary and solar photospheric magnetic fields from spacecraft observations
[AD-740309] 03 p0437 A72-13871
- Electromagnetic pulsar models features and predictions, using rotating neutron stars with strong dipolar magnetic fields
03 p0437 A72-13873

- Geomagnetic dipole field kinematic reversals due to cyclonic convective cell distribution fluctuations in earth core
06 p0807 A72-17895
- Neutral current sheath formation from plane dipole magnetic field extension by plasma flow, discussing solar corona streamers and geomagnetic tail
07 p1039 A72-18914
- Secular geomagnetic dipole moment decrease effect on inner proton belt proton energy distribution, comparing with radial diffusion influences
07 p1058 A72-19159
- Semiconductors cyclotron echo signals from dipole interactions of electrons with alternating magnetic fields, discussing frequency doubling and excitation mechanism
07 p1048 A72-19639
- Two dimensional model for plasma without magnetic field trapped near current sheet end in dipole magnetic field resembling geomagnetic tail
08 p1157 A72-21108
- Power integral method for electric and magnetic dipole antennas vlf/elf radiation patterns in cold magnetoplasma, emphasizing focusing effects of refractive index surface
09 p1279 A72-23009
- Radiation pattern of longitudinal magnetic dipole near circular cylinder parallel to flat screen
10 p1453 A72-24903
- Magnetosphere neutral layer plasma conductivity determination from model of linear magnetic dipole in conducting fluid flow
11 p1622 A72-25945
- Changes in total magnetic energy stored outside earth core accompanying earth dipole field decrease over 60 years period from paleomagnetic measurement
11 p1623 A72-26108
- Magnetospheric midday boundary width dependence on geomagnetic dipole axis orientation, discussing different positions for magnetosphere boundary
11 p1628 A72-26914
- Magnetosphere deformation by solar wind, comparing accuracy of free molecular flow and double dipole models
13 p1949 A72-29260
- Dipolar coordinate system for geomagnetic field dipole approximation in studies of diffusion and heat conduction in F region and outer ionosphere
14 p2102 A72-30652
- Wave pattern of three dimensional hydromagnetic perturbations produced by harmonic magnetic dipole in anisotropic plasma
14 p2102 A72-30661
- Hydromagnetic waves excited by transverse magnetic dipole in finite-conductivity plasma
14 p2102 A72-30662
- Eccentric geomagnetic dipole drift field as function of time dependent parameters, calculating potential components in spherical coordinates
14 p2103 A72-30667
- Magnetic dipole or small current loop over homogeneous flat earth, calculating transient electromagnetic field for airborne remote sensing
15 p2224 A72-31672
- Ionospheric models with constant electron density contours axially symmetrical to earth centered dipole magnetic field, discussing radio ray paths
15 p2230 A72-32263
- Stationary plasma flow interaction with dipole magnetic field to study geophysical phenomena in upper atmosphere
15 p2286 A72-32343
- Electromagnetic radiation frequency spectrum and mean power from accelerated magnetic dipoles in circular and Keplerian orbits, noting implications for pulsars
16 p2453 A72-33285
- Experimental methods for studying interactions between plasma streams and three dimensional magnetic dipole fields
16 p2454 A72-33384
- Magnetic dipole matrix elements for atomic transitions between Zeeman levels at microwave frequencies
17 p2585 A72-35769
- Magnetic dipole field interaction with plasma flow ions, noting qualitative model of solar wind flow past magnetosphere
17 p2593 A72-35905
- Capture zone in noninteracting particles rarefied flow around magnetic dipole with transfer into finite orbits under small perturbations
17 p2593 A72-35906
- Drift characteristics of the main eccentric geomagnetic dipole
18 p2689 A72-36872
- Neutral current sheath formation from plane dipole magnetic field extension by plasma flow, discussing solar corona streamers and geomagnetic tail
20 p2957 A72-39380
- Interaction of a steady plasma flow with a dipole magnetic field in the presence of a radial electric field.
21 p3093 A72-41388

- Earth main magnetic field description by cartography and analytic methods based on dipole or spherical harmonic series representations
23 p3283 A72-43366
- The Z sub e field, some of its properties, and its geophysical informativeness
23 p3283 A72-43373
- Semiconductors cyclotron echo signals from dipole interactions with alternating magnetic fields, discussing frequency doubling and excitation mechanism
24 p3431 A72-44571
- MAGNETIC DISPERSION**
- Annealing effects in plated-wire memory elements, discussing recrystallization in Permalloy films from grain size and magnetic dispersion observations
04 p0504 A72-15716
- Magnetic stress anisotropy field in plated cylindrical Permalloy films, determining relationships to circumferential composition variation, geometry and easy-axis dispersion
04 p0564 A72-15717
- Ion trajectories equations of motion solution for E x B type mass separator, presenting curves for mass species dispersion inside separator channel
10 p1509 A72-23942
- Dispersion signal recording for klystron AFC radio spectrometer by low frequency magnetic field modulation
22 p3175 A72-41900
- Use of the simulation method for the solution of a dispersion problem for the propagation of symmetrical magnetic waves in a rectangular waveguide filled with a nonhomogeneous plasma
23 p3263 A72-43450
- MAGNETIC DISTURBANCES**
- NT MAGNETIC STORMS**
- Equivalent current system from measured geomagnetic disturbance vectors, solving Biot-Savart formula derived nonlinear equations by Newton-Raphson iterative method
01 p0055 A72-10430
- Soviet-French Project Omega for near space disturbance studies, using ground and balloon measurements at conjugate points
01 p0063 A72-11075
- Solar cosmic ray cutoff rigidity increase during polar cap absorption related to geomagnetic perturbation onset
02 p0273 A72-11938
- Chapman uniform electrical conductivity core model for geomagnetic disturbance daily variations due to solar wind, noting error in analysis
02 p0222 A72-12794
- Inner magnetosheath hydromagnetic disturbances, presenting magnetometer data in inclination-declination coordinate system
03 p0348 A72-13510
- Auroral absorption prediction during disturbed conditions in communications as function of frequencies and radio ranges at different geomagnetic time and coordinates
05 p0626 A72-16009
- Upper atmosphere supplementary electron flux data relationship to geomagnetic disturbance obtained from high altitude balloon experiments
05 p0709 A72-16236
- F 1 region ion structure during ionospheric magnetic disturbances by numerical simulation of quiet and disturbed conditions based on electron concentration profiles
05 p0656 A72-16247
- Magnetic perturbations in near polar region and morning-night sectors of auroral oval as function of current sources and modulation by universal time
05 p0657 A72-16276
- Additional high energy electrons flux detection in upper atmosphere after magnetic perturbations
05 p0710 A72-16525
- Magnetic baylike disturbances and multiple midlatitude 6300-A auroral arcs during geomagnetic storm recovery phase and concurrent ionospheric current recovery
05 p0630 A72-16620
- Geomagnetic disturbances morphology, considering development and decay of magnetic storms and appearance of geomagnetic pulsations
06 p0802 A72-17367
- F region electron density variation above North America during geomagnetic disturbance on 28 May 1970
[AD-739792] 07 p0976 A72-19162
- Radio auroral electrojet aspect sensitivity and Farley two stream instability, discussing magnetic field distortion and orthogonal deviation as function of current strength and direction
07 p0976 A72-19163
- High time resolution of low latitude asymmetric disturbances in geomagnetic field by Fourier analysis for substorm activity studies
07 p0976 A72-19165
- Interplanetary origin of magnetospheric electric fields responsible for polar magnetic disturbances
07 p0979 A72-20382

Magnetic disturbance singularities searched for in horizontal intensity, showing field depressions around September 5 07 p0980 A72-20406

Ring current growth effects on midlatitude F region electron density change during large magnetic disturbances 08 p1152 A72-20706

Geomagnetic effect of solar wind rotational discontinuity observed by Explorer 34, noting high latitude nonstationary ionospheric current attenuation and magnetic disturbances 08 p1225 A72-20715

Solar unipolar magnetic regions relation to geomagnetic disturbances variability, discussing 11 year cycle 08 p1155 A72-20808

Geophysical data analysis for high latitude negative geomagnetic disturbances revealing geomagnetic pulsations during auroral arcs passage 08 p1155 A72-20809

Solar wind flux velocity diurnal variations relation to magnetic activity index based on Mariner 2 and 4, Pioneer 6 and Vela satellites data 08 p1226 A72-20821

Interplanetary magnetic field perturbations by solar wind and moon, noting lunar wake anomalies positive correlation with plasma beta value 09 p1387 A72-23003

Solar wind kinetic energy from flare associated solar wind disturbances relation to types 2 and 4 radio bursts, using satellite observations 09 p1378 A72-23399

Equatorial sporadic E sudden disappearance associated with magnetic field depressions, noting irregularities and electron velocities role 10 p1475 A72-24956

Ionospheric and magnetic disturbances effects on short wave radio links, using directional antennas and 1.5-24 MHz frequencies 11 p1594 A72-26279

Interplanetary magnetic field direction and high latitude ionospheric currents in dayside auroral regions, showing plasma drift induced magnetic disturbances 11 p1626 A72-26419

Magnetic disturbances recurrence relationship to even- and odd-numbered sunspot cycles, noting existence of 22-year solar cycle 12 p1803 A72-27773

Cosmic ray diffusion in radial divergent flow of magnetic discontinuities in interplanetary plasma, discussing isotropy in presence of regular magnetic field 13 p2029 A72-28591

Pc 5 type geomagnetic pulsations correlation with nighttime magnetosphere auroral magnetic disturbances from magnetograms obtained at Murmansk, College /Alaska/ and Tiksi 13 p1947 A72-28606

Solar cosmic ray cut-off rigidity increase during PCA related to geomagnetic perturbation onset 13 p2030 A72-29250

Ring current and polar electrojet effects on proton auroras oval during magnetic disturbances from H alpha line observation 13 p1952 A72-29659

Hyperfine magnetic field reduction produced in Fe-Cr alloy single crystal by Cr atoms observed by Mossbauer method, proposing spin disturbance mechanism 15 p2293 A72-32230

The perturbation of alternating geomagnetic fields by three-dimensional conductivity inhomogeneities 17 p2545 A72-34350

Auroral motion analysis based on baylike disturbances against quiet field background during polar substorm 17 p2550 A72-35858

Electron profiles during negative magnetic bays in the auroral zone 17 p2551 A72-35860

VLF hiss intensity, polarization, incidence angle and arriving direction observation at Antarctica station during magnetic disturbances 18 p2660 A72-36431

Ring current growth effects on midlatitude F region electron density change during large magnetic disturbances 19 p2790 A72-38334

Quasi-periodic variation in F 2 layer reflected signal field strength, noting predominance during periods with type 4 bursts, auroras and geomagnetic disturbances 19 p2792 A72-38639

The Harang discontinuity in auroral belt ionospheric currents. 20 p2920 A72-39980

Aspect-sensitive reflections from ionization irregularities in the F-region. 22 p3154 A72-42364

Sea level tropospheric pressure distribution persistence correlation to solar corpuscular radiation measured by planetary scale geomagnetic disturbance 22 p3219 A72-42517

Outer magnetosphere near midnight at quiet and disturbed times. 23 p3341 A72-44513

Energy releases in the upper atmosphere during geomagnetic disturbances. 24 p3396 A72-44847

Geomagnetic tail magnetic and electric fields ULF, VLF and ELF fluctuations, considering relationship to substorm processes 24 p3397 A72-44857

Polar cap magnetic field induced by currents along magnetospheric lines of force during polar substorm 24 p3397 A72-45087

Cosmic ray diffusion in radial divergent flow of magnetic discontinuities in interplanetary plasma, discussing isotropy in presence of regular magnetic field 24 p3435 A72-45091

Pc 5 type geomagnetic pulsations correlation with nighttime magnetosphere auroral magnetic disturbances from magnetograms obtained at Murmansk, College /Alaska/ and Tiksi 24 p3398 A72-45106

MAGNETIC DOMAINS

Single domain grain distribution deduction method obtained from Neel theory, applying to Apollo 11 lunar dust iron grains 01 p0125 A72-10071

Domain configuration observation of magnetic holograms in oriented MnBi films 03 p0359 A72-13447

Magnetostatic interactions of cylindrical magnetic domain propagation circuits in ferromagnetic overlay without in-plane fields [IEEE PAPER 2,1] 03 p0331 A72-13752

Logic functions for magnetic bubble devices based on interaction of circular magnetic domains in rare earth iron oxides, considering gates for dynamic memory [IEEE PAPER 2,3] 03 p0327 A72-13753

Low birefringent orthoferrites for optical devices, considering improvement in Faraday rotation detection of magnetic domains in single crystal platelets [IEEE PAPER 10,10] 03 p0360 A72-13760

Magnetic domain structure of Ni single crystals after plastic deformation as function of stress induced anisotropy of layer-like dislocations 07 p1020 A72-20411

Magnetic domains in cobalt and cementite observed by electron microscopy, investigating thin film thickness effect on temperature 10 p1496 A72-24088

Bloch walls and Landau domain configurations in iron whiskers from DC to 200 kHz by direct magnetization measurements 11 p1659 A72-25912

Diffraction of a laser beam by domains in yttrium iron garnet. 20 p2933 A72-39521

Gunn effect threshold and domain formation in transverse magnetic fields in indium antimonide. 20 p2960 A72-39566

Bubble and strip magnetic domains creation, annihilation and manipulation in epitaxial magnetic garnet films by laser beam thermal absorption induced local heating 22 p3185 A72-42612

MAGNETIC DRUMS

Error probability distribution of digital data magnetic recording in computer drum memory 16 p2367 A72-33262

Plated wire associative memory elements. 17 p2523 A72-35172

MAGNETIC EFFECTS

NT MAGNETIC RIGIDITY

Transient shock produced plasma flow interactions with transverse magnetic field 01 p0105 A72-10020

Similarity theory for electrostatic and magnetic collisionless shocks at zero ion temperature, using numerical simulation results 01 p0106 A72-10029

HF capacitive discharge plasma resonance under weak transverse magnetic field in vacuum 01 p0106 A72-10041

Rankine vortex conducting gas rotating about cylinder axis, investigating magnetic field effects on transverse waves 01 p0106 A72-10132

Two dimensional plasma under dc magnetic field, investigating thermal equilibrium with Liouville equation and BBGKY hierarchy 01 p0107 A72-10145

Flow characteristics, wave propagation and thermal stability of ferrofluids within uniform magnetic field 01 p0050 A72-10235

Magnetic transformation effect on creep behavior of fcc nickel-cobalt alloy compared with self diffusion data in Curie temperature vicinity 01 p0083 A72-10391

Magnetic declination effect on elevation control of F 2 layer maximum, considering east component of geomagnetic field from Capetown and Canberra observations 01 p0054 A72-10427

Ideally conducting plasma confined in vacuum by circularly polarized magnetic field, investigating MHD instabilities suppression by distributed automatic control system 01 p0109 A72-10503

Magnetic field effects on ruby laser radiation kinetics and spectral composition, studying crystal heating and light emission 01 p0080 A72-10577

Interplanetary magnetic field angular gradient and sectorial effects on solar wind, discussing wind velocity 01 p0118 A72-10583

Midlatitude vhf phase detection of magnetic field aligned ionospheric irregularities 01 p0031 A72-10916

Similarity models of interstellar loop structures, investigating magnetic field and energy losses effects and cosmic ray emission 01 p0131 A72-11011

Magnetoplasmadynamic supersonic ring duct as electromagnetic shock tube or plasma gun, emphasizing plasma flow-magnetic field interaction 01 p0110 A72-11204

MHD boundary layer calculation for conducting fluid along semiinfinite flat plate with transverse magnetic field, deriving momentum and kinetic energy integral equations 01 p0113 A72-11383

Strain gage and manganin pressure gage instrumentation for magnetic driven flyr plate facility [MDAC-WD-1700] 02 p2223 A72-11502

Nonuniform magnetic field effects in MHD slider bearing, showing inertia terms contribution dependence on Hartmann number [ASME PAPER 71-LUB-8] 02 p0235 A72-11533

Electron beam interaction with electromagnetic waves in longitudinal interaction devices during focusing by homogeneous magnetic and periodic electrostatic fields 02 p0189 A72-11564

Periodic magnetic field effects at gun cathode on electron beam focusing stability under nonoptimal conditions 02 p0190 A72-11572

Axisymmetric inviscid compressible transonic flow of electrically conducting, heat nonconducting gas in Laval nozzle in presence of meridional magnetic field, deriving equations for magnetic effects on dynamic flow characteristics 02 p0149 A72-11576

Quantum oscillations of minority Fermi surface carriers as function of magnetic field in Hall effect and thermoelectric power in pressure-annealed pyrolytic graphite 02 p0268 A72-11673

Rarefied plasma hydrodynamic equations for rotational discontinuities in solar wind, discussing magnetic field modulus jumpwise changes 02 p0272 A72-11915

Heat transfer from augmented flames and plasma jets based on magnetically rotated arcs, measuring transfer rate as function of electromagnetic torque 02 p0301 A72-12031

Parallel longitudinal resonant slots in rectangular waveguide broad wall, determining mutual impedance from magnetic field reaction 02 p0173 A72-12109

Viscous friction effects on phonon-electron interactions and dislocation velocity by deformation measurement of metallic crystals under pulsating magnetic fields 02 p0243 A72-12169

Weak dipole magnetic field effect on oscillation frequencies of conducting gaseous polytrope stars, using variational equation 02 p0260 A72-12310

Meteor trail forms diversity explanation from magnetic pressure and Reynolds number and plasma diffusion in magnetic fields, discussing geomagnetic effect on trail shape 02 p0282 A72-12336

Periodic solar flare modulation by pulsating structure, attributing radiation to synchrotron radiation emitted by electrons in magnetic tube embed in solar corona 02 p0274 A72-12412

Coulomb logarithm for hot plasma viscosity coefficient in magnetic field by quantum mechanical unified theory 02 p0267 A72-12770

MHD flow due to impulsive rotation of infinite disk, observing magnetic field strength effects on velocity components and boundary layer displacement thickness 02 p0267 A72-12772

Charged particle motion in strong magnetic field, considering magnetic moment and longitudinal adiabatic invariants 02 p0268 A72-12843

Magnetic field effect on Gunn diode oscillator frequency and output power, discussing strong field domain 02 p0196 A72-12885

Geomagnetic field effect on radar echoes from meteor trains during Geminid shower

03 p0345 A72-12982

Magnetic field role in Ap stars abundance peculiarities model, discussing rotational circulation, convection, accretion and mass loss effects on surface

03 p0416 A72-13010

Conducting fluid steady MHD pipe flow under transverse magnetic field, obtaining mass flow rate

03 p0394 A72-13241

Magnetic splitting of lines dependence on Paschen-Back effect for Li resonance doublet in sunspots

03 p0427 A72-13293

Filamentary magnetic structure production on plasma current sheath of coaxial deuterium operated accelerator for laboratory observations of solar flare processes

03 p0411 A72-13338

Coronal rotation determination by spectroscopic method for mean rotation rate vs heliographic latitude, confirming high latitude phenomena dependence of low latitude magnetic fields

03 p0432 A72-13352

Equilibrium state linear theta pinch plasma confinement dependence on nonuniform magnetic force lines curvature radius

03 p0396 A72-13655

Moving plasma beam capture by transverse magnetic field due to polarization space charges electrostatic separation

03 p0396 A72-13657

Microwave propagation through laminated metallic media with gyromagnetic effects, applying dc magnetizing field normal to film plate [IEEE PAPER 31,6]

03 p0323 A72-13784

Potentials, currents and velocity variation of rotating conducting disk system in liquid metal medium under uniform longitudinal magnetic field

03 p0397 A72-13996

Annular MHD channel laminar flow generation at supercritical Reynolds numbers by strong magnetic fields

03 p0398 A72-14005

Visual investigation of semibounded axisymmetric MHD flow of liquid eutectic K-Na alloy under strong magnetic field effect

03 p0399 A72-14014

Second harmonic generation, coherence lengths and second order susceptibilities near band edge in InSb as function of magnetic field

03 p0404 A72-14269

Absorption effects on circular polarization in synchrotron radiation, discussing frequency and magnetic field dependence

04 p0570 A72-14550

Uniform normal magnetic field effect upon MHD free convection from vertical wall with instantaneous heat source, considering shear stress

04 p0556 A72-14856

Interstellar electron density and magnetic field fluctuations effects on Faraday rotation and signal dispersion measure in radio band

04 p0487 A72-14901

Geomagnetic effects on lower ionosphere at lower midlatitude station, discussing long wave propagation

04 p0516 A72-14939

Planetary magnetic activity effects on hf cosmic noise absorption measurements at low and temperature latitudes

04 p0516 A72-14941

Ionospheric plasma drift instability, showing electric and magnetic fields, electron density and temperature effects

04 p0517 A72-14956

Finite Larmor radius effect on Rayleigh-Taylor plasma instability in vertical magnetic field, characterizing solution by variational principle

04 p0557 A72-15022

Nonuniform radial electric field effects on low beta magnetized plasma column stability from numerical analysis for weakly collisional regime

04 p0557 A72-15023

Time dependent hydromagnetic oscillations in contained rotating conducting fluid under magnetic field, using interior boundary layer expansion

04 p0549 A72-15115

Longitudinal ultrasonic sound attenuation in superconducting Mo-Re alloys as function of temperature, magnetic field and frequency, using evaporated thin film Cds transducers

04 p0562 A72-15295

Cylindrical grid-like antenna in anisotropic compressible homogeneous plasma, obtaining magnetic field effects on wave dispersion by numerical solution

04 p0488 A72-15306

Conducting incompressible fluid in laminar pipe flow under traveling magnetic field, investigating friction coefficient and energy balance

04 p0558 A72-15341

Magnetic field effect on heat transfer in steady plane laminar conducting incompressible viscoelastic liquid flow in channel with nonconducting walls

04 p0560 A72-15580

Magnetic damping comparison with internal viscous damping effect on circulatory elastic system equilibrium stability

05 p0689 A72-16061

Electrical conduction in orthogonal coordinates from nondipole geomagnetic field effect on conductivity tensor of ionospheric dynamo region

05 p0657 A72-16260

Magnetic storm disturbing effect on integral electron density in F2 layer and in topside ionosphere

05 p0657 A72-16262

Lower ionospheric currents fields, determining Hall conductivity and geomagnetic lines of force slope effects

05 p0657 A72-16266

Intestinal disbarteriosis and autoinfection occurrence in guinea pigs and rats under magnetic field effect, noting Escherichia population changes

05 p0622 A72-16647

Parallel and perpendicular magnetic field effects on optically injected electron-hole plasma diffusion in Ge from density measurement by infrared beam absorption technique

05 p0702 A72-17167

MHD flow of viscous fluid between two oscillating flat plates, observing velocity damping by magnetic field

05 p0699 A72-17179

Moderate Hartmann number MHD duct flow with applied transverse magnetic field, using numerical methods

06 p0859 A72-17619

Electron density distribution inhomogeneities from vhf Faraday rotation measurements, noting diurnal, seasonal, sunspot cycle and geomagnetic activity effects

06 p0806 A72-17642

Plane supersonic ionizing shock wave in magnetic field under small wave plane perturbation from equilibrium position, calculating stability from linearized equations

06 p0798 A72-17678

Force-free magnetic fields effects on plasma column stability

06 p0860 A72-17744

Stability of weakly ionized homogeneous plasma placed in weak microwave field and in constant magnetic field, expressing growth increments of longitudinal waves

06 p0861 A72-17902

Transverse ionizing shock waves in gaseous hydrogen at speeds to 4000 km/sec, presenting magnetic shock structure and magnetic field jump measurements [AD-738620]

06 p0863 A72-18531

Magnetic effects on Lorentz plasma collision processes, calculating electron distribution function in presence of strong arbitrarily oriented magnetic and weak electric fields

06 p0864 A72-18535

Shear layer finite thickness and magnetic field effects on Kelvin-Helmholtz MHD instability of earth magnetopause boundary [AD-746435]

07 p0974 A72-18892

Exponential conduction increase of semiconductors in strong magnetic fields, determining three dimensional random network resistance with percolation theory

07 p1047 A72-18918

Pulsar dynamics and electrodynamics for power derivation from rotational energy, discussing toroidal magnetic field induced nonhydrostatic stress in neutron star

07 p1068 A72-19001

Pitch angle distributions of energetic protons for different geomagnetic activity levels as function of invariant latitude and magnetic local time from ESRO IB satellite measurements

07 p1057 A72-19141

Sound velocity and attenuation variations with magnetic field from ultrasonic continuous wave spectrometry

07 p0984 A72-19321

Magnetic bremsstrahlung energy straggling and radiation reaction, calculating particle and emitted photon distribution

07 p1037 A72-19668

Temperature pulsation spectra of turbulent mercury flow in horizontal pipe at various Reynolds numbers, showing dependence on magnetic field

07 p1100 A72-19882

Reverse deflection and contraction of collisionless plasma beam during motion along curved magnetic field lines

07 p0979 A72-20378

Duskside magnetic activity relationship with bulge detection by whistler method, investigating plasmopause deformation

07 p0979 A72-20381

Plasma lf waves nonlinear spectral broadening in magnetic field based on degeneracy splitting

07 p1045 A72-20443

Refraction of electromagnetic wave with electric field perpendicular to applied magnetic field in anisotropic plasma cylinder cross section

07 p1046 A72-20507

He-Ne laser discharge gap oscillation modes observation, noting applied magnetic field, gas parameters and cathode type effects on stimulated emission

07 p1008 A72-20510

Geomagnetic effect of solar wind rotational discontinuity observed by Explorer 34, noting high latitude nonstationary ionospheric current attenuation and magnetic disturbances

08 p1225 A72-20715

Atmospherical model for plasma motion along surface of geomagnetic tail under action of interplanetary, magnetic lines of forces

08 p1153 A72-20722

Outer radiation belt parameters dependence on interplanetary magnetic field sectorial structure and solar wind velocity

08 p1226 A72-20811

Intraband multiphoton conduction-electron transfer probability in semiconductor under electromagnetic wave action in uniform magnetic field

08 p1216 A72-21066

Magnetic field effect on elf radio wave attenuation during propagation under six ionospheres, showing dependence of minimum on propagation path geomagnetic latitude

08 p1131 A72-21103

Steady state problem of energy spectrum of variable magnetic field accelerated electrons, considering synchrotron X ray emission of Crab pulsar and nebula

08 p1231 A72-21119

Moment of forces on spacecraft with low angular velocities in variable magnetic field, using electrodynamics equations

08 p1240 A72-21140

Induced nonuniform magnetic field effects on MHD channel flow between two infinite parallel plates, obtaining solution by perturbation theory

08 p1214 A72-21427

MGD equations for ideal plasma steady plane adiabatic flow in magnetic field, considering analogy to Chaplygin equations

08 p1214 A72-21645

Supersonic plasma flow in narrow rectangular channel and free incompressible inviscid conducting liquid jet motion within pulsating transverse magnetic field

08 p1214 A72-21652

Stagnation conditions of magnetoradiative supersonic flow through shock waves for temperature dependent specific heat parameter

08 p1255 A72-21795

Electron plasma fluctuations in semiconductor with nonparabolic conduction band under external electric and magnetic fields

08 p1218 A72-21877

Magnetic field effect on gain saturation in CW Ar laser associated with Zeeman splitting

08 p1184 A72-22036

Microwave induced dc voltages across unbiased Josephson tunnel junctions, showing power spectra dependence on magnetic field

09 p1367 A72-22458

Rotating stellar system with stars and interstellar gas within magnetic field, discussing gravitational and magnetic effects on gas pressure

09 p1384 A72-22511

Geomagnetic field effects on initially spherically symmetric ion cloud diffusive motion in earth upper atmosphere

09 p1297 A72-22577

MHD stability problems in radio galaxy structure and cosmic ray interaction with magnetic fields

09 p1386 A72-22751

Inhomogeneous superconductors and proximity effects, calculating conditions for vortex lattice pinning energy as increasing function of magnetic field and temperature

09 p1370 A72-22798

Hydrodynamic stability of electrically conducting hot viscous fluid surrounded by perfectly conducting rigid boundary in presence of magnetic field

09 p1359 A72-22825

Short plasmoids production in hydrogen plasma jets by applying pulsed multipole magnetic field generated in linear quadrupole system

09 p1362 A72-23203

Magnetic field effect on threshold pressure reduction for He and Ar gas breakdown by carbon dioxide laser radiation, taking into account inhibition of radial electron diffusion [AD-741539]

09 p1365 A72-23493

Perfectly conducting incompressible fluid motion past thin body in oblique field, discussing magnetic field influence on lift

09 p1365 A72-23559

Strong magnetic fields and electric current densities effects on acoustic oscillations and instability in stationary inhomogeneous low temperature plasma flow in crossed fields

10 p1517 A72-23838

- Input impedance of plane antenna immersed in plasma within magnetic field and propagating sheath waves 10 p1520 A72-24132
- Electromagnetic waves penetration through magnetized plasma into lower hybrid resonance region examined in geometrical optics approximation 10 p1521 A72-24352
- Dislocation structure analysis in ferromagnetic materials by magnetic techniques, discussing methods based on magnetization curve static properties and magnetic relaxation phenomena 10 p1487 A72-24574
- Cosmic ray ionization rate for hydrogen calculated for ambipolar diffusion efficiency in decoupling magnetic flux from gas during cloud collapse with angular momentum 10 p1544 A72-24664
- Combined plasma and magnetic field cumulation due to heavy conducting liner implosion, noting compression parameters for plane and cylindrical bodies 10 p1523 A72-24723
- Magnetic simulation of gravity for wind tunnel investigations of aircraft jetison processes, considering Froude number and relationships between model and full scale aircraft 10 p1462 A72-24775
- Linear wave dispersion in homogeneous beam plasma system, considering pressure anisotropies generated by external magnetic field 10 p1524 A72-24927
- Magnetometers for balloon-borne X ray astronomy payload azimuth determination, noting misorientation, earth and spurious magnetic fields effects on measurement effectiveness 10 p1530 A72-24954
- Sporadic E layer variations monitoring in 50 MHz band, examining diurnal, seasonal, magnetic and meteoroid showers relationships of oblique incidence paths 10 p1441 A72-25152
- Uniform and parallel magnetic field effects on hydromagnetic instability of two dimensional jet at small magnetic Reynolds numbers 11 p1693 A72-25521
- Small gap approximation for axial magnetic field effects on stability of nonrotationally symmetric disturbances in inviscid flow between concentric rotating cylinders 11 p1694 A72-25773
- Plasma equilibrium configurations, considering magnetically contained focus in external magnetic field 11 p1694 A72-25788
- Astronomical models of solar wind interaction with interstellar medium, determining magnetic field effects on shock wave 11 p1713 A72-25946
- Magnetic phenomena effects on superconductivity in simple and transition metals and dilute rare earth alloys 11 p1701 A72-26025
- Quasi-steady operation establishment in pulsed MPD arc jet, investigating ion density radial distribution and initial tank pressure and magnetic field effects on plasma front arrival [ALAA PAPER 72-496] 11 p1696 A72-26219
- Solenoid-produced local axial magnetic field influence on beat signal frequency characteristics in ring laser with nearly linearly polarized emission 11 p1650 A72-26357
- Rare gas ion laser excited by electrodeless microwave discharges, noting external magnetic field effects on output 11 p1651 A72-26571
- Ni powder artificial dielectric in waveguide transverse magnetic field, noting nonreciprocal nature of microwave attenuation and phase shift 11 p1607 A72-26786
- Magnetospheric midday boundary width dependence on geomagnetic dipole axis orientation, discussing different positions for magnetosphere boundary 11 p1628 A72-26914
- Predawn effect on hot and cold electrons at magnetoconjugate point in F 2 layer, discussing electron shock wave speed and thermal collisionless wave energy dissipation 11 p1628 A72-26916
- Magnetic field gradient in sunspot umbrae from magnetically split line profiles 12 p1867 A72-27206
- Unsteady viscous incompressible electrically conducting fluid flow generated by porous disk rotation, investigating transverse magnetic field effect 12 p1851 A72-27305
- Localized magnetic field for wind tunnel wall-plasma heat transfer minimization, preserving flow characteristics 12 p1852 A72-27684
- Remanent lunar magnetic field compression by solar wind from magnetic measurements at Apollo landing sites 12 p1871 A72-27691
- Magnetic field effect on ruby laser generated plasma in solid target, measuring thermal ion energy increase 12 p1852 A72-27879
- Geomagnetic field perturbation biological effects, studying geomagnetic storm field energy levels and magnetic flux variables relation to human sensitivity thresholds 12 p1773 A72-28210
- Magnetic storm strength ELF electromagnetic field effects on rabbits, dogs and bacteria, discussing changes in EEG, ECG and blood characteristics 12 p1763 A72-28214
- Signal propagation along homogeneous drifting electron beam focused by strong magnetic field, obtaining phase velocity and space charge density 13 p1914 A72-28373
- Plasma heating by HF electrostatic instabilities excitation with current across external magnetic field, estimating turbulence, ion collision frequencies and ion heating rates 13 p2009 A72-28426
- External magnetic field effect on two frequency quadrupole spin echo in polycrystalline specimen 13 p1915 A72-28473
- Probe triggered audio frequency plasma oscillation period dependence on applied magnetic field and discharge current 13 p2010 A72-28544
- Meteor-induced magnetic effect on cosmic ray intensity for meteor streams with orbits normal or parallel to interplanetary magnetic field lines of force 13 p2029 A72-28592
- Local perturbation generated waves in homogeneous plasma at rest subjected to uniform magnetic field 13 p2010 A72-28680
- Electromagnetic wave propagation in cylindrical plasma column of electrons and ions with and without applied uniform magnetic field in absence of collisions 13 p2010 A72-28681
- Effect of magnetic field superimposed on turbulent shear flow of electrically conducting fluid, discussing turbulent friction in plane flow 13 p2010 A72-28764
- Uniform vertical magnetic field effect on Ekman layer over horizontal plate at rest relative to rotating conducting liquid 13 p2011 A72-29006
- Meteor trail forms diversity explanation from magnetic pressure and Reynolds number and plasma diffusion in magnetic fields, discussing geomagnetic effect on trail shape 13 p2039 A72-29220
- Hall currents effect on unsteady MHD flow of electrically conducting fluid past flat plate imbedded in uniform external transverse magnetic field 13 p2012 A72-29225
- Rarefied plasma hydrodynamic equations for rotational discontinuities in solar wind, discussing magnetic field modulus jumpwise changes 13 p2030 A72-29227
- O-type synchronous electron beam waves interaction with electrostatically structured traveling wave, noting linear gain dependence on beam current and magnetic field 13 p1931 A72-29291
- Fluctuating electric current induced magnetic field effects on long wave nonequilibrium plasma instability associated with large scale closed cycle MHD generators 13 p2014 A72-29370
- Electroacoustomagnetic and Hall effects in semiconductors within strong electric field involving phonon production by supersonic electron drift 13 p2022 A72-29437
- Alternating magnetic field effect on collisionless nonhomogeneous magnetoplasma ion acoustic oscillations stability, examining parametric excitation of Langmuir oscillations 13 p2016 A72-29604
- Transverse magnetic field effect on electron temperature and energy distribution and spectral lines of gas discharge plasma 13 p2017 A72-29635
- VLF long distance radio propagation in earth-ionosphere waveguide, considering earth magnetic field effects in mode conversion and refraction error calculation 13 p1922 A72-29655
- Low temperature homogeneous plasma electric conductivity in magnetic field, noting monotonic decrease 13 p2018 A72-29892
- Visible light flash emission due to strong shock wave of laser spark, investigating strong external magnetic field effect and time variation of luminous intensity 13 p1972 A72-29983
- Density and electric field oscillations of plasma in stellarator, considering magnetic field strength effect, stabilization by ionic collisions and energy pumping mechanism 13 p2019 A72-29985
- Tangential MHD discontinuity stability for ideally conducting compressible fluid in magnetic and gravitational fields 13 p2020 A72-30068
- Range and frequency spread F diurnal and seasonal variations at magnetic equatorial station Thumba, noting geomagnetic activity effect 14 p2097 A72-30130
- He and Ar plasma transport by magnetic fields after expulsion from pulsed linear discharge 14 p2135 A72-30167
- Plasma capture by stellarator diverter magnetic field, noting stream length controllability by field pulse duration 14 p2135 A72-30168
- Sunspot formation due to magnetic flux concentration in active region and formation of invisible pores with suppressed granular motion 14 p2148 A72-30205
- Plasma heating in Tuman 2 toroidal magnetic trap by microwave injection at upper hybrid frequencies 14 p2137 A72-30311
- Experimental investigation of electrostatic cyclotron harmonic waves excited in inhomogeneous plasma column with axial magnetic field by RF capacitor field 14 p2138 A72-30398
- Cylindrical model of interplanetary magnetic field-moon interaction, taking into account solar wind flow boundary condition asymmetries 14 p2154 A72-30514
- Magnetic and electric field effects on steady state laminar MHD Couette flow of non-Newtonian fluids governed by Prandtl rheological law or Ostwald-de Waele power law 14 p2139 A72-30717
- Dc arc plasma, investigating applied magnetic field, trace elements and gap spacing effects on spectral line intensity spatial distribution 14 p2139 A72-30783
- Weber experiment gravitational signals correlation to solar and geomagnetic activity and cosmic ray intensity 14 p2160 A72-30886
- Uniform rotation and magnetic field effects on gravitational stability of interface between two semi-infinite homogeneous streams 15 p2284 A72-31593
- Transverse magnetic field effects on n-type GaAs Gunn diodes microwave power, coherence and dynamic I-V characteristics [ONERA, TP NO. 1051] 15 p2207 A72-31884
- Falkner-Skan problem extension to MHD flow past nonconducting body by imposing magnetic field with lines of force parallel to undisturbed streamlines 15 p2287 A72-32405
- Induced magnetic field effects on MHD flow between rotating coaxial [insulator/ cylinders, obtaining exact solution and graphical results 15 p2288 A72-32420
- Fast pressure gage with protection against magnetized plasma parasitic effects to measure neutral pressure 15 p2241 A72-32439
- Spectroscopic analysis of condensations density and intensity variations in solar eruptive prominences, discussing hypothetical magnetic field effects 15 p2318 A72-32781
- Quasi-linear approximation of absorption of oscillations excited by electron beam in nonuniform plasma, noting electron distribution change with heating under magnetic field 16 p2432 A72-32807
- Thermonuclear microexplosion ignition by bombarding dense target with intense relativistic electron beam, noting energy requirement reduction by self magnetic beam field 16 p2433 A72-32814
- Cylindrical antenna immersed in weakly ionized magnetoplasma, calculating steady magnetic field effect on electromagnetic and electroacoustic radiation resistances 16 p2434 A72-32860
- Quantum mechanics framework for electron movement perpendicular to intense magnetic field, predicting energy broadening with time for initially monoenergetic electron beam 16 p2422 A72-32881
- Shock wave generation by high current pulsed discharges, determining shock front velocity as function of magnetic pressure on current sheath 16 p2434 A72-32909
- Low energy outer zone electrons high latitude boundary variation with interplanetary magnetic field direction and with geomagnetic activity from Alouette and Explorer data 16 p2382 A72-32957
- Magnetic field effect on finite amplitude convection in fluids complying with Boussinesq approximation, discussing maximum Nusselt number shift 16 p2452 A72-33039
- Ionospheric electron content semiannual and seasonal variations as function of solar and geomagnetic activity from low and mid-northern latitude observations 16 p2385 A72-33378
- Magnetic field effect on polarization plane rotation and emission frequency shift of He-Ne ring laser at 3.39 micron wavelength 16 p2402 A72-33485

Plane hydromagnetic wave propagation in rotating fluid permeated by variable magnitude and direction magnetic field, observing wave-associated critical level

16 p2436 A72-33567

Solenoid-produced local axial magnetic field influence on beat signal frequency characteristics in ring laser with nearly linearly polarized emission

16 p2403 A72-33710

Cosmic ray isotopic data extraction via geomagnetic field, discussing magnetic effects on particle flux and finite resolution limitations of counters

16 p2447 A72-33728

Magnetic field effect on ruby laser generated plasma in solid target, measuring thermal ion energy increase

16 p2439 A72-33988

Magnetogasdynamic heat transfer to hemispherical body in supersonic low density plasma, noting magnetic field effects on heat flux

[AIAA PAPER 72-686] 16 p2346 A72-34056

Magnetoelastic buckling of beams and thin plates of magnetically soft material.

[ASME PAPER 72-APM-35] 17 p2624 A72-34311

Superconductivity.

17 p2594 A72-34565

Effect of a transverse magnetic field on the operation of a thermionic converter under undercompensated Knudsen conditions.

17 p2497 A72-34862

Electromagnetic waves penetration through magnetized plasma into lower hybrid resonance region examined in geometrical optics approximation

17 p2589 A72-34953

Russian book - Effect of magnetic fields on biological objects

17 p2502 A72-35001

Physical phenomena occurring in living objects under the action of constant magnetic fields

17 p2502 A72-35002

Magnetic field effects in enzymes, tissue respiration and some metabolism characteristics of an intact organism

17 p2503 A72-35003

Effects of magnetic fields on microorganisms

17 p2503 A72-35004

Mechanism of the biological action of a constant magnetic field

17 p2503 A72-35005

Action of a constant magnetic field on plant growth

17 p2503 A72-35006

Influence of a magnetic field on radiation-induced chromosome aberrations in plants

17 p2503 A72-35007

Pathologic-anatomic characterization of changes induced by magnetic fields in experimental animals

17 p2503 A72-35008

The magnetic field, infection and immunity

17 p2503 A72-35009

Effect of a magnetic field on the nervous system

17 p2503 A72-35010

Effect of a magnetic field on experimental tumors /direct and via nervous system/

17 p2503 A72-35011

Clinical hygienic and experimental data on magnetic field effects under working conditions

17 p2503 A72-35012

Methodical and methodological characteristics of a magneto-biological experiment

17 p2503 A72-35013

Generalization of basic equations of aerodynamics and electrodynamics.

17 p2539 A72-35043

Geomagnetically trapped alpha particles. I - Off-equator particles in the outer zone.

17 p2548 A72-35595

Geomagnetic effect on the neutral temperature of the F region during the magnetic storm of September 1969.

17 p2549 A72-35603

Transverse magnetic field effects on cylindrical hollow cathode discharge voltage-current characteristics, noting sustaining potential and recombination probability changes

17 p2593 A72-35886

Motion of a sphere in an electrically conducting rotating fluid.

18 p2714 A72-36123

The influence of magnetic pressure on the performance of a high-current discharge thermionic converter

18 p2646 A72-36195

The influence of a nonuniform transversal magnetic field on the power output of a gas laser.

18 p2715 A72-36338

On disturbances in a viscoelastic rod /of variable cross-section/ of Reiss type placed in a magnetic field.

18 p2711 A72-36752

Radial vibration of a composite cylindrical shell subjected to a magnetic field.

18 p2711 A72-36753

On axisymmetric vibration in a transversely isotropic finite cylindrical shell acted upon by a magnetic field.

18 p2711 A72-36755

Fast magnetoacoustic wave interaction with shock wave propagating in ideal electrically conducting gas, showing magnetic field stabilizing effect

18 p2711 A72-36812

Dependence of sporadic ionization in the high-latitude ionospheric E-region on magnetic activity

18 p2688 A72-36860

Lunar electrical conductivity.

18 p2729 A72-37000

Longitudinal waves in a perpendicular collisionless plasma shock. IV - Gradient B.

19 p2838 A72-37329

Beam-defocusing effect due to filament magnetic fields in electron guns of electron linear accelerators.

19 p2772 A72-37404

Permanent rotations of an equatorial satellite in the geomagnetic field

19 p2869 A72-37437

Effect of magnetic field on the performance of millimeter-wave detectors using bulk InSb.

19 p2772 A72-37570

Energy exchange processes in solar flares, noting initial derivation of energy from changing magnetic fields within solar atmosphere

19 p2850 A72-37782

Equations for electron and high-energy photon transfers in magnetic fields

19 p2837 A72-38059

Geomagnetic effect of solar wind rotational discontinuity observed by Explorer 34, noting magnetic storm initial phase relation to high latitude nonstationary ionospheric current attenuation

19 p2852 A72-38343

Atmospheric model for plasma motion along surface of geomagnetic tail under action of interplanetary magnetic lines of force

19 p2791 A72-38350

Hydromagnetic flow between two rotating disks with noncoincident parallel axes of rotation.

19 p2841 A72-38436

Effects of collisions on perpendicular longitudinal ion wave propagation in a magnetized plasma.

19 p2841 A72-38438

Heat conduction as mechanism for solar microwave bursts attenuation, noting effect of gyromagnetic absorption layers

19 p2852 A72-38497

Purification of hydrogen plasmoids by the magnetic field of an injector-diverter device

19 p2843 A72-38539

Investigation of the transport of electrode metal during welding in a carbon dioxide atmosphere

19 p2810 A72-38588

Ambipolar diffusion noise in a semiconductor in the presence of a magnetic field.

19 p2846 A72-38599

Critical current periodicity of Josephson junction interferometers.

19 p2846 A72-38601

Geomagnetic cutoffs for cosmic-ray protons for seven energy intervals between 1.2 and 39 Mev.

19 p2852 A72-38728

Faraday rotation by cosmic magnetic field in cosmology based on scalar-tensor theory of gravitation

20 p2969 A72-39264

Exponential conduction increase of semiconductors in strong magnetic fields, determining three dimensional random network resistance with percolation theory

20 p2960 A72-39384

Fabrication and properties of carbon-containing iron fibers and fiber sinter bodies

20 p2939 A72-39439

Gunn effect threshold and domain formation in transverse magnetic fields in indium antimonide.

20 p2960 A72-39566

Amplification of acoustic surface waves under transverse magnetic field in coupled intrinsic semiconductor-piezoelectric systems.

20 p2960 A72-39703

Effects of magnetic field on electron transport properties in gallium arsenide.

20 p2960 A72-39704

Single-cycle electron acceleration in focused laser fields.

20 p2934 A72-39720

Stellar emission and absorption line spectra formation in presence of magnetic field interpreted by radiative transfer equation solution, considering dwarf stars observation

20 p2956 A72-39753

Stability of laminar boundary layers on concave walls in presence of magnetic field.

20 p2958 A72-40066

Magnetic field effects on turbulent shear flow of electrically conducting fluid, discussing turbulence level, friction stress and heat exchange

21 p3089 A72-40260

Alternating magnetic field effect on ionoacoustic oscillations stability of collisionless nonhomogeneous magnetoplasma, examining parametric excitation of Langmuir oscillations

21 p3091 A72-40658

Influence of a magnetic field on the operation of an oscillator employing a two-base diode

21 p3032 A72-40791

OSO-4 observations of coronal EUV hole, considering association with regions of diverging magnetic fields

21 p3106 A72-41042

Influence of the terrestrial magnetic field on the motion of a satellite around its center of gravity

21 p3106 A72-41048

Quantum limit studies in single crystal and pyrolytic graphite.

21 p3097 A72-41186

Finite radial oscillations of uniformly rotating gravitating magnetized fluid cylinder model of star formation dynamics

21 p3109 A72-41331

Three-dimensional cosmic ray anisotropy in interplanetary space. III, IV.

21 p3101 A72-41385

Transverse magnetic field effect on unsteady incompressible laminar MHD boundary layer flow, noting cylindrical body oscillations in fluid

21 p3095 A72-41786

Magnetic field and suction effects on unsteady MHD free convection flow of conductive fluid around nonconductive porous flat plate

21 p3095 A72-41787

Magnetic-field-enhanced heating of plasmas with CO2 lasers.

22 p3210 A72-41969

Some aspects of flare properties versus magnetic boundary morphology.

22 p3217 A72-42038

Magnetic field change rate related to chromospheric activity in McMath Regions 8863, 10385 and 11415, discussing flare associated effects and total flux

22 p3217 A72-42039

Reflection and refraction of radio waves from the ionosphere in presence of time-varying irregularities.

22 p3154 A72-42302

Magnetic tension induced stress balance in plasma sheet, considering pressure gradient along geomagnetic tail axis, plasma flow kinetic energy and pressure anisotropy

22 p3211 A72-42408

Polar-cap electric field distributions related to the interplanetary magnetic field direction.

22 p3172 A72-42432

Neutron star model for magnetic field and superfluidity effects on cooling during pulsar stage

22 p3228 A72-42565

Propagation of Rayleigh waves on visco-elastic cylindrical surfaces placed in a magnetic field.

22 p3207 A72-42876

ULF wave observation by satellite, considering geomagnetic activity control of magnetospheric wave occurrence

22 p3174 A72-42902

August solar activity and its geophysical effects.

22 p3174 A72-42982

Plasma heating in Tuman 2 toroidal magnetic trap by microwave injection at upper hybrid frequencies

23 p3318 A72-43213

Sunspot formation due to magnetic flux concentration in active region and formation of invisible pores with suppressed granular motion

23 p3333 A72-43235

Determination of magnetic fields in plasmas from hydrogen spectral line profiles

23 p3318 A72-43313

The equatorial electrojet according to measurements from the Cosmos 321 satellite

23 p3328 A72-43369

Plane parallel nonuniform velocity plasma streams instability in absence and presence of magnetic field, comparing with ideal conductive liquid flows

23 p3320 A72-43518

Ion acoustic instability in collisionless shocks.

23 p3320 A72-43522

Perpendicular collisionless shock wave instability.

23 p3320 A72-43523

The effects of magnetic field oscillations on the boundary layer flow past a magnetized plate.

23 p3321 A72-43725

Relation between satellite radio signal scintillations and magnetic activity

23 p3264 A72-43850

Longitudinal magnetic field effect on the characteristics of a high frequency ion source

24 p3428 A72-45015

Meteor-induced magnetic effect on cosmic ray intensity for meteor streams with orbits normal or parallel to interplanetary magnetic field lines of force

24 p3435 A72-45092

Thermal cycling tests for natural remanent magnetism of lunar soil samples, proposing magnetization mechanism of material buried in regolith

24 p3443 A72-45373

Possible explanation of non-power-law radio spectra of cosmic radio sources.

24 p3446 A72-45477

MAGNETIC EQUATOR

Positive Fe ion concentration relationship to equatorial spread F from OGO 6 satellite observation near magnetic equator
01 p0062 A72-10902

Antiprotons abundance in primary cosmic radiation near geomagnetic equator from asymmetrical flux balloon measurements
03 p0407 A72-12992

Quiet day diurnal variability of equatorial geomagnetic field H component related to ionospheric dynamics
04 p0515 A72-14878

Equatorial ring current relation to polar electrojet during magnetosphere geomagnetic storm, discussing magnetosphere-ionosphere current systems
09 p1298 A72-22580

E and F region apparent and true drifts over magnetic equator correlated to solar activity, comparing electron density sensitivity to geomagnetic range
11 p1623 A72-26104

E region electron density distortion at magnetic equator by Sq current system, noting dependence on alpha coefficient profiles
13 p1952 A72-29663

Energetic particle flux observation at very low altitudes near geomagnetic equator, noting narrow distribution around 90-deg pitch angle
13 p2034 A72-30122

Range and frequency spread F diurnal and seasonal variations at magnetic equatorial station Thumba, noting geomagnetic activity effect
14 p2097 A72-30130

Quiet day daily geomagnetic field variability associated with equatorial ionospheric upheavals, noting longitudinal extent
19 p2794 A72-38869

Radar observations of equatorial spread F in a region of electrostatic turbulence.
23 p3286 A72-44528

Equatorial spread F - Recent observations and a new interpretation.
23 p3286 A72-44530

MAGNETIC FIELD INTENSITY
U MAGNETIC FLUX
MAGNETIC FIELDS

NT FORCE-FREE MAGNETIC FIELDS

NT GEOMAGNETISM

NT INTERPLANETARY MAGNETIC FIELDS

NT INTERSTELLAR MAGNETIC FIELDS

NT LUNAR MAGNETIC FIELDS

NT MAGNETOSTATIC FIELDS

NT NONUNIFORM MAGNETIC FIELDS

NT PALEOMAGNETISM

NT PLANETARY MAGNETIC FIELDS

NT SOLAR MAGNETIC FIELD

NT STELLAR MAGNETIC FIELDS

NT TRAPPED MAGNETIC FIELDS

Scattering cross section of electromagnetic wave by collisionless plasma perpendicular to applied magnetic field
01 p0105 A72-10025

Characteristic scale lengths of stationary ionic collisional shocks in Q device perpendicular to magnetic field, presenting shock thickness variation with Mach number and density
01 p0105 A72-10028

Electrostatic waves in longitudinally magnetized plasmas with random electron charge distribution and applied magnetic field, finding phase characteristics
01 p0106 A72-10128

Linear theory of transverse electromagnetic waves and instabilities in uniform plasma during propagation along magnetic field, considering multifluid and kinetic description
01 p0108 A72-10189

Collisionless plasma shock wave measurements in magnetic field, determining plasma temperature and free electron densities
01 p0108 A72-10236

Strong ionizing shock waves production in hydrogen and deuterium gases, measuring plasma electron temperature, axial electric field and density and magnetic field compression
01 p0108 A72-10237 [AD-734469]

Collisionless motion of solar wind ions in helical magnetic field, giving transfer function of charged particles
01 p0118 A72-10360

Magnetic field and plasma sheet variations observation by IMP 3 satellite in distant magnetotail during magnetospheric substorms
01 p0060 A72-10888

Meridional currents intensity in equatorial electrojet region, computing electric and magnetic fields
01 p0063 A72-10924

Electromagnetic instability of linearly polarized mode propagation perpendicular to magnetic field in two colliding plasma streams
01 p0110 A72-11112

Large amplitude linearly or elliptically polarized Alfvén wave propagation parallel to magnetic field, calculating nonlinear Landau damping rate
01 p0111 A72-11227

Numerical-integral equation approach to plane wave scattering from nonplanar conducting surface with sinusoidal height profile for magnetic field parallel to surface ridges
01 p0032 A72-11237 [AD-735574]

Nonaxisymmetric tubular spiral electron beam interaction with fast waves in cylindrical waveguide within longitudinal magnetic field
02 p0170 A72-11563

I-V characteristics and bandwidth properties of distributed emission amplifier within magnetic field, analyzing averaged electron trajectories and hf potential distribution
02 p0189 A72-11568

Extended Thomas-Fermi isolated atom model for pulsar outermost crust magnetic field effects, using pressure-density equations of state
02 p0277 A72-11903

Anomalous magnetic and gravitational fields energy spectra model, examining autocorrelation functions changes
02 p0217 A72-11932

Kubo bulk electrical conductivity of two dimensional guiding center plasma in strong dc magnetic field
02 p0263 A72-11966

Electromagnetic wave propagation perpendicular to applied uniform magnetic field in relativistic plasma, deriving dispersion relation for stability criterion
02 p0264 A72-12024

Lf drift-type and ion-acoustic oscillations in weakly ionized currentless plasma at low gas pressures in longitudinal magnetic field
02 p0265 A72-12291

Dispersion characteristics and frequency stabilization of 0.63 micron laser in magnetic field
02 p0180 A72-12583

Two stream instabilities of low density beam-plasma interaction in finite and zero magnetic fields
02 p0267 A72-12839

Tensor description of laser beam second harmonic generation in dc magnetic field, using group theory derivation of nonzero element relations for all crystallographical classes
03 p0365 A72-12963

Cylindrical gravitational waves propagation modes in hot plasma subject to axial magnetic field, investigating instability conditions
03 p0388 A72-13025

Neodymium laser plasma dispersion and diffusion in magnetic field, using electrostatic injection of LiH particles
03 p0393 A72-13081

Upstream influence on MHD flow velocity by Rankine body moving parallel to uniform magnetic field in conducting fluid
03 p0394 A72-13153

Calibration of polarimetric measurements in terms of magnetic fields, using Stokes parameters without line formation dependence
03 p0427 A72-13280

Coherence properties of polarized radiation in weak magnetic fields, considering scattering redistribution for normal Zeeman triplet
03 p0427 A72-13292

Radiation pattern from open ended parallel plate waveguide with arbitrary electric or magnetic aperture field distribution, using Wiener Hopf technique
03 p0331 A72-13409

Adiabatic charged particle orbits in magnetic null sheet with transverse electric and added normal magnetic fields
03 p0348 A72-13512

Induced current distribution in flat narrow conducting strip moving in inhomogeneous magnetic field, presenting current field and densities
03 p0311 A72-13564

Spreading currents in parabolic rotating coordinates, determining magnetic field components consistent with Laplace equation series expansion
03 p0311 A72-13565

Plasmoid transport in quadrupole and octupole magnetic fields, measuring plasma amounts in axial region charged particle densities and flux densities at vacuum chamber wall
03 p0395 A72-13568

Plasma flux interaction with axially symmetric magnetic field, investigating electrical polarization behavior
03 p0395 A72-13569

Plasma flow under inhomogeneous axially symmetric magnetic field, investigating axial component of poloidal Hall induction current
03 p0395 A72-13570

Bulk recombination effects on nonstationary pinching and collapse of electron-hole plasma by magnetic field in crystal
03 p0401 A72-13581

Power and gas consumption for inductive plasma formed in Ar atmosphere, measuring radial distribution of magnetic field axial component
03 p0395 A72-13652

Plasma beams injection into toroidal magnetic field along gradient or radius, using polarizational interaction
03 p0396 A72-13658

Plasma interchange instability in quadrupole and octupole magnetic fields determination by disturbance wavelength ratio to ion cyclotron radius
03 p0396 A72-13659

Stability of plane rotating galaxies in magnetic field parallel to axis of rotation, showing linearized MHD equations self conjugate for radial disturbance case
03 p0435 A72-13806

Magnetic field and current density distributions in cylindrical conduction MHD channel with arbitrary number of pole-electrode pairs
03 p0398 A72-14000

Time and coordinate dependence of magnetic field for steady symmetric flows of compressible conducting fluid at large Reynolds numbers, investigating self excitation conditions
03 p0398 A72-14001

Angular and linear velocities of plasmoid in coaxial accelerator under axisymmetric magnetic field
03 p0398 A72-14002

Laminar turbulent transition Reynolds number increase at finite perturbations in longitudinal magnetic field
03 p0398 A72-14003

Electric field intensity and pulsation spectra variation along rectangular channel in transverse magnetic field, noting current density changes
03 p0398 A72-14006

Dynamic and electromagnetic characteristics of MHD flow in square tube with walls differing in electroconductivity within oblique transverse magnetic field
03 p0398 A72-14007

Magnetic field distribution in linear MHD channel for large Reynolds numbers, determining current density and longitudinal field component
03 p0398 A72-14010

Free convective motion of conducting fluid past vertical plate in uniform transverse magnetic field, determining optimum dimensions of heat exchangers
03 p0399 A72-14011

Compression wave propagation from cylindrical cavity in weakly conducting magnetoelastic medium under unperturbed magnetic field
03 p0452 A72-14129

Rotationally symmetric force free magnetic field boundary value problem, using linear elliptic differential equation
03 p0400 A72-14352

Self consistent kinetic equations for evolution of particle distribution functions and wave intensity spectra of relativistic spatially homogeneous multippecies plasma in ambient magnetic field
04 p0553 A72-14401

Quasi-linear relaxation of fast ion beam in cold plasma moving transverse to magnetic field
04 p0554 A72-14403

Relativistic equations of motion of charged particle interacting with plane electromagnetic wave propagating at arbitrary angle to uniform magnetic field for magnetosphere model
04 p0554 A72-14406

Force free high beta plasma stability in homogeneous magnetic field and with inhomogeneous temperature and density
04 p0554 A72-14408

Magnetic and gravitational energy release by resistive MHD instabilities responsible for solar flares
04 p0571 A72-14578

Plasma density profiles by microwave interferometry technique in Sirius stellarator divertor for two magnetic field configurations and injection methods
04 p0555 A72-14619

Multimode Ne-He laser in strong magnetic field, discussing plasma-optical effects, emission cut-off magnetic field strength for various discharge levels and single-mode construction
04 p0530 A72-14656

Electromagnetic wave propagation across external magnetic field in contraststreaming thermally anisotropic plasmas, investigating plasma stability
04 p0556 A72-14942

Ar gas dc discharge plasma characteristics in crossed electric and magnetic fields, examining equivalent pressure concept
04 p0556 A72-14945

Electron heating by oscillating electric field in presence of steady magnetic field, solving Boltzmann transport equation for electron velocity distribution in plasma
04 p0556 A72-14947

Plasma column interaction with counter rotating hf magnetic fields of multipole configurations, calculating angular velocity
04 p0557 A72-15169

Toroidal plasma column in Tokamak systems, discussing field inhomogeneity role in maintaining equilibrium with conducting casing, confirming magnetic field and transformer iron core
04 p0557 A72-15171

Hf circularity polarized field strength and plasma density self consistent stationary distribution in weakly inhomogeneous constant magnetic field

04 p0558 A72-15175

High beta plasma lf wave parallel propagation to equilibrium magnetic field, deriving large scale length perturbations from coupled nonlinear partial differential equations

04 p0559 A72-15349

Electric or magnetic field tangential components at ground-air interface, discussing secondary electromagnetic sources

04 p0492 A72-15438

Nonstationary behavior of collisionless shock waves in plasma wind tunnel, suggesting interpretation of magnetosphere magnetic field structure near earth bow shock

04 p0559 A72-15468

Resonant transport properties of polyatomic gases in collinear static and oscillating magnetic fields, using microscopic kinetic equation

04 p0553 A72-15633

Two dimensional axisymmetric surface waves motion in inviscid incompressible homogeneous electrically conducting fluid under uniform magnetic and electric fields, considering surface tension effects

04 p0560 A72-15744

Monograph on design and characteristics of rotating plasma device under crossed electric and magnetic fields, covering dynamic behavior of hydrogen puff

05 p0642 A72-15798

Electromagnetic radiation modulators in millimeter and submillimeter wave range using gas-discharge plasma magneto-optical effects in alternating magnetic field

05 p0625 A72-15826

MHD squeeze film lubrication between electrically conducting parallel plates, showing graphically approach time under magnetic field in free space

05 p0665 A72-16031

Hypersonic axially symmetric laminar boundary layer electrically conducting fluid flow in blunt body stagnation region in presence of radial magnetic field

05 p0600 A72-16063

Book on electromagnetic waves in moving magnetoplasmas covering propagation in infinite and bounded plasmas subject to magnetic fields for nonrelativistic and relativistic velocities

05 p0695 A72-16396

Toroidal magnetic ring development and interaction with poloidal magnetic field, considering relationships to sunspots bright rings and spicules dynamics

05 p0719 A72-16512

Transfer equation system solution for nonscattering medium with stationary homogeneous magnetic field, considering boundary value problem in Fraunhofer line theory

05 p0690 A72-16513

Electromagnetic wave transmission and reflection by semiinfinite moving anisotropic plasma with parallel static magnetic field, considering incident H wave

05 p0696 A72-16623

Pulsed flat electrode erosion plasma accelerator, determining electric and magnetic fields distribution, current density and electron concentration

05 p0697 A72-16987

Boundary conditions and equations of plasma arc discharge in cylindrical diode with azimuthal magnetic field

05 p0697 A72-16988

Existence conditions for steady MHD shock waves propagating in collisionless plasma along magnetic field, observing dependence on pressure anisotropy

05 p0698 A72-17016

Anisotropic plasma stability to magnetosonic wave near ion cyclotron frequency propagating almost perpendicular to magnetic field

05 p0698 A72-17017

Relativistic electron pitch-angle diffusion driven by oblique lf whistler-mode turbulence in collisionless plasma immersed in static magnetic field

05 p0699 A72-17024

Coupled longitudinal and transverse plasma waves propagating normal to applied magnetic field, using three fluid model

05 p0700 A72-17230

Parametric plasma instability in hf electric field and constant magnetic field, noting longitudinal plasma oscillations growth

05 p0700 A72-17234

Ion charge composition in plasma-electron beam system in strong longitudinal magnetic field, noting multiply charged ions production under high temperature conditions

05 p0701 A72-17235

Stationary plasma flow interaction with axisymmetric spatially periodic magnetic field in presence of Hall effect, determining electric currents structure

05 p0701 A72-17241

Muon track curvatures in Wilson chamber magnetic field for calibrating ionization levels of logarithmic increase

06 p0811 A72-17293

Self induced electron beam collapse prevention by external magnetic field, determining required field strength by scaling law based on simple orbit model

06 p0854 A72-17418

Higher harmonics in lunar transfer functions for surface magnetic field tangential components, discussing lunar electrical conductivity models

06 p0875 A72-17448

Internal neutral sheet in geomagnetic tail from Explorer 34 magnetic field experiment, noting quasi-periodic structure and magnetic loop formation

06 p0803 A72-17450

Geomagnetic micropulsations on ground and magnetic field fluctuations in tail, noting field strength changes

06 p0804 A72-17455

Lf instability mode in partly ionized plasma due to electron temperature gradient aligned perpendicular to magnetic field, applying to E and F regions [AD-737931]

06 p0804 A72-17460

Cylindrical alkali metal plasma column structure in single ended Q device under axial magnetic field

06 p0854 A72-17503

Wake behind body moving in plasma parallel to magnetic field, observing coupling with parallel ion acoustic waves and with perpendicular Bernstein modes

06 p0875 A72-17525

Plasma perturbations and destabilization in curved magnetic field due to electronic electrical conductivity finiteness

06 p0860 A72-17684

Laser radiation intensity modulation by time varying magnetic field

06 p0825 A72-17685

Weakly ionized decaying afterglow plasma potential fluctuation and instability in magnetic field, using electrostatic probes

06 p0860 A72-17692

Longitudinal ambipolar acoustic instability effect on duration of plasma particle motion to wall across magnetic field, using phase method

06 p0860 A72-17693

Collisionless plasma oscillations in external uniform magnetic field, described by initial value problem for nonrelativistic linearized Vlasov-Maxwell equations

06 p0862 A72-18251

Closed magnetic fields of helical ring currents on concentric spheres surrounded by semiconductor /Tornado trap/

06 p0863 A72-18405

Magnetic field stability in Tornado-2 trap as function of helical currents on concentric sphere

06 p0863 A72-18406

Separatrix structure and stability of helical Tornado trap magnetic field from electron space charge measurements

06 p0863 A72-18407

Pulse reflection of polarized plane electromagnetic wave from cold plasma ionosphere model with vertical magnetic field

06 p0777 A72-18729

Gas laser emission fluctuations of total radiation energy, polarized field components and line widths in longitudinal magnetic field

07 p0999 A72-18911

Amplitron stability in optimal frequency regime, relating cut-off voltage and plate current as function of magnetic field, input power and geometrical parameters

07 p0953 A72-19014

Magnetized solar wind velocities and fields obtained by three dimensional model using perturbation technique with spherically symmetric boundary conditions

07 p1057 A72-19142

Lf oscillations of magnetic field at ATS 1, presenting local time and frequency distributions

07 p0975 A72-19160

Nonlinear Landau damping of longitudinal plasma waves in dc magnetic field, obtaining wave-particle interactions from Vlasov equation by perturbation theory and method of characteristics

07 p1041 A72-19505

Nonlinear Landau damping and growth of finite amplitude cyclotron harmonic plasma waves in magnetic field, measuring coupling coefficients by calibrated interferometer

07 p1041 A72-19506

Parallel current and sheath effects on collisional drift waves normal mode structure in Q machines with end plates, using slab plasma model with uniform magnetic field

07 p1042 A72-19511

Plasma layer growth and equilibrium magnetic fields for astron configurations, solving stream function by finite difference methods

07 p1042 A72-19512

Stationary high beta plasma shock waves generated in plasma wind tunnel by impinging on magnetic field, comparing with earth bow shock

07 p1042 A72-19617

Coordinate transformation for decoupling equations for tangential electric and magnetic field propagation

through series of uniform cylindrical layers with arbitrary properties

07 p0946 A72-19799

Statistical analysis of magnetic energy-density antenna performance in mobile communication, comparing two-crossed-slot design to three element unit

07 p0957 A72-19801

Quasi-nucleonic interactions of high energy protons in nuclear emulsion irradiated within pulsed magnetic field

07 p1038 A72-19869

Abrikosov and Mendelsohn models of nonideal superconductors of second kind in transverse magnetic field, discussing Landau-Ginzburg parameters and critical current density

07 p1049 A72-20153

Magnetoelastic vibrations of thin conducting plate in magnetic field, solving electrodynamic equations

07 p1095 A72-20315

Electric field in flow of medium with tensor conductivity due to Hall effect, studying eddy currents structure in magnetic field variation region

07 p1044 A72-20316

Lf convective oscillations in polytropic atmospheres within strong magnetic field, considering stability of quasi-adiabatic and quasi-isothermal motions

07 p1082 A72-20376

Magnetic field influence on shear viscosity of polyatomic gases, measuring rectangular cross section capillary flow resistance for different field orientations

07 p1038 A72-20398

Hall effect influence on magnetospheric boundary magnetic field generation by solar wind perturbation, using beam-magnetic field interface model

07 p0980 A72-20407

Optimal test conditions in magnetospheric control by electrical system for subsurface defects detection, obtaining tangential magnetic field on carbon steel plates

07 p0991 A72-20421

Transverse hydromagnetic plane waves existence in uniformly heated electrically conducting fluid under temperature gradient and magnetic field

07 p1045 A72-20442

Spark source generated electron beam interaction with plasma in uniform magnetic field, estimating HF longitudinal oscillation power

07 p1046 A72-20504

Ambipolar diffusion in weakly ionized unstable plasma afterglow in presence of uniform axial magnetic field

07 p1047 A72-20558

Magnetic field components of vertical currents at magnetosphere boundary and earth surface, using computerized Gaussian method

08 p1156 A72-20822

Unsteady flow of viscous incompressible electrically conducting fluid past infinite nonconducting plate within uniform transverse magnetic field

08 p1212 A72-21079

Magnetic field effect on elf radio wave attenuation during propagation under six ionospheres, showing dependence of minimum on propagation path geomagnetic latitude

08 p1131 A72-21103

Two dimensional model for plasma without magnetic field trapped near current sheet end in dipole magnetic field resembling geomagnetic tail

08 p1157 A72-21108

Solar wind tangential discontinuities and shock waves determination from flux velocity vector, magnetic field and particle density measurements

08 p1227 A72-21154

Electromagnetic wave polarization effect on linear transformation of waves in inhomogeneous magnetoactive plasma in magnetic field

08 p1212 A72-21245

Electrostatic ion wave Landau damping in magnetic field of Ar plasma QP machine

08 p1213 A72-21250

Charge separation effects on plasma shock wave profile in perpendicular propagation to magnetic field, using moment equations derived from Boltzmann equations for electrons and ions [AD-742533]

08 p1213 A72-21254

Molecular ordering in smectic A liquid crystals, evaluating spectrum hyperfine splitting as function of orientation to spectrometer magnetic field

08 p1217 A72-21490

Heisenberg ferromagnet thermodynamic properties in external magnetic field near Curie temperature, studying magnetization, susceptibility, entropy and magnetocaloric effect

08 p1217 A72-21520

Anisotropic conducting fluid flow in presence of traveling magnetic field, determining Hall effect via solution to electromagnetic field distribution boundary value problem

08 p1214 A72-21648

Slow and fast longitudinal ion acoustic waves in plasma cylinder under axial magnetic field

08 p1215 A72-21873

Quantizing magnetic field effect on electromagnetic wave propagation in multivalley n-type Si and Ge and PbTe semiconductors

08 p1218 A72-21878
Propagation time of charge diffusion across magnetic field in bounded plasma

08 p1215 A72-21879
Josephson effect /superconducting weak link/ devices for low frequency magnetic field sensing, noting applications in magnetocardiography and absolute noise thermometry

08 p1218 A72-21919
Hyperfine interactions of Fe cations in ilmenite determined by Mossbauer spectroscopy, noting internal magnetic field and quadrupole coupling constant

09 p1367 A72-22457
Magnetic field measurement methods and magnetometers performance in superconducting, thin film, resonance and fluxgate areas

09 p1308 A72-22465
Optimum pressure and field conditions for intense relativistic electron beam transport in longitudinal magnetic field

09 p1360 A72-22870
Two fluid MHD model to study cylindrical plasma condenser resonance properties in axial magnetic and alternating electric fields

09 p1360 A72-22952
Alfven waves development and high pressure plasma hydrodynamic and kinetic instabilities dependence on magnetic field to temperature gradients ratio

09 p1360 A72-22954
Hollow cylindrical cathode discharge sustaining potential reduction and recombination probability increase from transverse magnetic field and rising pressure and plasma density

09 p1361 A72-22957
Contractible current loop model for radius variations, induction current, temperature and inertia center velocity in plasmoid interacting with axially symmetric magnetic field

09 p1361 A72-23202
Plasmoids interaction in diverter magnetic field, investigating integral electron capture intensity

09 p1362 A72-23205
Plasma jet dynamics in axially symmetric magnetic field, obtaining magnetic field generated by conduction currents as function of plasma macroparameters

09 p1362 A72-23206
Moving plasma interaction with oblique magnetic field, establishing magnetization ranges for plasma density and velocity

09 p1362 A72-23208
Plasma flows interaction with plasma cylinder in diverter magnetic field, investigating plasma dynamics with electric probes, plasmascope and mass spectrograph

09 p1362 A72-23210
Plasma flow interaction with magnetic pulse field barrier from magnetic coil for short plasmoids formation

09 p1362 A72-23211
Single helix magnetic field with axial current, discussing field lines rotatory transformation and magnetic well and shear effect on plasma behavior

09 p1363 A72-23216
Double helix magnetic field in longitudinal and axial current fields of stellarators, noting rotatory transformation and shear of field lines

09 p1363 A72-23217
Multipole magnetic field configuration effectiveness in electromagnetic plasma trap, discussing electron losses critical angle and captured ions maximum density

09 p1363 A72-23221
Negative reabsorption coefficient for induced emission of neutron moving in medium in magnetic field

09 p1364 A72-23257
Oblique magnetic fields effect on compressible conductive fluids motion in presence of thin foil, noting lift values in hyperlipitic and double hyperbolic cases

09 p1365 A72-23360
Electrically conducting viscous incompressible fluid rotating with oscillating disk in magnetic field

09 p1366 A72-23575
LF drift-time and ion-acoustic oscillations in weakly ionized currentless plasma at low gas pressures in longitudinal magnetic field

10 p1517 A72-23765
German monograph on radiation characteristics of planar systems in aperture plane of parallel plate waveguide, obtaining relationship between electric and magnetic fields

10 p1434 A72-23775
Massive rotating objects with magnetic fields in galactic nuclei, considering similarities between Crab Nebula and quasars

10 p1535 A72-23908
Quiescent steady state plasma production by beam-plasma discharges in uniform magnetic fields, showing plasma density fluctuation relation to Penning effect

He-Ne laser output dependence on transverse magnetic field, ascribing magneto-optical effects to IR radiation decrease

10 p1490 A72-24046
Light polarization in anisotropic Zeeman laser under axial magnetic field

10 p1491 A72-24134
Relativistic Zeeman-Stark effect on molecular jet due to molecular translational motion in continuous magnetic field

10 p1514 A72-24135
Variable radio structure model using relativistic electron cloud outbursts in stationary magnetic field tubes for faster than light velocities

10 p1536 A72-24139
Velocity and magnetic field expressed by six scalar potentials from MHD equations system, noting compressible fluids flow

10 p1520 A72-24219
Microwave amplitude modulation during propagation through RF plasma under perpendicular low intensity time dependent magnetic field

10 p1520 A72-24345
Electromagnetic wave propagation perpendicular to magnetic field in two-component warm plasma, obtaining dispersion relations for transverse waves

10 p1520 A72-24350
Traveling wave mode ring laser operation, obtaining active medium polarization changes through longitudinal magnetic field excitation by capacitor discharge through spiral pump lamps

10 p1492 A72-24363
Conducting fluid laminar free convective flow over heated rotating horizontal plate in presence of strong magnetic field aligned with rotation vector

10 p1522 A72-24465
Joule dissipation effect on convective instability of current carrying fluid in magnetic field

10 p1522 A72-24533
Plane ionizing shock wave stability in MHD channel within magnetic field

10 p1522 A72-24542
Interacting viscous conducting media flow in inclined channel in presence of transverse magnetic field, using Moiseev asymptotic method for steady flows with wavy interface

10 p1522 A72-24546
Stability of superluminous and subluminal waves propagating transversely to external uniform magnetic field in streaming relativistic plasmas

10 p1522 A72-24608
Coma galaxy cluster X ray and radio source region magnetic field origin as primordial metagalactic flux or strong radio source remnant

10 p1542 A72-24617
Impurities effect on level density of electron gas within strong magnetic field, discussing included self energy

11 p1693 A72-25526
Electrical conductivity of two dimensional strongly magnetized guiding center plasma, using Liouville equation

11 p1693 A72-25563
Magnetic field generation in presence of turbulent velocity distribution, considering gyrotropy parameter equation and nonlinearity

11 p1686 A72-25716
Plasma column stabilization by constant longitudinal inhomogeneous magnetic and rotating HF electromagnetic fields, noting application to plasma convective instabilities

11 p1694 A72-25786
Controlled nuclear fusion plasma stabilization by electrostatic forces, reducing applied magnetic field

11 p1694 A72-25791
Ruby laser light scattering method for measuring magnetic field direction in Tokamak plasma, testing validity by numerical calculation of scattered spectrum

11 p1694 A72-25793
Hydromagnetic stability of isothermal stratified plasma atmosphere uniform flow over conducting liquid along magnetic field, discussing dispersion relation for static configuration

11 p1695 A72-26115
General relativity equations solution for interaction of gravitational radiation and conducting fluids in magnetic field, noting energy absorption in specified depth surface layer

11 p1720 A72-26116
Magnetic field and polar region geometry effects on hollow cathode thruster performance of Kaufman electric engine

11 p1706 A72-26167
Magnetic fields effect on anode heat losses in MPD accelerator arcs, noting minimal charge current density

11 p1711 A72-26225
Rayleigh problem in presence of magnetic field, discussing transpiration effects on MHD flow near oscillating flat plate

11 p1696 A72-26542
Resonant three wave interaction in magnetized spatially uniform plasma under constant magnetic field

11 p1698 A72-26603
Hydromagnetic stability of rotating nondissipative inviscid incompressible conducting fluid annulus permeated by radially varying magnetic field, considering axisymmetric and nonaxisymmetric disturbances

11 p1619 A72-26639
Slow and fast plane magnetoacoustic waves mutual transformation and reflection at plasma and magnetic field inhomogeneities

11 p1698 A72-26643
Electron gas in superstrong magnetic fields of gravitationally collapsed objects outer region, noting Wigner transition to ordered structure

11 p1699 A72-26704
Spreading currents in parabolic rotating coordinates, determining magnetic field components consistency with Laplace equation series expansion

11 p1607 A72-26752
Plasmoid transport in quadrupole and octupole magnetic fields, measuring axial charged particle and flux densities at vacuum chamber wall

11 p1699 A72-26755
Plasma flux interaction with axially symmetric magnetic field, investigating electrical polarization behavior

11 p1699 A72-26756
Plasma-ion beam system drift beam instability in longitudinal magnetic field, noting oscillations frequencies dependence

12 p1849 A72-27060
Pulsed flat electrode erosion plasma accelerator, determining electric and magnetic fields distribution, current density and electron concentration

12 p1850 A72-27131
Electron beam velocity distribution function fine structure for plasma-beam discharge in hydrogen within longitudinal magnetic field

12 p1850 A72-27261
Quiescent plasma production with axially homogeneous density distribution in skipping magnetic fields by electron cyclotron resonance discharge, noting high electron temperatures

12 p1851 A72-27400
Oscillation periods of rotating perfectly conducting liquid column in presence of axial magnetic field and uniform current

12 p1851 A72-27534
Ruby laser coherent light scattering by cylindrical electron beam under longitudinal magnetic field

12 p1820 A72-27586
Geomagnetic invariant coordinates and related field line parameters calculation via field model and fast numerical method

12 p1803 A72-27771
Inertial sensing principles interrelationship, stressing electric and magnetic procedures

12 p1809 A72-27788
Charged particles propagation in magnetic field and scattering medium with constant and variable transport paths, applying to proton propagation for solar flares

13 p2029 A72-28576
Kinetic approximation for bounded electron beam stability in plasma situated in magnetic field, deriving instability increments and dispersion relations

13 p2010 A72-28578
Polar cap magnetic field induced by currents along magnetospheric lines of force during polar substorm

13 p1946 A72-28587
Wave equations and photon absorption cross section of relativistic electron in magnetic field, taking into account relativistic energies

13 p2002 A72-28647
Dynamic thermo-magnetoelastic problems of long cylinder and infinite medium with hole under magnetic field, using variation method and Laplace transforms

13 p2056 A72-28882
Radial magnetic field geometry for total ion utilization in Kaufman thrusters, noting uniform current density and plasma generation and high electrical efficiency

13 p2027 A72-28948
Number density, particle, momentum and energy fluxes in model ion-exosphere with open magnetic field and asymmetric Maxwellian velocity distribution

13 p1948 A72-29115
Collisional plasma shock waves structure in electromagnetic shock tube with strong transverse bias magnetic field, using two fluid Navier-Stokes equations

13 p2011 A72-29119
Thermal equilibrium coefficient of ionized plasma spatial diffusion transverse to strong uniform dc magnetic field, extending Taylor-McNamara calculation scheme to three dimensions

13 p2011 A72-29120
Electromagnetic wave absorption in warm homogeneous plasma under static magnetic field parallel to surface, taking into account plasma-vacuum boundary conditions

13 p2012 A72-29123
Unsteady state propagation of weak nonlinear plasma waves in magnetic field, discussing shock wave formation and compression pulse evolution

Anomalous magnetic and gravitational fields energy spectra model, examining autocorrelation functions changes

13 p1949 A72-29244

Charged particle beams focusing in combined dual spiral system with homogeneous magnetic field along axis

13 p1932 A72-29292

Plasma wave measurements during OGO-5 dayside magnetosphere polar cusp encounters, discussing ULF magnetic field wave levels and VLF electric field amplitude ranges

13 p1950 A72-29380

Random homogeneous turbulence generation of rms weak magnetic field fluctuation in infinite medium with short correlation time

13 p2015 A72-29403

Nd laser irradiation of LiH particles in magnetic trap, investigating resultant plasma expansion and diffusion

13 p2015 A72-29431

Dispersion equations for electron and ion cyclotron waves propagating perpendicularly to magnetic field in plasma

13 p2016 A72-29602

Weakly ionized plasma decay within cylinder with electrically conducting walls in presence of longitudinal magnetic field, determining electric current dependence on cylinder length

13 p2016 A72-29603

He ions motion normal to magnetic field under induced electric field, analyzing resonance mechanism

13 p2016 A72-29606

Impulsive pulsations /Pi 2/ identification as geomagnetic field distension coincident with oscillatory component from high resolution Rb vapor magnetometer recordings

13 p1951 A72-29656

Plasma current layer formation due to electric field directed along magnetic field neutral line

13 p2017 A72-29699

Uniaxial compressive stress apparatus for InSb investigation at low temperatures in large magnetic fields

13 p1959 A72-29753

Steady barotropic inviscid flows of rarefied gas plasmas as free jet and within cylindrical channel in axisymmetric external magnetic field with Hall effect

13 p2018 A72-29823

Two dimensional mathematical model of magnetosphere with neutral sheet for oblique incidence of solar wind, noting magnetic field minimum energy

13 p1954 A72-29850

Mathematical model for magnetized solar wind with one fluid MHD and polytropic state equations, calculating magnetic field variables at earth

13 p2034 A72-29958

Critical superconductivity currents measurement in niobium based U shaped and coiled wires within steady magnetic field

13 p2007 A72-30013

Polar zone thermospheric temperature variations due to atmospheric cooling, H component variations and discrete perturbation

14 p2097 A72-30133

Current instability of electron-ion plasma in magnetic field produced by moving resonance charges

14 p2136 A72-30301

Isolated finite amplitude electrostatic oscillations production in thin plasma layer between two parallel metallic surfaces in magnetic field

14 p2136 A72-30302

Steady motion of dense electron beam in rarefied phonon plasma along magnetic field, analyzing polarization effects

14 p2136 A72-30305

Dynamic behavior of long-period oscillations of surface wave type in system of inhomogeneous ion beams moving in dense plasma along magnetic field

14 p2136 A72-30307

Plasma containment by superposed fields /sustained field/ technique application to theta pinch, studying hydrogen and helium discharge behavior

14 p2138 A72-30400

Near field effects on pulsar particle acceleration, relating electric and magnetic field magnitudes

14 p2156 A72-30568

Transverse particle diffusion across external homogeneous magnetic field under random isotropic large scale hydromagnetic turbulence

14 p2102 A72-30650

Spectrochemical trace analyses in electric arc plasma, examining external magnetic field effects on spectral line intensity variation

14 p2139 A72-30784

Diffraction of plane waves scattered by impedance structures in anisotropic medium, noting wedge shaped region with cold plasma under external magnetic field

14 p2086 A72-30809

Linear theory based analysis of compressible electroconductive fluid flow satisfying perfect gas equation in presence of thin profiles within quasi-aligned magnetic field

14 p2095 A72-30824

Magnetized nonuniform plasmas, discussing description to all orders in electron and ion temperatures of waves by operator method

14 p2139 A72-30879

Two counter streaming plasmas with anisotropic temperatures, deriving instability condition for ordinary mode electromagnetic propagation perpendicular to external magnetic field

14 p2140 A72-30935

Anisotropic homogeneous plasmas, deriving computer model to predict effects of circularly polarized parallel plasma waves in external uniform magnetic field direction on instabilities

14 p2140 A72-30938

Kinetic equations for turbulent magnetized plasma, considering wave-wave interactions and wave energy in terms of second order Markov differential equation

14 p2141 A72-30940

Gravitational radiation generation and detection, discussing Weber detector, interaction with electric and magnetic fields and gravitational astronomy

15 p2273 A72-31287

Zeeman triplet with unsplit upper level formation in isothermic atmosphere under magnetic field, considering Doppler and Lorentz frequency profiles of transitions

15 p2304 A72-31332

Numerical analysis of steady one dimensional quasi-shock waves in collisionless plasma within longitudinal uniform magnetic field, noting oscillations behind wave front

15 p2284 A72-31584

Electric and magnetic fields fluctuations in region between shock wave front and magnetosphere boundary, noting resulting energy dissipation

15 p2225 A72-31902

Correlated particle flux, magnetic field, electron intensity and riometer absorption measurements during recovery phase of polar magnetic substorm on 6 March 1970

15 p2226 A72-31946

Hyperfine magnetic field reduction produced in Fe-Cr alloy single crystal by Cr atoms observed by Mossbauer method, proposing spin disturbance mechanism

15 p2293 A72-32230

Geomagnetic substorm magneto-ionospheric effect, discussing electric field transmission, magnetic field variations and currents flowing in dynamo region

15 p2230 A72-32259

Solar flare and neutral sheet simulation by investigating behavior of plasma current through magnetic neutral point created by capacitor discharges

15 p2301 A72-32342

Stationary plasma flow interaction with dipole magnetic field to study geophysical phenomena in upper atmosphere

15 p2286 A72-32343

MHD Couette flow of electrically conducting viscous incompressible fluid in transverse magnetic field with time dependent suction or injection

15 p2286 A72-32396

Magnetic probe measurement of random fluctuations in transverse magnetic field caused by He plasma produced in arc discharge

15 p2287 A72-32408

Cooperative enhanced scattering cross section of far IR laser radiation from nonthermal theta pinch plasmas in weak magnetic field

15 p2288 A72-32417

Streaming MHD flow past sem infinite flat plate in presence of perpendicular uniform magnetic field, obtaining velocity field at large distances

15 p2288 A72-32480

Magnetized plasma discharge steady state problem of finite cylinder positive column in magnetic field, detailing radial and axial solutions

15 p2288 A72-32508

Three Josephson junction asymmetric feed quantum interferometer, discussing magnetic field sensitivity and amplitude variation increase

15 p2241 A72-32536

Skewed wire antennas electric and magnetic near fields prediction from computer programs based on matrix inversion method

15 p2209 A72-32567

Magnetic field profile optimization for beta-limitation in minimum-B mirror confined plasma in nuclear reactor

16 p2432 A72-32805

HF electrostatic instabilities driven by electron-ion relative drift velocity across external magnetic field for inhomogeneous plasma, noting Landau damping role

16 p2433 A72-32809

Ion acoustic, electron plasma and cyclotron harmonic waves parametric instabilities in magnetic field and applications to plasma heating

16 p2433 A72-32811

Plasma column formation by interaction with rotating HF electromagnetic field and longitudinal constant magnetic field

16 p2433 A72-32815

Magnetic configuration for plasma confinement in torsatron with helical windings and no toroidal field coils

16 p2433 A72-32816

Electromagnetic gain mechanisms with required energy supplied by static currents and magnetic fields in homogeneous plasmas

16 p2434 A72-32853

Two dimensional unsteady solutions to MHD equations, describing matter compression near zero line of magnetic field for solar flares and z pinch studies

16 p2435 A72-33151

Experimental methods for studying interactions between plasma streams and three dimensional magnetic dipole fields

16 p2454 A72-33384

Magnetic field rapid dissipation induced by stochastic topology of lines of force, discussing implications for hydromagnetic turbulence, solar activity and cosmic ray diffusion

16 p2378 A72-33454

Electric and magnetic field effects on auroras formation, noting similarity with thermonuclear reactor plasma

16 p2456 A72-33518

Magnetothermoelastic temperature distribution effects due to linear heat source in infinite circular cylinder acted upon by magnetic field

16 p2425 A72-33595

Equations of state and equilibrium for electron gas in strong magnetic field, discussing effects in pulsar crusts and atmospheres

16 p2460 A72-33929

Plasma motion relation to magnetic field line motion for perfect electroconductivity, noting comparison with total particle drift distance

16 p2439 A72-33931

Particle and energy fluxes across magnetic field in axisymmetric toroidal magnetic traps and plasmas with weak collisions, calculating radial electric field

16 p2440 A72-34153

Radiation from a magnetic line source covered with an anisotropic warm plasma slab

17 p2587 A72-34386

Thermomagnetic effect in a plasma placed in a non-homogeneous magnetic field

17 p2588 A72-34838

Closed magnetic fields of helical ring currents on concentric spheres surrounded by conductor /Tornado trap/

17 p2588 A72-34855

Magnetic field stability in Tornado-2 trap as function of helical currents on concentric spheres

17 p2588 A72-34856

Emission of coherent microwave radiation from a relativistic electron beam propagating in a spatially modulated field

17 p2589 A72-34874

Time correlation functions for gases of linear molecules in a magnetic field

17 p2589 A72-34894

Galactic cosmic rays anisotropy prediction as function of energy for various assumed source distributions and magnetic field configurations

17 p2599 A72-34924

Traveling wave mode ring laser operation, obtaining active medium polarization changes through longitudinal magnetic field excitation by capacitor discharge through spiral pump lamps

17 p2563 A72-34962

Russian book - Effect of magnetic fields on biological objects

17 p2502 A72-35001

Mechanism of the biological action of a constant magnetic field

17 p2503 A72-35005

Solution of the Boltzmann equation for a fully ionized plasma in an oscillatory electric field and a steady magnetic field. V - Explicit solution for a homogeneous plasma in a high-frequency electric field

17 p2589 A72-35057

Transverse diffusion and conductivity coefficients for a three-dimensional magnetized equilibrium plasma

17 p2592 A72-35379

Faraday rotation in connection with Hoyle theory of intergalactic magnetic field existence in steady state cosmology, considering cosmological model with cosmic magnetic field

17 p2614 A72-35504

Spectral dependence of diffusion in a magnetized plasma

17 p2592 A72-35623

Influence of reflected ions on the magnetic structure of a collisionless shock front

17 p2592 A72-35819

Alfven waves development and high pressure plasma hydrodynamic and kinetic instabilities dependence on magnetic field to temperature gradients ratio

17 p2593 A72-35883

A theoretical analysis of the acceleration of ions in axially symmetric crossed fields with an external source and sectioned electrodes

17 p2593 A72-35902

Calculation of the dependence of the charge density on the distribution of the potential in crossed symmetric electric and magnetic fields

17 p2593 A72-35903

Magnetic dipole field interaction with plasma flow ions, noting qualitative model of solar wind flow past magnetosphere

17 p2593 A72-35905

The influence of magnetic pressure on the performance of a high-current discharge thermionic converter

18 p2646 A72-36195

Combined Rayleigh and Kelvin instability of a Hall plasma with a vertical magnetic field.

18 p2715 A72-36502

Quasi-linear theory of plasmas situated in a weak UHF electric field and a constant magnetic field

18 p2715 A72-36654

Anisotropy and strong-coupling effects on the critical-magnetic-field curve of elemental superconductors.

18 p2719 A72-36710

Observational evidence for strength and structure of intergalactic magnetic fields, discussing primordial fields effects on galaxy formations and early universe evolution

18 p2726 A72-36728

Hydrodynamic stability of the gradient flow of a conducting fluid with a rheological power law in a transverse magnetic field

18 p2716 A72-36814

Circular-elliptical transformation of jet propagating in homogeneous slipstream within unperturbed uniform transverse magnetic field, using linearized three dimensional boundary layer equations

18 p2716 A72-36815

Hall phenomena in a plasma flow situated in a traveling magnetic field

18 p2716 A72-36816

Discontinuities in a collisionless plasma flow having a strong magnetic field.

18 p2717 A72-37042

Study of the mechanism of motion of nonequilibrium plasma inhomogeneities in a magnetic field

18 p2717 A72-37176

Propagation of electromagnetic waves in a rarefied plasma situated in an alternating magnetic field

18 p2717 A72-37177

Magnetic surface equation and collisional diffusion of finite beta tokamak plasma in low density regime

19 p2838 A72-37330

Equilibrium configurations of Vlasov plasmas carrying a current component along an external magnetic field.

19 p2839 A72-37332

Green function for temporal electromagnetic plasma wave echoes oblique to external magnetic field, calculating current density and damping term

19 p2839 A72-37333

The Rayleigh-Taylor problem with a vertical magnetic field, including the effects of Hall current and resistivity.

19 p2839 A72-37339

Classification of the magnetohydrodynamic motions of a rotating fluid

19 p2839 A72-37392

Angular distribution measurements of photoemitted electrons for InAs by means of magnetic field.

19 p2843 A72-37406

Drude theory of electromagnetic waves in an inclined magnetic field. I - One-band model of charge carriers.

19 p2840 A72-37510

Parametric excitation of electromagnetic waves.

19 p2834 A72-37718

The effect of contacts on microwave emission from InSb.

19 p2844 A72-37728

Radiation scattering matrix derivation with allowance for phase correlation, deriving method of radiation transfer equations solution for magnetic field

19 p2834 A72-37819

Propulsive performance of a 30 kW arc-jet thruster stabilized by vortex and magnetic forces.

19 p2848 A72-37925

Coherent radiation emission by indium antimonide in a transverse magnetic field

19 p2845 A72-38176

Solitary waves properties and propagation at right angles to magnetic field in two ion beam magnetized plasma

19 p2841 A72-38441

Magellanic clouds structure and dynamics from optical and radio observations, discussing interconnecting magnetic field existence

19 p2865 A72-38481

Unsteady weakly nonlinear waves in a multicompone plasma with allowance for weak dissipation

19 p2842 A72-38528

Effect of ionic viscosity on the stability of a finite-pressure plasma

19 p2842 A72-38529

Dipole antenna radiation in homogeneous plasma layer magnetized by normal uniform magnetic field, calculating radiation pattern

19 p2768 A72-38661

Pulse propagation in a magnetoplasma. I - Longitudinal propagation.

19 p2843 A72-38751

Propagation of Alfvén-gravitational waves in a stratified perfectly conducting flow with transverse magnetic field.

19 p2843 A72-38791

Differentially rotating magnetoid model for quasar and radio galaxies matter ejection and luminosity mechanisms in terms of magnetic field evolution and current sheet generation

20 p2965 A72-38903

Two dimensional linear polarization radio distribution maps of 3C 270 and 3C 452 radio galaxies, relating to source magnetic field structure

20 p2965 A72-38904

The Nyquist criterion for kinematic-dynamo action.

20 p2956 A72-38912

Some new methods of performing low frequency EMC measurements.

20 p2921 A72-38995

Moment of forces on spacecraft with low angular velocities in variable magnetic field, using electrodynamics equations

20 p2976 A72-39245

Solar wind tangential discontinuities and shock waves determination from flux velocity vector, magnetic field and particle density measurements

20 p2964 A72-39259

Transport phenomena in an electron-phonon system in strong magnetic fields at low temperatures

20 p2953 A72-39310

Determination of the magnetic field B in vacuum for general two-dimensional MHD-equilibria.

20 p2957 A72-39352

Plasma equilibrium in configurations with a helical magnetic axis with allowance for toroidality.

20 p2957 A72-39353

Gas laser emission fluctuations of total radiation energy, polarized field components and line widths in longitudinal magnetic field

20 p2931 A72-39377

Isotropically and anisotropically polarized He-Ne lasers output dependence on longitudinal magnetic fields, noting electron density radial redistribution in gas discharge plasma

20 p2932 A72-39411

Radiation from a particle in static electric and magnetic fields.

20 p2956 A72-39459

Spherical kinematic dynamo models with asymmetric magnetic fields based on mean field electrodynamics and on nearly axisymmetric limit

20 p2954 A72-39875

Computer simulation of RF-confinement of plasmas in an open-ended toroidal quadrupole.

21 p3089 A72-40191

Electrodynamical analysis of superconducting vortices interaction with cylindrical cavities (pinning), calculating critical currents in type II superconductors in external magnetic field

21 p3096 A72-40416

Isometric motion in relativistic magnetohydrodynamics.

21 p3091 A72-40567

The study of turbulence in theta-pinch plasma with azimuthal magnetic field.

21 p3091 A72-40571

Force free fields in type II superconductors.

21 p3096 A72-40573

Dispersion equations solved for electron and ion cyclotron waves propagating perpendicularly to magnetic field in plasma

21 p3091 A72-40656

Weakly ionized plasma decay within cylinder with electrically conducting walls in presence of longitudinal magnetic field, determining electric current dependence on cylinder length

21 p3091 A72-40657

He ions motion normal to magnetic field under induced electric field, analyzing resonance mechanism

21 p3091 A72-40660

Measurement of internal magnetic field distribution in axially magnetized YIG rods based on magnetoelastic resonance absorption.

21 p3097 A72-40692

Interaction of a steady plasma flow with a dipole magnetic field in the presence of a radial electric field.

21 p3093 A72-41388

Spatial measurement of the magnetic field direction in plasma.

21 p3094 A72-41633

Helical field experiments on a three-meter theta pinch.

21 p3094 A72-41636

Propagation of magnetohydrodynamic shock waves in a medium with diminishing density

21 p3094 A72-41653

Investigation of the interaction between a plasma flow and an axisymmetric magnetic field

21 p3094 A72-41655

The magnetic field of eddy currents above a surface crack in metal with excitation of them by an applied inductor.

21 p3057 A72-41722

Effect of a random magnetic field on the absorption line characteristics of stars

21 p3113 A72-41761

Trajectory equations of laminar electron flow in exponential magnetic field, calculating electrode shapes of magnetron injection electron gun

21 p3088 A72-41835

Accuracy of the conservation of the third adiabatic invariant of charged-particle motion in axisymmetric fields. II

22 p3217 A72-42209

Hydrodynamic instability of a plasma boundary with a magnetic field, taking viscosity into account

22 p3210 A72-42277

Self-consistent description of the magnetotail current system.

22 p3172 A72-42429

Boundary fluctuations of a plasma column with a current

22 p3211 A72-42655

Critical superconductivity currents measurement in niobium based U shaped and coiled wires within steady magnetic field

22 p3190 A72-42735

Electromagnetic disturbances within a degenerate electron plasma in a quantizing magnetic field

22 p3212 A72-43010

Injection of an electron beam into a plasma bounded by a conducting casing

22 p3213 A72-43105

Confinement time of plasma injected in magnetic field of racetrack with diverter, noting plasma equilibrium in toroidal magnetic field

22 p3213 A72-43106

Motion of plasmoids in a multipole magnetic field of toroidal configuration

22 p3214 A72-43120

Current instability of electron-ion plasma in magnetic field produced by moving resonance charges

23 p3317 A72-43203

Isolated finite amplitude electrostatic oscillations production in thin plasma layer between two parallel metallic surfaces in magnetic field

23 p3317 A72-43204

Steady motion of dense electron beam in rarefied phonon plasma along magnetic field, analyzing polarization effects

23 p3317 A72-43207

Dynamic behavior of long-period oscillations of surface wave type in system of inhomogeneous ion beams moving in dense plasma along magnetic field

23 p3317 A72-43209

Equilibrium equations for vortex lines with allowance for interaction with boundary of ideal superconductor, calculating extremum values of magnetic field

23 p3312 A72-43316

The $Z_{sub} e$ field, some of its properties, and its geophysical informativeness

23 p3283 A72-43373

Plasma diagnostics for electron-ion oscillation discharge in alternating positive-negative electrodes under axial magnetic field, noting electrons drift

23 p3319 A72-43403

Calculation of the parameters of a plasma accelerated in a high-frequency electric field and a static magnetic field

23 p3320 A72-43660

Plasma-beam interaction in limited geometry: Temperature effects

23 p3321 A72-43700

Laplace equation for homogeneous magnetic field perturbation by superconducting elliptical cylinder and by two parallel circular cylinders

23 p3313 A72-43779

Longitudinal dielectric tensor for an electron gas in a uniform magnetic field.

23 p3321 A72-43808

Method for solving the problem of radiation in an anisotropic plasma

23 p3321 A72-44220

Circularly polarized waves in magnetoplasmas containing negative ions.

23 p3323 A72-44533

Multicomponent plasmas with static magnetic field, deriving dielectric tensor and dispersion relation for wave propagation by linearization technique

24 p3428 A72-44967

Longitudinal magnetic field effect on the characteristics of a high frequency ion source

24 p3428 A72-45015

Charged particles propagation in magnetic field and scattering medium with constant and variable transport mean free path, applying to proton propagation for solar flares

24 p3435 A72-45076

Kinetic approximation for confined electron beam stability in plasma situated in magnetic field, deriving instability increments and dispersion relations

24 p3428 A72-45078

Superhigh-frequency heating of a plasma and longitudinal electron heat conductivity in a magnetic field

24 p3429 A72-45492

Current induced drift rate of plasma electrons in electric and magnetic fields, noting electron velocities in turbulent heating of plasma

24 p3429 A72-45507

Current-driven drift wave instability in a sheared magnetic field.

24 p3430 A72-45570

Thermal conductivity in dirty transition-metal superconductors near the upper critical field.

24 p3432 A72-45675

Plasma-ion beam system drift beam instability in longitudinal magnetic field, noting oscillations frequencies dependence

24 p3431 A72-45713

MAGNETIC FILMS

Domain configuration observation of magnetic holograms in oriented MnBi films

03 p0359 A72-13447

MnBi magnetic film optical memory system characteristics evaluation, considering laser power requirement, bit packing density and SNR

[IEEE PAPER 3,4]

03 p0332 A72-13754

Ten million bit magnetic film computer memory, discussing design, fabrication, performance and cost per bit

[IEEE PAPER 11,1]

03 p0327 A72-13761

Nondestructive readout in computer storage of plated wires on Permalloy film deposited substrates, testing design parameters effects on performance

[IEEE PAPER 11,2]

03 p0332 A72-13762

Plated-wire computer memory using thin Permalloy film on W wire substrate, testing nondestructive and destructive readout characteristics

[IEEE PAPER 11,3]

03 p0327 A72-13763

High speed easy rewrite read-only memory using plated wire with multilayered nondestructive readout magnetic thin film, testing performance

[IEEE PAPER 11,4]

03 p0332 A72-13764

Destructive readout computer memory of wire substrate electrodeposited with two thin Permalloy layers separated by Cu

[IEEE PAPER 11,5]

03 p0332 A72-13765

Iterative hysteretic model for calculating magnetization distribution in thin magnetic layer for digital recording systems

[IEEE PAPER 14,7]

03 p0328 A72-13769

Coupled-film closed-easy-axis arrays for large capacity NDRO multiple-write bulk memory, discussing disturb mechanisms limitation on performance and design

[IEEE PAPER 21,9]

03 p0328 A72-13780

Annealing effects in plated-wire memory elements, discussing recrystallization in Permalloy films from grain size and magnetic dispersion observations

04 p0504 A72-15716

Magnetic stress anisotropy field in plated cylindrical Permalloy films, determining relationships to circumferential composition variation, geometry and easy-axis dispersion

04 p0564 A72-15717

Bubble and strip magnetic domains creation, annihilation and manipulation in epitaxial magnetic garnet films by laser beam thermal absorption induced local heating

22 p3185 A72-42612

MAGNETIC FLUX

Dember-Hall voltage ratio for low magnetoconcentration in intrinsic semiconductor

01 p0113 A72-10044

Magnetospheric magnetic field distortions under quiet and slightly disturbed conditions, obtaining scalar intensity with OGO 3 and 5 rubidium vapor magnetometer

01 p0060 A72-10886

Solar magnetic fields time fluctuation determination using longitudinal, intensity and line of sight velocity measurements

03 p0356 A72-13278

Magnetic field strengths from umbral spectral lines in sunspots

03 p0428 A72-13301

Solar magnetic field structure determination in active regions from H alpha morphology obtained with chromospheric magnetograph, discussing emerging flux region role

03 p0428 A72-13304

Solar magnetic fields time fluctuation determination using longitudinal, intensity and line of sight velocity measurements

03 p0430 A72-13318

MHD processes responsible for solar flares in polarity boundaries of magnetic fields, determining magnetic energy change and flux

03 p0410 A72-13322

Solar proton flare connection with strong electric currents, discussing net magnetic flux changes and electric conductivity and field strength

03 p0410 A72-13326

Plasma jet formation within high pressure discharges in air at atmospheric pressure, discussing electrode configuration, current density and accelerating magnetic field strength

03 p0396 A72-13662

Polyphase signal generators, using reversed flux region propagation in saturable ring core controlled by switching transistors operation

[IEEE PAPER 17,5]

03 p0322 A72-13773

Two dimensional MHD turbulent flow generation in strong magnetic field

03 p0398 A72-14004

Inviscid incompressible conducting fluid motion under line sink in uniform strong magnetic field

[AD-740535]

04 p0550 A72-15343

Superposable and self-superposable MGD flows from nonlinear differential equations, considering entropy, flow velocity and magnetic field strength

05 p0694 A72-16030

Galactic high energy electron differential spectrum, estimating spatial distribution and random magnetic field intensity

05 p0709 A72-16237

Electromagnetic wave propagation in rectangular waveguide with periodic ferrite structure, presenting computer graphics for stop bandwidth vs magnetic field strength

05 p0627 A72-16342

Sunspot magnetic field strength rapid variation, discussing spot group development and flare activity

05 p0722 A72-17155

Plasma jet injection stoppage and reflection in strong transverse magnetic field, considering instability due to flow interactions

06 p0860 A72-17694

Magnetic flux determination in magnetosphere tail during substorm from auroral oval boundary and center location observation

06 p0807 A72-17985

Output power dependence on pressure and magnetic field strength in Kr ion laser for green, yellow and red lines

06 p0826 A72-18010

Geomagnetic field intensity fluctuations due to events in atmosphere, ionosphere, magnetosphere and in interplanetary space connected with solar activity

06 p0809 A72-18276

Nonlinear microwave absorption by plasma between cyclotron and hybrid frequencies for critical magnetic field

06 p0776 A72-18408

Magnetic and electric field intensities measurement with charged particle beams in coaxial high temperature plasma sources

06 p0863 A72-18415

Low latitude surface horizontal magnetic field intensity depression due to quiet time ring current in magnetosphere as function of solar wind velocity

07 p0155 A72-18884

Critical magnetic flux indications of microanomalous plasma diffusion in electron bombardment ion engines

07 p0154 A72-19614

Local structure of solar magnetic fields in sunspots as complexes of microspots

07 p1079 A72-20008

Optimal location of nonreciprocal disk shaped YIG element traveling wave quantum rub paramagnetic amplifier for weak magnetic levels

08 p1138 A72-20795

Impedance strip synthesis on symmetric cylindrical antenna excited by phased magnetic flux ring, determining radiation pattern for pure reactance conditions

08 p1131 A72-20932

Pulsar braking index and period-pulse width distribution calculations within proposed model leading to neutron star surface magnetic field strength estimates

08 p1235 A72-21389

Boltzmann equation solution in terms of irreducible spherical tensors and Talmi coefficients, calculating stress tensor for fully ionized plasma in strong magnetic field

09 p1341 A72-22681

Solar wind properties and discontinuity characteristics, describing particle densities, wind speed, magnetic field level and near earth electron and ion temperatures

09 p1377 A72-22756

Whistler damping factor dependence on magnetic field strength in geometrical optics approximation, emphasizing nonlinear effects at low frequencies in ionospheric propagation

09 p1282 A72-23516

Rb 87 line shift produced by rare buffer gases and molecular nitrogen measured from applied magnetic field magnitude and hyperfine structure of D lines

10 p1490 A72-24040

Geomagnetic field inflation during magnetic storm main phase, considering energy sources and injected proton plasma radial velocity

10 p1472 A72-24274

Semiconductor IC transducers for electrical readout of optical radiation, mechanical stress and magnetic field strength

10 p1448 A72-24282

Normal ionizing shock waves characteristics in He under varying conditions of magnetic field strength, discharge current and gas pressure

11 p1694 A72-25789

Electron bombardment ion thruster performance characteristics with variable magnetic baffle and hollow cathode

[AIAA PAPER 72-489]

11 p1710 A72-26214

Ar laser levels population inversion dependence on current density, discharge tube pressure and magnetic flux

11 p1649 A72-26350

Magnetic field line connection between F region irregularities causing scintillation and ionospheric conditions inducing spread E

11 p1625 A72-26405

Geomagnetic tail and substorm activity structure from IMP-3 magnetic data, discussing plasma sheet thickness changes and magnetic flux distribution

11 p1627 A72-26533

Physical properties of atoms, molecules and solid material in ultrastrong magnetic field, using quantum drift approximation

12 p1847 A72-27055

One-wavelength MHD induction generator operated on NaK flow system with various excitation conditions, calculating magnetic flux density and power by Fourier series

13 p1900 A72-29364

Drift dissipative instability in bounded gas discharge plasma within magnetic field, investigating oscillations dependence on gas pressure and field strength

13 p2016 A72-29605

Plasma ion heating by magnetoacoustic waves, presenting resonance peak-magnetic field intensity relations for various densities and ion energy

13 p2019 A72-29913

Energy storage in chromospheric magnetic flux ropes in solar flares, discussing kink perturbation instability suppression

13 p2049 A72-29936

Minimum magnetic field energy of two dimensional magnetosphere with neutral sheet for arbitrary dipole inclination to solar wind as function of potential difference on boundary points

14 p2101 A72-30643

Sense coil geometry and drive waveform effects on low level flux gate magnetometers sensor noise

15 p2233 A72-31507

Ar laser levels population inversion dependence on current density, discharge tube pressure and magnetic flux

16 p2402 A72-33703

Nonlinear microwave absorption by plasma between cyclotron and hybrid frequencies for critical magnetic field

17 p2588 A72-34858

Magnetic and electric field intensities measurement with charged particle beams in coaxial high temperature plasma sources

17 p2588 A72-34864

Rotary shocks and waves of relativistic magnetohydrodynamics

17 p2593 A72-35908

Earth surface magnetic field intensity variations in terms of magnetospheric resonator excitation, assuming three dimensional Alfvén waves

18 p2688 A72-36869

Generation of the large-scale magnetic field of the galaxy. II

19 p2864 A72-38079

A line-profile Stokesmeter - Preliminary results on non-sunspot fields.

20 p2971 A72-39761

On the filamentary nature of solar magnetic fields.

20 p2971 A72-39762

On the filamentary nature of active-region magnetic fields.

20 p2971 A72-39764

Flux vortices and transport currents in type II superconductors.

20 p2961 A72-39809

HF absorption of electromagnetic field in ionized oxygen plasma as function of dc discharge current

20 p2958 A72-39969

Sweet's mechanism for the destruction of magnetic flux.

20 p2955 A72-40017

A numerical solution for the near and far fields of an annular ring of magnetic current.

21 p3015 A72-40354

Drift dissipative instability in bounded gas discharge plasma within magnetic field, investigating oscillations dependence on gas pressure and field strength

21 p3091 A72-40659

Activity of the secular behavior of the geomagnetic field

22 p3168 A72-41924

Solar polar regions magnetic fields polarity and strength during 1960-1971

22 p3221 A72-42026

A possibly direct measurement of coronal magnetic field strengths.

22 p3222 A72-42042

Plasma sheet characteristics of geomagnetic tail at 60 earth radii, inferring spatial distribution of magnetic field magnitude and plasma energy density

22 p3211 A72-42407

An optical magnetic probe with pulsed detector voltage.

22 p3177 A72-42447

Numerical integration of integral equation for phased array radiation modeled by impedance fila-

- ments in conductive plane, noting excitation by magnetic flux 22 p3159 A72-42663
- Magnetic flux penetration into superconducting thin films. 23 p3323 A72-43271
- Electric field orientation, magnetic field strength and high voltage pulse delay effects on spark chamber track displacement from true particle trajectory 23 p3291 A72-44441
- Magnetic field fluctuations during substorms. 24 p3396 A72-44853
- Electron bremsstrahlung from hot plasma in the presence of strong magnetic field. 24 p3431 A72-45627
- Physical properties of atoms, molecules and solid material in ultrastrong magnetic field, using quantum drift approximation 24 p3427 A72-45708
- MAGNETIC FORMING**
- Al alloys degree of deformation dependence on pulse energy during extrusion by pulsed magnetic field, showing hardening effect 09 p1319 A72-22865
- Magnetic-explosive welding /magneweld/ process using capacitor discharge through wire coil, noting sintered Al powder and Zircaloy 2 applications 09 p1321 A72-23638
- Electrohydraulic and electromagnetic metal forming, using capacitor stored energy conversion into hydraulic shock waves or magnetic pressure to deform sheet metal components, pipes, etc 15 p2243 A72-31323
- MAGNETIC INDUCTION**
- Aligned fields in MHD shock polar equation, obtaining magnetic induction polar variables 01 p0106 A72-10135
- Geomagnetism, discussing world field distribution, secular variation, paleomagnetism, archaeomagnetism, origin, magnetic anomaly and earth electromagnetic induction 01 p0053 A72-10168
- Magnetosonic perturbations caused by ideally conducting sphere expansion in cold plasma, determining electric field and magnetic induction time dependences 02 p0217 A72-11939
- Filamentary magnetic structure production on plasma current sheath of coaxial deuterium operated accelerator for laboratory observations of solar flare processes 03 p0411 A72-13338
- Induced current distribution in flat narrow conducting strip moving in inhomogeneous magnetic field, presenting current field and densities 03 p0311 A72-13564
- Plasma flow under inhomogeneous axially symmetric magnetic field, investigating axial component of poloidal Hall induction current 03 p0395 A72-13570
- Variational problem of conducting fluid flow in MHD channel at large magnetic Reynolds numbers at induction saturation 03 p0397 A72-13999
- Anisotropic plasma rotational discontinuity theory, considering parallel and perpendicular components of plasma pressure and magnetic induction 05 p0695 A72-16074
- Neutral rotating mass shell surrounding concentric stationary electrically charged insulation, calculating induced dipole-like magnetic field from coupled linearized general relativity field equations 06 p0853 A72-18423
- Magnetic induction distribution in second species superconductor cylindrical samples after limited flux jumps, proposing instability propagation model 09 p1369 A72-22797
- Electron bombardment type simplified ion source with magnetic field induction by filament heating current, discussing design and characteristics 10 p1518 A72-23965
- Induced current distribution in flat narrow conducting strip moving in inhomogeneous magnetic field, presenting current field and densities 11 p1691 A72-26751
- Plasma flow under inhomogeneous axially symmetric magnetic field, investigating axial component of poloidal Hall induction current 11 p1699 A72-26757
- Steel components contact fatigue kinetics measurement by emf increase of inductive sensor 12 p1887 A72-28245
- Machine oil wear degree and Fe content determination by placing sample into induction coil and measuring coil Q at RF 13 p1957 A72-29142
- Magnetosonic perturbations caused by ideally conducting sphere expansion in cold plasma, determining electric field and magnetic induction time dependences 13 p1949 A72-29251
- Solid and composite rotor induction motors, comparing predicted characteristics based on analytical and numerical analyses 15 p2182 A72-31779
- Device for ac induction measurements in air, using the Gauss effect in germanium semiconductor diodes 17 p2529 A72-34767
- Voltagages induced in superconductors in the absence of transport currents. 18 p2719 A72-36744
- A kinematic theory of large magnetic Reynolds number dynamos. 19 p2833 A72-37248
- Some problems of electromagnetic induction in the equatorial electrojet region. II - The analysis of magnetic and telluric variations at Zaria, Nigeria. 19 p2789 A72-37772
- MAGNETIC INDUCTION PROBES**
- U MAGNETIC PROBES**
- MAGNETIC LENSES**
- Charged particle motion equations for fifth order spherical aberration of quadrupole-octupole lens with arbitrary electrode and pole shapes 05 p0638 A72-16989
- Rotationally symmetrical electromagnetic lenses of electron mirror and cathode lens type 10 p1513 A72-24977
- A design method for the electron beams of TWT's. 19 p2775 A72-38610
- Low light level optics for image forming photoemissive sensors, discussing refractive and catadioptric lenses and reflective systems with magnetic focusing 20 p2921 A72-39029
- Improvements in electro-optic circular-scan deflectors. 21 p3050 A72-40146
- Compression of high current relativistic electron beams using converging magnetic fields. 23 p3315 A72-43525
- MAGNETIC MATERIALS**
- NT FERROMAGNETIC FILMS**
- NT FERROMAGNETIC MATERIALS**
- NT MAGNETITE**
- NT PERMALLOYS [TRADEMARK]**
- Supermagnetization and ac core loss temperature dependence under slow temperature cycling in vacuum, noting anomalous Barkhausen effect 04 p0564 A72-15718
- Monograph on Co alloy permanent magnets covering principles, magnetization and testing, alnicos, magnet steel and miscellaneous alloy technology, fine particle magnets and applications 08 p1217 A72-21481
- Microstrip propagation and loss filling factor design formulas for magnetic substrates 11 p1599 A72-26991
- Magnetic recording head designs, covering information density, head-tape subsystems and head materials electrical and mechanical suitability 16 p2394 A72-33643
- Magnetic materials. 17 p2595 A72-34571
- Physicochemical properties of rare earth metals for alloying Al, Mg, Cu and Ti, noting getter and permanent magnet materials 22 p3191 A72-42806
- MAGNETIC MEASUREMENT**
- Skyllark rocket observations of sporadic E layer magnetic fields, winds and ionization indicating ion divergence region 01 p0052 A72-10086
- Magnetic survey worldwide earth coverage by land, sea and airplane measurements data 02 p0220 A72-12085
- Thermal zero signal instabilities and error reduction in devices using reluctance sensors 02 p0231 A72-12562
- Solar magnetic field measurements using electromagnetic radiation, atmospheric structure /MHD effects/ and energy equipartition 03 p0427 A72-13277
- Solar magnetic fields time fluctuation determination using longitudinal, intensity and line of sight velocity measurements 03 p0356 A72-13278
- Calibration of polarimetric measurements in terms of magnetic fields, using Stokes parameters without line formation dependence 03 p0427 A72-13280
- Magnetic atomic beam absorption filter for high resolution solar field observations 03 p0357 A72-13290
- Magnetic field measurements at different depths of solar atmosphere active regions by Crimean Astrophysical Observatory double magnetograph, showing close correlation 03 p0428 A72-13302
- Solar magnetic fields time fluctuation determination using longitudinal, intensity and line of sight velocity measurements 03 p0430 A72-13318
- Solar longitudinal magnetic field measurements in polar prominence, noting configuration similarity to arc 03 p0432 A72-13355
- Meridian and local vertical gyro errors effects on geomagnetic field elements determination accuracy 03 p0359 A72-13559
- Weak magnetic moments measurement under pressure and over wide temperature range by Faraday method, discussing magnetometer and cryogenic equipment modifications 04 p0522 A72-15478
- Wind tunnel six component magnetic balance system, describing ferromagnetic body forces and moments relationship to applied magnet fields and gradients [AIAA PAPER 72-164] 05 p0645 A72-16829
- Papers on geophysics covering magnetic measurements and natural vlf phenomena 06 p0802 A72-17366
- Geomagnetic field measurement, discussing variometers and magnetographs theory 06 p0812 A72-17370
- Geomagnetic field vector components measurement methods, considering data processing problems 06 p0812 A72-17371
- Geophysical applications of high resolution magnetometers to geomagnetic measurements, archaeological investigations and satellite sounding of planetary magnetic fields 06 p0812 A72-17374
- Magnetic vector directions determination in sunspots by fringe technique with corrections for instrumental polarization in line spectrum 06 p0889 A72-18326
- Dissipative magnetic parameters measurement in ferrite and insertion loss measurement in waveguide Y-circulators below microwave resonance 06 p0786 A72-18367
- Transverse ionizing shock waves in gaseous hydrogen at speeds to 4000 km/sec, presenting magnetic shock structure and magnetic field jump measurements [AD-738620] 06 p0863 A72-18531
- Imp 5 magnetic field measurements at high geomagnetic latitudes in outer magnetosphere near noon meridian, noting depressed field region centered on polar cusp 07 p0975 A72-19146
- Interplanetary magnetic sector structure at 1962-1969 solar maxima, noting Pioneer 9 magnetometer experiment observations 07 p1071 A72-19161
- Ultrasensitive measurement technique for low microwave susceptibility on ferrite samples featuring feedback scheme for signal klystron locking 07 p0955 A72-19320
- Pulsar rotation and dispersion from polarization and pulse arrival time observations, calculating magnetic field components in path to pulsars 07 p1072 A72-19343
- Transverse magnetic field measurement over sunspot in chromosphere, noting fan-shaped field line divergence 08 p1232 A72-21135
- Magnetic spectra measurement of powdered hexagonal ferrites in millimeter wavelength range during grinding and after heat treatment 08 p1218 A72-21875
- Magnetic field measurement methods and magnetometers performance in superconducting, thin film, resonance and fluxgate areas 09 p1308 A72-22465
- Ferromagnetic thin film magnetometers operation and performance characteristics for magnetic field measurement 09 p1308 A72-22467
- Resonance magnetometers for magnetic field measurement, discussing classification, operation principles and general properties 09 p1308 A72-22468
- Fluxgate magnetometry, discussing weak field sensors, low power devices and various applications 09 p1308 A72-22469
- Diamagnetic energy measurements on rotating plasma in crossed static electric and magnetic fields with short circuiting metal wall 10 p1519 A72-24097
- Search coil magnetometer for measurement of weak alternating magnetic fields encountered by Helios solar probe in space 11 p1632 A72-25804
- Magnetic field direction measurement in Tokamak toroidal plasma by laser light scattering, using Fabry-Perot interferometer 11 p1697 A72-26583
- Metagalactic magnetic field contributions to observed Faraday rotation measurements for distant extragalactic radio sources 13 p2039 A72-29088
- Aeros satellite magnetic properties, describing measurement procedures for component induced disturbance fields, dipole moments and eddy currents 13 p1940 A72-30080
- Sense coil geometry and drive waveform effects on low level flux gate magnetometers sensor noise 15 p2233 A72-31507
- Tansei satellite spin axis orientation measurement by two flux-gate magnetometers and sun sensor 15 p2272 A72-32334

Magnetic field distribution measurement in axisymmetric plasma column inside Tokamak device by alpha particle beam from radioisotope

16 p2434 A72-32818

Spin effects on satellite-borne cylindrical probe electron density measurements, considering satellite wake and geomagnetic field effects

16 p2389 A72-32962

Flux quantization in superconductors demonstrated by magnetometer probe measurement of magnetic field trapped in thin In film holes

16 p2441 A72-33225

Magnetic balance for magnetic saturation measurement and determination of retained austenite, Curie temperature, permeability and martensite content

16 p2391 A72-33237

Nondestructive test for measuring the state of heat treatment in closure welds.

18 p2695 A72-36672

The treatment of the Stokes parameters and measurement of magnetic field.

20 p2970 A72-39755

Investigation of the structure of a high-current discharge in a lithium plasma

22 p3209 A72-41878

A possibly direct measurement of coronal magnetic field strengths.

22 p3222 A72-42042

Simultaneous solar-wind plasma and magnetic-field measurements in the expected region of the extended geomagnetic tail.

22 p3170 A72-42405

Specific-heat and magnetic measurements in superconducting Ta-Nb alloys.

23 p3323 A72-43273

The equatorial electrojet according to measurements from the Cosmos 321 satellite

23 p3328 A72-43369

Magnetic anomalies in New Guinea-New Zealand region from geomagnetic measurements with proton magnetometer, noting effects of andesite-basalt volcanic processes and nuclear precession signal

23 p3284 A72-43380

Magnetism of meteorites - A review of Russian studies.

23 p3339 A72-44129

Pressure and magnetic field probe measurements in transverse shock waves in ionizing hydromagnetic regimes, investigating bow shock effects on accuracy

24 p3390 A72-44708

Approaches to verification and solution of magnetic particle inspection problems.

24 p3407 A72-44903

MAGNETIC MEMORIES

U MAGNETIC STORAGE

MAGNETIC METALS

U MAGNETIC MATERIALS

U METALS

MAGNETIC MIRRORS

Flutelike microinstabilities in mirror-confined homogeneous magnetized one-species plasma with broad perpendicular velocity distribution

04 p0559 A72-15354

Hydrogen plasma generation by microwave field in magnetic-mirror device due to electron cyclotron resonance, measuring transverse diffusion coefficient dependence on magnetic field

07 p1046 A72-20506

Velocity space instability in hot electron plasma created by adiabatic compression in pulsed magnetic mirror, observing radiation bursts below electron cyclotron frequency during compression

08 p1213 A72-21257

Colliding plasma flows motion and capture in transverse magnetic field with mirror configuration, noting polarization effect

09 p1362 A72-23209

Magnetic mirror system to study Lorentz ionization of highly excited hydrogen atoms with quantum numbers 6-7 in strong magnetic fields

09 p1363 A72-23222

Rotating low density plasma in magnetic mirror trap with Penning discharge, determining conditions for oscillations damping and plasma lifetime

10 p1521 A72-24354

Magnetic mirrors for highly stripped heavy ions production in hot electron plasmas by low voltage high current electron beam

10 p1524 A72-25035

Collisional distributions in mirror plasmas, using successive approximation technique for Fokker-Planck equation lowest eigenvalue and eigenmode

11 p1694 A72-25792

Electron density and temperature measurement from scattering of laser radiation in plasma within axisymmetric toroidal magnetic mirror machine

13 p2017 A72-29609

Dispersion relationship for electrostatic instability associated with electron beam trapped in magnetic mirror of magnetosphere, taking into account nonuniformity of magnetic field

15 p2283 A72-31434

Magnetic field profile optimization for beta-limitation in minimum-B mirror confined plasma in nuclear reactor

16 p2432 A72-32805

Stable mirror plasma machine, determining particle distribution near loss cone by asymptotic analysis based on transit to mean collision times ratio

16 p2432 A72-32808

Electron density and temperature measurement from laser radiation scattering in plasma within axisymmetric toroidal magnetic mirror machine

21 p3091 A72-40663

Interaction of a streaming plasma with a magnetic mirror.

21 p3094 A72-41635

External high-frequency modulation of an electron beam and heating of plasma ions in the case of beam-plasma instability in the magnetic trap

21 p3095 A72-41678

External high-frequency modulation of an ion beam and the absorption of beam-plasma instability oscillations in a plasma situated in a magnetic field of mirror configuration

21 p3095 A72-41683

MAGNETIC MOMENTS

Dynamo theory MHD equations numerical solution, showing rapid variation of electromagnetism field, hydrodynamic velocities and earth core magnetic moment

02 p0217 A72-11933

Electromagnetic wave scattering characteristics at arbitrarily configured body with dimensions smaller than primary field wavelength, determining electric and magnetic moments

02 p0181 A72-12595

Electron paramagnetic resonance investigation of III-V compound semiconductor crystals, observing large magnetic moments, heteropolar chemical bonding and impurities

13 p2021 A72-28572

Dynamo theory MHD equations numerical solution, showing rapid variation of electromagnetism field, hydrodynamic velocities and earth core magnetic moment

13 p1949 A72-29245

Mossbauer and X ray structural analysis of nickel ferrite-chromite magnetic moments, comparing with theoretical data

14 p2141 A72-30171

Magnetoelastic effects in elastic dielectric analysis based on continuum with single magnetic moment, noting magnetically saturated material

15 p2274 A72-31482

Paramagnetic phase induced moment system containing substitutional impurities, calculating mode energies by Green function method in random phase approximation

15 p2295 A72-32546

Surface effects on paramagnetic metals spin susceptibility models, including random-phase-approximation equation derivation and induced magnetic moment calculation

15 p2295 A72-32549

Induced electron emission dependence on polarization, frequency and intensity of second wave incident on electron with anomalous magnetic moment

16 p2424 A72-33365

Study of the Stark effect in the resonance lines of sodium by an atomic jet method

22 p3209 A72-43048

MAGNETIC PERMEABILITY

Pressure induced d band deformation effect on magnetic susceptibility of Ti-V and V-Cr alloys

03 p0370 A72-13087

Digital magnetic temperature transducer using permeability discontinuity at Curie temperature for high stability and reproducibility without calibration [IEEE PAPER 8, 5]

03 p0332 A72-13758

Second harmonic generation, coherence lengths and second order susceptibilities near band edge in InSb as function of magnetic field

03 p0404 A72-14269

Electron correlation effects on low temperature thermodynamics of amorphous semiconductors, predicting Curie law magnetic susceptibility and equilibrium electronic specific heat dependence on temperature

04 p0562 A72-15153

NMR behavior and magnetic susceptibility of intermetallic compound CeAl, noting exchange polarization of RKKY type between 4f electrons and conduction electrons

05 p0702 A72-16784

Electrical resistance, Hall coefficient and magnetic susceptibility of transition metal nitrides at low and room temperatures

06 p0827 A72-17386

Ultrasensitive measurement technique for low microwave susceptibility on ferrite samples featuring feedback scheme for signal klystron locking

07 p0955 A72-19320

Diamagnetic enhancement of magnetic susceptibility of amorphous semiconductors, considering mobility states and paramagnetic Van Vleck reduction

09 p1373 A72-23508

Magnetic susceptibility of ternary Al-Mn alloys with Ti, Va, Cr, Fe, Co, Ni, Cu and Zn, describing microstructure and aging experiments

10 p1494 A72-23832

Fcc lattice ferromagnetic alloys para-process susceptibility anomalous increase explanation by phase transition thermodynamic theory

13 p1977 A72-28911

Ionosphere radio wave propagation from fluid plasma wave and magnetically nonpermeable medium electrodynamics studies

15 p2193 A72-31281

Langmuir probe susceptance- and conductance-voltage measurements via in-phase and quadrature component plots as function of applied dc potential

15 p2241 A72-32515

Orbiting electron magnetic susceptibility derivation from many band Hamiltonian using Bloch representation to avoid decoupling transformation ambiguity

15 p2282 A72-32547

Surface effects on paramagnetic metals spin susceptibility models, including random-phase-approximation equation derivation and induced magnetic moment calculation

15 p2295 A72-32549

Magnetic balance for magnetic saturation measurement and determination of retained austenite, Curie temperature, permeability and martensite content

16 p2391 A72-33237

Magnetic shielding effectiveness of metal cylinder tubes with periodically imbedded annular transverse Bloch walls of high permeability

16 p2369 A72-33669

Special features of the operation of ferroperobs with low-permeability core moulds at small excitation fields.

19 p2804 A72-38760

Magnetism of meteorites - A review of Russian studies.

23 p3339 A72-44129

Application of a strongly doped semiconductor model to the study of thermodynamic and conductivity properties

24 p3432 A72-45068

MAGNETIC POLES

Electromagnetic emission from pulsar with magnetic force tube on surface of magnetosphere treated as rotating magnetic multipole

02 p0285 A72-12833

Solar polar magnetic fields, discussing inversion line location, observations, data analysis, general field and computer reduction

03 p0432 A72-13356

Magnetic monopole search in lunar samples by electromagnetic measurement, determining flux limits for cosmic radiation and pair production in proton-nucleon collisions

06 p0880 A72-17884

On the state of the geomagnetic field and its reversals.

17 p2548 A72-35323

H alpha loops incompatibility with stable filaments/prominences/ noting magnetic loops existence between regions of opposite polarity

17 p2617 A72-35704

Three dimensional seismic monitoring system developed from inertial guidance gyroscopes and accelerometers, noting pole shift observation, tilting during earth tides and earthquakes forecasting [AIAA PAPER 72-840]

20 p2923 A72-39088

Solar polar regions magnetic fields polarity and strength during 1960-1971

22 p3221 A72-42026

MAGNETIC PROBES

Fluxgate magnetometry, discussing weak field sensors, low power devices and various applications

09 p1308 A72-22469

Nanosecond response magnetic probes to measure fast disturbances in oblique shock waves within collisionless plasma, describing experimental technique

15 p2235 A72-31646

Magnetic probe measurement of random fluctuations in transverse magnetic field caused by He plasma produced in arc discharge

15 p2287 A72-32408

MAGNETIC PROPERTIES

NT ANTIFERROMAGNETISM

NT CURIE TEMPERATURE

NT DIAMAGNETISM

NT FERROMAGNETISM

NT GEOMAGNETISM

NT GYROFREQUENCY

NT GYROMAGNETISM

NT MAGNETIC EFFECTS

NT MAGNETIC INDUCTION

NT MAGNETIC MOMENTS

NT MAGNETIC PERMEABILITY

NT MAGNETIC RELAXATION

NT MAGNETIC RIGIDITY

NT MAGNETIC SUSPENSION

NT MAGNETOACOUSTICS

NT MAGNETOACTIVITY

NT MAGNETORESISTIVITY

NT MAGNETOSTRICTION

NT PALEOMAGNETISM

NT PARAMAGNETISM

NT POLARIZATION CHARACTERISTICS
NT RELUCTANCE
NT REMANENCE
NT SPIN-LATTICE RELAXATION
NT THERMOMAGNETIC EFFECTS

Short wave radio reception and signal path at magnetically conjugate point in Southern Hemisphere, using 40-110 msec delay times

Apollo 12 lunar crystalline rock and fines magnetic properties measurement, noting magnetic minerals composition

Lunar induced and permanent magnetism, discussing solar wind dynamic pressure effects and Apollo data

Large scale solar magnetic field properties, discussing rotation, patterns and effects on corona

Reliable Permalloy integrated magnetic memories with realizable low switching coefficients and square-loop properties, discussing design and fabrication

Lunar craters and maria origin from rock and sample chemical composition and magnetic differentiation

Nd-Dy alloy magnetic and structural properties over entire composition range

La superconductivity pressure dependence based on valency considerations, noting actinides metals and alloys localized magnetism explanation by simple model

Magnetic properties and paleomagnetic data of Permian Cutler and Elephant Canyon formations in Utah, discussing thermal demagnetization and origin of stable magnetization

Viking Lander magnetic properties investigation of Martian surface with implications for planetary composition and differentiation and atmospheric interaction

Magnetic properties, electrical resistivity and hardness of vacuum melted Ni-Fe-Ta alloys

Skew magnetic structure of ionizing shock waves with ohmic dissipation as dominant diffusion mechanism

Magnetic structure of ionizing oblique shock waves with transverse and normal components in zero magnetic Prandtl number limit

Magnetic structure of normal ionizing shock waves with zero transverse energetic component

Magnetovariometers design, operation and applications, discussing ferromagnetic materials properties effect on performance characteristics

Investigation method for shock wave induced demagnetization in YIG, noting impact study of magnetic properties

Aeros satellite magnetic properties, describing measurement procedures for component induced disturbance fields, dipole moments and eddy currents

Magnetization and temperature interrelationship in high constant magnetic field for Apollo 11, 12 and 14 rocks, obtaining magnetic hysteresis curves

Degenerate electron gas magnetic properties implications for metals, white dwarfs and neutron stars, discussing nonmagnetic state for thermal equilibrium

Structural rings impulsively loaded by magnetic pressure between two parallel current-carrying conductors

Magnetic materials.

Magnetic properties and texture of a thin strip of nickel-iron-molybdenum alloys

Magnetic properties of the powders of highly dispersed iron-cobalt-nickel alloys

MAGNETIC PUMPING

Electron-ion heating in high beta perpendicular collisionless shock waves by plasma cylinder magnetic compression using theta pinch

Nonthermal emission of a magnetoactive plasma in the field of super-high-frequency pumping wave

Parallel pumping of spin waves in yttrium garnet single crystals

Resonances in the collisionless heating of a plasma by transit time magnetic pumping.

MAGNETIC RECORDING

Long life magnetic tape recorder for onboard data storage in space flights, discussing two motor tape transport and static memories for improved reliability

Iterative hysteretic model for calculating magnetization distribution in thin magnetic layer for digital recording systems

Solar magnetogram recorded mean photospheric magnetic field cross correlation with interplanetary magnetic field

Error probability distribution of digital data magnetic recording in computer drum memory

Control equipment designs for phase error estimation of pulse sequences in multichannel magnetic recording systems

DAMIEN III digital magnetic tape recording system for aircraft flight test data acquisition, discussing components

Magnetic recording head designs, covering information density, head-tape subsystems and head materials electrical and mechanical suitability

Instantaneous velocity nonuniformity measurement of mechanism motion using phasemeters with magnetic data recording

Broadband magnetic tape predetection recording of data modulated carrier MHz radio telemetry signals, applying to Aris, Mercury and Gemini programs

MAGNETIC RELAXATION

NT SPIN-LATTICE RELAXATION

Proton and fluorine nuclear magnetic spin-lattice relaxations due to internal rotations in magnesium fluorosilicate hexahydrate

Dislocation structure analysis in ferromagnetic materials by magnetic techniques, discussing methods based on magnetization curve static properties and magnetic relaxation phenomena

Relaxation methods of magnetic and acoustic spectroscopy for studies of gravitational and inertial dipoles and quadrupoles in molecules and nuclei of solid bodies

MAGNETIC RESONANCE

NT ELECTRON

RESONANCE

NT FERROMAGNETIC RESONANCE

NT NUCLEAR MAGNETIC RESONANCE

NT PARAMAGNETIC RESONANCE

NT PROTON MAGNETIC RESONANCE

NT PROTON RESONANCE

Quasi-linear theory of magnetosphere gyroresonant wave-particle interactions, discussing particle distribution function anisotropy, wave packet effects, whistler mode, energy and pitch angle distributions, etc

Resonance magnetometers for magnetic field measurement, discussing classification, operation principles and general properties

Abrikosov vortex lattice in superconductors, calculating resonance linewidth and vacancy formation energy

In and Gd substitution effect in calcium-vanadium garnets as potential microwave materials, discussing magnetic properties, resonance linewidth and temperature stability

Earth surface magnetic field intensity variations in terms of magnetospheric resonator excitation, assuming three dimensional Alfvén waves

Theoretical study of the Zeeman spectrum and of the magnetic resonance in the evanescent wave of Fresnel - Case of the magnetic transverse mode

Pressure shift of the magnetic resonance line of neon in a He-Ne laser.

MAGNETIC RIGIDITY

Solar cosmic ray cutoff rigidity increase during polar cap absorption related to geomagnetic perturbation onset

Solar cosmic ray cut-off rigidity increase during PCA related to geomagnetic perturbation onset

MAGNETIC SHIELDING

Active shielding against radiation in space using charged particle deflection by electric and magnetic fields

Magnetic shielding effectiveness of metal cylinder tubes with periodically imbedded annular transverse Bloch walls of high permeability

MAGNETIC SIGNALS

Polarization and spatial and frequency characteristics of ground signal resulting from finite source Pc 1 micropulsation disturbance

Tunable wide field birefringent element / filter magnetograph/ to separate polarized magnetic signal from selected spectral line width

MAGNETIC SIGNATURES

Real time analog video magnetogram, describing differential photometer for electronic subtraction technique

Solar magnetic field fine structure from filter magnetograms, tabulating magnetic elements frequency distributions

Solar magnetic field variations in McMath Regions, using longitudinal magnetograms time sequences

Electric field aligned sheet currents of low energy electrons and protons near auroral arc, obtaining magnetic signatures

Pc 5 type geomagnetic pulsations correlation with nighttime magnetosphere auroral magnetic disturbances from magnetograms obtained at Murmansk, College /Alaska/ and Tiksi

Signatures for substorm development of the growth phase and expansion phase.

Energy spectrum of small scale solar magnetic fields.

Pc 5 type geomagnetic pulsations correlation with nighttime magnetosphere auroral magnetic disturbances from magnetograms obtained at Murmansk, College /Alaska/ and Tiksi

MAGNETIC SPECTROSCOPY

Superconducting magnetic spectrometer for cosmic ray nuclei spectrum analysis, describing design, calibration and operation

Digital pulse programmer with saturation burst sequence for pulsed nuclear magnetic resonance spectroscopy

Varian HR-60 NMR spectrometer probe with Dewared insert for low temperature operation

Magnetic-field variations in 78 Virginis, beta Coronae Borealis, and 73 Draconis.

Particle trajectory and time of flight measurement in search for anti-alpha particles in primary cosmic radiation, using magnetic spectrometer with spark chambers

MAGNETIC STARS

Observed light curve amplitude phase relations in Ap magnetic star UVB system, using oblique rotator model

Cosmic rays generation by charged particles acceleration in electromagnetic constant crossed fields during magnetic stars contraction to neutron star dimensions

Magnetic star theory, postulating stellar magnetic flux as slowly decaying relic of flux in prestar gas, considering dissipation processes and rotation

Dynamo theory of magnetic stars, proposing symmetrical rotator as alternative to skew rotator

Magnetic neutron stars /pulsars/ atmosphere, questioning vacuum approximation method applicability

Stellar MHD, discussing strongly magnetic stars identification and slow rotation origin based on oblique rotator model

Spectrophotometric investigation of Ap stars. I - Two-dimensional quantitative spectral classification

Spectral variabilities of magnetic peculiar A stars associated with atmospheric chemical composition anomalies, using inclined rotator model

MAGNETIC STORAGE

NT CORE STORAGE

NT MAGNETIC DRUMS

Magnetic bubble devices in memory hierarchies - IEEE Conference, Denver, April 1971

16 p2369 A72-33669

13 p1922 A72-29391

13 p2045 A72-29706

03 p0357 A72-13286

03 p0429 A72-13315

03 p0430 A72-13327

13 p1947 A72-28606

20 p2916 A72-39237

20 p2971 A72-39765

24 p3398 A72-45106

07 p0983 A72-19315

12 p1806 A72-27125

15 p2240 A72-32435

21 p3106 A72-41036

22 p3219 A72-42568

06 p0882 A72-18008

07 p1056 A72-19042

09 p1387 A72-22754

10 p1546 A72-24833

14 p2160 A72-30887

16 p2460 A72-33923

19 p2858 A72-37813

23 p3335 A72-43297

- Ten million bit magnetic film computer memory, discussing design, fabrication, performance and cost per bit
[IEEE PAPER 11,1] 03 p0327 A72-13761
- Nondestructive readout in computer storage of plated wires on Permalloy film deposited substrates, testing design parameters effects on performance
[IEEE PAPER 11,2] 03 p0332 A72-13762
- Plated-wire computer memory using thin Permalloy film on W wire substrate, testing nondestructive and destructive readout characteristics
[IEEE PAPER 11,3] 03 p0327 A72-13763
- High speed easy rewrite read-only memory using plated wire with multilayered nondestructive readout magnetic thin film, testing performance
[IEEE PAPER 11,4] 03 p0332 A72-13764
- Computerized design algorithm for ferrite core memory system, considering cross-temperature effect under worst driving conditions
[IEEE PAPER 11,8] 03 p0327 A72-13766
- Holographic optical techniques application to bulk magnetic storage for high information density and memory capacity and fast random access
[IEEE PAPER 19,4] 03 p0361 A72-13776
- Mathematical model for design of plated-wire magnetic memory cell, considering drive requirement minimization as criterion
[IEEE PAPER 21,1] 03 p0328 A72-13777
- Low cost large array of decoding magnetic switches with electrodeposited Au conductors and Permalloy memory elements featuring high output flux for low driving current
[IEEE PAPER 21,3] 03 p0328 A72-13778
- Reliable Permalloy integrated magnetic memories with realizable low switching coefficients and square-loop properties, discussing design and fabrication
[IEEE PAPER 21,4] 03 p0328 A72-13779
- Coupled-film closed-easy-axis arrays for large capacity NDRO multiple-write bulk memory, discussing disturb mechanisms limitation on performance and design
[IEEE PAPER 21,9] 03 p0328 A72-13780
- Magnetic bubble repertory dialer memory design, noting bit storage capacity and random access
[IEEE PAPER 28,1] 03 p0328 A72-13782
- Annealing effects in plated-wire memory elements, investigating Cu and Permalloy interdiffusion at low temperatures by X ray diffraction and electron beam microprobe
04 p0503 A72-15715
- Annealing effects in plated-wire memory elements, discussing recrystallization in Permalloy films from grain size and magnetic dispersion observations
04 p0504 A72-15716
- Mass storage systems technologies covering magnetic recording, surface wave acoustics, magneto-optic beam addressing, magnetic bubbles, switchable resistances and IC memories
09 p1283 A72-23413
- Storage characteristics of plated magnetic wire for nondestructive read and write
16 p2369 A72-33672
- MAGNETIC STORMS**
- Plasma sheet structures, dynamics and role in magnetospheric substorm onset as function of near earth and distant merging regions
01 p0052 A72-10082
- Geomagnetic storm field recovery near synchronous satellite ATS 1 in terms of ring current belt and plasma sheet variations
01 p0053 A72-10088
- Lower ionosphere ionization response to auroral particle fallout during 1968 substorms, using geomagnetic, VLF and balloon measurements
01 p0053 A72-10366
- Ionospheric composition of ions and neutral gases during magnetic storm, using coupled differential equations
01 p0054 A72-10425
- Decreasing period micropulsations during elementary magnetospheric substorms, discussing relation to ring current asymmetry development
01 p0059 A72-10602
- Earth magnetosphere boundary position, bow shock wave, transition region thickness and magnetopause currents magnetic fields during geomagnetic storms
01 p0059 A72-10605
- Auroral absorption and DR currents development during magnetic storms, discussing corpuscular fluxes arrival from magnetospheric tail into lower ionosphere
01 p0059 A72-10619
- High latitude magnetotail highly directed nearly monoenergetic positive ions population observation during geomagnetic storms, using Vela satellites electrostatic analyzers
01 p0060 A72-10887
- Magnetic field and plasma sheet variations observation by IMP 3 satellite in distant magnetotail during magnetospheric substorms
01 p0060 A72-10888
- Isolated magnetospheric substorms model, explaining electric field origin, cold plasma flow, magnetic field lines and particle phenomena
01 p0060 A72-10889
- Stable red arc 6300 Å emission calculation from satellite electron temperature and density data during geomagnetic storms
01 p0061 A72-10893
- Magnetospheric wave and particle phenomena correlation to convection electric fields in nighttime magnetosphere during isolated substorms
01 p0062 A72-10904
- ATS Faraday rotation measurement data on total electron content during geomagnetic storms, giving first midlatitude ionosphere average storm patterns and seasonal influence analysis
02 p0216 A72-11900
- DR-current belt dynamics during magnetic storm based on ground observation data on midlatitude red arcs
02 p0217 A72-11929
- Night sky upper ionospheric electron concentration perturbations during magnetic storm, noting latitudinal distribution
02 p0217 A72-11940
- Incomplete ring current decay during magnetic storm development, discussing field asymmetry based on global network synchronous observations and generation mechanism by protons
02 p0218 A72-11949
- Geomagnetic storms and anomaly observation by Satellite 1964 83C telemetry data transmission to ground stations network
02 p0219 A72-12083
- Plasma sheet positive ions flux enhancement detection at lunar distance during lunar eclipse and geomagnetic storm
02 p0283 A72-12452
- Damped geomagnetic pulsations associated with geomagnetic storms interpreted as interaction between hydromagnetic oscillations and solar wind induced magnetospheric motions, discussing modified mathematical model
02 p0222 A72-12872
- Geomagnetic field and interplanetary plasma parameters daily variations correlation, taking into account corrections for storm time effects
03 p0348 A72-13511
- Plasma sheet thinning in substorms correlated to auroral oval poleward expansion and associated phenomena in magnetotail
03 p0348 A72-13514
- Magnetic storm effects on neutral atmospheric composition above 400 km, discussing energy deposition
03 p0349 A72-13518
- Vertical motions of midlatitude F 2 layer during magnetospheric substorms, investigating electric field distribution
03 p0349 A72-13519
- Soviet book on calms and storms in upper atmosphere covering energy variations, auroras, geomagnetic storms, weather forecasting, etc
03 p0350 A72-13967
- Solar wind effects on storms and structure of magnetosphere and radiation belt maintenance
03 p0350 A72-14304
- Statistical analysis of low latitude F 2 layer disturbances associated with sudden commencement type geomagnetic storms, investigating critical frequencies
04 p0516 A72-14937
- Upper atmosphere and ionosphere magnetic storm phenomena, showing atomic to molecular concentration ratio decrease
04 p0516 A72-14938
- Ionospheric electron content changes during 25-26 May 1967 magnetic storm event from geostationary satellite monitoring
04 p0516 A72-14940
- Atmospheric density near 150 km altitude from Cosmos 316 orbital decay, noting density increases during geomagnetic storms
05 p0655 A72-16070
- Magnetic storm disturbing effect on integral electron density in F 2 layer and in topside ionosphere
05 p0657 A72-16262
- Auroral substorms development phases, noting auroral arcs latitudinal shifting during genesis phase
05 p0657 A72-16273
- Magnetic baylike disturbances and multiple midlatitude 6300-Å auroral arcs during geomagnetic storm recovery phase and concurrent ionospheric current system
05 p0630 A72-16620
- Geomagnetic disturbances morphology, considering development and decay of magnetic storms and appearance of geomagnetic pulsations
06 p0802 A72-17367
- Worldwide magnetic storm due to solar wind interaction with geomagnetic field, discussing field deformation
06 p0803 A72-17368
- VLF wave excitation during sudden storm commencement, causing magnetosphere trapped energetic electrons to diffuse and precipitate into lower ionosphere
06 p0803 A72-17451
- Geomagnetically trapped low energy proton flux distribution due to 17 April 1965 magnetic storm, noting adiabatic effects
06 p0803 A72-17452
- Geomagnetic storm associated quasi-sinusoidal magnetic field micropulsations due to Alfvén/drift instability or enhanced storm-time ring current
06 p0804 A72-17454
- Equatorward motion of midday auroras during magnetospheric substorms, using all sky photographs
06 p0805 A72-17463
- Solar flare effectiveness relation to magnetic field orientation from magnetic storms development analysis
06 p0873 A72-17984
- Ionospheric storms features based on F2 critical frequency data, investigating magnetosphere during geomagnetic storms
06 p0810 A72-18280
- Geomagnetic tail role in magnetospheric substorms, discussing solar wind energy storage, magnetic merging process and plasma sheet origin
07 p0977 A72-20032
- Geomagnetic phenomena associated with auroras and magnetic storms, investigating analog modeling experiment by stationary electrical discharges under laboratory conditions
07 p0980 A72-20457
- Shock wave excitation by moving solar wind discontinuity in geomagnetic tail as cause of active phase of magnetospheric substorm
08 p1153 A72-20716
- Geomagnetic field fluctuations during storms, considering Alfvén waves generation and propagation in solar wind and magnetosphere
08 p1153 A72-20717
- F 2 layer diffuse reflections and critical frequencies increase on ionogram recordings during Northern Hemisphere nighttime magnetic storm of 2 December 1967, noting cosmic radio emission decrease
08 p1154 A72-20738
- Vertical distribution of electron density seasonal anomaly and storm effects in daytime midlatitudes topside ionosphere from Alouette 1 data
08 p1155 A72-20814
- Midlatitude and equatorial geomagnetic micropulsations during 13-14 January 1967 world-wide magnetic storm from ground and satellite observations
08 p1157 A72-21107
- Ionospheric electron density nighttime changes as function of local time, height and latitude during geomagnetic storms
08 p1157 A72-21113
- Perturbation effects on F 2 layer and outer ionosphere electron density profiles during successive magnetic storms from Alouette 1 satellite data
08 p1157 A72-21145
- Polar magnetic substorm generation through ionospheric current intensification in westward electrojet localized region, noting interplanetary magnetic field role
08 p1159 A72-21494
- Auroral zone neutral wind velocity and atmospheric temperature correlations with geomagnetic activity, considering ion-neutral particle drag as accelerating mechanism during magnetic storms
08 p1161 A72-21535
- Upper atmospheric oxygen red line diurnal variations and midnight minimum, noting emission relation to kinetic temperature in magnetic storm
09 p1296 A72-22234
- Equatorial ring current relation to polar electrojet during magnetosphere geomagnetic storm, discussing magnetosphere-ionosphere current systems
09 p1298 A72-22580
- Geomagnetic field inflation during magnetic storm main phase, considering energy sources and injected proton plasma radial velocity
10 p1472 A72-24274
- Magnetic storm effects in atmospheric neutral composition, noting thermospheric wind circulation role due to Joule heating within auroral zone
10 p1476 A72-24957
- Geometric parameters variations of ionospheric N/h/ profiles and characteristics during magnetic storm, discussing prognosis procedures from solar activity, latitude and season
11 p1594 A72-26273
- F region N/h/ profiles and parameters deviations during ionospheric and magnetic storms, discussing perturbation index
11 p1594 A72-26275
- Ogo-5 observation of lower hybrid resonance noise, bursts, VLF hiss and whistlers near plasmapause during large magnetic storm
11 p1624 A72-26399
- Geomagnetic tail and substorm activity structure from IMP-3 magnetic data, discussing plasma sheet thickness changes and magnetic flux distribution
11 p1627 A72-26533
- Geomagnetic field perturbation biological effects, studying geomagnetic storm field energy levels and magnetic flux variables relation to human sensitivity thresholds
12 p1773 A72-28210

Upper atmosphere particle flux density determined from nocturnal electromagnetic absorption caused by geomagnetic storms, noting ionization process time lag in lower ionosphere
13 p1945 A72-28580

DR-current belt dynamics during magnetic storm based on ground observation data on midlatitude red arcs
13 p1948 A72-29241

Night sky upper ionospheric electron concentration perturbations during magnetic storm, noting latitudinal distribution
13 p1949 A72-29252

Incomplete ring current decay during magnetic storm development, discussing field asymmetry based on global network synchronous observations and generation mechanism by protons
13 p1949 A72-29261

Midnight auroral electrojet time variations relationship to midday auroras latitudinal shift during South Pole magnetospheric substorms
13 p1950 A72-29382

Low energy proton flux increases associated with geomagnetic storms due to interplanetary shock waves occurring during solar cosmic ray flare event decay
13 p2032 A72-29724

Global ionospheric electron density variations and associated thermospheric winds during 15-21 June 1965 geomagnetic storm from ground based and satellite data
13 p1953 A72-29805

Infrasonic excitation of red oxygen emission at 6300 A during geomagnetic storms at middle latitudes
14 p2098 A72-30146

Geomagnetic storms caused by quasi-stationary directed corpuscular streams resulting from solar chromosphere flares
14 p2147 A72-30487

Global electron concentration disturbances in low and middle latitude F2 during magnetic storm
14 p2100 A72-30635

Auroral electron spectrum space-time dynamics during magnetospheric substorms, using X ray bremsstrahlung balloon data
14 p2101 A72-30637

Expanding auroral bulge front photographs during auroral substorm, noting violent curl motions and arcs formation
15 p2223 A72-31439

Lower Arctic thermosphere neutral composition changes due to disturbances, considering atomic hydrogen, nitric oxide, hydroxyl, water vapor, nitrogen and oxygen
15 p2225 A72-31912

Unshocked solar wind detection by ATS 5 satellite during 8 March 1970 geomagnetic storm
15 p2299 A72-31960

Ionospheric ion temperatures and velocities and electron and neutral densities from incoherent scatter observations during 11 February 1969 magnetic storm
15 p2229 A72-32254

Geomagnetic substorm magneto-ionospheric effect, discussing electric field transmission, magnetic field variations and currents flowing in dynamo region
15 p2230 A72-32259

High latitude trapping boundary for 20 KeV electrons and 100 KeV protons during intense geomagnetic substorms, observing field-line motion
16 p2444 A72-32958

Solar flare producing regions statistical correlation to SC/SI events accounting for geomagnetic storms and Forbush decreases in terms of interplanetary streams
16 p2445 A72-33376

Model for magnetospheric substorm growth phase, noting daytime magnetopause convection onset, geomagnetic tail configurational changes and breakup with auroral electrojet development
16 p2387 A72-33903

Daytime irregular geomagnetic pulsation, Pid, and its relation to magnetospheric substorm.
17 p2546 A72-35062

Flaring-tail model explanation for geomagnetic tail configuration changes during magnetospheric substorm growth phase
17 p2548 A72-35589

Energetic electron intrusion into inner radiation zone during and after 2 September 1966 geomagnetic storm, noting radial diffusion role
17 p2601 A72-35596

Geomagnetic effect on the neutral temperature of the F region during the magnetic storm of September 1969.
17 p2549 A72-35603

Precipitation dynamics and energy spectrum of auroral electrons in the midnight sector during a magnetospheric substorm
17 p2550 A72-35854

Auroral substorm and proton auroras during moderate geomagnetic disturbances
17 p2550 A72-35857

Equatorial anomaly changes caused by ionospheric disturbances, noting diurnal variations of magnetic storm effect
17 p2551 A72-35868

Geomagnetic storms correlation with chromospheric flare series and with central meridian passages of recurrent positive plages
18 p2723 A72-36087

Comprehensive investigation of individual geomagnetic storms.
18 p2686 A72-36226

Geomagnetic activity and the solar situation in the neighbourhood of proton effects.
18 p2686 A72-36227

Sudden commencements of geomagnetic storms at the turn of two solar cycles.
18 p2686 A72-36228

Atmospheric model synthesis of observed electron temperatures and concentrations in tropical ionosphere during 8 March 1970 magnetic storm, noting F2 region features
18 p2686 A72-36296

North-south asymmetry in cosmic ray intensity increases before magnetic storms
18 p2722 A72-36851

Ionospheric magnetic disturbances during March 1970 related to solar flare corpuscular and proton fluxes, generating ring current and PCA absorption
18 p2688 A72-36857

Latitudinal energy distribution of geomagnetic disturbances
18 p2688 A72-36868

Measurements of MeV-electrons during the recovery-phase of a polar magnetic substorm on March 6, 1970.
19 p2789 A72-37409

Geomagnetic storms caused by quasi-stationary directional corpuscular streams resulting from solar chromosphere flares
19 p2851 A72-38316

Geomagnetic effect of solar wind rotational discontinuity observed by Explorer 34, noting magnetic storm initial phase relation to high latitude nonstationary ionospheric current attenuation
19 p2852 A72-38343

Shock wave excitation by moving solar wind discontinuity in geomagnetic tail as cause of active phase of magnetospheric substorm
19 p2791 A72-38344

Geomagnetic field fluctuations during storms, considering Alfvén waves generation and propagation in solar wind and magnetosphere
19 p2791 A72-38345

F 2 layer spread reflections and critical frequencies increase on ionogram recordings during Northern Hemisphere nighttime magnetic storm of 2 December 1967, noting cosmic radio emission decrease
19 p2791 A72-38366

Perturbation effects on F 2 layer and outer ionosphere electron density profiles during successive magnetic storms from Alouette 1 satellite data
20 p2916 A72-39250

Positive geomagnetic bays in evening high-latitudes and their possible connection with partial ring current.
21 p3049 A72-41387

On the physical mechanism of the magnetospheric substorm development.
22 p3169 A72-42012

Some topside electron density measurements from Ariel III satellite during the geomagnetic storm of 25-27 May 1967.
22 p3169 A72-42017

Magnetospheric substorm onset examined via simultaneous balloon X ray and electric field measurements, discussing ATS 5 observations
22 p3170 A72-42409

Coordinated observations of the magnetosphere - The development of a substorm.
22 p3171 A72-42410

Investigation of interaction between Pc 1 and 2 and Pc 5 micropulsations at the synchronous orbit during magnetic storms.
22 p3171 A72-42412

Statistical characteristics of storm-associated Pc 5 micropulsations observed at the synchronous equatorial orbit.
22 p3171 A72-42413

Geomagnetic storm and seasonal effects on spread of monthly distribution and average behavior of midlatitude F region electron peak density and slab thickness
22 p3172 A72-42434

Magnetic storm classification from geomagnetic field H and Z components behavior, associating with solar corpuscular flux
22 p3174 A72-42952

Families of geomagnetic storms, direction of the interplanetary magnetic field, and solar activity
23 p3283 A72-43371

Rocket measurements of electron influx during a major magnetic storm with type A aurora.
23 p3332 A72-44515

Quadruple conjugate pair observations of the sudden commencement absorption event on June 17, 1965.
23 p3286 A72-44526

Preconditions for the triggering of polar magnetic substorms by storm sudden commencements.
23 p3286 A72-44531

Symposium on the Morphology and Physics of Magnetospheric Substorms, Moscow, USSR, August 3, 1971, Proceedings.
24 p3395 A72-44846

Quiet, growth, expansive and recovery phases of auroral morphology, noting interplanetary magnetic field turning relation to substorm
24 p3396 A72-44848

Behavior of outer radiation zone and a new model of magnetospheric substorm.
24 p3396 A72-44850

Plasma sheet variations during substorms.
24 p3396 A72-44851

Magnetic field fluctuations during substorms.
24 p3396 A72-44853

Electric field variations during substorms - OGO-6 measurements.
24 p3396 A72-44854

Upper atmosphere particle flux density determined from nocturnal electromagnetic absorption caused by geomagnetic storms, noting ionization process time lag in lower ionosphere
24 p3397 A72-45080

MAGNETIC SUBSTORMS
U MAGNETIC STORMS
MAGNETIC SURVEYS
Papers on world geomagnetic survey 1957-1969 covering land, sea, airplane and polar-orbiting geophysical observatory satellite observations, magnetic anomalies and reference field
02 p0219 A72-12080

Geomagnetic survey by polar-orbiting OGO 2 and 4, discussing data acquisition and reduction results and accuracy
02 p0219 A72-12081

Geomagnetic survey by Cosmos-49 satellite as international program, discussing data analysis and observation accuracy
02 p0219 A72-12082

Magnetosphere and adjacent regions magnetic surveys by OGO 1 and 3 satellites, discussing magnetopause, bow shock, magnetosheath, geomagnetic tail, ring current and polar substorms
02 p0220 A72-12084

Magnetic survey worldwide earth coverage by land, sea and airplane measurements data
02 p0220 A72-12085

Conducting fluid convective motion in earth core estimated from geomagnetic field and time derivative data at earth surface
02 p0220 A72-12087

Latitudinal rotation direction daytime characteristics of pc 5 pulsation polarization based on global magnetic observations
18 p2689 A72-36870

Secular variation of the geomagnetic field in epoch 1965 to 1970 according to observatory and satellite data
18 p2689 A72-36871

Earth main magnetic field description by cartography and analytic methods based on dipole or spherical harmonic series representations
23 p3283 A72-43366

Some results of an analysis of Pc4-type steady geomagnetic pulsations at a network of stations
23 p3283 A72-43372

MAGNETIC SUSCEPTIBILITY
U MAGNETIC PERMEABILITY
MAGNETIC SUSPENSION
Electromagnetic suspension - Conference, Southampton, England, July 1971
10 p1460 A72-24756

Superconducting magnetic suspension and balance facility of supersonic wind tunnel for dynamic stability studies
10 p1460 A72-24757

Superconducting levitron machine for trapped hot plasma stability and confinement studies in vacuum, discussing construction and coil performance
10 p1460 A72-24758

Superconducting coil design for magnetic suspension of supersonic wind tunnel balance
10 p1460 A72-24759

Automatic electromagnetic suspensions using tuned RLC saturable reactor control
10 p1460 A72-24761

Electromagnetic remote model positioning sensing system for wind tunnels with magnetic suspension, using differential transformer action
10 p1461 A72-24762

Wind tunnel model magnetic suspension system with remote position sensor based on optical contrasts scanning analysis
10 p1461 A72-24763

Optical TV scanning for wind tunnel model position detection in magnetic suspension system for sphere low density drag measurements
10 p1461 A72-24764

[ONERA, TP NO. 988]
Aerodynamic force and moment measurements on model in magnetic wind tunnel balance system, using field equations
10 p1461 A72-24765

Data acquisition and reduction for model aerodynamics in superconducting magnetic suspension and balance of supersonic wind tunnel facility
10 p1461 A72-24766

Power supply for magnetic suspension system, using controlled rectifier and dc power amplifier circuits

10 p1461 A72-24767

Wind tunnel model remote position sensing and control systems, discussing drift reduction in magnetic suspension

10 p1461 A72-24768

Static aerodynamic characteristics of bulbous based cone models and slender wings at subsonic speed, using magnetic suspension and balance system

10 p1461 A72-24769

Aerodynamic data acquisition with magnetic balance on wind tunnel model delta and AGARD G wing planforms and body of revolution

10 p1462 A72-24770

Magnetic balance measurements of aerodynamic forces on spheres and slender cones in hypersonic low density wind tunnels, noting sting effect

10 p1462 A72-24771

Spheres drag coefficient measurements in laminar flow as function of Reynolds number, using wind tunnel model magnetic suspension system

10 p1419 A72-24772

Superconducting magnetic suspension systems safety aspects, discussing relief valves for He boil-off, flowmeters, cryostat temperature monitors, power supply diodes and safety interlocks

10 p1462 A72-24774

Iron rotational hysteresis effect in cold magnetic balance wind tunnel system for spinning aircraft configurations and subsonic flow regimes

10 p1462 A72-24776

Analysis of cryogenic suspensions for use in spacecraft

22 p3230 A72-42208

Residual drag torque on magnetically suspended rotating spheres.

23 p3315 A72-44540

MAGNETIC SWITCHING

Logic functions for magnetic bubble devices based on interaction of circular magnetic domains in rare earth iron oxides, considering gates for dynamic memory

03 p0327 A72-13753

Low cost large array of decoding magnetic switches with electrodeposited Au conductors and Permalloy memory elements featuring high output flux for low driving current

03 p0328 A72-13778

Reliable Permalloy integrated magnetic memories with realizable low switching coefficients and square-loop properties, discussing design and fabrication

03 p0328 A72-13779

Mass storage systems technologies covering magnetic recording, surface wave acoustics, magnetooptic beam addressing, magnetic bubbles, switchable resistances and IC memories

09 p1283 A72-23413

MAGNETIC TAPE RECORDERS

U MAGNETIC RECORDING

U TAPE RECORDERS

MAGNETIC TAPES

Moving window displays for IR scanner signals, producing images on magnetic video tape

02 p0228 A72-11852

Magnetic recording head designs, covering information density, head-tape subsystems and head materials electrical and mechanical suitability

16 p2394 A72-33643

Investigation of the strength and deformability of thin composite materials of magnetic recorder type. I. Strength and deformability at elevated temperatures

21 p3073 A72-41707

MAGNETIC TRANSDUCERS

Digital magnetic temperature transducer using permeability discontinuity at Curie temperature for high stability and reproducibility without calibration

03 p0332 A72-13758

Linear negative feedback dc current magnetic transducers for telemetry input signals, discussing operation principles and design

16 p2370 A72-33862

Application of N equalizing and compensating signals in a single-cell reciprocal magnetoelectric transducer

24 p3386 A72-45315

MAGNETIC TRAPS

U PLASMA CONTROL

MAGNETIC VARIATIONS

NT GEOMAGNETIC MICROPULSATIONS

NT GEOMAGNETIC PULSATIONS

NT NOCTURNAL VARIATIONS

Geomagnetic field and AU/AL index variations with UT during international quiet days at high latitudes interpreted as electrojet diurnal redistribution

02 p0217 A72-11930

Statistical characteristics of rough sea compared with variable magnetic fields near Crimean coast in Black Sea

02 p0218 A72-11951

Equatorial ionospheric drift measurements and relation to electrojet from H component geomagnetic field variations

02 p0221 A72-12459

Lunar surface magnetic field variations, considering solar wind effect

02 p0285 A72-12871

Five component electromagnetic field station to record geomagnetic field magnetic and electric components variations

05 p0643 A72-16253

Charged particles injection effects on magnetic perturbations relation to integral auroral luminance intensity from whole sky photometry measurements

05 p0658 A72-16277

Trapped particle motion response to collapsing dipole moment in secularly varying geomagnetic field

07 p1058 A72-19158

Geomagnetic variations propagation theory for LF electromagnetic and Alfvén waves diffraction at stratified earth in thin gyrotopical ionosphere

08 p1130 A72-20711

Geomagnetic field fluctuations during storms, considering Alfvén waves generation and propagation in solar wind and magnetosphere

08 p1153 A72-20717

Quasi-periodic ionospheric electron density fluctuations effects on electromagnetic waves propagation, noting effect on surface recordings as geomagnetic variations

08 p1156 A72-20824

Magnetic fluctuations in elf and vlf waves in space, discussing whistler phenomena and applications to magnetospheric probes

08 p1158 A72-21189

Geomagnetic field short term variations as function of solar activity from solar radiation data harmonic analysis, relating large amplitude fluctuation to seasonal variations

09 p1304 A72-23503

Semiannual and annual modulation of geomagnetic field horizontal intensity, suggesting two component model of generating mechanism

10 p1476 A72-24960

Geomagnetic field and magnetosphere variations due to solar wind interactions, using rocket, satellite and indirect measurements

11 p1621 A72-25841

Low latitude geomagnetic field diurnal variations caused by solar wind associated component, noting evening side depression

11 p1713 A72-26109

Ap stars with variable periods from magnetic and photometric data analysis

12 p1868 A72-27221

Abridged version of 1970 Soviet conference on constant geomagnetic field and paleomagnetism, reviewing secular variation data

13 p1946 A72-28588

AU and AL indices variations effect on geomagnetic field during international quiet days at high latitudes interpreted as electrojet diurnal redistribution

13 p1948 A72-29242

Statistical characteristics of rough sea compared with variable magnetic fields near Crimean coast in Black Sea

13 p1949 A72-29263

Geomagnetic activity index Ap correlation with daily magnetic variations during quiet sun year 1964

15 p2230 A72-32260

Geomagnetic and meteorological elements lunar daily variation calculation by modified Chapman-Miller method, estimating confidence limits for parameters reliability

16 p2384 A72-32972

Planetary waves in terms of geomagnetic secular variation due to earth core fluid oscillation under MHD forces, using thick shell model

16 p2385 A72-33342

Critical component of the interplanetary magnetic field responsible for large geomagnetic effects in the polar cap.

17 p2548 A72-35590

Geomagnetic activity annual variation investigation, showing 12-month wave existence

17 p2549 A72-35605

Spherical analyses of the principal geomagnetic field for the years 1550 through 1800

18 p2689 A72-36874

Some problems of electromagnetic induction in the equatorial electrojet region. II - The analysis of magnetic and telluric variations at Zaria, Nigeria.

19 p2789 A72-37772

Geomagnetic variations propagation theory for LF electromagnetic and Alfvén waves diffraction at stratified earth in thin gyrotopical ionosphere

19 p2765 A72-38339

Rotation period variation in long term behavior of interplanetary magnetic sector structure during nearly four solar cycles

19 p2868 A72-38731

Geomagnetic activity index Ap variation spectral data analysis, noting correlation to sunspot number variation

19 p2793 A72-38747

Lunar magnetic variations at Trelew /Argentina/.

19 p2794 A72-38860

Quiet day daily geomagnetic field variability associated with equatorial ionospheric upheavals, noting longitudinal extent

19 p2794 A72-38869

Seasonal, diurnal and magnetic dependence of ionospheric scintillation at 64 deg invariant latitude.

20 p2916 A72-39226

The interpretation of surface equatorial magnetic daily variations on disturbed days.

20 p2916 A72-39238

Activity of the secular behavior of the geomagnetic field

22 p3168 A72-41924

Short period geomagnetic variations, discussing origin by different solar activity mechanisms

22 p3173 A72-42544

The sunspot cycle and solar and lunar daily variations in H.

22 p3228 A72-42882

Solar-wind parameter variation, magnetic activity, and electrons in the magnetospheric tail and outer radiation belt

23 p3283 A72-43367

The Z sub e field, some of its properties, and its geophysical informativeness

23 p3283 A72-43373

The effects of magnetic field oscillations on the boundary layer flow past a magnetized plate.

23 p3321 A72-43725

The effect of change in the geomagnetic dipole moment on the rate of the earth's rotation.

23 p3285 A72-43819

Magnetic pulsation spectra in a nonisothermal plasma

23 p3323 A72-44483

Annual and solar-magnetic-cycle variations in the interplanetary magnetic field, 1926-1971.

23 p3286 A72-44504

Magnetic field fluctuations during substorms.

24 p3396 A72-44853

Abridged version of 1970 Soviet conference on constant geomagnetic field and paleomagnetism, reviewing secular variation data

24 p3397 A72-45088

MAGNETICALLY TRAPPED PARTICLES

NT ARTIFICIAL RADIATION BELTS

NT INNER RADIATION BELT

NT OUTER RADIATION BELT

NT PROTON BELTS

NT RADIATION BELTS

Magnetic field stability in Tornado-2 trap as function of helical currents on concentric sphere

06 p0863 A72-18406

Separatrix structure and stability of helical Tornado trap magnetic field from electron space charge measurements

06 p0863 A72-18407

Magnetospherically trapped particles sources, losses and transport processes, presenting time averaged proton, electron and alpha particle distributions in trapping and pseudo-trapping regions

07 p1062 A72-20028

Geomagnetically trapped protons, electrons and alpha particles verification and measurements in inner and outer radiation belts

07 p1062 A72-20227

Two dimensional model for plasma without magnetic field trapped near current sheet end in dipole magnetic field resembling geomagnetic tail

08 p1157 A72-21108

Multipole magnetic field configuration effectiveness in electromagnetic plasma trap, discussing electron losses critical angle and captured ions maximum density

09 p1363 A72-23221

Nonadiabatic and atmosphere induced energy losses as causes of proton capture in geomagnetic field

11 p1715 A72-26915

Energetic electron and proton trapping in lower solar atmosphere magnetic field, discussing particle injection, bremsstrahlung and gyro synchrotron radiation

13 p2046 A72-29719

Geomagnetically trapped protons pitch angle distribution from ESRO 2 semiconductor telescope measurements

15 p2300 A72-31991

Closed magnetic fields of helical ring currents on concentric spheres surrounded by conductor /Tornado trap/

17 p2588 A72-34855

Magnetic field stability in Tornado-2 trap as function of helical currents on concentric spheres

17 p2588 A72-34856

Separatrix shape, presence and position and electron lifetime and space charge in helical Tornado trap magnetic field

17 p2588 A72-34857

External high-frequency modulation of an electron beam and heating of plasma ions in the case of beam-plasma instability in the magnetic trap

21 p3095 A72-41678

Transformation of trapped charged particles to transit particles under the influence of a high-frequency electric field 24 p3429 A72-45494

MAGNETITE
Magnetite forms in Orgueil meteorite, observing platelets, stackings and framboids by scanning electron microscope 04 p0569 A72-14506
Electronic model for low temperature transition in magnetite with nonintegral average electron number on site 11 p1701 A72-26023

MAGNETIZATION
Anhyseretic contact printing magnetization simulation by computer with Preisach diagram modified by Onsager field effect [IEEE PAPER 14,2] 03 p0327 A72-13768
Iterative hysteretic model for calculating magnetization distribution in thin magnetic layer for digital recording systems [IEEE PAPER 14,7] 03 p0328 A72-13769
Supermendum magnetization and ac core loss temperature dependence under slow temperature cycling in vacuum, noting anomalous Barkhausen effect 04 p0564 A72-15718
Monograph on Co alloy permanent magnets covering principles, magnetization and testing, alnicos, magnet steel and miscellaneous alloy technology, fine particle magnets and applications 08 p1217 A72-21481
Pinning force of vortex lines and microstructural inhomogeneities in superconductors, using magnetization and critical current measurements 09 p1369 A72-22796
Magnetization and elastic stresses effect on Ni dislocations movement due to domain wall interactions 09 p1371 A72-22866
Magnetic properties and paleomagnetic data of Permian Cutler and Elephant Canyon formations in Utah, discussing thermal demagnetization and origin of stable magnetization 09 p1305 A72-23668
Lunar breccia and crystalline rocks thermoremanent magnetization characteristics, presenting alternating field and thermal demagnetization curves 14 p2154 A72-30507
Magnetization and temperature interrelationship in high constant magnetic field for Apollo 11, 12 and 14 rocks, obtaining magnetic hysteresis curves 14 p2155 A72-30517
Natural remanent magnetism creation in meteorites via shock passage in collisional fragments 16 p2451 A72-32990
Hard superconductors cylindrical samples irreversible magnetization and size effect calculation, comparing results with experiment on Nb-Ti alloy specimens 16 p2441 A72-33523
Low field magnetization measurements at 4.2 K on bulk and thin film niobium nitride, discussing Pauli spin paramagnetism and spin-orbit scattering 16 p2442 A72-33843
Possibility of using the eddy-current method to measure the local magnetization of an object. 19 p2805 A72-38761
Spin wave theory and sublattice magnetization of Cr obtaining wave velocity 21 p3097 A72-40626
Quantum-chemical model of organic ring-shaped molecule with persistent magnetization at microscopic level 22 p3150 A72-42318
Thermal stability of lunar rock remanence, indicating magnetization components acquired after initial cooling 22 p3226 A72-42535
Spontaneous magnetization of Ni foils in high pressure H gas, noting Hall voltage measurement in ferromagnetic foils and thin plates 23 p3324 A72-44140

MAGNETO-OPTICS
Optics for data processing, discussing magneto-optic and holographic memories in computer systems 01 p0035 A72-11315
Photosensitive magneto-optic films for large capacity computer memories 01 p0035 A72-11316
Data holder made of three thin ferromagnetic coupled films for magneto-optic computer memory 01 p0035 A72-11317
MnBi magnetic film optical memory system characteristics evaluation, considering laser power requirement, bit packing density and SNR [IEEE PAPER 3,4] 03 p0332 A72-13754
Thin film optical waveguides using magneto-optic GdIG as substrate, discussing computerized design for propagation mode converter efficiency [IEEE PAPER 3,6] 03 p0332 A72-13755
Magneto-optic storage density and read-write rate, discussing transducer cost, solid state injection lasers, holographic techniques and high activity data base applications [IEEE PAPER 19,1] 03 p0361 A72-13774

Holographic optical techniques application to bulk magnetic storage for high information density and memory capacity and fast random access [IEEE PAPER 19,4] 03 p0361 A72-13776
Mathematical model for reciprocal and nonreciprocal magneto-optical effects in magnetized ferrite-filled microstrip transmission lines 04 p0502 A72-15434
Electromagnetic radiation modulators in millimeter and submillimeter wave range using gas-discharge plasma magneto-optical effects in alternating magnetic field 05 p0625 A72-15826
Magneto-optical effects on circular polarization in sunspots within Fe I 6302.5 A line 05 p0719 A72-16514
Magneto-optical effect on CW radiation intensity of Ar laser with cell in magnetic field for various gain conditions 07 p1009 A72-20615
Mass storage systems technologies covering magnetic recording, surface wave acoustics, magneto-optic beam addressing, magnetic bubbles, switchable resistances and IC memories 09 p1283 A72-23413
He-Ne laser output dependence on transverse magnetic field, ascribing magneto-optical effects to IR radiation decrease 10 p1490 A72-24046
Muller matrix derivation for microwave light modulation studies in quasi-homogeneous magneto-optical and electro-optical media, taking into account finite light speed 10 p1493 A72-24914
Crossover and magneto-optical effects of line splitting in sunspot spectra, considering instrumental circular polarization 13 p2047 A72-29738
Magneto-optics materials for use in data storage, discussing quality evaluation based on figure of merit reflecting heat sensitivity and readout requirements 15 p2203 A72-32352
Magnetic materials. 17 p2595 A72-34571
Magneto-optic effects in Fraunhofer lines with Zeeman splitting 19 p2835 A72-38495
Polarimeter for recording of magneto-optical rotation dispersion and Kerr equatorial effect in visible, near UV and near IR spectral ranges 22 p3176 A72-42108
Electro-, magneto- and acousto-optical methods for laser Q-switching, discussing physical and operational principles 22 p3186 A72-42942
Electromagnetic radiation modulators in millimeter and submillimeter wave range using gas-discharge plasma magneto-optical effects in alternating magnetic field 23 p3319 A72-43434
Advanced optical storage techniques for computers. 23 p3288 A72-43876

MAGNETOACOUSTIC WAVES
Magnetosphere transmittance for fast magnetosonic waves, considering refraction, reflection and earth surface intersection 01 p0058 A72-10587
MHD channels magnetoacoustic and ionization instabilities effect on mean current density and electric field strength, determining effective electroconductivity and Hall parameter 01 p0110 A72-11208
One dimensional plane magnetoacoustic wave stability from synchronous flow in narrow flow gap MHD induction machine 02 p0265 A72-12263
Electroacoustic magnetic and Hall effects in semiconductors in strong electric field involving phonon production by supersonic electron drift 03 p0401 A72-13088
Short periodical pulsations in solar atmosphere related to magnetosound propagation in area of temperature minimum with directed perpendicular magnetic field 03 p0436 A72-13813
Anisotropic plasma stability to magnetosonic wave near ion cyclotron frequency propagating almost perpendicular to magnetic field 05 p0698 A72-17017
Dispersion relations for frequencies near first two harmonics of perpendicular magnetosonic waves in relativistic anisotropic plasmas 05 p0698 A72-17020
Magnetosonic, Alfvén, shock and infinitesimal waves and corresponding rays in relativistic hydrodynamics and magnetohydrodynamics, using tensor distributions 06 p0847 A72-17253
Weakly damped Alfvén ion-cyclotron waves and fast magnetoacoustic waves in infinite plasma cylinder inserted into current bearing finite coil 07 p1046 A72-20516

Cyclotron magnetoacoustic wave generation by planets and binary stars in circular orbits, deriving interstellar gas density variations 08 p1231 A72-21122
Electron Larmor radius effect on hf hose and mirror instabilities of fast magnetoacoustic and ion acoustic waves in nonisothermal plasma 08 p1215 A72-21874
Plasma filament equilibrium in Sirius stellarator during heating by fast magnetosonic wave 09 p1363 A72-23214
Magnetoacoustic wave propagation and reflection in equilibrium inhomogeneous plasma under nonuniform magnetic field 11 p1695 A72-26094
Slow and fast plane magnetoacoustic waves mutual transformation and reflection at plasma and magnetic field inhomogeneities 11 p1698 A72-26643
Magnetoacoustic waves interactions with energy particles in plasmasphere, demonstrating magnetosonic waveguide channel existence around earth below plasmasphere 13 p1947 A72-28605
Electroacoustomagnetic and Hall effects in semiconductors within strong electric field involving phonon production by supersonic electron drift 13 p2022 A72-29437
Plasma ion heating by magnetoacoustic waves, presenting resonance peak-magnetic field intensity relations for various densities and ion energy 13 p2019 A72-29913
Sounding rocket experiment on nonlinear interaction between two electron plasma waves and ion acoustic wave in ionosphere to investigate artificial realization feasibility 15 p2231 A72-32333
Ion acoustic, electron plasma and cyclotron harmonic waves parametric instabilities in magnetic field and applications to plasma heating 16 p2433 A72-32811
Nonlinear wave interaction in anisotropic plasmas, discussing helicon decay with acoustic wave emission and quasi-longitudinal waves with magnetoacoustic wave emission 16 p2436 A72-33478
Normal mode formulation of spin wave-helicon wave interactions in ferromagnetic semiconductors. 18 p2718 A72-36452
Fast magnetoacoustic wave interaction with shock wave propagating in ideal electrically conducting gas, showing magnetic field stabilizing effect 18 p2711 A72-36812
Nonlinear magnetosonic waves in a plasma with a finite conductivity. 21 p3090 A72-40485
Magnetosonic waves interactions with energy particles in plasmasphere, demonstrating magnetosonic waveguide channel existence around earth below plasmasphere 24 p3398 A72-45105

MAGNETOACOUSTICS
Moving plasma heating by fast large amplitude hf magnetoacoustic wave, noting Doppler effect resonance splitting 08 p1212 A72-21070

MAGNETOACTIVITY
NT MAGNETORESISTIVITY
Electromagnetic wave scattering by electron charge density fluctuations in plane waveguide with magnetoactive plasma, showing cross section spectrum function of plasma properties 02 p0183 A72-12766
Gyrosynchrotron radiation fields from mildly relativistic electrons in magnetoactive plasma, studying radiative transfer problem 14 p2138 A72-30556
Electromagnetic wave scattering by electron charge density fluctuations in plane waveguide with magnetoactive plasma, showing cross section spectrum function of plasma properties 20 p2903 A72-39072
Nonthermal emission of a magnetoactive plasma in the field of super-high-frequency pumping wave 21 p3090 A72-40407
Conditions for magnetoactive plasma longitudinal waves with phase velocity near light velocity existence, investigating increments during synchrotron instability due to relativistic particles 23 p3262 A72-43311
On the instability of nonlinear longitudinal oscillations of magnetoactive plasma. 23 p3320 A72-43524

MAGNETOCARDIOGRAPHY
Josephson effect /superconducting weak link/ devices for low frequency magnetic field sensing, noting applications in magnetocardiography and absolute noise thermometry 08 p1218 A72-21919
Mathematical, physical and engineering aspects of electro- and magnetocardiography, noting heart field nondipolar properties and heart vector determination difficulties 09 p1273 A72-23414

- Cryogenic Josephson junction magnetometer in magnetocardiography, discussing high ambient noise levels in unshielded environment
12 p1769 A72-27288
- Electrocardiography and magnetocardiography to determine flux and vortex sources respectively of heart electrical activity impressed current density
13 p1909 A72-28998
- MAGNETOELASTIC VIBRATIONS**
U MAGNETOELASTIC WAVES
MAGNETOELASTIC WAVES
NT MAGNETOACOUSTIC WAVES
Compression wave propagation from cylindrical cavity in weakly conducting magnetoelastic medium under unperturbed magnetic field
03 p0452 A72-14129
- Magnetoelastic vibrations of thin conducting plate in magnetic field, solving electrodynamic equations
07 p1095 A72-20315
- Exact solutions for plane thermoelastic and magnetoelastic wave frequency equations, determining specific loss extremum values
15 p2336 A72-32447
- Radial vibration of a composite cylindrical shell subjected to a magnetic field.
18 p2711 A72-36753
- MAGNETOELASTICITY**
U MAGNETOSTRICTION
MAGNETOELECTRIC MEDIA
Composite materials sum and product physical properties, considering magnetostrictive and piezoelectric interactions
18 p2717 A72-35996
- MAGNETOGASDYNAMICS**
U MAGNETOHYDRODYNAMICS
MAGNETOGRAMS
U MAGNETIC SIGNATURES
MAGNETOGRAPHS
U MAGNETOMETERS
U RECORDING INSTRUMENTS
MAGNETOHYDRODYNAMIC ACCELERATION
U PLASMA ACCELERATION
MAGNETOHYDRODYNAMIC FLOW
Transient shock produced plasma flow interactions with transverse magnetic field
01 p0105 A72-10020
- Interplanetary magnetic field angular gradient and sectorial effects on solar wind, discussing wind velocity
01 p0118 A72-10583
- Discrete ionospheric model of supersonic two dimensional low density plasma flow past large bodies, using quasi-neutrality condition
01 p0001 A72-10588
- Flowing plasma ionization density measurement by stagnation probe, comparing measured with calculated plasma sheath convection current values
[AD-738692] 01 p0110 A72-11189
- Electron thermal boundary layer effects on Langmuir probe measurements in subsonic cold plasma flow
01 p0071 A72-11191
- High velocity plasma generation in induction hydrodynamic shock tube and flow into rail type plasma accelerator, investigating possible T layer formation
01 p0110 A72-11203
- Magnetoplasma dynamic supersonic ring cut as electromagnetically shock tube or plasma gun, emphasizing plasma flow-magnetic field interaction
01 p0110 A72-11204
- Electron work function and electrode physicochemical properties and surface temperature on boundary layer formation and thickness at electrodes in MHD channel
01 p0009 A72-11206
- Electrically ionized striated plasma flow in annular channel, noting application to synchronous induction MHD generator
01 p0111 A72-11209
- Electrical properties of subsonic argon plasma stream seeded with uranium hexafluoride, using electrostatic probe
01 p0111 A72-11334
- German monograph on toroidal electric arc plasma with allowance for induced flow, covering tube wall heat transfer, electric field, MHD vortex development, mathematical model, etc
02 p0263 A72-11650
- Solar wind plasma spherically symmetrical outflow allowing for equations of motion of velocity components, discussing interplanetary field and single fluid MHD
02 p0278 A72-11914
- Fast hyperbolic MHD flow past point source, considering geometry and disturbances singularities of MHD Mach cones
02 p0266 A72-12369
- MHD flow development in parallel plate channel entrance region, obtaining numerical solution for velocity distribution, pressure drop and length at different Hartmann numbers
02 p0266 A72-12493

- Two dimensional MHD channel flow of inviscid fluid in circular nonuniform magnetic field
02 p0267 A72-12771
- MHD flow due to impulsive rotation of infinite disk, observing magnetic field strength effects on velocity components and boundary layer displacement thickness
02 p0267 A72-12772
- Upstream influence on MHD flow velocity by Rankine body moving parallel to uniform magnetic field in conducting fluid
03 p0394 A72-13153
- Conducting fluid steady MHD pipe flow under transverse magnetic field, obtaining mass flow rate
03 p0394 A72-13241
- Solar wind plasma flow through earth bow shock, deriving specific heats ratio based on one-fluid theory and conservation equations
03 p0412 A72-13509
- Plasmoid transport in quadrupole and octupole magnetic fields, measuring plasma amounts in axial region charged particle densities and flux densities at vacuum chamber wall
03 p0395 A72-13568
- Plasma flow under inhomogeneous axially symmetric magnetic field, investigating axial component of poloidal Hall induction current
03 p0395 A72-13570
- Moving plasma beam capture by transverse magnetic field due to polarization space charges electrostatic separation
03 p0396 A72-13657
- Cold plasma flow rate determination from emission inhomogeneities, using time of flight method and high speed streak photography for instantaneous velocity measurements
03 p0396 A72-13663
- Viscous electroconducting liquid two unidimensional Hartmann flows electromagnetic coupling under transverse magnetic field induction
03 p0396 A72-13790
- Compressible turbulent boundary layer equations for flow on B wall of MHD accelerator, including electron thermal nonequilibrium and finite rate ionization
03 p0397 A72-13923
- Decelerating MHD effect on rotational funnel flow excited by vortex line or radial converging currents
03 p0397 A72-13994
- Elliptic equations solutions for electromagnetic effect in MHD rectangular channels using relationship to Laplace equations
03 p0397 A72-13995
- Self similar solutions for unsteady shear flows of conducting Newtonian fluids with rheological power law under transverse magnetic field
03 p0397 A72-13997
- Plane mixing boundary layer flow of high temperature turbulent gas jet in longitudinal magnetic field
03 p0397 A72-13998
- Variational problem of conducting fluid flow in MHD channel at large magnetic Reynolds numbers at induction saturation
03 p0397 A72-13999
- Magnetic field and current density distributions in cylindrical conduction MHD channel with arbitrary number of pole-electrode pairs
03 p0398 A72-14000
- Time and coordinate dependence of magnetic field for steady symmetric flows of compressible conducting fluid at large Reynolds numbers, investigating self excitation conditions
03 p0398 A72-14001
- Two dimensional MHD turbulent flow generation in strong magnetic field
03 p0398 A72-14004
- Annular MHD channel laminar flow generation at supercritical Reynolds numbers by strong magnetic fields
03 p0398 A72-14005
- Dynamic and electromagnetic characteristics of MHD flow in square tube with walls differing in electroconductivity within oblique transverse magnetic field
03 p0398 A72-14007
- Steady laminar viscous conducting fluid flow in infinite rectangular channel in crossed electric and magnetic fields, deriving flow rate and potential distribution
03 p0398 A72-14008
- Steady flow of viscous incompressible conducting fluid in rectangular channel with sectional walls under longitudinal external magnetic field, deriving velocity distribution
03 p0398 A72-14009
- Magnetic field distribution in linear MHD channel for large Reynolds numbers, determining current density and longitudinal field component
03 p0398 A72-14010
- Free convective motion of conducting fluid past vertical plate in uniform transverse magnetic field, determining optimum dimensions of heat exchangers
03 p0399 A72-14011

- Axisymmetric rotational motion of electrically conducting fluid between dielectric disks in crossed electric and magnetic fields
03 p0399 A72-14012
- MHD boundary layer on rotating disk and on body of revolution in longitudinal flow at large Stewart numbers
03 p0399 A72-14013
- Visual investigation of semibounded axisymmetric MHD flow of liquid eutectic K-Na alloy under strong magnetic field effect
03 p0399 A72-14014
- Neutral current sheets in slow moving plasma with frozen-in magnetic field with null force line
03 p0438 A72-14070
- Supercritical stationary states of dissipative hydromagnetic rotating Couette flow between electrically insulating cylinders within axial magnetic field
04 p0554 A72-14405
- MHD approximation to solve natural convection problem in vertical channel under external inhomogeneous magnetic field, noting fluid flow rate
04 p0555 A72-14646
- Uniform normal magnetic field effect upon MHD free convection from vertical wall with instantaneous heat source, considering shear stress
04 p0556 A72-14856
- Magnetic field effect on heat transfer in steady plane laminar conducting incompressible viscoelastic liquid flow in channel with nonconducting walls
04 p0560 A72-15580
- Plasma velocity, gas pressure, wall heat flux and shock heated region extent measured in electrical discharge shock tube, discussing ionization relaxation process
05 p0693 A72-15849
- Cylindrical positive probe behavior in high speed collisionless mesothermal plasma flow
[ONERA, TP NO. 1000] 05 p0660 A72-15860
- General MHD duct flow problems solution using machine transformation and finite difference technique supplemented by successive overrelaxation [ASME PAPER 71-WA/APM-15]
05 p0694 A72-15965
- Superposable and self-superposable MGD flows from nonlinear differential equations, considering entropy, flow velocity and magnetic field strength
05 p0694 A72-16030
- Current collection characteristics of flush mounted electrostatic probes on sharp flat plate in ionized hypersonic flows
[AIAA PAPER 72-104] 05 p0696 A72-16814
- Argon plasma transient axial flow and heating characteristics in pinched column of linear z-pinch device with collapsing current sheets conversion to axial streaming velocity
[AIAA PAPER 72-208] 05 p0696 A72-16886
- One dimensional continuous electrode shock tube driven MHD accelerator, analyzing unsteady flow behind ionizing shock wave by method of characteristics [AIAA PAPER 72-102] 05 p0697 A72-16973
- MHD Couette flow stochastic processes optimal control synthesis by dynamic programming
05 p0653 A72-17131
- MHD flow of viscous fluid between two oscillating flat plates, observing velocity damping by magnetic field
05 p0699 A72-17179
- Poloidal Hall current calculation in hydrodynamic approximation for stationary weakly interacting and conducting cylindrical plasma flow with uniform transverse flow parameter distribution
05 p0701 A72-17240
- Stationary plasma flow interaction with axisymmetric spatially periodic magnetic field in presence of Hall effect, determining electric currents structure
05 p0701 A72-17241
- Polarization electric field and depolarization current measurements in plasma flows along toroidal solenoid with diverter
06 p0853 A72-17387
- Wake behind obstacle immersed in plasma flow of single ended Q-machine, using experiment as diagnostic of ion distribution function
06 p0856 A72-17526
- Magneto-viscous interactions in combustion plasma, measuring velocity distributions for ordinary hydrodynamic and MHD flow with transverse magnetic field
06 p0859 A72-17618
- Moderate Hartmann number MHD duct flow with applied transverse magnetic field, using numerical methods
06 p0859 A72-17619
- Hartmann number for velocity pulsation free transition from turbulent MHD flow to laminar, noting difference relative to linear stability theory
06 p0860 A72-17679
- Plasma jet injection stoppage and reflection in strong transverse magnetic field, considering instability due to flow interactions
06 p0860 A72-17694

Exact linear dielectric operator for stratified plasma streams with velocity gradients for diagnostics with electromagnetic waves 06 p0861 A72-17748

Steady two dimensional magnetodynamic flow past nonconducting wedge with perpendicular magnetic field at different shock attachment angles 06 p0861 A72-18113

Supersonic hydrogen plasma flow in collapsing postsunset upper ionosphere, noting nonvanishing temperature gradient effect on critical point location 07 p0974 A72-18899

Neutral current sheath formation from plane dipole magnetic field extension by plasma flow, discussing solar corona streamers and geomagnetic tail 07 p1039 A72-18914

Continuum plasma turbulent boundary layer structure in shear flow, showing electron to ion saturation currents ratio decrease from laminar case [AIAA PAPER 72-107] 07 p1040 A72-18953

Optimal control of hydromagnetic flow of electrically conducting fluid in equilibrium cylindrical configuration, using dynamic programming method 07 p1040 A72-18980

Dynamo action of magnetohydrodynamic fluid motions with two dimensional periodicity 07 p1042 A72-19611

Nonuniform plane parallel plasma streams instability with/without magnetic field, comparing with conducting fluid 07 p1042 A72-19618

Wall stabilized dc arc channel for plasma viscosity and flow characteristics studies, using pressure probe 07 p1043 A72-19877

Two channel high resolution spectrometric measurements of plasma velocity from intrinsic radiation in optical range by Doppler effect 07 p1044 A72-19885

Particle acceleration and plasma ejection in solar flares, using model of nonstationary cumulative flow near magnetic neutral line 07 p1060 A72-20014

Unsteady laminar viscous incompressible electrically conducting flow between nonconducting parallel flat plates with applied constant magnetic field 07 p1044 A72-20245

MHD dynamo model for incompressible real electrically conducting fluid unsteady flow 07 p1044 A72-20304

Electric field in flow of medium with tensor conductivity due to Hall effect, studying eddy currents structure in magnetic field variation region 07 p1044 A72-20316

Induced nonuniform magnetic field effects on MHD channel flow between two infinite parallel plates, obtaining solution by perturbation theory 08 p1214 A72-21427

MGD equations for ideal plasma steady plane adiabatic flow in magnetic field, considering analogy to Chaplygin equations 08 p1214 A72-21645

Inviscid conducting gas steady one-dimensional MHD flow, using three-dimensional phase diagram for differential equations analysis 08 p1214 A72-21646

Laminar MHD boundary layer lateral velocity component profile for conducting fluid injection at oblique incidence, considering drag force and pressure gradient effects 08 p1214 A72-21647

Supersonic plasma flow in narrow rectangular channel and free incompressible inviscid conducting liquid jet motion within pulsating transverse magnetic field 08 p1214 A72-21652

Steady flow of dual temperature plasma into vacuum from widening nozzle, taking into account electron thermal conductivity and heat exchange between components 08 p1214 A72-21653

Electric eddy currents formation during thermal acceleration of inviscid quasi-linear plasma in profiled channel 08 p1215 A72-21654

Two dimensional MHD conducting fluid flow past insulating cylinder in presence of arbitrarily oriented magnetic field, determining lift and drag coefficients for small Hartmann numbers 09 p1359 A72-22533

Convective heat transfer between jets produced by plasmatrons and heated substrate, showing independence of plasma flow rate 09 p1319 A72-23189

Pulsed plasma flow interaction with spatially periodic magnetic field generated by coaxial coils with alternating currents, noting MHD stability 09 p1362 A72-23207

Colliding plasma flows motion and capture in transverse magnetic field with mirror configuration, noting polarization effect 09 p1362 A72-23209

Plasma flows interaction with plasma cylinder in diverter magnetic field, investigating plasma dynamics with electric probes, plasmoscope and mass spectrograph 09 p1362 A72-23210

Plasma flow interaction with magnetic pulse field barrier from magnetic coil for short plasmoids formation 09 p1362 A72-23211

Perfectly conducting incompressible fluid motion past thin body in oblique field, discussing magnetic field influence on lift 09 p1365 A72-23559

Oblique magnetic fields effect on compressible conductive fluids motion in presence of thin foil, noting lift values in hyperlentic and double hyperbolic cases 09 p1365 A72-23560

Viscous boundary layer equations for MHD flow near rear stagnation point at small Reynolds number 09 p1296 A72-23674

Electromagnetic coupling between one dimensional laminar flows of viscous conducting fluid in presence of magnetic field, noting static and dynamic efficiencies dependence on Hartmann number 10 p1519 A72-24065

Velocity and magnetic field expressed by six scalar potentials from MHD equations system, noting compressible fluids flow 10 p1520 A72-24219

Steady state exact solutions of MHD equations for perfectly conducting self gravitating incompressible fluid, showing solutions existence for rotating planetary ellipsoid free liquid surface 10 p1539 A72-24328

Numerical solution for super-Alfvénic supersonic aligned MGD flow over cone with attached shock wave, obtaining surface pressure coefficients, current and vorticity distributions 10 p1418 A72-24463

Second order Cowley-Imai analogy application to transcribe gas dynamic perturbation solutions into magnetogasdynamic solutions for perfect gas axisymmetric super-Alfvénic flows 10 p1521 A72-24464

Joule dissipation effect on convective instability of current carrying fluid in magnetic field 10 p1522 A72-24533

Interacting viscous conducting media flow in inclined channel in presence of transverse magnetic field, using Moiseev asymptotic method for steady flows with wavy interface 10 p1522 A72-24546

Interaction solutions of steady crossed field MHD channel flows for perfect, singly ionizing monatomic and thermodynamically unspecified gases 10 p1523 A72-24789

Suction or injection interaction with rotation in three dimensional MHD flow between two porous nonconducting disks under magnetic field 10 p1524 A72-25039

Nonisothermal hydrogen plasma channel flow and radiative heat transfer combined with convective and conductive transfer between isothermal black parallel boundaries [AIAA PAPER 72-279] 11 p1692 A72-25219

Uniform and parallel magnetic field effects on hydromagnetic instability of two dimensional jet at small magnetic Reynolds numbers 11 p1693 A72-25521

T-tube plasma flow velocity measurement via shock wave attenuation recording technique 11 p1693 A72-25561

Stationary MHD aligned flows of ideal incompressible fluids with same streamline patterns in plane, axisymmetric and spatial flows 11 p1695 A72-25910

Magnetosphere neutral layer plasma conductivity determination from model of linear magnetic dipole in conducting fluid flow 11 p1622 A72-25945

Dynamic response of MHD flow under impulsive pressure gradient, obtaining approximate analytic solutions for conduits of arbitrary cross sections by complex variable approach 11 p1695 A72-26039

Sunspots contact region charged particles acceleration by plasma flow induced electric field, noting Fermi type mechanism 11 p1695 A72-26107

Hydromagnetic stability of isothermal stratified plasma atmosphere uniform flow over conducting liquid along magnetic field, discussing dispersion relation for static configuration 11 p1695 A72-26115

MPD thruster diagnostics and interpretation of electric current distribution, applying integral form of Maxwell equation for moving Hall probe [AIAA PAPER 72-498] 11 p1711 A72-26221

Magnetosphere fast electron precipitation investigated by simulation experiments with model created by plasma stream interaction with dipole magnetic field 11 p1714 A72-26531

Rayleigh problem in presence of magnetic field, discussing transpiration effects on MHD flow near oscillating flat plate 11 p1696 A72-26542

Method of characteristics for three dimensional supersonic flow of guiding center plasma, noting application to solar wind-moon interaction 11 p1573 A72-26601

Plasmoid transport in quadrupole and octupole magnetic fields, measuring axial charged particle and flux densities at vacuum chamber wall 11 p1699 A72-26755

Plasma flow under inhomogeneous axially symmetric magnetic field, investigating axial component of poloidal Hall induction current 11 p1699 A72-26757

Boundary conditions and equations of plasma arc discharge in cylindrical diode with azimuthal magnetic field 12 p1850 A72-27132

Oscillation periods of rotating perfectly conducting liquid column in presence of axial magnetic field and uniform current 12 p1851 A72-27534

Localized magnetic field for wind tunnel wall-plasma heat transfer minimization, preserving flow characteristics 12 p1852 A72-27684

Hydrodynamic approximation for solar wind nonuniformity in ecliptic plane, noting linear disturbances caused by nonuniform velocity of plasma flow from corona 13 p2029 A72-28577

Nonlinear transverse forced resonant oscillations in isotropic elastic body and ideally conducting compressible fluid flowing in external magnetic field 13 p2010 A72-28719

Effect of magnetic field superimposed on turbulent shear flow of electrically conducting fluid, discussing turbulent friction in plane flow 13 p2010 A72-28764

Growth rates of unstable electromagnetic waves propagating perpendicularly to symmetric counterstreaming finite temperature plasmas 13 p2012 A72-29129

Hall currents effect on unsteady MHD flow of electrically conducting fluid past flat plate imbedded in uniform external transverse magnetic field 13 p2012 A72-29225

Solar wind plasma spherically symmetrical outflow allowing for equations of motion of velocity components, discussing interplanetary field and single fluid MHD 13 p2039 A72-29226

Random phase approximation for nonlinear theory of MHD nonequilibrium plasma steady turbulent regime, noting ionization level rise by energy dissipation 13 p2013 A72-29359

Velocimeter design for MHD boundary layer flow velocity measurement, using Doppler frequency shift of laser light scattered from added macroscopic particles 13 p1957 A72-29360

Two dimensional laminar compressible flow of electrically conducting gas at thermodynamic equilibrium and perpendicular to magnetic field lines 13 p2013 A72-29362

Nonstationary laminar zero-discharge MHD Couette flow produced by sudden movement of highly conductive plate in closed volume filled with conducting liquid 13 p2016 A72-29607

Steady barotropic inviscid flows of rarefied gas plasmas as free jet and within cylindrical channel in axisymmetric external magnetic field with Hall effect 13 p2018 A72-29823

Slow viscous incompressible conducting fluid MHD flow between two nonparallel walls, obtaining velocity profile solution in power series for small Reynolds numbers 13 p2020 A72-30047

He and Ar plasma transport by magnetic fields after expulsion from pulsed linear discharge 14 p2135 A72-30167

Magnetic and electric field effects on steady state laminar MHD Couette flow of non-Newtonian fluids governed by Prandtl rheological law or Ostwald-de Waele power law 14 p2139 A72-30717

Heat transfer in MHD boundary layer flow of conducting incompressible fluid with aligned magnetic field on flat plate at high Prandtl number 14 p2141 A72-31068

Flow-plasma system described by hydrodynamic equations, comparing self oscillatory process features with other systems 14 p2141 A72-31129

Hydromagnetic channel flow stability computation via energy method, solving eigenvalue problem by direct forward numerical integration 15 p2283 A72-31212

Plasma velocity, gas pressure, wall heat flux and shock heated region length measured in electrical discharge shock tube without diaphragms, discussing ionization relaxation process 15 p2283 A72-31268

Approximate model of weak shock wave interaction with laminar MHD boundary layers for perfectly conducting supersonic streams 15 p2284 A72-31633

Convective heat transfer in fully developed MHD channel flow between two parallel electrically conducting plates

15 p2335 A72-31636

Characteristic parameters of stationary supersonic plasma flow in magnetic de Laval nozzle calculated for collisional and collisionless cases, measuring ion saturation currents

15 p2285 A72-32268

Stationary plasma flow interaction with dipole magnetic field to study geophysical phenomena in upper atmosphere

15 p2286 A72-32343

MHD Couette flow of electrically conducting viscous incompressible fluid in transverse magnetic field with time dependent suction or injection

15 p2286 A72-32396

Steady laminar MHD flow of viscous incompressible electrically conducting fluid between long concentric rotating porous cylinders under radial magnetic field

15 p2287 A72-32397

Falkner-Skan problem extension to MHD flow past nonconducting body by imposing magnetic field with lines of force parallel to undisturbed streamlines

15 p2287 A72-32405

End effect in current response of highly negative cylindrical Langmuir probe in collisionless plasma flow, discussing use for ion temperature determination

15 p2288 A72-32418

Induced magnetic field effects on MHD flow between rotating coaxial (insulator) cylinders, obtaining exact solution and graphical results

15 p2288 A72-32420

Streaming MHD flow past semiinfinite flat plate in presence of perpendicular uniform magnetic field, obtaining velocity field at large distances

15 p2288 A72-32480

Boundary layer ionization on flat plate and cylindrical plasma probes in high speed flow, considering ionized continuum flow and collisionless plasma

16 p2374 A72-32831

Asymptotic solution for inviscid conducting fluid flow past arbitrary wing profile in magnetic field

16 p2434 A72-32929

Perturbation theory for equations of motion of electrically and thermally conducting viscous compressible flow in homogeneous magnetic field, calculating fluctuation modes

16 p2435 A72-33008

Vorticity jump across stationary MHD discontinuity generalization from gas dynamics problem, noting results validity for shock and detonation waves

16 p2435 A72-33011

Skin friction effects due to Hall currents in conducting unsteady slip flow over porous flat plate under transverse magnetic field

16 p2435 A72-33108

Experimental methods for studying interactions between plasma streams and three dimensional magnetic dipole fields

16 p2454 A72-33384

Weakly ionized nonequilibrium plasma flow from gas discharge tube positive column, obtaining electron temperature axial decay rate from energy equation

16 p2437 A72-33655

Faraday ring currents induction by radial magnetic field in low pressure plasma supersonic ring channel flow driven by inductive hydrodynamic shock tube

16 p2437 A72-33749

Plane vortex sheet in incompressible inviscid and finitely conducting fluids, investigating discontinuity in density and conductivity on hydromagnetic stability

16 p2438 A72-33842

Russian book on magnetogasdynamic flow theory and calculations covering plasma flows and energy conversion in MHD channels of dc generator

16 p2438 A72-33873

Conducting fluid flow near neutral sheet in magnetic field, assuming cold polar wind plasma geomagnetic tail

16 p2438 A72-33930

Steady state magnetically balanced cross flow arc, calculating flow and temperature fields and boundary shape under assumption of two independent variables [AIAA PAPER 72-687]

16 p2439 A72-34055

Magnetogasdynamic heat transfer to hemispherical body in supersonic low density plasma, noting magnetic field effects on heat flux

16 p2346 A72-34056

Theoretical study of electromagnetic coupling in the forced oscillatory regime of two one-dimensional laminar flows of a viscous and electroconducting liquid in the presence of a transverse uniform magnetic field

17 p2587 A72-34281

Flow of a real gas in annular channels with curvilinear walls at large MHD-interaction parameters

17 p2587 A72-34457

Transverse edge effect in a rectangular MHD channel with a sectional side wall

17 p2587 A72-34458

Stabilization of magnetohydrodynamic flows by a distributed feedback system

17 p2587 A72-34459

Magnetohydrodynamic flow in the region of a conductivity discontinuity at the wall

17 p2587 A72-34460

Flow conditioning in electric discharge convection lasers.

17 p2562 A72-34638

Continuity, motion and Maxwell equations for steady MHD flow under constant magnetic flux

17 p2588 A72-34765

Experimental evidence for stationary population inversions of atomic levels in an expanding hydrogen plasma

[DFVLR-SONDDR-213] 17 p2589 A72-34898

On the motion of a perfectly conducting fluid past a thin body.

17 p2485 A72-35055

Critical point regularity conditions and asymptotic solutions to the time stationary, linearized, inhomogeneous solar wind flow problem.

17 p2599 A72-35095

Wall stabilized dc arc channel for plasma viscosity and flow characteristics studies, using pressure probe

17 p2590 A72-35127

Two channel high resolution spectrometric measurements of plasma velocity from intrinsic radiation in optical range by Doppler effect

17 p2590 A72-35133

Explorer 33 and 35 plasma observations of magnetosheath flow.

17 p2548 A72-35587

Experimental and two-dimensional computational study of end losses from a theta pinch.

17 p2592 A72-35628

Magnetic dipole field interaction with plasma flow ions, noting qualitative model of solar wind flow past magnetosphere

17 p2593 A72-35905

MHD inlet flow into channel, obtaining velocity profile numerical solution in Prandtl approximation with modified boundary conditions

18 p2714 A72-36121

Transition from sheath-convection to saturation-current behaviour of a Langmuir probe in a flowing plasma.

18 p2715 A72-36688

Solution of some mixed boundary value problems of conducting medium thermodynamics by the method of variable separation

18 p2715 A72-36802

Turbulence characteristics of flows with large velocity gradients in rectangular MHD channel with copper walls

18 p2715 A72-36813

Hydrodynamic stability of the gradient flow of a conducting fluid with a rheological power law in a transverse magnetic field

18 p2716 A72-36814

Hall phenomena in a plasma flow situated in a traveling magnetic field

18 p2716 A72-36816

Self-similar separation flows in a laminar magnetohydrodynamic boundary layer during injection and suction

18 p2716 A72-36886

Self-similar unsteady magnetogasdynamic flows of a radiating gas produced by the motion of a piston

18 p2716 A72-36897

Hydromagnetic boundary layer flow around an oscillating axisymmetric body.

18 p2683 A72-36932

The influence of geostrophic force on the stability of an heterogeneous conducting fluid with a radial gravitational force.

18 p2683 A72-36933

Discontinuities in a collisionless plasma flow having a strong magnetic field.

18 p2717 A72-37042

Determination of the separation parameter of an incompressible magnetohydrodynamic boundary layer by applying the dimensionality theory

18 p2717 A72-37181

Classification of the magnetohydrodynamic motions of a rotating fluid

19 p2839 A72-37392

Multiplicity theorem for aligned steady MHD flows of inviscid perfectly conducting gas, assuming constant density along streamline

19 p2840 A72-37405

German monograph - Behavior of an electric arc produced by an exploding wire in a granular medium

19 p2834 A72-37483

Numerical calculation of the lunar wake in a magnetohydrodynamic model.

19 p2864 A72-38435

Hydromagnetic flow between two rotating disks with noncoincident parallel axes of rotation.

19 p2841 A72-38436

Magnetohydrodynamic channel flow with an arbitrary inlet velocity profile.

19 p2842 A72-38446

Low beta model of collision dominated plasma flow effect on toroidal confinement, simulating Stellarator, Levitron and Tokamak

20 p2957 A72-39356

Neutral current sheath formation from plane dipole magnetic field extension by plasma flow, discussing solar corona streamers and geomagnetic tail

20 p2957 A72-39380

Magnetospheric shapes, flows and substorms in terms of magnetotail flux, solar wind pressure, dipole moment and plasma sheet interaction

20 p2919 A72-39546

Stationary adiabatic plasma flow in the magnetosphere.

20 p2919 A72-39547

Two phase flow types defined as flow problems of two-phase matter mixtures /solid, liquid, gas or plasma/ and interface interaction

20 p2915 A72-39971

The linear stability of flow in a circular pipe in the presence of a strong transverse magnetic field.

20 p2958 A72-40018

Magnetic field effects on turbulent shear flow of electrically conducting fluid, discussing turbulence level, friction stress and heat exchange

21 p3089 A72-40260

Isometric motion in relativistic magnetohydrodynamics.

21 p3091 A72-40567

Nonstationary laminar zero-discharge MHD Couette flow produced by sudden movement of highly conductive plate in closed volume filled with conducting liquid

21 p3091 A72-40661

Interaction of a steady plasma flow with a dipole magnetic field in the presence of a radial electric field.

21 p3093 A72-41388

Development of the AEDC-VKF tunnel J - A real gas high density, true velocity, hypersonic, aerodynamic test facility.

21 p3040 A72-41579

Interaction of a streaming plasma with a magnetic mirror.

21 p3094 A72-41635

Investigation of the interaction between a plasma flow and an axisymmetric magnetic field

21 p3094 A72-41655

Two dimensional MHD fluctuating flow of incompressible electrically conducting rarefied gas past infinite porous wall for slip-flow regime with variable suction

21 p3095 A72-41784

Transverse magnetic field effect on unsteady incompressible laminar MHD boundary layer flow, noting cylindrical body oscillations in fluid

21 p3095 A72-41786

Magnetic field and suction effects on unsteady MHD free convection flow of conductive fluid around nonconductive porous flat plate

21 p3095 A72-41787

Discontinuities propagation in quasi-linear hyperbolic partial differential equation systems, noting MHD flow and crystal optics equations

22 p3204 A72-41905

Anode heat transfer for a flowing argon plasma at elevated electron temperature.

22 p3210 A72-41952

Nonlinear transverse forced resonant oscillations in isotropic elastic body and ideally conducting compressible fluid flowing in external magnetic field

22 p3210 A72-42096

Approximate calculation of a laminar arc discharge in a cylindrical channel

22 p3210 A72-42285

Extremal bounds for mass flow rate of laminar MHD flow in circular and thin walled conducting pipes at high Hartmann number

22 p3210 A72-42315

Magnetic tension induced stress balance in plasma sheet, considering pressure gradient along geomagnetic tail axis, plasma flow kinetic energy and pressure anisotropy

22 p3211 A72-42408

A transpiration radiometer for measurement of total thermal radiation from a flowing plasma.

22 p3179 A72-42691

Motion of plasmoids in a multipole magnetic field of toroidal configuration

22 p3214 A72-43120

Polarizational interaction of opposed plasma flows in a linear octupolar magnetic field

22 p3214 A72-43121

Numerical treatment of a model of the hydromagnetic dynamo with a selected system of convection in the earth's core.

23 p3284 A72-43422

The effects of magnetic field oscillations on the boundary layer flow past a magnetized plate.

23 p3321 A72-43725

One dimensional steady conducting gas flow in nonaccelerating coordinate system under magnetic field, calculating pressure, density and temperature variations with boundary shock wave

23 p3281 A72-44265

Streamline and fieldline geometry with applications to MHD flow kinematic properties, discussing field and momentum relations decomposition in terms of sound velocity

23 p3322 A72-44270

- The equilibrium configuration of a slowly rotating mass of liquid in the presence of a poloidal magnetic field.
23 p3322 A72-44306
- Waves generated in the configuration of a magnetically confined and field-permeated axisymmetric jet.
23 p3322 A72-44307
- Magnetohydrodynamic flow between parallel rotating disks. I - Influence of finite wall-conductance.
23 p3322 A72-44400
- Modification of the Rankine-Hugoniot relations for shocks in space.
23 p3341 A72-44510
- Measurements of magnetotail plasma flow made with Vela 4B.
23 p3342 A72-44514
- A Lecher wire microwave interferometer for measurements of electron density and electron temperature in a flowing transient plasma.
23 p3292 A72-44543
- Pressure and magnetic field probe measurements in transverse shock waves in ionizing hydromagnetic regimes, investigating bow shock effects on accuracy
24 p3390 A72-44708
- MHD Couette flow between conducting walls with heat transfer.
24 p3428 A72-44970
- Hydrodynamic approximation for solar wind nonuniformity in ecliptic plane, noting linear disturbances caused by nonuniform velocity of plasma flow from corona
24 p3435 A72-45077
- Linearized analysis of magnetohydrodynamic channel entrance flow.
24 p3430 A72-45573
- On the unsteady magnetohydrodynamic flow over yawed infinite cylinder.
24 p3395 A72-45599
- MAGNETOHYDRODYNAMIC GENERATORS**
- Optimal conditions for energy conversion in MHD generator, observing ion seeding effect on plasma temperature
01 p0009 A72-11207
- Electrically ionized striated plasma flow in annular channel, noting application to synchronous induction MHD generator
01 p0111 A72-11209
- Plasma temperature and seed atom concentration in MHD generator ducts and combustion chambers by optical measurements, discussing boundary layer thickness, optical density, etc
01 p0072 A72-11218
- One dimensional plane magnetoacoustic wave stability from synchronous flow in narrow flow gap MHD induction machine
02 p0265 A72-12263
- Ambipolar diffusion influence on MHD generator electrical conductivity, discussing plasma radiation, electron escape generator geometry and efficiency and ignition temperature range
04 p0554 A72-14404
- Electron density and temperature fluctuations coupled through Ohm law for ionizable medium, applying to MHD generators and MPD arc thrusters [AIAA PAPER 72-101]
05 p0706 A72-16813
- NASA closed cycle MHD facility for power generation, discussing system components, design and operation [AIAA PAPER 72-103]
05 p0616 A72-16936
- Self regenerating molten seed electrodes for open cycle MHD power generators longevity, regulating combustion chamber and gas flow seeding
06 p0862 A72-18336
- Performance characteristics and limitations of electrode and insulation materials for open and closed cycle MHD generators, noting ceramic compositions for channel
09 p1335 A72-22401
- German monograph on gas dynamic properties of turbulent subsonic compressible flow of ideal gas at insulator walls in MHD generator
10 p1517 A72-23771
- MHD generator duct external loop electric current maximization by working material resistivity tensor optimal distribution
10 p1521 A72-24434
- Optical method based on spectral line center intensity recording to measure plasma temperature in MHD generators channels and combustion chambers
10 p1525 A72-25111
- Russian book on electrodynamic plasma acceleration covering charged particles motion in electromagnetic field and pulsed, MHD, steady and Hall accelerators
12 p1853 A72-28341
- Nonequilibrium MHD generator with electrode walls slanted away from magnetic field direction, predicting electrical performance for comparison with flat wall generator
13 p1899 A72-29352
- Linear nonequilibrium Faraday type MHD generator, predicting electrode configuration effects on voltage drops, axial leakages and current distribution
13 p1900 A72-29353
- Ionization turbulence effect on nonequilibrium plasma MHD generator performance, using I-V characteristics equation
13 p1900 A72-29354
- MHD power generators analytical modeling by digital technique for prediction of performance and efficiency as function of size and operating conditions [AD-741173]
13 p1900 A72-29355
- Thermal-to-electric power conversion efficiency of nonequilibrium MHD generator with Cs seeded noble gases, considering electrode configuration and gas dynamic effects
13 p1900 A72-29356
- Nonequilibrium Faraday MHD generator performance examined by double diaphragm shock tube within ionization region
13 p2013 A72-29357
- Time dependent and stationary two dimensional calculation of current and potential distributions in MHD generator preionizer and entrance region flow
13 p2013 A72-29358
- One-wavelength MHD induction generator operated on NaK flow system with various excitation conditions, calculating magnetic flux density and power by Fourier series
13 p1900 A72-29364
- Numerical analysis method for performance prediction of linear induction machines including liquid metal MHD pumps and generators and linear motors
13 p1900 A72-29365
- Electrothermal instability analysis for MHD generator, considering electron thermal conduction and wall boundaries effects for cases with current parallel or perpendicular to walls
13 p2014 A72-29366
- MHD laser discharge characteristics under generator conditions, emphasizing interaction of gas ionization instabilities and lasing radiation field
13 p2014 A72-29367
- Ionization stabilization in MHD generators by sensing electron density perturbation with linear feedback into nonequilibrium plasma
13 p2014 A72-29369
- Fluctuating electric current induced magnetic field effects on long wave nonequilibrium plasma instability associated with large scale closed cycle MHD generators
13 p2014 A72-29370
- Nonlinear model of ionization instability of MHD generators, assuming discharge structure with alternating layers of high and low electrical conductivity
13 p2014 A72-29371
- Mathematical model for ionized plasma response to sinusoidal perturbations, calculating dispersive waves in MHD generators with working fluid of potassium seeded argon
13 p2014 A72-29372
- Variable amplitude and phase velocity electromagnetic traveling wave field distribution in diverging MHD induction machine channel with liquid metal flow
16 p2435 A72-33282
- Electromagnetic field in MHD generator active zone approximated by cruciform plate, calculating secondary fields from Helmholtz equation
16 p2435 A72-33283
- Russian book on magnetogasdynamic flow theory and calculations covering plasma flows and energy conversion in MHD channels of dc generator
16 p2438 A72-33873
- Electromagnetic characteristics of MHD channels with nonconducting walls at finite magnetic Reynolds numbers
17 p2587 A72-34456
- Transverse edge effect in a rectangular MHD channel with a sectional side wall
17 p2587 A72-34458
- Electric fields in MHD channels in the case of anisotropic and nonuniform conductivity
18 p2716 A72-36817
- Optimum design of MHD generator combustion chamber, noting effects of heating temperature, oxygen enrichment degree and flow velocities
21 p2997 A72-41065
- Fission and fusion propulsion for deep space missions, discussing gas and colloid core reactors, controlled fusion, MHD and laser plasma systems
24 p3423 A72-45168
- Metal vapor plasma as working medium in MHD generator, discussing hydrodynamic relations, power efficiency and thermodynamic cycle
24 p3428 A72-45169
- MAGNETOHYDRODYNAMIC STABILITY**
- Two dimensional collisionless plasmas instability with neutral points, discussing sheet pinch with periodic structure
01 p0105 A72-10022
- Plasma hydrodynamic Buneman current instability under strong electric field, considering nonlinear stage in one dimensional case
01 p0105 A72-10024
- Steady motion effect on sunspot magnetic field stability related to force-free configurations and solar flare origin
01 p0118 A72-10083
- Plane and spherical geometry anisotropic plasma jet stability, considering uniform velocity streaming immersed in magnetic field surrounded by nonconducting medium
01 p0106 A72-10131
- Electron layer precession under magnetic field in background plasma, noting density effect on instability
01 p0107 A72-10144
- Linear theory of transverse electromagnetic waves and instabilities in uniform plasma during propagation along magnetic field, considering multifluid and kinetic description
01 p0108 A72-10189
- Nonlocal theory of electrostatic trapped particle instability in collisionless toroidal plasma, estimating particle mode nonlinear diffusion coefficient
01 p0108 A72-10239
- Nonlocal behavior of ion sound instability in collisionless nonuniform confined plasma shock wave
01 p0108 A72-10240
- Acoustic instability of plasma with current under equilibrium ionization and moderate neutral gas pressures
01 p0109 A72-10485
- MHD instabilities of plasma with current, using two fluid model in crossed magnetic-electric fields
01 p0109 A72-10486
- Ideally conducting plasma confined in vacuum by circularly polarized magnetic field, investigating MHD instabilities suppression by distributed automatic control system
01 p0109 A72-10503
- MHD waves nonlinear interaction in magnetosphere, calculating transverse Alfvén and magnetosonic and longitudinal acoustic wave decay instabilities
01 p0109 A72-10618
- Energy and momentum transfer between fields and particles in plasma crossed by transverse electromagnetic wave, investigating MHD stability
01 p0109 A72-10884
- Farley-Buneman instability nonlinear development mechanism in equatorial electrojet, noting turbulent vertical electron flux role
01 p0062 A72-10901
- Relativistic electron beams in plasma, considering electrostatic instability conditions and critical currents
01 p0109 A72-10975
- Electromagnetic instability of linearly polarized mode propagation perpendicular to magnetic field in two colliding plasma streams
01 p0110 A72-11112
- MHD channels magnetoacoustic and ionization instabilities effect on mean current density and electric field strength, determining effective electroconductivity and Hall parameter
01 p0110 A72-11208
- Unstable sound waves in uranium plasma, taking into account fission power density, radiation diffusion and ionization variations
01 p0112 A72-11336
- Plasma physics computer simulation of double stream and beam instabilities, wavelength nonlinearities and velocity distribution, using superparticle and Vlasov equation models
02 p0263 A72-11691
- Electromagnetic wave propagation perpendicular to applied uniform magnetic field in relativistic plasma, deriving dispersion relation for stability criterion
02 p0264 A72-12024
- Wall stabilized Ar arc plasma, investigating Boltzmann equilibrium existence between spectral energy levels
02 p0264 A72-12025
- Diffuse plasma resonances in space interpreted by wave-particle nonlinear interaction in weakly turbulent plasma, considering electrostatic electron cyclotron wave instability
02 p0265 A72-12366
- Inhomogeneous plasmas parametric instabilities excitation, observing threshold electric field power requirement
02 p0266 A72-12370
- Two stream instabilities of low density beam-plasma interaction in finite and zero magnetic fields
02 p0267 A72-12839
- Macroscopic geometry and velocity spaces of plasma collective modes involving long range force interaction between particles
02 p0267 A72-12841
- Rain type periodic solar radio bursts interpreted on basis of stream instability pulsating regime, considering plasma waves excitation
03 p0406 A72-12936
- Cylindrical gravitational waves propagation modes in hot plasma subject to axial magnetic field, investigating instability conditions
03 p0388 A72-13025
- Weakly turbulent plasma wave system, obtaining drift solution for stationary distribution stability
03 p0394 A72-13274
- Dash phenomenon in eruptive loop prominences representing solar flare process at all levels of atmosphere, discussing pinch effect instability
03 p0411 A72-13332

Plasma interchange instability in quadrupole and octupole magnetic fields determination by disturbance wavelength ratio to ion cyclotron radius

03 p0396 A72-13659

Fluctuations and diffusion correlation analysis in linear octupole magnetic confinement, determining dispersion relation for interchange instability

03 p0396 A72-13660

Linear and nonlinear MHD shock wave propagation and stability, investigating Hugoniot relation

03 p0396 A72-13688

Magnetoplasma with skin current characterized by current and electron temperature nonuniformity, analyzing instabilities for perturbations above ion gyrofrequency

03 p0396 A72-13713

Stability of plane rotating galaxies in magnetic field parallel to axis of rotation, showing linearized MHD equations self conjugate for radial disturbance case

03 p0435 A72-13806

Nonlinear ionization wave equation, calculating nonlinear response of unstable positive plasma column to weak pulse disturbance

03 p0399 A72-14346

Mathematical model for two-stream instability induced anomalous resistivity and heating in plasma with equal initial electron and ion temperatures in static electric field

04 p0554 A72-14402

Force free high beta plasma stability in homogeneous magnetic field and with inhomogeneous temperature and density

04 p0554 A72-14408

Magnetic and gravitational energy release by resistive MHD instabilities responsible for solar flares

04 p0571 A72-14578

Hf electric field influence on electron drift instability and slow ion-acoustic waves for inhomogeneous magnetized plasma stabilization

04 p0555 A72-14617

MHD equilibrium equations for axially asymmetric finite beta toroidal plasma with diffuse boundaries

04 p0556 A72-14854

Electromagnetic wave propagation across external magnetic field in contraststreaming thermally anisotropic plasmas, investigating plasma stability

04 p0556 A72-14942

Ionospheric plasma drift instability, showing electric and magnetic fields, electron density and temperature effects

04 p0517 A72-14956

Finite Larmor radius effect on Rayleigh-Taylor plasma instability in vertical magnetic field, characterizing solution by variational principle

04 p0557 A72-15022

Nonuniform radial electric field effects on low beta magnetized plasma column stability from numerical analysis for weakly collisional regime

04 p0557 A72-15023

Sufficient criteria for MHD stability derived from lowest eigenvalue bounds of Sturm-Liouville problem

04 p0557 A72-15168

Toroidal plasma column in Tokamak systems, discussing field inhomogeneity role in maintaining equilibrium with conducting casing, confirming magnetic field and transformer iron core

04 p0557 A72-15171

MHD stability of plasma boundary in transverse constant magnetic and hf circularly polarized fields

04 p0558 A72-15174

Hf circularly polarized field strength and plasma density self consistent stationary distribution in weakly inhomogeneous constant magnetic field

04 p0558 A72-15175

Ion-wave current instabilities theory, showing inhomogeneities generated by field aligned currents in collisionless plasma

04 p0559 A72-15350

One dimensional collisionless plasma instability driven by cold electron beam, determining limits from beam trapping

04 p0559 A72-15353

Flutelike microinstabilities in mirror-confined homogeneous magnetized one-species plasma with broad perpendicular velocity distribution

04 p0559 A72-15354

Plasma discharge instability in air in polyethylene and organic glass capillaries with evaporating walls, using time lapse filming

05 p0693 A72-15840

Vlasov equation stability properties of collisionless plasma and stellar gas, removing energy variation difficulties with multiple water bag model

05 p0694 A72-16060

Weak D type ionization waves stability in optically thick plasma layer behind front of interstellar gas

05 p0715 A72-16210

Longitudinal wave interaction and excitation by plasma instability in equatorial electrojet, considering energy transfer mechanism

05 p0656 A72-16242

Ion-acoustic instability in ionosphere in presence of fast particles inhomogeneity, estimating ions and electrons drift velocities

05 p0656 A72-16245

Plasma oscillations stabilization, considering nonlinear effects in phase velocity of plasma waves

05 p0695 A72-16416

Plasma stability in field of longitudinal monochromatic wave, examining satellites excitation by Langmuir wave

05 p0696 A72-16681

Turbulent heating in computer simulation of modified plasma two stream instability driven by relative electron-ion drifts across magnetic field

05 p0696 A72-16687

Low density plasma flute oscillations stabilization by feedback system with potential sensors and electrodes, deriving dispersion equation

05 p0697 A72-16983

Lf oscillations due to drift diffusion of current free weakly ionized inhomogeneous plasma in magnetic field

05 p0697 A72-16984

Whistler instability of electron plasmas with non-Maxwellian velocity distribution function

05 p0698 A72-17015

Anisotropic plasma stability to magnetosonic wave near ion cyclotron frequency propagating almost perpendicular to magnetic field

05 p0698 A72-17017

Longitudinal electrostatic waves in perpendicular collisionless plasma shock, investigating stability

05 p0698 A72-17021

MHD shock waves stability, showing Hall term effect on number of shock boundary conditions

05 p0699 A72-17025

Hot plasma transverse and longitudinal wave parametric excitation by intense laser light near plasma frequency, noting instability role in resonant coupling mechanism

05 p0699 A72-17172

Ion-acoustic waves and ionization waves instabilities in gas discharge plasmas

05 p0699 A72-17222

Laminar leading edge of collisionless plasma perpendicular shock structure and distribution functions, considering instability calculations

05 p0654 A72-17227

Electron temperature gradient instability in collisionless shocks propagating across magnetic field

05 p0700 A72-17228

Parametric plasma instability in hf electric field and constant magnetic field, noting longitudinal plasma oscillations growth

05 p0700 A72-17234

Geomagnetic storm associated quasi-sinusoidal magnetic field micropulsations due to Alfvén/drift instability or enhanced storm-time ring current

06 p0804 A72-17454

Lf instability mode in partly ionized plasma due to electron temperature gradient aligned perpendicular to magnetic field, applying to E and F regions

[AD-737931]

06 p0804 A72-17460

Heated lithium ion system /HELIOS/ facility for quiescent steady state plasma studies, noting MHD instabilities minimization

06 p0854 A72-17502

Plasma microinstabilities due to ion acoustic waves propagation with double-humped ion velocity distribution function in Q machine

06 p0855 A72-17516

Thermal noise and ion-acoustic waves excitation in Q machine two beam plasma with high temperature ratio in presence of inhomogeneous B-field, observing instability

06 p0856 A72-17517

Ion acoustic waves instability from electron-ion temperature difference in homogeneous collisional ionized plasma, using fluid equations perturbation analysis

06 p0856 A72-17524

Wave induced Q machine cesium plasma loss produced by current-driven collisional drift instability

06 p0857 A72-17527

Collisional drift instability dependence on parallel wavelength in potassium Q device plasma

06 p0857 A72-17528

Linear dispersion relation for pressure gradient driven drift waves instabilities from ion and electron thermal conductivity effects in collisional plasma

06 p0857 A72-17529

Electron temperature fluctuations associated with drift-type instability in Q device, discussing plasma diagnostic techniques

06 p0857 A72-17530

Dynamic stabilization of transverse Kelvin-Helmholtz instability driven by nonuniform plasma motion, using ac electric field near ion cyclotron frequency

06 p0857 A72-17531

Q-machine plasma column drift instability passive feedback control, regulating feedback drive current phase and amplitude by varying resonance circuit characteristics

06 p0857 A72-17532

Normal mode solutions for bounded systems from linear dispersion roots, discussing plasma waves and instabilities and damping effects in Q machines

06 p0858 A72-17537

Cross-field current driven ion acoustic instability in two plasma devices, causing neutral sheet phenomena, anomalous dispersion and ion heating

[AD-740261]

Plane supersonic ionizing shock wave in magnetic field under small wave plane perturbation from equilibrium position, calculating stability from linearized equations

06 p0798 A72-17678

Plasma perturbations and destabilization in curved magnetic field due to electronic electrical conductivity finiteness

06 p0860 A72-17684

Weakly ionized decaying afterglow plasma potential fluctuation and instability in magnetic field, using electrostatic probes

06 p0860 A72-17692

Longitudinal ambipolar acoustic instability effect on duration of plasma particle motion to wall across magnetic field, using phase method

06 p0860 A72-17693

Plasma jet injection stoppage and reflection in strong transverse magnetic field, considering instability due to flow interactions

06 p0860 A72-17694

Force-free magnetic fields effects on plasma column stability

06 p0860 A72-17744

Stability of weakly ionized homogeneous plasma placed in weak microwave field and in constant magnetic field, expressing growth increments of longitudinal waves

06 p0861 A72-17902

Numerical model for ion beam instability in nonisothermal plasma with electron temperature much greater than ion temperature

06 p0861 A72-17915

MHD convection in rotating electrically conducting viscous fluid layer within magnetic field, investigating linear stability

06 p0861 A72-18069

Magnetic field stability in Tornado-2 trap as function of helical currents on concentric sphere

06 p0863 A72-18406

Separatrix structure and stability of helical Tornado trap magnetic field from electron space charge measurements

06 p0863 A72-18407

Radial distribution of charged particle concentration fluctuation during decaying plasma instability development magnetic field

06 p0863 A72-18416

Soviet book on turbulent plasma theory covering stationary-turbulence spectra, instabilities, electromagnetic properties and wave propagation, particle stochastic acceleration, turbulent heating, etc

06 p0863 A72-18522

High-beta theta pinch plasma toroidal equilibrium by oscillating magnetic field superposition on main confining field

06 p0864 A72-18538

Contraststreaming electron beams instability in finite length one dimensional system with stationary neutralizing ion background, analyzing electrostatic waves space/time development by numerical simulation

06 p0865 A72-18540

Plasma density inhomogeneity effects on beam-plasma instability and Landau damping from digital simulation using charge sheet model

06 p0865 A72-18541

Plasma Dory-Guest-Harris type instability nonlinear evolution from numerical integration of Vlasov equation, using particle simulation and Fourier-Hermite transform methods

06 p0865 A72-18542

Weakly ionized plasma instability in strong nonuniform magnetic field with convective flow and steadily oscillating final state

06 p0865 A72-18543

Low frequency drift instability in local electron cyclotron resonance produced plasma, discussing oscillation fundamental frequency characteristics, wave propagation, density and potential waves, etc

07 p1039 A72-18799

Electrostatic wave instabilities at harmonics of electron cyclotron frequency in hot and cold anisotropic plasma with Maxwellian temperature distribution

07 p1039 A72-18824

Shear layer finite thickness and magnetic field effects on Kelvin-Helmholtz MHD instability of earth magnetopause boundary

07 p0974 A72-18892

Nonlinear monochromatic Alfvén wave propagation parallel to magnetic field in anisotropic plasma with long wavelength beam instability

07 p1039 A72-18915

Threshold condition for purely growing parametric instability in inhomogeneous plasma

07 p0975 A72-19153

Radiative cooling induced thermal instability mechanism for condensation in astrophysical plasma

07 p1040 A72-19348

Colliding plasmas transverse instabilities, investigating ion dynamic and electron beam induced return currents effects
07 p1041 A72-19508

Transverse electromagnetic instabilities in anisotropic plasmas, confirming by computer simulation energy constants derived from nonlinear Vlasov-Maxwell equations
07 p1041 A72-19509

Field free constricted plasma discharge stability between electrodes, obtaining critical current
07 p1042 A72-19606

Dispersion relation for uhf drift waves in nonuniform plasma with cold electrons drift through stationary ions, deriving plasma stability conditions
07 p1042 A72-19612

Hf instability on whistler branch of finite pressure plasma with nonmonotonic ion distribution function under Landau damping effect
07 p1042 A72-19615

Nonuniform plane parallel plasma streams instability with/without magnetic field, comparing with conducting fluid
07 p1042 A72-19618

Supraluminous wave instability in weakly turbulent plasmas, using Vlasov equations
07 p1043 A72-19619

Ion heating in high Mach number oblique collisionless shock waves, noting role of two-ion beam instability from digital simulation
07 p1043 A72-19665

Vibration modes and stability of nonequilibrium low density He-Cs plasma in magnetic field
07 p1043 A72-19876

Ionization change induced striation instability of low temperature plasma with ambipolar diffusion in transverse magnetic field
07 p1043 A72-19878

Hydrogen plasma ionization equilibrium and thermodynamic stability existence condition based on Saha equation
07 p1044 A72-19889

Rf excitation produced plasma instability, considering density fluctuation and drive frequency introduction by amplitude modulation
07 p1045 A72-20441

Stability conditions of dissipative trapped ion mode in axisymmetric toroidal confinement systems, investigating collisional damping rate
07 p1045 A72-20476

Growth rate and boundary of drift dissipative instability in plasma under linear theta pinch conditions
07 p1045 A72-20477

Anisotropic equilibrium solution to Vlasov equation for high beta theta pinch plasma column
07 p1045 A72-20478

Dynamic stabilization of MHD instabilities in plasma column by multipole hf fields, analyzing dispersion equation
07 p1045 A72-20479

Quasi-linear theory validity for turbulent collisionless plasmas, considering bump-in-tail and weak symmetric two-stream instabilities
07 p1045 A72-20481

Inhomogeneous high-collision finite pressure plasma stability, finding thermal instability development under uniform temperature and arbitrary pressure
07 p1046 A72-20514

Nonlinear ion acoustic instability in plasma for subharmonic and harmonic forcing oscillations similar to Van der Pol effect
07 p1046 A72-20541

Interplanetary medium physical parameters from spacecraft measurements, noting solar wind properties, magnetic fields and MHD discontinuities
08 p1228 A72-20826

Stability of steady large amplitude whistler wave supported by weak electrostatic waves in collisionless magnetoplasma, constructing distribution function via Vlasov equation solution
08 p1213 A72-21258

High energy electron beam interaction with dense plasma, investigating unstable waves growth by numerical methods
08 p1213 A72-21259

Electrostatic ion wave stability in electrogasdynamic channel flow from approximate numerical solution of dispersion equations
08 p1211 A72-21305

Electron Larmor radius effect on hf hose and mirror instabilities of fast magnetoacoustic and ion acoustic waves in nonisothermal plasma
08 p1215 A72-21874

MHD stability problems in radio galaxy structure and cosmic ray interaction with magnetic fields
09 p1386 A72-22751

Alfven waves development and high pressure plasma hydrodynamic and kinetic instabilities dependence on magnetic field to temperature gradients ratio
09 p1360 A72-22954

Axisymmetric MHD equilibria with elliptical cross sections and flat current profile, obtaining criterion for stability to localized modes by numerical computation
09 p1361 A72-23047

Ellipsoidal plasmoid equilibrium revolution frequency and potential energy and stability in external hf fields
09 p1362 A72-23204

Pulsed plasma flow interaction with spatially periodic magnetic field generated by coaxial coils with alternating currents, noting MHD stability
09 p1362 A72-23207

Plasma filament equilibrium in Sirius stellarator during heating by fast magnetosonic wave
09 p1363 A72-23214

Homogeneous plasma internal feedback mechanism and structure, discussing instabilities control by external feedback
09 p1365 A72-23474

Strong magnetic fields and electric current densities effects on acoustic oscillations and instability in stationary inhomogeneous low temperature plasma flow in crossed fields
10 p1517 A72-23838

Bounded plasma ionization instability inhomogeneity scale evaluation, assuming negligible electron energy losses due to heat conduction
10 p1517 A72-23844

Plane ionizing shock wave stability in MHD channel within magnetic field
10 p1522 A72-24542

MHD sheet pinch model time dependent nonequilibrium stability determined by equations of incompressible viscous resistive magnetofluid [AD-739661]
10 p1523 A72-24751

Superconducting levitron machine for trapped hot plasma stability and confinement studies in vacuum, discussing construction and coil performance
10 p1460 A72-24758

Parallel viscous modification of resistive tearing instability in Cartesian model of hard core pinch plasma confinement
10 p1523 A72-24795

Density fluctuations and ion acoustic two stream instability characteristics of RF generated plasma derived from electromagnetic scattering at 24 GHz
10 p1523 A72-24800

Collisionless thermalization of ion beam by interaction with plasma, noting acoustic instability growth
10 p1524 A72-24921

Nonlinear HF ionospheric instabilities classification on unified basis by coupled mode theory
10 p1440 A72-24936

Small scale sporadic E layer explained by means of cross field instability, proposing numerical solution based on realistic three dimensional perturbation
10 p1478 A72-25164

Three dimensional linear analysis of ionosphere cross field instability, noting potential as E region irregularities source
10 p1478 A72-25166

Perturbation technique application to nonlinear behavior of ion waves produced by two-beam instability in plasma
11 p1692 A72-25519

Uniform and parallel magnetic field effects on hydromagnetic instability of two dimensional jet at small magnetic Reynolds numbers
11 p1693 A72-25521

Plasma beam cyclotron instability theory based on computer simulation, noting stabilizing effect due to Landau damping
11 p1693 A72-25562

Plasma column stabilization by constant longitudinal inhomogeneous magnetic and rotating HF electromagnetic fields, noting application to plasma convective instabilities
11 p1694 A72-25786

Time dependent solutions of Tokamak equilibrium equations for plasma diffusive processes
11 p1694 A72-25787

Plasma equilibrium configurations, considering magnetically contained focus in external magnetic field
11 p1694 A72-25788

Plasma decay instabilities in finite amplitude Alfven wave field, discussing critical wave amplitude
11 p1694 A72-25790

Controlled nuclear fusion plasma stabilization by electrostatic forces, reducing applied magnetic field
11 p1694 A72-25791

Finite element method application to hydromagnetic plasma stability analysis, considering cylindrical plasma immersed in axial magnetic field and bounded by conducting shell
11 p1695 A72-25794

Longitudinal plasma oscillations nonlinear instability due to energy transformation into harmonics and subharmonics
11 p1695 A72-25795

Anomalous heating due to nonlinear parametric interaction between plasma and laser radiation, calculating laser power thresholds for nonlinear instability effects
11 p1695 A72-25857

Hydromagnetic stability of isothermal stratified plasma atmosphere uniform flow over conducting liquid along magnetic field, discussing dispersion relation for static configuration
11 p1695 A72-26115

Interplanetary plasma microinstabilities within framework of underlying electron-proton solar exosphere, discussing solar wind high beta effects
11 p1714 A72-26529

Plasma interchange instability and convection in gravitational field, showing viscosity and resistivity stabilization and critical Reynolds number
11 p1697 A72-26584

Absolute and convective plasma instabilities distinction in one dimensional linear infinite system, discussing saddle points method
11 p1697 A72-26585

Bounded systems dispersion relations interpretation for plasma waves and instabilities on finite cylinders, with emphasis on end plate damping and axial current effects on Q machines
11 p1697 A72-26597

Larmor frequency influence on Rayleigh-Taylor instability of viscous Hall plasma with magnetic field
11 p1698 A72-26604

Hydromagnetic stability of rotating nondissipative inviscid incompressible conducting fluid annulus permeated by radially varying magnetic field, considering axisymmetric and nonaxisymmetric disturbances
11 p1619 A72-26639

Plasma parametric instabilities excitation by radio waves in ionosphere, noting LF ionic and HF electrostatic wave growth
11 p1628 A72-26767

Plasma-ion beam system drift beam instability in longitudinal magnetic field, noting oscillations frequencies dependence
12 p1849 A72-27060

Low density plasma flute oscillations stabilization by feedback system with potential sensors and electrodes, deriving dispersion equation
12 p1850 A72-27127

LF oscillations due to drift-diffusion of current free weakly ionized inhomogeneous plasma in magnetic field
12 p1850 A72-27128

Thermal electron relativistic streaming effects on electromagnetic instability in magnetoplasmas
12 p1851 A72-27389

Electron wave sideband frequencies and wave-trapped electron oscillations as cause of plasma instability
12 p1851 A72-27430

Quasi-linear approximation equations for relativistic charged particles beam dissipative instability in collisional plasma, noting electrons heating at high collision frequencies
12 p1852 A72-27860

Stability properties for collisionless plasma and encounterless self gravitational stellar gas described by Vlasov equations
12 p1875 A72-27916

Self stabilization, measurement of two-ion beam instability generated by microturbulent ion heating in plasma with variable temperature ratio
13 p2007 A72-28428

Convective hydromagnetic stability of hot conducting fluid layer in magnetic field by Liapunov method
13 p2011 A72-28891

Parametric decay instability of Langmuir and acoustic plasma waves induced by incident electromagnetic wave near plasma frequency, noting application to ionospheric instabilities
13 p2012 A72-29126

Growth rates of unstable electromagnetic waves propagating perpendicularly to symmetric counterstreaming finite temperature plasmas
13 p2012 A72-29129

MHD laser discharge characteristics under generator conditions, emphasizing interaction of gas ionization instabilities and lasing radiation field
13 p2014 A72-29367

Cs seeded nonequilibrium MHD Ar plasma stability in fully ionized seed regime
13 p2014 A72-29368

Ionization stabilization in MHD generators by sensing electron density perturbation with linear feedback into nonequilibrium plasma
13 p2014 A72-29369

Fluctuating electric current induced magnetic field effects on long wave nonequilibrium plasma instability associated with large scale closed cycle MHD generators
13 p2014 A72-29370

Nonlinear model of ionization instability of MHD generators, assuming discharge structure with alternating layers of high and low electrical conductivity
13 p2014 A72-29371

Two point correlation description of MHD plasma properties subject to electrothermal instability, calculating electron number density and temperature fluctuations
13 p2015 A72-29373

Parametric instability of magnetoactive plasma relative to nonpotential oscillations excitation, deriving threshold value of HF field strength
13 p2016 A72-29601

Alternating magnetic field effect on collisionless nonhomogeneous magnetoplasma ion acoustic oscillations

tions stability, examining parametric excitation of Langmuir oscillations

13 p2016 A72-29604

Drift dissipative instability in bounded gas discharge plasma within magnetic field, investigating oscillations dependence on gas pressure and field strength

13 p2016 A72-29605

MHD stability in Hg vapor discharge plasma excited by standing microwave near electron cyclotron resonance, discussing electron energy anisotropy effect on LF oscillations

13 p2017 A72-29618

B type discrete radio aurora theoretical prediction based on drift gradient instability, comparing with observations

13 p1951 A72-29651

Stationary nonlinear ion acoustic oscillations in dense weakly ionized current carrying plasma, considering wave propagation velocity and instability process

13 p2019 A72-29988

Tangential MHD discontinuity stability for ideally conducting compressible fluid in magnetic and gravitational fields

13 p2020 A72-30068

Plasma instability theories for radio auroras, reviewing radar and radio observation systems and ion acoustic and drift gradient predictions

14 p2098 A72-30140

Current instability of electron-ion plasma in magnetic field produced by moving resonance charges

14 p2136 A72-30301

Dissipative instability produced by colliding ions and atoms in weakly ionized plasma

14 p2136 A72-30303

Dispersion of polyhedral nonrelativistic electron flow interacting with slow waves of magnetized cold plasma, observing instability in presence of Doppler effects

14 p2136 A72-30304

Kinetic instability bursts during heating of electron plasma in cylindrical resonator with standing electromagnetic waves

14 p2136 A72-30308

Kinetic instabilities during electron plasma heating in HF field of cylindrical resonator, discussing electron energy distribution function effect

14 p2137 A72-30309

LF and HF oscillations in plasma-electron beam system, investigating instability control

14 p2137 A72-30310

Non-Maxwellian inhomogeneous collisionless plasma equilibrium and stability, proposing statistical thermodynamic model

14 p2137 A72-30394

Ion viscosity tensor and ion thermal flux derived for microinstabilities of inhomogeneous collisional high pressure plasma, noting second derivatives of temperature

14 p2137 A72-30395

Wave pattern of three dimensional hydromagnetic perturbations produced by harmonic magnetic dipole in anisotropic plasma

14 p2102 A72-30661

Two counter streaming plasmas with anisotropic temperatures, deriving instability condition for ordinary mode electromagnetic propagation perpendicular to external magnetic field

14 p2140 A72-30935

Anisotropic homogeneous plasmas, deriving computer model to predict effects of circularly polarized parallel plasma waves in external uniform magnetic field direction on instabilities

14 p2140 A72-30938

Lagrangian complex amplitude derivation for monochromatic electrostatic wave in unmagnetized collisionless plasma, investigating nonlinear Landau damping effects on instability

14 p2140 A72-30939

Hydromagnetic channel flow stability computation via energy method, solving eigenvalue problem by direct forward numerical integration

15 p2283 A72-31212

Dispersion relationship for electrostatic instability associated with electron beam trapped in magnetic mirror of magnetosphere, taking into account nonuniformity of magnetic field

15 p2283 A72-31434

Monochromatic plasma wave excitation by cold electron beam, obtaining instability maximum amplitude and oscillation period

15 p2285 A72-32270

Mathematical model for modified ordinary electromagnetic wave propagation in presence of two cold counterstreaming plasma electron beams, noting instability regions and growth rate

15 p2286 A72-32274

Analytical solution of dispersion equation for ionization instability threshold in unbounded low temperature plasma, noting independence of relaxation rates

15 p2286 A72-32277

Radial transport instability during intense microbeam heating of thin plasma column, noting

maximum temperatures and phase coherence cut-off effect

15 p2286 A72-32306

MHD instabilities growth rates from diffuse linear pinch equations of motion solution

15 p2287 A72-32416

Finite beta plasma drift cone instability relationship to mirror ratio and plasma temperature changes

15 p2288 A72-32422

Solar flares induced magnetic field configurations, considering open and closed current sheets instabilities as flare sources

15 p2301 A72-32788

HF electrostatic instabilities driven by electron-ion relative drift velocity across external magnetic field for inhomogeneous plasma, noting Landau damping role

16 p2433 A72-32809

Ion acoustic, electron plasma and cyclotron harmonic waves parametric instabilities in magnetic field and applications to plasma heating

16 p2433 A72-32811

Rotating plasmas steady MHD equilibria without PS factor enhancement, considering cases of vanishing and nonvanishing toroidal current

16 p2433 A72-32817

Plasma accumulation in electrostatic potential well produced by electron space charges, determining diocotron instability as function of electron plasma and gyrofrequency ratio

16 p2434 A72-32819

Plasma wave excitation by monoenergetic relativistic electron beam, investigating beam-plasma wave synchronism during instability development

16 p2434 A72-32912

F region crossed field instability nonlinear theory based on energy transfer by mode coupling and absorption by linear damping with application to equatorial electrojet

16 p2384 A72-32976

Critical layer equations of plasma resistive instabilities, using sheet pinch model

16 p2436 A72-33577

Extraordinary wave instabilities in collision dominated plasma taking into account finite wave number, noting dispersion equation for refractive index larger than unity

16 p2436 A72-33653

Anomalous diffusion coefficient of axially decaying RF discharge collisional plasma under instability mode suppressed by feedback technique

16 p2437 A72-33657

Plasma stability in field of longitudinal monochromatic wave, examining satellites excitation by Langmuir wave

16 p2437 A72-33693

Random ionization waves convective instability in glow discharge positive column, calculating fluctuations spectrum as function of position along column for localized white noise source

16 p2437 A72-33747

Plane vortex sheet in incompressible inviscid and finitely conducting fluids, investigating discontinuity in density and conductivity on hydromagnetic stability

16 p2438 A72-33842

Alfvén wave firehose instability relaxation calculation to include nonlinear terms for explanation of solar wind temperature anisotropies by collisionless mechanism

16 p2449 A72-33933

Nonlinear theory of crossed field and two stream instabilities of nonthermal plasma motions in equatorial electrojet

16 p2387 A72-33937

Particle scattering due to Rosenbluth-Post convective plasma loss-cone instability distribution function

17 p2587 A72-34189

Magnetic field stability in Tornado-2 trap as function of helical currents on concentric spheres

17 p2588 A72-34856

Separatrix shape, presence and position and electron lifetime and space charge in helical Tornado trap magnetic field

17 p2588 A72-34857

Radial distribution of charged particle concentration fluctuation during decaying plasma instability development in magnetic field

17 p2588 A72-34865

Cerenkov instability and VLF emissions generated outside the plasmopause

17 p2547 A72-35063

Vibration modes and stability of nonequilibrium low density He-Cs plasma in magnetic field

17 p2589 A72-35126

Ionization change induced striation instability of low temperature plasma with ambipolar diffusion in transverse magnetic field

17 p2590 A72-35128

Hydrogen plasma ionization equilibrium and thermodynamic stability existence condition based on Saha equation

17 p2590 A72-35137

HF electrostatic wave instability induced in plasma by electron beam, noting resonant frequency Doppler shift

17 p2591 A72-35369

Slipping stream instability of a self-gravitating hydromagnetic gas cloud

17 p2613 A72-35501

Water bag model application to one dimensional inhomogeneous two-stream collisionless electron plasma stability computation, noting electrostatic modes

17 p2592 A72-35619

Electron cyclotron drift instability linear theory application to controlled fusion and collisionless shocks, proving anomalous resistance to current flow normal to magnetic field

17 p2592 A72-35624

A stability mechanism for the ion-acoustic waves

17 p2592 A72-35625

Beam-generated collisionless ion-acoustic shocks

17 p2592 A72-35626

Instability of electromagnetic cyclotron harmonic waves in plasmas

17 p2592 A72-35775

Alfvén waves development and high pressure plasma hydrodynamic and kinetic instabilities dependence on magnetic field to temperature gradients ratio

17 p2593 A72-35883

Dynamo instability and feedback in a stochastically driven system

18 p2678 A72-36013

Combined Rayleigh and Kelvin instability of a Hall plasma with a vertical magnetic field

18 p2715 A72-36502

The electromagnetic radiation near the ion plasma frequency emitted by a turbulently heated plasma

18 p2715 A72-36598

Observation of satellite modes in a beam-plasma instability

18 p2715 A72-36600

Quasi-linear theory of plasmas situated in a weak UHF electric field and a constant magnetic field

18 p2715 A72-36654

Hydrodynamic stability of the gradient flow of a conducting fluid with a rheological power law in a transverse magnetic field

18 p2716 A72-36814

Flute modes in a plasma in the presence of nonuniform electric fields

18 p2717 A72-37162

Nonlinear equations for explosive instabilities of three plasma waves interaction with mutually different linear damping

19 p2838 A72-37326

Longitudinal waves in a perpendicular collisionless plasma shock. IV - Gradient B

19 p2838 A72-37329

Nonlinear time evolution of firehose unstable MHD waves, noting quasi-linear theory truncation error for low wave numbers relaxation time and energy growth

19 p2839 A72-37334

Boundary conditions in the presence of Hall current or finite ion Larmor radius effects

19 p2839 A72-37338

Experimental indications of plasma instabilities induced by laser heating

19 p2840 A72-37549

Nonlinear saturation of the ion-acoustic instability

19 p2840 A72-37931

Hydrodynamic stability of periodic burning front for ideally conducting incompressible fluids in longitudinal or transverse magnetic field

19 p2882 A72-38457

Effect of ionic viscosity on the stability of a finite-pressure plasma

19 p2842 A72-38529

Stability of a plasma conductor with axial current, surrounded by cold gas with a pressure gradient

19 p2842 A72-38533

Electric discharge concept to uncouple electron density from temperature for production of stable uniform electric laser discharges

19 p2812 A72-38596

Continuum eigenmodes of an inhomogeneous plasma

20 p2956 A72-39015

MHD instability of two dimensional laminar boundary layer in incompressible electrically conducting fluid along concave wall with periodic three dimensional disturbances

20 p2957 A72-39328

Determination of the magnetic field B in vacuum for general two-dimensional MHD-equilibria

20 p2957 A72-39352

Plasma equilibrium in configurations with a helical magnetic axis with allowance for toroidality

20 p2957 A72-39353

Drift instabilities in an inhomogeneous collisionless plasma

20 p2957 A72-39355

Nonlinear monochromatic Alfvén wave propagation along magnetic field in anisotropic rarefied plasma with firehose instability

20 p2957 A72-39381

Finite sized optically thin radiating plasma stability analysis, deriving luminosity function for metastable state existence from mathematical model 20 p2958 A72-39456

Observation of superheat instability in a fully ionized current-carrying plasma. 20 p2958 A72-39854

Suppression of instabilities in a beam-plasma system by a modulation of the electron beam. 21 p3089 A72-40199

A system of disc-stabilized dc arc and solution nebulization device for the investigation of multicomponent plasmas. 21 p3039 A72-40213

Contribution to nonlinear theory of electron-beam kinetic instability in a plasma 21 p3090 A72-40408

Nonlinear ion sound in a fully ionized current-carrying plasma 21 p3090 A72-40411

Rayleigh-Taylor instability in a composite medium. 21 p3104 A72-40478

Nonlinear magnetosonic waves in a plasma with a finite conductivity. 21 p3090 A72-40485

The study of turbulence in theta-pinch plasma with azimuthal magnetic field. 21 p3091 A72-40571

Parametric instability of magnetoactive plasma relative to nonpotential oscillations excitation, deriving threshold value of HF field strength 21 p3091 A72-40655

Alternating magnetic field effect on ionoacoustic oscillations stability of collisionless nonhomogeneous magnetoplasma, examining parametric excitation of Langmuir oscillations 21 p3091 A72-40658

Drift dissipative instability in bounded gas discharge plasma within magnetic field, investigating oscillations dependence on gas pressure and field strength 21 p3091 A72-40659

MHD stability in Hg vapor discharge plasma excited by standing microwave near electron cyclotron resonance, discussing electron energy anisotropy effect on LF oscillations 21 p3091 A72-40671

Three-dimensional pattern of instability development during the interaction between a modulated electron beam and a plasma 21 p3092 A72-40800

Measurements of enhanced absorption of electromagnetic waves and effective collision frequency due to parametric decay instability. 21 p3092 A72-40829

Linear and nonlinear aspects of ion-sound current instability for solar atmosphere conditions of full ionization, noting implications for flare mechanism 21 p3100 A72-41040

Frictional effects with neutrals and the gravitational instability of a plasma. 21 p3093 A72-41332

Effects of parallel wavelength on the collisional drift instability. 21 p3093 A72-41627

Transverse velocity shear instabilities within a magnetically confined plasma. 21 p3093 A72-41628

Plasma heating by large-amplitude, low-frequency electric fields. 21 p3094 A72-41630

Helical field experiments on a three-meter theta pinch. 21 p3094 A72-41636

Low-frequency oscillations in a Penning-discharge plasma under conditions of a cyclotron ion source 21 p3095 A72-41682

External high-frequency modulation of an ion beam and the absorption of beam-plasma instability oscillations in a plasma situated in a magnetic field of mirror configuration 21 p3095 A72-41683

Influence of boundaries on the ionization instability of a plasma in a discharge of coaxial geometry 22 p3209 A72-41876

Influence of inelastic electron-energy losses on the development of ionization instability in a plasma 22 p3209 A72-41877

Uniform low temperature gas discharge plasma diagnostics in shielded volume, noting application of stable plasma generation effect for isotope analysis 22 p3210 A72-42152

Hydrodynamic instability of a plasma boundary with a magnetic field, taking viscosity into account. 22 p3210 A72-42277

Boundary fluctuations of a plasma column with a current 22 p3211 A72-42655

Larmor radius and collisional effects on the dynamic stability of a composite medium. 22 p3212 A72-42990

Wave propagation in plasma modulated by external electric field, noting dispersion equation for coupled waves and instability conditions 22 p3212 A72-43101

Surface drift vibrations of a weakly ionized plasma 22 p3212 A72-43102

Instability of a weakly ionized plasma with respect to vibrations with wavelengths of the order of the Debye radius 22 p3213 A72-43104

Confinement time of plasma injected in magnetic field of racetrack with diverter, noting plasma equilibrium in toroidal magnetic field 22 p3213 A72-43106

An ion-cyclotron instability of a plasma produced by a fast-ion beam 22 p3213 A72-43113

Electromagnetic emission during the development of a hydrodynamic beam instability in a bounded plasma 22 p3213 A72-43115

Current instability of electron-ion plasma in magnetic field produced by moving resonance charges 23 p3317 A72-43203

Dissipative instability produced by colliding ions and atoms in weakly ionized plasma 23 p3317 A72-43205

Dispersion of polyhelical nonrelativistic electron flow interacting with slow waves of magnetized cold plasma, observing instability in presence of Doppler effects 23 p3317 A72-43206

Kinetic instability bursts during heating of electron plasma in cylindrical resonator with standing electromagnetic waves 23 p3317 A72-43210

Kinetic instabilities during electron plasma heating in HF field of cylindrical resonator, discussing electron energy distribution function effect 23 p3317 A72-43211

LF and HF oscillations in plasma-electron beam system, investigating instability control 23 p3317 A72-43212

Conditions for magnetoactive plasma longitudinal waves with phase velocity near light velocity existence, investigating increments during synchrotron instability due to relativistic particles 23 p3262 A72-43311

Collisionless heating of plasma ions by an ion beam 23 p3318 A72-43321

Surface wave parametric excitation by weak HF electric field in semibounded plasma, calculating near threshold instability by dispersion equation 23 p3318 A72-43322

Nature of polar-aurora light intensity pulsations associated with P12-type geomagnetic pulsations 23 p3282 A72-43359

A current instability in the neutral layer of the tail of the earth's magnetosphere 23 p3283 A72-43368

Excitation of potential oscillations in a plasma by a flow of phased oscillators 23 p3319 A72-43401

Electron distribution fluctuation in two level system of unstable electron gas, noting periodic time dependence of population 23 p3319 A72-43406

Physical processes of weak, single wave and strong plasma turbulence and instabilities driven by oscillating fields 23 p3319 A72-43514

Plane parallel nonuniform velocity plasma streams instability in absence and presence of magnetic field, comparing with ideal conductive liquid flows 23 p3320 A72-43518

Ion acoustic instability in collisionless shocks. 23 p3320 A72-43522

Perpendicular collisionless shock wave instability. 23 p3320 A72-43523

On the instability of nonlinear longitudinal oscillations of magnetoactive plasma. 23 p3320 A72-43524

Strictional nonlinearity effect on uniform nonrelativistic monoenergetic beam interaction with isotropic bounded plasma, investigating plasma oscillations and stability 23 p3320 A72-43576

Plasma-beam interaction in limited geometry: Temperature effects 23 p3321 A72-43700

Quasi-linear theory for the low-frequency instability of a plasma placed in a weak SHF electric field 23 p3321 A72-44172

Electromagnetic instabilities produced by neutral-particle ionization in interplanetary space. 23 p3332 A72-44506

Parametric instabilities and anomalous heating of plasmas near the lower hybrid frequency. 23 p3323 A72-44545

The critical velocity of gas-plasma interaction and its possible heterogenic relevance. 24 p3429 A72-45468

Instability of a magnetically active plasma in the presence of a specified transverse velocity of the ions 24 p3429 A72-45488

High-frequency instabilities in a plasma with a nonlinear ion-acoustic wave 24 p3429 A72-45489

Anode sheath plasma current instabilities, examining electron and ion turbulent heating, plasma particle limiting energies and unsteady oscillation spectra 24 p3429 A72-45490

Current-driven drift wave instability in a sheared magnetic field. 24 p3430 A72-45570

Nonlinear instability of Bernstein modes pumped by an electromagnetic wave. 24 p3430 A72-45571

Plasma-ion beam system drift beam instability in longitudinal magnetic field, noting oscillations frequencies dependence 24 p3431 A72-45713

MAGNETOHYDRODYNAMIC TURBULENCE

NT PLASMA TURBULENCE

Solar coronal MHD disturbance off eastern limb correlation with complex radio event observed simultaneously with white light coronameter and Culgoora radioheliograph 02 p0276 A72-11647

Quasi-linear theory of relativistic particle acceleration by hydromagnetic turbulence for small gyration radius expansion, using Vlasov equation 02 p0265 A72-12301

Turbulent micro and macromotion velocities in solar photosphere from CN molecule vibrational band line contours 07 p1077 A72-19810

Random homogeneous turbulence generation of rms weak magnetic field fluctuation in infinite medium with short correlation time 13 p2015 A72-29403

Transverse particle diffusion across external homogeneous magnetic field under random isotropic large scale hydromagnetic turbulence 14 p2102 A72-30650

Postfrontal ion acoustic shock turbulence as function of Mach number and electron/ion temperature ratio, using particle in cell technique 15 p2281 A72-32424

Turbulent micro and macromotion velocities in solar photosphere from CN molecule vibrational band line contours 17 p2617 A72-35735

Energy spectrum of small scale solar magnetic fields. 20 p2971 A72-39765

On a resolution of the equations governing the second order correlation functions for an isotropic hydromagnetic turbulence. 22 p3212 A72-43100

MAGNETOHYDRODYNAMIC WAVES

NT ELECTROSTATIC WAVES

NT PLASMA WAVES

Aligned fields in MHD shock polar equation, obtaining magnetic induction polar variables 01 p0106 A72-10135

LF large scale oblique Alfvén wave propagation in turbulent ion acoustic plasma, investigating dispersion relation, Landau damping and interactions 01 p0107 A72-10137

Nonlinear hydromagnetic waves in finite beta collisionless plasma, calculating space-time evolution with nonlinear integrodifferential equation 01 p0107 A72-10143

Quasi-steady spectrum of hydromagnetic noise in proton belt, using random excited broad wave fields in nonisothermal magnetosphere 01 p0118 A72-10367

MHD waves nonlinear interaction in magnetosphere, calculating transverse Alfvén and magnetosonic and longitudinal acoustic wave decay instabilities 01 p0109 A72-10618

MHD boundary waves properties, noting application to traveling wave nonreciprocal devices and planar structures based on microwave integrated circuits 01 p0029 A72-10703

MHD wave modes nonlinear coupling by quantum field approach with Hamiltonian formulation, applying to solar coronal heating 01 p0129 A72-10797

Microscale MHD wave and stationary structure fluctuations in interplanetary medium solar wind, considering theoretical constraints 01 p0129 A72-10883

Magnetospheric wave and particle phenomena correlation to convection electric fields in nightside magnetosphere during isolated substorms 01 p0062 A72-10904

High speed interstellar gas dynamic resonant hydromagnetic wave interaction with cosmic ray shocks 01 p0121 A72-11140

Large amplitude linearly or elliptically polarized Alfvén wave propagation parallel to magnetic field, calculating nonlinear Landau damping rate 01 p0111 A72-11227

Hydromagnetic cylindrical blast wave propagation in self gravitating polytropic gas, obtaining graphs for velocity, pressure, density and magnetic field distributions 02 p0264 A72-12181

Magnetospheric hydromagnetic waves propagation characteristics, discussing isotropic/poloidal and guided/toroidal modes coupling in conjunction with hydromagnetic wedge model

02 p0268 A72-12870

Damped geomagnetic pulsations associated with geomagnetic storms interpreted as interaction between hydromagnetic oscillations and solar wind induced magnetospheric motions, discussing modified mathematical model

02 p0222 A72-12872

Acceleration phase of solar cosmic rays and relativistic electrons in solar flare of 7 July 1966, discussing MHD shock waves generation

03 p0407 A72-12942

Linear and nonlinear MHD shock wave propagation and stability, investigating Hugoniot relation

03 p0396 A72-13688

Ionospheric hydromagnetic and acoustic gravity wave interactions, examining stratified nonisothermal atmospheric model

04 p0516 A72-14934

Dispersion relation for MHD wave propagation through partially ionized magnetoplasma, discussing collision frequencies effects

04 p0556 A72-14943

Hydromagnetic whistler traveling wave tube amplification in magnetosphere, deriving temporal growth rate dependence on plasma parameters

04 p0517 A72-14950

Existence conditions for steady MHD shock waves propagating in collisionless plasma along magnetic field, observing dependence on pressure anisotropy

05 p0698 A72-17016

Nonlinear MHD wave trains in cold collisionless plasma investigated by numerical and analytical methods

05 p0698 A72-17018

MHD shock waves stability, showing Hall term effect on number of shock boundary conditions

05 p0699 A72-17025

Hall fields effect on interaction of MHD waves in inhomogeneous plasma, considering MHD wave dispersion

05 p0701 A72-17237

Magnetosonic, Alfvén, shock and infinitesimal waves and corresponding rays in relativistic hydrodynamics and magnetohydrodynamics, using tensor distributions

06 p0847 A72-17253

Circularly polarized hydromagnetic wave propagation upstream in solar wind, noting Doppler shifted whistler and slow electron cyclotron modes

06 p0872 A72-17449

Geoelectric field strengths deduction from mid-frequency slopes on diurnal incidence plot of pc 1 hydromagnetic whistlers

07 p0974 A72-18904

MHD shock normals calculation by magnetic coplanarity formula, applying to bow shock crossing of Pioneer 6

07 p1040 A72-19157

Hydromagnetic wave theory for solar wind, noting tangential discontinuities, perpendicular and Alfvén shocks and forward and reverse fast and slow shocks

07 p1058 A72-19354

Transverse hydromagnetic plane waves existence in uniformly heated electrically conducting fluid under temperature gradient and magnetic field

07 p1045 A72-20442

Weakly damped Alfvén ion-cyclotron waves and fast magnetoacoustic waves in infinite plasma cylinder inserted into current bearing finite coil

07 p1046 A72-20516

Geomagnetic variations propagation theory for LF electromagnetic and Alfvén waves diffraction at stratified earth in thin gyrotopical ionosphere

08 p1130 A72-20711

Geomagnetic field fluctuations during storms, considering Alfvén waves generation and propagation in solar wind and magnetosphere

08 p1153 A72-20717

Pulsars CP 0328 and NP 0531 twinkling explained by interstellar electron density fluctuations due to Alfvén wave passage and coupling of cosmic rays to interstellar gas

09 p1377 A72-22753

Alfvén waves development and high pressure plasma hydrodynamic and kinetic instabilities dependence on magnetic field to temperature gradients ratio

09 p1360 A72-22954

Van Allen proton belt model, considering ionosphere particle acceleration by stochastic interaction with hydromagnetic waves due to solar wind at magnetosphere shock front

10 p1529 A72-24245

Optimal control computation for nonlinear hyperbolic partial differential system by gradient and quasi-linearization techniques, noting MHD, fluid flow and electromagnetic wave propagation

10 p1456 A72-24453

Internal Alfvén gravity waves propagation in rotating Boussinesq inviscid adiabatic conducting fluid shear flow within transverse magnetic field, considering electromagnetic and Coriolis forces effects

10 p1511 A72-24470

Fast auroral hydromagnetic wave occurrence relation to substorm activity, suggesting role of enhanced particle population in magnetospheric region

10 p1476 A72-24962

Plasma decay instabilities in finite amplitude Alfvén wave field, discussing critical wave amplitude

11 p1694 A72-25790

Hydromagnetic waves propagation and horizontal group velocity westward from dawn terminator to dark hemisphere, inferring magnetospheric properties

11 p1625 A72-26414

Supergranular motions source of Alfvén waves dominating solar wind microstructure at earth orbit

11 p1724 A72-26530

Skew magnetic structure of ionizing shock waves with ohmic dissipation as dominant diffusion mechanism

11 p1618 A72-26605

Hydromagnetic wave scattering of high energy cosmic rays in highly ionized interstellar gas to confine cosmic rays to Milky Way

12 p1864 A72-27745

High frequency potential effect on fast transverse magnetic waves along plasma layer bounded by two conducting plates

12 p1785 A72-27855

Multilayer plasma model for MHD pulse propagation in ionospheric waveguide, noting approximation of Alfvén velocity distribution by plasma layers

13 p1946 A72-28585

LF oscillations and electron drift in frozen plasma under strong electromagnetic radiation, deriving formulas for coupled Alfvén and spiral waves

13 p2035 A72-28593

High latitude ionospheric transmission and reflection properties for oblique hydromagnetic plane waves at micropulsation frequencies for daytime and nighttime conditions

13 p1951 A72-29390

Alfvén wave transmission in sunspot umbral magnetic flux tube, noting standing progressive waves and energy dissipation in facular regions

13 p2049 A72-29937

Hydromagnetic waves excited by transverse magnetic dipole in finite-conductivity plasma

14 p2102 A72-30662

Earth core hydromagnetic oscillations with respect to geomagnetic secular variation time scales and role in dynamo process-produced geomagnetic field

15 p2222 A72-31279

Theory for plasma radiation from collisionless MHD shock waves applied to Type 2 solar radio bursts, comparing to type 4 bursts

16 p2446 A72-33461

Plane hydromagnetic wave propagation in rotating fluid permeated by variable magnitude and direction magnetic field, observing wave-associated critical level

16 p2436 A72-33567

MHD wave propagation and generation during spin-up of rotating viscous incompressible electrically conducting fluid

16 p2436 A72-33572

Plasmopause and geomagnetic micropulsations correlation from universal magnetospheric instability model, noting drift waves conversion to sound or Alfvén waves

16 p2387 A72-33906

Alfvén wave propagation in interplanetary medium for solar wind microscale fluctuations, using stationarity spherically symmetrical model

16 p2449 A72-33912

Alfvén wave firehose instability relaxation calculation to include nonlinear terms for explanation of solar wind temperature anisotropies by collisionless mechanism

16 p2449 A72-33933

Fermi acceleration effects in low energy particle transport in interplanetary space, assuming kinetic energy contained in Alfvén and bidirectional traveling waves

16 p2460 A72-33938

The propagation of non-axisymmetric Alfvén waves in an argon plasma

17 p2591 A72-35371

Detection of solar-wind electron plasma frequency fluctuations in an oblique nonlinear magnetohydrodynamic wave

17 p2602 A72-35610

Alfvén waves development and high pressure plasma hydrodynamic and kinetic instabilities dependence on magnetic field to temperature gradients ratio

17 p2593 A72-35883

Rotary shocks and waves of relativistic magnetohydrodynamics

17 p2593 A72-35908

Earth surface magnetic field intensity variations in terms of magnetospheric resonator excitation, assuming three dimensional Alfvén waves

18 p2688 A72-36869

Nonlinear time evolution of firehose unstable MHD waves, noting quasi-linear theory truncation error for low wave numbers relaxation time and energy growth

19 p2839 A72-37334

Geomagnetic variations propagation theory for LF electromagnetic and Alfvén waves diffraction at stratified earth in thin gyrotopical ionosphere

19 p2765 A72-38339

Geomagnetic field fluctuations during storms, considering Alfvén waves generation and propagation in solar wind and magnetosphere

19 p2791 A72-38345

Propagation of Alfvén-gravitational waves in a stratified perfectly conducting flow with transverse magnetic field

19 p2843 A72-38791

The effect of asymmetry on toroidal hydromagnetic waves in a dipole field

20 p2957 A72-39230

Nonlinear theory of particle motion in monochromatic Alfvén wave field application to Pc-1 geomagnetic pulsations evolution

20 p2917 A72-39408

Resonance between spin waves and magnetohydrodynamic waves in antiferromagnetic semiconductors and metals

21 p3096 A72-40415

Propagation of HM-waves with periods corresponding to periods of Pc1 micropulsations through the lower ionosphere

21 p3015 A72-40497

Linear and Alfvén waves propagation in incompressible beam-plasma systems, deriving dispersion law

21 p3092 A72-40994

Propagation of magnetohydrodynamic shock waves in a medium with diminishing density

21 p3094 A72-41653

Pc 1 hydromagnetic whistlers and emissions polarization characteristics measured in plane of earth surface

22 p3169 A72-42019

The heating of the solar plasma due to microwave phenomena correlated with type II meter bursts

22 p3222 A72-42041

ULF wave observation by satellite, considering geomagnetic activity control of magnetospheric wave occurrence

22 p3174 A72-42902

Nature of polar-aurora light intensity pulsations associated with Pi2-type geomagnetic pulsations

23 p3282 A72-43359

Magnetic pulsation spectra in a nonisothermal plasma

23 p3323 A72-44483

Instability of the whistler structure of oblique hydromagnetic shocks

24 p3428 A72-45013

Multilayer plasma model for MHD pulse propagation in ionospheric waveguide, noting approximation of Alfvén velocity distribution by plasma layers

24 p3397 A72-45085

LF oscillations and electron drift in frozen plasma under strong electromagnetic radiation, deriving formulas for coupled Alfvén and spiral waves

24 p3440 A72-45093

MAGNETOHYDRODYNAMICS

MHD equations for plasma of arbitrary collision frequency in weakly inhomogeneous magnetic field, considering collisional and resonant particle effects

01 p0108 A72-10241

Oscillatory hydromagnetic dynamo model of variable sign large scale solar magnetic field, using Benard convective cell with Coriolis velocity disturbance

01 p0128 A72-10585

Applied MHD and high temperature gas dynamics - Conference, Gdansk, Poland, May 1970

01 p0110 A72-11201

Nonuniform magnetic field effects in MHD slider bearing, showing inertia terms contribution dependence on Hartmann number

02 p0235 A72-11533

Rarefied plasma hydrodynamic equations for rotational discontinuities in solar wind, discussing magnetic field modulus jumpwise changes

02 p0272 A72-11915

Dynamo theory MHD equations numerical solution, showing rapid variation of electromagnetic field, hydrodynamic velocities and earth core magnetic moment

02 p0217 A72-11933

Geomagnetism theory of dynamos in homogeneous fluid masses, considering Rikitake self reversing, kinematic and hydromagnetic dynamo problems

02 p0220 A72-12088

Cascade connected electrode scheme for MHD applications, noting potential and current distributions and Hall voltage buildup

02 p0265 A72-12276

Solar corona MHD and plasma physical structure, considering macroscopic and microscopic properties

03 p0422 A72-13204

MHD processes responsible for solar flares in polarity boundaries of magnetic fields, determining magnetic energy change and flux

03 p0410 A72-13322

Radio-astronomical evidence for magnetohydrodynamic pulsations in corona, considering

solar radio burst model of pulsating structure due to synchrotron radiation

03 p0432 A72-13349

Solar magnetic field and solar cycle dynamo theory based on mean field MHD

03 p0433 A72-13361

Full lubrication characteristics, discussing pressure pump, viscosity, MHD, volume elasticity, centrifugal and rheodynamic techniques

03 p0365 A72-14299

Cylindrical blast wave propagation in MGD, deriving closed-form solutions for line explosion in medium with constant pressure, density and axial magnetic field

03 p0400 A72-14391

Plasma layer implosion in theta pinch, deriving modified snow flow equations from MHD equations

04 p0556 A72-14855

MHD squeeze film lubrication between electrically conducting parallel plates, showing graphically approach time under magnetic field in free space

05 p0665 A72-16031

Large scale alternating solar magnetic field generation by outer shell convective flow, constructing oscillator hydromagnetic dynamo model

05 p0715 A72-16232

Electron density and temperature temporal and radial profiles in megawatt MPD-arc thruster exhaust, using Thomson scattering technique

05 p0707 A72-16887

Spatio-temporal tensorial structure of fluid magnetodynamic equations in terms of electromagnetism and continuum mechanics

06 p0861 A72-18103

Magnetohydrodynamic theory of spherical drop deformation and drag under axisymmetric current distribution in conducting viscous incompressible fluid

06 p0864 A72-18533

Digital computer numerical procedure to solve dynamo theory MHD equations for earth nucleus, using combination of Fourier and finite difference methods for integration

08 p1155 A72-20810

Quasi-steady MPD propulsion systems for astronomical applications, describing electric energy storage bank, mass supply system, accelerator and operation principle

09 p1374 A72-22934

Two fluid MHD model to study cylindrical plasma condenser resonance properties in axial magnetic and alternating electric fields

09 p1360 A72-22952

Two fluid MHD model for flat plasma condenser in crossed magnetic and alternating electric fields, calculating impedance and disturbed plasma parameters

09 p1360 A72-22953

Clebsch transformation in relativistic MHD, considering Maxwell equations in vacuum and electromagnetic perfect fluid in isentropic flow

10 p1519 A72-24126

Current lines of relativistic fluid investigated by Ehlers method, applying to MHD Godel type universes

10 p1520 A72-24220

Godel metric type MHD universes, using Maxwell and conservation equations

10 p1524 A72-24857

Quasi-steady MPD thruster system, discussing gas injection, electronic synchronization and electrolytic pulse forming network

11 p1613 A72-26196

Optimization criteria for electric feeding in quasi-steady MPD thruster, discussing energy storage bank characteristics determination

11 p1709 A72-26197

Quasi-steady operation establishment in pulsed MPD arc jet, investigating ion density radial distribution and initial tank pressure and magnetic field effects on plasma front arrival

11 p1696 A72-26219

Mass, momentum and energy distribution measurement in quasi-steady MPD discharge, obtaining velocity vector profiles

11 p1696 A72-26220

Magnetogasdynamics intrinsic equations, determining geometrical and mechanical characteristics of axisymmetric and meridional plane motions

13 p2010 A72-28682

Uniform vertical magnetic field effect on Ekman layer over horizontal plate at rest relative to rotating conducting liquid

13 p2011 A72-29006

Rarefied plasma hydrodynamic equations for rotational discontinuities in solar wind, discussing magnetic field modulus jumpwise changes

13 p2030 A72-29227

Dynamo theory MHD equations numerical solution, showing rapid variation of electromagnetic field, hydrodynamic velocities and earth core magnetic moment

13 p1949 A72-29245

MHD - Conference, Argonne, Illinois, March 1972

13 p1899 A72-29351

Mathematical model for magnetized solar wind with one fluid MHD and polytropic state equations, calculating magnetic field variables at earth

13 p2034 A72-29958

Two dimensional unsteady solutions to MHD equations, describing matter compression near zero line of magnetic field for solar flares and z pinch studies

16 p2435 A72-33151

Stellar MHD, discussing strongly magnetic stars identification and slow rotation origin based on oblique rotator model

16 p2460 A72-33923

Combustion fronts velocity comparison with light speed in relativistic hydrodynamics and MHD

17 p2589 A72-34911

Two fluid MHD model for flat plasma condenser in crossed magnetic and alternating electric fields, calculating impedance and disturbed plasma parameters

17 p2593 A72-35882

Conservative difference schemes for linear and non-linear problems of mathematical physics, discussing gas dynamics and magnetogasdynamics problems requirements

19 p2833 A72-37383

Propagation of surface waves along a plane boundary between two magnetoactive plasmas

19 p2842 A72-38532

Thermoelasticity and magnetohydrodynamics equations and inequalities, covering Fourier law, stress relations, Bingham fluids, Ohms law, variational formulations and functional analysis

20 p2952 A72-39183

Radiation from an electric dipole in anisotropic media

24 p3424 A72-44706

MAGNETOHYDROSTATICS

Solar magnetic field distribution in sunspots surface layers, considering photospheric three dimensional magnetohydrostatic model

03 p0431 A72-13337

MAGNETOIONIC PLASMA

U PLASMAS [PHYSICS]

MAGNETOIONICS

Magnetoionic component with fluctuating elliptical polarization during wave reflection from F 2 layer, discussing suppression mechanism

01 p0028 A72-10593

Phase difference measurement between magnetoionic components returned from lower ionosphere due to pulsed radio signal, obtaining electron density profiles

01 p0063 A72-10914

Lorentz polarization effects on complex refractive index and wave polarization of magnetoionic theory

04 p0548 A72-14944

Magnetoionic mode reciprocity for oblique incident electromagnetic wave propagation through birefringent stratified media

04 p0492 A72-15445

Total flux and polarization of solar S-component at mm wavelengths, obtaining radio source optical depth by evaluation of QL propagation based on magnetoionic theory

07 p1069 A72-19080

Time dependent parallel and cross polarized electromagnetic pulse propagation in magnetoionic medium for normal incidence

09 p1280 A72-23231

Electromagnetic waves on a conducting infinite cylinder in a magnetoionic medium

17 p2517 A72-35399

Structure of ionospheric inhomogeneities according to simultaneous observations of two magnetoionic components

18 p2688 A72-36856

Group delay times of magnetoionic components for horizontal electron density profiles in magnetic meridian plane, noting comparison with ionospheric sounding data

23 p3283 A72-43361

Ray tracing in ionosphere and magnetoionic theory application to coupling in cold plasma waves, considering linear waves, electrodes, particles and echoes as exciters

23 p3319 A72-43516

MAGNETOMETERS

NT VARIOMETERS

Digital videomagnetograph providing real time display of line of sight component of solar magnetic fields

03 p0356 A72-13281

Kitt Peak 40 channel magnetograph using fiber optic probe for spectral and spatial resolution in weak photospheric field detection

03 p0356 A72-13282

Pressure scanning Fabry-Perot magnetometer using KDP crystal and Glan-Thompson prism with echelle interferometer spectrograph for polarized Zeeman components

03 p0356 A72-13283

Sacramento Peak magnetograph, discussing modified Doppler-Zeeman analyzer for separate measurements of circularly polarized line displacement

03 p0356 A72-13284

Systematic errors of Crimean vector magnetograph related to miscentering of spectral lines

03 p0357 A72-13285

Optics and electronics of digitized birefringent filter solar magnetograph to isolate magnetic sensitive lines

03 p0357 A72-13287

Absorption line formation in magnetic field for magnetograph interpretation of solar atmosphere

03 p0427 A72-13291

Magnetographic observations of magnetic fields in quiescent solar prominences, using Zeeman effect on H, He, and metal lines

03 p0428 A72-13298

Solar magnetic field structure determination in active regions from H alpha morphology obtained with chromosphere magnetograph, discussing emerging flux region role

03 p0428 A72-13304

Magnetograph scans of solar disk center supergranulation, showing downdrafts relation to magnetic field strength and chromosphere and photosphere brightness

03 p0429 A72-13307

High resolution magnetographic and spectrographic observations of plage fields and photospheric effects in weakly active regions

03 p0429 A72-13308

Plage magnetic fields associated with downward velocities from magnetograph filtergrams of opposite circular polarizations in CA I absorption line

03 p0429 A72-13312

Inner magnetosheath hydromagnetic disturbances, presenting magnetometer data in inclination-declination coordinate system

03 p0348 A72-13510

Weak magnetic moments measurement under pressure and over wide temperature range by Faraday method, discussing magnetometer and cryogenic equipment modifications

04 p0522 A72-15478

AEROS satellite active magnetic attitude control system, describing magnetometer system, sun and IR earth sensors, spin stabilization and axis and spin rate control torque generation

05 p0727 A72-16473

Geomagnetic field measurement, discussing variometers and magnetographs theory

06 p0812 A72-17370

Geomagnetic field vector components measurement methods, considering data processing problems

06 p0812 A72-17371

Three component airborne magnetometer design, discussing direction reference system and stabilized platform

06 p0812 A72-17372

Aeromagnetic surveying with airborne fluxgate magnetometer, discussing field data compilation and interpretation

06 p0812 A72-17373

Geophysical applications of high resolution magnetometers to geomagnetic measurements, archaeological investigations and satellite sounding of planetary magnetic fields

06 p0812 A72-17374

Rocket-borne vector magnetometer measurements of midlatitude ionospheric currents near sporadic E, noting nearly uniform vertical distribution

06 p0804 A72-17459

Earth bow shock magnetic field data correlation withOGO 5 flux gate magnetometer, using Tidman-Northrop theory

07 p0975 A72-19145

Proton 2 and 4 and Cosmos 196 orientation by quick response algorithm from onboard three component magnetometer readings

08 p1240 A72-21138

Magnetic field measurement methods and magnetometers performance in superconducting, thin film, resonance and fluxgate areas

09 p1308 A72-22465

Superconducting quantum flux sensors for measuring magnetic fields and susceptibility, voltage and resistance

09 p1308 A72-22466

Ferromagnetic thin film magnetometers operation and performance characteristics for magnetic field measurement

09 p1308 A72-22467

Resonance magnetometers for magnetic field measurement, discussing classification, operation principles and general properties

09 p1308 A72-22468

Fluxgate magnetometry, discussing weak field sensors, low power devices and various applications

09 p1308 A72-22469

Magnetometers for balloon-borne X ray astronomy payload azimuth determination, noting misorientation, earth and spurious magnetic fields effects on measurement effectiveness

10 p1530 A72-24954

Search coil magnetometer for measurement of weak alternating magnetic fields encountered by Helios solar probe in space

11 p1632 A72-25804

- Cryogenic Josephson junction magnetometer in magnetocardiography, discussing high ambient noise levels in unshielded environment 12 p1769 A72-27288
- Broadband superconducting quantum microwave magnetometer design, operation and performance 12 p1812 A72-28219
- Two gyro three axis stabilizer with gyrocompass effect for gravimeter or magnetometer sensor stabilization in towed gondola 13 p1957 A72-29271
- Impulsive pulsations (Pi/2) identification as geomagnetic field distortion coincident with oscillatory component from high resolution Rb vapor magnetometer recordings 13 p1951 A72-29656
- Photospheric network, magnetic fields, Ca emission and continuum faculae from multichannel magnetograph observations 13 p2045 A72-29705
- Tunable wide field birefringent element/filter magnetograph to separate polarized magnetic signal from selected spectral line width 13 p2045 A72-29706
- Apollo 16 lunar surface magnetometer cooling system variable conductance heat pipe/radiator design and thermal performance [AIAA PAPER 72-271] 14 p1271 A72-30828
- Sense coil geometry and drive waveform effects on low level flux gate magnetometers sensor noise 15 p2233 A72-31507
- Tansey satellite spin axis orientation measurement by two flux-gate magnetometers and sun sensor 15 p2272 A72-32334
- Optically pumped magnetometer error, predicting atomic g-factor modification by nonresonant RF fields 15 p2339 A72-32335
- Proton 2 and 4 and Cosmos 196 orientation by high speed algorithm from onboard three component magnetometer readings 20 p2976 A72-39243
- A line-profile Stokesmeter - Preliminary results on non-sunspot fields. 20 p2971 A72-39761
- Magnetic anomalies in New Guinea-New Zealand region from geomagnetic measurements with proton magnetometer, noting effects of andesite-basalt volcanic processes and nuclear precession signal 23 p3284 A72-43380
- Image motion in the Culgoora solar magnetograph - The role of vibration. 23 p3278 A72-43617
- MAGNETOMETRY**
U MAGNETIC MEASUREMENT
MAGNETOPOUSE
- Earth magnetosphere boundary position, bow shock wave, transition region thickness and magnetopause currents magnetic fields during geomagnetic storms 01 p0059 A72-10605
- Outer zone energetic electron precipitation, elf whistler and plasmopause location measurements by polar satellite OV-3-3 instruments 01 p0120 A72-10890
- Idealized model for small scale internal structure of magnetopause separating distorted geomagnetic field in magnetosphere from solar plasma flow in magnetosheath 02 p0218 A72-11977
- Solar proton entry observations over polar caps in relation to magnetosphere, magnetotail and magnetopause models 02 p0275 A72-12463
- Shear layer finite thickness and magnetic field effects on Kelvin-Helmholtz MHD instability of earth magnetopause boundary 07 p0974 A72-18892
- Hall effect influence on magnetospheric boundary magnetic field generation by solar wind perturbation, using beam-magnetic field interface model 07 p0980 A72-20407
- Spatial characteristics of magnetic field fluctuation in the magnetosheath. 17 p2545 A72-34474
- A three dimensional, analytical magnetospheric model with defined magnetopause. 19 p2789 A72-37410
- Model for the uneven illumination of polar caps by solar protons. 23 p3286 A72-44502
- Pioneer 8 observation of diffuse magnetosphere-magnetopause boundary, noting proton flux intensity and flow angle 23 p3341 A72-44512
- MAGNETOPLASMAS**
U PLASMAS [PHYSICS]
MAGNETORESISTANCE
U MAGNETORESISTIVITY
MAGNETORESISTIVITY
- Resistivity, thermoelectric power and magnetoresistance of carbon fibers derived from heat treated polyacrylonitrile 07 p1024 A72-20550
- Spectral distribution characteristics of geomagnetic field mean intensity variations, relating longitudinal

specific resistance and integral conductivity of top rock layer 09 p1296 A72-22236

Mobility-field characteristics of GaAs below Gunn threshold with magnetoresistance technique, relating to device performance and other material parameters 13 p2021 A72-28573

Electrical characterization of GaAs by Hall and magnetoresistance measurements, analyzing temperature dependence of carrier concentration 13 p2024 A72-30034

Tensor analysis for planar magnetoresistivity and Hall effect in Ni single crystal thin films, noting anisotropy effects in ferromagnetic crystals 15 p2294 A72-32386

Plasma magnetoresistance in variable magnetic field measured on n-type InSb sample for SHF inertialess power sensor development 16 p2436 A72-33482

LF circularly polarized electromagnetic waves/helicons/ resonance crystal plates, deriving magnetoresistivity and Hall coefficient 21 p3066 A72-40624

Galvanomagnetic properties of well-oriented graphite in relation to the structural imperfections. 21 p3073 A72-40691

MAGNETOSONIC RESONANCE

Magnetosonic perturbations caused by ideally conducting sphere expansion in cold plasma, determining electric field and magnetic induction time dependences 02 p0217 A72-11939

Magnetosonic perturbations caused by ideally conducting sphere expansion in cold plasma, determining electric field and magnetic induction time dependences 02 p0217 A72-11939

MAGNETOSPHERE

NT GEOMAGNETIC TAIL
 NT MAGNETOPOUSE

Drift shells and pitch angle evolution of energetic particle motion in magnetospheric model including convection electric field 01 p0117 A72-10077

Magnetosphere transmittance for fast magnetosonic waves, considering refraction, reflection and earth surface intersection 01 p0058 A72-10587

Hall effect and magnetic field characteristics in lower ionosphere by vertical magnetospheric currents, using gyrotropic model 01 p0059 A72-10590

Decreasing period micropulsations during elementary magnetospheric substorms, discussing relation to ring current asymmetry development 01 p0059 A72-10602

MHD waves nonlinear interaction in magnetosphere, calculating transverse Alfvén and magnetosonic and longitudinal acoustic wave decay instabilities 01 p0109 A72-10618

Open magnetosphere mathematical models application to dayside auroras, investigating interplanetary magnetic field topology 01 p0060 A72-10885

Magnetospheric magnetic field distortions under quiet and slightly disturbed conditions, obtaining scalar intensity with OGO 3 and 5 rubidium vapor magnetometer 01 p0060 A72-10886

Isolated magnetospheric substorms model, explaining electric field origin, cold plasma flow, magnetic field lines and particle phenomena 01 p0060 A72-10889

Magnetoionospheric wave and particle phenomena correlation to convection electric fields in nightside magnetosphere during isolated substorms 01 p0062 A72-10904

Magnetospheric diagnostics from ground stations data, considering dimensions, cusp, ring current, tail flux, electric fields, radiation zone, solar wind and interplanetary field 01 p0132 A72-11072

Pulsar magnetosphere axisymmetric and vacuum oblique rotator models, emphasizing electromagnetic field properties 01 p0134 A72-11159

Magnetospheric substorm model for auroral activity sudden increase and ionospheric current development explanation by shock wave excitation in magnetospheric tail neutral layer 02 p0217 A72-11927

Geomagnetic PDP pulsations oscillation frequency drift, considering proton motion characteristics in magnetospheric equatorial plane 02 p0217 A72-11931

Magnetosphere deformation by solar wind, comparing accuracy of free molecular flow and double dipole models 02 p0218 A72-11948

Long period geomagnetic pulsation generation at boundary of magnetosphere and incoming solar wind, considering possibility from idealized model 02 p0218 A72-11950

Magnetosphere and adjacent regions magnetic surveys by OGO 1 and 3 satellites, discussing magnetopause, bow shock, magnetosheath, geomagnetic tail, ring current and polar substorms 02 p0220 A72-12084

Vertical distribution of ionospheric and magnetospheric electric fields, estimating Joule heating 02 p0220 A72-12324

Magnetosphere model for low energy cosmic ray proton propagation mode to synchronous orbit satellite, calculating geomagnetic cutoffs and penetration regions [AD-741079] 02 p0274 A72-12453

Solar proton entry observations over polar caps in relation to magnetosphere, magnetotail and magnetopause models 02 p0275 A72-12463

Broadband geomagnetic micropulsations relations to magnetospheric, interplanetary and solar phenomena [AD-739038] 02 p0222 A72-12869

Magnetospheric hydromagnetic waves propagation characteristics, discussing isotropic/poleoidal and guided/toroidal modes coupling in conjunction with hydromagnetic wedge model 02 p0268 A72-12870

Damped geomagnetic pulsations associated with geomagnetic storms interpreted as interaction between hydromagnetic oscillations and solar wind induced magnetospheric motions, discussing modified mathematical model 02 p0222 A72-12872

Vertical motions of midlatitude F 2 layer during magnetospheric substorms, investigating electric field distribution 03 p0349 A72-13519

Trapped particles induced by fluctuating magnetospheric electric and magnetic fields, calculating radial diffusion and energy distribution and time variations 04 p0566 A72-14723

Geomagnetic micropulsation activity relationship to magnetospheric processes and interplanetary magnetic field, investigating time dependence of telluric current 04 p0515 A72-14927

Magnetospheric heat flux effect on height variation of electron and ion temperatures and ion composition in topside ionosphere 04 p0515 A72-14929

Hydromagnetic whistler traveling wave tube amplification in magnetosphere, deriving temporal growth rate dependence on plasma parameters 04 p0517 A72-14950

Nonstationary behavior of collisionless shock waves in plasma wind tunnel, suggesting interpretation of magnetosphere magnetic field structure near earth bow shock 04 p0559 A72-15468

Transverse electric field in ionosphere and magnetosphere during inhomogeneities consisting of fast electrons 05 p0656 A72-16246

Solar wind proton penetration through earth magnetosphere, taking into account drift, force lines curvature and nonstationary plasma boundary 05 p0709 A72-16255

Charged particle acceleration by nonstationary sinusoidal electric fields in earth magnetosphere based on mathematical model 05 p0709 A72-16256

Noncircular ionospheric current conversion into longitudinal currents in magnetosphere along lines of force of geomagnetic field 05 p0657 A72-16259

Magnetospheric field model, assuming magnetostatic problem solution facilitated by equation linearity 05 p0657 A72-16274

Magnetospheric current effects on geomagnetic field structure, noting electron and proton precipitation into auroral zone 05 p0657 A72-16275

Periodic quasi-noise spectrum and amplitude modulation of HF pulsed signals from earth in magnetosphere plasma 05 p0696 A72-16605

Magnetospheric electron cyclotron and Langmuir plasma frequencies ratio determination from satellite observed electron and ion density data 05 p0659 A72-16765

Cosmic plasma phenomena in astrophysics, discussing distribution, ionospheric disturbances, magnetospheric waves, solar wind, etc 05 p0723 A72-17217

Vlf phenomena of magnetospheric origin, presenting whistlers classification table 06 p0803 A72-17375

Vlf wave excitation during sudden storm commencement, causing magnetosphere trapped energetic electrons to diffuse and precipitate into lower ionosphere 06 p0803 A72-17451

Auroral zone vlf hiss and associated low energy electron precipitation in polar magnetosphere [AD-736327] 06 p0804 A72-17456

- Interplanetary magnetic field fluctuations correlation with trapped particles redistribution, deriving magnetospheric electric field properties
06 p0875 A72-17468
- Energetic charged particles penetration into magnetosphere by auroral simulation experiments with artificial solar wind, observing magnetic field microfluctuations behind collisionless shock front
06 p0805 A72-17469
- Magnetoguided whistler propagation, observing longitudinal current in ionospheric plasma
06 p0808 A72-18064
- Geomagnetic field intensity fluctuations due to events in atmosphere, ionosphere, magnetosphere and in interplanetary space connected with solar activity
06 p0809 A72-18276
- Magnetospheric structure models during quiet solar periods
06 p0809 A72-18277
- Electrodynamics of ionosphere and magnetosphere, discussing irregularities, red arc and auroral thermosphere density and temperature changes
06 p0809 A72-18279
- Ionospheric storms features based on F2 critical frequency data, investigating magnetosphere during geomagnetic storms
06 p0810 A72-18280
- Magnetospheric plasma sources, discussing wave-particle interactions and acceleration mechanisms
06 p0810 A72-18281
- Low latitude surface horizontal magnetic field intensity depression due to quiet time ring current in magnetosphere as function of solar wind velocity
07 p1055 A72-18884
- Magnetospheric field model from magnetosphere surface approximation by paraboloid of revolution
07 p0974 A72-18903
- Imp 5 magnetic field measurements at high geomagnetic latitudes in outer magnetosphere near noon meridian, noting depressed field region centered on polar cusp
07 p0975 A72-19146
- Solar wind discontinuities and shock waves in interplanetary medium at magnetospheric boundary related to geomagnetic impulses
07 p1061 A72-20024
- Spherical harmonic representations of geomagnetic field including magnetosphere and tail regions based on ground based and low altitude spacecraft measurements within several earth radii
07 p0977 A72-20026
- Particle motions in earth magnetospheric tail and core, estimating maximum rate of magnetic field annihilation and magnetic drift shell
07 p1062 A72-20027
- Auroral forms dynamics dependence on solar wind and DP intensity in magnetosphere
07 p0977 A72-20030
- Plasma sheet distribution in magnetosphere from low energy particle observations in equatorial region of magnetotail
07 p0977 A72-20031
- Quasi-linear theory of magnetosphere gyroresonant wave-particle interactions, discussing particle distribution function anisotropy, wave packet effects, whistler mode, energy and pitch angle distributions, etc
07 p0978 A72-20034
- Magnetospheric trapped particle diffusion coefficients and acceleration in earth radiation belts
07 p1062 A72-20035
- Magnetosphere If electric fields influence on trapped radiation region particle behavior, considering magnetic drift rates
07 p1062 A72-20036
- Electric field measurements in ionosphere and magnetosphere by double probe and electron and ion drift techniques
07 p0978 A72-20042
- Structural interactions between magnetosphere and ionosphere in terms of electrostatic field associated with plasma temperature difference
07 p0979 A72-20046
- Magnetosphere theory of pulsar electrodynamics, discussing unipolar inductor with iron sphere having uniform magnetization parallel to rotation axis
07 p1080 A72-20058
- Stability of electron beam injected into magnetospheric plasma at small and high altitudes
07 p0979 A72-20377
- Interplanetary origin of magnetospheric electric fields responsible for polar magnetic disturbances
07 p0979 A72-20382
- Space-time relationship derivation to estimate traveling time of discontinuities running against magnetosphere in unperturbed solar wind
08 p1153 A72-20714
- Geomagnetic field fluctuations during storms, considering Alfvén waves generation and propagation in solar wind and magnetosphere
08 p1153 A72-20717
- Magnetic field components of vertical currents at magnetosphere boundary and earth surface, using computerized Gaussian method
08 p1156 A72-20822
- Artificial magnetosphere interaction with 8 keV electrons in hydrogen plasma beam simulating solar wind, noting penetration caused by boundary instability
08 p1156 A72-20823
- Magnetic fluctuations in elf and vlf waves in space, discussing whistler phenomena and applications to magnetospheric probes
08 p1158 A72-21189
- Solar energetic particle access characteristics to magnetosphere from PCA riometer and satellite measurements, determining relationship between earth dipole field and interplanetary field
08 p1228 A72-21497
- Apollo 15 lunar subsatellite particle experiment subsystem design for studying magnetosphere dynamics, plasmas-moon interaction and solar flare physics
08 p1168 A72-21519
- RAE-1 measurements of lf radio phenomena in magnetosphere, solar corona and Galaxy, discussing design, calibration and performance
08 p1137 A72-21984
- Equatorial ring current relation to polar electrojet during magnetosphere geomagnetic storm, discussing magnetosphere-ionosphere current systems
09 p1298 A72-22580
- Thermal positive ion densities measurement in outer ionosphere and magnetosphere by OGO 1 satellite, relating plasmapause distribution and magnetic activity level
09 p1300 A72-23011
- Ionospheric and magnetospheric electric field measurements by rocket, satellite or balloon-borne electrostatic probes or by plasma drift methods
10 p1473 A72-24529
- Pulsar radiation mechanism study from magnetosphere structure model, taking into account neutron star evaporated gas accumulation in gravitation-centrifugal force balance region
10 p1544 A72-24672
- Magnetospheric electrons precipitation into ionosphere due to conjugate conductivity asymmetry caused by wind induced ions vertical redistribution, using atmospheric model
10 p1530 A72-24791
- Fast auroral hydromagnetic wave occurrence relation to substorm activity, suggesting role of enhanced particle population in magnetospheric region
10 p1476 A72-24962
- Geomagnetic field and magnetosphere variations due to solar wind interactions, using rocket, satellite and indirect measurements
11 p1621 A72-25841
- Interplanetary and magnetospheric magnetic force lines reconnection and effects on geomagnetic activity
11 p1718 A72-25933
- Penetrating particles effect on low energy scintillation spectrometers sensitivity in various regions of magnetosphere
11 p1632 A72-25934
- Magnetosphere neutral layer plasma conductivity determination from model of linear magnetic dipole in conducting fluid flow
11 p1622 A72-25945
- Dayside magnetosphere stably trapped radiation zone high latitude boundary determination from energetic electron intensity spatial distribution observation by Imp 3 satellite
11 p1713 A72-26106
- Radial profiles of ionized He flux and protons in magnetosphere, taking into account charge exchange processes and fluctuating electrostatic fields
11 p1624 A72-26397
- Magnetospheric equatorial compressional wave propagation to ground observed as transverse wave, noting plane of polarization
11 p1625 A72-26413
- Hydromagnetic waves propagation and horizontal group velocity westward from dawn terminator to dark hemisphere, inferring magnetospheric properties
11 p1625 A72-26414
- Magnetosheath pressure, magnetic field, temperature, particle density and stream velocity computed for earth bow shock in oblique interplanetary field with solar wind
11 p1723 A72-26526
- Magnetosphere fast electron precipitation investigated by simulation experiments with model created by plasma stream interaction with dipole magnetic field
11 p1714 A72-26531
- Geomagnetic activity index response time to fluctuations in interplanetary electric field azimuthal component, relating to magnetosphere average energy content
11 p1627 A72-26670
- Magnetospheric midday boundary width dependence on geomagnetic dipole axis orientation, discussing different positions for magnetosphere boundary
11 p1628 A72-26914
- Ionospheric irregularities-magnetospheric parameters relationship from satellite scintillation measurement, noting use as indirect electron precipitation indicator
12 p1803 A72-27772
- Analytic models of large scale electric fields in atmosphere, considering geomagnetic Sq current in lower atmosphere and inner magnetosphere
12 p1804 A72-27790
- Quasi-steady and sporadic corpuscular fluxes as basic solar activity effect on troposphere, showing magnetosphere interaction time relation to meridional atmospheric circulation changes
12 p1842 A72-28208
- Solar activity effects in magnetosphere and ionosphere relation to geomagnetic activity and biospheric development, noting 11 year geomagnetic perturbation cycles
12 p1805 A72-28209
- Polar cap magnetic field induced by currents along magnetospheric lines of force during polar substorm
13 p1946 A72-28587
- Magnetosonic waves interactions with energy particles in plasmasphere, demonstrating magnetosonic waveguide channel existence around earth below plasmasphere
13 p1947 A72-28605
- Magnetospheric substorm model for auroral activity sudden increase and ionospheric current development explanation by shock wave excitation in magnetospheric tail neutral layer
13 p1948 A72-29239
- Geomagnetic PDF pulsations oscillation frequency drift, considering proton motion characteristics in magnetospheric equatorial plane
13 p1949 A72-29243
- Magnetosphere deformation by solar wind, comparing accuracy of free molecular flow and double dipole models
13 p1949 A72-29260
- Long period geomagnetic pulsation generation at boundary of magnetosphere and incoming solar wind, considering possibility from idealized model
13 p1949 A72-29262
- Earth-solar wind bow shock structure from OGO-5 observations during passage from interplanetary medium into magnetosheath
13 p1950 A72-29379
- Plasma wave measurements during OGO-5 dayside magnetosphere polar cusp encounters, discussing ULF magnetic field wave levels and VLF electric field amplitude ranges
13 p1950 A72-29380
- Magnetosheath electron precipitation effect on dayside auroral-oval plasma density and conductivity, relating precipitation heat flux to solar wind energy density
13 p1950 A72-29381
- Midnight auroral electrojet time variations relationship to midday auroras latitudinal shift during South Pole magnetospheric substorms
13 p1950 A72-29382
- Magnetospheric ring current relation to polar magnetic substorm from charged particle measurements by satellites and magnetic field measurements at ground
13 p1952 A72-29658
- Time varying magnetospheric electric field spatial distribution effect on plasmasphere temporal evolution, considering fine structure due to periodic gusts in convection electric field
13 p1953 A72-29804
- Positively and negatively charged plasma components thermodynamic density fluctuations effect on ionospheric and magnetospheric slowly varying electric fields measurement
13 p1953 A72-29810
- Two dimensional mathematical model of magnetosphere with neutral sheet for oblique incidence of solar wind, noting magnetic field minimum energy
13 p1954 A72-29850
- Two dimensional equilibrium solution of plasma sheet, applying to tail magnetosphere problem
13 p1954 A72-29959
- Seasonal changes in magnetospheric directional fluxes at synchronous altitudes due to solar wind induced field line knee effect and drift shell asymmetry
14 p2097 A72-30131
- Nonlinear AM and FM due to bonded nature of quasi-monochromatic whistler packets in magnetosphere
14 p2085 A72-30448
- Three layer atmospheric model for neutral gas motion-produced ionosphere and magnetosphere currents, electromagnetic field and charged particle concentration perturbations
14 p2100 A72-30632
- Magnetospheric and ionospheric potential electric fields, using variational process based on transverse/longitudinal conductivity ratios in plasma
14 p2100 A72-30633
- Minimum magnetic field energy of two dimensional magnetosphere with neutral sheet for arbitrary dipole inclination to solar wind as function of potential difference on boundary points
14 p2101 A72-30643
- Magnetospheric electric fields estimation from electron fluxes intensity on early daylight side
14 p2102 A72-30660

Whistler waves amplification in magnetosphere, obtaining particles pitch angle and energy diffusion coefficients and one dimensional Fokker-Planck equation
15 p2194 A72-31427

Magnetosphere thermal plasma densities determination from hydromagnetic whistler digital sonograms and modified normalized dispersion curves
15 p2283 A72-31430

Whistler propagation in magnetosphere disturbed by ring current, explaining electron density decrease
15 p2194 A72-31433

Dispersion relationship for electrostatic instability associated with electron beam trapped in magnetic mirror of magnetosphere, taking into account nonuniformity of magnetic field
15 p2283 A72-31434

Electric and magnetic fields fluctuations in region between shock wave front and magnetosphere boundary, noting resulting energy dissipation
15 p2225 A72-31902

Whistler mode VLF signal transmission in ground transmitter and magnetically conjugate zones, observing spectrum broadening and AM in magnetosphere
15 p2197 A72-31919

Solar proton flux density angular and latitude distribution in polar regions magnetosphere from satellite observation
15 p2299 A72-31921

Whistlers nose frequency and minimum group time delay determined from model magnetosphere and from measurement, noting precision effect on electric field calculation accuracy
15 p2198 A72-31947

Rocket-observed energetic electron flux association with ground recorded plasmasphere whistler in terms of gyroresonant wave-particle interaction
15 p2198 A72-31948

Magnetospheric geometry derivation from ISIS-I observations of soft particles penetration into polar cap and auroral regions, discussing entry and energization mechanisms
15 p2227 A72-31953

Report to COSPAR on West German space program covering meteorology, aeronomy, ionospheric physics, magnetosphere, solar wind and radiation, solar system and life sciences
15 p2338 A72-32014

Review of symposium on D region, upper polar ionosphere, magnetosphere and wave-particle interactions
15 p2229 A72-32251

Geomagnetic substorm magneto-ionospheric effect, discussing electric field transmission, magnetic field variations and currents flowing in dynamo region
15 p2230 A72-32259

Magnetosphere description based on satellite observation data, discussing particle distributions, solar wind, shock wave, magnetic sheath and magnetopause
15 p2315 A72-32400

Pulsar rotating electromagnetic field vectors classification for magnetosphere models
16 p2450 A72-32866

Nightside magnetosphere convection electric field from motions of whistler ducts within plasmasphere, considering interplanetary magnetic field theta component
16 p2382 A72-32960

Mathematical model for magnetosphere surrounding rotating neutron star, noting computer programs for Maxwell and plasma equations solution
16 p2460 A72-33927

Pulsars radiation mechanism relationship to magnetospheric conditions, considering optical, X ray and gamma radiation
16 p2460 A72-33928

Indices of geomagnetic pulsations.
17 p2545 A72-34628

Daytime irregular geomagnetic pulsation, Pid, and its relation to magnetospheric substorm.
17 p2546 A72-35062

Association between quasi-periodic VLF emission and micropulsation.
17 p2516 A72-35065

Magnetospheric electron cyclotron and Langmuir plasma frequencies ratio determination from satellite observed electron and ion density data
17 p2548 A72-35268

Explorer 33 and 35 plasma observations of magnetosheath flow.
17 p2548 A72-35587

Flaring-tail model explanation for geomagnetic tail configuration changes during magnetospheric substorm growth phase
17 p2548 A72-35589

Critical component of the interplanetary magnetic field responsible for large geomagnetic effects in the polar cap.
17 p2548 A72-35590

Magnetospheric convection induced longitudinal or Fermi acceleration role in nighttime auroral particle flux production mechanism
17 p2601 A72-35592

Pitch-angle diffusion of radiation belt electrons within the plasmasphere.
17 p2602 A72-35597

Turbulence of electrostatic electron cyclotron harmonic waves observed by Ogo 5.
17 p2549 A72-35599

Book on ionosphere and magnetosphere covering solar radiation effects, ionospheric layers, currents and storms, charged particle movement and various wave propagations
17 p2550 A72-35850

Auroral zone splitting into various radiation intensity regions, discussing DR currents influence on particle motion in magnetosphere and structural relationship
17 p2550 A72-35856

Magnetosphere resonant oscillations space-time characteristics for arbitrary azimuthal number, noting frequency dependence on geomagnetic shell
17 p2551 A72-35859

Laboratory model information relating to modeled geophysical phenomena, noting magnetosphere study from plasma physics experiments
17 p2551 A72-35904

A new source for the large-scale electric fields in the magnetosphere.
18 p2686 A72-36623

Low latitude equatorial electrojet analysis based on three dimensional electric field equation for ionosphere and magnetosphere
18 p2687 A72-36854

Electron and proton acceleration in the outer magnetosphere regions during polar substorms
18 p2688 A72-36866

Sideband growth in nonlinear Landau wave-particle interaction.
19 p2838 A72-37327

A three dimensional, analytical magnetospheric model with defined magnetopause.
19 p2789 A72-37410

Magnetospheric and ionospheric conjugate point phenomena as solar events manifestations via solar wind shock wave interaction with geomagnetic field
19 p2790 A72-37858

Space-time relationship derivation to estimate traveling time of discontinuities running against magnetosphere in unperturbed solar wind
19 p2791 A72-38342

Geomagnetic field fluctuations during storms, considering Alfvén waves generation and propagation in solar wind and magnetosphere
19 p2791 A72-38345

Diurnal variation of the H+ flux between the ionosphere and the plasmasphere.
19 p2793 A72-38759

The propagation of very low-frequency waves in ducts in the magnetosphere. II.
20 p2916 A72-39192

Persistent particle anisotropies and magnetospheric models.
20 p2916 A72-39233

Signatures for substorm development of the growth phase and expansion phase.
20 p2916 A72-39237

Magnetosphere-ionosphere interactions; Proceedings of the Advanced Study Institute, Dalseter, Norway, April 14-23, 1971.
20 p2917 A72-39526

Magnetospheric interactions with topside ionosphere in terms of polar wind ion flows and density related to plasma temperature, F 2 region and cusp observations
20 p2918 A72-39537

Aircraft and spacecraft high latitude optical measurements of magnetosphere-related emissions, discussing red arcs, IR auroras, X ray pulsations, conjugate effects, etc
20 p2918 A72-39539

High latitude particle precipitation and source regions in the magnetosphere.
20 p2964 A72-39542

Ionospheric and magnetospheric electric field strength measurements in auroral and polar cap regions by Ba ion cloud and double floating probe techniques
20 p2918 A72-39543

Stationary adiabatic plasma flow in the magnetosphere.
20 p2919 A72-39547

Magnetic neutral sheet model in terms of self consistency between current and tail field in reversal region
20 p2919 A72-39548

VLF emission artificial triggering by whistler Morse pulses in magnetosphere, explained in terms of resonant trapped particle current and wave field behavior
20 p2903 A72-39549

Magnetospheric propagation of auroral hiss with whistler mode dispersive properties, suggesting burst source locations and mechanisms
21 p3048 A72-40399

Nonlinear theory of the monochromatic circularly polarized VLF and ULF waves in the magnetosphere.
21 p3015 A72-40480

Whistler propagation through magnetosphere.
21 p3049 A72-40975

Conjugate features of magnetospheric electron dynamics observed at balloon altitudes.
21 p3049 A72-41614

Rarefaction wave generation by solar wind shock wave interaction with magnetosphere, noting geomagnetic field weakening during magnetic storm
22 p3217 A72-41894

Sudden impulses in the geomagnetotail and the vicinity.
22 p3168 A72-42002

The equilibrium potential of a magnetospheric satellite in an eclipse situation.
22 p3168 A72-42003

DP-2 mode daily magnetic variation in polar cap based on magnetic and auroral records, noting relationship to magnetospheric substorms
22 p3168 A72-42005

On the physical mechanism of the magnetospheric substorm development.
22 p3169 A72-42012

Limits to energetic proton fluxes trapped in Jupiter's magnetosphere.
22 p3221 A72-42021

Nonadiabatic condition effects on ultrarelativistic electron energy losses in geomagnetic trap in remote magnetosphere regions
22 p3218 A72-42224

Longitudinal magnetospheric currents contribution to auroral electrojet from satellite observation data, noting magnetosphere electric field excitation of meridional Pedersen and Hall currents
22 p3169 A72-42225

Magnetohydrodynamic theory for the interaction of an interplanetary double-shock ensemble with the earth's bow shock.
22 p3170 A72-42404

Magnetospheric substorm onset examined via simultaneous balloon X ray and electric field measurements, discussing ATS 5 observations
22 p3170 A72-42409

Coordinated observations of the magnetosphere - The development of a substorm.
22 p3171 A72-42410

Upper limit of the torque of the solar wind on the earth.
22 p3219 A72-42427

Induction effect of slowly decaying ring current, estimating electric field strength by model consisting of earth dipole and symmetric ring
22 p3172 A72-42430

Injun 5 satellite measurements of magnetospheric convection electric fields via double probe technique, discussing substantiation with OGO 6 results
22 p3174 A72-42901

ULF wave observation by satellite, considering geomagnetic activity control of magnetospheric wave occurrence
22 p3174 A72-42902

Propagation of electromagnetic waves in a weakly ionized warm magnetoplasma.
22 p3155 A72-42991

Ray structures of polar auroras and their association with drift-current instability in a plasmoid
23 p3282 A72-43358

Some results of an analysis of Pc4-type steady geomagnetic pulsations at a network of stations
23 p3283 A72-43372

Generation threshold of anomalous resistance for longitudinal currents in the magnetosphere
23 p3284 A72-43379

Pioneer 8 observation of diffuse magnetosphere-magnetopause boundary, noting proton flux intensity and flow angle
23 p3341 A72-44512

Outer magnetosphere near midnight at quiet and disturbed times.
23 p3341 A72-44513

Symposium on the Morphology and Physics of Magnetospheric Substorms, Moscow, USSR, August 3, 1971, Proceedings.
24 p3395 A72-44846

Behavior of outer radiation zone and a new model of magnetospheric substorm.
24 p3396 A72-44850

Polar cap magnetic field induced by currents along magnetospheric lines of force during polar substorm
24 p3397 A72-45087

Magnetosonic waves interactions with energy particles in plasmasphere, demonstrating magnetosonic waveguide channel existence around earth below plasmasphere
24 p3398 A72-45105

MAGNETOSPHERIC ELECTRON DENSITY

Nonducted vlf wave propagation near plasmapause during whistlers based on diffusive equilibrium and collisionless models for magnetospheric electron density distribution
02 p0222 A72-12873

Magnetospheric electron cyclotron and Langmuir plasma frequencies ratio determination from satellite observed electron and ion density data
05 p0659 A72-16765

Magnetospherically trapped particles sources, losses and transport processes, presenting time averaged proton, electron and alpha particle distributions in trapping and pseudo-trapping regions
07 p1062 A72-20028

Whistler dispersion and occurrence rate characteristics at low latitudes during solar cycle, noting annual variations and magnetospheric electron density 11 p1623 A72-26105

Magnetospheric equator plane electron density profiles determination from plasmapause whistlers observed in UK 11 p1626 A72-26421

Low energy electron flux in magnetosphere, discussing relation to geophysical phenomena, solar wind, interplanetary magnetic field and charged particle longitudinal drift trajectories 15 p2225 A72-31903

Magnetosphere description based on satellite observation data, discussing particle distributions, solar wind, shock wave, magnetic sheath and magnetopause 15 p2315 A72-32400

Magnetospheric electron cyclotron and Langmuir plasma frequencies ratio determination from satellite observed electron and ion density data 17 p2548 A72-35268

Ring current effect on magnetospheric electron density profiles derived from plasmapause whistlers. 17 p2600 A72-35368

Radiation belt electron lifetimes and removal through pitch angle diffusion by plasmaspheric whistler waves in cyclotron harmonics 20 p2918 A72-39532

Properties of low energy particle impacts in the polar domain in the dawn and dayside hours. 20 p2964 A72-39541

Auroral electron and proton distribution in magnetosphere and precipitation pattern from satellite, rocket and ground based observations 20 p2920 A72-39976

Spatial and temporal variations of thermal plasma ion and electron densities as function of L at 3000-5700 km from polar orbiting OV 3-1 satellite observation 22 p3211 A72-42414

Solar-wind parameter variation, magnetic activity, and electrons in the magnetospheric tail and outer radiation belt 23 p3283 A72-43367

MAGNETOSPHERIC INSTABILITY

Plasma sheet structures, dynamics and role in magnetospheric substorm onset as function of near earth and distant merging regions 01 p0052 A72-10082

Quasi-steady spectrum of hydromagnetic noise in proton belt, using random excited broad wave fields in nonisothermal magnetosphere 01 p0118 A72-10367

Plasma electron and proton motion in equatorial plane of magnetosphere under geomagnetic disturbance generated electric field 01 p0058 A72-10586

Ion electromagnetic cyclotron modes growth rates in multicomponent magnetospheric plasmas, discussing instabilities enhancement 01 p0062 A72-10906

Inner magnetosheath hydromagnetic disturbances, presenting magnetometer data in inclination-declination coordinate system 03 p0348 A72-13510

Solar wind effects on storms and structure of magnetosphere and radiation belt maintenance 03 p0350 A72-14304

Radio auroral electrojet aspect sensitivity and Farley two stream instability, discussing magnetic field distortion and orthogonal deviation as function of current strength and direction 07 p0976 A72-19163

Vertical density gradients as source of two stream instability irregularities in radio aurora theory 07 p0976 A72-19164

Magnetospheric instabilities theory based on Vlasov equation and Landau damping 07 p0978 A72-20033

Shock wave excitation by moving solar wind discontinuity in geomagnetic tail as cause of active phase of magnetospheric substorm 08 p1153 A72-20716

Auroral plasma particle discharge during motion in strong inhomogeneous magnetic field, magnetospheric instability due to temperature anisotropy 11 p1715 A72-26904

Pc 5 type geomagnetic pulsations correlation with nighttime magnetosphere auroral magnetic disturbances from magnetograms obtained at Murmansk, College /Alaska/ and Tiksi 13 p1947 A72-28606

Auroral electron spectrum space-time dynamics during magnetospheric substorms, using X ray bremsstrahlung balloon data 14 p2101 A72-30637

Magnetospheric quasi-stationary pinch effect and filamentary structure due to electron streams parallel to geomagnetic field lines 14 p2103 A72-30664

Model for magnetospheric substorm growth phase, noting dayside magnetopause convection onset, geomagnetic tail configurational changes and breakup with auroral electrojet development 16 p2387 A72-33903

Plasmapause and geomagnetic micropulsations correlation from universal magnetospheric instability model, noting drift waves conversion to sound or Alfvén waves 16 p2387 A72-33906

Precipitation dynamics and energy spectrum of auroral electrons in the midnight sector during a magnetospheric substorm 17 p2550 A72-35854

Auroral absorption and magnetospheric plasma dynamics pattern from arctic stations atmospheric opacity data 18 p2688 A72-36859

Earth magnetosphere pinch effect related to geomagnetic field pulsations and polar aurora luminosity fluctuations 18 p2688 A72-36867

Earth surface magnetic field intensity variations in terms of magnetospheric resonator excitation, assuming three dimensional Alfvén waves 18 p2688 A72-36869

Shock wave excitation by moving solar wind discontinuity in geomagnetic tail as cause of active phase of magnetospheric substorm 19 p2791 A72-38344

Radial penetration of a hot plasma associated with a large-scale electric field in the magnetosphere, and some related problems. 20 p2916 A72-39228

Radiation belt protons and ion-cyclotron wave interactions accounting for magnetospheric ring current instabilities during storm at plasmapause 20 p2919 A72-39545

Magnetospheric shapes, flows and substorms in terms of magnetotail flux, solar wind pressure, dipole moment and plasma sheet interaction 20 p2919 A72-39546

Auroral space-time regularities relationship to magnetospheric variations, precipitating electron fluxes, magnetic tail formation and substorms 20 p2920 A72-39977

The generation and propagation of VLF emissions. 20 p2904 A72-39984

Earth outer radiation belt and unstable radiation zone dynamics during IQSY magnetically quiet and disturbed period based on Elektron-series satellite data 22 p3218 A72-42211

Midlatitude VLF emissions in magnetosphere due to plasma resonance instability near plasmapause, using ground, rocket and satellite observations, estimating electron energy 23 p3263 A72-43515

Plasma sheet variations during substorms. 24 p3396 A72-44851

Magnetic field fluctuations during substorms. 24 p3396 A72-44853

Pc 5 type geomagnetic pulsations correlation with nighttime magnetosphere auroral magnetic disturbances from magnetograms obtained at Murmansk, College /Alaska/ and Tiksi 24 p3398 A72-45106

MAGNETOSPHERIC ION DENSITY

NT MAGNETOSPHERIC PROTON DENSITY

Hydrogen ions concentration in dayside region of plasmasphere from OGO 5 satellite mass spectrometry, noting plasmapause position as function of magnetic activity 01 p0061 A72-10892

Magnetospheric electron cyclotron and Langmuir plasma frequencies ratio determination from satellite observed electron and ion density data 05 p0659 A72-16765

Whistling atmospherics generation mechanism, showing ionic sound excitation by hydromagnetic wave propagation through magnetospheric rapid plasma concentration change regions 08 p1155 A72-20807

Magnetospheric electron cyclotron and Langmuir plasma frequencies ratio determination from satellite observed electron and ion density data 17 p2548 A72-35268

Plasmapause nightside, dayside and bulge positive ion concentration measurements with OGO 5 mass spectrometer compared with magnetospheric convection model 20 p2919 A72-39544

Spatial and temporal variations of thermal plasma ion and electron densities as function of L at 3000-5700 km from polar orbiting OV 3-1 satellite observation 22 p3211 A72-42414

MAGNETOSPHERIC PROTON DENSITY

Magnetospherically trapped particles sources, losses and transport processes, presenting time averaged proton, electron and alpha particle distributions in trapping and pseudo-trapping regions 07 p1062 A72-20028

Magnetosphere description based on satellite observation data, discussing particle distributions, solar wind, shock wave, magnetic sheath and magnetopause 15 p2315 A72-32400

Magnetospheric particles and interplanetary magnetic field measurements for solar proton event of March 1970, noting polar cap structures 16 p2444 A72-32956

Auroral electron and proton distribution in magnetosphere and precipitation pattern from satellite, rocket and ground based observations 20 p2920 A72-39976

MAGNETOSTATIC AMPLIFIERS

Multidimensional function extremum for sectioned resonator type gyroamplifier efficiency optimization 08 p1172 A72-22050

MAGNETOSTATIC FIELDS

Magnetostatic interactions of cylindrical magnetic domain propagation circuits in ferromagnetic overlay without in-plane fields 03 p0331 A72-13752

Gyroresonance devices efficiency increase, discussing magnetostatic field distribution optimization in interaction space 04 p0502 A72-15575

Epitaxial YIG film separated from conductive plane by thin dielectric layer, considering magnetostatic propagation dispersion and insertion loss 15 p2294 A72-32502

Motion of ion-cloud in the ionosphere, field-aligned cloud with Gaussian distribution of ionization density. 17 p2546 A72-35060

The oriented elastic continuum as a model for the magnetoelectric body. 22 p3206 A72-42525

MAGNETOSTATICS

Magnetospheric field model, assuming magnetostatic problem solution facilitated by equation linearity 05 p0657 A72-16274

Microwave pulse frequency shift and frequency modulation in YIG bar magnetostatic delay line with adiabatically varying parameters 13 p1923 A72-30095

MAGNETOSTRICTION

Electrodynamics and magnetoelasticity nonlinear Emden-Fowler equation solutions, considering heavy current carrying filaments equilibrium and boundary value problems 07 p1035 A72-19975

Dynamic thermo-magnetoelastic problems of long cylinder and infinite medium with hole under magnetic field, using variation method and Laplace transforms. 13 p2056 A72-28882

Magnetoelastic coupling existence between shearing stresses and linear deformation, noting influence on Poynting effect experimental results 13 p1980 A72-29782

Magnetoelastic effects in elastic dielectric analysis based on continuum with single magnetic moment, noting magnetically saturated material 15 p2274 A72-31482

Magnetothermoelastic temperature distribution effects due to linear heat source in infinite circular cylinder acted upon by magnetic field 16 p2425 A72-33595

Magnetoelastic buckling of beams and thin plates of magnetically soft material. 17 p2624 A72-34311

Magnetoelastic amplitude modulator of millimeter waves based on an antiferromagnetic/hematite/ 17 p2529 A72-34842

Composite materials sum and product physical properties, considering magnetostrictive and piezoelectric interactions 18 p2717 A72-35996

Laminar composite materials with special physical properties 20 p2940 A72-39451

Electrodynamics and magnetoelasticity nonlinear Emden-Fowler equation solutions, considering current carrying heavy filaments equilibrium and boundary value problems 20 p2955 A72-40032

Measurement of internal magnetic field distribution in axially magnetized YIG rods based on magnetoelastic resonance absorption. 21 p3097 A72-40692

The oriented elastic continuum as a model for the magnetoelastic body. 22 p3206 A72-42525

Magnetostriction of porous nickel films 23 p3299 A72-43340

Magnetostriction of stainless steels as a function of heat treatment 23 p3300 A72-43596

A difference method for plane problems in magnetoelastodynamics. 23 p3321 A72-44051

MAGNETOTELLURIC PROFILING

U GEOMAGNETISM

U MAGNETIC SURVEYS

MAGNETOVARIOMETERS

U VARIOMETERS

Pulse modulator thyristor circuit design and optimum operating conditions for driving high peak power radar magnetron 02 p0195 A72-12694

Electrostatic field calculation for magnetron /injection/ electron gun with wedge shaped cathode 06 p0826 A72-18404

- Self consistent problem solution for planar magnetron diode with low cathode field and charge density not exceeding density of Brillouin zone
08 p1142 A72-21703
- Group and symmetry theory application to degenerate mode splitting in magnetron cavity systems with electromagnetic fields disturbances
08 p1142 A72-21740
- Vacuum tube developments for radar, TV and communication applications, discussing microwave, traveling wave, cathode ray, memory and vidicon tubes, magnetrons, klystrons and tetrodes
11 p1606 A72-26544
- Critical analysis of Mouthaan-Susskind diffusion theory for magnetron diode electron transport, noting theoretical results discrepancy with experimental data
13 p1931 A72-29289
- Magnetron crossed field amplifier multistage frequency multiplier HF field properties, obtaining numerical solutions for nonlinear governing equations
15 p2209 A72-32669
- Trajectory equations of laminar electron flow in exponential magnetic field, calculating electrode shapes of magnetron injection electron gun
21 p3088 A72-41835

MAGNETS

- NT CRYOGENIC MAGNETS
- NT ELECTROMAGNETS
- NT HIGH FIELD MAGNETS
- NT SUPERCONDUCTING MAGNETS
- Monograph on Co alloy permanent magnets covering principles, magnetization and testing, alnicos, magnet steel and miscellaneous alloy technology, fine particle magnets and applications
08 p1217 A72-21481

MAGNIFICATION

- N-wave dynamic magnification factors for sonic bangs response on complicated structures
04 p0464 A72-14849
- Holographic virtual image formation and magnification by classical geometrical optics laws application, deriving equivalent law of refraction
16 p2392 A72-33599

MAGNIFIERS

U MAGNIFICATION

MAGNITUDE

- General dimensional analysis as extension of conventional /restricted/ dimensional analysis of physical phenomena, using progressive homogeneity law and fundamental magnitudes
10 p1503 A72-23918

MAGNONS

- Quantum coherent spin wave interactions in ferromagnetics, showing retained emission field
07 p1007 A72-20125
- Heisenberg antiferromagnet with noncollinear sublattices and linear dislocation, considering coupled spin wave states and density
13 p2023 A72-29910
- Dynamic spin disorder effect on electrical and thermal conductivity, noting low resonant frequency in metal atom magnon spectrum
15 p2290 A72-31388
- Two-magnon Raman scattering in antiferromagnets, obtaining amplitude-renormalization factor by extended Dyson-Maleev graphical approach to include corrections in transition operator \hat{M}
15 p2295 A72-32548
- On the magnon interaction in haematite. I - Magnon energy of optical mode.
17 p2595 A72-35358
- Normal mode formulation of spin wave-helicon wave interactions in ferromagnetic semiconductors.
18 p2718 A72-36452
- Parallel pumping of spin waves in yttrium garnet single crystals
21 p3096 A72-40413
- Resonance between spin waves and magnetohydrodynamic waves in antiferromagnetic semiconductors and metals
21 p3096 A72-40415
- Direct fitting of spin wave energies to interatomic exchange parameters in the ferromagnetic rare earth metals.
21 p3097 A72-40625
- Spin wave theory and sublattice magnetization of Cr obtaining wave velocity
21 p3097 A72-40626

MAGNUS EFFECT

- Wind-tunnel Magnus testing of a canted fin or self-rotating configuration.
17 p2486 A72-35254
- Effects of rifling and N-vanes on the Magnus characteristics of bodies of revolution.
[AIAA PAPER 72-970] 22 p3135 A72-42341
- Spin induced boundary layer distortion on rotating cone at supersonic speeds via spark shadowgraphs, correlating Magnus and normal force measurements with boundary layer configurations
[AIAA PAPER 72-967] 22 p3135 A72-42343
- Correlation of Magnus force data for slender spinning cylinders.
[AIAA PAPER 72-966] 22 p3135 A72-42344

MAIN SEQUENCE STARS

- Stellar evolution in close binary systems, discussing post main sequence stage, hydrodynamical processes and dwarf binaries
03 p0437 A72-13868
- Metal-rich 1.19 solar mass main sequence star evolution to convection onset in core during He flash
04 p0577 A72-15283
- Long time behavior of neutron star magnetic fields, noting pulsar evidence for large internal fields in main sequence stars
09 p1389 A72-23393
- Main sequence star evolution relation to pulsar formation, discussing stellar core density at carbon ignition with respect to critical density limit
09 p1394 A72-23698
- Main sequence, red giant and white dwarf stars convective envelopes evolution, discussing mixing length theory inadequacy
10 p1545 A72-24826
- Structure of lower main sequence stars, considering ionization equilibrium in outer convection zone
10 p1546 A72-24835
- Secondary component of eclipsing binary beta Lyrae as massive main sequence star in rapid nonuniform motion, refuting black hole suggestion
11 p1717 A72-25869
- Evolution of extreme population I massive stars from main sequence to He exhaustion phase, discussing various development phases in H-R diagram
14 p2158 A72-30727
- Near-solar mass star secular stability during gravitational contraction and main sequence phases, considering static and quasi-static models
14 p2158 A72-30734
- Field stars near NGC 2168 /M 35/ cluster, segregating main sequence stars by proper motion dispersions with allowance for interstellar extinction
14 p2159 A72-30742
- B type main sequence star absolute energy flux envelope from ground based and OAO 2 observations, comparing with model atmosphere prediction
15 p2311 A72-31997
- Lower zero age main sequence star models uncertainties, comparing nonmixing and mixing length theory for various composition atmospheres
15 p2314 A72-32367
- Opacity corrections of main sequence stellar models of 2.25 solar masses in terms of Cox, Carson and Watson formulas
16 p2452 A72-33130
- Pre-main-sequence stars. II - Stellar polarization in NGC 2264 and the nature of circumstellar shells.
17 p2605 A72-34531
- Fundamental data for massive stars compared with theoretical models.
17 p2611 A72-35317
- Limb darkening for B-type main sequence stars in the infrared.
17 p2612 A72-35383
- The helium abundance in thirty-three main sequence B stars.
18 p2726 A72-36726
- Absolute magnitudes and color indexes of red giant concentration centers on a color-luminosity diagram
19 p2863 A72-38069
- Secular stability. I - A Population I star near the main sequence.
19 p2864 A72-38099
- Pulsating variables in the Pleiades cluster.
21 p3105 A72-41032
- Resonance effects on second order anharmonic pulsational amplitudes for polytropic main sequence evolutionary models, classifying Cepheid-type pulsators
24 p3437 A72-44832
- Iterative solution for adiabatic radial pulsation in massive main sequence star, noting transition to nonlinearity via Eddington stability integral extension
24 p3438 A72-44833

MAINTAINABILITY

- Task oriented maintainability engineering relationship to systems engineering and logistics support requirements
10 p1564 A72-23852
- Reliability and maintainability - Conference, San Francisco, January 1972
10 p1485 A72-23972
- Mathematical model as basis for equipment design-sensitive maintainability prediction technique, using information theory concepts of design interpretation
10 p1503 A72-23979
- Computer programmed instruction checklist for reliability and maintainability engineers requirements
10 p1443 A72-23981
- Multistage systems maintainability, presenting equations for optimum allocation of demonstration tests to repairable elements
10 p1443 A72-23982
- Statistical test plans with improved flexibility, application ease and efficiency for maintainability demonstration
10 p1504 A72-23998

- Spacecraft electronic equipment design criteria for maintainability and installation, discussing mockup zero g demonstration tests of new packaging concepts
[AIAA PAPER 72-235] 10 p1487 A72-24445
- Cost effectiveness determination for different levels of reliability and maintainability of training aircraft, using computer simulation
13 p2067 A72-28355

- Complete aircraft systems reliability and maintainability, discussing extraordinary variances causes, faulty data inferences and operational testing for equipment specifications validation
13 p1896 A72-28358

- OMEGA receiver integration into Navy P-3C airborne computerized navigation system, describing flight test, maintainability and laboratory simulation programs
13 p1999 A72-29202

- Bolkow 105C 5-place helicopter with twin turbine engine driven rigid glass-reinforced plastic rotor blades, emphasizing design philosophy of easy maintainability
13 p1898 A72-29871

- Concorde engines design for maintainability and reliability to reduce turnaround time, discussing diagnostic facilities and on-wing maintenance features
15 p2298 A72-32457

- Aircraft design for operational reliability and maintainability, emphasizing working relations coordination between manufacturer and operator
15 p2181 A72-32459

- Results of the reliability and maintainability demonstration of the OH-58A light observation helicopter.
[AHS PREPRINT 652] 17 p2491 A72-34507

- Aircraft hydraulic control systems modular design for maintainability, emphasizing component removal with minimum hydraulic fluid loss and air entrainment
22 p3140 A72-42294

- Aerospace vehicles preliminary design computer program to include cost, reliability, maintainability and safety parameters in addition to weight as performance determining factors
[SAWE PAPER 940] 23 p3342 A72-43480

- Man serviced spacecraft systems reliability and maintainability optimization methodology, developing parametric data based on failure modes analysis, components MTBF, duty cycles, redundancy and costs
[SAWE PAPER 943] 23 p3343 A72-43483

MAINTENANCE

NT AIRCRAFT MAINTENANCE

NT SPACE MAINTENANCE

- Field repair of Nb alloy panels with protective coatings designed as part of space shuttle thermal protection system
01 p0091 A72-10758
- Field repair of fused slurry silicide coating for oxidation protection of Nb alloys in space shuttle environment
01 p0075 A72-10759
- Multichannel communication system reliability, considering channel repair time random distribution
01 p0033 A72-11263
- Redundancy with repair for system mean time to first failure, presenting differential equation coefficients for Markov process
02 p0236 A72-11556

- Papers on metal fatigue damage covering basic mechanisms, detection, field practices for repair, avoidance and control
02 p0295 A72-12495

- Jet engine component overhaul procedures for fatigue damage repair, detailing distressed metal removal, replacement and welding techniques
02 p0271 A72-12499

- Metal fatigue damage avoidance, control and repair, considering design, metallurgical and service factors
02 p0296 A72-12500

- Computer simulation techniques in aerospace ground equipment design for maintenance testing of avionics systems
03 p0329 A72-14196

- Markov model random variation optimal periodicity in preventive maintenance operations, estimating distribution density and moments
04 p0527 A72-15574

- Boron-epoxy structure repair technology based on titanium plugs and fiberglass, discussing equipment, graphical design and nondestructive tests
08 p1193 A72-21691

- Stochastic rule for optimum moment of preventive maintenance of redundant technological systems, predicting system reliability
08 p1180 A72-22056

- Radio system failure prediction based on parameter variation a priori or a posteriori data, determining reliability and optimal preventive maintenance intervals
08 p1143 A72-22070

- Computer reliability in terms of design criteria to minimize faults incidence, discussing failures detection and correction, fault diagnosis and system maintenance
10 p1444 A72-23985

Prediction method for computing maintenance technician reliability as probability of equipment repair completion within given time

Decision making models application to systems configuration, reliability, repair level and spares optimization and availability analysis

Space shuttle thermal protection refurbishment labor costs and techniques, noting motion studies results for maintenance tasks in terms of manpower and performance time

Model for supervised repairable system reliability, assuming system life and repair times as exponential probability distributions with deterministic supervisor active and inactive times

Weapon system reliability improvement through integrated maintenance data collection and evaluation system, considering maintenance organization and operation

Military system and equipment Level of Repair optimization for minimum life cycle costs, considering weapon systems deployment, operation level and mobility requirements

Logical groupings of preventive maintenance and replacement policies for stochastically failing items to reduce cost under continuous surveillance

Allocating optimum time for systems malfunction search.

MAJORITY CARRIERS

Validity range of applied voltage relationship to majority carrier current in Schottky diodes, assessing minority carrier current importance

Laser induced chemical decomposition of copper maleate and fumarate and fragment reaction with low hydrocarbons, comparing with thermal heating

Single malfunction diagnosis models in systems failures, describing fixed and sequential testing schedules

Malfunction detection for space station environmental/thermal control and life support system, using onboard computer

Relay circuits malfunction due to interactions between coil induced currents and diode coil shunts, discussing circuit design and operating conditions

SIDERAL program organization and computational method application to calculation of malfunction by drift of linear analog equipment

Aircraft industry product support role in time delays minimization for aircraft operators, discussing malfunction report, minimum equipment decision and fault diagnosis

Incompressible fluid turbulent flow variational principles, discussing Malkus principle for maximum dissipation rate and minimum entropy production principle for convective and dissipative systems

Man-machine systems communication ambiguities due to information misinterpretation involving sense organs, previous experience and expectational bias

Synergic control of computer-manipulators, evaluating system

Hierarchically structured man machine control systems synthesis, outlining iterative procedure for optimizing functional

Time shortage as stress factor affecting mental activity of operator in man-flying vehicle system, discussing control signal handling efficiency

Unmanned systems flight testing by test bed vehicle conversion to man operated mode, discussing T-33A jet trainer conversion to drone operation

Computerized man machine systems human factors research simulator, discussing application to railroad train operations

Digital system automated design and analysis developments covering interactive graphic computer aided design, gate level simulation, synthesis, partitioning, interconnection and fault test generation

Interactive computerized design and programs for computer logic design block assignment to modules, comparing performance with manual solutions

Interactive computer graphics design aids to IC mask layouts, discussing hardware and software techniques including IMP program

CIRCAL-2 general purpose on-line circuit design computer program featuring multiple analysis, text editing, network representation and user-program interaction optimization capabilities

Algebraic scheme describing electric element and subnetwork interconnection into networks by wiring operators having conversation capability with computer

Book on discrete event computer simulation for complex systems synthesis and analysis covering random numbers use, languages, and interactive man machine applications

GPSS/360 interactive simulation program with report generator, selective output display and HELP blocks for model manipulation and real time viewing

Computer aided design in electronics, discussing interactive computing with time sharing teletype keyboards or CRT graphics and applications in IC, network analysis and optimization

Automated navigation aids interface with human operator, discussing Apollo flight experience and technology utilization in air and marine navigation

Man computer dialogue, considering human factors effects on interaction course

Instructor station design for automated flight training systems, considering human factors and informational requirements

Book on physiological approach to ergonomics covering muscular system, performance, work and fatigue, working efficiency and environment, man machine systems, etc

Interactive simulation language-8 for minicomputer and programming procedures for nonlinear differential equations solution, considering integration step size and computational accuracy and speeds

Hybrid computer and graphics terminals for real time dynamic man machine interaction, discussing AM communication system simulation

Computer interactive graphics for digital simulation of engineering fields modeled by partial differential equations boundary value problems

Soviet papers on industrial plants automatic control systems organization, design and technological arrangement, covering information handling requirements and man machine interfaces

Automated administrative control systems design, discussing man machine interactions in industrial and economic enterprises management

Man and technology in orientation and navigation Conferences, Essen, Germany, October 1971

Man machine systems in navigation, discussing problems of integrating man with high speed and high capacity electromechanical systems with allowance for human weaknesses and abilities

Development trends in airborne man machine flight control, discussing optimal division between human pilot and machine in relation to total system performance and economic factors

Human operator role in ATC systems analysis, evaluating tasks with respect to job demands and personal fulfillment

Operator mental processes during ATC task performance, discussing work load effect, mental representation and operator algorithm definition

Man machine decision making procedures for multicriterial aggregate estimates, using pairwise comparisons and linear programming

Man machine automatic control system structural synthesis, treating system operation as nonlinear programming problem

Interactive remote terminal as formatting tool for reliability engineer to free from computational labor and concentrate on conceptual problems

Human performance prediction dependence on task and equipment variables effects, using experimental data for performance classification system

Space shuttle flight crew/computer interface display and control functional requirements optimization by real time digital simulation

Unpowered shuttle orbiter piloted control during approach and landing, discussing energy management technique based on fixed base six degree of freedom simulation

Human operator role in space systems reliability, suggesting approaches to system design and program planning to exploit human potential

Optimum performance typewriter keyboard design, discussing biomechanical improvements in finger positioning facilitation, operator postural muscular strain reduction, etc

WINDCO interactive man-computer system for automated cloud motion tracking using precisely aligned digital ATS satellite pictures

Fault-tolerant digital computer logic design for dynamic and interactive recovery with data integrity after error, discussing hardware and software functions requirements

Visual display systems for man-machine communications, discussing applications, data processing, hardware designs and human engineering

Computer-aided interactive graphic displays for ATC, discussing subsystems, data processing flow and operational capabilities

Tactical ATC display system for airport surveillance, precision approach and landing and operator/aircraft/machine operations by using terminal Area Surveillance Radar

Human operator dynamic characteristics measurement, using pseudorandom binary signals and mathematical models in closed loop control system

Online identification on human describing function by iterative differential analyzer, noting application to man-machine systems and online adaptive control systems

Aircraft design interactive computer graphics technique, using human decision input response to computer output information

Book on human factors engineering covering systems design requirements and interface equipment for man machine interaction implementation

Systems, man and cybernetics - IEEE Conference, Anaheim, California, October 1971

Mathematical models for man-machine control behavior in biodynamic environments including manual control performance and interface elements

Pilots in aircraft systems management involving machine and air traffic environment

Automatic flight control systems value to aircraft pilot, stressing man machine interface

Soviet book on astronaut activity psychological features covering space flight living conditions, space and time perception psychophysiological mechanism changes and weightlessness effects

Man-machine systems communication ambiguities due to information misinterpretation involving sense organs, previous experience and expectational bias

Synergic control of computer-manipulators, evaluating system

Hierarchically structured man machine control systems synthesis, outlining iterative procedure for optimizing functional

Time shortage as stress factor affecting mental activity of operator in man-flying vehicle system, discussing control signal handling efficiency

Unmanned systems flight testing by test bed vehicle conversion to man operated mode, discussing T-33A jet trainer conversion to drone operation

Computerized man machine systems human factors research simulator, discussing application to railroad train operations

Digital system automated design and analysis developments covering interactive graphic computer aided design, gate level simulation, synthesis, partitioning, interconnection and fault test generation

Interactive computerized design and programs for computer logic design block assignment to modules, comparing performance with manual solutions

Interactive computer graphics design aids to IC mask layouts, discussing hardware and software techniques including IMP program

CIRCAL-2 general purpose on-line circuit design computer program featuring multiple analysis, text editing, network representation and user-program interaction optimization capabilities

Algebraic scheme describing electric element and subnetwork interconnection into networks by wiring operators having conversation capability with computer

Book on discrete event computer simulation for complex systems synthesis and analysis covering random numbers use, languages, and interactive man machine applications

GPSS/360 interactive simulation program with report generator, selective output display and HELP blocks for model manipulation and real time viewing

Computer aided design in electronics, discussing interactive computing with time sharing teletype keyboards or CRT graphics and applications in IC, network analysis and optimization

Automated navigation aids interface with human operator, discussing Apollo flight experience and technology utilization in air and marine navigation

Man computer dialogue, considering human factors effects on interaction course

Instructor station design for automated flight training systems, considering human factors and informational requirements

Book on physiological approach to ergonomics covering muscular system, performance, work and fatigue, working efficiency and environment, man machine systems, etc

Interactive simulation language-8 for minicomputer and programming procedures for nonlinear differential equations solution, considering integration step size and computational accuracy and speeds

Hybrid computer and graphics terminals for real time dynamic man machine interaction, discussing AM communication system simulation

Computer interactive graphics for digital simulation of engineering fields modeled by partial differential equations boundary value problems

Soviet papers on industrial plants automatic control systems organization, design and technological arrangement, covering information handling requirements and man machine interfaces

Automated administrative control systems design, discussing man machine interactions in industrial and economic enterprises management

Man and technology in orientation and navigation Conferences, Essen, Germany, October 1971

Man machine systems in navigation, discussing problems of integrating man with high speed and high capacity electromechanical systems with allowance for human weaknesses and abilities

Development trends in airborne man machine flight control, discussing optimal division between human pilot and machine in relation to total system performance and economic factors

Human operator role in ATC systems analysis, evaluating tasks with respect to job demands and personal fulfillment

Operator mental processes during ATC task performance, discussing work load effect, mental representation and operator algorithm definition

Man machine decision making procedures for multicriterial aggregate estimates, using pairwise comparisons and linear programming

Man machine automatic control system structural synthesis, treating system operation as nonlinear programming problem

Interactive remote terminal as formatting tool for reliability engineer to free from computational labor and concentrate on conceptual problems

Human performance prediction dependence on task and equipment variables effects, using experimental data for performance classification system

Space shuttle flight crew/computer interface display and control functional requirements optimization by real time digital simulation

Unpowered shuttle orbiter piloted control during approach and landing, discussing energy management technique based on fixed base six degree of freedom simulation

Human operator role in space systems reliability, suggesting approaches to system design and program planning to exploit human potential

Optimum performance typewriter keyboard design, discussing biomechanical improvements in finger positioning facilitation, operator postural muscular strain reduction, etc

dom numbers use, languages, and interactive man machine applications

GPSS/360 interactive simulation program with report generator, selective output display and HELP blocks for model manipulation and real time viewing

Computer aided design in electronics, discussing interactive computing with time sharing teletype keyboards or CRT graphics and applications in IC, network analysis and optimization

Automated navigation aids interface with human operator, discussing Apollo flight experience and technology utilization in air and marine navigation

Man computer dialogue, considering human factors effects on interaction course

Instructor station design for automated flight training systems, considering human factors and informational requirements

Book on physiological approach to ergonomics covering muscular system, performance, work and fatigue, working efficiency and environment, man machine systems, etc

Interactive simulation language-8 for minicomputer and programming procedures for nonlinear differential equations solution, considering integration step size and computational accuracy and speeds

Hybrid computer and graphics terminals for real time dynamic man machine interaction, discussing AM communication system simulation

Computer interactive graphics for digital simulation of engineering fields modeled by partial differential equations boundary value problems

Soviet papers on industrial plants automatic control systems organization, design and technological arrangement, covering information handling requirements and man machine interfaces

Automated administrative control systems design, discussing man machine interactions in industrial and economic enterprises management

Man and technology in orientation and navigation Conferences, Essen, Germany, October 1971

Man machine systems in navigation, discussing problems of integrating man with high speed and high capacity electromechanical systems with allowance for human weaknesses and abilities

Development trends in airborne man machine flight control, discussing optimal division between human pilot and machine in relation to total system performance and economic factors

Human operator role in ATC systems analysis, evaluating tasks with respect to job demands and personal fulfillment

Operator mental processes during ATC task performance, discussing work load effect, mental representation and operator algorithm definition

Man machine decision making procedures for multicriterial aggregate estimates, using pairwise comparisons and linear programming

Man machine automatic control system structural synthesis, treating system operation as nonlinear programming problem

Interactive remote terminal as formatting tool for reliability engineer to free from computational labor and concentrate on conceptual problems

Human performance prediction dependence on task and equipment variables effects, using experimental data for performance classification system

Space shuttle flight crew/computer interface display and control functional requirements optimization by real time digital simulation

Unpowered shuttle orbiter piloted control during approach and landing, discussing energy management technique based on fixed base six degree of freedom simulation

Human operator role in space systems reliability, suggesting approaches to system design and program planning to exploit human potential

Optimum performance typewriter keyboard design, discussing biomechanical improvements in finger positioning facilitation, operator postural muscular strain reduction, etc

Book on discrete event computer simulation for complex systems synthesis and analysis covering random numbers use, languages, and interactive man machine applications

GPSS/360 interactive simulation program with report generator, selective output display and HELP blocks for model manipulation and real time viewing

Computer aided design in electronics, discussing interactive computing with time sharing teletype keyboards or CRT graphics and applications in IC, network analysis and optimization

Automated navigation aids interface with human operator, discussing Apollo flight experience and technology utilization in air and marine navigation

Man computer dialogue, considering human factors effects on interaction course

Instructor station design for automated flight training systems, considering human factors and informational requirements

Book on physiological approach to ergonomics covering muscular system, performance, work and fatigue, working efficiency and environment, man machine systems, etc

Interactive simulation language-8 for minicomputer and programming procedures for nonlinear differential equations solution, considering integration step size and computational accuracy and speeds

Hybrid computer and graphics terminals for real time dynamic man machine interaction, discussing AM communication system simulation

Computer interactive graphics for digital simulation of engineering fields modeled by partial differential equations boundary value problems

Soviet papers on industrial plants automatic control systems organization, design and technological arrangement, covering information handling requirements and man machine interfaces

Automated administrative control systems design, discussing man machine interactions in industrial and economic enterprises management

Man and technology in orientation and navigation Conferences, Essen, Germany, October 1971

Man machine systems in navigation, discussing problems of integrating man with high speed and high capacity electromechanical systems with allowance for human weaknesses and abilities

Development trends in airborne man machine flight control, discussing optimal division between human pilot and machine in relation to total system performance and economic factors

Human operator role in ATC systems analysis, evaluating tasks with respect to job demands and personal fulfillment

Operator mental processes during ATC task performance, discussing work load effect, mental representation and operator algorithm definition

Man machine decision making procedures for multicriterial aggregate estimates, using pairwise comparisons and linear programming

Man machine automatic control system structural synthesis, treating system operation as nonlinear programming problem

Interactive remote terminal as formatting tool for reliability engineer to free from computational labor and concentrate on conceptual problems

Human performance prediction dependence on task and equipment variables effects, using experimental data for performance classification system

Computer aided iterative design of nonlinear single loop control system with sinusoidal describing function and time response display capability

11 p1601 A72-26042

Interactive computer graphics with three dimensional real time CRT display of air combat maneuvers for fighter pilot training

11 p1613 A72-26291

Integrated display system design with navigation update, weapon delivery, reconnaissance, bomb damage assessment, threat and terrain avoidance capabilities for multicrew military aircraft

11 p1684 A72-26292

Data display techniques in man operated automatic control system, assessing information volume versatility and operability

11 p1585 A72-26451

Aircraft microminiature ILS with transmitter and localizer antenna to provide pilot with bearing and glide slope information for alignment with runway

12 p1842 A72-27106

Interactive computer graphics technique for structural analysis, aiding engineering decisions by CRT graphical and numerical information display

12 p1787 A72-27864

Pilot-aircraft system model for relationship between weapons delivery accuracy and manual flight control system design, noting display, computation and control aids to pilot

12 p1773 A72-28121

Remotely manned vehicles /RMV/ application in aerial warfare, considering anti-aircraft defenses lethality increase, equipment costs and role of man during combat mission

13 p1896 A72-28451

Man machine system to repack weather information for easy assimilation, considering computer driven keyboard CRT displays

13 p1924 A72-28872

Pilot trainer transfer function identification for man-machine and on-line adaptive control system using analog/hybrid computer

14 p2091 A72-30721

Aircraft copilot assistance to pilot in flight phases, emphasizing takeoff and landing and man machine system reliability

14 p2072 A72-30815

Aerospace complex physical systems including human operator, discussing computerized design for behavior analysis by means of mathematical models

14 p2093 A72-30846

Russian book on man and computer covering interaction systems technological capabilities, mathematical aspects and applications

15 p2188 A72-31272

Aircraft inertial navigation system, discussing mode selection unit, digital computer and control display for operator communication with system

15 p2267 A72-31596

Graphic color display adapted to traffic control for direct operator-computer dialogue, noting instruction repertoire, switching device and input devices

16 p2420 A72-32894

Book on man machine system experiments covering ATC, air defense, logistics organizations, space flight, battlefield operation, police dispatching, communications, etc

16 p2359 A72-33796

Predictive model for human operator performance in short term visual information processing based on psychological research to obtain decision accuracy and response time

16 p2359 A72-33865

Computerized photographic imagery analysis system with interactive operator controls for processing option selection in image enhancement prior to pattern identification

17 p2520 A72-34407

Automated cloud tracking using precisely aligned digital ATIS pictures.

17 p2521 A72-34411

Pilot-fighter aircraft system mathematical model relating pilot performance to air to ground weapon delivery accuracy

17 p2493 A72-35564

Historical development of right and left hand patterns in horsemanship, land vehicle, ship and aircraft control and navigation

18 p2707 A72-37050

Man machine systems operational effectiveness augmentation through human factors engineering to enhance human operator capability for parallel data processing and decision making

19 p2761 A72-38308

Control center relation to process control computers in production engineering, discussing information flow and communication in man machine systems

19 p2761 A72-38310

Process control of the 100-m telescope - Communication of the observer with the computer-controlled telescope

19 p2804 A72-38487

Man machine automatic control system structural synthesis, treating system operation as nonlinear programming problem

19 p2782 A72-38521

Flight and centrifuge tested aircrew tilting supinating seats biomedical and technical adequacy as acceleration protective man machine system

19 p2761 A72-38707

Behavioural characteristics of men in the performance of some decision-making task components.

20 p2898 A72-39805

Area navigation systems integration into existing ATC and man/machine relationship problems, considering cockpit workload coordination

21 p3079 A72-40280

An area navigation system for a long range airplane.

21 p3079 A72-40281

Russian book - Space ergonomics.

21 p3004 A72-40300

Anthropotechnics /human engineering/ approach to man machine system optimization, discussing task allocation and adaptations of machine dynamics, displays and controls to human operator

21 p3009 A72-41403

Display device layout based on human operator manual control information requirements consideration, discussing functional categories, motion compatibility, indicators relation and integration

21 p3009 A72-41404

Prediction role in execution of manual control with display device to aid human operator adaptation

21 p3010 A72-41406

Display device design and human operator training based on visual and auditory sensation and perception principles, emphasizing fitting between man and information

21 p3010 A72-41407

Human operator decision making role in information presentation system determined by experiments using laboratory performance and test measures, field observation, electrical and biochemical measures

21 p3010 A72-41408

Prediction displays based on the extrapolation method.

21 p3010 A72-41409

Man machine system input via human controller output transformation, illustrating with spacecraft lateral position manual control problem

21 p3010 A72-41411

Manual workload determination by control characteristics, control-display relationships, demands for dexterity and sensitivity and speed and accuracy requirements

21 p3010 A72-41414

Man machine system functions and display and control role descriptions by flow diagrams, giving examples of keying and task in guided weapon system

21 p3011 A72-41415

Human or computer control role in teleoperator remote control mechanisms, discussing control modes, sensing and transmission time delay problems

21 p3011 A72-41416

Computerized supervisory control for interpretation of subgoal statements from human operator to permit teleoperator interaction with environment without long time delay

21 p3011 A72-41417

Lectures on theory of manual-vehicle control.

21 p3011 A72-41418

A method for the development and optimization of controller-models for man-machine systems.

21 p3011 A72-41420

Manual tracking control with continuously variable selective control gain in response to system state, noting intuitive optimization

21 p3011 A72-41425

Mental and physical workload measure and differentiation in man machine systems

21 p3012 A72-41427

Development and optimization of a nonlinear multiparameter human operator model.

22 p3149 A72-41949

Mathematical methods of man machine control system synthesis, using homeostasis and functional compatibility principle

22 p3162 A72-42243

German monograph - Control performance as a function of the transmission ratio and the Coulomb friction in the operational element.

22 p3152 A72-43052

Detection of hazards associated with aerospace operations.

23 p3287 A72-43424

Man machine control system synthesis, noting quality criteria and estimates for weighting function coefficients of optimization potential

24 p3376 A72-45508

Problems of complex object modeling based on heuristic self-organization

24 p3376 A72-45509

Invariant transformation of the control laws in ergatic systems

24 p3376 A72-45510

Formation of an optimizing functional in control systems

24 p3386 A72-45511

Mathematical description of a human operator in ergatic control systems

24 p3376 A72-45514

Algorithmic description of the generalized operational characteristic of a human operator

24 p3376 A72-45515

Estimate of the operational efficiency of a human operator in the follow-up mode of a closed-loop control system

24 p3376 A72-45516

Methodical aspects of studies of ergatic differential-game systems

24 p3376 A72-45517

Man in a control circuit during an information game synthesis

24 p3377 A72-45520

Experimental determination of the distribution rule for the time of failure-free operator action in the tracking mode /with pursuit/

24 p3377 A72-45521

Theoretical-experimental method for parametric synthesis of director-type control systems

24 p3377 A72-45522

Aircraft interception avoidance problem solved by differential game theory, discussing human operator decision making for random pursuit tracking

24 p3377 A72-45523

MANAGEMENT

NT CONFIGURATION MANAGEMENT

NT CONTRACT MANAGEMENT

NT DATA MANAGEMENT

NT ENGINEERING MANAGEMENT

NT FINANCIAL MANAGEMENT

NT INDUSTRIAL MANAGEMENT

NT INFORMATION MANAGEMENT

NT INVENTORY MANAGEMENT

NT LOGISTICS MANAGEMENT

NT PERSONNEL MANAGEMENT

NT PROCUREMENT MANAGEMENT

NT PRODUCTION MANAGEMENT

NT PROJECT MANAGEMENT

NT RESEARCH MANAGEMENT

NT SAFETY MANAGEMENT

NT SYSTEMS MANAGEMENT

NT WATER MANAGEMENT

NT WEAPON SYSTEM MANAGEMENT

Aerial photointerpretation in forest administration, discussing electronic data processing methods

09 p1302 A72-23291

MANAGEMENT ANALYSIS

Azur satellite project definition organizational structure and time schedule, noting management and implementation problems

05 p0752 A72-16136

MANAGEMENT INFORMATION SYSTEMS

Industrial R and D data collection to relate idea dispositions by management to subjective evaluation, considering urgency, predictability and expected time horizon roles

04 p0598 A72-15455

Electronic data processing for management information utilization

12 p1890 A72-27267

Management information system role in cost effective civil and military aircraft operations, discussing hardware modification and human resources and communication system adaptation

15 p2339 A72-32458

MANAGEMENT METHODS

Design review as management tool for complex systems quality and reliability assurance, discussing Skylab program

10 p1486 A72-24005

Apollo program management decisions based on reliability analysis, discussing incentive fees, testing optimization, engineering changes approval and flight readiness certification

10 p1486 A72-24007

Statistical-analytical cost models for spacecraft development and fabrication, taking into account various technical and management factors

10 p1564 A72-24026

Cost effective innovations in space programs management, discussing communication, problem solving and reward and punishment

10 p1564 A72-24451

Management alternatives evaluation methodology for capital expenditures on large facilities in terms of competitive capability enhancement for aerospace contracts

15 p2340 A72-32615

Problems confronting the engineer in charge of procurement of components intended for electronic aerospace systems

18 p2743 A72-37126

NDT application and development in industry, considering confidence in inspection techniques, framework and management resistance

24 p3408 A72-45295

MANAGEMENT PLANNING

NT PRODUCTION PLANNING

NT PROJECT PLANNING

Aircraft producibility considerations in preliminary design and production planning phases

01 p0074 A72-10245

Quality control function in configuration management, discussing hardware and software validity for decision formulation

NASA quality assurance program, discussing management planning, assessment, failure prevention and cost effectiveness

ATC system decision making problem and future technological and administrative improvements

European Space Research and Technology Center satellite project control system, describing critical path network analysis, work package cost control and project planning

Mathematical model for research payoff estimation by internal rate of return method used by large corporations for project evaluation

Product support functional organization, discussing support systems analysis and engineering, trainer design, technical proposals and publications, customer training, field service, etc

Industrial R and D data collection to relate idea dispositions by management to subjective evaluation, considering urgency, predictability and expected time horizon roles

DELTA flow chart and network method for R and D projects planning and scheduling

Interflug national economic control system, discussing objectives, costs, labor, science and technology, material and price management plans

In-house R and D laboratory organization cost effectiveness evaluation methods, discussing supervisory, program and special appraisals, visiting committees and natural competition

R and D management policies choices with respect to Bayesian decision-theoretic model in simulated environments

Technological forecasting method evaluation for R and D planning, fitting trend curves to sets of technological data

Technology transfer model in terms of donor-recipient activities for information implementation, forecasting and long range planning in developing countries and regional economics

Computer aided administrative control systems development for industrial enterprises management, covering product manufacture

Selection, arrangement and use of computers and peripheral equipment in automated administrative control management system within industrial enterprise

Industrial enterprises preparation for computerized administrative control systems introduction

Systems approach to technological forecasting for short range research, considering consumer, market and organizational resources

Reliability growth curves for product assessment as technical management forecasting technique

Work administration system for aerospace applications, considering contractual statements, corporate requirements, schedule accomplishment and cost effectiveness

Dynamic modeling application to technological forecasting, discussing mathematical simulation for R and D management planning in project selection and budget allocation

Technological forecasting and long range planning in transportation, considering roles of expert opinion, trend extrapolation, normative models and social impact

Optimization of diagnostic tests for monitoring industrial system efficiency, obtaining compromise between costs and utilization

Industrial enterprise training expense planning in terms of staff productivity and work time

Military R and D organization questionnaires data analysis to obtain relationship between job productivity, satisfaction, ability, age and salary

Aircraft maintenance operations and personnel requirements planning for optimal economic effectiveness, formulating relations between work productivity, downtime and aircraft utilization

Schedule analysis computer program algorithms for waterfall bar chart display and commodity flow processing and graphing through network

Lunar roving vehicle qualification program to meet performance specifications under lunar conditions, describing testing procedures and project management techniques

Resource analyses for R & D programs

French space program management planning, discussing orientation, operation and control of activities

Mathematical formulation of linear programming problem, reducing vector value optimal management plan determination to quadratic programming problem

Integration of safety engineering into a cost optimized development program

Planning and management requirements for aircraft jet engine control system research and development

NASA ICBM/IRBM space program major management decisions and highlights concerning Atlas, Titan and Thor

Simulation procedure for mission and maintenance planning of an air force wing

MANAGEMENT SYSTEMS

NT MANAGEMENT INFORMATION SYSTEMS
Aerospace management systems effectiveness in design, development, test and engineering areas, discussing cost, scheduling and technical performance factors

[AIAA PAPER 72-243]

MANDRELS
Inflatable mandrels use to manufacture filament wound casings examined in terms of suitable mandrel materials and required mechanical properties

Mandrel design for the filament winding process

MANEUVERABILITY
Air to air maneuverability of aircraft capable of in-flight thrust vectoring, indicating improved deceleration, normal acceleration g-force and turn rate

Dynamic control system parameters optimization for series of maneuvers under different degrees of informability

Combat jet helicopter maneuverability, considering aircraft flying characteristics, pilot capability, flight configuration, altitude and load factor

Fighter aircraft maneuverability, range and armament requirements, discussing canard vs delta configurations

General Dynamics model 401 air superiority single engine fighter design stressing light weight structure and maneuverability at high speeds and angles of attack

Helicopter maneuverability factors, discussing flight direction change ability, acceleration limitations and rotor thrust requirements

Design for air combat

Maneuver low control and relaxed static stability applied to a contemporary fighter aircraft

MANEUVERABLE SATELLITES
U MANEUVERABLE SPACECRAFT
U SATELLITES

MANEUVERABLE SPACECRAFT
NT APOLLO SPACECRAFT
NT LIFTING REENTRY VEHICLES
NT RENDEZVOUS SPACECRAFT

Rotating dumbbell shaped satellites orientation optimization by system of jets, calculating energy losses

MANEUVERS
NT EARTH ORBITAL RENDEZVOUS
NT ORBITAL RENDEZVOUS
NT SIDESLIP
NT SPACECRAFT DOCKING
NT SPACECRAFT MANEUVERS

Human and animal controlled self rotating maneuvers during free fall, comparing theoretical motion analysis with photographs of falling cats

SST operational maneuver effects on sonic boom, discussing steady flight and acceleration-to-cruise pressure signatures

Experimental investigation of an astronaut maneuvering scheme

ASW aircraft magnetic anomaly detection /MAD/ system range limitation due to residual maneuver noise, discussing real time compensation for geomagnetic gradient interference

MANGANESE

NT MANGANESE ISOTOPES

Fe XI to XV emission lines from transitions and isoelectronic spectra in manganese, chromium and vanadium

Manganese catalyst photoactivation process for oxygen photosynthetic evolution investigated in Mn-deficient Anacystis nidulans cells

Structural stabilization of austenitic steels with manganese, maintaining toughness and sensitivity to martensitic transformation by hammer hardening

Structural stabilization of austenitic steels with manganese, noting chemical purity and cleanliness conditions

Mn additions effects on austenitic stainless steels yield strength, work hardening characteristics, corrosion resistance and machinability

Mn content effect on mechanical properties and corrosion fatigue and stress corrosion cracking resistance of Al-Mg casting alloys

Solar spectrum Mg I multiplet lines hyperfine structures, examining emission lines with Fabry-Perot and Fourier transform spectrometers

Solar Mg abundance and hyperfine structure from oscillator strengths measurement by comparing absorption lines at furnace temperatures

Mg base alloys precipitation processes studied by electron microscopy, emphasizing Mn precipitation in Mg-Th alloy

The classification of transitions between levels of principal quantum numbers 3 and 4 in Fe IX to XVI and Mn VIII to XV

German monograph - Significance of the manganese-carbon ratio in the brittle-fracture behavior and weldability of high-strength fine-grained structural steels

MANGANESE ALLOYS
Al-Mn system constitution, discussing metastable phase, high and room temperature modifications and transformation equilibrium

Passivation velocity apparatus for testing Al-Mg alloy sensitivity to corrosion under voltage

High alloy chromium and manganese steels brittle fracture susceptibility, showing notch effects

Hardening of Fe-Mn-Ti ferritic and martensitic alloys, investigating microstructure and mechanical properties

Phase equilibria of Mo-Mn-C and W-Mn-C systems by X ray analysis, showing eutectoid decomposition involving rhombic modification

MnBi thin films as potential storage media within holographic optical memory system having write-in reference beam for readout

Aging effect on brittleness and hardening of Fe-Ni-Mn alloy at various temperatures

Magnetic susceptibility of ternary Al-Mn alloys with Ti, Va, Cr, Fe, Co, Ni, Cu and Zn, describing microstructure and aging experiments

Electron bombardment disordering of ordered Ni-Mn alloy along different crystallographic directions

Safe welding procedures for carbon manganese steels, noting hydrogen cracking association with hardening of heat affected zone

Relative valence effect of transition metal additions on alpha-gamma phase equilibrium in Fe-Cr-Mn system

Ni-Mn alloy phase transformation characteristics from neutron diffraction and small angle scattering studies, showing ordered nearly stoichiometric metastable phase for entire temperature range

Cr and V additions effects on Mn steels mechanical properties and wear resistance, noting strength limit increase

Microstructure and mechanical properties of heat resistant Fe-Mn-Al alloys at 650-1150 C

Al-Mu-Li alloys phases mechanical and thermal properties under tensile and fatigue tests at room and elevated temperatures 14 p2124 A72-31037

Composition, strength and plasticity of ultralight Mn-Li alloys with two-phase alpha-beta base 14 p2125 A72-31040

Structural and orientation study of sequentially evaporated MnBi thin films on glass substrates using electron diffraction and transmission microscopy 16 p2441 A72-33207

Texture of Ti-Sn and Ti-Mn alloy specimens observed by X ray reflection technique after hot rolling, annealing and cold rolling 16 p2407 A72-33529

Study of certain features of the electronic structure of the ternary alloys Ni3/Mn, Fe/ and Ni3/Mn, Co/ 17 p2568 A72-35518

Microstructure and differential thermal analyses of ternary system Co-Mn-Al, presenting phase diagrams 19 p2818 A72-37852

Ferromagnetic tau phase structure of Mn-Ac alloy with powder anisotropy related to platelet formation and twinning orientation 21 p3068 A72-40965

Strain hardening effect of Ni, Mn and Mo in Cr steel after high temperature annealing 23 p3301 A72-43742

High alloy chromium and manganese steels brittle fracture susceptibility, showing notch effects 24 p3414 A72-44941

MANGANESE COMPOUNDS

Effect of copper, cobalt and manganese salts on certain morphological-biochemical components of the blood in young sheep of the Hissar breed 20 p2893 A72-40075

MANGANESE IONS

Electron spin resonance of divalent Mn ion doped in thallous azide single crystals, investigating temperature effects on spin Hamiltonian parameters 22 p3152 A72-42716

MANGANESE ISOTOPES

Aluminum 26 and manganese 53 produced by solar-flare particles in lunar rock and cosmic dust. 20 p2970 A72-39472

MANGANESE 53

U MANGANESE ISOTOPES

MANGANESE 54

U MANGANESE ISOTOPES

MANGANESE 56

U MANGANESE ISOTOPES

MANIFOLDS

Bogoliubov-Mitropolski-Hale integral manifold theorem for perturbed nonlinear differential equations, using generalized variation of parameters formula 03 p0381 A72-12907

Missile destruct systems explosive transmission line manifolds, discussing designs for high reliability under severe environmental conditions 08 p1221 A72-20782

L-1011 TriStar cartridge valves and manifolds, reservoirs and hydraulic service center design for speedy maintenance and servicing 14 p2073 A72-31050

MANIFOLDS [MATHEMATICS]

Invariant manifolds in rigid body motion about fixed point, considering Euler-Poinsoit, Lagrange-Poisson and Kovalevskia cases 04 p0549 A72-15197

Differential equations of motion construction from given manifold, determining functional minimization of solution 04 p0550 A72-15544

Markov processes for local diffusions defined by second order differential operator delta with Holder coefficients on manifold 10 p1505 A72-24201

Differential geometry extremal problem of holomorphic embedding of complex curves in Kaehler manifold with constant holomorphic curvature, using Riemann surface moduli theory 10 p1506 A72-24862

Heat equation for insulated uniform body, examining definition and continuity of mapping from linear manifold of assumed boundary values 11 p1747 A72-26555

Dynamic control stability on given time interval, using Liapunov-like functions and integral manifolds in quadratic forms 13 p2004 A72-29471

System theory on group manifolds and coset spaces. 17 p2575 A72-34949

Criteria for nonlinear systems controllability in terms of state variable analytic function and derivatives, implying strong accessibility for manifolds including Euclidean spaces 18 p2673 A72-36616

Equivariant integrality theorems for differentiable manifolds. 22 p3199 A72-42310

A manifold imbedding algorithm for optimization problems. 23 p3268 A72-44197

Analytic continuation of functions over infinite dimensional domains, covering Banach manifolds, hypoanalytical mappings, convexity and topology 24 p3418 A72-44827

Spline functions application to approximation theory problem of determining diameters of subspaces and manifolds in Banach space 24 p3419 A72-45548

MANIPULATION

U MANIPULATORS

MANIPULATORS

Accuracy criterion for master mechanism position reproduction by slave mechanism of master-slave manipulator 07 p0914 A72-19261

Teleoperator manipulator for payload handling in space shuttle, noting design features and simulations of master-slave remote control system [AIAA PAPER 72-238] 13 p1909 A72-29075

In orbit servicing of spacecraft. 18 p2730 A72-36543

New modifications of manipulators for investigations using microelectrodes 22 p3149 A72-42073

Control simulation models of three dimensional joint angle motions, including circle, ellipse and straight line trajectories and orientations in space 22 p3162 A72-42187

Teleoperator technology development, discussing remote operators, mobile manipulators and autonomous robots for man capability extension and industrial application [ASME PAPER 72-AERO-18] 22 p3245 A72-43150

A teleoperator system for space application. 24 p3407 A72-45174

MANN-WHITNEY-WILCOXON U TEST

Noise statistics sensitivity of two sample Mann-Whitney nonparametric detector for radar application 05 p0629 A72-16570

MANNED LUNAR SURFACE VEHICLES

Manned-Unmanned Lunar Explorer (MULE) for NASA integrated program plan after 1980, discussing weight, locomotion system and mission capabilities [AIAA PAPER 72-369] 11 p1612 A72-25394

Implications of new transport vehicles and cost analysis of supplying and maintaining a manned lunar laboratory. 24 p3441 A72-45209

MANNED ORBITAL LABORATORIES

NT MANNED ORBITAL RESEARCH LABORATORIES

SkyLab experimental space station, discussing environment comfort, Apollo spacecraft rendezvous for crew rotation and onboard experiments in earth resources, biomedicine, astronomy, etc 06 p0893 A72-18611

Legal aspects of international manned orbiting laboratories, discussing space objects registry and liability for damage 07 p1103 A72-19461

Manned orbital laboratories within framework of space treaty 07 p1103 A72-19462

SkyLab earth resources experiment package, examining crew tasks [AIAA PAPER 72-234] 10 p1472 A72-24444

Design of Salyut manned orbital laboratory combined with Soyuz service module 12 p1876 A72-27107

Space Shuttle supported manned earth orbital laboratories for operational communication and navigation systems, discussing mission program, design and equipment [AIAA PAPER 72-533] 12 p1876 A72-27357

Space shuttle applications as spacecraft launcher, unmanned instrumentation platform and manned laboratory, discussing advantages to space research 13 p2051 A72-28935

Future orbital observatory modules for stellar and galactic astronomy. 24 p3453 A72-45533

MANNED ORBITAL RESEARCH LABORATORIES

MORL and Orbital Biomedical Laboratory projects, reviewing crew accommodation, spacecraft and booster requirements and biomedical measurements 05 p0724 A72-16177

MANNED ORBITAL SPACE STATIONS

U ORBITAL SPACE STATIONS

MANNED ORBITAL TELESCOPES

NT APOLLO TELESCOPE MOUNT

MANNED REENTRY

Parameters affecting communication and rescue time constraints for emergency astronaut return from low earth orbits 09 p1395 A72-23155

MANNED SPACE FLIGHT

NT APOLLO FLIGHTS

NT MANNED REENTRY

NT MERCURY FLIGHTS

Manned space station design for astronomy, space physics and biology, earth surveys, aerospace medicine, materials science and advanced technologies applications 01 p0135 A72-10937

Optimum duration of human circadian cycle with respect to energy cost during work hours, relating normal cycle change to prolonged space mission stresses 05 p0619 A72-16639

Soviet book on space exploration in U.S.S.R. covering Elektron, Proton and Cosmos research satellites, communication and meteorological satellites, lunar and manned spacecraft, etc 06 p0879 A72-17815

Space rescue - Conference, Konstanz, West Germany, October 1970 09 p1395 A72-23151

Manned space flight escape, rescue and survival systems based on onboard, prepositioned aid and earth launched concepts, considering earth orbit, lunar and interplanetary missions 09 p1395 A72-23152

Escape systems evolution for manned space flight, considering X-15, Mercury, Gemini and Apollo programs and future space stations and planetary missions 09 p1395 A72-23153

Parameters affecting communication and rescue time constraints for emergency astronaut return from low earth orbits 09 p1395 A72-23155

Terminal guidance systems and techniques application to manned space flight rescue operations, discussing emergency location and rescue spacecraft communication and guidance 09 p1396 A72-23158

Rest and activity patterns effect on space crews well-being and operational effectiveness during prolonged extraterrestrial missions, noting work load effect on long-haul transport aircrews 10 p1427 A72-23727

Design considerations and reliability analysis for long duration manned space missions, noting redundancy and inflight maintenance requirement [AIAA PAPER 72-239] 10 p1487 A72-24446

Medical evaluation of manned space flight physiological effects, considering Mercury, Gemini and Apollo programs 11 p1585 A72-26100

Diving operations medical aspects significance for manned planetary surface exploration in high density atmospheres, considering protective clothing, breathing apparatus and gas mixtures, etc 12 p1769 A72-27415

Computer and meteorological satellite effects on weather support for manned space missions, discussing Gemini 5 and Apollo 11 landing weather predictions and cloud climatology 13 p1989 A72-28804

NASA space plans for 1970s including lunar, planetary and universe explorations, cost reduction, human living and working capability, technology applications and international cooperation 14 p2162 A72-31136

Medical requirements for manned space flight, discussing physiological data monitoring and transmission, equipment miniaturization, telediagnosis, spacecraft environment protection, etc 16 p2358 A72-33562

Preventive and remedial space flight safety engineering, discussing escape capsules and onboard and earth-launched rescue systems 17 p2620 A72-34427

Long range planning for the development of space flight emergency systems. 17 p2620 A72-34428

The earth orbit shuttle as a space rescue vehicle. 17 p2620 A72-34437

Spacecrews rescue requirements, considering escape capsules earth-based and orbit-based rescue systems and flight hazards 17 p2620 A72-34438

Brief survey of the problems of space radiobiology and radiation safety in space flights. 17 p2509 A72-35376

International Space Rescue Symposium, 2nd, Mar del Plata, Argentina, October 9, 1969, Proceedings. 17 p2622 A72-35549

Iridium and tantalum foils for spaceflight neutron dosimetry. 17 p2558 A72-35901

Space technological advance effects on human extraterrestrial, scientific, economic and sociological progresses 19 p2867 A72-38545

Bosch CO2 reduction unit research and development. [ASME PAPER 72-ENAV-10] 20 p2896 A72-39167

An integrated medical system for long-duration space missions. 21 p3009 A72-41305

Space rescue operations planning requirements for 1980s manned satellite missions, discussing vehicles, equipment and various mission phases 24 p3449 A72-45129

Despinning and detumbling satellites in rescue operations. 24 p3450 A72-45160

Human organism and space flight stress endurance limits and manned space mission rescue capabilities requirements, considering cabin decompression, anoxia, radiation, onboard illness, etc 24 p3376 A72-45218

Comparative merits of manned and unmanned (automated) space exploration, considering lunar observatories, earth orbiting space stations and interplanetary missions 24 p3441 A72-45220

MANNED SPACE FLIGHT NETWORK

Apollo centralized ground support and communication system, describing network support team, mission control center, instrumentation support team and manned space flight network 13 p1940 A72-29860

MANNED SPACECRAFT

NT APOLLO SPACECRAFT

NT LUNAR MODULE

NT MANNED ORBITAL LABORATORIES

NT MANNED ORBITAL RESEARCH LABORATORIES

NT MERCURY SPACECRAFT

NT ORBITAL SPACE STATIONS

NT ORBITAL WORKSHOPS

NT SALYUT SPACE STATION

NT SOYUZ SPACECRAFT

NT SPACE SHUTTLES

NT SPACE STATIONS

NT VOSKHO MANNED SPACECRAFT

NT VOSTOK SPACECRAFT

Nighttime airglow layer effect application to autonomous navigation and orientation of piloted space vehicles 02 p0256 A72-12289

Optimum manned spacecraft electrical power distribution voltage and frequency selection, discussing corona, radiation and safety 03 p0313 A72-14187

UV sensitive fire detector in manned space vehicle, discussing simulation in aircraft flying zero gravity parabolas 06 p0814 A72-17584

International standardization of manned spacecraft components for rescue efforts and joint multinational space missions 09 p1395 A72-23154

Emergency reentry manned spacecraft remedial concepts, mission constraints and system designs in terms of cost effectiveness 09 p1396 A72-23159

Nighttime airglow layer effect application to autonomous navigation and orientation of piloted space vehicles 10 p1508 A72-23758

Fault tolerant redundancy for manned spacecraft computers considered as long term desirable solution from cost analysis 10 p1443 A72-23819

Human operator role in space systems reliability, suggesting approaches to system design and program planning to exploit human potential [AIAA PAPER 72-228] 10 p1430 A72-24439

Environmental control and life support subsystem conceptual design studies for shuttle launched 6-12 man crew modular space station [ASME PAPER 72-ENAV-22] 20 p2895 A72-39155

Bosch carbon dioxide reduction process for manned spacecraft oxygen recovery, analyzing carbon and water forming reactions with iron as catalyst [ASME PAPER 72-ENAV-9] 20 p2896 A72-39168

Integration of an automated onboard data management system with a manned spacecraft environmental thermal control and life support system. [ASME PAPER 72-ENAV-6] 20 p2896 A72-39171

Manned and unmanned space-based astronomical observatory systems pros and cons, discussing experiment management complexity and cost reduction 24 p3447 A72-45546

MANOMETERS

Pressure measuring method with piston manometers for absolute vacuum gage calibration 04 p0507 A72-14440

Combination flow-pressure measuring instrument based on rotating Flösdorf manometer with switching relay system 04 p0525 A72-15665

Thin walled Bourdon tube manometric spring deformation analysis by Ritz method in second approximation 09 p1397 A72-22349

Transit tube manometric system with fast particle beam ionization of residual gas molecules for vacuum measurements 09 p1364 A72-23226

Ultramicromanometer based on photomultiplier for low pressure Penning discharge light flux emission measurement 10 p1480 A72-24208

Vacuum gage calibration standardization by piston manometer method of pressure determination from direct force-area measurement 12 p1805 A72-27037

Mesosphere and lower thermosphere temperature measurement by rocket-borne manometer, relating temperature variations to corpuscular flux intensity and sun generated geomagnetic excitations 15 p2225 A72-31910

Pressure measuring instruments design, considering fluid, piston, spring, electrical and ultrasonic manometers 16 p2391 A72-33240

Kinetic theory of a modified Knudsen's absolute manometer. 22 p3175 A72-41941

MANPOWER

Space shuttle thermal protection refurbishment labor costs and techniques, noting motion studies results for maintenance tasks in terms of manpower and performance time [AIAA PAPER 72-374] 11 p1726 A72-25398

Aircraft maintenance operations and personnel requirements planning for optimal economic effectiveness, formulating relations between work productivity, downtime and aircraft utilization 14 p2174 A72-30822

MANTLE [EARTH STRUCTURE]

U EARTH MANTLE

MANUAL CONTROL

NT CONTROL STICKS

NT VISUAL CONTROL

Manual orbital control used on Soyuz spacecraft in orbital flight, investigating equations of motion and pilot work load 05 p0725 A72-16438

Dynamic manned vehicle cockpit simulator for visual and aural effects and acceleration changes, discussing STOL and VTOL characteristics 06 p0796 A72-18246

Design and operation of hand control of automatic camera for astrogodesy used for measuring artificial earth satellites orbits 08 p1165 A72-21021

Optimal solutions for apportionment between automatic and manual flight control, considering number and types of displays required 09 p1348 A72-22783

Unpowered shuttle orbiter piloted control during approach and landing, discussing energy management technique based on fixed base six degree of freedom simulation [AIAA PAPER 72-227] 10 p1551 A72-24438

Data display techniques in man operated automatic control system, assessing information volume versatility and operability 11 p1585 A72-26451

Pilot-aircraft system model for relationship between weapons delivery accuracy and manual flight control system design, noting display, computation and control aids to pilot 12 p1773 A72-28121

Target acquisition by systems with unlagged acceleration control or rate control with exponential time lag, discussing number of approach and control stick movements 13 p1911 A72-29819

Tracker recovery strategy during temporary target obscuration in pursuit tracking task, analyzing control stick movements 13 p1911 A72-29820

Historical development of right and left hand patterns in horsemanship, land vehicle, ship and aircraft control and navigation 18 p2707 A72-37050

An optimal model-following flight control system for manual control. 19 p2753 A72-38228

Relationships among isometric forces measured in aircraft control locations. 19 p2761 A72-38706

Displays and controls; Proceedings of the Advanced Study Institute, Berchtesgaden, West Germany, March 15-26, 1971. 21 p3009 A72-41402

Display device layout based on human operator manual control information requirements consideration, discussing functional categories, motion compatibility, indicators relation and integration 21 p3009 A72-41404

Human consciousness and choice role in biological control process automation to define differences between manual and automatic control systems 21 p3009 A72-41405

Prediction role in execution of manual control with display device to aid human operator adaptation 21 p3010 A72-41406

Man machine system input via human controller output transformation, illustrating with spacecraft lateral position manual control problem 21 p3010 A72-41411

A model for analysing the coordination of manual movements. 21 p3010 A72-41413

Manual workload determination by control characteristics, control-display relationships, demands for dexterity and sensitivity and speed and accuracy requirements 21 p3010 A72-41414

Man machine system functions and display and control role descriptions by flow diagrams, giving examples of keying and task in guided weapon system 21 p3011 A72-41415

Human or computer control role in teleoperator remote control mechanisms, discussing control modes, sensing and transmission time delay problems 21 p3011 A72-41416

Computerized supervisory control for interpretation of subgoal statements from human operator to permit teleoperator interaction with environment without long time delay 21 p3011 A72-41417

Lectures on theory of manual-vehicle control. 21 p3011 A72-41418

Some contributions to the theory of linear models describing the control behaviour of the human operation. 21 p3011 A72-41419

A method for the development and optimization of controller-models for man-machine systems. 21 p3011 A72-41420

Manual tracking control with continuously variable selective control gain in response to system state, noting intuitive optimization 21 p3011 A72-41425

Influence of stick efficiency on tracking error applying two slightly different control elements 21 p3012 A72-41429

Results of the investigation of different extrapolation displays. 21 p3012 A72-41431

Development and optimization of a nonlinear multiparameter human operator model. 22 p3149 A72-41949

Human operator dynamics for aural compensatory tracking. 22 p3149 A72-41950

German monograph - Control performance as a function of the transmission ratio and the Coulomb friction in the operational element. 22 p3152 A72-43052

An investigation of parameters and factors governing manual control of STOL aircraft in landing approach. [AIAA PAPER 72-987] 24 p3369 A72-45415

MANUALS

DC-10 nondestructive testing manual, detailing section/subject format, methods, planned area accessibility and aircraft maintenance 01 p0078 A72-11109

MANUFACTURING

NT LOW GRAVITY MANUFACTURING

NT SPACE MANUFACTURING

Aircraft design productivity to reduce production cost and enhance product profitability, using joint engineering and manufacturing team [SAE PAPER 710748] 01 p0074 A72-10247

Inconel 718 surface integrity from various manufacturing processes, tabulating data on surface finish effects on fatigue, microhardness and metallurgical properties [SME PAPER IQ 71-239] 01 p0076 A72-10967

Porous stainless steels as filter medium, describing manufacturing techniques, properties and applications 02 p0233 A72-11449

Industrial and biological processing possibilities under weightless condition, considering crystal growth, metal processing, vaccine production and electrophoresis in space manufacturing 02 p0278 A72-11961

Lunar mineral resources from analyses of moon samples, discussing solar cell and vacuum process manufacturing 05 p0722 A72-17099

Space shuttle payloads and space manufacturing candidate materials and methods, discussing float-zone refined semiconductors, electronic crystals, viral insecticides, vaccines and biological cells 06 p0824 A72-18622

Semifinished product production technology influence on heat resistant alloys mechanical properties, considering forging, rolling, casting, melting, diffusion welding and powder metallurgy 06 p0834 A72-18647

Automated detonator production facility features, describing modernization program 08 p1221 A72-20780

Book on digital and analog monolithic IC systems, covering manufacturing methods, component design, MOS logic, arithmetic, error correction, codes, applications, etc 09 p1286 A72-23044

Manufacturing process for dispersion strengthened nickel-chromium-thorium dioxide alloys for space shuttle thermal protection system panels, discussing joining optimization and mechanical properties 11 p1659 A72-26035

Production manufacturing processes improvements for composite materials 11 p1674 A72-26232

Inertia welded bimetallic fasteners for aerospace industrial applications, noting cost advantages [ASM PAPER W 72-32,5] 12 p1817 A72-28166

- Algorithm for optimal strategy in statistical plant control for machine parts production and assembly, discussing measuring equipment errors effects
13 p1965 A72-29168
- Semiconductor devices quality assurance based on electrical and mechanical performance tests at every stage of product manufacture from initial design
14 p2091 A72-31164
- Thin film resistor manufacture and evaluation for stability and long-life characteristics
14 p2091 A72-31171
- Manufacturing process for glass fiber chopped strand mats, discussing physical and electrical properties and applications to filament winding
16 p2414 A72-33303
- Resin selection for manufacture of chemically resistant glass fiber reinforced polyesters, considering structural factors of chain for susceptibility to alkaline hydrolysis
16 p2414 A72-33304
- Process computer system design, discussing structural units, data flow coordination with storage, input/output channels and periphery coupling problems
17 p2523 A72-35443
- The manufacture of multilayer reusable surface insulation materials for space shuttle.
[SME PAPER EM 72-714]
18 p2695 A72-36527
- INTERNEPCON '71; Proceedings of the International Electronic Packaging and Production Conference, Brighton, Sussex, England, October 19-21, 1971.
20 p2908 A72-39490
- Design and manufacturing considerations in hermetic microcircuit enclosures.
20 p2908 A72-39495
- A comparison of manufacturing techniques for hybrid microwave circuits.
20 p2908 A72-39496
- Industrial work study methods application to aerospace manufacturing for establishment of efficient work methods, facilities utilization and productivity controls
21 p3132 A72-41643
- Book - Industrial robots - A survey: Details of construction, performance, prices, and applications /Enlarged edition/
22 p3183 A72-43099
- ### MANY BODY PROBLEM
- Solution of N planets equations of motion around sun with recurrent power series in time
01 p0123 A72-10014
- Topological structure of anharmonically coupled many body problem, describing generalized Bose operators formulation
02 p0262 A72-12049
- Numerical instability of gravitational n-body problem considering differences between computed systems and exact solutions to differential equations
04 p0581 A72-15629
- Partial iterative refinements of parameters by reduced Newton-Raphson process based on generalized inverse, noting method use in gravitational n-body integration
04 p0581 A72-15630
- Differential equations systems formulation and numerical integration in gravitational problem of stellar n-bodies, discussing close approaches
05 p0713 A72-16052
- Book on orbital mechanics covering perturbation theory, many body problem, conic sections, orbit determination, canonical transformations and Hansen methods, moving coordinates, etc
06 p0879 A72-17820
- N-body problem equations of motion numerical integration methods supplemented by two body perturbation description and coordinate and time transformations
06 p0885 A72-18072
- Numerical integration of N-body problem integrodifferential equations, using integrals as constraints and for correction application in least squares procedure
06 p0885 A72-18074
- Statistical mechanics of N-body self gravitating system one dimensional model, using canonical and microcanonical ensembles
06 p0885 A72-18075
- Numerical experiments in collisionless stellar systems evolution by gravitational n-body calculations using computers
06 p0885 A72-18076
- N-body gravitational problem direct integration techniques, discussing fourth order polynomial method, computer algorithm and regularization procedure for two body encounters and close binaries
06 p0885 A72-18078
- N-body gravitational problem numerical integration treatment of close approaches, using transformations for eliminating differential equations of motion singularities
06 p0885 A72-18079
- Two point boundary value solution for N-body trajectories, comparing asymptotic with numerical integration solutions for several lunar and interplanetary trajectories
07 p1068 A72-18945
- Soviet book on celestial mechanics and astrodynamics covering classical and contemporary theory, many body problem, satellite perturbation, optimal and boundary value problems, etc
07 p1078 A72-19952
- Nonflat central configuration N point masses existence for any integer greater than four, disproving Wintner conjecture of finite number of integers
08 p1236 A72-21639
- Celestial mechanics considerations for many body problem with finite and infinite macroobjects motions correlation and conservation principles elucidation
08 p1236 A72-21641
- Generalized many body problem of interacting finite material points motion in isolated stellar systems
08 p1237 A72-21642
- Gravitational n body problem - IAU Conference, Cambridge, England, August 1970
12 p1872 A72-27890
- Numerical integration for many body systems equations of motion, noting Monte Carlo and Boltzmann moment methods for large systems
12 p1873 A72-27895
- Massless test star velocity vector deflection in stellar field from numerical integration on relaxation times
12 p1873 A72-27901
- Gravitational many body problem differential equation system formulation and numerical integration
12 p1874 A72-27902
- Integrals utilization in numerical integration of n body gravitational systems, discussing accuracy and reduced computation time
12 p1874 A72-27903
- Statistical mechanics of one dimensional model for many body self gravitating system with canonical and microcanonical ensembles, noting isothermal solution of Vlasov equation
12 p1846 A72-27907
- Numerical experimentation in collisionless systems for Jeans instability, static self consistent models and spiral patterns
12 p1874 A72-27908
- Relaxation processes enhancement by collective particle collisions effects in plasma, stressing application to stellar dynamics
12 p1853 A72-27915
- Fourth order polynomial method and computational algorithm for direct integration of n body systems, discussing two body encounters and binary systems
12 p1875 A72-27917
- Close approaches in numerical integration of gravitational many body problem, discussing smoothing and regularization
12 p1875 A72-27918
- Infinitesimal mass revolution around smallest primary of restricted four body problem, discussing element perturbation
14 p2161 A72-30913
- The collision singularity in a perturbed n-body problem.
17 p2609 A72-35107
- Use of multiple basis sets in the Brueckner-Goldstone many-body perturbation theory for atomic problems.
17 p2586 A72-35772
- Brueckner-Goldstone many-body perturbation calculation of helium photoionization.
17 p2586 A72-35773
- The one-dimensional N-body problem and rectilinear gas motion
17 p2584 A72-35909
- Many-body forces and the effect of the matter distribution in the universe to the gravitational constant.
18 p2728 A72-36800
- Problem of n bodies with a variable gravitational constant, and some dynamic characteristics of large-scale cosmic systems
19 p2863 A72-38077
- A form of the translational dynamical equations for relative motion in systems of many non-rigid bodies.
22 p3205 A72-42113
- The concept of reference loci applied to four-body dynamics.
24 p3440 A72-45137
- About the first integrals of the generalized problem of translatory-rotary motion of rigid bodies.
24 p3442 A72-45235
- Critical inclinations and eccentricities concepts for N planet problem, applying results to general three body problem
24 p3442 A72-45239
- ### MANY PARTICLE THEORY
- ### U MANY BODY PROBLEM
- ### MAPPING
- ### NT ICE MAPPING
- ### NT ORTHOPHOTOGRAHY
- ### NT SOIL MAPPING
- ERTS satellite return beam vidicon TV system and multispectral scanner images, describing photogrammetric and cartographic evaluations
01 p0065 A72-10449
- EROS program thematic mapping system for binary graphic overlays of open water, snow and ice, reflective IR vegetation and human works
01 p0066 A72-10460
- Grasslands mapping for ecosystem analysis, determining spectroradiance/reflectance characteristics by aerial and satellite-borne multispectral scanner imagery, aerial and ground photography and spectrometry
02 p0208 A72-11783
- Remote sensing for land use soil limitations recognition and mapping, using color encoded density slicing analysis
02 p0209 A72-11793
- Environments susceptibility to low resolution imaging for land-use mapping, relating landscapes spatial frequency distributions to expected ERTS resolutions
02 p0210 A72-11796
- Terrestrial radiation emission mapping from imagery produced by scanning radiometer, discussing remote sensors used to study surface energy phenomena
02 p0210 A72-11804
- ERTS return beam vidicon system geometric calibration for high resolution photomaps maps cartographic referencing and register, discussing optical and electronic distortion sources
02 p0225 A72-11818
- Narrow beam millimeter wave radiometer with real-time TV display for terrain mapping, analyzing contours blurring caused by antenna pattern and output integration
02 p0191 A72-11821
- Land pattern mapping from monom imagery analysis, using coordinate digitizer system with planimetric computer input
02 p0187 A72-11874
- Automatic geologic mapping with calibrated narrow band visible and near IR rock reflectivity data and computer processing
02 p0215 A72-11878
- Automated photometric wetland mapping using aerial color film microdensitometric analysis and computer techniques
02 p0215 A72-11886
- Hyperaltitude photography evaluation for geological mapping, comparing Gemini 4 and aerial photographs
02 p0216 A72-11891
- Satellite photography application to morphological cartography of Baja California
02 p0216 A72-11892
- Earth compartmentalization by meridians and parallels, discussing structuralization and latitude-longitude disymmetry
03 p0350 A72-13800
- Urban area aerial photography survey for large scale photomaps, discussing building feature examination and universal stereophotogrammetric instruments utilization
03 p0362 A72-14311
- Planicart stereoplotter for map compilation and revision in photogrammetry
06 p0815 A72-17756
- Satellite-borne multispectral photographic line-scan system with direct optoelectrical signal conversion for photogrammetric and cartographic applications
06 p0815 A72-17757
- Multiple projection assembly for topographic maps preparation by satellite photographs optical projection onto model surfaces, exemplifying by reverse lunar hemisphere
08 p1165 A72-21155
- U.S. Navy cartography, describing RA-3B Skywarrior capabilities and photographic instrumentation
08 p1169 A72-21699
- Sea surface roughness mapping by airborne microwave radiometry with correction for viewing angle and atmospheric effects
09 p1297 A72-22525
- Topographical stereo map plotting apparatus with auxiliary device for orthophoto production, describing design for combined photointerpretation-cartographic applications
09 p1313 A72-23309
- Automatic cloud cover mapping from satellite photographs, describing three step procedure of texture edge detection and cleaning, region coloring and map cleaning
10 p1478 A72-23782
- Linear processes coupling and cylindrical probability imaging through nonlinear mappings, noting relationship to Ito theory of stochastic integrals
10 p1505 A72-24072
- Geomagnetic Sq current electric field mapping into lower atmosphere, calculating equipotential surfaces
11 p1626 A72-26416
- Martian Sinus Meridiani and South Polar maps from mosaics of Mariner 6 and 7 wide angle photographs
12 p1871 A72-27664
- Apollo mapping camera system synchronized laser altimetry utilization in astro-photogrammetric triangulation
12 p1872 A72-27816

Nonsymmetrical stellar motion in galaxies, finding number of isolating integrals in systems with three degrees of freedom from four dimensional mapping 12 p1874 A72-27911

Photomaps plotting from high altitude photographs, presenting expressions for segment areas selection 13 p1954 A72-28496

Computerized reconstruction of orthogonal representations from cylindrical and conical mapped projections with known parameters and base 13 p1956 A72-28738

Large scale mapping by photogrammetric method based on contour points of outdated small scale aerial survey photographs, noting root-mean-square errors 13 p1959 A72-29633

Broad scale remote mapping of spectral composition of silicate rocks from thermal IR scanner data 14 p2099 A72-30321

Distortion corrections in geophysically traced gravitational, magnetic and geoelectric field maps, discussing automation 14 p2101 A72-30642

Cartographic and environmental surveys by Skylab orbiting stations and ERTS satellite using panoramic and mapping cameras and laser altimeter 15 p2232 A72-31247

Nonlinear electronic /transistor/ system mapping-on by matrix dynamic transform algorithms, comparing with Newton-Raphson method 15 p2210 A72-31491

Three dimensional transformation for continental scale geodetic grids photogrammetry by satellite method, noting scale alteration and Euler angles determination 16 p2387 A72-33799

Holographic photogrammetry and cartography 17 p2555 A72-35184

Transformation of points from sidelooking radar images into the map system. 17 p2555 A72-35336

Means of obtaining versions of orthogonal cartographic projections 17 p2548 A72-35361

The new Mariner 9 map of Mars. 18 p2729 A72-36988

Holography application in photogrammetric contour mapping, discussing topographic data acquisition, storage, retrieval and display problems 19 p2797 A72-37609

Method for transforming three-dimensional images on maps, plans, and other documents with the aid of an electronic computer 19 p2802 A72-38082

Multiple projection assembly for topographic maps preparation by satellite photographs optical projection onto model surfaces, exemplifying by reverse lunar hemisphere 20 p2924 A72-39260

Synthesis of threshold-logic networks using Karnaugh-mapping techniques. 21 p3037 A72-40636

Mars photographic mapping and UV/IR spectrometric investigation by Mariner 9, discussing Martian surface features and atmospheric composition 21 p3105 A72-40967

A new approach to automatic scanning of contour maps. 22 p3174 A72-43024

Analytic continuation of functions over infinite dimensional domains, covering Banach manifolds, hypoaanalytical mappings, convexity and topology 24 p3418 A72-44827

A thermal mapping technique for shock tunnels and a practical data reduction procedure. [AIAA PAPER 72-1031] 24 p3389 A72-45408

MAPS

NT ASTRONOMICAL MAPS

NT LUNAR MAPS

NT METEOROLOGICAL CHARTS

NT RADAR CLUTTER MAPS

NT RADAR MAPS

NT RELIEF MAPS

Image scale selection for topographic map revision in orthophotograph production considering economics and suitability 09 p1311 A72-22968

A square equal-area map of the world. 20 p2915 A72-38961

MARAGING

Maraging Fe-Ni-Co-Mo alloy ordered metastable omega phase formation during martensite aging from electron microscopic investigation, noting Co addition effects and precipitation 14 p2115 A72-30404

MARAGING STEELS

Constant high tensile stress and rapid aerodynamic heating effect on maraging steels and Ti and Al alloys, evaluating test and simulation procedures for design data development 01 p0084 A72-10749

Maraging and Ni steels stress corrosion cracking rates dependence on stress intensity factor, discussing measurements in salt and distilled water 01 p0086 A72-10995

Ni maraging steel microstructure effects on strength and fracture toughness 01 p0087 A72-11024

Press and sinter production of Ni maraging steel powder metallurgy parts 02 p0234 A72-11464

Quenched and tempered high strength and maraging steels delayed failure properties from notched-tensile sustained-load tests in distilled water 02 p0246 A72-12560

Maraging steel laminates stress corrosion cracking behavior, showing composite base plate and weld structure influence on crack propagation reduction 04 p0534 A72-15569

Stress corrosion crack growth in air melted and vacuum arc remelted nickel maraging steel, using stress wave analysis technique 05 p0674 A72-16327

Fatigue and fatigue-corrosion properties of high strength stainless maraging martensitic structural and stainless austenitic steels 05 p0680 A72-17206

Economical methods for cast maraging steel production, describing composition, heat treatment and mechanical properties 07 p1010 A72-18970

Maraging steel embrittlement by titanium carbonitrides lattices separation during cooling, suggesting rapid quenching and plastic deformation temperature reduction 07 p1012 A72-19677

Heat treatment effects on strength differential of high strength martensitic stainless and Ni maraging steels 07 p1015 A72-19926

Austenite stabilization in maraging steel by cumulative heat cycling, using dilatometric and X ray analysis techniques 07 p0998 A72-20483

Stable austenite formation during maraging steel aging at 300-750 C determined by X ray diffraction 07 p1022 A72-20525

German monograph on fracture formation and behavior in Ni maraging steel under repeated stress alternations, considering Al and Ti effects on steel strength 08 p1190 A72-22172

Fe-Ni alloys atom redistribution during aging before phase precipitation, discussing Mo and Co clusters in martensitic maraging steels 08 p1190 A72-22189

Welded high strength maraging steels fatigue performance, stressing nondestructive testing technique 09 p1332 A72-23617

Prototype fine wire feed unit and microplasma welding torch and equipment for butt welding of Ni maraging steel, testing welds mechanically 09 p1321 A72-23636

Fatigue and fatigue-corrosion properties of high strength stainless maraging, martensitic structural and stainless austenitic steels 11 p1660 A72-26141

Filler wires development for inert gas welding of stainless maraging steel 11 p1660 A72-26488

Coherent precipitate structure in Fe-Ni-Co-Mo maraging alloys, using electron microscopy 11 p1668 A72-26940

Electroslag and vacuum remelted maraging steel rolling contact, investigating fatigue life as function of lubricant film thickness/surface roughness ratio 12 p1816 A72-28109

Austenite grain growth characteristics of heat treated Ni maraging steel 13 p1976 A72-28673

Ni-Cr-Mo stainless maraging steel, investigating yield strength, toughness, corrosion resistance and weldability 14 p2113 A72-30270

Heat treatment and grain size effects on stress corrosion resistance and life duration of maraging steels, investigating crack initiation and propagation 14 p2117 A72-30539

Heat treatment hardening effect on stress corrosion resistance of ultrapure maraging and stainless steels, emphasizing hydrogen embrittlement 14 p2117 A72-30540

Plane strain fracture toughness tests of compact thick maraging steel specimens at various yield strength levels as function of aging 16 p2406 A72-33317

Fractographic lines in maraging steel - A link to fracture toughness. 18 p2700 A72-36584

Optimal composition equation with austenite retention index for high strength maraging stainless steel development for improved toughness 18 p2702 A72-36796

German monograph - Effect of molybdenum and degree of age hardening on the corrosion properties of maraging chromium steels 19 p2816 A72-37654

Tensile and compressive flow strength and work hardening behavior in maraging steels, attributing

strength differential to nonlinear elastic interactions between interstitials and dislocations 20 p2939 A72-39306

Load tests in air to evaluate maraging steels weldments for rocket motor case applications 20 p2942 A72-39955

Fracture toughness of the heat-affected zone in 14CrMoV69 steel and 18Ni maraging steel. 21 p3067 A72-40850

Strain hardening of maraging steels in liquid nitrogen 22 p3187 A72-41867

Contribution to the study of the creep behavior of 18 per cent-nickel maraging steel 24 p3415 A72-45600

MARIA

NT LUNAR MARIA

MARINE NAVIGATION

U SURFACE NAVIGATION

MARINE PROPULSION

NT UNDERWATER PROPULSION

Nuclear energy value to society, stressing usefulness for electric power generation and marine propulsion 03 p0387 A72-14376

Nuclear energy for power and transportation, discussing ship, submarine, air cushion vehicle, aircraft and rocket propulsion applications 05 p0688 A72-15777

MARINE TECHNOLOGY

Marine and aerospace engineering - Conference, Paris, May 1971 04 p0463 A72-15551

Self contained portable data acquisition system for marine, environmental and ecology research, using multiple analog recording and digital telemetry transmitter 06 p0797 A72-18613

Development and testing of a precise marine electrostatic gyroscope. 24 p3401 A72-44638

Weather satellites - Their role in the application of environmental services to the marine industries. 24 p3420 A72-44648

MARINER PROGRAM

Mariner 1969 Mars mission, emphasizing planetary encounter, surface and atmospheric data and search for extraterrestrial life 01 p0130 A72-10930

Satellite-star optical navigation data from Mariner program, describing objectives and performance of preflight and real time activities leading to successful performance 15 p2271 A72-32196

Mariner and Mars space probe data on Mars surface and atmosphere, suggesting possibility of tectonic activity 16 p2461 A72-34181

Coordinates of features on the Mariner 6 and 7 pictures of Mars. 24 p3436 A72-44695

Mariner spacecraft Jupiter-Saturn 1977 gravity assisted flyby, discussing mission objectives and trajectory options [AIAA PAPER 72-943] 24 p3444 A72-45438

Mariner Mars 1971 adaptive mission planning for scientific objectives flexibility based on planetary features observed, discussing plan change implementation [AIAA PAPER 72-944] 24 p3444 A72-45439

MARINER SPACE PROBES

Mars and Venus explorations, discussing Mariner probes, Mars craters, volcanism, polar areas, surface temperature and atmosphere and Venus radar astronomy and atmospheric model 03 p0440 A72-14305

Programming systems for onboard unmanned deep space probe computers, describing Mariner and outer planet Grand Tour Programs 07 p0949 A72-19295

Mariner Mars 1969 IR spectrometer for Mars atmosphere and surface spectra recording, describing design specifications and optimization for low light level sensitivity 09 p1313 A72-23326

Aeolian transport and surface roughness of Mars Hellas basin, using Mariner 1969 photographs 10 p1536 A72-24151

Mars observation by Mariner 9, discussing TV pictures of surface, UV and IR spectroscopy of atmosphere, S band experiment and Phobos and Deimos studies 10 p1538 A72-24309

Mars surface lineament systems from Mariner photographs, noting global and radial type associated with Hellas and South Pole basins 12 p1868 A72-27259

Mars craters degradation and density regional variations from Mariner 6 and 7 imagery, using numerical scoring method 14 p2149 A72-30318

Mars nonpolar region photometric and topographic characteristics from Mariner 6 and 7 UV spectrometer observations 15 p2311 A72-32084

Bistatic radar measurements of the surface of Mars with Mariner 1969. 21 p3110 A72-41453

The composition of the Martian atmosphere - Minor constituents. 21 p3110 A72-41458

MARINER SPACECRAFT

Mariner 9 experiments, discussing IR interferometric spectroscopy observations of Mars dust composition and pole flattening 06 p0889 A72-18340

Mariner 9 television reconnaissance of Mars surface and satellites, observing south polar cap and dark spots with crater features 06 p0889 A72-18341

Mariner 9 IR spectroscopy observations of Mars surface, indicating dust with silicon oxide content and atmospheric warming and water vapor over south polar cap 06 p0890 A72-18342

Brightness temperatures over Mars south polar cap from Mariner 9 IR radiometry, comparing to Mariner 6 and 7 06 p0890 A72-18343

Mariner 9 UV spectrometry observations of Mars airglow spectrum containing CO Cameron band and atomic oxygen and hydrogen lines 06 p0890 A72-18344

Mariner 9 radio occultation measurements of Mars day side atmosphere, indicating isothermal temperature, surface pressures and ionosphere properties 06 p0890 A72-18345

Mariner 9 radio tracking measurements of Mars gravity field and pole direction, comparing to moon and earth 06 p0890 A72-18346

Spacecraft planetary approach navigation with TV camera onboard Mariner 9 giving images of Mars natural satellites against star background, discussing optical data processing programs [AIAA PAPER 72-53] 07 p1032 A72-18946

Digital data transition tracking loop as practical implementation of optimum self bit synchronizer in Mariner spacecraft telemetry demodulators 10 p1437 A72-24687

Mars astrophysical observation from Mars 3, describing instruments and measurement results 15 p2308 A72-31901

Apparent difference in Martian night and day side surfaces atmospheric pressure based on Mariner spacecraft occultations, noting effects of topography and electron layer 15 p2310 A72-31973

Mariner spacecraft 1973 for flyby Venus and encounter Mercury, discussing launch and arrival conditions and aiming zones selection to maximize science return [AIAA PAPER 72-942] 21 p3113 A72-41578

Application of advanced filtering methods to the determination of the interplanetary orbit of Mariner 71. [AIAA PAPER 72-906] 24 p3443 A72-45427

Spacecraft navigation systems for Mariner Jupiter-Saturn 1977 Project, considering maneuvers, orbit determination and data requirements [AIAA PAPER 72-926] 24 p3423 A72-45432

MARINER VENUS-MERCURY 1973

Mariner Venus/Mercury 1973 flyby mission imaging experiment, discussing mission constraints, objectives and use of real time transmission vidicon camera and high resolution UV photography 04 p0568 A72-14494

Mariner spacecraft 1973 for flyby Venus and encounter Mercury, discussing launch and arrival conditions and aiming zones selection to maximize science return [AIAA PAPER 72-942] 21 p3113 A72-41578

MARINER 4 SPACE PROBE

Mariner 4 trajectory relation to proposed location of bow wave caused by solar wind interaction with Mars ionosphere, noting planet orbit aberration effects 09 p1385 A72-22581

MARINER 5 SPACE PROBE

Venus upper clouds composition from Mariner 5 occultation data analysis concerning temperature and pressure profiles, abundances, polarization characteristics, reflection and emission spectra 08 p1236 A72-21496

MARINER 6 SPACE PROBE

Nonthermal escape and predissociation mechanism for Mars low nitrogen concentration reflected in Mariner 6 and 7 UV spectrometric results 02 p0280 A72-12208

Mars surface topographic characteristics relationship to earth features, using Mariner 6 and 7 photographs 04 p0569 A72-14501

MARINER 7 SPACE PROBE

Nonthermal escape and predissociation mechanism for Mars low nitrogen concentration reflected in Mariner 6 and 7 UV spectrometric results 02 p0280 A72-12208

Mars surface topographic characteristics relationship to earth features, using Mariner 6 and 7 photographs 04 p0569 A72-14501

Mars south polar cap surface roughness and photometric function from Mariner 7 UV spectrometric experiment 10 p1531 A72-23708

The location of the Mountains of Mitchel and evidence for their nature in Mariner 7 pictures. 21 p3110 A72-41456

Mariner 7 ultraviolet spectrometer experiment - Topographic slopes of Mars' polar region. 21 p3110 A72-41457

MARINER 9 SPACE PROBE

Mariner 9 TV experiment image data display, processing and production for real time analysis, noting computer algorithms 15 p2236 A72-31982

Preflight and real time gravity sensing for Mariner 9 satellite orbit determination during Mars 1971 mission 15 p2270 A72-32186

Mars and its satellites as viewed by Mariner 9 17 p2607 A72-34752

A detailed analysis of Mariner nine TV navigation data. [AIAA PAPER 72-866] 20 p2977 A72-40061

Mars photographic mapping and UV/IR spectrometric investigation by Mariner 9, discussing Martian surface features and atmospheric composition 21 p3105 A72-40967

Mariner 9 spacecraft systems and photographs of Martian surface details 24 p3441 A72-45170

Maneuver design and implementation for the Mariner 9 mission. [AIAA PAPER 72-913] 24 p3443 A72-45429

Mariner 9 Mars orbital trajectory analysis from earth based radio data, considering gravity field, n-body perturbation and solar radiation pressure effects [AIAA PAPER 72-928] 24 p3443 A72-45434

MARKERS

Single Integrated Signal Device to aid in locating downed airmen awaiting rescue in dense jungle terrain by Search and Rescue aircraft 08 p1112 A72-21580

Inflight validation of laboratory scaled-down simulation experiments on optimal hierarchy of colors for markers and signals [AD-737901] 08 p1147 A72-21582

Rescue signaling devices design and operation, discussing pinpoint markers, rocket boosted panel markers, strobe units, antennas and balloon marker 08 p1112 A72-21584

MARKET RESEARCH

Commercial transport market and technology forecasting, considering all-cargo, STOL, SST and CTOI aircraft [SAE PAPER 710750] 01 p0002 A72-10249

Deterministic model for new product innovation adoption rate in commercial aircraft jet engine market 07 p1105 A72-20269

Mathematical models for passenger aircraft market forecast, discussing stock measurement and life expectancies 13 p2067 A72-30125

MARKETING

Air cargo growth potential, marketing and profitability, considering need for improvements in ground handling, rate structure, container standardization, documentation, etc 13 p1896 A72-28452

Helicopters technical and marketing projections for 1980s, emphasizing reliability, maintainability and maneuverability in design philosophy 17 p2491 A72-34926

MARKING

NT ISOTOPIC LABELING

Runway marking requirements for visibility under day and night conditions, considering night reflection value, color stability, durability, noninterference with flight operations, etc 17 p2535 A72-34243

MARKOV CHAINS

Markov chain successive approximation method for electromagnetic wave propagation in medium with random large discontinuities, using scalar parabolic equation 02 p0181 A72-12588

Target trajectory detector optimization, using data and Markovian chain apparatus 03 p0323 A72-13831

Optimal detection of Markov radio signals with intrapulse FM using nonlinear filtration theory 04 p0487 A72-15146

Accumulator type radar detector analysis by Markov chains method, discussing false alarm and detection probabilities 11 p1592 A72-25807

Simultaneous iteration for eigenvalue problem numerical solution by mutually orthogonal trial vectors close to required eigenvectors, applying to flutter analysis and Markov chains 11 p1679 A72-26959

Heuristic recognition algorithms with learning for homogeneous irreducible stationary Markov chain sequence of recognized objects 12 p1837 A72-27824

Limit distributions for sums of random values specified in a denumerable Markov chain with absorption 19 p2827 A72-38470

Convergence rate estimates for the sums of random values determined in a Markov chain with absorption 21 p3075 A72-41094

Uniform estimate of the residual term in a multidimensional limiting theorem for homogeneous Markov chains on the basis of a class of all measurable convex sets. I 23 p3307 A72-43344

MARKOV PROCESSES

NT MARKOV CHAINS

Three body ionic recombination as Markov process, deriving ion pairs quasi-equilibrium distribution equation identical to Bates-Flannery statistical theory 01 p0104 A72-10860

Semi-Markov process sojourn time within reducible subset of states, examining asymptotic behavior with algorithm developed for linear operators disturbances 01 p0094 A72-11265

Redundancy with repair for system mean time to first failure, presenting differential equation coefficients for Markov process 02 p0236 A72-11556

Second order Markov process statistical model for gravity anomalies in local region, applying to error analysis in inertial navigation system computerized simulation 02 p0207 A72-15596

Suboptimal nonlinear filter performance evaluation methods based on Kolmogorov equations for Markov process transition density function 04 p5055 A72-15040

Light transmission in medium with random inhomogeneities in Markov random process approximation, obtaining short wave field statistical characteristics 04 p0488 A72-15380

Markov model random variation optimal periodicity in preventive maintenance operations, estimating distribution density and moments 04 p0527 A72-15574

Run length encoding for removing redundancy from video signals, determining upper bound on compression ratio based on first order Markov model 06 p0773 A72-17488

Random vibrations nonlinear theory, investigating nonlinear systems response to random excitation via Markov processes modeling 06 p0896 A72-17966

Coupled detection-estimation of Gauss-Markov processes in white Gaussian noise, deriving Bayes optimal recursive rules 06 p0775 A72-18388

Nonlinear elastic systems with distributed parameters, obtaining single frequency mode random oscillations solution of boundary value problem by asymptotic method and Markov process 06 p0850 A72-18700

Gyroscopic error analysis, solving nonlinear equations by continuous Markov processes theory 06 p0819 A72-18724

Optimal receiver synthesis for radio signals with differentiable components of continuous Markov processes masked by phase interference and white noise 07 p0937 A72-18847

Signal detection in stationary, Markov and other noise background, discussing functional method of statistical and probabilistic representation 07 p0943 A72-19520

Orbit determination using Kalman-Bucy filter to estimate state and unmodeled acceleration approximated as first order stationary Gauss-Markov process 08 p1145 A72-20867

Random vibration theory and Markov processes in nonlinear stochastic systems with probability and asymptotic methods application 08 p1205 A72-20965

Algorithm for asymptotic behavior approximation of semi-Markov processes with splitting set of states by Markov chain 08 p1198 A72-20997

Markov type isotropic random Gaussian field analysis in n-dimensional Euclidean space 08 p1198 A72-20999

Markov processes in stellar dynamics, discussing relaxation and evaporation times and star velocity distribution for galactic cluster models 09 p1390 A72-23504

Reliability and time to failure prediction for degradation-prone systems via Markov processes theory 10 p1504 A72-23988

Fatou theorem at Martin boundary derived from Dynkin theory on excessive functions and exit space of Markov process 10 p1504 A72-24062

Markovian characteristics of time dependent excursions and independent incursions processes provided with limits to left and continuous to right, noting Poisson punctual process and Borel sets 10 p1505 A72-24114

Markov processes for local diffusions defined by second order differential operator delta with Holder coefficients on manifold 10 p1505 A72-24201

Time to failure determination in complex service systems, examining Markov processes 11 p1609 A72-25435

Reliability analysis of repairable redundant systems with random replenishment of reserves, using discrete time Markov process theory 11 p1600 A72-25440

Servo systems operational reliability analysis for variable intensity of fluctuating interference, discussing Markov process probability determination and Kolmogoroff equations solution 11 p1609 A72-25441

Russian papers on discrete control systems covering inertialess Markov objects, pulse amplitude and frequency modulation and statistical analysis 11 p1609 A72-25442

Recurrent algorithms for inertialess Markov objects identification based on statistical solutions theory 11 p1609 A72-25443

Time shared computer systems output maximization via degenerate exponential distribution function modeling, noting reducibility to Markov processes 11 p1601 A72-25900

Uniform Markov processes properties in Hilbert space, examining operator subgroups 12 p1836 A72-27071

Signal filtration algorithms and parameter estimation in additive non-Gaussian noise background by conditional Markov process theory 12 p1783 A72-27633

Russian papers on adaptive control systems covering automata and game theory, learning models, Markov processes and probability theory 12 p1787 A72-27921

Ergodic theorems for operators generated by Markov transients, examining asymptotic properties of stochastic learning model 12 p1787 A72-27924

Random number method for particle motion in homogeneous turbulence field, using Brownian motion Markov process for turbulence approximation 13 p1940 A72-28421

Van der Pol and nonlinear parametric oscillators fluctuations due to random noises analyzed by averaging method and discrete Markov processes 14 p2133 A72-31134

Alternant theorems for characterization of minimum solutions in multidimensional Chebyshev approximation of functions connected with Markov systems 15 p2261 A72-31497

Book - Elements of applied stochastic processes 17 p2575 A72-34624

Real and definite processes in complete probabilized space, showing Markov process as solution of stochastic differential equation 17 p2576 A72-35420

Reliability analysis of an intermittently used system with N types of failure. 18 p2693 A72-36024

Markovian plasma turbulence model to obtain convergent perturbation series for diffusion coefficient via trajectories in particle propagator 19 p2841 A72-38442

Optimal strategies for control of a semi-Markovian process by a set of observers 19 p2770 A72-38584

Pontryagin equations for Markov process limits probability, solving problem of one dimensional steady random process limits for given initial probability density function 22 p3205 A72-42227

Characteristics of filtering the Rayleigh parameter of pulse signals in the presence of noise 22 p3154 A72-42228

Optimal filtration algorithms of Markov parameters of discrete time signals in digital data transmission system with background noise, using Gaussian probability density approximation 23 p3264 A72-44005

MARS (PLANET)

Mariner 1969 Mars mission, emphasizing planetary encounter, surface and atmospheric data and search for extraterrestrial life 01 p0130 A72-10930

Review of papers on planetology given at Brighton symposium, covering moon, Venus, Mars and Jupiter 01 p0132 A72-11071

Martian internal structure, investigating oxidation rate of chondritic material 02 p0277 A72-11752

Martian radio emission at 8.57 mm during 1971 approach, comparing brightness temperature to Jupiter 02 p0280 A72-12196

Martian equatorial zone brightness distribution formula, noting agreement with observations near zero phase and 6-45 deg phase angles 02 p0282 A72-12328

Minimum velocity change noncoplanar two and three impulse orbital transfer from regressing oblate

earth assembly parking ellipse into flyby trans-Martian asymptotic velocity vector 03 p0434 A72-13634

Statistical processing of phase dependence of Martian integral brightness at 0.3-1.1 microns, noting abrupt reflectivity decrease 03 p0436 A72-13816

Extraterrestrial life on Mars and Venus and Jupiter atmospheres, discussing abiogenesis failures on life-supportable planets 04 p0471 A72-14805

Bright O, C and carbon dioxide emissions in Martian airglow from temperature profile models based on Mariner UV spectrometry 06 p0803 A72-17446

Mariner 9 experiments, discussing IR interferometric spectroscopy observations of Mars dust composition and pole flattening 06 p0889 A72-18340

Mariner 9 radio tracking measurements of Mars gravity field and pole direction, comparing to moon and earth 06 p0890 A72-18346

Mars internal structure models with chondrite as potential core-forming material, discussing absence of internal origin magnetic field 07 p1084 A72-20518

Venus, Mars, Jupiter and Saturn UV spectra from OAO-2 objective grating spectrophotometry, obtaining planetary albedos from G-type stars observations 09 p1382 A72-22288

Venus and Mars visible geocentric declinations from daytime observations with Wanschaff vertical circle compared to nighttime results 09 p1388 A72-23065

Viking Lander seismic investigations for Martian tectonic activity, internal structure and composition, core size and conditions of formation 10 p1540 A72-24389

Secular and periodic variations of orbital elements of Mars satellites due to oblateness and solar attraction 10 p1541 A72-24471

Mars and Venus instrumented spacecraft flight results, describing planetary topographies, atmospheres and magnetic fields 12 p1877 A72-27650

Martian equatorial zone brightness distribution formula, noting agreement with observations near zero phase and 6-45 deg phase angles 13 p2039 A72-29212

Mars and moon cores elastic properties inferred from hydrostatic equilibrium based on observed data for total mass, radius and moment of inertia 13 p2048 A72-29809

Mars upper cover temperature, representing diurnal variations at different areographic latitudes as harmonic series 14 p2148 A72-30207

Extraterrestrial life search, noting radio contact with civilizations, bioastronautics, Martian conditions and physicochemical experiments 14 p2076 A72-30694

Phobos and Deimos orbital characteristics, noting related Martian physical properties determination 15 p2302 A72-31277

Mars observations during 1971 opposition, noting south pole phenomena relation to Martian atmosphere changes 15 p2306 A72-31600

Mars and Venus automatic station data transmission systems for surface and atmosphere studies, discussing relay and direct transmission modes 15 p2203 A72-31823

Mars violet haze and blue clearing for Syrtis Major-Arabia from photographic and photoelectric data 15 p2311 A72-32086

Mars and its satellites as viewed by Mariner 9 17 p2607 A72-34752

Observations of the region of interaction between the solar-wind plasma and Mars 17 p2600 A72-35219

Observed seasonal change of the Martian polar cap. 17 p2615 A72-35679

Earth based Mars photographic observations with direct image transmission via TV system, determining rotation period 17 p2619 A72-35956

Exact positions of Mars as determined by the photographic method at Pulkovo in 1966 and 1967 19 p2859 A72-37914

Computer processed Mars photographic positional measurements with Pulkovo normal astrophotograph in 1965 19 p2861 A72-37985

Photoelectric transit observations of Saturn and Mars, showing culmination in universal ephemerides time 19 p2862 A72-37987

In-situ geochemical analysis of Martian and lunar composition via alpha particle activation technique, discussing Surveyor instrument performance 20 p2899 A72-39828

Mars upper cover temperature, representing diurnal variations at different areographic latitudes as harmonic series 23 p3333 A72-43237

The distribution of craters on the surfaces of the moon and Mars in relation to their origin 24 p3441 A72-45222

Photographic observations of Mars at the Main Astronomical Observatory, AN USSR during 1963-1967 24 p3448 A72-45686

MARS ATMOSPHERE

Radiative heat transfer equilibrium in Earth, Venus and Mars atmospheres, taking into account interaction with ground 01 p0058 A72-10561

Topography and Coriolis effects on Martian atmospheric circulation, incorporating low radiative time constant and large variations in analytical model 01 p0135 A72-11279

Nonthermal escape and predissociation mechanism for Mars low nitrogen concentration reflected in Mariner 6 and 7 UV spectrometric results 02 p0280 A72-12208

Martian atmosphere and surface, covering atmospheric composition, optical thickness and pressure, violet and yellow clouds, surface relief and topography 02 p0282 A72-12326

Mars short wave line spectra from measurement with reflector, estimating nitrogen dioxide content in atmosphere 03 p0436 A72-13815

Annual heat balance in Martian northern polar cap, considering atmospheric, ground and solar heat flux absorbed by snow 03 p0436 A72-13817

Mars and Venus explorations, discussing Mariner probes, Mars craters, volcanism, polar areas, surface temperature and atmosphere and Venus radar astronomy and atmospheric model 03 p0440 A72-14305

Mars atmospheric water vapor observations, examining spectroscopic plates water line strengths at 8200 A 04 p0569 A72-14497

Mars atmosphere diatomic oxygen upper limit abundance, using high dispersion spectroscopic data from 1969 apparition 04 p0569 A72-14498

Mars carbon dioxide distribution map determination of surface topography from spectrophotometric observations of equatorial region 04 p0569 A72-14499

Mars topographic map study of high velocity relief winds, showing seasonal and secular changes 04 p0569 A72-14502

Martian atmospheric volatiles history, noting initial chemical conditions favorable to abiotic organic synthesis 04 p0569 A72-14503

Reduced collision integrals for components of Venus and Mars type carbon dioxide atmospheres at 1000-11,000 K, using intermolecular interaction potentials 05 p0712 A72-15851

Mars Hellas area surface features, relating crater absence to surface age and white spot phenomena to water reservoir under permafrost layer 06 p0881 A72-17929

Martian atmospheric pressure determination from carbon dioxide bands spectroscopic measurements 06 p0884 A72-18032

Martian atmosphere evolution, stressing photochemical production of oxygen, carbon and nitrogen 06 p0889 A72-18275

Mariner 9 IR spectroscopy observations of Mars surface, indicating dust with silicon oxide content and atmospheric warming and water vapor over south polar cap 06 p0890 A72-18342

Mariner 9 UV spectrometry observations of Mars airglow spectrum containing CO Cameron band and atomic oxygen and hydrogen lines 06 p0890 A72-18344

Mariner 9 radio occultation measurements of Mars day side atmosphere, indicating isothermal temperature, surface pressures and ionosphere properties 06 p0890 A72-18345

Martian dust storm depth determination from carbon dioxide absorption and abundance observation on Mars by earth based spectroscopy 06 p0890 A72-18348

Mars, Venus and Jupiter atmosphere composition and structure from spectral analysis, discussing equilibrium temperature, radiative heat transfer, integrated density and adiabatic temperature gradient 07 p1073 A72-19353

Transcript of conference on origins of life covering cosmic evolution, abundance and distribution of biologically important elements, earth and Mars atmosphere evolution, etc 07 p1074 A72-19450

Mars* atmosphere temperature profiles inference from outgoing radiation spectral characteristics, constructing atmospheric model

08 p1232 A72-21147

Martian violet clouds photometric studies, determining monochromatic albedo, optical thickness and Junge parameter

08 p1237 A72-21827

Planetary atmosphere diffuse radiation from limb side, applying to Mars atmospheric emission

08 p1238 A72-21832

Planetary atmospheres composition diversity, discussing evolution of Mars, Venus, earth and Jupiter from primitive solar nebula

08 p1119 A72-22012

Mariner 4 trajectory relation to proposed location of bow wave caused by solar wind interaction with Mars ionosphere, noting planet orbit aberration effects

09 p1385 A72-22581

Carbon dioxide atmospheric models for Mars and Venus, discussing aeronomy, Mariner probes, gas dissociation by solar radiation, and electron density inconsistency

09 p1386 A72-22685

Mariner Mars 1969 IR spectrometer for Mars atmosphere and surface spectra recording, describing design specifications and optimization for low light level sensitivity

09 p1313 A72-23326

Theoretical model of large scale topographical effects on wind generation through temperature advection, applying to Mars atmosphere general circulation

10 p1531 A72-23707

Mars observation by Mariner 9, discussing TV pictures of surface, UV and IR spectroscopy of atmosphere, S band experiment and Phobos and Deimos studies

10 p1538 A72-24309

Martian atmosphere water vapor detection and mapping during Viking missions, discussing experimental approach and spectrometer choice

10 p1539 A72-24378

Mars atmospheric entry experiments for Viking 1975 mission, discussing onboard neutral gas mass spectrometer and retarding potential analyzer

10 p1540 A72-24381

Viking Lander imaging experiments with stereoscopic camera system to study Martian surface and atmospheric morphology, composition and evolution

10 p1540 A72-24382

Viking Lander mass spectroscopic analysis of organic compounds, water and volatile constituents of Martian atmosphere and surface

10 p1540 A72-24383

Viking Lander meteorology experiments to measure Martian atmosphere pressure, temperature, wind speed and direction and water vapor content

10 p1540 A72-24388

Viking Lander magnetic properties investigation of Martian surface with implications for planetary composition and differentiation and atmospheric interaction

10 p1541 A72-24391

Hypersonic base heating investigation on Mars atmosphere entry blunt bodies, taking into account gas composition and angle of attack effects

[AIAA PAPER 72-317]

11 p1568 A72-25251

Martian atmospheric pressure determination from carbon dioxide bands spectroscopic measurements

11 p1719 A72-25968

Carbon dioxide and dust effect on Martian atmospheric temperatures from time dependent calculations

12 p1865 A72-27033

Martian storm of 1971, describing development, decline, structure and photographic data

12 p1870 A72-27425

Mars surface particulate matter eroded by atmospheric winds, noting erosive and settling velocities and yellow clouds distribution

12 p2036 A72-28794

Martian atmosphere and surface, covering atmospheric composition, optical thickness and pressure, violet and yellow clouds, surface relief and topography

13 p2039 A72-29210

Mars atmospheric temperature, pressure and electron density from radio occultation measurement with Mariner 6 and 7, noting frozen carbon dioxide in middle atmosphere

13 p2039 A72-29335

Martian ionosphere electromagnetic wave propagation characteristics for E, F1 and F2 models, calculating refractive index for zero and nonzero collision frequencies

13 p1922 A72-29474

Pontyagin maximum principle for optimal terminal velocity control of automatic space probe descent in Mars atmosphere

14 p2162 A72-30456

Radiative transfer in Mars and above-cloud Venus carbon dioxide atmospheres, studying diurnal variations in temperature profile

14 p2160 A72-30897

Reduced collision integrals for components of Venus and Mars type carbon dioxide atmospheres at 1000-11,000 K, using intermolecular interaction potentials

15 p2302 A72-31270

Model Martian atmosphere, investigating effects of departures from electron density profile spherical symmetry on radio wave phase shift in bistatic radar occultation experiment

15 p2194 A72-31440

Mars observations during 1971 opposition, noting south pole phenomena relation to Martian atmosphere changes

15 p2306 A72-31600

Mars astrophysical observation from Mars 3, describing instruments and measurement results

15 p2308 A72-31901

Apparent difference in Martian night and day side surfaces atmospheric pressure based on Mariner spacecraft occultations, noting effects of topography and electron layer

15 p2310 A72-31973

Mars topography variations from earth based surface height radar ranging and Mariner spectrophotometric observation of Mars atmosphere

15 p2313 A72-32346

Probability for spore sterilization by aerodynamic heating, considering straight line and decaying circular orbital Mars entry trajectories

16 p2461 A72-34165

Mariner and Mars space probe data on Mars surface and atmosphere, suggesting possibility of tectonic activity

16 p2461 A72-34181

The spectrum of Mars between 8 and 13 microns.

17 p2606 A72-34575

Earth and Mars - Evolution of atmospheres and surface temperatures.

17 p2613 A72-35395

Electron temperature in the Martian ionosphere.

17 p2613 A72-35499

Mars Hellas region surface features, relating crater absence to surface age and atmospheric condensation-produced white spot phenomena to sub-permafrost water reservoir

18 p2730 A72-37154

Martian atmosphere atomic oxygen concentration estimation from Mariner 6 and 7 O I 1304 and 1356 A data analysis

19 p2868 A72-38734

Seasonal and latitudinal relation between Mars white clouds occurrence frequency and global water distribution, suggesting cloud composition as water vapor

20 p2968 A72-39241

Mars atmosphere temperature profiles inference from outgoing radiation spectral characteristics, constructing atmospheric model

20 p2968 A72-39252

Detection of molecular oxygen in the Martian atmosphere.

21 p3103 A72-40451

Numerical experiment of radiative-convective equilibrium of the Martian atmosphere.

21 p3105 A72-40772

Mars photographic mapping and UV/IR spectrometric investigation by Mariner 9, discussing Martian surface features and atmospheric composition

21 p3105 A72-40967

'Mars-2,' 'Mars-3' observatories exploring the 'red' planet.

21 p3109 A72-41318

The composition of the Martian atmosphere - Minor constituents.

21 p3110 A72-41458

Martian topography according to ground-based radar measurements and the CO2 absorption observed from the earth and from the Mariner 6 and 7 spacecraft

21 p3114 A72-41766

Martian surface relief and atmospheric properties from Mars probe observations, considering soil, dust storms, temperature distribution and life possibility

22 p3222 A72-42139

Martian light sources generated by suspended crystals producing parhelic halo in atmosphere, noting randomly oriented and gravitationally arranged suspensions

22 p3223 A72-42142

Stability of the Martian atmosphere.

22 p3224 A72-42292

Detection of molecular oxygen on Mars.

22 p3224 A72-42293

Development and performance analysis of a trajectory estimator for an entry through the Martian atmosphere.

[AIAA PAPER 72-953]

22 p3224 A72-42352

Mars - The effects of topography on baroclinic instability.

22 p3225 A72-42504

Mars atmosphere and surface observation by Soviet space probes Mars 2 and 3, investigating temperatures, chemical composition, dust storms and thermal radio emission

23 p3338 A72-43992

MARS ENVIRONMENT

NT MARS ATMOSPHERE

Mars biology likelihood from long winter model, suggesting north polar cap summer remnant vaporization as atmosphere, liquid water and greenhouse effect source

10 p1424 A72-23717

Antarctica dry valley microbiology investigation for Martian life model

12 p1802 A72-27258

Life on Mars, investigating ground based and probe observations of atmospheric composition and pressure, surface temperature and features and UV radiation

12 p1761 A72-27624

Viking mission gas exchange experiment for life detection in Martian soil, covering design of experiment

14 p2084 A72-30876

MARS LANDING

Mars 3 spacecraft structure and experiments, noting central hypergolic fuel tanks, S-band directional antenna and solar panels

06 p0892 A72-17400

Mars 1975 Viking mission profile, describing soft landing/orbiter probes and life detection experiments

12 p1877 A72-27687

Color band selection for Mars lander multispectral imaging system for surface constituent discrimination

15 p2307 A72-31809

Mars Viking 1975 mission objectives and navigation activities from trans-Mars injection through post-landing stationkeeping phase, considering trajectory dispersions

15 p2269 A72-32180

Landing-site and orientation determination for a spacecraft on Mars

21 p3103 A72-40302

Location estimation for spacecraft landed on Mars surface via statistical techniques application to earth based radio tracking data, taking into account ephemeris biases

[AIAA PAPER 72-903]

21 p3082 A72-41554

Evaluation of optical data for Mars approach navigation.

24 p3422 A72-44646

MARS PROBES

NT VIKING LANDER SPACECRAFT

NT VIKING MARS PROGRAM

NT VIKING ORBITER SPACECRAFT

Space crew radiation dosage calculation from Mars mission high impulse gas core nuclear rocket engine exhaust plume fission fragments

01 p0022 A72-11353

Soviet interplanetary spacecraft Mars 2 and 3, describing design, mission objectives, onboard systems and instrumentation

09 p1395 A72-22974

Mars and Venus probes entry into planetary atmospheres, discussing aerodynamics of trajectory control and soft landing

09 p1394 A72-23673

Life detection on earth from satellite 100 meter resolution photographs, discussing potential false positives and implications for Mars probes

10 p1471 A72-23718

Mars 3 probe design and mission details, covering trajectory correction lander separation, engine start-up, aerodynamic braking and dust storm data

14 p2151 A72-30477

Mariner and Mars space probe data on Mars surface and atmosphere, suggesting possibility of tectonic activity

16 p2461 A72-34181

Landing-site and orientation determination for a spacecraft on Mars

21 p3103 A72-40302

Martian surface relief and atmospheric properties from Mars probe observations, considering soil, dust storms, temperature distribution and life possibility

22 p3222 A72-42139

An integrated multi-purpose biology instrument utilizing a single detector, the mass spectrometer.

23 p3287 A72-43397

The results of Soviet research into Mars.

24 p3447 A72-45559

MARS SPACECRAFT

U MARINER SPACECRAFT

MARS SURFACE

Martian surface nature from Surveyor and Apollo missions data on lunar particle size distribution

01 p0132 A72-11037

Topography and Coriolis effects on Martian atmospheric circulation, incorporating low radiative time constant and large variations in analytical model

01 p0135 A72-11279

Martian atmosphere and surface, covering atmospheric composition, optical thickness and pressure, violet and yellow clouds, surface relief and topography

02 p0282 A72-12326

Annual heat balance in Martian northern polar cap, considering atmospheric, ground and solar heat flux absorbed by snow

03 p0436 A72-13817

Martian surface relief observation from earth distance, showing telescope resolution requirements above dense atmospheric layers

03 p0438 A72-13983

Mars and Venus explorations, discussing Mariner probes, Mars craters, volcanism, polar areas, surface temperature and atmosphere and Venus radar astronomy and atmospheric model

03 p0440 A72-14305

Central peaked Martian crater distribution from Mariners 6 and 7 photographs, comparing south polar region to equator

03 p0440 A72-14310

Mars carbon dioxide distribution map determination of surface topography from spectrophotometric observations of equatorial region

04 p0569 A72-14499

Mars surface features Schiaparelli nomenclature from Mediterranean Sea area classical geography

04 p0569 A72-14500

Mars surface topographic characteristics relationship to earth features, using Mariner 6 and 7 photographs

04 p0569 A72-14501

Mars topographic map study of high velocity relief winds, showing seasonal and secular changes

04 p0569 A72-14502

Radar observations of Martian craters and scarp during 1971 opposition

04 p0579 A72-15359

Radar observation of Mars surface, noting rugged terrain and craters

04 p0579 A72-15360

Southern Martian polar cap seasonal change, describing variation at vernal equinox and dry ice hypothesis

04 p0581 A72-15621

Carbon dioxide frost identification on Martian polar caps by Fourier spectroscopy

06 p0881 A72-17900

Mars Hellas area surface features, relating crater absence to surface age and white spot phenomena to water reservoir under permafrost layer

06 p0881 A72-17929

Mariner 9 television reconnaissance of Mars surface and satellites, observing south polar cap and dark spots with crater features

06 p0889 A72-18341

Mariner 9 IR spectroscopy observations of Mars surface, indicating dust with silicon oxide content and atmospheric warming and water vapor over south polar cap

06 p0890 A72-18342

Brightness temperatures over Mars south polar cap from Mariner 9 IR radiometry, comparing to Mariner 6 and 7

06 p0890 A72-18343

Martian crater abundance correlation with surface albedo, discussing relative age of light and dark terrains

08 p1230 A72-20983

Martian height gradients from 1.6 micron carbon dioxide band intensity, using telescopes with prismatic quartz spectrometer

08 p1231 A72-21125

Semitransparent particle model of Martian surface for reflective power at various incidence and reflection angles, discussing packing density and optical parameters

08 p1231 A72-21126

Brightness distribution and phase dependence measured for spheres with different colors and roughness for Mars surface optical parameters model validity

08 p1238 A72-21830

Mariner Mars 1969 IR spectrometer for Mars atmosphere and surface spectra recording, describing design specifications and optimization for low light level sensitivity

09 p1313 A72-23326

Lunar and Mars crater genetic similarities, discussing scale dependent effects and post-impact geologic development

10 p1531 A72-23704

Martian cratering by asteroid impact, discussing Palomar-Leiden asteroid statistics, Opik capture theory and evolutionary extrapolation limitations

10 p1531 A72-23705

Martian crater obliteration theory, suggesting filling by dust deposition

10 p1531 A72-23706

Mars south polar cap surface roughness and photometric function from Mariner 7 UV spectrometric experiment

10 p1531 A72-23708

Aeolian transport and surface roughness of Mars Hellas basin, using Mariner 1969 photographs

10 p1536 A72-24151

Mars observation by Mariner 9, discussing TV pictures of surface, UV and IR spectroscopy of atmosphere, S band experiment and Phobos and Deimos studies

10 p1538 A72-24309

Viking Mars Orbiter imaging experiment with high resolution contiguous coverage by vidicon cameras for landing sites selection and surface study

10 p1539 A72-24377

Viking Mars Orbiter IR thermal mapper /IRTM/ to study surface kinetic temperature, thermal balance, anomalous cooling regions, ground frosts and water vapor

10 p1539 A72-24379

Viking Lander imaging experiments with stereoscopic camera system to study Martian surface and atmospheric morphology, composition and evolution

10 p1540 A72-24382

Viking Lander mass spectroscopic analysis of organic compounds, water and volatile constituents of Martian atmosphere and surface

10 p1540 A72-24383

Viking Lander carbon 14 assimilation experiment for life detection in Martian soils

10 p1540 A72-24385

Viking Lander detection of metabolically produced radioactive labeled gas in Mars surface samples

10 p1540 A72-24386

Viking Lander light scattering experiment to detect microbial growth from aqueous turbidity changes in contact with Martian soil

10 p1430 A72-24387

Viking Lander physical properties experiments for Martian soil, studying bearing strength, cohesion, adhesion, grain size, porosity, thermal properties and internal friction

10 p1540 A72-24390

Viking Lander magnetic properties investigation of Martian surface with implications for planetary composition and differentiation and atmospheric interaction

10 p1541 A72-24391

Mars surface lineament systems from Mariner photographs, noting global and radial type associated with Hellas and South Pole basins

12 p1868 A72-27259

Life on Mars, investigating ground based and probe observations of atmospheric composition and pressure, surface temperature and features and UV radiation

12 p1761 A72-27624

Martian Sinus Meridiani and South Polar maps from mosaics of Mariner 6 and 7 wide angle photographs

12 p1871 A72-27664

Mars surface particulate matter eroded by atmospheric winds, noting erosive and settling velocities and yellow clouds distribution

13 p2036 A72-28794

Viking orbiter/lander spacecraft instrumentation for Mars soil biological life experiments, discussing pyrolytic and labeled release, light scattering and gas exchange techniques

13 p1956 A72-29024

Martian atmosphere and surface, covering atmospheric composition, optical thickness and pressure, violet and yellow clouds, surface relief and topography

13 p2039 A72-29210

Mars doublet cratering by impacting meteoroid breakup due to stresses in gravitational field, using Monte Carlo simulation

14 p2149 A72-30317

Mars craters degradation and density regional variations from Mariner 6 and 7 imagery, using numerical scoring method

14 p2149 A72-30318

Mars surface normal albedo distribution function from red light photometry data

14 p2152 A72-30489

Mars observations in 1965, 1967 and 1969 by 150 mm and 400 mm refracting telescopes noting surface map and drawings

15 p2305 A72-31397

Mars observations during 1971 opposition, noting south pole phenomena relation to Martian atmosphere changes

15 p2306 A72-31600

Color band selection for Mars lander multispectral imaging system for surface constituent discrimination

15 p2307 A72-31809

Apparent difference in Martian night and day side surfaces atmospheric pressure based on Mariner spacecraft occultations, noting effects of topography and electron layer

15 p2310 A72-31973

Mars nonpolar region photometric and topographic characteristics from Mariner 6 and 7 UV spectrometer observations

15 p2311 A72-32084

Surface roughness effects on Mars photometric properties, allowing for scattering in terms of Minnaert law

15 p2311 A72-32085

Unmanned remotely controlled planetary rovers for Mars surface exploration, discussing design concepts

15 p2214 A72-32316

Mars topography variations from earth based surface height radar ranging and Mariner spectrophotometric observation of Mars atmosphere

15 p2313 A72-32346

Mars integrated radio temperature relation to blanket electrical properties for 1971 opposition, assuming Martian soil properties independence from depth and temperature

15 p2315 A72-32730

Hellas-Hellepontos transition zone properties in origin model with impact and later isostatic subsidence

16 p2454 A72-33445

Mars surface mapping from spectrophotometric studies of surface materials photometric function, composition and distribution, suggesting color due to limonite-stained soil particles

16 p2457 A72-33616

Mariner and Mars space probe data on Mars surface and atmosphere, suggesting possibility of tectonic activity

16 p2461 A72-34181

Earth and Mars - Evolution of atmospheres and surface temperatures.

17 p2613 A72-35395

Saltation threshold velocity simulation by dynamic model with terrestrial and Martian surface applications, using particle trajectory equations for near ground-atmosphere interface

17 p2614 A72-35637

The new Mariner 9 map of Mars.

18 p2729 A72-36988

Mars Hellas region surface features, relating crater absence to surface age and atmospheric condensation-produced white spot phenomena to sub-permafrost water reservoir

18 p2730 A72-37154

Mars polar caps formation at aerographic latitudes, assuming water vapor condensation on ground and water presence in carbon dioxide snow

19 p2863 A72-38072

Mars surface normal albedo distribution function from red light photometry data

19 p2864 A72-38318

Secular and seasonal modifications of Mars surface, considering southern polar cap and 1971 dust storm

19 p2865 A72-38475

Sand deposition due to wind action in Martian craters, comparing to terrestrial analogs

20 p2969 A72-39389

Mars photographic mapping and UV/IR spectrometric investigation by Mariner 9, discussing Martian surface features and atmospheric composition

21 p3105 A72-40967

'Mars-2,' 'Mars-3' observatories exploring the 'red' planet.

21 p3109 A72-41318

Bistatic radar measurements of the surface of Mars with Mariner 1969.

21 p3110 A72-41453

Diurnal and seasonal behavior of discrete white clouds on Mars.

21 p3110 A72-41454

An orthographic photomap of the South Pole of Mars from Mariner 7.

21 p3110 A72-41455

The location of the Mountains of Mitchel and evidence for their nature in Mariner 7 pictures.

21 p3110 A72-41456

Mariner 7 ultraviolet spectrometer experiment - Topographic slopes of Mars' polar region.

21 p3110 A72-41457

Martian topography according to ground-based radar measurements and the CO2 absorption observed from the earth and from the Mariner 6 and 7 spacecraft

21 p3114 A72-41766

Martian surface relief and atmospheric properties from Mars probe observations, considering soil, dust storms, temperature distribution and life possibility

22 p3222 A72-42139

Specific effective scattering area of the lunar, Martian, and Venusian surfaces in the radio range

22 p3223 A72-42214

Mars - The effects of topography on baroclinic instability.

22 p3225 A72-42504

Biological instrumentation for the Viking 1975 mission to Mars.

23 p3259 A72-43396

Mars atmosphere and surface observation by Soviet space probes Mars 2 and 3, investigating temperatures, chemical composition, dust storms and thermal radio emission

23 p3338 A72-43992

Coordinates of features on the Mariner 6 and 7 pictures of Mars.

24 p3436 A72-44695

Mariner 9 spacecraft systems and photographs of Martian surface details

24 p3441 A72-45170

The results of Soviet research into Mars.

24 p3447 A72-45559

MARS 3 SPACECRAFT

Mars 3 spacecraft structure and experiments, noting central hypergolic fuel tanks, S-band directional antenna and solar panels

06 p0892 A72-17400

Mars atmosphere and surface observation by Soviet space probes Mars 2 and 3, investigating tempera-

- tures, chemical composition, dust storms and thermal radio emission
23 p3338 A72-43992
- MARS 69 PROJECT**
Mariner 1969 Mars mission, emphasizing planetary encounter, surface and atmospheric data and search for extraterrestrial life
01 p0130 A72-10930
Mariner Mars 1969 IR spectrometer for Mars atmosphere and surface spectra recording, describing design specifications and optimization for low light level sensitivity
09 p1313 A72-23326
- MARS 71 PROJECT**
Preflight and real time gravity sensing for Mariner 9 satellite orbit determination during Mars 1971 mission
15 p2270 A72-32186
- MARTENSITE**
Stress effects on TiNi compound martensitic transformation, investigating deformation as function of composition and heat treatment
01 p0087 A72-11023
Ultrasonic cavitation effects on martensitic specimens, observing plastic deformation, softening, phase transformations and decay
03 p0370 A72-13187
Tempered Fe-Cr-C-Co steels microstructural and mechanical properties, investigating martensite and bainite
03 p0375 A72-13929
Mo and C additives effects on austenite susceptibility to deformation martensite formation and steel resistance to hydroerosion
03 p0375 A72-13941
Dilatometric investigation of martensitic transformation in TiNi compound, observing plastic memory effect
03 p0377 A72-14021
Low temperatures and deformation rates effect on martensitic phase formation in Cr-Ni austenitic stainless steel under compression and tension
03 p0379 A72-14378
Hardening of Fe-Mn-Ti ferritic and martensitic alloys, investigating microstructure and mechanical properties
05 p0672 A72-16144
Face-centered orthorhombic martensite in Ti-V alloy, determining axial ratios and lattice parameters by transmission electron microscopy and X ray diffraction
05 p0676 A72-17102
Crystal structures and martensitic transformation mechanism of TiNi, using X ray diffraction and electrical resistivity measurements
06 p0827 A72-17421
Internal friction and plastic microstrains in martensitic transformation of Fe-Ni, Co-Ni, and Fe-Cr-Ni alloys
06 p0830 A72-18294
Austenitizing conditions effects on hardness and microstructure of tempered steel, emphasizing martensite structure and grain size changes produced by controlled heat treatment
07 p0995 A72-19486
Martensitic transformations induced by plastic deformation in Fe-Ni-Cr-C system, noting stacking fault energy dependence on temperature
07 p1015 A72-19928
Tensile strength enhancement of dislocated martensites in Fe alloys by precipitate dispersion in austenite prior to transformation
07 p1016 A72-19936
X ray study of martensite fine structure produced by plastic deformation in Fe-Ni alloy
08 p1188 A72-21788
Carbon effects on internal friction of low temperature Fe-Ni alloy during martensitic transformation
10 p1495 A72-24083
Internal friction peak in fresh tempered martensite from Fe-Ni-C alloy cooled to 77 K, suggesting hypothetical carbon atoms interactions with mobile dislocations
10 p1496 A72-24232
Co, Al and Mn additions effect on secondary hardening during aging in Fe-Mo-C martensite
11 p1655 A72-25511
High strength hypereutectoid steel with low carbon needle-like martensite matrix obtained by conventional heat treatment
12 p1827 A72-27100
Electron diffraction study of transformation twin rotations in Fe-Ni martensites, showing foil plane uncertainty effect with respect to image plane
13 p1975 A72-28666
Martensitic transformation in Cu-Al-Ni alloy thin film, investigating gamma-prime phase substructure formation and crystal growth pattern
13 p1976 A72-28907
Hardened coarse-grained steels recrystallization during fast heating, investigating martensite phase macro- and microstructural changes by X ray analysis
13 p1977 A72-28908

- Cu-Al-Ni alloys single crystals internal friction temperature dependence during martensitic transformations
13 p1977 A72-28912
Maraging Fe-Ni-Co-Mo alloy ordered metastable omega phase formation during martensite aging from electron microscopic investigation, noting Co addition effects and precipitation
14 p2115 A72-30404
Martensitic transformation athermal kinetics and accompanied martensite morphology change in Fe-Ni and Fe-Ni-Cr alloys
14 p2115 A72-30407
Premartensitic beta phase instability, lattice vibration and shape memory effect in noble metal base and Ti alloys
15 p2259 A72-32641
Magnetic balance for magnetic saturation measurement and determination of retained austenite, Curie temperature, permeability and martensite content
16 p2391 A72-33237
Quenching produced martensitic transformations from equilibrium beta phase region for Ti alloys with Ta
16 p2408 A72-33618
Precipitation reactions during tempering of Ti-Ta alloys, studying hcp and orthorhombic martensitic phases from electron microscope observations
16 p2408 A72-33619
The effect of plastic deformation on the martensite-to-austenite transition in an iron-nickel alloy
20 p2938 A72-39298
The effect of Si, Zr, Al and Mo on the structure and strength of Ti martensite
20 p2941 A72-37972
Habit plane interpretations of surface martensite transformation and orientation measurements compared with invariant plane strain (IPSS) theory
21 p3065 A72-40088
Single and double shear invariant plane crystallographic theories for martensitic transformations, calculating lattice deformations by combined Bain and complementary shear strains
21 p3065 A72-40089
Stress induced martensitic transformation relationship to shape memory effect compared with superelasticity, transformation plasticity and reversible linear change
21 p3065 A72-40091
Martensite formation temperature decrease and grain size reduction caused by martensite crystals interaction with barriers in Fe alloy containing austenite beta phase particles
21 p3070 A72-41679
Kinetic aspects of plastic strain induced martensite in polycrystalline Fe-Ni-C alloy from tensile tests on austenitic specimens
22 p3189 A72-42437
Thermoelastic martensite caused elastic vibration damping in Cu-Al-Ni alloy, observing shape memory effect
22 p3190 A72-42442
Martensitic transformation in filamentary cobalt crystals
22 p3192 A72-43017
Fe-Ni-C martensite reverse transformation to austenite during large and rapid applied shear, evaluating shear zone neighboring partially pierced hole
22 p3193 A72-43031
Enhanced strengthening of a spinodal Fe-Ni-Cu alloy by martensitic transformation
22 p3194 A72-43040
Martensitic transformation during deformation in titanium alloys with a metastable beta phase
23 p3300 A72-43591
- MARTENSITIC STAINLESS STEELS**
Plate microcracking of ferrous martensites containing Mn, Cr and Ni, discussing austenite grain size variations
05 p0678 A72-17119
Fatigue and fatigue-corrosion properties of high strength stainless maraging martensitic structural and stainless austenitic steels
05 p0680 A72-17206
Heat treatment effects on strength differential of high strength martensitic stainless and Ni maraging steels
07 p1015 A72-19926
Adiabatic reversion of Ni martensitic steel to austenite under shear in orthogonal cutting
07 p0996 A72-19934
High temperature nitriding of martensitically aging steels in ammonia-nitrogen mixtures, obtaining hard nonbrittle diffusion surface layers
07 p1020 A72-20418
Austeno-martensitic steel with 25 percent delta ferrite, examining microstructural changes due to aging at 550 C by thin slide electron microscopy
07 p1021 A72-20484
Internal friction measurements of tempered martensitic Cr steel quenched from 1100 C, connecting friction peaks with precipitation phenomena
07 p1021 A72-20486

- Martensite first stage decomposition mechanism and kinetics during tempering of quenched Re steels with varying carbon concentration
08 p1187 A72-21779
Fe-Ni alloys atom redistribution during aging before phase precipitation, discussing Mo and Co clusters in martensitic maraging steels
08 p1190 A72-22189
Soviet monograph on thermoplastic hardening of high strength martensitic steels and Ti alloys by ordering dislocation structure
09 p1327 A72-22520
Fe-Ni-C alloy mixed austeno-martensitic microstructure embrittlement, investigating mechanical properties after thermomechanical treatment
10 p1495 A72-24087
Fracture strength relation to austenite stability in steels with plastic deformation caused by strain induced austenite-martensite transformation
10 p1499 A72-24894
Fatigue and fatigue-corrosion properties of high strength stainless maraging, martensitic structural and stainless austenitic steels
11 p1660 A72-26141
Heat treatment effects on martensitic bainitic steel hardness, tensile strength and impact endurance, examining carbide and alpha phases
11 p1666 A72-26922
Tensile strength and martensitic transformation effect on stainless steel plastic deformation at cryogenic temperatures
15 p2253 A72-31521
Creep tests on Cr martensite stainless steel, showing inapplicability of Garofalo equation for stress dependence of secondary creep rate during variable stress experiment
16 p2412 A72-34112
Fine structure in quenched Fe-Al-C steels
20 p2938 A72-39300
Formation of deformation martensite in Fe-Ni-C alloys which do not undergo transformation on cooling
21 p3066 A72-40270
Deformation-induced martensitic transformation in isothermal and athermal Fe-Ni-C alloys
21 p3066 A72-40272
Strength of welded joints of high-strength stainless steels at cryogenic temperatures
21 p3061 A72-41365
Strain hardening of maraging steels in liquid nitrogen
22 p3187 A72-41867
- MARTIN MILITARY AIRCRAFT**
U MILITARY AIRCRAFT
MASCONS
Mascon free lunar gravitational potential calculations, showing hydrostatic equilibrium in early evolution
03 p0434 A72-13552
Lunar Mare Ibrum lava flow geology and nature, mascon origins and explosive, collapse and impact mechanisms for small crater origin
06 p0887 A72-18218
Moon model - An offset core
20 p2969 A72-39374
Dynamic model compensation algorithm accuracy for sequential estimation of time history of lunar satellite acceleration due to modeled surface mascons effects
24 p3440 A72-45139
- MASER OUTPUTS**
Microwave source four hundredth order harmonic mixing with laser radiation, using Josephson junction and maser
12 p1827 A72-28221
Buffer gas mixture and pumping light effects on shifts from ground state hyperfine frequency in Rb-85 maser frequency standard
14 p2109 A72-30196
Stellar OH radical emission amplification by maser effect raising low energy molecules to high energy by pumping
14 p2110 A72-30578
OH maser sources parametric down-conversion, deriving nonlinear current densities, electron cyclotron wave damping and parametric gain coefficient
21 p3064 A72-41030
Recoil effect on inverted molecules changing pumping conditions and gain for interstellar, OH maser intensity and radial velocity variations
21 p3102 A72-41773
- MASER RESONATORS**
U MASERS
MASERS
NT GAS MASERS
NT TRAVELING WAVE MASERS
Interstellar OH and water maser regions, deriving density, diameter and temperature
01 p0133 A72-11142
Quantum mechanical analysis of detuning in cascaded cavity molecular beam masers
03 p0368 A72-13747

Millimeter and submillimeter wave molecular beam masers amplification principles and Doppler and collisional broadening elimination capability
04 p0532 A72-15597

Signal detection in ruby element quantum paramagnetic amplifier operating at liquid nitrogen temperature
08 p1141 A72-21377

Ruby use for submillimeter range optically pumped quantum paramagnetic amplifier
08 p1183 A72-21770

Book on density matrix theory application to lasers and masers, covering quantum mechanics, perturbation theory, magnetism and magnetic resonance, statistical ensembles, etc
12 p1826 A72-28203

Interstellar OH maser size determination, discussing scattering by inhomogeneities in electron distribution
16 p2456 A72-33473

Russian book on microwave electronics covering linear-beam and cross-field backward and traveling wave amplifiers and oscillators, klystrons, masers, plasma devices, etc
17 p2532 A72-34650

Hydroxyl and water radio sources scale and geometry constraints placed by interstellar maser gain saturation relation to emission solid angle
21 p3062 A72-40565

Saturation protection of a maser amplifier by the pulse-modulated pumping method
21 p3063 A72-40785

Observations of sources of maser radio emission with an angular resolution of 0.0002 sec
21 p3101 A72-41751

Initial electron velocity and emitter surface roughness effects on oscillatory velocities dispersion in helical electron beams used in cyclotron resonance masers
22 p3208 A72-42664

Statistics of the radiation from astronomical masers
23 p3337 A72-43872

MASKING

Pitch shift of pure tone by masking tones and band limited noise
01 p0101 A72-10159

Visual masking effect due to light offset, investigating human identification response to tachistoscopic test stimuli on lighted background with simultaneous shut-off
02 p0166 A72-11550

Electrophysiology for auditory temporal masking mechanism study of cat cochlear nucleus and inferior colliculus single neurons
05 p0620 A72-17175

Interactive computer graphics design aids to IC mask layouts, discussing hardware and software techniques including IMP program
06 p0778 A72-17473

Programming system for automatic plotting of mask patterns for ICs
12 p1791 A72-27551

Masking functions for intensity discrimination of pulsed sinusoids with and without noise masker
13 p2006 A72-29772

Disparity-associated depth sensation masking, suggesting visual signal processing inhibitory mechanisms for crossed and uncrossed stimuli
15 p2184 A72-31366

Auditory induction of fainter by louder sounds as perceptual phenomenon cancelling masking effects
16 p2354 A72-33170

Energy detection model for transient overshoot in tonal signals masked by narrow band auditory stimuli, discussing masking produced by gated sinusoid
16 p2359 A72-33972

Effect of fringe on masking-level difference when gating from uncorrelated to correlated noise
21 p2997 A72-40346

Masking techniques for thin film and semiconductor devices and ICs fabrication, discussing conventional and computerized optical and electron beam systems
22 p3159 A72-42634

A means of reducing custom LSI interconnection requirements.
23 p3273 A72-44454

MASKS

NT OXYGEN MASKS

Gas mask-caused air flow resistance effects on respiratory and circulatory response to exercise, assessing maximal oxygen uptake
13 p1906 A72-29818

MASS

NT CRITICAL MASS

NT ELECTRON MASS

NT PARTICLE MASS

NT PLANETARY MASS

NT STELLAR MASS

Complex structures mass and stiffness matrices reduction by automatic condensation, calculating lowest eigenfrequencies and eigenmodes of substitute systems
[DGLR PAPER 71-108]
02 p0299 A72-12721

Inertial and gravitational mass equivalence principle verified for aluminum and platinum, using torsional pendulum with large relaxation time
03 p0388 A72-13076

Relativistic flight of decreasing mass, increasing acceleration and constant thrust rocket description from earth and rocket observer viewpoints, noting light flash transmission and arrival times
03 p0441 A72-13836

Gravitational and inertial masses equivalence principle verification by pendulum torsional oscillation experiment with laser beam
04 p0519 A72-15070

Mass concept for moving crack, relating stress concentrations of elastic field with crack inertia
05 p0673 A72-16306

Inertial and gravitational mass equivalence principle verified for Al and Pt, using torsional pendulum with large relaxation time
13 p2004 A72-29426

MASS BALANCE

Balance laws of micromorphic theory for polycrystalline mixtures, granular composites and fluid suspensions involving motions with wavelength comparable to intrinsic discontinuities in materials
01 p0102 A72-10320

Rotation and mass inclusion into study of energy barriers location effects on thermonuclear reaction dynamics
02 p0262 A72-11981

Gas turbine combustors performance model, using reaction rate equation from elementary mass balance equation
[ASME PAPER 71-WA/GT-5]
05 p0704 A72-15898

Angular velocity vector active damping during spin-up of electrically supported gyro with mass-unbalance readout, using Euler equations of motion
07 p0986 A72-19691

Mass and energy balance for electrode wire fusion in pulsed current MIG /metal inert gas/ welding, discussing pulse duration and amplitude requirements and shielding gas composition effect
09 p1321 A72-23644

Mass and energy balance in air cooled matrix type phosphoric acid cell, noting operational reliability and construction
16 p2351 A72-33889

Elastic vibrations in roller bearings. I - The rotating mass is balanced with respect to its own rotation axis
17 p2561 A72-35894

Unbalanced shafts vibration and stability characteristics, considering elastic and damping properties of sliding bearings oil films
18 p2731 A72-36069

Luminous intensity, visibility duration, condensation nuclei and mass balance of noctilucent clouds
18 p2686 A72-36504

An automatic mass-trim system for spinning spacecraft.
20 p2977 A72-39603

Balancing aerospace bodies on industrial balancing machines.
[SAWE PAPER 929]
23 p3293 A72-43469

Rotating aerospace vehicles dynamic balance error terms due to despun masses misalignment and aerodynamic effects
[SAWE PAPER 930]
23 p3342 A72-43470

Mass and heat budget estimations of the Atlantic SE trade wind flow at the equator.
24 p3420 A72-44756

Mathematical model for life support system optimization in terms of reduced mass minimization as quality criteria for energy conversion and metabolic processes
24 p3375 A72-45133

MASS DISTRIBUTION

Pultusk meteorite shower fragments number and mass estimates from numerical integration of differential equations
01 p0126 A72-10103

Galaxy clusters stability, obtaining mass distribution function from combined virial theorem and mass to light ratios
01 p0131 A72-11003

Computer calculation for atmospheric total mass and seasonal redistribution from pressure and temperature field data, discussing error sources
03 p0348 A72-13480

Globular clusters with inhomogeneous composition, deriving partial densities of masses
03 p0436 A72-13826

Vibration mode shapes and frequencies determination by finite element method using consistent and lumped masses formulations in differential equation solution, considering convergence rate
[AD-739820]
05 p0736 A72-16086

Time optimal control for pitch damping of gravity gradient stabilized satellite by mass distribution variation
05 p0727 A72-16465

Mass addition distribution and gas injectant effects on heat transfer rates, transition locations and surface pressures of sharp cone
[AIAA PAPER 72-183]
05 p0748 A72-16838

Rocket orbit in mass point gravitational field, studying KS variables separability, elliptic functions and equivalent problems
06 p0877 A72-17656

Protoplanetary bodies mass distribution by coagulation theory, using inverse power law
06 p0884 A72-18030

Mass distribution gravitationally equivalent to L1 lunar potential model for finite torus shaped shell region sampled by Apollo spacecraft
07 p1067 A72-18871

Spiral galaxies hypothesis for higher mass-luminosity ratio of outer parts from undetected cold neutral hydrogen, using model of NGC 300
07 p1068 A72-19071

Galactic nucleus explosive events and mass expulsion evidence from high velocity hydrogen survey with 20 ft horn reflector
07 p1070 A72-19086

Numerical solution of equations for asteroidal mass distribution under collisional fragmentation
07 p1071 A72-19180

Book on physical cosmology development covering universe expansion, steady state, isotropy, Hubble constant, cosmic time scale, mass density, etc
08 p1236 A72-21480

Optimal stabilization of permanent rotation of solid body with arbitrary mass distribution by controlled gyroscope
08 p1168 A72-21552

Nonflat central configuration N point masses existence for any integer greater than four, disproving Wintner conjecture of finite number of integers
08 p1236 A72-21639

Frost rule for meteoroid spatial sorting as basis for Allende meteorite shower stream field examination of fragment mass and position
08 p1237 A72-21651

Radar measurement of meteor bodies mass distribution parameter
08 p1239 A72-21889

Radio echo determination of meteor body distribution by mass with allowance for electron attachment and overestimated nighttime values
09 p1383 A72-22505

Galaxy NGC 253 mass and distance from neutral hydrogen spectral line observations with radio telescope
09 p1391 A72-23533

Velocity dispersions and discrepant red shifts in groups of galaxies, using virial theorem for galaxy mass calculations
10 p1534 A72-23903

Hyades member star BD plus 16.516 deg described as late evolution product of binary system with mass exchange and loss through planetary nebula phase
10 p1543 A72-24618

Distributed elastic system discrete model mass, stiffness and damping matrices derivation from dynamic test response data
[AIAA PAPER 72-346]
11 p1728 A72-25375

Protoplanetary bodies mass distribution by coagulation theory, using inverse power law
11 p1719 A72-25966

Mass, momentum and energy distribution measurement in quasi-steady MPD discharge, obtaining velocity vector profiles
[AIAA PAPER 72-497]
11 p1696 A72-26220

Computer calculation for atmospheric total mass and seasonal redistribution from pressure and temperature field data, discussing error sources
11 p1623 A72-26250

Shallow isotropic and orthotropic shells vibration, investigating dynamic rigidity for concentrated mass
12 p1878 A72-27079

Lognormal fragment mass distribution of Lowicz meteorite shower 1935
12 p1866 A72-27118

Sikhote-Alin meteorite shower individual specimens mass distribution with respect to distance from crater center
14 p2153 A72-30496

Lunar crust mass distribution relation to moments of inertia derivation from librations, inferring non-validity of lunar evolution fluid phase hypothesis
14 p2153 A72-30504

Charge and mass densities relation for stationary charged dust distribution in general relativity, investigating Einstein-Maxwell equations for stationary gravitational field
15 p2275 A72-31591

Earth-moon system mass from ratio of solar mass to sum of terrestrial and lunar masses, discussing solar attraction effects and radar distance measurements
15 p2306 A72-31598

Heavy body mass distribution gravitational effects in nonlocal linear theory, noting refractive index, rosette motion and perihelion advance
15 p2278 A72-32484

Vibration perturbation of slender rotating beam with end masses, using method of matched asymptotic expansions
[ASME PAPER 72-APM-B]
17 p2625 A72-34318

- Large amplitude vibration of a circular plate with concentric rigid mass. [ASME PAPER 71-APMW-11] 17 p2625 A72-34319
- Intergalactic ionized gas and member galaxies mass relationship in local group and nearby galactic clusters, considering gravitational potential 17 p2604 A72-34475
- Transverse vibrations of bars with concentrated additional masses 17 p2627 A72-34772
- Many-body forces and the effect of the matter distribution in the universe to the gravitational constant. 18 p2728 A72-36800
- Sikhote-Alin meteorite shower individual specimens mass distribution with respect to distance from crater center 19 p2864 A72-38325
- Vibrations of a concentrated mass on a ring coupled to a thin shell 20 p2981 A72-39908
- General relativity equations for hydrostatic equilibrium of spherical distribution of mass combined with equations of state for highly relativistic neutron star central regions 20 p2955 A72-40011
- The effects of discrete masses and elastic supports on continuous beam natural frequencies. 21 p3116 A72-40335
- Multiple scattering of bending waves by random inhomogeneities. 22 p3235 A72-42460
- The estimation of masses of individual galaxies in clusters of galaxies. 22 p3227 A72-42551
- New method for determining the distribution of delta-g anomalies for a sphere, horizontal cylinder, and vertical material half-line 22 p3173 A72-42574
- The parameters of a two-mass oscillatory system in which one of the masses is acted upon by a complex working resistance 23 p3312 A72-43352
- Balancing aerospace bodies on industrial balancing machines. [SAWE PAPER 929] 23 p3293 A72-43469
- Despun conical flight vehicles eccentric insulation mass properties history, deriving preflight and in-flight equations for weight, center of gravity coordinates and moments and products of inertia [SAWE PAPER 938] 23 p3342 A72-43478
- Structural mass properties mathematical modeling for dynamic structural analysis, describing matrix notation for finite element methods application [SAWE PAPER 944] 23 p3344 A72-43484
- The effect of meteoric ion processes on radio studies of meteoroids. 23 p3336 A72-43558
- Numerical models of elliptical galaxy based on rotational speed and integral equations for mass distribution 23 p3338 A72-44033
- Infinite rectangular elastic bar surface mass distribution effects on harmonic wave propagation modes, obtaining approximate solution by expanding displacement as power series 23 p3352 A72-44123
- Interplanetary objects in review - Statistics of their masses and dynamics. 24 p3435 A72-44688
- Determination of parameters related to the interior of Mercury. 24 p3436 A72-44696
- Particle fragmentation, mass distribution and chemical composition of cometary meteoroids in earth orbit, noting collisional erosion and similarity to stony meteorites 24 p3445 A72-45459
- MASS FILTERS**
- U FLUID FILTERS**
- MASS FLOW**
- Laminar flow between stationary and rotating disk with mass flow through concentric circular opening by finite difference method 02 p0203 A72-12098
- Self magnetic coaxial plasma accelerator integral output data, presenting mass velocities and thrust measurement [DGLR PAPER 71-103] 02 p0266 A72-12736
- Turbulence effects in stratified shearing flow, determining relationship between measured mass flux and overall Richardson number 06 p0798 A72-17762
- Laser plasma density and velocity distributions and mass flow from surface and plasma pressure in target heating process based on interferometric measurements 08 p1215 A72-21719
- Mass flow and current distribution in magnetic MPD accelerator thruster plumes calculated from meridional flow stream function equation 11 p1696 A72-26224 [AIAA PAPER 72-501]
- One-dimensional theory of flows with combustion 18 p2740 A72-36246

- Critical mass flow and nonequilibrium nozzle flow of vibrationally relaxing, ideal dissociating diatomic and singly ionizing monatomic gases, using steepest descent method 21 p3046 A72-41249
- Transverse mass flow past a sphere at small Reynolds numbers 21 p3047 A72-41664
- MASS FLOW FACTORS**
- Hydraulic servomechanism spool type control valve orifice flow characteristics, measuring mass flow for various spool determined port shapes 07 p0915 A72-20533
- MASS FLOW RATE**
- Kinetic energy correction in capillary viscometry, observing pressure drops and mass flow rates 02 p0202 A72-11724
- Conducting fluid steady MHD pipe flow under transverse magnetic field, obtaining mass flow rate 03 p0394 A72-13241
- Mass blocking of subsonic isentropic swirling flow through convergent axisymmetric nozzle, considering radial velocity component effect on vorticity 03 p0342 A72-13957
- Heat transfer in rectangular annular channel during external heating under supercritical pressure, discussing thermal flux, mass flow rates and enthalpy 03 p0457 A72-14152
- Electrical measurements on capillary-fed colloid thruster with Zener diode-like I-V characteristic and constant propellant mass flow rate 04 p0565 A72-15204
- Test facility for electric microthrusters, describing microbalance for thrust and propellant mass flow rate measurement 09 p1292 A72-23404
- Modular carbon dioxide laser design and operational features, reporting measured data on plasma tube current, pressure and gas mixture flow rate effects on power output 10 p1492 A72-24565
- Turbojet simulator for supersonic wind tunnel models, simulating inlet mass flow ratio and exhaust nozzle pressure ratio [ASME PAPER 72-GT-89] 11 p1705 A72-25664
- High efficiency hybrid rocket motor based on polyester fuel and RFNA oxidizer, determining correlation between burning rate, oxidizer and total flow rates 15 p2297 A72-31207
- Mass flow rate and mean density measurements in separated laminar boundary layers with large transverse density gradients, analyzing density difference effects on instability 16 p2379 A72-33571
- Compressible swirling flow through convergent-divergent nozzles. 17 p2485 A72-34999
- Centrifugal pumps performance instability, considering mass flow rate/pressure curve characteristics as function of impeller slip, fluid prerotation and hydraulic losses 18 p2694 A72-36042
- Influence of pressure, mass flow rate, and nozzle angle on the chemical relaxation in nozzles 19 p2880 A72-37494
- A study of the liquid-vapor phase change of mercury based on irreversible thermodynamics. [ASME PAPER 72-HT-A] 20 p2983 A72-39481
- Condensation on a downward-facing horizontal rippled surface. [ASME PAPER 72-HT-33] 20 p2983 A72-39485
- Equations of motion for the variable mass flow-variable exhaust velocity rocket. 21 p3112 A72-41559
- Extremal bounds for mass flow rate of laminar MHD flow in circular and thin walled conducting pipes at high Hartmann number 22 p3210 A72-42315
- The dynamical effects of stellar mass loss on diffuse nebulae. 22 p3224 A72-42380
- Solar system thin disk form planet formation in equatorial plane from nebula dust component, discussing gravitational effects and mass increase rate 23 p3335 A72-43261
- An experimental study of film cooling through a rearward-facing slot. 23 p3356 A72-43971
- MASS RATIOS**
- NT PAYLOAD MASS RATIO**
- NT PROPELLANT MASS RATIO**
- Periodic orbit families emanating from Lagrange triangular point L4 in restricted three body problem with mass ratio parameter equal to Routh critical mass ratio 01 p0123 A72-10013
- Inertial-gravitational mass ratio in classical and quantum case, proving equivalence principle non-validity for Brans-Dicke gravitation theory compared to Einstein theory 01 p0102 A72-10861
- Galactic evolution and cosmology implications of primordial solar D/H ratio, discussing deuterium production mechanisms 04 p0574 A72-14980

- Close binary system average gravity and effective temperature at Roche limit for 90 deg phase and both conjunctions, taking into account mass ratios and orbital inclination 06 p0882 A72-18002
- Impact interaction between free two body system with elastic spring coupling and fixed plane, considering mass ratio and velocity restitution coefficient 08 p0299 A72-21803
- Close binary stars system model for totally eclipsing AW UMa light curves and line profiles, noting very low mass ratio 10 p1550 A72-25195
- Spallation origin of anomalous He 3/He 4 ratio in 3 Centauri A, considering thermonuclear processes model 14 p2158 A72-30731
- Earth-moon system mass from ratio of solar mass to sum of terrestrial and lunar masses, discussing solar attraction effects and radar distance measurements 15 p2306 A72-31598
- Internal kinematics of two compact galaxies from spectroscopic observations, noting velocity dispersion, luminosity function and mass/light ratio 17 p2611 A72-35311
- A comparison of measurements of the charge spectrum of solar cosmic rays from nuclear emulsions and the Explorer 35 solid-state detector. 18 p2721 A72-35988
- Star cluster age relation to mass ratios of stars and interstellar hydrogen and dust 19 p2867 A72-38511
- Gross properties of five Scd galaxies as determined from 21-centimeter observations. 21 p3105 A72-41027
- A two-parameter survey of periodic orbits in the restricted problem of three bodies. 21 p3106 A72-41049
- Helicopter design figure of merit weight ratios definition in terms of rotor thrust coefficient, substituting pure airframe structure weight for conventionally used empty weight 23 p3250 A72-43463
- Dynamic behavior of three point mass system with variable body mass ratios and constant total system mass, applying results to stellar systems 24 p3442 A72-45240
- MASS SPECTRA**
- Artificial intelligence application to mass spectra interpretation, discussing heuristic Dendritic Algorithm based computer program to generate structural isomers 07 p0950 A72-19608
- Classification of mass spectra on computers /COM-SOC/ for compound characterization of complex mixtures with geochemical and environmental applications 07 p0980 A72-20393
- Electron impact induced aurene epoxides fragmentation, discussing ion formation, intermediates, thermal rearrangement and mass spectra 13 p1913 A72-29775
- Electron energy distribution, ions mass spectral composition and spatial charge concentration of currentless photoresonant Ce plasma obtained by associative ionization 14 p2136 A72-30175
- Solid bodies microanalysis by mass spectrum microscopy based on secondary ion-ion emission, discussing ion source and focusing systems 14 p2104 A72-30449
- Mass spectra stimulated by O+ and Ar+ interacting with a surface. 24 p3378 A72-45312
- MASS SPECTROMETERS**
- High resolution RF linear mass spectrometer for separation of ions formed by electron impact on organic molecules 01 p0064 A72-10043
- Positive H, HE and O ions in exosphere from mass spectrometers mounted on Elektron 4 satellite 01 p0053 A72-10368
- Miniaturized magnetic mass spectrometer for trace contaminants continuous monitoring and control, discussing applications to closed atmospheric systems in spacecraft and undersea environments [AIAA PAPER 71-1122] 01 p0068 A72-10558
- Equilibrium concentrations of negative ions in nighttime D region, comparing computations to mass spectrometric measurements 01 p0063 A72-10917
- Aeros satellite mass spectrometer, retarding potential analyzer and neutral gas thermograph onboard experiments, noting measurements and data transmission triggering by flight direction sensor [DGLR PAPER 71-093] 02 p0284 A72-12727
- Aeros satellite mass spectrometer design, discussing operation mode ion detection system, power supply, logarithmic electrometer and modulator 02 p0232 A72-12729
- Quadrupole mass spectrometer ultimate characteristics concerning resolution, range, recording speed, working pressure and sensitivity 03 p0360 A72-13665

Lunar mass spectrometer experiment, determining global distributions and diurnal variations of lunar atmosphere

04 p0509 A72-15103

Single breath diffusing capacity and alveolar dead space measurements for carbon 18 monoxide using respiratory mass spectrometer

04 p0480 A72-15215

Rocket-borne mass spectrometer with helium cooled electron bombardment ion source to reduce gas-wall interactions effects

04 p0524 A72-15538

Thermospheric structure between 100 and 400 km from rocket soundings and ground observations, noting mass spectrometers chemical reactions influence on atmosphere model accuracy

09 p1300 A72-23015

Mars atmospheric entry experiments for Viking 1975 mission, discussing onboard neutral gas mass spectrometer and retarding potential analyzer

10 p1540 A72-24381

Rocket-borne mass spectrometer tested in high velocity molecular beam facility for thermospheric atomic oxygen density measurement

11 p1634 A72-26422

Mass spectrometer measurements of hydrogen, helium, nitrogen, oxygen and nitrogen oxide ion concentrations vertical profiles in ionosphere at midlatitudes

11 p1628 A72-26906

Atmospheric ion composition analysis by RF mass spectrometer during rocket ionosphere sounding, discussing meteor ionization layers

15 p2225 A72-31915

Lower thermospheric neutral gas density and composition rocket-borne mass spectrometric measurements with liquid He cooled ion source

15 p2236 A72-31942

Satellite instrument to observe atmospheric composition by energy analysis of incoming gas stream, using velocity mass spectrometer for neutral particles measurement

15 p2236 A72-31966

Mesospheric and lower thermospheric composition from neutral atmospheric particles measured by rocket-borne instrument consisting of RF quadrupole mass spectrometer

15 p2228 A72-31967

An atomic oxygen beam system for the investigation of a mass spectrometer response in the upper atmosphere.

19 p2795 A72-37515

A simple combination mass spectrometer inlet and oxygen electrode chamber for sampling gases dissolved in liquids.

19 p2762 A72-38146

Dissociation of molecular ions formed by charge exchange in an in-line tandem mass spectrometer.

19 p2763 A72-38801

Nozzle beam-mass spectrometer system for studying one-atmosphere flames.

20 p2921 A72-38975

Electronic circuit for linearizing the transfer function of a photographic plate used in mass-spectrometry.

20 p2925 A72-39428

Helium-cooled mass spectrophotograph and frigen-cooled radiometer in a plasma wind tunnel

20 p2928 A72-39929

An integrated multi-purpose biology instrument utilizing a single detector, the mass spectrometer.

23 p3287 A72-43397

MASS SPECTROMETRY

U MASS SPECTROSCOPY

MASS SPECTROSCOPY

Mass spectrometric investigation of high power laser beam plasma on solid target, determining multicharged ion yield, energy, angular distribution and recombination effect

01 p0079 A72-10349

Mass spectroscopic analysis of addition effects of Xe, hydrogen and oxygen on CO-He laser discharge

01 p0079 A72-10517

Atomic/molecular oxygen concentration ratio semi-annual variation at 130 km altitude from mass spectroscopic data analysis

02 p0218 A72-11947

Ionospheric ion-molecule and ion-electron reaction rate constants determination from nighttime flight of rocket-borne ion mass spectrometer data least square fitting

03 p0347 A72-13396

Colorado Green River Formation oil shale extracts, determining nitrogenous compounds content with high resolution mass spectrometry

03 p0320 A72-13741

Mass spectrometric studies of solvent extractable acid methyl esters of oil shale from Colorado Green River Formation

03 p0320 A72-13742

Specific quantitative trace analysis technique for solids using spark source mass spectrometry

03 p0361 A72-13849

Apollo 11 lunar fines behavior and gas evolution characteristics from high vacuum differential thermal analysis and mass spectroscopy

04 p0569 A72-14504

Organic materials detection on planetary surfaces with in situ gas chromatography and mass spectrometry

04 p0573 A72-14808

Largest Apollo 15 lunar rock mass spectrometry analyses of noble gases with gas retention age estimation and spallation Kr data

06 p0888 A72-18267

Mass spectral analysis of aliphatic amino acid derivatives, obtaining diagnostic criteria for distinction of alpha, beta, gamma and N-methyl isomers

07 p0935 A72-18905

Gas content determination in metals by melting and vaporizing measured microvolumes using laser microprobe and magnetic mass spectrometer

07 p1006 A72-19549

Gaseous boron dioxide and oxyfluoride heat of formation determination by mass spectroscopy and molecular effusion technique

[AD-740421] 07 p0936 A72-19682

Teflon diffusion membrane for in vivo blood and intramycardial tissue gas tension measurement by mass spectroscopy without chemically bonded heparin surface

08 p1124 A72-20901

Mass spectroscopic measurement of inert gases in Lunik 16 fragments and dust samples

09 p1380 A72-22267

Eu and Sr distribution between coexisting feldspars in acidic rocks, using mass spectroscopic isotope dilution method

10 p1472 A72-24166

Viking Lander mass spectroscopic analysis of organic compounds, water and volatile constituents of Martian atmosphere and surface

10 p1540 A72-24383

Mass spectrometric analysis of positive ions in carbon dioxide laser systems with nitrogen-helium mixture

10 p1492 A72-24411

Rocket-borne mass spectrometric studies of composition of lower thermosphere

11 p1622 A72-25847

Chemical ionizing mass spectrometry with electron bombardment of reactant gas, discussing plasma chromatography

11 p1590 A72-26389

Atmospheric temperature measurement by neutral particle wake method, using satellite-borne mass spectrometer

11 p1634 A72-26408

High vacuum mass spectroscopic analysis of volatile products released under friction from solid synthetic resin lubricants with molybdenum disulfide as antifriction filler

12 p1835 A72-28199

Atomic/molecular oxygen concentration ratio semi-annual variation at 130 km altitude from mass spectroscopic data analysis

13 p1949 A72-29259

Mass spectroscopic determination of vapor composition during GaAs and GaP single crystals exposure to ruby laser radiation

14 p2109 A72-30316

Mass spectrometric techniques for collision processes in decaying nitrogen-helium and nitrogen-neon plasmas, obtaining ambipolar diffusion coefficients and reaction rate constants

15 p2283 A72-31299

Thermospheric composition global model for magnetically quiet conditions based onOGO-6 mass spectrometer measurements

15 p2227 A72-31954

Lower thermosphere neutral composition from February 1969 rocket-borne mass spectrometer measurements over Fort Churchill, Canada

16 p2383 A72-32965

IR mass spectrometric study of OBF in Ne and Ar matrices, discussing molecular structure

16 p2360 A72-33223

Positive and negative ions relative intensity measurement during nitrous oxide target molecules injection into sonic Ar plasma reaction channel, using quadrupole mass spectrometer

[AIAA PAPER 72-675] 16 p2440 A72-34064

Mass spectrometer sampling system for measuring effluent concentrations downwind of stacks at various positions in turbulent flow within atmospheric simulation facility

[AIAA PAPER 72-649] 17 p2536 A72-35478

Solid-body-surface and thin-layer analyses by the static method of secondary-ion mass spectroscopy

18 p2719 A72-36830

Lunar volcanic gas release rate estimation from orbiting Apollo spacecraft-borne mass spectrometer detection, noting atmospheric perturbation

19 p2868 A72-38736

Spacecraft atmosphere trace contaminant sensor system using mass spectrometric analysis of contaminants concentrated on sorbents in monitor inlet system

[ASME PAPER 72-ENAV-15] 20 p2896 A72-39162

Recent positive and negative ion composition measurements in the lower ionosphere by means of mass spectrometers.

20 p2917 A72-39528

Neutron activation and mass spectrometry methods for geochemical analysis of rare earth elements in meteoritic, lunar and terrestrial materials

20 p2899 A72-39835

The mass spectrographic measurement of gas separation with the aid of ambipolar effusion in neon-krypton mixtures

21 p3053 A72-40486

Chondrite and achondrite Nb abundance from spark source mass spectroscopic analysis

21 p3104 A72-40492

MASS TRANSFER

Flare region curved absorption lines interpreted as photospheric and chromospheric mass motions

01 p0129 A72-10800

Turbulence intensity effects on mass transfer from cylinders in cross flow at various Reynolds numbers

[ASME PAPER 70-WA/HT-3] 02 p0205 A72-12312

Solar wind induced atmospheric mass loss from magnetic field-free planets, using mass, momentum and energy conservation laws

02 p0275 A72-12465

Coronal magnetic fields effects on energy and mass flux from lower solar atmosphere levels into corona, discussing plasma instabilities, solar flares, radio bursts, etc

03 p0422 A72-13206

Global angular momentum balance, considering atmospheric frictional torques and fluxes, ocean water mass exchanges and seasonal variations effects

03 p0384 A72-14142

Heat and mass transfer equations for unsteady transpiration cooling, taking into account temperature gradient between coolant and surface

03 p0457 A72-14154

Heat and mass transfer processes in systems of bodies with variable phase boundaries, proposing difference scheme

03 p0458 A72-14159

Trimethylchlorosilane film boiling for silicon carbide deposit on vertical heated tungsten filaments, investigating mass transport rate

04 p0595 A72-14600

Quasi-linear parabolic equations loaded system first boundary value problem for heat and mass transfer equations inverse problems

04 p0540 A72-15545

Heat and mass transfer along axially conducting gas controlled heat pipes, discussing wall temperature profiles and condenser characteristics

[ASME PAPER 71-WA/HT-29] 05 p0745 A72-15882

Book on heat and mass transfer, covering research results over 1953-1969 on supersonic aircraft and missiles cooling problems, rarefied gas dynamics boundary layer flow, etc

05 p0747 A72-16399

Turbine blade local heat transfer coefficient calculation with digital computer program and naphthalene blade mass transfer in cascade flow

05 p0747 A72-16498

Heat and mass transfer blowing correction correlations for graphite and charring ablator reentry nosetip and heat shield applications

[AIAA PAPER 72-91] 05 p0748 A72-16810

Mass transfer effects on hypersonic turbulent boundary layer properties from profile measurements on porous cone

[AIAA PAPER 72-184] 05 p0650 A72-16839

Transient compressible heat and mass transfer in porous media, solving coupled nonlinear partial differential equations in finite difference form by iterative technique

[AIAA PAPER 72-23] 05 p0749 A72-16914

Analytical models for predicting mass transfer cooling effects on blade row efficiency of turbine airfoils

[AIAA PAPER 72-11] 05 p0707 A72-16943

Graphite ablation in combined convective and radiative heating, considering mass and energy transfer effects

[AIAA PAPER 72-88] 05 p0750 A72-16954

Shock wave deceleration and boundary layer mass loss effects on electron density and ionization levels of air in shock tube

05 p0700 A72-17225

Numerical solution of supersonic flow past blunt bodies with large mass injection, deriving finite difference equations

06 p0756 A72-18114

Reynolds analogy based correlation method for Stanton number prediction for turbulent heat and mass transfer in smooth tubes

06 p0903 A72-18186

Bulk vapor formation processes during laser beam heating of metals, considering effect on mass transfer

07 p1000 A72-18939

Heat and mass transfer in initial section of circular pipe under stabilized laminar flow, using modified Leveque method

07 p0968 A72-19883

Iterative solution of differential equations for steady plane flow with heat and mass transfer at high Reynolds numbers

07 p0971 A72-20098

Temperature fields and mass and heat transfer at surface of solid spherical particle in laminar viscous fluid flow

07 p0973 A72-20318

Modified mixing length velocity distribution predictions for turbulent boundary layers with uniform mass transfer for low and high Reynolds numbers

08 p1150 A72-21622

Heat and mass exchange in laminar boundary layer in air-carbon dioxide binary mixture under free convection on porous heated vertical surface

08 p1255 A72-21664

Soviet book on heat and mass transfer and friction in gradient fluid flows in variable cross sectioned ducts and at surface of bodies

08 p1152 A72-22022

Free turbulent jet heat and mass exchange and axial flow characteristics

09 p1292 A72-22235

Mass and energy exchange in tropical convective cloud systems from ATS cloud photographs

09 p1344 A72-22430

Burning process of low boiling Mg particle moving in relation to gaseous oxidizer, assuming heat and mass transfer occurrence by diffusion-conduction mechanism

09 p1411 A72-22888

Newton cooling law applicability to unsteady heat and mass transfer approximate calculation for ion exchange process

09 p1412 A72-23685

Heat and mass transfer analogy based on coefficients ratio and boundary layer theory

09 p1412 A72-23686

Book on heat and mass transfer analysis covering conduction, boundary layer and channel flow convection, thermal radiation, rarefied gas mechanics, thermophysical properties, etc

10 p1561 A72-23748

Nonthermal emission and ejection of matter from galactic nuclei, discussing radio, optical and IR synchrotron sources and background radiation

10 p1535 A72-23906

Thin liquid surface water film cooling tests for mass loss under simulated reentry heating and shear conditions

10 p1563 A72-24648

High mass transfer rate effect of foreign gas on transport coefficients in fully developed turbulent flow

11 p1614 A72-25231

Noncoincidence of maximum velocity and zero shear stress due to asymmetric turbulent velocity profiles, considering effect on momentum, heat and mass transfer in noncircular channels

11 p1618 A72-26534

Mass transfer effect on adiabatic wall enthalpy and recovery factors in laminar boundary layer flow at high injection rates, using self similar solutions

11 p1746 A72-26535

Laminar transition and turbulent natural convection mass transfer measurements on inclined and vertical surfaces by electromechanical method

11 p1635 A72-26536

Heat and momentum transfer of binary gas mixture flow in parallel plate channel with mass injection from porous wall, calculating velocity, pressure and temperature distributions

11 p1746 A72-26538

Turbulent gas flow mass transfer coefficient derived from Lapin relation between vertical velocity and concentration distributions in turbulent boundary layer near semipermeable surface

12 p1889 A72-28136

Papers on heat and mass transfer covering physicochemical conversions, transonic gas flow in closed channels, drying theory, turbulent flows, liquid evaporation, electrorheology, etc

13 p2063 A72-28626

Linearized steady motion of gas with mass sources and sinks, determining resonance onset conditions

13 p1893 A72-28731

Equilibrium diabatic Ekman layer geostrophic drag, heat and mass transfer coefficients, presenting velocity and temperature profiles

14 p2100 A72-30346

Radiation pressure on quasar outer envelope material as cause of mass outflow for masses less than gravitational force-determined critical value

14 p2155 A72-30552

Mass exchange and thermal time scales for shell source burning binary components with deep outer convective layers, interpreting numerical results from analytical model

14 p2159 A72-30739

Galactic tidal interactions, computing mass loss for hyperbolic collisions and giant system formation from density distribution models

14 p2161 A72-31043

Mass transfer effect on heat transfer to evaporating droplet, considering mass efflux shielding effect and forced convection flow field

14 p2172 A72-31051

Integral method application to convective flows with axial diffusion, obtaining heat and mass transfer characteristics

14 p2096 A72-31058

Free stream turbulence effect on mass transfer from circular cylinder in cross flow as function of Schmidt and Reynolds numbers, using electrochemical measurement method

14 p2096 A72-31061

Heat and mass transfer in steady viscous flow through curved circular tubes, investigating velocity and temperature profiles

14 p2173 A72-31064

Mass entrainment products effect on radiative and convective heat transfer during decomposition of graphite blunt body in steady hypersonic flow of radiating air

14 p2174 A72-31158

German monograph on mass transport in thin fluid layers covering diffusion, convection, laminar flow rate distribution, flame ionization and gas chromatography measurements, etc

15 p2216 A72-31350

Holographic determination of local convective mass transfer coefficients over flat plate normally impinged with laminar air jet, using swollen polymer transparent coating

15 p2239 A72-32349

Exact boundary layer calculations for heat and mass transfer on cones at angle of attack, considering Mach number, enthalpy ratio and cross flow effects

15 p2337 A72-32591

PTFE thin films interspersal with lumps and streaks from transfer to smooth surface during low speed sliding, discussing friction coefficient under various conditions

16 p2396 A72-32870

Thermodynamic properties of axisymmetric and planar stagnation flows of air with gas injection, taking into account mass transfer effects on heat transfer rate

16 p2477 A72-33428

Boundary conditions influence on heat and mass transfer in low temperature heat pipes with freon as working fluid

16 p2479 A72-33853

Book - The method of weighted residuals and variational principles: With application in fluid mechanics, heat and mass transfer

17 p2573 A72-34250

Measurement of the parameters and the structure of a wet vapor flow with interphase heat and mass transfer in the relaxation zone behind the front of a shock wave

17 p2637 A72-35130

Heat and mass transfer in initial section of circular pipe under stabilized laminar flow, using modified Leveque method

17 p2637 A72-35131

Flow over infinite wedge with mass transfer by boundary suction or injection, solving nonlinear boundary layer equations by parametric differentiation method

17 p2485 A72-35230

Arch prominence outside west limb on 24 April 1971, noting H α alpha monochromatic image, internal motion of matter and radio emission

17 p2614 A72-35503

Heat mass and momentum transport in free turbulent mixing

17 p2543 A72-35638

Turbulent boundary layer with discontinuity in wall temperature and concentration

17 p2638 A72-35746

Book - Investigation of nonstationary heat and mass transfer processes by the net-point method

18 p2740 A72-36248

Evolution of close binary systems with intermediate initial mass ratios

18 p2728 A72-36741

German monograph - A photometric method for measuring the concentration distribution in turbulent boundary layers

19 p2799 A72-37652

Burning of carbon particles in a supersonic chemically active gas flow

19 p2882 A72-38454

Investigation of the transport of electrode metal during welding in a carbon dioxide atmosphere

19 p2810 A72-38588

On the application of perturbation theory for the calculation of molecular constants due to small mass changes and on the determination of force constants from very heavy isotope substitution

19 p2763 A72-38806

The prediction of compressible turbulent boundary-layer flows with mass addition.

[ASME PAPER 72-HT-58]

20 p2914 A72-39658

An analytical solution of wall-temperature distribution for transpiration and local mass injection over a flat plate.

[ASME PAPER 72-HT-57]

20 p2985 A72-39659

Transient laminar free convection in closed spherical containers.

[ASME PAPER 72-HT-37]

Heat and mass transfer in the initial mixing region of confined coaxial laminar jets.

[ASME PAPER 72-HT-22]

A differential interferometer and its application to heat and mass transfer measurements.

[ASME PAPER 72-HT-12]

A two-equation model of turbulence applied to the prediction of heat and mass transfer in wall boundary layers.

[ASME PAPER 72-HT-15]

Prediction of turbulent boundary layer heat transfer with pressure gradient and mass transfer.

[ASME PAPER 72-HT-16]

Heat and mass transfer in Venturi tubes

20 p2928 A72-40048

Results of a study of heat and mass transfer during the purification of helium from nitrogen by the condensation method

21 p3127 A72-40130

Russian book - Heat and mass transfer: A reference book.

21 p3128 A72-40350

Unsteady state description of living corneal mass transport modes, elucidating cornea thickness control mechanism

21 p3001 A72-40912

Investigation by the mass transfer method of the diffusion of nickel at a $1/110^\circ$ surface of tungsten single crystals

21 p3068 A72-40955

Calculation of heat shield with local mass injection in hypersonic flow.

21 p3131 A72-41235

Studies on the convective heat transfer from a rotating disk. VI - Experiment on the laminar mass transfer from a stepwise discontinuous naphthalene disk rotating in a uniform forced stream.

22 p3243 A72-41946

A calculation procedure for heat, mass and momentum transfer in three-dimensional parabolic flows.

22 p3243 A72-41954

Flat compressible turbulent boundary layers of air, predicting foreign gas injection effects on mass and heat transfer Stanton numbers and skin friction

22 p3165 A72-41958

Arbitrary length thin liquid film cooling mass transfer data correlation, accounting for film roughness and entrainment effects

22 p3243 A72-41960

Numerical analysis of the natural convection in a porous medium between two concentric cylinders

22 p3244 A72-42640

Rate of molybdenum solution in carbon-saturated liquid iron.

22 p3193 A72-43027

Descriptive model of the turbulent motion of an isovolumetric fluid

23 p3279 A72-43699

Centaurus X-3 - Possible reactivation of an old neutron star by mass exchange in a close binary.

24 p3439 A72-44976

MAST SHOCK TUBES

U MAGNETIC ANNULAR SHOCK TUBES

MATCHING

Least squares and point matching techniques compared for solution of two dimensional steady state heat conduction problems with irregularly shaped boundaries

[ASME PAPER 71-HT-P]

Visual and haptic perception in angle reproduction matching task, noting performance differences relation to nature of form discrimination and task

10 p1433 A72-25126

MATERIAL ABSORPTION

Hydrogen diffusion kinetics in Nb under various temperatures during gas-metal absorption experiments, observing room temperature hardness profile

01 p0087 A72-11026

Nitrogen interaction with Ni-based melts at 1600 C, noting absorption rate dependence on nitrogen diffusion rates and melt viscosities

07 p1011 A72-19546

Thermodynamic analysis of metal surfaces covered by electropositive adsorbates.

18 p2656 A72-36126

Spacecraft functional properties degradation due to surface contamination with outgassing vapors, discussing contaminant materials transport and sorption characteristics

23 p3254 A72-43619

MATERIAL BALANCE

NT WATER BALANCE

MATERIAL REMOVAL [MACHINING]

U MACHINING

MATERIALS EROSION

U EROSION

MATERIALS HANDLING

NT GROUND HANDLING

NT PROPELLANT TRANSFER

NT REMOTE HANDLING

Vacuum handling system for lunar materials thermophysical properties measurements under contamination preventive conditions 04 p0509 A72-15496

Asbestos reinforced plastics safe handling and manipulation ensured by regulations provided precautions 11 p1583 A72-25549

Air cargo growth potential, marketing and profitability, considering need for improvements in ground handling, rate structure, container standardization, documentation, etc 13 p1896 A72-28452

Terminal handling environment and air cargo requirements for noncontainerized freight 16 p2372 A72-33175

Book - Industrial robots - A survey: Details of construction, performance, prices, and applications / Enlarged edition/ 22 p3183 A72-43099

Boeing 747-F cargo aircraft, describing onboard and ground facilities for freight handling and loading 23 p3278 A72-43245

Air freight ground handling and distribution terminal facilities and methods, discussing future technical and organizational developments for efficient handling of increased traffic volume 23 p3358 A72-43246

Feeder for the supply of powder materials to spraying setups 23 p3278 A72-43293

Flying crane helicopters utilization in construction industry for materials transport and structural erection work, discussing technical and economic aspects 23 p3251 A72-43637

The heavy lift helicopter - An operations research/technology/performance blend. 24 p3466 A72-44581

MATERIALS RECOVERY
NT WATER RECLAMATION
Rolling operations in vacuum for protection of metallic materials underprocessing 11 p1645 A72-26867

MATERIALS SCIENCE
Materials science historical development from ancient theories of structure of matter to modern atomic and field theories leading to general theory of elastic continuum 02 p0297 A72-12611

Transparent rain repellent polymer coatings, discussing water repellency theory, polymer chemical structures, adhesion to glass surfaces and evaluation methods 03 p0381 A72-14237

Materials research for investment cast turbine wheel, investigating Fe base specimens 05 p0666 A72-16496

Materials selection problems due to wide variety of new products, discussing technologically and economically optimal decisions on product design, development and future substitutions 06 p0906 A72-18255

Soviet book on nonmetallic material strength during nonuniform heating covering, load endurance, bending phenomena and thermal stability of fiberglass, pyroceramics and reinforced plastics 06 p0796 A72-18521

NASA materials science and manufacturing in space program involving space shuttle reusable equipment and weightlessness applications experiments 06 p0797 A72-18621

Laboratory metal corrosion testing, considering reasons, conditions and damage assessment 08 p1189 A72-22104

Electron microscopy and structure of materials - Conference, University of California, Berkeley, September 1971 11 p1666 A72-26926

Materials science - Conference, Los Angeles, April 1972 12 p1833 A72-28076

Macroparametric, microstructural and general rationales methods for fatigue resistant materials, noting crack propagation and fracture mechanics 14 p2120 A72-30612

Materials characteristics relevance for USAF technology, discussing processing conditions, environment simulation, real time techniques, ultrasonic and X ray inspection methods, etc 16 p2404 A72-32823

Carbon-carbon composite process and fabrication techniques, discussing heat treatment effects and physical properties correlation to material structure 17 p2561 A72-35666

Book - Treatise on materials science and technology, Volume I 18 p2718 A72-36392

Book - Annual review of materials science. Volume I 19 p2843 A72-37441

Isolator elastomers properties, discussing spring isolators, combination springs and pneumatic systems 19 p2806 A72-37550

Essential factors in reliability prediction and stress analysis of structural component with wide load and temperature variations 19 p2874 A72-37710

Time spectrum and angular distribution for positron annihilation studies of electron structure and phase transformations of materials 19 p2845 A72-38401

Japan Congress on Materials Research, 15th, Tokyo, Japan, September 1971, Proceedings. 20 p2935 A72-38877

Interamerican Conference on Materials Technology, 3rd, Rio de Janeiro, Brazil, August 14-17, 1972, Proceedings. 20 p2936 A72-39201

Structure-property relationships in polymeric materials. 20 p2944 A72-39212

Factors affecting acoustic emission response from materials. 20 p2924 A72-39279

Russian book - Handbook of aircraft materials. 21 p3072 A72-40459

Environmental characteristics and advantages of manufacturing in space, considering gravity, vacuum, temperature, pressure and radiation effects on materials and products processing 21 p3060 A72-40968

A non-equilibrium thermodynamic theory of simple materials based on a single-integral entropic functional. 21 p3124 A72-41505

The effect of a thermal and ultrahigh vacuum environment on the strength of precompressed granular materials. 22 p3173 A72-42528

Book - Fracture: An advanced treatise. Volume 7 - Fracture of nonmetals and composites. 23 p3345 A72-43501

Brittle ceramic materials strength, showing porosity effect dependence on Weibull homogeneity parameter value 23 p3306 A72-43750

Materials creep behavior and elevated temperature design. 24 p3453 A72-44553

Book - A review of the science of fibre reinforced plastics. 24 p3417 A72-44674

MATERIALS TESTS
Ground test determination of design data for low supersonic high density air deployable deceleration systems, considering high strain rate effects on parachute materials 01 p0005 A72-10313

Statistical methods application to parachute materials evaluation, using factorial experiments for multiple variables simultaneous effects analysis 01 p0005 A72-10317

Aerospace wire and cables testing methods standards for evaluating mechanical, electrical and chemical properties, coating thicknesses, continuity flaws, flammability, geometrical characteristics, etc [SAE AS 1198] 01 p0006 A72-10384

Structural sandwich panel design, establishing simple stress and deflection formulas under transverse loading based on tests evaluating balsa as laminate core 01 p0138 A72-10723

Impact sensitivity of space shuttle materials in liquid and gaseous oxygen at high pressures 01 p0102 A72-10772

Material characteristics effect on compaction behavior of metal powders, stressing density and pressure measurements 02 p0242 A72-11460

Polycarbonate yield locus from strain rate, creep, isotropy, isoclinic and reloading tests on perforated plates [SESA PAPER 1819] 02 p0248 A72-11501

Papers on metal fatigue damage covering basic mechanisms, detection, field practices for repair, avoidance and control 02 p0295 A72-12495

Acoustic emission techniques in defect structure materials tests, discussing fracture strength, crack propagation, fatigue, plastic deformation and creep in metals, composites and rocks 03 p0362 A72-13225

Flammability smoke hazards and combustion product toxicity tests of plastics [PI PAPER 2] 03 p0379 A72-13243

Aircraft interior materials selection relative to fire hazards and smoke emission properties [PI PAPER 18] 03 p0380 A72-13249

Thermography capabilities and limitations for design analysis and quality control in nondestructive testing of material test vehicle carbon-carbon composite cones 03 p0364 A72-14026

Nondestructive testing for materials inspection and monitored aircraft maintenance programs 03 p0364 A72-14201

MATERIALS TESTS
Materials spectral emission properties measurement, comparing with absolute black body model 04 p0596 A72-14652

Quality control of powdered metal parts, considering chemical, atomization, electrolytic and mechanical production stages, tool inspection and test patterns 06 p0822 A72-18070

Low temperature test facility for cryogenic and rocket materials under combined tension and torsion 06 p0797 A72-18648

Explosive shock loading effect on materials mechanical properties, describing test equipment 06 p0797 A72-18659

Two-fold congruency tests of penetrant inspection system sensitivity using hydrophilic and lipophilic removers/emulsifiers/ 07 p0995 A72-19650

Real time computer aided mechanical testing and data analysis system for composites, confirming computer analysis by motion pictures of thin walled graphite/epoxy composite fracture 07 p0965 A72-19734

Fatigue life gages to determine cumulative fatigue damage due to variable cyclic strain history on unmatched materials 08 p1163 A72-20915

Materials ideal strength calculation compared with test results 08 p1242 A72-21185

Flame resistant materials for aircraft fire fighter protective clothing from systems approach tests 08 p1126 A72-21585

Interlaminar shear testing of composite materials, discussing short beam, scissor and torsional methods [PI PAPER 7] 09 p1337 A72-22542

Material testing by holographic interferometry, discussing application to early detection of delayed cracking, fatigue damage and bond imperfections 10 p1482 A72-24575

Space and ground environments effect on cryogenic multilayer insulation materials, tabulating mechanical and thermophysical test data [AIAA PAPER 72-286] 11 p1741 A72-25225

Surface patterns from ablating, melting and flowing materials in supersonic flow of wind tunnel, rocket motor and flight test environments, comparing with theory [AIAA PAPER 72-313] 11 p1743 A72-25247

Venus probes thermal insulation materials development and testing under simulated Venus atmospheric conditions [AIAA PAPER 72-368] 11 p1744 A72-25393

Reusable external insulation materials for space shuttle thermal protection, evaluating local heat transfer at interface areas in plasma arc test facility [AIAA PAPER 72-388] 11 p1744 A72-25409

Composite materials testing and design - ASTM Conference, Anaheim, California, April 1971 11 p1670 A72-25452

Rolled polycrystalline metal samples principal anisotropy direction determination by acoustic measurements at ultrasonic frequencies 12 p1806 A72-27086

Long term high temperature test machine to record structural changes of materials 12 p1795 A72-27464

Fracture toughness of high strength alloys, discussing rocket motor cases, nondestructive test standards and subcritical crack growth 12 p1829 A72-27656

High modulus fiber composite circular tube specimens multiaxial load testing, noting gripping methods to reduce transitional strains 12 p1886 A72-28000

Material fatigue failure criterion during cyclic loading, noting energy dissipation and resonant frequency roles 12 p1888 A72-28250

Materials selection for contact and clearance type seals for various environment conditions [ASLE PREPRINT 72AM 23] 13 p1964 A72-28975

Thermostat for electrical measurements of high resistance materials in air up to 1200 C 13 p1957 A72-29274

Lightning current tests of aircraft glass/carbon fiber reinforced plastics materials 13 p1898 A72-30040

High speed testing of materials mechanical behavior over range of loading rates 14 p2165 A72-30441

Pure shear testing method and apparatus, verifying validity of method by chromoplastic test specimens 16 p2469 A72-33231

Testing method for materials exposed to explosive forming, noting applications in study of formability, heat treatment effects and crack initiation 16 p2391 A72-33235

Surface crack detection in ferrous and nonferrous metals, glass, ceramics and plastics by water-washable dye penetrants process 16 p2397 A72-33239

Evaluation of sublimed molybdenum collector coatings for additive diode operation. 18 p2646 A72-36202

- A mechanical pulsator for testing plastics with the capacity for adjusting cyclic and mean load during test 18 p2676 A72-37097
- New method for determining the integral radiative capacity of partially transparent materials at high temperatures 18 p2704 A72-37190
- Nondestructive testing of advanced composites. 19 p2799 A72-37669
- On the fatigue crack propagation in polymeric materials. 20 p2943 A72-38886
- On the plastic behaviour of time dependent materials - Theoretical and experimental investigation. 21 p3124 A72-41504
- Postoperative states of turbine disk alloys at 280-500 and 550-630 C, noting lower durability values 23 p3347 A72-43737
- Investigation of the state of the structure of turbine-disk materials after operation 23 p3302 A72-43965
- Ultrasonic defect detection and evaluation techniques, stressing limitations for defect geometry, size and nature 24 p3408 A72-45294

MATHEMATICAL ANALYSIS

U APPLICATIONS OF MATHEMATICS

MATHEMATICAL LOGIC

- NT ALGORITHMS
- NT AXIOMS
- NT BOOLEAN ALGEBRA
- NT BOOLEAN FUNCTIONS
- NT BOREL SETS
- NT EQUIVALENCE
- NT FORMULAS [MATHEMATICS]
- NT LATTICES [MATHEMATICS]
- NT SET THEORY
- NT THRESHOLD LOGIC
- Probabilistic logic method, concepts and elementary operations in combining Boolean algebra and probability theory 08 p1197 A72-20869
- Truth table classification and numerical identification of character patterns of elements in groups and clusters 09 p1265 A72-22644

MATHEMATICAL MODELS

- NT ANALOG SIMULATION
- NT DIGITAL SIMULATION
- NT THOMAS-FERMI MODEL
- NT VENEZIANO MODEL
- Planetary atmosphere IR radiative transfer model using matched asymptotic expansions method 01 p0125 A72-10099
- Warm inhomogeneous plasma models perturbation analysis, computing high frequency oscillation and eigenfrequencies and eigenfunctions formulas 01 p0106 A72-10134
- Model with large Lorentz factor and relativistic relations violations to explain theoretical estimate disparity with experimental data for high energy primary cosmic rays 01 p0118 A72-10156
- Sound propagation and absorption mechanism in liquid-base foams explored by bubble pulsation and coupling mathematical model and distributed parameter mechanical analog 01 p0115 A72-10161
- Shock isolator model, using passive elements and variable Coulomb friction force to minimize transmitted shock and relative displacement 01 p0047 A72-10218
- Kalman filtering process digital simulation by numerical integration of matrix differential equations describing linear system random process model and optimal filter 01 p0024 A72-10225
- Aerial focal plane shuttered camera high velocity images mathematical model based on collinearity equations, incorporating translational and rotational camera motion during exposure for image motion compensation 01 p0066 A72-10461
- Mathematics for pattern recognition, discussing perception, combinatorics and statistics, feature selection, cybernetic methods and fuzzy sets 01 p0034 A72-10465
- Microwave propagation on nonlinear transmission lines by examination of energy dissipation in shock front, considering distributed and lumped-parameter models 01 p0029 A72-10692
- Bipolar transistor model for device and circuit performance prediction, determining parameter from charge distribution by regional approximation technique 01 p0042 A72-10786
- Mathematical model of porosity gas transport test for automated fusion welding operation using mass spectrometer 01 p0076 A72-10815
- Planetary quarantine cost and mission success constraints, formulating mathematical models for international goals and implementation systems 01 p0019 A72-10819

- Open magnetosphere mathematical models application to dayside auroras, investigating interplanetary magnetic field topology 01 p0060 A72-10885
- Three dimensional roll-controlled missile trajectory model for simple time-sharing digital or analog simulation, using wind-to-inertial axis transformation 01 p0130 A72-10964
- Statistical model for communication probability estimate based on signal-to-interference and SNR criteria 01 p0031 A72-10997
- Physical inconsistencies of mechanico-mathematical concepts of metal deformation, considering friction forces, lubricant action and plastic tensors and deviators 01 p0102 A72-11077
- Atmospheric primary and secondary cosmic ray propagation with close reference to two-fire-ball, H-quantum and excited baryon models of multiple meson production 01 p0121 A72-11122
- Monte Carlo simulation on high energy cosmic ray propagation and multiplication in high altitude emulsion chamber observations, examining two-fire-ball and H-quantum models 01 p0121 A72-11123
- Hydraulic analogy application to heat conduction problems, considering seepage and network pipe flow models for complex heat flux phenomena representation 01 p0145 A72-11174
- Experimental development of homogeneous field of plane stresses gripped in biaxial traction, considering convex models under constraint 01 p0142 A72-11176
- Lateral spatial interactions of sensory receptors, discussing mathematical theory for monocular visual inputs described by real valued functions on continuum 01 p0021 A72-11196
- Spatially homogeneous rotating and expanding universe models, deriving Lagrangian function from Einstein field equations 01 p0103 A72-11260
- Energy spectrum equations for steady state turbulent convection model based on Heisenberg statistical theory, noting application to convection in planetary and stellar atmospheres 01 p0146 A72-11311
- Coaxial flow gaseous core nuclear reactor system dynamic analysis, developing mathematical model and equations solution by computer program 01 p0100 A72-11352
- Bidirectional scattering of electromagnetic waves from rough surfaces in plane of incidence restricted only by tangent plane approximation, comparing with other models 02 p0170 A72-11467
- Irredundant multiple output combinational logic network fault detection and diagnosis theorems derivation from structural models in labeled direct graph form 02 p0184 A72-11478
- Mathematical reliability modeling for fault tolerant digital computers, summarizing error masking and standby sparing reliability equations 02 p0184 A72-11481
- Ultrareliable fault-tolerant digital computer design with protective standby replacement and hybrid redundancy, presenting mathematical models for system reliability evaluation 02 p0185 A72-11487
- Reliable combinational logic networks, deriving conditions for fault locatability from directed graph formal model 02 p0185 A72-11491
- Three dimensional heat conduction behavior in laminated composites calculated from continuum model using asymptotic developments 02 p0300 A72-11547
- Second order Markov process statistical model for gravity anomalies in local region, applying to error analysis in inertial navigation system computerized simulation 02 p0207 A72-11596
- Creep theory by rheonomic body interpretation as controlled system with unknown vectors at input and output, obtaining stress-strain curves for experimental verification 02 p0289 A72-11620
- Aerodynamic multivariable function generation in real time simulation of high performance missile 02 p0186 A72-11656
- Mathematical model for control process as adaptive memory tracker, discussing digital simulation 02 p0186 A72-11659
- Single malfunction diagnosis models in systems failures, describing fixed and sequential testing schedules 02 p0186 A72-11689
- Plasma physics computer simulation of double stream and beam instabilities, wavelength nonlinearities and velocity distribution, using superparticle and Vlasov equation models 02 p0263 A72-11691

- Mathematical analogy between nonequilibrium and viscous inert transonic flows for reacting mixtures with relaxation and freezing 02 p0150 A72-11736
- Computerized statistical identification of aerial photograph ground patterns, comparing elliptical boundary condition with minimum distance to mean classification models 02 p0187 A72-11842
- Composite scattering theory mathematical model for radar backscattering cross section relation to ocean surface conditions and wind velocity 02 p0172 A72-11868
- Satellite-borne radar altimetry pulse compression, discussing signal return statistics, receiver models and detected waveshape relation to altitude, attitude and antenna beamwidth errors 02 p0172 A72-11870
- Thermal modeling for IR images geologic interpretation, discussing physical parameters role in materials natural environmental diurnal temperature behavior 02 p0214 A72-11877
- Extended Thomas-Fermi isolated atom model for pulsar outermost crust magnetic field effects, using pressure-density equations of state 02 p0277 A72-11903
- Three dimensional angle dependent model for three body problem, considering exact quantum mechanical reactive scattering cross sections 02 p0262 A72-11911
- Random processes models based on Poisson sequences extended to simultaneous asymmetry and probability density function excess, establishing asymptotic relationships 02 p0216 A72-11919
- Anomalous magnetic and gravitational fields energy spectra model, examining autocorrelation functions changes 02 p0217 A72-11932
- Oxygen distribution in human brain under counter-current capillary blood flow conditions, presenting mathematical simulation for transport in Krogh system 02 p0168 A72-12037
- Chlorella growth rate model, presenting specific photosynthetic and urea and carbon dioxide utilization rates 02 p0160 A72-12038
- Mathematical model for radiation damage cross section linear energy transfer dependence, explaining experimental values of relative biological effectiveness [CERN 71-16] 02 p0160 A72-12052
- Turbulent flow development in concentric annuli from modified Reichart integral equation model for eddy diffusivity of momentum 02 p0203 A72-12103
- Nonlinear theory of cascaded two-way coherent spacecraft tracking system model, obtaining steady state probability density functions of phase and Doppler error 02 p0174 A72-12137
- TWT small parameters measurement for gain calculation, using equivalent transmission line model 02 p0193 A72-12229
- Elastic continuous media nonlinear models approximation, obtaining Euler-Lagrange functions 02 p0259 A72-12234
- Isotropic incompressible turbulence numerical simulation, presenting algorithm for convolution sums calculation 02 p0205 A72-12367
- Helium shock wave two step collisional ionization model comparison to observed profile data from laser Fabry-Perot interferometer 02 p0266 A72-12368
- Gravity model for spacecraft orbit prediction with gravitational anomalies, discussing gravity dipoles and disturbing acceleration tangential component [AAS PAPER 71-375] 02 p0283 A72-12424
- Anelastic solid energy dissipation linear memory models based on viscoelasticity theory, applied to earth and metals experimental data and dynamic loading problems 02 p0294 A72-12447
- Solids static electrification models based on solid state physics, considering contact, deformation and cleavage charging processes 02 p0269 A72-12552
- Size determination for stationary space charge clouds in streaming media from theoretical model of tanks filled with electrostatically chargeable inflammable fluids 02 p0261 A72-12554
- Book on mathematical fluid dynamics covering viscous and ideal fluid motion, boundary theory, constitutive equations, hydrodynamics and kinematics 02 p0206 A72-12623
- Circular cylindrical sandwich panel and rectangular sandwich plates dynamic stability under periodic external loads derived from mathematical model 02 p0298 A72-12664
- Mathematical model for research payoff estimation by internal rate of return method used by large corporations for project evaluation 02 p0305 A72-12695

- Turbulent supersonic separated flow field analysis and pressure measurements for two dimensional and axisymmetric internal and external flow models [DGLR PAPER 71-076] 02 p0152 A72-12710
- Closed boundary layer separation regions in super- and hypersonic flow, deriving mathematical model for neutral stability curves calculation [DGLR PAPER 71-065] 02 p0153 A72-12715
- Chapman uniform electrical conductivity core model for geomagnetic disturbance daily variations due to solar wind, noting error in analysis 02 p0222 A72-12794
- Multivortex model of vortex sheet development on slender axisymmetric bodies at angle of attack 03 p0307 A72-12919
- Human arm arterial pressure and flow pulsations numerical analysis, constructing electrical analog circuit from mathematical model 03 p0317 A72-12951
- Mathematical models for man-machine control behavior in biodynamic environments including manual control performance and interface elements 03 p0318 A72-13162
- Differential and difference equations approximate solutions in finite state machine form, developing adaptive gain changer model in aircraft stability control system 03 p0338 A72-13164
- Finite element discrete model for large aspect ratio wing transverse vibrations, using inhomogeneous elements with various stiffness-length relations 03 p0442 A72-13189
- Statistical model of small scale discrete structure of magnetoplasma in solar active regions 03 p0430 A72-13335
- Homogeneous isotropic elastic medium free vibration in unbounded space, obtaining relativistic relations in wave field from mathematical model 03 p0389 A72-13425
- Equivalent circuit models in semiconductor transport for thermal, optical, Auger-impact and tunneling recombination-generation-trapping processes [AD-740495] 03 p0401 A72-13585
- Steels fatigue life tests as function of stress level, confirming Wohler curves mathematical model 03 p0373 A72-13673
- Optimization algorithms synthesis models, discussing conceptual-implementable transition 03 p0327 A72-13702
- Angular momentum conservation law compliance of generalized triple configuration model for spin-detonation nucleus, assuming transverse Chapman-Jouguet wave 03 p0342 A72-13734
- Iterative hysteretic model for calculating magnetization distribution in thin magnetic layer for digital recording systems [IEEE PAPER 14.7] 03 p0328 A72-13769
- Mathematical model for design of plated-wire magnetic memory cell, considering drive requirement minimization as criterion [IEEE PAPER 21.1] 03 p0328 A72-13777
- Plate under projectile impact, calculating motion response due to random initial velocity distribution over surface by stochastic model 03 p0447 A72-13852
- Combustible fuel-air mixture laminar and turbulent flame propagation mathematical model, with reference to detonation and prevention 03 p0456 A72-13876
- Isotopic heat source unit multiple elliptical orbit reentry unperturbed by solar-lunar gravitational forces, deriving analytical model of grazing trajectories, aerodynamic heating and thermochemical ablation 03 p0457 A72-13959
- Computer modeling technique for electromagnetic scattering and radiation problems in resonance region employing thin wire electric field integral equation 03 p0328 A72-14028
- Mathematical modeling methodology for communication receiver life cycle EMC decisions, considering analysis and prediction problems with emphasis on nonlinear circuits and systems 03 p0324 A72-14034
- Computer aided intrasystem electromagnetic compatibility prediction programs, discussing mathematical models and program philosophies 03 p0328 A72-14039
- LSI/MOS logic circuits radiation effects prediction from modeling studies of individual devices on test chip 03 p0334 A72-14087
- Statistical thermodynamics models for determining vacancy concentration and atoms and vacancies arrangement in metals and alloys under thermal equilibrium 03 p0378 A72-14255
- Hydrogen diffusivity in Fe with cavities at room temperature calculated by mathematical model and numerical methods 03 p0378 A72-14256
- Turbulent particle diffusion statistical mechanical model, using random walk 03 p0344 A72-14331
- Mathematical models of elastic shells and rods, discussing virtual work, operator classifications, deformations and constitutive equations 03 p0454 A72-14344
- Radar signal processing by digital computer modeling, presenting apparent target splitting probability and azimuth estimate distribution for shifting window target detectors 03 p0326 A72-14361
- Mathematical model for two-stream instability induced anomalous resistivity and heating in plasma with equal initial electron and ion temperatures in static electric field 04 p0554 A72-14402
- Two dimensional solar cell model with partial differential equation relating arbitrary point potential to cell parameters for I-V characteristics prediction 04 p0465 A72-14480
- ATC for North Atlantic air transportation, emphasizing collision risk model for safety standards assessment 04 p0544 A72-14484
- Computer model of dislocation motion acted on by viscous drag through point obstacle array for tensile stress and shock deformation tests [AD-737978] 04 p0584 A72-14528
- Microwave breakdown prediction models for antenna system in ionized reentry environment 04 p0486 A72-14531
- Kinetic-analytical models for nitric oxide formation in combustion processes, evaluating heterogeneous effects [WSCIP PAPER 71-28] 04 p0482 A72-14581
- Nuclear rocket time optimal start-up using distributed parameter system model with linear control and nonlinear state 04 p0547 A72-14672
- Analytical model for acoustic impedance of perforated plate liner with multiple frequency excitation, discussing effects of fluid motion, grazing flow and spectral excitation 04 p0548 A72-14699
- Human and animal controlled self rotating maneuvers during free fall, comparing theoretical motion analysis with photographs of falling cats 04 p0478 A72-14709
- Photochemical electron transfer evolution models, noting titanium and zinc oxides as photosensitizers 04 p0484 A72-14777
- Extended iterative weighted least squares estimation of coefficients for linearly independent component signals in linear model 04 p0539 A72-14913
- Large amplitude whistler mode wave packet multiple emissions model including wave-particle interactions 04 p0517 A72-14948
- Large linear time invariant dynamic control system optimum simplified model based on performance index connecting feedback errors 04 p0506 A72-15113
- Cyclic strain accumulation induced creep behavior prediction via plasticity model, considering non-homogeneous stress states [ASME PAPER 71-APM-NN] 04 p0589 A72-15179
- Fiber reinforced composites with transversely isotropic constituents, discussing various mathematical models for elastic constants calculation 04 p0590 A72-15189
- External biodynamic models for human mechanical response to various environmental forces, emphasizing injury mechanisms 04 p0481 A72-15266
- Bipropellant fuel droplets combustion in oxidizing atmospheres from spherico-symmetrical nonconvective quasi-steady state model, discussing supercritical pressures and forced convection probability 04 p0596 A72-15273
- Cross correlation model for interpreting empirical results on binaural noise masking level differences in sinusoidal signal detection, comparing with equalization-cancellation model 04 p0550 A72-15296
- Boltzmann equation collision integral statistical models, solving shock structure in monatomic gas 04 p0513 A72-15339
- Arrhenius model and graphical methods for temperature accelerated life tests in electrical insulation systems 04 p0500 A72-15364
- Mathematical model for reciprocal and nonreciprocal magneto-optical effects in magnetized ferrite-filled microstrip transmission lines 04 p0502 A72-15434
- Mountain barrier and convective area minimum size determination for numerical forecasting models, reducing primitive equations system to advection difference equation 04 p0544 A72-15459
- Markov model random variation optimal periodicity in preventive maintenance operations, estimating distribution density and moments 04 p0527 A72-15574
- Earth mantle shear velocity model derived from S waves travel time gradient direct measurement, disregarding deep depth lateral homogeneity assumption 04 p0519 A72-15578
- Book on similarity laws and modeling covering dimensional analysis, transformations, differential equations, gas flows and nonequilibrium processes 04 p0513 A72-15675
- Integrated data processing system organizational model methodology for individual firms, emphasizing interdependence on program groups 05 p0632 A72-15815
- Rarefied gases thermal energy diffusion model, using radiative transfer electrical network analog [ASME PAPER 71-WA/HT-4] 05 p0743 A72-15865
- Nonequilibrium stagnation heat transfer mathematical models for injecting He, Ar or H into ionizing air laminar viscous layers at low Reynolds numbers [ASME PAPER 71-WA/HT-18] 05 p0744 A72-15877
- Analytical model for living biological tissue transient heat transfer, taking into account conduction, storage, generation, convection and blood flow effects [ASME PAPER 71-WA/HT-36] 05 p0620 A72-15887
- Gas turbine combustors performance model, using reaction rate equation from elementary mass balance equation [ASME PAPER 71-WA/GT-5] 05 p0704 A72-15898
- Spiral groove shaft vacuum seals, presenting mathematical ballpark performance model [ASME PAPER 71-WA/PID-5] 05 p0664 A72-15914
- Theoretical model for turbulent mixing of confined jet, including wall boundary layer [ASME PAPER 71-WA/FE-31] 05 p0646 A72-15925
- Incompressible turbulent flow in parallel-plate channel with one porous bounding wall, using velocity slip model [ASME PAPER 71-WA/FE-1] 05 p0647 A72-15939
- Dutch monograph on heat transfer of gas with vibrational relaxation at shock tube end wall covering mathematical model, induced velocity effect on pressure, etc 05 p0648 A72-16045
- Computerized simulation techniques for plasmas, discussing electrostatic particle model properties and implications 05 p0694 A72-16058
- Pattern recognition by automatic clustering methods without fixed definitions for number and specification of classes, using sequential diagnosis 05 p0632 A72-16075
- Stability characteristics of finite difference schemes based on lumped-parameter model and numerical integrator for wave propagation in continuous media 05 p0735 A72-16081
- Pressure source model of sound radiated by sonic jet, deriving frequency spectra ratio and jet pressure 05 p0600 A72-16105
- Book on computer applications to engineering analysis covering mathematical models, numerical techniques, program usage, programming and design 05 p0632 A72-16106
- Quasi-steady continuous process adaptive optimal control, discussing algorithms and model for sensitivity matrix calculation and digital simulation for strategy 05 p0640 A72-16200
- Fluid motion model with gas bubbles, noting energy dependence on temperature and density 05 p0649 A72-16224
- Charged particle acceleration by nonstationary sinusoidal electric fields in earth magnetosphere based on mathematical model 05 p0709 A72-16256
- Generalized cellular automata simulation by mathematical model network of identical automata with two states 05 p0641 A72-16317
- Linear dynamic control system identification by local impulse response approximation, comparing with Goodman-Reswick model 05 p0641 A72-16319
- One dimensional bipolar junction transistor, comparing charge control and regional mathematical models for suitability in device and circuit computerized analysis and design 05 p0636 A72-16359
- Large launch vehicle attitude control system absolute stability mathematical model, using quadratic Liapunov function for exponential property description 05 p0728 A72-16475
- Mathematical model for blood leucocyte population changes after radiation exposure within Blair model leucocytes hemopoietic to cardiovascular systems transport 05 p0618 A72-16635
- Slat-airfoil combinations aerodynamics modeled by single point vortex to represent leading edge slat, discussing on-line computer graphics program [AIAA PAPER 72-221] 05 p0603 A72-16798
- Vortex production of intense localized heating to leeward regions of bodies in hypersonic flows, proposing flow field models [AIAA PAPER 72-77] 05 p0604 A72-16804

Finite difference integration based on theoretical model analysis of three dimensional turbulent boundary layer on sharp cone at angle of attack in supersonic flow
[AIAA PAPER 72-187] 05 p0650 A72-16842

Computerized analytical model of two dimensional multicomponent airfoil in viscous subsonic flow
[AIAA PAPER 72-2] 05 p0606 A72-16861

Atmospheric turbulence incompressible two dimensional model, comparing Navier-Stokes equations numerical integration results with finite difference simulation
[AIAA PAPER 72-152] 05 p0651 A72-16871

Analytical model of thermal/structural optimization for long term storage cryogenic propellant systems
[AIAA PAPER 72-142] 05 p0691 A72-16881

Theoretical model for radiating metallic gas produced around iron meteor entering earth atmosphere, presenting temperature, pressure and density distributions
[AIAA PAPER 72-204] 05 p0721 A72-16884

Turbulent boundary layer analogy mathematical model for turbulent mixing and buoyancy effects on aircraft trailing vortex wake motion and persistency
[AIAA PAPER 72-42] 05 p0607 A72-16903

Heat pipe temperature gradient initial conditions for ideal gas model, introducing two phase Mach number for choking phenomena analysis
[AIAA PAPER 72-22] 05 p0749 A72-16913

Mathematical model for radiative transfer properties of high albedo carbon dioxide and water cryodeposits on opaque substrate
[AIAA PAPER 72-58] 05 p0749 A72-16929

Analytical models for predicting mass transfer cooling effects on blade row efficiency of turbine airfoils
[AIAA PAPER 72-11] 05 p0707 A72-16943

Adaptive model following control systems design by hyperstability approach for flight control and simulation
[AIAA PAPER 72-95] 05 p0613 A72-16956

Finite difference model application to supersonic planar viscous near wake, determining parameter range by physical and numerical restraints
[AIAA PAPER 72-115] 05 p0609 A72-16971

Lattice gas critical point and nonanalytical three dimensional models comparison with experimental data
05 p0691 A72-17062

Multistage axial flow compressor adjustment by flow geometrical dimension changes obtaining influence coefficient from linearized mathematical model
05 p0708 A72-17064

Multistage gas turbine flow area dimension change influence coefficient calculation from discrete nonlinear mathematical model through equation linearization
05 p0708 A72-17065

Characteristic functional for random delayed events and cluster processes, using Blanc-Lapierre statistical model
05 p0693 A72-17079

Damping effect in discrete one dimensional nonlinear lattice model leading to weakly dissipative Korteweg-de Vries equation
06 p0838 A72-17301

Bright O₂ and carbon dioxide emissions in Martian airglow from temperature profile models based on Mariner UV spectrometry
06 p0803 A72-17446

Coordinated characterization and mathematical modeling for device, circuit and system designs and computer analysis, applying to bipolar transistor
06 p0778 A72-17477

One dimensional analysis computer program for junction device modeling, exemplifying hf bipolar transistor Fermi statistics effect and velocity limitation in high current density
06 p0779 A72-17478

Analytical model of Gunn diode oscillating in resonant mode with domain quenching, determining current harmonics
06 p0783 A72-17573

Numerical model for ion beam instability in nonisothermal plasma with electron temperature much greater than ion temperature
06 p0861 A72-17915

Blood flow mathematical formulation, considering tissues constitutive equations, geometrical configurations, arterial wave propagation, etc
06 p0768 A72-17959

Random vibrations nonlinear theory, investigating nonlinear systems response to random excitation via Markov processes modeling
06 p0896 A72-17961

ATC study by computerized simulation, using successive approximation models
06 p0845 A72-17975

Heart pacemaker activity during muscular exertion, developing mathematical model based on system dynamics transient processes analysis
06 p0764 A72-18059

Project management mathematical models for task scheduling, resource allocation, information planning and decision making
06 p0905 A72-18067

Flow in gas lubricated conical bearings, considering analytical and numerical solutions for axisymmetric flow model with temperature dependent viscosity and dissipation coefficients
06 p0801 A72-18124

Mathematical-physical model for laser pulsed radiation-induced pressure wave transmission through surface and internal biological tissues
06 p0768 A72-18150

EEG discharges virtual dipolar sources computation, using mathematical model with homogeneous spherical conductive medium to simulate human head
06 p0769 A72-18201

Mathematical modeling of discrete nonconservative dynamic elastic systems for finite sensitivity, using Liapunov stability
06 p0840 A72-18320

Linear four step model for photosynthetic molecular oxygen evolution, discussing oxidation states, flash yield oscillation damping and deactivation
06 p0770 A72-18424

Meteorological tests for mathematical models in study of climate changes
06 p0843 A72-18451

IMPATT diode oscillator injection locking behavior from model, comparing results with experiment
06 p0788 A72-18469

Turbulence model for near-wall boundary layer flows, solving differential equations for kinetic energy and length scale
06 p0802 A72-18527

Fiberglass reinforced plastics under constant strain rate, deriving failure models as random process for microscopic crack propagation
06 p0898 A72-18548

Diffused failure model as basis for plotting delayed fracture curves in space of principal stresses
06 p0898 A72-18552

Axiomatic determination of dynamic logic control systems based on Moore automaton elements and combined continuous and finite models
06 p0781 A72-18660

Artificial biped locomotion dynamic equilibrium, representing mathematical model by two nonlinear differential equations with variable coefficients
06 p0769 A72-18703

Coefficient matrix for estimation of numerical solution error bounds for finite element models
07 p1025 A72-18786

Nonlinear dynamic system mathematical model for unit mass particle escape trajectories from potential well, taking account of trapped motions and stable oscillations
07 p1025 A72-18807

Fluidic devices electrostatic modulation, verifying jet deflection analytical model by experimental results
07 p0913 A72-18819

Fluctuating and steady model for turbulent reactive and nonreactive flow, solving for turbulent kinetic energy and density by averaging procedure
[AIAA PAPER 72-68] 07 p0966 A72-18948

Magnetized solar wind velocities and fields obtained by three dimensional model using perturbation technique with spherically symmetric boundary conditions
07 p1057 A72-19142

Spacecraft charging at synchronous orbit, constructing mathematical model of ATSS
07 p1058 A72-19150

Metal clad dielectric slab waveguide for integrated optics, obtaining dispersion equation solution and propagation modes from simplified model
07 p0940 A72-19229

Mathematical model for dissipative dual-spin satellite analysis, making use of high speed rotor symmetry to permit quasi-holonomic transformation
07 p1085 A72-19280

Electrical cardiac activity computer simulation model including biophysically faithful conduction system and electrocardiograms for high fidelity production
07 p0929 A72-19313

Mathematical model for semicircular canal dynamic response to angular acceleration, emphasizing role of perilymph over endolymph in cupula displacement
07 p0917 A72-19491

Bilaterally symmetric vortex rings dynamic behavior, computing pointwise induced velocity via Biot-Savart law for hydrodynamic and Rankine vortex models
[AD-739139] 07 p0967 A72-19501

Mathematical model physical structure, effectiveness and limitations for circadian rhythms, discussing Princeton and modified biochemical models
07 p0930 A72-19530

Algorithm for low order linear state variable models construction from measured data
07 p0950 A72-19701

Linear multivariable discrete time cyclic system sensitivity model yielding sensitivity functions with

respect to any system parameters and initial conditions
07 p0961 A72-19706

Model-following control for nonlinear multivariable plants, considering implicit algorithm solution and application to variable stability aircraft control synthesis
07 p0961 A72-19708

Nonlinear wave propagation of laser beams in absorbing fluid media, comparing computer model calculation results with experiment on liquid carbon disulfide cell
07 p1006 A72-19837

Monatomic gas atoms scattering by solid surfaces, using classical three dimensional lattice model
07 p0969 A72-20064

Gas-solid surface interaction semicontinuous model, predicting accommodation coefficient as function of gas atoms initial energy on tungsten
07 p0970 A72-20081

Mathematical model for superheavy cosmic ray production by spallation on interstellar hydrogen, assuming single source for particle injection with given charge spectrum
07 p1062 A72-20197

Book on models of particles and moving conducting media covering generator electrodynamics, electron tubes, particle accelerators, plasma and electron beam simulation, ion propulsion, etc
07 p1036 A72-20203

Linear equations with periodic coefficients in mathematical models for systems with rotating components, discussing methods for obtaining closed form solutions
07 p0913 A72-20204

Analytical model for surface fatigue crack configuration during propagation into thick plate under cyclic loading
[AD-741575] 07 p1095 A72-20242

Deterministic model for new product innovation adoption rate in commercial aircraft jet engine market
07 p1105 A72-20269

MHD dynamo model for incompressible real electrically conducting fluid unsteady flow
07 p1044 A72-20304

Partial differential equation language /PDEL/ for batch and interactive digital simulation of PDE models
07 p0951 A72-20327

Stochastic simulation model for space shuttle fleet operations, using closed loop queueing system approach
07 p0965 A72-20330

Airfield surface system fast-time computer simulation model for airport planning systems analysis
07 p0965 A72-20341

Optimal selection of flawless nose cones from graphite billets, obtaining mathematical model based on ultrasonic reflection test data
07 p1086 A72-20350

Nonlinear model for computer simulation of human arterial system, using finite difference technique for pressure and flow calculations
07 p0934 A72-20357

Human performance and exhaustion predictive model from responses to exercise and environmental stresses, considering circulation, thermal regulation, work load and oxygen pressure effects
07 p0934 A72-20358

Numerical simulation of atmospheric turbulence in planetary boundary layer due to wind shear and/or unstable thermal stratification, noting buoyancy and planetary rotation effects
07 p1031 A72-20359

Computer simulation requirements for air and ground transportation system, emphasizing mathematical models capable of system performance relation to design parameters
07 p0952 A72-20362

Real time computer simulation of command and control in transportation systems, detailing models, and programming technique and ATC controller effectiveness evaluation
07 p0952 A72-20363

Venusian atmospheric circulation experiments with time dependent two layer primitive equations model, discussing hot house and Goody-Robinson radiation transfer implications
07 p1083 A72-20452

Interatomic force model for elastic properties of alpha quartz and alkali halides generalized for specified structure under arbitrary pressure
07 p0980 A72-20519

Mathematical model for multiple bearing supported isotropic undamped rotors with arbitrary stiffness and mass distribution, taking into account horizontal/vertical motion coupling
07 p1096 A72-20529

Circular elastoplastic beam under combined torsion and tension via Mindlin elastic model for materials with microstructure, taking into account work hardening
07 p1097 A72-20534

Acoustical theory application to jet engine noise reduction, developing mathematical model for blade shock wave spacing in noise generation process
07 p1055 A72-20542

Metals cold working mechanics about stress state and yield points, proposing theoretical model for mechanism and applications in extrusion molding, drawing and hollow forging

07 p0999 A72-20599

Geomagnetic field optimal model with expansion of spherical harmonic series by least squares method

07 p0980 A72-20657

Signal statistical model parameter evaluation by selection of operators in form of dimensionless quantile ratios

08 p1130 A72-20724

Hot wire ignitor modeling including measured H value and heat generation by explosive chemical reaction

08 p1219 A72-20754

Kalman filter estimator for nonlinear human pilot model parameters including time delay

08 p1145 A72-20861

Input binary sequence transformation in chain of series connected on-off neuron models, applying to n-stage linear filter analysis

08 p1138 A72-20870

Associative memory model using neuron synaptic weight change for storing input disturbances

08 p1138 A72-20871

Convective heat transfer from human form, using cylindrical model and aluminum statue physical replica in oven and wind tunnel air flow studies

08 p1123 A72-20892

Mathematical model of capacitive transducer for displacement measurement in open mesh grid structures

08 p1163 A72-20918

Spectral density estimates for discrete time models of steady nonGaussian random processes, noting dispersion in asymptotic expression

08 p1198 A72-20996

Thermomathematical model for calculating craters formed by short pulses in electro discharge machining

08 p1173 A72-21028

One dimensional model for drift transistor at low injection level with minority carrier mobility dependence on impurity concentration

08 p1140 A72-21063

Median true height atmospheric profile model synthesis from propagation parameters, using polynomial representations and alpha-Chapman layers

08 p1157 A72-21106

Two dimensional model for plasma without magnetic field trapped near current sheet end in dipole magnetic field resembling geomagnetic tail

08 p1157 A72-21108

Mathematical model of gravitational wave zone for ring emanated smooth axisymmetric toroidal pulse

08 p1158 A72-21177

Metallic matrix stress-strain properties from phenomenological model based on idealized behavior of system components, noting dependence on fiber volume content

08 p1185 A72-21183

Numerical modeling of Venus atmospheric circulation, taking into account short wave radiation absorption, boundary layer, mesoscale convection and horizontal friction

08 p1233 A72-21191

Stationary statistical model for microwave oscillator flicker frequency noise, leading to power spectral density and time domain frequency instability [ONERA, TP NO. 1085]

08 p1141 A72-21431

Metal cold working mechanics, discussing model based on equality of internal and external forces needed for plastic deformation

08 p1176 A72-21439

Fiberglass heat transfer mathematical model, noting scattering effect and thermal conductivity

08 p1191 A72-21452

Carrier based attack aircraft allocation model formulation and solution for maximum inflicted target damage, using sequential unconstrained minimization technique with nonlinear programming [AD-736073]

08 p1256 A72-21469

Graphical analysis of accelerated life test data on insulating fluids, capacitors, bearings and electronic devices, using inverse power law model

08 p1176 A72-21587

Phonon limited mean free path in Cd by limiting point method, proposing model with elastic anisotropy

08 p1217 A72-21592

Molecular beam continuum model for calculation of hypersonic flow past flat plate at zero incidence angle [AD-746387]

08 p1254 A72-21609

Mathematical model of solar radiation pressure effects on earth satellite orbit

08 p1237 A72-21643

Unsteady uniform turbulent flow of incompressible liquid in circular pipe, verifying mathematical model with velocity distribution calculations

08 p1151 A72-21666

Junction FET drain source capacitance theory based on two-region physical model, taking into account carrier drift velocity saturation effect

08 p1142 A72-21745

Glass fiber reinforced polymer composite model for tensile stress distribution in matrix and fibers and at bond interface

08 p1194 A72-21753

Soviet papers on human higher nervous activity physiology covering conditioned reflexes and adaptive behavior, neurotropic substance effects, mathematical and structural modeling, etc

08 p1118 A72-21834

Conditioned reflex activity, discussing biological and nervous system, electric analog simulation and mathematical and structural modeling

08 p1127 A72-21842

Mark VII ear performance calculation procedure for perceived loudness or noisiness levels relation to sound pressure, using experimental frequency weighting contours

08 p1127 A72-21895

Rarefied gas sealant viscoelastic performance prediction by analytical models, comparing results with experiments on multiple grooved samples

08 p1177 A72-21929

Radio system operational reliability analysis by mathematical methods with use of digital computer, discussing statistical modeling algorithm

08 p1143 A72-22065

Vibration modes of bladed turbine wheel, formulating mathematical model

08 p1224 A72-22132

Mathematical models for hydraulic position servo, deriving time optimal controllers

08 p1113 A72-22156

Turbulent flow model based on two equations for kinetic energy distribution and vorticity fluctuations, comparing flow and heat transfer prediction with experimental data

08 p1152 A72-22169

Submodel similarity relations in single indirect experiment design

08 p1257 A72-22176

Mathematical model for derivation of asperity or metal-metal contact load sharing of lubricated machine components in journal and roller bearings

09 p1317 A72-22248

Vaneless diffuser air flow calculation based on helical flow model with back currents in boundary layer

09 p1259 A72-22299

Spectrum shape of Doppler radar return from two dimensional random rough surface model using helmholtz integral approach and Kirchhoff approximation

09 p1277 A72-22314

German monograph on model concept for erosion mechanism involved in crystalline material surface bombardment covering particle elastic deformation during impact

09 p1397 A72-22324

German monograph on wall stabilized Ar arc column displacement by pulsed HF radiation heating covering power absorption determination based on theoretical model

09 p1358 A72-22341

Steady state global climatic model for earth-atmosphere-ocean system, discussing perturbations effect on stability

09 p1343 A72-22426

Filtered-equation pressure coordinate numerical weather prediction model in finite difference formulation, discussing various initialization procedures and boundary value specifications

09 p1343 A72-22427

Primitive equation multilayer model for winter precipitation prediction in U.S. northeast coastal region, noting correlation with observational data

09 p1344 A72-22428

Initially stationary axisymmetric disk of stars evolution calculated by gravitational potential solver for various values of velocity dispersion

09 p1383 A72-22460

Long distance communications multimode waveguides and probability distributions on symplectic group in extension of mathematical model with random inhomogeneities

09 p1277 A72-22474

Discrete model of dynamic forces between teeth of single stage transmission with parallel gear axes

09 p1404 A72-22772

Polyatomic ions interaction with neutral molecules in gases, calculating ion mobility as function of temperature from core model representation

09 p1355 A72-22788

Magnetic induction distribution in second species superconductor cylindrical samples after limited flux jumps, proposing instability propagation model

09 p1369 A72-22797

Mixing length model for turbulent boundary layer in incompressible flow with fluid injection at wall, extending solution to compressible case [ONERA, TP NO. 986]

09 p1294 A72-22818

Snow-plough model of plasma acceleration for determining time dependence, gas density distribution and energy transfer

09 p1359 A72-22819

Mathematical model of skin contact cooling tube device for human body thermoneutrality maintenance in various environments

09 p1270 A72-22821

Continuum model for cylindrical and spherical elastic laminated composites deformation, using balance and constitutive equations

09 p1405 A72-22992

Height integrated ionospheric conductivity calculated using numerical model and approximate formulas

09 p1300 A72-23017

Model of dynodes system with random electron-hole pairs number, calculating equations for mean fluxes transport and correlated noise fluctuations

09 p1280 A72-23116

German book on unsteady heat conduction and temperature field equalization covering mathematical treatment with Laplace transformations

09 p1412 A72-23175

Mathematical model and inelastic stress analysis for metal creep-fatigue interaction and progressive deformation in breeder reactors operation

09 p1407 A72-23200

Mathematical model of ion capture and annihilation by aerosol particles from ground level to 60 km

09 p1346 A72-23266

Ionospheric electron concentrations and temperatures determined by time dependent continuity equations model during 11 September 1969 solar eclipse

09 p1390 A72-23518

Collisionless plasma spherical probe RF sheath model based on quasi-static approximation and electrostatic theory

09 p1365 A72-23520

Mathematical model of block adjustment and star coordinate accuracy in photographic astrometry

09 p1392 A72-23541

Nonlinear systems optimal design mathematical modeling, discussing synthesis, manufacturing, production, exploitation and evaluation

09 p1343 A72-23610

Adjustable structure model for parameter adaptive control, noting convexity of performance index function over evaluation interval

10 p1455 A72-23793

Systems analysis and mathematical modeling role in planning transportation networks from control theory viewpoint

10 p1442 A72-23796

Turbulence models application to internal flow prediction, using two-, three- and five-equation models and shear stress hypothesis

10 p1463 A72-23854

Human left ventricle measurements, modeling, control and simulation for heart monitoring purposes, describing muscle performance mathematical model and stress effect prediction control system

10 p1429 A72-23924

Mathematical model as basis for equipment design-sensitive maintainability prediction technique, using information theory concepts of design interpretation

10 p1503 A72-23979

Bayes analysis application to Weibull distribution parameters estimation, using entropy concept for figure of merit to assess reliability analysis

10 p1444 A72-23987

Decision theory and cost-benefit modeling application to large government funded systems development programs, discussing Bayesian techniques

10 p1564 A72-23993

Stochastic models of human performance effectiveness functions reliability and correctability from error data generated by tracking and vigilance tasks

10 p1429 A72-24001

Decision making models application to systems configuration, reliability, repair level and spares optimization and availability analysis

10 p1486 A72-24006

Probability model of statistical independence relationships among two events and environmental event, examining all combinations of definition statements for reliability analysis

10 p1504 A72-24015

Statistical-analytical cost models for spacecraft development and fabrication, taking into account various technical and management factors

10 p1564 A72-24026

Cochlea enclosed two dimensional cavity potential flow model for fluid mechanical theory of hearing

10 p1430 A72-24295

Binary collision loaded-sphere molecular model for diatomic gases computer simulation, obtaining normal shock waves velocity, density and temperature profiles

10 p1466 A72-24297

Aerodynamic noise generation mechanism of ideally expanded supersonic jet based on large scale flow instabilities, deriving mathematical model

10 p1418 A72-24331

Absorbing sphere model for ion-ion recombination upper limit thermal energy reaction rate and total cross section energy dependence

10 p1515 A72-24342

Laminar flow dispersion coefficient for curved tubes and channels determined by mathematical model, permitting concentration distribution computation

10 p1468 A72-24371

Mathematical modeling for structural analysis and design from viewpoint of methodology, physical principles, simulation, optimization, constraints and control theory

[SMRT PAPER M 2/3] 10 p1556 A72-24393

Turbulence generated sound due to interaction with sound absorbent liners, investigating dynamic process via rigid boundary model with homogeneous array of circular orifices or pistons

10 p1511 A72-24424

Analytical design of pulse width modulated systems with time constant and delay for electronic control, using Z transform

10 p1457 A72-24458

Model for large signal losses prediction in charge coupled devices due to fast interface state trapping

10 p1526 A72-24625

Mathematical statistics application to complex systems modeling, considering group method of data handling, simulation and regression methods

10 p1457 A72-24634

Electronic circuits statistical optimization with Monte Carlo procedure, discussing methods and algorithms for accelerating evolutionary modeling

10 p1452 A72-24638

Glass network physical properties model, using physical chemistry description of crystal structure without regularly repeating lattice

10 p1502 A72-24735

Radio propagation over slightly roughened curved earth surface, using perturbation method and Taylor series in model calculation

10 p1439 A72-24743

MHD sheet pinch model time dependent nonequilibrium stability determined by equations of incompressible viscous resistive magnetofluid

[AD-739661] 10 p1523 A72-24751

Approximate model to reduce differential equation order for linear system of series connected elementary aperiodic components with different time constants

10 p1457 A72-24753

Mathematical model for compressed gas convection into lower atmosphere with substantial density changes

10 p1563 A72-24778

Mathematical model for arterial system pressure, blood flow and dimensional changes, examining cardiac ejection dynamics and vasculature mechanical properties and viscoelasticity

10 p1432 A72-24812

Universal mathematical model of n-plet atomic theory, obtaining existence criterion for photogeneous relation in relation age

10 p1506 A72-24851

Tensile ligament instability model for stress corrosion crack propagation velocity in austenitized steel tempered at 750 F

10 p1499 A72-24888

Mathematical model for supersonic crack propagation in cubic lattice, deriving velocity-applied stress relation

10 p1558 A72-24895

Mathematical description of frequency difference hologram obtained by superposition of two holograms of same object produced with light of different frequencies

10 p1483 A72-24915

Hubbard mathematical model for metal-insulator transition due to electrons correlations, noting schematic phase diagram and transition metal oxides

10 p1527 A72-24939

Random walk models replacing Fokker-Planck equation for many particle systems with Coulomb interactions

10 p1513 A72-25041

Linear dynamic control system identification by local impulse response approximation, comparing with Goodman-Reswick model

10 p1458 A72-25073

Model for I/O channel traffic in computer systems, obtaining closed solution for stationary probabilities of state

10 p1446 A72-25148

Retrieval model based on probability distribution defined on set of all admissible arrays of elements in loci set

10 p1446 A72-25191

Parameter identification method for mathematical extremal control model of complex structure for static plants based on regression analysis

10 p1458 A72-25192

Boundary layer model for laminar transient forced convection film boiling on isothermal flat plate, noting one dimensional conduction, intermediate and steady state regions

[AIAA PAPER 72-289] 11 p1741 A72-25227

Radiative heat transfer spectral, temperature and directional dependence on interacting opaque surfaces

system properties, noting models with accounted non-gas character

[AIAA PAPER 72-306] 11 p1742 A72-25240

Digital computer calculation of complex electric networks described by mathematical models, calculating flow distribution

11 p1577 A72-25282

Methods of moments, rational transform approximation, Taylor series expansion and modulating functions used for process identification model, determining system transfer functions

11 p1607 A72-25283

Accuracy and reliability in engineering design of discrete automata without memory/logic circuits/, using Boolean algebra for mathematical models

11 p1600 A72-25434

Equilibrium state dynamics of Burger turbulence model with two velocity components, using Fourier amplitude representation

11 p1615 A72-25553

Molecular scattering in free jet expansion, using spherical source and two component background gas mathematical models

11 p1615 A72-25558

Turbojet engine oil circuit contamination rate determination by spectrometric analysis, obtaining mathematical theory for data interpretation

[SAE PAPER 720303] 11 p1703 A72-25567

Steady state radial inlet pressure distortion index for axial flow compressor, examining radial velocity, continuity equation and mathematical model

[ASME PAPER 72-GT-109] 11 p1571 A72-25673

Relativistic homogeneous anisotropic models analogs construction in Newtonian cosmology

11 p1716 A72-25711

Mechano-acoustical network model for room-hallway-window system response to sonic booms or other transient loads, determining damping ratios

11 p1686 A72-25729

Ablation phase duration during spacecraft decelerated hypersonic reentry flight, using theoretical model based on quasi-steady assumptions

11 p1745 A72-25815

Single spiral vortex cavity termination model for second order solution of flat plate hydrofoil cavitation flow

11 p1616 A72-25879

Electronic model for low temperature transition in magnetite with nonintegral average electron number on site

11 p1701 A72-26023

Russian book on approximate solutions of boundary value problems covering elliptic differential equations and Ritz, moment, straight lines and probability modeling methods

11 p1677 A72-26065

Electrostatic ion thruster theoretical model, deriving ionization rate density as function of discharge current

[AIAA PAPER 72-432] 11 p1707 A72-26175

Resistorjet performance models for investigating energy losses in hydrogen, ammonia, methane and carbon dioxide nozzle flows

[AIAA PAPER 72-455] 11 p1708 A72-26191

Dynamic modeling application to technological forecasting, discussing mathematical simulation for R and D management planning in project selection and budget allocation

11 p1748 A72-26284

Narrow band process signal model for phase and amplitude difference distribution densities of alternating period compensation system output signal

11 p1596 A72-26310

Mathematical model of combustion region of steam boilers or gas turbines based on turbulent flow and transport equations

11 p1747 A72-26592

Mathematical model of weak coupling influence on damped harmonic oscillators with different eigenfrequencies applied to bounded plasma oscillations

11 p1698 A72-26600

Gabor-Nelson myocardium electrical activity model for mathematical construction of vectorcardiograph from ECG for comparison of various lead systems

11 p1588 A72-26629

Mathematical model of extracellular pH in brain tissue from blood and cerebrospinal fluid acid-base parameters for respiration central chemosensitive mechanism study

11 p1579 A72-26660

Pulsating heat source model for physical processes in metal surface layer under fatigue limit stress level, calculating critical volume to limit energy buildup

11 p1738 A72-26801

Computerized numerical model of mixed subsonic and supersonic gas flow with sonic transition in turbine curvilinear channel

11 p1574 A72-26967

Mathematical model of gas turbine parameters scatter and geometrical fabrication tolerances of flow through section

11 p1712 A72-26974

Perturbation procedure for weakly coupled oscillators in connection with statistical mechanics ergodic problem and nonlinear interaction models

12 p1844 A72-27248

Mathematical model for thermal lensing of IR laser window, discussing aberrations effect on diffraction-limited far field focus time

12 p1819 A72-27284

Kinetics and cavity intensity models for output characteristics of pulsed electric discharge carbon dioxide lasers

12 p1820 A72-27287

Nonlinear mathematical dc models of planar transistors for computerized IC design and analysis obtained by continuity equation approximate solution

12 p1789 A72-27313

Mathematical model to describe complete creep process in metal from hardening and brittle failure theories

12 p1828 A72-27322

Digital adaptive echo cancellation mathematical technique for voice circuits derived from satellite transmission

[AIAA PAPER 72-539] 12 p1780 A72-27362

Model for supervised repairable system reliability, assuming system life and repair times as exponential probability distributions with deterministic supervisor active and inactive times

12 p1814 A72-27555

Signal mathematical model in optical and acoustic pattern recognition

12 p1786 A72-27571

One stage approximation to color conversion model, predicting gain setting control dependence on achromatic contrast

12 p1809 A72-27681

Ekman boundary layer in two level quasi-geostrophic general circulation numerical model, representing physical characteristics of boundary layer turbulence increase with height

12 p1840 A72-27708

Jupiter and Saturn gravitational moments from available models, taking into account rotation, density and radius

12 p1871 A72-27744

Turbulence model based on transport equations for Reynolds stress tensor and energy dissipation rate, deriving simplified version for boundary layer flows

12 p1798 A72-27830

Computer model for evolution of isolated rotating disks of stars, noting gravitational two stream dynamic instability for infinite double periodic stellar systems

12 p1874 A72-27909

Ergodic theorems for operators generated by Markov transients, examining asymptotic properties of stochastic learning model

12 p1787 A72-27924

Lens MTF calculation in presence of diffraction patterns via image mathematical model construction yielding Fourier transform

12 p1810 A72-27937

Spectroscopy by synthesis of two or more fixed or moving diffraction gratings, obtaining transfer functions for total information increase

12 p1811 A72-27943

Mathematical model for hydraulic fatigue testing machine, analyzing nonlinear control stability of vibratory loading process

12 p1796 A72-27978

Combustion surface acoustic admittance model of blended solid propellant with allowance for foam zone inertia and solid/gas interface reactions

12 p1889 A72-27980

Pilot-aircraft system model for relationship between weapons delivery accuracy and manual flight control system design, noting display, computation and control aids to pilot

12 p1773 A72-28121

Statistical methods for friction and wear processes, noting Rayleigh distribution of wear particles, surface dispersion velocity, energy dissipation and friction force

12 p1818 A72-28186

Modified Van der Pol wave motion oscillator model for prediction of aortic dynamic response to negative g impact accelerations

12 p1765 A72-28271

Mathematical model for digital systems reliability, determining probability of success and of various failure modes

13 p1923 A72-28356

Mathematical models for complex system debugging in initial life period, noting maximum likelihood estimates for failure rate functions

13 p1962 A72-28365

Oscillations excitation, proposing models for percussive rotational action machines operation and dog tooth clutches processes

13 p1954 A72-28386

Interdiction bombing mission effectiveness model for bad and good weather aircraft type selection depending on weather conditions at target site

13 p1896 A72-28400

Mathematical model of reactive fluid flows during postignition transients in hybrid propellant rocket system
13 p2025 A72-28416

Explicit numerical modeling method for dynamics of dense high temperature laser-produced plasmas, discussing time scale for energy transfer from electrons to ions
13 p2009 A72-28424

Modeling process for mathematical representation of mechanical problems, deriving design information in digital or graphic form
13 p2000 A72-28450

Mathematical model for dynamic yield point dependence in strain rate based on similarity and dimensionality theories and Weierstrass theorem
13 p2054 A72-28458

Monte Carlo method for radiative transport theory problems, considering mathematical models of light scattering media and photon trajectory random elements
13 p2001 A72-28505

Exponential functions model for D region vertical distribution of electron density profiles, taking into account solar X- and cosmic rays
13 p1945 A72-28581

Multilayer plasma model for MHD pulse propagation in ionospheric waveguide, noting approximation of Alfvén velocity distribution by plasma layers
13 p1946 A72-28585

Gravitational theory strong discontinuity conditions, using basis variational equation for field and media model construction in general relativity theory
13 p2002 A72-28711

Conformally flat linear axial symmetry chromometrically invariant cosmological models, discussing various types of spaces realized during model evolution
13 p2036 A72-28759

Precipitation exceedance rates charts for various risks, using statistical models
13 p1989 A72-28811

Mathematical model for numerical simulation of warm fog modification by seeding hygroscopic particles, taking into account turbulent diffusion and horizontal wind advection
13 p1992 A72-28844

Multiscale numerical model for local weather development simulation, noting forecasting for long distance air travel
13 p1993 A72-28857

Mathematical two mass model for horizontal, angular and vertical vibrations of pneumatic wheel with allowance for inelastic tire resistance
13 p2003 A72-28918

Characteristic thrust concept introduced to classify propulsion system tasks related to geosynchronous communications spacecraft, developing approximate analytical models
[AIAA PAPER 72-514] 13 p2052 A72-28977

Random walk atomic migration model for radon diffusion through lunar regolith into atmosphere
13 p2038 A72-28995

Electrophysiologic data acquisition by multiple dipole type of inverse electrocardiographic procedure based on model data, noting favorable and unfavorable dipole array configuration
13 p1909 A72-28997

Mathematical random fluctuation models for noise and energy spectra of pulsed processes during current passage through semiconductors
13 p2021 A72-29064

Accelerated reliability, life, fatigue and performance tests of automatic systems components, noting mathematical models for minimum time techniques
13 p1965 A72-29172

Mathematical model for flow field inside raindrop under aerodynamic transient stresses before impingement at stagnation point of blunt body in supersonic flight
13 p1942 A72-29224

Random processes models based on Poisson sequences extended to simultaneous asymmetry and probability density function excess, establishing asymptotic relationships
13 p1948 A72-29231

Anomalous magnetic and gravitational fields energy spectra model, examining autocorrelation functions changes
13 p1949 A72-29244

Time history model of transient ignition to self sustained propellant burning, taking into account pressure effects and igniter heat flux
13 p2065 A72-29305

MHD power generators analytical modeling by digital technique for prediction of performance and efficiency as function of size and operating conditions
[AD-741173] 13 p1900 A72-29355

Nonlinear model of ionization instability of MHD generators, assuming discharge structure with alternating layers of high and low electrical conductivity
13 p2014 A72-29371

Mathematical model for ionized plasma response to sinusoidal perturbations, calculating dispersive waves

in MHD generators with working fluid of potassium seeded argon
13 p2014 A72-29372

Radar clutter models and comparison with measurements, discussing parameters for description and main functions for suppression
13 p1922 A72-29396

Human hand-arm system vibration characteristics, describing mechanical impedance measurements for mathematical modeling
13 p1910 A72-29559

Mathematical model for gas turbine engine inlet noise caused by shock wave impingement, noting dynamic wave system with overpressure and distortion
13 p2028 A72-29576

Acoustic environmental prediction model for near, mid and far field rocket engine noise
13 p2028 A72-29582

Analytical models for potential flow through smooth edged orifice, comparing acoustical inertance predicted and experimental values
13 p2006 A72-29770

Dynamics and thermodynamic interactions connected with large, mesoscale and small scale stratiform clouds, describing mathematical models
13 p1995 A72-29849

Two dimensional mathematical model of magnetosphere with neutral sheet for oblique incidence of solar wind, noting magnetic field minimum energy
13 p1954 A72-29850

Divided attention effect localization, using choice tracking task reaction times in sequential stage model for human information processing
13 p1911 A72-29852

Work hardening-recovery model of dislocation creep, deriving multiaxial mechanical equation of states for strain/time relationship under arbitrary temperature-stress sequences
13 p2061 A72-29872

Mathematical model for magnetized solar wind with one fluid MHD and polytropic state equations, calculating magnetic field variables at earth
13 p2034 A72-29958

Kalman filter stability analysis by mathematical modeling, using floating point computer algorithm
13 p1934 A72-30000

Mathematical model of atmospheric electric clouds, calculating electric charges and fields from convection and conductivity data
13 p1996 A72-30086

Mathematical models for passenger aircraft market forecast, discussing stock measurement and life expectancies
13 p2067 A72-30125

High velocity water jet generation dynamics, deriving equations of motion for mathematical model with nozzle profiles and liquid compressibility approximations
14 p2093 A72-30180

Two body model for three body problem of uniformly distributed and isotropically expanding gravitational matter of Einstein-Sitter universe, noting metagalaxy cooling rate
14 p2149 A72-30211

Mathematical model for compressed gas thermal convection into lower atmosphere with substantial density changes
14 p2170 A72-30215

Earth-moon system periodic orbits calculation by modified quasi-linearization combined with particular solutions method, using restricted three body model
14 p2149 A72-30232

Aircraft landing gear stress spectrum and design data during ground loading on airport runways, using linearized theory for model investigation
14 p2071 A72-30283

Non-Maxwellian inhomogeneous collisionless plasma equilibrium and stability, proposing statistical thermodynamic model
14 p2137 A72-30394

Porous cellular structure materials, investigating porosity effects on modulus of elasticity based on central monoporosity model
14 p2165 A72-30433

Lunar interior thermal history and current state from theoretical temperature models, taking into account initial conditions, heat sources, differentiation and simulated convection
14 p2155 A72-30519

Linear mathematical model for twin shaft gas turbine with isolated turbocompressor, calculating dynamic constants as function of operational modes
14 p2146 A72-30581

Myelinated nerve fiber mathematical model for action potential transmission mechanism analysis during relative refractory phases
14 p2079 A72-30597

Anomalous magnetic and gravitational field models autocorrelation function behavior dependence on circular cylindrical sources depth and spacing
14 p2101 A72-30647

Solid rocket propellants storage life analysis and prediction by mathematical modeling of physical-chemical failure generating processes
14 p2145 A72-30762

Modified geometrical model for sintering Ni-doped W, including surface tension effect at Ni-vapor interface
14 p2121 A72-30770

Aerospace complex physical systems including human operator, discussing computerized design for behavior analysis by means of mathematical models
14 p2093 A72-30846

Gas surface interactions models, computing scattering kernels by reduction to boundary value problem
14 p2134 A72-30880

Temperature-slip problem in rarefied gases, obtaining exact solution by generalized BGK scattering model and Wiener Hopf technique
14 p2095 A72-30882

Nonlinear interaction of resonant plasma oscillations with nonresonant wave pulse, using water bag model of electron plasma
14 p2140 A72-30936

Anisotropic homogeneous plasmas, deriving computer model to predict effects of circularly polarized parallel plasma waves in external uniform magnetic field direction on instabilities
14 p2140 A72-30938

Cooperative direction changing isomer movement on polymer chain lattice describing equations derivation procedure
14 p2125 A72-30962

Reichardt mixing model for turbulent boundary layer calculation in wall flow, noting supersonic and nonisothermal jet flow
14 p2095 A72-31002

Mathematical model for mechanical and electrical hysteresis, noting application to nonlinear ferromagnetic resonant circuit with saturable inductor
14 p2132 A72-31105

Nonlinear oscillation systems mathematical model, determining periodic mode parameters, self excitation and damping mechanisms by point mapping method
14 p2133 A72-31126

Rectangular plate nonlinear lumped-parameter model for large displacement amplitudes, deriving differential equations of motion via Hamilton principle and Euler equations
14 p2169 A72-31148

Mathematical model for computation of electronic circuit drift reliability and circuit production yields, discussing operational parameter allowance
14 p2091 A72-31165

Reliability modeling principles, concepts and implementation techniques for switching system design
14 p2091 A72-31167

Material constants for strain hardened polycrystalline metals calculated from mathematical model for plastic deformation
15 p2322 A72-31361

Linear systems theory for mathematical model of retinal image and ganglion cell excitation, calculating receptor layer luminance distributions for several stimulus patterns
15 p2184 A72-31367

Multimode optical fiber waveguide theoretical model to predict pulse propagation dispersion for comparison with measurements
15 p2194 A72-31546

Approximate model of weak shock wave interaction with laminar MHD boundary layers for perfectly conducting supersonic streams
15 p2284 A72-31633

Two dimensional incompressible turbulent boundary layer in arbitrary pressure gradient, obtaining mathematical model for solution by implicit finite difference method
15 p2217 A72-31718

Adaptive radar tracking processes in presence of clutter, comparing efficiencies via mathematical models
15 p2196 A72-31747

Software models to test operating conditions of logic nets, discussing application to network faults diagnostics
15 p2203 A72-31749

Theoretical model for HF mechanical waves interaction with crystal lattices based on measurements of high amplitude ultrasonic waves attenuation in metal crystals
15 p2292 A72-31835

MOS junction transistor turn-off behavior calculation based on model with carrier source and drain for channel formation
15 p2207 A72-31891

Mathematical adjustment model for lunar laser ranging, noting accuracy improvement of points coordinates and orientation parameters
15 p2310 A72-31971

Pageson balloon satellite orbital perturbations due to erratic solar radiation pressure induced accelerations, comparing modified Smith perturbation model calculations with photometric observations
15 p2228 A72-31975

Solar wind model dividing interplanetary space in one fluid and two fluid collisionless regions, discussing proton thermal anisotropy
15 p2300 A72-31996

ATC systems fast-time simulation, emphasizing importance of human operator performance realistic modeling
15 p2269 A72-32097

Solution kinetics of secondary phases in cast dendritic and nondendritic Mg-Zn and Mg-Zn-Zr alloys, using cylindrical and spherical diffusion models
15 p2257 A72-32119

Blade characteristics of axial flow fan with orifice fan guide investigation by theoretical model with flat plate parallel to wing tip surface
15 p2179 A72-32142

Thermodynamic perturbation and scaling theory for multidimensional spherical models of lattice structure in terms of field of critical phenomena
15 p2293 A72-32219

Amorphous semiconductors theories, discussing electron states and transport properties in terms of Cohen, Mott and Gubanov models
15 p2293 A72-32234

Lateral distribution, radiation spectra and pulse shapes calculated from mathematical models of cosmic ray showers radio emission, noting chemical composition of primary particle
15 p2230 A72-32262

Mathematical model for modified ordinary electromagnetic wave propagation in presence of two cold counterstreaming plasma electron beams, noting instability regions and growth rate
15 p2286 A72-32274

Finite element method for discrete models of composite materials, discussing nonlinear dynamic problems
15 p2330 A72-32296

Tight binding model for binding energy determination in transition atoms adsorption on same series transition metal substrate, using moments expansion technique
15 p2281 A72-32379

Surface effects on paramagnetic metals spin susceptibility models, including random-phase-approximation equation derivation and induced magnetic moment calculation
15 p2295 A72-32549

Particulate composite model deformation and failure behavior under plane uniaxial compressive stress, using finite element method
15 p2258 A72-32556

Mathematical models for electromagnetic interference in electronic equipment, discussing nonlinear circuit analysis
15 p2201 A72-32568

Structural averaging of stresses in finite element method hybrid stress model, using additional equilibrium equations
15 p2332 A72-32597

Analytical model for nonpenetrating impact caused head injuries, evaluating protective device effectiveness via energy absorption characteristics
15 p2191 A72-32602

Atmospheric motions prediction with numerical model based on discrete stratified fluid free oscillations
15 p2266 A72-32720

Probstein-Gold viscoelastic model of supersonic flow induced surface cross-hatching assessment against Dowell studies on plates and shells flutter
16 p2463 A72-32838

Harmonic oscillators with negative resistance elements, discussing simplified mathematical calculation for I-V characteristics nonlinearity and applications to various diodes and transistors
16 p2368 A72-32858

Reversible instantaneous deformations and internal energy in viscoelastic incompressible fluids, using Oldroyd and De Witt hydrodynamic models
16 p2376 A72-32937

Mathematical models for depolarized light scattering by particle pair in gas, noting molecular collisions effect
16 p2423 A72-32952

Mathematical model for fast transverse glow discharges for pumping high pressure gas lasers, noting short rise time of applied voltage pulse
16 p2399 A72-33012

Earth crust waveguide three layer model for electromagnetic wave propagation, showing mode relation to absorption conditions
16 p2362 A72-33074

Limit displacement or solids parameters optimization for perfectly locking bodies, presenting mathematical models based on extremum energy theorems
16 p2423 A72-33104

Two dimensional fibrous medium model for strain and stress analysis of structural plate formed by three dimensional grid of rods
16 p2467 A72-33115

Inverse transformations in mathematical models of elasticity and plasticity problems reducible to biharmonic equation
16 p2468 A72-33163

Theoretical model for computer calculation of transients in oscillator consisting of nonlinear amplifier with feedback through sequence of matched LC circuits
16 p2371 A72-33280

Mathematical models for radio attenuation in ice by electromagnetic absorption and reflection from interfaces, noting radar tracking
16 p2363 A72-33290

Mathematical model of atmospheric tides using Navier-Stokes equations for perfect gas in thermodynamic equilibrium
16 p2385 A72-33343

Mathematical model for reliability analysis of modularly redundant electronic systems with unequal failure rates for operating and standby units
16 p2398 A72-33344

Electronic circuit reliability prediction model with statistical dependence for detailed failure modes
16 p2371 A72-33345

Initiation mechanisms for explosive materials and experiments for hazard evaluation, discussing subdetonation reactions and mathematical models of explosive processes
16 p2442 A72-33353

Subcooling and acceleration effects on nucleate boiling heat flux, comparing heat transfer prediction models with experimental measurements
16 p2477 A72-33433

Approximation of mathematical models for continuous media with many degrees of freedom, local structure and interactions, discussing parameters similarity conditions
16 p2425 A72-33586

Mathematical model for atmospheric ions density fluctuation with time, noting absence of oscillating solutions
16 p2386 A72-33652

System models for R and D processes in terms of state variables and control vectors, deriving algorithm for optimization
16 p2482 A72-33864

Predictive model for human operator performance in short term visual information processing based on psychological research to obtain decision accuracy and response time
16 p2359 A72-33865

Nonparametric probability density function modeling algorithms comparison for convergence rate and limit cycle stability relative to implementation ease
16 p2367 A72-33867

Teflon-bonded hydrophobic gas diffusion electrode performance prediction by mathematical treatment of flooded catalyst agglomerate model
16 p2352 A72-33892

Model for VLF emissions triggered by whistlers and man-made radio signals, noting effects of wave packet and second order resonance
16 p2365 A72-33905

Mathematical model for magnetosphere surrounding rotating neutron star, noting computer programs for Maxwell and plasma equations solution
16 p2460 A72-33927

Earth bow shock wave structure model based on development of strong density gradient in magnetic field-free cosmic plasma
16 p2387 A72-33935

Structural information model for data compression algorithm synthesis, using piecewise signal approximation
16 p2395 A72-33954

Hybrid computer simulation of cochlea mathematical model, noting nonlinear damping
16 p2359 A72-33971

Mathematical model for deuterium slab solid and plasma under laser pulses irradiation, noting shock wave propagation and slab acceleration
16 p2439 A72-34027

Analytical model for crosshatch ablation patterns, geometric features and stability characteristics prediction based on viscoelastic melt layer interaction with gas boundary layer
16 p2480 A72-34030

Convective clouds fluid dynamic numerical modeling, considering plumes, thermals and vortex rings formation
16 p2419 A72-34083

Rheological model for creep under intermittent square wave stress pulses, taking into account time dependent dislocation density
16 p2412 A72-34113

Lift and drag on conical, cylindrical and spherical artificial satellites from spatial impulsive interaction model depending on gas temperature and surface conditions
16 p2347 A72-34167

A simulation method permitting the direct construction of an integrated fluidic circuit with predetermined frequency response curve
17 p2494 A72-34197

Communication satellite modeling into subsystems to formulate parametric relationships among power, mass and cost, comparing computerized design alternatives
17 p2512 A72-34263

Comparison of circuit call capacity of demand-assignment and preassignment operation.
17 p2512 A72-34270

Mathematical model for nonequilibrium gas composed of hard spherical nonattracting molecules, deriving gas dynamics theory in terms of multiple integrals
17 p2538 A72-34424

General purpose simulation system /GPSS/ to program discrete time dependent mathematical models related to transport and queueing processes
17 p2521 A72-34471

Simulation of an air cargo handling system
17 p2536 A72-34472

The reduction of false tracks during automatic tracking
17 p2522 A72-34826

The identification of parameters in nonlinear thermal networks with the aid of a Kalman filter
17 p2533 A72-34827

Discrete vortex model numerical simulation of Onsager negative temperature instability for interacting line vortices two dimensional motions
17 p2538 A72-34871

A new theoretical model for representing jet penetration into a subsonic stream
17 p2538 A72-34888

Mathematical model of nitric oxide formation by fuel droplet burning above fuel critical pressure, applying to diesel engine operations
17 p2511 A72-34901

Analysis and testing of compressible flow ejectors with variable area mixing tubes.
17 p2485 A72-34968

Russian book - Mathematical methods of modeling in space studies
17 p2607 A72-35026

A probabilistic model of a control computer complex for estimating the efficiency of communication of a computer with data sources and receivers
17 p2522 A72-35029

Flight vehicle, control system and perturbations models synthesis from variational problem solution via control functions improvement
17 p2621 A72-35037

Numerical integration of ordinary differential equations in a real-time modeling procedure
17 p2576 A72-35041

Mathematical models for metallic plastic strain hardening under cyclic loads, introducing internal state parameters
17 p2632 A72-35111

The fitting, calibration, and validation of simulation models.
17 p2523 A72-35226

Reflection of weak shock waves from permeable materials.
17 p2581 A72-35250

Intermediate-range gravity - A generally covariant model.
17 p2581 A72-35380

Flight tests correlation with mathematical models to predict electro-optical viewing systems capability for military missions
17 p2557 A72-35553

Pilot-fighter aircraft system mathematical model relating pilot performance to air to ground weapon delivery accuracy
17 p2493 A72-35564

Shock-wave structure using nonlinear model Boltzmann equations.
17 p2542 A72-35614

Verification of theory for plasma of finite-size particles.
17 p2592 A72-35618

Water bag model application to one dimensional inhomogeneous two-stream collisionless electron plasma stability computation, noting electrostatic modes
17 p2592 A72-35619

Phenomenological model for incoherent microwave scatter attenuation from turbulent plasma, establishing relation between plasma parameters and attenuation coefficient
17 p2517 A72-35622

Turbulence model equations for calculation of supersonic and hypersonic flows, representing Reynolds stresses and turbulent heat flux vector in terms of eddy viscosity
17 p2543 A72-35639

Stochastic model for unsteady rhythmic processes based on periodical correlation of random processes
17 p2534 A72-35777

Time-optimal mathematical models operating with low-frequency pulse-frequency-modulated input information converted to an intermediate digital code
17 p2524 A72-35786

Mathematical model for flow limitation in collapsible tube in relation to pressure in pulmonary and circulatory system
17 p2510 A72-35972

Electrodynamic generator nonlinear internal resistance determination as function of flow parameters

and model geometry via boundary conditions formulation 18 p2643 A72-35998

Approximations yielding closed equations for isotropic turbulence compared to laboratory and computer experiments, emphasizing Langevin type model equation for velocity 18 p2677 A72-36008

Low order model and error rates for two-dimensional turbulent motion prediction in atmosphere spectrum 18 p2677 A72-36009

Mathematical solution to equations of turbulent motion in viscous fluids asymptotic to strange attractors 18 p2678 A72-36015

Structure, analysis and synthesis of time series models, discussing kernel Hilbert space, spectral estimation, moving averages, identification, etc 18 p2678 A72-36023

Reliability analysis of an intermittently used system with N types of failure. 18 p2693 A72-36024

Self-consistent statistical models for the gravity anomaly, vertical deflections, and undulation of the geoid. 18 p2723 A72-36028

A geopotential model (APL 5.0-1967) determined from satellite Doppler data at seven inclinations. 18 p2685 A72-36029

Mathematical models for flow ejection and aorta pressures based on displacement ballistocardiography and time dependent incompressible flow theories respectively 18 p2649 A72-36035

Recursive bootstrap maximum likelihood estimators algorithms for identification of process modeled by stable linear difference equation under additive output measurement noise 18 p2672 A72-36056

Nonlinear dynamic feedback control systems modeling by parameter estimation scheme with polynomial representation for state variables 18 p2672 A72-36057

Feedback controller synthesis from nonlinear system modeling by linear equations, proving theorem relating stability properties 18 p2672 A72-36060

Model improvements for thermionic diode plasmas. 18 p2715 A72-36218

Conformally flat linear axisymmetric chronometrically invariant cosmological models, discussing various types of spaces realized during model evolution 18 p2724 A72-36237

Rate distortion theory model for visual communication fidelity assessment via weighted noise measurement and K rating 18 p2657 A72-36251

Q values from lunar seismic record measurements indicating separation of scattering and real loss parameters effects on energy propagation, discussing geophysical models 18 p2724 A72-36288

Mathematical modeling assumptions and procedures in experimental mechanics, considering transfer function, impedance and human factor roles 18 p2709 A72-36353

Mathematical model and simulation for contact problems involving elastic half spaces and viscoelastic and friction effects 18 p2734 A72-36371

Theoretical models for cavity and wake flows, outlining numerical methods for solving functional equations 18 p2679 A72-36387

Molecular and atomic interaction forces as interfacial free energy sources, discussing molecular attachment kinetics and surface configuration models 18 p2718 A72-36393

Resonant mode sound field radiated by nonuniform slender circular cross section free-free beams, using dipole array modeling 18 p2710 A72-36410

Sonic jet noise pressure source model for radiated sound power and jet pressure frequency spectra ratio derivation with application to noise suppression 18 p2680 A72-36414

Mathematical methods for improving the significance of scintigrams 18 p2652 A72-36425

A stochastic bioburden model for spacecraft sterilization. 18 p2652 A72-36442

Theoretical model for plane turbulent wakes subject to adverse, favorable and mixed pressure gradients based on Reynolds stress equation, describing experimental verification 18 p2680 A72-36477

Dual amplitude construction possibility from general field theory couplings and propagators, considering factorization on multiperipheral configuration in translational and rotational modes 18 p2713 A72-36516

Prediction of electron concentration reductions in re-entry flow fields due to electrophilic liquid and water injection. 18 p2730 A72-36537

[AIAA PAPER 72-670] Statistical model of chemical reactions in nonisothermal low pressure plasma. 18 p2715 A72-36567

An analytical description of the line element in the zone-fluctuation model of colour vision. I, II. 18 p2651 A72-36606

Linear homogeneous system of differential equations as model for perturbation problems including functions with retarded and/or advanced arguments 18 p2705 A72-36614

Mathematical model for internal atmospheric gravity waves breaking process modification by momentum exchange between wave and mean flow 18 p2687 A72-36630

Perturbation method in inelastic interaction model for transport processes in reacting gases described by Boltzmann kinetic equation 18 p2713 A72-36807

A vortex model for the study of the flow at the rotor blade of a helicopter 18 p2642 A72-36975

A mathematical model of cold propane flames 18 p2741 A72-37016

Dynamics of dissolution of gas bubbles or pockets in tissues. 18 p2655 A72-37027

Digital computer simulation of human systemic arterial pulse wave transmission - A nonlinear model. 18 p2655 A72-37028

Finite element models with rigid displacement for nonrigid structure analysis, noting curved beam and shells 18 p2739 A72-37173

Theoretical models for speed-accuracy tradeoff during difficult visual discrimination tasks under time pressure 18 p2655 A72-37220

Time-dependent ionization equilibrium and line radiation under flarelike conditions. 18 p2849 A72-37241

Optimal terminal rendezvous as a stochastic differential game problem. 18 p2869 A72-37284

Equilibrium configurations of Vlasov plasmas carrying a current component along an external magnetic field. 18 p2839 A72-37332

Scattering of Langmuir waves produced by a beam with finite transverse dimensions. 18 p2839 A72-37337

Mathematical model of class of complex control systems composed of structures obtained from aggregates of ordered sets and random operators 18 p2777 A72-37380

Two component reaction kinetics model for numerical analysis of combustion during two- and three dimensional supersonic steady flow of hydrogen-air fuel mixtures 18 p2880 A72-37389

A three dimensional, analytical magnetospheric model with defined magnetopause. 18 p2789 A72-37410

Models of neurons reacting to input signal alternation in space and time 18 p2759 A72-37424

Neuron mathematical model synthesis from algorithms to construct neural networks and single threshold element in network form 18 p2759 A72-37425

The thermal conductivity of a statistically isotropic heterogeneous medium. 18 p2880 A72-37462

A model of a nonlinear viscoelastic medium allowing for the effects of cumulative damage 18 p2871 A72-37528

Model reference adaptive control systems design based on optimal control, parametric optimization, stability and statistical estimation theory 18 p2778 A72-37722

Mathematical model of ideal incompressible gyroscopic fluid with internal angular momentum using kinematic equations 18 p2835 A72-37929

Effectiveness of using composite materials directionally reinforced by hollow fibers 18 p2823 A72-38002

STOL ride quality criteria - Passenger acceptance. [AIAA PAPER 72-790] 18 p2749 A72-38107

A method for increasing thrust reverser utilization on STOL aircraft. [AIAA PAPER 72-782] 18 p2752 A72-38141

An optimal model-following flight control system for manual control. 18 p2753 A72-38228

Variable stability simulation techniques for nonlinear, rate dependent systems. 18 p2780 A72-38241

An investigation of vehicle dependent aspects of terminal area ATC operation. 18 p2832 A72-38256

A biased filter for linear discrete dynamic systems. 19 p2781 A72-38273

Geophysical signal statistical model parameter evaluation by selection of operators in form of dimensionless quantile ratios 19 p2765 A72-38352

Adhesive wear theoretical model based on asperity interactions number, area and volume, considering implications for friction and surface temperature analysis 19 p2809 A72-38377

Numerical calculation of the lunar wake in a magnetohydrodynamic model. 19 p2864 A72-38435

Structure of ion acoustic solitons and shock waves in a two-component plasma. 19 p2841 A72-38440

Markovian plasma turbulence model to obtain convergent perturbation series for diffusion coefficient via trajectories in particle propagator 19 p2841 A72-38442

Nonlinear interaction of a small cold beam and a plasma. II. 19 p2841 A72-38444

Two state system analytic modelling as nonlinear heat transfer problem 19 p2882 A72-38445

Burke-Shumann-Zeldovich model for aerodynamic characteristics of straight jet laminar diffusion flames, considering free, semibounded and slipstream types 19 p2882 A72-38460

Certain problems in continuum mechanics for a deformed body of variable mass 19 p2835 A72-38471

Mathematical model for perfectly absorbing spherical Langmuir probe in collisionless plasma, obtaining plasma density and ion temperature 19 p2842 A72-38524

Linear acoustic model to predict axial flow turbomachinery aerodynamic sound generation including flow effects on radiation 19 p2788 A72-38568

Solution of the problem of the unsteady motion of a mixture in a flat duct using a quasi-homogeneous model with allowance for deposition on the walls 19 p2788 A72-38589

Model random medium with two kinds of dielectric layers stacked in arbitrary proportions, calculating electromagnetic wave propagation characteristics by transmission line analogy 19 p2767 A72-38613

Differential equations for digital model of linear quadrupole, discussing digital simulation of analog radio equipment circuits 19 p2775 A72-38659

Theory of spontaneous mode locking in lasers using a circuit model. 19 p2813 A72-38690

Collisionless solar wind protons - A comparison of kinetic and hydrodynamic descriptions. 19 p2853 A72-38732

The mechanics of an organized wave in turbulent shear flow. III - Theoretical models and comparisons with experiments. 19 p2789 A72-38794

A thermal stratification model of a cryogenic tank at supercritical pressures. 19 p2883 A72-38845

Book - An introduction to engineering systems. 20 p2945 A72-38925

A Monte Carlo model of turbulent mixing for the prediction of NO production in steady-flow combustors. [WSCI PAPER 72-8] 20 p2982 A72-38973

Antenna pattern analysis for compatibility prediction. 20 p2902 A72-39000

Mathematical model of seismic isolation block and pneumatic suspension for inertial guidance component tests to describe design factors effects on vibration behavior [AIAA PAPER 72-844] 20 p2950 A72-39085

Theoretical model for acoustic emission relationship to fiber cracking during rising load tensile test on fiber reinforced composites 20 p2925 A72-39285

Deformation of the earth by surface loads. 20 p2916 A72-39335

Low beta model of collision dominated plasma flow effect on toroidal confinement, simulating Stellarator, Levitron and Tokamak 20 p2957 A72-39356

Recent advances in R & D value measurement and project selection methods. 20 p2988 A72-39397

Electrostatic, reticular vorticity, turbulence effects and equivalences with tensional and spectral elastic fields. 20 p2953 A72-39419

Finite sized optically thin radiating plasma stability analysis, deriving luminosity function for metastable state existence from mathematical model 20 p2958 A72-39456

Earth density, surface wave velocity and other properties calculation from model consistent with physical and petrological mantle theories

20 p2917 A72-39475

Simple conduction model for the theoretical steady-state heat pipe performance.

20 p2984 A72-39607

An advanced stochastic model for threshold crossing studies of rotor blade vibrations.

20 p2885 A72-39622

Mathematical models for radiative heat transfer prediction in real enclosures, noting directional characteristics of heat exchanging surfaces

[ASME PAPER 72-HT-K]

20 p2984 A72-39652

Mathematical model for surface tension induced thermocapillary fluid flow influence on conductive heat transfer through condensate film broken by non-wetting strips

[ASME PAPER 72-HT-H]

20 p2985 A72-39654

An analysis of heat transfer in turbulent pipe flow with variable properties.

[ASME PAPER 72-HT-59]

20 p2985 A72-39657

Saturated liquid film boiling on vertical surface, calculating local heat transfer rates as function of height and superheat from turbulent vapor flow model

[ASME PAPER 72-HT-38]

20 p2986 A72-39668

A parametric study of the transient ablation of Teflon.

[ASME PAPER 72-HT-32]

20 p2986 A72-39671

A digital simulation system for heat transfer modelled by ordinary and partial differential equations.

[ASME PAPER 72-HT-25]

20 p2986 A72-39673

A two-equation model of turbulence applied to the prediction of heat and mass transfer in wall boundary layers.

[ASME PAPER 72-HT-15]

20 p2986 A72-39685

The calculation of low-Reynolds-number phenomena with a two-equation model of turbulence.

[ASME PAPER 72-HT-20]

20 p2914 A72-39688

Digital computer hierarchical structure based on tree model using request/service resources as nodes, examining parallel multiple-stream organizations effectiveness

20 p2906 A72-39735

Mathematical model for MOS transistor circuit analysis, noting parameters measurement and environmental effects representation

20 p2909 A72-39783

Mathematical model for moving radiometer system for reflected solar radiation measurement, discussing instrument time constant effect on surface emittance variations reproduction

20 p2927 A72-39795

Reliability prediction of a two-unit standby redundant system with standby failure.

20 p2929 A72-39855

Mathematical model for Venus phase anomaly, noting upper limit of reflecting layer for refraction effect

20 p2972 A72-39874

Spherical kinematic dynamo models with asymmetric magnetic fields based on mean field electrodynamics and on nearly axisymmetric limit

20 p2954 A72-39875

One dimensional migratory dynamo model for alpha effect turbulence controlled by increasing magnetic field, considering oscillatory antisymmetric solutions relation to solar cycle

20 p2972 A72-39877

Computerized long term weather forecasting via mathematical modeling of atmospheric processes based on meteorological parameters worldwide observational data

20 p2948 A72-39939

Dynamic adjustment of initial model fields by using complete equations of hydrothermodynamics

20 p2949 A72-39943

Characteristics of models of detonation spinning in various combustible media

20 p2987 A72-40045

Turbulent mixing of fluids of different density moving in a tube

21 p3044 A72-40129

Russian book - Mathematical modeling and electrical circuit theory, Number 8.

21 p3023 A72-40153

Solution of the general linear programming problem by electronic simulation using the regularization method

21 p3023 A72-40155

Inverse data transformation in control problems

21 p3036 A72-40156

Modeling a hybrid quasi-analog system on a computer

21 p3023 A72-40157

Digital simulation of the SEI-1 static electrointegrator for solving heat-type equations

21 p3127 A72-40160

Simulation of torsional vibrations of rods without concentrated masses

21 p3116 A72-40167

Simulation of flexural vibrations of rods without concentrated masses

21 p3116 A72-40168

Some problems in the mathematical simulation of blade vibrations in turbomachines

21 p3116 A72-40169

Accuracy of alpha-analog simulation of linear algebraic equations in the case of a nonzero discrepancy vector

21 p3074 A72-40170

Russian book - Mathematical modeling and electrical circuit theory.

21 p3036 A72-40176

Simulation of physically nonlinear multispin beams

21 p3116 A72-40180

Using the quasi-homogeneity of differential equations in modeling physical systems

21 p3083 A72-40377

Mathematical model of earth liquid core dynamo mechanism for magnetic field maintenance based on simple motions with spherical harmonic form

21 p3048 A72-40400

Mathematical model of two-component alga-bacteria biocenosis

21 p2997 A72-40431

Russian book - Hydrodynamic evolution model of the earth.

21 p3103 A72-40461

Further study of the severe storm with a rotating updraft configuration.

21 p3077 A72-40466

A method of calculating the parameters of a linearized transistor model

21 p3027 A72-40475

A contribution to the theory of finite antenna groups, taking into consideration radiation coupling

21 p3028 A72-40503

Theoretical model prediction for matched filter selectivity and noise effects on strained object deformation in optical correlation applications, comparing results with experiments

21 p3053 A72-40611

Void lattice model for Mo physical properties and equilibrium lattice spacing determination, calculating defect Green function

21 p3066 A72-40623

Current and voltage waveform measurements with sampling oscilloscope and capacitive voltage-divide probe to verify TRAPATT diode oscillator theoretical model

21 p3032 A72-40635

Failure diagnostics in mathematical models of automatic control systems

21 p3038 A72-40712

Crystalline lens optical structure in human eye, representing on and off axis imaging characteristics by mathematical model

21 p3007 A72-40737

Light pulse propagation through clouds - Models and experiments.

21 p3063 A72-40857

Canonic model representations for communication receiver to analyze and simulate input-output behavior as nonlinear signal processing black box

21 p3019 A72-40889

A mathematical model of the chemoreflex control of ventilation.

21 p3008 A72-40917

Mathematical models for temperature profiles and heat transfer rates in two-stream and multistream cross flow heat exchanger

21 p3128 A72-40931

Diffusion in the system K₂O-SrO-SiO₂. IV - Mobility model, electrostatic effects, and multicomponent diffusion.

21 p3097 A72-40935

Unsteady burning of reacting mixture of air and condensed-phase combustion products in closed variable volume, noting mathematical model for parameters calculation

21 p3128 A72-40977

Application of variational methods to the solution of some thermal shock problems

21 p3128 A72-40978

Two explanations of temporal changes in ability-skill relationships - A literature review and theoretical analysis.

21 p3008 A72-41015

Numerical model of NGC 7662 consistent with line strengths and ratios, considering double shell structure and central star flux deviation from black body

21 p3105 A72-41033

Mathematical model for dielectrics with time dependent polarization, noting relaxation time distribution function

21 p3085 A72-41074

Non-Hertzian contact stresses in a smoothly cradled heavy cylinder.

21 p3119 A72-41108

A model of low-frequency sound propagation in a lined duct.

21 p3085 A72-41112

Kullback-Leibler information function and the sequential selection of experiments to discriminate among several linear models.

21 p3075 A72-41187

Ground and torque relation to swivel angle and lateral displacement of wheel rim plane, using string model for tire

21 p2996 A72-41260

A method to calculate electric currents in quiescent prominences.

21 p3108 A72-41282

Determination of the limits of applicability of a continuous model when calculating a discrete polar lattice disk

21 p3122 A72-41346

Lectures on theory of manual-vehicle control.

21 p3011 A72-41418

Some contributions to the theory of linear models describing the control behaviour of the human operation.

21 p3011 A72-41419

The design of a nonlinear multi-parameter model for the human operator.

21 p3011 A72-41421

The functional organisation of object directed human intended-movement and the forming of a mathematical model.

21 p3011 A72-41422

The influence of a prediction display on the human transfer characteristics.

21 p3012 A72-41432

Application of wall corrections to transonic wind tunnel data.

[AIAA PAPER 72-1009]

21 p3041 A72-41591

Burgers model equation for shear flow turbulence with complex physical processes and nonlinearities in governing equations

21 p3047 A72-41637

Turbulent flow experimental and theoretical investigation, discussing Reynolds stress transport equations, shear layers and turbulence models in context of digital prediction methods

21 p3047 A72-41639

Phenomenological models of the electron-phonon interaction and the superconductivity criterion of metals

21 p3098 A72-41688

Physical model of the onset of turbulent burning of compacted systems in a half-closed volume

21 p3131 A72-41699

Optimum spatial filter for an anisotropic background-noise.

21 p3036 A72-41839

Electrodynamic mathematical model for electroconductivity of nonuniform plasma with Hall effect, calculating current distribution from Riemann problem solution

22 p3210 A72-41888

Development and optimization of a nonlinear multiparameter human operator model.

22 p3149 A72-41949

Transient oscillator analysis of a high-pressure electrically excited CO laser.

22 p3184 A72-41970

Resonant interaction of an electrostatic wave with electrons in a current sheet.

22 p3169 A72-42008

Gravitational theory strong discontinuity conditions, using fundamental variational equation for field and media model construction in general relativity theory

22 p3204 A72-42089

Nonlinear problems of analyzing the observability of the trajectories of spacecraft motion on the basis of measured data

22 p3223 A72-42203

Mathematical model for lattice-type error distribution of parallel channels communication system, noting metric for algebraic signal coding method

22 p3154 A72-42234

Mathematical methods of man machine control system synthesis, using homeostasis and functional compatibility principle

22 p3162 A72-42243

An analysis of aircraft lateral-directional handling qualities using pilot models.

[AIAA PAPER 72-962]

22 p3137 A72-42347

Equations of motion appropriate to the analysis of control configured vehicles.

[AIAA PAPER 72-952]

22 p3137 A72-42353

Error sensitivity of statistical models with pattern rearrangement for analysis of interplanetary scintillation in ecliptic plane

22 p3218 A72-42402

Induction effect of slowly decaying ring current, estimating electric field strength by model consisting of earth dipole and symmetric ring

22 p3172 A72-42430

Analytical model for a polarizable medium at radio and lower frequencies.

22 p3155 A72-42467

Extremum principles for a class of dynamic rigid-plastic problems.

22 p3235 A72-42522

The dynamics of the ascending flight of sounding rockets

[ONERA, TP NO. 1056]

22 p3231 A72-42582

Causality in the relativistic theory of elastic media in the three-dimensional case. 22 p3206 A72-42626

Pair-correlation and angular distribution functions calculations for one and two dimensional amorphous structures 22 p3197 A72-42797

Analytical model of the flash produced in aluminum-aluminum hypervelocity impacts. 22 p3207 A72-42867

Mathematical models from UV, IR and radio observations of chromosphere and transition region to corona, noting temperature effects of shock wave dissipation 22 p3229 A72-42903

Mathematical model for plastic deformation of polycrystalline materials with Hookes law elastic strains 22 p3242 A72-43135

Two body model for three body problem of uniformly distributed and isotropically expanding gravitational matter of Einstein-Sitter universe, noting metagalaxy cooling rate 23 p3334 A72-43241

Hydrodynamic and Wiener-Siegel hidden parameter models incapability for quantum mechanics reduction to classical mechanics, obtaining proofs to von Neumann theorem 23 p3312 A72-43298

Einstein equations reduction to friction systems in homogeneous cosmological models, investigating Bianchi models isotropization and statistical analysis 23 p3335 A72-43301

Model of degenerate semiconductor near semielectric phase transformation, noting superconducting state at low temperatures with corresponding impurity concentrations 23 p3323 A72-43317

A stability analysis for tethered aerodynamically shaped balloons. 23 p3250 A72-43332

Numerical treatment of a model of the hydromagnetic dynamo with a selected system of convection in the earth's core. 23 p3284 A72-43422

Electromagnetic induction in a half-space with a cylindrical inhomogeneity. 23 p3284 A72-43423

Structural mass properties mathematical modeling for dynamic structural analysis, describing matrix notation for finite element methods application [SAWE PAPER 944] 23 p3344 A72-43484

Probabilistic model for tensile strength of brittle fibers, discussing clamping effects at various gage lengths and Weibull flaw structure 23 p3305 A72-43490

Numerical simulation of the relaxation of a beam of charged particles in a strong electric field 23 p3315 A72-43530

Modeling a holographic process on a computer 23 p3287 A72-43531

Empirical support for a stochastic model of evolution. 23 p3254 A72-43565

Computer-controlled queuing system with service interruptions. 23 p3275 A72-43605

Isotropic materials nonlinear rheonomic behavior at small strains, deriving model structure deformation laws 23 p3345 A72-43623

Stochastic models for block triangulation by bundle approach, comparing theoretical accuracies obtained from different block adjustment methods 23 p3284 A72-43631

The dynamics and control of Eulerian turbomachines. [ASME PAPER 72-AUT-S] 23 p3279 A72-43633

Lumped parameter model description of distributed parameter fluid dynamic systems by bond graph techniques [ASME PAPER 72-AUT-J] 23 p3279 A72-43634

On the efficient reduction of truncation error in numerical weather prediction models. 23 p3311 A72-43675

Mathematical formulation of ice crystal formation and propagation mechanism in seeded supercooled convective clouds 23 p3311 A72-43722

Statistical strength and plasticity criterion for materials in a complex stress-strain state 23 p3349 A72-43953

Numerical models of elliptical galaxy based on rotational speed and integral equations for mass distribution 23 p3338 A72-44033

Properties of a superconducting point contact contained in a resonator 23 p3324 A72-44221

Elements of a theory of CW gasdynamic quantum generators. 23 p3297 A72-44225

Reliability analysis of a jet engine fuel system with the aid of an analog computer using operational data 23 p3326 A72-44282

Mathematical model for dynamics simulation of aircraft turboprop engines, using digital, analog and hybrid computers 23 p3327 A72-44288

A digital model of jet engine hydraulic fuel controller 23 p3327 A72-44291

Determination of the statistical characteristics of a turbine stage and a group of turbine stages 23 p3328 A72-44295

Charts for confidence limits and tests for failure rates. 23 p3294 A72-44395

Multiple collisions and an optical model of the inelastic interaction between cosmic particles and nuclei 23 p3330 A72-44413

Approximation for Monte Carlo method modeling of pion-nucleon and nucleon-nucleon inelastic collisions at high energies 23 p3317 A72-44414

Statistical forecasting models for USAF CONUS outbound cargo airlift requirements by averaging and exponential smoothing models 24 p3466 A72-44578

Lockheed airline system simulation and aircraft scheduling models. 24 p3466 A72-44579

Possibility of determining the lung ventilation volume by the mathematical modeling method 24 p3374 A72-44597

One-level fine-mesh limited-area grid numerical weather prediction atmospheric model, evaluating various finite difference schemes, boundary conditions and initialization methods 24 p3420 A72-44619

Time ratio models of equipment availability for using and procuring agencies, considering performance effectiveness criterion and suboptimization risk 24 p3467 A72-44659

Allocating optimum time for systems malfunction search. 24 p3406 A72-44661

Robert Bruce's spider problem extended - Reliability of adaptive experimental systems. 24 p3406 A72-44666

The problems of reliability growth and demonstration with military electronics. 24 p3384 A72-44670

Cumulative damage stochastic models and distributions of strength of steels and graphite. 24 p3412 A72-44673

A method for balancing geopotential and wind fields 24 p3420 A72-44765

Radiative transfer in a gray isothermal spherical layer. 24 p3461 A72-44805

Model potential calculations of lithium transitions. 24 p3426 A72-44808

A finite element model for shells based on the discrete Kirchhoff hypothesis. 24 p3457 A72-44876

Relative position of the rib within the chest and its determination on living subjects with the aid of a computer program. 24 p3372 A72-44957

Pulsed carbon dioxide laser medium composition, pressure and electrical parameters effects on output power, energy and efficiency from mathematical model solution of kinetic equations 24 p3409 A72-44966

Hyperbolic space criterion for cosmological model based on axioms conforming to special and general theory of relativity, noting coordinate transformation 24 p3439 A72-44969

Combustion product gas dynamic motion effects on detonation front propagation, discussing reacting blast wave and finite kinetic rate models and asymptotic results 24 p3391 A72-45027

Model for shock wave propagation through gas-liquid drop medium based on liquid phase atomization by boundary layer stripping 24 p3391 A72-45049

A theoretical model for the combustion of droplets in super-critical conditions and gas pockets. 24 p3463 A72-45050

Response of convectively controlled burning to non-linear disturbances. 24 p3464 A72-45055

Exponential functions model for D region vertical distribution of electron density profiles, taking into account solar X- and cosmic rays 24 p3397 A72-45081

Multilayer plasma model for MHD pulse propagation in ionospheric waveguide, noting approximation of Alfvén velocity distribution by plasma layers 24 p3397 A72-45085

Mathematical model for life support system optimization in terms of reduced mass minimization as quality criteria for energy conversion and metabolic processes 24 p3375 A72-45133

Flow model for the determination of the heat transfer on the base of vehicles with clustered H2-O2 rocket engines. 24 p3434 A72-45201

Frictionless core flow and friction layers at turbomachine walls and blades for real two dimensional cascade flow modeling 24 p3394 A72-45370

Jet stream formation from uniform distribution of grains in similar elliptical orbits, discussing models with numerical simulation 24 p3445 A72-45461

Problems of complex object modeling based on heuristic self-organization 24 p3376 A72-45509

Mathematical description of a human operator in ergatic control systems 24 p3376 A72-45514

Cross section parameters for electron impact excitation, noting mathematical models for aeronautical users 24 p3400 A72-45591

Mathematical model for secondary electron production fall-off, calculating ionization cross section from electron distribution 24 p3400 A72-45592

A power-law model for the multiple-integral theory of non-linear viscoelasticity. 24 p3460 A72-45696

MATHEMATICAL STATISTICS

U STATISTICAL ANALYSIS

MATHEMATICAL TABLES

Liapunov functions generation, using auxiliary functional differential equations table for invariance determination 06 p0838 A72-17378

Pade table for formal power series with notation for extension to Laurent series, relating algebraic theory to bigradient determinants and numerical analysis algorithms 11 p1676 A72-25501

Table of indefinite and definite integrals of products of error functions with transcendental and special functions 15 p2262 A72-31589

A table of solutions of the one-dimensional Burgers equation. 19 p2828 A72-38717

New method for determining the distribution of delta-g anomalies for a sphere, horizontal cylinder, and vertical material half-line 22 p3173 A72-42574

MATHEMATICS

Applied mathematics and mechanics - Conference, Mannheim, Germany, April 1971 15 p2323 A72-31451

MATHIEU EQUATION

U MATHIEU FUNCTION

MATHIEU FUNCTION

Harmonic waves propagation in infinite transverse isotropic cylinder with elliptic cross section, obtaining solution in terms of Mathieu functions 14 p2163 A72-30190

Special boundary value problems solution method for Mathieu differential equation, transforming Mathieu equation to Hill differential equation via Fourier series expansion 15 p2264 A72-32468

Integral equation for pressure distribution by rigid punch contact with elastic half space, solving by Mathieu function expansion in Fourier series 21 p3126 A72-41541

MATRICES

Pattern recognition by computerized local processing of binary matrix representations 01 p0018 A72-10476

MATRICES [CIRCUITS]

Analog matrix, input data and procedure for AI frame and Cu-clad printed circuit board module thermal resistance analysis using ECAIP program 01 p0035 A72-10380

Photosensitive MOS devices array as converters performing optical image data analysis, considering sensor sensitivity regulation 02 p0193 A72-12342

Destructive readout computer memory of wire substrate electrodeposited with two thin Permalloy layers separated by Cu [IEEE PAPER 11,5] 03 p0332 A72-13765

Coupled-film closed-easy-axis arrays for large capacity NDRO multiple-write bulk memory, discussing disturb mechanisms limitation on performance and design [IEEE PAPER 21,9] 03 p0328 A72-13780

MOS Si-gate arrays for static, dynamic and programmable read-only memories, investigating information storage reliability 03 p0336 A72-14282

Computer analysis of linear electric circuits without restrictions on network topology and component composition, using system matrix 04 p0495 A72-14464

Programmable cellular cascades and arrays synthesis for realizing arbitrary Boolean functions or parallel arithmetic operations

04 p0498 A72-15107

Thin film conductors, distributed film resistors and capacitors design and associated IC layout to form functional arrays

06 p0790 A72-18574

Photosensitive MOS devices array as converters performing optical image data analysis, considering sensor sensitivity regulation

08 p1143 A72-21948

Electroluminescent matrix display system with amorphous semiconductor threshold switches for isolation and memory, discussing performance and address waveforms

12 p1788 A72-27239

Active RC circuit synthesis by state model method, minimizing capacitances of admittance matrix for microelectronic circuit technology

15 p2210 A72-31595

Diffraction theory for large storage capacity holographic random access memory design, discussing geometric optimization of detector array and storage plate

15 p2238 A72-32159

Adjacent channel discrimination enhancement in Gray-scale binary coded two dimensional array, using checkerboard filter for pattern noise suppression

15 p2238 A72-32162

Minimum elements number on discrete two dimensional hologram with constant distance between emitters, considering reduction of matrix elements

15 p2242 A72-32665

Cellular-array arithmetic unit with multiplication and division

17 p2519 A72-34297

Investigation of the dependence of the electrical characteristics of a 'Fotovolt'-type high-voltage matrix photoconverter on the radiation intensity and temperature

17 p2498 A72-35511

Electrical properties and fabrication details of integral diode matrices with controllable avalanche breakdown produced from zone melted silicon under temperature gradient

19 p2774 A72-38416

Two dimensional microprogrammed cellular arrays logic organization and control structure for multifunctional digital subsystems

20 p2906 A72-39736

Disk and toroidal solid state computer storage cellular arrays without boundary cells, comparing read- and write-time characteristics with conventional organizations

20 p2910 A72-39966

Experimental investigation regarding Archimedean spiral antennas for the L-band, and radiator groups constructed from them whose radiation directions are controlled by a conduction matrix

21 p3028 A72-40510

Application of the transmission-line-matrix method to homogeneous waveguides of arbitrary cross-section

21 p3032 A72-40629

Parallelized algorithms for computer solution of spanning tree, distance and path problems on cellular array of identical modules containing memory and combinational logic

22 p3157 A72-43023

Gain measurements of matrix-type TEA CO₂ laser

23 p3296 A72-44072

MATRICES [MATHEMATICS]

NT ADJOINTS
NT CANONICAL FORMS
NT EIGENVALUES
NT EIGENVECTORS
NT JORDAN FORM

Spacecraft flight trajectory parameters from unknown second moment matrix of navigation measurement errors

01 p0127 A72-10352

Complex structures mass and stiffness matrices reduction by automatic condensation, calculating lowest eigenfrequencies and eigenmodes of substitute systems

[DGLR PAPER 71-108] 02 p0299 A72-12721

State space method application to power servomechanism analysis, discussing transition matrices and state equations

03 p0338 A72-13645

Covariance matrix of coordinate fluctuations of instantaneous radar center of reflection from set of scatterers

04 p0487 A72-15144

Matrix representation of nonlinear equation iterations based on polynomial methods, considering convergence and application to parallel computation

04 p0540 A72-15373

Matricial difference schemes based on numerical methods characterized by approximations for integrating stiff systems of differential equations

04 p0540 A72-15375

Modal theory of state observers for control of multivariable time-invariant linear systems with plant matrices possessing distinct eigenvalues

04 p0507 A72-15529

Multiple-input multiple-output linear time invariant feedback systems stability, investigating continuous-time case

04 p0507 A72-15694

N-port resistive network synthesis involving use of vectors, cones, bilinear inequalities and matrices

05 p0639 A72-15801

Analytical inversion of quasi-orthogonal matrix for Simpson method of state feedback gains calculation in multiloop linear mode control systems

05 p0639 A72-15807

Quasi-steady continuous process adaptive optimal control, discussing algorithms and model for sensitivity matrix calculation and digital simulation for strategy

05 p0640 A72-16200

Interplanetary spacecraft trajectory error analysis by closed form approximation to state transition matrix, enabling rapid estimation with computer program

05 p0718 A72-16443

Bounds on condition number for irregular meshes of finite elements expressed in terms of extremal eigenvalues of element matrices

[AD-739416] 05 p0682 A72-16540

Deflection function for symmetrical bending of unloaded annular plate, constructing stiffness, mass and stability coefficient matrices by function manipulation

05 p0739 A72-16550

Flight mechanics derivative transformations by matrix methods for changing coordinate or independent variable systems

[DFVLR-SONDDR-175] 05 p0612 A72-16706

Error covariance matrix square root calculation in orbit determination from ground based observations

05 p0720 A72-16752

Error covariance matrix evaluation at end of orbit extrapolation in terms of state vectors at measurement, discussing computation and interpretation

05 p0720 A72-16753

Finite periodic beam response to turbulent boundary layer pressure field fluctuation, using transfer matrix technique

[AIAA PAPER 72-171] 05 p0650 A72-16832

Generalized matrix inverse application to dynamic system state vector estimation, determining covariance matrix for comparison with optimal Kalman type procedure

05 p0641 A72-17089

Linear system digital simulation by matrix exponentiation with generalized hold order algorithm for accuracy improvement at less computer time

06 p0839 A72-17630

Complete measurement in holography using complex coefficients of conversion matrix of interaction between coherent beam and recorded object

06 p0817 A72-18014

Coefficient matrix for estimation of numerical solution error bounds for finite element models

07 p1025 A72-18786

Real rational function Cauchy index computed from integral functions of polynomial coefficients and signature of infinite class of matrices

07 p1026 A72-18817

Time-variable multivariable systems reduction to completely controllable and observable systems by subdivision and transformation procedures, using subsystems order matrices

07 p1026 A72-19271

Linear multivariable systems feedback invariant structure of controllable matrix pair under rich transformation group including regular linear coordinate and state-feedback transformations

07 p0960 A72-19700

Weighting matrices effect on optimal regulator for linear time invariant multivariable systems

07 p0961 A72-19713

Matrices of fundamental solutions constructed for loading singularities and Green method in unbounded micropolar elastic continuum

07 p1095 A72-20243

Linear first order differential equation transient response computer simulation using transition matrix method

07 p1028 A72-20340

Dynamic system time varying parameters on-line estimation using adaptive extended Kalman filter based on predicted error covariance matrix alteration

08 p1144 A72-20847

Significance criteria for comparing strength parameter against expectation from random group of vectors in variance matrix applications

09 p1341 A72-23023

Numerical algorithm for matrix case extension of transport problem in periodic media

09 p1342 A72-23368

Matrix notation for replacing vector analysis in control theory by introduction of differential operators similar to Hamiltonian operator

09 p1352 A72-23369

Revised algorithm for unconstrained optimization using quasi-Newton methods based on recurring factorization of approximation to Hessian matrix

10 p1502 A72-23723

Optimal probing signals design for state vector parameter estimation, considering Fisher information matrix function as optimality criterion

10 p1454 A72-23786

Muller matrix derivation for microwave light modulation studies in quasi-homogeneous magnetooptical and electrooptical media, taking into account finite light speed

10 p1493 A72-24914

Distributed elastic system discrete model mass, stiffness and damping matrices derivation from dynamic test response data

[AIAA PAPER 72-346] 11 p1728 A72-25375

Square matrix inverse computation by convergent power series method

11 p1678 A72-26368

Matrix and graphic test construction methods for optimal design of logic networks in automatic control systems

11 p1612 A72-26443

Regular matrices inversion for linear equations solution, using modified method of completing

11 p1678 A72-26495

Optimality and strategy efficiency in Gaussian elimination on sparse matrix, using graphical method

11 p1678 A72-26496

Automatic search for Huffman sequential logic circuit breakdown detection sequence, using VEGA program through matrices and graphs utilization

11 p1612 A72-26549

Linear multistep methods with variable matrix coefficients for asymptotic numerical integration of ordinary differential equations system

11 p1679 A72-26960

Supersonic aerodynamic influence coefficients matrices calculation for wings of arbitrary planform, constructing computer program

12 p1752 A72-28142

Transfer matrices determination for two terminal pair network derived from four terminal pair network, considering bandpass filters

13 p1931 A72-29060

Neuronal network numerical and analytic studies, using invariant imbedding and matrix Fredholm integral equation

13 p1986 A72-29400

Finite element displacement field with internal equilibrium application to nine degrees of freedom triangular bending element stiffness matrix calculation

14 p2168 A72-30930

Matrices and permutation rules for tetrahedral polynomial finite elements for Helmholtz equation, commenting on computer time and convergence rate

14 p2126 A72-30932

Slender rotating body aeroelastic behavior under inertial, gravitational, thrust, servocontrol, elastic and aerodynamic forces, presenting equilibrium equations in matrix form

15 p2319 A72-31210

Nonlinear electronic (transistor) system mapping-on by matrix dynamic transform algorithms, comparing with Newton-Raphson method

15 p2210 A72-31491

Algorithm to transpose large matrices in excess of direct access computer memory for external sequential storage

15 p2203 A72-31748

Generalized differential system for Hamiltonian, Hermitian and corresponding symmetric nonreal linear matrix differential equations systems

15 p2263 A72-31756

Nonlinear equations systems iterative solution methods convergence, generalizing Varga matrix splitting technique to nonlinear mappings in Banach space

15 p2264 A72-32465

Skewed wire antennas electric and magnetic near fields prediction from computer programs based on matrix inversion method

15 p2209 A72-32567

Numerical methods for Liapunov linear matrix equations solution in control systems analysis and design

15 p2265 A72-32798

Three dimensional orthogonal coordinate system transformation by simultaneous independent small angle axes rotation using transformation matrix

16 p2424 A72-33249

Sandwich structures buckling calculation by transfer matrices with allowance for cross section shearing

16 p2471 A72-33680

System theory on group manifolds and coset spaces

17 p2575 A72-34949

Monograph - The finite-element method in plate bending analysis

17 p2634 A72-35547

Book - Riccati differential equations

17 p2577 A72-35798

Functional relationships between the conventional steady-state error characteristics and the weighting matrices in the quadratic performance index.
18 p2672 A72-36058

On discrete-time Kalman filter in singular case and a kind of pseudo-inverse of a matrix.
18 p2672 A72-36059

Matrix coefficients calculation of state variables equations for network analysis and synthesis.
19 p2777 A72-37313

Formal extension of the possibilities of the method of integral transforms in the study of linear distributed systems with constant parameters.
19 p2834 A72-37432

Symmetric and innerwise matrices for the root-clustering and root-distribution of a polynomial.
19 p2825 A72-37851

Direct and inverse transformations between phase variable and canonical forms.
19 p2826 A72-38230

Decoupling of linear discrete time systems by state variable feedback.
19 p2827 A72-38563

A long line as a limit of an infinite quadrupole chain.
20 p2904 A72-39592

A modernized specialized computer for evaluating determinants.
21 p3036 A72-40161

Calculation of intensities of vibration-rotation of a diatomic molecule by the factorization method.
21 p3087 A72-40471

Nonlinear differential equation periodic solution approximation by pseudo-linear representation of nonlinear terms effects on single harmonic, using describing function matrix method.
21 p3076 A72-41314

Computational solutions of matrix problems over an integral domain.
21 p3076 A72-41315

Mathematical spectra theory application to matrix eigenvalue problem, obtaining explicit form of determinant characteristic polynomial by numerical methods.
21 p3076 A72-41781

Computer-aided vector Taylor series approximation of fundamental matrix of ordinary first order differential equations with variable coefficients.
21 p3076 A72-41785

Instability of the characteristic indices of systems of linear differential equations with almost periodic coefficients.
22 p3197 A72-41853

Structural mass properties mathematical modeling for dynamic structural analysis, describing matrix notation for finite element methods application [SAWE PAPER 944].
23 p3344 A72-43484

Formal solution of a system of differential equations of fractional rank with an irregular singular point.
23 p3308 A72-43579

Design of controllers for open-loop unstable multivariable system using inverse Nyquist array.
23 p3275 A72-43609

Iterative method of computing the limiting solution of the matrix Riccati differential equation.
23 p3275 A72-43610

Efficient method to multiply successively functions of the companion matrix and applying the method to evaluate transient response.
23 p3309 A72-43862

Ray optics applications to electromagnetics and other disciplines, discussing matrix representation for wavefront curvature and field computation simplification via transformations.
23 p3314 A72-44331

Use of the three-dimensional covariance matrix in analyzing the polarization properties of plane waves.
23 p3315 A72-44518

Determination of the covariance matrix of the spatial coordinates of points of a geometrical model.
24 p3397 A72-44867

MATRIX ALGEBRA
U MATRICES [MATHEMATICS]
MATRIX ANALYSIS
U MATRICES [MATHEMATICS]
MATRIX METHODS
Matrix calculation of forced atmospheric oscillations for Hall, Coriolis and Pedersen regions.
01 p0053 A72-10090

Matrix formulation of free-free modal synthesis procedures for dynamic analysis of composite structural systems, giving flow charts [SAE PAPER 710783].
01 p0137 A72-10274

Algorithms for mass and stiffness matrices synthesis from experimental vibration modes applied to cantilever beam [SAE PAPER 710787].
01 p0137 A72-10278

Pollution and environmental quality remote sensing, describing five dimensional sensor/applications matrix for decision guidance.
02 p0212 A72-11827

Noncircular cylindrical shells dynamic analysis using transfer matrix method.
02 p0293 A72-12372

Matrix method calculation for aerodynamic loads, transverse forces, bending moments, torques and twist of hinged main rotor blades in helicopter during forward flight.
02 p0294 A72-12440

Statistical linearization approach to determine approximate instantaneous correlation matrices of nonlinear structure response to nonwhite excitation.
02 p0298 A72-12663

Stiffness matrix method application to finite deformation theory, noting convergence through use of iterative interpolation in numerical calculations.
02 p0298 A72-12667

Strain anisotropy effect on thin walled tubular steel samples with combined bending and torsion, constructing matrix and stress vectors.
03 p0445 A72-13578

Antenna arrays near-field radiation pattern prediction, using Harrington matrix methods.
03 p0323 A72-14030

Wire antenna computer design to determine feed voltages for obtaining pattern synthesis and gain maximization, using matrix methods.
04 p0495 A72-14492

High frequency diffraction problems, using matrix formulation in spectral domain.
04 p0489 A72-15396

Vibration theory calculations using parametric matrix function method and associated operators.
04 p0550 A72-15543

Spacecraft attitude control system reliability and performance improvement through nonorthogonal coordinates application, using matrix technique.
05 p0728 A72-16477

Biaxial bending solution by tangent stiffness matrix method suitable for computer application.
06 p0897 A72-17967

Algorithm for bandwidth reduction of symmetric matrices for complex structural problems.
06 p0897 A72-17968

Dynamic matrix analysis of vibrating three dimensional frame structures, comparing discrete and continuous mass systems.
06 p0897 A72-17971

Iterative and direct modification procedures for structural analysis matrix displacement method, discussing computer program implementation.
07 p1089 A72-19329

Stress-strain state determination in elastic parallelepiped by net point method and matrix filtering.
07 p1091 A72-19754

Book on matrix structural analysis covering matrix algebra concepts, direct stiffness matrix methods, lifting surface, nonlinear truss and structural partitioning analysis, etc.
07 p1092 A72-19908

Nonlinear large amplitude vibration of beams for various support conditions, using finite element matrix displacement method.
08 p1245 A72-21626

Green matrix computation algorithm extensible to spherical and toroidal closed shells of revolution for stress-strain state determination.
08 p1246 A72-21672

Transfer matrix and dynamic stiffness techniques application to critical speed analysis in rotating machinery.
08 p1224 A72-22128

Transfer matrix method application to rocket vehicles structural dynamics, incorporating axial and aerodynamic lift forces in vibrational analysis.
09 p1397 A72-23499

Spectral line formation in atmosphere with plane parallel layers and frequency independent source function, using matrix approach for transfer equation solution.
10 p1535 A72-24058

Matrix displacement method for nonuniform beam vibration problems, using internal nodes concept.
11 p1735 A72-25740

Curved cylindrical shell finite element with reduced stiffness matrix, noting convergence for symmetrical and unsymmetrical loading.
11 p1735 A72-25896

Finite element method for buckling coefficients of isotropic rectangular plate subject to linearly varying axial compression, using general linear geometric matrix.
11 p1736 A72-25999

Jones matrix method for polarization natural states, frequencies and mode losses calculation in anisotropic optical resonators.
11 p1688 A72-26347

Matrix methods in structural dynamics, discussing frequency response, normal mode, Fourier, Newmark, difference and Houbolt methods.
12 p1882 A72-27338

Book on structural analysis covering statically indeterminate structures, force and displacement methods, flexibility and stiffness matrices, strain energy, virtual work, energy theorems, etc.
15 p2325 A72-31517

Orthogonal vibration damping matrix numerical evaluation, comparing Caughey series and direct approaches.
15 p2326 A72-31711

Temperature dependent elastoplastic wing assemblies and continua analysis via matrix displacement method.
16 p2471 A72-33791

Matrix progression method analysis of free vibration problem for cantilever thin circular cylindrical elastic shells, using Flugge equations.
16 p2475 A72-34173

Calculation of correlation matrices for linear systems subjected to nonwhite excitation. [ASME PAPER 71-APMW-10].
17 p2625 A72-34316

Freedoms retention determination eigenvalue analysis of complex structures large dynamic matrices deriving transformation vectors based on maximum swept volume deformation modes.
17 p2576 A72-35253

Monograph - The elastic flexural-torsional buckling of beam-columns by discrete element techniques.
17 p2634 A72-35548

Programmable computation method based on matrix formulation for numerical solution of differential equations in heat conduction and thermal stress problems.
17 p2635 A72-35898

Balancing of a flexible rotor by means of mode separation.
18 p2732 A72-36072

Higher vibration modes by matrix iteration.
18 p2736 A72-36772

FORTRAN subroutines for plate bending and plane stress elements stiffness and geometric matrices generation, taking into account anisotropic properties and linear thickness variations.
18 p2739 A72-37166

Bounds on the extremal eigenvalues of the finite element stiffness and mass matrices and their spectral condition number.
18 p2705 A72-37202

A general theory of polarization holography and its application to photoelastic analysis.
19 p2799 A72-37627

Structural-matrix methods for discrete automatic control system designs.
19 p2779 A72-38185

Book - An introduction to engineering systems.
20 p2945 A72-38925

Application of material formalisms to the specification of light polarization changing systems.
20 p2928 A72-40025

A consistent approach for treating distributed loading in the matrix force method.
21 p3122 A72-41261

Iteration process convergence improvement based on stiffness change expression as linear combination of two matrices in structural reanalysis.
22 p3235 A72-42602

Symmetrical bending of circular plates using finite elements.
22 p3236 A72-42605

Eigenvalue spectrum translation and frequency shifting by inertia and stiffness matrix modifications in iteration techniques.
22 p3207 A72-42850

Transfer matrix approach for determining stresses and displacements in elastostatics of laminated composites [ASCE PREPRINT 1674].
23 p3351 A72-44105

Butler-matrix fed arrays, discussing phase differences, scan steps and sectors, sidelobe structure and attenuation.
23 p3273 A72-44363

A method of computing numerically integrated stiffness matrices.
24 p3457 A72-44878

MATRIX STRESS CALCULATION
U MATRIX METHODS
MATRIX THEORY
Group matrix representation theory application to elastic spacecraft stabilization.
01 p0135 A72-10497

Two element matrix patterns generation with different degrees of internal constraint, developing objective complexity measures based on information theory or symmetry and grouping considerations.
01 p0013 A72-10715

Jones matrix representation of optical instruments applied to Fourier interferometers/spectrometers and spectropolarimeters/.
03 p0358 A72-13434

Time domain infinite matrices analysis methods for linear stationary and nonstationary multivariable systems, presenting recursion formulae.
06 p0792 A72-17310

Algorithm for bandwidth reduction of symmetric matrices for complex structural problems.
06 p0897 A72-17968

Density matrix equation solution in Liouville space, using variational procedure for laser mode equation and separable interaction method.
07 p1006 A72-19670

Toeplitz matrix in numerical solution of integral equation for cylindrical antenna and array, presenting rapid inversion algorithm by exploiting symmetry properties [AD-743577] 07 p0957 A72-19795

Linear inverse problem of coefficient matrix eigenvectors, implying surface waves and free oscillations for earth structure 08 p1159 A72-21495

Positive to quasi-stochastic matrix reduction by similar variation method, determining largest characteristic number and eigenvector 09 p1343 A72-23490

Algebraic dimensional analysis developed algorithm to generate optimized dimensionless products set associated with physical phenomenon, using matrix methods 10 p1443 A72-23916

Boundary value problems for overdetermined elliptical systems of differential equations with arbitrary sized rectangular matrix 10 p1506 A72-24777

Moore-Penrose pseudoinverse matrix computation, using single and multiple modulus arithmetic method for reduced roundoff error 11 p1676 A72-25505

Modal damping matrix off diagonal terms measurement in viscous damping exploration for dynamic analysis of linear structures 11 p1736 A72-25988

Complex square stochastic matrix spectral inverse, examining nonzero eigenvalues on unit circle 11 p1677 A72-26152

Polynomial theory problems, using Bezoutian matrix formed from polynomials a and b and matrix polynomial relating b to companion matrix of a 11 p1678 A72-26155

Square matrix inverse computation by convergent power series method 11 p1678 A72-26368

Inverse eigenvalue problem numerical solution for matrices and difference and differential equations, obtaining algorithms for parameters estimation 11 p1679 A72-26955

Book on density matrix theory application to lasers and masers, covering quantum mechanics, perturbation theory, magnetism and magnetic resonance, statistical ensembles, etc 12 p1826 A72-28203

Elementary formulas for scalar and matrix valued functions gradient calculation, including continuum mechanics application 15 p2262 A72-31587

Reduced density matrix dependence on nonzero boundary conditions, considering Salzburg-Kirkwood integral equations 15 p2282 A72-32448

Noninteractive compensation of linear multivariable control systems based on matrix block diagram technique 15 p2213 A72-32799

Matrix Riccati equation solution method in optimal control theory, noting boundary conditions implementation 15 p2265 A72-32803

Finite element method matrices in least squares approximation and elliptic partial differential equations, discussing numerical stability properties 17 p2573 A72-34219

Nonlinear generalizations of matrix diagonal dominance with application to Gauss-Seidel iterations. 17 p2573 A72-34220

On the Gaussian elimination method for inverting sparse matrices. 17 p2573 A72-34237

A sequential algorithm for covariance matrix calculations. 17 p2574 A72-34416

Magnetic dipole matrix elements for atomic transitions between Zeeman levels at microwave frequencies 17 p2585 A72-35769

Characteristic equation coefficients of monodromy matrix for linear system of second order homogeneous differential equations with periodic coefficients 21 p3075 A72-41092

Irreducible sparse matrix transformation to upper triangular form by row-column permutation formulated as linear integer programming problem 21 p3075 A72-41312

Reinforcement method algorithm for inversion of matrix with rational function terms 21 p3075 A72-41313

Gaussian elimination with floating point arithmetic, discussing algorithm for least squares scaling of matrices with less error than row and column norms equilibration 21 p3076 A72-41317

A constructive method of solving the Liapounov equation for complex matrices. 22 p3199 A72-42775

Reduction to diagonal form of some triangular-matrix classes in spaces of functions that are analytic in multicircular regions 23 p3308 A72-43581

Linear inequalities and P matrices, with applications to stability of nonlinear systems. 23 p3309 A72-43859

MATTER [PHYSICS]

Materials science historical development from ancient theories of structure of matter to modern atomic and field theories leading to general theory of elastic continuum 02 p0297 A72-12611

Hydrodynamics of matter-antimatter system embedded in thermal radiation, observing coalescence effect 03 p0416 A72-13013

Galactic superclusters and matter distribution in universe, considering systematic catalog errors and uncertainty of statistical tests 03 p0421 A72-13172

Equation of state for matter at 10-500 trillion g/cc, applying to baryon matter and neutron stars 04 p0571 A72-14557

Universe evolution, discussing constituents, matter and antimatter, quasars and radio stars in various galaxies 14 p2157 A72-30623

Electron and nuclear components and transformations of matter under extreme conditions of pressure and temperature exemplified in stellar /pulsar/ evolution 18 p2725 A72-36520

Kinetic equations for ultradense matter neutronization, noting stellar configuration of given mass with variable volume 21 p3086 A72-40096

Equation of state of neutron-star matter at sub-nuclear densities. 22 p3228 A72-42564

Joining of two semiclosed worlds and a cosmological model of matter-antimatter asymmetry. 23 p3336 A72-43489

Necessary conditions for steady state in radiation - Matter interaction and the role of entropy. 24 p3461 A72-44806

Physical properties of atoms, molecules and solid material in ultrastrong magnetic field, using quantum drift approximation 24 p3427 A72-45708

MATURE STREAMS

U STREAMS

MATURE VEGETATION

U VEGETATION

MAXIMUM LIKELIHOOD ESTIMATES

Error correction techniques of convolutional coding with Viterbi maximum likelihood decoding for communications systems design, using computer simulation 01 p0026 A72-10344

Optimal measurement programs for instrument controlled spacecraft trajectory sections, using maximum likelihood method 01 p0127 A72-10354

Adaptive maximum likelihood receiver for direct ranging navigation, comparing with phase locked receivers 05 p0686 A72-16560

Dynamic system observation accuracy in spacecraft trajectory measurement, deriving processing algorithm based on state-estimate error correlation matrix analysis with maximum likelihood procedure 05 p0721 A72-16760

Multiinput and multioutput linear and nonlinear dynamic system maximum likelihood identification based on state vector formulation and optimal filter use 07 p0959 A72-19286

On-line digital computer maximum likelihood estimate of Earth atmosphere profile ahead of flight vehicle using discrete measurements of density, temperature and pressure 08 p1156 A72-20853

Maximum likelihood estimates of covariance parameters of time discrete nonstationary linear systems from residuals measurement of suboptimal sequential filter 08 p1145 A72-20865

Taxonomy for incomplete data problems, developing unified analysis methods based on maximum likelihood estimate 08 p1199 A72-21199

Maximum likelihood estimate of carrier frequency and arrival direction of radio signals in background noise for large aperture antennas 08 p1133 A72-21373

Maximum likelihood estimation for Weibull distribution parameters from multicensored samples by Monte Carlo simulation 08 p1200 A72-21589

Bayes estimators for Poisson distribution random parameters and reliability function, using Monte Carlo method and maximum likelihood estimation 08 p1200 A72-21590

State estimation for nonlinear discrete-time system based on quantized data, presenting maximum likelihood estimate solution and Monte Carlo simulation results 09 p1290 A72-23095

Maximum likelihood method of combining system and component data for reliability estimates 10 p1444 A72-24016

Maximum likelihood receiver performance for optical detection of multimode laser or scattered radiation, considering photocounting distribution, decision threshold and error probability 10 p1452 A72-24681

Constant false alarm rate signal processors for several electromagnetic interference types, using distribution-free methods and maximum likelihood estimation in radar target detection 10 p1437 A72-24683

Stellar physical parameters computed from multicolor photometric data on extratmospheric magnitudes by maximum likelihood method 11 p1715 A72-25296

Mathematical models for complex system debugging in initial life period, noting maximum likelihood estimates for failure rate functions 13 p1962 A72-28365

Psychological criteria for flying personnel selection in civil aviation, noting performance prediction based on maximum likelihood estimates 14 p2080 A72-30816

Optimum processing structure /likelihood/ functional/ determination for signal sequence detection given noisy common background image sets 15 p2196 A72-31783

Joint maximum likelihood estimation of three parameters of Weibull distribution, obtaining modified quasi-linearization algorithm for nonlinear equations iterative solution 16 p2416 A72-33348

Dynamic system observation accuracy in spacecraft trajectory measurement, deriving processing algorithm based on state-estimate error correlation matrix analysis with maximum likelihood procedure 17 p2610 A72-35263

Recursive bootstrap maximum likelihood estimators algorithms for identification of process modeled by stable linear difference equation under additive output measurement noise 18 p2672 A72-36056

Maximum likelihood identification of time varying and random system parameters. 18 p2673 A72-36822

Recursive stochastic approximation of autocorrelation function for stationary random process based on mean-square error and maximum likelihood methods 19 p2824 A72-37285

Radar cross section fluctuation statistics description by generalized chi-square distribution, discussing target detection probabilities maximum likelihood estimates 19 p2763 A72-37293

Conditions for the effectiveness of adaptation algorithms based on an empirical Bayesian approach to statistics 19 p2825 A72-37440

Nonlinear on-line rapid estimation scheme with application to trajectory maneuvering vehicles. 19 p2781 A72-38258

A generalized method for the identification of aircraft stability and control derivatives from flight test data. 19 p2753 A72-38260

The observability of unforced physical systems by linear non-sequential estimators in the validation of linear error analysis. 20 p2910 A72-39123

Information criterion for optimal planning of reliability acceptance tests maximizing average effect 21 p3038 A72-40714

A bivariate normal theory maximum-likelihood technique when certain variances are known. 21 p3075 A72-40826

Radio pulse signal fixed source location estimate with nondirectional space diversity receivers in arbitrary configuration antenna array 23 p3263 A72-43430

Mean square invariant forecasters for the Weibull distribution. 24 p3418 A72-44664

MAXIMUM PRINCIPLE

German monograph on maximum principle application to optimum control of discrete problem 02 p0197 A72-11741

Jacketed tubular chemical reactor optimal startup control, presenting distributed maximum principle for diffusional parameter system 02 p0301 A72-12093

Second order parabolic equations C auchy problem solution with dissipation level, using maximum principle 04 p0538 A72-14626

Time optimal and fuel optimal control of spin stabilized space vehicle for body-fixed and gimbaled jets, using maximum principle 05 p0728 A72-16476

Differential equations system with right side dependent on constant parameters, obtaining approximate numerical solution by maximum principle of control theory 07 p1026 A72-18967

Aircraft optimal terminal guidance nonlinear feedback control law, deriving maximum principle by digital computer program 07 p1033 A72-19287

Soviet book on optimal trajectory synthesis covering second order linear control systems analysis based on Pontryagin maximum principle and Boltyanski theory 08 p1197 A72-20750

Adjoint control transformations advantages in optimal trajectories determination by Pontryagin maximum principle 10 p1547 A72-24879

Pontryagin maximum principle application to minimum deflection of cantilever beam under own weight 10 p1558 A72-24880

Optimal control problems characterized by nonlinear Volterra equations system, obtaining necessary conditions for extremality in maximum principle integral form 11 p1675 A72-25319

Associated system instability related to difficulties encountered in maximum principle application to optimization problems solution 13 p2003 A72-29069

Pontryagin maximum principle for optimal terminal velocity control of automatic space probe descent in Mars atmosphere 14 p2162 A72-30456

The maximum principle and controllability of nonlinear equations. 17 p2533 A72-34951

Optimality conditions of second and higher orders for discrete systems, discussing functional minimization and Pontryagin maximum principle limitations 17 p2534 A72-35725

Optimality conditions in a problem of heat transfer process control 18 p2741 A72-36809

Optimal control with partially specified input functions. 18 p2673 A72-36821

Necessary conditions for continuous parameter stochastic optimization problems. 22 p3198 A72-41932

A manifold imbedding algorithm for optimization problems. 23 p3268 A72-44197

Modelled time optimal control process investigation for system with relay components, noting Hausdorff maximum principle application for optimal linear control 24 p3386 A72-45389

Maximum principle and penalty function technique for flight optimization, noting optimal control for climbing flight 24 p3369 A72-45444

MAXIMUM USABLE FREQUENCY

Sporadic E layer shielding frequency correlation to limiting reflection frequency calculated by diurnal data from nine ground stations 02 p0221 A72-12522

Angles of arrival and skip distances prediction of radio waves near MUF, using monthly forecasts of quiet and perturbed ionospheric parameters and N/h profiles 11 p1594 A72-26276

HF radio signal reception behavior near maximum usable frequency during evening and at midnight, noting SNR 14 p2085 A72-30656

A study of the dependence of the maximum usable frequency on the electron content. 23 p3266 A72-44333

MAXWELL EQUATION

Book on microwave techniques covering Maxwell equations, electromagnetic wave propagation in conducting media, complex notation, plane polarized waves transmission and reflection, wave equations, etc 01 p0043 A72-11275

Nonlinear equations for M-type amplifiers derived from Maxwell equations 02 p0189 A72-11567

Radiative heat transfer across vacuum gap between two closely spaced metal bodies with arbitrary dielectric properties, solving Maxwell equations 02 p0300 A72-11672

Computer solution to vector variational formulation of electromagnetic Maxwell equations for dielectrically loaded rectangular waveguide 03 p0335 A72-12429

Guided gravitational wave possibility from analogy to Maxwell electromagnetic equations 04 p0574 A72-14979

Maxwell equation spinor formulation for Schwarzschild gravitational field effects on spherical electromagnetic waves propagation 05 p0689 A72-16165

Einstein and Einstein-Maxwell equations solutions by zero coupling transformations 09 p1349 A72-22201

Cylindrically guided hybrid TE and TM electromagnetic wave reflection and transmission from Maxwell equations and boundary value problems solution 09 p1278 A72-22605

Clebsch transformation in relativistic MHD, considering Maxwell equations in vacuum and electromagnetic perfect fluid in isentropic flow 10 p1519 A72-24126

Plane electromagnetic wave diffraction on ideally conducting convex body of large electrical dimensions, obtaining Maxwell equations asymptotic solution 10 p1436 A72-24577

MPD thruster diagnostics and interpretation of electric current distribution, applying integral form of Maxwell equation for moving Hall probe [AIAA PAPER 72-498] 11 p1711 A72-26221

Existence and uniqueness of general solutions of initial value problem for nonlinear Maxwell-Boltzmann equation with finite time interval 12 p1836 A72-27122

Electromagnetic plane field cumulation by heavy conducting shells implosion with quasi-relativistic velocity, solving Maxwell equations by characteristics method 12 p1851 A72-27396

Relativistic treatment of Dirac-Hestenes and Maxwell equations 13 p1987 A72-29787

Charge and mass densities relation for stationary charged dust distribution in general relativity, investigating Einstein-Maxwell equations for stationary gravitational field 15 p2275 A72-31591

Iterative procedure for Maxwell equations exact solution for anisotropic birefringent medium, applying result to limiting polarization problem 16 p2425 A72-33490

Maxwell equations solution for electromagnetic field in circular cylindrical tubes, deriving recursion formulas for computer processing 16 p2364 A72-33668

Continuity, motion and Maxwell equations for steady MHD flow under constant magnetic flux 17 p2588 A72-34765

Weak electromagnetic fields around a rotating black hole. 17 p2612 A72-35391

Isotropic, space-like, Maxwellian particles of real mass and of time-like velocity 18 p2710 A72-36472

Vlasov and Maxwell equations solution for surface waves dispersion in semiinfinite hot plasma 18 p2716 A72-36925

Analysis and prediction of coupling between collocated antennas. 20 p2902 A72-38999

Atmospheric turbulence induced optical effects due to refractive index fluctuations, solving Maxwell equations for instantaneous intensity distribution function 20 p2948 A72-39055

Vector wave solution of light beam propagating along lenslike medium. 20 p2903 A72-39266

Maxwell electromagnetic field theory review, emphasizing relationship between integral forms of Faraday and Ampere laws in conventional space and time concepts 20 p2904 A72-39778

Exact solutions of the Einstein-Maxwell equations for an accelerated charge. 20 p2955 A72-40008

On Maxwell's equations in three-dimensional anisotropic periodic media - Tensor formulation of the problem and the N-beam approximation. 20 p2962 A72-40019

Analytical model for a polarizable medium at radio and lower frequencies. 22 p3155 A72-42467

Equations of motion of a viscous fluid with relaxation properties 24 p3393 A72-45256

MAXWELL FLUIDS

Rheological properties of Maxwell fluid-St Venant solid model for solids, noting slip lines direction during plastic flow 02 p0259 A72-12238

Rectangular channel flow of two immiscible viscoelastic Maxwell fluids with transient pressure gradient, deriving interface velocity, flow rate and wall resistance components 04 p0514 A72-15705

Maxwell rheological creep model verification by tensile tests on Mg alloy at 150 C under step loadings, treating thermodynamics of ideal creep 16 p2412 A72-34111

MAXWELL-BOLTZMANN DENSITY FUNCTION

Quasi-static surface waves at Maxwellian plasma boundary with diffuse electron scattering, considering plasma electromagnetic oscillations 02 p0266 A72-12577

Electron and ion drift rate effect on floating double probe characteristics in Maxwellian plasmas 02 p0266 A72-12768

Initial viscous heat conducting gas dynamic state one dimensional decay problem solution, using kinetic theory with Boltzmann equation 04 p0512 A72-14982

Hard X ray emission by thermal plasma, applying relativistic corrections to photon bremsstrahlung Maxwell distribution and cross section 06 p0873 A72-18004

Linear analysis of gravitational perturbations in strongly collisional initially homogeneous and Maxwellian medium 10 p1536 A72-24138

Nonlinear analysis of gravitational stability perturbation based on Maxwellian velocity distribution 10 p1538 A72-24214

Ionized plasma electron velocity distribution function relaxation numerical calculation to validate local Maxwellian form during transport process 11 p1693 A72-25523

Bremsstrahlung photon emission rate from Maxwellian plasma, determining soft X ray diagnostic techniques applicability for laser produced plasmas 15 p2285 A72-32271

Solar wind heat flux measurements comparison with collision dominated heat transfer theory in ionized medium, noting deviations from Maxwellian velocity distribution 16 p2449 A72-33908

MAXWELLIAN DISTRIBUTION [DENSITY]

U MAXWELL-BOLTZMANN DENSITY FUNCTION

MCDONNELL MILITARY AIRCRAFT

U MILITARY AIRCRAFT

MEAN FREE PATH

Mean free path and particle size distribution in dispersion hardened nickel-thoria alloys, obtaining interparticle spacing by Scheil method 02 p0245 A72-12549

Energy transport within stellar structure, discussing radiative transfer and opacity relationship to mean free path of radiation 07 p1078 A72-19924

Solar protons propagation from instantaneous injection source and inhomogeneities interaction description by mean free path and scattering angle specification 07 p1063 A72-20627

Phonon limited mean free path in Cd by limiting point method, proposing model with elastic anisotropy 08 p1217 A72-21592

Topside ionosphere characteristics, discussing particle mean free path and geomagnetic field effects on conductivity, plasma anisotropies and latitudinal variations 10 p1473 A72-24704

Laser coupling through nonlinear gas filled absorber cell, discussing molecules mean free path 15 p2246 A72-31883

Rarefied gas flow problems, discussing mean free path effects on sharp nosed conical and bluff bodies drag and heat transfer coefficients 15 p2218 A72-32314

Studies of the free path of the current carriers in molybdenum 17 p2568 A72-35517

Charged particles propagation in magnetic field and scattering medium with constant and variable transport mean free path, applying to proton propagation for solar flares 24 p3435 A72-45076

MEAN TIME BETWEEN FAILURES

U MTBF

MEASURANDS

U MEASUREMENT

MEASURE AND INTEGRATION

NT BOREL SETS

NT FUNCTIONAL INTEGRATION

NT INTEGRAL CALCULUS

NT LEBESGUE THEOREM

NT NUMERICAL INTEGRATION

NT RUNGE-KUTTA METHOD

NT WEIGHTING FUNCTIONS

Integrability of rotating satellite differential equation of motion in axially symmetric gravitational field 01 p0122 A72-10008

Reproduction by substitutions of ordinary differential equations integrable in elementary and special functions 03 p0383 A72-14373

Computer program for construction and integration of chemical reaction rate equations, applying to nitric oxide formation and decomposition [WSCIP PAPER 71-27] 04 p0482 A72-14583

Asymptotic integration method solution of heat transfer equation with constant wall temperature for low speed slip flow regime [ASME PAPER 71-WA/HT-5] 05 p0599 A72-15866

Nonlinear differential equation of second order, investigating integrability criteria 06 p0838 A72-17553

Conditional expectation and integral of random closed convexity in probability space 06 p0839 A72-17555

Triaxial space station orbit around oblate earth, presenting equations of motion, Hamiltonian and integration methods

06 p0878 A72-17663

Iteration procedure for approximate integration of nonlinear system of partial differential equations with time lag, presenting upper and lower estimates

07 p1028 A72-20209

Coefficients estimation in nonlinear differential equations by direct integration followed by unconstrained nonlinear programming

08 p1197 A72-20854

Integral relations derivation for stationary and nonstationary potential motions in cases of zero and infinite conductivity, applying to wave expansion in cylindrical waveguide

08 p1212 A72-20966

Sretenskii-Chaplygin integral in polynomial form for solution to gyrostat motion problem

08 p1208 A72-21356

Third order nonlinear differential equation invariants use to obtain integrable forms

10 p1504 A72-24053

Integrability and identity relations for Newman-Penrose formalism equations in spinor description, assuming Einstein equations validity for vacuum

10 p1510 A72-24105

Rectilinear impulsive motion of compressible boundary layer on infinite plate, deriving integration method for differential equations of motion under energy dissipation neglect

10 p1465 A72-24203

Radar detection performance calculation with post-detection integration using single valued loss and ideal curves in terms of SNR

10 p1437 A72-24689

Nonlinear transformation for improper integral calculation, noting faster convergence than linear methods

10 p1506 A72-24997

Measurable multiapplications and convex integrals properties in complete probability and Banach spaces

11 p1678 A72-26476

Multistage pursuit-evasion game on circle, constructing player optimal strategies via measure theory

12 p1836 A72-27511

Fourth order polynomial method and computational algorithm for direct integration of n body systems, discussing two body encounters and binary systems

12 p1875 A72-27917

Dynamic equations integration with constraint factors, discussing Hamilton-Jacobi method applicability conditions

13 p2003 A72-28724

Delayed argument linear partial differential equations system integration, constructing asymptotic solution in nonresonant case

13 p1988 A72-30084

Steepest descent path of integral describing transient plane wave propagation in anisotropic cold plasma, relating to evanescent wave arrival

15 p2285 A72-32109

Integration of equations of motion for nonconservative holonomic systems with pulsed coupling factors

19 p2825 A72-38192

One realization of Liapunov's method for integrating linear equations

19 p2827 A72-38469

Book - Weak convergence of measures: Applications in probability.

20 p2946 A72-39730

Gas turbine engine performance measurement via parameters averaging method, noting integration time determination for given error limits

23 p3325 A72-43669

Integration scheme for two-dimensional impulsive waves in a linear acoustic medium.

23 p3314 A72-44250

MEASURE THEORY

U MEASURE AND INTEGRATION

MEASUREMENT

Standard linear estimation and control problem with quadratic loss, optimizing information rate by minimizing total measurements number through Riccati equation singular solution

08 p1144 A72-20859

Linear stochastic system optimal measurement strategy and matched Kalman type filter computation via transformation into deterministic control problem

18 p2674 A72-37100

MEASURING

U MEASUREMENT

MEASURING APPARATUS

U MEASURING INSTRUMENTS

MEASURING INSTRUMENTS

NT ACCELEROMETERS
NT ACTINOMETERS
NT ALTIMETERS
NT ANALYZERS
NT ANEMOMETERS
NT APPROACH INDICATORS
NT ATOMIC CLOCKS
NT ATTITUDE INDICATORS
NT BAYARD-ALPERT IONIZATION GAGES
NT BOLOMETERS

NT CALORIMETERS
NT CERENKOV COUNTERS
NT CHRONOMETERS
NT CINETHEODOLITES
NT CLOCKS
NT CLOUD HEIGHT INDICATORS
NT COMPARATORS
NT CONDUCTIVITY METERS
NT COUNTERS
NT DENSITOMETERS
NT DICKE RADIOMETERS
NT DIFFRACTOMETERS
NT DISTANCE MEASURING EQUIPMENT
NT DOSIMETERS
NT DYNAMOMETERS
NT EBERT SPECTROMETERS
NT ELECTRICAL CONDUCTIVITY METERS
NT ELECTRON COUNTERS
NT ELECTRON PROBES
NT ELECTROPHOTOMETERS
NT ELECTROSTATIC PROBES
NT ELLIPSOMETERS
NT ENGINE MONITORING INSTRUMENTS
NT ERGOMETERS
NT EXTENSOMETERS
NT FABRY-PEROT INTERFEROMETERS
NT FABRY-PEROT SPECTROMETERS
NT FIELD INTENSITY METERS
NT FLAME PROBES
NT FLIGHT LOAD RECORDERS
NT FLIGHT RECORDERS
NT FLOW DIRECTION INDICATORS
NT FLOWMETERS
NT FUEL GAGES
NT GEODIMETERS
NT GONIOMETERS
NT GRAVIMETERS
NT GRAVITY GRADIOMETERS
NT GYRO HORIZONS
NT GYROCOMPASSES
NT HELIOMETERS
NT HODOSCOPES
NT HOT-FILM ANEMOMETERS
NT HOT-WIRE ANEMOMETERS
NT HOT-WIRE FLOWMETERS
NT HYGROMETERS
NT HYSOMETERS
NT INDICATING INSTRUMENTS
NT INFRARED DETECTORS
NT INFRARED INSTRUMENTS
NT INFRARED SCANNERS
NT INFRARED SPECTROMETERS
NT INFRARED SPECTROPHOTOMETERS
NT INTERFEROMETERS
NT ION PROBES
NT ION TRAPS [INSTRUMENTATION]
NT IONIZATION GAGES
NT IONOSONDES
NT KNUDSEN GAGES
NT LASER ALTIMETERS
NT LASER RANGE FINDERS
NT LUNAR SEISMOGRAPHS
NT MACH-ZEHNDER INTERFEROMETERS
NT MAGNETIC PROBES
NT MAGNETOMETERS
NT MANOMETERS
NT MASS SPECTROMETERS
NT METEOROLOGICAL INSTRUMENTS
NT MICHELSON INTERFEROMETERS
NT MICROBALANCES
NT MICRODENSITOMETERS
NT MICROMETERS
NT MICROMILLIAMMETERS
NT MICROWAVE INTERFEROMETERS
NT MICROWAVE PLASMA PROBES
NT MICROWAVE PROBES
NT MICROWAVE RADIOMETERS
NT MICROWAVE REFLECTOMETERS
NT MICROWAVE SENSORS
NT MOISTURE METERS
NT MONOCHROMATORS
NT NEPHELOMETERS
NT NEUTRON COUNTERS
NT NEUTRON SPECTROMETERS
NT NOISE METERS
NT OCULOMETERS
NT OMEGA NAVIGATION SYSTEM
NT OPTICAL MEASURING INSTRUMENTS
NT OPTICAL PYROMETERS
NT OPTICAL RANGE FINDERS
NT OPTICAL SCANNERS
NT OSCILLOGRAPHS
NT OXYGEN ANALYZERS
NT PARTICLE TELESCOPES
NT PENNING GAGES
NT PHOTOMETERS
NT PIEZOELECTRIC GAGES
NT PIEZOMETERS
NT PLAN POSITION INDICATORS
NT PLASMA PROBES
NT PNEUMATIC PROBES
NT POLARIMETERS
NT POSITION INDICATORS
NT POTENTIOMETERS [INSTRUMENTS]
NT PRESSURE GAGES
NT PROFILOMETERS

NT PROPORTIONAL COUNTERS
NT PSYCHROMETERS
NT PYRANOMETERS
NT PYROHELIOMETERS
NT PYROMETERS
NT QUANTUM COUNTERS
NT RADIATION COUNTERS
NT RADIATION DETECTORS
NT RADIATION MEASURING INSTRUMENTS
NT RADIATION PYROMETERS
NT RADIO ALTIMETERS
NT RADIO DIRECTION FINDERS
NT RADIO FREQUENCY IMPEDANCE PROBES
NT RADIO INTERFEROMETERS
NT RADIOGONIOMETERS
NT RADIOMETERS
NT RADIOSONDES
NT RAIN GAGES
NT RANGE FINDERS
NT RATIOMETERS
NT RAWINSONDES
NT REFLECTOMETERS
NT REFRACTOMETERS
NT RESISTANCE THERMOMETERS
NT RESPIROMETERS
NT RHEOMETERS
NT RIOMETERS
NT SATELLITE-BORNE INSTRUMENTS
NT SCATTEROMETERS
NT SCINTILLATION COUNTERS
NT SEISMOGRAPHS
NT SEXTANTS
NT SHOCK MEASURING INSTRUMENTS
NT SIGNAL ANALYZERS
NT SILICON RADIATION DETECTORS
NT SOLAR SPECTROMETERS
NT SONDES
NT SPACECRAFT POSITION INDICATORS
NT SPARK CHAMBERS
NT SPECTROHELIOGRAPHS
NT SPECTROMETERS
NT SPECTROPHOTOMETERS
NT SPECTROPHOTOMETERS
NT SPECTROPHOTOMETERS
NT SPEED INDICATORS
NT STRAIN GAGES
NT TACHOMETERS
NT TEMPERATURE MEASURING INSTRUMENTS
NT TEMPERATURE PROBES
NT TENSIMETERS
NT TENSOMETERS
NT THEODOLITES
NT THERMAL CONDUCTIVITY GAGES
NT THERMOMETERS
NT THRESHOLD DETECTORS [DOSIMETERS]
NT TIME MEASURING INSTRUMENTS
NT TIMING DEVICES
NT TORQUEMETERS
NT TRANSMISSOMETERS
NT TURBULENCE METERS
NT ULTRAVIOLET SPECTROMETERS
NT ULTRAVIOLET SPECTROPHOTOMETERS
NT VACUUM GAGES
NT VARIOMETERS
NT VIBRATION METERS
NT VISCOMETERS
NT VOLTMETERS
NT WATTMETERS
NT WEATHER DATA RECORDERS
NT WEIGHT INDICATORS
NT WIND VANES

Fluidic device for measuring angular velocities based on pressure output proportional to shaft revolutions per unit time, discussing equivalent circuit

01 p0064 A72-10171

Ultrasonic rotameter for wind velocity circulation measurement, using cylindrical electroacoustic capacitor converter with solid dielectric for radiators and receivers

01 p0094 A72-10560

Instrument and technique for Gaussian mode laser beam parameters measurement

03 p0367 A72-13444

Universal perception meter for measurements in work psychology laboratories, discussing characteristics and operation

03 p0322 A72-13884

Hydraulic systems and components stationary operating conditions determination, discussing measuring apparatus, test equipment and interpretation methods

03 p0312 A72-13961

Ultrasonic resonance thickness gage sensitivity and accuracy, noting damper, piezoelectric plate, protector and frequency band influence

03 p0361 A72-13986

Book on EMI test instrumentation and automatic measuring systems covering shielded enclosures, emission and susceptibility antennas and spectrum analyzers

04 p0486 A72-14611

Automatic instrumental measurement of runway visual range at airport

04 p0508 A72-14679

- ALSEP lunar heat flow experiment, describing instrument for temperature and thermal conductivity measurements in lunar subsurface
11 p0577 A72-15098
- Computer servocontrolled granite stage and measuring microscope, discussing mechanical and optical construction, control electronics and applications
11 p0522 A72-15477
- Measuring apparatus for differential cross sections of charge transfer and elastic scattering of atomic projectiles by gas targets
11 p0553 A72-15539
- Low inertia instrument for ozone density measurement in atmosphere near ground
11 p0525 A72-15624
- Distortion measuring equipment for determining FM signal transmission errors due to amplitude and group delay frequency response deficiencies and AM/PM conversion
11 p0626 A72-16299
- Pyroelectric laser power meter with built-in calibration based on reference heating by If current, describing operation, design and testing
11 p0662 A72-16347
- Transit instrument system year-to-year stability in astronomical time determination, considering seasonal wave causes and star coordinate errors
11 p0885 A72-18037
- Measuring device for holographic virtual image reconstruction deformations due to relative orientation errors between reference beam and holographic plate
11 p0818 A72-18329
- Convective conductance meter for continuous measurement of outdoor exposed surface convection coefficient, using electrically heated plaques with known surface radiation properties
11 p0981 A72-18821
- Low pressure gauge with compensation of dry friction forces in servomechanism with respect to mean value
11 p0982 A72-18929
- Stress relaxation measurement assembly for polymer film and fiber samples under tensile stresses at 213-573 K
11 p0986 A72-19779
- Adhesives use for assembly of mechanical, optical, nucleonic and electronic instruments including printed and integrated circuits
11 p0992 A72-20576
- Fatigue life gages to determine cumulative fatigue damage due to variable cyclic strain history on unmatched materials
11 p1163 A72-20915
- Fatigue life gages planning and application to airplane cyclic fatigue test, describing automatic data acquisition system
11 p1163 A72-20916
- F-14 naval fighter aircraft flight test programs, discussing instrumentation and low-speed test results
11 p1108 A72-21005
- Component evaluation of linearity error of measuring instruments
11 p1284 A72-22241
- German monograph on electron beam focusing in partial pressure analyzer with two compartment ion source, eliminating residual gas-filament interaction
11 p1306 A72-22318
- Multihole flow probe measurement data evaluation by multidimensional approximation of calibration curves and surfaces
11 p1260 A72-22631
- Capacitance depth gage for thin liquid films thickness measurement, noting application to interface waves amplitude and frequency measurements
11 p1316 A72-23410
- Measuring instrument for minute pressure differences, noting accuracy
11 p1317 A72-23692
- FM measurement system with linear resistance-to-frequency converter realized in RC oscillator form, discussing design problems
11 p1482 A72-24598
- Electromagnetic position sensor for magnetically supported model in wind tunnel, discussing design, operation principles and performance
11 p1462 A72-24773
- Atmospheric temperature measurement up to 2 km height, reviewing sounding equipment and techniques
11 p1508 A72-25091
- Test assembly for Brinell microhardness measurements of metal and alloy surfaces under tension during vacuum heating and in protective gas media
11 p1612 A72-25490
- Transit instrument system year-to-year stability in astronomical time determination, considering seasonal wave causes and star coordinate errors
11 p1719 A72-25973
- Methyl alcohol-ethylene glycol self mixing antifreeze solution for precipitation gages
11 p1682 A72-26088
- Retarding potential analyzer errors and performance degradation due to grid plane potential depressions
11 p1634 A72-26411
- Measuring information systems optimization, considering first order system with time lag
11 p1611 A72-26436
- Discrete automatic monitoring and measuring systems with discrete random sequence and continuous process reconstructed output signals, deriving probability criteria for reading frequency determination
11 p1611 A72-26438
- Monotypic signal rejection by connecting line insertion to sensor and central electrical measuring device input galvanic decoupling
11 p1611 A72-26440
- Image-to-signal conversion by TV tube in automatic contactless measuring systems, producing mosaics of object by optical, X ray and ultrasonic techniques
11 p1634 A72-26460
- Thermistor anemometers design and measurement of displacement or dispersion coefficients
11 p1636 A72-26699
- Thermal conductivity measuring apparatus for small multispecimen thermoelectric materials
11 p1795 A72-27467
- Device for comparing powders friability to ascertain quality of compacts fabricated on automatic sintering presses, noting applications in ceramic, chemical and pharmaceutical industry
11 p1795 A72-27468
- Dynamic systems as models for electronic measuring instruments computerized development and design
11 p1791 A72-27579
- High temperature skin friction meter design for drag measurements, using motor-transducer air core assembly
11 p1812 A72-27959
- Light scattering media optical characteristics measurement techniques and equipment
11 p1955 A72-28515
- Ionospheric radio adsorption measuring device with readout data convenient for visual and computer processing, discussing block and circuit diagrams
11 p1955 A72-28602
- Instrument to measure thermodynamic, electrical and optical properties of gases and liquids, describing thermostat for 83-923 K range
11 p1956 A72-28633
- Compressor blade vibration indicator measurement by positioning one inductive sensor by rotor blades and another by toothed gear on rotor shaft
11 p1956 A72-28784
- Digital microwave power measuring device with automatic range selection
11 p1931 A72-29267
- Broadband correlation meter with multiplier using vacuum thermal converters for 1.5 KHz-15 MHz range and variable signal delay
11 p1961 A72-29920
- Microwave device phase and amplitude frequency response measuring equipment with wide range test pulse generation, discussing design and performance
11 p1934 A72-30091
- Apollo 15 manned lunar landing, discussing geological data and surface experiment package and instruments
11 p2310 A72-31983
- Sensor design and principles for atomic oxygen concentration measurement in dissociated gases, using Ag thin film electrical resistance change during oxidation
11 p2390 A72-33162
- Crack depth measuring instrument for fatigue crack propagation study in notch tests, noting application at high temperatures
11 p2391 A72-33234
- Instrumentation for space-time correlated measurement of explosion induced dynamic effects, discussing framing cameras, flash X-ray systems, pin switches and piezoresistive gages
11 p2392 A72-33360
- Computerized aircraft landing measurement system for civil airport, using optical, seismic and IR sensors
11 p2374 A72-33627
- Instrument for Hall and Gauss effects measurement in semiconductors and metals, noting instrument error analysis
11 p2529 A72-34758
- Contact-type level gauge with a transistorized decimal code converter
11 p2529 A72-34764
- Use of special gauges for determining crack growth rate in fatigue in the AU4G1 aluminum alloy
11 p2567 A72-34890
- Contactless parameter measurements of a vibrating bar.
11 p2554 A72-35148
- Digital methods of frequency measurement - A comparison.
11 p2530 A72-35363
- Dynamic characteristics of electrical measuring instruments and transducers, discussing static calibration curve, dynamic tests and parameters determination
11 p2557 A72-35757
- An equipment for measuring thermophysical quantities by means of heat-pulse methods in the temperature region between 20-300 C.
11 p2557 A72-35758
- Measuring instruments for gas pressure determination in vacuum systems, noting application of thermal conductivity or ionization characteristics of gas molecules
11 p2692 A72-36835
- Choice of parameters for measuring devices in a closed-loop linear control system
11 p2777 A72-37319
- Electromechanical measurement systems using analog transducers with ohmic resistance, electric and magnetic fields and digital/frequency and stochastic outputs
11 p2800 A72-37755
- Measurements of radiation flux at the moment of ignition of a solid propellant
11 p2800 A72-37759
- High-sensitivity resonant-quartz scales operating in high vacuum at very low temperature - Application to the study of gas-solid interactions
11 p2800 A72-37834
- Analysis of the performance of a single-half-period synchronous relay detector with an active-capacitance load
11 p2801 A72-37963
- Rational selection of structures and parameters for photoelectric meters and follow-up systems
11 p2801 A72-37964
- Investigation of the UIM-21 coordinate-measuring machine
11 p2802 A72-37988
- INTERKAMA 1971; International Congress with Exposition for Measurement Technology and Automation, 5th, Duesseldorf, West Germany, October 14-20, 1971, Reports
11 p2782 A72-38301
- Production measuring equipment and techniques for quality control, emphasizing measurement accuracy, speed and cost effectiveness maximization
11 p2802 A72-38304
- Measurement transducers in industrial process control, discussing requirements for dynamic properties, stability, linearity and computer applications
11 p2803 A72-38315
- Blade passage measurement with the aid of a graphite pin probe in the case of fluid flow engines
11 p2804 A72-38724
- Special features of the operation of ferroprobes with low-permeability core moulds at small excitation fields.
11 p2804 A72-38760
- Sensor selection for electromagnetic instrumentation system with sufficient sensitivity and bandwidth to demonstrate electroexplosive device compliance with MIL-E-6051D specified safety margin
11 p2962 A72-38979
- A small ELF electric field probe.
11 p2921 A72-38994
- The impact of gradiometer techniques on the performance of inertial navigation systems.
11 p2949 A72-39079
- A time-frequency localization system applied to acoustic certification of aircraft.
11 p2950 A72-39091
- An automated instrument for monitoring the quality of recovered water.
11 p2895 A72-39161
- A differential interferometer and its application to heat and mass transfer measurements.
11 p2927 A72-39683
- A new circuit for the contactless thickness measurement with the aid of pulse-excited LC measuring circuits
11 p2927 A72-39696
- Stress sensitive device based on anisotropic conductivity of multivalley semiconductor under uniaxial stress
11 p2961 A72-39713
- Installation for the simultaneous measurement of the functional properties of sliding contacts
11 p2928 A72-39936
- Apparatus for measurement and automatic graphical recording of variations of electrical characteristics of a metal-insulator-semiconducting structure
11 p3051 A72-40209
- A high-frequency dynamic phase metering instrument for ionospheric research.
11 p3051 A72-40214
- A meter giving the number of overshoots of the realization of a steady random process
11 p3058 A72-41732
- Recent progress regarding the measurement techniques in the hypersonic area
11 p3178 A72-42581
- Analysis of the structure of the flow downstream of a sudden widening
11 p3167 A72-42643
- International Aerospace Instrumentation Symposium, 18th, Miami, Fla., May 15-17, 1972, Proceedings.
11 p3178 A72-42676
- Comparative cut-bar thermal conductivity apparatus.
11 p3180 A72-42710
- Variable impedance transducer measuring instruments for in-flight aircraft performance tests under environmental thermal effects
11 p3180 A72-42711

Influence of noise on the accuracy of microwave phase meters 23 p3272 A72-43845

Experimental design algorithm based on information quantity optimization, noting measuring instrumentation synthesis adaptable to operational conditions 23 p3292 A72-44463

Ionospheric radio absorption measuring device with readout data convenient for visual and computer processing, discussing block and circuit diagrams 24 p3402 A72-45102

Optimal linear inertia-free processing of meter readouts with allowance for control-equipment signals 24 p3403 A72-45316

MECHANICAL DEVICES

German monograph on narrow band mechanical filter design, using resonant circuit and coupled four terminal network analogy 09 p1284 A72-22326

Hookes law formulation by multindex sequences for stereomechanical multiple system optimization 09 p1354 A72-23611

Jet compression role in high temperature mechanical energy conversion heat exchanger based on ejector principle 12 p1755 A72-27724

Mechanical fabrication of rectangular to cylindrical waveguide transitions for X band 13 p1932 A72-29475

Nondestructive technique for continuous recording of thickness or contour profiles, using mechanical probes 13 p2000 A72-29760

Structure-borne acoustic nondestructive testing for readiness assessment, fault isolation and automatic checkout of space vehicle mechanical devices 15 p2214 A72-31699

Mechanical system nonlinear perturbation effect on equations of motion solutions, deriving boundedness and stability conditions via inequality theorems 16 p2423 A72-33101

Low-explosive actuated mechanical devices to actuate switches and valves, sever cables or bolts, dispensing fluids, inflating bags or starting engines 16 p2442 A72-33359

Thermochemical techniques application to corrosion protection of metallic powders, mechanical parts and tools, describing chromizing, chromaluminizing, tantalizing and niobiumizing processes [ONERA, TP NO. 1049] 19 p2817 A72-37769

New modifications of manipulators for investigations using microelectrodes 22 p3149 A72-42073

Spectrally shaped transient forcing functions for frequency response testing 22 p3206 A72-42463

Evaluation of the danger of damage to mechanical systems exposed to random vibrations 24 p3459 A72-45449

MECHANICAL DRIVES

NT HELICOPTER PROPELLER DRIVE

Digital computer programmed numerical calculation based on admittance method for torsional forced vibration spectra of masses and stress distribution in transmission system 02 p0271 A72-12435

Gear transmission systems statistical characteristics under dynamic loads, noting normal Gaussian curve for operating conditions 04 p0585 A72-14614

Computer servocontrolled granite stage and measuring microscope, discussing mechanical and optical construction, control electronics and applications 04 p0522 A72-15477

Point contact realization between helical transmission wheels teeth 05 p0667 A72-17058

Multicircuit hf filters tuning drive with mechanical synchronization correction 06 p0774 A72-17749

Transmission locked differentials and variable ratio drive improvement effect on engine driven machine high speed performance and stability 08 p1113 A72-22097

Discrete model of dynamic forces between teeth of single stage transmission with parallel gear axes 09 p1404 A72-22772

Electromechanical system for wire drive along stellar right ascension of meridian circle of Odessa Astronomical Observatory 09 p1311 A72-23061

Mandelstam couplings theory for subdividing discrete mechanical system of three degrees of freedom gear transmission 09 p1409 A72-23614

German monograph on losses in gear pumps, discussing leakage, mechanical and hydraulic losses, measurement techniques and equipment, etc 10 p1422 A72-23774

Rolling radius of driven cylindrical wheel with solid rubber tire as function of normal load and tire dimensions 13 p2003 A72-28919

Nonlinear oscillations amplitude, frequency and instability regions of moving belt as function of longitudinal velocity 13 p1964 A72-29150

Dynamic structural analysis of system formed by engine, variable ratio differential and working machine, calculating differential ratio for constant shaft rotation speed 15 p2182 A72-31609

Gyroscope drive systems, discussing various ac and dc electric motor types and switching and control circuits 16 p2396 A72-34135

Use of digital computer graphics in gear design 17 p2520 A72-34338

Reduction of noise and acoustic-frequency vibrations in aircraft transmissions. 17 p2491 A72-34508

[AHS PREPRINT 661] Influence of coupling behavior on the quietness of multiply supported shaft systems 18 p2694 A72-36070

Optoelectronic speed control for replacing mechanical gear drives for precisely variable shaft speed ratios 21 p2997 A72-40259

Experimental procedure for determining the strength losses in the individual elements of wave-type toothed gears 22 p3182 A72-41866

MECHANICAL ENGINEERING

Electromagnetic field forces on finite conducting bodies, discussing heating rates and temperatures with ambient air convection and machine design recommendations 09 p1359 A72-22679

Design information for machinery to incorporate welding positions and joints, fatigue mechanisms, loads, combined stresses and plate and cast materials properties 09 p1409 A72-23621

Structural mechanics computer programs compendium covering subject oriented information according to structure type, load environment and analytical models 15 p2328 A72-31771

Mechanical and electrical technologies unification, discussing systems and balances 15 p2211 A72-31873

Experimental mechanics in research and development; Proceedings of the International Symposium, University of Waterloo, Waterloo, Ontario, Canada, June 12-16, 1972. Volumes I & 2. 18 p2732 A72-36352

Southeastern Conference on Theoretical and Applied Mechanics, 5th, North Carolina State University and Duke University, Raleigh and Durham, N.C., April 16, 17, 1970, Proceedings. 18 p2736 A72-37051

Israel Conference on Mechanical Engineering, 6th, Haifa, Israel, June 26, 27, 1972, Proceedings. 21 p3118 A72-40926

MECHANICAL IMPEDANCE

Mechanical impedance and phase angle time variation in restrained primate during prolonged sinusoidal vibration [ASME PAPER 71-WA/BHF-8] 05 p0616 A72-15946

Forced vibration and mechanical impedance of damped circular and annular membranes under central mass loads 05 p0739 A72-16615

Supine human body mechanical impedance under combined stress of vibration and sustained acceleration 12 p1765 A72-28270

Frequency method of mechanical impedance monitoring of natural frequency of transducer-article system under load in defectoscopy 13 p1956 A72-28923

Human hand-arm system vibration characteristics, describing mechanical impedance measurements for mathematical modeling 13 p1910 A72-29559

Human body or dummy mechanical impedance calculation by acceleration measurement at two point reference system with circular spring supporting mass 15 p2192 A72-32608

Signal analyzer for LF real time measurement of mechanical impedance by Fourier integral analysis 15 p2215 A72-32628

Liquid propellant rocket engines three dimensional nozzle admittance determination by impedance tube method from pressure distribution measurement, taking into account nozzle geometry effect [AIAA PAPER 72-666] 16 p2443 A72-34071

Damping coefficient measurement for sound waves inside cylindrical tube closed at one end and excited at other end by loudspeaker 17 p2582 A72-35426

Mathematical modeling assumptions and procedures in experimental mechanics, considering transfer function, impedance and human factor roles 18 p2709 A72-36353

Effect of electrode thickness on the frequency response of a piezoelectric transducer 18 p2693 A72-37218

Output impedance of a jet element 19 p2754 A72-37994

Measurement of specific mechanical impedance of the skin - Effects of static force, site of stimulation, area of probe, and presence of a surround. 21 p3005 A72-40347

New methods of measuring the parameters of multidimensional vibrations of linear mechanical systems 22 p3176 A72-42130

Low frequency measurement of mechanical impedance and frequency response. 22 p3164 A72-42700

Linear system proper frequencies and vibration dampings obtained by mathematical smoothing of mechanical admittance measurements 22 p3241 A72-43091

Useful range of a mechanical impedance technique for measurement of dynamic properties of materials. 23 p3294 A72-44126

On mechanical response of a non-uniform piezoelectric transducer under the influence of a body-force. 23 p3291 A72-44316

Frequency dependence of axially oscillated nozzles admittance real and imaginary parts for different Mach numbers, convergence angles and curvature radii, comparing theory and experiment 24 p3433 A72-45144

MECHANICAL MEASUREMENT

NT DISPLACEMENT MEASUREMENT

NT DRAG MEASUREMENT

NT FLOW MEASUREMENT

NT FRICTION MEASUREMENT

NT PRESSURE MEASUREMENTS

NT STRESS MEASUREMENT

NT THRUST MEASUREMENT

NT VELOCITY MEASUREMENT

NT VIBRATION MEASUREMENT

NT WIND MEASUREMENT

NT WIND VELOCITY MEASUREMENT

NT X RAY STRESS MEASUREMENT

Noncontact rotating shaft horsepower measurement, using phase displacement technique [ASME PAPER 72-GT-29] 11 p1630 A72-25625

Mechanical and electrical methods of measuring vibration rates, displacements, accelerations and time derivatives, examining magnetolectric and piezoelectric sensors characteristics 11 p1635 A72-26465

Thickness gage for continuous autographic record in nondestructive testing of irregular cross section specimens 13 p1959 A72-29759

Variable torque determination in precision work technology, discussing electronic measurements of length, shaft deformation, torsion angle and force 14 p2104 A72-30485

Systematic approach to study energy and information flow through measuring system in experimental mechanics, using transducer model 18 p2690 A72-36356

Photoelasticity, holography, moire and strain gage methods in European experimental mechanics research 18 p2733 A72-36357

Some uncommon electric transducers for the measurement of mechanical quantities. 18 p2690 A72-36369

Hybrid processing of empirical functions in mechanics 18 p2710 A72-36423

Application of N equalizing and compensating signals in a single-cell reciprocal magnetolectric transducer 24 p3386 A72-45315

MECHANICAL OSCILLATORS

NT GYROSCOPIC PENDULUMS

NT PENDULUMS

Self sustained oscillations of mechanical system with infinite number of degrees of freedom, considering application to diffusion in porous medium 02 p0258 A72-11496

Three-axis flight table with dc torque motors, discussing servo loops design and mechanical oscillations frequencies 02 p0257 A72-12541

Instability effect on aperiodic motion of nonlinear thermomechanical oscillator from periodic solutions 04 p0547 A72-14458

Optimal synthesis of multiparametric machine systems by LP search/determinate analog of random search/, applying to oscillatory models 06 p0821 A72-17726

Lightly damped nonlinear mechanical oscillators under random excitation, calculating stationary response frequency and autocorrelation by heuristic procedures 06 p0849 A72-18693

Mechanical systems with nonlinear position functions, elastic elements or self damping, investigating oscillation mode onset and stability conditions 06 p0850 A72-18701

Aerodynamic radial bearing analysis based on Reynolds equation, emphasizing gas bearing nonlinear oscillation stability 06 p0824 A72-18702

Mechanical system of elastically coupled bodies carrying identical vibrators, examining self synchronization behavior 06 p0850 A72-18713

Single frequency oscillations in nonlinear mechanical systems described by one dimensional mixed boundary value problems, using asymptotic methods 06 p0850 A72-18715

Nonlinear mechanical oscillation systems analysis by analog computer, exemplifying pendulum rotating about vertical axis 06 p0851 A72-18725

Autoparametric excitation in relation to divergence and flutter of autonomous mechanical cantilever systems under nonpotential circulatory forces 06 p0851 A72-18726

Optical bidirectional modulator for two beam spectrophotometer, using tuning fork as oscillatory system 07 p0988 A72-19962

Third-order resonance during oscillations of Hamiltonian system of nonlinearly coupled oscillators, obtaining equations of motion and phase portraits 07 p1035 A72-19978

Transcendental series solution of Chini-Painlevé nonlinear differential equations describing vehicle and meteorite oscillation during planetary atmospheric entry 07 p0964 A72-20594

German monograph on multielement linear mechanical oscillator analysis covering behavior of harmonically excited bar chains of arbitrary structure 09 p1350 A72-22337

Mechanical system with inertial vibration sensor and nonlinear spring, obtaining global asymptotic stability of zero solution of differential equations describing natural vibration 09 p1399 A72-22697

Holographic method for investigating piston type vibrations with phase modulated reference light beam 09 p1317 A72-23682

Inverted pendulum subjected to small amplitude sinusoidal periodic and stochastic base motion, determining stability boundaries by averaging method 12 p1844 A72-27247

Perturbation procedure for weakly coupled oscillators in connection with statistical mechanics ergodic problem and nonlinear interaction models 12 p1844 A72-27248

Multiple index Lagrange equations of motion of second kind, proving analogy between mechanical and stereomechanical effects 12 p1844 A72-27318

Linear oscillatory system, investigating effects of pulsed dynamic damper with mass vibrations bounded by limiters 12 p1887 A72-28235

Undesirable mechanical vibration control concepts for acoustic noise reduction, considering environment characteristics, attenuation degrees and passive and active control mechanisms 13 p2005 A72-29555

Random vibration of two multimodal mechanical systems with point coupling, obtaining power flow spectral density by statistical energy analysis 13 p2005 A72-29563

Mechanical oscillator model for experimental investigation of multistage electrical frequency multipliers subharmonic transient oscillations, considering energy flow under constant and/or phase modulated excitation 14 p2131 A72-30719

Generalized Thomson-Tait-Chetaev stability theorem for n-degrees-of-freedom mechanical oscillating systems with virtual nonconservative displacement forces 15 p2274 A72-31456

Single degree of freedom nonlinear mechanical system vibration characteristics calculation by averaging procedure, taking into account energy dissipation 16 p2424 A72-33279

Third-order resonance during oscillations of Hamiltonian system of nonlinearly coupled oscillators, obtaining equations of motion and phase portraits 20 p2956 A72-40034

The parameters of a two-mass oscillatory system in which one of the masses is acted upon by a complex working resistance 23 p3312 A72-43352

Experimental investigation of finite-amplitude acoustic oscillations in a closed tube. 23 p3314 A72-44124

MECHANICAL PROPERTIES

NT ABRASION RESISTANCE

NT AEROELASTICITY

NT AEROTHERMOELASTICITY

NT ANELASTICITY

NT BRITTLENESS

NT BULK MODULUS

NT COLD STRENGTH

NT COMPRESSIBILITY

NT COMPRESSIVE STRENGTH

NT CREEP PROPERTIES

NT CREEP RUPTURE STRENGTH

NT CREEP STRENGTH

NT DIMENSIONAL STABILITY

NT DUCTILITY

NT DYNAMIC MODULUS OF ELASTICITY

NT ELASTIC PROPERTIES

NT ELASTOPLASTICITY

NT ELECTROSTRICTION

NT FATIGUE LIFE

NT FIBER STRENGTH

NT FLEXIBILITY

NT FRACTURE STRENGTH

NT HARDNESS

NT HIGH STRENGTH

NT HYDROELASTICITY

NT IMPACT STRENGTH

NT MAGNETOSTRICTION

NT MICROHARDNESS

NT MODULUS OF ELASTICITY

NT NOTCH SENSITIVITY

NT NOTCH STRENGTH

NT PHOTOELASTICITY

NT PHOTOPLASTICITY

NT PHOTOVISCOELASTICITY

NT PIEZOELECTRICITY

NT PLASTIC PROPERTIES

NT POISSON RATIO

NT PROPORTIONAL LIMIT

NT RESILIENCE

NT SHEAR PROPERTIES

NT SHEAR STRENGTH

NT SHELL STABILITY

NT STEADY STATE CREEP

NT STIFFNESS

NT STRESS CYCLES

NT STRESS RATIO

NT STRESS RELAXATION

NT STRUCTURAL STABILITY

NT TENSILE CREEP

NT TENSILE PROPERTIES

NT TENSILE STRENGTH

NT THERMAL RESISTANCE

NT THERMOELASTICITY

NT THERMOPLASTICITY

NT THERMOVISCOELASTICITY

NT TOUGHNESS

NT VISCOELASTICITY

NT VISCOPLASTICITY

NT WELD STRENGTH

NT YIELD POINT

NT YIELD STRENGTH

Aerospace adhesives applications, discussing thermal and mechanical properties, and cryogenic, epoxy, urethane silicone and fluorocarbon types 01 p0090 A72-10188

High chromium ferritic stainless steels weldability and mechanical properties, showing C, N, Ti and residuals effects on recrystallization, toughness, tensile behavior and corrosion resistance 01 p0083 A72-10283

Parachute canopy fabrics and rigging lines cordage properties requirements, considering nylon, polypropylene, silk, cotton and nonwoven scrim-reinforced fabrics 01 p0005 A72-10314

High temperature strength degradation of graphite and boron reinforced epoxy composites after room temperature aging 01 p0090 A72-10728

Thermal and environmental exposure effects on high temperature mechanical properties of graphite/polyimide composites 01 p0090 A72-10730

High temperature testing of metal matrix composites mechanical properties, noting aerospace structural applications 01 p0084 A72-10732

Coextruded Be fiber-Ti alloy matrix composite sheets for light weight structures, describing ultrasonic inspection and mechanical properties 01 p0084 A72-10734

Aluminum stiffening structural sections selectively reinforced with boron/epoxy composite materials, discussing mechanical properties, cost effectiveness and stress distribution 01 p0139 A72-10737

Fiber reinforced filament wound composites for pressure vessel applications, investigating mechanical properties 01 p0090 A72-10741

Fe, Ni and Co based high temperature thin gauge sheet alloys, discussing chemical and mechanical properties, fabrication and availability 01 p0084 A72-10742

Dispersion strengthened Ni-Cr alloys processing technique and mill products development, noting increased strength at elevated temperatures 01 p0075 A72-10744

Bare and coated Nb alloy in high temperature vacuum conditions, discussing tensile and bend tests and mechanical properties 01 p0084 A72-10747

Multiple reentry effects on space shuttle thermal protective superalloys mechanical properties, present-

ing cyclic simulation results for different temperatures, pressures and stresses 01 p0084 A72-10754

Ti alloy honeycomb core sandwich panels fabricated by brazing or spot diffusion bonding, investigating elevated temperature effects on mechanical properties [ASM PAPER W 71-23,3] 01 p0086 A72-10875

Graphite filament reinforced plastics strength, performance properties, fabrication processes and tooling concepts [SME PAPER EM 71-205] 01 p0076 A72-10968

Unidirectional glass/graphite fiber-epoxy resin composite, discussing fabrication and performance tests for mechanical properties [SME PAPER EM 71-192] 01 p0092 A72-10971

Metals mechanical behavior, considering plastic deformability, strain hardening, cohesion and engineering performance prediction 01 p0086 A72-10985

Mo and Zr additions induced mechanical strength increase of Ni-Al-Nb alloys in cast and deformed states at 20-1100 C 01 p0088 A72-11081

Mechanical strength and performance of combined multicomponent bonded materials, including laminar, fiber, flake filled and metal matrix composites 01 p0093 A72-11086

Ti-Al-V alloy powders electrically activated pressure sintering /spark sintering/, considering mechanical properties and economic factors 02 p0240 A72-11428

Hydropressed sintered U-700 superalloy powder, noting weakened particle grain boundary conditions from mechanical properties and fracture studies 02 p0240 A72-11444

Composition, microstructure and mechanical properties of binder metal in cobalt bonded tungsten carbide 02 p0241 A72-11451

Carbon content effect on phase relationships and mechanical properties of sintered Fe-WC alloys, noting high strength 02 p0241 A72-11452

Corrosion effect on mechanical properties of sintered powder iron and bronze parts, describing test procedure for corrosion resistance determination 02 p0241 A72-11459

Sintering and heat treatment effects on mechanical properties of atomized and mixed powders of Ni-Mo steel 02 p0234 A72-11462

Low strength polymeric materials specimen geometry and lateral constraints effects on isothermal compressibility by compression tests [SESA PAPER 1935] 02 p0248 A72-11518

Lunar surface soil mechanical properties from computer simulation of Surveyor spacecraft observation data for each landing site, estimating cohesion 02 p0275 A72-11595

Soviet papers on strength and plasticity covering elasticity, creep, polymer mechanics, plates and shells, dynamic and high temperature stability, thermoelectricity, soil and free flowing media 02 p0288 A72-11601

Refractory materials strength testing equipment and techniques at high temperatures, covering creep, hardness, fatigue, ultrasonic, energy dissipation and loading tests 02 p0291 A72-11636

Thermoplasticity problems of materials with time dependent mechanical properties, obtaining approximate plastic deformation under cyclic loading 02 p0291 A72-11638

Macroscopic fracture mechanics of composite laminates, discussing flawed specimen static strength prediction 02 p0249 A72-11883

Microstructure and mechanical properties of iron base superalloys, examining precipitation hardening by gamma prime and secondary intermetallic compounds formation 02 p0245 A72-12505

Wrought superalloys microstructure and mechanical properties control by precipitating phases 02 p0245 A72-12506

Titanium and aluminum variations effects on eta and gamma prime solvus temperatures and on mechanical properties of iron-nickel superalloy 02 p0245 A72-12508

Temperature effects on strength and deformability of randomly reinforced fiberglass polyamides 02 p0250 A72-12678

Reinforcing fibers length effect on cross breaking strength and rupture area size at surface for silicoorganic glass reinforced plastic 02 p0250 A72-12681

Quenching effects on thoriated-dispersed Ni sheet plastic stress relaxation and room temperature mechanical properties 02 p0247 A72-12822

Superalloy compositions prealloyed powders strengthening by secondary gamma phase precipita-

tion, noting high temperature strength without ductility loss after thermomechanical treatment and aging
02 p0247 A72-12856

Tubular and rod extruded age hardenable Al alloys, determining mechanical anisotropic properties from yield loci and r values
03 p0369 A72-12957

Resistive force on moving dislocations at low temperature in solids and crystal defect studies by ultrasonic methods, determining temperature dependence of mechanical properties
03 p0362 A72-13224

Mechanical response of Al and Cu under complex strain histories conditions, using endochronic theory of viscoplasticity without yield surface
03 p0444 A72-13504

Tempered Fe-Cr-C-C steels microstructural and mechanical properties, investigating martensite and bainite
03 p0375 A72-13929

Soviet book on structural shape effects of machine parts on durability, covering production, gear transmissions shafts, axles, threaded joints, etc
03 p0364 A72-13966

Stress concentration at eccentric holes and effect on strength of full size rotating turbine disks
03 p0450 A72-14108

Alloying elements effects on aging response of austenitic-ferritic alloys in Fe-Cr-Mn-Ni base, determining mechanical properties dependence on processing and heat treatment
03 p0377 A72-14170

Alloy additions and heat treatment effects on mechanical properties and weldability of quenched and aged high strength Ni steels
03 p0378 A72-14173

Physicomechanical properties of metals at crystallization temperatures, considering density, viscosity, strength, hardness, elasticity and creep
03 p0378 A72-14219

Glass variables effect on polypropylene, polystyrene and Nylon-6 glass filled thermoplastic composites mechanical properties, discussing silane coupling agents and injection moulding machine conditions
04 p0537 A72-15085

Dislocation creep model for work hardening and recovery, deriving mechanical equation of states for various magnitudes and directions
04 p0589 A72-15160

Elastic stiffener bonded to elastic half plane with different mechanical properties, reducing governing integral equation to infinite system of linear algebraic equations
[ASME PAPER 71-APM-TT] 04 p0589 A72-15182

Substitutional dynamic strain aging effects on Fe-Nb alloys mechanical properties, attributing ductility reduction to work hardening and strain rate effects
04 p0534 A72-15576

Safe stressing of high strength and locally nonbrittle solid bodies, testing hard polymers at room temperature
04 p0593 A72-15656

Polyfluoroethylene-based composite materials mechanical properties, discussing strengthening mechanism of filler additions
05 p0682 A72-15989

Mechanical properties of heat treated hardened high strength steel, investigating microstructure relationship to breakdown characteristics
05 p0671 A72-15992

Metallurgical treatment control reliability in machine part mechanical properties quality evaluation
05 p0671 A72-15993

Strength margin estimation in materials sustaining cumulative static and damage under cyclic thermal loads
05 p0735 A72-15994

Large length-to-diameter ratio two layer blank bimetallic hard alloy product manufacture by extrusion die method, noting mechanical properties
05 p0666 A72-16098

Dissolved oxygen effect on structure and toughness of nonalloyed extruded steels, observing austenite recrystallization kinetics retardation after hot plastic deformation
05 p0672 A72-16143

Mechanical and microstructural properties of Be-base alloys consolidated by vacuum arc melting, reporting results of tensile tests, hardness measurements and microprobe analysis
05 p0674 A72-16389

Superalloys for gas turbine rotor and stator blades, testing long term heating effects on microstructure and mechanical and thermal fatigue properties
05 p0675 A72-16495

Strength analysis of hyperboloidal electric wire joint designs, expressing stress as function of contact loads
05 p0616 A72-17059

Alloying elements effects upon iron mechanical properties, investigating lattice parameters, temperature dependence of yielding and plastic flow, solid solution strengthening and softening, etc
05 p0676 A72-17101

Critique of microstructure effect on strength, toughness and stress corrosion cracking susceptibility of metastable beta titanium alloy, discussing recrystallization conditions
05 p0679 A72-17122

Mechanical, technological and physical properties of steel with and without molybdenum
05 p0679 A72-17204

Prolonged heatings effect on heat resistant magnesium alloys microstructure and mechanical properties
05 p0680 A72-17208

Homologous temperature method to compare mechanical properties of metals tested at different temperatures
06 p0827 A72-17399

Fe-Co alloy athermal transformation to bcc martensite at industrial cooling rates, investigating effects on mechanical properties
06 p0829 A72-17830

Fiber reinforced materials mechanical properties, showing strength dependence on stress-strain behavior of fibers and binders and fiber volumetric proportions
06 p0835 A72-18252

Structural and strength characteristics of carbon graphite materials, considering composites preparation and applications
06 p0836 A72-18361

Automatic testing machine for mechanical properties of metals under static loading
06 p0796 A72-18365

Anomalous temperature-strain rate dependence of Ni-Al intermetallic compound mechanical properties from plastic deformation mechanism
06 p0832 A72-18417

Isotropic and anisotropic materials strength criteria and boundary surfaces in invariant stress tensor spaces
06 p0898 A72-18553

Brittle strength characteristics of construction materials with cracks calculated by graphical analysis procedure, considering state of limiting equilibrium
06 p0899 A72-18560

Electrical contacts conduction principles, considering circuit voltage, current, variable resistance and resistive, mechanical, heating and adhesive properties
06 p0791 A72-18578

Carbon effects on strength, ductility, brittle transition and plastic strains of tungsten at high temperatures
06 p0833 A72-18634

Nonheat treated extruded Mo alloy under tension and vacuum conditions at various temperatures, investigating cylindrical samples size effects on mechanical properties
06 p0833 A72-18635

Semifinished product production technology influence on heat resistant alloys mechanical properties, considering forging, rolling, casting, melting, diffusion welding and powder metallurgy
06 p0834 A72-18647

Explosive shock loading effect on materials mechanical properties, describing test equipment
06 p0797 A72-18659

Thermocycling treatment influence on structural changes and strength in coarse grain Ni under creep tests
06 p0834 A72-18686

Structural changes, mechanical properties, electrical resistance and lattice constant during aging of Al alloys containing Mg, Li and Mn
06 p0834 A72-18743

Microstructural changes and mechanical properties of deformed Nb alloy during annealing process, observing low temperature plasticity increase
06 p0835 A72-18747

Economical methods for cast maraging steel production, describing composition, heat treatment and mechanical properties
07 p0100 A72-18970

Composite propeller blades with carbon fiber reinforced plastics spar for hovercraft, presenting mechanical properties test data for different composite configurations
07 p0912 A72-19062

Extruded superalloy powder structural shapes preparation by filled billet technique for improved chemical and mechanical properties
07 p0994 A72-19483

Cu contents effect on Ti-Cu alloys physical and mechanical properties, discussing beta phase decomposition during annealing
07 p0102 A72-19574

Real time computer aided mechanical testing and data analysis system for composites, confirming computer analysis by motion pictures of thin walled graphite/epoxy composite fracture
07 p0965 A72-19734

Oxygen effect on structure and mechanical, technological and corrosive properties of stainless steel melted in open and vacuum furnaces
07 p0103 A72-19739

Structure, hardness, density and electrical resistance of binary alloys V-Ti, V-Cr, V-Al and V-Sn
07 p0103 A72-19741

Mechanical properties of fiber reinforced heat resistant alloys
07 p0103 A72-19743

Heat resistant Nichrome composite alloy with tungsten filament reinforcement, discussing manufacture and mechanical properties at 1100 C
07 p0103 A72-19747

Cast and wrought Ti alloys Ar arc weldments microstructural and mechanical properties after different heat treatment sequences
07 p0103 A72-19750

Rupture strength of disk with surface crack under concentrated loads, applying integral equation to stressed state
07 p1092 A72-19777

Transition metals addition effect on Al-Cu alloy strength and aging characteristics, determining lattice constant increase by X ray microstructural analysis
07 p0104 A72-19841

High temperature strengthening of vacuum melted W-Ti alloys with Mo and Zr additions
07 p0104 A72-19843

Deformation rate and temperature effects on optimum strength and ductility of die forged and extruded Mo-Ti alloys
07 p0104 A72-19845

Book on materials low temperature mechanical properties covering metals, polymers, ceramics and composites, temperature effects on deformation processes, fracture mechanics, test methods, etc
07 p0105 A72-19909

Heat treatment effects on strength differential of high strength martensitic stainless and Ni maraging steels
07 p0105 A72-19926

Strength differential effect on microstructures of steels, using tensile and compressive stress-strain curves
07 p0105 A72-19927

Microstructure and high temperature mechanical properties of unidirectionally solidified pseudobinary Fe-Cr-Nb eutectic alloy
07 p0106 A72-19938

Carbide precipitation effect on strength of ausrolled hardenable hypoeutectoid and hypereutectoid stainless steels
07 p0106 A72-19943

Mechanical properties and structural strength evaluation methods for metallic materials at low temperatures, describing hydraulic and pneumatic testing facilities
07 p0107 A72-19930

Supermolecular structure artificial defects influence on mechanical strength of pyrographite
07 p0102 A72-20136

Chemically etched notches effect on Al-Mg alloy mechanical properties
07 p0108 A72-20139

Test temperature effect on phase composition, mechanical properties and resistance to cavitation of unstable austenitic steels, describing test facility
07 p0108 A72-20140

Nb and Nb alloys mechanical properties during plastic deformation and heat treatment, discussing grain size, dislocation structure and substructural changes effects
07 p0108 A72-20144

Metals and alloys breakdown toughness and mechanical properties predictions under various loading conditions, discussing interatomic bonds and plastic deformation zone size
07 p0109 A72-20146

Structural limitations of interstellar ramjet, investigating operation during travel in high matter number density space
07 p0104 A72-20249

Heat treatment of martensitically aging steels with Co, Ni and Mo, considering hardening effects and optimal conditions for high mechanical properties
07 p1020 A72-20414

Fe addition effects on structural and mechanical properties of heat resistant Ni-Cr alloys
07 p0102 A72-20416

Precipitation hardened Ni-Al alloy mechanical properties, relating ductility and strength to precipitate caused inhibition of microcrack initiation and propagation
07 p0101 A72-20438

Physicomechanical properties of steel with oxide, sulfide, silicon, phosphorus and mixed metal-non-metal inclusions
07 p0102 A72-20618

P-analytical functions application to strength analysis of zero moment shells of revolution with positive Gaussian curvature under concentrated loads
08 p1242 A72-20905

Soviet handbook on vibration absorbing properties of construction materials under cyclic straining, covering energy dissipation and dynamic strength
08 p1185 A72-20975

Materials ideal strength calculation compared with test results
08 p1242 A72-21185

Mellin transforms application to two dimensional elasticity problem for anisotropic wedge with continu-

ous mechanical characteristics under concentrated force

08 p1243 A72-21238

Monocrystals elastic anisotropy effects on polycrystalline sinter matrix minimum porosity, thermal conductivity, mechanical and elastic properties, thermal stress resistance and Hugoniot elastic limit

08 p1186 A72-21441

Thermal and mechanical properties of randomly reinforced fiber/resin composites including boron/epoxy, Thorne/epoxy and S glass/epoxy materials

08 p1192 A72-21682

Inorganic single crystal titanate whisker fibers with high modulus strength for plastic reinforcement, noting mechanical, thermal and physical properties

08 p1193 A72-21685

Composite processing, adhesive formulary, bonding processes and mechanical properties of low void content autoclave molded polyimide graphite composite stiffened titanium alloy structures

08 p1193 A72-21687

Graphite fiber reinforced composites with high mechanical strength and modulus at low weights, fatigue resistance, vibration damping and tailorable thermal expansion coefficient

08 p1193 A72-21689

Mechanical surface strengthening effect on small cycle fatigue life of Ti alloy weakened by stress raiser

08 p1186 A72-21725

Nondestructive determination of glass reinforced plastics normal elastic and shear moduli and strength characteristics by vibrational, pulsed and acoustic methods

08 p1195 A72-21773

Soviet papers on imperfections of crystalline structure effects on physical and mechanical properties of metals and alloys, covering radiation damage, microdeformations, X ray investigations, etc

08 p1187 A72-21785

Material properties nonuniformities effect on wound fiber glass reinforced plastic rings and cylinders thermoelastic residual stresses

08 p1196 A72-21858

Extremal mechanical properties directions in orthotropic glass fiber reinforced plastics symmetry planes

08 p1196 A72-21866

Copper, zinc and aluminum mechanical properties comparison by cyclic and steady state compressive load tests, noting stress-strain curve relationship to strain rate

08 p1188 A72-21921

Routine method for ultrathin carbon support film production for electron microscopy, noting mechanical stability and strength

08 p1172 A72-22020

Soviet book on corrosion cracking of carbon steels covering chemical composition, structure, mechanical properties, anode and cathode processes role and adsorption losses

08 p1190 A72-22163

Work hardening after ausforming and heat treatment effects on mechanical properties of metastable austenitic Ni-Cr steel

08 p1190 A72-22165

Surface active medium effect on free surface energy and strength of pyrographite in ethyl alcohol solution, using crack kinetics experiment

08 p1197 A72-22182

Mechanical properties anisotropy in heat resistant Ni alloys due to strengthening phase nonmetallic inclusions distribution, suggesting purification by vacuum melting

09 p1327 A72-22231

High temperature tests of graphite composites in air, determining material loss time dependence and correlation with observed strength data after oxidation

09 p1333 A72-22381

Thermomechanical treatment effects on microstructure and mechanical properties of Al alloy

09 p1327 A72-22470

Mg alloys compositions, melting points, mechanical properties and applications

09 p1327 A72-22479

Fiber thermoplastics matrix breakdown and mechanical properties enhancement, examining lateral and longitudinal strain during uniaxial tensile creep and recovery

[PI PAPER 4]

09 p1337 A72-22541

Pultrusion process for carbon fiber reinforced plastic, compared with wet lay up technique, noting mechanical properties

[PI PAPER 10]

09 p1318 A72-22545

Glass ceramics mechanical properties as function of temperature during bending, taking into account scale factor

09 p1337 A72-22742

Circumferential crack in closed shallow cylindrical shell under tension, computing stress singularities strength

09 p1404 A72-22912

Fiber composites mechanical properties - Conference, Teddington, England, November 1971

09 p1338 A72-23162

Strength and fracture energies and toughness in fibre reinforced ceramics

09 p1339 A72-23171

Plastic deformation effect on structure and properties of steel sheet under biaxial tension at liquid nitrogen temperature

09 p1330 A72-23187

Microstructure and mechanical behavior of unidirectionally solidified magnesium-magnesium nickelide eutectic composite over range of solidification rates

09 p1330 A72-23376

Thermomechanical strengthening of gamma prime precipitation hardened nickel base superalloy, emphasizing working operation and dislocation substructure

09 p1330 A72-23377

Stress-strain characteristics of metal ductile filaments with elastic brittle coatings, noting strengthening effect on anodic oxide coated aluminum

09 p1330 A72-23379

Beta-III Ti alloy mechanical properties dependence on heat treatment and elevated temperature exposure, illustrating associated microstructures

09 p1331 A72-23384

Diffusion bonding compared to other processes, discussing mechanical properties, metallurgical condition, fatigue, pressure, temperature and production problems

09 p1320 A72-23633

Fe-Ni-C alloy mixed austeno-martensitic microstructure embrittlement, investigating mechanical properties after thermomechanical treatment

10 p1495 A72-24087

Metal matrix composites deformation and mechanical properties prediction from component phases information, examining interface role, residual stress effect and thermal degradation

10 p1553 A72-24176

S glass/epoxy composites strength retention properties under long duration tensile load, proposing use of stress rupture data for reliable safe structural design

10 p1501 A72-24263

Fiber reinforced materials mechanical properties calculation, taking into account various fiber orientations and multiaxial loads

10 p1501 A72-24493

Sintering and aging effects on mechanical behavior of low carbon copper steel

10 p1488 A72-24696

Low temperature resistant stainless steels mechanical properties, microstructure and weldability, discussing compositions and heat treatments

10 p1498 A72-24838

High strength steel strip reinforced aluminum, discussing fabrication techniques and mechanical properties

10 p1498 A72-24839

Mechanical characteristics of natural and synthetic rubber, noting features of cork filled urethane

10 p1502 A72-24861

Filler metal paste application effect on Hastelloy sheet brazing quality, describing results in terms of mechanical properties and microstructural characteristics

11 p1637 A72-25342

Dimensional stability and micromechanical properties of materials for use in OAO, investigating residual stresses, creep properties and stress relaxation

[AIAA PAPER 72-325]

11 p1653 A72-25362

Beryllium sheet and foil application to lightweight space structures, discussing mechanical properties

[AIAA PAPER 72-404]

11 p1726 A72-25425

Empirical multiaxial strength criteria for anisotropic composite materials

11 p1731 A72-25455

Tubular specimens for testing mechanical characteristics of fiber reinforced composites under axial loading, discussing design, fabrication and end attachment problems

11 p1670 A72-25456

Mechanical behavior of three dimensional reinforced ablative composites, including carbon-phenolic, quartz-phenolic and quartz-carbon materials

11 p1670 A72-25459

Bolted connections strength in graphite fiber-epoxy resin composites reinforced by colaminated boron film

11 p1672 A72-25476

B-Al composite mechanical properties improvement through heat treatment and steel addition

11 p1653 A72-25478

Metal matrix composites, testing neutron irradiation effects on mechanical properties for nuclear application feasibility

11 p1654 A72-25483

Mn content effect on mechanical properties and corrosion fatigue and stress corrosion cracking resistance of Al-Mg casting alloys

11 p1658 A72-25850

Book on carbon fibers in composite materials covering fiber testing and mechanical properties

11 p1674 A72-25924

Luna 16 automatic probe drilling experiment, obtaining lunar rocks physicochemical properties for comparison with terrestrial rocks

11 p1613 A72-25938

Mechanical, technological and physical properties of steel with and without molybdenum

11 p1660 A72-26139

Prolonged heating effect on heat resistant Mg alloys microstructure and mechanical properties

11 p1660 A72-26143

Organic matrices in structural composites, considering mechanical behavior, processability and properties in adverse environments

11 p1674 A72-26230

Fiber-matrix composites overall strength optimization, emphasizing matrix and interface effects

11 p1674 A72-26231

Organic and metal matrix composites physical and mechanical properties and application to spacecraft and missile components, considering cost effectiveness

11 p1674 A72-26233

Microstructure and mechanical properties of heat treated friction welds at high temperatures

11 p1641 A72-26489

Tungsten alloy wires strength, creep properties and fatigue limit, investigating fracture characteristics

11 p1663 A72-26807

Test device for reinforced plastics mechanical properties under heating and pressure with allowance for gas permeability

11 p1613 A72-26813

Mo-Hf alloys high temperature mechanical properties improvement by internal diffusion nitriding, noting precipitates effects

11 p1644 A72-26843

Oxygen, carbon and boron effect on liquid phase sintering behavior and mechanical properties of Ni base superalloys

11 p1645 A72-26848

Microstructure and mechanical properties of dispersion strengthened Co alloys, investigating heat treatment effects

11 p1664 A72-26851

Mg addition effect on high temperature mechanical properties of nickel-alumina alloy, studying particle coarsening mechanism changes

11 p1664 A72-26856

W-Ni-Mo alloys obtained by powdered metals sintering, investigating mechanical properties, phase distribution and composition

11 p1666 A72-26876

Carbon and other inclusions effects on cast W strength at elevated temperatures from microscopic observation

11 p1666 A72-26877

Carbon and oxygen distribution and content effects on Mo mechanical properties and embrittlement

11 p1666 A72-26878

Luna 16 Sea of Abundance rock volume weight, destruction pattern, compressibility, shear strength and carrying ability, comparing to terrestrial rock

11 p1724 A72-26910

Dislocation structure and strength of Ti at low and intermediate temperatures, investigating strain, grain size and interstitial solute hardening

11 p1666 A72-26927

Coherent phases transformations in alloys, investigating mechanical properties dependence on microstructural features

11 p1667 A72-26929

Carbide precipitation effect on structure and high temperature strength of Co based alloys

11 p1667 A72-26932

Mechanical properties, microstructural characteristics and fracture behavior of beta Ti-V-Cr-Al alloy

11 p1667 A72-26933

Deformation characteristics and mechanical properties of superplastic alloys, stressing metallographic techniques

11 p1739 A72-26936

Mica glass ceramics mechanical properties and thermal shock behavior in terms of microstructural variables, discussing fracture propagation and secondary cracks formation

11 p1675 A72-26949

Glass sample mechanical strength testing, considering abrasion process, concentric ring stress calculation and laser light scattering techniques

12 p1832 A72-27007

Chemically strengthened glass for eject-through frangible canopy design in aircraft emergency escape systems, noting protection against ejection injuries

12 p1813 A72-27016

Polymer testing machine for simultaneous structural and mechanical properties measurement of specimens subjected to uniaxial tensile loads for broad temperature range

12 p1795 A72-27465

Flexible solar cell array module design technique, discussing electric welding procedure and equipment parameters effects on breaking strength and reliability

12 p1758 A72-28036

Fabrication, and physical, mechanical and ablation properties of three dimensional carbon-carbon cylinder composite materials

12 p1834 A72-28086

Fiber reinforced Mod 3 carbon-carbon composites mechanical and thermal properties comparison with polycrystalline bulk graphite

12 p1834 A72-28087

Resin bonded B-Al composites, discussing fabrication techniques and mechanical properties

12 p1815 A72-28098

Composite materials mechanical and thermal properties for ATS reflector supporting truss, noting graphite fiber reinforced epoxy plastic design, fabrication and tests

12 p1886 A72-28158

Fusion silicide protective coatings performance for Ta alloys under simulated reentry conditions, noting oxidation rate, ductile brittle bend transition temperature and mechanical properties

[ASM PAPER W 72-13,6] 12 p1835 A72-28162

Molecular-mechanical theory of external friction, taking into account surface roughness, time and temperature dependent mechanical properties and chemical processes

12 p1818 A72-28195

Low carbon steel prior plastic deformation effects on mechanical hysteresis loop shape

12 p1887 A72-28234

Engineering formula relating crack tip stress intensity coefficient to mechanical properties and structural element size

12 p1887 A72-28236

Crack and notch induced stress concentrations effect on steel mechanical properties at 20-293 K, using static and dynamic test methods

12 p1831 A72-28240

Rare earth metals addition effect on mechanical properties of electrolytic hydrogen-refined Cr, noting low temperature ductility

12 p1831 A72-28241

Russian book on hard alloys strength covering WC-Co and WC-TiC-Co alloys microstructure, thermal stresses and fracture mechanism

12 p1831 A72-28348

Haynes high strength heat resistant Ni-Cr-W alloy metallurgical and structural relationship, mechanical and physical properties, oxidation and corrosion behavior and fabrication processes

13 p1973 A72-28649

Mechanical properties of thick Be plate produced by diffusion bonding of thin sheets from ingot material

13 p1973 A72-28655

Ultrafine grained microstructures and mechanical properties of alloy steels developed by cold working followed by annealing

13 p1974 A72-28662

Mechanical properties of nitrified austenitic steels at low temperatures, noting improved tensile strength

13 p1977 A72-29017

Ti-V and Ti-Nb alloys mechanical strength and stress concentration resistance at low temperatures

13 p1977 A72-29018

Cr and V additions effects on Mn steels mechanical properties and wear resistance, noting strength limit increase

13 p1977 A72-29021

High temperature strength of low ductile refractory metals, describing test equipment

13 p1978 A72-29446

Borated steels strength under static bending, cyclic flexure and torsion and impact loads, correlating fatigue strength, residual stresses and core properties

13 p1979 A72-29477

High stress state mechanical properties of steels with different carbon contents and heat treatments

13 p1979 A72-29478

Combined thermal, vibrational and dimensional treatments effect on WC-Co alloy physical and mechanical properties, noting tensile and impact strength increase

13 p1979 A72-29480

Phase composition, structure and strength properties of aluminizing coatings on Ni-Al alloys, noting plasticity increase due to Ta addition

13 p1980 A72-29485

Effect on physical and mechanical properties of hard metals due to gas sorption by metallic films spray-coated on surfaces, describing vacuum apparatus

13 p1939 A72-29488

High strength carbon fiber reinforced plastics, discussing fabrication techniques, fiber structural, physical and mechanical properties and potential technological applications

13 p1984 A72-30075

Microstructure and mechanical properties of molecular cermets produced from slip-cast fused silica of different porosity by alumothermal reduction method

13 p1967 A72-30115

Cobalt-base superalloys powder-metallurgical fabrication techniques and related effects on physical and mechanical properties

13 p1982 A72-30126

Mechanical strength of interstitial solid tantalum-oxygen solutions obtained by electron beam fusion,

thermal cycling and saturation as function of temperature and oxygen contents

14 p2112 A72-30163

Optimal mechanical properties of Ti alloys with Cr, Mo, V, Nb and Ta additions, considering tensile strength, impact toughness, elongation and flattening

14 p2113 A72-30164

Ni-Cr-Mo stainless maraging steel, investigating yield strength, toughness, corrosion resistance and weldability

14 p2113 A72-30270

Ni, Si and Mn alloying effect on structural transformations, phase composition and mechanical properties of cast Cr-Ni steels

14 p2114 A72-30273

Sn alloying effect on heat resistant Ni-Cr alloys plastic strain resistance and strength at room and high temperatures

14 p2114 A72-30274

Hot worked Al alloy machine elements mechanical properties scattering, discussing quality control procedures

14 p2114 A72-30275

Aluminum-stainless steel and Ni-Mo composites prepared by dynamic hot pressing, determining bond strength between fibers and reinforced metal matrix

14 p2107 A72-30431

High speed testing of materials mechanical behavior over range of loading rates

14 p2165 A72-30441

High temperature mechanical properties - Conference, Clermont-Ferrand, France, October 1970

14 p2116 A72-30526

Welded Al alloys at temperatures above 100 C, discussing traditional and powder metallurgy and mechanical properties dependence on time, temperature and creep

14 p2116 A72-30528

Sintering and melting preparation effects on mechanical properties of refractory W-Re alloys, considering sigma phase in solid alpha solution

14 p2116 A72-30530

Chemical and mechanical properties relationship to stress corrosion in high strength Al-Cu and Al-Zn-Mg alloys, emphasizing grain boundaries cleavage energy

14 p2117 A72-30536

Heat resistant Ni alloys grain boundaries precipitates as function of composition and heat treatment, noting effects on mechanical properties

14 p2118 A72-30589

Quenching rate and alloying element content effects on precipitation extent and corrosion resistance of Al-Cu alloys, discussing microstructure, chemical composition and mechanical properties

14 p2119 A72-30604

Gamma radiation effects on composite propellants stability, investigating polyurethane, polybutadiene, silicone and polyisoprene binders mechanical properties

14 p2144 A72-30760

Carboxy-terminated polybutadiene/ammonium perchlorate base solid propellants aging properties under long time storage conditions at 243-353 K, considering mechanical, dimensional and combustion properties

14 p2145 A72-30763

Atmospheric humidity, temperature, vibrational and static loads effects on composite and double base rocket propellants strength and safety characteristics

14 p2145 A72-30764

Case bonded solid rocket propellants mechanical strength characteristics determination by photoelastic stress measurements or viscoelastic calculation

14 p2145 A72-30765

Polyester bonded explosives mechanical and thermal properties, noting need for desensitizing against shock and friction effects

14 p2145 A72-30768

Ta-W-Hf alloy mechanical properties impairment from oxygen contamination, noting hafnium dioxide precipitate in reaction zone

14 p2121 A72-30769

Iron carbide single crystal growth texture due to anisotropy of interatomic interactions associated with oriented covalent Fe-C bonds

14 p2121 A72-30774

Binary Al alloys intermetallic phases effects on microcracks nucleation and propagation at 300 C in uniaxial tension, considering alloying elements influence on mechanical properties

14 p2124 A72-31036

Heat treated light alloy bar deformation, temperature and time factor effects macrostructure and mechanical properties

14 p2124 A72-31038

Composition, strength and plasticity of ultralight Mn-Li alloys with two-phase alpha-beta base

14 p2125 A72-31040

Li addition effects on Mg mechanical properties temperature dependence and notch sensitivity of binary Mg-Li alloys

14 p2125 A72-31041

Combined heat treatment and machining effects on Mg-Nd alloys structure and mechanical properties, noting strain hardening mechanism

14 p2125 A72-31042

Material constants for strain hardened polycrystalline metals calculated from mathematical model for plastic deformation

15 p2322 A72-31361

Mechanical properties of composite materials, discussing elastic deformation and failure modes

15 p2260 A72-31442

Composite materials for engineering component and structure design, considering mechanical properties and cost-effective performance

15 p2260 A72-31443

High temperature oxidation resistance and mechanical properties of Fe-Al-Cr alloys with Ti and Mo additions

15 p2253 A72-31520

Plastic deformations accumulation and breakdown initiation in notched steel specimens, discussing effects of mechanical properties, geometry and heat treatment

15 p2256 A72-31607

Mechanical properties of high temperature steels and alloys for gas turbine rotors, disks and blades

15 p2256 A72-31703

Ultrasonic sound influence on metal physical and mechanical characteristics, utilizing in testing and manufacturing procedures

15 p2275 A72-31832

Complex Ca lubricants strength, colloidal and mechanical stability and thermal hardening relationship to dispersion medium viscosity

16 p2413 A72-33172

High strength fine grain structural steels fracture characteristics from notch-bar impact and tensile tests, determining inclusions effect on mechanical properties

16 p2406 A72-33236

Tensile strength, toughness and corrosion resistance of dross aluminized carbon steel specimens under static, cyclic and impact loads

16 p2406 A72-33267

Porosity effect on mechanical properties, airtightness, corrosion resistance and moisture absorption of glass fiber reinforced plastics

16 p2414 A72-33270

Flame retardant glass reinforced thermoplastic polyester Celanex processing and performance, considering flammability, and electrical/mechanical properties

16 p2415 A72-33420

Strain rate and temperature effects on supersaturated Al-Cu-Mg solid solution mechanical properties, considering ultimate tensile strength and hardening

16 p2407 A72-33443

Cold rotatory forging and subsequent heating effects on microstructure, texture and mechanical properties of dispersion hardened Ni specimens obtained by hot extrusion

16 p2407 A72-33530

Graphic procedure for strength test data conversion from test temperature to design temperature based on equivalent damageability concept

16 p2411 A72-33847

Carbon fibers for composite materials reinforcement, discussing mechanical properties and economic factors

17 p2569 A72-34188

Crack opening displacement and the rate of fatigue crack growth

17 p2565 A72-34255

The effect of firing temperature on properties of natural steatite and pyrophyllite

17 p2569 A72-34666

Carbon fibre composites with ceramic and glass matrices. I - Discontinuous fibres

17 p2570 A72-34668

Carbon fibre composites with ceramic and glass matrices. II - Continuous fibres

17 p2570 A72-34669

Transition metal-modified matrix resins for composite materials

17 p2570 A72-34672

Effect of end attachment on the strength of fiber reinforced composite cylinders.

[SESA PAPER 1994A]

17 p2630 A72-34817

Re applications technology, discussing production methods, mechanical and physical properties, plasma spraying, annealing and alloying techniques

17 p2567 A72-34825

High-temperature resistant cobalt alloys

17 p2567 A72-35173

Stress analysis of axisymmetric solids with asymmetric properties

17 p2632 A72-35227

Composite materials technology utilization in structural design, considering stiffness, strength, weight, fatigue properties, adhesive joining and structural reliability

17 p2633 A72-35283

Russian book on metal alloys structure and properties covering structural changes in solid bodies, metals

atomic structure, diffusion, phase transformations and composite materials
17 p2568 A72-35446

Mechanical properties of carbon filament wound carbon matrix composite from tensile tests, noting reinforcement efficiency
17 p2573 A72-35669

Physical-mechanical properties of beryllium oxide and investigation of its electrical resistance under irradiation in a reactor
18 p2703 A72-36147

The stability of structure of physical mechanical properties of molybdenum and tungsten after irradiation and thermal influence
18 p2698 A72-36153

Studies of physical-mechanical properties of monocrystal molybdenum and tungsten and electrical characteristics of TIC /thermionic converter/
18 p2698 A72-36154

The strength of fibre composites.
18 p2703 A72-36268

Coupled glass-fibre/polypropylene composite - An initial evaluation.
18 p2703 A72-36269

Substitutional-interstitial interactions in bcc alloys.
18 p2699 A72-36396

Kinetics and annealing and mechanical properties of W chemical vapor deposition, discussing high temperature tests
18 p2656 A72-36398

Phase stability and mechanical properties of carbide and boride strengthened chromium-base alloys.
18 p2700 A72-36579

The structure and properties of thermomechanically treated beta-III titanium.
18 p2700 A72-36586

Techniques to curb static austenite recrystallization rate in martensitic sheet steel during high temperature thermomechanical treatment through minute Ti or Zr additions
18 p2701 A72-36702

Effects of work hardening on the structural hardening of T-A6V6E2 titanium alloy
18 p2702 A72-36706

Transition metals physical and mechanical properties, production, refining and vacuum processing techniques
18 p2696 A72-36840

Russian book - Automation of the monitoring and study of metals
19 p2795 A72-37299

Program-controlled machine for the investigation of mechanical properties of materials under a complex stress.
19 p2795 A72-37575

Characterization of commercial titanium powders.
19 p2815 A72-37595

Investigation of the effect of some surface-active media on the variations in strength characteristics of steel U8 in a high strength state
19 p2817 A72-37738

Investigation of the influence of surface treatment purity and procedure on the strength of the Kh18Ni10T and Kh16N6 steels and the AMG6 alloy at normal and low temperatures
19 p2819 A72-38016

Inflatable mandrels use to manufacture filament wound casings examined in terms of suitable mandrel materials and required mechanical properties
19 p2808 A72-38167

A method of improving the physico-mechanical properties of filled epoxy compounds by treatment in an ultrasonic field
19 p2823 A72-38184

Electronic control systems for industrial applications, discussing electrical and mechanical properties, circuit reliability and mechanical design features
19 p2782 A72-38314

Computerized finite element three dimensional stress analysis, taking into account mechanical and thermal stresses
19 p2878 A72-38649

Strength factors of fiber reinforced composites under tension, compression, shear, bending and plane stress
20 p2944 A72-38947

Super-alpha Ti alloy development, measuring physical and mechanical properties
20 p2936 A72-39205

Reinforced metals - Mechanical property considerations.
20 p2936 A72-39210

Structure-property relationships in polymeric materials.
20 p2944 A72-39212

Factors affecting acoustic emission response from materials.
20 p2924 A72-39279

Influence of boron on the structure and certain properties of electron-beam melted molybdenum
20 p2939 A72-39313

Boron and carbon fibers fabrication and properties for composite materials reinforcing elements, noting

strength and stiffness dependence on stress orientation
20 p2944 A72-39437

The fiber and filament reinforcement of plastic and brittle matrix materials
20 p2944 A72-39438

Production and properties of carbon fiber-reinforced aluminum
20 p2940 A72-39442

Mechanical properties of boron fiber reinforced aluminum matrix composite, describing experimental and control techniques
20 p2940 A72-39447

Mechanical and microstructural properties of steels for effective surface cementation, suggesting Mo and Cr optimal contents
20 p2941 A72-39576

Mechanical properties improvement of Al alloys for machine construction applications, suggesting Ti, Zr and Be additions optimal rate
20 p2941 A72-39577

An interpretation of radiation effects on mechanical properties of carbon fibres based on a 'sheath' and 'core' model of fibre structure.
20 p2944 A72-39794

Mechanical properties of Ti-Mo alloys at low temperatures
20 p2942 A72-39824

Installation for the simultaneous measurement of the functional properties of sliding contacts
20 p2928 A72-39936

Russian book - Handbook of aircraft materials.
21 p3072 A72-40459

Extension Seminar on High Temperature Strength of Metals, Kyoto, Japan, August 21, 1971, Preprints.
21 p3068 A72-41007

The properties and structures of a heat resistant 1Cr-Mo-V steel and alloy A-286 after long time exposures at elev. temps.
21 p3069 A72-41012

Mechanical properties of titanium strengthened by monodirectional molybdenum wires
21 p3069 A72-41354

Random function theory method for estimation of tensile, compressive and shear strength and elastic constants of monodirectional fiberglass reinforced plastics
21 p3073 A72-41708

Investigation of the influence of multiple-pass welding on the mechanical properties of welded joints of VT6s and VT14 titanium alloys
22 p3182 A72-41861

Influence of temperature on the mechanical properties of metallic compounds
22 p3191 A72-42804

Binary and multicomponent Re alloys with W, Mo, Ni, Co and Cr, noting elastic and strength properties for torsional suspension structures
22 p3191 A72-42805

Alloying and impurity effects on mechanical and recrystallization properties of Ta obtained by arc, electron beam and zone melting
22 p3191 A72-42809

Effect of rare earth metals on the structure and properties of aluminum and its alloys
22 p3192 A72-42818

Deformable magnesium alloys with scandium and yttrium
22 p3192 A72-42820

Mechanical and thermophysical properties of heat resistant Nb alloys, noting application for thermionic cathodes
22 p3192 A72-42821

Effect of the process of crystallization of the liquid phase under pressure on the properties of Silumin
22 p3192 A72-42959

Fabrication and properties of graphite fiber reinforced magnesium.
22 p3193 A72-43035

The limiting strength of worn metal surfaces.
22 p3194 A72-43039

Enhanced strengthening of a spinodal Fe-Ni-Cu alloy by martensitic transformation.
22 p3194 A72-43040

Determination of the mechanical properties of steels by short-time rupture in hydrogen at high temperatures and pressures
22 p3195 A72-43160

Physico-mechanical properties of fiber carbides
23 p3299 A72-43291

Fiber composite columns under compression.
23 p3344 A72-43494

Mechanical properties of titanium alloys with isomorphous beta-stabilizing elements
23 p3300 A72-43590

Mechanical properties of heat and corrosion resistant nonmagnetic Ni-Cr-Nb spring alloys with W addition tested in aggressive and nitric acid base media
23 p3300 A72-43595

Diffusive metal coatings stress-strain state effect on composite Mo material strength, ductility and creep characteristics
23 p3306 A72-43732

Material properties, metallurgy, production technology and operational factors effects on machinery structural strength
23 p3347 A72-43733

Heat resistant steels long time strength determination by graph-analytical time-temperature extrapolation
23 p3301 A72-43739

Brittle ceramic materials strength, showing porosity effect dependence on Weibull homogeneity parameter value
23 p3306 A72-43750

Heat resistant ZhS6K alloy precision and ground cast specimens, determining short and long term strength and fatigue
23 p3301 A72-43761

Increasing the boundary strength of electron-beam-melted cast molybdenum by vanadium microadditions
23 p3302 A72-43967

Influence of the cooling rate after sintering on the structure and properties of the ZhGr1.5D2.5 cermet
23 p3303 A72-44014

Investigation of the process of D16-alloy quenching in liquid nitrogen
23 p3294 A72-44095

Dislocation-substructure-strengthening and mechanical-thermal treatment of metals.
23 p3304 A72-44299

Cumulative damage stochastic models and distributions of strength of steels and graphite.
24 p3412 A72-44673

Book - A review of the science of fibre reinforced plastics.
24 p3417 A72-44674

Two-dimensional problem of elasticity theory for an anisotropic inhomogeneous wedge
24 p3459 A72-45263

Relationship between the strength properties and the phase composition of annealed titanium alloys
24 p3414 A72-45383

A study of the hardening of the subspinoidal alloy Fe-Ni-Al
24 p3415 A72-45395

Soil mechanical properties at the Apollo 14 site.
24 p3447 A72-45556

Polyfluoroethylene-based composite materials mechanical properties, discussing strengthening mechanism of filler additions
24 p3417 A72-45731

Mechanical properties of heat treated hardened high strength steel, investigating microstructure relationship to failure characteristics
24 p3416 A72-45734

Metallurgical treatment control reliability in machine part mechanical properties quality evaluation
24 p3416 A72-45735

Strength margin estimation in materials sustaining cumulative static and cyclic damage under thermocyclic loads
24 p3460 A72-45736

V and Al addition effects on mechanical properties of oxygen rich Ti alloys
24 p3416 A72-45745

Structural and strength characteristics of carbon materials, considering composites preparation and applications
24 p3418 A72-45748

Automatic testing machine for mechanical properties of metals under static loading
24 p3389 A72-45751

Mechanical properties and structural strength evaluation methods for metallic materials at low temperatures, describing hydraulic and pneumatic testing facilities
24 p3416 A72-45756

Supermolecular structure artificial defects and bond strength influence on mechanical strength of pyrographite
24 p3418 A72-45761

Chemically etched notches effect on Al-Mg alloy mechanical properties
24 p3417 A72-45764

MECHANICAL RESONANCE
U RESONANT VIBRATION
MECHANICAL SHOCK
NT HYDRAULIC SHOCK

Averaging method for systems with shocks, assessing exact and approximate solutions discrepancy over finite time intervals
08 p1206 A72-20967

Low temperature shock effects on lunar glass spherules from two beam interferometry, discussing mechanical and thermal causes of fragmentation
14 p2149 A72-30266

New mechanical device for producing traumatic shock in dogs - Circulatory and respiratory responses.
22 p3142 A72-42490

MECHANICAL TWINNING
Ni-NiNb intermetallic unidirectional eutectic alloy crystal structure and high temperature behavior, considering mechanical twinning relationship to strain hardening and ductility
05 p0677 A72-17108

- Stress-strain behavior of steel under elastic compression at 4.2 K, observing discontinuous twinning
07 p1020 A72-20413
- Various restraint dislocation distributions effect on mechanical twinning behavior in purified Nb single crystals
10 p1497 A72-24824
- Slip and mechanical twinning in nickel-nickel niobide directionally solidified eutectic alloy, showing variation with temperature of stress-strain curves
11 p1667 A72-26935
- Mechanical twins formation process, distinguishing between deformation and strain and between crystal structure and lattice
20 p2961 A72-39991
- MECHANICS [PHYSICS]**
- Nonlinear mechanics and stability - Conference, Rome, February 1970
02 p0251 A72-11492
- Applied mechanics - Conference, University of Calgary, Canada, May 1971
02 p0292 A72-12001
- Book on applied mechanics covering hydrodynamics, biomechanics, transonic and hypersonic shock structures, random vibrations, plasticity, viscoplasticity, etc
06 p0896 A72-17958
- Nonlinear oscillations in mechanics - Conference, Kiev, U.S.S.R., August 1969
06 p0849 A72-18692
- Dimensional analysis proportionalities method parallel to formal similitude method for accelerative mechanics problems
10 p1503 A72-23919
- Modeling process for mathematical representation of mechanical problems, deriving design information in digital or graphic form
13 p2000 A72-28450
- Axiomatic development of mechanics from geometrically formulated kinematics to statics of rigid bodies and systems, using virtual rate of work and reaction principles
13 p2000 A72-28477
- Mechanics fundamentals in aerodynamical aircraft analysis, noting force concept and Newton theory
14 p2073 A72-30817
- Russian book on averaging method in nonlinear mechanics covering algorithms and schemes based on variables change, asymptotic methods and applications
15 p2273 A72-31274
- Applied mathematics and mechanics - Conference, Mannheim, Germany, April 1971
15 p2323 A72-31451
- Standardization of positive directions for parameters in materials strength theory, noting systems of coordinates, moments, forces, angles and stresses
15 p2325 A72-31502
- Inertial crosscouplings effect on orientation process dynamics of solid body investigated by nonlinear mechanics, noting centrifugal moments of inertia effects
15 p2275 A72-31730
- Papers on elasticity and thermoelasticity covering contact problems, stress effects on elastic wave propagation velocity, self excited thermal waves, diffraction, nonlinear thermoelasticity, etc
15 p2329 A72-32280
- Theory of nonlinear viscoelasticity and its applications
17 p2631 A72-35109
- Variational and probabilistic methods for multiphase media, noting applications in electrodynamics, nonlinear plasticity and mechanics
17 p2632 A72-35110
- Southeastern Conference on Theoretical and Applied Mechanics, 5th, North Carolina State University and Duke University, Raleigh and Durham, N.C., April 16, 17, 1970, Proceedings.
18 p2736 A72-37051
- Russian book - Problems of applied mathematics and mechanics
19 p2784 A72-37376
- Optical holography and holographic interferometry applications in solid mechanics, considering surface physics, bomb breakup, transverse wave propagation, nondestructive testing and vibration analysis
19 p2797 A72-37603
- Japan National Congress for Applied Mechanics, 20th, Tokyo, Japan, October 23, 24, 1970, Proceedings.
21 p3121 A72-41226
- Kepler second law based moment of gyration concept application to spacecraft and missiles mechanics and kinematics, proposing Skylab weightless environment experiment for validation [SAWE PAPER 931]
23 p3342 A72-43471
- Mechanical systems generalization using multilinear transformations and multiple index system flow formalism
24 p3424 A72-44624
- MECHANIZATION**
- Hybrid mechanical-electrical mechanizing techniques for aircraft flight control systems
17 p2493 A72-35576

MEDIA

- NT ANISOTROPIC FLUIDS
NT ANISOTROPIC MEDIA
NT ELASTIC MEDIA
NT INTERGALACTIC MEDIA
NT INTERPLANETARY DUST
NT INTERPLANETARY GAS
NT INTERPLANETARY MEDIUM
NT METEOROID DUST CLOUDS

MEDICAL ELECTRONICS

- Picoscale blood diagnostic device for red and white cell count, noting piston principle electronic operation
09 p1272 A72-23257
- Electromagnetic velocity and flow measurements techniques application to cardiovascular patients, discussing utilization problems
09 p1272 A72-23275

- Biological cell sorting by differential fluorescence generated electric signals via laser beam illuminated liquid stream
09 p1273 A72-23403

- NASA reliability and quality assurance methodology to improve hospital biomedical equipment, using space electric rocket test example
12 p1814 A72-27960

- Digital evoked brain potential detector using multichannel amplitude analyzers
13 p1908 A72-28645

- Considerations in the design of an automatic visual field tester.
18 p2654 A72-37013

- Needle type solid state detectors for in vivo measurement of tracer activity.
18 p2655 A72-37194

- 'VI-like' and 'AVF-like' leads for continuous electrocardiographic monitoring.
19 p2759 A72-37244

- An automatic measuring and recording system for clinical electro-oculography.
19 p2759 A72-37400

- Implantable blood pressure telemetry system.
19 p2762 A72-38824

- Techniques and procedure for differential ballistoscillography of extremities.
20 p2897 A72-39325

- Radiorespirometry in the case of work and sports activities
22 p3149 A72-42071

- Carotid displacement pulse first time derivative recording as noninvasive technique for heart function assessment
24 p3370 A72-44561

MEDICAL EQUIPMENT

- NT ARTIFICIAL HEART VALVES
NT CARDIOTACHOMETERS
NT PROSTHETIC DEVICES
NT RESPIRATORS

- Medical equipment advancements through NASA sponsored aerospace research program, describing prosthetic urethral valve, ear oximeter, radiation dosimeter and electromyographic muscle trainer
06 p0765 A72-18616

- Cardiac catheterization practice review, discussing pediatric and adult cardiology, risk reduction, diagnostic aids, relationship to radiology and laboratory equipment complexity
07 p0923 A72-20553

- Therapeutic electromedical equipment hazards due to electromagnetic interaction, considering implantation and simulation of human body
15 p2191 A72-32572

MEDICAL PERSONNEL

- NT PHYSICIANS

- Civil aeronautics environment relation to psychiatrists and medical psychologists treatment of air navigation personnel, discussing chemotherapeutic and psychotherapeutic treatment administration problems
07 p0927 A72-19243

MEDICAL PHENOMENA

- NT PHENOMENOLOGY

- Permanent flight unfitness attributable to air service, noting orthopedic traumatic sequelae, cardiovascular illnesses, psychological and ophthalmological causes
08 p1125 A72-21273

- Diving operations medical aspects significance for manned planetary surface exploration in high density atmospheres, considering protective clothing, breathing apparatus and gas mixtures, etc
12 p1769 A72-27415

- Statistical survey of barosinusitis incidence in U.S. Navy flying personnel during altitude chamber training, discussing diagnostic methods and clinical management
12 p1765 A72-28274

- USAF aircraft accidents/incidents involving aircrewmembers with medical waiver on various visual, cardiopulmonary and other chronic pathological and psychiatric conditions
12 p1776 A72-28315

- Review of aeromedical records for grounding USAF flying personnel during 1956-1970, noting increased age factor effect
12 p1776 A72-28316

MEDICAL SCIENCE

- NT ANESTHESIOLOGY
NT ENDOCRINOLOGY
NT HISTOLOGY
NT IMMUNOLOGY
NT NEUROLOGY
NT OTOLARYNGOLOGY
NT PATHOLOGY
NT PHENOMENOLOGY
NT PSYCHIATRY
NT RADIATION MEDICINE
NT RADIOBIOLOGY
NT RADIOLOGY
NT RADIOPATHOLOGY
NT SOCIAL PSYCHIATRY
NT SYMPTOMOLOGY
NT TOOTH DISEASES
NT UROLOGY

- Medical primatology - Conference, New York, September 1969
03 p0313 A72-13068

- Biotelemetry applications in medicine, animal experiments and ecology, including ergonometics, internal bleeding detection, fetal monitoring, animal brain implantations, animal movement tracking, etc
07 p0931 A72-19916

- Collaboration of World Health Organization and various international astronomical organizations for space technology applications to man-environment relationships and medical and communication sciences
07 p0933 A72-20300

- Clinical observations as a research method in physiology
17 p2504 A72-35017

- Pigs role as ideal experimental animal in human biomedical research, discussing investigations to emphasize similarities
18 p2649 A72-36440

- Russian book - Theory and practice of aviation medicine
19 p2760 A72-37447

MEDICAL SERVICES

- NASA sponsored medical R and D programs for space applications, stressing benefits to earthbound medical services
06 p0769 A72-18626

- Civil aviation physician duties for airline personnel and passenger benefit, discussing medical advice, health precautions, first aid training, etc
08 p1125 A72-21269

- A model corporate pilot physical program.
20 p2897 A72-39746

- Airport medical design guide /with comment on certain operational matters/.
22 p3150 A72-42500

- Application of planetary quarantine methodology and spacecraft sterilization technology to improved health care delivery.
24 p3375 A72-45148

MEDITERRANEAN SEA

- Mars surface features Schiaparelli nomenclature from Mediterranean Sea area classical geography
04 p0569 A72-14500

- Numerical wind profiles calculation over Mediterranean based on satellite photograph sequences of clouds
15 p2220 A72-31235

MEDIUM SCALE INTEGRATION

- Medium scale integration /MSI/ modules for arithmetic section in small, medium and process computers, emphasizing carry-lookahead procedure
13 p1926 A72-30053

- Techniques for control of long-term reliability of complex integrated circuits. II - A technique for the prediction of failure rates for MSI and LSI devices.
17 p2528 A72-34687

- Modularized digital controller for closed loop systems using MOS, MSI and LSI components
17 p2521 A72-34703

- High performance 16-bit computer organization.
17 p2523 A72-35580

MEETINGS**U CONFERENCES**

- MEISSNER EFFECT
U DIAMAGNETISM
U SUPERCONDUCTIVITY

MELLIN TRANSFORMS

- Direct method for dual and triple integral equations involving inverse Mellin transforms in potential mixed boundary value problems
01 p0094 A72-11390

- Mellin transforms application to two dimensional elasticity problem for anisotropic wedge with continuous mechanical characteristics under concentrated force
08 p1243 A72-21238

- Mellin transforms for finite elastic disk radial crack stress intensity factor and energy formulae in terms of Fredholm equation solution, considering constant loading case
11 p1738 A72-26724

- Inverse filtering for linear shift-variant imaging systems.
18 p2658 A72-36259

The torsion of a circular cylinder containing a symmetric array of edge cracks. 23 p3350 A72-44048

MELTING

NT ARC MELTING
NT FUSION [MELTING]
NT VACUUM MELTING

Melting atmosphere, atomizing media and consolidation techniques effects on Co base alloy powder products physical properties 02 p0240 A72-11436

Melting effect on recrystallization of overheated tempered steel, discussing rectification under conditions favoring formation of silicon-oxygen compounds 03 p0376 A72-14017

Hypersonic melting ablation waves simulation near stagnation region by frozen oil models [AIAA PAPER 72-92] 05 p0750 A72-16977

Gas content determination in metals by melting and vaporizing measured microvolumes using laser microprobe and magnetic mass spectrometer 07 p1006 A72-19549

Nonferrous metals melting, discussing solid and gaseous impurities removal, halide function and grain and Al-Si eutectic refinement method 07 p0999 A72-20570

BiTe crystal critical growth rate calculation based on theory for diffusional supercooling of melt with excess Te 08 p1217 A72-21338

Work hardening and recrystallization grain structure of sintered and electron bombardment melted Ta after annealing 11 p1644 A72-26839

Powder metallurgy versus melting and casting of high temperature alloys, tool steels and specialty alloys 11 p1646 A72-26869

Russian papers on physical chemistry of surface effects in melts covering binary and multicomponent alloys, silicates, oxides and salts at high temperatures 15 p2253 A72-31220

Metal melting heat relationship to diffusion activation energy with vacancy mechanism equal numerically to crystal internal energy maximum change 15 p2259 A72-32691

X-ray diffraction studies on liquids at very high pressures along the melting curve. I, II. 21 p3084 A72-40558

Influence of boron on the structure and properties of electron-beam melted molybdenum 24 p3414 A72-45380

Boron and carbon contents effect on elastic properties strength and ductility of electron beam melted Mo-B alloys 24 p3414 A72-45381

MELTING POINTS

Ta and Nb addition effects on W solid solution strengthening, determining W-Nb-Ta alloys phase diagram and melting point 03 p0375 A72-13943

Gamma irradiation effects on temperature of reversible solid-to-liquid phase transformation in Al 08 p1185 A72-21075

Powder materials heating and melting temperatures calculation in free turbulent nitrogen and argon plasma jets 08 p1181 A72-22098

Mg alloys compositions, melting points, mechanical properties and applications 09 p1327 A72-22479

Oxidation and substructural effects on low stress creep of Al near melting point 09 p1331 A72-23507

Melting points and phase diagrams for various tungsten oxide systems, noting alkaline earth and transition and trivalent metal tungstates 10 p1497 A72-24731

Surface patterns from ablating, melting and flowing materials in supersonic flow of wind tunnel, rocket motor and flight test environments, comparing with theory [AIAA PAPER 72-313] 11 p1743 A72-25247

Liquid Rb and Cs density and thermal expansion measurements near fusion point, discussing temperature dependence and gamma ray irradiation method 11 p1746 A72-26237

High melting point alloy and metal powder production by vacuum atomization, using rotary vane and electron beam melting techniques 11 p1645 A72-26860

Thermoplastic materials casting procedures to mold high melting point metal compound powders 11 p1645 A72-26861

Hf binary systems phase diagrams, noting components effect on melting point, polymorphous transformations and mutual solubility 14 p2122 A72-30979

Dynamic elastic moduli of diffusion saturated high melting point nitrides, carbides and borides of Ti, Zr, Nb, W, Mo and Ta 15 p2252 A72-31199

Graphite wetting with liquid V, Nb and Mo as function of metal melting point and sample temperature 15 p2243 A72-31223

Chemical inhomogeneity of high melting metals and alloys of Ti, Zr, Nb and Cr from radio isotopic and nuclear emission studies 15 p2255 A72-31576

Measurement of melting point and electrical resistivity /above 3600 K/ of tungsten by a pulse heating method. 20 p2941 A72-39722

Surface tension, density, and volume change on melting of Al₂O₃ systems, Cr₂O₃, and Sm₂O₃. 24 p3417 A72-44925

MEMBRANE ANALOGY

U MEMBRANE STRUCTURES
U STRUCTURAL ANALYSIS

MEMBRANE STRUCTURES

NT SKIN [STRUCTURAL MEMBER]

Free radicals participation in cell membrane biopotential generation mechanism, comparing properties of protein molecules with semiconductors 02 p0169 A72-12348

Axisymmetric circular membranes large deflections, solving nonlinear partial differential equations by iterative method in conjunction with finite difference approximations 02 p0296 A72-12526

Prismatic shells membrane and bending fields induced by concentrated forces, applying Fourier analysis to semiinfinite plates geometry 02 p0296 A72-12527

Beam theory application to cylindrical and conical shells bending, deriving flexibility functions from membrane equations 02 p0296 A72-12529

Stability control of rotating circular plates with edge slots and membrane stresses by finite element method [ASME PAPER 71-WA/AUT-2] 05 p0733 A72-15951

Forced vibration and mechanical impedance of damped circular and annular membranes under central mass loads 05 p0739 A72-16615

Teflon diffusion membrane for in vivo blood and intramyocardial tissue gas tension measurement by mass spectroscopy without chemically bonded heparin surface 08 p1124 A72-20901

Natural oscillation frequencies of piecewise homogeneous L-shaped membranes, determining eigenvalues of second order elliptical differential operator 08 p1241 A72-20903

Membrane and bending moment stresses distribution at elliptical hole in circular cylindrical shell, solving boundary value problems 08 p1243 A72-21234

Elastic-plastic deformation of thin membrane shells 08 p1244 A72-21290

Myocardium excitation-contraction mechanism in heart regulation, discussing surface membrane structure and cell action potential 09 p1264 A72-22222

Creep ratchetting deformation and rupture damage from thermal transient stress cycle and constant membrane force under high temperature metal creep conditions 09 p1406 A72-23197

Artificial heart-lungs model with contractile polymer membrane as synthetic muscles to react with gases and liquids, discussing design features 10 p1431 A72-24640

Book on continuous elements dynamics covering membrane, torsional, string and elastic beam vibration, four pole techniques, periodic forced motion and surface waves 10 p1557 A72-24674

Intermediate length open noncircular cylindrical shells analysis based on Vlasov semimembrane theory 10 p1559 A72-24992

Shearing stresses in rod under torsion, using Prandtl membrane analogy and moire interference fringes 13 p2053 A72-28397

Ionic and hydrophobic interactions effects on Micrococcus lysodeikticus membrane stabilization process 14 p2075 A72-30595

Transverse impacts of hard cones on elastic membranes for various apex angles, using high speed photography 15 p2323 A72-31445

Nonlinear stress-strain-curvature problem applied to noncircular cylindrical membrane shell under lateral pressure 16 p2464 A72-32917

Membrane and bending stress analysis for thin circular cylindrical shells with elliptic hole 16 p2464 A72-32918

Longitudinal and transverse waves propagation and decay in elastic membranes with allowance for coupling effects, using Hadamard method 16 p2465 A72-32983

Strain energy methods for stability of finitely deformed elastic membranes under conservative loading 16 p2465 A72-33002

Singular perturbation methods for deflections, frequencies and eigenmodes of statically loaded or freely vibrating circular or annular membrane 16 p2467 A72-33106

Three dimensional photoelastic analysis of edge loaded ring reinforced rotating shells with zero bending, assuming pure membrane stress field 18 p2733 A72-36365

The radiation of sound from vibrating composite membranes. 18 p2711 A72-36757

Stress analysis of shell junctions fabricated by the filament-winding method. 19 p2877 A72-38169

Spherelike deformations of a balloon. 19 p2878 A72-38716

Experiments concerning the contact surface in a membrane shock tube 20 p2911 A72-39017

The long fluid storage bag - A contact problem for a closed membrane. 20 p2980 A72-39691

On the asymptotically spherical deformations of arbitrary membranes of revolution fixed along an edge and inflated by large pressures - A nonlinear boundary layer phenomenon. 21 p3118 A72-40840

Nonlinear equilibrium equations for hinged flat circular and spherical membranes under large axisymmetric elastic deformations due to internal pressure 21 p3125 A72-41516

Hydrodynamic forces acting on rigid disk and circular membrane vibrating in ideal incompressible fluid, noting dependence on phase shift between vibration modes 21 p3126 A72-41552

Large deflections of flat arbitrary membranes. 22 p3235 A72-42604

A simple formula for the maximum stress in a twisted angle or channel. 22 p3240 A72-42894

Lower and upper bounds for the lowest characteristic value of the elastically supported membrane 23 p3347 A72-43717

The coupled transverse vibrations of a spinning membrane disk with a central hub. 23 p3355 A72-44367

Review and forecast of electron microscope studies of membrane systems in terms of fundamental problems of biomedical research and molecular biology 24 p3371 A72-44869

MEMBRANE THEORY

U MEMBRANE STRUCTURES
U STRUCTURAL ANALYSIS

MEMBRANES

NT CHOROID MEMBRANES

NT ION EXCHANGE MEMBRANE ELECTROLYTES

NT MEMBRANE STRUCTURES

NT SKIN [STRUCTURAL MEMBER]

Molecular evolution of biological membrane from lipid film to lipoprotein particle assembly, using bacterial biochemistry 04 p0469 A72-14786

Primitive earth model of ion selective enzymatic asymmetric synthetic membrane for accelerated nutrients and metabolites transfer studies 04 p0469 A72-14787

Ion selective accumulation model of carbohydrates diffusing through artificial polymer membranes, relating prebiological systems to catalytic microsystems 04 p0469 A72-14788

Origin and development of plasma membrane derived invaginations in Vinca rosea, observing endocytosis in plant cells 05 p0616 A72-15810

Hydrodynamic stability small perturbation theory, considering potential flow in contact with flexible membrane 07 p0969 A72-20067

Structure, function and origin of biological membranes, considering related surface phenomena 08 p1119 A72-22008

Oscillating membrane pressure gage for direct electrical measurements of fast and large pressure variations, noting insensitivity to interference 11 p1636 A72-26700

Neuron networks dynamic behavior in terms of linear differential equations for membrane potential changes and neuron threshold 12 p1772 A72-27925

Qualitative microscopic model for biologic postsynaptic membrane with tunneling chemical bonds, noting selective ionic conductivity as function of electric field 13 p1909 A72-28769

Numerical analytical determination of natural vibration frequencies for membrane elastically clamped along portion of contour, using method of summary representations 13 p2004 A72-29078

Radioprotectants /mexamine and cystamine/ effects on histo-hematic barrier permeability in rats under hypokinetic conditions

13 p1904 A72-29308

Lamellar structure and rhodopsin location in bleached and unbleached rod photoreceptor membranes of dark adapted frog retinas by X ray diffraction study

15 p2186 A72-32199

Hemoglobin-facilitated diffusion of oxygen - Interfacial and thickness effects.

18 p2650 A72-36569

Studies of the electron transport chain of extremely halophilic bacteria. VII - Solubilization properties of menadiene reductase.

19 p2755 A72-37649

Study of the conductivity of the motor neuron membrane during supraspinal stimulation

21 p2999 A72-40585

Unsteady state description of living corneal mass transport modes, elucidating cornea thickness control mechanism

21 p3001 A72-40912

The effect of membrane parameters on the properties of the nerve impulse.

22 p3140 A72-41936

MEMORY

Selective attention and short term memory encoding, using tachistoscopic visual display arrangements of capital letters

02 p0166 A72-11549

Human immediate memory adaptation to speed stress, discussing response time and performance accuracy relationship to stimuli complexity and input speed

06 p0766 A72-17716

Short-time memory and electrographic effective and trace processes relationship from visual and Rolandian cortical regions activity and Tarkhanov galvanocutaneous reaction

06 p0764 A72-17993

Hippocampus neuron reactions and memory function realization with incoming information and stored imprints comparison by brain

08 p1122 A72-22191

Review of biology and biochemistry of memory, suggesting molecular level mechanism of cerebral information processing

10 p1424 A72-23925

Sleep deprivation effects relation to work duration, time of day, circadian rhythm, memory function, task performance, environmental factors, drug use and age

11 p1580 A72-26678

Object code storage in the static portion of a short-term memory

19 p2759 A72-37423

Operative memory mechanism as visual system neuron chain storage of stimuli from image recognition time measurements

20 p2891 A72-38936

Characteristics of certain parameters of memory for visual signals in lower monkeys

21 p3001 A72-40804

Visual experience as a determinant of the response characteristics of cortical receptive fields in cats.

21 p3003 A72-41461

Some effects of cognitive similarity on proactive and retroactive interference in short-term memory.

22 p3142 A72-42548

Content and time aspects of short and long term memory operation theories, relating attention and memory spans

24 p3373 A72-45243

MEMORY STORAGE UNITS

U COMPUTER STORAGE DEVICES

U CORE STORAGE

MENISCI

Abastumani Observatory 70 cm meniscus telescope, determining performance from primary focus field data

03 p0359 A72-13498

MENTAL HEALTH

Psychiatric preventive intervention in emotional crisis situations during patients aeromedical evacuation and transportation, discussing personnel shortage

10 p1429 A72-23743

MENTAL PERFORMANCE

Soyuz 9 flight crew physiological data, discussing mental and physical performance and adaptation and readaptation to space-earth environments

01 p0020 A72-10933

Skill acquisition in performance of three phase code transformation task

01 p0021 A72-11193

Time sharing three phase code transformation multitask effects on sustained performance

01 p0021 A72-11194

Human mental and psychomotor performance measurements in compressed oxygen-helium atmosphere pressure chamber for dive between 100 and 1500 feet

02 p0166 A72-11701

Inert gas narcosis under hyperbaric conditions relationship to mental performance and auditory and visual evoked responses in man

02 p0166 A72-11705

A-1144

Human mental working capacity estimation relation to functional state, discussing brain performance tests

03 p0316 A72-13721

Operant conditioning for producing gross motor responses, discussing application to physical medicine and rehabilitation with mentally retarded Downs syndrome children

04 p0478 A72-14706

Short and long term mental and physical work effects on central nervous system and motor apparatus in young people

04 p0474 A72-15230

Time shortage as stress factor affecting mental activity of operator in man-flying vehicle system, discussing control signal handling efficiency

05 p0622 A72-16638

Psycho-physical theory of human mind, discussing molecular biological processes of neuron recording in terms of quantum mechanics

06 p0769 A72-18191

Mental rehearsal and physical practice relation to learning rate for rotary pursuit tracking skill acquisition

07 p0925 A72-18801

Sex differences of chronic effect of environmental stress on blood pressure and information processing in rats, observing neurotic hypertonic blood pressure irregularity

07 p0925 A72-20660

Operator mental processes during ATC task performance, discussing work load effect, mental representation and operator algorithm definition

09 p1270 A72-23129

Acceptable load standards in ATC tasks, defining moments of conscious brain control as mental load measure

09 p1271 A72-23139

Ergonomic simulators for testing individual mental working capacity, using stress-strain and fatigue relation

09 p1272 A72-23140

Visual search model from perceptual theory, animal studies and search data, discussing selection, inspection and naming single cued letters in visual array

09 p1270 A72-23647

Mental performance tests in sleep deprived subjects for indication of recuperative function of slow wave and REM sleep stages

11 p1580 A72-26682

Cumulative partial sleep deprivation effects on human performance in auditory vigilance, routine addition and running digit span tests, observing circadian rhythms

11 p1581 A72-26683

Project Pegasus vigilance tasks for mental performance aspects of time zone change effects on human circadian rhythms

11 p1589 A72-26695

Time zone transition induced circadian rhythm disturbance effect on military personnel mental and physiological performance

11 p1589 A72-26696

Vigilance effects for noise or vibration stimuli duration judgment task performed with or without simultaneous mental arithmetic task

14 p2080 A72-30964

Noise and vibration stress combined effects on human mental performance as function of time of day, taking into account circadian rhythm factor

14 p2081 A72-31083

Frontal cerebrum region and elementary mental activity

18 p2649 A72-36400

Manipulation of projected afterimages by means of the physiological theory imposed on the observer.

18 p2654 A72-36920

Mental and physical workload measure and differentiation in man machine systems

21 p3012 A72-41427

The function of external respiration in mental activity

22 p3150 A72-42284

Some data on the interrelations of conscious and unconscious reactions

23 p3257 A72-44076

Involuntary eye movements during the performance of mental tasks

23 p3260 A72-44077

Content and time aspects of short and long term memory operation theories, relating attention and memory spans

24 p3373 A72-45243

Learning and solving complex problems of reasoning - A test-theoretical investigation of the complexity of compound problems of predictive logic

24 p3373 A72-45244

MENTAL STRESS

U STRESS [PSYCHOLOGY]

MERCATOR PROJECTION

Polar navigation with transverse mercator technique for aircraft using secant geared ground position indicators

01 p0097 A72-10181

MERCURY [METAL]

NT MERCURY VAPOR

Excited Hg atom and electron concentration measurement behind shock front in nonstationary plasma by continuous displacement recording of interference bands

03 p0357 A72-13374

Fast acting nonmechanical self healing mercury fuse for high current circuit protection

03 p0335 A72-14203

Temperature pulsation spectra of turbulent mercury flow in horizontal pipe at various Reynolds numbers, showing dependence on magnetic field

07 p1100 A72-19882

Gaseous or solid particle Hg from fumaroles, suggesting natural and industrial sources of Hawaiian air pollution

09 p1305 A72-23648

Acoustic measurement of solid-liquid interface motion and solidification during freezing of Hg and paraffins

10 p1563 A72-25044

Optical radiation from Hg bombardment ion thrusters downstream regions due to excited atoms radiative decay, examining exhaust interference with star tracker

[AIAA PAPER 72-441]

11 p1707 A72-26182

Spacecraft thermal control coating damage by energetic Hg ion bombardment, using absorbance measurements

[AIAA PAPER 72-445]

11 p1746 A72-26183

Computer aided thermomechanical design of mercury bombardment ion thrusters, involving heat transfer, vibration and stress analysis

[AIAA PAPER 72-431]

12 p1860 A72-27420

Argon and mercury ion engines operation, performance and control, evaluating safety and ease of handling from laboratory test data

13 p2026 A72-28931

Energetic Hg ion bombardment erosive and chemical effects on spacecraft surfaces downstream of electrostatic rockets

[AIAA PAPER 72-446]

13 p1983 A72-28944

Combined hydrostatic suspension Hg cushion effects on gyrocompass response precision during irregular roll of platform

13 p1961 A72-30022

Mercury embrittlement of age-hardened Cu-1.9 wt pct cobalt and Cu-3.6 wt pct titanium.

20 p2938 A72-39296

A study of the liquid-vapor phase change of mercury based on irreversible thermodynamics.

[ASME PAPER 72-HT-A]

20 p2983 A72-39481

MERCURY [PLANET]

Computerized series solution of relativistic motion of planet Mercury for Schwarzschild and isotropic coordinates

02 p0260 A72-12306

Mariner Venus/Mercury 1973 flyby mission imaging experiment, discussing mission constraints, objectives and use of real time transmission vidicon camera and high resolution UV photography

04 p0568 A72-14494

Mercury isophotometric measurements in white and H alpha light during transit across sun on 9 May 1970

04 p0573 A72-14904

Mercury radar scattering properties, producing Fourier power spectrum from echo signals

06 p0880 A72-17864

Mercury trajectory across solar disk plotted by telephoto lens cameras, for determining position angles, disk contact times and relative angular velocity

06 p0882 A72-17934

Quantum and classical gravitation theory Mercury perihelion motion dependence on fourth order potential in scalar and Dirac fields

07 p1084 A72-20689

Relativistic explanation for excess motion of Mercury perihelion in terms of solar oblateness and interior rotation mechanism

[AD-745666]

11 p1715 A72-25350

Solar electric low thrust unmanned Mercury orbiter missions, considering spacecraft subsystems and ballistic and swingby trajectories

[AIAA PAPER 72-425]

11 p1721 A72-26170

Mercury topography and scattering characteristics from 3.8 cm radar observations, comparing to Mars and Venus

12 p1865 A72-27098

Contact time determinations during 9 May 1970 Mercury passage across solar disk

14 p2153 A72-30498

Unipolar steady electromagnetic bow shock interaction of Mercury with solar wind, calculating planetary surface temperature

15 p2303 A72-31305

Mercury magnitude determination near superior conjunction with aid of coronagraph photography and photometric calibration

15 p2312 A72-32090

Mercury diameter measurement by photoelectric Hertzprung method during transit on 9 May 1970

15 p2312 A72-32091

Mercury perihelion advance determination from radar echo delays measurement

16 p2453 A72-33190

Mercury trajectory across solar disk plotted by telephoto lens cameras to determine position angles, disk contact times and relative angular velocity
18 p2730 A72-37158

Photospheric faculae brightness influence on solar gravitational oblateness determination, considering criticism of Dicke-Goldenberg argument on Mercury excess perihelion motion
19 p2855 A72-37239

Right ascensions of the sun, Mercury, and Venus observed with the transit instrument at Nikolaev during 1966-1967
19 p2861 A72-37982

Declinations of the sun, Mercury, and Venus in the FK4 system as deduced from observations with the vertical circle of the Nikolaev Observatory during 1966-1967
19 p2861 A72-37983

Contact time determinations during 9 May 1970
Mercury passage across solar disk
19 p2864 A72-38327

Mission design and navigation for a 1977-1978 Venus Swingby/Mercury Orbiter.
[AIAA PAPER 72-941]
21 p3113 A72-41577

Determination of parameters related to the interior of Mercury.
24 p3436 A72-44696

Low thrust constant acceleration trajectories for a Mercury orbit.
24 p3441 A72-45208

MERCURY ALLOYS
Cadmium mercury telluride photovoltaic cell features, noting gigahertz range frequency response, heterodyne sensitivity, operating temperature and nonstoichiometric p-n junction preparation
07 p1003 A72-19224

MERCURY ARCS
Dense low temperature Ar and Hg plasmas, observing correlation between electrical conductivity and optical emission
10 p1517 A72-23835

Hg flow and hollow cathode temperature effects on ion thruster neutralizer stability and lifetime capability, using bell jar tests
[AIAA PAPER 72-422]
13 p2026 A72-28937

Hg fed hollow cathode ion thruster thermal and plasma heating characteristics, using Wiener-Kalman filtered temperature measurements
[AIAA PAPER 72-476]
13 p2027 A72-28947

Influence of single-pulse emission from a ruby laser on the plasma of a mercury vapor lamp
22 p3184 A72-42105

MERCURY COMPOUNDS
NT MERCURY TELLURIDES
Phase matched nonlinear frequency conversion of laser light in tetragonal mercury thiocyanate complex crystals
12 p1854 A72-27549

Mercuric chloride, bromide and iodide gas phase UV absorption spectra, discussing correlation with intermolecular charge transfer transitions
16 p2360 A72-32926

Venus high albedo, discussing compound reflecting layer and liquid Hg cloud models
24 p3436 A72-44692

MERCURY FLIGHTS
Guidance and navigation techniques for a solar electric Mercury orbiter.
[AIAA PAPER 72-917]
21 p3082 A72-41562

MERCURY LAMPS
Laser and mercury lamp outputs spatial coherence measurement by speckle patterns produced with ground glass as random inhomogeneous medium
17 p2565 A72-35752

MERCURY SPACECRAFT
Cruise guidance, trajectory and navigation analysis for solar electric Mercury orbiter, considering engine performance, thrust and terminal errors
[AIAA PAPER 72-427]
11 p1684 A72-26172

MERCURY TELLURIDES
L_f noise measurements of mercury telluride and Cd-Hg-Te semiconducting thin films using vacuum tube preamplifier and step-up transformer
02 p0268 A72-11523

Hall and resistance measurements on single crystal Hg-Te-In-Te alloy systems for high pressure phases in terms of conduction state, band structure and impurity effects
19 p2844 A72-37464

Mercury-cadmium telluride photoconductive detectors array for S-192 multispectral scanner for Skylab earth scanning experiments
23 p3288 A72-43879

Mercury-cadmium telluride multispectral photoconductive detectors, discussing fabrication techniques and performance characteristics
23 p3288 A72-43880

Mercury-cadmium telluride photodiode detectors for near IR laser receivers, discussing time response and I-V characteristics as function of temperature
23 p3296 A72-43881

MERCURY VAPOR
Mercury vapor physicochemical processes kinematics in shock tube, determining electron gas energy balance equations
03 p0395 A72-13572

Thin electrostatically self focusing electron streams in mercury vapor, analyzing energy distributions of ions and electrons ejected radially from beam
04 p0554 A72-14407

Mercury electron bombardment ion thrusters research program, discussing mission requirements, size, propulsion type and beam current range
04 p0565 A72-14434

Hg vapor condensation on cooled vertical steel cylinder at 70-185 C, considering heat flux relation to saturated vapor/cooling surface temperature difference
06 p0903 A72-18190

Cs and Hg vapors compressibility factor in supercritical range as function of density, considering charged particles and atoms polarization interactions in ionized metal vapors
07 p1040 A72-18943

Plasma diagnostics of inductively coupled RF Hg discharge in RIT-10 ion thruster
[AIAA PAPER 72-472]
11 p1709 A72-26203

Porous-tungsten mercury vaporizers design and tests for flow rate, liquid intrusion pressure level and mechanical strength
[AIAA PAPER 72-484]
11 p1710 A72-26210

Mercury vapor physicochemical processes kinematics in shock tube, determining electron gas energy balance equations and atom-atom collision cross sections
11 p1699 A72-26760

Model for mercury vapor electron bombardment ion thruster hollow cathodes operation and effects on thrust subsystem performance predictability
[AIAA PAPER 72-420]
13 p2026 A72-28936

Hg vapor absorptivity dependence on wave number, atomic density and temperature in 2537 A resonance line region, discussing measurement by magnetic scanning or monochromator
14 p2131 A72-30853

Contaminated Langmuir probes LF admittance measurements in mercury vapor plasma, considering dielectric relaxation in insulating layers
15 p2241 A72-32516

Ionization of mercury vapor and cesium vapor in a nuclear reactor.
18 p2713 A72-36208

Secondary ionization coefficients in a low-pressure discharge in mercury vapour.
19 p2836 A72-37459

Mercury Hall ion engine principles and design, discussing plasma ion acceleration, mercury evaporation and ionization and acceleration channel electrical and thermal insulation
20 p2963 A72-39937

MERIDIANS
U LATITUDE
U LONGITUDE
MERIDIONAL FLOW
Meridional thermospheric wind effect on auroral atomic oxygen red line profile, noting inadequacy of diffusion hypothesis
01 p0052 A72-10079

Meridional currents intensity in equatorial electrojet region, computing electric and magnetic fields
01 p0063 A72-10924

Tropospheric processes effects on Northern Hemisphere stratospheric meridional transformations in geopotential field and air circulation
02 p0253 A72-11732

Model calculation for seasonal effects on minor neutral constituents distribution in mesosphere and lower thermosphere, suggesting large scale meridional circulation role
09 p1274 A72-22354

Mass flow and current distribution in magnetic MPD accelerator thruster plumes calculated from meridional flow stream function equation
[AIAA PAPER 72-501]
11 p1696 A72-26224

A temperature adjustment process in a Boussinesq fluid via a buoyancy-induced meridional circulation.
21 p3044 A72-40112

Temporal behavior of hemispherically averaged geostrophic zonal and meridional flow from dynamic climatology studies of Northern Hemisphere large scale circulation
21 p3077 A72-40251

Direct observation of a complete unit of meridional circulation from the equatorial belt up to the polar front - Synthesis of concepts of the pseudofront, of the equatorial mesosystem, and of the subsidence well
21 p3078 A72-41344

Longitudinal magnetospheric currents contribution to auroral electrojet from satellite observation data, noting magnetosphere electric field excitation of meridional Pedersen and Hall currents
22 p3169 A72-42225

Application of cascade and actuator disc theories to computer aided design of fans.
24 p3363 A72-45359

Flow analysis in the axial-flow compressor impeller with meridional stream acceleration.
24 p3394 A72-45371

MEROMORPHIC FUNCTIONS
NT ELLIPTIC FUNCTIONS
NT RATIONAL FUNCTIONS
Bounded operators solution in locally convex topological vectorial spaces with meromorphic properties
13 p1987 A72-29778

MESON-NUCLEON INTERACTIONS
Meson exchange effects on solar pion-production process, using low energy Adler theorem with cross section correction factor
16 p2456 A72-33476

MESONS
NT MUONS
NT PIONS
Atmospheric primary and secondary cosmic ray propagation with close reference to two-fire-ball, H-quatum and excited baryon models of multiple meson production
01 p0121 A72-11122

Multiple meson production in 250 GeV nucleon-nucleon collisions in LiH targets, noting 40 per cent formation of heavy meson cluster fireballs
06 p0868 A72-17259

Time invariance violation in charge asymmetry experiment, showing K-meson decay rate difference reversal from world to antiparticle with particle unchanged
14 p2130 A72-30265

Static black hole noninteraction with exterior world by meson fields, noting baryon number conservation in general relativity
17 p2612 A72-35388

Characteristics of cosmic ray diurnal variation from Deep River neutron and meson data and temperature effects.
17 p2601 A72-35400

Atmospheric effects on the surface cosmic ray meson intensity recorded in London.
22 p3218 A72-42369

High energy nucleon inelastic collision characteristics dependence on secondary particle energy and meson velocity, using Wilson chamber measurement
23 p3291 A72-44445

Angular and impulse characteristics of negative-pion interactions at an energy of 60 GeV in the emulsion
23 p3292 A72-44446

MESOPAUSE
Noctilucent clouds in daytime - Circumpolar particulate layers near the summer mesopause.
22 p3173 A72-42515

MESOSPHERE
Ionospheric ion mobilities and densities measurements over Sardinia, using parachute mesosphere probe
01 p0055 A72-10436

Mesospheric OH volume density profile measurements by rocket-borne high resolution polarized Ebert-Fastie spectrometer
01 p0062 A72-10912

Mesosphere and lower thermosphere photochemical composition, allowing for molecular and eddy diffusion
03 p0345 A72-12980

Mesospheric models - Conference, Frascati, Italy, July 1970
03 p0345 A72-13376

Photochemical models of aeronomic formation and dissociation of hydrogen and ozone in mesosphere and stratosphere
03 p0346 A72-13377

Meridional model of oxygen and hydrogen compounds reactions in mesosphere and lower thermosphere, determining diurnal variations and vertical profiles
03 p0346 A72-13378

Oxygen, hydrogen and nitrogen constituents in mesosphere, investigating ionization process in D region at midlatitudes
03 p0346 A72-13379

Energy conversions and mean vertical motions in high latitude summer mesosphere and lower thermosphere, observing reaction kinetics
03 p0346 A72-13380

Dynamic modeling of stratospheric and mesospheric circulation and thermal structure
03 p0346 A72-13382

Mesosphere meteorological sounding by acoustic grenade and pitot probe techniques, investigating seasonal and latitudinal variations
03 p0383 A72-13384

Solar UV radiation role in mesosphere, investigating absorption cross sections of ozone and molecular oxygen
03 p0411 A72-13385

Meteorological elements, upper ionospheric data and solar radio emission intensities during winter stratospheric temperature rises
03 p0383 A72-13477

Atmospheric model for mesosphere odd-nitrogen concentration relation to NO dissociation rate and downward flux through mesopause

03 p0350 A72-13526

Free atmosphere vertical temperature structure at mesoscale, using continuous recording sonde [AD-739147]

04 p0519 A72-15158

Stratospheric rocket sounding on global scale for studies of atmospheric circulation in equatorial zone, polar regions and hemispheres

06 p0840 A72-17620

Laser radar observations of mesosphere and lower thermosphere optical scattering cross section variations due to tide-caused atmospheric density fluctuations

08 p1156 A72-21100

Semiannual latitude dependent mesospheric wind patterns from meteor trail observations, suggesting heat inputs from solar radiation and magnetic storm related auroral heating

08 p1159 A72-21227

Mesospheric temperature and wind profiles during stratospheric warming from rocket grenade experiments

08 p1160 A72-21533

Planetary scale circulation systems effects on photochemistry and transport processes of minor neutral constituents in mesosphere and lower thermosphere

09 p1274 A72-22353

Model calculation for seasonal effects on minor neutral constituents distribution in mesosphere and lower thermosphere, suggesting large scale meridional circulation role

09 p1274 A72-22354

Mesospheric ozone measurement for altitude profiles, comparing rocket and ground based observations of 1.27 micron emission band at twilight

09 p1296 A72-22355

Mesosphere region positively and negatively charged particles concentration and mobility measurements by sounding rocket experiments

09 p1375 A72-22361

Supersonic and subsonic measurements of mesospheric ionization at night, using Arcas rocket parachute borne nose-tip and blunt probes

09 p1296 A72-22362

Mesosphere ozone number densities from rocket photometric measurement of lunar UV radiation absorption

09 p1385 A72-22583

Day, night and sunset mesospheric nitric oxide concentrations during polar cap absorption from rocket measurements of cation composition and charged particle densities

[AD-741709]

09 p1300 A72-23026

Thermal stratification of mesosphere and lower thermosphere at low latitudes with allowance for turbulent mixing, showing molecular oxygen and ozone radiative heating prevalence

09 p1347 A72-23589

Mesospheric clouds composed of molecular complexes of extraterrestrial origin, considering chemical reactions, hydroxyl luminescence, thermospheric water vapor and auroras

09 p1347 A72-23590

Wind velocity distribution structural laws in vertical and horizontal planes for large mesospheric and atmospheric processes

09 p1347 A72-23591

Mesosphere and lower thermosphere heating and associated solar UV radiation absorption calculation based on diurnally varying photochemical diffusive model

10 p1475 A72-24943

Noctilucent cloud kinematics as indicators of mesospheric circulation and turbulence characteristics, discussing need for international scientific cooperation

10 p1476 A72-25006

Meteorological elements, upper ionospheric data and solar radio emission intensities during winter stratospheric temperature rises

11 p1682 A72-26247

Ground based synoptic measurement of mesospheric electron densities, noting variations relationship to solar radiation changes

11 p1626 A72-26424

Corpuscular radiation intensity relationship to midlatitude mesosphere temperature from rocket and balloon sounding and ground measurements

13 p2029 A72-28603

Mesosphere and stratosphere density and temperature variability with seasons and altitude

13 p1947 A72-28830

Rocket sounding of ozone diurnal variations in upper stratosphere and lower mesosphere

13 p1947 A72-28831

Daily difference analysis of magnitude, vertical and latitudinal structure of irregular mesospheric wind variations due to gravity waves

13 p1948 A72-28832

Semiannual equatorial wind oscillations in upper stratosphere and lower mesosphere dependence on temperature variations in high and middle latitudes

14 p2099 A72-30259

Aircraft atmospheric flow measurements of horizontal and vertical motions on mesoscales, using inertial reference system

14 p2127 A72-30300

Wind tunnel tests for correction of temperature profile data in stratosphere and lower mesosphere obtained from SKUA rocket sounding

14 p2105 A72-30807

Temperature and density data deviation from stratosphere and mesosphere mean season model values at high latitudes

15 p2225 A72-31907

Mesosphere and lower thermosphere temperature measurement by rocket-borne manometer, relating temperature variations to corpuscular flux intensity and sun generated geomagnetic excitations

15 p2225 A72-31910

Mesospheric air density and temperature measurements from rocket-borne resistance thermometers based on free molecular flow

15 p2225 A72-31911

Mesospheric and lower thermospheric composition from neutral atmospheric particles measurement by rocket-borne instrument consisting of RF quadrupole mass spectrometer

15 p2228 A72-31967

Electrical conductivity in mesosphere and upper stratosphere from rocket sounding by blunt probe technique, suggesting electron density profiles dependence on dissociative recombination variations

15 p2228 A72-31972

Molecular oxygen concentrations from solar Lyman alpha radiation absorption profile in mesosphere, using rocket-borne nitric oxide filled ion chamber

15 p2230 A72-32264

Summer upper mesosphere and lower thermosphere positive ion composition at high latitudes from Nike Cajun rocket soundings

16 p2383 A72-32966

Solar radiation induced molecular oxygen photodissociation rate as function of column density and temperature in mesosphere and lower thermosphere

16 p2383 A72-32967

Features of zonal circulation in the stratosphere and lower mesosphere of the equatorial region during the period of increasing solar activity [1967-1968]

19 p2790 A72-37999

The solar X-ray spectrum deduced from a proportional counter experiment and the resultant production of ionization in the mesosphere.

22 p3170 A72-42368

Ozone measurements in the mesosphere during the solar proton event of 2 November 1969.

22 p3173 A72-42509

Mesospheric noctilucent clouds: tables listing weather stations geographical coordinates, observation time periods, elevation above northern horizon and azimuth

22 p3173 A72-42575

Corpuscular radiation intensity relationship to midlatitude mesosphere temperature from rocket and balloon soundings and ground measurements

24 p3435 A72-45103

MESSAGES

Message distortions analysis in PCM communications systems due to phase fluctuations of synchronization signal

11 p1598 A72-26728

METABOLIC WASTES

NT HUMAN WASTES

NT URINE

Food ration effect on metabolite elimination rate in humans wearing isolation garment at rest or performing physical labor

05 p0622 A72-16644

Calorimetric measurements of human body temperature and of hot saline solution drinking effects on sweating rate

09 p1267 A72-23440

Viking Lander detection of metabolically produced radioactive labeled gas in Mars surface samples

10 p1540 A72-24386

High temperature biowaste resistojets with electrically conducting ceramic heaters, discussing lifetime and space station power systems adaptability [AIAA PAPER 72-454]

11 p1708 A72-26190

Human immunobiological status during prolonged maintenance in bioregenerative life support system, discussing possible allergic reaction to chlrella gaseous metabolites

13 p1910 A72-29312

Human waste management system evaluation in zero gravity flight tests, presenting design concept for collection by air flow technique

15 p2189 A72-31825

Myth of nitrogen equality in respiration - Its history and implications.

19 p2758 A72-38708

Bosch CO2 reduction unit research and development. [ASME PAPER 72-ENAV-10]

20 p2896 A72-39167

Influence of a high oxygen content on the rate of formation and elimination of gaseous wastes in albino rats

23 p3255 A72-43906

METABOLISM

NT ADRENAL METABOLISM

NT ASCORBIC ACID METABOLISM

NT CALCIUM METABOLISM

NT CARBOHYDRATE METABOLISM

NT CATABOLISM

NT ELECTROLYTE METABOLISM

NT ENZYME ACTIVITY

NT FERMENTATION

NT HORMONE METABOLISMS

NT HYPERGLYCEMIA

NT HYPOGLYCEMIA

NT LIPID METABOLISM

NT OXYGEN METABOLISM

NT PHOSPHORUS METABOLISM

NT PROTEIN METABOLISM

Long term bed rest effect on humans and primates, detailing cardiovascular metabolic and musculoskeletal physiological systems [AD-737557]

01 p0014 A72-10932

Starvation effects on male rats, mice and guinea pigs hepatic drug metabolism, discussing ethylmorphine, p-nitroanisole and aniline

01 p0015 A72-11262

Flavin photoreceptor participation in contemporary organism metabolic systems

04 p0469 A72-14781

Primitive earth model of ion selective enzymatic asymmetric synthetic membrane for accelerated nutrients and metabolites transfer studies

04 p0469 A72-14787

Preglycolitic energy metabolism in biochemical evolution, concerning anaerobic oxidation of pyruvate and acetaldehyde to acetate and ATP

04 p0471 A72-14799

Metabolic control of temperature compensation in circadian rhythm of *Euglena gracilis* strain

07 p0919 A72-19538

Yeast glycolytic pathway oscillations relation to concentration of diphosphopyridine nucleotide and other metabolites, noting analogy to behavioral and physiological rhythms

07 p0920 A72-19541

Glucose and fatty acid metabolic response during impending myocardial infarction in animals

07 p0921 A72-20175

Gaseous nitrogen production in humans under steady-state conditions, relating expired nitrogen minute volume increase after protein consumption to possible gastrointestinal and metabolic effects

08 p1122 A72-20882

Electrophysiological, neurophysiological, metabolic, vegetative, psychological, chemical and pathological aspects of sleep, noting disturbance and wakefulness mechanisms for various clinical disorders

09 p1264 A72-22223

Energetic motor activity rule hypothesis for physiological mechanisms of certain ontogenesis patterns, suggesting motor activity as excess anabolism induction factor

09 p1264 A72-22225

Work-rest schedules endocrine and metabolic effects on aircrews during 50 hour flight missions in C-141 aircraft, using urinary test techniques [AD-740992]

10 p1428 A72-23737

Thermodynamics of human body metabolism, discussing energy conversion calorimetric measurements, body size, food intake, age, sex, endocrine and nervous effects

11 p1584 A72-26072

Human body thermoregulatory processes under varying environmental conditions and metabolic rates, discussing role of blood circulation, sweating, nervous stimuli, hormones, etc

11 p1584 A72-26073

Dimensional analysis and similarity theories application to biological organisms relationships between body size and metabolism

11 p1585 A72-26074

Physical training effect on rat cardiac function and metabolic response to hypoxia

11 p1581 A72-26701

Energy metabolism and ATP balance characteristics during muscular activity as function of organism adaptation to activity

13 p1902 A72-28640

Diurnal changes in gas exchange and metabolic rate under normal and inverted day-night schedule conditions, studying human adaptation to shifted schedule

13 p1904 A72-29318

Human physiological function variations dependence on hyperthermia levels in high temperature environment

14 p2074 A72-30257

Red blood cell metabolite 1,3 diphosphoglycerate determination method by rapid deproteinization, concentration by precipitation and enzymatic reaction

15 p2190 A72-32488

Long term weightlessness-induced physiological response normalization by muscle bioelectrostimula-

tion, muscular tissue energy load increase and mineral metabolism stabilization

16 p2354 A72-33543
Cerebral blood flow and metabolic changes during wakefulness, sleep, coma and epileptic seizures in terms of homeostatic mechanisms

16 p2356 A72-33558
Thermal neutral temperature of rats in helium-oxygen, argon-oxygen, and air.

17 p2500 A72-34728
The uptake, metabolism and release of C/14-taurine by rat retina in vitro.

17 p2500 A72-34881
Metabolism of the hypoxic and ischaemic heart; Proceedings of the Symposium, Geneva, Switzerland, June 14-17, 1971. Part 1.

17 p2501 A72-34976
Normal and hypoxic myocardium mitochondrial metabolism process, studying electron transport system

17 p2501 A72-34978
The influence of exogenous ATP on cardiac metabolism in acute hypoxia.

17 p2501 A72-34987
Magnetic field effects in enzymes, tissue respiration and some metabolism characteristics of an intact organism

17 p2503 A72-35003
Book - Energy metabolism of human muscle.

20 p2893 A72-39700
Metabolic energy requirements for pushing loaded handcarts, measuring expenditure during treadmill and outdoor asphalt circuit walking

21 p3005 A72-40419
Muscle metabolism of ATP, CP, glycogen and lactates at rest and during submaximal and maximal exercise

21 p3005 A72-40421
Muscle metabolism during isometric exercise performed at constant force.

21 p3005 A72-40425
Determination of oxygen consumption by use of the paramagnetic oxygen analyzer.

21 p3006 A72-40429
Cortical metabolism regulation and effector systems of the adaptation process

21 p3000 A72-40760
Chemical energy transformation to mechanical energy and heat in muscles during exercise, considering energy sources for contraction, oxidations, glycolysis and alactic anaerobic mechanism

21 p3003 A72-41470
Specific ATP action on metabolism of isolated heart - Influence of pH, divalent cation concentration and stability of complexes.

22 p3147 A72-42986
Studies on weightlessness in a primate in the Biosatellite 3 experiment.

23 p3253 A72-43388
Cardiac output, hemodynamic and gas exchange variations as function of basal metabolism during bed rest in hypokinetic recumbent or antihorostatic position

23 p3255 A72-43915
Metabolic changes in healthy humans caused by prolonged bed rest in horizontal position, noting prevention by physical exercises and electric muscle stimulation

23 p3260 A72-43921
Biochemical and physiological evaluation of nourishment of subjects feeding on dehydrated products in test chamber with regenerative life support system, discussing metabolic data and hormone function

24 p3375 A72-45128

METAGALAXY

U UNIVERSE

METAL AIR BATTERIES

NT ZINC-OXYGEN BATTERIES

16 p2350 A72-33670
Metal-air batteries with alternately polarizable oxygen electrodes, discussing current state of technology

METAL ALLOYS

U ALLOYS

METAL BONDING

NT METAL-METAL BONDING

Bond zone wave formation in explosion cladding, predicting critical collision velocity and angle with fluid flow model

01 p0077 A72-11031
Composition, microstructure and mechanical properties of binder metal in cobalt bonded tungsten carbide

02 p0241 A72-11451
Au-Al wire bond, discussing intermetallic phase formation under elevated temperature treatments and reliability design limitations

03 p0364 A72-14284
Thermal deformation effects on metal bond fatigue failure modes in small signal transistors, micro and LSI circuits

03 p0365 A72-14291

Forging techniques and applications for YF-12A aircraft Ti alloy bulkhead production, considering diffusion bonding and die shimming

04 p0527 A72-14914
Fatigue strength optimization of bonded double strap metal joints, attributing stress concentration to plastic relaxation

05 p0731 A72-15791
[ASME PAPER 71-MET-Q]
Permanent electric connections by alloy and solid phase bonding and fusion welding, considering surface contamination, interface contact, activation energy and connection stability

06 p0822 A72-18581
Maximum allowable time between Ti metal surface preparation and agent application in adhesive bonding

07 p1024 A72-20254
Water effect at epoxy resin-steel interface on adhesive bond strength as function of vitrification temperature

08 p1196 A72-21863
Bonding conditions effects on wave mode formed at explosive bonded interfaces from experiments with bullets fired at thin metal targets

09 p1321 A72-23642
High alumina ceramics metallization and hard soldering to metals for manufacturing vacuum jacket of transmitting thermionic tubes

10 p1488 A72-24642
Adhesive bonded clad Al corrosion penetration rates from accelerated tests

11 p1656 A72-25600
[SAE PAPER 720344]
Solid state joining in gas turbine engines, discussing diffusion bonding, friction welding and coextrusion metal bonding

11 p1639 A72-25656
[ASME PAPER 72-GT-74]
Complex bipolar IC logic circuits realization by economical high speed techniques using metal bonding or cells available in library

11 p1606 A72-26548
Nonmetallized aluminum oxide ceramics brazing with metals under pressure using copper solder, noting optimum conditions for Kovar

15 p2243 A72-31225
Adhesive bonding of L-1011 body shell panels for improved fatigue strength and corrosion resistance

15 p2245 A72-32429
Fracture mechanics approach to adhesive joints.

17 p2633 A72-35282
Nondestructive ultrasonic inspection of braze bonds in high current electrical contact assemblies.

18 p2695 A72-36116
Acoustic emission technique as NDT method for quality control of brazed metal-ceramic bonding

18 p2695 A72-36458
Combined spot weld-adhesive bonding to join sheet metal parts with applications to propellant tanks and spacecraft and aircraft structures

18 p2695 A72-36526
[SME PAPER AD 72-710]
Use of the third-harmonic method for the selection of metal-bonded polycarbonate capacitors which are stable in time

18 p2669 A72-37115
Adhesion and transfer of PTFE to metals studied by Auger Emission Spectroscopy.

19 p2807 A72-37646
Holographic interference as a means for quality determination of adhesive bonded metal joints.

21 p3060 A72-41131
[ICAS PAPER 72-06]
On the diffusion of a load from a semi-infinite stringer bonded to a sheet.

22 p3238 A72-42833
Al powder bonding during compaction by explosively driven plates, measuring shock wave amplitudes, pressure drop, layer separation and critical pressures in spall plane

22 p3184 A72-43183
Diffusion bonded columbium panels for the shuttle heat shield.

24 p3406 A72-44889

METAL CARBIDES

U CARBIDES

METAL COATINGS

NT ALUMINUM COATINGS

NT GOLD COATINGS

NT NICKEL COATINGS

NT ZINC COATINGS

Niobium alloy for reentry vehicle heat shields, describing slurry coating process reliability

01 p0077 A72-10982
Diffusion aluminide protective coating formation mechanisms on Ni-base superalloys observed from microstructures and compositions in Ni-Al intermetallics

01 p0089 A72-11165
Lateral surface heat transfer effect on thermophysical characteristics in thin layer coatings, discussing temperature gradients in corundum and zirconium oxide on copper

02 p0304 A72-12864
Steel coatings produced by plasma jets on experimental machine parts, determining friction wear resistance by successive tests

03 p0363 A72-13548

NbN thin film stabilization by metal overlays with reduction in ac losses, discussing superconducting reversibility to normal transition

04 p0560 A72-14542
Ni-Cr-Al-Si and Fe-Cr-Al-Y oxidation resistant claddings for superalloys, comparing to commercial aluminide coatings by cyclic furnace and high velocity burner rig tests

04 p0533 A72-14700
Vacuum diffused Cr, Si, Ti and combined coatings effect on heat resistance of Nb and Nb alloys

04 p0534 A72-15660
Wear, bending and corrosion resistance of stainless steels with Cr thermal vacuum diffused coating

04 p0535 A72-15661
Ground plane curvature effect on aperture admittance of waveguide fed axial slot on teflon coated metal cylinder for underdense plasma

06 p0771 A72-17354
High temperature tests of creep rupture strength of W composite cast with heat resistant alloy coatings

06 p0829 A72-17947
Hot corrosion resistant Pt-Al coating for high temperature aircraft engine Ni alloy components, presenting cyclic sulfidation and thermal shock test results

07 p1012 A72-19573
Emission energy of positrons thermalized in moderators and coated with Au, suggesting Au negative work function existence

08 p1217 A72-21339
Residual shrinkage and thermal stresses in adhesion bond models of metal coatings and cemented seams

08 p1248 A72-21865
Metal deposition - Conference, Vilnius, Lithuanian SSR, April 1971

09 p1318 A72-22526
Metallic coatings effect on high-strength steels fatigue properties, noting beneficial effect of shot peening

10 p1494 A72-24024
Axial, circumferential and radial residual stresses calculation in polycrystalline coatings and cylindrical elements during surface layer removal by electrochemical processing

11 p1737 A72-26263
Residual stresses and stress relaxation determination in electrochemical galvanic coating with automatic strain curve plotter

11 p1613 A72-26264
Composite powders preparation by metals deposition from aqueous solution onto core materials by gaseous hydrogen at high temperature and pressure, noting coating application

11 p1646 A72-26875
Oxide thin films effects on surface layers deformation and wear resistance of coated metals under friction, noting electrical resistance changes in annealing

12 p1818 A72-28189
Russian papers on alloying and properties of heat resistant alloys covering creep, solid solution and dispersion hardening, chemical interactions and protective coatings

15 p2254 A72-31557
Re applications technology, discussing production methods, mechanical and physical properties, plasma spraying, annealing and alloying techniques

17 p2567 A72-34825
Work function change of tungsten /110/ planes as function of Mo coverage.

18 p2656 A72-36134
Evaluation of sublimed molybdenum collector coatings for additive diode operation.

18 p2646 A72-36202
Determination of the emission potential of cesium-coated surfaces at high temperatures with a plane-parallel cesium diode. I - Technology. II - Physical foundations and measurement results

19 p2754 A72-37779
Study of tungsten and molybdenum coatings obtained by arc discharge in a vacuum

19 p2808 A72-38186
Vacuum-friction temperature resistance and durability of a molybdenum-disulfide coating deposited on steel by the detonation method

19 p2809 A72-38290
Developments in the field of metallic diffusion protective layers employed against high-temperature corrosion

20 p2944 A72-39450
Structure and properties of nickel-phosphorus coatings as a function of the temperature and annealing time

20 p2929 A72-39583
A comparison of the effect of inward and outward diffusion aluminide coatings on the fatigue behavior of nickel-base superalloys.

21 p3067 A72-40916
Oxidation protection of tantalum and tantalum alloys at up to 1500 C

22 p3188 A72-41973
Investigation of the wear resistance carbonized chromium coatings on various brands of steel

22 p3195 A72-43159

- Diffusive metal coatings stress-strain state effect on composite Mo material strength, ductility and creep characteristics 23 p3306 A72-43732
- METAL COMBUSTION**
Chemical efficiency improvement of aluminum combustion with nitric acid in organic solid fuel 03 p0405 A72-13540
- Al powder burning in flame jets produced by ballistite powder N, using scanning spectrographic system for combustion temperatures, products and dynamics 06 p0903 A72-18209
- Superheating in Zr-oxygen combustion system during autoignition period 08 p1128 A72-21219
- Ignition delay time and combustion mechanism of Al-Mg alloys single particles in combustion products of oxidizer-fuel mixture 09 p1373 A72-22885
- Visual and motion picture studies of ignition and burning characteristics of Mg particle clusters in flames of gas mixtures 09 p1411 A72-22886
- Pressure effect on combustion rate of Mg particles in water vapors 09 p1411 A72-22887
- Burning process of low boiling Mg particle moving in relation to gaseous oxidizer, assuming heat and mass transfer occurrence by diffusion-conduction mechanism 09 p1411 A72-22888
- Autonomous combustion of Al sphere in controlled atmospheres oxygen-argon, nitrogen and air, identifying products 10 p1562 A72-24238
- Magnesium particle combustion in rarefied air during pressure changes, discussing combustion time decrease with pressure increase 14 p2170 A72-30236
- Boron reaction characteristics in ducted rockets under varying primary chamber conditions detailing various gaseous propellants effects 15 p2296 A72-32311
- Laser ignition and combustion of boron particles, developing oxide coating and droplet burning models for low and high temperature stages respectively 15 p2296 A72-32582
- Aerogel combustion kinetics and continuous flame formation on coal, Mg, Al and Al alloy powders, using track method 16 p2476 A72-33252
- Mg ignition in nitrous oxide at 600-800 C, determining induction period as function of particle mass and gas stream temperature 16 p2476 A72-33254
- Multicomponent system combustion of Al suspensions in kerosene, determining ignition temperature as function of metal particle size and concentration 16 p2476 A72-33256
- Al and Zr single thin strands burning rates at various total oxygen pressures, comparing photographic observation to computations 16 p2479 A72-34003
- Boron ignition and combustion in air-augmented rocket afterburners. 17 p2636 A72-34902
- Combustion propagation in cylindrical aluminum alloy specimens and some peculiarities of the aluminum combustion mechanism 19 p2847 A72-37362
- Influence of pressure on the combustion process of aluminum powders 19 p2847 A72-37368
- Induction period, particle size distribution and medium temperature effects on thermal ignition of metal particles under exothermal oxidation reaction on surface 20 p2987 A72-40040
- Burning of particles of an aluminum-magnesium alloy 20 p2987 A72-40041
- Propagation of the front of an exothermic reaction in condensed mixtures whose components interact through a high-melting layer 22 p3245 A72-43177
- Inflammation and burning of powdered aluminum in high-temperature gaseous media and in heterogeneous condensed systems 22 p3245 A72-43178
- Flow direction and velocity effects on metal burning rates of low carbon and Ni-Cr steels in pure oxygen, using diffusion model 22 p3245 A72-43185
- Measurement of the temperature of flames containing scattering particles on the basis of IR radiation 23 p3356 A72-43678
- METAL COMPOUNDS**
Cold pressed powdered boron nitride, Mo, W, Nb disulfides and diselenides, investigating thermal dissociation in He by X ray analysis 03 p0380 A72-13551
- Thermoplastic materials casting procedures to mold high melting point metal compound powders 11 p1645 A72-26861

- Current noise spectra in single crystals and polycrystals of transition metal compounds, discussing flicker noise origin 15 p2293 A72-32384
- Electron work function change of interstitial compounds of the 4a and 5a metals in dependence on the nonmetal content. 18 p2656 A72-36129
- Influence of temperature on the mechanical properties of metallic compounds 22 p3191 A72-42804
- METAL CORROSION**
U CORROSION
METAL CRYSTALS
Metal crystals dislocations movements and interactions with dislocation dipole under applied cyclic stresses for various configurations and starting conditions, using numerical methods 01 p0113 A72-10208
- Macrosonic metal crystal plastic deformation applications to aircraft and spacecraft materials production, considering internal friction and energy conversion into strain energy and heat 01 p0071 A72-11020
- Polycrystalline Mo work function calculation from electron emission microscopy, determining crystallographic grain orientation effects 01 p0071 A72-11027
- Critique of theoretical and experimental findings on slip geometry in bcc metals, especially Fe-Si alloy single crystals 01 p0089 A72-11300
- Viscous friction effects on phonon-electron interactions and dislocation velocity by deformation measurement of metallic crystals under pulsating magnetic fields 02 p0243 A72-12169
- Low energy He ion bombardment effects on Ni alloy single crystal surface, observing defect structure with stacking faults, tangled dislocations and carbide precipitation 04 p0533 A72-15159
- Flow stress measurements in disordered and partially ordered Ni-Ta alloy single crystals, correlating with ordered phase volume fraction and domain size 04 p0534 A72-15272
- Anodic layer thickness effect on fatigue crack initiation and fracture mode in mono and polycrystalline aluminum 05 p0672 A72-16015
- Internal friction changes in aluminum single crystal after uniaxial plastic deformation and irradiation 05 p0673 A72-16148
- Subgrain rotation induced angular anisotropy of plastic deformation of oriented Mo single crystals during rolling 05 p0674 A72-16354
- Age hardened Al-Cu single crystal anisotropy from stress-strain curves, using plane strain compression tests [AD-743602] 05 p0677 A72-17106
- Diffusive mobility of C in Mo single crystals and Mo-Re alloy, using autoradiography and electron microscopy 06 p0829 A72-17733
- Flux lines interaction with dislocations in twisted superconducting niobium single crystals, measuring flux gradient and dislocation arrangement 06 p0830 A72-18055
- Microscopic-macroscopic transition in heterogeneous metal polycrystals and multiphase composites at finite strain 06 p0897 A72-18068
- Low temperature slip discontinuity and strength of pure Al crystals as function of strain rate 06 p0831 A72-18355
- Crystallographic texture of Mo sheet, analyzing angular dependence of Young modulus 06 p0832 A72-18366
- Mo-Nb alloys single crystals work function, obtaining thermionic emission pattern 06 p0832 A72-18414
- X ray study of structural changes in Ni single crystals during recrystallization process after uniaxial deformation under compression loads with high loading rates 06 p0834 A72-18744
- Steady creep rates in Ni poly- and single crystals in presence of dislocation stresses 06 p0835 A72-18748
- Cu, Al and Pb bcc metals, investigating dislocation structure and creep characteristics change mechanism at transition from low to high temperature 07 p1014 A72-19822
- Magnetic domain structure of Ni single crystals after plastic deformation as function of stress induced anisotropy of layer-like dislocations 07 p1020 A72-20411
- X ray diffuse scattering from Al crystal at 100-500 V, considering phonon modes effects on anharmonicity and atomic deformation 08 p1186 A72-21591
- Soviet papers on imperfections of crystalline structure effects on physical and mechanical properties of

- metals and alloys, covering radiation damage, microdeformations, X ray investigations, etc 08 p1187 A72-21785
- Primary and secondary radiation damage to metals and alloys crystal lattices 08 p1187 A72-21786
- Impurities and temperature effects on microdeformation of Mo single crystals under dynamic loads 08 p1188 A72-21789
- Plastic deformation characteristics of Fe-Cr-Ni alloy single crystals at low temperatures 08 p1188 A72-21790
- Helium cryostat for X ray studies of phase transformations and structural changes in single metal crystals 08 p1169 A72-21792
- Metal single crystals use for corrosion tests, noting anisotropy, adsorption, oxidation and pitting 08 p1189 A72-22111
- Ti crystallographic and topographical features determination by hydrogen-ion microscopy, noting temperature effects on surface films and low index facets production 09 p1327 A72-22805
- Recrystallization of dispersion strengthened alloys with bcc lattice, deriving equations for grain size changes 09 p1328 A72-23031
- Subgrain growth during annealing of rolled samples of Mo-Ti-C alloy and of single crystal Mo purified by electron beam zone melting 09 p1329 A72-23034
- Elastoplastic deformation of Zn single crystals under uniaxial tensile loads, noting critical stresses relationship to current pulses 10 p1553 A72-23766
- Dislocations distribution in Al single crystals observed by X ray topography, noting effects of critical work hardening with annealing and secondary recrystallization 10 p1495 A72-24068
- Surface defects absence after intergranular creep from Al bicrystals grain boundaries observation by transmission electron microscopy 10 p1495 A72-24084
- Interaction forces between monovalent metal crystals determined from electrons quantified energy variations 10 p1525 A72-24136
- Various restrain dislocation distributions effect on mechanical twinning behavior in purified Nb single crystals 10 p1497 A72-24824
- Evaporation, superficial diffusion and oxidation role in grain junctions electromigration phenomenon in binary Al crystals traversed by high density continuous current 10 p1498 A72-24860
- Isotope effect calculation hydrogen and deuterium solubility in fcc metals, analyzing elastic vibrational spectrum of crystal with impurity atom in internode 10 p1498 A72-24873
- Subgrain rotation induced angular anisotropy of plastic deformation of oriented Mo single crystals during rolling 11 p1652 A72-25339
- Diffusive mobility of C in Mo single crystals and Mo-Re alloy, using autoradiography and electron microscopy 11 p1652 A72-25340
- Crystal grain size effect on fracture initiation in mild steel under triaxial stress, using notch tests at low temperatures 11 p1657 A72-25756
- Light figure microscope construction for crystal grain orientation determination in metal specimens 11 p1632 A72-25759
- Propulsion system based on ion tunneling through preferentially oriented metal crystal lattice [AIAA PAPER 72-480] 11 p1710 A72-26208
- Impurity atoms effects on grain boundary motion velocity, considering interactions with metal lattice vacancies 11 p1662 A72-26655
- Zone refined prism slip oriented Be single crystals deformation substructure analysis by synergetic method combining transmission electron microscopy, X ray topography and X ray diffraction profile analysis 11 p1666 A72-26928
- Rolled polycrystalline metal samples principal anisotropy direction determination by acoustic measurements at ultrasonic frequencies 12 p1806 A72-27086
- Critical resolved shear stress and solute atom concentrations relationship in solid solution hardening of metal crystals 12 p1853 A72-27101
- High purity Al single crystal orientation explained by Rowland transformation model, observing recrystallization grains 12 p1828 A72-27300
- Phase matched nonlinear frequency conversion of laser light in tetragonal mercury thiocyanate complex crystals 12 p1854 A72-27549

Second harmonic conversion of CW YAG-Nd laser radiation on lithium metaniobate crystals, discussing conversion coefficient optimization 12 p1825 A72-27886

Crystals deformation and orientation effects on Al polygonization process, noting dislocation densities dependence on stress axis orientation 13 p1972 A72-28464

Statistical adsorption kinetics model with electron desorption of oxygen on polycrystalline W, noting sticking coefficients 13 p1912 A72-28523

Electron paramagnetic resonance investigation of III-V compound semiconductor crystals, observing large magnetic moments, heteropolar chemical bonding and impurities 13 p2021 A72-28572

Ni single crystal growth by Czochralski method, investigating growth rate, direction and initial structures effects on substructure 13 p1976 A72-28906

Hydrostatic pressure effect on tensile creep and creep rupture of polycrystalline metals at high temperatures 13 p2058 A72-29450

Small amplitude plane wave speed variation with pressure for Na and K at absolute zero temperature, using crystal strain energy formulation 13 p2006 A72-29675

Plastic deformation in bcc metal single crystals, discussing glide and work hardening, dislocations, core structure and atomic calculations 13 p2061 A72-29874

Low and medium strain rates and temperature effects on bcc structure polycrystalline Nd and Mo, determining mechanical properties of yield and flow 14 p2114 A72-30367

Electric current pulses effect on Zn monocrystals plastic deformation before brittle rupture, noting critical normal stresses increase 14 p2115 A72-30411

Temperature dependent optical constants of Ti and W crystal surfaces cleaned by ion bombardment in ultrahigh vacuum 15 p2274 A72-31376

Steady creep and delayed fracture dependence on metal structure and composition, considering strain hardening at small strain rate and elevated temperature 15 p2254 A72-31559

Metal hardening level evaluation on basis of volume dislocation structure from stress field of dislocation loops 15 p2254 A72-31562

Alloying effects on high temperature softening due to crystal lattice, stacking fault energy and decreased mobility interactions 15 p2254 A72-31564

Polycrystalline Mo-Re alloy under cold longitudinal, transverse, cross and pack rolling, noting twin and dislocation microstructures 15 p2256 A72-31669

Theoretical model for HF mechanical waves interaction with crystal lattices based on measurements of high amplitude ultrasonic waves attenuation in metal crystals 15 p2292 A72-31835

Fcc metal defect structure due to ultrasonic fatigue observation via transmission electron microscopy for dislocations 15 p2256 A72-31836

Clean Ge crystal surface oxidation process investigation by LEED and conductivity measurements 15 p2292 A72-31868

Angular force models with electron-ion interaction applied to bcc and fcc metals, calculating phonon dispersion curves for V, Nb and Ta 15 p2258 A72-32226

Coherent potential approximation generalization for disordered alloy systems, showing different results for propagator and locator formalisms in multiple site approximation 15 p2293 A72-32229 [ONERA, TP NO. 1126]

Grain orientation and nonmetallic inclusion distribution and identification by color etching of single crystal and polycrystalline Mo 16 p2407 A72-33532

Deformed Cu-Au single crystal surface slip bands fine structure, determining separation distance between individual slip lines 16 p2408 A72-33774

Tensile deformation of Co single crystal in high temperature fcc phase, noting dislocations effect on work hardening 16 p2410 A72-33819

Second harmonic conversion of CW YAG-Nd laser radiation on lithium metaniobate crystals, discussing conversion coefficient optimization 16 p2404 A72-33995

Strengthening mechanism in metals during creep under variable stress for dislocation network structure studies 16 p2475 A72-34164

Work functions of some emitting and collecting refractory metal single crystals. 17 p2595 A72-34601

Orientation dependence of slip in tantalum single crystals. 17 p2567 A72-34748

Mo-Nb alloys single crystals work function, obtaining thermionic emission pattern 17 p2567 A72-34863

Effects of disorientation of grains on the viscoplastic behavior of fcc polycrystals 17 p2634 A72-35407

Work function dependence on crystal orientation for W with special emphasis to the variation near the /110/ orientation. 18 p2656 A72-36130

Work function, thermal stability, and atomic structure of electropositive films adsorbed on single crystals of metals 18 p2656 A72-36132

Impurity controlled deformation mechanism for softening control of interstitial bcc alloys, discussing low temperature and composition effects 18 p2699 A72-36341

Nucleation and growth of deformation twins in Mo-35 at. % Re alloy. 18 p2702 A72-36748

Surface energy and cleavage plane observation of brittle fracture for W single crystal in tension as function of orientation and temperature 18 p2702 A72-36750

Viscoplasticity of face-centered-cubic metals 18 p2703 A72-37017

The plastic deformation behavior of Mo single crystals under compression. 19 p2816 A72-37689

Estimation of the cleavage strength of polycrystalline metals from the internal energy 19 p2818 A72-38010

Electron microscope double contrast images to identify Burgers vectors of close packed metal crystal dislocations 19 p2846 A72-38590

Nickel single crystal target ionization by high voltage electron beam bombardment, using flight time mass spectroscopic analysis 19 p2835 A72-38666

Configuration determination method for metal crystal superdislocation anchored at two points and under stress in sliding plane, calculating critical stress related to double source unlocking 20 p2978 A72-39005

The influence of the surface orientation on yield in Mo single crystals. 20 p2935 A72-39007

A LEED investigation of the chemisorption of nitrous oxide on a tungsten /100/ surface. 20 p2898 A72-39188

Tensile and compressive stress coarsening effects on coherent gamma prime precipitate yield strength of Ni-base superalloy single crystals 20 p2938 A72-39299

Domain structures in metal crystals, investigating ordering in Ni-Mo alloys 20 p2962 A72-39997

Crystal structure and shear strength of solids and imperfections in metals in framework of X ray diffraction and dislocation theory 20 p2942 A72-39998

The mechanisms of diffusion in metals and alloys. 20 p2962 A72-39999

Recrystallized Al monocrystals applications to optics and X ray spectroscopy, describing preparation methods 21 p3065 A72-40085

Recrystallization and polygonization conditions in high purity metals, noting critical temperature and additives effect 21 p3065 A72-40093

Resonance between spin waves and magnetohydrodynamic waves in antiferromagnetic semiconductors and metals 21 p3096 A72-40415

Investigation by the mass transfer method of the diffusion of nickel at a /110/ surface of tungsten single crystals 21 p3068 A72-40955

Investigation of tantalum-compound films at the surface of acicular tungsten microcrystals 21 p3068 A72-40964

High energy electrons monokinetic beam propagation in Cu and Al crystals, investigating critical voltage effect on contrast 21 p3069 A72-41342

Theory of slow elastic-plastic deformation of polycrystalline metals with micro-stresses as latent variables descriptive of the state of the material. 21 p3124 A72-41508

Martensite formation temperature decrease and grain size reduction caused by martensite crystals interaction with barriers in Fe alloy containing austenite beta phase particles 21 p3070 A72-41679

Rheological properties of molybdenum and platinum of bamboo structure under bending loads 21 p3071 A72-41712

Gas adsorption by refractory metal single crystals. 22 p3187 A72-41940

Chemisorption of CO on tungsten /100/ - Combined flash desorption and electron stimulated desorption study. I. 22 p3152 A72-42297

Crystal structures and transition temperatures of polymorphous metals, discussing mechanical properties, thermal conditions for deformation and metal working by pressure 22 p3190 A72-42803

Physicochemical investigation of the thermionic emission properties of metals and alloys 22 p3191 A72-42811

Rotational hysteresis in single crystals of powdered nickel 22 p3192 A72-43011

Martensitic transformation in filamentary cobalt crystals 22 p3192 A72-43017

Deformation mechanism of aluminum and zinc single crystals during low-temperature cavitation 22 p3192 A72-43019

Determination of mosaic-block disorientations in the creep of aluminum by the method of low-angle X-ray scattering 23 p3299 A72-43341

Increasing the boundary strength of electron-beam-melted cast molybdenum by vanadium microadditions 23 p3302 A72-43967

Changes in the physical properties of metals subjected to elastoplastic deformation 23 p3303 A72-44199

Dislocation-substructure-strengthening and mechanical-thermal treatment of metals. 23 p3304 A72-44299

High-temperature creep of polycrystalline chromium. 23 p3304 A72-44449

Field-ion microscopic study of the interstitial plasticity of tungsten single crystals 23 p3304 A72-44484

Oxidation of W/110/. I - LEED study of the oxide formation at 1000 K. 24 p3378 A72-44952

A study of the effect of grain orientation misfit on the viscoplastic behavior of polycrystalline metals /fcc system/ 24 p3414 A72-45251

Energy spectra of Cs+ ions scattered by the surface of a tungsten single crystal 24 p3429 A72-45501

Low temperature slip discontinuity and strength of pure Al crystals as function of strain rate 24 p3416 A72-45742

Crystallographic texture of sheet Mo alloys, analyzing angular dependence of Young modulus 24 p3416 A72-45752

METAL CUTTING

Multilead electrical spark discharge machining for mass production technology, noting carburetor slot cutting and data processing equipment applications 01 p0078 A72-11097

Residual stress formation mechanism in two phase Ti alloys under cutting and plastic deformation, showing phase transformation composition and structure effects 03 p0363 A72-13467

Arc-air method application to groove planing, cutting and beveling, describing manual, semiautomatic and full-automatic units 07 p0994 A72-18932

Steel cutting suitability test, determining optimum cutting conditions for pure iron used in magnetic applications 07 p0994 A72-18973

High power carbon dioxide laser beam applications to deep penetration metal welding, including cutting tests 07 p0994 A72-19214

Adiabatic reversion of Ni martensitic steel to austenite under shear in orthogonal cutting 07 p0996 A72-19934

Plasma beam cutting of Al sheets, discussing heat effect on surface oxides and microstructure and plasmagenic gas influence 08 p1176 A72-21047

Plasma generator with Ar as ionizing medium for metal cutting and welding, discussing protection against secondary arc formation 08 p1176 A72-21048

German monograph on plasma arc machining and cutting of metallic materials on lathe as function of electric power and torch performance 09 p317 A72-22327

Electron beam machine for thin metal plates welding and cutting under space conditions, noting design features and performance 11 p1639 A72-25809

Leading angle effects on cutting force components, temperature and surface roughness in drawing of Ti alloys 13 p1963 A72-28746

Force distribution in refractory Ti alloy cutting with circular self turning blades, noting effects of feeding speed, cut area and cutter angle 13 p1966 A72-29467

Deep diffused layer sintering of metal-ceramic cutting alloys with variable Co content for increased wear resistance and tensile strength

13 p1982 A72-30112

Economics of material cutting and removal by plasma torches, presenting cutting rates as function of plate thickness for different materials

15 p2243 A72-31321

Some considerations on the residual stresses in orthogonal cut surface of aluminium.

20 p2978 A72-38884

Ti fabrication advances in forging, diffusion bonding, hot forming, chemical milling and laser cutting

21 p3061 A72-41335

Magnetic control of arc plasma and its application for welding.

24 p3406 A72-44777

Residual stress formation mechanism in two phase Ti alloys under cutting and plastic deformation, showing phase transformation composition and structure effects

24 p3407 A72-44942

METAL DRAWING

Tungsten wire deformation structure from swaging or rolling and drawing processes, noting cylindrical texture superimposed on fiber texture

03 p0375 A72-13933

Ferritic stainless steel metal ductility, investigating yield and fracture stresses after heat treatment

11 p1661 A72-26494

Deformation drawing textures of bcc metals, including W

11 p1644 A72-26838

Deformation limits in thin and thick walled metal blanks axisymmetric drawing process, determining stress-strain state based on prescribed velocity field

13 p1963 A72-28743

Leading angle effects on cutting force components, temperature and surface roughness in drawing of Ti alloys

13 p1963 A72-28746

Deep drawing of circular mild steel and aluminum sheets with polyurethane or rubber rings, examining strain distribution, shape and surface roughness

15 p2244 A72-32145

Deformation modes for deep drawing of extramild steel sheets, noting susceptibility and rupture criteria

16 p2396 A72-32872

Work hardening and anisotropy coefficients effects on deep drawing limit curves for extramild steel, noting rupture strain and deformation trajectories

16 p2396 A72-32873

METAL FATIGUE

Tensile and fatigue tests on steel, brass and aluminum with starter cracks, showing relation of strength and ductility to crack propagation and stress cycles

01 p0083 A72-10392

Inconel 718 surface integrity from various manufacturing processes, tabulating data on surface finish effects on fatigue, microhardness and metallurgical properties

[SME PAPER IQ 71-239]

01 p0076 A72-10967

Steel and Ti-Al-V alloy surface integrity during various machining methods, considering microstructures, residual stress profiles and fatigue characteristics

[SME PAPER IQ 71-237]

01 p0076 A72-10972

Ni, Fe and Ti alloys creep rupture characteristics in high temperature, high pressure gaseous hydrogen and helium

01 p0086 A72-10979

Cast high temperature Ni base alloy Udimet 500 low cycle fatigue, determining total stress and strain range vs fatigue life at elevated temperatures

01 p0087 A72-11030

Ti-Al-V alloy under vacuum fatigue tests, examining temperature and chemical environment effects on fatigue crack growth

01 p0087 A72-11034

Fatigue crack initiation and growth in sharply notched mild steel, showing specimen size, geometry and loading effects on fatigue life

01 p0142 A72-11098

Hot formed Cr-Ni-Mo and Ni-Mo prealloyed steel powders fatigue and toughness properties, determining hardness effects by varying draw temperature from 400 to 1000 F

02 p0240 A72-11435

Residual buckling strength of Al alloy elastic column with fatigue crack

[SESA PAPER 1914A]

02 p0288 A72-11511

Annealed pure Al polycrystals fatigue behavior data under elevated temperatures, using transmission electron microscopy

02 p0242 A72-11525

Automatic device for thermal and thermomechanical fatigue tests of steel specimens, noting crack nucleation and growth by hardening due to lattice defects

02 p0200 A72-11996

Impending metal fatigue failure holographic detection by optical correlation of coherent light reflection from deformed surface structure as function of time

02 p0294 A72-12442

Tension-compression cycling effects on fatigue crack growth in high strength alloys

[ASME PAPER 71-PVP-2]

02 p0294 A72-12469

Papers on metal fatigue damage covering basic mechanisms, detection, field practices for repair, avoidance and control

02 p0295 A72-12495

Metal fatigue mechanisms in subcreep temperature range, discussing response to cyclic loading including hardening, softening and inhomogeneous plastic strain development

02 p0295 A72-12496

Metal fatigue time and cycle dependent deformation and fracture mechanisms in creep range from cumulative damage law standpoint for lifetime prediction

02 p0295 A72-12497

Metal fatigue damage nondestructive detection, discussing inspection methods, equipment, advantages, limitations and test results

[AD-741977]

02 p0296 A72-12498

Jet engine component overhaul procedures for fatigue damage repair, detailing distressed metal removal, replacement and welding techniques

02 p0271 A72-12499

Metal fatigue damage avoidance, control and repair, considering design, metallurgical and service factors

02 p0296 A72-12500

Cumulative damage in metal fatigue, suggesting unified theory applicable to stress or strain controlled conditions

03 p0442 A72-12922

Automatic recording of cyclic creep and strain curves for metals under low cycle static tension

03 p0444 A72-13468

Austenitic steel under combined bending and torsion, showing fatigue strength dependence on temperature, load cycle asymmetry and stress concentration

03 p0371 A72-13469

Strain gage measurements of stress intensity factor for crack propagation in fatigue cracked thin metal sheets

03 p0444 A72-13542

Microfractographic fatigue fracture analysis of steels, aluminum, brass, nickel and molybdenum by scanning electron microscope

03 p0372 A72-13543

Soviet conference papers on fatigue of metals, alloys and composite materials covering breakdown mechanisms, failure kinetics, cyclic strength and hardening

03 p0372 A72-13587

Fatigue failure under cyclic stress, analyzing surface and temperature effects

03 p0372 A72-13588

Fatigue breakdown and energy dissipation dependence on stress during bending of cylindrical steel and iron specimens

03 p0372 A72-13589

Cyclic deformation and energy dissipation during fatigue breakdown in steels under tension-compression and torsion

03 p0372 A72-13590

Surface layers and aging influence on Bauschinger effect in profiled low carbon steel under low tension-compression load cycles

03 p0445 A72-13591

Secondary fatigue curves for determining service life of metal specimens under unsteady loads

03 p0445 A72-13592

Crack propagation rates during bending fatigue tests on flat hardened steel as function of stress intensity and plasticity area

03 p0445 A72-13593

Beta structure effect on cyclic fatigue strength in Ti alloy under various heat treatments

03 p0372 A72-13595

Optimal cyclic fatigue strength of low C steel from critical deformation rate during thermomechanical treatment

03 p0372 A72-13597

Stepwise thermomechanical treatment effect on improved cyclic fatigue strength of Ni-Cr sheet steel with tension and rolling deformations

03 p0372 A72-13598

Steels fatigue life tests as function of stress level, confirming Wohler curves mathematical model

03 p0373 A72-13673

Grain orientation effect on fatigue crack propagation in notched test specimens cut from cold rolled prestressed annealed brass plate

03 p0375 A72-13934

Fatigue cracks nucleation in steel bearings subjected to cyclic contact stresses

03 p0377 A72-14020

Corrosion fatigue cyclic crack growth rate above and below environmental threshold stress in steels as function of frequency and potentials, indicating hydrogen embrittlement

03 p0377 A72-14172

Cu single crystal fatigue life explanation by work hardening using statistical theory of slip

03 p0379 A72-14258

Ultrasonic fatigue at small strain amplitudes in Ti, deposing solitary slip band microcracks

04 p0533 A72-14539

Mean stress and overload effects on mild steel service life, using fatigue damage summation method

04 p0592 A72-15475

Impact fatigue testing apparatus, presenting results for stainless steel

04 p0524 A72-15549

Dislocation substructure in fatigued Al and Ni polycrystals surface layer and interior due to high and low stress cycling, discussing stacking fault energy influence

04 p0534 A72-15577

Titanium alloy microstructure effect on fatigue strength under symmetric bending load cycles in air and NaCl solution

04 p0535 A72-15663

Fatigue crack propagation rates for aluminum alloy plates under mode I extensional loads and transverse mode II bending loads

[ASME PAPER 71-MET-J]

05 p0732 A72-15793

Al and Al-Zr coating effects on heat resistant alloy turbine blades high temperature fatigue resistance under bending-torsion cyclic loads

05 p0671 A72-15990

Anodic layer thickness effect on fatigue crack initiation and fracture mode in mono and polycrystalline aluminum

05 p0672 A72-16015

High temperature low cycle fatigue of Cr-Mo-V steel, observing crack growth rate correlation with crack tip stress

05 p0673 A72-16321

Purity effect on fatigue crack growth in high strength steel at room temperature

05 p0674 A72-16325

Plastic zone formation and fatigue crack propagation rate during high cyclic bending of metals

05 p0674 A72-16326

Hydrogen environment effects on fatigue crack growth rates in Ti-Al-V weldments over low ambient temperature range

05 p0678 A72-17116

Zircaloy plastic properties and fatigue fracture modes under strain controlled push-pull cyclic loads, noting plastic anisotropy changes for warm cross rolled and recrystallized materials

05 p0678 A72-17120

Fatigue and fatigue-corrosion properties of high strength stainless maraging martensitic structural and stainless austenitic steels

05 p0680 A72-17206

High purity polycrystalline Al hf low strain fatigue measurements by piezoelectrically driven exponential horn, estimating critical point defect concentration

06 p0893 A72-17420

Microvolume decohesion hypothesis for crystal lattice defects explaining metal fatigue under variable stresses

06 p0829 A72-17743

Creep behavior during and immediately after loading of Nimonic 90 and H 46 Cr steel under various stresses, temperatures and rates

06 p0829 A72-17801

Semibrittle tears and fractures by progressive cracking in metallic structures, discussing metal fatigue and environmental stress

06 p0897 A72-18297

Slip band formation and crack initiation in Ti as function of cyclic loading frequency, considering plastic strain amplitude or distribution as causes

[DFVLR-SONDDR-149]

06 p0832 A72-18425

Refactory and structural steels and Al alloys, obtaining low cyclic plastic deformation and breaking stress curves

06 p0898 A72-18549

Deformation kinetics and failure of refractory Nb and Mo base alloys in plastic state under low cyclic fatigue

06 p0833 A72-18631

Nickel base alloy under axisymmetric tension compression tests, obtaining breaking load diagrams and fatigue and creep curves

06 p0833 A72-18638

Fractographic analysis of failure kinetics and crack formation in Al alloys, showing microfatigue intrusions and extrusions for various initial stress levels

06 p0834 A72-18653

Thermostable and heat resistant steels and alloys vibration loading frequency effects on fatigue at high temperatures

06 p0834 A72-18688

Static and fatigue strength in tension of welded joints composed of low carbon and austenitic steel

07 p0996 A72-19767

Static hydrogen fatigue of high strength steels, deriving relationship between time to cracking and tensile stresses magnitude for cadmium-plated steel

07 p1014 A72-19774

Test equipment with variable deflection and twist for metal fatigue microcrack initiation and growth detection

07 p0987 A72-19849

- Prestressing effect on stress corrosion resistance of fatigue precracked high strength steels
07 p1016 A72-19941
- Stepwise fatigue testing of high temperature alloy, noting strain hardening phenomena in prestressed samples
07 p1017 A72-20129
- Analytical model for surface fatigue crack configuration during propagation into thick plate under cyclic loading
[AD-741575] 07 p1095 A72-20242
- Metals and alloys for aerospace applications, emphasizing creep and fatigue properties and oxidation resistance at high temperatures
08 p1185 A72-21171
- Mechanical surface strengthening effect on small cycle fatigue life of Ti alloy weakened by stress raiser
08 p1186 A72-21725
- Machine metals fatigue life, creep theory and stress and strain kinetics in severe environments, formulating physical equations
08 p1246 A72-21805
- German monograph on computerized statistical analysis of Al alloy fatigue test data, considering welded samples and thin plates
08 p1188 A72-21848
- Fatigue striation formation and crack propagation mechanism in Al alloy films from electron microscope studies
09 p1328 A72-22917
- Crack propagation and substructure formation near fatigue crack in austenitic stainless steel observed by X ray diffraction and replica electron microscopy
09 p1329 A72-23148
- Metal creep fatigue analysis and life prediction by inelastic strain ranges partitioning into reversed tensile and compressive plasticity and creep components
09 p1406 A72-23198
- Time and cycles to failure diagrams for strain rate and hold periods effects on high temperature metal creep fatigue in design analysis
09 p1407 A72-23199
- Mathematical model and inelastic stress analysis for metal creep-fatigue interaction and progressive deformation in breeder reactors operation
09 p1407 A72-23200
- Welded structures fatigue, - Conference, Abington, England, July 1970
09 p1332 A72-23615
- Fracture mechanics application to welded structures fatigue, using crack propagation law
09 p1409 A72-23616
- Welded high strength maraging steels fatigue performance, stressing nondestructive testing technique
09 p1332 A72-23617
- Cumulative fatigue damage in Al-Zn-Mg alloy fillet welded joints, analyzing constant amplitude and programmed load fatigue test results
09 p1332 A72-23618
- Fatigue indicators with analytic or visual notched and cracked coupons techniques and strain multipliers for welded structures
09 p1316 A72-23620
- Design information for machinery to incorporate welding positions and joints, fatigue mechanisms, loads, combined stresses and plate and cast materials properties
09 p1409 A72-23621
- Diffusion bonding compared to other processes, discussing mechanical properties, metallurgical condition, fatigue, pressure, temperature and production problems
09 p1320 A72-23633
- Fatigue crack propagation theory based on linear accumulation of metallurgical damage in plastic region
10 p1553 A72-24098
- Transmission electron microscope examination of deformation microstructures adjacent to fatigue cracks in Al alloys
10 p1497 A72-24823
- Fatigue crack propagation relation to plasticized zone formation at crack tip in ferritic carbon steels and in Cr-Ni austenitic stainless steels
10 p1558 A72-24855
- Mean stress effect on fatigue crack propagation rate in half inch thick Al alloy specimens of high and low fracture toughness
10 p1498 A72-24884
- Carbon steel fatigue crack propagation rate dependence on strength and stress history, discussing conditions for crack nonpropagation
10 p1499 A72-24889
- Environmental sensitivity effect on crack propagation rates in steels and Al and Ti alloys, discussing corrosion fatigue
10 p1499 A72-24899
- Fatigue crack initiation and growth in filament reinforced Al alloys, noting interface crack tip stress distribution effects
11 p1654 A72-25480
- Test assembly design for microstructural studies of metal and alloy fatigue in vacuum during heating, describing electrical resistance measurement and stroboscopic illumination
11 p1612 A72-25492
- Ni fatigue crack propagation under low cyclic loads at high temperature in vacuum after annealing and mechanical treatment
11 p1655 A72-25497
- Liquid environments effect on mild steel fatigue strength, discussing effects of viscosity, compressibility and entry rate into cracks
11 p1656 A72-25738
- Locati and Prot methods for metal fatigue limits evaluated by axial and rotating bending tests on steel specimens
11 p1657 A72-25824
- Creep and low cycle fatigue dynamic behavior, noting stress concentration time dependence, strain hardening and local plastic deformations in dead annealed Al thin walled tubes
11 p1658 A72-25829
- Polycrystalline Mo fatigue behavior under cyclic stresses, discussing grain size effect on fatigue life and relationship between cycle dependent yield and French damage line
11 p1658 A72-25830
- Fatigue life cumulative damage prediction procedure for engineering metals subjected to complicated stress-strain histories, noting errors in average mean stress method
11 p1658 A72-25831
- Mn content effect on mechanical properties and corrosion fatigue and stress corrosion cracking resistance of Al-Mg casting alloys
11 p1658 A72-25850
- High power ultrasonics in metal fatigue studies, considering crack propagation and slip patterns for high and low frequencies
11 p1639 A72-26053
- Fatigue and fatigue-corrosion properties of high strength stainless maraging, martensitic structural and stainless austenitic steels
11 p1660 A72-26141
- Theoretical fatigue test procedure for reliability analysis of machine parts, calculating fatigue probability in load carrying components
11 p1640 A72-26244
- Fatigue properties of Ni-Al-W alloy with gamma-prime matrix, noting high endurance limit/yield strength ratio at room temperature
11 p1661 A72-26653
- Pulsating heat source model for physical processes in metal surface layer under fatigue limit stress level, calculating critical volume to limit energy buildup
11 p1738 A72-26801
- Cyclic loads frequency and environmental effects on fatigue crack propagation rate, comparing theoretical results with Al alloy thin plates experimental data
11 p1663 A72-26802
- Tungsten alloy wires strength, creep properties and fatigue limit, investigating fracture characteristics
11 p1663 A72-26807
- Diamond burnishing effect on surface quality and fatigue strength of steel, noting work hardening increase and compressive residual stresses buildup in surface layer
11 p1642 A72-26811
- Ti alloys fatigue strength, stress concentration sensitivity and grain sizes effects at normal and high temperature under cyclic loads
11 p1663 A72-26821
- Udimet 500 alloy dislocation substructure and fracture surface topography during deformation to failure in low cycle fatigue at high temperatures
11 p1667 A72-26938
- Low cycle fatigue deformation of lamellar eutectic and cast Ni-Sr alloys, noting microstructure and chemical composition effects on fracture energy
11 p1668 A72-26939
- Reversible stress effects in theory of plastic flow in strain hardened metals at high temperatures
12 p1879 A72-27159
- Fatigue failure tests of low carbon Mn steel, analyzing structural damage under cyclic loads in relation to temperature curve
12 p1829 A72-27458
- Cyclic stress ratio effects on stainless steel fatigue crack propagation at 1000 F, using linear elastic fracture mechanics
12 p1829 A72-27663
- Steel components contact fatigue kinetics measurement by emf increase of inductive sensor
12 p1887 A72-28245
- Metal fatigue strength testing under programmed temperature regimes, using HF induction generator
12 p1796 A72-28247
- High temperature low cycle fatigue of alloys as process of crack nucleation and growth to ultimate failure
13 p2058 A72-29445
- Microscopic substructure in high temperature fatigued fcc austenitic steel and aluminum, studying cross slip lines and crack initiation
13 p1979 A72-29448
- Temperature and strain rate dependence of austenitic stainless steel fracture by low cycle fatigue at high temperatures, studying striations with scanning electron microscopes
13 p1979 A72-29449
- Borated steels strength under static bending, cyclic flexure and torsion and impact loads, correlating fatigue strength, residual stresses and core properties
13 p1979 A72-29477
- Paint coatings aging effect on D16T type alloy corrosion fatigue in NaCl solution, noting protective efficiency decrease
13 p1984 A72-29486
- Aviation fuels and additives effect on steel endurance limit at room temperature
13 p1980 A72-29487
- Model for metal fatigue fracturing, noting crack initiation and two stages of propagation, emphasizing experimental fractographic /electron microscopy/ research
13 p2061 A72-29773
- Literature survey of fatigue behavior of Al alloy welded joints, discussing testing and analysis methods
14 p2113 A72-30250
- Resonance type facility using dynamic hysteresis loop method to test metal fatigue and anelasticity in torsion at room and high temperatures
14 p2092 A72-30443
- Fatigue crack growth rate in precracked steel samples observed at 100 C by etching technique, noting flow stress and yield in plastic zone
14 p2119 A72-30608
- Crystal lattice defects induced by cyclic straining in quenched Al-Zn alloy, noting fatigue effects on dislocations accumulation and grain boundary migration
14 p2120 A72-30610
- Fcc metal defect structure due to ultrasonic fatigue observation via transmission electron microscopy for dislocations
15 p2256 A72-31836
- Ultrasonic metal fatigue, discussing crack initiation and growth and frequency effects
15 p2256 A72-31837
- Microcrack initiation and propagation in ductile metals at low cycle and ultrasonic frequencies, investigating fatigue fracture mechanism by scanning electron microscope
15 p2256 A72-31838
- Metal fatigue tests at various frequencies to observe surface structure, dislocations in crack vicinity, plastic deformation and ultrasonic resonance techniques
15 p2257 A72-31839
- Rotating bending fatigue limit correlation with non-propagating crack for steel specimens with hole
15 p2329 A72-32140
- Prestraining effect on metal fatigue strength, showing increase relation to yield strength and ultimate strength
16 p2463 A72-32903
- Safe stress range for metal fatigue deformation preceding fracture under combined cyclic and steady push-pull loads
16 p2468 A72-33228
- Temperature effect on fatigue crack growth in high strength annealed Ti-Al-V alloy in water, oxygen/hydrogen and vacuum environments
16 p2406 A72-33320
- Deformation substructures in stainless steels under low cycle high strain fatigue tests evaluation for application as fuel cladding for fast breeder reactors
16 p2411 A72-33825
- Understressing and coaxing cycles effect on deeply notched carbon steel fatigue behavior, emphasizing crack initiation and breakdown
16 p2472 A72-33947
- Crack opening displacement and the rate of fatigue crack growth.
17 p2565 A72-34255
- Russian book on metal fatigue and inelasticity covering structural inhomogeneities, static and dynamic loading, failure mechanisms, deformation, temperature effects and test methods
17 p2566 A72-34649
- Effects of thickness on fatigue crack initiation and growth in notched mild steel specimens.
17 p2627 A72-34747
- Ultrasonic tests for incipient fatigue, hardness and elastic constants-tensile strength relationship in metals
18 p2690 A72-36125
- The effect of high vacuum on the low cycle fatigue law.
18 p2700 A72-36582
- The effects of environment on the elevated temperature fatigue behavior of nickel-base superalloy single crystals.
18 p2700 A72-36587
- Temperature effects on the strainrange partitioning approach for creep-fatigue analysis.
19 p2815 A72-37638
- Creep damage role in governing elevated temperature strain cycling fatigue lives of heat resistant stainless steel and cobalt alloy
19 p2817 A72-37712
- Evaluation of the tendency to brittle fracture of turbine rotors made from steels of medium strength
19 p2876 A72-38001
- Effect of the loading frequency on the fatigue strength of metals
19 p2818 A72-38012

Surface cold-working as a means of increasing the short-term fatigue endurance of machine elements
19 p2808 A72-38015

Relation between the reliability and allowable stress amplitude in fatigue design.
20 p2977 A72-38879

Microscopic substructure in face centered cubic metals fatigued at elevated temperatures.
20 p2935 A72-38880

Environmental acceleration of fatigue-crack growth in a high-strength steel.
20 p2935 A72-39140

Effect of thickness and orientation on fatigue crack growth rate in 4340 steel.
20 p2937 A72-39294

Thermal fatigue resistance of KHN70VMuT boronized alloy
20 p2941 A72-39585

Review - Fatigue-crack propagation in metallic and polymeric materials.
20 p2980 A72-39793

Vibrational shot peening as a method of increasing the fatigue strength of critical aircraft elements
20 p2929 A72-39802

Fatigue strength of welded aluminum-connections - Investigation with the aid of multiparameter life length lines
20 p2930 A72-39941

Fatigue-crack propagation characteristics of aluminum alloys in thick sections.
20 p2942 A72-39951

Metal fatigue crack propagation under cyclic loads, assuming specific energy dissipation as material constant
20 p2981 A72-39953

Criteria for valid plane strain fracture toughness testing dealing with straightness of fatigue crack front of metal specimens
20 p2981 A72-39958

Effect of notch root radius on the initiation and propagation of fatigue cracks.
20 p2981 A72-39960

Study of fatigue crack initiation from flaws using fracture mechanics theory.
20 p2981 A72-39961

Designing to avoid stress-corrosion and/or fatigue failures.
[AICHE PAPER 15C] 21 p3116 A72-40125

A comparison of the effect of inward and outward diffusion aluminate coatings on the fatigue behavior of nickel-base superalloys.
21 p3067 A72-40916

Fatigue cumulative damage in cases of rotating-bending and torsional multistep loading.
21 p3118 A72-40933

Isothermal deformation behavior of structural metals in laboratory creep, relaxation and low cycle fatigue tests at high temperatures
21 p3119 A72-41009

Temperature and strain rate dependencies of low cycle fatigue life at high temperatures of austenitic stainless steel, examining crack behavior and stress-strain relations
21 p3069 A72-41010

Low carbon steel S-N diagram for stresses ranging to fatigue limit, noting cyclic creep, macroplastic cyclic stress and fatigue failure
21 p3122 A72-41353

Influence of the cycling frequency and directional anisotropy on the fatigue strength of AMg6BM aluminum-alloy sheet
21 p3070 A72-41356

Resonant frequency, fatigue and energy dissipation relations for endurance limit determination in Al alloy specimens under vibrational loads
21 p3070 A72-41368

Book - Metal matrix composites.
21 p3070 A72-41528

Investigation of fatigue-failure mechanisms and inelastic deformation of metals in torsion
21 p3071 A72-41703

Facility for measuring and recording the electrical resistance of metallic samples during mechanical tests
21 p3043 A72-41718

Cyclic hardening of Al-Zn single crystals at constant plastic strain amplitude, observing similarity between fatigue hardening and work hardening
22 p3189 A72-42439

Brittle striation formation role in corrosion fatigue crack propagation mechanism in Al-Zn-Mg alloy from test in NaCl solution under reversed anodic-cathodic current
22 p3193 A72-43033

Effect of cyclic stress wave form on corrosion fatigue crack propagation in Al-Zn-Mg alloys.
22 p3194 A72-43043

Influence of the cycling frequency on the fatigue and corrosion fatigue of steel samples with bushings
22 p3242 A72-43155

Inelastic effects during metal fatigue
22 p3195 A72-43156

Investigation of the kinetics of low-cycle fatigue of steels in a hydrogen atmosphere and in vacuum
22 p3195 A72-43161

Gas turbine blades of cast ZhS6K heat resistant alloy, investigating structural strength from fatigue test data
23 p3347 A72-43734

Gas turbine blade models of heat resistant ZhS6K alloy under operational temperature variations, observing fatigue strength
23 p3347 A72-43735

Failure and crack formation in gas turbine engine compressor disks under variable stresses from fatigue tests, considering safety factors
23 p3347 A72-43736

Solid powder metallurgy tungsten alloys, determining scale factor effect on bending strength and fatigue limit
23 p3301 A72-43751

Fatigue strength of two phase Ti alloys, considering work hardening, electrochemical finishing, electropolishing and protective media
23 p3301 A72-43757

Heat resistant ZhS6K alloy precision and ground cast specimens, determining short and long term strength and fatigue
23 p3301 A72-43761

Energy dissipation in metals during high-frequency fatigue tests. I
23 p3302 A72-43963

Energy dissipation in metals during high-frequency fatigue tests. II
23 p3302 A72-43964

Machine with programmed load control for studying the fatigue and inelasticity of metals at room and elevated temperatures
23 p3278 A72-43969

Low cycle fatigue under biaxial strain controlled conditions.
23 p3354 A72-44259

Fatigue behavior of a titanium 8Al-1Mo-1V alloy in a dry argon environment.
23 p3304 A72-44261

Fatigue crack propagation in A514 base plate and welded joints.
23 p3354 A72-44309

A comparison of the axial and reversed-torsional strain cycling low-cycle fatigue strength of several structural materials.
23 p3304 A72-44397

The difference in the plastic deformation of the surface and bulk layers of polycrystalline iron under fatigue loading
23 p3304 A72-44490

Estimates of creep-fatigue interaction in irradiated and unirradiated austenitic stainless steels.
24 p3412 A72-44554

Fatigue-crack growth in 20% cold-worked Type 316 stainless steel at elevated temperatures.
24 p3435 A72-44555

The stress-strain relation in the low-cycle fatigue of metallic materials under rotating-beam bending.
24 p3454 A72-44626

The cyclic plastic strain and cumulative fatigue damage - Fatigue damage caused by the stress below the fatigue limit.
24 p3454 A72-44628

The application of Ti-6Al-4V titanium to helicopter fatigue loaded components.
24 p3366 A72-44732

Estimation of creep and fatigue behaviour under cyclic loading.
24 p3456 A72-44793

Plane-stress fracture toughness testing using a crack-line-loaded specimen.
24 p3456 A72-44810

Ultrasonic detection of fatigue damage.
24 p3457 A72-44820

Development and present-day state of the fatigue-damage theories.
24 p3457 A72-44873

Automatic recording of cyclic creep and strain curves for metals under low cycle static tension
24 p3458 A72-44943

Austenitic steel under combined bending and torsion, showing fatigue strength dependence on temperature, load cycle asymmetry and stress concentration
24 p3414 A72-44944

Al and Al-Zr coating effects on heat resistant alloy turbine blades high temperature fatigue resistance under bending-torsion cyclic loads
24 p3415 A72-45732

Stepwise fatigue testing of high temperature alloy, noting strain hardening phenomena in prestressed samples
24 p3416 A72-45755

Method for applying a fatigue crack to impact test specimens made from tough materials.
24 p3417 A72-45765

METAL FILMS

Au thin film effective optical constant calculation from measured reflection and transmission coefficients and thickness by approximate formulas
03 p0401 A72-13363

Superferromagnetism in thin polycrystalline Gd and Gd-Au films having Curie points near room temperature
03 p0401 A72-13583

Alloying elements and grain size effects on thermally induced surface reconstruction of Al film metalization on Si devices from thermal cycling tests
03 p0364 A72-14285

High resolution electron microscope observation of voids in amorphous Ge films, noting density dependence on substrate temperature
04 p0562 A72-15152

NbN film superconducting properties measured as function of thickness, discussing transition temperature, critical current and magnetic field
04 p0562 A72-15294

Al finished and Au plated triple calibration sphere as multispectral optical sensor for testing Cook hypothesis concerning satellite drag dependence on surface material
04 p0500 A72-15305

X ray spectral analysis of microchemical changes in surface films of titanium alloys during diffusive interaction with silicon carbide abrasive
04 p0534 A72-15654

Optical resonators using lossy anisotropic metal film linear polarizer for oscillation mode selection
[CLEA PAPER 6.3] 07 p1004 A72-19382

A-15 superconducting films preparation cosputtering method, noting alloying effects and crystal structure stability determinations applications
09 p1368 A72-22559

Noncrystalline Ge film preparation by rf sputtering onto substrate with explosive crystallization triggered by localized transient energy pulse at room temperature
09 p1369 A72-22625

Diffusion coefficient and distribution of Ti atoms in thin Al film from electric current vs time curves for oxidation of solid solution
09 p1329 A72-23036

Polymorphism in Ta vacuum condensates, observing beta-alpha phase transformation in films
09 p1329 A72-23041

Metal stress corrosion crack propagation rate theory based on film rupture mechanism
11 p1735 A72-25852

Transition temperature and other superconducting properties of annealed Nb-Al-Ge thin films
12 p1853 A72-27038

Low pressure hydrogen and titanium thin film reaction rate measurement, using flow technique
12 p1778 A72-27046

Vacuum deposition process relation to thin metal film properties, discussing current conducting mechanism
12 p1854 A72-27275

Epitaxial and textured Pb films on mica and glass, using reflection electron diffraction, etching and optical microscopy for structure study
12 p1854 A72-27289

Effect on physical and mechanical properties of hard metals due to gas sorption by metallic films spray-coated on surfaces, describing vacuum apparatus
13 p1939 A72-29488

Shielding metallic interlayer technique to protect MIS device against degradation due to ionizing radiation effects
13 p2023 A72-29836

High light transmission electrically conducting Hyviz and gold film laminates for aircraft windshields and window heating applications
13 p1898 A72-30038

Niobium and molybdenum carbide film deposition on steel substrates by open arc welding with partial carbon burnout
14 p2107 A72-30156

Electron work function for metallic sphere and thin film on dielectric substrate as function of radius, thickness and dielectric constant
15 p2290 A72-31222

Vacuum UV reflectance dependence of Re and W vapor-deposited films on substrate temperature during deposition, film thickness and aging in air
15 p2274 A72-31377

Strain analysis of thin metallic films on low modulus structural substrate by light intensity measurement
15 p2325 A72-31526

Soft X ray appearance potential spectrometer construction and operation for metal film diffusion detection in microcircuit technology
15 p2241 A72-32442

Sensor design and principles for atomic oxygen concentration measurement in dissociated gases, using Ag thin film electrical resistance change during oxidation
16 p2390 A72-33162

Structural and orientation study of sequentially evaporated MnBi thin films on glass substrates using electron diffraction and transmission microscopy
16 p2441 A72-33207

Diffusion limitation avoidance at high current densities by fuel cell preparation via Pt thin film sputtering on porous vycor substrates
16 p2352 A72-33893

Photoemissive properties of bismuth-cesium films
17 p2595 A72-34754

Theory for the excitation of SHF elastic waves by multiple-film transducers /Allowance for the influence of metallic and dielectric layers/
17 p2529 A72-34843

Contribution to the study of creep in thin permalloy films.
17 p2596 A72-35759

Off-axis hologram recording on thin bismuth film with picosecond pulse train from mode-locked Nd-glass laser
17 p2558 A72-35817

Work function, thermal stability, and atomic structure of electropositive films adsorbed on single crystals of metals
18 p2656 A72-36132

Crystal orientation effect on electron work function in chemical vapor deposited W layers on thermionic converter cylindrical emitters
18 p2717 A72-36142

Possibility of an inhomogeneous charge distribution in an adsorbed layer
18 p2713 A72-36176

On the radiation of discontinuous gold films by electric current transmission.
18 p2718 A72-36349

Laser machining of thin films. I - Irradiation characteristics of a focused Q-switched YAG laser beam.
18 p2695 A72-36518

Changes of electrical and structural properties of Au thin films obtained by sputtering during the annealing process.
18 p2720 A72-36955

Determination of the time of hole formation in a metallic film under the action of single-pulse laser radiation
19 p2812 A72-38540

Dependence of critical supercurrent on normal layer thickness in S-N-S structures.
19 p2846 A72-38631

Possible uses of plasma oscillations in thin metal films.
20 p2959 A72-39053

Investigation by the method of secondary ion-ion emission of the initial phase of the formation process of a silver vacuum condensate on a nickel substrate
21 p3068 A72-40960

Auger spectroscopic observation of Si-Au mixed-phase formation at low temperatures.
22 p3178 A72-42616

High value thin-film-on-silicon resistors for hybrid applications.
22 p3160 A72-42825

Magnetic flux penetration into superconducting thin films.
23 p3323 A72-43271

Electrical resistivity changes in nichrome films sintering of various thickness with different heat treatment conditions, noting heat stability and thermal shock tests
23 p3292 A72-43280

Magnetostriction of porous nickel films
23 p3299 A72-43340

Optical properties of thin cesium films over the wavelength range from 0.3 to 0.9 microns and their electrical resistance
24 p3426 A72-44801

METAL FINISHING
NT ELECTROPOLISHING
NT SHOT PEENING

Fatigue strength of two phase Ti alloys, considering work hardening, electrochemical finishing, electropolishing and protective media
23 p3301 A72-43757

METAL FOILS
Electrochemical thinning of metal disks for electron microscopic thin foils preparation
04 p0527 A72-15492

Dislocation loops in thin W foil due to ion irradiation, using electron microscopic analysis
09 p1331 A72-23505

Radiation damage in bcc metal Mo and W foils under energetic Au ion irradiation, noting vacancy dislocation loops
09 p1331 A72-23506

Lunar surface darkening caused by solar wind effect, noting Fe valence state changes evaluation from photoelectronic spectroscopy of foil samples exposed to ion bombardment
09 p1394 A72-23665

High intensity laser radiation absorption in plasma produced from thick metal targets and thin Au foil
10 p1490 A72-23967

Metallic foils effects on thermal joint resistance of interface between lathe turned and optically flat surfaces, noting optimal thickness
[AIAA PAPER 72-283] 11 p1685 A72-25223

Beryllium sheet and foil application to lightweight space structures, discussing mechanical properties
[AIAA PAPER 72-404] 11 p1726 A72-25425

Damping additions for plates using constrained thin viscoelastic sheets and metallic layers
11 p1688 A72-26063

High temperature low pressure reaction kinetics of nitrogen sorption by titanium foil, using ultrahigh vacuum microbalance
12 p1777 A72-27045

Be foil electrical resistance change during and after pulsed laser irradiation and annealing
12 p1853 A72-27067

Orientation and elongation effects on grain boundary correction term in foil surface energy measurement by zero creep, using virtual work method
15 p2258 A72-32637

Secondary electron emission and molecule passage during in-depth interaction of high energy molecular beam with thin gold foil
16 p2430 A72-33067

Iridium and tantalum foils for spaceflight neutron dosimetry.
17 p2558 A72-35901

Microcracks observed in hydrogenated niobium foil.
21 p3069 A72-41300

Spontaneous magnetization of Ni foils in high pressure H gas, noting Hall voltage measurement in ferromagnetic foils and thin plates
23 p3324 A72-44140

The direct study of crack formation in metals in a high-voltage electron microscope
24 p3401 A72-44717

Be foil electrical resistance change during and after pulsed laser irradiation and annealing
24 p3432 A72-45720

METAL FORGING
U FORGING

METAL FORMING
U FORMING TECHNIQUES
U METAL WORKING

METAL GRINDING
Electron microscope study of hard alloy surface layer formation characteristics during diamond grinding with electrolysis
12 p1814 A72-27766

METAL HALIDES
NT ALKALI HALIDES
NT ALUMINUM FLUORIDES
NT BARIUM FLUORIDES
NT CALCIUM FLUORIDES
NT CESIUM IODIDES
NT IRON CHLORIDES
NT LANTHANUM FLUORIDES
NT LITHIUM CHLORIDES
NT LITHIUM FLUORIDES
NT MAGNESIUM FLUORIDES
NT POTASSIUM CHLORIDES
NT SILVER BROMIDES
NT SILVER HALIDES
NT SODIUM CHLORIDES
NT SODIUM FLUORIDES
NT SODIUM IODIDES
NT TUNGSTEN FLUORIDES
NT URANIUM FLUORIDES

Metals and metal oxides powders mixture formation by mixed metal halides gelation in alcohol solution
02 p0233 A72-11455

METAL HARDENING
U HARDENING [MATERIALS]

METAL HYDRIDES
NT LITHIUM HYDRIDES

Solar MgH isotopic abundance ratios and photo-spheric lines, correcting previous overestimation for sunspot spectra analyses
07 p1071 A72-19179

Interstitial phases, crystal structure and chemical bonds of titanium, vanadium and niobium carbides, comparing with transition metal carbides
15 p2252 A72-31195

Chemical and spectroscopic activity of germanium tetrahydride in Jovian atmosphere in 4.7 micron window
15 p2312 A72-32094

Volumetric analysis of Th, Zr and Li hydrides precipitation in Mg alloys, determining rate equation and activation energy
15 p2257 A72-32118

Investigations concerning metal-hydride technology and hydrogen transport in the incore thermionic reactor /ITR/-core.
18 p2699 A72-36157

A possible problem in measuring hydrogen diffusivity at low temperatures by the Gorsky effect.
22 p3190 A72-42443

METAL INSULATOR SEMICONDUCTORS
U MIS [SEMICONDUCTORS]

METAL IONS
NT FERRIC IONS
NT MANGANESE IONS

Positive Fe ion concentration relationship to equatorial spread F fromOGO 6 satellite observation near magnetic equator
01 p0062 A72-10902

Garnet crystal structure type microwave ferrites with V and In ions, investigating ferromagnetic resonance linewidth reduction effect
03 p0400 A72-12971

Solar corona transition probabilities in intermediate coupling between Fe XVII configurations, including full configuration mixing
03 p0416 A72-13006

Electron impact broadening of ionized Be and Ba lines in electric shock tube plasma, measuring electron density and temperatures
03 p0393 A72-13020

Alkali ion scattering by NbTi alloy and SiC and components, comparing scattering coefficients
03 p0401 A72-13424

Quantum mechanical calculations of autoionization structure in ionization of Ba positive ions by electron impact
03 p0391 A72-13746

Photoluminescence of Er cations in CdS, observing group I co-dopants sensitizing behavior and broad-band emission spectra
04 p0563 A72-15472

Metallic ion convergent flow role in sporadic E layer formation in auroral and equatorial ionosphere
06 p0810 A72-18730

Zeeman patterns and energy level Lande g factors from spectrograms of As ion electrodeless discharge tubes in presence of 24,025 G magnetic field
07 p0987 A72-19832

Carbon like spectra and ground energy levels of Sc, Ti and V ions in 16-22 A range, using vacuum spark source
07 p1037 A72-19833

Mg ion excitation by electron collision in solar chromosphere studies, calculating scattering cross sections
07 p1081 A72-20234

Hyperfine interactions of Fe cations in ilmenite determined by Mossbauer spectroscopy, noting internal magnetic field and quadrupole coupling constant
09 p1367 A72-22457

Multiple charge Al and C ions X-UV spectra use for studying laser produced plasmas build up and expansion regions
09 p1359 A72-22830

Optical and inner shell X ray transitions in highly ionized Cu, Fe and Ti observed from point plasma source generated in linear vacuum discharge
09 p1360 A72-22833

Be and Mg ion generation and p-type layer electrical properties production by implantation in GaAs substrates
09 p1372 A72-23245

Tuned radar laser detection and ranging of high altitude Ba ion cloud by photon counting, discussing SNR requirement
10 p1440 A72-24963

Wind shear and midlatitude sporadic E layer theories, discussing metal ions production and loss
10 p1477 A72-25158

Metal ion sheaths in midlatitude sporadic E layer caused by vertical redistribution of neutral ionization, discussing wind shear discontinuities
10 p1477 A72-25159

Atmospheric metal ion chemistry, tabulating thermal energy binary and three body reaction rate data
10 p1434 A72-25160

Spacecraft thermal control coating damage by energetic Hg ion bombardment, using absorbance measurements
[AIAA PAPER 72-445] 11 p1746 A72-26183

Magnetically unaffected Fe I line profiles in sunspots from high resolution photographic spectra observation
12 p1867 A72-27205

Secondary autoionization reduction of recombination coefficient during dielectronic recombination process, considering importance in Fe ions
12 p1864 A72-27747

Monovalent K and Na and bivalent Ca and Mg plasma ion ratio effect on thrombocyte electrokinetic potential
13 p1901 A72-28635

West German-United States Barium Ion Cloud Project meteorological support at Wallops Station, discussing magnetospheric magnetic and electric fields
13 p1947 A72-28802

Energetic Hg ion bombardment erode and chemical effects on spacecraft surfaces downstream of electrostatic rockets
[AIAA PAPER 72-446] 13 p1983 A72-28944

Fourier transformation for natural abundance C 13 free induction decays of cyclic antibiotic valinomycin and K ion complex, noting chemical shift differences
13 p1913 A72-29862

Nickel ion charge sign and magnitude estimation in Ni-Cr alloy by electron transfer method
14 p2116 A72-30415

Fe and Ti ion bands in lunar pyroxenes and olivines single crystals polarized absorption spectra
14 p2154 A72-30510

Singly ionized Ca and Mg electron impact broadened resonance lines from rapid scanning Fabry-Perot spectrometer measurements in shock tube generated high temperature plasma
15 p2282 A72-32643

Solar Fe XIII IR lines intensity ratio at 10747 and 10798 Å, deriving electron density as function of dilution factor with allowance for proton impact effect
15 p2318 A72-32784

Solar corona Ca ion abundance from emission line measurements and electron density determination
15 p2318 A72-32785

Doubly ionized Mg, Ca and Ba atoms termolecular association rate constants with various molecular neutrals, comparing doubly charged with singly charged ions cluster reaction rates
16 p2360 A72-32924

Photoelectric observations of Fraunhofer ionized metal lines in sunspot spectrum relating to umbral dots
16 p2458 A72-33687

Charge carriers interaction with metal ions studied from electrical transport of Fe and Co in Fe-Cr alloy
17 p2569 A72-35521

Biomembrane hydration mechanism of Na-K ion pump of living cell based on fractionation at air-sea interface
18 p2649 A72-36441

Ion-atom scattering and interatomic potentials for ions of noble metals and period II elements incident on neon and argon with energies in the range 8-25 keV
19 p2837 A72-37883

Plasma formation on Al target surface by ruby laser beam irradiation, discussing electron and ion velocities as functions of beam power density
19 p2811 A72-38197

Fourier transform C-13 nmr analysis of some free and potassium-ion complexed antibiotics
20 p2898 A72-39399

Influence of cerium additions on the luminescence of europium and samarium ions in NaF single crystals
20 p2932 A72-39414

Metal ions effect on sporadic E layer formation, noting magnesium ions profile redistribution by vertical gradient in neutral particles wind
23 p3284 A72-43376

METAL JOINTS

NT SOLDERED JOINTS

NT SPOT WELDS

NT WELDED JOINTS

Book on vacuum brazing covering dissimilar metals joining, stress cracking, corrosion resistance, joint design, heat treatment and production engineering problems
01 p0073 A72-10165

Continuous seam diffusion bonding application to Ti and superalloys lap, butt and T joints production [ASME PAPER AD 71-264]
01 p0076 A72-10970

Impact effect on strength of glued metal joints mounted in groove cut in baseplate and pressed by yokes
01 p0144 A72-11380

Fatigue strength optimization of bonded double strap metal joints, attributing stress concentration to plastic relaxation [ASME PAPER 71-MET-Q]
05 p0731 A72-15791

Pipe joint flexible metal seal development and testing for Concorde Olympus 593 under thermal and pressure cycling
08 p1178 A72-21938

Ar-H microplasma welding of thin Cr steel sheets with narrow seams for aircraft engines and precision equipment casings
09 p1318 A72-22548

Thermal behavior of explosively welded metals, describing test facility for temperature measurements of joints
09 p1319 A72-22891

Tensile and fatigue tests of dissimilar metal joints made by friction pressure welding
09 p1321 A72-23640

Dimensionless thermal contact conductance parameter for determination of interstitial thermal contact materials effectiveness for metallic junctions [AIAA PAPER 72-284]
11 p1741 A72-25224

ESRO findings on optimal resistance welding of solar cell interconnections for silver coated metals and pure silver
12 p1814 A72-28030

A preliminary investigation of joining methods for aluminum-graphite composites.
17 p2561 A72-35665

German monograph - Contribution to the ultrasonic seam welding of metals
19 p2807 A72-37655

Calculation of the tightness of threshold joints of gas turbine engine rotor bearings
20 p2979 A72-39589

Theoretical interpretation of emf generation between noncompressed parts of bimetallic junction traversed by shock wave, taking into account radiation pressure of phonon gas
22 p3207 A72-43050

Non-destructive testing of adhesive bonded metal-to-metal joints. I.
24 p3408 A72-45289

METAL MATRIX COMPOSITES

Continuous casting of metallic tubular structural elements reinforced with boron filaments, stressing application to space shuttle structures
01 p0074 A72-10731

High temperature testing of metal matrix composites mechanical properties, noting aerospace structural applications
01 p0084 A72-10732

Metal matrix fabrication processes, considering plasma sprayed and diffusion bonded tapes and consolidated sheet material
01 p0074 A72-10733

Coextruded Be fiber-Ti alloy matrix composite sheets for light weight structures, describing ultrasonic inspection and mechanical properties
01 p0084 A72-10734

Buckling of boron/aluminum and graphite/resin fiber composite anisotropic plates, giving load vs fiber orientation angle for various plate aspect ratios
01 p0139 A72-10739

Space shuttle oriented polyimide reinforced Ti matrix composites properties, noting weight saving
01 p0139 A72-10785

Mechanical strength and performance of combined multicomponent bonded materials, including laminar, fiber, flake filled and metal matrix composites
01 p0093 A72-11086

Alumina dispersions structural stability in Fe and Ni based alloys metal matrices
02 p0241 A72-11445

Matrix hardening in dispersion strengthened powder products, discussing dispersion, grain boundary and solid solution hardening
02 p0241 A72-11457

Low cost metal matrix composition fabrication techniques, considering plasma spraying and continuous casting
03 p0364 A72-14236

High strength, stiffness and low density properties of boron/aluminum matrix composites in flight structures
04 p0585 A72-14745

Boron/aluminum composite sheet quality evaluation by radiography, ultrasonic C-scanning and micro-ohm resistance measurement, correlating with resistance weld strength
04 p0526 A72-14839

Ceramic whisker and fiber reinforcement of metals, discussing manufacturing and testing problems
04 p0533 A72-15088

Directionally solidified Al-AlNi intermetallic eutectic composites creep tests, identifying time dependent fracture mechanism
05 p0678 A72-17114

High temperature tests of creep rupture strength of W composite cast with heat resistant alloy coatings
06 p0829 A72-17947

Tensile strength of tungsten reinforced nickel, determining temperature effect on fibers deformation after vacuum rolling simultaneously with plastic matrix
06 p0832 A72-18362

Compressive strength of Cu-W fiber metal matrix composite as function of temperature, comparing to cermets
06 p0832 A72-18363

Scanning electron microscope for metal matrix composite materials structure examination, emphasizing matrix behavior, filament under load and interface
07 p1011 A72-19485

Mechanical properties of fiber reinforced heat resistant alloys
07 p1013 A72-19743

Nichrome matrix composites with W and Mo reinforcing fibers
07 p1013 A72-19744

Tungsten alloy filaments as reinforcing agent of heat resistant composite chromium alloy, investigating long term high temperature effects
07 p1013 A72-19745

Heat resistant Nichrome composite alloy with tungsten filament reinforcement, discussing manufacture and mechanical properties at 1100 C
07 p1013 A72-19747

Steady state creep model for high activation energy role in interstitial formation and migration in particle strengthened alloys
08 p1185 A72-20992

Metallic matrix stress-strain properties from phenomenological model based on idealized behavior of system components, noting dependence on fiber volume content
08 p1185 A72-21183

Composite processing, adhesive formulary, bonding processes and mechanical properties of low void content autoclave molded polyimide graphite composite stiffened titanium alloy structures
08 p1193 A72-21687

Helically bound wire reinforced sprayed Al tubes and rings, investigating failure mechanism dependence on fracture modes from tensile and bending tests
09 p1330 A72-23174

Microstructure and mechanical behavior of unidirectionally solidified magnesium-magnesium nickelide eutectic composite over range of solidification rates
09 p1330 A72-23376

Metastable austenitic steel fiber to increase Al matrix strength to density ratio and fracture toughness
09 p1331 A72-23385

Metal matrix composites deformation and mechanical properties prediction from component phases information, examining interface role, residual stress effect and thermal degradation
10 p1553 A72-24176

Elastoplastic analysis of unidirectional filament reinforced boron/aluminum and boron/epoxy composites under longitudinal loading, using finite element techniques
10 p1555 A72-24254

High strength steel strip reinforced aluminum, discussing fabrication techniques and mechanical properties
10 p1498 A72-24839

Compressive strength of Ti alloy airframe skin stringer panels reinforced with B-Al composite by brazing [AIAA PAPER 72-359]
11 p1729 A72-25387

B-Al metal matrix composites joining together and to Al and Ti, considering soldering, brazing, bonding and mechanical fastening [AIAA PAPER 72-360]
11 p1638 A72-25388

Space shuttle heat shield metallic refractory, superalloy and composite materials joining, discussing vacuum furnace brazing of Al/B matrix structures [AIAA PAPER 72-387]
11 p1638 A72-25408

Composite F-111 fuselage design, analysis and testing, considering graphite, boron and glass-epoxy and boron-aluminum systems
11 p1575 A72-25453

Fracture toughness of anisotropic heterogeneous filamentary boron/aluminum composites, correlating test results with acoustic emissions from filament breakage
11 p1672 A72-25470

Pendulum impact resistance of tungsten fiber-metal matrix composites, noting heat treatment and test temperature effects
11 p1653 A72-25473

B-Al composite mechanical properties improvement through heat treatment and steel addition
11 p1653 A72-25478

Off axis and transverse tensile properties of boron reinforced Al alloys, correlating metallurgical structures with stress-strain curves and fractographic studies
11 p1654 A72-25479

Fatigue crack initiation and growth in filament reinforced Al alloys, noting interface crack tip stress distribution effects
11 p1654 A72-25480

Critical aspect ratio of W fiber in copper matrix for stress rupture applications
11 p1654 A72-25482

Metal matrix composites, testing neutron irradiation effects on mechanical properties for nuclear application feasibility
11 p1654 A72-25483

High temperature metal fiber reinforced ceramic matrix composites for turbine vanes, showing strength toughness and crack depths dependence on interfacial bond [ASME PAPER 72-GT-51]
11 p1704 A72-25643

Tensile properties of continuously cast aluminum-carbon fiber composites, discussing fiber outgassing and metal coating for wetting promotion
11 p1659 A72-25859

Multilevel structural analysis for multilayered fiber-epoxy and metal matrix composites, using FORTRAN IV
11 p1601 A72-26033

Organic and metal matrix composites physical and mechanical properties and application to spacecraft and missile components, considering cost effectiveness
11 p1674 A72-26233

Young modulus of TiC-Co and TiC-Ni hard composites as function of volumetric fraction, using bending tests
11 p1660 A72-26487

Al alloy-graphite composites brazing and welding feasibility, tabulating spot welding parameters
11 p1641 A72-26491

Reinforcing fibers precise alignment and uniform distribution in metal matrix
11 p1645 A72-26854

Alloying addition effects on structural stability and particle-matrix cohesion in metal-alumina composites
11 p1665 A72-26864

Ordered growth and etching of uranium and zirconium oxide-tungsten fiber refractory composites, using X ray diffraction and scanning electron microscopy
11 p1668 A72-26943

Filament reinforced boron-aluminum composites multiple fracture behavior dependence on cross section geometry from tensile test
11 p1668 A72-26944

Metal matrix composites radiography in NDT, discussing parameters optimization and uses of microfilm, densitometers and high resolution vidicon tubes
12 p1813 A72-27199

Boron nitride coated boron fibers for metal matrix composite reinforcement, discussing surface nitriding process by heating
12 p1815 A72-28088

Metal matrix composites application to aircraft structures, describing design, analysis and fabrication of aircraft bulkhead with B-Al as main structural material 12 p1886 A72-28096

Resin bonded B-Al composites, discussing fabrication techniques and mechanical properties 12 p1815 A72-28098

Chemical interaction effects on single crystal sapphire filament strength in Ni and Ni alloy matrices during heat treatment in inert atmosphere 13 p1974 A72-28661

Fusion welding of Ti-W and Ti-graphite composites, determining weldability and effect of weld thermal energy on fiber matrix reactions 13 p1966 A72-29423

Diffusion kinetics and thermodynamic characteristics of solid phase interactions in systems cobalt-transition metal carbides 13 p1981 A72-30104

Dispersion hardening of Nb, Cr, Mo and W by inserting dispersed particles of refractory compounds into metal matrix 14 p2112 A72-30152

Aluminum-stainless steel and Ni-Mo composites prepared by dynamic hot pressing, determining bond strength between fibers and reinforced metal matrix 14 p2107 A72-30431

Refractory fiber metal reinforcement and matrix incorporation, considering SiC fiber reinforced Al 14 p2107 A72-30532

High temperature composite turbine blade materials, discussing service conditions and fiber/matrix selection, noting cast Ni and Mo based alloy fibers 14 p2125 A72-30533

Stress analysis of boron fiber-reinforced and isotropic Al panels under identical loading conditions 15 p2323 A72-31479

Steady state creep measurements of lead-phosphor bronze discontinuous fiber composites under nonuniform deformation, comparing to fiber and matrix alone 15 p2261 A72-32299

Steady state creep theory for discontinuous fiber composites, considering rigid and creeping fibers and sliding interface 15 p2261 A72-32300

Multifilamentary superconducting Nb-Sn composites wires in ductile metal matrix, determining transition temperature and critical current density 15 p2294 A72-32534

Temperature effect on bonding strength between ceramic whiskers or fibers and metal matrices attributed to thermal expansion coefficients disparity 16 p2413 A72-33206

Fracture-surface energy model for Cu-W fiber metal matrix composites, using plastic flow analysis 16 p2470 A72-33613

Plastic flow, yield strength and fracture of unidirectional Al-B fiber composite sheet under biaxial tension 16 p2411 A72-33821

Aluminum oxide high temperature equilibrium morphology in Ni matrix prepared via vapor deposition and internal oxidation methods 16 p2411 A72-33824

Thermal conductivity of W wire reinforced Cu as function of W content 16 p2411 A72-34017

Initial yield surface of a unidirectionally reinforced composite. [ASME PAPER 71-APMW-19] 17 p2623 A72-34301

One-dimensional wave pulses in steel-epoxy composites. [SESA PAPER 1945] 17 p2631 A72-34823

Ultrasonic wave propagation in metal-matrix composites. 17 p2560 A72-35287

Composites technology, costs and performance review covering metal matrix composites, ceramic reinforced plastics and whisker composites 17 p2571 A72-35652

Fractography of fiber reinforced metal composites. 17 p2560 A72-35654

Fracture of boron filaments in an aluminum matrix. 17 p2571 A72-35655

Sapphire filament mechanical property considerations of importance to Al2O3 reinforced metals. 17 p2572 A72-35658

Boron- and graphite-epoxy and boron-aluminum composites forming, processing and costs for aircraft structural materials 17 p2560 A72-35663

Fabrication of boron/aluminum tubes, I-beams, and other structural shapes from tape materials. 17 p2560 A72-35664

A preliminary investigation of joining methods for aluminum-graphite composites. 17 p2561 A72-35665

Fatigue of boron-aluminum and carbon-aluminum fibre composites. 18 p2701 A72-36625

Fracture behavior of stainless steel fibers in Sn-Pb alloy matrix. 19 p2820 A72-38373

The matrix fatigue behaviour of fibre composites subjected to repeated tensile loads - Application to B/Al 6061 composites. 20 p2936 A72-39208

Reinforced metals - Mechanical property considerations. 20 p2936 A72-39210

The transverse tensile properties of boron fiber reinforced aluminum matrix composites. 20 p2938 A72-39302

Production and properties of carbon fiber-reinforced aluminum 20 p2940 A72-39442

Problems and possibilities of the production of fiber-reinforced metallic components by thermal spraying 20 p2929 A72-39444

Mechanical properties of boron fiber reinforced aluminum matrix composite, describing experimental and control techniques 20 p2940 A72-39447

Prospects for the development of technically usable fiber-reinforced high-temperature materials 20 p2940 A72-39448

Transverse tensile properties of an unbonded model composite. 20 p2941 A72-39790

Interfacial characteristics of silicon carbide-coated boron-reinforced aluminium matrix composites. 20 p2941 A72-39791

The versatility of resistance welding machines for joining boron/aluminum composites. 21 p3060 A72-40847

Aircraft structures weight reduction through fiber-matrix composite materials, discussing anisotropic elastic and failure behavior of composite light shell structures [ICAS PAPER 72-38] 21 p3120 A72-41163

Bursting strength and toughness of wire reinforced composite tubes under uniaxial/hoop stress. 21 p3120 A72-41208

Bursting of wire reinforced composite tubes under biaxial tension stresses. 21 p3121 A72-41209

Changes in the phase composition of metal-glass materials depending on the sintering temperature 21 p3073 A72-41370

Metal fiber composites electrical resistivity as function of fiber volume proportion, evaluating vacuum cast Cu/W 21 p3073 A72-41373

Book - Metal matrix composites. 21 p3070 A72-41528

Fabricating aluminum matrix composites. I - A survey of aluminum matrix composites. 22 p3182 A72-41996

Spectroscopic study of the interaction of oxides with metallic surfaces. II - SiO2-Fe/Cu, Al, Ni, Co, Ti, W/ systems 22 p3189 A72-42197

Stress-strain diagrams and fracture characteristics of fiber-reinforced aluminum alloys 22 p3189 A72-42300

Superconducting alloys of niobium and vanadium 22 p3191 A72-42808

Fabrication and properties of graphite fiber reinforced magnesium. 22 p3193 A72-43035

Optimization of the range of elastic behavior of unidirectional composites by prestraining. 22 p3194 A72-43041

Composite Al- and Ni-base alloys strengthened by B and W/Mo fibers respectively for reduced weight wing spars and high temperature applications 22 p3197 A72-43139

Calculation of radial pressures in metal-fiber-reinforced materials during compacting 23 p3298 A72-43277

High strength boron and boric fiber reinforced aluminum composites. 23 p3299 A72-43491

Effects of hydrostatic stress on the yielding of cold rolled metals and fiber-reinforced composites. 23 p3299 A72-43496

Aluminum matrix composites fracture mechanism dependence on static loading conditions and reinforcing filament type, investigating failure modes in tension and compression tests 23 p3299 A72-43497

Fracture mechanics of composites. 23 p3345 A72-43509

Microstructural aspects of the fracture of two-phase alloys. 23 p3299 A72-43510

Fiber reinforced metallic matrix composite under creep, discussing rigidity, stress distribution, rupture strength and failure time 23 p3306 A72-43727

Fibers-matrix force interaction effects in metal composites, analyzing stress-strain state of reinforced plate 23 p3306 A72-43728

Diffusive metal coatings stress-strain state effect on composite Mo material strength, ductility and creep characteristics 23 p3306 A72-43732

Heat resistant Ni-base composite stiffened with W wires, investigating interaction between alloy and fibers from metallographic and X ray diffraction microscopy data 23 p3301 A72-43740

Thermal diffusion annealing improved Ni-B composite electrolytic coatings with uniform B distribution over bulk matrix 23 p3303 A72-44012

Some strength characteristics of graphite/zirconium carbide composites 23 p3307 A72-44013

Making a product from composites. II. 24 p3412 A72-44556

Fracture of WC-Co from a continuum viewpoint. 24 p3413 A72-44815

Precise alignment and uniform distribution of fibres in a metal matrix. 24 p3413 A72-44898

Utilization of advanced composite materials for spacecraft and space shuttle applications. 24 p3417 A72-45153

Fiber and filament reinforcement of plastic and brittle matrix materials 24 p3414 A72-45276

The effect of annealing temperature on certain properties of molybdenum and tungsten fibers 24 p3415 A72-45396

Tensile strength of tungsten reinforced nickel, determining temperature effect on fibers deformation after vacuum rolling simultaneously with plastic matrix 24 p3416 A72-45749

Compressive strength of Cu-W fiber metal matrix composite as function of temperature, comparing to cermets 24 p3416 A72-45750

METAL OXIDE SEMICONDUCTORS

Low driving power resistive gate MOSFET microwave switch with performance approaching P-I-N diode 01 p0038 A72-10658

Photosensitive MOS devices array as converters performing optical image data analysis, considering sensor sensitivity regulation 02 p0193 A72-12342

Failure modes of IC containing MOS devices, considering threshold voltage variations, oxide and silicon defects and leakage 02 p0194 A72-12443

Ferrite core memory for space flight devices, comparing 1 bit storage capacity power consumption with MOS cell [DGLR PAPER 71-090] 02 p0196 A72-12734

MOS transistor frequency and transient response characteristics for equivalent circuit synthesis, using Bessel functions in differential equation solution 02 p0196 A72-12761

Dual-gate MOS transistor structure, operational principles and electrical characteristics, noting suitable properties for use in low noise microwave amplifier 03 p0330 A72-12969

Two dimensional analysis of carrier circulation in MOS transistors for arbitrary polarization, including surface effects 03 p0330 A72-13166

Al, Mo and Cr radiation resistance as gate electrodes and corresponding MOS devices, discussing radiation behavior model revision 03 p0403 A72-14079

P-channel MOS devices radiation hardening by thermal silicon dioxide gate insulator optimization, applying to circuit fabrication 03 p0403 A72-14082

P-channel MOS/silicon-on-sapphire transistor logic circuits for aerospace systems, investigating radiation hardness and performance potential 03 p0334 A72-14086

LSI/MOS logic circuits radiation effects prediction from modeling studies of individual devices on test chip 03 p0334 A72-14087

Random access memory based on multichip array with MOS-bipolar device combinations by hybrid techniques, bypassing handling and cost limitations 03 p0329 A72-14185

MNOS transistors charge storage properties at high electric field strengths and current densities near gate insulator breakdown, determining reliable operating limits 03 p0336 A72-14277

Metal-alumina-oxide-semiconductor capacitor flat band bias voltage measurement before and after thermal stressing, noting potential barrier in structure model 03 p0336 A72-14278

MOS Si-gate arrays for static, dynamic and programmable read-only memories, investigating information storage reliability 03 p0336 A72-14282

N-channel MOS FET, measuring X ray irradiation effects on drain current and transfer characteristics at room temperature

05 p0634 A72-16033

MOS components technology with low threshold voltage, noting wafer surface planarity and smallness of parasitic capacitances and layer resistivity

05 p0702 A72-16181

N-channel Si MOS microwave transistor, discussing fabrication, design, power gain, stability, noise figure, equivalent circuit and applications

05 p0636 A72-16361

Si MOSFET substrate resistivity effect on surface state noise spectra

06 p0783 A72-17609

Electron irradiation effects on MOS structures at vlf, considering inversion layer cut-off frequency and surface state density

06 p0865 A72-17610

Microwave receiver double diffused MOS transistor /D-MOST/ device advantages over bipolar device

06 p0790 A72-18485

MOS inversion layer mobility theory and surface charge scattering mechanism

07 p0954 A72-19121

Switching characteristics of MOS channel transistors, solving nonlinear differential equations describing current and potential distribution

08 p1140 A72-21267

Junction and MOS FETs noise sources interaction with small signal model parameters and signal source admittance parameters, investigating amplifier If performance

08 p1141 A72-21428

MOS IC reliability based on p-channel enhancement mode transistors, discussing failure modes and mechanisms

08 p1142 A72-21588

Photosensitive MOS devices array as converters performing optical image data analysis, considering sensor sensitivity regulation

08 p1143 A72-21948

Book on digital and analog monolithic IC systems, covering manufacturing methods, component design, MOS logic, arithmetic, error correction, codes, applications, etc

09 p1286 A72-23044

MOS transistor low level background flicker noise equivalent voltage relationship to gate voltage and input capacitance and interface state density

09 p1286 A72-23108

P-channel MOS transistor LF background noise components analysis for different dependencies on gate bias and temperature

09 p1286 A72-23109

Six channel integrated MOS switch, discussing MOS transistor operation and circuits structure

09 p1288 A72-23363

Burn in technique in nonvolatile metal oxide semiconductor /MOS/ memory using ionizing radiation of reprogrammable electron beam

10 p1443 A72-23927

Ion implantation doping of MOSFET and IC for wafer production, using automatic vacuum pumpdown and cycle control

10 p1447 A72-23950

Reliability prediction for MOS/LSI devices based on chip circuit configurations evaluation, extrapolating bipolar IC failure rate model

10 p1447 A72-24009

Homogeneous computing media, examining microelectronic fabrication, interconnection and control problems for MOSFET, bipolar transistors and IC structures

10 p1448 A72-24277

MOS transistor current fluctuation relation to capture centers surface density, energy position and gate potential, determining spectral amplitude distribution

10 p1449 A72-24284

Multichannel integral commutators with MOSFET as switching elements, calculating transmission errors

10 p1449 A72-24288

Statistical analysis of MOS integrated circuits from initial data of electrophysical and geometric distribution laws and covariance matrix

10 p1449 A72-24289

MOS transistor logic circuits pulse noise stability dependence on transient response, emphasizing supply voltage effect

10 p1449 A72-24290

MOSFET for input impedance measuring amplifier, discussing input stage temperature drift and protection from overvoltage

10 p1482 A72-24599

Radio electronic equipment IC and microelectronics development trends, considering bipolar and MOS transistors applications in digital and analog computers and telemetry

10 p1454 A72-25176

Complementary metal oxide semiconductor applications, noting device power dissipation, high noise immunity, good switching speeds and cost reduction

11 p1701 A72-26386

MOS specifications and application to shift registers, considering maximum ratings, clock pulse level and width and pulse rate

11 p1611 A72-26387

High performance low power complementary MOS memories based on silicon-on-sapphire technology, noting quiescent power dissipation

11 p1606 A72-26565

Integrated metal-nitride-oxide-silicon /MNOS/ semiconductor storage units characteristics, design and operation in FETs

12 p1791 A72-27574

P channel MOS transistors hardening against ionizing radiation based on positive space charge density and electrode injection efficiency

13 p2023 A72-29837

Two dimensional numerical solution of semiconductor steady state transport equations, applying to MOS and bipolar transistors

14 p2142 A72-30847

MOS transistor injection level dependent theory, calculating drain region saturation conductance by iterative procedure

15 p2205 A72-31318

MOS junction transistor turn-off behavior calculation based on model with carrier source and drain for channel formation

15 p2207 A72-31891

Physical phenomena limitations on MOS IC miniaturization, considering gate oxide breakdown, drain source punch through, doping fluctuations, power dissipation and metal migration

16 p2370 A72-34102

Advances in LSI technology.

17 p2527 A72-34569

Modularized digital controller for closed loop systems using MOS, MSI and LSI components

17 p2521 A72-34703

Advantages of MOS/LSI computers in avionics systems.

17 p2523 A72-35579

French monograph - Experimental characterization and analysis of the effect of ionizing radiation on the electrical properties of MOS transistors

17 p2531 A72-35650

Current and capacitance transient responses of MOS capacitor. I - General theory and applications to initially depleted surface without surface states.

18 p2718 A72-36346

Thermal effects in JFET and MOSFET devices at cryogenic temperatures.

18 p2666 A72-36453

Limitations in microelectronics. II - Bipolar technology.

18 p2667 A72-36980

Si MOSFET elementary channel resistances before saturation onset from one dimensional theory, investigating current noise

18 p2668 A72-37037

Charge injection into the gate dielectric of MOS transistors during junction avalanche.

18 p2668 A72-37104

Industrial production of high-quality active semiconductor components

18 p2670 A72-37123

Quality and reliability evaluation method for integrated circuits using MOS transistors - Option: Circuits on request

18 p2671 A72-37141

Development of a complementary MOS technology of high reliability

18 p2671 A72-37142

A measuring method for MOST transconductance and its variation.

19 p2773 A72-37901

An elegant method for measuring MOST drain-source conductance in the saturated current region.

19 p2773 A72-37902

MOS transistor frequency and transient response characteristics for equivalent circuit synthesis, using Bessel functions in differential equation solution

20 p2907 A72-39067

Measurements of the field-effect and effective mobilities in MOS transistors.

20 p2907 A72-39272

A precise method for measuring low-frequency small-signal conductance parameters of an MOS transistor.

20 p2907 A72-39273

Differential negative resistance /DNR/ in n-channel MOSFETs of silicon.

20 p2961 A72-39711

Technology and performance of n-channel MOS-LSIs using depletion-type load elements.

20 p2961 A72-39712

Some results of testing M.O.S. transistors at elevated temperatures.

20 p2909 A72-39774

Mathematical model for MOS transistor circuit analysis, noting parameters measurement and environmental effects representation

20 p2909 A72-39783

Hybrid monostable delay circuit based on bipolar and low threshold voltage MOSFET transistor

20 p2910 A72-39788

Analysis of the characteristics of an MOS transistor as a switching element

21 p3025 A72-40163

The effects of X-ray irradiation on MAS diodes.

21 p3032 A72-40695

Carrier transport and storage effects in Au ion implanted SiO₂ structures.

21 p3097 A72-40699

Conductance associated with interface states in MOS tunnel structures.

21 p3032 A72-40701

The distribution of gate-channel capacitance between source and drain in the equivalent circuit of a MOS transistor

21 p3035 A72-41490

Forward and reverse characteristics of self-aligned double-diffused M.O.S. transistors.

22 p3160 A72-42754

MOS logic circuit design simplification by replacing series and parallel transistor networks by equivalent single transistor inverter circuit

23 p3271 A72-43843

Capacitance voltage characteristics instability of metal-aluminum oxide-silicon dioxide-silicon /MAOS/ structures, suggesting polarization effect in layer formed during deposition and annealing

23 p3324 A72-44070

On the determination of minority carrier lifetime and surface recombination velocity from the transient response of MOS capacitors.

23 p3324 A72-44071

Metal-oxide varistor - A new way to suppress transients.

23 p3272 A72-44100

Dependence of MOS transistor parameters on carrier mobility

23 p3272 A72-44139

MOS devices instability caused by water and hydroxyl molecules on silicon dioxide surface, noting optimal conditions for chemical stabilization

24 p3431 A72-44821

Circuit analysis and operation of analog multipliers with MOSFET, applying to industrial automatic control systems and measuring instruments

24 p3384 A72-44896

Shielded silicon gate complementary MOS integrated circuit.

24 p3385 A72-44972

Characteristics of P-channel MOS field effect transistors with ion-implanted channels.

24 p3385 A72-44981

METAL OXIDES

NT ALUMINUM OXIDES

NT ANATASE

NT BARIUM OXIDES

NT BERYLLIUM OXIDES

NT BISMUTH OXIDES

NT CALCIUM OXIDES

NT CERIUM OXIDES

NT CESIUM OXIDES

NT CHROMITES

NT CHROMIUM OXIDES

NT COBALT OXIDES

NT COPPER OXIDES

NT HAFNIUM OXIDES

NT HEMATITE

NT ILMENITE

NT IRON OXIDES

NT KAOLINITE

NT MAGNESIUM OXIDES

NT MAGNETITE

NT MOLYBDENUM OXIDES

NT NICKEL OXIDES

NT NIOBIUM OXIDES

NT POTASSIUM OXIDES

NT PYROPHYLLITE

NT RUTILE

NT SAPPHIRE

NT SCHEELITE

NT TANTALUM OXIDES

NT THORIUM OXIDES

NT TITANIUM OXIDES

NT TUNGSTEN OXIDES

NT URANIUM OXIDES

NT VANADIUM OXIDES

NT YTTRIUM OXIDES

NT ZINC OXIDES

NT ZIRCONIUM OXIDES

Metals and metal oxides powders mixture formation by mixed metal halides gelation in alcohol solution

02 p0233 A72-11455

Niobium anomalous oxidation below 600 C, noting suboxide formation between solid solutions and heat resistance reduction

02 p0243 A72-12214

Fine scale surface oxide film roughness effects on metal substrate-oxide film system hemispherical emittance

02 p0303 A72-12319

Transition metal oxides hot extrusion sintering, discussing temperature and pressure effects on compacting density

02 p0244 A72-12349

Refractory metal oxides hot microhardness and thermal stability over wide temperature range, noting softening rate variation with temperature
02 p0244 A72-12350

Metal oxide powder surface measurement using modified Kozeny-Karman formula, considering porous space, gas kinetic slip and air permeability effects
05 p0665 A72-16087

Hot pressing of sintered refractory metal oxide powders of Ti, Zr, U, Nb and Cr, showing improved compacting by raising temperature
06 p0822 A72-18427

Formation kinetics, phase composition and structure of oxide films in binary and ternary iron-base chromium aluminum alloys, studying hydrogen penetration characteristics
07 p1013 A72-19771

Catalytic action of metal oxides on isopropylbenzene hydroperoxide decomposition in liquid phase
08 p1129 A72-22094

Hubbard mathematical model for metal-insulator transition due to electrons correlations, noting schematic phase diagram and transition metal oxides
10 p1527 A72-24939

Book on binary metal oxides covering non-stoichiometry, electrical conductivity, diffusion theory, point defects, high temperature creep and electrochemical transport properties
10 p1527 A72-25075

Zirconium rich metal oxides mineral group in Apollo 14 and 15 lunar rocks from feldspar-phryic basalt and pyroxene ferrobasalt, noting optical and chemical properties
11 p1717 A72-25868

Transition series oxides metal-insulator phase transition based on electron phonon interaction model
11 p1701 A72-26024

Metal surface smoothing during electrochemical dissolution prior to polishing, involving electrolyte diffusion processes or semiconductor oxide film formation
11 p1640 A72-26259

Oxide content and sheet microstructure directionality effects on Be powder and ingot sheets notch strength, noting thickness dependence
[ASM PAPER W-72-12.6] 12 p1830 A72-28164

Oxide thin films effects on surface layers deformation and wear resistance of coated metals under friction, noting electrical resistance changes in annealing
12 p1818 A72-28189

High refractory gadolinium oxide-strontium oxide system phase diagram and transition temperature by X ray and differential thermal analyses
13 p1984 A72-30109

Conditions for obtaining high porosity materials of complex carbides by combined reduction-carbideization of metal oxides with soot in vacuum
13 p1967 A72-30114

Chain reaction mechanisms of fuel combustion in presence of metal oxides for ores reduction application
15 p2335 A72-31850

Oxide inclusions induced reductions in Nabarro-Herring creep and sintering rates of metals, discussing effect of inclusions diffusional mobility in metal matrix
15 p2257 A72-32112

High temperature oxide scale adherence on Fe-Cr-Al alloys with Y or Sc additions as promoting agents
16 p2410 A72-33817

The formation of metal-oxygen compounds for additive thermionic converters.
17 p2595 A72-34600

Chemical composition, refractivity and temperature dependence of blackness levels of aluminum oxide-chromium oxide-phosphorus oxide ceramic coatings flame sprayed on steel
21 p3072 A72-40384

Vapor phase formation during high temperature oxidation.
21 p3066 A72-40551

Phenomena and interpretation of the transients caused by temperature change on capacitance of metal-oxide-metal systems.
21 p3097 A72-40690

Excess metal buildup kinetics and work function of oxide thermionic cathode activated by emission current, noting effect of metal and oxygen concentrations
21 p2997 A72-40789

Growth rate of refractory oxide particles in nickel cermets
23 p3299 A72-43290

METAL PARTICLES
NT METAL POWDER
NT POWDERED ALUMINUM
Argon-hydrogen plasma seeded with submicron tungsten particles, measuring composition, temperature, radiant heat output and opacity
01 p0112 A72-11343

Mechanical constraints effects on loose spherical metal particles sintering rates, considering one, two and three dimensional arrays
02 p0232 A72-11433

Focused laser beam interaction with liquid metal particles, discussing fluid phase light screening effect,

droplet evaporation and mass expulsion characteristics
03 p0368 A72-13668

Photographic observations of W particle clusters high velocity impact against polystyrene, paraffin and W targets for energy dissipation in meteorite impact simulations
08 p1232 A72-21152

Maximum volatile solute vaporization escape prior to droplet solidification during metal vapor chemical release process
08 p1128 A72-21618

Ignition delay time and combustion mechanism of Al-Mg alloys single particles in combustion products of oxidizer-fuel mixture
09 p1373 A72-22885

Visual and motion picture studies of ignition and burning characteristics of Mg particle clusters in flames of gas mixtures
09 p1411 A72-22886

Pressure effect on combustion rate of Mg particles in water vapors
09 p1411 A72-22887

Burning process of low boiling Mg particle moving in relation to gaseous oxidizer, assuming heat and mass transfer occurrence by diffusion-conduction mechanism
09 p1411 A72-22888

Ignition and incendiarity of laser irradiated single micron size Mg particles suspended in stoichiometric methane air mixture
10 p1564 A72-25140

Phase structure of Cr rich Cr-Ni, Cr-Fe, Cr-Co and Cr-Ni-Fe alloy particles produced by evaporation in Ar using X ray diffraction
13 p1974 A72-28660

Metal particle decomposition products composition in slags from smelted Cr, Ti, Ni and Zr alloys, using X ray microanalysis
14 p2112 A72-30157

Reaction rate and activation energy of low temperature oxidation of Mg particles in nitrous oxide
16 p2476 A72-33253

Mg ignition in nitrous oxide at 600-800 C, determining induction period as function of particle mass and gas stream temperature
16 p2476 A72-33254

Photographic observations of W particle clusters high velocity impact against polystyrene, paraffin and W targets for energy dissipation in meteorite impact simulations
20 p2969 A72-39257

Heavy metal particle detection in noctilucent clouds by rocket experiments, using Pandora inflight shadowing technique
20 p2964 A72-39373

Condensed zinc particle size determined by a time discrete sampling apparatus.
20 p2913 A72-39608

Induction period, particle size distribution and medium temperature effects on thermal ignition of metal particles under exothermal oxidation reaction on surface
20 p2987 A72-40040

Electron diffusion across a shock wavefront in metals
22 p3208 A72-43184

METAL PLATES
Dynamic and plastic behavior of mild steel and Al wide beams and rectangular flat plates
02 p0291 A72-11964

Al and steel plate penetration, perforation and fragmentation under hard steel sphere impact at and above ballistic velocities, investigating velocity and strain histories
05 p0672 A72-16115

Dimpling behavior of metal plate with mode I edge crack, relating flaw depth, applied stress level and crack tip plastic zone
05 p0673 A72-16305

Environment acoustic resonant frequencies effect on flat steel plate vibration under direct and air flow vortex shedding excitations
06 p0894 A72-17768

Two dimensional dynamic thermal stresses in Al plate, allowing for Newtonian surface heat transfer
06 p0899 A72-18642

Al alloy plates and D-nosed specimens indentation and penetration under hail impact test
07 p1086 A72-18764

Acoustic loads effect on carrying capacity and vibration stability of longitudinally stiffened cylindrical metal panels, investigating fatigue strength and stress-strain state
07 p1091 A72-19760

Hypersonic gas flow around asymmetric triangular metal plate with blunt leading edges, using two layer model
07 p0909 A72-19985

X ray and resistance strain gage techniques for bar and metal plate simultaneous residual stress determination
07 p0993 A72-20606

Electrode vertex angle effect on fused weld bead geometry related to plate thickness in tungsten inert gas (TIG) welding
09 p1320 A72-23634

Thick steel plate diffusion welding in air with dead-weight loading and autogenous surface cleaning
11 p1637 A72-25343

Electron beam machine for thin metal plates welding and cutting under space conditions, noting design features and performance
11 p1639 A72-25809

Schlieren visualization of radiated wave fronts for Al plates illuminated with short acoustical pulses in water, comparing with Lamb theory
11 p1687 A72-26057

Al alloy plate material microstructural variations and specimen orientation effects on tensile and fracture toughness properties
12 p1830 A72-28080

Cumulative damage and structural changes in friction contact areas of steel plates under cyclic pulsed loads, noting microhardness distribution and surface layers microstructure
12 p1818 A72-28191

Surface roughness effects on seizure and friction of contacting metal plates under atmospheric pressure and vacuum
12 p1819 A72-28197

Mechanical properties of thick Be plate produced by diffusion bonding of thin sheets from ingot material
13 p1973 A72-28655

Fluid jets formation in collisions between metal plates for large angles at subsonic velocities
13 p1963 A72-28771

Powder combustion on metal plate at constant pressure based on two-phase model of condensed system thermal decomposition
13 p2065 A72-29879

Lamb acoustic surface wave method for rapid non-destructive evaluation of rolling texture in arbitrarily thick metal sheets and plates
14 p2107 A72-30615

The apparent heat transfer coefficient of plate heat exchangers
20 p2984 A72-39649

Experimental investigation of the stability of compressed heated three-layer plates beyond the proportional limit
20 p2981 A72-39920

Fluid jets formation region in subsonic collisions between metal plates at large angles
21 p3059 A72-40262

Stress-strain state of thin circular perforated Cu plate under uniform tensile load, showing applicability of small elastoplastic finite deformation theory
21 p3122 A72-41351

Mechanical properties of titanium strengthened by monodirectional molybdenum wires
21 p3069 A72-41354

Metal barrier maximum puncturable thickness dependence on high velocity meteorite particle impact parameters
22 p3234 A72-42217

Chladni's patterns for random vibration of a plate.
22 p3236 A72-42758

Energy measurement of primary particles from shower formation in solids, discussing ultrasonic waves generation in metal plates and electromagnetic waves excitation in ferrites
23 p3291 A72-44437

Non-steady shock waves in metals with phase transitions and hardening by explosion.
24 p3414 A72-45025

METAL POLISHING

NT ELECTROPOLISHING

METAL POWDER

NT POWDERED ALUMINUM

Chloride process produced tungsten powder for tungsten carbides production, discussing impurities, particle shape and size distribution, carburization behavior and applications
02 p0239 A72-11427

Ti-Al-V alloy powders electrically activated pressure sintering /spark sintering/, considering mechanical properties and economic factors
02 p0240 A72-11428

Dislocations forces during sintering of loose and cold-pressed metal powders, using photoelasticity for stress estimation and electron microscopy for defects structure
02 p0232 A72-11430

Metal powders sintering activation mechanism, considering heterogeneous metals particles diffusion flow, mutual solubility and crystal lattices distortion
02 p0232 A72-11432

Hot formed Cr-Ni-Mo and Ni-Mo prealloyed steel powders fatigue and toughness properties, determining hardness effects by varying draw temperature from 400 to 1000 F
02 p0240 A72-11435

Melting atmosphere, atomizing media and consolidation techniques effects on Co base alloy powder products physical properties
02 p0240 A72-11436

Ti powder technology, discussing pressed and sintered parts, forging and extrusion preforms and composites

02 p0233 A72-11437

High energy rate compacting methods in powder metallurgy, considering use of high explosives in water or air and impulse pressing of metal powders

02 p0233 A72-11438

Hot pressed Ti alloy powders, evaluating strength and toughness at cryogenic temperatures

02 p0240 A72-11439

Holes dispersion hardening in sintered metal powder, discussing dispersed particle effects

02 p0233 A72-11446

Metals and metal oxides powders mixture formation by mixed metal halides gelation in alcohol solution

02 p0233 A72-11455

Coextrusion of metal powder and ceramic dispersions clad alloyed Al as function of cartridge density and reactor core length

02 p0233 A72-11456

Matrix hardening in dispersion strengthened powder products, discussing dispersion, grain boundary and solid solution hardening

02 p0241 A72-11457

Material characteristics effect on compaction behavior of metal powders, stressing density and pressure measurements

02 p0242 A72-11460

Presintering effects on dimensional change of iron powder compacts, using dilatometric, thermogravimetric, differential thermal analyses and resistivity measurements

02 p0233 A72-11461

Sintering and heat treatment effects on mechanical properties of atomized and mixed powders of Ni-Mo steel

02 p0234 A72-11462

Oxygen determination in cemented carbides, metal powders and presintered and finished sintered products by vacuum fusion method, comparing with neutron activation method

02 p0245 A72-12548

Superalloy compositions prealloyed powders strengthening by secondary gamma phase precipitation, noting high temperature strength without ductility loss after thermomechanical treatment and aging

02 p0247 A72-12856

Metal powder materials at high loading rates, obtaining stress state diagram from Cauchy problem solution with inertia components in equilibrium equations

05 p0672 A72-16088

Temperature and compression rate effects on metal powder packing density, obtaining activation energy from Boltzmann equation

05 p0665 A72-16089

Metal powder hot compacting under vacuum and ultrasound action, considering porous body three dimensional viscous flow

05 p0665 A72-16091

Quality control of powdered metal parts, considering chemical, atomization, electrolytic and mechanical production stages, tool inspection and test patterns

06 p0822 A72-18070

Titanium powder metallurgy in ordnance applications, discussing hardware, weight economies and market development

06 p0822 A72-18071

Hot pressing /extrusion/ of rods from metal-ceramic Ti, using pure and cermet powders with tungsten carbide

06 p0822 A72-18426

Fe powder preform hot rolling, investigating mechanical properties, microstructure and internal oxidation resistance as function of final density

10 p1488 A72-24695

Slip casting process for ceramics, cermets and metal powders, discussing slurry preparation, deflocculating agents, binders and molding process

10 p1502 A72-24733

Thermal conductivity of two- and three phase solid mixtures of silicone rubber and Al, Pb, Ni and Bi powders, using line source method

11 p1744 A72-25264

Mercury porosimetry for iron powders void and internal particle porosity change as function of compacting pressure, noting compressibility improvement by precompacting and annealing

11 p1639 A72-25828

Russian book on powdered metals toxicity covering industrial dust, physiological effects, safety standards, electron configurations and crystalline structure

11 p1584 A72-26067

Iron base powders material requirements and forging processes, discussing powder composition, inclusions effect and preform densification

11 p1639 A72-26241

Ni powder artificial dielectric in waveguide transverse magnetic field, noting nonreciprocal nature of microwave attenuation and phase shift

11 p1607 A72-26786

Metal powder mixing, examining friction effects and optimal particle sizes, shapes and amounts

11 p1642 A72-26828

Refractory metal powders spherical agglomerates growth and strength in rotating tumbler, noting particle size dependence on binder

11 p1643 A72-26829

Continuous hot pressing of high density reactive ceramic and metal powder materials in alumina die

11 p1643 A72-26832

Explosive compaction of metal powders by direct method with emphasis on W

11 p1643 A72-26833

Mo powder sintering kinetics and disperse mechanism in isothermal and nonisothermal conditions

11 p1643 A72-26836

Microstructural properties of Ni-Al powder synthetic material from transmission and photoemission electron microscopy, discussing low and high temperature strength characteristics

11 p1645 A72-26855

High melting point alloy and metal powder production by vacuum atomization, using rotary vane and electron beam melting techniques

11 p1645 A72-26860

Chemical and physical activation mechanisms of sintering metal powder compacts

11 p1645 A72-26862

Fracture micromechanism in liquid-phase sintered W-Fe-Ni powder composites, using scanning electron microscopy

11 p1668 A72-26942

Oxide content and sheet microstructure directionality effects on Be powder and ingot sheets notch strength, noting thickness dependence

[ASM PAPER W 72-12.6] 12 p1830 A72-28164

Optimization of high temperature supersonic gas jets for metal powders production by melts atomization, discussing excess air ratio effect on gas parameters

13 p2025 A72-29133

Iron powder specific surface and particle size effect on shrinkage during sintering

13 p1966 A72-29800

General analysis and synthesis of alloys and materials with inhomogeneous physical properties, noting thermal physicochemical methods for laminates and metal powders

16 p2405 A72-33095

Notch sensitivity of sintered stainless steel powder as function of density from application of sharp crack fracture mechanics methods to plane strain fracture toughness

16 p2408 A72-33700

Electric spark activated hot pressing application for sintered composite structures, noting process parameters optimization for superalloy powders

16 p2411 A72-34093

The dry wear behaviour of porous cobalt

18 p2696 A72-36795

Hot forging of sintered stainless steel

19 p2815 A72-37592

Deformation, densification and material fracture characteristics for powder preform design for hot forging

19 p2806 A72-37593

Characterization of commercial titanium powders

19 p2815 A72-37595

Creep of porous nickel in oxidizing and neutral media

19 p2819 A72-38287

Strength properties of highly porous materials made of metallic fibers

19 p2820 A72-38288

Chromium-based powdered alloys used in highly alloyed steel welding

19 p2809 A72-38289

Mg-Al powder mixtures sintering and coining, describing fabrication procedure, microstructure and mechanical properties

21 p3067 A72-40832

Ferromagnetic tau phase structure of Mn-Ac alloy with powder anisotropy related to platelet formation and twinning orientation

21 p3068 A72-40965

Phase diagrams, microhardness and composition of sintered binary B compounds with Zr, Hf, Ta, Cr, Mo, W, Re, Fe, Ni, and Si

21 p3070 A72-41371

Particle temperature and flight velocity during gas-powder buildup

22 p3182 A72-42194

Gas permeability of high-porosity nickel cermet

22 p3188 A72-42196

Rotational hysteresis in single crystals of powdered nickel

22 p3192 A72-43011

German monograph - Contribution to the investigation of the fatigue strength of sintered iron

22 p3194 A72-43066

Iron-nickel-molybdenum carbonyl powders

23 p3298 A72-43276

Study of the process of powder knurling to articles

23 p3292 A72-43279

Characteristics of the state of particles of titanium and vanadium mononitrides after nitriding and heat treatment

23 p3298 A72-43282

Magnetic properties of the powders of highly dispersed iron-cobalt-nickel alloys

23 p3299 A72-43288

Thermophysical properties of highly porous thermochemically treated metal-ceramic iron

23 p3299 A72-43295

Influence of the nature of the particle distribution of the hardening phase in powders on the thermal stability of dispersion-strengthened nickel

23 p3302 A72-44011

Pores visualization in porous materials by liquid filling and subsequent solidification and basic material removal, observing porous samples of sintered W and nichrome powders

23 p3290 A72-44016

METAL PROPELLANTS

Metallized solid propellants burning rate augmentation by internal ballistics effect of spinning rocket motor, deriving relationship between burning rate, pressure level and acceleration

13 p2025 A72-29302

METAL SHEETS

Coextruded Be fiber-Ti alloy matrix composite sheets for light weight structures, describing ultrasonic inspection and mechanical properties

01 p0084 A72-10734

Fe, Ni and Co based high temperature thin gauge sheet alloys, discussing chemical and mechanical properties, fabrication and availability

01 p0084 A72-10742

Endurance tests of D16AlMo alloy sheets under high intensity acoustic, harmonic and electrodynamic vibrator loading

03 p0371 A72-13470

Strain gage measurements of stress intensity factor for crack propagation in fatigue cracked thin metal sheets

03 p0444 A72-13542

Sheet metal biaxial creep testing, using edge clamped circular diaphragm deflected by lateral hydrostatic pressure

03 p0373 A72-13649

Lamellar tearing and testing of steel sheets in direction of short side by Brodeau test

04 p0527 A72-15561

Bend tests for minimum radius/thickness ratio of Ti and Be alloy sheets in pressurized fluid

[ASME PAPER 71-WA/PT-8] 05 p0671 A72-15913

Crossing points computed curves from metal sheet response to pulsed eddy currents, suggesting independent lift-off distance variation possibility

05 p0666 A72-17049

Al sheet weld cracking, discussing hold-down, localized heating, welding speed and gap effects

06 p0820 A72-17702

Cr and U contents effect on high strength Cr-Mo-Va alloy steel sheet hot cracking susceptibility, using Huxley test method

06 p0820 A72-17704

Stress fields around moving weld arc on Al sheet from isotherm map, calculating compressive and tensile stresses from heat induced material expansion

06 p0820 A72-17705

Crystallographic texture of Mo sheet, analyzing angular dependence of Young modulus

06 p0832 A72-18366

Steel sheet creep, plastic deformation and service life under temperature and stress cycles

06 p0899 A72-18558

Temperature dependent directional differences of modulus of elasticity of Mo sheet, using resonance technique

06 p0833 A72-18632

Sheet metal fatigue test method for transverse 100-1000 Hz bending at normal and high temperatures, applying to 1.5 mm Ti alloy sheet

06 p0900 A72-18671

Spot and seam welding of Cr ferritic stainless steel thin sheets, discussing electric current loading in relation to sheet thickness and contact pressure

07 p0995 A72-19575

Vacuum hot press diffusion welding of nickel-chromium-thorium dioxide sheet, describing specimen preparation, welding procedure and welded joints photomicrographic microstructure

07 p0997 A72-20002

Plasma beam cutting of Al sheets, discussing heat effect on surface oxides and microstructure and plasmagenic gas influence

08 p1176 A72-21047

Ar-H microplasma welding of thin Cr steel sheets with narrow seams for aircraft engines and precision equipment casings

09 p1318 A72-22548

Optical mirror method for bending strains study in welding cycles with applications to sheet metal thermal stress strain rates

09 p1318 A72-22738

Metal inert gas (MIG) welding of thin sheets, using Si controlled rectifier power source

09 p1320 A72-23627

Ti alloy sheets diffusion brazing, describing chemical cleaning, auxiliary metal cladding, heating and pressure augmented fusion processes involved in high quality joints production

10 p1497 A72-24658

Beryllium sheet and foil application to lightweight space structures, discussing mechanical properties [AIAA PAPER 72-404]

11 p1726 A72-25425

Surface textures in rolled Al sheets, investigating friction and reduction

11 p1638 A72-25509

Elastic r-value variation in Ti sheet from direct measurement of width and thickness strains

11 p1659 A72-25895

Thermal conduction anomalies and electron phonon interaction in thin metallic sheet at low temperatures

12 p1888 A72-27182

Oxide content and sheet microstructure directionality effects on Be powder and ingot sheets notch strength, noting thickness dependence [ASM PAPER W 72-12.6]

12 p1830 A72-28164

Plane plastic deformation during single pass rolling of corrugated metal sheet, determining stress-strain fields for first and second passes

13 p1964 A72-29148

Iron content and stress level effect on flaking corrosion of Al alloy sheets, describing experimental technique

13 p1980 A72-29826

Flat Ti alloy sheet creep under variable loads at 300-400°C, comparing prediction with test data

14 p2116 A72-30434

Lamb acoustic surface wave method for rapid non-destructive evaluation of rolling texture in arbitrarily thick metal sheets and plates

14 p2107 A72-30615

Shock heating caused material phase transformation effects on bumper shield performance, studying thin metal sheets response to like-material spheres impact

14 p2168 A72-30921

Deep drawing of circular mild steel and aluminum sheets with polyurethane or rubber rings, examining strain distribution, shape and surface roughness

15 p2244 A72-32145

Anelastic damping of cold worked Nb sheet as function of vibration frequency, temperature, rolling rate and oxygen content

15 p2258 A72-32638

Deformation modes for deep drawing of extramild steel sheets, noting susceptibility and rupture criteria

16 p2396 A72-32872

Lamb wave technique for bond strength testing of laminated or clad metal sheets, calculating displacement and stress dispersion and amplitude distribution for different modes

16 p2391 A72-33230

German papers on crack propagation in metal sheets, resonant vibration of cylindrical shells and stress concentration in plastic plates

16 p2470 A72-33676

Crack propagation in Al-Cu-Mg alloy sheet under vibratory bending loads, noting crack length to loading cycles number relationship

16 p2408 A72-33677

Material thinout in deformed metal sheet specimens under explosive forming, using air cell effect

16 p2399 A72-33775

Ways of reducing porosity in argon-arc welding of thin titanium sheets.

18 p2695 A72-36428

Techniques to curb static austenite recrystallization rate in martensitic steel during high temperature thermomechanical treatment through minute Ti or Zr additions

18 p2701 A72-36702

Fabrication of Hastelloy B sheet by powder metallurgy using blends of elemental powders and homogenization/deformation processing.

19 p2815 A72-37596

Optimization of thermo-mechanical deformation parameters for Ti-6Al-4V.

19 p2821 A72-38385

Fe-Ni sheet with austenitic cube texture by rolling and annealing, investigating plastic deformation during martensitic transformation

21 p3065 A72-40090

Sheet metal economics in aircraft construction based on strength/weight and stiffness/weight comparison of Al alloys and Ti alloys in relation to cost and structural weight considerations

21 p3060 A72-41071

Influence of the cycling frequency and directional anisotropy on the fatigue strength of AMg6BM aluminum-alloy sheet

21 p3070 A72-41356

Influence of stress raisers in the form of circular holes on the endurance in symmetric bending of AMg6BM aluminum-alloy sheet

21 p3071 A72-41704

Composite materials obtained by depositing boron layers under vacuum on aluminum sheets

22 p3190 A72-42646

On the diffusion of a load from a semi-infinite stringer bonded to a sheet.

22 p3238 A72-42833

Studies on sizes and shapes of tensile test specimens for thin sheet materials of aluminum alloys.

22 p3195 A72-43125

Al alloy sheet panel tests for cracks emanating from stress concentration areas at holes or cutout edge

23 p3347 A72-43713

Width/thickness ratio effect on steel, brass and molybdenum sheet specimens plasticity and deformation under tension at room temperature

23 p3301 A72-43758

Experimental and theoretical study of the fracture of sheet materials in the presence of cracks

23 p3349 A72-43958

Structure of the 01420 alloy with zirconium

23 p3303 A72-44094

Fatigue crack closure at positive stresses.

24 p3457 A72-44819

Endurance tests of D16AMO alloy sheets under high intensity acoustic, harmonic and electrodynamic vibrator loading

24 p3414 A72-44945

Hydraulic sand blasting and annealing effects on Ti alloy sheet bending fatigue strength

24 p3416 A72-45744

Crystallographic texture of sheet Mo alloys, analyzing angular dependence of Young modulus

24 p3416 A72-45752

METAL SHELLS

Elastoplastic stress distribution in thin spherical metallic shells with cylindrical branch pipe under internal pressure

03 p0448 A72-13905

Plastic strain and rupture characteristics of thin walled tubular Ni samples under complex loading and biaxial tension

04 p0588 A72-15058

Approximate buckling load of orthotropic hyperbolic paraboloid metal shells, using energy approach

06 p0897 A72-17970

METAL SPRAYING

Problems and possibilities of the production of fiber-reinforced metallic components by thermal spraying

20 p2929 A72-39444

Particle temperature and flight velocity during gas-powder buildup

22 p3182 A72-42194

METAL STRIPS

Flattening, heat treatment and machining of narrow rectangular vacuum melt Mo strips for microwave devices

01 p0078 A72-11087

Thermomechanical conditions of plasticity-to-brittleness transition temperature for optimal rolling of cermet W strips

01 p0078 A72-11088

Equivalent dielectric properties of infinite two dimensional periodic metal tape structures in presence of electromagnetic waves propagating in various directions

05 p0628 A72-16410

Metal strip with circular hole under tension, calculating plastic strain and stress concentration coefficients

06 p0899 A72-18567

Stress-strain characteristics of metal ductile filaments with elastic brittle coatings, noting strengthening effect on anodic oxide coated aluminum

09 p1330 A72-23379

Dynamic stress concentration of notched strips.

21 p3117 A72-40715

Magnetic properties and texture of a thin strip of nickel-iron-molybdenum alloys

22 p3192 A72-43012

METAL SURFACES

Extruded anodized AlMgSi alloy matrix precipitate surface defects, noting wood grain effect, segregated bands, microstructural stains and heterogeneous zones

01 p0077 A72-11042

Extruded AlMgSi alloy manufacturing conditions effect on strength, surface finish and anodized appearance, discussing evenly distributed fine hardening precipitates, metal purity, etc

01 p0077 A72-11043

Breakdown surfaces of thin Ti alloy specimens under tension as function of composition and heat treatment temperature

01 p0088 A72-11079

Metal-semiconductor-metal Schottky barrier microwave diode impedance and shot noise calculation

02 p0191 A72-11894

Fine scale surface oxide film roughness effects on metal substrate-oxide film system hemispherical emittance

02 p0303 A72-12319

Ductile metal surface erosion by hard abrasive grains striking at grazing angles

03 p0373 A72-13650

Surface potential effects on splitting of p- and d-orbitals of atoms and ions approaching bcc and fcc substrates

03 p0393 A72-14340

Intermittent ion emission enhancement from tungsten surface in He-W field-ion microscope upon Ne addition to imaging gas

04 p0552 A72-14547

Dry heat resistance of bacillus spores on spacecraft metal surfaces for different pressures, atmospheres and materials

04 p0475 A72-15261

Filmform corrosion of steel, magnesium and aluminum coated and uncoated surfaces in humid and corrosive atmospheres

04 p0536 A72-15735

Scattering of arbitrarily impinging monochromatic electromagnetic waves by thin infinitely long isotropic, dielectric and metal rods of elliptic cross section

05 p0628 A72-16412

Smooth curved metal surfaces thermal conductance at high vacuum, verifying contacting surfaces plastic deformation

05 p0666 A72-16868

Elastic-plastic strain measurement on flat steel surfaces by moiré gratings, using electroluminescent source and crossing jig

06 p0818 A72-18323

Sputtered molybdenum disulfide lubrication on polished metal surfaces with low friction coefficient, strong adherence, high density and small particle size

06 p0824 A72-18607

Exoelectronic emission method for examining deformation induced structural changes and interactions with ambient medium of metals and alloys surfaces

07 p0989 A72-20157

Solid lubricant additives effects in oils and fats, discussing molybdenum disulfide and zinc pyrophosphate solid film formation on metal surfaces under contact friction conditions

07 p1024 A72-20395

Phase composition changes, crater formation and metal ejection during erosion by pulsed laser beam

07 p1009 A72-20610

Surface structure changes in metal worked by electroerosion, discussing temperature and electrical tension effects

08 p1174 A72-21036

Metal structure effect on anodic dissolution and surface microgeometry formation during electrochemical machining

08 p1175 A72-21040

Mechanical surface strengthening effect on small cycle fatigue life of Ti alloy weakened by stress raiser

08 p1186 A72-21725

Soviet book on temperature resistance of lubrication boundary layers and solid lubrication coatings during friction of metals and alloys

08 p1179 A72-22023

Corrosion tests by ellipsometer, discussing apparatus design and bare metal surface and thin film properties

08 p1172 A72-22110

German monograph on lattice and solid metal surface transport processes, discussing atom migration, activation energies, impurity atom diffusion, Kossel-Stranski model, etc

08 p1212 A72-22173

Amorphous chromate and phosphate conversion coatings of Al, providing inert surface for painting

09 p1317 A72-22480

Loading path effect on yield surfaces of pure Al at elevated temperatures under tension

09 p1328 A72-22993

Local level filling and Fermi distribution in metal semiconductor contact as function of voltage and level location

09 p1372 A72-23355

High intensity laser radiation absorption in plasma produced from thick metal targets and thin Au foil

10 p1490 A72-23967

Plasma coating formation mechanisms and parameters, studying metal surface and deposited particles temperatures, spraying time effects, etc

10 p1487 A72-24488

Metal adhesive forces to clean Fe surface measured with LEED and Auger emission spectroscopy, noting binding energy correlation to oxygen

10 p1497 A72-24821

Hail damage to aircraft, predicting metal surfaces dent depth and deformation shape with computer program

11 p1574 A72-25370

Test assembly for Brinell microhardness measurements of metal and alloy surfaces under tension during vacuum heating and in protective gas media

11 p1612 A72-25490

Hardcoat anodizing of Al surfaces, discussing preparation, racking, equipment and post treatments [SAE PAPER 720341]

11 p1638 A72-25598

Computational technique for crack growth prediction in metal subjected to variable amplitude cyclic loading, taking into account yield zone ahead of crack tip

11 p1735 A72-25876

Metal surface smoothing during electrochemical dissolution prior to polishing, involving electrolyte diffusion processes or semiconductor oxide film formation
11 p1640 A72-26259

Metal surface layer and microetching process along grain boundaries during electrochemical precision processing, verifying steel microcrack depths with mathematical model
11 p1640 A72-26260

Ti alloys processability by electrochemical method, showing output rate and surface quality improvement from increased current density and electrolyte temperature
11 p1640 A72-26261

Electrochemical precision metal processing accuracy, analyzing electrode gap size and surface nonuniformities effects on prescribed configuration
11 p1640 A72-26262

Pulsating heat source model for physical processes in metal surface layer under fatigue limit stress level, calculating critical volume to limit energy buildup
11 p1738 A72-26801

Helicopter rotor blade spars shot peening in centrifugal vibrator, optimizing Cr-Mo-Ni steel surfaces work hardening
11 p1642 A72-26820

X ray determination of thermal microstresses in metal specimens surfaces
12 p1807 A72-27447

Electron microscope study of hard alloy surface layer formation characteristics during diamond grinding with electrolysis
12 p1814 A72-27766

Low photon IR photovoltaic response of CdS-metal junction, noting energy conversion efficiency
12 p1855 A72-28009

Russian book on work hardening of surface components of heat resistant and Ti alloys for high temperature operation
12 p1816 A72-28156

Three dimensional heat propagation problem of copper electrode destruction under concentrated heat flux with allowance for metal evaporation
12 p1890 A72-28175

Physicochemical processes in metal surface layers subjected to contact friction with aircraft fuels presence, noting secondary compounds and thermal oxidation acceleration
12 p1817 A72-28183

Metal surface layers structural changes under external friction, noting hardening, softening and phase transformations of active layer material
12 p1818 A72-28190

Clean metallic surfaces adhesion coefficients in vacuum at 77-293 K as function of load, loading time and contact cycles
12 p1818 A72-28193

Low energy electron diffraction structures due to CO and oxygen adsorption on clean Re surfaces produced by Ar ion bombardment at 20 to 920°C
13 p2020 A72-28522

Temperature effects on synthetic rubber sliding friction characteristics against smooth steel surfaces under compression loads in vacuum and air at 10-140°C
13 p1962 A72-28554

Sulfur dioxide and carbon dioxide interaction with clean silver surface at ultrahigh vacuum, using Auger electron spectroscopy and work function measurement
13 p1912 A72-28684

High temperature contact creep tests in vacuum and in metal melts, noting adsorption effect on surfaces plastic deformation
13 p1963 A72-28768

Chemical reactions between solids during boundary friction, presenting literature review on mechanochemical or tribo-chemical reactions between solid lubricants and metal surfaces
[ASLE PREPRINT 72AM 1] 13 p1964 A72-28969

Ice adhesive shear strength to steel bearing surfaces coated with bonded solid lubricants, describing low temperature test apparatus and results
[ASLE PREPRINT 72AM 4] 13 p1964 A72-28970

Metal-dielectric-semiconductor junction transistor HF response analysis by digital computer, deriving switching time as function of impurity concentration and electrode voltage
13 p1932 A72-29294

Cu surface contamination effect on hot crack susceptibility and weldability of Co based superalloys
13 p1965 A72-29419

Rarefied gas flows effect on metals creep properties, examining molecular flow density distribution as function of specimen surface distance from nozzle
13 p1979 A72-29483

Effect on physical and mechanical properties of hard metals due to gas sorption by metallic films spray-coated on surfaces, describing vacuum apparatus
13 p1939 A72-29488

Hydrogen evolution and ferric ion corrosion inhibition by synergistic action of substituted thioureas and thioamides to minimize metal corrosion during acid cleaning
13 p1980 A72-29624

Antifriction phase structure of friction formed thin surface layer of sulfurized iron-graphite metal-ceramic materials, using transmission microscopy
13 p1967 A72-30108

Isolated finite amplitude electrostatic oscillations production in thin plasma layer between two parallel metallic surfaces in magnetic field
14 p2136 A72-30302

Temperature distribution of structural element with heat shield and metallic layer, determining ablation process for thermal flux at surface
14 p2170 A72-30593

Coating materials for metal surface wear inhibition by adhesive and abrasive interactions minimization, discussing laminar solids, plastics, ceramics and soft metals
[ASME PAPER 72-DE-48] 14 p2108 A72-30874

Temperature dependent optical constants of Ti and W crystal surfaces cleaned by ion bombardment in ultrahigh vacuum
15 p2274 A72-31376

Reactional diffusion in metal surface layers due to chemically active external media involving solid reaction products formation
15 p2255 A72-31570

Diffusion layer formation on metallic surfaces, discussing saturation, crystallization, phase structure, chemical reactions, thermal and contact conditions
15 p2255 A72-31571

Energy and angular distribution of hydrogen and rare gas ions backscattered from polycrystalline metal surfaces
15 p2276 A72-31852

Surface damage induced by ion bombardment of monocrystalline W and Mo, determining degradation rate dependence on collisional energy transfer
15 p2276 A72-31853

Absolute intensity LEED spectra for clean Ni surfaces, discussing measurement uncertainties
15 p2276 A72-31854

Kinematic intensity recovery from LEED data of specular and nonspecular beams from Ni(111) surface, noting multiple scattering interference elimination
15 p2276 A72-31855

Debye-Waller factors measurement for Mo and Cr surfaces near normal incidence based on LEED
15 p2292 A72-31857

Carbon monoxide adsorption on nickel surface, determining preferential orientation by extended Huckel calculations
15 p2276 A72-31867

Edge and surface modification of Nb alloys prior to coating with fused silicide for oxidation life extension
15 p2244 A72-32134

Optical nondestructive surface flaw detection for steel plates using oblique angle illumination combined with high pass spatial filter
15 p2238 A72-32153

Surface effects on paramagnetic metals spin susceptibility models, including random-phase-approximation equation derivation and induced magnetic moment calculation
15 p2295 A72-32549

Hydrogen atom ground state ionization probability derivation as function of electric field strength and distance to metal surface
15 p2279 A72-32699

Oxygen chemisorption effect on rare gas beams reflection from refractory metals polycrystalline surfaces, interpreting experimental results by simple correlation model
16 p2431 A72-33068

Carbon fibers reinforced polymer wear rate decrease in organic fluids associated with films development on steel counterface, noting application in lubricated systems
16 p2397 A72-33124

Molybdenum disulfide lubricating effectiveness due to surface film properties, suggesting chemical reaction effect with sliding metal surface
16 p2397 A72-33125

Mo and stainless Ni-Cr steel surfaces chemical composition determination by Auger electron spectroscopy during heating in high vacuum
16 p2406 A72-33251

Anodic oxide films separation from Al alloy surface using ethyl bromide at temperatures below 40°C
16 p2397 A72-33274

Field-ion microscopy as experimental metallurgical technique for metal surface atomic structure studies, discussing image formation, ionization and field evaporation
16 p2392 A72-33444

Conduction electron phonon scattering effect on electrical resistance of metallic contacts during pressure welding
16 p2370 A72-33952

Metal-insulator-metal tunnel junctions, investigating effect of nonparabolic band structure energy-momentum relation on I-V characteristics
16 p2370 A72-34101

Electron currents injected through dielectrics
17 p2529 A72-34753

Electric contact phenomena in ultra clean and specifically contaminated systems
18 p2717 A72-36115

Thermodynamic analysis of metal surfaces covered by electropositive adsorbates.
18 p2656 A72-36126

Electric contact between metal and n-type semiconductor, investigating contact pressure effects on electron tunneling and phonon conduction to provide band structure
18 p2718 A72-36488

An investigation of impurities segregation to the /001/ nickel surface during thermal treatment - Work function changes and Auger electron spectroscopy using the LEED camera.
18 p2720 A72-37022

Synthesis of a resin-metal damper whose characteristic shows minimum deviation from a constant-frequency response
19 p2806 A72-37429

A new morphological element on the viscous breakdown microsurface of hypoeutectoid steels
19 p2817 A72-37737

Investigation of the effect of some surface-active media on the variations in strength characteristics of steel U8 in a high strength state
19 p2817 A72-37738

Nature of ion generation during the action of laser emission on a solid body
19 p2811 A72-38193

A helium-neon laser active element with a metallic inner wall surface
19 p2814 A72-38785

The influence of the surface orientation on yield in Mo single crystals.
20 p2935 A72-39007

Developments in the field of metallic diffusion protective layers employed against high-temperature corrosion
20 p2944 A72-39450

Radiation heat transfer between closely spaced metal surfaces at low temperature - The impact of discrete modes of the radiation field.
[ASME PAPER 72-HT-O] 20 p2983 A72-39483

Image point formation in field ion microscopy of metal surfaces, using atom probe detection of noble gas apex adsorption
21 p3050 A72-40086

Electrochemical protection potential of metals and alloys in pitting, intergranular corrosion and stress corrosion cracking in presence of chlorides
21 p3065 A72-40087

Habit plane interpretations of surface martensite transformation and orientation measurements compared with invariant plane strain /IPS/ theory
21 p3065 A72-40088

An experimental investigation of yield surfaces at elevated temperatures.
21 p3117 A72-40678

Investigation of tantalum-compound films at the surface of acicular tungsten microcrystals
21 p3068 A72-40964

The magnetic field of eddy currents above a surface crack in metal with excitation of them by an applied inductor.
21 p3057 A72-41722

Antiscratch properties of nitrided layers of creep-resisting steels at high temperatures
22 p3187 A72-41868

Experimental setup for the investigation of the spectral radiative capability of metals
22 p3175 A72-41893

Surface effects during high-speed impact of metals
22 p3188 A72-42163

Spectroscopic study of the interaction of oxides with metallic surfaces. II - SiO₂-Fe /Cu, Al, Ni, Co, Ti, W/ systems
22 p3189 A72-42197

Nature of radiation defects formed by ruby laser emission on the surface of solids
22 p3185 A72-42273

Influence of the properties of the materials on junction tunnelling characteristics.
22 p3214 A72-42454

Photoelectron energy distributions from clean polycrystalline W, observing surface state
22 p3190 A72-42477

Photoemission from surface states on tungsten.
22 p3190 A72-42478

Brazing furnaces and heat treatment under vacuum
22 p3163 A72-42635

The limiting strength of worn metal surfaces.
22 p3194 A72-43039

Manifestation of the effect of adsorptive reduction in strength under conditions of selective transport during boundary friction
22 p3183 A72-43138

Isolated finite amplitude electrostatic oscillations production in thin plasma layer between two parallel metallic surfaces in magnetic field
23 p3317 A72-43204

Study of the dependence of the spectral and integral radiation properties of bodies on the surface roughness.
23 p3357 A72-44538

The kinetics of the reaction between oxygen and sulfur on a Ni(111) surface.
24 p3378 A72-44951

Transition of the oxide film on a molybdenum surface from the two-dimensional to the three-dimensional phase 24 p3432 A72-45503

Al and Ti alloy fatigue after temperature reduction to 253, 77 and 4 K as function of surface purity after machining 24 p3416 A72-45743

METAL VAPORS

NT MERCURY VAPOR

NT SODIUM VAPOR

Theoretical model for radiating metallic gas produced around iron meteor entering earth atmosphere, presenting temperature, pressure and density distributions [AIAA PAPER 72-204] 05 p0721 A72-16884

Negative hydrogen ion production during charge exchange between protons in thick Li, Na, K and Mg vapor jets 06 p0863 A72-18410

Bulk vapor formation processes during laser beam heating of metals, considering effect on mass transfer 07 p1000 A72-18939

Maximum volatile solute vaporization escape prior to droplet solidification during metal vapor chemical release process 08 p1128 A72-21618

Nonequilibrium ionization theories for high pressure discharge in inert gas-alkali metal vapor 10 p1515 A72-24414

Collisional ionization cross sections measurement for gaseous metal atoms in hydrogen-oxygen flames at 2000-2800 K 11 p1591 A72-26659

Chemical vapor deposition of W and Mo by hydrogen reduction of hexafluorides, noting crystal structure and microporosity 11 p1644 A72-26837

Phase composition and lattice constants of carbide films from vaporized Zr interaction on graphite surface at 1700 C 13 p1912 A72-28566

Vacuum gap discharge conditions as function of electron beam parameters and metal vapor pressure 13 p2017 A72-29611

Nonlinear radiation absorption and resonance molecular fluorescence of saturated diatomic Rb vapors excited by Q switched ruby laser 14 p2109 A72-30353

Liquid film condensation of low pressure metal vapors on isothermal vertical flat plates, obtaining equations for heat transfer rate prediction 14 p2173 A72-31059

Stefan problem of metal evaporation duration after intense heat flux termination as function of thermophysical properties 15 p2334 A72-31504

CW laser transitions in singly ionized Te vapor spectrum at 4843-9378 A, indicating charge transfer as dominant excitation mechanism 16 p2401 A72-33394

Ellipsometry for the study of equilibrium cesium adsorption. 17 p2552 A72-34599

Compatibility of brazed joints with potassium and vacuum. 17 p2567 A72-34938

Ultra-high vacuum coater for thin film research 18 p2676 A72-36839

Condensed zinc particle size determined by a time discrete sampling apparatus. 20 p2913 A72-39608

Vapor deposition in vacuum under conditions of constant vapor flow with the aid of electron emission current control 20 p2954 A72-39694

He-Cd lasers using recirculation geometry. 21 p3061 A72-40239

Design of high-temperature liquid-metal systems. [ASME PAPER 72-AERO-13] 22 p3204 A72-43149

Alkali metal vapor Q switches for synchronizing mode-locked laser pulse trains with external events. 23 p3297 A72-44189

Evaporation of metallic targets by intense optical radiation 23 p3297 A72-44485

Metal vapor plasma as working medium in MHD generator, discussing hydrodynamic relations, power efficiency and thermodynamic cycle 24 p3428 A72-45169

METAL WHISKER REINFORCEMENT

U WHISKER COMPOSITES

METAL WORKING

NT AUSFORMING

NT CLADDING

NT COINING

NT EXPLOSIVE FORMING

NT FORGING

NT MAGNETIC FORMING

NT METAL DRAWING

Integrity control procedures for machining, drilling and grinding of steel and Ti alloy aircraft parts, discussing nondestructive inspection method [SME PAPER IQ 71-238] 01 p0076 A72-10969

Soviet papers on deformation of metals and alloys covering rolling, mechanical properties and plastic deformation of W, Mo and Ni alloys 01 p0077 A72-11076

Physical inconsistencies of mechanico-mathematical concepts of metal deformation, considering friction forces, lubricant action and plastic tensors and deviators 01 p1012 A72-11077

Two component flow and optimal strength ratios between core and shell materials during extrusion of composite bimetallic specimens into circular tubes 01 p0077 A72-11078

Deformation and compression characteristics of W wire rolled from flattened vacuum melts 01 p0077 A72-11084

Plastic deformation, heat treatment and grinding of set blank W casts for strip and foil production 01 p0088 A72-11085

Flattening, heat treatment and machining of narrow rectangular vacuum melt Mo strips for microwave devices 01 p0078 A72-11087

Fabricable high strength Inconel 706 precipitation hardening superalloy, noting savings in Ni, Nb and Mo content 02 p0245 A72-12507

Superalloys ductility and workability improvements without sacrificing elevated temperature strength for aircraft engine applications 02 p0246 A72-12561

Rolled metals and alloys with various lattice types and packing defect energies, showing elastic properties isotropy and Young modulus anisotropy 03 p0371 A72-13188

Rolling workability of pure W single crystals grown by electron beam zone melting technique, discussing crack occurrence 03 p0374 A72-13718

Forming of 7075-T6 Al in high pressure environments, predicting fracture occurrence via finite element stress analysis computer programs and pressure dependent model [ASME PAPER 71-WA/PT-11] 05 p0671 A72-15912

Metallurgical treatment control reliability in machine part mechanical properties quality evaluation 05 p0671 A72-15993

Ti alloys evaluation technique of arc melting, processing and testing of miniature ingots, discussing alloying and microstructural effects and correlation with plate properties 05 p0674 A72-16390

Mechanical, technological and physical properties of steel with and without molybdenum 05 p0679 A72-17204

Adherent solid lubricant films electrochemical deposition, noting method application to metal forming techniques 06 p0824 A72-18606

Plastic strain and fracture of metals by specific internal energy change method, investigating mechanical work and heat release 06 p0900 A72-18691

Economical methods for cast maraging steel production, describing composition, heat treatment and mechanical properties 07 p1010 A72-18970

Stainless steels with improved formability developed through assessment of stress-strain curve slope and plastic strain ratio 07 p1011 A72-19477

Se and Te additions effects on low carbon steels formability and machinability from metallurgical examination and workability tests 07 p0994 A72-19480

Impurities and crystal lattice role in metal brittleness, discussing stress concentration and relaxation, crack initiation and plastic deformation 07 p1018 A72-20145

Metals and alloys breakdown toughness and mechanical properties predictions under various loading conditions, discussing interatomic bonds and plastic deformation zone size 07 p1019 A72-20146

Plastic stress-strain anisotropy of metals under forming for mild steel, austenitic stainless steel and Mg, showing nonconformability with Hill criterion 07 p1020 A72-20432

Metals cold working mechanics about stress state and yield points, proposing theoretical model for mechanism and applications in extrusion molding, drawing and hollow forging 07 p0999 A72-20599

Metal working technology - Conference, Timisoara, Rumania, October 1971 08 p1173 A72-21026

Dimensional metal working by material erosion involving stereomechanical energy transmission to surface of nonrigid mechanical body 08 p1173 A72-21027

Electrical erosion efficiency of metal working under increased pressure in discharge gap in air and water 08 p1174 A72-21029

Automatic control of electroerosion machining by process computer, using pulse-voltage-metal removal relation 08 p1174 A72-21030

Technological characterization of electric discharge machines by metal removal rate, volumetric electrode wastage and machined surface roughness 08 p1174 A72-21031

Dielectric sulfur activated liquids for high productivity electroerosion machining of steels and metallic carbides, comparing with petroleum 08 p1174 A72-21034

Surface structure changes in metal worked by electroerosion, discussing temperature and electrical tension effects 08 p1174 A72-21036

Metal working by plasma beam in turning machine, applying to high strength alloys 08 p1175 A72-21045

Metal cold working mechanics, discussing model based on equality of internal and external forces needed for plastic deformation 08 p1176 A72-21439

Thermal diffusivity and conductivity and specific heat of hard electrode graphite intermediate medium in hydraulic hot extrusion of metals 08 p1181 A72-22072

Metal forming - AIME Conference, Cleveland, October 1970 08 p1250 A72-22193

Plastic flow properties and stress measurement for metal working conditions with flat ring compression specimens and interfacial friction consideration 08 p1250 A72-22196

Workability tests from material deformation stress determination and fracture strain rate relation for forging, extrusion and rolling limits predictions 08 p1190 A72-22198

German monograph on plasma arc machining and cutting of metallic materials on lathe as function of electric power and torch performance 09 p1317 A72-22327

Al addition effect on thermal and mechanical stability, forgeability, cold workability, aging and oxidation resistance of Ti-Mo beta alloys 11 p1656 A72-25516

Metal forming techniques for gas turbine engines, considering isothermal, radial and powder metallurgy preform forgings, contoured cross and form rolling, and squeeze casting [ASME PAPER 72-GT-58] 11 p1638 A72-25649

Torsion testing machine for hot metal workability tests at constant strain rate 11 p1639 A72-25820

Numerical calculation of temperature distribution and tempering depth for inductive hardening process with automatic material feed, taking into account temperature dependent material properties 11 p1639 A72-25898

Mechanical, technological and physical properties of steel with and without molybdenum 11 p1660 A72-26139

Furnace technology review, stressing need for higher sintering temperatures, better automatic atmosphere controls and faster preforms transfer to forging operation 11 p1640 A72-26242

Hot isostatic pressing techniques for thin wall Be tubes manufacture 11 p1643 A72-26831

Solid state reactions in powder metallurgical production and working of Mo alloy, considering sintering process 11 p1644 A72-26846

Rolling operations in vacuum for protection of metallic materials underprocessing 11 p1645 A72-26867

Metal rolling speed effect on force and friction reduction by ultrasonic vibrations imposed on rollers, noting coefficient of friction dependence on deformation 12 p1814 A72-27645

Elastic deformations of porous Cu, Mo and W fiber materials after pressing and sintering due to residual stress relaxation 14 p2106 A72-30151

Squeeze casting for precision shaping mechanical properties, surface finish and cost reduction in metal working [ASME PAPER 72-DE-7] 14 p2108 A72-30862

Electrohydraulic and electromagnetic metal forming, using capacitor stored energy conversion into hydraulic shock waves or magnetic pressure to deform sheet metal components, pipes, etc 15 p2243 A72-31323

Kinetic forming of conical Al component from solid cylindrical billet, analyzing forming and inertia stresses, impact velocity and displacement-time history 15 p2244 A72-31708

Technical and economic aspects of explosive metal fabrication, considering requirements for close tolerances, nonsymmetrical shapes, large size workpieces and unusual material properties 16 p2398 A72-33354

- Fabrication of refractory metals.
17 p2559 A72-34187
- Metal working and testing of nuclear rocket engine components with Mo as structural material and uranium dioxide as fuel, discussing Mo-W interdiffusion
17 p2559 A72-34617
- Mathematical models for metallic plastic strain hardening under cyclic loads, introducing internal state parameters
17 p2632 A72-35111
- Testing the impact accuracy of the NEK-8 HERF machine
18 p2695 A72-36274
- Effects of combined high and low temperature deformation processing of beta III titanium.
18 p2701 A72-36590
- Transition metals physical and mechanical properties, production, refining and vacuum processing techniques
18 p2696 A72-36840
- Polish aircraft industry production and fabrication techniques, discussing metal working, digital controlled machining and cost reduction
18 p2696 A72-37010
- Thermochemical techniques application to corrosion protection of metallic powders, mechanical parts and tools, describing chromizing, chromaluminizing, tantalizing and niobiumizing processes [ONERA, TP NO. 1049]
19 p2817 A72-37769
- Dispersion hardening fabrication of hollow cooled blades of thin cermet layer and embedded plastic metal core, using aluminum oxynitrate in water-alcohol solution
19 p2809 A72-38282
- Metals and alloys solidification concepts, applying to casting techniques development
20 p2936 A72-39211
- Nucleation of new grains in recrystallization of cold-worked metals.
20 p2930 A72-39995
- Effects of hydrostatic stress on the yielding of cold rolled metals and fiber-reinforced composites.
23 p3299 A72-43496
- Fatigue-crack growth in 20% cold-worked Type 316 stainless steel at elevated temperatures.
24 p3435 A72-44555
- Making a product from composites. II.
24 p3412 A72-44556
- Metallurgical treatment control reliability in machine part mechanical properties quality evaluation
24 p3416 A72-45735

METAL-GAS SYSTEMS

- Hydrogen partial molar volume in metal-hydrogen two component systems under externally applied uniform hydrostatic stress field, using thermodynamic analysis
01 p0083 A72-10205
- Hydrogen chemical permeation through iron and steel as function of compressive and tensile stress
01 p0083 A72-10206
- Gas saturated surface layer deformation in rolled Ti alloys as function of specimen thickness reduction
01 p0077 A72-11080
- Phase oriented precipitation patterns of Ti in Ti-C-O system, discussing composition independence and dislocation networks
01 p0089 A72-11184
- Equilibrium states difference of ternary metal-boron-nitrogen systems, taking into account chemical bond type and crystal structure of boride and nitride atoms
14 p2112 A72-30154
- TiC high temperature oxidation and thermodynamic equilibria in air, using metallographic and X ray analyses
14 p2112 A72-30155
- Thermodynamics and phase relations in refractory metal solid solutions containing carbon, nitrogen, and oxygen.
18 p2699 A72-36576
- Relation between hydrogen embrittlement and the formation of hydride in the group V transition metals.
18 p2700 A72-36578
- Equilibria and degassing kinetics in the systems Mo-N, W-N, and Re-N
18 p2701 A72-36596
- Thermodynamic description of the metal-rich part of the system niobium-molybdenum-nitrogen
18 p2701 A72-36597
- Standard Ti bars samples for spectral determination of H concentration and distribution in Ti alloys, using mathematical statistical method
23 p3287 A72-43676
- Relationship between the electrical resistivity and solute concentration in the solid solution of tantalum-hydrogen system.
24 p3412 A72-44718
- Influence of oxygen and hydrogen on the strength of titanium alloys
24 p3414 A72-45379

METAL-METAL BONDING

- Continuous seam diffusion bonding application to Ti and superalloys lap, butt and T joints production [SME PAPER AD 71-264]
01 p0076 A72-10970

Bonding mechanisms and failure modes in thermocompression bonds of Au plated leads to Ti-Au metallized substrates, discussing Cu lead frames plated with Ni and Au
03 p0365 A72-14292

Ultrasonic bond formation between soft fcc metals, observing dislocation processes
04 p0526 A72-14837

Nondestructive examination of steel plate weld specimen, comparing ultrasonic and X ray techniques
04 p0527 A72-14840

Adhesive bonded components in aircraft and aerospace structures, discussing manufacturing, metal surface preparation, inspection and environmental exposure
06 p0835 A72-17325

Explosive welding of heat exchanger tubes and detonation produced compressive joining of cables as applications of explosive metalworking procedures
07 p0994 A72-18931

Plasma spraying process effects on carbon steel coatings structure and bonding, considering optimal parameters, properties control and phase transformations
07 p0996 A72-19966

B-Al metal matrix composites joining together and to Al and Ti, considering soldering, brazing, bonding and mechanical fastening [AIAA PAPER 72-360]
11 p1638 A72-25388

Aluminum-stainless steel and Ni-Mo composites prepared by dynamic hot pressing, determining bond strength between fibers and reinforced metal matrix
14 p2107 A72-30431

Lamb wave technique for bond strength testing of laminated or clad metal sheets, calculating displacement and stress dispersion and amplitude distribution for different modes
16 p2391 A72-33230

Slurry explosives for metal cladding, discussing applications to pipe joints, bearing sleeves, recoil rods, gun barrels and cylinder liners
16 p2398 A72-33357

Study of reliability of Al-Au thermocompressions by measurement of resistance
18 p2668 A72-37105

On some aspects of low-temperature and anodic oxidation of metals and semiconductors.
21 p3067 A72-40914

Bonded joints - Squeeze-out /flash/ effect on fatigue strength.
23 p3353 A72-44248

Investigation of the possibility of using radiant solar energy for welding and soldering of materials
24 p3407 A72-45126

Non-destructive testing of adhesive bonded metal-to-metal joints. I.
24 p3408 A72-45289

Non-destructive testing of adhesive bonded metal-to-metal joints. II.
24 p3408 A72-45290

METAL-WATER REACTIONS

- Partial pressure gage to measure water vapor-produced hydrogen content in metal samples, using reference gas evolution curves
12 p1807 A72-27451
- Temperature dependent aluminum-water reaction generation of free hydrogen and aluminum hydroxide
16 p2362 A72-34159
- Active corrosion in aqueous solutions, discussing reactions, adsorption, intergranular attack, pitting, crevice corrosion and stress corrosion cracking
19 p2815 A72-37446

METALLIC HYDROGEN

- Statistical mechanics of light elements at high pressure. II - Hydrogen and helium alloys.
21 p3106 A72-41044

METALLIC PLASMAS

- NT CESIUM PLASMA
NT URANIUM PLASMAS
Unstable sound waves in uranium plasma, taking into account fission power density, radiation diffusion and ionization variations
01 p0112 A72-11336
- Uranium arc plasma visible and near UV emission coefficients as function of U partial pressure and corresponding temperatures
01 p0112 A72-11337
- High temperature U plasma generation at near gas core reactor conditions by sliding spark discharge into capillary channel lined with sintered uranium dioxide
01 p0112 A72-11338
- Uranium and tungsten plasmas emission and absorption properties at shock tube generated pressures of 3-48 atm and temperatures of 7,000-12,000 K
01 p0112 A72-11339
- Organic dye lasers radiation nonlinear interaction with alkali metals spark discharge plasma, showing angular and spectral broadening
04 p0532 A72-15573
- Cylindrical alkali metal plasma column structure in single ended Q device under axial magnetic field
06 p0854 A72-17503

Density and flux measurements by Langmuir probes in uranium plasma produced in single ended Q device, noting application to isotope separation
06 p0855 A72-17506

Electrostatic wave propagation and damping in thermally ionized collisionless alkali plasma, determining electron and ion densities, electron temperature and ion distribution function
06 p0856 A72-17521

Collisional drift instability dependence on parallel wavelength in potassium Q device plasma
06 p0857 A72-17528

Collisionless drift waves in thermally ionized Li plasma column under variable shear magnetic field
06 p0857 A72-17535

Hf fluctuations in density gradient of alkali plasma within Q device
06 p0858 A72-17536

Single ended Q machine Ba plasma probe measurements of ion temperatures perpendicular to magnetic field, electron temperatures and plasma densities and potentials
06 p0859 A72-17550

Electrical conductivity of nonideal low temperature plasma as function of metalization densities, applying to semiconductors and mercury vapor systems
07 p1043 A72-19880

Absorption by Nd laser generated ionized Al plasma of extreme UV radiation due to inverse bremsstrahlung and photoionization
09 p1360 A72-22831

Heavy ion acceleration from strong electron beam in metallic plasma obtained with ruby laser and positive voltage pulses
10 p1524 A72-25034

Nonideal dense plasma properties, discussing electrostatic shielding, many particle clusters, phase transitions, metalization and electrical conductivity [AIAA PAPER 72-414]
11 p1695 A72-26164

Mercury vapor physicochemical processes kinematics in shock tube, determining electron gas energy balance equations and atom-atom collision cross sections
11 p1699 A72-26760

MHD stability in Hg vapor discharge plasma excited by standing microwave near electron cyclotron resonance, discussing electron energy anisotropy effect on LF oscillations
13 p2017 A72-29618

Electrical conductivity of nonideal low temperature plasma as function of metalization densities, applying to semiconductors and mercury vapor systems
17 p2590 A72-35129

Volt-ampere characteristics of Ba-Cs plasma thermionic converter with W emitter and Ta collector
18 p2646 A72-36199

Pulsed metallic-plasma generators.
20 p2958 A72-39781

MHD stability in Hg vapor discharge plasma excited by standing microwave near electron cyclotron resonance, discussing electron energy anisotropy effect on LF oscillations
21 p3091 A72-40671

Recombination continuum in a lithium plasma spectrum
22 p3210 A72-42171

Glow discharge in rare-gas and metal vapour mixture. I - Distribution functions and kinetic coefficients in He-Cd mixture discharge.
23 p3322 A72-44320

Metal vapor plasma as working medium in MHD generator, discussing hydrodynamic relations, power efficiency and thermodynamic cycle
24 p3428 A72-45169

METALLIZING

- Alloying elements and grain size effects on thermally induced surface reconstruction of Al film metalization on Si devices from thermal cycling tests
03 p0364 A72-14285
- Anodized aluminum metallization for reducing electromigration induced failure modes in silicon wafers
03 p0365 A72-14286
- Deposition of Ni-B coatings with specified electrical resistance onto fiberglass cloth reinforced plastics
09 p1318 A72-22528
- High alumina ceramics metalization and hard soldering to metals for manufacturing vacuum jacket of transmitting thermionic tubes
10 p1488 A72-24642
- Thermal analysis of high performance devices mounted on dielectric substrates.
17 p2527 A72-34677
- Plastic packages for complex microcircuits.
17 p2528 A72-34717
- Electrical conductivity of nonideal low temperature plasma as function of metalization densities, applying to semiconductors and mercury vapor systems
17 p2590 A72-35129
- Au alloys metalization system as alternative to aluminumizing for junction transistor reliability improvement, considering metal migration, microcracking and current leakage
18 p2666 A72-36554

Study of the process of niobium carbide production in a fluidized bed
23 p3293 A72-43294

METALLOGRAPHY

Metallographic and fractographic analyses of cracking in T53-L13 gas turbine engine compressor disks

01 p0085 A72-10816
Ti structures controlled path resistance welding, discussing welded joints metallographic and mechanical properties

07 p0996 A72-19996
Metallographic properties of vacuum brazed, heat treated and gas quenched Al alloys, low alloy steels and corrosion resistant steel alloys

07 p1017 A72-20001
Metallographic study of denuded zones from diffusional flow in hydrided Mg superplastic alloy with Zn and Zr

09 p1331 A72-23383
Advances in metallography - Conference, Leoben, Austria, October 1970

10 p1493 A72-23822
Soviet papers on high temperature metallography techniques and equipment covering test assemblies for fatigue and microhardness measurements

11 p1654 A72-25489
High temperature metallographic methods in microstructure study of austenitic heat resistant steel under plastic deformation and heat treatment

11 p1654 A72-25495
Metallographic examination of stainless steel specimens exposed to long term creep rupture tests, noting carbides precipitation and stress induced grain boundary migration

11 p1658 A72-25832
Deformation characteristics and mechanical properties of superplastic alloys, stressing metallographic techniques

11 p1739 A72-26936
Annealed and quenched Fe-Mo-Co system, defining phase relationships in Fe-rich corner at 2200, 2000 and 1800 F

13 p1973 A72-28650
Russian papers on phase diagrams of metallic systems covering thermodynamic, X ray and metallographic alloys analysis

14 p2122 A72-30976
Ce-N alloys phase diagram from durometric, X ray, metallographic and differential thermal analyses

14 p2123 A72-30991
Chemical inhomogeneity of high melting metals and alloys of Ti, Zr, Nb and Cr from radio isotopic and nuclear emission studies

15 p2255 A72-31576
Phase diagrams for W-Ta-Ti alloys at 1600 C from metallographic and X ray analysis

16 p2407 A72-33533
An electron microscopy study of carbide precipitation in vanadium.

18 p2699 A72-36577
Secondary recrystallization of nickel 270 work-hardened by tension

18 p2702 A72-36704
Investigation of defects and damage in metallic materials by metallographic examinations

20 p2941 A72-39573

METALLOIDS

NT ANTIMONY
NT ARSENIC
NT BORON
NT BORON ISOTOPES
NT GERMANIUM
NT SILICON
NT TELLURIUM

METALLOORGANIC COMPOUNDS

U ORGANOMETALLIC COMPOUNDS

METALLURGY

Monograph on electron beam welding covering space charge effect, equipment, metallurgical and mechanical aspects, production engineering, economics and applications

01 p0073 A72-10167
Cb alloy processing technology from ores to manufactured finished fabricated, joined and coated hardware, discussing reduction methods, annealing, forming, joining, etc

01 p0075 A72-10745
Metallurgical defects in hot extruded aluminum alloys, describing investigation methods and remedies

01 p0077 A72-11041
Selected microarea electron diffraction technique in high voltage electron microscopy, discussing applications in crystallography and metallurgy

04 p0523 A72-15490
Book on electrochemical machining covering metallurgical effects, electrolytes, tool design, rotating surfaces and operating costs

06 p0821 A72-17819
Metallurgy and metal science - Conference, Moscow, May 1968

07 p1011 A72-19543

Russian book on Nb in ferrous metallurgy covering physicochemical properties, steels, slags, ore reduction and smelting for Nb alloys production

11 p1659 A72-26048
Russian papers on electrochemical treatment of metals covering anode and cathode processes, electromechanical precision processing of machine parts and wear resistant electrolytic alloys

11 p1640 A72-26254
Haynes high strength heat resistant Ni-Cr-W alloy metallurgical and structural relationship, mechanical and physical properties, oxidation and corrosion behavior and fabrication processes

13 p1973 A72-28649
Superplastic alloys based on Al, Cu, Zn, Mg, Ti and carbon or stainless steels, discussing macroscopic properties and manufacturing cost reduction

14 p2120 A72-30622
Ultrasonic sound influence on metal physical and mechanical characteristics, utilizing in testing and manufacturing procedures

15 p2275 A72-31832
Russian book - Automation of the monitoring and study of metals

19 p2795 A72-37299
Physical and metallurgical factors causing embrittlement and creep rupture life reduction determined by tests, discussing crystal and grain boundary deformation and notch effects

19 p2874 A72-37711
Material properties, metallurgy, production technology and operational factors effects on machinery structural strength

23 p3347 A72-43733

METALS

NT ACTINIDE SERIES
NT ACTINIUM
NT ALKALI METALS
NT ALKALINE EARTH METALS
NT ALUMINUM
NT ALUMINUM COATINGS
NT ALUMINUM ISOTOPES
NT ANTIMONY
NT BARIUM
NT BARIUM ISOTOPES
NT BERYLLIUM
NT BERYLLIUM ISOTOPES
NT BISMUTH
NT CADMIUM
NT CALCIUM
NT CALCIUM ISOTOPES
NT CERIUM
NT CESIUM
NT CESIUM VAPOR
NT CHROMIUM
NT COBALT
NT DYSPROSIUM
NT ERBIUM
NT EUROPIUM
NT FERROUS METALS
NT GADOLINIUM
NT GALLIUM
NT GALLIUM ISOTOPES
NT GOLD
NT GOLD COATINGS
NT HAFNIUM
NT HOLMIUM
NT INDIUM
NT IRIDIUM
NT IRON
NT LANTHANUM
NT LEAD [ARSENAL]
NT LEAD ISOTOPES
NT LIQUID METALS
NT LIQUID POTASSIUM
NT LIQUID SODIUM
NT LITHIUM
NT LITHIUM ISOTOPES
NT LUTETIUM
NT MAGNESIUM
NT MAGNESIUM ISOTOPES
NT MANGANESE
NT MANGANESE ISOTOPES
NT MERCURY [METAL]
NT MERCURY VAPOR
NT METAL COATINGS
NT METAL CRYSTALS
NT METAL FILMS
NT METAL FOILS
NT METAL MATRIX COMPOSITES
NT METAL POWDER
NT METAL VAPORS
NT MOLYBDENUM
NT NEODYMIUM
NT NICKEL
NT NICKEL COATINGS
NT NIOBIUM
NT NOBLE METALS
NT NONFERROUS METALS
NT PALLADIUM
NT PLATINUM
NT PLUTONIUM ISOTOPES
NT POTASSIUM
NT POTASSIUM ISOTOPES
NT POWDERED ALUMINUM

NT PRASEODYMIUM
NT PROMETHIUM
NT RARE EARTH ELEMENTS
NT REFRACTORY METALS
NT RHENIUM
NT RHODIUM
NT RUBIDIUM
NT RUBIDIUM ISOTOPES
NT SAMARIUM
NT SCANDIUM
NT SILVER
NT SINTERED ALUMINUM POWDER
NT SODIUM
NT SODIUM VAPOR
NT STRONTIUM
NT STRONTIUM ISOTOPES
NT TANTALUM
NT TERBIUM
NT THALLIUM
NT THORIUM ISOTOPES
NT TIN
NT TIN ISOTOPES
NT TITANIUM
NT TITANIUM ISOTOPES
NT TRANSITION METALS
NT TRANSURANIAN ELEMENTS
NT TUNGSTEN
NT ULTRAPURE METALS
NT URANIUM
NT URANIUM ISOTOPES
NT VANADIUM
NT YTTERBIUM
NT YTTRIUM
NT ZINC COATINGS
NT ZIRCONIUM

Metals mechanical behavior, considering plastic deformability, strain hardening, cohesion and engineering performance prediction

01 p0086 A72-10985
Graphite, Mo, Ta and W thermal radiation total emittance measurement in 1200-2400 K range, evaluating recorded data by computer program

02 p0243 A72-12101
Metal ductile facies fracture study of cups formation from cracks by cleavage, noting roles of dislocations and inclusions

02 p0246 A72-12600
Quasi-static measurement and electron phonon interpretation of specific heat of metals at low temperature

03 p0456 A72-13843
Pure metals creep or self diffusion activation energy from hot-hardness data, noting temperature and elastic modulus effects

03 p0375 A72-13931
Metals thermophysical characteristics temperature dependence determination by analog computer, using one dimensional temperature fields in thin infinite plates and cylindrical or spherical surfaces

03 p0458 A72-14165
Physicomechanical properties of metals at crystallization temperatures, considering density, viscosity, strength, hardness, elasticity and creep

03 p0378 A72-14219
Statistical thermodynamics models for determining vacancy concentration and atoms and vacancies arrangement in metals and alloys under thermal equilibrium

03 p0378 A72-14255
Book on metallic and dielectric antennas covering planar, cylindrical and plasma types for symmetrical, dipole and ring excitations

04 p0497 A72-14612
Metal wear mechanism during electromechanical processing explained by configurational localization model

05 p0665 A72-16094
One dimensional two phase flow transpiration cooling through porous metals [AIAA PAPER 72-24]

05 p0749 A72-16915
Homologous temperature method to compare mechanical properties of metals tested at different temperatures

06 p0827 A72-17399
Automatic testing machine for mechanical properties of metals under static loading

06 p0796 A72-18365
Metals, insulators, semiconductors and ceramics thermophysical parameters measurement during monotonic heating or cooling at 123-3273 K

06 p0904 A72-18514
Small elastoplastic cyclic strain effects on internal friction and energy dissipation in metals during vibrations

06 p0834 A72-18679
Idealized model for anisotropy of metals inelastic characteristics due to plastic deformation, demonstrating applicability to polycrystalline materials

06 p0900 A72-18685
Test facility for studying temperature dependence of thermal diffusivity and true heat capacity of metals between minus 150 and plus 400 C

07 p0982 A72-18941

Gas content determination in metals by melting and vaporizing measured microvolumes using laser microprobe and magnetic mass spectrometer

07 p1006 A72-19549

Mechanical properties and structural strength evaluation methods for metallic materials at low temperatures, describing hydraulic and pneumatic testing facilities

07 p1017 A72-20130

Reversible hydrogen brittleness development conditions in metals, deriving equations for hydrogen content effect on plasticity dip

07 p1018 A72-20132

Nonferrous metals melting, discussing solid and gaseous impurities removal, halide function and grain and Al-Si eutectic refinement method

07 p0999 A72-20570

Laboratory metal corrosion testing, considering reasons, conditions and damage assessment

08 p1189 A72-22104

High temperature testing of metals, discussing specimen preparation and oxidation behavior evaluation by gravimetric, volumetric and optical techniques

08 p1189 A72-22107

Fluorescent X ray spectroscopy for K and L emission band structures of Mg, Al and V and metal compounds

09 p1370 A72-22839

Microscopic perturbations of metals electron density complex dynamic matrix, deriving electroconductivity and kinetic coefficients

09 p1329 A72-23039

Energy operator diagonalization of interacting valence electrons in semiconductor and metal models

09 p1352 A72-23356

Metal creep under multiaxial stress states, proposing technique for numerical stress analysis data collection

[SMRT PAPER L 1/3]

10 p1556 A72-24395

Metallic materials for delta wing space shuttle configuration with metallic thermal protection system

10 p1498 A72-24876

Inhomogeneous sink distribution effect on vacancy annealing kinetics and activation energy in metals

10 p1499 A72-24983

Space shuttle orbiter thermal protection system metal interaction with chemical environment during reentry, emphasizing degradation in dissociated oxygen

[AIAA PAPER 72-262]

11 p1590 A72-25206

Hexagonal metals stress corrosion cracking fractographs interpretation, noting striations as prominent feature of transgranular fractures

11 p1652 A72-25288

Pure metals bulk modulus pressure dependence from detonation generated shock wave data, using empirical relations between propagation velocity and material flow rate

11 p1662 A72-26741

Electrothermal NDT of metal structures by IR scanning camera or thermal image transducer

12 p1813 A72-27200

Mathematical model to describe complete creep process in metal from hardening and brittle failure theories

12 p1828 A72-27322

Electronic heating test arrangement for high temperature testing of metals and electrically conducting ceramics in vacuum, describing temperature control systems

12 p1796 A72-28249

Reversed creep deformation behavior of metals, observing acceleration at high temperatures due to grain boundary sliding enhancement

13 p1978 A72-29444

Cryogenic liquids cavitation erosion of plastic and cold-short metals at 77 K, determining vapor pressure effect

13 p1979 A72-29479

Reflectivity of metals at high temperatures based on Drude theory and electron-phonon scattering, detailing temperature dependence and optical constants

14 p2129 A72-30183

Shock induction melting and vaporization in metals, investigating initial porosity effect

14 p2113 A72-30185

Elastic effects in metal hardness testing with blunt indenter, considering indentation in rigid plastic manner

14 p2113 A72-30268

Metal creep activation energy determination during plastic deformation process, using temperature differential method

14 p2115 A72-30412

Degenerate electron gas magnetic properties implications for metals, white dwarfs and neutron stars, discussing nonmagnetic state for thermal equilibrium

14 p2158 A72-30728

Pavel stony meteorite microspectral analysis to obtain metallic elements weight percentages in chondrules, matrix and core, using laser source for local vaporization and excitation

14 p2159 A72-30785

Temperature aftereffect in heating and cooling of metals with cubic and noncubic lattices in relation to relaxation and hereditary deformation

14 p2143 A72-30952

Plastic deformation in metals and highly crystalline polymers as function of shear strain, strain rate, frequency and vibrational amplitude

15 p2328 A72-31840

Sound velocity and ultrasonic attenuation in anharmonic metal for collision dominated regime

15 p2277 A72-31889

Electron contribution to phonon damping in anharmonic metal for collision-free regime, evaluating relaxation times

15 p2277 A72-31890

Growth analysis curve of halo subdwarf Groombridge 1830 relative to sun, noting metal abundance

15 p2314 A72-32373

Metal melting heat relationship to diffusion activation energy with vacancy mechanism equal numerically to crystal internal energy maximum change

15 p2259 A72-32691

Metal fracture by electron pulse generated stress waves, noting intergranular fracture mechanism

16 p2472 A72-33845

Metal creep tests in thin walled ring shaped specimens for geometrical constancy under variable weights

16 p2472 A72-33850

Metal catalyst theory for electrocatalysis in alkaline hydrogen oxygen fuel cells, using Tafel equation

16 p2351 A72-33880

Instrument for Hall and Gauss effects measurement in semiconductors and metals, noting instrument error analysis

17 p2529 A72-34758

Metallic abundances in the solar chromosphere

17 p2613 A72-35498

Analysis of grain- and particle-size distributions in metallic materials

17 p2569 A72-35922

Dependence of emission on work function variation in metals under tension

18 p2699 A72-36350

New measurement and evaluation method for the determination of the diffusion coefficient of hydrogen in solid metals

18 p2692 A72-36841

Measurement of the damping capacity and dynamic modulus of high-damping metals under direct cyclic stresses

19 p2795 A72-37460

Effect of stress amplitude and number of vibration cycles on the damping decrement in metals

19 p2878 A72-38217

Metal-insulator-semiconductor-insulator-metal structure light pulse amplification investigating power gain and photocurrent dependences on applied voltage and applicability as radiation detector

20 p2960 A72-39517

Investigation of defects and damage in metallic materials by metallographic examinations

20 p2941 A72-39573

Autoclaves for the study of the effects of deformation on the high temperature aqueous corrosion of metals

21 p3039 A72-40216

Determination of copper, iron, cobalt, nickel, and manganese in biological samples of vegetable origin

23 p3260 A72-43924

Metallic solid material transient displacement field measurement by moire fringe photographic recording technique with computer program for data analysis

24 p3401 A72-44611

Temperature change direct measurement and annealing experiment via differential power analysis to determine stored energy release in metal plastic flow during compression

24 p3405 A72-44613

Automatic testing machine for mechanical properties of metals under static loading

24 p3389 A72-45751

Mechanical properties and structural strength evaluation methods for metallic materials at low temperatures, describing hydraulic and pneumatic testing facilities

24 p3416 A72-45756

Reversible hydrogen brittleness development conditions in metals, deriving equations for hydrogen content effect on plasticity dip

24 p3416 A72-45758

METAMORPHISM [GEOLOGY]

Shock transformed chondrite texture observed in thin plates by UV fluorescence

05 p0722 A72-17151

Alfanello meteorite inspection by optical microscopy for petrological features of shock metamorphism in chondrites

05 p0722 A72-17152

Shock metamorphism in Luna 16 soil sample, indicating regolith formation by meteorite impact

09 p1380 A72-22259

Savonoski crater, Alaska - A possible meteorite impact structure

19 p2790 A72-37861

Mineralogical and chemical researches on L-chondrites - Girsenti

19 p2858 A72-37862

Evidence for vapor fractionation in the origin of chondrules

23 p3339 A72-44134

METASTABILITY

U METASTABLE STATE

METASTABLE ATOMS

Metastable He atoms concentration in plasma from absorption characteristics at temperatures 4-300 K and pressures 1-70 mm Hg

05 p0696 A72-16612

Ground state and metastable atoms and ions optical pumping, presenting critical survey on pumping and relaxation mechanisms, light propagation and spin exchange

14 p2109 A72-30325

Metastable ²S/ atoms production by electron impact induced dissociative excitation of molecular deuterium, measuring total cross section via Lyman alpha flux

15 p2282 A72-32645

Fast metastable hydrogen atom beam production by proton beam-Cs vapor charge exchanges

16 p2429 A72-33057

Excitation transfer and Penning ionization reactions between helium metastables and carbon monoxide

18 p2713 A72-36563

Absolute detection and collisional destruction of 2.5-keV metastable hydrogen atoms produced by a charge-exchange process in cesium vapor

19 p2837 A72-37547

Metastable atomic oxygen deactivation in upper atmosphere by inelastic collisions and by spontaneous irradiation, noting airglow intensity dependence on red lines irradiation

19 p2792 A72-38633

Calculation of photoabsorption processes in helium

24 p3426 A72-45012

METASTABLE STATE

Transmission electron microscopic investigation of heterogeneous nucleation of Al-Ag alloys metastable gamma prime phase, noting association with four dislocation types

01 p0083 A72-10209

Al-Mn system constitution, discussing metastable phase, high and room temperature modifications and transformation equilibrium

01 p0088 A72-11045

Orion and planetary gaseous nebula helium atoms metastable triplet states population calculations

04 p0578 A72-15314

Semiconductor film compound decomposition, chemical composition and metastable modifications presence during condensation in vacuum, discussing defect formation in crystal structure

05 p0701 A72-15752

Collisional radiative model of population densities of metastable electron levels of orthohelium in low pressure rf helium plasma

05 p0694 A72-15998

Metastable Fe-Cr-Ni austenitic stainless steels, demonstrating step phenomenon at elastic limit

05 p0672 A72-16011

Dissociative excitation of CO and metastable fragments by electron impact on carbon dioxide, investigating cross sections

06 p0803 A72-17447

Ground state He long range interaction with triplet metastable He, discussing gerade and ungerade states

07 p1037 A72-19495

Metastable argon-carbon dioxide dissociation and electronic excitation of carbon monoxide or oxygen

07 p1037 A72-19496

Transition metals distribution of IV-VI and VIII groups in metastable refractory nickel alloys gamma and gamma-prime phases

07 p1012 A72-19678

Order-disorder transition in metastable splat cooled Ti-rich Ti-Fe alloys from phase formation, constitution and crystal chemistry viewpoint

09 p1330 A72-23378

Metastable austenitic steel fiber to increase Al matrix strength to density ratio and fracture toughness

09 p1331 A72-23385

Population inversion through metastable ion formation by atomic inner shell electrons photoionization, determining effectiveness relationship to emission source plasma composition

11 p1648 A72-26332

Pulsar speed increase mechanism as metastable flow state transition in neutron star superfluid core

11 p1724 A72-26705

Ti alloy metastable phases classification, including alpha-prime, secondary alpha, omega, beta and alpha phases

12 p1828 A72-27290

Liquid quenched Sb-transition metal binary alloy constitution, finding metastable phases in quenched Cr-Sb and Mn-Sb alloys

13 p1975 A72-28672

Ni-Mn alloy phase transformation characteristics from neutron diffraction and small angle scattering

studies, showing ordered nearly stoichiometric metastable phase for entire temperature range
13 p1976 A72-28903

Metastable coesite crystal growth in highly strained quartz under 5-20 kb pressures and 450-900 C
14 p2099 A72-30322

Ti alloy volume reduction during decomposition of metastable alpha-prime, alpha-two and beta phases after cooling from beta range
14 p2114 A72-30401

Maraging Fe-Ni-Co-Mo alloy ordered metastable omega phase formation during martensite aging from electron microscopic investigation, noting Co addition effects and precipitation
14 p2115 A72-30404

X ray and metallographic analyses of Ni-Mo, Ni-Ta, Ni-Nb, Ni-Zr and Ni-Ti alloys crystallized at high cooling rates, observing metastable phases
14 p2115 A72-30405

Mutual solid solubilities of rare earth metals with Zr extended by splat quenching, noting metastable low temperature allotropic forms of solid solutions
14 p2119 A72-30609

Phase diagrams of Ni-C and Co-C systems with metastable equilibrium lines, investigating microstructure and microhardness of carbide eutectic
14 p2123 A72-30990

Crystal lattice disarrangement by melting In-Ti alloy, noting fcc and bcc metastable phases formation during rapid crystallization
16 p2441 A72-33536

Lifetime and quenching of metastable CO produced by dissociative recombination of positive carbon dioxide ions in He afterglow
16 p2432 A72-33771

Nd-glass laser interaction with singly stimulated two-photon emission and anti-Stokes Raman scattering from metastable state He, calculating cross sections
17 p2565 A72-35831

Finite tested optically thin radiating plasma stability analysis, deriving luminosity function for metastable state existence from mathematical model
20 p2958 A72-39456

Metastable phases in very rapidly solidified aluminum-germanium alloys
21 p3070 A72-41644

Metastable growth patterns in some terrestrial and lunar rocks.
23 p3339 A72-44133

METAZOA

U ANIMALS

METEOR BURSTS

U METEOROID SHOWERS

METEOR CRATERS

U CRATERS

METEOR HAZARDS

U METEOROID HAZARDS

METEOR TRAILS

Wind profile determinations at 90-100 km from meteor trail drift and ionosphere inhomogeneity radar data, noting semidiurnal harmonics in wind components
01 p0058 A72-10563

Numerical analysis of radio echoes decay rate from randomly ionized meteor trails
01 p0130 A72-10913

Photometric meteor mass determination, using models relating radiation intensity, meteor velocity, atmospheric density and instantaneous luminous flux
02 p0282 A72-12334

Linear electron density distribution along faint meteor trail, discussing radio echo time-amplitude characteristics and ionization curve
02 p0282 A72-12335

Meteor trail forms diversity explanation from magnetic pressure and Reynolds number and plasma diffusion in magnetic fields, discussing geomagnetic effect on trail shape
02 p0282 A72-12336

Geomagnetic field effect on radar echoes from meteor trains during Geminid shower
03 p0345 A72-12982

Upper atmosphere He, Ne, Na and K atoms collisions with molecular oxygen, determining ejected electron energy during fast Na, K, Rb and Cs ionization for meteor phenomena modeling
03 p0438 A72-13980

Telescopic meteors light curves, showing maximum point brightness distribution in visible trajectory with respect to stellar magnitudes
03 p0438 A72-13985

Spectral line data on terminal flare and wake of double-station meteor 38421
04 p0574 A72-14922

Meteor observation and counting, discussing meteor stream formation along comet orbit
05 p0712 A72-15975

Antenna azimuthal radiation patterns and meteor radiant distribution effects on wind velocity measurement by radar observation of meteor trains
05 p0715 A72-16251

Wind velocity vertical component determination through meteor trail drift observation, presenting mean diurnal measurements data
05 p0657 A72-16272

Aerodynamic characteristics of hypersonic velocity meteor traveling in earth atmosphere and shock wave propagation generated by explosion in air and on ground
07 p1081 A72-20094

Galactic cosmic ray modulation region evaluation from meteoroid orbit, velocity and radioactive dating data
07 p1065 A72-20644

Radio meteors observability and wave reflection from trails, discussing velocities, deceleration and vertical distribution
08 p1130 A72-20712

Radar verification of sporadic E layer formation from meteoritic atoms and ions production by meteoritic ablation
08 p1154 A72-20728

Multicomponent meteoritic composition effects on meteor trails radio wave reflections, obtaining ionospheric electron concentration distribution
08 p1131 A72-20805

Semiannual latitude dependent mesospheric wind patterns from meteor trail observations, suggesting heat inputs from solar radiation and magnetic storm related auroral heating
08 p1159 A72-21227

Soviet papers on ionospheric propagation and meteor trail drifts during IQSY, covering Doppler frequencies recording and mountains effect on radio transmission
08 p1238 A72-21881

Air masses circulation in atmospheric upper layers during IQSY from meteor trail drifts observation by radar tracking method
08 p1161 A72-21882

Radio meteor measurements of ionospheric drifts by two separated stations, obtaining wind velocities mean hourly values correlation coefficient
08 p1238 A72-21883

One dimensional expansion of hot vapor and gases remaining behind meteor body
08 p1238 A72-21884

Mean monthly statistical characteristics of wind regime from meteor trail drifts observations
08 p1162 A72-21885

Optimal variant of meteor wind patrol radar station for atmospheric circulation study
08 p1147 A72-21886

Sectorial radio measurement of meteor trail drifts with If radar signals, determining Doppler shift sign and period
08 p1238 A72-21887

Diurnal and seasonal variation of ambipolar diffusion coefficient in meteor trail zone within upper atmosphere
08 p1238 A72-21888

Mountains located on meteor propagation path of radio waves, investigating effect on transmission region size
08 p1239 A72-21891

Meteor trails radar ranging system with circular vernier scanning and brightness indication with high accuracy
09 p1308 A72-22507

Leonid meteor trail drift measurements in upper atmosphere, comparing radar system with precise goniometric capabilities to photographic methods
09 p1383 A72-22509

Photometric parameters of Leonid meteor ionized trail and turbulent diffusion in M zone, determining electron attachment rate
09 p1384 A72-22510

Electron attachment, photodetachment and turbulent diffusion deionization effects on duration distribution of Geminid meteor radio echoes
09 p1384 A72-22512

Electron attachment rate relation to altitude in radar observation of meteor trails
09 p1384 A72-22513

Radio transmitter characteristics for radar sounding of upper atmosphere and meteor trails
09 p1278 A72-22874

Meteor trail photoobservations for atmospheric small scale turbulences vertical profile, determining eddy minima velocities and turbulent energy dissipation in M zone
09 p1393 A72-23650

Upper atmospheric dynamics and electrodynamic processes for evaluation of meteor trail radar observations in synoptic meteorology
10 p1473 A72-24702

Meteor trail winds over Europe, discussing continuous wave radar observations and measurement errors with respect to height and time
10 p1474 A72-24708

Radio meteor winds determination in Southern Hemisphere from vertically emitted continuous wave radiation, considering diurnal variations and wind and turbulence effects
10 p1474 A72-24709

Meteor trail wind radar measurements over Illinois, discussing scattering properties and monostatic vs multistatic coherent systems
10 p1474 A72-24710

Stanford pulse Doppler radar and digital data acquisition system for meteor trail wind measurements
10 p1438 A72-24711

Meteor trail radar operated under digital controller synchronization and programmed for alternate and simultaneous two orthogonal directions search
10 p1438 A72-24715

Meteor trail radar data processing for upper atmosphere research, proposing dissemination for dynamic synoptic exploration
10 p1438 A72-24716

Multiplicative noise envelope distribution for ionospheric scatter channel from single and diversity radio reception, noting meteor trails effects on electromagnetic wave propagation
12 p1782 A72-27627

Radar facility for weak meteor observation, describing antennas, transmitters, receivers, filters, calibration techniques and recording instruments
13 p1919 A72-29026

Aircraft measurements of radiation pattern of radar antenna system used for meteor height observation
13 p1919 A72-29027

Pulse radar equipment for meteor height measurement from nonsaturated trails by phase difference method
13 p1929 A72-29028

Optimal radar recording systems for meteor trail observations providing signal detection, processing and storage triggering and echo discrimination
13 p1929 A72-29030

Optimal selectivity digital recorders for meteor trails radar observations, considering input process quantization rate and spectral width selection
13 p1929 A72-29031

Atmospheric turbulence anisotropy from meteor trails radar observations statistics, presenting plots of velocity field transverse structure
13 p2038 A72-29036

Photometric meteor mass determination, using models relating radiation intensity, meteor velocity, atmospheric density and instantaneous luminous flux
13 p2039 A72-29218

Linear electron density distribution along faint meteor trail, discussing radio echo time-amplitude characteristics and ionization curve
13 p2039 A72-29219

Meteor trail forms diversity explanation from magnetic pressure and Reynolds number and plasma diffusion in magnetic fields, discussing geomagnetic effect on trail shape
13 p2039 A72-29220

Celestial pole region photographs obtained with TV equipment, emphasizing observations of faint meteoroids and gas trails
13 p2044 A72-29648

Upper atmosphere horizontal wind velocity from meteor trails radio echoes, noting structural function anisotropy
14 p2127 A72-30263

Meteoritic particle movement in earth atmosphere, discussing deceleration dependence on velocity, atmospheric density and surface evaporation reactive forces
14 p2152 A72-30493

Ejected lunar particles in meteoric sporadic background, noting brightness relation to yearly particle concentration
14 p2153 A72-30495

Perseid shower radiants observation in August 1969, indicating presence of one secondary and two main radiants
14 p2153 A72-30499

Fe light emission for simulated meteor conditions, measuring ionization and spectral emission cross sections for Fe reactions with nitrogen and oxygen for 350-2000 eV
14 p2156 A72-30562

Meteor trail drifts at 95 km over Turkmenistan from November 1969-August 1970 radar observations, comparing to Frunze, Dushanbe and Kharkov wind data
15 p2305 A72-31372

Signal generator designed for calibration and control of interferometric radar station to observe and study radar echoes induced by meteor trails
17 p2519 A72-35959

Determination of upper atmosphere parameters by measuring the ambipolar diffusion coefficient by the method of meteor trail radar observations
18 p2688 A72-36862

Determination of the predominant wind vector from meteor radar observations
19 p2857 A72-37740

Meteoritic particle motion in earth atmosphere, discussing deceleration dependence on velocity, atmospheric density and surface evaporation reactive forces
19 p2864 A72-38322

- Ejected lunar particles in meteoric sporadic background, noting brightness relation to yearly particle concentration 19 p2864 A72-38324
- Perseid shower radiants observation in August 1969, indicating presence of one secondary and two main radiants 19 p2864 A72-38328
- Radio meteors observability and wave reflection from trails, discussing velocities, deceleration and vertical distribution 19 p2765 A72-38340
- Radar verification of sporadic E layer formation from meteoric atoms and ions produced by meteoroid ablation 19 p2791 A72-38356
- Particle fragmentation, mass distribution and chemical composition of cometary meteoroids in earth orbit, noting collisional erosion and similarity to stony meteorites 24 p3445 A72-45459
- The possibility of a trans-Saturnian belt of particulate matter. 24 p3446 A72-45472

METEORITE COLLISIONS

- Crater 9 meteorite /Argentina/ entry trajectory and orbital calculations, determining masses and velocities from dynamic conditions at impact 02 p0275 A72-11599
- Comet collisions in planetary nebulae as source of organic compounds in universe in preplanetary era, noting nucleic acid bases in carbonaceous meteorites 04 p0471 A72-14802
- Photographic observations of W particle clusters high velocity impact against polystyrene, paraffin and W targets for energy dissipation in meteorite impact simulations 08 p1232 A72-21152
- Lunar regolith glassy particles formation processes modeling with molten soil samples, emphasizing liquid particles spattering with subsequent cooling during meteoritic impact 13 p2036 A72-28767
- Lunar rock and mineral shock melting and vaporization from hypervelocity meteoroid impacts, calculating entropy, phase changes and thermal equilibrium 14 p2155 A72-30520
- Photographic observations of W particle clusters high velocity impact against polystyrene, paraffin and W targets for energy dissipation in meteorite impact simulations 20 p2969 A72-39257
- Lunar regolith glassy particles formation processes modeling with molten soil samples, emphasizing liquid particles spattering with subsequent cooling during meteoritic impact 21 p3102 A72-40268
- Gas dynamics of the flight and explosion of meteorites. 24 p3439 A72-45020

METEORITE COMPRESSION TESTS

- U COMPRESSION TESTS
- U MECHANICAL PROPERTIES
- U METEORITES

METEORITE CRATERS

- Lunar crater population and distribution time development under meteoroid and solar wind bombardment, developing model for absolute formation ages 01 p0124 A72-10056
- Structure and characteristics of craters and pits in Sikhote-Alin iron meteorite shower, searching for meteor and meteorite dusts and micrometeorites 01 p0125 A72-10101
- Lunar far side crater Tsiolkovsky geology, indicating formation by meteoroid, asteroid or comet impact explosion 06 p0887 A72-18222
- Lunar crater origin mechanisms, considering single and multiple meteor impact and volcanic explosions, low velocity excavation, collapse and material emission 06 p0887 A72-18223
- Martian crater abundance correlation with surface albedo, discussing relative age of light and dark terrains 08 p1230 A72-20983
- Meteorite flux at lunar surface as function of position and earth-moon distance, applying to crater counting 10 p1531 A72-23703
- Stopfenheim Kuppel area as part of meteorite crater event forming Reis Kessel and Steinheim Basin from quartz grain shock feature analysis 10 p1537 A72-24159
- Impact glass-like objects as evidence of meteoritic origin of Lomar Crater /India/, discussing physical, chemical and optical properties 11 p1723 A72-26521
- Siberian Popigay river basin hollow as meteoritic explosion crater, discussing pseudovolcanic properties 13 p1947 A72-28754

- Transstructural topographic and gravity profiles of three Mauritanian meteorite craters, showing residual negative gravity anomalies 13 p1947 A72-28756
- Mars doublet cratering by impacting meteoroid breakup due to stresses in gravitational field, using Monte Carlo simulation 14 p2149 A72-30317
- Sikhote-Alin meteorite shower individual specimens mass distribution with respect to distance from crater center 14 p2153 A72-30496
- Geometric similitude of lunar and terrestrial craters. 17 p2615 A72-35681
- Displacements within impact craters. 17 p2549 A72-35686
- Savonoski crater, Alaska - A possible meteorite impact structure. 19 p2790 A72-37861
- Sikhote-Alin meteorite shower individual specimens mass distribution with respect to distance from crater center 19 p2864 A72-38325
- Sand deposition due to wind action in Martian craters, comparing to terrestrial analogs 20 p2969 A72-39389
- Lunar crater origins due to external impact of particles moving within earth-moon gravitational dipole during earliest history stage 22 p3226 A72-42538

METEORITES

- NT ACHONDrites
 - NT AUSTRALITES
 - NT BEDIASITES
 - NT BRUDERHEIM METEORITE
 - NT CARBONACEOUS METEORITES
 - NT CHONDrites
 - NT IRON METEORITES
 - NT ORGUEIL METEORITE
 - NT SIKHOTE-ALIN METEORITE
 - NT STONY METEORITES
 - NT TEKTITES
 - NT TUNGUSK METEORITE
- Age determination of Raco meteorite /Argentina/ by K-Ar method, noting olivine and rhombic pyroxene composition 01 p0126 A72-10104
- Chemical composition and morphology of silicate spherules, comparing to lunar rocks, meteorites and tektites 02 p0280 A72-12283
- Small meteor bodies fragmentation, using radar diffraction patterns 03 p0438 A72-13982
- Shock wave contributions from micrometeorites, meteorites and thunder to organic compounds formation in primeval atmosphere 04 p0572 A72-14760
- Lunar ejecta and meteorites experiment, determining speed, direction, mass and flux density of cosmic dust particles 04 p0509 A72-15102
- Meteorites fall in Germany, discussing composition, size and color classification, frequency and locations. 07 p1070 A72-19124
- Frost rule for meteoroid spatial sorting as basis for Allende meteorite shower strewn field examination of fragment mass and position 08 p1237 A72-21651
- Lunik 16 soil samples trace elements composition suggesting meteoritic component presence and similarity to Apollo soils 09 p1381 A72-22276
- Adsorption role in planetary primordial rare gas origin based on adsorptivity pattern of pulverized Allende meteoritic samples at 113 K 09 p1385 A72-22597
- Gas rich meteorites and lunar materials solar rare gases component observed and predicted relative abundance agreement indicating absence of fractionation in solar nebula formation 11 p1721 A72-26118
- Moonquakes and meteorite and manmade impacts as sources of seismic signals detected by Apollo lunar seismic stations 13 p2037 A72-28988
- Ferric ion traces evidenced in lunar and meteoritic titanates by charge transfer bands observations during heating, interpreting origin as caused by cosmic radiation 14 p2154 A72-30515
- The exposure time of the Kiffa meteorite 17 p2603 A72-34200
- Argon 37/argon 39 activity ratios in meteorites and the spatial constancy of the cosmic radiation. 18 p2723 A72-36027
- Ucra meteorite - Determination of differential atmospheric heating using its natural thermoluminescence. 19 p2858 A72-37859
- An isotopic criterion for estimating the length of meteorite orbits 22 p3223 A72-42160

- Magnetism of meteorites - A review of Russian studies. 23 p3339 A72-44129

- Accretion processes leading to formation of meteorite parent bodies. 24 p3444 A72-45454

METEORITIC COMPOSITION

- Pu-244 fission Xe isotopic composition parameters in achondrite meteorites, using lunar spallation systematics 01 p0124 A72-10058
- L-chondrite Assam, determining He, Ne and Ar concentrations and isotopic compositions and galactic and solar flare irradiation track densities 01 p0124 A72-10060
- Hibonite /Ca-Al-Ti-rich xenoliths/ from Leoville and Allende polymict brecciated HL group chondritic meteorites 01 p0125 A72-10067
- Iron River meteorite, discussing history, physical characteristics, element distribution and Widmanstätten structure 01 p0126 A72-10105
- Chemical analysis of iron meteorites, tabulating Ni, Co, P and C content 01 p0126 A72-10108
- Chondrules occurrence in iron meteorite, investigating bulk chemical composition and mineral properties 01 p0127 A72-10294
- Siderophilic element content relation to oxidation state of ordinary chondrites, using Ir/Ni concentrations from neutron activation analysis 02 p0277 A72-11896
- Oxygen isotope ratios in iron meteorites magnetite crust and cosmic spherules as indicators for atmospheric oxygen development 02 p0279 A72-12117
- Mineralogical and chemical compositions of Markovka chondrite 02 p0280 A72-12284
- Silicate microspherules distribution anomaly in peats of Tunguska meteorite fall area 02 p0281 A72-12293
- Organic cosmochemistry evolution, discussing radio astronomical observations, lunar soil samples, meteorite analysis and interstellar gas cloud molecules 03 p0320 A72-13171
- Xe and Kr abundance and isotopic composition in silicate inclusions of iron meteorites 03 p0435 A72-13690
- Al 26 production rates from Al, Si, S, Mg and Ca in Bruderheim chondrite by weighted least squares analysis 03 p0435 A72-13691
- Meteorite structure and chemical composition, describing investigation methods, origin and evolution 03 p0438 A72-13976
- Magnetite forms in Orgueil meteorite, observing platelets, stackings and framboids by scanning electron microscope 04 p0569 A72-14506
- Lunar Imbrian Basin formation, discussing micrometeorite component composition of Apollo 14 soil samples 05 p0715 A72-16160
- Alfianello meteorite inspection by optical microscopy for petrological features of shock metamorphism in chondrites 05 p0722 A72-17152
- Johnstown achondrite meteorite composition, presenting published and unpublished data on minor and trace elements 05 p0722 A72-17154
- Uranium content and radiogenic ages by fission track analysis in hypersthene, bronzite, amphibole and carbonaceous chondrites 06 p0878 A72-17791
- Meteorites fall in Germany, discussing composition, size and color classification, frequency and locations 07 p1070 A72-19124
- Oxygen isotopic temperatures and mineral compositions of equilibrated ordinary chondrites 07 p1076 A72-19588
- Oxygen isotopic abundances and equilibrium temperatures of meteoritic minerals, chondrules, meteorites and planets 07 p0985 A72-19589
- Organic origin of meteoritic hydrocarbons in early solar system related to Fischer-Tropsch reaction 07 p1076 A72-19590
- Meteorite genesis and formation processes from composition characteristics, discussing age determination methods and mineralogical classifications 07 p1082 A72-20302
- Xe and Kr mass fractionation and isotopic anomalies in ordinary chondrites, analyzing meteorite samples by mass spectrometry 07 p1084 A72-20497
- Multicomponent meteoritic composition effects on meteor trails radio wave reflections, obtaining ionospheric electron concentration distribution 08 p1131 A72-20805

Microscopic, chemical and morphological studies of ultralarge meteorite spherules in Yakut ASSR, noting composition 08 p1229 A72-20838

Volatile and siderophile elements in achondrites and ocean ridge basalts from radiochemical neutron activation analysis 09 p1385 A72-22598

Trapped He, Ne and Ar isotopic variations presence in meteorites due to rare gas ions implantation by solar wind and flares 09 p1385 A72-22599

Extraterrestrial abiogenic organic hollow spheres of Orgueil meteorite evaluated according to intrinsic and extrinsic criteria 09 p1385 A72-22640

Orgueil meteorite examination by mass spectroscopy and gas chromatography, identifying amino acids of extraterrestrial origin 09 p1393 A72-23549

Rare gases concentrations and isotope ratios in Haverø ureilite meteorite, including He, Ar, Ne, Kr and Xe 10 p1538 A72-24167

High C 13 content in carbonaceous phases of carbonaceous chondrites accounted for by Rayleigh distillation with oxidized and reduced forms of carbon 10 p1547 A72-24951

Allende carbonaceous chondrite composition analysis, suggesting formaldehyde presence and significance about possible origins 10 p1549 A72-25022

X ray fluorescence spectrometric analysis of carbonaceous chondrites for chemical subgroups 11 p1723 A72-26525

Thermal release patterns and activation energies of spallogenic He, Ne and Ar from Carbo iron meteorite 12 p1866 A72-27116

Nonprotein amino acids from spark discharges, comparing with Murchison meteorite amino acids 12 p1778 A72-27749

Handbook on elemental abundances in meteorites covering individual elements, emission and X ray spectrography, colorimetry, neutron activation and isotope dilution 12 p1876 A72-28204

Microprobe analysis of Timmersoi hypersthene chondrite from Niger Republic, noting equilibrium between olivine and orthopyroxene at 850 C 13 p2035 A72-28751

Microprobe analysis of Murchison and Vigarano meteorites, noting fractionation processes for Ca distribution in olivines 13 p2036 A72-28752

Xenolithic origin for silicate inclusions in anatase of Landes meteorite from West Virginia 13 p2036 A72-28753

Artificial meteor ablation on iron oxides by arc heated air plasma stream for product and environment identification studies 14 p2150 A72-30319

Sikhote-Alin meteorite shower individual specimens mass distribution with respect to distance from crater center 14 p2153 A72-30496

Neutron activation data for Ru, Os, Ir, Pt and Pu in iron meteorites, noting correlation 14 p2157 A72-30582

Ar-39/Ar-38 cosmic ray exposure age calculation from Sikhote-Alin meteorite fall fragment content of Ar-39, Ar-38, Ne-21 and He-3 14 p2157 A72-30584

Model for textural features and mineralogical composition of Ca and Al-rich inclusions in C3 chondrites during condensation in primitive solar nebula 14 p2157 A72-30585

Pavel stony meteorite microspectral analysis to obtain metallic elements weight percentages in chondrules, matrix and core, using laser source for local vaporization and excitation 14 p2159 A72-30785

Chondrule like spherules from supercooled molten oxide and silicate droplets by carbon dioxide laser heating compared with meteoritic chondrules 15 p2303 A72-31306

Abiotic origin of organic compounds in carbonaceous chondrites, analysing Murchison and Murray meteorites by combined gas chromatography-mass spectroscopy technique 15 p2306 A72-31625

Chondrite Pawel microspectral analysis with laser beam vaporization of sample from microzone 16 p2450 A72-32850

Enstatite chondrite Abee isotopic ratios of Gd, Sm and Eu comparison with terrestrial samples 16 p2457 A72-33566

Platinum and gold in chondritic meteorites. 17 p2610 A72-35149

The isotopic composition and elemental abundance of gallium in meteorites and in terrestrial samples. 18 p2723 A72-36061

Gas retention chronology of Petersburg and other meteorites. 18 p2723 A72-36062

Mineralogy, bulk chemistry and sample shape and mass of Seoni /India/ chondrite, observing extensive recrystallization 19 p2858 A72-37860

Mineralogical and chemical researches on L-chondrites - Gergenti. 19 p2858 A72-37862

Elemental abundances in stone meteorites. 19 p2858 A72-37863

Geochemistry of amino acid enantiomers - Gas chromatography of their diastereomeric derivatives. 19 p2762 A72-38224

Sikhote-Alin meteorite shower individual specimens mass distribution with respect to distance from crater center 19 p2864 A72-38325

Ordinary chondrite chemical and mineralogical properties establishment during solar system formation, noting fractionation events 20 p2969 A72-39334

Rocks and meteorites analysis techniques evaluation, using Apollo 11 fines results to evaluate activation analysis for geochemistry and cosmochemistry applications 20 p2899 A72-39827

Multielement neutron activation analysis of geological and lunar material using chemical group separations and high resolution gamma spectrometry. 20 p2899 A72-39830

Neutron activation techniques for nondestructive analysis of meteorites and lunar rocks, noting types of nuclear reactions for geochemical application 20 p2899 A72-39832

Non-destructive activation analysis of some elements in stony meteorites by proton- and bremsstrahlen-irradiation. 20 p2899 A72-39833

Neutron activation and mass spectrometry methods for geochemical analysis of rare earth elements in meteoritic, lunar and terrestrial materials 20 p2899 A72-39835

On the determination of trace elements in meteoritic phases by neutron activation analysis. 20 p2900 A72-39838

Elemental abundance trends in the australite strewn field by non-destructive neutron activation. 20 p2900 A72-39839

A re-examination of relationships among pyroxenepagioclase achondrites. 20 p2900 A72-39840

Coincidence counting applied to the activation analysis of meteorites and rocks. 20 p2900 A72-39841

Iron transport in chondrites - Evidence from the Warrenton meteorite. 21 p3104 A72-40491

Chondrite and achondrite Nb abundance from spark source mass spectroscopic analysis 21 p3104 A72-40492

Cosmic abundance of iron and nature of primitive material in meteorites. 22 p3220 A72-41963

Instrumental neutron-activation analysis of the troilite of the Sikhote-Alin meteorite 22 p3225 A72-42472

Depth distributions of cosmic ray produced radionuclides in chondrites and achondrites, determining aphelia from Al 26 activities 22 p3228 A72-42861

Isotopic compositions of rare gases in the carbonaceous chondrites Mokoia and Allende. 22 p3229 A72-42899

Chondrite Al-Ir abundance association for L compositional class consistent with Larimer condensation mechanism 23 p3335 A72-43266

Shock damaged zircon, corundum, rutile, monazite and quartz crystalline inclusions in Muong Nong-type indochinite /tektite/, noting production from detrital sedimentary materials as possible terrestrial origin 23 p3335 A72-43398

Spectrographic, photometric and chemical identification of Giacobinid /Draconid/ meteoroids, noting compositional similarity to carbonaceous and olivine-bronzite chondrites 23 p3336 A72-43600

Determination of Ni, Ga, and Ge in iron meteorites by X-ray fluorescence analysis. 23 p3262 A72-44128

Mundrabilla meteorites geographical location, external appearance, microstructure and chemical composition, suggesting shower occurrence 23 p3339 A72-44130

Rare earth and other abundances in the Murchison carbonaceous meteorite. 23 p3262 A72-44131

Minerals discovered in meteorites, tabulating formula and occurrence and plagioclase composition 23 p3262 A72-44132

Evidence for vapor fractionation in the origin of chondrules. 23 p3339 A72-44134

Determination of the coefficient of electron attachment to particles of meteor material 23 p3339 A72-44169

The chemical classification of iron meteorites. VI - A reinvestigation of irons with Ge concentrations lower than 1 ppm. 24 p3436 A72-44697

Irradiation history of grain aggregates in ordinary chondrites - Possible clues to the advanced stages of accretion. 24 p3444 A72-45455

Conditions in the early solar system, as inferred from meteorites. 24 p3445 A72-45458

Particle fragmentation, mass distribution and chemical composition of cometary meteoroids in earth orbit, noting collisional erosion and similarity to stony meteorites 24 p3445 A72-45459

METEORITIC DAMAGE

Tunguska explosion of 30 June 1908, determining air waves propagation velocity 03 p0438 A72-13981

Meteoritic cosmic catastrophe, interpreting flat depression in northern Siberian plateau Khatanga river basin 05 p0713 A72-15977

Apollo 14 lunar breccia samples, observing chondrules from meteoritic impact event 05 p0715 A72-16161

Shock metamorphism in Luna 16 soil sample, indicating regolith formation by meteorite impact 09 p1380 A72-22259

Siberian Popigay river basin hollow as meteoritic explosion crater, discussing pseudovolcanic properties 13 p1947 A72-28754

Lunar dumbbell shaped glass globules formation due to rotation and surface tension effects of ejecta from meteoric impacts 15 p2306 A72-31628

Lunar ash flows - Isothermal approximation. 18 p2723 A72-36026

Seismic data from lunar geophysical stations network, noting moonquakes and meteoroid impacts 18 p2724 A72-36283

Savoniski crater, Alaska - A possible meteorite impact structure. 19 p2790 A72-37861

Metal barrier maximum puncturable thickness dependence on high velocity meteorite particle impact parameters 22 p3234 A72-42217

Impact tests for aid in data interpretation of measured meteor particles impact on spacecraft structures, noting transducer response dependence on impact angle 22 p3234 A72-42218

METEORITIC DUST

U MICROMETEORIODS

METEORITIC IONIZATION

U ATMOSPHERIC IONIZATION

U METEOR TRAILS

METEORITIC MICROSTRUCTURES

Meteorite structure and chemical composition, describing investigation methods, origin and evolution 03 p0438 A72-13976

Shock transformed chondrite texture observed in thin plates by UV fluorescence 05 p0722 A72-17151

Phosphorus effect on Widmanstätten pattern in iron meteorites, using Fe-Ni-P phase diagram and cooling experiments 06 p0878 A72-17792

Mundrabilla meteorites geographical location, external appearance, microstructure and chemical composition, suggesting shower occurrence 23 p3339 A72-44130

METEOROID CONCENTRATION

Monte Carlo method application to meteor stream formation by meteor material ejection from comet nucleus, determining age of Draconids 02 p0282 A72-12333

Meteor count by naked eye and binocular visual observation in Crimea, obtaining luminosity functions 06 p0881 A72-17932

Frost rule for meteoroid spatial sorting as basis for Allende meteorite shower strewn field examination of fragment mass and position 08 p1237 A72-21651

Radio echo determination of meteor body distribution by mass with allowance for electron attachment and overestimated nighttime values 09 p1383 A72-22505

Meteorite flux at lunar surface as function of position and earth-moon distance, applying to crater counting 10 p1531 A72-23703

Monte Carlo method application to meteor stream formation by meteor material ejection from comet nucleus, determining age of Draconids 13 p2039 A72-29217

Ejected lunar particles in meteoric sporadic background, noting brightness relation to yearly particle concentration 14 p2153 A72-30495

Perseid shower radiants observation in August 1969, indicating presence of one secondary and two main radiants

14 p2153 A72-30499
Quadrantid underdense and dense meteors observations during sunrise on 16.67 MHz pulsed radar
15 p2312 A72-32197
Meteor count by naked eye and binocular visual observation in Crimea, obtaining luminosity functions
18 p2730 A72-37157
Ejected lunar particles in meteoric sporadic background, noting brightness relation to yearly particle concentration

19 p2864 A72-38324
Perseid shower radiants observation in August 1969, indicating presence of one secondary and two main radiants

19 p2864 A72-38328
Meteoroid bodies particle density from basal photographs, noting dependence on orbital parameters

20 p2969 A72-39395
Allowance for the striking angle of a meteoric body with penetration-depth and piezoelectric sensors in the evaluation of the spatial density of meteoric matter

22 p3234 A72-42219
Results of a comparison between radar meteor wind measurements and simultaneous lower ionosphere drift measurements in the same area.

22 p3154 A72-42361
Interplanetary objects in review - Statistics of their masses and dynamics.

24 p3435 A72-44688
The possibility of a trans-Saturnian belt of particulate matter.

24 p3446 A72-45472

METEOROID CRATERS

U METEORITE CRATERS

METEOROID DUST CLOUDS

Structure and characteristics of craters and pits in Sikhote-Alin iron meteorite shower, searching for meteor and meteorite dusts and micrometeorites

01 p0125 A72-10101

METEOROID HAZARDS

Pioneer 10 probe survival hazards during passage through asteroids belt and intense Jupiter radiation fields

10 p1551 A72-24272

METEOROID SHOWERS

NT DRACONID METEORIODS

NT GEMINID METEORIODS

NT LEONID METEORIODS

NT ORIONID METEORIODS

NT PERSEID METEORIODS

NT QUADRANTID METEORIODS

Structure and characteristics of craters and pits in Sikhote-Alin iron meteorite shower, searching for meteor and meteorite dusts and micrometeorites

01 p0125 A72-10101

Pultusk meteorite shower fragments number and mass estimates from numerical integration of differential equations

01 p0126 A72-10103

Meteor showers of March 1969, noting delta Lyrids, gamma Cygnids and beta Ursa Minorids observations

03 p0438 A72-13984

Sporadic E layer variations monitoring in 50 MHz band, examining diurnal, seasonal, magnetic and meteoroid showers relationships of oblique incidence paths

10 p1441 A72-25152

Lognormal fragment mass distribution of Lowicz meteorite shower 1935

12 p1866 A72-27118

Meteor streams secular perturbations computation by Gauss-Halphen-Goriachev method

14 p2161 A72-31078

Explorer 35 and OGO 3 data on picogram size dust particle distribution in cislunar and selenocentric space, showing fluctuations during meteor shower periods

15 p2309 A72-31937

Shower structure in sporadic meteor background from statistical analysis of radar range-time photographs, noting unidentified radiants activity

15 p2313 A72-32366

Determination of the coefficient of electron attachment to particles of meteor material

23 p3339 A72-44169

A meteor spectrum in the infrared region.

23 p3341 A72-44473

Meteor streams orbital elements dispersion from photographic data, and asteroid stream percentage variation with concentration of orbits to ecliptic plane.

24 p3445 A72-45462

METEORIODS

NT DRACONID METEORIODS

NT GEMINID METEORIODS

NT LEONID METEORIODS

NT METEOROID DUST CLOUDS

NT MICROMETEORIODS

NT ORIONID METEORIODS

NT PERSEID METEORIODS

NT QUADRANTID METEORIODS

NT RADIO METEORIODS

NT SPORADIC METEORIODS

Electron attachment rate determination by combined photographic and radar observation of meteors

01 p0128 A72-10601

Meteor spectrum analysis, presenting tables for Soviet observations

03 p0438 A72-13979

Meteor observation and counting, discussing meteor stream formation along comet orbit

05 p0712 A72-15975

Meteor passage time determination by optical shutter with wedge-shaped blades for light flux periodic intersection and production of two discontinuous lines for identification

06 p0816 A72-17930

Meteor streams effect on atmospheric motions turbulence intensity based on radar observations

06 p0842 A72-18045

Meteorite genesis and formation processes from composition characteristics, discussing age determination methods and mineralogical classifications

07 p1082 A72-20302

Galactic cosmic ray modulation region evaluation from meteoroid orbit, velocity and radioactive dating data

07 p1065 A72-20644

Wind measurements in lower thermosphere by meteor radar method, presenting models of prevailing circulation in meteor zone over Eurasia and Arctic

08 p1161 A72-21538

Radar measurement of meteor bodies mass distribution parameter

08 p1239 A72-21889

Meteor method for determining errors in rate measurement of electron attachment to neutral air particles based on nonexistent recombination, turbulent diffusion and photodetachment

09 p1383 A72-22503

Nighttime radar method of meteor radio echo observation to determine electron attachment rate to neutral air particles

09 p1383 A72-22504

Radar equipment complex in Dushanbe for upper atmosphere wind measurements in meteor physics studies

09 p1308 A72-22506

Multibeam indicator with block diagram description for meteor ranging radar and photofilm based recording system

09 p1308 A72-22508

Meteor-induced magnetic effect on cosmic ray intensity for meteor streams with orbits normal or parallel to interplanetary magnetic field lines of force

13 p2029 A72-28592

Celestial pole region photographs obtained with TV equipment, emphasizing observations of faint meteoroids and gas trails

13 p2044 A72-29648

Cosmic ray irradiations study of gas rich meteoroid aubrites by track method, comparing with lunar soils

15 p2303 A72-31308

Atmospheric ion composition analysis by RF mass spectrometer during rocket ionosphere sounding, discussing meteor ionization layers

15 p2225 A72-31915

Meteor passage time determination by optical shutter with wedge-shaped blades for light flux periodic intersection and production of two discontinuous lines for identification

18 p2693 A72-37155

The effect of meteoric ion processes on radio studies of meteoroids.

23 p3336 A72-43558

Flyby missions to comets, asteroids and meteors for obtaining solar system geological information, considering space dynamics feasibility

23 p3340 A72-44351

Interplanetary objects in review - Statistics of their masses and dynamics.

24 p3435 A72-44688

Meteor-induced magnetic effect on cosmic ray intensity for meteor streams with orbits normal or parallel to interplanetary magnetic field lines of force

24 p3435 A72-45092

Particle fragmentation, mass distribution and chemical composition of cometary meteoroids in earth orbit, noting collisional erosion and similarity to stony meteorites

24 p3445 A72-45459

METEOROLOGICAL BALLOONS

Balloon-borne radiometer-sonde measurement of stratospheric downward emission in absorption spectral region of water vapor rotational band

07 p0982 A72-19105

Eole satellite relay system for weather balloon location and data collection and transmission to ground stations

09 p1394 A72-22600

Upper wind measurement by balloon-borne targets or radiosondes tracking by primary and secondary radars and radio theodolites

13 p1917 A72-28697

Meteorological rising balloon systems accuracy limitation, noting response to wind field changes, aerodynamic self oscillations and radar tracking errors

13 p1990 A72-28817

Small scale atmospheric turbulent motions sensing by FPS-16 Radar-Jimsphere meteorological balloon system, analyzing wind velocity data from dual radar measurements

13 p1990 A72-28818

French tetrahedral and spherical meteorological balloons, discussing projects Eole and Essov to sound Southern Hemisphere and stratosphere respectively

13 p1897 A72-28828

Eole satellite observed meteorological balloon data analysis, obtaining mean zonal velocity, meridional velocity and temperature vs latitude from statistical estimates

15 p2266 A72-31980

Data system in Eole satellites program, discussing balloon localization, UHF information transmission and reception, distance measurement and data acquisition

15 p2268 A72-31981

Report to COSPAR on Argentina space program covering sounding rockets and balloons and Experimental Inter-American Meteorological Network meteorological rocket launchings

15 p2338 A72-32015

Behavior of spherical balloons in wind shear layers.

18 p2643 A72-36963

Wind tunnel investigation of shapes for balloon shelters.

20 p2885 A72-38967

METEOROLOGICAL CHARTS

Weather map numerical analysis for Northern Hemisphere, describing program with flow field for geopotential value checking

01 p0094 A72-10196

Digital simulation of general atmospheric circulation via spatial finite difference dense grid, considering surface properties and pressure distribution maps

02 p0252 A72-11652

Mesosphere meteorological sounding by acoustic grenade and pitot probe techniques, investigating seasonal and latitudinal variations

03 p0383 A72-13384

Computerized synoptic weather map forecasting of heavy snowfall in Colorado

04 p0542 A72-14685

Nimbus 4 satellite-borne selective chopper radiometer design characteristics, obtaining maps of stratospheric warmings in both hemispheres

08 p1173 A72-22168

Weather analysis for mountainous terrain from potential temperature surface maps and vertical cross sections

09 p1344 A72-22431

Precipitation exceedance rates charts for various risks, using statistical models

13 p1989 A72-28811

Gravity waves on leeward side of Continental Divide in Colorado, noting generation by winds and storms

14 p2128 A72-30343

Method of constructing a forecast chart of H sub 500 anomalies on the basis of several analogs

19 p2828 A72-38000

Annual height and temperature distribution charts of polar and tropical tropopause over Northern Hemisphere

23 p3310 A72-43534

METEOROLOGICAL FLIGHT

Operational aviation meteorological requirements, reviewing aircraft categories, ATC systems and avionics and navigational aids

10 p1508 A72-25078

East African low level cross equatorial air current exploration, using light aircraft-borne Doppler radar wind finding equipment

12 p1840 A72-27703

High level Canberra flight for three dimensional picture of wind and temperature fields, showing CAT, gravity waves and smooth flight characteristics

12 p1841 A72-27709

Thunderstorm penetration by F-100 aircraft to study turbulence hazard relation to updraft size and short period fluctuation-induced acceleration changes

13 p1992 A72-28852

Lower stratospheric turbulence and horizontal temperature gradients from RB-57F aircraft meteorological measurements

13 p1993 A72-28864

Aircraft laser radar measurements of atmospheric backscattering coefficients for cloud and underlying surface studies

15 p2266 A72-31908

Water vapor flux periodic and spatial variations from airborne measurements, confirming height variation of maximum spectral density wavelength for crosswind runs

18 p2706 A72-36632

Theoretical model, laboratory experiments and in situ measurements by instrumented sailplane for investigating cloud and precipitation formation physics relationship to atmospheric pollutants cleansing

23 p3311 A72-44263

METEOROLOGICAL INSTRUMENTS

NT CLOUD HEIGHT INDICATORS

NT IONOSONDES

NT RADIOSONDES
NT RAIN GAGES
NT RAWINSONDES
NT WEATHER DATA RECORDERS
NT WIND VANES

Meteorological information assistance for Concorde aircraft test flights, discussing high tropospheric turbulence and lower stratospheric temperature predictions and instruments 04 p0542 A72-14680

Standardized automatic telemetering hydrometeorological station, discussing structure, operation, working principles and sensors 10 p1462 A72-25009

Automatic remote transmitting meteorological station, discussing development, working principle, technological features and sensors 10 p1462 A72-25010

Air hygrometer with heated electrolytic sensor for atmospheric humidity determination by automatic meteorological stations 10 p1483 A72-25016

Sensors measurement accuracy for rainfall amount and duration determination by automatic remote transmitting meteorological station 10 p1483 A72-25017

Mean wind direction determining circuit for meteorological data collecting system 10 p1484 A72-25018

Classification of automatic meteorological ground stations networks in populated areas, discussing required equipment, data transmission, real time operation and costs 10 p1507 A72-25021

Meteorological observations and instrumentation - AMS Conference, San Diego, March 1972 10 p1507 A72-25076

Momentum anemometer for wind velocity and vorticity measurement, discussing design principle and performance advantages 10 p1484 A72-25089

Low cost meteorological sounding rocket evolution, including Arcas, Lokidart and Viper Dart systems for various altitude ranges 10 p1552 A72-25090

Airport meteorological instrumentation, discussing ground wind, visibility, cloud height, air temperature and humidity detectors and radar equipment 10 p1484 A72-25093

Precision radiometric techniques in meteorology and geostrophysics, discussing references, pyrohelimetric scale, transfer calibrations and solar radiation measurements 10 p1485 A72-25097

Automatic ceilometer systems for sky state reporting, discussing computerized cloud simulation model, instrumentation and data sampling 13 p1992 A72-28850

Aeronautical requirements for meteorological reporting and instruments at aerodromes, discussing surface wind, visibility, runway range, weather, temperature and pressure observations 13 p1938 A72-28868

Azimuth display of attenuation instrument used with weather radar to measure rain induced attenuation over slant paths 15 p2207 A72-32101

Measurement of unsteady hydrometeorological processes on inertial devices 19 p2830 A72-38774

Air temperature measurement errors due to instrument inertia under various meteorological conditions and atmospheric stratification 23 p3310 A72-43536

METEOROLOGICAL PARAMETERS

Acoustic echo sounder as real time monitor of airport environmental meteorological parameters 01 p0103 A72-11137

Microwave propagation anomalies due to meteorological factors, discussing superrefractive atmospheric layers effects on radar data reliability and undesirable echoes appearance on display screen 02 p0182 A72-12746

Meteorological elements, upper ionospheric data and solar radio emission intensities during winter stratospheric temperature rises 03 p0383 A72-13477

Stationary-nonstationary temporal sampling for synoptic meteorological networks, illustrating oceanic wind speed measurements 06 p0842 A72-18436

Meteorological tests for mathematical models in study of climate changes 06 p0843 A72-18451

Refractive index structural constant relationship to atmosphere mean meteorological parameters, observing phase difference fluctuations of radio propagation in atmospheric surface layer 06 p0778 A72-18750

Meteorological elements vertical profiles under cloud cover condition by solving heat and humidity transfer equations based on satellite data 07 p1029 A72-18860

Atmospheric attenuation due to rain based on links experiment and statistical study of equivalent precipitation for given path length and time percentage 07 p0939 A72-19188

Meteorological effects on cosmic rays, deriving muon and pion intensity and meteorological coefficient formulas and computer calculation scheme 07 p1066 A72-20654

Computerized numerical calculation of muons production spectrum, angular distribution and Coulomb scattering in determining meteorological factors effects on cosmic rays 07 p1067 A72-20655

Atmospheric pressure, temperature, humidity and 200-mb level changes effects on cosmic ray neutron component intensity, using multifactorial regression analysis 08 p1225 A72-20702

Internal atmospheric gravity wave effects on ionospheric parameters obtained by vertical sounding, considering electron concentration isoline pattern 08 p1154 A72-20735

Lin parameter and eddy viscosity of atmospheric vortex streets, using TIROS and Gemini data 08 p1200 A72-21621

Global radiation flux and energy sum calculation from turbidity factor and cloud cover parameters, comparing with measurements in tropics and polar region 08 p1201 A72-21797

Probabilistic-statistical method for recognition and short term forecasting of convective clouds, spring floods, hail, thunderstorms and showers 08 p1202 A72-22115

Hydrometeorological parameters spatial-temporal variations analysis and forecasting based on association functions and conditional probability distribution functions 08 p1202 A72-22116

Averaging period parameters determination for weather climatic norms forecasting with minimum mean square error 08 p1202 A72-22117

Atmospheric surface layer meteorological elements representative values determination as optimal filtration problem, examining data correlation with errors in initial statistical characteristics 08 p1203 A72-22121

Meteorological measurements representativeness and analog discrete filters synthesis with optimal data processing and weighting function averaging procedures 08 p1203 A72-22123

Rainfall rate estimation by radar reflectivity measurements based on atmospheric parameters obtained from radiosonde data 09 p1345 A72-22449

Parameterization of turbulent flux of momentum, heat and moisture at ground in baroclinic planetary boundary layer 09 p1346 A72-22810

Aspiration condenser spectrometry of small ion mobility as function of height and atmospheric conditions 09 p1346 A72-23267

Wind and temperature fields periodic updating, considering error reduction as function of time intervals between updates 09 p1348 A72-23659

Viking Lander meteorology experiments to measure Martian atmosphere pressure, temperature, wind speed and direction and water vapor content 10 p1540 A72-24388

Temperature indetermination and large scale weather patterns in winter from 70 year temperature records 10 p1507 A72-25003

Automatic hydrometeorological stations standardized sensors, describing data converters for atmospheric pressure, precipitation, humidity and wind and water and soil temperature measurements 10 p1483 A72-25014

Reference radiosondes for quality control of global high altitude temperature, pressure and humidity measurements, discussing dual soundings and synoptic comparison 10 p1484 A72-25077

Radar echo maximum intensity display by digital comparator with shift register video signals storage in National Severe Storms Laboratory 11 p1591 A72-25762

Snow accumulation determination from snow intensity based on visibility estimates, noting application to forecasting 11 p1682 A72-26085

Meteorological elements, upper ionospheric data and solar radio emission intensities during winter stratospheric temperature rises 11 p1682 A72-26247

Stochastic dynamic prediction of meteorological fields in deterministic and indeterminate atmosphere 12 p1838 A72-27020

Meteorological reference level location without wind information for use in numerical weather prediction 12 p1838 A72-27024

Millimeter to meter waves propagation conditions prediction in horizontally inhomogeneous coastal foreground by meteorological parameters, considering wind effects on refractivity 12 p1784 A72-27798

Earth atmosphere boundary layer nonstationary problems, considering diurnal changes of meteorological fields and nonperiodic evolution of elements from wind variations 12 p1841 A72-27988

Earth atmosphere general circulation model based on planetary boundary layer parameterization, considering surface stress and heat and moisture flux 13 p1988 A72-28442

F 2 layer parameter forecasting by computer based on series coefficients dependence on Wolf number 13 p1946 A72-28597

Parameterized daily profile characterization of global atmospheric conditions to minimize computer storage, discussing mathematical representations, wind, density and temperature profiles 13 p1989 A72-28806

Model determining system responses to nominal profiles of atmospheric parameters from orbital to 25 km altitudes 13 p1989 A72-28807

Cost analysis of high altitude meteorological network data with respect to research effectiveness and data reduction 13 p1990 A72-28820

Acoustic ray path method for computing atmospheric conditions effect on aircraft noise propagation, using digital computer 13 p1897 A72-28840

Low flight altitude atmospheric parameters spatial and temporal variability effects on aircraft flyover noise measurement 13 p1991 A72-28841

Synoptic meteorological parameters vs CAT encountered in stratosphere by XB-70 airplane, presenting frequency distributions and probability tables 13 p1994 A72-28867

Meteorological information requirements for V/STOL aircraft design, airport location, runway orientation, aircraft operations and ATC simulation 13 p1994 A72-28869

Stratospheric meteorological characteristics effects on Concorde supersonic flight performance, fuel consumption, dynamic behavior and passenger comfort 13 p1994 A72-28876

Thermospheric parameters seasonal and latitudinal variations calculation based on atmospheric model with components ionization and molecular oxygen dissociation as main heat sources 14 p2128 A72-30463

Precision frequency standards practical utility under field operating conditions, discussing propagation effects due to atmospheric and frequency parameters 15 p2199 A72-32066

Global meteorological data analysis using Gram-Schmidt generated orthogonal polynomial base functions 15 p2266 A72-32719

Geomagnetic and meteorological elements lunar daily variation calculation by modified Chapman-Miller method, estimating confidence limits for parameters reliability 16 p2384 A72-32972

Local climatic forecasts via influence equations based on past meteorological data as initial conditions, obtaining solution by operational analysis methods 16 p2418 A72-33379

Meteorological data analysis for CAT encounter of Boeing 747 flight over Nantucket Island on 4 November 1970 16 p2418 A72-33525

Stepwise multiple regression techniques for Nimbus 3 IR interferometer-spectrometer (IRIS) data inversion, obtaining radiation predictors of meteorological parameters 16 p2418 A72-33666

Russian book on atmosphere studies covering determination of periodic variations in meteorological elements to assess seasonal pressure, temperature and wind variations 17 p2546 A72-34975

Meteorological effects on SST performance, considering temperature, wind, turbulence, hydrometeors, ozone and radiation effects 17 p2577 A72-35790

Dependence of the optical transfer function of a turbulent atmosphere on the averaging time 18 p2707 A72-36968

High level atmospheric refraction of electromagnetic waves as function of elevation and meteorological element vertical stratification 19 p2764 A72-37349

Dynamic meteorological problems solution by four dimensional analysis, discussing information deficiency effect on boundary value problems analysis in numerical weather forecasting 19 p2828 A72-37997

Atmospheric pressure, temperature, humidity and 200-mb level changes effects on cosmic ray neutron

component intensity, using multifactorial regression analysis

19 p2852 A72-38330

Internal atmospheric gravity wave effects on ionospheric parameters obtained by vertical sounding, considering electron concentration soline pattern

19 p2791 A72-38363

Zenith angle dependence of the meteorological corrections coefficients for cosmic ray hard component.

19 p2852 A72-38632

The determination of the vertical structure of the atmosphere from satellite measurements

19 p2792 A72-38700

Atmospheric pressure, density and scale height calculated from H Lyman-alpha absorption allowing for the variation in cross-section with wavelength.

19 p2793 A72-38859

Photogrammetric refraction equation and integral interpretation for actual atmosphere, climate and weather conditions suitable for photographic flights

20 p2927 A72-39739

Computerized long term weather forecasting via mathematical modeling of atmospheric processes based on meteorological parameters worldwide observational data

20 p2948 A72-39939

On the hydrographic response to transient meteorological disturbances.

21 p3077 A72-40465

Ground humidity and wind velocity effects on terrestrial scintillation, considering adiabatic temperature stratification factor

21 p3007 A72-40738

Techniques for dealing with the effects of bad weather in satellite communications systems.

21 p3017 A72-40856

Climatology of the occurrences of thundery weather over Gauhati Airport.

22 p3202 A72-42887

Earth atmosphere boundary layer nonstationary problems, considering diurnal changes of meteorological fields and nonperiodic evolution of elements from wind variations

22 p3202 A72-43002

Allowance for the influence of orography in a dual-layer model of the atmosphere

23 p3310 A72-43343

Reproduction of the climatic distribution of meteorological elements on the basis of a nonadiabatic spectral model of the atmosphere

23 p3311 A72-43626

A method of calculating meteorological elements for mesoscale processes

24 p3420 A72-44633

Determination of refraction in the propagation of electromagnetic waves at the earth's surface

24 p3379 A72-44865

F 2 layer parameter forecasting by computer based on series coefficients dependence on Wolf number

24 p3398 A72-45097

METEOROLOGICAL PROBES

U SONDES

METEOROLOGICAL RADAR

Radar meteorology, discussing equipment design, radar observation station net need, aeronautical applications and laser devices utilization

02 p0254 A72-12783

Radar accuracy for precipitation measurements, discussing error sources

02 p0254 A72-12784

Remote meteorological elements sensing in terminal area, discussing radar, ceilings, thunderstorm warning, slant range visibility, low level winds and wind shear

04 p0543 A72-14692

Combined radar-acoustic system for lower atmosphere temperature sounding, considering use in air pollution studies and short range weather forecasting

05 p0663 A72-16690

Peak reading and thresholding in radar weather data processing, describing PPI map

06 p0843 A72-18440

Radar observing apparent land breeze front off Wallops Island, giving temperature and wind profiles

06 p0843 A72-18441

Broadbeam S band radar application to quantitative analysis of severe storms, calculating liquid water content

06 p0843 A72-18442

Aviation weather forecasting improvements due to radar, computer, satellites and high speed communications contributions

07 p1029 A72-18838

Meteorological radar measurements, noting missile tracking radio interferometer noise due to stochastic refractive ray bending and associated multipath conditions

08 p1136 A72-21978

Soviet papers on cloud seeding effects and meteorological radar studies covering precipitation formation, atmospheric model and reflected signal statistical characteristics

08 p1201 A72-21992

Meteorological radar signal reflectivity probability and quantization error dependence on incoherent storage device parameters from computer simulation

08 p1201 A72-21995

Cloud and precipitation dynamic processes effects on reflected radar signal statistical characteristics

08 p1137 A72-21996

Cloud and precipitation elementary processes effects on reflected radar signal fluctuation spectrum during hydrometeor formation

08 p1201 A72-21997

Automatic meteorological stations development in populated areas, foreseeing data gathering by sensors with satellite and radar efficiency taken into account

10 p1507 A72-25008

Single engine aircraft-borne weather radar with electronically scanned steerable phased array antenna [SAE PAPER 720315]

11 p1591 A72-25579

Wavelength choice for ground based operational weather radar systems as function of reflectivity dependence on scattering hydrometeors/raindrops, hailstones/

13 p1917 A72-28694

Meteorological formations investigation with lidar, discussing laser beam interaction with clouds, fog and precipitation with allowance for multiple scattering

13 p1995 A72-29595

Weather radar observations of Alps foothill region convective precipitation development and lifetime

13 p1996 A72-30088

Azimuth display of attenuation instrument used with weather radar to measure rain induced attenuation over slant paths

15 p2207 A72-32101

Airborne ground mapping and meteorological radar with steerable phased array antenna without mechanical scanners

15 p2200 A72-32216

Radar meteorology in the Soviet Union - 1970.

18 p2707 A72-36719

Studies of vertical motions in cloud systems by using a coherent pulse radar in the decimeter wavelength range

19 p2829 A72-38773

Investigation of moisture content in the atmosphere by the method of ground radar thermal measurements

20 p2949 A72-39945

Altitudinal dependence of upper atmosphere winds according to radar and ionosphere data

20 p2920 A72-40074

Aircraft radar for weather data, ground mapping, avoidance modes and independent landing monitor function, presenting straight and slant approach simulation data

21 p3080 A72-40290

METEOROLOGICAL ROCKETS

U SOUNDING ROCKETS

METEOROLOGICAL SATELLITES

NT AEROS SATELLITE

NT ELEKTRON SATELLITES

NT EOLE SATELLITES

NT ESSA SATELLITES

NT NIMBUS SATELLITES

NT SAN MARCO SATELLITE

NT SYNCHRONOUS METEOROLOGICAL

SATELLITE

NT TIROS SATELLITES

ESRO polar orbiting meteorological satellite, discussing design features and operational instruments

01 p0126 A72-10186

Atmospheric thermal sounding from meteorological satellites, reviewing measurement accuracy, equation kernel, spectral resolution, optimum measuring condition and interpretation techniques

01 p0070 A72-10959

Soyuz manned spacecraft meteorological observations, dealing cloud cover in various climatic zones, atmospheric turbidity and snow cover in mountain areas

02 p0253 A72-11731

AEROS aeronomy satellite solar cell array power supply system simulation tests under space conditions

04 p0466 A72-15650

Storm forecasts by meteorological satellites, describing TV monitoring of cyclones and hurricanes

05 p0683 A72-15978

Meteorological satellite stabilization and attitude control in synchronous equatorial orbit for two years life, emphasizing nutation damper optimal dynamic characteristics

05 p0725 A72-16437

Facsimile bandwidth compression by picture elements reduction with contrast preservation, discussing analog processing algorithm and application to weather satellite photographs

06 p0772 A72-17406

Meteorological satellites TV, visual and IR cloud imaging and atmospheric sounding techniques for short and long range weather forecasting

06 p0892 A72-18066

Meteorological satellites data gathering equipment including TV cameras, temperature humidity, ozone and radiation measuring devices, discussing data processing and evaluation for weather forecasting [DGLR PAPER 71-131]

06 p0892 A72-18231

Educational and social applications of communication and meteorological satellite data dissemination, discussing learning and teaching model development

06 p0777 A72-18624

Aviation weather forecasting improvements due to radar, computer, satellites and high speed communications contributions

07 p1029 A72-18838

Meteorological elements vertical profiles under cloud cover condition by solving heat and humidity transfer equations based on satellite data

07 p1029 A72-18860

Satellite system and data processing center feasibility for carrying out meteorological surveys in Mediterranean area

07 p0993 A72-20605

Meteosat geostationary satellite international program for earth cloud cover observation and meteorological data relays between ground stations as part of Global Atmospheric Research Program

08 p1241 A72-21204

Eole satellite relay system for weather balloon location and data collection and transmission to ground stations

09 p1394 A72-22600

Continuous scan diffraction spectrometer for thermal sounding experiment on Meteor satellite, presenting vertical temperature and humidity profiles

09 p1347 A72-23588

German-French DIAL aeronomy satellite project, describing geocoronal radiation, electron density and equatorial electrojet measurements

10 p1535 A72-24029

DIAL aeronomy satellite design and operational features, describing in-flight behavior

10 p1551 A72-24030

ESSA satellite observation of meridional circulation, noting roles of subsidence sinks, storm depressions and melting fronts

10 p1506 A72-24059

Automatic meteorological stations development in populated areas, foreseeing data gathering by sensors with satellite and radar efficiency taken into account

10 p1507 A72-25008

Military weather forecasting requirements by 1980, discussing decision making, data processing, satellite data, mission and terminal forecasts, display and computer flight planning

10 p1508 A72-25096

French-U.S. Eole meteorological satellite project to map Southern Hemisphere winds, describing system based on pressurized balloons for data acquisition

11 p1680 A72-25813

Weather satellite data use to obtain forecasts for aircraft and ships in Southern Hemisphere and for Antarctic research stations

11 p1683 A72-26896

Meteorological satellite information and communication aspects, stressing METEOSAT European project for permanent cloud cover observation in visible and IR bands

12 p1839 A72-27370

Space techniques application to meteorological prediction, noting Meteosat and Eole satellites capabilities

12 p1840 A72-27506

Hybrid forecast model for hydrometeors short range prediction based on meteorological satellites cloud pattern observations and quasi-Lagrangian advection analog

13 p1993 A72-28858

Global atmospheric circulation barotropic spectral model application to satellite asymptotic data continuous processing

14 p1217 A72-30258

Space technology development effect on meteorology progress, discussing earth resources technology satellites and meteorological satellites

15 p2220 A72-31234

Stable air clouds localization from meteorological satellite photographs, noting atmospheric air pollution

15 p2265 A72-31236

Geographical interpretations of ESSA and Nimbus weather satellite pictures for earth resources applications, noting ERTS project

15 p2221 A72-31248

Barbados oceanographic meteorological experiment /BOMEX/ sea air interaction program in equatorial Atlantic, using real time synchronous satellite information

15 p2225 A72-31808

Report to COSPAR on Australian space program covering earth atmosphere, cosmic and synchrotron radiation, X ray astronomy, weather satellites, deep space and sounding rockets

15 p2338 A72-32007

Use of satellites for the transmission of meteorological data and the tracking of observation stations

17 p2603 A72-34399

The collection of data by geostationary meteorological satellites

17 p2622 A72-35719

NASA developed geostationary weather and environmental satellite for launch in 1973, discussing

ground station equipment, antenna system and data collection service

- 23 p3343 A72-43551
- Weather satellites - Their role in the application of environmental services to the marine industries.
- 24 p3420 A72-44648
- Polar orbiting operational weather satellites.
- 24 p3451 A72-45197

METEOROLOGICAL SERVICES

Meteorological information assistance for Concorde aircraft test flights, discussing high tropospheric turbulence and lower stratospheric temperature predictions and instruments

- 04 p0542 A72-14680
- Aircraft in-flight monitoring instruments for meteorological service in U.S.

Automated meteorological telemetry and interrogation response system with terminal extensions for Paris airport

- 04 p0464 A72-14687
- Meteorological observations and instrumentation - AMS Conference, San Diego, March 1972
- 10 p1507 A72-25076

Aerospace and aeronautical meteorology - AMS Conference, Washington, D.C., May 1972

- 13 p1988 A72-28801
- West German-United States Barium Ion Cloud Project meteorological support at Wallops Station, discussing magnetospheric magnetic and electric fields
- 13 p1947 A72-28802

Computer and meteorological satellite effects on weather support for manned space missions, discussing Gemini 5 and Apollo 11 landing weather predictions and cloud climatology

- 13 p1989 A72-28804
- Man machine system to repackage weather information for easy assimilation, considering computer driven keyboard CRT displays
- 13 p1924 A72-28872

Pacific Ocean meteorological data collection from military and civil aircraft in-flight reports, discussing computer processing for daily analysis and monthly and seasonal means

- 13 p1994 A72-28874
- Worldwide weather data system as important factor for search and rescue operations implementation
- 17 p2488 A72-34432

Automatic position reporting, ATC communication, weather information and message identification via digital ground-air-ground data link, discussing operational and maintenance requirements

- 21 p3080 A72-40286
- Meteorological and takeoff and landing information transmission by proposed automated meteorological and information service, discussing air-ground data link
- 21 p3080 A72-40287

METEOROLOGICAL STATIONS

U WEATHER STATIONS

METEOROLOGY

- NT AEROLOGY
- NT HYDROMETEOROLOGY
- NT LONG RANGE WEATHER FORECASTING
- NT MICROMETEOROLOGY
- NT NUMERICAL WEATHER FORECASTING
- NT POLAR METEOROLOGY
- NT RADIO METEOROLOGY
- NT STATISTICAL WEATHER FORECASTING
- NT SYNOPTIC METEOROLOGY
- NT TROPICAL METEOROLOGY
- NT WEATHER FORECASTING

Nonmeteorological scientists and engineers views on meteorology and weather forecasting, discussing uses, problem areas and knowledgeability

- 03 p0384 A72-13637
- Tadzbakhsh method of meteorological data assimilation for numerical weather forecast analyses, testing validity under condition of one of three dependent variables being observed
- 03 p0384 A72-14141

Past meteorological data assimilation in dynamical analysis, computing initial condition with time sequential data for error reduction

- 04 p0541 A72-14455
- Various updating effects on meteorological data analysis accuracy, using balanced barotropic model
- 04 p0541 A72-14456

Meteorological fields matching by Sasaki method combined with optimum interpolation, using weighting functions

- 05 p0683 A72-16724
- Periodic aspects of nonphenemeral Euroatlantic blocking systems persistence, noting dominant role played by cyclonic vortices
- 05 p0684 A72-16794

Handbook on aviation meteorology covering atmospheric structure and composition, standard atmospheres, heat transfer, adiabatic processes, winds, cloud formations, precipitation, ice formation, fog, visibility, etc

- 08 p1200 A72-21479

Running average method of data smoothing effect on persistence tendency change in meteorological time series

- 10 p1507 A72-25004
- Large data processing systems for requirements of meteorology, environmentalogy, earth resources inventories and hydrology in 1980s
- 10 p1446 A72-25095

Space technology development effect on meteorology progress, discussing earth resources technology satellites and meteorological satellites

- 15 p2220 A72-31234
- Radiation measurements and thermal IR and photographic imaging techniques in meteorology and earth resources survey applications
- 15 p2221 A72-31241

Report to COSPAR on French space program covering ionospheric and magnetospheric physics, meteorology, earth resources and exobiology

- 15 p2337 A72-32003
- Report to COSPAR on West German space program covering meteorology, aeronomy, ionospheric physics, magnetosphere, solar wind and radiation, solar system and life sciences
- 15 p2338 A72-32014

Independent random test values effective sample numbers for mean and variance distributions in meteorological and geophysical statistical tests

- 16 p2385 A72-33382
- Bandpass-filtered geophysical and meteorological time series data statistical evaluation by comparison with filtered test series with same variance and autocorrelation function
- 16 p2363 A72-33383

The potentialities of space technology in relation to oceanography and surface meteorology.

- 19 p2790 A72-37924
- Dynamic programming technique for simultaneous measurement and dynamic control optimization for stochastic systems
- 19 p2779 A72-38233

A square equal-area map of the world.

- 20 p2915 A72-38961

METEORS

U METEORIODS

METERS

U MEASURING INSTRUMENTS

METHACRYLATE RESINS

U ACRYLIC RESINS

METHANE

Supersonic diffusion flame in duct configuration to study mixing with combustion of two parallel methane and air flows

- 03 p0405 A72-13545
- Jovian planets methane and ammonium absorption bands spectrophotometric investigation, noting Saturn spectral variations
- 03 p0436 A72-13819

Uranus IR spectral albedo, discussing methane absorption

- 04 p0580 A72-15365
- Slush, boiling methane and methane mixture characteristics, noting advantages as potential rocket, aircraft and motor vehicle fuels
- 04 p0564 A72-15542

Kr, Ar, methane and nitrogen physisorption isotherms on stainless steel in low pressure cryogenic baths calculating mean adsorption energies

- 05 p0624 A72-16395
- Photoelectric spectrophotometric measurements of Jupiter atmosphere optical properties and structure, showing methane absorption band intensity latitudinal variations
- 06 p0881 A72-17928

Methane pyrolysis in glow discharges /cold plasmas/, discussing chemical reactions initiated by high energy electrons inelastic collisions with gas molecules

- 07 p0937 A72-20286
- Frequency stability of free running methane stabilized He-Ne lasers with dc excitation, comparing to rf excitation
- 07 p1008 A72-20562

Methane contribution to thermal opacity in Uranus and Neptune atmospheres for atmospheric model synthesis

- 09 p1383 A72-22293
- Methane, hydrogen and oxygen adsorption and displacement on crystal surface of W investigated by thermal desorption and work function changes
- 09 p1276 A72-22807

Bromine additions effect on normal laminar flame propagation velocity of methane-air mixture at high pressures

- 09 p1411 A72-22889
- Carburization kinetics of Nb in acetylene or methane at high temperatures and low pressure
- 09 p1319 A72-22985

Flame structure studies of stabilizing region of near stoichiometric laminar burner methane-air flame

- 09 p1411 A72-23147
- Methane absorption line profile, intensity and width studied with magnetically tuned He-Ne laser
- 10 p1490 A72-24041

Temperature effects on kinetics of methane decomposition on carbon fiber at high temperatures, showing characteristics relationship to carbon gasification reactions

- 10 p1433 A72-24086
- Jupiter spectral observations, discussing presence of deuterated methane in atmosphere and comparison with solar spectra for telluric features identification
- 10 p1539 A72-24347

IR spectrophotometric data for Jupiter, determining limb darkening nature and ammonia and methane absorption variations over belts, zones and Red spot

- 10 p1548 A72-24971
- Stratospheric methane measurements over North America from solar absorption spectra observed from aircraft
- 11 p1622 A72-25911

Methane concentration of air sample from stratosphere measured by gas chromatography, discussing sample integrity, analysis method and results

- 12 p1802 A72-27505
- Shock heated methane-oxygen-argon mixtures ignition delay time from reaction kinetics calculations
- 12 p1778 A72-27852

Hydrogen atom exchange in ion-molecule reactions of methane and ethylene determined from reaction products distribution, using ion cyclotron resonance techniques

- 14 p2084 A72-30522
- Methane spectral band tetrahedral fine structure analysis, using vibration-rotation Hamiltonian
- 14 p2084 A72-30523

Methane collision broadened rotational fundamental line, calculating line width dependence on temperature

- 14 p2135 A72-30893
- Azomethane and azomethane-d6 IR and Raman spectra, discussing fundamental modes vibrational assignment based on band contours, isotopic shift ratios and group frequency correlations
- 16 p2360 A72-32923

Band model and scaling approximation validity for computation of transmission profile in V4 band of methane in Jovian atmosphere

- 16 p2461 A72-34099
- Photoelectric spectrophotometric measurements of Jupiter atmosphere optical properties and structure, showing methane absorption band intensity latitudinal variations
- 18 p2730 A72-37153

Aromatic hydrocarbons - Methane ignition inhibitors

- 19 p2879 A72-37364
- Influence of water vapor on the normal flame velocity of a methane-air mixture at high pressures
- 19 p2882 A72-38459

Detonation and burning characteristics of liquid oxygen-liquid methane mixtures.

- 19 p2848 A72-38834
- Jupiter atmosphere methane deuterium/hydrogen ratio estimate from exchange reaction and temperature studies
- 20 p2968 A72-39242

Resonance absorption of laser emission by methane behind the shock front

- 21 p3063 A72-40986
- New observations on the Kuiper bands of Uranus.
- 21 p3106 A72-41043

Jupiter atmospheric C12/C13 ratio for methane from equivalent width measurements in R[2] multiplet

- 21 p3107 A72-41273
- Chromium carbides synthesis by carburizing chromium hydroxide or oxalate in hydrogen-methane gas mixture at temperatures below 1000 C
- 22 p3188 A72-41974

Uranus methane brightening at limb and south pole explained by Rayleigh scattering and haze in upper atmosphere

- 22 p3228 A72-42573
- 3.39 micron resonance line absorption in shocked methane.
- 24 p3410 A72-45044

METHIONINE

Incorporation of methionine-S 35 in the proteins of the digestive organs of rabbits under the action of radiation and vibration

- 21 p2998 A72-40440

METHOD OF CHARACTERISTICS

Poincare-Lighthill-Kuo perturbation method and method of characteristics equivalence in one dimensional fluid motion due to ideal piston periodic oscillation

- 03 p0341 A72-13239
- Method of characteristics calculations of inviscid free jet flow with low specific heat ratios for perfect gas at 1.10 Mach number
- 03 p0309 A72-13926

Lagrange method extended to method of characteristics for solving first order hyperbolic partial differential equations, applying to ionospheric ion density distribution

- 04 p0539 A72-14885

Three dimensional supersonic flow about space shuttle, comparing method-of-characteristics and shock-capturing computations [AIAA PAPER 72-191] 05 p0729 A72-16845

Characteristic schemes comparison for three dimensional steady isentropic supersonic flow [AIAA PAPER 72-190] 05 p0605 A72-16846

Geometrical methods in fluid mechanics, solving quasi-linear nonelliptic systems by method of characteristics 07 p0969 A72-20063

Linearized method of characteristics application to supersonic flow past oscillating flat plate cascades with supersonic leading edge locus [AIAA PAPER 72-377] 11 p1730 A72-25401

Two dimensional cascades supersonic exit flow field, using Oswatitsch method of characteristics and conservation laws [ASME PAPER 72-GT-49] 11 p1570 A72-25641

Method of characteristics for solution of quasi-linear hyperbolic partial differential equations, analyzing frequency response 11 p1678 A72-26551

Method of characteristics for three dimensional supersonic flow of guiding center plasma, noting application to solar wind-moon interaction 11 p1573 A72-26601

Inward radial flow turbines under unsteady flow conditions with full and partial admission, predicting performance by method of characteristics 12 p1751 A72-27349

Electromagnetic plane field cumulation by heavy conducting shells implosion with quasi-relativistic velocity, solving Maxwell equations by characteristics method 12 p1851 A72-27396

Isoenergetic and irrotational planar supersonic cascade ideal gas flow computation by analytic method of characteristics 15 p2178 A72-31466

German monograph on supersonic flow past blunt sharp edged cones, comparing Van Dyke and method of characteristics results with schlieren photos and shadowgraphs 16 p2343 A72-33505

Supercritical pressure convergent nozzle performance prediction by time dependent method of characteristics solution to mixed flow problem, adapting Moretti-Abbott technique [AIAA PAPER 72-680] 16 p2346 A72-34061

The numerical solution of hyperbolic systems using bicharacteristics. 17 p2574 A72-34449

Method of characteristics application to supersonic jet and nozzle gas flow with allowance for equilibrium and nonequilibrium condensation 17 p2544 A72-35929

Conical and cylindrical shell deformation with nonlinear one dimensional wave processes, describing algorithm for method of characteristics application 18 p2735 A72-36664

A study of thermoelastic waves by the method of characteristics. 18 p2737 A72-37068

Method of characteristics for nonlinear equations of perturbed motion of fluid near contact point between shock and diffraction waves 20 p2912 A72-39023

Two dimensional underexpanded free jet flow into static medium, presenting wind tunnel nozzle experimental data and graphic solutions from method of characteristics 20 p2885 A72-39619

Method of characteristics for ideal gas flow in annular space of axisymmetric plug nozzle, noting flow visualization by schlieren photography 22 p3166 A72-42263

Use of characteristics for boundaries in time dependent finite difference analysis of multidimensional gas dynamics. 24 p3359 A72-44879

Method of characteristic application to curved beam motion under pulse type loading, investigating photoelastic fringe patterns and pulse propagation 24 p3458 A72-44888

Characteristics and constants of motion method for collisional kinetic equations. 24 p3426 A72-44984

METHODOLOGY

System methodology application to filter design for inertial reference unit calibration in digital test station for FB-111 aircraft navigation system 10 p1456 A72-23820

Analytical foundations of experimental mechanics - Trends in analytical mechanics. 18 p2732 A72-36354

METHODS

U METHODOLOGY

METHOXY SYSTEMS

Differential neurophysiological and psychological effects of subanesthetic concentrations of cyclopropane, diethyl ether, methoxyflurane and ethrane in conscious man 04 p0480 A72-15220

Molecular complexes of methoxyindoles with 1,3,5-trinitrobenzene and tetracyanoethylene /Spectroscopy/association constants/NMR/. 17 p2512 A72-35649

METHYL ALCOHOLS

Methanol and formaldehyde photoionization by UV irradiation, determining ion yields as function of wavelength by mass spectrometric analysis 07 p1038 A72-20498

Methyl alcohol-ethylene glycol self mixing antifreeze solution for precipitation gages 11 p1682 A72-26088

Miniaturized electronic system for controlling methanol concentration in aqueous electrolyte during fuel cell operation 12 p1755 A72-27723

Raney Pd-Ag catalysts for methanol oxidation in alkaline electrolyte in fuel cells 16 p2361 A72-33879

Alloying component effect on Pt catalytic activity in anodic oxidation of methanol for fuel cells 16 p2361 A72-33881

Electrodes converting hydrogen, methanol or oxygen for use in fuel cells with alkaline electrolyte, using Ag-Pd, Ni, Si and C catalysts 16 p2351 A72-33885

Effect of chloride on the anodic dissolution of titanium in methanolic solutions. 21 p3013 A72-40842

METHYL CHLORIDE

Photodissociation cross sections of methyl chloride and nitrous oxide cations, using ion cyclotron resonance technique 07 p0936 A72-19492

METHYL COMPOUNDS

NT METHYL NITRATE

NT METHYL POLYSILOXANE

Mass spectrometric studies of solvent extractable acid methyl esters of oil shale from Colorado Green River Formation 03 p0320 A72-13742

Molecular process and pressure effects on hydrogen formation in methyl acetylene photolysis at 1236 Å 11 p1590 A72-26011

Vibrational analysis of electronic absorption spectra of 3-methyldiazirine and 3-methyl-3-diazirine in vapor phase 18 p2657 A72-36566

METHYL NITRATE

Thermal conductivities of gaseous binary mixtures of methyl nitrate with helium, neon, argon and nitrogen 07 p1051 A72-19365

METHYL POLYSILOXANE

Methyl phenyl polysiloxane bonded solid film lubricants, discussing air curing at ambient temperatures and performance tests 06 p0836 A72-18592

METRIC SPACE

NT HILBERT SPACE

Gravitational field of bounded and isolated material in empty four-dimensional locally Minkowskian space-time, emphasizing radiation zone and gravitational waves 04 p0570 A72-14556

Steepest ascent method for function optimization in arbitrary direction by selecting distance metric and scale dependency 04 p0540 A72-15683

Euler-Lagrange equation construction to obtain phenomenological description of quasi-equilibrium systems in metrics, noting solution coincidence with Onsager equations 07 p1102 A72-20665

Toroidal gravitational waves in general relativity, considering analog to imploding-exploding cylindrical waves, linear field equations and symmetric metric 08 p1210 A72-21922

Minimal dynamic systems invariant Borel probabilistic measure with metric space and topological entropy equality 08 p1210 A72-22187

Metric tensors as alternate to coordinate transformation equations for computer program inputs in automatic problem formulation 10 p1443 A72-23923

Flat homogeneous isotropic relativistic cosmological two fluid model, using Robertson-Walker metric 15 p2307 A72-31795

Anisotropic and isotropic descriptions of physical process speeds in special relativity theory space-time metric 15 p2279 A72-32768

Regge calculus representation existence for solutions of initial value problem for spaces with axial symmetry 16 p2422 A72-32879

Conformally flat linear axisymmetric chronometrically invariant cosmological models, discussing various types of spaces realized during model evolution 18 p2724 A72-36327

Universe expansion induced electromagnetic wave backscattering absence in Robertson-Walker space-

time as consequence of motion equations conformal invariance 18 p2711 A72-36711

Polarization effects during electron scattering in the gravitational field of a rotating source 18 p2712 A72-36967

On the cosmological equations in a universe with small scale condensations. 22 p3220 A72-41998

Metric gravitation theories classified according to field type and interaction mode, constructing post-Newtonian limit 22 p3206 A72-42567

Trajectory bundles in metric space for objects motion study in dynamic pursuit games, noting Pontryagin and Pshenichnii methods for differential games solution 23 p3308 A72-43415

Estimates of derivative solutions of linear nonhomogeneous elliptic-type equations of arbitrary order near the domain boundary in the L2 metric 23 p3309 A72-44041

Degree of approximation of functions by integral operators in an infinite domain as related to the Hausdorff metric 23 p3310 A72-44163

A 'length and area principle' type inequality for images in which certain integral functionals remain bounded in an n-dimensional space 24 p3419 A72-45261

METROLOGY

German book on liquids flow rate measurement techniques covering physical principles of flow measurement including pressure, magnetic or inductive and ultrasonic methods 02 p0230 A72-12299

Metrology and radio performance of steerable antenna paraboloidal reflector, considering profile measurements by optical range finder and laser methods 04 p0493 A72-15518

Metrology and technology for sounds intense enough for physiological distress and mechanical structure damage, discussing accompanying high temperature and vibration [ONERA, TP NO. 1009] 05 p0661 A72-16024

Information theory in metrology, comparing measurement techniques and calculating quantity of measurement information 06 p0817 A72-18164

Papers on laser applications covering holography, metrology, geodesy, etc 07 p1007 A72-20220

Laser applications in metrology and geodesy, discussing use of beam directionality for alignment purposes, interference patterns and interferometry, modulated light methods, optical Doppler methods, etc 07 p1007 A72-20222

Temperature effects on low pressure calibration in vacuum gage metrology 09 p1312 A72-23249

Time metrology achievements review, discussing time unit development, atomic and molecular frequency standards, atomic clocks, time scales and time signal broadcasting 10 p1481 A72-24399

Metrological techniques reliability for industrial production processes, plotting quality control curves 11 p1637 A72-26823

Thermodynamic limiting relations between physical measurement accuracy and measurement performance energy dissipation, considering equilibrium and nonequilibrium dynamic models 13 p2003 A72-28761

Cloud height measurement with rotating beam ceilometers, discussing precision and representativeness 13 p1992 A72-28849

French book on industrial acoustics elements and metrology covering transmission, absorption, noise and complex sound measuring apparatus and preventive measures 15 p2275 A72-31524

Dynamic errors of a metering system with successive correction of the sensor's time constant for certain types of aperiodic input 17 p2557 A72-35787

Electro-optical TV technique with laser source illumination to provide engineering metrology and NDT procedure resembling real time holographic interferometry 20 p2930 A72-39038

Italian national time scale design and operation, discussing frequency standards, comparisons with national and international laboratories and time keeping 20 p2925 A72-39430

Analysis of the basic metrological characteristics of Vernier time-pulse converters 21 p3035 A72-41729

METROPOLITAN AREAS

U CITIES

MICA

NT BIOTITE

Epitaxial and textured Pb films on mica and glass, using reflection electron diffraction, etching and optical microscopy for structure study
12 p1854 A72-27289

Mica polymorph distribution among space groups from unit layer and stacking sequence characteristics
12 p1802 A72-27512

Radiometer with protective mica window for radiant flux densities measurement of near IR sources, noting reading independence of sources spectra characteristics
21 p3059 A72-41821

MICE
Relative biological effectiveness of energetic protons for somatic effects induction in mice during whole body irradiation, using mean energy of solar event protons
[CERN-71-16] 02 p0161 A72-12054

Mitotic index and aberrant mitose frequency in mice corneal and intestinal epithelial cells exposed to 50-630 MeV protons, estimating relative biological efficiency coefficients
[CERN-71-16] 02 p0161 A72-12055

MICHELSON INTERFEROMETERS
Multimode Q switched ruby laser temporal coherence, comparing theoretical with experimental results from Michelson two-beam interferometer measurements
01 p0080 A72-10849

Ultrasonic excitation induced vibration measurement for detecting incipient electrical breakdown in transducers, using laser-Michelson interferometer
01 p0081 A72-11018

Michelson interferometers with large interference fields for plasma diagnostics emphasizing structural rigidity, monochromatic light pulse power, instruments vibrations resistance, etc
02 p0223 A72-11402

Coarsely stabilized spacecraft-borne Michelson interferometer, obtaining high resolution by computerized spectrum reconstruction with fast Fourier transform
03 p0354 A72-13055

Separation measurement between two distant partially reflecting parallel surfaces using Michelson interferometer
03 p0358 A72-13435

Two dimensional time resolved and real time IR interferograms obtained with pulsed Nd doped glass laser illuminated Michelson interferometer
03 p0362 A72-14200

Relaxation processes in Michelson interferometer as integral part of carbon dioxide laser cavity in phase Q switching regime
04 p0530 A72-14990

Optical sweep generator using single frequency He-Ne lasers with Michelson interferometer for mode selection to provide smooth tuning throughout Doppler width
07 p1000 A72-19010

Field compensated Michelson spectrometer systems, discussing tolerances, usefulness, resolution luminosity products, stigmatism and astigmatism
09 p1513 A72-23328

Michelson interferometer application for continuous gas analysis in far IR
10 p1480 A72-24174

Nonrectilinearity evaluation of twin wave Michelson interferometer mirror displacement
10 p1481 A72-24498

Double passed Michelson interferometer with polarizing beam splitter, quarter wave plates and cube corner reflectors to obtain immunity to mirror misalignment
11 p1635 A72-26500

Q switched carbon dioxide laser based on PM by rotating mirror in one arm of Michelson interferometer, establishing phase relationships
13 p1968 A72-29287

Laser mode suppression arrangements consisting of Michelson interferometers with polarization prism as beam splitting element
18 p2697 A72-36112

High resolution Michelson interferometer for spectral investigations of lasers.
21 p3062 A72-40610

Identification and removal of phase errors in interferometry.
23 p3287 A72-43259

Measurement of small strain amplitudes in internal friction experiments by means of a laser interferometer.
24 p3402 A72-44947

Spaceborne astronomy by synthetic aperture optics for high resolution without cost and weight disadvantages of large telescopes, considering Michelson stellar interferometer
24 p3404 A72-45541

MICROANALYSIS
Microprobe analysis of Timmersoi hypersthene chondrite from Niger Republic, noting equilibrium between olivine and orthopyroxene at 850 C
13 p2035 A72-28751

Microprobe analysis of Murchison and Vigarano meteorites, noting fractionation processes for Ca distribution in olivines
13 p2036 A72-28752

Electron probe microanalysis of Mo-Pd system diffusion at 1000-1600 C, measuring chemical diffusion coefficient as function of temperature, concentration and activation energy
13 p1978 A72-29221

Solid bodies microanalysis by mass spectrum microscopy based on secondary ion-ion emission, discussing ion source and focusing systems
14 p2104 A72-30449

Chondrite Pawel microspectral analysis with laser beam vaporization of sample from microzone
16 p2450 A72-32850

Acute hypoxia of the myocardium - Ultrastructural changes.
17 p2501 A72-34982

Changes in energy stores in the hypoxic heart.
17 p2501 A72-34985

Morphological alterations in the ischaemic heart.
17 p2502 A72-34995

Microscopic and electron-microscopic investigation of the catalysis of ammonium perchlorate combustion
22 p3216 A72-43186

MICROBALANCES
Particle mass monitor system based on piezoelectric microbalance combined with electrostatic precipitator collector, considering applications to air quality monitoring, laboratory aerosol research, process control, etc
[AIAA PAPER 71-1100] 01 p0067 A72-10548

Test facility for electric microthrusters, describing microbalance for thrust and propellant mass flow rate measurement
09 p1292 A72-23404

Thermogravimetric design, using electromagnetic microbalances and turbomolecular pump for automatic sorption isotherm measurements in surface area and pore size analyses
11 p1636 A72-26788

Piezoelectric quartz crystal microbalance for material outgassing and optical element contaminant film measurements
12 p1806 A72-27043

Quartz microbalance studies of an adsorbed helium film.
18 p2719 A72-36675

Utilization of the CACTUS microaccelerometer as a detector of micrometeorite impacts
22 p3181 A72-43097

MICROBE
U MICROORGANISMS
MICROBEAMS
Electron microbeam testing for large microcircuit arrays, using analog voltage signal injection into isolated contact and digital voltmeter readout
10 p1446 A72-23938

Radial transport instability during intense microbeam heating of thin plasma column, noting maximum temperatures and phase coherence cut-off effect
15 p2286 A72-32306

MICROBIOLOGY
NT BACTERIOLOGY
Planetary quarantine microbiological and engineering problems, discussing cost, international policies, contamination and sterilization
01 p0019 A72-10818

Microbiological examination of space hardware, discussing viable organisms neutralization buried inside solid materials, sampling procedures and culture media
01 p0019 A72-10820

Terrestrial biosphere back contamination from outer space organisms, discussing microbiologic control and prevention requirements
01 p0020 A72-10825

Hereditary endosymbiotic model of microbial evolution of Precambrian prokaryotic and eukaryotic cells
04 p0471 A72-14800

Paleomicrobiological analysis of northwest Scotland Stoer Formation black shale pre-Paleozoic spheroidal unicellular fossils as probable form of marine phytoplankton
05 p0655 A72-16042

Thin layer chromatography technique for rapid quantification of bacterial cell adenosine triphosphate, using microscope ultraviolet photometer
06 p0763 A72-17872

Fine structure of *Pseudomonas saccharophila* at early and late log phase of growth, using electron microscopy and various culture techniques
07 p0922 A72-20238

Cellular evolution investigation using molecular biology, microbial physiology and ecology
08 p1119 A72-22011

Antarctica dry valley microbiology investigation for Martian life model
12 p1802 A72-27258

Modular microbiology laboratory design considerations and zero gravity experiments to investigate microbial culture systems behavior
12 p1765 A72-28280

Interval scanning photomicrography for recording growth of microbial cell populations during incubation
13 p1911 A72-29749

Optimal temperature control for microbial inactivation by composite environment of heat and gamma radiation, using quadratic technique
18 p2649 A72-36313

Microflora accumulation prevention methods during spacecraft flight, noting bacterial filters for air purification and wiping with disinfectants for surface contamination reduction
24 p3376 A72-45213

MICROCALORIMETERS
U CALORIMETERS
MICROCIRCUITS
U MICROELECTRONICS
MICROCLIMATOLOGY
Diurnal variation in energy balance microclimate across coastal beach, noting surface moisture effect
21 p3078 A72-40468

MICROCRACKS
Ultrasonic fatigue at small strain amplitudes in Ti, developing solitary slip band microcracks
04 p0533 A72-14539

Microfibrillar superlattice with vacancy defect and point dislocation in microcrack formation and propagation in nylon 6 fibers
05 p0681 A72-16308

Plate microcracking of ferrous martensites containing Mn, Cr and Ni, discussing austenite grain size variations
05 p0678 A72-17119

Thermally activated crystal microcrack initiation by fusion of leading and following dislocations
06 p0898 A72-18551

Test equipment with variable deflection and twist for metal fatigue microcrack initiation and growth detection
07 p0987 A72-19849

Crack initiation and propagation microscopic and phenomenological characteristics, discussing breakdown, plasticity and microcrack convergence
07 p1094 A72-20147

Precipitation hardened Ni-Al alloy mechanical properties, relating ductility and strength to precipitate caused inhibition of microcrack initiation and propagation
07 p1021 A72-20438

Tensile stress effect on formation of suboxide needles, microcracks and oxide wedges during low temperature Nb oxidation
11 p1658 A72-25854

Microcuts as equivalent mechanical stress concentrators for breakdown energy estimation in flat polymethyl methacrylate glass specimens under impact bending loads
13 p1983 A72-28563

Binary Al alloys intermetallic phases effects on microcracks nucleation and propagation at 300 C in uniaxial tension, considering alloying elements influence on mechanical properties
14 p2124 A72-31036

Microcrack initiation and propagation in ductile metals at low cycle and ultrasonic frequencies, investigating fatigue fracture mechanism by scanning electron microscope
15 p2256 A72-31838

Mechanical properties and residual stresses in and adjacent to interface of explosively welded Al-Zn-Mg alloy with steel, noting microcracks effect on weld strength
15 p2257 A72-32111

Two-phase crystal structure microdeformation measurement by combined holographic interferometry and X ray diffraction
18 p2690 A72-36358

Acoustic emission testing and microcracking processes.
20 p2924 A72-39277

Microcracks observed in hydrogenated niobium foil.
21 p3069 A72-41300

Fiber glass reinforced plastics elastoplastic behavior due to microcrack propagating across matrix, using elastic index of work done
22 p3232 A72-41943

Glass fracture mechanics, discussing microcrack stress concentration, Griffith theory, statistical failure theories, static fatigue and strength measurements
23 p3305 A72-43502

MICRODENSITOMETERS
Automated photometric wetland mapping using aerial color film microdensitometric analysis and computer techniques
02 p0215 A72-11886

Microdensitometer system analysis by partial coherence theory, determining optical transfer function for linear operation
07 p0987 A72-19830

- Partially coherent imaging in microdensitometer, investigating conditions for linear operation from difference between high and low contrast edge images
09 p1309 A72-22608
- Black and white aerial photographs quantitative evaluation for differentiation and identification of land use patterns by microdensitometry, using statistical methods
09 p1313 A72-23306
- Automation of aerial photointerpretation based on application of photometric, microdensitometric and digital computer technology
09 p1313 A72-23308
- MICROELECTRONICS**
NT LARGE SCALE INTEGRATION
NT MEDIUM SCALE INTEGRATION
Optimal design of logic networks in homogeneous microelectronic structures, using shortest link search and graph continuity parameters
01 p0034 A72-10300
- Book on microelectronics covering integrated circuits, semiconductors, p-n junctions, transistors, Schottky and MOS structures, epitaxy, ion implantation, photomechanical operation, fabrication techniques, etc
02 p0194 A72-12574
- Book on field effect electronics covering junction and insulated gate transistors and allied devices, monolithic and film IC and design techniques
03 p0333 A72-13846
- Microstrip double down-converter receiver in civil satellite earth stations for reduced interface problems, increased reliability and minimum initial cost
03 p0334 A72-14074
- Microelectronic computer system with image data cross correlation generation for real time video pattern abstraction, discussing design and operating characteristics
03 p0329 A72-14178
- Microcircuit failures due to electrical overstress, covering current density, thermally induced burn-out, junction shorts and second breakdown with nonuniform heat flow
03 p0336 A72-14290
- Thermal deformation effects on metal bond fatigue failure modes in small signal transistors, micro and LSI circuits
03 p0365 A72-14291
- Mathematical model for reciprocal and nonreciprocal magneto-optical effects in magnetized ferrite-filled microstrip transmission lines
04 p0502 A72-15434
- Planar coax micropackaging of minicomputers for aircraft navigation and military systems, noting environmental tests
05 p0632 A72-15772
- Microwires and microstrips fabrication from high strength deformation resistant aluminum alloys
05 p0680 A72-17207
- IC microcircuit for time-pulse voltage converter for conversion of dc voltage into electric pulses of length proportional to input signal
06 p0784 A72-17836
- Multilayer thin film microcircuits and printed circuits partial capacitance and potential coefficient approximate calculation by matrix method
07 p0953 A72-19016
- High power series voltage regulators, discussing power hybrid microelectronic design techniques
08 p1112 A72-21415
- IC technology review, considering computer applications and microelectronics prospects
08 p1142 A72-21843
- Reactivity evaporated titanium nitride resistors for thin film microcircuits, discussing nitrogen gas pressure and substrate temperature effects on electrical properties during evaporation
09 p1286 A72-22902
- Low energy scanning electron beam gun with retarding field mode for microelectronic device evaluation
10 p1446 A72-23936
- Electron microbeam testing for large microcircuit arrays, using analog voltage signal injection into isolated contact and digital voltmeter readout
10 p1446 A72-23938
- Computer controlled electron beam machine for microcircuit fabrication, using digital technique capable of working on complex patterns
10 p1459 A72-23956
- Electron image projection system using converter tube technique for microcircuit lithography, discussing performance tests and design changes
10 p1447 A72-23957
- Laser welding theory and applications to microelectronics, nuclear and aerospace fields
10 p1485 A72-23968
- Homogeneous computing media, examining microelectronic fabrication, interconnection and control problems for MOSFET, bipolar transistors and IC structures
10 p1448 A72-24277

- Electron-optical system with electro- and magneto-static lenses, ensuring large image reduction for producing printed microcircuits
10 p1482 A72-24589
- Monolithic, thin film and LSI technology development trends in microelectronics, noting heteroepitaxy, ion implantation and laser beam techniques
10 p1454 A72-25175
- Radio electronic equipment IC and microelectronics development trends, considering bipolar and MOS transistors applications in digital and analog computers and telemetry
10 p1454 A72-25176
- Microwires and microstrips fabrication from high strength deformation resistant Al alloys
11 p1660 A72-26142
- Common collector micropower monolithic transmitter for single or multichannel biomedical telemetry
11 p1586 A72-26563
- Monolithic micropower command receiver to extend lifetime of implanted biotelemetry system
11 p1586 A72-26564
- Micropower IC approach based on complementary transistor-transistor logic
11 p1606 A72-26566
- Automatic electrostatic contour welding of IC microcircuit metallic casings, using contact and electrode voltage feedback signals
13 p1963 A72-28921
- Reliability tests on miniature ceramic capacitors encapsulated by epoxy-novolac block polymer compounds
13 p1919 A72-29061
- Microelectronic devices liquid cooling by free and forced convection, investigating component size effects on heat transfer by boundary layer analysis and experiment
14 p2091 A72-31172
- Active RC circuit synthesis by state model method, minimizing capacitances of admittance matrix for microelectronic circuit technology
15 p2210 A72-31595
- Soft X ray appearance potential spectrometer construction and operation for metal film diffusion detection in microcircuit technology
15 p2241 A72-32442
- Nonideal component parts effect on behavior of digital microstrip closed circuit X band phase shifter, presenting detailed network analysis
15 p2201 A72-32471
- Computer thermal analysis of hybrid microcircuits.
17 p2521 A72-34679
- Microelectronic module application to LSI set for implementation of digital filters, division and square root operations, polynomials, matrix computations, etc
17 p2522 A72-34704
- Plastic packages for complex microcircuits.
17 p2528 A72-34717
- Laser beam welding of small components
17 p2559 A72-34925
- Russian book on radio component design covering radio equipment component properties, effects of geometry and materials, technological processes and microelectronics
17 p2531 A72-35496
- X- and Ku-band microelectronic phase shifters
17 p2531 A72-35767
- Optimization of the functions of a circuit with lumped and distributed RC parameters
17 p2535 A72-35785
- Report on Flip Chip and Beam Lead bonding for electronic circuits.
[SAE AIR 1141]
18 p2666 A72-36528
- Limitations in microelectronics. II - Bipolar technology.
18 p2667 A72-36980
- Survey of current component reliability problems and methods for prevention.
18 p2668 A72-37102
- Department of Defense Reliability Analysis Center.
18 p2676 A72-37131
- Applications of holographic nondestructive testing techniques in engineering.
19 p2806 A72-37608
- Frequency-selective networks suitable for microelectronic realization. II.
19 p2773 A72-37874
- Production of prototype hybrid micro-electronic modules using thin film substrates.
20 p2908 A72-39493
- Design and manufacturing considerations in hermetic microcircuit enclosures.
20 p2908 A72-39495
- Heat transfer coefficient measurement and thermal network analysis computer program for improving performance and reliability of microelectronic package/board and chip/substrate systems
20 p2908 A72-39497
- Microelectronic component system temperature distribution measurement by IR microscale and electrical technique to determine beam-lead IC thermal performance
20 p2908 A72-39498

- The computation of dynamic equilibrium temperature distributions on substrates having a temperature-dependent thermal conductivity.
20 p2908 A72-39499
- Electronic packaging techniques in housing spaceborne computer, digital telemetry and other microelectronics for protection against severe aerospace environment
20 p2909 A72-39767
- Microelectronic component reliability prediction technique with near Wiebull method accuracy in absence of detailed sampling life test results
20 p2930 A72-39857
- Potential measurement and stabilization of an isolated target using electron beams.
21 p3087 A72-40700
- Analysis and synthesis of visual phenomena in microscopic vision - with particular reference to visual acuity.
21 p3084 A72-40748
- Microelectronics developments and limitations, considering bipolar IC, metal-dielectric-semiconductor structures and optoelectronic communication links
21 p3033 A72-40940
- High value thin-film-on-silicon resistors for hybrid applications.
22 p3160 A72-42825
- National Electronic Packaging and Production Conference, Anaheim, Calif., February 8-10, 1972 and New York, N.Y., June 13-15, 1972, Proceedings of the Technical Program.
22 p3161 A72-43171
- Fine line multilayer system packaging using hybrid thick film processing and materials
22 p3161 A72-43174
- A survey of the costs of hermetic packaging and testing microcircuits.
22 p3161 A72-43175
- Information theory application for structural complexity measure of microelectronic logic circuits for digital computers, noting elements standardization for design quality criteria
23 p3269 A72-43441
- Microstrip matching networks synthesis for microwave integrated circuits, calculating passband of configurations with lumped and distributed elements
23 p3269 A72-43445
- MICROFIBERS**
Microfibrillar superlattice with vacancy defect and point dislocation in microcrack formation and propagation in nylon 6 fibers
05 p0681 A72-16308
- Microfiber extrusion of plasticized mixtures based on titanium and silicon carbides, showing optimum extrusion rate dependent on deformation and strengthening
13 p1967 A72-30105
- Isotropic fiber coarsening in unidirectionally solidified eutectic alloys, showing effect on alloy microstructure
16 p2409 A72-33802
- Effective separation technique for small diameter whiskers.
17 p2572 A72-35662
- MICROFILMS**
Vesicular films in electron and laser beam recording suitable for computer output microfilm duplication and graphic arts
10 p1488 A72-23930
- MICROGRAPHY**
U PHOTOMICROGRAPHY
MICROHARDNESS
Inconel 718 surface integrity from various manufacturing processes, tabulating data on surface finish effects on fatigue, microhardness and metallurgical properties
[SME PAPER IQ 71-239]
01 p0076 A72-10967
- Luna 16 lunar soil sample tests, comparing friction coefficients and microhardness with terrestrial analogs
02 p0280 A72-12286
- Refractory metal oxides hot microhardness and thermal stability over wide temperature range, noting softening rate variation with temperature
02 p0244 A72-12350
- Equilibrium state and microhardness of phase diagrams in Mg-rich region of Mg-Nd-Zn system
03 p0370 A72-13185
- Steels gas-powder facing with boron carbide, testing microhardness and wear resistance
03 p0363 A72-13547
- High temperature creep of niobium alloy, obtaining creep limit, microhardness and gas analysis data
06 p0833 A72-18637
- Stainless steel saturation with Al and Cr, investigating structure, microhardness, linear expansion and contact surface seizure reduction
07 p1020 A72-20419
- Nonstoichiometric solid solutions based on ZrC and NbC, investigating microhardness variation due to differing valences of atoms in metal sublattices
08 p1188 A72-22100

Sn additions influence on Te structural characteristics relation to microhardness and current carrier mobility variations
09 p1322 A72-22204

Crystalline ceramics compressive fracture strength and microhardness tests at room temperature, suggesting microplasticity role in failure mechanisms
09 p1334 A72-22388

Cermet coating with enhanced microhardness by Ni electroplating with fine corundum particles, presenting optimum electrolytes
09 p1318 A72-22527

Temperature dependence of Ge solubility in CdSb single crystals from microstructural observations and measurements of microhardness and electrical properties
09 p1372 A72-23480

Luna 16 lunar soil sample tests, comparing friction coefficients and microhardness with terrestrial analogs
10 p1532 A72-23755

Hot-stage optical microscopes for microhardness measurements at elevated temperatures, describing techniques to determine heat resistant alloys mechanical and physical properties temperature dependence
10 p1478 A72-23827

Al and oxygen effects on commercially pure Ti microhardness and microstructure, noting interstitial and substitutional atom inclusions effects on hexagonal cell dimensions
10 p1494 A72-23831

Soviet papers on high temperature metallography techniques and equipment covering test assemblies for fatigue and microhardness measurements
11 p1654 A72-25489

Test assembly for Brinell microhardness measurements of metal and alloy surfaces under tension during vacuum heating and in protective gas media
11 p1612 A72-25490

Temperature dependence of Ni and Ni alloys and solid solutions microhardness, noting strengthening effect of Ti, Cr, Al and B additions
11 p1654 A72-25491

Cumulative damage and structural changes in friction contact areas of steel plates under cyclic pulsed loads, noting microhardness distribution and surface layers microstructure
12 p1818 A72-28191

Microhardness anisotropy of hardened and aged Be single crystal as function of purity
13 p1978 A72-29023

Steels structural and microhardness changes by pulsed laser beam induced local heat treatment, noting needleshaped grain refinement
13 p1979 A72-29482

Aluminum oxide reproducible layers plastic deformability or microhardness from molecular beam scattering distribution
16 p2430 A72-33064

Phase diagrams, microhardness and composition of sintered binary B compounds with Zr, Hf, Ta, Cr, Mo, W, Re, Fe, Ni, and Si
21 p3070 A72-41371

MICROINDENTATION
U MICROHARDNESS
MICROINSTRUMENTATION
Microaccelerometer for satellite drag measurement and compensating thrust control
06 p0892 A72-18260

Electrolyte hydrostatic pressure measurement in limited volume biological compartments by fluid filled glass micropipette used in microtransducer capacity
11 p1587 A72-26623

MICROMANOMETERS
U MANOMETERS
MICROMETEOROLIDS
NT METEOROID DUST CLOUDS
Structure and characteristics of craters and pits in Sikhote-Alin iron meteorite shower, searching for meteor and meteorite dusts and micrometeorites
01 p0125 A72-10101

Fluorinated ethylene propylene encapsulated N/P Si solar cells, investigating simulated micrometeoroid exposure effects on I-V performance in shock tube
01 p0006 A72-10381

Interplanetary medium spherical solid component model from radio meteor orbit catalog, discussing density of interplanetary dust, meteor matter and cosmic fallout on sun
02 p0282 A72-12332

Shock wave contributions from micrometeorites, meteors, meteorites and thunder to organic compounds formation in primeval atmosphere
04 p0572 A72-14760

Lunar Imbrian Basin formation, discussing micrometeorite component composition of Apollo 14 soil samples
05 p0715 A72-16160

Micrometeoroid simulation by accelerated microparticles bombardment of metal targets, discussing energy partition as function of impact velocity
09 p1409 A72-23667

Book on earth environment covering atmospheric structure, terrestrial magnetic field, solar radiation, micrometeorites, ionosphere and van Allen belts
10 p1478 A72-25173

Surface orientation reconstruction of Apollo 14 lunar rocks from microstereoscopic studies of microcraters, soil covers and glass coatings, determining micrometeoroid erosion
11 p1719 A72-25975

Lunar glass particle micrometeorite crater morphology, showing radial fracture and spallation zone relationships
13 p2036 A72-28755

Interplanetary medium spherical solid component model from radio meteor orbit catalog, discussing density of interplanetary dust, meteor matter and cosmic fallout on sun
13 p2039 A72-29216

Meteorite particle movement in earth atmosphere, discussing deceleration dependence on velocity, atmospheric density and surface evaporation reactive forces
14 p2152 A72-30493

Micrometeorite flux observed by rocket-borne electroacoustic transducers
15 p2308 A72-31931

Micrometeorite and cosmic dust flux rates for near earth orbit and interplanetary space from satellite and ground based measurements
15 p2309 A72-31955

Lunar rock abrasion and catastrophic rupture lifetimes for near earth micrometeoroid flux determination, using hypervelocity impact tests
15 p2309 A72-31956

Satellite Prospero onboard micrometeoroid detector data analysis for near earth flux
15 p2310 A72-31987

A possible mechanism for the capture of micrometeoritic particles by the earth and other planets of the solar system.
17 p2619 A72-35939

Some space instruments for the study of micrometeoroids.
17 p2558 A72-35940

Meteorite particle motion in earth atmosphere, discussing deceleration dependence on velocity, atmospheric density and surface evaporation reactive forces
19 p2864 A72-38322

Chronology of first phases of formation of solar system solid objects, meteorites and primitive lunar rocks, describing models
19 p2867 A72-38548

Utilization of the CACTUS microaccelerometer as a detector of micrometeorite impacts
22 p3181 A72-43097

MICROMETEOROLOGY
Two dimensional dynamic model numerical simulation for micro- and macrostructures of moist convective clouds, comparing to field observations
12 p1839 A72-27028

Fine structure of temperature stratification in the troposphere and stratosphere
21 p3079 A72-41799

Time dependent one dimensional numerical model of hail-bearing cumulus cloud, using microphysical process parameterization and exponential raindrop and hailstone size distributions
22 p3201 A72-42513

MICROMETEORS
U MICROMETEOROLIDS
MICROMETERS
Stellar pair scale technique for determining multiplying factor of ocular micrometer drum in universal astronomical instrument
01 p0064 A72-10197

Comparison of several methods for determining the magnitude of turn for the screw of a positional contact micrometer in an astronomical universal instrument
19 p2795 A72-37347

Investigation of the screw turn magnitude of a contact micrometer attached to the Toepfer meridian circle on the basis of observed right ascensions of stars
19 p2802 A72-37975

A program of wide scale pairs for determining the micrometer screw turn magnitude of the Pulkovo ZTL-180 wide-angle zenith telescope
19 p2802 A72-37979

MICROMILLIAMMETERS
Quadratic logarithmic converter used with linear microammeter for decibel scale noise measurements
09 p1306 A72-22344

MICROMINIATURIZATION
NT LARGE SCALE INTEGRATION
Aircraft microminiature ILS with transmitter and localizer antenna to provide pilot with bearing and glide slope information for alignment with runway
12 p1842 A72-27106

Physical phenomena limitations on MOS IC miniaturization, considering gate oxide breakdown, drain source punch through, doping fluctuations, power dissipation and metal migration
16 p2370 A72-34102

Microminiaturization, microprogramming, multiprocessing, and processing and memory module design technology of aerospace computers in different size ranges
21 p3025 A72-41113

Physical limits of semiconductor devices miniaturization for electronic computers, considering thermal energy dissipation, electrical resistance and high current density induced electromigration effects
23 p3273 A72-44332

MICROMINIATURIZED ELECTRONIC DEVICES
NT MICROMODULES
MICROMODULES
Miniature modular wideband parametric amplifier for centimeter range, using IC optimal coupled circuit with passband dependent on diode time constant
07 p0956 A72-19570

Miniature modular wideband parametric amplifier for centimeter range, using Q optimal coupled circuit with passband dependent on diode time constant
22 p3158 A72-42088

Thermal design of hybrid modules and assemblies.
22 p3161 A72-43172

MICROORGANISMS
NT AEROBES
NT AMOEBA
NT ANAEROBES
NT BACILLUS
NT BACTERIA
NT BACTERIOPHAGES
NT CLOSTRIDIUM BOTULINUM
NT ESCHERICHIA
NT FLAGELLATA
NT HYDROGENOMONAS
NT PROTOZOA
NT PSEUDOMONAS
NT PSYCHROPHILES
NT SPORES
NT VIRUSES
Papars on planetary quarantine covering microbial survival in deep space, contamination by nonsterile flight hardware and sterilization
01 p0019 A72-10817

Planetary quarantine microbial contamination control, considering clean room concept and microbiological barrier techniques
01 p0019 A72-10821

Microbial survivability in deep space environmental simulation experiments, describing aerospace ecology and panspermia avoidance
01 p0019 A72-10823

Inorganic polyphosphates effect on phosphorus metabolism evolution in primary living organisms, noting polyphosphate glucokinase distribution in various microorganisms
04 p0470 A72-14797

Microorganism life in extreme high temperature, PH and solute concentration environments, noting salt effect on enzyme activity
04 p0471 A72-14801

Monograph on Jurassic and Cretaceous Hagias-tridae from Blake-Bahama Basin and Great Valley Sequence in California
04 p0519 A72-15255

Paleomicrobiological analysis of northwest Scotland Stoer Formation black shale pre-Paleozoic spheroidal unicellular fossils as probable form of marine phytoplankton
05 p0655 A72-16042

Protein-rich food substitute from microalgae cultures for human nutrition, describing experimental production, protein value determination, special diets and food shortage relief
06 p0768 A72-18159

Temperature effects on microorganism survival in deep space vacuum, using molecular sink test
09 p1265 A72-22641

Microorganisms effects on oxygen and compounds cycles, leading to changes in oxygen distribution in earth crust, hydrosphere, atmosphere and biomass
09 p1267 A72-23592

Hermetic chamber medico-engineering experiment for long term isolation effects on human intestinal microflora, showing reduction and disappearance of certain microbe populations
13 p1904 A72-29323

Environmental chamber simulation to show terrestrial microorganisms survival under Jovian atmospheric conditions
15 p2183 A72-31293

Effects of magnetic fields on microorganisms
17 p2503 A72-35004

A re-evaluation of material effects on microbial release from solids.
23 p3253 A72-43383

Effects of aeolian erosion on microbial release from solids.
23 p3253 A72-43384

Microflora accumulation prevention methods during spacecraft flight, noting bacterial filters for air purification and wiping with disinfectants for surface contamination reduction
24 p3376 A72-45213

MICROPARTICLES

- Analysis methods for microsize atmospheric aerosols and particulate contaminants from natural and industrial sources, discussing electron microscopy, electron probes, X-ray diffraction, etc [AIAA PAPER 71-1104] 01 p0067 A72-10550
- Micrometer particle formation by water vapor photolysis at 1500-1700 Å, noting particle production rate and implications to planetary atmosphere physics 02 p0220 A72-12207
- Fine oxide particle inclusions in mild steel weld metal deposited by carbon dioxide shielded metal arc process, using electron microscopy and diffraction pattern photography 06 p0820 A72-17706
- Enzymically synthesized homopolynucleotide and lysine-rich proteinoid microparticles effect on aminoacyl adenylate condensation as basis for genetic code origin 06 p0770 A72-17724
- Nonrelativistic quantum concept of electromagnetic field interaction with charged microparticles 11 p1692 A72-26093
- Dispersed particle shape effect on elastic behavior of magnesium oxide composites at low graphite concentrations 15 p2260 A72-31585
- Profile and depth of microcraters formed in glass. 18 p2736 A72-36972
- A method for the study of wear particles in lubricating oil. 19 p2803 A72-38376
- Craters formed in mineral dust by hypervelocity microparticles. 20 p2970 A72-39474
- Generalized integral equations of radiative heat exchange. 23 p3357 A72-44536
- MICROPHONES**
- Acoustic radiation pressure of small radius spherical obstacle in high level harmonic plane field for application to microphone calibration [ONERA, TP NO. 1008] 05 p0661 A72-16023
- Condenser microphones sensitivity and frequency response characteristics measurement at normal and elevated atmospheric pressures in hyperbaric chamber air and He-air environments 06 p0766 A72-17808
- Space-averaged sound pressure measurement by sequentially sampled microphone arrays, considering scanning rate and rms detector time constants effect 13 p1958 A72-29565
- A new approach to the measurement of very low acoustic noise levels. 20 p2953 A72-39554
- MICROPHOTOMETERS**
- U PHOTOMETERS**
- MICROPLASMAS**
- Zener diode surface and bulk breakdown mechanisms by scanning electron microscopy, discussing microplasma noise 03 p0336 A72-14289
- Ar-H microplasma welding of thin Cr steel sheets with narrow seams for aircraft engines and precision equipment casings 09 p1318 A72-22548
- Pulsed microplasma and intermediate current plasma welding of AL, comparing with tungsten arc and electron beam welding 09 p1320 A72-23628
- Prototype fine wire feed unit and microplasma welding torch and equipment for butt welding of Ni maraging steel, testing welds mechanically 09 p1321 A72-23636
- Far UV radiating hot dense microplasma production by laser heating for measuring by resonant absorption small quantities of gaseous element 21 p3093 A72-41341
- MICROPOLAR FLUIDS**
- Certain motions of micropolar fluids 17 p2538 A72-34771
- MICROPOROSITY**
- Neutron irradiation effect on submicroporosity formation and redistribution in structural graphite 09 p1340 A72-23482
- High temperature microporosity in W wire at 3000-3350 °C, using electron microscopy and fractography 13 p1973 A72-28651
- Micropores pinning effect on grain boundaries mobility during drawn tungsten wire recrystallization, determining pores induced repulsive force 15 p2257 A72-32116
- MICROPROGRAMMING**
- Modular avionic computer design concept to permit tailoring for diverse applications via microprogramming 17 p2524 A72-35581
- Microminiaturization, microprogramming, multiprocessing, and processing and memory module design technology of aerospace computers in different size ranges 21 p3025 A72-41113
- MICROPULSATIONS**
- NT GEOMAGNETIC MICROPULSATIONS**

Microscale MHD wave and stationary structure fluctuations in interplanetary medium solar wind, considering theoretical constraints 01 p0129 A72-10883

Periodic micropulsations in amplitude and bandwidth observed in long duration vlf whistler mode signals from ground stations, considering explanations 03 p0322 A72-13530

Geomagnetic micropulsation activity relationship to magnetospheric processes and interplanetary magnetic field, investigating time dependence of telluric current 04 p0515 A72-14927

High latitude ionospheric transmission and reflection properties for oblique hydromagnetic plane waves at micropulsation frequencies for daytime and nighttime conditions 13 p1951 A72-29390

Diurnal variations of micropulsation activity polarization parameters in horizontal plane, describing experimental technique 15 p2230 A72-32258

MICROCKET ENGINES

Ten mlb concentric tubes biowaste resistojet thrust performance for hydrogen, water, methane, carbon dioxide and biopropellant mixtures, discussing vibration, shock and acceleration tests [SAE PAPER 710769] 01 p0116 A72-10263

Two constituent gaseous propellant micropropulsion engines for satellite orbit correction and attitude control, discussing thermodynamic and reaction kinetics problems [DGLR PAPER 71-102] 02 p0271 A72-12711

Pulsed electric microthruster with solid fuel feed system, noting electrode geometry effects on performance and ablation patterns [AIAA PAPER 72-210] 05 p0705 A72-16799

Test facility for electric microthrusters, describing microbalance for thrust and propellant mass flow rate measurement 09 p1292 A72-23404

Parallel rail solid fuel pulsed electric microthruster performance, noting mathematical model for mass ablation and plasma acceleration mechanism [AIAA PAPER 72-458] 11 p1708 A72-26194

Solid propellant pulsed plasma microthruster performance tests, describing engine design and operation [AIAA PAPER 72-460] 13 p2026 A72-28945

Light scattering by the medium created by a spacecraft. I - Luminescence of the gas jets of the spacecraft microthrusters 22 p3230 A72-42216

MICROSCALES

U MICROBALANCES

MICROSCOPES

NT ELECTRON MICROSCOPES

NT ION MICROSCOPES

NT OPTICAL MICROSCOPES

Symmetrical three component pancreatic system with intermediate constant image plane and linear displacement of components 03 p0360 A72-13562

Automated microdynamometer for thin plastic specimens microtension tests with continuous microscopic observation and automatic diagram plotting 11 p1633 A72-26288

The effect exerted on pictorial-analytical measurements at the television microscope by subjective contrast enhancement with color filters 21 p3055 A72-40749

MICROSCOPY

Holography applications and processes, discussing holographic microscopy, particle analysis, high speed photography, data storage and retrieval, interferometry, nondestructive testing, etc 07 p0989 A72-20221

TV microscopic system for on-line measurement of cat omentum microvessels diameter relative to heart action 11 p1587 A72-26621

Investigation of the structural content and the determination of the optimal image of focus series in light and electron microscopy with the aid of Fraunhofer diffraction/structure spectroscopy/ 21 p3055 A72-40747

Analysis and synthesis of visual phenomena in microscopic vision - with particular reference to visual acuity. 21 p3084 A72-40748

MICROSEISMS

Continuous natural background sources of microseismic motions due to atmospheric and ocean loading, wind, flowing water and local disturbances [AIAA PAPER 72-819] 20 p2915 A72-39104

Stable microprecision test platforms construction and microseismic effects on motion sensing instrument calibration including gyroscopes and inertial navigation and guidance systems [AIAA PAPER 72-893] 20 p2911 A72-39110

The theory of motion of the horizontal pendulum with a Zoellner suspension and some indications for the instrumental design. 21 p3084 A72-40495

MICROSONICS

Telecommunications ultrasonic resonators, electromechanical and piezoelectric filters and microacoustic surface elastic wave devices 09 p1281 A72-23468

MICROSTRUCTURE

NT METEORITIC MICROSTRUCTURES

NT WIDMANSTATTEN STRUCTURE

Saint Venant problem solutions of cylindrical beam in linear theory of micropolar elasticity in terms of three functions 01 p0137 A72-10318

Electrochemical potential microstructure and stress intensity factor effect on aqueous stress corrosion crack propagation rate in high strength Ti alloy 01 p0085 A72-10776

Ni maraging steel microstructure effects on strength and fracture toughness 01 p0087 A72-11024

Beryllium microstructure and hexagonal close packed polycrystal material residual thermal stresses, calculating thermal expansion coefficients 01 p0087 A72-11028

Precipitation hardened Al-Cu alloy microstructure relation to fatigue and tensile properties, emphasizing particle size and distribution, moving dislocations and grain boundary effects 01 p0088 A72-11044

Ni base superalloy powder with refractory oxide particle dispersion, presenting high temperature creep, stress rupture, microstructure activation energy and processing history 02 p0240 A72-11442

Composition, microstructure and mechanical properties of binder metal in cobalt bonded tungsten carbide 02 p0241 A72-11451

Microstructure of prealloyed and premixed specimens of sintered steel 02 p0242 A72-11463

Continuum mechanics models of microscopically inhomogeneous elastic medium with microstructure, using moment theory 02 p0288 A72-11608

Hardened steel inhibited crack propagation mechanism, observing striation in microstructure on fracture surface 02 p0243 A72-12212

Inhomogeneous microstructure elastoplastic medium, examining strain and work in plastic deformation 02 p0293 A72-12427

Microstructure and mechanical properties of iron base superalloys, examining precipitation hardening by gamma prime and secondary intermetallic compounds formation 02 p0245 A72-12505

Wrought superalloys microstructure and mechanical properties control by precipitating phases 02 p0245 A72-12506

High strength low alloy type ferrite pearlite steel microstructural and compositional variations effect on work hardening, ductility and impact toughness 02 p0246 A72-12558

Equilibrium state and microhardness of phase diagrams in Mg-rich region of Mg-Nd-Zn system 03 p0370 A72-13185

Solid materials inelastic constitutive relations, developing internal variable thermodynamic formalism for microstructural rearrangements 03 p0446 A72-13710

Heat treated microstructures relation to equilibrium diagram in beta and alpha Ti alloys 03 p0374 A72-13715

Ta-Co system phase diagram from differential thermal, X ray, and microstructural analyses, determining composition, temperature, structural type and lattice constant 03 p0374 A72-13740

Tempered Fe-Cr-C-Co steels microstructural and mechanical properties, investigating martensite and bainite 03 p0375 A72-13929

Tungsten wire deformation structure from swaging or rolling and drawing processes, noting cylindrical texture superimposed on fiber texture 03 p0375 A72-13933

Fibrous structure of precipitates produced at bottom of trace due to friction in work hardened Al-Cu alloy solid solution 03 p0376 A72-13970

Structural features of heat resistant Ni-Cr alloy from electron diffraction microscopy, observing coherent lattice bond and plastic deformation 03 p0376 A72-14015

Substructure of cast alloys based on Al-Mg system from electron diffraction microscopy 03 p0377 A72-14023

Phosphorus-containing austenitic stainless steel, investigating quenching defects and precipitation from microstructure by transmission electron microscopy 03 p0379 A72-14260

X ray spectral analysis of microchemical changes in surface films of titanium alloys during diffusive interaction with silicon carbide abrasive 04 p0534 A72-15654

Titanium alloy microstructure effect on fatigue strength under symmetric bending load cycles in air and NaCl solution 04 p0535 A72-15663

Mechanical properties of heat treated hardened high strength steel, investigating microstructure relationship to breakdown characteristics 05 p0671 A72-15992

Holocene Bahamian oolites examination by scanning electron and light microscopy, observing aragonite crystals morphology, orientation and modification by boring activities of endolithic algae 05 p0654 A72-16037

Impact breccias in carbonate rocks of Sierra Madera /Texas/, investigating microstructure, chemical composition, petrography and mineralogy 05 p0654 A72-16038

Ni-based metal graphite materials, investigating sintering process control variables effects on structure and phase composition responses 05 p0665 A72-16090

Dissolved oxygen effect on structure and toughness of nonalloyed extramild steels, observing austenite recrystallization kinetics retardation after hot plastic deformation 05 p0672 A72-16143

Mechanical and microstructural properties of Be-base alloys consolidated by vacuum arc melting, reporting results of tensile tests, hardness measurements and microprobe analysis 05 p0674 A72-16389

Ti alloys evaluation technique of arc melting, processing and testing of miniature ingots, discussing alloying and microstructural effects and correlation with plate properties 05 p0674 A72-16390

Superalloys for gas turbine rotor and stator blades, testing long term heating effects on microstructure and mechanical and thermal fatigue properties 05 p0675 A72-16495

Large deflection microstructure continuum model for composite beam flexural wave propagation and free vibration, deriving equations of motion [AIAA PAPER 72-140] 05 p0741 A72-16937

Directionally solidified Al-AlNi intermetallic eutectic alloy microstructural characteristics and effects on creep fracture 05 p0678 A72-17115

Critique of microstructure effect on strength, toughness and stress corrosion cracking susceptibility of metastable beta titanium alloy, discussing recrystallization conditions 05 p0679 A72-17122

Impurities effect on microstructure alignment in unidirectionally solidified Al-AlNi eutectic intermetallic, noting fiberless region defects 05 p0679 A72-17123

Ductile fracture development in steel due to microcracks and pores formation 05 p0679 A72-17205

Prolonged heatings effect on heat resistant magnesium alloy microstructure and mechanical properties 05 p0680 A72-17208

Ti-Zr-O ternary alloys radiocrystallographic analysis, relating microstructure to composition and thermal treatment 06 p0827 A72-17569

Fe-Co alloy athermal transformation to bcc martensite at industrial cooling rates, investigating effects on mechanical properties 06 p0829 A72-17830

Incompressible micropolar fluid flow equations, deducing stable periodic solutions existence by energy method 06 p0799 A72-17917

Electron transmission microscope study of quenched Mo-N alloys supersaturated solid solution low temperature aging behavior, investigating recovery processes 06 p0830 A72-18056

Texture, mineralogy and metamorphic history of lunar anorthosite 15415 06 p0889 A72-18272

Internal friction and plastic microstrains in martensitic transformation of Fe-Ni, Co-Ni, and Fe-Cr-Ni alloys 06 p0830 A72-18294

Microstructure properties of heat resistant alloy for gas turbine blades as function of operational time 06 p0832 A72-18360

Thermocycling treatment influence on structural changes and strength in coarse grain Ni under creep tests 06 p0834 A72-18686

Aging kinetics in Co-Ni-Ti alloys, noting three dimensional periodically modulated structure development 06 p0834 A72-18742

Structural changes, mechanical properties, electrical resistance and lattice constant during aging of Al alloys containing Mg, Li and Mn 06 p0834 A72-18743

X ray study of structural changes in Ni single crystals during recrystallization process after uniaxial deformation under compression loads with high loading rates 06 p0834 A72-18744

Microstructural changes and mechanical properties of deformed Nb alloy during annealing process, observing low temperature plasticity increase 06 p0835 A72-18747

Rutile creep resistant substructure recovery at 1000-1040 C, discussing stress relaxation mechanism due to dislocation walls or subgrain boundaries migration 07 p1023 A72-18800

Scanning electron microscope for metal matrix composite materials structure examination, emphasizing matrix behavior, filament under load and interface 07 p1011 A72-19485

Austenitizing conditions effects on hardness and microstructure of tempered steel, emphasizing martensite structure and grain size changes produced by controlled heat treatment 07 p0995 A72-19486

Oxygen effect on structure and mechanical, technological and corrosive properties of stainless steel melted in open and vacuum furnaces 07 p1013 A72-19739

Gas saturation of Ti alloy in air and vacuum at 750-1050 C for 1-6 hr, discussing surface layer microstructure change after heat treatment 07 p1013 A72-19742

Phase and microstructure changes during nitriding process of Fe-Ti alloys, stressing Ti concentration effect 07 p1013 A72-19749

Cast and wrought Ti alloys Ar arc weldments microstructural and mechanical properties after different heat treatment sequences 07 p1013 A72-19750

Strength differential effect on microstructures of steels, using tensile and compressive stress-strain curves 07 p1015 A72-19927

Mechanical strength and microstructural characterization of sapphire ribbons and continuous filaments for composite materials 07 p1023 A72-19929

Hf addition effects on grain boundary structure of cast Ni-base superalloys 07 p1015 A72-19931

Environmental hydrogen embrittlement of Ti-Al alloy as function of test displacement rate and microstructure variation 07 p1016 A72-19933

Microstructure and high temperature mechanical properties of unidirectionally solidified pseudobinary Fe-Cr-Nb eutectic alloy 07 p1016 A72-19938

Plasma spraying process effects on carbon steel coatings structure and bonding, considering optimal parameters, properties control and phase transformations 07 p0996 A72-19966

Hf-Co-Al system phase equilibria determination by partial microstructural and X ray analysis 07 p1017 A72-19991

Vacuum hot press diffusion welding of nickel-chromium-thorium dioxide sheet, describing specimen preparation, welding procedure and welded joints photomicrographic microstructure 07 p0997 A72-20002

Time independent incompressible micropolar fluid flow existence 07 p0970 A72-20082

Thermoelastic characteristics and crystal phase distribution effect on microstructural stresses and thermal expansion of polycrystalline refractory materials 07 p1018 A72-20133

Nb and Nb alloys mechanical properties during plastic deformation and heat treatment, discussing grain size, dislocation structure and substructural changes effects 07 p1018 A72-20144

Nb-Ga system equilibrium phase diagram determination by differential thermal, tempering microstructural and X ray analysis techniques, discussing various compounds formation temperatures and characteristics 07 p1050 A72-20161

Rapidly and unidirectionally solidified Al alloys microstructure, discussing crystal dislocation origins and patterns 07 p1019 A72-20240

Heat treatment effect on elastic properties of steel clad material for devices in sulfuric acid, discussing structural changes and optimal conditions 07 p1020 A72-20415

Fe addition effects on structural and mechanical properties of heat resistant Ni-Cr alloys 07 p1020 A72-20416

Diffusion creep influence on grain boundary-adjacent precipitate free zone formation in Ni-Cr alloys subjected to high temperature tensile and creep tests 07 p1021 A72-20437

Internal oxidation behavior of Cu-Cr-Si ternary alloys microstructure comparison with Cu-Si binary alloys, discussing oxide-matrix interface nucleation 07 p1021 A72-20439

Austeno-martensitic steel with 25 percent delta ferrite, examining microstructural changes due to aging at 550 C by thin slide electron microscopy 07 p1021 A72-20484

Circular elastoplastic beam under combined torsion and tension via Mindlin elastic model for materials with microstructure, taking into account work hardening 07 p1097 A72-20534

Cast Nb-C alloys carbon solubilities of 1.4 and 0.25 percent at 2100 and 1200 C, showing molten microstructure and measuring procedures 07 p1023 A72-20669

Metal structure effect on anodic dissolution and surface microgeometry formation during electrochemical machining 08 p1175 A72-21040

X ray study of /Y-La-Ce/-Al-Si-B ternary systems structure at 500 C, noting binary compound presence 08 p1217 A72-21713

Precipitation effect on microstructure, coercive force, resistivity and cell formation changes in heterogeneous decomposition of supersaturated solid solutions and aging alloys 08 p1218 A72-21777

Explosive loading effect on Cr-Ni stainless steel structure with electron microscope study of gamma, alpha and epsilon phases 08 p1187 A72-21780

Ni-Cr-Nb alloys structure and phase composition changes from W-Mo additions and hardening by intermetallic Ni-Nb precipitated from supersaturated solid solution 08 p1187 A72-21782

Impurities and temperature effects on microdeformation of Mo single crystals under dynamic loads 08 p1188 A72-21789

Structural changes of nitrated steel diffusion zone, showing alpha solid solution and hard nitride phases mixture 08 p1188 A72-21880

Electron microscopy application to dynamic wear studies of Ni on Ni surface and subsurface topography and microstructure in nitrogen atmosphere 08 p1179 A72-21943

Ti-alloyed SiC based material microstructure investigation by X ray metallography, optical and electron microscopy 08 p1188 A72-22099

High temperature alloy deformation superplasticity and formability relation with microstructure, fine structure and load requirements for hot working with high strain rate 08 p1250 A72-22200

Oxide scale formation on zirconium diboride materials, observing microstructural features as function of temperature and reaction time [AD-737020] 09 p1333 A72-22380

Alumina microstructure, grain size and impurities effects on ballistic performance, discussing results in terms of microplasticity 09 p1334 A72-22390

Fractography of high boron ceramics under ballistic impact, suggesting macroscopic and microscopic textures relationship to stress states and microstructure 09 p1334 A72-22391

Ceramic materials stress-strain behavior dependence on microstructural factors, discussing point defects, pore size and grain boundaries 09 p1334 A72-22392

Sintered cadmium sulfide films microstructure analyzed by X rays, discussing structural changes effects on dark resistance and photosensitivity 09 p1366 A72-22414

Thermomechanical treatment effects on microstructure and mechanical properties of Al alloy 09 p1327 A72-22470

X ray method characteristics in thermal interphase microstresses determination, considering spherical silicon inclusion surrounded by concentric Al matrix envelope 09 p1309 A72-22638

Mathematical thermodynamic theory for plastic deformation induced internal structure changes in rheological material, describing homogeneous response by temperature and deformation gradients 09 p1403 A72-22761

Pinning force of vortex lines and microstructural inhomogeneities in superconductors, using magnetization and critical current measurements 09 p1369 A72-22796

Explosive strain hardening of hard metal-ceramic alloy, presenting photographs of carbide and cobalt phases structural changes after impact loading 09 p1337 A72-22892

Transmission electron microscope investigation of Al-Mg-Si alloy precipitation, showing Guinier-Preston zone visibility due to matrix elastic strain introduction 09 p1328 A72-22983

Extruded dispersion strengthened Mg-MgO alloys microstructure, discussing high temperature creep effect on dislocation structure changes 09 p1328 A72-22984

Microstructural transformations in preaged Ti alloys with unstable beta phase under external tensile stresses

09 p1328 A72-23032

Anomalous structural dependence of elastic limit in Mo, determining mechanisms responsible for deviations from Peck law

09 p1329 A72-23037

Crack propagation and substructure formation near fatigue crack in austenitic stainless steel observed by X ray diffraction and replica electron microscopy

09 p1329 A72-23148

Ni carbon steel microstructure changes in retained austenite phase and crack observation during low cycle fatigue testing

09 p1330 A72-23150

Aligned fibrous composites microstructural parameters, showing fiber thickness effect on fracture, fabrication, matrix cracking, creep resistance and fatigue

09 p1338 A72-23163

Plastic deformation effect on structure and properties of steel sheet under biaxial tension at liquid nitrogen temperature

09 p1330 A72-23187

Microstructure and mechanical behavior of unidirectionally solidified magnesium-magnesium nickel eutectic composite over range of solidification rates

09 p1330 A72-23376

Beta-III Ti alloy mechanical properties dependence on heat treatment and elevated temperature exposure, illustrating associated microstructures

09 p1331 A72-23384

Linear theory of elasticity application to wave propagation in homogeneous isotropic material with deformable microstructure, presenting approximate solution method

09 p1353 A72-23552

Photomicroscopy of sintered refractory alloys and nonmetals of B-Si-C-N system, discussing microstructural interactions between binder metal and refractory component

10 p1493 A72-23824

Electron microscopic, area diffraction and spectral analyses of carbide precipitates in Cr-Mo steels with different heat treatments and microstructures

10 p1494 A72-23828

Electron microscopic study of cyclically deformed Al, Cu, Al-Mg-Zn alloy and carbon steel dislocation structure

10 p1494 A72-23830

Al and oxygen effects on commercially pure Ti microhardness and microstructure, noting interstitial and substitutional atom inclusions effects on hexagonal cell dimensions

10 p1494 A72-23831

Magnetic susceptibility of ternary Al-Mn alloys with Ti, V, Cr, Fe, Co, Ni, Cu and Zn, describing microstructure and aging experiments

10 p1494 A72-23832

Fe-Ni-C alloy mixed austeno-martensitic microstructure embrittlement, investigating mechanical properties after thermomechanical treatment

10 p1495 A72-24087

Micrographic observation of Al and Al-Cu intermetallic dendrites shape at birth in liquid of nearly eutectic composition

10 p1496 A72-24239

Transmission electron microscope examination of deformation microstructures adjacent to fatigue cracks in Al alloys

10 p1497 A72-24823

Low temperature resistant stainless steels mechanical properties, microstructure and weldability, discussing compositions and heat treatments

10 p1498 A72-24838

Fracture energy and deformation of unidirectionally and randomly oriented lamellar Al-Cu eutectics from surface microstructure studies

10 p1499 A72-24893

Filler metal paste application effect on Hastelloy sheet brazing quality, describing results in terms of mechanical properties and microstructural characteristics

11 p1637 A72-25342

Acoustic emission monitoring of postweld heat treatment cracking in Rene 41 weldments, correlating relative crack susceptibility of different microstructures

11 p1653 A72-25345

Test assembly design for microstructural studies of metal and alloy fatigue in vacuum during heating, describing electrical resistance measurement and stroboscopic illumination

11 p1612 A72-25492

Ni and Ni alloys microstructure under tensile stress, determining Cr and Ti effects on plastic deformation at high temperature

11 p1654 A72-25494

High temperature metallographic methods in microstructure study of austenitic heat resistant steel under plastic deformation and heat treatment

11 p1654 A72-25495

Fe-Cr-Mn alloys structural changes during high temperature oxidation, noting subscale layer thickening and alpha phase detection after heat treatment

11 p1655 A72-25498

Microsegregation in Ti-Mo, Ti-V and commercial Ti alloys, investigating cooling rate and alloying elements contents effects

11 p1655 A72-25506

Al microsegregation in Ti-Al and commercial Ti alloys, investigating effects of cooling rate from beta phase and of Al content

11 p1655 A72-25507

Transitional microstructure of machined surface layer due to built-up edge disintegration

11 p1638 A72-25508

Hardened steel inhibited crack propagation mechanism, observing striation in microstructure on fracture surface

11 p1656 A72-25710

Cold rolled Zircaloy 2 sheet microstructure, microstrains and hardness by X ray diffraction and electron microscopy

11 p1657 A72-25757

Transitional ferrite phase formation in Fe-Cr-Ni alloy evidenced on electron micrographs and diffraction patterns

11 p1657 A72-25760

Ductile fracture development in steel due to microcracks and pores formation

11 p1660 A72-26140

Prolonged heating effect on heat resistant Mg alloys microstructure and mechanical properties

11 p1660 A72-26143

Microstructure and mechanical properties of heat treated friction welds at high temperatures

11 p1641 A72-26489

Supergranular motions source of Alfvén waves dominating solar wind microstructure at earth orbit

11 p1724 A72-26530

Low carbon ultrafine grain steel tensile behavior, noting critical grain size for stable/unstable plastic flow transition

11 p1661 A72-26651

Ti alloys fatigue strength, stress concentration sensitivity and grain sizes effects at normal and high temperature under cyclic loads

11 p1663 A72-26821

Ultrasonic oscillations effects on alloy castings grain size and heat resistance, suggesting waveguide direction for oriented solidification

11 p1642 A72-26822

Chemical composition, physical properties, microstructure and production of 1300 kg powder metallurgy forged billets

11 p1644 A72-26845

Microstructure and mechanical properties of dispersion strengthened Co alloys, investigating heat treatment effects

11 p1664 A72-26851

Microstructural properties of Ni-Al powder synthetic material from transmission and photoemission electron microscopy, discussing low and high temperature strength characteristics

11 p1645 A72-26855

Fog and cloud microstructure and density distributions from directional light scattering coefficient /halo indicatrix/

11 p1683 A72-26883

Electron microscopy and structure of materials - Conference, University of California, Berkeley, September 1971

11 p1666 A72-26926

Zone refined prism slip oriented Be single crystals deformation substructure analysis by synergetic method combining transmission electron microscopy, X ray topography and X ray diffraction profile analysis

11 p1666 A72-26928

Coherent phases transformations in alloys, investigating mechanical properties dependence on microstructural features

11 p1667 A72-26929

High temperature Ni base alloys microstructure via transmission electron microscopy and electron diffraction contrast theory, predicting yield and creep strength

11 p1667 A72-26931

Mechanical properties, microstructural characteristics and fracture behavior of beta Ti-V-Cr-Al alloy

11 p1667 A72-26933

Low cycle fatigue deformation of lamellar eutectic and cast Ni-Sr alloys, noting microstructure and chemical composition effects on fracture energy

11 p1668 A72-26939

Fracture micromechanism in liquid-phase sintered W-Fe-Ni powder composites, using scanning electron microscopy

11 p1668 A72-26942

Microstructural effects on high strength Mg, Al and Ti alloys stress corrosion crack growth in aqueous environments, discussing correlations relative to composition and preferred orientation

11 p1668 A72-26946

Dislocation bands in electrolytically hydrogen charged fcc Ni-Co alloy, describing band structure in terms of band axis and planes and Burgers vector

11 p1669 A72-26947

Mica glass ceramics mechanical properties and thermal shock behavior in terms of microstructural variables, discussing fracture propagation and secondary cracks formation

11 p1675 A72-26949

Shock deformation microstructures in Apollo 14 breccia and comparative terrestrial minerals, using transmission electron microscopy

11 p1724 A72-26951

Lunar and terrestrial pyroxenes phase structure electron microscopic investigation, using ion-thinned samples

11 p1725 A72-26952

Aitken condensation nuclei clouds microstructure and area contamination profiles, discussing small sources pollution and plumes polyfurcation [AIAA PAPER 71-1125]

11 p1628 A72-26989

Epitaxial and textured Pb films on mica and glass, using reflection electron diffraction, etching and optical microscopy for structure study

12 p1854 A72-27289

Nitride phase microstructure in ferrochromium nitrided in liquid state, comparing electrolytic etching and film coloration methods

12 p1829 A72-27454

Micromechanics of deformed continua, discussing atomic structure effects on stress concentrations in composite materials, framed structures and grids

12 p1884 A72-27640

Isothermal profiles for Nb-Zr-C and Nb-Ti-C alloys from microstructural and X ray analyses, noting Widmanstatten structure, and second phase formation

12 p1829 A72-27643

Al alloy plate material microstructural variations and specimen orientation effects on tensile and fracture toughness properties

12 p1830 A72-28080

Oxide content and sheet microstructure directionality effects on Be powder and ingot sheets notch strength, noting thickness dependence [ASM PAPER W 72-12.6]

12 p1830 A72-28164

Haynes high strength heat resistant Ni-Cr-W alloy metallurgical and structural relationship, mechanical and physical properties, oxidation and corrosion behavior and fabrication processes

13 p1973 A72-28649

Ultrafine grained microstructures and mechanical properties of alloy steels developed by cold working followed by annealing

13 p1974 A72-28662

Tempered or recrystallized chromium steels tensile behavior at 0 to 700 C, showing strength dependence on martensite transformation induced dislocation structure

13 p1975 A72-28667

Polycrystalline microstructure changes of corundum during high temperature creep tests, using optical microscopy

13 p1983 A72-28775

Hardened coarse-grained steels recrystallization during fast heating, investigating martensite phase macro- and microstructural changes by X ray analysis

13 p1977 A72-28908

Plane longitudinal displacement wave reflection from fixed surface in micropolar elastic half space, presenting reflection laws and amplitude ratios for specific cases

13 p2056 A72-29001

Microscopic substructure in high temperature fatigued fcc austenitic steel and aluminum, studying cross slip lines and crack initiation

13 p1979 A72-29448

Steels structural and microhardness changes by pulsed laser beam induced local heat treatment, noting needleshaped grain refinement

13 p1979 A72-29482

Phase composition, structure and strength properties of aluminizing coatings on Ni-Al alloys, noting plasticity increase due to Ta addition

13 p1980 A72-29485

Stress wave propagation and fracture in composites, discussing micromechanical and homogeneous-continuum theories

13 p2060 A72-29692

Directionally reinforced composites treated as homogeneous continuum with microstructure, deriving displacement equations of motion by Hamilton principle

13 p2060 A72-29694

Interacting continua theory for stress wave propagation in composites with microstructural stress and displacement fields, discussing elastic and viscoelastic materials behavior

13 p2060 A72-29695

High strength carbon fiber reinforced plastics, discussing fabrication techniques, fiber structural, physical and mechanical properties and potential technological applications

13 p1984 A72-30075

- Microstructure and mechanical properties of molecular cermets produced from slip-cast fused silica of different porosity by aluminothermal reduction method 13 p1967 A72-30115
- Ti-Mo-Ni system polythermal section microstructure, hardness, resistivity and thermal expansion characteristics 14 p2112 A72-30153
- Ni, Si and Mn alloying effect on structural transformations, phase composition and mechanical properties of cast Cr-Ni steels 14 p2114 A72-30273
- Microstructure effects on thermomechanically processed dispersion strengthened Ni alloys yield strength at various temperatures 14 p2114 A72-30368
- Al-Cu alloy structural changes after long term natural aging by X ray diffraction analysis 14 p2115 A72-30413
- Microstructural changes relationship to corrosion susceptibility in ternary Al alloy obtained from stress corrosion cracking tests and electron metallography, noting precipitate-free region 14 p2118 A72-30542
- Primary recrystallization in TD-nickel bars on sublight optical level identified by transmission electron microscopy examination of deformation and annealing substructures 14 p2119 A72-30601
- Macroparametric, microstructural and general rationales methods for fatigue resistant materials, noting crack propagation and fracture mechanics 14 p2120 A72-30612
- Modified Al-Si eutectic solidification behavior and microstructure, investigating LF mechanical vibration effects 14 p2120 A72-30617
- W-Nb-C system phase diagram from X ray and microstructural analyses, noting solid solubility, hardness and isothermal cross section 14 p2122 A72-30983
- Mo-W-C system high temperature phase equilibria from X ray and microstructural analysis, noting decrease of C solid solubility with temperature 14 p2123 A72-30984
- Mo-Ni-Al system phase equilibria at 600 C from X ray and microstructural analysis, noting hardness dependence on composition 14 p2123 A72-30985
- Nickel-trinickel alumide-trinickel niobumide system polythermal cross sections from X ray and microstructural analysis, noting electrical resistivity increase with Al content 14 p2123 A72-30988
- Laminated plate continuum theory with microstructure, studying one dimensional harmonic wave propagation in infinite laminate 14 p2169 A72-31147
- Electron microscope study of precipitated lines of austenitic steel containing V and N, noting heat treatment effect on fcc crystal structure 15 p2254 A72-31523
- Carbon distribution effect on cast Mo and alloys structure studied by electron microscopy, microdiffraction and X ray analysis, noting annealing from eutectic temperature 15 p2255 A72-31575
- Polycrystalline Mo-Re alloy under cold longitudinal, transverse, cross and pack rolling, noting twin and dislocation microstructures 15 p2256 A72-31669
- Electron microscopic investigation of Al-Mn alloy precipitate structure and morphology after annealing induced decomposition 15 p2257 A72-32114
- Dynamic boundary value problems for elastic materials with microstructure reduction to tensor equations of motion subject to initial and boundary conditions 15 p2329 A72-32283
- Nonlinear anisotropic elastic constitutive equations for micromorphic and micropolar mixtures, investigating plane wave propagation via field equations with restricted coupling 15 p2278 A72-32446
- Strain release method for investigating thermally activated microflow mechanisms in solids, discussing technique for activation energy and relaxation strength measurements 16 p2372 A72-32822
- Nitride precipitate platelets and dislocation loops formation in Nb-N alloys during aging at 535 C from electron microscope observations of structural changes 16 p2405 A72-32999
- Supermolecular scale microscopic dynamic model for solid body macroscopic friction and wear effects 16 p2398 A72-33367
- Cold rotatory forging and subsequent heating effects on microstructure, texture and mechanical properties of dispersion hardened Ni specimens obtained by hot extrusion 16 p2407 A72-33530
- Isotropic fiber coarsening in unidirectionally solidified eutectic alloys, showing effect on alloy microstructure 16 p2409 A72-33802
- Reliable nondestructive microstructure testing via surface ultrasonic waves 16 p2399 A72-33822
- Deformation substructures in stainless steels under low cycle high strain fatigue tests evaluation for application as fuel cladding for fast breeder reactors 16 p2411 A72-33825
- Alfven wave propagation in interplanetary medium for solar wind microscale fluctuations, using stationary spherically symmetrical model 16 p2449 A72-33912
- Microstructural damage effect on high temperature materials creep life, considering Robinson and Odqvist correlation laws 16 p2474 A72-34127
- The effect of firing temperature on properties of natural steatite and pyrophyllite. 17 p2569 A72-34666
- Carbon fibre composites with ceramic and glass matrices. I - Discontinuous fibres. 17 p2570 A72-34668
- Carbon fibre composites with ceramic and glass matrices. II - Continuous fibres. 17 p2570 A72-34669
- Flexure of micropolar elastic beams. 17 p2631 A72-35056
- Contributions to the study of the macro- and microstructures of semiconductor materials fabricated in our country 17 p2595 A72-35123
- Electron-microscopic investigation of the development of a cellular structure in molybdenum during hydroextrusion 17 p2569 A72-35524
- Structure, electrical conductivity and electron transport mechanisms in chalcogenide glasses 17 p2596 A72-35750
- Analysis of grain- and particle-size distributions in metallic materials. 17 p2569 A72-35922
- Geometric concepts for microstructure change processes dynamics, considering time variation determination of system topological and metrical properties and particle size distribution evolution 18 p2718 A72-36397
- The structure and properties of thermomechanically treated beta-III titanium. 18 p2700 A72-36586
- Microinhomogeneous elastic media with moduli tensor as coordinate random function, investigating stress and strain tensors 18 p2735 A72-36668
- The effect of dislocation tangles on superconducting properties. 18 p2719 A72-36746
- Quantitative microstructural measurements by room temperature photoemission electron microscopy, discussing relief contrast, edge effect, resolution and information depth 18 p2719 A72-36831
- New developments in the study of fiber superalloys obtained by directional solidification 18 p2702 A72-37015
- Variational principle based three dimensional elasticity theory of micropolar anisotropic sandwich plates, considering transverse shear and strains and rotatory inertia 18 p2737 A72-37057
- Effect of structural parameters and temperature on the effective thermal conductivity of plasma-sputtered aluminum oxide 18 p2696 A72-37188
- Some problems concerning microplastic deformation and isothermal transformation of Fe-Ni-C alloy. III - Effect of aging in the temperature range from 203 to 304 K on microplastic deformation at 77 K 19 p2814 A72-37419
- Some problems concerning microplastic deformation and isothermal transformation of Fe-Ni-C alloy. IV - Effect of transformation plasticity on microplastic deformation at 77 K 19 p2815 A72-37420
- Phenomenology and engineering significance of creep recovery in heat resistant steels, stressing ductility and microstructural effects 19 p2816 A72-37707
- A new morphological element on the viscous breakdown microsurface of hypoeutectoid steels 19 p2817 A72-37737
- Microstructure and differential thermal analyses of ternary system Co-Mn-Al, presenting phase diagrams 19 p2818 A72-37852
- Influence of the structure of VTZ-I and VT-18 alloys on the fatigue strength for an asymmetrical loading cycle 19 p2819 A72-38017
- Relations between mechanical properties and microstructures in TiC-Mo2C-Ni alloy. 19 p2821 A72-38375
- Structural features of plasma and gas-flame deposited aluminum oxide coatings 19 p2810 A72-38680
- Microscopic substructure in face centered cubic metals fatigued at elevated temperatures. 20 p2935 A72-38880
- Dislocation motion as a source of acoustic emission. 20 p2924 A72-39280
- Influence of boron on the structure and certain properties of electron-beam melted molybdenum 20 p2939 A72-39313
- Fog and cloud microstructure and particle size distributions from directional light scattering coefficient /halo indicatrix/ 20 p2948 A72-39570
- Mechanical and microstructural properties of steels for effective surface cementation, suggesting Mo and Cr optimal contents 20 p2941 A72-39576
- The effect of Si, Zr, Al and Mo on the structure and strength of Ti martensite. 20 p2941 A72-39792
- Beta to omega phase transformation and structure in Zr and Ti alloys bcc solid solutions by dark field electron microscopy, diffraction and ultrasonic technique 21 p3065 A72-40092
- Corundum polycrystalline microstructure changes during high temperature creep tests, using optical microscopy 21 p3072 A72-40269
- Investigation of the structural content and the determination of the optimal image of focus series in light and electron microscopy with the aid of Fraunhofer diffraction/structure spectroscopy/ 21 p3055 A72-40747
- Fracture toughness of the heat-affected zone in 14CrMoV69 steel and 18Ni maraging steel. 21 p3067 A72-40850
- Deformation microstructure of fine grained and plate-like structure two phase Ti alloys, noting plasticity decrease in beta phase presence 21 p3068 A72-40963
- Ferromagnetic tau phase structure of Mn-Ac alloy with powder anisotropy related to platelet formation and twinning orientation 21 p3068 A72-40965
- A study on the correlation between thermal fatigue and low-cycle fatigue at elevated temperatures. 21 p3119 A72-41008
- The properties and structures of a heat resistant 1Cr-Mo-V steel and alloy A-286 after long time exposures at elev. temps. 21 p3069 A72-41012
- The effect of alloying elements on creep rupture strength and microstructure of 12 percent chromium heat resisting steel. 21 p3069 A72-41014
- The influence of grain and twin boundaries in fatigue cracking. 21 p3069 A72-41350
- Metastable phases in very rapidly solidified aluminum-germanium alloys 21 p3070 A72-41644
- Structural and reaction kinetic characteristics of /W, Ti and Ta/C-Co systems, considering solubility, surface energy, diffusion, segregation and grain growth 21 p3071 A72-41849
- Peculiar absorption and emission microstructures in the type IV solar radio outburst of March 2, 1970. 22 p3217 A72-42044
- Light scattering studies in amorphous media. 22 p3206 A72-42798
- Effect of rare earth metals on the structure and properties of aluminum and its alloys 22 p3192 A72-42818
- Thermomechanical manipulation of precipitate shape in a titanium-base alloy. 22 p3194 A72-43044
- German monograph - Influence of programmed welding cycle temperatures on the microstructure formation and corrosion behavior of austenitic corrosion-resistant steels. 22 p3195 A72-43075
- Microscopic aspects of fracture in ceramics. 23 p3305 A72-43504
- Microstructural aspects of the fracture of two-phase alloys. 23 p3299 A72-43510
- X ray, microstructural and differential thermal analysis for binary Zr alloys, noting formation of ternary phases and solid solutions 23 p3300 A72-43588
- Investigation of the structural state of the InDk40T7 high-coercivity alloy 23 p3300 A72-43594
- Investigation of the state of the structure of turbine-disk materials after operation 23 p3302 A72-43965
- Increasing the boundary strength of electron-beam-melted cast molybdenum by vanadium microadditions 23 p3302 A72-43967
- Influence of the cooling rate after sintering on the structure and properties of the ZnGr1.5D2.5 cermet 23 p3303 A72-44014

- Structure of the 01420 alloy with zirconium
23 p3303 A72-44094
- Phase extraction and analysis in superalloys - Summary of investigations by ASTM Committee E-4 Task Group I.
23 p3304 A72-44257
- Mechanical properties of heat treated hardened high strength steel, investigating microstructure relationship to failure characteristics
24 p3416 A72-45734
- Microstructure properties of heat resistant alloy for gas turbine blades as function of operational time
24 p3416 A72-45747
- Thermoelastic characteristics and crystal phase distribution effect on microstructural stresses and thermal expansion of polycrystalline refractory materials
24 p3416 A72-45759
- MICROTHRUST**
- Ten mlb concentric tubes biowaste resistojet thrust performance for hydrogen, water, methane, carbon dioxide and biopropellant mixtures, discussing vibration, shock and acceleration tests
[SAE PAPER 710769] 01 p0116 A72-10263
- RF ion microthruster discharge vessel and plasma holder material investigation, considering quartz, boron nitride and aluminum oxide
[AIAA PAPER 72-473] 11 p1709 A72-26204
- Cs contact ion microthrusters, neutral fraction measurements, analytical methods and testing procedures
[AIAA PAPER 72-495] 11 p1711 A72-26218
- MICROTOPOGRAPHY**
- U. TERRAIN**
- MICROWAVE AMPLIFIERS**
- Transferred electron microwave oscillators / three-level and LSA relaxation types/ and amplifiers / reflection and traveling wave types/ fabrication, technology and performance capabilities
01 p0035 A72-10627
- Supercritically doped transferred electron microwave amplifiers stabilization mechanisms, considering cathode contact, anode diffusion current and active region temperature gradient roles
01 p0036 A72-10636
- Doping profile effects on reflection-type IMPATT diode microwave amplifiers, presenting power-gain vs frequency curves
01 p0037 A72-10643
- Broadband high efficiency mode /HEM/ TRAPATT amplifiers for S band, discussing bandpass and input-output characteristics with Ichebycheff filter
01 p0038 A72-10652
- Wideband microwave parametric amplifier using balanced circuits to relax isolation requirements between signal, idler and pump circuits
01 p0038 A72-10655
- Gain vs bandwidth characteristics of broadband microwave parametric amplifiers
01 p0038 A72-10656
- S band transistor power amplifier design and performance, noting application for 960 telephone channel radio relay system
01 p0038 A72-10657
- Computer program for design optimization of three-stage wideband low-noise integrated microwave amplifier
01 p0041 A72-10690
- Large signal nonlinear modeling and digital simulation of microwave transistor power amplifier and GaAs Gunn relaxation oscillator
01 p0041 A72-10691
- Gunn and IMPATT diodes applications for microwave power oscillators and amplifiers in radio link equipment
01 p0042 A72-10711
- Microwaves and optical generation and amplification - Conference, Amsterdam, September 1970, covering microwave tubes, solid state devices and quantum electronics
01 p0044 A72-11278
- Electron motion equations for threshold input signal of M type amplifiers with secondary emission cathode in interaction space
02 p0190 A72-11571
- Varactor diode microwave parametric amplifiers for radio astronomy interferometer, discussing system design features for gain and phase stabilities
02 p0192 A72-12043
- Dual-gate MOS transistor structure, operational principles and electrical characteristics, noting suitable properties for use in low noise microwave amplifier
03 p0330 A72-12969
- Book on microwave electronics covering electron beam microwave devices and solid state microwave oscillators and amplifiers
03 p0331 A72-13233
- Narrow band medium power X, Ku and C band solid state amplifiers, demonstrating TWT replacement with GaAs and avalanche diodes
03 p0334 A72-14072
- Gunn diode large signal admittance dependence on bias and frequency, discussing computer simulation and broadband oscillator and amplifier design
04 p0497 A72-14712

- High power reflection-type pulsed microwave amplifier using high efficiency antiparallel avalanche diode pair connected at transmission line ends
04 p0497 A72-14714
- Avalanche transit time diodes noise mechanisms and performance in microwave amplifier, oscillator and mixer applications
04 p0500 A72-15302
- Millimeter and submillimeter wave molecular beam masers amplification principles and Doppler and collisional broadening elimination capability
04 p0532 A72-15597
- Microstrip configuration for microwave GaAs IMPATT diode oscillators and power amplifiers
05 p0633 A72-15782
- Distributed unidirectional microwave IMPATT diode amplifier and CW tests for X and C band circuits
05 p0633 A72-15783
- Microwave IC power amplifiers for radio relay, telemetry, phased array radar and TWT replacement
05 p0634 A72-15784
- Frequency characteristics theory for two-stage electron tube microwave amplifiers coupled by transmission line on order of wavelength
05 p0634 A72-15827
- Ultralow noise microwave parametric amplifiers in communication satellite earth terminals, discussing technology basis of millimeter wave paramps
06 p0784 A72-17741
- Broadband uhf power amplifier for AM signals output power of 100 W, using eight parallel transistors
06 p0774 A72-17750
- Wideband tunnel diode microwave amplifier design with coaxial line, considering band-edge stability and impedance matching
06 p0785 A72-18310
- High power L-band microminiaturized hybrid type integrated transistor amplifier design and realization by computer
06 p0785 A72-18314
- Microwave thin film microstrip IC tunnel diode amplifiers for broadband high performance receivers, discussing design, construction and performance
06 p0786 A72-18374
- IMPATT diode microwave oscillators and amplifiers calculating noise sideband correlation factor at randomly large signal frequencies
06 p0788 A72-18464
- Medium power high gain, CW transferred electron microwave amplifiers at C band, describing bandwidth, saturation, intermodulation distortion and dynamic range characteristics
06 p0789 A72-18483
- Large signal analysis of stabilized supercritically doped transferred electron microwave amplifiers, considering diffusion and lattice temperature effects
06 p0790 A72-18484
- Power generation and low noise amplification devices development during past decade, considering avalanche diodes, transferred electron and acoustoelectric devices and microwave transistors
07 p0952 A72-18825
- Gigahertz reflection amplifiers with low cost avalanche transit time diodes, measuring characteristics of amplification by synchronization at center frequency
07 p0955 A72-19191
- Miniature modular wideband parametric amplifier for centimeter range, using IC optimal coupled circuit with passband dependent on diode time constant
07 p0956 A72-19570
- Waveguide cavity Gunn microwave power amplifiers, predicting maximum small signal gain and FM and AM noise performance
07 p0958 A72-19921
- Symmetrical amplitude-frequency characteristics of microwave reflection amplifiers with active resonators connected in series by nonhalf wave transmission line
08 p1138 A72-20791
- Five layer resonant transparent semiconductor device structures for microwave amplifiers, reactive elements, low current rectifiers and filters
08 p1139 A72-21059
- Transistor power amplifier for 2.5 GHz range directional transmitters, noting cooling problems elimination
08 p1140 A72-21306
- Multichannel junction gate FET /Gridistor/ for microwave power amplifier, discussing design, fabrication and performance
08 p1141 A72-21429
- Solid state microwave power amplifier with unidirectional transmission line loaded by negative resistance diode series, calculating large signal characteristics
08 p1142 A72-21558
- Millimeter wave pumped X band balanced diode type parametric amplifier using GaAs Schottky barrier varactors for operation at room temperature
09 p1289 A72-23417
- Supercritical CW GaAs transferred electron broadband reflection amplifier power gain and noise figure at 34 GHz
10 p1449 A72-24301

- CW circuit stabilized InP microwave reflection amplifiers in Q band, determining power gain and noise figure
10 p1450 A72-24308
- Multistage broadband microwave amplifier design based on bipolar transistors cascade coupling, using scattering parameters
10 p1451 A72-24572
- Transistorized microwave amplifier/limiter for upper part of decimeter wave range, suggesting limitation in automatic gain control transistor
10 p1451 A72-24588
- Nonlinear microwave power amplifiers with IMPATT diodes in stable and injection locked modes, predicting behavior for comparison with experiment
10 p1451 A72-24592
- Noise measurements of AM and FM microwave generators and amplifiers in nonlinear regime
10 p1452 A72-24643
- Stabilization bandwidth reduction in microwave parallel tuned tunnel diode amplifier circuits synthesis
10 p1453 A72-24910
- Minimum noise coefficients of M-type microwave beam amplifiers with crossed fields, taking into account delay system distributed losses
10 p1453 A72-24913
- Complex gain nonlinearity of transmitting microwave amplifiers in single and multicarrier operation
10 p1454 A72-25147
- High quality GaAs varactor diodes for double diode low noise wideband parametric amplifiers at idler frequencies up to 43 GHz without refrigeration
12 p1788 A72-27174
- Tunnel diode amplifier for 8 GHz band, considering gain, bandwidth, noise factor and stability characteristics
12 p1790 A72-27533
- Solid state InP sources for microwave transferred electron oscillators and amplifiers with improved conversion efficiencies, comparing with GaAs
13 p2020 A72-28432
- Microwave amplifier with internal negative feedback, using IF output for frequency modulation of mixer oscillator signal
13 p1930 A72-29057
- Parametric regeneration in Josephson superconducting point contacts for combination frequency signal amplification and conversion in microwave application
13 p1932 A72-29298
- Design and performance of microwave single stage relaxing avalanche diode reflection amplifier
14 p2088 A72-30918
- Transistorized microwave amplifiers with dissipative equalizing networks, describing transistor equivalent circuit
15 p2206 A72-31659
- Phase and gain response of wideband coaxial X band microwave avalanche diode amplifiers
16 p2368 A72-33073
- Parametric amplifiers for satellite microwave communication systems, discussing frequency stability, noise temperature and gain relationships
16 p2369 A72-33520
- Russian book on microwave electronics covering linear-beam and cross-field backward and traveling wave amplifiers and oscillators, klystrons, masers, plasma devices, etc
17 p2532 A72-34650
- Broadband high power L-band phased array amplifier chain.
17 p2528 A72-34710
- Modular I-band solid-state microwave amplifier.
17 p2528 A72-34711
- Series stabilization reflection type tunnel diode microwave amplifier synthesis with allowance for real circulator reactance
18 p2665 A72-36107
- Spaceflight-qualified tunable C-band parametric amplifier system.
19 p2770 A72-37253
- 18 GHz paramps with both liquid helium and room temperature operations and with triple-tuned gain characteristics.
19 p2770 A72-37254
- An X-band paramp with 0.85 dB noise figure /uncooled/ and 500 MHz bandwidth.
19 p2770 A72-37258
- A C-band all ferrite integrated wideband high power GaAs avalanche diode amplifier.
19 p2771 A72-37264
- Intermodulation characteristics of X-band IMPATT amplifiers.
19 p2771 A72-37265
- Millimeter-wave solid-state exciter-modulator-amplifier module for gigabit data-rate.
19 p2771 A72-37267
- Design considerations of a 3.1-3.5 GHz GaAs FET feedback amplifier.
19 p2771 A72-37269
- Single and dual gate GaAs FET integrated amplifiers in C band.
19 p2771 A72-37270

Dynamic behavior of nonlinear power amplifiers in stable and injection-locked modes.

19 p2773 A72-38293

Combinational distortions and cross distortions in parametric microwave systems

19 p2768 A72-38665

Microwave low noise amplifiers for use in radar systems.

20 p2907 A72-39220

Digital p-i-n diode microwave drive amplifier design guidelines, discussing sharp switching pulses and short circuit protection features

20 p2904 A72-39734

High-power microwave amplifier using IMPATT diodes.

20 p2909 A72-39776

IMPATT diode circuits operation as microwave amplifiers, presenting data on intermodulation distortion, amplitude to pulse modulation conversion and reliability

20 p2910 A72-39851

Low-noise parametric amplifiers for radio astronomical observations at 18 to 21 cm wavelengths

21 p3025 A72-40303

Low noise microwave parametric amplifier design for space communication receivers, using inverted diode balanced mixers

21 p3025 A72-40304

Miniature modular wideband parametric amplifier for centimeter range, using Q optimal coupled circuit with passband dependent on diode time constant

22 p3158 A72-42088

Frequency characteristics theory for two-stage electron tube microwave amplifiers coupled by transmission line on order of wavelength

23 p3268 A72-43435

Theory of microwave amplification with electron transfer

23 p3269 A72-43550

Linear theory of a microwave distributed amplifier based on an avalanche transit-time diode

23 p3271 A72-43776

Stability criteria for phase-locked oscillators.

23 p3272 A72-44192

Microwave phase shifting with gain using IMPATT diodes.

24 p3385 A72-44963

Reflection amplification in thin layers of n-GaAs.

24 p3385 A72-44971

MICROWAVE ANTENNAS

NT HORN ANTENNAS

NT LENS ANTENNAS

NT SLOT ANTENNAS

Pulse IMPATT diode Ka band microwave rf head mechanically steered antenna array for airborne monopulse tracker applications

01 p0039 A72-10661

Electronically scanned monopulse cavity backed quadratic spiral antenna array at 1.54-1.66 GHz for maritime satellite communications

01 p0039 A72-10662

X-band linear phased array tracking antenna with digital phase shifters and beam steering, evaluating beamwidth, gain and direction error

01 p0028 A72-10663

Multifunction integrated microwave array antenna design emphasizing interlacing multifrequency bands into single aperture and mutual interaction effects reduction between elements

01 p0039 A72-10667

Tubular traveling wave antenna array for radar applications and microwave television transmitters, describing computer program for design

01 p0039 A72-10668

Limited scan microwave antenna design, discussing angular coverage, feed motion and focal field distribution

01 p0039 A72-10670

Reflector antennas with very high front-to-back ratio - Theory and experiments on models.

01 p0029 A72-10673

Dielectric cone feeds design for microwave antennas, presenting radiation patterns

01 p0029 A72-10675

Short backfire antenna gain increase, considering construction case, reflector arrangement and circular polarization

01 p0040 A72-10684

Microwave breakdown prediction models for antenna system in ionized reentry environment

04 p0486 A72-14531

Modes propagating inside tubular microwave antenna, studying canonical problems by asymptotic and modal techniques

04 p0501 A72-15430

French book on antenna application to radars and space techniques covering UHF techniques, mathematical theories and apparatus development

05 p0626 A72-16287

Microwave antennas, feed systems, strip transmission lines and test instrumentation, examining radiation patterns, design and polarization characteristics

05 p0635 A72-16330

Polarization changes with distance from microwave antenna in near and intermediate zones for circularly and elliptically polarized fields in square and rectangular apertures

05 p0635 A72-16335

Dispersion and energy characteristics of azimuthally asymmetrical waves in microwave logarithmic or arithmetical spiral antenna deposited on isotropic magnetodielectric layer

05 p0636 A72-16338

Low cost automated digitized measurement for microwave antenna feed power gain and relative phase, using computer facilities

05 p0637 A72-16420

Microwave antenna efficiency measurement by integrated isotropic levels comparison, featuring elimination of error due to specular ground reflections

05 p0637 A72-16421

Four uhf antennas buried beneath refractory concrete, discussing design, fabrication and power gain and azimuthal pattern measurements

06 p0771 A72-17345

Multifrequency array antenna of interlaced open ended waveguide elements for L, S and C bands, reducing mutual interaction by cross polarization

06 p0782 A72-17360

Microwave holography using transmitting and receiving antenna for generation of synthetic aperture in angular direction

06 p0814 A72-17486

Papers on microwave engineering covering surface finish importance for waveguide propagation, parametric amplifiers and voltage breakdown of microwave antennas

06 p0783 A72-17737

Voltage breakdown of microwave antennas, discussing ionization rates in hot air and breakdown suppression by electron flow

06 p0783 A72-17739

Single slotted waveguide linear arrays, discussing microwave antenna design and feeding and cross polarization suppression

06 p0784 A72-17740

Microwave attenuation due to ohmic losses in periodic linear arrays of metallic cylinders, ribbons and slots in metallic ground plane

06 p0786 A72-18372

Step-scan landing system technique, using microwave fixed linear array for area coverage with pattern of narrow overlapping individually coded sequentially switched beams

06 p0846 A72-18397

K and Ka bands standard electromagnetic horn gain measurement and error analysis at different wavelengths by two-antenna method

07 p0957 A72-19784

X band microwave attenuation measurements in high density air plasma layer at aperture antenna in rectangular shock tube

07 p0949 A72-20560

Phased directional surface wave splitters and microwave and integrated optics elements based on single mode, dielectric and rectangular waveguides

08 p1131 A72-20935

Reflected signal and receiver noise interference error in antenna temperature and calibration measurements by artificial moon method in centimeter and decimeter bands

08 p1142 A72-21726

Microwave two reflector rectangular backfire antenna with dielectric surface wave structure as waveguide prolongation, obtaining far field radiation pattern

11 p1604 A72-25749

Microwave antenna radiation patterns from far field measurements by radio holograms with probe

11 p1598 A72-26718

Communication satellites microwave circular array antenna for wideband circularly polarized isotropic radiation

[AIAA PAPER 72-529]

12 p1789 A72-27419

Receiving and transmitting antennas directional gain effect on microwave long distance tropospheric propagation

12 p1783 A72-27632

Microwave horn and lens antennas radiation spatial coherence characteristics, noting effect on picture contrast

13 p1928 A72-28475

Pyramidal-horn primary element axial position effect on dual mirror Cassegrain microwave antenna main lobe pattern, obtaining optimal position

13 p1929 A72-29040

Narrow antenna radiation beam used for size and location determination of solar microwave radio burst observed with radio telescope

13 p2048 A72-29743

Microwave antenna near field apparent image and phase-amplitude distribution measurement with photocontrolled semiconductor panel

15 p2209 A72-32672

Fourier transform /subtractive/ holographic imaging technique for microwave antenna apertures

16 p2368 A72-33072

Blunt nose cone flow field characteristics microwave measurement at stagnation point during atmospheric reentry, using plasma diagnostic sensors with antennas and electrostatic probes

[AIAA PAPER 72-693]

16 p2345 A72-34049

A millimeter wave receiving antenna with an omni-directional or directional scannable azimuth pattern and a directional vertical pattern.

17 p2525 A72-34364

Broadband high power L-band phased array amplifier chain.

17 p2528 A72-34710

SHF airborne distributed phased array antenna system.

17 p2531 A72-35572

Antenna array analysis of arbitrarily-located, parallel center-fed dipoles with terminals in a common plane.

18 p2666 A72-36328

Low noise microwave receiving systems on a 64 m antenna.

19 p2763 A72-37255

Design of Cassegrain antennas employing dielectric cone feeds.

19 p2772 A72-37847

Prediction of near-field antenna coupling in the presence of obstacles.

20 p2902 A72-38998

Reflector profiles for the pencil-beam Cassegrain antenna.

20 p2903 A72-39221

Faraday rotation dual-mode ferrite reciprocal phaser with performance and cost advantages over toroidal type for microwave phased array applications

20 p2909 A72-39733

Radiation characteristics of dielectric cones.

20 p2904 A72-39773

A rectangular beam waveguide resonator and antenna.

21 p3026 A72-40358

Cross polarizing effects of a water film on a parabolic reflector at microwave frequencies.

21 p3027 A72-40375

Experimental investigation regarding Archimedean spiral antennas for the L-band, and radiator groups constructed from them whose radiation directions are controlled by a conduction matrix

21 p3028 A72-40510

Two-hybrid mode feed design procedure and performance for small and large f/D ratio reflectors of microwave telescope

21 p3029 A72-40515

A 3-meter Cassegrain antenna for the frequency range from 2.1 to 2.3 GHz

21 p3029 A72-40521

Luneburg lens spherical antenna microwave radiation pattern, computing Maxwell equations via Tai method

21 p3030 A72-40529

A dual frequency, dual polarized feed for radioastronomical applications.

21 p3034 A72-41400

Design of radiating elements for large planar arrays - Accomplishments and remaining challenges.

23 p3269 A72-43571

Geometrical optics approximation for angular error calculation of microwave antenna radome, noting boresight error proportionality to walls electrical thickness

23 p3271 A72-43837

MICROWAVE ATTENUATION

Rain droplet size distribution effects on microwave attenuation at millimeter wavelengths, comparing calculation with measurement

01 p0027 A72-10406

Waveguide channel microwave bandpass filters for radio relay systems, discussing methods of improving group delay in passband and attenuation at harmonic frequencies

01 p0041 A72-10694

Venus lower atmosphere from Venera 4, 5 and 6 and Mariner 5 data, evaluating greenhouse effect by microwave absorption and by nongray radiative model

01 p0129 A72-10795

Nonparabolic n-InSb semiconductors, presenting microwave conductivity dc field induced anisotropy

04 p0560 A72-14543

Circularly polarized microwave damping at electron cyclotron frequency in low density magneto cesium plasma, investigating power absorption coefficient and refractive index

04 p0555 A72-14853

Air-filled elliptical waveguide with nonmagnetic metal wall, determining dominant TE mode attenuation by perturbation method with Bessel function

04 p0491 A72-15426

Microwave attenuation due to ohmic losses in periodic linear arrays of metallic cylinders, ribbons and slots in metallic ground plane

06 p0786 A72-18372

Nonlinear microwave absorption by plasma between cyclotron and hybrid frequencies for critical magnetic field

06 p0776 A72-18408

- Microwave absorption by longitudinally inhomogeneous plasma, noting waveguide excitation in critical concentration region 06 p0776 A72-18409
- Atmospheric attenuation due to rain based on links experiment and statistical study of equivalent precipitation for given path length and time percentage 07 p0939 A72-19188
- Earth-space path attenuation statistics and fade duration at 15.3 GHz, using ATS 5 satellite transmission and radiometric sun/sky techniques 07 p0948 A72-20496
- X band microwave attenuation measurements in high density air plasma layer at aperture antenna in rectangular shock tube 07 p0949 A72-20560
- Microwave signal attenuation in II oscillation plasma beam discharge, comparing to braking cyclotron absorption effect 08 p1212 A72-20792
- Microwave absorption in high pressure hydrogen based on radio astronomical measurements of Uranus brightness temperature 08 p1239 A72-22088
- Microwave attenuation factor of TE and TM modes in hollow conducting elliptical waveguides, using first order perturbation formula for calculation 10 p1451 A72-24594
- Venus lower atmosphere enhanced microwave attenuation explained by water vapor and droplet layer, calculating mass density distributions 11 p1724 A72-26762
- Ni powder artificial dielectric in waveguide transverse magnetic field, noting nonreciprocal nature of microwave attenuation and phase shift 11 p1607 A72-26786
- Eigenfunctions, eigenvalues and microwave attenuation constants in square and rectangular waveguides with rounded corners 11 p1607 A72-26994
- Line-of-sight radio link attenuation by atmospheric precipitation and phase interference fading during multipath propagation in 7-15 GHz range 12 p1785 A72-27802
- Theoretical and measured rainfall attenuation of millimeter waves, correlating attenuation coefficients, rain rate and drop size distributions 12 p1785 A72-27803
- Microwave acoustic surface waves attenuation at solid and monatomic gas boundary, detailing frequency, molecular weight, pressure and temperature effects 15 p2278 A72-32505
- Molecular absorption of microwaves by atmospheric impurity gases ozone, carbon monoxide and nitrous oxide up to 20 km 16 p2364 A72-33483
- Microwave absorption in high pressure hydrogen based on radio astronomical measurements of Uranus brightness temperature 17 p2606 A72-34651
- Nonlinear microwave absorption by plasma between cyclotron and hybrid frequencies for critical magnetic field 17 p2588 A72-34858
- Microwave absorption by longitudinally inhomogeneous plasma, noting waveguide excitation in critical density region 17 p2588 A72-34859
- Phenomenological model for incoherent microwave scatter attenuation from turbulent plasma, establishing relation between plasma parameters and attenuation coefficient 17 p2517 A72-35622
- Absorption of the 4- to 6-millimeter wavelength band in the atmosphere. 18 p2689 A72-36961
- Heat conduction as mechanism for solar microwave bursts attenuation, noting effect of gyromagnetic absorption layers 19 p2852 A72-38497
- An ultra-broadband probe for RF radiation measurements. 20 p2921 A72-38993
- MICROWAVE CIRCUITS**
- Microwave module circuit design for airborne phased array radar with distributed power generation, reception and phase shift functions, considering performance, reliability and cost 01 p0028 A72-10660
- Computerized optimization procedure for microwave circuits without tuning elements, applying to high pass filter design 01 p0040 A72-10686
- Microwave oriented circuit analysis program /MODMAN/ to handle nonlinear, time-varying, lumped and distributed elements in time domain, using transmission line modeling algorithm 01 p0045 A72-10687
- Computer program for microwave circuit scattering matrix sensitivity, applying to stripline elliptic low pass filters and thin-film negative resistance transistor amplifier 01 p0034 A72-10688
- REDAP 31 network analysis program for design of S-band phase shifter with P-I-N diodes for phase array antennas 01 p0040 A72-10689
- Coaxial connector standard interfaces for optimum microwave performance, discussing single connector reflection coefficient measurement equipment and procedures 01 p0041 A72-10693
- Nonreciprocal microwave ferrite device design, outlining loss-free, cyclic symmetrical, multipoint junction circulator theory 01 p0041 A72-10695
- Ferrite-loaded waveguide Y-junction field mode identification by eigenvalue phase-frequency characteristics measurement, applying to millimeter wave circulator synthesis 01 p0041 A72-10697
- Hybrid microwave integrated circuits, discussing distributed circuits with strip transmission lines and lumped element circuits with inductors and capacitors 01 p0045 A72-10698
- GaAs, Si and alumina performance as substrates in integrated microwave circuits 01 p0046 A72-10700
- Directional couplers design for broadband microwave integrated circuits 01 p0046 A72-10702
- Interference control in microwave circuit design, discussing coupling element, antenna terminals, radiated interference susceptibility and electromagnetic environments 02 p0189 A72-11558
- Dual gate GaAs microwave FET, measuring second gate voltage effects on power gain and noise 02 p0191 A72-11893
- Metal-semiconductor-metal Schottky barrier microwave diode impedance and shot noise calculation 02 p0191 A72-11894
- Dual-gate MOS transistor structure, operational principles and electrical characteristics, noting suitable properties for use in low noise microwave amplifier 03 p0330 A72-12969
- GaAs Schottky barrier and germanium backward diodes in microwave integrated circuit applications, describing design and performance as frequency changers and low level detectors 03 p0334 A72-14073
- Low cost ferrite remanence microwave phase shifter design using periodic loading structures 04 p0497 A72-14716
- Lumped capacitors, inductors, resistors and gyrators for use at microwave frequencies, discussing design and applications up to X band 04 p0497 A72-14717
- Gaussian envelope microwave pulse generation using absorption p-i-n diode modulator, predicting performance by digital simulation 04 p0498 A72-14718
- Reciprocal dual mode millimeter wavelength phase shifter design for use in phased array antennas, calculating phase shift and insertion loss vs frequency 04 p0498 A72-14719
- Wideband microwave acoustic delay line design featuring superior bandwidth, phase linearity, spurious echo and insertion loss characteristics 04 p0521 A72-14720
- Distributed unidirectional microwave IMPATT diode amplifier and CW tests for X and C band circuits 05 p0633 A72-15783
- Hf and microwave hybrid circuits encapsulation, discussing hermetic seals formation 05 p0634 A72-16182
- Coaxial and stripline wideband microwave hybrid ring junctions equivalent to magic Tees with improved electrical properties 05 p0636 A72-16344
- N-channel Si MOS microwave transistor, discussing fabrication, design, power gain, stability, noise figure, equivalent circuit and applications 05 p0636 A72-16361
- Conical cavity resonator design for submillimeter wave electron beam devices, investigating mode and resonant frequency dependence on cavity size 05 p0636 A72-16364
- Microwave lumped element impedance measurements from 1 to 12 GHz by resonant transmission line frequency and Q perturbation technique 05 p0637 A72-16419
- Multicircuit hf filters tuning drive with mechanical synchronization correction 06 p0774 A72-17749
- L- and X-band Y junction waveguide circulators for medium and peak high powers in radar applications, discussing operation principle and design 06 p0785 A72-18311
- Microwave frequency multiplier construction by hybrid circuits based on quasi-lumped components, calculating characteristics from equivalent circuit 06 p0785 A72-18313
- Bulk semiconductor material complex microwave conductivity and dielectric constant measurements by cavity perturbation techniques 06 p0786 A72-18371
- Microwave biased millimeter and submillimeter wave detector with n-type InSb, using down conversion process and free carrier absorption for detection 06 p0866 A72-18384
- Harmonic power extraction from series-stacked high efficiency avalanche diodes at superhigh frequencies on simple microstrip circuits 06 p0788 A72-18468
- Microwave parametric amplification and conversion in circuits with Josephson junctions, describing stable oscillation measurements 06 p0866 A72-18477
- Microwave IC front end receiver synthesis for radio relay system, considering low noise figure achievement by Si Schottky barrier diodes 07 p0955 A72-19356
- IR radiation detection by microwave biased photoconductor, lead-tin telluride photovoltaic detector and thermal imaging pyroelectric detector and array system 07 p1034 A72-19425
- Schottky barrier semiconductor devices characteristics, fabrication and application to pulse microwave diodes and IC elements 08 p1139 A72-21053
- Small signal microwave transistors design with arsenic and phosphorus diffused emitters, comparing performance in terms of power gain-bandwidth product, maximum frequency and noise figure 08 p1142 A72-21743
- Microwave transistor noise factor measurement for various geometries and parameter values correlation with predictions 09 p1286 A72-23104
- Junction transistor equivalent circuit small signal parameters determination at VHF and UHF 10 p1450 A72-24324
- Schottky barrier crystal microwave video diodes design and fabrication to maximize burnout resistance and dynamic range for given detection sensitivity 10 p1450 A72-24553
- X band high power ferrite phase shifter design and performance 10 p1451 A72-24595
- Wideband microwave device with diode and single component correction circuits Q factors measurement from frequency dependence of input traveling wave coefficients 10 p1453 A72-24918
- High conversion efficiency microwave second harmonic generator using negative resistance nonlinearity of n-type GaAs 11 p1591 A72-25741
- Lossless distributed rectangular microwave structure with dielectrics interposed between two conductive metallic layers, noting existence of transmission zeros and filter properties 11 p1607 A72-26990
- Pulsed IMPATT diode oscillators, pulse power capabilities, considering microwave circuit, dc and pulse biasing, power limitation and circuit anomalies 13 p1931 A72-29109
- Microwave circuits for multiplexing applications, discussing optimal design in terms of economic, mechanical and electrical parameters 13 p1934 A72-30089
- Schottky diode microwave down-converter conversion loss calculation as function of image terminal with consideration of barrier capacitance, series resistance and voltage drop 14 p2088 A72-30586
- Nonlinear microwave circuit feedback model analysis by describing function in control theory, applying to oscillator phase locking problem 15 p2210 A72-31355
- Microwave waveguide semiconductor modulator with p-n-n diode as control element, taking into account semiconductor control element conductivity change along waveguide wall 15 p2206 A72-31662
- German monograph on microwave broadband tunnel diode mixers theory and design, taking into account parasitic elements as part of filter networks 16 p2368 A72-33507
- Microwave integrated circuits. 17 p2527 A72-34570
- Ceramic waveguide microwave integrated circuits. 17 p2534 A72-35570
- Microwave power junction transistor design factors effects on long and short term reliability and MTBF 18 p2666 A72-36552
- Microwave junction transistor geometric design factors effect on reliability and performance, comparing overlay, interdigitated, mesh and inverse overlay structures 18 p2666 A72-36553
- Low noise high power bipolar and field effect transistors monolithic integration potentials for microwave applications 19 p2771 A72-37261

P-i-n variable attenuator with low phase shift.
19 p2773 A72-38294

A comparison of manufacturing techniques for hybrid microwave circuits.
20 p2908 A72-39496

Low noise compact down converter for 12 GHz to UHF based on waveguide mounting microwave ICs, measuring conversion loss for GaAs Schottky diode
21 p3033 A72-40885

Automatic measurement of microwave-cavity parameters using stable sampled control loops.
21 p3034 A72-41465

Variable-bandwidth frequency-modulation chirp pulse compression using a longitudinal acoustic-wave convolver at 1.3 GHz.
21 p3023 A72-41468

Computation of single-conductor and symmetric and asymmetric two-conductor stripline characteristics by the relaxation method.
21 p3036 A72-41831

Microstrip matching networks synthesis for microwave integrated circuits, calculating passband of configurations with lumped and distributed elements
23 p3269 A72-43445

Accuracy of measuring the noise figure of microwave two-ports
23 p3273 A72-44313

MICROWAVE COUPLING
NT COUPLING CIRCUITS

Mutual microwave coupling effects on element VSWR in linear dipole log periodic antenna array
01 p0043 A72-11242

Top wall and multiple branch hybrid junction waveguide couplers for millimeter wavelengths, measuring insertion loss performance
06 p0787 A72-18378

LSA oscillators performance and control optimization, discussing multiaxis radial microwave cavity effectiveness in oscillation starting and coupling to coaxial transmission line
06 p0789 A72-18481

Rectangular and orthogonal circular waveguides hybrid junction with magnetized ferrite resonators along axes, discussing design and applications
07 p0952 A72-18844

Q factor over temperature range of microwave resonator coupled with drifting indium antimonide plasma
09 p1285 A72-22895

Multimode dielectric slab waveguide power coupling due to core-cladding interface irregularities, obtaining power distribution and radiation losses
11 p1603 A72-25270

Rare gas ion laser excited by electrodeless microwave discharges, noting external magnetic field effects on output
11 p1651 A72-26571

Decoupled formulation of vector wave equation in orthogonal curvilinear coordinates, applying to ferrite-filled and curved waveguide of general cross section
11 p1607 A72-26995

Scattering matrix derivation for parallel plate waveguide array terminated in infinite plane, determining neighboring guides TEM modes mutual coupling
13 p1921 A72-29345

Signal distortion minimization for random waveguides with frequency-dependent optimum coupling based on transfer function covariance and impulse response time domain statistics
15 p2194 A72-31352

Multimode dielectric waveguide with random coupling, discussing pulse dispersion improvement and loss penalty from power spectrum derivation
20 p2901 A72-38923

Prediction of near-field antenna coupling in the presence of obstacles.
20 p2902 A72-38998

A quasi-optical directional coupler.
20 p2907 A72-39222

Reflectivity dependence of triple polarization grid on elements spacing and wires orientation, noting bandwidth of ray guide matching transformer
23 p3269 A72-43446

MICROWAVE EMISSION

Extragalactic radio source 3C 1202 microwave flux density variations suggesting superrelativistic expansion
17 p2611 A72-35295

The effect of contacts on microwave emission from InSb.
19 p2844 A72-37728

Microwave emission from geological materials - Observations of interference effects.
20 p2917 A72-39477

Some characteristics of microwave type IV radio bursts and the acceleration of solar cosmic rays.
23 p3328 A72-43616

MICROWAVE EQUIPMENT

NT BACKWARD WAVE TUBES
NT CATHODE RAY TUBES
NT CELESCOPES
NT COLD CATHODE TUBES
NT GAS DISCHARGE TUBES
NT GYRATORS

NT HORN ANTENNAS
NT IMAGE ORTHICONS
NT IMAGE TUBES
NT KLYSTRONS
NT LENS ANTENNAS
NT MAGNETRONS
NT MICROWAVE AMPLIFIERS
NT MICROWAVE ANTENNAS
NT MICROWAVE FILTERS
NT MICROWAVE INTERFEROMETERS
NT MICROWAVE OSCILLATORS
NT MICROWAVE PLASMA PROBES
NT MICROWAVE PROBES
NT MICROWAVE RADIOMETERS
NT MICROWAVE TUBES
NT ORTHICONS
NT PHOTOMULTIPLIER TUBES
NT PICTURE TUBES
NT PLANOTRONS
NT SLOT ANTENNAS
NT THERMIONIC DIODES
NT TRAVELING WAVE TUBES
NT VIDICONS

Ferrite microwave devices design, covering non-reciprocal circuit and electrical tuner
01 p0041 A72-10696

MHD boundary waves properties, noting application to traveling wave nonreciprocal devices and planar structures based on microwave integrated circuits
01 p0029 A72-10703

Equivalent circuit model for electroacoustic surface microwave transducer, discussing radiation properties determination from excitation fields distribution
01 p0041 A72-10704

Zinc oxide longitudinal acoustic microwave transducer, measuring untuned insertion loss and electroacoustic coupling constant
01 p0042 A72-10705

Thick overlay elastic rectangular microwave guides, investigating layer thickness effect, energy partition and higher modes
01 p0042 A72-10706

Frequency planning for Symphonie German-French telecommunication satellite microwave equipment
01 p0030 A72-10710

Flattening, heat treatment and machining of narrow rectangular vacuum melt Mo strips for microwave devices
01 p0078 A72-11087

Microwave half blinder for sidelobe reduction in large horn reflector antennas in E plane radiation for horizontal polarization
01 p0043 A72-11243

Temperature compensated high dielectric constant material, discussing low loss at microwave frequencies, reproducibility and mechanical properties
01 p0044 A72-11308

Gain and bandwidth properties of microwave and optical devices with isotropic active medium, investigating transmission coefficient
02 p0189 A72-11566

Two stage resonant slow wave structure synthesis for microwave device applications, deriving conditions for required dispersion and coupling impedance characteristics
02 p0190 A72-11574

Prototype compact ruggedized crystal-controlled L-band artillery telemetry transmitter design and performance
02 p0192 A72-12156

Navy uhf telemetry transmitter production system, discussing test program contribution to quality control
02 p0177 A72-12322

Microwave aircraft landing system development, discussing contract definition, feasibility, prototype development, management planning and program costs
02 p0304 A72-12377

Microwave precision coaxial connectors in terms of dimensional specifications, material properties, surface characteristics and other parameters for transmission standards effects
03 p0330 A72-13230

Book on microwave semiconductor devices, considering point contact crystal, varactor, Schottky-barrier, tunnel, backward and p-i-n diodes, transistors, Gunn effect devices and integrated circuits
03 p0333 A72-13845

Semiconductor devices potential interference and biological exposure hazards in microwave leakage field, considering shielding and filtering methods for reducing susceptibility
03 p0320 A72-14032

Solid state tunnel diode amplifier-rectifier expander for microwave pulse regenerators
03 p0335 A72-14184

High speed digital communication at millimeter wavelengths, discussing system requirements, digital computer use, transmission data rate and equipment development
04 p0485 A72-14481

ATC technology impact on flight operations and public value of aviation, discussing microwave landing system economic aspects
04 p0544 A72-14810

Aircraft landing microwave guidance and control systems, considering general dynamic model for aircraft translational motion determination in earth fixed coordinate system
04 p0545 A72-14821

Submillimeter waves development, discussing materials research, lasers, semiconductor and electron tube sources, system components and applications in space communication, imagery, metrology and sensing
04 p0550 A72-15591

Millimeter and submillimeter wave applications, considering environment remote sensing, radar communication, tracking and imagery, wideband communication, plasma diagnostics and spectroscopy
04 p0550 A72-15592

Microwave-range optical heterodyne system with magnetically tuned /Zeeman effect/ laser emissions mixing and AFC
05 p0668 A72-16345

Proposed microwave ILS, discussing continuous step and Doppler scanned radar scanning beams
06 p0846 A72-18396

Microwave Doppler scanning landing guidance system with radar beam comparison and signal format simplification suggestion
06 p0846 A72-18398

Microwave instrument landing systems based on continuous radar scanning technique, using pulse format for data transmission
06 p0846 A72-18399

IMPATT driven pumps replacement of klystron for parametric amplifiers producing over 100 mW at 38-40 GHz with good stability and noise performance
06 p0788 A72-18470

Microwave receiver double diffused MOS transistor /D-MOST/ device advantages over bipolar device
06 p0790 A72-18485

Microwave signals detection with virtual cathode in klystron repeller by electrons screening at velocity modulated electron beam
08 p1136 A72-21766

Solid state microwave devices, discussing varactor, varistor, tunnel, Gunn, IMPATT and TRAPATT diodes and power transistors characteristics and applications
09 p1285 A72-22567

Noncontacting measurements by miniature CW Doppler radar with semiconductor microwave generator
09 p1285 A72-22691

Microwave equipment and technology application for instrument landing, terminal ATC, millimeter wave CAT detection and satellite communications
10 p1509 A72-24036

Microwave equipment for electron density profiles determination used in ionization relaxation start study of shock induced Ar plasma
10 p1519 A72-24067

Microwave frequency mixer using two inverted tunnel diodes in series connection
10 p1450 A72-24519

Three centimeter balanced ring modulator with carrier and sideband suppression using amplitude and phase relations
11 p1605 A72-26321

Self balanced microwave static calorimeter with substantial delay time, discussing system instability conditions
11 p1634 A72-26450

Microwave power transistors and active two terminal devices performance, describing representative applications
11 p1607 A72-26983

Spatial and time dependence of electron velocity in short channel microwave FET, using Monte Carlo method
12 p1790 A72-27434

Maximum transmission delay in microwave TWT delay lines as function of electron beam size, current, shape and velocity distribution
12 p1782 A72-27436

Cryogenic microwave equipment for solids study provided with adiabatic demagnetization cooling system, noting relaxation time measurement in magnetic fields
12 p1796 A72-27856

Broadband superconducting quantum microwave magnetometer design, operation and performance
12 p1812 A72-28219

Regional microwave ground distribution facility for TV service organized for satellite relay transmitted video signals accommodation
13 p1918 A72-28984

[AIAA PAPER 72-557]

Digital microwave power measuring device with automatic range selection
13 p1931 A72-29267

Mechanical fabrication of rectangular to cylindrical waveguide transitions for X band
13 p1932 A72-29475

Telecommunication satellites microwave components, emphasizing reliability requirements in multiplex systems
13 p1933 A72-29835

Microwave device phase and amplitude frequency response measuring equipment with wide range test pulse generation, discussing design and performance 13 p1934 A72-30091

Microwave pulse frequency shift and frequency modulation in YIG bar magnetostatic delay line with adiabatically varying parameters 13 p1923 A72-30095

Ferrite materials for microwave applications, discussing frequency and temperature limit extension, power level increase and loss reduction 14 p2088 A72-30833

Microwave semiconductor device technology review and development prospects in terms of fabrication processes and materials 14 p2088 A72-30834

Correlation between internal noise sources of microwave transistors at low collector currents 14 p2088 A72-30917

Microwave scale model of ILS glide path, considering interference and aircraft taxing effects 14 p2129 A72-30944

Nonlinear plasma oscillations effect on electron bunching in microwave devices, noting space charge waves of finite amplitude 14 p2089 A72-31106

In and Gd substitution effect in calcium-vanadium garnets as potential microwave materials, discussing magnetic properties, resonance linewidth and temperature stability 15 p2293 A72-32243

Calculations showing the reduction in the frequency dependence of a two-element array antenna fed by microwave transistors. 17 p2514 A72-34369

Microwave Doppler radar spectrum-based design parameters. 17 p2515 A72-34422

Microwave technology - A five year prospective. 17 p2528 A72-34709

The absolute calibration of periodic microwave phase shifters without a standard phase shifter. 17 p2531 A72-35470

Design of a 14/12 GHz transponder for the Communications Technology Satellite. 18 p2660 A72-36540

Microwave varactors for communications satellites. 18 p2670 A72-37122

Microwave and optoelectronic devices performance and component reliability, considering varactors, p-i-n, avalanche and Gunn diodes, ICs, FETs, light emitters and liquid crystals 18 p2720 A72-37137

Physical parameters and structure of microwave power transistors, noting scanning electron microscope analysis of fine structure 18 p2671 A72-37144

High burnout gallium arsenide Schottky barrier diodes. 19 p2770 A72-37259

Room temperature operation of microwave acoustic delay lines with magnesium aluminate spinel, discussing acoustic mode conversion and shear wave piezoelectric transducers 19 p2800 A72-37875

High power microwave nanosecond pulse generator with waveguide standing wave resonator, noting power gain and pulse shape 19 p2776 A72-38672

Microwave landing system effect on the flight guidance and control system. 20 p2952 A72-40057

ILS replacement by microwave landing system, considering landing phase range from acquisition to touchdown, terminal approach handling by airborne navigation system and economic advantages 21 p3081 A72-40294

Design and frequency characteristics of cylindrical waveguide diode for microwave range, noting semiconductor junction effect on device efficiency 21 p3036 A72-41837

Mathematical description and calculation of the steady-state regime of a microwave power stabilizer with a semiconductor attenuator 23 p3270 A72-43766

Ferrite component for waveguide commutator used as microwave switching element and modulator, noting application in navigation instruments and avionics 23 p3270 A72-43768

Possible impact of area navigation upon MLS requirements for azimuth angular coverage and range. 24 p3422 A72-44643

Solid state microwave devices, discussing varactor, varistor, tunnel, Gunn, IMPATT, and TRAPATT diodes and power transistors characteristics and applications 24 p3384 A72-44746

MICROWAVE FILTERS

Computerized optimization procedure for microwave circuits without tuning elements, applying to high pass filter design 01 p0040 A72-10686

Waveguide channel microwave bandpass filters for radio relay systems, discussing methods of improving

group delay in passband and attenuation at harmonic frequencies 01 p0041 A72-10694

Hybrid IC at 30 GHz, considering IMPATT oscillators, circulators, frequency multipliers and filters configuration and performance 01 p0046 A72-10699

Quasi-optical 30-60 GHz varactor doubler circuit filters, waveguide tuners and mounts for frequency multipliers 04 p0507 A72-15617

Dissipative loss effects on frequency response and miniaturization limits for minimum loss conditions in microwave filters with Chebyshev characteristics 05 p0638 A72-17188

Multicircuit hf filters tuning drive with mechanical synchronization correction 06 p0774 A72-17749

Weighted acoustic surface wave dispersive microwave filter apodized interdigital array design modification for phase error correction to reduce distortion 06 p0787 A72-18380

Unified design charts for communication systems filter networks with inverse Chebyshev and elliptic function responses 06 p0787 A72-18400

Steepened microwave bandpass filters with bypass and flattened reflection coefficient and delay, discussing design and implementation 07 p0954 A72-19175

Narrow bandpass waveguide filters synthesis, using orthogonal mode cavities to realize negative coupling elements 10 p1451 A72-24591

Lossless distributed rectangular microwave structure with dielectrics interposed between two conductive metallic layers, noting existence of transmission zeros and filter properties 11 p1607 A72-26990

Susceptance inductive loaded evanescent mode waveguide filters with reduced length, using quartz tuned elements 12 p1792 A72-27697

Ferrite microwave limiter-filters and circulators using resonant rotation of polarization plane 13 p1927 A72-28409

Minimum amplitude and phase distortion selective bandpass filters/equalizers for satellite communications, noting realizability in UHF and microwave bands 14 p2089 A72-31048

Inexpensive microwave high density channel filters to meet amplitude and phase requirements without external equalization 15 p2210 A72-31181

German monograph on microwave broadband tunnel diode mixers theory and design, taking into account parasitic elements as part of filter networks 16 p2368 A72-33507

YIG filter banks for ECM and communications. 19 p2772 A72-37523

Dissipative loss effects on frequency response and miniaturization limits for minimum loss conditions in microwave filters with Chebyshev characteristics 19 p2775 A72-38624

Microwave filters in antenna circuit feeder systems of space vehicles 21 p3026 A72-40318

Microwave filter of interdigital or comb construction, calculating attenuation coefficient relationship to impedance of slabline with cylindrical inner conductor 21 p3032 A72-40628

Correction of diffraction errors in acoustic-surface-wave pulse-compression filters. 21 p3034 A72-41464

MICROWAVE FREQUENCIES

NT C BAND

NT EXTREMELY HIGH FREQUENCIES

NT SUPERHIGH FREQUENCIES

Natural and artificial snowpacks microwave brightness temperature variations with snow depth, free water content and underlying material characteristics 02 p0212 A72-11832

Wideband spectrum utilization above 10 GHz for high speed digital communications and ecological monitoring 02 p0176 A72-12182

Microwave photoconductivity and photodiode effect in organic semiconductors 04 p0561 A72-15083

Frequency characteristics theory for two-stage electron tube microwave amplifiers coupled by transmission line on order of wavelength 05 p0634 A72-15827

Ultrasensitive measurement technique for low microwave susceptibility on ferrite samples featuring feedback scheme for signal klystron locking 07 p0955 A72-19320

Hydrogen plasma generation by microwave field in magnetic-mirror device due to electron cyclotron resonance, measuring transverse diffusion coefficient dependence on magnetic field 07 p1046 A72-20506

Antimony compounds single crystal whiskers permittivity determination at microwave frequencies from power reflection and transmission coefficients 09 p1366 A72-22417

Chemistry and performance characteristics of flash photolysis and microwave discharge initiated CW carbon disulfide/oxygen lasers 09 p1325 A72-23236

Radar IF voltage in-phase and quadrature components detection thresholds, evaluating square and octagonal approximations to circle for false alarm probabilities 10 p1438 A72-24693

Sea foam emission and reflection characteristics at microwave frequencies from radiometric measurements, correlating data as functions of frequency and angle 10 p1475 A72-24749

Low noise power level measurement at microwave frequencies, noting Nyquist equation applicability and cooled-to-uncooled element connections effects in receivers 12 p1779 A72-27175

Microwave breakdown calculation on symmetrically excited conical reentry vehicle based on variational technique, comparing with experimental data 13 p1916 A72-28536

Analog simulation of Josephson superconducting junctions dc characteristics for two mixed microwave frequencies, discussing signal detection sensitivity improvement 13 p2021 A72-28648

Polarization method for measuring small phase difference variations in microwave range, developing rules for optimum selection of multiplication factor 13 p1928 A72-28790

Phase error magnitudes due to individual microwave elements imperfections and multiple reflections in phase difference measurements by polarization method in microwave range 13 p1928 A72-28791

Titanium nitride powder obtained by hydrogen reduction of titanium tetrachloride in nitrogen flow heated in microwave electrodeless discharge 13 p1967 A72-30111

Plasma heating in Tuman 2 toroidal magnetic trap by microwave injection at upper hybrid frequencies 14 p2137 A72-30311

High microwave voltage effects on p-i-n junction conductance under inverse dc bias, noting role of hole generation and accumulation by impact ionization 15 p2206 A72-31643

Piezoelectric substrate covered with semiconductor layers, calculating sound amplification characteristics at microwave frequencies 15 p2197 A72-31895

Microwave measurements on high permittivity materials with slotted waveguides excited in E mode 15 p2207 A72-31894

Low cost microwave scanning beam landing systems for interim instrument landing system replacement in civil aviation 15 p2272 A72-32217

Oxygen molecule parameters from frequency data in microwave, submillimeter and IR spectroscopy 15 p2283 A72-32654

Millimeter-wavelength frequency multipliers employing gallium arsenide diodes 17 p2529 A72-34851

A revision of Jupiter brightness temperatures in the frequency interval 18.5-24.0 GHz /1968/. 17 p2610 A72-35119

Multifunction microwave apertures - Concepts and potential. 17 p2531 A72-35574

Magnetic dipole matrix elements for atomic transitions between Zeeman levels at microwave frequencies 17 p2585 A72-35769

He-Ne laser radiation modulator at 1.5 GHz using X and Z cut lithium niobate crystals in toroidal microwave cavity 18 p2697 A72-36113

UHF and microwave dielectric properties of an amorphous semiconductor. 18 p2718 A72-36311

Quasi-linear theory of plasmas situated in a weak UHF electric field and a constant magnetic field 18 p2715 A72-36654

Numerical analysis of microwave heat generation in disc-shaped Luneberg lenses. 21 p3032 A72-40627

MHD stability in Hg vapor discharge plasma excited by standing microwave near electron cyclotron resonance, discussing electron energy anisotropy effect on LF oscillations 21 p3091 A72-40671

Study of the thermal self-focusing of electromagnetic waves in a plasma 22 p3211 A72-42652

Plasma heating in Tuman 2 toroidal magnetic trap by microwave injection at upper hybrid frequencies 23 p3318 A72-43213

Low frequency oscillations of cesium and mercury vapor plasmas, noting intensity distribution, radiation

pattern and polarization characteristics of microwave emission

23 p3319 A72-43411

Frequency characteristics theory for two-stage electron tube microwave amplifiers coupled by transmission line on order of wavelength

23 p3268 A72-43435

Influence of noise on the accuracy of microwave phase meters

23 p3272 A72-43845

MICROWAVE IMAGERY

Diffraction theory of microwave holography, presenting computer aided imaging approach for alleviating optically reconstructed image distortion

01 p0068 A72-10707

Microwave hologram CW radar system, discussing theory and flight test imagery, optical processors and alignment procedures

02 p0171 A72-11819

Microwave holography using transmitting and receiving antenna for generation of synthetic aperture in angular direction

06 p0814 A72-17486

Subtractive microwave holography application to plasma discharge diagnostics

07 p0981 A72-18889

Low energetic efficiency of semiconductor microwave scanning converters for radio images of fog obscured objects

13 p1932 A72-29297

Airborne microwave hologram radar system, discussing along- and cross-track direction resolution realization by synthetic aperture technique and phased receiving array respectively

15 p2196 A72-31788

Microwave holographic imaging techniques for aircraft landing aids and airport security applications, discussing real time operation

19 p2798 A72-37625

Experimental investigation of direct quasi-optical radiovision of small objects

19 p2768 A72-38673

Image quality of binary and multigradation microwave holograms, noting HF components and background noise

21 p3055 A72-40794

Dark field method for phase diffraction grating visualization by microwave holography, using radio lens for object microwave spectrum formation

21 p3055 A72-40795

MICROWAVE INTERFEROMETERS

Microwave holographic interferometry with optical wave front reconstruction for visual mapping of large objects deformation

01 p0072 A72-11236

Varactor diode microwave parametric amplifiers for radio astronomy interferometer, discussing system design features for gain and phase stabilities

02 p0192 A72-12043

Plasma density profiles by microwave interferometry technique in Sirius stellerator divertor for two magnetic field configurations and injection methods

04 p0555 A72-14619

High resolution Galactic center interferometric observations at 5 GHz, showing compact components in Sagittarius A

04 p0580 A72-15511

High resolution stabilized superheterodyne microwave interferometer, noting noise figure and dynamic range

07 p0993 A72-20590

Interferometer investigations of Cassiopeia linear polarization at centimeter wavelengths, explaining results by source model incorporating Faraday depolarization

12 p1865 A72-27094

Microwave interferometry as plasma diagnostic technique to measure electron densities in partially ionized dense gases

14 p2103 A72-30177

Comparative electron density measurements in positive low pressure He discharge column with Langmuir probes and microwave interferometer and cavity

14 p2105 A72-30808

Ku band radio interferometer for discrete radio sources mapping, discussing construction and incorporated PDP-8 computer for pointing, tracking, delay compensation and data analysis

15 p2207 A72-32107

How to measure surface and atmospheric conditions on Venus by microwave interferometry

17 p2611 A72-35321

Precision interferometric observations of Venus at 11.1-centimeter wavelength

17 p2611 A72-35322

A new, earth-based radar technique for the measurement of lunar topography

18 p2659 A72-36277

Two-frequency microwave holographic interferometry

20 p2927 A72-39784

The measurement of the local electron density by means of direct reading microwave interferometer

21 p3056 A72-41220

A Lecher wire microwave interferometer for measurements of electron density and electron temperature in a flowing transient plasma

23 p3292 A72-44543

MICROWAVE OSCILLATORS

NT BACKWARD WAVE TUBES

NT GAS DISCHARGE TUBES

Tunnel diode microwave oscillator design by circle diagrams of operational and load characteristics

01 p0035 A72-10048

Microwave Gunn oscillator frequency modulation in quenched domain mode, calculating signal admittance as function of bias voltage and amplitude

01 p0035 A72-10224

Transferred electron microwave oscillators /three-level and LSA relaxation types/ and amplifiers /reflection and traveling wave types/ fabrication, technology and performance capabilities

01 p0035 A72-10627

Planar Gunn effect devices for microwave oscillators, discussing impedance matching and diode conductivity profile effect on output power

01 p0028 A72-10628

Transferred electron microwave oscillator diodes with n-n-n structure by liquid phase epitaxy, reducing high resistance layer in interfaces and crystal defects

01 p0036 A72-10629

High power Q-band pulsed Gunn diode microwave oscillator constructed from thin GaAs sandwich layers grown by vapor phase epitaxy

01 p0036 A72-10630

Liquid phase epitaxial GaAs transferred electron microwave oscillators with high dc to rf conversion efficiencies dependent on frequencies

01 p0036 A72-10631

Bulk InP three level transferred electron microwave oscillators, observing current-controlled instabilities and operation modes

01 p0036 A72-10632

CW and pulsed InP transferred electron microwave oscillators, discussing fabrication techniques and electrical properties

01 p0036 A72-10633

High efficiency transferred electron microwave oscillators operated in short LSA mode, noting pulse-operated diode power appearance time delay behavior

01 p0036 A72-10634

L-band Gunn oscillator using nonsinusoidal device voltage /switching mode/, comparing efficiency and output power with sinusoidal mode

01 p0036 A72-10635

Electronic tuning of transverse Gunn effect microwave oscillators by varying voltage on third electrode incorporated between cathode and anode

01 p0036 A72-10637

Output power, efficiency and fundamental frequency resistance of Gunn microwave self oscillator in single and multiresonant mode

01 p0037 A72-10638

Lf noise spectrum of Gunn oscillators due to direct modulation of rf admittance for constant voltage bias source

01 p0037 A72-10639

Gunn diode microwave oscillator postcoupling to waveguide, deriving theory based on equivalent circuit for load impedance assessment

01 p0037 A72-10640

CW X-band Gunn oscillator in coaxial cavities, investigating frequency variation with ambient temperature

01 p0037 A72-10641

Microwave oscillator detector Gunn diode as inexpensive alarm device for Doppler radar application

01 p0028 A72-10642

AM and FM noise reduction of cavity and injection stabilized microwave Gunn and avalanche diode oscillators

01 p0037 A72-10644

Phase locked IMPATT diode microwave oscillator transients for reflection amplifier or pulse modulated source applications

01 p0037 A72-10646

Wideband modulation feedback technique for IMPATT diode oscillator AM-FM noise suppression

01 p0037 A72-10647

Synchronized multiple microwave oscillators power and noise characteristics at microwave and millimeter frequencies, discussing magic T configuration

01 p0037 A72-10648

CW power of single cavity multiple IMPATT diode oscillator at 9.1 GHz, comparing with moding of multiple device oscillators

01 p0038 A72-10649

X band power, bandwidth, efficiency and temperature performance of one watt CW microwave integrated avalanche diode oscillator

01 p0038 A72-10650

Resonant traveling wave IMPATT oscillators wave propagation and power output characteristics, taking into account metal conductor and semiconductor substrate losses

01 p0038 A72-10651

Voltage and current waveforms monitoring on sampling oscilloscope for TRAPATT microwave oscillator performance optimization

01 p0038 A72-10653

MICROWAVE OSCILLATORS

Microwave TRAPATT oscillator efficiency, using avalanche diode in coaxial cavity, slug and tapered sleeve

01 p0038 A72-10654

Hybrid IC at 30 GHz, considering IMPATT oscillators, circulators, frequency multipliers and filters configuration and performance

01 p0046 A72-10699

Gunn and IMPATT diodes applications for microwave power oscillators and amplifiers in radio link equipment

01 p0042 A72-10711

Low noise phase locked power microwave sources for solid state radio links with 960 voice channels, discussing design

01 p0006 A72-10712

Phase stable locked local oscillators for K band radiometers for long baseline interferometric measurements, emphasizing construction technique

01 p0044 A72-11307

High efficiency GaAs transferred electron device operation and microwave oscillator design by simple static I-V characteristics description for time domain computer simulation

02 p0193 A72-12230

Book on microwave electronics covering electron beam microwave devices and solid state microwave oscillators and amplifiers

03 p0331 A72-13233

CW avalanche diode microwave oscillator frequency modulation, using injected rf signal

03 p0334 A72-14075

High intensity ionizing gamma ray pulsed radiation effects on Gunn diode microwave oscillator failure modes

03 p0334 A72-14089

Ionizing radiation effects in cavities of microwave Gunn oscillators, noting large dose rate effects on circuit performance

03 p0335 A72-14094

Three terminal voltage-tunable Gunn effect microwave oscillator, discussing depletion depth and electric field control modes for frequency

04 p0496 A72-14479

Gunn diode large signal admittance dependence on bias and frequency, discussing computer simulation and broadband oscillator and amplifier design

04 p0497 A72-14712

Gunn diode microwave oscillator with moving reflector as self-excited mixer and load variation detector, analyzing performance by I-V characteristics model

04 p0497 A72-14713

Si p-n-p and Cr-n-p junction transit time diode oscillators microwave and dc characteristics comparison, noting similarity

04 p0499 A72-15206

Avalanche transit time diodes noise mechanisms and performance in microwave amplifier, oscillator and mixer applications

04 p0500 A72-15302

Transit time and LSA oscillations at millimeter and submillimeter wavelengths in n-type GaAs

04 p0563 A72-15593

Electron tube with Fabry-Perot cavity resonator with grooved and smooth mirrors for millimeter and submillimeter wave generation

04 p0503 A72-15598

Josephson junction as 100 GHz oscillator-mixer for heterodyne frequency conversion in millimeter and submillimeter regions, observing I-V characteristics

04 p0503 A72-15604

Large signal IMPATT diode microwave oscillator lumped model, considering steady state oscillation

04 p0503 A72-15672

Microstrip configuration for microwave GaAs IMPATT diode oscillators and power amplifiers

05 p0633 A72-15782

Computer simulation in optimized 5-GHz Gunn diode oscillator design

05 p0633 A72-16360

CW millimeter wave power generation with spiraling electron beams, investigating energy spread effects on performance limitation

05 p0636 A72-16363

Vapor-grown GaAs transfer electron microwave oscillator, discussing design, fabrication and CW power conversion efficiency

05 p0637 A72-16366

Fast frequency switching for shift keying pulse code modulation with two cavity modes for Gunn oscillator frequency states

05 p0631 A72-17072

Noise spectra of double sided CW silicon TRAPATT oscillator comparable to silicon IMPATT oscillator

06 p0783 A72-17482

Noise effect in IMPATT and Gunn diode oscillators on phase/frequency fluctuation using series/parallel connected multiple active devices

06 p0783 A72-17483

Analytical model of Gunn diode oscillating in resonant mode with domain quenching, determining current harmonics

06 p0783 A72-17573

Double heat sinking high power CW TRAPATT diode oscillators using integral metallic heat spreaders
06 p0784 A72-17788

InP transferred electron microwave oscillators, observing higher efficiency than IMPATT and GaAs devices
06 p0784 A72-18063

Transistorized automatic feedback power level control for centimeter band reflex klystron oscillator for electron paramagnetic resonance studies
06 p0784 A72-18166

Microwave IC oscillators design for broadband high performance receivers, exemplifying thin film Gunn effect, step- and varactor-tuned transistor oscillators
06 p0786 A72-18373

K band Gunn oscillator with high frequency stability, discussing construction, performance, output power and frequency saturation effect
06 p0786 A72-18375

IMPATT diode avalanche region microwave self oscillation mechanism explanation by cavity resonator and feedback theories
06 p0787 A72-18383

GaAs IMPATT diode with plated heat sink for microstrip circuit applications, exemplifying X band oscillator experiment
06 p0787 A72-18385

Transferred electron effect in GaAs, presenting three level solid state microwave oscillator advantages
06 p0866 A72-18454

High efficiency microwave avalanche diode oscillators circuit design in TRAPATT mode
06 p0787 A72-18455

System potential of microwave solid state generation and amplification, comparing IMPATT, TRAPATT, Gunn, LSA, transistor and transistor-multiplier devices
06 p0787 A72-18456

Computer simulation data on pulsed IMPATT microwave oscillator performance improvement via double-drift diodes and second harmonic tuning
06 p0788 A72-18463

IMPATT diode microwave oscillators and amplifiers calculating noise sideband correlation factor at randomly large signal frequencies
06 p0788 A72-18464

Pulsed and CW solid state microwave oscillator EM noise as function of power level and locking parameters
06 p0788 A72-18465

IMPATT diode oscillator injection locking behavior from model, comparing results with experiment
06 p0788 A72-18469

X band IMPATT and Gunn oscillator, calculating injection lock time, modulation bandwidth, noise and FM suppression and dynamic response
06 p0788 A72-18471

Transferred electron microwave oscillators design for various peak and average power levels, considering tradeoff between operating mode and device configuration
06 p0789 A72-18475

S band module with Gunn diode oscillators in series connection used as phased array radar 250 W power sources with efficient heat sink
06 p0789 A72-18476

Varactor tuned high performance Gunn oscillators, emphasizing specifications for level power output with frequency, tuning linearity and rate
06 p0789 A72-18479

Solid state Ku-band local Gunn oscillator for airborne radar applications, discussing design and batch process fabrication
06 p0789 A72-18480

LSA oscillators performance and control optimization, discussing multi-axis radial microwave cavity effectiveness in oscillation starting and coupling to coaxial transmission line
06 p0789 A72-18481

High power GaAs LSA transmitter oscillator refinements, noting pulsers development to change load and thermal environment frequency stability
06 p0789 A72-18482

Power generation and low noise amplification devices development during past decade, considering avalanche diodes, transferred electron and acoustoelectric devices and microwave transistors
07 p0952 A72-18825

Transit effects in grid plate gap of triode for generating microwave oscillations in regime similar to IMPATT diode
07 p0953 A72-19015

Low noise Ku band klystron oscillators for Doppler radar, discussing FM noise induced frequency deviation, spurious modulation and countermeasures
07 p0954 A72-19049

Low frequency modulation noise generation due to conductance fluctuations in Gunn oscillators, measuring noise spectra temperature dependence
07 p0954 A72-19050

Si p-n-p punchthrough X band oscillator, discussing wideband tuning and low noise properties and applications
07 p0955 A72-19252

Resonator second harmonic influence on Gunn oscillator parameters for transit and hybrid modes, discussing bias voltage, harmonic amplitudes, phase difference, doping level and frequency
07 p0955 A72-19254

YIG tuning of X band Gunn effect stripline oscillator circuit, noting application to microwave ICs
07 p0955 A72-19357

Gunn diode microwave oscillator thermal resistance reduction for increased output power and efficiency
07 p0958 A72-20685

IMPATT diode microwave oscillator stabilized by two external resonant circuits, investigating self oscillation characteristics
08 p1138 A72-20745

Optimal output power of avalanche transit time diode oscillator in millimeter band as function of electric field and diode geometry
08 p1141 A72-21378

Stationary statistical model for microwave oscillator flicker frequency noise, leading to power spectral density and time domain frequency instability
08 p1141 A72-21431

Digital frequency shift keying modulation of Gunn microwave oscillator by cavity placed between output and transmission line
08 p1141 A72-21432

German monograph on frequency noise of microwave transistor power oscillators covering generation mechanism and spectral density determination
09 p1285 A72-22340

Inexpensive solid state microwave sources development and applications considering spectrum allocations, health hazards and reliability problems
09 p1285 A72-22595

Cavity resonator frequency detuning effects on FM and AM noise in cavity stabilized Gunn microwave oscillator
09 p1285 A72-22651

Subharmonically injected phase locked microwave IMPATT oscillator
09 p1285 A72-22894

Random frequency FM noise model for microwave Gunn effect oscillators
09 p1288 A72-23122

Bulk effect diodes combination with YIG elements to provide oscillator operation up to 18 GHz, discussing design, circuit diagrams and performance
10 p1448 A72-24037

Double balanced frequency converter design for selective microwave generation by combination of CW or swept signal with local oscillator source
10 p1448 A72-24038

Short and long term frequency stability improvement in X band klystron oscillator stabilized by high Q superconducting cavity
10 p1449 A72-24303

Power-combining methods for synchronous detuned solid state microwave oscillators with stable large signal locking characteristics, noting feasibility
10 p1449 A72-24306

Coupled line microstrip circuit for high power and efficiency L and S band TRAPATT diode oscillators
10 p1450 A72-24307

CW X band Gunn microwave oscillators, measuring frequency variation relationship to ambient temperature
10 p1450 A72-24555

GaAs abrupt junction IMPATT diode large signal operation analysis, noting oscillation efficiency HF fall-off characteristics
10 p1450 A72-24557

YIG tuned Gunn oscillator phase locking and shifting over 3 GHz range in X band, using feedback control
10 p1451 A72-24596

Computer simulation for TRAPATT circuit response to periodic current impulse, noting avalanche diode microwave oscillation efficiency
10 p1458 A72-24935

Bulk negative resistance devices equivalent noise temperature derivation via diffusion-impedance field noise formula, obtaining Gunn oscillators SNR approximate value
10 p1454 A72-25106

Multi-axis radial circuits for transferred electron microwave oscillator performance optimization to obtain wideband CW amplification, discussing LSA tests
11 p1604 A72-25745

Si Pd-n-p-plus/ transit time diode microwave oscillator, discussing fabrication, FM noise spectrum and bias current fluctuation
11 p1604 A72-25748

High efficiency CW performance of InP transferred electron microwave oscillator with anomalous I-V characteristics temperature dependence
11 p1604 A72-25750

Epitaxial InP diode for high efficiency circuit controlled microwave oscillator, discussing solution growth technique, layers electrical properties and I-V performance
12 p1854 A72-27162

Stacked TRAPATT diodes oscillator with microstripline circuit to obtain 1 kw peak power at 1 GHz
12 p1788 A72-27163

Continuous wave Doppler radar with microwave oscillator for ATC measurements and surveillance
12 p1789 A72-27403

Encapsulation influence on Gunn effect devices from circuit analysis of wideband tunable transferred electron microwave oscillators
12 p1790 A72-27440

K band Read avalanche diodes fabricated by epitaxial deposition and diffusion processes, measuring capacitance-voltage characteristics and oscillator power efficiency
12 p1790 A72-27441

Microwave and optical quantum electronic sources for frequency standards, noting primary Cs reference and multimode laser-RF oscillator beat technique
12 p1824 A72-27867

C and X band CW GaAs Schottky barrier IMPATT oscillators with nichrome as barrier metal, noting high power efficiency and low noise performance
12 p1793 A72-27966

Microwave source four hundredth order harmonic mixing with laser radiation, using Josephson junction and maser
12 p1827 A72-28221

Solid state InP sources for microwave transferred electron oscillators and amplifiers with improved conversion efficiencies, comparing with GaAs
13 p2020 A72-28432

Pulsed IMPATT diode oscillators, pulse power capabilities, considering microwave circuit, dc and pulse biasing, power limitation and circuit anomalies
13 p1931 A72-29109

CW Gunn oscillator cavity loading and bias voltage effects on external negative differential conductance
13 p1933 A72-29825

Liquid and two phase liquid-gaseous hydrogen density determination via dielectric constant measurement by open-ended microwave cavity
14 p2103 A72-30197

Millimeter and submillimeter radiation produced by diffraction phenomena during charged particle passage near periodic structures, discussing physical properties and oscillator development
14 p2088 A72-30598

Microwave power generation via semiconductor devices, discussing circuit problems due to negative resistance
14 p2088 A72-30832

CW oscillator model for laser amplifier, including nonlinear effect of gain saturation
14 p2111 A72-30896

Correlation measurements of LF current noise and frequency fluctuations in Gunn oscillators, emphasizing generation-recombination noise component
14 p2088 A72-30916

Amplitude and frequency characteristics of avalanche diode microwave oscillator loaded with resonant circuits, noting Q value effect on self oscillations
14 p2089 A72-31109

Self oscillations of microwave autodyne oscillator loaded by two resonant cavities, noting radio spectroscopic applications
14 p2089 A72-31110

Two cavity self exciting SHF microwave oscillator with resistance coupling through low Q-factor resonant diaphragm, noting frequency stability
14 p2090 A72-31121

Prototype local oscillator for X band communication satellite, discussing electrical and mechanical characteristics and temperature and noise measurements
15 p2204 A72-31182

EHF double-drift IMPATT oscillator small and large signal behavior analysis with computer program, noting second harmonic tuning and single frequency operation possibilities
15 p2204 A72-31314

Equivalent circuit characterization of waveguide-mounted IMPATT diode oscillators and associated circuit parasitics at millimeter wave frequencies
15 p2205 A72-31315

Generalized locking equation for microwave oscillator bandwidth prediction for arbitrary cavity configurations and waveforms, considering strong harmonics presence
15 p2205 A72-31358

High efficiency X band pulse operation of transferred electron oscillator in hybrid mode, noting high material quality and optimum impedance match
15 p2206 A72-31548

Pulsed IMPATT diode oscillators RF oscillations growth rate and frequency shift behavior during build-up period, comparing equivalent circuit derived electrical properties with measurements
15 p2208 A72-32472

Gunn diode elements design, operation, performance, efficiency, heat dissipation, lifetime and applications as microwave oscillators
15 p2208 A72-32500

Avalanche generation process interpretation for nontransit frequency oscillations association with current runaway in bulk InP microwave diode oscillators
16 p2369 A72-33755

High efficiency and power S-band pulsed oscillator using avalanche diode and microstrip circuit
16 p2369 A72-33759

Frequency stabilized self-oscillating microwave up-converter with transferred electron diodes, noting maximum power output and bandwidth
16 p2369 A72-33764

Microwave and optical quantum electronic sources for frequency standards, noting primary Cs reference and multimode laser-RF oscillator beat technique
16 p2403 A72-33976

Noise-to-carrier ratio and rms frequency deviation evaluation for X band Gunn and Si and GaAs avalanche diode oscillators
16 p2370 A72-34177

Simple Doppler radar using the CL8630 Gunn effect oscillator for the observation of small rotating objects.
17 p2524 A72-34245

BARITT, IMPATT, TRAPATT and Gunn diodes, discussing power, noise and thermal dissipation problems
17 p2526 A72-34465

Pulsed Impatt diode oscillator circuit design and operation frequency prediction for high Q coaxial structures from equivalent circuit
17 p2526 A72-34466

Avalanche diode oscillators.
17 p2526 A72-34563

Russian book on microwave electronics covering linear-beam and cross-field backward and traveling wave amplifiers and oscillators, klystrons, masers, plasma devices, etc
17 p2532 A72-34650

Characteristics of Gunn elements CGY 11 to 14 and their application as microwave oscillators. II
17 p2530 A72-35150

Superconducting-cavity-stabilised oscillator of high stability.
17 p2530 A72-35386

Electrical characteristics of bulk n-InP oscillators.
18 p2666 A72-36456

Frequency/temperature characteristics of Gunn devices.
18 p2667 A72-36684

Frequency-modulation sensitivity and frequency-pushing factor of a Pd-n-p/+/- punchthrough microwave diode.
18 p2667 A72-36686

LSA diode relaxation oscillator loading effect on oscillation damping, calculating optimum loading as function of conductance
18 p2667 A72-36690

The behaviour of a Gunn oscillator in the domain-delayed mode.
18 p2667 A72-36945

Synchronization and noise performance of mutually coupled oscillators.
18 p2668 A72-37036

Thermal modulation and FM noise of Gunn oscillators.
18 p2668 A72-37038

Endurance test results for microwave avalanche diode oscillators
18 p2671 A72-37146

Improved injection locking of microwave FM-oscillators.
19 p2771 A72-37262

K-band high power single-tuned IMPATT oscillator stabilized by hybrid-coupled cavities.
19 p2771 A72-37263

A 22 percent C.W. efficiency solid state microwave oscillator.
19 p2771 A72-37266

German monograph - Measurement of 'oscillation impedances' and optimization of frequency noise effects of microwave-semiconductor oscillators tunable over a wide frequency range
19 p2772 A72-37477

Some tuning characteristics and oscillation conditions of a waveguide-mounted transferred-electron diode oscillator.
19 p2772 A72-37569

The effect of junction temperature on the output power of a silicon IMPATT diode.
19 p2773 A72-38145

An analytical equivalent circuit representation for waveguide-mounted Gunn oscillators.
19 p2773 A72-38291

A solid-state transponder source using high-efficiency silicon avalanche oscillators.
19 p2774 A72-38400

Some problems of microwave electromagnetic oscillation phase control by using an inductance transistor
19 p2776 A72-38670

Acousto-optic modulation with coupled Gunn oscillator-piezoelectric structure.
20 p2960 A72-39702

A general analysis of noise in Gunn oscillators.
20 p2909 A72-39782

Current and voltage waveform measurements with sampling oscilloscope and capacitive voltage-divide probe to verify TRAPATT diode oscillator theoretical model
21 p3032 A72-40635

Analysis of large-signal noise in Read oscillators.
21 p3032 A72-40698

Temperature effects on modulation sensitivity and vibrational spectra in Gunn diode oscillators, suggesting frequency stability improvement method
21 p3032 A72-40792

Intermodulation distortion of FDM-FM in injection locked oscillator.
21 p3020 A72-40899

A regenerative high multiplicity tunnel-diode frequency multiplier
21 p3034 A72-41122

Effects of tunneling on an IMPATT oscillator.
21 p3034 A72-41382

Calculation of the electronic readjustment of a tunnel-diode oscillator by a varactor
22 p3159 A72-42246

Low temperature characteristics of the Gunn diode.
22 p3159 A72-42307

Plasma diagnostics by means of microwave cavity resonators
22 p3212 A72-42950

Frequency-variable semiconductor-oscillator in the microwave region.
23 p3272 A72-43948

Stability criteria for phase-locked oscillators.
23 p3272 A72-44192

A single-tuned oscillator circuit for Gunn diode characterizations.
23 p3272 A72-44194

Signal frequency distortions in frequency-modulated oscillators with feedback delay
23 p3266 A72-44209

Reciprocal synchronization of generators connected by a long line section
23 p3272 A72-44210

Amplitude dependence of frequency in oscillators.
24 p3385 A72-44964

Frequency stability of Gunn oscillators with variation of ambient temperature.
24 p3385 A72-44980

MICROWAVE PHOTOGRAPHY
Meteorological precipitation and earth surface under cloud characteristics from airborne microwave radiation measurements using millimeter and centimeter waves
02 p0216 A72-11889

Swept frequency resolution and optical processing in propellant grain flaw detection by microwave holography, using Vander Lugt filter imaging
19 p2798 A72-37626

MICROWAVE PLASMA PROBES
Double Langmuir probe, microwave cavity and upper hybrid frequency measurements of plasma density in hydrogen, helium, neon and argon
01 p0110 A72-11190

Microwave measurements of plasma parameters in medium pressure gas discharges in absence of constant magnetic field and in weak electromagnetic field
01 p0072 A72-11215

Electron density microwave measurements in helium-neon laser plasma, discussing population inversion during glow discharge
01 p0081 A72-11216

Spatial distribution of plasma density from phase shift measurement in millimeter waves based on microwave multichannel probes
02 p0263 A72-11412

FM homodyne phase meter with klystron oscillator for measuring plasma electron concentration, presenting block diagrams of meter, detector and oscillator
02 p0223 A72-11414

Direct phase measuring and measured phase compensating microwave devices designed for plasma diagnostics applications
02 p0223 A72-11416

Phase measurements at if in microwave plasma diagnostics, examining phase stabilization processes
02 p0223 A72-11417

Passive electric microwave probe with balancing capacitance for studying waveguide fields at high microwave power levels in radiative plasma accelerators
02 p0223 A72-11418

Numerical method for cylindrical microwave cavities calibration for plasma diagnostics, noting computer programs applicability for arbitrary electron density radial distributions
05 p0662 A72-16418

Self action penetration of electromagnetic wave through dense collisionless plasma layer in high vacuum, using antenna microwave probes
05 p0695 A72-16601

Hydrogen plasma production, using linearly polarized microwaves with superimposed magnetic field
13 p2010 A72-28683

Heat-pipe plasma oven for microwave and spectroscopic measurements.
20 p2912 A72-39433

Calibration procedure to correct for the effects of dielectric containers in microwave plasma density measurements.
21 p3056 A72-41377

Spatial measurement of the magnetic field direction in plasma.
21 p3094 A72-41633

Electron density and temperature in microwave plasmas at higher pressures.
22 p3211 A72-42479

A Lecher wire microwave interferometer for measurements of electron density and electron temperature in a flowing transient plasma.
23 p3292 A72-44543

MICROWAVE PROBES
NT MICROWAVE PLASMA PROBES
Remote passive microwave sensing of ocean surface wind fields, discussing sea microwave brightness temperature dependence on wind speed
02 p0214 A72-11864

Microwave time of flight method for measuring electron drift velocity in GaAs semiconductor
12 p1855 A72-27667

Ultrabroadband probe design for microwave radiation intensity measurement in harmful exposure study
15 p2191 A72-32574

MICROWAVE RADIATION
U MICROWAVES
MICROWAVE RADIOMETERS
Atmospheric humid cover measurement with airborne/spaceborne microwave radiometric sounding, considering radiothermal radiation models
02 p0253 A72-11733

Earth surface and atmosphere remote sensing by airborne microwave measurements, noting ocean surface emittance dependence on temperature, surface conditions and pollution
02 p0207 A72-11779

Subsurface discontinuity detection by microwave radiometry, noting microwave temperature correlation with moisture patterns
02 p0209 A72-11792

Ground based passive remote sensing of low altitude vertical temperature profiles by microwave radiometry
02 p0211 A72-11807

Narrow beam millimeter wave radiometer with real-time TV display for terrain mapping, analyzing contours blurring caused by antenna pattern and output integration
02 p0191 A72-11821

Oil spills remote detection by multispectral photography, IR scanner imagery and microwave radiometry
02 p0226 A72-11830

Passive microwave remote sensing, discussing thermal imaging, radiometer tracking and image deterioration due to antenna imperfections
02 p0214 A72-11865

Microwave measurement and interpretation of oceanic thermal emission in terms of molecular temperature
02 p0214 A72-11866

Surface temperature measurement by microwave radiometry, noting sensitivity reduction due to moisture effects for resolution cell size targets
02 p0214 A72-11867

Soil surface moisture content and temperature profile determination by remote microwave sensing
02 p0214 A72-11871

Calibration technique for low energy IR radiometers, calculating detector field of view energy content or photons number from mirror reflectivity and temperature
03 p0359 A72-13441

Dicke-type microwave radiometer for daily measurements of 2800 MHz solar flux, discussing antenna system and dynamic range
04 p0522 A72-15163

Radar and radiometric millimeter wave signal systems in near earth environment for remote detection purposes
04 p0494 A72-15610

Combined FM CW radar and radiometer at millimeter wavelengths, investigating objects signatures measurement
04 p0494 A72-15611

Microwave and IR radiometer surveillance of oil spills, discussing sources tracking, sea surface oil volume and flow rate determination and terminal location prediction
05 p0658 A72-16599

Earth resources applications of multispectral remote sensing techniques for airborne and satellite-borne imaging systems, discussing microwave radiometer augmentation of visual and IR data
06 p0813 A72-17430

Airborne or satellite-mounted millimeter wave radiometer for atmospheric water vapor determination noting accuracy advantage over IR measurement
06 p0814 A72-17589

Microwave radiometer and scatterometer sensing for earth surface and subsurface measurements
06 p0815 A72-17784

Superheterodyne radiometers for millimeter and submillimeter waves, using Mach-Zehnder inter-

- ferometer frequency mixer for parasitic signal suppression
08 p1140 A72-21265
- Sea surface roughness mapping by airborne microwave radiometry with correction for viewing angle and atmospheric effects
09 p1297 A72-22525
- Calibrator for millimeter wave horn radiometers, using radiation from lead immersed in liquid nitrogen
09 p1310 A72-22652
- Constraint on astrophysical sources of gravitational waves, using microwave radiometers
11 p1721 A72-26124
- Microwave radiometer performance analysis, deriving input noise power relation to instrument indication in terms of noise parameters
14 p2105 A72-30587
- Microwave radiometry for celestial body emitted or reflected radiation observation, discussing radar cartography with emphasis on side-looking and synthetic aperture radars advantages
15 p2232 A72-31251
- Microwave /60 GHz/ radiometer for air temperature measurement outside aircraft during icing conditions
16 p2393 A72-33631
- Microwave spectrograph with broadband superheterodyne total-power radiometer for time-shared recording solar burst dynamic spectra
17 p2552 A72-34191
- Solar tracking via automatic 5-GHz radiometer with paraboloid antenna, using continuous polar axis rotation in one direction
18 p2691 A72-36433
- S-band radiometer design for high absolute precision measurement.
19 p2794 A72-37252
- Ground-based sensing of temperature profiles from angular and multi-spectral microwave emission measurements.
23 p3285 A72-44147
- Remote sensing of earth resources by microwave radiometry.
24 p3402 A72-45107
- ### MICROWAVE REFLECTOMETERS
- Visual/graphical recording microwave reflectometer for measuring reflection coefficient along waveguide component, based on Fourier transform evaluation by real time analog method
06 p0786 A72-18369
- RF time domain nonreal time reflectometer operating as nanosecond radar with pulse spectrum lines reflections measured and stored for echo computation
19 p2770 A72-37256
- ### MICROWAVE RESONANCE
- Resonance rail line scattering range using flat parallel conductor transmission line for radar cross section measurement
01 p0032 A72-11251
- Garnet crystal structure type microwave ferrites with V and In ions, investigating ferromagnetic resonance linewidth reduction effect
03 p0400 A72-12971
- Arbitrarily located inclined resonant slot in waveguide antenna, obtaining condition for circularly polarized radiation from scattering parameters analysis
04 p0499 A72-15205
- Vibration-rotation double resonance transitions in symmetrical top molecules in millimeter range under chopped laser radiation
04 p0532 A72-15615
- Temperature inhomogeneity effect on plasma column microwave resonant behavior in presence of axial magnetic field, ascribing spectral shifts to electron density and temperature profiles changes
06 p0854 A72-17417
- Dielectric substrate layer surface wave parasitic resonance effects on microstripline waveguide conductor
07 p0958 A72-18855
- Ionization wave propagation in inert gas due to microwave resonance quanta diffusion, explaining plasmaguide phenomena
07 p1040 A72-18916
- Resonator second harmonic influence on Gunn oscillator parameters for transit and hybrid modes, discussing bias voltage, harmonic amplitudes, phase difference, doping level and frequency
07 p0955 A72-19254
- Shf resonator small resonant frequency shift and Q factor changes measurement based on FM signal envelope shape analysis
07 p1046 A72-20508
- End holes effects on dielectric constant measurement of long glass tubes by cylindrical microwave resonant cavity
08 p1164 A72-20940
- YIG-tuned microwave transistor oscillator design and performance, considering resonance phenomena and magnetic circuit effects on applications
08 p1139 A72-20985
- Microwave resonators excited in coupled and E sub zero modes, determining equivalent circuit and Sommerfeld resonator Q factor and guide wavelength
11 p1605 A72-26369
- Mode chart and unloaded quality factor of elliptic microstrip resonator operating in inverse or radial TM modes
11 p1607 A72-26996
- Dual resonant cavity absorption cell composed of Fabry-Perot interferometers excited by microwave sources, observing spectroscopic double resonance effects
12 p1806 A72-27264
- Ferrite loaded X band waveguide Y junctions eigenvalue frequency dependence measurement to identify modal resonance and arrange displacement for circular operation
12 p1790 A72-27508
- Rietz-Kantorovich method reduction of scalar problem for wave propagation along direction surface to boundary value problem, discussing parametric resonance and periodic waveguides
14 p2132 A72-31118
- Millimeter band open cavity resonator using trihedral reflector diffraction grating and inclination control for mode selection
16 p2364 A72-33491
- Natural frequencies of a cylindrical microwave cavity containing a coaxial cylindrical dielectric sample
17 p2513 A72-34334
- Propagation of ionization wave in rarefied noble gases due to microwave resonance quanta diffusion, explaining plasmaguide phenomena
20 p2957 A72-39382
- Plasma diagnostics by means of microwave cavity resonators
22 p3212 A72-42950
- Problem of error estimation during solution of internal boundary value problems in microwave electrodynamics
23 p3265 A72-44201
- ### MICROWAVE SCATTERING
- Pulsar PSR 0833-45 linear polarization measurements at 300 and 1420 MHz, showing frequency invariance with interstellar scattering and Faraday rotation allowance
01 p0133 A72-11119
- Nonlinear scattering of microwave signals incident on unmagnetized cold plasma column
06 p0859 A72-17547
- Deschamps graphical method application to multipoint waveguide junction scattering coefficient measurement with averaging and least square fitting for error reduction
06 p0787 A72-18379
- Airborne radar measurement of 2.25 cm backscatter from sea surface, obtaining wind speed by computerized clustering data analysis techniques
09 p1296 A72-22312
- Backscattering by turbulent irregularities derived in context of single scattering corresponding to weak microwave reflections observed in atmospheric sounding
09 p1280 A72-23412
- Multistage broadband microwave amplifier design based on bipolar transistors cascade coupling, using scattering parameters
10 p1451 A72-24572
- Electromagnetic wave diffraction by dielectric steps in waveguides, calculating microwave scattered field by modified residue calculus technique
10 p1451 A72-24593
- Density fluctuations and ion acoustic two stream instability characteristics of RF generated plasma derived from electromagnetic scattering at 24 GHz
10 p1523 A72-24800
- Spatial distribution of electron beam excited plasma wave spectrum, determining wavenumber, amplitude and frequency by incoherent microwave scattering
11 p1693 A72-25564
- Superhigh frequency electromagnetic waves diffraction by conducting screen circular aperture with phase change by dielectric disk and multiple internal reflections, noting patterns and backscattering apparatus
11 p1597 A72-26371
- Characteristics of nonuniform regions responsible for microwave signals auroral scattering, noting observations with two sidelobe radio interferometer
13 p1946 A72-28584
- Electron density effect on microwave scattering from turbulent plasma, observing change from volume to surface scattering at critical density value
13 p2012 A72-29130
- Galactic structure, ionized gas distribution and radio source diameter studies from interstellar scattering at 81.5 MHz, comparing with pulsars
13 p2050 A72-29962
- Statistical correlation of X-band microwave scattering by overdense intermittently turbulent ionized Ar jet with flux fluctuations from electrostatic probe observations
16 p2440 A72-34065
- Phenomenological model for incoherent microwave scatter attenuation from turbulent plasma, establishing relation between plasma parameters and attenuation coefficient
17 p2517 A72-35622
- Microwave-analogy tests regarding light scattering at cosmic dust particles
19 p2804 A72-38507
- Lunar radar backscattering measurement of 0.86 cm circularly polarized radiation, noting echo polarization ratio and depolarization variations with incidence angle
19 p2868 A72-38735
- Microwave scattering from a radially propagating ion acoustic wave in a positive column.
21 p3089 A72-40201
- Stationary expressions for scattering coefficients of rectangular waveguides with dielectric plugs constituting a finite planar array.
21 p3027 A72-40371
- Study of microwave scattering in a plasma-beam discharge
23 p3321 A72-44212
- Characteristics of nonuniform regions responsible for microwave signals auroral scattering, noting observations with two sidelobe radio interferometer
24 p3397 A72-45084
- ### MICROWAVE SENSORS
- Microwave spectrometer remote sensing of atmospheric temperature and water vapor, discussing cloud, topography and sea state effects and multiple regression statistical method
02 p0228 A72-11859
- Microwave temperature sensor for radiation environment use, discussing cavity resonator design and operation, thermal cycling tests and comparative radiometer technique
07 p0993 A72-20677
- Plasma magnetoresistance in variable magnetic field measured on n-type InSb sample for SHF inertialess power sensor development
16 p2436 A72-33482
- ### MICROWAVE SPECTRA
- Trace gas pollutant monitoring by microwave rotational absorption spectroscopy, discussing test results with Gunn diode cavity spectrometer
01 p0023 A72-10524
- H I radio recombination line observation in H II region NGC 2024 microwave spectrum, detailing radiation frequency dependence
01 p0133 A72-11143
- Radio variable sources PKS 0727-11 and 1514-24 observation at 2295 MHz, presenting flux measurements and drift curves
01 p0134 A72-11161
- Millimeter and submillimeter microwave spectrometric studies of high temperature plasmas and noise emission, discussing instrumentation and absolute measurements
02 p0223 A72-11409
- Stratospheric and lower mesospheric temperature measurement by ground based passive microwave sensing, calculating oxygen absorption band lines brightness temperature emission spectra
02 p0213 A72-11861
- Vacuum UV spectra of free plasma column in microwave field at high pressures for discharge in helium-deuterium mixture
03 p0394 A72-13084
- Interstellar molecular microwave observations, emphasizing theoretical production rates and modes
03 p0419 A72-13119
- Diffuse cosmic background radiation measurements, emphasizing microwave and X ray spectra and excitation mechanism
03 p0409 A72-13138
- Solar turbulent magnetic field in lower corona associated with expanding limb microwave burst of 30 March 1969
03 p0410 A72-13325
- Submillimeter wave stratospheric emission spectra measurement by aircraft- or balloon-borne phase modulated Fourier spectrometry, noting SNR and small errors
03 p0348 A72-13399
- Oso-3 satellite observation of solar flare associated EUV bursts, comparing with microwave radio bursts [AD-739641]
03 p0413 A72-13529
- Microwave spectrometer crystal current leveler for broadband video detector and rotary wave attenuator control
04 p0524 A72-15541
- Solar microwave bursts impulsive and gradual rise and fall type comparison, noting frequency response and distribution
05 p0713 A72-16022
- Partial solar eclipse observation at 9 mm wavelength on 25 February 1971, noting limb brightening
05 p0718 A72-16509
- Magnetic field decay in solar microwave burst region evaluated from circular polarization degree time profile
06 p0891 A72-18505
- Microwave radiation intensity and spectral frequencies of Knudsen discharge in cesium plasma
07 p1046 A72-20515
- Atmospheric vertical temperature profile inference from ground based measurement of microwave thermal emission spectrum from atmospheric oxygen
08 p1161 A72-21824

Microwave induced dc voltages across unbiased Josephson tunnel junctions, showing power spectra dependence on magnetic field 09 p1367 A72-22458

Spectrum studies of extragalactic diffuse background radiation fields consisting of X ray and thermal or microwave background 10 p1529 A72-23914

Simultaneous observations of radio flares from beta Persei on 25-25 January 1972 at 2.8, 3.7 and 11.1 cm, noting spectral characteristics different from quasi-steady component 10 p1547 A72-24945

High resolution observation of stratospheric submillimeter thermal emission spectrum by helium-cooled InSb electron bolometer on board Comet 2E aircraft 10 p1476 A72-25023

Holographic Fourier spectroscopy for microwave radiation spectra of toroidal plasma with turbulent heating 12 p1850 A72-27135

Heavily obscured galaxy IC 10 21-cm line observation with radio telescope and neutral hydrogen diameter measurement for distance estimation 12 p1868 A72-27215

Interstellar atomic hydrogen observations in radio nebula W 3 direction, noting 21-cm absorption line profile coincidence with Cn alpha recombination line in radial velocity 12 p1868 A72-27219

Dual resonant cavity absorption cell composed of Fabry-Perot interferometers excited by microwave sources, observing spectroscopic double resonance effects 12 p1806 A72-27264

Microwave recombination lines from emitters with mass greater than 12 amu in Orion B and W3A regions 13 p2041 A72-29415

Vacuum UV spectra of free plasma column in microwave high pressure discharge in helium-deuterium mixture 13 p2015 A72-29434

Galactic background continuous radiation observation at 15 GHz, determining brightness temperature and thermal radiation component 15 p2313 A72-32348

Radio maps of extragalactic sources at 2.7 and 5.0 GHz presented with physical data for various components 16 p2458 A72-33718

Soft X-ray and microwave observations of hot regions in solar flares. 17 p2608 A72-35089

Possible long-period oscillations in solar radio emission at microwaves. 17 p2608 A72-35091

Spectral observations of Venus in the frequency interval 18.5-24.0 GHz - 1964 and 1967-68. 17 p2610 A72-35120

The electromagnetic radiation near the ion plasma frequency emitted by a turbulently heated plasma. 18 p2715 A72-36598

Microwave celestial water-vapor sources. 18 p2729 A72-36990

The structure of the Crab Nebula at 2.7 and 5 GHz. I. 19 p2855 A72-37340

Expanding ring in Galactic center from analysis of microwave spectroscopic data, measuring expansion and rotation velocities 20 p2972 A72-39860

Low-temperature part of a spectrometer for gigahertz-ultrasonics and ultrasonic paramagnetic resonance. 21 p3051 A72-40215

Dark field method for phase diffraction grating visualization by microwave holography, using radio lens for object microwave spectrum formation 21 p3055 A72-40795

Observations of linear polarization of radio sources at 7.2 cm. 21 p3109 A72-41326

Application of holographic Fourier spectroscopy to the analysis of the microwave radiation spectrum 21 p3058 A72-41733

Spectral analysis of microwave pulses by a ferrite transducer 22 p3158 A72-42119

Brightness temperature of the terrestrial sky at 2.66 GHz. 22 p3173 A72-42516

Cross correlated interstellar scintillation patterns of circumpolar pulsar PSR 0329+54 at 408 MHz, interpreting transverse velocities in Galaxy 23 p3334 A72-43253

Microwave generation with high energy electrons in magnetic undulator with transverse electromagnetic field, calculating frequency distribution of undulator radiation 23 p3265 A72-44158

Observations of the interplanetary medium and of the structure of radio sources using higher moments of interplanetary scintillations. 24 p3437 A72-44830

Microwave spectrum of compressed O2-foreign gas mixtures in the 48-81 GHz region. 24 p3378 A72-44871

Microwave observations of a partially ionized interstellar cloud. 24 p3447 A72-45551

MICROWAVE SWITCHING

Low driving power resistive gate MOSFET microwave switch with performance approaching P-I-N diode 01 p0038 A72-10658

Moderate power GaAs FET switching experiment, obtaining rise and fall times 07 p0952 A72-18826

Microwave diode switch operating at 35 GHz for spin lattice relaxation time measurement, discussing insertion loss, and rise and decay times characteristics 16 p2369 A72-33623

The use of semiconductor diodes to protect a radar receiver 18 p2663 A72-37217

S-band high power microstrip switches with p-i-n diodes for spacecraft radio systems 19 p2770 A72-37257

A multi-channel rotary joint for spacecraft applications. 19 p2770 A72-37260

Semiconductor diodes for microwave power control 21 p3033 A72-40939

MICROWAVE TRANSMISSION

Rain, snow and hail precipitation effects on radio link signal attenuation, scattering and fading along various transmission paths at millimeter and centimeter wavelengths 01 p0027 A72-10407

FM radio link superposed parabolic antenna systems adjustment for space diversity reception for scatter propagation and broadband multichannel transmission in 1.9 GHz range 01 p0027 A72-10410

Microwave propagation on nonlinear transmission lines by examination of energy dissipation in shock front, considering distributed and lumped-parameter models 01 p0029 A72-10692

Microwave communication via satellites, discussing FDMA and TDMA transponders design 01 p0029 A72-10709

Book on microwave techniques covering Maxwell equations, electromagnetic wave propagation in conducting media, complex notation, plane polarized waves transmission and reflection, wave equations, etc 01 p0043 A72-11275

Real time programmable video data compression system for microwave transmission of ATS satellite pictures between acquisition station and central computer processing 02 p0173 A72-12128

Circuit design techniques used for wideband signal processing systems, considering 1000 MB/S microwave communication link 02 p0176 A72-12163

Signal modification of microwaves propagating transversely in underdense turbulent plasma jet 02 p0265 A72-12365

Microwave propagation anomalies due to meteorological factors, discussing superrefractive atmospheric layers effects on radar data reliability and undesirable echoes appearance on display screen 02 p0182 A72-12746

Millimeter wave pulse signal transmission path length modulator with P-I-N diode switch, discussing system design and experimental results 02 p0196 A72-12798

Microwave propagation through laminated metallic media with gyromagnetic effects, applying dc magnetizing field normal to film plate [IEEE PAPER 31.6] 03 p0323 A72-13784

Angle modulation distortions and measurements in broadband FM microwave links 04 p0485 A72-14466

Zwischenmedium concept application to electromagnetic diffraction problems in waveguides with one or more interfaces and continuity condition met by orthogonal expansion 04 p0488 A72-15378

Intermodulation noise distortion due to multipath transmission over FM/FDM microwave links, deriving distortion probability distribution for Nakagami-Rice randomly distributed signal reception 04 p0493 A72-15517

Cut-off frequencies of degenerate LSE and LSM modes in rectangular waveguides containing dielectric layers in H plane 04 p0502 A72-15526

Semiconductor slab electroconductivity measurement based on circularly polarized microwave propagation in circular waveguide 04 p0502 A72-15533

Millimeter wave and laser space-to-space communication links comparison, considering ehf system based on size, weight, power consumption and communication parameters calculations 04 p0493 A72-15609

Pollution free electrical power generation from solar energy, discussing microwave transmission to earth, power shortages, thermal pollution and solar cell manufacture cost [ASME PAPER 71-WA/SOL-2] 05 p0614 A72-15892

Microwave dispersive line structures with nonlinear phase characteristics, considering use of empty waveguide segment near cut-off 06 p0785 A72-18312

Radio attenuation above 10 GHz based on theoretical model of equivalent precipitation on path using intensity spatial distribution function within rain cell 07 p0940 A72-19189

High resolution measurement of microwave refraction including arrival and fire angles on short line-of-sight tropospheric paths 07 p0946 A72-19790

Integral relations derivation for stationary and nonstationary potential motions in cases of zero and infinite conductivity, applying to wave expansion in cylindrical waveguide 08 p1212 A72-20966

Microwave transmission loss prediction formula for obliquely incident plane wave leakage through perforated flat metal plate 08 p1135 A72-21559

Fixed frequency or wideband real time measurements of microwave reflection and transmission coefficients and fields in open or closed structures 09 p1289 A72-23425

UHF band satellite TV broadcasting system with FM, calculating required field strength and transmitter power 10 p1435 A72-24033

Microwave amplitude modulation during propagation through RF plasma under perpendicular low intensity time dependent magnetic field 10 p1520 A72-24345

Microwave diagnostics of P doped Si semiconductor crystal prism determining relation between complex permittivity and reflection factor by variational method 10 p1450 A72-24404

Microwaves propagation through circular waveguide partially filled with lossless cold electron plasma dielectric, presenting computed dispersion curves for waveguide and plasmaguide modes 10 p1522 A72-24677

Complex gain nonlinearity of transmitting microwave amplifiers in single and multicarrier operation 10 p1454 A72-25147

Single sideband AM microwave analog transmission systems using frequency division multiplex techniques 11 p1595 A72-26289

Lossless distributed rectangular microwave structure with dielectrics interposed between two conductive metallic layers, noting existence of transmission zeros and filter properties 11 p1607 A72-26990

Skylab communications system, discussing voice, data, TV and command mission requirements and microwave instrumentation [AIAA PAPER 72-543] 12 p1781 A72-27366

Receiving and transmitting antennas directional gain effect on microwave long distance tropospheric propagation 12 p1783 A72-27632

GaAs semiconductor devices role in microwave communications, discussing physical properties and potential applications 12 p1792 A72-27736

Microwave radio link transmission loss Rayleigh-like long term distribution explained by two-path propagation model 12 p1784 A72-27796

Ground terminals spatial diversity for earth satellite mm wave communication systems to avoid attenuations by rainfall 13 p1989 A72-28810

Wall-impedance waveguide propagation constant determination from Rayleigh-Schroedinger power expansion of perturbed eigenvalues 15 p2194 A72-31549

SHF signal propagation through troposphere at low elevation angles, comparing fading measurements in winter and summer 15 p2194 A72-31550

Microwave propagation delay due to atmosphere in satellite-to-earth communication based on spherical smoothly varying model and geometrical optics techniques 15 p2200 A72-32102

Slant path radar attenuation events due to rain during summers at 10 GHz, obtaining statistics on frequency of occurrence, extent in azimuth and duration 15 p2200 A72-32103

Microwave transmission phenomenon and application to NDT, discussing various methods and examples 16 p2391 A72-33233

Love wave tapping in isotropic microacoustic surface waveguide by partial transduction into bulk wave at discontinuity 16 p2428 A72-34178

Experimental investigation of the parameters of a statistical Gaussian field model for centimeter waves beyond the radio horizon

17 p2515 A72-34834

Determination of the dielectric constants of microwave-striplines

17 p2530 A72-35429

Controversy surrounding Sirio satellite project related to microwave atmospheric propagation above 10 GHz with possible application in earth-to-space communication systems

17 p2623 A72-35918

UHF radio signals refraction angles and group delay times for biexponential model of ionospheric electron density profile

18 p2657 A72-36101

Simplified method of calculating microwave diffraction loss over spherical earth.

18 p2660 A72-36517

Reflection of microwave through laboratory plasma.

18 p2716 A72-36947

Calculation of the transmission factor of a parametric microwave transistor multiplier

19 p2774 A72-38423

Electromagnetic compatibility and interference problems of radar altimeters, collision avoidance systems and air and marine mobile satellite communication equipment in 1600 MHz region

20 p2901 A72-38977

A variation-iteration technique for the design of wall-impedance waveguides.

20 p2903 A72-39429

Wave scattering at a step in a circular multiwave waveguide

21 p3016 A72-40781

Experimental investigation of the propagation of electromagnetic waves in a rectangular waveguide partially filled with n -InSb in the presence of a transverse magnetic field

21 p3016 A72-40796

Geostationary satellite direct TV broadcasting system extension to 12 GHz band, considering receiving installations, antennas, performance and costs

21 p3018 A72-40876

Reliability aspects of fading in microwave line of sight using digital transmission.

21 p3019 A72-40887

Automatic landing and microwave guidance system potential.

21 p3040 A72-41072

Magneto-microwave free-carrier absorption in germanium in the Faraday configuration.

21 p3097 A72-41379

Propagation loss of centimeter and millimeter waves in rainfall.

21 p3023 A72-41833

State of the art in the detection of intelligent extraterrestrial signals.

24 p3441 A72-45190

MICROWAVE TUBES

NT BACKWARD WAVE TUBES

NT CATHODE RAY TUBES

NT CELESCOPES

NT COLD CATHODE TUBES

NT GAS DISCHARGE TUBES

NT IMAGE ORTHICONS

NT IMAGE TUBES

NT KLYSTRONS

NT MAGNETRONS

NT MICROWAVE OSCILLATORS

NT ORTHICONS

NT PHOTOMULTIPLIER TUBES

NT PICTURE TUBES

NT PLANOTRONS

NT THERMIONIC DIODES

NT TRAVELING WAVE TUBES

Grid controlled 100 W microwave transmitter power triode for space applications, noting high reliability and stability through use of metal dispenser cathode

01 p0009 A72-11223

Spatially periodic coupled cavity slow wave structures for multibeam microwave tube stabilization without absorber

02 p0190 A72-11575

Electron tube with Fabry-Perot cavity resonator with grooved and smooth mirrors for millimeter and submillimeter wave generation

04 p0503 A72-15598

Optimal hf triode oscillation tripler with allowance for power limitation by thermal losses on plate and grid electrodes

05 p0638 A72-17184

Twin triodes type parameters stability in microwave region as function of cathode service life and temperature

09 p1284 A72-22243

Broadband electrostatically focused klystron for airborne radar application, discussing focusing cell design, amplification and efficiency

10 p1446 A72-23821

Noise temperature and admittance of space charge limited double cathode tube with transit time effects at microwave frequencies

10 p1454 A72-25105

Vacuum tube developments for radar, TV and communication applications, discussing microwave, traveling wave, cathode ray, memory and vidicon tubes, magnetrons, klystrons and tetrodes

11 p1606 A72-26544

Experimental determination of ion density trapped by electron beam.

21 p3034 A72-41463

MICROWAVES

NT DECIMETER WAVES

NT MICROWAVE EMISSION

NT MILLIMETER WAVES

Type 3 and 3/5 solar radio bursts coupling with microwave bursts, considering connection with H alpha flares and X ray emission

01 p0118 A72-10414

Microwave emission characteristics of oil slicks, showing dependence on oil type, film thickness and sea state

[AIAA PAPER 71-1071]

01 p0057 A72-10533

Microwaves - Conference, Stockholm, August 1971, Volumes 1 and 2

01 p0035 A72-10626

Book on microwave techniques covering Maxwell equations, electromagnetic wave propagation in conducting media, complex notation, plane polarized waves transmission and reflection, wave equations, etc

01 p0043 A72-11275

Chronic microwave irradiation effects on experimental animal blood forming systems, examining peripheral blood count changes and nuclei and mitosis abnormalities in erythroblastic and lymphoid cells

02 p0158 A72-11708

Satellite solar power stations, considering energy conversion, microwave generators and beam transfer to earth

02 p0155 A72-11770

Polarization distribution and inversion of solar impulsive microwave bursts at 17 GHz

03 p0407 A72-12940

Microwave solar radio bursts occurrence and intensity distribution at 19 GHz during July 1967-December 1969

03 p0407 A72-12941

Papers on microwave advances covering precision coaxial connectors, O-type linear beam devices, electron dynamics and energy conversion and junction circulators

03 p0424 A72-13229

Cataractogenesis from microwave radiation exposure, discussing protection, legislation and Western and Soviet literature review

06 p0767 A72-17877

Third harmonic generation in Ge induced by conduction nonlinearity during bulk heating of charge carriers by microwave fields

07 p1047 A72-19023

Cosmos 243 microwave radiation analysis over cultivated terrain, showing radio brightness temperature dependence on soil temperature and humidity effect on emissivity

09 p1297 A72-22495

Microwave, X ray and corpuscular emission by gas discharges in coaxial plasma gun, measuring pressure and current distribution

09 p1362 A72-23212

Atmospheric humidity vertical profile determination by measuring microwave radiation from satellite

11 p1620 A72-25274

Lower atmosphere vertical temperature profiles determination from clear air ground based measurements of microwave thermal emission by oxygen

11 p1591 A72-25764

Lunar microwave emission, constructing thermophysical models for radio observations and brightness temperature variations

12 p1869 A72-27327

Statistical analysis of solar microwave bursts, examining radiation source development and emission mechanism

12 p1872 A72-27814

Neuroendocrine responses in microwave radiation exposed rats, correlating thyroid and thyrotropic activity

12 p1767 A72-28321

MHD stability in Hg vapor discharge plasma excited by standing microwave near electron cyclotron resonance, discussing electron energy anisotropy effect on LF oscillations

13 p2017 A72-29618

Flux density variations incidence among extragalactic sources found by 3.8 cm sky survey

13 p2048 A72-29830

Earth velocity through microwave background, discussing absolute and relative motion, inertial frame and distant matter distribution and Mach principle

14 p2157 A72-30624

Standardization of microwave irradiation experiments on animals, discussing power density level evaluations and local vs whole-body irradiation effects

14 p2080 A72-30746

Microwave induced cutaneous heat and pain perception thresholds, noting usefulness as possible radiation hazard warning

15 p2188 A72-31506

Irradiation system for animal and human subjects exposure to controlled microwave radiation in environmental tests

15 p2191 A72-32573

Microwaves interaction with ultrashort laser pulse generated traveling refractive index changes in liquids with orientational Kerr effect

15 p2252 A72-32652

Microwave modulated incoherent light for large volume scenes holography, noting object image reconstruction by coherent light transillumination of hologram

15 p2242 A72-32675

Expanding loops of H alpha filaments in peculiar galaxy M 82 investigated by microwave radio map, suggesting thermal and nonthermal radiation sources

15 p2317 A72-32757

Time-of-flight measurements of molecular and atomic beams produced by cooled microwave discharge source, using hydrogen, helium, argon and nitrogen

16 p2430 A72-33061

Cosmic microwave background radiation origin by energy dissipation associated with primordial chaotic universe

16 p2459 A72-33770

Microwave radiation - Biophysical considerations and standards criteria.

17 p2507 A72-34299

Emission of coherent microwave radiation from a relativistic electron beam propagating in a spatially modulated field.

17 p2589 A72-34874

X ray sources associated with galactic clusters resulting from relativistic electrons Compton scattering on microwave background radiation

17 p2599 A72-35072

Short cesium plasma discharge diode as physical model for thermionic converter, studying ionization, recombination and microwave radiation

18 p2714 A72-36212

Observations on microwave hazards to USAF personnel.

18 p2653 A72-36522

Observation of linear polarization of solar microwave bursts.

18 p2722 A72-36997

International Microwave Symposium, Arlington Heights, Ill., May 22-24, 1972, Proceedings.

19 p2770 A72-37251

Microwave hologram radar imagery.

19 p2764 A72-37602

Nonthermal emission of a magnetoactive plasma in the field of super-high-frequency pumping wave

21 p3090 A72-40407

Deposition of finishes and dyes in materials dried using microwave heating.

22 p3183 A72-42480

Progress in the efficiency of free-space microwave power transmission.

22 p3140 A72-42481

Comparison of microwave-induced constant-voltage steps in Pb and Sn Josephson junctions.

23 p3323 A72-43272

MICROWEIGHING

U WEIGHT MEASUREMENT

MICTURITION

U URINATION

MDAIR COLLISIONS

Vertical dipole antenna design for CW Doppler radar midair collision avoidance system

05 p0629 A72-16571

Aircraft midair collision prevention in dense air traffic environments, suggesting problem solution based on proximity warning system

08 p1204 A72-21090

Aircraft collision near misses under IFR and VFR conditions, discussing ATC coordination, equipment failure and personal and planning problems

09 p1349 A72-22977

Pilot warning systems for visual midair collision avoidance, noting reaction to imminent threats, scanning patterns and display sector size effects [SAE PAPER 720312]

11 p1583 A72-25576

Collision avoidance techniques for midair collisions reduction, discussing airborne and ground based systems

15 p2272 A72-32213

Midair collision causes and prevention, considering pilot responsibilities, anticollision devices and procedures

19 p2831 A72-37800

Design, operation and performance of time-frequency midair collision avoidance system, noting air traffic controller backup for departure, enroute and arrival control

21 p3081 A72-40295

Operation principles, capabilities and tests of midair collision avoidance system with aircraft separation control by nonsynchronous techniques

21 p3081 A72-40296

- Midair collision prevention independent of ATC, discussing aircraft lighting, collision avoidance systems and proximity warning indicator
21 p3081 A72-40297
- Air traffic, collision risks, defense zones, airspace structure and central planning agency for flight safety problems reform
[DGLR PAPER 72-038] 24 p3467 A72-44617
- Midair collision prevention for Army aircraft.
24 p3422 A72-44645
- SECANT midair collision avoidance system based on nonsynchronous microsec pulse transmission and receiving via randomly selected frequency, describing modular components and operating principles
24 p3422 A72-44647
- MIDAS SATELLITES**
U.S. reconnaissance satellites development, discussing RAND project, Agena, Discoverer, Samos and Midas
12 p1876 A72-27109
- MIDCOURSE GUIDANCE**
White Sands Missile Range and Range-Rate system design and verification to meet midcourse tracking requirements under severe target dynamics
08 p1133 A72-21402
- Interplanetary spacecraft midcourse guidance stochastic control, deriving algorithm for computing optimum velocity correction and execution time with allowance for correction-dependent errors
10 p1508 A72-23778
- Optimum aim point biasing in case of a planetary quarantine constraint.
20 p2968 A72-39196
- An approximation to midcourse correction direction errors.
22 p3203 A72-42870
- Analysis of the Radio Astronomy Explorer lunar orbit mission.
[AIAA PAPER 72-940] 24 p3444 A72-45437
- MIDCOURSE TRAJECTORIES**
Maneuver strategies for multi-planet missions.
[AIAA PAPER 72-914] 24 p3443 A72-45431
- MIDDLE EAR**
Cat and rabbit middle ear muscles contraction by electric stimulation of motor nerves, noting sound transmission reduction
08 p1115 A72-21136
- Cat middle ear muscles motor units (twitch tension and contraction time in response to motor neuron threshold stimulation
08 p1116 A72-21137
- Stapedectomy postoperative complications as flying hazard, discussing pilot reaction to middle ear pressure changes
14 p2082 A72-31094
- MIDLATITUDE ATMOSPHERE**
Midlatitude D layer observations during sunspot minimum, emphasizing atmospheric ionization and ozonospheric parameters
01 p0055 A72-10433
- Radio communication accuracy characteristics in calculation of maximum frequency, skip distance and emission angle by transmission curves for midlatitude ionosphere
01 p0028 A72-10600
- Midlatitude ionospheric trough characteristics from computer analysis of Ariel 3 electron density data, correlating with geomagnetic phenomena
01 p0120 A72-10921
- Middle geographic latitude sporadic E-layer initial height variations during 1957-1968 solar cycle
01 p0064 A72-11103
- DR-current belt dynamics during magnetic storm based on ground observation data on midlatitude red arcs
02 p0217 A72-11929
- Midlatitude ionospheric radio wave absorption measurements, using radio astronomical polarization method
02 p0172 A72-11945
- Cosmic noise ionospheric absorption measurements with riometers, showing mid and low latitudinal variation
02 p0221 A72-12464
- Vertical motions of midlatitude F 2 layer during magnetospheric substorms, investigating electric field distribution
03 p0349 A72-13519
- Long wave radiation and surface friction effects on midlatitude cyclone development in eight-level primitive equation orographic model
03 p0385 A72-14229
- Auroral behavior observation at midlatitude station, exhibiting correlation with solar activity as regards solar cycle recurrence and phase
[AD-739061] 04 p0515 A72-14882
- Geomagnetic effects on lower ionosphere at lower midlatitude station, discussing long wave propagation
04 p0516 A72-14939
- Magnetic baylike disturbances and multiple midlatitude 6300-A auroral arcs during geomagnetic storm recovery phase and concurrent ionospheric current system
05 p0630 A72-16620
- Ionospheric ion density distribution at 600 km height and medium and low latitudes from Cosmos 184 satellite data analysis
05 p0659 A72-16766
- Rocket-borne vector magnetometer measurements of midlatitude ionospheric currents near sporadic E, noting nearly uniform vertical distribution
06 p0804 A72-17459
- Variance spectral techniques in detecting wave modes of synoptic scale tropospheric wind in midlatitudes and tropics
06 p0841 A72-17634
- Midlatitude F region wavelike disturbances detection by hf radio echo techniques, discussing correlation with jet stream associated tropopause wind patterns
07 p0974 A72-18885
- Midlatitude geomagnetic micropulsations polarization and spectral characteristics, explaining behavior in terms of MHD wave propagation theories
07 p0975 A72-19152
- Ring current growth effects on midlatitude F region electron density change during large magnetic disturbances
08 p1152 A72-20706
- Vertical distribution of electron density seasonal anomaly and storm effects in daytime midlatitudes topside ionosphere from Alouette 1 data
08 p1155 A72-20814
- Midlatitude and equatorial geomagnetic micropulsations during 13-14 January 1967 world-wide magnetic storm from ground and satellite observations
08 p1157 A72-21107
- Seasonal variation in ionospheric horizontal drift velocities under normal E and sporadic E conditions for middle latitudes
08 p1157 A72-21115
- Wind shear theory of midlatitude sporadic E formation, using wind profiles from artificial luminous cloud observations
08 p1161 A72-21540
- Model calculation for electron production rates due to photoionization and particle precipitation below 100 km at midlatitude during solar minimum and maximum years
09 p1375 A72-22357
- Nightglow evidence of precipitating energetic electrons in midlatitude nighttime D region based on intensity determination from satellite and rocket data
09 p1375 A72-22358
- Midlatitude auroral zone positive ion mass spectrometer observations in E region, noting diurnal variation and sporadic E events
09 p1375 A72-22364
- Synoptic measurement of midlatitude D region electron density diurnal and seasonal variations under quiet conditions, using differential absorption partial reflection experiment
09 p1376 A72-22372
- Tropical storms generated midlatitudinal cloud bands relation to autumnal large scale circulation, analyzing heat and moisture injection effects
09 p1344 A72-22429
- Vlf hiss with lower hybrid resonance cut-off recorded by Alouette 1, emphasizing midlatitude events and electromagnetic energy transportation by multion duct in topside ionosphere
09 p1279 A72-23007
- VLF waves propagation dependence on ionospheric horizontal electron density gradients associated with midlatitude depression from FR-1 satellite observation
10 p1472 A72-24060
- Sporadic E layer critical frequency relationship to ionospheric wind direction for midlatitudes in summer period
10 p1472 A72-24079
- Midlatitude sporadic E layer observed by rocket and radio sounding, deriving plasma frequency from peak electron density
10 p1477 A72-25156
- Wind shear and midlatitude sporadic E layer theories, discussing metal ions production and loss
10 p1477 A72-25158
- Metal ion sheaths in midlatitude sporadic E layer caused by vertical redistribution of neutral ionization, discussing wind shear discontinuities
10 p1477 A72-25159
- F 2 layer midlatitude local centers of anomalous noontime ionization during winter and summer solstices
11 p1623 A72-26283
- Strong pitch angle scattering of energetic electrons in presence of electrostatic waves due to ion cyclotron instability above midlatitude ionospheric trough region
11 p1714 A72-26398
- Midlatitude stable auroral red arcs observation from OV1-10, showing generation at plasmopause due to turbulent dissipation of ring current energy
11 p1624 A72-26401
- Mass spectrometer measurements of hydrogen, helium, nitrogen, oxygen and nitrogen oxide ion concentrations vertical profiles in ionosphere at midlatitudes
11 p1628 A72-26906
- Electron precipitation in upper atmosphere at midlatitudes from positive ionized nitrogen molecules electrophotometric observation and night airglow and geomagnetic field measurements
12 p1802 A72-27302
- Seasonal atmospheric composition changes relation to midlatitude F 2 layer seasonal anomaly during high solar activity
12 p1803 A72-27776
- Corpuscular radiation intensity relationship to midlatitude mesosphere temperature from rocket and balloon sounding and ground measurements
13 p0229 A72-28603
- DR-current belt dynamics during magnetic storm based on ground observation data on midlatitude red arcs
13 p1948 A72-29241
- Midlatitude ionospheric radio wave absorption measurements, using radio astronomical polarization method
13 p1920 A72-29257
- Infrasonic excitation of red oxygen emission at 6300 A during geomagnetic storms at middle latitudes
14 p2098 A72-30146
- Midlatitude upper atmosphere wind, tide and turbulence measurements, using radar observations of meteor trails
14 p2099 A72-30248
- Composition of radiation excess over primary cosmic ray background recorded by Cosmos satellites below midlatitude belt region
14 p2147 A72-30626
- Midlatitude VLF emissions intensity relationship to dayside auroral particle precipitation flux
15 p2194 A72-31437
- Midlatitude nighttime sporadic E layer relationship to geomagnetic field, considering wind shear theory
15 p2224 A72-31798
- Polar/midlatitude model of atmospheric density variations from LOGACS low altitude satellite accelerometer experiment
15 p2229 A72-32000
- Imposed southern boundary experimentation for large scale Northern Hemisphere midlatitude atmospheric flow numerical prediction, discussing factors contributing to model success
15 p2267 A72-32726
- Ionospheric electron content semiannual and seasonal variations as function of solar and geomagnetic activity from low and mid-northern latitude observations
16 p2385 A72-33378
- Ionospheric ion density distribution at 600 km height and medium and low latitudes from Cosmos 184 satellite data analysis
17 p2548 A72-35269
- Midlatitude red arc observations by satellite and ground station, suggesting thermal conduction theory of formation from ionospheric electron and ion temperatures and densities
18 p2685 A72-35989
- Ring current growth effects on midlatitude F region electron density change during large magnetic disturbances
19 p2790 A72-38334
- Mid-latitude D-region ionization associated with the 'slot' in radiation belt electrons.
20 p2964 A72-39533
- Magnetically symmetric detection of the midlatitude electron density trough by Ariel 3 satellite.
22 p3170 A72-42372
- Geomagnetic storm and seasonal effects on spread of monthly distribution and average behavior of midlatitude F region electron peak density and slab thickness
22 p3172 A72-42434
- Relative movements of mid-latitude trough and scintillation boundary.
23 p3282 A72-43267
- Midlatitude VLF emissions in magnetosphere due to plasma resonance instability near plasmopause, using ground, rocket and satellite observations, estimating electron energy
23 p3263 A72-43515
- Corpuscular radiation intensity relationship to midlatitude mesosphere temperature from rocket and balloon soundings and ground measurements
24 p3435 A72-45103
- Tropospheric wave motions with baroclinic basic flow in equatorial latitudes.
24 p3399 A72-45485
- MIDLATITUDES**
U TEMPERATE REGIONS
MIE SCATTERING
NT RAYLEIGH SCATTERING
Extinction curves for Mie scattering by interstellar grains, including refractive index differences in vacuum UV for methane, ammonia and water ice absorption
02 p0284 A72-12633
- Mie scattering by spherical particles in low loss glasses for fiber optic waveguides, discussing angular dependence
03 p0359 A72-13445

Spherical scatterers extinction efficiency effect on photometer optical systems transmittances, using Mie equation and numerical methods

07 p0987 A72-19831

Mie scattering models of zodiacal light based on spherical particles, commenting on inadequacy for nonspherical particles at elongations above 120 deg

19 p2792 A72-38506

Light attenuation coefficient measurement in water of various turbidity with AR and Kr lasers, interpreting results by Mie scattering theory

20 p2931 A72-39270

MIE THEORY

U MIE SCATTERING

MIGRATION

Binary alloys concentration distribution determination in migrating liquid-solid plane phase interfaces range during crystallization

07 p1022 A72-20571

Laser stimulated Raman scattering and IR absorption on crystal defects leading to atomic migration in solids

11 p1647 A72-26144

MILITARY AIR FACILITIES

Military weather forecasting requirements by 1980, discussing decision making, data processing, satellite data, mission and terminal forecasts, display and computer flight planning

10 p1508 A72-25096

Integrated civil/military ATC system for upper airspace control (UAC) center at Karlsruhe

16 p2421 A72-34108

Mediator plan for joint civil/military ATC organization at London center, discussing sectorization, control and radar facilities, flight plan processing and communications

16 p2421 A72-34109

Design of a military air cargo transportation system by use of a large scale mathematical programming model

24 p3466 A72-44577

Statistical forecasting models for USAF CONUS outbound cargo airlift requirements by averaging and exponential smoothing models

24 p3466 A72-44578

MILITARY AIRCRAFT

Industry assisted state of art assessment of high lift turbofan configurations for USAF STOL tactical transport technology program

[SAE PAPER 710758]

01 p0003 A72-10255

Military aircraft inertial navigation system design, discussing gyroscope, gyro compassing alignment, accuracy and performance

04 p0545 A72-15666

Conventional open and closed loop servo analysis methods applied to Naval aircraft approach power compensator systems, using pilot model concepts

[AIAA PAPER 72-124]

05 p0612 A72-16922

Civil and military aircraft forced diversion, discussing legal counters and aircraft restoration

05 p0753 A72-17166

Military aircraft operations and logistics computerized simulation for support and maintenance cost estimates

06 p0758 A72-17974

Structural demonstration flight testing (U.S. Navy/ of new aircraft, presenting maneuver checklist

06 p0759 A72-18489

National Environmental Policy Act (PL 91-190) impact on Army aircraft turbine engine development in terms of performance, additional cost and time

07 p1053 A72-18773

French, British, Italian, U.S., German and Israeli military aircraft, presenting design and performance data

07 p0913 A72-20308

Linear programming application to aircraft selection for tactical airlift fleet contingency planning

[AD-736074]

08 p1256 A72-21468

Naval aircraft optimal repair and replacement policies determination for operation cost minimization by dynamic programming

[AD-736094]

08 p1256 A72-21470

Survival rates in USAF accidents during 1965-69, noting visual sighting as primary rescue factor

08 p1109 A72-21564

Aircraft fuel system gunfire vulnerability and fire and explosion protection techniques

08 p1112 A72-21579

Mitsubishi XT-2 jet trainer aircraft, presenting design, structural and performance data

10 p1421 A72-25107

Propulsion system design for military VTOL aircraft, emphasizing subsonic cruise to maximum thrust ratio and exhaust downwash characteristics

[ASME PAPER 72-GT-73]

11 p1704 A72-25655

Propulsion control systems design for military and commercial V/STOL aircraft, considering power management performance with minimum weight and maximum reliability and maintainability

[ASME PAPER 72-GT-79]

11 p1705 A72-25659

Integrated display system design with navigation update, weapon delivery, reconnaissance, bomb damage

assessment, threat and terrain avoidance capabilities for multicrew military aircraft

11 p1684 A72-26292

Structural design and optical problems of external vision and cockpit transparencies in military aircraft

12 p1753 A72-27002

Emergency escape from high performance military aircraft in flight and on ground, using explosive cord for transparent canopy material breakup

12 p1753 A72-27017

Anthropometric data utilization for military pilot/aircraft compatibility evaluation, discussing cockpit exclusion code development and implementation

12 p1777 A72-28324

Tethered autostabilized rotor platform for military surveillance, target location and communication, discussing flight vehicle, tethering cable, ground station and guidance-control system

13 p1898 A72-30078

Management information system role in cost effective civil and military aircraft operations, discussing hardware modification and human resources and communication system adaptation

15 p2339 A72-32458

Fokker VTOL transport aircraft designs, considering payload, range, runway conditions, noise, military capabilities and operational costs

16 p2347 A72-33048

Low level night operations of Army aircraft

[AHS PREPRINT 631]

17 p2488 A72-34481

Status of U.S. Navy stall/post-stall/spin flight testing

19 p2749 A72-38104

Investigation of the commonality in development of military and commercial STOL transports

[AIAA PAPER 72-808]

19 p2750 A72-38114

Tactical aircraft weapon system development, describing navigation, target acquisition, release point guidance and delivery modes

[AIAA PAPER 72-896]

20 p2951 A72-39107

STOL performance criteria for military transport aircraft

[AIAA PAPER 72-806]

20 p2889 A72-40055

Military aircraft construction, design and economic requirements, discussing fighter payloads, armament efficiency and fire control systems

24 p3369 A72-45450

MILITARY AVIATION

Instrument landing systems specifications for civil and military aviation, suggesting replacement type development based on existing configurations

12 p1842 A72-27110

Ejection injuries from U.S. Navy aircraft, discussing statistical distribution of vertebral, shoulder, arm/hand, knee, leg, head and face injuries

12 p1774 A72-28273

Statistical survey of barosinusitis incidence in U.S. Navy flying personnel during altitude chamber training, discussing diagnostic methods and clinical management

12 p1765 A72-28274

USAF V-51R noise protector earplugs modification to allow for pressure equalization during aircraft climb and descent

12 p1774 A72-28276

Central nervous system symptoms and simple bends in gas decompression sickness cases during USAF operational flying

12 p1775 A72-28283

Change in Naval Flight Officer operational role due to modern equipment design in weapons systems, sensors and navigational aids

12 p1775 A72-28291

USAF aircraft accidents/incidents involving aircrewmembers with medical waiver on various visual, cardiopulmonary and other chronic pathological and psychiatric conditions

12 p1776 A72-28315

Review of aeromedical records for grounding USAF flying personnel during 1956-1970, noting increased age factor effect

12 p1776 A72-28316

Air Force Global Weather Central computer simulation of specific aircraft flight plans, using update weather information for specified route profile

13 p1924 A72-28873

Flight psychiatry in NATO countries, discussing organization and facilities with respect to military and civil aviation

13 p1911 A72-29858

Military aviation navigator training, discussing objectives, methods, instructors and equipment

15 p2272 A72-32207

USAF Academy air navigation training program, discussing systems development course and descriptive and applied astronomy

15 p2272 A72-32210

Military systems cost reduction via civil avionics procurement techniques, discussing cost-reliability design criteria

15 p2338 A72-32215

Time parameter in military air operations, discussing weapon systems R and D, all-weather capa-

bility, communications, reliability and maintainability, manpower training, etc

15 p2339 A72-32453

ATC system organization in terms of optimal operating conditions for civil and military airspace users, discussing navigation systems, human factors, equipment reliability, etc

15 p2272 A72-32455

An air traffic controller's view on area navigation and ATS requirements related thereto

21 p3081 A72-40299

Midair collision prevention for Army aircraft

24 p3422 A72-44645

Simulation procedure for mission and maintenance planning of an air force wing

24 p3365 A72-44663

Naval helicopters applications to search and rescue, ASW, ground support and other roles, considering reliability and maintenance

24 p3365 A72-44685

Keratoconus incidence in USAF flying personnel, discussing diagnosis, etiology and therapy

24 p3378 A72-45663

Paranasal sinus barotrauma in military flying personnel, discussing radiographic diagnostic methods and hypobaric test procedures for flight status restoration time determination

24 p3378 A72-45664

MILITARY HELICOPTERS

General aviation patient transportation, investigating military helicopter airlift performance

01 p0022 A72-11298

Flight testing of Army helicopters terrain following and/or avoidance systems concepts for operational capability, performance and cost evaluation

05 p0686 A72-16658

Rotary wing aircraft design features and performance, discussing military and civilian helicopters and future developments

05 p0612 A72-16734

Attack helicopters engine failure problems, discussing flight test results in transition from powered high speed flight to autorotational flight

08 p1108 A72-21011

Combat jet helicopter maneuverability, considering aircraft flying characteristics, pilot capability, flight configuration, altitude and load factor

10 p1421 A72-24923

Hydrofluidic stability augmentation system (HYSAS) development for military helicopters, discussing test program and technical feasibility

12 p1754 A72-27407

Military transport helicopter optimum secondary power system, considering onboard auxiliary power unit, electric or hydraulic engine start system, environmental control, etc

17 p2494 A72-34480

Flight test evaluation of a forward looking radar system for search and rescue applications

17 p2490 A72-34499

Critical review of Mil-F-83300 V/STOL flying qualities specifications as applied to helicopter design and missions, suggesting inappropriateness for Navy helicopters

17 p2490 A72-34503

Helicopter/ship dynamic interface testing for launch and recovery capabilities under sea environment conditions, discussing visual landing aids, wind, visibility and ship motions

17 p2491 A72-34505

Results of the reliability and maintainability demonstration of the OH-58A light observation helicopter

17 p2491 A72-34507

Hydrofluidic stability augmentation system for U.S. Army helicopters, emphasizing reliability, maintainability and reduced cost

17 p2492 A72-34928

Low level light TV camera with Si intensifier target tube for fire control system to improve AH-1G Cobra helicopter night reconnaissance and attack capabilities

17 p2557 A72-35555

Naval helicopters applications to search and rescue, ASW, ground support and other roles, considering reliability and maintenance

24 p3365 A72-44685

MILITARY PSYCHIATRY

U MILITARY PSYCHOLOGY

MILITARY PSYCHOLOGY

Wake-sleep cycle importance in military service, considering drugs effects on wakefulness

07 p0922 A72-20383

California psychological inventory as a predictor of success in the Naval flight program

24 p3377 A72-45655

MILITARY SPACECRAFT

NT MIDAS SATELLITES

Earth satellite legal aspects under space treaty, discussing orbiting military remote sensing devices, national obligations and security issues

07 p1105 A72-19476

Electric propulsion systems assessment for military spacecraft, discussing ion, colloid, pulsed and quasi-steady plasma thrusters

[AIAA PAPER 72-493]

11 p1711 A72-26217

Reliability role in commercial and military telecommunication satellite system planning, discussing economic factors, earth station redundancies and maintenance, spare levels and control systems
13 p2051 A72-28352

Military geostationary communication satellite Skynet 2 subsystems design development and testing
13 p2052 A72-29856

Satellites for long distance telecommunications, noting ATIS, Intelsat, military systems and Canadian domestic system Amik
14 p2085 A72-30363

Error correcting codes applied to satellite channels.
21 p3018 A72-40874

MILITARY TECHNOLOGY

Parachute designs and applications to escape systems, paratrooping, supply dropping, aircraft braking, weapons systems stabilization, flight testing aids and sport
01 p0003 A72-10302

Paratroop type parachutes breathing oscillations and stability characteristics, using high speed cinematography and kinetheodolites to track during steady state descent
01 p0004 A72-10307

Tactical optical ground communication systems, discussing use of GaAs and carbon dioxide lasers and ultrawideband data links
04 p0485 A72-14482

Missile systems of U.S., U.S.S.R. and other nations, discussing ground-to-ground, ground-to-air, air-to-ground and air-to-air missiles
05 p0728 A72-16740

Military pulsed range finder design involving modularity, cooling, optical system and solid state receiver. [CLEA PAPER 9.2]
07 p0942 A72-19384

Leads and booster explosives replacements for tetryl, discussing military specifications and safety criteria of various newly developed compounds and mixtures
08 p1220 A72-20770

Soviet book on radio receiver design covering military applications, bandwidth requirements, network synthesis and AM, FM, SSB, Doppler, phase metering, PCM and radar equipment
11 p1604 A72-26045

Military R and D organization questionnaires data analysis to obtain relationship between job productivity, satisfaction, ability, age and salary
12 p1891 A72-27655

Worldwide satellite navigation system for precise position and velocity of military aircraft, ships and ground vehicles
13 p1996 A72-28758

U.S. Army missile systems rocket motors life cycle reliability programs based on propellant laboratory analyses, motors static tests and field firings statistical evaluation
14 p2146 A72-30759

Navy program for composites technology development in aircraft structures, discussing design, reliability and cost
[ASME PAPER 72-DE-3] 14 p2073 A72-30860

Materials characteristics relevance for USAF technology, discussing processing conditions, environment simulation, real time techniques, ultrasonic and X ray inspection methods, etc
16 p2404 A72-32823

Military system and equipment Level of Repair optimization for minimum life cycle costs, considering weapon systems deployment, operation level and mobility requirements
16 p2482 A72-33793

Book on man machine system experiments covering ATC, air defense, logistics organizations, space flight, battlefield operation, police dispatching, communications, etc
16 p2359 A72-33796

Dc power supply for military electronics applications, describing circuit design for well regulated and filtered output dc voltage from various ac dc sources
17 p2497 A72-34708

Flight tests correlation with mathematical models to predict electro-optical viewing systems capability for military missions
17 p2557 A72-35553

USAF development of electrostatic gyros for inertial air navigation, noting flight tests and associated airborne digital computer
17 p2578 A72-35558

Aircraft FDM and TDM systems, considering signal processing, cable requirements and applications to aircraft weapon systems and telemetry
[SAE AIR 1207] 18 p2692 A72-36529

Department of Defense Reliability Analysis Center.
18 p2676 A72-37131

Defense Documentation Center independent R and D data bank for evolution and maintenance of creative technology oriented defense industry
21 p3132 A72-40974

The design and operation of the Air Force Flight Dynamics Laboratory Ballistic Impact Test Facility. [AIAA PAPER 72-998]
21 p3041 A72-41584

Effects of projectile damage on critical helicopter components.
24 p3454 A72-44609

The problems of reliability growth and demonstration with military electronics.
24 p3384 A72-44670

Observations on designing to combat fatigue and its effects on the economics of civil transport aircraft.
24 p3368 A72-44745

MILKY WAY GALAXY

Milky Way Galaxy spiral structure determination, presenting arms anatomy, gas and star kinetics and radio astronomy data
03 p0417 A72-13104

He production from H to maintain Galactic luminosity, discussing interstellar gas enrichment
03 p0419 A72-13116

Cepheid variables compared for Milky Way and Small and Large Magellanic Clouds, discussing amplitudes, period-luminosity relations and light curves
03 p0425 A72-13255

Magellanic Clouds cepheid variables compared to Milky Way cepheids, discussing evolution tracks
03 p0425 A72-13261

Magellanic Clouds and Galactic nucleosynthesis from chemical composition
03 p0426 A72-13263

Stellar orbits in galactic symmetry plane, using gravitational potential theories
03 p0434 A72-13496

Galactic plane 100 micron survey, detecting continuum radio sources, bright and dark nebula and IR stars
04 p0570 A72-14524

High resolution Galactic center interferometric observations at 5 GHz, showing compact components in Sagittarius A
04 p0580 A72-15511

Large aperture ratio wide field VCN-UV camera exploration of night sky, presenting isophotes of zodiacal light and Milky Way
04 p0525 A72-15685

Gravitational intensification due to focusing of massive rotating gravitational wave emitting oblate object in galactic center
06 p0880 A72-17887

Cyclonic turbulence generation of large scale magnetic field of Galaxy, using Steenbeck differential rotation mechanism
06 p0883 A72-18017

High radial velocity neutral hydrogen outside galactic plane, noting inability to correlate with radio spurs, absorption and emission regions
07 p1069 A72-19082

Faint planetary nebulae classification and measurement in northern Milky Way between Cygnus and Perseus from Schmidt camera survey
07 p1070 A72-19084

Stellar extinction and genesis with Galaxy, discussing L1 role in nucleosynthesis and degenerate star structure theory
07 p1073 A72-19427

Stellar dynamical and density wave theories for spiral pattern persistence in Galaxy with differential rotation
07 p1074 A72-19430

Long period Cepheids in galactic spherical component, confirming two groups according to spectral characteristics
09 p1384 A72-22514

Precessional corrections, solar motion and galactic rotation determination from proper motions by maximum likelihood method, taking into account stars visual magnitude
09 p1391 A72-23535

Cassiopeia region galactic structure study via objective prism, cataloging stars radial velocities and distances
09 p1391 A72-23539

Galactic center radio, IR, X ray, gamma ray and molecular spectral features, considering models for source component emission mechanisms and energy densities
10 p1533 A72-23887

Spectral indications of activity in galactic center, discussing radio source Sagittarius A and expanding hydrogen clouds
10 p1541 A72-24568

Galactic plane distance effect on interstellar reddening in north galactic polar cap, discussing line blanketing and surface gravity role
10 p1546 A72-24834

Satellite photometric observation of diffuse celestial sources such as Milky Way, zodiacal light and gegenschein
10 p1546 A72-24863

Gravitational wave antenna response to linear, mixed and randomly polarized sources, discussing Weber signals galactic nucleus source
11 p1717 A72-25882

Gravitational wave observation interpretations, discussing Weber theory of galactic nucleus isotropic radiation and synchrotron radiation sources in terms of black hole existence
11 p1717 A72-25883

Cyclonic turbulence generation of large scale magnetic field of Galaxy, using Steenbeck differential rotation mechanism
11 p1718 A72-25953

Diffuse galactic light observation, suggesting emanation from discrete sources
11 p1720 A72-26113

Galactic center region neutral hydrogen self absorbing cold cloud, discussing matter, spatial and radial velocity distributions and cloud temperature and density
12 p1867 A72-27208

Hydromagnetic wave scattering of high energy cosmic rays in highly ionized interstellar gas to confine cosmic rays to Milky Way
12 p1864 A72-27745

Milky Way spiral structure and star distribution, discussing photometric methods
12 p1875 A72-27967

Interstellar gas motions and density and temperature variations, discussing galactic structure, radiation fields and cosmic ray effects
13 p2038 A72-29009

Stellar population in Galactic nuclear bulge, considering interstellar reddening and variable stars
13 p2038 A72-29011

Habing galactic model extension and confirmation from observations of high velocity neutral hydrogen clouds and outer spiral arm structure
13 p2048 A72-29817

Galactic astronomy - Conference, State University of New York, Stony Brook, June-July 1968, covering Galactic structure, spiral shape theories, star migration, etc
14 p2152 A72-30486

Galactic spiral arm hypothesis for positive velocity neutral hydrogen clouds above galactic plane, surveying distribution
14 p2158 A72-30732

Spiral structure density wave model of inner parts of Galaxy, calculating density, potential and velocity perturbation and dispersion in gas and stars
14 p2161 A72-30914

Relativistic theory gravitational analogue to electromagnetic radiation, suggesting black hole collision as galactic center flux mechanism
15 p2273 A72-31286

Spherical mirror camera for southern galaxy planar photometry, discussing photographic calibration methods
15 p2306 A72-31597

Lunar orbital photography of astronomical and geophysical phenomena during Apollo 15 flight, noting solar corona and Milky Way
15 p2236 A72-31974

Distribution of high velocity hydrogen near Galactic center due to free-free emission from exploding hot gas or cosmic ray pressure
15 p2317 A72-32756

Book on stellar astronomy covering H-R diagram, solar system, nuclear energy sources, Milky Way Galaxy, quasars, cosmology, planetology, etc
16 p2453 A72-33275

The gravitational acceleration perpendicular to the galactic plane.
17 p2603 A72-34441

On the kinematic distribution of galactic neutral hydrogen.
17 p2606 A72-34572

High energy gamma radiation from the galactic centre region.
18 p2722 A72-36998

Central galactic plane, interstellar medium and spiral arm conditions for star formation in Milky Way
19 p2855 A72-37249

Kinematics of faint M stars near the north galactic pole, and the mass density in the solar neighbourhood.
19 p2855 A72-37341

Soft X-ray emission from intergalactic gas in the neighbourhood of the Galaxy.
19 p2855 A72-37345

Extragalactic origin of the transient X-ray sources.
19 p2856 A72-37502

Pulsars as stellar population, considering physical models, pulse emission radiation mechanism and use in galaxy studies
19 p2865 A72-38476

Density wave detection by local hydrogen gas and young stars radial velocities comparison with Lin theory of galactic spiral structure
19 p2866 A72-38494

Galactic structure at galactic longitudes from 230 to 355 deg on the basis of photoelectric UVB H beta photometry of 55 southern open star clusters
19 p2867 A72-38513

Interstellar gas electron temperature determination from recombination line spectra observations along galactic ridge
20 p2971 A72-39858

Expanding ring in Galactic center from analysis of microwave spectroscopic data, measuring expansion and rotation velocities
20 p2972 A72-39860

Structure and motions in the Carina spiral feature.
20 p2973 A72-39880

- A study of the interstellar extinction in the Carina-Centaurus region. 20 p2973 A72-39881
- Circular polarisation measurements of the zodiacal light. 20 p2920 A72-39899
- Wide-angle photographs of the southern sky as a contribution to the planar photometry of the Galaxy. 21 p3102 A72-40275
- Nebulae of the Southern Milky Way - An atlas. 21 p3114 A72-41847
- Red variables in globular clusters, in the galactic centre and in the solar neighbourhood. 22 p3222 A72-42135
- Spiral and halo structure of our galaxy on the basis of optical distance determinations. 22 p3222 A72-42136
- Estimate for the frequency of novae in the Andromeda Nebula and our Galaxy. 23 p3333 A72-43229
- Cross correlated interstellar scintillation patterns of circumpolar pulsar PSR 0329+54 at 408 MHz, interpreting transverse velocities in Galaxy. 23 p3334 A72-43253
- Calculation of stellar and diffuse radiation for a plane-parallel semiinfinite model of the Galaxy. 23 p3338 A72-44027
- On the possible existence of different interstellar extinction laws in the spiral arms and in the field regions. 24 p3438 A72-44836
- An H I velocity-longitude diagram for the Southern Milky Way. 24 p3438 A72-44845
- Emission and absorption spectral behavior observation by millimeter radio telescopes for molecules in interstellar space of Milky Way galaxy spiral arms. 24 p3439 A72-44905
- Spectral classification of stars with respect to non-broadened low-dispersion spectra. III - Classification method and criteria. 24 p3447 A72-45678
- ### MILLIMETER WAVES
- Rain droplet size distribution effects on microwave attenuation at millimeter wavelengths, comparing calculation with measurement. 01 p0027 A72-10406
- Synchronized multiple microwave oscillators power and noise characteristics at microwave and millimeter frequencies, discussing magic T configuration. 01 p0037 A72-10648
- Millimeter and submillimeter microwave spectrometric studies of high temperature plasmas and noise emission, discussing instrumentation and absolute measurements. 02 p0223 A72-11409
- Millimeter wave sky noise temperature measurement with 16 and 35 GHz radiometers, including antenna loss and rain and cloud effects. 02 p0171 A72-11665
- Low loss reactive wall rectangular and circular waveguides with periodic dielectric structures for millimeter wave and high power applications. 02 p0190 A72-11678
- Low loss wideband circular wave guide bend characteristics and branching filters for millimeter wave large capacity digital transmission. 02 p0190 A72-11682
- Dielectric surface waveguides for millimeter and optical wavelength applications, discussing technologies, materials, fabrication and measurement. 02 p0191 A72-11683
- Beam guides for optical and millimeter wave communication, discussing optical pipelines and iris, lens and reflector waveguides. 02 p0191 A72-11684
- Mm and sub mm wave generation by semiconductor devices, showing power vs frequency plots for IMPATT, Gunn and LSA oscillator diodes. 02 p0268 A72-11694
- Narrow beam millimeter wave radiometer with real-time TV display for terrain mapping, analyzing contours blurring caused by antenna pattern and output integration. 02 p0191 A72-11821
- Solid state components for millimeter wave systems, including IMPATT diode power sources and amplifiers, P-I-N diode modulators and switches and Schottky barrier mixers. 02 p0192 A72-12183
- ATS-F satellite short and long term data processing, detailing millimeter wave propagation experiment. 02 p0177 A72-12384
- Millimeter wave pulse signal transmission path length modulator with P-I-N diode switch, discussing system design and experimental results. 02 p0196 A72-12798
- Solar active region properties at millimeter wavelengths, suggesting chromospheric magnetic field measurement possibility from polarization. 03 p0432 A72-13348
- High speed digital communication at millimeter wavelengths, discussing system requirements, digital computer use, transmission data rate and equipment development. 04 p0485 A72-14481
- Point contact Josephson junctions arrangement for millimeter and submillimeter region, showing mechanical stability. 04 p0561 A72-14919
- Millimeter and submillimeter wave applications, considering environment remote sensing, radar communication, tracking and imagery, wideband communication, plasma diagnostics and spectroscopy. 04 p0550 A72-15592
- CW 100 GHz Si IMPATT diodes with nearly abrupt junctions, discussing output power and dc and small signal analyses. 04 p0502 A72-15594
- Millimeter and submillimeter wave molecular beam masers amplification principles and Doppler and collisional broadening elimination capability. 04 p0532 A72-15597
- Electron tube with Fabry-Perot cavity resonator with grooved and smooth mirrors for millimeter and submillimeter wave generation. 04 p0503 A72-15598
- Horn lens antennas for millimeter wave radiometric applications, discussing medium gain polystyrene lens design to obtain low peak sidelobes. 04 p0503 A72-15608
- Millimeter wave and laser space-to-space communication links comparison, considering ehf system based on size, weight, power consumption and communication parameters calculations. 04 p0493 A72-15609
- Radar and radiometric millimeter wave signal systems in near earth environment for remote detection purposes. 04 p0494 A72-15610
- Combined FM CW radar and radiometer at millimeter wavelengths, investigating objects signatures measurement. 04 p0494 A72-15611
- Visible displays of millimeter and submillimeter wave images for all-weather ground surveillance, discussing image conversion [AD-736578]. 04 p0494 A72-15612
- Vibration-rotation double resonance transitions in symmetrical top molecules in millimeter range under chopped laser radiation. 04 p0532 A72-15615
- Electromagnetic radiation modulators in millimeter and submillimeter wave range using gas-discharge plasma magneto-optical effects in alternating magnetic field. 05 p0625 A72-15826
- Dispersion characteristics of laminated cylindrical dielectric waveguide in millimeter band, noting application to permittivity measurement. 05 p0627 A72-16341
- CW millimeter wave power generation with spiraling electron beams, investigating energy spread effects on performance limitation. 05 p0636 A72-16363
- Partial solar eclipse observation at 9 mm wavelength on 25 February 1971, noting limb brightening. 05 p0718 A72-16509
- Venus 8.2 mm radio emission dependence on sun-light phase angle, considering implications regarding day/night atmospheric temperature variations. 06 p0884 A72-18031
- Total atmospheric water vapor content from solar radiation absorption observation at millimeter wavelengths. 06 p0817 A72-18091
- Millimeter wave GaAs avalanche diode oscillator processing on plated Cu heat sinking block resulting in epitaxially grown p-n junctions. 06 p0788 A72-18467
- GaAs and Si millimeter wave Schottky barrier mixer diodes fabrication, noting low noise broadband mixer/preamp. 06 p0790 A72-18486
- Ring-plane type slow wave structure hot tested near 3 cm for scale modeling in mm range. 07 p0938 A72-18854
- Total flux and polarization of solar S-component at mm wavelengths, obtaining radio source optical depth by evaluation of QL propagation based on magnetoionic theory. 07 p1069 A72-19080
- Millimeter wave techniques for laser stabilization to frequency standards, using phase locked HCN laser and high resolution IR spectrometer [CLEA PAPER 6,7]. 07 p1004 A72-19383
- Millimeter and submillimeter band frequency conversion in nonlinear bulk n-InSb semiconductor at liquid helium temperature. 08 p1140 A72-21060
- Superheterodyne radiometers for millimeter and submillimeter waves, using Mach-Zehnder interferometer frequency mixer for parasitic signal suppression. 08 p1140 A72-21265
- Optimal output power of avalanche transit time diode oscillator in millimeter band as function of electric field and diode geometry. 08 p1141 A72-21378
- Magnetic spectra measurement of powdered hexagonal ferrites in millimeter wavelength range during grinding and after heat treatment. 08 p1218 A72-21875
- Aperture filtering effects on amplitude scintillation power spectra of paraboloid radio telescope over millimeter wave propagation path. 08 p1136 A72-21982
- Calibrator for millimeter wave horn radiometers, using radiation from load immersed in liquid nitrogen. 09 p1310 A72-22652
- Millimeter wave pumped X band balanced diode type parametric amplifier using GaAs Schottky barrier varactors for operation at room temperature. 09 p1289 A72-23417
- Venus 8.2 mm radio emission dependence on sun-light phase angle, considering implications for day/night atmospheric temperature variations. 11 p1719 A72-25967
- Short term frequency instability in mm wave reflex klystrons, obtaining rms frequency drift. 11 p1605 A72-26319
- Theoretical and measured rainfall attenuation of millimeter waves, correlating attenuation coefficients, rain rate and drop size distributions. 12 p1785 A72-27803
- Ground terminals spatial diversity for earth satellite mm wave communication systems to avoid attenuations by rainfall. 13 p1989 A72-28810
- Solar radial brightness distribution, using mm observations during 7 March 1970 solar eclipse for improved angular resolution. 13 p2042 A72-29531
- Solar radio emission map at 1.2 mm wavelength obtained with He cooled Ge bolometer connected radio telescope. 13 p2046 A72-29716
- Upper atmosphere mm emission spectrum from aircraft observation, comparing with rocket and ground based data. 13 p1923 A72-29963
- Millimeter wave scattering at turbulent density discontinuities in plasma from electrodeless inductive discharge. 14 p2136 A72-30174
- Millimeter and submillimeter radiation produced by diffraction phenomena during charged particle passage near periodic structures, discussing physical properties and oscillator development. 14 p2088 A72-30598
- Millimeter wave third harmonic generation and frequency multiplication in n-type InSb at 77 K. 14 p2142 A72-30799
- High resolution atmospheric millimeter wave spectrum of attenuated solar radiation from sea level observations, using Fourier type IR techniques. 15 p2224 A72-31671
- Lunar eclipse observations at millimeter wavelengths on 10 February 1971, determining surface cooling for Copernicus, Mare Serenitatis and highland region. 15 p2311 A72-32087
- Millimeter band open cavity resonator using trihedral reflector diffraction grating and inclination control for mode selection. 16 p2364 A72-33491
- Plasma electron density measurements using flat plate and semifocal millimeter wave Fabry-Perot interferometers [AIAA PAPER 72-672]. 16 p2440 A72-34067
- A millimeter wave receiving antenna with an omnidirectional or directional scannable azimuth pattern and a directional vertical pattern. 17 p2525 A72-34364
- Polarization measurements of radio sources at 9.55-mm wavelength. 17 p2603 A72-34439
- Magnetoelastic amplitude modulator of millimeter waves based on an antiferromagnetic/hematite/. 17 p2529 A72-34842
- Slowly varying component spectrum of the solar radio emission at millimetre wavelengths. 17 p2617 A72-35708
- Composite quasi-optical-broad waveguide transmission lines for millimeter and submillimeter waves with spectrum phase correction. 18 p2664 A72-36106
- Absorption of the 4- to 6-millimeter wavelength band in the atmosphere. 18 p2689 A72-36961
- Millimeter-wave solid-state exciter-modulator-amplifier module for gigabit data-rate. 19 p2771 A72-37267
- Effect of magnetic field on the performance of millimeter-wave detectors using bulk InSb. 19 p2772 A72-37570
- Radio astronomical observations in the 0.9 to 1.5 mm band using a 22-m radio telescope with an n-InSb receiver. 19 p2858 A72-37803

Structure of solar active zones in the mm wave range 19 p2866 A72-38496

A development study for a 65-m radio telescope for the mm wave range 19 p2804 A72-38510

A variation-iteration technique for the design of wall-impedance waveguides. 20 p2903 A72-39429

Spherical reflector as possible antenna for millimeter wave astronomy, discussing feed design for spherical aberration corrections 21 p3029 A72-40519

Dielectric coating effects on millimeter wave diffraction pattern of gratings, noting sharp anomalous dips in transmission intensity for P and S polarizations 21 p3031 A72-40604

Experimental investigation of a millimeter-wavelength n-InSb frequency converter at 4.2 K 21 p3016 A72-40786

The 20 and 30 GHz communications system for the ATSF millimeter wave experiment. 21 p3019 A72-40882

Atmospheric transmissivity in the 49- to 72-GHz band - Analysis and laboratory measurements. 21 p3021 A72-40906

Millimeter absorption features corresponding with H alpha dark filaments on disk and emissive regions in solar prominences, discussing electron temperatures and densities 22 p3221 A72-42035

Electromagnetic radiation modulators in millimeter and submillimeter wave range using gas-discharge plasma magneto-optical effects in alternating magnetic field 23 p3319 A72-43434

Radiation patterns and structural design of two mirror millimeter wave Cassegrain antennas with horn radiator 23 p3271 A72-43778

The quiet sun brightness distributions at millimeter wavelengths and chromospheric inhomogeneities. 24 p3438 A72-44840

MILLING [MACHINING]

Co and carbide containing alloys, investigating milling and sintering temperature effects on technological and physical properties 06 p0829 A72-17831

Milling, band grinding, final manual polishing and tumbler polishing effects on fatigue life and surface finish of steel compressor blades 06 p0824 A72-18651

WC powder milling and sintering, investigating strain and dislocation density effects on behavior by scanning electron microscope 08 p1176 A72-21440

The effect of mixed milling on the sintering of WC-Co hardmetals. 22 p3188 A72-41975

MINERAL OILS

Free and dissolved water contents determination in light petroleum products by modified Karl Fischer method using ethylene glycol solvent mixture 05 p0702 A72-16669

Lubricating mixtures of mineral oil with inorganic phosphates, hydroxides and sulfides, discussing lubrication mechanism and physical properties 06 p0837 A72-18603

Remote sensing of oil pollution on water by laser induced fluorescence, using airborne spectroscopy [AIAA PAPER 71-1076] 07 p0981 A72-18822

Properties of pyrolytic oil hydrogenated aromatic fraction, noting suitability for jet fuels applications 14 p2145 A72-31075

MINERALOGY

Chondrules occurrence in iron meteorite, investigating bulk chemical composition and mineral properties 01 p0127 A72-10294

Mineralogical and chemical compositions of Markovka chondrite 02 p0280 A72-12284

Electron microprobe analysis of plagioclase points and pyroxene grains of Apollo 15415 anorthositic genesis rock 02 p0282 A72-12411

Impact breccias in carbonate rocks of Sierra Madera /Texas/, investigating microstructure, chemical composition, petrography and mineralogy 05 p0654 A72-16038

Mineralogical and petrologic study of lunar anorthosite slide 15415,18 06 p0888 A72-18271

Texture, mineralogy and metamorphic history of lunar anorthosite 15415 06 p0889 A72-18272

Meteorite genesis and formation processes from composition characteristics, discussing age determination methods and mineralogical classifications 07 p1082 A72-20302

Opaque mineralogy of Luna 16 soil sample, emphasizing compositional variations of Fe-Ti-Cr-Al-Mg spinels 09 p1380 A72-22261

Luna 16 rock sample B-1 petrology, mineralogy and chemistry, noting fine grained ophitic basalt nature 09 p1380 A72-22262

Crystallization sequence, petrology and mineralogy of Apollo 12 basalt sample 12009 10 p1537 A72-24160

Zirconium rich metal oxides mineral group in Apollo 14 and 15 lunar rocks from feldspar-phryic basalt and pyroxene ferrobasalt, noting optical and chemical properties 11 p1717 A72-25868

Electron spectroscopy for chemical analysis /ESCA/ technique for nondestructive elemental analysis of lunar and terrestrial minerals 16 p2454 A72-33447

Lunar rock 12052 euhedral clinopyroxenes composed of honey yellow pigeonite cores overgrown by dark brown augite 16 p2454 A72-33448

Study by Mossbauer spectrometry of the iron distribution in mineralogical fractions separated from lunar rocks brought back by Apollo 12 17 p2607 A72-34917

Rock size, mineralogy and fines size distribution in lunar regolith 17 p2615 A72-35683

Petrologic comparisons of lunar terra materials. 17 p2615 A72-35684

Mineralogy, bulk chemistry and sample shape and mass of Seoni /India/ chondrite, observing extensive recrystallization 19 p2858 A72-37860

Mineralogical and chemical researches on L-chondrites - Girenti. 19 p2858 A72-37862

Ordinary chondrite chemical and mineralogical properties establishment during solar system formation, noting fractionation events 20 p2969 A72-39334

Phenocryst fabric in lunar basalt sample 12052 from the Ocean of Storms. 21 p3106 A72-41115

Changes in the phase composition of metal-glass materials depending on the sintering temperature 21 p3073 A72-41370

Czech book - Moldavites and tektites. 21 p3111 A72-41536

IR reflectance [or emittance] remote spectroscopy of mineral particulate surfaces, discussing particle size, surface roughness, porosity and mixing ratios effects 22 p3178 A72-42526

Mineralogy, petrology and chemistry of lunar rock 12039. 23 p3339 A72-44127

Minerals discovered in meteorites, tabulating formula and occurrence and plagioclase composition 23 p3262 A72-44132

MINERALS

NT ANATASE

NT ARAGONITE

NT ASBESTOS

NT BIOTITE

NT CALCITE

NT CHROMITES

NT COESITE

NT DOLOMITE [MINERAL]

NT ENSTATITE

NT FAYALITE

NT FELDSPARS

NT FLUORITE

NT FORSTERITE

NT GARNETS

NT GRAPHITE

NT HEMATITE

NT ILMENITE

NT KAOLINITE

NT MAGNETITE

NT MICA

NT OLIVINE

NT PEROVSKITES

NT PROUSTITE

NT PYROPHYLLITE

NT PYROXENES

NT QUARTZ

NT SCHEELITE

NT SPINEL

NT TALC

NT TROILITE

NT WURTZITE

NT ZINCBLENDE

Book on Apollo 11 lunar rocks and minerals covering mineralogy, petrology, chemical and isotope analyses, bioscience, organic geochemistry, physical properties and measurements 01 p0122 A72-10001

Visible and near IR reflectance spectra of soil mineralized trees, using multispectral photographic filters 02 p0209 A72-11789

Apollo 12 lunar crystalline rock and fines magnetic properties measurement, noting magnetic minerals composition 02 p0278 A72-12026

Amino acid-phosphate anhydrides polymerization in presence of clay minerals, noting reactions superposition and monomer diffusion 04 p0483 A72-14774

Geochemistry of lunar opaque minerals in Apollo 14 crystalline rocks, including FeNi metal, ilmenite, spinels, schreibersite, baddeleyite, fayalite and tranquillityite 10 p1538 A72-24164

U, Th, Pb and rare earth elements abundances and Pb 207/Pb 206 ages of Apollo lunar minerals by ion microprobe mass analysis 12 p1866 A72-27114

U bearing phase zirkelite in Apollo 12 and 14 lunar rocks, using electron microprobe 15 p2303 A72-31303

Chain reaction mechanisms of fuel combustion in presence of metal oxides for ores reduction application 16 p2461 A72-34163

Lunar rock 14310 whitlockite richness in rare earth elements relative to associated apatite 16 p2454 A72-33446

Diopside and Cr-Zr-armalcolite occurrence on moon from Apollo 14166.6 fines, using petrographic and electron microprobe examination 16 p2461 A72-34163

Craters formed in mineral dust by hypervelocity microparticles. 20 p2970 A72-39474

Osarsite, a new osmium-ruthenium sulfarsenide from California. 22 p3172 A72-42450

Shock damaged zircon, corundum, rutile, monazite and quartz crystalline inclusions in Muong Nong-type indochinite /tektite/, noting production from detrital sedimentary materials as possible terrestrial origin 23 p3335 A72-43398

MINES

Chromosome aberrations and germination speedup in Soyuz 5 carried oat seeds, noting stimulating effect by preflight ethylenimine treatment 05 p0623 A72-16777

MINES [EXCAVATIONS]

Subsurface electromagnetic fields of current carrying cable line source on flat earth conducting half space, considering mine rescue operations 01 p0060 A72-10840

Measurements of gradients of gravity in mines. 21 p3048 A72-40500

MINIATURE ELECTRONIC EQUIPMENT

Miniaturized micropower biomultiplexer telemetry system utilizing hybrid techniques 02 p0192 A72-12133

Minority carrier diffusion effect on current gain in miniature bipolar transistors 04 p0498 A72-15132

Planar coax micropackaging of minicomputers for aircraft navigation and military systems, noting environmental tests 05 p0632 A72-15772

Noncontacting measurements by miniature CW Doppler radar with semiconductor microwave generator 09 p1285 A72-22691

Electron microscope interfaced computer for generating, registering and fabricating microelectronic device and circuit patterns 10 p1459 A72-23955

Miniaturized electronic system for controlling methanol concentration in aqueous electrolyte during fuel cell operation 12 p1755 A72-27723

Voltage controlled miniaturized n-type negative resistance circuit based on junction transistor and FET without internal bias 21 p3038 A72-40998

Miniaturized IC semiconductor device fabrication and failure under electrical load, using scanning electron microscope 21 p3035 A72-41492

Miniaturized piezoelectric transducer electronics versus charge amplifiers - A comparison of the two systems in vibration and pressure applications. 22 p3159 A72-42702

Minicomputers application for long distance data transmission, noting multipurpose use of VT 1010/B computer in satellite operation program 24 p3382 A72-45391

MINIATURIZATION

NT MICROMINIATURIZATION

NT SUBMINIATURIZATION

Dissipative loss effects on frequency response and miniaturization limits for minimum loss conditions in microwave filters with Chebyshev characteristics 05 p0638 A72-17188

Vacuum mold preparation and flexural testing of miniature carbon fiber reinforced composite specimens 11 p1671 A72-25468

Miniature high gain photomultiplier for pulse counting applications in close-packed arrays and mosaics for scintillation imaging and spectrum analyzing 15 p2234 A72-31534

Electric relay spring design for miniaturization, deriving relation between length and thickness to minimize fiber stress under constant contacting force 19 p2775 A72-38617

Dissipative loss effects on frequency response and miniaturization limits for minimum loss conditions in microwave filters with Chebyshev characteristics
19 p2775 A72-38624

Viscously damped miniature piezoresistive biaxial accelerometer for operation in single cavity to 250 F
22 p3179 A72-42701

MINIMA

An algorithm for determining the absolutely minimum form of weakly determined functions
23 p3308 A72-43349

MINIMAX TECHNIQUE

Optimal nonlinear discrete filters with finite memory for polynomial signals, discussing synthesis with aid of minimax method
04 p0505 A72-14998

Minimax solution of linear regulator problem, presenting algorithm for numerical computation
05 p0682 A72-16451

Minimax terminal state estimator existence and structure for linear discrete system, applying to stochastic pursuit evasion games of LQG variety
07 p1027 A72-19283

Programmed minimax target acquisition in rendezvous game between conflictingly controlled motion and given set of vectors
07 p1028 A72-19969

Minimax optimal control problems with incomplete information, using dynamic programming and phase space location measurements
07 p0963 A72-19970

Optimal strategies conditions for game problems in conflictingly controlled system, discussing minimax technique and Bellman equation solution
07 p1028 A72-19971

Minimax feedback control of uncertain discrete time dynamic systems with set description, using dynamic programming
10 p1456 A72-23806

Variational minimum principle for two elastic bodies frictionless contact, discussing Hertzian and non-Hertzian normal half space problems
11 p1690 A72-26667

Spacecraft motion stabilization about mass center and optimal angular velocity control using minimax technique
11 p1684 A72-26903

Binary PSK signals optimized on minimax and quadratic criteria, noting design of coders and decoders on shift registers with external logic
13 p1914 A72-28415

Numerical algorithm for guaranteed minimax [max-min] estimates for multistep decision making processes, using ALGOL 60
13 p1924 A72-28708

Algorithm for minimax parameter optimization by linear and quadratic programming with application to earth orbiting satellite orbital transfer
16 p2366 A72-33191

On behavior strategy solutions in two-person zero-sum finite extended games with imperfect information. I - A method for determination of minimally complex behavior strategy solutions.
17 p2574 A72-34343

Minimax method of optimizing electric circuits in the absence of constraints on the variable parameters
19 p2777 A72-37309

Frequency response optimization of electric filters, modulators and impedance matching circuits using minimax criterion, noting nonlinear programming sequence
19 p2771 A72-37310

Optimal avoidance control to transfer dynamic system from initial to terminal state in maximin distance problem
19 p2778 A72-37724

Minimax technique for direct synthesis of Kalman-like filter under large uncertainties in a priority statistics of plant and measurement noises
20 p2907 A72-39120

Programmed minimax target acquisition in rendezvous game between conflict controlled motion and given set of vectors
20 p2947 A72-40026

Minimax technique in optimal control problems with incomplete information on phase vector, using dynamic programming and system position measurement refinements
20 p2911 A72-40027

Optimal strategies conditions for game problems in conflict controlled system, discussing minimax technique and Bellman equation solution
20 p2947 A72-40028

Optimal minimax regulation of a dynamic system.
23 p3276 A72-43860

MINIMIZATION

U OPTIMIZATION

MINIMUM DRAG

Optimal airfoil profile for minimum drag in supersonic linearized gas flow with allowance for random fabrication errors and surface melting and sublimation at high temperatures
05 p0610 A72-17136

Minimum drag bodies of revolution in supersonic flow obtained by combining steepest descent method with integral flow model
14 p2069 A72-30231

Optimum nonslender bodies of revolution minimum drag in free molecular flow under integral constraints
15 p2180 A72-32395

V-wings and diamond ring-wings of minimum induced drag.
21 p2992 A72-41263

Determination of slender bodies of minimum total drag in hypersonic flow using Newton-Busemann pressure coefficient law.
23 p3249 A72-44267

MINKOWSKI SPACE

Gravitational field of bounded and isolated material in empty four-dimensional locally Minkowskian space-time, emphasizing radiation zone and gravitational waves
04 p0570 A72-14556

Quasar luminosity due to unique big bang in specific space-time region, considering Minkowskian geometry
06 p0878 A72-17669

Space-time model locally identical with Minkowski space in geometrical and causality features, implying non-Doppler red shift and cosmology
12 p1868 A72-27218

Minkowski space-times for impulsive gravitational waves, considering idealized plane fronted wave form and limiting case of Robinson-Trautman null spherically fronted wave
20 p2955 A72-40007

Interaction between weak gravitational waves and a gas
21 p3084 A72-40402

Hyperbolic space criterion for cosmological model based on axioms conforming to special and general theory of relativity, noting coordinate transformation
24 p3439 A72-44969

MINORITY CARRIERS

Minority carriers similarity in graphite natural single crystals and pyrolytic samples
01 p0114 A72-11035

Quantum oscillations of minority Fermi surface carriers as function of magnetic field in Hall effect and thermoelectric power in pressure-annealed pyrolytic graphite
02 p0268 A72-11673

Minority carriers localized surface distribution effect on helicon propagation modes reflectivity in semiconductor
03 p0402 A72-13797

Minority carrier diffusion effect on current gain in miniature bipolar transistors
04 p0498 A72-15132

One dimensional model for drift transistor at low injection level with minority carrier mobility dependence on impurity concentration
08 p1140 A72-21063

Validity range of applied voltage relationship to majority carrier current in Schottky diodes, assessing minority carrier current importance
10 p1448 A72-24108

Cosmic radiation effects and damage on solar cells, discussing shielding, stability improvement, space environments, minority carrier lifetime and photosensitivity spectral distribution
10 p1422 A72-24312

Minority carrier diffusion length in liquid epitaxial GaP, noting dependence on dominant impurity and substrate growth orientation from Schottky diode photocurrent technique
10 p1526 A72-24551

Recombination diffusion length of minority carriers in thin layer cuprous sulfide solar cells
12 p1856 A72-28011

Electron irradiation of Li doped Ge at low temperatures, measuring Hall effect and minority carriers diffusion length
12 p1857 A72-28055

Effects of junction depth on the radiation damage of silicon solar cells.
17 p2594 A72-34388

Determination of the parameters of minority carriers in semiconductor photocells from a spectral sensitivity curve
17 p2498 A72-35512

Stability of the dynamic parameters of a transistor in a small signal mode superimposed on a static injection mode
17 p2594 A72-35801

Short-circuit current in silicon solar cells - Dependence on cell parameters.
19 p2753 A72-37567

Minority-carrier trapping and the luminescence time response of semiconductors.
19 p2844 A72-37946

Cooling associated with minority carriers exclusion effect in semiconductors, discussing influence of electroconductivity and forbidden bandwidth
21 p3097 A72-40788

On the determination of minority carrier lifetime and surface recombination velocity from the transient response of MOS capacitors.
23 p3324 A72-44071

MINUTEMAN ICBM

Computerized bias optimization of telemetry timing accuracy applied to Minuteman system
02 p0174 A72-12144

Minuteman HERO / hazards of electromagnetic radiation to ordnance/ preflight testing, describing ordnance monitoring system based on fiber optic data links
08 p1220 A72-20767

Three solid stage Minuteman ICBM, discussing all-inertial guidance system, ablative reentry vehicle and management arrangements
23 p3358 A72-44357

MINUTEMAN MISSILES

U MINUTEMAN ICBM

MIRAGE 3 AIRCRAFT

Mirage 3E liquid propellant auxiliary rocket engine, discussing intercept performance enhancement
05 p0705 A72-16708

MIRRORS

NT TELESCOPES

NT FRESNEL REFLECTORS

NT MAGNETIC MIRRORS

NT PARABOLOID MIRRORS

NT ROTATING MIRRORS

Laser with convex-plane resonator and cross sectional variable mirror transmission, showing effective transverse mode selection and diffraction divergence
02 p0239 A72-12767

Spectrophotometer and tristimulus mask calorimeter using double grating mirror dispersion system
03 p0358 A72-13427

Enhanced He-Ne laser frequency and output power stabilities obtained by constructing mirror and gas discharge tube as integral unit
04 p0529 A72-14603

Gas lasers mode locking, describing use of amplitude and frequency modulation and moving mirrors
04 p0530 A72-14738

Cast telescope mirror design with light metallic structures, examining possibilities offered by composite high modulus fiber structures
05 p0660 A72-15855

Cylindrical mirror electron energy analyzer, discussing theory, operation and design parameters [AD-745599]
07 p0984 A72-19322

Cer-Vit glass mirror replacement for AFCRL lunar laser observatory inverted Dall-Kirkham Cassegrain telescope, noting one arc sec resolution from wire and null optics tests
07 p0985 A72-19410

Anastigmatic optical systems with two high aperture ratio mirrors for UV image tubes
08 p1169 A72-21952

Ruby laser radiation modulation by mirror ultrasonic vibrations, discussing mechanism
09 p1326 A72-23681

Holographic correction of reflecting refracting telescope objective mirror deformation aberrations, noting interferometric attachment
10 p1479 A72-24049

Nonrectilinearity evaluation of twin wave Michelson interferometer mirror displacement
10 p1481 A72-24498

Optical mirrors contamination by condensation of outgassed spacecraft materials in vacuum under UV irradiation, describing test apparatus and results with various materials
11 p1637 A72-25208

Frequency stabilization of He-Ne two mode laser with internal mirror plasma tube
11 p1646 A72-25303

Double passed Michelson interferometer with polarizing beam splitter, quarter wave plates and cube corner reflectors to obtain immunity to mirror misalignment
11 p1635 A72-26500

Pulsed RF hydrogen plasma heating in mirror machine near ion cyclotron frequency and harmonics
11 p1699 A72-26703

Astronomical reflector telescope design, describing thermal effects on Al mirror and image intensification
12 p1807 A72-27428

Solid state laser resonator inhomogeneous dielectric and mirror elements matching effects on Q factor and output power
12 p1822 A72-27609

Approximate analytical method for diffraction losses and corrections to lower transverse modes and resonance condition in symmetrical stable cavities with round spherical mirrors
13 p1970 A72-29679

Spherical mirror camera for southern galaxy planar photometry, discussing photographic calibration methods
15 p2306 A72-31597

Operational tests of the AFCRL 152-cm telescope.
17 p2555 A72-35198

A gas laser with external mirrors generating non-polarized radiation
17 p2563 A72-35308

Determination of the quality of the reflective properties of mirrors used in photoelectric converter assemblies
17 p2498 A72-35510

- Holographic interferometer employing spherical mirrors. 18 p2692 A72-36699
- Excitation of a confocal spherical laser resonator. 19 p2810 A72-37403
- Reduction of the effect of mount deformation on the flexure of the telescope mirror 19 p2801 A72-37967
- Method for determining thermal strains in astronomical mirrors 19 p2801 A72-37968
- Scatterplate, artificial hologram, moire and null lens methods for aspheric mirror testing for space astronomy and laser communication 20 p2922 A72-39033
- Properties of metal interference filters for 1200-3000 A, of dichroic mirrors for 1700-3000 A and of multielectric narrow passband interference filters for 2000-3000 A 20 p2923 A72-39051
- Laser with convex-plane resonator and cross sectional variable mirror transmission, showing effective transverse mode selection and diffraction divergence 20 p2931 A72-39073
- Exit slit mirror system in rocket-borne scanning Ebert grating spectrometer, discussing imaging properties and required adjustments 21 p3053 A72-40606
- Investigation of optical inhomogeneities in large fields by holographic methods 22 p3176 A72-42106
- Spectrum of stimulated emission in a resonator with plane mirrors 22 p3184 A72-42154
- A large multiple mirror telescope (MMT) project. 22 p3180 A72-42988
- ## MIS [SEMICONDUCTORS]
- Metal-insulator-metal tunneling junction, calculating effect of localized impurity states in barrier on tunneling current 03 p0404 A72-12627
- MIS semiconductors radiation-hardening mechanisms and radiation effects on electrical properties and degradation 03 p0405 A72-12481
- Vacuum technology - Conference, Boston, October 1971 12 p1805 A72-27034
- Shielding metallic interlayer technique to protect MIS device against degradation due to ionizing radiation effects 13 p2023 A72-29836
- Binary information storage with bipolar transistors, tunnel diodes, MIS and glass semiconductors, considering Gunn effect devices application 20 p2905 A72-39425
- Apparatus for measurement and automatic graphical recording of variations of electrical characteristics of a metal-insulator-semiconducting structure 21 p3051 A72-40209
- Microelectronics developments and limitations, considering bipolar IC, metal-dielectric-semiconductor structures and optoelectronic communication links 21 p3033 A72-40940
- Measurement of substrate impurity profile of MIS field-effect transistors. 21 p3035 A72-41488
- ## MISALIGNMENT
- Misalignment effect on load distribution and fatigue life of tapered roller bearings [ASME PAPER 71-LUB-6] 02 p0234 A72-11532
- Control axes misalignment effects on spinning satellite wobble damping and requirements for active momentum exchange controllers 02 p0286 A72-12267
- Random filament misalignment effects on rigidity and tensile strength of unidirectional graphite composites under shear loading 08 p1192 A72-21681
- Random filament misalignment effect on reinforced composite strength, discussing bundle, tensile and shear strengths 11 p1673 A72-25486
- PSK signal cross-correlated receiver output SNR in presence of random misalignments with respect to carrier frequency and arrival signal time 13 p1921 A72-29283
- An automatic mass-trim system for spinning spacecraft. 20 p2977 A72-39603
- ## MISCIBILITY
- ## U SOLUBILITY
- ## MISFRES
- ## U FIRING (IGNITING)
- ## MISMATCH
- ## U IMPEDANCE MATCHING
- ## MISORIENTATION
- ## U MISALIGNMENT
- ## MISS DISTANCE
- Miss distance simulation for SAM guided by proportional navigation, using ASIM programming language for digital computer 03 p0386 A72-13611
- ## MISSILE ANTENNAS
- Unpredicted structural vibration in Comet and Electra aircraft, Graf Zeppelin dirigible, missile antennas, etc 02 p0292 A72-12002
- Electra method of plasma diagnosis around reentry vehicle head, describing onboard antennas impedance measurements and use of triple Langmuir probe mounted on telescopic mast 10 p1552 A72-24659
- ## MISSILE BODIES
- Finned missiles nonlinear rolling motion characteristics at large angles of attack, solving differential equation of motion by global nonlinear least squares method [AIAA PAPER 72-980] 22 p3134 A72-42333
- Periodicity in exothermic hypersonic flows about blunt projectiles. 24 p3463 A72-45035
- ## MISSILE CASES
- ## U MISSILE BODIES
- ## MISSILE COMPONENTS
- ## NT MISSILE ANTENNAS
- ## NT MISSILE BODIES
- Numerical control component insertion for missile IC electronic module, tabulating producer-user survey data for designs usage and machine tools 17 p2532 A72-35923
- ## MISSILE CONFIGURATIONS
- Minimum ballistic factor missile shapes. 19 p2746 A72-37522
- Generalized subharmonic response of a missile with slight configurational asymmetries. 22 p3134 A72-42339
- The effects of protuberances and scaling parameters on the aerodynamic characteristics of an air-to-air cruciform missile. [AIAA PAPER 72-969] 22 p3231 A72-42342
- Occurrence and inhibition of large yawing motions during high-incidence flight of slender missile configurations. [AIAA PAPER 72-968] 24 p3364 A72-45411
- ## MISSILE CONSTRUCTION
- ## U MISSILE STRUCTURES
- ## MISSILE CONTROL
- Three dimensional roll-controlled missile trajectory model for simple time-sharing digital or analog simulation, using wind-to-inertial axis transformation 01 p0130 A72-10964
- Harpoon air-sea/sea-sea all-weather missile system, describing two phase guidance system based on inertial platform initial phase and radar terminal guidance 07 p1085 A72-20312
- Hybrid computer simulation for telemetry data collected during missile flight control system model post-flight verification and hardware performance analysis 07 p1085 A72-20332
- Tactical missile controlled test vehicle flight test analysis by six-degree-of-freedom digital simulation 07 p1086 A72-20351
- Cassiopeia attitude control apparatus flight tests on Tacite rocket, describing aiming accuracy, target acquisition and gas consumption 15 p2321 A72-31824
- Rotating body linear dynamic control by complex transfer function approach with application to stability conditions for controlled gyro and homing missiles 17 p2583 A72-35528
- Gas bearing gyroscope for fluidic guidance and control system, satisfying missile and recoverable booster requirements 18 p2648 A72-36557
- Proportional navigation with a maneuvering target. 19 p2830 A72-37290
- Discrete optimal terminal control, with application to missile guidance. 19 p2780 A72-38257
- A versatile Kalman technique for aircraft or missile state estimation and error analysis using radar tracking data. [AIAA PAPER 72-838] 20 p2950 A72-39089
- A new approach to a cruise navigator evaluation using sparse reference data. [AIAA PAPER 72-835] 20 p2950 A72-39092
- Computer simulation aided airborne attack missile launch system design for safe separation from carrier aircraft, discussing ejection and control systems design [AIAA PAPER 72-828] 20 p2951 A72-39099
- Virtual target steering - A unique air-to-surface missile targeting and guidance technique. [AIAA PAPER 72-826] 20 p2951 A72-39100
- Development and optimization of the SRAM guidance and control software. [AIAA PAPER 72-824] 20 p2951 A72-39102
- A simulation technique used in the development of a flight control system for an aerodynamically controlled missile. [AIAA PAPER 72-858] 20 p2976 A72-39136
- Aerodynamic characteristics of the slotted fin. 21 p2992 A72-41262
- ## MISSILE DEFENSE
- Parallel processing of ballistic missile defense radar data with PEPE. 24 p3383 A72-45667
- ## MISSILE DEFENSE SYSTEMS
- ## U MISSILE SYSTEMS
- ## MISSILE DESIGN
- Guided weapon systems design under cost restrictive conditions, discussing conceptual design planning and performance tradeoffs against cost and reliability 01 p0147 A72-11155
- Joint venture and international collaboration in guided weapon systems design, development and production, discussing cost sharing coordination between governments and contractors 01 p0147 A72-11156
- Missile destruct systems explosive transmission line manifolds, discussing designs for high reliability under severe environmental conditions 08 p1221 A72-20782
- Simply supported skew plates stability under combined loading, noting wing and tail design applications for high speed aircraft and missiles 10 p1555 A72-24196
- Minimum ballistic factor missile shapes. 19 p2746 A72-37522
- NASA ICBM/IRBM space program major management decisions and highlights concerning Atlas, Titan and Thor 23 p3358 A72-44356
- Three solid stage Minuteman ICBM, discussing all-inertial guidance system, ablative reentry vehicle and management arrangements 23 p3358 A72-44357
- ## MISSILE DETECTION
- ## NT RADAR DETECTION
- ## MISSILE ENGINE CASES
- ## U ROCKET ENGINE CASES
- ## MISSILE GUIDANCE
- ## U MISSILE CONTROL
- ## MISSILE LAUNCHERS
- Computer simulation aided airborne attack missile launch system design for safe separation from carrier aircraft, discussing ejection and control systems design [AIAA PAPER 72-828] 20 p2951 A72-39099
- ## MISSILE RANGES
- Telemetry standards for transmitting, receiving and signal processing equipment at missile test ranges 02 p0176 A72-12164
- White Sands Missile Range and Range-Rate system design and verification to meet midcourse tracking requirements under severe target dynamics 08 p1133 A72-21402
- ## MISSILE ROLL CONTROL
- ## U LATERAL CONTROL
- ## U MISSILE CONTROL
- ## MISSILE SILOS
- The use of an expansion tube with cold gas to determine rocket engine starting transient pressures during silo launch. [AIAA PAPER 72-997] 21 p3040 A72-41583
- ## MISSILE SIMULATION [MATH MODELS]
- ## U MATHEMATICAL MODELS
- ## U MISSILES
- ## MISSILE SIMULATORS
- RF simulator design for missile systems performance tests, discussing requirements, target array and anechoic chamber [AIAA PAPER 72-861] 20 p2911 A72-39125
- ## MISSILE SIMULATORS [TRAINING]
- ## U MISSILES
- ## U TRAINING SIMULATORS
- ## MISSILE STABILIZATION
- ## U MISSILE CONTROL
- ## U STABILIZATION
- ## MISSILE STAGING
- ## U MISSILES
- ## U STAGE SEPARATION
- ## MISSILE STORAGE
- Evaluation of guided missile system in-service reliability. 24 p3448 A72-44658
- ## MISSILE STRUCTURES
- Lightweight low pressure plastic hose assemblies in aircraft and missile petroleum base fuel and synthetic lubricating oil systems at 395-710 R and up to 200 psi [SAE ARP 1180] 01 p0006 A72-10388
- Data generation for engineering design with advanced composites. 17 p2571 A72-35653
- ## MISSILE SYSTEMS
- Missile systems of U.S., U.S.S.R. and other nations, discussing ground-to-ground, ground-to-air, air-to-ground and air-to-air missiles 05 p0728 A72-16740
- Earthbound missile propulsion systems, reviewing turbojet and ramjet engines, liquid, solid and hybrid propellant rocket engines and composite propulsion systems for special applications 05 p0705 A72-16741
- Polaris and Poseidon missile systems reliability assessment, discussing test programs, analytical techniques and data management 10 p1551 A72-24013
- U.S. Army missile systems rocket motors life cycle reliability programs based on propellant laboratory analyses, motors static tests and field firings statistical evaluation 14 p2146 A72-30759

Weapon system program choice for development in aerospace industry, considering cost effectiveness and ranking illustrated on stand-off tactical interdiction missiles

16 p2482 A72-33598

Computer simulation aided airborne attack missile launch system design for safe separation from carrier aircraft, discussing ejection and control systems design

[AIAA PAPER 72-828]

20 p2951 A72-39099

RF simulator design for missile systems performance tests, discussing requirements, target array and anechoic chamber

[AIAA PAPER 72-861]

20 p2911 A72-39125

MISSILE TEST LABORATORIES

U LABORATORIES

U MISSILE TESTS

MISSILE TEST RANGES

U MISSILE RANGES

MISSILE TESTS

Sidewall reflection induced boresight error in anechoic chamber used for missile test or simulation

08 p1141 A72-21421

Polaris and Poseidon missile systems reliability assessment, discussing test programs, analytical techniques and data management

10 p1551 A72-24013

RF simulator design for missile systems performance tests, discussing requirements, target array and anechoic chamber

[AIAA PAPER 72-861]

20 p2911 A72-39125

Evaluation of guided missile system in-service reliability.

24 p3448 A72-44658

MISSILE TRACKING

White Sands Missile Range and Range-Rate system design and verification to meet midcourse tracking requirements under severe target dynamics

08 p1133 A72-21402

Meteorological radar measurements, noting missile tracking radio interferometer noise due to stochastic refractive ray bending and associated multipath conditions

08 p1136 A72-21978

Lidar application to aircraft and missile tracking and ranging, describing results obtained with ONERA experimental equipment

10 p1436 A72-24655

Nonlinear filtering for random signals in statistically unknown noise, noting application to satellite orbit determination, aircraft navigation and missile tracking

11 p1611 A72-25986

Missile tracking laws for inhomogeneous linear-quadratic performance optimization

11 p1593 A72-25992

Refraction correction of rocket tracking radar inputs in near real time.

18 p2661 A72-36636

MISSILE TRAJECTORIES

Missile trajectory stochastic optimal control systems with fuel constraint by mean path deviation optimization

05 p0725 A72-16452

Hypersonic missile trail conductivity measurement on ballistic test stand, calculating electron concentration decrease

14 p2069 A72-30312

Proportional navigation with a maneuvering target.

19 p2830 A72-37290

Virtual target steering - A unique air-to-surface missile targeting and guidance technique.

[AIAA PAPER 72-826]

20 p2951 A72-39100

Free-flight projectiles aerodynamic characteristics and trajectories from yawsonde and radar track data, obtaining best fit coefficients by equations of motion numerical integration

[AIAA PAPER 72-978]

22 p3134 A72-42335

Hypersonic missile trail conductivity measurement on ballistic test stand, calculating electron concentration decrease

23 p3247 A72-43214

SAM-D control test vehicle trajectory planning and flight test analysis.

24 p3451 A72-45338

MISSILE VIBRATION

Vibration analysis of shaft supported low aspect ratio control surfaces on guided rockets, using Rayleigh-Ritz method

07 p1097 A72-20602

The effects of frictional drag on missile vibrations - A finite difference solution.

21 p3118 A72-40929

MISSILE WINGS

U LOW ASPECT RATIO WINGS

MISSILES

NT AIR TO AIR MISSILES

NT AIR TO SURFACE MISSILES

NT ANTITANK MISSILES

NT BALLISTIC MISSILES

NT INTERCONTINENTAL BALLISTIC MISSILES

NT INTERMEDIATE RANGE BALLISTIC MISSILES

NT MINUTEMAN ICBM

NT POLARIS MISSILES

NT POSEIDON MISSILES

NT RAMJET MISSILES

NT SURFACE TO AIR MISSILES

NT SURFACE TO SURFACE MISSILES

Aerodynamic multivariable function generation in real time simulation of high performance missile

02 p0186 A72-11656

Coning motion, autorotation, and vortex systems of slender flight vehicles

22 p2321 A72-42904

MISSILRY

U MISSILES

MISSILE PLANNING

Planetary quarantine cost and mission success constraints, formulating mathematical models for international goals and implementation systems

01 p0019 A72-10819

Delta and Thor/Agenda satellite launch vehicles, discussing costs, performance and mission planning based on booster design flexibility, incorporating computer programmed strapdown inertial guidance

01 p0136 A72-10953

Helios solar probe mission, describing project management, data reception system, trajectory monitoring and international cooperation

[DGLR PAPER 71-052]

02 p0284 A72-12720

German-American interplanetary solar probes Helios A and B mission characteristics and ground operations system, discussing planning phase

[DGLR PAPER 71-122]

02 p0285 A72-12741

Mission analysis of Helios spacecraft swingby past Venus to acquire extraelectric trajectory

[AIAA PAPER 72-50]

05 p0721 A72-16951

Earth resources technology satellite program, discussing mission requirements, payload, orbital characteristics, earth stations, data processing, system design and international features

[DGLR PAPER 71-139]

06 p0892 A72-18230

Regional communications coverage by controlled satellite constellations with low altitude circular orbits, developing analog or digital simulation method for mission planning

07 p0945 A72-19690

Skylab launch and mission program, describing modular components, crew training, checkout, launch and docking procedures, flight plan and crew working schedules, rescue and reentry procedures, etc

08 p1240 A72-21008

Linear programming procedure for efficiency and cost optimization in aerial survey mission

08 p1165 A72-21164

Skylab S-193 altimeter experimental mission objectives and spacecraft instrumentation, considering precision designs, oceanographic surface remote sensing and electromagnetic scattering measurement

09 p1306 A72-22317

Soviet interplanetary spacecraft Mars 2 and 3, describing design, mission objectives, onboard systems and instrumentation

09 p1395 A72-22974

Complex system mission worth optimization by redundancies discussing MISDGRAD computer program to evaluate cost-reliability for mission without maintenance

10 p1550 A72-23994

Design considerations and reliability analysis for long duration manned space missions, noting redundancy and inflight maintenance requirement

[AIAA PAPER 72-239]

10 p1487 A72-24446

Multimission capability of solar electric propulsion /SEP/ spacecraft, analyzing payload variations, propellant requirements, thrusting time limitations and throttling range

[AIAA PAPER 72-51]

10 p1552 A72-25125

Solar electric propulsion upper stage for multiple space exploration missions, discussing spacecraft performance, configurations and program plans

[AIAA PAPER 72-464]

11 p1709 A72-26199

Spacecraft nuclear electric propulsion system multimission performance evaluation, discussing launch mode and vehicle capability factors in system size selection

[AIAA PAPER 72-503]

11 p1685 A72-26226

Mars 1975 Viking mission profile, describing soft landing/orbiter probes and life detection experiments

12 p1877 A72-27687

German aeronomy research satellite Aeros mission objectives, discussing orbit layout, onboard equipment and operation

13 p2050 A72-30079

Mars 3 probe design and mission details, covering trajectory correction lander separation, engine start-up, aerodynamic braking and dust storm data

14 p2151 A72-30477

Deep space navigation requirements for interplanetary missions /1978-1990/

15 p2269 A72-32178

Resource allocation for minimum cost launch vehicle assignment to space missions, using network and dynamic programming algorithm

16 p2482 A72-33498

Long range planning for the development of space flight emergency systems.

17 p2620 A72-34428

Spacecraft rescue and recovery capabilities assessment based on anticipated U.S. space programs,

discussing mission design, recovery response, weather prediction and communications

17 p2620 A72-34429

Linear programming procedure for efficiency and cost optimization in aerial survey mission

17 p2521 A72-34455

Mission operations for unmanned nuclear electric propulsion outer planet exploration with a thermionic reactor spacecraft.

17 p2606 A72-34578

Lunar landing sites selection approach for Apollo missions, examining mission design requirements, launch vehicle considerations and lunar composition

19 p2857 A72-37700

Mission design and navigation for a 1977-1978 Venus Swingby/Mercury Orbiter.

[AIAA PAPER 72-941]

21 p3113 A72-41577

Two early missions to comets in 1977-1980 as precursors to more ambitious missions in 1984-1986, discussing exploration objectives and spacecraft configurations

23 p3340 A72-44352

Simulation procedure for mission and maintenance planning of an air force wing.

24 p3365 A72-44663

Space rescue operations planning requirements for 1980s manned satellite missions, discussing vehicles, equipment and various mission phases

24 p3449 A72-45129

Rescue operation capability for Skylab, discussing mission requirements, response time and vehicle configuration

24 p3449 A72-45132

Optimization of altitude and inclination change schedules during low thrust ascent to geosynchronous orbit.

24 p3440 A72-45150

NASA space science, exploration and applications plans and policies in view of space shuttle capabilities, emphasizing cost reduction

24 p3440 A72-45162

The Scout launch vehicle system.

24 p3450 A72-45165

Study of shuttle-based systems for high-energy planetary missions.

24 p3441 A72-45189

Design and operation objectives and constraints for German scientific spacecrafts, discussing orbital performance and reliability and quality control requirements

24 p3451 A72-45206

Mission objectives, hardware development and international cooperation aspects in U.S. future space flight programs, discussing space shuttle, space tug, Apollo 17 and Skylab

24 p3441 A72-45216

Mission strategy for combined comet-asteroid flybys.

[AIAA PAPER 72-939]

24 p3444 A72-45436

Mariner spacecraft Jupiter-Saturn 1977 gravity assisted flyby, discussing mission objectives and trajectory options

[AIAA PAPER 72-943]

24 p3444 A72-45438

Mariner Mars 1971 adaptive mission planning for scientific objectives flexibility based on planetary features observed, discussing plan change implementation

[AIAA PAPER 72-944]

24 p3444 A72-45439

Space astronomical observatory mission planning, analysis and operation and data utilization in terms of space and ground facility instruments and support subsystems

24 p3382 A72-45536

Unmanned OAO spacecraft series and experiment packages, discussing space astronomy scientific achievements, mission plans and space shuttle role

24 p3453 A72-45535

HEAO satellite to carry instruments required in high energy astrophysics missions, discussing observational objectives, configuration and experiments

24 p3453 A72-45538

MITOCHONDRIA

Normal and hypoxic myocardium mitochondrial metabolism process, studying electron transport system

Acute hypoxia of the myocardium - Ultrastructural changes.

17 p2501 A72-34978

Effect of chronic hypoxia on the kinetics of energy transformation in heart mitochondria.

17 p2502 A72-34993

Cytoplasmic heredity theory linking mitochondria origin to bacteria

19 p2758 A72-38549

Helium effect on cardiac mitochondria of mice.

19 p2759 A72-38712

Hypoxic acclimation effects on rats heart, liver and kidney mitochondria, measuring cytochrome oxidase and succinic dehydrogenase activities

22 p3144 A72-42673

MITOSIS

Mitotic index and aberrant mitose frequency in mice corneal and intestinal epithelial cells exposed to 50-630

MeV protons, estimating relative biological efficiency coefficients
[CERN-71-16] 02 p0161 A72-12055
Hypoxia effect on diurnal mitotic activity rhythm of marrow erythropoiesis system of guinea pigs in pressure chamber 05 p0618 A72-16631
Hyperoxia effect on kidney blood flow erythroproietic properties in rabbits, noting inhibiting effect on erythroblast cells mitotic activity in bone marrow culture 06 p0765 A72-18061
Pulsed and continuous rf irradiation effects on mitotic activity and chromosomal aberrations in regenerating rat liver tissue 07 p0917 A72-19443
Mitosis duration and mitotic activity diurnal rhythms in esophageal epithelium of rats given thyroxine 07 p0924 A72-20623

MIXED CRYSTALS
Optically pumped semiconductor lasers, discussing two photon absorption, emission from compounds and mixed crystals and smooth frequency variation 07 p1006 A72-20118
Two photon absorption of ruby laser emission in mixed zinc cadmium sulfide crystals, plotting laser light damping vs beam power density 09 p1322 A72-22212
Electronic configuration effect on wetting characteristics of hard material mixed crystals, investigating transition metals carbides, nitrides and oxides 11 p1665 A72-26873
Room temperature negative photoconductivity of p-type ZnTe-CdTe solid solutions mixed crystals within model with electron and hole capture levels 14 p2141 A72-30173

MIXED FLOW
U MULTIPHASE FLOW
MIXERS
Integrated receiver module for satellite transponders, including tunnel diode amplifier, Schottky barrier mixer, Gunn oscillator and low pass filter 01 p0041 A72-10701
GaAs and Si millimeter wave Schottky barrier mixer diodes fabrication, noting low noise broadband mixer/preamp 06 p0790 A72-18486

MIXING
NT COLLOIDING
NT DISSOLVING
NT HOMOGENIZING
NT LAMINAR MIXING
NT SIGNAL MIXING
NT SUSPENDING [MIXING]
NT TURBULENT MIXING
Fuel injection, mixing and combustion processes investigation in model cylindrical swirl chamber, describing flow visualization method for turbulence observation 15 p2297 A72-32297

MIXING CIRCUITS
Gunn diode microwave oscillator with moving reflector as self-excited mixer and load variation detector, analyzing performance by I-V characteristics model 04 p0497 A72-14713
Josephson junction as 100 GHz oscillator-mixer for heterodyne frequency conversion in millimeter and submillimeter regions, observing I-V characteristics 04 p0503 A72-15604
Computational model of post mixer spectra of periodic FM altimeters with area target returns, using radar scattering coefficient 05 p0637 A72-16568
Conversion coefficients of optical heterodyne receiver mixer for various amplitude-phase distributions of interfering signal 07 p1000 A72-19012
Parametric converter mixers with FM and AM signal and pump oscillator, investigating SNR behavior 07 p0956 A72-19658
Multiplication and mixing of electromagnetic waves in optically nonlinear anisotropic crystal media 07 p1007 A72-20119
Microwave frequency mixer using two inverted tunnel diodes in series connection 10 p1450 A72-24519
Input match conditions for broadband mixer conversion loss minimization, comparing optimization procedures 15 p2208 A72-32392
German monograph on microwave broadband tunnel diode mixers theory and design, taking into account parasitic elements as part of filter networks 16 p2368 A72-33507
Frequency conversion and limiter action for an angle-modulated wave with amplitude fluctuation in a half-wave linear mixer. 23 p3265 A72-44179

MIXING LENGTH FLOW THEORY
Turbulent boundary layer fluid dynamic behavior under transpiration and acceleration effects, presenting mean velocity profile data, skin friction and mixing length model [ASME PAPER 71-HT-F] 02 p0205 A72-12315
Two and three dimensional turbulent boundary layer development in incompressible and compressible flows, obtaining boundary layer equations similarity solutions via mixing length model [DGLR PAPER 71-066] 02 p0206 A72-12719
Turbulent mixing length formulation and velocity profiles for non-Newtonian power law fluids, determining friction factor for pipe flow at high Reynolds numbers 03 p0343 A72-14318
Finite difference schemes for surface and planetary boundary layer solutions using grid spacings proportional to mixing length and eddy viscosity 03 p0386 A72-14337
Planetary boundary layer mixing length flow hypothesis with dependence on Reynolds tangential stress permitting turbulent diffusion coefficient maximum values computation 04 p0519 A72-15458
Longitudinal curvature effects on laminar and turbulent boundary layer flows predicted from Navier-Stokes equations, noting mixing length assumption validity [ASME PAPER 71-WA/FE-37] 05 p0645 A72-15920
Pressure gradient effect on mixing length for equilibrium turbulent boundary layers, calculating eddy viscosity [AIAA PAPER 72-213] 05 p0651 A72-16855
Modified mixing length velocity distribution predictions for turbulent boundary layers with uniform mass transfer for low and high Reynolds numbers 08 p1150 A72-21622
Mixing length model for computing three dimensional turbulent boundary layers with small cross flow [ONERA, TP NO. 985] 09 p1294 A72-22817
Mixing length model for turbulent boundary layer in incompressible flow with fluid injection at wall, extending solution to compressible case 09 p1294 A72-22818
Two and three dimensional turbulent boundary layers integral calculation method, presenting similarity solutions based on extended mixing length model 10 p1469 A72-24653
Main sequence, red giant and white dwarf stars convective envelopes evolution, discussing mixing length theory inadequacy 10 p1545 A72-24826
Compressible turbulent boundary layer with arbitrary pressure gradients on solid or permeable surfaces, using extended mixing length theory 11 p1616 A72-25917
Book on turbulence covering Reynolds stresses, kinetic theory of gases, vorticity dynamics and mixing length models 11 p1616 A72-25925
Dynamic and thermal laminar compressible boundary layers on flat plate, noting interaction of two quasi-steady flows [ONERA, TP NO. 1068] 12 p1797 A72-27167
Turbulent mixing length velocity, temperature pulsations and viscous sublayer thickness in steady incompressible fluid flow past infinite plate 12 p1799 A72-28179
Massive red supergiants radial pulsations from adiabatic theory application to convective envelope models based on mixing length theory and H-He ionization zones 14 p2159 A72-30743
Mixing length theory derivation of barotropic planetary boundary layer profiles for geostrophic wind deviations, Reynolds stress, eddy viscosity and turbulent kinetic energy dissipation 15 p2224 A72-31675
Lower zero age main sequence star models uncertainties, comparing nonmixing and mixing length theory for various composition atmospheres 15 p2314 A72-32367
Turbulent mixing layers analytical and experimental mean velocity profiles, discussing Goetler eddy viscosity theory 16 p2374 A72-32832
Mixing processes of newly made elements in Galaxy, taking into account thermodynamics, galactic structure and nucleosynthesis parameters 18 p2727 A72-36732
Free gas jets turbulent mixing flow, considering development of submerged air jet with action of mechanical turbulence generator ahead of nozzle 20 p2913 A72-39367
A gradient method of expanding a group data handling method to new plants not studied by experiments 22 p3162 A72-42242
Mixing between stellar envelope and core in advanced phases of evolution. IV - Effect of super-adiabaticity in convective envelope. 23 p3335 A72-43486
Turbulent mixing of three plane isothermal jets with various velocity ratios, showing jet initial length shortening due to initial turbulence increase 23 p3279 A72-43657

Contributions to the study of turbulent flow in the vicinity of a flat wall 24 p3394 A72-45443

MIXTURES
NT ADMIXTURES
NT AEROSOLS
NT AQUEOUS SOLUTIONS
NT BINARY MIXTURES
NT COLLOIDAL PROPELLANTS
NT COLLOIDS
NT DETONABLE GAS MIXTURES
NT DISPERSIONS
NT EUTECTIC ALLOYS
NT EUTECTICS
NT FOG
NT GAS MIXTURES
NT LIQUID-GAS MIXTURES
NT METAL MATRIX COMPOSITES
NT NUCLEAR EMULSIONS
NT PHOTOGRAPHIC EMULSIONS
NT SLURRIES
NT SMOKE
NT SOLID SOLUTIONS
NT SOLID SUSPENSIONS
NT SOLUTIONS
Extremum search algorithm in multicomponent mixture optimization problem, using gradient method adaptation 13 p1924 A72-28460
Thermodynamic parameters and reacting multicomponent mixture composition, using state equations and energy conservation equations for reaction kinetics 21 p3013 A72-40989

MOBILE LOUNGES
Passenger transfer in airports with total separation between aircraft and permanent buildings for independent functioning, noting Dulles Airport mobile lounges 16 p2374 A72-34143

MOBILITY
NT ATOMIC MOBILITIES
NT ELECTRON MOBILITY
NT HOLE MOBILITY
NT IONIC MOBILITY
Elastic-plastic-viscous model for creep analysis of rheo-mobile materials, taking into account cracks and other defects 16 p2412 A72-34116
Measurement of mobility in high-resistivity semiconductor layers by the van Heek method 17 p2530 A72-35067

MODAL RESPONSE
Matrix formulation of free-free modal synthesis procedures for dynamic analysis of composite structural systems, giving flow charts [SAE PAPER 710783] 01 p0137 A72-10274
Direct-iterative eigensolution technique for simultaneous determination of structural system lowest frequencies and modal patterns, using reduced generalized coordinates and Stodola-Vianello method [SAE PAPER 710784] 01 p0137 A72-10275
Moving load effect on circular cylindrical shell in acoustic medium, discussing free axisymmetric vibration mode, shape and frequencies 02 p0290 A72-11627
Thick orthotropic off-axis laminated plates vibration equations solution, presenting natural frequencies spectra and modal functions 02 p0249 A72-11988
Dynamic analysis of shallow shells with doubly-curved triangular finite element, investigating natural frequencies, mode shapes and convergence 04 p0585 A72-14844
Free solid body kinetic moment vector effects on long period motion in resonant state during transition from rotational to somersaulting mode 06 p0849 A72-18699
Mode conversion effects on Gaussian laser beam in acousto-optical modulation for optical communications 07 p1004 A72-19225
Modal matching method evaluating planar surface waveguide junction transmission and reflection coefficients, comparing to integral equation method 07 p0955 A72-19253
Circular semiinfinite dielectric rod antenna, determining near- and far-zone fields, gain and beamwidth under excitation by HE/sub 11/ hybrid mode 07 p0956 A72-19782
Ideal liquid small oscillations natural frequencies and mode shapes in shell of revolution under weak gravitational field 08 p1148 A72-20956
Nonlinear modal response analysis of plate structures under random acoustic excitation, using finite element method and perturbation technique 08 p1245 A72-21607
Axisymmetric MHD equilibria with elliptical cross sections and flat current profile, obtaining criterion for stability to localized modes by numerical computation 09 p1361 A72-23047
Nonlinear microwave power amplifiers with IMPATT diodes in stable and injection locked modes, predicting behavior for comparison with experiment 10 p1451 A72-24592

Modal damping matrix off diagonal terms measurement in viscous damping exploration for dynamic analysis of linear structures 11 p1736 A72-25988

Radiation resistance for natural modes of rectangular panel from far field acoustic radiation energy distribution 11 p1687 A72-26059

Mode locked ruby laser having triangular ring cavity with four prisms to obtain reliable single-transverse-mode Q switched and normal operation 11 p1647 A72-26150

Ferrite loaded X band waveguide Y junctions eigenvalue frequency dependence measurement to identify modal resonance and arrange displacement for circulator operation 12 p1790 A72-27508

Structural evaluations and dynamic testing of solar electric propulsion components, surveying power conditioning panel modal frequencies by holographic interferometry technique [ALAA PAPER 72-442] 13 p1899 A72-28941

Zero moment stress effect on modal density spectrum of fluctuating thin cylindrical shells and cylindrical panels 15 p2327 A72-31737

Complex structures dynamic analysis by component mode technique, treating modal characteristics as random variables 15 p2331 A72-32555

Dynamically loaded elastic, viscous, plastic and rigid, viscoplastic structures instantaneous mode responses definitions and characterization by variational criteria with isometric constraints [ASME PAPER 72-APM-17] 17 p2628 A72-34799

Spectral theory of Taylor vortices. I - Structure of unstable modes. 19 p2788 A72-38550

Modal control theory for distributed parameter systems with multiengine assignment implemented for one dimensional diffusion equation 21 p3037 A72-40642

Linear distributed parameter systems modal analysis and design for low sensitivity optimal feedback control, using linear differential operators 21 p3037 A72-40646

Transient test techniques for modal survey testing. 22 p3163 A72-42698

Method of measuring modal characteristics of a structure subjected to a random excitation 22 p3242 A72-43095

MODE OF VIBRATION

U VIBRATION MODE

MODE SHAPES

U MODAL RESPONSE

MODE TRANSFORMERS

Thin film optical waveguides using magneto-optic GdIG as substrate, discussing computerized design for propagation mode converter efficiency [IEEE PAPER 3,6] 03 p0332 A72-13755

MODELS

NT AIRCRAFT MODELS

NT ANALOG SIMULATION

NT ASTRONOMICAL MODELS

NT ATMOSPHERIC MODELS

NT BREADBOARD MODELS

NT DIGITAL SIMULATION

NT DYNAMIC MODELS

NT ENVIRONMENT MODELS

NT MATHEMATICAL MODELS

NT REFERENCE ATMOSPHERES

NT SCALE MODELS

NT SPACECRAFT MODELS

NT THOMAS-FERMI MODEL

NT VECTOR DOMINANCE MODEL

NT WIND TUNNEL MODELS

Plastic model shells design, construction and instrumentation for elastic stability studies in NDT, discussing deformation measurements for critical condition prediction 22 p3163 A72-42694

MODEMS

SSB signal generation without Nyquist filter or auxiliary equipment for PM modems in data transmission 15 p2195 A72-31620

MODERATION [ENERGY ABSORPTION]
NT THERMALIZATION [ENERGY ABSORPTION]

MODERATORS

Investigations concerning metal-hydride technology and hydrogen transport in the incore thermionic reactor I/TR-core. 18 p2699 A72-36157

MODES

NT COUPLED MODES

NT LASER MODES

NT PROPAGATION MODES

NT UNCOUPLED MODES

NT VIBRATION MODE

MODIFIERS

U ADDITIVES

MODULATION

NT AMPLITUDE MODULATION

NT DELTA MODULATION

NT FEEDBACK FREQUENCY MODULATION

NT FM/PM [MODULATION]

NT FREQUENCY MODULATION

NT FREQUENCY SHIFT KEYING

NT INTERMODULATION

NT IONOSPHERIC CROSS MODULATION

NT LIGHT MODULATION

NT PHASE MODULATION

NT PHASE SHIFT KEYING

NT PULSE AMPLITUDE MODULATION

NT PULSE CODE MODULATION

NT PULSE DURATION MODULATION

NT PULSE FREQUENCY MODULATION

NT PULSE FREQUENCY MODULATION

NT PULSE FREQUENCY MODULATION

NT PULSE FREQUENCY MODULATION

NT PULSE FREQUENCY MODULATION

NT PULSE POSITION MODULATION

NT PULSE TIME MODULATION

NT TRAVELING WAVE MODULATION

NT ULTRASONIC LIGHT MODULATION

NT VELOCITY MODULATION

Read avalanche diode noise theory, showing carrier current modulation and lf and hf noise coupling in nonlinear regime 03 p0333 A72-13848

Mathematical expectation of angularly modulated signal in unsteady linear random noise, using Marchenko formula 07 p0939 A72-19020

Direct broadcasting communication satellites, discussing frequency allocation, modulation and data processing systems 07 p0948 A72-20266

Nonstationary and asymmetric cosmic ray modulation theory, discussing moving boundary problem and solar wind model with spherical singularity 07 p1065 A72-20643

Galactic cosmic ray modulation region evaluation from meteoroid orbit, velocity and radioactive dating data 07 p1065 A72-20644

Differential equation solution for plane self focusing and one dimensional self modulation of waves interacting in nonlinear media 08 p1209 A72-21718

Modulated electromagnetic wave transmission in dispersive medium with cubic nonlinearity, discussing solitary wave and instabilities in two-wave interaction 09 p1352 A72-23475

Technical standards for educational and community TV by satellite, considering picture quality requirement, modulations, SNR, threshold and fade margin, and channel width 10 p1435 A72-24034

Equivalent baseband and passband delay line and transversal equalizers derivation for linear modulation systems, obtaining relationship between tap coefficients 15 p2211 A72-31844

Digital communication system for analog signal transmission by digital modulation techniques, presenting detection schemes 15 p2201 A72-32565

Electron interferometer based on second order interference effects from laser modulated electron beam, applying quantum mechanical analysis 16 p2402 A72-33398

Grid modulation information encoding technique for image features extraction with simple Fourier filtering to replace heuristic method 16 p2365 A72-33752

A comparison of voice communication techniques for aeronautical and marine applications. 17 p2512 A72-34267

Rigidity dependence of cosmic ray modulation function at 2-13 Gv from C-130 aircraft survey flights data. 17 p2602 A72-35606

The theoretical amplification limit of modulation amplifiers with correlation detection 18 p2668 A72-37035

Uniqueness of the solution for identification of linear systems by the modulating function method 19 p2779 A72-38086

Acousto-optic modulation with coupled Gunn oscillator-piezoelectric structure. 20 p2960 A72-39702

Reductive perturbation method application to Vlasov equation governing one dimensional motion of collisionless plasmas, investigating nonlinear modulation of plasma waves 21 p3089 A72-40188

Effects of Landau damping on nonlinear wave modulation in plasma. 21 p3089 A72-40189

Temperature effects on modulation sensitivity and vibrational spectra in Gunn diode oscillators, suggesting frequency stability improvement method 21 p3032 A72-40792

Measurement of a radio signal nonenergetic parameter at high additive and modulation noise levels 21 p3022 A72-41117

External high-frequency modulation of an electron beam and heating of plasma ions in the case of beam-plasma instability in the magnetic trap 21 p3095 A72-41678

External high-frequency modulation of an ion beam and the absorption of beam-plasma instability oscillations in a plasma situated in a magnetic field of mirror configuration 21 p3095 A72-41683

Modulation transfer function for solar telescopes and atmospheric turbulence. 22 p3175 A72-42047

Influence of modulating /multiplicative/ noise on signal processing in a phased-array-antenna/receiver system 23 p3265 A72-44205

Nature of the long-term and short-term modulations of cosmic-ray intensity. 23 p3332 A72-44521

MODULATORS

VLF modulation/demodulation system performance prediction by atmospheric noise model, comparing results with measurements 01 p0025 A72-10327

Millimeter wave pulse signal transmission path length modulator with P-I-N diode switch, discussing system design and experimental results 02 p0196 A72-12798

Robust delta modulator configuration with minimal mean square error from signal statistics estimates, discussing design and performance by digital simulation 04 p0486 A72-14486

Gaussian envelope microwave pulse generation using absorption p-i-n diode modulator, predicting performance by digital simulation 04 p0498 A72-14718

Electromagnetic radiation modulators in millimeter and submillimeter wave range using gas-discharge plasma magneto-optical effects in alternating magnetic field 05 p0625 A72-15826

Optimum adaptive variable step size delta modulator-demodulator producing minimum error for Markov-Gaussian source 06 p0772 A72-17404

Performance characteristics of electro-optical material cadmium telluride for intracavity modulator of carbon dioxide lasers 07 p1003 A72-19223

T equivalent circuit magnetic modulator system with split excitation windings on four separate cores magnetized by HF source, noting null drift due to hysteresis 11 p1603 A72-25281

Three centimeter balanced ring modulator with carrier and sideband suppression using amplitude and phase relations 11 p1605 A72-26321

Microwave waveguide semiconductor modulator with p-n diode as control element, taking into account semiconductor control element conductivity change along waveguide wall 15 p2206 A72-31662

Liquid opticoacoustical modulator for laser radiation control operating on pulse amplitude modulated ultrasonic traveling waves with membrane partitions 16 p2400 A72-33081

Magnetoelastic amplitude modulator of millimeter waves based on an antiferromagnetic/hematite/ 17 p2529 A72-34842

Contactless relay circuits employing a branched-core magnetic modulator with second-harmonic output 19 p2771 A72-37302

Frequency response optimization of electric filters, modulators and impedance matching circuits using minimax criterion, noting nonlinear programming sequence 19 p2771 A72-37310

Space applications of Fabry-Perot modulator as alternative to mechanical devices, presenting optical and electrical performance data for different temperatures 21 p3055 A72-40824

Solid state laser sources, light modulators and silicon avalanche photodiode detectors for fiber optical communication, discussing performance and limitations from system design viewpoint 21 p3018 A72-40866

Electromagnetic radiation modulators in millimeter and submillimeter wave range using gas-discharge plasma magneto-optical effects in alternating magnetic field 23 p3319 A72-43434

Local-oscillator-circuit optimisation for minimum distortion in double-balanced modulators. 23 p3270 A72-43603

Ferrite component for waveguide commutator used as microwave switching element and modulator, noting application in navigation instruments and avionics 23 p3270 A72-43768

MODULATORS-DEMODULATORS

MODULES

NT COMMAND SERVICE MODULES

NT ELECTRONIC MODULES

NT LUNAR MODULE

NT MICROMODULES

NT SERVICE MODULES

NT SPACECRAFT MODULES
 Modular fluidic elements in pneumatic logic system based on Coanda effect
 02 p0156 A72-11999

Flexible solar cell array module design technique, discussing electric welding procedure and equipment parameters effects on breaking strength and reliability
 12 p1758 A72-28036

Completely modular thermionic reactor ion propulsion system /trips/.
 18 p2721 A72-36177

MODULUS OF ELASTICITY
NT DYNAMIC MODULUS OF ELASTICITY
 Nondestructive determination of temperature dependence of elastic moduli of Al alloy and Ni and stainless steels by resonant frequency method
 01 p0084 A72-10518

High modulus high strength graphite composites for aerospace structures, noting materials, machining properties and applications
 [SME PAPER EM 71-191] 01 p0092 A72-10965

Stress waves propagation in woven-fabric composites, obtaining dynamic moduli and vibration damping coefficients by resonance technique
 [AD-736006] 02 p0291 A72-11984

Directional solidification of off-eutectic Al-Be alloy, obtaining ultimate strength, elastic modulus and concentration perturbation caused by freezing rate changes
 [AD-738212] 02 p0242 A72-11985

Ultrasonic measurement of orthotropic laminated composites elastic moduli, describing stress-strain response
 [AD-736007] 02 p0249 A72-11994

Hereditarily elastic body model with various tensile and compressive strengths, using elasticity theory with differing moduli
 02 p0294 A72-12429

Steels modulus of elasticity dependence on prestressing level produced by transverse and longitudinal tension
 03 p0371 A72-13462

Rigid and compliant walls longitudinal curvature and compliance effects on incompressible laminar boundary layer hydrodynamic stability
 03 p0342 A72-13854

Elastic plates with moduli of elasticity variable in tension and compression, deriving plane stress-strain relations
 03 p0451 A72-14118

Variable-modulus isotropic material finite elastic deformation, deriving two dimensional stress concentration by dual series expansion
 03 p0452 A72-14132

Heat treatable Al alloys tensile and compressive moduli of elasticities data from USAF programs, comparing to long-accepted typical values
 03 p0378 A72-14175

Elasticity theory relations for material with tension- and compression-varying modulus of elasticity, representing elastic strain energy as quadratic form potential
 04 p0586 A72-15009

German monograph on refractory materials elasticity modulus determination at elevated temperatures, describing device based on characteristic vibrations frequency relation to temperature
 04 p0510 A72-15698

First and second order moduli of elasticity for finitely deformed elastic materials, deriving acceleration waves propagation condition and growth equation
 05 p0735 A72-16028

Tensor calculus theorem application to elastic isotropic materials finite deformation, considering acceleration waves propagation and moduli of elasticity
 05 p0735 A72-16029

Preferred orientation effects on X ray stress measurement of Young modulus and Poisson ratio of Al alloy
 06 p0829 A72-17793

Crystallographic texture of Mo sheet, analyzing angular dependence of Young modulus
 06 p0832 A72-18366

Temperature dependent directional differences of modulus of elasticity of Mo sheet, using resonance technique
 06 p0833 A72-18632

High temperature tests of short time strength, hardness and moduli of elasticity of W-Mo alloys subject to plastic deformation and annealing
 06 p0833 A72-18633

Unidirectionally and cross rolled Ti alloys elastic properties anisotropy during cooling, discussing Young modulus distribution
 06 p0834 A72-18666

Elastic unbounded homogeneous layer separation from half plane under normal load pressures, determining contact area with base for elastic moduli relationships
 08 p1243 A72-21233

Carbon fibers elastic modulus inference from electrical conductivity inverse correlation with sound propagation rates
 08 p1191 A72-21498

Elastic filler rigidity effect on cylindrical glass fiber reinforced plastic shells stability loss and critical load value under axial compression
 08 p1245 A72-21503

Nondestructive determination of glass reinforced plastics normal elastic and shear moduli and strength characteristics by vibrational, pulsed and acoustic methods
 08 p1195 A72-21773

Contact problem of semiinfinite plate deflection on linearly deformed half space with depth dependent elasticity modulus
 08 p1247 A72-21808

Transient strain in axially impacted hollow non-homogeneous cone with axially varying modulus of elasticity and density
 10 p1555 A72-24195

Linear equations relating elastic compliance coefficients of anisotropic two-phase fiber reinforced composites
 10 p1556 A72-24262

Cross-ply laminates effective elastic moduli relations based on generalized Hooke's law
 10 p1556 A72-24264

Linear anisotropic composites with periodic spatial structure, determining elastic moduli and electrical conductivity variational bounds
 10 p1556 A72-24346

Random elastic modulus variability of building materials test pieces under compression and tensile loads
 10 p1557 A72-24403

Ring assembly with hinged cross section and uniform radial and transverse loads, determining deflection dependence on bulkheads and rigidity of supports
 [AIAA PAPER 72-355] 11 p1729 A72-25384

Young modulus of TiC-Co and TiC-Ni hard composites as function of volumetric fraction, using bending tests
 11 p1660 A72-26487

Longitudinal propagation of elastic disturbance in conical rod, discussing Young modulus, material density and periodic and impulsive stress
 11 p1737 A72-26589

Nb-Ti alloy elasticity modulus temperature dependence, considering foreign atoms interactions with dislocations
 11 p1662 A72-26737

Screw dislocation with free surface interaction in inhomogeneous elastic medium with continuously varying elastic moduli
 12 p1881 A72-27253

Electronic system for continuous automatic recording of internal friction and modulus of elasticity at high temperatures
 12 p1807 A72-27462

Stress relaxation in anelastic materials, calculating spectra, complex modulus of elasticity and internal friction
 12 p1883 A72-27541

Particulate fillers bulk effects on epoxy resin compositions flexural, compressive and tensile strengths and moduli
 12 p1834 A72-28089

Laplace transformation for mechanical response of piezoelectric composite transducer under action of thermal field and electric potential, noting time dependent modulus of elasticity
 13 p1955 A72-28621

Normal modulus of elasticity of filamentary silicon nitride crystals with three orientations, calculating elastic plibilities
 13 p1984 A72-30117

Porous cellular structure materials, investigating porosity effects on modulus of elasticity based on central monoporous model
 14 p2165 A72-30433

High modulus composites structural design applications, considering fatigue performance vs cost
 [ASME PAPER 72-DE-24] 14 p2167 A72-30866

Finite element method with compliance equations determining energy release rates and stress intensity factors for complex crack configurations and loadings
 14 p2168 A72-30908

Dynamic elastic moduli of diffusion saturated high melting point nitrides, carbides and borides of Ti, Zr, Nb, W, Mo and Ta
 15 p2252 A72-31199

Upper and lower bounds for complex elastic moduli of composite materials with isotropic linear viscoelastic phases behaving as homogeneous isotropic materials
 16 p2468 A72-33199

Approximate method for composite materials effective elastic moduli determination from uniform stress-strain field or as second derivative of average strain energy
 17 p2625 A72-34322

Plane problem of thermal creep at high temperatures
 17 p2636 A72-34473

Microinhomogeneous elastic media with moduli tensor as coordinate random function, investigating stress and strain tensors
 18 p2735 A72-36668

A photoelastic material with variable modulus of elasticity.
 19 p2822 A72-37731

Variations as a function of the temperature of the moduli of elasticity of monocrystalline P-type GaSb
 19 p2846 A72-38542

Determination of the elastic modulus of the left-ventricle myocardium with the aid of X-ray kymography
 20 p2893 A72-38940

Young and shear moduli of binary Fe base alloys as functions of composition and temperature by ultrasonic pulse echo technique
 20 p2937 A72-39287

Contribution of the invar anomaly and the elinvar effect to the formation of the thermal stability of the modulus of elasticity of iron-nickel invars
 21 p3068 A72-40952

Dependence of linear elasticity solutions on the elastic constants. II - Dependence on the shear modulus in elastostatics.
 21 p3119 A72-41106

Connexions between the moduli for anisotropic elastic materials.
 21 p3119 A72-41107

Dynamic inelastic properties of materials. I - Damping characteristics of fiber composites. II - Representation of time dependent characteristics of metals.
 [ICAS PAPER 72-28] 21 p3069 A72-41153

Stress differentiation procedure for screen technique studies in dynamic photoelasticity, giving expressions for elastic modulus and Poisson coefficient
 21 p3123 A72-41363

The modulus of elasticity of plastic materials at stress times between .001 and 10,000,000 seconds
 22 p3197 A72-42859

The use of a torsion machine to measure the shear strength and modulus of unidirectional carbon fibre reinforced plastic composites.
 23 p3306 A72-43562

Useful range of a mechanical impedance technique for measurement of dynamic properties of materials.
 23 p3294 A72-44126

Compliance calibrations of a contoured and face grooved double cantilever beam specimen.
 24 p3413 A72-44817

Steels modulus of elasticity dependence on prestressing level produced by transverse and longitudinal tension
 24 p3413 A72-44937

Crystallographic texture of sheet Mo alloys, analyzing angular dependence of Young modulus
 24 p3416 A72-45752

MOHR CIRCLES

U FRACTURE MECHANICS

MOIRE EFFECTS

Noncoherent moire contour-sum contour-difference and vibration analysis of three dimensional objects using grid projection and offset camera
 03 p0358 A72-13438

Elastic-plastic strain measurement on flat steel surfaces by moire gratings, using electroluminescent source and crossing jig
 06 p0818 A72-18323

Transient high speed deformations analysis of annealed Al under impact loads by three dimensional moire fringe techniques
 07 p0983 A72-19131

Double beam Mach-Zehnder interferometer, discussing optical element imperfection induced degradation elimination by Moire technique
 07 p0985 A72-19406

Experimental determination of torsional stresses in rod from moire patterns, describing facility and procedure
 07 p1091 A72-19762

Vibration measurement based on moire pattern fringes motion due to line gratings respective displacement, noting high accuracy and resolution
 09 p1315 A72-23388

Real time hologram-moire interferometry for visualization of turbulence phenomena in liquid flow through cylindrical pipe
 11 p1629 A72-25317

Retina visual acuity testing by zero and first order moire fringes, using square-wave amplitude gratings
 12 p1772 A72-27953

Shearing stresses in rod under torsion, using Prandtl membrane analogy and moire interference fringes
 13 p2053 A72-28397

Sensitivity limits in moire picture application to holographic interferometry
 13 p1958 A72-29514

Experimental development by holography of three dimensional moire fringes for very large deformations study
 13 p1960 A72-29781

Composite materials stress analysis techniques, discussing strain gages, photoelastic coatings moire and holographic applications
 [ASME PAPER 72-DE-6] 14 p2167 A72-30861

Principle of control of aspherical surfaces by holography and moires
 17 p2554 A72-34912

Photoelasticity, holography, moire and strain gage methods in European experimental mechanics research

18 p2733 A72-36357

Holographic interferometry analyzed from the point of view of moire patterns.

18 p2690 A72-36362

Flat beam linear vibration analysis from mode measurement and moire technique, applying to prototype turbine compressor blade

18 p2734 A72-36375

Use of a projected-ruling moire method for vibration and deflection measurements of three-dimensional structures.

19 p2799 A72-37629

Scatterplate, artificial hologram, moire and null lens methods for aspheric mirror testing for space astronomy and laser communication

20 p2922 A72-39033

Moire screens coded with pseudo-random sequences.

23 p3289 A72-43892

Mapping of large dynamic deflections of structures.

24 p3454 A72-44606

Metallic solid material transient displacement field measurement by moire fringe photographic recording technique with computer program for data analysis

24 p3401 A72-44611

MOISTURE

Surface moisture effect on dielectric properties of ultrafine barium titanate particulates of varying particle size

[ACSPAPER 7-E-69F] 02 p0269 A72-12416

Electrical measurement of moisture effects on adhesive bond strength, insulation resistance and hydrophilicity of cast epoxy and organosilicon adhesives

12 p1833 A72-27449

MOISTURE CONTENT

NT ATMOSPHERIC MOISTURE

Topmost soil layer moisture content measurement by reflected visible light polarization enhancement

02 p0209 A72-11794

Surface temperature measurement by microwave radiometry, noting sensitivity reduction due to moisture effects for resolution cell size targets

02 p0214 A72-11867

Soil surface moisture content and temperature profile determination by remote microwave sensing

02 p0214 A72-11871

Free and dissolved water contents determination in light petroleum products by modified Karl Fischer method using ethylene glycol solvent mixture

05 p0702 A72-16669

Gas dynamic laser technology advances, discussing water content, temperature and Na effects and nozzle design

[AIAA PAPER 72-143] 05 p0669 A72-16895

White thick layer anodic zirconium oxide water content determination by volumetric and thermogravimetric analysis of heated samples

05 p0667 A72-17051

Specific moisture contents in stratosphere over European Soviet Union from balloon measurements

06 p0806 A72-17734

Broadband S band radar application to quantitative analysis of severe storms, calculating liquid water content

06 p0843 A72-18442

Epoxy and polyester resin fatigue fracture tests for cyclic stress and moisture effects

08 p1192 A72-21680

Slag powdery material moisture content determination by absolute pyridine adsorption method of moisture extraction

12 p1813 A72-27450

Remote measurement of cloud ice and water content from Raman scattering of ground based laser signal

12 p1840 A72-27547

Cloud statistics stratification by climatological regime, month and time of day, extending simulation to drop size distributions and liquid water content

13 p1989 A72-28808

Coastal and inland fog microphysical features, discussing visibility, liquid water content, drop size distributions and haze droplet concentrations

13 p1991 A72-28842

Fluctuations of water vapour content in the troposphere as derived from interferometric observations of celestial radio sources.

17 p2545 A72-34690

Multispectral photography in soil moisture determination and soil series differentiation.

18 p2686 A72-36320

Cloud liquid water content measurement via digital radar system, presenting two dimensional display of storm system characteristics

21 p3077 A72-40250

MOISTURE DETECTORS

U MOISTURE METERS

MOISTURE METERS

NT HYGROMETERS

NT PSYCHROMETERS

Radiometric method for atmospheric moisture data retrieval above radiosonde hygrometer cut-off or during malfunction, inferring average moisture decrease through radiative transfer equation

09 p1307 A72-22441

Gage for solids and liquids moisture content measurement based on phase shift of UHF electromagnetic wave propagating through tested material, noting specimen thickness optimization

12 p1807 A72-27466

MOL [ORBITAL LABORATORIES]

U MANNED ORBITAL LABORATORIES

MOLDAVITE

Czech book - Moldavites and tektites.

21 p3111 A72-41536

MOLDING MATERIALS

Epoxy- and polyimide-graphite composites electrical dissipation factor and capacitance measurements as guide to molding quality, describing equipment

02 p0250 A72-12609

Explosives injection molding into stainless steel, aluminum, plastic and rubber tubes, considering applications to fuse and detonation transfer trains and small warheads

08 p1221 A72-20781

Thermoplastic polypropylene sandwich molds stiffness variation with time, noting three point bending and creep tests

11 p1673 A72-25550

Thermoplastic materials casting procedures to mold high melting point metal compound powders

11 p1645 A72-26861

Pure metal unidirectional solidification as function of liquid superheat, metal/mold heat transfer coefficient and mold material

16 p2399 A72-33804

Effects of modification and additional elements on the solidification of Al-Si alloy - Studies on the solidification of Al-Si alloys in a shell mold. II.

21 p3067 A72-40937

MOLECULAR ABSORPTION

Molecular continuity relationship relating discrete absorption oscillator strengths to photodissociation cross sections

01 p0104 A72-11115

Boundary effects on light incoherent scattering by dispersing molecules, using quantum statistics

04 p0490 A72-15398

Atmospheric molecular and aerosol absorption effects on submillimeter radio wave propagation using laser, BWT and liquid He receiver-transmitter devices

04 p0551 A72-15607

Molecular sieve adsorption sampler for stratospheric carbon 14 measurements from balloon collected carbon dioxide samples

06 p0807 A72-17824

Molecular gases absorption coefficients measurement in extreme UV, analyzing photoionization curves in energy range far beyond threshold

09 p1356 A72-22829

Intracavity gas cell for carbon monoxide laser oscillations restriction to lines coincident with atmospheric transmission bands, noting absorption by atmospheric water vapor

12 p1823 A72-27837

Luminous molecular absorption cross sections in aeronomy, considering photodissociation, actinic solar radiation attenuation and UV to IR analysis

14 p2097 A72-30135

Nonlinear radiation absorption and resonance molecular fluorescence of saturated diatomic Rb vapors excited by Q switched ruby laser

14 p2109 A72-30353

IR absorption coefficients of oxygen atom and molecule fields due to free-free electron transfers at specific elastic scattering cross sections

15 p2274 A72-31409

Molecular oxygen concentrations from solar Lyman alpha radiation absorption profile in mesosphere, using rocket-borne nitric oxide filled ion chamber

15 p2230 A72-32264

Molecular adsorption on semiconducting surfaces, discussing conditions for formation of local surface levels in forbidden gap

15 p2296 A72-32760

Molecular absorption of microwaves by atmospheric impurity gases ozone, carbon monoxide and nitrous oxide up to 20 km

16 p2364 A72-33483

Atmospheric transmissivity in the 49- to 72-GHz band - Analysis and laboratory measurements.

21 p3021 A72-40906

Calculation of the radiation of two plane isothermal layers of carbon dioxide and/or water vapor

22 p3242 A72-41884

Nonlinear molecular absorption cell for frequency stabilization of carbon dioxide laser radiation, discussing stability limit dependence on amplification, absorptivity and Q value

22 p3184 A72-42102

Total absorption cross sections of several gases of aeronomic interest at 584 Å.

22 p3152 A72-42419

Slab band absorptance for molecular gas radiation.

23 p3316 A72-44327

MOLECULAR BEAMS

Oscillation transient in molecular Q switched ammonia beam maser following Stark voltage pulse in resonant cavity

01 p0081 A72-11186

Ammonia beam maser with electret focuser providing semipermanent molecular separation under high vacuum for use in relaxation studies

01 p0081 A72-11187

Supersonic oxygen molecules nozzle beam reactive scattering on barium atoms, detailing exothermic reaction energy in barium oxide formation

02 p0170 A72-11912

Quantum mechanical analysis of detuning in cascaded cavity molecular beam masers

03 p0368 A72-13747

Molecular beams - Conference, Cannes, June-July 1971

03 p0392 A72-14051

Skimmer design optimization for maximum nozzle beam intensity yields in hypersonic flow

03 p0362 A72-14052

Nonsteady molecular beam approximation for strong shock structure problem, considering Boltzmann equation

03 p0399 A72-14053

Apparatus for emission spectroscopic studies on high density molecular jets excited by slow electron bombardment

03 p0392 A72-14054

Spatial distribution of gaseous nitrogen molecules scattered from metal surface, estimating beam capture coefficient

03 p0392 A72-14056

Digital computer simulation of rarefied gas molecular beam-rough metal surface interaction

03 p0392 A72-14057

Impulsive spatial interaction model between monoenergetic molecular beam and rough isotropic rigid metal surface in free molecule flow

03 p0392 A72-14058

Effective cross sections of ion collisions with gaseous target and argon atoms collision with argon target by molecular beam intensity attenuation method

03 p0392 A72-14060

Random method solution of Boltzmann equation for pseudoshock/relaxation mixing/, applying to random collisions of molecular beams

04 p0551 A72-14519

Millimeter and submillimeter wave molecular beam masers amplification principles and Doppler and collisional broadening elimination capability

04 p0532 A72-15597

Neutral unexcited gas atoms or molecules scattering at solid surfaces, interpreting molecular beam experimental results in terms of classical dynamics

07 p0969 A72-20065

Gas-surface interactions study by molecular beam technique, discussing measurement and target surface conditions control methods

07 p0969 A72-20069

Molecular beam continuum model for calculation of hypersonic flow past flat plate at zero incidence angle [AD-746387]

08 p1254 A72-21609

Molecular beam velocity distribution measurement from integral quantity, obtaining precise results in noisy environment and probability density function by numerical deconvolution

09 p1356 A72-22793

Adiabatic transition experimental implementation by molecular beam irradiating field frequency variation

10 p1491 A72-24210

Low energy elastic scattering cross section measurements for helium-nitrogen system, using two collimated aerodynamically intensified crossed molecular beams

10 p1515 A72-24338

Radiative displacement of molecular beam sidebands by spatiotemporal modulation of irradiating RF field

10 p1492 A72-24858

Elastic, inelastic and reactive scattering experiments with low, high and intermediate energy molecular beams

11 p1691 A72-25675

Molecular beams - Conference, Cannes, France, June-July 1971

16 p2429 A72-33051

Atomic and molecular beams fluid dynamic applications in rarefied gas flows exemplified by satellite drag coefficient measurement

16 p2429 A72-33052

Supersonic molecular jet improvement via expansion chamber residual gas pressure reduction and nozzle stagnation pressure increase

16 p2429 A72-33053

Gas mixtures separation in Kantrowitz-Grey underexpanded molecular jet background as function of rarefaction degree, using electron beam fluorescence technique for concentration measurements

16 p2429 A72-33054

Thermal molecular jets mixing produced by Knudsen effusion from porous wall, obtaining Boltzmann

equation approximate solution by moment method via assumed distribution function

16 p2429 A72-33055

Velocity distributions of molecular beams evaporating into vacuum from polycrystalline hexachlorobenzene and sulfur surfaces

16 p2429 A72-33058

High resolution spectroscopic studies of high density molecular beam production and emission spectrum excitation, using Ebert-Fastie vacuum spectrometer

16 p2430 A72-33059

High and medium energy molecular beam detection for large dispersion angle collision cross sections determination, using photographic plates

16 p2389 A72-33060

Time-of-flight measurements of molecular and atomic beams produced by cooled microwave discharge source, using hydrogen, helium, argon and nitrogen

16 p2430 A72-33061

Perturbations effects on plane symmetry supersonic molecular beam intensity as function of nozzle-skimmer geometry and nozzle pressures

16 p2430 A72-33062

Spatial distribution of nitrogen molecular beam scattering from solid nitrogen surface as function of beam energy and incidence angle

16 p2430 A72-33063

Aluminum oxide reproducible layers plastic deformability or microhardness from molecular beam scattering distribution

16 p2430 A72-33064

Face centered solid crystal cell spatial distribution effect on body surface-reflected molecular beam intensity distribution

16 p2430 A72-33066

Secondary electron emission and molecule passage during in-depth interaction of high energy molecular beam with thin gold foil

16 p2430 A72-33067

Oxygen chemisorption effect on rare gas beams reflection from refractory metals polycrystalline surfaces, interpreting experimental results by simple correlation model

16 p2431 A72-33068

Aerodynamic coefficients determination from momentum and energy exchange between low velocity molecular jet and solid surfaces, describing time of flight measurement technique

16 p2390 A72-33069

Differential collision cross sections for argon pairs with neon, methane and ethane at angular region of two crossed nozzle molecular beams

16 p2431 A72-33070

Nitrogen molecular beam rotational excitation by collision with argon beam, describing electron beam spectrographic experimental method and numerical simulation technique

16 p2431 A72-33071

Fcc in thin films and bcc in thick vacuum condensates deposited from Nb molecular beams obtained by evaporation and condensation in mass spectrometer

16 p2407 A72-33528

Velocity distribution and Mach number in a supersonic molecular beam of plane symmetry

17 p2486 A72-35423

Hydrogen and nitrogen desorption phenomena associated with a stainless steel 304 low energy electron diffraction /LEED/ and molecular beam assembly.

19 p2762 A72-38023

Properties of the electrostatic field of a system of annular electrets and possibilities of its application for focusing in molecular generators

19 p2804 A72-38538

Nozzle beam-mass spectrometer system for studying one-atmosphere flames.

20 p2921 A72-38975

[WSCI PAPER 72-9]

Molecular-beam-stabilized argon laser.

23 p3296 A72-43817

Electron impact ionization of ions trapped in a hollow electron beam.

23 p3316 A72-44343

MOLECULAR BIOLOGY

Cytochrome c X ray structure and molecular evolution rates, using amino acid sequence comparative data

02 p0158 A72-11763

Chemical evolution and life origin - Conference, Pont-a-Mousson, France, April 1970, Volume 1, Molecular evolution

04 p0467 A72-14751

Molecular paleontology of fossil organic remnants in Molluscan shell proteins

04 p0467 A72-14753

Molecular evolution of biological membrane from lipid film to lipoprotein particle assembly, using bacterial biochemistry

04 p0469 A72-14786

Genetic code numerical structure association with logarithmic optimization rule for hierarchy of structures from molecular biology experiments

04 p0470 A72-14794

Volumetric analysis of blood oxygen and CO, showing combination with hemoglobin without significant molecular volume increase

05 p0619 A72-16786

Psycho-physical theory of human mind, discussing molecular biological processes of neuron recording in terms of quantum mechanics

06 p0769 A72-18191

Conformal electron interactions in biopolymer and hypermolecular biological systems, discussing calcium ions effects, enzyme activity, muscle contractions and information theory

07 p0915 A72-18803

Molecular aspects of structural and functional circadian rhythms in chloroplasts of unicellular alga Acetabularia, emphasizing protein synthesis role

07 p0919 A72-19540

Statistical, physical and biotic theories on molecular chirality origin, considering catalytic processes and asymmetric processes with circularly polarized light

08 p1129 A72-22007

Cellular evolution investigation using molecular biology, microbial physiology and ecology

08 p1119 A72-22011

Review of biology and biochemistry of memory, suggesting molecular level mechanism of cerebral information processing

10 p1424 A72-23925

Evolutionary significance of primary amino acid or nucleotide base sequences of DNAs within various phylogenetic groups

12 p1759 A72-27160

Liver and muscle type isozymes of DPN-linked glycerol-3-P dehydrogenase in chickens in terms of tissue distribution, ontogeny and avian evolution

12 p1759 A72-27161

Ionic and hydrophobic interactions effects on Micrococcus lysodeikticus membrane stabilization process

14 p2075 A72-30595

Low molecular active hormones isolation from cat blood, obtaining eluates with phosphate buffer by chromatography

14 p2077 A72-30971

Molecular complexes of methoxyindoles with 1,3,5-trinitrobenzene and tetracyanoethylene /Spectroscopy/association constants/NMR/.

17 p2512 A72-35649

The resonance mechanism of the biological action of vibration

20 p2897 A72-39409

Biology and molecular biophysics progress review, discussing synthetic semibiological systems, molecular pathology, free radicals and longevity

22 p3142 A72-42474

Empirical support for a stochastic model of evolution.

23 p3254 A72-43565

Recently published protein sequences. I.

23 p3254 A72-43570

The state of water in muscle tissue as determined by proton nuclear magnetic resonance.

24 p3371 A72-44774

Review and forecast of electron microscope studies of membrane systems in terms of fundamental problems of biomedical research and molecular biology

24 p3371 A72-44869

Nucleic acid hybridization with RNA immobilized on filter paper.

24 p3379 A72-45773

MOLECULAR BONDS

U CHEMICAL BONDS

MOLECULAR CHAINS

Nonmetallic material properties effects on structural design for reliability, considering molecular chain folding, polymer crystallization, entropic molecular segregation, adhesion and intermolecular forces

01 p0092 A72-10986

Linear polyethylene irradiation, investigating chain scission processes importance, critical conditions for gelation and sol/gel partitioning

04 p0484 A72-15258

Ionizing radiation as effective energy in primordial organic synthesis, discussing small molecule formation and subsequent condensation into polypeptides and polynucleotides

05 p0617 A72-16127

Solid thermal motion influence on atom colliding with solid surface linear semifinite atomic chain, presenting accommodation coefficient calculation method

06 p0853 A72-18140

Free and stressed polymer molecules nonlinear vibrations, estimating three- and four-phonon processes contribution to linear chain vibration bands half width by numerical methods

08 p1195 A72-21851

Cooperative direction changing isomer movement on polymer chain lattice describing equations derivation procedure

14 p2125 A72-30962

Monte Carlo studies of the relaxation of vector end-to-end length in random-coil polymer chains.

20 p2898 A72-39599

Statistical mechanics of polymerized materials.

22 p3197 A72-42796

Polypophosphate and trimetaphosphate formation under potentially prebiotic conditions.

23 p3261 A72-43566

Recently published protein sequences. I.

23 p3254 A72-43570

MOLECULAR COLLISIONS

Fluid immersed body velocity fluctuations due to irregular molecular impacts

01 p0001 A72-10234

Molecular collision model, comparing generalized phase shift approximation method with classical trajectory calculations for rotational inelasticity

03 p0391 A72-13857

Upper atmosphere He, Ne, Na and K atoms collisions with molecular oxygen, determining ejected electron energy during fast Na, K, Rb and Cs ionization for meteor phenomena modeling

03 p0438 A72-13980

Spatial distribution of gaseous nitrogen molecules scattered from metal surface, estimating beam capture coefficient

03 p0392 A72-14056

Effective cross sections for charged and excited particles formation from He, Ne and Ar ion collisions with CO molecules, using mass spectrometry

03 p0393 A72-14065

Random method solution of Boltzmann equation for pseudoshock /relaxation mixing/, applying to random collisions of molecular beams

04 p0551 A72-14519

Scattering function of ellipsoidal gas molecules with translational and rotational degrees of freedom

04 p0552 A72-14629

Collision induced vibration-rotation transition probabilities for molecular motions, using state averaged potentials

06 p0851 A72-17299

Lyman alpha radiation emission cross sections due to H/2p and H/2s/ formation in protons and hydrogen atoms collisions with hydrogen molecules

07 p1038 A72-20678

Temperature dependence of scattering cross sections for cold and hot neutrons colliding with oxygen and deuterium molecules

08 p1211 A72-21872

Ion quadrupole effects in ion-molecule collisions, calculating capture cross sections and ion trajectories

09 p1354 A72-22658

Polyatomic ions interaction with neutral molecules in gases, calculating ion mobility as function of temperature from core model representation

09 p1355 A72-22788

Spectroscopic moments of molecular collision induced far IR and Raman spectra, stressing gas dimers contribution

09 p1276 A72-22859

Foreign gas collisional broadening of nitrous oxide absorption lines, obtaining optical collision cross sections

09 p1276 A72-23332

Collision operator behavior in linear Boltzmann equation model of molecular gas in Hilbert space

10 p1510 A72-24102

Binary collision loaded-sphere molecular model for diatomic gases computer simulation, obtaining normal shock waves velocity, density and temperature profiles

10 p1466 A72-24297

Attractive well potential effects on vibrational transition probability during atom-diatom molecule collinear collision

10 p1514 A72-24335

Reduced mass and asymmetry differences effects on elastic collision integrals and thermal diffusion factors for isotopic hydrogen molecules

10 p1515 A72-24340

Intermolecular collisions distribution on centerline of freely expanding axisymmetrical jet, using ellipsoidal statistical model and simplified transport equations

11 p1615 A72-25557

Population inversion in exothermal decomposition reactions of multiatomic molecules for chemical and collision laser systems

13 p1912 A72-28778

Internal rarefied gas flow, taking into account molecular backscattering due to wall surface roughness

13 p1942 A72-29117

IR radiation amplification due to high pressure colliding reacting molecular gas phototransitions

13 p1971 A72-29917

Na atoms D line radiation excited in collisions with molecular gases, noting transfer cross section dependence on kinetic energy for given quantum number change

13 p2009 A72-30063

Ion-molecule collision frequencies in gases by phase coherent pulsed ion cyclotron resonance spectrometry [ONERA, TP NO. 1071]

14 p2133 A72-30524

Simultaneous vibration-translation and vibration-vibration exchanges between colliding carbon dioxide and nitrous oxide excited molecules

15 p2280 A72-31686

- Generalized phase shift effect on classical limit of rotational excitation collision cross sections related to transport properties of diatomic gas molecules
16 p2428 A72-32925
- Mathematical models for depolarized light scattering by particle pair in gas, noting molecular collisions effect
16 p2423 A72-32952
- Nitrogen molecular beam rotational excitation by collision with argon beam, describing electron beam spectrographic experimental method and numerical simulation technique
16 p2431 A72-33071
- Molecular and atomic mechanisms for hydrogen-iodine exchange reaction dynamics, using classical trajectory analysis
16 p2360 A72-33581
- Vibrational energy transfer probabilities for inelastic collisions between diatomic molecules, considering system represented by harmonic oscillators coupled by time dependent interaction potential
16 p2431 A72-33582
- Entropy and chemical change. I - Characterization of product/and reactant/ energy distributions in reactive molecular collisions: Information and entropy deficiency.
17 p2511 A72-34738
- Triple collision effects in the transport properties for a gas of hard spheres.
17 p2585 A72-35157
- Excitation of molecular vibration on collision - Simultaneous vibrational and rotational transitions in hydrogen + argon at high collision velocities.
17 p2585 A72-35467
- Electron loss in atom-molecule collisions.
21 p3087 A72-40473
- Computer-graphics studies of dipole-dipole collisions - Evidence for neutral collisional complexes.
21 p3087 A72-40559
- Shapes and widths of ammonia lines collision-broadened by hydrogen.
21 p3013 A72-40817
- Collisional excitation of carbon monoxide in interstellar clouds.
22 p3227 A72-42553
- Molecular gas presence effect on electron energy balance in atomic gases, noting inelastic collisions loss factor in heated Ar plasma containing nitrogen molecules
22 p3213 A72-43110
- Charge state variation processes in hydrogen atom collisions with H₂ molecules
23 p3315 A72-43304
- A kinetic-theory description of a chemically reacting gas.
23 p3357 A72-44272
- Variation in the hyperfine state of a hydrogen atom during its collision with unsaturated hydrocarbons in the gaseous phase
23 p3317 A72-44477
- Classical calculations of H₂O rotational excitation in energetic atom-molecule collisions.
24 p3427 A72-45309
- MOLECULAR DIFFUSION**
- Mesosphere and lower thermosphere photochemical composition, allowing for molecular and eddy diffusion
03 p0345 A72-12980
- Molecular diffusion laser gain determination from interaction kinetics between diatomic and cold working gases, examining annihilation processes
10 p1491 A72-24360
- Molecular and eddy diffusion transport velocities for helium and hydrogen distributions in upper atmosphere
11 p1622 A72-25845
- Random walk atomic migration model for radon diffusion through lunar regolith into atmosphere
13 p2038 A72-28995
- Adiabatic effect of slow rotational molecular diffusion on perturbed angular correlations of gamma radiation for radioactive studies in viscous media
13 p2008 A72-29863
- Concentration profile derivation for fluid flow near rotating disk with chemical reactions, considering concentration gradient and barodiffusion effects
13 p1944 A72-30049
- Molecular diffusion laser gain determination from interaction kinetics between diatomic and cold working gases, examining annihilation processes
17 p2563 A72-34959
- Hemoglobin-facilitated diffusion of oxygen - Interfacial and thickness effects.
18 p2650 A72-36569
- On the role of density gradients in the continuum theory of mixtures.
18 p2712 A72-37076
- Analytical and low-speed experimental diffusion-thermo effects in turbulent binary boundary layers. [ASME PAPER 72-HT-56]
20 p2985 A72-39660
- Variance reduction in Monte Carlo analysis of rarefied gas diffusion.
21 p3046 A72-41183
- Effect of a flow with a stagnation point on the rate of variation of the total entropy of a fluid mixture
24 p3465 A72-45074

- MOLECULAR DISSOCIATION**
- U DISSOCIATION**
- MOLECULAR ELECTRONICS**
- NT LARGE SCALE INTEGRATION
- NT MEDIUM SCALE INTEGRATION
- Cyanide and carbon molecules and isotopes electronic systems opacity probability distribution functions for stellar equilibrium model atmospheres calculations
03 p0416 A72-13012
- Book on electronic processes in noncrystalline materials covering liquid metals, semimetals and semiconductors, Hall effect, phonons and polarons, thermoelectricity, photoconductivity, etc
06 p0866 A72-18516
- MOLECULAR ENERGY LEVELS**
- NT INTERMOLECULAR FORCES
- Interstellar OH formation through inverse predissociation from continuum to vibrational level of repulsive molecular state originating from asymptotic atomic ground state
01 p0133 A72-11141
- Pulsed nitrous oxide molecular laser upper energy level relaxation time measurement by afterglow pulse-gain technique
04 p0529 A72-14601
- Carbon dioxide-nitrogen-water or He mixtures expansion through supersonic nozzles, showing population inversion of vibrational energy levels
04 p0513 A72-15337
- Deactivation of A-state nitrogen molecules in auroras, reinterpreting rocket observations of nitrogen Vegard-Kaplan system in terms of atmospheric model based on mass spectrometer measurements
05 p0655 A72-16072
- Neutral monatomic rarefied gas-surface interaction at energy levels 0.1-10 eV, using Boltzmann equation
07 p0969 A72-20061
- Number of molecular hydrogen ion vibrational levels, using phase function method for scattering length and potential energy
08 p1211 A72-21293
- Binary system molar energy diagram plotting, covering superheated, saturation and liquid phase regions
08 p1255 A72-22170
- Molecular energy levels population inversions calculated from vibrational temperatures in carbon dioxide laser discharge plasma
11 p1649 A72-26339
- Boltzmann distribution of nitrogen ions according to rotational energy levels in nitrogen ionization by slow electrons impact
12 p1847 A72-27050
- Stellar OH radical emission amplification by maser effect raising low energy molecules to high energy by pumping
14 p2110 A72-30578
- Energy curves of negative carbon dioxide ion as function of bending angle
14 p2134 A72-30749
- Rutile titanium dioxide molecular orbital energy level diagram deduction from X ray emission and absorption band spectra, noting Ti and O states roles
15 p2295 A72-32539
- Molecular adsorption on semiconducting surfaces, discussing conditions for formation of local surface levels in forbidden gap
15 p2296 A72-32760
- Isotopic effect in photodissociation processes of triplet excited molecules
19 p2838 A72-38779
- Organic dye laser molecular sublevel relaxation effects on steady state pi pulse behavior and spectral hole burning from resonance radiation propagation analysis
20 p2932 A72-39503
- Energy exchange processes in a low temperature N₂-CO transfer laser.
22 p3184 A72-41993
- Photochemistry of the airglow continuum.
22 p3153 A72-42889
- Boltzmann distribution of nitrogen ions according to rotational energy levels in nitrogen ionization by slow electrons impact
24 p3427 A72-45703
- MOLECULAR EXCITATION**
- Collision excited carbon dioxide molecule vibrational relaxation rate constant based on statistical model
01 p0104 A72-10493
- Pulsed laser emission in carbon monoxide, calculating molecular excited state populations
02 p0237 A72-11471
- Resonance electron spectrometry experiments on electron collisions involving vibrational excitation, deactivation and attachment in molecular oxygen
03 p0347 A72-13391
- Rotational excitation of polyatomic molecule by electron collision attributed to polarization and electrostatic forces
04 p0552 A72-14852
- Vibrationally excited oxygen molecules formation and decomposition in upper atmosphere, calculating day and night equilibrium concentrations
05 p0657 A72-16252

- Dissociative excitation of CO and metastable fragments by electron impact on carbon dioxide, investigating cross sections
06 p0803 A72-17447
- Molecular nitrogen photoelectron impact excitation of Herman-Kaplan upper electronic state, considering cascade contribution to low lying states in electron auroras and dayglow
06 p0806 A72-17647
- Adiabatic-nuclei theory application to diatomic molecules excitation by electron impact, approximating fixed nuclei phase shifts dependence on internuclear separation
06 p0852 A72-17826
- Electron energy distribution in carbon monoxide lasers, considering excitation effects on exchange processes, power transfer to vibration levels and vibrationally excited molecules influence
07 p0999 A72-18883
- Atomic selective two step photoionization and molecular photodissociation by tunable laser radiation, experimenting on Rb vapor and HCl respectively [CLEA PAPER 12.4]
07 p1005 A72-19395
- Optically pumped gas lasers with electron transitions to molecular excited state and resonant absorption lines
07 p1006 A72-19634
- Carbon dioxide-air-helium molecular systems population excitation rates with current, gas composition and partial pressures dependence
08 p1183 A72-22028
- Excitation accompanying photoionization in atoms and molecules and relationship to electron correlation observed from rare gases inner and valence shell satellite lines measurements
09 p1356 A72-22835
- Post-threshold translational energy dependence of endoergic cross sections for vibrational excitation and reactive scattering of diatomic molecules by atomic or molecular impact
09 p1357 A72-22858
- Excitation and relaxation of upper laser state in carbon dioxide discharge from Q spoiled pulse-produced fluorescence measurements
09 p1326 A72-23577
- Electron impact excitation of nitric oxide in vacuum UV, measuring absolute cross sections for emission features [AD-742536]
10 p1515 A72-24341
- Chemical laser with deuterium and nitrogen fluorides mixture, examining excited molecules emission spectra
11 p1649 A72-26351
- Evanescent photons absorption and emission in light excited molecules fluorescence
11 p1691 A72-26745
- Light absorption by molecular crystals with dual zone of exciton states
12 p1847 A72-27226
- Electron impact excitation spectrum of molecular oxygen, investigating angular behavior of differential scattering cross sections and energy dissipation
12 p1848 A72-27851
- Effect of pumping radiation absorption by electron-excited molecules on organic compounds lasing efficiency
12 p1825 A72-27885
- Nonlinear light amplification in molecular nitrogen amplifier as function of input pulse delay relative to excitation start
13 p1969 A72-29522
- Hydroxyl vibration levels excitation rates calculation from transition probabilities and band sequence nightglow intensity measurements
13 p1954 A72-29816
- Absolute cross sections for Werner band system excitation of molecular hydrogen by electron impact, discussing relative spectral response calibration
13 p2009 A72-30065
- Quantum mechanical calculation of interaction potential energy surface role in vibrational excitation of diatomic molecules
14 p2134 A72-30750
- Hydrogen molecule highly excited electronic levels, developing transition probabilities estimation method
14 p2135 A72-30888
- Simultaneous vibration-translation and vibration-vibration exchanges between colliding carbon dioxide and nitrous oxide excited molecules
15 p2280 A72-31686
- Diatomic molecular vibrational excitation and dissociation effects on imploding shock waves, comparing shock tube data to prediction
15 p2192 A72-32148
- Transversely excited pulsed carbon dioxide laser with and without hydrogen addition, observing gain spatial and temporal dependence
15 p2251 A72-32529
- Metastable ²S/ atoms production by electron impact induced dissociative excitation of molecular deuterium, measuring total cross section via Lyman alpha flux
15 p2282 A72-32645

- High power carbon dioxide lasers review covering CW, Q switched and pulsed atmospheric pressure lasers and various excitation techniques
16 p2399 A72-32848
 - High energy resolution spectrometric measurement of relative emission cross section for electron impact excited molecular nitrogen second positive system bands
16 p2428 A72-32922
 - Generalized phase shift effect on classical limit of rotational excitation collision cross sections related to transport properties of diatomic gas molecules
16 p2428 A72-32925
 - Nitrogen molecular beam rotational excitation by collision with argon beam, describing electron beam spectrographic experimental method and numerical simulation technique
16 p2431 A72-33071
 - Hydrogen direct photoionization and photoexcited autoionization cross sections calculation for radiation in 600-800 Å region
16 p2431 A72-33579
 - Chemical laser with deuterium and nitrogen fluorides mixture, examining excited molecules emission spectra
16 p2402 A72-33704
 - Effect of pumping radiation absorption by electron-excited molecules on organic compounds lasing efficiency
16 p2404 A72-33992
 - Dissociative excitation of vacuum ultraviolet emission features by electron impact on molecular gases, III - CO₂
17 p2585 A72-34734
 - Rotational excitation of rigid rotor in argon-nitrogen system, measuring energy transfer moments by particle-body and perturbation technique
17 p2585 A72-34740
 - Rates of interaction of vibrationally excited hydroxyl ($v = 9$) with diatomic and small polyatomic molecules.
17 p2511 A72-35648
 - Tunable Raman excitation and vibrational relaxation in diatomic molecules.
17 p2586 A72-35802
 - Excitation of a long-pulse CO₂ laser with a short-pulse longitudinal electron beam.
17 p2565 A72-35815
 - Spectroscopic determination of the rotational temperature in a rarefied supersonic flow in glowing-discharge excited nitrogen.
17 p2544 A72-35928
 - Excitation modes and operating characteristics of electric discharge convection lasers
[AIAA PAPER 72-722] 17 p2565 A72-35962
 - Vibrationally excited nitrogen in upper atmosphere
18 p2688 A72-36865
 - Vibrational excitation in N₂ by electron impact in the 15-35-eV region.
19 p2837 A72-37546
 - Evaluation of rotational temperature at high vibrational temperature in electron beam fluorescence technique.
19 p2803 A72-38434
 - Isotopic effect in photodissociation processes of triplet excited molecules
19 p2838 A72-38779
 - Two-step photodissociation of ammonia molecules excited by laser radiation.
21 p3013 A72-40724
 - Analytic expressions for electron energy transfer rates for nitrogen and oxygen vibrational excitation in ionosphere, applying to atmospheric and ionospheric computer modeling
22 p3168 A72-42001
 - Collisional excitation of carbon monoxide in interstellar clouds.
22 p3227 A72-42553
 - Pulse energy and temporal/spatial distribution of carbon dioxide laser pumped by energy transfer from vibrationally excited DF produced by deuterium-fluorine chain reaction
22 p3185 A72-42617
 - Superradiant laser excitation at 3371 Å in molecular nitrogen second positive band system by high energy electron beam, noting 6 nsec pulse outputs to 24 MW
22 p3186 A72-42623
 - Coulomb approximation method for photoionization cross sections of hydrogen molecule singly excited states
22 p3208 A72-42718
 - Application of gasdynamic flows in laser technology
22 p3187 A72-43176
 - Effect of fluorescence observation geometry on lifetime measurement, including the development of an approximation to the detector collection efficiency integral.
23 p3288 A72-43884
 - Electronic excitation of N₂ and dissociative excitation of O₂ by proton impact.
23 p3317 A72-44250
 - Optically pumped gas lasers with electron transitions to molecular excited state and resonant absorption lines
24 p3408 A72-44566
 - Molecular crystals stationary Raman oscillators quantum model, deriving coupled nonlinear equations for excited modes polariton operators
24 p3409 A72-44912
- MOLECULAR FLOW**
- NT SLIP FLOW
- NT TRANSITION FLOW
- German monograph on gas type and nozzle flow conditions effect on condensed molecular jets properties
03 p0391 A72-13275
- Reference transfer method for in situ calibration of ionization gases, determining pressure ratio of molecular gas flow through fixed orifices
10 p1480 A72-24147
- Rarefied gas flows effect on metals creep properties, examining molecular flow density distribution as function of specimen surface distance from nozzle
13 p1979 A72-29483
- Hydrodynamic and molecular velocity characteristics of rarefied gas motion between infinite plane parallel emitting and absorbing surfaces, using Boltzmann equation
14 p2096 A72-31025
- Molecular flux distribution in cylindrical vacuum chambers with various inlet and pumping configurations under assumption of Knudsen law validity, describing computer program
15 p2183 A72-32382
- Study by phase detection of the velocity of a molecular jet
18 p2714 A72-37200
- Determination of the probability for passage of molecules through the working rotor of a turbomolecular vacuum pump with nonparallel walls of the channel between vanes
22 p3139 A72-41862
- MOLECULAR GASES**
- NT DIATOMIC GASES
- NT POLYATOMIC GASES
- Absorption cell heterodyne method for nondispersive IR detection of trace gases with molecular vibrational-rotational spectrum
01 p0023 A72-10532
- Triatomic hydrogen positive ions dissociation at 410, 510 and 550 keV in molecular hydrogen gas, measuring atoms yield as function of target thickness
01 p0104 A72-11148
- Electrically excited tunable IR molecular gas lasers with rotational lines overlapping due to high pressure broadening
03 p0366 A72-12965
- Scattering function of ellipsoidal gas molecules with translational and rotational degrees of freedom
04 p0552 A72-14629
- Molecular nitrogen dayglow emission in F region, noting volume emission rates, integrated overhead intensities and solar activity effects
04 p0518 A72-14959
- Atomic and molecular hydrogen mixture viscosity measurement, considering mutual diffusion coefficient, collision cross sections and interaction potentials
04 p0553 A72-15637
- Carbon dioxide laser Q switching by molecular gases intracavity Stark modulation with sine or square wave electric field, using methyl chloride and difluoroethane
05 p0669 A72-16609
- Intermolecular interaction potential parameters determination from gas compressibility data based on equation of state in kinetic theory
05 p0692 A72-17068
- Stable molecules spatial concentration profiles in high intensity combustion chamber, using quartz sampling probe and gas chromatograph
05 p0751 A72-17088
- Thermal conductivity of argon, helium, hydrogen, nitrogen, carbon dioxide, methane and ethane gases at high temperature and pressure
07 p1099 A72-19620
- Thermomolecular pressure gradients and temperatures in flow between parallel plates for statistical gas models at arbitrary Knudsen numbers
07 p1101 A72-20513
- Noble and molecular gases addition in reactions induced in ethylene by carbon dioxide-nitrogen-helium laser
07 p1009 A72-20693
- Molecular gases absorption coefficients measurement in extreme UV, analyzing photoionization curves in energy range far beyond threshold
09 p1356 A72-22829
- Kinetic equations derivation for rarefied chemically reacting monatomic or stable molecular gases
10 p1514 A72-23845
- Collision operator behavior in linear Boltzmann equation model of molecular gas in Hilbert space
10 p1510 A72-24102
- 50 MW laser amplifier at 3371 Å in molecular nitrogen via transverse electron pumping
10 p1491 A72-24225
- Binary collision loaded-sphere molecular model for diatomic gases computer simulation, obtaining normal shock waves velocity, density and temperature profiles
10 p1466 A72-24297
- Stellar absorption spectral line fineness indication for cold interstellar molecular clouds between observer and star
10 p1546 A72-24848
- IR radiation amplification due to high pressure colliding reacting molecular gas phototransitions
13 p1971 A72-29917
- Na atoms D line radiation excited in collisions with molecular gases, noting transfer cross section dependence on kinetic energy for given quantum number change
13 p2009 A72-30063
- Diatomic-monomeric molecular gas mixtures oscillation and rotation energies relaxation equations, taking into account transport and chemical reaction processes
14 p2083 A72-30327
- Quantum kinetic equation for monatomic and molecular gases optical characteristics calculation, considering spontaneous emission spectrum of atoms
14 p2110 A72-30358
- Hydrogen molecule highly excited electronic levels, developing transition probabilities estimation method
14 p2135 A72-30888
- Laser coupling through nonlinear gas filled absorber cell, discussing molecules mean free path
15 p2246 A72-31883
- Potential energy curves for exothermic reaction between oxygen cations and nitrogen molecules to form nitric oxide and atomic nitrogen
16 p2360 A72-32921
- Doubly ionized Mg, Ca and Ba atoms termolecular association rate constants with various molecular neutrals, comparing doubly charged with singly charged ions cluster reaction rates
16 p2360 A72-32924
- Numerically computed momentum and energy accommodation coefficients and angular distributions of gas molecules reflected from solid crystalline surfaces applied to satellite drag calculation
16 p2430 A72-33065
- Pulsed emission at pulse front in molecular hydrogen, deuterium and nitrogen at near IR electronic transitions, analyzing spectral, temporal and energy characteristics
16 p2401 A72-33298
- Interstellar molecular hydrogen formation on water, ice and solid CO, using laboratory adsorption energy measurements
16 p2461 A72-34160
- Mathematical model for nonequilibrium gas composed of hard spherical nonattracting molecules, deriving gas dynamics theory in terms of multiple integrals
17 p2538 A72-34424
- Time correlation functions for gases of linear molecules in a magnetic field.
17 p2589 A72-34894
- Molecular equilibrium abundances in interstellar H I gas clouds, noting formation dependence on gas density and degree of interstellar radiation extinction
19 p2854 A72-37230
- Detection of molecular oxygen in the Martian atmosphere.
21 p3103 A72-40451
- Molecular abundances and gas-to-electron pressure ratios as function of temperatures and pressures in solar composition gaseous mixture of late type stellar atmospheres
21 p3110 A72-41446
- Detection of molecular oxygen on Mars.
22 p3224 A72-42293
- Variation in the hyperfine state of a hydrogen atom during its collision with unsaturated hydrocarbons in the gaseous phase
23 p3317 A72-44477
- Transport properties of a gas of diatomic molecules. V - GPS calculation of the rotational relaxation time of the Ar-N₂ system.
24 p3427 A72-45307
- Multiphoton dissociation, predissociation, and autoionization of the hydrogen molecule.
24 p3427 A72-45476

MOLECULAR INTERACTIONS

NT MOLECULAR COLLISIONS

- Photochemical ion-molecule reactions in ionosphere by air exhaust device and RF mass spectrometer observation in geophysical rocket experiment
01 p0068 A72-10591
- Laboratory measurements of D region ion-molecule reactions using flowing afterglow system
03 p0347 A72-13388
- Model intermolecular interaction potentials constants determination for extrapolating thermodynamic properties of gases at high temperatures and pressures
05 p0692 A72-15842
- Reduced collision integrals for components of Venus and Mars type carbon dioxide atmospheres at 1000-11,000 K, using intermolecular interaction potentials
05 p0712 A72-15851

Free molecular flow heat transfer to rough surface, discussing surface/molecule interaction model for digital simulation

[ASME PAPER 71-WA/HT-8] 05 p0743 A72-15868
Intermolecular interaction potential parameters determination from gas compressibility data based on equation of state in kinetic theory

05 p0692 A72-17068
Small distance range anisotropic intermolecular interaction potentials for carbon dioxide and nitrogen oxide from beams elastic scattering data

06 p0852 A72-17983
Gas-surface interactions study by molecular beam technique, discussing measurement and target surface conditions control methods

07 p0969 A72-20069
Quantum mechanical transport equation for radiation interactions with molecules subject to perturber atom collisions, describing macroscopic density matrix evolution

[AD-739082] 07 p1039 A72-20683
Hydrogen protons and atoms interaction with hydrogen and nitrogen molecules, showing electron transfers agreement with Franck-Condon principle

08 p1210 A72-20835
Nonspherical and nonadditive interactions contribution to third virial coefficient of polyatomic gas, discussing anisotropy, shape factor, and intermolecular forces

08 p1211 A72-21292
Spectroscopic measurements of light emission from carbon dioxide positive ions and carbon monoxide in metastable He interaction with carbon dioxide

09 p1354 A72-22667
Molecular scattering in free jet expansion, using spherical source and two component background gas mathematical models

11 p1615 A72-25558
Molecular process and pressure effects on hydrogen formation in methyl acetylene photolysis at 1236 Å

11 p1590 A72-26011
Solar activity effects on biosphere processes, discussing radiation-induced molecular activation mechanisms in water and biological plasma calcium ion concentration changes

12 p1763 A72-28213
Inversion population distribution during nonexcited carbon dioxide and excited nitrogen molecules plane jets interaction in diffusion carbon dioxide laser

14 p2109 A72-30314
Hydrogen atom exchange in ion-molecule reactions of methane and ethylene determined from reaction products distribution, using ion cyclotron resonance techniques

14 p2084 A72-30522
Quasi-classical mechanical approximation in molecular scattering, using Monte Carlo methods for Jacobian determinant evaluation

14 p2134 A72-30836
Model intermolecular interaction potentials constants determination for extrapolating thermodynamic properties of gases at high temperatures and pressures

15 p2280 A72-31261
Reduced collision integrals for components of Venus and Mars type carbon dioxide atmospheres at 1000-11,000 K, using intermolecular interaction potentials

15 p2302 A72-31270
Secondary electron emission and molecule passage during in-depth interaction of high energy molecular beam with thin gold foil

16 p2430 A72-33067
Particle excitation processes in solar corona, ionosphere and astrophysics, discussing electron affinities, ion-molecule reactions, forbidden atomic transitions and Fe II problem

16 p2432 A72-34150
Molecular and atomic interaction forces as interfacial free energy sources, discussing molecular attachment kinetics and surface configuration models

18 p2718 A72-36393
Nonequilibrium transport equations for chemically reacting inhomogeneous gas mixtures, using Hermitian tensor polynomials of molecular velocities

18 p2713 A72-36895
Ion mobilities and ion-molecule reaction rates in oxygen.

19 p2836 A72-37457
Laboratory positive and negative ion composition measurements compared with D region ion-molecule reaction observations

20 p2917 A72-39527
Application of statistical methods to studies of the surface properties of polymers

21 p3072 A72-40080
Limiting properties of solutions of the Boltzmann equation.

21 p3086 A72-40264
Repulsive potential determination for alkali cations, halide anions and anisotropic molecules from scattering experiments and bond energy data

21 p3087 A72-40555
Scattering cross section glory undulations relationship to potential energy of interaction of two

molecules with minimum containing one or more bound states

21 p3087 A72-40561
Molecular orbital calculation of the isotropic hyperfine interactions in triatomic nitrogen radicals.

21 p3013 A72-40564
Predvoditelev critical revision of hydrodynamic and heat transfer theory based on Navier-Stokes and Boltzmann equations, developing statistical system of molecular interactions

22 p3165 A72-41951
Inversion population distribution during nonexcited carbon dioxide and excited nitrogen molecules plane jets interaction in diffusion carbon dioxide laser

23 p3294 A72-43217
Filler quantity and type effects on mechanical energy losses in polymers, discussing molecular interaction and chemical bond influences

23 p3306 A72-43731
Exact solution of the equations of molecular optics for refraction and reflection of an electromagnetic wave on a semi-infinite dielectric.

23 p3313 A72-43803
Laser-source spectroscopy. II - Experimental study of line broadening for the 00 1-10 0, 02 0/ transition of CO₂ disturbed by N₂: Application of the theory of Anderson, Tsao, and Cornette to the calculation of pure and N₂-disturbed CO₂ linewidths

23 p3298 A72-44535
Early stage condensation in planetary formation, discussing atomic and molecular reactions in interstellar space and earth outer atmosphere properties

24 p3444 A72-45452
Evidence for protonated cyclopropane intermediates in crossed-beam ion molecule reactions.

MOLECULAR IONS

Triatomic hydrogen positive ions dissociation at 410, 510 and 550 keV in molecular hydrogen gas, measuring atoms yield as function of target thickness

01 p0104 A72-11148
Hydrogen molecular ion g tensor calculation, determining approximate ground state wave functions

03 p0391 A72-13152
Elastic scattering without dissociation of nitrogen molecular ions by noble gas targets in 0.3-3 keV range, analyzing energy loss

03 p0393 A72-14357
Number of molecular hydrogen ion vibrational levels, using phase function method for scattering length and potential energy

08 p1211 A72-21293
Secondary molecular ion emission of Li as function of atoms number

11 p1701 A72-26506
Nitric oxide and oxygen molecular ion composition of lower ionosphere during solar eclipses from rocket measurements

[AD-744403] 12 p1801 A72-27150
Model potential method for calculating positively charged diatomic sodium molecular ions potential energy curves and resonance charge transfer cross sections

12 p1848 A72-28350
Diatomic carbon negative ion search in HD 201626 and solar spectra, noting rotational lines coincidence with absorption features

13 p2038 A72-29010
Electron impact induced aurene epoxides fragmentation, discussing ion formation, intermediates, thermal rearrangement and mass spectra

13 p1913 A72-29775
Relative cross sections for gas phase photodetachment of electrons from amide and arsenide ions using ion cyclotron resonance spectrometer

13 p1914 A72-30064
Atmospheric desorbed water molecules and ions number density vertical distribution in lower ionosphere and thermosphere

15 p2225 A72-31913
Lifetime and quenching of metastable CO produced by dissociative recombination of positive carbon dioxide ions in He afterglow

16 p2432 A72-33771
Emission spectra of comet tail carbon monoxide molecular ion indicating constant or slowly varying electron transition moment

17 p2618 A72-35826
Dissociation of molecular ions formed by charge exchange in an in-line tandem mass spectrometer.

19 p2763 A72-38801
Electronic and nuclear magnetic resonances of the oxygen and hydrogen labile negative molecular ions.

20 p2956 A72-39189
Oxygen ion anticorrelation to molecular ion concentrations from OGO 6 observations in F 2 region

22 p3169 A72-42016
Photoionization of N₂, O₂, NO, CO, and CO₂ by soft X rays.

24 p3426 A72-45302
MOLECULAR ORBITALS

Allowed states of electronic complexes and impurity molecules in crystals determination in molecular orbital scheme of molecular electronic calculations

03 p0392 A72-13864

Molecular orbital calculation of the isotropic hyperfine interactions in triatomic nitrogen radicals.

21 p3013 A72-40564

MOLECULAR OSCILLATIONS

Carbon dioxide and hydrogen mixtures in shock tube, noting rotational- and translational-vibrational energy transfer role from relaxation time measurement

02 p0203 A72-12028
Two dimensional molecular dynamics digital simulation of Ar liquid-vapor interface at triple point, yielding strongly oscillatory density profile

03 p0393 A72-14263
Nonisothermal gas layer IR radiation in multiatomic molecular vibrational-rotational band range, determining lowest level energy for wide line spectrum

04 p0547 A72-14651
High power tunable IR gas lasers based on anharmonic molecules vibrational-rotational transitions excitation at gas pressures of 10 atm

06 p0825 A72-17786
Free and stressed polymer molecules nonlinear vibrations, estimating three- and four-phonon processes contribution to linear chain vibration bands half width by numerical methods

08 p1195 A72-21851
IR emission of oxygen reaction with carbon oxysulfide, investigating molecular vibrational transitions

10 p1510 A72-24133
Spontaneous radiative dissociation in molecular hydrogen vibrational levels as function of emission wavelength, discussing fluorescent spectra, radiation lifetimes and centrifugal distortion

13 p2008 A72-30058
Diatomic-monatomic molecular gas mixtures oscillation and rotation energies relaxation equations, taking into account transport and chemical reaction processes

[DFVLR-SONDDR-198] 14 p2083 A72-30327
Intermolecular hydrogen bond study of hydroxyl group in caranol and caranol-o₂ compounds, listing IR absorption bands for valence oscillations

15 p2192 A72-32100
Vibrational excitation in N₂ by electron impact in the 15-35-eV region.

19 p2837 A72-37546
Questions in the theory of monomolecular decay of a one-component gas and the dissociation constant of CO₂ at high temperatures

21 p3088 A72-41657
Molecular vibration levels inversion ratios increase by vibrationally cold CO addition to CW CO chemical laser, observing R-branch emission lines

22 p3185 A72-42616
Measurement of thermal relaxation time of vibration of polyatomic molecules by the impact tube method

24 p3402 A72-45045
High speed mixing of nitrogen vibrationally excited with carbon dioxide

24 p3464 A72-45065

MOLECULAR OSCILLATORS

Molecular continuity relationship relating discrete absorption oscillator strengths to photodissociation cross sections

01 p0104 A72-11115
Precision timekeeping, discussing atomic standards and Cs and Rb controlled molecular oscillators stability, cost and size

04 p0521 A72-14835
Electron impact cross section and energy deposition in molecular hydrogen, using generalized oscillator strength in Born-Bethe approximation

07 p1038 A72-20566
Transient oscillator analysis of a high-pressure electrically excited CO laser.

22 p3184 A72-41970
Fluctuations in a quantum frequency standard

23 p3271 A72-43842
Laser frequency measurement by comparison with stable molecular oscillator Doppler shift produced by reflection of UHF modulated coherent optical signal

MOLECULAR PHYSICS

Dense cloud and protostar molecules from molecular line emission, considering mass effects in stellar evolution

03 p0419 A72-13120
Hydrodynamic asymptotic characteristics of autocorrelation function for molecule velocity in classical liquid, obtaining Lagrangian diffusion coefficient

05 p0692 A72-16684
Gases for carbon dioxide laser lines modulation by molecular Stark effect, presenting data for fluoroethane, monomethylamine, methyl mercaptan, vapors methanol and trichloroethylene

07 p1001 A72-19193
Relativistic Zeeman-Stark effect on molecular jet due to molecular translational motion in continuous magnetic field

10 p1514 A72-24135
Physical properties of atoms, molecules and solid material in ultrastrong magnetic field, using quantum drift approximation

12 p1847 A72-27055

Russian book - Macromolecules at the boundary between phases.

21 p3071 A72-40077

Dark dust nebulae and bright H II clouds, considering light molecules, stellar birth region, radio and IR astronomy

22 p3220 A72-41995

Quantum-chemical model of organic ring-shaped molecule with persistent magnetization at microscopic level

22 p3150 A72-42318

Molecular mechanical aspects of the isothermal rupture of elastomers.

23 p3305 A72-43507

Physical properties of atoms, molecules and solid material in ultrashort magnetic field, using quantum drift approximation

24 p3427 A72-45708

MOLECULAR PUMPS

Thermogravimetric design, using electromagnetic microbalances and turbomolecular pump for automatic sorption isotherm measurements in surface area and pore size analyses

11 p1636 A72-26788

Flow phenomena in turbomolecular pumps

18 p2696 A72-36837

Determination of the probability for passage of molecules through the working rotor of a turbomolecular vacuum pump with nonparallel walls of the channel between vanes

22 p3139 A72-41862

MOLECULAR RELAXATION

Collision excited carbon dioxide molecule vibrational relaxation rate constant based on statistical model

01 p0104 A72-10493

Carbon dioxide and hydrogen mixtures in shock tube, noting rotational- and translational-vibrational energy transfer role from relaxation time measurement

02 p0203 A72-12028

Hydrogen shock waves density profiles measurement, noting uncoupled translational and rotational relaxation processes

02 p0263 A72-12360

Relaxation and heating rate due to solar radiation absorption by 2.7 and 4.3 micron vibration-rotation bands of carbon dioxide

03 p0347 A72-13387

CW longitudinal flow carbon monoxide chemical laser system analysis, discussing vibrational levels, population densities, excitation and relaxation processes and dynamic model

03 p0368 A72-13858

Pulsed nitrous oxide molecular laser upper energy level relaxation time measurement by afterglow pulse-gain technique

04 p0529 A72-14601

Submillimeter wave sulfur dioxide molecular laser, investigating lasing lines, plasma decay and relaxation, line interactions and signal temporal behavior

04 p0532 A72-15595

Master equation for vibrational relaxation of diatomic dilute gases, discussing restrictions on experimental initial conditions and scattering cross sections

04 p0553 A72-15634

Dutch monograph on heat transfer of gas with vibrational relaxation at shock tube end wall covering mathematical model, induced velocity effect on pressure, etc

05 p0648 A72-16045

Plasma physics collective phenomena enhancing effect on relaxation processes, emphasizing relevance to stellar dynamics

[AD-739801]

05 p0714 A72-16059

Surface catalytic properties effect on multicomponent gas hypersonic boundary layer with simultaneous vibrational-dissociative relaxation, considering plate and blunt body laminar boundary layer

06 p0757 A72-18130

Nonequilibrium thermodynamics description of rarified gas relaxation phenomena for very fast flow processes with translational temperatures

06 p0902 A72-18137

Neutron irradiation effect on grain boundary relaxation in Al and Al-Li alloy by internal friction investigation

06 p0830 A72-18292

Hydrogen halide rotational relaxation to thermal distribution without intermediate quantum number peak, discussing IR chemiluminescence data correction method

07 p0936 A72-19673

Vibrational relaxation in nonequilibrium and expansion nozzle flows

08 p1148 A72-21015

Nonlinear vibrational relaxation equations for expanding carbon dioxide-helium-nitrogen laser gas mixture, obtaining mode temperatures and gain coefficients by Runge-Kutta technique

08 p1149 A72-21261

Excitation and relaxation of upper laser state in carbon dioxide discharge from Q spoiled pulse-produced fluorescence measurements

09 p1326 A72-23577

Kinetic equations solution for homogeneous multiatomic gas relaxation, proving solution existence and uniqueness

10 p1516 A72-24629

Combined translational and internal relaxation theory of sound propagation in polyatomic gases, using 17 moment approximation

11 p1687 A72-26054

Raman effect application to study of gas vibration relaxation downstream of shock wave

12 p1888 A72-27180

Chemical laser dynamics review, discussing population inversion, molecular vibrational relaxation and reactions initiation methods

12 p1822 A72-27605

CO-He laser vibrational population distribution and small signal gain measurements, comparing with prediction based on V-V anharmonic exchange relaxation

12 p1827 A72-28222

Collisional relaxation and rotational intensity distributions in aeronomic spectra, including radiative losses effects from weak interaction model

13 p2008 A72-30057

Diatomic-monatomic molecular gas mixtures oscillation and rotation energies relaxation equations, taking into account transport and chemical reaction processes

[DFVLR-SONDDR-198]

14 p2083 A72-30327

Relaxation methods of magnetic and acoustic spectroscopy for studies of gravitational and inertial dipoles and quadrupoles in molecules and nuclei of solid bodies

14 p2143 A72-30963

Interferometric investigation of impurities effects on electron density distribution in ionization-relaxation zone behind shock waves in monatomic gas

15 p2215 A72-31213

German monograph on wave expansion in gases with thermodynamic relaxation covering steady dispersed compression wave development in piston barrel for two component mixtures

[DFVLR-SONDDR-184]

15 p2218 A72-31768

Light scattering by monatomic and polyatomic gases, superimposing effects due to rotational and translational molecular relaxation

16 p2428 A72-32944

Room temperature vibrational relaxation measurements in gases subsequent to laser pumping by picosecond pulse generated transient stimulated Raman scattering

16 p2401 A72-33389

HF vibrational relaxation measurements using the combined shock tube-laser-induced fluorescence technique.

17 p2511 A72-34735

Measurement of the parameters and the structure of a wet vapor flow with interphase heat and mass transfer in the relaxation zone behind the front of a shock wave.

17 p2637 A72-35130

Tunable Raman excitation and vibrational relaxation in diatomic molecules.

17 p2586 A72-35802

Vibrational relaxation of the bending mode of shock-heated CO₂ by laser-absorption measurements.

18 p2697 A72-36562

Numerical and shock tube experiments for variation of bound electron temperature and nonequilibrium chemical and radiative relaxation behind normal shock waves in air, using atom-molecule collision model

18 p2681 A72-36564

Influence of pressure, mass flow rate, and nozzle angle on the chemical relaxation in nozzles

19 p2880 A72-37494

Intramolecular interactions and vibronic spectra of polyatomic molecules. IV - Electronic relaxations: Configurational and relaxational spectra - The four-level arrangement

19 p2838 A72-38778

IR chemiluminescence technique /method of arrested relaxation/ to measure spectral energy distribution among Cl and HI and DI reaction products

19 p2763 A72-38802

Energy distribution among reaction products. VI - F + H₂, D₂.

19 p2763 A72-38804

Organic dye laser molecular sublevel relaxation effects on steady state pi pulse behavior and spectral hole burning from resonance radiation propagation analysis

20 p2932 A72-39503

Monte Carlo studies of the relaxation of vector end-to-end length in random-coil polymer chains.

20 p2898 A72-39599

Critical mass flow and nonequilibrium nozzle flow of vibrationally relaxing, ideal dissociating diatomic and singly ionizing monatomic gases, using steepest descent method

21 p3046 A72-41249

Special features of photoresonance perturbation relaxation in a low-temperature discharge plasma

23 p3319 A72-43409

Measurement of thermal relaxation time of vibration of polyatomic molecules by the impact tube method

24 p3402 A72-45045

Catalytic efficiencies of H₂O, D₂O, NO, and HCl in the vibrational relaxation of HF and DF.

24 p3378 A72-45306

MOLECULAR ROTATION

Self broadened rotational half widths for Lorentzian line shape and slit function in CO fundamental, using line center transmission measurements

01 p0104 A72-10095

Kinetic equation for gases with rotational degrees of freedom under equality of probabilities of direct and inverse transitions and stereoisomerism of molecules

01 p0050 A72-10350

High precision rotational constants and transition frequencies in ground state interstellar molecule cyanoacetylene

01 p0023 A72-11147

Rotation and mass inclusion into study of energy barriers location effects on thermonuclear reaction dynamics

02 p0262 A72-11981

Nonisothermal gas layer IR radiation in multiatomic molecular vibrational-rotational band range, determining lowest level energy for wide line spectrum

04 p0547 A72-14657

Vibration-rotation double resonance transitions in symmetrical top molecules in millimeter range under chopped laser radiation

04 p0532 A72-15615

Artificial barium oxide clouds band spectrum analysis, calculating rotational and vibrational temperatures in total wavelength region

05 p0655 A72-16069

Collision induced vibration-rotation transition probabilities for molecular motions, using state averaged potentials

06 p0851 A72-17299

Hydrogen halide rotational relaxation to thermal distribution without intermediate quantum number peak, discussing IR chemiluminescence data correction method

07 p0936 A72-19673

Molecular rotation stimulation and deactivation of diatomic molecule addition to monatomic gas, discussing energy exchange in rarefied gas flow

08 p1211 A72-21656

Dynamic model of night time hydroxyl rotational temperature variations from airborne and ground measurements

09 p1298 A72-22587

Shock tube rotational relaxation time measurements in cryogenic hydrogen, using laser schlieren optical system

11 p1691 A72-26008

Ion dipole capture cross sections at low ion and rotational energies compared with reaction cross sections for ammonia and water parent-ion collisions

11 p1692 A72-26014

Carbon dioxide laser vibrational-rotational band small signal gain factor dependence on time elapsing after breakdown of equilibrium distribution

13 p2008 A72-29503

Adiabatic effect of slow rotational molecular diffusion on perturbed angular correlations of gamma radiation for radioactive studies in viscous media

13 p2008 A72-29863

Diatomic-monatomic molecular gas mixtures oscillation and rotation energies relaxation equations, taking into account transport and chemical reaction processes

[DFVLR-SONDDR-198]

14 p2083 A72-30327

CW tunable semiconductor laser measurement of CO laser amplifier gain line shape for several vibration-rotation lines

15 p2245 A72-31382

Optically pumped pulsed hydrogen fluoride gas laser, observing anisotropic ultrahigh gain emission in rotational transitions

15 p2251 A72-32531

Generalized phase shift effect on classical limit of rotational excitation collision cross sections related to transport properties of diatomic gas molecules

16 p2428 A72-32925

Nitrogen molecular beam rotational excitation by collision with argon beam, describing electron beam spectrographic experimental method and numerical simulation technique

16 p2431 A72-33071

Hydrogen and hydrocarbon diatomic molecules and cations rotational state upper limits determination, noting potential energy functions

16 p2432 A72-34098

Rotational excitation of rigid rotor in argon-nitrogen system, measuring energy transfer moments by particle-body and perturbation technique

17 p2585 A72-34740

Spectroscopic determination of the rotational temperature in a rarefied supersonic flow in glowing-discharge excited nitrogen.

17 p2544 A72-35928

Rate constant determination for reaction product molecule in vibrational and rotational quantum states, obtaining spectral energy distribution

19 p2763 A72-38803

Calculation of intensities of vibration-rotation of a diatomic molecule by the factorization method

21 p3087 A72-40471

Coriolis constants for prolate symmetric top molecules from gas phase Raman band contours observation, noting comparison with IR spectroscopy

22 p3209 A72-42719

Influence of steric effects and compressibility on nonlinear response to laser pulses and the diameters of self-trapped filaments.

23 p3296 A72-43873

Transport properties of a gas of diatomic molecules. V - GPS calculation of the rotational relaxation time of the Ar-N₂ system.

24 p3427 A72-45307

MOLECULAR SPECTRA

NT ELECTRONIC SPECTRA

NT RAMAN SPECTRA

NT VIBRATIONAL SPECTRA

Microwave measurement and interpretation of oceanic thermal emission in terms of molecular temperature

02 p0214 A72-11866

Interstellar molecular microwave observations, emphasizing theoretical production rates and modes

03 p0419 A72-13119

Molecular oxygen photoelectron spectra at autoionizing resonance frequencies, comparing with Franck-Condon calculations

04 p0552 A72-14892

White dwarf Grw plus 70 deg 8247 circular polarization spectral structure with molecular absorption bands coincident with Minkowski bands

04 p0580 A72-15368

Vertically oriented double crystal attachment to vacuum X ray spectrograph for enhanced resolution of ionic solids and solutions molecular spectra

07 p0983 A72-19317

Formaldehyde concentration into cloud formation compared to atomic hydrogen from analysis of molecular lines near galactic center

08 p1235 A72-21386

Tabulation of calculated rotational line intensities relative to integrated vibration-rotation band intensity for various electron transitions of nitrous oxide

09 p1276 A72-22665

Ultrasoft X ray absorption spectra features of inner atomic shell photoionization in molecules

09 p1356 A72-22827

Molecular X ray emission spectra interpretation based on singly ionized states observation by photoelectron spectroscopy and transition probability calculation

09 p1357 A72-22838

Abundance in cold stellar atmospheres, noting effect on atmospheric thermal stratification and energy transfer from molecular spectra

11 p1722 A72-26432

Interstellar free radicals and molecules spectra, noting catalyzers, temperature and abundances role

11 p1722 A72-26434

Absorption spectrum of molecular nitrogen in 730-980 A band, investigating absorption cross sections and optical oscillator strengths

12 p1848 A72-27853

Hydroxyl vibration levels excitation rates calculation from transition probabilities and band sequence nightglow intensity measurements

13 p1954 A72-29816

Methane spectral band tetrahedral fine structure analysis, using vibration-rotation Hamiltonian

14 p2084 A72-30523

Molecular band model for inhomogeneous radiating gases nonuniform transfer paths based on single collision broadened spectral line growth

14 p2135 A72-30891

Methane collision broadened rotational fundamental line, calculating line width dependence on temperature

14 p2135 A72-30893

Fundamental and overlapping bands integrated intensities and nitrogen broadened half widths of rotational lines in nitrous oxide obtained from absorption measurements

14 p2135 A72-30895

Carbon 12/13 isotope ratio measurement for interstellar ionized CH molecules toward stars with strong interstellar lines

17 p2604 A72-34524

Spectroscopy of pulsed HF chemical lasers using an infrared vidicon camera tube.

17 p2562 A72-34641

The identification of the 1-0 and 2-1 bands of HCl in the infrared sunspot spectrum.

17 p2611 A72-35299

Application of dispersion techniques to molecular band intensity measurements. I - Principles of 'fringe shift' and 'fringe slope' band analysis procedures.

17 p2586 A72-35832

Fringe shift and slope analysis of interferometric spectrogram formed by NO-gamma system spectral band

17 p2586 A72-35833

On circumstellar molecules in the Pleiades.

19 p2856 A72-37508

Quenching of fluorescence and the photoeffect in anthracene crystals

19 p2847 A72-38782

Rate constant determination for reaction product molecule in vibrational and rotational quantum states, obtaining spectral energy distribution

19 p2763 A72-38803

Vibration spectra of the isomorphous proustite-pyrrargyrite series.

20 p2932 A72-39506

Interstellar molecules and dense clouds.

20 p2970 A72-39600

Ground and low-lying excited electronic states of FeH.

21 p3096 A72-40563

Dipole moment derivative of triatomic hydrogen ion electronic ground state, considering fundamental spectrum observation in hydrogen gas in local thermodynamic equilibrium

22 p3209 A72-42720

Laser magnetic resonance of the O₂ molecule using the 337-micron HCN laser.

22 p3209 A72-42896

Study of the variation of the intensity of vibration-rotation spectra of hydrogen halide molecules under the action of compressed foreign gases

22 p3209 A72-43047

Emission and absorption spectral behavior observation by millimeter radio telescopes for molecules in interstellar space of Milky Way galaxy spiral arms

24 p3439 A72-44905

Measurement of longitudinal relaxation times for spin-decoupled protons.

24 p3427 A72-45400

Titanium oxide molecular spectrum band intensities measurement for vibrational temperature of M supergiant stars, noting atomic absorption effect on measurement accuracy

24 p3448 A72-45681

MOLECULAR SPECTROSCOPY

NT RAMAN SPECTROSCOPY

Air pollutant detection by multiple slit correlation spectrometry and laser absorption technique, noting sensitivity enhancement by laser output increase

04 p0530 A72-14894

Laser source spectroscopic determination of pure and nitrogen perturbed carbon dioxide transition lines half-widths

10 p1491 A72-24227

High resolution spectroscopic studies of high density molecular beam production and emission spectrum excitation, using Ebert-Fastie vacuum spectrometer

16 p2430 A72-33059

Strict allowance for the variation of the system of normal coordinates in the theory for the vibronic spectra of polyatomic molecules

19 p2838 A72-38777

Pulsed photoexcitation /flash photolysis/ spectrophotometers in terms of light sources, recording sensitivity enhancement, data processing, laser use and performance requirements

21 p3058 A72-41726

MOLECULAR STRUCTURE

Phenolic-novolac prepolymer molecular structure and pyrolysis reactions thermokinetic parameters, presenting statistical methods for estimating char yield

01 p0023 A72-11261

Vibrational IR and Raman spectra of dimethylaminodichlorophosphine, determining molecular structure symmetry in liquid and solid phases

04 p0481 A72-14444

Artificial intelligence applications for chemical inference, discussing modified heuristic DENDRAL computer program for cyclic structure and linear molecule identification

07 p0936 A72-19498

Supermolecular structure artificial defects influence on mechanical strength of pyrographite

07 p1024 A72-20136

Nonspherical and nonadditive interactions contribution to third virial coefficient of polyatomic gas, discussing anisotropy, shape factor, and intermolecular forces

08 p1211 A72-21292

Molecular ordering in smectic A liquid crystals, evaluating spectrum hyperfine splitting as function of orientation to spectrometer magnetic field

08 p1217 A72-21490

Temperature effects on blood electrobioluminescence, relating luminescence peaks to protein and lipid molecular structure changes

09 p1268 A72-23694

Molecular structure and thermomechanical properties of polyimide and polyamide resins used for precision parts

12 p1833 A72-27406

Organic semiconductors for photovoltaic cell applications, discussing structural characteristics, improved charge transfer and crystallographic conductivity mechanisms

12 p1856 A72-28015

Plasticizers and modifiers effect on epoxy polymers structure from electron microscopy and IR spectroscopy, observing chemical reactions between aliphatic resin and hardening agent

13 p1983 A72-28689

Crystalline polymers behavior as multiphase composite solid, calculating supermolecular structures effects on stiffness properties

14 p2163 A72-30181

Protein biosynthesis R and D, discussing rate control, structure and medical and nutritional applications

14 p2076 A72-30600

IR mass spectrometric study of OBF in Ne and Ar matrices, discussing molecular structure

16 p2360 A72-33223

The interference function of molten metals

17 p2568 A72-35175

Freeze etching techniques in electron microscopic investigations of biological cells molecular structure

18 p2653 A72-36829

Strict allowance for the variation of the system of normal coordinates in the theory for the vibronic spectra of polyatomic molecules

19 p2838 A72-38777

Friction and molecular structure - The behaviour of some thermoplastics.

20 p2945 A72-39974

Calculation of the surface properties of elastic polymer molecules in athermal solutions by the Guggenheim method

21 p3095 A72-40078

Electron microscope investigation of the effect of fillers on the formation of supramolecular structures and on the type of breakdown in amorphous and crystalline polymers

21 p3072 A72-40084

Supermolecular structure artificial defects and bond strength influence on mechanical strength of pyrographite

24 p3418 A72-45761

MOLECULAR THEORY

Molecular processes in interstellar space and life origin, discussing radio astronomy observations, catalytic action and hydroxyl radicals in galaxies

01 p0128 A72-10398

Molecular dynamic techniques for simulating one dimensional shock wave motion in three dimensional solid, using rare gas solid model

12 p1881 A72-27282

Oxygen molecule parameters from frequency data in microwave, submillimeter and IR spectroscopy

15 p2283 A72-32654

The molecular-kinetic theory of polymer adhesion

23 p3307 A72-43930

MOLECULAR WEIGHT

Partial molar enthalpy measurement of oxygen mixture in substoichiometric Zr at 1300 C, using Tian-Calvet microcalorimeter

02 p0170 A72-12167

Polymer fractionation in simulated Jovian atmosphere according to molecular weight, suggesting substance responsible for red color

04 p0572 A72-14773

Radioimmunoassay and gel filtration determination of molecular size and immunochemical reactivity of parathyroid hormone in gland extracts, peripheral circulation and parathyroid effluent blood

04 p0473 A72-15228

Ultrahigh enthalpy gas generation by steady multicomponent flow process with kinetic energy transfer from low molecular weight gas to higher weight working medium

05 p0750 A72-16979

Irradiation effects on linear polyethylene molecular weight fractions in molten and crystalline states, determining sol-gel partitioning to establish critical conditions for gelation

09 p1337 A72-22550

On the application of perturbation theory for the calculation of molecular constants due to small mass changes and on the determination of force constants from very heavy isotope substitution.

19 p2763 A72-38806

MOLECULES

NT DIATOMIC MOLECULES

NT POLYATOMIC MOLECULES

NT TRIATOMIC MOLECULES

Review of NASA Ames Research Center 1971 conference on interstellar molecules and origin of life

09 p1265 A72-22645

MOLEIRE FORMULA

U COSMIC RAY SHOWERS

U SECONDARY COSMIC RAYS

U SPATIAL DISTRIBUTION

MOLLUSKS

Marine gastropod mollusk synaptic transmission mechanism, discussing various chemical transmitters, two phase potential, receivers, electrical interaction and electrophysiological conditioning

06 p0764 A72-17996

MOLNIYA SATELLITES

Molniya 1 satellite slow neutron monitor with photomultiplier scanned scintillator, noting limiting effect of geomagnetic perturbations

14 p2105 A72-30628

Aerodynamic drag at high latitudes observed from Molniya satellites orbit analysis, suggesting upper atmosphere density change

15 p2229 A72-31989

MOLTEN SALT ELECTROLYTES

Rechargeable high energy density battery with Al and Cl electrodes and molten aluminum chloride-alkali chloride eutectic electrolyte

16 p2352 A72-33896

The reduction of chlorine on carbon in AlCl₃-KCl-NaCl melts.

21 p3013 A72-40843

The aluminum electrode in AlCl₃-alkali-halide melts.

21 p3013 A72-40844

MOLTEN SALT NUCLEAR REACTORS

Design of high-temperature liquid-metal systems. [ASME PAPER 72-AERO-13]

22 p3204 A72-43149

MOLYBDATES

Raman scattering techniques applied to problems in solid state physics.

21 p3096 A72-40602

MOLYBDENUM

Polycrystalline Mo work function calculation from electron emission microscopy, determining crystallographic grain orientation effects

01 p0071 A72-11027

Flattening, heat treatment and machining of narrow rectangular vacuum melt Mo strips for microwave devices

01 p0078 A72-11087

Molybdenum-zirconium oxide cermets oxidation behavior, noting change of Mo oxidation characteristic from linear to parabolic time law above molybdenum oxide melting point

02 p0246 A72-12550

Molybdenum-uranium dioxide cermet fuel pins fission heating at 1145 K in forced convection He cooled reactor, measuring dimensional changes and U 235 burnup

04 p0546 A72-14424

Subgrain rotation induced angular anisotropy of plastic deformation of oriented Mo single crystals during rolling

05 p0674 A72-16354

Ni-Mo-N system alpha-solid solution thermodynamic analysis, deriving reaction enthalpies/entropies, free energy and interaction coefficients

05 p0676 A72-16795

Bcc Mo and Nb after cold working observing internal friction relaxation peaks as function of stress, strain, temperature and strain rate

06 p0831 A72-18296

Crystallographic texture of Mo sheet, analyzing angular dependence of Young modulus

06 p0832 A72-18366

Temperature dependent directional differences of modulus of elasticity of Mo sheet, using resonance technique

06 p0833 A72-18632

Cast electron-beam remelted Mo, investigating carbon and zirconium carbide additions effects on cold shortness and low temperature plasticity

06 p0833 A72-18645

Nichrome matrix composites with W and Mo reinforcing fibers

07 p1013 A72-19744

Surface processes effect on hydrogen penetration and diffusion into thick Mo membranes

07 p1014 A72-19772

High temperature tensile tests of Mo with helical and circular V grooves, discussing stress concentration sensitivity relations for grooved and smooth samples

07 p1018 A72-20141

Thermodynamics of Mo silicidation reactions from gas phase in silicon chloride and hydrogen media, discussing glow discharge maximum yield

07 p0937 A72-20417

Mo single crystal internal dislocation friction and ultrasound damping dependence on oscillation amplitude, exposure time and annealing temperature

08 p1185 A72-21073

Impurities and temperature effects on microdeformation of Mo single crystals under dynamic loads

08 p1188 A72-21789

Impurities effect on Mo plastic properties and toughness, suggesting lower vacuum arc welding rates and increased electron beam zone refining runs

09 p1326 A72-22228

Subgrain growth during annealing of rolled samples of Mo-Ti-C alloy and of single crystal Mo purified by electron beam zone melting

09 p1329 A72-23034

Anomalous structural dependence of elastic limit in Mo, determining mechanisms responsible for deviations from Petch law

09 p1329 A72-23037

Radiation damage in bcc metal Mo and W foils under energetic Au ion irradiation, noting vacancy dislocation loops

09 p1331 A72-23506

Carbon dioxide absorption kinetics on monocrystalline Mo from Auger spectroscopy and slow electrons diffraction

10 p1525 A72-24137

Levitator calorimetry for solid and liquid Mo enthalpy measurement, calculating specific heat and heat of fusion

10 p1496 A72-24243

Oxygen adsorption effects on Mo orientation contrasts and emission image under electron microscope

10 p1513 A72-24875

High temperature gradients in pulsed heated Mo specimen under vacuum, using photomicrographic technique

11 p1629 A72-25267

Subgrain rotation induced angular anisotropy of plastic deformation of oriented Mo single crystals during rolling

11 p1652 A72-25339

Grain size and carbon content effects on recrystallized Mo wire ductility at room and low temperatures

11 p1657 A72-25758

Polycrystalline Mo fatigue behavior under cyclic stresses, discussing grain size effect on fatigue life and relationship between cycle dependent yield and French damage line

11 p1658 A72-25830

Mo powder sintering kinetics and disperse mechanism in isothermal and nonisothermal conditions

11 p1643 A72-26836

Chemical vapor deposition of W and Mo by hydrogen reduction of hexafluorides, noting crystal structure and microporosity

11 p1644 A72-26837

Sintered Mo diffusion weld strength dependence on contact surface flatness and smoothness

11 p1644 A72-26847

Temperature, oxygen pressure and exposure time effects on oxidation characteristics of molybdenum-zirconium oxide cermets

11 p1665 A72-26865

Carbon and oxygen distribution and content effects on Mo mechanical properties and embrittlement

11 p1666 A72-26878

Photometric determination of Mo in Ni based steels and alloys in molybdenum-unithiol complex form, noting temperature and aqueous solution pH effects

12 p1828 A72-27445

Time-temperature-precipitation (TTP) diagrams and phase instabilities of high temperature exposed Mo containing austenitic stainless steels

13 p1974 A72-28658

Mo influence on gamma prime phase precipitate in wrought Ni-base superalloys, considering solvus temperature, weight fraction and lattice parameters

13 p1975 A72-28669

Mo addition effect on Al and Ti diffusion from intermetallic compounds into Ni matrix, noting increased high temperature stress rupture life

13 p1975 A72-28670

Electron probe microanalysis of Mo-Pd system diffusion at 1000-1600 C, measuring chemical diffusion coefficient as function of temperature, concentration and activation energy

13 p1978 A72-29221

Current breaks due to capacitor discharges in W and Mo wires, noting duration proportional to wire mass

13 p2007 A72-29980

Mo single crystal weakening after hot rolling and annealing, showing decreased dislocation density and hardness recovery by electron microscopy

14 p2112 A72-30160

Hydrogen gas solubility measurement in solid Mo at atmospheric pressure and 905-1521 C, noting quasiregular linearity of Arrhenius plot

14 p2113 A72-30246

Low and medium strain rates and temperature effects on bcc structure polycrystalline Nd and Mo, determining mechanical properties of yield and flow

14 p2114 A72-30367

Mo addition effect on high temperature creep resistance and diffusion activation energy of Nb alloys tested in torsion and tension at 1100-1500 C in vacuum

14 p2116 A72-30436

High temperature composite turbine blade materials, discussing service conditions and fiber/matrix selection, noting cast Ni and Mo based alloy fibers

14 p2125 A72-30533

Dislocation substructures effect on relaxation and internal friction peak in cold rolled Mo single crystals after annealing

14 p2122 A72-30956

Zr-Cu-Mo system phase diagram from microscopy, X ray analysis and mechanical tests, noting beta solid solution transformation into alpha, omega and beta phase mixtures

14 p2122 A72-30978

Y and La action on oxidation rates of Cr and Mo at high temperature in air

15 p2252 A72-31191

Surface damage induced by ion bombardment of monocrystalline W and Mo, determining degradation rate dependence on collisional energy transfer

15 p2276 A72-31853

Debye-Waller factors measurement for Mo and Cr surfaces near normal incidence based on LEED

15 p2292 A72-31857

Oxygen monolayer amounts adsorption on yttrium films and molybdenum foil investigated by Auger electron spectroscopy, observing growth of shifted peaks

15 p2292 A72-31860

Mo and stainless Ni-Cr steel surfaces chemical composition determination by Auger electron spectroscopy during heating in high vacuum

16 p2406 A72-33251

Grain orientation and nonmetallic inclusion distribution and identification by color etching of single crystal and polycrystalline Mo

16 p2407 A72-33532

Mo and W simultaneous addition effects on Ni-Cr-Nb alloy properties, noting heat resistance increase and Nb solid solubility decrease

16 p2408 A72-33534

Metal working and testing of nuclear rocket engine components with Mo as structural material and uranium dioxide as fuel, discussing Mo-W interdiffusion

17 p2559 A72-34617

Studies of the free path of the current carriers in molybdenum

17 p2568 A72-35517

Electron-microscopic investigation of the development of a cellular structure in molybdenum during hydroextrusion

17 p2569 A72-35524

Work function change of tungsten /110/ planes as function of Mo coverage.

18 p2656 A72-36134

Incore thermionic reactor cylindrical Mo emitter covered with two CVD W layers, discussing first layer adhesion and diffusion characteristics and work function stability

18 p2707 A72-36135

Behavior of tungsten-clad Mo-UO₂ fuel under neutron irradiation at high temperature.

18 p2708 A72-36143

The vapor deposition of high work function materials in a gas discharge.

18 p2656 A72-36149

The stability of structure of physical mechanical properties of molybdenum and tungsten after irradiation and thermal influence

18 p2698 A72-36153

Studies of physical-mechanical properties of monocrystal molybdenum and tungsten and electrical characteristics of TIC/thermionic converter/

18 p2698 A72-36154

Room temperature ductility of different types of molybdenum after differing annealing

18 p2698 A72-36155

Evaluation of sublimed molybdenum collector coatings for additive diode operation.

18 p2646 A72-36202

Analysis of primary creep of molybdenum at high temperatures.

18 p2700 A72-36580

An integral test of the inelastic cross sections of Pb and Mo using measured neutron spectra.

19 p2837 A72-37634

German monograph - Effect of molybdenum and degree of age hardening on the corrosion properties of maraging chromium steels

19 p2816 A72-37654

The plastic deformation behavior of Mo single crystals under compression.

19 p2816 A72-37689

Anisotropy of angular distribution of radiation due to positron annihilation on the surface of Mo single crystals.

19 p2844 A72-37691

Study of tungsten and molybdenum coatings obtained by arc discharge in a vacuum

19 p2808 A72-38186

Strength and plasticity of molybdenum during short-term tests

19 p2819 A72-38218

Effect of molybdenum on the properties of TiC-Ni cermet hard alloys

19 p2819 A72-38283

The influence of the surface orientation on yield in Mo single crystals.

20 p2935 A72-39007

Influence of boron on the structure and certain properties of electron-beam melted molybdenum

20 p2939 A72-39313

Vapor deposition effects on high density Mo, W and Nb obtained by carbonyls pyrolysis or chlorides and fluorides reduction

20 p2941 A72-39821

Void lattice model for Mo physical properties and equilibrium lattice spacing determination, calculating defect Green function

21 p3066 A72-40623

- Mechanical properties of titanium strengthened by monodirectional molybdenum wires
21 p3069 A72-41354
- Rheological properties of molybdenum and platinum of bamboo structure under bending loads
21 p3071 A72-41712
- Effect of voids on angular correlation of positron annihilation photons in molybdenum.
22 p3187 A72-41967
- Rate of molybdenum solution in carbon-saturated liquid iron.
22 p3193 A72-43027
- Diffusive metal coatings stress-strain state effect on composite Mo material strength, ductility and creep characteristics
23 p3306 A72-43732
- Electric resistance and enthalpy of molybdenum and tungsten
23 p3272 A72-44167
- Study of the dependence of the spectral and integral radiation properties of bodies on the surface roughness.
23 p3357 A72-44538
- The effect of annealing temperature on certain properties of molybdenum and tungsten fibers
24 p3415 A72-45396
- High temperature tensile tests of Mo with helical and circular V grooves, discussing stress concentration sensitivity relations for grooved and smooth samples
24 p3417 A72-45766
- MOLYBDENUM ALLOYS**
- Powder metallurgy processed Mo alloy, investigating destructive and nondestructive tests, structural grain size and hardness, wedge density and metallography
02 p0241 A72-11454
- Sintering and heat treatment effects on mechanical properties of atomized and mixed powders of Ni-Mo steel
02 p0234 A72-11462
- Al-Mo alloys under high temperature, determining phase equilibria and intermetallic phases
03 p0370 A72-12961
- Nb-Mo-N solid solution nitrogen solubility equilibrium at various temperatures and pressures
03 p0370 A72-12962
- Fine structure of Mo-Re alloys single crystals in solid solution region as function of Re content
03 p0377 A72-14019
- Carbon impurity effects on molybdenum ingot formation, detailing crystal growth, size reduction and length
04 p0533 A72-14987
- Longitudinal ultrasonic sound attenuation in superconducting Mo-Re alloys as function of temperature, magnetic field and frequency, using evaporated thin film CdS transducers
04 p0562 A72-15295
- Quaternary Mo-Zr-Cr-C system, investigating fcc phase liquidation from phase diagram by chemical, metallographic and X ray analyses
05 p0666 A72-16099
- Electron microscopic examination of molybdenum alloy thin plates aging at 700 C observing nucleation and precipitated phase
05 p0673 A72-16147
- Mo- and Ta-base refractory alloys creep tests, determining interactions between creep strength, fatigue life and strain aging by fatigue vibration application
05 p0677 A72-17111
- Mechanical, technological and physical properties of steel with and without molybdenum
05 p0679 A72-17204
- Diffusive mobility of C in Mo single crystals and Mo-Re alloy, using autoradiography and electron microscopy
06 p0829 A72-17733
- Electron transmission microscope study of quenched Mo-Ni alloys supersaturated solid solution low temperature aging behavior, investigating recovery processes
06 p0830 A72-18056
- Mo-Nb alloys single crystals work function, obtaining thermionic emission pattern
06 p0832 A72-18414
- Phase equilibria of Mo-Mn-C and W-Mn-C systems by X ray analysis, showing eutectoid decomposition involving rhombic modification
06 p0833 A72-18432
- Deformation kinetics and failure of refractory Nb and Mo base alloys in plastic state under low cyclic fatigue
06 p0833 A72-18631
- High temperature tests of short time strength, hardness and moduli of elasticity of W-MO alloys subject to plastic deformation and annealing
06 p0833 A72-18633
- Nonheat treated extruded Mo alloy under tension and vacuum conditions at various temperatures, investigating cylindrical samples size effects on mechanical properties
06 p0833 A72-18635
- Temperature and deformation velocity effects on elasticity and tensile strength of Mo and Nb alloys
06 p0833 A72-18636
- Nb-Mo alloys behavior in aggressive boron containing medium at high temperatures, relating boride phases growth rate to component percentages
07 p1012 A72-19680
- High temperature strengthening of vacuum melted W-Ti alloys with Mo and Zr additions
07 p1014 A72-19843
- Age hardening of Mo alloys with titanium and zirconium carbides at high temperatures after quenching
07 p1014 A72-19844
- Deformation rate and temperature effects on optimum strength and ductility of die forged and extruded Mo-Ti alloys
07 p1014 A72-19845
- Long-time isothermal temper embrittlement in Ni-Cr-Mo-V steels, noting tensile ductility decrease and intergranular fracture
07 p1015 A72-19932
- Corrosion resistance decrease and embrittlement in Ni-Mo cermet alloys after heat treatment from electrical resistance measurement
07 p1017 A72-19965
- Heat treatment of martensitically aging steels with Co, Ni and Mo, considering hardening effects and optimal conditions for high mechanical properties
07 p1020 A72-20414
- C and Re effects on brittleness threshold temperature and plasticity of Mo-Re alloy
09 p1326 A72-22227
- Mo-Zr solid solutions internal bonding, discussing diffusion controlled process and hardness dependence on Zr
10 p1494 A72-23833
- Diffusive mobility of C in Mo single crystals and Mo-Re alloy, using autoradiography and electron microscopy
11 p1652 A72-25340
- Microsegregation in Ti-Mo, Ti-V and commercial Ti alloys, investigating cooling rate and alloying elements contents effects
11 p1655 A72-25506
- Elastic constants of dilute Mo-Re alloys with bcc structure, determining randomly distributed point defects low concentration effects with T-matrix method
11 p1656 A72-25724
- Mechanical, technological and physical properties of steel with and without molybdenum
11 p1660 A72-26139
- X ray analysis of internal friction strains in nickel molybdenide during ordering process at 650-700 C, using torsional pendulum method for friction measurements
11 p1662 A72-26654
- Fe-Mo solid solutions transient creep behavior as function of applied stress, noting temperature effect
11 p1662 A72-26656
- Mo-Hf alloys high temperature mechanical properties improvement by internal diffusion nitriding, noting precipitates effects
11 p1644 A72-26843
- Arc cast vacuum melted Mo base alloy properties, production and applications to heat pipes, aerospace structures and pressure vessels
11 p1644 A72-26844
- Solid state reactions in powder metallurgical production and working of Mo alloy, considering sintering process
11 p1644 A72-26846
- Mo corner of Mo-B phase diagram constructed from microstructural analysis and microhardness, melting point and lattice constant measurements
12 p1828 A72-27291
- X ray spectral analysis of Ti-Mo system alloys, investigating K and L lines and electronic structure
13 p1972 A72-28491
- Annealed and quenched Fe-Mo-Co system, defining phase relationships in Fe-rich corner at 2200, 2000 and 1800 F
13 p1973 A72-28650
- Ni-Mo-W alloys hardness rating and corrosion resistance to sulfuric and hydrochloric acids, discussing dispersion hardening, quenching and aging treatments
14 p2114 A72-30272
- Electron microscopic and X ray analyses of ordering kinetics in Ni-Mo alloys, noting lattice type change and complex domain structure formation causes
14 p2115 A72-30409
- Heterogeneous order-disorder transformation in Ni-Mo alloy at 78 K after annealing, using ion field emission microscopy
14 p2116 A72-30416
- Alpha solid solution of nitrogen in Nb-Mo alloys, obtaining excess partial quantities and activity and interaction coefficients at high temperatures
14 p2121 A72-30773
- Mo-Ni-Al system phase equilibria at 600 C from X ray and microstructural analysis, noting hardness dependence on composition
14 p2123 A72-30985
- Ni-Al-Nb-Mo system phase diagram from X ray and microstructural analysis, noting solid solubility and dependence of hardness and electrical resistivity on components
14 p2123 A72-30989
- Rare earth metals interactions with V, Nb and Mo alloys, describing procedures for interstitial impurities removal
15 p2252 A72-31190
- Carbon distribution effect on cast Mo and alloys structure studied by electron microscopy, microdiffraction and X ray analysis, noting annealing from eutectic temperature
15 p2255 A72-31575
- Polycrystalline Mo-Re alloy under cold longitudinal, transverse, cross and pack rolling, noting twin and dislocation microstructures
15 p2256 A72-31669
- Transition metals additives effect on binary Mo alloys softening, noting influence of temperature and electron concentration change
15 p2258 A72-32135
- Ti-Mo binary solid solution, investigating superconducting transition temperature, lattice instability and electron-to-atom ratio by calorimetric measurements
15 p2295 A72-32544
- Nb-Mo alloys elastic constants anomalous temperature dependence, proposing phase changes role and relationship to neutron diffraction and specific heat
16 p2405 A72-33167
- Boron concentrations in Mo-Hf alloy samples from neutron activation analysis, measuring Li 8 beta radiation with plastic scintillation detector
16 p2391 A72-33238
- C diffusion mobility and coefficients in W-Mo steels gamma and alpha phases, discussing ionization effect on activation energy increase
16 p2408 A72-33538
- Investigations aimed at eliminating the susceptibility to thermal cracking of the high corrosion resistant NiMo 30 nickel-molybdenum alloy/Remanit HB/
17 p2559 A72-34394
- Low-temperature properties of nitrogen-alloyed austenitic chromium-nickel /molybdenum/ steels and chromium-manganese-nickel steels and their applicability as low-temperature ductile steels
17 p2566 A72-34395
- Mo-Nb alloys single crystals work function, obtaining thermionic emission pattern
17 p2567 A72-34863
- Complexonometrical analysis of molybdenum aluminides and Cu-Mo alloys without preliminary separation of components
18 p2655 A72-36097
- Gravimetric and polarographic determination of W in binary W-Mo alloys, noting methods accuracy
18 p2655 A72-36098
- Creep of different molybdenum alloys at high temperature and under strong stresses
18 p2698 A72-36144
- Thermodynamic description of the metal-rich part of the system niobium-molybdenum-nitrogen
18 p2701 A72-36597
- Nucleation and growth of deformation twins in Mo-35 at. % Re alloy.
18 p2702 A72-36748
- Creep tests on 2-1/4 per cent chromium 1 per cent molybdenum steel in bainitic condition.
19 p2817 A72-37713
- Study of the structural stability and mechanical properties of molybdenum subjected to the prolonged action of temperature and stress
19 p2818 A72-38013
- Aging characteristics of Ti-Mo base beta alloys.
19 p2820 A72-38371
- Elastic constants of niobium-molybdenum alloys in the temperature range -190 to +100 C.
19 p2821 A72-38591
- Interdiffusion in nickel-molybdenum and palladium-molybdenum systems
20 p2939 A72-39315
- Effect of twins produced by annealing on high-temperature failure of chromium-nickel-molybdenum steel
20 p2939 A72-39316
- Mechanical and microstructural properties of steels for effective surface cementation, suggesting Mo and Cr optimal contents
20 p2941 A72-39576
- Carbide hardening of chromium-molybdenum-vanadium steel
20 p2941 A72-39578
- Mechanical properties of Ti-Mo alloys at low temperatures
20 p2942 A72-39824
- Domain structures in metal crystals, investigating ordering in Ni-Mo alloys
20 p2962 A72-39997
- Microalloying effect on creep and stress rupture characteristics of hot rolled and annealed Mo alloys
21 p3070 A72-41355
- Solid-state reactions during the production of TZM molybdenum alloy by powder metallurgical methods
22 p3187 A72-41972
- Investigation of phase equilibria in alloys of silicon with molybdenum and titanium
22 p3188 A72-42150

Study of the properties of porous materials of nickel-molybdenum and nickel-chromium-molybdenum alloys 22 p3188 A72-42193

Oxidation rate anisotropy investigation on coupon specimen of Ta-Mo alloy at 950 C 22 p3190 A72-42770

Niobium and molybdenum alloys containing borides and carbides of the IV-a group metals 22 p3191 A72-42814

Phase compositions, impurity effects, crystallization and production of plastic W and Mo alloys and heat resistant W-based alloys 22 p3192 A72-42815

Magnetic properties and texture of a thin strip of nickel-iron-molybdenum alloys 22 p3192 A72-43012

Influence of alloying elements on ordering in alloys of the nickel-molybdenum system 22 p3192 A72-43016

Cast heterophase Mo and alloys fracture strength and plastic characteristics, investigating crystal growth texture, orientation and substructure 23 p3301 A72-43741

Strain hardening effect of Ni, Mn and Mo in Cr steel after high temperature annealing 23 p3301 A72-43742

Mo alloy under impact tests, investigating notch sharpness effects on cold shortness threshold and strength 23 p3301 A72-43756

Increasing the boundary strength of electron-beam-melted cast molybdenum by vanadium microadditions 23 p3302 A72-43967

Metalceramic alloy of the B2Zr type 23 p3302 A72-44010

Influence of boron on the structure and properties of electron-beam melted molybdenum 24 p3414 A72-45380

Boron and carbon contents effect on elastic properties strength and ductility of electron beam melted Mo-B alloys 24 p3414 A72-45381

Crystallographic texture of sheet Mo alloys, analyzing angular dependence of Young modulus 24 p3416 A72-45752

MOLYBDENUM CARBIDES

Niobium and molybdenum carbide film deposition on steel substrates by open arc welding with partial carbon burnout 14 p2107 A72-30156

Molybdenum carbide needle formation, growth in kinetics and morphology Fe-C-Mo alloy from lattice parameters measurements 14 p2120 A72-30618

Relations between mechanical properties and microstructures in TiC-Mo2C-Ni alloy. 19 p2821 A72-38375

MOLYBDENUM COMPOUNDS

NT MOLYBDATES

NT MOLYBDENUM DISULFIDES

NT MOLYBDENUM OXIDES

Antioxidation coatings of Ta and Ta alloys for high temperature long term operation, emphasizing sintered molybdenum disilicide 11 p1663 A72-26840

Iron-nickel-molybdenum carbonyl powders 23 p3298 A72-43276

MOLYBDENUM DISULFIDES

Ultralow sliding friction during bombardment of polypropylene, molybdenum disulfide and graphite surfaces with charged helium atoms at room temperature in vacuum chamber 02 p0249 A72-12282

Graphite and molybdenum disulfide surface and lubricating properties, examining basal plane proportion relationship with edge sites 02 p0236 A72-12847

Sputtered molybdenum disulfide film lubrication, discussing adherence to metal surfaces, particle size, friction experiments and tensile tests 02 p0236 A72-12848

Tungsten, molybdenum and tantalum disulfides oxidation rate determination by fluidized bed technique, calculating kinetic and diffusive processes activation energy 03 p0370 A72-13184

Molybdenum disulfide and layer lattice materials lubricating mechanism and effectiveness from sulfur atoms strong polarization, using scanning electron microscope 06 p0822 A72-18157

Molybdenum disulfide lubricating film and wear-in study by scanning electron microscopy and testing machine 06 p0836 A72-18586

Lubrication with thin molybdenum disulfide solid film under various temperatures and atmospheric pressures, examining friction and lifetime 06 p0823 A72-18587

Molybdenum disulfides with varying purity level evaluated as solid lubricants and as lubricant additives in standard lubricating testing devices 06 p0836 A72-18588

Impurity content, particle size and abrasion resistance role in abrasiveness of molybdenum disulfide 06 p0836 A72-18589

Wear behavior of molybdenum disulfide and antimony trioxide bonded solid film lubricant with air curing silicone resin, noting temperature and pretreatment effects 06 p0823 A72-18593

Basal plane and edge surface areas measurement in graphitized molybdenum disulfide powders 06 p0837 A72-18601

Graphite and molybdenum disulfide, investigating temperature effect, thermal stability and oxidation effect on weight by TGA and DTA 06 p0837 A72-18602

Molybdenum disulfide lubricating effectiveness improvement with finer particles at aggravated sliding conditions, suggesting surface roughness qualifications 06 p0837 A72-18605

Sputtered molybdenum disulfide lubrication on polished metal surfaces with low friction coefficient, strong adherence, high density and small particle size 06 p0824 A72-18607

Graphite and molybdenum disulfide powders lubricating properties relation to surface crystalline orientation 06 p0824 A72-18608

Radioactive molybdenum disulfide lubrication films distribution on nitrated steel and on magnesium pig iron 07 p0996 A72-19775

Solid lubricant additives effects in oils and fats, discussing molybdenum disulfide and zinc pyrophosphate solid film formation on metal surfaces under contact friction conditions 07 p1024 A72-20395

Superconductivity observation in Na, K and Rb intercalates of molybdenum disulfide comparing transition temperatures 09 p1368 A72-22561

Ultralow sliding friction during bombardment of polypropylene, molybdenum disulfide and graphite surfaces with charged helium atoms at room temperature in vacuum chamber 11 p1639 A72-25707

Molybdenum disulfide addition effect on compounded model greases lubricating performance, determining oxidation stability, rust preventive behavior and consistency 12 p1832 A72-27047

Molybdenum disulfide lubricating effectiveness due to surface film properties, suggesting chemical reaction effect with sliding metal surface 16 p2397 A72-33125

Lubrication with solids. 19 p2807 A72-37771

Evidence of crystal structure in some sputtered MoS2 films. 19 p2823 A72-37897

Investigation of the lubricant properties of molybdenum disulfide, graphite, and phthalocyanine 19 p2823 A72-38094

Vacuum-friction temperature resistance and durability of a molybdenum-disulfide coating deposited on steel by the detonation method 19 p2809 A72-38290

MOLYBDENUM OXIDES

Differential thermal and X ray analyses of ignition and preignition solid-solid reactions in Zr-Mo trioxide delay system over 440-475 C 08 p1219 A72-20756

Low-temperature reduction of molybdenum and tungsten oxides 20 p2941 A72-39820

Transition of the oxide film on a molybdenum surface from the two-dimensional to the three-dimensional phase 24 p3432 A72-45503

MOLYBDENUM SULFIDES

NT MOLYBDENUM DISULFIDES

MOMENT DISTRIBUTION

Thin walled prismatic structural members under uneven axial moment distribution, formulating force deflection equations for torsional-flexural behavior 01 p0141 A72-11049

Closed quasi-linear cubic theory of viscoelasticity for bodies with force and moment physical nonlinearity 03 p0454 A72-14218

Lasing onset moments distribution over emitting surface of injection lasers at room temperature 04 p0531 A72-15082

Grad moment method application to radiative transfer in medium with relativistic differential motions, obtaining Eddington approximation and Thomas radiative-viscosity terms 04 p0579 A72-15322

Multimoment solutions to convective heat transfer from sphere, discussing maximum drag coefficient and validity at all Knudsen numbers [ASME PAPER 71-WA/HT-1] 05 p0743 A72-15863

Time optimal control of system with distributed moments, deriving conditions for existence of fast response solution 05 p0683 A72-17134

Waveguide integral equation numerical solution by moment method, suggesting algorithm for detecting and alleviating relative convergence behavior [AD-745595] 06 p0775 A72-18368

Inverse integral Fourier transforms to solve steady periodic motions of wing close to solid surface, deriving equations of lift and principal moment 08 p1108 A72-21701

Nonuniform non-Lambertian diffusely scattering surface optical transfer characteristics and initial irradiance distribution inside sphere, discussing spherical harmonic moment measurement 09 p1309 A72-22610

Bending theory of homogeneous isotropic micropolar cantilever beam loaded by moments at edges 09 p1399 A72-22700

Violation effect of moment equilibrium about normal in shell of revolution and helical shell theory, discussing distribution 10 p1560 A72-25171

Jupiter and Saturn gravitational moments from available models, taking into account rotation, density and radius 12 p1871 A72-27744

Zero moment stress effect on modal density spectrum of fluctuating thin cylindrical shells and cylindrical panels 15 p2327 A72-31737

An inverse problem in the momentless theory of shells of revolution situated in a temperature field 22 p2322 A72-41895

Interplanetary scintillation of radio sources observed through solar corona, deriving higher central moments from skewness coefficient of probability density function 24 p3437 A72-44831

Solution of a boundary-value thermoelasticity problem for a turbine blade by the polymoment method 24 p3460 A72-45623

MOMENTS

NT BENDING MOMENTS

NT DIPOLE MOMENTS

NT DISTRIBUTION MOMENTS

NT ELECTRIC MOMENTS

NT LOADING MOMENTS

NT MAGNETIC MOMENTS

NT MOMENTS OF INERTIA

NT PITCHING MOMENTS

NT ROLLING MOMENTS

NT STABILITY DERIVATIVES

NT STANDARD DEVIATION

NT TORQUE

NT VARIANCE [STATISTICS]

NT YAWING MOMENTS

Stresses, strains and moments interrelationship in axisymmetrically loaded circular cylindrical shell under unsteady creep conditions 09 p1401 A72-22729

Control surface dynamic hinge moment coefficients estimation based on system state measurements from flight tests, using least squares criterion [AIAA PAPER 72-379] 11 p1730 A72-25403

Second order moments of system with parametric excitation by filtered white noise calculated with Fokker-Planck equation, giving condition for mean-square-stability 14 p2131 A72-30711

Techniques for power spectrum moment estimation. 21 p3021 A72-40911

MOMENTS OF INERTIA

Moment of inertia of earth atmosphere relative to earth axis of rotation 06 p0808 A72-18038

Zero moment theory application to cylindrical shells with elliptical geometries under constant transverse loads 07 p1087 A72-18992

Natural inertia moment effect of balance weight at wing tip on critical flutter rate 08 p1242 A72-21092

Moment of forces on spacecraft with low angular velocities in variable magnetic field, using electro-dynamics equations 08 p1240 A72-21140

Gyrostad inertial motion under nonholonomic constraint of mass center coincidence with fixed point 08 p1208 A72-21360

Nonspinning satellite earth-pointing attitude control for elliptic orbits using active regulation of pitch moment of inertia 08 p1204 A72-21605

Accelerated aperiodic actuation of pendulous mass surface gyrocompass to meridian direction, using inertial moment from rotor start-up 10 p1481 A72-24496

Moment of inertia of earth atmosphere relative to earth axis of rotation 11 p1622 A72-25974

- Equations of motion for torsional vibrations in system with nonlinear elastic term and variable moments of inertia, noting analog computer simulation
11 p1739 A72-26982
- Lunar mass, gravitational field and moments of inertia from Lunar Orbiter spacecraft Doppler tracking data
13 p2037 A72-28989
- Asymmetrical mechanics theory of nematic liquid crystals, noting relation for local moment of inertia and tensor analysis of kinematic characteristics
13 p2022 A72-29497
- Optimal efficiency of satellite passive nutation damper, noting system moment of inertia and flywheel axis relationship and viscous friction coefficient
14 p2162 A72-30458
- Lunar crust mass distribution relation to moments of inertia derivation from librations, inferring nonvalidity of lunar evolution fluid phase hypothesis
14 p2153 A72-30504
- Elastic damping of spin stabilized space stations nutational oscillations induced by time-variant moments of inertia
15 p2319 A72-31458
- Body of revolution motion in fixed center Newtonian field, investigating plane trajectories of center of inertia
15 p2307 A72-31677
- Inertial crosscouplings effect on orientation process dynamics of solid body investigated by nonlinear mechanics, noting centrifugal moments of inertia effects
15 p2275 A72-31730
- Stability analysis of gyrostat satellites possible equilibria under gravitational torques, considering inertia, equilibrium and angular momentum parameters
15 p2321 A72-32586
- The masses, densities and moments of inertia of Uranus and Neptune.
20 p2967 A72-39184
- Moment of forces on spacecraft with low angular velocities in variable magnetic field, using electrodynamics equations
20 p2976 A72-39245
- Determination of parameters related to the interior of Mercury.
24 p3436 A72-44696
- MOMENTUM**
NT ANGULAR MOMENTUM
Pressure determination in kinematic pairs of spatial landing gear mechanism, describing rotatory and spherical pairs reactions to various combinations of momenta
05 p0614 A72-17057
- Mass, momentum and energy distribution measurement in quasi-steady MPD discharge, obtaining velocity vector profiles
[AIAA PAPER 72-497]
11 p1696 A72-26220
- MOMENTUM ENERGY**
U KINETIC ENERGY
MOMENTUM PRECESSION
U PRECESSION
MOMENTUM THEORY
Flow momentum losses during gas mixture chemically nonequilibrium expansion in nozzle
01 p0145 A72-10487
- Energy-momentum tensor for radiation and radiative viscosity in optically thick matter having Thomson scattering with photon absorption and emission processes
01 p0129 A72-10798
- MHD boundary layer calculation for conducting fluid along semiinfinite flat plate with transverse magnetic field, deriving momentum and kinetic energy integral equations
01 p0113 A72-11383
- Limited three body problem applied to planetary angular momentum increment due to accretion of particles in heliocentric orbits, discussing planet rotation laws
02 p0282 A72-12330
- Nonlinear development of instability wave in turbulent wake behind thin body based on integrals of mean flow momentum and kinetic energy equations
02 p0152 A72-12351
- Boundary layer of gas-particle flows with pressure gradient, numerically integrating momentum equation for cascade particulate flow
[AIAA PAPER 72-87]
05 p0604 A72-16808
- Helicopter rotor boundary layer, comparing analytical shear stress and velocity distributions obtained by momentum integral techniques with hot wire probe experimental data
[AIAA PAPER 72-38]
05 p0607 A72-16900
- Closed system equilibrium correlation functions relationships based on total momentum conservation, discussing application to solids or liquids electrical conductivity via nuclei dynamics
07 p1035 A72-19669
- Gravitational field potential energy-momentum pseudotensor component determination in general relativity theory
08 p1207 A72-21301

- Turbulent boundary layer characteristics of rotating helical blade in annulus contained fluid, calculating boundary layer growth and streamline angles via momentum integral equations
10 p1466 A72-24296
- Critique of general momentum theory of propeller actuator disk model, showing flow field determination from nonlinear elliptic differential equation solution
11 p1572 A72-25998
- Newton-Busemann pressure law derived for hypersonic rotationally symmetric flow from momentum theory considerations and plane flows
12 p1751 A72-27120
- Impulse and kinetic momentum equations for dynamics of variable mass solid using mechanical model
12 p1846 A72-27543
- Flux functions and balance laws for linear momentum in continuum mechanics, deriving traction vector and differential equilibrium equation
12 p1846 A72-27570
- Momentum consideration aided air resistance calculations for cylinder, discussing position effects
13 p1893 A72-28705
- Nonfriction vortices generation by jet flow in stationary fluid, using conservation of momentum principle
15 p2219 A72-32554
- Lagrange equations of second kind for rigid systems, using balances of linear and angular momenta for mass point or rigid body
16 p2466 A72-33021
- Gravitational field potential energy-momentum pseudotensor component determination in general relativity theory
17 p2580 A72-34659
- Approximate calculation of the magnitude of the momentum during the passage of a material particle past an elongated homogeneous biaxial ellipsoid
17 p2618 A72-35812
- A simple quadrature method for computing laminar boundary layers.
22 p3165 A72-42110
- Approximate equations of the flow behind a detonation with lateral confinement
24 p3463 A72-45041
- MOMENTUM TRANSFER**
Momentum exchange coefficient for surface layer neutrally stable flow after surface roughness change, noting error possibility in flow estimates for heterogeneous terrain
01 p0094 A72-10827
- Energy and momentum transfer between fields and particles in plasma crossed by transverse electromagnetic wave, investigating MHD stability
01 p0109 A72-10884
- Control axes misalignment effects on spinning satellite wobble damping and requirements for active momentum exchange controllers
02 p0286 A72-12267
- Temperature dependent gas internal diatomic laminar heat transfer, investigating continuity, energy, momentum for two dimensional flow between heated parallel plates
[ASME PAPER 71-HT-N]
02 p0302 A72-12317
- Global angular momentum balance, considering atmospheric frictional torques and fluxes, ocean water mass exchanges and seasonal variations effects
03 p0384 A72-14142
- Planetary boundary layer mixing length flow hypothesis with dependence on Reynolds tangential stress permitting turbulent diffusion coefficient maximum values computation
04 p0519 A72-15458
- Plasma ion collision transport analogy with turbulent velocity space momentum transfer, explaining confined plasma runaway electron absence in strong electric fields
04 p0560 A72-15469
- Orbiting space vehicle life extension by momentum management using gravity gradient torques
05 p0727 A72-16467
- Angular momentum and Li diffusive transport induced by mild thermally driven turbulence associated with Goldreich-Schubert-Fricke instability, discussing solar rotation slowdown
[AD-735988]
05 p0720 A72-16718
- Thermal and momentum diffusivity measurements in turbulent stratified flow, obtaining velocity and temperature profiles
[AIAA PAPER 72-80]
07 p0966 A72-18950
- Atmospheric eddy flux spatial variations in constant flux layer, noting heat and momentum flux variability of less than 10 percent
07 p1030 A72-19107
- Energy and momentum removal from troposphere and lower atmosphere by mountain lee wave breaking, discussing effects on atmospheric circulation evolution and maintenance
08 p1203 A72-22167
- Trailing vortex core decay with axial injection as function of momentum flux parameter
09 p1261 A72-23623

- Momentum transfer theory for ion drift velocity in multicomponent gas mixture at arbitrary electric field strengths
10 p1519 A72-24096
- Gravitational field angular momentum transfer analogy with Einstein gravitational energy transfer in general relativity
10 p1511 A72-24246
- Relativistic heavy ion in plasma, calculating energy loss based on electron scattering and momentum transfers
10 p1515 A72-24344
- Numerical solution of two massive rigid bodies impact with variable slipping direction using Routh momentum change theorem
11 p1735 A72-25769
- Internal gravity waves effects on energy budgets and vertical angular momentum transport over mountainous terrain in southwestern U.S. from handheld camera pictures on Apollo 9
11 p1682 A72-26472
- Noncoincidence of maximum velocity and zero shear stress due to asymmetric turbulent velocity profiles, considering effect on momentum, heat and mass transfer in noncircular channels
11 p1618 A72-26534
- Heat and momentum transfer of binary gas mixture flow in parallel plate channel with mass injection from porous wall, calculating velocity, pressure and temperature distributions
11 p1746 A72-26538
- Modified gas dynamic functions of total momentum of plane boundary layer for arbitrarily oriented control surfaces and for stratified flows with potential layer
11 p1574 A72-26973
- Heat and momentum transfer properties and storm propagation speed under steady convective overturning in shear, considering cumulonimbus convection scale of atmospheric motion
12 p1840 A72-27704
- Atmospheric surface layer turbulent transfer mechanisms, studying direct measurements of momentum, heat and moisture turbulent fluxes
12 p1840 A72-27705
- Limited three body problem applied to planetary angular momentum increment due to accretion of particles in heliocentric orbits, discussing planet rotation laws
13 p2039 A72-29214
- Large scale motion of turbulent boundary layer during relaminarization under strong pressure gradient, obtaining fluctuating velocity components and tangential Reynolds stress
13 p1944 A72-30028
- High momentum transfer collisions importance for anisotropic part of distribution function in Lorentz and single component plasmas
14 p2134 A72-30802
- Ar and K electron cross section determination for momentum transfer, using dc conductivity measurement of high pressure plasma
14 p2134 A72-30803
- Momentum transport in thermal incompressible turbulent boundary layers with constant wall temperature, using dimensional analysis and Stratford model
14 p2096 A72-31055
- Momentum and energy equations for pool film boiling heat transfer from horizontal cylinder to saturated liquids, using integral boundary layer analysis
14 p2173 A72-31067
- Langmuir waves scattering by denser plasma ions as dominant turbulent process momentum exchange between dynamic plasmas, applying to galaxies expansion into intergalactic media
15 p2285 A72-32269
- Plasma containment in toroidal systems investigated on basis of fluid model containing inertia, momentum transfer, ionic collisions and thermal conductivity effects
15 p2285 A72-32273
- X ray Brillouin scattering investigation of phonon phenomena for small momentum transfers with Bragg condition nearly satisfied
15 p2250 A72-32308
- Numerically computed momentum and energy accommodation coefficients and angular distributions of gas molecules reflected from solid crystalline surfaces applied to satellite drag calculation
16 p2430 A72-33065
- Aerodynamic coefficients determination from momentum and energy exchange between low velocity molecular jet and solid surfaces, describing time of flight measurement technique
16 p2390 A72-33069
- Energy and momentum losses of high temperature gas flow through externally cooled tube, solving laminar flow differential equations numerically on digital computer
16 p2378 A72-33430
- Spiral structure generation by outward angular momentum transfer, considering gravitational stress tensor, star-spiral wave momentum transfer and galactic secular evolution
16 p2457 A72-33683

Dankwert liquid film surface layer renewal concept as refinement of Reynolds theory of correlation between convective heat transfer and momentum transfer

17 p2637 A72-35050

Heat mass and momentum transport in free turbulent mixing.

17 p2543 A72-35638

The bounding theory of turbulence and its physical significance in the case of turbulent Couette flow.

18 p2677 A72-36006

Mathematical model for internal atmospheric gravity waves breaking process modification by momentum exchange between wave and mean flow

18 p2687 A72-36630

A technique for position sensing and improved momentum evaluation of microparticle impacts in space.

19 p2795 A72-37518

Momentum transfer and plasma formation above a surface with a high-power CO₂ laser.

19 p2811 A72-37864

Momentum transport by gravity waves in a perfectly conducting shear flow.

19 p2788 A72-38792

The indirect determination of stability, heat and momentum fluxes in the atmospheric boundary layer from simple scalar variables during dry unstable conditions.

20 p2947 A72-38964

Collisionless momentum transfer interactions in laser produced plasma on solid target, refuting Wright model

21 p3090 A72-40339

Linear momentum transfer effects in molecular dissociation produced by electron impact.

21 p3087 A72-40557

Theory of laminar film condensation of flowing vapor.

21 p3128 A72-40950

Wave energy exchanger for hybrid propulsion system.

21 p3100 A72-41172

One dimensional variable slip and homogeneous model predictions of momentum flux in two phase two component low quality flow

21 p3130 A72-41179

A calculation procedure for heat, mass and momentum transfer in three-dimensional parabolic flows.

22 p3243 A72-41954

Evanescent and internal gravity wave propagation effects on atmospheric dynamics, considering momentum transfer, energy dissipation and turbulence

22 p3168 A72-41964

Transfer equations for stellar systems

23 p3338 A72-44035

Atmospheric boundary layer definition by height of maximum vertical kinetic energy flux, considering stable and unstable stratifications

24 p3421 A72-44954

Chemical explosion energy distribution between gases and propelled mass, discussing momentum and kinetic energy transfer

24 p3463 A72-45040

MONATOMIC GASES

Boundary conditions for monatomic gas flow in constant cross section channel with heat supply and ionization

01 p0111 A72-11211

Monatomic He-Ar binary gas mixtures heat transfer to cylinders in low Reynolds number flow, considering internal energy effects

02 p0303 A72-12358

Low density monatomic gas supersonic spherical source flow, presenting departure from translational equilibrium

02 p0205 A72-12359

Shock wave structure in monatomic gases, using Fokker-Planck model for particle collisions and Mott-Smith distribution for shock front

04 p0512 A72-15162

Boltzmann equation collision integral statistical models, solving shock structure in monatomic gas

04 p0513 A72-15339

Steady normal shock wave analysis in binary inert monatomic gas mixtures using kinetic theory moment method

04 p0513 A72-15340

Numerical simulation of gas atom scattering from solid surface and satellite drag coefficient calculation

07 p0910 A72-20106

Numerical determination of particle number and mass flux density in monatomic rarefied gas flow through circular orifice at finite pressure ratio

07 p0972 A72-20107

Molecular rotation stimulation and deactivation of diatomic molecule addition to monatomic gas, discussing energy exchange in rarefied gas flow

08 p1211 A72-21656

Kinetic equations derivation for rarefied chemically reacting monatomic or stable molecular gases

10 p1514 A72-23845

Steady two dimensional flow of monatomic rarefied gas past seminfinit beam

10 p1418 A72-24543

Zeeman effects in hyperfine structure of atomic iodine photodissociation laser emission, noting magnetic fields effect on time behavior

11 p1692 A72-26558

Hypersonic flow of nonequilibrium ionized monatomic inviscid radiating gas past axisymmetric blunt body with allowance for electron and ion temperatures difference

13 p1895 A72-29877

Diatomic-monatomic molecular gas mixtures oscillation and rotation energies relaxation equations, taking into account transport and chemical reaction processes

[DFVLR-SONDDER-198] 14 p2083 A72-30327

Quantum kinetic equation for monatomic and molecular gases optical characteristics calculation, considering spontaneous emission spectrum of atoms

14 p2110 A72-30358

Interferometric investigation of impurities effects on electron density distribution in ionization-relaxation zone behind shock waves in monatomic gas

15 p2215 A72-31213

Monatomic ionized gas thermodynamic properties direct computation by numerical method without iteration or numerical differentiation

15 p2335 A72-31714

Thermal force exerted on spherical particle between two flat plates in stagnant monatomic rarefied gas, using moment solution to Boltzmann equation

15 p2336 A72-32403

Microwave acoustic surface waves attenuation at solid and monatomic gas boundary, detailing frequency, molecular weight, pressure and temperature effects

15 p2278 A72-32505

Spherical source jet flow expansion of single monatomic gas into vacuum on basis of BGK kinetic equation

16 p2375 A72-32887

Light scattering by monatomic and polyatomic gases, superimposing effects due to rotational and translational molecular relaxation

16 p2428 A72-32944

Theory of sound propagation in mixtures of monatomic gases.

17 p2583 A72-35613

Shock-wave structure using nonlinear model Boltzmann equations.

17 p2542 A72-35614

French monograph - An asymptotic theory of the Boltzmann equation and its application to the study of near continuum flows

19 p2785 A72-37489

Limiting properties of solutions of the Boltzmann equation.

21 p3086 A72-40264

Electron-energy distribution in a low-temperature plasma

22 p3213 A72-43118

MONAURAL SIGNALS

Monaural prestimulatory loudness adaptation measurement by delayed and single simultaneous balance methods, discussing intensity, frequency and duration effects

08 p1127 A72-21896

MONITORS

Particle mass monitor system based on piezoelectric microbalance combined with electrostatic precipitator collector, considering applications to air quality monitoring, laboratory aerosol research, process control, etc

[AIAA PAPER 71-1100] 01 p0067 A72-10548

Voltage and current waveforms monitoring on sampling oscilloscope for TRAPATT microwave oscillator performance optimization

01 p0038 A72-10653

Acoustic echo sounder as real time monitor of airport environmental meteorological parameters

01 p0103 A72-11137

Long distance monitoring method for short wavelength radio transmission to remote countries

02 p0182 A72-12671

Ultrasonic transducer monitoring of decompression-caused gas bubbles in rat thigh muscle tissue for decompression sickness time course development studies

07 p0921 A72-20183

Explosive/pyrotechnics performance monitoring for acceptance, lot qualification, comparison testing and system design guidelines

08 p1219 A72-20760

ATC radar performance monitoring, considering advances in radar signal processing and digital display techniques

08 p1134 A72-21525

Aircraft maintenance and reliability monitoring and control on scheduled airlines, considering component failure rate and mode analysis, sampling inspection and remedial action

09 p1261 A72-22901

Picoampere charged particle beam symmetry and magnitude monitor consisting of four transmission ion chambers

09 p1315 A72-23405

MONOCHROMATIC RADIATION

Hardware monitor and associated analysis programs to evaluate real time satellite command and control digital computer system performance

10 p1442 A72-23817

Structural Acoustic Monitor system for airframe structural proof testing, providing multichannel recording and aural monitoring of acoustic data derived from aircraft mounted accelerometers

10 p1459 A72-24146

Russian papers on automatic monitoring and electrical measurement methods covering optical systems, control devices, diagnostic test optimization, bionic applications, etc

11 p1611 A72-26435

Effectiveness and reliability criteria for information and monitoring systems performance evaluation, suggesting use of revenue ratio

11 p1611 A72-26437

Discrete automatic monitoring and measuring systems with discrete random sequence and continuous process reconstructed output signals, deriving probability criteria for reading frequency determination

11 p1611 A72-26438

Optimization of diagnostic tests for monitoring industrial system efficiency, obtaining compromise between costs and utilization

11 p1611 A72-26441

Rank correlation coefficient method for complex control plants parameters selection, applying to aircraft power system monitoring

11 p1612 A72-26442

Low cost real time computerized C 14 radiopospirometry telemetering system for monitoring human metabolism data during space missions

12 p1774 A72-28277

Aircraft CRT electronic displays discussing operational flexibility versus control and monitor complexities, economics, reliability and human factors

15 p2182 A72-32636

Nondestructive monitoring techniques to optimize performance and service tests, considering penetrating radiation, electromagnetic induction, ultrasonics, holography, microwaves, acoustic emission and thermal monitoring

16 p2397 A72-33219

Photodiode-operational amplifier circuit for pulsed laser systems energy variations monitoring, noting insensitivity to ambient light conditions

16 p2402 A72-33607

Monitor and regulator for automatic speed control and flow velocity measurement in wind tunnel

16 p2392 A72-33609

'VI-like' and 'aVF-like' leads for continuous electrocardiographic monitoring.

19 p2759 A72-37244

Methods for monitoring the parameters of phased antenna arrays.

19 p2767 A72-38622

Computerized supervisory control for interpretation of subgoal statements from human operator to permit teleoperator interaction with environment without long time delay

21 p3011 A72-41417

Computer-operated data acquisition and control system for automatic diagnostic monitoring of propulsion research instrument

22 p3216 A72-42684

Development of a digital control system for a spacecraft propulsion test facility.

22 p3163 A72-42685

An advanced strain level counter for monitoring aircraft fatigue.

22 p3179 A72-42688

Signal quality monitoring of computer data transmission.

[ASME PAPER 72-AERO-1] 22 p3156 A72-43146

Multipoint real time all-day computerized noise monitoring system for diagnostic evaluation of airport, discussing design and applications

24 p3387 A72-44684

MONKEYS

Chlorpromazine tranquilizer influence on squirrel monkeys in electric shock tests, shifting postevent aggressivity to pre event anticipation

07 p0916 A72-18975

Space medical urological problems from experience with Biosatellite 3 monkey, discussing closed catheter conduit system, urinary calcium changes in immobilized animals and urinary diuresis

10 p1424 A72-23728

MONOCHROMATIC RADIATION

Monochromatic waves propagating in uniform magnetoplasma, considering resonant interaction with electrostatic approximation

01 p0107 A72-10138

Monochromatic electromagnetic field diffraction problems in homogeneous medium, presenting computer aided numerical analysis

02 p0171 A72-11690

Null electromagnetic field propagation in general relativity, applying to Stokes parameters definitions for monochromatic light

02 p0259 A72-12178

Solar coronal monochromatic optical emission, inferring electron density and ionization or temperature distributions and variations with time

03 p0422 A72-13208

Solar corona shape, structure and brightness changes during 11 year cycle from monochromatic and total eclipse white light observations

03 p0423 A72-13210

Monochromatic radio emission from decilight years distant stars, discussing search experiment by low noise multichannel receivers

03 p0436 A72-13827

Solar energy exchange by thermal radiation, investigating monochromatic emission factors at 0.3-15 micron

04 p0596 A72-14702

Laser coherent monochromatic light for cybernetics research in pattern classification, discussing fingerprints and letters

04 p0531 A72-15137

Dye laser monochromatic coherent light wavelength tuning with minimized optical cavity degradation and without external optics

04 p0531 A72-15502

Planetary nebulae NGC 2392, 6210, 6826, 6720 and 6853 observations, presenting monochromatic photographs and isophotic contours

05 p0713 A72-16021

Elliptical polarization and depolarization coefficients for monochromatic radio waves reflected from F 2 ionosphere using Stokes parameters

05 p0656 A72-16241

Scattering of arbitrarily impinging monochromatic electromagnetic waves by thin infinitely long isotropic, dielectric and metal rods of elliptic cross section

05 p0628 A72-16412

Nonlinear propagation effects of monochromatic circularly polarized vlf waves /whistlers, heli cons/ along field lines in magnetosphere

05 p0658 A72-16603

Monochromatic radiation pulse transfer in absorbing plasma, deriving heat wave propagation velocity

05 p0696 A72-16680

Plasma stability in field of longitudinal monochromatic wave, examining satellites excitation by Langmuir wave

05 p0696 A72-16681

Monochromatic light beam propagation in optically nonhomogeneous medium containing matter in near critical state, determining exciting wave electric field strength

05 p0691 A72-16683

Nonlinear monochromatic Alfvén wave propagation parallel to magnetic field in anisotropic plasma with long wavelength beam instability

07 p1039 A72-18915

One- and two-conductor transmission lines electromagnetically coupled to rocket, deriving current bounds in load impedances under incident plane monochromatic wave

07 p0956 A72-19556

Commercial radiographic system with data enhancement based on monochromatic blue film, noting image quality and exposure range

07 p0991 A72-20425

Semiregular variable CH Cygni observations from 1967 to 1969 with continuous spectrum variations comparison to monochromatic brightness changes

08 p1233 A72-21278

Narrow band signal envelope analysis of astronomically observed quasi-monochromatic emission sources

08 p1135 A72-21731

Monochromatic absorption coefficients determination for Ar heated in wall-stabilized arc at high temperatures and pressures

10 p1517 A72-23836

Stimulated monochromatic electromagnetic wave scattering derived from analysis of nonlinear interactions in magnetoactive plasma

12 p1849 A72-27063

Plane monochromatic electromagnetic wave scattering by rotating metallic cylinder, noting frequency shift dependence on cylinder translational motion velocity

13 p1914 A72-28370

Numerical methods to solve boundary value problems of monochromatic transport equations in light scattering media optics

13 p2001 A72-28504

Solar corona intensification analysis based on ionized Fe monochromatic emission spectra, investigating spectral lines behavior as function of temperature and electron density

13 p2047 A72-29736

Quasi-monochromatic wave interaction with second harmonic in weakly nonlinear medium, obtaining exact nonstationary solutions

13 p1971 A72-29911

Nonlinear damping of potential monochromatic waves in inhomogeneous plasma, obtaining resonance particle distribution function

13 p1923 A72-29984

Nonlinear AM and FM due to bonded nature of quasi-monochromatic whistler packets in magnetosphere

14 p2085 A72-30448

Monochromatic brightness coefficient measurements for Jupiter and Saturn disk centers and Uranus geometric albedo

14 p2152 A72-30491

Lagrangian complex amplitude derivation for monochromatic electrostatic wave in unmagnetized collisionless plasma, investigating nonlinear Landau damping effects on instability

14 p2140 A72-30939

Opponent color responses of monkey optic tract fibers to monochromatic lights, using chromatic adaptation and microelectrode recording

15 p2184 A72-31369

Submillimeter plane monochromatic waves propagation in ground layer of turbulent atmosphere, deriving received signals levels fluctuations

15 p2195 A72-31653

Monochromatic plasma wave excitation by cold electron beam, obtaining instability maximum amplitude and oscillation period

15 p2285 A72-32270

Monochromatic radio wave propagation in interplanetary plasma, deriving frequency spectrum and phase and amplitude fluctuations

15 p2202 A72-32656

Coherent CW radiation by tunable GaAs injection laser in external dispersive cavity at 77 K, discussing monochromatic output spectral analysis by Fabry-Perot interferometer

16 p2401 A72-33393

Monochromatic electromagnetic wave reflection and transmission at oblique incidence on sharp plasma boundary of moving ionization source

16 p2363 A72-33481

Monochromatic radiation pulse transfer in absorbing plasma, deriving heat wave propagation velocity

16 p2437 A72-33692

Plasma stability in field of longitudinal monochromatic wave, examining satellites excitation by Langmuir wave

16 p2437 A72-33693

Monochromatic light beam propagation and scattering in optically nonhomogeneous medium containing matter in near critical state, determining exciting wave electric field strength

16 p2426 A72-33694

Monochromatic carbon dioxide TEA laser

17 p2564 A72-35424

Multicomponent structure of Nd-glass laser radiation, observing active medium gain band portions interrelationships in free running and stimulated emission operation modes

17 p2564 A72-35507

Radio galaxies monochromatic luminosity-spectral index relationship from 3CR spectra studied at 10 MHz to 10,700 MHz

18 p2726 A72-36621

Experimental observations of the instability of stellar images from a bichromatic two-channel television system

19 p2860 A72-37956

Monochromatic brightness coefficient measurements for Jupiter and Saturn disk centers and Uranus geometric albedo

19 p2864 A72-38320

Influence of roughness on the thermal radiation emitted by opaque surfaces - Model test

19 p2881 A72-38393

Measurement of electron concentration in the plasma of a pulsed erosion-type accelerator

19 p2843 A72-38535

Nonlinear monochromatic Alfvén wave propagation along magnetic field in anisotropic rarefied plasma with firehose instability

20 p2957 A72-39381

Measurements of a mode-competition discriminant in a single-frequency argon ion ring laser

21 p3062 A72-40240

Nonlinear theory of the monochromatic circularly polarized VLF and ULF waves in the magnetosphere.

21 p3015 A72-40480

Pulsed monochromatic laser with toluene, xylene, ethanol, isoamyl alcohol and dimethylformamide solutions of organic dyes, discussing wavelength variations and power outputs

21 p3064 A72-41736

Holographic system resolving capacity increase by oblique illumination of object, analyzing plane monochromatic wave transmission through one dimensional semitransparent body

21 p3058 A72-41791

Monochromatic plasma waves linear and nonlinear coupling, discussing LF modulation partial transfer /Luxembourg effect/ and application to ionospheric diagnostics

23 p3319 A72-43517

Ionization structure and coarse and fine analyses in planetary nebulae spatial spectroscopic diagnostics based on line profile monochromatic intensity integral equation inversion

23 p3339 A72-44236

Visual sensitivity measurement in retinal areas with stepwise change from one monochromatic light to another, discussing eye movements effects and perception thresholds

23 p3258 A72-44385

Spectral composition and phase function of plane monochromatic light wave scattering by electrons in high temperature plasma

23 p3322 A72-44465

Utilization of a composite resonator for improving the monochromaticity of a semiconductor laser with electron-beam excitation

23 p3297 A72-44468

Stimulated monochromatic electromagnetic wave scattering derived from analysis of nonlinear interactions in magnetoactive plasma

24 p3431 A72-45716

MONOCHROMATIZATION

Michelson interferometers with large interference fields for plasma diagnostics emphasizing structural rigidity, monochromatic light pulse power, instruments vibrations resistance, etc

02 p0223 A72-11402

Application of the moving-slit X-ray automonochromatization method in structural studies of planar diodes and an attempt to correlate electrical properties with lattice defects.

17 p2595 A72-34749

MONOCHROMATORS

Solar UV flux measurements by balloon-borne grating monochromator, using FM-FM analog and PCM telemetry systems for computerized data analysis

03 p0409 A72-13051

Fabry-Perot spectrometer/premonochromator assembly integral transmissivity as function of spectral tuning noting selectivity by amplitude modulation

08 p1172 A72-22035

Astronomical spectroscopy using ultraviolet resolution single Fabry-Perot interferometer in tandem with echelle Hilger monochromator

12 p1811 A72-27942

Cs vapor photoionization by sequential method via thermally tunable Ga-As laser and arc-lamp monochromator radiation

17 p2585 A72-34614

MONOCLINAL VALLEYS

U VALLEYS

MONOCOQUE CYLINDERS

U CYLINDRICAL SHELLS

MONOCOQUE STRUCTURES

MONOCOQUE STRUCTURES

Vibration and buckling analysis of doubly curved composite monocoque plates and shells of positive and negative Gaussian curvature, examining stacking sequence effect

02 p0292 A72-11990

Papers on aerospace structure by N. J. Hoff covering aircraft framework, stress analysis, structural stability, shell theories, bending, buckling, monocoque and sandwich structures, etc

04 p0591 A72-15238

Russian book - Design principles in aircraft construction.

22 p3136 A72-42074

MONOCRYSTALS

U SINGLE CRYSTALS

MONOCULAR VISION

Functional organization of visual cortex in monkeys, discussing monocular and binocular responses, trigger and stimulus abstraction

01 p0011 A72-10467

Lateral spatial interactions of sensory receptors, discussing mathematical theory for monocular visual inputs described by real valued functions on continuum

01 p0021 A72-11196

Stereoscopic depth movement perception sensitivity compared to monocular movement

02 p0169 A72-12209

Objects visual detection probability distribution as function of angular size, contrast and search time, comparing binocular and monocular searches effectiveness

07 p0931 A72-19919

Response latencies and correlation in single units and visual evoked potentials in cat striate cortex following monocular and binocular stimulations

11 p1582 A72-26771

Monocular and biocular magnifiers for night vision equipment.

20 p2921 A72-39030

On a long-term temporal aspect of stereoscopic depth sensation.

23 p3258 A72-44381

Visual stimuli distance estimation with head stationary or moving, discussing performance after monocular motion parallax training

24 p3374 A72-44557

MONOLITHIC CIRCUITS

U INTEGRATED CIRCUITS

MONOMERS

Cation polymerization of beta-propiolactone without initial kinetics dependence on monomers concentration, relating acyl ion bonding and electron donor groups

09 p1275 A72-22496

Addition type polyimide-graphite fiber composites fabrication from monomeric reactant solutions to improve mechanical properties and thermal stability
12 p1834 A72-28091

Polymerization characteristics of 4-ferrocenyl-1, 3-pentadiene monomer, discussing synthesis on molar scale
17 p2512 A72-35934

Fiber optics development and physical foundations, discussing reflection, optical waveguides, vibrational modes during light transmission and fabrication from inhomogeneous glass and mixed monomers
24 p3425 A72-44782

MONOPLANES
NT BUCCANEER AIRCRAFT
NT ELECTRA AIRCRAFT

MONOPOLE ANTENNAS
First order admittance of coaxially driven infinite monopole antenna, obtaining Green function expansion
01 p0043 A72-11247

Vertically polarized logarithmically periodic monopole antenna for incoming wave front reception with low elevation angles in 1.5 to 30 MHz frequency range
02 p0195 A72-12697

Admittance calculation for vertical monopole antenna driven by coaxial line, approximating current distribution by polynomial with complex coefficients
04 p0501 A72-15429

Monopole antenna with lumped mutual coupling between driven and folded sections, noting staggered resonant frequencies and bandwidth broadening from input impedance analysis
06 p0782 A72-17355

Broadband cylindrical monopole antenna with adjustable quasi-distributed capacitive loading, comparing theoretical and experimental admittances
11 p1604 A72-25744

Active loop dipole aerials with height reduction properties at resonance, investigating transistor configurations in loop monopole aerial
12 p1792 A72-27699

Input impedances and current distributions of cylindrical monopole antennas of various lengths in hot lossy plasma as function of plasma density
13 p2009 A72-28538

Numerical analysis of surface current density distribution and electromagnetic fields of conducting body, noting radiation patterns of radial dipole and quarter wavelength monopole
13 p1916 A72-28541

Rod antenna near field energy flow direction and intensity characterization by time independent and dependent components of Poynting vector
13 p1932 A72-29398

Combination antenna unit with vertical monopole and two perpendicular slots in horizontal plane to yield steerable cardioid-shaped pattern for vertically polarized waves
15 p2206 A72-31776

Monopole antenna height reduction by transistor amplifier incorporation in antenna structure
15 p2208 A72-32391

Analysis of antennas on finite circular cylinders with conical or disk end caps.
17 p2525 A72-34361

The monopole slot - A small broad-band unidirectional antenna.
17 p2525 A72-34367

Engineering approach to the design of tapered dielectric-rod and horn antennas.
17 p2530 A72-35362

Analysis and prediction of coupling between collocated antennas.
20 p2902 A72-38999

Application of an agar-agar chamber for the study of electromagnetic waves in an inhomogeneous medium.
21 p3015 A72-40359

Computer-aided numerical solution for electric field structure of rod and plate, calculating field distortion by rod antennas and near lightning rod
21 p3086 A72-41671

MONOPOLES
Air shower cores or relativistic monopoles as sources of straight lightning, considering thundercloud conditions over ocean and land areas
03 p0350 A72-14100

Magnetic monopole search in lunar samples by electromagnetic measurement, determining flux limits for cosmic radiation and pair production in proton-nucleon collisions
06 p0880 A72-17884

Electromagnetic waves scattering by uniformly moving objects in free space, considering two dimensional monopoles and dipoles
09 p1282 A72-23523

Geomagnetic data testing by including monopole term in spherical harmonic reduction
13 p1951 A72-29394

Photoconductivity in depleted surface layer of quasi-monopolar semiconductors with arbitrary diffusion to Debye lengths ratio, noting n-type low resistance gallium arsenide
15 p2296 A72-32694

MONOPROPELLANTS
NT AEROZINE
Dissolved gases effect on liquid surface state during high pressure liquid monopropellant strand combustion
08 p1222 A72-22046

MONOPULSE ANTENNAS
Pulse IMPATT diode Ka band microwave rf head mechanically steered antenna array for airborne monopulse tracker applications
01 p0039 A72-10661

Bearing estimation performance of monopulse tracking with passive linear arrays, using computer simulation for various integration times and input S/N ratios
06 p0774 A72-17809

Optimization of monopulse antenna performance indices for specified sidelobe envelope function and/or specified pattern nulls
13 p1915 A72-28530

Cross coupling in a five horn monopulse tracking system.
17 p2513 A72-34356

L band optimum monopulse high power feed using dominate and higher order waveguide modes to develop sum and difference patterns
17 p2526 A72-34421

Five-horn feed system design for improving large steerable antenna monopulse performance, discussing weight and cost reductions by focal length selection
17 p2526 A72-34467

Combination of sum and difference diagrams of a dipole group in front of a parabolic reflector for a two-plane monopulse method
21 p3029 A72-40517

MONOPULSE RADAR
Low angle monopulse radar tracking errors due to multipath, considering amplitude variation across antenna aperture and reduction by target-image resolution
02 p0178 A72-12391

Ground secondary radar interrogator system using monopulse technique for bearing measurement, accuracy and interference reduction
04 p0493 A72-15523

Angular coordinates and slope determination from monopulse radar measurements of two unresolved targets
05 p0629 A72-16578

Bearing azimuth measurement accuracy improvement by ATC beacon system/secondary surveillance radar using monopulse technique
18 p2662 A72-37047

Optimisation of slope of difference-mode radiation pattern in sum-and-difference-comparison monopulse radar.
23 p3264 A72-43606

MONOTONE FUNCTIONS
Monotonicity theorems for functionals and transformations in stochastic models of queueing, reliability and optimality problems
09 p1343 A72-23565

Solutions for multivalued evolution equations, considering monotonic maximal operator on finite dimensional Hilbert space
10 p1504 A72-24061

Cosmic objects and phenomena frequency distribution functions monotone decrease with respect to importance, considering star clusters, binaries, lunar craters, solar activity, etc
14 p2160 A72-30912

Non-monotonicity of temporal recognition of brief duration.
18 p2651 A72-36912

Certain algorithms for obtaining an approximate solution of incorrect problems on a set of monotonic functions
19 p2828 A72-38846

MONTE CARLO METHOD
Elliptic and parabolic partial differential difference equations solution using modified random walk Monte Carlo technique
01 p0093 A72-10858

Monte Carlo simulation on high energy cosmic ray propagation and multiplication in high altitude emulsion chamber observations, examining two-fire-ball and H-quantum models
01 p0121 A72-11123

Monte Carlo methods for hybrid computer solution of nonlinear parabolic partial differential equations with two spatial dimensions
02 p0186 A72-11657

Monte Carlo method application to meteor stream formation by meteor material ejection from comet nucleus, determining age of Draconids
02 p0282 A72-12333

Ionospheric photoelectron fluxes and motions simulated by Monte Carlo technique, including transport effects, elastic and inelastic collisions and energy losses
03 p0412 A72-13517

Rarefied gas heat transfer problem between two parallel plates of different temperatures, evaluating

nonlinear Boltzmann equation with Monte Carlo techniques
04 p0595 A72-14599

Orthogonal expansion of estimators and estimands in Hermite series for Monte Carlo computation
04 p0540 A72-15631

System natural frequency standard deviation estimator, using Monte Carlo method
[ASME PAPER 71-WA/APM-8] 05 p0734 A72-15972

Optimal sequential multiple decision procedures for radar receiver using Monte Carlo method
05 p0628 A72-16565

Flexible elastic plate nonlinear vibration response and noise transmission from turbulent boundary layer by Monte Carlo technique, discussing subsonic and supersonic flow regions
[AIAA PAPER 72-199] 05 p0651 A72-16850

Data uncertainties effects on thermal analysis, discussing Monte Carlo method combination with sensitivity analysis
[AIAA PAPER 72-60] 05 p0749 A72-16930

Nuclear-electron cascades longitudinal evolution calculation in ionization calorimeter for primary nucleons and pions, using Monte Carlo method
06 p0811 A72-17260

Monte Carlo scheme for dynamic evolution of spherical stellar systems
06 p0885 A72-18080

Direct simulation Monte Carlo method for rarefied gas dynamics, discussing computer display units use for flow visualization
07 p0973 A72-20344

Monte Carlo digital simulation of probabilistic buckling behavior of indeterminate structure under initial stresses due to random geometric lack-of-fit
07 p1095 A72-20348

Combined signal detection and trajectory estimation functions optimization application to Monte Carlo simulation for trajectory moving across two dimensional grid
08 p1144 A72-20858

Discrete-time nonlinear estimators digital implementations by computerized Monte Carlo method, comparing with alternative techniques
08 p1145 A72-20864

Maximum likelihood estimation for Weibull distribution parameters from multicensored samples by Monte Carlo simulation
08 p1200 A72-21589

Bayes estimators for Poisson distribution random parameters and reliability function, using Monte Carlo method and maximum likelihood estimation
08 p1200 A72-21590

Hybrid Monte Carlo techniques with digital and analog computers and minimal interface, simulating random walks for partial differential equations solution
08 p1138 A72-21602

Book on heat transfer by thermal radiation, covering black body radiation, electromagnetic theory, energy exchange, Monte Carlo solution, and absorbing and emitting media
09 p1411 A72-23046

State estimation for nonlinear discrete-time system based on quantized data, presenting maximum likelihood estimate solution and Monte Carlo simulation results
09 p1290 A72-23095

Monte Carlo and convolution methods for statistical analysis of ladder filters, describing programs for determining attenuation probabilistic distribution as function of components dispersions
09 p1289 A72-23679

Bayesian analysis application to reliability and life parameter estimation for Weibull failure model, using Monte Carlo simulation
10 p1503 A72-23978

Transport theory Boltzmann equation and Monte Carlo methods applied to semiconductor negative differential mobility calculation
10 p1526 A72-24398

Observation errors effects on satellite attitude best least squares estimate based on direction measurements, using Monte Carlo method computer simulation
10 p1438 A72-24692

Monte Carlo random walk methods for directional emittance of one dimensional absorbing-scattering slab with reflecting boundaries, considering refractive index, optical thickness and albedo
[AIAA PAPER 72-309] 11 p1743 A72-25243

Numerical integration for many body systems equations of motion, noting Monte Carlo and Boltzmann moment methods for large systems
12 p1873 A72-27895

Dynamical evolution of spherical star cluster under effect of internal encounters, using Monte Carlo models
12 p1873 A72-27896

Monte Carlo scheme for dynamical evolution of spherical star clusters, considering stellar dense core, spurious relaxation and escape
12 p1875 A72-27919

- Hybrid computer Monte Carlo solution algorithm for parabolic partial differential equations with time varying boundary conditions, applying to ferromagnetic rod magnetization problem 12 p1787 A72-28119
- Monte Carlo method for radiative transport theory problems, considering mathematical models of light scattering media and photon trajectory random elements 13 p2001 A72-28505
- Atmospheric model for random density variations effects on space shuttle reentry parameters, using Monte Carlo trajectories for delta wing orbiter 13 p1990 A72-28814
- Monte Carlo simulation for imperfect second order hybrid phase locked loop in radio frequency interference and Gaussian noise backgrounds, employing digital computer simulation model 13 p1935 A72-29104
- Monte Carlo method application to meteor stream formation by meteor material ejection from comet nucleus, determining age of Draconids 13 p2039 A72-29217
- Quasi-classical mechanical approximation in molecular scattering, using Monte Carlo methods for Jacobian determinant evaluation 14 p2134 A72-30836
- Upward and downward radiative transfer in atmosphere-ocean system model calculated by Monte Carlo method, noting turbidity effect on radiance 15 p2224 A72-31673
- Computerized Monte Carlo techniques for nonlinear error analysis of system behavior, using random number generators for input distribution simulation 15 p2264 A72-32184
- Monte Carlo simulation method for flow field around two dimensional or axisymmetric body immersed in hypersonic rarefied gas flow 16 p2342 A72-32882
- Monte Carlo treatment of Lyman-alpha radiation in a plane-parallel atmosphere. 17 p2598 A72-34538
- Study of high energy /25-10,000 GeV/ interactions with a multilayer cloud chamber using Monte Carlo simulations for energy calibration. 17 p2585 A72-34922
- Monte Carlo calculation of radial and time dependence of isophote diagrams for Cerenkov light in 0.1 to 1 TeV extensive air shower 17 p2599 A72-35142
- Hybrid computer Monte Carlo solution algorithm for parabolic partial differential equations with time varying boundary conditions, applying to ferromagnetic rod magnetization problem 19 p2770 A72-38620
- Monte Carlo trajectory calculations of the three-body recombination and dissociation of diatomic molecules. 19 p2838 A72-38805
- A Monte Carlo model of turbulent mixing for the prediction of NO production in steady-flow combustors. [WSCIPAPER 72-8] 20 p2982 A72-38973
- Monte Carlo studies of the relaxation of vector end-to-end length in random-coil polymer chains. 20 p2898 A72-39599
- Application of the Monte-Carlo method to the calculations of the configuration of a heat source whose material is subjected to the action of electron beams 21 p3127 A72-40135
- Transfer of resonance-line radiation in differentially expanding atmospheres. I - General considerations and Monte Carlo calculations. 21 p3106 A72-41037
- Variance reduction in Monte Carlo analysis of rarefied gas diffusion. 21 p3046 A72-41183
- Kullback-Leibler information function and the sequential selection of experiments to discriminate among several linear models. 21 p3075 A72-41187
- On the calculation of variances of solutions to linear simultaneous equation. 21 p3075 A72-41233
- The application of Monte Carlo methods to the nonlinear filtering problem. 23 p3274 A72-43541
- Approximation for Monte Carlo method modeling of pion-nucleon and nucleon-nucleon inelastic collisions at high energies 23 p3317 A72-44414
- Ranking the reliability of two designs by Monte Carlo techniques. 24 p3383 A72-44655
- MOON**
- Critique of Brown lunar theory, discussing planetary orbits, earth and moon figure effects and second order terms 01 p0122 A72-10009
- Review of papers on planetology given at Brighton symposium, covering moon, Venus, Mars and Jupiter. 01 p0132 A72-11071
- Solar wind and geomagnetic tail interaction with moon, discussing lunar Mach cone evidence for anisotropic wave propagation in magnetized collisionless warm plasma 07 p1061 A72-20025
- Lunar center of mass position with respect to visible hemisphere physical surface calculated from photogrammetric analysis and Lunar Orbiter I data 08 p1232 A72-21158
- Soviet papers on physics of moon and planets covering Martian violet clouds, UV absorption levels in Jupiter and Saturn disks, etc 08 p1237 A72-21826
- Lunar motion as plane restricted three body problem in celestial mechanics 11 p1722 A72-26478
- Solar eclipse timings by photoelectric, photographic and visual observation for comparison of Newcombe sun tables and improved lunar ephemeris reference systems 13 p2041 A72-29527
- Mars and moon cores elastic properties inferred from hydrostatic equilibrium based on observed data for total mass, radius and moment of inertia 13 p2048 A72-29809
- Star catalog zero-point improvement by Bessel method modification for lunar observation data reduction 14 p2149 A72-30210
- Cylindrical model of interplanetary magnetic field-moon interaction, taking into account solar wind flow boundary condition asymmetries 14 p2154 A72-30514
- Moon radius from Lunar Orbiter I angular velocity data obtained from camera image motion compensator sensor /V/H sensor/ 17 p2603 A72-34207
- Ephemeris time, lunar orbital elements and FK4 equinox correction from the observations of the moon by the method of equal altitudes. 17 p2603 A72-34274
- New orbital elements for moon and planets. 17 p2609 A72-35106
- Positions of the major planets and the moon observed at the 0.33 M photographic equatorial 19 p2858 A72-37856
- Lunar center of mass position with respect to visible hemisphere physical surface calculated from photogrammetric analysis and Lunar Orbiter I data 20 p2969 A72-39263
- Recent developments in the theory of the motion of the moon. 21 p3102 A72-40124
- Lunar thermal history model, considering nonuniform initial composition, radioactive element partitioning and melt cutoff value 22 p3225 A72-42529
- Lunar albedo and temperature distribution from simultaneous photoelectric and far IR brightness temperature measurements of sunlit lunar surface 22 p3226 A72-42536
- Star catalog zero-point improvement by Bessel method modification for lunar observation data reduction 23 p3333 A72-43240
- Discrepancy between Brown theory and Griffith values for lunar perigee and node mean motions partial derivatives with respect to moon mean motion 24 p3442 A72-45241
- MOON ILLUSION**
- Parallel swing with affixed luminous disks test for induced vestibular stimulation effects on moon illusion, noting eye movement factors 20 p2893 A72-38900
- MOON-EARTH TRAJECTORIES**
- Cosmic proton and neutron produced recoil proton energy spectra measurements along earth-moon-earth trajectory with nuclear emulsions aboard Zond 5 and 7 [CERN-71-16] 02 p0273 A72-12074
- MOONMOBILES**
- U LUNAR SURFACE VEHICLES
- U MANNED LUNAR SURFACE VEHICLES
- MOONQUAKES**
- Anomalous lunar tide vs latitudinal or declinational tidal wave for moonquakes recorded at Apollo 12 landing site 16 p2457 A72-33565
- MORAINAL LAKES**
- U LAKES
- MORL**
- U MANNED ORBITAL RESEARCH LABORATORIES
- MORPHINE**
- Starvation effects on male rats, mice and guinea pigs hepatic drug metabolism, discussing ethylmorphine, p-nitroanisole and aniline 01 p0015 A72-11262
- MORPHOLOGICAL INDEXES**
- Thyroid glands iodine concentrations, blood proteins and morphological changes in rats with acute hypoxic hypoxia and pulmonary edema 07 p0924 A72-20620
- Auroral particle precipitation /keV electrons and protons/ morphology from ESRO IA particle spectrometer measurement, discussing particle populations in day and night magnetospheres 12 p1864 A72-27786
- MORPHOLOGY**
- NT GEOMORPHOLOGY
- NT ISOMORPHISM
- NT LUNG MORPHOLOGY
- NT POLYMORPHISM
- Global morphology of integrated product with respect to D and E regions electron concentration height and collision frequency 03 p0345 A72-12981
- Exercise and denervation effects on intrafusal muscle fibers morphology, noting 25-33 percent cross-sectional area atrophy in nuclear bag and chain fibers 04 p0472 A72-14895
- Small lunar maria craters morphological maturity as function of age and dimensions 05 p0722 A72-17041
- Bond zones morphology and composition in Invar based explosive welds, using metallographic and electron microprobe techniques 06 p0820 A72-17707
- Graphite morphology in metallic materials from scanning electron micrographs, discussing sulfur contents effect in tempered cast iron 10 p1500 A72-23825
- Co-Cu alloy phase formation and separation morphology changes with temperature and anomalous diffusive X ray scattering in solid solutions 13 p1976 A72-28905
- Rat adrenal cortex morphology after 24 hour transverse acceleration stress, studying changes in lipid, ascorbic acid and RNA content and acid phosphatase activity 13 p1904 A72-29310
- Martensitic transformation athermal kinetics and accompanied martensite morphology change in Fe-Ni and Fe-Ni-Cr alloys 14 p2115 A72-30407
- Elliptical and barred spiral Markarian galaxies, discussing starlike and diffuse spectra dependence on morphology 15 p2304 A72-31327
- New experimental data on the morpho-physiological analysis of the adaptation phenomenon in the somatic reflex arch 17 p2504 A72-35023
- Morpho-functional changes in the endocrine system during oxygen starvation 21 p2998 A72-40447
- Adrenal morphology changes in rats subjected to hypokinesia 23 p3255 A72-43905
- Mechanism of adaptation to hypoxic hypoxia 23 p3255 A72-43907
- MORPHOTROPISM**
- U ISOMORPHISM
- MORTALITY**
- Incidence rates of myocardial infarction and sudden death from coronary heart disease for adult black and white populations in Nashville 02 p0156 A72-11425
- Intraventricular conduction defects incidence and mortality in acute myocardial infarction, noting left anterior hemiblock dominance 09 p1266 A72-23273
- Analysis of survival and cause of death statistics for mice under single and duration-of-life gamma irradiation. 23 p3254 A72-43394
- MORTARS [MATERIAL]**
- Boron/potassium nitrate parachute mortar design for aircraft and spacecraft applications, comparing with high-low propellant 08 p1221 A72-20783
- MOS [SEMICONDUCTORS]**
- U METAL OXIDE SEMICONDUCTORS
- MOSFET**
- U FIELD EFFECT TRANSISTORS
- MOSS [SPACE STATIONS]**
- U ORBITAL SPACE STATIONS
- MOSSBAUER EFFECT**
- Lunar basalts 10044 and 12021 Fe oxidation state in plagioclase and distribution in crystal structure, using Mossbauer spectroscopy 01 p0124 A72-10064
- Mossbauer spectra measurement of metallic iron, sodium nitroprusside, sodium ferrocyanide and ferrocyanide absorbers at 78-293 K, fitting temperature dependences and resonant velocity to models 01 p0114 A72-10324
- Miniature vacuum furnace for Mossbauer spectroscopic samples heating to 1000 C, discussing temperature control, use of inert atmospheres, etc 04 p0523 A72-15481
- Critique of paper on heat capacity and thermal conductivity of Apollo 11 lunar rocks at liquid helium temperatures, noting constraints imposed by Mossbauer data 07 p1084 A72-20521
- Mossbauer gamma radiation diffraction by Y-Fe garnet crystals with Mossbauer nuclei in magnetic and electric field nodes 08 p1217 A72-21767
- Hyperfine interactions of Fe cations in ilmenite determined by Mossbauer spectroscopy, noting internal magnetic field and quadrupole coupling constant 09 p1367 A72-22457

- Mossbauer lines diffusion broadening and weakening in crystals impurity atoms nuclear spectra
09 p1371 A72-23030
- Defects high temperature diffusion effect on Mossbauer spectral lines width and positions in crystals with quantum transfer between multiplet sublevels in fine structure
09 p1372 A72-23038
- X ray and Mossbauer spectral analyses of thermomagnetically treated nickel ferrite samples containing Co, investigating ordering mechanism
13 p2020 A72-28490
- Mossbauer and X ray structural analysis of nickel ferrite-chromite magnetic moments, comparing with theoretical data
14 p2141 A72-30171
- Hyperfine magnetic field reduction produced in Fe-Cr alloy single crystal by Cr atoms observed by Mossbauer method, proposing spin disturbance mechanism
15 p2293 A72-32230
- Mossbauer spectroscopy theory and application to steel technology, discussing spectral characteristics of various iron phases and corrosion and stress effects
16 p2405 A72-32824
- Study by Mossbauer spectrometry of the iron distribution in mineralogical fractions separated from lunar rocks brought back by Apollo 12
17 p2607 A72-34917
- MOTILITY**
U LOCOMOTION
- MOTION AFTEREFFECTS**
Reaction time to visual orientation change, obtaining aftereffects as function of orientation specific adaptation duration and separation angle between inspection and test lines
08 p1124 A72-20986
- MOTION EQUATIONS**
U EQUATIONS OF MOTION
- MOTION PERCEPTION**
U SPACE PERCEPTION
- MOTION PICTURES**
Motion picture technique for studying vapor bubbles formation, determining temperature fluctuations on heated surface below active region
03 p0457 A72-14153
- Synchronization system for remote control and performance checking of motion picture projectors with running film, discussing recording equipment and stroboscopic pulsed illuminator operations
04 p0521 A72-14711
- FORTAN digital simulation of ATC radar beacon system making possible computer generated movie display
07 p0950 A72-19301
- Turbulent earth atmosphere optical inhomogeneities determination from solar limb image characteristics in motion pictures of solar disk edge
09 p1305 A72-22233
- Radiation transfer equations solved in isotropic light scattering approximation, relating transfer function to motion picture film optical properties
13 p1955 A72-28519
- Discontinuity of seen motion reduces the visual motion aftereffect.
19 p2760 A72-37600
- Role of eye movements in the perception of apparent motion.
23 p3259 A72-43804
- MOTION SICKNESS**
Navigators, pilots and airman trainees response to Coriolis accelerations, investigating nystagmus sensitivity coefficient relationship to motion sickness resistance
01 p0021 A72-11286
- Human vestibular stability under frontal and sagittal head tilts in rotating chairs, discussing motion sickness onset
05 p0622 A72-16640
- Galvanic skin response techniques for palmar and dorsal sweat detection during motion sickness by vestibular stimulation, comparing arousal and thermal sweat response
07 p0933 A72-20185
- Loudness function correlations to illusory spiral aftereffect persistence, motion sickness susceptibility and auditory reaction time in individuals
08 p1128 A72-22138
- Motion sickness experience correlations to vestibular tests in pilots and nonpilots
12 p1764 A72-28257
- Vision influence on acute motion sickness elicitation in slow rotation room, comparing with vestibular factors
12 p1764 A72-28258
- Environmental temperature effect on motion sickness sweating, discussing nausea and discomforting symptomatology prediction
12 p1775 A72-28302
- Experimental motion sickness studies in slow rotation room simulating rotating spacecraft conditions, noting relation between subject susceptibility and number of head motions
16 p2354 A72-33542
- Influence of high temperature on the onset of motion sickness
21 p3004 A72-41749
- Influence of vision on susceptibility to acute motion sickness studied under quantifiable stimulus-response conditions.
24 p3377 A72-45659
- MOTION SICKNESS DRUGS**
Antimotion sickness drugs effectiveness based on acetylcholine or norepinephrine induced changes of balance between vestibular and reticular neurons
10 p1427 A72-23726
- MOTION STABILITY**
NT AERODYNAMIC STABILITY
NT AIRCRAFT STABILITY
NT ATTITUDE STABILITY
NT BOUNDARY LAYER STABILITY
NT DIRECTIONAL STABILITY
NT FLAME STABILITY
NT FLOW STABILITY
NT GYROSCOPIC STABILITY
NT HOVERING STABILITY
NT LATERAL STABILITY
NT LONGITUDINAL STABILITY
NT MAGNETOHYDRODYNAMIC STABILITY
NT ROTARY STABILITY
NT SPACECRAFT STABILITY
- Stability of and motion about L4 in restricted three body problem with 3 to 1 commensurability between long and short periods of motion
01 p0122 A72-10010
- Stability relative to part of variables of n-dimensional vector equation, considering applications to solid bodies with fluid filled cavities and gyrostat satellite optimal stabilization
02 p0251 A72-11494
- Unperturbed motion asymptotic stability and instability theorems, considering Liapunov function method
02 p0260 A72-12432
- Motion stability of sphere and homogeneous semi-infinite rotating cylinder in circular orbits and monoenergetic streams, integrating by trajectories
02 p0285 A72-12832
- Finite time motion stability of systems with small parameter, using method of averaging and matching principle
03 p0390 A72-13910
- Linear nongyroscopic conservative system stability from modified Lagrange equations of motion, using pseudo degree of freedom concepts and vibration method
03 p0362 A72-14394
- Instability effect on aperiodic motion of nonlinear thermomechanical oscillator from periodic solutions
04 p0547 A72-14458
- Plane physical pendulum motion stability under randomly oscillating suspension point with allowance for viscous friction
04 p0549 A72-15055
- Steady state angular motion stability of passive magnetically stabilized satellites, using Liapunov method
05 p0726 A72-16464
- Flexible antennas effect on three dimensional motion stability of gravity gradient satellite, using coupled rigid-elastic analysis
05 p0727 A72-16470
- Nonlinear motion stability of finite amplitude wave solution in thin viscous incompressible liquid film
06 p0801 A72-18142
- Mechanical systems with nonlinear position functions, elastic elements or self damping, investigating oscillation mode onset and stability conditions
06 p0850 A72-18701
- Nonlinear resonance oscillations of flexible rod and elastic cylindrical shell under potential and nonpotential forces, investigating motion instability
06 p0900 A72-18704
- Sensitivity functions for differential equations describing aircraft perturbed motion, noting dependence on time derivatives, system parameters and coordinates
07 p1032 A72-18977
- Parachute design for very high altitude sounding rockets, discussing stability and descent velocity requirements and test methods
07 p1085 A72-19604
- Reduction principle validity in perturbed motion stability theory for near-critical systems with gyro horizon application
07 p1035 A72-19972
- Perturbed motion differential equations for stability and integration problems in mechanics
08 p1205 A72-20964
- Saturn ring motion stability factors for atomized material resistance to gravitational field, discussing ring thickness, density and other parameters
08 p1231 A72-21128
- Distant stellar satellites existence possibility based on maximum distance estimation for material particle motion stability with respect to sun or another star
08 p1231 A72-21133
- Bounded circular-space three body problem, obtaining Lagrangian solutions for triangular motion configuration stability
08 p1232 A72-21134
- Liquid fuel elastic rocket motion stability in supersonic flight, using vibration and thrust vector control equations for dynamic properties description
08 p1241 A72-21633
- Liapunov stability of circular equatorial motions of light bodies in Kerr gravitational field of massive rotating body, using geodesic lines equations
08 p210 A72-22071
- Asymptotic motion stability for part of periodic and continuous systems variables, deriving solution uniqueness sufficient conditions
09 p1350 A72-22206
- Motion stability of linear discrete deterministic and random systems over finite time interval
09 p1291 A72-23428
- Upper bounds on lumped and continuous dynamic systems motion under loads and perturbations, discussing structure stability conditions
[ASME PAPER 71-APMW-3] 10 p1554 A72-24188
- Stability of superluminal and subluminal waves propagating transversely to external uniform magnetic field in streaming relativistic plasmas
10 p1522 A72-24608
- Oscillation modes and stability region of harmonic oscillators with homogeneous nonlinear rheological differential equations of motion
10 p1513 A72-24998
- Body center of mass position for stable fall in viscous fluid, determining terminal velocity as function of body geometry
10 p1470 A72-25067
- Periodic motions stability of nonlinear control systems with energy consumption, using contact transformations
10 p1458 A72-25074
- Spacecraft motion stabilization about mass center and optimal angular velocity control using minimax technique
11 p1684 A72-26903
- Inverted pendulum subjected to small amplitude sinusoidal periodic and stochastic base motion, determining stability boundaries by averaging method
12 p1844 A72-27247
- Simultaneous nonhomogeneous internal and external friction effects on nonconservative force systems motion stability, considering cantilever beam compression
12 p1845 A72-27321
- Runaway stars trajectories stability tested from clusters study, noting preservation of energy, velocity and position and reproducibility
12 p1873 A72-27900
- Orbital and rotational motion stability of solid body containing elastic rods and fluid-filled cavity
13 p2002 A72-28715
- Control parameters required for stabilization of motion in systems with nonholonomic couplings by dynamic programming method of summary representations
13 p2003 A72-29068
- Nonlinear oscillations amplitude, frequency and instability regions of moving belt as function of longitudinal velocity
13 p1964 A72-29150
- Liapunov functions and integral inequalities for study of finite time stability of motion, noting small parameter system subjected to continuous disturbances
13 p2004 A72-29496
- Dynamic system motion stability estimation with Liapunov function in quadratic form, applying to circular satellite orbit stability in axisymmetric gravitational field
14 p2161 A72-31079
- Axisymmetric flight vehicles motion stability and transient behavior via Liapunov method, taking into account nonlinear characteristics
15 p2318 A72-31203
- Liapunov function application to stability of unperturbed motion of differential equations with respect to part of variables
16 p2422 A72-32940
- Pasquill method adequacy for atmospheric stability conditions discrimination and prediction of horizontal and vertical turbulence intensities
16 p2419 A72-33943
- Study of the stability of certain relative equilibria of a symmetrical satellite
17 p2620 A72-34282
- Russian book - Introduction to the theory of stability of motion
18 p2711 A72-36523
- Motion stability of inertial navigation gyroscopic system with gyro horizon compass, noting constant and time dependent coefficients of motion equations
19 p2830 A72-37320
- Reduction principle validity in perturbed motion stability theory for near-critical systems with gyro horizon application
20 p2955 A72-40029
- Numerical stabilization of the differential equations of Keplerian motion.
21 p3106 A72-41050
- Non-linear rotor bearing behavior.
21 p3061 A72-41518

Instability of the equilibrium position of a multidimensional system consisting of 'neutrally' unstable subsystems

21 p3126 A72-41546

Long term stability of earth and lunar orbiters - Theory and analysis.

[AIAA PAPER 72-936]

21 p3112 A72-41574

Asymptotic motion stability analysis with respect to part of variables, using Liapunov functions for solution boundedness conditions

22 p3204 A72-41901

Orbital and rotational motion stability of rigid body containing elastic rods and fluid-filled cavity

22 p3204 A72-42092

Frequency stability criterion for variable-structure automatic control systems

22 p3162 A72-42185

Helicopter rotor blade flapping motion stability, applying perturbation technique to linear equations of motion for different advance ratios and Lock numbers [AIAA PAPER 72-955]

22 p3137 A72-42351

Atmospheric frontal motion stability via two-layer homogeneous incompressible fluid model, solving eigenvalue problem by small perturbation method

22 p3201 A72-42505

Stability of motion at collinear libration centers in the restricted problem of three bodies with allowance for light pressure

24 p3437 A72-44762

Iterative solution for adiabatic radial pulsation in massive main sequence star, noting transition to non-linearity via Eddington stability integral extension

24 p3438 A72-44833

MOTIVATION

Management enhancement of researchers motivation in times of economic uncertainty, stressing security related aspects of employment

06 p0905 A72-17396

Motivation in vigilance, studying effects of subject self evaluation and experimenter knowledge of results/ controlled feedback

06 p0766 A72-17711

Terminal area ATC specialists and trainees job attitude and motivation from questionnaire on challenge, tasks, salary, work schedule, etc

06 p0766 A72-17865

Incentive contracts with price differential acceptance test plans to motivate producer to product improvement, defining admissible strategies in terms of risk limitation

13 p2066 A72-28354

Conditioned slow negative potential of human brain cortex dependence on motivation, emphasizing punishment avoidance conditions

16 p2353 A72-33097

Self-paced ergometer performance - Effects of pedal resistance, motivational contingency and inspired oxygen concentration.

18 p2653 A72-36911

Employee motivation programs as a means of cost reduction in aerospace industries.

24 p3468 A72-45221

MOTOR SYSTEMS (BIOLOGY)

U EFFERENT NERVOUS SYSTEMS

MOTORS

NT ELECTRIC MOTORS

NT SERVOMOTORS

NT SYNCHRONOUS MOTORS

NT TORQUE MOTORS

Variable rigidity effects of ball bearings on axial loading stability and failure of gyromotor supports

15 p2235 A72-31898

MOUNTAIN INHABITANTS

Respiration control during hyperoxia, discussing chemoreceptor significance in minute volume respiration rate reduction mechanism from Pamir mountain aborigines oxygen breathing reaction studies

08 p1120 A72-22076

Native highlander and lowlander chemoreflex ventilatory response to transient carbon dioxide inhalation at low and high altitudes

12 p1762 A72-27728

High altitude natives cerebral arterial-venous oxygen difference measurement during ambient air and oxygen breathing, showing chronic hypoxia effect on cerebral blood flow

14 p2079 A72-30704

Mountain inhabitants cardiocirculatory adaptation to chronic hypoxia, studying coronary flow and myocardial oxygen consumption and efficiency

15 p2187 A72-32498

Ventilatory peripheral chemoreflex response to hypoxia during physical exercise in native highlanders and altitude-acclimated lowlanders

17 p2499 A72-34345

Pulmonary gas exchange in Andean natives at high altitude.

18 p2650 A72-36570

Vascular headache of acute mountain sickness.

22 p3150 A72-42491

Adaptive processes responsible for natural acclimatization of human organism to low ambient pressures at high altitudes

22 p3143 A72-42584

Anatomy of the coronary circulation at high altitude.

22 p3144 A72-42594

Resistance and capacitance vessels of the skin in permanent and temporary residents at high altitude.

22 p3144 A72-42595

MOUNTAINS

NT HIMALAYAS

Mountain stations wind measurement usefulness for small aircraft traffic guidance

04 p0544 A72-15625

Mountains located on meteor propagation path of radio waves, investigating effect on transmission region size

08 p1239 A72-21891

Weather analysis for mountainous terrain from potential temperature surface maps and vertical cross sections

09 p1344 A72-22431

Numerical shallow fluid model for air flow across orographic variable grid barrier, using idealized Andes Mountains range

12 p1838 A72-27023

Winds aloft forecast use to predict southwestern mountain lee wave behavior for general aviation cross country flights

13 p1993 A72-28863

Atmospheric boundary layer and diffusion over three dimensional mountainous terrain by laboratory simulation with meteorological wind tunnel and scale model

[AIAA PAPER 72-648]

16 p2419 A72-34085

Medical and technical aspects of rescue and survival of astronauts in high mountain and mountainous remote areas.

17 p2507 A72-34434

Structure of Sierra Madera, Texas, as a guide to central peaks of lunar craters.

21 p3049 A72-41114

Ka-26 helicopter operational flight testing in high mountain environment, discussing takeoff, landing and climb performance as function of altitude dependent engine characteristics

23 p3251 A72-43638

Certain characteristics of the muon and electron components of extensive air showers at mountain level

23 p3331 A72-44425

MOUNTING

NT RIGID MOUNTING

Solar array for San Marco C satellite to study neutral atmosphere structure, discussing interior mounting design features

12 p1758 A72-28038

Laser ranging instrument for satellite distance measurement, discussing four-axial mounting, guiding telescope, receiving optics and performance

15 p2247 A72-31935

Reduction of the effect of mount deformation on the flexure of the telescope mirror

19 p2801 A72-37967

High power pulsed ruby laser and sapphire rods optical contacting technique

21 p3063 A72-40622

MOUNTS

U SUPPORTS

MOUTH

Influence of ionizing radiation on the tooth organ

22 p3141 A72-41987

MOVING TARGET INDICATORS

MTI radar system design philosophy for target detection in land clutter environment

02 p0178 A72-12390

Radar measurement accuracy in log-normal clutter of fluctuating targets in random noise or intentional interference

02 p0178 A72-12401

Pulse and Doppler microwave radars comparison with respect to accuracy of moving targets velocity measurements and power characteristics

05 p0661 A72-16034

Electronic scanning steerable phased array radar beam pointing capability improvement for moving target detection probability

06 p0772 A72-17423

Criterion for estimating radar capability to resolve two targets with differential motion, noting application to synthetic aperture radars and Doppler filters

08 p1134 A72-21424

Digital MTI detection filter using on-line adaptive procedure for adjustment

10 p1456 A72-23804

Detection probability for moving small targets embedded in random white noise on TV display, comparing machine processed pattern recognition techniques and human performances

12 p1843 A72-27933

Recursive digital MTI radar filter design in z plane, detailing spectrum rolloff and flat passband in amplitude response

16 p2369 A72-33758

Design of nonrecursive digital moving-target-indicator radar filters.

18 p2667 A72-36687

Weighting factor and transmission time optimization in video MTI radar.

21 p3022 A72-41088

Effect of envelope limiting in pulse-compression moving-target-indicator radar systems.

24 p3380 A72-45577

MRKOS COMET

Observation and feature variations of comet 1969e before and during the perihelion passage.

24 p3445 A72-45463

MSRE REACTORS

U MOLTEN SALT NUCLEAR REACTORS

MTBF

Redundancy configuration effect on electronic system reliability, discussing MTBF and cost analysis

02 p0194 A72-12444

Aircraft flight control system MTBF field operational and MIL-STD-781 testing, establishing data baseline for reliability predictions

05 p0638 A72-16662

Confidence level determination in terms of reliability index (MTBF) for MIL-STD-781 truncated sequential probability ratio tests

10 p1444 A72-23985

Training cockpit TL-29 mean time of failure-free operation from measurement data during development tests and two year guarantee, calculating avionics devices reliability

14 p2092 A72-30288

Microwave power junction transistor design factors effects on long and short term reliability and MTBF

18 p2666 A72-36552

Reliability prediction of a two-unit standby redundant system with standby failure.

20 p2929 A72-39855

Evaluation of the mean time to tracking failure in a nonlinear pulsed servo with irregular signal input

21 p3038 A72-40708

Prior distributions fitted to observed reliability data.

22 p3182 A72-41980

Determining optimum burn-in and replacement times using Bayesian decision theory.

22 p3182 A72-41982

MTI RADAR

U MOVING TARGET INDICATORS

MUFFLERS

Sound field measurement in circular and rectangular air duct with sound-absorbing walls (mufflers), deriving empirical formula for attenuation frequency characteristics

09 p1354 A72-23683

MULLITES

Reusable external thermal insulation mullite for space shuttle vehicle, presenting conductivity, expansion coefficient, specific heat, stability, tensile strength and strain capability

01 p0091 A72-10762

Mullite as part of aluminum oxide-silicon dioxide system, discussing formation, structure, physical chemistry, additives effects and high alumina refractories

10 p1501 A72-24729

The manufacture of mullite reusable surface insulation materials for space shuttle.

[SME PAPER EM 72-714]

18 p2695 A72-36527

MULTICHANNEL COMMUNICATION

Molniya-Orbit communication satellite system, discussing operational quality, maintenance, television transmission facsimile, sound broadcast and multichannel telephony

01 p0023 A72-10046

Wideband data transmission on group-band communication channels, using dual single-sideband modulation with basic transmission rate of 48 kbit/sec

01 p0024 A72-10113

Orthogonal convolutional coding with on-off signaling and Viterbi decoding for synchronous multiple access communication with bound bit error rate

01 p0026 A72-10343

FM radio link superposed parabolic antenna systems adjustment for space diversity reception for scatter propagation and broadband multichannel transmission in 1.9 GHz range

01 p0027 A72-10410

S band transistor power amplifier design and performance, noting application for 960 telephone channel relay system

01 p0038 A72-10657

Low noise phase locked power microwave sources for solid state radio links with 960 voice channels, discussing design

01 p0006 A72-10712

Multichannel communication system reliability, considering channel repair time random distribution

01 p0033 A72-11263

Time division multiple access systems for communication satellites, discussing performance and application in Intelsat network

01 p0033 A72-11301

Time division multiple access system with 100/50 M bit/s channel capacity for Symphonie and Intelsat satellite speech channels

01 p0033 A72-11302

Time division multiple access systems for satellite transmission, discussing burst transmission control problem associated with transmitting end synchronization

01 p0033 A72-11303

Time division multiple access systems transmitting and receiving end synchronization control criteria derivation, discussing code pattern selection for reliable detection

01 p0033 A72-11304

Switching operations in TDMA system, noting availability of signaling channels with broadcast mode

01 p0033 A72-11305

Spectral characteristics of ionospheric signal by phase lags introduced in multichannel field recorder

02 p0172 A72-11926

Multichannel space station communications using PCM-PSK-PM interplex modulation for reducing cross modulation loss

02 p0174 A72-12131

Intermodulation noise in multichannel frequency division multiplex telemetry systems due to nonlinearities in transmitter-receiver links and tape recorder

02 p0175 A72-12145

Multichannel high-speed high-density digital recorder, describing tape transport and signal system

02 p0187 A72-12151

Communication satellites multiple access, using time division multiplex method

02 p0181 A72-12607

Multiple access techniques in satellite telecommunication systems, discussing clean mesh type network

02 p0182 A72-12699

Graphical and tubular methods for frequency assignment to avoid intermodulation interference in channelized bands

03 p0325 A72-14046

Communication satellites performance improvement by time division multiple access techniques and use of frequencies above 10 GHz for localized coverage through highly directive beams

04 p0494 A72-15676

Time division multiple access (TDMA) satellite communication system optimal design, discussing earth stations, satellites and transmission path characteristics

05 p0626 A72-16298

Exercise ECG multichannel radio telemetry equipment, discussing sources of malfunction and unreliability and remedial procedures

05 p0621 A72-16610

Signal coding for discrete information in multichannel systems using multiple differential phase shift keying

06 p0773 A72-17500

Multichannel communication system in adaptive system based on random parameter extremum criterion, deriving average usage time of extremal channel

07 p0938 A72-19008

FM mf equipment for 2700-channel Hertzian beam, considering thermal noise, intermodulation and equivalent distortion of amplifiers, discriminator, limiter, etc

07 p0954 A72-19190

Digital decision directed suboptimal receiver design for random multipath channel communication with intersymbol interference, predicting performance for steady state probability of correct decision

07 p0941 A72-19272

TDMA satellite communication system with convolutional encoding and Viterbi decoding, evaluating data buffering and control configurations

07 p0941 A72-19297

Error probability estimates in two channel diversity reception systems with allowance for fading correlation and incomplete signal separation

09 p1278 A72-22572

Multiple access to communication satellites in time division multiplex, discussing burst phase control and ground station receiving-transmitting systems

09 p1278 A72-22852

Multichannel integral commutators with MOSFET as switching elements, calculating transmission errors

10 p1449 A72-24288

Frequency measurements of square wave signal with unknown amplitude by two mismatched channels, comparing rms error with effective estimate variance

10 p1436 A72-24509

Multichannel monopulse Nd glass laser design characteristics, describing input generator, preamplifier and amplifier channel beam distribution

11 p1651 A72-26363

Clock synchronization of multichannel radio communications systems using orthogonal signals with overlapping transmission spectra

11 p1598 A72-26727

Noise immunity and code sequence rejection probability in real multifrequency communications systems with multipositional frequency shift keying

11 p1598 A72-26729

Intelsat 4 satellite communication transponder design for broadband multicarrier operation, using frequency and pulse modulation techniques

[AIAA PAPER 72-535] 12 p1780 A72-27358

Intelsat V satellite system with large telephone channels capacity and full earth station network connectivity, discussing system concepts and technology

[AIAA PAPER 72-536] 12 p1780 A72-27359

TDMA system for Intelsat 4 and subsequent satellites, discussing automatic synchronization acquisition, terrestrial network-satellite transmission channel modular interface, etc

[AIAA PAPER 72-538] 12 p1780 A72-27361

Intelsat satellite time division multiple access system (TDMA) using semiconductor technology with burst synchronization

[AIAA PAPER 72-546] 12 p1781 A72-27369

Aircraft and water vehicles mobile communications via stationary satellite, discussing optimum multiple access and repeater configuration

[AIAA PAPER 72-565] 12 p1781 A72-27376

AM/PM conversion and transfer in nonlinear signal transmission systems, calculating coefficients as function of multicarrier powers for intelligible crosstalk

12 p1782 A72-27554

Bandpass filter harmonic signal phase shift distortion effect on transient response in PSK of multichannel transmission

12 p1783 A72-27630

Intelsat 3 global multichannel wideband multiple access communication system, describing technological advancements in communication performance, attitude control and testing procedures

[AIAA PAPER 72-534] 13 p1918 A72-28982

Self adaptive two channel iteration servosystems for input reconstruction by successive approximations, determining signal and noise error operators

13 p1936 A72-29155

Spectral characteristics of ionospheric signal by phase lags introduced in multichannel field recorder

13 p1920 A72-29238

Inexpensive microwave high density channel filters to meet amplitude and phase requirements without external equalization

15 p2210 A72-31181

Multimode fiber optics data transmission through high electrical noise environments for send-receive communication links

15 p2198 A72-32059

Time division demultiplexing technique using two channel simulation of twenty-four channel digital optical PCM communication system

15 p2200 A72-32163

Incoherent receiver noise stability in multichannel system with channel frequency separation, deriving formula for receiver error probability

15 p2209 A72-32668

Multichannel monopulse Nd glass laser design characteristics, describing input generator, preamplifier and amplifier channel beam distribution

16 p2403 A72-33715

Random multiple access data transmission systems with feedback for message confirmation and retransmission in event of errors, evaluating channel capacity

16 p2372 A72-33794

Intelsat satellite SPADE demand-assignment multiple access system design for increased communication flexibility and efficiency

17 p2512 A72-34269

Correlation functions and reconstruction error for quantized Gaussian signals transmitted over discrete memoryless channels

17 p2516 A72-35333

Intelsat 4 multichannel communication network earth station equipment components and characteristics experimental system (SPADE) study to realize demand assignment

18 p2659 A72-36272

YIG filter banks for ECM and communications

19 p2772 A72-37523

Limitations of technological state-of-the-art with satellite and space communications above 10 GHz

19 p2765 A72-37940

Predictive filtering of multi-channel time series records with application to Doppler radar data

19 p2781 A72-38272

Satellite communications in Japan

19 p2766 A72-38603

Simulation of the process of reducing the redundancy of multichannel telemetry information on a digital computer by the method of adaptive break down into discrete elements and associative sorting

21 p3014 A72-40313

Computer simulation of a digital satellite communications system utilizing TDMA and coherent quadrature signalling

21 p3020 A72-40895

Bandwidth economy for multiplexed digital signals

21 p3020 A72-40897

Suppressed clock pulse duration modulation for noisy voice communication channels with hard limiting satellite repeaters, discussing system design and test data

21 p3020 A72-40898

Commercial satellite communication system development, considering external constraints, orbital geometry, frequency allocations, multiple access transmission techniques, and satellite and earth station designs

21 p3021 A72-40921

Mathematical model for lattice-type error distribution of parallel channels communication system, noting metric for algebraic signal coding method

22 p3154 A72-42234

Parameter estimation of reflected signal in multichannel communication system with discrete readings, considering receiver with optimal signal processing under low noise level

22 p3154 A72-42239

Asymptotic methods of calculating the effectiveness of one variant procedure of selecting operational subchannels in an adaptive multichannel communications system

23 p3266 A72-44207

Optimal signal processing in systems with multiple reception elements /channels/

23 p3266 A72-44219

Error probability estimates in two channel diversity reception systems of digital data transmission with allowance for fading correlation and incomplete signal separation

24 p3379 A72-44751

MULTICHANNEL RECEIVERS

U MULTICHANNEL COMMUNICATION
U RECEIVERS

MULTICHANNEL TRANSMITTERS
U MULTICHANNEL COMMUNICATION
U TRANSMITTERS

MULTILAYER INSULATION

Space shuttle cryogenic tanks self evacuating multilayer insulation, evaluating thermal and dynamic performance

01 p0139 A72-10778

Multilayer insulation materials for reusable space vehicles thermal protection and radiation shielding, tabulating thermal conductivity values for various materials

01 p0092 A72-10780

Two-layer dielectric loaded cylindrical antenna with wall airgap, calculating radiation pattern by boundary value approach

06 p0775 A72-18240

Space and ground environments effect on cryogenic multilayer insulation materials, tabulating mechanical and thermophysical test data

[AIAA PAPER 72-286] 11 p1741 A72-25225

Multilayer insulation apparent thermal conductivity measurement at low compressive loads, describing test calorimeter and experimental technique

[AIAA PAPER 72-367] 11 p1670 A72-25392

Damping additions for plates using constrained thin viscoelastic sheets and metallic layers

11 p1688 A72-26063

Heat losses due to spacecraft installation discontinuities on aluminized Mylar multilayer insulation, predicting blanket performance

[AIAA PAPER 72-285] 14 p2171 A72-30829

Analytical prediction of pressure-time relationship during evacuation of multilayer insulation thermal protection systems, taking into account outgassing effects

14 p2172 A72-30925

Statistical solution to unsteady heat conduction through flat multilayer insulating wall, using random walk method

16 p2477 A72-33407

Fine line multilayer system packaging using hybrid thick film processing and materials

22 p3161 A72-43174

MULTILAYER STRUCTURES

U LAMINATES

MULTILOOP SYSTEMS

U CASCADE CONTROL

MULTIMODE RESONATORS

Multimode cavity for simultaneous oxygen/argon plasma excitation and electron density measurements, noting gas pressure effect

08 p1213 A72-21323

Three resonant mode waveguide circulator adjustment with eigenvalues associated to resonant field patterns

15 p2208 A72-32388

Resonator dielectric waveguide structure in electron beam pumped semiconductor laser, noting reduction of diffraction losses and of laser action threshold

17 p2562 A72-34660

Frequency detection with digital resonators without damping

19 p2773 A72-37939

Magnitude of the attenuation troughs of a two-branch filter with multiple-frequency quartz resonators

23 p3272 A72-44170

MULTIPATH TRANSMISSION

Wideband FSK receiver for space telemetry, calculating error probability in multipath signal fading due to planetary surface reflections

01 p0025 A72-10329

- Electromagnetic wave line-of-sight propagation based on geometrical optics for different refractivity profiles above sea, noting earth surface reflection role
01 p0026 A72-10404
- Rain, snow and hail precipitation effects on radio link signal attenuation, scattering and fading along various transmission paths at millimeter and centimeter wavelengths
01 p0027 A72-10407
- Centimeter waves fading due to interference from tropospheric multipath propagation
01 p0027 A72-10412
- Low angle monopulse radar tracking errors due to multipath, considering amplitude variation across antenna aperture and reduction by target-image resolution
02 p0178 A72-12391
- Intermodulation noise distortion due to multipath transmission over FM/FDM microwave links, deriving distortion probability distribution for Nakagami-Rice randomly distributed signal reception
04 p0493 A72-15517
- AM/PM distortion intermodulation in FM/FDM radio systems during two-path propagation, using Fourier series method for noise power spectra calculation
06 p0775 A72-18239
- Digital decision directed suboptimal receiver design for random multipath channel communication with intersymbol interference, predicting performance for steady state probability of correct decision
07 p0941 A72-19272
- Multipath angle error reduction using multiple radar target signal processor with angle tracking of wave fronts
08 p1134 A72-21408
- Adaptive multibeam experiment for aeronautical and maritime services [AMEAMS], discussing NASA ATS-G satellite application to small mobile terminal communications system
12 p1842 A72-27383
- Microwave radio link transmission loss Rayleigh-like long term distribution explained by two-path propagation model
12 p1784 A72-27796
- Line-of-sight radio link attenuation by atmospheric precipitation and phase interference fading during multipath propagation in 7-15 GHz range
12 p1785 A72-27802
- Adaptive reception of weak repetitive signals on background of intense fluctuating noise, synthesizing adaptive detection system for multipath propagation and small SNR
15 p2195 A72-31658
- A mode-averaging diversity combiner
17 p2513 A72-34360
- Error rate of phase-shift keying in the presence of discrete multipath interference
17 p2516 A72-35334
- On an anomaly in long-range short-wave propagation from the equatorial region to central Europe
18 p2657 A72-36232
- Digital simulation for radio frequency interference and specular multipath effects on FM spread spectrum demodulation with feedback and phase lock loops
18 p2659 A72-36317
- MULTIPHASE FLOW**
NT TWO PHASE FLOW
- Thermodynamic equilibrium variational theory for multiphase systems subject to nonhydrostatic stress, considering diffusion and phase transformations
03 p0455 A72-12908
- Multiphase Stefan problems for bounded and unbounded temperature fields with variable phase volume
06 p0904 A72-18401
- Three phase bidirectional pulsating flow hydraulic control system, discussing design, performance and applications
08 p1114 A72-22162
- Single- and multiphase theories of slowly varying nonlinear dispersive waves, noting stability solutions to large scale variations and shocks
09 p1351 A72-22942
- Small scale flow and surface effects in multiphase media hydromechanics, obtaining entropy production in mixture for interphase transformations characterization
10 p1468 A72-24430
- Steady state lumped linear formulation of heat transfer in multichannel parallel-and-mixed-flow heat exchangers
14 p2173 A72-31065
- Multiphase Stefan problems for bounded and unbounded temperature fields with variable phase volume
17 p2636 A72-34852
- MULTIPLE DEGREES OF FREEDOM**
U DEGREES OF FREEDOM
- MULTIPLE OUTPUT PROGRAMS**
Executive job handling program for operation with fault tolerant multiprocessor in real time control environment
10 p1442 A72-23816

- MULTIPLETS**
U FINE STRUCTURE
- MULTIPLEX TRANSMISSION**
U MULTIPLEXING
- MULTIPLEXERS**
U MULTIPLEXING
- MULTIPLEXING**
NT FREQUENCY DIVISION MULTIPLEXING
NT TIME DIVISION MULTIPLEXING
- Analog FM multiplex signal intermodulation formula based on time-variable electromagnetic waves tropospheric scatter propagation
01 p0027 A72-10411
- Format logic design for airborne memory controlled PCM telemetry multiplex digital and analog data system
02 p0187 A72-12130
- Miniaturized micropower biomultiplexer telemetry system utilizing hybrid techniques
02 p0192 A72-12133
- Data transmission and distribution systems interface, using semiconductor technology in multiplexing, asynchronous data transfer, A-D and D-A data conversion and sensor signal conditioning
02 p0194 A72-12404
- Multiplex FM recording system parameters effect on system design, considering SNR, deviation ratio, wow and flutter, tape speed errors, crosstalk and FM filters
02 p0230 A72-12409
- Interrogation frequency effects in random access analog multiplexers operating on flying capacitor at very high sampling frequencies
02 p0195 A72-12692
- Doubly multiplexing dispersive spectrometer, noting high SNR and Littrow mode operation
03 p0359 A72-13446
- High resolution Hadamard transform IR spectrometer with single slit and multiplex scan operation modes determined by signal strength, noise characteristics and scanning time
09 p1313 A72-23327
- Computerized and analytic techniques for estimating multiplexed systems output probability distribution, considering system effectiveness, reliability and survivability
10 p1486 A72-23977
- Optimal detection of rectangular radio signal pulse envelope distortions by multiplex fluctuations over white noise background
10 p1436 A72-24516
- Switching behavior and attenuation of space division multiplex crosspoint circuit with end marking, discussing realization in thick film technology
11 p1604 A72-25908
- Energy spectra of mixed discrete random processes in statistical multiplexing systems with pulse position, delta and pulse code modulation
13 p1919 A72-29054
- Telecommunication satellites microwave components, emphasizing reliability requirements in multiplex systems
13 p1933 A72-29835
- Microwave circuits for multiplexing applications, discussing optimal design in terms of economic, mechanical and electrical parameters
13 p1934 A72-30089
- Time sharing radio communication system analysis with amplitude modulated carrier, noting power reduction, sideband content and multiplexing
15 p2201 A72-32566
- FM/FM multiplex receiver with carrier and subcarrier demodulators, deriving average click rate, output noise spectrum and SNR from Rice model
16 p2362 A72-33212
- Methods using Walsh functions for multiplexing and transmitting signals
19 p2765 A72-37942
- New technique of image multiplexing using random diffuser
21 p3050 A72-40145
- Bandwidth economy for multiplexed digital signals
21 p3020 A72-40897
- Bistable trigger stages composed of digital multiplexer with IC logic modulus replacing NAND or NOR circuits
23 p3267 A72-43990
- MULTIPLICATION**
Binary multiplication algorithms adaptable to IC functional elements for ultrahigh speed operations
11 p1602 A72-26547
- Fixed point computer mean square errors in multiplication as function of number of digital order
16 p2367 A72-33959
- Cellular-array arithmetic unit with multiplication and division
17 p2519 A72-34297
- Some properties of iterative square-rooting methods using high-speed multiplication
19 p2769 A72-37577
- Efficient method to multiply successively functions of the companion matrix and applying the method to evaluate transient response
23 p3309 A72-43862

MULTIPLIER PHOTOTUBES **U PHOTOMULTIPLIER TUBES** **MULTIPLIERS**

- Floating point cellular logic multiplier with variable dynamic range suitable for scientific satellites, missiles, desk calculators and cellular computers
04 p0499 A72-15208
- Multiplier method for discrete optimization problems with equality constraints, applying to time optimal control for V/STOL aircraft
06 p0794 A72-18387
- Wide dynamic range analog multiplier with variable transconductance divider in operational transistor amplifier feedback path
11 p1603 A72-25742
- Quadratic optimal control problem solution via multipliers method, generating minimizing convergent sequence of arcs
12 p1794 A72-27509
- Classical isoperimetric problem approximation via multipliers method, generating minimizing convergent sequence of arcs
12 p1836 A72-27510
- Broadband correlation meter with multiplier using vacuum thermal converters for 1.5 KHz-15 MHz range and variable signal delay
13 p1961 A72-29920
- Nonlinear characteristics of semiconductor diode multiplier circuits for frequency converters
16 p2370 A72-33951
- Strain multiplier with S-N fatigue life gages, discussing design and performance
22 p3179 A72-42708
- Circuit analysis and operation of analog multipliers with MOSFET, applying to industrial automatic control systems and measuring instruments
24 p3384 A72-44896
- Allowable regions for stability multiplier characteristics
24 p3420 A72-45787
- MULTIPOLAR FIELDS**
Plasma interchange instability in quadrupole and octupole magnetic fields determination by disturbance wavelength ratio to ion cyclotron radius
03 p0396 A72-13659
- Fluctuations and diffusion correlation analysis in linear octupole magnetic confinement, determining dispersion relation for interchange instability
03 p0396 A72-13660
- Multipole magnetic field configuration effectiveness in electromagnetic plasma trap, discussing electron losses critical angle and captured ions maximum density
09 p1363 A72-23221
- Electric multipole moments calculation by quasi-static method for homogeneous quasi-neutral oblate plasmoid during resonance
13 p2020 A72-30014
- Geomagnetic field multipoles effects on radiation belt particle motion for analysis of true anomalies
15 p2222 A72-31280
- Nonlinear equations of discrete elastic Cosserat media from multipolar media equations, studying small rotation theory
16 p2425 A72-33591
- Motion of plasmoids in a multipole magnetic field of toroidal configuration
22 p3214 A72-43120
- Polarizational interaction of opposed plasma flows in a linear octupolar magnetic field
22 p3214 A72-43121
- MULTIPOLES**
Multipole methods for electromagnetic scattering from conducting cylinder over dielectric half space, noting application to radar cross sections
01 p0030 A72-10842
- Plasma column interaction with counter rotating hf magnetic fields of multipole configurations, calculating angular velocity
04 p0557 A72-15169
- Multipole network characteristics of optical link assemblies /optons/ using photosensitive element and light source
08 p1139 A72-21057
- Plasma injected into closed multipole magnetic trap, investigating plasma wave locking time and characteristic life
09 p1362 A72-23213
- Multipole synthesis compensating mutual coupling for orthonormalized radiation patterns in ring antenna array
11 p1598 A72-26711
- Correction to nonlinear refractivity calculation for cubic lattice crystal with allowance for higher induced multipoles
12 p1855 A72-27620
- Electric multipole moments calculation by quasi-static method for homogeneous quasi-neutral oblate plasmoid during resonance
13 p2020 A72-30014
- Multipole expansion of sound radiation from moving rigid bodies
18 p2710 A72-36404

Electric multipole moments calculation by quasi-static method for homogeneous quasi-neutral oblate plasma spheroid during electromagnetic interaction under resonance conditions

22 p3212 A72-42729

A rapid assay of dipolar and extrapolar content in the human electrocardiogram.

23 p3259 A72-43811

MULTIPROGRAMMING

Aerospace guidance multiprocessor with memory units attached to time-multiplexed data bus, predicting performance in terms of queueing theory, Markov process and simulation

12 p1786 A72-27433

Operational software for computerized process control, considering operations system, translator, supervision and auxiliary and service programs

21 p3024 A72-41000

Multiprogrammed virtual memory digital computer systems analysis and design, discussing component characteristics, operating system structure and mathematical description techniques

23 p3267 A72-43987

MULTIROPPELLANTS

U ROCKET PROPELLANTS

MULTISPECTRAL BAND SCANNERS

ERTS satellite return beam vidicon TV system and multispectral scanner images, describing photogrammetric and cartographic evaluations

01 p0065 A72-10449

ERTS satellite image processing for multispectral scanning system, discussing distortion from geometrical properties

01 p0066 A72-10458

Aerial multispectral scanners and ground data stations for water quality measurements and pollution abatement

[ALAA PAPER 71-1096] 01 p0067 A72-10545

Multichannel multispectral scanner system for NASA C-130 earth resources aircraft, describing electronic equipment and calibration sources

01 p0048 A72-10946

IR scanner for Indian land areas and oceans thermal mapping, using satellite-borne multispectral photography

02 p0225 A72-11777

Water depth attenuation coefficients and bottom reflectance characteristics from large area multispectral scanner measurements for discharge and concentrations monitoring

02 p0211 A72-11812

Southern corn leaf blight detectability by remote sensing based on pattern recognition technique application to multispectral color and IR photographic and scanner data

02 p0212 A72-11814

Forest vegetation distributional and statistical parameters ecological analysis by multiband remote sensing in areas devoid of ground control

02 p0212 A72-11815

Aerial multispectral scanner data determination with filtering and smoothing along flight line over extended areas, deriving algorithm for cloud-shadowed area detection

02 p0212 A72-11817

Orbiting multispectral scanner with independent land and oceanographic spectrometers for ground controlled dual mode operation

02 p0226 A72-11823

Natural resources multispectral remote sensing for national emergencies, discussing various imaging techniques

02 p0212 A72-11828

Oil slicks aerial photographic and multispectral scanner investigation, discussing detection effectiveness of UV, blue, green and IR imagery

02 p0226 A72-11829

Object proportions estimation algorithms in single resolution element of airborne multispectral scanner

02 p0227 A72-11839

Data compression and random noise effects on pattern recognition and picture quality of multispectral scanner data

02 p0227 A72-11840

Multispectral scanner data preprocessing to improve automated recognition by reducing atmospheric and sensor induced signal variability

02 p0227 A72-11841

Multispectral scanner data training sets size effect on correlation between soil reflectance and organic matter content obtained from ground truth

02 p0227 A72-11845

Pattern recognition of multispectral scanner remote sensor data, using table look-up approach for processing simplicity and time reduction

02 p0227 A72-11846

Airborne high resolution multispectral TV camera system, describing special objective configuration for improved ground resolution

02 p0227 A72-11850

Multichannel multispectral airborne IR imaging system and video data processing for U.S. geological survey

02 p0227 A72-11851

Extended wavelength field spectroradiometry for multispectral scanner data interpretation in airborne observations

02 p0228 A72-11853

Automatic classification over extended remote sensing test sites, examining causes of variation in multispectral scanner data response

02 p0228 A72-11875

Digital computer mapping of terrain by clustering techniques, using color IR film emulsion layers as three band spectrometer

02 p0215 A72-11879

Automatic soil type mapping, using multispectral remote sensing and computerized pattern recognition

02 p0215 A72-11881

ERTS multispectral scanner data telemetry decom-mutator/processor capable of decommutating five spectral bands of digital video data

02 p0175 A72-12162

Earth resources applications of multispectral remote sensing techniques for airborne and satellite-borne imaging systems, discussing microwave radiometer augmentation of visual and IR data

06 p0813 A72-17430

Performance tests of return beam vidicon multispectral television camera system for ERTS program

07 p0986 A72-19657

Multispectral remote sensing techniques, equipment and applications, discussing color and IR camera, line scanning and radar systems and automated interpretation devices

09 p1312 A72-23304

Photointerpretation and computerized radiometric analysis of ERTS multispectral TV and scanner imagery of Israel

15 p2221 A72-31242

Color band selection for Mars lander multispectral imaging system for surface constituent discrimination

15 p2307 A72-31809

Melting snow and ice packs detection by multispectral/visible and near IR/ remote sensing from earth satellites

16 p2387 A72-33999

Suitability of the normal density assumption for processing multispectral scanner data.

22 p3157 A72-43025

Mercury-cadmium telluride photoconductive detectors array for S-192 multispectral scanner for Skylab earth scanning experiments

23 p3288 A72-43879

Mercury-cadmium telluride multispectral photoconductive detectors, discussing fabrication techniques and performance characteristics

23 p3288 A72-43880

Nimbus limb radiometer, Apollo fine sun sensor, and Skylab multispectral scanner.

23 p3288 A72-43882

MULTISPECTRAL PHOTOGRAPHY

NT INFRARED PHOTOGRAPHY

NT RADAR PHOTOGRAPHY

Forestry and agricultural applications of multiband photography, considering photointerpretation of black and white, color and IR photographs

01 p0057 A72-10459

Air pollution circulation patterns remote sensing, describing multispectral stereo image pairs digital cross correlation

[ALAA PAPER 71-1106] 01 p0067 A72-10551

Soyuz 6 multispectral aerogeophysical measurements of Usturt plateau and Caspian and Aral Seas, discussing remote sensing information yield on earth water/land and atmosphere properties

02 p0208 A72-11785

High altitude aircraft and Apollo 9 multispectral photography and simulated ERTS-A imagery evaluation, comparing with ground observations in Arizona

02 p0210 A72-11799

Environmental analysis of Lake Tahoe Basin from small scale multispectral aerial imagery, discussing color enhancement usefulness for interpretation and management of natural resources

02 p0210 A72-11800

Computer enhancement of multispectral satellite-and air-photographs and imagery for earth resources

02 p0186 A72-11801

Oil spills remote detection by multispectral photography, IR scanner imagery and microwave radiometry

02 p0226 A72-11830

Multispectral photographic data preprocessing and computerized simulation of ERTS data channel to make terrain maps, testing classification accuracy improvement possibility

02 p0215 A72-11880

Hybrid system to process multispectral photographic data from aircraft and spacecraft sensors, assessing data quality, cost effectiveness and delay reduction

02 p0228 A72-11883

Chesapeake Bay aquatic ecosystems observations, using satellite remote sensing multispectral photography and imagery

02 p0215 A72-11885

MULTISTAGE ROCKET VEHICLES

RADAM /Radar Amazon/ side-looking radar imagery and multiband aerial photography for mineral, vegetation, soil and water resources mapping in Brazil

02 p0216 A72-11890

Si monolithic multispectral image photosensor array for satellite application, presenting fabrication and spectral response data

04 p0500 A72-15304

Radio quiet quasar PHL 957 absorption line spectra obtained at telescope with Cassegrain image tube and multichannel spectrometer and integrating TV camera

05 p0720 A72-16714

Satellite-borne multispectral photographic line-scan system with direct optoelectrical signal conversion for photogrammetric and cartographic applications

06 p0815 A72-17757

Multispectral TV camera systems for satellite recording of earth surface electromagnetic radiation at separate wavelengths

[DGLR PAPER 71-135] 06 p0817 A72-18232

Image resolutions for ERTS return beam vidicon TV, Skylab multispectral cameras and Gemini/Apollo photographs

06 p0818 A72-18328

ERTS A and B satellite systems for multispectral imaging of earth surface, discussing sensors, operational control and data processing requirements and implementation

07 p1085 A72-19276

Return beam vidicon multispectral camera system for ERTS A and B, describing camera system design and performance characteristics in terms of ERTS mission purpose

07 p0986 A72-19601

Earth science and technical applications of multispectral photography and digital image processing techniques

08 p1166 A72-21334

Multiband color aerial photography interpretation for forest appraisal in U.S.S.R.

09 p1302 A72-23285

Multiband aerial photography application to vegetal cover determination, evaluating film types, seasons and scales

09 p1302 A72-23287

Multiband photointerpretation of forested land units, using aerial black and white photographs and film-filter combinations

09 p1302 A72-23288

Multispectral remote sensing techniques, equipment and applications, discussing color and IR camera, line scanning and radar systems and automated interpretation devices

09 p1312 A72-23304

Crop classification by airborne multispectral observations, suggesting sample regions selection method for spectral signatures identification based on statistical similarities

11 p1628 A72-26985

Photogrammetric camera system imaging characteristics comparison with aerial reconnaissance, multispectral and return beam vidicon systems, noting economic benefits due to smaller scale imagery

12 p1805 A72-27819

Apollo 9, Skylab and Earth Resources Technology Satellite-borne multiband cameras performance requirements and tolerances comparison, considering geometric and spectroradiometric properties

16 p2395 A72-34103

Multispectral angular reflectivity effect on optimum filter combinations for spaceborne multiband photography sensing mission in visible and near IR regions

16 p2395 A72-34104

Multispectral photography in soil moisture determination and soil series differentiation.

18 p2686 A72-36320

ERTS-borne return beam vidicon camera using high resolution TV sensors coaligned to view identical scene in different spectral bands

19 p2795 A72-37576

Multicolor photometry of the NGC 5194/5195 double system

19 p2858 A72-37812

Earth resources technology satellites /ERTS/ program requirements, considering coverage, spectral characteristics, system performance, photographic interpretation and information extraction

24 p3398 A72-45115

High resolution multispectral camera system for ERTS A & B.

24 p3402 A72-45182

MULTISTAGE COMPRESSORS

U TURBOCOMPRESSORS

MULTISTAGE ROCKET VEHICLES

NT ATLAS CENTAUR LAUNCH VEHICLE

NT BLACK KNIGHT ROCKET VEHICLE

NT DIAMANT LAUNCH VEHICLE

NT ELDO LAUNCH VEHICLE

NT SATURN LAUNCH VEHICLES

NT SCOUT LAUNCH VEHICLE

NT SKYLARK ROCKET VEHICLE

NT THOR AGENA LAUNCH VEHICLE

Stages optimum selection for step rocket moving in plane gravitational field

13 p2051 A72-28384

- Two stage solid propellant sounding rocket, discussing engine design, operation and tests
13 p2052 A72-29859
- Reusable two-stage meteorological rocket vehicle, discussing design, performance, second stage recovery technique and cost
17 p2619 A72-34185
- Considerations regarding the choice of the number of stages in long-range or high-altitude rockets
20 p2977 A72-39596
- Ascent acceleration maximization of variable mass particle, calculating optimal parameters of multistage rocket
22 p3204 A72-42066
- Dynamic behavior of M-4S rocket devices for strap-on booster separation and nose cone and flare deployment
22 p3232 A72-43143
- Multistage rocket optimal control, deriving conditions for existence of minimum of performance index function of mass, position and velocity initial and final values
23 p3343 A72-44264
- MULTIVARIATE STATISTICAL ANALYSIS**
NT BIVARIATE ANALYSIS
NT CORRELATION
NT COVARIANCE
NT DISCRETE FUNCTIONS
NT ORTHOGONALITY
NT REGRESSION ANALYSIS
Multivariate algorithms of optimum content and form for cardiovascular risk assessment in pilots and air transport personnel
12 p1764 A72-28264
- Kennedy Space Center area afternoon convective thunderstorm activity and associated weather phenomena prediction via multivariate regression analysis
13 p1989 A72-28803
- Computerized analytical system for side-looking radar imagery interpretation by isodensitracer scanned density data multivariate analysis applied to environmental discrimination
15 p2198 A72-32064
- Extension of analytical design techniques to multivariable feedback control systems.
23 p3274 A72-43539
- Output-feedback control law for randomly distributed multivariable system.
23 p3275 A72-43608
- MULTIVIBRATORS**
NT FLIP-FLOPS
Book on transistors in pulse circuits covering switching diodes and circuits, multivibrators, blocking oscillators, etc
05 p0640 A72-16288
- Base resistance coupled transistorized multivibrator design characterized by superior frequency stability regardless of wide voltage fluctuation
13 p1934 A72-30017
- Multivibrator with p-n-p and n-p-n transistors, noting circuit diagram, operation and power dissipation
20 p2906 A72-38898
- Linearization of relaxation-time control in a transistorized multivibrator
23 p3270 A72-43765
- MUONS**
Cerenkov radiation detection by human eye, discussing relativistic muons passage through vitreous humor and retina
02 p0272 A72-11754
- Absorbed doses at various depths in water target exposed to charged pions, muons and electron beams, using Monte Carlo program
02 p0162 A72-12063
- Atmospheric temperature effect on solar diurnal variation of muon component, considering asymptotic characteristics of cosmic ray anisotropy
05 p0709 A72-16257
- Electron and muon density fluctuations, trajectory distribution and azimuthal symmetry in cosmic ray air showers
06 p0870 A72-17279
- Extensive air shower spectra based on electron and muon number
06 p0871 A72-17283
- Extensive air shower characteristics and muon counts at different level observations relative to particle number and primary energy spectra
06 p0871 A72-17284
- High energy cosmic ray interactions at one TeV, including X process, horizontal showers and muon poor showers
06 p0871 A72-17285
- High energy muon energy and angular distributions from electron-photon cascades, using emulsion chamber with X ray films
06 p0871 A72-17286
- Energy spectrum of muon formed electromagnetic cascades in vertical cosmic radiation flux
06 p0871 A72-17287
- Spectral calculations of electromagnetic and nuclear showers of cosmic ray muons interacting with substance
06 p0871 A72-17288
- Muon densities in penetrating high energy particles, comparing with extensive atmospheric showers
06 p0871 A72-17289
- Muon generated cascade showers in iron, using ionization calorimeter and hodoscope detectors
06 p0871 A72-17290
- Muon track curvatures in Wilson chamber magnetic field for calibrating ionization levels of logarithmic increase
06 p0811 A72-17293
- Cosmic ray muon intensity in interplanetary magnetic field, revealing sidereal variation due to motion of solar system relative to local galactic rotation frame
06 p0873 A72-17648
- Cosmic ray muons integral energy spectrum and angular distribution at sea level represented by power law, using primary interaction model
07 p1063 A72-20475
- Meteorological effects on cosmic rays, deriving muon and pion intensity and meteorological coefficient formulas and computer calculation scheme
07 p1066 A72-20654
- Computerized numerical calculation of muons production spectrum, angular distribution and Coulomb scattering in determining meteorological factors effects on cosmic rays
07 p1067 A72-20655
- Muon telescopes calibration for cosmic rays rigid component variations by data comparison with variable aperture telescope
08 p1162 A72-20720
- Temperature effects elimination from underground muon intensity measurements
08 p1226 A72-20813
- Inelasticity fluctuations effect on cosmic ray showers development, proposing criteria for lateral electron distribution and relative abundance of hadrons and muons
10 p1529 A72-24213
- Muon rich showers interpretation, allowing for combined influence of types I and II fluctuations
10 p1529 A72-24229
- Nucleonic cascade model analysis of underground vertical muon curve for primary cosmic ray nucleon spectrum below 40 TeV
10 p1529 A72-24417
- Sea level absolute vertical cosmic ray muon intensity from range spectrometer measurements within tropic zone
12 p1864 A72-28225
- Scaling hypothesis and limiting fragmentation mechanism for cosmic ray muon production, noting energy independent charge ratio
15 p2298 A72-31289
- Underground delayed shower particles small pulse events interaction analysis for muons and pions compared with quark behavior
16 p2450 A72-34140
- An improved measurement of the charge ratio of cosmic ray muons in the range 10-300 GeV/c
17 p2599 A72-34920
- The absolute vertical cosmic-ray muon intensity at sea level.
17 p2600 A72-35147
- Scintillation telescopes for muon angular distribution, designing test device for photomultiplier tubes section
17 p2556 A72-35437
- Short- and long-range terrestrial telecommunication using energetic collimated beams of muons
17 p2519 A72-35837
- Yields of gamma rays emitted following capture of negative muons by Si28 and Mg24.
19 p2837 A72-38026
- Muon telescopes calibration for cosmic rays hard component variations by data comparison with variable aperture standard telescope
19 p2803 A72-38348
- Zenith angle dependence of the meteorological corrections coefficients for cosmic ray hard component.
19 p2852 A72-38632
- Cosmic ray muon sea level momentum spectra and charge ratios geomagnetic latitude dependence measurements by spark chamber technique
19 p2853 A72-38754
- The muon flux of cosmic rays at sea level.
20 p2964 A72-39349
- Energy spectrum and composition of primary cosmic radiation at energies from 50 to 5000 TeV
23 p3330 A72-44422
- Investigation of EAS characteristics at sea level with the aid of the classical method and by the method of recording radio emission
23 p3330 A72-44423
- Certain characteristics of the muon and electron components of extensive air showers at mountain level
23 p3331 A72-44425
- Muon component near the axis of an extensive air shower
23 p3331 A72-44426
- Energy spectrum and angular distribution of cascades with an energy greater than 0.3 TeV, formed by cosmic muons
23 p3331 A72-44427
- Energy spectra and angular distributions of cosmic ray muons with an energy of 2 to 10 TeV
23 p3331 A72-44428
- Energy dependence of muon-nucleon inelastic interaction, calculating photonuclear cross section for high energy interactions in iron
23 p3331 A72-44429
- A study of the mechanisms of formation of penetrating particle groups by the spark calorimeter method
23 p3291 A72-44430
- Fluctuations of the spatial distribution of the number of particles in showers generated by muons in heavy material
23 p3331 A72-44431
- Angular distribution of high-energy cosmic-ray muons
23 p3331 A72-44434
- Device for studying the photonuclear interaction of superhigh-energy muons
23 p3291 A72-44440
- Primary cosmic ray nucleon spectrum from sea-level muon spectrum and scaling hypothesis parameters.
23 p3332 A72-44458
- Stopping rate of negative cosmic-ray muons near sea level.
23 p3332 A72-44501
- Gamma-neutrino angular correlations in muon capture.
24 p3427 A72-45774
- MUSCLES**
NT MYOCARDIUM
Fast and slow human muscle fibers temporal response characteristics, using tensometric recording
03 p0317 A72-13989
- Spinal reflexes through electric stimulation of gastrocnemius and soleus human leg muscles, attributing increased tendon reflex amplitudes to gamma motoneurons hyperactivation
04 p0467 A72-14704
- Exercise and denervation effects on intrafusal muscle fibers morphology, noting 25-33 percent cross-sectional area atrophy in nuclear bag and chain fibers
04 p0472 A72-14895
- Daily prolonged exercises effects on human muscle glycogen utilization, noting reduced lactate accumulation and increased free fatty acid levels
04 p0480 A72-15213
- Regulation of sweat secretion on skin surfaces overlying active and nonactive muscle tissue during skin or core temperature alterations
04 p0480 A72-15216
- Muscle blood flow relation to oxygen consumption from measurements during bicycle ergometer exercises, using Xe 133 clearance method
08 p1123 A72-20888
- Endurance exercise effect on respiratory capacity in white, red and intermediate muscles in rats, relating fiber type to oxidative capacity
08 p1115 A72-21083
- Stepwise adaptation to high mountain conditions effect on brain and sural muscle oxidation processes in rats
08 p1121 A72-22085
- Alternative heating local heat clearance probes for human muscle blood flow measurement
09 p1273 A72-23442
- Continuous and intermittent maximal exercise effects on human muscle intracellular and capillary blood pH
10 p1425 A72-24477
- Forearm skin and muscle blood flow change measurements during whole body heating, using plethysmography, isotopic labeling and blood sampling techniques
11 p1587 A72-26617
- Liver and muscle type isozymes of DPN-linked glycerol-3-P dehydrogenase in chickens in terms of tissue distribution, ontogeny and avian evolution
12 p1759 A72-27161
- Rat vena porta muscle cells spontaneous activity intensified by direct current depolarization and inhibited by hyperpolarization, noting effects of calcium and sodium ions
13 p1902 A72-28638
- Cold adaptation effects on rat skeletal muscle tissue Vant-Hoff coefficient, considering phosphorylation and oxidation rate, P/O and mitochondrial ATP-ase activity
13 p1902 A72-28639
- Potassium, sodium and calcium ion distribution in skeletal muscle subcellular organoids, discussing lipid, protein and nucleic acid binding
14 p2076 A72-30670
- Muscle cell ATP, creatine phosphate and lactate concentration changes relation to oxygen uptake during and after exercise
14 p2080 A72-30705
- Long term weightlessness-induced physiological response normalization by muscle bioelectrostimulation, muscular tissue energy load increase and mineral metabolism stabilization
16 p2354 A72-33543

Biological systems activity in controlling extremal problems of nervous and muscular systems, noting external stimulation minimization
19 p2761 A72-38577

The state of water in muscle tissue as determined by proton nuclear magnetic resonance.
24 p3371 A72-44774

MUSCULAR FATIGUE
Human oxygen intake and blood lactic acid removal kinetics during recovery from mild steady work on bicycle ergometer
10 p1426 A72-24989

Dynamic bioelectric impedance level of tissue area between active electromyograph electrodes related to human skeletal muscle fatigue
13 p1905 A72-29332

MUSCULAR FUNCTION
NT SPASMS
Frog Rana temporaria striated muscle tension response recording during sudden fiber length alteration, suggesting force generation mechanism
01 p0009 A72-10017

Discharge patterns in motor nerve fibers during human voluntary muscle contractions
01 p0013 A72-10624

Optimum muscle work conditions experiments with rabbits, correlating total work performance and power output with muscle temperature variations
02 p0160 A72-12013

Training effect on oxygen consumption in negative muscular work, considering connective tissue strengthening and muscle viscosity changes
03 p0315 A72-13676

Human muscular electrical activity in various body positions, noting potentials during natural and unaccustomed postures
03 p0317 A72-13990

Electromyographic determination of muscular compliance during arm movements, using on-line analog computer
04 p0478 A72-14708

Prolonged muscular work effects on erythrocyte 2,3-DPG generation relation to oxyhemoglobin affinity
04 p0472 A72-14898

Stochastic signal method for measuring dynamic viscoelastic properties of isometric frog sartorius muscle at rest and contraction, using white noise vibrations
04 p0480 A72-15221

Hemodynamic and blood oxygen parameter changes comparison in dogs during hypoxia at rest and muscle activity in various oxygen concentrations
04 p0474 A72-15232

Heat production increase by muscular contractions due to noradrenaline in cold adapted rats
05 p0620 A72-17215

Coleoptera flight muscle system anatomy, presenting instantaneous lift forces measurement systems
06 p0755 A72-17563

Heart pacemaker activity during muscular exertion, developing mathematical model based on system dynamics transient processes analysis
06 p0764 A72-18059

Electromyogram study of antagonist muscles reactions to Achilles tendon percussion or whole body sudden motion via test stand jerking
07 p0915 A72-18864

Cardiac acceleration by voluntary muscle contractions of minimal duration in men due to vagal tone inhibition
07 p0929 A72-19442

Myoepithelial mechanism of high frequencies pulsatile discharge of human sweat glands
07 p0930 A72-19444

Vagal control of ventilation and respiratory muscles during elevated pressures in cats
07 p0917 A72-19446

Book on physiological approach to ergonomics covering muscular system, performance, work and fatigue, working efficiency and environment, man machine systems, etc
07 p0930 A72-19875

Acceleration tolerance increase by static forearm muscular contraction exercise comparison to g-suit protection during human centrifuge tests
[AD-739063] 08 p1114 A72-20887

Cat and rabbit middle ear muscles contraction by electric stimulation of motor nerves, noting sound transmission reduction
08 p1115 A72-21136

Cat middle ear muscles motor units twitch tension and contraction time in response to motor neuron threshold stimulation
08 p1116 A72-21137

Motor unit potential histogram study of human motoneuron activity patterns during voluntary muscular contractions
08 p1116 A72-21472

Myocardium excitation-contraction mechanism in heart regulation, discussing surface membrane structure and cell action potential
09 p1264 A72-22222

Force-velocity relations in cat papillary muscles isotonic relaxation, discussing effects of preloads and afterloads, temperature and stimulation frequency
09 p1265 A72-22864

Functional organization of monkey cortical efferent zones in distal forelimb muscle control from intracortical microstimulation studies, showing stimulation thresholds distribution
09 p1267 A72-23582

Peripheral afferent input to monkey cortical efferent zones of distal forelimb muscle control, using single microelectrode for intracranial stimulation and cellular discharge recording
09 p1267 A72-23583

Artificial heart-lungs model with contractile polymer membrane as synthetic muscles to react with gases and liquids, discussing design features
10 p1431 A72-24640

Human body biochemical energy conversion processes during muscular activity, discussing nutrition, circulation and respiration roles
11 p1585 A72-26075

Speed and mechanical work measurements during knee bending and immediate or delayed leg extension exercise, showing muscle elastic potential energy utilization
11 p1587 A72-26615

Electromyogram and myogram responses in phasic stretch reflex under prestrain conditions as index of fusimotor activity level in normal humans
11 p1588 A72-26632

Human motoneuron discharge time relations during isometric muscle contraction, measuring adjacent action potential and mean interspike intervals
12 p1761 A72-27653

Irreversibility mechanism in postpartum ductus arteriosus closure in guinea pigs, studying vessel cellular changes and smooth muscle response to oxygen pressure
12 p1762 A72-27826

Inspiration, expiration and hand muscle control comparison in psychophysical category production method for human voluntary breathing regulation investigation
12 p1763 A72-27843

Energy metabolism and ATP balance characteristics during muscular activity as function of organism adaptation to activity
13 p1902 A72-28640

Supraspinal effects on different work regimes of supplementary respiratory muscles, using interference electromyograms cross correlation analysis
13 p1905 A72-29328

Contractile responses of guinea pig, rat and human isolated ventricular myocardium to increased stimulation frequency
13 p1907 A72-30044

Temperature and extracellular Ca level effects on mammalian ventricular myocardium force-frequency relationships, determining contractile tension, velocity and phase duration
13 p1907 A72-30045

Delayed growth of rats carcasses and skeletal muscles during prolonged hypokinesia, comparing effects on flexor muscles to ankle joint extensors
14 p2074 A72-30378

Prolonged bed rest induced muscular activity restriction effect on arterial and venous tone in different body areas
14 p2074 A72-30385

Human leg muscle reflex excitability changes during angular acceleration, suggesting vestibular apparatus as coordination means in quasi-static and dynamic movement control
14 p2075 A72-30388

Surface electrode position effect on electromyogram recording of electrical activity during repeated biceps and triceps brachii contractions
15 p2190 A72-32489

Surface electrode distance, area and pressure effects on electromyogram recording of large skeletal muscle electrical activity during defined muscular tensions
15 p2190 A72-32490

Hill model for myocardium activity, taking into account contractile state variations and characteristic force-velocity curve
15 p2187 A72-32492

Human heart physiopathology from cardiac performance analysis, treating heart as pump and muscle
15 p2187 A72-32493

Apexocardiograms and carotid pulse measurements as indicators of cardiac function and myocardial contractility
15 p2190 A72-32494

Hypokinesia and motor activity of humans in industrial societies, noting prolonged inactivity and posture maintaining effects
16 p2353 A72-33098

Increase in skeletal muscle performance during emotional stress in man.
17 p2500 A72-34942

Effects of hypoxia and ischemia on myocardial contraction - Alterations in the time course of force and ischemia-dependent inhomogeneity of contractility.
17 p2502 A72-34996

Interrelation of interoceptors and exteroceptors in the process of urination and defecation reflex act maturation in ontogeny
17 p2504 A72-35022

Servo action in human voluntary movement.
18 p2654 A72-36999

Computerized statistical simulation of automatism of spontaneously active smooth muscle strip, neglecting individual cell spontaneous activity
19 p2757 A72-37949

Vertical posture control mechanisms in man
19 p2757 A72-37992

Automatically controlled delay in self-excited pulsating systems based on artificial muscles
19 p2761 A72-38464

Influence of rhythmical photostimulation on lower-order monkeys with hyperkinesia of post-encephalitic origin
20 p2890 A72-38930

Significance of the nature of an increase in physical strain as it affects the adaptation of an organism to intense muscular activity
20 p2891 A72-38933

The silent period in man during muscle lengthening produced by loading
20 p2892 A72-39590

Book - Energy metabolism of human muscle.
20 p2893 A72-39700

Muscle metabolism of ATP, CP, glycogen and lactates at rest and during submaximal and maximal exercise
21 p3005 A72-40421

Muscle metabolism during isometric exercise performed at constant force.
21 p3005 A72-40425

Synchronization in the work of motor neurons during arbitrary motor activity of various types
21 p2999 A72-40595

Cortical metabolism regulation and effector systems of the adaptation process
21 p3000 A72-40760

A model for analysing the coordination of manual movements.
21 p3010 A72-41413

The foot as input device for control operation.
21 p3012 A72-41428

Physical and chemical identification methods for biochemical reactions and energy balance of muscular contraction and shaking
21 p3003 A72-41469

Chemical energy transformation to mechanical energy and heat in muscles during exercise, considering energy sources for contraction, oxidations, glycolysis and alactic anaerobic mechanism
21 p3003 A72-41470

Effects of physical exercise on spinal reflectivity in man
21 p3003 A72-41524

Dependence of muscle efficiency on oxygen concentration in the venous blood
22 p3141 A72-42157

Blood flow, oxygen uptake, and capillary filtration in resting skeletal muscle.
22 p3150 A72-42668

Analysis of femoral venous blood during maximum muscular exercise.
22 p3145 A72-42742

Sensorimotor mechanism of proprioceptors in muscles and tendons, considering reflexive control of position and motion
22 p3146 A72-42781

Functional insufficiency of the neuromuscular system caused by weightlessness and hypokinesia.
23 p3253 A72-43387

Metabolic changes in healthy humans caused by prolonged bed rest in horizontal position, noting prevention by physical exercises and electric muscle stimulation
23 p3260 A72-43921

Influence of the nervous system and its mediators on the spontaneous contractile activity of a smooth muscle
24 p3370 A72-44590

Changes in certain hemodynamic indices during muscular strain in people with differing capacity to perform work
24 p3370 A72-44591

The reflex and mechanical response of the inspiratory muscles to an increased airflow resistance.
24 p3372 A72-44958

General index for the assessment of cardiac function.
24 p3372 A72-45011

MUSCULAR STRENGTH
Contractile and muscle-like fibers and autopulsation systems for polymer engine and spring action studies
19 p2760 A72-38200

MUSCULAR TONUS
Human and monkey muscle tonic vibration reflex response to vibratory stimulation dependent on

- frequency range, electromyograph discharge interval length, etc 02 p0163 A72-12250
- Techniques and procedure for differential ballistoscillography of extremities. 20 p2897 A72-39325
- Breathing rate response to oral instructions in relationship to nervous system, bronchial muscle tonus and gas metabolism rate reflex-type changes 21 p3001 A72-40761
- Functional insufficiency of the neuromuscular system caused by weightlessness and hypokinesia. 23 p3253 A72-43387

MUSCULOSKELETAL SYSTEM

- NT BONES
- NT CEREBRUM
- NT CHIN
- NT COLLAGENS
- NT CONNECTIVE TISSUE
- NT CONSTRUCTORS
- NT CRANIUM
- NT FEMUR
- NT INTRACRANIAL CAVITY
- NT JOINTS [ANATOMY]
- NT PELVIS
- NT SCIATIC REGION
- NT STERNUM
- NT TIBIA
- NT ULNA
- NT VERTEBRAL COLUMN
- Long term bed rest effect on humans and primates, detailing cardiovascular metabolic and musculoskeletal physiological systems [AD-737557] 01 p0014 A72-10932
- Free oxygen content and diffusion coefficient in adrenalectomized rat skeletal muscles after physical strain 03 p0317 A72-13991
- Confinement, physical deconditioning and hypercapnia effects on human musculoskeletal protein by chromatographic method for quantifying urinary peptides and free amino acids 06 p0767 A72-17869
- Book on physiological approach to ergonomics covering muscular system, performance, work and fatigue, working efficiency and environment, man machine systems, etc 07 p0930 A72-19875
- Corticosterone content in blood plasma, cerebral cortex and skeletal muscles during hypoxia adaptation in rats 08 p1121 A72-22083
- Pure biocarbons for skeletal fixation of limb prosthetic devices, noting load bearing applications dependence on brittle characteristics 12 p1773 A72-28095
- Electrical components of cardiac and skeletal muscle impedance, calculating rectangular stimulating current mean value 13 p1908 A72-28461
- Prevention of weightlessness effects on blood hydrostatic pressure, musculoskeletal system and sensorimotor performance, discussing space flight training and space environment simulation tests 13 p1909 A72-28787
- Dynamic bioelectric impedance level of tissue area between active electromyograph electrodes related to human skeletal muscle fatigue 13 p1905 A72-29332
- Increase in skeletal muscle performance during emotional stress in man. 17 p2500 A72-34942
- Techniques and procedure for differential ballistoscillography of extremities. 20 p2897 A72-39325
- Effect of hypoxia on the condition of skeleton muscles in rats under hypokinesia 21 p2998 A72-40433
- Blood flow, oxygen uptake, and capillary filtration in resting skeletal muscle. 22 p3150 A72-42668
- MUTATIONS
- Molecular evolutionary changes in amino acids of proteins due to mutant random fixation, comparing human and fish hemoglobin chains 02 p0158 A72-11761
- Evolutionary rate of cistrons in vertebrates, discussing hemoglobin and cytochrome c changes involving amino acid mutant substitution 02 p0158 A72-11762
- Amino acid code comparisons of polypeptide chains of globins due to mutations during vertebrate evolution from ancestral gene 02 p0159 A72-11764
- Space flight effects on chlorella cell survival and mutability in Zond automatic stations 05 p0623 A72-16775
- Dose response curves for pink somatic mutations in *Tradescantia* after neutron and X ray irradiation 15 p2186 A72-31723
- Blue green algae *Anacystis nidulans* UV light-sensitive mutants photorecovery capacity following irradiation 16 p2356 A72-33673

- Space flight effects on chlorella cell survival and mutability in Zond automatic stations 17 p2504 A72-35278
- Soyuz 5 satellite vehicle space flight factors effect on chlorella cells, investigating survival rates and mutability 17 p2505 A72-35279
- Empirical support for a stochastic model of evolution. 23 p3254 A72-43565
- Amino acid substitution correlation with genetic code in human, bovine, ovine, porcine and salmon calcitonins, suggesting mutation occurrence time during evolution 23 p3254 A72-43568

MYELIN

- Myelinated nerve fiber mathematical model for action potential transmission mechanism analysis during relative refractory phases 14 p2079 A72-30597

MYLAR [TRADEMARK]

- Heat losses due to spacecraft installation discontinuities on aluminized Mylar multilayer insulation, predicting blanket performance [AIAA PAPER 72-285] 14 p2171 A72-30829

MYOCARDIUM

- Incidence rates of myocardial infarction and sudden death from coronary heart disease for adult black and white populations in Nashville 02 p0156 A72-11425
- Canine and human ventricular myocardium microelectrophysiological studies of postextrasystolic T wave change relation to cellular repolarization and contractile potentiation magnitude 02 p0157 A72-11474
- High altitude hypoxia effects on rat myocardium lactic dehydrogenase isozyme complement and anoxic tolerance 02 p0165 A72-12834
- Xenon 133 myocardial clearance method accuracy and reliability in determining high and low left coronary artery blood flow under different hemodynamic conditions 03 p0319 A72-13181
- Myocardial blood flow measurement by Xe 133 clearance method after direct application of isotope into subendocardial and subepicardial layers of left ventricle 03 p0315 A72-13182
- Familial cardiomyopathy detection by electrocardiography noting arrhythmias, ventricular hypertrophy, abnormal Q waves and intraventricular conduction defects 04 p0466 A72-14443
- Regional myocardial contraction mechanics during transient ischemia and reoxygenation in anesthetized dogs 04 p0476 A72-15719
- Helium-cold hypothermia induction and maintenance effect on hamster myocardia, with ventricle analysis of hypoxic damage, glycogen and catecholamines 04 p0476 A72-15720
- Hemodynamic response to hypoxia in dogs with experimental myocardial infarction, discussing changes in cardiac output, stroke volume, left ventricular pressure and systemic vascular resistance 05 p0617 A72-16152
- Myorelaxant 3,5-dimethyl-4-bromopyrazol injection effect on rabbit and dog heart during direct extracardiac nerve stimulation 05 p0618 A72-16358
- Myokinase activity determination as diagnostic test for human myocardial infarction, comparing to creatine phosphokinase activity test 05 p0618 A72-16388
- Asymmetrical hypertrophic cardiomyopathy symptoms simulating mitral stenosis, suggesting electrocardiography, chest X ray and hemodynamic studies as diagnostic procedures 06 p0761 A72-17380
- Sudden death in myocardial infarction, discussing heart electrical stability, neural control, arrhythmias and cardiac conduction disturbances 06 p0761 A72-17381
- Coronary artery disease and vessel involvement severity predictions from electrocardiographic and vectorcardiographic patterns of anterior wall myocardial infarction 07 p0931 A72-19994
- ECG evidence of myocardial ischemia in patients without arteriographic evidence of coronary artery disease, studying myocardial oxygen supply 07 p0920 A72-19995
- ECG and VCG in diagnosis of myocardial infarction and QRS changes 07 p0920 A72-20174
- Glucose and fatty acid metabolic response during impending myocardial infarction in animals 07 p0921 A72-20175
- Stretch activation of myogenic oscillation of isolated contractile structures of heart muscle in ATP salt solution 07 p0923 A72-20427

- Myocardium catecholamine level reduction by heart hyperfunction from aortic coarctation during moderate thyroidin doses 07 p0924 A72-20622
- Hyperbaric chamber tests for hemodynamic response to oxygen inhalation at 1 and 2 atm pressure for myocardial infarction treatment assessment 08 p1114 A72-20891
- Myocardial infarction effects on drug tolerance and hemodynamic changes due to digitalis doses, discussing toxic arrhythmias 08 p1115 A72-21082
- Beta-adrenergic inhibitors effects on coronary blood flow and myocardial oxygen consumption of normal and coronary artery disease patients 08 p1118 A72-21549
- Ventricular myocardium contractile function disorder diagnosis by phase coordinate method with intracardial hemodynamics application 08 p1122 A72-22186
- Myocardium excitation-contraction mechanism in heart regulation, discussing surface membrane structure and cell action potential 09 p1264 A72-22222
- Intraventricular conduction defects incidence and mortality in acute myocardial infarction, noting left anterior hemiblock dominance 09 p1266 A72-23273
- Assessment of regional myocardial temperature changes effect on blood flow measurements by heated cross-thermocouples in dogs 10 p1432 A72-25071
- Serum petidase activity determination as enzymatic diagnostic test for myocardial infarction 11 p1579 A72-25851
- Myocardium biopulse-controlled cardiosynchronizer as key component of biocontrol systems for cardiological studies 11 p1585 A72-26455
- Chronic hypoxia adapted rat myocardial tissue sensitivity to increased carbon dioxide tension 11 p1579 A72-26616
- Hemodynamic variables relation to coronary blood flow and myocardial oxygen consumption during upright bicycle exercise 11 p1587 A72-26618
- Gabor-Nelson myocardium electrical activity model for mathematical construction of vectorcardiograph from ECG for comparison of various lead systems 11 p1588 A72-26629
- Myocardial infarction stress effect on serum cortisol, plasma free fatty acid and urinary catecholamine levels 11 p1582 A72-26787
- High altitude hypoxia preadaptation effects on left ventricle myocardium noradrenaline concentration in rats with experimental vitium cordis 12 p1761 A72-27648
- Hemodynamic effects of angiographic contrast medium in patients with and without heart disease, discussing myocardial performance during first ten beats 12 p1762 A72-27732
- Electrical components of cardiac and skeletal muscle impedance, calculating rectangular stimulating current mean value 13 p1908 A72-28461
- Heart enzyme activity under experimental myocardial ischemia in rabbits determined for blood, left and right ventricles and atrium 13 p1901 A72-28463
- Physiological evaluation of diastole mechanism in rat hypertrophied myocardium as function of heart rate, Ca ion concentrations and temperature 13 p1901 A72-28521
- Contractile responses of guinea pig, rat and human isolated ventricular myocardium to increased stimulation frequency 13 p1907 A72-30044
- Temperature and extracellular Ca level effects on mammalian ventricular myocardium force-frequency relationships, determining contractile tension, velocity and phase duration 13 p1907 A72-30045
- Platelet aggregates role in intramyocardial vessel circulation impedance in patients dying suddenly of coronary artery disease 15 p2186 A72-31770
- Hill model for myocardium activity, taking into account contractile state variations and characteristic force-velocity curve 15 p2187 A72-32492
- Human heart physiopathology from cardiac performance analysis, treating heart as pump and muscle 15 p2187 A72-32493
- Apexocardiograms and carotid pulse measurements as indicators of cardiac function and myocardial contractility 15 p2190 A72-32494
- Mountain inhabitants cardiocirculatory adaptation to chronic hypoxia, studying coronary flow and myocardial oxygen consumption and efficiency 15 p2187 A72-32498

Baboon heart endocardial structure dynamic behavior, comparing left ventricle septum and epicardium contractile force and intramyocardial pressure changes

15 p2187 A72-32748

Serial ECG change detection and description in myocardial infarction survivors, using computer analysis to find best diagnostic discriminants from multiple criteria

16 p2357 A72-34008

Myocardial lipid and carbohydrate metabolism in fasting men during prolonged exercise.

17 p2499 A72-34347

Thyroidal influence on myocardial changes induced by simulated high altitude.

17 p2500 A72-34730

Normal and hypoxic myocardium mitochondrial metabolism process, studying electron transport system

17 p2501 A72-34978

Myocardial protein synthesis in acute myocardial hypoxia and ischemia.

17 p2501 A72-34980

Acute myocardial anoxia - Anatomical changes and their possible relation to immunological processes.

17 p2501 A72-34981

Acute hypoxia of the myocardium - Ultrastructural changes.

17 p2501 A72-34982

Extracellular acid-base changes in the dog myocardium during hypoxia and local ischemia, measured by means of glass micro-electrodes.

17 p2501 A72-34983

Changes of intracellular myocardial electrolytes in experimental hypertension.

17 p2501 A72-34984

The intramyocardial oxygen pressure at normoxia and hypoxia.

17 p2501 A72-34986

Myocardial ultrastructure in acute and chronic hypoxia.

17 p2502 A72-34988

Myocardial metabolic changes in chronic hypoxia.

17 p2502 A72-34989

Anoxic tolerance of the heart muscle in different types of chronic hypoxia.

17 p2502 A72-34991

Ion alterations during myocardial ischemia.

17 p2502 A72-34994

Morphological alterations in the ischaemic heart.

17 p2502 A72-34995

Effects of hypoxia and ischemia on myocardial contraction - Alterations in the time course of force and ischemia-dependent inhomogeneity of contractility.

17 p2502 A72-34996

Induction of ventricular arrhythmias by elevation of arterial free fatty acids in experimental myocardial infarction.

17 p2502 A72-34997

Effect of nicotinic acid on myocardial metabolism in man at rest and during exercise.

17 p2506 A72-35968

Analysis of left ventricular wall motion by reflected ultrasound - Application to assessment of myocardial function.

19 p2755 A72-37497

Coronary collateral circulation and myocardial blood flow reserve.

19 p2755 A72-37500

Prognostic value of an electrocardiographic sign in acute myocardial infarction.

19 p2756 A72-37871

Systematic detection of myocardial infarction in the course of medical screening of flight personnel

19 p2757 A72-37881

Influence of inotropic alteration on the severity of myocardial ischemia after experimental coronary occlusion.

19 p2758 A72-38552

Determination of the elastic modulus of the left-ventricle myocardium with the aid of X-ray kymography

20 p2893 A72-38940

An indirect method for evaluation of left ventricular function in acute myocardial infarction.

20 p2892 A72-39462

Cardiac hypertrophy, capillary and muscle fiber density, muscle fiber diameter, capillary radius and diffusion distance in the myocardium of growing rats adapted to a simulated altitude of 3500 m.

21 p3003 A72-41624

Myocardium automatism, excitability, conductivity and contractility under cooling, noting complete inhibition at 9-3 deg C

22 p3141 A72-42072

Succinic and lactic dehydrogenases activities in homogenates from myocardial tissues of guinea pigs, rabbits and dogs in high altitude environments

22 p3144 A72-42592

Coronary blood flow and myocardial metabolism in man at high altitude.

22 p3144 A72-42593

Factors limiting the increase in stroke volume obtainable by positive inotropism - Investigations regard-

ing the sufficient heart in the case of continued postextrasystolic potentiation

22 p3145 A72-42748

Cardiocirculatory adaptation to chronic hypoxia. II - Comparative study of myocardial metabolism of glucose, lactate, pyruvate and free fatty acids between sea level and high altitude residents.

22 p3148 A72-43022

Effects of coronary arteriography on myocardial blood flow.

23 p3256 A72-43933

Collagen in human myocardium as a function of age.

23 p3256 A72-43935

General index for the assessment of cardiac function.

24 p3372 A72-45011

Clinical and anatomic implications of intraventricular conduction blocks in acute myocardial infarction.

24 p3374 A72-45691

MYOELECTRIC POTENTIALS

Motor unit potential histogram study of human motoneuron activity patterns during voluntary muscular contractions

08 p1116 A72-21472

Myocardium excitation-contraction mechanism in heart regulation, discussing surface membrane structure and cell action potential

09 p1264 A72-22222

Human motoneuron discharge time relations during isometric muscle contraction, measuring adjacent action potential and mean interspike intervals

12 p1761 A72-27653

MYOELECTRICITY

NT MYOELECTRIC POTENTIALS
Myocardium biopulse-controlled cardiosynchronizer as key component of biocontrol systems for cardiological studies

11 p1585 A72-26455

Gabor-Nelson myocardium electrical activity model for mathematical construction of vectorcardiograph from ECG for comparison of various lead systems

11 p1588 A72-26629

Electrical components of cardiac and skeletal muscle impedance, calculating rectangular stimulating current mean value

13 p1908 A72-28461

Surface electrode position effect on electromyogram recording of electrical activity during repeated biceps and triceps brachii contractions

15 p2190 A72-32489

Surface electrode distance, area and pressure effects on electromyogram recording of large skeletal muscle electrical activity during defined muscular tensions

15 p2190 A72-32490

MYOGLOBIN

Hemoglobin-facilitated diffusion of oxygen - Interfacial and thickness effects.

18 p2650 A72-36569

MYSTERE 20 AIRCRAFT

The Dassault Mystere 20.

19 p2748 A72-37900

N

N-N JUNCTIONS

Schottky barrier and n-n heterojunction diodes hf noise, considering ideality factor effect

07 p0955 A72-19358

S-type negative resistance segment formation on rectilinear branch of I-V characteristics of p-n-n structure

14 p2089 A72-30969

N-P JUNCTIONS

U P-N JUNCTIONS

N-P-N JUNCTIONS

Avalanche injected current relationship to emitter-base junction breakdown damage in planar n-p-n gated transistors

03 p0336 A72-14279

High temperature GaAs bipolar transistor n-p-n junction fabrication by vapor phase growth technique, considering I-V characteristics dependence on procedure

06 p0783 A72-17607

Complementary monolithic IC n-p-n and p-n-p transistor circuit structure with high sheet and low saturation resistance

11 p1606 A72-26567

Monoplastic solid encapsulant for n-p-n and p-n-p silicon planar passivated signal transistors

17 p2528 A72-34715

Multivibrator with p-n-p and n-p-n transistors, noting circuit diagram, operation and power dissipation

20 p2906 A72-38898

Boron p-type region impurity concentration calculation technique to establish anomalous base profile in n-p-n bipolar transistors

20 p2908 A72-39567

Emitter-dip model of diffusion anomalies of n-p-n Si HF transistors doped with B and P

21 p3035 A72-41489

N-TYPE SEMICONDUCTORS

Transferred electron microwave oscillator diodes with n-n structure by liquid phase epitaxy, reducing high resistance layer in interfaces and crystal defects

01 p0036 A72-10629

Transverse photoconductivity and dark I-V characteristics of n-GaAs compensated with Cr in high electric field at room temperature

03 p0401 A72-13586

Annealing defects in n-type silicon, observing anomalous heat treatment temperatures of A and E centers

04 p0560 A72-14529

Nonparabolic n-InSb semiconductors, presenting microwave conductivity dc field induced anisotropy

04 p0560 A72-14543

Transit time and LSA oscillations at millimeter and submillimeter wavelengths in n-type GaAs

04 p0563 A72-15593

N- and p-type semiconductors energy band structure bending near interface

05 p0702 A72-16197

Hopping electroconductivity of n-type GaS single crystals, observing frequency dependence

06 p0866 A72-18181

Microwave biased millimeter and submillimeter wave detector with n-type InSb, using down conversion process and free carrier absorption for detection

06 p0866 A72-18384

Carrier wave growth during propagation through negative differential mobility n-type GaAs under nonuniform dc bias conditions

07 p1047 A72-19044

Energy spectrum of radiation defects in proton bombarded n-type Si crystals from Hall effect and electroconductivity measurements

07 p1049 A72-19901

Millimeter and submillimeter band frequency conversion in nonlinear bulk n-InSb semiconductor at liquid helium temperature

08 p1140 A72-21060

Quantizing magnetic field effect on electromagnetic wave propagation in multivalley n-type Si and Ge and PbTe semiconductors

08 p1218 A72-21878

Electron and hole recombination at deep impurity centers during nonequilibrium current carriers excitation by Nd-glass laser light in p- and n-type germanium

09 p1322 A72-22214

Au-Si and Al-Si p diodes noise operating in avalanche with charges injected by radiation

09 p1287 A72-23113

Piezoresistance magnitude and temperature dependence changes of electron irradiated n-type silicon due to oxygen vacancy complex /A center/

09 p1372 A72-23239

Internal Q switching and long time delay emission in electron beam excited p-type and n-type GaAs lasers, indicating optical absorption traps

10 p1489 A72-23947

Electric field profile in n-type GaAs layer biased above transferred electron threshold for small signal amplifier operation

10 p1450 A72-24554

High conversion efficiency microwave second harmonic generator using negative resistance nonlinearity of n-type GaAs

11 p1591 A72-25741

Recombination parameters in low resistivity gamma irradiated n-type Ge, obtaining energy levels and temperature dependence of electron and hole capture probabilities

12 p1857 A72-28056

Li defect interactions in electron irradiated n-type single crystal Si from electron paramagnetic resonance measurements

12 p1858 A72-28063

Introduction rate and annealing of defects produced in Li-diffused float zone n-type Si by 30 MeV electrons and fission neutrons

12 p1858 A72-28064

Electron irradiation of n-type Si or Te doped GaAs, determining carrier removal rate, mobility changes and annealing characteristics

12 p1858 A72-28067

Annealing behavior of electrical properties and photoluminescence spectra in electron irradiated n-type GaAs semiconductors

12 p1859 A72-28068

Carrier concentration Hall mobility and photoconductivity in n- and p-type CdTe after neutron and electron bombardment

12 p1859 A72-28072

Quasi-linear approximation of input impedance of epitaxial n-type Si unijunction transistors for predominant drift conditions

13 p1927 A72-28406

Laser light induced high-low impedance switch in Cd doped n-type Si diodes with p-p-n junctions and negative resistance

13 p1928 A72-28676

Negative photoconductivity effect in high resistance n-type indium phosphide single crystals, noting

photocurrent spectral distribution and I-V characteristics 13 p2022 A72-29647

Zr oxidation kinetics at 440-850 C for 3 min maximum exposure time, observing time oxide change relationship to activation energy 14 p2113 A72-30247

Quasi-discrete acceptor states in zero gap n-type semiconductors, showing noncompensation at low temperatures 14 p2142 A72-30360

Millimeter wave third harmonic generation and frequency multiplication in n-type InSb at 77 K 14 p2142 A72-30799

Carrier wave behavior in n-type GaAs slab under crossed dc electric and magnetic fields, investigating traveling space charge amplifier magnetic control 14 p2143 A72-30941

High resistance n-type InP crystals electrical conductivity and photoconductivity characteristics at 80 K, discussing photosensitivity spectral distribution and temperature dependence 15 p2290 A72-31371

Electrical conductivity, reluctance and Hall effect of n-type semiconductors determined at extremely low temperatures 15 p2291 A72-31389

Transverse magnetic field effects on n-type GaAs Gunn diodes microwave power, coherence and dynamic I-V characteristics [ONERA, TP NO. 1051] 15 p2207 A72-31884

Tunable monochromatic IR laser based on magneto-Raman scattering from conduction electrons in n-type InSb, discussing physical processes and experimental techniques 15 p2250 A72-32393

Photoconductivity in depleted surface layer of quasi-monopolar semiconductors with arbitrary diffusion to Debye lengths ratio, noting n-type low resistance gallium arsenide 15 p2296 A72-32694

N-type GaAs absorption spectra construction from transmission spectra, considering effects of irradiation by fast protons, electrons, neutrons and alpha particles 16 p2441 A72-33368

Plasma magnetoresistance in variable magnetic field measured on n-type InSb sample for SHF inertialess power sensor development 16 p2436 A72-33482

Electrical characteristics of bulk n-InP oscillators. 18 p2666 A72-36456

Electric contact between metal and n-type semiconductor, investigating contact pressure effects on electron tunneling and phonon conduction to provide band structure 18 p2718 A72-36488

New efficient method for calculating hot electron effects applied to n-Ge. 19 p2844 A72-37686

Quantum efficiency and radiative lifetime of the band-to-band recombination in heavily doped n-type GaAs. 19 p2844 A72-37947

Differential negative resistance (DNR) in n-channel MOSFETs of silicon. 20 p2961 A72-39711

Technology and performance of n-channel MOSLSs using depletion-type load elements. 20 p2961 A72-39712

Small-signal admittance of the insulator-n type-gallium-arsenide interface region. 20 p2909 A72-39775

Fast-neutron-compensated n-germanium as a model of amorphous semiconductors. 20 p2961 A72-39853

Solid state physics experiment for conduction electrons effective mass determination in ultrapure n-type InSb by means of magnetophonon effect 21 p3096 A72-40203

Determination of conduction anisotropies in semiconductors. 21 p3097 A72-40697

Experimental investigation of a millimeter-wavelength n-InSb frequency converter at 4.2 K 21 p3016 A72-40786

Experimental investigation of the propagation of electromagnetic waves in a rectangular waveguide partially filled with n-InSb in the presence of a transverse magnetic field 21 p3016 A72-40796

Magneto-microwave free-carrier absorption in germanium in the Faraday configuration. 21 p3097 A72-41379

Plasma echo-type oscillations in n-type InSb semiconductor, noting conduction band nonparabolicity effects 21 p3098 A72-41687

Theory of microwave amplification with electron transfer 23 p3269 A72-43550

NACELLES

Propulsion system optimization in transonic transport aircraft design, considering nacelle integration,

engine choice, noise attenuation and technology utilization [SAE PAPER 710762] 01 p0115 A72-10259

Engine fan-compressor maximum noise reduction for given aircraft configuration by acoustic linings on nacelle inlet and exhaust walls 07 p1054 A72-19268

Subsonic powered nacelle wind tunnel model for investigation of geometric variables effect on pressure drag [ASME PAPER 72-GT-14] 11 p1568 A72-25613

Balloon-nacelle for small scale photography and multispectral photometric ground measurements, describing automatic adjustment device for photographic lens diaphragm 16 p2349 A72-33633

Performance of low pressure ratio ejectors for engine nacelle cooling. 18 p2721 A72-36530

Balloon nacelle for terrain photography from very high altitudes 24 p3403 A72-45229

NAMING

NT NORMS

NAPHTHALENE

Turbine blade local heat transfer coefficient calculation with digital computer program and naphthalene blade mass transfer in cascade flow 05 p0747 A72-16498

Radical concentrations in gamma irradiated poly(ethylene 2,6-naphthalene dicarboxylate) by ESR spectrum analysis 10 p1433 A72-23847

Electron spin resonance of gamma-irradiated poly(ethylene 2,6-naphthalene dicarboxylate). 20 p2898 A72-39400

Studies on the convective heat transfer from a rotating disk. VI - Experiment on the laminar mass transfer from a stepwise discontinuous naphthalene disk rotating in a uniform forced stream. 22 p3243 A72-41946

NARCOLEPSY

IR pupillography for screening narcoleptics and fatigue prone individuals from driver and pilot training applicants 12 p1777 A72-28323

NARCOSIS

Inert gas narcosis under hyperbaric conditions relationship to mental performance and auditory and visual evoked responses in man [AD-736736] 02 p0166 A72-11705

Acute hypercapnia neurotropic effect in rabbits, describing carbon dioxide inhalation period, pre-narcotic and narcotic stages and recovery phase 02 p0160 A72-12015

NARCOTICS

NT MORPHINE

Central nervous system pharmacology, discussing somniferous, narcotic and neurotropic substances effects on brain activity 08 p1127 A72-21841

NASA PROGRAMS

NT APOLLO PROJECT

NT EARTH RESOURCES PROGRAM

NT GLOBAL ATMOSPHERIC RESEARCH PROGRAM

NT HELIOS PROJECT

NT MARINER PROGRAM

NT ROVER PROJECT

NT SKYLAB PROGRAM

NT TILT ROTOR RESEARCH AIRCRAFT PROGRAM

NT VIKING MARS PROGRAM

Jet noise reduction technology, hardware and tests for NASA Quiet Engine Program to develop low noise subsonic civil transport aircraft propulsion system [SAE PAPER 710774] 01 p0116 A72-10266

Experiment sensors impact on on-orbit vehicle configurations and operations in NASA program, synthesizing and cost analyzing common module sets 01 p0135 A72-10945

NASA earth resources satellite R and D program for acquiring data on agriculture, forestry, geography, geology, hydrology, mineralogy and marine resources 01 p0063 A72-10949

NASA quality assurance program, discussing management planning, assessment, failure prevention and cost effectiveness 02 p0304 A72-11554

NASA/MSFC earth observation aircraft program radar scatterometers, presenting system evaluation 02 p0172 A72-11849

NASA spacecraft instrumentation for high energy phenomena measurements, discussing collimated proportional counters, wire grid digitized spark chambers and modulation and slit collimators 03 p0353 A72-13038

NASA closed cycle MHD facility for power generation, discussing system components, design and operation [AIAA PAPER 72-103] 05 p0616 A72-16936

Skylink project as prospective joint American-Soviet space mission, combining Skylab and Soyuz spacecraft 05 p0731 A72-17092

NASA space applications program review, discussing potential of communication, navigation and earth observation satellites 06 p0893 A72-18610

Medical equipment advancements through NASA sponsored aerospace research program, describing prosthetic urethral valve, ear oximeter, radiation dosimeter and electromyographic muscle trainer 06 p0765 A72-18616

NASA materials science and manufacturing in space program involving space shuttle reusable equipment and weightlessness applications experiments 06 p0797 A72-18621

NASA sponsored medical R and D programs for space applications, stressing benefits to earthbound medical services 06 p0769 A72-18626

NASA programs phased planning and quality assurance techniques, noting cost effectiveness 07 p1102 A72-19126

Book on NASA technology transfer program covering regional university-based dissemination center evaluation and comparison with other transfer mechanisms 07 p1102 A72-19182

Biomedical transducers for NASA space program, discussing spray-on electrodes and telemetering for ECG respiration and body temperature 07 p0931 A72-19917

ERTS program, discussing orbit selection and sensor equipment 07 p1085 A72-20305

NASA research and applications module (RAM) for interim space station development and possible missions with space shuttle 08 p1240 A72-20978

NASA space programs, discussing future Apollo, Skylab, orbiting space station, space shuttle and deep space projects 08 p1230 A72-21002

Global NASA communications network (NASCOM) reliability, discussing design and performance goals 10 p1435 A72-23992

NASA ERTS and Skylab programs review, presenting information on spacecraft design, orbits, attitudes, sensors, image characteristics, data handling and processing, etc 10 p1539 A72-24323

Manned-Unmanned Lunar Explorer (MULE) for NASA integrated program plan after 1980, discussing weight, locomotion system and mission capabilities [AIAA PAPER 72-369] 11 p1612 A72-25394

NASA aerodynamic technology program, emphasizing airframe and engine development for next generation subsonic CTOL jet transport requirements [SAE PAPER 720319] 11 p1575 A72-25582

NASA quiet engine program, discussing noise reduction technology for subsonic civil transport aircraft propulsion system [ASME PAPER 72-GT-96] 11 p1705 A72-25667

Large space telescope (LST) project, discussing instrumentation, observation program and operational characteristics 11 p1630 A72-25681

Short and long range contributions of NASA space program to life quality improvement, discussing land and crop surveys, communications and environment modification 11 p1748 A72-26098

NASA space program impact on U.S. technology, discussing performance levels, precision, reliability and industry stimulation 11 p1748 A72-26099

NASA program to develop heat resistant materials for aerospace applications, discussing refractory carbides, nitrides and borides temperature dependent behavior and properties 11 p1664 A72-26857

Weather forecasting support of NASA programs involving earth oriented viewing and sensing experiments from aircraft and spacecraft 13 p1990 A72-28816

NASA program for acquisition, analysis and dissemination of space propagation and interference data for space systems designers, operators and regulatory agencies [AIAA PAPER 72-577] 13 p1918 A72-28985

NASA space plans for 1970s including lunar, planetary and universe explorations, cost reduction, human living and working capability, technology applications and international cooperation 14 p2162 A72-31136

European programs on space stations, tugs, shuttles, propulsion and avionics and consideration for participation in NASA programs for 1970s and 1980s 14 p2175 A72-31137

European space project priority in terms of technological competition, budget limitation and participation in NASA post-Apollo program 14 p2175 A72-31138

U.S. industry views on NASA plans for 1970s, emphasizing interplanetary nuclear propulsion, space transportation, shuttle costs and economics 14 p2175 A72-31139

- U.S.-U.S.S.R. space cooperation, considering Eisenhower and Kennedy initiatives, NASA-Soviet Agency negotiations and current situation
14 p2176 A72-31145
- Apollo lunar exploration program survey, reviewing information on lunar crust composition and thickness, lunar evolutionary processes and chronology and extraterrestrial particle fluxes
15 p2309 A72-31970
- Report to COSPAR on U.S. space program covering stellar astronomy, lunar and planetary research under atmospheric physics, earth and life sciences, etc
15 p2337 A72-32006
- NASA teleoperator-robot development program, discussing technology and design studies related to space shuttle and stations, satellites and planetary vehicles
15 p2190 A72-32315
- NASA/General Electric joint development of low noise propulsion technology, describing demonstrator engine A design, components development and aerodynamic/acoustic performance evaluation [AIAA PAPER 72-657]
16 p2443 A72-34077
- NASA R and D for STOL short haul transportation systems, discussing propulsive lift, blown flap and augmentor wing concepts, noise reduction, etc
17 p2487 A72-34238
- Spacecraft rescue and recovery capabilities assessment based on anticipated U.S. space programs, discussing mission design, recovery response, weather prediction and communications
17 p2620 A72-34429
- Survival equipment for life raft in conjunction with Mercury, Gemini, Apollo, Skylab and space shuttle NASA programs
17 p2620 A72-34433
- Space shuttle program, discussing configurational concepts, payload carrying capacity variants and cost reduction design changes
17 p2621 A72-34869
- NASA technology transfer from information dissemination and service to product development, noting firemen breathing system
17 p2639 A72-35506
- NASA R and D programs for quiet STOL aircraft and engines development
18 p2721 A72-36503
- Space science advances and NASA Planetary Program, noting solar system evolution, life origin and Skylab and Space Shuttle programs
19 p2855 A72-37274
- Potential applications of NASA-developed technology to problems of the environment. [ASME PAPER 72-ENAV-23]
20 p2895 A72-39154
- Flight safety research, discussing NASA aviation hazards R and D programs involving fire, lightning and static, steep approaches, aircraft wakes, fog and visibility
20 p2888 A72-39742
- European participation in space shuttle and space tug programs, discussing funding and technical aspects
21 p3103 A72-40456
- NASA Quiet Engine program R and D on conventional takeoff and landing subsonic cruise aircraft engine noise [ICAS PAPER 72-48]
21 p3100 A72-41173
- NASA's quiet engine programs.
22 p3217 A72-43152
- Development of planetary quarantine in the United States.
23 p3259 A72-43382
- NASA developed geostationary weather and environmental satellite for launch in 1973, discussing ground station equipment, antenna system and data collection service
23 p3343 A72-43551
- Explorer satellites and Pioneer space probes development program, discussing launching rockets, reentry tests, payloads, radio communication, Van Allen belts discovery, etc
23 p3358 A72-44353
- NASA ICBM/IRBM space program major management decisions and highlights concerning Atlas, Titan and Thor
23 p3358 A72-44356
- NASA space science, exploration and applications plans and policies in view of space shuttle capabilities, emphasizing cost reduction
24 p3440 A72-45162
- United States Space Nuclear Electric Power Program.
24 p3424 A72-45179
- NASA's management concept for the Space Shuttle Program.
24 p3468 A72-45194
- Potential contributions of the United States space program to exploration of the solar system.
24 p3445 A72-45467
- ### NATIONAL AIRSPACE UTILIZATION SYSTEM
- Aircraft proximity control for ATC system using national secondary surveillance radar (SSR) for CAS-PWI functions
06 p0844 A72-17330
- Air traffic flow control - Problems and approaches.
19 p2832 A72-38254
- ### NATIONAL AVIATION SYSTEM
- National Aviation System technology, discussing wide body jets, smokeless turbopfans, all-weather operational capability, collision avoidance and noise reduction
04 p0597 A72-14824
- Nationwide real time automated ATC system interconnected by data transmission links, discussing radar signal acquisition/transfer and computer complex
06 p0845 A72-18283
- Air traffic flow control - Problems and approaches.
19 p2832 A72-38254
- ### NATURAL FREQUENCIES
- #### U RESONANT FREQUENCIES
- ### NATURAL GAS
- Combustion products thermodynamic parameters for natural gas burning in oxygen atmosphere, plotting gas temperature and flow rates against pressure and excess oxidant ratio
13 p2065 A72-29451
- ### NATURAL SATELLITES
- #### NT EUROPA
- #### NT IAPETUS
- #### NT IO
- #### NT MOON
- #### NT PHOBOS
- #### NT TITAN
- Io modulation of Jupiter decametric emissions, using cyclotron magnetosphere model and coupling by whistler mode electromagnetic waves
01 p0125 A72-10084
- Jupiter outer satellite origin, considering capture orbit dimensions based on three body elliptical problem
02 p0275 A72-11594
- Outer planets satellites physics and chemistry, discussing steady state thermal models based on energy equilibrium between internal radioactive decay and surface radiation
04 p0568 A72-14495
- Jupiter outer satellite group formation theory, suggesting asteroid-larger satellite collision
04 p0569 A72-14496
- Jupiter-induced perturbations in orbital elements of Callisto artificial satellite, noting correction requirement due to Jupiter polar flattening
04 p0572 A72-14634
- Jovian decametric radiation observations, showing satellite Io relative position correlated to highest frequency
04 p0581 A72-15515
- Jupiter mass from discrete time observations of J1X satellite positions and velocities, using sequential Kalman-Bucy filter
06 p0876 A72-17580
- Astronomical model for Jovian decametric radio emission control by Io satellite based on two surface sources on planet and particle interaction with plasma
06 p0891 A72-18504
- Spacecraft planetary approach navigation with TV camera onboard Mariner 9 giving images of Mars natural satellites against star background, discussing optical data processing programs [AIAA PAPER 72-53]
07 p1032 A72-18946
- Maximum cut-off frequency of Io controlled Jovian decametric radiation as function of lambda coordinates
07 p1059 A72-19599
- Photoelectric measurements of brightness of Galilean satellites of Jupiter as function of solar phase angle
08 p1238 A72-21831
- Telescope observations of occultations of stars by outer planets, natural satellites and asteroids
09 p1387 A72-22977
- Negative search for post-eclipse brightening of Io and Europa satellites in 1970 based on single beam photometric observation
10 p1532 A72-23714
- Secular and periodic variations of orbital elements of Mars satellites due to oblateness and solar attraction
10 p1541 A72-24471
- Photoelectric observation of beta Scorpis occultation by Jovian satellite Io, noting Fresnel diffraction effects
10 p1548 A72-24969
- Occultation of beta Scorpis by Jupiter and Io to determine Jovian equatorial radius and oblateness
10 p1548 A72-24970
- Three body problem study of satellite capture by planets in elliptical orbits, deriving orbital elements in terms of mass ratio and planetary orbit eccentricity
12 p1865 A72-27096
- Jupiter occultations of multiple star beta Scorpis and Io close approach to beta sub 2 Sco
12 p1871 A72-27757
- Titan and Galilean satellites effective temperatures from broadband observations, suggesting low surface emissivity or high opacity for Titan
13 p2041 A72-29417
- Jupiter decametric radiation modulation by photoelectron emission by satellite Io, describing future probe experimental test
14 p2156 A72-30558
- Comets formation from Jupiter satellite Io surface eruption using particle trajectory analysis and comet orbital elements calculation
15 p2305 A72-31391
- Callisto radio emission analysis by ice body model, noting brightness temperature calculation of ice surface
15 p2308 A72-31904
- Io effects on Jupiter decametric radio bursts, discussing ionosphere vs solid surface for required conductivity
16 p2455 A72-33465
- Solar wind velocity near Jupiter correlated to Io geocentric phase during radio bursts, noting plasma-sphere models
16 p2459 A72-33904
- Titan spectrum absorption features, estimating hydrogen abundances
17 p2606 A72-34540
- Sheath effects and related charged-particle acceleration by Jupiter's satellite Io.
17 p2611 A72-35320
- Influence of the Galilean Jovian satellites on the motion of an artificial satellite of Callisto
17 p2618 A72-35811
- Temperature sounding experiments for the Jovian planets.
18 p2726 A72-36641
- Electrodynamic effects of Jupiter's satellite Io.
21 p3104 A72-40483
- Role of the swarm of satellite-particles on the origin of the earth's rotation
22 p3220 A72-41916
- Origin and evolution of the earth-moon system.
22 p3227 A72-42540
- Book on moons and planets covering celestial mechanics, solar system origin, stellar formation, comets, asteroids, meteorites, planetary interiors, surfaces, atmospheres, etc
22 p3228 A72-42750
- The physical properties of the Jovian atmosphere inferred from eclipses of the Galilean satellites. II - 1971 apparition.
24 p3435 A72-44689
- The determination of the diameter of Io from its occultation of beta Scorpis C on May 14, 1971.
24 p3436 A72-44700
- Observation of the occultation of beta Sco C by Io.
24 p3436 A72-44702
- Luni-solar perturbations of the geostationary vehicle at arbitrary latitude.
24 p3448 A72-44990
- Ground observation for outer planets natural satellites ephemeris, using astrometric telescopes, photographic and plate reduction techniques [AIAA PAPER 72-904]
24 p3443 A72-45426
- ### NAUSEA
- Environmental temperature effect on motion sickness sweating, discussing nausea and discomforting symptomatology prediction
12 p1775 A72-28302
- ### NAVIER-STOKES EQUATION
- Difference analog of nonlinear hydrodynamic boundary value problem from Navier-Stokes steady state theory
01 p0050 A72-10576
- Inertia effects in fully developed axisymmetric laminar flow between two parallel rotating walls, solving Navier-Stokes equation in nonlinear form [ASME PAPER 71-LUB-J]
02 p0234 A72-11529
- Nonlinearity effects on two dimensional steady supersonic dissipative flow governed by Navier-Stokes equations, obtaining expressions for flows past thin airfoil and wedge
02 p0203 A72-11976
- Secondary periodic solution for Navier-Stokes type evolution problems, observing stabilities [ONERA, TP NO. 1035]
03 p0389 A72-13786
- Navier-Stokes equation analysis of three dimensional steady radial expansion of viscous heat-conducting compressible fluid from spherical sonic source into vacuum
03 p0343 A72-14247
- Laminar viscous flow past finite flat plate at high Reynolds numbers, solving Navier-Stokes equations
04 p0511 A72-14859
- Pressure and convective heat transfer distribution at air inlet central body surface, reducing Navier-Stokes equations to partial differential equations with similar solutions
04 p0596 A72-14971
- German monograph on two dimensional unsteady boundary layer calculation with unstable effects, using Navier-Stokes equations
04 p0512 A72-15245
- Navier-Stokes equations numerical solution by computerized simulation for viscous channel flow with diaphragm orifice reducing cross section
04 p0513 A72-15644
- Navier-Stokes equations solution by finite difference methods for steady incompressible laminar vapor flow in symmetrical and unsymmetrical heat pipes, calculating pressure losses [ASME PAPER 71-WA/HT-15]
05 p0744 A72-15874

Longitudinal curvature effects on laminar and turbulent boundary layer flows predicted from Navier-Stokes equations, noting mixing length assumption validity [ASME PAPER 71-WA/FE-37] 05 p0645 A72-15920

Navier-Stokes equations solution for unsteady viscous flow around oscillating elliptic airfoil in turbomachinery flutter analysis, obtaining pressure and shear stress distributions 05 p0600 A72-16002

Navier-Stokes equations asymptotic solution for compressible weightless conducting fluid flow in plane channel with intense blowing from walls 05 p0648 A72-16219

Numerical simulations of three dimensional homogeneous isotropic turbulence at wind tunnel Reynolds numbers, solving Navier-Stokes equations for incompressible flow 05 p0649 A72-16685

Two dimensional turbulence stationary states from statistical equilibria for Navier-Stokes equation 05 p0649 A72-16686

Navier-Stokes equations numerical solution for laminar incompressible flow past paraboloid of revolution at zero angle of attack [ALAA PAPER 72-110] 05 p0604 A72-16818

Numerical solution to Navier-Stokes equations for viscous annular flow between rotating long eccentric cylinders [ALAA PAPER 72-113] 05 p0605 A72-16821

Atmospheric turbulence incompressible two dimensional model, comparing Navier-Stokes equations numerical integration results with finite difference simulation [ALAA PAPER 72-152] 05 p0651 A72-16871

Unsteady axisymmetric incompressible pipe flow stability near piston, using Navier-Stokes equations solution with finite difference forms 05 p0653 A72-17006

Two-dimensional asymptotic solutions to Navier-Stokes equations for weak vortex discontinuity flow with vanishing viscosity 06 p0798 A72-17680

Navier-Stokes equation solution for laminar incompressible flow past parabolic cylinder, investigating skin friction and pressure drag 06 p0798 A72-17782

Perturbation methods for laminar flows near leading edge, discussing approximations of Navier-Stokes equations and domain connection 06 p0756 A72-18108

Small parameter method solution of two dimensional incompressible flow Navier-Stokes equations, exemplifying application to viscous incompressible flow past seminfinit plate 06 p0801 A72-18127

Convergent finite difference schemes for Navier-Stokes equations initial boundary value problems, using Temam systems approximation method 06 p0840 A72-18132

Coolant flow and heat transfer in rotating circular cylindrical enclosure, solving Navier-Stokes and energy equations by finite difference formulation 06 p0802 A72-18189

Navier-Stokes equations numerical solution for viscous incompressible fluid in circular cylinder with rotating top disk, computing secondary flow at Reynolds numbers to 400 06 p0802 A72-18526

Difference method for numerical integration of Navier-Stokes equations for two dimensional incompressible steady flow along flat thin plate 07 p0908 A72-19170

Hydrodynamic stability problems with reference to Navier-Stokes equation solutions, discussing linearization principle application 07 p0969 A72-20066

Navier-Stokes equation numerical solution methods, expressing boundary conditions by separate equations for vorticity and stream function 07 p0970 A72-20077

Invariant free boundary problems of Navier-Stokes equations with nonzero vector of volume forces, investigating liquid layer flow on vertical cylinder surface 07 p0972 A72-20105

Generalized Navier-Stokes equations for incompressible turbulent flow time mean values, using nonlinear phenomenological theory 07 p0972 A72-20109

Unsteady gas flow in thrust bearing with spiral grooves, presenting Navier-Stokes and discontinuity equation 08 p1176 A72-21167

Navier-Stokes equations numerical solution for symmetric laminar incompressible flow past parabolic cylinder, presenting surface pressure, friction and pressure drag results 10 p1465 A72-24291

Finite amplitude disturbances effect on plane Poiseuille flow hydrodynamic stability, presenting numerical method for solving parabolic partial differential equations derived from Navier-Stokes equation 10 p1468 A72-24422

Navier-Stokes equations system integration for axisymmetric vortex flow of viscous incompressible three component fluid 10 p1471 A72-25134

Turbulent flow time averaged description by Navier-Stokes equations, determining Reynolds number dependent stress tensor coefficients 11 p1615 A72-25722

Wind velocities field in vortices leeward of islands derived from Navier-Stokes equation for isolated axisymmetric viscous vortex 12 p1839 A72-27032

Collisional plasma shock waves structure in electromagnetic shock tube with strong transverse bias magnetic field, using two fluid Navier-Stokes equations 13 p2011 A72-29119

Navier-Stokes equation for rotating liquid axial flow past porous plate, noting velocity distribution for suction and thinning effect for blowing 13 p1942 A72-29127

Binary gas mixture slipping rate determination from joined solution of Hamel kinetic model linearized equations, and Navier-Stokes and Boltzmann equations 14 p2096 A72-31013

Two dimensional viscous flow past seminfinit flat plate and smooth obstacle, using Navier-Stokes equations for lift force relationship investigation 15 p2216 A72-31312

Navier-Stokes equation for unsteady asymptotic suction flow over flat plate, plotting velocity distribution profiles 15 p2178 A72-31406

Finite difference solution to Navier-Stokes equations for axisymmetric flow of incompressible viscous fluid 15 p2216 A72-31446

Ideal gas supersonic axial flow past circular cylinder, solving Navier-Stokes equations by Van Dyke matched asymptotic expansions method 15 p2178 A72-31463

Kinematic eddy viscosity for incompressible two dimensional turbulent flow, obtaining Navier-Stokes equations and conditions for equilibrium and nonequilibrium boundary layers 15 p2216 A72-31470

Three dimensional boundary layer instability, obtaining linearized perturbation equation on basis of Navier-Stokes equation 15 p2216 A72-31471

Shock wave propagation in gas with discrete velocity distribution, comparing solutions based on Euler, exact and Navier-Stokes equations respectively 16 p2375 A72-32861

Mathematical model of atmospheric tides using Navier-Stokes equations for perfect gas in thermodynamic equilibrium 16 p2385 A72-33343

Turbulent solutions of certain linear and nonlinear partial differential equations 17 p2537 A72-34194

Solution of the two-dimensional, unsteady, compressible Navier-Stokes equations using a second-order accurate numerical scheme. 17 p2538 A72-34646

Numerical calculation of the supersonic flow of a viscous fluid about a parabolic obstacle 17 p2484 A72-34887

A modified Navier-Stokes equation, and its consequences on sound dispersion. 17 p2540 A72-35146

The flow caused by the differential rotation of a right circular cylindrical depression in one of two rapidly rotating parallel planes. 17 p2540 A72-35189

General closed form solutions to Burger equation with forcing terms in Navier-Stokes equation for turbulence studies 18 p2677 A72-36004

Invariant solutions of the Navier-Stokes equations describing motions with a free boundary. 18 p2679 A72-36234

A new method of analysis in laminar-flow theory. 18 p2681 A72-36551

Numerical study of a viscous gas flow in the wake of a plane body 18 p2642 A72-36804

A comparison of the solutions of Prandtl's and Navier-Stokes equations in a superposed fluctuating flow. 18 p2684 A72-37084

Proper equations and similar approximations in the hypersonic merged layer. 20 p2885 A72-39621

Large-scale instabilities of turbulent wakes. 21 p3044 A72-40116

Two-dimensional stationary problem with a free boundary for the Navier-Stokes equations 21 p3047 A72-41663

Predvoditelev critical revision of hydrodynamic and heat transfer theory based on Navier-Stokes and Boltzmann equations, developing statistical system of molecular interactions 22 p3165 A72-41951

Numerical solution to the Navier-Stokes equations in the problem of a gas flow past a rectangle 22 p3166 A72-42252

Boundary value problems of viscous fluid dynamic system generated by Navier-Stokes equations, using Hopf theory 22 p3208 A72-43137

Navier-Stokes evolution inequality bounded solution existence and uniqueness theorems for two dimensional space 22 p3200 A72-43201

Periodic solutions of a nonlinear mixed problem for the Navier-Stokes equations 24 p3418 A72-44780

A theory of homogeneous, isotropic turbulence of incompressible fluids. 24 p3392 A72-45245

Kinetic theory of turbulent flow. 24 p3394 A72-45563

NAVIGATION

NT AIR NAVIGATION

NT ALL-WEATHER AIR NAVIGATION

NT ASTRONAVIGATION

NT CELESTIAL NAVIGATION

NT DECCA NAVIGATION

NT DIGITAL NAVIGATION

NT DOPPLER NAVIGATION

NT HYBRID NAVIGATION SYSTEMS

NT HYPERBOLIC NAVIGATION

NT INERTIAL NAVIGATION

NT INTERPLANETARY NAVIGATION

NT LORAN

NT LORAN C

NT LORAN D

NT OMEGA NAVIGATION SYSTEM

NT POLAR NAVIGATION

NT RADAR NAVIGATION

NT RADIO NAVIGATION

NT SHORAN

NT SPACE NAVIGATION

NT SURFACE NAVIGATION

NT TACAN

NT VHF OMNIRANGE NAVIGATION

Circumpolar region object position autonomous determination from arbitrarily zenith-oriented moving horizontal platform position coordinates 04 p0545 A72-15002

Man and technology in orientation and navigation Conferences, Essen, Germany, October 1971 09 p1348 A72-22776

Man machine systems in navigation, discussing problems of integrating man with high speed and high capacity electromechanical systems with allowance for human weaknesses and abilities 09 p1269 A72-22777

NAVIGATION AIDS

NT AIRPORT BEACONS

NT BEACONS

NT GYROCOMPASSES

NT LASER ALTIMETERS

NT MAGNETIC COMPASSES

NT NAVIGATION INSTRUMENTS

NT RADAR BEACONS

NT RADIO BEACONS

NT RADIO DIRECTION FINDERS

Broadband beam scanned linear waveguide antenna array design with FMCW short range high resolution radar for airport navigation aid in fog 01 p0039 A72-10669

Air transportation system design for safety and efficiency, discussing navigation facilities and surveillance systems employment for blunder prevention 01 p0098 A72-11117

Inertial navigation role in automatic ATC systems, discussing path control accuracies, environmental conditions, noise and air pollution, etc 01 p0098 A72-11118

Airfield Vehicle Obstacle Indication Device short range high-definition radar system for aircraft navigation aid 02 p0173 A72-12042

Optimal stochastic /Kalman/ filters application to integrated air and submarine navigation systems, discussing measurement errors modeling as bias and colored noise 02 p0256 A72-12050

Airborne pictorial navigation systems for visual indication of aircraft position in addition to digital readout 02 p0256 A72-12106

Soviet book on course-indicating systems and automatic navigation aids for civil aviation aircraft covering design, operation principles, error analysis and reliability 02 p0256 A72-12298

Radio aids to maritime and aerial navigation - Conference, Trieste, June 1971 02 p0257 A72-12640

L band in satellite system for aerial navigation aid, discussing position accuracy, data transmission and voice communication and modulation methods 02 p0257 A72-12642

Radio aids for air navigation and traffic control in Italy, discussing facilities development 02 p0257 A72-12748

Maritime and aerial navigation radio aids, discussing recent technological advances 02 p0258 A72-12750

Satellite navigational aid system technical and operational characteristics, emphasizing voice communications links in L band 03 p0386 A72-12972

Operational requirements of instrument landing systems, interferometers, correlation protected instruments, landing guidance systems and navigation aids 03 p0386 A72-13421

Automated navigation aids interface with human operator, discussing Apollo flight experience and technology utilization in air and marine navigation 06 p0846 A72-18288

Low light television camera tubes application to navigation safety in congested areas, reconnaissance and other watchkeeping system 07 p1032 A72-19070

V/STOL development for short haul air transportation, discussing requirements for quiet pollution-free operation, ATC systems, navigation and landing aids 08 p1108 A72-21010

Area navigation systems, discussing VOR/DME, Doppler and inertial systems, CRT displays, data links, etc 08 p1204 A72-21523

Automated navigation management in cockpit, considering modular navigation /MONA/ dual channel system of L-1011 TriStar 09 p1349 A72-23450

Area navigation for Chicago-New York region, evaluating Decca Omnitrac 1A RNAV system installation in Boeing 727 aircraft 09 p1349 A72-23467

Operational aviation meteorological requirements, reviewing aircraft categories, ATC systems and avionics and navigational aids 10 p1508 A72-25078

Loran-Omega course and track equipment /LO-CATE/ of integrated upper air meteorological sounding systems, describing radiosonde navigational aids 10 p1484 A72-25086

Integrated display system design with navigation update, weapon delivery, reconnaissance, bomb damage assessment, threat and terrain avoidance capabilities for multicrew military aircraft 11 p1684 A72-26292

Skyguide airborne computer navigation system for airline applications, discussing system components, flight crew monitoring and optimization 11 p1684 A72-26999

VOR and Doppler VOR ground station equipment based on reliable solid state radio transmitters and signal generating devices for aircraft navigation 12 p1779 A72-27104

Detection range, color, brightness and flash subjective response tests to evaluate light signals for nighttime sea navigation and visual collision avoidance 12 p1777 A72-28326

Great circle intermediate waypoint computation method for inertial navigation equipped aircraft 15 p2271 A72-32205

Hybrid area navigation and microwave instrument landing system, discussing approach control and terminal guidance 15 p2271 A72-32206

ICAO assistance to member states in various transport airports and navigation facilities economics including accounting and financial statistics 16 p2481 A72-33334

V/STOL flight control - Trend and requirements. 17 p2487 A72-34240

The Omega navigation system - Its history, application and versatility. 17 p2578 A72-35559

OMEGA air and maritime navigation system development, test phase and application potential, discussing operational modes, propagation parameters, solar activity effects and signal loss 19 p2831 A72-37796

Precision navigation for approach and landing operations. 19 p2832 A72-38253

Space shuttle terminal navigation with conventional navigation aids. 20 p2950 A72-39095

Reduction of air traffic congestion due to corridor effect of present airway route pattern through area navigation /R-NAV/ based on VOR/DME inputs 20 p2952 A72-39750

An area navigation system for a long range airplane. 21 p3079 A72-40281

Statistical synthesis of navigation aids systems with unsteady random interferences, obtaining optimization criterion by least squares method 22 p3202 A72-42232

NAVIGATION INSTRUMENTS

NT ATTITUDE INDICATORS

NT GYRO HORIZONS

NT GYROCOMPASSES

NT MAGNETIC COMPASSES

NT RADIO ALTIMETERS

NT RADIO DIRECTION FINDERS

Error probability distributions in navigational statistics involving single or identical and diverse instruments or operators 01 p0096 A72-10176

Human factors engineering of aircraft cockpit data entry keyboards on area navigation control and display units 01 p0020 A72-11138

Apollo lunar roving vehicle design requirements based on environmental conditions, emphasizing wheel drive control and steering systems optimization and navigational instrumentation 05 p0643 A72-16428

Incorrect or unmodeled error sources effects on arbitrary linear navigation filters design and performance [AIAA PAPER 72-14] 05 p0688 A72-16911

Onboard orbital navigation system analysis on space shuttle radio range and range rate measurement data relative to ground beacon, using Kalman filter 08 p1203 A72-20856

Astrolabe design and operation for reconnaissance and simultaneous determination of latitude and longitude 08 p1165 A72-21022

Flight testing of automated modular area navigation system for L-1011, describing computer, data storage and control-display units and electronic automatic chart system 10 p1509 A72-24271

Self organizing control system for optimal performance of navigation instruments, using adaptive algorithm for statistical error filtration 13 p1996 A72-29157

Small aircraft navigation over 10-400 mile course segments by raw OMEGA phase information dc presentation on conventional ID-249 course deviation indicator 13 p1999 A72-29201

Landmark navigation with angle measurements for roving vehicle guidance on lunar and planetary surfaces 15 p2268 A72-31790

Configuration and flight test of the only operational Air Force area navigation system. 17 p2578 A72-35557

Contribution of Danjon's astrolabe to the study of proper motions 18 p2726 A72-36727

Landmark navigation rule, a new navigation device. 19 p2830 A72-37296

Development of STOLAND, a versatile navigation, guidance and control system. 19 p2831 A72-38106

Design of a reduced-state suboptimal filter for self-calibration of a terrestrial inertial navigation system. [AIAA PAPER 72-849] 20 p2949 A72-39080

Error analysis of hybrid aircraft inertial navigation systems. [AIAA PAPER 72-848] 20 p2950 A72-39081

An adaptive technique for a redundant-sensor navigation system. [AIAA PAPER 72-863] 20 p2952 A72-39134

A detailed analysis of Mariner nine TV navigation data. [AIAA PAPER 72-866] 20 p2977 A72-40061

Modular navigation /MONA/ dual channel automatic area navigation system, describing computer, flight data storage and control/display units 21 p3079 A72-40277

TCE-71A area navigation system based on modular design with provision for 20 waypoints parameter storage, describing computer, control display and automatic data entry units 21 p3079 A72-40278

Operational implementation of area navigation. 21 p3079 A72-40279

Present status of self-contained navigation systems combining Doppler velocity sensors and attitude/heading references. 21 p3079 A72-40282

ILS replacement by microwave landing system, considering landing phase range from acquisition to touchdown, terminal approach handling by airborne navigation system and economic advantages 21 p3081 A72-40294

Application of external information about the linear velocity of an object for correcting inertial navigation systems 24 p3423 A72-45319

NAVIGATION SATELLITES

NT NAVSTAR SATELLITES

NT TRANSIT SATELLITES

Geometry and latitude/longitude differentials approximations for position fixing by Doppler signals and earth satellites 01 p0097 A72-10182

Uhf aeronautical satellite system, presenting ATC trends, international aspects, available flight levels, weather conditions and long haul conflicts 02 p0257 A72-12383

Satellite navigational aid system technical and operational characteristics, emphasizing voice communications links in L band 03 p0386 A72-12972

Flight navigation technology current state and development trends, discussing transition from Doppler to inertial systems, use of computers and satellites, collision avoidance, etc 05 p0687 A72-16737

Spacecraft, aircraft and ship navigation by satellites, noting Navy Navigation Satellite System 05 p0687 A72-16747

Single satellite angle system and multiple satellite ranging and range difference systems in short haul air navigation, comparing with VORTAC 06 p0844 A72-17335

NASA space applications program review, discussing potential of communication, navigation and earth observation satellites 06 p0893 A72-18610

Trends in civil ATC discussing plans to increase terminal capacity, surveillance system and use of multiple synchronous satellites for ocean travel efficiency improvement 12 p1842 A72-27103

Correlation technique for position location in surveillance and navigation by phase extraction from range tones using synchronous satellites [AIAA PAPER 72-564] 12 p1842 A72-27375

Russian book on flight navigation cybernetics covering Doppler, astro and radio inertial schemes and satellite systems 12 p1843 A72-28344

OMEGA navigation system operation aboard NOAA ship Discoverer in conjunction with satellite system, noting Trans-Atlantic tracklines 13 p1998 A72-29194

Navy navigation satellite system, discussing time and frequency role, TIMATION satellite time standard and application for user equipment clock signal comparison 15 p2268 A72-32070

Technical and operational aspects of L-band satellite system for air navigation, discussing verbal communication, direction finding and noise interference problems 16 p2421 A72-34138

Ranging signals for aeronautical satellite systems 17 p2516 A72-35220

Geostationary satellite system for air navigation via voice and data communication, discussing ground facilities and avionics 21 p3080 A72-40284

Navigation satellite system based on triangular distance measurement between two satellites and aircraft, noting simplification of air- and satellite-borne equipment requirements 21 p3080 A72-40285

A hybrid navigation concept using a spinning satellite-borne interferometer and self-contained equipment. 21 p3082 A72-41083

The role of time/frequency in Navy navigation satellites. 22 p3202 A72-42749

Theoretical and practical comparison between two minute Doppler and short Doppler satellite position fix accuracy. 22 p3203 A72-42947

Potential of the navy navigation satellite system in predicting ionospheric characteristics. 24 p3447 A72-45555

NAVIGATORS

Navigators, pilots and airman trainees response to Coriolis accelerations, investigating nystagmus sensitivity coefficient relationship to motion sickness resistance 01 p0021 A72-11286

Civil aeronautics environment relation to psychiatrists and medical psychologists treatment of air navigation personnel, discussing chemotherapeutic and psychotherapeutic treatment administration problems 07 p0927 A72-19243

Military aviation navigator training, discussing objectives, methods, instructors and equipment 15 p2272 A72-32207

Electronic displays with weapon aiming sensors in aircraft navigator-attack systems 15 p2273 A72-32634

A new approach to a cruise navigator evaluation using sparse reference data. [AIAA PAPER 72-835] 20 p2950 A72-39092

NAVION AIRCRAFT

Effects of variations in lift and drag response to longitudinal control on the ease and quality of landing. 24 p3368 A72-45333

NAVSTAR SATELLITES

Spacecraft, aircraft and ship navigation by satellites, noting Navy Navigation Satellite System 05 p0687 A72-16747

NAVY

Critical review of Mil-F-83300 V/STOL flying qualities specifications as applied to helicopter design and missions, suggesting inappropriateness for Navy helicopters [AHS PREPRINT 643] 17 p2490 A72-34503

Polaris submarine-weapon system autonomous organization and management technique based on team

- combining Navy and civilian contractors in close working relationship 23 p3358 A72-44358
- NEAR INFRARED RADIATION**
- Visible and near IR reflectance spectra of soil mineralized trees, using multispectral photographic filters 02 p0209 A72-11789
- Water molecules absorption lines in sunspots umbral near IR spectrum, noting improved spectrometric apparatus 05 p0719 A72-16515
- Earth upper atmosphere outgoing thermal radiation radiance calculation in near IR spectrum 06 p0808 A72-18041
- Ground based IR astronomical telescope detectors, relating F number and optical requirements to near, far, and intermediate IR observation 10 p1481 A72-24249
- III-V metal photocathodes for near IR and shorter wavelengths, noting performance improvements over conventional cathodes 11 p1630 A72-25683
- Laser emission in near IR by flash lamp pumped fluorescent dyes, presenting oscillograms 11 p1651 A72-26505
- Venus atmosphere IR synthetic spectra of carbon dioxide band and water line formation for isotropic scattering, comparing with terrestrial clouds 13 p2040 A72-29410
- Stimulated luminescence in activated Nd glass by pulsed laser radiation at 1060 nm wavelength 13 p1969 A72-29519
- Human eye relative luminous efficiency for near IR and UV coherent light, using ruby laser pumped tunable dye laser primary and second harmonic outputs 15 p184 A72-31380
- Sky spectral brightness, transmittance and indicatrix measurements at near IR wavelengths 15 p2222 A72-31398
- Avalanche photodiode with n-p-pi-p double diffused reach-through structure for visible and near-IR regions, noting high efficiency, low noise and gain stability 15 p2248 A72-32036
- Near IR airglow observation by sound rocket to determine layer height diurnal variation and rocket axis zenith angle 15 p2231 A72-32328
- Pulsed emission at pulse front in molecular hydrogen, deuterium and nitrogen at near IR electronic transitions, analyzing spectral, temporal and energy characteristics 16 p2401 A72-33298
- Flowing air glow discharge near IR emission spectrum as function of pressure, noting atomic lines 16 p2427 A72-34097
- Multispectral angular reflectivity effect on optimum filter combinations for spaceborne multiband photography sensing mission in visible and near IR regions 16 p2395 A72-34104
- Near-infrared photometry of Mira variables. 18 p7229 A72-37018
- Grid polarisers for use in the near infrared. 20 p2922 A72-39046
- The employment of a novel Quntacon photomultiplier for increasing the sensitivity of older flame photometers in the near IR 20 p2927 A72-39697
- Radiometer with protective mica window for radiant flux densities measurement of near IR sources, noting reading independence of sources spectra characteristics 21 p3059 A72-41821
- Mercury-cadmium telluride photodiode detectors for near IR laser receivers, discussing time response and I-V characteristics as function of temperature 23 p3296 A72-43881
- Circular and linear dichrometer for the near infrared. 23 p3289 A72-43899
- Observation of M 82 in the near infrared 24 p3446 A72-45487
- NEAR ULTRAVIOLET RADIATION**
- Uranium arc plasma visible and near UV emission coefficients as function of U partial pressure and corresponding temperatures 01 p0112 A72-11337
- Brightness correlation and mapping of weak photospheric magnetic fields and faculae using CN 3883-A spectroheliograms 03 p0414 A72-12927
- High spectral resolution balloon-borne spectrograph for near UV solar Mg II resonance lines 03 p0354 A72-13053
- Solc-type tunable birefringent filter for near UV spectrum, discussing optical design and transmission characteristics 03 p0355 A72-13058
- Human eye relative luminous efficiency for near IR and UV coherent light, using ruby laser pumped tunable dye laser primary and second harmonic outputs 15 p2184 A72-31380

NEAR WAKES

- Finite difference model application to supersonic planar viscous near wake, determining parameter range by physical and numerical restraints [AIAA PAPER 72-115] 05 p0609 A72-16971
- Supersonic near wake flow around blunt and sharp cones with trailing edge turbulent boundary layer 06 p0757 A72-18141
- Laminar near wake solutions for slender ablating cone under supersonic atmospheric entry conditions including boundary layer reactions [AIAA PAPER 72-116] 07 p0907 A72-18954
- Book on steady laminar supersonic and hypersonic wakes covering near and far region solutions, boundary layer separation, etc 09 p1261 A72-23029
- About the interaction between a satellite and its environmental ionospheric plasma. 21 p3090 A72-40454
- Base mounted cylinders effect on near wake of axisymmetric blunt base in supersonic flow [AIAA PAPER 72-1013] 21 p2993 A72-41594
- NEBULAE**
- NT CASSIOPEIA A
- NT CRAB NEBULA
- NT PLANETARY NEBULAE
- Galactic II astronomy, discussing findings on emission from H II regions of Orion Nebula and late and early type stars 02 p0276 A72-11643
- Planetary mass distribution in solar system from gravitational contraction of nebula formed by accretion of ring shaped particle cloud 02 p0282 A72-12311
- Dust continuous spectrum and Balmer line intensity ratio in Orion Nebula from slit spectroscopy observations [AD-745076] 02 p0284 A72-12631
- Reflection nebulae genetic relationship to illuminating stars from catalogs based on Palomar Observatory Sky Survey 02 p0284 A72-12639
- Emission nebulae in Magellanic Clouds observed at 408 MHz, calculating electron density and total mass 02 p0285 A72-12796
- He abundances in gaseous nebulae by optical and radio observation, discussing hydrogen and helium recombination spectra interpretation 03 p0419 A72-13115
- Gum Nebula size, emission features and expansion dynamics, discussing Zeta Puppis UV spectrum and Vela X radio emission 03 p0440 A72-14364
- Galactic plane 100 micron survey, detecting continuum radio sources, bright and dark nebula and IR stars 04 p0570 A72-14524
- Faust project history, scientific objectives and present status, discussing stars, nebulae, quasars point sources and galactic photometry 04 p0583 A72-15691
- Radio emitting giant loops in the Galaxy, considering supernova radiation induced nebulae model to explain spectral and polarization properties 06 p0876 A72-17649
- Interstellar gas motion model of nebulae formation by Wolf-Rayet stars 06 p0883 A72-18016
- Galactic cepheid RS Puppis and surrounding ring-structured nebula luminous variations and evolution, using reflecting shell model 07 p1069 A72-19079
- Radio emission of Lupus region believed to contain supernova of 1006 A.D., noting strong polarization 07 p1076 A72-19607
- Isophote equidensity role in astronomical photometric investigation of solar corona, galactic nebulas, comets and extragalactic stellar systems 07 p1082 A72-20301
- Photoelectric Fabry-Perot measurements of M8 and M42 nebulae H alpha and forbidden N II emission lines profiles, determining temperatures and turbulent motions 09 p1390 A72-23528
- OH emission source and H II region bright knots coincidence in NGC 7538 nebula, suggesting physical model 09 p1392 A72-23548
- Interstellar gas motion model of nebulae formation by Wolf-Rayet stars 11 p1718 A72-25952
- Interstellar anomalous 6 centimeter formaldehyde absorption in diffuse dark nebulae, discussing quantum mechanics of collisional pumping process 11 p1720 A72-26112
- Chemical equilibrium models of low temperature condensation from solar nebula relating to planetary composition 15 p2311 A72-32083
- Galactic nebulae electron temperature and density from forbidden line emissions interpreted in terms of transition probabilities and collision strengths 18 p2723 A72-36090

- Bright nebulae near concentrations of high-velocity gas. 19 p2856 A72-37504
- Study of a faint nebula identified as the HB-21 radio source 19 p2862 A72-38054
- Two quantum induced photon-plasmon transition probability for hydrogen atom in processes of nebulas and stellar chromospheres 19 p2837 A72-38058
- Transfer of resonance-line radiation in differentially expanding atmospheres. I - General considerations and Monte Carlo calculations. 21 p3106 A72-41037
- Interstellar nitrogen-15 and U169.3 - Possibly a new methanol line. 21 p3107 A72-41272
- Various ground configuration level intervals from gaseous nebulae and solar coronal forbidden transitions observations and laboratory investigations of resonance lines 21 p3108 A72-41286
- A spectral study of the nebula NGC 7635 and the star BD +60.2522 deg 21 p3113 A72-41755
- Nebulae of the Southern Milky Way - An atlas. 21 p3114 A72-41847
- Dark dust nebulae and bright H II clouds, considering light molecules, stellar birth region, radio and IR astronomy 22 p3220 A72-41995
- The non-spherical nebulae of Nova Delphini 1967, Nova Vulpeculae 1968/I, and Nova Serpentis 1970. 22 p3221 A72-41999
- The dynamical effects of stellar mass loss on diffuse nebulae. 22 p3224 A72-42380
- Gum nebula origin as ionized hydrogen cloud from prehistorical supernova explosion, discussing different ionization mechanisms 22 p3227 A72-42543
- The peculiar O6f star HD 148937 and the symmetrically surrounding nebulae. 22 p3227 A72-42557
- Internal dust effects on nebulae structure and spectrum, solving radiation transfer equation for spherical models with nonisotropic scattering 22 p3227 A72-42558
- Spectrophotometric study of the cometary nebula NGC 2261 22 p3229 A72-42961
- Estimate for the frequency of novae in the Andromeda Nebula and our Galaxy. 23 p3333 A72-43229
- Investigation of several nebulae in Cassiopeia with a Fabry-Perot interferometer. 23 p3333 A72-43233
- Solar system thin disk model planet formation in equatorial plane from nebula dust component, discussing gravitational effects and mass increase rate 23 p3335 A72-43261
- Russian book - Problems of the physics of nebulas and unsteady stars. 23 p3338 A72-44026
- Polarization of emission in the IC 4592 and IC 4601 nebulae 23 p3338 A72-44032
- Orion nebula continuum spectrum energy distribution from spectrophotometric measurements, comparing color temperature with previously obtained data 24 p3438 A72-44839
- NECK [ANATOMY]**
- Neck proprioception effects and otolith organ activity in perceived visual target elevation under centrifuging stress 12 p1776 A72-28305
- NEGATIVE CONDUCTANCE**
- Theorems derived for bulk semiconductor device static negative differential resistance exhibition 01 p0114 A72-10790
- Dynamic negative differential conductivity in bulk semiconductors, analyzing relation to impulse responses 04 p0562 A72-15129
- Transport phenomena theory for semiconductors in strong electric fields, examining negative differential conductivity and nonmonotonic current behavior 07 p1048 A72-19637
- Transverse negative differential conductivity in semiconductors, discussing effect of locations and shapes of energy surfaces in k-space and favorable crystal orientations 11 p1701 A72-25856
- Energy absorption inelastic surface mechanisms effect on I-V characteristics profile for bounded semiconductors with negative differential conductivity 13 p2023 A72-29991
- Free carrier mobility dependence on excitation light intensity in CdSe single crystals with negative photoconductivity 14 p2141 A72-30169

- Room temperature negative photoconductivity of p-type ZnTe-CdTe solid solutions mixed crystals within model with electron and hole capture levels
14 p2141 A72-30173
- Gunn effect - Bulk instabilities.
17 p2594 A72-34562
- New measurement method of Gunn-diode impedance.
17 p2529 A72-35000
- The behaviour of a Gunn oscillator in the domain-delayed mode.
18 p2667 A72-36945
- The negative space-charge density distribution and the potential distribution in a Penning discharge cell
23 p3324 A72-44211
- Transport phenomena theory for semiconductors in strong electric fields, examining negative differential conductivity and nonmonotonic current behavior
24 p3427 A72-44569
- NEGATIVE FEEDBACK**
NT SENSORY FEEDBACK
Balanced negative feedback circuits for reducing nonlinear distortions in distributed gain power amplifiers
02 p0193 A72-12223
- Elimination of spherical cavity resonators natural frequencies degeneration through symmetry disrupting disturbance, using group theory for fields and frequencies calculations
08 p1209 A72-21737
- Microwave amplifier with internal negative feedback, using IF output for frequency modulation of mixer oscillator signal
13 p1930 A72-29057
- Forced oscillations in RC amplifier with negative feedback through nonlinear bandpass filter with varicaps
13 p1931 A72-29266
- Linear negative feedback dc current magnetic transducers for telemetry input signals, discussing operation principles and design
16 p2370 A72-33862
- SNR improvement by negative feedback and deterioration by positive feedback in amplifiers, discussing input circuit thermal noise
21 p3034 A72-41123
- Reciprocal synchronization of generators connected by a long line section
23 p3272 A72-44210
- NEGATIVE RESISTANCE CIRCUITS**
Thermal effects on reversible threshold switching in amorphous semiconductor thin films involving current controlled negative resistance
02 p0268 A72-12202
- Receptor membrane pulse generation electronic model with tunnel diode negative resistance circuit
12 p1771 A72-27578
- Microwave power generation via semiconductor devices, discussing circuit problems due to negative resistance
14 p2088 A72-30832
- End line matching for high gain traveling wave amplifier constructed from heterogeneous transmission line sections with negative resistance
18 p2665 A72-36110
- Stabilization of relaxation oscillators with components having an S-shaped current-voltage characteristic
20 p2906 A72-38891
- Voltage controlled miniaturized n-type negative resistance circuit based on junction transistor and FET without internal bias
21 p3038 A72-40998
- Multiloop LC oscillators with negative resistance and nonlinear capacitances
23 p3271 A72-43838
- Negative resistance, transit time and limited space charge accumulation modes of semiconductor devices operation with electron transitions
23 p3272 A72-44138
- NEGATIVE RESISTANCE DEVICES**
Punch-through transit time negative resistance semiconductor device utilizing injection from Schottky barrier, deriving small signal theory for microwave impedance
01 p0042 A72-10787
- Waveguide structures partially filled with bulk negative differential conductivity media, describing wave propagation characteristics and power distributions
04 p0501 A72-15427
- Three layer bipolar transistor structure with negative resistance region in I-V characteristics
04 p0503 A72-15668
- High power negative resistance amplifiers, calculating relationship among output, gain, gain compression and efficiency for comparison with GaAs avalanche diode amplifier experiment
07 p0958 A72-19920
- Solid state microwave power amplifier with unidirectional transmission line loaded by negative resistance diode series, calculating large signal characteristics
08 p1142 A72-21558
- Bulk negative resistance devices equivalent noise temperature derivation via diffusion-impedance field noise formula, obtaining Gunn oscillators SNR approximate value
10 p1454 A72-25106
- High conversion efficiency microwave second harmonic generator using negative resistance nonlinearity of n-type GaAs
11 p1591 A72-25741
- Small signal theory of emitter current limited injection in negative mobility semiconductors at zero doping limit
12 p1788 A72-27165
- Laser light induced high-low impedance switch in Cd doped n-type Si diodes with p-p-n junctions and negative resistance
13 p1928 A72-28676
- CW Gunn oscillator cavity loading and bias voltage effects on external negative differential conductance
13 p1933 A72-29825
- Negative photoconductivity in CdSe single crystals due to free carrier mobility decrease after surface treatment in gas discharge, noting neutron traps role
13 p2024 A72-30046
- S-type negative resistance segment formation on rectilinear branch of I-V characteristics of p-n-n structure
14 p2089 A72-30969
- GaAs Gunn diode LSA operation mode in multiloop circuit to extend high frequency limit
15 p2207 A72-31888
- Gunn diode elements design, operation, performance, efficiency, heat dissipation, lifetime and applications as microwave oscillators
15 p2208 A72-32500
- Negative resistance devices, stability under open and short circuits from dc I-V characteristic shape
16 p2368 A72-32857
- Harmonic oscillators with negative resistance elements, discussing simplified mathematical calculation for I-V characteristics nonlinearity and applications to various diodes and transistors
16 p2368 A72-32858
- Arc discharge transition from diffusion to arc mode, presenting theory on I-V characteristics negative resistance section and on hysteresis causes
18 p2714 A72-36207
- Stability of injection-locked oscillators.
18 p2665 A72-36265
- Improved geometry for a semiconductor surface-wave oscillator.
18 p2667 A72-36685
- Dynamic behavior of nonlinear power amplifiers in stable and injection-locked modes.
19 p2773 A72-38293
- Effect of the filling of the capture levels with increasing current on the formation of negative resistance under double injection conditions
19 p2846 A72-38574
- Four-terminal Si controlled switches, discussing negative resistance and linear amplification I-V characteristics and applications in oscillators and modulators
20 p2907 A72-39274
- Harmonic oscillation characteristics of avalanche Si diode with nonlinear and negative resistance characteristics
20 p2908 A72-39705
- Differential negative resistance / DNR / in n-channel MOSFETS of silicon.
20 p2961 A72-39711
- Electronic superregeneration in semiconductor photosensitive structures with negative resistance
23 p3268 A72-43345
- Theory of microwave amplification with electron transfer
23 p3269 A72-43550
- Stability criteria for phase-locked oscillators.
23 p3272 A72-44192
- Noise properties of the injection-limited Gunn diode.
24 p3385 A72-44962
- NEMBUTAL (TRADEMARK)**
Nembutal barbiturate effects on afferent signals transmission and thalamocortical level of somatosensory system
08 p1116 A72-21195
- NEODYMIUM**
Mode locked oscillation in ring cavity Nd glass laser, showing satellite pulse and spectral broadening due to self phase modulation
02 p0238 A72-12203
- Picosecond pulse production and measurement from mode locked Nd glass laser
02 p0238 A72-12492
- Neodymium laser plasma dispersion and diffusion in magnetic field, using electrostatic injection of LiH particles
03 p0393 A72-13081
- Pinched vortex tube high current arc discharges for continuous pumping of ion crystal YAG-Nd lasers
06 p0825 A72-17839
- Single pulse Nd laser with KDP cascade multipliers and tunable frequency converter using organic dye solution
06 p0825 A72-17841
- Temporal characteristics of emission line broadening in lasers with dispersive resonators for Nd ion activated phosphate glasses and disordered crystals
06 p0826 A72-18011
- Stimulated emission cross section, loss coefficient and terminal level lifetime of high power Nd-phosphorus oxychloride liquid lasers
07 p1004 A72-19226
- Energy transfer rates and spectral line inhomogeneity of narrow band oscillation phosphate glass and inorganic liquid lasers with Nd
07 p1004 A72-19227
- Continuous TEM power from single longitudinal mode Nd-YAG laser pumped with tungsten-iodine lamp
07 p1004 A72-19235
- Neodymium-glass laser emission spectral and temporal correlations during Q switching by rotating prisms and passive shutter
07 p1006 A72-19633
- Spectroluminescent and lasing properties of Nd ions in anisotropic scheelite crystal structures
07 p1007 A72-20121
- Nd smooth pulsed laser action with narrow spectral line and emission amplification from Nd doped phosphate and silicate glass rods
08 p1183 A72-22027
- Nd glass absorption of flash pump emission energies with varying discharge parameters, Xe pressure and glass thickness
08 p1184 A72-22030
- Giant pulse amplification with neodymium-phosphorus oxychloride liquid laser amplifier
09 p1323 A72-22655
- High power Nd-glass laser systems, discussing oscillator and amplifier operating parameters optimization
10 p1489 A72-23945
- Spectroscopic and stimulated emissive properties of neodymium ions in potassium yttrium tungstate crystals at 77 and 300 K
11 p1701 A72-26362
- Multichannel monopulse Nd glass laser design characteristics, describing input generator, preamplifier and amplifier channel beam distribution
11 p1651 A72-26363
- Angular spectra and frequency characteristics of quasi-continuous monomode and two mode Nd-YAG lasers with spherical resonator
12 p1819 A72-27054
- High power Nd glass laser with stepwise pulse amplification for intensive heating of solid target plasmas
12 p1849 A72-27061
- Frequency tuning and intracavity high efficiency extraction of second harmonic radiation from prism type Nd laser
12 p1825 A72-27885
- Nd-YAG laser bibliography covering oscillation, dynamics, engineering, materials and harmonic generation
12 p1826 A72-27957
- High power monopulse Nd laser, obtaining single longitudinal frequency stabilized mode with anisotropic spar or quartz plates
13 p1971 A72-29922
- Phononless lines shift and broadening and electron phonon interaction in lanthanum trifluoride-Nd crystal, obtaining temperature dependence of non-radiative transition probability
14 p2142 A72-30359
- High energy storage laser material Nd-doped silicate oxyapatite refractivity temperature dependence characteristics measurement
15 p2249 A72-32167
- Spiking response of luminescent diode pumped CW Nd-YAG laser to sinusoidal modulation, showing agreement with relaxation oscillation resonance prediction
15 p2250 A72-32526
- Multichannel monopulse Nd glass laser design characteristics, describing input generator, preamplifier and amplifier channel beam distribution
16 p2403 A72-33715
- Frequency tuning and intracavity high efficiency extraction of second harmonic radiation from prism type Nd laser
16 p2404 A72-33994
- Breakdown of some transparent dielectrics under the action of neodymium and ruby lasers in free light emission modes
19 p2810 A72-37542
- Quantum yield variations of Nd ion activated glass as function of electron beam energy and intensity, noting nuclear particles effect on laser radiation
19 p2823 A72-38205
- Properties of stimulated neodymium laser emission under the action of Co 60 gamma emission
19 p2812 A72-38214
- Amplification of mode-locked trains with a liquid laser amplifier, Nd³⁺/POCl₃:ZrCl₄.
20 p2934 A72-39642

- A stable neodymium-glass laser harmonic generator
21 p3064 A72-41739
- Unidirectional single frequency traveling wave CW
pumped Nd-YAG ring laser, noting spatial hole burning
elimination
22 p3185 A72-42614
- Neodymium-glass laser emission spectral and temporal
correlations during Q switching by rotating
prisms and passive shutter
24 p3408 A72-44565
- Angular spectra and frequency characteristics of
quasi-continuous monomode and two mode Nd-YAG
lasers with spherical resonator
24 p3412 A72-45707
- High power Nd glass laser with stepwise pulse
amplification for intensive heating of solid target plasmas
24 p3431 A72-45714

NEODYMIUM ALLOYS

- Ti-Nd and Ti-Nd-Al alloys heat treatment effects on
tensile and bending strengths
02 p0244 A72-12245
- Nd-Dy alloy magnetic and structural properties over
entire composition range
08 p1217 A72-21596
- Thermal and microstructural analysis of phase
interactions in Mg alloys of Mg-Nd-Y system
14 p2124 A72-31028
- Phase diagram of the neodymium-erbium system
19 p2846 A72-38473

NEODYMIUM COMPOUNDS

- Spectral heterogeneous lasing media with asymmetric
luminescence bands, considering neodymium
phosphate and germanate glass
06 p0824 A72-17392
- Giant pulse radiation in Q factor modulated Nd glass
laser frequency stabilization by molecular Cs vapor
15 p2245 A72-31411
- Laser effect in solution of neodymium oxide in mixture
of phosphorus oxychloride and heavy water,
presenting preparation procedure
15 p2246 A72-31680

NEON

NT NEON ISOTOPES

- Isotopic composition of trapped helium, neon and
argon in carbonaceous chondrites, observing covariance
based on mass-dependent fractionation
03 p0414 A72-12904
- Pulsed current changes in positive column of He and
Ne discharges, observing gradient and electron
concentration transient behavior
03 p0399 A72-14348
- Neon lower laser level spontaneous emission double
resonance phenomena, discussing depopulation rates
and resonance line profile changes
04 p0531 A72-15138
- Galactic nucleus IR measurements in terms of forbidden
NE II emission line at 12.8 microns
07 p1081 A72-20229
- Subnanosecond light pulse generation by Ne laser at
5401 Å by amplified spontaneous emission
09 p1323 A72-22869
- Nonlinear effects in optical pumping of Ne transition
by laser line
10 p1491 A72-24109
- Absolute differential cross sections of electrons
elastically scattered on neon atom.
18 p2713 A72-36952
- The use of known helium line cross sections for investigation
of unknown transition in neon.
18 p2713 A72-36954
- Ion-atom scattering and interatomic potentials for
ions of noble metals and period II elements incident on
neon and argon with energies in the range 8-25 keV.
19 p2837 A72-37883
- Pressure shift of the magnetic resonance line of
neon in a He-Ne laser.
19 p2811 A72-37930
- Interpretation of experimental differential elastic
scattering cross section for H⁺/+ Ne.
20 p2956 A72-39721
- Transition probabilities and collision-induced transitions
in excited levels of neon.
21 p3061 A72-40136
- The mass spectrographic measurement of gas
separation with the aid of ambipolar effusion in neon-
krypton mixtures
21 p3053 A72-40486
- Nonlinear interaction of p and s ionization waves in
neon.
21 p3090 A72-40487
- Apparent constant wavelength oscillations in a
bounded plasma.
23 p3320 A72-43577
- New lines of neon ions in the range 50-200 Å.
23 p3315 A72-43802
- Frequency stabilization of pure neon laser.
23 p3296 A72-43951
- Nonlinear effects in the dynamic behavior of the
positive column from a low-voltage low-pressure
discharge
24 p3428 A72-44965

NEON ISOTOPES

- L-chondrite Assam, determining He, Ne and Ar
concentrations and isotopic compositions and galactic
and solar flare irradiation track densities
01 p0124 A72-10060

Optical hyperfine structure of Ne 21 excited states
and quadrupole moment obtained by laser induced line
narrowing techniques
10 p1515 A72-24601

Ar-39/Ar-38 cosmic ray exposure age calculation
from Sikhote-Alin meteorite fall fragment content of
Ar-39, Ar-38, Ne-21 and He-3
14 p2157 A72-30584

Pure Ne laser and its fundamental characteristics.
23 p3296 A72-43946

NEON 19

U NEON ISOTOPES

NEOPENTANE

- Organophosphorus antiwear additives in neopentyl
polyol ester lubricants on 440C stainless steel surfaces,
using four ball wear test machine
[AD-740055] 02 p0250 A72-12849
- Chromatographic analysis of reaction products of
HCl-accelerated neopentane pyrolysis, showing tert-
butyl chloride formation
10 p1434 A72-24235

NEOPLASMS

NT CANCER

NT LEUKEMIAS

NEPHELOMETERS

- Atmospheric aerosol chemical composition analysis
by nephelometer light scattering measurement of
suspended particle mass concentration, visibility and
size distribution and scattering-humidity relationship
[ALAA PAPER 71-1101] 01 p0058 A72-10549
- NEPTUNE (PLANET)
Methane contribution to thermal opacity in Uranus
and Neptune atmospheres for atmospheric model
synthesis
09 p1383 A72-22293

Jupiter, Saturn, Uranus, Neptune and Pluto state of
knowledge, noting angular momentum fraction, red
spot, albedos, densities, atmospheric compositions,
natural satellites, etc
12 p1870 A72-27345

Uranus, Neptune and Pluto disk temperature observations
via National Radio Astronomy Observatory
interferometer
16 p2455 A72-33464

Secular variations of the first order of elements for
the four major planets - Comparison with Le Verrier
and Gaillot
18 p2727 A72-36734

The masses, densities and moments of inertia of
Uranus and Neptune.
20 p2967 A72-39184

Invalidity of Neptune predicted position derivation
from perturbations on Uranus via method neglecting
eccentricity
21 p3111 A72-41474

NERNST GENERATORS

U THERMOMAGNETIC COOLING

NERNST HEAT THEOREM

U NERNST-ETTINGSHAUSEN EFFECT

NERNST-ETTINGSHAUSEN EFFECT

- Ni-Co alloys Nernst-Ettingshausen and Hall effects
anomalous constants relationship determination from
emf and electrical conductivity measurements
13 p1977 A72-28910
- Adiabatic conditions influence on charge carriers
dispersion determination of semiconductors based on
Nernst-Ettingshausen effect
15 p2291 A72-31390

Temperature dependence of the thermal electromotive
force and of the Nernst-Ettingshausen effect in
nickel-cobalt alloys
22 p3187 A72-41855

NERVA (ENGINE)

U NUCLEAR ENGINE FOR ROCKET VEHICLES

NERVES

HIS bundle electrocardiography for arrhythmia studies,
discussing conducting tissue potential recording,
ventricular delay and block site determination and
electrophysiological effects of drugs
02 p0157 A72-11473

Vestibular nuclei bulbar complex evoked potentials
under visceral and somatic nerves electric stimulation
in anesthetized cats
02 p0164 A72-12512

Exercise and denervation effects on intrafusal
muscle fibers morphology, noting 25-33 percent cross-
sectional area atrophy in nuclear bag and chain fibers
04 p0472 A72-14895

Adrenergic innervation of internal carotid arteries in
extra- and intracranial regions in dogs, using
luminescence method
08 p1121 A72-22184

German monograph on Ranvier node steady state I-
V characteristics transition range and control by altered
external solutions and morphological effects on
nerve fiber
09 p1264 A72-22336

Photically induced and spontaneously discharged
neuron impulse propagation through direct pathways
from superior colliculus to dorsal and ventral lateral
geniculate nuclei in cats
09 p1265 A72-22863

Cerebrospinal fluid pH change effects on cat
respiratory response before and after vagotomy,
showing vagal activity relation to central chemical
control of respiration
12 p1762 A72-27825

Vagus nerve regeneration in humans after stomach
cancer surgery
13 p1903 A72-28779

Statistical activity analysis procedure for random
nerve network model, determining representative
point trajectory in phase space via similarity matrix
13 p1909 A72-29176

Myelinated nerve fiber mathematical model for action
potential transmission mechanism analysis during
relative refractory phases
14 p2079 A72-30597

Cat cerebellum cortex evoked response impulses in
teraction during stimulation of hypothalamus and
peripheral nerves
14 p2076 A72-30669

Cerebral cortex electric shock stimulation effects on
phrenic nerve discharges in bivagotomized and curarized
cats
14 p2077 A72-30842

Acquired complete right bundle branch block
without overt cardiac disease - Clinical and
hemodynamic study of 37 patients.
17 p2505 A72-35821

Effects of vagotomy and increased blood pressure
on the incidence of decompression-induced pulmonary
hemorrhage.
18 p2650 A72-36446

Electrical stimulation of vestibular nuclei - Effects
on light-evoked activity of lateral geniculate nucleus
neurons.
19 p2758 A72-38220

Study of bilateral cortical nerve connections
between the preorel gyrus and various cortical regions
20 p2891 A72-39323

Propriospinal ducts of the lateral funiculus and their
possible role in transmission of pyramidal stimuli
21 p2999 A72-40583

Localization and structural-functional organization
of the system of vagus nerve nuclei constituting the
'cardiac center' of the medulla oblongata
21 p3004 A72-41673

Computation of the shape and velocity of a nerve
pulse
22 p3149 A72-42156

Continuous recording of His bundle electrogram
during selective coronary cineangiography in man.
23 p3255 A72-43813

H-V intervals in left bundle-branch block - Clinical
and electrocardiographic correlations.
24 p3374 A72-45690

Clinical and anatomic implications of intraventricular
conduction blocks in acute myocardial infarction.
24 p3374 A72-45691

NERVOUS SYSTEM

NT AFFERENT NERVOUS SYSTEMS

NT AUTONOMIC NERVOUS SYSTEM

NT AXONS

NT BRAIN

NT BRAIN STEM

NT CENTRAL NERVOUS SYSTEM

NT CEREBELLUM

NT CEREBRAL CORTEX

NT CEREBRUM

NT DIENCEPHALON

NT EFFERENT NERVOUS SYSTEMS

NT GANGLIA

NT HIPPOCAMPUS

NT MYELIN

NT NERVES

NT NEUROGLIA

NT NEURONS

NT PERIPHERAL NERVOUS SYSTEM

NT SPINAL CORD

NT SPINE

NT SYMPATHETIC NERVOUS SYSTEM

NT SYNAPSES

NT THALAMUS

Soviet book on physiology of conditioned reflexes
covering brain and nervous system, tonic reflexes,
functional models, inhibition localization, etc
01 p0011 A72-10295

Human nervous system properties responsible for
individual behavioral differences, discussing
methodological problems in future research from
biological criteria viewpoint
08 p1118 A72-21839

Conditioned reflex activity, discussing biological
and nervous system, electric analog simulation and
mathematical and structural modeling
08 p1127 A72-21842

Effects of long periods of clinical death from
drowning or lethal blood loss on higher nervous activity
in reanimated dogs
13 p1902 A72-28642

Statistical activity analysis procedure for random
nerve network model, determining representative
point trajectory in phase space via similarity matrix
13 p1909 A72-29176

Effect of a magnetic field on experimental tumors
/direct and via nervous system/
17 p2503 A72-35011

- New experimental data on the morpho-physiological analysis of the adaptation phenomenon in the somatic reflex arch 17 p2504 A72-35023
- Vasomotor reflex locking level 17 p2504 A72-35025
- Biological systems activity in controlling extremal problems of nervous and muscular systems, noting external stimulation minimization 19 p2761 A72-38577
- Changes in the functional state of analysors in flying personnel during long flights 21 p3006 A72-40445
- Critique of Pavlov conditioned reflex role in higher nervous activity and association principle role in psychic activity 21 p3001 A72-40811
- A model for analysing the coordination of manual movements. 21 p3010 A72-41413
- Some data on the interrelations of conscious and unconscious reactions 23 p3257 A72-44076
- Influence of the nervous system and its mediators on the spontaneous contractile activity of a smooth muscle 24 p3370 A72-44590
- ## NETS
- ### NT NEURAL NETS
- ## NETWORK ANALYSIS
- ### NT CRITICAL PATH METHOD
- Large-signal IC equivalent circuit model for DC, linear and nonlinear transient time circuit analysis of lateral p-n-p transistors, including isolation junction interactions 01 p0044 A72-10126
- Microwave oriented circuit analysis program (MODMAN) to handle nonlinear, time-varying, lumped and distributed elements in time domain, using transmission line modeling algorithm 01 p0045 A72-10687
- Irredundant multiple output combinational logic network fault detection and diagnosis theorems derivation from structural models in labeled direct graph form 02 p0184 A72-11478
- Circuit theory optimization techniques in computer aided electric circuits and devices design, discussing algorithms, sequential methods, convergence speed, topologies, system responses, etc 02 p0197 A72-11688
- Computer aided circuit design and analysis, emphasizing algebra of structural numbers as synthesis technique without system structure restriction 02 p0186 A72-11693
- Network sensitivity analysis emphasizing first, higher and mixed higher derivatives computation and iterative synthesis techniques 02 p0197 A72-12114
- Affined RC or RL networks, investigating real and equal or imaginary, conjugate and inverse voltage and current transmittances 02 p0197 A72-12240
- Dc, ac and transient models of IC operational amplifier for computer aided circuit design and analysis applications 03 p0329 A72-14180
- Microcircuit failures due to electrical overstress, covering current density, thermally induced burn-out, junction shorts and second breakdown with nonuniform heat flow 03 p0336 A72-14290
- Computer analysis of linear electric circuits without restrictions on network topology and component composition, using system matrix 04 p0495 A72-14464
- Circular network analysis by conformal mapping method, evaluating physical and geometric magnitudes in turbine driven machinery 04 p0461 A72-14514
- Implicit equations in nonlinear network analysis, deriving conditions for existence of unique solutions 04 p0540 A72-15695
- Computer aided linear circuit design for network synthesis, analysis, optimization and data storage noting MARTHA program 05 p0639 A72-15785
- One dimensional bipolar junction transistor, comparing charge control and regional mathematical models for suitability in device and circuit computerized analysis and design 05 p0636 A72-16359
- Photomultiplier operation pulsed control in semiconductor circuit for background cosmic radiation noise error minimization in atmospheric shower station 06 p0811 A72-17294
- Digital system automated design and analysis developments covering interactive graphic computer aided design, gate level simulation, synthesis, partitioning, interconnection and fault test generation 06 p0778 A72-17471
- CIRCAL-2 general purpose on-line circuit design computer program featuring multiple analysis, text editing, network representation and user-program interaction optimization capabilities 06 p0778 A72-17474
- Coordinated characterization and mathematical modeling for device, circuit and system designs and computer analysis, applying to bipolar transistor 06 p0778 A72-17477
- One dimensional analysis computer program for junction device modeling, exemplifying hf bipolar transistor Fermi statistics effect and velocity limitation in high current density 06 p0779 A72-17478
- Computer aided steady state response analysis for nonlinear electric circuits with periodic input, using Newton algorithm with rapid convergence 06 p0779 A72-17480
- Linear network sensitivity and group delay evaluation without topology or component restraints, using computer technique 06 p0793 A72-17594
- Two dimensional network class port behavior equivalence to three layer structures of linear passive isotropic materials based on depth and surface properties analysis 06 p0793 A72-17595
- GERT simulation program as stochastic network analysis technique for modeling policies and processes in performance tests and checkout 06 p0780 A72-17977
- Algorithm for constructing linear and nonlinear differential and algebraic equations of state variables of nonlinear electronic circuits 07 p0958 A72-18846
- Direct coupled waveguide cavity resonator equalizer networks, determining reflection coefficient, phase, amplitude and time delay characteristics by scattering matrix theory 07 p0955 A72-19327
- Digital simulation for predicting performance of data communication networks with computerized switching centers, detailing space shuttle interior communication system 07 p0952 A72-20364
- Input binary sequence transformation in chain of series connected on-off neuron models, applying to n-stage linear filter analysis 08 p1138 A72-20870
- German monograph on multielement linear mechanical oscillator analysis covering behavior of harmonically excited bar chains of arbitrary structure 09 p1350 A72-22337
- Linear IC amplifier analysis by admittance parameters of equivalent two terminal pair network as function of frequency, temperature and supply voltage 09 p1285 A72-22342
- Linear analysis and synthesis of three dimensional interference system stationary in space and time domains 09 p1278 A72-22573
- Stability degree analysis of linear feedback control systems with dead time, presenting proportional and integral compensation diagrams produced with digital computer program 09 p1291 A72-23370
- Electronic circuits statistical optimization with Monte Carlo procedure, discussing methods and algorithms for accelerating evolutionary modeling 10 p1452 A72-24638
- Book on logarithmic video amplifiers covering design, analysis, performance and applications 10 p1452 A72-24698
- Digital computer calculation of complex electric networks described by mathematical models, calculating flow distribution 11 p1577 A72-25282
- Nonlinear resistive network analysis by piecewise linear mappings, studying Lipschitz condition and global homomorphism 11 p1608 A72-25360
- Computerized filter design, discussing frequency analysis and synthesis programs for quadrupole eigenmodes and transfer function 11 p1604 A72-26089
- Phase metering information converters with digital analog computation, discussing analysis of prototype semiconductor model with ten-digit binary codes 11 p1602 A72-26449
- Linear multiple section binary filters analysis and synthesis, discussing mesh functions spectra for signal measurement in automatic control systems 11 p1612 A72-26452
- Transistorized measuring amplifiers optimal initial regimes calculation with generalized junction voltage method, noting circuits analysis and internal feedback loops 11 p1605 A72-26467
- IC lateral p-n-p multijunction transistor frequency characteristics analysis, noting parasitic effects, cutoff frequencies and power gain 12 p1788 A72-27311
- Linear approximations and grapho-analytical method for neuronist line analysis, noting conditions for tunnel diode parameters 12 p1789 A72-27397
- Iterative solution for linear and nonlinear dc networks with independent voltage sources, noting convergence conditions 12 p1794 A72-27398
- Encapsulation influence on Gunn effect devices from circuit analysis of wideband tunable transferred electron microwave oscillators 12 p1790 A72-27440
- Antoniou bridge type gyrator circuit stability, showing sensitivity to resistors ratio variations 12 p1792 A72-27698
- TV network distribution systems cost, comparing video tape shipping, terrestrial interconnection with delay for time zones and indirect and direct satellite transmission [ALAA PAPER 72-552] 13 p1918 A72-28983
- Circuit of two parallel connected vacuum pentodes with different reactances to provide exact voltage division of ac signals by another 13 p1930 A72-29045
- Transfer matrices determination for two terminal pair network derived from four terminal pair network, considering bandpass filters 13 p1931 A72-29060
- Circuit theory - Conference, University of Missouri, Rolla, May 1972 13 p1935 A72-29101
- Nonlinear harmonic analysis of reflex klystrons with high electron conductance, using average method in second approximation 13 p1931 A72-29290
- Interaction between generating lines in coupled channels with arbitrary line broadening, studying radiation generation regimes in cascade circuit 13 p1970 A72-29680
- Electromagnetic processes computation in circuits with SHF currents by reduction to integral equation, using dipoles system representation 13 p1937 A72-29945
- Nonsingular feedback control system phase-amplitude frequency response graphical analysis using real circle diagram 13 p1937 A72-29974
- Variable saturation of series LC circuit, discussing current response, ferromagnetic jump, symmetry and subharmonic oscillations 14 p2090 A72-31116
- Regenerative semiconductor parametric amplifier under dc through p-n junction, analyzing nonlinear phenomena 14 p2090 A72-31124
- Lumped approximation to distributed RC notch networks for linear IC, deriving open circuit voltage transfer functions and root locus graphs 14 p2092 A72-31170
- Multiple port waveguide circulators bandwidth performance calculation to include higher order cylindrical and evanescent modes 15 p2205 A72-31356
- Low storage numerical solution of waveguide problem based on impulse analysis, using random walk technique to eliminate large matrix processing 15 p2194 A72-31542
- Reflector networks analysis for optimal operation of electronic scanning antenna in illuminated grating 15 p2195 A72-31670
- Computer program for symbolic network functions, using numerical algorithms for branches not represented by symbolic parameters 15 p2211 A72-31845
- Nonideal component parts effect on behavior of digital microstrip closed circuit X band phase shifter, presenting detailed network analysis 15 p2201 A72-32471
- Mathematical models for electromagnetic interference in electronic equipment, discussing nonlinear circuit analysis 15 p2201 A72-32568
- Three section stepped structure to satisfy requirements for multifunction matching four-pole in signal network with active semiconductor component 15 p2210 A72-32708
- Passive and active electric circuit analysis by structural numbers method with computer time and space advantages, noting application to transistor circuits 16 p2370 A72-32851
- Laguerre filters parameters choice for correlator input networks application, noting output SNR improvement 16 p2368 A72-33089
- Stress and parametric change analysis for failure mode identification and reliability screen tests of LSI circuits, noting MOS inverter operation and RAM mechanization 17 p2528 A72-34706
- Parametric resonance in an oscillatory circuit with a nonlinear p-n junction capacitance 17 p2533 A72-34757
- Calculation of steady modes of operation of RC circuits with jumpwise varying parameters 17 p2533 A72-34761
- The identification of parameters in nonlinear thermal networks with the aid of a Kalman filter 17 p2533 A72-34827

A recognition method for technical diagnosis of analog electronic circuits

17 p2522 A72-34913

DC analysis of linearized electronic circuits with the aid of electronic computers

17 p2524 A72-35977

Fundamental, harmonic and combination frequency components amplitude analysis via dual input describing function for nonlinear element response under two incommensurate frequency sinusoidal signals

18 p2671 A72-36051

Development of a continuous linear model of a d-c to d-c flyback converter.

18 p2643 A72-36073

Digital simulation of stiff linear dynamic systems.

18 p2663 A72-36315

Minimax method of optimizing electric circuits in the absence of constraints on the variable parameters

19 p2777 A72-37309

Programming method for computer analysis of linear passive circuits powered by voltage sources

19 p2777 A72-37311

Determination of linear circuit sensitivity to circuit parameter changes in the equations of state variables

19 p2777 A72-37312

Matrix coefficients calculation of state variables equations for network analysis and synthesis

19 p2777 A72-37313

Feedback influence coefficient on amplifier gain, using recurrent difference concept

19 p2777 A72-37314

Admissible changes in the parameters of a matching four-terminal network

19 p2772 A72-37315

Equivalent circuits and oriented graphs for network analysis and synthesis of nonlinear transducers used in control systems

19 p2777 A72-37316

French monograph - Contribution to the study of the behavior of bipolar transistors during high frequency dynamic operation

19 p2772 A72-37485

Frequency-selective networks suitable for microelectronic realization. II.

19 p2773 A72-37874

Frequency detection with digital resonators without damping

19 p2773 A72-37939

Amplitude and harmonic oscillation characteristics of quaternary RC parametron using tunnel diodes

19 p2773 A72-38211

Adaptive control systems fundamental functions, principles, characteristics and applicability

19 p2782 A72-38312

Digital computer algorithm for electronic circuit calculations

19 p2774 A72-38422

A six-phase bridge rectifier circuit with a reduced number of controlled rectifiers and a rigid external characteristic during high-level regulation

19 p2774 A72-38585

Eigenfrequencies of monolithic filters.

19 p2774 A72-38608

A large-signal theory for current-driven frequency multipliers.

19 p2775 A72-38609

Mathematical model for MOS transistor circuit analysis, noting parameters measurement and environmental effects representation

20 p2909 A72-39783

Integral equations of a multipoint network with a digital control automaton

21 p3036 A72-40154

Possibility of developing combination method for calculating, with a controlled quantization step, the response of a nonlinear network

21 p3074 A72-40184

Digital filters with cyclically variable coefficients

21 p3025 A72-40221

Communication network vertex and mixed cutset definitions and computation from interchange graph of given finite connected undirected graph without loops and multiple edges

21 p3015 A72-40634

Digital command system second-order subcarrier tracking loop performance.

21 p3038 A72-40870

Communication receivers interference modeling - Nonlinear transfer functions from circuit analysis - Mild excitations.

21 p3019 A72-40890

Digraphs application to electronic linear networks analysis, developing computer program

21 p3024 A72-40992

Network algebra simplification through computerized minimization of Boolean functions, describing FORTRAN IV program

21 p3038 A72-41001

Shaping circuit for complex RF pulse consisting of simultaneous equilength square pulses with different frequencies, discussing carrier frequencies selection

21 p3022 A72-41118

The mathematical synthesis and analysis of fluid logic networks.

22 p3161 A72-42049

Complex amplitude four-pole network nonlinear conversion of sum of sinusoidal oscillations

22 p3158 A72-42083

Network analysis and frequency response of LF filter with distributed RC structure and voltage converter

22 p3158 A72-42120

Generalized numbers method for analysis and synthesis of linear circuits described by signal flow graph, noting algorithms for computer programming

23 p3269 A72-43443

Numerical integration of nonlinear differential equations in nonlinear circuits analysis, obtaining information on unsteady processes from calculation with controlled level time quantization step

23 p3269 A72-43444

Error analysis of linear and nonlinear elements in hydraulic control circuits of flight vehicles, calculating accuracy of frequency response determination

23 p3252 A72-43671

An estimate of expected critical-path length in PERT networks.

23 p3308 A72-43806

Linear electronic networks analysis and synthesis via equations of variable states, noting structural features of circuits without component related degeneration

23 p3271 A72-43844

Asilomar Conference on Circuits and Systems, 5th, Pacific Grove, Calif., November 8-10, 1971, Record.

23 p3276 A72-43851

An algorithm to obtain the steady state response of nonlinear periodic systems.

23 p3267 A72-43852

NETWORK SYNTHESIS

Tunnel diode microwave oscillator design by circle diagrams of operational and load characteristics

01 p0035 A72-10048

Time optimal phase locked AFC system synthesis based on Po ntryagin maximum principle, comparing computerized and experimental transient response

01 p0024 A72-10049

Optimal design of logic networks in homogeneous microelectronic structures, using shortest link search and graph continuity parameters

01 p0034 A72-10300

Network synthesis of cascaded threshold logic elements to separate binary patterns into two classes by iterative computation of parameters

01 p0034 A72-10474

Distributed impedance controller synthesis for stabilization of plane fluid flows, investigating Rayleigh-Taylor instability

01 p0050 A72-10504

High stability and power IMPATT oscillator design for line-of-sight communication links, avoiding spurious resonances and mode jumping

01 p0037 A72-10645

Microwave module circuit design for airborne phased array radar with distributed power generation, reception and phase shift functions, considering performance, reliability and cost

01 p0028 A72-10660

Ferrite microwave devices design, covering nonreciprocal circuit and electrical tuner

01 p0041 A72-10696

Directional couplers design for broadband microwave integrated circuits

01 p0046 A72-10702

Efficiency/reliability design requirements of driven transistor synchronous rectifiers in low output voltage applications

01 p0042 A72-11053

Integrated electronics digital-analog solar cell array control unit, discussing circuit design and radiation hardening

01 p0042 A72-11059

Phase stable locked local oscillators for K band radiometers for long baseline interferometric measurements, emphasizing construction technique

01 p0044 A72-11307

Minimum length fault tests design for irredundant combinational logic circuits containing single faults based on Boolean difference function

02 p0185 A72-11485

Interference control in microwave circuit design, discussing coupling element, antenna terminals, radiated interference susceptibility and electromagnetic environments

02 p0189 A72-11558

High perveance electron guns with control grids and low voltage beam modulation, considering design, operation, structural and control characteristics

02 p0189 A72-11562

Computer aided circuit design and analysis, emphasizing algebra of structural numbers as synthesis technique without system structure restriction

02 p0186 A72-11693

Circuit design techniques used for wideband signal processing systems, considering 1000 MB/S microwave communication link

02 p0176 A72-12163

Reactive two terminal pair network synthesis for shaping sawtooth current pulses in inductive load for given input function

02 p0193 A72-12222

High efficiency GaAs transferred electron device operation and microwave oscillator design by simple static I-V characteristics description for time domain computer simulation

02 p0193 A72-12230

Linear aperture antennas approximate synthesis method, determining radiation pattern characteristics by solution of extremal problems in theory of linear integral operators

02 p0195 A72-12592

Computer programs and program systems for IC synthesis, emphasizing models, analysis methods, optimized design and monolithic and hybrid IC configurations

02 p0197 A72-12668

Multiple access techniques in satellite telecommunication systems, discussing clean mesh type network

02 p0182 A72-12699

Optimal synthesis of pulse repetition frequency control and filtering circuits of radar range finder in Gaussian approximation

02 p0183 A72-12759

MOS transistor frequency and transient response characteristics for equivalent circuit synthesis, using Bessel functions in differential equation solution

02 p0196 A72-12761

Active all-pass circuits transfer function and synthesis, including delay lines, phase correctors and wide-band phase shifter applications

03 p0338 A72-13169

Self consistent junction circulator theory, considering lossless ferrite loaded symmetric n-port junction and numerical design procedures

03 p0330 A72-13232

Linear time optimal control system with retardations in controls, discussing controllability, existence and uniqueness, synthesis techniques and dynamic programming

03 p0338 A72-13406

Linear radio receiver circuit synthesis for output signal structure and rotational choice, using reduction algorithm

03 p0323 A72-13894

Limiting approximation theorems for synthesis of linear circuits and signals in time-frequency domains

03 p0338 A72-13896

Dc, ac and transient models of IC operational amplifier for computer aided circuit design and analysis applications

03 p0329 A72-14180

Self oscillating dc-to-dc converters performance and design, considering switching frequency, duty cycles, line and load regulation and peak-to-peak ripple

04 p0465 A72-14487

RC network synthesis technique using grounded gyrator and summing amplifier, applying to thin film RC networks and IC operational amplifiers

04 p0504 A72-14570

Optical birefringent networks synthesis, describing use of building blocks of polarizers, birefringent crystals and optical compensators

04 p0548 A72-14737

Control system synthesis from transient process estimates with Liapunov functions, proposing optimality criteria based on Gaussian minimum constraint principle extension

04 p0505 A72-14997

Optimal nonlinear discrete filters with finite memory for polynomial signals, discussing synthesis with aid of minimax method

04 p0505 A72-14998

Linear dynamic system sensitivity models simplification conditions application to adaptive nonsearching system synthesis algorithms

04 p0505 A72-14999

Programmable cellular cascades and arrays synthesis for realizing arbitrary Boolean functions or parallel arithmetic operations

04 p0498 A72-15107

Synthesis of currents along linear antennas, reducing to solution of integral equation

04 p0500 A72-15406

Capacitor-fed parallel chopper as phase sensitive demodulator, discussing design, stability, linearity and wide dynamic frequency range

04 p0507 A72-15522

Computer aided linear circuit design for network synthesis, analysis, optimization and data storage noting MARTHA program

05 p0639 A72-15785

N-port resistive network synthesis involving use of vectors, cones, bilinear inequalities and matrices

05 p0639 A72-15801

Synthesis method for optimized single-stage reflection type phase shifters, determining transformation coefficient

05 p0634 A72-15831

Logical synthesis of hybrid off-on control systems with proportional and binary variables, presenting example of fluid power, electronic and fluidic implementation

[ASME PAPER 71-WA/FLCS-1]

05 p0640 A72-15919

Linear single and multiloop control system synthesis for sensitivity reduction by introducing signals proportional to sensitivity functions with analyzer
05 p0640 A72-16207

Model reference adaptive control system synthesis in presence of random perturbations, considering error signal derivative use to form parameter adjustment algorithm
05 p0640 A72-16208

Radio signal electron-phonon detector design and experimental realization, considering requirements for minimum transduction and surface wave propagation loss
05 p0626 A72-16281

Nonlinear spatial filter synthesis by one-to-one signal-to-reference beam ratio and optimum exposure condition
05 p0663 A72-16676

Optimally sensitive closed loop control synthesis for systems containing uncertain time varying parameters, applying to stochastic systems
06 p0792 A72-17309

CIRCAL-2 general purpose on-line circuit design computer program featuring multiple analysis, text editing, network representation and user-program interaction optimization capabilities
06 p0778 A72-17474

Algebraic scheme describing electric element and subnetwork interconnection into networks by wiring operators having conversation capability with computer
06 p0778 A72-17475

Microwave frequency multiplier construction by hybrid circuits based on quasi-lumped components, calculating characteristics from equivalent circuit
06 p0785 A72-18313

Unified design charts for communication systems filter networks with inverse Chebyshev and elliptic function responses
06 p0787 A72-18400

High efficiency microwave avalanche diode oscillators circuit design in TRAPPATT mode
06 p0787 A72-18455

Optimal receiver synthesis for radio signals with differentiable components of continuous Markov processes masked by phase interference and white noise
07 p0937 A72-18847

Steepened microwave bandpass filters with bypass and flattened reflection coefficient and delay, discussing design and implementation
07 p0954 A72-19175

Suboptimal Kalman filter design for system state estimation in presence of plant dynamics uncertainties and measurements noise, optimizing tradeoff between sensitivity and estimation error
07 p0959 A72-19302

Microwave IC front end receiver synthesis for radio relay system, considering low noise figure achievement by Si Schottky barrier diodes
07 p0955 A72-19356

Optimal Bayesian system synthesis for simultaneous discrimination and parameter estimation of several signals in noise background
07 p0943 A72-19516

Algorithm for asynchronous multilevel sequential circuits design, stressing NOR networks
07 p0963 A72-20387

Quantization errors effect on recursive filter design for strapdown inertial navigation systems, developing suboptimal linear minimum variance
08 p1144 A72-20848

Numerically exact nonlinear filter synthesis, describing confidence intervals for error performance statistical inferences
08 p1144 A72-20850

Hybrid computer synthesis and simulation algorithm for optimal discrete nonlinear filters, giving timing, accuracy and equipment requirement estimates
08 p1137 A72-20851

Transcendent Si power rectifier with high current and power dissipation capacity, discussing design, fabrication and performance tests
08 p1111 A72-21413

Circuits for pulse rise time discrimination in proportional counters with different gas mixtures
08 p1167 A72-21511

Radio communication system optimization from viewpoints of global synthesis, including economics and partial synthesis based on noise stability, precision and reliability
08 p1136 A72-21845

Digital filter synthesis for radar signal processing applications, discussing frequency sampling method extension with advantage of known waveform and reduced computations
08 p1146 A72-21916

German monograph on optimal design of HF bandpass filters with lumped elements, covering LC coupled two- and four-circuit systems
09 p1284 A72-22328

Linear analysis and synthesis of three dimensional interference system stationary in space and time domains
09 p1278 A72-22573

Horn antenna synthesis for determining impedance boundary conditions at walls for aperture field distribution
09 p1285 A72-22574

Polynomial filter design with three layer RC distributed elements and operational amplifiers, investigating active elements effects on response
09 p1290 A72-23354

Digital computer prepared optimal controls setting diagrams for single loop, linear and concentrated parameter control circuit design
09 p1291 A72-23372

Phased array radar systems synthesis based on life cycle cost minimization, taking into account high-speed digital data processing
09 p1280 A72-23374

Stationary Kalman-Bucy filter synthesis from filter coefficients and correlation matrix of filtration errors, discussing random process estimation application
09 p1289 A72-23434

DESMAG computer program extension with graphic terminal to functional network conception and implantation
09 p1283 A72-23469

Numerical linear interpolator design with ICs, noting application to digital filters and sampled data systems
09 p1289 A72-23677

Flow control circuits design based on unvented bistable fluid amplifiers
10 p1422 A72-23970

Bulk effect diodes combination with YIG elements to provide oscillator operation up to 18 GHz, discussing design, circuit diagrams and performance
10 p1448 A72-24037

Integrated circuits fabrication and design, describing internal physical processes, input and output signal values, functional operations and topological features
10 p1448 A72-24283

Nonlinear filtering synthesis of optimal receiver for pseudorandom phase shift keyed signal with arbitrary modulation angle and white noise background
10 p1436 A72-24510

Narrow bandpass waveguide filters synthesis, using orthogonal mode cavities to realize negative coupling elements
10 p1451 A72-24591

FM measurement system with linear resistance-to-frequency converter realized in RC oscillator form, discussing design problems
10 p1482 A72-24598

Pulse width modulated regulating dc-to-dc converter with small number of transistors to improve circuit reliability
10 p1452 A72-24680

Network synthesis for various second and third order sinusoidal oscillators consisting of linear passive or active RC circuits and amplifier
10 p1452 A72-24802

Voltage-frequency converter network design and operation, presenting circuit diagram
10 p1453 A72-24817

Stabilization bandwidth reduction in microwave parallel tunnel diode amplifier circuits synthesis
10 p1453 A72-24910

Linear constant systems synthesis with structural constraints in state space form, applying to RC filter circuit
10 p1453 A72-25101

Stationary weighting pattern synthesis by linear time varying dynamic system, noting feedback system input-output mapping property
11 p1608 A72-25321

Lumped-distributed active network function sensitivity formulas in terms of immittance parameters
11 p1610 A72-25747

Switching behavior and attenuation of space division multiplex crosspoint circuit with end marking, discussing realization in thick film technology
11 p1604 A72-25908

Soviet book on radio receiver design covering military applications, bandwidth requirements, network synthesis and AM, FM, SSB, Doppler, phase metering, PCM and radar equipment
11 p1604 A72-26045

Computerized filter design, discussing frequency analysis and synthesis programs for quadrupole eigenmodes and transfer function
11 p1604 A72-26089

Matrix and graphic test construction methods for optimal design of logic networks in automatic control systems
11 p1612 A72-26443

Linear multiple section binary filters analysis and synthesis, discussing mesh functions spectra for signal measurement in automatic control systems
11 p1612 A72-26452

Electronic filters realization by error function minimization, discussing parameter space algorithmic search and complex plane optimization methods
11 p1606 A72-26550

Multipole synthesis compensating mutual coupling for orthonormalized radiation patterns in ring antenna array
11 p1598 A72-26711

Radiation pattern forming circuit with compensated mutual coupling in phased antenna arrays, noting synthesis by matched multipoles
11 p1598 A72-26712

Criterion selection and minimum margin search for optimization of complex electronic circuit parameters described by mathematical models
11 p1612 A72-26736

Polish monograph on minimal representations and identification of Boolean function symmetry in combinational logic network synthesis, using two dimensional topological model
12 p1793 A72-27224

Multivalued logical function synthesis with multistage logical network through hypercomplex representation and linear transformation
12 p1794 A72-27497

Matching two port network synthesis for prescribed damping poles and impedances
12 p1794 A72-27573

Integrated metal-nitride-oxide-silicon (M/NOS)/semiconductor storage units characteristics, design and operation in FETs
12 p1791 A72-27574

Computer aided circuit design by TRAPPATT diode model consisting of nonlinear capacitance shunted by voltage- and current-controlled switch
12 p1791 A72-27672

RC network synthesis for accurate realization of complex transmission zeros without capacitor adjustment
12 p1794 A72-27696

Dicke radiometer for 100 meter radio telescope, discussing demodulator design with dc coupling for difference signal and individual switching phases
12 p1792 A72-27807

Optimal reception system synthesized for FM signal with phase fluctuation masked by narrow band AM and white noise
13 p1914 A72-28414

Additional operator method application to nonlinear servosystems self adjusting circuits design, presenting system simulation results
13 p1935 A72-28611

Method to obtain optimal efficiency gyroamplifier circuits with short waveguide selector by prior grouping of electronic oscillators
13 p1928 A72-28799

Subtraction circuit design for impulse noise elimination at front end of aircraft oriented OMEGA navigation system receiver
13 p1999 A72-29204

Microwave circuits for multiplexing applications, discussing optimal design in terms of economic, mechanical and electrical parameters
13 p1934 A72-30089

Graphical design technique based on Nyquist plane construction using circle criterion for nonlinear systems controller synthesis
14 p2091 A72-30375

Narrow band retuned dc pumped amplifier-filter design based on diffron, considering electron beam interaction
14 p2088 A72-30798

Two-variable resonant ladder network synthesis for prescribed amplitude response with closed-form solution, illustrating with waveguide bandstop filter
14 p2091 A72-30945

Optimal filter synthesis for linear time varying parameter control systems, using computer-aided solution of multidimensional Riccati equations
14 p2090 A72-31120

Inexpensive microwave high density channel filters to meet amplitude and phase requirements without external equalization
15 p2210 A72-31181

Distributed lumped active network configuration and design chart for realizing all-pass voltage transfer function
15 p2210 A72-31508

Active RC circuit synthesis by state model method, minimizing capacitances of admittance matrix for microelectronic circuit technology
15 p2210 A72-31595

Open circuit voltage transfer function synthesis to realize arbitrary real rational function in complex variable, using generalized positive impedance converter
15 p2211 A72-31847

Reliability-maximizing digital computer synthesis based on multiple redundant network design, discussing majority structure distribution optimization technique
15 p2203 A72-32174

Lossless low pass ladder network synthesis in terms of reflection coefficient poles and zeros with application to bandpass matching problem
15 p2212 A72-32248

Linear radio receiver circuit synthesis for output signal structure and rational selection, using reduction algorithm
15 p2202 A72-32705

Limiting approximation theorems for synthesis of linear circuits and signals in time-frequency domains 15 p2212 A72-32707

Voltage and current generalized immittance converter realization, using with current conveyor for simulation 16 p2367 A72-32856

Computer algorithms for adaptive optimal synthesis of complex electronic systems, using stochastic approximation and gradient search with data storage 16 p2367 A72-33265

German monograph on microwave broadband tunnel diode mixers theory and design, taking into account parasitic elements as part of filter networks 16 p2368 A72-33507

Circuit synthesis for random numbers probabilistic digital transducers reduced to synthesis of random binary signal converters, noting method description with Boolean functions 16 p2372 A72-34012

State space technique application to discrete linear control systems synthesis, discussing time-optimal and quadratic-cost problems, and pole assignment method 17 p2532 A72-34246

Bandpass filters set synthesis in crab eye configuration, noting design principles and telephone techniques 17 p2524 A72-34295

Advances in LSI technology. 17 p2527 A72-34569
Relationship between antenna synthesis for a given radiation pattern and the synthesis of spatial signal processing systems 17 p2515 A72-34832

Radio pulse shaping network synthesis composed of lumped elements, noting pulse duration limitation by network efficiency 17 p2533 A72-34837

An algorithm for the automatic synthesis of nearly optimal 2-level and-or combinational circuits. 17 p2533 A72-35058

Design of nonlinear networks with a prescribed small-signal behavior. 17 p2533 A72-35199

Threshold logic network synthesis with specific threshold-gate sensitivities. 17 p2533 A72-35364

Binomial electronic filter design for nonnegative impulse transient response to obtain fast rise times via in-line pole-zero configuration 18 p2672 A72-36053

Feedback controller synthesis from nonlinear system modeling by linear equations, proving theorem relating stability properties 18 p2672 A72-36060

Series stabilization reflection type tunnel diode microwave amplifier synthesis with allowance for real circulator reactance 18 p2665 A72-36107

The use of linear programming to design digital filters from impulse-response specifications. 18 p2663 A72-36304

Synthesis of networks containing three-layer rectangular distributed RC elements and nonideal operational amplifiers 18 p2673 A72-36791

Design of digital filters using state-space realization. 18 p2674 A72-36943

Linear electric circuits optimal synthesis as nonlinear programming of network parameters, discussing approximation algorithms 19 p2776 A72-37306

Computerized design of electric filters with given frequency response, discussing attenuation characteristic approximation by Chebyshev method 19 p2776 A72-37307

Electric circuits design by combined network synthesis and optimization methods, noting approximation by nonlinear programming 19 p2776 A72-37308

Matrix coefficients calculation of state variables equations for network analysis and synthesis 19 p2777 A72-37313

Equivalent circuits and oriented graphs for network analysis and synthesis of nonlinear transducers used in control systems 19 p2777 A72-37316

On the performance and design of self-oscillating dc-to-dc converters. 19 p2754 A72-37850

Design considerations in the measurement of electron temperature in the ionosphere. 19 p2801 A72-37926

Algorithm for linear multivariable systems synthesis via combined dynamic feedforward compensation and linear state variable feedback 19 p2779 A72-38232

Stationary Kalman-Bucy filter synthesis from filter coefficients and correlation matrix of filtration errors, discussing random process estimation application 19 p2782 A72-38517

Nonlinear programming in computerized electronic circuits design, discussing optimization methods and real time operation 19 p2782 A72-38578

Oscillatory circuits synthesis by wave resistance determination of homogeneous line segments for given resonant frequencies spectrum 19 p2768 A72-38660

Optimal synthesis of pulse repetition frequency control and filtering circuits of radar range finder in Gaussian approximation 20 p2902 A72-39065

MOS transistor frequency and transient response characteristics for equivalent circuit synthesis, using Bessel functions in differential equation solution 20 p2907 A72-39067

Synthesis and analysis of a fly-by-wire flight control system for an F-4 aircraft. 20 p2887 A72-39119

[ALAA PAPER 72-880] Minimax technique for direct synthesis of Kalman-like filter under large uncertainties in a priority statistics of plant and measurement noises 20 p2907 A72-39120

[ALAA PAPER 72-878] Synthesis of passive matching two-ports with given apparent resistances. III 20 p2907 A72-39424

Transformation of reactive ladders into digital circuits. 20 p2910 A72-39427

New active all-pass network with linear group delay. 20 p2910 A72-39431

A frequency transformation chart for RC-active band-pass filters. 20 p2907 A72-39432

A high-frequency dynamic phase metering instrument for ionospheric research. 21 p3051 A72-40214

Russian book - Design principles for multiple-valued physical circuits. 21 p3027 A72-40386

Antenna radiation patterns synthesis from individual elements amplitude and phase characteristics, using method based on steepest descent technique 21 p3028 A72-40506

Synthesis of threshold-logic networks using Karnaugh-mapping techniques. 21 p3037 A72-40636

Synthesis of feedback systems with large plant ignorance for prescribed time-domain tolerances. 21 p3037 A72-40643

Frequency-sampling and transversal digital filter equalizers optimal design from specified unit impulse time response, using linear programming algorithm 21 p3033 A72-40900

Low cost design of linear pulse stretcher circuit for short duration pulse time measurement in nuclear instrumentation and computing counters 21 p3033 A72-40997

Network algebra simplification through computerized minimization of Boolean functions, describing FORTRAN IV program 21 p3038 A72-41001

Correction of diffraction errors in acoustic-surface-wave pulse-compression filters. 21 p3034 A72-41464

The mathematical synthesis and analysis of fluid logic networks. 22 p3161 A72-42049

Design equations for comb type bandpass filter formed by cascade connection of symmetrical networks containing coupled waveguides and coaxial lines 22 p3158 A72-42125

Optimal frequency-difference communications system with manipulated amplitudes 22 p3154 A72-42237

Voltage generalized-immittance converter synthesis with RC circuits for obtaining current transfer function proportional to square of s with application to filter design 22 p3140 A72-42303

Symbol synchronization advances impact on PCM bit synchronizers design, discussing symbol detection and timing extraction circuits 22 p3155 A72-42706

Reliability-maximizing digital computer synthesis based on redundant network design, discussing majority structure optimal allocation technique 22 p3157 A72-43008

Synthesis method for phase and loss optimized single-stage reflection type phase shifters, determining transformation coefficient 23 p3268 A72-43439

Computation of optimal parameter domains of components in the design of electronic circuits 23 p3268 A72-43440

Generalized numbers method for analysis and synthesis of linear circuits described by signal flow graph, noting algorithms for computer programming 23 p3269 A72-43443

Microstrip matching networks synthesis for microwave integrated circuits, calculating passband of configurations with lumped and distributed elements 23 p3269 A72-43445

Local-oscillator-circuit optimisation for minimum distortion in double-balanced modulators. 23 p3270 A72-43603

Calculation of the nonlinear dynamic regime of a two-terminal pair network with a weak nonlinearity 23 p3270 A72-43772

Digital filter realizations using a special-purpose stored-program computer. 23 p3267 A72-43815

MOS logic circuit design simplification by replacing series and parallel transistor networks by equivalent single transistor inverter circuit 23 p3271 A72-43843

Linear electronic networks analysis and synthesis via equations of variable states, noting structural features of circuits without component related degeneration 23 p3271 A72-43844

An approach for generation of second order RC-active filters. 23 p3276 A72-43863

Digital filter design using observers. 23 p3276 A72-43864

Optimal design of a class of nonlinear networks. 23 p3276 A72-43865

Synthesis of hyperstable discrete model reference adaptive systems. 23 p3276 A72-43867

RC, RL and RLC networks associated tunnel diode circuits normalized graphs, design method and stability consideration 23 p3272 A72-43988

Discrete-antenna synthesis theory in the case of uniform approximation to a given radiation pattern 23 p3266 A72-44213

Stochastic coder electronic circuit for random numbers conversion into electrical voltages and vice versa, noting compactness and low cost 23 p3273 A72-44460

Book - Electronic integrated systems design. 23 p3274 A72-44475

Book on complete technological system reliability assessment covering performance requirement and achievement, transfer characteristics, sampling, estimation, confidence, synthesis problem, etc 23 p3294 A72-44499

Linear analysis and synthesis of three dimensional interference system stationary in space and time domains 24 p3379 A72-44752

Synthesis of horn antenna with impedance boundary conditions on walls and specified aperture field distribution 24 p3384 A72-44753

A near-time-optimal control circuit with a large number of relay elements 24 p3387 A72-45699

NEUMANN PROBLEM

Laplace equation internal Dirichlet and Neumann boundary value problems solution procedure for thermal potential of steady temperature field 07 p1098 A72-18988

Poisson equation boundary value problems summary representation formulas for three layer annular sector with Dirichlet or Neumann conditions 08 p1205 A72-20963

Laplace operator eigenvalue computation for simply connected region with homogeneous Dirichlet and Neumann boundary conditions and finite difference problem 09 p1340 A72-22296

Algorithms for eigenvalue spectrum determination in Dirichlet and Neumann problems for Helmholtz equation in configuration domains 12 p1847 A72-27985

Neumann problem for eigenvalues with homogeneous boundary conditions, using R-functions for complex-type regions 13 p1987 A72-29792

Steady state temperature field and heat flux at wall for metallic coolant flow in thin walled axisymmetric pipe with nonhomogeneous Neumann boundary condition 16 p2477 A72-33413

NEURAL NETS

Neurophysiology of auditory pattern recognition of simple and complex sounds, using cats data on cochlear nerve neural mechanism 01 p0012 A72-10482

Neural tissues excitability relationship to precellular organization, considering polyphosphate distribution in vertebrate tissues 04 p0470 A72-14789

Multichannel IC spike height discriminator for separating electrical activity of neural units recorded with microelectrode 04 p0481 A72-15223

Cats cochlea and cochlear nucleus neural responses in auditory masking of low frequency tones, showing phase locked cells progressive desynchronization with intensity 04 p0475 A72-15251

- Nerve structures localized cooling device using vacuum insulated closed circuit controlled cryogenic probe with cooling range of plus/minus 20 C
04 p0481 A72-15252
- Human visual system selective adaptability to speed, size and orientation, suggesting motion analysis by visual cortex neural subsystems
06 p0761 A72-17603
- Input binary sequence transformation in chain of series connected on-off neuron models, applying to n-stage linear filter analysis
08 p1138 A72-20870
- Associative memory model using neuron synaptic weight change for storing input disturbances
08 p1138 A72-20871
- Adaptive neural nets of threshold logic units as models of perception and memory in biological systems
09 p1273 A72-23580
- Visual cortex neuronal background activity in unanesthetized rabbits under stimulation and depression of lateral geniculate body and mesencephalic reticular formation, considering synaptic organization
12 p1761 A72-27646
- Neuron networks dynamic behavior in terms of linear differential equations for membrane potential changes and neuron threshold
12 p1772 A72-27925
- Coherent brain model for evolution mechanisms of biological resonance in neuron network signal flow
13 p1908 A72-28455
- Neuronal network numerical and analytical studies, using invariant imbedding and matrix Fredholm integral equation
13 p1986 A72-29400
- Automata with behavior defined by input stimuli sequence and independent on initial state, considering neuron nets as example
15 p2203 A72-32173
- Object code storage in the static portion of a short-time memory
19 p2759 A72-37423
- Models of neurons reacting to input signal alternation in space and time
19 p2759 A72-37424
- Neuron mathematical model synthesis from algorithms to construct neural networks and single threshold element in network form
19 p2759 A72-37425
- A possible anatomical basis for descending control of impulse transmission through the dorsal horn
21 p2998 A72-40578
- Visual information space-time dependent filtering by retinal and geniculate body neural nets
22 p3142 A72-42299
- Preprocessing of nerve pulse sequences for analysis by digital computer
23 p3261 A72-44349
- NEURISTORS**
- Hybrid neuristor transmission lines with planar p-n-p semiconductor structures, discussing development, testing and electrical parameters
10 p1448 A72-24281
- Linear approximations and grapho-analytical method for neuristor line analysis, noting conditions for tunnel diode parameters
12 p1789 A72-27397
- NEUROGLIA**
- Proton irradiation effects on monkey central nervous system, showing inflammatory reaction and neuroglial astrocyte glycogen accumulation
13 p1906 A72-29833
- NEUROLOGY**
- Motoneuron pool fraction determination in human monosynaptic response of healthy and neuropathological subjects, comparing diagnostic methods
07 p0924 A72-20619
- Acceleration stress effects on splanchnic blood flow due to organ displacement and neurogenic vasoconstriction in vascular beds
12 p1765 A72-28285
- Workload modification effects on pilot neurological changes during Boeing 707 letdown, approach and landing
12 p1775 A72-28290
- Neurologic oxygen toxicity - Effects of switch of inert gas and change of pressure.
19 p2758 A72-38704
- Study of bilateral cortical nerve connections between the precentral gyrus and various cortical regions
20 p2891 A72-39323
- NEUROMUSCULAR TRANSMISSION**
- Discharge patterns in motor nerve fibers during human voluntary muscle contractions
01 p0013 A72-10624
- Human and monkey muscle tonic vibration reflex response to vibratory stimulation dependent on frequency range, electromyograph discharge interval length, etc
02 p0163 A72-12250
- Lateral geniculate body neurons activity during nystagmic eye movements in cats after vestibular stimulation related to visuo-motor mechanisms counteracting illusory shifts
03 p0315 A72-13623
- Spinal reflexes through electric stimulation of gastrocnemius and soleus human leg muscles, attributing increased tendon reflex amplitudes to gamma motoneurons hyperactivation
04 p0467 A72-14704
- Human neuromuscular coordination control optimization, discussing preprogrammed open-loop control with feedback monitoring loop
04 p0477 A72-14705
- Human arm muscle motor neuron reflex response to rectangular pulse excitation of ulnar nerve
04 p0476 A72-15587
- Marine gastropod mollusk synaptic transmission mechanism, discussing various chemical transmitters, two phase potential, receivers, electrical interaction and electrophysiological conditioning
06 p0764 A72-17996
- Phase relations between alpha waves in EEG and automated rhythmic motoric activity as function of subject behavioral activity and thalamic pacemaker zones
07 p0916 A72-19109
- Field and intracellular potentials in cat trochlear nucleus following vestibular nerve and nuclei stimulation for synaptic organization study of vestibulo-ocular reflex
07 p0923 A72-20501
- Stimulation transmission tracts, synaptic mechanisms and tonic activity of cat sympathetic ganglia
07 p0924 A72-20617
- Motoneuron pool fraction determination in human monosynaptic response of healthy and neuropathological subjects, comparing diagnostic methods
07 p0924 A72-20619
- Cat and rabbit middle ear muscles contraction by electric stimulation of motor nerves, noting sound transmission reduction
08 p1115 A72-21136
- Cat middle ear muscles motor units twitch tension and contraction time in response to motor neuron threshold stimulation
08 p1116 A72-21137
- Motor unit potential histogram study of human motoneuron activity patterns during voluntary muscular contractions
08 p1116 A72-21472
- Bulbar respiratory neuron discharge pattern response to nasal and tracheal receptor stimulation in cats, relating changes in neuronal activity and intratracheal pressure
08 p1117 A72-21473
- High pressure gas mixture breathing effects on intercostals externi muscles electrical activity and respiratory cycle time in rats
08 p1121 A72-22082
- Myocardium excitation-contraction mechanism in heart regulation, discussing surface membrane structure and cell action potential
09 p1264 A72-22222
- Laryngeal motoneuron activity during Hering-Breuer reflexes, noting inspiratory fibers firing inhibition and activation during lung inflation
09 p1266 A72-22975
- Functional organization of monkey cortical efferent zones in distal forelimb muscle control from intracortical microstimulation studies, showing stimulation thresholds distribution
09 p1267 A72-23582
- Peripheral afferent input to monkey cortical efferent zones of distal forelimb muscle control, using single microelectrode for intracranial stimulation and cellular discharge recording
09 p1267 A72-23583
- Human motoneuron discharge time relations during isometric muscle contraction, measuring adjacent action potential and mean interspike intervals
12 p1761 A72-27653
- Neuronal mechanisms of muscular motor activity control, analyzing cerebrum-motoneuron connections, spinal potentials, monosynaptic responses and depolarization
13 p1907 A72-29981
- Description of an easy and simplified test for electromyographic diagnosis of latent spasmophilia in flight personnel
19 p2760 A72-37878
- Propriospinal ducts of the lateral funiculus and their possible role in transmission of pyramidal stimuli
21 p2999 A72-40583
- Synaptic suprasegmental control mechanisms of spinal cord motor neurons
21 p2999 A72-40584
- Study of the conductivity of the motor neuron membrane during supraspinal stimulation
21 p2999 A72-40585
- Synaptic potentials of sensor and motor neurons of trigeminal nuclei during corticofugal stimulation
21 p2999 A72-40587
- Influence of a preceding afferent stimulation on the pyramidal activation of spinal motor neurons
21 p2999 A72-40588
- Role of pyramidal and extrapyramidal components of cortically-induced efferent stimuli in the mechanism of cortical motor activity coordination
21 p2999 A72-40591
- Synchronization in the work of motor neurons during arbitrary motor activity of various types
21 p2999 A72-40595
- Role of efferent influences of temporo-rhino-encephalic cerebral structures in pre-adjustment alterations of spinal motor neuron excitability
21 p2999 A72-40596
- Cortical metabolism regulation and effector systems of the adaptation process
21 p3000 A72-40760
- Computation of the shape and velocity of a nerve pulse
22 p3149 A72-42156
- Tactile information transmission for orientation and motor control, discussing somatic sensitivity peripheral mechanism
22 p3146 A72-42778
- Functional insufficiency of the neuromuscular system caused by weightlessness and hypokinesia.
23 p3253 A72-43387
- NEURON TRANSMISSION**
- U BIOELECTRICITY**
- NEURONS**
- Postsynaptic electric potential responses to click of auditory cortex neurons in cats
02 p0158 A72-11757
- Visual cortex neuron responses to light flashes under hypothalamic and reticular electric stimulation in rats
02 p0158 A72-11758
- Neurosecretory cell functional activity of supraoptic and paraventricular hypothalamic nuclei in rats after electrical stimulation of midbrain reticular formation
02 p0158 A72-11759
- Synaptic mechanisms of vestibulospinal and reticulospinal effect on transmission to lumbar motoneurons in monkeys
02 p0158 A72-11760
- Noceptive chemical action in cat skin vessels, showing fiber types for impulse transmission
02 p0164 A72-12511
- Cerebral neurons population electric stimulation effect on deep sleep duration in Parkinsonism patients
04 p0476 A72-15585
- Electrophysiology for auditory temporal masking mechanism study of cat cochlear nucleus and inferior colliculus single neurons
05 p0620 A72-17175
- Marine gastropod mollusk synaptic transmission mechanism, discussing various chemical transmitters, two phase potential, receivers, electrical interaction and electrophysiological conditioning
06 p0764 A72-17996
- Psycho-physical theory of human mind, discussing molecular biological processes of neuron recording in terms of quantum mechanics
06 p0769 A72-18191
- Neuronal systems short-latency paired interactions detection method, obtaining histogram for action potentials
07 p0934 A72-20624
- Hypothalamic single neuron unit discharge pattern response to acoustic, light and somatosensory stimulation in cats
08 p1116 A72-21471
- Motor unit potential histogram study of human motoneuron activity patterns during voluntary muscular contractions
08 p1116 A72-21472
- Neurophysiological mechanisms responsible for conditioned reflexes, considering cells, reaction relationship to animal behavior, neuronal stimuli interactions, internal inhibitions and trace process reproduction
08 p1118 A72-21835
- Hippocampus neuron reactions and memory function realization with incoming information and stored imprints comparison by brain
08 p1122 A72-22191
- Protein biosynthesis inhibitors retardation of noradrenaline and serotonin induced hyperpolarization of neuron membranes in cortical sensorimotor region of rabbits
08 p1122 A72-22192
- Photically induced and spontaneously discharged neuron impulse propagation through direct pathways from superior colliculus to dorsal and ventral lateral geniculate nuclei in cats
09 p1265 A72-22863
- Single lateral geniculate neuron recording during receptive field-centered flashing spot variations for intensity response function comparison with optic neurons in cats
10 p1427 A72-25177
- Cortico-subcortical connections transection effect on cat lateral geniculate body and visual cortex neurons spontaneous activity
12 p1761 A72-27652
- Human motoneuron discharge time relations during isometric muscle contraction, measuring adjacent action potential and mean interspike intervals
12 p1761 A72-27653

Illumination code efficiency in impulse activity of neurons of outer geniculate body of cat visual system, emphasizing pulse per group technique

13 p1903 A72-28780

Visual cortex neuron reactions to antidromic stimulation of cat pyramidal tract, noting axon activation increased discrimination in analysis

13 p1903 A72-28781

Neuronal mechanisms of muscular motor activity control, analyzing cerebrum-motoneuron connections, spinal potentials, monosynaptic responses and depolarization

13 p1907 A72-29981

Human spinal segment functional state before voluntary movement during water immersion, using H-reflex for spinal cord motoneuron excitability evaluation

14 p2073 A72-30255

Organ cell lysosomes polymorphic properties and formation by Golgi complex, discussing role in neurocyte structure restitution following gamma irradiation

14 p2075 A72-30594

Cat bulbar respiratory neuron discharge modification by single electric shock stimulation of cerebral cortex

14 p2077 A72-30843

Sperry neuronal specificity hypothesis for nerve cell connections formation between eye and brain during embryonic development, proposing systems matching theory

17 p2504 A72-35070

Nuclein acid contents in cholinergic and adrenergic spinal cord neurons and in their glial satellite-cells during hypoxic hypoxia and a post-hypoxia period

19 p2756 A72-37742

Influence of cooling of the sensorimotor region of the cerebral cortex on the neurons of the mesencephalic reticular formation

20 p2890 A72-38926

RNA content in the cortex neurons in connection with the change in its function during the emergence of an animal from hypothermia

20 p2890 A72-38928

Device for eliminating the artifact of electrical stimulation when recording evoked pulse activity of neurons

20 p2893 A72-38938

Neuronal fiber and synaptic axonal contact structure of cat spinal gray matter in corticospinal, rubrospinal and reticulospinal terminal zones by Golgi method

21 p2998 A72-40579

Morphological changes in spinal cord neurons of animals due to the decreased intensity of supraspinal stimulation

21 p2998 A72-40580

The ultrastructure of the lateral basilar region of the spinal cord.

21 p2998 A72-40581

Neuronal organization of descending systems of the spinal cord

21 p2998 A72-40582

Intracellular study of rubrospinal neurons and of their synaptic activation during the stimulation of the sensorimotor cortical region

21 p2998 A72-40586

Synaptic potentials of sensor and motor neurons of trigeminal nuclei during corticofugal stimulation

21 p2999 A72-40587

Patterns of spontaneous and reflexly-induced activity in phrenic and intercostal motoneurons.

21 p3003 A72-41462

Electromyographic investigation of diaphragm cross contraction following spinal cord section in cats, noting diaphragm motoneurons excitation by breathing center pulses

22 p3142 A72-42281

Reactions of auditory cortex neurons to geniculocortical fiber stimulation

22 p3145 A72-42723

Dependence of inhibitory areas of inferior colliculus neurons on the time characteristics of acoustic stimuli

22 p3145 A72-42724

Effect of a polarizing current on the activity of neurons of the respiratory center

22 p3145 A72-42725

Changes in the impulse activity of cortical neurons during selective reinforcement of a chosen range of their interspike intervals

23 p3257 A72-44087

Synaptic events during specific and nonspecific inhibition of visual cortex neurons

23 p3257 A72-44088

Neuronal and focal reactions of the parietal associative cortex to various peripheral stimuli

23 p3257 A72-44089

Responses of anterior suprasylvian gyrus neurons to peripheral stimuli of different modalities

23 p3257 A72-44090

Post-synaptic potentials of motor neurons of the facial nerve nucleus evoked by afferent and corticofugal pulse stimulation

23 p3257 A72-44091

Classification of neurons in the lumbosacral section of the spinal cord according to their discharge during evoked locomotion

23 p3257 A72-44092

Elaboration of steady changes in the firing rate of cortical neuron populations

24 p3370 A72-44587

Cat hypothalamus regions neurons background activity characterized by single nonrhythmic spikes with large interspike intervals, noting frequency of discharge bursts

24 p3370 A72-44588

Pulse activity of neurons in the thermal regulation center of the anterior hypothalamus during chill shivering

24 p3371 A72-44594

First-breath response of medullary inspiratory neurons to the mechanical loading of inspiration.

24 p3372 A72-44595

Temperature-sensitive neurons in the brain stem - Their responses to brain temperature at different ambient temperatures.

24 p3373 A72-45232

NEUROPHYSIOLOGY

Soviet book on physiology of conditioned reflexes covering brain and nervous system, tonic reflexes, functional models, inhibition localization, etc

01 p0011 A72-10295

Psychology of visual form perception in relation to neurophysiological principles of lateral interaction and organization, considering retinal images, aftereffects, binocular vision, etc

01 p0011 A72-10469

Neuronal mechanisms of binocular vision and space perception from tests on cats and men, discussing neurophysiological models of stereopsis

01 p0012 A72-10479

Neurophysiology of auditory pattern recognition of simple and complex sounds, using cats data on cochlear nerve neural mechanism

01 p0012 A72-10482

Split human cerebrum physiology, discussing corpus callosum as interhemispheric nervous process transfer, and right and left hemispheres functional differentiation and asymmetry

02 p0157 A72-11544

Retinal annulus onset and offset thresholds, discussing neural signals delay characteristics

02 p0164 A72-12488

Differential neurophysiological and psychological effects of subanesthetic concentrations of cyclopropane, diethyl ether, methoxyflurane and ethrane in conscious man

04 p0480 A72-15220

Neuroelectric signal recognition system with computerized compensation for variations due to small random changes, slow trends and interference potentials

04 p0481 A72-15253

Ecdysone hormonal control of *Drosophila* circadian rhythms and synchronizing mechanisms, discussing light stimulation and neurohormone secretion

07 p0919 A72-19537

Thalamus functional and organizational anatomy studies from improved neurophysiological research methods, emphasizing cytoarchitectural differentiation functional significance

07 p0922 A72-20274

Comparative EEG characteristics of frontal and occipital human brain cortex, relating psychophysiological and neurophysiological factors

08 p1116 A72-21196

Soviet papers on human higher nervous activity physiology covering conditioned reflexes and adaptive behavior, neurotropic substance effects, mathematical and structural modeling, etc

08 p1118 A72-21834

Neurophysiological mechanisms responsible for conditioned reflexes, considering cells, reaction relationship to animal behavior, neuronal stimuli interactions, internal inhibitions and trace process reproduction

08 p1118 A72-21835

Brain structures role in fixation of temporal relationships in information memory function of central nervous system

08 p1118 A72-21836

Conditioned reflex mechanisms responsible for regulation of emotions in higher order animal and human neurophysiology

08 p1118 A72-21837

Physiology of sleep phases and dreams, discussing data on highly organized and interacting neurohumoral mechanisms exhibiting alternating forms of brain bioelectric activity

08 p1118 A72-21838

Human nervous system properties responsible for individual behavioral differences, discussing methodological problems in future research from biological criteria viewpoint

08 p1118 A72-21839

Soviet book on psychic phenomena and brain, covering cybernetics, dialectical materialist implications, consciousness, psychophysiology and cerebral neurodynamic structures

08 p1121 A72-22164

Electrophysiological, neurophysiological, metabolic, vegetative, psychological, chemical and pathological aspects of sleep, noting disturbance and wakefulness mechanisms for various clinical disorders

09 p1264 A72-22223

Neurophysiological mechanisms of sleep, studying sleep and wakefulness state evoked potentials relation to cortex and subcortical activity levels

09 p1264 A72-22224

German monograph on Ranvier node steady state I-V characteristics transition range and control by altered external solutions and morphological effects on nerve fiber

09 p1264 A72-22336

Antimotion sickness drugs effectiveness based on acetylcholine or norepinephrine induced changes of balance between vestibular and reticular neurons

10 p1427 A72-23726

Neural effects on human visual resolution of horizontal and vertical gratings resulting from early abnormal visual inputs due to astigmatism

10 p1430 A72-24348

Russian book on visual sensor signal dynamics covering nerve signal transformation, light stimuli responses, afferent flow, bionics, neurocybernetics and communication theory

11 p1584 A72-26049

Intraelectroretinographic analysis of light signal spatial summation at different retinal nerve levels in frogs

11 p1585 A72-26454

Effects of long periods of clinical death from drowning or lethal blood loss on higher nervous activity in reanimated dogs

13 p1902 A72-28642

Functional organization and neurophysiological mechanisms of return corticothalamic system in anesthetized cats, showing axon terminal presynaptic depolarization

13 p1902 A72-28762

Pancreas insular apparatus biosynthesis of neurohumoral mechanism compounds stimulating coronary ectasia hormones discharge from brain into blood in cats with alloxan diabetes

14 p2077 A72-30973

Slow neural recovery processes during sleep, characterizing cerebral neurons synchronized and desynchronized sleep phases for mammals

16 p2355 A72-33557

Evidence for the role of the transient neural 'off-response' in perception of light decrement - A psychophysical test derived from neuronal data in the cat.

17 p2500 A72-34884

New experimental data on the morpho-physiological analysis of the adaptation phenomenon in the somatic reflex arch

17 p2504 A72-35023

Bioelectric activity of the medulla oblongata during hypothermia and bloodletting

17 p2504 A72-35024

Neuroinhibition in the regulation of emesis.

18 p2650 A72-36449

Operative memory mechanism as visual system neuron chain storage of stimuli from image recognition time measurements

20 p2891 A72-38936

General principles and detail similarities in visual pattern analysis by single neuron operation, computer programs and psychological perception

20 p2891 A72-39275

Negative /painful/ stimulus cessation relation to emotionally positive zone activation in rat brain during self stimulation experiments

20 p2892 A72-39410

Anatomy, pathology, etiology, diagnosis and therapy of posterior tibial nerve compression lesion, discussing tarsal tunnel syndrome

21 p3005 A72-40396

Russian book - Neurophysiological background of tactile perception.

21 p2998 A72-40464

Russian book - Mechanisms of descending control of spinal cord activities.

21 p2998 A72-40577

Morphological changes in spinal cord neurons of animals due to the decreased intensity of supraspinal stimulation

21 p2998 A72-40580

Neuronal organization of descending systems of the spinal cord

21 p2998 A72-40582

Cerebrum sections and related afferent processes as activator of automatic neuron mechanism control of motor activity, discussing segmentary spinal cord changes

21 p2999 A72-40593

Russian book - Cortico-visceral interrelations in physiology, biology and medicine.

21 p3000 A72-40752

Role of afferent and efferent connections in the formation and reproduction of trace processes in man
21 p3001 A72-40807

Critique of Pavlov conditioned reflex role in higher nervous activity and association principle role in psychic activity
21 p3001 A72-40811

Effect of neurohomologous phospholipids associated with other substances on experimental intoxication by asymmetrical dimethylhydrazine. II - Biochemical aspects of the pyridoxine-phospholipid association
21 p3009 A72-41195

The effect of size, retinal locus, and orientation on the visibility of a single afterimage.
21 p3003 A72-41253

Analysis of the activity evoked in the cerebellar cortex by stimulation of the visual pathways.
21 p3003 A72-41460

Effect of vibration on the permeability of the blood-brain barrier
22 p3149 A72-42070

Neurophysiological mechanisms of the extinction of the orientating reflex
22 p3142 A72-42280

Ocular and induced visual effects of systemic and topical drugs in terms of eye neuroanatomy and pharmacology, stressing glaucoma therapy
22 p3150 A72-42499

Subjective and objective sensory physiology, discussing transformation processes in sensory receptors and nerves, psychophysical scaling methods, chemoreceptors and peripheral adaptation
22 p3146 A72-42777

Temperature sensitivity neurophysiological mechanism, discussing cold and heat sensitive receptors localized distribution in human skin and thermoregulatory function
22 p3146 A72-42779

Pain perception anatomical and neurophysiological mechanism, discussing human response to mechanical, thermal and chemical pain inducing stimuli
22 p3146 A72-42780

Olfactory perception neurophysiological mechanism, discussing receptor cells sensory thresholds and time, temperature and humidity effects
22 p3146 A72-42782

Taste organs neurophysiological structure and function, considering stimuli and excitation parameters effects on perception threshold
22 p3146 A72-42783

Cerebral auditory system acoustic information processing, discussing ganglia and cochlea neurophysiological functions in response to afferent stimulations
22 p3146 A72-42786

Human vocal apparatus anatomical and neural structure, considering linguistic sounds composition
22 p3147 A72-42789

Limbico-neocortical, cardiovascular and hormonal system vegetative shifts associated with emotional behavior response, presenting neurogenic stress model for animals
22 p3148 A72-43166

Nervous mechanisms of the acoustic stress reaction
22 p3148 A72-43169

Nervous-emotional stress as a problem of modern work physiology
22 p3148 A72-43170

Preprocessing of nerve pulse sequences for analysis by digital computer
23 p3261 A72-44349

Influence of the sympathetic nervous system on the presynaptic inhibition of the dorsal surface potential of the spinal cord
24 p3370 A72-44589

Influence of the nervous system and its mediators on the spontaneous contractile activity of a smooth muscle
24 p3370 A72-44590

NEUROSCIENCE
U NEUROLOGY
NEUROSES
Extraversion, neuroticism, and color preferences.
18 p2653 A72-36903

NEUROTROPISM
Acute hypercapnia neurotropic effect in rabbits, describing carbon dioxide inhalation period, preanesthetic and narcotic stages and recovery phase
02 p0160 A72-12015

Central nervous system pharmacology, discussing somniferous, narcotic and neurotropic substances effects on brain activity
08 p1127 A72-21841

NEUTRAL BEAMS
NT MOLECULAR BEAMS
NT NEUTRON BEAMS
Neutral Cr beam excited states radiative lifetime measurement by beam foil method
03 p0390 A72-13016

NEUTRAL PARTICLES
NT FAST NEUTRONS
NT NEUTRONS
NT THERMAL NEUTRONS

Plasma ion temperature and neutral collision frequency determination by Langmuir probes [AD-739452]
02 p0264 A72-12262

Weakly ionized turbulent gas flow in pipe, comparing neutral and plasma fluctuations with laser beam scintillations
04 p0558 A72-15331

Ionospheric neutral composition variations as function of height, local time and solar activity
05 p0656 A72-16235

Neutral atoms pressure distribution along capillary and pressure compensating channel during discharge in argon ion laser
05 p0670 A72-16990

Internal neutral sheet in geomagnetic tail from Explorer 34 magnetic field experiment, noting quasi-periodic structure and magnetic loop formation
06 p0803 A72-17450

Combustion product plasma electrical conductivity dependence on neutral component density fluctuation
07 p1044 A72-19888

Planetary scale circulation systems effects on photochemistry and transport processes of minor neutral constituents in mesosphere and lower thermosphere
09 p1274 A72-22353

Model calculation for seasonal effects on minor neutral constituents distribution in mesosphere and lower thermosphere, suggesting large scale meridional circulation role
09 p1274 A72-22354

Meteor method for determining errors in rate measurement of electron attachment to neutral air particles based on nonexistent recombination, turbulent diffusion and photodetachment
09 p1383 A72-22503

Nighttime radar method of meteor radio echo observation to determine electron attachment rate to neutral air particles
09 p1383 A72-22504

Frictioned force modification of lower thermosphere vertical neutral gas velocities with resulting atomic oxygen and molecular nitrogen density-height distribution deviation from barometric law
09 p1298 A72-22582

Effective photoionization sections of neutral atoms, discussing photon energy effects, subshell periodicity and continuum functions phase shift
09 p1356 A72-22828

Target jet density variations effect on vacuum in neutral atom beam ionization region of fast neutral particle magnetic trap
09 p1363 A72-23223

Charged to neutral particle transformation capacity of wide aperture recharge target formed by supersonic gas jets in magnetic trap with annular nozzle
09 p1363 A72-23224

Charged and neutral particles radial distribution across positive isothermal plasma column in high current discharges
10 p1521 A72-24355

Ionization movement of charged and neutral particles in F 2 region coupled to air movement by collision drag forces
11 p1621 A72-25839

Neutral gases density and flux distribution in lunar atmosphere, using kinetic theory of gases
11 p1722 A72-26394

Atmospheric neutral density measurement near 400 km during daytime by microphone density gage on OGO 6
11 p1625 A72-26407

Atmospheric temperature measurement by neutral particle wake method, using satellite-borne mass spectrometer
11 p1634 A72-26408

Electron temperature determination from rate of ionization due to collisions between electrons and neutral particles in plasma
11 p1697 A72-26586

Neutral gas velocity distribution, transverse drift velocity, particle and energy densities in column under free fall conditions, considering wastage by ionization processes
11 p1698 A72-26645

Neutral atoms pressure distribution along capillary and pressure compensating channel during discharge in argon ion laser
12 p1819 A72-27133

Upper atmosphere neutral particle pressure, temperature and density profiles during 7 March 1970 solar eclipse from pitot tube soundings
12 p1800 A72-27144

Neutral upper ionosphere temperature measurement with manometer device onboard Cosmos 320 satellite, noting equatorial fluctuations at 250 km
13 p1955 A72-28586

Wind profiles, turbulence, and temperature and density distribution of neutral upper atmosphere obtained via sounding with Skylark rockets carrying chemical seeding payloads
15 p2223 A72-31435

Satellite instrument to observe atmospheric composition by energy analysis of incoming gas stream,

using velocity mass spectrometer for neutral particles measurement
15 p2236 A72-31966

Mesospheric and lower thermospheric composition from neutral atmospheric particles measurement by rocket-borne instrument consisting of RF quadrupole mass spectrometer
15 p2228 A72-31967

Atmospheric stratification, wind profiles and vertical density distribution of ions and neutral particles determined by rocket sounding
15 p2228 A72-31968

Solar flare and neutral sheet simulation by investigating behavior of plasma current through magnetic neutral point created by capacitor discharges
15 p2301 A72-32342

Neutral atom concentration measurement in Cs ion beam, using high sensitivity detection gage to obtain emission indicatrices
16 p2434 A72-32862

Charged and neutral particles radial distribution across positive isothermal plasma column in high current discharges
17 p2589 A72-34955

Combustion product plasma electrical conductivity dependence on neutral component density fluctuation
17 p2590 A72-35136

Hot rarefied neutral gas existence in interstellar space on basis of data collected in 21 cm hydrogen line
19 p2865 A72-38480

IR emission of nitrogen layer heated by reflected shock wave, noting absorption cross sections under free-free electron transitions in neutral particle fields
19 p2835 A72-38776

Free fall column theory allowing for 'neutral gas reduction' by ionization processes, and application of this theory to noble gas ion lasers
21 p3090 A72-40488

Bond energy electrostatic potential calculation and equilibrium and rate constants prediction for alkali and halide ions association with neutrals
21 p3087 A72-40556

Frictional effects with neutrals and the gravitational instability of a plasma.
21 p3093 A72-41332

Elastic electron-neutral interaction in argon in the vicinity of the Ramsauer minimum
22 p3211 A72-42642

Physical and chemical properties and stratification of neutral matter in comet atmospheres, discussing neutral gas dynamics and surface brightness distribution in comet images
23 p3335 A72-43299

Metal ions effect on sporadic E layer formation, noting magnesium ions profile redistribution by vertical gradient in neutral particles wind
23 p3284 A72-43376

Study of the angular distribution of charged and neutral pions during inelastic interactions in the energy region above 1 TeV
23 p3291 A72-44443

Relationship between the energies of charged and neutral particles generated in the energy region above 100 GeV
23 p3332 A72-44447

Electromagnetic instabilities produced by neutral-particle ionization in interplanetary space.
23 p3332 A72-44506

Interaction of the solar wind with the neutral component of the interstellar gas.
23 p3332 A72-44507

Neutral upper ionosphere temperature measurement with manometer device onboard Cosmos 320 satellite, noting equatorial fluctuations at 250 km
24 p3402 A72-45086

Steady-state distribution of the charged and neutral particle concentration in a bounded high-temperature turbulent plasma
24 p3429 A72-45493

Charged and neutral cosmic rays radioactive isotope and momentum distribution measuring techniques in high energy particle astronomy observatories /HEAO/
24 p3404 A72-45540

Theoretical models of the D-region.
24 p3399 A72-45580

The development of a theoretical model of the atmosphere and the ionosphere.
24 p3399 A72-45585

NEUTRALIZERS
Hollow cathode neutralizer for electron bombardment ion thruster, discussing performance from SERT II flight
05 p0706 A72-16853

[AIAA PAPER 72-207]
Rectifier tube cathode as colloid thruster electron gun type neutralizer, discussing efficiency and accelerated life tests
11 p1711 A72-26228

[AIAA PAPER 72-511]
Hg flow and hollow cathode temperature effects on ion thruster neutralizer stability and lifetime capability, using bell jar tests
13 p2026 A72-28937

[AIAA PAPER 72-422]
Theory of the dynamic vibration neutralizer with motion-limiting stops.
17 p2625 A72-34317

[ASME PAPER 71-APMW-14]

NEUTRINOS

- Neutrino flux from solar models differing in opacity, equations of state and nuclear cross section factors
01 p0122 A72-11146
- Spectroscopic He abundance in population II stars from viewpoint of big-bang cosmology, taking into account neutrino emission according to photon-neutrino coupling theory
02 p0281 A72-12303
- Solar model for capture rate in C1 37 neutrino experiment, comparing different stellar evolution programs
04 p0566 A72-14562
- Neutrino emission process effects on solar C-N-O cycle energy generation and C12/C13 abundance ratio
04 p0567 A72-14911
- Neutron star evolution theories, emphasizing neutrino emission processes and stellar collapse
07 p1080 A72-20056
- Neutrino interactions in lepton era of universe and hot big bang cosmology according to proton-neutrino coupling theory
07 p1084 A72-20538
- Stellar evolution from precarbon-burning contraction to presupernova stage with and without neutrino production by electron neutrino interaction
10 p1545 A72-24825
- Closed rotating cosmologies containing matter described by the kinetic theory - Entropy production in the collision time approximation.
17 p2618 A72-35823
- Ion-ion correlation effects on electron-nucleus neutrino bremsstrahlung.
18 p2723 A72-36089
- Experimental nuclear physics and theoretical solar structure and evolution explanations of disagreement between calculated and observed solar neutrino flux
18 p2722 A72-37007
- Variation of evolved blue/red ratio for supergiants as function of stellar mass, discussing status of astrophysical test for neutrino emission
19 p2854 A72-37235
- Unsteady hydrodynamic accretion on a neutron star
19 p2862 A72-38053
- Stellar energy-loss rates in a convergent theory of weak and electromagnetic interactions.
20 p2972 A72-39868
- An upper limit on the neutrino rest mass.
21 p3088 A72-40830
- Approximation of energy generation and nucleosynthesis during hydrostatic carbon burning in massive stars, noting neutrino-dominated evolution effects
22 p3228 A72-42562
- Solar neutrino flux dependence on gravitational effects, discussing Brans-Dicke gravitation theory and general relativity equations
22 p3229 A72-42957
- Solar neutrino and dilaton theory of non-Newtonian gravity.
23 p3329 A72-44315
- On the physical nature of cosmic neutrino absorption. I - Cosmological models with continuous creation. II - Cosmological models without continuous creation.
24 p3439 A72-44974
- Gamma-neutrino angular correlations in muon capture.
24 p3427 A72-45774
- NEUTRON ABSORBERS**
High neutron absorption doping material selection for enhancing explosive mixtures neutron radiographic image without interference with chemical reaction
08 p1220 A72-20769
- NEUTRON ACTIVATION ANALYSIS**
Na and K trace amounts detection in Al based solid rocket propellants by neutron activation analysis, using gamma ray spectroscopy for nondestructive analysis
02 p0270 A72-11959
- Lunar rock 12013 sawdust and fragment composition from neutron activation analysis, comparing to Java tektite J2
05 p0722 A72-17127
- Apollo 6 photogrammetric, photometric and neutron activation analysis of smoke plume, determining eddy diffusivity
06 p0819 A72-18439
- Bulk and rare earth abundances in Luna 16 soil levels A and D by sequential instrumental neutron activation analysis
09 p1381 A72-22275
- Neutron activation data for Ru, Os, Ir, Pt and Pu in iron meteorites, noting correlation
14 p2157 A72-30582
- Boron concentrations in Mo-Hf alloy samples from neutron activation analysis, measuring Li 8 beta radiation with plastic scintillation detector
16 p2391 A72-33238
- Platinum and gold in chondritic meteorites.
17 p2610 A72-35149
- Gas retention chronology of Petersburg and other meteorites.
18 p2723 A72-36062

Instrumental neutron activation analysis of igneous rock abundances in petrogenic and stratigraphic problems, applying to Colombia River basalts and Apollo 11 rock samples
20 p2899 A72-39829

Multielement neutron activation analysis of geological and lunar material using chemical group separations and high resolution gamma spectrometry.
20 p2899 A72-39830

Neutron activation and neutron-capture gamma ray analyses of igneous rock trace elements, discussing Tyrone Igneous Series granites
20 p2899 A72-39831

Neutron activation techniques for nondestructive analysis of meteorites and lunar rocks, noting types of nuclear reactions for geochemical application
20 p2899 A72-39832

Neutron activation and mass spectrometry methods for geochemical analysis of rare earth elements in meteoritic, lunar and terrestrial materials
20 p2899 A72-39835

On the determination of trace elements in meteoritic phases by neutron activation analysis.
20 p2900 A72-39838

Elemental abundance trends in the australite strewn field by non-destructive neutron activation.
20 p2900 A72-39839

Coincidence counting applied to the activation analysis of meteorites and rocks.
20 p2900 A72-39841

Neutron activation analysis of tin in geochemical and cosmochemical material, using 40 minute Sn-123.
20 p2900 A72-39843

Instrumental neutron-activation determination of cobalt and certain other elements in plant materials
22 p3183 A72-42471

Instrumental neutron-activation analysis of the trolite of the Sikhote-Alin meteorite
22 p3225 A72-42472

Simultaneous neutron-activation analyses of scandium, cobalt, iron, and zinc in biological objects with the aid of a total-absorption gamma spectrometer
23 p3259 A72-43347

NEUTRON BEAMS

Depth-dose experiments with monodirectional 14 MeV neutrons in low scatter environment, describing test facility
02 p0162 A72-12068

Neutron radiography visual examination method, using uniform intensity neutron beam from nuclear reactor source
06 p0816 A72-17998

NEUTRON COUNTERS

NT NEUTRON SPECTROMETERS

Scintillation counter to determine neutrons number and distribution in time in pulses generated in hot plasma
02 p0263 A72-11419

Neutron albedo flux recording instrument with composite scintillation crystal and photomultiplier scanning to monitor near space
02 p0273 A72-11934

Solar neutrons search near solar maximum with plastic scintillator counter, discussing irregular excess in counting rate
05 p0719 A72-16524

Space anisotropy responsible for solar semidirectional variation of cosmic ray intensity studied with data from worldwide network of neutron monitor stations
09 p1377 A72-22929

Solar proton event classification system with index of three digits representing proton flux, absorption and sea level neutron monitor response measurements
11 p1714 A72-26425

Neutron albedo flux recording instrument with composite scintillation crystal and photomultiplier scanning to monitor near space
13 p2030 A72-29246

Molnira 1 satellite slow neutron monitor with photomultiplier scanned scintillator, noting limiting effect of geomagnetic perturbations
14 p2105 A72-30628

Two new methods to increase the contrast of track-etch neutron radiographs.
19 p2833 A72-37636

Change in the eleven-year modulation at the time of the June 8, 1969, Forbush decrease.
22 p3172 A72-42424

NEUTRON CROSS SECTIONS

Temperature dependence of scattering cross sections for cold and hot neutrons colliding with oxygen and deuterium molecules
08 p1211 A72-21872

NASA-Lewis experiences with multigroup cross sections and shielding calculations.
19 p2833 A72-37633

An integral test of the inelastic cross sections of Pb and Mo using measured neutron spectra.
19 p2837 A72-37634

Anomalous high concentration of lunar rock Xe-131 relation to Ba-130 nonthermal neutron-capture cross section in resonance energy region
20 p2967 A72-39180

NEUTRON DECAY

X ray observation inconsistency with matter creation in steady state universe due to inner bremsstrahlung from neutron decay
11 p1713 A72-26125

NEUTRON DETECTORS

U NEUTRON COUNTERS

NEUTRON DIFFRACTION

Niobium nitride neutronographic structural study with diffractometer after foil nitriding and rapid cooling
07 p1023 A72-20670

Neutron diffraction study of inorganic materials atomic structure, examining symmetry properties and group arrangements of hydrogen compounds
09 p1358 A72-23478

NEUTRON DISTRIBUTION

Scintillation counter to determine neutrons number and distribution in time in pulses generated in hot plasma
02 p0263 A72-11419

Cosmic ray neutrons angular distribution and energy spectrum at 3200 m altitude, using ionization calorimeter and proportional counters
02 p0275 A72-12828

Earth albedo neutrons energy and angular distributions, suggesting neutron source of inner radiation belt trapped protons
11 p1712 A72-25880

Characteristics of cosmic ray diurnal variation from Deep River neutron and meson data and temperature effects.
17 p2601 A72-35400

Gd and Sm isotope composition in Apollo 15 soils and drill stem samples, discussing lunar sedimentary processes dating from neutron capture dependence on depth
18 p2729 A72-36974

NEUTRON EMISSION

Stilbene scintillator detector for gamma ray spectrometry in energy range 0.5-5 MeV, separating gamma rays from neutrons by pulse shape discrimination technique
03 p0408 A72-13031

Gamma ray and neutron emissions from sun, considering acceleration of charged particles in solar atmosphere
04 p0566 A72-14724

X ray spectrum and D-D neutrons emission from high temperature plasma produced by two pulsed Nd-glass laser systems
07 p1041 A72-19394

Negative reabsorption coefficient for induced emission of neutron moving in medium in magnetic field
09 p1364 A72-23357

Short laser pulses for plasma heating, considering turbulent heating mechanisms, neutron yield and electromagnetic radiation
09 p1364 A72-23444

NEUTRON FLUX

U FLUX [RATE]

NEUTRON FLUX DENSITY

Cosmic ray neutron leakage flux and energy spectrum measurements in 0.01-10 MeV range by OGO 6 satellite-borne neutron detector
01 p0119 A72-10877

Epithermal neutrons energy spectra in atmospheric equilibrium layers at 57 geomagnetic N, noting agreement with experimental error limits
02 p0273 A72-11918

Neutron cosmic ray spectrograph method of separating recorded data by energies, using statistical analysis of data combinations with different dead times
02 p0229 A72-11936

Altitude effects on high energy neutrons and galactic gamma rays flux and spectrum variations from balloon flight studies
06 p0873 A72-17639

Diurnal, sporadic and yearly variations in cosmic ray flux based on neutron component data, noting relation to solar activity cycles
07 p1066 A72-20647

Epithermal neutron differential flux spectrum in equilibrium layers of atmosphere at 57 degrees north
07 p1066 A72-20652

Atmospheric pressure, temperature, humidity and 200-mb level changes effects on cosmic ray neutron component intensity, using multifactorial regression analysis
08 p1225 A72-20702

Solar cosmic ray energy spectrum from calculation of secondary emission neutron component generation multiplicities
08 p1225 A72-20723

Gd and Sm isotopic composition measurement in Luna 16 soil with largest low energy neutron fluence
09 p1380 A72-22265

Boltzmann neutron transport equation solution for homogeneous slabs and spheres, noting dominant critical eigenfunction existence and total flux boundedness, continuity and positivity
09 p1358 A72-23072

- Neutron flux and energy spectra from crossed field acceleration model of plasma focus and z-pinch discharges
11 p1693 A72-25565
- Earth albedo neutrons energy and angular distributions, suggesting neutron source of inner radiation belt trapped protons
11 p1712 A72-25880
- Epithermal neutrons energy spectra in atmospheric equilibrium layers at 57 geomagnetic N, noting agreement with experimental error limits
13 p2030 A72-29230
- Neutron cosmic ray spectrograph method of separating recorded data by energies, using statistical analysis of data combinations with different dead times
13 p1957 A72-29248
- Diurnal cosmic ray neutron variation dependence on interplanetary magnetic field based on neutron monitor data
16 p2449 A72-33940
- Solar cosmic ray anisotropy 27-day variations during IGY from global network stations neutron component data
18 p2722 A72-36876
- Atmospheric pressure, temperature, humidity and 200-mb level changes effects on cosmic ray neutron component intensity, using multifactorial regression analysis
19 p2852 A72-38330
- Solar cosmic ray energy spectrum from calculation of secondary emission neutron component production multiplicities
19 p2852 A72-38351
- Balloon-borne telescope search for solar neutrons and gamma rays during enhanced solar activity periods
21 p3101 A72-41298
- NEUTRON IRRADIATION**
- Reactor source neutron radiography for nondestructive testing, noting hydrogen detection, boron fiber imaging and photographic or electronic color enhancement
01 p0069 A72-10807
- High peak power LSA epitaxial GaAs diode relaxation oscillator breakdown under neutron irradiation
01 p0044 A72-11309
- Excess Xe 131 in lunar Ba feldspar rocks, discussing results of reactor irradiation experiments with fast and epithermal neutrons
03 p0414 A72-12901
- Li-diffused Si compared to conventionally doped materials under neutron irradiation, considering carrier removal
03 p0403 A72-14078
- Gamma and neutron radiation effects on bipolar transistor current gain response predicted from multiple linear regression analysis
03 p0335 A72-14091
- Matched Si junction FET under neutron burst and pulsed gamma radiation, investigating device parameters degradation
03 p0335 A72-14093
- Ni-C solid solution, determining room temperature neutron irradiation effects on C distribution during decomposition
03 p0378 A72-14251
- Visual discrimination task-trained monkeys performance and physiology after pulsed mixed gamma-neutron irradiation, noting blood pressure and respiratory and heart rate changes
06 p0763 A72-17873
- Neutron irradiation effect on grain boundary degradation in Al and Al-Li alloy by internal friction investigation
06 p0830 A72-18292
- Neutron irradiation induced material degradation and circuit failure in high power GaAs Gunn diode oscillator operating in LSA relaxation mode
06 p0788 A72-18472
- Endurance limit of construction materials under fast and thermal neutron irradiation in reactor channel
06 p0834 A72-18682
- Neutron damage effects on red and green output of GaP light emitting diodes at 300 K
07 p1047 A72-19043
- Cosmic radiation effects in Concorde prototype cabin, using photographic dosimeters for neutron dose measurement and nuclear emulsions for all charged particle recordings
07 p0927 A72-19241
- Neutron irradiation produced lattice disorder in Li doped float zone melted n-p type Si solar cells
08 p1216 A72-21182
- Neutron irradiation effect on submicroporosity formation and redistribution in structural graphite
09 p1340 A72-23482
- Thermal neutron radiography industrial applications, describing nondestructive testing techniques
10 p1216 A72-23813
- Neutron capture effects on Gd isotopic composition and irradiation histories of lunar rocks from Apollo sites, using mass spectroscopic measurements
10 p1536 A72-24154
- Metal matrix composites, testing neutron irradiation effects on mechanical properties for nuclear application feasibility
11 p1654 A72-25483
- Neutron irradiation effects on GP zones and precipitates in ternary Al alloy, measuring X ray small angle scattering and electrical resistivity
11 p1655 A72-25514
- Visual image indicator used beside and behind objects for neutron radiography quality determination and radiographs series grading
11 p1632 A72-25822
- Irradiation produced defects and electrical properties of n and p-type Si, discussing radiation damage due to neutron and ion implantation
12 p1857 A72-28058
- EPR for point defects produced in Si by fast neutron irradiation, emphasizing damage cluster model
12 p1858 A72-28060
- Introduction rate and annealing of defects produced in Li-diffused float zone n-type Si by 30 MeV electrons and fission neutrons
12 p1858 A72-28064
- IR absorption bands in mechanically and chemically polished GaAs single crystals irradiated with varying neutron and electron doses
12 p1859 A72-28069
- Carrier concentration Hall mobility and photoconductivity in n- and p-type CdTe after neutron and electron bombardment
12 p1859 A72-28072
- Russian book on penetrating radiation effect on radio components covering resistors and capacitors electrophysical characteristics and parameters changes under gamma and neutron radiation
12 p1793 A72-28342
- Permanent operational characteristics changes of Si and Ge transistors bombarded by gamma and neutron radiation
13 p1928 A72-28700
- Defect annealing in neutron irradiated Si by deep trap concentrations, using space charge limited current (SCLC)
13 p2022 A72-29630
- Radiation effects measurement on neutron, proton and electron irradiated Li-drifted Si detectors by IR response technique, comparing characteristics with photovoltage effect
15 p2234 A72-31538
- Radiation damage effects in Li compensated Si nuclear particle detectors induced by irradiation with electrons, protons and fast neutrons
15 p2291 A72-31539
- Dose response curves for pink somatic mutations in Tradescantia after neutron and X ray irradiation
15 p2186 A72-31723
- Neutron irradiation effects on structural materials brittle fracture initiation and propagation mechanisms, discussing residual elements influence on radiation defect stabilization
15 p2258 A72-32486
- Electron trapping data in neutron irradiated high purity Si, using space charge limited current measurements
15 p2294 A72-32514
- Charpy impact tests of neutron irradiated nuclear reactor component steels to determine ductile/brittle transition temperature, describing setup and gas heating and cooling procedures
16 p2373 A72-33222
- Effect of fast-neutron irradiation on ceramics and ceramic-metal seals.
17 p2559 A72-34591
- Implications of ceramic-insulator irradiation results for thermionic reactor design.
17 p2496 A72-34592
- Radiation damage to refractory metals as related to thermionic applications.
17 p2566 A72-34595
- Iridium and tantalum foils for spaceflight neutron dosimetry.
17 p2558 A72-35901
- Neutron irradiation effects on thermionic converter materials, performance and service life
18 p2707 A72-36140
- Behavior of tungsten-clad Mo-UO₂ fuel under neutron irradiation at high temperature.
18 p2708 A72-36143
- Physical-mechanical properties of beryllium oxide and investigation of its electrical resistance under irradiation in a reactor
18 p2703 A72-36147
- In-core thermionic converter emitters irradiation tests to determine fuel, fission gas venting system and emission layer performances
18 p2708 A72-36158
- Thermionic fuel element triple diode configuration, processing, assembly and performance during neutron irradiation testing in reactor
18 p2708 A72-36159
- Breeder reactor testing of fast neutron irradiation effect on alumina and yttria cylinders for thermionic fuel rod designs
18 p2708 A72-36161
- Thermal neutron radiography as NDT technique for industrial inspection, noting advantages for low atomic number and radioactive materials
18 p2695 A72-36457
- Thermal release Xe analysis of neutron irradiated white inclusion samples from Allende carbonaceous meteorite, noting iodine and plutonium isotopes abundance
18 p2728 A72-36971
- Viscoelastic analysis of graphite under neutron irradiation and temperature distribution.
18 p2704 A72-37088
- Polyacrylonitrile based carbon fiber strengthening by fast neutron irradiation at high temperatures
22 p3196 A72-41965
- Effect of voids on angular correlation of positron annihilation photons in molybdenum.
22 p3187 A72-41967
- Dielectric dispersion of irradiated BaTiO₃ near the phase transition.
22 p3215 A72-42934
- NEUTRON PHYSICS**
- Neutronic studies for the French thermoelectronic program
18 p2645 A72-36179
- Equation of state of neutron-star matter at sub-nuclear densities.
22 p3228 A72-42564
- NEUTRON SCATTERING**
- Water absorber lateral scattering effect on absorbed dose from 400 MeV neutron and proton beams [CERN-71-16]
02 p0162 A72-12062
- Phonon dispersion curves from inelastic neutron scattering for actinide and transition metals carbides, noting superconducting properties
09 p1369 A72-22564
- Very-high-frequency gravitational radiation from neutron stars.
21 p3111 A72-41484
- Inelasticity of cosmic neutron interactions in carbon
21 p3102 A72-41840
- Coherent/incoherent elastic/inelastic neutron scattering in amorphous solids, presenting neutron intensity and correlation functions
22 p3206 A72-42799
- NEUTRON SPECTRA**
- Neutron production mechanism and energy spectrum in thermal plasma focus by time of flight spectrometry
01 p0109 A72-10243
- Neutron energy spectrum of radiative pion captured by carbon 12, using gamma and neutron counters
05 p0692 A72-16688
- K-neutral pion inelasticity factor measurement for nucleon interactions in carbon corresponding to primary neutron energy transferred to pions
06 p0869 A72-17269
- Altitude effects on high energy neutrons and galactic gamma rays flux and spectrum variations from balloon flight studies
06 p0873 A72-17639
- Epithermal neutron differential flux spectrum in equilibrium layers of atmosphere at 57 degrees north
07 p1066 A72-20652
- Neutron capture effect on isotopic composition variations of Sm in Apollo lunar samples, comparing with terrestrial abundance
10 p1537 A72-24156
- Effect of neutron spectra on the swelling of ceramic insulators and implications for thermionic reactor design.
18 p2703 A72-36146
- An integral test of the inelastic cross sections of Pb and Mo using measured neutron spectra.
19 p2837 A72-37634
- NEUTRON SPECTROMETERS**
- Resonance neutron transmission for nondestructive absorption spectroscopic evaluation of quantitative chemical or isotopic composition at depth in large samples
01 p0069 A72-10806
- Neutron cosmic ray spectrograph method of separating recorded data by energies, using statistical analysis of data combinations with different dead times
02 p0229 A72-11936
- Short and long term spectral modulation of primary cosmic rays above 2 GV during solar cycle 19 descending phase, presenting neutron monitors calibration procedure
06 p0874 A72-18160
- Neutron cosmic ray spectrograph method of separating recorded data by energies, using statistical analysis of data combinations with different dead times
13 p1957 A72-29248
- NEUTRON STARS**
- NT PULSARS**
- Pulsar nature and radiation mechanism, examining rotating neutron stars structure and atmospheric dynamics
01 p0131 A72-10973

Astronomical research, discussing Venus exploration, stellar evolution quasar structure, Maffei galaxies, black holes, dwarfs and neutron star model

01 p0133 A72-11099

Pulsar theory, discussing rotating neutron star principle, kinetic energy, structure, atmosphere, radiation mechanics and supernovae remnants

03 p0417 A72-13103

Neutron star surface structure and cooling calculations for pulsar cosmic ray production through surface material acceleration

03 p0421 A72-13136

Crab Nebula optical pulsar NP 0532 polarization minima delay mechanism, suggesting relativistic radiation from region orbiting relativistically around neutron star

03 p0434 A72-13553

Electromagnetic pulsar models features and predictions, using rotating neutron stars with strong dipolar magnetic fields

03 p0437 A72-13873

Equation of state for matter at 10-500 trillion g/cc, applying to baryon matter and neutron stars

04 p0571 A72-14557

Relaxation time estimation for electron velocity relative to dilute vortex core array in rotating neutron superfluid, applying to pulsar slowdown rate

04 p0571 A72-14590

Pulsar model, discussing polar radiation diagram formation with source motion around neutron star

04 p0573 A72-14903

Gravitational waves proposed origin, considering black holes, star collapse, white dwarf and neutron star formation and galaxy center neutron star clustering

04 p0576 A72-15074

Tesseral equilibrium shapes of rotating neutron stars emitting gravitational radiation pulses

05 p0719 A72-16602

Neutron star and white dwarf strong magnetic field generation mechanism involving thermodynamic equilibrium states of electron gas

05 p0723 A72-17162

Galactic nuclei and quasars as IR source, noting critical accretion of gas at neutron stars

06 p0883 A72-18015

Microscopic calculations for nuclear forces, compressibility of neutron matter and maximum mass of neutron stars based on solid state model at high densities

06 p0891 A72-18507

Isolated pulsar or neutron star upper mass limit based on consideration of rotational energy, by ejection of low energy cosmic rays or photons

06 p0891 A72-18508

Pulsar dynamics and electrodynamics for power derivation from rotational energy, discussing toroidal magnetic field induced nonhydrostatic stress in neutron star

07 p1068 A72-19001

Loop structure of Monoceros supernova remnant, predicting thermal soft X ray point source as cooling neutron star

07 p1073 A72-19421

Pulsars suggested as rotating neutron stars based on collapsed star magnetic field strength, mass-radius relation and radio flux emission

07 p1080 A72-20055

Neutron star evolution theories, emphasizing neutrino emission processes and stellar collapse

07 p1080 A72-20056

Pulsar model based on neutron star rotation with skew magnetic field, considering radiated particle acceleration responsible for high energy activity in supernova remnants

07 p1080 A72-20057

Pulsar and quasar energy sources, discussing Crab nebula, rotating neutron stars and gravitational collapse role

08 p1233 A72-21208

Pulsar braking index and period-pulse width distribution calculations within proposed model leading to neutron star surface magnetic field strength estimates

08 p1235 A72-21389

Black body X ray sources creation due to neutron stars rotational energy dissipation by strain hysteresis in crust

09 p1382 A72-22284

Long time behavior of neutron star magnetic fields, noting pulsar evidence for large internal fields in main sequence stars

09 p1389 A72-23393

Neutron star properties, formation theories, crust composition and internal structure, examining interior neutron behavior, fermion systems superfluidity, magnetic field effects and stellar dynamics

10 p1533 A72-23890

Pulsar radiation mechanism study from magnetosphere structure model, taking into account neutron star evaporated gas accumulation in gravitation-centrifugal force balance region

10 p1544 A72-24672

Cold static superdense model for white dwarf and neutron stars, using relativity theory and variational principles for stellar structure in hydrostatic equilibrium

11 p1715 A72-25528

Pulsar rotational models, considering white dwarves, neutron stars, oblique rotators, etc

11 p1718 A72-25907

Galactic nuclei and quasars as IR sources, noting critical accretion of gas at neutron stars

11 p1718 A72-25951

Pulsar speed increase mechanism as metastable flow state transition in neutron star superfluid core

11 p1724 A72-26705

Stellar gravitational collapse to neutron stars and black holes, discussing gravitational wave emission from Galactic center

12 p1875 A72-27958

Low mass neutron star source of pulsed X radiation in binary Centaurus X-3 ejected during low energy supernova explosion

14 p2156 A72-30570

Degenerate electron gas magnetic properties implications for metals, white dwarfs and neutron stars, discussing nonmagnetic state for thermal equilibrium

14 p2158 A72-30728

Magnetic neutron stars /pulsars/ atmosphere, questioning vacuum approximation method applicability

14 p2160 A72-30887

Radio emission due to relativistic electrons spiral orbit motion in rotating pulsating neutron star

15 p2304 A72-31333

Rotating neutron stars stability and radial pulsations by energy method, allowing for relativistic effects

15 p2304 A72-31335

Rotating white dwarfs and neutron stars quasi-radial pulsations frequencies, discussing central densities critical values

15 p2304 A72-31336

Flare mechanism of pulsar radiation near magnetic poles of rotating neutron stars

15 p2298 A72-31627

Vela pulsar speedup explanation by corequake release of elastic energy stored within solid neutron lattice

16 p2450 A72-32869

Neutron star acceleration of He, Fe and supernova debris into cosmic ray flux throughout Galaxy, discussing magnetic and superfluidity effects

16 p2448 A72-33745

Mathematical model for magnetosphere surrounding rotating neutron star, noting computer programs for Maxwell and plasma equations solution

16 p2460 A72-33927

Fermi lectures by Dyson on neutron stars and pulsars origin and structure, using perfect gas and realistic models

16 p2460 A72-33974

Pulsating X ray sources with 1 sec periods as stars with central densities between neutron stars and white dwarfs

17 p2599 A72-35074

Formation of neutron star spots and its connection with pulsars. I.

17 p2613 A72-35502

Single body and stellar cluster models of quasars and galactic nuclei stability, noting neutron and collapsing star lifetimes

19 p2862 A72-38052

Unsteady hydrodynamic accretion on a neutron star

19 p2862 A72-38053

Neutron-rich nuclei in a Fermi gas

19 p2837 A72-38060

Effects of nuclear reactions on the stability of degenerate stars

19 p2864 A72-38100

Neutron star matter properties and model calculations, investigating magnetic field decay

19 p2865 A72-38482

On the acceleration of charged particles to cosmic ray energies.

19 p2852 A72-38483

Stability of nonradial vibrational modes of relativistic neutron stars.

20 p2972 A72-39869

General relativity equations for hydrostatic equilibrium of spherical distribution of mass combined with equations of state for highly relativistic neutron star central regions

20 p2955 A72-40011

Neutron star detection based on nearby pulsar soft thermal X ray flux observations

21 p3107 A72-41218

Very-high-frequency gravitational radiation from neutron stars.

21 p3111 A72-41484

Self similar procedure derived for gas fall to solid surface in constant gravitational field, applying to initial phase of neutron star matter accretion

21 p3113 A72-41753

Equation of state of neutron-star matter at sub-nuclear densities.

22 p3228 A72-42564

Neutron star model for magnetic field and superfluidity effects on cooling during pulsar stage

22 p3228 A72-42565

Accretion disc models for compact X-ray sources.

24 p3435 A72-44828

Centaurus X-3 - Possible reactivation of an old neutron star by mass exchange in a close binary.

24 p3439 A72-44976

Radiation pressure supported stars, degenerate dwarfs, neutron stars and black holes high energy observations from space platforms

24 p3446 A72-45536

NEUTRON TRANSMUTATION

U NUCLEAR REACTIONS

NEUTRONS

NT FAST NEUTRONS

NT THERMAL NEUTRONS

Pyramidal tract neuron reactions to antidromic and afferent stimuli in cats, determining somatosensor cortical neurons responses by intra- and extracellular potential outlets

02 p0159 A72-11768

Explosive p-process nucleosynthesis limiting conditions in supernova envelopes, using proton capture and neutron photodisintegration rates

04 p0579 A72-15318

Atmospheric neutron production by cosmic rays, calculating Cd-In ratio

05 p0662 A72-16258

Probabilistic integral multiplicity of generation of primary cosmic ray particles from count rate and primary spectrum relationship, using definition for neutron component calculations

07 p1067 A72-20656

Si burning in stellar explosions, discussing initial composition and neutron enrichment

10 p1544 A72-24666

Negative photoconductivity in CdSe single crystals due to free carrier mobility decrease after surface treatment in gas discharge, noting neutron traps role

13 p2024 A72-30046

Kinetic equations for ultradense matter neutronization, noting stellar configuration of given mass with variable volume

21 p3086 A72-40096

Neutron production in exploding-wire discharges.

21 p3089 A72-40338

Universe evolution study from contemporary chemical composition of cosmic matter, noting concentration changes of protons, neutrons and He 4

22 p3222 A72-42140

The threshold of disintegration of nuclei in a degenerate electron-neutron gas

22 p3209 A72-42963

NEWTON SECOND LAW

Mechanical systems generalization using multilinear transformations and multiple index system flow formalism

24 p3424 A72-44624

NEWTON THEORY

Particle escape within Newtonian gravitational system of three point masses, discussing necessary conditions

01 p0122 A72-10007

Newtonian quasi-static crack propagation theory application to nonlinear structures, considering slender beams, plates and circular cylindrical shells

02 p0292 A72-12029

Power law bodies lift and drag coefficients interrelationship under Newtonian nonaffine similarity laws, presenting rules for equivalent transformations identification

02 p0151 A72-12273

Newton laws and solution existence of two and three body problems in remote universe

03 p0388 A72-13174

Relativistic cosmological model, showing relation to fluid dynamics in Newtonian theory and space-time dependence on causality condition

03 p0426 A72-13267

Newtonian theory for maximum lift drag ratio of blunt-cone cylinder bodies, optimizing rocket reentry nose shape

05 p0602 A72-16535

Nonsymmetrical aerodynamic damping moments on 10 deg cone at supersonic speeds and large angles of attack, comparing Newtonian theory prediction with wind tunnel test results

05 p0609 A72-16947

Stationary stars rigid and differential rotation angular velocity limits, showing analogous conditions in general relativity

06 p0882 A72-18001

Homogeneous isotropic Newtonian and Robertson-Walker cosmological models, discussing radiative transfer and optics

07 p1074 A72-19431

Hypersonic vehicles lateral dynamics during great circle flight, using linearized equations of motion and Newtonian theory for stability derivatives estimation

08 p1110 A72-21603

Newton cooling law applicability to unsteady heat and mass transfer approximate calculation for ion exchange process

09 p1412 A72-23685

- Relativistic homogeneous anisotropic models
analogous construction in Newtonian cosmology
11 p1716 A72-25711
- Newtonian hydrodynamic equations derived from
scalar-tensor theory field equations for cosmic fluid
nonlinear effects during galaxy formation
11 p1717 A72-25866
- Potential or gravitational energy in Newtonian
physics based on Maxwell definition, noting energy
transfer
12 p1843 A72-27187
- Structural and integral parameters for rotating stellar
configurations within Newton gravitation theory,
giving equations for gravitational potential, outer surface
geometry and multipole moments
13 p2035 A72-28677
- Relativistic and Newtonian theory compared for orbiting
satellite matter release criteria and subrelativistic
change effects during gravitational collapse of central
dense core
13 p2040 A72-29407
- Mechanics fundamentals in aerodynamical aircraft
analysis, noting force concept and Newton theory
14 p2073 A72-30817
- Study of the stability of certain relative equilibria of
a symmetrical satellite
17 p2620 A72-34282
- General relativistic planetary structures comparison
with Newton gravitational theory, deriving field equations
for spherically symmetric planets with explicit
pressure and density distributions
18 p2728 A72-36751
- Linear pulsations and stability of differentially
rotating stellar models. I - Newtonian analysis. II -
General relativistic analysis.
19 p2855 A72-37247
- Metric gravitation theories classified according to
field type and interaction mode, constructing post-
Newtonian limit
22 p3206 A72-42567
- The topology of the regularized integral surfaces of
the 3-body problem.
23 p3309 A72-43982
- Solar neutrino and dilaton theory of non-Newtonian
gravity.
23 p3329 A72-44315
- About the first integrals of the generalized problem
of translatory-rotary motion of rigid bodies
24 p3442 A72-45235
- NEWTON-BUSEMANN LAW**
Newton-Busemann pressure law derived for hyper-
sonic rotationally symmetric flow from momentum
theory considerations and plane flows
12 p1751 A72-27120
- Determination of slender bodies of minimum total
drag in hypersonic flow using Newton-Busemann
pressure coefficient law.
23 p3249 A72-44267
- NEWTON-RAPHSON METHOD**
Equivalent current system from measured geomagnetic
disturbance vectors, solving Biot-Savart formula
derived nonlinear equations by Newton-Raphson
iterative method
01 p0055 A72-10430
- Partial iterative refinements of parameters by
reduced Newton-Raphson process based on generalized
inverse, noting method use in gravitational n-
body integration
04 p0581 A72-15630
- Some properties of iterative square-rooting methods
using high-speed multiplication.
19 p2769 A72-37577
- Existence of a unique solution for a class of non-
linear systems of equations and its calculation by iterative
methods
19 p2827 A72-38546
- Finite difference and extended Newton methods
application to transient and steady state creep deformation
in shells of revolution under high temperature and
high stress
22 p3235 A72-42482
- Treatment of the flutter equation by functional analysis,
using the Newton method
22 p3240 A72-42907
- NEWTONIAN FLUIDS**
Self similar solutions for unsteady shear flows of
conducting Newtonian fluids with rheological power law
under transverse magnetic field
03 p0397 A72-13997
- Newtonian fluid laminar free convection over
curved wall with arbitrary temperature variation, investigating
similarity solutions existence by method of
free parameters
04 p0596 A72-15193
- Forebody blowing induced dynamic instability effect
on slender cones at hypersonic speeds, presenting
theory based on unsteady imbedded Newtonian flow
concepts
05 p0607 A72-16919
- Forced convective heat transfer for laminar flow of
Newtonian fluid inside noncircular duct, taking into
account viscous dissipation and work compression
07 p1100 A72-19628
- Transpiration cooling of laminar tangential Newtonian
flow in annuli, obtaining temperature distribution
07 p1100 A72-19631
- Viscosity measurement error estimates for Newtonian
incompressible fluid flow through deformed
capillary tube
07 p0991 A72-20535
- Nonvertical alignment effect on performance of
falling cylinder Newtonian fluid filled viscometer
07 p0992 A72-20552
- Heat transfer in laminar and turbulent Newtonian
fluid flow in narrow channels with allowance for temperature
dependence of viscosity and energy dissipation
08 p1148 A72-20955
- Concentric double and single screw seals in laminar
Newtonian fluid flow operation, using mathematical
methods for optimum thread geometry and maximum
sealing coefficients
08 p1178 A72-21930
- Tacky adhesive tearing between two flexible strips,
solving Newtonian viscous fluid slow flow problem by
iterative numerical scheme
12 p1798 A72-27831
- Viscoplastic media flow rate in noncircular tube
from Newtonian fluid velocity profile, using Green
formula
12 p1799 A72-27981
- Classical flow problem solution by fixed point approach,
using quasi-Lipschitz conditions for Newtonian
potential gradients
15 p2216 A72-31468
- Flows between stationary surfaces of revolution,
having similarity solutions.
17 p2537 A72-34304
- Boundary value problem approximate solution for
Stokes flow of unbounded viscous Newtonian fluid
past single body, applying algorithm to spheroidal
shapes
19 p2784 A72-37369
- Fluid dynamic forces exerted by Newtonian fluid
axisymmetric creeping flow on accelerating body of
arbitrary shape, calculating pressure gradient via Navier-
Stokes equation
23 p3347 A72-43726
- NICHROME (TRADEMARK)**
Nichrome matrix composites with W and Mo reinforcing
fibers
07 p1013 A72-19744
- Heat resistant Nichrome composite alloy with tungsten
filament reinforcement, discussing manufacture and
mechanical properties at 1100 C
07 p1013 A72-19747
- High porosity nichrome fiber materials sintering at
1000-1350 C, considering size, electric conductivity,
shear strength, interfibrillar contact and briquet quality
13 p1967 A72-30105
- Reliability of nichrome film resistors deposited in
vacuum by sublimation on a glass substrate
18 p2669 A72-37117
- Strength properties of highly porous materials made
of metallic fibers
19 p2820 A72-38288
- Electrical resistivity changes in nichrome films sintering
of various thickness with different heat treatment
conditions, noting heat stability and thermal
shock tests
23 p3292 A72-43280
- Pores visualization in porous materials by liquid
filling and subsequent solidification and basic material
removal, observing porous samples of sintered W and
nichrome powders
23 p3290 A72-44016
- NICKEL**
Plastic strain and rupture characteristics of thin
walled tubular Ni samples under complex loading and
biaxial tension
04 p0588 A72-15058
- Dislocation substructure in fatigued Al and Ni
polycrystals surface layer and interior due to high and
low stress cycling, discussing stacking fault energy influence
04 p0534 A72-15577
- Mono- and polycrystalline Ni high temperature
creep kinetics, investigating substructural changes
05 p0671 A72-16000
- Electron density profiles as function of position in
enhanced coronal region from Ni XV and Fe XIII
emission lines observation
05 p0719 A72-16517
- Tensile strength of tungsten reinforced nickel,
determining temperature effect on fibers deformation
after vacuum rolling simultaneously with plastic
matrix
06 p0832 A72-18362
- Composite plasma sprayed coatings of Cu, Ni and
boron nitride, noting antifriction and wear characteristics
06 p0822 A72-18429
- Thermocycling treatment influence on structural
changes and strength in coarse grain Ni under creep
tests
06 p0834 A72-18686
- X ray study of structural changes in Ni single
crystals during recrystallization process after uniaxial
deformation under compression loads with high loading
rates
06 p0834 A72-18744
- Steady creep rates in Ni poly- and single crystals in
presence of dislocation stresses
06 p0835 A72-18748
- Magnetic domain structure of Ni single crystals
after plastic deformation as function of stress induced
anisotropy of layer-like dislocations
07 p1020 A72-20411
- Small impurity amounts effect on packing defect
density and deformation energy in Ni
08 p1188 A72-21791
- Electron microscopy application to dynamic wear
studies of Ni on Ni surface and subsurface topography
and microstructure in nitrogen atmosphere
08 p1179 A72-21943
- Magnetization and elastic stresses effect on Ni
dislocations movement due to domain wall interactions
09 p1371 A72-22866
- Nonstabilized Ni-P thin films electrical conductivity
at 50-280 C, using mass spectrographic, thermal differential,
X ray diffraction and electron microdiffraction analyses
10 p1495 A72-24076
- Powder metallurgy Ni-Cr thoria cleaning by reduction
with atmosphere of hydrogen plus HCl or HBr
10 p1488 A72-24697
- Ni fatigue crack propagation under low cyclic loads
at high temperature in vacuum after annealing and
mechanical treatment
11 p1655 A72-25497
- Ni powder artificial dielectric in waveguide transverse
magnetic field, noting nonreciprocal nature of
microwave attenuation and phase shift
11 p1607 A72-26786
- Ni additive effects on tungsten trioxide reduction
with hydrogen and W powder sinterability
11 p1643 A72-26835
- Microstructural properties of Ni-Al powder
synthetic material from transmission and photoemission
electron microscopy, discussing low and high
temperature strength characteristics
11 p1645 A72-26855
- Ni single crystal growth by Czochralski method,
investigating growth rate, direction and initial structures
effects on substructure
13 p1976 A72-28906
- Cs vapors thermal conductivity at various temperatures
and pressures, using low emissivity Ni cylinders
13 p2065 A72-29896
- Modified geometrical model for sintering Ni-doped
W, including surface tension effect at Ni-vapor interface
14 p2121 A72-30770
- Absolute intensity LEED spectra for clean Ni surfaces,
discussing measurement uncertainties
15 p2276 A72-31854
- Kinematic intensity recovery from LEED data of
specular and nonspecular beams from Ni(111) surface,
noting multiple scattering interference elimination
15 p2276 A72-31855
- Carbon monoxide adsorption on nickel surface,
determining preferential orientation by extended
Huckel calculations
15 p2276 A72-31867
- Tensor analysis for planar magnetoresistivity and
Hall effect in Ni single crystal thin films, noting
anisotropy effects in ferromagnetic crystals
15 p2294 A72-32386
- Cold rotatory forging and subsequent heating effects
on microstructure, texture and mechanical properties
of dispersion hardened Ni specimens obtained by hot
extrusion
16 p2407 A72-33530
- Aluminum oxide high temperature equilibrium
morphology in Ni matrix prepared via vapor deposition
and internal oxidation methods
16 p2411 A72-33824
- Gas shielded arc welding of Ni, discussing current
density, energy, arc length and preheating temperature
effects on welds porosity
18 p2695 A72-36427
- Plastic anisotropy quantitative calculation formula
verified on Cu, Ni and Al, discussing physical sense of
coefficients
18 p2735 A72-36475
- Influence of twinned growth crystals on the texture
of nickel work hardened in tension
18 p2702 A72-36703
- Secondary recrystallization of nickel 270 work-
hardened by tension
18 p2702 A72-36704
- An investigation of impurities segregation to the
/001/ nickel surface during thermal treatment - Work
function changes and Auger electron spectroscopy
using the LEED camera.
18 p2720 A72-37022
- Creep of porous nickel in oxidizing and neutral
media
19 p2819 A72-38287

Deformation and fracture of dispersion-strengthened nickel charged with hydrogen.

20 p2935 A72-39004

Adhesion characteristics of alpha-aluminum oxide-nickel system from shear strength measurements, investigating effects of sintering parameters and Ti and Zr alloying components

20 p2940 A72-39445

The plastic behavior of pure and dispersion-hardened nickel in the temperature range from 20 to 600 C

20 p2940 A72-39455

Effect of cold work on the oxidation of nickel at high temperature.

21 p3067 A72-40846

Oxidation of TD nickel at 1050 and 1200 C as compared to three grades of nickel of different purity.

21 p3067 A72-40915

Investigation by the mass transfer method of the diffusion of nickel at a $\{110\}$ surface of tungsten single crystals

21 p3068 A72-40955

Investigation by the method of secondary ion-ion emission of the initial phase of the formation process of a silver vacuum condensate on a nickel substrate

21 p3068 A72-40960

Gas permeability of high-porosity nickel cermet

22 p3188 A72-42196

Rotational hysteresis in single crystals of powdered nickel

22 p3192 A72-43011

Growth rate of refractory oxide particles in nickel cermets

23 p3299 A72-43290

Determination of Ni, Ga, and Ge in iron meteorites by X-ray fluorescence analysis.

23 p3262 A72-44128

Spontaneous magnetization of Ni foils in high pressure H gas, noting Hall voltage measurement in ferromagnetic foils and thin plates

23 p3324 A72-44140

The kinetics of the reaction between oxygen and sulfur on a Ni $\{111\}$ surface.

24 p3378 A72-44951

Tensile strength of tungsten reinforced nickel, determining temperature effect on fibers deformation after vacuum rolling simultaneously with plastic matrix

24 p3416 A72-45749

NICKEL ALLOYS

NT HASTELLOY [TRADEMARK]

NT INCONEL [TRADEMARK]

NT NICHROME [TRADEMARK]

NT UDIMET ALLOYS

NT WASPALOY

Ni-Cr-Al alloys high temperature oxidation, detailing surface reactions and continuous oxide layer formation [ECS PAPER 114]

01 p0082 A72-10172

Thermal conductivity, electrical resistivity, Lorentz ratio and thermopower of Ti, Al and Ni alloys for aerospace structures over 4-300 K range

01 p0113 A72-10173

Magnetic transformation effect on creep behavior of fcc nickel-cobalt alloy compared with self diffusion data in Curie temperature vicinity

01 p0083 A72-10391

Dispersion strengthened Ni-Cr alloys processing technique and mill products development, noting increased strength at elevated temperatures

01 p0075 A72-10744

High temperature high strength Ni alloys with Ti, Nb and Hf additions, using modified Hastelloy N

01 p0084 A72-10746

TD nickel as construction material for rocket thrust chambers, discussing spin-forming, welding, machining, electric discharge machining and electroforming operations

01 p0075 A72-10753

Arc jet simulation tests of thorium dispersed Ni and Co alloys for space shuttle Metallic Thermal Protection System, determining material degradation

01 p0086 A72-10978

Ni, Fe and Ti alloys creep rupture characteristics in high temperature, high pressure gaseous hydrogen and helium

01 p0086 A72-10979

Stress effects on TiNi compound martensitic transformation, investigating deformation as function of composition and heat treatment

01 p0087 A72-11023

Mo and Zr additions induced mechanical strength increase of Ni-Al-Nb alloys in cast and deformed states at 20-1100 C

01 p0088 A72-11081

Ductility enhancement in directionally solidified Ni base Mar-M200 alloy by Hf additions increasing gamma-gamma prime eutectic

01 p0089 A72-11104

Thoriated Ni-Cr alloys oxidation kinetics at high temperatures, discussing oxide formations as function of CR content

01 p0089 A72-11164

Diffusion aluminide protective coating formation mechanisms on Ni-base superalloys observed from microstructures and compositions in Ni-Al intermetallics

01 p0089 A72-11165

Ni base superalloy powder with refractory oxide particle dispersion, presenting high temperature creep, stress rupture, microstructure activation energy and processing history

02 p0240 A72-11442

Powder metallurgy advantages for Ni-based superalloys, presenting thermomechanical process results

02 p0240 A72-11443

Alumina dispersions structural stability in Fe and Ni based alloys metal matrices

02 p0241 A72-11445

Thorium oxide dispersion strengthened Ni powder metallurgy alloys, noting thermomechanical processing effects on tensile strength

02 p0241 A72-11447

Anodic polarization curves of Ni-Fe alloys relating reaction to attack at controlled voltage of gamma joints and Ni content, using electron microprobe

02 p0243 A72-12168

Eutectic Ni-Cr alloy temperature effects on deformation rate on plasticity, noting superplasticity point

02 p0244 A72-12243

Titanium and aluminum variations effects on eta and gamma prime solvus temperatures and on mechanical properties of iron-nickel superalloy

02 p0245 A72-12508

Mean free path and particle size distribution in dispersion hardened nickel-thoria alloys, obtaining interparticle spacing by Scheil method

02 p0245 A72-12549

Gamma prime precipitate hardened Ni base alloys, attributing strengthening mechanism to coherency strains and precipitates antiphase boundary energy

02 p0247 A72-12817

Quenching effects on thorium-dispersed Ni sheet plastic stress relaxation and room temperature mechanical properties

02 p0247 A72-12822

Powdered chromium carbide-nickel alloys phosphorus addition effects on sintering temperature, shrinkage, density and hardness

03 p0372 A72-13546

Vapor pressure and partial thermodynamic functions of Co-Ni alloys, observing negative deviations from Raoult law

03 p0374 A72-13928

Nb-Co-Sn and Nb-Ni-Sn ternary systems, investigating intermetallic compounds existence by X ray analysis

03 p0375 A72-13944

Structural features of heat resistant Ni-Cr alloy from electron diffraction microscopy, observing coherent lattice bond and plastic deformation

03 p0376 A72-14015

Dilatometric investigation of martensitic transformation in TiNi compound, observing plastic memory effect

03 p0377 A72-14021

Ni-C solid solution, determining room temperature neutron irradiation effects on C distribution during decomposition

03 p0378 A72-14251

Short range order and nucleation of long range order in Ni-rich Ni-Nb alloys, observing electrical resistivity changes dependence on solute concentration

03 p0379 A72-14338

Grain size and precipitate parameters effect on creep properties of Ni-Cr alloys

03 p0379 A72-14339

Quenched and tempered Ni-Cr-Nb-Co alloy, describing cellular precipitation mechanism

04 p0533 A72-14977

Low energy He ion bombardment effects on Ni alloy single crystal surface, observing defect structure with stacking faults, tangled dislocations and carbide precipitation

04 p0533 A72-15159

Flow stress measurements in disordered and partially ordered Ni-Ta alloy single crystals, correlating with ordered phase volume fraction and domain size

04 p0534 A72-15272

Ni alloy stress rupture data correlation and extrapolation from computerized evaluations of time-temperature parameters relative abilities

[ASME PAPER 71-WA/MET-4] 05 p0670 A72-15905

Order-disorder reaction in Ni-V, Ni-V-Nb and Ni-V-Ta alloys, estimating critical temperature

05 p0671 A72-15999

Ni-based metal graphite materials, investigating sintering process control variables effects on structure and phase composition responses

05 p0665 A72-16090

Ni-Cr thick films triode sputtering technique with temperature control by low-energy electron bombardment heating, presenting phase diagram

05 p0675 A72-16393

INCO 713C and IN 100 cast Ni base alloy gas turbine blades under thermal fatigue tests

05 p0675 A72-16497

Binary and ternary alloys of Cr and Fe with Ni, determining interaction coefficient and molar enthalpy for Cr at 1600 C by mass spectrometry

05 p0676 A72-17103

Ni-NiNb intermetallic unidirectional eutectic alloy crystal structure and high temperature behavior, considering mechanical twinning relationship to strain hardening and ductility

05 p0677 A72-17108

Sequential sulfidation and oxidation effects on sulfur self propagation in Ni-Cr alloy

05 p0677 A72-17110

Directionally solidified Al-AlNi intermetallic eutectic composites creep tests, identifying time dependent fracture mechanism

05 p0678 A72-17114

Directionally solidified Al-AlNi intermetallic eutectic alloy microstructural characteristics and effects on creep fracture

05 p0678 A72-17115

Plastic flow stress around dislocations on Ni-Al intermetallic cube and octahedral cross slip systems

05 p0678 A72-17118

Impurities effect on microstructure alignment in unidirectionally solidified Al-AlNi eutectic intermetallic, noting fiberless region defects

05 p0679 A72-17123

Fe effect on dispersion hardened Ni alloys with various quantities of Nb and Ti during cryogenic operation

05 p0679 A72-17202

Superplasticity relation to heat resistance in metal systems Ni-Cr, Ni-Cr-W-Ti-Al and Ti-Si

05 p0680 A72-17212

Crystal structures and martensitic transformation mechanism of TiNi, using X ray diffraction and electrical resistivity measurements

06 p0827 A72-17421

Ni-Al alloy, investigating Y addition effect on vacancy agglomeration suppression during oxidation

06 p0829 A72-17787

Internal friction spectrum peaks in Fe-Ni alloy at 20-1100 C upon heating and cooling, explaining by grain boundary relaxation and martensitic transformations

06 p0830 A72-18293

Anomalous temperature-strain rate dependence of Ni-Al intermetallic compound mechanical properties from plastic deformation mechanism

06 p0832 A72-18417

Hardening mechanisms of interaction between superlattice dislocations and point defects in Ni-Al intermetallic compound mechanical properties strain rate and temperature dependence

06 p0832 A72-18420

Damping characteristics of Ni base heat resistant alloys at high temperatures, showing increase with cyclic strain amplitude

06 p0833 A72-18630

Nickel base alloy under axisymmetric tension compression tests, obtaining breaking load diagrams and fatigue and creep curves

06 p0833 A72-18638

Aging kinetics in Co-Ni-Ti alloys, noting three dimensional periodically modulated structure development

06 p0834 A72-18742

Critical cleavage stresses dependence on ordering degree in Ni-Cr alloy

06 p0835 A72-18745

Nitrogen interaction with Ni-based melts at 1600 C, noting absorption rate dependence on nitrogen diffusion rates and melt viscosities

07 p1011 A72-19546

Nitrogen interaction with liquid binary Ni alloys, investigating solubility as function of temperature and pressure and titanium nitrides existence conditions

07 p1011 A72-19547

Rare earth metals microadditions influence on Ni grain boundaries free energy and compounds formation

07 p1012 A72-19676

Transition metals distribution of IV-VI and VIII A groups in metastable refractory nickel alloys gamma and gamma-prime phases

07 p1012 A72-19678

Aluminized layer phase and chemical composition on heat resistant iron and nickel alloys

07 p1013 A72-19748

Heat resistant weldable precipitation hardened Ni base alloy, discussing intermetallic phase hardening

07 p1014 A72-19842

Hf addition effects on grain boundary structure of cast Ni-base superalloys

07 p1015 A72-19931

Jerky flow /serrated yielding/ in Co-Ni-Cr-C fcc alloys during tensile testing, noting no correlation to dislocation-precipitate interactions

07 p1016 A72-19940

Corrosion resistance decrease and embrittlement in Ni-Mo cermet alloys after heat treatment from electrical resistance measurement

07 p1017 A72-19965

Vacuum hot press diffusion welding of nickel-chromium-thorium dioxide sheet, describing specimen

preparation, welding procedure and welded joints photomicrographic microstructure 07 p0997 A72-20002

Ni-Cr-Ti alloy hardening during intermetallic phases precipitation, discussing atom segregations, Guinier-Preston zones and fcc and hcp lattices 07 p1019 A72-20152

Fe addition effects on structural and mechanical properties of heat resistant Ni-Cr alloys 07 p1020 A72-20416

Kinetic data analysis of internal oxidation in dilute Ni-Be alloys, deriving activation energy and diffusivity of oxygen in Ni 07 p1021 A72-20435

Diffusion creep influence on grain boundary-adjacent precipitate free zone formation in Ni-Cr alloys subjected to high temperature tensile and creep tests 07 p1021 A72-20437

Precipitation hardened Ni-Al alloy mechanical properties, relating ductility and strength to precipitate caused inhibition of microcrack initiation and propagation 07 p1021 A72-20438

Electrode potential gradients during dimensional electrochemical treatment of Ni and Ni based alloys 08 p1175 A72-21041

Dispersion strengthening of electrolytically deposited nickel-aluminum oxide alloys, comparing tensile tests to theoretical values 08 p1186 A72-21442

Ni-Cr-Nb alloys structure and phase composition changes from W-Mo additions and hardening by intermetallic Ni-Nb precipitated from supersaturated solid solution 08 p1187 A72-21782

X ray study of martensite fine structure produced by plastic deformation in Fe-Ni alloy 08 p1188 A72-21788

Plastic deformation characteristics of Fe-Cr-Ni alloy single crystals at low temperatures 08 p1188 A72-21790

Fe-Ni alloys atom redistribution during aging before phase precipitation, discussing Mo and Co clusters in martensitic maraging steels 08 p1190 A72-22189

High strength Ni alloy hot working properties evaluation from extrusion simulation by torsion testing, considering stress-strain-time relations, microstructure, recrystallization and ductility 08 p1190 A72-22199

Mechanical properties anisotropy in heat resistant Ni alloys due to strengthening phase nonmetallic inclusions distribution, suggesting purification by vacuum melting 09 p1327 A72-22231

Ceramic fiber reinforced Ni base alloy for gas turbine blades, improving creep resistance at high temperatures 09 p1335 A72-22396

Analytic determination of Nb low content in highly alloyed Ni base alloys 09 p1276 A72-22637

X ray K absorption edges in binary solid solutions of Co, Fe and Ni with localized hole increases 09 p1371 A72-22846

Parabolic oxidation kinetics of Ni-Ti alloy compound at elevated temperatures 09 p1330 A72-23358

Microstructure and mechanical behavior of unidirectionally solidified magnesium-magnesium nickelide eutectic composite over range of solidification rates 09 p1330 A72-23376

Thermomechanical strengthening of gamma prime precipitation hardened nickel base superalloy, emphasizing working operation and dislocation substructure 09 p1330 A72-23377

Environment and grain size effect on steady state creep and creep rupture properties of Ni-W solid solution 09 p1331 A72-23381

Protective aluminum oxide scale development on Ni-Cr-Al alloy, describing transient oxidation stage 09 p1332 A72-23584

Samaria distribution effect on Ni-Cr alloy oxidation rate for various oxygen pressures, discussing behavior of electroplated and bulk specimens 09 p1332 A72-23585

Differential sputtering yield of Ni-Cu alloy solid solution bombarded by Ar ions 10 p1495 A72-24057

Electron bombardment disordering of ordered Ni-Mn alloy along different crystallographic directions 10 p1514 A72-24075

Carbon effects on internal friction of low temperature Fe-Ni alloy during martensitic transformation 10 p1495 A72-24083

Nb-W equilibrium phase diagram estimation from known phase diagrams of Ni-Nb, Ni-W and Ni-Nb-W systems via Guggenheim quasi-chemical model application to Ni-Nb-W thermodynamic properties 10 p1496 A72-24233

Electrochemical and stress corrosion tests of Ti-Ni alloys in acidic chloride solutions at ambient and elevated temperatures [NACE PAPER 30] 10 p1497 A72-24321

Chloride ion concentration effect on polarization behavior of Fe-Ni alloy, noting cathodic curve parallel shift in noble potential direction 11 p1652 A72-25290

Superplasticity relation to heat resistance in metal systems Ni-Cr, Ni-Cr-W-Ti-Al and Ti-Si 11 p1727 A72-25338

Temperature dependence of Ni and Ni alloys and solid solutions microhardness, noting strengthening effect of Ti, Cr, Al and B additions 11 p1654 A72-25491

Ni and Ni alloys microstructure under tensile stress, determining Cr and Ti effects on plastic deformation at high temperature 11 p1654 A72-25494

Titanium oxide, carbide and nitride fractional determination in Ti-Ni alloy, noting optimum extraction conditions 11 p1655 A72-25513

Manufacturing process for dispersion strengthened nickel-chromium-thorium dioxide alloys for space shuttle thermal protection system panels, discussing joining optimization and mechanical properties 11 p1659 A72-26035

Temperature and strain rate effects on superplasticity of Ni-Cr eutectic alloy 11 p1659 A72-26129

Fe effect on plasticity and ductility of dispersion hardened Ni alloys with various quantities of Nb and Ti at cryogenic temperature 11 p1660 A72-26137

Young modulus of TiC-Co and TiC-Ni hard composites as function of volumetric fraction, using bending tests 11 p1660 A72-26487

Fatigue properties of Ni-Al-W alloy with gamma-prime matrix, noting high endurance limit/yield strength ratio at room temperature 11 p1661 A72-26653

X ray analysis of internal friction strains in nickel molybdenide during ordering process at 650-700 C, using torsional pendulum method for friction measurements 11 p1662 A72-26654

Cold working effect on precipitation-recrystallization interaction in Cu-Ni-Zn alloy, discussing superposed strengthening mechanism during annealing 11 p1641 A72-26738

Cold working effect on Cu-Ni-Si-Mg and Cu-Ni-Si-Cr alloys age hardening behavior, presenting hardness and tensile strength vs aging time at 350 and 400 C 11 p1662 A72-26743

Oxygen, carbon and boron effect on liquid phase sintering behavior and mechanical properties of Ni base superalloys 11 p1645 A72-26848

Dispersed phase nickel-thoria alloy production method based on organometallic compounds, avoiding high temperature and solvent elimination difficulties 11 p1664 A72-26849

Dispersion strengthened nickel-chromium-thoria alloy production methods, noting halogen gas phase diffusion process 11 p1645 A72-26850

High temperature effects on stability, corrosion behavior, structure and protective effectiveness of Al coatings on Ni and Co alloys 11 p1664 A72-26852

Mg addition effect on high temperature mechanical properties of nickel-alumina alloy, studying particle coarsening mechanism changes 11 p1664 A72-26856

Ordered crystallization casting of Ni superalloys for turbine blades, using power down and high rate solidification processes 11 p1646 A72-26894

High temperature Ni base alloys microstructure via transmission electron microscopy and electron diffraction contrast theory, predicting yield and creep strength 11 p1667 A72-26931

Slip and mechanical twinning in nickel-nickel-niobide directionally solidified eutectic alloy, showing variation with temperature of stress-strain curves 11 p1667 A72-26935

Compression creep in ordered binary and ternary ordered bcc Ni alloys investigated by transmission electron microscopy 11 p1667 A72-26937

Low cycle fatigue deformation of lamellar eutectic and cast Ni-Sr alloys, noting microstructure and chemical composition effects on fracture energy 11 p1668 A72-26939

Dislocation bands in electrolytically hydrogen charged fcc Ni-Co alloy, describing band structure in terms of band axis and planes and Burgers vector 11 p1669 A72-26947

Electron microscope study of commercial Ni superalloys, discussing intermetallic compound and carbide precipitation hardening 12 p1827 A72-27137

Photometric determination of Mo in Ni based steels and alloys in molybdenum-unithiol complex form, noting temperature and aqueous solution pH effects 12 p1828 A72-27445

Electrochemical conditions for separation of gamma prime phase from heat resistant Ni alloys by electrolysis 12 p1828 A72-27446

Tensile plastic deformation effect on structural evolution of Ti-Ni alloy under anisothermal heat treatment 12 p1830 A72-27738

Chemical interaction effects on single crystal sapphire filament strength in Ni and Ni alloy matrices during heat treatment in inert atmosphere 13 p1974 A72-28661

Electron diffraction study of transformation twin rotations in Fe-Ni martensites, showing foil plane uncertainty effect with respect to image plane 13 p1975 A72-28666

High temperature steady state tensile creep behavior of Ni-W solid solutions, showing creep rate relation to stress and stacking fault energy 13 p1975 A72-28668

Mo influence on gamma prime phase precipitate in wrought Ni-base superalloys, considering solvus temperature, weight fraction and lattice parameters 13 p1975 A72-28669

Mo addition effect on Al and Ti diffusion from intermetallic compounds into Ni matrix, noting increased high temperature stress rupture life 13 p1975 A72-28670

Ni-Mn alloy phase transformation characteristics from neutron diffraction and small angle scattering studies, showing ordered nearly stoichiometric metastable phase for entire temperature range 13 p1976 A72-28903

Optical interband transition energies in Ni and Ni based alloys, measuring light conductivity at various spectral energies 13 p1976 A72-28904

Ni-Co alloys Nemst-Ettingshausen and Hall effects anomalous constants relationship determination from emf and electrical conductivity measurements 13 p1977 A72-28910

Fcc lattice ferronickel alloys para-process susceptibility anomalous increase explanation by phase transition thermodynamic theory 13 p1977 A72-28911

Phase composition, structure and strength properties of aluminumizing coatings on Ni-Al alloys, noting plasticity increase due to Ta addition 13 p1980 A72-29485

Ti-Ni alloy strengthening by titanium nickelide intermetallic epsilon phase formation control via heat treatment 13 p1981 A72-29829

Sintering of binary systems Co-Ni Co-Fe and Fe-Ni with infinite mutual solubility at different temperatures 13 p1966 A72-29954

Metal particle decomposition products composition in slags from smelted Cr, Ti, Ni and Zr alloys, using X ray microanalysis 14 p2112 A72-30157

Phase precipitated helicoidal dislocations and vacancy-type stacking faults in aged austenite Fe-Ni-Ti alloy, using electron microscope diffraction contrast analysis 14 p2112 A72-30162

Ni-Mo-W alloys hardness rating and corrosion resistance to sulfuric and hydrochloric acids, discussing dispersion hardening, quenching and aging treatments 14 p2114 A72-30272

Sn alloying effect on heat resistant Ni-Cr alloys plastic strain resistance and strength at room and high temperatures 14 p2114 A72-30274

Microstructure effects on thermomechanically processed dispersion strengthened Ni alloys yield strength at various temperatures 14 p2114 A72-30368

X ray and metallographic analyses of Ni-Mo, Ni-Ta, Ni-Nb, Ni-Zr and Ni-Ti alloys crystallized at high cooling rates, observing metastable phases 14 p2115 A72-30405

Martensitic transformation athermal kinetics and accompanied martensite morphology change in Fe-Ni and Fe-Ni-Cr alloys 14 p2115 A72-30407

Electron microscopic and X ray analyses of ordering kinetics in Ni-Mo alloys, noting lattice type change and complex domain structure formation causes 14 p2115 A72-30409

Nickel ion charge sign and magnitude estimation in Ni-Cr alloy by electron transfer method 14 p2116 A72-30415

Heterogeneous order-disorder transformation in Ni-Mo alloy at 78 K after annealing, using ion field emission microscopy 14 p2116 A72-30416

High temperature composite turbine blade materials, discussing service conditions and fiber/matrix selection, noting cast Ni and Mo based alloy fibers 14 p2125 A72-30533

Ni additions effect on Fe-Cr alloys oxidation behavior at high temperatures during varied exposure time periods, noting dichromium trioxide scale formation

14 p2118 A72-30545

Accelerated intergranular corrosion and grain boundary precipitation mechanisms in stainless steel Fe-Ni-Cr alloy, using Huey, acid and Strauss tests

14 p2118 A72-30548

Heat resistant Ni alloys grain boundaries precipitates as function of composition and heat treatment, noting effects on mechanical properties

14 p2118 A72-30589

Primary recrystallization in TD-nickel bars on sublight optical level identified by transmission electron microscopy examination of deformation and annealing substructures

14 p2119 A72-30601

Coarse grain transformation in TD-nickel bar subjected to deformation and annealing, noting abnormal growth caused by thermomechanical effects

14 p2119 A72-30602

Mo-Ni-Al system phase equilibria at 600 C from X ray and microstructural analysis, noting hardness dependence on composition

14 p2123 A72-30985

Nickel-trinickel alumide-trinickel niobiumide system polythermal cross sections from X ray and microstructural analysis, noting electrical resistivity increase with Al content

14 p2123 A72-30988

Ni-Al-Nb-Mo system phase diagram from X ray and microstructural analysis, noting solid solubility and dependence of hardness and electrical resistivity on components

14 p2123 A72-30989

Phase diagrams of Ni-C and Co-C systems with metastable equilibrium lines, investigating microstructure and microhardness of carbide eutectic

14 p2123 A72-30990

Alloying characteristics of heat resistant Ni base Ni-Cr-Al-Ti-Nb-Mo disk alloy

15 p2255 A72-31566

Dispersion hardening Ni base alloys for gas turbine blades, considering composition, structure, gamma phase and embrittlement avoidance

15 p2255 A72-31568

Dispersion hardening /aging/ effect on embrittlement of Ni base alloys in cold worked pipes during heat treatment

15 p2255 A72-31569

Mobile dislocation density and strain rate sensitivity of bcc Fe-Ni alloys from deformation onset to high temperature plateau

15 p2258 A72-32639

Aircraft gas turbine engine Ni base alloy disks and shafts thermomechanical treatment, considering yield strength and high and low cycle fatigue resistance

16 p2406 A72-33299

Mo and W simultaneous addition effects on Ni-Cr-Nb alloy properties, noting heat resistance increase and Nb solid solubility decrease

16 p2408 A72-33534

C concentration and temperature dependence of graphite wetting by liquid Ni and Co and melts of Ni-C and Co-C alloys, noting nonequilibrium effect

16 p2415 A72-33537

Ternary Ni-Cr-Al superalloys oxidation at 800-1300 C as function of composition, temperature, oxygen pressure and reaction time

16 p2410 A72-33811

Investigations aimed at eliminating the susceptibility to thermal cracking of the high corrosion resistant NiMo 30 nickel-molybdenum alloy /Remanit HB/

17 p2559 A72-34394

Susceptibility of the NiCr 15 Fe chromium-nickel alloy /Remanit 1675 SEW and Thermax 1675/ to intercrystalline corrosion

17 p2566 A72-34396

Study of certain features of the electronic structure of the ternary alloys Ni3/Mn, Fe/ and Ni3/Mn, Co/

17 p2568 A72-35518

The effects of environment on the elevated temperature fatigue behavior of nickel-base superalloy single crystals.

18 p2700 A72-36587

Grain-boundary relaxations in an Fe-Ni-Cr alloy.

18 p2700 A72-36588

Composition dependence of density in NiTi and CoTi.

18 p2701 A72-36592

Diffusion in the nickel-rich, Ni-Al solid solution at 1260 C.

18 p2701 A72-36593

Behavior of Fe-21.6 Ni, Fe-18.4 Ni-15.0 Co, Fe-16.8 Ni-5.0 Mo subjected to cumulative thermal cycling at 300 C/hr

18 p2701 A72-36701

Hot corrosion of experimental aluminum-coated cobalt-base alloys.

18 p2702 A72-36797

Self-diffusion of cobalt in the ternary system Co-Ni-Fe

19 p2814 A72-37416

The effect of Mo, Al, and C on phase transformations in Ni alloys

19 p2814 A72-37417

Some problems concerning microplastic deformation and isothermal transformation of Fe-Ni-C alloy. III - Effect of aging in the temperature range from 203 to 304 K on microplastic deformation at 77 K

19 p2814 A72-37419

Some problems concerning microplastic deformation and isothermal transformation of Fe-Ni-C alloy. IV - Effect of transformation plasticity on microplastic deformation at 77 K

19 p2815 A72-37420

Comparison of experimental and theoretical thermal fatigue lives for five nickel-base alloys.

19 p2815 A72-37639

Effect of molybdenum on the properties of TiC-Ni cermet hard alloys

19 p2819 A72-38283

Relations between mechanical properties and microstructures in TiC-Mo2C-Ni alloy.

19 p2821 A72-38375

Phase composition and isothermal cross section diagrams of Cr-Ni-B system at 800 C, using X ray and microstructural analyses

19 p2822 A72-38678

Self-diffusion of cobalt in coarse grained polycrystalline Ni-Co alloys at low temperature

20 p2935 A72-39016

The mechanism of oxidation of Ni-Cr-Al alloys.

20 p2937 A72-39214

The internal oxidation of Ni-Cr-Al alloys.

20 p2937 A72-39215

Formation of voids and dislocation loops in near-stoichiometric NiAl by aging at 700 to 900 C, and some effects on alloy properties.

20 p2937 A72-39288

The effect of elastic anisotropy on dislocations in Ni3Fe.

20 p2937 A72-39293

The effect of plastic deformation on the martensite-to-austenite transition in an iron-nickel alloy.

20 p2938 A72-39298

Tensile and compressive stress coarsening effects on coherent gamma prime precipitate yield strength of Ni-base superalloy single crystals

20 p2938 A72-39299

Decomposition, solubility and coherent phase stability of modulated structure Co-Ni-Ti system at high nucleation temperatures

20 p2939 A72-39312

Investigation of solid solution decay in cobalt-titanium, iron-cobalt-titanium-aluminum and iron-nickel-titanium-aluminum alloys

20 p2939 A72-39314

Interdiffusion in nickel-molybdenum and palladium-molybdenum systems

20 p2939 A72-39315

Powder-metallurgical production of dispersion-hardened nickel and cobalt alloys

20 p2929 A72-39454

Deformation and failure characteristics of joints in a Ni-Al system under the action of high thermal pulses

20 p2942 A72-39822

Domain structures in metal crystals, investigating ordering in Ni-Mo alloys

20 p2962 A72-39997

Fe-Ni sheet with austenitic cube texture by rolling and annealing, investigating plastic deformation during martensitic transformation

21 p3065 A72-40090

Some results of an investigation of the tungsten-nickel-boron ternary system

21 p3066 A72-40393

Ni alloys weld testing for hot cracking resistance, describing vareststraint test method

21 p3060 A72-40848

A comparison of the effect of inward and outward diffusion aluminate coatings on the fatigue behavior of nickel-base superalloys.

21 p3067 A72-40916

Contribution of the invar anomaly and the elinvar effect to the formation of the thermal stability of the modulus of elasticity of iron-nickel invars

21 p3068 A72-40952

Calorimetric investigation of atom ordering effects in a Ni2Cr alloy

21 p3068 A72-40958

Changes in the structure of nickel-beryllium alloys during deformation, recrystallization, and aging

21 p3068 A72-40959

Diffusion of cobalt in Ni-Co alloys at temperatures up to 1000 C

21 p3070 A72-41645

Martensite formation temperature decrease and grain size reduction caused by martensite crystals interaction with barriers in Fe alloy containing austenite beta phase particles

21 p3070 A72-41679

Temperature dependence of the thermal electromotive force and of the Nernst-Ettingshausen effect in nickel-cobalt alloys

22 p3187 A72-41855

Study of the properties of porous materials of nickel-molybdenum and nickel-chromium-molybdenum alloys

22 p3188 A72-42193

Kinetic aspects of plastic strain induced martensite in polycrystalline Fe-Ni-C alloy from tensile tests on austenitic specimens

22 p3189 A72-42437

Thermoelastic martensite caused elastic vibration damping in Cu-Al-Ni alloy, observing shape memory effect

22 p3190 A72-42442

Alloys of thorium with certain transition metals. VI - The constitution of thorium-nickel alloys containing 50-96% nickel.

22 p3190 A72-42769

Influence of temperature on the mechanical properties of metallic compounds

22 p3191 A72-42804

Magnetic properties and texture of a thin strip of nickel-iron-molybdenum alloys

22 p3192 A72-43012

Influence of alloying elements on ordering in alloys of the nickel-molybdenum system

22 p3192 A72-43016

Carbide phases in nickel-based heat-resistant alloys

22 p3192 A72-43018

Grain size and temperature effects on Cr and Al diffusion coefficients and mobility in Ni-20Cr and thoria dispersed NiCr alloys from measurement at 1038-1200 C

22 p3193 A72-43028

Aluminized thoria dispersed NiCr and Ni-20Cr alloys with protective alumina scales from pack diffusion, observing oxidation resistance by isothermal and cyclic oxidation tests

22 p3193 A72-43030

Constitution of the Ni-Cr-Fe system from 0 to 40 pct Fe including some effects of Ti, Al, Si, and Nb.

22 p3194 A72-43038

Composite Al- and Ni-base alloys strengthened by B and W/Mo fibers respectively for reduced weight wing spars and high temperature applications

22 p3197 A72-43139

Thermoelectric properties of alloys of the gallium-nickel system under standard conditions

22 p3215 A72-43191

Titanium carbonitrides alloying with Ni in nitrogen atmosphere, noting N concentration effect on cermet wear resistance

23 p3298 A72-43281

Magnetic properties of the powders of highly dispersed iron-cobalt-nickel alloys

23 p3299 A72-43288

Flow-stress recovery of nickel-aluminum alloys.

23 p3299 A72-43563

Recovery of high temperature deformed Ni-Al alloys.

23 p3300 A72-43564

Investigation of the structural state of the InNDK40T7 high-coercivity alloy

23 p3300 A72-43594

Mechanical properties of heat and corrosion resistant nonmagnetic Ni-Cr-Nb spring alloys with W addition tested in aggressive and nitric acid base media

23 p3300 A72-43595

Desulfurization of cobalt, nickel, and their eutectic carbon alloys during noncrucible zone melting in vacuum

23 p3300 A72-43647

Phase diagrams from X ray analysis of rapidly crystallized Ni-Sn alloys, noting crystal lattices and phase transformation

23 p3300 A72-43648

Heat resistant Ni-base composite stiffened with W wires, investigating interaction between alloy and fibers from metallographic and X ray diffraction microscopy data

23 p3301 A72-43740

Strain hardening effect of Ni, Mn and Mo in Cr steel after high temperature annealing

23 p3301 A72-43742

Energy dissipation in metals during high-frequency fatigue tests. II

23 p3302 A72-43964

Investigation of the state of the structure of turbine-disk materials after operation

23 p3302 A72-43965

Influence of the nature of the particle distribution of the hardening phase in powders on the thermal stability of dispersion-strengthened nickel

23 p3302 A72-44011

Estimation of creep and fatigue behaviour under cyclic loading.

24 p3456 A72-44793

The creep of dispersion-strengthened Ni-Co alloys.

24 p3413 A72-44923

A study of the hardening of the subspinoidal alloy Fe-Ni-Al

24 p3415 A72-45395

Growth kinetics of dispersed thoria in Ni and Ni-Cr alloys.

24 p3415 A72-45480

NICKEL CADMIUM BATTERIES

Charging methods for Ni-Cd batteries used in satellites, noting life increase and weight reduction
01 p0007 A72-11054
Electrical power subsystem for Initial Defense Communications Satellite Program/Augmentation, noting solar cells for power conversion and Ni-Cd batteries for energy storage
01 p0008 A72-11066
A comparison of sealed and vented Ni/Cd battery characteristics.
17 p2498 A72-35567
Thermal conductivity measurements of nickel-cadmium aerospace cells. II - Component conductivities.
21 p2997 A72-40841

NICKEL COATINGS

Cermet coating with enhanced microhardness by Ni electroplating with fine corundum particles, presenting optimum electrolytes
09 p1318 A72-22527
Deposition of Ni-B coatings with specified electrical resistance onto fiberglass cloth reinforced plastics
09 p1318 A72-22528
Developments in vacuum braze coating of aero-engine nozzle guide vanes.
17 p2559 A72-34937
Structure and properties of nickel-phosphorus coatings as a function of the temperature and annealing time
20 p2929 A72-39583
Magnetostriction of porous nickel films
23 p3299 A72-43340
Thermal diffusion annealing improved Ni-B composite electrolytic coatings with uniform B distribution over bulk matrix
23 p3303 A72-44012

NICKEL COMPOUNDS

NT NICKEL OXIDES
X ray and Mossbauer spectral analyses of thermomagnetically treated nickel ferrite samples containing Co, investigating ordering mechanism
13 p2020 A72-28490
Mossbauer and X ray structural analysis of nickel ferrite-chromite magnetic moments, comparing with theoretical data
14 p2141 A72-30171
Photocolorimetric determination of boron in nickel and titanium borides via Magnezone I in alkaline medium, determining solution pH, reaction time, light absorption, etc
18 p2655 A72-36099
Certain physical properties of the borides of cobalt and nickel
21 p3068 A72-40953
Iron-nickel-molybdenum carbonyl powders
23 p3298 A72-43276
Complex compounds of cobalt and nickel with hydrazine
23 p3262 A72-44165

NICKEL OXIDES

Antiferromagnetic dispersion, absorption and light scattering in NiO and other face centred cubic crystals.
20 p2960 A72-39458

NICKEL PLATE

Ni plating by chemical reduction method in boron hydride solution, deducing stabilizing effect of sulfur compounds and Pb salts from catalyst poisoning theory
11 p1641 A72-26265

NICKEL STEELS

Nondestructive determination of temperature dependence of elastic moduli of Al alloy and Ni and stainless steels by resonant frequency method
01 p0084 A72-10518
Maraging and Ni steels stress corrosion cracking rates dependence on stress intensity factor, discussing measurements in salt and distilled water
01 p0086 A72-10995
Ni maraging steel microstructure effects on strength and fracture toughness
01 p0087 A72-11024
Stress corrosion cracking of Cr-Ni austenitic stainless steel with Mo and Cu additions in boiling sulfuric medium
01 p0089 A72-11181
Sintering and heat treatment effects on mechanical properties of atomized and mixed powders of Ni-Mo steel
02 p0234 A72-11462
Press and sinter production of Ni maraging steel powder metallurgy parts
02 p0234 A72-11464
Temperature-time dependent torsional strength and fracture failure of Cr-Ni steel microalloyed with La and Ce as function of grain boundaries
02 p0243 A72-12010
Temperature dependence of low temperature endurance of Cr-Ni steels in bending fatigue tests
03 p0371 A72-13463
Stepwise thermomechanical treatment effect on improved cyclic fatigue strength of Ni-Cr sheet steel with tension and rolling deformations
03 p0372 A72-13598

Hydrogen charging of iron-chrome-nickel austenitic stainless alloys, investigating crack initiation in Inconel 600
03 p0373 A72-13600

Alloy additions and heat treatment effects on mechanical properties and weldability of quenched and aged high strength Ni steels
03 p0378 A72-14173

Potential change under pitting corrosion and repassivation on Cr-Ni steels alloyed with V, Si, Mo and Re
04 p0535 A72-15730

Hardened and tempered Ni-Cr-Mo steel, testing rest periods caused fatigue life increase in terms of cycles to failure
06 p0895 A72-17802

Boron addition effects on scaling resistance of Ni-Cr steel at high temperatures
07 p1012 A72-19738

Long-time isothermal temper embrittlement in Ni-Cr-Mo-V steels, noting tensile ductility decrease and intergranular fracture
07 p1015 A72-19932

Adiabatic reversion of Ni martensitic steel to austenite under shear in orthogonal cutting
07 p0996 A72-19934

Aging effect on brittleness and hardening of Fe-Ni-Mn alloy at various temperatures
07 p1016 A72-19939

Heat treatment of martensitically aging steels with Co, Ni and Mo, considering hardening effects and optimal conditions for high mechanical properties
07 p1020 A72-20414

Hydrogen embrittlement of stable austenitic Ni-Cu steel, observing intergranular decohesion in fractured specimens by microfractography, electron microscopy and X ray crystallography
07 p1021 A72-20485

Carbon determination in Cr-Ni steels and Ni alloys by layerwise spectral analysis, using electrode gap with He
07 p0993 A72-20609

Explosive loading effect on Cr-Ni stainless steel structure with electron microscope study of gamma, alpha and epsilon phases
08 p1187 A72-21780

German monograph on fracture formation and behavior in Ni maraging steel under repeated stress alternations, considering Al and Ti effects on steel strength
08 p1190 A72-22172

Quenched and tempered Ni carbon steel retained austenite transformation and crack observation by X ray diffraction under low cycle fatigue testing
09 p1329 A72-23149

Ni carbon steel microstructure changes in retained austenite phase and crack observation during low cycle fatigue testing
09 p1330 A72-23150

Prototype fine wire feed unit and microplasma welding torch and equipment for butt welding of Ni maraging steel, testing welds mechanically
09 p1321 A72-23636

Fe-Ni-C alloy mixed austeno-martensitic microstructure embrittlement, investigating mechanical properties after thermomechanical treatment
10 p1495 A72-24087

Magnetic properties, electrical resistivity and hardness of vacuum melted Ni-Fe-Ta alloys
11 p1655 A72-25512

Transitional ferrite phase formation in Fe-Cr-Ni alloy evidenced on electron micrographs and diffraction patterns
11 p1657 A72-25760

Coherent precipitate structure in Fe-Ni-Co-Mo maraging alloys, using electron microscopy
11 p1668 A72-26940

Photometric determination of Mo in Ni based steels and alloys in molybdenum-unithiol complex form, noting temperature and aqueous solution pH effects
12 p1828 A72-27445

Austenite grain growth characteristics of heat treated Ni maraging steel
13 p1976 A72-28673

Austenite deformation effect on thermal stability and hardness of Ni steels at various C and Ni concentrations
13 p1977 A72-29019

Ni-Cr-Mo stainless maraging steel, investigating yield strength, toughness, corrosion resistance and weldability
14 p2113 A72-30270

Ni, Si and Mn alloying effect on structural transformations, phase composition and mechanical properties of cast Cr-Ni steels
14 p2114 A72-30273

Co, Mo, Ti and Al alloying effects on aging and hardening processes in Ni steel from hardness, thermal emf and electrical resistance measurements
14 p2115 A72-30408

Cr-containing Fe-alloy and Ni steels, investigating thermal cycling effects on thermal resistance by factorial program
14 p2118 A72-30546

Transformation induced plasticity /trip/ Ni-C steel strengthening by thermal cycling between martensite and reverted austenite
16 p2399 A72-33815

Incoloy low cycle fatigue tests at high temperatures and different strain rates, discussing fatigue life at 10 and 60 min hold times
16 p2410 A72-33820

Low-temperature properties of nitrogen-alloyed austenitic chromium-nickel /molybdenum/ steels and chromium-manganese-nickel steels and their applicability as low-temperature ductile steels
17 p2566 A72-34395

Contribution to the study of the stabilization of corrosion-resistant chromium-nickel austenitic steels
18 p2702 A72-37014

Fe-Ni-C alloys internal damping, martensitic structure and mechanical properties after quenching and tempering, discussing Mo and Cr additions
19 p2806 A72-37418

Effect of twins produced by annealing on high-temperature failure of chromium-nickel-molybdenum steel
20 p2939 A72-39316

Formation of deformation martensite in Fe-Ni-C alloys which do not undergo transformation on cooling.
21 p3066 A72-40270

Deformation-induced martensitic transformation in isothermal and athermal Fe-Ni-C alloys.
21 p3066 A72-40272

Nickel-titanium intermetallic phase effect on recrystallization of dispersion hardening high melting point steel during furnace and induction heating
21 p3071 A72-41789

German monograph - Determination of the diffusion coefficient of hydrogen in the binary iron-nickel system at 25 and 58 C.
22 p3194 A72-43057

German monograph - The causes of hot crack formation in welded joints of austenitic steel with 16 percent chromium and 16 percent nickel.
22 p3195 A72-43079

Investigation of the thermal fatigue of Kh18NiOT steel under complex stress-strain state conditions
23 p3301 A72-43956

Influence of the chemical composition of Kh25Ni16G7AR steel on its heat resistance
23 p3303 A72-44098

Corrosion and electrochemical properties of Kh15Ni5D2T and Kh15Ni4AM3 oxidized steels
23 p3303 A72-44099

Temperature dependence of low temperature endurance of Cr-Ni steels in bending fatigue tests
24 p3413 A72-44938

Measurement of stacking fault energy in CrMnNi austenitic steel by the method of extended nodes
24 p3415 A72-45397

NICOTINE

Separation of central effects of CO₂ and nicotine on ventilation and blood pressure.
21 p3001 A72-40918

NICOTINIC ACID

Effect of nicotinic acid on myocardial metabolism in man at rest and during exercise.
17 p2506 A72-35968

NIGHT

Nighttime ground surface temperature prediction by net flux radiometer
05 p0684 A72-16792

Energy spectra of positive ion bursts on lunar night side from Apollo 12 and 14 Alsep suprathermal ion detectors data
06 p0872 A72-17462

NIGHT AIRGLOW

U AIRGLOW

U NIGHT SKY

NIGHT E LAYER

U E REGION

U NIGHT SKY

NIGHT F LAYER

U F REGION

U NIGHT SKY

NIGHT SKY

Tweaks contribution to atmospheric radio noise background, discussing nighttime ionospheric source information
01 p0056 A72-10444

Daytime and nighttime sporadic F layer regularities correlation with other ionospheric phenomena based on vertical sounding data
01 p0059 A72-10611

Nighttime sodium layer observation by tuned laser beam resonance scattering technique, measuring seasonal variation in Na abundance and height distribution
01 p0063 A72-10915

Equilibrium concentrations of negative ions in nighttime D region, comparing computations to mass spectrometric measurements
01 p0063 A72-10917

Nighttime ionosphere dynamical behavior, discussing motions effect on OI emission intensity
01 p0063 A72-10919

Lower ionospheric nighttime absorption as ionization processes indicator, discussing relationship to geomagnetic activity

02 p0216 A72-11921

Night sky upper ionospheric electron concentration perturbations during magnetic storm, noting latitudinal distribution

02 p0217 A72-11940

Nighttime ionospheric radio wave propagation, determining geomagnetic latitude variations effects on absorption and reflection

02 p0218 A72-11944

Quadrantid meteoritic shower upper atmosphere contamination effects on twilight and night sky brightness

02 p0283 A72-12467

Nighttime radio satellite scintillation from ionospheric irregularities heights associated with magnetic activity at subauroral latitudes

02 p0221 A72-12468

Ray path and absorption calculation for mf and hf radio wave oblique propagation through model ionosphere in nighttime, noting E region ionization role

02 p0184 A72-12875

Thumba night time equatorial E region electron density profiles from rocket-borne Langmuir probe experiments

04 p0517 A72-14957

Van Rhijn height and intensity variations of 5577 A emission in night E layer airglow

04 p0518 A72-14960

Nighttime radio absorption from lower ionospheric ionization by Sco X-1 and Tau X-1 X rays, using full wave admittance method

04 p0519 A72-15161

Large aperture ratio wide field VCN-UV camera exploration of night sky, presenting isophotes of zodiacal light and Milky Way

04 p0525 A72-15685

Nighttime polar atmospheric structure and temperature variations due to gas kinetic and electron energy changes

05 p0656 A72-16240

Terrestrial atmospheric effects on quasar red shift measurements, considering night sky emission lines and atmospheric window size limits

05 p0723 A72-17159

Nighttime plasmopause and thermal ion plasma structures relationship to micropulsations, considering excitation in post storm recovery and diurnal plasma bulge regions

06 p0804 A72-17453

Quantum efficiency at 6300 and 6364 A of recombination mechanism in nighttime F layer, obtaining ionospheric electron density profiles

07 p0974 A72-18893

Nighttime ionospheric dynamo current modulation due to galactic X ray ionization, observing diurnal sidereal time variation in geomagnetic field

07 p1056 A72-18898

Supersonic hydrogen plasma flow in collapsing post sunset upper ionosphere, noting nonvanishing temperature gradient effect on critical point location

07 p0974 A72-18899

Forbush decreases in galactic cosmic ray flux and associated vlf nighttime ionospheric propagation phenomena

07 p1056 A72-18900

F 2 layer diffuse reflections and critical frequencies increase on ionogram recordings during Northern Hemisphere nighttime magnetic storm of 2 December 1967, noting cosmic radio emission decrease

08 p1154 A72-20738

Nighttime and sunrise period ionospheric electron density profiles with respect to time after sunset and solar zenith angle

08 p1226 A72-21102

Neutral wind influence on lower ionosphere nighttime electron and NO ion density profiles

08 p1157 A72-21112

Ionospheric electron density nighttime changes as function of local time, height and latitude during geomagnetic storms

08 p1157 A72-21113

Nighttime D region ionization production by cosmic X rays from various celestial sources and galactic background

09 p1375 A72-22359

Supersonic and subsonic measurements of mesospheric ionization at night, using Arcas rocket parachute borne nose-tip and blunt probes

09 p1296 A72-22362

Laboratory ionization chamber measurement of ion chemistry and production rates from partial simulation of disturbed nighttime ionosphere at 300 K

09 p1275 A72-22368

Nocturnal F region electrodynamic drift at conjugate point sunrise time, discussing dynamo electrostatic field normal component change as cause of ionospheric vertical movement

09 p1297 A72-22576

Star sky simulation in testing and training stands, using spherical mirror, collimator and imbedded spheres

09 p1310 A72-22949

Inferred perturbation effects of Arecibo large nighttime gravity wave on neutral atmosphere velocity and temperature

09 p1300 A72-23021

Equatorial Faraday rotation measurements for night ionospheric electron density peak structures during equinoctial months, using ATSC geostationary satellite radiation

10 p1476 A72-24958

Nighttime E region electron density variation effects on MF and HF radio wave propagation, discussing ionospheric absorption detection experiments

11 p1593 A72-26070

Twilight and nighttime ionospheric temperatures from oxygen 6300 and 5577 A spectral line profiles obtained with Fabry-Perot interferometers

11 p1625 A72-26406

Daytime and nighttime electron temperatures from topside resonances, using oblique echo theory

11 p1625 A72-26409

F region parameters relationship to night sky optical emission, considering electron distribution produced by dissociative recombination

12 p1802 A72-27308

Lower ionospheric nighttime absorption as ionization processes indicator, discussing relationship to geomagnetic activity

13 p1948 A72-29233

Night sky upper ionospheric electron concentration perturbations during magnetic storm, noting latitudinal distribution

13 p1949 A72-29252

Nighttime ionospheric radio wave propagation, determining geomagnetic latitude variations effects on absorption and reflection

13 p1949 A72-29256

HF radio signal reception behavior near maximum usable frequency during evening and at midnight, noting SNR

14 p2085 A72-30656

Midlatitude nighttime sporadic E layer relationship to geomagnetic field, considering wind shear theory

15 p2224 A72-31798

Nighttime F region vertical velocity estimation, using electron density profiles vs true height

15 p2231 A72-32267

Magnetospheric convection induced longitudinal or Fermi acceleration role in nighttime auroral particle flux production mechanism

17 p2601 A72-35592

Rocket radiometers measurement of oxygen IR atmospheric system altitude profile at night, noting auroral enhancement possibility

22 p3170 A72-42365

Rocket measurement after sunset for altitude distribution of 1.27 micron band nightglow emission from diatomic oxygen molecules

22 p3172 A72-42435

Observations of the airglow continuum.

22 p3174 A72-42888

Outer magnetosphere near midnight at quiet and disturbed times.

23 p3341 A72-44513

NIGHT VISION

Color defective vision performance predictions during day and night tests of aviation color signal light discrimination

06 p0767 A72-17871

Landolt ring radioactive plague night vision tester comparison with electoretinography and Goldmann-Weekers dark adaptometry apparatus from special tests of night blind patients

12 p1777 A72-28332

Human vision sensitivity to covert IR illuminators for image intensification during night observation

15 p2189 A72-32046

Lightweight man-portable uncooled semiconductor laser illuminator design for field use in night vision applications

15 p2248 A72-32047

Low level night operations of Army aircraft. [AHS PREPRINT 631]

17 p2488 A72-34481

Monocular and binocular magnifiers for night vision equipment.

20 p2921 A72-39030

Night vision performance measure based on object recognition experiments with optical instruments, noting improvement with image intensifier

21 p3007 A72-40741

IR night vision instruments range calculation, taking into account atmospheric optics and electro-optical image converter characteristics

21 p3059 A72-41816

NIGHTGLOW

Nighttime airglow layer effect application to autonomous navigation and orientation of piloted space vehicles

02 p0256 A72-12289

F2 layer 6300 A night airglow emission photometric data on 31 January 1968, showing large electron content and movements

04 p0517 A72-14958

Lower ionosphere 5577 and 5893 A and hydroxyl band emissions interrelationships, observing atomic O and vertical eddy transport effects

04 p0518 A72-14961

Oxygen Herzberg bands excitation in nightglow, obtaining quenching reaction rate coefficients

07 p0976 A72-19579

Earth horizons nighttime, twilight and daytime visual observations from manned Soyuz spacecraft, discussing upper atmosphere emission layer structure and aureole development

08 p1158 A72-21148

Nightglow evidence of precipitating energetic electrons in midlatitude nighttime D region based on intensity determination from satellite and rocket data

09 p1375 A72-22358

Dynamic model of night time hydroxyl rotational temperature variations from airborne and ground measurements

09 p1298 A72-22587

Nighttime airglow layer effect application to autonomous navigation and orientation of piloted space vehicles

10 p1508 A72-23758

Hydroxyl vibration levels excitation rates calculation from transition probabilities and band sequence nightglow intensity measurements

13 p1954 A72-29816

Seasonal features of nocturnal 6300 A emission variation and decay coefficient in nightglow related to recombination coefficient for F layer ionization

14 p2097 A72-30132

Nightglow small scale intensity fluctuations of 5577 A atomic oxygen emission due to turbulent transport of horizontal wind observed with photometers

14 p2098 A72-30143

Nightglow ground based spectrophotometric observations of hydroxyl emission intensity and rotational temperature variations related with solar and geophysical activity

14 p2098 A72-30144

Sounding rocket observation for emission height of night airglow continuum near 6050 A, using photoelectric photometers

15 p2231 A72-32329

Semidiurnal variation in O I 5577 A nightglow due to lunar tidal dynamics effect in E and F regions

16 p2383 A72-32971

Observation of the intensity ratio between /5,1/ and /9,4/ bands of OH emission in the night airglow.

17 p2546 A72-35059

Atomic oxygen green line emission in nightglow from OGO-F photometer observations, calculating tropical F region electron density spatial distribution

17 p2549 A72-35604

Nocturnal and semiannual variations of the intensity of 5577 A emission of atomic oxygen.

19 p2789 A72-37511

Nightglow observations and ionospheric soundings for red oxygen line intensity relation to F region parameters

19 p2792 A72-38638

Earth horizons nighttime, twilight and daytime visual observations from manned Soyuz spacecraft, discussing upper atmosphere emission layer structure and aureole development

20 p2916 A72-39253

Rocket measurement after sunset for altitude distribution of 1.27 micron band nightglow emission from diatomic oxygen molecules

22 p3172 A72-42435

NIMBUS SATELLITES

Nimbus 3 and 4 satellite technological and meteorological performance, discussing atmospheric temperature humidity and ozone vertical sounding for numerical weather forecasting models

01 p0130 A72-10955

Nimbus satellite image dissector camera system for continuous meteorological scanning, noting special suitability for cloud and ice features discrimination from brightness changes

08 p1171 A72-21967

CAT probabilities relationship to temperature radiance gradients determined by IR spectrometers on-board Nimbus satellites

23 p3310 A72-43614

NIMBUS 2 SATELLITE

Sea surface temperature determination on Nimbus 2 satellite, using three channels in medium resolution IR radiometer

15 p2224 A72-31674

NIMBUS 3 SATELLITE

Autumnal stratospheric temperature variations in northern and southern hemispheres from Nimbus 3 IR spectrometer

11 p1680 A72-25761

Stepwise multiple regression techniques for Nimbus 3 IR interferometer-spectrometer /IRIS/ data inversion, obtaining radiation predictors of meteorological parameters

16 p2418 A72-33666

NIMBUS 4 SATELLITE

Nimbus 4 vertical atmospheric sounding techniques, obtaining temperature, water vapor and ozone profiles with Michelson IR interferometer
 01 p0095 A72-10957

Total ozone estimation by interpolation from Nimbus 4 satellite data on backscattered UV earth radiance attenuation
 01 p0096 A72-11285

Nimbus 4 satellite selective chopper IR radiometer atmospheric temperature measurements from earth surface to 50 km altitude, describing instrument design, operation and performance
 07 p1029 A72-19097

Nimbus 4 satellite-borne selective chopper radiometer design characteristics, obtaining maps of stratospheric warmings in both hemispheres
 08 p1173 A72-22168

Regional geologic features of Alaska and Western Canada from Nimbus 4 satellite image dissection camera system /IDCS/ photographs
 10 p1477 A72-25109

NIMONIC ALLOYS

Nimonic 75 sliding pin and rotating disk frictional force, wear rate and surface temperature
 06 p0830 A72-18156

X ray diffraction patterns of aging nimonic alloys, noting effects of atomic volume difference between precipitation phase and matrix
 13 p1976 A72-28766

X ray diffraction patterns of aging nimonic alloys, noting effects of atomic volume difference between precipitation phase and matrix
 21 p3065 A72-40267

Dilatometric studies of volume compression effect during aging of nimonic alloy showing linear dependence of matrix lattice constant on gamma prime phase
 21 p3068 A72-40957

NIMPHE [ENGINE]

U HYDRAZINE ENGINES

NIOBATES

Tunable optical and IR radiation source by rotating lithium niobate crystal in front of Q switched ruby laser
 04 p0550 A72-15599

Optical holographic storage in lithium niobate single crystals, noting erasability and rewritability
 07 p0981 A72-18890

Temperature dependence of destruction threshold of lithium niobate surface under laser irradiation, noting ferroelectric properties effects
 12 p1853 A72-27069

Discrete ten stage system for laser beam deflection based on electro-optical effect in lithium niobate crystals
 12 p1808 A72-27595

Longitudinal electro-optical effect in oblique cut lithium niobate crystal with minimum half wave voltage between incident beam and optical axis angle
 12 p1855 A72-27603

He-Ne laser light modulation with lithium niobate crystals, noting lower light power and modulator volume requirements, better mechanical properties and lower thermal sensitivity
 13 p1969 A72-29632

Undoped lithium niobate for holographic storage applications, reviewing physics and recording performance
 15 p2239 A72-32353

Transition metal doped lithium niobate for holographic storage, measuring recording sensitivity, maximum diffraction efficiency and erase behavior
 15 p2239 A72-32354

He-Ne laser radiation modulator at 1.5 GHz using X and Z cut lithium niobate crystals in toroidal microwave cavity
 18 p2697 A72-36113

Fracture of nonlinear KDP and LiNbO3 crystals by ruby laser radiation
 19 p2812 A72-38537

Electro-optic KTN /potassium tantalate niobate/ crystals for modulators, deflectors, phase shifters and polarization rotator devices
 20 p2922 A72-39047

Use of oblique-cut lithium niobate in optical-beam control systems.
 24 p3411 A72-45606

Profile of a parametric luminescence line emitted by lithium niobate crystals.
 24 p3432 A72-45614

Temperature and angular widths of the phase-matching curve of a lithium niobate crystal.
 24 p3432 A72-45615

Temperature dependence of destruction threshold of lithium niobate surface under laser irradiation, noting ferroelectric properties effects
 24 p3432 A72-45722

NIONIUM

Hydrogen diffusion kinetics in Nb under various temperatures during gas-metal absorption experiments, observing room temperature hardness profile
 01 p0087 A72-11026

Niobium anomalous oxidation below 600 C, noting suboxide formation between solid solutions and heat resistance reduction
 02 p0243 A72-12214

Oxygen determination in Nb with reduction fusion, determining metallic bath temperature, nature and composition effects on extraction efficiency
 03 p0374 A72-13674

Oxygen and/or nitrogen interstitial solute pick-up effects on yield stress during Nb annealing, discussing Hall-Petch plot parameter values
 05 p0676 A72-16730

Ni-Mo-N system alpha-solid solution thermodynamic analysis, deriving reaction enthalpies/entropies, free energy and interaction coefficients
 05 p0676 A72-16795

Flux lines interaction with dislocations in twisted superconducting niobium single crystals, measuring flux gradient and dislocation arrangement
 06 p0830 A72-18055

Bcc Mo and Nb after cold working observing internal friction relaxation peaks as function of stress, strain, temperature and strain rate
 06 p0831 A72-18296

V, Nb and Ta deoxidizing capability in liquid Fe from oxide phase formation identification by electronographic and X ray analyses
 07 p1011 A72-19545

Steady state high temperature niobium creep in torsion under rarefied oxygen infiltration conditions, discussing surface interactions kinetics
 07 p1012 A72-19679

Reflection electron diffraction and ellipsometric studies of oxidation of niobium crystal surface, showing oxygen absorption in lattice and oxide film formation stages
 07 p1017 A72-19944

Absorbed oxygen concentration variation with depth in Nb during oxidation
 07 p1022 A72-20555

Ta, Nb and La superconductivity, investigating surface contamination effects on electron tunneling characteristics
 09 p1367 A72-22554

Analytic determination of Nb low content in highly alloyed Ni base alloys
 09 p1276 A72-22637

Carburization kinetics of Nb in acetylene or methane at high temperatures and low pressure
 09 p1319 A72-22985

Various restrain dislocation distributions effect on mechanical twinning behavior in purified Nb single crystals
 10 p1497 A72-24824

Bending stress in oxygen presaturated Nb during oxidation, cooling, dissolution and annealing, using thin film model
 11 p1658 A72-25853

Tensile stress effect on formation of suboxide needles, microcracks and oxide wedges during low temperature Nb oxidation
 11 p1658 A72-25854

Carbon solubility in Nb at 1500-2150 C, determining saturation concentrations from electrical resistivity vs reaction time curves
 11 p1662 A72-26740

Superconductive behavior of cold-worked sintered Nb wires, examining effects of aluminum oxide addition on residual resistivity, magnetization behavior and critical current density
 11 p1662 A72-26742

High temperature dislocation rearrangement in lightly cold deformed Nb as function of time and temperature, using etch pit technique for evaluation
 12 p1827 A72-27136

Niobium diffusion into copper as function of time and temperature, obtaining rates by electrical resistance measurements
 12 p1828 A72-27448

Nb superconducting resonant cavities application to linear accelerator and RF particle separator structures in GHz region for wall energy loss reduction
 13 p1922 A72-29348

Low and medium strain rates and temperature effects on bcc structure polycrystalline Nd and Mo, determining mechanical properties of yield and flow
 14 p2114 A72-30367

Hydrogen adsorption and absorption by niobium, investigating sticking probability and heat of solution
 15 p2276 A72-31864

Decarburization kinetics of Nb wires with dissolved carbon in high temperature oxygen flow, monitoring electrical resistivity and CO partial pressure
 15 p2244 A72-32113

Anelastic damping of cold worked Nb sheet as function of vibration frequency, temperature, rolling rate and oxygen content
 15 p2258 A72-32638

Oxygen and nitrogen atoms effect on defects recovery in cold rolled Nb during annealing
 16 p2406 A72-33208

Fcc in thin films and bcc in thick vacuum condensates deposited from Nb molecular beams obtained by evaporation and condensation in mass spectrometer
 16 p2407 A72-33528

Computed performance data for a thermionic converter having a CI-CVD-W emitter and a polycrystalline Nb collector.
 17 p2521 A72-34613

Grain-size dependence of Snoek peaks in niobium.
 17 p2566 A72-34671

The effects of composition and annealing conditions on the stability of columbium /niobium/-treated low-carbon steels.
 20 p2938 A72-39301

Vapor deposition effects on high density Mo, W and Nb obtained by carbonyls pyrolysis or chlorides and fluorides reduction
 20 p2941 A72-39821

Anomalous line broadening in the low temperature X-ray diffraction pattern of niobium.
 20 p2942 A72-39989

Chondrite and achondrite Nb abundance from spark source mass spectroscopic analysis
 21 p3104 A72-40492

Nb heat pipe design with Na coolant for high temperature operation, discussing slopes effect on transmitted power
 21 p3129 A72-41051

Microcracks observed in hydrogenated niobium foil.
 21 p3069 A72-41300

Hydrogen cold work peak measurements in Nb, showing hydrogen atoms-dislocations binding energy extent and temperature effects on internal friction
 22 p3189 A72-42440

Ultrasonic evidence against multiple energy gaps in superconducting niobium.
 22 p3190 A72-42476

Niobium superconductive tunnel diode integrated circuit arrays.
 22 p3161 A72-43090

NIONIUM ALLOYS

Nb alloys bend ductility at various temperatures, showing silicide coatings and electron beam and gas tungsten arc welding effects on mechanical properties
 01 p0083 A72-10284

Cb alloy processing technology from ores to manufactured finished fabricated, joined and coated hardware, discussing reduction methods, annealing, forming, joining, etc
 01 p0075 A72-10745

Bare and coated Nb alloy in high temperature vacuum conditions, discussing tensile and bend tests and mechanical properties
 01 p0084 A72-10747

Larson-Miller parameter application to N6 base alloys creep rupture data, discussing extrapolation method limitations
 01 p0084 A72-10748

Nb alloy silicide coating thickness data correlation by thermoelectric, metallographic and pointed micrometer techniques, discussing state of art in thickness control, penalties and substrate independence
 01 p0075 A72-10750

Coated Nb alloys as reradiative thermal protection system skin materials for space shuttle, investigating flaw growth
 01 p0085 A72-10757

Field repair of Nb alloy panels with protective coatings designed as part of space shuttle thermal protection system
 01 p0091 A72-10758

Field repair of fused slurry silicide coating for oxidation protection of Nb alloys in space shuttle environment
 01 p0075 A72-10759

High temperature carbide dispersion strengthened Nb alloys, using heat and thermomechanical treatments
 01 p0085 A72-10863

Nondestructive tests of Nb alloy radiative thermal protection heat shield design for space shuttle requirements
 01 p0048 A72-10980

Niobium alloy for reentry vehicle heat shields, describing slurry coating process reliability
 01 p0077 A72-10982

Mo and Zr additions induced mechanical strength increase of Ni-Al-Nb alloys in cast and deformed states at 20-1100 C
 01 p0088 A72-11081

Niobium-oxygen-nitrogen system solid solution, noting gas composition effects on hardness and electrical resistivity
 03 p0369 A72-12958

Nb-Mo-N solid solution nitrogen solubility equilibrium at various temperatures and pressures
 03 p0370 A72-12962

Nb-Ti-B ternary system melts hardened in vacuum, determining solidus temperature and surface from phase diagram
 03 p0370 A72-13186

Alkali ion scattering by NbTi alloy and SiC and components, comparing scattering coefficients
 03 p0401 A72-13424

Nb-Co-Sn and Nb-Ni-Sn ternary systems, investigating intermetallic compounds existence by X ray analysis
 03 p0375 A72-13944

Short range order and nucleation of long range order in Nisrich Ni-Nb alloys, observing electrical resistivity changes dependence on solute concentration

03 p0379 A72-14338

Quenched and tempered Ni-Cr-Nb-Co alloy, describing cellular precipitation mechanism

04 p0533 A72-14977

Nb-Ti alloy critical current density increase dependence on temperature, discussing evidence supporting rigidly pinned vortex lattice model

04 p0562 A72-15292

Vacuum diffused Cr, Si, Ti and combined coatings effect on heat resistance of Nb and Nb alloys

04 p0534 A72-15660

Order-disorder reaction in Ni-V, Ni-V-Nb and Ni-V-Ta alloys, estimating critical temperature

05 p0671 A72-15999

Nb-Zr alloy vacuum chamber tests for oxygen reaction rates, showing oxide surface film relation to sticking probability

05 p0674 A72-16391

Nb-O and Nb-N alloys, investigating oxygen and nitrogen solute-hardening effects on room temperature flow stress

05 p0675 A72-16729

Nb alloy oxidation behavior dependence on temperature in 550-1316 C range

05 p0676 A72-16732

Ni-NbNb intermetallic unidirectional eutectic alloy crystal structure and high temperature behavior, considering mechanical twinning relationship to strain hardening and ductility

05 p0677 A72-17108

Mo-Nb alloys single crystals work function, obtaining thermionic emission pattern

06 p0832 A72-18414

Deformation kinetics and failure of refractory Nb and Mo base alloys in plastic state under low cyclic fatigue

06 p0833 A72-18631

Temperature and deformation velocity effects on elasticity and tensile strength of Mo and Nb alloys

06 p0833 A72-18636

High temperature creep of niobium alloy, obtaining creep limit, microhardness and gas analysis data

06 p0833 A72-18637

Nb and Nb-Zr alloy tubular and sheet samples cyclic loading tests, determining heat treatment effects on notch sensitivity and fatigue strength

06 p0834 A72-18646

Microstructural changes and mechanical properties of deformed Nb alloy during annealing process, observing low temperature plasticity increase

06 p0835 A72-18747

Nb-Mo alloys behavior in aggressive boron containing medium at high temperatures, relating boride phases growth rate to component percentages

07 p1012 A72-19680

Diffusion kinetics in Nb-Al system for varying time and temperatures

07 p1015 A72-19930

Microstructure and high temperature mechanical properties of unidirectionally solidified pseudobinary Fe-Cr-Nb eutectic alloy

07 p1016 A72-19938

Nb and Nb alloys mechanical properties during plastic deformation and heat treatment, discussing grain size, dislocation structure and substructural changes effects

07 p1018 A72-20144

Precipitation hardening of quenched superconducting Nb-Al alloys, examining polycrystalline and single crystal samples and intermetallic phases

07 p1050 A72-20155

Nb-Ga system equilibrium phase diagram determination by differential thermal, tempering microstructural and X ray analysis techniques, discussing various compounds formation temperatures and characteristics

07 p1050 A72-20161

Precipitates dispersion and fluxoid pinning/critical current density/ in superconducting Nb-Hf alloy during aging, using transmission electron microscopy

07 p1020 A72-20409

Cast Nb-C alloys carbon solubilities of 1.4 and 0.25 percent at 2100 and 1200 C, showing molten microstructure and measuring procedures

07 p1023 A72-20669

Critical supercurrents in heat treated and cold worked Nb-Ti wires, proposing pinning model based on enhancement of Ginzburg-Landau parameter in cell walls

08 p1186 A72-21594

Phase diagrams, superconducting properties and annealing critical temperature of Nb-Al-Ge alloys, establishing four phase peritectic equilibria

08 p1218 A72-21778

Ni-Cr-Nb alloys structure and phase composition changes from W-Mo additions and hardening by intermetallic Ni-Nb precipitated from supersaturated solid solution

08 p1187 A72-21782

Electron microscopic investigation of niobium-oxygen alloys with Zr and Hf additions, measuring oxygen solubility

08 p1187 A72-21787

Cast Nb alloys plasticity enhancement by heat treatment, discussing solid solution decay kinetics and carbides composition of Nb-Mo-Zr-C system

09 p1327 A72-22229

X ray diffraction and chemical phase analysis of Nb alloys in cast and heat treated state, considering hardening mechanism

09 p1327 A72-22636

Nb-Al-Ge alloy superconductor deposits structure, transition temperature and critical current densities after preparation by triode sputtering and heat treatment

09 p1369 A72-22795

Soft X ray emission spectra from Al-Nb and Al-Pd alloys, deducing electron state density near Al ions

09 p1371 A72-22848

Nb-W equilibrium phase diagram estimation from known phase diagrams of Ni-Nb, Ni-W and Ni-Nb-W systems via Guggenheim quasi-chemical model application to Ni-Nb-W thermodynamic properties

10 p1496 A72-24233

Russian book on Nb in ferrous metallurgy covering physicochemical properties, steels, slags, ore reduction and smelting for Nb alloys production

11 p1659 A72-26048

Ti-Nb and Ti-Nb-Al alloys heat treatment effects on tensile and bending strengths

11 p1659 A72-26131

Nb-Ti alloy elasticity modulus temperature dependence, considering foreign atoms interactions with dislocations

11 p1662 A72-26737

Transmission and scanning electron microscope observations of Nb-Hf alloys fracture morphology, noting precipitate free zone

11 p1667 A72-26934

Slip and mechanical twinning in nickel-nickel niobide directionally solidified eutectic alloy, showing variation with temperature of stress-strain curves

11 p1667 A72-26935

W addition effect on Co-Nb alloys, noting phase structure transformation from cubic to hexagonal due to mean electron density increase

12 p1829 A72-27642

Isothermal profiles for Nb-Zr-C and Nb-Ti-C alloys from microstructural and X ray analyses, noting Widmanstatten structure, and second phase formation

12 p1829 A72-27643

Two phase and three phase composition of ternary alloys Nb-C-Re at 2000 C from X ray, metallographic and chemical analysis

13 p1973 A72-28567

Ti-V and Ti-Nb alloys mechanical strength and stress concentration resistance at low temperatures

13 p1977 A72-29018

Critical superconductivity currents measurement in niobium based U shaped and coiled wires within steady magnetic field

13 p2007 A72-30013

Tungsten and carbon combined solubility in solid niobium at 2000, 1700 and 1100 C

14 p2113 A72-30165

Mo addition effect on high temperature creep resistance and diffusion activation energy of Nb alloys tested in torsion and tension at 1100-1500 C in vacuum

14 p2116 A72-30436

Metallurgical and superconducting properties of beta-tungsten structure niobium aluminide with high critical temperature

14 p2119 A72-30607

Alpha solid solution of nitrogen in Nb-Mo alloys, obtaining excess partial quantities and activity and interaction coefficients at high temperatures

14 p2121 A72-30773

Nb-Ti-Zr-Hf system phase diagram from X ray analysis, observing beta solid solution below solid curve

14 p2122 A72-30977

Phase composition of Nb-O-Hf and Nb-O-Zr ternary alloys, noting O solubility decrease

14 p2122 A72-30980

Ni-Al-Nb-Mo system phase diagram from X ray and microstructural analysis, noting solid solubility and dependence of hardness and electrical resistivity on components

14 p2123 A72-30989

Ru-Nb-Zr alloys phase diagrams from physicochemical analysis, noting components interaction

14 p2123 A72-30993

Rare earth metals interactions with V, Nb and Mo alloys, describing procedures for interstitial impurities removal

15 p2252 A72-31190

High temperature steady creep of Nb and niobium-aluminum oxide alloys at 850-1400 C

15 p2254 A72-31561

Dispersion hardening of Nb-Zr-O and Nb-Hf-O alloys, discussing composition and heat treatment effects on aging, recrystallization temperature and grain growth

15 p2255 A72-31567

Edge and surface modification of Nb alloys prior to coating with fused silicide for oxidation life extension

15 p2244 A72-32134

Multifilamentary superconducting Nb-Sn composite wires in ductile metal matrix, determining transition temperature and critical current density

15 p2294 A72-32534

Heat capacity data analysis for solid solutions of superconducting Nb-Ti system, investigating electronic structure

15 p2296 A72-32692

K and L lines of X ray emission spectra of Ti in alloys with Nb, noting atomic structure change during alloy formation

15 p2259 A72-32701

Nitride precipitate platelets and dislocation loops formation in Nb-N alloys during aging at 535 C from electron microscope observations of structural changes

16 p2405 A72-32999

Nb-Mo alloys elastic constants anomalous temperature dependence, proposing phase changes role and relationship to neutron diffraction and specific heat

16 p2405 A72-33167

Mo and W simultaneous addition effects on Ni-Cr-Nb alloy properties, noting heat resistance increase and Nb solid solubility decrease

16 p2408 A72-33534

Solid phase reaction kinetics in zirconium beryllide alloys with Ta and Nb at 900-1400 C, noting Be diffusion effect

16 p2408 A72-33535

Si stabilization of laves and intermediate phases in Nb-Fe-Si and Nb-Co-Si systems

16 p2409 A72-33805

Precipitation hardening effects on yield strength, toughness and ductile to brittle transition temperature of low alloy steels containing Nb

16 p2409 A72-33809

As-quenched and aged form of omega phase in Ti-Nb alloys investigated by electron microscopy and X ray diffraction

16 p2410 A72-33818

Electron diffraction patterns of previously deformed Ti-Nb alloy containing unequal populations of omega phase variants, noting anisotropy

17 p2566 A72-34673

Mo-Nb alloys single crystals work function, obtaining thermionic emission pattern

17 p2567 A72-34863

Interstitial and substitutional dynamic strain aging of Fe-Nb alloy and Al-Nb bearing steel at 295-950 K

18 p2699 A72-36342

Thermodynamic description of the metal-rich part of the system niobium-molybdenum-nitrogen

18 p2701 A72-36597

Nitrogen interactions in Nb-Zr alloys, investigating interior friction spectra peaks

18 p2702 A72-36707

Characteristics of temperature dependences for the thermal conductivity coefficients of niobium-zirconium solid solutions

19 p2817 A72-37739

Elastic constants of niobium-molybdenum alloys in the temperature range -190 to +100 C

19 p2821 A72-38591

The low strain tensile behavior of U-7.5 wt pct Nb-2.5 wt pct Zr

20 p2938 A72-39303

Phase precipitation structure of superconducting Nb-Ti alloys after cold working and low temperature annealing

21 p3067 A72-40951

Fabrication studies of Nb3Al superconductors

21 p3097 A72-41182

Study of the hot pressing kinetics for niobium-cemented tungsten and titanium carbide alloys

22 p3182 A72-42191

Critical superconductivity currents measurement in niobium based U shaped and coiled wires within steady magnetic field

22 p3190 A72-42735

Superconducting alloys of niobium and vanadium

22 p3191 A72-42808

Niobium and molybdenum alloys containing borides and carbides of the IV-a group metals

22 p3191 A72-42814

Mechanical and thermophysical properties of heat resistant Nb alloys, noting application for thermionic cathodes

22 p3192 A72-42821

Characteristics of superconducting niobium-tin alloys obtained by the vacuum evaporation method

22 p3192 A72-43013

Superconducting transition temperature increase in Nb-Al-Si alloys as function of composition under tetragonal lattice crystallization

22 p3192 A72-43020

Specific-heat and magnetic measurements in superconducting Ta-Nb alloys

23 p3323 A72-43273

Antifriction and electrical properties of WSe2-NbSe2 quasi-binary alloys

23 p3299 A72-43292

Mechanical properties of heat and corrosion resistant nonmagnetic Ni-Cr-Nb spring alloys with W addition tested in aggressive and nitric acid base media 23 p3300 A72-43595

Diffusion bonded columbium panels for the shuttle heat shield. 24 p3406 A72-44889

NIOBIUM CARBIDES

Physical properties of monocarbides of Zr, Nb and alloys in homogeneity range, explaining electronic structure relationship to composition changes 02 p0241 A72-11453

X ray diffraction analysis of dilute Nb-C alloys epsilon phase, discussing Bravais lattice and unit cell dimensions 03 p0375 A72-13932

Niobium carbide thermodynamic properties tabulated for 0-3000 K, deriving equation for heat capacity from low temperature experiments 06 p0832 A72-18430

Niobium carbide coatings for carbon steels and cermets, comparing with titanium carbide coatings 08 p1186 A72-21724

Nonstoichiometric solid solutions based on ZrC and NbC, investigating microhardness variation due to differing valences of atoms in metal sublattices 08 p1188 A72-22100

Niobium carbide resistors properties, investigating temperature dependence of electrical resistance and thermal stability 09 p1331 A72-23483

Plane titanium and niobium carbide precipitation in microalloyed steels during heat treatment above 1300 C, noting eutectic sulfide effect 12 p1827 A72-27102

Shock wave reduction, microcracks and dislocation density of hot pressed titanium, zirconium and niobium carbide powders, using X ray crystal analysis 13 p1982 A72-30110

Niobium and molybdenum carbide film deposition on steel substrates by open arc welding with partial carbon burnout 14 p2107 A72-30156

Niobium carbide coatings for carbon steels and cermets, comparing with titanium carbide coatings 17 p2567 A72-35124

Systems of niobium monocarbide with transition metals. 20 p2942 A72-39985

Study of the process of niobium carbide production in a fluidized bed 23 p3293 A72-43294

Some technological factors influencing the ductility of thermoplastic dross and the properties of niobium-carbide-based finished products 23 p3293 A72-44009

NIOBIUM COMPOUNDS

NT NIOBATES

NT NIOBIUM CARBIDES

NT NIOBIUM OXIDES

NT NIOBIUM STANNIDES

Intercalation complexes of Lewis bases and layered tantalum and niobium disulfide superconductors, noting critical temperatures 01 p0113 A72-10018

Niobium trifluoride synthesis, noting semiconductor and paramagnetic properties 02 p0243 A72-12170

NbN thin film stabilization by metal overlays with reduction in ac losses, discussing superconducting reversibility to normal transition 04 p0560 A72-14542

NbN film superconducting properties measured as function of thickness, discussing transition temperature, critical current and magnetic field 04 p0562 A72-15294

Enthalpy measurements of niobium silicides at 1200-2200 K by mixing method, using isothermal calorimeter 06 p0833 A72-18431

Niobium nitride neutronographic structural study with diffractometer after foil nitriding and rapid cooling 07 p1023 A72-20670

NbN family high transition temperature values application to phonon spectrum prediction based on superconductivity microscopic theory 09 p1369 A72-22565

Atomic radius ratios and lattice constants in intermetallic compounds Laves phases, presenting semistatistically calculated values for niobium diferide based on rigid sphere model 10 p1527 A72-24978

Low field magnetization measurements at 4.2 K on bulk and thin film niobium nitride, discussing Pauli spin paramagnetism and spin-orbit scattering 16 p2442 A72-33843

Influence of hydraulic extrusion on the composition and properties of the Nb3Sn compound 23 p3323 A72-43597

NIOBIUM OXIDES

Tensile stress effect on formation of suboxide needles, microcracks and oxide wedges during low temperature Nb oxidation 11 p1658 A72-25854

Conditions and mechanism of formation of suboxide phases in the niobium-oxygen system 21 p3066 A72-40381

Observation on phenomena associated with a slowly varying surface barrier at niobium oxide and aluminum interface. 21 p3097 A72-40702

NIOBIUM STANNIDES

Uniaxial stress effect on monocrystalline niobium stannide superconducting transition temperature, considering crystal structure 04 p0562 A72-15293

NITRATE ESTERS

Liquid nitrate ester sensitivity and dissolved water desensitization, using thermal initiation and drop weight impact tests 09 p1373 A72-23145

Nitrate ester propellants self ignition hazard and ballistic stability, describing heat generation test at various temperatures for long term storage 14 p2144 A72-30754

NITRATES

NT AMMONIUM NITRATES

NT CELLULOSE NITRATE

NT METHYL NITRATE

NT NITROGLYCERIN

Boron/potassium nitrate parachute mortar design for aircraft and spacecraft applications, comparing with high-low propellant 08 p1221 A72-20783

Vacuum thermal decompositions of the nitrate salts of hydrazine. 19 p2848 A72-38876

NITRIC ACID

Chemical efficiency improvement of aluminum combustion with nitric acid in organic solid fuel 03 p0405 A72-13540

Vertical distribution of nitric acid vapor concentration in lower stratosphere from balloon sounding 11 p1622 A72-26086

Atmospheric nitric acid vapor radiation absorption measurements at various partial pressures 12 p1805 A72-27993

Development of a solid fuel on a polyurethane basis for a hybrid rocket propulsion system with 98% nitric acid as oxidizer 20 p2962 A72-39416

Atmospheric nitric acid vapor radiation absorption measurements at various partial pressures 22 p3174 A72-43007

NITRIC OXIDE

Airborne and spaceborne remote measurement and mapping of atmospheric nitric oxide, describing system configuration with mono or bistatic and pulsed or CW laser [ALAA PAPER 71-1112] 01 p0068 A72-10556

Vertical concentration profile and diurnal variations of N and NO vs solar activity from satellite horizon airglow experiment 02 p0217 A72-11925

Dissociative recombination coefficients of water vapor and nitric oxide in determining D region electron densities 03 p0347 A72-13389

Atmospheric model for mesosphere odd-nitrogen concentration relation to NO dissociation rate and downward flux through mesopause 03 p0350 A72-13526

Reaction kinetics of NO and CO formation in lean premixed hydrocarbon-air flames 04 p0594 A72-14409

Kinetic-analytical models for nitric oxide formation in combustion processes, evaluating heterogeneous effects [WSCIPAPER 71-28] 04 p0482 A72-14581

NO formation in spherical diffusion flames around hydrocarbon fuel drops burning in air [WSCIPAPER 71-29] 04 p0482 A72-14582

Computer program for construction and integration of chemical reaction rate equations, applying to nitric oxide formation and decomposition [WSCIPAPER 71-27] 04 p0482 A72-14583

Fluorescence polarization and intensities of nitric oxide vibrational bands from Cd line and continuum excitation for spectrometer calibration 04 p0552 A72-14893

Nitric oxide formation rate in combustion products of propane-air and hydrogen-air diluent flames 07 p0935 A72-19361

Atmospheric ozone photochemistry, discussing pure oxygen and moist atmospheres, NO mechanism, tracer applications, stratospheric dynamics and Umkehr observations 07 p0979 A72-20228

Vacuum UV excitation cross sections measurement by electron impact on nitric oxide, tabulating threshold energies and transition probabilities 09 p1357 A72-22857

Day, night and sunset mesospheric nitric oxide concentrations during polar cap absorption from rocket measurements of cation composition and charged particle densities 09 p1300 A72-23026

NO ion production rate in D region in relation to electron densities 09 p1300 A72-23027

Electron impact excitation of nitric oxide in vacuum UV, measuring absolute cross sections for emission features [AD-742536] 10 p1515 A72-24341

Neutral atmosphere effects on lower ionosphere, considering D region atomic oxygen, nitric oxide and water vapor and electron density distributions 10 p1474 A72-24712

Vertical concentration profile and diurnal variations of N and NO vs solar activity from satellite horizon airglow experiment 13 p1948 A72-29237

Photochemical model of N and NO distribution based on E region ion composition 15 p2226 A72-31916

Nitric oxide gas release by rocket in auroral glow to determine atomic oxygen densities in ionosphere via observation of auroral light emission 15 p2226 A72-31936

Potential energy curves for exothermic reaction between oxygen cations and nitrogen molecules to form nitric oxide and atomic nitrogen 16 p2360 A72-32921

Mathematical model of nitric oxide formation by fuel droplet burning above fuel critical pressure, applying to diesel engine operations 17 p2511 A72-34901

The reaction of hydrogen peroxide with nitrogen dioxide and nitric oxide. 17 p2511 A72-35466

Fringe shift and slope analysis of interferometric spectrogram formed by NO-gamma system spectral band 17 p2586 A72-35833

A Monte Carlo model of turbulent mixing for the prediction of NO production in steady-flow combustors. [WSCIPAPER 72-8] 20 p2982 A72-38973

Theoretical investigation of nitric oxide and its role in D-region ionization. 20 p2918 A72-39531

NITRIDES

NT ALUMINUM NITRIDES

NT BORON NITRIDES

NT SILICON NITRIDES

NT TANTALUM NITRIDES

NT TITANIUM NITRIDES

NT ZIRCONIUM NITRIDES

Germanium nitride thermolysis, discussing allotropic alpha and beta phases stability and activation energies 01 p0023 A72-10191

Physical properties of transition metal nitrides, carbonitrides and nitride-based cemented hard alloys, discussing carbides stability in presence of high pressure nitrogen 02 p0241 A72-11450

NbN thin film stabilization by metal overlays with reduction in ac losses, discussing superconducting reversibility to normal transition 04 p0560 A72-14542

Sputtering sources fabrication by plasma spraying for nitride films deposition with Ta-Hf mixtures 04 p0527 A72-15494

Electrical resistance, Hall coefficient and magnetic susceptibility of transition metal nitrides at low and room temperatures 06 p0827 A72-17386

Uranium mononitride as nuclear reactor fuel for space vehicle power supply applications, discussing fabrication techniques and irradiation behavior 09 p1349 A72-22406

NbN family high transition temperature values application to phonon spectrum prediction based on superconductivity microscopic theory 09 p1369 A72-22565

Equilibrium states difference of ternary metal-boron-nitrogen systems, taking into account chemical bond type and crystal structure of boride and nitride atoms 14 p2112 A72-30154

Dynamic elastic moduli of diffusion saturated high melting point nitrides, carbides and borides of Ti, Zr, Nb, W, Mo and Ta 15 p2252 A72-31199

Nitride precipitate platelets and dislocation loops formation in Nb-N alloys during aging at 535 C from electron microscope observations of structural changes 16 p2405 A72-32999

Low field magnetization measurements at 4.2 K on bulk and thin film niobium nitride, discussing Pauli spin paramagnetism and spin-orbit scattering 16 p2442 A72-33843

Evaluations of uranium-nitride fueled converters. 17 p2497 A72-34609

NASA research on refractory carbides, nitrides and borides, discussing electronic and defect structures, hot extrusion, uranium nitride, cermets for bearings and composite evaluation 18 p2701 A72-36594

Hot pressing of transition metal nitrides and their properties 19 p2808 A72-38281

NITRIDING

- Heat treatment, quenching and aging caused metastable and stable alpha and beta structures effects on nitrogen diffusion rate in Ti alloy during nitriding 02 p0244 A72-12248
- Phase and microstructure changes during nitriding process of Fe-Ti alloys, stressing Ti concentration effect 07 p1013 A72-19749
- High temperature nitriding of martensitically aging steels in ammonia-nitrogen mixtures, obtaining hard nonbrittle diffusion surface layers 07 p1020 A72-20418
- Niobium nitride neutronographic structural study with diffractometer after foil nitriding and rapid cooling 07 p1023 A72-20670
- Structural changes of nitrified steel diffusion zone, showing alpha solid solution and hard nitride phases mixture 08 p1188 A72-21880
- Heat treatment produced metastable and stable alpha and beta structures effects on nitrogen diffusion rate in Ti alloy during nitriding 11 p1660 A72-26134
- Mo-Hf alloys high temperature mechanical properties improvement by internal diffusion nitriding, noting precipitates effects 11 p1644 A72-26843
- Nitride phase microstructure in ferrochromium nitrified in liquid state, comparing electrolytic etching and film coloration methods 12 p1829 A72-27454
- Boron nitride coated boron fibers for metal matrix composite reinforcement, discussing surface nitriding process by heating 12 p1815 A72-28088
- Mechanical properties of nitrified austenitic steels at low temperatures, noting improved tensile strength 13 p1977 A72-29017
- Internal nitridation zones and growth kinetics for Cr and Cr-Ti alloys at 1000-1400 C, using Maak analysis 16 p2409 A72-33807
- Low-temperature properties of nitrogen-alloyed austenitic chromium-nickel/molybdenum/steels and chromium-manganese-nickel steels and their applicability as low-temperature ductile steels 17 p2566 A72-34395
- The nitriding behaviour of austenitic stainless steels containing titanium. 21 p3066 A72-40686
- Antiscratch properties of nitrified layers of creep-resisting steels at high temperatures 22 p3187 A72-41868
- Characteristics of the state of particles of titanium and vanadium mononitrides after nitriding and heat treatment 23 p3298 A72-43282
- NITRILES**
NT ACRYLONITRILES
 Laboratory simulation of Jovian atmospheric reactions, observing amino nitriles formation 04 p0572 A72-14764
- Nitriles, nitrogen bases and porphyrin-like pigments catalytic synthesis products analysis by mass spectroscopy gas and other chromatographies 14 p2157 A72-30583
- NITRITES**
 Reactions of aniline with isoamyl nitrite and phenyldiazonium borofluoride with caustic potash, investigating kinetics of chemical polarization of products nuclei 09 p1275 A72-22497
- NITRO COMPOUNDS**
NT NITROBENZENES
NT NITROGLYCERIN
NT NITROMETHANE
NT TETRYL
NT TRINITROTOLUENE
NITROAMINES
 Dinitroxydiethyl nitramine burning, describing experimental facilities used to determine temperature profile of combustion front 09 p1411 A72-22884
- NITROBENZENES**
NT TRINITROTOLUENE
 Molecular complexes of methoxyindoles with 1,3,5-trinitrobenzene and tetracyanoethylene /Spectroscopy/association constants/NMR/ 17 p2512 A72-35649
- NITROCELLULOSE**
U CELLULOSE NITRATE
NITROGEN
NT LIQUID NITROGEN
NT NITROGEN ATOMS
NT NITROGEN IONS
NT NITROGEN ISOTOPES
NT SOLID NITROGEN
 Electric quadrupole to magnetic dipole f-values for CO fourth positive and nitrogen Lyman-Birge-Hopfield systems, using curve of growth method 01 p0103 A72-10092

- Differential thermal radiation scattering coefficients of submicron W refractory particles in hydrogen and nitrogen at temperatures to 1080 K 01 p0112 A72-11341
- Nonthermal escape and predissociation mechanism for Mars low nitrogen concentration reflected in Mariner 6 and 7 UV spectrometric results 02 p0280 A72-12208
- Shock wave impact at flat/spherical end surface of cylindrical body in supersonic nitrogen flow, using pulsed ruby laser for shadow photography 02 p0151 A72-12280
- Non-Boltzmann molecular nitrogen vibrational distribution in aurora during electron bombardment as function of altitude 02 p0221 A72-12456
- Lung ventilation nonuniformity determination by single calm breath method, showing nitrogen concentration in alveolar phases 02 p0165 A72-12515
- Seigel state equation validity limit application to isentropic hydrogen and nitrogen steady and unsteady flow expansions at high pressure 02 p0206 A72-12597
- Cross-excited carbon-dioxide-nitrogen laser with pulse sharpening effect due to self-Q-switching, finding optimal nitrogen mixing ratio for peak power 02 p0239 A72-12827
- Niobium-oxygen-nitrogen system solid solution, noting gas composition effects on hardness and electrical resistivity 03 p0369 A72-12958
- Nb-Mo-N solid solution nitrogen solubility equilibrium at various temperatures and pressures 03 p0370 A72-12962
- Altitude, photon wavelength and solar activity effects on photoionization yield of ionospheric monatomic and diatomic oxygen and nitrogen via Monte Carlo simulation 03 p0345 A72-12983
- Oxygen, hydrogen and nitrogen constituents in mesosphere, investigating ionization process in D region at midlatitudes 03 p0346 A72-13379
- Atmospheric model for mesosphere odd-nitrogen concentration relation to NO dissociation rate and downward flux through mesopause 03 p0350 A72-13526
- Spatial distribution of gaseous nitrogen molecules scattered from metal surface, estimating beam capture coefficient 03 p0392 A72-14056
- Oxygen and oxygen-nitrogen mixtures dc and hf discharges, evaluating traveling low field domains in positive column 03 p0400 A72-14350
- Pulmonary RC network and multiple breath nitrogen washout time constants mathematical relationship for breathing mechanics measurement, discussing lung compliance and resistance 04 p0478 A72-14862
- Molecular nitrogen dayglow emission in F region, noting volume emission rates, integrated overhead intensities and solar activity effects 04 p0518 A72-14959
- Height profiles for volume emission rate and intensity of second positive band of nitrogen molecule excited by photoelectron impact, noting solar activity effects 04 p0518 A72-14962
- Underexpanded nitrogen jet from sonic orifice, investigating axial rotational temperature distribution 04 p0597 A72-15335
- Nitrogen to carbon dioxide vibrational energy transfer time measurement in gas dynamic laser 04 p0531 A72-15352
- Nitrogen heat pipe axial temperature distribution and vapor pressure measurement, noting effective thermal conductivity variation with power load and inclination angle [ASME PAPER 71-WA/HT-28] 05 p0744 A72-15881
- Deactivation of A-state nitrogen molecules in auroras, reinterpreting rocket observations of nitrogen Vegard-Kaplan system in terms of atmospheric model based on mass spectrometer measurements [AD-737434] 05 p0655 A72-16072
- Ar, Kr, methane and nitrogen physisorption isotherms on stainless steel in low pressure cryogenic baths calculating mean adsorption energies 05 p0624 A72-16395
- Nb-O and Nb-N alloys, investigating oxygen and nitrogen solute-hardening effects on room temperature flow stress 05 p0675 A72-16729
- Oxygen and/or nitrogen interstitial solute pick-up effects on yield stress during Nb annealing, discussing Hall-Petch plot parameter values 05 p0676 A72-16730
- Ni-Mo-N system alpha-solid solution thermodynamic analysis, deriving reaction enthalpies/entropies, free energy and interaction coefficients 05 p0676 A72-16795
- Molecular nitrogen photoelectron impact excitation of Herman-Kaplan upper electronic state, considering

- cascaade contribution to low lying states in electron auroras and dayglow 06 p0806 A72-17647
- Trimethylphosphite interaction with acetyl- and benzoyl-p-quinone in dry nitrogen atmosphere, noting phosphate formation through intermediate bipolar ion 06 p0770 A72-17986
- Electron beam induced dissociative excitation of vacuum UV emission from atomic nitrogen multiplets, using normal incidence monochromator and pulse counting techniques [AD-736008] 07 p1036 A72-18925
- Thermal conductivities of gaseous binary mixtures of methyl nitrate with helium, neon, argon and nitrogen 07 p1051 A72-19365
- Vibrationally excited nitrogen photoionization spectrum obtained with quadrupole mass spectrometer in flowing nitrogen afterglow 07 p1037 A72-19434
- Nitrogen interaction with Ni-based melts at 1600 C, noting absorption rate dependence on nitrogen diffusion rates and melt viscosities 07 p1011 A72-19546
- Nitrogen interaction with liquid binary Ni alloys, investigating solubility as function of temperature and pressure and titanium nitrides existence conditions 07 p1011 A72-19547
- Na deactivation effect on carbon dioxide-nitrogen gas dynamic laser gain 07 p1008 A72-20564
- Gaseous nitrogen production in humans under steady-state conditions, relating expired nitrogen minute volume increase after protein consumption to possible gastrointestinal and metabolic effects 08 p1122 A72-20882
- Population inversion development and breakdown in active medium produced by plasma generation during pulsed discharge in molecular nitrogen laser 08 p1183 A72-21716
- High power electron beam pumped nitrogen super-radiant laser with 60 kW output 09 p1323 A72-22624
- Nitrogen adsorption kinetics on bulk W targets investigated by ultrahigh vacuum, molecular beam, reflexion detector method 09 p1276 A72-22806
- Pressure, temperature and nozzle size effects on molecular cluster formation in expanding supersonic jets of rare gases, nitrogen and carbon dioxide 09 p1294 A72-22853
- Lasing length, power and efficiency of cw HF chemical laser with nitrogen or He diluent [AD-742962] 09 p1325 A72-23241
- 50 MW laser amplifier at 3371 A in molecular nitrogen via transverse electron pumping 10 p1491 A72-24225
- Low energy elastic scattering cross section measurements for helium-nitrogen system, using two collimated aerodynamically intensified crossed molecular beams 10 p1515 A72-24338
- Shock wave impact at flat/spherical end surface of cylindrical body in supersonic nitrogen flow, using pulsed ruby laser for shadow photography 11 p1571 A72-25702
- Electrically excited carbon dioxide-nitrogen laser using high repetition rate discharge pulses from pin electrode array transition to supersonic flow 11 p1647 A72-26147
- High pressure electroionization carbon dioxide and nitrogen filled carbon dioxide lasers 11 p1652 A72-26793
- Nitrogen solubility, degassing kinetics and diffusion coefficients for Mo-N, W-N and Re-N systems for 1300-3050 C 11 p1663 A72-26841
- High temperature low pressure reaction kinetics of nitrogen sorption by titanium foil, using ultrahigh vacuum microbalance 12 p1777 A72-27045
- High temperature solubility and diffusion coefficient of nitrogen in rhenium 12 p1827 A72-27138
- Absorption spectrum of molecular nitrogen in 730-980 A band, investigating absorption cross sections and optical oscillator strengths 12 p1848 A72-27853
- Chlorella population age structure and cell requirements correlation with nutrient medium nitrogen and phosphorus absorption 13 p1909 A72-29311
- Vibrational relaxation mechanism in supersonic flows of chemically reacting carbon dioxide-nitrogen mixture, using numerical integration 13 p1913 A72-29502
- Nonlinear light amplification in molecular nitrogen amplifier as function of input pulse delay relative to excitation start 13 p1969 A72-29522
- Resonance scattering and direct photoelectron excitation contribution to molecular nitrogen first positive bands emission in day airglow from rocket measurements 13 p1953 A72-29808

Nonequilibrium dissociating inviscid nitrogen flow pattern over spheres and circular cylinders, obtaining temperature, pressure and density fields 13 p1895 A72-30032

Low carbon and nitrogen concentrations in chromium ferritic stainless steel obtained with gas rinsing at reduced pressure, noting weldability and corrosion resistance 14 p2119 A72-30606

Photoelectron precipitation induced dissociation of atmospheric nitrogen molecules during moderate solar activity 14 p2102 A72-30659

Four-parallel-compartment lung model for emptying pattern study, using expired nitrogen concentration data to calculate alveolar dilution ratio and emptying rate 14 p2079 A72-30703

Alpha solid solution of nitrogen in Nb-Mo alloys, obtaining excess partial quantities and activity and interaction coefficients at high temperatures 14 p2121 A72-30773

First positive and first negative nitrogen emission excitation kinetic mechanisms, investigating shock tube measurements of nonequilibrium radiation 14 p2134 A72-30837

Anomalous excitation of nitrogen positive bands in seeded Ar free plasma jet, measuring oscillator strengths of atoms 14 p2140 A72-30899

Ce-N alloys phase diagram from durometric, X ray, metallographic and differential thermal analyses 14 p2123 A72-30991

Molecular nitrogen pulsed laser wavelength measurements, observing IR bands, stimulated emission lines and population inversion mechanisms 15 p2249 A72-32151

Nitrogen molecular beam rotational excitation by collision with argon beam, describing electron beam spectrographic experimental method and numerical simulation technique 16 p2431 A72-33071

Nitrogen existence in galactic cosmic ray sources, considering formation from CNO cycle hydrogen and He burning and ejection from normal stars 16 p2448 A72-33739

Coupling of free electron and nitrogen vibrational temperature nonequilibrium in weakly ionized nozzle expansions of shock heated nitrogen [AIAA PAPER 72-683] 16 p2380 A72-34059

Nitrogen plasma jet flow, attributing discrepancies in electrical conductivity and velocity to shock effects on probe measurements [AIAA PAPER 72-671] 16 p2440 A72-34069

Combustion process in mixing gas jets of different density, using argon and nitrogen for internal flow and air for external jet 16 p2381 A72-34169

Regression analysis for steady state N2 inequality in O2 consumption calculations. 17 p2507 A72-34542

Effects of nitrogen and helium upon pulmonary damage after rapid decompression to 2 torr. [AD-746093] 17 p2508 A72-34544

N2 positive and N2+/- band systems and the energy spectra of auroral electrons. 17 p2545 A72-34634

Breakdown in argon and nitrogen under the influence of a 0.35-micron picosecond laser pulse. 17 p2564 A72-35508

Determination of the quenching of O(1D) by molecular nitrogen using the ionospheric modification experiment. 18 p2685 A72-35991

Equilibria and degassing kinetics in the systems Mo-N, W-N, and Re-N 18 p2701 A72-36596

Thermodynamic description of the metal-rich part of the system niobium-molybdenum-nitrogen 18 p2701 A72-36597

Proton capture mean lifetimes in fast C-N cycle, presenting nitrogen/carbon abundance ratio variation with temperature 18 p2721 A72-36650

Nitrogen interactions in Nb-Zr alloys, investigating interior friction spectra peaks 18 p2702 A72-36707

Vibrationally excited nitrogen in upper atmosphere 18 p2688 A72-36865

Vibrational excitation in N2 by electron impact in the 15-35-eV region. 19 p2837 A72-37546

Pulse nitrogen laser at high repetition rate. 19 p2813 A72-38696

Neurologic oxygen toxicity - Effects of switch of inert gas and change of pressure. 19 p2758 A72-38704

Myth of nitrogen equality in respiration - Its history and implications. 19 p2758 A72-38708

IR emission of nitrogen layer heated by reflected shock wave, noting absorption cross sections under free-free electron transitions in neutral particle fields 19 p2835 A72-38776

The influence of interstitial nitrogen on the asymmetry of the yield stress of tantalum. 20 p2935 A72-39006

Exploratory investigation of Y, La, and Hf coatings for nitridation protection of chromium alloys. 20 p2944 A72-39290

Results of a study of heat and mass transfer during the purification of helium from nitrogen by the condensation method 21 p3127 A72-40130

Molecular orbital calculation of the isotropic hyperfine interactions in triatomic nitrogen radicals. 21 p3013 A72-40564

Angular distribution of electrons elastically scattered from N2. 21 p3088 A72-40777

Critical flow rate and pressure ratio for nitrogen flowing through convergent-divergent nozzle at stagnation conditions, emphasizing thermodynamic critical region 21 p3046 A72-41180

Nitrogen excretion as a measure of protein metabolism in man under different conditions of renal function. 21 p3003 A72-41523

Nitrogen temperature determination in arc tunnel air flows. [AIAA PAPER 72-1022] 21 p3042 A72-41600

Energy exchange processes in a low temperature N2-CO transfer laser. 22 p3184 A72-41993

OI 6300 and 5577 A, NI 5200 A and H beta 4861 A emission line measurement during 8-9 March 1970 auroral arc event 22 p3169 A72-42018

Airglow observations with a Hadamard photometer. 22 p3169 A72-42023

Thermospheric atomic oxygen and molecular nitrogen densities from OGO 6 neutral atmospheric composition experiment, comparing with prediction by Jacchia models 22 p3172 A72-42431

Spontaneous self mode locking in transversely excited nitrogen laser operation in first positive system 22 p3186 A72-42618

Drift velocities, diffusion coefficients, and temperatures of photoions in argon, nitrogen, and oxygen 22 p3209 A72-42926

German monograph - Ionization of nitrogen-oxygen gas mixtures by shock waves. 22 p3209 A72-43073

Molecular gas presence effect on electron energy balance in atomic gases, noting inelastic collisions loss factor in heated Ar plasma containing nitrogen molecules 22 p3213 A72-43110

Titanium carbonitrides alloying with Ni in nitrogen atmosphere, noting N concentration effect on cermets wear resistance 23 p3298 A72-43281

Second positive system of nitrogen bands in the day airglow from Cosmos-224 data 23 p3282 A72-43356

Visual perception of accelerated nitrogen nuclei interacting with the human retina. 23 p3256 A72-43940

Electronic excitation of N2 and dissociative excitation of O2 by proton impact. 23 p3317 A72-44520

Laser-source spectroscopy. II - Experimental study of line broadening for the 00 1-/10 0, 02 0/ transition of CO2 disturbed by N2: Application of the theory of Anderson, Tsao, and Cornette to the calculation of pure and N2-disturbed CO2 linewidths 23 p3298 A72-44535

On the use of a Fabry-Perot interferometer for the study of Raman spectra of gases under high resolution. 24 p3426 A72-44904

High speed mixing of nitrogen vibrationally excited with carbon dioxide 24 p3464 A72-45065

Electron scattering by molecules with and without vibrational excitation. IV - Elastic scattering and excitation of the first vibrational level for N2 and CO at 20 eV. 24 p3427 A72-45304

Electron scattering by molecules with and without vibrational excitation. V - Elastic scattering and non-resonant vibrational excitation of N2 at 30-83 eV. 24 p3427 A72-45305

Transport properties of a gas of diatomic molecules. VI - Classical trajectory calculations of the rotational relaxation time of the Ar-N2 system. 24 p3427 A72-45308

NITROGEN ATOMS

Vertical concentration profile and diurnal variations of N and NO vs solar activity from satellite horizon airglow experiment 02 p0217 A72-11925

Vertical concentration profile and diurnal variations of N and NO vs solar activity from satellite horizon airglow experiment 13 p1948 A72-29237

Oxygen and nitrogen atoms effect on defects recovery in cold rolled Nb during annealing 16 p2406 A72-33208

Theory of dispersion in relation to light shifts. 24 p3409 A72-44921

NITROGEN COMPOUNDS

NT ALUMINUM NITRIDES

NT AMIDES

NT AMMONIA

NT AMMONIUM NITRATES

NT AZIDES [INORGANIC]

NT AZO COMPOUNDS

NT BORON NITRIDES

NT CELLULOSE NITRATE

NT CYANAMIDES

NT CYANO COMPOUNDS

NT GUANINES

NT HYDROGEN CYANIDES

NT IMINES

NT LIQUID AMMONIA

NT METHYL NITRATE

NT MORPHINE

NT NICOTINE

NT NITRATE ESTERS

NT NITRATES

NT NITRIC ACID

NT NITRIC OXIDE

NT NITRIDES

NT NITRITES

NT NITROAMINES

NT NITROBENZENES

NT NITROGEN DIOXIDE

NT NITROGEN FLUORIDES

NT NITROGEN OXIDES

NT NITROGEN TETROXIDE

NT NITROGLYCERIN

NT NITROMETHANE

NT NITROUS OXIDES

NT POLYIMIDES

NT RDX

NT RESERPINE

NT SILICON NITRIDES

NT SUCCINIMIDES

NT TANTALUM NITRIDES

NT TETRYL

NT TITANIUM NITRIDES

NT TRINITROTOLUENE

NT TRYPTOPHAN

NT UREAS

NT URIC ACID

NT XANTHINES

NT ZIRCONIUM NITRIDES

Colorado Green River Formation oil shale extracts, determining nitrogenous compounds content with high resolution mass spectrometry 03 p0320 A72-13741

Nitriles, nitrogen bases and porphyrin-like pigments catalytic synthesis products analysis by mass spectroscopy gas and other chromatographies 14 p2157 A72-30583

NITROGEN DIOXIDE

Remote sensing of regional vertical air column pollutants, discussing sulfur dioxide and nitrogen dioxide measurements by correlation spectrometer [AIAA PAPER 71-1060] 01 p0057 A72-10529

Thermal conductivity measurement of dissociating nitrogen dioxide over 548-792 K and 1-30 atm 02 p0170 A72-12091

Heat transfer of nonequilibrium dissociating nitrogen dioxide in round tube, allowing for finite reaction velocity 02 p0303 A72-12861

Nitrogen dioxide producing chemiluminescent radiative and three-body recombination reaction at low pressures, determining airglow and oxygen atoms decay time by resonance fluorescence method 03 p0347 A72-13395

Mars short wave line spectra from measurement with reflector, estimating nitrogen dioxide content in atmosphere 03 p0436 A72-13815

Mass spectroscopic rate constants for reactions of negative ions of rhenium and tungsten oxides with chlorine and nitrogen dioxide 04 p0484 A72-15639

Nitrogen dioxide photodissociation by pulsed ruby laser at 6943 A, noting single photon energy relationship to dissociation energy 07 p0937 A72-20676

D region negative ion reaction schemes, discussing reaction rates of nitrogen dioxide with hydrogen 09 p1275 A72-22592

The reaction of hydrogen peroxide with nitrogen dioxide and nitric oxide. 17 p2511 A72-35466

Burning rates of organic perchlorates of aliphatic, aromatic and heterocyclic amines and amidines with explosive compounds containing nitrogen dioxide group as oxidizer 22 p3153 A72-43181

Effect of fluorescence observation geometry on lifetime measurement, including the development of an approximation to the detector collection efficiency integral. 23 p3288 A72-43884

NITROGEN FLUORIDES

- Chemical laser with deuterium and nitrogen fluorides mixture, examining excited molecules emission spectra 11 p1649 A72-26351
- Chemical laser with deuterium and nitrogen fluorides mixture, examining excited molecules emission spectra 16 p2402 A72-33704

NITROGEN IONS

- Midday oval, cusp region and polar cap auroral electron precipitation at low magnetic activity, presenting intensity vs altitude profiles for nitrogen ion line emissions 03 p0350 A72-13531
- Elastic scattering without dissociation of nitrogen molecular ions by noble gas targets in 0.3-3 keV range, analyzing energy loss 03 p0393 A72-14357
- Forbidden O I and molecular nitrogen ions emission lines ratio variation with height in aurora 03 p0352 A72-14382
- Radial density profiles and emittance for nitrogen ion beams from Penning-type cyclotron ion source with hot filament 10 p1516 A72-25028
- Boltzmann distribution of nitrogen ions according to rotational energy levels in nitrogen ionization by slow electrons impact 12 p1847 A72-27050
- Vertical distribution of atomic nitrogen ions in F region produced by dissociative photoionization and charge transfer, suggesting undiscovered source at 300 km altitude 13 p1954 A72-29815
- Airglow and auroral OI and NI allowed and spin forbidden transitions for above 9 eV excitation potential lines 14 p2098 A72-30145
- Dayglow nitrogen ion 3914 A emission profiles for average solar activity at 110-240 km heights from Cosmos 224 observations 23 p3282 A72-43357
- Boltzmann distribution of nitrogen ions according to rotational energy levels in nitrogen ionization by slow electrons impact 24 p3427 A72-45703

- Boltzmann distribution of nitrogen ions according to rotational energy levels in nitrogen ionization by slow electrons impact 24 p3427 A72-45703

- Boltzmann distribution of nitrogen ions according to rotational energy levels in nitrogen ionization by slow electrons impact 24 p3427 A72-45703

- Boltzmann distribution of nitrogen ions according to rotational energy levels in nitrogen ionization by slow electrons impact 24 p3427 A72-45703

- Boltzmann distribution of nitrogen ions according to rotational energy levels in nitrogen ionization by slow electrons impact 24 p3427 A72-45703

- Boltzmann distribution of nitrogen ions according to rotational energy levels in nitrogen ionization by slow electrons impact 24 p3427 A72-45703

- Boltzmann distribution of nitrogen ions according to rotational energy levels in nitrogen ionization by slow electrons impact 24 p3427 A72-45703

- Boltzmann distribution of nitrogen ions according to rotational energy levels in nitrogen ionization by slow electrons impact 24 p3427 A72-45703

- Boltzmann distribution of nitrogen ions according to rotational energy levels in nitrogen ionization by slow electrons impact 24 p3427 A72-45703

- Boltzmann distribution of nitrogen ions according to rotational energy levels in nitrogen ionization by slow electrons impact 24 p3427 A72-45703

- Boltzmann distribution of nitrogen ions according to rotational energy levels in nitrogen ionization by slow electrons impact 24 p3427 A72-45703

- Boltzmann distribution of nitrogen ions according to rotational energy levels in nitrogen ionization by slow electrons impact 24 p3427 A72-45703

- Boltzmann distribution of nitrogen ions according to rotational energy levels in nitrogen ionization by slow electrons impact 24 p3427 A72-45703

- Boltzmann distribution of nitrogen ions according to rotational energy levels in nitrogen ionization by slow electrons impact 24 p3427 A72-45703

- Boltzmann distribution of nitrogen ions according to rotational energy levels in nitrogen ionization by slow electrons impact 24 p3427 A72-45703

- Boltzmann distribution of nitrogen ions according to rotational energy levels in nitrogen ionization by slow electrons impact 24 p3427 A72-45703

- Boltzmann distribution of nitrogen ions according to rotational energy levels in nitrogen ionization by slow electrons impact 24 p3427 A72-45703

- Boltzmann distribution of nitrogen ions according to rotational energy levels in nitrogen ionization by slow electrons impact 24 p3427 A72-45703

- Boltzmann distribution of nitrogen ions according to rotational energy levels in nitrogen ionization by slow electrons impact 24 p3427 A72-45703

- Boltzmann distribution of nitrogen ions according to rotational energy levels in nitrogen ionization by slow electrons impact 24 p3427 A72-45703

- Boltzmann distribution of nitrogen ions according to rotational energy levels in nitrogen ionization by slow electrons impact 24 p3427 A72-45703

- High pressure CO and N plasmas production by uncoupling electron temperature from number density, measuring electron-ion recombination rates 10 p1518 A72-23962

- Radial temperature distribution determination in nitrogen plasma jet from continuous spectral background intensity measurement 10 p1519 A72-24131

- Mass spectrometric techniques for collision processes in decaying nitrogen-helium and nitrogen-neon plasmas, obtaining ambipolar diffusion coefficients and reaction rate constants 15 p2283 A72-31299

- Distribution function for free electrons in a molecular-nitrogen plasma. 17 p2593 A72-35891

- Spectral intensity measurements from high-pressure nitrogen plasmas. 19 p2840 A72-37836

- Parameters influencing the theoretical calculation of the thermal conductivity of a nitrogen plasma 23 p3321 A72-43692

- Disequilibria created by an electric field in a nitrogen plasma 23 p3321 A72-43695

- Spectroscopic measurements for atmospheric nitrogen and helium arcs. 23 p3322 A72-44326

- Spectroscopic measurements for atmospheric nitrogen and helium arcs. 23 p3322 A72-44326

- Spectroscopic measurements for atmospheric nitrogen and helium arcs. 23 p3322 A72-44326

- Spectroscopic measurements for atmospheric nitrogen and helium arcs. 23 p3322 A72-44326

- Spectroscopic measurements for atmospheric nitrogen and helium arcs. 23 p3322 A72-44326

- Spectroscopic measurements for atmospheric nitrogen and helium arcs. 23 p3322 A72-44326

- Spectroscopic measurements for atmospheric nitrogen and helium arcs. 23 p3322 A72-44326

- Spectroscopic measurements for atmospheric nitrogen and helium arcs. 23 p3322 A72-44326

- Spectroscopic measurements for atmospheric nitrogen and helium arcs. 23 p3322 A72-44326

- Spectroscopic measurements for atmospheric nitrogen and helium arcs. 23 p3322 A72-44326

- Spectroscopic measurements for atmospheric nitrogen and helium arcs. 23 p3322 A72-44326

- Spectroscopic measurements for atmospheric nitrogen and helium arcs. 23 p3322 A72-44326

- Spectroscopic measurements for atmospheric nitrogen and helium arcs. 23 p3322 A72-44326

- Spectroscopic measurements for atmospheric nitrogen and helium arcs. 23 p3322 A72-44326

- Spectroscopic measurements for atmospheric nitrogen and helium arcs. 23 p3322 A72-44326

- Spectroscopic measurements for atmospheric nitrogen and helium arcs. 23 p3322 A72-44326

- Spectroscopic measurements for atmospheric nitrogen and helium arcs. 23 p3322 A72-44326

- Spectroscopic measurements for atmospheric nitrogen and helium arcs. 23 p3322 A72-44326

- Spectroscopic measurements for atmospheric nitrogen and helium arcs. 23 p3322 A72-44326

- Spectroscopic measurements for atmospheric nitrogen and helium arcs. 23 p3322 A72-44326

- Spectroscopic measurements for atmospheric nitrogen and helium arcs. 23 p3322 A72-44326

- Atmospheric carbon monoxide and nitrous oxide telluric line contours and line centers optical thickness, measuring solar radio emission transmissivity 11 p1628 A72-26881

- Enhanced turbulent diffusion of nitrous oxide in parallel wall duct with obstructions for high Reynolds numbers 12 p1797 A72-27536

- Nitrous oxide band intensities, half widths and pressure broadening coefficients 13 p2008 A72-30059

- Fundamental and overlapping bands integrated intensities and nitrogen broadened half widths of rotational lines in nitrous oxide obtained from absorption measurements 14 p2135 A72-30895

- Simultaneous vibration-translation and vibration-vibration exchanges between colliding carbon dioxide and nitrous oxide excited molecules 15 p2280 A72-31686

- Reaction rate and activation energy of low temperature oxidation of Mg particles in nitrous oxide 16 p2476 A72-33253

- Mg ignition in nitrous oxide at 600-800 C, determining induction period as function of particle mass and gas stream temperature 16 p2476 A72-33254

- Positive and negative ions relative intensity measurement during nitrous oxide target molecules injection into sonic Ar plasma reaction channel, using quadrupole mass spectrometer [AIAA PAPER 72-675] 16 p2440 A72-34064

- Comments upon shock-initiated oxidations by nitrous oxide. 17 p2511 A72-34905

- Gas induced osmosis as factor in pulmonary homeostasis, showing differential water retention in lungs ventilated with normoxic nitrous oxide compared with air 17 p2506 A72-35970

- Neurologic oxygen toxicity - Effects of switch of inert gas and change of pressure. 19 p2758 A72-38704

- Nitrous oxide production from ozone photolysis reaction with molecular nitrogen 19 p2762 A72-38753

- A LEED investigation of the chemisorption of nitrous oxide on a tungsten (100) surface. 20 p2898 A72-39188

- Atmospheric carbon monoxide and nitrous oxide telluric line contours and optical thickness in line centers, measuring solar radio emission transmissivity 20 p2919 A72-39568

- Theoretical interpretation of the optical and electron scattering spectra of polyatomic molecules. III - N₂O and the discovery of resonant phenomena in the B region at 6.8 eV. 24 p3426 A72-45301

- Theoretical interpretation of the optical and electron scattering spectra of polyatomic molecules. III - N₂O and the discovery of resonant phenomena in the B region at 6.8 eV. 24 p3426 A72-45301

- Theoretical interpretation of the optical and electron scattering spectra of polyatomic molecules. III - N₂O and the discovery of resonant phenomena in the B region at 6.8 eV. 24 p3426 A72-45301

- Theoretical interpretation of the optical and electron scattering spectra of polyatomic molecules. III - N₂O and the discovery of resonant phenomena in the B region at 6.8 eV. 24 p3426 A72-45301

- Theoretical interpretation of the optical and electron scattering spectra of polyatomic molecules. III - N₂O and the discovery of resonant phenomena in the B region at 6.8 eV. 24 p3426 A72-45301

- Theoretical interpretation of the optical and electron scattering spectra of polyatomic molecules. III - N₂O and the discovery of resonant phenomena in the B region at 6.8 eV. 24 p3426 A72-45301

- Theoretical interpretation of the optical and electron scattering spectra of polyatomic molecules. III - N₂O and the discovery of resonant phenomena in the B region at 6.8 eV. 24 p3426 A72-45301

- Theoretical interpretation of the optical and electron scattering spectra of polyatomic molecules. III - N₂O and the discovery of resonant phenomena in the B region at 6.8 eV. 24 p3426 A72-45301

- Theoretical interpretation of the optical and electron scattering spectra of polyatomic molecules. III - N₂O and the discovery of resonant phenomena in the B region at 6.8 eV. 24 p3426 A72-45301

- Theoretical interpretation of the optical and electron scattering spectra of polyatomic molecules. III - N₂O and the discovery of resonant phenomena in the B region at 6.8 eV. 24 p3426 A72-45301

- Theoretical interpretation of the optical and electron scattering spectra of polyatomic molecules. III - N₂O and the discovery of resonant phenomena in the B region at 6.8 eV. 24 p3426 A72-45301

- Theoretical interpretation of the optical and electron scattering spectra of polyatomic molecules. III - N₂O and the discovery of resonant phenomena in the B region at 6.8 eV. 24 p3426 A72-45301

- Theoretical interpretation of the optical and electron scattering spectra of polyatomic molecules. III - N₂O and the discovery of resonant phenomena in the B region at 6.8 eV. 24 p3426 A72-45301

- Theoretical interpretation of the optical and electron scattering spectra of polyatomic molecules. III - N₂O and the discovery of resonant phenomena in the B region at 6.8 eV. 24 p3426 A72-45301

discussing need for international scientific cooperation
10 p1476 A72-25006

Nike-Apache rocket-borne particle collection and photometry of noctilucent clouds, obtaining single-shadowed particle size distributions and inflight shadowing surface data
15 p2226 A72-31923

Rocket-borne laser radar for aerosol observation in upper atmosphere, noting light scattering layer relation to noctilucent cloud appearance
15 p2231 A72-32331

Noctilucent cloud research, discussing morphology, rocket studies and ice particle theory
16 p2386 A72-33605

Luminous intensity, visibility duration, condensation nuclei and mass balance of noctilucent clouds
18 p2686 A72-36504

Heavy metal particle detection in noctilucent clouds by rocket experiments, using Pandora inflight shadowing technique
20 p2964 A72-39373

First approximation for spacecraft observations of noctilucent clouds from circular orbits with optimal optical axis orientations
21 p3049 A72-41438

Noctilucent clouds in daytime - Circumpolar particulate layers near the summer mesopause.
22 p3173 A72-42515

Mesospheric noctilucent clouds tables listing weather stations geographical coordinates, observation time periods, elevation above northern horizon and azimuth
22 p3173 A72-42575

NOCTURNAL VARIATIONS
Upper atmosphere particle flux density determined from nocturnal electromagnetic absorption caused by geomagnetic storms, noting ionization process time lag in lower ionosphere
13 p1945 A72-28580

Nocturnal and semiannual variations of the intensity of 5577 A emission of atomic oxygen.
19 p2789 A72-37511

Upper atmosphere particle flux density determined from nocturnal electromagnetic absorption caused by geomagnetic storms, noting ionization process time lag in lower ionosphere
24 p3397 A72-45080

NODES (STANDING WAVES)
Matrix displacement method for nonuniform beam vibration problems, using internal nodes concept
11 p1735 A72-25740

Helicopters vibration reduction through fuselage nodalization, discussing analysis method and dynamic scale model and full scale flight test results
[AHS PREPRINT 611] 17 p2489 A72-34487

NOISE (SOUND)
NT AERODYNAMIC NOISE
NT AIRCRAFT NOISE
NT ENGINE NOISE
NT JET AIRCRAFT NOISE
NT ROCKET ENGINE NOISE
NT SONIC BOOMS
NT THERMAL NOISE
Environmental noise induced human fatigue, considering physiological and psychological effects
01 p0016 A72-10050

Pitch shift of pure tone by masking tones and band limited noise
01 p0101 A72-10159

High and low pass filtered clicks lateralization tests, suggesting lateral position discrimination dependence on IF content and cochlear partition apical end
04 p0550 A72-15297

Transportation noises - Conference, University of Washington, Seattle, March 1969
07 p0931 A72-20162

Noise rating methods for speech communication effectiveness evaluation, presenting charts and tables for intelligibility limits with various communication techniques and equipment
07 p0932 A72-20167

Noise effects on human attention and work efficiency in extroverted and introverted individuals
08 p1128 A72-22137

Noise and vibration control engineering - Conference, Purdue University, Indiana, July 1971
13 p2005 A72-29553

French book on industrial acoustics elements and metrology covering transmission, absorption, noise and complex sound measuring apparatus and preventive measures
15 p2275 A72-31524

Fan noise estimation from equation involving delivery volume and pressure to correct ratings to generated sound power levels
16 p2377 A72-33323

LF whole body vibration effects on rat escape conditioning in terms of frequency, amplitude and controls for noise and activation
16 p2357 A72-33868

Blowdown wind tunnel internal and external noise fields prediction by empirical method, considering valves, burners, turbulent boundary layers and exhaust jets as sources
[AIAA PAPER 72-668] 16 p2374 A72-34070

NOISE ATTENUATION
U NOISE REDUCTION
NOISE ELIMINATION
U NOISE REDUCTION
NOISE GENERATORS
Noise reduction by acoustic interference, using sound generators operating in antiphase mode to noise input
02 p0262 A72-12897

Fluctuating flow in idealized model of turbulent shear layer composed of many discrete two dimensional vortices, analyzing noise generation
[AIAA PAPER 72-155] 05 p0609 A72-16955

Digital system for wideband Gaussian noise generation using simultaneously generated PN-sequence with analog summation of independent binary waveforms
07 p0941 A72-19284

Circular jets sound generation analysis, using Lighthill equation and Michalke spectral method [DEVL-SONDIR-179] 07 p0910 A72-20100

Acoustical theory application to jet engine noise reduction, developing mathematical model for blade shock wave spacing in noise generation process
07 p1055 A72-20542

Junction and MOS FETs noise sources interaction with small signal model parameters and signal source admittance parameters, investigating amplifier If performance
08 p1141 A72-21428

Pressure sensor measurements of fluctuating aerodynamic forces on rotor blades related to compressor noise generation
[ASA PAPER H 6] 08 p1107 A72-21486

LF noise generator with Rice variable amplitude probability distribution law, using shielded vacuum tube superregenerative amplifier
09 p1285 A72-22345

Two dimensional dynamic model for background noise generation in bipolar transistors, using equivalent circuit
09 p1286 A72-23105

Aerodynamic noise generation mechanism of ideally expanded supersonic jet based on large scale flow instabilities, deriving mathematical model
10 p1418 A72-24331

Russian monograph on self oscillatory noise generation during gas jet ejection covering single, parallel, supersonic, flat and cylindrical jets stability
11 p1617 A72-26066

Theory of a coaxial gas-discharge generator loaded by a spiral line
17 p2529 A72-34841

Variable strong atmospheric radio noise production under fair weather conditions without manmade signals, noting peaks before midnight and sunrise
22 p3173 A72-42885

NOISE HAZARDS
U HAZARDS
U NOISE [SOUND]
NOISE INJURIES
Hearing damage scaling methods, discussing audiometric frequencies effect and damage risk criteria
07 p0932 A72-20169

Physiological and psychological effects of noise noting vulnerability of circulatory apparatus, neurovegetative system and stomach
14 p2079 A72-30696

NOISE INTENSITY
Aircraft engine noise effects in airport vicinities, discussing measurement scales, turbofan sources, noise reduction and future air traffic
02 p0154 A72-12022

Jet noise suppression near airports, discussing noise physical description, source relation to engine technology and ICAO certification standards
03 p0309 A72-13097

Electromagnetic noise and effects on communication systems, considering statistical parameters definition and measurements
03 p0324 A72-14036

Aircraft and other transient noise levels temporal characteristics effect on noise assessment
04 p0464 A72-14843

Cats cochlea and cochlear nucleus neural responses in auditory masking of low frequency tones, showing phase locked cells progressive desynchronization with intensity
04 p0475 A72-15251

Pyroelectric detector noise equivalent power limitation factors, discussing heterodyne systems and pulsed submillimeter lasers detection
04 p0551 A72-15602

Metrology and technology for sounds intense enough for physiological distress and mechanical structure damage, discussing accompanying high temperature and vibration
[ONERA, TP NO. 1009] 05 p0661 A72-16024

Aerospace vehicle noise induced structural vibration, presenting propellers, turbojet engine exhausts and sonic boom waves
05 p0739 A72-16597

Duration effect on judged acceptability of noise, discussing interpretation and meaning of laboratory determinations
06 p0766 A72-17765

Reconstruction errors, quantization noise and channel bandwidth in high order digital to analog conversion
06 p0779 A72-17783

Airport surrounding communities survey on attitudes toward aircraft noise, noting daily activity disturbance, emotional reactions, economic effects, noise abatement awareness, etc
06 p0767 A72-17870

Optimal signal detection relative to Neumann-Pearson criterion invariant with respect to amplitude and random noise intensity in radio location
07 p0938 A72-19019

Noise level measurement scales, units datum points and mathematical formulas, suggesting method of quasi-peak level above masked threshold
07 p1035 A72-20164

Perceived noise level correction for background noise effects based on frequency band SNR
07 p0932 A72-20170

Loudness and noisiness judgment contours, considering experimental subjective and objective conditions, subject age and sex and sound field characteristics
07 p0932 A72-20171

Mark VII ear performance calculation procedure for perceived loudness or noisiness levels relation to sound pressure, using experimental frequency weighting contours
08 p1127 A72-21895

Microwave transistor noise factor measurement for various geometries and parameter values correlation with predictions
09 p1286 A72-23104

Noise characteristics and mechanisms in avalanche diodes and transferred electron devices
09 p1287 A72-23115

CW circuit stabilized InP microwave reflection amplifiers in Q band, determining power gain and noise figure
10 p1450 A72-24308

Optimal antennas statistical synthesis for minimum noise power for given signal gain
10 p1436 A72-24505

Minimum noise coefficients of M-type microwave beam amplifiers with crossed fields, taking into account delay system distributed losses
10 p1453 A72-24913

Human performance under intense noise, measuring effects on muscle tension, metabolism, respiration rate, visual accommodation, saccadic eye movement and dark adaptation
11 p1583 A72-25728

Auditory sensation overall loudness prediction for steady broad-band noise from summation of weighted intensities of power spectrum sub-bands
11 p1686 A72-25800

Aircraft flyover house noise reduction data, noting application to indoors noise level estimation
[SAE AIR 1081] 11 p1686 A72-26029

Complementary metal oxide semiconductor applications, noting device power dissipation, high noise immunity, good switching speeds and cost reduction
11 p1701 A72-26386

Noise immunity and code sequence rejection probability in real multifrequency communications systems with multipositional frequency shift keying
11 p1598 A72-26729

Low noise power level measurement at microwave frequencies, noting Nyquist equation applicability and cooled-to-uncooled element connections effects in receivers
12 p1779 A72-27175

Noise characteristics of regenerative amplifier with direct coupling to load
13 p1929 A72-28897

Aircraft noise sources, showing noise intensity relationship to airfoil velocity and pressure ratio
13 p1897 A72-29568

Masking functions for intensity discrimination of pulsed sinusoids with and without noise masker
13 p2006 A72-29772

Microwave radiometer performance analysis, deriving input noise power relation to instrument indication in terms of noise parameters
14 p2105 A72-30587

White background noise intensity effects on human visual target detection performance considering display difficulty levels, target location, detection time and error
14 p2083 A72-31156

Preferences for signaled over unsignaled noise from subjectively rated noise intensity experiments, discussing preparatory response vs information cognitive control interpretations
15 p2187 A72-32763

Fan noise estimation from equation involving delivery volume and pressure to correct ratings to generated sound power levels
16 p2377 A72-33323

- Design requirements for a quiet helicopter.
[AHS PREPRINT 604] 17 p2488 A72-34484
- Cavitation study of pump with semiopen impeller, obtaining hydraulic performance, flow photographs and noise level 17 p2561 A72-35899
- Synchronization and noise performance of mutually coupled oscillators. 18 p2668 A72-37036
- Thermal modulation and FM noise of Gunn oscillators. 18 p2668 A72-37038
- Correlation between the reliability of silicon bipolar transistors and their excess background noise 18 p2669 A72-37110
- Effect of temperature on the base resistance and the noise factor of a bipolar junction transistor. 19 p2773 A72-37848
- Mean value of noisy signal quantized by analog/digital converter, noting input noise level relation to estimate accuracy 20 p2904 A72-39785
- Separation and detection of signals in the presence of nonadditive noise 21 p3023 A72-41746
- Aircraft noise duration correction for effective perceived noise level [EPNL] computation, eliminating mathematical anomaly incurred by present FAA and ICAO prescribed method 22 p3139 A72-42909
- German monograph - Studies of the ground effect on the noise levels and their frequency distribution in the near field of an engine jet directed vertically against the ground. 22 p3217 A72-43060
- Statistical analysis of the sound level distribution of aircraft noise as a function of time 23 p3252 A72-44337
- Community noise levels of the L-1011 Tristar Jet Transport. 24 p3365 A72-44677
- NOISE MEASUREMENT**
U ACOUSTIC MEASUREMENTS
NOISE METERS
- California airport noise standards instrumentation, discussing battery operated measurement of hourly and community noise equivalent levels 07 p0985 A72-19490
- Quadratic logarithmic converter used with linear microammeter for decibel scale noise measurements 09 p1306 A72-22344
- ELF wideband noise receiver for atmospheric waveshape magnetic tape recording, computer processing and system simulation 12 p1791 A72-27637
- Microwave radiometer performance analysis, deriving input noise power relation to instrument indication in terms of noise parameters 14 p2105 A72-30587
- A new approach to the measurement of very low acoustic noise levels. 20 p2953 A72-39554
- Multipoint real time all-day computerized noise monitoring system for diagnostic evaluation of airport, discussing design and applications 24 p3387 A72-44684
- NOISE POLLUTION**
- Portable detector-recorder for automobile, blast furnace, railroad car, engine room and helicopter infrasonic noise measurements, discussing peak frequencies and subjective effects 01 p0101 A72-10157
- Air transportation evolution and relation to atmospheric and noise pollution 03 p0459 A72-14151
- Aircraft operations effects on community noise pollution, discussing ATC airline operational procedures modifications in terms of noise reduction 04 p0464 A72-14819
- New York-New Jersey megalopolis offshore jetport feasibility, considering noise, air-water pollution, land conservation, cost, etc 13 p1938 A72-28792
- Acoustical environment pollution control, considering noise annoyance effects due to industry and construction, surface and air traffic, alarm devices, radio and TV, etc 13 p2067 A72-29554
- Private and governmental regulatory aspects of environmental noise abatement and control, discussing legal efforts and trends at local, state and federal levels 15 p2340 A72-32614
- Noise pollution measurements parameter selection based on human reactions and attitudes, discussing psychoacoustic experiments, ratings and acoustic instruments 16 p2390 A72-33165
- Hypersonic transports commercial applications, examining economic and noise and air pollution aspects [ICAS PAPER 72-32] 21 p2995 A72-41157
- VTOL aircraft noise reduction through design methods and flight path management in terminal area,

- evaluating acoustical annoyance to surrounding community [ICAS PAPER 72-34] 21 p2995 A72-41159
- Aircraft gas turbine engines environmental effects, considering thermal radiation, acoustic emissions and exhaust gases in relation to propulsion system design parameters 23 p3328 A72-44296

NOISE PROPAGATION

- Turbojet engine noise causes and reduction techniques, noting U.S. antinoise standards 04 p0465 A72-14925
- Radiative noise effect on threshold current, output power and quantum yield of injection laser, evaluating noise loss factor 04 p0531 A72-15077
- Flexible elastic plate nonlinear vibration response and noise transmission from turbulent boundary layer by Monte Carlo technique, discussing subsonic and supersonic flow regions [AIAA PAPER 72-199] 05 p0651 A72-16850
- Cross flow effect on lifting fan noise at subsonic blade tip speeds, analyzing radiation pattern change due to inlet flow distortion 05 p0608 A72-16921
- Acoustic ray path method for computing atmospheric conditions effect on aircraft noise propagation, using digital computer 13 p1897 A72-28840
- Supersonic jet noise and sonic boom sources, propagation and reduction, considering airport community disturbances, aircraft cabin noise and fatigue problems 13 p1898 A72-29578
- Acoustic environmental prediction model for near, mid and far field rocket engine noise 13 p2028 A72-29582
- Sudden decreases of atmospheric due to solar flares effects on lower ionosphere, discussing noise propagation 15 p2230 A72-32256
- Transient acoustic point source disturbance transmission in two dimensional idealized jet, noting velocity profile effects on noise radiated to far field 18 p2679 A72-36406
- Tone noise from rotor/stator interactions in high speed fans. 24 p3433 A72-44917
- NOISE REDUCTION**
- Liquid-base foam sound absorbing properties for jet aircraft noise reduction 01 p0115 A72-10160
- Acoustic power radiated by jet aircraft fuselage structure exposed to turbulent boundary layer pressure field, evaluating noise reduction treatments 01 p0002 A72-10216
- Jet aircraft turbofan engine fan compressor noise reduction by acoustic linings, giving R and D results [BAS PAPER 71 SA6] 01 p0115 A72-10223
- Jet noise reduction technology, hardware and tests for NASA Quiet Engine Program to develop low noise subsonic civil transport aircraft propulsion system [SAE PAPER 710774] 01 p0116 A72-10266
- FM communication system multiterminal phase lock loop state equations derivation from phase model, predicting noise improvement characteristics by analog and digital simulation 01 p0044 A72-10328
- AM and FM noise reduction of cavity and injection stabilized microwave Gunn and avalanche diode oscillators 01 p0037 A72-10644
- Wideband modulation feedback technique for IMPATT diode oscillator AM-FM noise suppression 01 p0037 A72-10647
- Substorm electron drift relationship to cosmic noise absorption on auroral zone morning side, calculating electron energy loss 01 p0063 A72-10918
- STOL aircraft for solving noise reduction and land use problems in future transportation systems, discussing airport location and layout for growing air traffic 01 p0005 A72-11153
- Earplugs effect on passenger speech reception and intelligibility in rotary wing aircraft, noting protection against noise annoyance, fatigue and deafening 01 p0022 A72-11294
- High speed jet noise source physical properties interpretation by theory and scale-model experiments for supersonic transport aircraft noise suppression problem 02 p0154 A72-11973
- Aircraft engine noise effects in airport vicinities, discussing measurement scales, turbofan sources, noise reduction and future air traffic 02 p0154 A72-12022
- Papers on noise and vibration control covering acoustics in free space, outdoors, small enclosures and rooms, measurement, analysis and design problems 02 p0258 A72-12100

- Noise reduction by acoustic interference, using sound generators operating in antiphase mode to noise input 02 p0262 A72-12897

- Jet noise suppression near airports, discussing noise physical description, source relation to engine technology and ICAO certification standards 03 p0309 A72-13097

- Circular polarization parasitical signal reduction in variable profile antennas by curved wire grating, noting application to solar magnetic field studies by radio methods 03 p0331 A72-13289

- Short haul operating systems in air transportation environments, discussing terminal vs cruise configurations, costs and noise abatement 03 p0309 A72-13422

- Air breathing propulsion systems for reducing engine noise level, discussing stoichiometric gas turbine engines, V/STOL propfans and variable-geometry supersonic inlet and exhaust nozzles 03 p0406 A72-13486

- Noise reduction in pulse width modulated converters with rms voltage values digital readout, using active or passive filters methods 03 p0331 A72-13557

- NASA Quiet Engine experimental program for jet aircraft noise reduction, discussing aerodynamic and acoustic evaluation and tests of three fans 03 p0406 A72-13679

- French jet aircraft noise reduction research facilities, discussing in-flight and overfly noise measurements, various silencer configurations and Concorde engine tests 03 p0406 A72-13680

- Cloud interference-free sea surface temperatures, using techniques to reduce noise effect in Nimbus IR radiometer data 03 p0385 A72-14227

- Aircraft operations effects on community noise pollution, discussing ATC airline operational procedures modifications in terms of noise reduction 04 p0464 A72-14819

- Aircraft industry noise reduction efforts to meet FAA requirements for CTOL and STOL aircraft, emphasizing turbofan and compressor noise suppression and/or attenuation 04 p0565 A72-14820

- National Aviation System technology, discussing wide body jets, smokeless turbofans, all-weather operational capability, collision avoidance and noise reduction 04 p0597 A72-14824

- Sound propagation in acoustic ducts with shear flow and wall lining by Ritz-Galerkin technique 04 p0511 A72-14848

- Flight helmet optimal fitting technique, using automatic recording audiometer and noise source for acoustic leakage detection 04 p0479 A72-14873

- Turbojet engine noise causes and reduction techniques, noting U.S. antinoise standards 04 p0465 A72-14925

- Telemetry systems with discrete compression-expansion function, calculating noise stability improvement as compared to linear and nonlinear signal conversion operations 04 p0487 A72-15000

- Jet aircraft noise reduction, discussing engine design modifications 04 p0465 A72-15167

- Sound attenuation in lined rectangular ducts with uniform steady flow, considering aircraft engine noise reduction 04 p0565 A72-15267

- Cross correlation model for interpreting empirical results on binaural noise masking level differences in sinusoidal signal detection, comparing with equalization-cancellation model 04 p0550 A72-15296

- Avalanche transit time diodes noise mechanisms and performance in microwave amplifier, oscillator and mixer applications 04 p0500 A72-15302

- Rocket-borne mass spectrometer with helium cooled electron bombardment ion source to reduce gas-wall interactions effects 04 p0524 A72-15538

- Aircraft noise measurement units and methods, discussing engine design for noise reduction 05 p0611 A72-16026

- Leaning vanes for fan noise reduction, discussing rotor-stator plane fluctuating pressure amplitude decrease and radial distribution modification [AIAA PAPER 72-126] 05 p0706 A72-16823

- Jet engine silencing plug nozzle suppressor configurations acoustic and thrust performance measurements [AIAA PAPER 72-160] 05 p0706 A72-16826

- Twilight atmospheric sounding in oxygen absorption bands to reduce noise level in secondary light scattering 06 p0807 A72-17943

Rotorcraft based on VTOL concept for aircraft noise reduction in urban transportation
06 p0758 A72-18248

X band IMPATT and Gunn oscillator, calculating injection lock time, modulation bandwidth, noise and FM suppression and dynamic response
06 p0788 A72-18471

Hybrid computer method of nonstationary spectrum analysis of aircraft noise, applying to flyover and jet aircraft noise abatement under operational conditions
07 p0911 A72-18778

Externally blown flap noise tests at various nozzle exhaust velocities for STOL aircraft noise reduction [AIAA PAPER 72-129]
07 p0908 A72-18962

Engine fan-compressor maximum noise reduction for given aircraft configuration by acoustic linings on nacelle inlet and exhaust walls
07 p1054 A72-19268

PCM systems low pass filter characteristics from PAM off-band signals noise attenuation calculations
07 p0943 A72-19435

Hovercraft noise and vibration source and reduction for improved crew and passenger comfort
07 p0912 A72-19648

Jet noise intensity reduction by screen across nozzle exit, using acoustic and hot wire measurements
07 p0968 A72-19873

Turbojet and turbofan engines noise signatures and sonic boom effects, discussing frequency spectra, atmospheric attenuation and noise suppression systems
07 p0912 A72-20163

Design criteria for transportation system noise regulation, considering ambient noise, hearing damage, speech interference and subjective reactions
07 p0932 A72-20173

Aircraft noise protective earplug design, employing perforated and slit modifications for additional protection without tympanic membrane pressure excess risk
07 p0933 A72-20187

Laser telemetry performance, considering means of noise reduction
07 p0947 A72-20256

Interference rejection method for high speed analog to digital converters, noting application to on-line computer systems
07 p0948 A72-20386

Acoustical theory application to jet engine noise reduction, developing mathematical model for blade shock wave spacing in noise generation process
07 p1055 A72-20542

Operational and equivalent circuit characteristics of low noise hf and shf transistors in wideband amplifiers
08 p1139 A72-21052

Sonic boom minimization, obtaining positive phase signature pressures as function of altitude, Mach number, weight and length
08 p1110 A72-21903

Helicopter noise and vibration testing and cabin soundproofing for improved comfort
08 p1128 A72-22141

Aerodynamic noise produced by gas jet flow around airfoil, discussing sound reduction
10 p1417 A72-24107

Hot water ejector application to environmental control, considering noise suppression, air and gas purification and dust particles precipitation
10 p1460 A72-24491

Estimate of effectiveness of utilization of composite signals to combat external interference with available a priori data
10 p1436 A72-24580

Commercial applications of quiet light aircraft technology, discussing cost and noise reduction [SAE PAPER 720339]
11 p1576 A72-25596

Noise reduction effects of wake interaction between rotor blade rows in axial flow compressor, cancelling velocity defect at stator position [ASME PAPER 72-GT-15]
11 p1569 A72-25614

Low pressure ratio Q-FAN propulsor noise reduction tests on wind tunnel model, discussing source components and design configurations [ASME PAPER 72-GT-40]
11 p1569 A72-25634

NASA quiet engine program, discussing noise reduction technology for subsonic civil transport aircraft propulsion system [ASME PAPER 72-GT-96]
11 p1705 A72-25667

Aircraft flyover house noise reduction data, noting application to indoors noise level estimation [SAE AIR 1081]
11 p1686 A72-26029

Transistorized amplifier input elements design for biopotentials recording, providing minimum noise at high input impedance
11 p1585 A72-26468

Atmospheric pressure noise reducer for active microbarograph array, evaluating performance in field tests
11 p1613 A72-26510

STOL aircraft role in civil aviation, discussing short range operation, ATC, reduced noise and weather capability
12 p1754 A72-27518

Future short haul aircraft transportation systems, discussing aircraft forms, noise reduction technology and runway requirements
12 p1754 A72-27660

Statistical characteristics of IR receivers with parametric carrier frequency conversion, describing noise index minimization technique
12 p1846 A72-27889

USAF V-51R noise protector earplugs modification to allow for pressure equalization during aircraft climb and descent
12 p1774 A72-28276

Subtraction circuit design for impulse noise elimination at front end of aircraft oriented OMEGA navigation system receiver
13 p1999 A72-29204

Noise and vibration control engineering - Conference, Purdue University, Indiana, July 1971
13 p2005 A72-29553

Undesirable mechanical vibration control concepts for acoustic noise reduction, considering environment characteristics, attenuation degrees and passive and active control mechanisms
13 p2005 A72-29555

Noise and vibration control in industrial and aerospace environments, discussing materials and techniques for structural vibration damping
13 p2059 A72-29557

Building soundproofing codes for airport zoning ordinances, emphasizing wider latitude in land use options
13 p2067 A72-29561

Noise control by Helmholtz resonators, considering equivalent circuits via feedback schemes
13 p2005 A72-29567

Fiberglass performance as duct liner in presence of spinning modes from free field measurements, noting ineffectiveness for plane wave attenuation
13 p2028 A72-29573

Fan engine compressor noise measurement by spinning mode synthesizer for use in duct liner optimization
13 p2028 A72-29574

Supersonic jet noise and sonic boom sources, propagation and reduction, considering airport community disturbances, aircraft cabin noise and fatigue problems
13 p1898 A72-29578

Bibliography on noise control covering surface transportation, machinery and aircraft noise, industrial criteria, biodynamics, legislation and measurement
13 p2006 A72-29588

Noise suppression by time exposure oscilloscope photography to enhance repetitive electric signals obscured by noise of equal amplitude
13 p1959 A72-29754

French book on industrial acoustics elements and metrology covering transmission, absorption, noise and complex sound measuring apparatus and preventive measures
15 p2275 A72-31524

Avalanche photodiodes for Nd and injection lasers radiation detection, reducing noise equivalent power
15 p2247 A72-32035

Adjacent channel discrimination enhancement in Gray-scale binary coded two dimensional array, using checkerboard filter for pattern noise suppression
15 p2238 A72-32162

Low noise aircraft-engine configuration feasibility, discussing turbofan engine noise reduction
15 p2181 A72-32322

Holographic precoded TV system, discussing coherent light noise elimination and redundancy effects on image quality
15 p2239 A72-32356

RB 211 three-shaft turbofan engine for L-1011 airliner, describing design for noise reduction
15 p2298 A72-32428

Private and governmental regulatory aspects of environmental noise abatement and control, discussing legal efforts and trends at local, state and federal levels
15 p2340 A72-32614

U.S. federal regulation on occupational noise exposure control for hearing loss prevention, discussing noise measurement, reduction and periodic tests
16 p2358 A72-33324

STOL aircraft for civil transport applications, considering optimum design concepts, noise reduction and terminal facility requirements
16 p2348 A72-33331

Twilight atmospheric sounding in oxygen absorption bands to reduce noise level in secondary light scattering
16 p2386 A72-33784

Statistical characteristics of IR receivers with parametric carrier frequency conversion, describing noise index minimization technique
16 p2427 A72-33998

STOL aircraft minimum noise takeoff trajectories determination, taking into account engine thrust and listeners distance from noise source [AIAA PAPER 72-665]
16 p2349 A72-34072

NASA/General Electric joint development of low noise propulsion technology, describing demonstrator engine A design, components development and aerodynamic/acoustic performance evaluation [AIAA PAPER 72-657]
16 p2443 A72-34077

Leading edge serrations effect on rotor noise and aerodynamic characteristics, noting vortex and rotational noise reduction and overall efficiency decrease [AIAA PAPER 72-655]
16 p2349 A72-34079

Sonic boom alleviation by flow field alteration near supersonic aircraft, considering finite rise times, reduced overpressures and shock pressure rises [AIAA PAPER 72-653]
16 p2349 A72-34081

Jet noise reduction by screen placed across jet flow, investigating acoustic properties, velocity and pressure in mixing zone [AIAA PAPER 72-644]
16 p2381 A72-34088

Acoustic attenuation and thrust loss incurred by shrouded multiube supersonic jet noise suppressor [AIAA PAPER 72-642]
16 p2381 A72-34090

NASA R and D for STOL short haul transportation systems, discussing propulsive lift, blown flap and augmentor wing concepts, noise reduction, etc
17 p2487 A72-34238

Bayesian recursive linear Kalman filtering technique for image estimation with noise background elimination, proposing time invariant dynamic model to provide stationary statistics
17 p2520 A72-34403

Design requirements for a quiet helicopter. [AHS PREPRINT 604]
17 p2488 A72-34484

Reduction of noise and acoustic-frequency vibrations in aircraft transmissions. [AHS PREPRINT 661]
17 p2491 A72-34508

Digital correlator for change detection in picture element processing with CDC 1700 computer to obtain spatial alignment accuracy
17 p2556 A72-35538

Bayesian recursive estimation by Kalman filtering for enhancement of image corrupted by additive random noise
17 p2557 A72-35539

Externally blown flap impingement noise. [AIAA PAPER 72-664]
17 p2487 A72-35961

Tracking radar system rain clutter reduction by backscatter polarization technique for signal phase and magnitude adjustment
18 p2659 A72-36310

Sonic jet noise pressure source model for radiated sound power and jet pressure frequency spectra ratio derivation with application to noise suppression
18 p2680 A72-36414

NASA R and D programs for quiet STOL aircraft and engines development
18 p2721 A72-36503

Internal noise reduction in hovercraft.
18 p2642 A72-36574

Spatial diversity technique based on predetector equal-gain combining for fast fading reduction of AM radio receiver, using phase shifter
18 p2661 A72-36845

The theoretical amplification limit of modulation amplifiers with correlation detection
18 p2668 A72-37035

Forward flight effects on mixer nozzle design and noise considerations for STOL externally blown flap systems. [AIAA PAPER 72-792]
19 p2746 A72-38109

Flight evaluation of three-dimensional area navigation for jet transport noise abatement. [AIAA PAPER 72-814]
19 p2750 A72-38116

Aircraft noise problem in piston engine to turbofan jumbo jet transports, discussing need for noise reduction research [AIAA PAPER 72-815]
19 p2750 A72-38117

Jet aircraft noise sources in subsonic and supersonic exhaust mixing process, suppressing noise via turbofan exhaust speed reduction
19 p2849 A72-38380

Ionosonde receiver with automatic noise suppression and digital-analogue recording of the first ionospheric reflection.
19 p2805 A72-38867

Interference suppression design of switching circuits utilizing slewing rates.
20 p2906 A72-38982

Frequency assignment for collocated transmitters using the branch-and-bound technique.
20 p2901 A72-38986

Minimisation of the solar array generated electrical interference on the GEOS satellite.
20 p2889 A72-38990

An algorithm for linearly constrained adaptive array processing.
20 p2904 A72-39777

Quiet engine design for V/STOL and reduced takeoff and landing /RTOL/ aircraft, discussing various engine noise sources, countermeasures and tolerance levels
20 p2963 A72-39819

Supersonic aircraft wing form influence on sonic boom, discussing supersonic wind tunnel tests for noise reduction
20 p2888 A72-39931

Thermal imaging with pyroelectric IR detector arrays, discussing signal processing by digital technique to eliminate voltage offset variations effects in preamplifiers
20 p2928 A72-39968

- ATS F and G radio link with ground stations, discussing telemetry and command functions with redundancy for RF interference minimization
21 p3019 A72-40883
- A model of low-frequency sound propagation in a lined duct.
21 p3085 A72-41112
- Noise radiation from V/STOL aircraft.
[ICAS PAPER 72-22] 21 p2995 A72-41147
- VTOL aircraft noise reduction through design methods and flight path management in terminal area, evaluating acoustical annoyance to surrounding community
[ICAS PAPER 72-34] 21 p2995 A72-41159
- NASA Quiet Engine program R and D on conventional takeoff and landing subsonic cruise aircraft engine noise
[ICAS PAPER 72-48] 21 p3100 A72-41173
- Noise control technology for jet-powered STOL vehicles.
[ICAS PAPER 72-50] 21 p2995 A72-41175
- Analysis of noise immunity of two-channel eddy-current flow detector.
21 p3057 A72-41723
- Jet noise generation theory (Lighthill-Ffowcs Williams) verification by model tests, discussing means of reducing or eliminating shock cells
[ICAS PAPER 72-55] 21 p3047 A72-41852
- NASA's quiet engine programs.
22 p3217 A72-43152
- Noise resistance of optical communication lines with radio and optical AGC systems
23 p3264 A72-43770
- Supersonic aircraft focused sonic boom suppression by slowing down during turning flight, obtaining conditions for focus cut-off at ground by atmospheric refraction
23 p3251 A72-44125
- NOISE SPECTRA**
- Quasi-steady spectrum of hydromagnetic noise in proton belt, using random excited broad wave fields in nonisothermal magnetosphere
01 p0118 A72-10367
- VLF noise spectra in earth-ionosphere cavity due to thunderstorm discharges, noting resonance level splitting by geomagnetic field
01 p0028 A72-10598
- LF noise spectrum of Gunn oscillators due to direct modulation of rf admittance for constant voltage bias source
01 p0037 A72-10639
- Millimeter and submillimeter microwave spectrometric studies of high temperature plasmas and noise emission, discussing instrumentation and absolute measurements
02 p0223 A72-11409
- Dc excited argon laser anode oscillation noise, discussing relation to ballast resistance, suppression conditions and current fluctuation frequency response to laser fluctuation
02 p0239 A72-12826
- Tube wall temperature and acoustic noise spectra dependence on thermal flux density in bubble coalescence
03 p0458 A72-14162
- Optimal digital Kalman filtering for systems with continuous input noise by autocorrelation function matching
[ASME PAPER 71-WA/AUT-21] 05 p0640 A72-15952
- Periodic quasi-noise spectrum and amplitude modulation of LF pulsed signals from earth in magnetosphere plasma
05 p0696 A72-16605
- Turbobfan multiple pure tone noise analysis, discussing rotor geometry, relative Mach number and incidence angle effect on sound emission
[AIAA PAPER 72-127] 05 p0706 A72-16824
- Jet flap type exhaust flows acoustic and fluid dynamic characteristics, measuring sound power output and noise spectra for various configurations
[AIAA PAPER 72-130] 05 p0608 A72-16920
- Aerodynamic noise measurement, discussing physical units, spectral analysis, conversion and correction formulas
05 p0614 A72-17195
- Noise spectra of double sided CW silicon TRAPATT oscillator comparable to silicon IMPATT oscillator
06 p0783 A72-17482
- Cylindrical plasma ion-acoustic resonance measurements from various excitation methods for noise component identification
06 p0856 A72-17523
- Si MOSFET substrate resistivity effect on surface state noise spectra
06 p0783 A72-17609
- Kalman-Bucy colored noise filtering discrete time results and continuous time linear minimum variance estimation by calculus of variations
06 p0793 A72-17955
- Hybrid computer method of nonstationary spectrum analysis of aircraft noise, applying to flyover and jet aircraft noise abatement under operational conditions
07 p0911 A72-18778

- Spectral measurements of jet turbulence noise in core and annular mixing region, using subsonic test experiments
[AIAA PAPER 72-158] 07 p0966 A72-18957
- Low frequency modulation noise generation due to conductance fluctuations in Gunn oscillators, measuring noise spectra temperature dependence
07 p0954 A72-19050
- Schottky barrier and n-n heterojunction diodes hf noise, considering ideality factor effect
07 p0955 A72-19358
- Turbojet and turbofan engines noise signatures and sonic boom effects, discussing frequency spectra, atmospheric attenuation and noise suppression systems
07 p0912 A72-20163
- Standard procedures development for perceived noisiness or noise annoyance evaluation, taking into account spectral complexity, spectra weighting, time integration and onset duration
07 p0932 A72-20166
- Stationary statistical model for microwave oscillator flicker frequency noise, leading to power spectral density and time domain frequency instability
[ONERA, TP NO. 1085] 08 p1141 A72-21431
- Frequency response of spectral noise amplitude in chalcogenide glass switches
09 p1366 A72-22215
- German monograph on frequency noise of microwave transistor power oscillators covering generation mechanism and spectral density determination
09 p1285 A72-22340
- Statistical noise characteristics and conditional signal distribution function measurements at output of standard FM demodulator
09 p1277 A72-22570
- Band limited background noise variance measurements by analog and digital techniques
09 p1280 A72-23103
- Resonance occurrence in generation-recombination noise spectrum of Co 60 gamma irradiated Ge single crystals, investigating Hall effect
09 p1372 A72-23112
- Model of dynodes system with random electron-hole pairs number, calculating equations for mean fluxes transport and correlated noise fluctuations
09 p1280 A72-23116
- LF noise spectral density measurements in avalanche diodes as function of frequency, considering mean square voltage drift
09 p1287 A72-23118
- LF originated background noise in Gunn oscillators, developing evolution equation for oscillator weakly perturbed by noise
09 p1288 A72-23121
- Noise of high electric field biased gallium arsenide diodes, calculating LF power spectrum
09 p1288 A72-23123
- Instantaneous frequency statistical characteristics of passive noise spectra and fluctuating signals reflected from nonpoint moving radar targets
10 p1436 A72-24514
- High efficiency low noise volume /Lippmann-Bragg/ holograms recorded on photographic plate, using bleaching-darkening procedure
11 p1629 A72-25316
- Si Pd-n-p/plus/ transit time diode microwave oscillator, discussing fabrication, FM noise spectrum and bias current fluctuation
11 p1604 A72-25748
- Spectral density of frequency deviating process for performance predictions from oscillator testing and frequency noise calibration, discussing sample averages convergence to statistical values
11 p1593 A72-25892
- Spatial noise in holographic images of diffusely scattering objects with allowance for recording apparatus resolving capacity
12 p1810 A72-27871
- Measurement of spatially coherent and incoherent structure of axial compressor-generated noise modes propagating in duct
[ONERA, TP NO. 1045] 12 p1861 A72-28049
- Mathematical random fluctuation models for noise and energy spectra of pulsed processes during current passage through semiconductors
13 p2021 A72-29064
- Optimal random search noise recognition systems with Bayes teaching technique
13 p1924 A72-29162
- Parametric resonance suppression in annular laser by steady noise perturbation, discussing beat signal spectrum
13 p1968 A72-29505
- Noise generated by free flow turbulence incident on rotor or stator in axial flow fans and compressors, noting sound spectrum dependence
13 p2028 A72-29575
- Digital data processing techniques for aircraft engine noise data reduction, analyzing fan noise spectrum
13 p1925 A72-29840
- Tu-104 turboprop aircraft flight noise measurements and spectral changes at different distances from land-

- ing strip, evaluating public nuisance and resident reactions
14 p2072 A72-30446
- Lf white noise voltage theory of avalanche diode extended to small multiplication M values and unequal hole and electron avalanche ionization coefficients
15 p2206 A72-31642
- Thermodynamic plasma density fluctuation induced electric noise field measurement as means to determine plasma density and electron and ion temperatures
15 p2284 A72-31943
- Current noise spectra in single crystals and polycrystals of transition metal compounds, discussing flicker noise origin
15 p2293 A72-32384
- Gaussian beam laser Doppler velocimeter system under high scattering center concentrations and steady flow conditions, deriving noise spectral densities and SNR
16 p2390 A72-33210
- FM/FM multiplex receiver with carrier and subcarrier demodulators, deriving average click rate, output noise spectrum and SNR from Rice model
16 p2362 A72-33212
- Spatial noise in holographic images of diffusely scattering objects with allowance for recording apparatus resolving capacity
16 p2395 A72-33980
- The estimation of nonstationary spectra from moving acoustic source distributions.
[AIAA PAPER 72-667] 17 p2583 A72-35486
- Acoustic power spectrum of a subsonic jet
17 p2541 A72-35544
- Low energy auroral electron precipitation associated ELF noise band observation by polar-orbiting satellite INJUN 5
17 p2517 A72-35593
- The effects of electron bombardment on the noise properties of field effect transistors.
18 p2666 A72-36322
- Quantum noise in semiconductor lasers.
18 p2697 A72-36345
- Temperature dependence of low-frequency excess noise in junction-gate FET's.
18 p2666 A72-36454
- Characteristic features of ELF-noise spectra during the excitation of the earth-ionosphere resonator by cosmic sources
18 p2662 A72-36861
- Si MOSFET elementary channel resistances before saturation onset from one dimensional theory, investigating current noise
18 p2668 A72-37037
- Ambipolar diffusion noise in a semiconductor in the presence of a magnetic field.
19 p2846 A72-38599
- Frequency instability due to discrete noise in frequency synthesizers.
19 p2775 A72-38618
- Theoretical and experimental investigations of a second-order phase-coordinate receiver
19 p2775 A72-38658
- Polar ionosphere ELF/VLF noise distribution from Alouette 2 electric dipole observations
20 p2903 A72-39538
- A general analysis of noise in Gunn oscillators.
20 p2909 A72-39782
- Observation of quantum-phase and quantum-amplitude noise for a laser below and above threshold.
20 p2934 A72-39813
- Analysis of large-signal noise in Read oscillators.
21 p3032 A72-40698
- A numerical evaluation and experimental study of the intermodulation noise spectra of traveling wave tubes.
21 p3033 A72-40880
- Signal voltage density, pulse shape and noise power spectrum analysis of matched filter configurations in IR scanning system model
21 p3033 A72-41078
- Signal voltage density, pulse shape and noise power spectrum analysis of running integrator output in IR scanner model
21 p3056 A72-41086
- Discrete component of the noise spectrum of a supersonic annular jet
21 p3045 A72-41100
- Tu-104 turboprop aircraft flight noise measurements and spectral changes at different distances from landing strip, evaluating annoyance factors and resident reactions
21 p3009 A72-41110
- Description and use of a method for characterizing noise sources in jets
[ICAS PAPER 72-35] 21 p3046 A72-41160
- Parametric method of statistical synthesis with incomplete initial information on signal and noise distribution, discussing signal detection in white noise with unknown spectral density
22 p3154 A72-42230
- Current noise and conductance-temperature characteristics of thin discontinuous Pt films on glass sub-

strate interpreted by quantum mechanical electron tunneling model
22 p3214 A72-42453

General transport theory of noise in pn junction-like devices. I Three-dimensional Green's function formulation.
22 p3160 A72-43083

General transport theory of noise in pn junction-like devices. II - Carrier correlations and fluctuations for high injection.
22 p3160 A72-43084

Statistical analysis of the sound level distribution of aircraft noise as a function of time
23 p3252 A72-44337

Basic directivity and spectra of jet noise with improved correction for refraction.
24 p3389 A72-44678

Statistical noise characteristics and conditional signal distribution function measurements at output of standard FM demodulator
24 p3379 A72-44749

Noise properties of the injection-limited Gunn diode.
24 p3385 A72-44962

External noise effect on capture conditions in ring laser, noting capture bandwidth narrowing with noise spectral density increase
24 p3410 A72-45423

NOISE STORMS
Statistical tests for spectral correlation analysis of continuum VHF radio emission fluctuations from noise storms
21 p3102 A72-41778

NOISE SUPPRESSORS
U NOISE REDUCTION
NOISE TEMPERATURE
Radome enclosed Haystack parabolic antenna characteristics as radio astronomical instrument, discussing gain, polarization, interference susceptibility and noise temperature
[AD-737166] 01 p0032 A72-11233

Millimeter wave sky noise temperature measurement with 16 and 35 GHz radiometers, including antenna loss and rain and cloud effects
02 p0171 A72-11665

Josephson effect /superconducting weak link/ devices for low frequency magnetic field sensing, noting applications in magnetocardiography and absolute noise thermometry
08 p1218 A72-21919

Alternating Josephson effect and junctions applications to radiation generators and detectors, electromotive force regulators, oscillators, mixers and noise thermometers
09 p1370 A72-22799

Noise temperature and admittance of space charge limited double cathode tube with transit time effects at microwave frequencies
10 p1454 A72-25105

Bulk negative resistance devices equivalent noise temperature derivation via diffusion-impedance field noise formula, obtaining Gunn oscillators SNR approximate value
10 p1454 A72-25106

Earth station parabolic antenna gain-noise temperature ratio measurement using radio star and Applications Technology Satellite technique
[AIAA PAPER 72-528] 12 p1779 A72-27354

Microwave radiometer performance analysis, deriving input noise power relation to instrument indication in terms of noise parameters
14 p2105 A72-30587

Antennas scattering coefficients measurement by ground and atmospheric radiation, permitting antenna noise temperature components determination
15 p2206 A72-31652

Parametric amplifiers for satellite microwave communication systems, discussing frequency stability, noise temperature and gain relationships
16 p2369 A72-33520

SHF airborne distributed phased array antenna system.
17 p2531 A72-35572

An X-band paramp with 0.85 dB noise figure /uncooled/ and 500 MHz bandwidth.
19 p2770 A72-32758

Schottky diode frequency converter characteristics, considering series resistance, housing reactance, barrier layer capacitance, noise sources and noise temperature
19 p2773 A72-37937

A general analysis of noise in Gunn oscillators.
20 p2909 A72-39782

Low-noise parametric amplifiers for radio astronomical observations at 18 to 21 cm wavelengths
21 p3025 A72-40303

Variation of tropospheric slant-path attenuation in the UK at 11.75 and 17 GHz.
22 p3155 A72-42751

Accuracy of measuring the noise figure of microwave two-ports
23 p3273 A72-44313

NOISE THRESHOLD

Impulse noise reproduction for temporary threshold shift and impulse noise measurements, considering rise time, frequency response and limitations of tape recorders
04 p0521 A72-14847

Noise threshold improvement of PCM signals for satellite transmission, using quality detector and error detecting codes
10 p1441 A72-25102

Audiometric determination of human temporary threshold shifts due to steady state and impulsive noise
11 p1583 A72-25873

Amplitude-time quantization of radar pulse signals in analog-digital converter, improving noise threshold and ranging accuracy
11 p1595 A72-26294

Binaural frequency discrimination in masking level difference /MLD/ noise under homophasic and antiphase conditions
13 p2006 A72-29771

Coherent IR heterodyne receivers with quantum noise threshold sensitivity for laser communications and radar transmission
15 p2198 A72-32063

Threshold noise of an FM receiver at small signal-to-noise ratios
22 p3154 A72-42236

Reciprocal mean-square error and signal-to-noise ratio as distinct performance measures in below-threshold communication.
23 p3265 A72-44177

Cumulants of multidimensional response of linear and nonlinear systems to Poisson distributed impulses, estimating joint probability distribution and evaluating threshold statistics
23 p3314 A72-44368

NOISE TOLERANCE

Rating scale judgments of aircraft noise based on surveys around airport
03 p0309 A72-12956

Psychophysical comparison methods for evaluating noisiness or annoyance values of sounds
07 p0932 A72-20168

Community response prediction to noise based on laboratory tests of individual acceptability judgments.
07 p0932 A72-20172

Human performance under intense noise, measuring effects on muscle tension, metabolism, respiration rate, visual accommodation, saccadic eye movement and dark adaptation
11 p1583 A72-25728

Acoustical environment pollution control, considering noise annoyance effects due to industry and construction, surface and air traffic, alarm devices, radio and TV, etc
13 p2067 A72-29554

Noise and vibration stress combined effects on human mental performance as function of time of day, taking into account circadian rhythm factor
14 p2081 A72-31083

Individual functions and intersubject differences of noise annoyance susceptibility, noting relationship to Rorschach test
16 p2357 A72-32987

NOMENCLATURES

Mars surface features Schiaparelli nomenclature from Mediterranean Sea area classical geography
04 p0569 A72-14500

Extension of lunar nomenclature to the far side of the moon
17 p2610 A72-35213

NOMINAL VALUES

U APPROXIMATION

NOMOGRAPHS

Tunnel diode microwave oscillator design by circle diagrams of operational and load characteristics
01 p0035 A72-10048

Nomogram determination of frequency characteristics of closed loop linear automatic control systems
02 p0197 A72-12563

Gravity data free air and Bouguer correction /elevation correction/ by nomographic alignment chart
06 p0809 A72-18148

Optimal nomographic determination of surface gyrocompass parameters ensuring minimum period of undamped precession oscillations
09 p1307 A72-22346

Fermi level and scattering phase function nomograms for semiconductors with parabolic and isotropic energy bands, noting charge transfer effects
11 p1700 A72-25781

Onboard turbogenerator igniter operating conditions determination from fuel-air ratio obtained from nomogram
12 p1861 A72-28145

Lifetime nomogram for evaporating drop at vapor combustion, applying thermomechanical and aerodynamic decay to jet engine combustion chamber [DFVLR-SONDDR-203] 16 p2477 A72-33422

NONCONSERVATIVE FORCES

Nomographic correction method for quantization error limited data systems, modifying root-summed-squared error analysis for non-Gaussian distribution
16 p2367 A72-33863

Nomogram for heat detector size determination from thermal inertia index and Biot number
16 p2395 A72-33968

A method of solving the problem of choosing an optimal transfer orbit with the aid of an invariant nomographic scale
17 p2610 A72-35217

A nomogram for determining the phase difference of an elliptically polarized wave
18 p2663 A72-37219

A nomogram for look angles to geostationary satellites.
19 p2869 A72-37298

Solar altitude nomogram for estimating terrestrial ground objects heights from shadow length on aerial photographs
22 p3181 A72-43196

NONADIABATIC CONDITIONS

U ADIABATIC CONDITIONS

NONADIABATIC THEORY

Supplemental internal gaseous film cooling combined with external cooling of combustion chamber walls, analyzing effectiveness via nonadiabatic model [AICHE PREPRINT 3] 18 p2741 A72-36550

Viscous non-adiabatic laminar flow through a supersonic nozzle - Experimental results and numerical calculations.
[ASME PAPER 72-HT-49] 20 p2985 A72-39662

Application of variational methods to the solution of some thermal shock problems
21 p3128 A72-40978

Nonadiabatic condition effects on ultrarelativistic electron energy losses in geomagnetic trap in remote magnetosphere regions
22 p3218 A72-42224

NONAXISYMMETRY

U ASYMMETRY

NONCONDUCTORS

U ELECTRICAL INSULATION

NONCONSERVATIVE FORCES

Nonconservative radiative transfer in spherically symmetric system, calculating linearly polarized electron scattering atmosphere
01 p0102 A72-11127

Nonconservative stability problems, obtaining eigenvalues with adjoint variational methods [AD-742170] 04 p0583 A72-14446

Mathematical modeling of discrete nonconservative dynamic elastic systems for finite sensitivity, using Liapunov stability
06 p0840 A72-18320

Galerkin method application to nonconservative nonself-adjoint aeroelasticity problems based on interpretation as mathematical formulation of virtual work principle
07 p1025 A72-18788

Linear mechanical elastic systems divergence with infinitely large frequency onset, noting discrete cantilever beam under nonconservative forces [ASME PAPER 71-APM-DDD] 10 p1555 A72-24189

Simultaneous nonhomogeneous internal and external friction effects on nonconservative force systems motion stability, considering cantilever beam compression
12 p1845 A72-27321

Numerical analysis methods for solution stability of reduced field equations describing perturbed motion of body under nonconservative loads
13 p2001 A72-28485

Averaging variational Euler-Lagrange equation for nonlinear waves with dispersion in nonconservative system
13 p2003 A72-28774

Generalized Thomson-Tait-Chetaev stability theorem for n-degrees-of-freedom mechanical oscillating systems with virtual nonconservative displacement forces
15 p2274 A72-31456

Unsymmetrical coupled columns stability under nonconservative lateral and end loading, using finite element method
15 p2331 A72-32557

A comparison of approximate methods for solving non-conservative problems of elastic stability.
17 p2634 A72-35410

An approximate analysis of non-linear non-conservative systems subjected to step function excitation.
17 p2582 A72-35412

Some properties pertaining to the stability of circulatory systems.
18 p2737 A72-37060

Integration of equations of motion for nonconservative holonomic systems with pulsed coupling factors
19 p2825 A72-38192

The post-flutter oscillations of discrete symmetric structural systems with circulatory loading.
21 p3120 A72-41207

On the destabilizing effect in a non-conservative system with slight internal and external damping.
21 p3124 A72-41483

Stability of elastoplastic rod under external conservative and nonconservative forces, discussing nonconservative component effect and critical load magnitude 22 p3234 A72-42149

NONDESTRUCTIVE TESTS NT PRELAUNCH TESTS

Nondestructive determination of temperature dependence of elastic moduli of Al alloy and Ni and stainless steels by resonant frequency method 01 p0084 A72-10518

NDT program for detectability changes of tight defects in Al as function of applied load 01 p0085 A72-10756

Nondestructive evaluation in aerospace, weapon systems and nuclear applications Conference, San Antonio, April 1971 01 p0075 A72-10801

Acoustic emission tests of nuclear pressure vessels and piping, detecting weld slag, porosity, fatigue microcracking and stress corrosion cracking 01 p0048 A72-10802

Acoustic emission characteristics from nuclear reactor irradiated steels during tensile and wedge opening load tests 01 p0068 A72-10803

Acoustic emission evaluation of damage of filament wound composite materials under tensile loading applied to spherical test shapes 01 p0069 A72-10804

Nondestructive identification of alloy elements by nondispersive X ray fluorescence spectroscopy using Si/Li detectors and radioisotope sources for mobile applications 01 p0069 A72-10805

Resonance neutron transmission for nondestructive absorption spectroscopic evaluation of quantitative chemical or isotopic composition at depth in large samples 01 p0069 A72-10806

Reactor source neutron radiography for nondestructive testing, noting hydrogen detection, boron fiber imaging and photographic or electronic color enhancement 01 p0069 A72-10807

Radiographic detection of small flaws in bulk graphite and carbon/carbon composites, improving image quality and sensitivity by contrasting liquid impregnation 01 p0069 A72-10808

Nondestructive radiographic tests for void and unbond detection in Scout solid propellant rocket motors 01 p0114 A72-10812

Nondestructive radioactive gas penetrant tests for porosity and fatigue damage in jet engine castings 01 p0069 A72-10813

Portable self contained ultrasonic field inspection equipment for nondestructive crack detection in T53 gas turbine compressor disks 01 p0076 A72-10814

Integrity control procedures for machining, drilling and grinding of steel and Ti alloy aircraft parts, discussing nondestructive inspection method [SME PAPER IQ 71-238] 01 p0076 A72-10969

Nondestructive tests of Nb alloy radiative thermal protection heat shield design for space shuttle requirements 01 p0048 A72-10980

DGS diagrams for defect size determination in ultrasonic NDT 01 p0070 A72-11016

Automatic ultrasonic testing equipment for NDT tests of helicopter rotor blades 01 p0071 A72-11021

DC-10 nondestructive testing manual, detailing section/subject format, methods, planned area accessibility and aircraft maintenance 01 p0078 A72-11109

NDT holographic interference pattern technique to determine Advanced Test Reactor fuel element swage joint tightness 01 p0078 A72-11110

Point density measurement and crack detection in P/M green compacts with interconnected porosity by pneumatic tests, noting application to quality control 02 p0233 A72-11458

Graphite-epoxy conductive polymers as fatigue damage indicators of structures under cyclic strain [SESA PAPER 1915] 02 p0287 A72-11509

NERVA fuel quality control, discussing planning, nondestructive tests, computer data acquisition and certification systems 02 p0258 A72-11552

Subsurface discontinuity detection by microwave radiometry, noting microwave temperature correlation with moisture patterns 02 p0209 A72-11792

Na and K trace amounts detection in Al based solid rocket propellants by neutron activation analysis, using gamma ray spectroscopy for nondestructive analysis 02 p0270 A72-11959

Impending metal fatigue failure holographic detection by optical correlation of coherent light reflection from deformed surface structure as function of time 02 p0294 A72-12442

Metal fatigue damage nondestructive detection, discussing inspection methods, equipment, advantages, limitations and test results [AD-741977] 02 p0296 A72-12498

Acoustic emission techniques in defect structure materials tests, discussing fracture strength, crack propagation, fatigue, plastic deformation and creep in metals, composites and rocks 03 p0362 A72-13225

TV time lapse interferometry and contouring for photoelastic nondestructive testing, comparing with photographic techniques 03 p0358 A72-13436

Ultrasonic flaw detector pulse transducers operation using electrodynamic and capacitance receivers 03 p0361 A72-13987

Ultrasonic defectoscope sensitivity, discussing statistical character of random signal level distribution and test conditions 03 p0364 A72-13988

NDT for detecting density variation, local anomalies regions and completeness of copper-infiltrated W powder rocket nozzle inserts 03 p0364 A72-14025

Thermography capabilities and limitations for design analysis and quality control in nondestructive testing of material test vehicle carbon-carbon composite cones 03 p0364 A72-14026

Nondestructive testing for materials inspection and monitored aircraft maintenance programs 03 p0364 A72-14201

Boron/aluminum composite sheet quality evaluation by radiography, ultrasonic C-scanning and micro-ohm resistance measurement, correlating with resistance weld strength 04 p0526 A72-14839

Nondestructive examination of steel plate weld specimen, comparing ultrasonic and X ray techniques 04 p0527 A72-14840

Stress measurement at surface of polycrystalline bodies by nondestructive X ray diffraction method 04 p0525 A72-15553

Crossing points computed curves from metal sheet response to pulsed eddy currents, suggesting independent lift-off distance variation possibility 05 p0666 A72-17049

Ultrasonic acoustic holography for real time nondestructive testing of cracks, voids, nonbonds and other defects in metals, ceramics and plastics [SAE PAPER 720173] 06 p0811 A72-17319

Acoustic emission systems application to materials nondestructive testing, discussing single and multiple piezoelectric transducer arrays with on-line computer analysis [SAE PAPER 720175] 06 p0819 A72-17323

Spacecraft incipient failure detection, stressing acoustic energy release techniques 07 p0964 A72-18829

X ray, ultrasonic and eddy current nondestructive testing of aircraft structure for maintenance and special problems 07 p0994 A72-18840

Micrographic evaluation of inclusions in austenitic stainless steel tubes ensuring surface quality control 07 p0994 A72-18972

Two-fold congruency tests of penetrant inspection system sensitivity using hydrophilic and lipophilic removers/emulsifiers/ 07 p0995 A72-19650

Nondestructive tests of welded joint heterogeneities and corrosion cavities by densitometric photometric differentiation of radiographs 07 p0995 A72-19674

Holography applications and processes, discussing holographic microscopy, particle analysis, high speed photography, data storage and retrieval, interferometry, nondestructive testing, etc 07 p0989 A72-20221

Nondestructive testing - Conference, Trieste, Italy, May 1971 07 p0991 A72-20420

Optimal test conditions in magnetoscopic control by electrical system for subsurface defects detection, obtaining tangential magnetic field on carbon steel plates 07 p0991 A72-20421

Nondestructive ultrasonic determination of defects in structural steel blanks 07 p0991 A72-20423

Bulk conductors dc field distribution applications to electrical resistivity measurements and nondestructive testing 07 p0998 A72-20461

Nondestructive testing of electroexplosive devices, considering bridgewire-explosive interface and faults-abnormalities interrelationship 08 p1220 A72-20764

Nondestructive testing techniques - ISA Conference, Chicago, October 1971 08 p1163 A72-20914

Holographic interferometry for nondestructive testing, discussing applicability to laminate structures 08 p1164 A72-20924

Nondestructive determination of glass reinforced plastics normal elastic and shear moduli and strength characteristics by vibrational, pulsed and acoustic methods 08 p1195 A72-21773

Betatron electron beam evaluation for flaw detection in laminated materials by radiographic and radiometric methods 08 p1177 A72-21774

Gamma radiation source energy and activity determination for radiometric flaw detection in steel 08 p1177 A72-21775

High pressure bulk modulus test rig for composite material specimen nondestructive test, discussing measurement method and errors 09 p1315 A72-23391

Welded high strength maraging steels fatigue performance, stressing nondestructive testing technique 09 p1332 A72-23617

Thermal neutron radiography industrial applications, describing nondestructive testing techniques 10 p1485 A72-23813

Diffusion bonded joints tensile strength determination from ultrasonic pulse echo and attenuation measurements, discussing contamination and SNR effects 10 p1485 A72-23814

Delayed pulse echo and through-transmission ultrasonic techniques for nondestructive inspection and quality control of braze bonds in high current electric contact assemblies 10 p1487 A72-24173

Visual image indicator used beside and behind objects for neutron radiography quality determination and radiographs series grading 11 p1632 A72-25822

Multifrequency ultrasonic pulse echo interference effect applying to flaw detection in metals 11 p1687 A72-26051

NDT of diffusion formed coatings on refractory alloys and superalloys, stressing eddy current technique 11 p1641 A72-26287

NDT application to aircraft design and reliability, discussing fatigue life analysis and in-service monitoring for structural elements, components and airframes 12 p1813 A72-27198

Metal matrix composites radiography in NDT, discussing parameters optimization and uses of microfilm, densitometers and high resolution vidicon tubes 12 p1813 A72-27199

Electrothermal NDT of metal structures by IR scanning camera or thermal image transducer 12 p1813 A72-27200

Fracture toughness of high strength alloys, discussing rocket motor cases, nondestructive test standards and subcritical crack growth 12 p1829 A72-27656

Frequency method of mechanical impedance monitoring of natural frequency of transducer-article system under load in defectoscopy 13 p1956 A72-28923

Optimal level of recording defects in ultrasonic flaw detection, taking into account inspection conditions and defect size probability distribution 13 p1956 A72-28924

Thickness gage for continuous autographic record in nondestructive testing of irregular cross section specimens 13 p1959 A72-29759

Nondestructive technique for continuous recording of thickness or contour profiles, using mechanical probes 13 p2000 A72-29760

Reliability of nondestructive ultrasonic testing methods of quality control, discussing defect size distribution and detectability coefficient 14 p2106 A72-30149

Radiation defectoscopy methods based on calculating perturbations in gamma radiation field due to inhomogeneities 14 p2106 A72-30150

Fatigue life tests of structural sandwich plates with honeycomb layer, considering temperature effects, material scattering and defects inside honeycomb by nondestructive methods 14 p2164 A72-30280

Leak detection in pressurized installations via NDT, discussing uses of fluid tracers, thermal and acoustic sensors, halogen detectors, He mass spectrometers and radioactive tracers 14 p2104 A72-30374

Lamb acoustic surface wave method for rapid nondestructive evaluation of rolling texture in arbitrarily thick metal sheets and plates 14 p2107 A72-30615

Carbon fiber reinforced plastics nondestructive testing by ultrasonic compressional and shear wave resonance 14 p2107 A72-30856

- Continuous NDT of coalescers /jet fuel filters/ by liquid crystals, detecting split seams, cap leaks, cracks, material imperfections and epoxy filled voids [ASME PAPER 72-DE-25] 14 p2108 A72-30867
- Heat flux nondestructive inspection methods for laminate and sandwich structures and electronic components 15 p2232 A72-31322
- Structure-borne acoustic nondestructive testing for readiness assessment, fault isolation and automatic checkout of space vehicle mechanical devices 15 p2214 A72-31699
- Optical nondestructive surface flaw detection for steel plates using oblique angle illumination combined with high pass spatial filter 15 p2238 A72-32153
- Ultrasonic flaw detector data analysis, discussing digital computer interface and encoders 16 p2397 A72-33202
- Nondestructive monitoring techniques to optimize performance and service tests, considering penetrating radiation, electromagnetic induction, ultrasonics, holography, microwaves, acoustic emission and thermal monitoring 16 p2397 A72-33219
- Nondestructive vibration analysis of mechanical structures, using digital computer technique for sound wave spectrum analysis 16 p2397 A72-33220
- Microwave transmission phenomenon and application to NDT, discussing various methods and examples 16 p2391 A72-33233
- Surface crack detection in ferrous and nonferrous metals, glass, ceramics and plastics by water-washable dye penetrants process 16 p2397 A72-33239
- Nondestructive vibration tests of fatigue crack damage in composite structures, investigating glass reinforced epoxy and polyester laminates 16 p2414 A72-33318
- Reliable nondestructive microstructure testing via surface ultrasonic waves 16 p2399 A72-33822
- Holographic nondestructive testing with impact excitation. 17 p2555 A72-35197
- Ultrasonic wave propagation in metal-matrix composites. 17 p2560 A72-35287
- Nondestructive ultrasonic inspection of braze bonds in high current electrical contact assemblies. 18 p2695 A72-36116
- Thermal neutron radiography as NDT technique for industrial inspection, noting advantages for low atomic number and radioactive materials 18 p2695 A72-36457
- Acoustic emission technique as NDT method for quality control of brazed metal-ceramic bonding 18 p2695 A72-36458
- Nondestructive test for measuring the state of heat treatment in closure welds. 18 p2695 A72-36672
- Factors governing radiographic crack detectability in steel weld specimens. 18 p2695 A72-36673
- Detection of defects in semiconductor structures by means of recording the temperature and electric fields. 18 p2693 A72-37106
- Applications of holographic nondestructive testing techniques in engineering. 19 p2806 A72-37608
- Holometric deformation measurement on carbon carbon biaxial test specimens. 19 p2822 A72-37616
- Swept frequency resolution and optical processing in propellant grain flow detection by microwave holography, using Vander Lugt filter imaging 19 p2798 A72-37626
- Application of video techniques and speckle pattern interferometry to engineering measurement. 19 p2799 A72-37628
- Nondestructive testing of advanced composites. 19 p2799 A72-37669
- IAD-3 amplitude-phase impedance defectoscope. 19 p2805 A72-38765
- Electro-optical TV technique with laser source illumination to provide engineering metrology and NDT procedure resembling real time holographic interferometry 20 p2930 A72-39038
- Acoustic emission experiments design based on piezoelectric transducer, discussing signal detection and data acquisition methods 20 p2924 A72-39278
- Crack growth behavior correlation to acoustic emission signal amplitude distribution in high strength steel heat treated to different fracture toughness values 20 p2924 A72-39282
- Infrared testing of solar cell arrays. 20 p2890 A72-39339
- Neutron activation techniques for nondestructive analysis of meteorites and lunar rocks, noting types of nuclear reactions for geochemical application 20 p2899 A72-39832
- Non-destructive activation analysis of some elements in stony meteorites by proton- and bremsstrahlen-irradiation. 20 p2899 A72-39833
- Elemental abundance trends in the australite strewn field by non-destructive neutron activation. 20 p2900 A72-39839
- Non-destructive examination of fibre reinforced polymers with special reference to continuous carbon fibre reinforcement. 21 p3073 A72-41169
- Use of stress wave emission for nondestructive testing of materials and articles. 21 p3061 A72-41720
- Bilateral version of an ultrasonic velocimetric method of defectoscopy. 21 p3057 A72-41721
- The magnetic field of eddy currents above a surface crack in metal with excitation of them by an applied inductor. 21 p3057 A72-41722
- Analysis of noise immunity of two-channel eddy-current flaw detector. 21 p3057 A72-41723
- Plastic model shells design, construction and instrumentation for elastic stability studies in NDT, discussing deformation measurements for critical condition prediction 22 p3163 A72-42694
- Nondestructive stability evaluation of large shell structures by direct computer controlled testing. 22 p3157 A72-42695
- The importance of service inspection in aircraft fatigue. 24 p3367 A72-44740
- Bonded honeycomb structures. II - Bonded joints and non-destructive testing. 24 p3407 A72-45288
- Non-destructive testing of adhesive bonded metal-to-metal joints. I. 24 p3408 A72-45289
- Non-destructive testing of adhesive bonded metal-to-metal joints. II. 24 p3408 A72-45290
- Electromagneto-acoustic non-destructive testing in the Soviet Union. 24 p3408 A72-45291
- NDT techniques selection, economics and organization for aircraft industry, considering ultrasonic holographic and adhesion tests 24 p3408 A72-45292
- A bibliographical survey of acoustic emission. 24 p3408 A72-45293
- Ultrasonic defect detection and evaluation techniques, stressing limitations for defect geometry, size and nature 24 p3408 A72-45294
- NDT application and development in industry, considering confidence in inspection techniques, framework and management resistance 24 p3408 A72-45295
- NONELECTROLYTES**
- Nonequilibrium transitions for thermodynamic systems with generalized forces and flows by linear transformations, applying to nonelectrolyte solutions with concentration and temperature gradients 07 p1097 A72-18806
- NONEQUILIBRIUM CONDITIONS**
- Nonlinear oscillations stochastic instability in dynamic systems, discussing nonequilibrium statistical mechanics 03 p0390 A72-14316
- Radiative transfer and chemical nonequilibrium phenomena for radiating flow field predictions behind high altitude hypervelocity normal shock waves 05 p0603 A72-16545
- Nonequilibrium chemistry effects on electrical properties of solid propellant rocket motors turbulent afterburning exhaust plumes, describing free electron sources 07 p0935 A72-19359
- Statistical-hydrodynamic description of nonequilibrium gas dynamics of single component and binary mixtures and systems with chemical reactions 07 p0968 A72-19886
- Kinetic theory and nonequilibrium distribution functions of reacting gases with simultaneous reactions 07 p1035 A72-20114
- Beam-foil-gas spectroscopy and relative cross section measurements for studying steady state nonequilibrium processes 10 p1434 A72-24325
- Relativistic counterpart of Poincare condition for angular velocity of rigidly rotating star, discussing equilibrium disturbance effects 10 p1549 A72-25058
- Chemical lasers diatomic and multitatomic molecules dissociation in nonequilibrium conditions, discussing vibrational energy exceeding gas temperature 11 p1646 A72-25713
- Competition criteria for chemical reactions selection in nonequilibrium computer calculations on combustion systems properties, noting seeded flames and rocket exhausts 13 p1912 A72-28548
- Plasticity, elastic relaxation and stress-strain relation characterization for Schofield-Scott Blair media, using nonequilibrium thermodynamics method 15 p2331 A72-32482
- Diatomic gas flow behind blast wave, discussing vibrational nonequilibrium effects and solution of governing equations via characteristics method 16 p2378 A72-33440
- Coupling of free electron and nitrogen vibrational temperature nonequilibrium in weakly ionized nozzle expansions of shock heated nitrogen [AIAA PAPER 72-683] 16 p2380 A72-34059
- Mathematical model for nonequilibrium gas composed of hard spherical nonattracting molecules, deriving gas dynamics theory in terms of multiple integrals 17 p2538 A72-34424
- Applications of an improved formalism for the analysis of transport phenomena in gaseous mixtures and plasmas. 17 p2587 A72-34615
- Statistical-hydrodynamic description of nonequilibrium gas dynamics of single component and binary mixtures and systems with chemical reactions 17 p2540 A72-35134
- The two-particle correlation function in nonequilibrium statistical mechanics. 17 p2581 A72-35164
- Nonequilibrium thermodynamics with rate equations as nonlinear solid mechanics foundation, noting viscoelastic, viscoplastic and plastic behavior 18 p2732 A72-36076
- Nonequilibrium transport equations for chemically reacting inhomogeneous gas mixtures, using Hermitian tensor polynomials of molecular velocities 18 p2713 A72-36895
- Nonlinear oscillations stochastic instability in dynamic systems, discussing nonequilibrium statistical mechanics 19 p2836 A72-38814
- Low-temperature photoluminescence of GaAs under conditions of strong interaction of the nonequilibrium carriers. 19 p2847 A72-38821
- One dimensional stationary gas flow across normal shock wave, taking into account nonequilibrium factors and momentum, mass and energy transport 20 p2914 A72-39970
- Nonequilibrium phenomena in electron tunneling in normal metal-insulator-metal junctions. 21 p3096 A72-40343
- A non-equilibrium thermodynamic theory of simple materials based on a single-integral entropic functional. 21 p3124 A72-41505
- Spectroscopic measurements for atmospheric nitrogen and helium arcs. 23 p3322 A72-44326
- NONEQUILIBRIUM DRAG**
- U FRICTION DRAG**
- NONEQUILIBRIUM FLOW**
- Numerical analysis of nonequilibrium gas mixture flow through nozzle 02 p0149 A72-11589
- Mathematical analogy between nonequilibrium and viscous inert transonic flows for reacting mixtures with relaxation and freezing 02 p0150 A72-11736
- Electron temperature profile across nonequilibrium stagnation point boundary layer in partially ionized gas, investigating charged particles interaction with body in ionosphere 02 p0262 A72-12268
- Laminar three dimensional boundary layer nonequilibrium effects at hypersonic wing swept leading edge with intensively cooled surface, considering sweep induced crossflow effect [VPI-E-71-23] 02 p0152 A72-12422
- Slender projectile supersonic flight in fluid with nonequilibrium transformations, comparing theoretical shock decay angle with Wegener-Klikoff measurements 03 p0307 A72-13158
- Nonequilibrium stagnation heat transfer mathematical models for injecting He, Ar or H into ionizing air laminar viscous layers at low Reynolds numbers [ASME PAPER 71-WA/HT-18] 05 p0744 A72-15877
- Low Reynolds number nonequilibrium stagnation heat transfer with helium, argon and hydrogen injection into air boundary and thin viscous shock layers [ASME PAPER 71-WA/HT-19] 05 p0744 A72-15878
- Integral computation for nonequilibrium compressible turbulent boundary layers using moment, momentum and skin friction equations [ASME PAPER 71-WA/APM-12] 05 p0647 A72-15968
- Vector analysis of three dimensional nonequilibrium dissociative gas flow quantity variations along stream lines 05 p0652 A72-17001
- Curved shocks discontinuities in nonequilibrium dissociative gas flows, investigating flow gradient variables 05 p0653 A72-17080

- Nonequilibrium dissociating gases high speed laminar mixing layers, comparing approximate closed form solution with numerical solution
[VPI-E-71-22] 05 p0653 A72-17150
- Nonequilibrium transitions for thermodynamic systems with generalized forces and flows by linear transformations, applying to nonelectrolyte solutions with concentration and temperature gradients
07 p1097 A72-18806
- Monatomic ionized radiating gas nonequilibrium flow in blunt body stagnation region behind shock wave during hypersonic atmospheric reentry
07 p0909 A72-20083
- Vibrational relaxation in nonequilibrium and expansion nozzle flows
08 p1148 A72-21015
- Simple waves in one dimensional unsteady nonequilibrium dissociative gas dynamics, discussing internal, chemical bond and dissociation energies
11 p1616 A72-25982
- Nonequilibrium dissociating inviscid nitrogen flow pattern over spheres and circular cylinders, obtaining temperature, pressure and density fields
13 p1895 A72-30032
- Pseudo-one dimensional dissociating nonequilibrium nozzle flow, presenting governing equations transformation via similarity parameter for oxygen
16 p2375 A72-32906
- Pohlhausen type integral method for dissociative binary mixture nonequilibrium laminar boundary layer on flat plate, using Crocco relationship between enthalpy and velocity profile
16 p2378 A72-33436
- Viscous shock layer analysis application to blunt nosed reentry vehicle plasma layer nonequilibrium flow species distribution, considering electron density
[AIAA PAPER 72-689] 16 p2346 A72-34053
- Nonequilibrium steady quasi-one dimensional expanding nozzle flow of chemically reacting gas mixture, using time dependent finite difference technique
[AIAA PAPER 72-684] 16 p2480 A72-34058
- Generalized relations for determining specific impulse losses in nonequilibrium two-phase nozzle flows
20 p2914 A72-39909
- Computation of three-dimensional non-equilibrium supersonic flows.
[ICAS PAPER 72-37] 21 p2992 A72-41162
- Critical mass flow and nonequilibrium nozzle flow of vibrationally relaxing, ideal dissociating diatomic and singly ionizing monatomic gases, using steepest descent method
21 p3046 A72-41249
- Development of the AEDC-VKF tunnel J - A real gas high density, true velocity, hypersonic, aerodynamic test facility.
[AIAA PAPER 72-993] 21 p3040 A72-41579
- Weak shock wave propagation in a relaxing gas.
24 p3391 A72-45042
- Laminar high speed mixing of nonequilibrium dissociating gases.
24 p3392 A72-45056
- Study of a reactive nozzle flow associated with solid gas-phase interaction.
24 p3433 A72-45063
- ### NONEQUILIBRIUM IONIZATION
- Nonequilibrium effects on ionization growth in molecular hydrogen, tabulating experimental data for comparison with Monte Carlo computation
02 p0267 A72-12793
- Strong normal shock wave structure upstream and downstream of discontinuity due to nonequilibrium radiation and collisional ionization
06 p0902 A72-18106
- Nonequilibrium ionization theories for high pressure discharge in inert gas-alkali metal vapor
10 p1515 A72-24414
- Nonequilibrium partially ionized viscous shock layer on blunt body, determining electron temperature and electron-ion density profiles
11 p1744 A72-25560
- Ionization turbulence effect on nonequilibrium plasma MHD generator performance, using I-V characteristics equation
13 p1900 A72-29354
- Nonequilibrium ionization phenomena effects on electric conductivity of combustion gas-particle plasma generated by aluminized fuel seeded with potassium nitrate
13 p2013 A72-29363
- Hypersonic flow of nonequilibrium ionized monatomic inviscid radiating gas past axisymmetric blunt body with allowance for electron and ion temperatures difference
13 p1895 A72-29877
- Nonequilibrium relaxation phenomena in the near-emitter region of the thermionic converter.
18 p2647 A72-36209
- Influence of boundaries on the ionization instability of a plasma in a discharge of coaxial geometry
22 p3209 A72-41876
- Influence of inelastic electron-energy losses on the development of ionization instability in a plasma
22 p3209 A72-41877
- Kinetics of impact-radiative ionization and recombination
23 p3318 A72-43296
- ### NONEQUILIBRIUM PLASMAS
- Electron and population densities in inhomogeneous nonequilibrium plasmas with photoabsorption, using radiative transport equation
02 p0266 A72-12441
- Electron temperature measurements in ionospheric isotropic nonequilibrium plasma by electrostatic probes and radar backscatter
03 p0349 A72-13520
- Nonequilibrium plasma production by induced electric field in helium and argon streams in magnetic field
05 p0700 A72-17229
- Fast electron-cyclotron wave excitation with infinite phase velocity along magnetic field in nonequilibrium electron plasma
06 p0862 A72-18402
- Vibration modes and stability of nonequilibrium low density He-Cs plasma in magnetic field
07 p1043 A72-19876
- H Balmer lines H alpha/H beta ratios as electron temperature indicators in nonequilibrium plasmas
09 p1359 A72-22666
- Nonequilibrium ionization theories for high pressure discharge in inert gas-alkali metal vapor
10 p1515 A72-24414
- T Tauri type variable stars spectral features relation to evolutionary sequences, noting stellar atmosphere nonthermal equilibrium plasma region effects
10 p1549 A72-25056
- Nonequilibrium MHD generator with electrode walls slanted away from magnetic field direction, predicting electrical performance for comparison with flat wall generator
13 p1899 A72-29352
- Linear nonequilibrium Faraday type MHD generator, predicting electrode configuration effects on voltage drops, axial leakages and current distribution
13 p1900 A72-29353
- Ionization turbulence effect on nonequilibrium plasma MHD generator performance, using I-V characteristics equation
13 p1900 A72-29354
- Random phase approximation for nonlinear theory of MHD nonequilibrium plasma steady turbulent regime, noting ionization level rise by energy dissipation
13 p2013 A72-29359
- Cs seeded nonequilibrium MHD Ar plasma stability in fully ionized seed regime
13 p2014 A72-29368
- Ionization stabilization in MHD generators by sensing electron density perturbation with linear feedback into nonequilibrium plasma
13 p2014 A72-29369
- Fluctuating electric current induced magnetic field effects on long wave nonequilibrium plasma instability associated with large scale closed cycle MHD generators
13 p2014 A72-29370
- Nonequilibrium plasma wave scattering cross section dependence on energy bands shape and field orientation in semiconductors
13 p2023 A72-29992
- Nonequilibrium relativistic plasma fluctuations with direct movement of particles, considering isotropic velocity distribution of particles
15 p2289 A72-32695
- Weakly ionized nonequilibrium plasma flow from gas discharge tube positive column, obtaining electron temperature axial decay rate from energy equation
16 p2437 A72-33655
- Fast electron cyclotron wave excitation with infinite phase velocity along magnetic field in nonequilibrium electron plasma
17 p2588 A72-34853
- Vibration modes and stability of nonequilibrium low density He-Cs plasma in magnetic field
17 p2589 A72-35126
- Nonequilibrium energy constants associated with large-amplitude electron whistlers.
17 p2517 A72-35620
- Polarization and interferometric investigations of discharge modes in thermionic energy converters
18 p2647 A72-36219
- Study of the mechanism of motion of nonequilibrium plasma inhomogeneities in a magnetic field
18 p2717 A72-37176
- Dispersive waves in a slightly ionized nonequilibrium plasma.
21 p3092 A72-41223
- Kinetic equation for electron distribution in high temperature laser plasma, calculating nonequilibrium conditions for strong field and plasma parameters
23 p3318 A72-43323
- Magnetic pulsation spectra in a nonisothermal plasma
23 p3323 A72-44483
- ### NONEQUILIBRIUM RADIATION
- Nonstationary radiation transfer with one dimensional anisotropic scattering, deriving Bessel function expressions for quantum exit from semiinfinite medium
02 p0262 A72-12830
- Two dimensional time dependent nonlinear radiative transfer and nonequilibrium diffusion in arbitrary geometry by synthesis method
05 p0746 A72-15996
- Strong normal shock wave structure upstream and downstream of discontinuity due to nonequilibrium radiation and collisional ionization
06 p0902 A72-18106
- Long wave fluctuations in nonequilibrium gas with pair collisions, using Bogoliubov equations for simultaneous correlation functions
15 p2282 A72-32450
- ### NOEUCLEDIAN GEOMETRY
- ### U DIFFERENTIAL GEOMETRY
- ### NONFERROUS METALS
- Russian papers on light and nonferrous alloys structure and properties covering phase diagrams, alloying effects, reduction, crystallization and recrystallization, solid solutions decomposition, etc
14 p2123 A72-31027
- ### NONFLAMMABLE MATERIALS
- Nonflammable coolants for Saturn instrument unit environmental control systems, considering component materials compatibility with selected dielectric fluids
01 p0091 A72-10769
- Flame resistance requirements of high temperature resistant and highly chlorinated fibers
[PI PAPER 11] 03 p0380 A72-13245
- Phosphorus compounds incorporation in polyurethane foams and polyesters for flame retardancy
[PI PAPER 12] 03 p0380 A72-13246
- Fire retardant capabilities of bromine and chlorine compounds in polymers
[PI PAPER 13] 03 p0380 A72-13247
- Weibull distribution government of dispersion of destructive temperature gradients characteristic of fireproof ceramic materials heat resistance
21 p3074 A72-41713
- ### NONGRAY ATMOSPHERES
- Venus lower atmosphere from Venera 4, 5 and 6 and Mariner 5 data, evaluating greenhouse effect by microwave absorption and by nongray radiative model
01 p0129 A72-10795
- Book on stellar atmospheric physics covering gray and nongray atmospheres, radiation emission and absorption, transfer equation, Eddington approximation, spectral lines formation, etc
10 p1532 A72-23725
- Jupiter atmospheric greenhouse effect modeled by two layer emission, deriving temperatures from non-gray step function approximation of IR absorption
15 p2312 A72-32096
- Mechanical equilibrium equation of nongray stellar matter, approximating electron pressure vs temperature in early stellar atmospheres
21 p3109 A72-41435
- Mean coefficient of opacity in stellar atmosphere model calculations
21 p3110 A72-41443
- ### NONGRAY GAS
- Nongray treatment of nonisothermal IR radiative transfer problem in terms of mean absorption coefficient
09 p1354 A72-22668
- IR radiative energy transfer to laminar flow of non-gray absorbing emitting gases through circular tube
10 p1563 A72-25038
- Transient radiative heat transfer in a non-gray medium.
19 p2880 A72-37835
- Slab band absorbance for molecular gas radiation.
23 p3316 A72-44327
- Semigray approximation to nongray radiative transfer, taking into account mean absorption coefficient variation with spatial position and photon propagation direction
23 p3314 A72-44328
- ### NONHOLONOMIC EQUATIONS
- Motion equations of gyrostat with nonholonomic constraint under gravitational force
08 p1208 A72-21359
- Gyrostat inertial motion under nonholonomic constraint of mass center coincidence with fixed point
08 p1208 A72-21360
- Linear invariant solution to gyrostat motion under nonholonomic constraint
08 p1208 A72-21361
- Virtual displacement application to nonholonomic systems with arbitrary constraints to derive Lagrange and Appell equations of motion
10 p1513 A72-24995
- Control parameters required for stabilization of motion in systems with nonholonomic couplings by dynamic programming method of summary representations
13 p2003 A72-29068
- Relation between the first integrals of a nonholonomic mechanical system and a corresponding system freed of constraints
22 p3204 A72-41902

Motion of a solid with a nonholonomic constraint around a fixed point in a conservative force field 23 p3313 A72-43800

Equations of motion of nonlinear nonholonomic mechanical systems of variable mass with impulsive constraint factors 23 p3313 A72-43848

NONHOMOGENEITY

U INHOMOGENEITY

NONISENTPICITY

Nonisentropic flow behavior behind propagating self similar blast wave [AD-745485] 08 p1252 A72-21260

NONISOTHERMAL PROCESSES

U ISOTHERMAL PROCESSES

NONISOTROPIC PLATES

U ANISOTROPIC PLATES

NONISOTROPY

U ANISOTROPY

NONLINEAR EQUATIONS

NT DUFFING DIFFERENTIAL EQUATION

NT QUADRATIC EQUATIONS

Nonlinear effects due to crack front plastic yield and slow crack extension in energy release rate and fracture toughness calculations 01 p0140 A72-10993

Step-by-step algorithmic numerical solution for nonlinear Volterra integro-differential equation, considering convergence 01 p0093 A72-11105

Sixth order nonlinear differential equation isolated equilibrium point stability determination, constructing Liapunov function 01 p0094 A72-11125

Nonlinear equations for M-type amplifiers derived from Maxwell equations 02 p0189 A72-11567

Monte Carlo methods for hybrid computer solution of nonlinear parabolic partial differential equations with two spatial dimensions 02 p0186 A72-11657

Liquid motion in circular cylinder with elastic bottom under longitudinal excitation, representing dynamic and kinematic free surface conditions as nonlinear equations 02 p0204 A72-12254

Axisymmetric circular membranes large deflections, solving nonlinear partial differential equations by iterative method in conjunction with finite difference approximations 02 p0296 A72-12526

Variational solutions of nonlinear free boundary integrodifferential Euler equations for rotating star models 02 p0252 A72-12540

Bogoliubov-Mitropolski-Hale integral manifold theorem for perturbed nonlinear differential equations, using generalized variation of parameters formula 03 p0381 A72-12907

Nonlinear differential second order equation system development for gyroscopic coupling of forced nonlinear oscillators 03 p0389 A72-13631

Soviet book on nonlinear problems of inhomogeneous shallow shell theory covering bending, stability, bearing capacity, plasticity criteria, compressibility, etc 03 p0454 A72-14225

Nonlinear ionization wave equation, calculating nonlinear response of unstable positive plasma column to weak pulse disturbance 03 p0399 A72-14346

Nonlinear elliptical equations first boundary value problem, presenting approximation capacity and convergence of straight line procedure 04 p0538 A72-14625

Nonlinear heat conduction equation explicit solution in combustion theory with allowance for gas dynamics model equation and resulting Cauchy problem solution 04 p0595 A72-14643

Nonlinear differential equations systems solution by A-stable numerical integration techniques 04 p0539 A72-14732

Cauchy problem for nonlinear biharmonic equation in Euclidean n-space, deriving a priori inequality estimate by logarithmic convexity of functional F 04 p0539 A72-15044

Matrix representation of nonlinear equation iterations based on polynomial methods, considering convergence and application to parallel computation 04 p0540 A72-15373

Quasi-linear parabolic equations loaded system first boundary value problem for heat and mass transfer equations inverse problems 04 p0540 A72-15545

Superposable and self-superposable MGD flows from nonlinear differential equations, considering entropy, flow velocity and magnetic field strength 05 p0694 A72-16030

Nonlinear transient coupled thermoviscoelasticity problems solution by finite element method and iterative solution for integrodifferential equation 05 p0736 A72-16085

Rectangular variable thickness plate deflection under uniform lateral pressure, solving nonlinear partial differential equations with variable coefficients by iterative procedure 05 p0738 A72-16533

Nonlinear differential equation of second order, investigating integrability criteria 06 p0838 A72-17553

Numerical integration solution of nonlinear equations and two point boundary value problems, using quasi-linearization and imbedding methods 06 p0839 A72-17957

Autonomous two body system described by nonlinear differential equations of motion, obtaining free relative vibration solution in terms of elliptic functions 06 p0849 A72-18694

Gyroscopic error analysis, solving nonlinear equations by continuous Markov processes theory 06 p0819 A72-18724

Power series method with Cauchy formula for nonlinear partial differential equations solution in unsteady periodic temperature oscillations 06 p0905 A72-18727

Algorithm for constructing linear and nonlinear differential and algebraic equations of state variables of nonlinear electronic circuits 07 p0958 A72-18846

Tangent methods for nonlinear equations iterative solution using alternate tangent and derivative values 07 p1026 A72-19039

Averaging techniques for nonlinear integral and integrodifferential equations, considering standard equations with and without rapid and slow variables, asymptotic series application to unsolved problems 07 p1027 A72-19609

Electrodynamics and magnetoelasticity nonlinear Emden-Fowler equation solutions, considering heavy current carrying filaments equilibrium and boundary value problems 07 p1035 A72-19975

Nonlinear difference schemes for quasi-linear transfer equation in gas dynamics and shock wave computations 07 p0971 A72-20085

Gas dynamics K-wave interaction in nonlinear media described by nonlinear partial differential equations 07 p0972 A72-20103

Iteration procedure for approximate integration of nonlinear system of partial differential equations with time lag, presenting upper and lower estimates 07 p1028 A72-20209

Self similar invariant group solutions to Bellman nonlinear partial differential equation for optimal correction problems of control systems motion with random disturbances 07 p0963 A72-20322

Truncation error correction based on Richardson extrapolation in finite difference approximation of nonlinear partial differential operators 07 p1101 A72-20328

Transcendental series solution of Chini-Painleve nonlinear differential equations describing vehicle and meteorite oscillation during planetary atmospheric entry 07 p0964 A72-20594

Goodman-Lance method of adjoints extension for solving boundary value problems of nonlinear differential equation systems 08 p1197 A72-20786

Coefficients estimation in nonlinear differential equations by direct integration followed by unconstrained nonlinear programming 08 p1197 A72-20854

Switching characteristics of MOS channel transistors, solving nonlinear differential equations describing current and potential distribution 08 p1140 A72-21267

Nonlinear differential equations system stability conditions for arbitrary initial perturbations of zero solution, using Liapunov functions 08 p1199 A72-21461

Asymptotic method solution for boundary value problems for nonlinear differential equations describing transonic and slow supersonic flow past thin bodies 08 p1108 A72-21709

Nonlinear beam and plate analysis, obtaining smooth elastic-plastic transition through modified Richard moment-rotation equation application 08 p1249 A72-21923

Hilbert space filling curves for solutions of sets of nonlinear equations 09 p1340 A72-22244

Equilibrium statistics of randomly forced two dimensional viscous flow three mode representation constructed by numerical integration of nonlinear equations system 09 p1293 A72-22459

Riemann invariants method for plasticity theory application to first order quasi-linear systems, considering plastic flow in arbitrary die 09 p1403 A72-22760

Approximate method for nonlinear differential equations of motion solution in flight dynamics, applying to control surface buzz and slender wing oscillations 09 p1262 A72-23453

Numerical solutions of linear and nonlinear hydrostatic primitive equations for frontogenesis forced by nondivergent horizontal wind, noting discontinuities prediction 09 p1347 A72-23651

Third order nonlinear differential equation invariants use to obtain integrable forms 10 p1504 A72-24053

Sobolov-Orlicz anisotropic spaces application to calculus of variations equations with strongly nonlinear coefficients 10 p1505 A72-24215

Numerical solution of nonlinear integrodifferential equation governing finite amplitude wave propagation on concentrated vortices 10 p1468 A72-24419

Algorithms for spatially varying parameters estimation in nonlinear partial differential equations from noisy observations, noting diffusivity in heat equation 10 p1506 A72-24457

Oscillation modes and stability region of harmonic oscillators with homogeneous nonlinear rheological differential equations of motion 10 p1513 A72-24998

Nonlinear differential equations cycle properties and frequency, using Leray-Schauder theorem for cycle existence proof 11 p1675 A72-25325

Perturbation method for asymptotic solutions of initial value problems for hyperbolic wave equations with small nonlinearities 11 p1676 A72-25355

Geometric interpretation of solution existence for nonlinear ordinary differential equations with linear and nonlinear boundary conditions, analyzing funnel of solutions 11 p1676 A72-25503

Boundary value problems to initial value problems transformation method extended by physical parameters invariant properties, noting fluid mechanics nonlinear equations 11 p1616 A72-25878

Control theory application to nonlinear elastic analysis of trusses, partitioning structure into statically determinate stages 11 p1736 A72-25989

Coupled nonlinear equations of motion of large deflections of impacted helical springs, comparing with streak photographs 11 p1688 A72-26061

Method of characteristics for solution of quasi-linear hyperbolic partial differential equations, analyzing frequency response 11 p1678 A72-26551

Nonlinear integral equations solution for heavily loaded actuator disk induced flow field, taking into account blade tip vortices and thrust coefficient effects 11 p1573 A72-26577

Dynamic stability of rapidly heated shallow cylindrical shells, formulating nonlinear equations 12 p1877 A72-27076

Nonlinear equilibrium equations and elastic stability of cylindrical shell weakened by circular hole 12 p1878 A72-27080

Existence and uniqueness of general solutions of initial value problem for nonlinear Maxwell-Boltzmann equation with finite time interval 12 p1836 A72-27122

Equation difference minimization techniques for ordinary nonlinear differential equations approximate periodic solution generation, noting error bounding procedure validity 12 p1836 A72-27240

Nonlinear stochastic partial differential equations solution by graph technique, calculating correlation function and phase change spectrum in phase locked circuit 12 p1837 A72-27575

Variational problems in automatic control theory, presenting existence theorems for solution of boundary value problems for nonlinear differential equations with deviating argument 12 p1837 A72-27995

Differentiation method for complex root calculation for system of nonlinear equations with analytic functions 13 p1985 A72-28710

Shock waves internal structure in gas of elastic spheres, solving nonlinear Boltzmann equation 13 p1944 A72-30029

Variational problem solution for solid strained body with nonlinear stress-strain relation, applying finite element method 14 p2130 A72-30189

Gradient catastrophe /solution derivative discontinuity/ occurrence time for quasi-linear hyperbolic differential equations describing elastic string oscillations 14 p2130 A72-30194

Relaxation method for thermal computation programs to solve nonlinear heat exchange equations for

steady state temperature distribution, discussing numerical instability due to linearization

14 p2170 A72-30684

Polynomial spline function for approximate solution of Cauchy problem for nonlinear differential equations of order n

14 p2126 A72-30716

Russian book on averaging method in nonlinear mechanics covering algorithms and schemes based on variables change, asymptotic methods and applications

15 p2273 A72-31274

Nonlinear differential equations of motion of complex configuration, developing stable solution method

15 p2261 A72-31489

Approximate periodic solutions of second order nonlinear differential equations via step function

15 p2262 A72-31553

Boundary value problem solution uniqueness relation to existence for nonlinear differential equations of arbitrary order satisfying solution compactness condition

15 p2263 A72-31753

Boundary value problems for discrete spectrum of nonlinear ordinary differential operators on unbounded intervals

15 p2263 A72-31760

Nonlinear Boltzmann equation prediction of time correlation functions with long asymptotic time tails

15 p2278 A72-32307

Nonlinear equations systems iterative solution methods convergence, generalizing Varga matrix splitting technique to nonlinear mappings in Banach space

15 p2264 A72-32465

Liapunov functions for nonlinear autonomous difference equations stability analysis, defining difference gradient, principal sum and definite sum

15 p2265 A72-32802

Joint maximum likelihood estimation of three parameters of Weibull distribution, obtaining modified quasi-linearization algorithm for nonlinear equations iterative solution

16 p2416 A72-33348

Variational principles application to nonlinear heat transfer problems, using Euler-Lagrange equation

16 p2478 A72-33435

Nonlinear equations of discrete elastic Cosserat media from multipolar media equations, studying small rotation theory

16 p2425 A72-33591

Onsager irreversibility theory extension to nonlinear constitutive relations and with allowance for inclusion of all thermodynamic variables

16 p2479 A72-33826

Stability of a class of systems of nonlinear differential equations

17 p2574 A72-34348

Approximate solutions of problems involving simultaneous multifunctional nonlinear partial differential equations, noting rectangular plate deflection under lateral pressure

17 p2627 A72-34780

The maximum principle and controllability of nonlinear equations.

17 p2533 A72-34951

Variational principles in nonlinear viscoelasticity.

17 p2633 A72-35402

Book - Nonlinear partial differential equations in engineering, Volume 2

17 p2576 A72-35449

A priori estimates and nonlinear parabolic equations of arbitrary order.

17 p2577 A72-35796

Three point distribution function related to lower order functions for closure of hierarchy of equations for turbulent probability distribution functions

18 p2677 A72-36005

Cameron-Martin-Wiener /C-M-W/ representations of nonlinear random process tested on Burger turbulence for real fluid problem

18 p2677 A72-36010

Steady state response of nonlinear beam under periodic loading, using finite element techniques for nonlinear differential equation

18 p2732 A72-36078

The Cauchy problem for the nonlinear Boltzmann equation in general relativity

18 p2710 A72-36471

Note on the 'alpha'-constant stiffness method for the analysis of non-linear problems.

18 p2739 A72-37172

Nonlinear equations for explosive instabilities of three plasma waves interaction with mutually different linear damping

19 p2838 A72-37326

Nonlinear equations solutions for interior ballistics parameters of solid rocket propellants combustion during rocket engine nozzle opening

19 p2878 A72-37352

Optimal control of plant described by nonlinear hyperbolic equations with variable initial conditions of system, noting constraints on plant phase coordinates

19 p2777 A72-37434

Asymptotic method application to wave propagation in nonlinearly elastic rods, describing displacement field by perturbation series

19 p2875 A72-37885

Numerical integration of nonlinear convective flow equations for arbitrary atmospheric temperature and wind profiles, discussing cloud streets formation

19 p2828 A72-37998

A certain property of standard Fredholm-type nonlinear integro-differential equations

19 p2825 A72-38178

Solution of nonlinear integro-differential Volterra equations and their systems with the aid of power series

19 p2825 A72-38196

Investigation of the solution of a two-dimensional nonlinear Volterra integral equation

19 p2825 A72-38203

Convergence of a multipoint iteration method for solving nonlinear equations

19 p2826 A72-38215

Lyapunov functions for quadratic differential equations with applications to adaptive control.

19 p2826 A72-38264

Waveguides of arbitrary cross section by solution of a nonlinear integral eigenvalue equation.

19 p2773 A72-38292

Investigation of generalized and classical solutions of a mixed boundary value problem in a finite domain for one class of nonlinear second-order parabolic equations

19 p2827 A72-38448

Approximate integration of a nonlinear system of differential equations with time lag

19 p2827 A72-38468

Existence of a unique solution for a class of nonlinear systems of equations and its calculation by iterative methods

19 p2827 A72-38546

German Book - Introduction into nonlinear optics, Volume I

19 p2813 A72-38775

Method of characteristics for nonlinear equations of perturbed motion of fluid near contact point between shock and diffraction waves

20 p2912 A72-39023

Solution of a boundary value problem for a class of nonlinear ordinary differential equations by the method of successive approximations

20 p2945 A72-39463

A modified gradient technique for solving boundary and initial value problems.

20 p2946 A72-39618

Electrodynamics and magnetoelasticity nonlinear Emden-Fowler equation solutions, considering current carrying heavy filaments equilibrium and boundary value problems

20 p2955 A72-40032

Decomposition of multidimensional nonlinear equations of heat-conduction type and construction of nonlinear electrical integrators

21 p3128 A72-40181

Electrical modeling of nonlinear problems of thermal engineering

21 p3128 A72-40182

Nonlinear differential equation periodic solution approximation by pseudo-linear representation of nonlinear terms effects on single harmonic, using describing function matrix method

21 p3076 A72-41314

Non-linear elastic constitutive equations.

21 p3125 A72-41514

Nonlinear equilibrium equations for hinged flat circular and spherical membranes under large axisymmetric elastic deformations due to internal pressure

21 p3125 A72-41516

Non-linear rotor bearing behavior.

21 p3061 A72-41518

Group properties and invariant solutions of electric-field equations in the case of nonlinear Ohm's laws

21 p3086 A72-41654

Reissner nonlinear equations for stability analysis of shallow shells of revolution, noting critical loads range and error analysis

22 p3232 A72-41856

Investigation with the aid of a Fourier method of the classical solution of a multidimensional composite problem for a class of hyperbolic equations of the second order with a nonlinear operator right-hand part

22 p3198 A72-41897

Solution method for some boundary problems of nonlinear hyperbolic-type equations and propagation of weak shock waves

22 p3164 A72-41904

Time evaluation of discontinuity occurrence in solutions of boundary problems for second-order hyperbolic quasi-linear systems

22 p3198 A72-41912

A collocation solution of the nonlinear equations for axisymmetric bending of shallow spherical shells.

22 p3232 A72-41938

A priori estimates and Harnack's inequality for general solutions of second-order degenerate quasi-linear parabolic equations

22 p3198 A72-42159

On the solution of non-linear simultaneous equations with particular reference to fluid-dynamics.

22 p3199 A72-42325

Diatomic molecular dissociation in pure gas and mixtures with inert diluent, expressing as set of coupled quadratically nonlinear differential equations [AICHE PAPER 6B]

22 p3208 A72-42400

Three dimensional thermoelastodynamic theory for elastic beams, deriving nonlinear motion equations by combined expansion and variational methods

22 p3235 A72-42523

Asymptotic method for nonlinear wave systems of periodic structure

22 p3155 A72-42657

On the perturbation method in the stability analysis of continuous systems.

22 p3206 A72-42842

Vertical asymptotes and bounds for certain solutions of a class of second order differential equations.

22 p3199 A72-42914

Nonlinear natural vibrations of rectangular plates and cylindrical panels

22 p3242 A72-43134

Calculation of transient processes in a capacitance parametron by the phase approximation method

23 p3312 A72-43351

Widely convergent method for finding multiple solutions of simultaneous nonlinear equations.

23 p3308 A72-43400

Numerical integration of nonlinear differential equations in nonlinear circuits analysis, obtaining information on unsteady processes from calculation with controlled level time quantization step

23 p3269 A72-43444

Problem of the spatial localization of thermal disturbances in nonlinear heat-conduction theory

23 p3356 A72-43529

Representation of the solution of a nonlinear differential equation in the form of a path integral

23 p3308 A72-43580

Nonlinear mechanics perturbation method for Liapunov functions construction, noting application to nonlinear differential equations

23 p3308 A72-43582

Method of equivalent turns in the kinematics of inertial systems

23 p3311 A72-43583

Equilibrium equations and deformation of elastoplastic thin isotropic cylindrical shell with circular hole, noting nonlinear partial differential equations for plate displacements

23 p3345 A72-43587

Influence of a nonlinearity in a coherent accumulator of pulse signals on the gain in the signal-to-noise ratio

23 p3264 A72-43762

The internal boundary value problem for the Boltzmann equation in the steady state and weakly nonlinear

23 p3280 A72-43820

Asymptotic behavior of solutions of nonlinear parabolic equations.

23 p3309 A72-43979

A priori bounds and upper and lower solutions for nonlinear second-order boundary-value problems.

23 p3309 A72-43980

Dual extremum variational principles relevant to nonlinear heat transfer, applying to temperature distribution on thin walled spherical spacecraft surface

24 p3465 A72-45474

A numerical integration method useful for studying ionospheric phenomena.

24 p3399 A72-45582

Application of the method of mechanical quadratures to the approximate solution of nonlinear singular integral equations

24 p3419 A72-45646

Straightforward difference scheme for nonlinear parabolic equations in polar coordinates

24 p3420 A72-45649

NONLINEAR FEEDBACK

Self oscillating dc-dc converter analysis and optimal design, modeling by single loop nonlinear feedback system

04 p0465 A72-14571

Control system stability with nonlinear feedback in steady equilibrium state

07 p0963 A72-20321

Hammerstein form nonlinear systems class invertibility and reproducibility criteria derivation, noting decoupling possibility by dynamic precompensation and nonlinear state feedback

10 p1502 A72-23781

Computerized synthesis technique for nonlinear feedback control systems, incorporating circle and Popov criteria

13 p1936 A72-29107

Saturating nonlinear feedback systems stability under bounded input excitation, discussing error signals magnitude and duration

15 p2212 A72-32246

Effect of nonlinearity in the feedback circuit of a recirculation-type comb filter

20 p2906 A72-38893

Stabilities and settling times of nonlinear and time-varying feedback systems.

22 p3161 A72-41937

NONLINEAR FILTERS

Learning-identification of unknown nonlinear discrete systems, using local estimation results for global function learning

01 p0046 A72-11199

Distributed systems modeled by partial differential equations, identifying unknown parameters by Galerkin method using steepest descent method and nonlinear filter

04 p0505 A72-14674

Optimal nonlinear discrete filters with finite memory for polynomial signals, discussing synthesis with aid of minimax method

04 p0505 A72-14998

Suboptimal nonlinear filter performance evaluation methods based on Kolmogorov equations for Markov process transition density function

04 p0505 A72-15040

Optimal nonlinear logical filters for noise protection of space vehicle servosystems

05 p0726 A72-16460

Nonlinear spatial filter synthesis by one-to-one signal-to-reference beam ratio and optimum exposure condition

05 p0663 A72-16676

Numerically exact nonlinear filter synthesis, describing confidence intervals for error performance statistical inferences

08 p1144 A72-20850

Hybrid computer synthesis and simulation algorithm for optimal discrete nonlinear filters, giving timing, accuracy and equipment requirement estimates

08 p1137 A72-20851

Optimal filtering for state estimation of nonlinear dynamic models observed with discrete noisy observations by retaining second order terms in series approximation

08 p1145 A72-20863

Nonlinear filter dynamics for stochastic optimal control for quadratic cost functional, evaluating performance

08 p1145 A72-20866

Nonlinear filtering synthesis of optimal receiver for pseudorandom phase shift keyed signal with arbitrary modulation angle and white noise background

10 p1436 A72-24510

Nonlinear filtering for random signals in statistically unknown noise, noting application to satellite orbit determination, aircraft navigation and missile tracking

11 p1611 A72-25986

Integrated inductorless quadratic bandpass filters for constant bandwidth wide frequency range, using IC analog multipliers network

13 p1927 A72-28403

Forced oscillations in RC amplifier with negative feedback through nonlinear bandpass filter with varicaps

13 p1931 A72-29266

Bayesian estimation for nonlinear filtration of nonstationary non-Gaussian radio signals, deriving second central moments and parameter estimate errors

15 p2195 A72-31656

Regenerative nonlinear RC amplifier oscillations due to series opposed varicap diode capacitance

18 p2665 A72-36109

Nonlinear double T-shaped RC filter

19 p2774 A72-38417

Effect of nonlinearity in the feedback circuit of a recirculation-type comb filter

20 p2906 A72-38893

Real time estimation of trajectory for lifting reentry vehicle of shuttle orbiter type, discussing iterated nonlinear filter and adaptive filter

20 p2966 A72-39126

Optimal frequency-difference communications system with manipulated amplitudes

22 p3154 A72-42237

The application of Monte Carlo methods to the nonlinear filtering problem.

23 p3274 A72-43541

Some numerical results using Kalaba's new approach to optimal control and filtering.

23 p3274 A72-43543

Integrated navigation systems and Kalman filtering - A perspective.

24 p3386 A72-44642

NONLINEAR PROGRAMMING

Nonlinear programming iteration scheme for fuel-time optimization of satellite orbital rendezvous terminal phase

03 p0437 A72-13838

Coefficients estimation in nonlinear differential equations by direct integration followed by unconstrained nonlinear programming

08 p1197 A72-20854

Carrier based attack aircraft allocation model formulation and solution for maximum inflicted target damage, using sequential unconstrained minimization technique with nonlinear programming

08 p1256 A72-21469

Nonlinear programming analysis of free vibration of simply supported beam

08 p1249 A72-22136

Man machine automatic control system structural synthesis, treating system operation as nonlinear programming problem

09 p1291 A72-23438

Nonlinear programming and parameter optimization algorithms for constrained feedback control system design

10 p1441 A72-23790

Nonlinear programming solution of optimal control problems, using methods of centers and feasible directions

10 p1455 A72-23797

Flight vehicle structures optimum design for random vibration environment, presenting formulation as nonlinear programming problem

11 p1736 A72-26003

Path arrangement optimization method for fluid distribution network with separable and concave cost function, using simplex method in nonlinear programming

13 p2053 A72-28423

Computerized optimal design by nonlinear programming for minimum weight elastic plates crossed with rigid ribs for vibrational loading to meet natural frequencies condition

14 p2165 A72-30576

Linear electric circuits optimal synthesis as nonlinear programming of network parameters, discussing approximation algorithms

19 p2776 A72-37306

Electric circuits design by combined network synthesis and optimization methods, noting approximation by nonlinear programming

19 p2776 A72-37308

Frequency response optimization of electric filters, modulators and impedance matching circuits using minimax criterion, noting nonlinear programming sequence

19 p2771 A72-37310

Man machine automatic control system structural synthesis, treating system operation as nonlinear programming problem

19 p2782 A72-38521

Nonlinear programming in computerized electronic circuits design, discussing optimization methods and real time operation

19 p2782 A72-38578

The branch and boundary method as a regular method of solving irregular problems of mathematical programming. I

22 p3198 A72-42188

Minimum weight elastic structure designs under dynamic loads with nonlinear constraints on stress displacements and natural oscillation frequencies

22 p3236 A72-42737

A survey of methods of feasible directions for the solution of optimal control problems.

23 p3274 A72-43537

NONLINEAR SYSTEMS

Random background noise effect on nonlinear self oscillation envelope passage time moments, discussing relationship between amplitude and frequency stabilities

01 p0035 A72-10032

Duffing type quasi-linear differential equation system, obtaining ultraharmonic resonance by small parameter and harmonic balance methods for comparison with analog computer solutions

01 p0101 A72-10034

Imperfect nonlinear system elastic buckling critical load calculation by higher order approximation, using perturbation approach and discrete coordinate diagonalized system

01 p0136 A72-10035

Nonlinear hydromagnetic waves in finite beta collisionless plasma, calculating space-time evolution with nonlinear integrodifferential equation

01 p0107 A72-10143

French monograph on extremum values of function with two variables and nonlinear feedback control systems stability, using associate recurrence solutions properties

01 p0044 A72-10164

Frequency conditions of absolute stability for closed automatic control system with nonlinear unsteady units

01 p0045 A72-10499

Controllability of dynamic systems with motion described by nonlinear differential equations

01 p0045 A72-10500

Error fluctuation component spectral density determination in closed automatic nonlinear system for controlling random vibration spectrum

01 p0045 A72-10505

Difference analog of nonlinear hydrodynamic boundary value problem from Navier-Stokes steady state theory

01 p0050 A72-10576

Learning-identification of unknown nonlinear discrete systems, using local estimation results for global function learning

01 p0046 A72-11199

Step width for gradient projection method in Hilbert space for optimal linear control problems with quadratic functional

01 p0047 A72-11386

Nonlinear mechanics and stability - Conference, Rome, February 1970

02 p0251 A72-11492

Structural analysis of cable stayed bridge scale model with fractional and full loading, showing system linear behavior with small displacements and real nonlinearities, respectively

02 p0199 A72-11515

Nonlinear systems absolute stability calculation, considering time lag, backlash type nonlinearity and process controller

02 p0196 A72-11674

Elastic continuous media nonlinear models approximation, obtaining Euler-Lagrange functions

02 p0259 A72-12234

Self-correcting incremental solution procedure for nonlinear structural mechanics, noting application to systems with many degrees of freedom

02 p0260 A72-12272

Asymptotic method for investigating multiwave interaction processes in one dimensional weakly nonlinear distributed systems with slowly changing parameters

02 p0261 A72-12585

Frequency fluctuations in nonlinear self oscillating system in presence of periodic nonstationary random noise effects

02 p0195 A72-12586

Statistical linearization approach to determine approximate instantaneous correlation matrices of nonlinear structure response to nonwhite excitation

02 p0298 A72-12663

Free flight simulation tests for V/STOL aircraft nonlinear attitude control system adaptation to helicopter pitch and roll control

02 p0155 A72-12714

Describing function method for nonlinear systems under stochastic input, considering statistical optimizations/linearization and self oscillation under noise

03 p0337 A72-13074

Neighboring optimal feedback control for multiinput nonlinear dynamical systems with discontinuous control, applying to minimum time satellite attitude acquisition problem solution

03 p0338 A72-13407

Frequency criteria for stability of nonlinear multivariable RLC networks with bounded solutions approaching equilibrium

03 p0338 A72-13411

Tunnel diode quartz oscillator frequency stability improvement and dc power requirement reduction using nonlinear feed circuits

03 p0331 A72-13555

Nonlinear thermoviscoelasticity problem exact solution expressed as product of two functions, formulating conditions

03 p0445 A72-13576

Additive type composite oscillations in nonlinear damped vibratory system with two degrees of freedom, presenting modified Galerkin method

03 p0382 A72-13628

Read avalanche diode noise theory, showing carrier current modulation and lf and hf noise coupling in nonlinear regime

03 p0333 A72-13848

Mathematical modeling methodology for communication receiver life cycle EMC decisions, considering analysis and prediction problems with emphasis on nonlinear circuits and systems

03 p0324 A72-14034

Nonlinear oscillations stochastic instability in dynamic systems, discussing nonequilibrium statistical mechanics

03 p0390 A72-14316

Closed-loop nonlinear sampled-data systems with sampler and finite Hankel transformable distributed elements, deriving frequency domain stability criteria

04 p0504 A72-14662

Nonlinear stochastic systems stability conditions description by Volterra integral equation, applying to distributed parameter feedback control system with nonlinear amplifier of random gain

04 p0504 A72-14663

Sequential interpolating estimation algorithm derivation for distributed-parameter noisy dynamic systems described by nonlinear partial differential equations

04 p0538 A72-14669

Nonlinear plant and observation models with white Gaussian noise and continuous data, obtaining state vector a posteriori probability density for optimal prediction

04 p0506 A72-15112

Third order nonlinear van der Pol oscillating systems, discussing digital computer verification for existence of stable limit cycles in state space trajectory plots

05 p0639 A72-15806

Stationary nonlinear dynamic systems identification, using modified differential approximation technique
[ASME PAPER 71-WA/AUT-11]

05 p0682 A72-15955

Single- and many degree of freedom nonlinear structural systems transient dynamic response by presentation of equations of motion, damping and restoring force functions

05 p0736 A72-16082

Quasi-periodic solution of nonlinear differential system in case of resonance, concerning Duffing equation

05 p0682 A72-16120

Probabilistic output analysis of dynamic nonlinear system with random characteristics by functional Volterra series

05 p0641 A72-16315

Nonlinear multivariable and linear systems optimal control in aerospace field, discussing use of performance indexes for fuel consumption, process evolution time or combination

05 p0725 A72-16453

Optimal closed loop control of stochastic nonlinear systems by expanded cost function applied to reduced terminal error atmospheric entry problem

05 p0685 A72-16462

Nonlinear control systems of vehicles angular orientation, investigating dynamic properties by method of harmonic linearization

05 p0727 A72-16474

Controlled motion dynamics of spacecraft performing maneuvers, applying point transformation to third-order nonlinear system moving about center of mass in lateral motion

05 p0730 A72-17029

Optimal control of one dimensional physical system with delayed argument described by nonlinear first order hyperbolic partial differential equations, using maximum principle

05 p0691 A72-17138

Optimal control algorithm for nonlinear stochastic systems ensuring probability-wise stability and minimum error, using Liapunov theory and dynamic programming

05 p0691 A72-17141

Nonlinear optimal control problems with undetermined final time, using conjugate-gradient method

06 p0792 A72-17312

Third order nonlinear systems phase plane analysis, noting applicability to unity feedback closed-loop systems with linear memory

06 p0792 A72-17313

Suboptimal feedback control for nonlinear dynamic processes, presenting control algorithm based on linear plant optimal solution

06 p0792 A72-17314

Nonlinear stochastic systems analysis by extended Volterra-functional method for first and higher order linear plants with constant or time varying parameters

06 p0838 A72-17376

Higher order nonlinear autonomous oscillation system limit cycle and stability determination by numerical solution based on Andronov point transformation and Liapunov theory

06 p0838 A72-17377

Computer aided steady state response analysis for nonlinear electric circuits with periodic input, using Newton algorithm with rapid convergence

06 p0779 A72-17480

Validity proof of asymptotic methods in oscillation theory of one dimensional nonlinear dynamic systems described by hyperbolic and parabolic differential equations

06 p0839 A72-17681

Random vibrations nonlinear theory, investigating nonlinear systems response to random excitation via Markov processes modeling

06 p0896 A72-17961

Frequency criterion of weak instability in nonlinear control systems

06 p0794 A72-18304

Nonlinear oscillations in mechanics - Conference, Kiev, U.S.S.R., August 1969

06 p0849 A72-18692

Lightly damped nonlinear mechanical oscillators under random excitation, calculating stationary response frequency and autocorrelation by heuristic procedures

06 p0849 A72-18693

Nonlinear self excited oscillations in uniformly distributed oscillators interacting with traveling transverse or surface waves of elastic body

06 p0849 A72-18698

Nonlinear elastic systems with distributed parameters, obtaining single frequency mode random oscillations solution of boundary value problem by asymptotic method and Markov process

06 p0850 A72-18700

Mechanical systems with nonlinear position functions, elastic elements or self damping, investigating oscillation mode onset and stability conditions

06 p0850 A72-18701

Aerodynamic radial bearing analysis based on Reynolds equation, emphasizing gas bearing nonlinear oscillation stability

06 p0824 A72-18702

Nonlinear resonance oscillations of flexible rod and elastic cylindrical shell under potential and nonpotential forces, investigating motion instability

06 p0900 A72-18704

Elastic systems nonlinear oscillations with moving inertial loads, noting standing waves superposition

06 p0901 A72-18706

Nonlinear solid body system rotating and oscillating parts effect on spatial vibration stability, deriving excitation-natural frequencies relationship

06 p0850 A72-18711

Single frequency oscillations in nonlinear mechanical systems described by one dimensional mixed boundary value problems, using asymptotic methods

06 p0850 A72-18715

Nonlinear self oscillation solution for systems with two degrees of freedom, comparing with harmonic linearization method for error of small parameter method

06 p0851 A72-18721

Nonlinear mechanical oscillation systems analysis by analog computer, exemplifying pendulum rotating about vertical axis

06 p0851 A72-18725

Perturbation theorems proving for nonlinear systems of differential equations with integral solution of linearized equation

06 p0840 A72-18739

Numerical algorithm for Galerkin solutions of nonlinear ordinary differential equations in dynamic system applications

07 p1025 A72-18785

Nonlinear dynamic system mathematical model for unit mass particle escape trajectories from potential well, taking account of trapped motions and stable oscillations

07 p1025 A72-18807

Stability analysis of steady control systems acted upon by random signal in single valued one dimensional nonlinearity form, using statistical linearization

07 p0959 A72-18989

System parameters random step changes effect on nonlinear system steady vibration stability

07 p1088 A72-19172

Book on asymptotic behavior and stability in ordinary differential equations covering linear and nonlinear systems, Liapunov and analytical-topological methods

07 p1026 A72-19184

Cross modulation relationship to intermodulation product based on third order distortions in nonlinear system

07 p0941 A72-19255

Real time near optimal closed loop control solution to fixed time nonlinear differential game by periodically updating to two point boundary value problem

07 p1027 A72-19278

Multiinput and multioutput linear and nonlinear dynamic system maximum likelihood identification based on state vector formulation and optimal filter use

07 p0959 A72-19286

Quasi-time optimal nonlinear controller for steerable antennas or telescopes in target acquisition or slew mode, predicting performance by digital simulation

07 p0959 A72-19288

Hyperstable algorithm for multiinput and output systems identification through equation error method, representing scheme as equivalent time varying nonlinear feedback system

07 p1027 A72-19290

Singular perturbation of absolute stability of Lure-Postnikov nonlinear systems described by differential equations with small parameters at higher derivatives

07 p1027 A72-19293

Harmonic oscillations sum conversion by two terminal pair network with complex nonlinearity

07 p0956 A72-19565

Model-following control for nonlinear multivariable plants, considering implicit algorithm solution and application to variable stability aircraft control synthesis

07 p0961 A72-19708

Optimal control on nonlinear multivariable plant with common constraint on control action, presenting linear programming algorithm

07 p0962 A72-19717

Nonlinear multivariable system optimal control with respect to time and fuel consumption, discussing Gauss-Newton and Davidson methods and application to geostationary satellite

07 p0962 A72-19719

Geometrical methods in fluid mechanics, solving quasi-linear nonelliptic systems by method of characteristics

07 p0969 A72-20063

Nonlinear controls for single axis gyro platforms, using time optimal Luenberger observers

07 p0989 A72-20278

Sequential testing of actual and calculated error covariances consistency in recursive nonlinear estimators, noting method application to linear filters

08 p1197 A72-20857

Discrete-time nonlinear estimators digital implementations by computerized Monte Carlo method, comparing with alternative techniques

08 p1145 A72-20864

Conditional mean state estimate approximation for nonlinear systems by parallel computation to reduce computer time

08 p1145 A72-20868

Random vibration theory and Markov processes in nonlinear stochastic systems with probability and asymptotic methods application

08 p1205 A72-20965

Parametric oscillations of nonlinear systems prone to self excitation, using asymptotic method

08 p1206 A72-21243

Nonlinear system of differential equations for gravity perturbation on geometrical form of thin axisymmetric cavity in heavy fluid

08 p1151 A72-21705

Nonlinear dynamic response of deformable solids under time and space dependent thermal and mechanical loads determined by finite element method

08 p1248 A72-21822

Nonlinear closed loop system reduction of differential trajectory sensitivity to continuous variations or external disturbance

09 p1340 A72-22245

Mechanical system with inertial vibration sensor and nonlinear spring, obtaining global asymptotic stability of zero solution of differential equations describing natural vibration

09 p1399 A72-22697

Nonlinear systems controllers design based on Liapunov functions and time domain ratio criterion, presenting digital computer algorithm

09 p1290 A72-23090

Generalized polynomial operators for nonlinear systems analysis, presenting local invertibility theorem

09 p1341 A72-23092

State estimation for nonlinear discrete-time system based on quantized data, presenting maximum likelihood estimate solution and Monte Carlo simulation results

09 p1290 A72-23095

Quasi-harmonic vibrations of dynamic system with arbitrary number of degrees of freedom and finite number of discrete nonlinearities, using Van der Pol method

09 p1352 A72-23178

Stability regions of phase-locked AFC with nonlinear control circuit, describing system dynamics by differential equations

09 p1290 A72-23180

Nonlinear dynamics of flight vehicle - Conference, University of Technology, Loughborough, England, March 1972

09 p1407 A72-23451

Nonlinear dynamic motion response analysis of flight vehicles typified by continuously changing vibration damping and frequency

09 p1262 A72-23452

Beecham-Kryloff-Bogoliubov approximation method application to a degree of freedom nonlinear systems, using averaged kinetic energy and virtual work terms in Lagrange equation

09 p1342 A72-23454

Single degree of freedom systems with nonlinear spring characteristics of skew symmetric form, discussing 1/2 subharmonic oscillation analysis by harmonic balance method

09 p1342 A72-23455

Liapunov functional stability analysis in structural dynamics problems including wave equations with nonlinear damping

09 p1407 A72-23457

Random vibration of linearly elastic lumped mass systems containing, nonlinear damping to ideal stationary Gaussian white noise excitation

09 p1408 A72-23460

General structure steady state response under harmonic forcing in internal resonance relation, noting inertial nonlinearity effects on autoparametric interactions and energy flow

09 p1408 A72-23462

Applied nonlinear mechanics problems solutions by variable scale method, choosing transformations for linearization of differential equations

09 p1343 A72-23602

Nonlinear vibrations under random excitation, discussing equivalent linearization and small parameter perturbation methods and Fokker-Planck equation

09 p1353 A72-23604

Nonlinearity effects on random vibration displacement and frequency characteristics of one degree of freedom system, using Fokker-Planck equation

09 p1353 A72-23605

Zaidenberg correlation method for nonlinear systems dynamic properties under random excitation, determining statistically equivalent linearized terms for equations of motion

09 p1353 A72-23607

Nonlinear systems optimal design mathematical modeling, discussing synthesis, manufacturing, production, exploitation and evaluation

09 p1343 A72-23610

Hartman-Olech theorem to prove asymptotic stability of mechanical system with nonlinear elastic characteristic, analyzing differential equations of motion 09 p1343 A72-23612

Hammerstein form nonlinear systems class invertibility and reproducibility criteria derivation, noting decoupling possibility by dynamic precompensation and nonlinear state feedback 10 p1502 A72-23781

Optimal estimates for nonlinear dynamic systems with time delay, using calculus of variations 10 p1454 A72-23784

Differential geometric methods to extend linear system theory to nonlinear classes, considering differential equations, controllability, optimal control, stochastic processes and bilinear system problems 10 p1503 A72-23788

Compression of data from measurements in real time nonlinear estimation to reduce data processing requirements without performance deterioration, applying to reentry vehicle tracking 10 p1442 A72-23802

Optimal nonlinear estimation problem with nonlinear plant and observation models obtaining state vector a posteriori probabilities for prediction and smoothing via partition theorem [AD-736521] 10 p1455 A72-23803

Stochastic nonlinear system one-step optimal dual control instead of separation control policy for performance improvement 10 p1456 A72-23810

Optimal closed loop control of discrete stochastic nonlinear systems, considering guidance and navigation for space and terrestrial vehicles 10 p1456 A72-23811

Optimal closed loop control of discrete stochastic nonlinear systems, obtaining solution by cost function in power series around deterministic trajectory 10 p1457 A72-24499

Antisymmetric pseudorandom signal performance in measurement of second order kernels in Volterra series representation of nonlinear system by cross correlation 10 p1439 A72-24805

Periodic motions stability of nonlinear control systems with energy consumption, using contact transformations 10 p1458 A72-25074

Optimal control problems characterized by nonlinear Volterra equations system, obtaining necessary conditions for extremality in maximum principle integral form 11 p1675 A72-25319

Global controllability of nonlinear differential systems during linear system perturbation, discussing controllable and uncontrollable parts splitting and null domain nature 11 p1608 A72-25323

Nonlinear resistive network analysis by piecewise linear mappings, studying Lipschitz condition and global homomorphism 11 p1608 A72-25360

Nonstationary nonlinear multidegree-of-freedom systems resonant response analysis by asymptotic method, investigating gyroscopic system for combination differential resonances [AIAA PAPER 72-401] 11 p1629 A72-25422

Longitudinal and transverse vibrations and transient response of elastically coupled nonlinear mechanical system 11 p1732 A72-25534

Accuracy improvement of nonlinear systems phase trajectories graphic construction, noting second order ordinary differential equations solution 11 p1733 A72-25547

Probabilistic output analysis of dynamic nonlinear system with random characteristics by functional Volterra series 11 p1610 A72-25798

Suboptimal feedback control law synthesis for nonlinear systems, using second order approximation to optimal control 11 p1610 A72-25872

Computer aided iterative design of nonlinear single loop control system with sinusoidal describing function and time response display capability 11 p1601 A72-26042

Static deflection effect on nonlinear spring mass system step function response, considering approximate calculation of oscillation period 11 p1688 A72-26372

Equations of motion for torsional vibrations in system with nonlinear elastic term and variable moments of inertia, noting analog computer simulation 11 p1739 A72-26982

Natural vibration modes of coupled spring-mass nonlinear system with two degrees of freedom from stability analysis 12 p1844 A72-27245

Perturbation procedure for weakly coupled oscillators in connection with statistical mechanics ergodic problem and nonlinear interaction models 12 p1844 A72-27248

AM/PM conversion and transfer in nonlinear signal transmission systems, calculating coefficients as function of multicarrier powers for intelligible crosstalk 12 p1782 A72-27554

Mathematical model for hydraulic fatigue testing machine, analyzing nonlinear control stability of vibratory loading process 12 p1796 A72-27978

Fourth order normal modes and resonances of nonlinear vibrations, applying to gyro horizon compass sensitive element gimbal motion 13 p2000 A72-28382

Stability and oscillation in linear and nonlinear systems, examining existence of T-periodic solutions /harmonic forced vibrations/ 13 p2000 A72-28484

Averaging technique for nonlinear viscoelastic dynamic problems, considering forced oscillations of oscillator with weakly nonlinear hereditary elastic characteristics 13 p2054 A72-28551

Popov frequency criterion analog for stochastic nonlinear continuous systems with random parameters and disturbances, investigating stability 13 p1935 A72-28608

Additional operator method application to nonlinear servosystems self adjusting circuits design, presenting system simulation results 13 p1935 A72-28611

Shock wave solutions of nonlinear hyperbolic system of conservation laws, considering case of zero viscosity 13 p1940 A72-28616

Differential systems perturbation method by association with easy-to-integrate reduced system, applying to nonlinear mechanics 13 p1987 A72-29780

Transients analysis for nonlinear branched dynamic systems by integral manifold and small parameter method 13 p2007 A72-29997

Linearization method to determine changes in principal harmonic resulting from nonlinear device characteristic deformation due to HF components 13 p1937 A72-30019

Frequency criterion of weak instability in nonlinear control systems 13 p1937 A72-30072

Absolute stability of nonlinear automatic control systems based on root locus trajectories and Popov line hodographs 13 p1937 A72-30094

Graphical design technique based on Nyquist plane construction using circle criterion for nonlinear systems controller synthesis 14 p2091 A72-30375

Parameter resonances influenced by nonlinear damping amplitude-limiting due to vibrating systems nonlinearities with periodic coefficients 14 p2131 A72-30712

Nonlinear resonant circuits analysis, noting steady state operation of ferroresonant circuit with staircase response curve and synchronization conditions 14 p2132 A72-31103

Short signal pulse shaping based on phase and amplitude selective properties of distributed parametric amplifiers operating under nonlinear conditions 14 p2090 A72-31112

Laser amplifier nonlinear properties by simplification of partial differential equations of amplitude and phase behavior, considering signal pulse deformation 14 p2111 A72-31113

Nonlinear autooscillatory systems forced vibration under random perturbations, calculating dynamic processes by statistical linearization 14 p2132 A72-31114

Nonlinear coupled cyclotron oscillators excitation by external sine wave force, analyzing amplitude/phase variation and negative absorption 14 p2132 A72-31115

Ferroresonant circuit with inductor, resistor, nonlinear ferrocapacitor and voltage source, deriving oscillation stability condition 14 p2090 A72-31119

Van der Pol oscillator periodic pulling behavior under weak perturbation near natural frequency, analyzing Fourier frequency spectrum 14 p2132 A72-31122

Van der Pol oscillator acted upon by weak random noise, evaluating oscillations envelope dispersion from probability density function and phase derivation 14 p2132 A72-31123

Nonlinear oscillation systems mathematical model, determining periodic mode parameters, self excitation and damping mechanisms by point mapping method 14 p2133 A72-31126

Nonlinear self excited oscillations with negative hysteresis in automatic control systems 14 p2091 A72-31127

Quasi-conservative optimal nonlinear self excited oscillation systems theory for automatic control, telemechanics and computer applications 14 p2133 A72-31130

Nonlinear approximation of slowly changing standing waves in self excited parametric oscillators with distributed and bulk structures 14 p2090 A72-31131

Nonlinear variable transformation method to determine locking band and transition processes in automatic phase and frequency control systems 14 p2087 A72-31132

Nonlinear processes in oscillatory systems with semiconductor diodes, calculating amplitude and phase characteristics in steady state and transient conditions 14 p2090 A72-31133

Van der Pol and nonlinear parametric oscillators fluctuations due to random noises analyzed by averaging method and discrete Markov processes 14 p2133 A72-31134

Rectangular plate nonlinear lumped-parameter model for large displacement amplitudes, deriving differential equations of motion via Hamilton principle and Euler equations 14 p2169 A72-31148

Nonlinear microwave circuit feedback model analysis by describing function in control theory, applying to oscillator phase locking problem 15 p2210 A72-31355

Nonlinear electronic /transistor/ system mapping-on by matrix dynamic transform algorithms, comparing with Newton-Raphson method 15 p2210 A72-31491

Parameter-dependent linear and nonlinear equation systems solution by approximation polynomials, developing numerical algorithms 15 p2261 A72-31496

Partial differential equations of motion for nonlinear mechanical systems solved by Lanczos formula, discussing prismatic cylinder oscillations under uniformly distributed transverse load 15 p2275 A72-31729

Nonlinear systems normal mode vibrations analysis by group theory using symmetry properties 15 p2275 A72-31732

Globally controllable nonlinear differential systems arising from linear system under perturbation 15 p2264 A72-31762

Optical field emission effects on photoelectron emission nonlinearity from metal cathode using ultrashort mode locked laser pulses 15 p2250 A72-32303

Mathematical models for electromagnetic interference in electronic equipment, discussing nonlinear circuit analysis 15 p2201 A72-32568

Automatic control theory trends /1950-1970/, discussing nonlinear, discontinuous and adaptive systems, optimization problems, Liapunov stability theory, etc 15 p2212 A72-32576

High speed deterministic adaptive controller for linear and nonlinear plants, identifying control law from state and input data by linear regression procedure 15 p2212 A72-32794

Limit set configuration of optimal nonlinear feedback control scheme in n-dimensional state space 15 p2213 A72-32797

Damping perturbation of high order nonlinear autonomous Liapunov system, reducing system equations integration to quadratures via transformation to lower order quasi-linear nonautonomous system 16 p2422 A72-32938

Finite element method application to nonlinear dynamic problems exemplified by study of plastic deformation behavior of cylindrical billet under impact of heavy rigid body 16 p2466 A72-33019

Group perturbation method for accuracy analysis of nonlinear stochastic automatic control systems, noting computer time reduction 16 p2371 A72-33091

Observability conditions for nonlinear and unsteady linear systems, noting control systems design 16 p2371 A72-33092

Nonlinear vibration damper system subject to forced vibrations considered as stochastic processes in form of white noise and stationary and ergodic processes 16 p2467 A72-33144

Averaging and Ritz methods for solution approximation of nonlinear periodic and combined resonances in vibrating systems with multiple degrees of freedom 16 p2424 A72-33145

Single degree of freedom nonlinear mechanical system vibration characteristics calculation by averaging procedure, taking into account energy dissipation 16 p2424 A72-33279

Optimal filtering estimate of noisy nonlinear partial differential distributed parameter system, using least squares and invariant imbedding techniques 16 p2416 A72-33575

Nonlinear generalizations of matrix diagonal dominance with application to Gauss-Seidel iterations 17 p2573 A72-34220

Application of statistical linearization techniques to nonlinear multidegree-of-freedom systems.
[ASME PAPER 71-WA/APM-5] 17 p2624 A72-34315

State dependent state variable feedback method to control multiple input multiple output nonlinear and/or time varying systems
17 p2532 A72-34420

Nonlinear system consisting of gas filled tube with pressure sensitive heat source, noting oscillation evolution due to equilibrium perturbation
[ASME PAPER 72-APM-21] 17 p2580 A72-34796

Design of nonlinear networks with a prescribed small-signal behavior.
17 p2533 A72-35199

An approximate analysis of non-linear non-conservative systems subjected to step function excitation.
17 p2582 A72-35412

Russian book on numerical methods in optimal control systems theory covering functional extremum, dynamic programming, control synthesis and statistical linearization of nonlinear systems
17 p2533 A72-35458

Stability and transient behavior of composite nonlinear systems.
17 p2534 A72-35530

Numerical solution of an optimal control problem with a probability criterion.
17 p2534 A72-35531

Reachable sets and singular arcs for minimum fuel problems based on norm-invariant systems.
17 p2534 A72-35533

Equivalent predictions of the circle criterion and an optimum quadratic form for a second-order system.
17 p2577 A72-35534

New description of a first harmonic approximation for nonlinear distributed parameter systems
17 p2534 A72-35722

Fundamental, harmonic and combination frequency components amplitude analysis via dual input describing function for nonlinear element response under two incommensurate frequency sinusoidal signals
18 p2671 A72-36051

Nonlinear dynamic feedback control systems modeling by parameter estimation scheme with polynomial representation for state variables
18 p2672 A72-36057

Feedback controller synthesis from nonlinear system modeling by linear equations, proving theorem relating stability properties
18 p2672 A72-36060

The effects of damping on a non-linear system with two degrees of freedom.
18 p2709 A72-36080

Nonlinear current oscillations in a plasma diode
18 p2714 A72-36205

Output signal-to-noise ratio of a nonlinear device and bandpass filter.
18 p2666 A72-36334

Criteria for nonlinear systems controllability in terms of state variable analytic function and derivatives, implying strong accessibility for manifolds including Euclidean spaces
18 p2673 A72-36616

Computation of optimal controls by a method combining quasi-linearization and quadratic programming.
18 p2673 A72-36824

Hopscotch algorithm for numerical integration of nonlinear hyperbolic partial differential equation systems based on finite difference method
18 p2705 A72-37020

Digital computer simulation of human systemic arterial pulse wave transmission - A nonlinear model.
18 p2655 A72-37028

Maximal contraction points of autonomous nonlinear system phase trajectories, using van der Pol differential equations
18 p2674 A72-37149

Minimax method of optimizing electric circuits in the absence of constraints on the variable parameters
19 p2777 A72-37309

Equivalent circuits and oriented graphs for network analysis and synthesis of nonlinear transducers used in control systems
19 p2777 A72-37316

Extension of the frequency-type unconditional stability criterion of controlled systems with one nonlinear nonstationary element
19 p2777 A72-37431

Stability of nonlinear automatic systems with double pulse modulation, discussing systems with linear and nonlinear pulse elements
19 p2777 A72-37435

Nonsymmetric oscillations in certain symmetric nonautonomous systems
19 p2777 A72-37436

Variational method in the control system invariance problem
19 p2778 A72-37990

Evaluation of the coefficients of influence of initial information and model errors on optimization results
19 p2779 A72-37996

A circle criterion for nonlinear stochastic feedback systems.
19 p2779 A72-38235

Variable stability simulation techniques for nonlinear, rate dependent systems.
19 p2780 A72-38241

Distributed parameter linear and nonlinear systems analysis, deriving theorem for solution stability of linear partial differential equations
19 p2826 A72-38247

Hyperstability concepts and their application to discrete control systems.
19 p2780 A72-38248

Nonlinear on-line rapid estimation scheme with application to trajectory maneuvering vehicles.
19 p2781 A72-38258

Decoupling and synthesis of certain nonlinear systems.
19 p2827 A72-38275

Study of the stability of a polar coordinate compensator
19 p2783 A72-38581

Nonlinear oscillations stochastic instability in dynamic systems, discussing nonequilibrium statistical mechanics
19 p2836 A72-38814

Difference schemes with a divergent operator for a general system of second-order hyperbolic equations
19 p2828 A72-38854

Dynamic nonlinear system direct statistical analysis by Covariance Analysis Describing Function Technique with linearization, giving illustrative examples [AIAA PAPER 72-875] 20 p2905 A72-39124

Heuristic description for harmonic oscillator as quantized model of anharmonicity applied to excitation fields involving particle clusters and multibody configuration
20 p2953 A72-39398

Dynamic models for hydraulic machine parts, discussing resonant properties of one degree of freedom system and dynamic characteristics of nonlinear parametric systems
20 p2953 A72-39421

Nonlinear system described by three generalized coordinates, noting dynamic response stability equivalence to two degrees of freedom system
20 p2953 A72-39553

Iterative solution of nonlinear structural problems, using convergence criteria based on displacement quantities
20 p2946 A72-39625

Book - Some aspects of the optimal control of distributed parameter systems.
20 p2946 A72-39731

Possibility of developing combination method for calculating, with a controlled quantization step, the response of a nonlinear network
21 p3074 A72-40184

Use of the multidimensional Laplace transform for the analysis of nonlinear systems with variable parameters
21 p3036 A72-40185

Using the quasi-homogeneity of differential equations in modeling physical systems
21 p3083 A72-40377

Necessary conditions for optimality in a general class of non-linear mixed boundary value control problems.
21 p3037 A72-40644

Bounded-input bounded-output stability of nonlinear discrete systems by a method of comparison.
21 p3037 A72-40645

Geometric criterion for the design of a non-oscillatory dynamical system.
21 p3037 A72-40647

State vector moments of nonlinear mechanical systems under stochastic excitation, using Fokker-Planck equation for transition probability and differential equations derivation
21 p3084 A72-40679

Trajectory synthesis of optimal control
21 p3037 A72-40704

Absolute instability of nonlinear pulse-amplitude modulated control systems - Frequency criteria
21 p3038 A72-40707

Evaluation of the mean time to tracking failure in a nonlinear pulsed servo with irregular signal input
21 p3038 A72-40708

The behaviour of the solutions of the equations of motion of a mechanical system, with a parameter occurring as a coefficient of each derivative.
21 p3084 A72-40812

Canonic model representations for communication receiver to analyze and simulate input-output behavior as nonlinear signal processing black box
21 p3019 A72-40889

Analysis of impact vibrations by delta-function method - Case of one degree-of-freedom system. I - Perfectly elastic collision.
21 p3121 A72-41238

The design of a nonlinear multi-parameter model for the human operator.
21 p3011 A72-41421

A comparison of the effects of small nonlinearities on several estimation schemes.
[AIAA PAPER 72-905] 21 p3076 A72-41555

Propagation of electromagnetic disturbances and the stability of stationary states in media with a nonlinear Ohm's law
21 p3086 A72-41651

An algorithm in the gradient method for synthesis of nonlinear control systems
21 p3039 A72-41804

Cross-modulation in tuning circuits with nonlinear capacitances.
21 p3039 A72-41830

Stabilities and settling times of nonlinear and time-varying feedback systems.
22 p3161 A72-41937

Development and optimization of a nonlinear multiparameter human operator model.
22 p3149 A72-41949

Complex amplitude four-pole network nonlinear conversion of sum of sinusoidal oscillations
22 p3158 A72-42083

Synthesis of statistically optimal multiloop control systems containing essentially nonlinear elements
22 p3162 A72-42182

Variational method for invariance problem solution for optimal finite state of nonlinear dynamic systems under external disturbances
22 p3162 A72-42240

Self focusing effect on wave beam propagation in optical lens waveguides, discussing system nonlinearity
22 p3186 A72-42656

Theory of thermal fluctuations in nonequilibrium systems
22 p3206 A72-42659

Decision surface estimate of nonlinear system stability domain by Lie series method.
23 p3274 A72-43540

Singular small parameter perturbation effect on absolute stability of high order derivatives in Lure-Postnikov nonlinear systems
23 p3274 A72-43544

Polynomial operators for nonlinear systems analysis.
23 p3308 A72-43599

Decoupling and diagonalization conditions determination for nonlinear multivariable time-varying differential equations system by state feedback, giving illustrative examples
23 p3275 A72-43611

Stability bounds for nonlinear systems designed via frequency domain stability criteria.
[ASME PAPER 72-AUT-1] 23 p3275 A72-43636

Application of an electronic computer to the calculation of the locking band in nonlinear phase-lock automatic frequency control systems
23 p3264 A72-43763

Parallel-type varactor frequency multipliers. I - Spectral analysis of the voltage at a partially forward-biased varactor
23 p3270 A72-43764

Optimal parallel-type varactor frequency multiplier calculation for reverse-biased conditions in terms of nonlinear conductance loss and diffusion capacitance Q factor
23 p3270 A72-43774

Equations of motion of nonlinear nonholonomic mechanical systems of variable mass with impulsive constraint factors
23 p3313 A72-43848

An algorithm to obtain the steady state response of nonlinear periodic systems.
23 p3267 A72-43852

Sufficient condition formulation for Lure type nonlinear continuous control system exponential absolute stability
23 p3309 A72-43854

Regions of absolute ultimate boundedness for discrete-time systems.
23 p3309 A72-43857

Nonlinear nonautonomous dynamic systems practical stability conditions for specified settling time, verifying constant matrix Hurwitz property
23 p3309 A72-43858

Linear inequalities and P matrices, with applications to stability of nonlinear systems.
23 p3309 A72-43859

Optimal design of a class of nonlinear networks.
23 p3276 A72-43865

Linearizing compensation for nonlinear control system transformation into linear system without approximation, discussing differential operator matrix definition and random noise effects
23 p3277 A72-43945

Controllability properties of right invariant nonlinear systems described by evolution differential equation in Lie group
23 p3309 A72-43981

Qualitative investigation of nonlinear pulse systems by the point mapping method
23 p3277 A72-44006

Approximate harmonic linearization method of stability analysis of nonlinear periodic systems, identifying fictitious oscillations due to computation errors
23 p3277 A72-44007

Stabilization of the motion of certain nonlinear systems by a linear approximation 23 p3313 A72-44045

Cumulants of multidimensional response of linear and nonlinear systems to Poisson distributed impulses, estimating joint probability distribution and evaluating threshold statistics 23 p3314 A72-44368

Equivalence conditions for classes of linear and non-linear distributed parameter systems. 23 p3277 A72-44369

Non-linear free vibration of a beam with time-dependent material properties. 23 p3355 A72-44374

Non-linear flexural vibration of orthotropic skew plates. 23 p3355 A72-44375

Nonlinear differential equations control systems, determining conditions for observability of initial state and vector of constant parameters extended from time-varying linear systems 23 p3310 A72-44548

Analytical designing of regulators for second-order nonlinear systems 24 p3387 A72-45519

The first initial-boundary value problem for a nonuniform parabolic equation. 24 p3419 A72-45631

Allowable regions for stability multiplier characteristics. 24 p3420 A72-45787

NONLINEARITY

MHD waves nonlinear interaction in magnetosphere, calculating transverse Alfvén and magnetosonic and longitudinal acoustic wave decay instabilities 01 p0109 A72-10618

Closed quasi-linear cubic theory of viscoelasticity for bodies with force and moment physical nonlinearity 03 p0454 A72-14218

Chebyshev approximation by nonlinear families on general compact space with local Haar condition 04 p0539 A72-14730

Nonlinear phenomena in transition region through resonance of dense inhomogeneous plasma in alternating electromagnetic field 04 p0489 A72-15390

Implicit equations in nonlinear network analysis, deriving conditions for existence of unique solutions 04 p0540 A72-15695

Quasi-linearized solution to nonlinear Volterra equations in design of structures under creep deformations 06 p0897 A72-18318

Amplifier amplitude characteristic nonlinearity effect on dynamic properties of autooscillatory temperature controller 07 p0981 A72-18926

Small parameter method application to quasi-linear problems solution in nonstationary heat conduction with substantial nonlinearities and weak perturbation, analyzing error 07 p1098 A72-18937

Solution uniqueness in physically nonlinear viscoelasticity dynamic theory 08 p1195 A72-21761

Thermal stress-strain state analysis of nonlinear elastic medium by small parameter method 09 p1400 A72-22717

Nonlinear effects in optical pumping of Ne transition by laser line 10 p1491 A72-24109

Nonlinear transformation for improper integral calculation, noting faster convergence than linear methods 10 p1506 A72-24997

Complex gain nonlinearity of transmitting microwave amplifiers in single and multicarrier operation 10 p1454 A72-25147

Magnetic field generation in presence of turbulent velocity distribution, considering gyrotropy parameter equation and nonlinearity 11 p1686 A72-25716

Nonlocal elasticity theory from global equilibrium and second thermodynamics laws, deriving constitutive equations from Clausius-Duhem inequality and Gibbs thermodynamics 11 p1738 A72-26721

Nonlinear interactions between synthesized plasma positive and negative ion beams, discussing effect on individual velocity distribution functions 12 p1849 A72-27058

Regenerative semiconductor parametric amplifier under dc through p-n junction, analyzing nonlinear phenomena 14 p2090 A72-31124

Nonlinear regression method for nonlinear least squares problem compared to other solution techniques, discussing convergence theorems and computational results 15 p2262 A72-31632

Computerized Monte Carlo techniques for nonlinear error analysis of system behavior, using random number generators for input distribution simulation 15 p2264 A72-32184

Ionized and neutral atmospheres coupled ionospheric continuity and motion equations, discussing nonlinear force effects on F2 height and electron density 15 p2230 A72-32257

Nonlinear thermoelasticity theory extension via entropy production inequality theorem, deriving expressions for stress tensor and heat conduction vector 16 p2465 A72-32980

Linearization and perturbation procedures to calculate nonlinear effects in fluid stability problems with application to nonlinear critical layer 16 p2377 A72-33338

Nonlinearity effects on finite amplitude, plane uniform oblique shock wave reflection, using inviscid gas analogous solution techniques 16 p2426 A72-33661

Nonlinear flexural vibrations of a clamped circular plate. [ASME PAPER 72-APM-18] 17 p2628 A72-34798

Focusing of intense electromagnetic waves in ducts with saturating nonlinearity. 18 p2659 A72-36293

On the numerical solution of a class of nonlinear problems in dynamic coupled thermoelasticity. 18 p2738 A72-37078

Effect of a junction capacitance nonlinearity on the spectral characteristics of a tunnel diode current 20 p2906 A72-38897

Nonlinear theory of particle motion in monochromatic Alfvén wave field application to Pc-1 geomagnetic pulsations evolution 20 p2917 A72-39408

Russian book - Introduction to nonlinear electrodynamics. 22 p3204 A72-42076

Calculation of the nonlinear dynamic regime of a two-terminal pair network with a weak nonlinearity 23 p3270 A72-43772

Spectrophotometer linearity testing using the double-aperture method. 23 p3289 A72-43894

Standardization of resistance and capacitance elements nonlinearity measurement procedure, proposing constant amplitude supply voltage 24 p3386 A72-45392

Nonlinear interactions between synthesized plasma positive and negative ion beams, discussing effect on individual velocity distribution functions 24 p3431 A72-45711

NONNEWTONIAN FLOW

Non-Newtonian pipe flow turbulence measurements by laser anemometer, describing optical system and signal processing instrumentation [AD-742872] 11 p1646 A72-25554

Flow of a non-Newtonian fluid in a tube with sinusoidal deformation. 21 p3044 A72-40192

On the vortex street behind a circular cylinder in non-Newtonian flows. 21 p2992 A72-41227

NONNEWTONIAN FLUIDS

Turbulent mixing length formulation and velocity profiles for non-Newtonian power law fluids, determining friction factor for pipe flow at high Reynolds numbers 03 p0343 A72-14318

Non-Newtonian real fluids flow characteristics, determining stress-deformation relationship by tensor analysis, with application to lubrication theory 04 p0528 A72-15742

Turbulent flow and heat transfer characteristics of non-Newtonian fluids on flat plate, measuring velocity and temperature distributions 05 p0648 A72-16003

Plane Couette flow of incompressible non-Newtonian viscous fluid between parallel plates, using minimum entropy production variational principle 06 p0798 A72-17779

Non-Newtonian Reiner-Rivlin fluid flow between two coaxial porous cylinders with longitudinal pulses applied to inner cylinder at finite time intervals 10 p1468 A72-24402

Second order fluids plane Poiseuille flow instability to finite amplitude disturbances, noting implications to Toms friction pressure reduction phenomenon in pipe flow 10 p1470 A72-25065

Magnetic and electric field effects on steady state laminar MHD Couette flow of non-Newtonian fluids governed by Prandtl rheological law or Ostwald-de Waele power law 14 p2139 A72-30717

Velocity distributions for slow steady rotational motion of non-Newtonian inelastic viscous fluid contained between two concentric spheres, using successive approximations 15 p2217 A72-31689

Dilatant suspensions impact energy absorbent properties, considering application to ejection seat cushions for occupant acceleration attenuation 15 p2191 A72-32604

Pulsatile flow of linear viscoelastic fluids in elastic-viscous tubes. 23 p3280 A72-43823

Stability of the laminar flow of a 'power-law' non-Newtonian fluid in the boundary layer on a flat plate 24 p3393 A72-45255

NONOHMIC EFFECT

On the theory of electrical conductivity in semiconducting thin films under a high electric field. 20 p2959 A72-39216

NONOSCILLATORY ACTION

Geometric criterion for the design of a non-oscillatory dynamical system. 21 p3037 A72-40647

NONPARAMETRIC STATISTICS

Nonparametric constant false alarm rate /CFAR/ radar extractor for target detection in background noise, using sign test 05 p0629 A72-16569

Noise statistics sensitivity of two sample Mann-Whitney nonparametric detector for radar application. 05 p0629 A72-16570

Signal detection in noise, investigating quantiles position optimization in nonparametric test statistics 07 p0943 A72-19519

NONREFLECTION

U ENERGY ABSORPTION

NONRELATIVISTIC MECHANICS

Nonrelativistic quantum concept of electromagnetic field interaction with charged microparticles 11 p1692 A72-26093

Hydrodynamic equations for incompressible fluid in steady relativistic state extended to nonrelativistic velocities case, noting transition from Euler to Predvoditelev equations 23 p3279 A72-43686

NONRESONANCE

Spherically specularly reflecting nonresonant cavities for use as absorption cells in far IR spectroscopy, predicting performance 11 p1629 A72-25301

Nonresonant mode and nutation damping of rotational-vibrational motion of free solid body with elastic elements 12 p1846 A72-27968

Optically pumped magnetometer error, predicting atomic g-factor modification by nonresonant RF field 15 p2239 A72-32335

NONRIGIDITY

U FLEXIBILITY

NONSTABILIZED OSCILLATION

Instability effect on aperiodic motion of nonlinear thermomechanical oscillator from periodic solutions 04 p0547 A72-14458

Power series method with Cauchy formula for nonlinear partial differential equations solution in unsteady periodic temperature oscillations 06 p0905 A72-18727

Nonstable oscillating motions positive measure set in dynamic system with noncompact phase space, considering elastically rebounded falling sphere on horizontal plate 08 p1210 A72-22188

Instability of rotational and gravitational modes of oscillation. 21 p3078 A72-40773

NONSYNCHRONIZATION

Dual mode - An efficient encoding method of nonsynchronous data signals on PCM. 21 p3023 A72-41827

SECANT midair collision avoidance system based on nonsynchronous microsec pulse transmission and receiving via randomly selected frequency, describing modular components and operating principles 24 p3422 A72-44647

NONUNIFORM FLOW

Nonhomogeneous fluid geostrophic flow, establishing relationship between velocity and density fields 01 p0051 A72-11230

Nonuniform flow along axial turbomachine blades, presenting pressure loss evaluation method under boundary layer effect on external walls 01 p0002 A72-11271

Average stagnation pressure measurement in low velocity ducted gas flow with nonuniform velocity profiles, discussing mathematical technique and computer program [ASME PAPER 71-WA/PUR-1] 05 p0645 A72-15910

Suspended compression shock construction near supersonic point in plane nonuniform ideal gas flow by hodograph technique 05 p0600 A72-16213

Hingeless rotor helicopter blade steady state response with nonuniform inflow and elastic blade bending [AIAA PAPER 72-65] 05 p0741 A72-16933

Internal compressible spatially nonuniform ducted flow performance, defining diffuser efficiency, loss coefficient and static pressure rise coefficient [AIAA PAPER 72-85] 05 p0652 A72-16960

Nonuniform propeller stream effects on aerodynamic characteristics of high aspect ratio wing, using airfoil theory [AD-745477] 07 p0908 A72-19092

- Nonuniform vortex flow of compressible gas past cascade of plates, noting monochromatic pressure waves at harmonics of plate vibration frequency
10 p1418 A72-24538
- Statistical theory of nonuniform turbulent incompressible fluid flow, presenting approximate formulas of nonisotropic two point correlation tensors
13 p1941 A72-28629
- Slender profile in nonuniform flow, deriving lift, normal force distribution and moment from vortex and source distribution induced flow field
13 p1894 A72-29005
- Inhomogeneous two phase flow past sphere, comparing structural and hydrodynamic characteristics on basis of X ray photographs
13 p2066 A72-30003
- Cylindrical pitot tube displacement effects on stagnation point and static pressure angle in impeller nonuniform peripheral flow
14 p2094 A72-30720
- Investigation of the influence of nonuniform conditions at the inlet and of secondary flows on the flow parameters in arbitrarily twisted channels
21 p3045 A72-41067
- Inhomogeneous two phase flow past sphere, comparing structural and hydrodynamic characteristics on basis of X ray photographs
22 p3167 A72-42726
- Simultaneous measurements of temperature and velocity in heated flows.
23 p3292 A72-44541
- Nonsymmetric flow in Laval-type rocket nozzles, deriving formulae for optimum nozzle design with neutralized lateral forces and turning couples
24 p3359 A72-44675
- ### NONUNIFORM MAGNETIC FIELDS
- MHD equations for plasma of arbitrary collision frequency in weakly inhomogeneous magnetic field, considering collisional and resonant particle effects
01 p0108 A72-10241
- Magnetospheric magnetic field distortions under quiet and slightly disturbed conditions, obtaining scalar intensity with OGO 3 and 5 rubidium vapor magnetometer
01 p0060 A72-10886
- Nonuniform magnetic field effects in MHD slider bearing, showing inertia terms contribution dependence on Hartmann number
[ASME PAPER 71-LUB-8] 02 p0235 A72-11533
- Two dimensional MHD channel flow of inviscid fluid in circular nonuniform magnetic field
02 p0267 A72-12771
- Faraday rotation as perturbation for analytic solution of system of differential equations for line formation in inhomogeneous magnetic fields
03 p0427 A72-13295
- Equilibrium state linear theta pinch plasma confinement dependence on nonuniform magnetic force lines curvature radius
03 p0396 A72-13655
- MHD approximation to solve natural convection problem in vertical channel under external inhomogeneous magnetic field, noting fluid flow rate
04 p0555 A72-14646
- Nonrelativistic charged particle resonating with circularly polarized transverse electromagnetic wave in nonuniform magnetic field, showing Fresnel diffraction pattern-like motion
04 p0557 A72-14951
- Thermal noise and ion-acoustic waves excitation in Q machine two beam plasma with high temperature ratio in presence of inhomogeneous B-field, observing instability
06 p0856 A72-17517
- Weakly ionized plasma instability in strong nonuniform magnetic field with convective flow and steadily oscillating final state
06 p0865 A72-18543
- Induced nonuniform magnetic field effects on MHD channel flow between two infinite parallel plates, obtaining solution by perturbation theory
08 p1214 A72-21427
- Plasma injection in magnetic trap along curvilinear inhomogeneous magnetic field, showing long plasmoids polarization and drift reduction by depolarization currents
09 p1363 A72-23218
- Magnetoacoustic wave propagation and reflection in equilibrium inhomogeneous plasma under nonuniform magnetic field
11 p1695 A72-26094
- Induced current distribution in flat narrow conducting strip moving in inhomogeneous magnetic field, presenting current field and densities
11 p1691 A72-26751
- Plasma flow under inhomogeneous axially symmetric magnetic field, investigating axial component of poloidal Hall induction current
11 p1699 A72-26757
- Auroral plasma particle discharge during motion in strong inhomogeneous magnetic field, magnetospheric instability due to temperature anisotropy
11 p1715 A72-26904
- Dispersion relationship for electrostatic instability associated with electron beam trapped in magnetic mirror of magnetosphere, taking into account nonuniformity of magnetic field
15 p2283 A72-31434
- Thermomagnetic effect in a plasma placed in a nonhomogeneous magnetic field
17 p2588 A72-34838
- The influence of a nonuniform transversal magnetic field on the power output of a gas laser.
18 p2715 A72-36338
- ### NONUNIFORM PLASMAS
- Warm inhomogeneous plasma models perturbation analysis, computing high frequency oscillation and eigenfrequencies and eigenfunctions formulas
01 p0106 A72-10134
- Electrostatic wave-particle interactions in inhomogeneous collisionless plasma, calculating resonant distribution function, charge densities and trapping periods
01 p0107 A72-10136
- Periodic inhomogeneous plasma electrostatic waves, considering dispersion relation and longitudinal oscillations
01 p0107 A72-10141
- Nonlocal behavior of ion sound instability in collisionless nonuniform confined plasma shock wave
01 p0108 A72-10240
- Multifrequency interferometer for inhomogeneous plasma density soundings, determining time dependence, spatial distribution and plasma layer size
02 p0263 A72-11413
- Nonuniform plasmas resonant wave-particle interactions, using linearized Vlasov equation
02 p0264 A72-12119
- Frequency variations from uniformly moving source in homogeneous and inhomogeneous isotropic plasmas, calculating source-to-transmitted-wave group velocity ratio from Doppler curves slopes
02 p0264 A72-12120
- Inhomogeneous plasmas parametric instabilities excitation, observing threshold electric field power requirement
02 p0266 A72-12370
- Electron and population densities in inhomogeneous nonequilibrium plasmas with photoabsorption, using radiative transport equation
02 p0266 A72-12441
- Second harmonic emission from plasma hybrid resonance region during electromagnetic wave normal incidence on nonhomogeneous magnetoactive plasma layer
02 p0180 A72-12578
- Right handed circularly polarized electromagnetic wave propagation in hot inhomogeneous plasma, deriving local dispersion equation by WKB methods
03 p0393 A72-12949
- Magnetoplasma with skin current characterized by current and electron temperature nonuniformity, analyzing instabilities for perturbations above ion gyrofrequency
03 p0396 A72-13713
- Hf electric field influence on electron drift instability and slow ion-acoustic waves for inhomogeneous magnetized plasma stabilization
04 p0555 A72-14617
- Electromagnetic wave propagation across external magnetic field in contraststreaming thermally anisotropic plasmas, investigating plasma stability
04 p0556 A72-14942
- Nonlinear phenomena in transition region through resonance of dense inhomogeneous plasma in alternating electromagnetic field
04 p0489 A72-15390
- Electromagnetic absorption heating in cold randomly inhomogeneous plasma, discussing consequences of thermal particle motion neglect
04 p0489 A72-15393
- Electromagnetic wave propagation and stability in inhomogeneous collisionless plasma under static magnetic field
04 p0490 A72-15401
- LF oscillations due to drift diffusion of current free weakly ionized inhomogeneous plasma in magnetic field
05 p0697 A72-16984
- Hall fields effect on interaction of MHD waves in inhomogeneous plasma, considering MHD wave dispersion
05 p0701 A72-17237
- Pulsed FM radio pulse signal reflection from inhomogeneous plasma or ionosphere calculating electron collision loss effects on distortion
06 p0854 A72-17487
- Dynamic stabilization of transverse Kelvin-Helmholtz instability driven by nonuniform plasma motion, using ac electric field near ion cyclotron frequency
06 p0857 A72-17531
- Microwave absorption by longitudinally inhomogeneous plasma, noting waveguide excitation in critical concentration region
06 p0776 A72-18409
- Plasma density inhomogeneity effects on beam-plasma instability and Landau damping from digital simulation using charge sheet model
06 p0865 A72-18541
- Threshold condition for purely growing parametric instability in inhomogeneous plasma
07 p0975 A72-19153
- Dispersion relation for uhf drift waves in nonuniform plasma with cold electrons drift through stationary ions, deriving plasma stability conditions
07 p1042 A72-19612
- Nonuniform plane parallel plasma streams instability with/without magnetic field, comparing with conducting fluid
07 p1042 A72-19618
- Electrostatic oscillations of multivelocity electron streams in hot inhomogeneous plasma
07 p1046 A72-20502
- Inhomogeneous high-collision finite pressure plasma stability, finding thermal instability development under uniform temperature and arbitrary pressure
07 p1046 A72-20514
- Long radio waves slant incidence on isotropic inhomogeneous ionospheric plasma
08 p1131 A72-20737
- Charged particles nonlinear oscillations in nonhomogeneous plasma, noting amplitude limitation and heating by external hf field energy absorption
08 p1212 A72-21210
- Electromagnetic wave polarization effect on linear transformation of waves in inhomogeneous magnetoactive plasma in magnetic field
08 p1212 A72-21245
- Dielectric permeability tensor operator for surface wave-electron beam interaction in relativistic nonuniform plasma stream with cylindrical geometry
09 p1359 A72-22769
- Electromagnetic wave propagation obliquely incident on thermal inhomogeneous plasma at frequencies near second electron cyclotron harmonic
09 p1365 A72-23521
- Inhomogeneous plasma effect on helical slow wave systems approximated by anisotropically conducting plane
10 p1522 A72-24518
- Inhomogeneous rarefied plasma, investigating nonlocal, linear and nonlinear effects on electromagnetic wave reflection and transmission
11 p1694 A72-25717
- Magnetoacoustic wave propagation and reflection in equilibrium inhomogeneous plasma under nonuniform magnetic field
11 p1695 A72-26094
- Nonlinear waves in nonuniform plasma, extending Butler and Gribbon formulation for Vlasov-Poisson equations
11 p1697 A72-26598
- Nonlinear wave interaction in plasma with random inhomogeneities, using quasi-hydrodynamic approximation
12 p1849 A72-27062
- LF oscillations due to drift-diffusion of current free weakly ionized inhomogeneous plasma in magnetic field
12 p1850 A72-27128
- Diagnostic procedures for nonhomogeneous plasma based on geometrical optics approximation, irradiating plasma by plane wave at oblique incidence
13 p2013 A72-29295
- Alternating magnetic field effect on collisionless nonhomogeneous magnetoplasma ion acoustic oscillations stability, examining parametric excitation of Langmuir oscillations
13 p2016 A72-29604
- Plasma inhomogeneity in crossed electromagnetic field, comparing motion velocity to ion component transverse drift rate in polarized electric field
13 p2019 A72-29893
- Nonlinear damping of potential monochromatic waves in inhomogeneous plasma, obtaining resonance particle distribution function
13 p1923 A72-29984
- Quasi-hydrodynamic equations for transverse waves in inhomogeneous plasma, using geometric optics approximation
13 p2019 A72-29986
- Non-Maxwellian inhomogeneous collisionless plasma equilibrium and stability, proposing statistical thermodynamic model
14 p2137 A72-30394
- Ion viscosity tensor and ion thermal flux derived for microinstabilities of inhomogeneous collisional high pressure plasma, noting second derivatives of temperature
14 p2137 A72-30395
- Electrostatic cyclotron harmonic waves propagation in inhomogeneous electron plasma slab, deriving RF electric field
14 p2138 A72-30397
- Experimental investigation of electrostatic cyclotron harmonic waves excited in inhomogeneous plasma column with axial magnetic field by RF capacitor field
14 p2138 A72-30398

Wave pattern of three dimensional hydromagnetic perturbations produced by harmonic magnetic dipole in anisotropic plasma 14 p2102 A72-30661

Electromagnetic waves backscattering in magnetoactive plasma containing random inhomogeneities of electron density, calculating field spatial-time and cross correlation functions 14 p2086 A72-30789

Electromagnetic waves propagation in inhomogeneous moving cold electron plasma without external magnetic field and collisions, investigating dynamo-optical effects 14 p2086 A72-30790

Magnetized nonuniform plasmas, discussing description to all orders in electron and ion temperatures of waves by operator method 14 p2139 A72-30879

Solitons propagation in two ion streams plasma for cold and finite temperature ions, noting periodic waves condition 15 p2286 A72-32276

Singly scattered radiation in weakly inhomogeneous turbulent plasma for incidence angles greater than critical angle, calculating backscattered wave depolarization from radiative transport equation 15 p2288 A72-32425

Quasi-linear approximation of absorption of oscillations excited by electron beam in nonuniform plasma, noting electron distribution change with heating under magnetic field 16 p2432 A72-32807

HF electrostatic instabilities driven by electron-ion relative drift velocity across external magnetic field for inhomogeneous plasma, noting Landau damping role 16 p2433 A72-32809

Langmuir wave coupling in inhomogeneous plasma due to combined density gradient and external HF electric field 16 p2436 A72-33654

Scattering of electromagnetic waves from an inhomogeneous magnetoplasma column moving in the axial direction. 17 p2587 A72-34359

Microwave absorption by longitudinally inhomogeneous plasma, noting waveguide excitation in critical density region 17 p2588 A72-34859

Investigation of two types of collisionless linear dampings of electromagnetic waves in a non-homogeneous magnetized plasma. 17 p2588 A72-34870

Critical point regularity conditions and asymptotic solutions to the time stationary, linearized, inhomogeneous solar wind flow problem. 17 p2599 A72-35095

Water bag model application to one dimensional inhomogeneous two-stream collisionless electron plasma stability computation, noting electrostatic modes 17 p2592 A72-35619

Growth rate and frequency dispersion characteristics of drift waves in an RF collisional plasma. 18 p2716 A72-36924

Amplitude limits to the theory of resonant absorption in cold plasmas. 18 p2716 A72-36960

Discontinuities in a collisionless plasma flow having a strong magnetic field. 18 p2717 A72-37042

Study of the mechanism of motion of nonequilibrium plasma inhomogeneities in a magnetic field 18 p2717 A72-37176

Long radio waves oblique incidence on isotropic inhomogeneous ionospheric plasma 19 p2766 A72-38365

Potential created by a point charge oscillating in an inhomogeneous plasma 19 p2842 A72-38522

Continuum eigenmodes of an inhomogeneous plasma. 20 p2956 A72-39015

Drift instabilities in an inhomogeneous collisionless plasma 20 p2957 A72-39355

Parametric excitation of Bernstein waves in inhomogeneous magneto-plasmas. 21 p3089 A72-40187

Alternating magnetic field effect on ionoacoustic oscillations stability of collisionless nonhomogeneous magnetoplasma, examining parametric excitation of Langmuir oscillations 21 p3091 A72-40658

Excitation of volume ion-acoustic oscillations in an inhomogeneous dense plasma by the field of an electromagnetic wave. 21 p3092 A72-40836

Absorption of an obliquely incident extraordinary wave in a weakly inhomogeneous plasma in the hybrid resonance region 21 p3095 A72-41694

Electrodynamical mathematical model for electroconductivity of nonuniform plasma with Hall effect, calculating current distribution from Riemann problem solution 22 p3210 A72-41888

Coupled fields in inhomogeneous warm plasmas with static pressure gradients. I. 22 p3210 A72-42313

Transport of RF energy to the lower hybrid resonance in an inhomogeneous plasma. 22 p3212 A72-42898

Theoretical study and wind tunnel simulation of the electrical phenomena of reentry 22 p3231 A72-43092

Surface drift vibrations of a weakly ionized plasma 22 p3212 A72-43102

Diffusive spreading of weak plasma discontinuities in the presence of two kinds of positive ion 23 p3283 A72-43363

Use of the simulation method for the solution of a dispersion problem for the propagation of symmetrical magnetic waves in a rectangular waveguide filled with a nonhomogeneous plasma 23 p3263 A72-43450

Plane parallel nonuniform velocity plasma streams instability in absence and presence of magnetic field, comparing with ideal conductive liquid flows 23 p3320 A72-43518

Perpendicular collisionless shock wave instability. 23 p3320 A72-43523

Method for solving the problem of radiation in an anisotropic plasma 23 p3321 A72-44220

Anode sheath plasma current instabilities, examining electron and ion turbulent heating, plasma particle limiting energies and unsteady oscillation spectra 24 p3429 A72-45490

Current-driven drift wave instability in a sheared magnetic field. 24 p3430 A72-45570

Nonlinear wave interaction in plasma with random inhomogeneities, using quasi-hydrodynamic approximation 24 p3431 A72-45715

NONUNIFORMITY

Thin shell theory analysis of thin walled cylindrical shell necking phenomenon as tensile deformation nonuniformity 08 p1248 A72-21821

NONVISCIOUS FLOW
U TURBULENT FLOW
NOON

Airborne optical measurement comparison with satellite observation for auroral emissions and particle precipitation at noon, suggesting electron precipitation role 19 p2868 A72-38738

NORADRENALINE

Ground and flying activity endurance training effect on urinary excretion of noradrenaline and adrenaline 04 p0478 A72-14868

Heat production increase by muscular contractions due to noradrenaline in cold adapted rats 05 p0620 A72-17215

Hypothalamus increased noradrenaline turnover after adrenal glands demedullation in rats given disulfiram inhibitor 07 p0924 A72-20621

Protein biosynthesis inhibitors retardation of noradrenaline and serotonin induced hyperpolarization of neuron membranes in cortical sensorimotor region of rabbits 08 p1122 A72-22192

High altitude hypoxia preadaptation effects on left ventricle myocardium noradrenaline concentration in rats with experimental vitium cordis 12 p1761 A72-27648

Adrenaline and noradrenaline metabolic stages and production mechanism under various physiological and pathological conditions, noting application to flight emotional stress detection 21 p3002 A72-41196

NOREPINEPHRINE

Epinephrine and norepinephrine effects on cerebral blood circulation volume and oxygen tension in tissues 02 p0165 A72-12517

Antimotion sickness drugs effectiveness based on acetylcholine or norepinephrine induced changes of balance between vestibular and reticular neurons 10 p1427 A72-23726

Modifications of the rate of renewal of norepinephrine in various peripheral organs of the rat during exposure and acclimatization to cold 23 p3258 A72-44244

NORMAL DENSITY FUNCTIONS

Gaussian periodic data optimal smoothing, describing convolution kernel and computer program 03 p0381 A72-13200

Multidimensional Gaussian distribution integrals evaluation for correlator analysis, discussing fix error probability and variance 03 p0387 A72-14189

Error distribution computation for combined Rayleigh-Gaussian statistics data, applying to antenna radiation beam-pointing example 04 p0500 A72-15303

Rice exceedance statistics application to atmospheric turbulence, indicating strong nonGaussian second order distributions [AIAA PAPER 72-136] 05 p0684 A72-16969

Markov type isotropic random Gaussian field analysis in n-dimensional Euclidean space 08 p1198 A72-20999

Clutter correlated lognormal random variables generation from statistically independent Gaussian random variables for radar simulations 08 p1134 A72-21423

Fresnel diffraction integrals for irradiance and power distribution calculations of Gaussian beams focused through annular apertures 09 p3352 A72-23334

HF radio waves scattering by spherical electron cloud with Gaussian density distribution 09 p1282 A72-23515

Solute dispersion distribution over tube cross section with flowing solvent, comparing with Gaussian distribution 10 p1466 A72-24330

Feature selection from pattern recognition of Gaussian distributed classes by mapping of vector samples from n dimensional space to m dimensional space via transformation matrix 10 p1445 A72-24461

Computer approximate computation of multidimensional normal distribution, examining error measure, random processes and correlation coefficient 11 p1676 A72-25429

Expected value of two dimensional Gaussian random array gain, assuming two dimensional isotropic noise field of single frequency 11 p1604 A72-26040

Target position information for radar energy potential calculation and detection quality, describing transmitter power reduction for normal range distribution density 11 p1596 A72-26313

Least squares method algorithm for estimating unsteady harmonic signal parameter in presence of normally distributed additive noise 13 p1915 A72-28435

Automated problem solving in continuous stochastic processes, using nonergodic representation of Gaussian process with continuous spectral density 15 p2204 A72-32588

Statistical analysis of position-fixing general theory for systems with Gaussian errors. 17 p2578 A72-34294

Book - Elements of applied stochastic processes 17 p2575 A72-34624

Experimental investigation of the parameters of a statistical Gaussian field model for centimeter waves beyond the radio horizon 17 p2515 A72-34834

Motion of ion-cloud in the ionosphere, field-aligned cloud with Gaussian distribution of ionization density. 17 p2546 A72-35060

Correlation functions and reconstruction error for quantized Gaussian signals transmitted over discrete memoryless channels. 17 p2516 A72-35333

A bivariate normal theory maximum-likelihood technique when certain variances are known. 21 p3075 A72-40826

Spherical focusing transducers with Gaussian surface velocity distribution. 21 p3057 A72-41477

Geometrical interpretation of Gaussian beam optics. 23 p3288 A72-43877

NORMAL DISTRIBUTIONS

U NORMAL DENSITY FUNCTIONS

NORMAL FORCE DISTRIBUTION

U FORCE DISTRIBUTION

NORMAL SHOCK WAVES

Steady normal shock wave analysis in binary inert monatomic gas mixtures using kinetic theory moment method 04 p0513 A72-15340

Radiative transfer and chemical nonequilibrium phenomena for radiating flow field predictions behind high altitude hypervelocity normal shock waves 05 p0603 A72-16545

Strong normal shock wave structure upstream and downstream of discontinuity due to nonequilibrium radiation and collisional ionization 06 p0902 A72-18106

Cylindrical tube geometry and electrode separation effects on normal ionizing shock waves, showing speed proportional to azimuthal drive and axial magnetic fields 10 p1470 A72-24794

Electron beam fluorescence method for normal shock wave velocity distribution in Ar-He mixtures 11 p1615 A72-25556

Supersonic turbine stator and rotor blading design corrected for boundary layer displacement thickness, discussing limitations due to normal shock wave at flow separation [ASME PAPER 72-GT-63] 11 p1571 A72-25653

- Normal ionizing shock waves characteristics in He under varying conditions of magnetic field strength, discharge current and gas pressure
11 p1694 A72-25789
- Magnetic structure of normal ionizing shock waves with zero transverse energetic component
11 p1618 A72-26607
- Aerodynamic normal shock noise measurements on nose cylinder bodies in transonic flow [AIAA PAPER 72-669]
16 p2346 A72-34068
- Analytical investigation of normal shock waves in water near the thermodynamic critical point.
17 p2543 A72-35635
- One dimensional stationary gas flow across normal shock wave, taking into account nonequilibrium factors and momentum, mass and energy transport
20 p2914 A72-39970
- Pressure jump across normal ionizing shock waves.
21 p3045 A72-40566

NORMALIZING

- Computer aided renormalized perturbation method for inhomogeneously loaded waveguide performance calculation
06 p0786 A72-18377
- Dense convexes class characterization in real seminormalized space on basis of decomposition family concept
13 p1987 A72-29779
- Long term weightlessness-induced physiological response normalization by muscle bioelectrostimulation, muscular tissue energy load increase and mineral metabolism stabilization
16 p2354 A72-33543

NORMALIZING [STATISTICS]

- Criterion for signals records legibility obtained by analog recorders, deriving relationship between normalized root-mean-square error and apparent frequency
09 p1316 A72-23663
- Solar X-ray data normalization, using conversion factors independent of incident photons spectrum
13 p2034 A72-29941
- Fluctuation renormalized transport coefficients in corrected nonlinear transport equations derivation from generalized Fokker-Planck equation
15 p2337 A72-32653

NORMS

- Error bounds relationship to norm in approximate numerical solutions of initial value problems for ordinary differential equations
11 p1679 A72-26957
- Ideas of individual on group members majority behavior in various situations, noting norm concept confirmation from psychological tests on reference groups
13 p1903 A72-28796
- Norms of the successive overrelaxation method.
17 p2574 A72-34448
- Reachable sets and singular arcs for minimum fuel problems based on norm-invariant systems.
17 p2534 A72-35533
- Evaluation of the norm of a function in terms of its Fourier coefficients, convenient in problems of approximation theory
24 p3419 A72-45549

NORTH AMERICAN MILITARY AIRCRAFT

- U MILITARY AIRCRAFT
NORTHERN HEMISPHERE
NT ARCTIC REGIONS
- Weather map numerical analysis for Northern Hemisphere, describing program with flow field for geopotential value checking
01 p0094 A72-10196
- Tropospheric processes effects on Northern Hemisphere stratospheric meridional transformations in geopotential field and air circulation
02 p0253 A72-11732
- Numerical weather prediction, discussing automatic forecasting, error sources, models and four-day validity in Northern Hemisphere
02 p0254 A72-12781
- Tropical east-west atmospheric circulation geometrical, thermal and intensity characteristics during northern summer
03 p0384 A72-14143
- Northern Hemisphere mean zonal flow across arbitrary horizontal surfaces, evaluating vertical transports of kinetic energy
04 p0541 A72-14454
- Ozone content and vertical distribution variations as causes of winter stratospheric warmings in Northern Hemisphere
07 p0973 A72-18861
- Baroclinic primitive equation prediction model for nontropical part of Northern Hemisphere with allowance for moisture exchange, radiative heat influx and cloud formation processes
11 p1683 A72-26886
- Hydrodynamic theory of atmospheric action center formation due to pressure migration for Northern troposphere two level meteorological forecasting
14 p2127 A72-30261

- Long term atmospheric pressure fluctuations in relationship to solar activity over Northern Hemisphere, confirming 22 year cycle
14 p2101 A72-30648
- Explorer 19 satellite drag evidence for neutral exosphere He concentration asymmetry between Northern and Southern Hemispheres over entire solar activity cycle
15 p2228 A72-31977
- Imposed southern boundary experimentation for large scale Northern Hemisphere midlatitude atmospheric flow numerical prediction, discussing factors contributing to model success
15 p2267 A72-32726
- Temporal behavior of hemispherically averaged geostrophic zonal and meridional flow from dynamic climatological studies of Northern Hemisphere large scale circulation
21 p3077 A72-40251
- Stratospheric general circulation patterns from geographical, vertical and annual distribution for Northern Hemisphere temperatures, geopotential heights and winds
21 p3078 A72-41611
- A diagnostic study of the vorticity balance at 200 mb in the tropics during the Northern summer.
22 p3201 A72-42507

NORTHROP MILITARY AIRCRAFT

- U MILITARY AIRCRAFT
NOSE [ANATOMY]
Otorhinolaryngological organ response during hypokinetic antiorthostatic bed rest for control, exercising and muscular electric-stimulated groups
23 p3256 A72-43917

NOSE CAPS

- U NOSE CONES
NOSE CONES
NT ABLATIVE NOSE CONES
NT ROCKET NOSE CONES
- Newtonian theory for maximum lift drag ratio of blunt-cone cylinder bodies, optimizing rocket reentry nose shape
05 p0602 A72-16535
- Surface heat transfer and pressure measurements for downstream effects of transpiration cooled nose tip, using nitrogen as injectant fluid [AIAA PAPER 72-185]
05 p0605 A72-16840
- Transitional and turbulent heat transfer measurements on yawed blunt cone nosetip in supersonic air flow at various angles of attack
07 p0964 A72-18960
- Boundary layer transition on slender cone in hypersonic flow as function of nose bluntness, free stream Reynolds number and angle of attack [AIAA PAPER 72-216]
07 p0908 A72-18961
- Conical and spherical nose shapes effects on drag and static stability at Mach 10
07 p0908 A72-19695
- Optimal selection of flawless nose cones from graphite billets, obtaining mathematical model based on ultrasonic reflection test data
07 p1086 A72-20350
- Thermal stress measurement and thermoelastic behavior of carbon-carbon-materials for reentry nose cones, describing gage mounting, temperature compensation and data recording
08 p1164 A72-20921

- Aerodynamic normal shock noise measurements on nose cylinder bodies in transonic flow [AIAA PAPER 72-669]
16 p2346 A72-34068
- Prediction of nose shape effects on nonlinear stability characteristics of slender cones.
20 p2886 A72-39628
- Hypersonic leading edge problem - Wedges and cones.
24 p3364 A72-45778

NOSE WHEELS

- Electromechanical nose wheel steering system for general aviation aircraft ground maneuverability improvement, describing design
01 p0006 A72-10963

NOSES [FOREBODIES]

- NT ABLATIVE NOSE CONES
NT NOSE CONES
NT ROCKET NOSE CONES
- Iterative solutions for three dimensional turbulent boundary layers on rotating nose-body, using streamline and cross flow momentum equations
01 p0002 A72-11397
- Al alloy plates and D-nosed specimens indentation and penetration under hail impact test
07 p1086 A72-18764
- Nose bluntness effect on bodies of revolution pitching moment characteristics in incompressible flow at various angles of attack
11 p1573 A72-26576

NOTATION

U CODING

NOTCH SENSITIVITY

- Waspaloy sheet creep rupture time dependent sensitivity to sharp-edged notches at 1000-1400 deg F, optimizing smooth and notched specimen yield strengths [ASME PAPER 71-WA/MET-3]
05 p0670 A72-15906

- Nb and Nb-Zr alloy tubular and sheet samples cyclic loading tests, determining heat treatment effects on notch sensitivity and fatigue strength
06 p0834 A72-18646

- Chemically etched notches effect on Al-Mg alloy mechanical properties
07 p1018 A72-20139

- Fatigue indicators with analytic or visual notched and cracked coupons techniques and strain multipliers for welded structures
09 p1316 A72-23620

- Tensile strength, plastic properties and notch sensitivity from low temperature tests of binary Ti alloys, noting effects of Sn content and temperature
12 p1831 A72-28239

- Stress-service life relations for duralumin samples from impact and nonimpact tensile tests with cyclic axial loads, noting notch sensitivity
13 p1978 A72-29147

- Li addition effects on Mg mechanical properties temperature dependence and notch sensitivity of binary Mg-Li alloys
14 p2125 A72-31041

- Notch toughness criteria of metals with S shape transition temperature curve, considering experimental design and impact test model
16 p2406 A72-33322

- Notch sensitivity of sintered stainless steel powder as function of density from application of sharp crack fracture mechanics methods to plane strain fracture toughness
16 p2408 A72-33700

- Thermal and mechanical stresses concentration near peripheral notches on ring-shaped graphite, noting notch sensitivity relationship to tip curvature and graphite grain size
23 p3306 A72-43755

- Chemically etched notches effect on Al-Mg alloy mechanical properties
24 p3417 A72-45764

NOTCH STRENGTH

- Elastic equilibrium of infinite wedge with apical asymmetric notch, reducing to Hilbert problem for holomorphic vectors
07 p1093 A72-19976
- Tensile strength of notched carbon and glass fiber reinforced epoxy resin composites as function of crack size
10 p1500 A72-24253
- Low temperature mechanical properties of Ti-base alloys, examining notched samples impact strength as function of temperature and notch depth
11 p1663 A72-26806
- Oxide content and sheet microstructure directionality effects on Be powder and ingot sheets notch strength, noting thickness dependence [ASM PAPER W 72-12.6]
12 p1830 A72-28164
- Cylindrical samples with deep circular hyperbolic notch, investigating cyclic inelastic strain induced stress redistribution effects on load bearing capacity
12 p1830 A72-28229
- Notch stress concentration in disk with elastic core under tension, using finite element method
13 p2060 A72-29600
- Understressing and coaxing cycles effect on deeply notched carbon steel fatigue behavior, emphasizing crack initiation and breakdown
16 p2472 A72-33947
- Some considerations on the residual stresses in orthogonal cut surface of aluminium.
20 p2978 A72-38884

NOTCH TESTS

- NT CHARPY IMPACT TEST
- Finite element analysis of creep due to stress and strain in double edge notched plates and round bars
01 p0138 A72-10519
- Crack angle effect on high strength metals fracture toughness, using Al alloys and tool steel ASTM-type single edge notch tension specimens
01 p0086 A72-10988
- Fatigue crack initiation and growth in sharply notched mild steel, showing specimen size, geometry and loading effects on fatigue life
01 p0142 A72-11098
- Crack opening displacement concept for fracture toughness testing, presenting elastic and plastic notch tip stress and deformation relationships in plane strain
02 p0292 A72-12005
- Quenched and tempered high strength and maraging steels delayed failure properties from notched-tensile sustained-load tests in distilled water
02 p0246 A72-12560
- Crack notched three point loaded bend specimens plain strain fracture toughness determination, showing relation between elastic work and stress intensity factor
03 p0442 A72-12960
- Deformation kinetics relationship to scale effect in notched samples during elastoplastic loading phase
03 p0443 A72-13455
- Stress concentration coefficients calculation at sharp cracks and notches for rods in tension, compression and combined bending and torsion
03 p0443 A72-13457

- Ductility relationship to plasticity characteristics in cylindrical steel samples with short notch under tension 03 p0443 A72-13458
- Plane strain fracture toughness of notched high strength Al and Ti alloys at low temperatures 03 p0371 A72-13464
- High alloy chromium and manganese steels brittle fracture susceptibility, showing notch effects 03 p0371 A72-13466
- Grain orientation effect on fatigue crack propagation in notched test specimens cut from cold rolled prestressed annealed brass plate 03 p0375 A72-13934
- Fatigue test curves of notched Al alloys under bending with rotation 05 p0676 A72-17086
- Fatigue behavior of notched or cracked aircraft structure parts, examining service life prediction problem 06 p0895 A72-17811
- Notch length effect on stress concentration in polymethyl methacrylate sample from tensile, impact and bending tests 08 p1196 A72-21867
- Notched bend test crack opening displacement gage for continuous measurement of apparent rotation axis and true displacement location at crack tip 10 p1483 A72-24885
- Al alloy notch-bend and compact-tension specimens thickness and crack length effects on plane-strain fracture toughness test results 10 p1498 A72-24886
- Ti alloys fracture strength in air and sea water obtained by bending tests of notched specimens, noting stress corrosion resistance enhancement by Mo addition 10 p1499 A72-24891
- Photoelastic investigation of star shaped models for loading direction influence on shear stress distribution at notch tip region in uniform tensile field 10 p1559 A72-24897
- Specimen preparation effects on fracture strength measurements, noting critical stress intensity factor for single edge notch and compact tension high strength steel samples 11 p1657 A72-25825
- Fracture toughness anisotropy and crack sensitivity of Al alloys extruded bars notched cylindrical samples 11 p1659 A72-26130
- Stepwise compression loading effect on yield stress of carbon and alloy steels in cylindrical samples with end plane cylindrical notches filled with solid lubricant 12 p1831 A72-28237
- Crack and notch induced stress concentrations effect on steel mechanical properties at 20-293 K, using static and dynamic test methods 12 p1831 A72-28240
- Unsteady loading effects in high temperature fatigue tests of refractory alloys for turbine blades, noting steady and programmed notch tests 13 p1980 A72-29494
- Fatigue limit and Woehler curve determined from notch tests, noting relation between fatigue damage and residual stresses in notched parts 13 p1980 A72-29673
- Plastic deformations accumulation and breakdown initiation in notched steel specimens, discussing effects of mechanical properties, geometry and heat treatment 15 p2256 A72-31607
- Crack depth measuring instrument for fatigue crack propagation study in notch tests, noting application at high temperatures 16 p2391 A72-33234
- Effects of thickness on fatigue crack initiation and growth in notched mild steel specimens. 17 p2627 A72-34747
- Strength and plasticity of molybdenum during short-term tests 19 p2819 A72-38218
- An analytical approach to the non propagating crack problem using the finite element method. 20 p2977 A72-38882
- Fatigue tests at low cyclic loads of smooth and notched Ti alloy specimens, noting surface hardening effect on service life 20 p2941 A72-39580
- Effect of notch root radius on the initiation and propagation of fatigue cracks. 20 p2981 A72-39960
- Dynamic stress concentration of notched strips. 21 p3117 A72-40715
- Plastic deformation in annealed aluminum bar containing circumferential semicircular notch. 21 p3118 A72-40719
- Book - Effect of notches on low-cycle fatigue: A literature survey. 22 p3242 A72-43145
- Plane elastostatic analysis of V grooved rectangular plates notch angle and specimen geometry effects on stress intensity factors and fracture toughness measurements 23 p3346 A72-43703
- Crack opening displacement relationship to notch root contraction from fracture toughness tests, describing plastic deformation mechanism at notch tip 23 p3346 A72-43704
- Load distribution in a single-edge-notch tensile specimen. 23 p3306 A72-43710
- Mo alloy under impact tests, investigating notch sharpness effects on cold shortness threshold and strength 23 p3301 A72-43756
- Computation of post-yield behaviour in notch-bend and tension testpieces. 24 p3456 A72-44796
- Deformation kinetics relationship to scale effect in notched samples during elastoplastic loading phase 24 p3458 A72-44930
- Stress concentration coefficients calculation at sharp cracks and notches for engine parts in tension, compression and combined bending and torsion 24 p3458 A72-44932
- Ductility relationship to plasticity characteristics in cylindrical steel samples with short notch under tension 24 p3458 A72-44933
- Plane strain fracture toughness of notched high strength Al and Ti alloys at low temperatures 24 p3413 A72-44939
- High alloy chromium and manganese steels brittle fracture susceptibility, showing notch effects 24 p3414 A72-44941
- NOTCHED METALS**
- U NOTCH TESTS
- NOTCHED STEEL**
- U NOTCH TESTS
- U STEELS
- NOTCHES**
- Heat transfer and temperature profiles in separated flow generated by transverse rectangular notch in flat plate 02 p0303 A72-12700
- Plane theory of elasticity for infinite triangular wedge with notched apex, reducing problem to non-homogeneous Hilbert problem 05 p0737 A72-16301
- Plastic slip in notched half plane undergoing antiplane deformation, using screw dislocation continuous distribution theory 09 p1403 A72-22747
- Stress concentration in symmetrical U-notched plates, comparing data with Baratta, Neal, Neuber and Heywood formulas 14 p2167 A72-30904
- A hyperboloidal notch in a transversely isotropic material under pure shear. 21 p3119 A72-41105
- NOVAE**
- Astronomical catalog of 42 novae, presenting tables of exact positions 03 p0433 A72-13489
- Short lived X ray burst precursor of X ray nova Centaurus XR-4, investigating event intensity 06 p0881 A72-17899
- VV Pup binary light variations correlation with primary component variable disk dimensions, considering nova-like processes 06 p0882 A72-18003
- High speed photometry of nova variables with white dwarf and late-type binary star flickering, using Cassegrain focus 06 p0889 A72-18332
- Classification-dispersion spectrograms of early decline of Nova Serpentis 1970, discussing diffuse enhanced absorption system behavior 07 p1071 A72-19338
- N Her 1963 distance, absolute magnitude, stellar mass and explosion-ejected shell mass, using maximum and relative intensity calculation methods 08 p1229 A72-20840
- Nova outbursts hydrodynamic processes, studying mass loss mechanism based on direct shock wave ejection and pulsational instability 09 p1382 A72-22283
- Delphinus Nova positions determination from plates obtained with photographic telescope with/without diffraction gratings 09 p1389 A72-23067
- Nova Delphini evolution from metallic absorption lines observations before December 1967 maximum, obtaining dispersion variation with wavelength 14 p2159 A72-30741
- Novae and background stars relative proper motions, deriving and tabulating absolute proper motions via statistical transformation 19 p2860 A72-37970
- A preliminary model for the shell ionisation of the nova RS Ophiuchi. 19 p2866 A72-38504
- Hydrodynamic model of white dwarf envelope thermonuclear runaway evolution producing nova outburst, computed for various CNO nuclei initial abundances 20 p2966 A72-38908
- Photoelectric light curve of Nova Vulpeculae 1968 N. 1. 20 p2973 A72-39883
- The spectrum of N Del 67 and some remarks on chemical composition of the novae envelopes. 21 p3109 A72-41436
- The non-spherical nebulae of Nova Delphini 1967, Nova Vulpeculae 1968/I/, and Nova Serpentis 1970. 22 p3221 A72-41999
- Estimate for the frequency of novae in the Andromeda Nebula and our Galaxy. 23 p3333 A72-43229
- Identification of four novae and a super-nova in Palomar Sky Atlas. 23 p3341 A72-44474
- NOXIOUS MATERIALS**
- U CONTAMINANTS
- NOZZLE COEFFICIENT**
- U NOZZLE FLOW
- NOZZLE DESIGN**
- Aladin 2 noiseless STOL jet aircraft project, describing exhaust nozzle configuration, design and economics 02 p0155 A72-12503
- Externally water cooled conical nozzle throat wall thickness design for high pressure and temperature argon flow medium [DGLR PAPER 71-095] 02 p0299 A72-12702
- Nozzle boundary layer effects on resistojets performance, presenting conical design model in heater stagnation conditions 03 p0405 A72-12973
- Gas dynamic laser technology advances, discussing water content, temperature and Na effects and nozzle design [AIAA PAPER 72-143] 05 p0669 A72-16895
- Ejector nozzle design criteria, analyzing primary/secondary flow interactions and diameter, spacing and temperature ratio effects [AIAA PAPER 72-46] 05 p0609 A72-16963
- Pyrolytic graphite coated rocket nozzle design, discussing substrate properties, coating thickness, erosion rates and rocket tests 10 p1500 A72-24199
- Carbon-carbon composite ring structure tested for processing cycle, design properties and ablative performance in solid rocket nozzle environment 11 p1673 A72-25488
- Russian book on theory of ramjet and rocket ramjet engines covering supersonic diffuser operational principles and design, nozzle, combustion chamber and ejector 12 p1862 A72-28346
- Russian book on solid propellant rocket engines covering combustion chamber and nozzle layouts, working cycle and thrust control 16 p2443 A72-33350
- Extendible variable profile nozzle for various flow regimes operation, developing numerical design algorithm 18 p2641 A72-36661
- Forward flight effects on mixer nozzle design and noise considerations for STOL externally blown flap systems. [AIAA PAPER 72-792] 19 p2746 A72-38109
- Method of calculating pneumatic spray nozzles 23 p3325 A72-44015
- Nonsymmetric flow in Laval-type rocket nozzles, deriving formulae for optimum nozzle design with neutralized lateral forces and turning couples 24 p3359 A72-44675
- Thrust stand for evaluation of thrust vectoring nozzle performance. [AIAA PAPER 72-1029] 24 p3389 A72-45406
- NOZZLE EFFICIENCY**
- Computer program for biowaste resistojets nozzle performance prediction, taking into account viscous effect at low Reynolds number 11 p1708 A72-26187
- Supercritical pressure convergent nozzle performance prediction by time dependent method of characteristics solution to mixed flow problem, adapting Moretti-Abbett technique [AIAA PAPER 72-680] 16 p2346 A72-34061
- Supersonic aircraft engine inlet performance in terms of pressure recovery, discussing oblique shock wave formation ahead of entrance to improve efficiency 24 p3360 A72-44991
- NOZZLE EXPANSION**
- U GAS EXPANSION
- U NOZZLE FLOW
- NOZZLE FLOW**
- Gas turbine nozzles aerodynamic throat area air flow measurement, describing accuracy, standards, reference nozzles and mounting flanges [SAE ARP 1195] 01 p0065 A72-10390
- Flow momentum losses during gas mixture chemically nonequilibrium expansion in nozzle 01 p0145 A72-10487
- Optical emission spectrum of Ba and CuO combustion products during nozzle expansion into vacuum 01 p0146 A72-11312

Liquid and solid particle trajectory calculation in two phase Laval nozzle flows, determining density, velocity and temperature

02 p0149 A72-11588

Numerical analysis of nonequilibrium gas mixture flow through nozzle

02 p0149 A72-11589

Nozzle boundary layers effect on reattachment position of two dimensional jet to adjacent flat plate, noting Reynolds number influence

02 p0150 A72-11729

Hypersonic two component gas mixture nozzle flow with condensation or evaporation discontinuity, determining Pitot pressure limits

02 p0230 A72-12255

Nonstationary temperature field determination in stream turbine casing-connector nozzle by difference method based on heat balances, comparing results with electric analog studies

02 p0303 A72-12534

Externally water cooled conical nozzle throat wall thickness design for high pressure and temperature argon flow medium

[DGLR PAPER 71-095]

02 p0299 A72-12702

Flow characteristics of pin type nozzles in constant pressure carburetors of Otto cycle engines

02 p0206 A72-12853

German monograph on gas type and nozzle flow conditions effect on condensed molecular jets properties

03 p0391 A72-13275

Rocket acceleration effect on internal isentropic nozzle flow, giving formulas for thermodynamic variables

03 p0441 A72-13627

Mass blocking of subsonic isentropic swirling flow through convergent axisymmetric nozzle, considering radial velocity component effect on vorticity

03 p0342 A72-13957

Skimmer design optimization for maximum nozzle beam intensity yields in hypersonic flow

03 p0362 A72-14052

Nozzle and cavity wall cooling limitations on uranium plasma nuclear rocket specific impulse, discussing wall heat flux and transpirational cooling by propellant flow

03 p0387 A72-14383

Flow development in gas nozzles with depressive networks, describing geometric and functional characteristics

04 p0510 A72-14467

Thermal nozzle combustion effects on supersonic flow of chemically reacting gas in thermodynamic equilibrium

05 p0599 A72-15846

Convergent conical nozzle shape effect on propulsive performance and compressible flow field internal characteristics

[ASME PAPER 71-WA/FE-3]

05 p0647 A72-15937

Flow calculations for subsonic and transonic portions of ring nozzles and plane curvilinear channels

05 p0601 A72-16226

Finite difference calculations for two dimensional unsteady inviscid expanding flow of perfect gas through nozzle, obtaining flow field patterns

05 p0603 A72-16539

Rapid expansion nozzles for gas dynamic laser working gas vibrational energy freezing to obtain population inversion, considering size and shape effects on performance

[AIAA PAPER 72-148]

05 p0669 A72-16965

Nonadiabatic real gas nozzle flow with friction and heat transfer to wall, obtaining solution by Runge-Kutta method

05 p0610 A72-17066

Population inversion of carbon dioxide molecules in gas flow expanding from nozzle

06 p0852 A72-17904

Plane irrotational flow of fluid with arbitrary thermodynamic properties in throat of Laval nozzle, solving flow equations

07 p0972 A72-20111

Vibrational relaxation in nonequilibrium and expansion nozzle flows

08 p1148 A72-21015

Steady flow of dual temperature plasma into vacuum from widening nozzle, taking into account electron thermal conductivity and heat exchange between components

08 p1214 A72-21653

Mixed subsonic-supersonic flows solution for choked isentropic flow in convergent-divergent nozzle, comparing results with series solution

10 p1561 A72-23721

Numerical prediction of subsonic and supersonic flow through convergent-divergent nozzle

10 p1416 A72-23874

Steady inviscid irrotational transonic flow in two dimensional symmetric and axially symmetric nozzle throats

10 p1417 A72-23875

Plane transonic gas flows through Laval nozzle and symmetrical wedge-shaped profile, solving boundary

value problem by reduction to singular integral equation

10 p1418 A72-24433

Aerodynamic throttling effect due to air jet flow interaction in throat region of mainstream two dimensional nozzle flow

10 p1419 A72-24845

Resistojet performance models for investigating energy losses in hydrogen, ammonia, methane and carbon dioxide nozzle flows

[AIAA PAPER 72-455]

11 p1708 A72-26191

Critical discharge regimes of two phase steam/water mixture flow from nozzles, using counterpressure effect

11 p1619 A72-26674

Turbine nozzle vanes edge losses dependence on profile edge thickness, allowing flow velocity variation

12 p1861 A72-28135

Steady flow of compressible heat conducting fluid, discussing effect of small transfer coefficient on isentropic sonic singularity in Laval nozzle

14 p2171 A72-30713

Thermal nozzle combustion effects on supersonic flow of chemically reacting gas in thermodynamic equilibrium

15 p2334 A72-31265

Transient flow induced in convergent-divergent nozzles by shock front impingement, investigating nozzle shape and Mach number effects on formation process of reflected shock

15 p2179 A72-32143

Transient flow induced by shock front impingement on Laval nozzles observed by schlieren method, noting time variations of temperature and pressure

15 p2179 A72-32144

Characteristic parameters of stationary supersonic plasma flow in magnetic de Laval nozzle calculated for collisional and collisionless cases, measuring ion saturation currents

15 p2285 A72-32268

Pseudo-one dimensional dissociative nonequilibrium nozzle flow, presenting governing equations transformation via similarity parameter for oxygen

16 p2375 A72-32906

Inverse Laval problem of three dimensional subsonic and supersonic flows in nozzles and ducts of variable cross section in terms of asymptotic series

16 p2342 A72-32930

Supersonic molecular jet improvement via expansion chamber residual gas pressure reduction and nozzle stagnation pressure increase

16 p2429 A72-33053

Water vapor condensation in jet turbulent mixing zone of confluent high velocity high temperature gas streams for finite axisymmetric nozzle

16 p2377 A72-33260

Three dimensional supersonic nozzle exhaust flow field numerical analysis based on reference plane characteristics, deriving difference equations for three coordinate systems

[AIAA PAPER 72-704]

16 p2344 A72-34040

Nonequilibrium steady quasi-one dimensional expanding nozzle flow of chemically reacting gas mixture, using time dependent finite difference technique

[AIAA PAPER 72-684]

16 p2480 A72-34058

Coupling of free electron and nitrogen vibrational temperature nonequilibrium in weakly ionized nozzle expansions of shock heated nitrogen

[AIAA PAPER 72-683]

16 p2380 A72-34059

Supercritical pressure convergent nozzle performance prediction by time dependent method of characteristics solution to mixed flow problem, adapting Moretti-Abbott technique

[AIAA PAPER 72-680]

16 p2346 A72-34061

Supersonic jet noise mechanisms and scaling laws, studying acoustic fields for rectangular and axisymmetric nozzle configurations

[AIAA PAPER 72-641]

16 p2381 A72-34091

Influence of contraction section shape and inlet flow direction on supersonic nozzle flow and performance

17 p2483 A72-34204

Subsonic, transonic, and supersonic nozzle flow by the inverse technique

17 p2483 A72-34206

Flow in an accelerated rocket nozzle - Effect of variation of total mass. II

17 p2621 A72-34918

Compressible swirling flow through convergent-divergent nozzles

17 p2485 A72-34999

Air film cooling in a nonadiabatic wall conical nozzle

17 p2638 A72-35493

Density distribution in a high-pressure gas jet measured by laser-induced gas breakdown

17 p2486 A72-35630

Method of characteristics application to supersonic jet and nozzle gas flow with allowance for equilibrium and nonequilibrium condensation

17 p2544 A72-35929

Swirling flows vortex breakdown in nozzles, diffusers and combustion chambers, considering analogy to boundary layer separation

18 p2641 A72-36385

Determination of the stream function of a perturbation associated with a plane jet

18 p2680 A72-36470

A through-type counting method for two-dimensional and spatial supersonic flows. II

18 p2642 A72-36810

Structure of turbulent underexpanded jets expelled into a submerged space and into a slipstream

18 p2642 A72-36884

Nonlinear development of capillary waves in a fluid jet

18 p2682 A72-36885

Analysis of a transonic flow in elliptic nozzles

18 p2642 A72-36898

Turbulent diffusion in Laval nozzle, studying mixing of weakly heated jet coaxial with main flow in subsonic flow region

20 p2913 A72-39368

Viscous non-adiabatic laminar flow through a supersonic nozzle - Experimental results and numerical calculations

[ASME PAPER 72-HT-49]

20 p2985 A72-39662

Generalized relations for determining specific impulse losses in nonequilibrium two-phase nozzle flows

20 p2914 A72-39909

Interaction between the droplets of a polydispersed condensate in a nozzle flow

20 p2915 A72-40046

Experimental CW chemical laser studies

[AIAA PAPER 72-712]

21 p3063 A72-40920

Critical flow rate and pressure ratio for nitrogen flowing through convergent-divergent nozzle at stagnation conditions, emphasizing thermodynamic critical region

21 p3046 A72-41180

Critical mass flow and nonequilibrium nozzle flow of vibrationally relaxing, ideal dissociating diatomic and singly ionizing monatomic gases, using steepest descent method

21 p3046 A72-41249

Perturbation analysis of aerodynamic test flow in Ludwig tubes, investigating nonsteady coupling effects on nozzle turbulent boundary layer

[AIAA PAPER 72-994]

21 p2993 A72-41580

Pressure transmitter for flow parameter measurements of aerodynamic nozzles and static pressure taps rotating on turbine rotor blades

22 p3176 A72-42250

Method of characteristics for ideal gas flow in annular space of axisymmetric plug nozzle, noting flow visualization by schlieren photography

22 p3166 A72-42263

Numerical integration of three dimensional flow equations for supersonic jets of ideal gas exhausted from elliptical and rectangular nozzles

22 p3133 A72-42264

Flow equations for axisymmetric compressible conical flow in Busemann nozzle, noting numerical method for integral lines construction for given Mach number

22 p3134 A72-42288

Modified Newton-Kantorovich variational method for calculating flows in subsonic and transonic portions of circular nozzles, noting savings in computer time

23 p3248 A72-43659

Flow parameters and geometric factors effect on wake structure behind nozzle cascades with cooling air ejection through blade trailing edges, evaluating energy losses due to flow mixing process

23 p3248 A72-43665

Experimental investigation of the structure of turbulent jets expelled from a rectangular nozzle and nozzles with a limited head

23 p3280 A72-44020

An experimental study of flows in planar nozzles

[ASME PAPER 72-FLCS-2]

23 p3249 A72-44066

Nonsymmetric flow in Laval-type rocket nozzles, deriving formulae for optimum nozzle design with neutralized lateral forces and turning couples

24 p3359 A72-44675

Various efficiencies of fluid flows and application to the hypersonic ramjet

24 p3360 A72-44993

Water tunnel study of turbulent boundary layers structure in incompressible fluid with longitudinal pressure gradient at inlet section of converging and diverging nozzles

24 p3390 A72-45006

Instabilities in the reaction zones of detonation waves

24 p3462 A72-45029

Formation of a jet of shock-heated gas outflowing into evacuated space

24 p3391 A72-45046

Study of a reactive nozzle flow associated with solid gas-phase interaction

24 p3433 A72-45063

Frequency dependence of axially oscillated nozzles admittance real and imaginary parts for different

- Mach numbers, convergence angles and curvature radii, comparing theory and experiment 24 p3433 A72-45144
- Effect of a line energy source at the boundary of a supersonic flow. 24 p3361 A72-45187
- Mach reflection from overexpanded nozzle flows. 24 p3365 A72-45794
- ### NOZZLE GEOMETRY
- Gas turbine nozzles aerodynamic throat area air flow measurement, describing accuracy, standards, reference nozzles and mounting flanges [SAE ARP 1195] 01 p0065 A72-10390
- Thermal and I-V characteristics of dc plasmatron with vortex stabilized arc, interelectrode insert and diverging arc channel for various nozzle diameters 05 p0694 A72-15854
- Convergent conical nozzle shape effect on propulsive performance and compressible flow field internal characteristics [ASME PAPER 71-WA/FE-3] 05 p0647 A72-15937
- Jet engine silencing plug nozzle suppressor configurations acoustic and thrust performance measurements [AIAA PAPER 72-160] 05 p0706 A72-16826
- Large scale high aspect ratio multielement suppressor nozzle arrays testing for augmentor wings and internally blown flaps [AIAA PAPER 72-131] 05 p0612 A72-16888
- Steady heat conduction of cooled gas turbine hollow nozzle blades with gas temperature variation along cascade 08 p1223 A72-20948
- Pulsed carbon dioxide laser operation, measuring pulse energy variation with gas pressure, expansion nozzle shape and output mirror transmission 09 p1323 A72-22980
- High velocity water jet generation dynamics, deriving equations of motion for mathematical model with nozzle profiles and liquid compressibility approximations 14 p2093 A72-30180
- Approximate analytical solution for spherical particle acceleration in uniform gas flow, examining nozzle geometry and particle size effects 14 p2095 A72-30924
- Two stream ejector propulsion performance, measuring nozzle geometry effect on discharge coefficient for 2-90 deg convergence angles [ONERA, TP NO. 1050] 15 p2177 A72-31208
- Thermal and I-V characteristics of dc plasmatron with vortex stabilized arc, interelectrode insert and diverging arc channel for various nozzle diameters 15 p2283 A72-31271
- Perturbations effects on plane symmetry supersonic molecular beam intensity as function of nozzle-skimmer geometry and nozzle pressures 16 p2430 A72-33062
- Axisymmetric jet impact on ground board for different nozzle configurations and heights in VTOL aircraft aerodynamic studies 16 p2377 A72-33404
- Liquid propellant rocket engines three dimensional nozzle admittance determination by impedance tube method from pressure distribution measurement, taking into account nozzle geometry effect [AIAA PAPER 72-666] 16 p2443 A72-34071
- Supersonic jet noise mechanisms and scaling laws, studying acoustic fields for rectangular and axisymmetric nozzle configurations [AIAA PAPER 72-641] 16 p2381 A72-34091
- Influence of contraction section shape and inlet flow direction on supersonic nozzle flow and performance. 17 p2483 A72-34204
- Effect of nozzle throat radius of curvature on gasdynamic laser gain. 17 p2561 A72-34210
- Shape factors for nozzle corner cracks evaluated from epoxy-model pressure vessels. 17 p2630 A72-34814
- Servo pump nozzle area controls for gas turbines. 18 p2694 A72-36048
- Extendible variable profile nozzle for various flow regimes operation, developing numerical design algorithm 18 p2641 A72-36661
- Analysis of a transonic flow in elliptic nozzles 18 p2642 A72-36898
- Influence of pressure, mass flow rate, and nozzle angle on the chemical relaxation in nozzles 19 p2880 A72-37494
- Importance of nozzle geometry to high-pressure gas-dynamic lasers. 19 p2811 A72-37867
- Optimal arrangement of conical nozzles in a segment of a partial supersonic turbine stage. 20 p2963 A72-39913
- Flow parameters and geometric factors effect on wake structure behind nozzle cascades with cooling air ejection through blade trailing edges, evaluating energy losses due to flow mixing process 23 p3248 A72-43665
- Experimental investigation of the structure of turbulent jets expelled from a rectangular nozzle and nozzles with a limited head 23 p3280 A72-44020
- An experimental study of flows in planar nozzles. [ASME PAPER 72-FLCS-2] 23 p3249 A72-44066
- Frequency dependence of axially oscillated nozzles admittance real and imaginary parts for different Mach numbers, convergence angles and curvature radii, comparing theory and experiment 24 p3433 A72-45144
- Jet pumps for compressible fluids at supersonic velocities. 24 p3393 A72-45362
- Axisymmetric nozzles shape for thrust optimization, comparing maximum thrust circular arc and conical nozzles performances 24 p3365 A72-45784
- ### NOZZLE INSERTS
- NDT for detecting density variation, local anomalies regions and completeness of copper-infiltrated W powder rocket nozzle inserts 03 p0364 A72-14025
- Aircraft engines high pressure turbine guide vanes air cooling by internal insert, analyzing thermal stresses [AIAA PAPER 72-7] 05 p0707 A72-16864
- ### NOZZLE THRUST COEFFICIENTS
- Convergent-divergent nozzles thrust model measurement on supersonic aircraft afterbody [ONERA, TP NO. 978] 05 p0642 A72-15856
- Thrust stand for evaluation of thrust vectoring nozzle performance. [AIAA PAPER 72-1029] 24 p3389 A72-45406
- Axisymmetric nozzles shape for thrust optimization, comparing maximum thrust circular arc and conical nozzles performances 24 p3365 A72-45784
- ### NOZZLE WALLS
- Externally water cooled conical nozzle throat wall thickness design for high pressure and temperature argon flow medium [DGLR PAPER 71-095] 02 p0299 A72-12702
- Side force and shock wave induced by obstacle on rocket engine nozzle wall, investigating pressure distribution 07 p1055 A72-20250
- Shock wave interactions with nozzle wall turbulent boundary layer, discussing shock strength variation to produce unseparated, incipient and fully separated flow fields [AIAA PAPER 72-715] 16 p2380 A72-34033
- ### NOZZLES
- Hot water rocket engine design and operation principles, discussing high pressure tank and nozzle characteristics 15 p2297 A72-31830
- ### NRX-A REACTOR
- ### U NUCLEAR ENGINE FOR ROCKET VEHICLES
- ### NUCLEAR AUXILIARY POWER UNITS
- ### NT SPACE POWER REACTORS
- ### NT SPACE POWER UNIT REACTORS
- Uranium mononitride as nuclear reactor fuel for space vehicle power supply applications, discussing fabrication techniques and irradiation behavior 09 p1349 A72-22406
- ### NUCLEAR BINDING ENERGY
- Resistometric investigation of Ge addition effect on Al-Zn alloy clustering kinetics, determining Ge atom-vacancy binding energy 02 p0247 A72-12821
- Tight binding model for binding energy determination in transition atoms adsorption on same series transition metal substrate, using moments expansion technique 15 p2281 A72-32379
- Oxygen molecule electron affinity role in ion chemistry of lower ionosphere, noting binding energy of ground state 17 p2585 A72-34260
- ### NUCLEAR CAPTURE
- ### NT ELECTRON CAPTURE
- ### NUCLEAR DEFORMATION
- X ray diffuse scattering from Al crystal at 100-500 V, considering phonon modes effects on anharmonicity and atomic deformation 08 p1186 A72-21591
- ### NUCLEAR ELECTRIC POWER GENERATION
- ### NT NUCLEAR AUXILIARY POWER UNITS
- ### NT NUCLEAR POWER PLANTS
- ### NT NUCLEAR POWER REACTORS
- ### NT SPACE POWER REACTORS
- ### NT SPACE POWER UNIT REACTORS
- ### NT THERMONUCLEAR POWER GENERATION
- Laser beam power transmission to lunar bases or spacecraft from nuclear fueled satellite power station, discussing achievable ranges and efficiencies 17 p2611 A72-35328
- An out-of-core thermionic-converter system for nuclear space power. 18 p2645 A72-36187
- On-board nuclear power plants in space 24 p3423 A72-45119
- United States Space Nuclear Electric Power Program. 24 p3424 A72-45179
- ### NUCLEAR ELECTRIC PROPULSION
- Comet rendezvous and outer planet exploration mission operations by unmanned nuclear electric propulsion /NEP/ system with incore thermionic reactors for electric power generation [AIAA PAPER 72-428] 11 p1722 A72-26173
- Spacecraft nuclear electric propulsion system multi-mission performance evaluation, discussing launch mode and vehicle capability factors in system size selection [AIAA PAPER 72-503] 11 p1685 A72-26226
- Nuclear electric propulsion systems performance evaluation for various escape missions 17 p2606 A72-34577
- Mission operations for unmanned nuclear electric propulsion outer planet exploration with a thermionic reactor spacecraft. 17 p2606 A72-34578
- Thermionic reactor system for auxiliary power and electric propulsion. 17 p2494 A72-34579
- Thermionic reactors design based on flashlight and external fuel concepts for nuclear electric propulsion 17 p2494 A72-34580
- Thermionic reactor power conditioner design for nuclear electric propulsion. 17 p2495 A72-34582
- ### NUCLEAR EMULSIONS
- Nuclear emulsion and solid track threshold dosimetry for ion spectrum division of heavy relativistic particles in primary cosmic rays [CERN-71-16] 02 p0162 A72-12065
- Dispersion energy relation for ultrahigh energy nuclear reactions in cosmic ray emulsion 03 p0410 A72-13148
- Nuclear photoemulsions under bombardment by pion beam of 60 GeV/c momentum, investigating pion-nucleon interactions involving recoil protons 06 p0851 A72-17273
- Pulsed and hf electric field effects on ionizing particle recording in nuclear and photographic emulsions 06 p0816 A72-17833
- Cosmic radiation effects in Concorde prototype cabin, using photographic dosimeters for neutron dose measurement and nuclear emulsions for all charged particle recordings 07 p0927 A72-19241
- Quasi-nucleonic interactions of high energy protons in nuclear emulsion irradiated within pulsed magnetic field 07 p1038 A72-19869
- Primary cosmic rays antineutrino content upper limit from emulsions investigations with balloons and satellites 14 p2148 A72-30885
- Isotopic abundance analysis of primary cosmic radiation with nuclear emulsion technique, discussing mass measurements in Be, C, O, Ne, Mg and Fe tracks 16 p2447 A72-33731
- A comparison of measurements of the charge spectrum of solar cosmic rays from nuclear emulsions and the Explorer 35 solid-state detector. 18 p2721 A72-35988
- General characteristics of proton-nucleon and coherent interactions at an energy of 67 GeV 23 p3317 A72-44415
- High energy inelastic collisions of pions and protons with nuclear emulsion nucleons, noting pion pulse spectra 23 p3317 A72-44417
- Recording high-energy particle interactions by the method of the controlled emulsion stack of large volume 23 p3291 A72-44438
- Angular and impulse characteristics of negative-pion interactions at an energy of 60 GeV in the emulsion 23 p3292 A72-44446
- ### NUCLEAR ENERGY
- Nuclear energy value to society, stressing usefulness for electric power generation and marine propulsion 03 p0387 A72-14376
- Closed type gas turbines heated with nuclear energy, calculating heat transmitter dynamic behavior with computer program 07 p1055 A72-20598
- Laser heating of plasma based on thermal conductivity mechanism, considering nuclear microfusion energy recovery 08 p1213 A72-21303
- Nuclear science and power systems - IEEE-NASA-AEC Conference, San Francisco, November 1971 08 p1166 A72-21506
- Heat transfer research review, discussing gas turbines, aeronautics, astronautics, nuclear power, thermal pollution and controlled fusion challenges 09 p1412 A72-23684
- Laser conductive heating of plasma with accounted nuclear fusion energy, assuming plane thermal wave 10 p1522 A72-24722

Nuclear energy sources in overdense celestial bodies
19 p2862 A72-38061

NUCLEAR ENERGY LABORATORIES
U LABORATORIES

NUCLEAR ENGINE FOR ROCKET VEHICLES
NERVA fuel quality control, discussing planning, nondestructive tests, computer data acquisition and certification systems
02 p0258 A72-11552

Nuclear rocket propulsion program, discussing solid refractory core technology, Rover project and NERVA engine development and tests
15 p2273 A72-31811

NERVA flight engine control system design.
21 p3083 A72-40764

NUCLEAR EXPLOSION EFFECT
Radiation-hardened components, circuits and systems.
18 p2665 A72-36308

Quasi-static loading of the earth by propagating air waves.
22 p3172 A72-42468

Stratospheric concentration of radioactive carbon from 1961-62 nuclear tests by balloon measurements over European U.S.S.R. territory during 1967-69
23 p3286 A72-44492

NUCLEAR EXPLOSIONS
NT THERMONUCLEAR EXPLOSIONS
Point explosion in cosmic spheroid with exponential density distribution, observing shock wave propagation along symmetry axis direction
07 p1075 A72-19583

Papers on high temperature physics and chemistry covering peaceful nuclear explosions, radiative transfer, hydrodynamics, stellar opacity and solar He abundance
07 p1078 A72-19922

Long term A3 absorption associated with nuclear explosion caused artificial radiation belts, discussing electron precipitation role in D region ionization
15 p2299 A72-31933

NUCLEAR FISSION
Molybdenum-uranium dioxide cermet fuel pins fission heating at 1145 K in forced convection He cooled reactor, measuring dimensional changes and U 235 burnup
04 p0546 A72-14424

Symmetric fission of superheavy nuclei, observing overabundance of rare earth elements
10 p1515 A72-24526

Release of fission products from high temperature fuel materials
18 p2707 A72-36137

Transuranium elements in HD 25354.
22 p3224 A72-42381

Uranium distribution in basalt fragments of five lunar samples.
23 p3261 A72-43399

Fission and fusion propulsion for deep space missions, discussing gas and colloid core reactors, controlled fusion, MHD and laser plasma systems
24 p3423 A72-45168

NUCLEAR FORCES
U NUCLEAR BINDING ENERGY

NUCLEAR FUEL ELEMENTS
Nuclear light bulb engine concept, detailing radiant heat transfer calculations in fuel and buffer gas regions
01 p0099 A72-11345

Minicavity reactor rocket engine combining high specific impulse of central gaseous fueled cavity and low weight NERVA type fuel elements in driver region external to moderator-reflector zone
01 p0100 A72-11358

Conductive heat transfer from rib roughened surfaces in gas cooled reactor fuel elements
04 p0595 A72-14596

Design features, fabrication technology and in-pile testing of thermionic reactor fuel elements
17 p2495 A72-34584

Sizing an external-fueled in-core thermionic reactor.
17 p2495 A72-34588

Cythere capsule for irradiation of experimental fuel elements under geometric and thermal conditions representative of thermionic converters
17 p2579 A72-34619

Thermionic converters fuel tests by uranium dioxide-Mo cermet irradiation, noting fission gas retention and metallic matrix deformation
18 p2708 A72-36141

State of development of diodes for incore thermionic fuel elements.
18 p2708 A72-36150

Thermionic fuel element development status summary.
18 p2708 A72-36151

Multicell thermionic fuel element fabrication technology.
18 p2708 A72-36152

Ceramic-to-metal seal development for thermionic fuel elements.
18 p2695 A72-36156

Thermionic fuel element triple diode configuration, processing, assembly and performance during neutron irradiation testing in reactor
18 p2708 A72-36159

Reactor testing and performance of in-pile thermionic fuel elements, noting neutron radiographs
18 p2708 A72-36160

Breeder reactor testing of fast neutron irradiation effect on alumina and yttria cylinders for thermionic fuel rod designs
18 p2708 A72-36161

Pure and thoriated W compatibility with uranium carbide alloys at 1800 C, noting thermal gradient and thoria noneffects
18 p2699 A72-36163

Thermionic fuel cladding development, compatibility, stability and performance for uranium carbide-tungsten and uranium oxide-tungsten systems at high temperatures under irradiation
18 p2709 A72-36164

High-voltage thermionic reactor using double-sheath fuel elements.
18 p2644 A72-36171

Measurements with thermionic fuel elements in the ITR critical facility.
18 p2645 A72-36181

NUCLEAR FUELS
NT CERAMIC NUCLEAR FUELS
NDT holographic interference pattern technique to determine Advanced Test Reactor fuel element swage joint tightness
01 p0078 A72-11110

Injection geometry and inlet flow conditions application to open cycle gas nuclear reactor engine, evaluating fuel containment from cylindrical and spherical chambers experiments
01 p0100 A72-11350

Thermal environment and fuel region simulation for nuclear light bulb engine, using rf induction heater and uranium and tungsten hexafluorides injection
01 p0113 A72-11355

Split-core heat pipe reactor for out-of-core thermionic power systems, using center gap for fuel reactivity control
04 p0546 A72-14425

Cylindrical nuclear fueled capsules heat transfer gaps, determining dimensional changes with neutron radiographs
04 p0546 A72-14428

Uranium mononitride as nuclear reactor fuel for space vehicle power supply applications, discussing fabrication techniques and irradiation behavior
09 p1349 A72-22406

Design of an external-fueled thermionic diode for in-pile testing.
17 p2495 A72-34585

Out-of-core evaluations of a nonfueled and a UO₂-fueled cylindrical thermionic converter.
17 p2497 A72-34608

Evaluations of uranium-nitride fueled converters.
17 p2497 A72-34609

Metal working and testing of nuclear rocket engine components with Mo as structural material and uranium dioxide as fuel, discussing Mo-W interdiffusion
17 p2559 A72-34617

Release of fission products from high temperature fuel materials
18 p2707 A72-36137

Behavior of tungsten-clad Mo-UO₂ fuel under neutron irradiation at high temperature.
18 p2708 A72-36143

State of development of an actinium fueled thermionic generator.
18 p2644 A72-36169

Results of a preliminary experimental investigation of a vapor transport fuel pin.
19 p2832 A72-37631

Developmental status of thermionic materials.
19 p2833 A72-38575

The impact of aerospace technology on energy conversion in the 70's.
17 p2495 A72-34588

[ASME PAPER 72-AERO-11] 22 p3140 A72-43147

NUCLEAR FUSION
NT CONTROLLED FUSION
He abundances in universe, discussing stellar structure and evolution, He production, variable stars and globular clusters H-R diagrams shape
03 p0418 A72-13112

He production from H to maintain Galactic luminosity, discussing interstellar gas enrichment
03 p0419 A72-13116

Helium production within supermassive stars and disks and little bangs, discussing conversion from hydrogen
03 p0419 A72-13117

Magellanic Clouds and Galactic nucleosynthesis from chemical composition
03 p0426 A72-13263

Nuclear astrophysics review, discussing chemical elements and isotopes abundance and cosmic nucleosynthesis
03 p0437 A72-13842

High temperature dense plasma formation by laser heating of gas target, noting fusion reaction in deuterium-tritium mixture
03 p0399 A72-14066

Nucleosynthesis model for gamma ray astronomy, covering explosive events
03 p0413 A72-14275

Early solar system nucleosynthesis of Al 26, discussing silicon and carbon burning and spallation
04 p0567 A72-14912

Nuclear fusion by laser radiation, discussing plasma heating mechanisms and limitations in DD reaction production
04 p0557 A72-15172

Metal-rich 1.19 solar mass main sequence star evolution to convection onset in core during He flash
04 p0577 A72-15283

Explosive p-process nucleosynthesis limiting conditions in supernova envelopes, using proton capture and neutron photodisintegration rates
04 p0579 A72-15318

Nuclear microfusion energy recovery threshold increase during laser pulse heating process of D-T plasma
05 p0695 A72-16280

Energy dependence of solar proton-proton reaction, generating p-p wave function from Schroedinger equation
05 p0718 A72-16501

Elemental synthesis and energy sources in stellar evolution, hydrogen, helium and advanced burning stages, p-p cycle, e process and nuclear equilibrium
06 p0876 A72-17585

Galactic evolution model, tracing stellar and supernova nucleosynthesis influence on interstellar gas composition
06 p0886 A72-18082

Stellar extinction and genesis with Galaxy, discussing Li role in nucleosynthesis and degenerate star structure theory
07 p1073 A72-19427

Elemental nucleosynthesis, considering cosmological, stellar, galactic and solar system evolution and atomic nuclei energetic levels
07 p1083 A72-20466

Laser heating of plasma based on thermal conductivity mechanism, considering nuclear microfusion energy recovery
08 p1213 A72-21303

Laser heating of plasma based on heat conduction mechanism of spherical thermal wave, taking into account nuclear fusion heat generation
09 p1365 A72-23553

Laser heating and fusion energy recovery of D-T plasma by mechanical-magnetic cumulation, considering cylindrical wave system
09 p1365 A72-23553

Main sequence star evolution relation to pulsar formation, discussing stellar core density at carbon ignition with respect to critical density limit
09 p1394 A72-23698

Si burning in stellar explosions, discussing initial composition and neutron enrichment
10 p1544 A72-24666

Closed form solution for spherical and cylindrical wave propagation in laser conductively heated plasma, considering account of nuclear fusion energy recovery
10 p1522 A72-24721

Laser conductive heating of plasma with accounted nuclear fusion energy, assuming plane thermal wave
10 p1522 A72-24722

Averaged equations for laser heating of two temperature plasma with allowance for nuclear fusion energy, noting inequality of ion and electron temperatures
12 p1851 A72-27395

Evolution of extreme population I massive stars from main sequence to He exhaustion phase, discussing various development phases in H-R diagram
14 p2158 A72-30727

Fusion reactor RF heating below 100 MHz, discussing coil structures and arcing and cooling problems in main fusion region
16 p2433 A72-32813

Laser heating of two temperature plasma based on conductive heat transfer, taking into account nuclear fusion energy
16 p2434 A72-32876

Nitrogen existence in galactic cosmic ray sources, considering formation from CNO cycle hydrogen and He burning and ejection from normal stars
16 p2448 A72-33739

The potential of a laser-induced fusion device as a thermal-neutron source.
17 p2591 A72-35353

Thermonuclear fusion spacecraft propulsion systems operation principles, interplanetary orbit-to-orbit mission capabilities and environmental safeguard problems
17 p2598 A72-35953

Mixing processes of newly made elements in Galaxy, taking into account thermodynamics, galactic structure and nucleosynthesis parameters
18 p2727 A72-36732

- Hydrostatic oxygen burning in stars. II.
19 p2854 A72-37236
Averaged equations of the combined process of hydrodynamic expansion and conduction heating of plasma, the recovered energy of nuclear fusion being taken into consideration. I - The plane problem.
19 p2841 A72-38095
Alternative description of the conduction-type laser heating process of two-temperature plasma in the spherically symmetric case, the nuclear fusion energy being taken into consideration.
19 p2841 A72-38096
Recent developments in the history of the nucleosynthesis of the solar system.
20 p2971 A72-39837
The possibility of producing plasma regions at thermonuclear fusion conditions in a supersonic flow by means of high power electron beam.
21 p3092 A72-41224
Averaged equations of simultaneous hydrodynamic expansion and thermal heating of two-temperature plasma, taking the recovery of thermonuclear fusion into account. I - The plane problem. II - The spherical problem.
21 p3093 A72-41476
The problem of conductivity-type laser heating of two-temperature plasma, the nuclear fusion energy being taken into consideration, in the spherically symmetric case.
21 p3093 A72-41480
Averaged equations of laser heating of Z-pinch plasma the nuclear fusion energy being taken into consideration.
21 p3093 A72-41481
Nucleosynthesis theory for advanced thermonuclear evolution models of massive stars from helium burning through final hydrodynamic stages
22 p3227 A72-42561
Approximation of energy generation and nucleosynthesis during hydrostatic carbon burning in massive stars, noting neutrino-dominated evolution effects
22 p3228 A72-42562
Studies of heavy-element synthesis in the galaxy. I - Separation of r- and s-process abundances.
22 p3228 A72-42563
Alternative description of laser plasma heating for spherical thermal wave, the fusion energy being taken into account.
22 p3211 A72-42629
Averaged equations for joint treatment of hydrodynamic expansion and conduction-type heating of plasma, the energy of nuclear fusion being taken into consideration. II - Spherical problem.
22 p3211 A72-42630
Averaged equations of laser heating of plasma in a focus-type system taking into account the heat of nuclear fusion.
23 p3322 A72-44223
Averaged equations of laser heating of two-temperature plasma in a focus-type system taking into account the heat of nuclear fusion.
23 p3322 A72-44224
- NUCLEAR INTERACTIONS**
NT ELECTRON CAPTURE
NT SPIN-ORBIT INTERACTIONS
High energy nucleon tissue doses calculation based on averaged characteristics of nuclear interactions [CERN-71-16]
02 p0162 A72-12067
Inelastic nuclear interactions between 200-GeV cosmic ray particles and polyethylene targets, correlating similarity property, angular momentum spectra and secondary particle pairs
06 p0868 A72-17258
Particle multiplicity and momentum spectra for high energy inelastic nuclear interactions in Wilson chamber with polyethylene target
06 p0868 A72-17261
Spectral calculations of electromagnetism and nuclear showers of cosmic ray muons interacting with substance
06 p0871 A72-17288
Microscopic calculations for nuclear forces, compressibility of neutron matter and maximum mass of neutron stars based on solid state model at high densities
06 p0891 A72-18507
Papers on high energy cosmic ray and nuclear interactions covering extensive air showers, cloud chamber data, electron-photon cascades, solar activity effects, etc
07 p1060 A72-19863
Inelastic high energy multiple interactions between cosmic ray particles and atomic nucleus targets, using Wilson chamber and ionization calorimeter
07 p0988 A72-19864
Radiation measuring instruments assembly for extensive air showers and cosmic ray particle nuclear interactions at high energies
07 p0988 A72-19868
Quasi-nucleonic interactions of high energy protons in nuclear emulsion irradiated within pulsed magnetic field
07 p1038 A72-19869
- Pion generation during collective interactions between nucleons of heavy cosmic ray nuclei, using Proton 4 satellite data
08 p1228 A72-22179
Pion generation during collective interactions between nucleons in heavy cosmic ray nuclei, using Proton 4 satellite data
18 p2721 A72-36235
Effective cross section of the inelastic interaction of hadrons with lead-atom nuclei at energies from 3 to 30 TeV
23 p3330 A72-44410
Nuclear interactions in the atmosphere at energies greater than 100 TeV
23 p3330 A72-44411
Multiple collisions and an optical model of the inelastic interaction between cosmic particles and nuclei
23 p3330 A72-44413
Energy dependence of muon-nucleon inelastic interaction, calculating photonuclear cross section for high energy interactions in iron
23 p3331 A72-44429
- NUCLEAR MAGNETIC RESONANCE**
NT PROTON MAGNETIC RESONANCE
NT PROTON RESONANCE
Nuclear magnetic resonance of Al 27 in topaz /aluminum fluorosilicate/, determining nuclear quadrupolar coupling constant and asymmetry parameter
04 p0564 A72-15638
NMR behavior and magnetic susceptibility of intermetallic compound CeAl, noting exchange polarization of RKKY type between 4f electrons and conduction electrons
05 p0702 A72-16784
High resolution NMR spectrometer conversion from continuous wave to Fourier transform operation, permitting computer systems and pulse amplifiers use
09 p1316 A72-23408
Digital pulse programmer with saturation burst sequence for pulsed nuclear magnetic resonance spectroscopy
12 p1806 A72-27125
Hydrated iron silicon fluoride internal motion pressure dependence examined by wide-line and NMR techniques, noting corrections of second moments for bulk paramagnetic effects
13 p1914 A72-30061
Varian HR-60 NMR spectrometer probe with Dewared insert for low temperature operation
15 p2240 A72-32435
Molecular complexes of methoxyindoles with 1,3,5-trinitrobenzene and tetracyanoethylene /Spectroscopy/association constants/NMR/.
17 p2512 A72-35649
Classical nonlinear electronic relaxation oscillators as EPR and NMR signal detectors, reconstructing resonance lines from absorption induced oscillator waveform changes
18 p2662 A72-36993
Electronic and nuclear magnetic resonances of the oxygen and hydrogen labile negative molecular ions.
20 p2956 A72-39189
Fourier transform C-13 nmr analysis of some free and potassium-ion complexed antibiotics.
20 p2898 A72-39399
A simple, low power, multiple pulse NMR spectrometer.
21 p3056 A72-41005
Investigation of the influence of cobalt on the redistribution of the atoms of the alloying elements in iron-base alloys by the NGR method
22 p3188 A72-42162
Structural characteristics of high resolution NMR spectra, noting interrelationships between line positions and intensities
23 p3290 A72-44171
Analysis of a nuclear magnetic resonance blood flowmeter for pulsatile flow.
24 p3401 A72-44574
- NUCLEAR PARTICLES**
NT ALPHA PARTICLES
NT ANTINEUTRONS
NT ANTIPARTICLES
NT ANTIPROTONS
NT BETA PARTICLES
NT BOSONS
NT MESONS
NT NUCLEONS
NT PHOTOELECTRONS
NT PHOTONS
NT PIONS
NT POSITRONS
Primary cosmic ray nuclear component, discussing Cosmos 163 measurements
01 p0119 A72-10603
Cosmic ray heavy nuclear component during solar activity minimum, using Cerenkov counters onboard Elektron satellites
07 p1060 A72-19872
Radiation damage effects in Li compensated Si nuclear particle detectors induced by irradiation with electrons, protons and fast neutrons
15 p2291 A72-31539
- Quantum yield variations of Nd ion activated glass as function of electron beam energy and intensity, noting nuclear particles effect on laser radiation
19 p2823 A72-38205
Weak decay, branching ratio and decay probability of strongly interacting particle event observed by Niu in cosmic nuclear jet shower
19 p2853 A72-38808
Nuclear particle fluxes and radioactive isotopes production rate distribution from cosmic rays data along orbits, calculating iron meteorite dimensions prior to atmosphere entry
22 p3220 A72-41919
- NUCLEAR PHYSICS**
NT FIELD THEORY [PHYSICS]
NT PLASMA PHYSICS
NT QUANTUM THEORY
NT REACTOR PHYSICS
Nuclear astrophysics review, discussing chemical elements and isotopes abundance and cosmic nucleosynthesis
03 p0437 A72-13842
Japanese cosmological studies covering evolutionary cosmology, astrophysics, relativity, nuclear physics and metagalactic phenomena
13 p2038 A72-29083
German book on vacuum technology covering theory, measurement techniques and applications in nuclear physics research facilities, electronic tubes, space environment simulation, mass transfer, etc
18 p2709 A72-36250
Experimental nuclear physics and theoretical solar structure and evolution explanations of disagreement between calculated and observed solar neutrino flux
18 p2722 A72-37007
- NUCLEAR POWER**
U NUCLEAR ENERGY
NUCLEAR POWER GENERATION
U NUCLEAR ELECTRIC POWER GENERATION
NUCLEAR POWER PLANTS
Permanent manned lunar stations electrical power systems, discussing nuclear energy, solar cells and electrochemical power cells
15 p2214 A72-31814
Probabilistic analysis of aircraft crash-caused structural damage to nuclear power plant, using Monte Carlo method and yield line theory for perforation and collapse modes
16 p2421 A72-33600
- NUCLEAR POWER REACTORS**
NT SPACE POWER REACTORS
NT SPACE POWER UNIT REACTORS
Gas-core reactor power transient analysis.
19 p2833 A72-37632
- NUCLEAR PROPELLED AIRCRAFT**
Nuclear energy for power and transportation, discussing ship, submarine, air cushion vehicle, aircraft and rocket propulsion applications
05 p0688 A72-15777
- NUCLEAR PROPULSION**
NT NUCLEAR ELECTRIC PROPULSION
Electrical and nuclear propulsion plasma containment problems, discussing simulation experiments and scaling devices feasibility
01 p0117 A72-10938
Mini-cavity gas core reactor concept for low thrust high impulse probe propulsion, using U 233 or 235 fuel
04 p0546 A72-14422
Transoceanic helium cooled thermal reactor powered air cushion freighter of gross weight 4500 metric tons, discussing design and performance characteristics
04 p0464 A72-14431
Controlled thermonuclear fusion for space propulsion, discussing magnetic-confinement and laser-plasma fusion engines
04 p0556 A72-14889
Nuclear energy for power and transportation, discussing ship, submarine, air cushion vehicle, aircraft and rocket propulsion applications
05 p0688 A72-15777
Current and future rocket and spacecraft propulsion systems based on chemical propellants, nuclear thermoelectric, electrostatic and electromagnetic power generators
05 p0705 A72-16743
Space technology developments during 1970s and 1980s, discussing solar system exploration, space shuttle systems, cost effectiveness, international cooperation, nuclear propulsion systems, etc
13 p2051 A72-28453
U.S. industry views on NASA plans for 1970s, emphasizing interplanetary nuclear propulsion, space transportation, shuttle costs and economics
14 p2175 A72-31139
Nonchemical space propulsion systems for lunar and planetary flights, discussing fission, fusion and electric rockets
15 p2297 A72-31810
Nuclear rocket propulsion program, discussing solid refractory core technology, Rover project and NERVA engine development and tests
15 p2273 A72-31811

Small power nuclear propulsion engines for Europa launching systems, discussing heat exchange reactor using hydrogen propellant 15 p2273 A72-31812

Thermonuclear fusion spacecraft propulsion systems operation principles, interplanetary orbit-to-orbit mission capabilities and environmental safeguard problems 17 p2598 A72-35953

Gas-core reactor power transient analysis. 19 p2833 A72-37632

Fission and fusion propulsion for deep space missions, discussing gas and colloid core reactors, controlled fusion, MHD and laser plasma systems 24 p3423 A72-45168

Development and testing of a radioisotope-fueled thruster for spacecraft propulsion. 24 p3434 A72-45178

Nuclear safety in nuclear power and propulsion devices for space. 24 p3424 A72-45180

On the utilization of thermonuclear propulsion for an upper stage of the Europa III launcher 24 p3424 A72-45227

NUCLEAR QUADRUPOLE RESONANCE

Frequency marker measurement of nuclear quadrupole resonance (NQR) signal in pulsed radio spectrometer compared with zero beat method 16 p2390 A72-33078

EPR transitions of quadrupole interaction of cubic imperfections with ground-vibronic-state degeneracy /Jahn-Teller effect/ 16 p2431 A72-33725

NUCLEAR RADIATION

NT BETA PARTICLES

NT FAST NEUTRONS

NT GAMMA RAY BEAMS

NT GAMMA RAYS

NT NEUTRON BEAMS

NT POST-BLAST NUCLEAR RADIATION

NT SPALLATION

NT THERMAL NEUTRONS

Fiber reinforced plastic composite seals for liquid hydrogen and nuclear radiation environments, stressing polyquinoxaline fitness 01 p0075 A72-10773

Nuclear pumped laser, noting electrically excited carbon dioxide laser experiment and high temperature multiple ionized plasma concepts 01 p0082 A72-11329

Nuclear radiation enhancement of carbon dioxide laser performance, discussing low pressure CW and high pressure pulsed discharges 01 p0082 A72-11330

Nuclear and space radiation effects - Conference, University of New Hampshire, Durham, July 1971. 03 p0402 A72-14076

Nuclear radiation interference and damage effects in galactic and solar cosmic ray measurements during charged particle experiments by deep space missions 03 p0438 A72-14085

Solar flare, galactic and magnetically trapped /Van Allen/ nuclear particle radiation environments calculation for three outer planet Grand Tour missions 03 p0413 A72-14095

Nuclear radiation effects on ceramic cemented strain gages and polyimide encapsulated epoxy bonded gages 08 p1164 A72-20922

Metal matrix composites, testing neutron irradiation effects on mechanical properties for nuclear application feasibility 11 p1654 A72-25483

Semiconductor devices application to gamma ray, X ray and nuclear radiations detection and analysis 15 p2235 A72-31644

Needle type solid state detectors for in vivo measurement of tracer activity. 18 p2655 A72-37194

NUCLEAR RADIATION SPECTROSCOPY

Multielement neutron activation analysis of geological and lunar material using chemical group separations and high resolution gamma spectrometry. 20 p2899 A72-39830

Coincidence counting applied to the activation analysis of meteorites and rocks. 20 p2900 A72-39841

NUCLEAR REACTIONS

NT ANNIHILATION REACTIONS

NT CONTROLLED FUSION

NT ELECTRON CAPTURE

NT ELECTRON SCATTERING

NT HIGH ENERGY INTERACTIONS

NT NEUTRON EMISSION

NT NEUTRON SCATTERING

NT NUCLEAR FISSION

NT NUCLEAR FUSION

NT NUCLEAR INTERACTIONS

NT NUCLEAR SCATTERING

NT PHOTONUCLEAR REACTIONS

NT PHOTOPRODUCTION

NT POSITRON ANNIHILATION

NT PROTON SCATTERING

NT PROTON-PROTON REACTIONS

NT RADIOACTIVE DECAY

NT RESONANCE SCATTERING

NT SPALLATION

NT SPIN-ORBIT INTERACTIONS

NT THERMONUCLEAR REACTIONS

Book on nuclear reactions in stellar surfaces and relations with stellar evolution covering high energy L elements formation, Li-Be observations and thermonuclear and spallative theories 01 p0122 A72-10002

Carbon dioxide laser pumping with nuclear reactions, indicating improved laser performance due to additional ionization by energetic charged particles 01 p0082 A72-11331

Primary cosmic ray interaction with tissues, emphasizing biological effects and nuclear reactions induced radioactivity in astronaut body 03 p0313 A72-12911

Dispersion energy relation for ultrahigh energy nuclear reactions in cosmic ray emulsion 03 p0410 A72-13148

Nuclear reactions in anomalous element abundances production for peculiar A stars, considering surface diffusion and surface and internal nuclear processes 03 p0437 A72-13872

X ray and gamma astronomy, discussing satellite-borne experiments for electromagnetic and nuclear reaction rates and antimatter existence in cosmic radiation 04 p0582 A72-15692

Type R Corona Borealis variable stars luminosity variations attributed to formation of carbon layer from He nuclear transformation process at stellar core-envelope boundary 08 p1231 A72-21086

Nuclear reaction-produced high energy ion beams for gas laser pumping and output enhancement 10 p1489 A72-23948

Algorithmic calculation for composition changes due to nuclear reactions and convective mixing during stellar evolution 15 p2314 A72-32374

Li, Be and B nuclei production via nuclear spallation reactions generated by Galactic cosmic ray bombardment of interstellar gas 16 p2448 A72-33737

Electron and nuclear components and transformations of matter under extreme conditions of pressure and temperature exemplified in stellar /pulsar/ evolution 18 p2725 A72-36520

Effects of nuclear reactions on the stability of degenerate stars. 19 p2864 A72-38100

Kinetic equations for ultradense matter neutronization, noting stellar configuration of given mass with variable volume 21 p3086 A72-40096

Turbulent plasma 'caldrons' in galactic nuclei 21 p3114 A72-41772

The threshold of disintegration of nuclei in a degenerate electron-neutron gas 22 p3209 A72-42963

Nuclear reactions in a degenerate electron-nuclear plasma 22 p3209 A72-42964

General characteristics of proton-nucleon and coherent interactions at an energy of 67 GeV 23 p3317 A72-44415

NUCLEAR REACTOR CONTROL

Controlled thermonuclear fusion for space propulsion, discussing magnetic-confinement and laser-plasma fusion engines 04 p0556 A72-14889

Singular controls calculation based on Poisson brackets, applying to nuclear reactor 06 p0849 A72-18300

Singular controls calculation based on Poisson brackets, applying to nuclear reactor 13 p1937 A72-29440

Dynamics and control of an incore-thermionic-reactor in the power region. 18 p2644 A72-36174

Feedback synthesis of an incore thermionic reactor control system for space. 18 p2645 A72-36186

Control of the incore thermionic reactor /ITR/ by movable reflector elements. 18 p2645 A72-36189

NUCLEAR REACTOR MATERIALS

U REACTOR MATERIALS

NUCLEAR REACTORS

NT ASTRON THERMONUCLEAR REACTOR

NT BREEDER REACTORS

NT ENGINEERING TEST REACTORS

NT GAS COOLED REACTORS

NT GASEOUS FISSION REACTORS

NT HIGH TEMPERATURE NUCLEAR REACTORS

NT MOLTEN SALT NUCLEAR REACTORS

NT NUCLEAR POWER REACTORS

NT SPACE POWER REACTORS

NT THERMAL REACTORS

NT WATER COOLED REACTORS

Acoustic emission tests of nuclear pressure vessels and piping, detecting weld slag, porosity, fatigue microcracking and stress corrosion cracking 01 p0048 A72-10802

Acoustic emission characteristics from nuclear reactor irradiated steels during tensile and wedge opening load tests 01 p0068 A72-10803

Energy release and accelerating inner stream effects on flow field near fuel injection in gas core reactor, basing Euler equations energy diffusion term on radial radiative transport 01 p0100 A72-11351

Minicavity reactor rocket engine combining high specific impulse of central gaseous fueled cavity and low weight NERVA type fuel elements in driver region external to moderator-reflector zone 01 p0100 A72-11358

Split core heat pipe nuclear reactor dynamics, describing shutdown mechanisms, ramp reactivity inputs fuel melting temperature and wall heat flux 04 p0546 A72-14421

Nuclear Brayton space power systems, discussing efficiency, isotope decay and reactor design 04 p0546 A72-14423

Water radiolysis within sealed Al capsules in nuclear reactor, calculating pressure rise due to water decomposition via predictive models derived by multiple regression analysis 04 p0546 A72-14429

Power supply and converters for satellite and spacecraft, discussing fuel cells, radioisotopes, nuclear reactors, etc 05 p0615 A72-16745

Fluid discharge rate relationship to space fraction for fluidized layers in reactor 13 p1943 A72-29786

Finite element method for nonlinear analysis of nuclear reactor structures, noting elasticity, viscoelasticity and elastoplasticity problems [SMRT PAPER M 2/2] 14 p2166 A72-30724

Magnetic field profile optimization for beta-limitation in minimum-B mirror confined plasma in nuclear reactor 16 p2432 A72-32805

Fusion reactor RF heating below 100 MHz, discussing coil structures and arcing and cooling problems in main fusion region 16 p2433 A72-32813

Completely modular thermionic reactor ion propulsion system /trips/. 18 p2721 A72-36177

Critical experiment ITR - Methods of nuclear design calculation and theoretical interpretation of experimental data. 18 p2709 A72-36185

Ionization of mercury vapor and cesium vapor in a nuclear reactor. 18 p2713 A72-36208

A small, 1400 K, reactor for Brayton space power systems. 19 p2833 A72-37635

NUCLEAR RELAXATION

Photoabsorption and simple and multiple excitations of rare gases internal atomic layers under X ray action, relating electron transition and relaxed core energies 09 p1357 A72-22836

Nuclear and dipole relaxation at polymer-polymer interfaces 23 p3307 A72-43931

NUCLEAR RESEARCH AND TEST REACTORS

NT HIGH TEMPERATURE NUCLEAR REACTORS

NUCLEAR ROCKET ENGINES

Thermonuclear microbomb ignition with intense relativistic electron beams for rocket propulsion, discussing achievable exhaust velocities and system optimization 01 p0117 A72-11222

High temperature gaseous U fission plasma core reactor engine concepts for space propulsion 01 p0099 A72-11327

Nuclear gas core and fusion rocket engines performance potential for various space missions, comparing capabilities in terms of payload ratio 01 p0099 A72-11328

Radiant heat attenuation of W seeded hydrogen aerosol at high pressure and temperature for gas core nuclear rocket propellant application 01 p0112 A72-11340

Shock tube technique for opacity measurement at high pressures in seeded hydrogen for gas core nuclear rockets 01 p0099 A72-11342

Simulation of nuclear light bulb engine propellant radiative heating, using argon seeded with micronized carbon particles and 500 kw dc arc as radiant energy source 01 p0099 A72-11344

Nuclear light bulb engine concept, detailing radiant heat transfer calculations in fuel and buffer gas regions 01 p0099 A72-11345

- Induction plasma heating simulation of open cycle gas core nuclear rocket engine, describing plasma forming material feed, permeable walls and propellant seeding
01 p0112 A72-11346
- Design of 6000 Mw open cycle gas core nuclear rocket engine with hydrogen as propellant, considering critical U 235 mass, major reactor components and specific impulse
01 p0099 A72-11347
- Open cycle gas core nuclear rocket engine, determining scaling laws for buoyancy force effect on fuel containment at various flow parameters
01 p0099 A72-11348
- Open cycle gas core nuclear rocket engine flow studies to obtain maximum system reactivity at low uranium/coolant gas loss ratio
01 p0100 A72-11349
- Injection geometry and inlet flow conditions application to open cycle gas nuclear reactor engine, evaluating fuel containment from cylindrical and spherical chambers experiments
01 p0100 A72-11350
- Space crew radiation dosage calculation from Mars mission high impulse gas core nuclear rocket engine exhaust plume fission fragments
01 p0022 A72-11353
- Nuclear light bulb rocket engine design and performance, presenting start-up, steady state operation, shutdown, dynamic response and control
01 p0100 A72-11354
- Thermal environment and fuel region simulation for nuclear light bulb engine, using rf induction heater and uranium and tungsten hexafluorides injection
01 p0113 A72-11355
- Transparent fused silica wall irradiation induced optical absorption and heat deposition in nuclear light bulb engine
01 p0103 A72-11356
- Minicavity reactor rocket engine combining high specific impulse of central gaseous fueled cavity and low weight NERVA type fuel elements in driver region external to moderator-reflector zone
01 p0100 A72-11358
- Flow characteristics of colloid core reactor rocket engine, studying two component vortex flows with solid to gas mass density ratios over 100
[AD-735527] 01 p0100 A72-11359
- Nozzle and cavity wall cooling limitations on uranium plasma nuclear rocket specific impulse, discussing wall heat flux and transpirational cooling by propellant flow
03 p0387 A72-14383
- Nuclear rocket time optimal start-up using distributed parameter system model with linear control and nonlinear state
04 p0547 A72-14672
- Controlled thermonuclear fusion for space propulsion, discussing magnetic-confinement and laser-plasma fusion engines
04 p0556 A72-14889
- Nuclear energy for power and transportation, discussing ship, submarine, air cushion vehicle, aircraft and rocket propulsion applications
05 p0688 A72-15777
- Gas core nuclear rocket reactor program for 60 day Mars, shuttle and Skylab applications
05 p0688 A72-15778
- Minimum time thrust start-up of nuclear rocket as optimal control problem with integrodifferential constraints, using Pontryagin maximum principle and calculus of variations
11 p1685 A72-25870
- Nuclear rocket for space tug, comparing performance and operational costs with chemical propulsion
13 p2000 A72-28926
- Two phase propellant flow rate through simulated rotating liquid core nuclear rocket fuel bed under high centrifugal acceleration
14 p2129 A72-30923
- Small power nuclear propulsion engines for Europa launching systems, discussing heat exchange reactor using hydrogen propellant
15 p2273 A72-31812
- Mission operations for unmanned nuclear electric propulsion outer planet exploration with a thermionic reactor spacecraft
17 p2606 A72-34578
- Thermionic reactor system for auxiliary power and electric propulsion
17 p2494 A72-34579
- Thermionic reactors design based on flashlight and external fuel concepts for nuclear electric propulsion
17 p2494 A72-34580
- Constant voltage and constant emitter-temperature control schemes dynamics in thermionic reactor, showing closed loop responses to load changes, converter failures and reactivity perturbations
17 p2494 A72-34581
- Thermionic reactor power conditioner design for nuclear electric propulsion
17 p2495 A72-34582
- Design features, fabrication technology and in-pile testing of thermionic reactor fuel elements
17 p2495 A72-34584
- Sizing an external-fueled in-core thermionic reactor
17 p2495 A72-34588
- Development of the insulating multilayer collector system for ITR /Status report/
17 p2559 A72-34594
- Metal working and testing of nuclear rocket engine components with Mo as structural material and uranium dioxide as fuel, discussing Mo-W interdiffusion
17 p2559 A72-34617
- Investigations concerning metal-hydride technology and hydrogen transport in the incore thermionic reactor /ITR/-core.
18 p2699 A72-36157
- Thermionic reactor electric propulsion system requirements.
18 p2720 A72-36167
- Auxiliary power and electric propulsion applications of thermionic reactor power systems in manned and unmanned space missions
18 p2644 A72-36168
- Controlled dc to dc converter for a space-qualified thermionic-reactor.
18 p2644 A72-36170
- High-voltage thermionic reactor using double-sheath fuel elements.
18 p2644 A72-36171
- Electronic temperature-flattening of thermionic reactors.
18 p2644 A72-36172
- Aspects on the modular lay-out of incore thermionic reactors.
18 p2645 A72-36175
- Significance of the results of the ITR critical experiments for the calculation of an incore-thermionic reactor.
18 p2645 A72-36180
- A comparison of thermionic reactor designs employing a common thermionic fuel element.
18 p2645 A72-36183
- Feedback synthesis of an incore thermionic reactor control system for space.
18 p2645 A72-36186
- Control of the incore thermionic reactor /ITR/ by movable reflector elements.
18 p2645 A72-36189
- Developmental status of thermionic materials.
19 p2833 A72-38575
- Nuclear rocket reactor and radioisotope power technology for propulsion and electricity requirements in spacecraft and space stations
24 p3423 A72-45166
- Thermionic reactor systems for space applications.
24 p3423 A72-45177
- NUCLEAR SCATTERING**
NT NEUTRON SCATTERING
NT RESONANCE SCATTERING
Analysis of pion-helium scattering for the pion charge form factor.
19 p2837 A72-37922
- Possibilities of determining complex form factors from experiments with polarized particles
21 p3086 A72-40100
- NUCLEAR SHIELDING**
U RADIATION SHIELDING
NUCLEAR SPIN
Proton and fluorine nuclear magnetic spin-lattice relaxations due to internal rotations in magnesium fluorosilicate hexahydrate
04 p0564 A72-15636
- NUCLEAR SUBMARINES**
U SUBMARINES
NUCLEAR-ELECTRIC MOMENTS
U ELECTRIC MOMENTS
NUCLEATE BOILING
NT LEIDENFROST PHENOMENON
Dry areas occurrence on heating surface in pool boiling near burnout heat flux, discussing nucleate and film boiling stability and hysteresis
07 p1099 A72-19621
- Nucleate pool boiling three component heat flux theory, taking into account latent heat transport, molecular heat conduction and turbulent convection
11 p1746 A72-26539
- High Jakob numbers effect on bubble growth rates during nucleate boiling, taking into account liquid inertia
14 p2172 A72-31053
- Subcooling and acceleration effects on nucleate boiling heat flux, comparing heat transfer prediction models with experimental measurements
16 p2477 A72-33433
- Convective heat exchange of metastable liquid during suspension of boiling
19 p2881 A72-38037
- NUCLEATION**
NT CLOUD SEEDING
Transmission electron microscopic investigation of heterogeneous nucleation of Al-Ag alloys metastable gamma prime phase, noting association with four dislocation types
01 p0083 A72-10209
- Short range order and nucleation of long range order in Ni-rich Ni-Nb alloys, observing electrical resistivity changes dependence on solute concentration
03 p0379 A72-14338
- Electron microscopic examination of molybdenum alloy thin plates aging at 700 C observing nucleation and precipitated phase
05 p0673 A72-16147
- Supercooled water drops freezing by contact nucleation with AgI and silicate particles, determining effective temperature in updraft wind tunnel experiments
09 p1345 A72-22445
- Nucleation mechanism for weld solidification in electron beam and tungsten-inert gas welding processes
09 p1332 A72-23641
- Binary Al alloys intermetallic phases effects on microcracks nucleation and propagation at 300 C in uniaxial tension, considering alloying elements influence on mechanical properties
14 p2124 A72-31036
- Thermal flux transmitted from hot surface to boiling fluid near nucleation site measured simultaneously with bubble growth rate
14 p2172 A72-31056
- Zinc oxide effect on alumina dispersion, energy of formation, nucleation and particle size reduction, calculating critical nucleus radii
16 p2476 A72-33255
- Luminous intensity, visibility duration, condensation nuclei and mass balance of noctilucent clouds
18 p2686 A72-36504
- Nucleation of new grains in recrystallization of cold-worked metals.
20 p2930 A72-39995
- Thin film deposition of carbon on polypropylene, noting morphological templates role in enhancement of polymer nucleation during recrystallization
23 p3305 A72-43269
- Electron-microscope study on the recrystallization in technically pure aluminum.
24 p3412 A72-44719
- NUCLEI**
Cloud and Aitken nuclei vertical distribution upwind and downwind of urban pollution sources from simultaneous airborne observations
09 p1345 A72-22443
- Reactions of aniline with isosamyl nitrite and phenyldiazonium borofluoride with caustic potash, investigating kinetics of chemical polarization of products nuclei
09 p1275 A72-22497
- Collapse of massless nonrotating gas particle nonuniform spheroidal shell contracting around gravitating massive point nucleus, interpreting galactic evolution
24 p3438 A72-44844
- NUCLEI [NUCLEAR PHYSICS]**
NT ALPHA PARTICLES
NT DEUTERONS
NT HEAVY NUCLEI
Cosmic Li, Be and B nuclei charge and isotopic composition measured by particle telescopes, finding L/M ratio
01 p0121 A72-11120
- Heavier-than-helium cosmic ray nuclei composition inferring galactic confinement of particles, path lengths and transit times
03 p0409 A72-13137
- Bevatron nuclear fragmentation of N 14 nuclei, discussing isotopic fragments identification
03 p0391 A72-13692
- Interstellar propagation of 2-8 Z galactic cosmic ray nuclei at 10-1000 MeV/nucleon, analyzing differential kinetic energy spectra
04 p0567 A72-15323
- Nuclear charge composition and energy spectra measurement for hydrogen, helium and medium nuclei in 12 April 1969 solar particle event
04 p0567 A72-15325
- High energy cosmic ray pions and nucleons interactions with atomic nuclei, using ionization calorimeter and spark chambers system
06 p0869 A72-17267
- Adiabatic-nuclei theory application to diatomic molecules excitation by electron impact, approximating fixed nuclei phase shifts dependence on inter-nuclear separation
06 p0852 A72-17826
- Perturbation theory oscillatory wave function for second order correction to oxygen 16 nucleus bonding energy
08 p1211 A72-21067
- Angular distributions of proton polarization during elastic scattering by V, Cr, Ni and Co nuclei in high energy region
08 p1211 A72-21093
- Inclusive isotope spectra of secondary nuclei produced by Bevatron heavy ion fragmentation in carbon and polyethylene targets, noting partial differential cross sections
10 p1517 A72-25144

- Cosmic ray proton and He nuclei differential energy spectra measurements by balloon-borne ionization spectrometer 11 p1712 A72-25881
- Cosmic ray nuclei charge and isotope composition measurement, discussing data for Li, Be, B and 15-30Z nuclei 16 p2447 A72-33727
- Cosmic ray nuclei isotope identification with cryogenic magnet plus plastic scintillators to measure charge composition and rigidity 16 p2447 A72-33732
- Neutron-rich nuclei in a Fermi gas 19 p2837 A72-38060
- Spatial spark jitter measurements of highly charged nuclei for optical spark chambers. 21 p3055 A72-41003
- Investigation of hadron interactions with atomic nuclei at energies greater than 100 GeV 23 p3329 A72-44404
- Multiplicity of particles generated in inelastic interactions of nucleons with LiH nuclei at energies from 150 to 550 GeV 23 p3329 A72-44405
- Multiple collisions and an optical model of the inelastic interaction between cosmic particles and nuclei 23 p3330 A72-44413

NUCLEIC ACIDS

NT RIBONUCLEIC ACIDS

- Site binding model of nucleic acid-protein interactions for chemical evolution and genetic code studies 02 p0159 A72-11765
- Nucleic acid, protein and cell primordial sequence, ribosomes and genetic code for life origin, discussing experiments on homopolyamine acids reaction with mononucleotides 04 p0468 A72-14775
- Proteobionts formation by random aggregation and reproduction from proteins and nucleic acids macromolecules 04 p0469 A72-14782
- Protein evolution, discussing biological group amino and nucleic acid structure variations from phylogenetic tree of cytochrome c data 04 p0470 A72-14791
- Comet collisions in planetary nebulae as source of organic compounds in universe in preplanetary era, noting nucleic acid bases in carbonaceous meteorites 04 p0471 A72-14802
- Genetic organization emergence, considering pretranslational evolution in nontranslational protein synthesis, nucleic acid evolution and gene origin 08 p1119 A72-22010
- Abiogenic formation of nucleic acid bases and nucleosides in photochemically synthesized self sustaining coacervates 12 p1761 A72-27657
- Role of the synthesis of nucleic acids and proteins in the adaptation of the organism to altitude hypoxia. 17 p2502 A72-34990
- Nuclein acid contents in cholinergic and adrenergic spinal cord neurons and in their glial satellite-cells during hypoxic hypoxia and a post-hypoxia period 19 p2756 A72-37742

NUCLOGENESIS

- Amino acid code comparisons of polypeptide chains of globins due to mutations during vertebrate evolution from ancestral gene 02 p0159 A72-11764
- Site binding model of nucleic acid-protein interactions for chemical evolution and genetic code studies 02 p0159 A72-11765
- Nucleotides condensation in aqueous system in prebiotic conditions, investigating effects of imidazole, cyanamide and polymorphine 04 p0483 A72-14766
- DNA primary structure variability relation to origin and evolution, discussing taxon scale in existing animal, plant and microorganism systems 04 p0470 A72-14792

NUCLEON-NUCLEON INTERACTIONS

- Multiple meson production in 250 GeV nucleon-nucleon collisions in LiH targets, noting 40 per cent formation of heavy meson cluster fireballs 06 p0868 A72-17259
- K-neutral pion inelasticity factor measurement for nucleon interactions in carbon corresponding to primary neutron energy transferred to pions 06 p0869 A72-17269

NUCLEON-NUCLEON SCATTERING

- Approximation for Monte Carlo method modeling of pion-nucleon and nucleon-nucleon inelastic collisions at high energies 23 p3317 A72-44414

NUCLEONICS

- Observability of hyperfine structure and Lamb, nuclear-volume shifts in 1sn1-1sn' transitions of helium-like ions. 19 p2837 A72-37544

NUCLEONS

- High energy nucleon tissue doses calculation based on averaged characteristics of nuclear interactions [CERN-71-16] 02 p0162 A72-12067

Nuclear-electron cascades longitudinal evolution calculation in ionization calorimeter for primary nucleons and pions, using Monte Carlo method 06 p0811 A72-17260

Inelasticity factor dependence on particle energy spectra to explain nucleon flux calculations and Proton satellite data, considering scattering cross sections 06 p0869 A72-17264

High energy cosmic ray pions and nucleons interactions with atomic nuclei, using ionization calorimeter and spark chambers system 06 p0869 A72-17267

Secondary particles in pion-nucleon and coherent interactions, measuring momentum from multiple Coulomb scattering 06 p0870 A72-17272

Nuclear photoemulsions under bombardment by pion beam of 60 GeV/c momentum, investigating pion-nucleon interactions involving recoil protons 06 p0851 A72-17273

Pion-nucleon high energy interactions, determining inelasticity coefficient distribution 06 p0851 A72-17274

Primary cosmic radiation nucleonic component composition comparison with elements natural abundance, discussing mechanism of matter injection into cosmic ray accelerator 07 p1059 A72-19586

Extensive atmospheric showers and high energy transfer from interacting nucleons to electron photon cascades 07 p1060 A72-19867

Three dimensional cosmic ray anisotropy and density distribution at earth orbit and in interplanetary space with allowance for primary particle and nucleon energy spectrum 07 p1065 A72-20645

Nucleon and electromagnetic component generation, energy spectrum and diffusion during solar flares 07 p1066 A72-20651

High energy hadrons time structure in extensive air showers, considering production of nucleon-antinucleon pairs in particle interactions 07 p1067 A72-20687

Quantum gravitation theory and Mercury perihelion motion, calculating three body potentials from treatment of celestial bodies as nucleon assemblies 07 p1084 A72-20690

Pion generation during collective interactions between nucleons of heavy cosmic ray nuclei, using Proton 4 satellite data 08 p1228 A72-22179

Scaling of energy spectrum of particles emitted in high energy nucleon-nucleon collisions 10 p1529 A72-24527

The absorption length for solar particles in the earth's atmosphere - Solar proton event November 18, 1968. 17 p2602 A72-35760

Pion generation during collective interactions between nucleons in heavy cosmic ray nuclei, using Proton 4 satellite data 18 p2721 A72-36235

Pion exchange and the cosmic-ray nucleon cascade. 19 p2851 A72-37923

The threshold of disintegration of nuclei in a degenerate electron-neutron gas 22 p3209 A72-42963

High altitude cosmic ray pion and nucleon interaction characteristics at high energies, using spark chamber, Cerenkov absorption spectrometer and ionization calorimeter measurements 23 p3329 A72-44402

Multiplicity of particles generated in inelastic interactions of nucleons with LiH nuclei at energies from 150 to 550 GeV 23 p3329 A72-44405

Collective interactions of the nucleons of heavy nuclei in high-energy cosmic rays 23 p3330 A72-44408

Ionization calorimeter for neutral pion production investigation in high energy hadrons interaction, noting energy transfer identity for nucleon and pion interactions 23 p3330 A72-44409

High energy inelastic collisions of pions and protons with nuclear emulsion nucleons, noting pion pulse spectra 23 p3317 A72-44417

Low-energy nucleons in extensive air showers 23 p3331 A72-44424

Energy dependence of muon-nucleon inelastic interaction, calculating photonuclear cross section for high energy interactions in iron 23 p3331 A72-44429

Characteristics of pion and nucleon interaction with carbon and aluminum nuclei over the energy range from 30 to 300 GeV 23 p3331 A72-44435

High energy nucleon inelastic collision characteristics dependence on secondary particle energy and meson velocity, using Wilson chamber measurement 23 p3291 A72-44445

Primary cosmic ray nucleon spectrum from sea-level muon spectrum and scaling hypothesis parameters. 23 p3332 A72-44458

NUCLEOSIDES

NT ADENINES
NT ADENOSINE DIPHOSPHATE [ADP]
NT ADENOSINE TRIPHOSPHATE [ATP]
NT ADENOSINES

Inorganic phosphates-nucleoside hypohydrous thermal reaction mechanism, discussing thermal polymerization of orthophosphates for phosphorylation and condensing agents in primordial synthesis 04 p0483 A72-14770

Abiogenic formation of nucleic acid bases and nucleosides in photochemically synthesized self sustaining coacervates 12 p1761 A72-27657

Studies in prebiotic synthesis. VII - Solid-state synthesis of purine nucleosides. 23 p3262 A72-43567

NUCLEOSYNTHESIS

U NUCLEAR FUSION

NUCLEOTIDES

NT ADENINES
NT ADENOSINE DIPHOSPHATE [ADP]
NT ADENOSINE TRIPHOSPHATE [ATP]
NT ADENOSINES

Site binding model of nucleic acid-protein interactions for chemical evolution and genetic code studies 02 p0159 A72-11765

Nucleotides condensation in aqueous system in prebiotic conditions, investigating effects of imidazole, cyanamide and polymorphine 04 p0483 A72-14766

Biochemical processes and structures interrelation, using nucleoprotein coacervate models and ribonuclease and polynucleotide phosphorylase enzymes 04 p0469 A72-14783

Enzymically synthesized homopolynucleotide and lysine-rich proteinoid microparticles effect on aminoacyl adenylate condensation as basis for genetic code origin 06 p0770 A72-17724

Evolutionary significance of primary amino acid or nucleotide base sequences of DNAs within various phylogenetic groups 12 p1759 A72-27160

NUCLIDES

NT ALUMINUM ISOTOPES
NT ARGON ISOTOPES
NT BARIUM ISOTOPES
NT BERYLLIUM ISOTOPES
NT BORON ISOTOPES
NT CALCIUM ISOTOPES
NT CARBON ISOTOPES
NT CESIUM VAPOR
NT DEUTERIUM
NT GALLIUM ISOTOPES
NT HELIUM ISOTOPES
NT HYDROGEN ISOTOPES
NT IODINE ISOTOPES
NT ISOTOPES
NT KRYPTON ISOTOPES
NT LEAD ISOTOPES
NT LITHIUM ISOTOPES
NT LUTETIUM
NT MANGANESE ISOTOPES
NT NEON ISOTOPES
NT NITROGEN ISOTOPES
NT OXYGEN ISOTOPES
NT PLUTONIUM ISOTOPES
NT POTASSIUM ISOTOPES
NT RADIOACTIVE ISOTOPES
NT RADON ISOTOPES
NT RUBIDIUM ISOTOPES
NT STRONTIUM ISOTOPES
NT TELLURIUM
NT THORIUM ISOTOPES
NT TIN ISOTOPES
NT TITANIUM ISOTOPES
NT TRANSURANIUM ELEMENTS
NT TRITIUM
NT URANIUM ISOTOPES
NT XENON ISOTOPES

Bremsstrahlung from cylindrical beta sources. 21 p3088 A72-41383

NULL HYPOTHESIS

Cyclic phenomena periodicity by expected mean square deviation statistical analysis of observational data samples, using null hypothesis and unequally spaced sample intervals 04 p0574 A72-14908

NULL REFERENCE GLIDE PATH

U GLIDE PATHS

NULL ZONES

Null electromagnetic field propagation in general relativity, applying to Stokes parameters definitions for monochromatic light 02 p0259 A72-12178

Adiabatic charged particle orbits in magnetic null sheet with transverse electric and added normal magnetic fields 03 p0348 A72-13512

Phased antenna array blind spot detection and elimination, describing aperture match with inductive irises 04 p0486 A72-14493

Global controllability of nonlinear differential systems during linear system perturbation, discussing controllable and uncontrollable parts splitting and null domain nature 11 p1608 A72-25323

Exact solutions of the Einstein-Maxwell equations for an accelerated charge. 20 p2955 A72-40008

NUMBER THEORY

NT ARITHMETIC

NT CONGRUENCES

NT DIOPHANTINE EQUATION

NT DIVIDING [MATHEMATICS]

NT INTEGERS

NT MULTIPLICATION

NT SUBTRACTION

Equivariant integrality theorems for differentiable manifolds. 22 p3199 A72-42310

NUMERICAL ANALYSIS

NT APPROXIMATION

NT BORN APPROXIMATION

NT BORN-OPPENHEIMER APPROXIMATION

NT CHEBYSHEV APPROXIMATION

NT DIFFERENCE EQUATIONS

NT ERROR ANALYSIS

NT FINITE DIFFERENCE THEORY

NT HARTREE APPROXIMATION

NT INTERPOLATION

NT ITERATION

NT ITERATIVE SOLUTION

NT LEAST SQUARES METHOD

NT MONTE CARLO METHOD

NT NEWTON-RAPHSON METHOD

NT NOMOGRAPHS

NT NUMERICAL INTEGRATION

NT OSEEN APPROXIMATION

NT PADE APPROXIMATION

NT PARTICLE IN CELL TECHNIQUE

NT POHLHAUSEN METHOD

NT RAYLEIGH-RITZ METHOD

NT RELAXATION METHOD [MATHEMATICS]

NT RITZ AVERAGING METHOD

NT RUNGE-KUTTA METHOD

NT SCHWARTZ METHOD

NT SOMMERFELD APPROXIMATION

NT TRUNCATION ERRORS

Feautrier numerical solutions to transfer equation of polarized continuum radiation from sunspot in chromosome 01 p0101 A72-10096

Mathematical analysis of separation standards and aircraft navigational collision risk for parallel tracks in radar monitored systems 01 p0096 A72-10178

Weather map numerical analysis for Northern Hemisphere, describing program with flow field for geopotential value checking 01 p0094 A72-10196

Metal crystals dislocations movements and interactions with dislocation dipole under applied cyclic stresses for various configurations and starting conditions, using numerical methods 01 p0113 A72-10208

Modified implicit continuous fluid Eulerian technique for numerical solution of time dependent fluid flow for Mach numbers from zero to infinity 01 p0049 A72-10226

Fluid flow numerical solution by contour dynamics methodology with flow features resolution advantage. 01 p0049 A72-10227

Simplified Marker and Cell method extension for numerical solution of almost three dimensional incompressible flow and internal obstacle treatment 01 p0049 A72-10228

Alternating directional implicit numerical solution for three dimensional steady low density hypersonic flow over finite width flat plate [AD-736572] 01 p0049 A72-10230

Large scale structural systems dynamic response analysis, discussing numerical techniques with emphasis on computer codes usage [SAE PAPER 710780] 01 p0137 A72-10272

Correspondence principle application to numerical solution for plane boundary value problem of linear viscoelasticity theory based on Kelvin point force solution to field equations 01 p0138 A72-10512

Numerical analysis of radio echoes decay rate from randomly ionized meteor trails 01 p0130 A72-10913

Step-by-step algorithmic numerical solution for nonlinear Volterra integro-differential equation, considering convergence 01 p0093 A72-11105

Numerical method for wave propagation and dynamic stresses in viscoelastic cylinders under internal and external loads 01 p0144 A72-11375

Survey and bibliography of extrapolation processes in numerical analysis based on polynomial or rational functions 02 p0252 A72-11546

Incompressible nonself similar turbulent and transitional flows numerical analysis in wakes, jets and boundary layers, using turbulent viscosity equations 02 p0202 A72-11587

Numerical analysis of nonequilibrium gas mixture flow through nozzle 02 p0149 A72-11589

Associative array digital processors application to numerical solution of partial differential equations, illustrating methodology on weather forecasting equations 02 p0186 A72-11658

Monochromatic electromagnetic field diffraction problems in homogeneous medium, presenting computer aided numerical analysis 02 p0171 A72-11690

Hollow waveguide problem considering numerical solution with scalar field approximation, Green function and conformal transformation 02 p0191 A72-11692

Stiffness matrix method application to finite deformation theory, noting convergence through use of iterative interpolation in numerical calculations 02 p0298 A72-12667

Stress-strain state determination for plane orthotropic bodies by optical polarization method, discussing numerical methods for stress and strain tensor components 03 p0445 A72-13580

Current lines and temperature fields in square cavity with one movable wall and viscous flow and heat transfer, solving equations numerically 03 p0456 A72-13629

Rigid/plastic media plane and axially symmetric deformations determination, using principal and slip line numerical analysis methods 03 p0446 A72-13704

Plastic torsion of prismatic and anisotropic rods, emphasizing inhomogeneity problems numerical solution 03 p0447 A72-13853

Hydrogen diffusivity in Fe with cavities at room temperature calculated by mathematical model and numerical methods 03 p0378 A72-14256

Numerical method and computerized design for feedback controller pulse transfer function in overall error criterion minimization, comparing results with sampled error method 03 p0329 A72-14355

Human body kinematics numerical analysis, obtaining space-time resolution by photogrammetric restitution and electronic data processing of photographic recordings 04 p0478 A72-14710

Shooting and imbedding methods for theoretical analysis and approximate numerical solution of two-point boundary value problems involving n-vector-valued functions [AD-743615] 04 p0539 A72-15043

Numerical fluctuations minimization during luminosity functions and density evolution derivations from data subject to observational selection, applying to 3CR quasars 04 p0577 A72-15284

Buckling of radially constrained imperfect circular ring loaded within perfect rigid circular boundary, obtaining numerical solution by discrete treatment 04 p0591 A72-15286

Spacecraft antenna radiation pattern numerical analysis using combined electric and magnetic integral equations 04 p0500 A72-15407

Numerical instability of gravitational n-body problem considering differences between computed systems and exact solutions to differential equations 04 p0581 A72-15629

Navier-Stokes equations numerical solution by computerized simulation for viscous channel flow with diaphragm orifice reducing cross section 04 p0513 A72-15644

Wilf-type quadrature formulas with preassigned nodes, featuring existence of error bound without derivatives 05 p0632 A72-15816

Approximate numerical method for calculating flow profiles in arteries from local pressure measurements, taking into account Navier-Stokes equations nonlinear terms [ASME PAPER 71-WA/BHF-3] 05 p0621 A72-15948

Numerical method for cylindrical microwave cavities calibration for plasma diagnostics, noting computer programs applicability for arbitrary electron density radial distributions 05 p0662 A72-16418

Higher order nonlinear autonomous oscillation system limit cycle and stability determination by numerical solution based on Andronov point transformation and Liapunov theory 06 p0838 A72-17377

Moderate Hartmann number MHD duct flow with applied transverse magnetic field, using numerical methods 06 p0859 A72-17619

Soviet book on qualitative methods in celestial mechanics covering differential equations of motion averaging schemes, Newton type convergence method, three body problems, etc 06 p0879 A72-17821

Kalman and linear numerical filtering, discussing data processing from wind tunnel and rocket flight tests 06 p0774 A72-17847

Waveguide integral equation numerical solution by moment method, suggesting algorithm for detecting and alleviating relative convergence behavior [AD-745595] 06 p0775 A72-18368

Beams and square plates nonlinear vibration response to random concentrated driving force solved numerically on digital computer 06 p0901 A72-18718

Computer simulated data analysis procedure for improved resolution of optical instrument by integral equation numerical solution 06 p0840 A72-18738

Coefficient matrix for estimation of numerical solution error bounds for finite element models 07 p1025 A72-18786

Numerical analysis of computing velocity distribution in vortex row cascade profiles by method of singularities 07 p0965 A72-18787

Round-off error analysis in numerical solutions of finite element equations in dynamic models 07 p1025 A72-18796

Hf diffusion type chemical laser fluid dynamic and optical properties, discussing computerized numerical analysis [AIAA PAPER 72-146] 07 p1001 A72-19063

Numerical solution of equations for asteroidal mass distribution under collisional fragmentation 07 p1071 A72-19180

Feasible solutions to automatic control problems satisfying multiple state and control variable inequality constraints, discussing algorithmic numerical implementation 07 p0959 A72-19281

Toeplitz matrix in numerical solution of integral equation for cylindrical antenna and array, presenting rapid inversion algorithm by exploiting symmetry properties [AD-743577] 07 p0957 A72-19795

Heat transfer steady state and transient response problems nodal formulation and numerical solution on digital computer 07 p1101 A72-19918

Navier-Stokes equation numerical solution methods, expressing boundary conditions by separate equations for vorticity and stream function 07 p0970 A72-20077

Transonic flow past wing airfoils, obtaining numerical solution by fitting mixed initial boundary conditions 07 p0909 A72-20079

Numerical determination of particle number and mass flux density in monatomic rarefied gas flow through circular orifice at finite pressure ratio 07 p0972 A72-20107

Numerical analysis of passing screw dislocation arrays under stress for computerized work hardening model 07 p1097 A72-20556

Computerized numerical nodal analysis of heat transfer away from bridgewire of electroexplosive device to meet all- and no-fire requirements 08 p1219 A72-20753

Digital computer numerical procedure to solve dynamo theory MHD equations for earth nucleus, using combination of Fourier and finite difference methods for integration 08 p1155 A72-20810

High energy electron beam interaction with dense plasma, investigating unstable waves growth by numerical methods 08 p1213 A72-21259

Numerical solution of disintegration and surface stability of gas bubbles under nonspherical free oscillation 08 p1149 A72-21295

Numerical analysis of capture area ratio effect on shock wave propagation from free stream into moving flowing duct 08 p1150 A72-21619

German monograph on optimum principle for numerical representation of surfaces, discussing association with elasticity theory extremal requirements 09 p1340 A72-22319

Axisymmetric MHD equilibria with elliptical cross sections and flat current profile, obtaining criterion for stability to localized modes by numerical computation 09 p1361 A72-23047

Spatial filtering techniques and numerical classification methods for pattern recognition in automated photointerpretation 09 p1312 A72-23305

Numerical solution of turbulent recirculating flow, using energy equation to estimate eddy viscosity distribution

10 p1464 A72-23869

Metal creep under multiaxial stress states, proposing technique for numerical stress analysis data collection

[SMRT PAPER L 1/3] 10 p1556 A72-24395

Structural design systematology of statics and dynamics numerical approximate procedures based on variational principles and differential equations

[SMRT PAPER M 7/4] 10 p1505 A72-24397

Numerical solution of nonlinear integrodifferential equation governing finite amplitude wave propagation on concentrated vortices

10 p1468 A72-24419

Stiffened panels initial buckling under longitudinal compression, presenting results obtained by numerical methods

10 p1558 A72-24843

Numerical solution of two massive rigid bodies impact with variable slipping direction using Routh momentum change theorem

11 p1735 A72-25769

Numerical stability in linear algebraic equations, considering mapping from input data to desired output information

11 p1677 A72-25861

Numerical calculation of temperature distribution and tempering depth for inductive hardening process with automatic material feed, taking into account temperature dependent material properties

11 p1639 A72-25898

Numerical analysis applications - Conference, University of Dundee, Scotland, March 1971

11 p1679 A72-26953

Integral equation numerical solution applications to rectangular solid capacitance calculation and mixed boundary value problems

11 p1679 A72-26954

Inverse eigenvalue problem numerical solution for matrices and difference and differential equations, obtaining algorithms for parameters estimation

11 p1679 A72-26955

Recursive algorithm for numerical solution of Sturm-Liouville problem with periodic boundary conditions

11 p1679 A72-26958

Representational method for evolution type partial differential equations numerical solution, noting relationship to finite element method

11 p1679 A72-26961

Plane Poiseuille flow Orr-Sommerfeld problem numerical solutions comparison and computer program implementation

12 p1797 A72-27192

Helmholtz equation numerical solution for potential field problems with arbitrary boundary conditions of wave propagation, diffusion and thermal conduction in mathematical physics

12 p1846 A72-27553

Numerical methods for inverse solution to turbulent swirling boundary layer combustion flow problem

13 p2063 A72-28420

Numerical analysis methods for solution stability of reduced field equations describing perturbed motion of body under nonconservative loads

13 p2001 A72-28485

Numerical methods to solve boundary value problems of monochromatic transport equations in light scattering media optics

13 p2001 A72-28504

Numerical description of electromagnetic radiation from open-ended flanged waveguides, giving truncation corrected expressions for field behavior in aperture perimeter vicinity

13 p1915 A72-28520

Numerical analysis of surface current density distribution and electromagnetic fields of conducting body, noting radiation patterns of radial dipole and quarter wavelength monopole

13 p1916 A72-28541

Nonlinearity effect on electron plasma wave dispersion relation, using numerical simulation and theoretical analysis by perturbation expansion and Hamilton variational principle

13 p2011 A72-29121

Numerical analysis method for performance prediction of linear induction machines including liquid metal MHD pumps and generators and linear motors

13 p1900 A72-29365

Digital data processing techniques for aircraft engine noise data reduction, analyzing fan noise spectrum

13 p1925 A72-29840

Relaxation method for thermal computation programs to solve nonlinear heat exchange equations for steady state temperature distribution, discussing numerical instability due to linearization

14 p2170 A72-30684

Holomorphic rational functions involving error bounds without derivatives solution by numerical differentiation procedure

14 p2126 A72-30709

Two dimensional numerical solution of semiconductor steady state transport equations, applying to MOS and bipolar transistors

14 p2142 A72-30847

Arbitrary cascade profiles aerodynamic characteristics calculation via integral equation numerical solution for attached potential incompressible fluid problem

14 p2070 A72-31014

Numerical calculation of stresses and displacements in variable radius bodies of revolution under axially symmetric torsional load, using Fredholm type integral equation

15 p2324 A72-31480

Low storage numerical solution of waveguide problem based on impulse analysis, using random walk technique to eliminate large matrix processing

15 p2194 A72-31542

Numerical analysis of steady one dimensional quasi-shock waves in collisionless plasma within longitudinal uniform magnetic field, noting oscillations behind wave front

15 p2284 A72-31584

Bairstow Method extension with restored convergence for multiple quadratic factors using interval arithmetic

15 p2262 A72-31631

Orthogonal vibration damping matrix numerical evaluation, comparing Caughey series and direct approaches

15 p2326 A72-31711

Monatomic ionized gas thermodynamic properties direct computation by numerical method without iteration or numerical differentiation

15 p2335 A72-31714

Thin circular loop antenna input admittance and current distribution calculation comparison

15 p2209 A72-32673

Numerical methods for Liapunov linear matrix equations solution in control systems analysis and design

15 p2265 A72-32798

Numerical method for force-free magnetic field structures in solar active regions, discussing rotation effects

16 p2455 A72-33462

Sea level wind and pressure data adjustment to governing dynamical equations by numerical variational analysis, using Sasaki matching technique

16 p2419 A72-33941

Numerical construction of the Hill functions.

17 p2573 A72-34216

Rate of convergence of several conjugate gradient algorithms.

17 p2573 A72-34218

Block five diagonal matrices and the fast numerical solution of the biharmonic equation.

17 p2574 A72-34446

On the numerical solution of elliptic partial differential equations by the method of lines.

17 p2575 A72-34647

Discrete vortex model numerical simulation of Onsager negative temperature instability for interacting line vortices two dimensional motions

17 p2538 A72-34871

The evaluation of the stress intensity factors for cracks subjected to tension, torsion, and flexure by an efficient numerical technique.

17 p2631 A72-34966

A comparison of numerical methods for determining stress intensity factors.

17 p2631 A72-34973

Particle interactions in real and numerically simulated plasmas, considering effects of macroparticles formation via idealized clustering

17 p2590 A72-35143

Russian book on numerical methods in optimal control systems theory covering functional extremum, dynamic programming, control synthesis and statistical linearization of nonlinear systems

17 p2533 A72-35458

Numerical solution of an optimal control problem with a probability criterion.

17 p2534 A72-35531

Verification of theory for plasma of finite-size particles.

17 p2592 A72-35618

Programmable computation method based on matrix formulation for numerical solution of differential equations in heat conduction and thermal stress problems

17 p2635 A72-35898

Numerical calculation of energy storage, wave dispersion and propagation in waveguides of periodic resonator chains at high frequencies

18 p2657 A72-36105

Effective dimensional reduction in the computation of linear, discrete, time-delay problems.

18 p2672 A72-36302

Theoretical models for cavity and wake flows, outlining numerical methods for solving functional equations

18 p2679 A72-36387

A basic theorem in the computation of ellipsoidal error bounds.

18 p2705 A72-36602

The numerical solution of Fredholm integral equations of the second kind with singular kernels.

18 p2705 A72-36603

A numerical method for coupled differential equations.

18 p2705 A72-37174

Numerical prediction of the diffusion of exhaust products of supersonic aircraft in the stratosphere

19 p2748 A72-37824

Numerical solutions in the simplest problem of the calculus of variations.

19 p2827 A72-38382

The Galerkin method for the numerical solution of Fredholm integral equations of the second kind.

19 p2827 A72-38384

The possible use of Laguerre polynomials for representing the vertical structure of numerical models of the atmosphere.

19 p2829 A72-38562

Marcum Q function parameters approximations for error probabilities computation in multilevel frequency shift keying and differentially coherent phase shift keying systems

20 p2903 A72-39426

Book - Functional analysis and approximation theory in numerical analysis.

20 p2946 A72-39729

An inverse problem in boundary-layer flows - Numerical determination of pressure gradient for a given wall shear.

21 p3043 A72-40108

A numerical solution for the near and far fields of an annular ring of magnetic current.

21 p3015 A72-40354

Numerical analysis of microwave heat generation in disc-shaped Luneberg lenses.

21 p3032 A72-40627

Computation of three-dimensional non-equilibrium supersonic flows.

[ICASP PAPER 72-37] 21 p2992 A72-41162

Conformal mapping procedure for numerical generation of airfoils with local curvature singularities, presenting test problem results for zero trailing edge angle

21 p2992 A72-41259

Numerical solution of a boundary value problem arising in the deflection of beams and shells.

21 p3122 A72-41311

Computational solutions of matrix problems over an integral domain.

21 p3076 A72-41315

The motion of a viscous fluid past an impulsively started semi-infinite flat plate.

21 p3046 A72-41316

Regularized linear problem with perturbed equation as solution, presenting error overestimate

21 p3076 A72-41336

Eigenvalue numerical solution for dispersion relation and propagation characteristics of nonlocal drift waves in cylindrical plasma based on two fluid model

21 p3093 A72-41495

Orbit prediction for artificial satellites via numerical averaging technique, presenting algorithm for planetary equations solution

[AIAA PAPER 72-934] 21 p3112 A72-41572

Computer-aided numerical solution for electric field structure of rod and plate, calculating field distortion by rod antennas and near lightning rod

21 p3086 A72-41671

Mathematical spectra theory application to matrix eigenvalue problem, obtaining explicit form of determinant characteristic polynomial by numerical methods

21 p3076 A72-41781

Time dependent one dimensional numerical model of hail-bearing cumulus cloud, using microphysical process parameterization and exponential raindrop and hailstone size distributions

22 p3201 A72-42513

Clamped circular rigid-plastic plates subjected to central blast loading.

22 p3235 A72-42601

Numerical solution of bending stresses in elastic cantilever plates under surface and edge loads, noting boundary layer, load concentration and sweep back effects

22 p3236 A72-42609

Numerical analysis of the natural convection in a porous medium between two concentric cylinders

22 p3244 A72-42640

Analysis of the transient response of shell structures by numerical methods.

22 p3237 A72-42762

Multimoded components wavefront arrival angle from measurements of signal induced in linear array, discussing numerical calculation from linear equation solution and polynomial roots

23 p3264 A72-43601

Numerical determination of the stress concentration around a hole in a circular cylindrical shell

23 p3348 A72-43799

Results of a numerical solution of a complex dispersion equation for the HE-sub 11 wave in a two-layer circular waveguide 23 p3273 A72-44214

Numerical evaluation of elastic stress intensity factors by the boundary-integral equation method. 23 p3353 A72-44233

Numerical analysis of global satellite triangulation grid projects 24 p3397 A72-44868

Numerical analysis of natural frequency spectrum of plastic plate free vibrations in compressible inviscid fluid 24 p3459 A72-45003

Frequency multiplication with a traveling-wave tube. II - Numerical analysis of a traveling-wave frequency multiplier by the large-signal theory. 24 p3386 A72-45285

A general theory of convergence for numerical methods. 24 p3419 A72-45300

NUMERICAL CONTROL

Nd-YAG laser system generating gold conductor patterns on ceramic substrates, using numerical control system for Si production 07 p1002 A72-19213

Closed line magnetic confinement device filled with laser produced hydrogen plasma, discussing laser beam high speed numerical control for injected pellet interception [CLEA PAPER 12,1] 07 p1040 A72-19392

Numerically controlled machine tools accuracy, discussing feed spindle and displacement/angle measuring system errors determination through angular step transducers and laser interferometer 07 p0995 A72-19684

Large automated tape placement machine tool design and construction for laying up aircraft structures from composite materials 08 p1177 A72-21690

Sequential control using computer program for signal processing, noting machine tool, die casting, elevator and warehouse applications 09 p1290 A72-22240

Deterministic methods to calculate quantization error in digital control system 11 p1610 A72-25976

Floating point arithmetic operators with variable dynamic range and multiple precision, noting word method for numerical data processing in computation and process control 12 p1787 A72-27666

Astronomical pointing of radio telescopes using on-line computer 12 p1793 A72-27813

Numerically controlled composite tape laying machine, discussing production run simulation, raw material quality effect and control corrective devices 12 p1815 A72-28078

Control optimization avoiding stability problem by integrating matrix Riccati equation 13 p1937 A72-30074

Measuring technique importance for aircraft R and D, emphasizing quartz tensometer, digital control and signal processing 14 p2092 A72-30286

Optimal state space synthesis of discrete linear computer controlled systems with quadratic cost function, using Liapunov, Pontryagin, and Bellman techniques 15 p2212 A72-32765

Die-casting machine design trends, considering uses of elbow lever and hydraulic systems and programmed control 16 p2399 A72-34142

Computerized photographic imagery analysis system with interactive operator controls for processing option selection in image enhancement prior to pattern identification 17 p2520 A72-34407

Book on Soviet astronomical reflecting telescopes, paraboloid mirrors, computer control, microphotometers and image converters 17 p2553 A72-34623

A method of using a control computer in a system controlling onboard spacecraft equipment 17 p2522 A72-35027

A probabilistic model of a control computer complex for estimating the efficiency of communication of a computer with data sources and receivers 17 p2522 A72-35029

Analysis of a control computer complex as a multiphase queuing system 17 p2522 A72-35030

Process computer system design, discussing structural units, data flow coordination with storage, input/output channels and periphery coupling problems 17 p2523 A72-35443

Numerical control component insertion for missile IC electronic module, tabulating producer-user survey data for designs usage and machine tools 17 p2532 A72-35923

Computer control of aircraft landing. 17 p2578 A72-35950

The AEG 60-50 process computer in special research field 55 at the Rhein-Westphalian Technische Hochschule at Aachen 18 p2664 A72-36680

Program-controlled machine for the investigation of mechanical properties of materials under a complex stress. 19 p2795 A72-37575

Development of a digital control system for a spacecraft propulsion test facility. 19 p2783 A72-37641

Computers and automatic drafting machines as aids in artwork production for printed circuits 19 p2809 A72-38307

Process control of the 100-meter telescope - Astronomical concept 19 p2803 A72-38485

Process control of the 100-m telescope - Communication of the observer with the computer-controlled telescope 19 p2804 A72-38487

Advanced fighter controls flight simulator for all-systems compatibility testing. 20 p2911 A72-39090

[AIAA PAPER 72-837] Operational software for computerized process control, considering operations system, translator, supervision and auxiliary and service programs 21 p3024 A72-41000

Dynamic characteristics, stability and steady state accuracy for orbital gyroscope with digital control, noting bit density requirements of onboard computer 22 p3202 A72-42207

Electrical components in gas turbine control systems. 22 p3216 A72-42521

Digital computer controlled testing equipment for separately driven coaxial gas turbine low and high pressure compressors, emphasizing reliability and flexibility in system design 22 p3157 A72-42682

Computer-operated data acquisition and control system for automatic diagnostic monitoring of propulsion research instrument 22 p3216 A72-42684

Development of a digital control system for a spacecraft propulsion test facility. 22 p3163 A72-42685

Nondestructive stability evaluation of large shell structures by direct computer controlled testing. 22 p3157 A72-42695

Computer control of the General Dynamics High Speed Wind Tunnel. 22 p3157 A72-42697

Computer-controlled queuing system with service interruptions. 23 p3275 A72-43605

Qualitative investigation of nonlinear pulse systems by the point mapping method 23 p3277 A72-44006

The use of minimum order state observers in digital flight-control systems. 24 p3382 A72-45343

Parallel Element Processing Ensemble (PEPE)/digital computer for real time radar data processing and control, discussing system design and applications 24 p3383 A72-45666

A prognosis on fault-tolerant digital control systems. 24 p3383 A72-45672

NUMERICAL FLOW VISUALIZATION

Numerical shallow fluid model for air flow across orographic variable grid barrier, using idealized Andes Mountains range 12 p1838 A72-27023

Numerical simulation of three dimensional shape-preserving convective elements from buoyancy release in incompressible fluid, using Navier-Stokes equations 12 p1839 A72-27027

Two dimensional dynamic model numerical simulation for micro- and macrostructures of moist convective clouds, comparing to field observations 12 p1839 A72-27028

Numerical model of global scale propagating waves in equatorial stratosphere generated by tropospheric heat sources for Kelvin and Rossby-gravity modes 12 p1839 A72-27029

NUMERICAL INTEGRATION

NT RUNGE-KUTTA METHOD

Kalman filtering process digital simulation by numerical integration of matrix differential equations describing linear system random process model and optimal filter 01 p0024 A72-10225

Aircraft stability coefficient determination by numerical integration fitting to differential equations of motion 01 p0005 A72-11136

Numerical solution for swirling ideal gas flow in Laval nozzle, determining swirling effects on nozzle performance 02 p0149 A72-11583

Asymptotic methods application to differential equations in nonlinear solar convection theory at high

Rayleigh number, noting discrepancy from numerical integration 02 p0276 A72-11644

Stellar systems existence with positive total energy, using numerical integration of equations of motion for members of Orion Trapezium 03 p0435 A72-13808

Numerical integration of element T (transit time through perihelion/ in perturbations of near parabolic comet orbits 03 p0436 A72-13829

Orthogonal polynomials in several variables relation to approximate multiple integration, extending Stroud theorem for two-dimensional regions cubature formulas to n-dimension 04 p0539 A72-14731

Nonlinear differential equations systems solution by A-stable numerical integration techniques 04 p0539 A72-14732

Matricial difference schemes based on numerical methods characterized by approximations for integrating stiff systems of differential equations 04 p0540 A72-15375

Differential equations systems formulation and numerical integration in gravitational problem of stellar n-bodies, discussing close approaches 05 p0713 A72-16052

Stability characteristics of finite difference schemes based on lumped-parameter model and numerical integrator for wave propagation in continuous media 05 p0735 A72-16081

Boundary layer of gas-particle flows with pressure gradient, numerically integrating momentum equation for cascade particulate flow [AIAA PAPER 72-87] 05 p0604 A72-16808

Compressibility and total enthalpy difference effects on laminar free shear layer from numerical integration of equations of motion 05 p0653 A72-17011

Numerical integration solution of nonlinear equations and two point boundary value problems, using quasi-linearization and imbedding methods 06 p0839 A72-17957

N-body problem equations of motion numerical integration methods supplemented by two body perturbation description and coordinate and time transformations 06 p0885 A72-18072

Numerical integration of N-body problem integrodifferential equations, using integrals as constraints and for correction application in least squares procedure 06 p0885 A72-18074

N-body gravitational problem direct integration techniques, discussing fourth order polynomial method, computer algorithm and regularization procedure for two body encounters and close binaries 06 p0885 A72-18078

N-body gravitational problem numerical integration treatment of close approaches, using transformations for eliminating differential equations of motion singularities 06 p0885 A72-18079

Plasma Dory-Guest-Harris type instability nonlinear evolution from numerical integration of Vlasov equation, using particle simulation and Fourier-Hermite transform methods 06 p0865 A72-18542

Numerical solution of integral equations with singular and weakly singular kernels by weighted residuals method 07 p1025 A72-18781

Numerical approximation of Pochhammer-Chree longitudinal vibration modes in elastic cylinders by quadratic spline functions 07 p1087 A72-18797

Singular integral equations numerical solution from Gauss-Chebyshev formulas for mixed boundary value problems 07 p1026 A72-18808

Difference method for numerical integration of Navier-Stokes equations for two dimensional incompressible steady flow along flat thin plate 07 p0908 A72-19170

Digital simulation of two dimensional or marginally turbulent three dimensional flows by discretization and numerical integration, noting Galerkin method efficiency in avoiding errors 07 p0951 A72-20355

Numerical integration of unsteady heat conduction equations for gas turbine rotor with shrouded blades, using grid method 08 p1223 A72-20950

Numerical simulation of two dimensional and marginal three dimensional turbulent flows, discussing variable eddy viscosity model, discretization, numerical integration and Galerkin methods 08 p1200 A72-21492

Equilibrium statistics of randomly forced two dimensional viscous flow three mode representation constructed by numerical integration of nonlinear equations system 09 p1293 A72-22459

Ordinary differential operators eigenvalues calculation, noting numerical integration scheme for initial value problem

09 p1340 A72-22461

Numerical integration of viscous and inviscid fluid flow equations, comparing various methods with exact solution

09 p1293 A72-22463

Numerical integration of primitive equations for barotropic atmosphere, using spherical polar coordinates

09 p1346 A72-22809

Numerical algorithm for matrix case extension of transport problem in periodic media

09 p1342 A72-23368

Numerical solutions of linear and nonlinear hydrostatic primitive equations for frontogenesis forced by nondivergent horizontal wind, noting discontinuities prediction

09 p1347 A72-23651

Fifth order modified Runge-Kutta integration algorithm, presenting truncation error estimation method and computation procedure flow chart

10 p1505 A72-24091

Coupling of interstitial liquid and porous elastic medium deformation, calculating solidification by numerical integration of partial differential equations system of Lamé type

10 p1465 A72-24116

Navier-Stokes equations numerical solution for symmetric laminar incompressible flow past parabolic cylinder, presenting surface pressure, friction and pressure drag results

10 p1465 A72-24291

Linear multistep methods with variable matrix coefficients for asymptotic numerical integration of ordinary differential equations system

11 p1679 A72-26960

Numerical integration for many body systems equations of motion, noting Monte Carlo and Boltzmann moment methods for large systems

12 p1873 A72-27895

Binary evolution in star cluster models from numerical methods of direct integration, noting domination by heavy binary and double star formation and disruption

12 p1873 A72-27899

Massless test star velocity vector deflection in stellar field from numerical integration on relaxation times

12 p1873 A72-27901

Gravitational many body problem differential equation system formulation and numerical integration

12 p1874 A72-27902

Integrals utilization in numerical integration of n body gravitational systems, discussing accuracy and reduced computation time

12 p1874 A72-27903

Close approaches in numerical integration of gravitational many body problem, discussing smoothing and regularization

12 p1875 A72-27918

Time constant limited stability of numerical integration procedures for systems of kinetic equations, examining causes and effects of stiffness

13 p1985 A72-28419

Atmospheric motion equations numerical integration, presenting conservative finite difference approximation for quasi-uniform spherical grids derived from regular polyhedrons

13 p1985 A72-28445

Digital computer estimates of random processes spectral density by statistical correlation method, calculating errors in numerical integration techniques

13 p1937 A72-29495

Numerical integration of boundary layer equations through region of reverse flow past parallel flat plate with negative surface velocity

13 p1944 A72-30033

Error sources in numerical integration of spacecraft equations of motion in solar and planetary gravitational fields, suggesting methods for improving accuracy

14 p2151 A72-30453

Linear stiff differential equations subdominant solutions, developing numerical integration algorithm

14 p2126 A72-30525

Numerical integration of equations of motion in finite element methods, investigating explicit methods stability

15 p2326 A72-31717

Fast numerical solution for supersonic flow past flat-faced blunt body by integration from stagnation point, noting computing time on CDC 6600

16 p2341 A72-32840

A method of solving partial differential equations for boundary layers

17 p2537 A72-34195

The numerical solution of hyperbolic systems using bicharacteristics.

17 p2574 A72-34449

Initial value techniques in free-surface hydrodynamics.

17 p2538 A72-34644

Single point and multipoint methods for numerical integration of differential equations, discussing solution efficiency improvement via automatic step selection

17 p2576 A72-35040

Numerical integration of ordinary differential equations in a real-time modeling procedure

17 p2576 A72-35041

Numerical evaluation of Chapman's grazing incidence integral $ch/X, \chi_i$.

17 p2549 A72-35609

Computerized numerical integration for nonlinear bending of tapered slender cantilever beams under concentrated tip loads

17 p2635 A72-35975

Numerical solution of Volterra integral equation.

18 p2705 A72-36601

A-stable, accurate averaging of multistep methods for stiff differential equations.

18 p2705 A72-37019

Hopscotch algorithm for numerical integration of nonlinear hyperbolic partial differential equation systems based on finite difference method

18 p2705 A72-37020

Integral equation method for solution of boundary value problems of structural mechanics. I - Ordinary differential equations. II - Elliptic partial differential equations.

18 p2739 A72-37169

Numerical integration of nonlinear convective flow equations for arbitrary atmospheric temperature and wind profiles, discussing cloud streets formation

19 p2828 A72-37998

Numerical integration method with recurrent power series for motion and variational equations of elliptic restricted three body problem

19 p2862 A72-38019

Control theory stability criteria applied to discrete time feedback systems, investigating numerical integration methods for initial value problems solution

19 p2826 A72-38250

Numerical calculation of third virial coefficient in equation of state of real gases eliminating errors associated with substitution of integration infinite integral

19 p2838 A72-38462

Book - Astrodynamics: Orbit correction, perturbation theory, integration

19 p2868 A72-38723

Numerical gas dynamic calculations by difference method with two moving curve families, noting water mass impact on plane solid wall

19 p2789 A72-38851

An intermediate matching technique for solving two point boundary value problems using the perturbation method.

20 p2910 A72-39198

Fractional steps method of difference schemes for approximate numerical solution of parabolic and elliptic initial boundary value problems

20 p2945 A72-39327

Numerical integration of gamma ray photopeak digital data from nondestructive activation analysis

20 p2899 A72-39834

An application of the shooting method to the stability problem for a stratified, rotating boundary layer.

21 p3043 A72-40106

A method of numerical integration for trajectories with variational equations.

[AIAA PAPER 72-910]

21 p3111 A72-41557

Numerical integration of three dimensional flow equations for supersonic jets of ideal gas exhausted from elliptical and rectangular nozzles

22 p3133 A72-42264

Numerical solution of integral equations of the first kind, using a priori information about the function to be restored

22 p3198 A72-42276

Numerical integration of integral equation for phased array radiation modeled by impedance filaments in conductive plane, noting excitation by magnetic flux

22 p3159 A72-42663

Linear multistep methods for a class of functional differential equations.

22 p3199 A72-42774

An approximation to midcourse correction direction errors.

22 p3203 A72-42870

Numerical integration of nonlinear differential equations in nonlinear circuits analysis, obtaining information on unsteady processes from calculation with controlled level time quantization step

23 p3269 A72-43444

A method of computing numerically integrated stiffness matrices.

24 p3457 A72-44878

Satellite orbital motion numerical integration method, using Picard iteration relative to reference orbit to calculate short-term anomalous period intervals

[AIAA PAPER 72-909]

24 p3443 A72-45428

A numerical integration method useful for studying ionospheric phenomena.

24 p3399 A72-45582

NUMERICAL WEATHER FORECASTING

Kennedy Space Center thunderstorm forecasting system, discussing data processing with conditional and exposure period probabilities and nonlinear predictors multiple regression equations

01 p0094 A72-10826

Nimbus 3 and 4 satellite technological and meteorological performance, discussing atmospheric temperature humidity and ozone vertical sounding for numerical weather forecasting models

01 p0130 A72-10955

Weather forecasting, discussing statistical entropy, numerical and statistical methods and computer technology utilization

02 p0254 A72-12777

Numerical weather prediction, discussing automatic forecasting, error sources, models and four-day validity in Northern Hemisphere

02 p0254 A72-12781

Satellite measurements of tropospheric and earth surface state parameters for long term numerical weather forecasting, discussing data fluctuations

02 p0255 A72-12789

Tadzbakhsh method of meteorological data assimilation for numerical weather forecast analyses, testing validity under condition of one of three dependent variables being observed

03 p0384 A72-14141

Closure schemes and retention of third moments in stochastic dynamic equations for numerical weather prediction, discussing imperfect forcing effects and kinetic energy relations

03 p0385 A72-14230

Short period height and long period kinetic energy oscillations in 10-level primitive equation model for circulation prediction in tropical region

03 p0385 A72-14232

CAT, cloud cover and icing forecasting for aviation in terms of numerical model and real atmosphere

04 p0542 A72-14689

Mountain barrier and convective area minimum size determination for numerical forecasting models, reducing primitive equations system to advection difference equation

04 p0544 A72-15459

Numerical two layer model of frontal motions development in atmosphere

06 p0840 A72-17384

Stochastic dynamic equations for atmospheric prediction and numerical weather forecasting, using barotropic model

06 p0841 A72-17633

Linearized two level model for atmospheric motion equations systems, using Psi-balanced system for 24 hour forecast

08 p1156 A72-20995

Numerical forecasting model with precipitation as function of vertical velocity and humidity distribution, noting orographic influence and atmosphere static stability

08 p1200 A72-21796

Filtered-equation pressure coordinate numerical weather prediction model in finite difference formulation, discussing various initialization procedures and boundary value specifications

09 p1343 A72-22427

Primitive equation multilayer model for winter precipitation prediction in U.S. northeast coastal region, noting correlation with observational data

09 p1344 A72-22428

Numerical solutions of linear and nonlinear hydrostatic primitive equations for frontogenesis forced by nondivergent horizontal wind, noting discontinuities prediction

09 p1347 A72-23651

Nonlinear medium range numerical weather forecasting method based on atmospheric spectral model

11 p1683 A72-26884

Stochastic dynamic prediction of meteorological fields in deterministic and indeterminate atmosphere

12 p1838 A72-27020

Meteorological reference level location without wind information for use in numerical weather prediction

12 p1838 A72-27024

F 2 layer parameter forecasting by computer based on series coefficients dependence on Wolf number

13 p1946 A72-28597

Thunderstorm encounter probability at SST altitudes for selected cross country routes, using radar observation data

13 p1992 A72-28853

Mathematical criteria for probable and potential aircraft icing occurrence, using radiosonde and empirical climatological data

13 p1993 A72-28856

Multiscale numerical model for local weather development simulation, noting forecasting for long distance air travel

13 p1993 A72-28857

Winds aloft forecast use to predict southwestern mountain lee wave behavior for general aviation cross country flights

13 p1993 A72-28863

Book on dynamic meteorology covering synoptic disturbance model, numerical weather prediction and baroclinic waves origin 15 p2266 A72-31875

Atmospheric motions prediction with numerical model based on discrete stratified fluid free oscillations 15 p2266 A72-32720

Imposed southern boundary experimentation for large scale Northern Hemisphere midlatitude atmospheric flow numerical prediction, discussing factors contributing to model success 15 p2267 A72-32726

Semiimplicit time integration algorithm in atmospheric baroclinic models for short range weather forecasting in Canada 16 p2418 A72-33665

Convective clouds fluid dynamic numerical modeling, considering plumes, thermals and vortex rings formation [AIAA PAPER 72-651] 16 p2419 A72-34083

Some observed properties of atmospheric turbulence. 18 p2705 A72-36019

Spatial variations in atmospheric predictability. 18 p2706 A72-36627

Numerical methods of solving weather forecasting problems 19 p2828 A72-37386

Dynamic meteorological problems solution by four dimensional analysis, discussing information deficiency effect on boundary value problems analysis in numerical weather forecasting 19 p2828 A72-37997

Computer program for numerical analysis of atmospheric fronts in lower troposphere based on models for spatial distribution of hydrothermal characteristic in air mass 19 p2829 A72-38771

Numerical climatic-change experiments - The effect of man's production of thermal energy. 20 p2947 A72-38962

Computerized long term weather forecasting via mathematical modeling of atmospheric processes based on meteorological parameters worldwide observational data 20 p2948 A72-39939

Thermodynamic conditions for the development of convective clouds and a method of forecasting the quantity of rainfall 22 p3202 A72-42953

Reproduction of the climatic distribution of meteorological elements on the basis of a nonadiabatic spectral model of the atmosphere 23 p3311 A72-43626

On the efficient reduction of truncation error in numerical weather prediction models. 23 p3311 A72-43675

One-level fine-mesh limited-area grid numerical weather prediction atmospheric model, evaluating various finite difference schemes, boundary conditions and initialization methods 24 p3420 A72-44619

F 2 layer parameter forecasting by computer based on series coefficients dependence on Wolf number 24 p3398 A72-45097

Incorporation of steep mountains into numerical forecasting models. 24 p3421 A72-45486

NUSSELT NUMBER

Temperature effects on hot-wire anemometer calibrations, plotting Nusselt number variation with Reynolds number 07 p0990 A72-20369

Heat transfer coefficient, maximum Nusselt number and particle thermal conductivity effect for gas fluidized beds, using surface renewal-penetration theory [ASME PAPER 71-HT-Z] 08 p1251 A72-20879

Evaluation of Collis-Williams and Davies-Fisher heat transfer formulas for flow past fine wires based on Nusselt vs Reynolds number relationship 10 p1562 A72-24294

Fluid flow and heat transfer in tube bank with two cylinders in cross flow, determining static pressure, Nusselt number and drag coefficients 11 p1743 A72-25259

Forced convection and thermal boundary condition in parallel and tapered passages, discussing Nusselt numbers for exponentially decreasing wall heat fluxes 14 p2173 A72-31062

Magnetic field effect on finite amplitude convection in fluids complying with Boussinesq approximation, discussing maximum Nusselt number shift 16 p2452 A72-33039

Nusselt number dependence on Rayleigh number for steady convection in porous medium, explaining heat transport abrupt change by breakdown of Darcy law 18 p2740 A72-36484

Calculus of variations and finite difference method for combined free and forced convective heat transfer through vertical noncircular ducts, calculating Nusselt number 18 p2741 A72-36926

Buoyancy effects on laminar heat transfer in the thermal entrance region of horizontal rectangular channels with uniform wall heat flux for large Prandtl number fluid. 22 p3243 A72-41956

NUTATION

Earthquake excitation of Chandler wobble in earth rotation 03 p0351 A72-14365

Earth motion nutations, considering external forces effects from sun and moon 04 p0575 A72-15030

Earth nutation tables, comparing precession-nutations and tidal potential 04 p0575 A72-15031

Combined rotational motions of free solid and coupled elastic bodies oscillations around center of mass with nutation passive dampers 06 p0850 A72-18707

Terrestrial pole motion components, discussing variations in Chandler wobble period and sidereal motion direction and average annual motion along ellipse 07 p0976 A72-19815

German monograph on optimal guidance of spin stabilized space bodies for combined attitude and angular velocity control and time optimal nutation damping 08 p1241 A72-21847

Elastic dislocation theory of Chandler wobble excitation by earthquakes 09 p1299 A72-22802

Free nutations of earth from 1904-1941 latitude observations at Pulkovo, noting diurnal variations with almost identical amplitudes 09 p1388 A72-23058

Earth free diurnal nutation parameters comparison based on determinations from latitude observations at various observations 09 p1388 A72-23059

Stochastic atmospheric density fluctuations effect on circular-orbiting satellite roll-yaw oscillations stability 15 p2319 A72-31457

Elastic damping of spin stabilized space stations nutational oscillations induced by time-variant moments of inertia 15 p2319 A72-31458

Frequency shift and mode shapes for equatorial vibrations of flexible boom on spin stabilized satellite, applying to thermal flutter resonance and nutational stability 15 p2320 A72-31803

Optimum design parameters for a spin-stabilized spacecraft nutation damper. 17 p2619 A72-34208

Variations of the earth's gravity field due to the free nutation. 17 p2544 A72-34272

Terrestrial pole motion components, discussing variations in Chandler wobble period and sidereal motion direction and average annual motion along ellipse 17 p2549 A72-35740

Determination of the aberration constant and the coefficients of short-period nutation terms from observations by the Pulkovo polar tube during the period from 1953 to 1964 19 p2861 A72-37976

Preliminary results of discussions of latitude observations by the prismatic astrolabe in Pulkovo /1963.2-1968.7/ 19 p2861 A72-37977

Attitude stability and performance of a dual-spin satellite with nutation damping. 19 p2862 A72-38022

Earth precession, nutation, polar axis displacement and rotation period reduction, discussing solid core existence within liquid core, elasticity and polar displacement 23 p3341 A72-44462

Motion of a rotationally symmetrical gyro with an arbitrary number of vessels containing liquid 24 p3395 A72-45578

NUTATION DAMPERS

SAS-A satellite attitude control and determination systems, discussing momentum wheel development, nutation damper and magnetic torquing 03 p0442 A72-14398

Universal ball-in-tube nutation dampers for spinning satellites, noting cost savings 05 p0729 A72-16756

Intelsat 4 nutation dynamics and gyrostat stabilization technique for precision pointing in international telecommunication, discussing damper and fuel sloshing [AIAA PAPER 72-537] 12 p1780 A72-27360

Autotracking antenna effect on dual spin spacecraft nutational stability, using averaging, eigenvalues and digital simulation techniques 12 p1876 A72-27379

[AIAA PAPER 72-571] 12 p1876 A72-27379

Nonresonant mode and nutation damping of rotational-vibrational motion of free solid body with elastic elements 12 p1846 A72-27968

Optimal efficiency of satellite passive nutation damper, noting system moment of inertia and flywheel axis relationship and viscous friction coefficient 14 p2162 A72-30458

Nutational stability of a dual-spin satellite under the influence of applied reaction torques. [AIAA PAPER 72-885] 20 p2976 A72-39116

NUTATIONAL OSCILLATION

U NUTATION

NUTRIENTS

Dihydroxyacetone /DHA/ as nutrient in growing fats diet, showing unsuitability of regenerated DHA-containing formose mixtures for space crew diets 16 p2354 A72-33371

NUTRITION

Apollo 14 food system, describing new items, improvements in production methods, packaging and preparation with emphasis on rehydratable foods 02 p0166 A72-11706

Spinal mesenteric vascular reflexes of vasoconstriction effect of pressure drop in coeliac artery relation to Rein nutritional hepatic reflex 04 p0473 A72-15125

Protein-rich food substitute from microalgae cultures for human nutrition, describing experimental production, protein value determination, special diets and food shortage relief 06 p0768 A72-18159

Higher nervous activity of monkeys two years after the extirpation of the dorsolateral frontal cortex 21 p3001 A72-40803

NUTRITIONAL REQUIREMENTS

NT CALORIC REQUIREMENTS

Chlorella population age structure and cell requirements correlation with nutrient medium nitrogen and phosphorus absorption 13 p1909 A72-29311

NYLON [TRADEMARK]

Parachute canopy fabrics and rigging lines cordage properties requirements, considering nylon, polypropylene, silk, cotton and nonwoven scrim-reinforced fabrics 01 p0005 A72-10314

Webbing joints stitching strain, considering nylon and flax yarns stretching properties and various stitching patterns strengths 01 p0005 A72-10315

Nylon parachute materials failure mechanics, considering friction, light, chemical and thermal effects 01 p0005 A72-10316

Design against fatigue failure in thermoplastics. 24 p3457 A72-44816

NYLON RESINS

U POLYAMIDE RESINS

NYQUIST DIAGRAM

Discrete time systems with periodic feedback gain, deriving stability conditions and Nyquist plot from linear operator spectral theory 11 p1608 A72-25318

Graphical design technique based on Nyquist plane construction using circle criterion for nonlinear systems controller synthesis 14 p2091 A72-30375

The Nyquist criterion for kinematic-dynamic action. 20 p2956 A72-38912

Design of controllers for open-loop unstable multivariable system using inverse Nyquist array. 23 p3275 A72-43609

NYSTAGMUS

Navigators, pilots and airman trainees response to Coriolis accelerations, investigating nystagmus sensitivity coefficient relationship to motion sickness resistance 01 p0021 A72-11286

Vestibular system tests using optokinetic, caloric, positional and rotational stimuli 01 p0022 A72-11292

Lateral geniculate body neurons activity during nystagmic eye movements in cats after vestibular stimulation related to visuo-motor mechanisms counteracting illusory shifts 03 p0315 A72-13623

Eye movement control device for electronystagmography, describing construction, line drawing and basic circuits 03 p0319 A72-13724

Alcohol ingestion effects on tracking performance during angular acceleration, observing nystagmic eye movements and eye-hand coordination 04 p0477 A72-14474

Nystagmus and illusory phenomena in man under simultaneous rotation in two perpendicular planes as function of vestibular excitation 09 p1267 A72-23593

Nystagmus eye movements relationship to oculogyril illusion from test involving vestibular stimulation and visual stimuli velocity estimates 12 p1776 A72-28304

Alcohol ingestion effect on vestibular responses to angular acceleration and Coriolis stimulation, discussing nystagmus and subjective responses 14 p2082 A72-31090

Effects of different alcohol dosages and display illumination on tracking performance during vestibular stimulation. 17 p2508 A72-34554

Vestibular labyrinth reactions and nystagmus thresholds in dogs during negative angular acceleration

tions and simulated chronic galactic radiation from Co 60 gamma source

21 p2998 A72-40439

O

O RING SEALS

Polyurethane O ring seals for high pressure applications, discussing stress relaxation /creep/ behavior, resilience and wear and abrasion resistance

08 p1173 A72-21023

Thermocracking and thermal stresses in packing rings of face-type mechanical seals under dry friction

08 p1177 A72-21927

Reciprocating O ring seal sliding friction behavior prediction by elastohydrodynamic theory, noting dwell time, acceleration rate and previous deceleration effects

12 p1816 A72-28110

O STARS

Early O and Of spectroscopic and photometric data, evaluating atmospheric properties, surface gravities and temperature scales

01 p0131 A72-11009

Circumstellar dust formation hypothesis based on O stars mean circumstellar extinction, explaining Ca and Na abundance in interstellar gas

02 p0284 A72-12636

Line spectrum of Of star zeta Puppis at 3150-8600 A, comparing absorption spectrum to 9 Sgr

03 p0416 A72-13014

Spectrographic observation of hot OB subdwarf HD 149382

03 p0435 A72-13799

Interstellar Ca II, H and K optical absorption lines of bright O and early B stars in Orion region

05 p0723 A72-17200

Non-LTE atmospheric model calculations for H, He I and II spectra of O stars, discussing He abundances

08 p1239 A72-21949

Spectral types and magnitudes of O and WC stars of binary gamma Velorum system

09 p1382 A72-22282

OB star distribution in Puppis from UVB and H beta photometry, noting correlation with hydrogen concentration

10 p1542 A72-24615

Ca II K line profiles in front of distant OB stars, using pressure scanned Fabry-Perot interferometer and coude spectrograph

10 p1542 A72-24616

Perseus two armed spiral shock model based on O associations, young open clusters, H II regions, interstellar absorption lines and 21 cm hydrogen maps

11 p1720 A72-26110

The peculiar O6f star HD 148937 and the symmetrically surrounding nebulae.

22 p3227 A72-42557

Individual reddening laws of O-type stars. I - Computation method, first results

24 p3437 A72-44829

OAO

Absolute UV calibration of rocket photometers used to update OAO calibration for determining energy distribution of reference stars

03 p0355 A72-13065

OAO space telescope of 120 inches aperture, discussing structural design, geometric configuration and stabilization and pointing control system

[AIAA PAPER 72-201] 05 p0663 A72-16800

Dimensional stability and micromechanical properties of materials for use in OAO, investigating residual stresses, creep properties and stress relaxation

[AIAA PAPER 72-325] 11 p1653 A72-25362

OAO IR instruments development to observe IR stars, diffuse galactic objects, galactic center and extragalactic objects

24 p3446 A72-45534

Unmanned OAO spacecraft series and experiment packages, discussing space astronomy scientific achievements, mission plans and space shuttle role

24 p3453 A72-45535

OAO 2

Orbiting astronomical observatory - Review of scientific results.

18 p2731 A72-36555

OAO 3

Self priming high capacity spiral artery heat pipe with ammonia as working fluid for flight on OAO 3, discussing development models analysis, design and testing

[AIAA PAPER 72-258] 11 p1725 A72-25203

OAO 3 satellite Copernicus onboard equipment, discussing UV reflecting and X ray telescopes, attitude sensor, star tracker, solar sensor and computer

22 p3231 A72-42985

OAO-A

U OAO

OBESITY

ECG P-wave-like deflections caused by strong diaphragmatic action potentials in obese woman with fever and erysipelas

13 p1908 A72-28569

OBLATE SPHEROIDS

Rotating earth oblateness and equator ellipticity influence on near-equatorial synchronous satellite behavior, using nonlinear mechanics asymptotic method

03 p0436 A72-13835

Triaxial space station orbit around oblate earth, presenting equations of motion, Hamiltonian and integration methods

06 p0878 A72-17663

Prolate and oblate spheroids flow field generated by axial translatory oscillations in still incompressible viscous fluid from Stokes linearized equations, deriving formulas for drag

10 p1418 A72-24462

Relativistic explanation for excess motion of Mercury perihelion in terms of solar oblateness and interior rotation mechanism

11 p1715 A72-25350

Linearized stability analysis of collapsing uniform nonrotating oblate gaseous spheroid, noting subcondensation growth rate dependence on shape and size

15 p2313 A72-32364

Photographic flow visualization of steady recirculating wakes behind sphere and oblate spheroids for low Reynolds numbers

15 p2180 A72-32419

Photospheric faculae brightness influence on solar gravitational oblateness determination, considering criticism of Dicke-Goldenberg argument on Mercury excess perihelion motion

19 p2855 A72-37239

Faculae and the solar oblateness

19 p2855 A72-37240

Decomposition of the force function of two homogeneous spheroids with noncoinciding symmetry planes

21 p3114 A72-41771

A non imaging approach to solar oblateness measurements.

22 p3222 A72-42046

Electric multipole moments calculation by quasi-static method for homogeneous quasi-neutral oblate plasma spheroid during electromagnetic interaction under resonance conditions

22 p3212 A72-42729

OBLIQUE SHOCK WAVES

Solar wind reverse and forward oblique shock waves, examining discontinuities from Pioneer 6 plasma and magnetic field data

01 p0120 A72-10882

Ion heating in high Mach number oblique collisionless shock waves, noting role of two-ion beam instability from digital simulation

07 p1043 A72-19665

Plane oblique shock wave diffraction on wedge moving in homogeneous gas flow at supersonic speed, reducing boundary value problem to Hilbert problem

07 p0910 A72-20317

Magnetic structure of ionizing oblique shock waves with transverse and normal components in zero magnetic Prandtl number limit

11 p1618 A72-26606

Nanosecond response magnetic probes to measure fast disturbances in oblique shock waves within collisionless plasma, describing experimental technique

15 p2235 A72-31646

Small-amplitude near-steady oblique shock waves in cold collisionless plasma, considering magnetoacoustic and Alfvén waves

15 p2287 A72-32414

Nonlinearity effects on finite amplitude, plane uniform oblique shock wave reflection, using inviscid gas analogous solution techniques

16 p2426 A72-33661

Pressure distribution on a yawed wedge interacted by an oblique shock.

17 p2485 A72-35239

Analytical solutions for straight oblique shock waves in radiating gases.

17 p2542 A72-35616

Particle motion behind oblique shock wave in two phase supersonic wedge flow, deriving expressions for particle trajectories and velocity equalization time

17 p2487 A72-35926

A contribution to the gas dynamics of oblique shocks with change of total enthalpy.

18 p2682 A72-36725

On the conditions for the appearance of the Mach effect in the reflection of an oblique shock wave in supersonic flow

21 p3046 A72-41339

Two-dimensional model for thermal compression.

22 p3136 A72-42868

Earth collisionless plasma bow shock oblique structure assessment by pulsation index I_p devised from empirical results

23 p3341 A72-44511

Pressure fluctuations resulting from the interaction between a shock wave and a turbulent boundary layer.

24 p3359 A72-44682

Supersonic aircraft engine inlet performance in terms of pressure recovery, discussing oblique shock wave formation ahead of entrance to improve efficiency

24 p3360 A72-44991

Instability of the whistler structure of oblique hydromagnetic shocks.

24 p3428 A72-45013

Gas dynamics problems of oblique shock waves around aerodynamic bodies, noting exact quasi-explicit and approximate explicit solutions

24 p3394 A72-45445

OBSERVATION

U OCCULTATION

OBSERVATION

NT SATELLITE OBSERVATION

NT VISUAL OBSERVATION

Optimal control of observation processes, formulating solvability conditions in terms of ordinary differential equations

16 p2370 A72-32927

Optimization of noise impeding observation of dynamic system subjected to random perturbations, discussing optimal control based on least square estimate

16 p2371 A72-33090

Nonlinear differential equations control systems, determining conditions for observability of initial state and vector of constant parameters extended from time-varying linear systems

23 p3310 A72-44548

OBSERVATION AIRCRAFT

Results of the reliability and maintainability demonstration of the OH-58A light observation helicopter. [AHS PREPRINT 652]

17 p2491 A72-34507

OBSERVATORIES

NT ASTRONOMICAL OBSERVATORIES

NT GEOPHYSICAL OBSERVATORIES

NT HEAO

NT LUNAR OBSERVATORIES

NT OAO

NT OGO

NT OGO-A

NT OGO-B

NT OGO-D

NT OGO-E

NT OSO

NT OSO-E

NT OSO-G

NT OSO-H

NT SOLAR OBSERVATORIES

OBSIDIAN

NT MOLDAVITE

OBSTACLES

U BARRIERS

OBSTRUCTING

U BLOCKING

OCCIPITAL LOBES

Spatio-temporal scalp mapping localization of human visual evoked responses to half field light adapted stimulation, comparing to half-field stimulation

01 p0015 A72-11185

Occipital and vertex visual evoked response relation to sensory information, perception and stimulation

06 p0763 A72-17723

Factor analysis of frontal and occipital brain regions EEG indices interzonal variability, relating autocorrelation function parameters to neuron ensembles force level

06 p0764 A72-18057

Occipital electroencephalographic response to slowly repeated aperiodic light flashes, discussing alpha wave and rhythmic afteractivity amplitude changes

07 p0916 A72-19041

Comparative EEG characteristics of frontal and occipital human brain cortex, relating psychophysiological and neurophysiological factors

08 p1116 A72-21196

Occipital EEG activity during fluctuations of perception under stabilized image and simplified stimulus conditions.

17 p2506 A72-34247

OCCLUDED FRONTS

U FRONTS [METEOROLOGY]

OCCULTATION

NT LUNAR OCCULTATION

NT RADIO OCCULTATION

NT SOLAR ECLIPSES

NT STELLAR OCCULTATION

Mariner 9 radio occultation measurements of Mars day side atmosphere, indicating isothermal temperature, surface pressures and ionosphere properties

06 p0890 A72-18345

Venus upper clouds composition from Mariner 5 occultation data analysis concerning temperature and pressure profiles, abundances, polarization characteristics, reflection and emission spectra

08 p1236 A72-21496

Periodic intensity and period variations of X ray pulsating source Cen X-3 caused by occulting binary system from Uhuru satellite observation

09 p1382 A72-22289

Model Martian atmosphere, investigating effects of departures from electron density profile spherical symmetry on radio wave phase shift in bistatic radar occultation experiment

15 p2194 A72-31440

Apparent difference in Martian night and day side surfaces atmospheric pressure based on Mariner

spacecraft occultations, noting effects of topography and electron layer

15 p2310 A72-31973

OCCUPATION

Terminal area ATC specialists and trainees job attitude and motivation from questionnaire on challenge, tasks, salary, work schedule, etc

06 p0766 A72-17865

OCEAN BOTTOM

Regulating amplifier with optoelectronic coupler for sonar sea bed layer measurements

09 p1284 A72-22239

OCEAN CURRENTS

Declinational component of geomagnetic lunar tide diurnal variations, noting effects of electric currents induced in oceans

11 p1622 A72-26103

Oceanic and atmospheric flow geostrophic adjustment by means of gravity-inertial wave propagation from initially imbalanced regions

15 p2222 A72-31278

Nonrotating Hadley cells turbulence from steady one dimensional flow instabilities in thin nonrotating differentially heated atmosphere or ocean

15 p2219 A72-32722

Geophysical fluid dynamics approach to dynamical processes in ocean and atmospheric motions, discussing equations of motion, vorticity, geostrophism, Ekman layer, Rossby waves, etc

16 p2377 A72-33336

OCEAN SURFACE

Atmospheric water vapor role in waveguide effects above sea on millimeter and centimeter propagation along transhorizon and beyond horizon paths

01 p0026 A72-10403

Electromagnetic wave propagation anomalies over sea, comparing calculated and measured field strengths based on simultaneous refractivity vertical distribution measurement

01 p0026 A72-10405

Synthetic aperture radar application to oil spill detection and monitoring for ocean surface, demonstrating feasibility

01 p0057 A72-10534

Computer programs for global disk and landmarks registration of cloud motions from satellite data for ocean weather monitoring applications

01 p0070 A72-10871

Earth surface and atmosphere remote sensing by airborne microwave measurements, noting ocean surface emissance dependence on temperature, surface conditions and pollution

02 p0207 A72-11779

Automated operational procedure for sea surface temperature determination from ITOS IR data, discussing error analysis

02 p0211 A72-11810

Synoptic sea surface temperature mapping off Eastern United States using NASA ITOS satellite IR imagery data

02 p0211 A72-11813

Remote passive microwave sensing of ocean surface wind fields, discussing sea microwave brightness temperature dependence on wind speed

02 p0214 A72-11864

Composite scattering theory mathematical model for radar backscattering cross section relation to ocean surface conditions and wind velocity

02 p0172 A72-11868

Ocean wave height measurements with nanosecond radar, using ground truths to relate radar measurements to actual sea conditions

02 p0172 A72-11869

Space TV images use in hydrospherical temperature discontinuity front location, examining cloud cover distributions over Sea of Japan

02 p0214 A72-11872

Cloud interference-free sea surface temperatures, using techniques to reduce noise effect in Nimbus IR radiometer data

03 p0385 A72-14227

Near sea level atmospheric effects on submillimeter radiation absorption in terms of dielectric coefficient theory

04 p0551 A72-15606

Microwave and IR radiometer surveillance of oil spills, discussing sources tracking, sea surface oil volume and flow rate determination and terminal location prediction

05 p0658 A72-16599

Mt/hf/vhf scattering from sea, deriving received power and spectral energy density dependence on grazing angle, frequency, range and surface impedance

06 p0770 A72-17338

Altitude dependent turbulence characteristics in atmospheric boundary layer over wavy ocean surface from wind pulsation measurements

06 p0841 A72-17624

Coherence function and phase shift dependence of free ocean surface on angular energy distribution in two dimensional wind induced wave spectrum

06 p0841 A72-17625

Image enhancement techniques for sea-ice mapping from satellite IR data, discussing gray scale contrast augmentation scheme for visual quantitative information

06 p0807 A72-17825

Remote sensing of oil pollution on water by laser induced fluorescence, using airborne spectroscopy [AIAA PAPER 71-1076]

07 p0981 A72-18822

Atmospheric turbulence measurements over sea from 30 m to 1 km, examining rms vertical velocity variations with altitude

07 p1030 A72-19104

Airborne radar measurement of 2.25 cm backscatter from sea surface, obtaining wind speed by computerized clustering data analysis techniques

09 p1296 A72-22312

Sea surface roughness mapping by airborne microwave radiometry with correction for viewing angle and atmospheric effects

09 p1297 A72-22525

HF radio wave backscatter from sea surface to obtain gravity wave structure information

10 p1438 A72-24739

Electromagnetic theory of HF radio ground wave backscattering from gently rippled sea surfaces, discussing approximations for separated scattering and receiving antennas case

10 p1438 A72-24742

Airborne IR radiometric measurements of upward vertical radiance from tropical sea surface at 10-12 microns, noting absorption coefficient dependence on water vapor

10 p1474 A72-24747

Sea foam emission and reflection characteristics at microwave frequencies from radiometric measurements, correlating data as functions of frequency and angle

10 p1475 A72-24749

Doppler spectral width of radar signal reflected from sea surface as function of illuminated region dimensions, waviness scale and emission factors

10 p1439 A72-24904

Gulf Stream surface front structure, temperature and salinity observation from ship, aircraft and satellite

11 p1620 A72-25348

Global sea surface temperature distribution determination with ITOS 1 radiation measurements and composite histogram, discussing RMS errors

11 p1620 A72-25763

Joint ocean-atmosphere model response to solar zenith angle seasonal variation, noting snow cover and ocean surface effects on lower troposphere warming

11 p1620 A72-25766

Tropical hurricane model describing initial whirlwind and self exciting wind velocity development and dependence on ocean surface temperature

11 p1682 A72-26879

Nonregular oceanic level fluctuations dependence on atmospheric pressure and tangential wind stress, deriving fluctuation spectrum from linear hydrodynamic model

11 p1682 A72-26882

Satellite altimetry based on ocean backscattering, analyzing received signal model and altitude errors

13 p1955 A72-28533

Acoustically scaled simulation of sonic boom N-wave energy penetration into ocean for flat air-water interface

13 p1951 A72-29587

Satellite anemometry for ocean waves and weather forecasting, discussing Skylab microwave radiometer-scatterometer potential design

15 p2221 A72-31239

Upward and downward radiative transfer in atmosphere-ocean system model calculated by Monte Carlo method, noting turbidity effect on radiance

15 p2224 A72-31673

Sea surface temperature determination on Nimbus 2 satellite, using three channels in medium resolution IR radiometer

15 p2224 A72-31674

Sea clutter measurement at low grazing angles by high resolution radar, noting non-Rayleigh probability density and variation with frequency, pulsewidth and polarization

15 p2196 A72-31786

Skylab radar altimeter for earth surface features remote sensing with high range resolution mode for ocean wave height determination

15 p2236 A72-31995

Sea surface wind-caused waves spectral component phase velocity measurement method based on statistical treatment of synchronous continuous records of surface elevation

16 p2417 A72-33291

Sea surface albedo for short wave solar radiation in terms of sun altitude and atmospheric transmittance, noting wind and surface roughness effects

18 p2687 A72-36642

S-band radiometer design for high absolute precision measurement.

19 p2794 A72-37252

German monograph - A proposal for a radar device with two simultaneously emitted radar frequencies which has a reduced susceptibility to disturbances produced by sea echoes

19 p2764 A72-37481

Continuous natural background sources of microseismic motions due to atmospheric and ocean loading, wind, flowing water and local disturbances [AIAA PAPER 72-819]

20 p2915 A72-39104

Nonperiodic oceanic level fluctuations dependence on atmospheric pressure and tangential wind stress, deriving fluctuation spectrum from linear hydrodynamic model

20 p2948 A72-39569

Allowance for the ocean surface temperature in monthly weather forecasts for the Northern Atlantic Ocean

20 p2949 A72-39946

Wind profile development above a locally adjusted sea surface.

22 p3202 A72-42600

Primary cosmic ray nucleon spectrum from sea-level muon spectrum and scaling hypothesis parameters.

23 p3332 A72-44458

OCEANOGRAPHY

IR scanner for Indian land areas and oceans thermal mapping, using satellite-borne multispectral photography

02 p0225 A72-11777

Orbiting multispectral scanner with independent land and oceanographic spectrometers for ground controlled dual mode operation

02 p0226 A72-11823

Geodetic and oceanographic applications of radar equipped satellites in polar orbits for measuring heights along geoid

06 p0809 A72-18259

Stationary-nonstationary temporal sampling for synoptic meteorological networks, illustrating oceanic wind speed measurements

06 p0842 A72-18436

Meteorological satellites and Gemini and Apollo earth photographs, showing annual and diurnal oceanographic, hydrologic and geologic dynamic features

06 p0810 A72-18614

Holographic weak signal enhancement technique in presence of strong noise for seismic and oceanographic applications

07 p0992 A72-20563

Color enhanced black and white IR satellite images for oceanographic applications

11 p1620 A72-25346

Gulf Stream surface front structure, temperature and salinity observation from ship, aircraft and satellite

11 p1620 A72-25348

Satellite IR telescensors in oceanography for data acquisition on ocean state, circulation, surface temperature, salinity, pollution, etc

15 p2221 A72-31238

Barbados oceanographic meteorological experiment /BOMEX/ sea air interaction program in equatorial Atlantic, using real time synchronous satellite information

15 p2225 A72-31808

Barbados Oceanographic and Meteorological Experiment to compare synoptic scale-measured vertical vapor fluxes over tropical ocean

16 p2417 A72-33169

Radar imaging systems application to cartography, geology, hydrology, biogeography, oceanography and geography, emphasizing remote sensing in cloudy environments

16 p2364 A72-33634

Physical and numerical experiments on layered convection in a density-stratified fluid.

17 p2543 A72-35764

The potentialities of space technology in relation to oceanography and surface meteorology.

19 p2790 A72-37924

OCEANS

NT ARCTIC OCEAN
NT ATLANTIC OCEAN
NT INDIAN OCEAN
NT PACIFIC OCEAN

OCTAHEDRAL RESEARCH SATELLITES

U ENVIRONMENTAL RESEARCH SATELLITES

OCTAHEDRITE

U ANATASE
U MINERALS

OCTANES

Liquid n-octane, n-decane and n-undecane densities and adiabatic/isothermal compressibilities from sound velocity measurements at high pressures and 30-140 C

02 p0261 A72-12829

OCULOGRAPHIC ILLUSIONS

Sjoberg hypothesis for zero gravity produced inversion illusion mechanism in aircraft parabolic flight, noting otolith membrane deflection result of force on maculae

02 p0167 A72-11710

Lateral geniculate body neurons activity during nystagmic eye movements in cats after vestibular stimulation related to visuo-motor mechanisms counteracting illusory shifts

03 p0315 A72-13623

Contrast vision enhancement in Hermann grid with variable figure-ground ratio, using Baumgartner receptive field hypothesis

03 p0315 A72-13624

Pilot and nonpilot vestibular sensitivity to rotation, determining oculogular illusion and rotation perception thresholds

06 p0767 A72-17867

Nystagmus and illusory phenomena in man under simultaneous rotation in two perpendicular planes as function of vestibular excitation

09 p1267 A72-23593

Nystagmus eye movements relationship to oculogular illusion from test involving vestibular stimulation and visual stimuli velocity estimates

12 p1776 A72-28304

OCULOMETERS

EEG and electrooculogram recording of chimpanzee sleep, noting rapid eye movement stages

01 p0009 A72-10074

OCULOMOTOR NERVES

Optic nerve axon diameters in central and peripheral cat retina related to conduction velocity groups

03 p0315 A72-13622

Lateral geniculate body neurons activity during nystagmic eye movements in cats after vestibular stimulation related to visuo-motor mechanisms counteracting illusory shifts

03 p0315 A72-13623

Alcohol ingestion effects on tracking performance during angular acceleration, observing nystagmic eye movements and eye-hand coordination

04 p0477 A72-14474

Oculomotor accommodation and convergence as distance perception cues, showing size perception change relation to glasses adaptation

06 p0765 A72-17411

Oculomotor cue-based distance perception, discussing glasses adaptation-caused accommodation and convergence changes in stereoscopic depth perception

06 p0765 A72-17414

Phase shifts of circadian rhythm of optic nerve potentials from isolated eye of sea hare in darkness

07 p0919 A72-19534

Eye movements and dynamic visual acuity as function of tracking velocity, analyzing pursuit and saccadic component by electrooculography

13 p1912 A72-30043

An objective test for evaluating the functional state of the oculomotor system during somnolence states

19 p2756 A72-37876

Involuntary eye movements during the performance of mental tasks

23 p3260 A72-44077

Conjugate and disjunctive optokinetic eye movements in the rabbit, evoked by rotatory and translatory motion.

23 p3257 A72-44243

Eye movements evoked by collicular stimulation in the alert monkey.

24 p3371 A72-44906

ODORS

Single olfactory bulb units under cyclic stimulation, observing activity related to inhalation cycle and odor quality

05 p0617 A72-16162

OFF-ON CONTROL

Solid rocket on-off and acceleration control, discussing motor concepts, thrust modulation and potential technology applications [SAE PAPER 710767]

01 p0116 A72-10262

Orthogonal convolutional coding with on-off signaling and Viterbi decoding for synchronous multiple access communication with bound bit error rate

01 p0026 A72-10343

Time optimal bang-bang response control of two pole single phase static inverter, giving output current transient response data

01 p0008 A72-11062

Bang-bang automatic control of linear plant with discontinuous characteristics element, investigating periodic function oscillation

05 p0639 A72-15757

Logical synthesis of hybrid off-on control systems with proportional and binary variables, presenting example of fluid power, electronic and fluidic implementation [ASME PAPER 71-WA/FLCS-1]

05 p0640 A72-15919

Spacecraft precision off-on attitude control by pure jet torquing, using electronics based on control system idealized model

05 p0726 A72-16459

On-off control system stability with feedback proportional to square of velocity, determining system frequency response

06 p0793 A72-17316

Phase-plane analysis of transient response of on-off control system relative to sinusoidal inputs

06 p0795 A72-18714

Bistable hydraulic servomechanisms limit cycle stable oscillations from bang-bang control and cavitation effects, discussing valve driving gear hysteresis and time lag

08 p1113 A72-22155

Loaded hydraulic cylinder response to step inputs in on-off servos with three position valves, considering cavitation effect on system natural frequency [ASME PAPER 72-AUT-A]

10 p1423 A72-25052

Nonlinear control system optimal bang-bang controls computation, noting algorithm obtained by parameter optimization

11 p1577 A72-26666

Dynamic motion analysis of digital servo system with proportional bang-bang control by trajectory mapping on phase plane

15 p2211 A72-31895

Numerical solution of an optimal control problem with a probability criterion.

17 p2534 A72-35531

OGEE WINGS

U VARIABLE SWEEP WINGS

OGO

NT OGO-A

NT OGO-B

NT OGO-D

NT OGO-E

Magnetospheric magnetic field distortions under quiet and slightly disturbed conditions, obtaining scalar intensity with OGO 3 and 5 rubidium vapor magnetometer

01 p0060 A72-10886

Bidirectional reflectance at several wavelengths from moonlit earth observations by airglow photometer on OGO-4 satellite

03 p0433 A72-13428

Earth bow shock magnetic field data correlation with Ogo 5 flux gate magnetometer, using Tidman-Northrop theory

07 p0975 A72-19145

Electric field variations during substorms - OGO-6 measurements.

24 p3396 A72-44854

OGO-A

Thermal positive ion densities measurement in outer ionosphere and magnetosphere by OGO 1 satellite, relating plasmopause distribution and magnetic activity level [AD-742186]

09 p1300 A72-23011

OGO-B

Geomagnetic survey by polar-orbiting OGO 2 and 4, discussing data acquisition and reduction results and accuracy

02 p0219 A72-12081

OGO-D

Geomagnetic survey by polar-orbiting OGO 2 and 4, discussing data acquisition and reduction results and accuracy

02 p0219 A72-12081

OGO-E

French Lyman alpha photometer experiment on OGO 5 satellite, describing geocoronal observations, extraterrestrial emission and Bennett and Encke comets hydrogen envelopes

04 p0582 A72-15684

OGO-E plasmopause crossing correlation with ground observations of Pi geomagnetic micropulsations

08 p1159 A72-21223

Electron plasma oscillations distribution upstream from earth bow shock, evaluating OGO-E plasma wave detector data

09 p1300 A72-23019

Ogo-5 observation of lower hybrid resonance noise, bursts, VLF hiss and whistlers near plasmopause during large magnetic storm

11 p1624 A72-26399

Plasma wave measurements during OGO-5 dayside magnetosphere polar cap encounters, discussing ULF magnetic field wave levels and VLF electric field amplitude ranges

13 p1950 A72-29380

Nuclear composition telescope measurements on-board OGO 5 satellite, observing presence of geomagnetically trapped carbon, nitrogen and oxygen nuclei

16 p2382 A72-32959

OGO-1

U OGO-A

OGO-2

U OGO-B

OH-6 HELICOPTER

Hughes 500 and OH-6 helicopter tail rotor cambered blades, comparing thrust and stall characteristics with symmetrical blades

14 p2072 A72-30290

OHMIC DISSIPATION

Microwave attenuation due to ohmic losses in periodic linear arrays of metallic cylinders, ribbons and slots in metallic ground plane

06 p0786 A72-18372

Joule dissipation effect on convective instability of current carrying fluid in magnetic field

10 p1522 A72-24533

Ohmic and internal friction loss minimization in stationary rotating incompressible plasmas, assuming magnetic and velocity fields as Trkal fields

10 p1524 A72-24928

Skew magnetic structure of ionizing shock waves with ohmic dissipation as dominant diffusion mechanism

11 p1618 A72-26605

Joule heating power density in NbZr superconductor hollow cylinder, estimating temperature changes and instability locations

13 p2023 A72-29855

Lighthill method for ohmic dissipation pulsation effect on sound field generated by turbulent flow of conducting fluid

14 p2141 A72-31001

Thermospheric density annual and semiannual variations due to solar heat input into ozone layer and Joule heating, discussing decomposition into Fourier terms

15 p2229 A72-32255

OHMS LAW

Electron density and temperature fluctuations coupled through Ohm law for ionizable medium, applying to MHD generators and MPD arc thrusters [AIAA PAPER 72-101]

Plasma rotation during theta pinch collapse, determining ion azimuthal velocity from fields and pressure gradient measurements via Ohms law

08 p1213 A72-21255

Ohmic law generalization in electrodynamics for electrically conductive fluid medium in turbulent motion, taking into account Hall effect

10 p1524 A72-24931

Propagation of electromagnetic disturbances and the stability of stationary states in media with a nonlinear Ohm's law

21 p3086 A72-41651

Group properties and invariant solutions of electric-field equations in the case of nonlinear Ohm's laws

21 p3086 A72-41654

OIL ADDITIVES

Solid lubricant additives effects in oils and fats, discussing molybdenum disulfide and zinc pyrophosphate solid film formation on metal surfaces under contact friction conditions

07 p1024 A72-20395

Antiwear properties of mixed anhydrides of alkyl xanthogene and phosphorus containing acids for use as oil lubricant additives

09 p1336 A72-22499

Antioxidative and antiwear action of S-containing and S-free phosphoric acid ester additives in lubricating oils

12 p1835 A72-28201

OIL EXPLORATION

Heat losses in oil wells hot liquid injections, modifying Orveanu approximation method for exact solution

04 p0597 A72-15743

OILS

NT FUEL OILS

NT LUBRICATING OILS

NT MINERAL OILS

Microwave emission characteristics of oil slicks, showing dependence on oil type, film thickness and sea state

[AIAA PAPER 71-1071] 01 p0057 A72-10533

Synthetic aperture radar application to oil spill detection and monitoring for ocean surface, demonstrating feasibility

[AIAA PAPER 71-1072] 01 p0057 A72-10534

Remote airborne sensors for sea water oil pollution surveillance in near UV, thermal IR and microwave regions

[AIAA PAPER 71-1073] 01 p0057 A72-10535

Sky light polarization, cloudiness and view angle effects on oil remote detection over water surface, describing passive radiometric techniques [AIAA PAPER 71-1075] 01 p0057 A72-10536

Oil slicks aerial photographic and multispectral scanner investigation, discussing detection effectiveness of UV, blue, green and IR imagery

02 p0226 A72-11829

Oil spills remote detection by multispectral photography, IR scanner imagery and microwave radiometry

02 p0226 A72-11830

Colorado Green River Formation oil shale extracts, determining nitrogenous compounds content with high resolution mass spectrometry

03 p0320 A72-13741

Mass spectrometric studies of solvent extractable acid methyl esters of oil shale from Colorado Green River Formation

03 p0320 A72-13742

Microwave and IR radiometer surveillance of oil spills, discussing sources tracking, sea surface oil volume and flow rate determination and terminal location prediction

05 p0658 A72-16599

Airborne optical detection of oil on water based on reflected sunlight, investigating contrast and absorption bands

05 p0658 A72-16689

Turbojet engine oil circuit contamination rate determination by spectrometric analysis, obtaining mathematical theory for data interpretation [SAE PAPER 720303]

11 p1703 A72-25567

Oil spills remote sensing in marine environment, using laser excited fluorescence for detection, identification and quantification

15 p2251 A72-32623

Remote sensing system for oil pollution spectral signature properties, analyzing UV, IR, visible light, radar and microwave data

15 p2242 A72-32624

OLEIC ACID

Negative slip reversal effect formation mechanism during friction, discussing elimination via oleic acid

08 p1181 A72-22092

Negative slip reversal effect formation mechanism during friction, discussing elimination via oleic acid as lubricant additive

17 p2559 A72-34663

OLFACTORY PERCEPTION

Single olfactory bulb units under cyclic stimulation, observing activity related to inhalation cycle and odor quality

05 p0617 A72-16162

Olfactory receptor models sensitivity, discussing threshold dependence on adsorbed odoriferous agent amount and exposure time

11 p1585 A72-26453

Amygdala projection to accessory olfactory bulb in rats, discussing main bulb, olfactory tubercle, pyriform cortex accessory bulb and amygdala relationships

11 p1581 A72-26770

German book - Somatic sensitivity, smell and taste.

22 p3145 A72-42776

Olfactory perception neurophysiological mechanism, discussing receptor cells sensory thresholds and time, temperature and humidity effects

22 p3146 A72-42782

The effect of electrical stimulation of the olfactory bulbs on the behaviour of cats and on the electrical activity of the neo- and archepaleocortex

22 p3147 A72-42960

OLIVINE

Microprobe analysis of Timmersoi hypersthene chondrite from Niger Republic, noting equilibrium between olivine and orthopyroxene at 850 C

13 p2035 A72-28751

Microprobe analysis of Murchison and Vigarano meteorites, noting fractionation processes for Ca distribution in olivines

13 p2036 A72-28752

Lunar interior temperature profile estimation from electrical conductivity distribution based on forsteritic olivine composition

14 p2153 A72-30505

Fe and Ti ion bands in lunar pyroxenes and olivines single crystals polarized absorption spectra

14 p2154 A72-30510

Temperature dependent Mg and Fe hyperfine doublets in lunar olivine, indicating slow cooling crystallization

15 p2303 A72-31302

Olivine-garnet reaction in peridotites from Tanzania.

17 p2551 A72-35937

Compositional characteristics of olivines from Apollo 12 samples.

18 p2723 A72-36063

Activity-composition relations in the fayalite-forsterite solid solution between 900 and 1300 C at low pressures.

20 p2915 A72-39178

Lunar temperature profiles from electrical conductivity profile of olivine single crystal as lunar interior material representative sample

20 p2967 A72-39179

Iron transport in chondrites - Evidence from the Warren meteorite.

21 p3104 A72-40491

OMEGA NAVIGATION SYSTEM

X ray stars atmospheric ionization effects by vlf phase tracking relative to Omega navigation accuracy, diurnal shift variations and astrophysical data

04 p0486 A72-14877

OMEGA system application to airborne long range navigation, describing aircraft position determination technique for extended flight over water without line-of-sight radio navigation aids

05 p0686 A72-16655

Omega system in short range navigation supplementing VORTAC for coverage at low altitudes in mountain areas

06 p0844 A72-17334

Omega radio navigation system lanning problem, discussing ambiguity resolution by multiple state vector Kalman filter

08 p1144 A72-20860

Loran-Omega course and track equipment /LO-CATE/ of integrated upper air meteorological sounding systems, describing radiosonde navigational aids

10 p1484 A72-25086

Radiosonde balloon tracking errors in upper atmosphere wind measurement with Loran C, Omega and radar transmitters

10 p1441 A72-25092

OMEGA navigation system - Conference, Washington, D.C., November 1971

13 p1997 A72-29180

OMEGA short term range precision for broad ocean area navigation, using four range least squares position solution

13 p1997 A72-29181

Loran/OMEGA course and track equipment /LO-CATE/ for remote object tracking by retransmission technique, eliminating search from search and rescue missions

13 p1997 A72-29182

Wind profiles determination by Locate System in connection with OMEGA navigation system as sensing device

13 p1997 A72-29183

OMEGA receiver with digital solid state circuits for remote unmanned platform positioning, discussing ship to shore tests and design features

13 p1925 A72-29184

OMEGA phase shifts in auroral region due to solar phenomena, discussing methods eliminating PCA induced errors

13 p1997 A72-29185

Navigation accuracy of corrected OMEGA close to transmitter, using aircraft flight test at 500 nm range

13 p1997 A72-29186

Polynomial surface approximation to OMEGA sky wave corrections for small computer compatible with automatic receiver

13 p1925 A72-29187

Design characteristics and in-flight performance tests of computerized airborne OMEGA receiver, noting time independent one mile accuracy

13 p1997 A72-29188

AN/ARN-99 OMEGA lane ambiguity resolution for receiver location, using multiple state vector Kalman filter approach

13 p1997 A72-29189

Sky wave correction /Swanson/ model and computer program for real time propagation prediction for airborne OMEGA system

13 p1997 A72-29190

Airborne OMEGA navigation system performance, discussing transmission facilities, three frequency receiver, flight tests and optimization of receiving antenna

13 p1998 A72-29191

Aircraft applications of composite signal OMEGA configuration with phase data combined at separate carrier with weighting coefficients, discussing advantages over uncompensated navigation systems

13 p1998 A72-29192

OMEGA navigation system in civil maritime application, discussing single frequency, composite, difference and differential configurations and sky wave corrections

13 p1998 A72-29193

OMEGA navigation system operation aboard NOAA ship Discoverer in conjunction with satellite system, noting Trans-Atlantic tracklines

13 p1998 A72-29194

FAA airborne OMEGA development program covering signal monitoring, airborne data collection and system operational evaluation

13 p1998 A72-29195

Operational advantages of low cost VLF/OMEGA digital navigation system for various aircraft types

13 p1998 A72-29196

OMEGA effect on oceanic airway safety, noting improvement over inertial navigation systems

13 p1998 A72-29197

Preproduction OMEGA aircraft receivers and antennas development and flight testing, noting signal loss problems in high noise or precipitation static environments

13 p1998 A72-29198

Aeronautical navigation/guidance standardization in conjunction with OMEGA, covering sensor and computer equipment life cycles

13 p1999 A72-29199

Polar region performance of OMEGA navigation system, noting addition of selectable grid reference, multiple parallel DR system, manual celestial computation and bearing resolver

13 p1999 A72-29200

Small aircraft navigation over 10-400 mile course segments by raw OMEGA phase information dc presentation on conventional ID-249 course deviation indicator

13 p1999 A72-29201

OMEGA receiver integration into Navy P-3C airborne computerized navigation system, describing flight test, maintainability and laboratory simulation programs

13 p1999 A72-29202

Test flights into weather at midlatitudes and tropical systems with airborne OMEGA navigation system, discussing E field and H field antennas

13 p1999 A72-29203

Subtraction circuit design for impulse noise elimination at front end of aircraft oriented OMEGA navigation system receiver

13 p1999 A72-29204

Hardware and software integration of OMEGA and LORAN C and D receivers based on hyperbolic navigation systems compatibility

13 p1999 A72-29205

Avionics equipment for signal processing onboard civil aircraft to improve flight safety, discussing uses of OMEGA navigation system and digital computers

15 p2193 A72-31178

VLF signal role in long range time dissemination, communication and navigation, comparing conventional and modern techniques with emphasis on OMEGA system accuracy

15 p2199 A72-32068

Time of delay signal information addition to OMEGA worldwide VLF navigation system by digital code applicable for clock resetting and timing for automatic data recording

15 p2199 A72-32077

The Omega navigation system - Its history, application and versatility.

17 p2578 A72-35559

OMEGA air and maritime navigation system development, test phase and application potential, discussing operational modes, propagation parameters, solar activity effects and signal loss

19 p2831 A72-37796

Implementation status of the Omega Navigation System.

22 p3203 A72-42945

Automatic transmission and application of sky wave corrections with differential OMEGA navigation, discussing test equipment, procedures and results

22 p3203 A72-42948

Application of differential OMEGA to remote environmental sensing.

24 p3421 A72-44639

Satellite relay and Omega navigation system for distress signal transmission and reception in global rescue alarm network serving ships, aircraft and spacecraft

24 p3467 A72-45134

OMNIDIRECTIONAL ANTENNAS

NT MONOPOLE ANTENNAS

NT TURNSTILE ANTENNAS

A millimeter wave receiving antenna with an omnidirectional or directional scannable azimuth pattern and a directional vertical pattern.

17 p2525 A72-34364

A polydirectional antenna in polygon reflector design with cosecant-type elevation directional diagram for providing television in the 12-GHz frequency range

21 p3029 A72-40524

Turnstile antennas polydirectional emission and polarization characteristics, discussing relationship formulation by Scott-Soo Hoo theorem

21 p3030 A72-40531

An antenna principle with universally polydirectional radiation for large spin-stabilized flight devices

21 p3030 A72-40532

Broad-band television transmitting antenna with polydirectional characteristics for the UHF-region

21 p3031 A72-40542

Horizontally polarized polydirectional or beam antenna, which is slightly out of round and consists of beam units, for television and FM radio

21 p3031 A72-40544

OMNIRANGE NAVIGATION

U VHF OMNIRANGE NAVIGATION

ON-LINE PROGRAMMING

Online identification on human describing function by iterative differential analyzer, noting application to man-machine systems and online adaptive control systems

02 p0169 A72-12661

Human neuromuscular coordination control optimization, discussing preprogrammed open-loop control with feedback monitoring loop

04 p0477 A72-14705

On-line digital spectrum analysis based on fast Fourier transform algorithm, exemplifying by plasma density fluctuations correlation

04 p0496 A72-15488

Slat-airfoil combinations aerodynamics modeled by single point vortex to represent leading edge slat, discussing on-line computer graphics program [AIAA PAPER 72-221]

05 p0603 A72-16798

Acoustic emission systems application to materials nondestructive testing, discussing single and multiple piezoelectric transducer arrays with on-line computer analysis

[SAE PAPER 720175]

06 p0819 A72-17323

Bubble chamber high energy particle tracks semiautomatic measuring device, using small on-line computer for data processing

06 p0813 A72-17438

CIRCAL-2 general purpose on-line circuit design computer program featuring multiple analysis, text editing, network representation and user-program interaction optimization capabilities

06 p0778 A72-17474

Interference rejection method for high speed analog to digital converters, noting application to on-line computer systems

07 p0948 A72-20386

Instantaneous velocity vector determination in two dimensional flow by hot-wire anemometer and on-line digital computer technique

10 p1478 A72-23877

Analog and hybrid computers automated programming, setup and checking facilities for off and on-line program preparation and debugging

10 p1445 A72-24090

Rotating analyzer astronomical photopolarimeter automation by on-line computer control system

11 p1600 A72-25695

Astronomical pointing of radio telescopes using on-line computer

12 p1793 A72-27813

Process computer technology, discussing data recognition, on-line open loop operation and system characteristics

13 p1926 A72-30051

Parameter identification of a class of multiple input/multiple output linear discrete-time systems

19 p2826 A72-38269

On-line identification of multivariable stochastic feedback systems

19 p2781 A72-38270

An interactive approach for the generation and verification of test sequences in a logic system

24 p3382 A72-44662

ONBOARD COMPUTERS

U AIRBORNE/SPACEBORNE COMPUTERS

ONBOARD EQUIPMENT

NT AIRBORNE EQUIPMENT

NT AIRBORNE/SPACEBORNE COMPUTERS

NT AIRCRAFT EQUIPMENT

NT SPACECRAFT ELECTRONIC EQUIPMENT

Pilot role in automated ATC system using onboard situation display with navigation and collision avoidance devices

06 p0844 A72-17332

Outer planets Grand Tour trajectory correction requirements, examining combined radio/onboard navigation system and delta V estimates

[ALAA PAPER 72-54] 07 p1068 A72-18947

Mars atmospheric entry experiments for Viking 1975 mission, discussing onboard neutral gas mass spectrometer and retarding potential analyzer

10 p1540 A72-24381

Onboard turbogenerator igniter operating conditions determination from fuel-air ratio obtained from nomogram

12 p1861 A72-28145

Preventive and remedial space flight safety engineering, discussing escape capsules and onboard and earth-launched rescue systems

17 p2620 A72-34427

Military transport helicopter optimum secondary power system, considering onboard auxiliary power unit, electric or hydraulic engine start system, environmental control, etc

[AHS PREPRINT 664] 17 p2494 A72-34480

A horizon sensor with a bolometer and electrooptical modulators

17 p2556 A72-35385

Area navigation and its affect on aircraft operation and systems design

[ALAA PAPER 72-754] 19 p2831 A72-38125

The on-board computer of the Astronomical Netherlands Satellite [ANSI]

24 p3382 A72-45163

Extraterrestrial electromagnetic radiation and particle flux characteristics of low and medium energy, considering onboard spacecraft measuring instruments and data processing systems

24 p3404 A72-45398

ONBOARD NAVIGATION

U NAVIGATION

ONE DIMENSIONAL FLOW

One dimensional unsteady flow in turbine engines rotating and static vane cascades, discussing vibrations propagation

02 p0202 A72-11584

One dimensional plane magnetoacoustic wave stability from synchronous flow in narrow flow gap MHD induction machine

02 p0265 A72-12263

Poincare-Lighthill-Kuo perturbation method and method of characteristics equivalence in one dimensional fluid motion due to ideal piston periodic oscillation

03 p0341 A72-13239

One dimensional Boltzmann equation with linearized small perturbation, determining secondary conditions

03 p0399 A72-14347

Similar unsteady one dimensional motion of viscous heat conducting gas due to sudden energy release at surface

[ASME PAPER 71-WA/HT-3] 05 p0743 A72-15864

Conservation equations for blast waves one dimensional nonsteady flow field, considering Eulerian space and time profiles

[ASME PAPER 71-WA/APM-1] 05 p0745 A72-15974

One dimensional two phase flow transpiration cooling through porous metals

[ALAA PAPER 72-24] 05 p0749 A72-16915

Inviscid conducting gas steady one-dimensional MHD flow, using three-dimensional phase diagram for differential equations analysis

08 p1214 A72-21646

One dimensional expansion of hot vapor and gases remaining behind meteor body

08 p1238 A72-21884

Boundary value solutions and computer programs for one dimensional laminar flame propagation equations

08 p1129 A72-22040

Electromagnetic coupling between one dimensional laminar flows of viscous conducting fluid in presence of magnetic field, noting static and dynamic efficiencies dependence on Hartmann number

10 p1519 A72-24065

Simple waves in one dimensional unsteady nonequilibrium dissociative gas dynamics, discussing internal, chemical bond and dissociation energies

11 p1616 A72-25982

Hot-wire measurement of vector velocity modulus and sign in one dimensional unsteady gas flow

12 p1806 A72-27178

Possible regimes and solutions for adiabatic one dimensional compressible gas flow in convergent and divergent ducts with friction

12 p1797 A72-27348

Numerical algorithm for Boltzmann equation solution with application to shock structure in one dimensional flow

13 p1985 A72-28617

One dimensional unsteady flow of dense magnetized plasma, investigating time evolution of temperature profile in wall layer and thermal conductivity

13 p2018 A72-29876

Pseudo-one dimensional dissociative nonequilibrium nozzle flow, presenting governing equations transformation via similarity parameter for oxygen

16 p2375 A72-32906

Nonequilibrium steady quasi-one dimensional expanding nozzle flow of chemically reacting gas mixture, using time dependent finite difference technique

[ALAA PAPER 72-684] 16 p2480 A72-34058

Theoretical study of electromagnetic coupling in the forced oscillatory regime of two one-dimensional laminar flows of a viscous and electroconducting liquid in the presence of a transverse uniform magnetic field

17 p2587 A72-34281

Steady state heat transfer in one dimensional flow involving simultaneous convective and diffusive transport via finite difference formulation

18 p2741 A72-37171

Linearized problem of one-dimensional periodic gas flow in a pipe

19 p2786 A72-37666

One dimensional stationary gas flow across normal shock wave, taking into account nonequilibrium factors and momentum, mass and energy transport

20 p2914 A72-39970

One dimensional variable slip and homogeneous model predictions of momentum flux in two phase two component low quality flow

21 p3130 A72-41179

Equations of plane potential electrohydrodynamic flow, noting jet and quasi-one dimensional flows of charged particles in curvilinear electrostatic field

22 p3210 A72-42269

One-dimensional shock waves in heat conducting materials with memory. I - Thermodynamics

23 p3314 A72-44341

ONISOTROPY

U ANISOTROPY

ONSAGER PHENOMENOLOGICAL COEFFICIENT

Discrete vortex model numerical simulation of Onsager negative temperature instability for interacting line vortices two dimensional motions

17 p2538 A72-34871

ONSAGER RELATIONSHIP

Euler-Lagrange equation construction to obtain phenomenological description of quasi-equilibrium systems in metrics, noting solution coincidence with Onsager equations

07 p1102 A72-20665

Onsager irreversibility theory extension to nonlinear constitutive relations and with allowance for inclusion of all thermodynamic variables

16 p2479 A72-33826

Negative temperatures in two dimensional vortex motion

18 p2681 A72-36669

OPACITY

Cepheid variables mass discrepancy from evolution and pulsation theories, emphasizing opacity changes, luminosity values and effective temperature

01 p0133 A72-11128

Shock tube technique for opacity measurement at high pressures in seeded hydrogen for gas core nuclear rockets

01 p0099 A72-11342

Fresnel diffraction on opaque half plane screens with statistically rough surfaces, using Kirchhoff approximation

02 p0183 A72-12755

Missing solar UV opacity from band adsorption coefficient comparison between photospheric diatomic molecules and metals and hydrogen

04 p0579 A72-15327

Energy transport within stellar structure, discussing radiative transfer and opacity relationship to mean free path of radiation

07 p1078 A72-19924

Transparent and opaque materials fracture mechanism analogies under laser beam action, determining dislocation structure

08 p1185 A72-22093

Methane contribution to thermal opacity in Uranus and Neptune atmospheres for atmospheric model synthesis

09 p1383 A72-22293

Geochemistry of lunar opaque minerals in Apollo 14 crystalline rocks, including FeNi metal, ilmenite, spinels, schreibersite, baddeleyite, fayalite and tranquillityite

10 p1538 A72-24164

Mean opacities and effective absorption coefficients measurement using wide bandwidths and path lengths

14 p2131 A72-30900

Opacity corrections of main sequence stellar models of 2.25 solar masses in terms of Cox, Carson and Watson formulas

16 p2452 A72-33130

Transparent and opaque crystal surface fracture mechanism analogies under laser beam action, determining dislocation structure

17 p2562 A72-34664

Radiative opacity and calculation of stellar models

18 p2728 A72-36766

Influence of roughness on the thermal radiation emitted by opaque surfaces - Model test

19 p2881 A72-38393

Fresnel diffraction on opaque half plane screens with statistically rough surfaces, using Kirchhoff approximation

20 p2902 A72-39061

On the influence of the opacity values on static stellar models. I - Horizontal branch stars

20 p2973 A72-39879

Mean coefficient of opacity in stellar atmosphere model calculations

21 p3110 A72-41443

OPEN PIT MINES

U MINES [EXCAVATIONS]

OPENINGS

NT APERTURES

NT IRISES [MECHANICAL APERTURES]

NT PORTS [OPENINGS]

NT SLITS

Buckling of shells with cutouts - Experiment and analysis

17 p2634 A72-35405

OPERATING SYSTEMS [COMPUTERS]

Simultaneous operation of digital computer units to reduce input times and prolong useful computer operation time

13 p1925 A72-29944

Multiprogrammed virtual memory digital computer systems analysis and design, discussing component characteristics, operating system structure and mathematical description techniques

23 p3267 A72-43987

OPERATING TEMPERATURE

Thermal resistance estimation for machine parts of heat resistant alloys under real working conditions

06 p0833 A72-18559

Metallic four-lip seal performance, discussing force cycle, mechanical spring-back, reusability at room and higher temperatures and thermal shock behavior

08 p1179 A72-21939

Cesium oxide system stable phases as sources of Cs and oxygen vapors in thermionic energy converters, increasing power and reservoir operating temperature

09 p1263 A72-22959

Semiconductor laser thermal resistance and time constant evaluation, obtaining operating temperature range and maximum attainable pulse width

11 p1647 A72-25808

Cesium oxide system stable phases as sources of Cs and oxygen vapors in thermionic energy converters, increasing power and reservoir operating temperature

17 p2498 A72-35888

Experimental technique for determination of roller bearing preload to optimize dynamic characteristics and minimize operating temperature

19 p2810 A72-38650

OPERATIONAL HAZARDS

Rotary wing and VTOL aircraft induced downwash effects on ground personnel, considering injuries, body heat loss, work capability impairment and sound pressure effects
14 p2072 A72-30425
The onboard authority of the aircraft commanding officer as provided by the 1963 Tokyo Convention
17 p2639 A72-35763
Detection of hazards associated with aerospace operations.
23 p3287 A72-43424
Apollo/Saturn 5 spacecraft liquid propellants safety procedures in event of fire on explosion in operations building at Kennedy Space Center
23 p3343 A72-43552

OPERATIONAL PROBLEMS

Operational stability of rocket engine with combustion chamber having charge of two propellant types with different burning rate dependences on pressure
06 p0867 A72-18206
Prediction of weather induced airline operating delays, discussing fog, snow, freezing rain, thunderstorms, crosswind, headwinds, CAT, wind shear, wet runways and tail winds
07 p1030 A72-19597
Man machine automatic control system structural synthesis, treating system operation as nonlinear programming problem
09 p1291 A72-23438
Aircraft transparencies from civil operator viewpoint, considering replacement cost of flight deck and cabin windows
12 p1753 A72-27005
Hypersonic commercial aircraft operational problems, considering passenger physiology limits flight profile, sonic pollution, traffic demands, route structure, etc
14 p2073 A72-30830
International cooperation in space operations and exploration - AAS Conference, Washington, D.C., March 1971
14 p2175 A72-31135
Earth resources survey systems, discussing benefits, ground truth problem, data analysis, experimental satellites, operational system, and developing countries needs and activities
14 p2175 A72-31142
Aircraft CRT electronic displays discussing operational flexibility versus control and monitor complexities, economics, reliability and human factors
15 p2182 A72-32636
Man machine automatic control system structural synthesis, treating system operation as nonlinear programming problem
19 p2782 A72-38521
Human engineering requirements in aircraft system development.
21 p3011 A72-41423
Material properties, metallurgy, production technology and operational factors effects on machinery structural strength
23 p3347 A72-43733
The space tug orbital operations.
24 p3451 A72-45196

OPERATIONS RESEARCH

NT CRITICAL PATH METHOD
NT DYNAMIC PROGRAMMING
NT GAME THEORY
NT LINEAR PROGRAMMING
NT MINIMAX TECHNIQUE
NT NONLINEAR PROGRAMMING
NT SADDLE POINTS [GAME THEORY]
Cybernetic system effectiveness analysis with operations research and statistical theory based on stochastic treatment
11 p1608 A72-25428
Operations research and reliability - Conference, Turin, Italy, June-July 1969
13 p1961 A72-28351
An operations research approach to solve complex and unstructured problems illustrated for the case of cost-plus-award fee contracts.
17 p2639 A72-35341
Optimal design of indeterminate truss using geometric programming.
23 p3354 A72-44256
The application of operational research to transport problems; Proceedings of the Conference, Sandefjord, Norway, August 14-18, 1972.
24 p3466 A72-44576
The heavy lift helicopter - An operations research/technology/performance blend.
24 p3466 A72-44581
Applications of operational research in the airline industry.
24 p3466 A72-44583

OPERATOR PERFORMANCE

Time shortage as stress factor affecting mental activity of operator in man-flying vehicle system, discussing control signal handling efficiency
05 p0622 A72-16638
Response surface methodology /RSM/ techniques application to operator target acquisition performance

prediction, describing multivariables functional relationship by multiple regression polynomial equation
06 p0773 A72-17714
Dynamic response and functional state of human operator subjected to harmonic and random vibrational excitations, discussing biodynamic nonlinear oscillatory system model construction
06 p0770 A72-18728
Human operator role in ATC systems analysis, evaluating tasks with respect to job demands and personal fulfillment
09 p1270 A72-23127
Operator mental processes during ATC task performance, discussing work load effect, mental representation and operator algorithm definition
09 p1270 A72-23129
Operator, task level and workload effects on operative strategy, showing controllers methods modification in ATC center
09 p1270 A72-23130
Landing sequence strategy variations for individual ATC operators, indicating dependence on flight progress data variation, existing maneuvering conditions and controller personality traits
09 p1271 A72-23131
Pilot and ATC radar controller workload variations relation, discussing distraction stress effects
09 p1271 A72-23132
Time analyses of ATC approach controller tasks, developing flow diagram for task component sequencing and quantifying
09 p1271 A72-23133
ATC operator stress factor evaluation from information theory analysis of radio telecommunication information content
09 p1271 A72-23134
ATC task analysis by subjective rating of work load, discussing information processing measures, scoring method and observer rating procedure
09 p1271 A72-23135
Acceptable load standards in ATC tasks, defining moments of conscious brain control as mental load measure
09 p1271 A72-23139
Individual style differences between operators of simulated aircraft control
09 p1273 A72-23579
Operator independence test for human performance reliability modelling based on symptom detection and fault location of sonar system failure
10 p1429 A72-24002
Human operator role in space systems reliability, suggesting approaches to system design and program planning to exploit human potential [AIAA PAPER 72-228]
10 p1430 A72-24439
Pressure suit effects on psychomotor skills, testing manual dexterity, tracking skills, hand strength, steadiness and coordination for pressurized, unpressurized and shirtsleeve conditions
10 p1431 A72-24796
Optimum performance typewriter keyboard design, discussing biomechanical improvements in finger positioning facilitation, operator postural muscular strain reduction, etc
10 p1433 A72-25114
Multichannel information processing task complexity relation to operator performance for rapidly increasing input conditions
10 p1433 A72-25115
Short sleep period and oxygen breathing effects on arousal level of air traffic controller during detection task performance
11 p1588 A72-26686
Work-rest scheduling and sleep loss effect on operator performance in watchkeeping and active multiple visual tasks
11 p1589 A72-26689
Change in Naval Flight Officer operational role due to modern equipment design in weapons systems, sensors and navigational aids
12 p1775 A72-28291
Tracker recovery strategy during temporary target obscuration in pursuit tracking task, analyzing control stick movements
13 p1911 A72-29820
Compensatory tracking task performance with continuous error information feedback via visual, auditory or electrocutaneous displays
14 p2083 A72-31152
ATC systems fast-time simulation, emphasizing importance of human operator performance realistic modeling
15 p2269 A72-32097
An objective test for evaluating the functional state of the oculomotor system during somnolence states
19 p2756 A72-37876
Man machine systems operational effectiveness augmentation through human factors engineering to enhance human operator capability for parallel data processing and decision making
19 p2761 A72-38308
Visual optical system evaluation from viewpoint of human operator target detection under field conditions

in terms of resolution, transfer functions, aberration and eye movements
20 p2893 A72-39041
An assembly for studying the perceptive motor reactions of man under one-dimensional follow-up conditions
21 p3008 A72-40810
The design of a nonlinear multi-parameter model for the human operator.
21 p3011 A72-41421
A psychologist's laboratory approach to a human factors problem.
21 p3012 A72-41430
The influence of a prediction display on the human transfer characteristics.
21 p3012 A72-41432
Human operator dynamics for aural compensatory tracking.
22 p3149 A72-41950
German monograph - Control performance as a function of the transmission ratio and the Coulomb friction in the operational element.
22 p3152 A72-43052
The simultaneous action of stimulants and tranquilizers on the efficiency of a human operator
23 p3260 A72-43923
Mathematical description of a human operator in ergatic control systems
24 p3376 A72-45514
Algorithmic description of the generalized operational characteristic of a human operator
24 p3376 A72-45515
Estimate of the operational efficiency of a human operator in the follow-up mode of a closed-loop control system
24 p3376 A72-45516
Methodical aspects of studies of ergatic differential-game systems
24 p3376 A72-45517
Man in a control circuit during an information game synthesis
24 p3377 A72-45520
Experimental determination of the distribution rule for the time of failure-free operator action in the tracking mode /with pursuit/
24 p3377 A72-45521
Aircraft interception avoidance problem solved by differential game theory, discussing human operator decision making for random pursuit tracking
24 p3377 A72-45523

OPERATORS [MATHEMATICS]
Semi-Markov process sojourn time within reducible subset of states, examining asymptotic behavior with algorithm developed for linear operators disturbances
01 p0094 A72-11265
Time operator method in creep theory for orthotropic bodies, obtaining asymptotic solutions for laminar orthotropic rod and elastic plate vibration problems
02 p0289 A72-11617
Topological structure of anharmonically coupled many body problem, describing generalized Bose operators formulation
02 p0262 A72-12049
Quasi-linear tensor operator derived in form of series converging inside circle, proving theorem concerning reciprocity conditions and existence of potential
03 p0445 A72-13579
Nonhomogeneous media electrodynamics with varying permittivity and permeability, solving nonstationary equations by differential operators
03 p0389 A72-13654
Multiplication operator unidimensional perturbation by independent variable, considering spectral function density poles and branch points
03 p0382 A72-13728
Liapunov functionals synthesis for continuous system stability study, discussing linear combinations of moments of governing partial differential operators
04 p0538 A72-14671
Edge-coding operators for two dimensional binary picture black-white boundary pattern recognition suitable for use in parallel processing systems
04 p0496 A72-15203
Closure approximation in hierarchy stochastic differential operator equations in statistical mechanics
04 p0540 A72-15257
Vibration theory calculations using parametric matrix function method and associated operators
04 p0550 A72-15543
Continuous linear elastic systems characteristic vibrations differential operator eigenvalues lower bounds calculation, obtaining Green integral operator first invariant upper bound via stress function
04 p0540 A72-15706
Multidimensional time dependent flow field analysis by split finite difference operator technique, using star mesh of quadrilateral cells
05 p0609 A72-16950
Continuous linear probability functions characterization, applying to p-radonizing operators
06 p0838 A72-17554

Exact linear dielectric operator for stratified plasma streams with velocity gradients for diagnostics with electromagnetic waves

06 p0861 A72-17748

Density matrix equation solution in Liouville space, using variational procedure for laser mode equation and separable interaction method

07 p1006 A72-19670

Algebraic algorithm for reducing to state form multivariable control systems defined by linear constant differential operators

07 p0950 A72-19702

Control theory of dynamic multiconnected systems with differential operators, time lags and hereditary components

07 p0962 A72-19721

Boundary value problems in supporting surfaces vibrations theory, constructing Green function from part of differential operator

07 p1093 A72-19984

Truncation error correction based on Richardson extrapolation in finite difference approximation of nonlinear partial differential operators

07 p1101 A72-20328

Signal statistical model parameter evaluation by selection of operators in form of dimensionless quantile ratios

08 p1130 A72-20724

Natural oscillation frequencies of piecewise homogeneous L-shaped membranes, determining eigenvalues of second order elliptical differential operator

08 p1241 A72-20903

Multiple completeness characteristics of eigenvectors and adjoint vectors of polynomial operator packets in separable Hilbert space

08 p1198 A72-21096

Algebraic structures of operator nodes with reduced elements

08 p1198 A72-21097

Integral operators functions approximation for elasticity and materials aging equations, noting transcendental functions in solutions

08 p1243 A72-21239

Bergman operators construction for second order linear partial differential equations

08 p1199 A72-21288

Operator approach solution to boundary value problems with infinite defect for differential equations with deviating argument, considering Fredholm alternative validity and compressed mappings application

08 p1199 A72-21465

Ordinary differential operators eigenvalues calculation, noting numerical integration scheme for initial value problem

09 p1340 A72-22461

Generalized polynomial operators for nonlinear systems analysis, presenting local invertibility theorem

09 p1341 A72-23092

Matrix notation for replacing vector analysis in control theory by introduction of differential operators similar to Hamiltonian operator

09 p1352 A72-23369

Rayleigh-Ritz method supplement for optimal evaluation of eigenvalue bounds for semibounded self adjoint operators

09 p1353 A72-23484

Functional analytical formulation of steady creep processes, using error estimations in solution of equations with monotonic potential operators in Banach spaces

09 p1409 A72-23567

Solutions for multivalued evolution equations, considering monotonic maximal operator on finite dimensional Hilbert space

10 p1504 A72-24061

Spectral continuity conditions of linear operator, noting application to elliptical operators approximation in separable Hilbert spaces

10 p1505 A72-24070

Collision operator behavior in linear Boltzmann equation model of molecular gas in Hilbert space

10 p1510 A72-24102

Stability criteria for continuous dynamic system under parametric excitation derived by Liapunov direct method, using time dependent functionals and Rayleigh operators quotients

10 p1510 A72-24187

Markov processes for local diffusions defined by second order differential operator delta with Holder coefficients on manifold

10 p1505 A72-24201

Discrete time systems with periodic feedback gain, deriving stability conditions and Nyquist plot from linear operator spectral theory

11 p1608 A72-25318

Finite difference approximation of eigenvalues of singular differential operators in Hilbert space

11 p1678 A72-26556

Uniform Markov processes properties in Hilbert space, examining operator subgroups

12 p1836 A72-27071

Quasi-projection operators for calculating electron resonances in multitarget scattering tested on He ion autoionization system

12 p1847 A72-27385

Floating point arithmetic operators with variable dynamic range and multiple precision, noting word method for numerical data processing in computation and process control

12 p1787 A72-27666

Ergodic theorems for operators generated by Markov transients, examining asymptotic properties of stochastic learning model

12 p1787 A72-27924

Generalized Fourier transformation method for mixed boundary value problems of second order parabolic differential equation in unbounded region, noting singular differential operator

12 p1837 A72-27998

Additional operator method application to nonlinear servosystems self adjusting circuits design, presenting system simulation results

13 p1935 A72-28611

Difference scheme application to Laplace operator eigenvalues determination for regions composed of rectangles, using summary representation formulas

13 p1986 A72-29082

Weakly complete projecting convex cone, considering operators subalgebra representation

13 p1987 A72-29776

Bounded operators solution in locally convex topological vectorial spaces with meromorphic properties

13 p1987 A72-29778

Linear functional equations with constant coefficients for generalized partial derivative operators introduced in certain spaces of functions of many complex variables

13 p1987 A72-30083

Operator identities unification and classification, presenting reformulation as algebraic closure properties of graphs

14 p2125 A72-30229

Eigenvalues examination for self adjoint singular differential operators in Hilbert space by finite difference methods

14 p2126 A72-30619

Magnetized nonuniform plasmas, discussing description to all orders in electron and ion temperatures of waves by operator method

14 p2139 A72-30879

Elastic body stress concentration problem formulation as singular integral operator eigenvalue problem for half space

15 p2323 A72-31478

Iteration methods to compute inverse for nonsingular linear operator on Banach space

15 p2261 A72-31495

Boundary value problems for discrete spectrum of nonlinear ordinary differential operators on unbounded intervals

15 p2263 A72-31760

Two-magnon Raman scattering in antiferromagnets, obtaining amplitude-renormalization factor by extended Dyson-Maleev graphical approach to include corrections in transition operator M

15 p2295 A72-32548

Triple and quadruple integral equations solution in analogy to Fourier-Bessel series with mixed boundary values, using Erdelyi, Kober, Sneddon and Srivastav operators

16 p2416 A72-33663

Book - Approximation of elliptic boundary-value problems

17 p2574 A72-34622

Self-adjusting hybrid schemes for shock computations.

17 p2575 A72-34648

Means of converting the solutions of partial differential equations, obtained in operator form, to solutions of conventional form when the differential operators are expressed in general form

17 p2577 A72-35789

Relationship between finite differences and quadratures of a Green's function for a second-order ordinary differential operator

17 p2577 A72-35803

Investigation of a solution to an almost everywhere multidimensional mixed problem of a class of second-order hyperbolic equations with a nonlinear operator-containing right side

17 p2577 A72-35841

Investigation of a strongly generalized solution to a multidimensional mixed problem of a class of second-order hyperbolic equations with a nonlinear operator-containing right side

17 p2577 A72-35843

Necessary and sufficient conditions for space linear operator factorization, noting summation operators theory

18 p2704 A72-36462

Compact self adjoint differential operators in family of Hilbert interpolation spaces, applying perturbation theorem to boundary value problems

18 p2704 A72-36511

Interpolation theorems for nonlinear operators acting on locally convex spaces constituting projective and inductive limits of Banach spaces

18 p2704 A72-36513

Nonzero solutions of boundary value problems for second order ordinary and delay-differential equations.

18 p2705 A72-36617

Differential inequalities for semilinear hyperbolic operators with two independent variables.

18 p2705 A72-36618

Wyld diagram method extended to turbulence decay, considering operators expressed as integrals with kernels

19 p2785 A72-37469

Heat-conduction equations for multilayer shells

19 p2881 A72-38158

Solution of certain systems of partial differential equations in linear commutative differential operators

19 p2825 A72-38183

Problem of the eigenvalues of certain unbounded and nonsymmetrical operators and their applications to ordinary differential equations

19 p2825 A72-38195

Geophysical signal statistical model parameter evaluation by selection of operators in form of dimensionless quantile ratios

19 p2765 A72-38352

Investigation of a mixed boundary value problem for one class of second-order hyperbolic equations with a nonlinear operator-type right-hand side

19 p2827 A72-38447

Difference schemes with a divergent operator for a general system of second-order hyperbolic equations

19 p2828 A72-38854

Certain properties of differential operators with variable coefficients dependent on the domain format

20 p2946 A72-39465

Expansion of a theory of elasticity operator in a series of eigenfunctions

20 p2979 A72-39467

Group properties of ordinary linear second-order differential equations

20 p2946 A72-39471

Operator to minimize information loss, deleterious truncation and aliasing effects introduced by linear interpolation

21 p3077 A72-40104

Stability of solutions to the Hill equation with an operator coefficient having a negative mean value

21 p3074 A72-40256

Linear distributed parameter systems modal analysis and design for low sensitivity optimal feedback control, using linear differential operators

21 p3037 A72-40646

Book on nonhomogeneous boundary value problems covering Hilbert theory for trace and interpolation spaces, elliptic operators and variational equations

21 p3076 A72-41526

Book on nonhomogeneous boundary value problems for different classes of linear evolution parabolic operators, with applications to optimal control problems

21 p3076 A72-41527

Investigation with the aid of a Fourier method of the classical solution of a multidimensional composite problem for a class of hyperbolic equations of the second order with a nonlinear operator right-hand part

22 p3198 A72-41897

Certain necessary conditions for the local solvability of first-order differential equations with infinitely differentiable coefficients

22 p3198 A72-42158

Linear multistep methods for a class of functional differential equations.

22 p3199 A72-42774

Existence and uniqueness theorems of elliptic equations with eigenfunction exponential decrease at infinity and 2m order self adjoint differential operator in n-dimensional Euclidean space

23 p3307 A72-43223

Conditions for complete continuity of integral operators with stationary features in a space of continuous functions

23 p3307 A72-43224

Direct methods of qualitative spectral analysis for the singular Sturm-Liouville equation with an unrestricted operator potential

23 p3308 A72-43578

Polynomial operators for nonlinear systems analysis.

23 p3308 A72-43599

Recent results in convolution feedback systems.

23 p3276 A72-43861

Linearizing compensation for nonlinear control system transformation into linear system without approximation, discussing differential operator matrix definition and random noise effects

23 p3277 A72-43945

Cauchy problem for abstract Love equations

23 p3309 A72-44042

Dirichlet series in eigenvalues of boundary value problems for an arbitrary second-degree elliptic differential operator 23 p3309 A72-44043

Degree of approximation of functions by integral operators in an infinite domain as related to the Hausdorff metric 23 p3310 A72-44163

Boundary value problems for multidimensional hyperbolic equations with degeneration 23 p3310 A72-44487

The growth of entire solutions of differential equations of finite and infinite order. 24 p3418 A72-44725

The superharmonic functions in the axiomatics of M. Brelot associated with a degenerate elliptical operator 24 p3418 A72-44825

Dispersion relations of scalar hereditary theory of nonlinear viscoelasticity, representing integral operators as orthonormalized function series in Fourier space 24 p3459 A72-45264

OPERATORS (PERSONNEL)

NT AIRCRAFT PILOTS

NT PILOTS (PERSONNEL)

NT TEST PILOTS

Frankfurt Airport air traffic controller opinion survey of attitudes toward work and working environment 09 p1271 A72-23138

Invariant transformation of the control laws in ergatic systems 24 p3376 A72-45510

OPHTHALMODYNAMOMETRY

Eye mark recorder system for eyeball movement studies, describing operational principle and various optical systems 06 p0813 A72-17433

Ophthalmoscopic, photocalibrometric and ophthalmodynamometric examinations of test subjects visual acuity during bed rest in hypokinetic antihostatic position 23 p3255 A72-43916

OPHTHALMOLOGY

NT EYE EXAMINATIONS

Optic disk drusen and Marcus Gunn pupillary phenomenon relation to visual field defects, discussing need for calibrated perimetry and binocular field testing 07 p0933 A72-20190

Sight impairment-caused flight personnel disqualification analysis, establishing eye disease structure, sight damage preconditions and ophthalmological practice inadequacies 14 p2080 A72-30748

Eagle eye retinal image quality determination by ophthalmoscopic method, comparing to human visual acuity 15 p2186 A72-31724

An automatic measuring and recording system for clinical electro-oculography. 19 p2759 A72-37400

Quantitative determination of fluorescence within the eye without disrupting the integrity of the eyeball 20 p2893 A72-38941

The use of high refractive index glasses of low dispersion for the correction of medium and high ametropia. 21 p3084 A72-40731

Determination of corneal configuration by the measurement of its derivatives. 21 p3055 A72-40745

Ocular and induced visual effects of systemic and topical drugs in terms of eye neuroanatomy and pharmacology, stressing glaucoma therapy 22 p3150 A72-42499

OPTICAL ABSORPTION

U ELECTROMAGNETIC ABSORPTION

U LIGHT TRANSMISSION

OPTICAL AMPLIFIERS

U LIGHT AMPLIFIERS

OPTICAL COMMUNICATION

Incoherent optical communications fixed receiver passband, determining SNR for pulse time and code modulation with discrete time 01 p0024 A72-10198

Information feedback application to AM laser communication system, predicting multiplicative error, background shot noise and photon arrival fluctuation effects on continuous parameter transmission [AD-736731] 01 p0025 A72-10326

Dielectric surface waveguides for millimeter and optical wavelength applications, discussing technologies, materials, fabrication and measurement 02 p0191 A72-11683

Beam guides for optical and millimeter wave communication, discussing optical pipelines and iris, lens and reflector waveguides 02 p0191 A72-11684

Imperfect timing degradation of direct detection /noncoherent/ optical system using pulse position modulation bits 02 p0174 A72-12141

Modulation/demodulation techniques for optical one-gigabit/sec intersatellite data transmission link system, comparing per-unit data costs for system selection 02 p0174 A72-12142

Optical communication technique based on fiber optic light pipes and time, space or wavelength division multiplexing 03 p0325 A72-14050

Tactical optical ground communication systems, discussing use of GaAs and carbon dioxide lasers and ultrawideband data links 04 p0485 A72-14482

Lens type beam waveguide for optical trunk communication, discussing transmission medium, terrain layout, bandwidth, terminal equipment, misalignment and multibeam application 04 p0497 A72-14483

Millimeter wave and laser space-to-space communication links comparison, considering chf system based on size, weight, power consumption and communication parameters calculations 04 p0493 A72-15609

He-Ne laser controlled frequency shift in wideband optical heterodyne communications systems with Currie low reflection mirror 05 p0668 A72-16346

Wideband electro-optic FM of laser light for optical communication, discussing modulator design, construction and testing 05 p0631 A72-16961

[AIAA PAPER 72-177]

Optical data transmission system with dielectric single-mode glass fiber waveguide, PCM semiconductor laser diode transmitter and avalanche photodiode receiver 06 p0774 A72-17770

Harmonically modulated reflected light signals phase shift and demodulation, assuming single scattering 06 p0848 A72-18047

Incoherent optical system model with photodetectors governed by Laguerre counting statistics obtaining error probabilities for comparison with Poisson counting 06 p0776 A72-18394

Soviet book on laser communication statistical theory covering coherent and noncoherent optical signal detection and discrimination, SNR optimal reception, beam scanning, etc 06 p0777 A72-18518

Gaussian rf noise effect on optical detection signal fluctuations in optically pumped frequency standards 07 p0938 A72-19013

Carbon dioxide laser IR radiation modulation by application of Stark effect in various molecular absorbers, showing absence of saturation 07 p1000 A72-19035

Mode conversion effects on Gaussian laser beam in acousto-optical modulation for optical communications 07 p1004 A72-19225

Wave propagation in thin film optical waveguides with gyrotropic and anisotropic substrates, deriving TE and TM mode conversion conditions 07 p0940 A72-19230

[AD-739120]

Picosecond pulse distortion under multimode conditions in optical fiber communication systems 07 p0940 A72-19231

High sensitivity wideband heterodyne receiver system for spaceborne and ground-based IR laser communications 07 p0940 A72-19238

Wideband laser communication for space applications, comparing carbon dioxide and Nd-YAG systems on basis of SNR 07 p0941 A72-19239

Laser communication systems for terrestrial and space data transmission, discussing line-of-sight requirements and atmospheric effects 07 p0947 A72-20225

Laser telemetry performance, considering means of noise reduction 07 p0947 A72-20256

Aberration introduced by high satellite velocities, investigating application to laser telemetry 07 p0947 A72-20258

Tracking efficiency of laser telemetry on reflector carrying satellites 07 p0947 A72-20259

Tracking efficiency calculation for laser telemetry with laser reflector on nonstabilized satellite 07 p0947 A72-20260

Optical signal heterodyne reception, discussing atmospheric distortion effects reduction 08 p1131 A72-20749

Industrial applications of lasers, considering programmable machining, distance measurement, computer memories, communication, night clubs, machine shops, aircraft manufacture and tunnel boring machine alignment 08 p1182 A72-21207

Optimal continuous recording of amplitude-phase distributions on spatial carrier frequency for light wave modulation and optical antenna simulation 08 p1132 A72-21263

Gaussian noise quasi-optimal filtering in optical communication system, evaluating signal timing accuracy in detector-amplifier circuits 08 p1136 A72-21914

Laser pulse propagation measurements on multimode glass fibers to evaluate communication potential 09 p1323 A72-22868

Material dispersion contribution to signal envelope delay distortion in weakly guiding dielectric optical fiber waveguides 09 p1314 A72-23340

Receivers for PPM optical communication and pulsed signal detection in background light, evaluating upper bounds on error probability based on photoelectron Poisson statistics 11 p1591 A72-25311

Narrow pulse optical communication digital systems with PPM and on-off keying, investigating timing error effects on bit error probabilities 11 p1592 A72-25885

Weak signals detection at visible wavelengths with background noise, examining photoelectric recording and optimal detection characteristics of receiver 11 p1596 A72-26314

GaAs injection laser optical link assembly with silicon photodiode and optical transistor, noting applicability to optical data processing 11 p1648 A72-26328

Video information transmission over planar and rectangular multimode waveguides under excitation by coherent light, calculating field distribution by geometrical optics approximation 11 p1633 A72-26330

Angular variation and spot dancing of laser beam in atmospheric propagation, obtaining standard deviation 12 p1782 A72-27493

Surface wave propagation mechanism on dielectric bodies noting compatibility with physical properties involved with optical cables for commercial transmission systems 12 p1782 A72-27556

Optical communications with FDM digital data channels, examining signal optimal reception and noise stability 14 p2084 A72-30331

Optical communications photodetector sensitivity assessed from input power ratio of ideal and actual detector, noting amplitude modulated systems 15 p2235 A72-31621

Incoherent optical communications fixed receiver passband, determining SNR for pulse time and code modulation with discrete time 15 p2195 A72-31622

Laser communication lines in atmospheric ground layer, comparing SNR for direct-reception and superheterodyne video systems 15 p2247 A72-31887

Optical PCM communication system with megabits/sec information rate based on dye laser with combined frequency-time division multiplexing 15 p2198 A72-32060

Computer simulation for performance of carbon dioxide laser heterodyne communication system with photoconductive n-type mercury-cadmium telluride detector/mixer 15 p2198 A72-32062

Coherent IR heterodyne receivers with quantum noise threshold sensitivity for laser communications and radar transmission 15 p2198 A72-32063

Time division demultiplexing technique using two channel simulation of twenty-four channel digital optical PCM communication system 15 p2200 A72-32163

Quasi-optical transmission line stability improvement, investigating pulsating light beam concept 15 p2202 A72-32663

Computer technique to synthesize binary holograms for wave beams analysis in quasi-optical communication channels 15 p2242 A72-32674

Feedback averaging procedure application to M-ary polarization modulated laser communication system, obtaining error rate improvement over systems without feedback 16 p2362 A72-33215

Variable rate optical communication schemes over earth/space link neutralizing atmospheric turbulence effects 17 p2514 A72-34415

Laser systems. 17 p2562 A72-34567

Theory of optimum M-ary laser detection. 18 p2661 A72-36683

Optical communications in Japan. 19 p2766 A72-38602

An optical communication system using envelope modulation. 19 p2766 A72-38604

Coherent optical signal superregenerative amplification in Q switched gas laser, calculating sensitivity of He-Ne laser light amplifier 19 p2813 A72-38663

- Calculation of pulsed signal amplitudes at linear filter output in optical communication systems
19 p2768 A72-38671
- Experimental effects of finite transmitter-apertures on scintillations.
20 p2932 A72-39500
- Optical communication with distant spacecraft, discussing electro-optical transducers, light sources and receivers
21 p3014 A72-40321
- Optical communication channel optimization with binary signals preamplified in optical parametric amplifier, noting amplifier gain and SNR
21 p3016 A72-40783
- Direct-detection optical receivers for angle-modulated signals.
21 p3017 A72-40858
- Receiver processing for direct-detection optical communication systems.
21 p3017 A72-40859
- Solid state laser sources, light modulators and silicon avalanche photodiode detectors for fiber optical communication, discussing performance and limitations from system design viewpoint
21 p3018 A72-40866
- Optical direct detection using avalanche devices.
21 p3018 A72-40867
- Hybrid digital transmission systems based on optical fiber waveguides and analog repeaters, noting YAG laser light modulation by phase shift keyed sub-carrier
21 p3018 A72-40868
- Injection laser and light emitting diode techniques to transmit digital data in local distribution
21 p3018 A72-40869
- Ground, satellite, terrestrial glass fiber channel and waveguide radiation systems for laser communications
21 p3023 A72-41398
- A new optical PCM communication system
22 p3186 A72-42939
- Noise resistance of optical communication lines with radio and optical AGC systems
23 p3264 A72-43770
- Automatic acquisition and tracking system for laser communication.
23 p3265 A72-44176
- Broad-band information transfer with the aid of laser-beam coupling fields
23 p3266 A72-44359
- The precise simulation of image transfer systems with the aid of an optical convolution obtained with a rotating slit of prescribed form
23 p3261 A72-44361
- Image formation using antenna properties of optical heterodyne receivers.
23 p3409 A72-44802
- Threshold characteristics of receivers with optical quantum amplifiers.
24 p3412 A72-45617
- OPTICAL CORRECTION PROCEDURE**
- Aberration correction in collimator of Schmidt spectrograph camera by changing surface geometry and grating positioning
03 p0362 A72-14358
- Self calibration of surveying cameras for three dimensional object photography without control points, using homologous ray method
06 p0815 A72-17754
- Film flatness in airborne cameras, reducing large area and short period photogrammetric deviations
06 p0815 A72-17758
- Digital image processing for TV camera noise suppression and photometric and geometric distortions calibration and rectification
08 p1172 A72-21977
- Drobyshev stereograph corrector operation for aerial photographs processing with transformed beam of stereoprojector
09 p1308 A72-22483
- Correction procedures for spherical surface transformation on plane for high altitude aerial photographs
09 p1310 A72-22948
- Holographic correction of reflecting refracting telescope objective mirror deformation aberrations, noting interferometric attachment
10 p1479 A72-24049
- Image deformation sources correction in space photography, discussing stationary and moving cameras and panoramic and complex sensing systems
12 p1809 A72-27817
- Film flatness in airborne cameras, reducing large area and short period photogrammetric deviations
12 p1809 A72-27818
- Artificial compensation holograms for complex optical objective substitution, using interference fringe image technique
13 p1958 A72-29513
- Aplanatic mirror-lens telescope systems with spherical optics, discussing isochromatic corrective lens specifications
14 p2104 A72-30497
- Error corrections for UV photometric measurements with light filters involving Bouguer formula
15 p2233 A72-31400

- Correction formulas for aerial photograph distortions due to internal refraction of light rays in separation of gas media by lateral surface of circular cylinder
15 p2277 A72-32124
- Variable area modulation dual signal recording onto single input device for coherent optical correlators
15 p2249 A72-32165
- Composite quasi-optical-broad waveguide transmission lines for millimeter and submillimeter waves with spectrum phase correction
18 p2664 A72-36106
- Polarization offset angle effect on isochromatic fringe visibility of holographic photoelasticity recordings, noting reference beam ellipticity adjustment
18 p2733 A72-36360
- Remotely sensed data processing by scanner/printer designed for photograph scanning, geometric correction and photographic printing of corrected image
18 p2691 A72-36495
- Russian book - Refraction of light rays in the atmosphere
19 p2834 A72-37448
- Lateral chromatic aberration of a double-meniscus telescope in Chile
19 p2801 A72-37919
- Experimental investigation of optical aberrations, due to temperature deformation and convective fluxes, by using a nonequal-arm interferometer with a coherent light source
19 p2801 A72-37920
- Design of a system for automatic compensation of atmospheric dispersion
19 p2801 A72-37962
- Aplanatic mirror-lens telescope systems with spherical optics, discussing isochromatic corrective lens specifications
19 p2803 A72-38326
- Computer aided analysis of hologram optical elements for aberration and dispersion reduction and recording on thick media
20 p2922 A72-39036
- Scattering from inhomogeneous cylindrically symmetric lenses with a line infinity in the index of refraction.
21 p3050 A72-40148
- Spectrophotometer linearity testing using the double-aperture method.
23 p3289 A72-43894
- A simple method of hologram transmission by using random phase reference - Principle and computer simulation.
23 p3290 A72-43949
- Motion thresholds for fovea and peripheral retina with/without correction for peripheral refractive error
23 p3260 A72-43978
- Spectrometer for absolute stellar spectrometry
23 p3290 A72-44039
- Optical alignment of planes and straight lines in space by reflecting prism systems and double ray bundles with mirror symmetry
24 p3424 A72-44768
- The influence of the atmosphere on the wavelength of the He-Ne laser and the solution of corrections of the laser interferometer.
24 p3409 A72-44771
- Optical system chromatic aberration correction relationship to focus plane position in white light based on Strehl and Hopkins criteria
24 p3425 A72-44772
- Linear corrector for laser beam intensity distribution transformation into random distribution with rectangular envelope, noting uniform energy distribution result of spatial fluctuations averaging
24 p3411 A72-45608
- OPTICAL COUPLING**
- Tunable multiple wavelength organic dye laser using optical feedback through partially transparent mirrors
03 p0367 A72-13443
- Output coupling apertures effect on carbon dioxide laser spatial coherence, considering resonator mode structure
05 p0667 A72-16001
- Passive nonlinear output coupler for mode-locked high power picosecond pulse laser, using optical Kerr effect
05 p0670 A72-17190
- Carbon dioxide lasers and GaAs electro-optical crystals 110-MHz bandwidth with coupling modulation technique
07 p1005 A72-19413
- Optical coupling effects in frequency stabilized He-Ne lasers, finding instabilities for interferometric length measurement
07 p1005 A72-19414
- Two coupled lasers theory, obtaining fields equations of motion
07 p1009 A72-20681
- Multipole network characteristics of optical link assemblies /optrons/ using photosensitive element and light source
08 p1139 A72-21057
- Steady state plane wave theory of intracavity coupled parametric oscillator upconverter, obtaining efficiency, pump power transmission and optimum output coupling
09 p1325 A72-23086
- Stable single frequency Ar laser radiation with coupled transitions emission
11 p1650 A72-26356
- Critical values for two surface optical systems of refracting imaginary case modules in coupling and lens design
11 p1691 A72-26746
- Light power coupling efficiency from GaAs injection laser into single- and multimode fibers
12 p1820 A72-27507
- Optical interaction of inhomogeneously excited semiconductor injection laser diodes, noting power efficiency increase with inhomogeneity
12 p1822 A72-27606
- Gas laser asynchronous coupling modulation, examining dependence on lasing threshold, optical spectrum and transition line shape
15 p2246 A72-31660
- Laser coupling through nonlinear gas filled absorber cell, discussing molecules mean free path
15 p2246 A72-31883
- Light emitting diodes, photodiodes and photon coupled pair temperature compensation schemes, including uses of n-p-n transistors, operational amplifier and thermistor-resistor network
15 p2247 A72-32034
- Stable single frequency Ar laser radiation with coupled transitions emission
16 p2403 A72-33709
- Variable output coupling device for far infrared laser.
17 p2562 A72-34643
- Visual aid-to-eye direct coupling, evaluating partial coherence effects on imagery optical performance by computer program
20 p2931 A72-39050
- Laser beam periodic coupler design based on radiation property reciprocity theorem, suggesting use of reflecting layers and long wavelength gratings
23 p3288 A72-43888
- Broad-band information transfer with the aid of laser-beam coupling fields
23 p3266 A72-44359
- A new method of optical coupling of two laser cavities which permits stable generation of ultrashort optical pulses
24 p3410 A72-45075

OPTICAL DATA PROCESSING

- Crop discrimination with manual and automatic computerized side-looking radar imagery analysis for microtexture pattern recognition
01 p0065 A72-10451
- Data correlation and annotation of earth resources remote survey pictorial records
01 p0065 A72-10453
- Digital computer program high speed algorithm for high resolution images geometric correction, discussing application to ERTS return beam vidicon images
01 p0065 A72-10454
- Agriculture and natural vegetation remote sensing programs, discussing dichotomous keys for side-looking airborne radar imagery analysis
01 p0056 A72-10457
- ERTS satellite image processing for multispectral scanning system, discussing distortion from geometrical properties
01 p0066 A72-10458
- Pattern recognition, invariance, redundancy and information reduction in computer aided image processing
01 p0034 A72-10475
- Two dimensional digital pictorial signal processing - Conference, University of Missouri, Columbia, October 1971
01 p0069 A72-10865
- Computer image processing for photorecognition, enhancement and calibration applications
01 p0070 A72-10870
- WINDCO interactive man-computer system for automated cloud motion tracking using precisely aligned digital ATS satellite pictures
01 p0070 A72-10872
- Transfer function compensation technique for processing sampled imagery data prior to recording on hard copy to remove degrading effect for quality improvement
01 p0046 A72-10873
- Optics for data processing, discussing magneto-optic and holographic memories in computer systems
01 p0035 A72-11315
- Remote sensor viewing angle effect on detectability of geological faults in side-looking airborne radar image data by optical spatial frequency analysis
02 p0209 A72-11791
- Sea waves energy spectra from optical Fourier analysis of ocean photographs under particular skylight irradiance
02 p0211 A72-11809

- Natural formations optical spectral reflectance optimal coding with speedy digital computer processing advantage for remote sensing of earth surface
02 p0187 A72-11811
- Aerial multispectral scanner data determination with filtering and smoothing along flight line over extended areas, deriving algorithm for cloud-shadowed area detection
02 p0212 A72-11817
- Microwave hologram CW radar system, discussing theory and flight test imagery, optical processors and alignment procedures
02 p0171 A72-11819
- Digital fast transform methods application to satellite image processing, comparing with nontransform algorithms
02 p0227 A72-11843
- Multichannel multispectral airborne IR imaging system and video data processing for U.S. geological survey
02 p0227 A72-11851
- Crop, soil and geological mapping from digitized multispectral satellite photography, discussing data processing requirements and surface features distinguishable from satellite altitudes
02 p0214 A72-11876
- Multispectral photographic data preprocessing and computerized simulation of ERTS data channel to make terrain maps, testing classification accuracy improvement possibility
02 p0215 A72-11880
- Hybrid system to process multispectral photographic data from aircraft and spacecraft sensors, assessing data quality, cost effectiveness and delay reduction
02 p0228 A72-11883
- Digital picture processing techniques for increased detail resolution, applying equidensity film methods [DFVLR-SONDDR-170]
02 p0229 A72-12018
- Improved Tiros operational satellite visual and IR scanning radiometer data processing for polar and mercator map projection
02 p0173 A72-12127
- Photosensitive MOS devices array as converters performing optical image data analysis, considering sensor sensitivity regulation
02 p0193 A72-12342
- Real time coherent optical processor of pulse Doppler radar signals with Fresnel diffraction masks for PCW target range rate determination
03 p0322 A72-13437
- Spatial pulse modulation of optical signals for use in picture transmission, cinematography and holography
03 p0358 A72-13440
- Microelectronic computer system with image data cross correlation generation for real time video pattern abstraction, discussing design and operating characteristics
03 p0329 A72-14178
- Passive airborne mapping of radiation sources, using fixed side-looking multilobed and scanning fan beam antenna pattern with coherent optical processing of film records
04 p0495 A72-14491
- Edge-coding operators for two dimensional binary picture black-white boundary pattern recognition suitable for use in parallel processing systems
04 p0496 A72-15203
- Optical image recording, transformation, readout, transmission and data processing techniques and instruments, discussing transfer function, cut-off frequency and information quantity concepts and holography
04 p0525 A72-15700
- Geodetic determination of geoid shape by computerized laser-effect space telemetry ground stations
04 p0495 A72-15724
- Photogrammetric coordinate relation of points on lunar surface and stereo panoramas of scanning photographs by Luna 9 and 13 orbiters
05 p0660 A72-15832
- Bayes theorem based iterative method for image restoration by treating degraded images as probability-processing functions, noting adaptability to computer processing
05 p0690 A72-16671
- Hough transformation for detection of lines and curves in pictures, using angle radius instead of slope intercept parameters for efficient computation
05 p0664 A72-17164
- Image data coding by adaptive block classification and quantization of source output symbols, evaluating performance
06 p0772 A72-17402
- Facsimile bandwidth compression by picture elements reduction with contrast preservation, discussing analog processing algorithm and application to weather satellite photographs
06 p0772 A72-17406
- Cellular electronic logic circuit planar array representing objects inertial motion, applying to traffic control, image processing and artificial intelligence
06 p0779 A72-17496
- Nematic liquid crystals application to real time optical data processing
06 p0847 A72-17565
- Upper bound on rate distortion function for discrete ergodic sources with memory, applying to pictorial data processing
06 p0776 A72-18390
- Spacecraft planetary approach navigation with TV camera onboard Mariner 9 giving images of Mars natural satellites against star background, discussing optical data processing programs [AIAA PAPER 72-53]
07 p1032 A72-18946
- Image processing of diagnostic echocardiogram by ultrahigh speed analog to digital converter interfacing digital computer
07 p0928 A72-19312
- Human binocular visual system fusional information processing, evaluating compensatory eye movements role in overcoming retinal image disparity
07 p0929 A72-19314
- MnBi thin films as potential storage media within holographic optical memory system having write-in reference beam for readout [CLEA PAPER 18,1]
07 p0950 A72-19399
- Strain biased transparent ferroelectric electro-optic ceramics for coherent transducers /page compositors/ for holographic memories and optical data processing [CLEA PAPER 18,6]
07 p0950 A72-19401
- Holographic information storage with reference wave modulation by Fabry-Perot interferometer, using two coherent sources
07 p0985 A72-19417
- Holography applications and processes, discussing holographic microscopy, particle analysis, high speed photography, data storage and retrieval, interferometry, nondestructive testing, etc
07 p0989 A72-20221
- Placeholder for on site wet processing of holograms in real time holographic interferometry, obtaining undistorted reconstructed image by liquid gate immersion
07 p0992 A72-20581
- Earth science and technical applications of multispectral photography and digital image processing techniques
08 p1166 A72-21334
- Planetary and lunar surface relief reconstruction from photographic imagery, discussing statistical morphological characteristics determination from relief
08 p1238 A72-21833
- Photosensitive MOS devices array as converters performing optical image data analysis, considering sensor sensitivity regulation
08 p1143 A72-21948
- Digital image processing for TV camera noise suppression and photometric and geometric distortions calibration and rectification
08 p1172 A72-21977
- Rectification process for transformation of single photograph orientation into setting value, noting reduced accidental residual errors
09 p1311 A72-22967
- Optical image filtering to simplify and facilitate automatic aerial photointerpretation processes
09 p1313 A72-23310
- Reversible photodimerization of polycyclic aromatic hydrocarbons as basis for optical information storage, discussing monomer and photodimer photosensitivity, thermal stability and refractive index specifications
09 p1314 A72-23331
- Fourier transform plane irradiance distribution for random phase data masks in holographic data recording, discussing phase quantization level change effects
09 p1314 A72-23335
- Three stage retinal model for visual monitoring method applied to computerized photointerpretation of aerial photographs
09 p1284 A72-23624
- Remotely sensed imagery data photointerpretation by gray tone texture context feature extraction, noting identification accuracy
10 p1442 A72-23812
- Radiographic image enhancement based on mathematical concepts of image convolution, Fourier transformation and spatial frequency filtering, discussing hardware and computer needs [LA-DC-72-57]
10 p1481 A72-24322
- Rapid data input system for Minsk 22 digital computers using photographic film read by photoelectric scanning system
10 p1445 A72-24495
- Image dissector system fabrication for two dimensional area scanning, applying to photograph digitization
11 p1631 A72-25688
- Camac modular instrumentation data handling system for interfacing to digital computers and hardware controllers, noting astronomical data acquisition application
11 p1601 A72-25700
- GaAs injection laser optical link assembly with silicon photodiode and optical transistor, noting applicability to optical data processing
11 p1648 A72-26328
- Computerized image analysis, establishing desirable scene characteristics for biomedical display in automated system
11 p1602 A72-26388
- Scanning photoelectric image conversion /photoanalyzing/ systems for data telemetry from remote optical sensors
11 p1634 A72-26461
- Character recognition experiments to determine attention control and temporal-spatial capacity limitation during visual information processing
12 p1768 A72-27074
- Phi-spatial filter method for straight or curved line geometric feature extraction of characters, using coherent optical system
12 p1820 A72-27494
- Optical correlation technique, converting input data into area charts with binary valued density
12 p1820 A72-27495
- Signal mathematical model in optical and acoustic pattern recognition
12 p1786 A72-27571
- Lens evaluation procedure based on optical transfer function data, discussing computer displays and merit parameters
12 p1810 A72-27936
- Dispersive optical imaging systems for chromatic aberration correction, considering broadband holographic reconstruction and generation, optical information processing and diffraction pattern achromatization
12 p1811 A72-27950
- Language description of remotely sensed image data, noting application to artificial intelligence, linguistic analysis and retrieval
13 p1924 A72-28525
- Modified run-length encoding system for text and drawing documents to obtain higher data reduction ratio
13 p1922 A72-29349
- Photoemulsion diffraction efficiency from latent holographic image signal formed during beam incidence on one or both photoplate sides
13 p1959 A72-29685
- Automatic digitizing and recording of analog information from oscilloscope photographs
13 p1959 A72-29755
- Computer controlled ground truth station for environmental agricultural aerial photographic remote sensors data processing, discussing system components, printout format and computer program
15 p2213 A72-31249
- Optimum processing structure /likelihood functional/ determination for signal sequence detection given noisy common background image sets
15 p2196 A72-31783
- Mariner 9 TV experiment image data display, processing and production for real time analysis, noting computer algorithms
15 p2236 A72-31982
- Spacecraft onboard compact low-power coherent optical data processing system, using GaAs laser and paraboloid mirror segments
15 p2248 A72-32052
- Two dimensional optical phased array beam steering based on membrane light modulation and high speed digital techniques
15 p2248 A72-32053
- Diffraction theory for large storage capacity holographic random access memory design, discussing geometric optimization of detector array and storage plate
15 p2238 A72-32159
- Coherent light signal optoelectronic processing techniques application to engineering components displacement measurement and vibration amplitude real time imaging
15 p2238 A72-32168
- Grid modulation information encoding technique for image features extraction with simple Fourier filtering to replace heuristic method
16 p2365 A72-33752
- Two Dimensional Digital Signal Processing Conference, University of Missouri, Columbia, Mo., October 6-8, 1971, Proceedings.
17 p2520 A72-34401
- Fast computational techniques for generalized two dimensional Wiener filtering.
17 p2532 A72-34402
- Bayesian recursive linear Kalman filtering technique for image estimation with noise background elimination, proposing time invariant dynamic model to provide stationary statistics
17 p2520 A72-34403
- Image enhancement by computer programs, discussing digital filtering, fast Fourier transform algorithm, data management and large matrix handling
17 p2520 A72-34404

Pattern recognition computer programs for input data preprocessing with characterization and transformation through layered recognition cone

17 p2520 A72-34405

Frequency domain design of two-dimensional finite impulse response digital filters.

17 p2532 A72-34406

Computerized photographic imagery analysis system with interactive operator controls for processing option selection in image enhancement prior to pattern identification

17 p2520 A72-34407

Computer processed image enhancement applications to spacecraft returned photoreconnaissance, discussing data transmission and resolution vs recognition and color quality

17 p2520 A72-34408

Texture measurements in earth resources data management system by automatic photointerpretation with analog and digital techniques, discussing data processing rate requirements

17 p2520 A72-34409

Computer program algorithm for processing local landmark and cloud motion data recorded by satellite observation

17 p2520 A72-34410

Automated cloud tracking using precisely aligned digital ATS pictures.

17 p2521 A72-34411

Sampled imagery transfer function compensation by inverse function, noting truncation effects on processing array SNR performance

17 p2521 A72-34412

Laser computer technology - Today and tomorrow.

III

17 p2523 A72-35186

Texture synthesis by image processing equipment consisting of digital computer and input/output unit, noting image signatures of constant parameter areas

17 p2555 A72-35338

Encoding and decoding of color information using two-dimensional spatial filtering.

17 p2556 A72-35537

Digital correlator for change detection in picture element processing with CDC 1700 computer to obtain spatial alignment accuracy

17 p2556 A72-35538

Bayesian recursive estimation by Kalman filtering for enhancement of image corrupted by additive random noise

17 p2557 A72-35539

Application of factorial analysis of correspondences to the compression of image signals

17 p2517 A72-35671

Experimental study of image coding by complex Haar and Hadamard transformations

17 p2518 A72-35673

Adaptive compression of prediction of differential coding images

17 p2518 A72-35674

Range coding application to TV and videophone images, stressing plug memory

17 p2518 A72-35675

Image processing by digital computer.

18 p2663 A72-36247

Rate distortion theory model for visual communication fidelity assessment via weighted noise measurement and K rating

18 p2657 A72-36251

Intraframe coding for picture transmission.

18 p2657 A72-36252

Video data transmission minimum channel capacity requirement calculation from rate distortion function of source with known probability distribution

18 p2657 A72-36253

Picture coding via linear transformation and quantization on subpictures with applications to monochromatic image processing

18 p2658 A72-36254

Recent developments in digital image processing at the image processing laboratory at the Jet Propulsion Laboratory.

18 p2658 A72-36255

Image processing in the context of a visual model.

18 p2658 A72-36256

Image restoration - The removal of spatially invariant degradations.

18 p2658 A72-36257

Space-variant image motion degradation and restoration.

18 p2658 A72-36258

Inverse filtering for linear shift-variant imaging systems.

18 p2658 A72-36259

Role of recursive estimation in statistical image enhancement.

18 p2658 A72-36260

Data structures and computational organization in digital image enhancement.

18 p2658 A72-36262

Computational algorithms compared for spatial frequency image filtering, considering tradeoffs between direct convolution and fast Fourier transform under equal point-spread functions assumption

18 p2658 A72-36263

Generalized multi-dimensional sampling theory and applications in optical systems.

18 p2672 A72-36333

Digital techniques for image data processing and analysis, discussing data sampling, conversion, computer implementation, image matching, etc

18 p2664 A72-36490

Coherent optical terrain-relief determination using a matched filter.

18 p2691 A72-36491

Epipolar scanning to convert image correlation from two dimensional to one dimensional task for application to photogrammetric automation

18 p2691 A72-36492

The image-processing system for the Earth Resources Technology Satellite.

18 p2674 A72-36496

The precision-processing subsystem for the Earth Resources Technology Satellite.

18 p2674 A72-36497

A new computer-assisted stereocomparator.

18 p2664 A72-36499

Resolution of optical-memory matrices prepared from photochromatic materials when using a focused beam to record information

18 p2692 A72-36658

Geometrical study of the shape and orientation of the tail of Comet Bennett /1969/

18 p2728 A72-36764

Error reduction in digitally generated holographic memories via parity sequence interlacing with true data sequence for spectrum shaping

19 p2796 A72-37581

Synthetic aperture radar data processing via tilted plane optical system, explaining technique in terms of holographic analogy

19 p2796 A72-37584

Experimental investigation of direct quasi-optical radiovision of small objects

19 p2768 A72-38673

Optical information processing analysis for coherent optics and holography, discussing characteristic spectral bands, sampling and signal averaging

20 p2922 A72-39035

Radio astronomical event visible image generation by electro-optical processing comparing SNR performance and electronic complexity with conventional technique

20 p2904 A72-39787

New technique of image multiplexing using random diffuser.

21 p3050 A72-40145

Russian book - Principles of holography and coherent optics.

21 p3052 A72-40388

Theoretical model prediction for matched filter selectivity and noise effects on strained object deformation in optical correlation applications, comparing results with experiments

21 p3053 A72-40611

Digital computer synthesis of Fourier holograms of transparencies, noting significance to digital filtering method development for optical signal processing

21 p3054 A72-40670

A measurement of the surface strain distribution by optical differentiation method.

21 p3056 A72-41239

Light emitting diodes /LED/ materials characteristics, heterojunction band structures and optical spectral ranges, considering application to information processing

21 p3035 A72-41649

Effect of the video signal shaping mechanism in a photosensitive scanistor sensor on the optical data processing accuracy

21 p3058 A72-41735

Small-size phase holograms for binary data storage

21 p3058 A72-41744

Real time analog computation at light speed and rapid access data storage in optical data processing systems, considering coherent electro-optical instrumentation

22 p3180 A72-42713

A fast opto-electronic transducer

22 p3180 A72-42944

Suitability of the normal density assumption for processing multispectral scanner data.

22 p3157 A72-43025

German monograph - Contributions to the study of the astigmatic image.

22 p3207 A72-43067

Modeling a holographic process on a computer

23 p3287 A72-43531

Advanced optical storage techniques for computers.

23 p3288 A72-43876

Conditions for space invariance in optical data processors used with coherent or noncoherent light.

23 p3288 A72-43887

A cathode-ray tube with a semiconductor laser screen

23 p3272 A72-43925

Simplified, low-noise processing technique for photographic phase holograms.

24 p3401 A72-44804

Noise characteristics of a digital system of light-beam deflection

24 p3410 A72-45323

Viewing Phobos and Deimos for navigating Mariner 9.

[AIAA PAPER 72-927]

24 p3423 A72-45433

OPTICAL DENSITY

Laser beam deflection as temperature sensor in optically inhomogeneous medium discussing gas density and temperature gradient relations

04 p0531 A72-15136

Inverse boundary value problem of optically inhomogeneous layer nonuniform profile construction from optical field distribution

10 p1510 A72-24050

Optical correlation technique, converting input data into area charts with binary valued density

12 p1820 A72-27495

Crowded photographic emulsions, predicting granularity of multilayer sandwich as function of layers number

12 p1808 A72-27676

Whole blood flow dependence on optical density from light transmission measurement, showing photometric effects of red cell aggregation, deformation and orientation

15 p2185 A72-31639

Radiation intensity angular distribution from optically thick plane cloud layer reflection, relating photon survival probability and scattering functions

16 p2426 A72-33780

Radiant energy transfer in dispersive medium of low optical density under LTE and radiant equilibrium

16 p2427 A72-33859

Screen equidensities in aerial photograph interpretation

17 p2555 A72-35337

Optical system parameters for electrophotographic print quality, discussing aberration effect on image optical density

21 p3059 A72-41818

Phototropic borosilicate glass optical density variation by exposure to UV or blue light, considering utilization for digital data storage and/or cathode ray tubes

22 p3180 A72-42941

OPTICAL DEPOLARIZATION

On depolarization of visible light from water clouds for a monostatic lidar.

18 p2706 A72-36648

OPTICAL EMISSION

U LIGHT EMISSION

OPTICAL EMISSION SPECTROSCOPY

Ozone photolysis in UV region, determining primary products from oxygen optical emission detection using time-resolved flow system

03 p0320 A72-13398

Spectroscopic measurements of light emission from carbon dioxide positive ions and carbon monoxide ion metastable He interaction with carbon dioxide

09 p1354 A72-22667

Stimulated emission and spectroscopic properties of activated ferroelectric crystal laser, noting Stark effect

09 p1323 A72-22981

Spectroscopic device for pulsed light or plasma source temperature measurement, noting operation in 2000-4000 C range

11 p1635 A72-26468

Crystal growth, physical and spectroscopic properties and laser performance of Nd and Ho doped crystals with apatite structure

12 p1825 A72-27927

Small spectral width emission from dye laser with interference filter and quartz plate Fabry-Perot interferometer for spectroscopic investigations

14 p2110 A72-30674

Extensive air showers at zenith, measuring associated UHF radio pulses with optical Cerenkov emission receiver as trigger source

14 p2147 A72-30858

Sounding rocket observation for emission height of night airglow continuum near 6050 A, using photoelectric photometers

15 p2231 A72-32329

Spectral image formation and aberration by spherical concave grating for point light source, using geometric optics method

15 p2278 A72-32337

Ar plasma radiation dispersion by plane grating, measuring ionic spectral lines and continuous spectrum intensity variation

15 p2286 A72-32340

Large sunspot umbra high resolution spectrogram obtained by beam splitter with monochromator polarization optics, noting blends near Zeeman lines

15 p2317 A72-32775

Dissociative excitation of vacuum ultraviolet emission features by electron impact on molecular gases III - CO₂.

17 p2585 A72-34734

Aircraft and spacecraft high latitude optical measurements of magnetosphere-related emissions

discussing red arcs, IR auroras, X ray pulsations, conjugate effects, etc 20 p2918 A72-39539

High-resolution spectroscopy using magnetic-field-tuned semiconductor lasers. 20 p2933 A72-39561

Investigations on spectroscopy by nonlinear Zeeman-resonances of a multimode laser. 20 p2934 A72-39845

Experimental setup for the investigation of the spectral radiative capability of metals 22 p3175 A72-41893

Interferometric spectropolarimetry - Alternate experimental methods. 23 p3289 A72-43890

Experimental studies of injection lasers - Spontaneous spectrum at room temperature. 24 p3409 A72-44713

OPTICAL EQUIPMENT

NT ASTRONOMICAL TELESCOPES

NT BALLISTIC CAMERAS

NT BINOCULARS

NT CAMERAS

NT CELESTIALS

NT CINETHODOLITES

NT COLLIMATORS

NT DIFFRACTOMETERS

NT EBERT SPECTROMETERS

NT ELECTROPHOTOMETERS

NT ELLIPSOIDOMETERS

NT EYEPIECES

NT FRAMING CAMERAS

NT GEODIMETERS

NT HELIOMETERS

NT HIGH SPEED CAMERAS

NT IMAGE CONVERTERS

NT IMAGE TUBES

NT INFRARED SPECTROMETERS

NT INFRARED SPECTROPHOTOMETERS

NT LALLEMAND CAMERAS

NT MICRODENSITOMETERS

NT MICROWAVE REFLECTOMETERS

NT MULTISPECTRAL BAND SCANNERS

NT NEPHELOMETERS

NT OPTICAL GYROSCOPES

NT OPTICAL MEASURING INSTRUMENTS

NT OPTICAL MICROSCOPES

NT OPTICAL PYROMETERS

NT OPTICAL RADAR

NT OPTICAL RANGE FINDERS

NT OPTICAL SCANNERS

NT PANORAMIC CAMERAS

NT PHOTOGRAPHIC RECTIFIERS

NT PHOTOMETERS

NT POLARIMETERS

NT PRISMATIC BARS

NT PRISMS

NT PYROHELIOMETERS

NT REFLECTOMETERS

NT REFRACTOMETERS

NT SCHMIDT CAMERAS

NT SEXTANTS

NT SPECTROHELIOGRAPHS

NT SPECTROPHOTOMETERS

NT SPECTROSCOPIC TELESCOPES

NT STRATOSCOPE TELESCOPES

NT STROBOSCOPES

NT TELEVISION CAMERAS

NT THEODOLITES

NT TRANSMISSOMETERS

NT ULTRAVIOLET SPECTROMETERS

NT ULTRAVIOLET SPECTROPHOTOMETERS

NT WIDE ANGLE LENSES

NT X RAY TELESCOPES

Gain and bandwidth properties of microwave and optical devices with isotropic active medium, investigating transmission coefficient

Anglo-Australian astronomical optical telescope construction, summarizing project organization, components and system design

Space vehicles guidance with UV optical systems, describing photometric celestial images with various receptors and different wavelength bandwidth selection

Integral image tube optical systems for far UV narrow band and broad bandpass photography from spacecraft outside atmosphere

Low birefringent orthoferrites for optical devices, considering improvement in Faraday rotation detection of magnetic domains in single crystal platelets [IEEE PAPER 10,10]

Prolate spheroidal functions application to optical system performance characteristics, discussing laser modes, signals maximal concentration, image data extrapolation, etc

Optical acoustic field recordings application to turbulent characteristics measurement for transparent media

Laser interferometer for quality control of optical parts and instruments

Photo-optical instrumentation - Conference, Tokyo, June 1970

Eye mark recorder system for eyeball movement studies, describing operational principle and various optical systems

Photo-optical techniques in biomedical data acquisition, discussing cineangiography and X ray tomography applications in cardiological research work

Two-mirror optical system to study energy dissipation in elastic systems subjected to cyclic straining and vibrations

Double beam Mach-Zehnder interferometer, discussing optical element imperfection induced degradation elimination by Moire technique

Lunar laser reflectors specifications and fabrication procedures, discussing lunar environment simulator and optical test equipment, techniques and results

Quartz crystal oscillator device for continuous monitoring and controlling thin film thickness in optical and electronic applications, noting temperature effects on crystal oscillating frequency

Binocular observation of astronomical objects, discussing binocular design of astronomical telescopes

Multiple projection assembly for topographic maps preparation by satellite photographs optical projection onto model surfaces, exemplifying by reverse lunar hemisphere

First order imagery in neighborhood of base ray transversing arbitrary optical system, discussing relationships among anamorphic nature, astigmatism and image rotation

Uniform plane wave theory of internal upconversion and frequency doubling in optical parametric oscillators

Thin organosilicon films for integrated optical circuits and devices, discussing transparency and loss characteristics and refractive index control

Optical mirrors contamination by condensation of outgassed spacecraft materials in vacuum under UV irradiation, describing test apparatus and results with various materials [AIAA PAPER 72-267]

Thin Se film for recording mode structure of 10.6 micron carbon dioxide laser emission, describing optical equipment

Temperature distribution and heat dissipation calculations for CW and pulsed laser optical elements

Optical acoustic field recordings application to turbulent characteristics measurement for transparent media of fluid flows

Book on coherent optical computers covering lens design, power sources, computation mathematics, modulation, detection, digital techniques and applications

Computer designed optical integrating devices for semiconductor laser arrays, considering diode, collection, projection and zoom parameters

Optical modeling of antenna radiation patterns from radio hologram of Fresnel region field

Optical system production acceptance test based on modulation transfer function, discussing instrument design and test philosophy

Glass choice for two lens uncemented objectives, calculating surface and aberration coefficients

Precision laser system for micromachining applications, describing optical system

Coma, astigmatism and spectral line curvature derivation for spherical mirror-concave grating assembly, calculating mounting resolution in terms of wavelength

Polarization optical method for analyzing local stress concentrations in structural members.

Application of the optical transfer function to visual instruments.

Significance of OTF methods in assessing lenses to be used with partially coherent illumination.

Multiple projection assembly for topographic maps preparation by satellite photographs optical projection onto model surfaces, exemplifying by reverse lunar hemisphere

Phase holograms wave front formation as replacement of optical elements with aspherical surfaces and multilens objectives

Optical devices to produce transmitted image rotation about axis, comparing derotation systems and roll and high-speed prisms

Optoelectronic speed control for replacing mechanical gear drives for precisely variable shaft speed ratios

Possibilities of optical elements design using phase holograms.

Visual performance when using optical instruments; Symposium, Munich, West Germany, July 21-23, 1971, Technical Papers.

Viewing stereoscopically through binocular optical systems.

Optical system parameters for electrophotographic print quality, discussing aberration effect on image optical density

Determination of optical transfer functions by Fourier transformation in spatially incoherent light

Flat optical surfaces production methods for Fabry-Perot interferometers, describing Otte polishing process and quality test methods

Experimental determination of some optical characteristics of a double magnetic prism-electrostatic mirror system

Comparison of theoretical and experimental results concerning spatial filtering in coherent optics

Noise resistance of optical communication lines with radio and optical AGC systems

Optical system chromatic aberration correction relationship to focus plane position in white light based on Strehl and Hopkin criteria

Human observation error effect on astronomical refraction calculation from time determination of solar limbs passages across optical instrument reticle

Measurement of the optical transfer function of an onboard objective in the space environment

OPTICAL FILTERS

NT INFRARED FILTERS

NT ULTRAVIOLET FILTERS

Red interference filter design for high performance prominence telescope for H alpha line observation

Feature classifying filter for pattern recognition system simulated on computer for line printed numerals

Gas filter correlation spectral analysis technique for measuring pollutant concentrations in presence of interfering gases, describing application to hydrochloric and hydrofluoric acids monitoring [AIAA PAPER 71-1049]

Correlation filters alignment for optical character recognition, discussing kinematic mounting and in position techniques

Fabry-Perot interferometers as narrow band optical filters, discussing transmission and construction for various wavelengths

Filters and color effects on lunar occultation of stars and appropriate deconvolution procedures

Optics and electronics of digitized birefringent filter solar magnetograph to isolate magnetic sensitive lines

Narrow band electrically controlled interferential polarization filter with fine tuning capability for solar physical research, discussing design and operation

Fourier transform lens design in coherent optical fielding systems

Optical birefringent networks synthesis, describing use of building blocks of polarizers, birefringent crystals and optical compensators

Eclipsing variable binary A1 Draconis BV photoelectric observations, using wideband filters

Complex filter properties of Fresnel hologram with converging beam for optical filtration of three dimensional objects in Fourier or image planes

Rhodamine 6G dye laser tuning by variable birefringence filter using lead lanthanum zirconate titanate electrooptic ceramics for wavelength selection

07 p1002 A72-19203

Photometer using rotating wedge interference filter as wavelength scanning element near 6300 Å for high altitude sounding rocket application

07 p0985 A72-19403

Gaussian noise quasi-optimal filtering in optical communication system, evaluating signal timing accuracy in detector-amplifier circuits

08 p1136 A72-21914

Passive optical shutter implementation for unidirectional emission from traveling wave ruby laser, using diffraction grating

08 p1184 A72-22037

Two dimensional optical signals Fourier transform properties and local frequency filtering methods

09 p1351 A72-22982

Multichannel signal processing system for spatial optical filters synthesized by orthogonal functions

09 p1314 A72-23342

Solid state laser with slow relaxation bleachable filter, calculating modes self synchronization probability statistics relationship to relaxation time

10 p1492 A72-24512

Laser emission spectrum broadening due to saturable dye filter bleaching, discussing amplitude and phase modulation contributions

11 p1649 A72-26341

Optoacoustic processing of large time-bandwidth signals, calculating insertion loss vs delay time

12 p1810 A72-27935

Opaque scatterers disadvantages in interferometric images recording of transparent objects obtained by double exposure holography, noting phase type diffraction gratings

13 p1958 A72-29616

Semiconducting glass filter time dependent transition, absorption coefficient and luminescent spectral dependences, using monopolised ruby laser

13 p1971 A72-29909

Error corrections for UV photometric measurements with light filters involving Bouguer formula

15 p2233 A72-31400

Spectral transmittance enhancement in Fabry-Perot narrow band light filter by wavelength shifted dielectric mirror technique

15 p2233 A72-31414

Simulated Nimbus orbital electron, proton and UV radiation effects on wide bandpass glass and narrow bandpass thin film interference filters and fused silicas

15 p2277 A72-32157

Q switched and free emission mode locking of neodymium glass and ruby lasers via liquid bleachable dye filter

16 p2400 A72-33296

Multispectral angular reflectivity effect on optimum filter combinations for spaceborne multiband photography sensing mission in visible and near IR regions

16 p2395 A72-34104

Use of amplitude filter to improve the partially space coherent diffraction of a defocused circular aperture.

19 p2833 A72-37402

Calculation of pulsed signal amplitudes at linear filter output in optical communication systems

19 p2768 A72-38671

Theoretical model prediction for matched filter selectivity and noise effects on strained object deformation in optical correlation applications, comparing results with experiments

21 p3053 A72-40611

Opaque scatterers disadvantages in interferometric images recording of transparent objects obtained by double exposure holography, noting phase type diffraction gratings

21 p3054 A72-40669

The effect exerted on pictorial-analytical measurements at the television microscope by subjective contrast enhancement with color filters

21 p3055 A72-40749

Improved holographic matched filter systems for pattern recognition using a correlation method.

22 p3177 A72-42445

German monograph - Contributions to the study of the astigmatic image.

22 p3207 A72-43067

Tilting-filter measurements in dayglow rocket photometry.

23 p3289 A72-43893

OPTICAL GENERATORS

U LASERS

OPTICAL GYROSCOPES

Single isotope He-Ne laser gyro comparison with multiisotope system, noting strong mode competition in ring laser

07 p1005 A72-19402

Laser gyro operational principles, discussing passive Sagnac and active ring laser interferometers, readout, errors due to null shift, lock-in and mode pulling, etc

07 p1007 A72-20223

Multimode ring laser gyro phase modulation theory based on oppositely directed traveling waves

09 p1324 A72-23084

Multimode ring laser gyro with intracavity phase modulation, discussing experimental results concerned with lock-in at low rotation rates

09 p1324 A72-23085

OPTICAL HETERODYNING

Absorption cell heterodyne method for nondispersive IR detection of trace gases with molecular vibrational-rotational spectrum

01 p0023 A72-10532

Gaseous pollutants remote detection by IR heterodyne radiometer with tunable lasers

[AIAA PAPER 71-1079] 01 p0080 A72-10538

Carbon dioxide laser IR heterodyne radiometer for remote sensing of atmospheric pollution

[AIAA PAPER 71-1083] 01 p0067 A72-10540

Microwave-range optical heterodyne system with magnetically tuned /Zeeman effect/ laser emissions mixing and AFC

05 p0668 A72-16345

He-Ne laser controlled frequency shift in wideband optical heterodyne communications systems with Currie low reflection mirror

05 p0668 A72-16346

Three frequency IR laser signal heterodyne detection with 40-MHz if narrow-band reception, measuring SNR

05 p0669 A72-16607

Conversion coefficients of optical heterodyne receiver mixer for various amplitude-phase distributions of interfering signal

07 p1000 A72-19012

Sensitivity of optical autodyne quantum receiver in presence of output noise, using photomultiplier signal model

07 p1000 A72-19022

Wideband IR heterodyne receiver in spatially coherent array, discussing signal conversion efficiency, beam crossover control, mixer characteristics and microwave antenna comparison

07 p0940 A72-19237

High sensitivity wideband heterodyne receiver system for spaceborne and ground-based IR laser communications

07 p0940 A72-19238

Optical signal heterodyne reception, discussing atmospheric distortion effects reduction

08 p1131 A72-20749

Sensitivity threshold of optical heterodyne receiver as function of laser radiation amplitude spectrum, using photodetector output noise

08 p1181 A72-20794

Single band optical mixer heterodyne spectrum analyzer for laser radiation image spectrum suppression

08 p1182 A72-21375

Reciprocity theorem for antenna directivity pattern measurement of optical superheterodyne receiver for carbon dioxide laser radiation

08 p1140 A72-21376

Microwave and optical quantum electronic sources for frequency standards, noting primary Cs reference and multimode laser-RF oscillator beat technique

12 p1824 A72-27867

Computer simulation for performance of carbon dioxide laser heterodyne communication system with photoconductive n-type mercury-cadmium telluride detector/mixer

15 p2198 A72-32062

Interfering beams amplitude modulation, applying optical heterodyne techniques

15 p2202 A72-32676

Microwave and optical quantum electronic sources for frequency standards, noting primary Cs reference and multimode laser-RF oscillator beat technique

16 p2403 A72-33976

IR heterodyne radiometer SNR and spectral resolution, noting application to solar physics and air pollution detection

17 p2555 A72-35196

Image formation using antenna properties of optical heterodyne receivers.

24 p3409 A72-44802

OPTICAL ILLUSION

Poggendorff illusion depth processing theory, noting noncollinear line resolution effects on projective relationships within figure

01 p0013 A72-10714

Psychophysical perceived orientation experiments on Poggendorff illusion/transversal interrupted by parallel lines/

01 p0013 A72-10717

Visual persistence and perceptual moment hypotheses for time-dependent visual illusion from viewing moving stroboscopically illuminated object

05 p0621 A72-16150

Geometric central projection properties of optical illusions, including Muller-Lyer, Zollner and Hering configurations

05 p0689 A72-16194

Anisotropic responses to dot and line visual stimuli, obtaining judgments on apparent straightness for various visual field locations and dot densities

10 p1427 A72-25183

On the apparent orbit of the Pulfrich pendulum.

18 p2653 A72-36608

Division and orientation in the vertical-horizontal illusion.

18 p2651 A72-36913

Mach band measurement by psychological compensation technique, causing band disappearance by changes in stimulus pattern luminance and brightness distribution relations

19 p2760 A72-37827

Book - Aspects of motion perception.

21 p3012 A72-41531

Visual angle and apparent size of objects in peripheral vision.

22 p3152 A72-42932

OPTICAL MASER MODULATION

U LIGHT MODULATION

OPTICAL MASERS

U LASERS

OPTICAL MEASUREMENT

NT ASTRONOMICAL PHOTOMETRY

NT COLORIMETRY

NT ELECTROPHOTOMETRY

NT OPTOMETRY

NT PHOTOMETRY

NT POLARIMETRY

NT SPECTROPHOTOMETRY

NT STELLAR SPECTROPHOTOMETRY

NT TELEPHOTOMETRY

NT ULTRAVIOLET PHOTOMETRY

NT VISUAL PHOTOMETRY

Planetary mass estimation from radar and optical observation data analysis of sun and planets

[AD-737167] 01 p0127 A72-10292

Atmospheric aerosol chemical composition analysis by nephelometer light scattering measurement of suspended particle mass concentration, visibility and size distribution and scattering-humidity relationship

[AIAA PAPER 71-1101] 01 p0058 A72-10549

Optical/electrical apparatus for measuring high brightness temperatures in 6,000-100,000 K range

01 p0068 A72-10620

Active and passive parameters correlations of solid state laser ruby crystals and Nd glass, using mechanical, thermal, chemical, optical, spectroscopic and electrical measurements

01 p0081 A72-11183

Plasma temperature and seed atom concentration in MHD generator ducts and combustion chambers by optical measurements, discussing boundary layer thickness, optical density, etc

01 p0072 A72-11218

Papers on plasma diagnostics, Volume 1, Optical techniques

02 p0263 A72-11400

Solid body surface strain field optical determination, using diffraction gratings

[SESA PAPER 1751] 02 p0199 A72-11512

Absolute gravity acceleration determination using free-falling laser interferometer apparatus with rotation-insensitive mirror at different sites

02 p0207 A72-11597

Remote sensing applications to operational weather forecasting including ground optical measurement of cloud base height and radar observation of precipitation

02 p0253 A72-11825

Classical optical measurement and holographic methods of flow field visualization, discussing operating principles, measurement sensitivity, three dimensional and depth-focusing properties

02 p0230 A72-12300

Optical visualization and probe measurements on combustion characteristics of liquid fuel in compression-ignition engine swirl chamber

02 p0271 A72-12436

Impending metal fatigue failure holographic detection by optical correlation of coherent light reflection from deformed surface structure as function of time

02 p0294 A72-12442

Optical interference measurement of various shaped elastic plates deflection and application to thermal stress problems

02 p0306 A72-12824

He abundances in gaseous nebulae by optical and radio observation, discussing hydrogen and helium recombination spectra interpretation

03 p0419 A72-13115

HCN laser amplifier gain measurement at IR wavelengths in gas mixtures by recording with pyroelectric receiver

03 p0368 A72-13667

Two photon method of measuring ultrashort pulses and nonlinear optical effectiveness of lasers in synchronized mode

03 p0369 A72-14063

Gas lasers application to precise length measurements via absorbing medium resonance determined wavelength

04 p0530 A72-14734

Digital measurement of pulsed laser energy, using planar vacuum photodiode detector with photocurrent capacitive integration and voltmeter display

04 p0530 A72-14921

Optical image recording, transformation, readout, transmission and data processing techniques and in-

struments, discussing transfer function, cut-off frequency and information quantity concepts and holography

04 p0525 A72-15700

Europe-Africa geodetic link in spatial triangulation of passive Pageos satellite, discussing laser telemetry operation

04 p0520 A72-15725

High accuracy laser reflector telemetric measurement for earth-moon distance variation in time by correlation method

04 p0495 A72-15727

Holographic measurements of dioptric powers and glass defects in thin transparent sheet under vertical or oblique parallel and divergent light

05 p0662 A72-16190

Laser interferometer for quality control of optical parts and instruments

05 p0668 A72-16191

Optical interference technique for experimental stress analysis of cracked structures, obtaining crack shape relationship to stress intensity factor

05 p0666 A72-16322

Airborne optical detection of oil on water based on reflected sunlight, investigating contrast and absorption bands

05 p0658 A72-16689

Holographic measurement for optical transfer function of lenses, considering negative black and white photographic indicator emulsion effect

05 p0663 A72-16728

Bubble chamber high energy particle tracks semiautomatic measuring device, using small on-line computer for data processing

06 p0813 A72-17438

Wide angle lenses off-axis modulation transfer function measurement, explaining extrapolation method with MTF and conversion diagrams

06 p0813 A72-17439

Optical observation program for upper atmosphere and interplanetary space investigations, discussing zodiacal light, earth atmosphere composition and stratification, interplanetary dust clouds, etc

06 p0881 A72-17927

Complete measurement in holography using complex coefficients of conversion matrix of interaction between coherent beam and recorded object

06 p0817 A72-18014

Single fiber reinforced plate initial stress distribution due to linear expansion coefficients difference between matrix and fiber, using optical polarization

06 p0836 A72-18557

Two phase flow model of water droplets velocity in air stream, using Fresnel biprism and laser differential scheme

07 p1000 A72-18940

Displacement and profile diffractographic measurement using changes in far field diffraction patterns of slit aperture between test and reference object

[CLEA PAPER 11,5]

07 p0984 A72-19390

Laser interferometers for displacement, length, gas refractivity, laser wavelength and relative object position measurements

[CLEA PAPER 15,1]

07 p1005 A72-19396

Vibrational amplitude measurement of diffuse surface by modulation of projected fringes in optical field

07 p0985 A72-19407

Gas content determination in metals by melting and vaporizing measured microvolumes using laser microprobe and magnetic mass spectrometer

07 p1006 A72-19549

Nonlinear wave propagation of laser beams in absorbing fluid media, comparing computer model calculation results with experiment on liquid carbon disulfide cell

07 p1006 A72-19837

Optical losses, reflectivity and transmissivity measurements of He-Ne laser Fabry-Perot resonator elements, using laser output power dependence on element losses

07 p1006 A72-19905

Light absorptivity measurement in low loss liquid with interferometer based on refractivity dependence on temperature change due to absorption

09 p1309 A72-22602

Refractivity measurement of pure hexagonal structure 2H SiC over visible range, determining birefringence from curve fitting of data to Cauchy dispersion equation

09 p1309 A72-22603

Optical measurement of point velocity on surface of moving solid, applying to Mylar foil accelerated by plasma gun

09 p1310 A72-22773

Vibration measurement based on moire pattern fringes motion due to line gratings respective displacement, noting high accuracy and resolution

09 p1315 A72-23388

Supersonic Ar, He and molecular nitrogen jets, determining electron temperature and concentration and atomic state population in shock waves region by spectroscopic measurement

10 p1517 A72-23837

Air pollution monitoring by remote optical sensing techniques based on light scattering measurements, noting suitability of high power laser probes

10 p1480 A72-24100

Precise optical positions of nine compact radio sources in AGK 3 catalog

10 p1536 A72-24140

Interferometric testing of optical systems, discussing test plates, Fizeau, Lloyd moire, transmission, Twyman-Green, shearing, Ronchi, scatter fringe, grazing and holographic methods

10 p1482 A72-24567

Optical method based on spectral line center intensity recording to measure plasma temperature in MHD generators channels and combustion chambers

10 p1525 A72-25111

IR refractivity measurement for atmospheric aerosol substances and sea salts

[AD-744397]

11 p1620 A72-25306

Coordinate transformation equations derivation to determine third orthogonal velocity component from measurements at common point by two rotationally displaced laser Doppler velocimeter systems

11 p1629 A72-25308

Reflecting surface roughness measurement by holographic interferometry, applying to lapped steel specimens

11 p1629 A72-25309

Light absorption and scattering factors in whole blood related to hemoglobin concentration, discussing oxygen saturation, cardiac output and pathological conditions

11 p1588 A72-26630

In situ measurement of objective lens data for high resolution electron microscope, using Bragg reflex images of crystallites with known orientation

12 p1807 A72-27528

Optical Kerr constant measurement in liquid phosphoryl chloride and toluene and glasses, noting nonlinear refractivity

12 p1823 A72-27756

Tracer particle motion behavior in laser anemometry for turbulent flow, comparing liquids with gases for accuracy

12 p1809 A72-27763

Crystal characteristics of optical detectors for direct measurement of high power laser radiation

12 p1824 A72-27874

Radial temperature and water vapor concentration profiles of radiating combustion source from optical method, using IR band model

12 p1811 A72-27945

Minor planets orbital elements determination accuracy from planets coincident optical observations

13 p2035 A72-28439

Optical measurement of crosswind from effects produced by atmospheric turbulence and wind velocity relationships

13 p1994 A72-28870

Optimal optical measurement for two dimensional object position on plane in Gaussian background noise, calculating mean square error for false identification probability determination

13 p1920 A72-29280

TV speckle pattern recording for coherent laser light measurement of mechanical vibrations in micrometer range

13 p1961 A72-30026

German monograph on optical transmission measurement interferometer with plane-parallel birefringent crystal plates covering plate combination selection based on interference pattern mathematics

15 p2233 A72-31525

Strain analysis of thin metallic films on low modulus structural substrate by light intensity measurement

15 p2325 A72-31526

Sine, square and triangular wave targets for optical transfer function measurements, comparing modulations in partial coherent light under different illumination conditions

15 p2246 A72-31613

Vehicle orientation degrees of freedom remote measurement with mounted passive devices and polarization-modulated light, discussing data reduction and system accuracy

15 p2267 A72-31780

Transient phase object high sensitivity measurement by He-Ne laser beam transmission through differential interferometer and signal detection with p-i-n photodiode

15 p2235 A72-31784

Planetary nebulae RF observations comparison with optically determined H-beta intensity for extinction coefficients

15 p2307 A72-31797

Roll angle detector for angular position measurement of two independent bodies, using optical-mechanical-electrical system

15 p2268 A72-32043

Laser Doppler velocimeter designs for atmospheric applications, discussing illuminating techniques, SNR, performance comparison and system selection

15 p2237 A72-32051

Time transfer measurement between two locations using nearly simultaneous reception times from optical pulsar signal transmission

15 p2199 A72-32076

Optical nondestructive surface flaw detection for steel plates using oblique angle illumination combined with high pass spatial filter

15 p2238 A72-32153

High energy storage laser material Nd-doped silicate oxyapatite refractivity temperature dependence characteristics measurement

15 p2249 A72-32167

Photochromic crystal materials erase mode recording characteristics measurement, using Ar laser for optical recording and readout

15 p2240 A72-32361

Optical measurements of electric fields turbulence level in gun plasma, noting compatibility with spatial Landau damping

15 p2287 A72-32409

Oil spills remote sensing in marine environment, using laser excited fluorescence for detection, identification and quantification

15 p2251 A72-32623

Optical measurement for simultaneous determination of transparent isotropic medium thermal diffusivity and conductivity

16 p2389 A72-32947

Angular measurement error for group and repetition techniques as function of observation time, deriving formulas for comparison in terms of economy and efficiency

16 p2389 A72-33030

Correlation function measurements of optical gravity center roaming of spatially limited light beams in turbulent atmosphere

16 p2364 A72-33486

Atmospheric turbulence from illuminance and intensity fluctuation measurements at focused light beam

16 p2364 A72-33488

Focused light beam intensity fluctuations measurement during passage through turbulent atmosphere, discussing random walks effects on dispersion

16 p2364 A72-33494

Radio sources reidentification in field of Coma Cluster of galaxies by Schmidt telescope

16 p2458 A72-33719

Pulsar radio and optical observations, discussing periods, pulse shapes at various frequencies and marching subpulses

16 p2460 A72-33925

Crystal characteristics of optical detectors for direct measurement of high power laser radiation

16 p2403 A72-33983

Optical timing of the Crab pulsar, NP 0532.

17 p2605 A72-34535

New orbital elements for moon and planets.

17 p2609 A72-35106

Laser and mercury lamp outputs spatial coherence measurement by speckle patterns produced with ground glass as random inhomogeneous medium

17 p2565 A72-35752

An optical method for the determination of constrained zones at crack-tips.

18 p2733 A72-36368

Ultrasonic velocity measurement by small power He-Ne laser visualization of standing waves in Fresnel diffraction region

18 p2697 A72-36416

New measurements of the polarization of photospheric light near the solar limb

18 p2727 A72-36739

Optical observation program for upper atmosphere and interplanetary space investigations, discussing zodiacal light, earth atmosphere composition and stratification, interplanetary dust clouds, etc

18 p2730 A72-37152

Correlation study of geodetic refraction effect on astronomical refraction anomalies for solar light source observation at large zenith distances

19 p2855 A72-37348

Measurement of three-dimensional refractive-index fields by holographic interferometry.

19 p2798 A72-37621

Two new methods to increase the contrast of track-etch neutron radiographs.

19 p2833 A72-37636

A program of wide scale pairs for determining the micrometer screw turn magnitude of the Pulkovo ZTL-180 wide-angle zenith telescope

19 p2802 A72-37979

Ground based optical astronomy developments, emphasizing faint objects positional observation, trigonometric parallaxes, data analysis and measuring techniques

19 p2865 A72-38477

Airborne optical measurement comparison with satellite observation for auroral emissions and particle precipitation at noon, suggesting electron precipitation role

19 p2868 A72-38738

Pulsed and repetitively Q switched ruby and Nd laser design characteristics for optical applications and holography

20 p2930 A72-39027

- Scatterplate, artificial hologram, moire and null lens methods for aspheric mirror testing for space astronomy and laser communication 20 p2922 A72-39033
- Optical measurement of wave front lens or mirror surface contours by laser unequal path interferometer combined with computer data reduction 20 p2922 A72-39034
- Three axis angular deviations measurement by flexure monitor system for spacecraft, using pulsed light sources, autocollimator and porro reflectors [AIAA PAPER 72-855] 20 p2951 A72-39106
- An analysis of the spectral scanning technique for determining the temperature distribution in a semi-transparent medium. 20 p2986 A72-39677
- Optical measurements in a pulsating flame. [ASME PAPER 72-HT-8] 20 p2926 A72-39679
- A new test of the second postulate of special relativity sensitive to first-order effects. 21 p3085 A72-41214
- A high-frequency transmitted power meter using a laser signal 21 p3064 A72-41730
- An arrangement for the holographic study of electrical explosions of wires 21 p3058 A72-41742
- An immersion interferometer for monitoring the quality of second-order aspherical surfaces 21 p3058 A72-41808
- Simultaneous recording of laser radiation and signal related to secondary processes, using ruby luminescence for oscillograph triggering 22 p3185 A72-42274
- GaAs light emitting diodes intensity fluctuations measurements at .025-20 kHz. 23 p3297 A72-44190
- Evaluation of optical data for Mars approach navigation. 24 p3422 A72-44646
- New optical measurements of planetary diameters. II - Planet Venus. 24 p3436 A72-44694
- An experimental investigation of radiative properties of aluminum oxide particles. 24 p3461 A72-44809
- Measurement of the angular divergence and of the refraction of a laser beam in the ground layer of the atmosphere. 24 p3380 A72-45611
- OPTICAL MEASURING INSTRUMENTS**
- NT CINETHEODOLITES
- NT DIFFRACTOMETERS
- NT EBERT SPECTROMETERS
- NT ELECTROPHOTOMETERS
- NT ELLIPSOMETERS
- NT GEODIMETERS
- NT INFRARED SPECTROMETERS
- NT INFRARED SPECTROPHOTOMETERS
- NT MICRODENSITOMETERS
- NT MICROWAVE REFLECTOMETERS
- NT NEPHELOMETERS
- NT OCULOMETERS
- NT OPTICAL PYROMETERS
- NT OPTICAL RANGE FINDERS
- NT OPTICAL SCANNERS
- NT PHOTOMETERS
- NT POLARIMETERS
- NT REFLECTOMETERS
- NT REFRACTOMETERS
- NT SEXTANTS
- NT SPECTROPHOTOMETERS
- NT THEODOLITES
- NT TRANSMISSOMETERS
- NT ULTRAVIOLET SPECTROMETERS
- NT ULTRAVIOLET SPECTROPHOTOMETERS
- Laser radar application to air pollution measurement, discussing techniques and instrumentation utilizing elastic, Raman and fluorescence scattering [AIAA PAPER 71-1056] 01 p0028 A72-10527
- Laser optical anemometry system, describing fringe, Doppler and reference beam operation modes 01 p0081 A72-11168
- Plasma diagnostics facilities design, circuit diagrams and operation based on Q switched ruby laser and optical recording system 02 p0237 A72-11407
- High spatial resolution solar X-ray and far UV instruments, employing glancing incidence optics 03 p0353 A72-13045
- Photomultiplier signal for water axial velocity in glass pipe, providing turbulent liquid flow information and laser Doppler velocimeter evaluation 04 p0520 A72-14438
- Cloud base altitude measurement by optical telemetry using TNN 1000 apparatus, noting reduced maintenance 04 p0521 A72-14691
- Meteor passage time determination by optical shutter with wedge-shaped blades for light flux periodic intersection and production of two discontinuous lines for identification 06 p0816 A72-17930
- Computer simulated data analysis procedure for improved resolution of optical instrument by integral equation numerical solution 06 p0840 A72-18738
- Autocollimating photokeratoscope for human in vivo corneal shape measurements for contact lens fitting and dioptric image examination 07 p0987 A72-19826
- Displacement measuring instrument based on holographic interferometry using He-Ne laser with split beam for interference fringes on photographic plate 07 p0987 A72-19848
- Semiconductor structure investigation by measuring photoresponses to optical probe motion 07 p1049 A72-19963
- Laser probes for acoustic surface wave amplitude and phase measurements 07 p1008 A72-20385
- Systematic errors in scan-and-measure devices for tracking cameras photographs analysis, discussing correction during measurements 08 p1209 A72-21913
- German monograph on inertial platform stabilization by optical sensors for space vehicle guidance covering aircraft position determination 09 p1394 A72-22334
- Geodetic optical distance measuring instruments with electro-optical polarization modulators, comparing characteristics of four possible configurations 09 p1314 A72-23336
- Pulsed laser sensitometer using multiple imaging technique to retrieve average energy distribution from photographic plate optical density 09 p1325 A72-23346
- Multiple reflection absorption cell for gaseous air pollutants IR radiation measurements over wide temperature, pressure and distance ranges [AIAA PAPER 72-276] 11 p1619 A72-25216
- Two-laser optical distance measuring instrument with atmospheric refractivity correction, noting accuracy 11 p1646 A72-25305
- Avalanche photodiode optical detector noise amplitude distribution as function of operating conditions 13 p1971 A72-29924
- Methane absorption stabilized 30 meter laser strain meter with Fabry-Perot geometry for earth tide, nuclear explosion and free earth oscillation observation 14 p2109 A72-30323
- Laser Doppler velocimetry system design for optical measurement of intrablade flow velocity in turbomachinery 15 p2237 A72-32045
- Optical system production acceptance test based on modulation transfer function, discussing instrument design and test philosophy 16 p2389 A72-32847
- Optical sensors for spacecraft attitude determination, discussing operation principles based on solar radiation, albedo, IR contrast and stellar radiation detection 16 p2389 A72-32849
- Gaussian beam laser Doppler velocimeter system under high scattering center concentrations and steady flow conditions, deriving noise spectral densities and SNR 16 p2390 A72-33210
- Laser interferometric calibration for vibration measurement, discussing operation principle and detector error 16 p2391 A72-33248
- Two beam optical recording instrument for atmospheric IR transmissivity, discussing spectrophotometers with changeable NaCl, KBr and LiF prisms 16 p2392 A72-33294
- A diffraction transducer for vibration analysis. 17 p2626 A72-34722
- Optical method for measuring the velocity of particles entrained in a flow 17 p2554 A72-34892
- A laser velocimeter for Reynolds stress and other turbulence measurements. 17 p2555 A72-35235
- Laser velocimeter measurement of Reynolds stress and turbulence in dilute polymer solutions. 17 p2541 A72-35252
- Optical path meter for contactless measurement of body mechanical deflection 17 p2556 A72-35442
- Simple two-dimensional laser velocimeter optics. 17 p2558 A72-35845
- Method for calibration and verification of automatic liquidborne particle counter/light method/. [SAE ARP 1192] 18 p2692 A72-36533
- Facility and procedure for measuring the spectral transmittance of the atmosphere in the range from 0.48 to 12 microns with moderate resolution 18 p2692 A72-36965
- Meteor passage time determination by optical shutter with wedge-shaped blades for light flux periodic intersection and production of two discontinuous lines for identification 18 p2693 A72-37155
- German monograph - Development and testing of a laser autocollimator 19 p2810 A72-37480
- Twyman-Green interferometer to test large aperture optical systems. 19 p2811 A72-37590
- A photoelectric method for measuring the temperature pulsations of solids 19 p2799 A72-37664
- Experimental investigation of nonstationary heat exchange for flow around a flat plate 19 p2880 A72-37665
- Using ring lasers as rate sensors. 19 p2812 A72-38223
- Theoretical considerations of significance to the design of optical anemometers. [ASME PAPER 72-HT-7] 20 p2926 A72-39678
- Active spectroscopy of Raman scattering of light with the aid of a quascontinuously tunable parametric generator. 20 p2934 A72-39852
- Transparent film thickness, refractivity and birefringence measurements by white light interferometric gage, noting performance insensitivity to chemical composition, film temperature and haze level 21 p3053 A72-40601
- A measurement of the surface strain distribution by optical differentiation method. 21 p3056 A72-41239
- Investigation of the operation of a vane anemometer in vacuum with the aid of an optical transducer for the rotational frequency 21 p3059 A72-41820
- Optical pyrometers with dual spectral ratios to eliminate instrument error due to selective radiation 22 p3175 A72-41887
- Noise-cancelling signal difference method for optical velocity measurements. 22 p3177 A72-42394
- Self-aligning comparison beam methods for one-, two- and three-dimensional optical velocity measurements. 22 p3177 A72-42395
- Measurement of the electron density distribution in plasmas from the bending of a gas laser beam. 22 p3211 A72-42396
- An optical magnetic probe with pulsed detector voltage. 22 p3177 A72-42447
- Fluid velocity measurement of oscillatory flow generated from vortex shedding by laser Doppler system, discussing frequency tracker design, continuous detection problem and application 22 p3178 A72-42677
- Laser Doppler velocimeter operating in forward- and back-scatter modes for supplementing wind tunnel flow field measurements in subsonic, transonic and supersonic regimes 22 p3179 A72-42678
- Electro-optical design and performance parameters of polluted air liquid droplet size distribution measurement by pulsed junction diode laser light external scattering 22 p3179 A72-42680
- Circular and linear dichrometer for the near infrared. 23 p3289 A72-43899
- Measurement of the modulation transfer functions of focusing screens. 24 p3425 A72-44770
- A laser interferometer for combustion, aerodynamics and heat transfer studies. 24 p3402 A72-44950
- OPTICAL METHODS**
- U OPTICS**
- OPTICAL MICROSCOPES**
- Computer servocontrolled granite stage and measuring microscope, discussing mechanical and optical construction, control electronics and applications 04 p0522 A72-15477
- High resolution portable hologram microscope based on pulsed ruby laser to avoid vibration degrading effects [CLEA PAPER 15,7] 07 p0984 A72-19398
- Hot-stage optical microscopes for microhardness measurements at elevated temperatures, describing techniques to determine heat resistant alloys mechanical and physical properties temperature dependence 10 p1478 A72-23827
- Light figure microscope construction for crystal grain orientation determination in metal specimens 11 p1632 A72-25759
- OPTICAL MODULATION**
- U LIGHT MODULATION**
- OPTICAL PATHS**
- Electromagnetic wave line-of-sight propagation based on geometrical optics for different refractivity profiles above sea, noting earth surface reflection role 01 p0026 A72-10404
- Computer program for atmospheric effects on IR radiation, calculating transmission and radiance spectra for various remotely sensed atmospheric, path and target conditions 02 p0187 A72-11862

Atmospheric refractive index inhomogeneity statistics from interferometer measurements of distance-dependent phase fluctuations in near-ground horizontal optical propagation paths under turbulence conditions
09 p1354 A72-23696

Optical path calculation in ionosphere and troposphere, determining term due to astronomical refraction with respect to frequency
10 p1475 A72-24859

Ambiguity of radar phase measurement above sea within radio horizon, noting optimal relation between wavelength and optical paths difference of direct and reflected ray
12 p1784 A72-27799

Luminosity distribution in plane of image produced by radiation from plane parallel plate, taking into account rays real path
13 p1955 A72-28498

Beam trajectory distortions due to turbulent air refractive index fluctuations in optical transmission line
15 p2197 A72-31885

Turbulent divergence of laser beams along oblique atmospheric path for vertical refractive index distribution, using Markov coherence model
16 p2364 A72-33489

Design of an inexpensive, 30 cm diameter, long path difference interferometer.
17 p2553 A72-34640

Optical path meter for contactless measurement of body mechanical deflection
17 p2556 A72-35442

Interferometric investigation of the phase fluctuations of coherent optical emission in the atmosphere
22 p3186 A72-42661

Determination of the refractive index of air by a dispersion method based on the use of radio waves
22 p3155 A72-42722

Study of target edge response viewed through atmospheric turbulence over water.
23 p3289 A72-43896

Transmission losses in glass and plastic single mode and liquid core optic fibers for long distance data links and image transmission
24 p3380 A72-45252

OPTICAL POLARIZATION

Nonlinear photoelasticity, elastoplasticity and creep problems studies by optical polarization methods, comparing transparent model and photoelastic coating techniques
02 p0289 A72-11613

Narrow band electrically controlled interferential polarization filter with fine tuning capability for solar physical research, discussing design and operation
03 p0357 A72-13369

Stress-strain state determination for plane orthotropic bodies by optical polarization method, discussing numerical methods for stress and strain tensor components
03 p0445 A72-13580

Optical birefringent networks synthesis, describing use of building blocks of polarizers, birefringent crystals and optical compensators
04 p0548 A72-14737

Q switched high power laser pulse compression based on optical polarization change on passing through Kerr-active medium
07 p1000 A72-19038

Pulsed ruby laser mode structure effects on quartz damage, noting dependence on propagation and polarization directions with crystal
07 p1001 A72-19196

Optical resonators using lossy anisotropic metal film linear polarizer for oscillation mode selection [CLEA PAPER 6.3]
07 p1004 A72-19382

Scorpius X-1 linear optical polarization, comparing intrinsic to interstellar theories
08 p1235 A72-21390

Electro-optical Q switching of solid state laser sources without linear energy polarization in optical resonator
09 p1326 A72-23422

Polarization modes of anisotropic optical traveling wave resonator using half wave plate and Faraday rotation cell
12 p1824 A72-27870

GaAs laser array Fabry-Perot structure to produce uniform TE polarization in emitted light
12 p1827 A72-28223

Vehicle orientation degrees of freedom remote measurement with mounted passive devices and polarization-modulated light, discussing data reduction and system accuracy
15 p2267 A72-31780

Coherence narrowing during multiple scattering of resonance radiation in atomic vapor, treating polarization transfer in terms of classical tensors
15 p2281 A72-32221

Photoelasticity with stress induced optical activity analysis using Stokes parameters, discussing rotational effects in scattered light problems
15 p2277 A72-32235

LF spectrum of depolarized light scattered from liquids composed of molecules with anisotropic polarizabilities, noting sharp line spectra with VH shear doublets
16 p2429 A72-32951

Mathematical models for depolarized light scattering by particle pair in gas, noting molecular collisions effect
16 p2423 A72-32952

Radio source Oj 287 photometric and polarimetric observations, noting optical intensity and plane polarization variability
16 p2452 A72-33134

Feedback averaging procedure application to M-ary polarization modulated laser communication system, obtaining error rate improvement over systems without feedback
16 p2362 A72-33215

Optical circular polarization search in quasars, Seyfert galaxies nuclei, BL Lac and OJ 287
16 p2456 A72-33472

Bidirectional optical scattering from dielectric materials of various pigmentation and surface roughnesses, obtaining cross section data to determine angular, spectral and polarization behavior
16 p2427 A72-33839

Polarization modes and phase shifts of normal oscillation modes in anisotropic optical traveling wave resonator with Brewster winders half wave plate and Faraday rotation cell
16 p2403 A72-33979

Poincare sphere application to polarimetry and two- and three-dimensional photoelasticity by scatter light photoelastometry
18 p2691 A72-36381

Optical polarization effects in a gas laser.
18 p2697 A72-36487

Brightness matrix of a flat powdered layer with opaque particles in the single-scattering approximation
19 p2836 A72-38783

Polarization effect of attenuation of opposed-wave competition in ring lasers
20 p2932 A72-39412

The redistribution function of polarized light in the presence of collisions and of small magnetic fields - Discussion of the polarization of the solar line Ca I 4227 A.
20 p2971 A72-39756

Influence of polarization of laser fields on nonlinear interference effects
21 p3062 A72-40405

Quartz and calcite spectral emission polarization calculation from Fresnel equation, comparing results with field measurements with broadband IR radiometer
21 p3097 A72-40603

Dielectric coating effects on millimeter wave diffraction pattern of gratings, noting sharp anomalous dips in transmission intensity for P and S polarizations
21 p3031 A72-40604

Skylight intensity, polarization and airglow measurements during the total solar eclipse of 30 May 1965.
22 p3170 A72-42371

Interstellar circular polarization.
23 p3336 A72-43556

Discovery of interstellar circular polarization in the direction of the Crab Nebula.
23 p3336 A72-43557

Approximate formulae for mixed modulated coherent and partially polarized chaotic light.
24 p3425 A72-44769

Analysis of the polarization properties of TW laser emission
24 p3411 A72-45497

OPTICAL PROPERTIES

NT ABSORPTANCE

NT ABSORPTIVITY

NT BIREFRINGENCE

NT BRIGHTNESS

NT COLOR

NT DICHROISM

NT LUMINOSITY

NT OPACITY

NT OPTICAL REFLECTION

NT PHOSPHORESCENCE

NT PHOTOCONDUCTIVITY

NT PHOTOELECTRIC EFFECT

NT PHOTOELECTRIC EMISSION

NT PHOTOIONIZATION

NT PHOTOVISCOELASTICITY

NT PHOTOVOLTAIC EFFECT

NT RADIANCE

NT REFLECTANCE

NT REFRACTIVITY

NT SKY BRIGHTNESS

NT SPECTRAL REFLECTANCE

NT STELLAR LUMINOSITY

NT STIGMATISM

NT TRANSLUCENCE

NT TRANSMISSIVITY

NT TRANSMITTANCE

NT TRANSPARENCE

NT TURBIDITY

OPTICAL POLARIZATION

High performance aerospace vehicles transparent materials, discussing glasses, plastics and optical coatings, solar properties, refractive index, UV transmittance and radiation damage susceptibility
01 p0091 A72-10765

Fused silica optical transmittance at elevated temperatures during high energy electron bombardment, noting optical absorption at short wavelengths
01 p0103 A72-11357

Optical distortion induced by heated windows in high power laser systems, deriving figures of merit for window materials
02 p0237 A72-11470

Air holography interferometry for acrylic model materials inspection and selection for optical flatness, comparing with photoelasticity [SESA PAPER 1941]
02 p0224 A72-11516

Birefringent filter theory and optical properties, discussing transmission profile and error sources
03 p0352 A72-12947

Rocket plume contamination effect on transmitting and reflecting materials optical properties, noting predominant absorption and scattering effects [AIAA PAPER 72-56]
05 p0750 A72-16967

Thermodynamic equilibrium, transport and optical properties and quantum effects in nonideal plasmas, using Monte Carlo method
05 p0700 A72-17223

Handbook on lasers and optical technology covering gas, dye, liquid, injection and insulating crystal lasers, materials, sources, transmission, hazards and holographic recording
06 p0826 A72-17945

Inorganic photochromic and cathodochromic recording materials in single crystal and powder forms, considering color change properties during light or electron beam exposures
06 p0866 A72-17950

Hf diffusion type chemical laser fluid dynamic and optical properties, discussing computerized numerical analysis [AIAA PAPER 72-146]
07 p1001 A72-19063

Optical properties of paraboloid-hyperboloid mirror X ray telescopes evaluated by ray tracing method, noting resolution and focal plane curvature approximation
07 p0985 A72-19405

Temperature and physical state effects on rubidium optical constants at 0.3-2.4 microns
07 p1050 A72-20522

Optical transmission, reflection and absorption of thin rubidium films for parallel and perpendicularly polarized monochromatic radiation, investigating volume and surface plasma oscillations
07 p1050 A72-20523

Optical and electrical characteristics of gas discharge plasma in pulsed radiation sources as function of power dissipation
07 p1047 A72-20611

Band averaged optical constants and IR characteristics of thin plastic films with/without metal substrate, using transmittance measurements [ASME PAPER 70-WA/HT-15]
08 p1205 A72-20874

Semitransparent particle model of Martian surface for reflective power at various incidence and reflection angles, discussing packing density and optical parameters
08 p1231 A72-21126

Optical properties changes of Al alloys containing impurities, noting band structure modification and tendency toward free electron response
08 p1186 A72-21593

Brightness distribution and phase dependence measured for spheres with different colors and roughness for Mars surface optical parameters model validity
08 p1238 A72-21830

Turbulent earth atmosphere optical inhomogeneities determination from solar limb image characteristics in motion pictures of solar disk edge
09 p1305 A72-22233

Recrystallization effects on thin ZnTe film structure, electrical and optical properties
09 p1367 A72-22421

Electron phonon coupling and IR optical constants relationship to superconductivity in transition metals
09 p1369 A72-22566

Optical properties of Gd polycrystals in IR, explaining frequency dependence of complex permittivity
09 p1372 A72-23040

Optical simulation of plastic strain distribution with models prepared from organic glass, investigating birefringence effect
09 p1406 A72-23182

Optical properties of nematic and cholesteric liquid crystals, noting application for visualization and display systems
09 p1373 A72-23598

Optical properties of nuclei of normal, Seyfert and N-type galaxies and quasars from spectrographic and photometric observations
10 p1534 A72-23902

Cosmic epoch dependent evolution of radio sources with identified optical counterparts
10 p1535 A72-23912

Ground based IR astronomical telescope detectors, relating F number and optical requirements to near, far, and intermediate IR observation

10 p1481 A72-24249

Selective surfaces and coatings for solar energy conversion systems, discussing semiconductor photoconverters, white-black surfaces, cooling systems and optimal optical properties

10 p1422 A72-24315

Zinc oxide as refractory material, discussing optical, elastic and electro- and photoconductivity properties

10 p1501 A72-24732

Russian book on radar studies of moon covering lunar motion, dimensions, mass, density and surface layer thermal and optical properties

11 p1720 A72-26047

Electrostatic rocket exhaust materials deposits effects on solar cells optical, thermal and electrical performance characteristics, using optical thin film theory

[AIAA PAPER 72-447]

11 p1578 A72-26184

Dielectric and optical constants of p-type GaSb single crystals, interpreting singularities by energy bands diagram

11 p1689 A72-26485

Impact glass-like objects as evidence of meteoritic origin of Lomar Crater /India/, discussing physical, chemical and optical properties

11 p1723 A72-26521

Two dimensional characteristic and distribution functions of monomode laser radiation random processes with nonlinear optics application

11 p1651 A72-26716

Optical transparencies - Conference, London, June 1971

12 p1752 A72-27001

Optical quality requirements for aircraft transparencies, considering resolution, haze, halation, light transmission, distortion, binocular deviation, double images, scratches and inclusions

12 p1832 A72-27003

Optical qualities of aircraft windshields and direct vision windows, considering color, light transmission, faults, heating, distortion, inside reflections and double images

12 p1832 A72-27004

Piezoelectric quartz crystal microbalance for material outgassing and optical element contaminant film measurements

12 p1806 A72-27043

Solar absorptance and thermal emittance of thermal control coatings contaminated by thruster exhaust in vacuum environment

[AIAA PAPER 72-263]

12 p1846 A72-27865

Monoenergetic electrons and low energy protons radiation damage effect on Si solar cell electrical and optical properties

12 p1759 A72-28046

Statistical Coulomb potential and thermodynamic, kinetic and optical properties of nonideal dense plasma

12 p1853 A72-28173

Light propagation patterns in absorbing and scattering medium with radiation density dependent optical properties

13 p2002 A72-28510

Light scattering media optical characteristics measurement techniques and equipment

13 p1955 A72-28515

Radiation transfer equations solved in isotropic light scattering approximation, relating transfer function to motion picture film optical properties

13 p1955 A72-28519

Instrument to measure thermodynamic, electrical and optical properties of gases and liquids, describing thermostat for 83-923 K range

13 p1956 A72-28633

Experimental method to directly determine frequency-contrast and phase-frequency characteristics of optical objectives from boundary curve

13 p2003 A72-28798

Au film optical refractivity, absorptivity and transmittance in visible and UV ranges of Au-GaAs and Au-GaP photoelectric converters

14 p2141 A72-30224

Quantum kinetic equation for monatomic and molecular gases optical characteristics calculation, considering spontaneous emission spectrum of atoms

14 p2110 A72-30358

Schlieren method for qualitative study of optical inhomogeneities produced by temperature field in cylindrical solid body

14 p2106 A72-31162

Temperature dependent optical constants of Ti and W crystal surfaces cleaned by ion bombardment in ultrahigh vacuum

15 p2274 A72-31376

Heavily doped ruby optical properties review, discussing N-lines, absorption and fluorescence spectra, interactions with phonon and photon fields and ionic reactions

16 p2441 A72-33522

Influence of the transverse distribution of pumping on the energetics and the profile of thermo-optical distortions in a rhodamine 6G laser

17 p2563 A72-35302

Attachment for studying optical properties of highly cooled crystals in the vacuum ultraviolet region

17 p2555 A72-35309

Determination of the parameters of a satellite camera

17 p2556 A72-35360

Determination of the quality of the reflective properties of mirrors used in photoelectric converter assemblies

17 p2498 A72-35510

Wave-guiding properties of stripe-geometry double heterostructure injection lasers

18 p2698 A72-36981

Investigation of the optical and pyrometric behavior of surface coatings for the Helios probe

19 p2880 A72-37493

Effect of optical constants on the energy distribution in homogeneous particles illuminated by a parallel beam of light

19 p2812 A72-38216

Constitutive equations and optical yielding of anisotropic perfectly plastic dielectrics

19 p2878 A72-38799

Application of optimization techniques over flat surfaces, determining optical constants of thin films

20 p2959 A72-39052

Some optical properties of liquid crystals

20 p2961 A72-39850

Application of matrix formalisms to the specification of light polarization changing systems

20 p2928 A72-40025

Photographic material characteristics for adequate diffraction efficiency and contrast and noise levels and acceptable nonlinear distortions of holograms, noting optical transfer function optimization

21 p3052 A72-40389

Output power saturation with increasing discharge current in powerful argon CW lasers

21 p3062 A72-40404

Study of the diffusing properties of the retina - Application to the optical system of the eye

21 p3007 A72-40736

Corrugated image screens advantages over flat screens, determining light intensity per corrugation, maximum viewing angle and reflection factor

21 p3055 A72-40743

Pure and compensated Ge and Si far IR spectral properties at liquid He temperatures for bolometer detector application

21 p3013 A72-40822

Optical properties of transmission echelette high-pass filters

21 p3055 A72-40823

Space applications of Fabry-Perot modulator as alternative to mechanical devices, presenting optical and electrical performance data for different temperatures

21 p3055 A72-40824

Optical properties and structure of the Jovian atmosphere. V - Probable structure of the ammonium aerosol layer

22 p3219 A72-41914

Investigation of optical inhomogeneities in large fields by holographic methods

22 p3176 A72-42106

Change in the sign of the thermal lens of glass laser rods during variation of the thermo-optical constant of glass

23 p3296 A72-43926

Optical constants of cesium in the wavelength range from 0.3 to 2.5 microns and their dependence on temperature and state of matter

24 p3426 A72-44800

Optical properties of thin cesium films over the wavelength range from 0.3 to 0.9 microns and their electrical resistance

24 p3426 A72-44801

OPTICAL PUMPING

Two dimensional scanning electron beam pumped laser, describing production of coherent emission

01 p0079 A72-10522

Carbon dioxide laser pumping with nuclear reactions, indicating improved laser performance due to additional ionization by energetic charged particles

01 p0082 A72-11331

Laser pumped organic dye laser frequency-time characteristics, noting noncoincidence of amplification and photon density maxima

02 p0238 A72-12118

Laser pumping pulse shape effects on second harmonic emission waveform during nonlinear crystal excitation by ultrashort light pulse

03 p0366 A72-13368

Superradiative properties of high gain flashlamp-pumped dye laser amplifier, determining small signal amplification as function of pumping power and frequency

03 p0369 A72-14393

Water vapor laser pumping by upper lasing level excitation through direct electron impact, explaining mechanism by model

[AD-735585]

04 p0529 A72-14587

CW CO laser by discharging premixed carbon disulfide-oxygen flame, suggesting chemical pumping mechanism and flame laser possibility

04 p0529 A72-14589

Emission spectrum and intensity variation of organic dye solutions excited by nitrogen laser pulsed radiation

04 p0529 A72-14655

Short duration high peak power laser pulses generation and measurement, examining active and passive mode locking, chirping, pulse compression and optical pumping

04 p0530 A72-14735

Pinched vortex tube high current arc discharges for continuous pumping of ion crystal YAG-Nd lasers

06 p0825 A72-17839

Carbon dioxide laser pumping at atmospheric pressure by electron beam controlled electrical discharge, discussing measured electrical and laser properties

07 p0999 A72-18875

Optically pumped indium-gallium-arsenides laser coherent emission at room temperature, measuring total power conversion efficiency

[AD-737941]

07 p0999 A72-18882

Gaussian rf noise effect on optical detection signal fluctuations in optically pumped frequency standards

07 p0938 A72-19013

Continuously pumped repetitively Q switched Nd:yttrium-aluminum trioxide laser, discussing mode selection technique based on gain excess over hold-off loss

07 p1000 A72-19045

Flashlamp pumped dye-doped polymethyl methacrylate laser thermal and photochemical effects decrease and peak power output increase by light converter

07 p1002 A72-19206

Transient gain measurements on laser dyes of flashlamp pumped rhodamine 6G-ethanol solutions with air and nitrogen

07 p1002 A72-19208

Dye laser system with narrow linewidth oscillator, transverse mode selector, power amplifier and nitrogen pumping, noting 50 kw and 5 nsec pulse generation capability

07 p1002 A72-19208

Atmospheric pressure carbon dioxide-nitrogen-helium lasers with high output energy densities, using auxiliary discharge for volumetric excitation

07 p1003 A72-19217

Lamp pumped IR solid state laser obtaining 20 W output and 4 percent efficiency from transition of He ion in sensitized YAG

07 p1004 A72-19234

Optically pumped gas lasers with electron transitions to molecular excited state and resonant absorption lines

07 p1006 A72-19634

Optically pumped semiconductor lasers, discussing two photon absorption, emission from compounds and mixed crystals and smooth frequency variation

07 p1006 A72-20118

Ruby laser emission losses for free lasing modes and threshold and above threshold pumping

07 p1007 A72-20122

Output characteristics of Q switched liquid laser as function of pumping pulse, cavity mirror reflectivity and cavity length

07 p1008 A72-20544

Wavelength tunable dye laser pumped by dual pulse lamps with Fabry-Perot interferometer in resonator

07 p1009 A72-20614

Pulse rate and pumping power effects on emission spectra and I-V characteristics of multielement GaAs injection lasers

08 p1181 A72-20796

Ruby use for submillimeter range optically pumped quantum paramagnetic amplifier

08 p1183 A72-21770

Organic dyes molecular photodecay effect on output and power losses of laser activated by flash pumped white light

08 p1184 A72-22029

Nd glass absorption of flash pump emission energies with varying discharge parameters, Xe pressure and glass thickness

08 p1184 A72-22030

Rhodum solution laser emission pulse characteristics relation to pumping energy distribution over container end surface

08 p1184 A72-22048

Self mode locking operation of transversely excited atmospheric pressure carbon dioxide pulsed laser with helical pumping

08 p1184 A72-22075

Resonator dielectric waveguide structure in electron beam pumped semiconductor laser, noting reduction of diffraction losses and of laser action threshold

08 p1184 A72-22089

High power electron beam pumped nitrogen super-radiant laser with 60 kW output 09 p1323 A72-22624

Flashlamp and laser pumped cresyl violet laser emission characteristics between 620 and 710 nm, noting self mode locking in 3 component solution 09 p1324 A72-23048

CW Kr arc lamps for high power Nd-YAG laser pumping, testing operating life and electrical and spectral characteristics as function of design 09 p1324 A72-23080

Steady state plane wave theory of intracavity coupled parametric oscillator upconverter, obtaining efficiency, pump power transmission and optimum output coupling 09 p1325 A72-23086

Nuclear reaction-produced high energy ion beams for gas laser pumping and output enhancement 10 p1489 A72-23948

Nonlinear effects in optical pumping of Ne transition by laser line 10 p1491 A72-24109

50 MW laser amplifier at 3371 Å in molecular nitrogen via transverse electron pumping 10 p1491 A72-24225

Traveling wave mode ring laser operation, obtaining active medium polarization changes through longitudinal magnetic field excitation by capacitor discharge through spiral pump lamps 10 p1492 A72-24363

Rb87 vapor laser with optical pumping, measuring nitrogen or nitrogen argon mixture buffer gas partial pressure effect on power output 10 p1493 A72-24911

Vortex discharge in Ar as optical pumping source for ionic crystal CW lasers, comparing efficiency with YAG-Nd crystal pumping 11 p1648 A72-26331

Pumping conditions relationship to tube filling in Nd-YAG pulsed laser 11 p1649 A72-26344

Multilayer dielectric reflective coatings performance in solid state laser pumping systems 11 p1649 A72-26345

Total emitted power calculated for transversely pumped pulsed molecular nitrogen laser at 3371 Å 11 p1651 A72-26504

Laser emission in near IR by flash lamp pumped fluorescent dyes, presenting oscillograms 11 p1651 A72-26505

Laser emission intensity enhancement based on stimulated Brillouin scattering effect by raising pumping level, energy density and pulse duration 12 p1821 A72-27587

Absorption spectrum of Cr cations in magnesium aluminate spinel crystals excited by strong optical pumping 12 p1854 A72-27596

Temperature gradient and thermoelastic stresses in Nd-YAG laser active elements under continuous pumping conditions, noting refractivity radial distribution 12 p1822 A72-27614

Singly and doubly resonant pulsed optical parametric oscillators driven by time-dependent pump, deriving output power rise time by steady state analysis 12 p1792 A72-27751

Multielement electron beam pumped semiconductor laser using emitting GaAs disks with vapor deposited dielectric mirror coatings 12 p1824 A72-27876

Pumping current pulse duration effect on lasing threshold of injection lasers with diffusion junctions and heterojunctions in GaAs-AlAs system 12 p1824 A72-27877

Computer simulation of pulsed hydrofluoric acid laser pumped by chain reaction, investigating cavity and chemical parameters effects on laser pulse 12 p1826 A72-27938

Short term instability of frequency standard using AFC of quartz crystal oscillator by phase locking to optically pumped Rb 87 vapor clock 13 p1968 A72-29296

Energy conversion efficiency of xanthene dye laser pumped by mode-locked Nd-glass laser second harmonic, discussing effect of excited molecules transition to triplet state 13 p1970 A72-29686

Superradiant laser emission from organic dyes rhodamine 6G and B with coaxial flashlamp pumping source, relating input threshold energy to dye concentration 13 p1971 A72-29864

Wide tuning range organic dye laser design, using nitrogen laser line as transverse pumping source 13 p1971 A72-29869

Xenon filled coaxial pulse tube for pumping organic dye solutions, obtaining intensive light flashes 13 p1971 A72-29923

Buffer gas mixture and pumping light effects on shifts from ground state hyperfine frequency in Rb-85 maser frequency standard 14 p2109 A72-30196

Ground state and metastable atoms and ions optical pumping, presenting critical survey on pumping and relaxation mechanisms, light propagation and spin exchange 14 p2109 A72-30325

Molecular iodine photolysis in photodissociative laser due to selective pumping, noting recombination-like storage mechanism 14 p2110 A72-30354

Flashlamp pumped tunable narrowband traveling wave dye ring laser, stabilizing emission frequency by intracavity Fabry-Perot etalon 14 p2110 A72-30675

Efficiency of pulsed tubular pumping lamps made of quartz glass investigated by active element luminescence measurement, noting dependence on current density 15 p2246 A72-31425

Photon loss coefficients and gain measurement in CdS electron beam pumped lasers, noting absorption mechanism and efficiency 15 p2246 A72-31668

High power CW Nd-YAG laser efficiency improvement by optical pump wavelength, power coupling and balance factors, noting krypton arc lamp contribution 15 p2247 A72-32029

Flashlamp pumped cryptocyanine Q switched high peak power ruby lasers, noting UV radiation responsible for methanolic solution photochemical decomposition 15 p2249 A72-32156

Optically pumped magnetometer error, predicting atomic g-factor modification by nonresonant RF field 15 p2239 A72-32335

Optically pumped pulsed hydrogen fluoride gas laser, observing anisotropic ultrahigh gain emission in rotational transitions 15 p2251 A72-32531

Stimulated emission in molecular iodine vapor phase laser optically pumped by Q switched Nd-YAG laser second harmonics 15 p2251 A72-32538

Mathematical model for fast transverse glow discharges for pumping high pressure gas lasers, noting short rise time of applied voltage pulse 16 p2399 A72-33012

Short flash characteristics of spiral pumping lamp for dye laser 16 p2400 A72-33079

Pumping current pulse duration effect on lasing threshold of injection lasers with diffusion junctions and heterojunctions in GaAs-AlAs system 16 p2404 A72-33986

Resonator dielectric waveguide structure in electron beam pumped semiconductor laser, noting reduction of diffraction losses and of laser action threshold 17 p2562 A72-34660

Traveling wave mode ring laser operation, obtaining active medium polarization changes through longitudinal magnetic field excitation by capacitor discharge through spiral pump lamps 17 p2563 A72-34962

Influence of the transverse distribution of pumping on the energetics and the profile of thermo-optical distortions in a rhodamine 6G laser 17 p2563 A72-35302

Saturated absorption in optically pumped semiconductor lasers 17 p2563 A72-35303

Output fluctuations of CW-pumped Nd:YAG lasers. 17 p2564 A72-35345

Atmospheric pressure carbon dioxide pulsed IR laser to obtain 80 W peak power by optical pumping with TEA HBr laser and filter 17 p2565 A72-35816

CW optically pumped tunable dye laser wavelength ranges, linewidth, mode purity, polarization and power output characteristics 17 p2565 A72-35947

Dynamics of the optical-pumping cycle of F centers in alkali halides - Theory and application to detection of electron-spin and electron-nuclear-double-spin resonance in the relaxed-excited state. 18 p2719 A72-36709

Bandwidth and threshold calculations for angletuned parametric oscillators. 19 p2813 A72-38689

Experimental achievement of optical pumping of a carbon dioxide molecular laser 19 p2814 A72-38790

Influence of gas pressure in arc lamps on the pumping efficiency of CW garnet lasers. 20 p2933 A72-39513

Control circuit for a power supply of a laser pump lamp. 20 p2933 A72-39524

Frequency-tunable stimulated IR parametric fluorescence produced by barium sodium niobate crystal pumped with picosecond pulses from frequency-doubled mode locked Nd-glass laser 20 p2933 A72-39560

Continuously tunable dye laser to obtain output wavelength variation by changing pump laser beam incidence angle on prism lateral face 20 p2933 A72-39563

Pump laser design for an infrared upconverter. 20 p2934 A72-39873

Flash lamp optimal operating parameters determination by impedance matching to driving circuit and spectral matching to material of optically pumped solid state pulsed lasers 21 p3061 A72-40204

The effect of pump coherence on frequency conversion and parametric amplification. 21 p3014 A72-40238

The beam-plasma discharge laser 21 p3062 A72-40406

Optical elements of a laser-pumped dye laser 21 p3064 A72-41737

Exciton condensation in a momentum space under the action of optical pumping 22 p3185 A72-42161

German monograph - Amplification measurements and investigation of 'super radiation' characteristics in the case of optically pumped rubies. 22 p3187 A72-43065

Stimulated emission with pumping by a pulsed electron beam formed in a direct discharge 23 p2925 A72-43319

Dynamic thermo-optical distortions compensation in lamp pumped rhodamine 6G liquid laser by introducing auxiliary dish with dye into cavity 23 p2925 A72-43679

Evanescent-field-pumped dye laser. 23 p2926 A72-43816

Properties of a pulsed LiIO3 doubly resonant parametric oscillator. 23 p2927 A72-44187

Fluorescent organic dyes solutions for Nd:YAG laser output performance improvement 23 p2927 A72-44191

Optical signal envelopes recording and reproduction with parametric superregenerative frequency converters, noting optical pumping by continuous wave YAG laser emission 23 p2929 A72-44471

Optically pumped gas lasers with electron transitions to molecular excited state and resonant absorption lines 24 p3408 A72-44566

Theory of dispersion in relation to light shifts. 24 p3409 A72-44921

Flashlamp-pumped dye lasers for investigations of the upper atmosphere. 24 p3409 A72-44948

Wideband parametric up-conversion of infrared waves into visible region using tunable dye laser pumping. 24 p3410 A72-45286

Kinetics, spectrum, and specific loss properties of radiation emitted by rhodamine 6G in the case of pumping by a self-constricting discharge 24 p3410 A72-45417

Pulsed laser employing a rhodamine 6G solution in ethyl alcohol with an output energy of 110 J 24 p3411 A72-45498

Time dependence of the divergence of the radiation emitted by a rhodamine laser pumped by a pinched discharge. 24 p3411 A72-45612

OPTICAL PYROMETERS

Electrical conductivity of pyrographite at high temperatures along and across deposition plane, using optical pyrometer measurements 02 p0251 A72-12860

Three color optical pyrometer with microsecond resolution time based on three-wavelength double ratio method, displaying temperature/time relationship on cathode ray oscilloscope 04 p0522 A72-15476

Radiation thermometry trends, considering photodetectors, optical pyrometers and filters [ASME PAPER 71-WA/TEMP-3] 05 p0661 A72-15909

OPTICAL RADAR

Optical radar target range estimation, determining suboptimum post detection signal processing algorithms in photon counting mode 01 p0024 A72-10047

Lidar measurements of atmospheric aerosol distributions over large areas including urban haze, scattering layers, trade wind inversion and Sahara dust stream in Caribbean [AIAA PAPER 71-1055] 01 p0057 A72-10526

Laser radar application to air pollution measurement, discussing techniques and instrumentation utilizing elastic, Raman and fluorescence scattering [AIAA PAPER 71-1056] 01 p0028 A72-10527

Monostatic and bistatic lidar and solar radiometer sensing techniques for remote measuring of aerosol size distributions 01 p0066 A72-10528

FM/CW laser radar technique for smoke plume opacity remote measurement, discussing eye safety [AIAA PAPER 71-1081] 01 p0080 A72-10539

Smoke plume opacity or particulate content measurement by laser backscatter, using Q switched ruby and Nd lidars [AIAA PAPER 71-1087] 01 p0058 A72-10544

Hydrometeors linear depolarization ratios measurements by monostatic lidar, using different size water drops and ice crystal clouds

01 p0095 A72-10830

Air pollution measurements by laser radar, using coherence properties to discriminate between backscatter due to molecular atmospheric constituents and pollutant particulates

02 p0212 A72-11816

Laser station coordinate and Geos B satellite position compensation with simultaneous optical and laser observations

02 p0219 A72-12045

CAT detection by airborne laser Doppler radar and ground based ultrasensitive microwave Doppler radar methods

04 p0543 A72-14822

Raman laser radar (LIDAR) for remote probing, discussing design, construction, testing, atmospheric scattering, and intensity and polarization measurements

06 p0824 A72-17588

Low energy per pulse high repetition rate laser radar capabilities for atmospheric density measurement above 30 km

06 p0775 A72-18093

Airborne ruby lidar application to cirrus and haze layers measurements, deriving optical parameters

06 p0777 A72-18448

Air pollutant monitoring and remote analysis by Raman, fluorescence and resonance backscattering, Rayleigh scattering and absorption laser radar techniques

06 p0827 A72-18460

FM-CW radar range measurement by carbon dioxide laser, considering laser output nonlinear variation due to frequency pulling/pushing and refractivity changes

07 p0940 A72-19205

Angle scintillation in laser radar return from retroreflector, comparing measurement with theoretical derivation in terms of phase fluctuation parameter [CLEA PAPER 2.1]

07 p0942 A72-19377

Spaceborne laser radar for target acquisition and tracking in spacecraft rendezvous and docking applications

[CLEA PAPER 9.5]

07 p0943 A72-19387

Suboptimum linear quadratic algorithm for optical radar signals postdetection processing and target range estimation

07 p0943 A72-19522

Laser radar observations of mesosphere and lower thermosphere optical scattering cross section variations due to tide-caused atmospheric density fluctuations

08 p1156 A72-21100

Narrow-band pulsed laser radar photocount distribution statistics in thermal background radiation, noting detection performance dependence on signal and noise absolute level and SNR

08 p1134 A72-21420

Relation for detector-aperture size for spatially coherent detection with dependent scattering applied to realistic laser radar signal signatures

09 p1278 A72-22618

GaAs lidar reflectance of fair weather cumulus clouds at 0.903 micron from aircraft observation

09 p1280 A72-23349

CW carbon dioxide laser Doppler radar for remote measurement of atmospheric wind velocity and turbulence, obtaining Doppler signal via homodyned radiation scattered by airborne particles

09 p1315 A72-23407

Laser radar technique for invisible air pollutants remote sensing systems, comparing Raman backscattering resonance scattering and absorption schemes

10 p1489 A72-23952

Lidar application to aircraft and missile tracking and ranging, describing results obtained with ONERA experimental equipment

10 p1436 A72-24655

Tuned laser radar detection and ranging of high altitude Ba ion cloud by photon counting, discussing SNR requirement

10 p1440 A72-24963

Cloud height measurements and instrumentation, discussing rotating and fixed beam triangulation and French lidar and ruby laser ranging ceilometers

10 p1484 A72-25094

Atmospheric water vapor measurements by Raman backscatter from pulsed laser radar, comparing with meteorological tower data

11 p1680 A72-25347

Atmospheric constituents dimension, composition and dynamics from optical radar echo observation of laser light scattering

11 p1592 A72-25849

Slant range visibility measurements by lidar for aircraft landing operations under low clouds and fog at coastal region

13 p1992 A72-28847

Meteorological formations investigation with lidar, discussing laser beam interaction with clouds, fog and precipitation with allowance for multiple scattering

13 p1995 A72-29595

Gas temperature from Raman rotational line intensities generated by lidar techniques applied to inelastic Raman scattering

15 p2232 A72-31373

Aircraft laser radar measurements of atmospheric backscattering coefficients for cloud and underlying surface studies

15 p2266 A72-31908

First and second order backscattering, beam divergence, angular field of view, field size and receiver distance of water clouds illuminated by continuous lidar beam

15 p2200 A72-32154

STRADA landing trajectory recording system for real time flight path restitution during approach and landing, using computer and lidar techniques

16 p2420 A72-32895

Directivity pattern accuracy effects on angular coordinate determination by scanning active optical radars

16 p2362 A72-33188

Airport runway fog dispersal in UK, discussing cost projection for chemical seeding system combined with lidar remote sensing

16 p2418 A72-33500

Upper atmospheric trace constituents global mapping by laser radar probing from satellite, discussing feasibility and comparison with ground based system

16 p2365 A72-34074

IR carbon dioxide laser radar with heterodyne detection, measuring SNR and atmospheric scattering coefficients for various weather conditions

17 p2516 A72-35192

Remote measurements of the atmosphere using Raman scattering.

17 p2547 A72-35195

Complex index of refraction of airborne fly ash determined by laser radar and collection of particles at 13 km.

18 p2661 A72-36637

Measurement of aerosol motion and wind velocity in the lower troposphere by Doppler optical radar.

18 p2706 A72-36638

On depolarization of visible light from water clouds for a monostatic lidar.

18 p2706 A72-36646

Clear air turbulence detection possibility by optical laser radar and turbulent fluctuation correlations

23 p3264 A72-43898

Laser radar /lidar/ for mapping aerosol structure.

23 p3298 A72-44542

Rocket-borne GaAs laser radar system with scatter light detector and data processor for upper atmosphere aerosol and pollution measurements

24 p3409 A72-44778

OPTICAL RANGE FINDERS

NT LASER RANGE FINDERS

FM-CW radar range measurement by carbon dioxide laser, considering laser output nonlinear variation due to frequency pulling/pushing and refractivity changes

07 p0940 A72-19205

Lidar application to aircraft and missile tracking and ranging, describing results obtained with ONERA experimental equipment

10 p1436 A72-24655

Q switched YAG-Nd laser implementation into target designators and range finders, stressing temperature insensitive design with electronic compensation and thermal equalization

12 p1825 A72-27928

Laser ranging instrument for satellite distance measurement, discussing four-axial mounting, guiding telescope, receiving optics and performance

15 p2247 A72-31935

Timing requirements in geodetic measurements with optical and electronic equipment, considering lunar laser ranging technique for high accuracy

15 p2229 A72-32075

Laser tracking measurements of distance to light reflector mounted on Lunokhod 1, describing equipment and procedure

16 p2404 A72-33997

Laser systems.

17 p2562 A72-34567

Two channel high resolution spectrometric measurements of plasma velocity from intrinsic radiation in optical range by Doppler effect

17 p2590 A72-35133

OPTICAL REFLECTION

Goos-Hanchen nonpolarized light effect for laser beam separation into rectilinearly polarized beams during reflection

01 p0101 A72-10042

Reflection nebulae genetic relationship to illuminating stars from catalogs based on Palomar Observatory Sky Survey

02 p0284 A72-12639

Separation measurement between two distant partially reflecting parallel surfaces using Michelson interferometer

03 p0358 A72-13435

Jupiter and Venus cloudy atmosphere reflected sunlight circular polarization measurement, noting sense variations with phase angle and location on disk

03 p0439 A72-14150

Spectral analysis of light reflected from Nd laser produced deuterium plasma, observing Doppler shift

07 p1039 A72-18888

Angle scintillation in laser radar return from retroreflector, comparing measurement with theoretical derivation in terms of phase fluctuation parameter [CLEA PAPER 2.1]

07 p0942 A72-19377

Optical losses, reflectivity and transmissivity measurements of He-Ne laser Fabry-Perot resonator elements, using laser output power dependence on element losses

07 p1006 A72-19901

Semitransparent particle model of Martian surface for reflective power at various incidence and reflection angles, discussing packing density and optical parameters

08 p1231 A72-21126

Ground based Raman laser backscatter measurement of stratospheric water vapor content, noting 1 ppm accuracy

08 p1161 A72-21825

Focal length determination for on-axis parabolic mirrors by He-Ne laser reflection

09 p1315 A72-23352

Laser reflection studies of surface morphology of growing or evaporating crystals

09 p1326 A72-23409

Radiative transfer theory for passage wall surface roughness effects on light transmission and reflection [ALAA PAPER 72-303]

11 p1742 A72-25237

Measurement of light pressure-force on Echo I satellite based on satellite surface reflection and stellar magnitude as function of phase angle

11 p1718 A72-25939

Titanium dioxide thin film antireflection coating to minimize reflection losses in Si solar cells, discussing fabrication and optical and electrical characteristics

12 p1757 A72-28028

Reflectometer based on quasi-optical transmission line using conversion of incident and reflected waves into opposed circularly polarized components

13 p1954 A72-28375

High angular resolution optical system to measure light reflection from rough surfaces

13 p2002 A72-28513

Spectral changes of light reflected back from plasma during heating by mode locked Nd laser, noting equidistant lines presence

14 p2138 A72-30444

Lunar physical libration measurement from Apollo laser experiment with retroreflectors, assessing obtained data

14 p2154 A72-30516

Optical anisotropy effects in birefringent materials by reflected shadow method and extension of theory for constrained zones around cracked plates under plane stress

14 p2167 A72-30905

Circularly polarized photon echo decay measurement as function of Cr concentration in ruby, noting relationships to temperature, pulse separation and external magnetic field

15 p2295 A72-32545

Light transmission, reflection and environmental problems of hydrophilic coatings for fog and frost protection in aviation instrument window design

22 p3196 A72-42519

Sunlight scattering by double reflection on rough and absorbing surfaces, deriving fractional circular polarization from models for comparison with observation

23 p3334 A72-43254

OPTICAL RESONANCE

Gas lasers application to precise length measurements via absorbing medium resonance determined wavelength

04 p0530 A72-14734

Neon lower laser level spontaneous emission double resonance phenomena, discussing depopulation rates and resonance line profile changes

04 p0531 A72-15138

Optical resonators using lossy anisotropic metal film linear polarizer for oscillation mode selection [CLEA PAPER 6.3]

07 p1004 A72-19382

Quasar 3C 273 light variation periodicities search, noting confidence level concerning resonance periods

07 p1073 A72-19424

Diffraction losses and corrections for lower order transverse modes and resonance conditions in optical resonators with cylindrical mirrors

08 p1133 A72-21371

He-Ne laser with absorption cell, investigating high contrast power resonances due to Lamb dip at nonuniformly broadened absorption line center

11 p1649 A72-26340

Jones matrix method for polarization natural states, frequencies and mode losses calculation in anisotropic optical resonators

11 p1688 A72-26347

Power resonance and frequency stabilization of gas laser with nonlinear absorption cell, considering He-Ne laser with Fabry-Perot resonator
12 p1820 A72-27584

Singly and doubly resonant pulsed optical parametric oscillators driven by time-dependent pump, deriving output power rise time by steady state analysis
12 p1792 A72-27751

Resonant interaction and self transparency effect of coherent ultrashort light pulse passing through semiconductor
12 p1824 A72-27868

Laser resonator transverse and longitudinal mode selection techniques, considering single frequency stabilization, gain saturation theory and applications
12 p1826 A72-27964

Coherent laser light propagation in resonance media with level splitting, determining Lorentz and broadened resonance lines
13 p1969 A72-29515

Spectral line profile of optical transition spontaneous radiation during resonance with strong field on adjacent transition
14 p2110 A72-30781

Hg vapor absorptivity dependence on wave number, atomic density and temperature in 2537 A resonance line region, discussing measurement by magnetic scanning or monochromator
14 p2131 A72-30853

Spiking response of luminescent diode pumped CW Nd-YAG laser to sinusoidal modulation, showing agreement with relaxation oscillation resonance prediction
15 p2250 A72-32526

Resonant interaction and self transparency effect of coherent ultrashort light pulse passing through semiconductor
16 p2403 A72-33977

Excitation of a confocal spherical laser resonator.
19 p2810 A72-37403

Balloon-borne UV spectrophotometer observation of Mg II resonance doublet at 2795 and 2802 A in stellar spectra, comparing to Ca II line widths
20 p2965 A72-38907

Unstable resonator theory with geometrical optics and diffraction approximation, applying to laser mode selection and beam divergence reduction
20 p2932 A72-39501

Organic dye laser molecular sublevel relaxation effects on steady state pi pulse behavior and spectral hole burning from resonance radiation propagation analysis
20 p2932 A72-39503

Investigations on spectroscopy by nonlinear Zeeman-resonances of a multimode laser.
20 p2934 A72-39845

Book - Introduction to optical electronics.
23 p3295 A72-43650

3.39 micron resonance line absorption in shocked methane.
24 p3410 A72-45044

OPTICAL RESONATORS
U LASERS
OPTICAL SCANNERS
NT FLYING SPOT SCANNERS
NT MULTISPECTRAL BAND SCANNERS
Global satellite horizon-scanning monitoring technique permitting scattered solar radiation horizon profile conversion into aerosol vertical distribution
[AIAA PAPER 71-1111] 01 p0058 A72-10555

Green and blue-green algae reflectance and transmittance characteristics, selecting spectral bands for multispectrum scanning of algal suspensions in water bodies
02 p0213 A72-11857

Bulk data storage and retrieval with scanning laser and electron beams, discussing spot formation focal sensitivity, noise, beam deflection, speed and media environment
[IEEE PAPER 19,2] 03 p0368 A72-13775

Oscillating slot-and-bar and sinusoidal reticle scanners for measuring optical image velocity
03 p0326 A72-14202

German monograph on sky scanner for short term sky spectral density distribution using glass fiber bundles for spectral components simultaneous measurement
07 p0983 A72-19266

Photometer using rotating wedge interference filter as wavelength scanning element near 6300 A for high altitude sounding rocket application
07 p0985 A72-19403

Design and operation of scanning laser based on exciting electron beam directional variation, discussing laser characteristics for various operating modes
08 p1182 A72-21268

Systematic errors in scan-and-measure devices for tracking camera photographs analysis, discussing correction during measurements
08 p1209 A72-21913

Space astronomy experiments with TV scanning, discussing data from Telescope catalog of UV observations and photometric and astrometric accuracy
08 p1170 A72-21957

Laser beams cross-sectional power distribution measurement by spinning disk scanner, using dual beam oscilloscope for laser beam profile display
10 p1489 A72-23949

Optical TV scanning for wind tunnel model position detection in magnetic suspension system for sphere low density drag measurements
[ONERA, TP NO. 988] 10 p1461 A72-24764

Lick observatory image-dissector scanner for faint astronomical spectra, describing design and performance of system based on individual photon pulse counting and memory storage
11 p1631 A72-25691

Image tube scanner photon loss probability, considering effects of system gain, aperture time and sweep rate via computer simulation
11 p1631 A72-25694

Long wave radio and acoustic holograms recording by complex scanning for transmission over communication channels
11 p1636 A72-26714

Photosensor aperture shape and line scan spacing effect in reducing facsimile camera aliasing
12 p1807 A72-27408

Astronomical spectroscopy using ultravariable resolution single Fabry-Perot interferometer in tandem with echelle Hilger monochromator
12 p1811 A72-27942

High speed and resolution laser scanning by optomechanical methods, discussing theoretical bandwidth, resolution limits, position error correction measures and performance optimization
15 p2248 A72-32037

High speed facsimile transmission system based on LR70 laser scanner, presenting typical system output image
15 p2248 A72-32041

High-speed image scanning devices using acoustic surface waves and photodiode array.
18 p2658 A72-36267

Generalized multi-dimensional sampling theory and applications in optical systems.
18 p2672 A72-36333

Epipolar scanning to convert image correlation from two dimensional to one dimensional task for application to photogrammetric automation
18 p2691 A72-36492

Remotely sensed data processing by scanner/printer designed for photograph scanning, geometric correction and photographic printing of corrected image
18 p2691 A72-36495

Early data from the ultraviolet sky-scan telescope in the TD1 satellite.
19 p2857 A72-37524

A system for programmed control of the motion of the carriage of a microphotometer along two coordinates
19 p2801 A72-37966

Improvements in electro-optic circular-scan deflectors.
21 p3050 A72-40146

Pressure-scanned echelle grating plus Fabry-Perot stellar spectrophotometer.
21 p3053 A72-40609

Use of air bearings in the construction of a scanning Fabry-Perot interferometer.
21 p3054 A72-40621

Effect of the video signal shaping mechanism in a photosensitive scanistor sensor on the optical data processing accuracy
21 p3058 A72-41735

A fast opto-electronic transducer
22 p3180 A72-42944

A new approach to automatic scanning of contour maps.
22 p3174 A72-43024

Optical considerations for an acoustooptic deflector.
23 p3288 A72-43885

OPTICAL SENSORS
U OPTICAL MEASURING INSTRUMENTS
OPTICAL SIGNALS
U OPTICAL COMMUNICATION
OPTICAL SPECTRUM
U LIGHT [VISIBLE RADIATION]
OPTICAL THICKNESS
Electron energy equation and recombination radiation loss for atomic radiating optically thin plasmas, using Kramers-Unsöld approximation
01 p0106 A72-10097

Invariant imbedding theory of aerosols multiple scattering induced telephotometric errors, determining scattering coefficients relative to optical thickness by Monte Carlo method
[AIAA PAPER 71-1062] 01 p0066 A72-10531

Energy-momentum tensor for radiation and radiative viscosity in optically thick matter having Thomson scattering with photon absorption and emission processes
01 p0129 A72-10798

Optically thin radiation effects on local heat transfer in gas flow narrow duct thermal entrance region, presenting Nusselt number variations terms for uniform and parabolic velocity profiles
02 p0303 A72-12321

Martian atmosphere and surface, covering atmospheric composition, optical thickness and pressure, violet and yellow clouds, surface relief and topography
02 p0282 A72-12326

Saturn radio emission and brightness temperature measurements, determining rings optical thickness upper limit
03 p0438 A72-13977

Weak D type ionization waves stability in optically thick plasma layer behind front of interstellar gas
05 p0715 A72-16210

Radiation intensity angular distribution from optically thick plane cloud layer reflection, relating photon survival probability and scattering functions
06 p0807 A72-17939

Multilayer heat reflective coating optical thickness effect on temperature distributions, taking into account interlayer contact resistance and thermal radiation volume absorption
06 p0904 A72-18511

Total flux and polarization of solar S-component at mm wavelengths, obtaining radio source optical depth by evaluation of QL propagation based on magnetotonic theory
07 p1069 A72-19080

Atmospheric aerosols optical thickness evaluation from solar radiation integral intensity
07 p1031 A72-19855

He ionization and excitation in optically thick solar prominences, considering recombination excitation for observed triplet-level populations at 5000-10,000 K electron temperature
08 p1231 A72-21123

Scattered light coherence in optically thin vapors and ideal gases in energy level crossing experiment formulated in terms of autocorrelation function
08 p1206 A72-21294

Martian violet clouds photometric studies, determining monochromatic albedo, optical thickness and Junge parameter
08 p1237 A72-21827

Luminous filaments model of density condensations optically thick to ionizing radiation in planetary nebulae
10 p1550 A72-25197

Monte Carlo random walk methods for directional emittance of one dimensional absorbing-scattering slab with reflecting boundaries, considering refractive index, optical thickness and albedo
[AIAA PAPER 72-309] 11 p1743 A72-25243

Atmospheric carbon monoxide and nitrous oxide telluric line contours and line centers optical thickness, measuring solar radio emission transmissivity
11 p1628 A72-26881

Radiation propagation in optically thin anisotropic noncrystalline media, obtaining explicit formulas for Stokes parameters of transmitted and scattered radiation
12 p1865 A72-27052

Anisotropic light scattering layer radiation intensity dependence on optical coordinate, obtaining integral equations for seminfinte and finitely thick layers
13 p2001 A72-28502

Asymptotic and exact methods for light scattering problems in radiative transport theory, discussing finitely thick plane layer luminescence
13 p2001 A72-28503

Martian atmosphere and surface, covering atmospheric composition, optical thickness and pressure, violet and yellow clouds, surface relief and topography
13 p2039 A72-29210

Total line intensities interpretation from optically thin gases, considering matter partitioning bivariate distribution function and chemical composition
13 p2008 A72-29930

Sunspot area east-west asymmetry dependence on location in chromospheric facula or plage, considering solar atmosphere optical and geometric depth changes
15 p2318 A72-32787

Optically thick plasma temperature profile determination by extended brightness emissivity method
16 p2440 A72-34100

On the dependence of the linear velocity of solar rotation on latitude and optical depth.
17 p2607 A72-35076

Source function for radiative fields produced by uniform parallel irradiation of scattering absorbing medium of finite optical thickness, using radiative transfer linearity
19 p2834 A72-37837

Absorption line profile and equivalent line width derivation for planetary atmosphere with low and high optical thicknesses, assuming arbitrary scattering coefficients
19 p2863 A72-38071

Atmospheric carbon monoxide and nitrous oxide telluric line contours and optical thickness in line centers, measuring solar radio emission transmissivity
20 p2919 A72-39568

Asymptotic theory of an optically thick radiating gas flow past a smooth boundary at moderate radiation strength.
21 p2989 A72-40196

- Transparent film thickness, refractivity and birefringence measurements by white light interferometric gage, noting performance insensitivity to chemical composition, film temperature and haze level
21 p3053 A72-40601
- Method of calculation of the emission coefficient of a cylindrical plasma starting from the experimental profile of the intensity
21 p3092 A72-41198
- Steady radiating gas flow past a semi-infinite flat plate at a constant temperature for an optically thick case.
21 p3131 A72-41497
- Connection of the brightness indicatrices with the optical thickness of the atmosphere
22 p3200 A72-41874
- Determination of the optical thickness of polymer fracture surface layers from interference phenomena.
23 p3307 A72-44317
- Transfer effects on X-ray lines in optically thick celestial sources.
24 p3435 A72-44843
- Radiation propagation in optically thin anisotropic noncrystalline media, obtaining explicit formulas for Stokes parameters of transmitted and scattered radiation
24 p3425 A72-45705
- OPTICAL TRACKING**
- Southern radio sources optical identification by photography using fiber optics image tube
02 p0285 A72-12795
- Satellite tracking by combined optimal estimation and control techniques with Kalman filter, considering radio antenna and optical tracking systems
02 p0285 A72-12812
- Moving display visibility effect on pilot tracking performance, discussing dependence on illumination intensity and color
04 p0477 A72-14445
- Alcohol ingestion effects on tracking performance during angular acceleration, observing nystagmic eye movements and eye-hand coordination
04 p0477 A72-14474
- International Satellite Geodesy Experiment based on laser telemetry technique, discussing ground stations network and tracking cameras
04 p0520 A72-15726
- Automatic optical tracking instrumentation at rocket launching station Tanegashima, describing automatic cinephotodolite
06 p0795 A72-17432
- Horizontal and vertical eye motions temporal relations in tracking light spot, discussing saccadic system orthogonal interaction mechanism
06 p0761 A72-17601
- GEOS satellite orbit determination and prediction errors from optical tracking systems and gravity models, estimating resonant coefficients
06 p0877 A72-17653
- Moving target resolution threshold in retina, discussing visual acuity relation to target angular velocity during ocular pursuit
07 p0926 A72-19029
- Dynamic visual acuity and eye movement data for moving targets, deriving retinal target image position and velocity errors during ocular pursuit
07 p0926 A72-19030
- Moving visual stimuli apparatus with independent control over size, shape, background intensity, orientation and velocity of motion, describing cat neuronal sensitivity studies
07 p0926 A72-19032
- Afterimage apparent motion preceding smooth eye movement association with target tracking, noting unequal impairment occurrence over entire visual field
07 p0927 A72-19034
- Control optimization of pulsed laser automatic tracking system, analyzing angular and temporal distribution of signals
07 p0942 A72-19386 [CLEA PAPER 9,4]
- Satellite angular coordinates determination by laser ranging from single station, using echo recording by Schmidt telescope
07 p0947 A72-20255
- Tracking efficiency of laser telemetry on reflector carrying satellites
07 p0947 A72-20259
- Tracking efficiency calculation for laser telemetry with laser reflector on nonstabilized satellite
07 p0947 A72-20260
- Laser tracking of magnetically and gravity gradient stabilized satellites, noting latitude effect on efficiency
07 p0947 A72-20263
- Laser ranging techniques application to ground baseline measurements, discussing maximum range of satellites tracking laser system
07 p0947 A72-20264
- Lidar application to aircraft and missile tracking and ranging, describing results obtained with ONERA experimental equipment
10 p1436 A72-24655
- Rotating mirror image position sensor for high angular resolution optical tracking, discussing performance

improvement by computer generated variable density spatial filter
11 p1591 A72-25312

Laser tracking measurements of distance to light reflector mounted on Lunokhod 1, describing equipment and procedure
12 p1825 A72-27888

Circadian rhythms of visual accommodation responses and physiological correlations during target tracking, recording monocular focus state by IR optometer
12 p1767 A72-28306

Semiautomatic tracking device for satellites comprising laser telemetry equipment
13 p1939 A72-29674

Eye movements and dynamic visual acuity as function of tracking velocity, analyzing pursuit and saccadic component by electrooculography
13 p1912 A72-30043

Laser ranging instrument for satellite distance measurement, discussing four-axial mounting, guiding telescope, receiving optics and performance
15 p2247 A72-31935

Transverse wind self-induced thermal lens effects on target image quality in laser beam tracking systems
15 p2249 A72-32164

Effects of different alcohol dosages and display illumination on tracking performance during vestibular stimulation.
17 p2508 A72-34554

Laser systems.
17 p2562 A72-34567

Nonholographic coherent optical correlation for automatic stereoperception.
18 p2691 A72-36493

Investigation of the atmospheric boundary layer and clouds by the laser tracking method
18 p2698 A72-36969

Visual optical system evaluation from viewpoint of human operator target detection under field conditions in terms of resolution, transfer functions, aberration and eye movements
20 p2893 A72-39041

An assembly for studying the perceptive motor reactions of man under one-dimensional follow-up conditions
21 p3008 A72-40810

Fluid velocity measurement of oscillatory flow generated from vortex shedding by laser Doppler system, discussing frequency tracker design, continuous detection problem and application
22 p3178 A72-42677

Automatic acquisition and tracking system for laser communication.
23 p3265 A72-44176

Optoelectronic flight path tracking systems
24 p3380 A72-45274

OPTICAL TRANSITION

Gas dynamic lasers theory based on two fluid model of optically active medium, investigating medium velocity effect on lasing mechanism
01 p0081 A72-11210

Optical and inner shell X ray transitions in highly ionized Cu, Fe and Ti observed from point plasma source generated in linear vacuum discharge
09 p1360 A72-22833

Semiconductor laser threshold current dependence on doping degree and temperature based on optical transition model and energy band theory
11 p1647 A72-26327

Optical interband transition energies in Ni and Ni based alloys, measuring light conductivity at various spectral energies
13 p1976 A72-28904

Photoelectric emission usefulness for investigation of energy parameters and optical transitions of semiconductor surfaces
15 p2276 A72-31865

CW laser transitions in singly ionized Te vapor spectrum at 4843-9378 Å, indicating charge transfer as dominant excitation mechanism
16 p2401 A72-33394

Stable single frequency Ar laser radiation with coupled transitions emission
16 p2403 A72-33709

The use of known helium line cross sections for investigation of unknown transition in neon.
18 p2713 A72-36954

OPTICAL WAVEGUIDES

Optical waveguide maximum length determination based on self focusing pulse channel growth rate relationship to striction nonlinearity
12 p1823 A72-27619

Dielectric slab surrounding medium gain effects on bound modes amplification via estimation of evanescent surface wave interactions in optical waveguide by perturbation theory
21 p3062 A72-40605

Hybrid digital transmission systems based on optical fiber waveguides and analog repeaters, noting YAG laser light modulation by phase shift keyed sub-carrier
21 p3018 A72-40868

Fundamental transverse electric field /TE-sub 0/ mode selection for thin-film asymmetric light guides.
22 p3186 A72-42622

Self focusing effect on wave beam propagation in optical lens waveguides, discussing system nonlinearity
22 p3186 A72-42656

Evanescent-field-pumped dye laser.
23 p3296 A72-43816

OPTICS

Objects optical granularity in diffuse coherent light, noting similarity to image formation in diffuse incoherent light
01 p0073 A72-11313

Symmetrical three component pancreatic system with intermediate constant image plane and linear displacement of components
03 p0360 A72-13562

Isoplanatic instrument wave aberration determination, using longitudinal defocusing
03 p0360 A72-13563

Book on optics covering gas lasers, power output vs frequency, picosecond laser pulses, Q switching principles, mode locking, optical propagation through turbulent atmosphere, etc
04 p0548 A72-14733

Book on holographic technology covering fundamentals of holography and classical optics, diffraction theory, Huygens principle, lasers, illumination sources, holographic interferometry, etc
04 p0522 A72-15271

Inverse scattering by ray optics for conducting wedge, considering TE and TM edge diffracted fields
04 p0551 A72-15671

Herzberger fundamental optical invariant for rotationally symmetric systems, using partial differential equations [AD-738406]
05 p0690 A72-16672

Atmospheric heating and kinetic cooling nonlinear effects on IR carbon dioxide laser beam propagation, comparing digital simulation results with geometrical optics [CLEA PAPER 2,6]
07 p0942 A72-19381

Homogeneous isotropic Newtonian and Robertson-Walker cosmological models, discussing radiative transfer and optics
07 p1074 A72-19431

Digitized SEC vidicon detector for OSO-H satellite coronagraph, describing optics
08 p1170 A72-21959

Learning systems mathematical scheme to identify classes invariant with respect to transformation groups, realizing functionals with coherent and incoherent optics
09 p1282 A72-22218

Physical optics approximation study of gravitational waves effect on electromagnetic propagation, noting unobservability of local scintillation effect
09 p1351 A72-22683

Optical mirror method for bending strains study in welding cycles with applications to sheet metal thermal stress strain rates
09 p1318 A72-22738

Zeiss aerial photographic lens systems imaging quality characteristics in visible and near IR spectral ranges
09 p1313 A72-23311

Laser beam induced thermal blooming in absorbing gases from combined fluid dynamics and eikonal geometric optics theory, considering wind effects
09 p1352 A72-23333

Diagnostic procedures for nonhomogeneous plasma based on geometrical optics approximation, irradiating plasma by plane wave at oblique incidence
13 p2013 A72-29295

Iterative-zonal method for radiative heat transfer calculations with capability to numerically determine radiation characteristics of optically and energetically homogeneous zones
13 p2065 A72-29643

Holographic virtual image formation and magnification by classical geometrical optics laws application, deriving equivalent law of refraction
16 p2392 A72-33599

German Book - Introduction into nonlinear optics, Volume 1
19 p2813 A72-38775

Atmospheric turbulence induced optical effects due to refractive index fluctuations, solving Maxwell equations for instantaneous intensity distribution function
20 p2948 A72-39055

Unstable resonator theory with geometrical optics and diffraction approximation, applying to laser mode selection and beam divergence reduction
20 p2932 A72-39501

Geometrical optics approximation for angular error calculation of microwave antenna radome, noting boresight error proportionality to walls electrical thickness
23 p3271 A72-43837

Geometrical interpretation of Gaussian beam optics
23 p3288 A72-43877

Ray optics applications to electromagnetics and other disciplines, discussing matrix representation for wavefront curvature and field computation simplification via transformations 23 p3314 A72-44331

Future giant-aperture orbital space telescope design based on active optics and electro-optical techniques, discussing laser interferometry and precise servomechanisms roles 24 p3405 A72-45544

OPTIMAL CONTROL

NT TIME OPTIMAL CONTROL

Soviet book on reliable logic units design covering adaptive redundant and nonredundant control systems, threshold functions, optimal adaptation algorithms, restoring circuits, etc 01 p0033 A72-10296

High order optimality conditions of singular controls, considering Pontryagin maximum principle, Bellman dynamic programming and functional analysis 01 p0044 A72-10297

Optimal control algorithm for spacecraft descent in atmosphere at speed near escape velocity, using game theory 01 p0135 A72-10298

Optimal metric programmable high speed sequential decoder for convolutional code deep space channels 01 p0026 A72-10340

Optimal control of material point motion in thin spherical layer of central gravitational field, solving by approximation 01 p0127 A72-10355

Optimal flight of material point in central field of forces subject to controlled small thrust 01 p0127 A72-10356

Optimal control for thrusting rocket guidance with controllable steering angle rate during insertion into circular orbit, using flat earth approximation 01 p0097 A72-10383

Multidimensional variable structure systems synthesis for automatic optimization of inertialless technological plants in presence of constraints 01 p0045 A72-10498

Gradient method for optimization control system construction with cross couplings between channels 01 p0045 A72-10501

Closed linear systems optimal stabilization determining transfer function from Wiener Hopf equation 01 p0045 A72-10572

Minimum propellant impulsive optimal spacecraft guidance and trajectory problem, developing deterministic theory in discrete linear quadratic form with second order perturbation analysis 01 p0130 A72-10929

Step width for gradient projection method in Hilbert space for optimal linear control problems with quadratic functional 01 p0047 A72-11386

German monograph on maximum principle application to optimum control of discrete problem 02 p0197 A72-11741

Jacketed tubular chemical reactor optimal startup control, presenting distributed maximum principle for diffusional parameter system 02 p0301 A72-12093

Optimal stabilization of permanent rotation of solid body with arbitrary mass distribution by controlled gyroscope 02 p0230 A72-12337

Optimal stabilization law for ensuring gyroscope equilibrium position asymptotic stability in rms error, aperiodicity and system transient response time 02 p0230 A72-12338

Extremal system with second control loop for search signal frequency regulation to optimize primary loop operation, determining system dynamic errors under random drift 02 p0197 A72-12340

Stochastic linear-quadratic-Gaussian problem role in optimal closed loop control system design, emphasizing philosophy, modeling and problem formulation [AD-738763] 02 p0198 A72-12801

Linear and quadratic programming procedures in optimal control problems of stochastic and deterministic system design 02 p0198 A72-12807

Discrete-time linear quadratic stochastic control system with perfect measurements of state, obtaining optimal solution by dynamic programming 02 p0198 A72-12808

Satellite tracking by combined optimal estimation and control techniques with Kalman filter, considering radio antenna and optical tracking systems 02 p0285 A72-12812

Bibliography on linear-quadratic-Gaussian problems covering quadratic criteria, state estimation, stochastic control, computations and applications 02 p0198 A72-12813

Optimal control algorithm synthesized from linear sampling theory for inertial platform alignment, requiring systematic error free optimal digital computer 02 p0258 A72-12899

Linear multivariable interacting feedback control system optimal design by heuristic approach to determine input-output pairing and controller settings for satisfactory disturbance attenuation 03 p0337 A72-12905

Pulse shaped small parameter variation effects on performance index of minimum fuel control systems with initial and final manifolds 03 p0337 A72-12906

Neighboring optimal feedback control for multiinput nonlinear dynamical systems with discontinuous control, applying to minimum time satellite attitude acquisition problem solution 03 p0338 A72-13407

Weak solutions of degenerate partial differential equation of dynamic programming, investigating relation to value function of stochastic optimal control problem 03 p0382 A72-13701

Analytic solution for optimal control circular orbit escape with constant thrust rocket, using Euler-Lagrange equations and perturbation technique 03 p0347 A72-13839

Approximation method for determination of distributed parameter systems optimal control, considering state and control variable constraints 03 p0338 A72-13917

Finite memory uncertain stochastic controller, developing optimal and suboptimal algorithms 03 p0329 A72-14181

Numerical method and computerized design for feedback controller pulse transfer function in overall error criterion minimization, comparing results with sampled error method 03 p0329 A72-14355

Optimization programs for linear control systems with nonconvex constraints on phase coordinates applied to material point transfer 04 p0504 A72-14624

Closed-loop temperature distribution optimal control by heater-sensor spatial configuration design for highest steady state temperature stiffness under heat flux disturbance 04 p0504 A72-14661

Iterative procedure for computing optimal controls in distributed parameter systems described by linear parabolic differential equations, applying to metal slab temperature profile problem 04 p0504 A72-14664

Dual variational principles application to distributed parameter system suboptimal control strategy evaluation, considering control variable and feedback gain as piecewise function of time 04 p0505 A72-14665

Distributed parameter control system optimal control problems, formulating existence with minimum norm technique 04 p0505 A72-14667

Kalman type optimal filter for linear distributed-parameter systems under white Gaussian and boundary noise, obtaining Wiener-Hopf equation by calculus of variations 04 p0505 A72-14668

Linear distributed parameter system optimal boundary control by direct method using linear combination of finite number of orthonormal functions 04 p0505 A72-14670

Discrete system high order optimality sufficient conditions and methods for singular and nonsingular controls study 04 p0505 A72-14996

Control system synthesis from transient process estimates with Liapunov functions, proposing optimality criteria based on Gaussian minimum constraint principle extension 04 p0505 A72-14997

Extremal problems of natural vibration spectrum optimal control in mechanical systems with constraints, using mathematical programming methods 04 p0586 A72-15004

Suboptimal nonlinear filter performance evaluation methods based on Kolmogorov equations for Markov process transition density function 04 p0505 A72-15040

Minimal order precompensator with state feedback for decoupling linear time-invariant multivariable control system, discussing design parameters determination from linear equations 04 p0506 A72-15109

Optimal control systems with terminal state constraints, presenting algorithm based on constraint-space conjugate gradient method for function minimization 04 p0506 A72-15111

Nonlinear plant and observation models with white Gaussian noise and continuous data, obtaining state vector a posteriori probability density for optimal prediction 04 p0506 A72-15112

Large linear time invariant dynamic control system optimum simplified model based on performance index connecting feedback errors 04 p0506 A72-15113

Detection characteristics of optimal interperiod processing radar pulse systems for arbitrary correlation of signal and noise fluctuations 04 p0487 A72-15145

Optimal detection of Markov radio signals with intrapulse FM using nonlinear filtration theory 04 p0487 A72-15146

Optimal two stage signal search in frequency vs arrival time indeterminacy plane of communication system 04 p0487 A72-15148

Necessary conditions for inequality-type mixed constraint optimal control, using abstract multiplier rule for Banach space of continuous and bounded measurable functions 04 p0506 A72-15201

High speed helicopter elastic rotor blade suboptimal motion controller decreasing flapping motion and bending loads despite small control angles and vertical gusts 04 p0465 A72-15504

Electric network scattering matrix and associated incident and reflected wave variables concepts applications in linear optimal control problem 04 p0507 A72-15528

Optimal control of linear systems /continuous and discrete/, using quadratic performance criterion 04 p0507 A72-15667

Adaptive control algorithm with disturbance prediction for solution of deterministic and stochastic optimization problems of linear equation of state and quadratic performance criteria 05 p0639 A72-15759

Distributed parameter state regulator system, investigating order of spatial discretization error in finite difference approximation to optimal response, control and performance cost 05 p0639 A72-15805

Optimal digital Kalman filtering for systems with continuous input noise by autocorrelation function matching [ASME PAPER 71-WA/AUT-21] 05 p0640 A72-15952

Computational algorithm for optimal control problem with variable terminal point constrained on state space surface, using iteration technique for satisfying transversality condition [ASME PAPER 71-WA/AUT-6] 05 p0640 A72-15957

Quasi-steady continuous process adaptive optimal control, discussing algorithms and model for sensitivity matrix calculation and digital simulation for strategy 05 p0640 A72-16200

Optimal dynamic system design for maneuvers with complete statistical information applied to limited power space flight 05 p0641 A72-16313

Optimal control synthesis for linear systems with quadratic functional under random white noise 05 p0641 A72-16314

Apollo lunar roving vehicle design requirements based on environmental conditions, emphasizing wheel drive control and steering systems optimization and navigational instrumentation 05 p0643 A72-16428

Spacecraft reentry trajectory parameter selection and optimal control algorithm under random atmospheric density variation 05 p0685 A72-16429

Airborne computer programmed adaptive optimal control for subsonic vehicle automatic landing with aerodynamic performance 05 p0685 A72-16430

Nonlinear and digital synthesis of computerized optimal control systems for long-life orbital stations and laboratories 05 p0724 A72-16434

Meteorological satellite stabilization and attitude control in synchronous equatorial orbit for two years life, emphasizing nutation damper optimal dynamic characteristics 05 p0725 A72-16437

Missile trajectory stochastic optimal control systems with fuel constraint by mean path deviation optimization 05 p0725 A72-16452

Nonlinear multivariable and linear systems optimal control in aerospace field, discussing use of performance indexes for fuel consumption, process evolution time or combination 05 p0725 A72-16453

KS-transformation based regularization technique modification for minimal fuel consumption rocket trajectory control during space maneuver 05 p0726 A72-16454

Optimal control problem formulation as nonlinear two point boundary value problems, comparing linear systems and Riccati equations for solution 05 p0726 A72-16455

Optimal closed loop control of stochastic nonlinear systems by expanded cost function applied to reduced terminal error atmospheric entry problem 05 p0685 A72-16462

Hierarchically structured man machine control systems synthesis, outlining iterative procedure for optimizing functional

05 p0727 A72-16471

Optimization algorithms for jet transport aircraft inertially based flight trajectory control in turbulent atmosphere, comparing with ILS

05 p0685 A72-16472

Penalty function method validity for singular solutions to optimal trajectory control problems with state variable inequality constraints

05 p0641 A72-16531

Optimality conditions for safe time in linear pursuit problems within n-dimensional Euclidean space

05 p0683 A72-16584

Control system design computerized optimization technique based on high speed repetitive simulations and gradient minimization, considering application to reusable and expendable boost vehicles

[AIAA PAPER 72-98]

05 p0729 A72-16812

MHD Couette flow stochastic processes optimal control synthesis by dynamic programming

05 p0653 A72-17131

Optimal averaging of control in distributed random parameter system described by hyperbolic partial differential equations, considering boundary values on characteristics as control functions

05 p0683 A72-17133

Statistical solution of analytical design of optimal control system maintaining coarseness/universality/with minimum quality loss

05 p0691 A72-17135

Optimal control of system described by parabolic partial differential equations with constraints on change rate of boundary conditions

05 p0683 A72-17137

Optimal control of one dimensional physical system with delayed argument described by nonlinear first order hyperbolic partial differential equations, using maximum principle

05 p0691 A72-17138

Optimal control of systems described by stochastic differential equations with delayed argument, using Kozhevnikov mean principle

05 p0683 A72-17140

Optimal control algorithm for nonlinear stochastic systems ensuring probability-wise stability and minimum error, using Liapunov theory and dynamic programming

05 p0691 A72-17141

Minimal energy stochastic controller design for electrically driven vehicles, using dynamic programming

06 p0795 A72-17304

Adaptive control for linear discrete time stochastic systems with unknown gain parameters, considering open loop feedback optimal control using quadratic performance index

[AD-739126]

06 p0791 A72-17305

Optimally sensitive closed loop control synthesis for systems containing uncertain time varying parameters, applying to stochastic systems

06 p0792 A72-17309

Linear time-varying control system synthesis for specific input and maximum admissible error, considering various weighting functions and constraints

06 p0792 A72-17311

Suboptimal feedback control for nonlinear dynamic processes, presenting control algorithm based on linear plant optimal solution

06 p0792 A72-17314

Optimal linear multivariable control systems design with prescribed eigenvalues, presenting method for corresponding weighting matrix elements

06 p0792 A72-17315

Optimum adaptive variable step size delta modulator-demodulator producing minimum error for Markov-Gaussian source

06 p0772 A72-17404

Second variational algorithm for iterative solution of unconstrained optimal control problems, examining linearized feedback control

06 p0839 A72-17592

Extremal field properties in optimal control problem applied to aircraft flight over assigned distance with minimum fuel consumption

06 p0758 A72-17727

Regularization theorems for epsilon solutions to Bellman functions in optimal quick response problems

06 p0847 A72-17728

Control, prediction and risk optimization in scheduling problems with incomplete random information

06 p0793 A72-17729

Conjugate gradient iterative method for optimal control problems with state variable constraint, noting optimal trajectory cases

06 p0793 A72-17953

Optimal final value control systems in phase-variable canonical form, discussing feedback gain singularity structure for single and multiple input systems

06 p0793 A72-17954

Discrete stochastic differential games with quadratic payoff function, deriving deterministic, randomized and game optimal control strategies

06 p0793 A72-17956

Suboptimal security solution of linear quadratic pursuit evasion game with state dependent, control dependent and additive noises, deriving equations for state estimation

06 p0794 A72-18151

Suboptimal stochastic control strategies class based on game theory and optimin principle, investigating completeness in closed discrete-time systems

06 p0794 A72-18167

Optimal control systems synthesis with allowance for given reliability, finding extremal value of quality function with constraint on probability of fail-safe operation

06 p0794 A72-18305

Stochastic optimal control for operations of plants with pure lag and two point estimate of performance index investigating systems stability

06 p0795 A72-18662

Optimal control of hydromagnetic flow of electrically conducting fluid in equilibrium cylindrical configuration, using dynamic programming method

07 p1040 A72-18980

Optimal control of distributed parameter systems with incomplete state information by dynamic programming and Liapunov methods

07 p1034 A72-18981

Time behavior of single axis gyro platforms, considering linear and nonlinear-suboptimal control

07 p0983 A72-19169

Real time near optimal closed loop control solution to fixed time nonlinear differential game by periodically updating to two point boundary value problem

07 p1027 A72-19278

Optimal thrust reversing in pursuit evasion games between two aircraft in horizontal plane, considering cost functions and termination criteria

07 p0912 A72-19282

Multiinput and multioutput linear and nonlinear dynamic system maximum likelihood identification based on state vector formulation and optimal filter use

07 p0959 A72-19286

Aircraft optimal terminal guidance nonlinear feedback control law, deriving maximum principle by digital computer program

07 p1033 A72-19287

Approximating trajectory solution to state constrained optimal control problems, discussing convergence

07 p0959 A72-19289

Dynamic programming for optimal stochastic control problem with Gaussian shot noise involving parabolic or elliptic differential equation in unbounded domain, discussing iterative solution and quasi-linearization

07 p1027 A72-19292

Control optimization of pulsed laser automatic tracking system, analyzing angular and temporal distribution of signals

[CLEA PAPER 9.4]

07 p0942 A72-19386

Dynamic control system parameters optimization for series of maneuvers under different degrees of informability

07 p0959 A72-19652

Minimal order controller for decoupling of linear multivariable systems with low order control devices and reduced control effort

07 p0960 A72-19697

Linear dynamic control systems controllability and observability quality analysis and optimization, considering determinant, trace and maximal eigenvalue

07 p0960 A72-19699

Linear multivariable system design based on relationship between performance index parameters and optimal response in frequency domain, exemplifying gas turbine feedback controller design

07 p0961 A72-19710

Multivariable linear systems control structure via optimal control theory with quadratic criterion, permitting compensation for nonzero mean value and slowly varying perturbations

07 p0961 A72-19711

Weighting matrices effect on optimal regulator for linear time invariant multivariable systems

07 p0961 A72-19713

Eigenvalue sensitivity in optimal feedback control systems with state estimation

07 p0962 A72-19716

Optimal control on nonlinear multivariable plant with common constraint on control action, presenting linear programming algorithm

07 p0962 A72-19717

Optimal control of lumped and distributed parameter systems with time lag, considering approach with extrapolator insertion and suboptimal solution based on system dynamic equation

07 p0962 A72-19718

Optimal control of linear multivariable plants with one or more quality criteria, considering control channels and game theory

07 p0962 A72-19720

Optimal multivariable control systems theory, considering linear programming, maximum principle and differential games

07 p0963 A72-19724

Minimax optimal control problems with incomplete information, using dynamic programming and phase space location measurements

07 p0963 A72-19970

Optimal strategies conditions for game problems in conflictingly controlled system, discussing minimax technique and Bellman equation solution

07 p1028 A72-19971

Optimal alignment and calibration of gyro-stabilized platforms, using Kalman filter and minimal weighted squared errors

07 p0989 A72-20280

Self similar invariant group solutions to Bellman nonlinear partial differential equation for optimal correction problems of control systems motion with random disturbances

07 p0963 A72-20322

Integrated systems approach to computer simulation with functional modules to achieve control processor independent expansion and optimization

07 p0951 A72-20331

Optimal test conditions in magnetoscopic control by electrical system for subsurface defects detection, obtaining tangential magnetic field on carbon steel plates

07 p0991 A72-20421

External disturbance accommodation in optimal control, based on characterization of waveform modes, applying to linear-quadratic regulator problem

07 p0963 A72-20591

Operational optimization of ion traps with dc amplifiers mounted on nonoriented earth satellite, proposing control circuit

07 p0993 A72-20664

Soviet book on optimal trajectory synthesis covering second order linear control systems analysis based on Pontryagin maximum principle and Bolyanski theory

08 p1197 A72-20750

Compensated Kalman filter as suboptimal state estimator to eliminate steady state bias errors in use with mismatched asymptotic time-invariant case

08 p1144 A72-20845

Standard linear estimation and control problem with quadratic loss, optimizing information rate by minimizing total measurements number through Riccati equation singular solution

08 p1144 A72-20859

Nonlinear filter dynamics for stochastic optimal control for quadratic cost functional, evaluating performance

08 p1145 A72-20866

Electroerosion machining with optimal control of electrical parameters, number of passes and electrode wear, using nonlinear programming and critical path method

08 p1174 A72-21032

Complex erosion machining control and optimization, investigating current and tension effects

08 p1175 A72-21042

Pontryagin maximum principle application to optimal linear filtration for multivariable systems with signal processing

08 p1133 A72-21374

Optimal controllers analytic design for linear steady controlled differential equations system

08 p1145 A72-21467

Optimal stabilization of permanent rotation of solid body with arbitrary mass distribution by controlled gyroscope

08 p1168 A72-21552

Optimal stabilization law for ensuring gyroscope equilibrium position asymptotic stability in rms error, aperiodicity and system transient response time

08 p1168 A72-21553

Extremal system with second control loop for search signal frequency regulation to optimize primary loop operation, determining system dynamic errors under random drift

08 p1146 A72-21555

Sequential reliability control and analysis in low run production with plan optimization and tests number reduction

08 p1181 A72-22069

German monograph on optimal attitude control of satellites with rotors and simultaneous spin reduction, covering motion equations for stable equilibrium and circular orbit

09 p1394 A72-22330

Optimal and quasi-optimal automatic control systems synthesis by cross section method

09 p1290 A72-22489

Optimal answer-back communications systems using feedback channel for error checking

09 p1277 A72-22568

Optimal control of two shaft gas turbine engine in helicopter, using cybernetic equipment

09 p1374 A72-22862

Epsilon technique for optimal control computation in pursuit and evasion problems, reducing dynamic to nondynamic optimization problem

09 p1342 A72-23253

Digital computer prepared optimal controls setting diagrams for single loop, linear and concentrated parameter control circuit design

09 p1291 A72-23372

Numerical algorithm for optimal coefficient equations in analytical design of complex control plants
10 p1291 A72-23426

Optimal control synthesis for linear passive stationary plants with symmetrical coefficient matrices of minimized functional
10 p1291 A72-23431

Singular control problems calculation in trajectory optimization using sufficient conditions for control values set form
10 p1291 A72-23432

Algorithms for optimal adaptive control of steady motions of single channel discrete extremal systems with independent search, studying quality functional behavior
10 p1291 A72-23437

Interplanetary spacecraft midcourse guidance stochastic control, deriving algorithm for computing optimum velocity correction and execution time with allowance for correction-dependent errors
10 p1508 A72-23778

Quadratic performance index generation for optimal design of completely controllable, scalar linear system with state feedback
10 p1454 A72-23783

Optimal probing signals design for state vector parameter estimation, considering Fisher information matrix function as optimality criterion
10 p1454 A72-23786

Differential geometric methods to extend linear system theory to nonlinear classes, considering differential equations, controllability, optimal control, stochastic processes and bilinear system problems
10 p1503 A72-23788

Nonlinear programming and parameter optimization algorithms for constrained feedback control system design
10 p1441 A72-23790

Quadratic cost, nonlinear optimal adaptive stochastic control of linear plant and measurement models excited by white Gaussian noise and with unknown parameters
10 p1455 A72-23792

Nonlinear programming solution of optimal control problems, using methods of centers and feasible directions
10 p1455 A72-23797

Recursive minimum variance linear filter and controller for systems with white state-dependent noise
10 p1455 A72-23800

Optimal nonlinear estimation problem with nonlinear plant and observation models obtaining state vector a posteriori probabilities for prediction and smoothing via partition theorem
10 p1455 A72-23803

Near optimal closed loop control laws for fixed time pursuit-evasion differential game between two aircraft in vertical plane, using dynamic modeling
10 p1421 A72-23805

Stochastic projected gradient algorithm to maximize SNR subject under linear or nonlinear constraints, applying to detector antenna array processing
10 p1456 A72-23808

Adaptive optimal antenna array detection of unknown spatial location radar targets, noting tradeoff between array size and signal energy with respect to performance
10 p1434 A72-23809

Stochastic nonlinear system one-step optimal dual control instead of separation control policy for performance improvement
10 p1456 A72-23810

Optimal closed loop control of discrete stochastic nonlinear systems, considering guidance and navigation for space and terrestrial vehicles
10 p1456 A72-23811

Optimal control computation for nonlinear hyperbolic partial differential system by gradient and quasi-linearization techniques, noting MHD, fluid flow and electromagnetic wave propagation
10 p1456 A72-24453

Modified sweep variation method for optimal control programs, solving two point boundary value problem by linear perturbation technique
10 p1551 A72-24455

Sensitivity comparison of equivalent open and closed loop optimal control systems, extending performance index formulas to instantaneous and isoperimetric constraints
10 p1456 A72-24456

Minimum fuel continuous low thrust orbit transfer problem of optimal control, solving boundary value problem with Multiple Substitution Polynomials and Marquardt method
10 p1552 A72-24486

Optimal closed loop control of discrete stochastic nonlinear systems, obtaining solution by cost function in power series around deterministic trajectory
10 p1457 A72-24499

Steady state operation of automatic control system to stabilize random vibration spectra, noting maximum control accuracy at optimum loop gain
10 p1457 A72-24635

Equivalence conditions for optimal control problems for stochastic and deterministic plants in cases of nonrandomized strategies
10 p1457 A72-24637

Adjoint control transformations advantages in optimal trajectories determination by Pontryagin maximum principle
10 p1547 A72-24879

Optimal filter for narrow band stochastic signal processing, using Wiener theory
10 p1441 A72-25103

Optimal control of linear stochastic feedback systems described by functional differential equations
10 p1458 A72-25145

Linear continuous time systems optimal dual control problem solution by reduction to partial differential equation in finite domain with suitable boundary conditions
10 p1458 A72-25170

Optimal control problems characterized by nonlinear Volterra equations system, obtaining necessary conditions for extremality in maximum principle integral form
11 p1675 A72-25319

Optimality conditions for dynamic control systems, considering multidimensional singular controls and state space transformations
11 p1608 A72-25324

Extremal field properties in optimal control problem applied to aircraft flight over assigned distance with minimum fuel consumption
11 p1574 A72-25329

Control, prediction and risk optimization in scheduling problems with incomplete random information
11 p1608 A72-25331

Optimal control design for digital guidance system, conducting efficiency and reliability analyses
11 p1600 A72-25437

Pulsed perturbation and Q coupled extremal control systems with noise distortion, obtaining optimal transfer functions with Kolmogoroff-Wiener method
11 p1610 A72-25448

Linear maximization of turbine disk natural vibration frequencies combination, solving optimal control problem via Pontryagin maximum principle
11 p1734 A72-25727

Optimal dynamic system design for maneuvers with complete statistical information applied to limited power space flight
11 p1610 A72-25796

Optimal control synthesis for linear systems with quadratic functional under random white noise
11 p1610 A72-25797

Suboptimal feedback control law synthesis for nonlinear systems, using second order approximation to optimal control
11 p1610 A72-25872

Spacecraft reentry into random medium atmosphere, determining optimal control procedure for prescribed arrival region and time with simulation equation
11 p1686 A72-25930

Spacecraft interplanetary guidance trajectory correction, deriving algorithm for optimal accuracy and minimum fuel expenditure
11 p1718 A72-25931

Flight mechanics of point with limited power propulsion system and energy storage unit, investigating variational maximum payload problem with singular control optimization
11 p1727 A72-25932

Missile tracking laws for inhomogeneous linear-quadratic performance optimization
11 p1593 A72-25992

Book on sensitivity theory covering continuous and sampled data systems, linear, nonlinear and self exciting dynamic systems, optimal systems, large systems, controllability, etc
11 p1611 A72-26021

Matrix and graphic test construction methods for optimal design of logic networks in automatic control systems
11 p1612 A72-26443

Spacecraft motion stabilization about mass center and optimal angular velocity control using minimax technique
11 p1684 A72-26903

Quadratic optimal control problem solution via multipliers method, generating minimizing convergent sequence of arcs
12 p1794 A72-27509

Classical isoperimetric problem approximation via multipliers method, generating minimizing convergent sequence of arcs
12 p1836 A72-27510

Optimal allocation of tasks and resources, using asymptotic properties of stochastic approximation method
12 p1837 A72-27823

Multiple input automata with optimal response to any input set, using maximum mean gain as criteria for response selection
12 p1787 A72-27923

Flight vehicle motion described by linear differential equations with variable parameters, discussing programmed optimal control solution by functional analysis
12 p1755 A72-28128

Suboptimal controls of linear multidimensional plants with variable parameters, considering asymptotic stability
13 p1935 A72-28609

Algorithmic method in ALGOL 60 for successive approximations of optimal control problems, discussing improved convergence
13 p1935 A72-28707

Optimizing functional for combined control of dynamic control plant, synthesizing stabilization system for maximal transient damping
13 p1935 A72-28713

Optimal algorithms for analysis, synthesis and correcting filter of self adaptive control systems
13 p1936 A72-29154

Self organizing control system for optimal performance of navigation instruments, using adaptive algorithm for statistical error filtration
13 p1996 A72-29157

Two step adaptive control of multidimensional linear static system, using first and second step ratio and optimization equations
13 p1936 A72-29159

Statistical superoptimal search strategies of self optimizing systems, applying to one dimensional step type and multiextremal problems
13 p1936 A72-29160

Optimal random search noise recognition systems with Bayes teaching technique
13 p1924 A72-29162

Algorithm for optimal strategy in statistical plant control for machine parts production and assembly, discussing measuring equipment errors effects
13 p1965 A72-29168

Optimal viability of complex system with ambient medium interaction, using stochastic game theory
13 p1936 A72-29174

Dynamic programming for optimal statistical control of self adaptive systems with fixed learning experiments, noting structural constraints for suboptimality
13 p1965 A72-29178

Optimal control systems synthesis with allowance for given reliability, finding extremal value of quality function with constraint on probability of fail-safe operation
13 p1937 A72-30073

Control optimization avoiding stability problem by integrating matrix Riccati equation
13 p1937 A72-30074

Pontryagin maximum principle for optimal terminal velocity control of automatic space probe descent in Mars atmosphere
14 p2162 A72-30456

Spacecraft optimal control after transfer from hyperbolic trajectory to planetary satellite orbit by atmospheric drag, minimizing engine thrust
14 p2129 A72-30470

Optimal filter synthesis for linear time varying parameter control systems, using computer-aided solution of multidimensional Riccati equations
14 p2090 A72-31120

Quasi-conservative optimal nonlinear self excited oscillation systems theory for automatic control, telemechanics and computer applications
14 p2133 A72-31130

Linear control systems optimal synthesis using ALGOL program for digital computers minimizing error square integral
15 p2210 A72-31687

Optimal feedback controller design based on cooperative game described by quadratic cost functional under linear differential equation constraints, applying to satellite terminal rendezvous
15 p2267 A72-31789

Suboptimal feedback control for aircraft gust alleviation design, using indirect perturbation information through normal acceleration factor measurement
15 p2181 A72-32025

Optimal controller design for parabolic type second-order linear stationary systems, discussing integro-differential equation solution possibility
15 p2211 A72-32170

Infinite dimensional system optimal discrete-time feedback controller calculation by n-dimensional system approximation using recurrence relations with functional analysis
15 p2212 A72-32245

Automatic control theory trends /1950-1970/, discussing nonlinear, discontinuous and adaptive systems, optimization problems, Liapunov stability theory, etc
15 p2212 A72-32576

Flexible launch vehicle optimal and constrained-optimal control for performance index minimization, using sensors and constant feedback gains
15 p2321 A72-32585

Random vibration optimal control by transfer function estimation, using relative phase information in cross spectral density functions to sort out self noise 15 p2215 A72-32629

Optimal state space synthesis of discrete linear computer controlled systems with quadratic cost function, using Liapunov, Pontryagin, and Bellman techniques 15 p2212 A72-32765

Sensitivity design of multiple input controller for dynamic optimization applied to linear systems with quadratic performance index 15 p2212 A72-32795

Limit set configuration of optimal nonlinear feedback control scheme in n-dimensional state space 15 p2213 A72-32797

Matrix Riccati equation solution method in optimal control theory, noting boundary conditions implementation 15 p2265 A72-32803

Optimal control of observation processes, formulating solvability conditions in terms of ordinary differential equations 16 p2370 A72-32927

Discontinuity problems in optimal control of systems describable by ordinary differential equations, deriving Weierstrass optimality conditions 16 p2371 A72-32939

Optimization of noise impeding observation of dynamic system subjected to random perturbations, discussing optimal control based on least square estimate 16 p2371 A72-33090

Perturbation extremum controller with simple coincidence logic, discussing fluidic implementation and performance in simulated plant control 16 p2350 A72-33193

Optimal invariant control system synthesis for inertial plants with nonminimal phases and random perturbation compensation 16 p2371 A72-33263

Computer algorithms for adaptive optimal synthesis of complex electronic systems, using stochastic approximation and gradient search with data storage 16 p2367 A72-33265

Optimal filtering estimate of noisy nonlinear partial differential distributed parameter system, using least squares and invariant imbedding techniques 16 p2416 A72-33575

Spacecraft free fall trajectory calculation, using numerical optimization procedure based on Hamilton principle for two point boundary value problems 16 p2460 A72-34021

Perturbation method for two point boundary value problem for fluid flow applied to optimal reentry control problem 16 p2462 A72-34166

Computational difficulties reduction in optimal control and estimation problems, discussing controllability and observability 17 p2574 A72-34417

Phase locked loop model based on AGC circuitry, devising optimum control strategies 17 p2532 A72-34419

Optimal and quasi-optimal automatic control systems synthesis by cross section method 17 p2533 A72-34652

Controllability, observability and optimal feedback control of affine hereditary differential systems. 17 p2533 A72-34950

Controlled systems with discontinuous couplings and means of optimization of their control 17 p2621 A72-35035

Control function improvement method for flight dynamics variational problems solution, discussing dynamic programming, trajectories with uncontrolled elements and coordinate transformation 17 p2607 A72-35036

Optimal deterministic guidance for bounded-thrust spacecrafts. 17 p2609 A72-35101

An automated gradient projection algorithm for optimal control problems. 17 p2576 A72-35244

Russian book on numerical methods in optimal control systems theory covering functional extremum, dynamic programming, control synthesis and statistical linearization of nonlinear systems 17 p2533 A72-35458

Optimal aerodynamic attitude stabilization of near-earth satellites. 17 p2622 A72-35488

Optimal regulator inverse problem analysis for multi-input systems with integral type performance indices, using state variable canonical form 17 p2534 A72-35527

Limit-cycle bounds of a satellite attitude-control system. 17 p2622 A72-35529

Numerical solution of an optimal control problem with a probability criterion. 17 p2534 A72-35531

Reachable sets and singular arcs for minimum fuel problems based on norm-invariant systems. 17 p2534 A72-35533

Time-optimality of a class of extremal systems with statistical signal processing 17 p2518 A72-35782

Computer control of aircraft landing. 17 p2578 A72-35950

State feedback control law for linear multiinput multioutput time-invariant dynamic system under disturbance to obtain output with zero steady state error 18 p2672 A72-36054

Stochastic optimal path selection via N discrete points set, discussing probability distributions and computer requirements 18 p2672 A72-36055

Functional relationships between the conventional steady-state error characteristics and the weighting matrices in the quadratic performance index. 18 p2672 A72-36058

Optimal temperature control for microbial inactivation by composite environment of heat and gamma radiation, using quadratic technique 18 p2649 A72-36313

Optimal signal design for digital center of gravity feedback communications over white noise channels, using energy ratio functions 18 p2659 A72-36316

Parabolic switching boundaries method for optimal fuel consumption control of manned orbital space vehicles 18 p2672 A72-36325

Second order differential guidance game, formulating strategy for optimal feedback control 18 p2673 A72-36660

Minimum fuel control of second order system in n-dimensional Euclidean space, examining Pontryagin maximum principle applicability 18 p2673 A72-36696

Optimal control of plants whose transfer functions contain zeros. 18 p2673 A72-36724

Optimality conditions in a problem of heat transfer process control 18 p2741 A72-36809

Hill-climbing controller for plants with any dynamics and rapid drifts. 18 p2673 A72-36819

Optimal control with partially specified input functions. 18 p2673 A72-36821

Optimal filtering in linear distributed-parameter systems. 18 p2673 A72-36823

Computation of optimal controls by a method combining quasi-linearization and quadratic programming. 18 p2673 A72-36824

Optimal control laws for stochastic problems involving intentional errors, caution and probing 18 p2674 A72-36825

Optimal minimal-order observers for discrete-time systems - A unified theory. 18 p2674 A72-37099

Linear stochastic system optimal measurement strategy and matched Kalman type filter computation via transformation into deterministic control problem. 18 p2674 A72-37100

Modifications and extensions of the sequential gradient-restoration algorithm for optimal control theory. [AD-736265] 19 p2776 A72-37246

Optimal terminal rendezvous as a stochastic differential game problem. 19 p2869 A72-37284

Optimally sensitive adaptive control techniques for systems with unknown time-varying parameters, suggesting applicability to ATC 19 p2776 A72-37289

Sufficient conditions for two stage stochastic optimal control difference approximation by finite dimensional extremum problem sequences 19 p2777 A72-37318

Certain problems of the theory of hierarchical control systems 19 p2824 A72-37379

Optimal control of plant described by nonlinear hyperbolic equations with variable initial conditions of system, noting constraints on plant phase coordinates 19 p2777 A72-37434

French monograph - Optimal impulse corrections for near-circular orbits - Comparison of various thruster configurations 19 p2856 A72-37491

Model reference adaptive control systems design based on optimal control, parametric optimization, stability and statistical estimation theory 19 p2778 A72-37722

Optimal avoidance control to transfer dynamic system from initial to terminal state in maximum distance problem [ASME PAPER 72-AUT-D] 19 p2778 A72-37724

Homogeneous linear partial differential equation for optimal control with boundary condition formed by terminal component, noting weighting functions for linear plant 19 p2778 A72-37989

Optimization of control and observation processes in a dynamic system at random disturbances 19 p2778 A72-37991

Evaluation of the coefficients of influence of initial information and model errors on optimization results 19 p2779 A72-37996

Optimal selection of stability augmentation parameters for excellent pilot acceptance. 19 p2752 A72-38227

An optimal model-following flight control system for manual control. 19 p2753 A72-38228

Dynamic programming technique for simultaneous measurement and dynamic control optimization for stochastic systems 19 p2779 A72-38233

Pontryagin Minimum Principle application to stochastic optimal control problems formulated around linear systems with Gaussian noise and general cost criteria 19 p2779 A72-38234

Optimal decentralized control of two coupled linear stochastic systems, introducing fake plant white noise for weak coupling effects compensation 19 p2779 A72-38236

Linear control system design with parameter uncertainties, using stochastic control approach based on minimization of state vector-dependent quadratic performance index expected value 19 p2780 A72-38239

Invariant poles feedback control of flexible, highly variable spacecraft. 19 p2869 A72-38240

Suboptimal stochastic control of a class of linear distributed parameter regulators. 19 p2780 A72-38243

Discrete optimal terminal control, with application to missile guidance. 19 p2780 A72-38257

Nonlinear on-line rapid estimation scheme with application to trajectory maneuvering vehicles. 19 p2781 A72-38258

Investigation of data rate requirements for low visibility approach with a scanning beam landing guidance system. 19 p2832 A72-38259

Asymptotic series solution of optimal systems with small time-delay. 19 p2826 A72-38268

Feedback loop equations and discrete measuring point methods for synthesis of optimal control systems with location dependent controlled variables 19 p2782 A72-38311

Optimal recurrent and nonrecurrent algorithms for polynomial diverging functions of learning and recognition in form of adaptive threshold elements 19 p2769 A72-38465

Optimal control synthesis for linear passive stationary plants with symmetrical coefficient matrices of minimized functional 19 p2782 A72-38514

Singular control problems calculation in trajectory optimization using sufficient conditions for control values set form 19 p2782 A72-38515

Algorithms for optimal adaptive control of steady motions of single channel discrete extremal systems with independent search, studying quality functional behavior 19 p2782 A72-38520

Comparison of the quality of empirical and optimal adaptation algorithms in multiple-alternative choice problems 19 p2828 A72-38583

Optimal strategies for control of a semi-Markovian process by a set of observers 19 p2770 A72-38584

Optimal delay control circuit adjustment by approximate calculation with quadratic error integral and ITAE criterion dependence on loop amplification 19 p2783 A72-38643

Design of a reduced-state suboptimal filter for self-calibration of a terrestrial inertial navigation system. [AIAA PAPER 72-849] 20 p2949 A72-39080

Optimum aiding of inertial navigation systems using air data. [AIAA PAPER 72-847] 20 p2950 A72-39082

Attitude control of a spinning Skylab. [AIAA PAPER 72-889] 20 p2975 A72-39112

Problem of the analytical design of controllers for parabolic and hyperbolic equations 20 p2946 A72-39468

Coincidence of the mapping point with the slip plane in the modified differential descent method 20 p2946 A72-39470

Response of discrete linear systems to forcing functions with inequality constraints. 20 p2910 A72-39604

Book - Some aspects of the optimal control of distributed parameter systems. 20 p2946 A72-39731

Performance improvement of amplitude-constrained minimum-variance controller by minimising sum of variance. 20 p2911 A72-39772

- Solution to the encounter avoidance problem in a linear differential game 20 p2947 A72-39865
- Optimization of controlled plants sequence with stochastic process described by partial differential equations, noting hydropneumatic system of liquid fuel jet engine 20 p2947 A72-39903
- Heat flux and friction force minimization problems equivalence in optimal control of incompressible boundary layer on isothermal plate 20 p2914 A72-39918
- Minimax technique in optimal control problems with incomplete information on phase vector, using dynamic programming and system position measurement refinements 20 p2911 A72-40027
- Optimal strategies conditions for game problems in conflict controlled system, discussing minimax technique and Bellman equation solution 20 p2947 A72-40028
- Linear estimation stochastic filtering and deterministic linear optimal regulation duality concept extension to problems with inequality constraints 21 p3074 A72-40228
- Using the quasi-homogeneity of differential equations in modeling physical systems 21 p3083 A72-40377
- Optimal single stage control law applicable to linear multivariable systems based on discrete-time analysis, discussing real time simulation on hybrid computer 21 p3037 A72-40637
- A computational technique for optimal control problems having singular arcs. 21 p3037 A72-40641
- Necessary conditions for optimality in a general class of non-linear mixed boundary value control problems. 21 p3037 A72-40644
- Linear distributed parameter systems modal analysis and design for low sensitivity optimal feedback control, using linear differential operators 21 p3037 A72-40646
- Trajectory synthesis of optimal control 21 p3037 A72-40704
- Selection of an optimal control law for time-lag control systems subjected to random load disturbances 21 p3038 A72-40705
- Optimal risk equation and solution existence and uniqueness of dual control problems with unknown parameter and additive disturbances 21 p3038 A72-40706
- A method for the development and optimization of controller-models for man-machine systems. 21 p3011 A72-41420
- Book on nonhomogeneous boundary value problems for different classes of linear evolution parabolic operators, with applications to optimal control problems 21 p3076 A72-41527
- Performance optimization of satellite semipassive aerodynamic attitude controller for near-earth orbits, considering damping time and pointing error [ALAA PAPER 72-923] 21 p3082 A72-41567
- Optimal invariant conversion of information from a turbine flow meter and a capacitive fuel gauge 21 p3058 A72-41801
- An algorithm in the gradient method for synthesis of nonlinear control systems 21 p3039 A72-41804
- Necessary conditions for continuous parameter stochastic optimization problems. 22 p3198 A72-41932
- Compatible controllers for time-varying linear plants. 22 p3161 A72-41939
- Development and optimization of a nonlinear multiparameter human operator model. 22 p3149 A72-41949
- A design procedure for intermediate-order observer-estimators for linear discrete-time dynamical systems. 22 p3161 A72-41994
- Optimal controller design for parabolic type second-order linear stationary systems, discussing integro-differential equation solution possibility 22 p3162 A72-42079
- Optimizing functional for combined control of dynamic control plant, synthesizing stabilization system for maximal transient damping 22 p3162 A72-42091
- Optimal receivers for measuring time lags of pulse signals in the presence of fading 22 p3154 A72-42123
- Linear dynamic control system synthesis methods based on aggregation and suboptimal control by decomposition, considering quadratic performance criterion 22 p3162 A72-42177
- Mathematical formulation of linear programming problem, reducing vector value optimal management plan determination to quadratic programming problem 22 p3198 A72-42179
- Liapunov function method in control problems of distributed parameter systems /Survey/ 22 p3205 A72-42180
- An application of the theory of Lie groups in the optimal control problem for linear dynamic systems with time-variable coefficients 22 p3162 A72-42181
- Synthesis of statistically optimal multiloop control systems containing essentially nonlinear elements 22 p3162 A72-42182
- Synthesis problems of optimum quick-response engine control systems 22 p3216 A72-42190
- Variational method for invariance problem solution for optimal finite state of nonlinear dynamic systems under external disturbances 22 p3162 A72-42240
- Optimal control of complex time lag systems with series connected lumped and distributed parameters described by linear differential equations 22 p3162 A72-42241
- On the convergence of difference approximations in distributed parameter optimal control problems. 22 p3162 A72-42486
- Control and estimation separation in stochastic optimization, discussing Wonham observer matrix reversibility and replacement in closed and closed-open loop systems 22 p3163 A72-42740
- Optimal random disturbance intensity control of dynamic systems, minimizing error with respect to observed and controlled plant coordinates 23 p3274 A72-43221
- Approximate optimal control solution to boundary value problem for one dimensional heat conduction equation, using Fredholm linear integral and degenerate kernels 23 p3274 A72-43526
- A survey of methods of feasible directions for the solution of optimal control problems. 23 p3274 A72-43537
- Adaptive filtering algorithms for Kalman filter optimal gain estimation, discussing Bayesian, maximum likelihood, correlation and covariance matching methods relationship 23 p3274 A72-43542
- Some numerical results using Kalaba's new approach to optimal control and filtering. 23 p3274 A72-43543
- On discrete linear time-invariant systems with singular transition matrix. 23 p3275 A72-43545
- Control of jump parameter systems with discontinuous state trajectories. 23 p3275 A72-43547
- Optimization of contraction-mapping algorithm for calculating optimal controls. 23 p3275 A72-43607
- Output-feedback control law for randomly distributed multivariable system. 23 p3275 A72-43608
- Optimally sensitive control for distributed parameter systems. 23 p3275 A72-43612
- A direct method for computing optimal feedback control for linear systems. 23 p3275 A72-43613
- Stochastically optimal terminal control system synthesis for loss function dependence on finite phase coordinates of dynamic system, considering soft landing of flight vehicle 23 p3275 A72-43781
- Optimal control of stochastic systems with continuous and discontinuous random disturbances, obtaining problem solution conditions for linear system via dynamic programming 23 p3276 A72-43782
- Asilomar Conference on Circuits and Systems, 5th, Pacific Grove, Calif., November 8-10, 1971, Record. 23 p3276 A72-43851
- Regulator vector selection algorithm for largest estimate of exponential absolute control stability region based on Popov frequency condition reformulation 23 p3276 A72-43853
- Optimal, on-line linear filtering with noisy, time-delayed observations. 23 p3276 A72-43855
- Reduced order observers design for optimal control of linear discrete time stochastic systems, considering velocity-aided tracking filter 23 p3276 A72-43856
- Optimal minimax regulation of a dynamic system. 23 p3276 A72-43860
- The optimal control of merging aircraft - Implementation of the hybrid air traffic controller. 23 p3277 A72-43868
- Atmospheric density from spacecraft drag data by successive optimization of control laws, using quadratic programming 23 p3277 A72-44003
- Optimal filtration algorithms of Markov parameters of discrete time signals in digital data transmission system with background noise, using Gaussian probability density approximation 23 p3264 A72-44005
- The inverse problem of optimal process theory and the synthesis of linear optimal systems in the case of restricted phase coordinates 23 p3277 A72-44008
- Achievement of given motion by impulse correction under arbitrary disturbances /difference models/ 23 p3313 A72-44044
- Application of quadratic optimization to supersonic inlet control. 23 p3251 A72-44195
- A manifold imbedding algorithm for optimization problems. 23 p3268 A72-44197
- A learning approach to the parameter-adaptive self-organizing control problem. 23 p3277 A72-44198
- Optimal gyroresonator control in electric oscillating field by HF magnetic Lorentz force in terms of relativistic electron trajectory drifts 23 p3290 A72-44200
- Multistage rocket optimal control, deriving conditions for existence of minimum of performance index function of mass, position and velocity initial and final values 23 p3343 A72-44264
- Optimal synthesis of a two-parameter continuous controller for a jet engine with an afterburner 23 p3326 A72-44284
- Allowable region of approach height and desirable approach path of aircraft for safe landing, presenting optimal control trajectories 23 p3252 A72-44497
- A computational successive improvement scheme for adaptive optimal control processes. 23 p3268 A72-44549
- Optimum reception algorithms in communication systems with decision feedback in presence of noise in forward and return channel 24 p3379 A72-44747
- Aerodynamic solar semipassive hybrid system for continuous three dimensional attitude control of axisymmetric satellite in near-earth orbits, discussing operation, design and optimization 24 p3450 A72-45146
- Optimal three dimensional maneuvering of a rocket powered hypervelocity vehicle. 24 p3450 A72-45151
- Duality in problems of the calculus of variations and optimal control 24 p3419 A72-45390
- Maximum principle and penalty function technique for flight optimization, noting optimal control for climbing flight 24 p3369 A72-45444
- Formation of an optimizing functional in control systems 24 p3386 A72-45511
- Selection of an optimizing functional in control system synthesis 24 p3387 A72-45512
- Automatic complex control systems with digital computer application for optimal control of production systems, selecting optimality criterion from hierarchically distributed local criteria 24 p3387 A72-45513
- Parametric optimization of the equivalent transfer function of a system with the aid of the error integral 24 p3387 A72-45700
- Comparison of linear and Riccati equations used to solve optimal control problems. 24 p3420 A72-45776
- Omega-Dot law for time optimum approximation of rotating satellites wobble damping with control moment gyroscopes, calculating wobble rates by energy sink method 24 p3453 A72-45777

OPTIMIZATION

- NT FLIGHT OPTIMIZATION
- NT OPTIMAL CONTROL
- NT TIME OPTIMAL CONTROL
- NT TRAJECTORY OPTIMIZATION
- Optimal psychomotor performance in relation to thermal comfort conditions in man, using complex dual tests and subjective rating scales 01 p0016 A72-10117
- Optimum cylindrical handle size determination by muscle electromyography, considering gripping task, routine performance and fatigue test 01 p0017 A72-10119
- Airline Propulsion Team approach to DC-10 aircraft power plant design for maximum operational effectiveness [SAE PAPER 710778] 01 p0116 A72-10270
- Optimal design of logic networks in homogeneous microelectronic structures, using shortest link search and graph continuity parameters 01 p0034 A72-10300
- Optimal measurement programs for instrument controlled spacecraft trajectory sections, using maximum likelihood method 01 p0127 A72-10354
- Linear antenna array optimal power pattern synthesis by best approximation, using weighting function in man-machine iteration 01 p0029 A72-10665
- Computerized optimization procedure for microwave circuits without tuning elements, applying to high pass filter design 01 p0040 A72-10686

Clutter suppression by amplitude weighted pulse trains in coherent radar, obtaining optimum weights and signal-to-clutter gain as function of Doppler frequency

01 p0030 A72-10789

Signal flow graph theory based computer diagnosis using blocking gate approach, constructing algorithm for gates optimal locations determination for maximum faults distinguishability

02 p0184 A72-11479

Circuit theory optimization techniques in computer aided electric circuits and devices design, discussing algorithms, sequential methods, convergence speed, topologies, system responses, etc

02 p0197 A72-11688

Optimum power allocation in design of phase-coherent receiver having bandpass limiter, extending technique from single channel to two channel system

02 p0174 A72-12136

Computerized bias optimization of telemetry timing accuracy applied to Minuteman system

02 p0174 A72-12144

Optimization methods in digital data transmission systems, discussing equalization circuits for base band channel using metallic lines

02 p0182 A72-12691

Optimal synthesis for radiator coordinates and complex amplitudes of linear antenna array for given radiation pattern

02 p0196 A72-12756

Optimal radiative capacity of star shaped radiator with mirror reflecting surfaces for vacuum cooling of elongated finned bodies

02 p0304 A72-12867

Optimization algorithms synthesis models, discussing conceptual-implementable transition

03 p0327 A72-13702

Complex determinate and indeterminate structures weight minimization subject to design constraints relative to size, allowable stress, natural frequencies, etc

03 p0446 A72-13703

Analytical optimization of point to point communication above spherical ground, obtaining frequency minimizing transmission losses

03 p0325 A72-14193

Multipurpose optimal design of elastic structures with piecewise uniform cross section for load states and prescribed stiffness by energy methods

03 p0455 A72-14386

Robust delta modulator configuration with minimal mean square error from signal statistics estimates, discussing design and performance by digital simulation

04 p0486 A72-14486

Genetic code numerical structure association with logarithmic optimization rule for hierarchy of structures from molecular biology experiments

04 p0470 A72-14794

Computational efficiency of minimization algorithm for solving eigenvalue problem arising from dynamic structural analysis by finite element method

04 p0585 A72-14845

Herringbone grooved gas bearing load carrying capacity optimization, considering lubricant film thickness, groove width and length ratios and angle

04 p0527 A72-14915

Optimal nonlinear discrete filters with finite memory for polynomial signals, discussing synthesis with aid of minimax method

04 p0505 A72-14998

Random search method application to optimal design of closed circular cylindrical shells under axial compressive loading

04 p0587 A72-15020

Discrete time systems unknown parameter identification, considering unified error function minimization approach

04 p0506 A72-15106

Statically indeterminate and determinate elastic beams optimal design for maximum-minimum deflection under distributed load

04 p0590 A72-15192

Antenna arrays performance optimization, emphasizing directivity and signal to noise power ratio

04 p0499 A72-15301

Upper and lower bounds for expected value and variance of minimum material weight necessary for random resistance structure able to support assigned loads

04 p0593 A72-15648

Optimal temperature fields in locally heated orthotropic cylindrical shells, determining rigidities effect

04 p0593 A72-15655

Steepest ascent method for function optimization in arbitrary direction by selecting distance metric and scale dependency

04 p0540 A72-15683

Optimization algorithm for simultaneous solutions to bivalent 0-1 Knapsack problems with linear target function and linear restrictions, using ALGOL

05 p0632 A72-15817

Synthesis method for optimized single-stage reflection type phase shifters, determining transformation coefficient

05 p0634 A72-15831

Flow rate metering by multiple Venturi systems, discussing internal fluid mechanics for design optimization

[ASME PAPER 71-WA/FE-27] 05 p0661 A72-15926

Composite multilayer fibrous shell structural design optimization, using nonlinear mathematical programming methods

[ASME PAPER 71-WA/DE-12] 05 p0733 A72-15943

Hybrid representation for structural component by vibration modes with free or fixed connection points and boundary conditions selection to optimize accuracy

05 p0736 A72-16084

Automatic plastic minimum weight design of structural frames comparing with linear programming techniques

05 p0737 A72-16117

Optimization algorithm in measurement conditions selection for satellite thermal sounding of atmosphere in 15 micron carbon dioxide band

05 p0655 A72-16174

Direct and inverse problems of sensitivity theory, discussing solvability conditions, search optimization and applicability in automatic control

05 p0640 A72-16206

Recurrent algorithms for optimal signal detection on background of random noise, using Markov processes

05 p0627 A72-16406

Iterative method for approximate determination of local minima in fuel optimal finite thrust orbit transfer

05 p0719 A72-16541

Two parameter trajectory measurement optimal planning reduced to quadratic programming based on linear programming generalization for continuous case

05 p0721 A72-16758

Algorithms for optimal planning of trajectory measurement times during sampling several parameters

05 p0641 A72-16759

Analytical model of thermal/structural optimization for long term storage cryogenic propellant systems

[AIAA PAPER 72-142] 05 p0691 A72-16881

Optimal reversion coefficient determination for passenger aircraft engine thrust reversal

05 p0614 A72-17060

Optimal averaging of discontinuous processes with distributed parameters, taking into account random disturbances and measurement errors

05 p0683 A72-17130

Laminar flow airfoils for gliders, optimizing profiles for favorable velocity and pressure distribution

05 p0610 A72-17194

Supersynthesis antenna array design by analytical approach involving isolation and separate optimization of parameters effects on spatial frequency component sampling

06 p0771 A72-17341

CIRCAL-2 general purpose on-line circuit design computer program featuring multiple analysis, text editing, network representation and user-program interaction optimization capabilities

06 p0778 A72-17474

Computer search for optimum narrow band FM and PM systems bandpass filters, noting low index angle modulated signals

06 p0783 A72-17484

Optimal synthesis of multiparametric machine systems by LP search /determinate analog of random search/, applying to oscillatory models

06 p0821 A72-17726

Dynamic system optimal design with various degrees of maneuver parameters information, considering space flight mechanics problem of payload maximization for limited propulsive power

06 p0849 A72-18306

Broadband parametric amplifier design using computerized optimization procedure based on Gauss-Newton iteration technique

06 p0786 A72-18376

Multiplier method for discrete optimization problems with equality constraints, applying to time optimal control for V/STOL aircraft

06 p0794 A72-18387

Source permutation code optimum encoding for long block length, comparing performance with rate distortion function bound and various quantization schemes

06 p0776 A72-18391

LSA oscillators performance and control optimization, discussing multiaxis radial microwave cavity effectiveness in oscillation starting and coupling to coaxial transmission line

06 p0789 A72-18481

Resin bonded solid lubricant film thickness optimization from statistical analysis of bench and machine element test data

06 p0823 A72-18591

Optimization problems in gravitational attraction, considering homogeneous ellipsoids interaction and free particle simple harmonic motion

06 p0851 A72-18740

Inlet duct and turbofan engine compatibility without stalling and surge conditions obtained by design optimization and wind tunnel testing

07 p1052 A72-18761

Algorithm selection for optimization solutions by finite, ad hoc, conjugate, Newton and restricted step methods

07 p1025 A72-18783

Optimal rigid-plastic limit load analysis of spherical shells under nonsymmetrical loadings, using SUMT and Rosenbrock method

07 p1087 A72-18791

Optimal receiver synthesis for radio signals with differentiable components of continuous Markov processes masked by phase interference and white noise

07 p0937 A72-18847

Passive radio interference filtration analysis, obtaining SNR maximization by ambiguity function partial volume minimization

07 p0937 A72-18848

Optimal radio signal processing system on background of correlated interference, calculating detection characteristics

07 p0937 A72-18850

Rain induced flood mathematical model, optimizing parameters and applying to hydrological forecasts

07 p1029 A72-18862

Steel cutting suitability test, determining optimum cutting conditions for pure iron used in magnetic applications

07 p0994 A72-18973

Radiative heat transfer characteristics of optimal geometry radiating stainless steel fin

07 p1098 A72-18997

Optimal signal detection relative to Neumann-Pearson criterion invariant with respect to amplitude and random noise intensity in radio location

07 p0938 A72-19019

Optimality criterion for beams and frames with segmentwise constant cross sections and alternative loading exceeding plastic load carrying capacity

07 p1088 A72-19119

Signal design for coherent M-ary communication systems by stochastic gradient algorithm for minimizing error rate

07 p0959 A72-19285

Suboptimal Kalman filter design for system state estimation in presence of plant dynamics uncertainties and measurements noise, optimizing tradeoff between sensitivity and estimation error

07 p0959 A72-19302

Optimal Bayesian system synthesis for simultaneous discrimination and parameter estimation of several signals in noise background

07 p0943 A72-19516

Asymptotically optimal rank algorithms for signal resolution at phase and amplitude detectors outputs

07 p0943 A72-19518

Signal detection in noise, investigating quantiles position optimization in nonparametric test statistics

07 p0943 A72-19519

Aerospace subsystem alternate designs and cost effectiveness evaluation and optimization, considering algorithm of three functions with minimal coupling

07 p1105 A72-19552

Optimal PSK signals selection and synthesis from random sequences ensuring minimum value of maximum side peak of autocorrelation function

07 p0943 A72-19564

Optimization algorithm for minimum margin efficiency of electronic circuits, applying to IC TTL gate and transistorized bistable multivibrator /flip-flop/

07 p0944 A72-19568

Multivariable plant optimization, considering oil field operations, n-paired transeiver power loads, Laplace and Poisson equations described systems and interindustrial balance

07 p0962 A72-19722

Minimum weight design of elastic sandwich beam with segmentwise constant stiffness under displacement and stress constraints, using iterative solution and finite element analysis

07 p1092 A72-19825

Optimum exposure time for sintering in Ar flow of porous rolled product of Ti powders determined from physicochemical properties changes

07 p0996 A72-19964

Optimum lasing conditions and spectral characteristics of organic dye lasers at 3,100-11,000 Å

07 p1009 A72-20613

Estimation-correlation principle and optimal detector for incomplete a priori information signal reception on random and white noise background

08 p1131 A72-20790

Biased estimator as alternative to linear unbiased estimator for dynamic system model states and parameters optimization and regulation, noting squared errors sum

08 p1144 A72-20852

Optimal filtering for state estimation of nonlinear dynamic models observed with discrete noisy observations by retaining second order terms in series approximation

08 p1145 A72-20863

Optimization for maximum productivity of electric spark machining with vibrating electrode, noting erosion product removal difficulties 08 p1174 A72-21033

Optimization criteria for electroerosion machining, determining objective functions 08 p1175 A72-21039

Linear programming procedure for efficiency and cost optimization in aerial survey mission 08 p1165 A72-21164

Thin walled box beam optimal design, noting cross section areas and dimensions with permissible walls and flanges safety and stability 08 p1243 A72-21240

Optimality conditions for nonconvex optimization problems from linear programming solution 08 p1199 A72-21285

Optimal synthesis of four radar waveform classes with distinct resolution properties based on target environment analysis 08 p1133 A72-21403

Naval aircraft optimal repair and replacement policies determination for operation cost minimization by dynamic programming [AD-736094] 08 p1256 A72-21470

German book on control technology development covering historic periods, symbols and representations, stability, integral transformations, computers, servos, relays and multivariable systems, optimization, etc 08 p1145 A72-21478

Plastics optimal reinforcement in given stressed state by determining shortest path from stress point to strength region 08 p1244 A72-21502

Optimal design of anisotropic composite material annular plates by numerical method 08 p1246 A72-21673

Radio communication system optimization from viewpoints of global synthesis, including economics and partial synthesis based on noise stability, precision and reliability 08 p1136 A72-21845

Optimal variant of meteor wind patrol radar station for atmospheric circulation study 08 p1147 A72-21886

Sonic boom minimization, obtaining positive phase signature pressures as function of altitude, Mach number, weight and length 08 p1110 A72-21903

Optimum directive gain of circular Taylor patterns for planar aperture antenna design 08 p1143 A72-21987

Multidimensional function extremum for sectioned resonator type gyroamplifier efficiency optimization 08 p1172 A72-22050

Stochastic rule for optimum moment of preventive maintenance of redundant technological systems, predicting system reliability 08 p1180 A72-22056

Reliability of redundant schemes with quorum element, noting optimal parameters for known failure damages 08 p1180 A72-22059

Economic factors influence on reliability optimization of complex radio systems and elements 08 p1143 A72-22066

Radio system failure prediction based on parameter variation a priori or a posteriori data, determining reliability and optimal preventive maintenance intervals 08 p1143 A72-22070

Hydrodynamic models and computational schemes optimization in statistical weather forecasting 08 p1202 A72-22114

Optimal gradient minimization scheme for finite element eigenvalue and eigenvector problems, including effect of round-off errors and termination criterion 08 p1200 A72-22140

German monograph on optimal design of gyroscope using spherical static gas bearing 08 p1173 A72-22174

German monograph on optimum principle for numerical representation of surfaces, discussing association with elasticity theory extremal requirements 09 p1340 A72-22319

German monograph on optimal design of HF band-pass filters with lumped elements, covering LC coupled two- and four-circuit systems 09 p1284 A72-22328

German monograph on ring shaped continuous beams calculation, deriving optimum support under torsional stress 09 p1397 A72-22335

Optimal nomographic determination of surface gyrocompass parameters ensuring minimum period of undamped precession oscillations 09 p1307 A72-22346

Zirconia ceramics for high performance storage heaters, discussing operating conditions, optimal properties for heater design, engineering evaluation tests and in-service performance 09 p1333 A72-22383

Sigma algebra and statistics system for optimal stopping of stochastic processes for continuous time case 09 p1340 A72-22424

Two point boundary value problems solved by finite difference method using optimal sequence of nodes 09 p1341 A72-22464

Optimization of load-carrying elastic lattice structures designed on prescribed surface 09 p1402 A72-22746

Development trends in airborne man machine flight control, discussing optimal division between human pilot and machine in relation to total system performance and economic factors 09 p1270 A72-22781

Optimal solutions for apportionment between automatic and manual flight control, considering number and types of displays required 09 p1348 A72-22783

Stochastic approximation for identification of element with second order lag, noting convergence with optimum parameter 09 p1291 A72-23371

Deterministic optimization of aircraft undercarriage suspension characteristics for taxing induced vibration minimization, discussing damping and stiffness functions and hybrid computer solution 09 p1407 A72-23458

Energy transfer optimization in electromagnetic wave transmission through dispersive dielectric media 09 p1365 A72-23522

Monotonicity theorems for functionals and transformations in stochastic models of queueing, reliability and optimality problems 09 p1343 A72-23565

Minimum time duration rocket interception, calculating trajectory parameters and target orbits in Earth gravitational field 09 p1393 A72-23573

Nonlinear systems optimal design mathematical modeling, discussing synthesis, manufacturing, production, exploitation and evaluation 09 p1343 A72-23610

Hookes law formulation by multindex sequences for stereomechanical multiple system optimization 09 p1354 A72-23611

Revised algorithm for unconstrained optimization using quasi-Newton methods based on recurring factorization of approximation to Hessian matrix 10 p1502 A72-23723

German monograph on flight performance optimization of solid propellant rockets covering thrust values, burning time, rocket design and orbits within earth atmosphere 10 p1550 A72-23770

Optimum bounding filter design based on error covariance for Kalman-Bucy and Wiener filters with inaccurately known parameters, obtaining performance figure of merit 10 p1454 A72-23785

Optimal tracking filter for processing sensor data of imprecisely determined origin in surveillance system by minimizing effects of correlation uncertainties 10 p1455 A72-23787

Low speed performance and boundary layer growth in optimal annular diffuser with uniform center body diameter and conically diverging wall 10 p1415 A72-23856

Algebraic dimensional analysis developed algorithm to generate optimized dimensionless products set associated with physical phenomenon, using matrix methods 10 p1443 A72-23916

High power Nd-glass laser systems, discussing oscillator and amplifier operating parameters optimization 10 p1489 A72-23945

Multistage systems maintainability, presenting equations for optimum allocation of demonstration tests to repairable elements 10 p1443 A72-23982

Permanent state operation optimization for fluid amplifier with jet interaction 10 p1422 A72-24125

MHD generator duct external loop electric current maximization by working material resistivity tensor optimal distribution 10 p1521 A72-24434

Econometric approach to space shuttle design for optimum operational redundancy levels, using payload-cost effectiveness criterion [AIAA PAPER 72-242] 10 p1551 A72-24448

Terminal control solution in terms of finite dimensional minimization of convex function, applying to time optimal control and minimum energy problems 10 p1457 A72-24459

Optimal configuration of lifting bodies for hypersonic speeds, noting negligible effect of blunt leading edges 10 p1418 A72-24536

Electronic circuits statistical optimization with Monte Carlo procedure, discussing methods and algorithms for accelerating evolutionary modeling 10 p1452 A72-24638

Stochastic optimization of airborne laser seeker system design parameters to maximize target acquisition probability through regression analysis of data from computerized model 10 p1437 A72-24682

Weak signal turnaround transponder design for pseudonoise coded ranging systems, discussing bandwidth optimization and performance comparison between various receiver configurations 10 p1452 A72-24688

Optimum thickness variation in annular strip /curved beam/ under bending moment at constant stress based on Mises-Hencky yield criterion 10 p1558 A72-24847

Pontryagin maximum principle application to minimum deflection of cantilever beam under own weight 10 p1558 A72-24880

Modulating /multiplicative/ noise effects on output signal characteristics of receiver designed for optimal reception on background of Gaussian noise 10 p1439 A72-24906

Minimum noise coefficients of M-type microwave beam amplifiers with crossed fields, taking into account delay system distributed losses 10 p1453 A72-24913

Optimal distribution of resources in automatic systems for detection and measurement of random concentrated noises number in assigned frequency range 10 p1440 A72-24917

Statistical linearization of stochastic differential equations for optimal terms in mean square distance 10 p1506 A72-24993

Aircraft maintenance optimization, considering safety, reliability, punctuality and cost factors 10 p1422 A72-25108

Linear optimization of holographic process, investigating application to three dimensional diffusive object 11 p1629 A72-25315

Algorithm for optimal binary search tree construction with minimum weighted and restricted maximum path lengths 11 p1676 A72-25354

Automated optimization for preliminary design of supersonic aircraft wings, noting flutter, stresses and resonant frequency as dynamic constraints [AIAA PAPER 72-333] 11 p1727 A72-25368

Optimal parameters selection for natural vibrations maximum damping rate, applying method to two mass electromechanical system 11 p1686 A72-25533

Transport aircraft aerodynamic design technology application to general aviation propeller driven twin engine aircraft, discussing wing loading and aspect ratio optimization [SAE PAPER 720337] 11 p1576 A72-25595

Multiaxis radial circuits for transferred electron microwave oscillator performance optimization to obtain wideband CW amplification, discussing LSA tests 11 p1604 A72-25745

Optimum decision rule for sync word location in binary data frame, noting sum maximization of correlation and energy correction terms 11 p1592 A72-25888

Flight vehicle structures optimum design for random vibration environment, presenting formulation as nonlinear programming problem 11 p1736 A72-26003

Overall characteristics of optimal quasi-steady plasma thruster system, discussing mass, burning time and thrust variations as function of power supply and pulse duration [AIAA PAPER 72-456] 11 p1708 A72-26192

Optimization criteria for electric feeding in quasi-steady MPD thruster, discussing energy storage bank characteristics determination [AIAA PAPER 72-462] 11 p1709 A72-26197

Fiber-matrix composites overall strength optimization, emphasizing matrix and interface effects 11 p1674 A72-26231

Optimal synthesis and analysis of quasi-deterministic signal detection system with simultaneous parameter measurement on background noise 11 p1596 A72-26312

Optimal active layer thickness in heterogeneous injection lasers, estimating minimal threshold currents 11 p1649 A72-26346

Measuring information systems optimization, considering first order system with time lag 11 p1611 A72-26436

Optimization of diagnostic tests for monitoring industrial system efficiency, obtaining compromise between costs and utilization 11 p1611 A72-26441

Optimality and strategy efficiency in Gaussian elimination on sparse matrix, using graphical method 11 p1678 A72-26496

Electronic filters realization by error function minimization, discussing parameter space algorithmic search and complex plane optimization methods 11 p1606 A72-26550

Aluminum-silicon Schottky diode clamped transistor-transistor logic circuits parameters optimization for high switching speed and IC applications 11 p1606 A72-26568

Nonlinear control system optimal bang-bang controls computation, noting algorithm obtained by parameter optimization

11 p1577 A72-26666

Optimum synthesis of antenna array of slot radiators with passive elements, using nonlinear programming

11 p1597 A72-26708

Optimal sum-difference characteristics of nonseparable convex slot spherical antennas for maximum directive gain and minimum spatial sidelobe radiation

11 p1598 A72-26713

Criterion selection and minimum margin search for optimization of complex electronic circuit parameters described by mathematical models

11 p1612 A72-26736

Path connection algorithms for optimal IC layout on circuit board, using digital computer

11 p1607 A72-26784

Computer calculation of minimum weight ribbed plates under axial compression by random search method and linear programming

12 p1878 A72-27083

Probability minimization and detection of errors in computerized analysis of civil engineering frameworks, noting graphical output advantages

12 p1786 A72-27190

Metal matrix composites radiography in NDT, discussing parameters optimization and uses of microfilm, densitometers and high resolution vidicon tubes

12 p1813 A72-27199

Equation difference minimization techniques for ordinary nonlinear differential equations approximate periodic solution generation, noting error bounding procedure validity

12 p1836 A72-27240

Prager-Shield theory for optimal plastic design extended to multicomponent cost functions and load conditions, applying to fiber reinforced plate

12 p1881 A72-27243

Structural weight optimization with piecewise concave cost functionals defined on set in Euclidean space for anisotropic cylindrical shells

12 p1881 A72-27254

Modular computer program for digital transmission systems, applying to optimization of filters in multitransponder satellite and ground stations

12 p1786 A72-27323

Optical and electronic imaging systems optimization for solar system exploration, discussing effects on public support for national funding

12 p1807 A72-27346

Multistage pursuit-evasion game on circle, constructing player optimal strategies via measure theory

12 p1836 A72-27511

Analog measuring data transmission systems optimization by computers, noting improvement of dynamic response and linearity in digital systems

12 p1786 A72-27580

Lens parameters selection and prisms position optimization in light beam to avoid premature damage

12 p1808 A72-27623

Computerized antenna array design, using Automated Engineering and Scientific Optimization Program

12 p1792 A72-27735

Emission of density modulated electron flux passing over diffraction structures formed by half planes and combs with oblique teeth, discussing optimum emitted power conditions

12 p1793 A72-27858

Cocuring technique optimization for primary aircraft components composite materials, discussing mechanical and dimensional properties test data, production cost analysis and cure time

12 p1815 A72-28077

Algorithms for combinatorial problem optimal solution based on implicit enumeration method, applying to assembly line balancing

12 p1837 A72-28117

Data file optimal arrangement by programmed procedures formulated as combinatorial problem, using branch-and-bound method for solution

12 p1787 A72-28118

Binary logic circuits with interconnected repeaters and inverters, discussing signal level selection to ensure maximum noise stability

12 p1786 A72-28120

Gas turbine units with constant pressure cycle, discussing design and optimization method

12 p1862 A72-28149

Reliability requirements and optimization for complex systems, discussing method to improve component reliability of aircraft weapon system

13 p1961 A72-28353

System reliability demonstration test cost minimization for one-shot electroexplosive device

13 p2024 A72-28367

Optimal parameters of electro-optical signal processor for phased array antennas, noting optical subsystem correspondence to optoacoustical spectrum analyzer

13 p1926 A72-28374

Stages optimum selection for step rocket moving in plane gravitational field

13 p2051 A72-28384

Binary PSK signals optimized on minimax and quadratic criteria, noting design of coders and decoders on shift registers with external logic

13 p1914 A72-28415

Path arrangement optimization method for fluid distribution network with separable and concave cost function, using simplex method in nonlinear programming

13 p2053 A72-28423

Optimal design of elastic structures, emphasizing stability and response under applied static and dynamic loads

13 p2054 A72-28487

Computer program analysis of errors in mutual orientation elements on aerial photographs with different lengthwise overlaps, discussing error minimization

13 p1955 A72-28497

Optimization of monopulse antenna performance indices for specified sidelobe envelope function and/or specified pattern nulls

13 p1915 A72-28530

Random retrieval algorithms in finite set of preset movement directions, considering quadratic function minimization

13 p1924 A72-28610

Algorithm and computer program to calculate low run multiple nomenclature production process optimal parameters

13 p1962 A72-28741

Polarization method for measuring small phase difference variations in microwave range, developing rules for optimum selection of multiplication factor

13 p1928 A72-28790

Optimal matched Wiener discrete filters investigated with operator-matrix concepts

13 p1918 A72-28894

Optimal cross section selection of rectangular beams in oblique bending by nonlinear programming and learning algorithm

13 p2056 A72-28914

Optimal level of recording defects in ultrasonic flaw detection, taking into account inspection conditions and defect size probability distribution

13 p1956 A72-28924

Thermal storage type resistors design for satellite attitude control, discussing heat loss minimization

13 p2026 A72-28927

Pyramidal-horn primary element axial position effect on dual mirror Cassegrain microwave antenna main lobe pattern, obtaining optimal position

13 p1929 A72-29040

Associated system instability related to difficulties encountered in maximum principle application to optimization problems solution

13 p2003 A72-29069

Optimal design of thin walled minimum weight aircraft shell structures, using linear programming

13 p2058 A72-29143

Overestimation in optimization problems calculated by regressive equation, comparing with actual effect in static process

13 p1936 A72-29158

Two phase algorithm for selecting optimal sets of characteristics for image recognition systems

13 p1925 A72-29164

Optimal multistep sampling procedures for production quality control, discussing methods for minimization of error probabilities and total sampling volume

13 p1965 A72-29167

Fiber glass reinforced plastic structure design based on anisotropy, calculating optimum angle between reinforcement and horizontal axis

13 p2058 A72-29463

Computer method of link formation in multiple nomenclature aircraft production lines, minimizing idle time

13 p1966 A72-29464

Signal discretization frequency upper bounds determination to satisfy prescribed level of mean square error in continuous signal restoration

13 p1925 A72-30021

Microwave circuits for multiplexing applications, discussing optimal design in terms of economic, mechanical and electrical parameters

13 p1934 A72-30089

Minimum drag bodies of revolution in supersonic flow obtained by combining steepest descent method with integral flow model

14 p2069 A72-30231

Heliocentric orbit from modified Laplace and Leuschner method with optimal time interval between five successive observations

14 p2149 A72-30233

Outgoing 15 micron carbon dioxide band radiation measurement optimization for atmospheric thermal sounding by satellite

14 p2099 A72-30243

Kalman filter application to inertial navigation systems optimal alignment, discussing linear systems

representation in state space and filter algorithm recursive equations

14 p2129 A72-30330

Gravitational stabilization systems parameters determination for minimum amplitude of satellite eccentric vibrations

14 p2162 A72-30457

Pulsed motion of gravity gradient vehicle in central gravity field, presenting expressions of optimized attitude control

14 p2162 A72-30473

GaAs varactor diode design optimization based on calculation of cut-off frequency vs carrier concentration with consideration of skin effect

14 p2088 A72-30588

Operating conditions of photometers for optimum photomultiplier photon counting photometry, considering measurement precision dependence on experimental parameters

14 p2105 A72-30733

Complex systems optimization with respect to vector-valued cost function without prespecified constraints or criteria weighting, deriving algorithm for characteristic set of noninferior solutions

14 p2087 A72-30825

Liquid propellant rocket performance, stability and compatibility prediction techniques, noting effect on design time and cost

14 p2146 A72-30919

Sandwich beams structural optimization for given deflection by iterative finite element procedure

14 p2168 A72-30927

Optimal plastic design of doubly symmetric closed ring and frame structures of idealized sandwich section under uniform internal pressure

15 p2322 A72-31346

Signal distortion minimization for random waveguides with frequency-dependent optimum coupling based on transfer function covariance and impulse response time domain statistics

15 p2194 A72-31352

Coupled flexural longitudinal vibrations of circular arc girder with symmetrical cross section, discussing optimal design

15 p2324 A72-31487

Alternant theorems for characterization of minimum solutions in multidimensional Chebyshev approximation of functions connected with Markov systems

15 p2261 A72-31497

Celestial Thomson-scattering X ray polarimeter design for OSO-1, optimizing sensitivity in 4-24 keV energy range by Monte Carlo simulation computer program

15 p2234 A72-31540

Optimal segment boundaries with composite error function in piecewise approximation chosen by dynamic program in scalar state variable, noting uniqueness properties

15 p2262 A72-31634

Reflector networks analysis for optimal operation of electronic scanning antenna in illuminated grating

15 p2195 A72-31670

Computer method of optimal turbomachine disk design, using local search techniques to determine disk minimum weight

15 p2328 A72-31746

Dynamic optimization procedure for bivalent knapsack problem solution involving large number of variables

15 p2203 A72-31750

Optimization of heat pipe with wick and annulus liquid flow, investigating effect of pressure loss and recovery in vapor passage

15 p2335 A72-31767

Jointly optimal filters for fixed range radar filter-sampler-filter system, determining impulse response function forms

15 p2207 A72-31793

Single crystal scheelite material for Nd doped intermediate gain laser host substance, considering optimum growth conditions, lasing parameter and Nd concentration

15 p2292 A72-32030

Reliability-maximizing digital computer synthesis based on multiple redundant network design, discussing majority structure distribution optimization technique

15 p2203 A72-32174

Fraunhofer holograms wavelength dependent distortion reduction by system parameters optimization, applying to color holotape

15 p2239 A72-32357

Input match conditions for broadband mixer conversion loss minimization, comparing optimization procedures

15 p2208 A72-32392

Optimum nonslender bodies of revolution minimum drag in free molecular flow under integral constraints

15 p2180 A72-32395

Structural design optimization procedure based on sequence of linearizations with iterative convergence through series of least critical intermediate solutions in hyperspace

15 p2331 A72-32551

Magnetic field profile optimization for beta-limitation in minimum-B mirror confined plasma in nuclear reactor 16 p2432 A72-32805

Weight minimization for simple structures with single natural frequency constraint, solving nonlinear two point boundary value problem by variational and numerical methods 16 p2463 A72-32834

Analog simulation method for highly redundant structure optimization based on reproducing structure mechanical behavior in stabilized stress states 16 p2463 A72-32899

Structural design optimization by geometric programming, illustrating computerized technique on two bar truss and ship bulkhead problem 16 p2366 A72-32913

Optimal plane elastic trusses under alternative loads, designing for smallest total volume of bars with upper stress bound 16 p2466 A72-33017

Limit displacement or solids parameters optimization for perfectly locking bodies, presenting mathematical models based on extremum energy theorems 16 p2423 A72-33104

Algorithm for minimax parameter optimization by linear and quadratic programming with application to earth orbiting satellite orbital transfer 16 p2366 A72-33191

Iterative computational procedure for system parameter identification and optimization, using multilevel technique 16 p2371 A72-33192

Thin walled elastic structures optimization by overall and local buckling coincidence, discussing compression column design 16 p2468 A72-33200

Nondestructive monitoring techniques to optimize performance and service tests, considering penetrating radiation, electromagnetic induction, ultrasonics, holography, microwaves, acoustic emission and thermal monitoring 16 p2397 A72-33219

Photographic-oscillographic study of discharges in atmospheric pressure helium-carbon dioxide mixtures, discussing discharge paths nonuniformity and energy input maximization 16 p2435 A72-33391

Military system and equipment Level of Repair optimization for minimum life cycle costs, considering weapon systems deployment, operation level and mobility requirements 16 p2482 A72-33793

System models for R and D processes in terms of state variables and control vectors, deriving algorithm for optimization 16 p2482 A72-33864

Exact differential equation derived for optimal design of straight nonprismatic column subject to creep buckling 16 p2474 A72-34132

Optimal design of static laterally loaded fiber reinforced plates, determining optimum load-path directions at all plate points 16 p2475 A72-34174

Mixed-mode propulsion - Optimum burn profile for two-mode systems. 17 p2596 A72-34212

On behavior strategy solutions in two-person zero-sum finite extended games with imperfect information. I - A method for determination of minimally complex behavior strategy solutions. 17 p2574 A72-34343

Phase optimization of antenna array gain with constrained amplitude excitation. 17 p2513 A72-34355

A fast numerical method for determining the optimum SNR of an array subject to a Q factor constraint. 17 p2514 A72-34372

Fast computational techniques for generalized two dimensional Wiener filtering. 17 p2532 A72-34402

Linear programming procedure for efficiency and cost optimization in aerial survey mission 17 p2521 A72-34455

Optimized 100 We multicell thermionic power supply design with high reliability, noting isomite converter performance characteristics 17 p2495 A72-34583

Problem of antenna parameter optimization in the presence of random errors 17 p2529 A72-34831

Functional equations for optimal spacecraft or rocket interception by similar vehicle within limits of dense atmosphere 17 p2621 A72-35121

Multilevel hierarchical structural design optimization, proposing component by component ascent method of dynamic programming 17 p2533 A72-35171

Design of nonlinear networks with a prescribed small-signal behavior. 17 p2533 A72-35199

Two parameter trajectory measurement optimal planning reduced to quadratic programming based on linear programming generalization for continuous case 17 p2610 A72-35261

Algorithms for optimal planning of trajectory measurement times during sampling several parameters 17 p2533 A72-35262

An operations research approach to solve complex and unstructured problems illustrated for the case of cost-plus-award fee contracts. 17 p2639 A72-35341

Invariant imbedding and optimum beam design with displacement constraints. 17 p2634 A72-35406

Asymptotically optimal procedures for certain types of moments of cutoff and terminal decisions in sequential estimation 17 p2576 A72-35419

Equivalent predictions of the circle criterion and an optimum quadratic form for a second-order system. 17 p2577 A72-35534

Optimal smoothing for continuous-time systems with multiple time delays. 17 p2534 A72-35536

Optimality conditions of second and higher orders for discrete systems, discussing functional minimization and Pontryagin maximum principle limitations 17 p2534 A72-35725

Optimization of the functions of a circuit with lumped and distributed RC parameters 17 p2535 A72-35785

Techniques for generating highly reliable redundant systems. 18 p2663 A72-36309

Practical problems and solutions in modeling physical systems with time-domain input-output measurements or specifications. 18 p2663 A72-36327

Optimal distributions for semi-circular arrays of isotropic radiators. 18 p2666 A72-36330

Adaptive nonlinear optimization of the signal-to-noise ratio of an array subject to a constraint. 18 p2660 A72-36507

Quality assurance of transistor chips for the user 18 p2669 A72-37120

A finite element approach to optimal design of plastic structures in plane stress. 18 p2739 A72-37165

Natural frequencies and dynamic response constraints in optimal structural design, considering mathematical programming aspects 18 p2739 A72-37167

Electric circuits design by combined network synthesis and optimization methods, noting approximation by nonlinear programming 19 p2776 A72-37308

Minimax method of optimizing electric circuits in the absence of constraints on the variable parameters 19 p2777 A72-37309

French monograph - Contribution to the study of extremal control systems 19 p2778 A72-37487

Specific fuel consumption and specific thrust optimization methods in turbofan cycles, noting optimum fan pressure ratio increase with turbine inlet temperature 19 p2848 A72-37746

Optimization of self-acting step thrust bearings for load capacity and stiffness. 19 p2807 A72-37895

Linear programming application to the solution of some optimum problems of reliability theory 19 p2825 A72-37995

Necessary and sufficient conditions for differentiable non-scalar-valued functions to attain extrema. 19 p2826 A72-38244

Modified Ritz method to find optimum boundaries to elliptic systems governed by Laplace or Poisson equation 19 p2826 A72-38246

Linear dynamic systems parameter identification via optimal input design, noting eigenfunction dependence on positive self adjoint operator 19 p2781 A72-38271

Data file optimal arrangement for retrieval by programmed procedures formulated as combinatorial problem, using branch-and-bound method for solution 19 p2770 A72-38619

Binary logic circuits with interconnected repeaters and inverters, discussing signal level selection to ensure maximum noise stability 19 p2767 A72-38621

Experimental technique for determination of roller bearing preload to optimize dynamic characteristics and minimize operating temperature 19 p2810 A72-38650

Certain algorithms for obtaining an approximate solution of incorrect problems on a set of monotonic functions 19 p2828 A72-38846

Application of optimization techniques to the problem of determining optical constants of thin films. 20 p2959 A72-39052

Optimal synthesis for radiator coordinates and complex amplitudes of linear antenna array for given radiation pattern 20 p2907 A72-39062

Development and optimization of the SRAM guidance and control software. [AIAA PAPER 72-824] 20 p2951 A72-39102

Memory requirements and computation times for implementing reduced consensus algorithms. 20 p2905 A72-39434

Considerations regarding the choice of the number of stages in long-range or high-altitude rockets 20 p2977 A72-39596

Modified Hestenes method of Lagrange multipliers for numerical iterative solution of mathematical programming problems in function minimizing noting improved convergence 21 p3074 A72-40226

Optimization of acoustic linings in presence of wall shear layers. 21 p3083 A72-40334

Reflector optimization of backfire antennas with the aid of the theory of the Fresnel zones 21 p3031 A72-40541

Broad-band television transmitting antenna with polydirectional characteristics for the UHF-region 21 p3031 A72-40542

Existence theorems in multidimensional problems of optimization with distributed and boundary controls. 21 p3074 A72-40548

Optimum diopter value for a view-finder of photographic camera. 21 p3054 A72-40729

Optimal search in the presence of Poisson-distributed false targets. 21 p3075 A72-40837

Frequency-sampling and transversal digital filter equalizers optimal design from specified unit impulse time response, using linear programming algorithm 21 p3033 A72-40900

Network algebra simplification through computerized minimization of Boolean functions, describing FORTRAN IV program 21 p3038 A72-41001

Comparison of design procedures of vibration absorbers for systems with random excitations. 21 p3121 A72-41230

Characterization and algorithm for optimal solution of stochastic linear programming to minimize cost 21 p3075 A72-41234

Optimal compression of constant-thickness media in a plane stress state 21 p3123 A72-41391

Anthropotechnics/human engineering/ approach to man machine system optimization, discussing task allocation and adaptations of machine dynamics, displays and controls to human operator 21 p3009 A72-41403

Algorithm for solving the schedule planning problem in mass production [AD-742589] 21 p3132 A72-41790

Determining optimum burn-in and replacement times using Bayesian decision theory. 22 p3182 A72-41982

Optimal PSK signals selection and synthesis from random sequences, ensuring minimum value of maximum side peak of autocorrelation function 22 p3153 A72-42082

Optimization algorithm for minimum margin efficiency of electronic circuits, applying to IC TTL gate and transistorized bistable multivibrator /flip-flop/ 22 p3158 A72-42086

Cylindrical shells of optimal torsional stiffness 22 p3233 A72-42112

A minimization method of describing classes in pattern recognition 22 p3198 A72-42178

Integration of aerospace vehicle performance and design optimization. [AIAA PAPER 72-948] 22 p3137 A72-42355

The influence of production imperfections on design of optimum structures. 22 p3239 A72-42841

Optimum design of circular sandwich plates. 22 p3239 A72-42843

Dangerous structural failure characteristics due to idealized design optimization, discussing shell buckling instabilities 22 p3240 A72-42895

Reliability-maximizing digital computer synthesis based on redundant network design, discussing majority structure optimal allocation technique 22 p3157 A72-43008

Optimization of the range of elastic behavior of unidirectional composites by prestraining. 22 p3194 A72-43041

German monograph - A search procedure for electronic radar. 22 p3156 A72-43054

Book - Computer simulation of dynamic systems. 22 p3157 A72-43081

Minimization of finite automata 22 p3157 A72-43082

Aeroelastic optimization of a panel in high Mach number supersonic flow. 23 p3343 A72-43327

Synthesis method for phase and loss optimized single-stage reflection type phase shifters, determining transformation coefficient 23 p3268 A72-43439

Aircraft synthesis analysis program /ASAP/ for computerized aircraft design, enabling large number of trade-off studies for design optimization [SAWE PAPER 907] 23 p3250 A72-43454

Structural design optimization via area ratio method, developing shape factor design charts [SAWE PAPER 937] 23 p3344 A72-43477

Finite element method optimization of orthotropic layered shells of revolution under mechanical and thermal loadings, considering stress-strain relationships [SAWE PAPER 939] 23 p3344 A72-43479

Space subsystems cost optimization technique for minimization of total spacecraft plus boost cost, studying orbital logistics spacecraft [SAWE PAPER 941] 23 p3342 A72-43481

Local-oscillator-circuit optimisation for minimum distortion in double-balanced modulators. 23 p3270 A72-43603

Optimisation of slope of difference-mode radiation pattern in sum-and-difference-comparison monopulse radar. 23 p3264 A72-43606

Minimum weight structural design, generalizing method for deriving sufficient optimality conditions with examples for specified maximum deflection and critical nonconservative loading parameters 23 p3347 A72-43719

Optimal search with uncertain sweep width. 23 p3308 A72-43805

Design optimization of an integrated-circuit direct access memory unit 23 p3267 A72-43841

Optimal design of a class of nonlinear networks. 23 p3276 A72-43865

Equipment assembly design optimization by operational versions determination and criteria evaluation for optimal conditions, noting rotary wing design 23 p3294 A72-44024

Optimal equalization of discrete signals passed through a random channel. 23 p3265 A72-44178

Estimates of unknown parameter from quantized observations given as sequence of evenly distributed random values, noting optimal grouping equations for general distribution function 23 p3266 A72-44218

Optimal signal processing in systems with multiple reception elements /channels/ 23 p3266 A72-44219

Optimal design of indeterminate truss using geometric programming. 23 p3354 A72-44256

Dynamic programming and the optimum design of rotating disks. 23 p3356 A72-44550

Optimal cost effective sequencing model for component reliability tests, applying to complex electronic equipment 24 p3467 A72-44654

Allocating optimum time for systems malfunction search. 24 p3406 A72-44661

Mathematical model for life support system optimization in terms of reduced mass minimization as quality criteria for energy conversion and metabolic processes 24 p3375 A72-45133

Thrust-weight ratio optimization for spacecraft orbit inclination change maneuver, deriving motion kinematics via point mass gravitational model 24 p3440 A72-45167

Space shuttle design evolution for program cost minimization, discussing refurbishment, payload impact, management cost and mission specifications and objectives 24 p3450 A72-45171

The space tug optimum cost evaluation. 24 p3468 A72-45212

Minimum-time entry of space vehicles into a planetary atmosphere 24 p3452 A72-45442

Optimization of spacecraft reentry into a planetary atmosphere 24 p3453 A72-45597

Computer algorithm for breakpoints and forcing functions determination for optimal curve fitting by piecewise differential approximation 24 p3419 A72-45632

Axisymmetric nozzles shape for thrust optimization, comparing maximum thrust circular arc and conical nozzles performances 24 p3365 A72-45784

OPTIMUM CONTROL

U OPTIMAL CONTROL

OPTIMUM THRUST PROGRAMMING

U THRUST PROGRAMMING

OPTOMETRY

Head mounted monkey eye orientation measuring system for performance of brightness discrimination tasks 03 p0318 A72-13073

Visual acuity measurement methods, comparing angular acuity by Beyne optometer and morphoscopic acuity by Mercier optometric scale 07 p0927 A72-19246

Visual acuity measurement by dynamic and static tests as function of target velocity and exposure time 13 p1911 A72-30042

OR-GATES

U GATES [CIRCUITS]

ORBIT CALCULATION

Autonomous Hamiltonian system with two degrees of freedom, investigating origin and periodic orbits stability with two time variable method 01 p0123 A72-10030

Crater 9 meteorite /Argentina/ entry trajectory and orbital calculations, determining masses and velocities from dynamic conditions at impact 02 p0275 A72-11599

Satellite orbit determination accuracy from radio interferometer tracking data containing systematic errors, using digital computer techniques on Symphonie transfer orbit [DFVLR-SONDDR-212] 02 p0182 A72-12744

Relative stellar orbit determination in clusters NGC 5460, 5617, 6067, 6405 and 6494, presenting gravitational potential, orbital elements and anomalistic period 03 p0434 A72-13495

Orbit distributions of hypothetical comets from Jovian surface eruptions, calculating orbital elements with computer 03 p0439 A72-14240

Book on orbit determination, space navigation and celestial mechanics covering two body problem integration, units and constants, perturbation theory, orbit correction, etc 05 p0712 A72-15862

Artificial earth satellites orbit plane determination accuracy in terms of local vertical sensor errors and gyroscope drift 05 p0717 A72-16441

Error covariance matrix square root calculation in orbit determination from ground based observations 05 p0720 A72-16752

Error covariance matrix evaluation at end of orbit extrapolation in terms of state vectors at measurement, discussing computation and interpretation 05 p0720 A72-16753

Book on orbital mechanics covering perturbation theory, many body problem, conic sections, orbit determination, canonical transformations and Hansen methods, moving coordinates, etc 06 p0879 A72-17820

Orbit determination using Kalman-Bucy filter to estimate state and unmodeled acceleration approximated as first order stationary Gauss-Markov process 08 p1145 A72-20867

Hill variable modification of Brouwer satellite theory algorithm for simplified orbital element and perturbation calculations and orbital eccentricity generalization 08 p1237 A72-21749

Visual binary star investigations, considering parallaxes, masses, absolute magnitudes and orbit computation 09 p1390 A72-23502

Satellite coordinates calculation for arbitrary inclinations and orbit eccentricity below Laplace limit 10 p1543 A72-24633

Nonlinear filtering for random signals in statistically unknown noise, noting application to satellite orbit determination, aircraft navigation and missile tracking 11 p1611 A72-25986

Near circular orbit elements determination as functions of satellite initial speed and coordinates deviation by mathematical expectation procedure 11 p1724 A72-26912

Minor planets orbital elements determination accuracy from planets coincident optical observations 13 p2035 A72-28439

Earth shadow effects on light artificial satellite orbital motion 13 p2051 A72-28440

Trans-Plutonian planet effect on Halley comet, considering perihelion errors and comet residuals 13 p2038 A72-29012

Earth-moon system periodic orbits calculation by modified quasi-linearization combined with particular solutions method, using restricted three body model 14 p2149 A72-30232

Heliocentric orbit from modified Laplace and Leuschner method with optimal time interval between five successive observations 14 p2149 A72-30233

Geostationary artificial satellite orbital parameters calculation, taking into account lunar, solar and light pressure perturbations 14 p2150 A72-30451

Optimum elliptic orbit characteristics of planetary artificial satellite based on earth-planet-earth flight 14 p2151 A72-30472

Computer calculation of artificial satellite ephemerides from Smithsonian mean orbital elements, comparing observed and computed topocentric equatorial coordinates 14 p2087 A72-30480

Spectroscopic binary orbital elements calculated by FORTRAN IV computer programs, considering period, radial velocity Fourier coefficients and element improvement by least squares method 14 p2159 A72-30736

Direct periodic orbits in planar restricted barycentric three body problem, using Poincare variables and Hamiltonian function 15 p2307 A72-31763

Orbit determination strategy, detailing optimization criterion correlation with measurement errors 15 p2307 A72-31817

Skyнет 1 synchronous satellite orbit determinations and longitude acceleration due to tesseral harmonics of earth gravity, using tracking station range data 15 p2321 A72-31949

The orbit of Cosmos 307 rocket and its use in atmospheric research. 17 p2545 A72-34632

Russian book - Mathematical methods of modeling in space studies 17 p2607 A72-35026

New orbital elements for moon and planets. 17 p2609 A72-35106

Existence proof and boundary regions for multiple solutions in minor planets circular orbits determination 18 p2723 A72-36085

Accuracy of outer-planet ephemerides. 19 p2857 A72-37683

Relativity gyroscope experiment at arbitrary orbit inclinations. 20 p2972 A72-39870

Collision periodic orbits calculation in restricted three body problem 20 p2973 A72-39885

New method of calculating disturbed ephemeris of minor planets 21 p3102 A72-40095

Representation of the coordinates of a satellite of a spheroidal planet with the aid of series expansions 21 p3102 A72-40099

Russian book - Algorithms for calculation of navigation data on spacecraft position. 21 p3103 A72-40460

Satellite orbit computations using gravity anomalies. 21 p3104 A72-40493

Invalidity of Neptune predicted position derivation from perturbations on Uranus via method neglecting eccentricity 21 p3111 A72-41474

First order theory of satellite orbit determination with time difference data for synchronous equatorial spacecraft, applying to VLBI experiments with ATS-3 [AIAA PAPER 72-924] 21 p3112 A72-41568

Orbit prediction for artificial satellites via numerical averaging technique, presenting algorithm for planetary equations solution [AIAA PAPER 72-934] 21 p3112 A72-41572

Long-term orbit prediction using two-variable asymptotic expansions and the automated manipulation capabilities of the FORMAC language. [AIAA PAPER 72-938] 21 p3113 A72-41576

Orbit of the visual double star ADS 7896 equals JDS 2052 equals A 2768 21 p3114 A72-41848

Terminal orbit of comet 1937 V /Finisler/ 22 p3220 A72-41917

Equations for 15th-order geopotential coefficients from the orbit of Transit 1B. 22 p3169 A72-42009

Least squares method for satellite motion parameters determination in orbital plane, using altimeter distance to planet surface measurements 22 p3223 A72-42202

Transcendental equations solution for satellite Kepler orbit determination from coordinates, velocity and time components, using Lambert-Euler relation 22 p3223 A72-42204

Velocity space maps and transforms of tracking observations, for orbital trajectory state analysis. 24 p3440 A72-45135

Thrust-weight ratio optimization for spacecraft orbit inclination change maneuver, deriving motion kinematics via point mass gravitational model 24 p3440 A72-45167

The estimation of accuracy of short-term atmosphere density prediction. 24 p3398 A72-45173

Discrepancy between Brown theory and Griffith values for lunar perigee and node mean motions partial derivatives with respect to moon mean motion 24 p3442 A72-45241

Application of advanced filtering methods to the determination of the interplanetary orbit of Mariner '71. [AIAA PAPER 72-906] 24 p3443 A72-45427

Spacecraft navigation systems for Mariner Jupiter-Saturn 1977 Project, considering maneuvers, orbit determination and data requirements
[AIAA PAPER 72-926] 24 p3423 A72-45432

Mariner 9 Mars orbital trajectory analysis from earth based radio data, considering gravity field, n-body perturbation and solar radiation pressure effects
[AIAA PAPER 72-928] 24 p3443 A72-45434

ORBIT DECAY

Atmospheric density near 150 km altitude from Cosmos 316 orbital decay, noting density increases during geomagnetic storms
05 p0655 A72-16070

Gas-surface interaction parameters and atmospheric density determination from satellite drag induced orbital decay measurements
07 p0910 A72-20116

Geopotential harmonics of fifteenth order obtained from decaying satellite orbits analysis
15 p2311 A72-32001

Long term stability of earth and lunar orbiters - Theory and analysis.
[AIAA PAPER 72-936] 21 p3112 A72-41574

A thermospheric model from satellite orbital decay densities and incoherent scatter temperatures.
24 p3400 A72-45595

ORBIT EQUATIONS

U ORBITAL MECHANICS

ORBIT PERTURBATION

NT SATELLITE PERTURBATION

Satellite in eccentric Keplerian orbit transgressing Roche limit about rigid sphere, considering time dependent evolution problem with various centrifugal and tidal forces
01 p0134 A72-11145

Draconitic-sidereal orbital period difference estimation formula for near-circular orbit satellites with air drag
02 p0279 A72-12048

Gravity model for spacecraft orbit prediction with gravitational anomalies, discussing gravity dipoles and disturbing acceleration tangential component
[AAS PAPER 71-375] 02 p0283 A72-12424

Numerical integration of element T /transit time through perihelion/ in perturbations of near parabolic comet orbits
03 p0436 A72-13829

Rotating earth oblateness and equator ellipticity influence on near-equatorial synchronous satellite behavior, using nonlinear mechanics asymptotic method
03 p0436 A72-13835

Jupiter-induced perturbations in orbital elements of Callisto artificial satellite, noting correction requirement due to Jupiter polar flattening
04 p0572 A72-14634

Long period perturbations arising in orbits of artificial satellites with large surface to mass ratio under solar radiation pressure and earth oblateness effects
04 p0572 A72-14637

General perturbations theory for canonical systems extended to noncanonical systems, applying to perturbed Kepler motion
04 p0573 A72-14875

Earth motion nutations, considering external forces effects from sun and moon
04 p0575 A72-15030

Book on orbital mechanics covering perturbation theory, many body problem, conic sections, orbit determination, canonical transformations and Hansen methods, moving coordinates, etc
06 p0879 A72-17820

Earth gravitational field determination based on long periodic perturbations in orbital motion of satellites, estimating tesseral coefficients errors
07 p0976 A72-19817

Stellar perturbations of eccentric orbits of long period comets
07 p1081 A72-20232

Planetary perturbation of orbits of long period comets with large perihelion distances
07 p1081 A72-20236

Outer planet mass determination limitations from mutual motion perturbations
08 p1236 A72-21636

Stability solutions of collective oscillations of spherical star cluster rotating in near circular orbits in self consistent field
08 p1239 A72-22180

Dynamic system motion stability estimation with Liapunov function in quadratic form, applying to circular satellite orbit stability in axisymmetric gravitational field
14 p2161 A72-31079

Asteroids and comets orbit perturbation equations for small eccentricity values
14 p2161 A72-31080

Upper atmosphere density from orbital drag on Cannon Ball II and Musket Ball satellites
15 p2227 A72-31963

Pagcos balloon satellite orbital perturbations due to erratic solar radiation pressure induced accelerations, comparing modified Smith perturbation model calculations with photometric observations
15 p2228 A72-31975

Secular and long term periodic perturbation effects of third body upon particle motion in three body problem, discussing mass motion in Jovian gravitational field
15 p2312 A72-32120

Earth gravitational field determination based on long periodic perturbations in orbital motion of synchronous satellites, estimating tesseral coefficients errors
17 p2550 A72-35742

Stability solutions of collective oscillations of spherical star cluster rotating in near circular orbits in self consistent field
18 p2724 A72-36236

Interaction between attitude libration and orbital motion of a rigid body in a near Keplerian orbit of low eccentricity.
20 p2968 A72-39197

Cometary parent bodies transfer to short period orbits by Jupiter caused gravitational disturbances, noting qualitative analysis of orbits evolution
22 p3219 A72-41913

Correction of the orbits of 161 minor planets
24 p3437 A72-44763

ORBITAL ELEMENTS

Orbital elements and onboard transmitter frequency drift of active satellite from Doppler and angle data recorded at single receiving station
02 p0171 A72-11664

Draconitic-sidereal orbital period difference estimation formula for near-circular orbit satellites with air drag
02 p0279 A72-12048

Sporadic meteor orbital parameters measurement by continuous radar, determining out-of-atmosphere rate
02 p0283 A72-12524

Relative stellar orbit determination in clusters NGC 5460, 5617, 6067, 6405 and 6494, presenting gravitational potential, orbital elements and anomalistic period
03 p0434 A72-13495

Numerical integration of element T /transit time through perihelion/ in perturbations of near parabolic comet orbits
03 p0436 A72-13829

Orbit distributions of hypothetical comets from Jovian surface eruptions, calculating orbital elements with computer
03 p0439 A72-14240

Comet orbits with perihelion distances and inclinations from Jupiter, calculating osculating orbital elements and distributions
03 p0439 A72-14241

Jupiter-induced perturbations in orbital elements of Callisto artificial satellite, noting correction requirement due to Jupiter polar flattening
04 p0572 A72-14634

Astronomical constants - IAU Conference, Heidelberg, August 1970
04 p0574 A72-15025

Planetary mass errors effects on orbit determinations, discussing Ceres mass from influence on Pallas orbit
04 p0575 A72-15035

Lunar elements and fundamental constants corrections from meridian observations for nodal period, determining corrections to solar mean anomaly and eccentricity
06 p0875 A72-17298

Jacobian matrix partial derivatives for orbital motion representation by time step power series
06 p0877 A72-17651

Soviet book on geometrical space geodesy covering satellite observation, Keplerian laws, two body problem and orbit element determination
06 p0879 A72-17817

Periodic comets orbital elements and nongravitational parameters, discussing mass loss rates, time effects and nuclear core-mantle model
06 p0880 A72-17863

Computer program for photometric orbital elements determination of eclipsing binary stars
06 p0883 A72-18022

Restricted two body problem anomalistic and sidereal orbital periods in coordinate and proper time, noting cosmological constant
06 p0884 A72-18035

Orbital elements from radial velocity measurements for single line K giant binary star 4 Ursae Minoris
07 p1071 A72-19337

Statistical and probabilistic analyses of comet groups existence with similar orbital elements, considering gravitational capture by trans-Neptunian planets
07 p1075 A72-19559

Secular perturbations of artificial earth satellites Keplerian orbital elements from arbitrary-order zonal harmonics in geopotential series expansion
07 p1078 A72-19982

Evolutionary processes /tidal dissipation, close approach and collision/ responsibility for commensurability relations between orbital periods and orbital-spin periods in solar system
07 p1083 A72-20465

Comets heliographic coordinates and angles quadrants from orbital elements
08 p1229 A72-20832

Longitude dependent perturbation inducing portion of geopotential as function of artificial earth satellite orbital elements
08 p1158 A72-21160

Orbital elements evolution for two body problem with decreasing mass according to Jeans mode
08 p1236 A72-21638

Satellite orbital inclination change due to rotating upper atmosphere with day-to-night density variation, deriving resonance conditions
08 p1241 A72-21640

Hill variable modification of Brouwer satellite theory algorithm for simplified orbital element and perturbation calculations and orbital eccentricity generalization
08 p1237 A72-21749

Near earth satellite orbit parameters correction, discussing least squares approach
09 p1387 A72-22770

Lunar limb charts comparison, computing corrections to orbital elements and systematic and random errors
09 p1388 A72-23056

Venus and Mars visible geocentric declinations from daytime observations with Wanschaff vertical circle compared to nighttime results
09 p1388 A72-23065

Pallada, Vesta, Irida and Harmony asteroids positions computed from observations with 400 mm photographic telescope
09 p1389 A72-23066

Secular and periodic variations of orbital elements of Mars satellites due to oblateness and solar attraction
10 p1541 A72-24471

Solar radiation pressure effects on orbital evolutions of light artificial earth satellites
10 p1543 A72-24632

Computer program for photometric orbital elements determination of eclipsing binary stars
11 p1718 A72-25958

Restricted two body problem anomalistic and sidereal orbital periods in general relativistic coordinate and proper time, noting cosmological constant
11 p1719 A72-25971

Near circular orbit elements determination as functions of satellite initial speed and coordinates deviation by mathematical expectation procedure
11 p1724 A72-26912

Minor planets orbital elements determination accuracy from planets coincident optical observations
13 p2035 A72-28439

Sub-Mercurial planet Vulcan observation data, calculating orbital elements, angular size and velocity radial distance and object diameter
14 p2149 A72-30234

Statistical data processing method for accuracy evaluation of satellite orbits parameters obtained from onboard measurements of two stars angular positions
14 p2151 A72-30454

Data processing method for optimal prediction of spacecraft orbital elements, using dynamic and quadratic programming
14 p2151 A72-30455

Spectroscopic binary orbital elements calculated by FORTRAN IV computer programs, considering period, radial velocity Fourier coefficients and element improvement by least squares method
14 p2159 A72-30736

Phobos and Deimos orbital characteristics, noting related Martian physical properties determination
15 p2302 A72-31277

Comets formation from Jupiter satellite Io surface eruption using particle trajectory analysis and comet orbital elements calculation
15 p2305 A72-31391

Earth satellite orbit motion in terms of probability densities and distributions for large populations and single satellites
15 p2307 A72-31692

Program for orbital determination and prediction of satellite positions from observations at one station
15 p2268 A72-31941

Radio meteor orbit inclination angle dispersions for semimajor axis intervals compared with photographic meteors
16 p2456 A72-33514

Relative orbit inclination dispersions of minor planets, fireballs and photographic and radio meteors, indicating common origin
16 p2456 A72-33515

Atmospheric absorption height determination from orbital elements during solar radiation satellite observation
16 p2386 A72-33603

Solar radiation pressure effects on balloon satellite behavior, noting orbital eccentricity variations
16 p2463 A72-34182

Ephemeris time, lunar orbital elements and FK4 equinox correction from the observations of the moon by the method of equal altitudes.
17 p2603 A72-34274

Longitude dependent perturbation inducing portion of geopotential as function of artificial earth satellite orbital elements

17 p2545 A72-34451

The orbit of Cosmos 307 rocket and its use in atmospheric research.

17 p2545 A72-34632

Equinoctial orbit elements position and velocity vectors partial derivatives matrices for two body problem, discussing application to general and special perturbations

17 p2609 A72-35104

New orbital elements for moon and planets.

17 p2609 A72-35106

Secular variations of the first order of elements for the four major planets - Comparison with Le Verrier and Gailliot

18 p2727 A72-36734

On the effects of gravitational absorption on orbits of artificial earth satellites.

18 p2728 A72-36761

Meteoroid bodies particle density from basal photographs, noting dependence on orbital parameters

20 p2969 A72-39395

Determination of the orbits of artificial satellites by the integrated Doppler effect method

20 p2974 A72-40023

Equinoctial orbit elements - Application to artificial satellite orbits.

[AIAA PAPER 72-937]

21 p3112 A72-41575

Secular perturbations in the motion of artificial earth satellites

21 p3114 A72-41770

Orbit of the visual double star ADS 7896 equals JDS 2052 equals A 2768

21 p3114 A72-41848

An isotopic criterion for estimating the length of meteorite orbits

22 p3223 A72-42160

The dependence on inclination of the planetary perturbations of the orbits of long-period comets.

22 p3224 A72-42378

The estimation of masses of individual galaxies in clusters of galaxies.

22 p3227 A72-42551

Discrepancy between Brown theory and Griffith values for lunar perigee and node mean motions partial derivatives with respect to moon mean motion

24 p3442 A72-45241

Meteor streams orbital elements dispersion from photographic data, and asteroid stream percentage variation with concentration of orbits to ecliptic plane

24 p3445 A72-45462

Observation and feature variations of comet 1969e before and during the perihelion passage.

24 p3445 A72-45465

On the existence of a resonance-captured 'quasi-satellite' of the earth.

24 p3446 A72-45471

ORBITAL LAUNCHING

Extending the utility of the Space Shuttle as a space rescue vehicle.

24 p3449 A72-45130

Study of shuttle-based systems for high-energy planetary missions.

24 p3441 A72-45189

ORBITAL MECHANICS

NT KEPLER LAWS

Consecutive collision orbits characterized by particle ejection from mass along x axis in restricted three body problem

01 p0122 A72-10006

Critique of Brown lunar theory, discussing planetary orbits, earth and moon figure effects and second order terms

01 p0122 A72-10009

Recurrence relation derived for homogeneous normalized satellite inclination function with three parameters in series expansion for geogravitational potential

01 p0123 A72-10012

Periodic orbit families emanating from Lagrange triangular point L4 in restricted three body problem with mass ratio parameter equal to Routh critical mass ratio

01 p0123 A72-10013

Hori perturbation theory equivalence to von Zeipel theory established to third order approximations in perturbed elliptic motions

01 p0129 A72-10796

Motion stability of sphere and homogeneous semi-infinite rotating cylinder in circular orbits and monoenergetic streams, integrating by trajectories

02 p0285 A72-12832

Liapunov stability of rigorous particular solutions /corresponding to libration points/ of three body problem, determining motions of satellite influenced by two spherical bodies

03 p0436 A72-13823

Comet hypotheses, examining orbit axes and perihelions spatial distribution as possible interstellar origin

03 p0438 A72-13978

Conditionally periodic motions of particle in gravitational field of axisymmetric oblate planet, describing

canonical transformations for Hamiltonian function reduction to normal form

04 p0572 A72-14638

Spatial motion of two thread-coupled bodies along satellite circular orbit, discussing system equilibrium position stability and phase trajectories

04 p0582 A72-15003

German monograph on Poincare orbit stability in restricted three body problem, using canonical mappings of annulus and perturbation method

05 p0689 A72-16044

Collisionless stellar dynamics, considering Lin wave interactions for orbital theory

05 p0713 A72-16053

GEOS satellite orbit determination and prediction errors from optical tracking systems and gravity models, estimating resonant coefficients

06 p0877 A72-17653

Book on orbital mechanics covering perturbation theory, many body problem, conic sections, orbit determination, canonical transformations and Hansen methods, moving coordinates, etc

06 p0879 A72-17820

Hamilton-Jacobi equation for bounded plane circular three body problem with construction of algebraic partial integrals and periodic orbits

06 p0850 A72-18709

Short period comets orbital evolution and major planets gravitational effects, discussing cometary cloud formation, diffusion, motion and discovery

07 p1078 A72-19981

Gravitational system dynamics, discussing massive-light star mixtures with collisions and systems with equal mass objects

08 p1231 A72-21121

Flexibly stabilized satellite orientation determination by stellar sensors and magnetic damping of rotation

08 p1240 A72-21139

Librational transverse oscillations boundary value problems of heavy thread on orbiting satellite, determining equilibrium and eigenfunctions

08 p1240 A72-21142

Aerodynamic and gravitational effects on relative motion of two orbiting point masses connected by flexible nonexpandable thread

08 p1240 A72-21143

Planar restricted three body problem periodic solutions with bridges connecting direct and retrograde circular orbits

11 p1721 A72-26153

Infinitesimal mass revolution around smallest primary of restricted four body problem, discussing element perturbation

14 p2161 A72-30913

Orbital correction problems for vehicle around spherical planet, considering velocity, fuel consumption and trajectory optimization

15 p2308 A72-31819

Fourier analysis for geopotential resonance effect on satellite orbits, calculating 13th harmonic influence on GEOS 2 and BE-C mean longitude

15 p2309 A72-31939

Aerodynamic drag at high latitudes observed from Molniya satellites orbit analysis, suggesting upper atmosphere density change

15 p2229 A72-31989

Singularity of noncircular cross section zero velocity torus circumscribing area with three dimensional orbit of stationary stellar system star

16 p2460 A72-34014

Further periodic solutions of the three-dimensional restricted problem. II.

17 p2604 A72-34444

Long-term prediction of artificial satellite motion along almost circular orbits allowing for a random number of zonal harmonics

17 p2607 A72-35033

The determination of zonal harmonic coefficients of the terrestrial potential

19 p2790 A72-38173

Terrestrial and lunar orbital and rotational motion behavior, discussing kinematic theory and ground and space vehicle based observation techniques

19 p2865 A72-38479

Three body problem second kind periodic orbit existence proof based on Weinstein theorem

19 p2867 A72-38553

Book - Astrodynamics: Orbit correction, perturbation theory, integration

19 p2868 A72-38723

Loosely stabilized satellite orientation determination by stellar sensors and magnetic damping of rotation

20 p2976 A72-39244

Librational transverse oscillations boundary value problems of heavy thread on orbiting satellite, determining equilibrium and eigenfunctions

20 p2977 A72-39247

Aerodynamic and gravitational effects on relative motion of two orbiting point masses connected by flexible nonexpandable thread

20 p2977 A72-39248

Near parabolic orbit and short periodic comets motion, discussing circumsolar cloud and nongravitational disturbances

20 p2974 A72-40068

Comparison of the classical and the global solutions of the ideal resonance problem.

21 p3085 A72-41047

A two-parameter survey of periodic orbits in the restricted problem of three bodies.

21 p3106 A72-41049

The concept of reference loci applied to four-body dynamics.

24 p3440 A72-45137

Critical inclinations and eccentricities concepts for N planet problem, applying results to general three body problem

24 p3442 A72-45239

ORBITAL MOTION

U ORBITS

ORBITAL POSITION ESTIMATION

Geodetic latitude and altitude from geocentric coordinates.

17 p2547 A72-35103

Equinoctial orbit elements position and velocity vectors partial derivatives matrices for two body problem, discussing application to general and special perturbations

17 p2609 A72-35104

Photographic observation of artificial earth satellites without the aid of time recording devices. II

17 p2517 A72-35384

Least squares method for satellite motion parameters determination in orbital plane, using altimeter distance to planet surface measurements

22 p3223 A72-42202

On application of Kalman filtering technique to on-line orbit estimation of a launching vehicle.

22 p3203 A72-43142

ORBITAL RENDEZVOUS

NT EARTH ORBITAL RENDEZVOUS

Nonlinear programming iteration scheme for fuel-time optimization of satellite orbital rendezvous terminal phase

03 p0437 A72-13838

European reusable space tug, discussing computer controlled attitude stabilization and maneuvering system design for orbital rendezvous and docking

05 p0725 A72-16446

Relative motion of active interceptor spacecraft approaching passive craft in central gravitational field using dimensionless differential equations similarity coefficients method

05 p0728 A72-16592

Spacecraft soft orbital rendezvous guidance involving orbital transfer maneuver for velocity vector directional coincidence to reduce terminal relative velocity

05 p0729 A72-16757

Elliptical orbiting spacecraft minimum fuel consumption rendezvous maneuver, formulating variational extremum problem with constraints

14 p2150 A72-30329

Optimal feedback controller design based on cooperative game described by quadratic cost functional under linear differential equation constraints, applying to satellite terminal rendezvous

15 p2267 A72-31789

Spacecraft soft orbital rendezvous guidance involving orbital transfer maneuver for velocity vector directional coincidence to reduce terminal relative velocity

17 p2622 A72-35260

Relative motion of active interceptor spacecraft approaching passive craft in central gravitational field, using dimensionless differential equations similarity coefficients method

19 p2869 A72-37564

The space tug orbital operations.

24 p3451 A72-45196

ORBITAL SHOTS

Titan 3 family systems analysis for delivering multiple communication satellites to geostationary orbits [AIAA PAPER 72-570]

12 p1870 A72-27378

ORBITAL SIMULATORS

U SPACE SIMULATORS

ORBITAL SPACE STATIONS

NT EOSS

NT HALO ORBIT SPACE STATION

NT ORBITAL WORKSHOPS

NT SALYUT SPACE STATION

Nonlinear and digital synthesis of computerized optimal control systems for long-life orbital stations and laboratories

05 p0724 A72-16434

Space shuttle, tug and orbital station transportation system benefits and applications, noting European economic implications

08 p1229 A72-20977

NASA research and applications module /RAM/ for interim space station development and possible missions with space shuttle

08 p1240 A72-20978

NASA space programs, discussing future Apollo, Skylab, orbiting space station, space shuttle and deep space projects

Human role in space shuttle on-orbit maintenance vs space station modules earth return, considering feasibility and cost effectiveness
[AIAA PAPER 72-229]

Space tools and support equipment for earth orbital systems maintenance, replacement and repair, discussing Skylab requirements and teleoperator applications
[AIAA PAPER 72-230]

Report to COSPAR on 1971 Soviet space programs, discussing moon, planets, cosmic radiation, interplanetary medium, magnetosphere, upper atmosphere, meteorological, orbital station and biomedical studies

Astronomical observations from astrophysical observatory onboard orbital space station controlled by astronaut, discussing telescope orientation outside of spacecraft

Parabolic switching boundaries method for optimal fuel consumption control of manned orbital space vehicles

Theory of an experiment in an orbiting space laboratory to determine the gravitational constant.

The Space Station Prototype Program - The development of a regenerative life support system for extended-duration missions.

The space tug orbital operations.

Astronomy from a space platform; Proceedings of the Symposium, Philadelphia, Pa., December 27, 28, 1971.

Space astronomical observatory mission planning, analysis and operation and data utilization in terms of space and ground facility instruments and support subsystems

Electronic imaging devices for astronomy from a space platform.

Future giant-aperture orbital space telescope design based on active optics and electro-optical techniques, discussing laser interferometry and precise servomechanisms roles

Orbital transfer

U TRANSFER ORBITS

ORBITAL VELOCITY

Minimum velocity change noncoplanar two and three impulse orbital transfer from regressing oblate earth assembly parking ellipse into flyby trans-Martian asymptotic velocity vector

Orbital correction problems for vehicle around spherical planet, considering velocity, fuel consumption and trajectory optimization

Equinoctial orbit elements position and velocity vectors partial derivatives matrices for two body problem, discussing application to general and special perturbations

ORBITAL WORKERS

MORL and Orbital Biomedical Laboratory projects, reviewing crew accommodation, spacecraft and booster requirements and biomedical measurements

Human role in space shuttle on-orbit maintenance vs space station modules earth return, considering feasibility and cost effectiveness

[AIAA PAPER 72-229]

ORBITAL WORKSHOPS

In orbit servicing of spacecraft.

[AIAA PAPER 72-731]

ORBITALS

NT ELECTRON ORBITALS

NT MOLECULAR ORBITALS

NT SLATER ORBITALS

Surface potential effects on splitting of p- and d-orbitals of atoms and ions approaching bcc and fcc substrates

High energy particle and photon orbital and vortical motions in Kerr metric outside equatorial plane in gravitational field

Resonant diffusion in the presence of strong plasma turbulence.

ORBITER PROJECT

Outer planet low thrust orbiter missions, comparing three body numerical results with two methods of patching together two body solutions

ORBITING ASTRONOMICAL OBSERVATORY

U OAO

ORBITING FROG OTOLITH

OFO A orbital flight recording of bullfrog vestibular gravity sensor nerve fiber pulses for assessing necessity of artificial gravity during prolonged weightlessness

23 p3254 A72-43391

ORBITING GEOPHYSICAL OBSERVATORY

U OGO

ORBITING SATELLITES

U ARTIFICIAL SATELLITES

ORBITING SOLAR OBSERVATORY

U OSO

ORBITS

NT APHELIONS

NT APOGEES

NT CIRCULAR ORBITS

NT EARTH ORBITS

NT ECCENTRIC ORBITS

NT ELLIPTICAL ORBITS

NT EQUATORIAL ORBITS

NT INTERPLANETARY TRANSFER ORBITS

NT LUNAR ORBITS

NT PARKING ORBITS

NT PERIGEEES

NT PERIHELIONS

NT PLANETARY ORBITS

NT POLAR ORBITS

NT SATELLITE ORBITS

NT SOLAR ORBITS

NT SPACECRAFT ORBITS

NT STATIONARY ORBITS

NT TRANSFER ORBITS

NT TROJAN ORBITS

NT TWENTY-FOUR HOUR ORBITS

Collision periodic orbits calculation in restricted three body problem

20 p2973 A72-39885

ORDER-DISORDER TRANSFORMATIONS

Cation distribution observation over nonequivalent lattice sites in shocked orthopyroxene, noting Mg and Fe order-disorder

Order-disorder transition cooling effects on V carbide superlattice domain structure, using electron and optical microscopy

Alloying and heat treatment ordering effect on hydrogen diffusion coefficients, penetrability and solubility in Pd-Al alloys

Short range order and nucleation of long range order in Ni-rich Ni-Nb alloys, observing electrical resistivity changes dependence on solute concentration

Order-disorder reaction in Ni-V, Ni-V-Nb and Ni-V-Ta alloys, estimating critical temperature

Laser pulse heating inability to quench in disorder in Fe-Al alloy

Neutron irradiation produced lattice disorder in Li doped float zone melted n-p type Si solar cells

Soviet monograph on thermoplastic hardening of high strength martensitic steels and Ti alloys by ordering dislocation structure

Order-disorder transition in metastable splat cooled Ti-rich Ti-Fe alloys from phase formation, constitution and crystal chemistry viewpoint

Electron bombardment disordering of ordered Ni-Mn alloy along different crystallographic directions

Epitaxy and vacancy structure of TiSe with type B8 ordering

Ordering degree effect on elementary excitation spectrum gaps in nonideally ordered solid systems, obtaining Green functions for valence and conduction electrons calculations

X ray analysis of internal friction strains in nickel molybdenide during ordering process at 650-700 C, using torsional pendulum method for friction measurements

Ordered crystallization casting of Ni superalloys for turbine blades, using power down and high rate solidification processes

Ordered growth and etching of uranium and zirconium oxide-tungsten fiber refractory composites, using X ray diffraction and scanning electron microscopy

Hydrostatic pressure effect on itinerant antiferromagnetic ordering in Cr-Fe alloys with Ru and Mn additions

Lattice disorder effects in ion implanted Si and compound semiconductors, using IR and EPR measurements

Ordering in fcc lattice ternary alloys with allowance for atoms interactions, noting phase transformation critical temperature and superlattices existence

12 p1828 A72-27432

12 p1859 A72-28074

13 p1976 A72-28691

Temperature dependent electron density of state and dc resistivity of disordered binary alloys, using single band thermal disorder model

Electron microscopic and X ray analyses of ordering kinetics in Ni-Mo alloys, noting lattice type change and complex domain structure formation causes

Heterogeneous order-disorder transformation in Ni-Mo alloy at 78 K after annealing, using ion field emission microscopy

Model with lamellae and tie molecules disordered alignments to explain relation between stress-strain behavior and bond fracture in highly oriented polymer fibers

Solid-state phase transformations.

In vitro of the mechanism of radiative recombination in study of monocrystalline arsenic selenide.

Domain structures in metal crystals, investigating ordering in Ni-Mo alloys

Calorimetric investigation of atom ordering effects in a Ni2Cr alloy

Influence of alloying elements on ordering in alloys of the nickel-molybdenum system

Contribution to the study of phenomena of ordering of defects in single crystals of alumina- or zirconia-base refractory materials

23 p3302 A72-44000

ORDINATES

U COORDINATES

ORDNANCE

Titanium powder metallurgy in ordnance applications, discussing hardware, weight economies and market development

Minuteman HERO /hazards of electromagnetic radiation to ordnance/ preflight testing, describing ordnance monitoring system based on fiber optic data links

Flight mechanics of spin stabilized rotating disks for special ordnance delivery, considering aerodynamic parameters relation to dynamic stability and orientation

[AIAA PAPER 72-982]

ORGAN WEIGHT

Elastic lung shaped model for distribution analysis of weight induced stresses, strains and surface pressures in lung

Adrenal morphology changes in rats subjected to hypokinesia

23 p3255 A72-43905

ORGANIC CHEMISTRY

Organic cosmochemistry evolution, discussing radio astronomical observations, lunar soil samples, meteorite analysis and interstellar gas cloud molecules

Carbon chemistry of Apollo 14 size-fractionated fines, noting solar wind activity effect

Simulation study of lunar carbon chemistry, noting hydrocarbon production by solar wind interaction with fines

Chemical evolution in microenvironment reactions system due to dominant energy or mass parameter, discussing complex organic molecule synthesis

Life beyond solar system, discussing planetary formation and prebiological organic chemistry developments and interstellar communication

Life origin and primordial organic chemistry, considering Darwinian evolution, spontaneous generation, primitive atmospheres, interstellar matter, energy sources, macromolecular synthesis, moon and Jupiter

Atmospheric organic vapor effects on electric contact erosion, deriving showering arc duration, gap breakdown, arc number and energy

Chemical evolution and the origin of life - Bibliography supplement 1970.

Complex organic molecules in interstellar space, discussing molecular identification reliability, prebiological organic synthesis, interstellar and planetary biology and UV natural selection

Quantum-chemical model of organic ring-shaped molecule with persistent magnetization at microscopic level

22 p3150 A72-42318

ORGANIC COMPOUNDS

NT ADENINES

NT ADENOSINE DIPHOSPHATE [ADP]

NT ADENOSINE TRIPHOSPHATE [ATP]

NT ADENOSINES
 NT AMINO ACIDS
 NT CARBON TETRAFLUORIDE
 NT FATTY ACIDS
 NT FLUOROCARBONS
 NT FLUOROXYHYDROCARBONS
 NT GLUTATHIONE
 NT LEUCINE
 NT METHIONINE
 NT NUCLEOTIDES
 NT OLEIC ACID
 NT ORGANIC LIQUIDS
 NT OXIDASE
 NT PEPTIDES
 NT PROTOPROTEINS
 NT SEROTONIN
 NT THYROXINE
 NT TRYPTOPHAN

Gas bubble damage centers in organic glass produced by quasi-steady ruby laser pulse induced high temperature heating, using high speed photography 01 p0079 A72-10373

Apollo 12 retrieved Surveyor 3 TV camera mirror surface and camera-shroud organic contamination attributed to spacecraft outgassing and engine exhaust products 03 p0415 A72-12948

Martian atmospheric volatiles history, noting initial chemical conditions favorable to abiotic organic synthesis 04 p0569 A72-14503

Shock wave contributions from micrometeorites, meteors, meteorites and thunder to organic compounds formation in primeval atmosphere 04 p0572 A72-14760

Comet collisions in planetary nebulae as source of organic compounds in universe in preplanetary era, noting nucleic acid bases in carbonaceous meteorites 04 p0471 A72-14802

Chemical evolution of carbonaceous chondrite organic compounds, discussing similarity to terrestrial abiogenic material 04 p0484 A72-14804

Organic materials detection on planetary surfaces with in situ gas chromatography and mass spectrometry 04 p0573 A72-14808

Ionizing radiation as effective energy in primordial organic synthesis, discussing small molecule formation and subsequent condensation into polypeptides and polynucleotides 05 p0617 A72-16127

Burning rates dependence on pressure in mixtures of ammonium perchlorate with succinic, glutaric, adipic, azelaic, sebacic, fumaric and aminosuccinic acids 06 p0867 A72-18210

Organic origin of meteoritic hydrocarbons in early solar system related to Fischer-Tropsch reaction 07 p1076 A72-19590

Polyethylene oxidative degradation study with gas chromatographic techniques, obtaining aliphatic and organic compounds at 75-200 C in varying oxygen concentrations 08 p1128 A72-21425

Cosmic sources of organic compounds from chemical evolution viewpoint, discussing comets, interstellar space, prestellar nebulae and cool stellar atmospheres 08 p1120 A72-22014

Viking Lander mass spectroscopic analysis of organic compounds, water and volatile constituents of Martian atmosphere and surface 10 p1540 A72-24383

Nd laser second harmonic generation by organic crystalline powders, noting suitability of benzophenone, xanthone, benzimidazole and resorcin 12 p1823 A72-27854

Vapor-liquid equilibrium analysis of water soluble volatile organic compounds in closed airtight systems by gas chromatography 13 p1910 A72-29326

Urease-active colloidal organo-complex extraction from Dublin clay loam soil, describing filtration procedure 13 p1913 A72-29399

Abiotic origin of organic compounds in carbonaceous chondrites, analysing Murchison and Murray meteorites by combined gas chromatography-mass spectroscopy technique 15 p2306 A72-31625

Rhodamine 6G photodegradation resistance improvement in cooled solid matrices of polymethylmethacrylate, investigating time and temperature dependence of bleaching by linearly polarized lasers 16 p2401 A72-33386

Electrochemical development of high energy batteries using organic solvents, organic cathode depolarizers and fused salts 16 p2351 A72-33888

Quinones as reversible redox couples for rechargeable cathodes, noting air regeneration capacity in organic electrolytes 16 p2352 A72-33898

Transition metal complex organic dye solution for Nd-glass laser Q-switching and mode locking, noting high photochemical stability 21 p3062 A72-40244

ORGANIC LASERS

Laser generator research, discussing metallic vapor, heterojunction semiconductor, liquid, neodymium and organic colorant types 02 p0237 A72-11696

Aqueous solutions specular reflectance measurement, using organic dye laser spectrophotometer at 360-650 nm and reflectometer equipped spectrophotometer at 0.2-20 micron wavelengths 02 p0226 A72-11831

Laser pumped organic dye laser frequency-time characteristics, noting noncoincidence of amplification and photon density maxima 02 p0238 A72-12118

Tunable multiple wavelength organic dye laser using optical feedback through partially transparent mirrors 03 p0367 A72-13443

Passively mode locked Rhodamine 6G dye laser, obtaining frequency tuning with intracavity Fabry-Perot filter and transform limited duration picosecond pulses 03 p0368 A72-13605

Superradiative properties of high gain flashlamp-pumped dye laser amplifier, determining small signal amplification as function of pumping power and frequency 03 p0369 A72-14393

Emission spectrum and intensity variation of organic dye solutions excited by nitrogen laser pulsed radiation 04 p0529 A72-14655

Dye laser monochromatic coherent light wavelength tuning with minimized optical cavity degradation and without external optics 04 p0531 A72-15502

Organic dye lasers radiation nonlinear interaction with alkali metals spark discharge plasma, showing angular and spectral broadening 04 p0532 A72-15573

Rhodamine 6G dye laser tuning by variable birefringence filter using lead lanthanum zirconate titanate electrooptic ceramics for wavelength selection 07 p1002 A72-19203

Flashlamp pumped dye-doped polymethyl methacrylate laser thermal and photochemical effects decrease and peak power output increase by light converter 07 p1002 A72-19206

Transient gain measurements on laser dyes of flashlamp pumped rhodamine 6G-ethanol solutions with air and nitrogen 07 p1002 A72-19208

Dye laser system with narrow linewidth oscillator, transverse mode selector, power amplifier and nitrogen pumping, noting 50 kw and 5 nsec pulse generation capability 07 p1002 A72-19209

Pulsed dye lasers logarithmic detector circuit with two ultrafast photodiodes, eliminating intensity variations problem 07 p1005 A72-19415

Repetitive dye laser with monochromatic beam of tunable wavelength, noting spectroscopic applications 07 p1009 A72-20588

Optimum lasing conditions and spectral characteristics of organic dye lasers at 3,100-11,000 Å 07 p1009 A72-20613

Wavelength tunable dye laser pumped by dual pulse lamps with Fabry-Perot interferometer in resonator 07 p1009 A72-20614

Organic dyes molecular photodecay effect on output and power losses of laser activated by flash pump white light 08 p1184 A72-22029

Rhodium solution laser emission pulse characteristics relation to pumping energy distribution over container end surface 08 p1184 A72-22048

Absorption spectra and detection sensitivity enhancement by organic dye laser quenching with broadband cavity 09 p1323 A72-22601

Tunable dye laser system with narrow band filter for Raman spectroscopy of gases 09 p1326 A72-23351

Fast coaxial flash lamp pumped liquid dye laser /LDL for photolysis and biophysical and biochemical applications 09 p1326 A72-23406

Four-photon parametric frequency selection within broad stimulated emission lines during coherent light interaction, considering dye solution laser pumping 11 p1648 A72-26335

Quasi-stationary supersonic plasma flare generation by lamp-pumped rhodamine laser, studying shock wave structure by high speed cinematography 12 p1825 A72-27882

Effect of pumping radiation absorption by electron-excited molecules on organic compounds lasing efficiency 12 p1825 A72-27883

Picosecond pulse efficient second harmonic generation by crystals inside high power dye mode locked Nd-glass laser folded cavity 12 p1826 A72-28220

Plasma spectral absorption coefficients determination by organic dye laser with tunable radiation frequency 13 p2015 A72-29504

Electron transfer frequencies and triplet-triplet transition spectra of polyphenyl compound molecule scintillators for UV lasers, using chaotic phase method 13 p1968 A72-29509

Energy conversion efficiency of xanthene dye laser pumped by mode-locked Nd-glass laser second harmonic, discussing effect of excited molecules transition to triplet state 13 p1970 A72-29686

Superradiant laser emission from organic dyes rhodamine 6G and B with coaxial flashlamp pumping source, relating input threshold energy to dye concentration 13 p1971 A72-29864

Wide tuning range organic dye laser design, using nitrogen laser line as transverse pumping source 13 p1971 A72-29869

Small spectral width emission from dye laser with interference filter and quartz plate Fabry-Perot interferometer for spectroscopic investigations 14 p2110 A72-30674

Flashlamp pumped tunable narrowband traveling wave dye ring laser, stabilizing emission frequency by intracavity Fabry-Perot etalon 14 p2110 A72-30675

Optical PCM communication system with megabits/sec information rate based on dye laser with combined frequency-time division multiplexing 15 p2198 A72-32060

Electrical pumping discharge confined by liquid wall of vortex channel in dye laser solution 15 p2251 A72-32528

Short flash characteristics of spiral pumping lamp for dye laser 16 p2400 A72-33079

CW dye laser output tuning by mirror-grating combination with interspersed output coupling element, noting orders of magnitude reduction of fluorescence background intensity 16 p2401 A72-33388

Rhodamine laser radiation effects on absorbing materials investigated by high speed cinematography and shock wave structure 16 p2404 A72-33991

Effect of pumping radiation absorption by electron-excited molecules on organic compounds lasing efficiency 16 p2404 A72-33992

Influence of the transverse distribution of pumping on the energetics and the profile of thermo-optical distortions in a rhodamine 6G laser 17 p2563 A72-35302

Tunable output dye and semiconductor lasers application to absorption spectroscopy and air pollution monitoring 17 p2564 A72-35381

CW optically pumped tunable dye laser wavelength ranges, linewidth, mode purity, polarization and power output characteristics 17 p2565 A72-35947

Wavelength tunable UV dye laser pumped by the fourth harmonic of Nd:YAG laser. 19 p2810 A72-37407

Organic dye laser molecular sublevel relaxation effects on steady state pi pulse behavior and spectral hole burning from resonance radiation propagation analysis 20 p2932 A72-39503

Energy characteristics of the laser action in rhodamine 6G pumped by a pinched discharge. 20 p2933 A72-39512

Continuously tunable dye laser to obtain output wavelength variation by changing pump laser beam incidence angle on prism lateral face 20 p2933 A72-39563

Pulsed monochromatic laser with toluene, xylene, ethanol, isoamyl alcohol and dimethylformamide solutions of organic dyes, discussing wavelength variations and power outputs 21 p3064 A72-41736

Optical elements of a laser-pumped dye laser 21 p3064 A72-41737

Investigation of amplification spectra and triplet-triplet absorption in a laser with a rhodamine 6G solution 21 p3064 A72-41743

Wavelength tuning of an intracavity pumped CW mode-locked dye laser. 22 p3184 A72-41989

Effects of thermo-optical distortion on the radiation loss magnitude and spatial-angular radiation characteristics for a lamp-pumped rhodamine-6G laser 22 p3185 A72-42173

A new optical PCM communication system 22 p3186 A72-42939

Use of light transformers in organic dye lasers 23 p3295 A72-43413

Dynamic thermo-optical distortions compensation in lamp pumped rhodamine 6G liquid laser by introducing auxiliary dish with dye into cavity
23 p3295 A72-43679

Evanescent-field-pumped dye laser.
23 p3296 A72-43816

Ultrasensitive response of a CW dye laser to selective extinction.
23 p3297 A72-44186

Fluorescent organic dyes solutions for Nd:YAG laser output performance improvement
23 p3297 A72-44191

The efficient generation of coherent radiation continuously tunable from 2500 Å to 3250 Å.
24 p3409 A72-44803

Flashlamp-pumped dye lasers for investigations of the upper atmosphere.
24 p3409 A72-44948

Wideband parametric up-conversion of infrared waves into visible region using tunable dye laser pumping.
24 p3410 A72-45286

Kinetics, spectrum, and specific loss properties of radiation emitted by rhodamine 6G in the case of pumping by a self-constricting discharge
24 p3410 A72-45417

Rhodamine laser emission spectral band control by plane parallel plates and polarizing prisms, noting band widening by resonator loss modulation with Fabry-Perot interferometer
24 p3410 A72-45418

Pulsed laser employing a rhodamine 6G solution in ethyl alcohol with an output energy of 110 J
24 p3411 A72-45498

Time dependence of the divergence of the radiation emitted by a rhodamine laser pumped by a pinched discharge.
24 p3411 A72-45612

ORGANIC LIQUIDS
Room temperature nonaqueous organic solvent electrochemical cell, producing open-circuit potential of 4.5 V
03 p0311 A72-12924

ORGANIC LITHIUM COMPOUNDS
IR-spectroscopic investigation of the effectiveness of oxidation inhibitors in lubricants
19 p2823 A72-38092

ORGANIC MATERIALS
High transition temperature alloys, layered intermetallic and organic superconductors development and properties
01 p0113 A72-10163

Thermally stable organic polymer fiber production methods and performance evaluation in high temperature environments, discussing structure types, flammability and tensile properties
02 p0248 A72-11771

Multispectral scanner data training sets size effect on correlation between soil reflectance and organic matter content obtained from ground truth
02 p0227 A72-11845

Carbon isotopic studies of organic matter in Precambrian rocks
09 p1304 A72-23496

Organic matrices in structural composites, considering mechanical behavior, processability and properties in adverse environments
11 p1674 A72-26230

Organic and metal matrix composites physical and mechanical properties and application to spacecraft and missile components, considering cost effectiveness
11 p1674 A72-26233

Fiberglass replacement by organic fiber for L-1011 interior sandwich panels and laminates, considering Nomex fiber in woven fabric
12 p1835 A72-28099

Weld solidification synthesis with crystalline organic materials, investigating substructure size, growth rate and thermal gradients
13 p1966 A72-29424

Ruby laser emission second harmonic generation effectiveness in organic polycrystals from comparison to lithium niobate
13 p1970 A72-29689

Xenon filled coaxial pulse tube for pumping organic dye solutions, obtaining intensive light flashes
13 p1971 A72-29923

Book - Solid lubricants and self-lubricating solids.
21 p3073 A72-41529

Variation of the output of radioluminescence of organic scintillators with energy loss and the number of charges of ionizing particles
22 p3180 A72-42938

ORGANIC NITRATES
NT CELLULOSE NITRATE
NT NITROGLYCERIN

ORGANIC PHOSPHORUS COMPOUNDS
Organophosphorus antiwear additives in neopentyl polyol ester lubricants on 440C stainless steel surfaces, using four ball wear test machine [AD-740055]
02 p0250 A72-12849

Inorganic phosphates-nucleoside hypohydrous thermal reaction mechanism, discussing thermal

polymerization of orthophosphates for phosphorylation and condensing agents in primordial synthesis
04 p0483 A72-14770

Physiological effects of transfusing 2,3-diphosphoglycerate (DPG)/depleted red cells with high oxygen affinity in anemic hypoxic patients
04 p0473 A72-15211

Kinetics of heat inactivation of phosphoglycerate kinase in soluble fraction from hydrogenomonas facilis
07 p0922 A72-20237

Red blood cell metabolite 1,3 diphosphoglycerate determination method by rapid deprotonization, concentration by precipitation and enzymatic reaction
15 p2190 A72-32488

Structure-property relationships in flame retardant systems - Relative effects of alkyl phosphates, phosphonates and phosphites on cellulose flammability.
20 p2987 A72-39698

Cortical effects mechanisms in animal vegetative systems, noting biological oxidation and organic phosphorus compound studies
21 p3000 A72-40759

ORGANIC SEMICONDUCTORS
Impurity, surrounding gas and pressure effects on organic semiconducting material electrical conductivity, discussing carrier origin and number, and measurement techniques
01 p0113 A72-10125

Organic semiconductor developments in chemistry and physicochemistry of multiconjugate systems and polymer complexes with charge transfer
01 p0114 A72-11074

Microwave photoconductivity and photodiode effect in organic semiconductors
04 p0561 A72-15083

Space charge limited current theory of thin film organic semiconductor systems, investigating energy spectrum of traps and free carrier capture kinetics
11 p1700 A72-25783

Charge carrier photoproduction and energy structure of trans-bis-indonylene (TBB)/semiconductor thin films
11 p1700 A72-25784

Photoemission from tetracene organic semiconductor due to electron capture defect ionization by excitons
11 p1700 A72-25785

Organic semiconductors for photovoltaic cell applications, discussing structural characteristics, improved charge transfer and crystallographic conductivity mechanisms
12 p1856 A72-28015

Semiconductor properties of iodine and bromine molecular complexes of /1-phenyl-3-isindolyl-/ /1-phenyl-3-pseudoisindolylidene-/ phenylmethane and /1-p-tolyl-3-isindolyl-/ /1-p-tolyl-3-pseudoisindolylidene-/ phenylmethane.
19 p2847 A72-38641

ORGANIC SILICON COMPOUNDS
Thin organosilicon films for integrated optical circuits and devices, discussing transparency and loss characteristics and refractive index control
09 p1314 A72-23339

Electrical measurement of moisture effects on adhesive bond strength, insulation resistance and hydrophilicity of cast epoxy and organosilicon adhesives
12 p1833 A72-27449

ORGANISMS
Gravitational biology theory problems, discussing possibility of applying relativistic phenomena to living organisms in inertial or inertialess systems
02 p0160 A72-12016

Foresight, forecast and prognosis concepts in physiology, discussing intuition role and relation between molecular and cellular processes and organism activity
02 p0163 A72-12346

Flavin photoreceptor participation in contemporary organism metabolic systems
04 p0469 A72-14781

Biochemical functions of organisms in evolution of biosphere, discussing redox reactions, elementary compositions and metal compounds role in photosynthesis
04 p0470 A72-14796

ORGANIZATIONS
Book on IATA organization and functions, discussing international aviation history, conference machinery, enforcement of conference resolutions, air transportation economics, public corporations, etc
10 p1564 A72-23846

ORGANIZING
Organizational changes due to electronic data processing /EDP/ introduction into INTERFLUG material-technical supply
12 p1890 A72-27273

ORGANOMETALLIC COMPOUNDS
NT CARBOXYHEMOGLOBIN
NT CHLOROPHYLLS
NT FERROCENES
NT HEMOGLOBIN
NT ORGANIC LITHIUM COMPOUNDS
NT OXYHEMOGLOBIN

NT PORPHINES

Lattice expansion of metal chalcogenide superconducting organometallic structures with aromatic or aliphatic Lewis bases sandwiched into van der Waal gap
08 p1216 A72-21214

Dispersed phase nickel-thoria alloy production method based on organometallic compounds, avoiding high temperature and solvent elimination difficulties
11 p1664 A72-26849

Qualitative determination of organometallic substances in solid propellants by thin layer chromatography
23 p3262 A72-43598

ORGANOMETALLIC POLYMERS
Metal polymer interface synthesis based on linearly cyclic organoelementary high molecule compounds, analyzing heat and thermal oxidation resistances
05 p0680 A72-16202

ORGANS
NT BLADDER
NT KIDNEYS
NT LIVER
NT LUNGS
NT PITUITARY GLAND
NT SPLEEN
NT TESTES

A new model for estimating space proton dose to body organs.
17 p2508 A72-35354

Modifications of the rate of renewal of norepinephrine in various peripheral organs of the rat during exposure and acclimatization to cold
23 p3258 A72-44244

Quantitative evaluation of the kinetics of free-radical processes in animal organs under hypoxic conditions
24 p3371 A72-44596

ORIGINE METEORITE
Magnetite forms in Orgueil meteorite, observing platelets, stackings and framboids by scanning electron microscope
04 p0569 A72-14506

Extraterrestrial abiogenic organic hollow spheres of Orgueil meteorite evaluated according to intrinsic and extrinsic criteria
09 p1385 A72-22640

Orgueil meteorite examination by mass spectroscopy and gas chromatography, identifying amino acids of extraterrestrial origin
09 p1393 A72-23549

ORIENTATION
Magnesium alloys torsional vibration damping correlation with texture orientation resulting from fabrication method
03 p0375 A72-13930

Nonlinear control systems of vehicles angular orientation, investigating dynamic properties by method of harmonic linearization
05 p0727 A72-16474

Reaction time to visual orientation change, obtaining aftereffects as function of orientation specific adaptation duration and separation angle between inspection and test lines
08 p1124 A72-20986

Adjustment to subjective horizontal, vertical and 45 deg tilt in dark as function of age in 3-20 year old subjects
08 p1124 A72-20989

Moving and inertial trihedron orientation determination from absolute angular velocity vector, solving Poisson equations system
08 p1205 A72-21802

Aerial stereopair photograph orientation for geodetic coordinate adjustment in terms of collinearity, coplanarity and scaling
09 p1308 A72-22486

Spacecraft orientation angle measurement by inertial sensors, analyzing equipment kinematic efficiency and limitations
11 p1684 A72-26913

Inertial crosscouplings effect on orientation process dynamics of solid body investigated by nonlinear mechanics, noting centrifugal moments of inertia effects
15 p2275 A72-31730

Carbon monoxide adsorption on nickel surface, determining preferential orientation by extended Huckel calculations
15 p2276 A72-31867

Stabilized retinal image techniques to examine functional relationships between nonstabilized grating pattern orientation adaptation and stabilized line stimuli fading rates
16 p2358 A72-33646

Orientation dependence of slip in tantalum single crystals.
17 p2567 A72-34748

Vestibular and optical stimuli interaction in human orientation, testing via Barany chair on rotating platform surrounded by optokinetic drum
21 p3007 A72-40751

Body orientation under vertical sinusoidal vibration.
21 p3008 A72-41019

Signal detection analysis of meridional variations to vertical and horizontal gratings. 23 p3259 A72-44389

ORIFICE FLOW

Navier-Stokes equations numerical solution by computerized simulation for viscous channel flow with diaphragm orifice reducing cross section 04 p0513 A72-15644

Mean and fluctuating temperature dependence of gas discharging from orifice to atmosphere on pressure vessel wall heat transfer [ASME PAPER 71-WA/HT-32] 05 p0745 A72-15884

Flow field quantities for nearly free axisymmetric steady molecular gas flow through circular orifice from high pressure region into vacuum 06 p0800 A72-18118

Numerical determination of particle number and mass flux density in monatomic rarefied gas flow through circular orifice at finite pressure ratio 07 p0972 A72-20107

Hydraulic servomechanism spool type control valve orifice flow characteristics, measuring mass flow for various spool determined port shapes 07 p0915 A72-20533

Reference transfer method for *in situ* calibration of ionization gages, determining pressure ratio of molecular gas flow through fixed orifices 10 p1480 A72-24147

Analytical models for potential flow through smooth edged orifice, comparing acoustical inductance predicted and experimental values 13 p2006 A72-29770

Core axial density distribution in gas jets freely expanding into vacuum from double concentric orifices, using electron beam fluorescence technique 15 p2218 A72-32150

Computer simulation by Monte Carlo technique of particulate fluxes in divergent conical Knudsen cell orifices, considering specular reflection and surface diffusion effects 15 p2218 A72-32380

Three-dimensional wall jet originating from a circular orifice. 19 p2747 A72-38811

Study of the flow of a heavy fluid with free surface from a symmetrical tank 20 p2913 A72-39417

Turbulent interaction of air jets issuing from perforated surfaces into free space, determining three dimensional flow field via Reichardt free turbulence theory 23 p3248 A72-43625

Boundary layer flow on a circular cylinder moving in a fluid at rest. 23 p3248 A72-43715

Temperature freezing in spherical or cylindrical expansion into a vacuum. 23 p3357 A72-44498

ORIFICES

Stress concentration near elliptic and square orifices in plates with nonlinear viscoelastic hereditary creep properties 08 p1244 A72-21242

ORION CONSTELLATION

Orion A and M17 radio recombination line width increases, discussing Stark broadening functional dependence on principal quantum number 01 p0131 A72-11010

Galactic IR astronomy, discussing findings on emission from H II regions of Orion Nebula and late and early type stars 02 p0276 A72-11643

Dust continuous spectrum and Balmer line intensity ratio in Orion Nebula from slit spectroscopy observations [AD-745076] 02 p0284 A72-12631

Stellar systems existence with positive total energy, using numerical integration of equations of motion for members of Orion Trapezium 03 p0435 A72-13808

Cas A, Tau A, Cyg A and Orion Nebula absolute flux density measurements at centimeter wavelengths 04 p0578 A72-15313

Orion and planetary gaseous nebula helium atoms metastable triplet states population calculations 04 p0578 A72-15314

Zeta Orionis spectra at 922-1453 A from rocket spectroscopy, matching lines with stellar atmosphere models 07 p1072 A72-19346

Far UV view of Orion from Aerobee rocket-borne electromagnetic camera photographs of Orion-Monoceros-Canis Major region 08 p1164 A72-20994

ORIONID METEORIDS

Orionid meteor head echoes variations with diurnal radiant motion compared to Perseid meteors 09 p1389 A72-23395

ORLICZ SPACE

Solvability of the first boundary value problem of higher-order elliptic quasi-linear equations with discontinuous and rapidly increasing Orlicz-class coefficients 17 p2577 A72-35842

ORNITHOPTER AIRCRAFT
U RESEARCH AIRCRAFT
OROGRAPHY

Long wave radiation and surface friction effects on midlatitude cyclone development in eight-level primitive equation orographic model 03 p0385 A72-14229

Mountain barrier and convective area minimum size determination for numerical forecasting models, reducing primitive equations system to advection difference equation 04 p0544 A72-15459

Major and trace element abundances in orogenic area volcanic rocks, considering geographic and stratigraphic relations and composition 05 p0658 A72-16721

Numerical forecasting model with precipitation as function of vertical velocity and humidity distribution, noting orographic influence and atmosphere static stability 08 p1200 A72-21796

Numerical shallow fluid model for air flow across orographic variable grid barrier, using idealized Andes Mountains range 12 p1838 A72-27023

Response of the tropical atmosphere to local, steady forcing. 21 p3077 A72-40248

Allowance for the influence of orography in a dual-layer model of the atmosphere 23 p3310 A72-43343

Incorporation of steep mountains into numerical forecasting models. 24 p3421 A72-45486

ORRERIES

U ASTRONOMICAL MODELS

ORTHICONS

NT IMAGE ORTHICONS

A fast opto-electronic transducer 22 p3180 A72-42944

ORTHOGONAL FUNCTIONS

NT WALSH FUNCTION

Time and frequency domain properties of orthogonal nonrecursive binomial sequences, discussing digital filters synthesis 03 p0381 A72-13408

Spatial transformation in geodesy, considering point in space as position function for orthogonal and curvilinear coordinates 03 p0351 A72-14329

Orthogonal polynomials in several variables relation to approximate multiple integration, extending Stroud theorem for two-dimensional regions cubature formulas to n-dimension 04 p0539 A72-14731

Orthogonal expansion of estimators and estimands in Hermite series for Monte Carlo computation 04 p0540 A72-15631

Antenna synthesis problems approximate solution with reactive factor /supergain ratio/, involving radiation pattern and aperture current expansion as orthogonal functions 05 p0634 A72-15819

Orthogonal functions representation of received signals in ideal signal sequences transmission in linear systems with matched filters and frequency band limitation 08 p1132 A72-21326

Orthonormalized exponential functions use in hydrometeorology 08 p1202 A72-22119

Statistical analysis of temperature characteristics based on natural orthogonal components expansion for weather forecasting application 08 p1203 A72-22120

Multichannel signal processing system for optical filters synthesized by orthogonal functions 09 p1314 A72-23342

Atmospheric optics inverse problem solution, comparing orthogonal functions series expansion and regularization method algorithms 12 p1841 A72-27992

Orthogonalization method application to problems of diffraction on several bodies through reduction to integral equations 13 p1920 A72-29278

Orthogonal projection method for nonstationary heat conduction boundary value problem with thermal conductivity and specific heat as prescribed functions of position 14 p2126 A72-31049

Relations between Haar and Walsh/Hadamard transforms to yield orthogonal transforms with common fast algorithm 15 p2264 A72-32081

Global meteorological data analysis using Gram-Schmidt generated orthogonal polynomial base functions 15 p2266 A72-32719

Orthogonal functions application to flexible rotors balance, expressing deflections vs angular velocity as sum of eigenvectors 18 p2731 A72-36066

Correlator with orthogonal filters for acoustic diagnostics, noting Laguerre functions variations in signal pairs autocorrelation 22 p3176 A72-42133

Atmospheric optics inverse problem solution, comparing orthogonal functions series expansion and statistical regularization method algorithms 22 p3202 A72-43006

Antenna synthesis problems approximate solution with reactive factor /supergain ratio/, involving radiation pattern and aperture current expansion as orthogonal functions 23 p3268 A72-43427

Schauder bases in certain spaces of holomorphic functions 24 p3418 A72-44826

ORTHOGONAL MULTIPLEXING THEORY

Error probabilities estimates for communication systems using orthogonal multiposition signals in information transmission, noting techniques applicability to diversity reception systems with self selection 13 p1918 A72-28893

Performance characterization for L-orthogonal signal transmission and detection, discussing tradeoffs between error probability, SNR and bandwidth by numerical evaluation 23 p3265 A72-44180

ORTHOGONALITY

Radio wave polarization orthogonality recovery by using differential phase shifter and attenuator in radio communication systems 02 p0183 A72-12799

Geomagnetic field-hf sky wave orthogonality conditions, discussing ray tracing for signals reflected in ionosphere 05 p0630 A72-16619

Orthogonality conditions for VLF height gains in vertically inhomogeneous anisotropic earth ionosphere waveguide 09 p1282 A72-23517

Pi-theorem alternative formulation, defining independent dimensionless products in terms of universal constants, governing equations and initially and additionally specified physical quantities 10 p1503 A72-23920

Axisymmetric shock wave propagation in continuous inhomogeneous medium, taking into account shock geometry orthogonality conditions and flow hydrodynamics behind shock 11 p1616 A72-25864

Free and forced vibrations of circular plates with associated rigidities and masses, obtaining orthogonality condition for natural vibration modes 13 p2059 A72-29501

Orthogonality condition application to continuum mechanics systems with zero free energy, viscoelastic materials and chemical problems 14 p2130 A72-30419

Time dependent orthogonal coordinate system rotation by unit vector along effective axis, obtaining angular velocity and effective angle interpretation 15 p2275 A72-31590

Orthogonal vibration damping matrix numerical evaluation, comparing Caughey series and direct approaches 15 p2326 A72-31711

Poisson equations solution in orthogonal curvilinear coordinate systems to allow Laplace and Helmholtz equations separability, applying to hydrodynamic, electrostatic, electromagnetic and MHD problems 15 p2278 A72-32249

Exponential representation of isotropy groups of simple solids, noting conditions for conjugation of unimodular to orthogonal group subgroups 16 p2423 A72-33111

Piezoelectric waveguide generalized treatment via field representation by sum of normal mode waves, using modified orthogonality relation 16 p2369 A72-33761

Analysis of discrete automatic control systems with variable parameters by the method of orthogonal expansions. I, II 19 p2778 A72-37438

ORTHONORMAL FUNCTIONS

Linear distributed parameter system optimal boundary control by direct method using linear combination of finite number of orthonormal functions 04 p0505 A72-14670

Radio signal parameters with unknown envelope approximated by orthonormal function series during white noise background reception 05 p0625 A72-15823

Incompressible laminar flow in conduit with arbitrary cross section, time varying pressure gradient and initial velocity, constructing finite series solution by orthonormalizing procedure [ASME PAPER 71-WA/FE-22] 05 p0646 A72-15927

Radio signal parameters with unknown envelope approximated by orthonormal function series during white noise background reception 23 p3263 A72-43431

ORTHOPHOTOGRAPHY

An orthographic photomap of the South Pole of Mars from Mariner 7. 21 p3110 A72-41455

ORTHOSTATIC TOLERANCE

Human tilt tolerance relation to aerobic capacity, weight, height and physical fitness, determining correlation coefficient between heart rate and orthostatic response

10 p1428 A72-23733

Prolonged water immersion effects on renal function and plasma volume in trained and untrained subjects, noting deleterious effect on orthostatic tolerance and work capacity

10 p1428 A72-23738

Tilt table tests for orthostatic tolerance, measuring heart rate, blood pressure and responses of fainters and nonfainters

21 p3008 A72-41020

Lower-body negative pressure as a method of preventing shifts associated with changes in the hydrostatic pressure of blood

23 p3256 A72-43919

Comparative study of regional hemodynamics during tilt test and lower body negative pressure exposure

24 p3373 A72-45131

Induction of hemodynamic deterioration by the hypogravic state - An evaluation of mechanisms and prevention

24 p3373 A72-45199

Response to daily lower body negative pressure (LBNP) exposure 1-70mm Hg, with emphasis on plasma renin activity, sodium and potassium excretion

24 p3377 A72-45658

ORTHOTROPIC CYLINDERS

Time operator method in creep theory for orthotropic bodies, obtaining asymptotic solutions for laminar orthotropic rod and elastic plate vibration problems

02 p0289 A72-11617

Orthotropicity orientation effect on supersonic flutter of infinite-length thin heterogeneous circular cylindrical structures in axisymmetric gas flow

04 p0584 A72-14520

Saint Venant problem for orthotropic almost cylindrical beams, investigating elongation, bending due to couple and transversal loads and torsion due to torque

04 p0594 A72-15747

Stress functions for anisotropic elastic body with uniformly propagating circumferential crack, considering axially orthotropic cylinder

10 p1553 A72-23744

Radial and circular thermal stresses in free and end-constrained orthotropic cylinders with axisymmetric temperature distributions, determining relation between temperature and thermoelastic coefficients

13 p2055 A72-28561

Three dimensional axisymmetric problem for stressed state of elastic homogeneous cylindrical orthotropic bodies of revolution, using method based on small parameters

13 p2062 A72-29948

Thermal circular and radial stresses in elastic orthotropic cylinders with anisotropic expansion coefficients

19 p2872 A72-37535

Three-dimensional vibrations of orthotropic cylinders

19 p2873 A72-37693

Stability of a twisted orthotropic cylindrical shell with a jump-wise variable wall rigidity

21 p3118 A72-40815

ORTHOTROPIC PLATES

Laminated orthotropic plates and shallow shells structural analysis using finite element program

01 p0140 A72-10984

Time operator method in creep theory for orthotropic bodies, obtaining asymptotic solutions for laminar orthotropic rod and elastic plate vibration problems

02 p0289 A72-11617

Stress-strain characteristics of stochastically reinforced materials of high rigidity orthotropic elastic layers alternating with isotropic elastic or viscoelastic layers

02 p0248 A72-11623

Flexible viscoelastic orthotropic plates and shells obeying linear heredity relations, solving stability and bending problems by Laplace transform

02 p0290 A72-11625

Thick orthotropic off-axis laminated plates vibration equations solution, presenting natural frequencies spectra and modal functions

02 p0249 A72-11988

Elastoplastic problem of stress concentration in orthotropic plate with circular hole under balanced biaxial tension of infinity

02 p0293 A72-12428

Square orthotropic and isotropic plates stability with square hole under uniformly distributed load

02 p0299 A72-12685

Stresses due to initial elastic deformations in orthotropic thin plate strip, expressing Dirac function by Fourier series and integral

03 p0444 A72-13505

Stress-strain state determination for plane orthotropic bodies by optical polarization method, discussing numerical methods for stress and strain tensor components

03 p0445 A72-13580

Thermal stress concentration at heat insulated holes in orthotropic plate, assuming external-load free contour

03 p0452 A72-14134

Free vibration and buckling of orthotropic skew plates with different edge conditions, using Ritz variational method

04 p0584 A72-14508

Thickness function corresponding to constant velocity loading condition for orthotropic annular circular plate with uniform stress

04 p0591 A72-15279

Elasticity theory equations for orthotropic plate bending, derived from combination variational and difference-differential procedures

05 p0741 A72-17144

Frequency analysis of tapered rectangular orthotropic plates, determining bounds

07 p1092 A72-19945

Elastic properties of bonded orthotropic layer plates, finding good agreement with fiberglass reinforced plastic laminates

07 p1097 A72-20596

Central crack in plane orthotropic rectangular sheet under tension, showing stress intensity factors dependence on geometric and elastic constants

09 p1404 A72-22915

Microelastic stress mechanics of thinly laminated orthotropic multilayered plates, taking into account skin effect

09 p1405 A72-22994

Three dimensional dynamic analysis of multilayered orthotropic viscoelastic plates, taking into account skin effect

09 p1405 A72-22995

Piston exerting pressure on liquid filled cylinder, determining deformation state based on thin elastic orthotropic plate theory

10 p1556 A72-24266

Orthotropic point-supported rectangular panel vibration and flutter analysis for natural frequencies land flutter boundaries, applying to space shuttle design

11 p1728 A72-25379

[AIAA PAPER 72-350] Stress concentrations around circular openings and failure criteria for orthotropic and anisotropic composite laminated plates subjected to uniaxial, biaxial and shear loading

11 p1732 A72-25474

Flexural vibration of rectangular orthotropic plates with clamped, simply supported and/or free edges, presenting solution method for coupled characteristic equation pairs

11 p1735 A72-25737

Thermal stress distribution in orthotropic plates with variable heat transfer coefficient, using Fourier and Laplace transforms

12 p1878 A72-27084

Stress calculation in inflexible overlapping cemented joint of orthotropic layers, taking into account joining geometry and elastic properties anisotropy

13 p1962 A72-28396

Two dimensional reinforced plastic material anisotropic creep derivation from orthotropic plate time functions and stress tensor invariants

13 p2034 A72-28437

Boundary values for bending of plates with weak orthotropy from Vekua plate theory

13 p2062 A72-29951

Bending deflections of rectangular plates with laminated orthotropic layers analysis by finite element displacement, comparing with carbon fiber reinforced plastic structures

14 p2167 A72-30905

Elastic bending of rectangular continuous orthotropic plate with variable rigidities and elastic foundation coefficients for discontinuous boundary conditions along one edge

16 p2467 A72-33118

Stress-strain diagrams for orthotropic glass fiber reinforced plastic plates with circular hole under uniaxial tensile load

16 p2471 A72-33681

Elastic sandwich plates analysis with core layer as orthotropic Cosserat surface supporting force and moment stresses

16 p2471 A72-33787

Transverse vibration frequencies and mode shapes of clamped or supported orthotropic plates by energy method, using Rayleigh-Ritz technique

17 p2626 A72-34327

On natural vibrations and waves in laminated orthotropic plates

17 p2581 A72-34803

[ASME PAPER 72-APM-14] Shear deformation in heterogeneous anisotropic plates

17 p2633 A72-35294

Buckling of orthotropic, curved, sandwich panels subjected to edge shear loads

18 p2735 A72-36770

The dynamic characteristics of clamped rectangular plates of orthotropic material

18 p2737 A72-37067

Analysis of an inclined crack centrally placed in an orthotropic rectangular plate

19 p2870 A72-37221

Book - Analysis of plates.

21 p3125 A72-41530

Stability of orthotropic stiffened composite plates.

23 p3352 A72-44109

Large deflection of rectangular orthotropic plates.

23 p3352 A72-44111

Non-linear flexural vibration of orthotropic skew plates.

23 p3355 A72-44375

Vibration frequencies and modes determination for clamped rectangular plates of orthotropic material, using weighted residual technique and polynomial approximation

24 p3455 A72-44683

On the use of a coordinate transformation for analysis of axisymmetric vibration of polar orthotropic annular plates.

24 p3457 A72-44883

ORTHOTROPIC SHELLS

NT CYLINDRICAL SHELLS

Laminated orthotropic plates and shallow shells structural analysis using finite element program

01 p0140 A72-10984

Natural vibrations of closed crosswise reinforced orthotropic circular cylindrical shells, using digital computer solution

01 p0142 A72-11363

Flexible viscoelastic orthotropic plates and shells obeying linear heredity relations, solving stability and bending problems by Laplace transform

02 p0290 A72-11625

Elastic equilibrium in circular conical orthotropic shells of linearly variable thickness, investigating stresses under arbitrary loads

02 p0297 A72-12615

Infinitely long orthotropic cylindrical shell partially filled with elastic media under compression load, determining local stability

02 p0299 A72-12688

Computer program for buckling loads of shallow stiffened eccentrically orthotropic sandwich shells

02 p0299 A72-12703

[DGLR PAPER 71-109] Rupture induced perturbation loads in pressurized orthotropic circular cylindrical shells

02 p0299 A72-12704

Anisotropic shell supercritical deformation, deriving formula for lower critical load for shallow orthotropic spherical segment under external pressure

03 p0447 A72-13729

Critical load and stability analysis for three layer orthotropic cylindrical shell with filler under nonuniform external pressure

03 p0448 A72-13906

Optimal temperature fields and stress-strain state in orthotropic conical and cylindrical shells subject to local heating

04 p0588 A72-15051

Critical load limit and stability of elastic isotropic and orthotropic cylindrical shells, using net-point method for end conditions

04 p0588 A72-15053

Thermoelasticity theory coupled linear equations for thin orthotropic shells, taking into account rotatory inertia and lateral shear

04 p0588 A72-15060

Optimal temperature fields in locally heated orthotropic cylindrical shells, determining rigidities effect

04 p0593 A72-15655

Elastic equilibrium of circular conical orthotropic shells with linearly varying thickness, determining real and complex roots of stress state characteristic equation

04 p0594 A72-15710

Circular conical orthotropic shells of linearly variable thickness loaded by distributed and concentrated forces and moments, analyzing stress-strain state by numerical methods

04 p0594 A72-15749

Approximative buckling load of orthotropic hyperbolic paraboloid metal shells, using energy approach

06 p0897 A72-17970

Orthotropic hinged cylindrical shell stability under uniform external pressure, deriving linearized three dimensional differential equations

08 p1246 A72-21711

Orthotropic circular cylindrical elastic shell vibration mode shape analysis by Vlasov equations, using asymptotic method

08 p1247 A72-21813

Elastic shell geometry and rigidity effects on critical load in pure bending within structurally orthotropic theory, taking into account reinforcing rib eccentricity

08 p1247 A72-21816

Stress-strain state produced by asymmetric physical and thermal loads in thin orthotropic viscoelastic shells of revolution

09 p1399 A72-22702

Thermoelastic problem of open orthotropic multilayer shell of revolution, obtaining one dimensional boundary value problem solutions by numerical orthogonalization method

09 p1400 A72-22712

Thermal stress distribution in orthotropic cylindrical shell weakened by circular hole, obtaining general solution by small parameter method

09 p1400 A72-22715

Torsional behavior of twisted elastic orthotropic cylindrical shells after stability loss, using energy method

09 p1404 A72-22771

Bubnov-Galerkin method for dynamic stability of closed thin walled orthotropic cylindrical shell loaded by variable external pressure

11 p1739 A72-26977

Shallow isotropic and orthotropic shells vibration, investigating dynamic rigidity for concentrated mass

12 p1878 A72-27079

Linearized elastic equilibrium stability equations for orthotropic cylindrical shell under critical axial compression

12 p1885 A72-27970

Proximate equations of two dimensional orthotropic shell theory obtained by asymptotic integration method, examining anisotropy effect

13 p2053 A72-28391

Static deformation of laminar orthotropic shells of revolution with variable rigidity, using integral correlation method

13 p2061 A72-29795

Truncated orthotropic conical shells thermostability at different temperature gradients, using Ritz method

14 p2163 A72-30193

Differential equations for shallow orthotropic shells with variable thickness obtained by Bubnov-Galerkin variational method, presenting error assessment

14 p2163 A72-30195

Schaefer equilibrium and compatibility equations and Reissner constitutive equations for orthotropic cylindrical shells reduction to four simultaneous third-order equations

16 p2466 A72-33023

On a laminated orthotropic shell theory including transverse shear deformation.

17 p2629 A72-34807

Buckling and vibration analysis for stiffened orthotropic shells of revolution.

17 p2632 A72-35242

Heat-conduction equations for multilayer shells

19 p2881 A72-38158

Torsional vibration of an orthotropic cylindrical shell.

22 p3240 A72-42881

Finite element method optimization of orthotropic layered shells of revolution under mechanical and thermal loadings, considering stress-strain relationships

23 p3344 A72-43479

ORTHOTROPISM

Viscoelastic parameters calculation for orthotropic composite materials reinforced by unidirectional fibers, giving time dependence of relaxation functions

01 p0142 A72-11177

Distortional energy theory for predicting failure of orthotropic materials exposed to three dimensional stress state

05 p0732 A72-15942

Plane harmonic waves propagation in stressed polycrystalline bodies with slight orthotropy in unstressed state, substantiating theory for initial stress determination by ultrasonic technique

07 p1090 A72-19753

Extremal mechanical properties directions in orthotropic glass fiber reinforced plastics symmetry planes

08 p1196 A72-21866

Plane stress solution for thin walled cantilever beam with end load extended for beam width effects in composite orthotropic beam bending

16 p2463 A72-32841

Rheological characteristics of orthotropically reinforced polymer materials

19 p2822 A72-37531

On the solution of plane, orthotropic elasticity problems by an integral method.

23 p3350 A72-44056

Acceleration waves in orthotropic elastic materials.

23 p3354 A72-44342

Orthotropic photoelasticity methods application to concentrated force on half plane edge and to stress distribution on elliptical hole boundary in tensile strip

24 p3455 A72-44790

Linear fracture mechanics in orthotropic materials.

24 p3457 A72-44818

OSCILLATING CYLINDERS

Unsteady supersonic aerodynamic forces on oscillating circular cylindrical shell calculated using linearized equation of potential flow

02 p0151 A72-12256

Equations of motion for oscillating heavy symmetrical gyroscope with cylindrical cavity partially filled with inviscid incompressible liquid

05 p0664 A72-17145

Flow stability of viscous fluid in annular space between rotating inner and axially oscillating coaxial outer cylinder, using perturbation method

07 p0971 A72-20089

Damping measurements of hydrodynamic vibrations of cylinder excited by random pressure field of liquid flow

10 p1465 A72-24073

Non-Newtonian Reiner-Rivlin fluid flow between two coaxial porous cylinders with longitudinal pulses applied to inner cylinder at finite time intervals

10 p1468 A72-24402

Coupled electroelastic vibrations of piezoceramic cylinders from polycrystalline electrostriction theory, taking into account mechanical and dielectric losses

14 p2132 A72-31117

Partial differential equations of motion for nonlinear mechanical systems solved by Lanczos formula, discussing prismatic cylinder oscillations under uniformly distributed transverse load

15 p2275 A72-31729

Linearized supersonic flow past harmonically vibrating cylindrical body, solving boundary value problem by cylindrical integral transformation

16 p2342 A72-32878

Heat generation in oscillating torsional spring modeled by viscoelastic hollow cylinder subjected to sinusoidal shear stresses, calculating stress and temperature distribution and displacement

17 p2635 A72-34232

Composite sphere and cylinder vibrations, considering radial and rotatory/torsional vibrations

18 p2735 A72-36756

Three-dimensional vibrations of orthotropic cylinders.

19 p2873 A72-37693

Comet tail wave motion explanation via consideration as plasma cylinder with free boundary tangential discontinuity surface immersed in interplanetary plasma

22 p3221 A72-42011

OSCILLATING FLOW

Ion oscillation theory for electrodynamic channel Poiseuille and Hagen-Poiseuille type flows, using transport and dispersion equations in various ionized media

01 p0111 A72-11214

Gas flow fluctuations near stagnation point on hot wall, taking into account laminar boundary layer compressibility effects

04 p0462 A72-15178

Oscillating torus shaped crucible viscometer, discussing oscillating viscous liquid fluid dynamic problem

04 p0522 A72-15480

Free oscillations of liquid masses contained in tanks, analyzing variational and Ritz methods

04 p0513 A72-15557

Nonlinear oscillations of liquid in movable conical containers, presenting approximate procedures for solving weight boundary value problem of eigenvalues

07 p0972 A72-20211

Fluid oscillator temperature sensor, noting fast dynamic response and application in high temperature environments

08 p1164 A72-20926

Viscous incompressible flow past circular cylinder at Reynolds numbers 100-1000, obtaining oscillatory drag, lift and torque by governing equations numerical solution

08 p1107 A72-21251

Gas flow effect on undulating flow of viscous fluid film down vertical wall, using Fourier series

10 p1469 A72-24532

Oscillation periods of rotating perfectly conducting liquid column in presence of axial magnetic field and uniform current

12 p1851 A72-27534

Coordinate perturbation and multiple scale techniques application to supersonic flow field around two dimensional wing and oscillations in closed tube

16 p2379 A72-33576

Oscillating flapped vane system for large amplitude uniform sinusoidal lateral gust generation in semiopen jet wind tunnel

16 p2374 A72-33699

Evaluation of Reissner's correction for finite span aerodynamic effects.

18 p2736 A72-36774

Fluid oscillations in a partially filled cylindrical tank with a spring supported elastic floor.

18 p2684 A72-37062

Oscillatory flow of a viscous fluid in a flexible walled two dimensional channel.

18 p2684 A72-37064

Visualization study of flow near the trailing edge of an oscillating airfoil.

20 p2886 A72-40067

A similarity solution for viscous internal waves.

21 p3044 A72-40118

Investigation of the self-oscillations of a continuous medium arising at a stability loss in operation steadiness

22 p3164 A72-41907

Time-periodic solutions of boundary layer equation systems

22 p3164 A72-41908

Fluid velocity measurement of oscillatory flow generated from vortex shedding by laser Doppler system, discussing frequency tracker design, continuous detection problem and application

22 p3178 A72-42677

Transverse oscillations of a jet in a jet-splitter system.

[ASME PAPER 72-FLCS-1] 23 p3281 A72-44065

Tidal waves of a two-layer liquid in a cylindrical basin of revolution rotating about its axis

24 p3392 A72-45073

Effects of upstream unsteadiness on hypersonic flow past a wedge.

24 p3364 A72-45565

OSCILLATION DAMPERS

Energy-phase time transformations of damped Liapunov system applied to nonlinear spring pendulum and betatron transient oscillations

01 p0103 A72-11387

Meteorological satellite stabilization and attitude control in synchronous equatorial orbit for two years life, emphasizing nutation damper optimal dynamic characteristics

05 p0725 A72-16437

Magnetic damper for gravity gradient stabilized satellite rotational and librational motions, deriving formula for calculating damping coefficients

05 p0726 A72-16463

Combined rotational motions of free solid and coupled elastic bodies oscillations around center of mass with nutation passive dampers

06 p0850 A72-18707

Gunn domain oscillations suppression by dielectric surface loading of transversely thin GaAs diodes

10 p1526 A72-24305

Linear oscillatory system, investigating effects of pulsed dynamic damper with mass vibrations bounded by limiters

12 p1887 A72-28235

Small amplitude libration stability and damping system for gravitationally stabilized tethered orbiting radio interferometer satellite system

16 p2462 A72-34020

Optimum design parameters for a spin-stabilized spacecraft nutation damper.

17 p2619 A72-34208

Synthesis of a resin-metal damper whose characteristic shows minimum deviation from a constant-frequency response

19 p2806 A72-37429

Attitude stability and performance of a dual-spin satellite with nutation damping.

19 p2862 A72-38022

OSCILLATIONS

NT ELECTRON OSCILLATIONS

NT H WAVES

NT HARMONIC OSCILLATION

NT MOLECULAR OSCILLATIONS

NT NONOSCILLATORY ACTION

NT NONSTABILIZED OSCILLATION

NT PLASMA OSCILLATIONS

NT PRESSURE OSCILLATIONS

NT SELF OSCILLATION

NT STABLE OSCILLATIONS

NT TRANSIENT OSCILLATIONS

NT TRANSVERSE OSCILLATION

NT UNDAMPED OSCILLATIONS

NT WING OSCILLATIONS

Pupil size spontaneous oscillation /Hippus/, discussing development by repeated light step and accommodation and disappearance due to mental activity

02 p0164 A72-12490

Oscillation periods of single degree of freedom variable mass point, using stiffening hypothesis

03 p0390 A72-14220

Nonlinear oscillations stochastic instability in dynamic systems, discussing nonequilibrium statistical mechanics

03 p0390 A72-14316

Toroidal oscillations of spherical planetary models, presenting regular eigenfunction form near center

03 p0352 A72-14381

Plane periodic oscillations of solid body on elliptic orbit, characterizing stability of motion equations periodic solutions

04 p0582 A72-14632

Polytropic masses oscillations under rapid uniform rotation, using variational principle

04 p0579 A72-15320

Nonlinear oscillations in mechanics - Conference, Kiev, U.S.S.R., August 1969

06 p0849 A72-18692

Elastic systems nonlinear oscillations with moving inertial loads, noting standing waves superposition

06 p0901 A72-18706

Oscillations and acoustic emission by interacting elastic shells in connecting medium, using quadratures with Green function

07 p1034 A72-18922

Hologram interference fringe relationship to nonlinearity of simple oscillations

07 p0987 A72-19836

Lf convective oscillations in polytropic atmospheres within strong magnetic field, considering stability of quasi-adiabatic and quasi-isothermal motions 07 p1082 A72-20376

Asymptotic approximation method for damping force as function of velocity from successive oscillations amplitudes measurement 07 p1096 A72-20474

Krylov-Bogoliubov asymptotic method for oscillation analysis in time lag systems under pulse inputs 08 p1206 A72-20970

Autonomous linear second order equations system reduction to Poincare normal form in oscillations theory 08 p1206 A72-21169

Stability solutions of collective oscillations of spherical star cluster rotating in near circular orbits in self consistent field 08 p1239 A72-22180

Avalanche diode background noise in linear and nonlinear regimes, emphasizing source dependence on oscillation level 09 p1287 A72-23117

Prolate and oblate spheroids flow field generated by axial translatory oscillations in still incompressible viscous fluid from Stokes linearized equations, deriving formulas for drag 10 p1418 A72-24462

Oscillation criteria for fourth order differential equation conjugate point location relationship in terms of existence of solution with two double zeros 11 p1678 A72-26159

Static deflection effect on nonlinear spring mass system step function response, considering approximate calculation of oscillation period 11 p1688 A72-26372

Inhomogeneous strings oscillations determination in nonstationary inverse boundary value problems with integral equations 11 p1689 A72-26381

Oscillating membrane pressure gage for direct electrical measurements of fast and large pressure variations, noting insensitivity to interference 11 p1636 A72-26700

Varied states superimposed on finite elements in discrete elasticity, noting small oscillations superposition on arbitrary motion of elastic system 12 p1845 A72-27393

Oscillations excitation, proposing models for percussive rotational action machines operation and dog tooth clutches processes 13 p1954 A72-28386

Equations of motion and phase trajectory analysis for resonant oscillations of beam-pendulum system 13 p2003 A72-28721

Stability criteria for limiting oscillatory motion of coasting sounding rocket exiting atmosphere 13 p2051 A72-28886

Nonlinear oscillations amplitude, frequency and instability regions of moving belt as function of longitudinal velocity 13 p1964 A72-29150

Oscillations and acoustic emission by interacting elastic shells in connecting medium, using quadratures with Green function 13 p2004 A72-29208

Impulsive pulsations /Pi 2/ identification as geomagnetic field distension coincident with oscillatory component from high resolution Rb vapor magnetometer recordings 13 p1951 A72-29656

Gradient catastrophe /solution derivative discontinuity/ occurrence time for quasi-linear hyperbolic differential equations describing elastic string oscillations 14 p2130 A72-30194

Nonlinear oscillations theory application to electronics and electrical engineering - Conference, Kiev, August-September 1969 14 p2089 A72-31101

Oscillations in ferromagnetic resonant circuit of parametric amplifier with constant capacitance and periodically variable inductance modulated by input signal 14 p2089 A72-31107

Quasi-conservative optimal nonlinear self excited oscillation systems theory for automatic control, telematics and computer applications 14 p2133 A72-31130

Coupled oscillations of inviscid homogeneous liquid with free surface under vacuum or gas filled space in elastic cylindrical container 15 p2217 A72-31472

Second order delay differential equations, investigating oscillatory behavior of stable and unstable equations solutions and nonoscillatory solution existence 15 p2264 A72-31765

Nonlinear system consisting of gas filled tube with pressure sensitive heat source, noting oscillation evolution due to equilibrium perturbation [ASME PAPER 72-APM-21] 17 p2580 A72-34796

Spacecraft oscillatory motion as function of attitude control impulse and slave mechanism efficiency 17 p2622 A72-35205

Exact solution for dynamic oscillations of re-entry bodies. 17 p2622 A72-35231

Stability solutions of collective oscillations of spherical star cluster rotating in near circular orbits in self consistent field 18 p2724 A72-36236

Nonlinear oscillations stochastic instability in dynamic systems, discussing nonequilibrium statistical mechanics 19 p2836 A72-38814

Steady solutions of generalized Korteweg-de Vries equation for oscillatory solitary waves in dispersive media 21 p3089 A72-40197

Scattering cross section glory undulations relationship to potential energy of interaction of two molecules with minimum containing one or more bound states 21 p3087 A72-40561

Periodic wave of oscillating and stationary two dimensional bodies immersed in uniform incompressible stream, investigating semiinfinite vortex trails relationship to oscillating airfoils 21 p2989 A72-40651

Velocity oscillations in the solar atmosphere. 21 p3107 A72-41278

Comparison of three oscillatory techniques for comets at incidence. 21 p3042 A72-41595

A new method for the evaluation of slotted wind tunnel interference parameters applicable to subsonic oscillatory tests. 21 p3043 A72-41642

The parameters of a two-mass oscillatory system in which one of the masses is acted upon by a complex working resistance 23 p3312 A72-43352

Motion of a solid with a nonholonomic constraint around a fixed point in a conservative force field 23 p3313 A72-43800

Problems of interference between oscillating surfaces in subsonic flow 23 p3248 A72-43809

Buildup of oscillations in crossed-field backward-wave oscillators. 24 p3385 A72-44973

On zeros of solutions of the second-order linear differential equation with retardation. 24 p3419 A72-45577

OSCILLATORS

NT AUTODYNES
NT CRYSTAL OSCILLATORS
NT GYROSCOPIC PENDULUMS
NT HARMONIC OSCILLATORS
NT MAGNETRONS
NT MECHANICAL OSCILLATORS
NT MICROWAVE OSCILLATORS
NT MICROWAVE TUBES
NT MOLECULAR OSCILLATORS
NT PENDULUMS
NT PHANTASTRONS
NT PLANOTRONS
NT RELAXATION OSCILLATORS
NT SYNCHRONIZED OSCILLATORS
NT VACUUM TUBE OSCILLATORS
RF intrinsic and up or down-converted modulation noise mutual relationship with application to IMPATT diode oscillators 01 p0035 A72-10114

High Q oscillator with simulated inductor circuit consisting of negative immittance converter and RC elements 01 p0035 A72-10127

High stability and power IMPATT oscillator design for line-of-sight communication links, avoiding spurious resonances and mode jumping 01 p0037 A72-10645

Physical interpretations of physiological control, covering history, biochemical oscillator viewpoint of life and conferences 02 p0160 A72-12039

Stability and perturbation of oscillator system with frequency fixed by all pass ring transmission function with delayed amplitude regulation 03 p0331 A72-13410

Tunnel diode quartz oscillator frequency stability improvement and dc power requirement reduction using nonlinear feed circuits 03 p0331 A72-13555

Nonlinear differential second order equation system development for gyroscopic coupling of forced nonlinear oscillators 03 p0389 A72-13631

Book on transistors in pulse circuits covering switching diodes and circuits, multivibrators, blocking oscillators, etc 05 p0640 A72-16288

Electron tube present and future applications as oscillators, high power and hf amplifiers and optoelectronic converters 06 p0784 A72-17775

Millimeter wave GaAs avalanche diode oscillator processing on plated Cu heat sinking block resulting in epitaxially grown p-n junctions 06 p0788 A72-18467

Magnetic-transistor master oscillator with digital analog converter as programmer for needed output voltage frequency shifts 07 p0946 A72-19959

LF originated background noise in Gunn oscillators, developing evolution equation for oscillator weakly perturbed by noise 09 p1288 A72-23121

High power Nd-glass laser systems, discussing oscillator and amplifier operating parameters optimization 10 p1489 A72-23945

Spectral density of frequency deviating process for performance predictions from oscillator testing and frequency noise calibration, discussing sample averages convergence to statistical values 11 p1593 A72-25892

Absorption spectrum of molecular nitrogen in 730-980 A band, investigating absorption cross sections and optical oscillator strengths 12 p1848 A72-27853

FM distortion in injection phase locked oscillator amplifiers from generalized Alder equation 12 p1793 A72-27965

Self excited oscillator using emitter follower circuit and distributed active RC phase shifter network 13 p1927 A72-28404

Transit time, retarded domain and suppressed domain mode simulation of Gunn oscillator, using LF analog 13 p1927 A72-28405

Single frequency generation stability of one dimensional model of traveling wave laser using inhomogeneously broadened active material 13 p1967 A72-28470

Averaging technique for nonlinear viscoelastic dynamic problems, considering forced oscillations of oscillator with weakly nonlinear hereditary elastic characteristics 13 p2054 A72-28551

Method to obtain optimal efficiency gyroamplifier circuits with short waveguide selector by prior grouping of electronic oscillators 13 p1928 A72-28799

Spurious oscillations in external excitation oscillators due to internal feedback in transistor, investigating frequency dependence of stability coefficient in cascade with common emitter 13 p1929 A72-28896

Transistorized oscillators for variable-frequency generators designed to feed synchronous motor drives of equatorial telescopes 14 p2073 A72-30683

Stability conditions for damped single degree of freedom oscillator system under stationary narrow-band random excitation, obtaining approximate solution by perturbation method 14 p2131 A72-30718

Nonlinear coupled cyclotron oscillators excitation by external sine wave force, analyzing amplitude/phase variation and negative absorption 14 p2132 A72-31115

Nonlinear approximation of slowly changing standing waves in self excited parametric oscillators with distributed and bulk structures 14 p2090 A72-31131

Minimum values estimation of amplitude fluctuations dispersion and spectral line width for conventional and quartz crystal controlled oscillators 15 p2210 A72-32735

Theoretical model for computer calculation of transients in oscillator consisting of nonlinear amplifier with feedback through sequence of matched LC circuits 16 p2371 A72-33280

Nonlinear and phase delay distortion of FM modulation in tuned and detuned injection phase-locked oscillator-amplifiers 16 p2369 A72-33760

Improved geometry for a semiconductor surface-wave oscillator. 18 p2667 A72-36685

A thermal oscillator using the thermo-electric /Seebeck/ effect in silicon. 18 p2667 A72-36978

Switching curves and lobesweeping in origin seeking time optimal control for Duffing oscillator, using Pontryagin maximum principle 19 p2777 A72-37373

Approximate calculation of the maximum efficiency of an O-type oscillator with a resonance delay system in the presence of losses 19 p2774 A72-38412

Oscillatory circuits synthesis by wave resistance determination of homogeneous line segments for given resonant frequencies spectrum 19 p2768 A72-38660

Self excited LC and RC oscillator networks based on FETs, discussing frequency tuning and FM methods 20 p2906 A72-38899

Oscillator strength for sulfur monoxide transition band systems calculated from radiative lifetime with Franck-Condon factors

20 p2966 A72-38916

The detection of gravitational waves by electromagnetic oscillators.

20 p2974 A72-40024

Possibility of employing a transistorized self-excited oscillator with a thermistor as radio sensor of temperature

21 p3058 A72-41792

Influence of instantaneous and prolonged pulses on the oscillations of timing-device oscillators

21 p3059 A72-41815

Radiation of an oscillator moving parallel with the interface of two media

21 p3036 A72-41843

Radiation of an oscillating charge in a three-dimensional periodically inhomogeneous medium

21 p3023 A72-41844

Investigation of electrical processes in high frequency condensed-spark generators

22 p3139 A72-42169

German monograph - Stability conditions for a linear homogeneous ordinary differential equation of second order with stochastic parameter excitation.

22 p3199 A72-43055

Computation of the maximum oscillation frequency of bipolar transistors

23 p3269 A72-43448

Application of logarithmic characteristics to calculate wideband load matching of an oscillator

23 p3271 A72-43836

Multiloop LC oscillators with negative resistance and nonlinear capacitances

23 p3271 A72-43838

Excitation of oscillations in transistor oscillators

23 p3271 A72-43840

Master oscillator/power amplifier laser systems output beam divergence and far field brightness, comparing to Gaussian plane waves

23 p3296 A72-43901

OSCILLOGRAMS

U OSCILLOGRAPHIS

OSCILLOGRAPHIS

Cu electrical resistance and heat content oscillographic measurement, using high voltage pulse method

07 p0981 A72-18804

Multichannel oscillograph for real time biomedical studies of LF physiological processes

09 p1270 A72-22881

Two coordinate oscillograph recording device with automatic reversing for stress-strain tests under static and cyclic loads

11 p1637 A72-26814

Cast Al alloys tendency to brittle failure in percussive bending tests estimated from force strain oscillograms

14 p2124 A72-31035

Techniques and procedure for differential ballistooscillography of extremities.

20 p2897 A72-39325

OSCILLOSCOPES

Storage oscilloscope interface for small computers, describing graphic display characteristics and line cursor and character generators

03 p0329 A72-14177

Three color optical pyrometer with microsecond resolution time based on three-wavelength double ratio method, displaying temperature/time relationship on cathode ray oscilloscope

04 p0522 A72-15476

Display device for engine rotational speed nonuniformity parameters indication on oscilloscope without supplementary computation

05 p0662 A72-16125

Cardiac cycle intervals measurement with multibeam cathode oscilloscope synchronized with multichannel polycardiographic automatic recording machine

09 p1272 A72-23192

High tension exciter output voltage measurement based on cathode ray oscilloscope and high voltage probe, stressing calibration procedure [SAE AIR 1092]

11 p1604 A72-26028

Noise suppression by time exposure oscilloscope photography to enhance repetitive electric signals obscured by noise of equal amplitude

13 p1959 A72-29754

Automatic digitizing and recording of analog information from oscilloscope photographs

13 p1959 A72-29755

Registers and digital circuits with FETs and integrated operational amplifiers to permit analog measurements storage for display on CRT oscilloscope

15 p2204 A72-32499

Optical design and production of low cost oscilloscope camera incorporating reliable setting for correct exposure and focus

20 p2921 A72-39031

The random-sampling procedure in oscilloscope technology

23 p3273 A72-44348

OSCULATORY INTERPOLATION

U ORBIT CALCULATION

U ORBIT PERTURBATION

OSEEN APPROXIMATION

Laminar viscous flow past semiinfinite flat plate at zero incidence, using Oseen approximation in matching leading edge and potential flow regions

11 p1615 A72-25522

Third order extension of perturbation method to solve Oseen equations for two dimensional steady viscous flow past cylindrical body at low Reynolds number

14 p2095 A72-30722

OSMIUM COMPOUNDS

Erichmanite /natural osmium disulfide/ chemical analysis and X ray data, noting osmium abundance

03 p0351 A72-14369

Passive Q factor modulation in carbon dioxide laser by resonance absorption saturation in osmium tetroxide vapors, noting vapor pressure effects

11 p1650 A72-26355

Passive Q factor modulation in carbon dioxide laser by resonance absorption saturation in osmium tetroxide vapors, noting vapor pressure effects

16 p2402 A72-33708

The distribution of the long wave photoreceptors in the compound eye of the honey bee as revealed by selective osmic staining.

17 p2500 A72-34877

Osarsite, a new osmium-ruthenium sulfarsenide from California.

22 p3172 A72-42450

OSMOSIS

Early diagnostics of cerebral arteriosclerosis in flying personnel, investigating hypertension, neurocirculatory dystonia and myocarditic cardiocirculatory effects on flight performance

06 p0765 A72-18198

Improperly controlled learning processes relationship to hypertonic blood pressure irregularities pathogenesis in rats, investigating negative emotional reactions effects

07 p0925 A72-20659

Sex differences of chronic effect of environmental stress on blood pressure and information processing in rats, observing neurotic hypertonic blood pressure irregularity

07 p0925 A72-20660

Radial diffusion and convection capillary model for analysis of tissue protein concentration and colloidal osmotic pressure changes during transcapillary fluid movement

08 p1114 A72-20896

Influence of hyperosmolality on left ventricular stiffness.

17 p2499 A72-34727

Influence of thermal, osmotic, and chemical stimulations on food and water intake

17 p2504 A72-35016

Gas induced osmosis as factor in pulmonary homeostasis, showing differential water retention in lungs ventilated with normoxic nitrous oxide compared with air

17 p2506 A72-35970

Electro-osmotic energy conversion in the glass/n-propanol system.

21 p2997 A72-41384

OSMOTIC PRESSURE

U OSMOSIS

OSO

Solar observation survey, considering sounding rockets, OSO, balloons, orbiting observatories, spectral resolution, spectral features and solar flare

03 p0409 A72-13050

Real time ground control optimization of data acquisition of solar spectra scans from OSO 6

03 p0417 A72-13060

Space environment and astronomical studies with sounding rockets, satellites and orbiting solar observations

10 p1548 A72-24974

Description and in-orbit performance of the Orbiting Solar Observatory control system.

[AIAA PAPER 72-852]

20 p2975 A72-39077

Zodiacal light, airglow and lightning monitoring by wide field broad bandpass OSO-5 experiment, obtaining height profile, cell size and intensity variations of nightglow

21 p3054 A72-40619

Star scanner attitude determination for the OSO-7 spacecraft.

[AIAA PAPER 72-922]

21 p3082 A72-41566

OSO pointing accuracy improvement through dual spin stabilization, discussing OSO design evolution 1962-72

24 p3449 A72-45145

OSO and Skylab astronomical instruments technology, emphasizing precision pointing, spatial and spectral resolution and photometric efficiency problems

24 p3405 A72-45545

OSO-E

High energy solar and celestial X ray experiment with OSO 5, measuring spectrum as function of time, intensity and spatial distribution

03 p0353 A72-13044

OSO-G

OSO-G satellite spectroheliograms of chromospheric, transition zone and coronal lines, indicating magnetic field spread with height

03 p0432 A72-13351

Gamma ray spectrometer with antiCompton shield for OSO-7 spacecraft

08 p1167 A72-21515

OSO-H

OSO-H solar X ray instrument for solar flares energy release investigation via thermal and nonthermal electrons X ray emission

08 p1167 A72-21514

Optimal pulse height analyzer with quadratic transfer function for gamma ray spectrometer on OSO-H

08 p1167 A72-21516

Digitized SEC vidicon detector for OSO-H satellite coronagraph, describing optics

08 p1170 A72-21959

OSO-1

Celestial Thomson-scattering X ray polarimeter design for OSO-1, optimizing sensitivity in 4-24 keV energy range by Monte Carlo simulation computer program

15 p2234 A72-31540

OSO-3

Multiplicative factors for energy scale corrections of OSO-3 ion chamber for solar X-ray monitoring

13 p1033 A72-29748

OTOLARYNGOLOGY

Prophylactic otolaryngological investigation of vestibular analyzer function in aviation medicine

15 p2186 A72-31769

Otorhinolaryngological organ response during hypokinetic antiorthostatic bed rest for control, exercising and muscular electric-stimulated groups

23 p3256 A72-43917

OTOLITH ORGANS

Sjoberg hypothesis for zero gravity produced inversion illusion mechanism in aircraft parabolic flight, noting otolith membrane deflection result of force on maculae

02 p0167 A72-11710

Human centrifuge tests for gravito-inertial force effect on ocular counterrolling in normal and deaf subjects

02 p0159 A72-11956

Neck proprioception effects and otolith organ activity in perceived visual target elevation under centrifuging stress

12 p1776 A72-28305

The vestibular apparatus. I - The physics and physiology of the otoliths and the semicircular canals

22 p3146 A72-42787

OTTO CYCLE

Flow characteristics of pin type nozzles in constant pressure carburetors of Otto cycle engines

02 p0206 A72-12853

OUTCROPS

Tectonic dewatering and strain in the Michigamme Slate, Michigan.

18 p2686 A72-36223

OUTER PLANET MISSIONS

U GRAND TOURS

OUTER PLANET SPACECRAFT

U OUTER PLANETS EXPLORERS

OUTER PLANETS EXPLORERS

STAR self testing and repairing fault tolerant digital computer for outerplanet exploration spacecraft, discussing architecture, reliability analysis, software and peripheral system automatic maintenance

02 p0184 A72-11482

Outer planets Grand Tour trajectory correction requirements, examining combined radio/onboard navigation system and delta V estimates [AIAA PAPER 72-54]

07 p1068 A72-18947

Comet rendezvous and outer planet exploration mission operations by unmanned nuclear electric propulsion /NEP/ system with inciner thermionic reactors for electric power generation

[AIAA PAPER 72-428]

11 p1722 A72-26173

Outer Planet Grand Tours Missions radio science experiments for planetary and satellite atmospheres and surfaces, celestial mechanics, relativity, interplanetary medium and solar corona

12 p1870 A72-27347

Trajectory shaping advantages for outer planet orbiter solar electric propulsion, considering radiation belt constraints, dual launch and target orbit geometries

[AIAA PAPER 72-423]

13 p2036 A72-28938

Mission operations for unmanned nuclear electric propulsion outer planet exploration with a thermionic reactor spacecraft.

17 p2606 A72-34578

High accuracy approach guidance system for outer planet exploration.

[AIAA PAPER 72-867]

20 p2951 A72-39132

Earth-based navigation capabilities for outer planet missions.

[AIAA PAPER 72-925]

24 p3423 A72-45430

- Spacecraft navigation systems for Mariner Jupiter-Saturn 1977 Project, considering maneuvers, orbit determination and data requirements [AIAA PAPER 72-926] 24 p3423 A72-45432
- The possibility of a trans-Saturnian belt of particulate matter. 24 p3446 A72-45472
- OUTER RADIATION BELT**
- Outer zone energetic electron precipitation, elf whistler and plasmopause location measurements by polar satellite OV-3-3 instruments 01 p0120 A72-10890
- Inner and outer belt electron differential energy spectra from Cosmos 228 satellite data, discussing fluxes of precipitating and quasi-captured particles 02 p0272 A72-11916
- Geomagnetically trapped protons, electrons and alpha particles verification and measurements in inner and outer radiation belts 07 p1062 A72-20227
- Outer radiation belt parameters dependence on interplanetary magnetic field sectorial structure and solar wind velocity 08 p1226 A72-20811
- Inner and outer belt electron differential energy spectra from Cosmos 228 satellite data, discussing fluxes of precipitating and quasi-captured particles 13 p2030 A72-29228
- Quasi-periodical intensity pulsations in trapped and precipitating electrons in earth outer radiation belt 15 p2299 A72-31914
- Geomagnetically trapped alpha particles. I - Off-equator particles in the outer zone. 17 p2548 A72-35595
- Studies of outer belt and slot region protons at low altitudes. 19 p2853 A72-38740
- Motion and diffusion of energetic particles in the outer zone. 20 p2916 A72-39231
- Earth outer radiation belt and unstable radiation zone dynamics during IQSY magnetically quiet and disturbed period based on Elektron-series satellite data 22 p3218 A72-42211
- Solar-wind parameter variation, magnetic activity, and electrons in the magnetospheric tail and outer radiation belt 23 p3283 A72-43367
- OUTGASSING**
- Toxicological control and chemical analysis of outgassing products from nonmetallics in high temperature oxygen atmosphere, investigating use within LM crew compartment 01 p0019 A72-10771
- ESRO 1 satellite residual gas outgassing rate and composition measurements during thermal heat balance tests, using mass spectrometer 09 p1263 A72-23260
- Optical mirrors contamination by condensation of outgassed spacecraft materials in vacuum under UV irradiation, describing test apparatus and results with various materials [AIAA PAPER 72-267] 11 p1637 A72-25208
- Piezoelectric quartz crystal microbalance for material outgassing and optical element contaminant film measurements 12 p1806 A72-27043
- Analytical prediction of pressure-time relationship during evacuation of multilayer insulation thermal protection systems, taking into account outgassing effects 14 p2172 A72-30925
- Impurity effects in carbon fibres. 17 p2569 A72-34667
- Toxicological evaluation of some synthetic materials designed for airtight space equipment 21 p2998 A72-40434
- Backscattering of desorbed gas molecules from spacecraft 23 p3284 A72-43618
- Spacecraft functional properties degradation due to surface contamination with outgassing vapors, discussing contaminant materials transport and sorption characteristics 23 p3254 A72-43619
- OUTLETS**
- Gas turbine engine combustion chamber, investigating swirl vane air flow rate effects on circumferential nonuniformity of gas temperature field at outlet 12 p1861 A72-28132
- OUTLETS (GEOLOGY)**
- U ESTUARIES**
- OUTPUT**
- NT LASER OUTPUTS**
- NT MASER OUTPUTS**
- OVERCAST**
- U CLOUD COVER**
- OVERESTIMATION**
- U ESTIMATING**
- OVEREXPOSURE**
- U RADIATION DOSAGE**

OVERPRESSURE

- Characteristic overpressure concept for sonic bangs effect on structures and dynamic magnification factor engineering formula 06 p0758 A72-17858
- Mathematical model for gas turbine engine inlet noise caused by shock wave impingement, noting dynamic wave system with overpressure and distortion 13 p2028 A72-29576
- Maximum overpressures of supersonic aircraft maneuvering-produced sonic booms occurring at geometrical-aoustic ray focus points/caustic cusps/ 13 p1898 A72-29586
- Sonic boom effects on sleep - A field experiment on military and civilian populations. 23 p3261 A72-44370
- OVERTONES**
- U HARMONICS**
- OXALATES**
- Chromium carbides synthesis by carburizing chromium hydroxide or oxalate in hydrogen-methane gas mixture at temperatures below 1000 C 22 p3188 A72-41974
- OXIDASE**
- Coacervate drops oxidoreductases and stability in primitive prebiological systems, using polyphenol oxidase-carbohydrate-histone-quinones 04 p0469 A72-14784
- Mechanical vibration induced physiological changes in rats, determining plasma Ca, Mg and inorganic phosphate concentration and xanthine oxidase activity response to frequency and g-levels 13 p1910 A72-29560
- OXIDATION**
- NT ELECTROCHEMICAL OXIDATION**
- NT PHOTOOXIDATION**
- Ni-Cr-Al alloys high temperature oxidation, detailing surface reactions and continuous oxide layer formation [ECS PAPER 114] 01 p0082 A72-10172
- Thoriaated Ni-Cr alloys oxidation kinetics at high temperatures, discussing oxide formations as function of Cr content 01 p0089 A72-11164
- Martian internal structure, investigating oxidation rate of chondritic material 02 p0277 A72-11752
- Niobium anomalous oxidation below 600 C, noting suboxide formation between solid solutions and heat resistance reduction 02 p0243 A72-12214
- Molybdenum-zirconium oxide cermets oxidation behavior, noting change of Mo oxidation characteristic from linear to parabolic time law above molybdenum oxide melting point 02 p0246 A72-12550
- Titanium disilicide oxidation mechanism at various temperatures, discussing surface quality effect, growth rate and protective mechanism 03 p0369 A72-12925
- Tungsten, molybdenum and tantalum disulfides oxidation rate determination by fluidized bed technique, calculating kinetic and diffusive processes activation energy 03 p0370 A72-13184
- Nonequilibrium subsolidus reduction of lunar spinels at low oxygen fugacities based on Cr-Al ulvöspinel and olivine decomposition 03 p0439 A72-14298
- Carbon monoxide oxidation by hydroxyl radicals at high and low temperatures from transition state theory, confirming flame and shock tube results [WSCIP PAPER 71-36] 04 p0482 A72-14584
- Ti anodic behavior in anhydrous liquid ammonia, noting oxidation by halogen intermediary 04 p0484 A72-14976
- Zr alloys hydride distribution after oxidation in steam at 550 C, discussing hydrogen uptake 04 p0534 A72-15362
- IR spectroscopy analysis of oxidation treatment, chemical and structural changes during carbon fiber formation from acrylic precursors 05 p0680 A72-16076
- Soot oxidation rate from diffusion flame measurements extrapolated for gas turbine combustion chambers 05 p0747 A72-16368
- Nb-Zr alloy vacuum chamber tests for oxygen reaction rates, showing oxide surface film relation to sticking probability 05 p0674 A72-16391
- Ordinary and macroporous structured polycondensation oxidation-reduction polymers synthesis, discussing application to organic impurities removal from atmospheric moisture condensates 05 p0622 A72-16645
- Catalytic oxidation of gaseous products formed during thermal treatment of human wastes, considering hopcalite, Cu-Cr, Cu-Co, Pt and Pd 05 p0622 A72-16646
- Sequential sulfidation and oxidation effects on sulfur self propagation in Ni-Cr alloy 05 p0677 A72-17110

- Self ignition in hydrogen oxidation kinetics, considering convection, molecular diffusion, mixing and pressure 05 p0625 A72-17213
- Ni-Al alloy, investigating Y addition effect on vacancy agglomeration suppression during oxidation 06 p0829 A72-17787
- Graphite and molybdenum disulfide, investigating temperature effect, thermal stability and oxidation effect on weight by TGA and DTA 06 p0837 A72-18602
- Surface and thermal effects on hydrogen oxidation, calculating explosion limits and slow reaction rates 07 p0935 A72-19370
- Product of net branching factor and induction period in hydrocarbon oxidation at low temperatures, tabulating results 07 p1051 A72-19374
- Mg dispersion hardening techniques, exploring internal oxidation of alloys containing rare earths 07 p1011 A72-19481
- Reflection electron diffraction and ellipsometric studies of oxidation of niobium crystal surface, showing oxygen absorption in lattice and oxide film formation stages 07 p1017 A72-19944
- Kinetic data analysis of internal oxidation in dilute Ni-Be alloys, deriving activation energy and diffusivity of oxygen in Ni 07 p1021 A72-20435
- Internal oxidation behavior of Cu-Cr-Si ternary alloys microstructure comparison with Cu-Si binary alloys, discussing oxide-matrix interface nucleation 07 p1021 A72-20439
- Absorbed oxygen concentration variation with depth in Nb during oxidation 07 p1022 A72-20555
- Superheating in Zr-oxygen combustion system during autoignition period 08 p1128 A72-21219
- Polyethylene oxidative degradation study with gas chromatographic techniques, obtaining aliphatic and organic compounds at 75-200 C in varying oxygen concentrations 08 p1128 A72-21425
- Electrochemical tests, noting electric potential, current and electrode impedance measurements for corrosion rate and oxidizing power evaluation 08 p1189 A72-22105
- High temperature testing of metals, discussing specimen preparation and oxidation behavior evaluation by gravimetric, volumetric and optical techniques 08 p1189 A72-22107
- Metal single crystals use for corrosion tests, noting anisotropy, adsorption, oxidation and pitting 08 p1189 A72-22111
- Parabolic oxidation kinetics of Ni-Ti alloy compound at elevated temperatures 09 p1330 A72-23358
- Cyclic oxidation kinetics of Hastelloy X sheet and wire specimens for high temperature alloy evaluation in transpiration cooled engine components manufacture 09 p1331 A72-23476
- Oxidation and substructural effects on low stress creep of Al near melting point 09 p1331 A72-23507
- Protective aluminum oxide scale development on Ni-Cr-Al alloy, describing transient oxidation stage 09 p1332 A72-23584
- Samaria distribution effect on Ni-Cr alloy oxidation rate for various oxygen pressures, discussing behavior of electroplated and bulk specimens 09 p1332 A72-23585
- High C 13 content in carbonaceous phases of carbonaceous chondrites accounted for by Rayleigh distillation with oxidized and reduced forms of carbon 10 p1547 A72-24951
- Space shuttle orbiter thermal protection system metal interaction with chemical environment during reentry, emphasizing degradation in dissociated oxygen [AIAA PAPER 72-262] 11 p1590 A72-25206
- Fe-Cr-Mn alloys structural changes during high temperature oxidation, noting subscale layer thickening and alpha phase detection after heat treatment 11 p1655 A72-25498
- Bending stress in oxygen presaturated Nb during oxidation, cooling, dissolution and annealing, using thin film model 11 p1658 A72-25853
- Tensile stress effect on formation of suboxide needles, microcracks and oxide wedges during low temperature Nb oxidation 11 p1658 A72-25854
- Temperature, oxygen pressure and exposure time effects on oxidation characteristics of molybdenum-zirconium oxide cermets 11 p1665 A72-26865
- Fusion silicide protective coatings performance for Ta alloys under simulated reentry conditions, noting oxidation rate, ductile brittle bead transition temperature and mechanical properties [ASM PAPER W 72-13,6] 12 p1835 A72-28162

Physicochemical processes in metal surface layers subjected to contact friction with aircraft fuels presence, noting secondary compounds and thermal oxidation acceleration

12 p1817 A72-28183

Reclaimed surface, ground and sewage water oxidizability measurement, studying oxidation kinetics of potassium bichromate distilled urine condensate admixtures

13 p1910 A72-29313

High purity aluminum-aluminum oxide reversible oxidation, discussing mechanism based on electron charging due to beam

13 p1980 A72-29827

TiC high temperature oxidation and thermodynamic equilibria in air, using metallographic and X ray analyses

14 p2112 A72-30155

Lower oxide mechanism in reduction-oxidation reactions during Ti steels electrosmelting with slag and gas phases

14 p2112 A72-30158

Zr oxidation kinetics at 440-850 C for 3 min maximum exposure time, observing type oxide change relationship to activation energy

14 p2113 A72-30247

Creep rate dependence on high temperature oxidation in austenitic steel, noting preformed oxide layer and environment cycling effects

14 p2117 A72-30537

Stress relieving heat treatment for service failure prevention of stressed austenitic stainless steel components of high temperatures, noting cracking regulation by oxidation mechanism

14 p2117 A72-30538

Co-Cr alloy high temperature oxidation kinetics reduction by Y addition, presenting metallographic study

14 p2118 A72-30543

Disilicide coated Ta-W alloy system oxidation behavior at 927-1482 C, using thermogravimetric, X ray diffraction and electron microprobe analyses

14 p2121 A72-30771

Octahedral TiC single crystals oxidation at high temperature in oxygen, carbon dioxide and mixtures, investigating oxygen partial pressure effects on kinetics

14 p2121 A72-30772

Zirconium diboride oxidation processes at temperatures above 520 C, noting zirconium oxide formation

14 p2121 A72-30850

Y and La action on oxidation rates of Cr and Mo at high temperature in air

15 p2252 A72-31191

Refractory steels heat resistance improvement by surface saturation with Be and subsequent oxidation in air at 900-1000 C, comparing with aluminized steels

15 p2255 A72-31574

Low energy electron spectroscopy measurement of thin oxide layer growth on Al surface, noting oxidation uniformity dependence on residual gas water content

15 p2276 A72-31859

Clean Ge crystal surface oxidation process investigation by LEED and conductivity measurements

15 p2292 A72-31868

Edge and surface modification of Nb alloys prior to coating with fused silicide for oxidation life extension

15 p2244 A72-32134

Reaction rate and activation energy of low temperature oxidation of Mg particles in nitrous oxide

16 p2476 A72-33253

Carbon monoxide oxidation reactions temperature dependence, correlating high to low temperature results via transition state theory

16 p2360 A72-33511

Ternary Ni-Cr-Al superalloys oxidation at 800-1300 C as function of composition, temperature, oxygen pressure and reaction time

16 p2410 A72-33811

Quinones as reversible redox couples for rechargeable cathodes, noting air regeneration capacity in organic electrolytes

16 p2352 A72-33898

The formation of metal-oxygen compounds for additive thermionic converters.

17 p2595 A72-34600

High temperature oxidation of ammonia.

17 p2511 A72-34904

Comments upon shock-initiated oxidations by nitrous oxide.

17 p2511 A72-34905

IR-spectroscopic investigation of the effectiveness of oxidation inhibitors in lubricants

19 p2823 A72-38092

Formation of hydrogen from amine oxidation and pyrolysis.

19 p2883 A72-38874

Development of a spacecraft wet oxidation waste processing system.

[ASME PAPER 72-ENAV-3] 20 p2896 A72-39174

The mechanism of oxidation of Ni-Cr-Al alloys.

20 p2937 A72-39214

The internal oxidation of Ni-Cr-Al alloys.

20 p2937 A72-39215

Internal oxidation in carburized layers of alloyed steels

20 p2929 A72-39584

Induction period, particle size distribution and medium temperature effects on thermal ignition of metal particles under exothermal oxidation reaction on surface

20 p2987 A72-40040

Detonation shock wave study of liquid fuel droplets in gaseous oxidizing agent flow, using schlieren and scanning photography

20 p2962 A72-40044

Reversible changes in polyethylene coating adhesion due to thermo-oxidative destruction of polyethylene

21 p3072 A72-40082

Vapor phase formation during high temperature oxidation.

21 p3066 A72-40551

Cortical effects mechanisms in animal vegetative systems, noting biological oxidation and organic phosphorus compound studies

21 p3000 A72-40759

Strengthening of tungsten by powder metallurgical internal oxidation.

21 p3067 A72-40833

Effects of scale porosity, second-phase oxides, and doping in the high-temperature oxidation of cobalt and dilute cobalt-chromium alloys.

21 p3067 A72-40845

Effect of cold work on the oxidation of nickel at high temperature.

21 p3067 A72-40846

Auger spectroscopic observation of Si-Au mixed-phase formation at low temperatures.

22 p3178 A72-42616

Respiratory chain components correlation to tension production at various oxygen pressures in guinea pig ductus arteriosus, investigating light absorption changes

22 p3144 A72-42670

Oxidation rate anisotropy investigation on coupon specimen of Ta-Mo alloy at 950 C

22 p3190 A72-42770

German monograph - Gas-phase precipitation and high-temperature oxidation of titanium carbide.

22 p3194 A72-43053

Production and properties of materials of the Si3N4-Cr2O3 system

23 p3298 A72-43283

Influence of the oxidation of finely dispersed graphite powders on their compactibility

23 p3307 A72-44018

Alpha aluminum whiskers growth in multilayer ceramic composition following vapor-liquid-solid phase

23 p3303 A72-44152

Oxidation of W(110)/ I - LEED study of the oxide formation at 1000 K.

24 p3378 A72-44952

Field repair of fused slurry silicide coating for oxidation protection of Nb alloys in space shuttle environment

01 p0075 A72-10759

Oxidation screening at 2200 F of Ni, Fe and Co wrought alloys for space shuttle thermal protection system, noting microstructural changes

01 p0085 A72-10781

Space shuttle thermal protection system, discussing oxidation resistant coatings, refractory metals, heat shield technology, ballistic reentry programs, weight and cost

01 p0135 A72-10935

Ni-Cr-Al-Si and Fe-Cr-Al-Y oxidation resistant claddings for superalloys, comparing to commercial aluminide coatings by cyclic furnace and high velocity burner rig tests

04 p0533 A72-14700

Metal polymer interface synthesis based on linearly cyclic organoelementary high molecule compounds, analyzing heat and thermal oxidation resistances

05 p0680 A72-16202

Nb alloy oxidation behavior dependence on temperature in 550-1316 C range

05 p0676 A72-16732

Gas turbine superalloys high temperature oxidation resistance by fiber strengthening, rare earth alloying, precipitation hardening and intermetallic compounds

06 p0828 A72-17611

Oxidation and hot corrosion tests of coated Ta and Ta based alloys between 800 and 1500 C in still air and in oxidizing gas stream

06 p0828 A72-17614

Oxidation resistant solid lubricants for high temperature air and gaseous environments applications, considering oxide and fluoride coatings with silicate additives for wear life improvement

06 p0837 A72-18600

Metals and alloys for aerospace applications, emphasizing creep and fatigue properties and oxidation resistance at high temperatures

08 p1185 A72-21171

Thermodynamics of ceramic oxide corrosion by sulphur and oxygen bearing atmospheres, considering

formation products and furnace refractory materials choice

09 p1333 A72-22377

Hot pressed baron nitride and composite oxidation tests in atmospheric arc jet, noting fabrication and composition effects on thermal shock and oxidation resistance

09 p1333 A72-22379

High temperature tests of graphite composites in air, determining material loss time dependence and correlation with observed strength data after oxidation

09 p1333 A72-22381

Vehicle components oxidation in thermal control coatings, investigating resistance to oxidation by UV photoproduct ZnO electronic holes

[AIAA PAPER 72-264] 11 p1699 A72-25207

Al addition effect on thermal and mechanical stability, forgeability, cold workability, aging and oxidation resistance of Ti-Mo beta alloys

11 p1656 A72-25516

Hot pressed silicon nitride with high strength and good oxidation and thermal shock resistance for gas turbine applications

[ASME PAPER 72-GT-19] 11 p1673 A72-25618

Transition metals silicides additions effect on sintering and oxidation resistance at high temperatures of Ti and Zr diborides

11 p1665 A72-26874

Molybdenum disulfide addition effect on compounded model greases lubricating performance, determining oxidation stability, rust preventive behavior and consistency

12 p1832 A72-27047

Aromatic polyimide binder for compression moldable high performance composites preparation with thermal curing to obtain good thermal-oxidative stability and toughness

12 p1834 A72-28090

Al inhibitive of Ti oxidation at 800-1000 C due to interatomic bonds, lower oxygen solubility and diffusion rates

14 p2113 A72-30166

Thin oxidation resistant alloy claddings for superalloys, comparing performance with aluminide coatings by cyclic furnace and high velocity burner rig tests

14 p2113 A72-30271

Ni additions effect on Fe-Cr alloys oxidation behavior at high temperatures during varied exposure time periods, noting dichromium trioxide scale formation

14 p2118 A72-30545

W and Nb effect on Ta base alloys high temperature oxidation behavior

14 p2118 A72-30547

High temperature oxidation resistance and mechanical properties of Fe-Al-Cr alloys with Ti and Mo additions

15 p2253 A72-31520

Apiezone lubricants physicochemical properties comparison, noting aromatic hydrocarbons effect on thermo-oxidation stability and polyisoprene rubber type polymer additive effect on adhesiveness

16 p2413 A72-33171

Thermosetting polybutadienes as co-curing plasticizers for thermoplastics reinforcement, noting oxidation resistance at room and moderately elevated temperatures

16 p2415 A72-33416

Oxidizability of boron-carbon compounds at high temperatures, determining chemical composition effect on oxidation resistance

18 p2703 A72-36095

Oxidation resistance at high temperatures of refractory materials based on silicon nitride and carbide in various concentrations, showing time and temperature dependence

18 p2703 A72-36096

German monograph - The effect of alloying elements on the dry high temperature oxidation of cobalt in the temperature range from 800 C to 1000 C in air and pure oxygen

19 p2816 A72-37656

Creep of porous nickel in oxidizing and neutral media

19 p2819 A72-38287

Inconel alloy 617 - A new high-temperature alloy.

19 p2821 A72-38388

Multi-cycle plasma arc evaluation of oxidation inhibited carbon-carbon material for shuttle leading edges.

[ASME PAPER 72-ENAV-26] 20 p2894 A72-39151

On some aspects of low-temperature and anodic oxidation of metals and semiconductors.

21 p3067 A72-40914

Oxidation of TD nickel at 1050 and 1200 C as compared to three grades of nickel of different purity.

21 p3067 A72-40915

Oxidation protection of tantalum and tantalum alloys at up to 1500 C

22 p3188 A72-41973

Aluminized thorium dispersed NiCr and Ni-20Cr alloys with protective alumina scales from pack diffusion, observing oxidation resistance by isothermal and cyclic oxidation tests

22 p3193 A72-43030

Effect of oxygen on the scale resistance of titanium-tin alloys 23 p3300 A72-43592

Corrosion and electrochemical properties of Kh15N5D2T and Kh15N4AM3 oxidized steels 23 p3303 A72-44099

OXIDES

NT ALUMINUM OXIDES

NT ANATASE

NT ANHYDRIDES

NT BARIUM OXIDES

NT BERYLLIUM OXIDES

NT BISMUTH OXIDES

NT BORON OXIDES

NT CALCIUM OXIDES

NT CARBON DIOXIDE

NT CARBON MONOXIDE

NT CERIUM OXIDES

NT CESIUM OXIDES

NT CHROMITES

NT CHROMIUM OXIDES

NT COBALT OXIDES

NT COESITE

NT COPPER OXIDES

NT ENSTATITE

NT HAFNIUM OXIDES

NT HEAVY WATER

NT HEMATITE

NT HYDROGEN PEROXIDE

NT ILMENITE

NT IRON OXIDES

NT MAGNESIUM OXIDES

NT MAGNETITE

NT METAL OXIDES

NT MOLYBDENUM OXIDES

NT NICKEL OXIDES

NT NIOBATES

NT NIOBIUM OXIDES

NT NITRIC OXIDE

NT NITROGEN DIOXIDE

NT NITROGEN OXIDES

NT NITROGEN TETROXIDE

NT NITROUS OXIDES

NT PEROXIDES

NT POTASSIUM OXIDES

NT PYROXENES

NT QUARTZ

NT RUTILE

NT SAPPHIRE

NT SCHEELITE

NT SILICON DIOXIDE

NT SILICON OXIDES

NT SULFUR OXIDES

NT TANTALUM OXIDES

NT THORIUM OXIDES

NT TITANIUM OXIDES

NT TUNGSTEN OXIDES

NT URANIUM OXIDES

NT VANADIUM OXIDES

NT YTTRIUM OXIDES

NT ZINC OXIDES

NT ZIRCONIUM OXIDES

Thermodynamics of ceramic oxide corrosion by sulphur and oxygen bearing atmospheres, considering formation products and furnace refractory materials choice 09 p1333 A72-22377

Oxide scale formation on zirconium diboride materials, observing microstructural features as function of temperature and reaction time [AD-737020] 09 p1333 A72-22380

Thermal shock resistant composite materials with carbide or oxide matrices based on concept of crack propagation prevention, noting superiority from thermal simulation tests 09 p1334 A72-22384

Stoichiometry effect on high temperature creep in oxides, relating impurities, point defects concentration and diffusion 09 p1335 A72-22397

Papers on high temperature oxides covering refractory glasses, glass-ceramics, mullite, oxide spinels, glass networks theory and physical chemistry principles application 10 p1501 A72-24726

Oxide spinels crystallographic structure determination, stability relationships, covalent bondings and physical properties 10 p1501 A72-24730

I-V characteristics of metal-semiconductor-metal structures based on oxide glasses, noting temperature dependence and current limitation 13 p2021 A72-28688

Chondrule like spherules from supercooled molten oxide and silicate droplets by carbon dioxide laser heating compared with meteoritic chondrules 15 p2303 A72-31306

Ultrasonic device with magnetostriction vibrator for suspension coating oxide cathodes, noting superiority to spray coating by compressed air 16 p2374 A72-33969

Comparative evaluation of zinc borate 2:3:3.5 with antimony oxide using various fire testing methods 20 p2898 A72-39699

Oxidizers

NT FLOX

NT HIGH ENERGY OXIDIZERS

NT LIQUID OXYGEN

NT ROCKET OXIDIZERS

Active ingredient oxidizing potential and pressure effects on burning rate of explosive substances 02 p3032 A72-12292

Heterogeneous composite solid propellants ignition behavior under exposure to hot oxidizing gas, using gas phase model with species and energy radial diffusion 07 p1051 A72-19726

Quench combustion studies with two dimensional propellant sandwiches with ammonium perchlorate oxidizer and various binders, using high pressure combustion vessel for deflagration characteristics determination 07 p1051 A72-19727

Burning process of low boiling Mg particle moving in relation to gaseous oxidizer, assuming heat and mass transfer occurrence by diffusion-conduction mechanism 09 p1411 A72-22888

Active ingredient oxidizing potential and pressure effects on burning rate of explosive substances 10 p1561 A72-23767

Ammonium perchlorate burning rate temperature dependence as function of pressure and oxidizer particles size, noting low pressure deflagration limit [ONERA, TP NO. 1079] 13 p2025 A72-29669

Ignition moment of solid propellant particles monodispersive aggregate uniformly distributed in gaseous oxidizer 19 p2879 A72-37359

Development of a solid fuel on a polyurethane basis for a hybrid rocket propulsion system with 98% nitric acid as oxidizer 20 p2962 A72-39416

Burn-up rate of a solid-propellant slab in contact with a solid-oxidizer layer 22 p3245 A72-43180

Burning rates of organic perchlorates of aliphatic, aromatic and heterocyclic amines and amidines with explosive compounds containing nitrogen dioxide group as oxidizer 22 p3153 A72-43181

OXIMETRY

Ear oximeter design for human subject blood oxygen saturation estimation during increased g-loads 12 p1774 A72-28278

OXYFLUORIDES

Gaseous boron dioxide and oxyfluoride heat of formation determination by mass spectroscopy and molecular effusion technique [AD-740421] 07 p0936 A72-19682

IR mass spectrometric study of OFB in Ne and Ar matrices, discussing molecular structure 16 p2360 A72-33223

OXYGEN

NT HIGH PRESSURE OXYGEN

NT LIQUID OXYGEN

NT OXYGEN ATOMS

NT OXYGEN ISOTOPES

NT OXYGEN PLASMA

NT OZONE

Oxygen effect on dynamic elastic modulus of titanium-oxygen alloys by density and longitudinal ultrasonic wave velocity measurements 01 p0083 A72-10393

Pulmonary functional inhomogeneities effects on steady state oxygen and CO diffusing capacity estimates in gas transfer resistances terms 01 p0014 A72-10847

Upper atmosphere neutral oxygen density diurnal variations from incoherent scatter and satellite drag data, noting deviations from Jacchia static diffusion model predictions 01 p0062 A72-10911

Oxygen content and stoichiometry effects on metal carbides grain growth in liquid phase sintering, discussing carbide-metal interface solution reaction as rate controlling mechanism 02 p0240 A72-11434

Stratospheric and lower mesospheric temperature measurement by ground based passive microwave sensing, calculating oxygen absorption band lines brightness temperature emission spectra 02 p0213 A72-11861

Supersonic oxygen molecules nozzle beam reactive scattering on barium atoms, detailing exothermic reaction energy in barium oxide formation 02 p0170 A72-11912

Atomic oxygen layer height and peak concentration in earth upper atmosphere, considering solar dissociative radiation and turbulent diffusion for equinox conditions 02 p0217 A72-11924

Partial molar enthalpy measurement of oxygen mixture in substoichiometric Zr at 1300 C, using Tian-Calvet microcalorimeter 02 p0170 A72-12167

Continuum UV radiation absorption by vibrationally excited molecular oxygen in Schumann-Runge system 02 p0221 A72-12457

Oxygen determination in cemented carbides, metal powders and presintered and finished sintered products by vacuum fusion method, comparing with neutron activation method 02 p0245 A72-12548

Stress induced oxygen diffusion in alpha Zr, attributing temperature dependent internal friction peak to oxygen-titanium interactions 02 p0247 A72-12818

Niobium-oxygen-nitrogen system solid solution, noting gas composition effects on hardness and electrical resistivity 03 p0369 A72-12958

Altitude, photon wavelength and solar activity effects on photoionization yield of ionospheric monatomic and diatomic oxygen and nitrogen via Monte Carlo simulation 03 p0345 A72-12983

Oxygen, hydrogen and nitrogen constituents in mesosphere, investigating ionization process in D region at midlatitudes 03 p0346 A72-13379

Molecular oxygen photodissociation in Schumann-Runge bands, discussing determination of solar radiation penetration depth into chemosphere 03 p0412 A72-13386

Resonance electron spectroscopy experiments on electron collisions involving vibrational excitation, deactivation and attachment in molecular oxygen 03 p0347 A72-13391

Quantum yield observations for photochemistry of ozone and singlet molecular oxygen in atmosphere 03 p0347 A72-13393

Oxygen determination in Nb with reduction fusion, determining metallic bath temperature, nature and composition effects on extraction efficiency 03 p0374 A72-13674

Quenching rate of vibrationally excited hydroxyl with molecular oxygen in fast flows for airglow studies in upper atmosphere 03 p0321 A72-13899

Oxygen and oxygen-nitrogen mixtures dc and hf discharges, evaluating traveling low field domains in positive column 03 p0400 A72-14350

Oxygen hazards, mishaps and safety programs in NASA operations, considering material, design, cleaning and procedural deficiencies and failures 04 p0564 A72-14436

Molecular oxygen photoelectron spectra at autoionizing resonance frequencies, comparing with Franck-Condon calculations 04 p0552 A72-14892

Intensity-height profiles for molecular oxygen first and second negative bands in F region, using equilibrium velocity distribution of photoelectrons 04 p0518 A72-14963

Crack corrosion in metals and metal alloys, considering electrochemical reaction kinetics as function of oxygen concentration and pH 04 p0536 A72-15738

Dissolved oxygen effect on structure and toughness of nonalloyed extramild steels, observing austenite recrystallization kinetics retardation after hot plastic deformation 05 p0672 A72-16143

Vibrationally excited oxygen molecules formation and decomposition in upper atmosphere, calculating day and night equilibrium concentrations 05 p0657 A72-16252

Oxygen ions vertical flux altitude distribution in F layer from incoherent scatter radar measurements, noting existence in protonosphere during daytime [AD-737929] 05 p0629 A72-16616

Nb-O and Nb-N alloys, investigating oxygen and nitrogen solute-hardening effects on room temperature flow stress 05 p0675 A72-16729

Oxygen and/or nitrogen interstitial solute pick-up effects on yield stress during Nb annealing, discussing Hall-Petch plot parameter values 05 p0676 A72-16730

Molecular oxygen dissociation rate constant determination during interaction with He atoms in cylindrical shock tube 06 p0852 A72-17686

Linear four step model for photosynthetic molecular oxygen evolution, discussing oxidation states, flash yield oscillation damping and deactivation 06 p0770 A72-18424

Polybenzimidazole fabric treatment for flammability reduction in oxygen atmospheres 07 p1023 A72-19055

Oxygen effect on structure and mechanical, technological and corrosive properties of stainless steel melted in open and vacuum furnaces 07 p1013 A72-19739

Kinetic data analysis of internal oxidation in dilute Ni-Be alloys, deriving activation energy and diffusivity of oxygen in Ni 07 p1021 A72-20435

Self diffusion coefficients of carbon and oxygen in dolomite 07 p0937 A72-20520

Absorbed oxygen concentration variation with depth in Nb during oxidation 07 p1022 A72-20555

Electron microscopic investigation of niobium-oxygen alloys with Zr and Hf additions, measuring oxygen solubility 08 p1187 A72-21787

Temperature dependence of scattering cross sections for cold and hot neutrons colliding with oxygen and deuterium molecules 08 p1211 A72-21872

Diatomic oxygen and carbon dioxide density profiles effects on photoionization rates in D region [AD-741091] 09 p1274 A72-22356

Embryogenesis of fertile chicken eggs in pure oxygen at reduced pressure 09 p1265 A72-22642

Methane, hydrogen and oxygen adsorption and displacement on crystal surface of W investigated by thermal desorption and work function changes 09 p1276 A72-22807

Microorganisms effects on oxygen and compounds cycles, leading to changes in oxygen distribution in earth crust, hydrosphere, atmosphere and biomass 09 p1267 A72-23592

Oxygen jet-carbon dioxide laser beam cutting in mild and stainless steels, noting speed and material thickness limitations 09 p1321 A72-23639

Steady state model for Venus atmosphere water vapor loss, noting hydrogen and oxygen escape due to dynamic outflow of constituents from upper region 09 p1393 A72-23657

Al and oxygen effects on commercially pure Ti microhardness and microstructure, noting interstitial and substitutional atom inclusions effects on hexagonal cell dimensions 10 p1494 A72-23831

Chemisorbed oxygen effect on electrical properties of monocrystalline cadmium sulfide thin plates with high resistivity 10 p1525 A72-24211

Oxygen adsorption effects on Mo orientation contrasts and emission image under electron microscope 10 p1513 A72-24875

Oxygen chemisorption surface states effects on electrical conductivity of CdS single crystals and evaporated films 11 p1701 A72-25855

Carbon and oxygen distribution and content effects on Mo mechanical properties and embrittlement 11 p1666 A72-26878

Electron impact excitation spectrum of molecular oxygen, investigating angular behavior of differential scattering cross sections and energy dissipation 12 p1848 A72-27851

Gaseous buffering for oxygen fugacity control in high temperature gas systems at one atmosphere 12 p1778 A72-28104

Ear oximeter design for human subject blood oxygen saturation estimation during increased g-loads 12 p1774 A72-28278

Statistical adsorption kinetics model with electron desorption of oxygen on polycrystalline W, noting sticking coefficients 13 p1912 A72-28523

Atmospheric oxygen concentration latitudinal and diurnal variations from incoherent scatter and satellite drag data, noting compatibility with Jacchia model 13 p1951 A72-29389

Combustion products thermodynamic parameters for natural gas burning in oxygen atmosphere, plotting gas temperature and flow rates against pressure and excess oxidant ratio 13 p2065 A72-29451

Mechanical strength of interstitial solid tantalum-oxygen solutions obtained by electron beam fusion, thermal cycling and saturation as function of temperature and oxygen contents 14 p2112 A72-30163

Co-Cr alloy oxidation as function of temperature and oxygen partial pressure, discussing solid state diffusion 14 p2118 A72-30544

Ta-W-Hf alloy mechanical properties impairment from oxygen contamination, noting hafnium dioxide precipitate in reaction zone 14 p2121 A72-30769

Phase composition of Nb-O-Hf and Nb-O-Zr ternary alloys, noting O solubility decrease 14 p2122 A72-30980

Oxygen monolayer amounts adsorption on yttrium films and molybdenum foil investigated by Auger electron spectroscopy, observing growth of shifted peaks 15 p2292 A72-31860

Ionospheric molecular oxygen density measurements during solar grazing ray absorption experiment on Ariel 3 satellite 15 p2226 A72-31950

Decarburization kinetics of Nb wires with dissolved carbon in high temperature oxygen flow, monitoring electrical resistivity and CO partial pressure 15 p2244 A72-32113

Lateral diffusion measurement for mass identified positive ions in oxygen, noting spiralling, charge exchange and collisions effects on ion-molecule system 15 p2281 A72-32224

Molecular oxygen concentrations from solar Lyman alpha radiation absorption profile in mesosphere, using rocket-borne nitric oxide filled ion chamber 15 p2230 A72-32264

Oxygen molecule parameters from frequency data in microwave, submillimeter and IR spectroscopy 15 p2283 A72-32654

Potential energy curves for exothermic reaction between oxygen cations and nitrogen molecules to form nitric oxide and atomic nitrogen 16 p2360 A72-32921

Solar radiation induced molecular oxygen photodissociation rate as function of column density and temperature in mesosphere and lower thermosphere 16 p2383 A72-32967

Solar radiation absorption measurements in 2150 A region as function of altitude to obtain oxygen and ozone densities 16 p2384 A72-32975

Metal-air batteries with alternately polarizable oxygen electrodes, discussing current state of technology 16 p2350 A72-33670

Cubic sodium tungsten bronze electrocatalytic activity increase for oxygen reduction by traces of Pt 16 p2361 A72-33883

Organic catalysts for oxygen reduction, discussing phthalocyanines, Pfeiffer complexes and porphyrins 16 p2361 A72-33884

Electrodes converting hydrogen, methanol or oxygen for use in fuel cells with alkaline electrolyte, using Ag-Pd, Ni, Si and C catalysts 16 p2351 A72-33885

Oxygen molecule electron affinity role in ion chemistry of lower ionosphere, noting binding energy of ground state 17 p2585 A72-34260

Oxygen adsorption effect in Cs-W thermionic converter system, comparing statistical-mechanical model analytical results with Alleau-Bacal experimental data 17 p2496 A72-34597

Measurements of molecular oxygen in the thermosphere. 17 p2546 A72-34694

High temperature solid-solubility limit and phase studies in the system tantalum-oxygen. 17 p2567 A72-34731

Thermospheric molecular oxygen from solar extreme-ultraviolet occultation measurements. 17 p2614 A72-35602

W/100% work function change during adsorption of oxygen, cesium, and oxygen-cesium co-adsorption 18 p2656 A72-36128

Thermionic converter I-V performance improvement via oxygen addition, examining feasibility of cesium oxide-cesium solution as source 18 p2647 A72-36204

Effect of low-pressure oxygen on the creep properties of W-25 pct Re. 18 p2700 A72-36581

Hydrostatic oxygen burning in stars. II. 19 p2854 A72-37236

Ion mobilities and ion-molecule reaction rates in oxygen. 19 p2836 A72-37457

Oxygen diffusion coefficient variation with temperature observed during dissolution in alpha-zirconium, noting oxygen content effect on oxygen atom elementary jump length 19 p2817 A72-37795

Environmental acceleration of fatigue-crack growth in a high-strength steel. 20 p2935 A72-39140

Electronic and nuclear magnetic resonances of the oxygen and hydrogen labile negative molecular ions. 20 p2956 A72-39189

The effect of oxygen on tantalum-sodium compatibility. 20 p2938 A72-39297

Conditions and mechanism of formation of suboxide phases in the niobium-oxygen system 21 p3066 A72-40381

Detection of molecular oxygen in the Martian atmosphere. 21 p3103 A72-40451

Cross sections calculations for electron-oxygen scattering using the polarized orbital close coupling theory. 21 p3087 A72-40472

Excess metal buildup kinetics and work function of oxide thermionic cathode activated by emission current, noting effect of metal and oxygen concentrations 21 p2997 A72-40789

The nature of solid solutions of the titanium-vanadium-oxygen and titanium-vanadium-aluminum-oxygen systems 21 p3068 A72-40962

Optimum design of MHD generator combustion chamber, noting effects of heating temperature, oxygen enrichment degree and flow velocities 21 p2997 A72-41065

Detection of molecular oxygen on Mars. 22 p3224 A72-42293

Rocket radiometers measurement of oxygen IR atmospheric system altitude profile at night, noting auroral enhancement possibility 22 p3170 A72-42365

Equimolar oxyhydrogen detonation wave behavior near pressure limit, considering unsteadiness caused by tube length 22 p3244 A72-42485

Laser magnetic resonance of the O₂ molecule using the 337-micron HCN laser. 22 p3209 A72-42895

Drift velocities, diffusion coefficients, and temperatures of photoions in argon, nitrogen, and oxygen 22 p3209 A72-42926

German monograph - Ionization of nitrogen-oxygen gas mixtures by shock waves. 22 p3209 A72-43073

Flow direction and velocity effects on metal burning rates of low carbon and Ni-Cr steels in pure oxygen, using diffusion model 22 p3245 A72-43185

Adsorbed oxygen inhibition of reactions of hydrogen with tungsten. 23 p3298 A72-43270

Electronic excitation of N₂ and dissociative excitation of O₂ by proton impact. 23 p3317 A72-44520

On the use of a Fabry-Perot interferometer for the study of Raman spectra of gases under high resolution. 24 p3426 A72-44904

The kinetics of the reaction between oxygen and sulfur on a Ni(111) surface. 24 p3378 A72-44951

Influence of oxygen and hydrogen on the strength of titanium alloys 24 p3414 A72-45379

V and Al addition effects on mechanical properties of oxygen rich Ti alloys 24 p3416 A72-45745

OXYGEN AFTERGLOW

Low-temperature measurements of the three-body electron-attachment coefficient in O₂. 19 p2837 A72-37545

Formation and loss of O₂⁺/+ and O₄⁺/+ ions in krypton-oxygen afterglow plasmas. 23 p3316 A72-44345

OXYGEN ANALYZERS

Semiautomatic measurement of human oxygen uptake, discussing apparatus and accuracy 10 p1432 A72-24991

Aviator breathing oxygen contaminant detector using gas chromatography and portable IR analyzer 12 p1773 A72-28253

A simple combination mass spectrometer inlet and oxygen electrode chamber for sampling gases dissolved in liquids. 19 p2762 A72-38146

Determination of oxygen consumption by use of the paramagnetic oxygen analyzer. 21 p3006 A72-40429

A critical assessment of an open circuit technique for measuring oxygen consumption. 23 p3260 A72-43937

Acrylamide polymerization - New method for determining the oxygen content in blood. 24 p3376 A72-45376

OXYGEN ATOMS

Seasonal variation in lower thermosphere atomic oxygen concentration deduced from static diffusion models, using incoherent scatter and orbital decay temperature measurements 01 p0062 A72-10907

Nighttime ionosphere dynamical behavior, discussing motions effect on OI emission intensity 01 p0063 A72-10919

Atomic/molecular oxygen concentration ratio semi-annual variation at 130 km altitude from mass spectroscopic data analysis 02 p0218 A72-11947

Atomic oxygen coupled electron excitation and ionization by electron-atom and atom-atom collisions in nonequilibrium relaxation zone behind shock wave 02 p0207 A72-12896

Oxygen and hydrogen atoms production in atmosphere by photodissociation, investigating terrestrial hydrogen escape efficiency 03 p0346 A72-13381

Nitrogen dioxide producing chemiluminescent radiative and three-body recombination reaction at low pressures, determining airglow and oxygen atoms decay time by resonance fluorescence method 03 p0347 A72-13395

Forbidden O I and molecular nitrogen ions emission lines rate variation with height in aurora 03 p0352 A72-14382

Energetic electrons absorption cross sections in weakly ionized atomic oxygen gas, showing energy losses through excitation 05 p0655 A72-16071

Intensity ratio and effective lifetime of excited oxygen atoms in pulsating aurora from auroral intensity and absorption observations, noting diurnal variations 07 p0974 A72-18897

Scattering cross section for excited oxygen atoms produced by electron impact dissociation of molecular oxygen 07 p1037 A72-18964

Extreme UV absorption cross sections ratios for atomic oxygen in upper atmosphere, observing solar radiation attenuation with satellite instruments 09 p1297 A72-22578

Phase angle measurements of frequency-oxygen atom lifetime relationship in pulsating auroras 09 p1298 A72-22589

Neutral atmosphere effects on lower ionosphere, considering D region atomic oxygen, nitric oxide and water vapor and electron density distributions 10 p1474 A72-24712

Space shuttle orbiter thermal protection system metal interaction with chemical environment during reentry, emphasizing degradation in dissociated oxygen [AIAA PAPER 72-262] 11 p1590 A72-25206

Heat conduction and radiative transfer equations of IR cooling by atomic O in thermosphere 11 p1622 A72-25848

Rocket-borne mass spectrometer tested in high velocity molecular beam facility for thermospheric atomic oxygen density measurement 11 p1634 A72-26422

Upper atmosphere atomic oxygen distribution calculated for D and E region aeronomy problems solution 13 p1947 A72-28604

Atomic oxygen layer height and peak concentration in earth upper atmosphere, considering solar dissociative radiation and turbulent diffusion for equinox conditions 13 p1948 A72-29236

Atomic/molecular oxygen concentration ratio semi-annual variation at 130 km altitude from mass spectroscopic data analysis 13 p1949 A72-29259

Ionospheric oxygen ions loss rate in charge exchange reactions with hydrogen, molecular nitrogen and oxygen and atomic oxygen photoionization rate 13 p1953 A72-29811

Auroral spectroscopic and excitation processes, discussing atomic oxygen production, emission ratios and electron energy spectrum, UV and IR emissions, composition and temperature measurements 14 p2098 A72-30138

Nitric oxide gas release by rocket in auroral glow to determine atomic oxygen densities in ionosphere via observation of auroral light emission 15 p2226 A72-31936

Oxygen atom electron affinity calculation by symmetry-adapted pair correlation approximation, using pseudonatural orbitals (PSNO) technique 15 p2282 A72-32644

Sensor design and principles for atomic oxygen concentration measurement in dissociated gases, using Ag thin film electrical resistance change during oxidation 16 p2390 A72-33162

Oxygen and nitrogen atoms effect on defects recovery in cold rolled Nb during annealing 16 p2406 A72-33208

Decay rate coefficients at 250-370 K for three-body recombination kinetics of O and CO, considering CO, carbon dioxide and nitrogen as third body 17 p2511 A72-34736

Determination of the quenching of O(1D) by molecular nitrogen using the ionospheric modification experiment 18 p2685 A72-35991

An atomic oxygen beam system for the investigation of mass spectrometer response in the upper atmosphere 19 p2795 A72-37515

Atomic oxygen-ozone gas phase reaction rate constant direct measurement in steady state flow system at 269-409 K under excess ozone conditions 19 p2762 A72-38221

Metastable atomic oxygen deactivation in upper atmosphere by inelastic collisions and by spontaneous irradiation, noting airglow intensity dependence on red lines irradiation 19 p2792 A72-38633

Martian atmosphere atomic oxygen concentration estimation from Mariner 6 and 7 O I 1304 and 1356 A data analysis 19 p2868 A72-38734

Utilization of photorecombination of radicals and atoms in continuous-wave lasers 20 p2932 A72-39508

Thermospheric atomic oxygen and molecular nitrogen densities fromOGO 6 neutral atmospheric composition experiment, comparing with prediction by Jacchia models 22 p3172 A72-42431

Determination of the detonation velocity of isoatomic mixtures 24 p3462 A72-45032

Upper atmosphere atomic oxygen distribution calculated for D and E region aeronomy problems solution 24 p3398 A72-45104

Mass spectra stimulated by O+ and Ar+ interacting with a surface. 24 p3378 A72-45312

OXYGEN BREATHING

Human mental and psychomotor performance measurements in compressed oxygen-helium atmosphere pressure chamber for dive between 100 and 1500 feet 02 p0166 A72-11701

Human blood carboxyhemoglobin saturation relation to inspired air oxygen and CO concentrations from small closed rebreathing system tests [AD-740929] 04 p0472 A72-14863

Respiratory adaptation to pure oxygen excess pressure after cockpit depressurization from flight simulator tests with pressure-suited pilots, presenting ECG reactions 05 p0623 A72-16749

Hypoxia pretreatment for decreased pulmonary oxygen toxicity during high pressure oxygen breathing in rats 07 p0917 A72-19328

Inhaled oxygen pressure variation effects on adenosines, glucose, lactate and pyruvate levels in rat brains, noting anoxic limit value relation to age 07 p0924 A72-20658

Oxygen intake and cardiac output measurements during various treadmill and bicycle ergometer exercises, relating exercise type to heart rate and arteriovenous oxygen differences 08 p1123 A72-20885

Hyperbaric chamber tests for hemodynamic response to oxygen inhalation at 1 and 2 atm pressure for myocardial infarction treatment assessment 08 p1114 A72-20891

Respiration control during hyperoxia, discussing chemoreceptor significance in minute volume respiration rate reduction mechanism from Pamir mountain aborigines oxygen breathing reaction studies 08 p1120 A72-22076

Pure oxygen atmosphere effects at 450 and 600 mm Hg on rats in vitro liver and adipose tissue lipid synthesis, measuring food intake and plasma components 10 p1424 A72-23739

Cardiovascular responses to positive pressure oxygen breathing from blood pressure and heart and respiratory rate measurements 11 p1584 A72-26017

Hyperoxia effect on human airways resistance during high pressure oxygen breathing 11 p1586 A72-26614

Short sleep period and oxygen breathing effects on arousal level of air traffic controller during detection task performance 11 p1588 A72-26686

Arterial blood gas tensions, using sequential phased dilution for pilot oxygen delivery 12 p1764 A72-28255

Suppression effects of hyperoxic breathing gases on red blood cell and erythropoietin hormone production following blood loss 12 p1766 A72-28298

High altitude natives cerebral arterial-venous oxygen difference measurement during ambient air and oxygen breathing, showing chronic hypoxia effect on cerebral blood flow 14 p2079 A72-30704

Hemodynamic changes in man during immersion with the head above water. 17 p2507 A72-34543

Effects of in vivo inhalation of 100% oxygen at reduced pressure on serum and red cell lipids. [AD-746090] 17 p2508 A72-34553

USAF custom fit oxygen mask program. 17 p2508 A72-34559

Hypercapnia with relief of hypoxia in normal individuals with increased work of breathing. 21 p3005 A72-40420

OXYGEN COMPOUNDS

Meridional model of oxygen and hydrogen compounds reactions in mesosphere and lower thermosphere, determining diurnal variations and vertical profiles 03 p0346 A72-13378

IR emission of oxygen reaction with carbon oxysulfide, investigating molecular vibrational transitions 10 p1510 A72-24133

Fluorescence and absorption spectra from oxygen sulfur dichloride photodissociation in vacuum UV, discussing So formation 11 p1590 A72-26012

Russian book - Water in the universe 19 p2789 A72-37743

OXYGEN CONSUMPTION

Hypophysectomy in rats, resulting in prolonged red blood cell survival due to oxygen consumption decrease and altered erythrocyte enzymatic processes 01 p0010 A72-10075

Human exercise capacity assessment from maximal oxygen intake estimates and Harvard step test 01 p0016 A72-10116

Coronary blood flow measurement in various hemodynamic conditions by argon technique, determining oxygen consumption and coronary vascular resistance 03 p0315 A72-13183

Training effect on oxygen consumption in negative muscular work, considering connective tissue strengthening and muscle viscosity changes 03 p0315 A72-13676

Serum enzyme activity changes response to constant test exercise, discussing relation to maximum oxygen uptake 04 p0472 A72-14897

Physiological effects of transfusing 2,3-diphosphoglycerate (DPG) depleted red cells with high oxygen affinity in anemic hypoxic patients 04 p0473 A72-15211

Hemodynamic and blood oxygen parameter changes comparison in dogs during hypoxia at rest and muscle activity in various oxygen concentrations 04 p0474 A72-15232

Pilots oxygen uptake vs flight time and altitude as indicator of physical condition, noting large fluctuations and differences for individual pilots and different flights 05 p0623 A72-16748

Maximum aerobic power response and oxygen consumption to training stimulus intensity, duration and frequency, using bicycle ergometer exercise 07 p0916 A72-18965

Maximal oxygen intake prediction in acute moderate hypoxia during exercise, showing heart rate linearity with work load 07 p0916 A72-18966

Maximum oxygen intake during exercise on treadmill compared with bicycle ergometer, analyzing circulatory dynamic factors and cardiac output relation to oxygen transport capacity 07 p0922 A72-20251

Muscle blood flow relation to oxygen consumption from measurements during bicycle ergometer exercises, using Xe 133 clearance method 08 p1123 A72-20888

Beta-adrenergic inhibitors effects on coronary blood flow and myocardial oxygen consumption of normal and coronary artery disease patients 08 p1118 A72-21549

Hypoxic and normoxic gas mixture breathing during intense muscular activity, relating oxygen consumption and carbon dioxide elimination magnitudes and motor performance 08 p1121 A72-22081

Aerobic work capacity indices of gas exchange pulse rate, pulmonary ventilation and acid base balance in runners, determining maximum oxygen utilization 09 p1268 A72-23596

Oxygen consumption and body temperature in anesthetized, paralyzed and artificially ventilated dogs cooled in water bath at 34 C, measuring hypercapnia and beta-adrenergic blockade effects [AD-740991] 10 p1424 A72-23735

Semiautomatic measurement of human oxygen uptake, discussing apparatus and accuracy 10 p1432 A72-24991

Physical work capacity comparison during bicycle ergometry and treadmill walking tests, measuring oxygen uptake, ventilatory parameters and excess carbon dioxide production 11 p1579 A72-26095

Maximal oxygen uptake and heart rate during ladder climbing, inclined treadmill running and cycling ergometer tests 11 p1586 A72-26612

Hemodynamic variables relation to coronary blood flow and myocardial oxygen consumption during upright bicycle exercise 11 p1587 A72-26618

Isotopic labeled microspheres for cat uveal and retinal blood flow and oxygen consumption determination, studying increased intraocular pressure and carbon dioxide tension effects 12 p1763 A72-27841

Crowding phenomenon effect on blood cell oxygen consumption, using Cartesian diver technique for polymorphonuclear leukocyte, lymphocyte and platelet measurements 12 p1763 A72-27842

Cold adaptation effects on rat skeletal muscle tissue Vant-Hoff coefficient, considering phosphorylation and oxidation rate, P/O and mitochondrial ATP-ase activity 13 p1905 A72-29324

Pulmonary oxygen transport dynamic model representing lung gas-side airway and alveolar regions and blood-side capillary bed 13 p1909 A72-28996

Six day bed rest effect on external respiration and subcutaneous tissue oxygen metabolism, noting oxygen consumption decline 13 p1905 A72-29324

Gas mask-caused air flow resistance effects on respiratory and circulatory response to exercise, assessing maximal oxygen uptake 13 p1906 A72-29818

- Work capacity evaluation from fatigue, biological rhythm, tissue respiration and oxygen consumption studies, discussing pharmacological stimulation effects
14 p2078 A72-30376
- Sweating relation to body temperature after exhaustive exercise for various oxygen uptakes and ambient temperatures
14 p2079 A72-30702
- High altitude natives cerebral arterial-venous oxygen difference measurement during ambient air and oxygen breathing, showing chronic hypoxia effect on cerebral blood flow
14 p2079 A72-30704
- Muscle cell ATP, creatine phosphate and lactate concentration changes relation to oxygen uptake during and after exercise
14 p2080 A72-30705
- Energy cost [oxygen consumption] prediction for treadmill and various levels terrain walking at two speeds under three different pack loads
14 p2080 A72-30706
- Mountain inhabitants cardiocirculatory adaptation to chronic hypoxia, studying coronary flow and myocardial oxygen consumption and efficiency
15 p2187 A72-32498
- Regression analysis for steady state N2 inequality in O2 consumption calculations.
17 p2507 A72-34542
- Cell proliferation in lungs of mice exposed to elevated concentrations of oxygen.
17 p2499 A72-34548
- Thermal neutral temperature of rats in helium-oxygen, argon-oxygen, and air.
17 p2500 A72-34728
- Ion alterations during myocardial ischemia.
17 p2502 A72-34994
- Thermoregulation during positive and negative work at different environmental temperatures.
18 p2650 A72-36559
- Self-paced ergometer performance - Effects of pedal resistance, motivational contingency and inspired oxygen concentration.
18 p2653 A72-36911
- Coronary collateral circulation and myocardial blood flow reserve.
19 p2755 A72-37500
- Influence of inotropic alteration on the severity of myocardial ischemia after experimental coronary occlusion.
19 p2758 A72-38552
- Determination of oxygen consumption by use of the paramagnetic oxygen analyzer.
21 p3006 A72-40429
- Comparative studies of the respiratory functions of mammalian blood.
21 p3002 A72-40919
- Cardiac output, arterial and mixed-venous O2 saturation, and blood O2 dissociation curve in growing rats adapted to a simulated altitude of 3500 m.
21 p3003 A72-41623
- Influence of intracellular convection on the oxygen release by human erythrocytes.
21 p3003 A72-41625
- Dependence of muscle efficiency on oxygen concentration in the venous blood
22 p3141 A72-42157
- The function of external respiration in mental activity
22 p3150 A72-42284
- Oxygen consumption in liquid breathing mice.
22 p3142 A72-42488
- Blood flow, oxygen uptake, and capillary filtration in resting skeletal muscle.
22 p3150 A72-42668
- Effect of activity and temperature on metabolism and water loss in snakes.
22 p3144 A72-42669
- Analysis of femoral venous blood during maximum muscular exercise.
22 p3145 A72-42742
- Oxygen uptake kinetics for various intensities of constant-load work.
22 p3145 A72-42743
- Excitation contraction correlates in true ischemia.
23 p3255 A72-43814
- Influence of a high oxygen content on the rate of formation and elimination of gaseous wastes in albino rats
23 p3255 A72-43906
- A critical assessment of an open circuit technique for measuring oxygen consumption.
23 p3260 A72-43937
- Physiologic effects of passive hyperventilation on oxygen delivery and consumption.
23 p3258 A72-44365
- OXYGEN DEFICIENCY**
U HYPOXIA
OXYGEN DETECTORS
U OXYGEN ANALYZERS
OXYGEN ISOTOPES
Oxygen isotope ratios in iron meteorites magnetite crust and cosmic spherules as indicators for atmospheric oxygen development
02 p0279 A72-12117

- Oxygen and hydrogen stable isotopes utilization for studying water vapor in precipitations, constructing meteorological model
05 p0684 A72-16793
- Oxygen isotopic temperatures and mineral compositions of equilibrated ordinary chondrites
07 p1076 A72-19588
- Oxygen isotopic abundances and equilibrium temperatures of meteoritic minerals, chondrules, meteorites and planets
07 p0985 A72-19589
- Perturbation theory oscillatory wave function for second order correction to oxygen 16 nucleus bonding energy
08 p1211 A72-21067
- Oxygen 18/16 composition of Lunik 16 soil, comparing with Apollo soils
09 p1381 A72-22277
- Pionic X ray fields and transitions in Li 6, Be 9, C 12 and O 16, obtaining 2p level absorption broadening
10 p1515 A72-24418
- Cross section measurement for low energy proton reactions with N 14 and O 16 targets observing Be 7 and C 11 in N 14
16 p2447 A72-33735
- Energy difference measurement between 2S and 2P levels of multiply charged O 16 positive ion, using Stark quenching technique
16 p2432 A72-33768
- OXYGEN MASKS**
Custom fit oxygen mask for life support of crew members
08 p1126 A72-21567
- Physiological evaluation of modified jet transport passenger oxygen mask from altitude chamber experiments
08 p1126 A72-21571
- Disposable emergency oxygen mask for air passengers based on continuous flow, phase dilution principle, describing altitude chamber tests with human subjects to study physiological responses
13 p1908 A72-28702
- USAF custom fit oxygen mask program.
17 p2508 A72-34559
- Continuous flow general aviation oxygen masks.
18 p2653 A72-36536
- OXYGEN METABOLISM**
Ventilatory and metabolic responses of unanesthetized dogs exposed to various carbon dioxide concentrations at 2 and 18 C, discussing oxygen uptake relation to cold
02 p0159 A72-11954
- Hypoxia, hyperoxia and hypercapnia short period effect on rat brain oxygen supply, measuring blood gas values, tissue oxygen partial pressure time variations, etc
02 p0159 A72-11957
- External respiration gas metabolism and energy consumption measurements for test pilots during parabolic trajectory flights in weightlessness simulation experiments
02 p0163 A72-12347
- Free oxygen content and diffusion coefficient in adrenalectomized rat skeletal muscles after physical strain
03 p0317 A72-13991
- Manganese catalyst photoactivation process for oxygen photosynthetic evolution investigated in Mn-deficient *Anacystis nidulans* cells
05 p0624 A72-15811
- Human breathing metabolic simulation device for evaluating respiratory diagnostic, monitoring, support and resuscitation equipment
06 p0769 A72-18618
- CO hypoxia effect on oxygen transport during exercise, discussing changes in cardiac and respiratory functions and work capacity
08 p1114 A72-20893
- Cardiorespiratory functions in child swimmers and nonathletes during growth, relating training to oxygen transport system dimensions
08 p1123 A72-20894
- Laughing gull metabolism dependence on flight speed and angle during wind tunnel tests from oxygen consumption, carbon dioxide production and aerodynamic forces analyses
08 p1115 A72-21080
- Endurance exercise effect on respiratory capacity in white, red and intermediate muscles in rats, relating fiber type to oxidative capacity
08 p1115 A72-21083
- Stepwise adaptation to high mountain conditions effect on brain and sural muscle oxidation processes in rats
08 p1121 A72-22085
- Human oxygen intake and blood lactic acid removal kinetics during recovery from mild steady work on bicycle ergometer
10 p1426 A72-24989
- Six day bed rest effect on external respiration and subcutaneous tissue oxygen metabolism, noting oxygen consumption decline
13 p1905 A72-29324

- High gravity, cold and starvation space stress effects on oxidative metabolism of ethylmorphine, aniline and p-nitroanisole in male rat liver
15 p2185 A72-31700
- Myocardial metabolic changes in chronic hypoxia.
17 p2502 A72-34989
- Blood oxygenating ability of helium- and argon-oxygen environments relative to air, using alveolar gas equation to predict arterial oxygen pressure
18 p2649 A72-36438
- Hypoxic theory for atherosclerosis formation, noting blood plasma protein concentration effects on oxygen diffusion
18 p2651 A72-37030
- Lack of effect of high altitude on hemoglobin oxygen affinity.
21 p3006 A72-40443
- Human plasma free fatty acids relation to lactic acid concentration and maximum aerobic power, noting carbohydrate availability as exercise capacity limiter
21 p3003 A72-41520
- Coronary blood flow and myocardial metabolism in man at high altitude.
22 p3144 A72-42593
- Blood flow, oxygen uptake, and capillary filtration in resting skeletal muscle.
22 p3150 A72-42668
- Effect of activity and temperature on metabolism and water loss in snakes.
22 p3144 A72-42669
- Physiologic effects of passive hyperventilation on oxygen delivery and consumption.
23 p3258 A72-44365
- Gas exchange mechanism in lung alveoles and capillaries, discussing cell metabolism for oxygen uptake and carbon dioxide formation
24 p3371 A72-44599
- OXYGEN PLASMA**
Multimode cavity for simultaneous oxygen/argon plasma excitation and electron density measurements, noting gas pressure effect
08 p1213 A72-21323
- Semiconductor materials etching and surface coating with protective silicon dioxide film in low temperature oxygen plasma
11 p1700 A72-25777
- HF absorption of electromagnetic field in ionized oxygen plasma as function of dc discharge current
20 p2958 A72-39969
- OXYGEN PRODUCTION**
Chlorate based oxygen generator assembly, discussing tests, advantages and applications
04 p0482 A72-14566
- Molecular oxygen evolution Mn catalyst photocatalysis as two-quantum process, discussing kinetic model computer simulation
04 p0484 A72-15740
- Closed loop life support systems, discussing manned ninety day test in space station simulator, Soviet experiments and water and oxygen regeneration
10 p1432 A72-24973
- Bioengineering models of energy and mass exchange of algae under varying ambient conditions, noting mass cultivation possibility for oxygen regeneration in closed environments
20 p2893 A72-38959
- Bosch carbon dioxide reduction process for manned spacecraft oxygen recovery, analyzing carbon and water forming reactions with iron as catalyst
[ASME PAPER 72-ENAV-9] 20 p2896 A72-39168
- Six-month test program of two water electrolysis systems for spacecraft cabin oxygen generation.
[ASME PAPER 72-ENAV-5] 20 p2896 A72-39172
- Regeneration of oxygen from carbon dioxide and water.
24 p3375 A72-45183
- System design of a near-self-supporting lunar colony.
24 p3388 A72-45192
- OXYGEN RECOMBINATION**
Oxygen ionization and ion mobility measurements in air by open proportional counting chamber with electron counter and exoelectron emitter
09 p1305 A72-22203
- OXYGEN REGULATORS**
Proportional-integral control of reactants supply for hydrazine-oxygen fuel cells with pulse controlled solenoids
06 p0867 A72-18290
- OXYGEN SENSORS**
U OXYGEN ANALYZERS
OXYGEN SPECTRA
Meridional thermospheric wind effect on auroral atomic oxygen red line profile, noting inadequacy of diffusion hypothesis
01 p0052 A72-10079
- UV airglow in 1304 A line of oxygen from Cosmos 215 satellite
01 p0053 A72-10362
- Atomic/molecular oxygen concentration ratio semi-annual variation at 130 km altitude from mass spectroscopic data analysis
02 p0218 A72-11947

Ozone photolysis in UV region, determining primary products from oxygen optical emission detection using time-resolved flow system

03 p0320 A72-13394

Late twilight airglow vacuum UV spectra from sounding rocket observation, noting conjugate-point electron excitation role in O I emissions

03 p0350 A72-13525

Mars atmosphere diatomic oxygen upper limit abundance, using high dispersion spectroscopic data from 1969 apparition

04 p0569 A72-14498

F2 layer 6300 A night airglow emission photometric data on 31 January 1968, showing large electron content and movements

04 p0517 A72-14958

Lower ionosphere 5577 and 5893 A and hydroxyl band emissions interrelationships, observing atomic O and vertical eddy transport effects

04 p0518 A72-14961

Twilight atmospheric sounding in oxygen absorption bands to reduce noise level in secondary light scattering

06 p0807 A72-17943

Oxygen telluric lines contours shape analysis, allowing for atmospheric nonisothermicity and inhomogeneity

06 p0852 A72-18050

Oxygen Herzberg bands excitation in nightglow, obtaining quenching reaction rate coefficients

07 p0976 A72-19579

Auroral F region electron density enhancement relation to sporadic F2 and red oxygen emission

08 p1226 A72-21111

Atmospheric vertical temperature profile inference from ground based measurement of microwave thermal emission spectrum from atmospheric oxygen

08 p1161 A72-21824

Upper atmospheric oxygen red line diurnal variations and midnight minimum, noting emission relation to kinetic temperature in magnetic storm

09 p1296 A72-22234

Chemical bond effect on K emission spectrum of oxygen and fluorine

09 p1275 A72-22522

Line intensity variation simulation in Raman spectrum of oxygen with allowance for spin splitting of rotational levels

09 p1358 A72-23049

Forbidden O I lines brightness and shadow bands properties during 7 March 1970 solar eclipse, comparing with rocket measurements

12 p1800 A72-27143

Atomic/molecular oxygen concentration ratio semi-annual variation at 130 km altitude from mass spectroscopic data analysis

13 p1949 A72-29259

Seasonal features of nocturnal 6300 A emission variation and decay coefficient in nightglow related to recombination coefficient for F layer ionization

14 p2097 A72-30132

Nightglow small scale intensity fluctuations of 5777 A atomic oxygen emission due to turbulent transport of horizontal wind observed with photometers

14 p2098 A72-30143

Airglow and auroral OI and NI allowed and spin forbidden transitions for above 9 eV excitation potential lines

14 p2098 A72-30145

Infrasonic excitation of red oxygen emission at 6300 A during geomagnetic storms at middle latitudes

14 p2098 A72-30146

Incoherent scatter and filter photometer search for 6300 A predawn enhancement by magnetically conjugate photoelectron impact excitation, comparing with ionospheric electron density

14 p2098 A72-30148

IR absorption coefficients of oxygen atom and molecule fields due to free-free electron transfers at specific elastic scattering cross sections

15 p2274 A72-31409

Semidiurnal variation in O I 5777 A nightglow due to lunar tidal dynamics effect in E and F regions

16 p2383 A72-32971

Atmospheric transmittance calculation from 0.76-micron oxygen band fine structure parameters

16 p2417 A72-33289

Twilight atmospheric sounding in oxygen absorption bands to reduce noise level in secondary light scattering

16 p2386 A72-33784

Atomic oxygen green line emission in nightglow from OGO-F photometer observations, calculating tropical F region electron density spatial distribution

17 p2549 A72-35604

Absorption of the 4- to 6-millimeter wavelength band in the atmosphere.

18 p2689 A72-36961

French monograph - Determination of the absolute value of the absorption in the bands of the Schumann-Runge system of molecular oxygen

19 p2836 A72-37476

Nocturnal and semiannual variations of the intensity of 5777 A emission of atomic oxygen.

19 p2789 A72-37511

Measurement of the equivalent widths of oxygen A-band absorption lines at different pressures

19 p2837 A72-37959

Nightglow observations and ionospheric soundings for red oxygen line intensity relation to F region parameters

19 p2792 A72-38638

Martian atmosphere atomic oxygen concentration estimation from Mariner 6 and 7 O I 1304 and 1356 A data analysis

19 p2868 A72-38734

Oxygen abundances of three population II horizontal-branch stars.

21 p3109 A72-41330

OI 6300 and 5577 A, NI 5200 A and H beta 4861 A emission line measurement during 8-9 March 1970 auroral arc event

22 p3169 A72-42018

Airglow observations with a Hadamard photometer.

22 p3169 A72-42023

Theoretical calculations of the F-region tropical ultraviolet airglow intensity.

22 p3171 A72-42418

Rocket measurement after sunset for altitude distribution of 1.27 micron band nightglow emission from diatomic oxygen molecules

22 p3172 A72-42435

Photochemistry of the airglow continuum.

22 p3153 A72-42889

Tilting-filter measurements in dayglow rocket photometry.

23 p3289 A72-43893

Ground-based sensing of temperature profiles from angular and multi-spectral microwave emission measurements.

23 p3285 A72-44147

Microwave spectrum of compressed O2-foreign gas mixtures in the 48-81 GHz region.

24 p3378 A72-44871

OXYGEN SUPPLY EQUIPMENT

NT OXYGEN MASKS
Soviet book on civil aircraft high altitude equipment covering air conditioning systems, oxygen equipment and cabin pressurization

02 p0156 A72-12295

Extravehicular life support systems for shuttle, space station, lunar base and Mars missions, considering thermal control, carbon dioxide control and oxygen supply subsystems

10 p1430 A72-24441

LOX supply systems installation for civil transport aircraft crew and/or passenger breathing oxygen

11 p1584 A72-26030

Contaminant analysis in gaseous oxygen generated by chlorate candle combustion, using Draeger tubes

12 p1779 A72-28254

Integrated water vapor electrolysis oxygen generator and hydrogen depolarized carbon dioxide concentrator development.

20 p2896 A72-39170

Six-month test program of two water electrolysis systems for spacecraft cabin oxygen generation.

20 p2896 A72-39172

Calculation procedures for some parameters of space suit gas medium supply systems

21 p3006 A72-40449

OXYGEN SYSTEMS

U OXYGEN SUPPLY EQUIPMENT
OXYGEN TENSION
NT HYPOXEMIA
Oxygen distribution in human brain under counter-current capillary blood flow conditions, presenting mathematical simulation for transport in Krogh system

02 p0168 A72-12037

Epinephrine and norepinephrine effects on cerebral blood circulation volume and oxygen tension in tissues

02 p0165 A72-12517

Free oxygen content and diffusion coefficient in adrenalectomized rat skeletal muscles after physical strain

03 p0317 A72-13991

Inhaled oxygen pressure variation effects on adenosines, glucose, lactate and pyruvate levels in rat brains, noting anoxic limit value relation to age

07 p0924 A72-20658

Rebreathing technique to estimate human mixed venous oxygen and carbon dioxide tension changes at start of exercise under respiratory stress and natural conditions

08 p1122 A72-20883

In vitro measurements of oxygen tension effect on teleost and amphibian retinal lactate dehydrogenase activity, discussing acetazolamide produced hypoxia effects

10 p1424 A72-23729

Pressure sensitivity of Na-K-Mg ATPase activity from rat intestine, investigating inhibiting effects of oxygen, nitrogen and helium tension increases

10 p1424 A72-23731

High altitude acclimatization effects on human lung diffusing capacity for carbon monoxide at different oxygen tensions

10 p1425 A72-24476

Pathological significance of high oxygen tension exposure effects on acid soluble collagen extracted from mouse skin

12 p1760 A72-27483

Carbon monoxide laser output power variation as function of oxygen tension

12 p1823 A72-27755

Irreversibility mechanism in postpartum ductus arteriosus closure in guinea pigs, studying vessel cellular changes and smooth muscle response to oxygen pressure

12 p1762 A72-27826

Arterial blood gas tensions, using sequential phased dilution for pilot oxygen delivery

12 p1764 A72-28255

Human centrifuge studies of high positive acceleration effects on blood oxygenation and arterial oxygen and carbon dioxide tension

12 p1766 A72-28287

Solid combustibles flame spread rates in compressed atmospheres, noting dependence on oxygen concentration

14 p2170 A72-30340

The intramyocardial oxygen pressure at normoxia and hypoxia.

17 p2501 A72-34986

Interaction of chronic hypoxia and hypercapnia upon blood gases and acid base status.

17 p2504 A72-35166

Respiratory frequency and alveolar oxygen and carbon dioxide tension relationship to hypercapnia in man

17 p2506 A72-35965

Effects of diffusion impairment on O2 and CO2 time courses in pulmonary capillaries.

17 p2506 A72-35967

Blood oxygenating ability of helium- and argon-oxygen environments relative to air, using alveolar gas equation to predict arterial oxygen pressure

18 p2649 A72-36438

Pulmonary gas exchange in Andean natives at high altitude.

18 p2650 A72-36570

Hypoxic pulmonary steady-state diffusing capacity for CO and alveolar-arterial O2 pressure differences in growing rats after adaptation to a simulated altitude of 3500 m.

21 p3003 A72-41622

Oxygen consumption in liquid breathing mice.

22 p3142 A72-42488

Morphometric evaluation of changes in lung structure due to high altitude.

22 p3143 A72-42585

Respiratory chain components correlation to tension production at various oxygen pressures in guinea pig ductus arteriosus, investigating light absorption changes

22 p3144 A72-42670

Influence of elevated partial oxygen pressure on the sympathetic-adrenal and acetylcholine systems

24 p3371 A72-44595

Experimental studies on the alkali-acid equilibrium in the blood gases under the chronic action of low concentrations of lead.

24 p3374 A72-44824

In vivo hemolysis due to hyperoxia - Role of H2O2 accumulation.

24 p3374 A72-45651

OXYGEN TOXICITY

U HYPEROXIA

OXYGEN 18

Beam maser spectrometric measurements of normal, C-13 and O-18 formaldehyde transitions, determining coupling constants for all rotational transitions hyperfine structure

16 p2431 A72-33132

OXYGENATION

Regional myocardial contraction mechanics during transient ischemia and reoxygenation in anesthetized dogs

04 p0476 A72-15719

Human centrifuge studies of high positive acceleration effects on blood oxygenation and arterial oxygen and carbon dioxide tension

12 p1766 A72-28287

Hemoglobin-facilitated diffusion of oxygen - Interfacial and thickness effects.

18 p2650 A72-36569

OXYHEMOGLOBIN

Prolonged muscular work effects on erythrocyte 2,3-DPG generation relation to oxyhemoglobin affinity

04 p0472 A72-14898

Volumetric analysis of blood oxygen and CO, showing combination with hemoglobin without significant molecular volume increase

05 p0619 A72-16786

Immunochemical properties of human oxyhemoglobin comparison with complex of dog hapto-globin and human hemoglobin reactions in anti-hemoglobin serum

09 p1268 A72-23695

Physiologic effects of passive hyperventilation on oxygen delivery and consumption.

23 p3258 A72-44365

OZONE

Vertical ozone distribution model using four variable parameters for stratospheric studies, climatology, scattering or radiometric measurements from ground or satellite
 01 p0059 A72-10834

Nimbus 4 vertical atmospheric sounding techniques, obtaining temperature, water vapor and ozone profiles with Michelson IR interferometer
 01 p0095 A72-10957

Inhaled ozone effect on chromosome aberrations break frequencies in circulating blood lymphocytes of irradiated Chinese hamsters
 01 p0015 A72-11149

Gas flow visualization technique using fluorescent plate with UV irradiated ozone tracer, noting application to wall attachment fluidic elements
 01 p0072 A72-11198

Total ozone estimation by interpolation from Nimbus 4 satellite data on backscattered UV earth radiance attenuation
 01 p0096 A72-11285

Atmospheric ozone pressure variations in high altitude cyclones, anticyclones, troughs and crests at low pressure levels
 02 p0207 A72-11734

Cosmos 65 global ozone contour data similarity with geomagnetic L shells configuration, discussing South Pacific region depletion area
 02 p0221 A72-12466

Upper atmosphere ozone, aerosol and neutral constituent density profiles estimation by recursive filtering algorithm for satellite observation data
 02 p0222 A72-12811

Quantum yield observations for photochemistry of ozone and singlet molecular oxygen in atmosphere
 03 p0347 A72-13393

Ozone photolysis in UV region, determining primary products from oxygen optical emission detection using time-resolved flow system
 03 p0320 A72-13394

Low inertia instrument for ozone density measurement in atmosphere near ground
 04 p0525 A72-15624

French monograph on atmospheric ozone utilization as tracer for troposphere-stratosphere exchanges covering investigations at various locations
 05 p0654 A72-15799

Ozone content and vertical distribution variations as causes of winter stratospheric warmings in Northern Hemisphere
 07 p0973 A72-18861

Atmospheric ozone photochemistry, discussing pure oxygen and moist atmospheres, NO mechanism, tracer applications, stratospheric dynamics and Umkehr observations
 07 p0979 A72-20228

Environmental chamber tests for ozone exposure effects on human pulmonary function at rest and during bicycle exercise
 08 p1122 A72-20884

Vertical ozone distribution observed by Umkehr and IR methods
 08 p1159 A72-21226

Mesospheric ozone measurement for altitude profiles, comparing rocket and ground based observations of 1.27 micron emission band at twilight
 09 p1296 A72-22355

Mesosphere ozone number densities from rocket photometric measurement of lunar UV radiation absorption
 09 p1385 A72-22583

Stratospheric ozone photochemistry through nitrogen oxides and hydrogen compounds reactions, noting controlling effect of water vapor
 09 p1298 A72-22674

Horizontal ozone distribution in middle stratospheric macrosynoptic situations, considering anticyclonic side and jet stream delta region
 09 p1301 A72-23194

IR absorption spectrum of gaseous ozone, obtaining mechanical anharmonicity coefficients and zero order wave numbers
 10 p1511 A72-24226

Spectrophotometric measurements of sky radiance distribution to determine atmospheric pollution, ozone content and radiation attenuation by clouds
 10 p1476 A72-25085

Rocket sounding of ozone diurnal variations in upper stratosphere and lower mesosphere
 13 p1947 A72-28831

Turbulence effects on electron, ion, aerosol, water vapor and ozone concentration in atmospheric layers
 15 p2222 A72-31395

Tropospheric meridional ozone profiles between Europe and South Africa from measurements aboard commercial airliners, noting seasonal variations
 16 p2382 A72-32889

Solar radiation absorption measurements in 2150 Å region as function of altitude to obtain oxygen and ozone densities
 16 p2384 A72-32975

Stratospheric pollution by SST exhaust gases, discussing water vapor and nitrogen oxides effects on ozone concentration
 17 p2597 A72-35327

Atomic oxygen-ozone gas phase reaction rate constant direct measurement in steady state flow system at 269-409 K under excess ozone conditions
 19 p2762 A72-38221

Nitrous oxide production from ozone photolysis reaction with molecular nitrogen
 19 p2762 A72-38753

Modified Dobson ozone spectrophotometer with revised electronic design circuitry, considering high voltage power supply, photomultiplier tube circuit, amplifier and electromechanical phase sensitive rectifier
 20 p2921 A72-38968

A rocket measurement of the vertical distribution of atmospheric ozone.
 23 p3285 A72-44242

OZONOMETRY

Ozone observation and daily and seasonal variations at Cologne, noting longitudinal variations for monthly means
 06 p0808 A72-18146

Total ozone measurements by selective transmission filter ozoneometer comparable to Dobson spectrophotometer
 09 p1307 A72-22453

Atmospheric ozone inference from satellite IR horizon radiance measurements
 12 p1799 A72-27030

Ozone photochemical reactions measurements for quantum yield of UV photolysis in strong Hartley band with water vapor chain decomposition effects
 14 p2083 A72-30134

Distribution of total ozone content in the atmosphere according to spacecraft observations
 21 p3050 A72-41797

Ozone measurements in the mesosphere during the solar proton event of 2 November 1969.
 22 p3173 A72-42509

OZONOSPHERE

Midlatitude D layer observations during sunspot minimum, emphasizing atmospheric ionization and ozonospheric parameters
 01 p0055 A72-10433

Two dimensional meridional ozone model for seasonal ozone concentration behavior at 15-45 km, taking into account advective and turbulent effects
 03 p0351 A72-14360

Atmospheric ozone and the history of life.
 18 p2686 A72-36626

A rocket measurement of the vertical distribution of atmospheric ozone.
 23 p3285 A72-44242

P

P WAVES

Elastic singlet p wave phase shift calculation for electron scattering by H atom and He cation, using time dependent Hartree-Fock perturbation theory
 09 p1355 A72-22786

Many electron pseudopotential method for electron-atom scattering, calculating singlet s wave and p wave phase shifts
 12 p1848 A72-27429

Elastic wave diffraction by rigid ellipsoid, deriving scattering cross section for incident P wave from integral equation solution
 16 p2426 A72-33659

P-I-N DIODES

U DIODES

U P-I-N JUNCTIONS

P-I-N JUNCTIONS

Low driving power resistive gate MOSFET microwave switch with performance approaching P-I-N diode
 01 p0038 A72-10658

REDAP 31 network analysis program for design of S-band phase shifter with P-I-N diodes for phase array antennas
 01 p0040 A72-10689

P-I-N diodes power handling characteristics in high power solid state TR switches
 01 p0042 A72-10708

Solid state components for millimeter wave systems, including IMPATT diode power sources and amplifiers, P-I-N diode modulators and switches and Schottky barrier mixers
 02 p0192 A72-12183

Book on microwave semiconductor devices, considering point contact crystal, varactor, Schottky-barrier, tunnel, backward and p-i-n diodes, transistors, Gunn effect devices and integrated circuits
 03 p0333 A72-13845

Gaussian envelope microwave pulse generation using absorption p-i-n diode modulator, predicting performance by digital simulation
 04 p0498 A72-14718

Digital loaded-line phase shifters for phased array antennas, discussing lossy microstrips effects and P-I-N diode switching shortcomings in design requirements
 07 p0954 A72-19048

High microwave voltage effects on p-i-n junction conductance under inverse dc bias, noting role of hole generation and accumulation by impact ionization
 15 p2206 A72-31643

X- and Ku-band microelectronic phase shifters
 17 p2531 A72-35767

The use of semiconductor diodes to protect a radar receiver
 18 p2663 A72-37217

S-band high power microstrip switches with p-i-n diodes for spacecraft radio systems
 19 p2770 A72-3725

P-i-n variable attenuator with low phase shift.
 19 p2773 A72-38294

Digital p-i-n diode microwave drive amplifier design guidelines, discussing sharp switching pulses and short circuit protection features
 20 p2904 A72-39734

Semiconductor diodes for microwave power control
 21 p3033 A72-40939

P-N JUNCTIONS

Fluorinated ethylene propylene encapsulated N/P Si solar cells, investigating simulated micrometeoroid exposure effects on I-V performance in shock tube
 01 p0006 A72-10381

Mode guiding improvement in p-n junction of symmetrical AlGaAs-GaAs heterojunction laser diode with narrow active region, obtaining low room temperature threshold current
 01 p0080 A72-10788

Dc flow through p-n junction by modified Melehy force field method, discussing space charge variation in depletion layer
 03 p0338 A72-13866

N-p silicon solar cells damage at room temperature by proton and deuteron irradiation, considering particle mass and energy functions and illuminating light wavelength effects
 04 p0561 A72-14574

Avalanche breakdown voltage of Gaussian Si planar p-n junctions for design and impurity diffusion evaluation
 04 p0562 A72-15126

Space charge recombination in forward biased diffused p-n junction silicon diodes
 04 p0562 A72-1512

Millimeter wave GaAs avalanche diode oscillator processing on plated Cu heat sinking block resulting in epitaxially grown p-n junctions
 06 p0788 A72-1846

Semiconductor device physical behavior, discussing energy levels, impurity conduction, p-n junction capacitance and bipolar and unipolar transistor I-V characteristics
 06 p0790 A72-18575

Cadmium mercury telluride photovoltaic cell features, noting gigahertz range frequency response, heterodyne sensitivity, operating temperature and nonstoichiometric p-n junction preparation
 07 p1003 A72-19224

Electrical breakdown in reverse biased semiconductor p-n junctions involving Zener effect and avalanche mechanisms
 07 p1048 A72-19821

IMPATT diode thermal resistance measurement from heat diffusion effect on small signal impedance of p-n junction
 07 p0958 A72-20684

Physical and operational characteristics of Si and Ge photoelectric semiconductor devices with p-n junctions, discussing photodiodes, phototransistors, mosaic arrays and coordinate sensitive structures
 08 p1139 A72-21055

Flow graph analysis of optimal operation of frequency multipliers with idler circuits using nonlinear n-p junction capacitance
 08 p1140 A72-21061

Reverse biased p-n diffused junction design with two impurities in nonhomogeneous semiconductors, calculating depleted space charge region thickness
 08 p1140 A72-21062

Barrier capacitance effect on transient characteristics of light diodes, obtaining time dependence of p-n junction volume charge voltage and recombination emission intensity
 09 p1284 A72-22211

Avalanche carrier multiplication influence on semiconductor device p-n junction quality, discussing current distribution and I-V characteristics during avalanche breakdown
 10 p1446 A72-23849

Lead tin telluride photovoltaic p-n junction diode and lasers, discussing n-type layer fabrication by proton bombardment
 10 p1450 A72-24552

Width of space charge layer of reverse-biased p-n junction in p-n-p structure effect on current density, mobile charge carriers and constituent transistors gain coefficients
 10 p1526 A72-24584

Electrical properties of Te/p-Si/N heterodiodes at room and liquid air temperatures
10 p1527 A72-24937

Book on semiconductors covering electrical properties, energy band structure, impurities, epitaxial growth, silicon dioxide, surface properties, p-n junctions and measurement techniques
10 p1528 A72-25123

Si Pd-n-p/plus/ transit time diode microwave oscillator, discussing fabrication, FM noise spectrum and bias current fluctuation
11 p1604 A72-25748

Time dependent light emission from mesoplasmas in Si p-n junctions in pulse mode, showing carrier heating effect
11 p1700 A72-25780

Heterojunction p-GaAs-n-ZnSe diodes electrical and photovoltaic properties, showing space charge limited current effects
11 p1606 A72-26624

P-n junction diodes fabricated by ion implantation doping, calculating I-V characteristics for comparison with measured breakdown voltages
12 p1789 A72-27312

Internal parameters of injection lasers based on diffusion and epitaxial p-n junctions and heterojunctions in GaAs-AlAs system at 300 K
12 p1825 A72-27878

Photovoltaic effects in solar cell p-n homojunctions and heterojunctions at low and high excitation levels
12 p1855 A72-28006

P-n thin film solar cell based on thermally and electrochemically stable II-IV semiconductors with graded energy gaps
12 p1756 A72-28013

Pulsed Si p-n junction mesoplasma dynamic I-V characteristics explained by mechanism based on hot carrier annihilation
12 p1853 A72-28113

Varactor broken voltage-capacitance curve due to uncompensated impurities concentration change at p-n junction
13 p1926 A72-28379

P-n-p-n junction thyristor turnoff process under reverse anode voltage at high injection level, examining current voltage curve and switching time constant
13 p1932 A72-29293

Forward voltage vs temperature characteristics for Si planar p-n junction diodes, determining zero temperature energy gaps for silicon, germanium and GaAs
13 p1933 A72-29824

N region capture centers effects on small signal impedance in p-n-n diode structure during passage of strong dc current
13 p1933 A72-29977

S-type negative resistance segment formation on rectilinear branch of I-V characteristics of p-n structure
14 p2089 A72-30969

Regenerative semiconductor parametric amplifier under dc through p-n junction, analyzing nonlinear phenomena
14 p2090 A72-31124

Avalanche photodiode with n-p-pi double diffused reach-through structure for visible and near-IR regions, noting high efficiency, low noise and gain stability
15 p2248 A72-32036

Near junction doping characteristics of p-n GaP red emitting diodes by scanning electron microscope correlated with electrical and electroluminescent measurements
15 p2208 A72-32521

Internal parameters of injection lasers based on diffusion and epitaxial p-n junctions and heterojunctions in GaAs-AlAs system at 300 K
16 p2404 A72-33987

Si p-n junction solar cell fill factor for electric power available to load, noting discrepancy between calculated and measured values due to recombination
17 p2494 A72-34264

Effects of junction depth on the radiation damage of silicon solar cells.
17 p2594 A72-34388

Forced oscillations in a circuit with a nonlinear p-n junction capacitance
17 p2533 A72-34756

Parametric resonance in an oscillatory circuit with a nonlinear p-n junction capacitance
17 p2533 A72-34757

Preparation and properties of nonheat-treated single crystal Cu₂S-CdS heterojunctions.
17 p2595 A72-35331

Determination of the parameters of minority carriers in semiconductor photocells from a spectral sensitivity curve
17 p2498 A72-35512

The capacitances of aniso-type heterojunctions with continuously varying energy band gap and electron affinity in the transition region.
18 p2719 A72-36944

Effect of a junction capacitance nonlinearity on the spectral characteristics of a tunnel diode current
20 p2906 A72-38897

Effects of impurities on gamma-irradiated silicon crystal examined by photovoltaic effect of p-n junction diode.
21 p3097 A72-40693

A theoretical investigation on the generation current in silicon p-n junctions under reverse bias.
21 p3097 A72-40703

Electrical fluctuations in ideal straight-staggered nondegenerate diodes
21 p3033 A72-40945

GaP /Zn-O/ diodes light emission efficiency increase by forward bias, relating to precipitation in n and p layers
22 p3159 A72-42613

General transport theory of noise in pn junction-like devices. I Three-dimensional Green's function formulation.
22 p3160 A72-43083

General transport theory of noise in pn junction-like devices. II - Carrier correlations and fluctuations for high injection.
22 p3160 A72-43084

Frequency dependent deep level trap admittance and field effect transcapacitance of p-n junctions calculated by truncated space charge approximation
22 p3161 A72-43086

Linear theory of a microwave distributed amplifier based on an avalanche transit-time diode
23 p3271 A72-43776

X-band silicon double-drift IMPATT diodes using multiple epitaxy.
23 p3273 A72-44334

P-N-P JUNCTIONS

Large-signal IC equivalent circuit model for DC, linear and nonlinear transient time circuit analysis of lateral p-n-p transistors, including isolation junction interactions
01 p0044 A72-10126

Static I-V characteristics and gain properties of lateral p-n-p transistors, using multijunction analysis
02 p0189 A72-11522

Si p-n-p and Cr-n-p junction transit time diode oscillators microwave and dc characteristics comparison, noting similarity
04 p0499 A72-15206

Si p-n-p punchthrough X band oscillator, discussing wideband tuning and low noise properties and applications
07 p0955 A72-19252

Ion implantation for varicaps and p-n-p bipolar transistors fabrication, examining implanted impurities profiles
10 p1449 A72-24285

Alloy p-n-p junction transistor diffusion capacity variation with emitter current as function of temperature at 80-320 K
10 p1451 A72-24558

Complementary monolithic IC n-p-n and p-n-p transistor circuit structure with high sheet and low saturation resistance
11 p1606 A72-26567

IC lateral p-n-p multijunction transistor frequency characteristics analysis, noting parasitic effects, cutoff frequencies and power gain
12 p1788 A72-27311

Electro-optical regenerative assembly with p-n-p structure, emphasizing positive feedback and I-V characteristics
13 p1933 A72-29976

Properties of a composite transistor
17 p2530 A72-35066

Multivibrator with p-n-p and n-p-n transistors, noting circuit diagram, operation and power dissipation
20 p2906 A72-38898

P-n-p and p-n-p-n transistors and thyristors with lateral structure geometry, discussing operational characteristics and effects of structural modification on semiconductor parameters
23 p3271 A72-43835

P-N-P-N JUNCTIONS

Thyristors junction area current rise time extension, discussing emitter field regional delay times as function of p-n-p-n structural properties
08 p1140 A72-21266

Hybrid neuristor transmission lines with planar p-n-p-n semiconductor structures, discussing development, testing and electrical parameters
10 p1448 A72-24281

Static and impedance characteristics and equivalent circuit of p-n-p-n inductance diode, using ambipolar diffusion length
12 p1790 A72-27499

The static current-voltage characteristic of four-layer structures in two-collector operation at a low injection level
19 p2846 A72-38573

P-n-p and p-n-p-n transistors and thyristors with lateral structure geometry, discussing operational characteristics and effects of structural modification on semiconductor parameters
23 p3271 A72-43835

P-TYPE SEMICONDUCTORS

Density waves propagation and amplification in p-InSb electron-hole plasmas, investigating dependence on frequency and injection level
04 p0561 A72-14851

N- and p-type semiconductors energy band structure bending near interface
05 p0702 A72-16197

Hysteresis loops during breakdown in reverse bias segment of p-PbS point contact diodes I-V curves
05 p0638 A72-17177

IR luminescence and photoconductivity in p-type GaSe single crystals alloyed with Sn and Ge impurities
08 p1216 A72-21069

Thermally stimulated autophotocurrent emission from Cr-alloyed p-type GaAs electrode, determining spectral distribution and light and electric field effects on current
08 p1216 A72-21071

Temperature dependence of intrinsic light absorption band edge characteristics in p-type InSb
09 p1366 A72-22213

Electron and hole recombination at deep impurity centers during nonequilibrium current carriers excitation by Nd-glass laser light in p- and n-type germanium
09 p1322 A72-22214

Au-Si n and Al-Si p diodes noise operating in avalanche with charges injected by radiation
09 p1287 A72-23113

Solid state sinusoidal signal generator based on current density oscillation effect in high resistivity p-type InSb with transmutation doping
09 p1288 A72-23191

Be and Mg ion generation and p-type layer electrical properties production by implantation in GaAs substrates
09 p1372 A72-23245

Internal Q switching and long time delay emission in electron beam excited p-type and n-type GaAs lasers, indicating optical absorption traps
10 p1489 A72-23947

Emitter conduction bands with negative electron affinity energy from surface barrier lowering of Cs p-type semiconductors
10 p1526 A72-24351

Microwave diagnostics of P doped Si semiconductor crystal prism determining relation between complex permittivity and reflection factor by variational method
10 p1450 A72-24404

Temperature dependence of internal quantum efficiency of spontaneous emission as function of beam voltage in electron beam excited p-type GaAs
10 p1526 A72-24559

Thin film tunnel triode using p-type amorphous semiconductors to achieve injected current amplification
10 p1451 A72-24624

Dielectric and optical constants of p-type GaSb single crystals, interpreting singularities by energy bands diagram
11 p1689 A72-26485

Annealing effects on gamma ray irradiated Li compensated p-type B doped Si semiconductor
12 p1858 A72-28065

Carrier concentration Hall mobility and photoconductivity in n- and p-type CdTe after neutron and electron bombardment
12 p1859 A72-28072

Room temperature negative photoconductivity of p-type ZnTe-CdTe solid solutions mixed crystals within model with electron and hole capture levels
14 p2141 A72-30173

Zr oxidation kinetics at 440-850 C for 3 min maximum exposure time, observing type oxide change relationship to activation energy
14 p2113 A72-30247

Be doped p-type Si piezoresistance and hole transport properties dependence on temperature, crystal orientation and doping concentration
16 p2442 A72-33834

Theory of photon-induced hopping on acceptors in p-type germanium.
17 p2595 A72-34750

Emitter conduction bands with negative electron affinity energy from surface barrier lowering of Cs p-type semiconductors
17 p2595 A72-34952

Normal mode formulation of spin wave-helicon wave interactions in ferromagnetic semiconductors.
18 p2718 A72-36452

Properties of 1 MeV electron-irradiated defect centers in p-type silicon.
19 p2844 A72-37687

Photoluminescence and photoconductivity of hole-type cadmium telluride single crystal films
19 p2845 A72-38403

Variations as a function of the temperature of the moduli of elasticity of monocrystalline P-type GaSb
19 p2846 A72-38542

Subthreshold radiation effect in silicon
20 p2959 A72-38953

Boron p-type region impurity concentration calculation technique to establish anomalous base profile in n-p-n bipolar transistors

20 p2908 A72-39567

Magneto-microwave free-carrier absorption in germanium in the Faraday configuration.

21 p3097 A72-41379

Influence of a surface space charge on certain photoelectric properties of p-type gallium arsenide

21 p3098 A72-41684

Influence of irradiation by 1.2-MeV electrons on the electrophysical properties of p-Si single crystals grown in a hydrogen atmosphere

21 p3098 A72-41686

I-V, spectral and temperature characteristics of autophotocathode emission in p-type silicon cathodes with varying acceptor concentrations

21 p3098 A72-41692

Electroconductivity anisotropy effect on transverse Denber effect angular dependence and spectral distribution in p-type CdSb lattice

21 p3098 A72-41693

Effect of increasing beam voltage on the internal quantum efficiency of spontaneous emission in electron-beam-excited p-type GaAs.

22 p3185 A72-42308

Pulsed room temperature laser action of Si-doped double heterostructure GaAs p type diodes within 9100-9500 A wavelengths, discussing threshold current densities and power efficiency

22 p3186 A72-42621

Characteristics of P-channel MOS field effect transistors with ion-implanted channels.

24 p3385 A72-44981

P-3 AIRCRAFT

OMEGA receiver integration into Navy P-3C airborne computerized navigation system, describing flight test, maintainability and laboratory simulation programs

13 p1999 A72-29202

P-1127 AIRCRAFT

Flying experience with the SC1 research aircraft and the P1127 prototype at the Royal Aircraft Establishment, Bedford, England.

22 p3136 A72-42324

PACIFIC ISLANDS

NT JAPAN

PACIFIC OCEAN

Tropospheric wind estimation from ATS 1 satellite cloud motions over equatorial Pacific

01 p0060 A72-10856

Wind, pressure and temperature diurnal and semidiurnal variations to 30 km altitude over tropical western Pacific, considering atmospheric model based on linearized equations of motion

07 p1029 A72-19099

Time-spectral characteristics and geographic variations of large scale cloud activity in tropical Pacific

12 p1837 A72-27018

Pacific Ocean meteorological data collection from military and civil aircraft in-flight reports, discussing computer processing for daily analysis and monthly and seasonal means

13 p1994 A72-28874

PACKAGES

NT APOLLO LUNAR SURFACE EXPERIMENTS PACKAGE

NT EASEP

NT INSTRUMENT PACKAGES

PACKAGING

NT ELECTRONIC PACKAGING

Air cargo intermodal and interline containers handling in warehouse storage, transportation and distribution, considering total pack and interlock requirements

16 p2372 A72-33174

PACKING DENSITY

MnBi magnetic film optical memory system characteristics evaluation, considering laser power requirement, bit packing density and SNR [IEEE PAPER 3.4]

03 p0332 A72-13754

Holographic optical techniques application to bulk magnetic storage for high information density and memory capacity and fast random access [IEEE PAPER 19.4]

03 p0361 A72-13776

Temperature and compression rate effects on metal powder packing density, obtaining activation energy from Boltzmann equation

05 p0665 A72-16089

Transition metals and alloys electron structure and packing defect energy theory, discussing crystal atomic interactions and brittle breakdown

07 p1049 A72-20148

Semitransparent particle model of Martian surface for reflective power at various incidence and reflection angles, discussing packing density and optical parameters

08 p1231 A72-21126

Small impurity amounts effect on packing defect density and deformation energy in Ni

08 p1188 A72-21791

Fast IC signal delay time reduction by high packing density, discussing yield, power dissipation and cost problems

09 p1290 A72-22820

Limitations in microelectronics. II - Bipolar technology.

18 p2667 A72-36980

Advanced optical storage techniques for computers.

23 p3288 A72-43876

PACKINGS (SEALS)

Thermocrazing and thermal stresses in packing rings of face-type mechanical seals under dry friction

08 p1177 A72-21927

PADE APPROXIMATION

Ground state energy of interacting electrons for entire density range from two-point Pade approximation

04 p0549 A72-15229

Pade table for formal power series with notation for extension to Laurent series, relating algebraic theory to bigradient determinants and numerical analysis algorithms

11 p1676 A72-25501

Approximate representation of a type of transcendental polynomials describing wave systems with fractional rational functions

19 p2834 A72-37751

PAGEOS SATELLITE

Europe-Africa geodetic link in spatial triangulation of passive Pageos satellite, discussing laser telemetry operation

04 p0520 A72-15725

Pageos balloon satellite orbital perturbations due to erratic solar radiation pressure induced accelerations, comparing modified Smith perturbation model calculations with photometric observations

15 p2228 A72-31975

PAIN

Negative /painful/ stimulus cessation relation to emotionally positive zone activation in rat brain during self stimulation experiments

20 p2892 A72-39410

PAIN SENSITIVITY

Nociceptive chemical action in cat skin vessels, showing fiber types for impulse transmission

02 p0164 A72-12511

Analgesic electrical stimulation in rat brainstem with other sensory modes unaffected

04 p0475 A72-15361

Cardiac membrane pain sensitivity in vagotomized cats under sensitizing acetylcholine influence during reduced cholinesterase activity

13 p1905 A72-29329

Microwave induced cutaneous heat and pain perception thresholds, noting usefulness as possible radiation hazard warning

15 p2188 A72-31506

Vicarious influence effect on eliciting pain in individuals subjected to previously reported nonpainful electric shocks

18 p2654 A72-36916

Pain perception anatomical and neurophysiological mechanism, discussing human response to mechanical, thermal and chemical pain inducing stimuli

22 p3146 A72-42780

PAINTS

Paint coatings aging effect on D16T type alloy corrosion fatigue in NaCl solution, noting protective efficiency decrease

13 p1984 A72-29486

Factors affecting phase-change paint heat-transfer data reduction with emphasis on wall temperatures approaching adiabatic conditions. [ALAA PAPER 72-1030]

24 p3389 A72-45407

PAIR PRODUCTION

Electron emission in strong electromagnetic waves within quantum electrodynamics, discussing energy losses and electron pair production

03 p0415 A72-13003

Vacuum UV irradiation of silicon dioxide, discussing positive charging for photon energies above threshold for electron-hole pair creation

03 p0403 A72-14080

High energy hadrons time structure in extensive air showers, considering production of nucleon-antinucleon pairs in particle interactions

07 p1067 A72-20687

Nonthermal ultrarelativistic plasmas covariant analysis with quantum electrodynamics and Green function theory of nonequilibrium statistical mechanics, discussing electron-positron pair production and annihilation

10 p1525 A72-25100

Ion pair production rate and electron number density in ionospheric D region from ground based and rocket measurements, discussing two ion model

15 p2229 A72-32252

Oxygen atom electron affinity calculation by symmetry-adapted pair correlation approximation, using pseudonatural orbitals /PSNO/ technique

15 p2282 A72-32644

Pulsar properties correlation with radially oscillating coherent plasma of electron-positron pair production by strong electric field around central object

19 p2859 A72-37892

Stellar energy-loss rates in a convergent theory of weak and electromagnetic interactions.

20 p2972 A72-39868

Particle production in inelastic high energy interactions, noting correlation between particle pairs and groups

23 p3330 A72-44407

PALEOMAGNETISM

Geomagnetism, discussing world field distribution, secular variation, paleomagnetism, archaeomagnetism, origin, magnetic anomaly and earth electromagnetic induction

01 p0053 A72-10168

Magnetic properties and paleomagnetic data of Permian Cutler and Elephant Canyon formations in Utah, discussing thermal demagnetization and origin of stable magnetization

09 p1305 A72-23668

Changes in total magnetic energy stored outside earth core accompanying earth dipole field decreases over 60 years period from paleomagnetic measurement

11 p1623 A72-26108

Abridged version of 1970 Soviet conference on constant geomagnetic field and paleomagnetism, reviewing secular variation data

13 p1946 A72-28588

On the applicability of lunar breccias for paleomagnetic interpretations.

22 p3226 A72-42532

Magnetism of meteorites - A review of Russian studies.

23 p3339 A72-44129

Abridged version of 1970 Soviet conference on constant geomagnetic field and paleomagnetism, reviewing secular variation data

24 p3397 A72-45088

PALEONTOLOGY

Molecular paleontology of fossil organic remnants in Molluscan shell proteins

04 p0467 A72-14753

Monograph on Jurassic and Cretaceous Hagiastriidae from Blake-Bahama Basin and Great Valley Sequence in California

04 p0519 A72-15255

Paleomicrobiological analysis of northwest Scotland Stoor Formation black shale pre-Paleozoic spheroidal unicellular fossils as probable form of marine phytoplankton

05 p0655 A72-16042

Precambrian paleobiological history from fossil records, discussing heterotrophic living systems and eucaryote emergence in evolutionary organization development

08 p1162 A72-22000

Ultrastructure and geologic relations of some two-aeon old Nostocacean algae from northeastern Minnesota.

17 p2544 A72-34336

PALLADIUM

Electron probe microanalysis of Mo-Pd system diffusion at 1000-1600 C, measuring chemical diffusion coefficient as function of temperature, concentration and activation energy

13 p1978 A72-29221

Thermodynamic properties of liquid Co and Pd metals by levitation calorimetry, including specific heat, heats of fusion and surface emissivities

16 p2480 A72-34025

PALLADIUM ALLOYS

Alloying and heat treatment ordering effect on hydrogen diffusion coefficients, penetrability and solubility in Pd-Ag alloys

03 p0376 A72-14016

Soft X ray emission spectra from Al-Nb and Al-Pd alloys, deducing electron state density near Al ions

09 p1371 A72-22848

Diffusion measurements during annealing of Pd-V, Pd-Ti and metal-ceramic systems by microprobe

11 p1664 A72-26853

Interdiffusion in nickel-molybdenum and palladium-molybdenum systems

20 p2939 A72-39315

Phase diagrams, solubility and alloying of Pt, Pd, Ru, Ir and Rh with noble, alkali earth, rare earth and transition metals

22 p3191 A72-42810

PALLADIUM COMPOUNDS

Phase diagram of Ti-Pd system, using metallographic, X ray and differential thermal analyses

13 p1982 A72-30116

Pd-Al intermetallic compound contact materials.

18 p2698 A72-35985

PALMAR SWEAT INDEX

Galvanic skin response techniques for palmar and dorsal sweat detection during motion sickness by vestibular stimulation, comparing arousal and thermal sweat response

07 p0933 A72-20185

PAM (MODULATION)

U PULSE AMPLITUDE MODULATION

PANCREAS

Parenterally introduced protein hydrolyzates and aminopeptides influence on human pancreas enzyme secretion activity

09 p1268 A72-23595

Noninvasive polygraphic technique to assess cardiovascular responses to intravenous glucagon injection 13 p1901 A72-28570

Pancreas insular apparatus biosynthesis of neurohumoral mechanism compounds stimulating coronary ectasia hormones discharge from brain into blood in cats with alloxan diabetes 14 p2077 A72-30973

PANEL FLUTTER

Rigid boundary effect on thin panel flutter speed, determining aerodynamic forces via linearized potential theory 03 p0443 A72-13402

Flutter of thin homogeneous isotropic cylindrical panels from analog computer study 04 p0593 A72-15646

Minimum weight panel designs subject to supersonic flutter constraint, approximating governing differential equations by difference equations [AIAA PAPER 72-170] 05 p0741 A72-16908

Nonlinear mode coupling in equations of motion for thin panel vibration as function of membrane stretching-bending energy ratio 09 p1408 A72-23465

Hypersonic nonlinear aerodynamic loading effect on panel flutter, examining stability for various initial conditions [AIAA PAPER 72-345] 11 p1728 A72-25374

Orthotropic point-supported rectangular panel vibration and flutter analysis for natural frequencies and flutter boundaries, applying to space shuttle design [AIAA PAPER 72-350] 11 p1728 A72-25379

Computerization of panel flutter boundary calculations with aerodynamic forces derived from linear three dimensional unsteady potential flow theory [AIAA PAPER 72-403] 11 p1731 A72-25424

Cylindrical panel natural vibrations, describing motion of base with dynamic elasticity equations 11 p1733 A72-25539

Pressure law for flow between two parallel plates describing medium action on plates, noting plate flutter analogy to buckling 13 p2056 A72-29002

Panel-flutter analysis of a thermal protection-shield concept for the space shuttle. 20 p2980 A72-39623

Nonlinear natural vibrations of rectangular plates and cylindrical panels 22 p3242 A72-43134

Aeroelastic optimization of a panel in high Mach number supersonic flow. 23 p3343 A72-43327

Supersonic flutter of plane, rectangular, anisotropic, heterogeneous structures 24 p3459 A72-45440

PANELS

NT CURVED PANELS

NT RECTANGULAR PANELS

NT WING PANELS

Ti alloy honeycomb core sandwich panels fabricated by brazing or spot diffusion bonding, investigating elevated temperature effects on mechanical properties [ASM PAPER W 71-23,3] 01 p0086 A72-10875

Circular cylindrical sandwich panel and rectangular sandwich plates dynamic stability under periodic external loads derived from mathematical model 02 p0298 A72-12664

Dynamic buckling of shallow circular cylindrical hinged panel under axial compression 08 p1249 A72-22087

Vibration characteristics of unidirectional filamentary boron-epoxy composite panels, obtaining nodal patterns, natural frequencies and damping coefficients 11 p1732 A72-25477

Dynamic buckling of shallow circular cylindrical hinged panel under axial compression 17 p2626 A72-34665

Buckling of plates and cylindrical panels under the action of axial dynamic compression 22 p3232 A72-41923

Diffusion bonded columbium panels for the shuttle heat shield. 24 p3406 A72-44889

PANORAMIC CAMERAS

Panoramic aerial cameras with revolving objective or mirror, presenting formulas for photoimage plots geometric characteristics 09 p1308 A72-22487

Cartographic and environmental surveys by Skylab orbiting stations and ERTS satellite using panoramic and mapping cameras and laser altimeter 15 p2232 A72-31247

Central band-type wide angle camera shutter design, noting stress examination in machine parts by optical method 21 p3052 A72-40306

PANORAMIC SCANNING

Photogrammetric coordinate relation of points on lunar surface and stereo panoramas of scanning photographs by Luna 9 and 13 orbiters 05 p0660 A72-15832

PAPILLAE

Human taste papillae sensitivity to chemical stimuli, showing stable quality and intensity response patterns 05 p0620 A72-17129

Force-velocity relations in cat papillary muscles isotonic relaxation, discussing effects of preloads and afterloads, temperature and stimulation frequency 09 p1265 A72-22864

PARABOLIC ANTENNAS

Radio telescopes quality criteria, noting performance dependence on antennas dimensions and distribution 01 p0047 A72-10194

FM radio link superposed parabolic antenna systems adjustment for space diversity reception for scatter propagation and broadband multichannel transmission in 1.9 GHz range 01 p0027 A72-10410

Radome enclosed Haystack parabolic antenna characteristics as radio astronomical instrument, discussing gain, polarization, interference susceptibility and noise temperature [AD-737166] 01 p0032 A72-11233

Prime focus paraboloid antenna performance with cylindrical hybrid mode feeds, detailing radiation patterns and distribution 02 p0173 A72-12110

ATS F and G ground station mobile terminal, discussing system flexibility, utility and reliability features and parabolic antenna design 04 p0485 A72-14478

Frequency characteristics of selectively reflecting screens in multichannel parabolic mirror antennas and determination of Fresnel coefficients dependence on polarized plane wave incidence angle 04 p0499 A72-15241

Radiation pattern of radio astronomical paraboloidal reflector antenna in Dwingeloo, Netherlands, determining directivity and beam efficiency 04 p0501 A72-15423

Optimal design of directive dielectric loaded circular waveguide antenna for parabolic reflectors and radar detection 06 p0782 A72-17356

Interferometric measurement at 1415 MHz of radio telescope paraboloidal antenna radiation pattern, using cosmic radio sources with known flux density as signal source 07 p0945 A72-19789

Parabolic antenna instantaneous phase center calculations, using radiation patterns from aperture field and current distribution methods 08 p1138 A72-20744

Aperture filtering effects on amplitude scintillation power spectra of paraboloid radio telescope over millimeter wave propagation path 08 p1136 A72-21982

Hoghorn parabolic antenna design, presenting relations for dimensions, aperture field and radiation patterns calculation by computer 09 p1284 A72-22242

Radiation pattern determination parabolic Cassegrain radio telescope reflector antennas from Fresnel zone emission source, using holographic technique 10 p1482 A72-24783

Earth station parabolic antenna gain-noise temperature ratio measurement using radio star and Applications Technology Satellite technique [AIAA PAPER 72-528] 12 p1779 A72-27354

Directional and mode characteristics of coaxial exciter for high area utilization and low halation paraboloid antennas 12 p1793 A72-27812

Electromagnetic cylindrical wave diffraction by linear emitter in parabolic cylinder with slots 13 p1917 A72-28709

Design of parabolic reflector antenna with pyramidal horn radiator closed by quadratic waveguide, calculating radiation pattern 13 p1929 A72-29039

Parabolic, Cassegrain, spherical and horn-parabolic axisymmetric mirror antennas, calculating primary radiating element orientation effects on radiation polarization characteristics 13 p1931 A72-29277

Radiation pattern reconstruction of radio telescope parabolic Cassegrain reflector antennas from Fresnel zone emission source, using holography and optical processing 14 p2103 A72-30221

A new project of 8-cm radioheliograph. 18 p2691 A72-36434

Coaxial exciter for parabolic antennas with high area efficiency and small halation 21 p3029 A72-40514

Combination of sum and difference diagrams of a dipole group in front of a parabolic reflector for a two-plane monopulse method 21 p3029 A72-40517

Near-field Cassegrain antennas of high surface efficiency for satellite communication links 21 p3029 A72-40520

Focus field and horn exciter regarding parabolic antennas with small f/D-relation 21 p3029 A72-40523

Low noise receiver for satellite broadcasting. 21 p3019 A72-40886

A dual frequency, dual polarized feed for radioastronomical applications. 21 p3034 A72-41400

PARABOLIC BODIES

Navier-Stokes equations numerical solution for laminar incompressible flow past paraboloid of revolution at zero angle of attack 05 p0604 A72-16818

Steady two dimensional symmetric viscous flow past parabolic cylinder in uniform stream, correlating calculated nose skin friction with boundary layer theory 05 p0610 A72-17012

Navier-Stokes equation solution for laminar incompressible flow past parabolic cylinder, investigating skin friction and pressure drag 06 p0798 A72-17782

Equilibrium equations for thin walled shallow paraboloid shell of revolution, solving boundary value problem for edge fastened loaded circular planform region 07 p1091 A72-19757

Navier-Stokes equations numerical solution for symmetric laminar incompressible flow past parabolic cylinder, presenting surface pressure, friction and pressure drag results 10 p1465 A72-24291

Numerical calculation of the supersonic flow of a viscous fluid about a parabolic obstacle 17 p2484 A72-34887

PARABOLIC DIFFERENTIAL EQUATIONS

Elliptic and parabolic partial differential difference equations solution using modified random walk Monte Carlo technique 01 p0093 A72-10858

Monte Carlo methods for hybrid computer solution of nonlinear parabolic partial differential equations with two spatial dimensions 02 p0186 A72-11657

Markov chain successive approximation method for electromagnetic wave propagation in medium with random large discontinuities, using scalar parabolic equation 02 p0181 A72-12588

Hybrid computer for solving complex problems in distributed parameter systems in terms of parabolic differential equations 02 p0188 A72-12655

Quasi-linear parabolic equations, investigating conditions for Cauchy-Dirichlet problem solution 03 p0383 A72-14380

Second order parabolic equations C auchy problem solution with dissipation level, using maximum principle 04 p0538 A72-14626

Iterative procedure for computing optimal controls in distributed parameter systems described by linear parabolic differential equations, applying to metal slab temperature profile problem 04 p0504 A72-14664

Hyperbolic and parabolic partial differential equations behavior comparison by studying point-to-point time optimal control for heat conduction and vibrating string motion 04 p0505 A72-14673

Quasi-linear parabolic equations loaded system first boundary value problem for heat and mass transfer equations inverse problems 04 p0540 A72-15545

Similarity and finite difference solutions of parabolic differential equations, exemplifying by heat conduction and boundary layer equations [ASME PAPER 71-WA/APM-6] 05 p0682 A72-16151

Optimal control of system described by parabolic partial differential equations with constraints on change rate of boundary conditions 05 p0683 A72-17137

Regularity of nonunique solutions of degenerate elliptic-parabolic partial differential equations systems without compactness requirement for associated differential quadratic form 06 p0839 A72-17627

Validity proof of asymptotic methods in oscillation theory of one dimensional nonlinear dynamic systems described by hyperbolic and parabolic differential equations 06 p0839 A72-17681

Large deformations of incompressible isotropic materials with parabolic stress-strain relations, deriving constitutive equation from strain energy function 06 p0848 A72-17919

Dynamic programming for optimal stochastic control problem with Gaussian shot noise involving parabolic or elliptic differential equation in unbounded domain, discussing iterative solution and quasi-linearization 07 p1027 A72-19292

Parabolic differential equation system for boundary layer behavior of steady plane gas flow 08 p1107 A72-20911

Convergence and stability criteria of monotonic difference schemes for linear parabolic differential equations with interface boundary conditions

08 p1199 A72-21286

Boundary value problem for degenerate quasi-linear parabolic differential equation, showing solution existence and smoothness dependence on region width

09 p1342 A72-23485

Total variation of parabolic equations solutions, noting upper bound and explicit results for Cauchy and mixed problems

09 p1343 A72-23587

Finite amplitude disturbances effect on plane Poiseuille flow hydrodynamic stability, presenting numerical method for solving parabolic partial differential equations derived from Navier-Stokes equation

10 p1468 A72-24422

Generalized Fourier transformation method for mixed boundary value problems of second order parabolic differential equation in unbounded region, noting singular differential operator

12 p1837 A72-27998

Hybrid computer Monte Carlo solution algorithm for parabolic partial differential equations with time varying boundary conditions, applying to ferromagnetic rod magnetization problem

12 p1787 A72-28119

Successive approximation for solving parabolic equation with abstract function, using Chaplygin method for Cauchy boundary value problem in Banach space

13 p1987 A72-29646

Many-term formulas for parabolic differential equations solution in boundary layer theory, using linearized second order ordinary differential equations

15 p2216 A72-31467

Optimal controller design for parabolic type second-order linear stationary systems, discussing integro-differential equation solution possibility

15 p2211 A72-32170

Parabolic differential equations to define exponential spatial decay of heat equation solutions, replacing Edelstein energy estimate by time-independent estimate

16 p2475 A72-33005

The approximate solution of parabolic initial-boundary value problems by weighted least-squares methods.

17 p2573 A72-34217

A priori estimates and nonlinear parabolic equations of arbitrary order.

17 p2577 A72-35796

Approximation by fractional steps of control problems governed by parabolic equations and with boundary control

19 p2825 A72-37786

Investigation of generalized and classical solutions of a mixed boundary value problem in a finite domain for one class of nonlinear second-order parabolic equations

19 p2827 A72-38448

Hybrid computer Monte Carlo solution algorithm for parabolic partial differential equations with time varying boundary conditions, applying to ferromagnetic rod magnetization problem

19 p2770 A72-38620

A boundary value problem for a mixed-type equation with two perpendicular parabolic-degeneration lines

19 p2828 A72-38630

A table of solutions of the one-dimensional Burgers equation.

19 p2828 A72-38717

Fractional steps method of difference schemes for approximate numerical solution of parabolic and elliptic initial boundary value problems

20 p2945 A72-39327

Problem of the analytical design of controllers for parabolic and hyperbolic equations

20 p2946 A72-39468

A method for determining the motion in a laminar boundary layer.

21 p3045 A72-40813

Book on nonhomogeneous boundary value problems for different classes of linear evolution parabolic operators, with applications to optimal control problems

21 p3076 A72-41527

Steady state or periodic solution to initial-boundary value problems for heat conduction equation with nonlinear terms and boundary conditions

21 p3131 A72-41667

Asymptotic representation of the solution of a boundary value problem for a biharmonic equation degenerating into a fourth-order parabolic equation

22 p3198 A72-41899

A calculation procedure for heat, mass and momentum transfer in three-dimensional parabolic flows.

22 p3243 A72-41954

Optimal controller design for parabolic type second-order linear stationary systems, discussing integro-differential equation solution possibility

22 p3162 A72-42079

A priori estimates and Harnack's inequality for general solutions of second-order degenerate quasilinear parabolic equations

22 p3198 A72-42159

Book - The method of fractional steps: The solution of problems of mathematical physics in several variables

22 p3208 A72-43200

Asymptotic behavior of solutions of nonlinear parabolic equations.

23 p3309 A72-43979

The first initial-boundary value problem for a nonuniform parabolic equation.

24 p3419 A72-45631

Straightforward difference scheme for nonlinear parabolic equations in polar coordinates

24 p3420 A72-45649

PARABOLIC FLIGHT

Sjoberg hypothesis for zero gravity produced inversion illusion mechanism in aircraft parabolic flight, noting otolithic membrane deflection result of force on maculae

02 p0167 A72-11710

Two step spacecraft reentry guidance involving skip trajectory at parabolic speeds, proposing algorithm for running coordinate and speed vector components values

11 p1684 A72-26896

Spacecraft roll stabilization during parabolic earth atmosphere reentry, developing single parameter multistep algorithm

11 p1684 A72-26897

Parabolic velocity atmospheric reentry navigation algorithm for spacecraft control, demonstrating guidance accuracy to landing point

11 p1684 A72-26899

PARABOLIC REFLECTORS

NT PARABOLOID MIRRORS

Feed requirements and design of Effelsberg radio telescope with parabolic reflector operating down to 1 cm wavelengths

01 p0040 A72-10676

Metrology and radio performance of steerable antenna paraboloidal reflector, considering profile measurements by optical range finder and laser methods

04 p0493 A72-15518

Radio telescope for cosmic radio emission reception at 50-2 cm wavelengths, describing parabolic and auxiliary reflectors

07 p0965 A72-20299

Conical scalar horn for paraboloidal reflector illumination, discussing half flare angle calculation for prescribed sidelobe realization

10 p1435 A72-24302

Arecibo Observatory radio-radar telescope design and operation, discussing reflector wire mesh surface, computer control and data acquisition, ionosphere and pulsar studies and interferometry

10 p1459 A72-24310

Isolation between two orthogonally polarized beams radiated by single paraboloidal reflector, discussing polarization coupling to earth receiving antenna

12 p1789 A72-27356

Waveguides for primary and hybrid mode horns for secondary feeders of deep paraboloid reflector radio telescope in Effelsberg, West Germany

12 p1793 A72-27811

Design of parabolic reflector antenna with pyramidal horn radiator closed by quadratic waveguide, calculating radiation pattern

13 p1929 A72-29039

Parabolic reflector fed by log-periodic dipole antenna array, predicting combined effects of feed phase center lateral and axial displacement on secondary performance

15 p2205 A72-31541

The analysis of deployable umbrella parabolic reflectors.

17 p2524 A72-34351

Technique for compensating for reflector-antenna-surface errors with long correlation lengths.

18 p2667 A72-36691

Cross polarizing effects of a water film on a paraboloid reflector at microwave frequencies.

21 p3027 A72-40375

Combination of sum and difference diagrams of a dipole group in front of a parabolic reflector for a two-plane monopulse method

21 p3029 A72-40517

Spherical reflector as possible antenna for millimeter wave astronomy, discussing feed design for spherical aberration corrections

21 p3029 A72-40519

A 3-meter Cassegrain antenna for the frequency range from 2.1 to 2.3 GHz

21 p3029 A72-40521

A polydirectional antenna in polygon reflector design with cosecant-type elevation directional diagram for providing television in the 12-GHz frequency range

21 p3029 A72-40524

Main-reflector-rim diffraction in back direction.

21 p3032 A72-40632

German monograph - Electromagnetic wave propagation inside a paraboloid of revolution subjected to different types of excitation.

22 p3156 A72-43070

Simple small primary feed for large opening angles and high aperture efficiency.

24 p3385 A72-44961

PARABOLIC VELOCITY U ESCAPE VELOCITY PARABOLOID MIRRORS

Long wavelength focusing collector for X ray astronomy with effective bandpass of 100-280 eV determined by low energy transmitting contour windows and paraboloid mirror reflectivity

03 p0353 A72-13040

Optical properties of paraboloid-hyperboloid mirror X ray telescopes evaluated by ray tracing method, noting resolution and focal plane curvature approximation

07 p0985 A72-19405

Focal length determination for on-axis parabolic mirrors by He-Ne laser reflection

09 p1315 A72-23352

Paraboloid and elliptical mirrors in 100 m radio telescope for Helios space probe signals reception, noting device compatibility for data exchange with NASA

13 p1939 A72-28964

Spacecraft onboard compact low-power coherent optical data processing system, using GaAs laser and paraboloid mirror segments

15 p2248 A72-32052

Book on Soviet astronomical reflecting telescopes, paraboloid mirrors, computer control, microphotometers and image converters

17 p2553 A72-34623

Design of an inexpensive, 30 cm diameter, long path difference interferometer.

17 p2553 A72-34640

PARABOLOIDS U PARABOLIC BODIES PARACHUTE DESCENT

Paratroop type parachutes breathing oscillations and stability characteristics, using high speed cinematography and kinetheodolites to track during steady state descent

01 p0004 A72-10307

Parachutes flow characteristics in low speed free descent, discussing glide angle effect on total drag and water channel flow pattern studies

01 p0004 A72-10309

Parachute opening shock and filling time calculation based on aerodynamic drag, air mass and effective porosity time functions, using momentum and continuity equations

01 p0004 A72-10310

Parachute inflation loads and times, presenting calculation method based on unsteady pressure distribution on decelerating inflating parabolic shell of revolution with unsteady starting vortex

01 p0004 A72-10311

Heart and respiration rates response to free fall parachuting, using FM/FM telemetry

02 p0167 A72-11709

Parachuting and aerial towing physiological and force data FM telemetry for biomedical response assessment leading to human engineered equipment improvement and midair retrieval system development

02 p0168 A72-12138

Human coagulating and anticoagulating blood system changes due to emotional stress during parachute jumps, noting plasma recalcification time increase

04 p0474 A72-15233

Thermodynamic parameters correlation of planetary atmosphere with planetary probe parachute descent rate applied to Venera 5 and 6 data

05 p0721 A72-16769

Parachute design for very high altitude sounding rockets, discussing stability and descent velocity requirements and test methods

07 p1085 A72-19604

Boron/potassium nitrate parachute mortar design for aircraft and spacecraft applications, comparing with high-low propellant

08 p1221 A72-20783

Emergency systems for helicopter crew and passenger survivability improvement, discussing use of ejection seats, extraction systems parachute bail-out and shaped explosive charges

08 p1109 A72-21581

Physiological index changes in parachutists of various ages, considering plasma recalcification, blood prothrombin, heparin time, fibrinolytic activity, pressure and heart beat

11 p1590 A72-26988

Pulse-sounding position finding device for light parachute probes conducting ionospheric studies, discussing design features

13 p1922 A72-29350

Planetary atmosphere thermodynamic parameters correlation between spacecraft parachute descent rate and measured data, noting Venera spacecraft example

17 p2610 A72-35272

Investigation of the parachute inflation aid utilizing liquid vapor pressure. 22 p3139 A72-43141

PARACHUTE FABRICS
Ground test determination of design data for low supersonic high density air deployable deceleration systems, considering high strain rate effects on parachute materials 01 p0005 A72-10313
Parachute canopy fabrics and rigging lines cordage properties requirements, considering nylon, polypropylene, silk, cotton and nonwoven scrim-reinforced fabrics 01 p0005 A72-10314
Nylon parachute materials failure mechanics, considering friction, light, chemical and thermal effects 01 p0005 A72-10316
Statistical methods application to parachute materials evaluation, using factorial experiments for multiple variables simultaneous effects analysis 01 p0005 A72-10317

PARACHUTES
NT DRAG CHUTES
NT RECOVERY PARACHUTES
NT RIBBON PARACHUTES
Parachutes and related technologies - Conference, London, September 1971 01 p0003 A72-10301
Parachute designs and applications to escape systems, paratrooping, supply dropping, aircraft braking, weapons systems stabilization, flight testing aids and sport 01 p0003 A72-10302
Nonporous rigid parachute models three component measurements, using low speed wind tunnel for testing skirt length effects on aerodynamic characteristics 01 p0003 A72-10303
Industrial parachute R and D in UK, discussing management, technical staff requirements and government/industry liaison 01 p0004 A72-10304
Axial cords effects on parachute drag and stability characteristics and opening time, discussing wind tunnel and balloon drop tests results 01 p0004 A72-10306
Ionospheric ion mobilities and densities measurements over Sardinia, using parachute mesosphere probe 01 p0055 A72-10436
Lower D region ion density measurement with parachuted blunt probe consisting of disk-shaped collector with guard ring at bottom 03 p0347 A72-13398
Parachute design for very high altitude sounding rockets, discussing stability and descent velocity requirements and test methods 07 p1085 A72-19604
Pneumatically assisted parachute deployment at high altitudes with low accelerations 10 p1421 A72-24273
Incompressible potential flow model of porous parachute canopy flow field, using Stokes stream function for axisymmetric vortex sheet in uniform steady stream 12 p1755 A72-28123

PARACHUTING
U PARACHUTE DESCENT
PARACHUTING INJURY
Chin-sternum-heart syndrome from partial parachute failure, with close reference to atrial endocardial and myocardial lacerations 02 p0167 A72-11711

PARADOXES
Heat conduction in infinite incompressible fluid with turbulent velocity field, deriving physically impossible growth in time of long-wavelength modes of average temperature 16 p2424 A72-33127

PARAFFINS
Acoustic measurement of solid-liquid interface motion and solidification during freezing of Hg and paraffins 10 p1563 A72-25044

PARAGLIDERS
NT FLEXIBLE WINGS
NT PARAWINGS

PARALLAX
RR Lyrae stars absolute magnitude determination by statistical parallaxes method 03 p0421 A72-13139
Three dimensional hologram synthesis from two dimensional pictures with parallax preservation [AD-736057] 03 p0359 A72-13448
Pinhole, fly-eye and holographic stereogram methods, examining resolution relationships, horizontal and vertical parallax and aberrations 05 p0663 A72-16673
Visual binary star investigations, considering parallaxes, masses, absolute magnitudes and orbit computation 09 p1390 A72-23502
Extragalactic eclipsing binaries parallax determination by Gaposchkin method, noting application to distance determination of nearby galaxies 10 p1549 A72-25057

Visual depth perception response functions for sine and square wave modulated binocular parallax 17 p2498 A72-34293
Ground based optical astronomy developments, emphasizing faint objects positional observation, trigonometric parallaxes, data analysis and measuring techniques 19 p2865 A72-38477
Visual stimuli distance estimation with head stationary or moving, discussing performance after monocular motion parallax training 24 p3374 A72-44557

PARALLEL PLATES
Temperature dependent gas internal diatomic laminar heat transfer, investigating continuity, energy, momentum for two dimensional flow between heated parallel plates [ASME PAPER 71-HT-N] 02 p0302 A72-12317
MHD flow development in parallel plate channel entrance region, obtaining numerical solution for velocity distribution, pressure drop and length at different Hartmann numbers 02 p0266 A72-12493
Velocity and temperature distributions for unsteady plane Poiseuille flow of viscous incompressible fluid between two parallel plates 03 p0340 A72-13000
Radiation pattern from open ended parallel plate waveguide with arbitrary electric or magnetic aperture field distribution, using Wiener Hopf technique 03 p0331 A72-13409
Separation measurement between two distant partially reflecting parallel surfaces using Michelson interferometer 03 p0358 A72-13435
Rarefied gas heat transfer problem between two parallel plates of different temperatures, evaluating nonlinear Boltzmann equation with Monte Carlo techniques 04 p0595 A72-14599
Lens waveguides characteristics, analyzing Gaussian beams propagation through periodic system of thin plane-parallel nonlinear dielectric plates 04 p0489 A72-15389
Confined laminar jet mixing of two uniform streams flowing in parallel plate channel, obtaining velocity field from linearized governing equation [ASME PAPER 71-WA/APM-2] 05 p0647 A72-15973
MHD squeeze film lubrication between electrically conducting parallel plates, showing graphically approach time under magnetic field in free space 05 p0665 A72-16031
Plane Couette flow of incompressible non-Newtonian viscous fluid between parallel plates, using minimum entropy production variational principle 06 p0798 A72-17779
Parallel plate waveguide radiation into dielectric or plasma layer, using Hilbert formulation 06 p0791 A72-18734
Heat transfer in thermal entrance region with turbulent flow between parallel plates, solving energy equation by difference methods 07 p1099 A72-19622
Open ended parallel plate waveguide, calculating radiation pattern variation with diaphragm dimension 07 p0945 A72-19663
Tensile load elastostatic transfer from rectangular cross section web to two infinite parallel sheets, deriving Cauchy type integral equation for adhesive bond force density 07 p1095 A72-20241
Al alloys welding with Pb sheathed linear ribbon RDX explosives by parallel plate process, achieving high weld strength 08 p1173 A72-20779
Induced nonuniform magnetic field effects on MHD channel flow between two infinite parallel plates, obtaining solution by perturbation theory 08 p1214 A72-21427
Steady state and temperature relaxation of rarefied gas between two plane parallel plates 08 p1211 A72-21871
Ruby laser power output losses at 80 K with spectral line suppression dependence on surface reflection coefficient of plane parallel plate in resonator 08 p1183 A72-22026
German monograph on radiation characteristics of planar systems in aperture plane of parallel plate waveguide, obtaining relationship between electric and magnetic fields 10 p1434 A72-23775
Computer storage array of isolated electrodes imbedded between capacitor parallel plates, discussing read-write cycle time, expected performance and experimental techniques 10 p1443 A72-23933
Heat transfer between alternating hot and cold parallel plates of constant temperature situated in low density gas 10 p1562 A72-24537
Kinetic model for polyatomic gas heat transfer between parallel plates, considering boundary value problem with arbitrary accommodation coefficients 11 p1744 A72-25559

Diffusion with convection for parallel wall Couette flow, using Airy functions 11 p1618 A72-26591
Luminosity distribution in plane of image produced by radiation from plane parallel plate, taking into account rays real path 13 p1955 A72-28498
Nonuniform inlet velocity profile effect on laminar flow development between parallel plates, solving equations by finite difference method 13 p1941 A72-28706
Uniform suction effect at stationary plate on longitudinal and transverse velocities of plane Couette flow between parallel plates 13 p1941 A72-28884
Pressure law for flow between two parallel plates describing medium action on plates, noting plate flutter analogy to buckling 13 p2056 A72-29002
Scattering matrix derivation for parallel plate waveguide array terminated in infinite plane, determining neighboring guides TEM modes mutual coupling 13 p1921 A72-29345
Numerical integration of boundary layer equations through region of reverse flow past parallel flat plate with negative surface velocity 13 p1944 A72-30033
Interferometric investigation of temperature fields and heat transfer in air layers between vertical, inclined and horizontal parallel walls 14 p2170 A72-30251
German monograph on optical transmission measurement interferometer with plane-parallel birefringent crystal plates covering plate combination selection based on interference pattern mathematics 15 p2233 A72-31525
Convective heat transfer in fully developed MHD channel flow between two parallel electrically conducting plates 15 p2335 A72-31636
Steady state electron mean energy variation between parallel plates in Ar and He calculated by Monte Carlo simulation for comparison 15 p2285 A72-32222
Flow theory improvement for laminar radial flow between parallel plates, considering inertial effects 15 p2219 A72-32479
Time behavior of two dimensional laminar free convection flow between heated vertical parallel plates, calculating temperature and velocity distributions as function of Grashof number 16 p2477 A72-33426
On the behavior of thin-wire antennas and scatterers arbitrarily located within a parallel-plate region 17 p2513 A72-34365
Certain motions of micropolar fluids 17 p2538 A72-34771
Unsteady temperature distribution for laminar flow in a porous straight channel 17 p2541 A72-35434
Hydromagnetic flow between two rotating disks with noncoincident parallel axes of rotation 19 p2841 A72-38436
Radiation heat transfer between closely spaced metal surfaces at low temperature - The impact of discrete modes of the radiation field. 20 p2983 A72-39483
Subharmonic generation in plane-parallel plate for light wave propagation perpendicularly to plate, noting frequency division near multiplicative resonance 23 p3295 A72-43408

PARALLEL PROCESSING [COMPUTERS]
Parallel digital computer application to radar tracking data processing, discussing system design for efficiency maximization and performance, desensitization in traffic level fluctuation 15 p2203 A72-31781
Array processor design for massive computation, discussing special purpose satellite computer for communication with main memory through multiple module access units 16 p2366 A72-33242
Univac 1832 multiprocessor avionics computer for airborne ASW, discussing input/output controllers and interfaces and IC design features 16 p2367 A72-33245
Solution of the problem of a fast Fourier transform in a homogeneous associative parallel processor 19 p2779 A72-37993
Future trends of airborne computers. 20 p2905 A72-39109
Digital computer hierarchical structure based on tree model using request/service resources as nodes, examining parallelor multiple-stream organizations effectiveness 20 p2906 A72-39735
Microminiaturization, microprogramming, multiprocessing, and processing and memory module design technology of aerospace computers in different size ranges 21 p3025 A72-41113
Digital data system with real time displays and multiprocessing capability for multitest of aircraft struc-

ture with operational manpower reduction, assessing performance 22 p3163 A72-42696

Parallelized algorithms for computer solution of spanning tree, distance and path problems on cellular array of identical modules containing memory and combinational logic 22 p3157 A72-43023

German monograph - Iterative algorithms for ordinary differential equations and their suitability for parallel processing by means of symbol manipulation. 22 p3200 A72-43063

Parallel Element Processing Ensemble (PEPE)/digital computer for real time radar data processing and control, discussing system design and applications 24 p3383 A72-45666

Parallel processing of ballistic missile defense radar data with PEPE. 24 p3383 A72-45667

PARALLELEPIPEDS

Stress-strain state determination in elastic parallelepiped by net point method and matrix filtering 07 p1091 A72-19754

Unsteady heat conductivity equation for finite dimensions parallelepiped, noting temperature dependence of specific heat and thermal conductivity 08 p1252 A72-21321

Solid deformable body mean stress determination by statistical summation of stress squares on faces of parallelepiped rotated within Euler angle limits 12 p1887 A72-28233

Castiglione variational theorem for algebraic equation solution of thermal stresses determination in elastic parallelepiped, using Maxwell stress functions as cosine binomial series 24 p3459 A72-45267

PARALLELOGRAMS

Linear uncoupled quasi-static thermoelasticity theory for thermal bending of nonuniformly heated parallelogram-shaped plates 09 p1400 A72-22710

Thermal buckling of parallelogram shaped plate under stationary temperature field and uniformly distributed forces, deriving critical load 09 p1402 A72-22733

PARAMAGNETIC AMPLIFIERS

U MASERS

PARAMAGNETIC RESONANCE

NT ELECTRON

Low-temperature part of a spectrometer for gigahertz-ultrasonics and ultrasonic paramagnetic resonance. 21 p3051 A72-40215

PARAMAGNETISM

Niobium trifluoride synthesis, noting semiconductor and paramagnetic properties 02 p0243 A72-12170

Russian book on transition metals and alloys electron structure and electronic properties covering paramagnetism, positron annihilation, magnetic transformations and electron heat capacity 11 p1659 A72-26069

Paramagnetic phase induced moment system containing substitutional impurities, calculating mode energies by Green function method in random phase approximation 15 p2295 A72-32546

Surface effects on paramagnetic metals spin susceptibility models, including random-phase-approximation equation derivation and induced magnetic moment calculation 15 p2295 A72-32549

Low field magnetization measurements at 4.2 K on bulk and thin film niobium nitride, discussing Pauli spin paramagnetism and spin-orbit scattering 16 p2442 A72-33843

PARAMETERIZATION

Stability theorems reformulation with one-parameter families of Liapunov functions, discussing applications to Matrosov and Rouche asymptotic stability theorems 02 p0251 A72-11495

Discrete time systems unknown parameter identification, considering unified error function minimization approach 04 p0506 A72-15106

Prandtl layer turbulence spectra parameterization from wind vector data, considering functional dependence on mean wind velocity, height and thermal stratification 04 p0544 A72-15623

Loitsiankii parametric method application to universalize isothermal laminar boundary layer partial differential equations in Crocco variables 05 p0649 A72-16221

Small parameter method solution of two dimensional incompressible flow Navier-Stokes equations, exemplifying application to viscous incompressible flow past semiinfinite plate 06 p0801 A72-18127

Parametric solution of Brans-Dicke cosmological equations for flat Friedmann type expanding universe for time, density, expansion parameter and scalar field 07 p1074 A72-19525

Computed and observed color indices of intermediate band UPXYZVS and wideband UVB photometric systems, evaluating response curve validity for parameter determination 11 p1715 A72-25295

Optimal parameters selection for natural vibrations maximum damping rate, applying method to two mass electromechanical system 11 p1686 A72-25533

Earth atmosphere general circulation model based on planetary boundary layer parameterization, considering surface stress and heat and moisture flux 13 p1988 A72-28442

Parameterized daily profile characterization of global atmospheric conditions to minimize computer storage, discussing mathematical representations, wind, density and temperature profiles 13 p1989 A72-28806

Thermal stress distribution determination in isotropic plate with rigid circular insert, using small parameter technique 13 p2056 A72-28913

Rectangular plate nonlinear lumped-parameter model for large displacement amplitudes, deriving differential equations of motion via Hamilton principle and Euler equations 14 p2169 A72-31148

Iterative computational procedure for system parameter identification and optimization, using multilevel technique 16 p2371 A72-33192

Parametric cost estimating aids DOD in systems acquisition decisions. 17 p2639 A72-34461

Analysis of discrete automatic control systems with variable parameters by the method of orthogonal expansions. I, II 19 p2778 A72-37438

PARAMETERS

U INDEPENDENT VARIABLES

PARAMETRIC AMPLIFIERS

Parametric amplification of laser waves with amplitude and phase modulation under exponential signal growth applied to Raman scattering picosecond pulse field 01 p0079 A72-10346

Wideband microwave parametric amplifier using balanced circuits to relax isolation requirements between signal, idler and pump circuits 01 p0038 A72-10655

Gain vs bandwidth characteristics of broadband microwave parametric amplifiers 01 p0038 A72-10656

Varactor diode microwave parametric amplifiers for radio astronomy interferometer, discussing system design features for gain and phase stabilities 02 p0192 A72-12043

Inhomogeneous plasmas parametric instabilities excitation, observing threshold electric field power requirement 02 p0266 A72-12370

Computer aided design of single tuned parametric amplifiers, stressing voltage gain-bandwidth product 04 p0497 A72-14715

Papers on microwave engineering covering surface finish importance for waveguide propagation, parametric amplifiers and voltage breakdown of microwave antennas 06 p0783 A72-17737

Ultralow noise microwave parametric amplifiers in communication satellite earth terminals, discussing technology basis of millimeter wave paramps 06 p0784 A72-17741

Broadband parametric amplifier design using computerized optimization procedure based on Gauss-Newton iteration technique 06 p0786 A72-18376

IMPATT driven pumps replacement of klystron for parametric amplifiers producing over 100 mW at 38-40 GHz with good stability and noise performance 06 p0788 A72-18470

Microwave parametric amplification and conversion in circuits with Josephson junctions, describing stable oscillation measurements 06 p0866 A72-18477

Miniature modular wideband parametric amplifier for centimeter range, using IC optimal coupled circuit with passband dependent on diode time constant 07 p0956 A72-19570

Parametric oscillations of nonlinear systems prone to self excitation, using asymptotic method 08 p1206 A72-21243

Uniform plane wave theory of internal upconversion and frequency doubling in optical parametric oscillators 09 p1324 A72-23079

Steady state plane wave theory of intracavity coupled parametric oscillator upconverter, obtaining efficiency, pump power transmission and optimum output coupling 09 p1325 A72-23086

Millimeter wave pumped X band balanced diode type parametric amplifier using GaAs Schottky barrier varactors for operation at room temperature 09 p1289 A72-23417

High quality GaAs varactor diodes for double diode low noise wideband parametric amplifiers at idler frequencies up to 43 GHz without refrigeration 12 p1788 A72-27174

Singly and doubly resonant pulsed optical parametric oscillators driven by time-dependent pump, deriving output power rise time by steady state analysis 12 p1792 A72-27751

Optimal design of broad passband in unilateral parametric balance amplifier 13 p1928 A72-28789

Parametric regeneration in Josephson superconducting point contacts for combination frequency signal amplification and conversion in microwave application 13 p1932 A72-29296

Parametric resonance suppression in annular laser by steady noise perturbation, discussing beat signal spectrum 13 p1968 A72-29505

Alfven waves parametric amplification in magnetized plasma, showing dependence on wave frequency and phase and perturbation field strength 14 p2137 A72-30396

Oscillations in ferromagnetic resonant circuit of parametric amplifier with constant capacitance and periodically variable inductance modulated by input signal 14 p2089 A72-31107

Gravity waves parametric generation on liquid surface, presenting threshold values for space distribution of amplitudes and phases 14 p2097 A72-31111

Short signal pulse shaping based on phase and amplitude selective properties of distributed parametric amplifiers operating under nonlinear conditions 14 p2090 A72-31112

Regenerative semiconductor parametric amplifier under dc through p-n junction, analyzing nonlinear phenomena 14 p2090 A72-31124

Nonlinear approximation of slowly changing standing waves in self excited parametric oscillators with distributed and bulk structures 14 p2090 A72-31131

Van der Pol and nonlinear parametric oscillators fluctuations due to random noises analyzed by averaging method and discrete Markov processes 14 p2133 A72-31134

Three-frequency parametric traveling wave amplifier gain and conversion factors calculation by numerical method with allowance for fast and slow space charge wave effects 15 p2206 A72-31661

Parametric amplifiers for satellite microwave communication systems, discussing frequency stability, noise temperature and gain relationships 16 p2369 A72-33520

Optical second harmonic generation and parametric oscillation. 17 p2594 A72-34566

Spaceflight-qualified tunable C-band parametric amplifier system. 19 p2770 A72-37253

18 GHz paramps with both liquid helium and room temperature operations and with triple-tuned gain characteristics. 19 p2770 A72-37254

An X-band paramp with 0.85 dB noise figure /uncooled/ and 500 MHz bandwidth. 19 p2770 A72-37258

German monograph - Multiple tuning of cooled parametric amplifiers 19 p2772 A72-37651

Parametric amplification and frequency conversion in a dual section TWT 19 p2774 A72-38411

Self-excited parametric oscillations at the second harmonic in a parametric system with a triple-post ferromagnetic core 19 p2774 A72-38586

Combinational distortions and cross distortions in parametric microwave systems 19 p2768 A72-38665

Bandwidth and threshold calculations for angle-tuned parametric oscillators. 19 p2813 A72-38689

Microwave low noise amplifiers for use in radar systems. 20 p2907 A72-39220

The effect of pump coherence on frequency conversion and parametric amplification. 21 p3014 A72-40238

Low-noise parametric amplifiers for radio astronomical observations at 18 to 21 cm wavelengths 21 p3025 A72-40303

Low noise microwave parametric amplifier design for space communication receivers, using inverted diode balanced mixers 21 p3025 A72-40304

Optical communication channel optimization with binary signals preamplified in optical parametric amplifier, noting amplifier gain and SNR 21 p3016 A72-40783

Low noise receiver for satellite broadcasting.
21 p3019 A72-40886

OH maser sources parametric down-conversion, deriving nonlinear current densities, electron cyclotron wave damping and parametric gain coefficient
21 p3064 A72-41030

Miniature modular wideband parametric amplifier for centimeter range, using Q optimal coupled circuit with passband dependent on diode time constant
22 p3158 A72-42088

Properties of a pulsed LiIO₃ doubly resonant parametric oscillator.
23 p3297 A72-44187

Theory of pulsed internal optical parametric oscillators.
24 p3409 A72-44714

Analysis of a single-loop parametric amplifier by the phase plane method
24 p3384 A72-44893

Parametric preamplifiers for transistorized nuclear-emission detectors and their capabilities
24 p3402 A72-44894

PARAMETRIC DIODES
Optoelectronic elements for information system applications, discussing photomultipliers, photodiodes, photoresistors, avalanche and photoparametric diodes response and bandwidth characteristics
08 p1169 A72-21844

PARAMETRIC FREQUENCY CONVERTERS
Microwave parametric amplification and conversion in circuits with Josephson junctions, describing stable oscillation measurements
06 p0866 A72-18477

Parametric converter mixers with FM and AM signal and pump oscillator, investigating SNR behavior
07 p0956 A72-19658

Statistical characteristics of IR receivers with parametric carrier frequency conversion, describing noise index minimization technique
12 p1846 A72-27889

Parametric regeneration in Josephson superconducting point contacts for combination frequency signal amplification and conversion in microwave application
13 p1932 A72-29298

Controllable matched filter model for single circuit and twin circuit parametric converters
15 p2207 A72-31886

Statistical characteristics of IR receivers with parametric carrier frequency conversion, describing noise index minimization technique
16 p2427 A72-33998

Calculation of the transmission factor of a parametric microwave transistor multiplier
19 p2774 A72-38423

Optical signal envelopes recording and reproduction with parametric superregenerative frequency converters, noting optical pumping by continuous wave YAG laser emission
23 p3292 A72-44471

Wideband parametric up-conversion of infrared waves into visible region using tunable dye laser pumping.
24 p3410 A72-45286

PARAMETRIC OSCILLATORS
U PARAMETRIC AMPLIFIERS
PARAMETRONS
Calculation of transient processes in a capacitance parametron by the phase approximation method
23 p3312 A72-43351

PARANASAL SINUSES
Case report on dive decompression induced maxillary sinus barotrauma due to sinus pressure buildup caused by ostium blockage
22 p3150 A72-42497

Paranasal sinus barotrauma in military flying personnel, discussing radiographic diagnostic methods and hypobaric test procedures for flight status restoration time determination
24 p3378 A72-45664

PARAPSYCHOLOGY
U EXTRASENSORY PERCEPTION
PARATHYROID GLAND
Radioimmunoassay and gel filtration determination of molecular size and immunochemical reactivity of parathyroid hormone in gland extracts, peripheral circulation and parathyroid effluent blood
04 p0473 A72-15228

PARAWINGS
Buoyancy systems and parawings application in short haul passenger transportation, discussing VTOL and STOL operations
16 p2348 A72-33183

PARKING ORBITS
Minimum velocity change noncoplanar two and three impulse orbital transfer from regressing oblate earth assembly parking ellipse into flyby trans-Martian asymptotic velocity vector
03 p0434 A72-13634

PARKINSON DISEASE
Cerebral neurons population electric stimulation effect on deep sleep duration in Parkinsonism patients
04 p0476 A72-15585

PARTIAL DIFFERENTIAL EQUATIONS

NT BIHARMONIC EQUATIONS
NT BURGER EQUATION
NT ELLIPTIC DIFFERENTIAL EQUATIONS
NT FOKKER-PLANCK EQUATION
NT GAUSS EQUATION
NT LIOUVILLE EQUATIONS
NT PARABOLIC DIFFERENTIAL EQUATIONS
NT VLASOV EQUATIONS
Invariant imbedding technique application to linear partial differential equations boundary value problems conversion to Cauchy problem via generalized Riccati transformations
01 p0093 A72-11116

Associative array digital processors application to numerical solution of partial differential equations, illustrating methodology on weather forecasting equations
02 p0186 A72-11658

Axisymmetric circular membranes large deflections, solving nonlinear partial differential equations by iterative method in conjunction with finite difference approximations
02 p0296 A72-12526

Hyperbolic partial differential equations solution by hybrid computer, simulating wave propagation by track hold circuits
02 p0188 A72-12656

Weak solutions of degenerate partial differential equation of dynamic programming, investigating relation to value function of stochastic optimal control problem
03 p0382 A72-13701

Hsu-Howe iterative hybrid method for partial differential equations solution by time sharing analog components, using dynamic scaling and incremental formulations for reduced sensitivity
04 p0495 A72-14418

Two dimensional solar cell model with partial differential equation relating arbitrary point potential to cell parameters for I-V characteristics prediction
04 p0465 A72-14480

Sequential interpolating estimation algorithm derivation for distributed-parameter noisy dynamic systems described by nonlinear partial differential equations
04 p0538 A72-14669

Liapunov functionals synthesis for continuous system stability study, discussing linear combinations of moments of governing partial differential operators
04 p0538 A72-14671

Distributed systems modeled by partial differential equations, identifying unknown parameters by Galerkin method using steepest descent method and nonlinear filter
04 p0505 A72-14674

Lagrange method extended to method of characteristics for solving first order hyperbolic partial differential equations, applying to ionospheric ion density distribution
04 p0539 A72-14885

Pressure and convective heat transfer distribution at air inlet central body surface, reducing Navier-Stokes equations to partial differential equations with similar solutions
04 p0596 A72-14971

Continuous media stationary motion stability using initial boundary value problem of partial differential equations in perturbations
[ASME PAPER 71-WA/APM-17]
05 p0647 A72-15963

Loitsiankii parametric method application to universalize isothermal laminar boundary layer partial differential equations in Crocco variables
05 p0649 A72-16221

Discrete elasticity theory constitutive and motion equations, considering finite difference and partial differential equations
05 p0737 A72-16297

Rectangular variable thickness plate deflection under uniform lateral pressure, solving nonlinear partial differential equations with variable coefficients by iterative procedure
05 p0738 A72-16533

Herzberger fundamental optical invariant for rotationally symmetric systems, using partial differential equations
[AD-738406]
05 p0690 A72-16672

Finite element algorithm derived for partial differential equation system governing laminar three dimensional boundary layer flow of multicomponent compressible fluid
[AIAA PAPER 72-108]
05 p0604 A72-16817

Transient compressible heat and mass transfer in porous media, solving coupled nonlinear partial differential equations in finite difference form by iterative technique
[AIAA PAPER 72-23]
05 p0749 A72-16914

Group velocity and numerical error propagation in partial differential and finite difference equations of gas dynamics
[AIAA PAPER 72-153]
05 p0652 A72-16952

Optimal averaging of control in distributed random parameter system described by hyperbolic partial differential equations, considering boundary values on characteristics as control functions
05 p0683 A72-17133

Optimal control of one dimensional physical system with delayed argument described by nonlinear first order hyperbolic partial differential equations, using maximum principle
05 p0691 A72-17138

Hybrid computer solution of partial differential equations by invariant imbedding application to serial method
06 p0839 A72-17631

Jacobian matrix partial derivatives for orbital motion representation by time step power series
06 p0877 A72-17651

Mixed boundary value problem of partial differential equations describing nonlinear viscoelastic vibration of clamped rods, examining asymptotic solution stability
06 p0901 A72-18716

Power series method with Cauchy formula for nonlinear partial differential equations solution in unsteady periodic temperature oscillations
06 p0905 A72-18727

Multidimensional Fourier transforms application to theoretical physics partial differential equations, using singular delta function for homogeneous equations general integral
07 p1027 A72-19436

Sufficient conditions definition for existence of solution for heat conduction equation coupling to telegrapher equation
07 p1028 A72-19897

Wave diffusion related to phenomena governed by linear hyperbolic partial differential equations of second order, presenting Cauchy problem solution
07 p1035 A72-20090

Gas dynamics K-wave interaction in nonlinear media described by nonlinear partial differential equations
07 p0972 A72-21013

Iteration procedure for approximate integration of nonlinear system of partial differential equations with time lag, presenting upper and lower estimates
07 p1028 A72-20209

Elastic body dynamics partial differential equations transformation into boundary value problem for Monge-Ampere equation
07 p1095 A72-20218

Self similar invariant group solutions to Bellman nonlinear partial differential equation for optimal correction problems of control systems motion with random disturbances
07 p0963 A72-20322

Partial differential equation language (PDEL/ for batch and interactive digital simulation of PDE models
07 p0951 A72-20327

Truncation error correction based on Richardson extrapolation in finite difference approximation of nonlinear partial differential operators
07 p1101 A72-20328

Computer interactive graphics for digital simulation of engineering fields modeled by partial differential equations boundary value problems
07 p0951 A72-20337

Iterative solution of Cauchy problem of partial differential equations nonlinear system with time lag, formulating uniqueness theorem
08 p1198 A72-20904

Liapunov theorem for polynomial solution existence for first order inhomogeneous system of linear partial differential equations
08 p1205 A72-20958

Bergman operators construction for second order linear partial differential equations
08 p1199 A72-21288

Hybrid Monte Carlo techniques with digital and analog computers and minimal interface, simulating random walks for partial differential equations solution
08 p1138 A72-21602

Geometrical characterization of steady nondissipative compressible fluid flow described by first order partial differential equations system
09 p1295 A72-23366

Coupling of interstitial liquid and porous elastic medium deformation, calculating solidification by numerical integration of partial differential equations system of Lamé type
10 p1465 A72-24116

Algorithms for spatially varying parameters estimation in nonlinear partial differential equations from noisy observations, noting diffusivity in heat equation
10 p1506 A72-24457

Partial differential equation for thin walled circular cylindrical shells, deriving solutions for displacement and stresses in terms of surface coordinates low degree polynomials
10 p1557 A72-24560

Linear continuous time systems optimal dual control problem solution by reduction to partial differential equation in finite domain with suitable boundary conditions
10 p1458 A72-25170

ferential equations, considering boundary values on characteristics as control functions
05 p0683 A72-17133

Optimal control of one dimensional physical system with delayed argument described by nonlinear first order hyperbolic partial differential equations, using maximum principle
05 p0691 A72-17138

Hybrid computer solution of partial differential equations by invariant imbedding application to serial method
06 p0839 A72-17631

Jacobian matrix partial derivatives for orbital motion representation by time step power series
06 p0877 A72-17651

Mixed boundary value problem of partial differential equations describing nonlinear viscoelastic vibration of clamped rods, examining asymptotic solution stability
06 p0901 A72-18716

Power series method with Cauchy formula for nonlinear partial differential equations solution in unsteady periodic temperature oscillations
06 p0905 A72-18727

Multidimensional Fourier transforms application to theoretical physics partial differential equations, using singular delta function for homogeneous equations general integral
07 p1027 A72-19436

Sufficient conditions definition for existence of solution for heat conduction equation coupling to telegrapher equation
07 p1028 A72-19897

Wave diffusion related to phenomena governed by linear hyperbolic partial differential equations of second order, presenting Cauchy problem solution
07 p1035 A72-20090

Gas dynamics K-wave interaction in nonlinear media described by nonlinear partial differential equations
07 p0972 A72-21013

Iteration procedure for approximate integration of nonlinear system of partial differential equations with time lag, presenting upper and lower estimates
07 p1028 A72-20209

Elastic body dynamics partial differential equations transformation into boundary value problem for Monge-Ampere equation
07 p1095 A72-20218

Self similar invariant group solutions to Bellman nonlinear partial differential equation for optimal correction problems of control systems motion with random disturbances
07 p0963 A72-20322

Partial differential equation language (PDEL/ for batch and interactive digital simulation of PDE models
07 p0951 A72-20327

Truncation error correction based on Richardson extrapolation in finite difference approximation of nonlinear partial differential operators
07 p1101 A72-20328

Computer interactive graphics for digital simulation of engineering fields modeled by partial differential equations boundary value problems
07 p0951 A72-20337

Iterative solution of Cauchy problem of partial differential equations nonlinear system with time lag, formulating uniqueness theorem
08 p1198 A72-20904

Liapunov theorem for polynomial solution existence for first order inhomogeneous system of linear partial differential equations
08 p1205 A72-20958

Bergman operators construction for second order linear partial differential equations
08 p1199 A72-21288

Hybrid Monte Carlo techniques with digital and analog computers and minimal interface, simulating random walks for partial differential equations solution
08 p1138 A72-21602

Geometrical characterization of steady nondissipative compressible fluid flow described by first order partial differential equations system
09 p1295 A72-23366

Coupling of interstitial liquid and porous elastic medium deformation, calculating solidification by numerical integration of partial differential equations system of Lamé type
10 p1465 A72-24116

Algorithms for spatially varying parameters estimation in nonlinear partial differential equations from noisy observations, noting diffusivity in heat equation
10 p1506 A72-24457

Partial differential equation for thin walled circular cylindrical shells, deriving solutions for displacement and stresses in terms of surface coordinates low degree polynomials
10 p1557 A72-24560

Linear continuous time systems optimal dual control problem solution by reduction to partial differential equation in finite domain with suitable boundary conditions
10 p1458 A72-25170

Satellite orbit tracking data accuracy estimation by partial differentiation, using Doppler and interferometric methods

11 p1593 A72-26097

Method of characteristics for solution of quasi-linear hyperbolic partial differential equations, analyzing frequency response

11 p1678 A72-26551

Representational method for evolution type partial differential equations numerical solution, noting relationship to finite element method

11 p1679 A72-26961

Nonlinear stochastic partial differential equations solution by graph technique, calculating correlation function and phase change spectrum in phase locked circuit

12 p1837 A72-27575

Russian papers on functional analysis covering approximate solution of linear integral equations, averaging principle for partial differential equations and boundary value problems

12 p1837 A72-27994

Asymptotic approximation methods for boundary layers in singular perturbation theory for linear elliptic partial differential equations in two independent variables

13 p1940 A72-28425

Liapunov direct stability method extension to partial differential equations, using functional analysis and wave equation example

13 p1985 A72-28483

Asymptotically bilateral solutions to partial differential equations, using fictitious regions and auxiliary unsteady problem methods

13 p1987 A72-29472

Partial differential equations for longitudinal, torsional and transverse vibrations of bars with variable composition

13 p2006 A72-29885

Linear functional equations with constant coefficients for generalized partial derivative operators introduced in certain spaces of functions of many complex variables

13 p1987 A72-30083

Delayed argument linear partial differential equations system integration, constructing asymptotic solution in nonresonant case

13 p1988 A72-30084

Partial differential equations of motion for nonlinear mechanical systems solved by Lanczos formula, discussing prismatic cylinder oscillations under uniformly distributed transverse load

15 p2275 A72-31729

Dissipative systems of ordinary differential equations concepts extension to functional and partial differential equations

15 p2263 A72-31754

Control theory of second order linear hyperbolic partial differential equations, discussing relation to harmonic and spectral analysis

15 p2263 A72-31757

Complex conjugate fourth order partial differential equations for circular cylindrical shells deformation, comparing accuracy with Fluegge, Morley and Novozhilov equations

15 p2331 A72-32559

First eigenvalue and first eigenfunction properties of linear elliptic partial differential equation in variational form with discontinuous coefficients, considering Dirichlet problem

16 p2416 A72-33502

Optimal filtering estimate of noisy nonlinear partial differential distributed parameter system, using least squares and invariant imbedding techniques

16 p2416 A72-33575

Turbulent solutions of certain linear and nonlinear partial differential equations

17 p2537 A72-34194

A method of solving partial differential equations for boundary layers

17 p2537 A72-34195

Finite element method matrices in least squares approximation and elliptic partial differential equations, discussing numerical stability properties

17 p2573 A72-34219

Search density function optimality for randomly moving target in n dimensional space with location probability density function satisfying given partial differential equation

17 p2574 A72-34340

Asymptotic solutions of inhomogeneous initial boundary value problems for weakly nonlinear partial differential equations.

17 p2574 A72-34342

Use of fast Fourier transforms for solving partial differential equations in physics.

17 p2575 A72-34645

Conditions for the uniqueness of the solution to the Cauchy problem for special systems of equations with variable coefficients

17 p2575 A72-34775

Approximate solutions of problems involving simultaneous multifunctional nonlinear partial differential

equations, noting rectangular plate deflection under lateral pressure

[ASME PAPER 72-APM-47] 17 p2627 A72-34780

Dissipative periodic process theory for application to elasticity and distributed parameter and hereditary systems defined by partial and functional differential equations

17 p2575 A72-34867

Three-dimensional small-signal analysis of bipolar transistors.

17 p2530 A72-35099

Book - Nonlinear partial differential equations in engineering, Volume 2

17 p2576 A72-35449

Means of converting the solutions of partial differential equations, obtained in operator form, to solutions of conventional form when the differential operators are expressed in general form

17 p2577 A72-35789

Hopscotch algorithm for numerical integration of nonlinear hyperbolic partial differential equation systems based on finite difference method

18 p2705 A72-37020

Optimal control of plant described by nonlinear hyperbolic equations with variable initial conditions of system, noting constraints on plant phase coordinates

19 p2777 A72-37434

Linear partial differential equations with random forcing.

19 p2825 A72-37573

Homogeneous linear partial differential equation for optimal control with boundary condition formed by terminal component, noting weighting functions for linear plant

19 p2778 A72-37989

Solution of certain systems of partial differential equations in linear commutative differential operators

19 p2825 A72-38183

Identification of parameters in nonlinear boundary conditions of distributed systems with linear fields.

19 p2780 A72-38245

Distributed parameter linear and nonlinear systems analysis, deriving theorem for solution stability of linear partial differential equations

19 p2826 A72-38247

Certain properties of differential operators with variable coefficients dependent on the domain format.

20 p2946 A72-39465

Optimization of controlled plants sequence with stochastic process described by partial differential equations, noting hydropneumatic system of liquid fuel jet engine

20 p2947 A72-39903

Numerical solution of quasi-conservative hyperbolic systems - The cylindrical shock problem.

21 p3043 A72-40101

Decomposition of multidimensional nonlinear equations of heat-conduction type and construction of nonlinear electrical integrators

21 p3128 A72-40181

Classes of uniqueness of solutions to the Cauchy problem

21 p3074 A72-40255

Limiting equation for solving a boundary value problem in a multilayer domain

21 p3074 A72-40258

Partial derivatives of dispersion curves for higher modes of Love waves in a single-layered medium.

21 p3084 A72-40496

A method for determining the motion in a laminar boundary layer.

21 p3045 A72-40813

Partial differential equation solution for plane electromagnetic wave diffraction by infinite dielectric cylinder of arbitrary cross section

21 p3085 A72-41199

A system of linear equations with partial derivatives

21 p3077 A72-41822

Solution method for some boundary problems of nonlinear hyperbolic-type equations and propagation of weak shock waves

22 p3164 A72-41904

Discontinuities propagation in quasi-linear hyperbolic partial differential equation systems, noting MHD flow and crystal optics equations

22 p3204 A72-41905

Certain necessary conditions for the local solvability of first-order differential equations with infinitely differentiable coefficients

22 p3198 A72-42158

On the perturbation method in the stability analysis of continuous systems.

22 p3206 A72-42842

Equilibrium equations and deformation of elastoplastic thin isotropic cylindrical shell with circular hole, noting nonlinear partial differential equations for plate displacements

23 p3345 A72-43587

Optimally sensitive control for distributed parameter systems.

23 p3275 A72-43612

Boundary value problems for a mixed-composite type of equation in an unbounded domain

23 p3308 A72-43628

Asymptotic behavior of solutions of systems of conservative differential equations

23 p3308 A72-43693

Equivalence conditions for classes of linear and non-linear distributed parameter systems.

23 p3277 A72-44369

Partial differential heat conduction equation for temperature distribution in rectangular plate, comparing with finite difference solution

24 p3465 A72-45268

PARTIAL PRESSURE

NT HYPOXEMIA

NT OXYGEN TENSION

Upper atmosphere neutral oxygen density diurnal variations from incoherent scatter and satellite drag data, noting deviations from Jacchia static diffusion model predictions

01 p0062 A72-10911

Vagal control of ventilation and respiratory muscles during elevated pressures in cats

07 p0917 A72-19446

Carbon dioxide-air-helium molecular systems population excitation rates with current, gas composition and partial pressures dependence

08 p1183 A72-22028

German monograph on electron beam focusing in partial pressure analyzer with two compartment ion source, eliminating residual gas-filament interaction

09 p1306 A72-22318

Direct single electrode measurement of carbon dioxide partial pressure in liquids and gases, using pH changes due to gas diffusion

09 p1317 A72-23671

Co-Cr alloy oxidation as function of temperature and oxygen partial pressure, discussing solid state diffusion

14 p2118 A72-30544

Transversely excited pulsed carbon dioxide-nitrogen-helium laser with electrical discharge determined optimum partial pressure

15 p2249 A72-32236

The measurement of partial pressure in vacuum technology and vacuum physics

18 p2692 A72-36836

PARTICLE ACCELERATION

Extragalactic cosmic ray hypothesis plausibility from viewpoints of energy supply, acceleration process efficiency, galactic nucleus activity and intergalactic space

01 p0122 A72-11260

Quasi-linear theory of relativistic particle acceleration by hydromagnetic turbulence for small gyroradius expansion, using Vlasov equation

02 p0265 A72-12307

Acceleration phase of solar cosmic rays and relativistic electrons in solar flare of 7 July 1966 discussing MHD shock waves generation

03 p0407 A72-12941

Neutron star surface structure and cooling calculations for pulsar cosmic ray production through surface material acceleration

03 p0421 A72-13136

Ions acceleration during current passage through plasma, discussing maximum energies, threshold current and electron beam flux density

03 p0396 A72-13661

Heavy nuclei enrichment in solar accelerated particles, discussing differential energy spectra, photospheric and coronal abundances, satellite observation and agreement with galactic cosmic rays

04 p0568 A72-15366

Charged particle acceleration by nonstationary sinusoidal electric fields in earth magnetosphere based on mathematical model

05 p0709 A72-16256

Magnetospheric plasma sources, discussing wave-particle interactions and acceleration mechanisms

06 p0810 A72-18281

Cosmic rays generation by charged particles acceleration in electromagnetic constant crossed fields during magnetic stars contraction to neutron star dimensions

07 p1056 A72-19042

Active region sources of solar proton streams, discussing 27-day recurrence, acceleration and confinement in interplanetary space

07 p1060 A72-20010

Solar discrete particle events classification and emission and acceleration mechanisms in relation to flare development

07 p1060 A72-20011

Particle acceleration and plasma ejection in solar flares, using model of nonstationary cumulative flow near magnetic neutral line

07 p1060 A72-20014

Magnetospheric and polar substorms model for auroral particles acceleration and geomagnetic tail current diversion to auroral oval night side

07 p0977 A72-20029

Magnetospheric trapped particle diffusion coefficients and acceleration in earth radiation belts

07 p1062 A72-20035

Solar cosmic ray heavy nuclei acceleration independence from solar activity phenomena, based on Elektron 4 satellite observation

07 p1064 A72-20632

Auroral ionosphere radio self emission at supercritical frequencies from accelerated protons charge exchange effects, comprising radio bursts, storms and amplifications

08 p1153 A72-20713

Plasma emitter shape determination in accelerating electric field for charged particle flux production

09 p1358 A72-22490

Low energy ions and negative particle fluxes simultaneous enhancements due to Apollo 14 lunar module impact, suggesting solar wind and gas cloud interaction as acceleration mechanism

09 p1388 A72-23018

Micrometeoroid simulation by accelerated microparticles bombardment of metal targets, discussing energy partition as function of impact velocity

09 p1409 A72-23667

Galactic and universal theories of cosmic ray source mechanisms, energy requirements, particle composition, propagation through interstellar matter and acceleration in supernovae remnants

10 p1533 A72-23889

Ion acceleration by relativistic electron-beam-formed plasma, explaining ion energy dependence on neutral gas pressure by potential well model

10 p1518 A72-23961

Van Allen proton belt model, considering ionosphere particle acceleration by stochastic interaction with hydromagnetic waves due to solar wind at magnetosphere shock front

10 p1529 A72-24245

Sunspots contact region charged particles acceleration by plasma flow induced electric field, noting Fermi type mechanism

11 p1695 A72-26107

Ionization and associated energy loss effects on particles acceleration in solar atmosphere, emphasizing Fermi mechanisms

12 p1863 A72-27303

Near field effects on pulsar particle acceleration, relating electric and magnetic field magnitudes

14 p2156 A72-30568

Approximate analytical solution for spherical particle acceleration in uniform gas flow, examining nozzle geometry and particle size effects

14 p2095 A72-30924

Acceleration and recombination effects on ion energy spectra, discussing energy distributions of hydrogen, zirconium, lithium, and deuterium ions in laser plasmas

16 p2428 A72-32910

Solar radio bursts time sequence and positions observation during 24 January 1971 proton event, noting relation to relativistic particles acceleration into interplanetary field

16 p2445 A72-33045

Low energy cosmic ray deuteron and He 3 source spectra observation implications for adiabatic deceleration in solar cavity, discussing interstellar propagation

16 p2448 A72-33743

Neutron star acceleration of He, Fe and supernova debris into cosmic ray flux throughout Galaxy, discussing magnetic and superfluidity effects

16 p2448 A72-33745

Electromagnetic wave propagation in uniform and nonuniform plasmas with enough strength to cause relativistic electron velocities, considering linear polarization and nonlinear penetration effects

16 p2438 A72-33926

Fermi acceleration effects in low energy particle transport in interplanetary space, assuming kinetic energy contained in Alfvén and bidirectional traveling waves

16 p2460 A72-33938

Plasma emitter shape determination in accelerating electric field for charged particle flux production

17 p2588 A72-34653

Magnetospheric convection induced longitudinal or Fermi acceleration role in nighttime auroral particle flux production mechanism

17 p2601 A72-35592

Auroral electron acceleration by longitudinal electric field due to protons defreezing above ionosphere

17 p2550 A72-35852

Electron and proton acceleration in the outer magnetosphere regions during polar substorms

18 p2688 A72-36866

Equations of motion in the linear approximation.

19 p2835 A72-38174

Auroral ionosphere radio self emission at supercritical frequencies from accelerated protons charge exchange effects, comprising radio noise bursts, storms and amplifications

19 p2790 A72-38341

On the acceleration of charged particles to cosmic ray energies.

19 p2852 A72-38483

On the acceleration time of particles in the solar atmosphere.

19 p2852 A72-38634

Energy spectrum and composition of pulsar-accelerated cosmic rays.

20 p2964 A72-39343

Single-cycle electron acceleration in focused laser fields.

20 p2934 A72-39720

Exact solutions of the Einstein-Maxwell equations for an accelerated charge.

20 p2955 A72-40008

Formation of intense charged particle beams in a current-carrying plasma.

21 p3092 A72-40834

Solar soft X-rays and solar activity. II - Observational assessment of the role of the type III acceleration mechanism in establishment of the soft X-ray source volume.

21 p3101 A72-41294

Solar flare associated relativistic electron acceleration relationship to cosmic ray and type 4 radio burst production

22 p3217 A72-42010

Electron and plasma particle acceleration by moving pulsed laser, noting appearance of fast particles, hard radiation and neutrons

23 p3295 A72-43312

Some characteristics of microwave type IV radio bursts and the acceleration of solar cosmic rays.

23 p3328 A72-43616

Ion acceleration during expansion of a rarefied plasma

23 p3322 A72-44482

PARTICLE ACCELERATOR TARGETS

Multiple meson production in 250 GeV nucleon-nucleon collisions in LiH targets, noting 40 per cent formation of heavy meson cluster fireballs

06 p0868 A72-17259

Micrometeoroid simulation by accelerated microparticles bombardment of metal targets, discussing energy partition as function of impact velocity

09 p1409 A72-23667

Inclusive isotope spectra of secondary nuclei produced by Bevatron heavy ion fragmentation in carbon and polyethylene targets, noting partial differential cross sections

10 p1517 A72-25144

PARTICLE ACCELERATORS

NT BETATRONS

NT BEVATRON

NT CYCLOTRONS

NT ELECTRON ACCELERATORS

NT ION ACCELERATORS

NT LINEAR ACCELERATORS

NT VAN DE GRAAFF ACCELERATORS

Spark calorimeter calibration by particle accelerator induced high energy pions, noting neutral and charged particles track detectors high geometric resolution

06 p0811 A72-17292

Collective self fields generated from intense electron beams for high energy positive particle acceleration and Astron hot plasma confinement for fusion control

10 p1523 A72-24788

Dished accelerator grids design, fabrication and operation in electron bombardment ion thruster, studying ion extraction capability and discharge chamber performance

[AIAA PAPER 72-486]

11 p1710 A72-26212

PARTICLE BEAMS

NT ATOMIC BEAMS

NT ELECTRON BEAMS

NT ION BEAMS

NT MOLECULAR BEAMS

NT NEUTRAL BEAMS

NT NEUTRON BEAMS

NT PION BEAMS

NT PROTON BEAMS

Transit tube manometric system with fast particle beam ionization of residual gas molecules for vacuum measurements

09 p1364 A72-23226

Picoampere charged particle beam symmetry and magnitude monitor consisting of four transmission ion chambers

09 p1315 A72-23405

Beam-foil-gas spectroscopy and relative cross section measurements for studying steady state nonequilibrium processes

10 p1434 A72-24325

Converging or diverging high intensity charged particle beams arbitrary profile shaping, obtaining solution via Laplace equation through reduction to Cauchy problem

10 p1521 A72-24362

Quasi-linear approximation equations for relativistic charged particles beam dissipative instability in collisional plasma, noting electrons heating at high collision frequencies

12 p1852 A72-27860

Charged particle beams focusing in combined dual spiral system with homogeneous magnetic field along axis

13 p1932 A72-29292

Nonlinear theory of interaction between restricted relativistic particle beam and plasma, determining field amplitudes and beam radii

13 p2019 A72-29989

Spectrometer entrance slit diffraction effects on observed fast beam spectral line width

15 p2280 A72-31383

Converging or diverging high intensity charged particle beams arbitrary profile shaping, obtaining solution via Laplace equation through reduction to Cauchy problem

17 p2589 A72-34961

Short- and long-range terrestrial telecommunication using energetic collimated beams of muons

17 p2519 A72-35837

Formation of intense charged particle beams in a current-carrying plasma.

21 p3092 A72-40834

PARTICLE CHARGING

Frictional electrification from supersonic particle impact, determining particle charge and concentration, body intercepting area and velocity variations with speed

02 p0261 A72-12555

Powder concentration effects on corona particle charging efficiency of aerosols for electrogasdynamic generators

06 p0760 A72-18335

PARTICLE CLOUDS

U CLOUDS

PARTICLE COLLISIONS

Ordinary electromagnetic waves propagating in plasma, calculating thermal and particle collisional corrections with moment approach

01 p0107 A72-10140

Reactive and nonreactive channels full particle scattering amplitudes using coupled integral equations

02 p0262 A72-11910

Frictional electrification from supersonic particle impact, determining particle charge and concentration, body intercepting area and velocity variations with speed

02 p0261 A72-12555

Collision integral for classical electron plasma, concerning Born-Bogoliubov-Green-Kirkwood-Yvon equations for long range interaction potential and motions of multiple particles

03 p0399 A72-14069

Collisional radiative recombination applicability to time dependent electron density decay in helium afterglow before reaching quasi-steady state

04 p0555 A72-14579

Vibrationally inelastic scattering of CO cations by Ar collision, measuring ion energy, mass and angular distribution with high resolution ion beam apparatus

05 p0693 A72-17169

Single collision beam experiments, swarms, Townsend current and capture processes in negative ions

05 p0693 A72-17219

Cosmic ray hadrons inelastic collision cross sections and partial K-neutral pion inelasticity factor in ionization calorimeter

06 p0868 A72-17262

Multiple production processes hydrodynamic-type models validated by high energy particle collision collective interactions

06 p0869 A72-17265

Coupled equations for collision amplitudes in three body system involving particle redistribution

06 p0851 A72-17391

Hydrogen atom emission spectrum calculation in uniform rotating electric field, applying to charged particles collisions and Stark broadening of plasma H lines

10 p1514 A72-24039

Linear analysis of gravitational perturbations in strongly collisional initially homogeneous and Maxwellian medium

10 p1536 A72-24138

Electron-neutral collisions effects on wavelength and damping of electrostatic waves propagation in Ar and He plasmas

10 p1525 A72-25143

Numerical solution of two massive rigid bodies impact with variable slipping direction using Routh momentum change theorem

11 p1735 A72-25769

Collisional distributions in mirror plasmas, using successive approximation technique for Fokker-Planck equation lowest eigenvalue and eigenmode

11 p1694 A72-25792

Charged particle thermodynamics in ionosphere, considering energy exchange due to collisions or thermal conductivity

11 p1621 A72-25837

Interstellar anomalous 6 centimeter formaldehyde absorption in diffuse dark nebulae, discussing quantum mechanics of collisional pumping process

11 p1720 A72-26112

Electron temperature determination from rate of ionization due to collisions between electrons and neutral particles in plasma

11 p1697 A72-26586

Galactic disk systems relaxation time due to particle encounters, discussing validity of Boltzmann-Vlasov equation

12 p1872 A72-27894

Relaxation processes enhancement by collective particle collisions effects in plasma, stressing application to stellar dynamics

12 p1853 A72-27915

Disturbed ionospheric electron and ion kinetics, detailing dissociative recombination as regulating process for temporal evolution

14 p2102 A72-30654

Cross section determination of proton production in collisions of electrons and hydrogen ions

14 p2134 A72-30801

High momentum transfer collisions importance for anisotropic part of distribution function in Lorentz and single component plasmas

14 p2134 A72-30802

Mass spectrometric techniques for collision processes in decaying nitrogen-helium and nitrogen-neon plasmas, obtaining ambipolar diffusion coefficients and reaction rate constants

15 p2283 A72-31299

Collisions role in nonlinear mode coupling and harmonic generation associated with electromagnetic wave in plasma, describing plasma electron distribution function by kinetic equation

15 p2195 A72-31679

Sound velocity and ultrasonic attenuation in anharmonic metal for collision dominated regime

15 p2277 A72-31889

Anisothermal magnetoplasma with non-Maxwellian particle distribution function, calculating electrical conductivity collisional factor from convergent classical kinetic equation

15 p2287 A72-32410

Multispecies magnetoplasma as electrical conductivity tensor collisional factor from quantum mechanical convergent kinetic equation

15 p2287 A72-32411

Ionization energy loss of relativistic heavy nuclei for close collisions as function of charge, computing Born approximation corrections via Mott exact cross section

15 p2282 A72-32647

Stable mirror plasma machine, determining particle distribution near loss cone by asymptotic analysis based on transit to mean collision times ratio

16 p2432 A72-32808

Charged particle energy dissipation in cold collisional plasma, discussing collisions effect on power spectrum

16 p2436 A72-33651

Rotating plasma-neutral gas collision interaction studies, determining particle energy and velocity in partially ionized plasmas

16 p2438 A72-33916

Particle scattering due to Rosenbluth-Post convective plasma loss-cone instability distribution function

17 p2587 A72-34189

Rotational excitation of rigid rotor in argon-nitrogen system, measuring energy transfer moments by particle-body and perturbation technique

17 p2585 A72-34740

A review of the unified theory of relaxations in plasmas.

17 p2590 A72-35159

Soft collision plasma scattering function, conductivity and particle energy loss from simplified Fokker-Planck collision model

17 p2592 A72-35621

Growth rate and frequency dispersion characteristics of drift waves in an RF collisional plasma.

18 p2716 A72-36924

A technique for position sensing and improved momentum evaluation of microparticle impacts in space.

19 p2795 A72-37518

Metastable atomic oxygen deactivation in upper atmosphere by inelastic collisions and by spontaneous irradiation, noting airglow intensity dependence on red lines irradiation

19 p2792 A72-38633

Particle charging behind shock waves in suspensions.

20 p2914 A72-39627

Collision periodic orbits calculation in restricted three body problem

20 p2973 A72-39885

Possibilities of determining complex form factors from experiments with polarized particles

21 p3086 A72-40100

A comparison of some particle-in-cell plasma simulation methods.

21 p3089 A72-40105

Determination of the characteristics of the averaged motion of the carrier medium in turbulent gas flow with suspended particles

21 p3044 A72-40126

Transition probabilities and collision-induced transitions in excited levels of neon.

21 p3061 A72-40136

Lateral deviation of radio waves reflected from ionosphere.

21 p3022 A72-41321

Book - Excitation in heavy particle collisions.

21 p3088 A72-41525

Particle collisions integral in Boltzmann equation for arbitrary distribution function, with particular attention to two dimensional flows

22 p3205 A72-42266

Long wave oscillations attenuation by charged particle collisions in one- and two-component hot and cold Boltzmann plasma, using kinetic and polarization vector equations

23 p3318 A72-43325

Characteristics and constants of motion method for collisional kinetic equations.

24 p3426 A72-44984

PARTICLE COUNTERS

U RADIATION COUNTERS

PARTICLE DECAY

U RADIOACTIVE DECAY

PARTICLE DENSITY [CONCENTRATION]

NT ELECTRON DENSITY [CONCENTRATION]

NT ELECTRON DENSITY PROFILES

NT ELECTRON DISTRIBUTION

NT ION DENSITY [CONCENTRATION]

NT IONOSPHERIC ELECTRON DENSITY

NT IONOSPHERIC ION DENSITY

NT MAGNETOSPHERIC ELECTRON DENSITY

NT MAGNETOSPHERIC ION DENSITY

NT MAGNETOSPHERIC PROTON DENSITY

NT PLASMA DENSITY

NT PROTON DENSITY [CONCENTRATION]

Concentration distribution in turbulent flow as function of velocity field, deriving differential equations from characteristic functionals to describe diffusion process

01 p0049 A72-10190

Mesospheric OH volume density profile measurements by rocket-borne high resolution polarized Ebert-Fastie spectrometer

01 p0062 A72-10912

Solid particle influence on underexpanded gas jet shock structures, using schlieren photographs

03 p0342 A72-13840

Self consistent kinetic equations for evolution of particle distribution functions and wave intensity spectra of relativistic spatially homogeneous multispecies plasma in ambient magnetic field

04 p0553 A72-14401

Vertical extensive air showers at aircraft heights, constructing integral spectrum based on particle number

06 p0870 A72-17280

Numerical determination of particle number and mass flux density in monatomic rarefied gas flow through circular orifice at finite pressure ratio

07 p0972 A72-20107

Extraterrestrial magnetic spheroid concentrations observed in October 1967 and 1969 proposing relationship to rainfall frequency

08 p1226 A72-21109

Solar wind tangential discontinuities and shock waves determination from flux velocity vector, magnetic field and particle density measurements

08 p1227 A72-21154

Solar wind properties and discontinuity characteristics, describing particle densities, wind speed, magnetic field level and near earth electron and ion temperatures

09 p1377 A72-22756

Gas discharge plasma detection characteristics, examining electron and ion densities and collision rates dependence on electromagnetic field frequency and amplitude

09 p1361 A72-22956

Target jet density variations effect on vacuum in neutral atom beam ionization region of fast neutral particle magnetic trap

09 p1363 A72-23223

Equations of state for ultrahigh densities, obtaining relativistic statistical thermodynamics description of hadronic interactions

10 p1533 A72-23891

Deionization mechanism of expanding plasma cloud produced by arc burning in vacuum, discussing charged particle concentration and ion thermal velocity

10 p1521 A72-24356

Real time measurements of ground level and airborne particle concentrations and diffusion in 10-100 km range

11 p1681 A72-26081

Nonideal dense plasma properties, discussing electrostatic shielding, many particle clusters, phase transitions, metallization and electrical conductivity [AIAA PAPER 72-414]

11 p1695 A72-26164

Neutral gas velocity distribution, transverse drift velocity, particle and energy densities in column under free fall conditions, considering wastage by ionization processes

11 p1698 A72-26645

Thermospheric ion, electron and neutral particle concentration, composition and temperature changes during 7 March 1970 solar eclipse from rocket measurements

12 p1778 A72-27152

Nature and requirements of electrostatic inertial plasma confinement, deriving potential and particle densities as function of radius, grid voltage and current

12 p1850 A72-27281

Number density, particle, momentum and energy fluxes in model ion-exosphere with open magnetic field and asymmetric Maxwellian velocity distribution

13 p1948 A72-29115

Homogeneous plasma column generation by HF generator, probing for electron temperature and charged particle concentration

13 p2015 A72-29507

Positively and negatively charged plasma components thermodynamic density fluctuations effect on ionospheric and magnetospheric slowly varying electric fields measurement

13 p1953 A72-29810

Three layer atmospheric model for neutral gas motion-produced ionosphere and magnetosphere currents, electromagnetic field and charged particle concentration perturbations

14 p2100 A72-30632

Turbulence effects on electron, ion, aerosol, water vapor and ozone concentration in atmospheric layers

15 p2222 A72-31395

Atmospheric desorbed water molecules and ions number density vertical distribution in lower ionosphere and thermosphere

15 p2225 A72-31913

Anisothermal magnetoplasma with non-Maxwellian particle distribution function, calculating electrical conductivity collisional factor from convergent classical kinetic equation

15 p2287 A72-32410

Giant hygroscopic atmospheric dust particle concentration variations measured with light scattering monitor, noting frontal passage dependence on prefrontal concentration

16 p2386 A72-33604

Deionization mechanism of expanding plasma cloud produced by arc burning in vacuum, discussing charged particle concentration and ion thermal velocity

17 p2589 A72-34955

Statistical mechanics of magneto-active plasma.

17 p2590 A72-35144

Effect of a distributed sand roughness on the spectrum of wall pressure pulsations in a turbulent flow in a tube

17 p2541 A72-35542

Gas discharge plasma detection characteristics, examining electron and ion densities and collision rates dependence on electromagnetic field frequency and amplitude

17 p2593 A72-35885

Method for calibration and verification of automatic liquidborne particle counter/light method. [SAE ARP 1192]

18 p2692 A72-36533

Complex index of refraction of airborne fly ash determined by laser radar and collection of particles at 13 km.

18 p2661 A72-36637

Ignition moment of solid propellant particles monodisperse aggregate uniformly distributed in gaseous oxidizer

19 p2879 A72-37359

Solar wind tangential discontinuities and shock waves determination from flux velocity vector, magnetic field and particle density measurements

20 p2964 A72-39259

The muon flux of cosmic rays at sea level.

20 p2964 A72-39349

Meteoroid bodies particle density from basal photographs, noting dependence on orbital parameters

20 p2969 A72-39395

Angular distribution of interstellar atomic hydrogen.

23 p3315 A72-38334

Investigation of the angular distribution of particles on the basis of Cosmos-219 satellite data

23 p3343 A72-44174

Determination of the physical properties of atmospheric aerosol particles above the Atlantic

24 p3420 A72-44757

Steady-state distribution of the charged and neutral particle concentration in a bounded high-temperature turbulent plasma

24 p3429 A72-45493

PARTICLE DETECTORS

U RADIATION COUNTERS

PARTICLE DIFFUSION

NT ELECTRON DIFFUSION

NT IONIC DIFFUSION

Metal powders sintering activation mechanism, considering heterogeneous metals particles diffusion flow, mutual solubility and crystal lattices distortion

02 p0232 A72-11432

Astronomical model for solar cosmic ray bursts propagation including anisotropic particle diffusion along interplanetary magnetic field

03 p0407 A72-12944

- High temperature creep activation energies relationship to diffusion in TiC, ZrC and UC
03 p0371 A72-13461
- Turbulent particle diffusion statistical mechanical model, using random walk
03 p0344 A72-14331
- Trapped particles induced by fluctuating magnetospheric electric and magnetic fields, calculating radial diffusion and energy distribution and time variations
04 p0566 A72-14723
- Diffusion and fallout of polluting particulates emitted by aircraft engines, discussing effect of wing-tip vortices, plume visibility and monitoring, simulation and modeling
[ASME PAPER 71-WA/AV-2] 05 p0704 A72-15950
- Brownian particle sedimentation rate and diffusion coefficient determination by holographic double exposure interferometry
06 p0816 A72-17982
- Diffusion models of energetic solar particles in interplanetary medium, considering impulsive emission from solar flares
07 p1061 A72-20023
- Magnetospheric trapped particle diffusion coefficients and acceleration in earth radiation belts
07 p1062 A72-20035
- Upper atmosphere minor component distribution rearrangement, investigating transition time to diffusion equilibrium
08 p1155 A72-20803
- Solar cosmic ray diffusion in interplanetary medium, describing solar flare proton and heavy nuclei propagation in terms of time of arrival measurements
08 p1227 A72-21157
- One dimensional atmospheric turbulent diffusion model and semiempirical equation, considering jumplike changes in particle velocity
08 p1201 A72-21999
- Nonlinear initial boundary value problem for time dependent convection-diffusion equation with ionization and recombination reactions
09 p1341 A72-22472
- Approximate expression for charge exchange spreading of proton beam precipitating into atmosphere, showing dependence on atmospheric structure, collision data and primary particle energy
09 p1377 A72-22591
- Real time measurements of ground level and airborne particle concentrations and diffusion in 10-100 km range
11 p1681 A72-26081
- Recombination diffusion length of minority carriers in thin layer cuprous sulfide solar cells
12 p1856 A72-28011
- Combined photon and particle diffusion of two level system with ground and excited atomic states and photon emission-formed radiation field
13 p2001 A72-28509
- Cosmic ray diffusion in radial divergent flow of magnetic discontinuities in interplanetary plasma, discussing isotropy in presence of regular magnetic field
13 p2029 A72-28591
- Galactic cosmic ray anisotropy due to radial and diffusive streaming in direction of interplanetary magnetic field, using neutron monitor data
13 p1033 A72-29747
- Transverse particle diffusion across external homogeneous magnetic field under random isotropic large scale hydromagnetic turbulence
14 p2102 A72-30650
- Oxide inclusions induced reductions in Nabarro-Herring creep and sintering rates of metals, discussing effect of inclusions diffusional mobility in metal matrix
15 p2257 A72-32112
- Microscopic theory of weakly ionized plasma conductivity, showing particle diffusion function or transition probability description by linear Boltzmann equation
15 p2287 A72-32412
- Quantum mechanics variational methods reformulation for turbulent diffusion of marked particles
16 p2379 A72-33570
- Diffusion propagation and source distribution effects on cosmic ray charge composition and anisotropy in galactic disk, considering nuclear fragmentation
16 p2448 A72-33742
- Spatial diffusion dynamics, spin, and the Pauli equation
17 p2573 A72-34193
- Geomagnetically trapped alpha particles. I - Off-equator particles in the outer zone.
17 p2548 A72-35595
- Influence of carrier diffusion on the intrinsic response time of semiconductor avalanches.
18 p2717 A72-36083
- Propagation of an impurity in a laminar flow in a circular tube
18 p2682 A72-36892
- Motion and diffusion of energetic particles in the outer zone.
20 p2916 A72-39231
- Solar cosmic ray diffusion in interplanetary medium, describing solar flare proton and heavy nuclei propagation in terms of time of arrival measurements
20 p2964 A72-39262
- Determination of the duration of the diffusional motion of charges in a plasma with allowance for bulk ionization
22 p3213 A72-43116
- Parasitic pitch angle diffusion of radiation belt particles by ion cyclotron waves.
23 p3333 A72-44527
- High temperature creep activation energies relationship to diffusion in TiC, ZrC and UC
24 p3413 A72-44936
- Cosmic ray diffusion in radial divergent flow of magnetic discontinuities in interplanetary plasma, discussing isotropy in presence of regular magnetic field
24 p3435 A72-45091
- Steady-state distribution of the charged and neutral particle concentration in a bounded high-temperature turbulent plasma
24 p3429 A72-45493
- Wave growth in a strongly turbulent plasma.
24 p3430 A72-45568
- PARTICLE EMISSION**
NT ELECTRON EMISSION
NT FIELD EMISSION
NT ION EMISSION
NT NEUTRON EMISSION
NT PHOTOELECTRIC EMISSION
NT SECONDARY EMISSION
NT THERMIONIC EMISSION
- Smoke plume opacity or particulate content measurement by laser backscatter, using Q switched ruby and Nd lidars
[AIAA PAPER 71-1087] 01 p0058 A72-10544
- Spectral and polarization characteristics of type 4 bursts with respect to energetic particle emission and solar-terrestrial phenomena
03 p0407 A72-12938
- Neutrino emission process effects on solar C-N-O cycle energy generation and C 12/C 13 abundance ratio
04 p0567 A72-14911
- Azur satellite for investigating polar regions, inner radiation belt and solar particle emission
05 p0715 A72-16135
- Fast electron gun with subnanosecond switching times and 100 mA peak beam current for delayed coincidence studies of atomic decays
13 p1933 A72-29761
- Measurements of radon emanation from Apollo 11, 12, and 14 fines.
18 p2728 A72-36970
- Variation of evolved blue/red ratio for supergiants as function of stellar mass, discussing status of astrophysical test for neutrino emission
19 p2854 A72-37235
- PARTICLE ENERGY**
NT ELECTRON ENERGY
NT ELECTRON STATES
NT PROTON ENERGY
- Cosmic ray energetic spectrum variation from observed latitudinal effects during 1954-1962 solar activity cycle
01 p0119 A72-10607
- Parallel electric field evidence near auroral ionosphere deduced from low energy particles, energy spectra and angular distribution
01 p0061 A72-10895
- High energy nucleon tissue doses calculation based on averaged characteristics of nuclear interactions
[CERN-71-16] 02 p0162 A72-12067
- Depth-dose experiments with monodirectional 14 MeV neutrons in low scatter environment, describing test facility
[CERN-71-16] 02 p0162 A72-12068
- Induction heated low density supersonic free plasma jet diagnosis, determining velocities and heavy particle temperatures
02 p0265 A72-12361
- Electrostatic analyzer for very low energy particles, calculating trajectories
03 p0392 A72-14055
- Solar effects contradictory relationships with earth atmosphere, discussing geomagnetic disturbance, annual variations, stratospheric transport and high energy particles
05 p0656 A72-16233
- Polar cap absorption event, investigating solar high energy protons precipitation effects
05 p0709 A72-16239
- Energetic solar flare particles release from sun, describing satellite observations of solar electromagnetic radiation
05 p0710 A72-16522
- Correlation energy calculation for system of fermions by means of variational method
05 p0702 A72-16785
- Energetic charged particles penetration into magnetosphere by auroral simulation experiments with artificial solar wind, observing magnetic field microfluctuations behind collisionless shock front
06 p0805 A72-17469
- Boltzmann integrals for inelastic collisions and radiative processes in stationary monatomic plasma, using Grad 8-moment approximation of particles momentum distribution functions
06 p0861 A72-18174
- Electron photon cascade energy measurement by photometering blackened spots on X ray films
07 p0988 A72-19870
- Ionization loss effects on cosmic ray lifetime in galactic interstellar medium, noting dependence on particle energy
07 p1064 A72-20637
- Quarter thickness variation and particle temperature dependence on height and frequency in summer daytime F region
08 p1155 A72-20815
- Emission energy of positrons thermalized in moderators and coated with Au, suggesting Au negative work function existence
08 p1217 A72-21339
- Particle detector assembly for low energy heavy mass cosmic ray nuclei identification
08 p1167 A72-21508
- High energy cosmic ray hadrons energy measurement using glass scintillator ionization spectrometer
09 p1309 A72-22523
- Solar atmosphere low energy positron production by solar particle fluxes demodulated according to cosmic ray transport equations
09 p1378 A72-23022
- Target jet density variations effect on vacuum in neutral atom beam ionization region of fast neutral particle magnetic trap
09 p1363 A72-23223
- Scaling of energy spectrum of particles emitted in high energy nucleon-nucleon collisions
10 p1529 A72-24527
- Neutron flux and energy spectra from crossed field acceleration model of plasma focus and z-pinch discharges
11 p1693 A72-25565
- Elastic, inelastic and reactive scattering experiments with low, high and intermediate energy molecular beams
11 p1691 A72-25675
- Fast charged particle flux measurement in inner radiation belt by Cosmos 137 satellite in January-February 1967
11 p1713 A72-25947
- Craters produced by high speed hardened spherical particles, investigating depth and diameter relationship to impact speed
11 p1738 A72-26919
- Number density, particle, momentum and energy fluxes in model ion-exosphere with open magnetic field and asymmetric Maxwellian velocity distribution
13 p1948 A72-29115
- Time evolution of chromosphere layer heated by energetic particle stream during solar flare, noting cooling by Lyman continuum radiation transfer
13 p2032 A72-29721
- Energetic particle flux observation at very low altitudes near geomagnetic equator, noting narrow distribution around 90-deg pitch angle
13 p2034 A72-30122
- Microscopic processes within high energy ion acceleration in laser-produced plasmas, discussing transient electric field role
14 p2136 A72-30178
- Nonlinear interaction between oscillations produced by monoenergetic particles beam passing through plasma
14 p2136 A72-30306
- Maximum ion energy dependence on radiation density in laser plasma
14 p2137 A72-30315
- Magnetospheric geometry derivation from ISIS-1 observations of soft particles penetration into polar cap and auroral regions, discussing entry and energization mechanisms
15 p2227 A72-31953
- Stellar winds and breezes classification using energy flux and particles kinetic and thermal energies for criteria, noting coronal temperature effects
15 p2313 A72-32298
- The geometric factor of a cylindrical plate electrostatic analyzer.
17 p2553 A72-34639
- An improved measurement of the charge ratio of cosmic ray muons in the range 10-300 GeV/c.
17 p2599 A72-34920
- Investigation of energetic charged particles and VLF emissions on the 'Interkosmos-3' satellite
17 p2600 A72-35209
- Evidence for solar particle production above approximately 75 GeV.
17 p2600 A72-35365
- Black hole rotational energy extraction by super-radiant scattering with impinging wave amplification and by floating particle orbits with zero net radiation reaction
19 p2857 A72-37720

Effect of optical constants on the energy distribution in homogeneous particles illuminated by a parallel beam of light

19 p2812 A72-38216

On the acceleration time of particles in the solar atmosphere.

19 p2852 A72-38634

Coordinate system for use with high-latitude energetic-particle phenomena.

19 p2853 A72-38729

Properties of low energy particle impacts in the polar domain in the dawn and dayside hours.

20 p2964 A72-39541

Composition of cosmic-ray nuclei at high energies.

20 p2965 A72-39716

Change of solar flare proton to alpha ratios during an energetic storm particle event.

21 p3101 A72-41297

Experimental determination of some optical characteristics of a double magnetic prism-electrostatic mirror system

22 p3180 A72-42937

Nonlinear interaction between oscillations produced by monoenergetic particles beam passing through plasma

23 p3317 A72-43208

Maximum ion energy dependence on radiation density in laser plasma

23 p3318 A72-43218

High energy inelastic interactions in cosmic ray showers from Wilson chamber and ionization calorimeter observations, noting secondary particles occurrence dependence on primary energy

23 p3330 A72-44406

EAS Cerenkov glow and the relation of shower strength to the primary-particle energy

23 p3330 A72-44419

Low-energy nucleons in extensive air showers

23 p3331 A72-44424

Energy spectra and angular distributions of cosmic ray muons with an energy of 2 to 10 TeV

23 p3331 A72-44428

Angular distribution of high-energy cosmic-ray muons

23 p3331 A72-44434

Energy measurement of primary particles from shower formation in solids, discussing ultrasonic waves generation in metal plates and electromagnetic waves excitation in ferrites

23 p3291 A72-44437

Coherent cross section effects on primary particle energy in inelastic proton interaction with carbon nuclei at 20-600 GeV

23 p3332 A72-44439

Relationship between the energies of charged and neutral particles generated in the energy region above 100 GeV

23 p3332 A72-44447

Influence of the polarization of incident radiation on the distribution of the energy absorbed in a particle

24 p3424 A72-44621

Degenerate electron gas self energy approximation by dielectric function, calculating quasi-particle and plasmaron properties

24 p3428 A72-44797

PARTICLE FLUX

U FLUX (RATE)

PARTICLE FLUX DENSITY

NT ELECTRON FLUX DENSITY

NT NEUTRON FLUX DENSITY

NT PROTON FLUX DENSITY

Longitudinal variations of inner radiation belt particle flux density at low altitudes from Proton 2 satellite data

01 p0119 A72-10604

Rocket-borne measurement of particle fluxes and currents in auroral arc, determining pitch-angle distribution of electron and proton energies

01 p0120 A72-10897

Polar cap region solar particle fluxes from Esro 1/Aurorae satellite recordings, noting north-south asymmetry

03 p0348 A72-13506

Lunar ejecta and meteorites experiment, determining speed, direction, mass and flux density of cosmic dust particles

04 p0509 A72-15102

Cascade nozzle gas particle flow properties, discussing flow pressure experiments and theory at different streamlines

05 p0602 A72-16490

Inelasticity factor dependence on particle energy spectra to explain nucleon flux calculations and Proton satellite data, considering scattering cross sections

06 p0869 A72-17264

Muon densities in penetrating high energy particles, comparing with extensive atmospheric showers

06 p0871 A72-17289

Light generator aided autonomous calibration of Cerenkov spectrometer for continuous primary cosmic nuclear flux measurements

06 p0815 A72-17832

Scintillation crystal light yield dependence on emission energy in particle flux measurements with semiconductor spectrometer

06 p0816 A72-17835

Cosmic ray nuclei intensity and energy spectrum measurement in nuclear emulsions stack, noting no charge dependence in solar modulation process

07 p1059 A72-19582

Multichannel modular spectrometer with electrostatic analyzers for low energy electron and proton flux measurement

07 p0988 A72-19954

Spectrometers with electrostatic analyzers alternating with shielding and suppressing gratings for low energy electron flux measurement

07 p0988 A72-19955

Plasma sheet distribution in magnetosphere from low energy particle observations in equatorial region of magnetotail

07 p0977 A72-20031

Pulsar production rate relationship to high energy cosmic ray origin and number density

07 p1081 A72-20059

Geomagnetically trapped protons, electrons and alpha particles verification and measurements in inner and outer radiation belts

07 p1062 A72-20227

Primary cosmic rays alpha particles and protons energy spectra similarity and intensity difference at .05 to 1.6 TeV, using Proton satellites data

07 p1064 A72-20631

Meteorological effects on cosmic rays, deriving muon and pion intensity and meteorological coefficient formulas and computer calculation scheme

07 p1066 A72-20654

Probabilistic integral multiplicity of generation of primary cosmic ray particles from count rate and primary spectrum relationship, using definition for neutron component calculations

07 p1067 A72-20656

Primary cosmic ray high energy gamma quanta flux measurements on Cosmos 208 satellite-borne instruments

08 p1225 A72-20798

Visual aurora and Explorer 40 satellite simultaneous observations of VLF radio noise, noting hiss associated with light emissions and associated charged particle flux

[AD-740047]

09 p1299 A72-23006

Energetic particle flux measurement on spacecraft based on statistics of overflowing register counting Poisson process

09 p1312 A72-23261

Fast auroral hydromagnetic wave occurrence relation to substorm activity, suggesting role of enhanced particle population in magnetospheric region

10 p1476 A72-24962

Fast charged particle flux measurement in inner radiation belt by Cosmos 137 satellite in January-February 1967

11 p1713 A72-25947

Heavy ions from interplanetary dust, estimating contribution to solar wind flux

11 p1713 A72-26393

Simultaneous Esro satellites observation of spatial and temporal particle flux variations over polar caps

11 p1714 A72-26418

Solar wind distortion of stellar anisotropy of galactic cosmic rays, associating annual particle density variation with earth revolution about sun

13 p2029 A72-28590

Energetic particle flux observation at very low altitudes near geomagnetic equator, noting narrow distribution around 90-deg pitch angle

13 p2034 A72-30122

Midlatitude VLF emissions intensity relationship to dayside auroral particle precipitation flux

15 p2194 A72-31437

Micrometeorite flux observed by rocket-borne electroacoustic transducers

15 p2308 A72-31931

Correlated particle flux, magnetic field, electron intensity and riometer absorption measurements during recovery phase of polar magnetic substorm on 6 March 1970

15 p2226 A72-31946

Micrometeorite and cosmic dust flux rates for near earth orbit and interplanetary space from satellite and ground based measurements

15 p2309 A72-31955

Lunar rock abrasion and catastrophic rupture lifetimes for near earth micrometeoroid flux determination, using hypervelocity impact tests

15 p2309 A72-31956

Satellite Prospero onboard micrometeoroid detector data analysis for near earth flux

15 p2310 A72-31987

Lunar surface microerosion relationship to interplanetary dust particle flux distributions, investigating sputter erosion and lunar rocks lifetimes

15 p2310 A72-31988

Interplanetary particles intensity relationship with solar activity based on Heos A1 observations during 1969-1971

15 p2300 A72-31992

Stable mirror plasma machine, determining particle distribution near loss cone by asymptotic analysis based on transit to mean collision times ratio

16 p2432 A72-32808

Exobase atomic hydrogen densities for zero ballistic net flux as function of temperature distribution, noting support of McAfee hypothesis by OGO-4 polar UV observations

16 p2384 A72-32979

Interstellar absorption of Crab Nebula soft X ray from Aerobee rocket photographic scan, estimating average volume densities for H, O, Ne, Si and Mg

16 p2445 A72-33129

Cosmic ray isotopic data extraction via geomagnetic field, discussing magnetic effects on particle flux and finite resolution limitations of counters

16 p2447 A72-33721

HEAO experiment proposal for Be to Sn flux and energy spectra and Be to Fe isotopic composition of galactic primary cosmic rays

16 p2447 A72-33733

Particle and energy fluxes across magnetic field in axisymmetric toroidal magnetic traps and plasmas with weak collisions, calculating radial electric field

16 p2440 A72-34153

The solar wind H and He/+/- content.

17 p2598 A72-34627

The absolute vertical cosmic-ray muon intensity at sea level.

17 p2600 A72-35147

Entry of high-energy solar protons into the distant geomagnetic tail.

17 p2601 A72-35588

Velocity and flux dependence of the solar-wind helium abundance.

17 p2602 A72-35607

A method of calculating the pitch angle distributions of particle fluxes based on rocket and satellite data.

17 p2558 A72-35840

Possibility of estimating an energetic particle stream in the ionospheric D region at sunrise and under daytime conditions

18 p2688 A72-36858

Zenith angle dependence of the meteorological corrections coefficients for cosmic ray component.

19 p2852 A72-38632

Diurnal variation of the H+ flux between the ionosphere and the plasmasphere.

19 p2793 A72-38759

Observations of the radial gradient of galactic cosmic radiation over a solar cycle.

20 p2964 A72-39333

High latitude particle precipitation and source regions in the magnetosphere.

20 p2964 A72-39542

Particle flux measurements from rockets during a solar cosmic-ray flare in April, 1969

22 p3218 A72-42226

Association between interplanetary shock waves and delayed solar particle events.

23 p3332 A72-44503

Annual variation of the interplanetary He+ velocity distribution at 1 AU.

23 p3332 A72-44505

Energy and mass content of high-speed solar-wind streams.

23 p3332 A72-44508

Nature of the long-term and short-term modulations of cosmic-ray intensity.

23 p3332 A72-44521

Behavior of outer radiation zone and a new model of magnetospheric substorm.

24 p3396 A72-44850

Solar wind distortion of stellar anisotropy of galactic cosmic rays, associating annual particle density variation with earth revolution about sun

24 p3435 A72-45090

PARTICLE IN CELL TECHNIQUE

Numerical solutions to gas dynamic problems with large deformations by particle in cell method

06 p0800 A72-18102

A comparison of some particle-in-cell plasma simulation methods.

21 p3089 A72-40105

PARTICLE INTENSITY

Cosmic ray muon intensity in interplanetary magnetic field, revealing sidereal variation due to motion of solar system relative to local galactic rotation frame

06 p0873 A72-17648

Galactic cosmic ray particle intensity decrease relationship to low energy proton flux increase based on interplanetary Zond 3 and Venera probes measurements

07 p1063 A72-20626

Converging or diverging high intensity charged particle beams arbitrary profile shaping, obtaining solution via Laplace equation through reduction to Cauchy problem

10 p1521 A72-24362

Penning ion source for multiply charged ions high intensity beams generation, describing axial type design with electron focusing magnetic coil

10 p1516 A72-25030

Sea level absolute vertical cosmic ray muon intensity from range spectrometer measurements within tropic zone 12 p1864 A72-28225

Converging or diverging high intensity charged particle beams arbitrary profile shaping, obtaining solution via Laplace equation through reduction to Cauchy problem 17 p2589 A72-34961

Liquid scintillation counters application in search for relativistic quarks in cosmic rays, setting upper confidence limits on particle intensity 17 p2601 A72-35471

Geometric factor of a cosmic ray detector - Equivalence of alternative analytical derivations. 22 p3178 A72-42647

PARTICLE INTERACTIONS

NT ELECTRON CAPTURE

NT ELEMENTARY PARTICLE INTERACTIONS

NT ION ATOM INTERACTIONS

NT MOLECULAR COLLISIONS

NT MOLECULAR INTERACTIONS

NT NUCLEAR INTERACTIONS

NT SPIN-ORBIT INTERACTIONS

Electron beam interaction with electromagnetic waves in longitudinal interaction devices during focusing by homogeneous magnetic and periodic electrostatic fields 02 p0189 A72-11564

Auroral current generation by ionization and space charge transport interaction between charged particles and atmospheres 02 p0273 A72-11928

Macroscopic geometry and velocity spaces of plasma collective modes involving long range force interaction between particles 02 p0267 A72-12841

Fast particle interaction with intergalactic matter, discussing relaxation of power law cosmic ray spectra 04 p0570 A72-14553

Transport coefficients of relativistic gas by method of moments, assuming constant differential cross section of particle interactions in center of mass system 04 p0547 A72-14630

Large amplitude whistler mode wave packet multiple emissions model including wave-particle interactions 04 p0517 A72-14948

Ground state energy of interacting electrons for entire density range from two-point Pade approximation 04 p0549 A72-15229

Book on auroras, discussing primary particle-atmosphere interactions, H line emission, geometry, intensity, height and atmospheric temperature determination from auroral spectra 04 p0519 A72-15356

Second virial coefficient, temperature derivatives and additive components for $12/7$ potential of charged particle interaction in gas 05 p0692 A72-15841

Cosmic ray particle high energy inelastic interactions, discussing pion and nucleon interaction angular and energy characteristics and muon production mechanism 06 p0869 A72-17270

Nuclear photoemulsions under bombardment by pion beam of 60 GeV/c momentum, investigating pion-nucleon interactions involving recoil protons 06 p0851 A72-17273

Pion-nucleon high energy interactions, determining inelasticity coefficient distribution 06 p0851 A72-17274

Solid thermal motion influence on atom colliding with solid surface linear semiinfinite atomic chain, presenting accommodation coefficient calculation method 06 p0853 A72-18140

Magnetospheric plasma sources, discussing wave-particle interactions and acceleration mechanisms 06 p0810 A72-18281

Cs and Hg vapors compressibility factor in supercritical range as function of density, considering charged particles and atoms polarization interactions in ionized metal vapors 07 p1040 A72-18943

Semiautomatic stereophotographic processing of cosmic ray shower particle interaction data from Wilson chamber 07 p0988 A72-19865

Extensive atmospheric showers and high energy transfer from interacting nucleons to electron photon cascades 07 p1060 A72-19867

Electron beam welding induced secondary X rays observation with pinhole X ray movie camera to determine beam-metal interactions during penetration 07 p0997 A72-20003

Quasi-linear theory of magnetosphere gyroresonant wave-particle interactions, discussing particle distribution function anisotropy, wave packet effects, whistler mode, energy and pitch angle distributions, etc 07 p0978 A72-20034

Neutrino interactions in lepton era of universe and hot big bang cosmology according to proton-neutrino coupling theory 07 p1084 A72-20538

Auroral charged particle fluxes electrodynamic interaction with atmosphere, determining ion formation rate and electron concentration and conductivity 08 p1155 A72-20804

Ferroelectrics with strong hydrogen bonds, deriving self consistent optical phonon frequency and coupled proton-phonon vibration spectrum 09 p1366 A72-22221

High energy particle and ionizing radiation effects on glasses in aerospace environment 09 p1336 A72-22402

Interaction forces between monovalent metal crystals determined from electrons quantified energy variations 10 p1525 A72-24136

Incompressible fluid jet propagation beyond charged particle source exit section, investigating electrohydrodynamic interaction parameter 10 p1522 A72-24549

Random walk models replacing Fokker-Planck equation for many particle systems with Coulomb interactions 10 p1513 A72-25041

Particle-proton total cross section from cosmic ray data on proton-air inelastic cross sections 11 p1712 A72-25884

Natural oscillations of magnetosphere and trapped radiation transport by electromagnetic pulses as possible mechanism for disturbances from thermonuclear explosion reaction on particles in natural radiation belt 11 p1712 A72-25935

Nonlinear interactions between synthesized plasma positive and negative ion beams, discussing effect on individual velocity distribution functions 12 p1849 A72-27058

Time structure of massive interacting particles with energies above 20 GeV near axes of cosmic ray showers of energy above 100 TeV 12 p1864 A72-27737

Computer simulation of plasmas by following actual orbits of particles interacting through electrostatic forces 12 p1852 A72-27914

Direct particle theory of weak interactions, considering two component spinors and leptonic decay 13 p2007 A72-28500

Ordering in fcc lattice ternary alloys with allowance for atoms interactions, noting phase transformation critical temperature and superlattices existence 13 p1976 A72-28691

Auroral current generation by ionization and space charge transport interaction between charged particles and atmosphere 13 p2030 A72-29240

Electron beam-helicons interaction in semiconductor plasma, determining instabilities onset conditions for unbounded system 14 p2141 A72-30172

Relativistic plasma particle correlation function based on transverse electromagnetic field energy density treatment by enlarged Bogoliubov hypothesis 14 p2140 A72-30881

Bound states and Coulomb interaction of continuum particles effects on thermodynamic properties of cesium plasma calculated on computer for different pressures and temperatures 15 p2283 A72-31259

Second virial coefficient, temperature derivatives and additive components for $12/7$ potential of charged particle interaction in gas 15 p2280 A72-31260

Review of symposium on D region, upper polar ionosphere, magnetosphere and wave-particle interactions 15 p2229 A72-32251

Electromagnetic field-two level atoms coherent interactions, using semiclassical approximation 15 p2250 A72-32305

Underground delayed shower particles small pulse events interaction analysis for muons and pions compared with quark behavior 16 p2450 A72-34140

Particle excitation processes in solar corona, ionosphere and astrophysics, discussing electron affinities, ion-molecule reactions, forbidden atomic transitions and Fe II problem 16 p2432 A72-34150

Master equations for finite systems. 17 p2576 A72-35153

Superposition principle in test particle method for reducing plasma cloud kinetic theory to determination of conditional probability function involving Vlasov equation 17 p2591 A72-35163

VLF wave propagation and its interaction with the magnetoplasma. 17 p2516 A72-35357

On the magnon interaction in haematite. I - Magnon energy of optical mode. 17 p2595 A72-35358

Whistler side-band growth due to nonlinear wave-particle interaction. 17 p2517 A72-35601

Radiant interchange among suspended particles and its effect on thermal relaxation in gas-particle mixtures. 17 p2638 A72-35643

[DFVLR-SONDDR-210] Approximate calculation of the magnitude of the momentum during the passage of a material particle past an elongated homogeneous biaxial ellipsoid 17 p2618 A72-35812

Accretionary processes in the early solar system - An experimental approach. 17 p2618 A72-35836

Geomagnetic activity and the solar situation in the neighbourhood of proton effects. 18 p2686 A72-36227

Weak decay, branching ratio and decay probability of strongly interacting particle event observed by Niu in cosmic nuclear jet shower 19 p2853 A72-38808

Weinberg model application to hot universe of weakly interacting particles at nonzero temperature, noting long range character 21 p3084 A72-40726

Interactions between stars and local dust formations 21 p3113 A72-41758

Energy degradation calculation for electron interaction with carbon dioxide molecules, discussing relationship with Mariner UV data 22 p3171 A72-42421

The threshold of disintegration of nuclei in a degenerate electron-neutron gas 22 p3209 A72-42963

Ionization calorimeter for neutral pion production investigation in high energy hadrons interaction, noting energy transfer identity for nucleon and pion interactions 23 p3330 A72-44409

Recording high-energy particle interactions by the method of the controlled emulsion stack of large volume 23 p3291 A72-44438

The concepts of mean force, mean velocity, and ensemble velocity for a particle ensemble 24 p3425 A72-45070

Nonlinear interactions between synthesized plasma positive and negative ion beams, discussing effect on individual velocity distribution functions 24 p3431 A72-45711

PARTICLE MASS

NT ELECTRON MASS

Particle mass monitor system based on piezoelectric microbalance combined with electrostatic precipitator collector, considering applications to air quality monitoring, laboratory aerosol research, process control, etc [AIAA PAPER 71-1100] 01 p0067 A72-10548

Lunar ejecta and meteorites experiment, determining speed, direction, mass and flux density of cosmic dust particles 04 p0509 A72-15102

Mass-zero spin-two particle field theory of gravitational interaction with covariance under full conformal group 09 p1355 A72-22684

Reduced mass and asymmetry differences effects on elastic collision integrals and thermal diffusion factors for isotopic hydrogen molecules 10 p1515 A72-24340

Cosmological models with astrophysical and geophysical properties by introducing particles mass field and dimensionless coupling constant in conformally invariant gravitational theory 10 p1541 A72-24475

Finite rest masses of wave quanta in material media, discussing dispersion and Einstein formulas equivalence, Doppler effect, gravitational red shift and radio photon trajectories 10 p1512 A72-24790

Time structure of massive interacting particles with energies above 20 GeV near axes of cosmic ray showers of energy above 100 TeV 12 p1864 A72-27737

Finite particle propagator constructed by path integral method, deriving infinitesimal propagator in relativistic quantum mechanics from mass nature consideration in Machian cosmological sense 13 p2001 A72-28499

Proton accretion effect on circumstellar dust grains mass, noting impossibility of grain formation in H II region 13 p2048 A72-29790

Poincare noninvariance of Stigma equation as alternative to Dirac equation for spin one-half finite mass particles 15 p2780 A72-31519

Isotropic, space-like, Maxwellian particles of real mass and of time-like velocity 18 p2710 A72-36472

Finite range gravitation theory extension to generally covariant massive two-tensor field gravitation theory containing eight dynamically independent degrees of freedom 20 p2953 A72-39342

Longitudinal electric waves absorption in interstellar space due to electron-heavy particle collisions, considering photon rest mass

20 p2969 A72-39348

An upper limit on the neutrino rest mass.

21 p3088 A72-40830

PARTICLE MOTION

Drift shells and pitch angle evolution of energetic particle motion in magnetospheric model including convection electric field

01 p0117 A72-10077

Hot magnetoplasmas cyclotron radiation, investigating thermal particle motion effects

01 p0107 A72-10142

Optimal control of material point motion in thin spherical layer of central gravitational field, solving by approximation

01 p0127 A72-10355

Optimal flight of material point in central field of forces subject to controlled small thrust

01 p0127 A72-10356

Collisionless motion of solar wind ions in helical magnetic field, giving transfer function of charged particles

01 p0118 A72-10360

Plasma electron and proton motion in equatorial plane of magnetosphere under geomagnetic disturbance generated electric field

01 p0058 A72-10586

Euler and Lagrange methods of calculation for agglomeration of particles due to velocity drop disparities among particles in Laval nozzles

02 p0149 A72-11593

Geomagnetic PDP pulsations oscillation frequency drift, considering proton motion characteristics in magnetospheric equatorial plane

02 p0217 A72-11931

Charged particle motion in strong magnetic field, considering magnetic moment and longitudinal adiabatic invariants

02 p0268 A72-12843

Particle motion in uniform acceleration field via Schwarzschild line element of general relativity, applying to clock paradox

03 p0388 A72-13227

Adiabatic charged particle orbits in magnetic null sheet with transverse electric and added normal magnetic fields

03 p0348 A72-13512

Collision integral for classical electron plasma, concerning Born-Bogoliubov-Green-Kirkwood-Yvon equations for long range interaction potential and motions of multiple particles

03 p0399 A72-14069

Relativistic equations of motion of charged particle interacting with plane electromagnetic wave propagating at arbitrary angle to uniform magnetic field for magnetosphere model

04 p0554 A72-14406

Conditionally periodic motions of particle in gravitational field of axisymmetric oblate planet, describing canonical transformations for Hamiltonian function reduction to normal form

04 p0572 A72-14638

Cauchy-Poisson problem of infinitely deep fluid wave motion resulting from initial particle velocities and horizontal equilibrium surface change

04 p0511 A72-14648

Nonrelativistic charged particle resonating with circularly polarized transverse electromagnetic wave in nonuniform magnetic field, showing Fresnel diffraction pattern-like motion

04 p0557 A72-14951

Hydrodynamic equations for non-Lagrangian statistical mechanical particle systems with three degrees of freedom under frictional and velocity dependent forces

04 p0512 A72-15202

Charged particle motion equations for fifth order spherical aberration of quadrupole-octupole lens with arbitrary electrode and pole shapes

05 p0638 A72-16989

Plasma heating and compression with nonadiabatic charged particle motion in uniform magnetic field

05 p0701 A72-17239

Potential around moving test particle in quiescent plasma, discussing energy loss, transport properties and gravitational analog

06 p0859 A72-17549

Longitudinal ambipolar acoustic instability effect on duration of plasma particle motion to wall across magnetic field, using phase method

06 p0860 A72-17693

Field-dynamic equilibrium of macroparticle motion in central field, comparing with Schroedinger equation

06 p0890 A72-18418

Optimization problems in gravitational attraction, considering homogeneous ellipsoids interaction and free particle simple harmonic motion

06 p0851 A72-18740

Convective heat transfer coefficient for particles of arbitrary shape in flow at low Reynolds number, using equivalent radius method

07 p1098 A72-18985

Trapped particle motion response to collapsing dipole moment in secularly varying geomagnetic field

07 p1058 A72-19158

Micron sized particle velocity relaxation measurement in shock wave, using laser Doppler methods [CLEA PAPER 11,3]

07 p1005 A72-19389

Equations of free particle motion, gas energy, distribution evolution and cosmic indeterminacy for Friedmann universe filled with uniform density and pressure ideal gas

07 p1074 A72-19429

Particle motions in earth magnetospheric tail and core, estimating maximum rate of magnetic field annihilation and magnetic drift shell

07 p1062 A72-20027

Book on models of particles and moving conducting media covering generator electrodynamics, electron tubes, particle accelerators, plasma and electron beam simulation, ion propulsion, etc

07 p1036 A72-20203

Distant stellar satellites existence possibility based on maximum distance estimation for material particle motion stability with respect to sun or another star

08 p1231 A72-21133

Particle motion in conformal spaces in general relativity, deriving gravitational potential and proper energy of mass point

08 p1209 A72-21369

Negative reabsorption coefficient for induced emission of neutron moving in medium in magnetic field

09 p1364 A72-23357

Topside ionosphere characteristics, discussing particle mean free path and geomagnetic field effects on conductivity, plasma anisotropies and latitudinal variations

10 p1473 A72-24704

Ionization movement of charged and neutral particles in F 2 region coupled to air movement by collision drag forces

11 p1621 A72-25839

Auroral plasma particle discharge during motion in strong inhomogeneous magnetic field, magnetospheric instability due to temperature anisotropy

11 p1715 A72-26904

Tracer particle motion behavior in laser anemometry for turbulent flow, comparing liquids with gases for accuracy

12 p1809 A72-27763

Theory of magnetotail elongation based on magnetosphere neutral layer drift motion due to electric current from trapped charge carriers inside surrounding plasma sheath

12 p1802 A72-27770

Russian book on geomagnetic field cosmic rays covering charged particle motion theory, extraionosphere currents, magnetosphere tail and solar wind effects, etc

12 p1864 A72-28345

Random number method for particle motion in homogeneous turbulence field, using Brownian motion Markov process for turbulence approximation

13 p1940 A72-28421

Finite particle propagator constructed by path integral method, deriving infinitesimal propagator in relativistic quantum mechanics from mass nature consideration in Machian cosmological sense

13 p2001 A72-28499

Geomagnetic PDP pulsations oscillation frequency drift, considering proton motion characteristics in magnetospheric equatorial plane

13 p1949 A72-29243

Relativistic analysis for synchrotron gravitational radiation emitted by particle in circular orbit around Schwarzschild black hole, noting astrophysical implications

13 p2007 A72-30123

Meteorite particle movement in earth atmosphere, discussing deceleration dependence on velocity, atmospheric density and surface evaporation reactive forces

14 p2152 A72-30493

Earth capture of dust particles moving in ecliptic plane heliocentric orbits, using three gravitational bodies analysis

14 p2153 A72-30494

Auroral electron spectrum space-time dynamics during magnetospheric substorms, using X ray bremsstrahlung balloon data

14 p2101 A72-30637

Geomagnetic field multipoles effects on radiation belt particle motion for analysis of true anomalies

15 p2222 A72-31280

Relaxation oscillations in dynamic systems describing turbulence in fluid, rigid body and particle motions

15 p2263 A72-31755

Dynamic particle field in-line holographic recordings using IR film and p-n junction GaAs lasers

15 p2237 A72-32056

Secular and long term periodic perturbation effects of third body upon particle motion in three body problem, discussing mass motion in Jovian gravitational field

15 p2312 A72-32120

Nonequilibrium relativistic plasma fluctuations with direct movement of particles, considering isotropic velocity distribution of particles

15 p2289 A72-32695

Lorentz-covariant procedure for equations of structure and motion of particles represented by singularities in Einstein relativistic field theory

16 p2422 A72-32880

Spherical particle accelerated motion in stationary viscous fluid, using numerical integration technique for velocity and displacement computations

16 p2375 A72-32907

Plasma motion relation to magnetic field line motion for imperfect electroconductivity, noting comparison with total particle drift distance

16 p2439 A72-33933

Dispersive motions in the ionosphere.

17 p2546 A72-34696

Transverse diffusion and conductivity coefficients for a three-dimensional magnetized equilibrium plasma.

17 p2592 A72-35379

Lunar local surface magnetic fields production mechanism, considering convection currents due to ionization of volcanic-ash-particle flow by electrodynamics model

17 p2614 A72-35586

Approximate calculation of the magnitude of the momentum during the passage of a material particle past an elongated homogeneous biaxial ellipsoid

17 p2618 A72-35812

Auroral zone splitting into various radiation intensity regions, discussing DR currents influence on particle motion in magnetosphere and structural relationship

17 p2550 A72-35856

Capture zone in noninteracting particles rarefied flow around magnetic dipole with transfer into finite orbits under small perturbations

17 p2593 A72-35906

Particle motion behind oblique shock wave in two phase supersonic wedge flow, deriving expressions for particle trajectories and velocity equalization time

17 p2487 A72-35926

On motions with a history of constant deformation

18 p2680 A72-36463

Measurement of aerosol motion and wind velocity in the lower troposphere by Doppler optical radar.

18 p2706 A72-36639

Anomalous motion of radiating particles in strong fields.

18 p2713 A72-36715

Pulses of gravitational radiation of a particle falling radially into a Schwarzschild black hole.

18 p2711 A72-36714

Meteorite particle motion in earth atmosphere, discussing deceleration dependence on velocity, atmospheric density and surface evaporation reactive forces

19 p2864 A72-38322

Earth capture of dust particles moving in ecliptic plane heliocentric orbits, using three gravitational bodies analysis

19 p2864 A72-38323

Radiation of charged particle moving uniformly in a nonstationary magnetoactive plasma

19 p2843 A72-38570

Motion and diffusion of energetic particles in the outer zone.

20 p2916 A72-39231

High energy particle and photon orbital and vortical motions in Kerr metric outside equatorial plane in gravitational field

20 p2953 A72-39341

Heuristic description for harmonic oscillator as quantized model of anharmonicity applied to excitation fields involving particle clusters and multibody configuration

20 p2953 A72-39398

Nonlinear theory of particle motion in monochromatic Alfvén wave field application to Pc-1 geomagnetic pulsations evolution

20 p2917 A72-39408

Motion of particles injected from the surface into stagnation-point flow.

20 p2913 A72-39611

Note on the symmetries of certain material tensors for a particle in Stokes flow.

21 p3044 A72-40113

Improved criteria for hyperbolic-elliptic motion in the general three-body problem.

21 p3109 A72-41333

Charged particle uniform motion in sinusoidally space-time periodic medium, determining Cerenkov and transition radiation field spectrum from Brillouin diagram

21 p3088 A72-41378

Hamiltonian analysis of charged particle motion in the pulsar rotating magnetic field.

21 p3111 A72-41472

Reflector-analyzers for studies of rarefied low-energy plasmas

21 p3058 A72-41731

Radiation of an oscillator moving parallel with the interface of two media 21 p3036 A72-41843

Accuracy of the conservation of the third adiabatic invariant of charged-particle motion in axisymmetric fields. II 22 p3217 A72-42209

Radiation from a free electron interacting with a circularly polarized laser pulse. 23 p3296 A72-43875

Improved calculation of resonant frequencies of Helmholtz resonators. 23 p3315 A72-44372

S-system motion effect on angular distribution of secondary high energy particle cluster in showers formed by primary and neutral particles, considering nucleon collision line 23 p3331 A72-44436

PARTICLE PRODUCTION

NT PAIR PRODUCTION

Neutron production mechanism and energy spectrum in thermal plasma focus by time of flight spectrometry 01 p0109 A72-10243

Atmospheric primary and secondary cosmic ray propagation with close reference to two-fire-ball, H-quantum and excited baryon models of multiple meson production 01 p0121 A72-11122

Monte Carlo simulation on high energy cosmic ray propagation and multiplication in high altitude emulsion chamber observations, examining two-fire-ball and H-quantum models 01 p0121 A72-11123

Micrometer particle formation by water vapor photolysis at 1500-1700 Å, noting particle production rate and implications to planetary atmosphere physics 02 p0268 A72-12207

Atmospheric neutron production by cosmic rays, calculating Cd-In ratio 05 p0662 A72-16258

Ion charge composition in plasma-electron beam system in strong longitudinal magnetic field, noting multiply charged ions production under high temperature conditions 05 p0701 A72-17235

Multiple meson production in 250 GeV nucleon-nucleon collisions in LiH targets, noting 40 per cent formation of heavy meson cluster fireballs 06 p0868 A72-17259

Particle multiplicity and momentum spectra for high energy inelastic nuclear interactions in Wilson chamber with polyethylene target 06 p0868 A72-17261

Multiple production processes hydrodynamic-type models validated by high energy particle collision collective interactions 06 p0869 A72-17265

Particle creation by strong rapidly changing gravitational fields in gravitational collapse of heavy star and in initial singularity 07 p1068 A72-19000

Particle production and vacuum polarization, in anisotropic gravitational field, discussing energy momentum tensor values and collapse behavior 07 p1034 A72-19632

Mathematical model for superheavy cosmic ray production by spallation on interstellar hydrogen, assuming single source for particle injection with given charge spectrum 07 p1062 A72-20197

Solar protons propagation from instantaneous injection source and inhomogeneities interaction description by mean free path and scattering angle specification 07 p1063 A72-20627

Nucleon and electromagnetic component generation, energy spectrum and diffusion during solar flares 07 p1066 A72-20651

Computerized numerical calculation of muons production spectrum, angular distribution and Coulomb scattering in determining meteorological factors effects on cosmic rays 07 p1067 A72-20655

Probabilistic integral multiplicity of generation of primary cosmic ray particles from count rate and primary spectrum relationship, using definition for neutron component calculations 07 p1067 A72-20656

Radio absorption in lower ionosphere obtained from vertical distribution of electron density and production rates from solar protons energy spectrum 08 p1226 A72-20816

Solar atmosphere low energy positron production by solar particle fluxes demodulated according to cosmic ray transport equations 09 p1378 A72-23022

Stellar evolution from precarbon-burning contraction to presupernova stage with and without neutrino production by electron neutrino interaction 10 p1545 A72-24825

Cosmic ray experiment jet shower event with possible new particle existence 11 p1712 A72-25867

X ray observation inconsistency with matter creation in steady state universe due to inner bremsstrahlung from neutron decay 11 p1713 A72-26125

Scaling hypothesis and limiting fragmentation mechanism for cosmic ray muon production, noting energy independent charge ratio 15 p2298 A72-31289

Resonant and semiweak process production cross sections for massive Lee-Wick spin-zero and spin-one bosons at high energies 15 p2280 A72-31290

Energetic electrons generation and relaxation in narrow belt near 2.8 L measured with Cosmos 137 Cerenkov counter 15 p2299 A72-31909

Metastable ²S/ atoms production by electron impact induced dissociative excitation of molecular deuterium, measuring total cross section via Lyman alpha flux 15 p2282 A72-32645

Meson exchange effects on solar pion-production process, using low energy Adler theorem with cross section correction factor 16 p2456 A72-33476

Li, Be and B nuclei production via nuclear spallation reactions generated by Galactic cosmic ray bombardment of interstellar gas 16 p2448 A72-33737

Test of scale invariance in pion production at high energies using cosmic ray primary nucleon and sea level muon intensities. 17 p2599 A72-34875

Evidence for solar particle production above approximately 75 GeV. 17 p2600 A72-35365

Magnetospheric convection induced longitudinal or Fermi acceleration role in nighttime auroral particle flux production mechanism 17 p2601 A72-35592

Neutron production in exploding-wire discharges. 21 p3089 A72-40338

Production of light elements in the solar system. 23 p3335 A72-43487

Multiplicity of particles generated in inelastic interactions of nucleons with LiH nuclei at energies from 150 to 550 GeV 23 p3329 A72-44405

Particle production in inelastic high energy interactions, noting correlation between particle pairs and groups 23 p3330 A72-44407

Multifireball theory of particle production in inelastic high energy interactions, using elastic scattering amplitude for inelastic processes model 23 p3316 A72-44412

General characteristics of proton-nucleon and coherent interactions at an energy of 67 GeV 23 p3317 A72-44415

A study of the mechanisms of formation of penetrating particle groups by the spark calorimeter method 23 p3291 A72-44430

Fluctuations of the spatial distribution of the number of particles in showers generated by muons in heavy material 23 p3331 A72-44431

Coherent cross section effects on primary particle energy in inelastic proton interaction with carbon nuclei at 20-600 GeV 23 p3332 A72-44439

Relationship between the energies of charged and neutral particles generated in the energy region above 100 GeV 23 p3332 A72-44447

Particle production and vacuum polarization in anisotropic gravitational field, discussing energy momentum tensor values and collapse behavior 24 p3424 A72-44564

PARTICLE SIZE DISTRIBUTION

Rain droplet size distribution effects on microwave attenuation at millimeter wavelengths, comparing calculation with measurement 01 p0027 A72-10406

Monostatic and bistatic lidar and solar radiometer sensing techniques for remote measuring of aerosol size distributions [AIAA PAPER 71-1057] 01 p0066 A72-10528

Radiative, segregation and evaporation processes of ice particles surrounding early type stars of Orion association, justifying ice particle model for dust grains 01 p0129 A72-10794

Martian surface nature from Surveyor and Apollo missions data on lunar particle size distribution 01 p0132 A72-11037

Visibility relationships to atmospheric liquid water content in fog derived from fog drop size distribution model 01 p0096 A72-11281

Atmospheric aerosols size/altitude distribution via sun aureole sky brightness and airborne particle counterpoint sampling measurements 02 p0213 A72-11860

Venus cloud reflected radiation flux and polarization by Monte Carlo technique, using models with different particle size distributions 02 p0280 A72-12193

Surface moisture effect on dielectric properties of ultrahigh barium titanate particulates of varying particle size [ACS PAPER 7-E-69F] 02 p0269 A72-12416

Mean free path and particle size distribution in dispersion hardened nickel-thoria alloys, obtaining interparticle spacing by Scheil method 02 p0245 A72-12549

Cobalt-rare earth single particles hysteresis loops interpretation, considering coercive force relationship to particle size [IEEE PAPER 22.1] 03 p0402 A72-13781

Sedimentology of Apollo 11 and 12 soils, investigating grain size distribution 03 p0440 A72-14325

Grain size and precipitate parameters effect on creep properties of Ni-Cr alloys 03 p0379 A72-14339

Luna 16 sampled lunar rock size distribution near craters in Sea of Rains from Lunokhod panoramic pictures 04 p0576 A72-15068

Polydisperse spray device with controllable drop size distribution for two phase detonation research 04 p0509 A72-15486

Impurity content, particle size and abrasion resistance role in abrasiveness of molybdenum disulfide 06 p0836 A72-18589

Molybdenum disulfide lubricating effectiveness improvement with finer particles at aggravated sliding conditions, suggesting surface roughness qualifications 06 p0837 A72-18605

Sputtered molybdenum disulfide lubrication on polished metal surfaces with low friction coefficient, strong adherence, high density and small particle size 06 p0824 A72-18607

IR radiation radiative transfer calculation for selected spectral intervals due to various model cloud droplet size distribution 07 p0980 A72-20456

Particle mass spatial distribution effect on particulate damping of combustion acoustic vibrations in solid rocket propellants 08 p1224 A72-21617

Burning rate dependence on oxidizer particle size of ammonium or potassium perchlorate mixtures with organic fuels 09 p1373 A72-23146

Environment and grain size effect on steady state creep and creep rupture properties of Ni-W solid solution 09 p1331 A72-23381

Aluminum nitride amount and particle size measurement at austenitic grain coarsening temperatures in low carbon steels 11 p1656 A72-25755

Metal powder mixing, examining friction effects and optimal particle sizes, shapes and amounts 11 p1642 A72-26828

Theoretical and measured rainfall attenuation of millimeter waves, correlating attenuation coefficients, rain rate and drop size distributions 12 p1785 A72-27803

Particle size distribution functions reconstruction from scattered radiation data, discussing accuracy and applicability of small angle, spectral transparency and complete indicatrix methods 13 p1955 A72-28514

Cloud statistics stratification by climatological regime, month and time of day, extending simulation to drop size distributions and liquid water content 13 p1989 A72-28808

Coastal and inland fog microphysical features, discussing visibility, liquid water content, drop size distributions and haze droplet concentrations 13 p1991 A72-28842

Catalytic effects on ammonium perchlorate combustion pressure limits, noting distribution, concentration and particle size effects 13 p2025 A72-29303

Ammonium perchlorate burning rate temperature dependence as function of pressure and oxidizer particles size, noting low pressure deflagration limit [ONERA, TP NO. 1079] 13 p2025 A72-29669

Optimum dispersion time and size particle determination for zirconium diboride powder grinding in vibrating mill, using gas flow ratio method 13 p1967 A72-30101

Approximate analytical solution for spherical particle acceleration in uniform gas flow, examining nozzle geometry and particle size effects 14 p2095 A72-30924

Nike-Apache rocket-borne particle collection and photometry of noctilucent clouds, obtaining single-shadowed particle size distributions and inflight shadowing surface data 15 p2226 A72-31923

Explorer 35 and OGO 3 data on picogram size dust particle distribution in cislunar and selenocentric

space, showing fluctuations during meteor shower periods

15 p2309 A72-31937

Zinc oxide effect on alumina dispersion, energy of formation, nucleation and particle size reduction, calculating critical nucleus radii

16 p2476 A72-33255

Hail size distribution and concentration in thunderstorm updraft regions from aircraft and S band radar observations

16 p2419 A72-33946

Development of moldable carbonaceous materials for ablative rocket nozzles.

17 p2572 A72-35668

Rock size, mineralogy and fines size distribution in lunar regolith

17 p2615 A72-35683

Analysis of grain- and particle-size distributions in metallic materials.

17 p2569 A72-35922

Laser IR radiation attenuation in natural and artificial fogs, noting dependence on particle size distribution

18 p2697 A72-36102

Geometric concepts for microstructure change processes dynamics, considering time variation determination of system topological and metrical properties and particle size distribution evolution

18 p2718 A72-36397

Method for calibration and verification of automatic liquidborne particle counter/light method/

[SAE ARP 1192] 18 p2692 A72-36533

Complex index of refraction of airborne fly ash determined by laser radar and collection of particles at 13 km.

18 p2661 A72-36637

Acceleration effects on burning velocity of aluminumized condensed rocket propellant systems, calculating particle size and slag mass

19 p2847 A72-37360

Error of the statistical method for determining the dependence of the combustion characteristics of particles upon particle size

19 p2879 A72-37363

Grain size distribution in recrystallized alpha-titanium.

19 p2820 A72-38297

A method for the study of wear particles in lubricating oil.

19 p2803 A72-38376

Fog and cloud microstructure and particle size distributions from directional light scattering coefficient /halo indicatrix/

20 p2948 A72-39570

Dust particle sizes in cometal atmospheres and the heliocentric distance

20 p2970 A72-39726

Approximate determination of the change in the aerosol distribution spectrum in a Venturi coagulator tube

20 p2928 A72-40039

Induction period, particle size distribution and medium temperature effects on thermal ignition of metal particles under exothermal oxidation reaction on surface

20 p2987 A72-40040

Device for measuring the kinetic characteristics of particle combustion

20 p2928 A72-40050

Propagation loss of centimeter and millimeter waves in rainfall.

21 p3023 A72-41833

Hail formation model based on injection of finite embryo size classes into horizontally homogeneous steady nondivergent updraft, considering growth and accumulation zones

22 p3201 A72-42514

IR reflectance [or emittance] remote spectroscopy of mineral particulate surfaces, discussing particle size, surface roughness, porosity and mixing ratios effects

22 p3178 A72-42526

Electro-optical design and performance parameters of polluted air liquid droplet size distribution measurement by pulsed junction diode laser light external scattering

22 p3179 A72-42680

Theoretical approach to the fracture of two-phase glass-crystal composites.

23 p3306 A72-43560

Stability of Al₃Mg₂ particles against diffusive coagulation in aluminum-magnesium alloys

23 p3301 A72-43649

Influence of the nature of the particle distribution of the hardening phase in powders on the thermal stability of dispersion-strengthened nickel

23 p3302 A72-44011

An experimental investigation of radiative properties of aluminum oxide particles.

24 p3461 A72-44809

Two-phase detonations with bimodal drop distributions.

24 p3463 A72-45052

Fraunhofer single beam holography application to gas/liquid mixture high velocity flow cross section determination, observing liquid component effects on droplet dispersion composition

24 p3405 A72-45624

PARTICLE SPIN

NT ELECTRON SPIN

NT ISOTOPIC SPIN

NT NUCLEAR SPIN

Mass-zero spin-two particle field theory of gravitational interaction with covariance under full conformal group

09 p1355 A72-22684

Resonant and semiwave process production cross sections for massive Lee-Wick spin-zero and spin-one bosons at high energies

15 p2280 A72-31290

PARTICLE TELESCOPES

Gathering power, geometrical factor and directional response of single and multielement particle telescopes

06 p0811 A72-17317

Semidiurnal lunar variation, solar and sidereal effects on cosmic radiation intensity, using zenith pointed particle telescopes

06 p0873 A72-17490

Muon telescopes calibration for cosmic rays rigid component variations by data comparison with variable aperture telescope

08 p1162 A72-20720

Electron scattering effects on response of cosmic ray particle telescopes from pulse height and counting rate measurements

08 p1167 A72-21510

Semidiurnal cosmic ray anisotropy, eliminating atmospheric effects and global isotropic variations in cosmic ray telescope

09 p1377 A72-22928

Satellite-borne semiconductor particle detector telescope for C and Mn isotopes identification in heavy primary cosmic rays, considering scintillation counter and mass resolutions

16 p2389 A72-32883

Nuclear composition telescope measurements on-board OGO 5 satellite, observing presence of geomagnetically trapped carbon, nitrogen and oxygen nuclei

16 p2382 A72-32959

Scintillation telescopes for muon angular distribution, designing test device for photomultiplier tubes selection

17 p2556 A72-35437

Muon telescopes calibration for cosmic rays hard component variations by data comparison with variable aperture standard telescope

19 p2803 A72-38348

Balloon-borne telescope search for solar neutrons and gamma rays during enhanced solar activity periods

21 p3101 A72-41298

PARTICLE THEORY

CP-noninvariance model of baryon interaction and charge asymmetry of universe, postulating kappa particle /neutral massive fermion/

06 p0875 A72-17275

French book on wave mechanics reinterpretation covering double solution theory, particle thermodynamics, guidance dynamics, etc

06 p0847 A72-17813

Elementary particle theory and field equations in cosmological spaces, using four dimensional conformal imbeddings

06 p0891 A72-18421

Ideal gas many particle distribution functions in microspace from solution of chain of integrodifferential equations

09 p1354 A72-22220

Thermodynamic quantities expression in terms of S matrix to formulate questions pertaining to statistical mechanics-particle physics boundary, applying to cosmology

09 p1355 A72-22750

Direct particle theory of weak interactions, considering two component spinors and leptonic decay

13 p2007 A72-28500

Improved calculation of resonant frequencies of Helmholtz resonators.

23 p3315 A72-44372

PARTICLE TRACKS

U PARTICLE TRAJECTORIES

PARTICLE TRAJECTORIES

NT ELECTRON TRAJECTORIES

Liquid and solid particle trajectory calculation in two phase Laval nozzle flows, determining density, velocity and temperature

02 p0149 A72-11588

Electrostatic analyzer for very low energy particles, calculating trajectories

03 p0392 A72-14055

High energy cosmic ray track angular azimuthal distribution in lunar silicate rocks

04 p0577 A72-15154

Fission origin of cosmic ray fossil tracks in augite achondrite high-uranium-concentration meteorite Angra dos Reis

05 p0714 A72-16078

Muon track curvatures in Wilson chamber magnetic field for calibrating ionization levels of logarithmic increase

06 p0811 A72-17293

Bubble chamber high energy particle tracks semiautomatic measuring device, using small on-line computer for data processing

06 p0813 A72-17438

Computerized simulation of high intensity beam charged particle trajectories in electromagnetic fields with rotational symmetry, applying to ion extraction

06 p0852 A72-17491

Cascade wind tunnel and water table determination for trajectories and velocities of suspended particles in fluid flow through axial compressor stage

07 p0907 A72-18756

Nonlinear dynamic system mathematical model for unit mass particle escape trajectories from potential well, taking account of trapped motions and stable oscillations

07 p1025 A72-18807

Wide gap spark chamber feeding technique for compensation of charged particle track drift due to avalanches

07 p0988 A72-19956

Solar protons propagation from instantaneous injection source and inhomogeneities interaction description by mean free path and scattering angle specification

07 p1063 A72-20627

Solar cosmic ray diffusion in interplanetary medium, describing solar flare proton and heavy nuclei propagation in terms of time of arrival measurements

08 p1227 A72-21157

Particle track densities in Lunik 16 soil column grains from Sea of Plenty, noting surface irradiation and regolith age

09 p1380 A72-22268

Fossil track densities and thermoluminescence measurements of Luna 16 feldspar crystal samples compared to Apollo 12 samples

09 p1381 A72-22270

Plasma turbulent diffusion effects on particle trajectories in phase space as Wiener process

09 p1358 A72-22294

Ion quadrupole effects in ion-molecule collisions, calculating capture cross sections and ion trajectories

09 p1354 A72-22658

Ion trajectories equations of motion solution for E x B type mass separator, presenting curves for mass species dispersion inside separator channel

10 p1509 A72-23944

Gas-particle flow trajectories, velocities and pressure distribution in axial flow turbine stage, using cascade tunnel and high speed photographic techniques

11 p1571 A72-25648

Toroidal plasmas heating by neutral injection, discussing ion acceleration, charge exchange and fast ion trajectories

11 p1697 A72-26585

Computer simulation of plasmas by following actual orbits of particles interacting through electrostatic forces

12 p1852 A72-27914

Monte Carlo method for radiative transport theory problems, considering mathematical models of light scattering media and photon trajectory random elements

13 p2001 A72-28505

DR ring current belt formation due to electron and proton gradient drift in inhomogeneous geomagnetic field, calculating charged particles trajectories

14 p2101 A72-30646

Comets formation from Jupiter satellite Io surface eruption using particle trajectory analysis and comet orbital elements calculation

15 p2305 A72-31391

Game problem of impulse controlled soft rendezvous of two material particles under attractive forces

16 p2422 A72-32928

Heavy cosmic ray nuclei tracks in etched plastic sheets flown in satellites and balloons, discussing detector response as function of velocity

16 p2447 A72-33730

Capture zone in noninteracting particles rarefied flow around magnetic dipole with transfer into finite orbits under small perturbations

17 p2593 A72-35906

Two new methods to increase the contrast of track-etch neutron radiographs.

19 p2833 A72-37636

Black hole rotational energy extraction by super-radiant scattering with impinging wave amplification and by floating particle orbits with zero net radiation reaction

19 p2857 A72-37720

Markovian plasma turbulence model to obtain convergent perturbation series for diffusion coefficient via trajectories in particle propagator

19 p2841 A72-38442

Solar cosmic ray diffusion in interplanetary medium, describing solar flare proton and heavy nuclei propagation in terms of time of arrival measurements

20 p2964 A72-39262

Solar wind noble gases and solar flare emitted Fe group nuclei energetic tracks in chondrite Weston, considering galactic cosmic ray generated tracks

22 p3228 A72-42863

Determination of characteristic magnitudes of toroidal electrostatic analyzers - Application to the optimization of analyzers used in space physics

22 p3180 A72-42935

Relativistic test particle escape from circular orbit around central mass due to mass loss, considering orbiting body corrections due to general relativity

23 p3335 A72-43265

East-west asymmetry of cosmic rays at the sea level in the range of geomagnetic latitudes from 50 N to 20 S

23 p3328 A72-43355

A study of the mechanisms of formation of penetrating particle groups by the spark calorimeter method

23 p3291 A72-44430

Electric field orientation, magnetic field strength and high voltage pulse delay effects on spark chamber track displacement from true particle trajectory

23 p3291 A72-44441

Electronic detection of ionizing-particle tracks in liquid argon

23 p3291 A72-44442

Meteor streams orbital elements dispersion from photographic data, and asteroid stream percentage variation with concentration of orbits to ecliptic plane

24 p3445 A72-45462

PARTICLES

NT AEROSOLS
NT ALPHA PARTICLES
NT ANIONS
NT ANTINEUTRONS
NT ANTIPARTICLES
NT ANTIPROTONS
NT ARGON PLASMA
NT ARTIFICIAL RADIATION BELTS
NT BETA PARTICLES
NT BOSONS
NT CATIONS
NT CESIUM PLASMA
NT CHARGED PARTICLES
NT COLD PLASMAS
NT COLLISIONLESS PLASMAS
NT CONDUCTION ELECTRONS
NT CORPUSCULAR RADIATION
NT COSMIC PLASMA
NT CYCLOTRON RADIATION
NT DEUTERIUM PLASMA
NT DEUTERONS
NT DROPS [LIQUIDS]
NT ELECTRON BEAMS
NT ELECTRON PLASMA
NT ELECTRON PRECIPITATION
NT ELECTRON RADIATION
NT ELECTRONS
NT ELEMENTARY PARTICLES
NT FAST NEUTRONS
NT FERMIONS
NT FERRIC IONS
NT FINES
NT FOG
NT FREE ELECTRONS
NT HADRONS
NT HELIUM PLASMA
NT HIGH ENERGY ELECTRONS
NT HOT ELECTRONS
NT HYDROGEN PLASMA
NT INNER RADIATION BELT
NT ION CYCLOTRON RADIATION
NT LEPTONS
NT LIGHT BEAMS
NT MAGNETICALLY TRAPPED PARTICLES
NT MANGANESE IONS
NT MESONS
NT METAL IONS
NT METAL PARTICLES
NT METALLIC PLASMAS
NT MICROPARTICLES
NT NEUTRAL PARTICLES
NT NEUTRINOS
NT NEUTRONS
NT NONEQUILIBRIUM PLASMAS
NT NONUNIFORM PLASMAS
NT NUCLEAR PARTICLES
NT NUCLEONS
NT OUTER RADIATION BELT
NT OXYGEN PLASMA
NT PHOTOELECTRONS
NT PHOTONS
NT PIONS
NT PLASMA CLOUDS
NT PLASMA JETS
NT PLASMA LAYERS
NT PLASMA SHEATHS
NT PLASMA SLABS
NT PLASMAS [PHYSICS]
NT POLLEN
NT POSITRONS
NT POWDER [PARTICLES]
NT POWDERED ALUMINUM
NT PRIMARY COSMIC RAYS
NT PROTON BELTS
NT PROTONS

NT QUARKS
NT RADIATION BELTS
NT RAINDROPS
NT RAREFIED PLASMAS
NT RECOIL PROTONS
NT RELATIVISTIC PARTICLES
NT RELATIVISTIC PLASMAS
NT ROTATING PLASMAS
NT SOLAR CORPUSCULAR RADIATION
NT SOLAR COSMIC RAYS
NT SOLAR PROTONS
NT SOLAR WIND
NT SOOT
NT STELLAR WINDS
NT TACHYONS
NT THERMAL NEUTRONS
NT THERMAL PLASMAS
NT TOROIDAL PLASMAS
NT TRAPPED PARTICLES

Thermal IR radiation attenuation by atmospheric particulates, comparing computer simulated brightness temperatures with airborne radiometer and Nimbus 3 observed data

02 p0213 A72-11863

Optical method for measuring the velocity of particles entrained in a flow

17 p2554 A72-34892

Determination of the characteristics of scattering particles in the Venusian atmosphere on the basis of photometric measurements

22 p3223 A72-42215

PARTICULATE FILTERS

U FLUID FILTERS

PARTICULATE SAMPLING

Atmospheric aerosols size/altitude distribution via sun aureole sky brightness and airborne particle counterpoint sampling measurements

02 p0213 A72-11860

Forecasting technique for accumulated particulate contamination on spacecraft assemblies, discussing cleanliness optimization and test procedures

07 p0915 A72-18763

Condensed zinc particle size determined by a time discrete sampling apparatus.

20 p2913 A72-39608

Gaseous and particulate iodine in the marine atmosphere.

22 p3173 A72-42469

Gaseous and particulate bromine in the marine atmosphere.

22 p3173 A72-42470

PARTITIONS [MATHEMATICS]

Automatic classification algorithms using heuristic, partitioning and variational techniques

09 p1283 A72-23429

Centered Gaussian process oscillations /Brownian motion/, obtaining divergence rate in sequence of finite partitions

10 p1504 A72-24054

Scalar and vector partitions of forecasts probability score in two state situation

11 p1681 A72-26078

Electronic partition functions cut-off criteria effect on translational and reactive thermal conductivity and viscosity of thermal plasmas

11 p1698 A72-26602

Diatom molecules partition functions derivation by classical and quantum mechanical theories for simple harmonic oscillator and square-well potential

15 p2280 A72-31693

Approximations and bifurcations in flight dynamic system, investigating singular point motion over trajectory during partition process

19 p2748 A72-37553

PARTITIONS [STRUCTURES]

Book on matrix structural analysis covering matrix algebra concepts, direct stiffness matrix methods, lifting surface, nonlinear truss and structural partitioning analysis, etc

07 p1092 A72-19908

PARTS

U COMPONENTS

PAS

Symphonic satellite stability during perigee, apogee and orbital transfer, considering propellant motion in tank and spinning top containing liquid

02 p0287 A72-12717

PASCHEN SERIES

Magnetic splitting of lines dependence on Paschen-Back effect for Li resonance doublet in sunspots

03 p0427 A72-13293

Planetary nebula IC 418 reddening constant from Paschen line intensities of IR spectrum

04 p0570 A72-14554

Paschen beta emission line equivalent width variation in IR spectra of omicron Ceti

11 p1716 A72-25679

PASSBANDS

U BANDPASS FILTERS

U BANDWIDTH

PASSENGER AIRCRAFT

NT ELECTRA AIRCRAFT
NT EUROPEAN AIRBUS

Passenger aircraft onboard automated inertial navigation devices, emphasizing accelerometer and gyroscope design and construction

01 p0096 A72-10070

VFW-614 short range twin jet passenger transport aircraft, analyzing service performance and economic efficiency requirements influence on design characteristics

03 p0310 A72-13643

Airbus A-300 B design and characteristics for passenger transport on short and medium haul routes

05 p0612 A72-16694

Optimal reversion coefficient determination for passenger aircraft engine thrust reversal

05 p0614 A72-17060

Future civil air transport trends, considering passenger and cargo growth, travel frequency per capita income and STOL market

08 p1257 A72-22150

Mathematical models for passenger aircraft market forecast, discussing stock measurement and life expectancies

13 p2067 A72-30125

Airbus design features, noting passenger number, operational range and propulsion engine number and location

14 p2072 A72-30813

Buoyancy systems and parawings application in short haul passenger transportation, discussing VTOL and STOL operations

16 p2348 A72-33183

The air bus as the aircraft of near future. II

17 p2492 A72-35439

The DHC-7, first generation transport category STOL - Particular design challenges.

[AIAA PAPER 72-809]

19 p2750 A72-38115

Instruments installation effect on soviet passenger aircraft pilot performance, discussing Tupolev aircraft control systems

21 p2994 A72-40173

Airlines requirements for European airbus, discussing design of aircraft structure, control, pressurized cabin and propulsion system

21 p2994 A72-40174

Minimum operational costs of passenger and cargo transport aircraft, considering effects of flight distance, wind conditions and optimum speed and altitude

23 p3252 A72-44338

Systems approach to airport passenger terminal planning.

24 p3387 A72-44585

PASSENGERS

Airport terminal flow and interface transportation systems, discussing access, passenger traffic and cargo handling and government controls

03 p0339 A72-13414

Prolonged jet flight effect on passenger interstitial and intracellular fluid volumes from plasma, extracellular and total body water measurements, noting dehydration and foot swelling

06 p0767 A72-17866

Crew members handling of emotionally disturbed aircraft passengers

07 p0926 A72-18836

Air/ground interface simulation in GPSS/360 for passenger transfer between airport terminal and aircraft

07 p1106 A72-20342

Passenger behavioral inaction in survivable aircraft accidents, suggesting maladaptive behavior counteraction by leadership and/or training

13 p1908 A72-28727

Hierarchical system of helicopter service terminals, calculating passenger lots for single and multiloop arrangements under given stochastic input conditions

15 p2337 A72-31498

Major civil airport passenger and cargo terminal complex design and layout planning, discussing various facilities and equipment requirements

16 p2373 A72-33329

Passenger transfer in airports with total separation between aircraft and permanent buildings for independent functioning, noting Dulles Airport mobile lounges

16 p2374 A72-34143

Airport terminal design - The passenger's point of view.

17 p2535 A72-34225

Kansas City International Airport facilities and features, discussing decentralized passenger processing system

17 p2535 A72-34242

STOL ride quality criteria - Passenger acceptance. [AIAA PAPER 72-790]

19 p2749 A72-38107

PASSIVATION

U PASSIVITY

PASSIVE SATELLITES

NT BEACON SATELLITES

NT PAGESO SATELLITE

Solar radiation pressure effects on balloon satellite behavior, noting orbital eccentricity variations

16 p2463 A72-34182

PASSIVITY

- Passivation velocity apparatus for testing Al-Mg alloy sensitivity to corrosion under voltage
02 p0246 A72-12599

PATCHING

U MAINTENANCE

PATHOGENESIS

- Pathogenesis of in-flight illusory acceleration sensations, discussing amino acid level, protein metabolism rate and pyridoxin metabolism
05 p0619 A72-16642
- Arterial hypoxemia development during hypoxic ontogenesis early stages related to age in dogs
09 p1266 A72-22879
- Electron microscope study of hyperoxia-induced pathogenetic ultrastructural changes in rat lung
12 p1761 A72-27531

PATHOGENS

- Aliphatic hydrocarbons in phytopathogenic fungi spores, discussing similarity to higher plant alkanes, functional roles and species distribution and occurrence
13 p1906 A72-29834

PATHOLOGICAL EFFECTS

- High energy proton irradiation late pathological effects on rabbit brains, discussing brain lesions and radiation dosages
02 p0161 A72-12056
- Aseptic bone necrosis pathology from radiographic studies in dogs with decompression sickness noting articular cartilage erosion and joint dysplasia and exostosis
06 p0764 A72-17876

- Cortical synthesis and information handling properties of evoked potential in human normal and pathological behavior
08 p1119 A72-21840

- Electrophysiological, neurophysiological, metabolic, vegetative, psychological, chemical and pathological aspects of sleep, noting disturbance and wakefulness mechanisms for various clinical disorders
09 p1264 A72-22223

- Pathological significance of high oxygen tension exposure effects on acid soluble collagen extracted from mouse skin
12 p1760 A72-27483

- Case report of pilot near-syncope episode with bradycardia due to hyperactive right carotid sinus reflex
12 p1771 A72-27487

- Physiological effects on anesthetized and conscious dogs during exposure at 80,000 ft for different decompression rates, discussing cardiovascular, biochemical and pathological effects
12 p1768 A72-28322

- Myocardial protein synthesis in acute myocardial hypoxia and ischemia.
17 p2501 A72-34980

- Pathologic-anatomic characterization of changes induced by magnetic fields in experimental animals
17 p2503 A72-35008

- Neuropathological evaluation of monkeys exposed to body-alone X-radiation.
18 p2649 A72-36439

- Reflex and conditional movement observation of central nervous system function restitution in Macaca mulatta monkeys with cortical lesions, studying pathological forced grasping
18 p2651 A72-36977

- Effect of hyperoxic media on the stability of rats during acute carbon monoxide exposure
21 p2998 A72-40437

- Adrenaline and noradrenaline metabolic stages and production mechanism under various physiological and pathological conditions, noting application to flight emotional stress detection
21 p3002 A72-41196

- Changes produced in the nerve structures of the stellate ganglion by total X-ray irradiation
22 p3140 A72-41925

- Influence of ionizing radiation on the tooth organ
22 p3141 A72-41987

- Chronic altitude sickness pathology based on anatomical and histological findings in abnormal mountain inhabitants autopsies, comparing with cardiovascular system morphology in normal people
22 p3143 A72-42586

- Heart function and pulmonary circulation in humans suffering from chronic mountain sickness
22 p3143 A72-42587

- Transarterial leakage - A possible mechanism of high altitude pulmonary oedema.
22 p3143 A72-42588

- Analysis of survival and cause of death statistics for mice under single and duration-of-life gamma irradiation.
23 p3254 A72-43394

- Adrenal morphology changes in rats subjected to hypokinesia
23 p3255 A72-43905

- Natural aging and radiation-induced life shortening in *Drosophila melanogaster*.
24 p3373 A72-45279

PATHOLOGY

NT HUMAN PATHOLOGY

- Clinical death period and reanimation concepts, noting erroneous interpretations of irreversible histological alterations, revival attempt period and organism self reanimation potential
09 p1266 A72-22876

PATTERN DISTRIBUTION

U DISTRIBUTION (PROPERTY)

PATTERN RECOGNITION

NT CHARACTER RECOGNITION

- Crop discrimination with manual and automatic computerized side-looking radar imagery analysis for microtexture pattern recognition
01 p0065 A72-10451

- Pattern recognition in biological and technical systems - Conference, Berlin, April 1970
01 p0017 A72-10463

- Mathematics for pattern recognition, discussing perceptrons, combinatorics and statistics, feature selection, cybernetic methods and fuzzy sets
01 p0034 A72-10465

- Neuron responses in cat visual system/retina, geniculate body, primary, secondary and tertiary visual cortex/ to simple visual stimulus pattern
01 p0011 A72-10466

- Psychology of visual form perception in relation to neurophysiological principles of lateral interaction and organization, considering retinal images, aftereffects, binocular vision, etc
01 p0011 A72-10469

- Feature classifying filter for pattern recognition system simulated on computer for line printed numerals
01 p0034 A72-10473

- Network synthesis of cascaded threshold logic elements to separate binary patterns into two classes by iterative computation of parameters
01 p0034 A72-10474

- Pattern recognition, invariance, redundancy and information reduction in computer aided image processing
01 p0034 A72-10475

- Pattern recognition by computerized local processing of binary matrix representations
01 p0018 A72-10476

- Object size erroneous perception by apparent distance alteration
01 p0012 A72-10478

- Neurophysiological hearing mechanisms of inner ear in peripheral auditory pattern recognition
01 p0012 A72-10481

- Neurophysiology of auditory pattern recognition of simple and complex sounds, using cats data on cochlear nerve neural mechanism
01 p0012 A72-10482

- Auditory pathway neuron discharge response to complex sound stimuli and frequency discrimination of pattern recognition in cats
01 p0012 A72-10483

- Two element matrix patterns generation with different degrees of internal constraint, developing objective complexity measures based on information theory or symmetry and grouping considerations
01 p0013 A72-10715

- Human pattern analysis by stabilized retinal image fragmentation as function of fade frequencies for angle and line stimuli in different orientations
01 p0014 A72-10721

- Pattern recognition computer programs for transforming and characterizing input scene through successive layers of recognition cone
01 p0046 A72-10867

- Operator interactive computer controlled electro-optical system for photographic image enhancement prior to target or pattern identification
01 p0070 A72-10869

- Southern corn leaf blight detectability by remote sensing based on pattern recognition technique application to multispectral color and IR photographic and scanner data
02 p0212 A72-11814

- Data compression and random noise effects on pattern recognition and picture quality of multispectral scanner data
02 p0227 A72-11840

- Multispectral scanner data preprocessing to improve automated recognition by reducing atmospheric and sensor induced signal variability
02 p0227 A72-11841

- Computerized statistical identification of aerial photograph ground patterns, comparing elliptical boundary condition with minimum distance to mean classification models
02 p0187 A72-11842

- Airborne sensors terrain classification, considering sample points clustering approach and signature analysis
02 p0227 A72-11844

- Pattern recognition of multispectral scanner remote sensor data, using table look-up approach for processing simplicity and time reduction
02 p0227 A72-11846

- Automatic soil type mapping, using multispectral remote sensing and computerized pattern recognition
02 p0215 A72-11881

- Urban geographic social-spatial pattern determination with aerial photographic interpretation
02 p0229 A72-12019

- Microelectronic computer system with image data cross correlation generation for real time video pattern abstraction, discussing design and operating characteristics
03 p0329 A72-14178

- Laser coherent monochromatic light for cybernetics research in pattern classification, discussing fingerprints and letters
04 p0531 A72-15137

- Edge-coding operators for two dimensional binary picture black-white boundary pattern recognition suitable for use in parallel processing systems
04 p0496 A72-15203

- Pattern recognition by automatic clustering methods without fixed definitions for number and specification of classes, using sequential diagnosis
05 p0632 A72-16075

- Hough transformation for detection of lines and curves in pictures, using angle radius instead of slope intercept parameters for efficient computation
05 p0664 A72-17164

- Human visual system multiple channels sensitivity to patterns at low luminance or high drift rates, noting retinal ganglion cells selective sensitivity
06 p0761 A72-17602

- Nonsupervised learning algorithm steady state behavior for multicategory pattern classification by analysis and digital computer simulations
06 p0780 A72-18256

- Recognition algorithms of moving objects for patterns alone and in symbolic and motion context, indicating possible recognition mechanism degradation
06 p0780 A72-18257

- Automatic recognition of aircraft by Fourier harmonics of slope densities of silhouettes
07 p0949 A72-19053

- Pattern recognition through atmospheric turbulence by reflected coherent light power spectrum recording technique, using Wiener-Khinchin theorem
07 p0982 A72-19054

- Light variation threshold amounts for flicker and flickering pattern detection as function of variation frequency
09 p1269 A72-22615

- Spatial filtering techniques and numerical classification methods for pattern recognition in automated photointerpretation
09 p1312 A72-23305

- Potential function criterion for feature selection in pattern recognition, obtaining upperbound estimate of misrecognition probability
09 p1342 A72-23419

- Probability density functions shape estimation by deterministic heuristic and entropy maximization algorithms
10 p1442 A72-23798

- Remotely sensed imagery data photointerpretation by gray tone texture context feature extraction, noting identification accuracy
10 p1442 A72-23812

- Feature selection from pattern recognition of Gaussian distributed classes by mapping of vector samples from n dimensional space to m dimensional space via transformation matrix
10 p1445 A72-24461

- Computerized image analysis, establishing desirable scene characteristics for biomedical display in automated system
11 p1602 A72-26388

- Image visual recognition during voluntary saccadic eye movements, noting stimuli visible luminance change effect
12 p1760 A72-27310

- Stochastic time varying patterns classification by Kalman filter, discussing optimum dichotomizer with supervised learning
12 p1790 A72-27498

- Signal mathematical model in optical and acoustic pattern recognition
12 p1786 A72-27571

- Pattern recognition in mental process automation, noting character transformations, written symbols content analysis and syntactic description
12 p1786 A72-27576

- Contrast enhancement for switch-on and -off modes of bar patterns, noting spatial transients due to primary image interaction with negative afterimage
12 p1808 A72-27679

- Heuristic recognition algorithms with learning for homogeneous irreducible stationary Markov chain sequence of recognized objects
12 p1837 A72-27824

- Detection probability for moving small targets embedded in random white noise on TV display, comparing machine processed pattern recognition techniques and human performances
12 p1843 A72-27933

- Optimal random search noise recognition systems with Bayes teaching technique
13 p1924 A72-29162

Image discretization accuracy in recognition system, considering two dimensional object reconstruction on element network

13 p1925 A72-29163

Two phase algorithm for selecting optimal sets of characteristics for image recognition systems

13 p1925 A72-29164

Indirect statistical quality control procedure for piece goods in batch based on image recognition technique for data classification

13 p1965 A72-29175

Human flexible processing accomplishment in speeded recognition task with visual stimulus dimension relevancy contingent upon other dimension stimuli values

13 p1911 A72-29832

Pattern recognition computer programs for input data preprocessing with characterization and transformation through layered recognition cone

17 p2520 A72-34405

Computer processed image enhancement applications to spacecraft returned photoreconnaissance, discussing data transmission and resolution vs recognition and color quality

17 p2520 A72-34408

Texture measurements in earth resources data management system by automatic photointerpretation with analog and digital techniques, discussing data processing rate requirements

17 p2520 A72-34409

Three dimensional model images information content increasing in coherent light interference shadow marking, noting automatic systems for distant objects recognition

17 p2529 A72-34844

Learning strategy-based pattern recognition system for automatic classification of terrain type from aerial photography

18 p2691 A72-36494

Perception of tachistoscopic binary patterns, examining reproduction accuracy with respect to pattern length and fixation and end-segregation reference points

18 p2653 A72-36914

Effect of set size, age, and mode of stimulus presentation on information-processing speed

18 p2654 A72-36922

Stochastic analogs of finite-converging learning algorithms for recognition systems

19 p2769 A72-37421

Optimal recurrent and nonrecurrent algorithms for polynomial dividing functions of learning and recognition in form of adaptive threshold elements

19 p2769 A72-38465

Signal recognizing algorithms for class of large number of normal distributions with unknown probabilities, using statistical complex hypothesis verification

19 p2770 A72-38466

Selection of characteristics for automatic classification of welding defects in radiographic testing

19 p2805 A72-38763

Probability threshold of data element similarity as separation criterion for automatic multiparameter biomedical data classification

20 p2893 A72-38937

Dynamic electromagnetic scattering pattern of flying object, constructing quasi-ergodicity condition to compute standard statistical descriptions for recognition

20 p2903 A72-39071

An electronic model of visual receptive fields

20 p2897 A72-39271

General principles and detail similarities in visual pattern analysis by single neuron operation, computer programs and psychological perception

20 p2891 A72-39275

Book - Fundamentals of pattern recognition

20 p2905 A72-39575

Perceptual differentiation of sequential visual patterns

21 p3008 A72-41021

Adaptive signal-discrimination system using signals for observation of the channel characteristics

21 p3023 A72-41838

A minimization method of describing classes in pattern recognition

22 p3198 A72-42178

Improved holographic matched filter systems for pattern recognition using a correlation method

22 p3177 A72-42445

Application of computer mathematics procedures for prediction of phase diagrams

22 p3191 A72-42812

Suitability of the normal density assumption for processing multispectral scanner data

22 p3157 A72-43025

Decision surface estimate of nonlinear system stability domain by Lie series method

23 p3274 A72-43540

Continuous ECG monitoring method /scattergram/ for arrhythmia pattern recognition in intensive care units

23 p3260 A72-43938

Atmospheric density from spacecraft drag data by successive optimization of control laws, using quadratic programming

23 p3277 A72-44003

PATTERN REGISTRATION

TV speckle pattern recording for coherent laser light measurement of mechanical vibrations in micrometer range

13 p1961 A72-30026

Reconstruction of phase holograms by means of a helium-cadmium laser

23 p3292 A72-44469

PATTERNS

Stabilized retinal image techniques to examine functional relationships between nonstabilized grating pattern orientation adaptation and stabilized line stimuli fading rates

16 p2358 A72-33646

PATTERSON MAP

Solution of the inverse heat conduction problem by using the regularization method to increase the peaks of the self-contraction function /Patterson's function/

19 p2880 A72-37753

PAVEMENTS

Airport apron surface pavement strain measurements under field loading conditions, considering static and dynamic loads with finite element method

01 p0047 A72-10192

Lime, cement, fly ash and sand combination airport pavement design and testing, discussing material structural and chemical properties, compressive strength, costs, etc

02 p0200 A72-12023

Concrete airport pavement thickness determination methods comparison, noting design life dependence on safety factors

18 p2675 A72-36786

Airfield flexible pavement design - A state of the art paper

18 p2675 A72-36787

Systems approach to integrated planning of airfield pavements design, construction, operation and maintenance, emphasizing need for mathematical models, constitutive parameters and limiting criteria

18 p2675 A72-36788

Airlines and aircraft manufacturers requirements for airport pavement evaluation/data system, discussing relationships between strength, landing gear design, aircraft weight, range, etc

18 p2675 A72-36789

PAYLOAD MASS RATIO

Algol 3 solid propellant rocket motor design for Scout D and E launch vehicles first stage, considering high total impulse, payload/mass capability and propellant grains

01 p0115 A72-10261

Nuclear gas core and fusion rocket engines performance potential for various space missions, comparing capabilities in terms of payload ratio

01 p0099 A72-11328

PAYLOADS

Composite materials application for space shuttle structures, relating structural weight to payloads

01 p0090 A72-10727

Space shuttle optimal boost trajectories, showing payload increase by flying pitch profiles optimization

02 p0286 A72-12423

Three-axis attitude control and stabilization system for sounding rocket payload, discussing performance from simulation and ground test results

05 p0728 A72-16478

Dynamic system optimal design with various degrees of maneuver parameters information, considering space flight mechanics problem of payload maximization for limited propulsive power

06 p0849 A72-18306

Space shuttle payloads and space manufacturing candidate materials and methods, discussing float-zone refined semiconductors, electronic crystals, viral insecticides, vaccines and biological cells

06 p0824 A72-18622

High performance sounding rockets design, discussing Skylark propulsion system improvement and new rocket vehicle design for 200 kg payload capability with existing motor hardware

08 p1241 A72-21172

Sounding rocket payloads environmental testing, discussing test techniques for shock, vibration, temperature, humidity, pressure, contamination, corrosion effects during handling, storage, launch, flight and recovery

08 p1241 A72-21173

Multimission capability of solar electric propulsion /SEP/ spacecraft, analyzing payload variations, propellant requirements, thrusting time limitations and throttling range

10 p1552 A72-25125

Spacecraft propulsion into orbit by ground based high-power lasers via thrust generation by material evaporation, emphasizing advantages in launching small payloads

13 p2025 A72-28454

Teleoperator manipulator for payload handling in space shuttle, noting design features and simulations of master-slave remote control system

[AIAA PAPER 72-238] 13 p1909 A72-29075

Equipment for ground and sea recovery of sounding rocket payloads, discussing airbrakes, buoy and parachute assemblies

15 p2319 A72-31690

Parachute systems and flotation gear used to recover sounding rocket payloads and components after water landings

15 p2320 A72-31691

Apollo 15 orbital science payload instruments for exploring lunar origin and evolution to relate to earth history

15 p2310 A72-31984

Space shuttle payload design for weight and cost reduction, discussing refurbishable modular design concept

15 p2321 A72-32317

Space shuttle program, discussing configurational concepts, payload carrying capacity variants and cost reduction design changes

17 p2621 A72-34869

Space shuttle configuration, discussing payload accommodation requirements, accessories, mission operations and reusable tug

[AIAA PAPER 72-737] 18 p2731 A72-36546

Constrained payload-optimum extremal ascent trajectories for space shuttle vehicles

[AIAA PAPER 72-829] 20 p2966 A72-39097

Stability of dual spin spacecraft containing tracking payloads

[AIAA PAPER 72-890] 20 p2975 A72-39111

RAM - A concept for reducing space payload costs

[SAWE PAPER 942] 23 p3343 A72-43482

Explorer satellites and Pioneer space probes development program, discussing launching rockets, reentry tests, payloads, radio communication, Van Allen belts discovery, etc

23 p3358 A72-44353

Operational support of space shuttle transportation and payload systems with modular checkout and test equipment, noting service life and economy of operations

24 p3388 A72-45111

Space shuttle design evolution for program cost minimization, discussing refurbishment, payload impact, management cost and mission specifications and objectives

24 p3450 A72-45171

Study of shuttle-based systems for high-energy planetary missions

24 p3441 A72-45189

The effect of space shuttle payload design techniques on total space program cost

24 p3451 A72-45210

The space tug optimum cost evaluation

24 p3468 A72-45212

The Symphonie transponder in the integration phase

24 p3380 A72-45273

PCM (MODULATION)

U PULSE CODE MODULATION

PCM TELEMETRY

Format logic design for airborne memory controlled PCM telemetry multiplex digital and analog data system

02 p0187 A72-12130

Frame synchronization performance tests for PCM telemetry system, considering code selection, frame length and data recovery

02 p0175 A72-12147

PCM/PM 136 MHz telemetry system of SAS-A satellite, describing operation in record and playback modes

03 p0326 A72-14396

Europa 2 launch vehicle standardized PCM/FM and FM/PM telemetry system compared with Europa 1

05 p0630 A72-16751

Telemetric frame synchronization with the aid of distributed and concentrated frame periods

21 p3024 A72-40329

Particle, plasma and field detectors for rocket investigations in and above atmosphere, considering PCM telemetry system and balloon-borne X ray telescope system

21 p3057 A72-41617

Frame synchronization in time-multiplexed PCM telemetry with variable frame length

23 p3265 A72-44182

PDM (MODULATION)

U PULSE DURATION MODULATION

PDP 8 COMPUTER

Logic character generator for CRT text display and DEC PDP 8/S graphics

11 p1601 A72-26290

PEARLITE

Hardenability and pearlite stee isothermal transformation properties of direct-quenching low Cr case-hardening steels, discussing Mn, Mo and Ni alloying effects on machinability

07 p0995 A72-19571

Austenite formation kinetics in Fe-C ferritic-pearlitic structure at 855 C, comparing experimental data with theoretical calculations

11 p1662 A72-26744

On a method of analysis of the strain energy changes taking place during the rotatory bending fatigue test of carbon steels and an effect of the pearlite patches to these changes.

20 p2935 A72-38881

PEARSON DISTRIBUTIONS

Statistical method of Pearson moments applied to temperature regimes effects on ruby laser output energy distribution

13 p1968 A72-29506

PECLET NUMBER

Forced heat convection from sphere immersed in inviscid fluid stream at small Peclet number, using matched asymptotic expansions

11 p1747 A72-26669

Galerkin boundary method as variational approach to low Peclet number heat transfer in laminar flow

13 p2063 A72-28418

Heat transfer to two dimensional laminar flow, calculating axial conduction and fluid preheating effects on adiabatic forced convection at low Peclet number

15 p2336 A72-32478

PEDALS

Foot forces exerted at various aircraft brake-pedal angles, observing 20 degree zone with maximum effectiveness

[AD-733551] 01 p0018 A72-10567

The foot as input device for control operation.

21 p3012 A72-41428

PEDOLOGY

U SOIL SCIENCE

PEENING

NT SHOT PEENING

PELTIER EFFECTS

Test apparatus and technique for assessing Peltier thermoelectric cooling device operational characteristics

12 p1755 A72-27721

Thermoelectric generators theory, design and performance characteristics, discussing Seebeck, Peltier and Thomson effects

15 p2182 A72-31375

Compound tellurides and their alloys for Peltier cooling - A review.

22 p3215 A72-43088

PELVIS

Hypergravity effects on bats spatial orientation, noting resistance to head-pelvis and pelvis-head accelerations

13 p1907 A72-30015

PENALTIES

Legal problems of aircraft hijacking, discussing jurisdiction, duty to prosecute, penalties, extradition, sanctions and international criminal tribunal

05 p0752 A72-15833

Hague convention on aircraft hijacking, discussing international extradition, prosecution and punishment

05 p0752 A72-15836

PENDULOUS GYROSCOPES

U GYROSCOPIC PENDULUMS

PENDULUMS

NT GYROSCOPIC PENDULUMS

Energy-phase time transformations of damped Liapunov system applied to nonlinear spring pendulum and betatron transient oscillations

01 p0103 A72-11387

Plane physical pendulum motion stability under randomly oscillating suspension point with allowance for viscous friction

04 p0549 A72-15055

Gravitational and inertial masses equivalence principle verification by pendulum torsional oscillation experiment with laser beam

04 p0519 A72-15070

Nonlinear mechanical oscillation systems analysis by analog computer, exemplifying pendulum rotating about vertical axis

06 p0851 A72-18725

Existence and branching of analytical solutions to equations describing oscillatory-rotatory motions of system of two pendulums with different masses

07 p1036 A72-20217

Subharmonic oscillations excited by horizontal vibrations of mathematical pendulum suspension

07 p1036 A72-20232

Dynamic characteristics of strongly damped pendulum, assessing vibrations effects on vertical determination accuracy

08 p1206 A72-20974

Pendulum impact resistance of tungsten fiber-metal matrix composites, noting heat treatment and test temperature effects

11 p1653 A72-25473

Inverted pendulum subjected to small amplitude sinusoidal periodic and stochastic base motion, determining stability boundaries by averaging method

12 p1844 A72-27247

Asymptotic stability of mechanical system with two mathematical pendulums and rod subjected to axial

follower, correcting aerodynamic and dissipative forces

12 p1847 A72-27979

Equations of motion and phase trajectory analysis for resonant oscillations of beam-pendulum system

13 p2003 A72-28721

On the apparent orbit of the Pulfrich pendulum.

18 p2653 A72-36608

Instability conditions for holonomic system with stationary constraints, applying to pendulum and to rectilinear motion of material point

20 p2955 A72-40033

The theory of motion of the horizontal pendulum with a Zoellner suspension and some indications for the instrumental design.

21 p3084 A72-40495

Energy transfer in vibration damping of pendulum with elastic suspension, noting periodic regimes and transient oscillations

21 p3086 A72-41547

Influence of instantaneous and prolonged pulses on the oscillations of timing-device oscillators

21 p3059 A72-41815

Electronically-damped pendulum acceleration measuring device with analog restoring mechanism. I

24 p3403 A72-45271

PENETRANTS

Nondestructive radioactive gas penetrant tests for porosity and fatigue damage in jet engine castings

01 p0069 A72-10813

Two-fold congruency tests of penetrant inspection system sensitivity using hydrophilic and lipophilic removers/emulsifiers/

07 p0995 A72-19650

Surface crack detection in ferrous and nonferrous metals, glass, ceramics and plastics by water-washable dye penetrants process

16 p2397 A72-33239

PENETRATING PARTICLES

U CORPUSCULAR RADIATION

PENETRATION BALLISTICS

U TERMINAL BALLISTICS

PENICILLIN

Ti leaching from granitic rocks by Penicillium, simplicissimum, discussing extraterrestrial life detection

05 p0616 A72-15809

PENNING DISCHARGE

Plasma beam production with Penning type discharge, demonstrating anisotropic electron temperature

03 p0395 A72-13566

Plasma sheath drift origin of hot ions in modified Penning discharge

04 p0551 A72-14439

PIG discharge system with plasma feed from duoplasmatron ion source for steady state operation with ion energies 1.5-5 keV

08 p1214 A72-21435

Quiescent steady state plasma production by beam-plasma discharges in uniform magnetic fields, showing plasma density fluctuation relation to Penning effect

10 p1519 A72-24022

Ultramicromanometer based on photomultiplier for low pressure Penning discharge light flux emission measurement

10 p1480 A72-24208

Rotating low density plasma in magnetic mirror trap with Penning discharge, determining conditions for oscillations damping and plasma lifetime

10 p1521 A72-24354

Penning ion source for multiply charged ions high intensity beams generation, describing axial type design with electron focusing magnetic coil

10 p1516 A72-25030

Plasma beam production with Penning type discharge, demonstrating anisotropic electron temperature

11 p1699 A72-26753

Low-frequency oscillations in a Penning-discharge plasma under conditions of a cyclotron ion source

21 p3095 A72-41682

The negative space-charge density distribution and the potential distribution in a Penning discharge cell

23 p3324 A72-44211

PENNING EFFECT

Electron cyclotron resonance in Penning ion source, measuring electron temperature from X ray emission spectra

10 p1516 A72-25029

Excitation transfer and Penning ionization reactions between helium metastables and carbon monoxide.

18 p2713 A72-36563

PENNING GAGES

Performance characteristics of various types of PIG sources for multiply charged heavy ions production

10 p1516 A72-25027

PENTACHLORIDES

U CHLORIDES

PENTANES

NT NEOPENTANE

PENTOBARBITAL SODIUM

NT RESERPINE

Dose dependent hyperglycemia and hypolipemia response to pentobarbital sodium injection in rats from plasma glucose and fatty acid analysis

08 p1116 A72-21187

PENTODES

Circuit of two parallel connected vacuum pentodes with different reactances to provide exact voltage division of ac signals by another

13 p1930 A72-29045

PENUMBRAS

Prominent Zeeman multiplets in photosphere, penumbra, umbra and sunspot spectra, presenting ratios for temperature sensitivity measurements

03 p0415 A72-12933

Fine structure of magnetic field distribution in umbra and penumbra of sunspots

03 p0428 A72-13299

Sunspots penumbral and umbral areas ratio in eleven year solar activity cycle, noting larger umbras at second maximum

07 p1082 A72-20295

Bright point intensity distribution on CN spectroheliogram of sunspot penumbra on 4 July 1970

13 p2045 A72-29710

Spectroheliograph study of fine structure of Evershed effect, determining radial velocity in penumbra along dark filaments and interfilamentary space

13 p2047 A72-29739

Lunar eclipse of 25 September 1965, observing penumbra densities and isophotes in B and V spectral regions by photoelectric photometry

14 p2161 A72-30915

PEPTIDES

Amino acid code comparisons of polypeptide chains of globins due to mutations during vertebrate evolution from ancestral gene

02 p0159 A72-11764

Energy transfer conditions of transdehydration reactions on primeval earth leading to transphosphorylation, transacylation and peptide synthesis

04 p0468 A72-14768

Atmospheric model for proteins abiogenesis, considering heteropolypeptides formation from hydrogen cyanide and water

04 p0468 A72-14772

Antibiotic polypeptide synthesis of gramicidin S and tyrocidine, using primitive model of sequential addition of amino acids on polyenzymes

04 p0470 A72-14790

Conversion of angiotensin to angiotensin 2 in dog pulmonary circulation, studying peptide synthesis, radioimmunoassay and in vivo and plasma in vitro metabolism

04 p0475 A72-15465

Dipeptidyl aminopeptidase I preparation from beef spleen and rat liver, discussing contamination with catheptic carboxypeptidase C and Ser-Met dipeptidase

07 p0935 A72-18906

Parenterally introduced protein hydrolyzates and aminopeptides influence on human pancreas enzyme secretion activity

09 p1268 A72-23595

Diastereometric S-prolyl dipeptide derivatives adaptation to gas chromatographic quantitative estimation of R- and S-leucine enantiomers

11 p1590 A72-26366

Biochemical analysis of cat brain regions for gamma-aminobutyric, aspartic and glutamic acids, glycogen and phosphatidopeptide concentrations during paradoxical sleep deprivation

16 p2356 A72-33559

Dipeptidyl aminopeptidase. I - Application in sequencing of peptides.

17 p2511 A72-35167

Evolutionary clock - Nonconstancy of rate in different species.

19 p2758 A72-38551

Recently published protein sequences. I.

23 p3254 A72-43570

PERCENTAGE

U RATIOS

PERCEPTION

NT AUDITORY PERCEPTION

NT AUTOKINESIS

NT BINAURAL HEARING

NT CONSCIOUSNESS

NT CRITICAL FLICKER FUSION

NT EXTRASENSORY PERCEPTION

NT KINESTHESIA

NT OLFACTORY PERCEPTION

NT PAIN

NT PAIN SENSITIVITY

NT PROPRICEPTION

NT SENSORY PERCEPTION

NT SOUND LOCALIZATION

NT SPACE PERCEPTION

NT TACTILE DISCRIMINATION

NT TASTE

NT VERTICAL PERCEPTION

NT VISUAL DISCRIMINATION

NT VISUAL PERCEPTION

Universal perception meter for measurements in work psychology laboratories, discussing characteristics and operation

03 p0320 A72-13884

Adaptive neural nets of threshold logic units as models of perception and memory in biological systems

- 09 p1273 A72-23580
Statistical periodic analysis of cyclic activity in human perceptual-motor performance
13 p1911 A72-29845
Space environment weightlessness induced perceptual deprivation, considering hand-eye coordination, visual judgments and motion and time perception
16 p2355 A72-33549
Developmental relationships between field independence and fixity-mobility.
18 p2651 A72-36906

PERCEPTORS

U SELF ORGANIZING SYSTEMS

PERCEPTUAL SPEED

U PERCEPTUAL TIME CONSTANT

PERCEPTUAL TIME CONSTANT

- Time perception distortion level in simulated and real flight due to task complexity-related pilot emotional stress
14 p2078 A72-30392
Non-monotonicity of temporal recognition of brief duration.
18 p2651 A72-36912
Threshold excitation, temporal summation, and impulse response function in the retina of the cat - Temporal receptive fields of retinal ganglion cells
19 p2758 A72-38648

PERCHLORATES

NT AMMONIUM PERCHLORATES

NT POTASSIUM PERCHLORATES

Barium perchlorate thermal decomposition mechanism, presenting pressure-time and weight-loss curves

- 07 p1051 A72-19360
Burning rates of organic perchlorates of aliphatic, aromatic and heterocyclic amines and amidines with explosive compounds containing nitrogen dioxide group as oxidizer
22 p3153 A72-43181

PERCHLORIC ACID

Thermal decomposition of perchloric acid vapor in Pyrex reaction vessels at 279-471 C, using flow technique

- 09 p1276 A72-23143

PERFLUORO COMPOUNDS

Rust inhibited chemically inert perfluorinated polymer greases for liquid fueled rocket engines, discussing lubricating and nonreactive properties under high pressure operating conditions

- 06 p0837 A72-18604

PERFORATED PLATES

Momentum jet and electric discharge from same hole in plane wall bounding viscous incompressible conducting fluid, investigating flow field with similarity solutions

- 01 p0107 A72-10139
Ductile tensile cracking macroscopic simulation with perforated pure Al specimens, determining fracture energy as function of hole size and pattern
01 p0086 A72-10987

Carrying capacity solutions for perforated circular plates of rigid plastic material by kinematic method

- 01 p0143 A72-11366
Polycarbonate yield locus from strain rate, creep, isotropy, isoclinic and reloading tests on perforated plates

[SESA PAPER 1819] Stress and failure analysis of glass-epoxy composite plate with circular hole under uniaxial tension by finite element method

- 02 p0248 A72-11501
[SESA PAPER 1942] Stress tensor asymmetry effects on stress concentration at curvilinear holes in elastic plates under tension

02 p0289 A72-11611
Wake blockage paradox in two dimensional perforated wall wind tunnel, investigating interference velocity distribution

- 02 p0151 A72-12271
Elastoplastic problem of stress concentration in orthotropic plate with circular hole under balanced biaxial tension of infinity

02 p0293 A72-12428
Circularly symmetrical disks with circular hole and loaded by pressure at edges, calculating linear and power-law strain hardening

- 02 p0297 A72-12535
Stress distribution for anisotropic elastic plate containing two or more arbitrary elliptical holes

02 p0298 A72-12674
Square orthotropic and isotropic plates stability with square hole under uniformly distributed load

- 02 p0299 A72-12685
Thermal stress concentration at circular heat-insulated hole in plate with elastoplastic strains, assuming temperature independent mechanical properties

03 p0445 A72-13575
Stress concentration around reinforced curvilinear hole in elastic infinite plate, discussing ring reinforcement rigidity effects

- 03 p0447 A72-13730

Temperature stresses near thermally insulated square holes in unbounded plane, determining temperature distribution

- 03 p0449 A72-13914
Soviet papers on stress concentration near holes in plate and shell structures

03 p0449 A72-14101
Approximate solution for stress concentration near oval shaped hole in nonlinearly elastic plate, using small parameter and boundary perturbation methods

- 03 p0449 A72-14105
Stress concentration near free hole in circular thick compressed plate, using plane elasticity theory

03 p0450 A72-14107
Edge temperature effects on contact stress concentration in anisotropic plate with elliptic hole under mixed boundary conditions of thermoelasticity

- 03 p0450 A72-14109
Stress concentration and stability of plates and shells weakened by holes

03 p0450 A72-14110
Stress concentration at hole in plates after stability loss, using branching and small parameter method

- 03 p0450 A72-14111
Anisotropic plate with hole stiffened at edge by thin isotropic ring, calculating thermal stress distribution

03 p0450 A72-14113
Stress concentration of isotropic rotating multiply connected circular and elliptic plates weakened by two circular holes

- 03 p0450 A72-14114
Pressurized vessel bottoms weakened by central hole with edge stiffened by elastic ring, determining stress-strain state and stress concentration

03 p0451 A72-14120
Stress concentration at circular holes in polyurethane plates under plane compression wave, obtaining interference fringes

- 03 p0451 A72-14121
Transversely isotropic plates with elastic circular insert, calculating stress concentration at holes under bending

03 p0451 A72-14123
Diffusion saturation effects on thermal stress concentration in plate with circular hole under edge heating and lateral surface heat transfer

- 03 p0451 A72-14124
Time effects on stress concentration around circular and elliptical holes in infinite plate with nonlinear creep

03 p0451 A72-14126
Stress concentration around circular hole in infinite semibrittle plate under omnidirectional tension at infinity or pressure at hole contour

- 03 p0452 A72-14127
Stress concentration at circular, elliptical, square, rectangular and triangular holes in isotropic plates stiffened by discontinuous elements under uniaxial tension

03 p0452 A72-14133
Thermal stress concentration at heat insulated holes in orthotropic plate, assuming external-load free contour

- 03 p0452 A72-14134
Stress-strain state of transverse isotropic plate with hole under bending and torsional moments

03 p0452 A72-14136
Dynamic stress concentration at circular hole generated by plane bending wave propagation in thin plate, analyzing dependence on vibration frequency

- 03 p0453 A72-14139
Optimum variable thickness reinforcement around circular hole in flat elastic sheet under radial tension

04 p0583 A72-14463
Analytical model for acoustic impedance of perforated plate liner with multiple frequency excitation, discussing effects of fluid motion, grazing flow and spectral excitation

- 04 p0548 A72-14699
Variable thickness plate under cylindrical bending, considering stress concentration around circular hole

04 p0586 A72-14991
Forced vibrations of elastic plate with infinite series of identical circular holes, discussing elastic wave diffraction and stresses at/near holes

- 04 p0587 A72-15017
Circular disks, rings and perforated plates steady state field components, evolving forced and free vibration natural frequency equations

04 p0592 A72-15505
Disturbances in infinite plate of viscoelastic material due to impulsive radial forces and twist on inner surface of circular hole, using Laplace transformation

- 04 p0594 A72-15709
Complex potentials for nonlinear elasticity, creep and small elastoplastic deformations, applying to stress concentration at curvilinear hole in infinite plate

05 p0742 A72-17183
Stress concentrations at circular holes and inclusions in elastoplastic strain hardening plate under tension and shear

- 06 p0897 A72-18316

Low frequency biaxial load effect on stress concentration factors for circular and elliptical holes in Plexiglas plates

- 06 p0898 A72-18350
Approximate trigonometric solution to thermoelastic boundary value problem of plate with doubly periodic system of holes under unsteady temperature and thermal stress fields

06 p0899 A72-18363
Stress-strain state in elastic plate with small radial cracks and circular hole under hydrostatic tension

- 07 p1091 A72-19765
Stressed state of isotropic nonlinear plate with doubly periodic system of curvilinear holes

07 p1094 A72-20208
Stressed state approximate determination for isotropic slab with randomly positioned circular holes

- 07 p1094 A72-20210
Stressed state of infinite isotropic plate weakened by curvilinear hole with elastic plug, using asymptotic integration method

07 p1094 A72-20212
Stressed state of isotropic plate with curvilinear holes under tension, using computer techniques

- 07 p1094 A72-20215
Three dimensional stressed state of isotropic plate with elliptical holes under tension, solving boundary value problems

07 p1095 A72-20216
Biharmonic boundary value problems solution by summary representations method and conformal mapping for plane with two circular holes

- 08 p1242 A72-20906
Longitudinal plane harmonic elastic wave scattering and stress concentration at rough circular hole boundary in thin isotropic plate

08 p1243 A72-21230
Stress concentration and elastohereditary values at curvilinear hole in fiberglass reinforced plastic plate under bending moment

- 08 p1243 A72-21237
Stress concentration near elliptic and square orifices in plates with nonlinear viscoelastic hereditary creep properties

08 p1244 A72-21242
Thermal stresses in anisotropic annular, circular and perforated plates with temperature dependent coefficients for lateral surfaces heat removal

- 08 p1245 A72-21505
Microwave transmission loss prediction formula for obliquely incident plane wave leakage through perforated flat metal plate

08 p1135 A72-21559
Plane stability of isotropic plate with straight line series of holes reinforced by complex elements or multicomponent rings, determining stress concentration

- 08 p1246 A72-21710
Elasticity theory doubly periodic problem for unbounded anisotropic plate weakened by system of identical arbitrary holes with self balanced loads

08 p1246 A72-21807
Perforated flexible polymer plates stressed state problem with boundary conditions and viscoelastic and creep properties effects

- 08 p1248 A72-21861
Mixed boundary elasticity solutions for plane with cuts on real axis, using hyperelliptic Riemann surface

10 p1553 A72-23768
Plane harmonic compression waves scattering by circular holes in thin elastic plate, calculating dynamic stresses concentration

- 10 p1554 A72-24179
Stress concentrations around circular openings and failure criteria for orthotropic and anisotropic composite laminated plates subjected to uniaxial, biaxial and shear loading

11 p1732 A72-25474
Perforated plates plastic deformation, stresses and strains near holes, using strain gauge data in biaxial tensile tests

- 11 p1733 A72-25540
Linear contingency method for elasticity theory of anisotropic plate with elliptic hole, deriving boundary value problems solutions

11 p1733 A72-25543
Bending of simply supported thin square plate clamped around central circular hole and under uniformly distributed transverse load

- 11 p1736 A72-25985
Equilibrium equations of infinite strip with circular hole, using plane multiply connected domain method for stress field

12 p1878 A72-27087
Stress-strain state approximation for isotropic strip with circular hole, noting method adaptability to computer computations

- 12 p1880 A72-27232
Stress concentration in infinite elastic isotropic disk with circular hole under internal tensile loading

12 p1882 A72-27320
Green function for stress distribution in plane shaped disk with edge loaded circular hole, noting conformal mapping for arbitrary shape

- 12 p1883 A72-27391

Stress-strain state in pure bending for infinite elastic strip with circular central hole, using integral Fourier transforms

13 p2053 A72-28390

Stress-strain concentrations near circular holes in fiberglass reinforced plastic plates under various types of load as function of hole diameter/plate width ratio, anisotropy and load

13 p1983 A72-28560

Quasi-static thermoviscoelasticity problem for infinite plate with circular hole, investigating plate surface heat transfer and material viscosity effect on temperature stresses

13 p2061 A72-29796

Anisotropic plate with doubly periodic system of elastic ring stiffened elliptic holes, calculating stresses at holes due to tensile forces applied at infinity

14 p2165 A72-30685

Point heat source induced thermal stresses in elliptic plate with circular holes, determining stress-strain field by two dimensional elasticity theory

14 p2166 A72-30689

Elastoplastic stress concentration near elliptic hole in plate loaded in smallest axis direction

15 p2325 A72-31606

Equilibrium equations for boundary value problems in Vekua theory with moments allowance for plate with circular hole under bending and torsion

15 p2333 A72-32682

Rigidity effect of reinforcing rings on stressed state of physically nonlinear perforated elastic plates

15 p2333 A72-32683

Analytical solution of stress distribution and load endurance of perforated square plate supported at corners, comparing with photoelastic observations

16 p2470 A72-33410

Strain energy release rate for radial cracks emanating from a pin loaded hole.

17 p2623 A72-34254

On the extension of an infinite elastic plate containing an axisymmetric hole.

[ASME PAPER 72-APM-G] 17 p2624 A72-34313

An asymptotic solution for the large deflection of a circular plate with a central hole.

18 p2732 A72-36081

Infinite plate with a supported reinforced circular hole.

18 p2738 A72-37071

An analytical approach to the non propagating crack problem using the finite element method.

20 p2977 A72-38882

Russian book - Plates strengthened by composite rings and elastic cover pieces.

21 p3116 A72-40385

Theoretical and experimental investigations, conducted with the aid of a plate containing holes, concerning the simulation of a statistically arranged antenna group

21 p3028 A72-40505

Stresses around one hole or two holes subjected to internal pressures in semi-infinite or infinite medium.

21 p3118 A72-40717

A study of stress around non-central holes in a rotating tapered disc.

21 p3118 A72-40775

Thermoelastic problems for multiply-connected plates with heat dissipation at both plane surfaces.

21 p3121 A72-41237

Stress-strain state of thin circular perforated Cu plate under uniform tensile load, showing applicability of small elastoplastic finite deformation theory

21 p3122 A72-41351

Stress concentration around curvilinear holes in plates according to Reissner's theory

21 p3126 A72-41543

Influence of stress raisers in the form of circular holes on the endurance in symmetric bending of AM6BM aluminum-alloy sheet

21 p3071 A72-41704

Stress-strain state of an isotropic half-plane with an elliptic hole, deformed by concentrated loads

22 p3233 A72-42057

Stress-strain state at holes in plates in the case of asymmetric buckling modes

22 p3233 A72-42059

Stress concentration at an elliptic hole in an elastoplastic body

22 p3233 A72-42060

Velocity distribution in turbulent air flow over perforated plates with gas injection in turbulent boundary layer

22 p3166 A72-42256

Bending of a rectangular plate with a clamped edge and an internal symmetric cut

22 p3234 A72-42291

On the effect of the form of the strain energy function on the solution of a boundary-value problem in finite elasticity.

22 p3236 A72-42606

Versatile stretching of a disc shaped as a plane with elliptic aperture.

22 p3236 A72-42627

The stretching of a disc shaped as a semi-infinite plate with half-elliptic edge sector.

22 p3236 A72-42628

Stress concentration around holes in plates and shells.

22 p3238 A72-42834

Extensional vibration of a certain type of composite circular plate with a central hole.

22 p3240 A72-42879

Stress concentration around a circular hole in an elastoplastic medium under the action of a temperature field and omnidirectional tension

23 p3344 A72-43418

Steady thermoelastic state in an infinite plate with a moving parabolic cut

23 p3345 A72-43586

Temperature distribution in a perforated stiffener

23 p3356 A72-43684

Al alloy sheet panel tests for cracks emanating from stress concentration areas at holes or cutout edge

23 p3347 A72-43713

Approximate stress-strain state determination in plate weakened by arbitrarily oriented rectilinear cracks and circular holes in elasticity theory

23 p3349 A72-43801

Stress distributions in a semi-infinite plate with a row of circular holes.

23 p3355 A72-44398

PERFORATED SHELLS

Stress analysis of pressurized ribbed cylindrical shell with intersecting reinforced circular hole under internal pressure

[ASME PAPER 71-PVP-8] 02 p0294 A72-12470

Stress concentration in shallow cylindrical shell with circular hole under axial tension, torsion and internal pressure loading

[ASME PAPER 71-PVP-9] 02 p0295 A72-12472

Soviet papers on stress concentration near holes in plate and shell structures

03 p0449 A72-14101

Stress concentration around circular and elliptical holes in isotropic three layer spherical shells with rigid and lightweight fillers

03 p0449 A72-14104

Stress concentration and stability of plates and shells weakened by holes

03 p0450 A72-14110

Stress concentration at hypotrochoid hole in cylindrical shell under internal pressure and axial tensile stresses

03 p0453 A72-14138

Nonlinear elastoplastic deformations of flexible shells of revolution, calculating stress concentration at circular hole in spherical shell

04 p0588 A72-15049

Stress-strain state of thin ellipsoidal shell with central stiffened hole, using small elastoplastic deformation theory

04 p0588 A72-15050

Stress distribution at hole in multilayer anisotropic shells of composite glass-plastic or cermet material

04 p0588 A72-15052

Stress concentration around elliptic hole in infinitely long circular cylindrical shell under torsional loads

04 p0589 A72-15122

Perturbation solution for stress concentration around elliptic hole in cylindrical shell under torsional loading

04 p0589 A72-15123

Slot length effect on buckling load of cylindrical shell with circular holes

05 p0739 A72-16543

Elastoplastic stressed state of thin cylindrical shells with circular hole, using small strain theory

07 p1092 A72-19896

Membrane and bending moment stresses distribution at elliptical hole in circular cylindrical shell, solving boundary value problems

08 p1243 A72-21234

Critical values of compressive loads applied to mid-section of cylindrical shell weakened by circular holes

08 p1244 A72-21241

Successive approximations method for stress concentration problem at hole in cylindrical shell

08 p1247 A72-21818

Thermal stress distribution in orthotropic cylindrical shell weakened by circular hole, obtaining general solution by small parameter method

09 p1400 A72-22715

Pressure loaded shallow spherical shells with reinforced circular holes, noting stress concentration increase due to reinforcement bead eccentricity

11 p1734 A72-25736

Nonlinear equilibrium equations and elastic stability of cylindrical shell weakened by circular hole

12 p1878 A72-27080

Optimal weight and load capacity of ellipsoidal cylindrical shell of revolution of constant thickness with central circular hole under uniform internal pressure

12 p1885 A72-27977

Stress distribution in circular cylindrical shell weakened by two identical holes on common generatrix

12 p1886 A72-27984

Circular cylindrical shell under distributed edge load along circular hole contour, calculating stress concentration by trigonometric series solution for shallow shell equation

12 p1886 A72-28130

Shear strains and elastic anisotropy of transversely isotropic cylindrical shell with circular hole under uniform internal pressure, using shallow shell equations

14 p2165 A72-30438

Stress concentrations in cylindrical shells with cutouts under uniformly distributed axial tensile load, presenting exact solution of differential equation

15 p3238 A72-32138

Differential equations for stress-strain state of circular cylindrical shell with circular holes resting on elastic base under external pressure

15 p3233 A72-32686

Membrane and bending stress analysis for thin circular cylindrical shells with elliptic hole

16 p2464 A72-32918

Asymptotic singular perturbation solution to thick spherical shell with circular hole under axisymmetric external pressure

16 p2474 A72-34157

Stresses in a circular cylindrical shell having two circular cutouts.

20 p2982 A72-40063

Stress distribution in a cylindrical shell with reinforced holes

21 p3126 A72-41542

Calculation of the stress concentration at the joint between a cylindrical casing and a branch pipe for internal pressure

21 p3127 A72-41710

On the application of the mixed finite element methods to the stress concentration problems of cylindrical shells with a circular cutout or a crack.

22 p3232 A72-41942

Stress concentration around holes in plates and shells.

22 p3238 A72-42834

Stresses in a circular cylindrical shell with arbitrary holes.

22 p3238 A72-42837

Equilibrium equations and deformation of elastoplastic thin isotropic cylindrical shell with circular hole, noting nonlinear partial differential equations for plate displacements

23 p3345 A72-43587

Numerical determination of the stress concentration around a hole in a circular cylindrical shell

23 p3348 A72-43799

Stress concentration of a cylindrical shell with one or two circular holes.

23 p3355 A72-44399

PERFORATION

Stresses in a perforated, continuously loaded cantilever beam.

21 p3117 A72-40452

PERFORMANCE

Receiver performance characteristics and failure mechanism in presence of interference, discussing measurement methods for interference susceptibility

02 p0192 A72-12150

Modified quasi-linearization algorithm for solving nonlinear two-point boundary value problems based on performance index and cumulative error in differential equations

04 p0539 A72-15045

Antenna arrays performance optimization, emphasizing directivity and signal to noise power ratio

04 p0499 A72-15301

Antenna design and performance in random fields, using statistical description of fields

04 p0500 A72-15394

Adjustable structure model for parameter adaptive control, noting convexity of performance index function over evaluation interval

10 p1455 A72-23793

Sensitivity comparison of equivalent open and closed loop optimal control systems, extending performance index formulas to instantaneous and isoperimetric constraints

10 p1456 A72-24456

Hydraulic vortex amplifiers with and without diffusers, discussing supply pressure and liquid viscosity effects on system performance

11 p1578 A72-26980

Magnetovariometers design, operation and applications, discussing ferromagnetic materials properties effect on performance characteristics

12 p1792 A72-27739

EUV open channel photomultipliers satellite-borne long term performance degradation, attributing sensitivity loss to grating contamination

15 p2235 A72-31645

Centrifugal pumps performance instability, considering mass flow rate/pressure curve characteristics as function of impeller slip, fluid prerotation and hydraulic losses

18 p2694 A72-36042

German monograph - Computational and experimental investigations regarding the operational characteristics of a three-stage axial-flow compressor with high performance per stage

19 p2745 A72-37490

Improving diffuser performance by artificial means.
20 p2885 A72-39624

PERFORMANCE CHARACTERISTICS

U PERFORMANCE

PERFORMANCE DECREMENT

U PERFORMANCE

PERFORMANCE PREDICTION

NT PREDICTION ANALYSIS TECHNIQUES

VLF modulation/demodulation system performance prediction by atmospheric noise model, comparing results with measurements
01 p0025 A72-10327

Bipolar transistor model for device and circuit performance prediction, determining parameter from charge distribution by regional approximation technique
01 p0042 A72-10786

Supercapacitor balloons /tetroons/ performance characteristics, determining ascent rates and superpressure, stress and volume perturbations due to forced change in height
01 p0005 A72-10829

Metals mechanical behavior, considering plastic deformability, strain hardening, cohesion and engineering performance prediction
01 p0086 A72-10985

ERTS return beam vidicon imagery simulation, predicting resolvability of ground targets as function of target size, contrast, spectral distribution and radiance level
02 p0226 A72-11833

Signals detection under unknown direction and arrival time conditions, developing performance evaluation method based on detection probability-false alarm curves
02 p0180 A72-12573

Pulse shaped small parameter variation effects on performance index of minimum fuel control systems with initial and final manifolds
03 p0337 A72-12906

Quadrupole mass spectrometer ultimate characteristics concerning resolution, range, recording speed, working pressure and sensitivity
03 p0360 A72-13665

P-channel MOS/silicon-on-sapphire transistor logic circuits for aerospace systems, investigating radiation hardness and performance potential
03 p0334 A72-14086

Two dimensional solar cell model with partial differential equation relating arbitrary point potential to cell parameters for I-V characteristics prediction
04 p0465 A72-14480

Self oscillating dc-to-dc converters performance and design, considering switching frequency, duty cycles, line and load regulation and peak-to-peak ripple
04 p0465 A72-14487

Prolate spheroidal functions application to optical system performance characteristics, discussing laser modes, signals maximal concentration, image data extrapolation, etc
04 p0548 A72-14741

Suboptimal nonlinear filter performance evaluation methods based on Kolmogorov equations for Markov process transition density function
04 p0505 A72-15040

Arc driven shock tubes performance prediction, presenting correlation equations for velocity calculation
[AD-738275] 04 p0510 A72-15499

Nonrecursive and recursive adaptive equalizers for digital communication, discussing computerized simulation of performance
04 p0493 A72-15520

Gas turbine combustors performance model, using reaction rate equation from elementary mass balance equation
[ASME PAPER 71-WA/GT-5] 05 p0704 A72-15898

Forming of 7075-T6 Al in high pressure environments, predicting fracture occurrence via finite element stress analysis computer programs and pressure dependent model
[ASME PAPER 71-WA/PT-11] 05 p0671 A72-15912

Spiral groove shaft vacuum seals, presenting mathematical ballpark performance model
[ASME PAPER 71-WA/PID-5] 05 p0664 A72-15914

Bistable fluidic amplifiers switching dynamics, developing analytic performance prediction method from flow visualization studies
[ASME PAPER 71-WA/FLCS-8] 05 p0615 A72-15916

CW millimeter wave power generation with spiraling electron beams, investigating energy spread effects on performance limitation
05 p0636 A72-16363

Sail rotors for hovering platform, calculating rotor performance based on ideal two-dimensional flexible airfoil section characteristics
[AIAA PAPER 72-66] 05 p0612 A72-16925

Mach 2.65 axisymmetric mixed-compression inlet system diffuser and boundary layer bleed system performance estimates confirmed by tests
[AIAA PAPER 72-45] 05 p0609 A72-16959

presence of thermal noise and intersymbol interference
06 p0772 A72-17408

M-ary orthogonal signal phase noncoherent detection in sequential decision feedback, comparing performance with optimal coherent reception
06 p0773 A72-17596

Pyramidal horn antenna with mesh conducting surface comparing response with geometrically similar horn with continuous walls
06 p0783 A72-17600

Wide range bias dependence of planar bipolar transistor dc and small signal current gain, comparing analytical findings with Si junction experiment
06 p0783 A72-17608

Response surface methodology /RSM/ techniques application to operator target acquisition performance prediction, describing multivariable functional relationship by multiple regression polynomial equation
06 p0773 A72-17714

Fatigue behavior of notched or cracked aircraft structure parts, examining service life prediction problem
06 p0895 A72-17811

Color defective vision performance predictions during day and night tests of aviation color signal light discrimination
06 p0767 A72-17871

Microwave frequency multiplier construction by hybrid circuits based on quasi-lumped components, calculating characteristics from equivalent circuit
06 p0785 A72-18313

Computer aided renormalized perturbation method for inhomogeneously loaded waveguide performance calculation
06 p0786 A72-18377

Quasi-time optimal nonlinear controller for steerable antennas or telescopes in target acquisition or slew mode, predicting performance by digital simulation
07 p0959 A72-19288

Selective attention dichotic listening test as flying proficiency prediction criteria, discussing omission and intrusion errors
07 p0929 A72-19351

Metals and alloys breakdown toughness and mechanical properties predictions under various loading conditions, discussing interatomic bonds and plastic deformation zone size
07 p1019 A72-20146

Aircraft preliminary design procedure with integrated performance simulation, using time sharing computer facility
07 p0913 A72-20353

Numerically exact nonlinear filter synthesis, describing confidence intervals for error performance statistical inferences
08 p1144 A72-20850

Nonlinear filter dynamics for stochastic optimal control for quadratic cost functional, evaluating performance
08 p1145 A72-20866

Coherent radar pulse train clutter performance prediction for targets with range acceleration effects on Doppler response
08 p1133 A72-21405

Rarefied gas sealant viscoelastic performance prediction by analytical models, comparing results with experiments on multiple grooved samples
08 p1177 A72-21929

Hydrodynamically lubricated mechanical seal design, predicting duty variation effects on performance
08 p1179 A72-21942

Single mode He-Ne laser output, predicting intensity correlation function form and decay time near threshold
[AD-742154] 09 p1324 A72-23081

Quadratic performance index generation for optimal design of completely controllable, scalar linear system with state feedback
09 p1454 A72-23783

Prediction method for computing maintenance technician reliability as probability of equipment repair completion within given time
09 p1486 A72-24000

Human performance prediction dependence on task and equipment variables effects, using experimental data for performance classification system
09 p1429 A72-24003

Maximum likelihood receiver performance for optical detection of multimode laser or scattered radiation, considering photocounting distribution, decision threshold and error probability
09 p1452 A72-24681

Radar detection performance calculation with post-detection integration using single valued loss and ideal curves in terms of SNR
09 p1437 A72-24689

Antisymmetric pseudorandom signal performance in measurement of second order kernels in Volterra series representation of nonlinear system by cross correlation
10 p1439 A72-24805

PERFORMANCE PREDICTION

Vortex fluid amplifier design with asymmetrical flow fields, discussing effects of geometrical parameters variations on performance characteristics
10 p1423 A72-25053

Momentum anemometer for wind velocity and vorticity measurement, discussing design principle and performance advantages
10 p1484 A72-25089

Vigilance performance prediction for difficulty-matched auditory and loosely and closely coupled visual intensity discrimination tasks
10 p1433 A72-25127

Hub and shroud boundary layer growth in centrifugal compressor vaneless diffusers, comparing predicted and measured performance at high pressure ratio per stage
[ASME PAPER 72-GT-54] 11 p1570 A72-25645

Fluidic proportional and digital amplifiers environmental effects on sensitivity of gain, noise and null shift based on dependence on Reynolds number
[ASME PAPER 72-GT-84] 11 p1577 A72-25660

Spectral density of frequency deviating process for performance predictions from oscillator testing and frequency noise calibration, discussing sample averages convergence to statistical values
11 p1593 A72-25892

Computer program for biowaste resistojet nozzle performance prediction, taking into account viscous effect at low Reynolds number
[AIAA PAPER 72-450] 11 p1708 A72-26187

Inward radial flow turbines under unsteady flow conditions with full and partial admission, predicting performance by method of characteristics
12 p1751 A72-27349

Glass fiber reinforced thermoplastic resins chemical and hydrolytic resistance, noting composites and polymers long term performance prediction in aggressive environments
12 p1833 A72-27405

Aerospace guidance multiprocessor with memory units attached to time-multiplexed data bus, predicting performance in terms of queueing theory, Markov process and simulation
12 p1786 A72-27433

Factor analysis of grades for successful performance skill identification during undergraduate and graduate jet pilot training
12 p1769 A72-27472

ATS F/G spacecraft thermal control design verification by chamber thermal balance tests and performance prediction mathematical model of earth viewing module and orbital environment
12 p1877 A72-27527

Intensified electron bombarded Si camera tube performance in low light level TV systems, predicting sensor resolution vs irradiance characteristics
12 p1810 A72-27934

Reliability prediction of system with components having independent and constant rate failures
13 p1961 A72-28357

Strike aircraft reliability prediction in cost effectiveness analyses, showing failure probability distribution with time
13 p1896 A72-28360

Model for mercury vapor electron bombardment ion thruster hollow cathodes operation and effects on thrust subsystem performance predictability
[AIAA PAPER 72-420] 13 p2026 A72-28936

Nonequilibrium MHD generator with electrode walls slanted away from magnetic field direction, predicting electrical performance for comparison with flat wall generator
13 p1899 A72-29352

Linear nonequilibrium Faraday type MHD generator, predicting electrode configuration effects on voltage drops, axial leakages and current distribution
13 p1900 A72-29353

MHD power generators analytical modeling by digital technique for prediction of performance and efficiency as function of size and operating conditions
[AD-741173] 13 p1900 A72-29355

Numerical analysis method for performance prediction of linear induction machines including liquid metal MHD pumps and generators and linear motors
13 p1900 A72-29365

Sunspot cycle 21 behavior prediction, explaining solar activity forecasting based on 80 year cycle
13 p2046 A72-29727

Energy cost /oxygen consumption/ prediction for treadmill and various levels terrain walking at two speeds under three different pack loads
14 p2080 A72-30706

Psychological criteria for flying personnel selection in civil aviation, noting performance prediction based on maximum likelihood estimates
14 p2080 A72-30816

Adhesive and abrasive wear technology assessment, considering design equations use for prediction
[ASME PAPER 72-DE-2] 14 p2108 A72-30859

Liquid propellant rocket performance, stability and compatibility prediction techniques, noting effect on design time and cost
14 p2146 A72-30919

Pilot landing performance prediction criteria based on day and night carrier qualification trials and flight training

14 p2081 A72-31084

Multiple port waveguide circulators bandwidth performance calculation to include higher order cylindrical and evanescent modes

15 p2205 A72-31356

Generalized locking equation for microwave oscillator bandwidth prediction for arbitrary cavity configurations and waveforms, considering strong harmonics presence

15 p2205 A72-31358

Parabolic reflector fed by log-periodic dipole antenna array, predicting combined effects of feed phase center lateral and axial displacement on secondary performance

15 p2205 A72-31541

Computer model study of FET with submicrometer gates, noting gain-bandwidth product increase with decreasing gate length

15 p2205 A72-31544

Solid and composite rotor induction motors, comparing predicted characteristics based on analytical and numerical analyses

15 p2182 A72-31779

Limited energy source operational time comparison for continuous and pulse mode operations

15 p2196 A72-31785

Laser Doppler velocimeter designs for atmospheric applications, discussing illuminating techniques, SNR, performance comparison and system selection

15 p2237 A72-32051

Aerodynamic properties prediction procedure for thin jet-flapped airfoil in incompressible inviscid flow bounded by different types of boundaries

15 p2179 A72-32147

Collection efficiency of conical and blunted axisymmetric power law bodies in hypersonic flight through dust clouds and of impact angle and velocity

15 p2180 A72-32580

Crash helmet performance prediction through maximum strain criteria, using brain injury biodynamic model

15 p2192 A72-32607

Automatic systems design for monitoring dynamic control systems, noting feedback control system performance prediction based on subsystems characteristics

16 p2371 A72-33085

Perturbation extremum controller with simple coincidence logic, discussing fluidic implementation and performance in simulated plant control

16 p2350 A72-33193

Performance criteria for transform data coding schemes evaluation under computational constraints, presenting numerical examples for Fourier, Walsh, Haar and Karhunen-Loeve transforms

16 p2366 A72-33214

Teflon-bonded hydrophobic gas diffusion electrode performance prediction by mathematical treatment of flooded catalyst agglomerate model

16 p2352 A72-33892

Aerodynamic stall characteristic prediction from static experimental data for airfoils, noting boundary layer effects

[AIAA PAPER 72-682]

16 p2346 A72-34060

Supercritical pressure convergent nozzle performance prediction by time dependent method of characteristics solution to mixed flow problem, adapting Moretti-Abbott technique

[AIAA PAPER 72-680]

16 p2346 A72-34061

Components creep-rupture life prediction for multiaxial stress from uniaxial test data, discussing crack initiation and propagation phases stress states

16 p2412 A72-34114

An electromagnetic analysis of a cylindrical homogeneous lens.

17 p2525 A72-34362

Simulation models for airports performance evaluation through replication of traffic units actual movement

17 p2535 A72-34414

Pulsed Impatt diode oscillator circuit design and operation frequency prediction for high Q coaxial structures from equivalent circuit

17 p2526 A72-34466

The wake geometry of a hovering helicopter rotor and its influence on rotor performance.

[AHS PREPRINT 620]

17 p2484 A72-34497

Digital simulation for sampled electro-optical imaging system performance prediction and optimization

17 p2557 A72-35553

Flight tests correlation with mathematical models to predict electro-optical viewing systems capability for military missions

17 p2557 A72-35553

Performance of low pressure ratio ejectors for engine nacelle cooling.

[SAE AIR 1191]

18 p2721 A72-36530

Microwave junction transistor geometric design factors effect on reliability and performance, comparing overlay, interdigitated, mesh and inverse overlay structures

18 p2666 A72-36553

Effect of magnetic field on the performance of millimeter-wave detectors using bulk InSb.

19 p2772 A72-37570

Influence of plasma kinetic processes on electrically excited CO₂ laser performance.

19 p2812 A72-38598

Differentially coherent detection scheme with error-correcting capability by means of decision patterns.

19 p2766 A72-38605

Visual aid-to-eye direct coupling, evaluating partial coherence effects on imagery optical performance by computer program

20 p2931 A72-39050

Double-ended, folded-path and double-reflecting transmissometers operation principles, and measurement error sources consideration for relative merits and disadvantages

20 p2923 A72-39054

Thermal scale models utilization to predict spacecraft radiator system performance, presenting criteria for modeling fluid system with combined convection, conduction and radiation effects

[ASME PAPER 72-ENAV-29]

20 p2894 A72-39148

Simple conduction model for theoretical steady-state heat pipe performance.

20 p2984 A72-39607

Performance improvement of amplitude-constrained minimum-variance controller by minimising sum of variance.

20 p2911 A72-39772

Performance of antennas in random fields.

21 p3026 A72-40355

Theoretical model prediction for matched filter selectivity and noise effects on strained object deformation in optical correlation applications, comparing results with experiments

21 p3053 A72-40611

Analysis of large-signal noise in Read oscillators.

21 p3032 A72-40698

Two explanations of temporal changes in ability-skill relationships - A literature review and theoretical analysis.

21 p3008 A72-41015

Team size and decision rule in the performance of simulated monitoring teams.

21 p3008 A72-41016

Shadow shields for minimizing radiant heat transfer into cryogenic propellant tanks on interplanetary missions, predicting performance for comparison with scale model experiment

21 p3130 A72-41181

Integration of aerospace vehicle performance and design optimization.

[AIAA PAPER 72-948]

22 p3137 A72-42355

Performance prediction of large-scale integrated logic circuits.

22 p3160 A72-42824

Two-dimensional model for thermal compression.

22 p3136 A72-42868

Empty weight and cruise performance of very large subsonic jet transports.

[SAWE PAPER 919]

23 p3251 A72-43466

Performance characterization for L-orthogonal signal transmission and detection, discussing tradeoffs between error probability, SNR and bandwidth by numerical evaluation

23 p3265 A72-44180

Book on complete technological system reliability assessment covering performance requirement and achievement, transfer characteristics, sampling, estimation, confidence, synthesis problem, etc

23 p3294 A72-44499

A concept of service life for estimating the reliability of machines and devices

24 p3405 A72-44623

The calculation of elastic tanks partially filled with liquids for prediction of the Pogo effect

24 p3392 A72-45152

Application of cascade and actuator disc theories to computer aided design of fans.

24 p3363 A72-45359

Prediction of velocity profiles for turbulent boundary layers on the blading of radial impellers.

24 p3393 A72-45360

An approximate method for the calculation of the characteristics of axial-flow fans.

24 p3363 A72-45369

California psychological inventory as a predictor of success in the Naval flight program.

24 p3377 A72-45655

PERFORMANCE TESTS

Supersonic ribbon parachute testing by transonic wind tunnel, rocket sled and water channel simulator

01 p0004 A72-10305

Test program to evaluate metallic materials candidates for space shuttle booster thermal protection system

01 p0085 A72-10755

Completely sealed off room temperature CO laser system, discussing performance and continuous wave power

01 p0080 A72-10852

Nimbus 3 and 4 satellite technological and meteorological performance, discussing atmospheric

temperature humidity and ozone vertical sounding for numerical weather forecasting models

01 p0130 A72-10955

Unidirectional glass/graphite fiber-epoxy resin composite, discussing fabrication and performance tests for mechanical properties

[SME PAPER EM 71-192]

01 p0092 A72-10971

Random and algorithmic procedures employing three-valued logic system for sequential circuits fault detection test sequence generation

02 p0185 A72-11486

Multispectral photographic data preprocessing and computerized simulation of ERTS data channel to make terrain maps, testing classification accuracy improvement possibility

02 p0215 A72-11880

Bias and spread in extreme value theory inter-performance tests of communications systems, comparing with bit error rate tests

02 p0173 A72-12129

ECG telemetry systems parameters, discussing manufacturers specifications and standardized laboratory performance test data

02 p0169 A72-12139

Frame synchronization performance tests for PCM telemetry system, considering code selection, frame length and data recovery

02 p0175 A72-12147

One-way error correcting system with 1/3 rate interleaved block code, testing code performance over 1300 km vhf ionoscatter path and 1500 km hf path

02 p0175 A72-12153

Ti-Al-Mo alloys thermomechanical treatment, investigating alloy composition effects on hardening

02 p0244 A72-12246

Navy uhf telemetry transmitter production system, discussing test program contribution to quality control

02 p0177 A72-12322

Optimal smoothing application to testing of inertial navigation systems, gyros and component failure detection during mission

02 p0258 A72-12810

Nozzle boundary layer effects on resistojets performance, presenting conical design model in heater stagnation conditions

03 p0405 A72-12973

Time shared performance test monitor function, operation and self repair of corporate fed array radars with computer control for long time internal reliability

03 p3321 A72-13165

Abastumani Observatory 70 cm meniscus telescope, determining performance from primary focus field data

03 p0359 A72-13498

Ten million bit magnetic film computer memory, discussing design, fabrication, performance and cost per bit

[IEEE PAPER 11.1]

03 p0327 A72-13761

Nondestructive readout in computer storage of plated wires on Permalloy film deposited substrates, testing design parameters effects on performance

[IEEE PAPER 11.2]

03 p0332 A72-13762

High speed easy rewrite read-only memory using plated wire with multilayered nondestructive readout magnetic thin film, testing performance

[IEEE PAPER 11.4]

03 p0332 A72-13764

Isolated antenna system for shielded enclosure measurements at 20-200 MHz, discussing associated circuits design and performance tests

03 p0333 A72-14037

Pioneer F and G space probe EMC specification limits, comparing computer analysis prediction and system test data

03 p0329 A72-14048

Synchronization system for remote control and performance checking of motion picture projectors with running film, discussing recording equipment and stroboscopic pulsed illuminator operations

04 p0521 A72-14711

Gallium-doped Ge bolometers and triglycine sulfate pyroelectric far IR detector, testing performance as functions of frequency and temperature

04 p0525 A72-15601

Military aircraft inertial navigation system design, discussing gyroscope, gyro compassing alignment, accuracy and performance

04 p0545 A72-15666

Arterial and grooved Wick cryogenic nitrogen heat pipe performance tests, comparing elevation sensitivity, priming and heat transfer characteristics

[ASME PAPER 71-WA/HT-42]

05 p0745 A72-15889

Gas turbine procurement standard rating and performance indicators, noting dependence on ambient conditions

[ASME PAPER 71-WA/GT-1]

05 p0703 A72-15894

Spherical air bearing supported test facility for satellite attitude control system performance testing, discussing motion simulator and automatic balancing system

05 p0643 A72-16435

Satellite attitude control with gimbaled reaction wheel digital system, discussing logic and computerized design, implementation, fabrication and performance tests

05 p0726 A72-16458

Three-axis attitude control and stabilization system for sounding rocket payload, discussing performance from simulation and ground test results

05 p0728 A72-16478

Supersonic axial flow shock-in-rotor type compressor performance tests, discussing factors responsible for low efficiency

05 p0601 A72-16481

Circular arc blades two dimensional cascade performance test data for various cambers comparison with potential theory data

05 p0602 A72-16485

Large scale high aspect ratio multielement supersonic nozzle arrays testing for augmentor wings and internally blown flaps

[AIAA PAPER 72-131] 05 p0612 A72-16888

Image data coding by adaptive block classification and quantization of source output symbols, evaluating performance

06 p0772 A72-17402

Raman laser radar /LIDAR/ for remote probing, discussing design, construction, testing, atmospheric scattering, and intensity and polarization measurements

06 p0824 A72-17588

GERT simulation program as stochastic network analysis technique for modeling policies and processes in performance tests and checkout

06 p0780 A72-17977

InP transferred electron microwave oscillators, observing higher efficiency than IMPATT and GaAs devices

06 p0784 A72-18063

Top wall and multiple branch hybrid junction waveguide couplers for millimeter wavelengths, measuring insertion loss performance

06 p0787 A72-18378

Carrier suitability testing for aircraft landing, considering landing gear and supporting structure under simulated shipboard conditions

06 p0759 A72-18497

Semiconductor device IC encapsulation, thermal design, stress analysis, testing and applications

06 p0791 A72-18577

Semipermanent and permanent pressure connections in electronic systems, discussing design and performance evaluation

06 p0791 A72-18580

Economical performance of single rim supersonic turbine stage with repeated low level admission of working body

07 p0908 A72-18986

Gigahertz reflection amplifiers with low cost avalanche transit time diodes, measuring characteristics of amplification by synchronization at center frequency

07 p0955 A72-19191

High voltage axially pulsed carbon dioxide laser performance test, determining output energy dependence on tube parameters

07 p1001 A72-19197

Performance tests of return beam vidicon multispectral television camera system for ERTS program

07 p0986 A72-19657

Explosive/pyrotechnics performance monitoring for acceptance, lot qualification, comparison testing and system design guidelines

08 p1219 A72-20760

Aluminum plated pyrotechnics physical properties and performance for electroexplosive device applications, describing particle size distribution and loading pressure dependence of density

08 p1221 A72-20772

Transcendent Si power rectifier with high current and power dissipation capacity, discussing design, fabrication and performance tests

08 p1111 A72-21413

Sealed-off He-Se laser construction and performance, comparing with He-Cd, He-Zn and He-Ne lasers

08 p1182 A72-21437

Flame resistant materials for aircraft fire fighter protective clothing from systems approach tests

08 p1126 A72-21585

Metallic four-lip seal performance, discussing force cycle, mechanical spring-back, reusability at room and higher temperatures and thermal shock behavior

08 p1179 A72-21939

Workability tests from material deformation stress determination and fracture strain rate relation for forging, extrusion and rolling limits predictions

08 p1190 A72-22198

Zirconia ceramics for high performance storage heaters, discussing operating conditions, optimal properties for heater design, engineering evaluation tests and in-service performance

09 p1333 A72-22383

Alumina microstructure, grain size and impurities effects on ballistic performance, discussing results in terms of microplasticity

09 p1334 A72-22390

Performance characteristics and limitations of electrode and insulation materials for open and closed cycle MHD generators, noting ceramic compositions for channel

[AD-737019] 09 p1335 A72-22401

Magnetic field measurement methods and magnetometers performance in superconducting, thin film, resonance and fluxgate areas

09 p1308 A72-22465

CW Kr arc lamps for high power Nd-YAG laser pumping, testing operating life and electrical and spectral characteristics as function of design

09 p1324 A72-23080

Pulsed arc TIG welding with modulation of current from standard power source, comparing performance with steady dc method

09 p1320 A72-23632

Low speed performance and boundary layer growth in optimal annular diffuser with uniform center body diameter and conically diverging wall

10 p1415 A72-23856

Electric discharge carbon dioxide laser performance in terms of optical beam quality, electrical efficiency and gas utilization

10 p1489 A72-23943

Electron image projection system using converter tube technique for microcircuit lithography, discussing performance tests and design changes

10 p1447 A72-23957

Multistage systems maintainability, presenting equations for optimum allocation of demonstration tests to repairable elements

10 p1443 A72-23982

Reliability program for SAAB 37 Viggen airborne computer, discussing prototype and components operating tests and failure rates

10 p1443 A72-23984

Bulk effect diodes combination with YIG elements to provide oscillator operation up to 18 GHz, discussing design, circuit diagrams and performance

10 p1448 A72-24037

CW circuit stabilized InP microwave reflection amplifiers in Q band, determining power gain and noise figure

10 p1450 A72-24308

Three dimensional wind tunnel investigation of vortex augmented unswept wing with leading edge cusp flap and split upper and lower trailing edge flaps

11 p1568 A72-25584

Liquid metal regenerator design and test evaluation for gas turbine engine fuel consumption improvement

[ASME PAPER 72-GT-33] 11 p1704 A72-25629

Cascade technology for centrifugal compressor vane diffuser design, comparing performance results with conventional diffuser data

[ASME PAPER 72-GT-39] 11 p1569 A72-25633

Multiaxis radial circuits for transferred electron microwave oscillator performance optimization to obtain wideband CW amplification, discussing LSA tests

11 p1604 A72-25745

Engine ignition electronic system for triggering detonators in Aeros aeronomy satellite blastoff and release devices, discussing prototypes acceptance tests

11 p1610 A72-25803

GaAs solar batteries for spacecraft power supplies, comparing effectiveness with Si cells for optimum utilization

11 p1578 A72-25940

Ion thruster performance calibration investigating double ion content, back ingestion, beam spreading and propellant flow rate

11 p1709 A72-26206

Optimization of diagnostic tests for monitoring industrial system efficiency, obtaining compromise between costs and utilization

11 p1611 A72-26441

Vibrating string accelerometer sea gravity meter with electronics for digital readout, discussing performance tests

11 p1635 A72-26499

Atmospheric pressure noise reducer for active microbarograph array, evaluating performance in field tests

11 p1613 A72-26510

Quadrupole ion pump performance characteristics, presenting pumping speed as function of pressure at different peak voltages

12 p1805 A72-27040

Technological parameters effects on resistance values dispersion of thick film resistors, reviewing stability test performance

12 p1788 A72-27274

Performance and environmental tests of large lightweight solar array unit, measuring structural members displacements with electro-optical instruments

[AIAA PAPER 72-569] 12 p1755 A72-27377

Silicon solar cells antireflection coatings for performance loss minimization, obtaining improvement with titanium dioxide compared to silicon monoxide coatings

12 p1757 A72-28027

Integral diode cell for solar arrays compared with bypass configuration, discussing design, advantages and electrical performance test data

12 p1757 A72-28031

Cocuring technique optimization for primary aircraft components composite materials, discussing

mechanical and dimensional properties test data, production cost analysis and cure time

12 p1815 A72-28077

Composite materials application to gas turbine fan guide vane fabrication, noting economic factors and prototypes performance in engine tests

12 p1815 A72-28100

Detection range, color, brightness and flash subjective response tests to evaluate light signals for nighttime sea navigation and visual collision avoidance

12 p1777 A72-28326

Incentive contracts with price differential acceptance test plans to motivate producer to product improvement, defining admissible strategies in terms of risk limitation

13 p2066 A72-28354

Solid propellant pulsed plasma microthruster performance tests, describing engine design and operation

[AIAA PAPER 72-460] 13 p2026 A72-28945

Accelerated reliability, life, fatigue and performance tests of automatic systems components, noting mathematical models for minimum time techniques

13 p1965 A72-29172

Design characteristics and in-flight performance tests of computerized airborne OMEGA receiver, noting time independent one mile accuracy

13 p1997 A72-29188

Thin oxidation resistant alloy claddings for superalloys, comparing performance with aluminide coatings by cyclic furnace and high velocity burner rig tests

14 p1113 A72-30271

Training cockpit TL-29 mean time of failure-free operation from measurement data during development tests and two year guarantee, calculating avionic devices reliability

14 p2092 A72-30281

Microwave radiometer performance analysis, deriving input noise power relation to instrument indication in terms of noise parameters

14 p2105 A72-30587

Semiconductor devices quality assurance based on electrical and mechanical performance tests at every stage of product manufacture from initial design

14 p2091 A72-31164

Low power TTL IC in plastic and hermetic packages tested for reliability via critical dc parameters measurement in initial and post-stress states

14 p2091 A72-31168

Prototype local oscillator for X band communication satellite, discussing electrical and mechanical characteristics and temperature and noise measurements

15 p2204 A72-31182

Large astronomical telescopes construction, discussing aspherical surfaces control, grinding, polishing and optical testing procedures

15 p2234 A72-31612

Ultrasonic sound influence on metal physical and mechanical characteristics, utilizing in testing and manufacturing procedures

15 p2275 A72-31832

Worldwide distress alarm, identification and position location system for downed aircraft, discussing GRAN feasibility tests

15 p2272 A72-32214

Lunar roving vehicle qualification program to meet performance specifications under lunar conditions, describing testing procedures and project management techniques

15 p2214 A72-32613

Optical system production acceptance test based on modulation transfer function, discussing instrument design and test philosophy

16 p2389 A72-32847

Nondestructive monitoring techniques to optimize performance and service tests, considering penetrating radiation, electromagnetic induction, ultrasonics, holography, microwaves, acoustic emission and thermal monitoring

16 p2397 A72-33219

Piezoelectric shock transducers system performance tests, assessing previously recorded shock signatures

16 p2393 A72-33636

Sailplane performance measured in flight

17 p2487 A72-34215

Focusing properties and efficiency of EHF waveguide lens with Al honeycomb as guiding medium, noting design considerations and performance test results

17 p2525 A72-34368

Development of a full-length external-fuel thermionic converter for in-pile testing

17 p2495 A72-34590

Comparison of computer-acquired performance data from several fixed spaced planar diodes

17 p2496 A72-34605

Performance comparison of thermionic converters with several collector materials

17 p2497 A72-34606

Cylindrical diode characteristics with sublimed electrode surfaces

17 p2527 A72-34607

- Performance measurement in helicopter training and operations. 17 p2509 A72-35550
[PP-10-72]
- A relative performance analysis of atmospheric laser Doppler velocimeter methods. 17 p2558 A72-35949
- Thermionic converters performance and life tests, discussing test equipment and diffusion effect on emitter stability 18 p2643 A72-36139
- In-core thermionic converter emitters irradiation tests to determine fuel, fission gas venting system and emission layer performances 18 p2708 A72-36158
- Thermionic fuel element triple diode configuration, processing, assembly and performance during neutron irradiation testing in reactor 18 p2708 A72-36159
- Reactor testing and performance of in-pile thermionic fuel elements, noting neutron radiographs 18 p2708 A72-36160
- Attitude instruments, pitch and roll. I - Minimum performance standard for equipment. 18 p2692 A72-36534 [SAE AS 1162]
- Operation and performance characteristics of flying spot scanning X ray imaging systems for rapid film safe parcel inspection 18 p2692 A72-36671
- Acceptance testing of the MKL capacitor for space application 18 p2669 A72-37119
- Gauges for ultrahigh vacuum. 19 p2803 A72-38390
- Significance of OTF methods in assessing lenses to be used with partially coherent illumination. 20 p2931 A72-39049
- RF simulator design for missile systems performance tests, discussing requirements, target array and anechoic chamber [AIAA PAPER 72-861] 20 p2911 A72-39125
- Compression distillation unit design and development for integrated water and waste management system onboard spacecraft, describing reliability and performance tests [ASME PAPER 72-ENAV-1] 20 p2897 A72-39176
- Some results of testing M.O.S. transistors at elevated temperatures. 20 p2909 A72-39774
- Tilt-propotor VTOL aircraft design evaluation based on aerodynamic and aeroelastic model and full scale performance tests [AIAA PAPER 72-803] 20 p2889 A72-40054
- Viking 2 rocket engines for Europa 3 first stage propulsion, describing engine components design and functions and performance test results 22 p3216 A72-42649
- Variable impedance transducer measuring instruments for in-flight aircraft performance tests under environmental thermal effects 22 p3180 A72-42711
- Gas turbine engine performance measurement via parameters averaging method, noting integration time determination for given error limits 23 p3325 A72-43669
- Developing a synthetic turbine oil. 23 p3306 A72-43810
- Development and testing of a precise marine electrostatic gyroscope. 24 p3401 A72-44638
- Experimental performance of coaxial injectors in thrust-variable LO2/GH2-rocket engines. 24 p3434 A72-45181
- PERIDOTITE**
Olivine-garnet reaction in peridotites from Tanzania. 17 p2551 A72-35937
- PERIGEE-APOGEE SATELLITES**
U PAS
- PERIGEEES**
Extremum of satellite orbit perigee or apogee height in Hohmann transfer 05 p0713 A72-16006
- Observational bias source in lunar transient events correlation with perigee and tidal stresses, using statistical analysis for 1947-1967 period 14 p2150 A72-30324
- Discrepancy between Brown theory and Griffith values for lunar perigee and node mean motions partial derivatives with respect to moon mean motion 24 p3442 A72-45241
- Explorer 34 satellite orbit perturbation, noting earth gravitational tesseral harmonic effect on perigee passage time 24 p3399 A72-45557
- PERIHILIONS**
Numerical integration of element T /transit time through perihelion/ in perturbations of near parabolic comet orbits 03 p0436 A72-13829
- Comet hypotheses, examining orbit axes and perihelions spatial distribution as possible interstellar origin 03 p0438 A72-13978

- Comet orbits with perihelion distances and inclinations from Jupiter, calculating osculating orbital elements and distributions 03 p0439 A72-14241
- Planetary perturbation of orbits of long period comets with large perihelion distances 07 p1081 A72-20236
- Quantum and classical gravitation theory Mercury perihelion motion dependence on fourth order potential in scalar and Dirac fields 07 p1084 A72-20689
- Quantum gravitation theory and Mercury perihelion motion, calculating three body potentials from treatment of celestial bodies as nucleon assemblies 07 p1084 A72-20690
- Relativistic explanation for excess motion of Mercury perihelion in terms of solar oblateness and interior rotation mechanism 11 p1715 A72-25350 [AD-745666]
- Mercury perihelion advance determination from radar echo delays measurement 16 p2453 A72-33190
- Observation and feature variations of comet 1969e before and during the perihelion passage. 24 p3445 A72-45465

PERIOD EQUATIONS**U PERIODIC FUNCTIONS****PERIODIC FUNCTIONS****NT TANGENTS****NT TRIGONOMETRIC FUNCTIONS**

- Nonautonomous systems periodic solutions through Liapunov functions construction, considering application to nth-order dynamic systems forced oscillations 02 p0251 A72-11498
- Secondary periodic solution for Navier-Stokes type evolution problems, observing stabilities [ONERA, TP NO. 1035] 03 p0389 A72-13786
- Nonhomogeneous elastic structure with quasi-periodic coefficients, deriving mechanical model by continuum spectral theory 04 p0594 A72-15745
- Bang-bang automatic control of linear plant with discontinuous characteristics element, investigating periodic function oscillation 05 p0639 A72-15757
- Dynamic systems stability under periodic impulsive parametric excitation, deriving simple closed-form analytic stability criteria for special cases from general theory [ASME PAPER 71-WA/APM-19] 05 p0733 A72-15961
- Periodic integral convolution equations in elasticity theory and mathematical physics, demonstrating solution existence 05 p0739 A72-16589
- Time independent or periodic Hamiltonian conservative differential equations, studying open, oscillating, limited and abnormal trajectories [ONERA, TP NO. 1046] 06 p0877 A72-17661
- Quasi-periodic n-degrees of freedom solutions to Hamiltonian systems with 2n plus 2 variables, noting applicability to planar three body problem 06 p0839 A72-17882
- Incompressible micropolar fluid flow equations, deducing stable periodic solutions existence by energy method 06 p0799 A72-17917
- Linear equations with periodic coefficients in mathematical models for systems with rotating components, discussing methods for obtaining closed form solutions 07 p0913 A72-20204
- Radial gas bearing air lubrication theory, proving existence and uniqueness theorems for Reynolds equation periodic solution 07 p0998 A72-20473
- Elasticity theory doubly periodic problem for unbounded anisotropic plate weakened by system of identical arbitrary holes with self balanced loads 08 p1246 A72-21807
- Asymptotic almost periodic differential equations solved by introducing semiseparated conditions concept 09 p1340 A72-22246
- Numerical algorithm for matrix case extension of transport problem in periodic media 09 p1342 A72-23368
- Haag synchronization theory generalization through precision improvement and extension to almost periodical systems 10 p1510 A72-24123
- Discrete time systems with periodic feedback gain, deriving stability conditions and Nyquist plot from linear operator spectral theory 11 p1608 A72-25318
- Recursive algorithm for numerical solution of Sturm-Liouville problem with periodic boundary conditions 11 p1679 A72-26958
- Equation difference minimization techniques for ordinary nonlinear differential equations approximate periodic solution generation, noting error bounding procedure validity 12 p1836 A72-27240

- Periodic solutions of forced oscillatory system with hysteresis damping 12 p1844 A72-27246

- Steady bifurcating time periodic solutions stability for flows in bounded domain with complex conjugate simple eigenvalues at critical Reynolds number 12 p1837 A72-27712
- Periodic waveform expression in truncated Fourier series, determining polynomial coefficients relationship to amplitude density function 13 p1920 A72-29108
- Periodic two-parameter solution families of dynamic systems having first integral, showing stability and bifurcation existence criteria relationships to dimensionality and Hamiltonian systems 15 p2261 A72-31309
- Variational calculus methods for periodic solutions of autonomously perturbed Hamiltonian systems of differential equations 15 p2263 A72-31759
- Further periodic solutions of the three-dimensional restricted problem. II. 17 p2604 A72-34444
- Convergence of Rothe's method in the construction of bounded almost periodic and periodic solutions to a parabolic boundary value problem 19 p2824 A72-37433
- Periodic integral convolution equations in elasticity theory and mathematical physics, demonstrating solution existence 19 p2872 A72-37561
- Critical current periodicity of Josephson junction interferometers. 19 p2846 A72-38601
- Approximation of partial sums of multiple conjugate Fourier series of functions whose measure of continuity is given in the mean by Poisson integrals 20 p2945 A72-39394
- Nonlinear differential equation periodic solution approximation by pseudo-linear representation of nonlinear terms effects on single harmonic, using describing function matrix method 21 p3076 A72-41314
- Time-periodic solutions of boundary layer equation systems 22 p3164 A72-41908
- The rotating noncircular shaft as stability problem of a linear periodic system 23 p3347 A72-43718
- Approximation of continuous periodic functions by Faward sums 24 p3419 A72-45547
- PERIODIC ORBITS**
U ORBITS
- PERIODIC OSCILLATIONS**
U OSCILLATIONS
- PERIODIC PROCESSES**
U CYCLES
- PERIODIC VARIATIONS**
NT ANNUAL VARIATIONS
NT DIURNAL VARIATIONS
NT NOCTURNAL VARIATIONS
- Lunar tidal variations of ionospheric electron density at fixed heights for different solar hours over Huan-cayo and Puerto Rico 01 p0053 A72-10089
- Cosmic ray density distribution inside cosmic ray modulating spherical cone in solar wind, noting modulation depth quasi-periodic variation 01 p0119 A72-10606
- Middle geographic latitude sporadic E-layer initial height variations during 1957-1968 solar cycle 01 p0064 A72-11103
- Periodicities from power spectrum analysis of light curve of RR Tauri variable [AD-739638] 02 p0281 A72-12302
- Source motion effects on Doppler period variations of high velocity pulsars, considering first and second time derivatives 02 p0281 A72-12309
- DT Cyg and T Vul cepheid variables light curves and periodic variations from photoelectric observations 03 p0416 A72-13018
- Periodic micropulsations in amplitude and bandwidth observed in long duration vlf whistler mode signals from ground stations, considering explanations 03 p0322 A72-13530
- Cyclic phenomena periodicity by expected mean square deviation statistical analysis of observational data samples, using null hypothesis and unequally spaced sample intervals 04 p0574 A72-14908
- Pulsar CP 0328 wideband rf spectrum long term periodicity, considering origin during propagation through interstellar medium 04 p0580 A72-15369
- Markov model random variation optimal periodicity in preventive maintenance operations, estimating distribution density and moments 04 p0527 A72-15574
- Periodic aspects of nonephemeral Euroatlantic blocking systems persistence, noting dominant role played by cyclonic vortices 05 p0684 A72-16794

Computer aided steady state response analysis for nonlinear electric circuits with periodic input, using Newton algorithm with rapid convergence
06 p0779 A72-17480

Quasar 3C 273 light variation periodicities search, noting confidence level concerning resonance periods
07 p1073 A72-19424

Dynamo action of magnetohydrodynamic fluid motions with two dimensional periodicity
07 p1042 A72-19611

Terrestrial pole motion components, discussing variations in Chandler wobble period and sidereal motion direction and average annual motion along ellipse
07 p0976 A72-19815

Pulsar periods measurement with pulse arrival time calculation based on source position
07 p1080 A72-20052

Stratospheric cosmic ray short period variations at 30 km by spectral density method
07 p1066 A72-20653

Quasi-periodic ionospheric electron density fluctuations effects on electromagnetic waves propagation, noting effect on surface recordings as geomagnetic variations
08 p1156 A72-20824

Pleiades flare stars with slow cyclical variations from 1969-1970 observations
08 p1233 A72-21276

Periodic motion of gyroscope, using geometrical method of analysis
08 p1207 A72-21348

Goriachev-Chaplygin solution to gyroscopic motion of body around fixed point for periodic motion
08 p1208 A72-21355

RR Lyrae variables period-luminosity relations explained by linearized pulsation calculations for quenching of first harmonic
08 p1235 A72-21388

Periodic intensity and period variations of X ray pulsating source Cen X-3 caused by occulting binary system from Uhuru satellite observation
09 p1382 A72-22289

Periodic variations of 12 Cepheids from 4 to 45 days
09 p1384 A72-22515

Photoelectric observation of eclipsing contact binary 44 i Bootis period changes
09 p1391 A72-23534

Microorganisms effects on oxygen and compounds cycles, leading to changes in oxygen distribution in earth crust, hydrosphere, atmosphere and biomass
09 p1267 A72-23592

Secular and periodic variations of orbital elements of Mars satellites due to oblateness and solar attraction
10 p1541 A72-24471

Visual observations of eclipsing period elements of nova-like variable V Sagittae for estimate of total magnitude of uneclipsed binary
10 p1545 A72-24829

Chandlerian wobble period correlation to damping coefficient of earth polar motion for 10 yr intervals during 1900-1970
10 p1475 A72-24871

Short period terms in earth rotation rate and polar motion, considering data truncation effects on periodograms
10 p1475 A72-24872

Atmospheric wind velocity time variations at 80-100 km altitudes from ionospheric drift data, finding planetary oscillation periodicities relationship to solar activity cycle
11 p1620 A72-25273

Perturbation method study of governing differential equations for wave reflection by periodic two-dimensional topography
11 p1685 A72-25358

Sporadic E layer cyclic variations during solar activity cycle, noting time dependence of occurrence probability and critical frequency
11 p1623 A72-26281

Paris Observatory Danjon astrolabe observation of latitude variations, obtaining periodograms by Fourier analysis
12 p1868 A72-27217

Solar activity relation to geophysical phenomena, discussing atmospheric circulation and climatic variation cyclicity and sunspot corpuscular fluxes
12 p1842 A72-28207

Abridged version of 1970 Soviet conference on constant geomagnetic field and paleomagnetism, reviewing secular variation data
13 p1946 A72-28588

Regular cyclic fading of HF and VHF radio signals due to ionospheric scintillation, noting consistency with two ray interference formula
13 p1952 A72-29665

Flux density variations incidence among extragalactic sources found by 3.8 cm sky survey
13 p2048 A72-29830

Nonlinear dispersive wave propagation problems singly and multiply periodic solutions, using perturbation and numerical approximation methods
14 p2130 A72-30227

X ray source Cygnus X-1 pulsation periodicity analysis, showing random shot noise characteristics
14 p2156 A72-30571

Long term atmospheric pressure fluctuations in relationship to solar activity over Northern Hemisphere, confirming 22 year cycle
14 p2101 A72-30648

Pulsars distance computation, considering period-luminosity relationship and uncertainties inherent in dispersion measure /DM/ method
14 p2159 A72-30738

Monthly mean pattern variations for equatorial stratospheric easterly and westerly winds, noting continuity of low latitude regimes
14 p2129 A72-30806

Oscillations in ferromagnetic resonant circuit of parametric amplifier with constant capacitance and periodically variable inductance modulated by input signal
14 p2089 A72-31107

Dispersion equation determining periodic structures natural modes propagation constants, using induced electromotive and magnetomotive forces method
15 p2195 A72-31655

Subsonic wind tunnel for pulsed flows with speed modulation as periodic function of time
16 p2372 A72-32898

Radio source Oj 287 photometric and polarimetric observations, noting optical intensity and plane polarization variability
16 p2452 A72-33134

OSO 1 observation of 300 second oscillation in solar transition region and coronal extreme UV emission line intensity
16 p2453 A72-33137

Uhuru satellite data on periodic pulsating X ray source in Hercules, interpreting intensity variations as occulting binary star system effect
16 p2446 A72-33475

Periodic perturbation effect on oscillatory system behavior at frequencies approaching resonance
16 p2426 A72-33789

Criterion for unique periodic solution of perturbed Liénard equation for small amplitude periodic perturbation
17 p2574 A72-34400

Dissipative periodic process theory for application to elasticity and distributed parameter and hereditary systems defined by partial and functional differential equations
17 p2575 A72-34867

Russian book on atmosphere studies covering determination of periodic variations in meteorological elements to assess seasonal pressure, temperature and wind variations
17 p2546 A72-34975

Observation of the intensity ratio between /5,1/ and /9,4/ bands of OH emission in the night airglow
17 p2546 A72-35059

Association between quasi-periodic VLF emission and micropulsation.
17 p2516 A72-35065

Possible long-period oscillations in solar radio emission at microwaves.
17 p2608 A72-35091

Controllably periodic perturbations of autonomous systems.
17 p2576 A72-35200

Terrestrial pole motion components, discussing variations in Chandler wobble period and sidereal motion direction and average annual motion along ellipse
17 p2549 A72-35740

Identification of periodicities in the structure of natural stochastic processes
17 p2534 A72-35783

Spectral properties of periodically correlated random processes
17 p2535 A72-35784

Period changes in eclipsing variables. II - The system VW Cephei.
18 p2723 A72-36084

Mean period of fluctuations near the wall in turbulent flows.
18 p2682 A72-36721

The Chandlerian wobble from 1900 to 1970.
18 p2727 A72-36731

Solar activity centers characteristics cyclic variations in decreasing and increasing parts of sunspot activity cycles, discussing latitude-longitude distribution
19 p2851 A72-37906

Short-period pulsar intensity variations at 70 to 115 MHz
19 p2862 A72-38056

Three body problem second kind periodic orbit existence proof based on Weinstein theorem
19 p2867 A72-38553

Quasi-periodic variation in F 2 layer reflected signal field strength, noting predominance during periods with type 4 bursts, auroras and geomagnetic disturbances
19 p2792 A72-38639

Rotation period variation in long term behavior of interplanetary magnetic sector structure during nearly four solar cycles
19 p2868 A72-38731

Seasonal, diurnal and magnetic dependence of ionospheric scintillation at 64 deg invariant latitude.
20 p2916 A72-39226

Radiation models and explanations for absence of ground level gamma ray background periodic fluctuations
20 p2964 A72-39386

Straight fins with periodic base temperature variation, calculating design parameters effects on heat transfer rates, temperature distributions and efficiencies
20 p2983 A72-39484

[ASME PAPER 72-HT-E] Response of linear periodically time varying systems to random excitation.
20 p2974 A72-39892

A statistical method for the determination of the rate of changes of period for eclipsing binaries.
20 p2974 A72-39892

Secondary fluctuations in the light curve of epsilon Aur.
20 p2974 A72-39898

Search for high frequency optical variability in X-ray sources.
21 p3100 A72-40685

Magnetic-field variations in 78 Virginis, beta Coronae Borealis, and 73 Draconis.
21 p3106 A72-41036

Thermal oscillations in the high solar photosphere.
21 p3107 A72-41275

Atmospheric model for numerical simulation of five minute oscillation field properties of solar granular convection-excited gravity waves
21 p3107 A72-41277

Transition metals thermal conductivity periodic variations relation to free Fermi surfaces and valence electrons localization variations
21 p3070 A72-41646

Description of global-scale circulation cells in the tropics with a 40-50 day period.
22 p3201 A72-42506

Quantum impulse autocorrelation function of one dimensional harmonic crystal lattice, noting periodic time dependence at high and low temperatures
23 p3312 A72-43405

An algorithm to obtain the steady state response of nonlinear periodic systems.
23 p3267 A72-43852

Radial velocity periodic variability determination from shell star 88 Herculis hydrogen lines, obtaining hypothetical spectroscopic binary elements
23 p3340 A72-44237

Abridged version of 1970 Soviet conference on constant geomagnetic field and paleomagnetism, reviewing secular variation data
24 p3397 A72-45088

PERIODICITY
U PERIODIC VARIATIONS
PERIODICITY [BIOLOGY]
U RHYTHM [BIOLOGY]
PERIPHERAL CIRCULATION
Physical conditioning effect on central and peripheral circulatory responses to arm work, measuring cardiac output at 80 percent maximum aerobic power
04 p0473 A72-14900

Blood circulation minute volume and peripheral resistance changes during human aging process, accounting for body weight
08 p1120 A72-22073

Forearm skin and muscle blood flow change measurements during whole body heating, using plethysmography, isotopic labeling and blood sampling techniques
11 p1587 A72-26617

Water filled volume and strain gage phlethysmography for forearm blood flow measurement during isometric exercise
11 p1587 A72-26622

Peripheral venous renin activity during 70 deg tilt and lower body negative pressure.
19 p2758 A72-38703

Resistance and capacitance vessels of the skin in permanent and temporary residents at high altitude.
22 p3144 A72-42595

Rheographic investigation of cerebral, pulmonary and peripheral circulation during bed rest in antiorthostatic position
23 p3255 A72-43914

Comparative study of regional hemodynamics during tilt test and lower body negative pressure exposure.
24 p3373 A72-45131

PERIPHERAL NERVOUS SYSTEM
EEG study of cortical aftereffects to peripheral stimulation in cats
07 p0915 A72-18866

Russian book - Neurophysiological background of tactile perception.
21 p2998 A72-40464

Pyramidal control of the activity of interneurons related to various types of peripheral afferents
21 p2999 A72-40589

Subjective and objective sensory physiology, discussing transformation processes in sensory receptors and nerves, psychophysical scaling methods, chemoreceptors and peripheral adaptation
22 p3146 A72-42777

Tactile information transmission for orientation and motor control, discussing somatic sensitivity peripheral mechanism

22 p3146 A72-42778

PERMALLOYS [TRADEMARK]

Nondestructive readout in computer storage of plated wires on Permalloy film deposited substrates, testing design parameters effects on performance [IEEE PAPER 11, 2]

03 p0332 A72-13762

Plated-wire computer memory using thin Permalloy film on W wire substrate, testing nondestructive and destructive readout characteristics [IEEE PAPER 11, 3]

03 p0327 A72-13763

Low cost large array of decoding magnetic switches with electrodeposited Au conductors and Permalloy memory elements featuring high output flux for low driving current [IEEE PAPER 21, 3]

03 p0328 A72-13778

Reliable Permalloy integrated magnetic memories with realizable low switching coefficients and square-loop properties, discussing design and fabrication [IEEE PAPER 21, 4]

03 p0328 A72-13779

Annealing effects in plated-wire memory elements, investigating Cu and Permalloy interdiffusion at low temperatures by X ray diffraction and electron beam microprobe

04 p0503 A72-15715

Annealing effects in plated-wire memory elements, discussing recrystallization in Permalloy films from grain size and magnetic dispersion observations

04 p0504 A72-15716

Magnetic stress anisotropy field in plated cylindrical Permalloy films, determining relationships to circumferential composition variation, geometry and easy-axis dispersion

04 p0564 A72-15717

Contribution to the study of creep in thin permalloy films.

17 p2596 A72-35759

PERMEABILITY

NT DIELECTRIC PERMEABILITY

Hydrogen chemical permeation through iron and steel as function of compressive and tensile stress

01 p0083 A72-10206

Nonhomogeneous media electrodynamics with varying permittivity and permeability, solving nonstationary equations by differential operators

03 p0389 A72-13654

Active Na-K transport and passive permeability temperature adaptation in ground squirrel erythrocytes

04 p0475 A72-15546

Permeable porous plate surface properties effect on boundary layer stability

09 p1293 A72-22408

Optimal flexible ferrite keeper for ferromagnetic thin film memories performance improvement, noting requirements for high permeability, low loss factor and dielectric constant, etc

11 p1601 A72-25899

Effect of vibration on the permeability of the blood-brain barrier

22 p3149 A72-42070

Gas permeability of high-porosity nickel cermet

22 p3188 A72-42196

PERMEATING

New measurement and evaluation method for the determination of the diffusion coefficient of hydrogen in solid metals

18 p2692 A72-36841

PERMITTIVITY

Nonhomogeneous media electrodynamics with varying permittivity and permeability, solving nonstationary equations by differential operators

03 p0389 A72-13654

Dispersion characteristics of laminated cylindrical dielectric waveguide in millimeter band, noting application to permittivity measurement

05 p0627 A72-16341

Pulsating point charge potential in cold homogeneous boundless magnetoplasma with complex permittivity tensor coefficients for quadrupole probes theory

06 p0859 A72-17638

Antimony compounds single crystal whiskers permittivity determination at microwave frequencies from power reflection and transmission coefficients

09 p1366 A72-22417

Optical properties of Gd polycrystals in IR, explaining frequency dependence of complex permittivity

09 p1372 A72-23040

Dielectric tensor for electromagnetic waves in weakly inhomogeneous anisotropic media, taking into account permittivity and conductivity fluctuations

09 p1280 A72-23230

Microwave diagnostics of P doped Si semiconductor crystal prism determining relation between complex permittivity and reflection factor by variational method

10 p1450 A72-24404

Q switched ruby laser radiation spatial coherence, considering modes relationship to permittivity inhomogeneities and changes due to holes burning in population inversion

12 p1821 A72-27591

Electromagnetic wave diffraction on ideally conducting homogeneous bodies of revolution with arbitrary complex permittivity and permeability, using variables separation method

13 p1920 A72-29279

Electromagnetic wave propagation in nondispersing media with spatial-time fluctuations of dielectric permittivity, calculating scattered field by perturbation method

14 p2086 A72-30796

Microwave measurements on high permittivity materials with slotted waveguides excited in E mode

15 p2207 A72-31894

Antarctic ice sheet complex permittivity in VLF band from reduction of measurement data with buried dipole antenna under snow surface

15 p2200 A72-32104

Determining electrical ground constants from the mutual impedance of small coplanar loops.

17 p2514 A72-34371

Formation of fluorine-containing solid solutions based on barium titanate

19 p2845 A72-38407

Permittivity measurement of nonmagnetic materials samples in waveguide systems with an unknown movable reflecting load

24 p3404 A72-45504

PERMUTATIONS

Matrices and permutation rules for tetrahedral polynomial finite elements for Helmholtz equation, commenting on computer time and convergence rate

14 p2126 A72-30932

On the Gaussian elimination method for inverting sparse matrices.

17 p2573 A72-34237

Irreducible sparse matrix transformation to upper triangular form by row-column permutation formulated as linear integer programming problem

21 p3075 A72-41312

PEROVSKITES

Sintered prepolarized perovskite type ferroelectric ceramics adiabatic depolarization and energy conversion under shock wave action

10 p1422 A72-24128

Ceramic dielectrics capacitors, considering perovskites and barium titanate physicochemical properties

11 p1702 A72-26545

Pyrochlore and perovskite preparation and structure in bismuth rhodium oxide system, discussing variable position parameter, occupancy factor and structure stability

13 p2022 A72-29375

PEROXIDES

NT HYDROGEN PEROXIDE

Gaseous diethyl peroxide spontaneous ignition during decomposition in cylindrical vessel, investigating diluents and temperature effects on self heating

02 p0301 A72-12027

Epithelial follicle and mast cell role in peroxidase activity of thyroid gland during experimental burn development

13 p1905 A72-29330

Lipid peroxidation on the human skin surface following erythrogenic UV irradiation

19 p2757 A72-38087

PERSEID METEORIDS

Perseid shower radiants observation in August 1969, indicating presence of one secondary and two main radiants

14 p2153 A72-30499

Perseid shower radiants observation in August 1969, indicating presence of one secondary and two main radiants

19 p2864 A72-38328

PERSONALITY TESTS

Group composition and n-dominance personality trait effects on decision and communication task efficiency in laboratory triads

08 p1125 A72-21200

Personality correlates of lateral eye movement and handedness.

18 p2653 A72-36905

California psychological inventory as a predictor of success in the Naval flight program.

24 p3377 A72-45655

PERSONNEL

NT AIRCRAFT PILOTS

NT ASTRONAUTS

NT COSMONAUTS

NT FLIGHT CREWS

NT FLYING PERSONNEL

NT GROUND CREWS

NT INSTRUCTORS

NT MEDICAL PERSONNEL

NT NAVIGATORS

NT OPERATORS [PERSONNEL]

NT ORBITAL WORKERS

NT PHYSICIANS

NT PILOTS [PERSONNEL]

NT SCIENTISTS

NT SPACECREWS

NT TEST PILOTS

Terminal area ATC specialists and trainees job attitude and motivation from questionnaire on challenge, tasks, salary, work schedule, etc

06 p0766 A72-17865

PERSONNEL DEVELOPMENT

Earth Resources Survey /ERS/ program personnel training and education, discussing trainee selection, knowledge categories and training methods for remote sensing

02 p0304 A72-11855

PERSONNEL MANAGEMENT

Social factors of labor organization and control in scientific teams for industry

02 p0304 A72-11728

Individuals with high information potential in informal communications networks of government R and D organizations, discussing personal characteristics

12 p1891 A72-27654

Military R and D organization questionnaires data analysis to obtain relationship between job productivity, satisfaction, ability, age and salary

12 p1891 A72-27655

Heuristic procedure solution for least cost commercial airline crew scheduling, emphasizing combinatorial space size reduction

24 p3466 A72-44584

Employee motivation programs as a means of cost reduction in aerospace industries.

24 p3468 A72-45221

PERSONNEL SELECTION

NT PILOT SELECTION

Earth Resources Survey /ERS/ program personnel training and education, discussing trainee selection, knowledge categories and training methods for remote sensing

02 p0304 A72-11855

Education and training of personnel for photointerpretation, discussing psychological, physiological and methodological aspects of aerial photointerpretation

09 p1272 A72-23298

Soviet space crews selection and training based on professional and scientific background, emphasizing psychological qualities for working compatibility in space environment

09 p1274 A72-23672

Aptitude screening test of ATC training applicants, using directional heading determination under aural distraction

12 p1773 A72-28252

Brief vestibular disorientation test technique for assessment of potential nonpilot airborne specialists or naval flight officers

12 p1773 A72-28256

Potential coronary heart disease susceptibility indicators in ATC population, using Framingham age/obesity parameters

12 p1764 A72-28265

Sight impairment-caused flight personnel disqualification analysis, establishing eye disease structure, sight damage preconditions and ophthalmological practice inadequacies

14 p2080 A72-30748

Psychological criteria for flying personnel selection in civil aviation, noting performance prediction based on maximum likelihood estimates

14 p2080 A72-30816

Systematic detection of myocardial infarction in the course of medical screening of flight personnel

19 p2757 A72-37881

The Macruz index and its clinical evaluation in electrocardiography with regard to the selection and control of air crews

21 p3009 A72-41193

PERSPIRATION

Peripheral modifications to exercise induced central drive for sweating, determining rates as functions of internal temperature

04 p0479 A72-15212

Human temperature regulation during upright and supine exercise, showing nonlinear relationships between perspiration and skin and core temperatures

07 p0922 A72-20275

Human diaphoretic system physiology, discussing skin surface sweat excretion intensity relation to optimal balancing process in thermoregulation

14 p2076 A72-30672

Sweating relation to body temperature after exhaustive exercise for various oxygen uptakes and ambient temperatures

14 p2079 A72-30702

Monograph on hot environments stress covering heat exchange at skin surface, clothing effect, body temperature regulation and sweating control

15 p2185 A72-31515

Heat strain in hot and humid environments.

22 p3150 A72-42492

PERT

An estimate of expected critical-path length in PERT networks.

23 p3308 A72-43806

Cost estimation for engineering proposals in competitive bidding, discussing cost variability quantification methods based on PERT assumptions

24 p3468 A72-45478

PERTURBATION

NT ORBIT PERTURBATION
 NT SATELLITE PERTURBATION
 Nonlinear differential equations system stability conditions for arbitrary initial perturbations of zero solution, using Liapunov functions 08 p1199 A72-21461
 Small perturbation stability of discontinuous solution of equations of motion for solid fuel combustion processes 08 pl253 A72-21463
 Small gap approximation for axial magnetic field effects on stability of nonrotationally symmetric disturbances in inviscid flow between concentric rotating cylinders 11 pl694 A72-25773
 Approximation for mechanical system equilibrium perturbation anharmonic analysis based on Fourier series with real multiplication factors of fundamental pulsation 12 p1845 A72-27542
 Two dimensional Lagrangian hydrodynamic code for stability of shock acceleration perturbed interface between two gases of different density 13 p1942 A72-29114
 Oscillations of spacecraft with on-off attitude control under constant perturbation moment, calculating energy expenditures for desired orientation maintenance 14 p2162 A72-30459
 Determination of the stream function of a perturbation associated with a plane jet 18 p2680 A72-36470

PERTURBATION THEORY
 Warm inhomogeneous plasma models perturbation analysis, computing high frequency oscillation and eigenfrequencies and eigenfunctions formulas 01 p0106 A72-10134
 Hori perturbation theory equivalence to von Zeipel theory established to third order approximations in perturbed elliptic motions 01 p0129 A72-10796
 Coriolis acceleration effects on flight of projectiles fired from earth surface, discussing horizontal and vertical velocities 01 p0132 A72-11050
 Ion oscillation theory for electrogasdynamic channel Poiseuille and Hagen-Poiseuille type flows, using transport and dispersion equations in various ionized media 01 p0111 A72-11214
 Electromagnetic wave scattering from rough surfaces by Kirchhoff approach and small perturbation method, discussing validity near grazing angle 01 p0032 A72-11249
 Hypersonic source flow past wedges and cones, calculating flow nonuniformities effects on shock shape, velocity, pressure and density by perturbation analysis 01 p0033 A72-11394
 Relativistic nonlinear gravitational instability theory for hydrodynamical system of equations applicable to early cosmic expansion, deriving density perturbations associated with rotational and gravitational waves 02 p0275 A72-11524
 Steady sonic flow around three dimensional obstacles by pseudo-axisymmetrical flow approach, revealing singular perturbation of lift downstream at infinity 02 p0150 A72-12096
 Variational perturbation problem solution in power series form for elliptic functional description of elastic continuous medium state by Euler-Lagrange equations 02 p0259 A72-12233
 Normal electromagnetic wave propagation in randomly inhomogeneous medium in presence of super-refraction, deriving phase fluctuation spectra by perturbation method 02 p0180 A72-12587
 Rupture induced perturbation loads in pressurized orthotropic circular cylindrical shells 02 p0299 A72-12704
 Series summations for perturbation theory of multiple photon ionization probabilities of atoms applied to hydrogen and helium 03 p0391 A72-13080
 Perturbation induced long waves boundary effects in ideal incompressible fluid in uniformly rotating basin with stepwise depth difference, using Schwarz symmetry principle 03 p0340 A72-13094
 Kinetic theory application to initially nonuniform gas relaxation to equilibrium, obtaining macroscopic velocity, density and temperature solutions by multitime scale perturbation methods 03 p0340 A72-13155
 Poincare-Lighthill-Kuo perturbation method and method of characteristics equivalence in one dimensional fluid motion due to ideal piston periodic oscillation 03 p0341 A72-13239
 Faraday rotation as perturbation for analytic solution of system of differential equations for line formation in inhomogeneous magnetic fields 03 p0427 A72-13295

Multiplication operator unidimensional perturbation by independent variable, considering spectral function density poles and branch points 03 p0382 A72-13728
 One dimensional Boltzmann equation with linearized small perturbation, determining secondary conditions 03 p0399 A72-14347
 Ultralong wave baroclinic instability, obtaining linearized perturbation equations from layered geostrophic hydrostatic adiabatic model 04 p0541 A72-14451
 General perturbations theory for canonical systems extended to noncanonical systems, applying to perturbed Kepler motion 04 p0573 A72-14875
 Air-filled elliptical waveguide with nonmagnetic metal wall, determining dominant TE mode attenuation by perturbation method with Bessel function 04 p0491 A72-15426
 Fabry-Perot open resonators, determining eigenvalues, resonant frequencies and diffraction losses by asymptotic perturbation method 04 p0502 A72-15436
 Step-by-step perturbation method for calculating vibration modes of aerospace structure [ONERA, TP NO. 968] 04 p0592 A72-15552
 Pulsar planetary systems observation from perturbation of pulse arrival time 05 p0712 A72-15771
 Weakly divergent beam propagation of electromagnetic waves in statistically inhomogeneous nonlinear medium with dielectric constant dependence, using small perturbation method 05 p0625 A72-15818
 Continuous media stationary motion stability using initial boundary value problem of partial differential equations in perturbations [ASME PAPER 71-WA/APM-17] 05 p0647 A72-15963
 German monograph on Poincare orbit stability in restricted three body problem, using canonical mappings of annulus and perturbation method 05 p0689 A72-16044
 Structure, controllability and synthesis of n-dimensional invariant systems under perturbation vector, using governing equations 05 p0641 A72-16352
 Perturbation theory, saturation and relaxation effects in electron and ion plasma wave echoes 05 p0699 A72-17220
 Static perturbation technique functional form for postbuckling equilibrium path analysis by asymptotic approximation, noting relationship to Koiter method 05 p0742 A72-17244
 Electromagnetic wave scattering by underdense plasma layer, considering perturbation calculation for Gaussian, sech squared and parabolic density distribution 06 p0853 A72-17350
 Ion density perturbations propagation through plasma with double-humped Maxwellian ion velocity distribution in single-ended Q machine 06 p0855 A72-17515
 Perturbations in Godel universe, considering Einstein equations in relativistic cosmology 06 p0876 A72-17564
 Hamiltonian algorithms based on Lie transforms and von Zeipel method, discussing application to non-Hamiltonian system perturbation solution 06 p0839 A72-17660
 Book on orbital mechanics covering perturbation theory, many body problem, conic sections, orbit determination, canonical transformations and Hansen methods, moving coordinates, etc 06 p0879 A72-17820
 Perturbation methods for laminar flows near leading edge, discussing approximations of Navier-Stokes equations and domain connection 06 p0756 A72-18108
 Bulk semiconductor material complex microwave conductivity and dielectric constant measurements by cavity perturbation techniques 06 p0786 A72-18371
 Computer aided renormalized perturbation method for inhomogeneously loaded waveguide performance calculation 06 p0786 A72-18377
 Nonlinear self oscillation solution for systems with two degrees of freedom, comparing with harmonic linearization method for error of small parameter method 06 p0851 A72-18721
 Perturbation theorems proving for nonlinear systems of differential equations with integral solution of linearized equation 06 p0840 A72-18739
 Weakly damped harmonic oscillator, using perturbation methods for approximate solution to boundary value problem differential equation 07 p1034 A72-18816
 Small parameter method application to quasi-linear problems solution in nonstationary heat conduction

with substantial nonlinearities and weak perturbation, analyzing error 07 p1098 A72-18937
 Solar chromosphere radiative transfer and thermal conduction coupling, applying singular perturbation method to Frisch analysis 07 p1070 A72-19087
 Magnetized solar wind velocities and fields obtained by three dimensional model using perturbation technique with spherically symmetric boundary conditions 07 p1057 A72-19142
 Monograph on boundary layer generation, presenting two dimensional singular perturbation method 07 p0967 A72-19265
 Singular perturbation of absolute stability of Lure-Postnikov nonlinear systems described by differential equations with small parameters at higher derivatives 07 p1027 A72-19293
 Multivariable linear systems control structure via optimal control theory with quadratic criterion, permitting compensation for nonzero mean value and slowly varying perturbations 07 p0961 A72-19711
 Stress-strain state of homogeneous isotropic medium bounded by noncanonical surfaces of revolution, using perturbation method 07 p1091 A72-19755
 Reduction principle validity in perturbed motion stability theory for near-critical systems with gyro horizon application 07 p1035 A72-19972
 Hydrodynamic stability small perturbation theory, considering potential flow in contact with flexible membrane 07 p0969 A72-20067
 Matched asymptotic expansions method application to problems with two independent perturbation parameters, considering application to boundary layer and hypersonic flow theory 07 p0970 A72-20076
 Perturbation solution to nonlinear nonuniform torsion of thin walled open elastic beams with strain hardening dependent on torque-rotation behavior 07 p1096 A72-20431
 Solar wind plasma parameter spatial perturbation problem solution by method of characteristics 08 p1225 A72-20721
 Perturbation theory oscillatory wave function for second order correction to oxygen 16 nucleus bonding energy 08 p1211 A72-21067
 Linear time optimal problem with analytical perturbations of initial conditions, determining optimal control switching points from convergent series representation 08 p1145 A72-21466
 Nonlinear modal response analysis of plate structures under random acoustic excitation, using finite element method and perturbation technique 08 p1245 A72-21607
 Second order libration solution of ideal resonance problem, using Lie series perturbation technique 08 p1236 A72-21637
 Nonlinear system of differential equations for gravity perturbation on geometrical form of thin axisymmetric cavity in heavy fluid 08 p1151 A72-21705
 Hill variable modification of Brouwer satellite theory algorithm for simplified orbital element and perturbation calculations and orbital eccentricity generalization 08 p1237 A72-21749
 Perturbation solution of deceleration trajectory in ballistic reentry through rotating atmosphere with winds, assuming constant gravitational field and square law drag force 09 p1395 A72-22924
 Perturbation analysis of nonlinear free flexural vibrations of circular cylindrical shell, using Donnell equations 09 p1405 A72-22998
 Microscopic perturbations of metals electron density complex dynamic matrix, deriving electroconductivity and kinetic coefficients 09 p1329 A72-23039
 Book on perturbation theory in celestial mechanics, covering disturbing function, Lagrange method and Delaunay theory 09 p1389 A72-23246
 Book on perturbation theory in celestial mechanics, covering absolute perturbation, Hill lunar theory and application to Jupiter satellites 09 p1389 A72-23247
 Nonlinear vibrations under random excitation, discussing equivalent linearization and small parameter perturbation methods and Fokker-Planck equation 09 p1353 A72-23604
 Equation of isovolumetric fluid pulsed and potential flow in convergent duct solved by perturbation method 10 p1465 A72-24118
 Lie transformations for perturbed canonical system of differential equations solution, proposing parameter

ter square root series development for resonance problems of celestial mechanics

10 p1536 A72-24119

Linear analysis of gravitational perturbations in strongly collisional initially homogeneous and Maxwellian medium

10 p1536 A72-24138

Upper bounds on lumped and continuous dynamic systems motion under loads and perturbations, discussing structure stability conditions

[ASME PAPER 71-APMW-3] 10 p1554 A72-24188

Perturbation method for stability boundaries of Hill equation with three independent parameters

10 p1505 A72-24190

Nonlinear analysis of gravitational stability perturbation based on Maxwellian velocity distribution

10 p1538 A72-24214

Two dimensional low Mach number sound field from line vortex passage around rigid half plane edge, calculating space-time variation by perturbation methods

10 p1468 A72-24370

Modified sweep variation method for optimal control programs, solving two point boundary value problem by linear perturbation technique

10 p1551 A72-24455

Second order Cowley-Imai analogy application to transcribe gas dynamic perturbation solutions into magnetogasdynamic solutions for perfect gas axisymmetric super-Alfvénic flows

10 p1521 A72-24464

Perturbation analysis for forced flow past semi-infinite flat plate parallel to uniform mainstream, calculating two dimensional laminar film condensation by boundary layer theory

10 p1469 A72-24563

Rapid perturbation growth conditions for expanding universe, discussing background density decrease with time

10 p1543 A72-24661

Radio propagation over slightly roughened curved earth surface, using perturbation method and Taylor series in model calculation

10 p1439 A72-24743

Confocal spherical laser resonator deformation analysis based on perturbation method, investigating forced oscillation

10 p1493 A72-25150

Global controllability of nonlinear differential systems during linear system perturbation, discussing controllable and uncontrollable parts splitting and null domain nature

11 p1608 A72-25323

Structure, controllability and synthesis of n-dimensional invariant systems under perturbation vector, using governing equations

11 p1608 A72-25328

Perturbation method for asymptotic solutions of initial value problems for hyperbolic wave equations with small nonlinearities

11 p1676 A72-25355

Perturbation method study of governing differential equations for wave reflection by periodic two-dimensional topography

11 p1685 A72-25358

Pulsed perturbation and Q coupled extremal control systems with noise distortion, obtaining optimal transfer functions with Kolmogoroff-Wiener method

11 p1610 A72-25448

Fluid dynamics layer-type singular perturbation problems, constructing inner and outer asymptotic approximations with overlapping domains of validity

11 p1615 A72-25502

Vlasov perturbation theory of nonlinear plasma wave with Landau damping based on Korteweg-de Vries equation

11 p1692 A72-25517

Perturbation technique application to nonlinear behavior of ion waves produced by two-beam instability in plasma

11 p1692 A72-25519

Asymptotic behavior of unperturbed linear and nonlinear perturbed functional differential equations

11 p1677 A72-25524

Nonlinear theory of gravitational instability in expanding universe, discussing density and velocity perturbations amplification at intermediate stage

11 p1715 A72-25527

First order asymptotic matching computational hyperbola for calculation of perturbed moon-centered hyperbola parameters in earth-moon trajectory

11 p1720 A72-25996

Symmetric discrete elastic conservative structural systems stability boundary estimation through reduction to linear equation recursive solution, using perturbation method

12 p1880 A72-27242

Perturbation procedure for weakly coupled oscillators in connection with statistical mechanics ergodic problem and nonlinear interaction models

12 p1844 A72-27248

Perturbation theory for electromagnetic radiation in weakly anisotropic magnetoplasma, calculating Green

function for delta function source oriented parallel to static magnetic field

12 p1783 A72-27668

Viscous flow stability between two rotating nonconcentric cylinders, obtaining approximate solution to eigenvalue problem by perturbation method

12 p1799 A72-27846

Small perturbations in collisionless stellar dynamics, discussing linear modes for flat axisymmetric galaxy and effects introduced by nonlinear theory of spiral structure

12 p1874 A72-27904

Airplane sideslip and yaw rate perturbations by continuous random vertical and side gusts, using low pass filtered white noise representation for mathematical modeling

12 p1755 A72-28125

Book on density matrix theory application to lasers and masers, covering quantum mechanics, perturbation theory, magnetism and magnetic resonance, statistical ensembles, etc

12 p1826 A72-28203

Asymptotic approximation methods for boundary layers in singular perturbation theory for linear elliptic partial differential equations in two independent variables

13 p1940 A72-28425

Space-time correlation of field amplitude and phase in plane waveguide with statistically irregular boundary, using Born approximation and perturbation theory method

13 p1928 A72-28471

Numerical analysis methods for solution stability of reduced field equations describing perturbed motion of body under nonconservative loads

13 p2001 A72-28485

Quadrature solution for variable mass point motion under perturbing force in trajectory plane normal to velocity vector

13 p2003 A72-28725

Torsional waves far-field structure in infinite elastic rod of elliptical cross section, using perturbation method

13 p2057 A72-29004

Nonlinearity effect on electron plasma wave dispersion relation, using numerical simulation and theoretical analysis by perturbation expansion and Hamilton variational principle

13 p2011 A72-29121

Error analysis of ionospheric parameter measurement by satellite transmitted or reflected multiple frequency pulsed radiation signal, using perturbation method

13 p1920 A72-29276

Perturbation theory of hydrogen and helium atoms multiphoton ionization probabilities, proposing series summation method

13 p2007 A72-29430

Elastic waves propagation in randomly inhomogeneous fiber reinforced or layered composites from perturbation methodology for electron and vibrational waves in disordered media

13 p2061 A72-29697

Differential systems perturbation method by association with easy-to-integrate reduced system, applying to nonlinear mechanics

13 p1987 A72-29780

Given motion realization in presence of constantly acting perturbations by pulsed correction, applying to signal transmission accuracy implementation

13 p2007 A72-30082

Radiation defectoscopy methods based on calculating perturbations in gamma radiation field due to inhomogeneities

14 p2106 A72-30150

Nonlinear dispersive wave propagation problems singly and multiply periodic solutions, using perturbation and numerical approximation methods

14 p2130 A72-30227

Waldman-Snyder equation application to sound absorption and dispersion in dilute polyatomic gases, presenting truncation procedure for perturbation function expansion in irreducible Cartesian tensors

14 p2131 A72-30673

Stability conditions for damped single degree of freedom oscillator system under stationary narrow-band random excitation, obtaining approximate solution by perturbation method

14 p2131 A72-30718

Third order extension of perturbation method to solve Oseen equations for two dimensional steady viscous flow past cylindrical body at low Reynolds number

14 p2095 A72-30722

Electromagnetic wave propagation in nondispersing media with spatial-time fluctuations of dielectric permittivity, calculating scattered field by perturbation method

14 p2086 A72-30796

Infinitesimal mass revolution around smallest primary of restricted four body problem, discussing element perturbation

14 p2161 A72-30913

Spiral structure density wave model of inner parts of Galaxy, calculating density, potential and velocity perturbation and dispersion in gas and stars

14 p2161 A72-30914

Meteor streams secular perturbations computation by Gauss-Halphen-Goriachev method

14 p2161 A72-31078

Asteroids and comets orbit perturbation equations for small eccentricity values

14 p2161 A72-31080

Nonlinear autooscillatory systems forced vibration under random perturbations, calculating dynamic processes by statistical linearization

14 p2132 A72-31114

Van der Pol oscillator periodic pulling behavior under weak perturbation near natural frequency, analyzing Fourier frequency spectrum

14 p2132 A72-31122

Three dimensional boundary layer instability, obtaining linearized perturbation equation on basis of Navier-Stokes equation

15 p2216 A72-31471

Isentropic perfect gas steady compressible flow finite element analysis through nonlinear equations linearization based on perturbation theory

15 p2217 A72-31719

Variational calculus methods for periodic solutions of autonomously perturbed Hamiltonian systems of differential equations

15 p2263 A72-31759

Thermodynamic perturbation and scaling theory for multidimensional spherical models of lattice structure in terms of field of critical phenomena

15 p2293 A72-32219

Quantitative measure for sensitivities of natural frequencies to perturbations leaving modes invariant

15 p2278 A72-32279

Radiative stellar envelopes circulation velocity calculation for various cylindrical rotation laws using perturbation method

15 p2314 A72-32371

Nonlinear stability theory for plane Poiseuille flow under finite amplitude perturbations, solving Orr-Sommerfeld boundary value problem via finite difference method

15 p2218 A72-32469

Perturbation scheme for branching analysis of post-buckling behavior in elastic spherical shells

16 p2465 A72-33001

Perturbation theory for equations of motion of electrically and thermally conducting viscous compressible flow in homogeneous magnetic field, calculating fluctuation modes

16 p2435 A72-33008

Perturbations effects on plane symmetry supersonic molecular beam intensity as function of nozzle-skimmer geometry and nozzle pressures

16 p2304 A72-33062

Group perturbation method for accuracy analysis of nonlinear stochastic automatic control systems, noting computer time reduction

16 p2371 A72-33091

Mechanical system nonlinear perturbation effect on equations of motion solutions, deriving boundedness and stability conditions via inequality theorems

16 p2423 A72-33101

Singular perturbation methods for deflections, frequencies and eigenmodes of statically loaded or freely vibrating circular or annular membrane

16 p2467 A72-33106

Optimal invariant control system synthesis for inertial plants with nonminimal phases and random perturbation compensation

16 p2371 A72-33263

Linearization and perturbation procedures to calculate nonlinear effects in fluid stability problems with application to nonlinear critical layer

16 p2377 A72-33338

Coordinate perturbation and multiple scale techniques application to supersonic flow field around two dimensional wing and oscillations in closed tube

16 p2379 A72-33576

Stellar magnetic oblique rotator internal motion field construction by perturbation technique estimating energy dissipation and turbulent viscosity

16 p2458 A72-33721

Coupled thermoelastic theory for thin plates, using perturbation method to find free vibration frequencies of plates under various boundary conditions

16 p2471 A72-33785

Periodic perturbation effect on oscillatory system behavior at frequencies approaching resonance

16 p2426 A72-33789

Transonic airfoil section design to given surface pressure distribution, applying finite difference procedures to transonic small disturbance equations [AIAA PAPER 72-679]

16 p2346 A72-34062

Perturbation methods for density stratified viscous flow past flat plate, using boundary layer and low Reynolds number approximations [AIAA PAPER 72-646]

16 p2381 A72-34086

Perturbation method for two point boundary value problem for fluid flow applied to optimal reentry control problem

16 p2462 A72-34166

Hamiltonian for first order wave function in charge exchange perturbation theory 17 p2584 A72-34259

Analysis of wave propagation in elastic cylindrical shells by the perturbation method. 17 p2623 A72-34307

Criterion for unique periodic solution of perturbed Liénard equation for small amplitude periodic perturbation 17 p2574 A72-34400

Flight vehicle, control system and perturbations models synthesis from variational problem solution via control functions improvement 17 p2621 A72-35037

Controllably periodic perturbations of autonomous systems. 17 p2576 A72-35200

Nonspherical perturbations of relativistic gravitational collapse. I - Scalar and gravitational perturbations. II - Integer-spin, zero-rest-mass fields. 17 p2612 A72-35390

Perturbation theory for torsional earth oscillations - Second approximation 17 p2548 A72-35475

Use of multiple basis sets in the Brueckner-Goldstone many-body perturbation theory for atomic problems. 17 p2586 A72-35772

Brueckner-Goldstone many-body perturbation calculation of helium photoionization. 17 p2586 A72-35773

The exact evaluation of certain partial sums of the second order energies of atoms. I - The ground and the singly excited states. 17 p2586 A72-35829

Thermal and gravitational instability in universe, obtaining equation for growth rate of density contrast 17 p2618 A72-35910

Coordinate transformation for perturbation analysis of elastic structural system imperfections influence on elastic buckling 18 p2732 A72-36079

Linear homogeneous system of differential equations as model for perturbation problems including functions with retarded and/or advanced arguments 18 p2705 A72-36614

Field fluctuations of a laser beam propagating in a turbulent atmosphere 18 p2661 A72-36656

On disturbances in a viscoelastic rod /of variable cross-section/ of Reiss type placed in a magnetic field. 18 p2711 A72-36752

Perturbation method in inelastic interaction model for transport processes in reacting gases described by Boltzmann kinetic equation 18 p2713 A72-36807

Alternate singular perturbation theory of high Reynolds number flow over flat plate to eliminate asymptotic matching and composite solution for accuracy improvement 18 p2684 A72-37083

Range correction computations for weapons dropped from aircraft. 19 p2747 A72-37286

Intrinsically transonic /almost equal frozen and equilibrium sound velocities/ flows of chemically active gas mixture, developing nonlinear perturbation theory 19 p2745 A72-37390

Perturbations development in laminar flow and transition to turbulent flow based on nonlinear theory of hydrodynamic stability 19 p2785 A72-37468

Undisturbed eccentric anomaly difference as the independent variable in the perturbation differential equations. 19 p2856 A72-37520

On the adiabatic invariants of a quantified system perturbed by a coherent wave 19 p2834 A72-37789

Optimization of control and observation processes in a dynamic system at random disturbances 19 p2778 A72-37991

Rotatory perturbations in anisotropic cosmology 19 p2864 A72-38078

Applicability of the small parameter method to the estimation of stresses in nonhomogeneous elastic media 19 p2876 A72-38153

A stability theory for perturbed difference equations. 19 p2826 A72-38249

Solar wind plasma parameter spatial perturbation problem solution by method of characteristics 19 p2852 A72-38349

The Poincare Lighthill perturbation technique and its generalizations. 19 p2827 A72-38383

Markovian plasma turbulence model to obtain convergent perturbation series for diffusion coefficient via trajectories in particle propagator 19 p2841 A72-38442

Low-frequency vibrations in a rarefied bounded plasma 19 p2842 A72-38530

Book - Astrodynamics: Orbit correction, perturbation theory, integration 19 p2868 A72-38723

On the application of perturbation theory for the calculation of molecular constants due to small mass changes and on the determination of force constants from very heavy isotope substitution. 19 p2763 A72-38806

An intermediate matching technique for solving two point boundary value problems using the perturbation method. 20 p2910 A72-39198

Rotational perturbation of three bodies in space tied by flexible elastic ropes, relating physical parameters to stable motion regions boundaries 20 p2977 A72-39246

Vector wave solution of light beam propagating along lenslike medium. 20 p2903 A72-39266

MHD instability of two dimensional laminar boundary layer in incompressible electrically conducting fluid along concave wall with periodic three dimensional disturbances 20 p2957 A72-39328

Beams on bilinear elastic foundations. 20 p2980 A72-39692

Galaxy formation in generic dust filled anisotropic cosmology, analyzing density perturbations growth rate 20 p2972 A72-39872

Tidal perturbation of the non-radial oscillations of a star. 20 p2974 A72-39895

Reduction principle validity in perturbed motion stability theory for near-critical systems with gyro horizon application 20 p2955 A72-40029

New method of calculating disturbed ephemeris of minor planets 21 p3102 A72-40095

A similarity solution for viscous internal waves. 21 p3044 A72-40118

Optical propagation in space-time-modulated media using many-space-scale perturbation theory. 21 p3014 A72-40142

Reductive perturbation method application to Vlasov equation governing one dimensional motion of collisionless plasmas, investigating nonlinear modulation of plasma waves 21 p3089 A72-40188

Perturbation theory for field moments in inhomogeneous media 21 p3016 A72-40780

Gravitational perturbations as source for solar oblateness fluctuations, considering density in upper convective zone 21 p3106 A72-41039

Comparison of the classical and the global solutions of the ideal resonance problem. 21 p3085 A72-41047

Numerical stabilization of the differential equations of Keplerian motion. 21 p3106 A72-41050

Synthesis of Tolubinskii's integral method and the perturbation method in nonstationary transport problems with nonlinear boundary conditions 21 p3129 A72-41053

Application of methods in perturbation theory to the calculation of the natural vibrations of rod systems 21 p3119 A72-41097

The post-flutter oscillations of discrete symmetric structural systems with circulatory loading. 21 p3120 A72-41207

Stellar evaporation in globular clusters passing through galactic plane, considering gravitational perturbation increase of total energy within system 21 p3107 A72-41269

Regularized linear problem with perturbed equation as solution, presenting error overestimate 21 p3076 A72-41336

Invalidity of Neptune predicted position derivation from perturbations on Uranus via method neglecting eccentricity 21 p3111 A72-41474

Satellite vibration-rotation motions studied via canonical transformations. [AIAA PAPER 72-919] 21 p3115 A72-41564

Long-term orbit prediction using two-variable asymptotic expansions and the automated manipulation capabilities of the FORMAC language. [AIAA PAPER 72-938] 21 p3113 A72-41576

Perturbation analysis of aerodynamic test flow in Ludwig tubes, investigating unsteady coupling effects on nozzle turbulent boundary layer [AIAA PAPER 72-994] 21 p2993 A72-41580

Propagation of electromagnetic disturbances and the stability of stationary states in media with a non-linear Ohm's law 21 p3086 A72-41651

The total pulsation-frequency spectrum of a polytropic atmosphere 21 p3114 A72-41779

Fluidic implementation of a perturbation extremum controller. 22 p3139 A72-42050

Quadrature solution for variable mass point motion under perturbing force in trajectory plane normal to velocity vector 22 p3205 A72-42101

Airborne towed cargo carrying bodies dynamic stability for single-point suspension system, using linearized small perturbation analysis [AIAA PAPER 72-986] 22 p3136 A72-42328

Helicopter rotor blade flapping motion stability, applying perturbation technique to linear equations of motion for different advance ratios and Lock numbers [AIAA PAPER 72-955] 22 p3137 A72-42351

The dependence on inclination of the planetary perturbations of the orbits of long-period comets. 22 p3224 A72-42378

Atmospheric frontal motion stability via two-layer homogeneous incompressible fluid model, solving eigenvalue problem by small perturbation method 22 p3201 A72-42505

The estimation of masses of individual galaxies in clusters of galaxies. 22 p3227 A72-42551

Continuum and finite element branching studies of the circular plate. 22 p3235 A72-42603

On the perturbation method in the stability analysis of continuous systems. 22 p3206 A72-42842

Singular small parameter perturbation effect on absolute stability of high order derivatives in Lure-Postnikov nonlinear systems 23 p3274 A72-43544

Nonlinear mechanics perturbation method for Liapunov functions construction, noting application to nonlinear differential equations 23 p3308 A72-43582

Stresses around an axial crack in a pressurized cylindrical shell. 23 p3346 A72-43705

Perturbation of the shape of the cavity during motion in a ponderable liquid 23 p3280 A72-43797

Gravitational instability of perturbed and unperturbed matter distribution in form of density and velocity fluctuations associated with continuity relationship between wavelength and rotation direction 23 p3338 A72-44036

Differential equations of motion of two mutually perturbing bodies, noting series expansion of perturbation function for close commensurability of mean motions 24 p3437 A72-44761

Small disturbances propagation effect on self similar flow due to point explosion in medium with density varying according to distance from center 24 p3390 A72-44786

Stokes series for perturbing potential determination from gravity anomalies expressed as sum of two convergent series 24 p3418 A72-44858

Electric dipole moment of diatomic molecules by configuration interaction. IV. 24 p3426 A72-44870

On exponential-asymptotic stability properties of Boltzmann's equation and a class of its modifications. 24 p3426 A72-44911

Smoked foil observation technique for transient behavior produced by perturbing equilibrium configuration detonation waves 24 p3462 A72-45033

Weak shock wave propagation in a relaxing gas. 24 p3391 A72-45042

The concept of reference loci applied to four-body dynamics. 24 p3440 A72-45137

Celestial mechanics ideal resonance problem global solution via Bohlman-von Zeipel perturbation technique, modifying Hamiltonian expansion point and separatix and libration region singularities suppression method 24 p3440 A72-45138

Discrepancy between Brown theory and Griffith values for lunar perigee and node mean motions partial derivatives with respect to moon mean motion 24 p3442 A72-45241

A general theory of convergence for numerical methods. 24 p3419 A72-45300

Perturbation methods in atmospheric flight mechanics. 24 p3368 A72-45350

A linear asymptotic theory for anisotropic shells. 24 p3460 A72-45473

PETROGRAPHY

Impact breccias in carbonate rocks of Sierra Madera /Texas/, investigating microstructure, chemical composition, petrography and mineralogy 05 p0654 A72-16038

Mineralogic and petrologic study of lunar anorthosite slide 15415.18 06 p0888 A72-18271

Geological setting, petrography and history of Apollo 15 anorthosite sample, tracing fragmentation and thermal metamorphic events 11 p1722 A72-26239

Broad scale remote mapping of spectral composition of silicate rocks from thermal IR scanner data
14 p2099 A72-30321

Thermal expansion measurements of simulated volcanic and nonvolcanic lunar rocks as function of temperature
15 p2222 A72-31258

Morphology and petrography of volcanic ashes.
18 p2685 A72-36222

PETROLOGY

NT PETROGRAPHY

Lunik 16 core-tube soil sample petrology and chemical composition
01 p0126 A72-10107

Electron microprobe analysis of plagioclase points and pyroxene grains of Apollo 15415 anorthositic genesis rock
02 p0282 A72-12411

High temperature thermal properties of solid and liquid metals and rocks and minerals, discussing earth heat balance and measurement methods for heat capacity and conductivity
04 p0596 A72-14653

Northeast Bank, Southern California Borderland volcanic petrology and geologic history, investigating basaltic rocks, hyaloclastites and fossil fragments
04 p0520 A72-15589

Ti leaching from granitic rocks by *Penicillium*, simplicissimum, discussing extraterrestrial life detection
05 p0616 A72-15809

Alfianello meteorite inspection by optical microscopy for petrological features of shock metamorphism in chondrites
05 p0722 A72-17152

Chemical, geochronological and petrogenetic analyses of Apollo 15 lunar mare basalt rock from Hadley Rille, comparing with Apollo 12 and 14 basalts
06 p0888 A72-18264

Petrological analysis of Mare Fecunditatis regolith returned from Luna 16 mission
09 p1379 A72-22254

Optical petrographic, electron microprobe and single crystal X ray diffraction analysis of basaltic and monomineralic soil fragments of Lunik 16 core sample from Sea of Fertility
09 p1379 A72-22257

Luna 16 rock sample B-1 petrology, mineralogy and chemistry, noting fine grained ophitic basalt nature
09 p1380 A72-22262

Lunik 16 lunar soil samples petrogenesis and chemical composition, comparing to Apollo regoliths
09 p1381 A72-22271

Crystallization sequence, petrology and mineralogy of Apollo 12 basalt sample 12009
10 p1537 A72-24160

Petrologic comparisons of lunar terra materials.
17 p2615 A72-35684

Olivine-garnet reaction in peridotites from Tanzania.
17 p2551 A72-35937

Earth density, surface wave velocity and other properties calculation from model consistent with physical and petrological mantle theories
20 p2917 A72-39475

Instrumental neutron activation analysis of igneous rock abundances in petrogenic and stratigraphic problems, applying to Colombia River basalts and Apollo 11 rock samples
20 p2899 A72-39829

Czech book - Moldavites and tektites.
21 p3111 A72-41536

Lunar interior composition constraints from chemical composition of igneous rocks on surface
22 p3226 A72-42533

Occurrence of chromian, hercynitic spinel /'pleonaste' in Apollo-14 samples and its petrologic implications.
22 p3153 A72-42862

Mineralogy, petrology and chemistry of lunar rock 12039.
23 p3339 A72-44127

Chemical composition of Luna 16 and Luna 20 rock samples from Sea of Fertility and Apollonius Crater
24 p3440 A72-45109

PFM [MODULATION]

U PULSE FREQUENCY MODULATION

PH

Intracellular pH prime regulation in rat brain during acute and sustained hypercapnia, discussing cellular bicarbonate accumulation
01 p0012 A72-10623

Phosphate solubilization and activation on primitive earth, using apatite solubility as function of pH
04 p0483 A72-14769

Microorganism life in extreme high temperature, PH and solute concentration environments, noting salt effect on enzyme activity
04 p0471 A72-14801

Grain boundary region constituents corrosion behavior and solution chemistry within stress corrosion cracks in Al alloys observed from pH changes
04 p0535 A72-15733

Crack corrosion in metals and metal alloys, considering electrochemical reaction kinetics as function of oxygen concentration and pH
04 p0536 A72-15738

Acid-base balance shift during muscular exertion, determining pH and bicarbonate content variation by Astrup micromethod
06 p0765 A72-18062

Direct single electrode measurement of carbon dioxide partial pressure in liquids and gases, using pH changes due to gas diffusion
09 p1317 A72-23671

Continuous and intermittent maximal exercise effects on human muscle intracellular and capillary blood pH
10 p1425 A72-24477

Electrolyte temperature, pH and mixing rate effects on anodic dissolution of steels and brass in electrochemical precision processing, using thermokinetic data processing
11 p1640 A72-26257

Cerebrospinal fluid pH change effects on cat respiratory response before and after vagotomy, showing vagal activity relation to central chemical control of respiration
12 p1762 A72-27825

PH FACTOR

Mathematical model of extracellular pH in brain tissue from blood and cerebrospinal fluid acid-base parameters for respiration central chemosensitive mechanism study
11 p1579 A72-26660

Respiration control by extracellular pH in medullary tissue, studying chemoreceptor response to hydrogen ion concentration in cat cerebrospinal fluid
11 p1579 A72-26661

PHANTASTRONS

Oscillation development time in phantastron oscillator, using linearization of nonlinear term
10 p1450 A72-24517

PHARMACOLOGY

Abdominal injected barbamyol somnifacient and toxic effect on mice subjected to hypokinesia and isolation
05 p0622 A72-16650

Central nervous system pharmacology, discussing somniferous, narcotic and neurotropic substances effects on brain activity
08 p1127 A72-21841

Russian book on pathophysiological principles of air and space pharmacology covering stress and fatigue reduction and pilots and astronauts performance improvement
12 p1772 A72-27926

Medication effects on pilot performance, covering tranquilizers, sedatives, antibiotics, stimulants, antihistamine and hypotension drugs
13 p1909 A72-28750

Work capacity evaluation from fatigue, biological rhythm, tissue respiration and oxygen consumption studies, discussing pharmacological stimulation effects
14 p2078 A72-30376

Effect of Acetazolamide /Diamox/ at different dose levels on survival time of rats under acute hypoxia and on Na⁺/K⁺-ATP-ase activity of rat tissue microsomes.
17 p2499 A72-34546

Pharmacological effects on the central adrenergic regulation mechanisms of blood circulation
17 p2504 A72-35019

The effect of chlordiazepoxide on visual field, extraocular muscle balance, colour matching ability and hand-eye co-ordination in man.
17 p2505 A72-35915

Studies of the influence of theophylline on the vasodilating action of different medications on the cerebral and coronary circulation of man
18 p2651 A72-36799

Apparatus for programmed oral administration of drugs to large primates in altered environments.
18 p2654 A72-36921

Influence of inotropic alteration on the severity of myocardial ischemia after experimental coronary occlusion.
19 p2758 A72-38552

Ocular and induced visual effects of systemic and topical drugs in terms of eye neuroanatomy and pharmacology, stressing glaucoma therapy
22 p3150 A72-42499

PHASE ANGLE

U PHASE SHIFT

PHASE CHANGES

U PHASE TRANSFORMATIONS

PHASE COHERENCE

Coded multiple FSK in presence of random variable phase, predicting optimum reception performance relationship to phase distribution and SNR
01 p0025 A72-10330

Multimode Q switched ruby laser temporal coherence, comparing theoretical with experimental results from Michelson two-beam interferometer measurements
01 p0080 A72-10849

Optimum power allocation in design of phase-coherent receiver having bandpass limiter, extending technique from single channel to two channel system
02 p0174 A72-12136

Nonlinear theory of cascaded two-way coherent spacecraft tracking system model, obtaining steady state probability density functions of phase and Doppler error
02 p0174 A72-12137

Distribution moments mathematical method for partially coherent light beam propagation through random phase screens in linear and nonlinear media
02 p0181 A72-12589

Plane wave intensity fluctuations behind random phase screen, discussing phase structural function relation to field statistical properties and fluctuation dispersion
02 p0181 A72-12590

Recovered carrier phase ambiguity resolution in four-phase PSK digital satellite communications system
06 p0772 A72-17409

M-ary orthogonal signal phase noncoherent detection in sequential decision feedback, comparing performance with optimal coherent reception
06 p0773 A72-17596

Phase coherent frequency synthesizer as modulation source for multiple feature communication system, noting noise resistance, navigation capability, Doppler correction and transmitter to receiver ranging
06 p0777 A72-18619

Hybrid carrier and modulation tracking loops exploiting sideband coherency for phase coherent tracking, telemetry and command system performance improvements
07 p0939 A72-19066

Diffraction efficiency of phase holograms formed by surface deformation of light sensitive dichromated gelatin films
12 p1808 A72-27600

Emulsion response and phase effects on two point resolution in coherent holographic imaging systems, using Rayleigh criterion
15 p2237 A72-32058

Differentially coherent detection scheme with error-correcting capability by means of decision patterns.
19 p2766 A72-38605

Phase holograms wave front formation as replacement of optical elements with aspherical surfaces and multilens objectives
20 p2926 A72-39519

Signal transmission and detection in differentially encoded coherent multiple phase shift keyed digital communication systems, discussing carrier suppression-induced resolution ambiguity
21 p3017 A72-40861

Investigation of optical inhomogeneities in large fields by holographic methods
22 p3176 A72-42106

PHASE CONTRAST

Experiments on the phase contrast transfer functions of a superconducting lens
17 p2594 A72-34284

PHASE CONTROL

Statistical synthesis of antenna arrays using phase amplitude distribution equivalent to reference array radiation pattern
02 p0196 A72-12758

Active all-pass circuits transfer function and synthesis, including delay lines, phase correctors and wide-band phase shifter applications
03 p0338 A72-13169

Polyphase signal generators, using reversed flux region propagation in saturable ring core controlled by switching transistors operation
03 p0322 A72-13773

Phase stabilization of synchronized tracking oscillator with resonant frequency regulated by output voltage
03 p0333 A72-13895

Gas dynamic laser analysis based on phase cancellation model, showing flow induced phase nonuniformity minimization for far field intensity improvement
05 p0669 A72-16857

Phase-plane analysis of transient response of on-off control system relative to sinusoidal inputs
06 p0795 A72-18714

Multiple access to communication satellites in time division multiplex, discussing burst phase control and ground station receiving-transmitting systems
09 p1278 A72-22852

FM mode locked Nd-YAG pulsed laser controlled bistable phase position operation, using modulator cut as Brewster angle prism
09 p1325 A72-23089

Fourier transform plane irradiance distribution for random phase data masks in holographic data recording, discussing phase quantization level change effects
09 p1314 A72-23335

Function space linear bounded phase coordinate control problems under regularity and normality conditions discussing solution existence and uniqueness conditions
11 p1608 A72-25322

Nonlinear variable transformation method to determine locking band and transition processes in automatic phase and frequency control systems
14 p2087 A72-31132

Phase stabilization of synchronized tracking oscillator with resonant frequency regulated by output voltage
15 p2209 A72-32706

Single frequency and mode carbon dioxide laser frequency and power stabilization by phase control with electronic servosystem
16 p2402 A72-33621

Phase optimization of antenna array gain with constrained amplitude excitation.
17 p2513 A72-34355

Some problems of microwave electromagnetic oscillation phase control by using an inductance transistor
19 p2776 A72-38670

Partially coherent light for image formation of objects with amplitude, phase and complex variations, discussing system concepts, coherence control, apodization and techniques
20 p2931 A72-39048

Statistical synthesis of antenna arrays using phase amplitude distribution equivalent to reference array radiation pattern
20 p2907 A72-39064

A solid-state 'flux-drive' control circuit for latching-ferrite-phaser applications.
23 p3275 A72-43574

PHASE DETECTORS
NT SYNCHROSCOPES
Precision phase indicating pulsed optical range finder, using uncooled semiconductor laser
01 p0080 A72-10621

Midlatitude vhf phase detection of magnetic field aligned ionospheric irregularities
01 p0031 A72-10916

Phase measurements at if in microwave plasma diagnostics, examining phase stabilization processes
02 p0223 A72-11417

Capacitor-fed parallel chopper as phase sensitive demodulator, discussing design, stability, linearity and wide dynamic frequency range
04 p0507 A72-15522

M-ary orthogonal signal phase noncoherent detection in sequential decision feedback, comparing performance with optimal coherent reception
06 p0773 A72-17596

Phase locked AFC system, calculating phase detector response effects on dynamic properties
07 p0943 A72-19524

Earth location effect in Fresnel diffraction zone on comparator performance, measuring phase difference fluctuations in turbulent atmospheric boundary layer radio waves
09 p1284 A72-22232

Radar IF voltage in-phase and quadrature components detection thresholds, evaluating square and octagonal approximations to circle for false alarm probabilities
10 p1438 A72-24693

Synchronous detector technique for statistical properties improvement in phase comparison AM radio altimeter signal
11 p1633 A72-26304

Second order phase lock AFC system transient response duration calculation for rectangular and sawtooth characteristics of phase detector, using averaging method
13 p1921 A72-29284

Book on phase locked and frequency feedback systems covering FM and multiple loop principles, limiter-discriminator operation, phase detection techniques, etc
15 p2210 A72-31500

Turbine blade trailing edge wall thickness measurement by phase sensitive eddy current technique
16 p2397 A72-33201

A method of phase detection of the beat signal in FM-CW radar.
17 p2514 A72-34383

Study by phase detection of the velocity of a molecular jet
18 p2714 A72-37200

Phase detector data distortion in phase-lock loop receivers.
19 p2763 A72-37297

Analysis of the performance of a single-half-period synchronous relay detector with an active-capacitance load
19 p2801 A72-37963

A simple reference generator for lock-in amplifiers.
21 p3025 A72-40206

A high-frequency dynamic phase metering instrument for ionospheric research.
21 p3051 A72-40214

An irregular signal phase discriminator
21 p3033 A72-40943

Influence of noise on the accuracy of microwave phase meters
23 p3272 A72-43845

PHASE DEVIATION

Normal electromagnetic wave propagation in randomly inhomogeneous medium in presence of super-refraction, deriving phase fluctuation spectra by perturbation method
02 p0180 A72-12587

Inhomogeneous nonstationary medium caused electromagnetic wavefront phase disturbance reduction in holography by averaging
04 p0522 A72-15381

Spherical reflector antenna phase aberration correction by planar array feeds, discussing synthesis procedure for mean square error minimization
06 p0781 A72-17344

Angle scintillation in laser radar return from retroreflector, comparing measurement with theoretical derivation in terms of phase fluctuation parameter [CLEA PAPER 2,1]
07 p0942 A72-19377

Message distortions analysis in PCM communications systems due to phase fluctuations of synchronization signal
11 p1598 A72-26728

Linear product demodulator for quadrature double sideband signal, evaluating channel noise and phase jitter effect on carrier
13 p1920 A72-29105

Instrumental errors estimation in photomultipliers and photodiodes during measurement of short time phase fluctuations in quasi-harmonic signals
15 p2246 A72-31424

PHASE DIAGRAMS

Al-Mo alloys under high temperature, determining phase equilibria and intermetallic phases
03 p0370 A72-12961

Equilibrium state and microhardness of phase diagrams in Mg-rich region of Mg-Nd-Zn system
03 p0370 A72-13185

Nb-Ti-B ternary system melts hardened in vacuum, determining solidus temperature and surface from phase diagram
03 p0370 A72-13186

Heat treated microstructures relation to equilibrium diagram in beta and alpha Ti alloys
03 p0374 A72-13715

Ta-Ra-B ternary alloy, investigating phase equilibria and isothermal cross sections with X ray analysis
03 p0374 A72-13739

Ta-Co system phase diagram from differential thermal, X ray, and microstructural analyses, determining composition, temperature, structural type and lattice constant
03 p0374 A72-13740

Ta and Nb addition effects on W solid solution strengthening, determining W-Nb-Ta alloys phase diagram and melting point
03 p0375 A72-13943

Y-Mn-Al ternary alloy solid solution phase diagram isothermal section construction from X ray structural data
03 p0376 A72-13945

Quaternary Mo-Zr-Cr-C system, investigating fcc phase liquation from phase diagram by chemical, metallographic and X ray analyses
05 p0666 A72-16099

Phase equilibria of Mo-Mn-C and W-Mn-C systems by X ray analysis, showing eutectoid decomposition involving rhombic modification
06 p0833 A72-18432

Phase diagram of Ta-B system by thermal, X ray and microstructural analyses
06 p0833 A72-18434

Hf-B system alloys phase diagram and impurities effect, discussing synthesis and heat treatment regime
07 p1010 A72-18857

Phase diagrams of yttrium, erbium and ytterbium oxides at 1500-2400 C, using annealing and quenching method with differential thermal analysis
07 p1047 A72-18858

Hf-Co-Al system phase equilibria determination by partial microstructural and X ray analysis
07 p1017 A72-19991

Equilibrium diagram of Cr-Va alloy produced by arc melting under Ar atmosphere, using high temperature differential thermal analysis
07 p1019 A72-20160

Nb-Ga system equilibrium phase diagram determination by differential thermal, tempering microstructural and X ray analysis techniques, discussing various compounds formation temperatures and characteristics
07 p1050 A72-20161

Phase diagrams, superconducting properties and annealing critical temperature of Nb-Al-Ge alloys, establishing four phase peritectic equilibria
08 p1218 A72-21778

Ti-Ce-S alloys phase equilibria with isothermal cross section, discussing eutectic alloys anomalous structure and cerium monosulfide preparation method
08 p1187 A72-21784

Binary system molar energy diagram plotting, covering superheated, saturation and liquid phase regions
08 p1255 A72-22170

Cathodic processes in Al electrodeposition from ethyl pyridine bromide electrolyte, discussing phase equilibrium and electrical conductivity dependence on solution composition
09 p1318 A72-22529

X ray diffraction and chemical phase analysis of Nb alloys in cast and heat treated state, considering hardening mechanism
09 p1327 A72-22636

Nb-W equilibrium phase diagram estimation from known phase diagrams of Ni-Nb, Ni-W and Ni-Nb-W systems via Guggenheim quasi-chemical model application to Ni-Nb-W thermodynamic properties
10 p1496 A72-24233

Melting points and phase diagrams for various tungsten oxide systems, noting alkaline earth and transition and trivalent metal tungstates
10 p1497 A72-24731

Hubbard mathematical model for metal-insulator transition due to electrons correlations, noting schematic phase diagram and transition metal oxides
10 p1527 A72-24939

Deformable wrought stainless steels phase diagram for structural state estimation from chemical composition, considering various austenite, martensite and ferrite combinations
11 p1659 A72-26127

Relative valence effect of transition metal additions on alpha-gamma phase equilibrium in Fe-Cr-Mn system
12 p1827 A72-27099

Mo corner of Mo-B phase diagram constructed from microstructural analysis and microhardness, melting point and lattice constant measurements
12 p1828 A72-27291

Phase composition and lattice constants of carbide films from vaporized Zr interaction on graphite surface at 1700 C
13 p1912 A72-28566

Two phase and three phase composition of ternary alloys Nb-C-Re at 2000 C from X ray, metallographic and chemical analysis
13 p1973 A72-28567

Annealed and quenched Fe-Mo-Co system, defining phase relationships in Fe-rich corner at 2200, 2000 and 1800 F
13 p1973 A72-28650

Phase structure of Cr rich Cr-Ni, Cr-Fe, Cr-Co and Cr-Ni-Fe alloy particles produced by evaporation in Ar using X ray diffraction
13 p1974 A72-28660

Phase diagram of cast and annealed Cr-Sc alloys by differential thermal, X ray, metallographic and microhardness analyses
13 p1981 A72-29953

High refractory gadolinium oxide-strontium oxide system phase diagram and transition temperature by X ray and differential thermal analyses
13 p1984 A72-30109

Phase diagram of Ti-Pd system, using metallographic, X ray and differential thermal analyses
13 p1982 A72-30116

Russian papers on phase diagrams of metallic systems covering thermodynamic, X ray and metallographic alloys analysis
14 p2122 A72-30976

Nb-Ti-Zr-Hf system phase diagram from X ray analysis, observing beta solid solution below solid curve
14 p2122 A72-30977

Zr-Cu-Mo system phase diagram from microscopy, X ray analysis and mechanical tests, noting beta solid solution transformation into alpha, omega and beta phase mixtures
14 p2122 A72-30978

Hf binary systems phase diagrams, noting components effect on melting point, polymorphous transformations and mutual solubility
14 p2122 A72-30979

Phase composition of Nb-O-Hf and Nb-O-Zr ternary alloys, noting O solubility decrease
14 p2122 A72-30980

Interaction of W with transition metals in ternary and multicomponent alloy systems, noting phase diagrams
14 p2122 A72-30981

Phase diagram of quaternary W-Mo-Nb-Ta alloy system, noting dependence of hardness on composition and temperature
14 p2122 A72-30982

W-Nb-C system phase diagram from X ray and microstructural analyses, noting solid solubility, hardness and isothermal cross section
14 p2122 A72-30983

Mo-W-C system high temperature phase equilibria from X ray and microstructural analysis, noting decrease of C solid solubility with temperature
14 p2123 A72-30984

Ti-Si system phase diagram and equilibrium states, noting crystal lattices and thermograms
14 p2123 A72-30986

Cr-N alloy phase diagram from thermal and X ray analysis, metallographic observation and hardness tests, noting melts crystallization
14 p2123 A72-30987

Ni-Al-Nb-Mo system phase diagram from X ray and microstructural analysis, noting solid solubility and dependence of hardness and electrical resistivity on components

14 p2123 A72-30989

Phase diagrams of Ni-C and Co-C systems with metastable equilibrium lines, investigating microstructure and microhardness of carbide eutectic

14 p2123 A72-30990

Ce-N alloys phase diagram from durometric, X ray, metallographic and differential thermal analyses

14 p2123 A72-30991

Phase diagrams of Ru binary and ternary systems, noting admixtures interactions

14 p2123 A72-30992

Ru-Nb-Zr alloys phase diagrams from physicochemical analysis, noting components interaction

14 p2123 A72-30993

Binary systems phase diagrams qualitative and quantitative analysis based on free atoms electron state energy ratios, formulating solid solubility criterion

14 p2123 A72-30994

Temperature measuring instrument with thermocouple for differential thermal analysis equipment used in phase diagram construction

14 p2106 A72-30995

Russian papers on light and nonferrous alloys structure and properties covering phase diagrams, alloying effects, reduction, crystallization and recrystallization, solid solutions decomposition, etc

14 p2123 A72-31027

Phase equilibrium of Mg base solid solutions of Mg-Li-Sn system at 200-500 C, analyzing microstructure, microhardness and electrical resistivity

14 p2124 A72-31029

Russian papers on rare earth metals and alloys covering physical properties, phase diagrams and industrial applications

15 p2252 A72-31183

Scandium alloys properties based on phase diagrams, noting corrosion resistance

15 p2289 A72-31186

Sm and Eu binary alloys, investigating physicochemical interactions and phase diagrams

15 p2289 A72-31187

Phase diagrams of Hf-Ce and Hf-Er alloys, plotting hardness and electroconductivity curves

15 p2289 A72-31188

Phase diagrams of rare earth ternary alloys with transition metals and Si, noting semiconductor properties

15 p2289 A72-31189

Composition diagrams and properties of intermetallic compounds of magnesium in binary and ternary systems

15 p2252 A72-31196

Electronic structure of binary phase diagrams of group III-VI transition metals, using valence separation and condensed state model

15 p2252 A72-31198

Mo, W, Nb, Ti, V and N complex alloying to harden cast heat resistant austenitic steel, discussing phase composition and stress-rupture strength

15 p2254 A72-31563

Phase diagrams for W-Ta-Ti alloys at 1600 C from metallographic and X ray analysis

16 p2407 A72-33533

Cd effect on alpha-beta transformation temperature and phase equilibrium in Ti rich end of Ti-Cd phase diagram, using metallographic and X ray techniques

16 p2409 A72-33806

Liquidus temperatures and isothermals in Al corner of Al-Ti-B alloy phase diagram, using differential thermal analysis

16 p2409 A72-33808

High temperature solid-solubility limit and phase studies in the system tantalum-oxygen

17 p2567 A72-34731

Influence of isothermic reaction levels on the diffusion growth of compounds with a binary equilibrium diagram

19 p2817 A72-37792

Microstructure and differential thermal analyses of ternary system Co-Mn-Al, presenting phase diagrams

19 p2818 A72-37852

Concentration dependences and equilibrium values of the impurity distribution coefficients in bismuth telluride

19 p2845 A72-38177

Phase diagrams of AlSb-GaSb and InAs-GaAs systems, noting mixing energy for liquid and solid phases

19 p2845 A72-38207

Phase equilibria in the hafnium-niobium-boron and tantalum-chromium-boron systems

19 p2819 A72-38285

Peritectic interaction and phase diagrams of quasi-binary semiconductor CdS-CdTe and CdP-CdSe systems

19 p2845 A72-38404

Phase diagram of the neodymium-erbium system

19 p2846 A72-38473

Phase diagram of the chromium-holmium system

19 p2821 A72-38474

Phase composition and isothermal cross section diagrams of Cr-Ni-B system at 800 C, using X ray and microstructural analyses

19 p2822 A72-38678

Systems of niobium monocarbide with transition metals.

20 p2942 A72-39985

Phase diagram study of Cr-Ga alloys, investigating intermetallic compounds presence and polymorphic transformation and temperature effects

20 p2942 A72-39987

Phase diagram, isomorphism and temperature dependence of hexagonal, monoclinic and triclinic modifications of Sr-Ba polycrystalline aluminosilicates

21 p3072 A72-40382

Phase diagrams, microhardness and composition of sintered binary B compounds with Zr, Hf, Ta, Cr, Mo, W, Re, Fe, Ni, and Si

21 p3070 A72-41371

Crystallization and structure of hypereutectic iron-carbon-chromium alloys

21 p3071 A72-41788

Investigation of phase equilibria in alloys of silicon with molybdenum and titanium

22 p3188 A72-42150

Alloys of thorium with certain transition metals. VI - The constitution of thorium-nickel alloys containing 50-96% nickel.

22 p3190 A72-42769

Application of computer mathematics procedures for prediction of phase diagrams

22 p3191 A72-42812

Plotting of composition vs property curves for superconducting systems with a digital computer by the method of simplex arrays

22 p3191 A72-42813

Phase compositions, impurity effects, crystallization and production of plastic W and Mo alloys and heat resistant W-based alloys

22 p3192 A72-42815

Constitution of the Ni-Cr-Fe system from 0 to 40 pct Fe including some effects of Ti, Al, Si, and Nb.

22 p3194 A72-43038

X ray and differential thermal analysis for phase diagrams of binary alloys of samarium oxides and gadolinium oxides with calcium oxides, noting solid solutions formation

23 p3304 A72-43250

Phase diagrams from X ray analysis of rapidly crystallized Ni-Sn alloys, noting crystal lattices and phase transformation

23 p3300 A72-43648

Investigation of the influence of the gas medium on the phase composition and certain properties of refractory materials containing zirconium

23 p3306 A72-43690

High temperature interaction between W and ZrC constructing isothermal structure

23 p3303 A72-44151

Relationship between the strength properties and the phase composition of annealed titanium alloys

24 p3414 A72-45383

Three-phase equilibria of cast and annealed V-Zr-Cr alloy by X ray, metallographic and melting point analyses

24 p3414 A72-45384

PHASE ERROR

Nonlinear theory of cascaded two-way coherent spacecraft tracking system model, obtaining steady state probability density functions of phase and Doppler error

02 p0174 A72-12137

Planar phased array antennas with uniform current amplitudes, calculating beam-pointing error dependence on array geometry, phase errors and scan angle

03 p0325 A72-14179

Two channel radio interferometry, determining limiting accuracy characteristics under arbitrary phase error

05 p0660 A72-15829

Weighted acoustic surface wave dispersive microwave filter apodized interdigital array design modification for phase error correction to reduce distortion

06 p0787 A72-18380

Pulse overlapping effects on phase jittering in carrier regeneration with quaternary phase shift keying

07 p0945 A72-19662

Phase errors and main lobe orientation changes during beam scanning of two reflector Cassegrain antennas

08 p1139 A72-20934

Phase errors in range finding measurements with radio waves reflection from underlying surface

09 p1277 A72-22481

Phase and amplitude error effects on image reconstruction in conventional and weak signal enhancement holography

09 p1312 A72-23242

Phase error magnitudes due to individual microwave elements imperfections and multiple reflections in

phase difference measurements by polarization method in microwave range

13 p1928 A72-28791

Instrument errors of RF phase comparison altimeter for meteor height measurements, using radar tracked aircraft flights calibration

13 p1957 A72-29029

Sinusoidal signal and stationary quasi-white Gaussian noise mixture effects on stochastic phase locked AFC system operation, noting phase error probability density function

13 p1921 A72-29285

Asymptotic formula for approximation of mean cycle-slip time of phase locked loops with low SNR and steady state phase error

16 p2371 A72-33211

Control equipment designs for phase error estimation of pulse sequences in multichannel magnetic recording systems

16 p2367 A72-33264

Russian book - Methods of measurement-information conversion and separation from harmonic signals

19 p2764 A72-37449

Identification and removal of phase errors in interferometry.

23 p3287 A72-43259

Two channel radio interferometry, determining limiting accuracy characteristics under arbitrary phase error

23 p3287 A72-43437

A high-accuracy radio direction finder with a moving antenna

23 p3270 A72-43769

Influence of noise on the accuracy of microwave phase meters

23 p3272 A72-43845

PHASE LOCK DEMODULATORS

Parameter regions for proper operation of multifilter phase lock loops used for demodulation by digital and analog computer techniques

03 p0339 A72-14194

Digital phase locked loop realization for near-optimum demodulation of continuous-time FM signal using stochastic estimation theory

16 p2362 A72-33213

PHASE LOCKED SYSTEMS

Time optimal phase locked AFC system synthesis based on Pontryagin maximum principle, comparing computerized and experimental transient response

01 p0024 A72-10045

FM communication system multifilter phase lock loop state equations derivation from phase model, predicting noise improvement characteristics by analog and digital simulation

01 p0044 A72-10328

AFC for suppressed-carrier SSB voice signal reception, using phase locking procedure or comparative zero-crossing-rate measurement

01 p0025 A72-10333

Phase locked IMPATT diode microwave oscillator transients for reflection amplifier or pulse modulated source applications

01 p0037 A72-10646

Low noise phase locked power microwave sources for solid state radio links with 960 voice channels, discussing design

01 p0006 A72-10712

Phase stable locked local oscillators for K band radiometers for long baseline interferometric measurements, emphasizing construction technique

01 p0044 A72-11307

Transient characteristics of phase lock automatic frequency control system with integrating filter, using nonlinear phase-plane method

02 p0176 A72-12224

Acquisition time for sideband modulated noiseless phase lock loops

03 p0325 A72-14191

Submillimeter wavelength HCN laser stabilization, describing AFC and phase locking

04 p0532 A72-15596

Stability conditions and effective bandwidths of first and second degree pulsed phase locked AFC systems with proportionately integrating filter, using Z transform method

05 p0625 A72-15825

Unlimited phase locked loop analysis for AM signal by Fokker-Planck equation

05 p0637 A72-16554

Phase locked loop bandwidth, acquisition time and SNR for Doppler tracking deep space communications for Venus and Jupiter probes

05 p0629 A72-16575

Pulsed and CW solid state microwave oscillator EM noise as function of power level and locking parameters

06 p0788 A72-18465

X band IMPATT and Gunn oscillator, calculating injection lock time, modulation bandwidth, noise and FM suppression and dynamic response

06 p0788 A72-18471

Phase lock loop receiving system digital simulation for estimating mean time to indicate lock and probability distribution function for wide SNR range

07 p0939 A72-19065

Phase locking loop synchronized quartz oscillator for integral frequency multiplication in wideband carrier frequency systems 07 p0954 A72-19174

First passage time boundary value problem for first order phase locked loop systems, determining probability density function of time to cycle-slip 07 p0959 A72-19273

Millimeter wave techniques for laser stabilization to frequency standards, using phase locked HCN laser and high resolution IR spectrometer [CLEA PAPER 6,7] 07 p1004 A72-19383

Phase locked AFC system, calculating phase detector response effects on dynamic properties 07 p0943 A72-19524

Subharmonically injected phase locked microwave IMPATT oscillator 09 p1285 A72-22894

Stability regions of phase-locked AFC with nonlinear control circuit, describing system dynamics by differential equations 09 p1290 A72-23180

YIG tuned Gunn oscillator phase locking and shifting over 3 GHz range in X band, using feedback control 10 p1451 A72-24596

Capture range and acquisition time analysis of phase locked loop with active filter 10 p1458 A72-24934

Phase noise and transient times for binary quantized digital phase locked loops in white Gaussian noise 11 p1592 A72-25886

Error analysis of measurement-type servo systems with constant product /or quotient/ of dependent and independent variables applying to phase loop AFC operation 11 p1595 A72-26301

Nonlinear stochastic partial differential equations solution by graph technique, calculating correlation function and phase change spectrum in phase locked circuit 12 p1837 A72-27575

FM distortion in injection phase locked oscillator amplifiers from generalized Alder equation 12 p1793 A72-27965

Monte Carlo simulation for imperfect second order hybrid phase locked loop in radio frequency interference and Gaussian noise backgrounds, employing digital computer simulation model 13 p1935 A72-29104

Second order phase lock AFC system transient response duration calculation for rectangular and sawtooth characteristics of phase detector, using averaging method 13 p1921 A72-29284

Sinusoidal signal and stationary quasi-white Gaussian noise mixture effects on stochastic phase locked AFC system operation, noting phase error probability density function 13 p1921 A72-29285

Short term instability of frequency standard using AFC of quartz crystal oscillator by phase locking to optically pumped Rb 87 vapor clock 13 p1968 A72-29296

Vibration stability and interference transfer function of onboard transponder with phase lock AFC used in Doppler system for measuring spacecraft trajectory parameters 13 p1958 A72-29456

Nonlinear microwave circuit feedback model analysis by describing function in control theory, applying to oscillator phase locking problem 15 p2210 A72-31355

Book on phase locked and frequency feedback systems covering FM and multiple loop principles, limiter-discriminator operation, phase detection techniques, etc 15 p2210 A72-31500

Estimation-correlation principle application to harmonic signal receiver with unknown carrier frequency, using searching phase locked AFC circuit as estimation unit 15 p2202 A72-32667

Asymptotic formula for approximation of mean cycle-slip time of phase locked loops with low SNR and steady state phase error 16 p2371 A72-33211

Nonlinear and phase delay distortion of FM modulation in tuned and detuned injection phase-locked oscillator-amplifiers 16 p2369 A72-33760

Phase locked loop model based on AGC circuitry, devising optimum control strategies 17 p2532 A72-34419

Hybrid injection locking of higher power CO₂ lasers. 17 p2564 A72-35343

Determination of the locking range from the reactive power balance of the oscillator. 17 p2530 A72-35430

Phase detector data distortion in phase-lock loop receivers. 19 p2763 A72-37297

Capture of a signal with a linearly varying frequency in an astatic phase autotuning system 19 p2766 A72-38420

Nonautonomous phase system of equations with a small parameter, containing invariant tori and rough homoclinic curves 19 p2828 A72-38579

Digital command system second-order subcarrier tracking loop performance. 21 p3038 A72-40870

Near optimum digital phase locked loops. 21 p3038 A72-40871

Decision directed phase locked loops acquisition properties improvement technique for PCM bit synchronizer of random nonreturn to zero data 21 p3038 A72-40872

Phase locked feedback circuit for FM demodulation, discussing all digital circuit design and voltage controlled oscillator algorithm to avoid analog implementation problems 21 p3018 A72-40873

Detection of whistler mode signals from VLF transmitter in Australia. 21 p3023 A72-41386

Investigation of the threshold properties of a phase-lock AFC detecting a sinusoidally frequency modulated signal against a noise background 22 p3154 A72-42231

Stability conditions and effective bandwidths of first and second degree pulsed phase locked AFC systems with proportionately integrating filter, using Z transform method 23 p3263 A72-43433

Application of an electronic computer to the calculation of the locking band in nonlinear phase-lock automatic frequency control systems 23 p3264 A72-43763

Fluctuations in a quantum frequency standard 23 p3271 A72-43842

Stability criteria for phase-locked oscillators. 23 p3272 A72-44192

PHASE MODULATION

NT FM/PM (MODULATION)

NT PHASE SHIFT KEYING

RF interference in angle-modulated system with predetection linear bandpass filter, calculating output power spectral density in baseband 01 p0045 A72-10332

Parametric amplification of laser waves with amplitude and phase modulation under exponential signal growth applied to Raman scattering picosecond pulse field 01 p0079 A72-10346

Solid state oscillator phase and frequency synchronization by injection of stable sinusoidal uhf signal modulated by 0-180 deg phase jump 02 p0194 A72-12569

Power spectrum analysis of multilevel digital signals phased modulated by arbitrary pulse shapes, giving examples for rectangular and raised-cosine pulses 02 p0183 A72-12797

Interference polarization filter by modulation and phase detection for passband narrowing and secondary maxima attenuation, discussing application to photoelectric recording system 03 p0356 A72-13096

PCM/PM 136 MHz telemetry system of SAS-A satellite, describing operation in record and playback modes 03 p0326 A72-14396

High speed digital communication over space to earth satellite links by quadriphase modulation, discussing modulator, receiver and system technology for maximizing data transfer 04 p0485 A72-14477

Statistical properties of random-phase modulated laser beams, calculating coherence functions of optical fields 04 p0528 A72-14580

Relaxation processes in Michelson interferometer as integral part of carbon dioxide laser cavity in phase Q switching regime 04 p0530 A72-14990

Quasi-monochromatic radio signal propagation for arbitrary amplitude and phase envelopes in nonlinear medium with nonlinearity caused by plasma heating 05 p0627 A72-16404

Algebraic prediction formalism for ring laser mode coupling by phase modulation 05 p0668 A72-16566

Amplitude and phase modulated radar pulse train representation by complex number sequences, discussing generation, processing, and Z transform application to combination codes 06 p0773 A72-17495

AM/PM distortion intermodulation in FM/FDM radio systems during two-path propagation, using Fourier series method for noise power spectra calculation 06 p0775 A72-18239

Binary single sideband phase modulation with simultaneous AM by signal and Hilbert transformation 06 p0776 A72-18395

Variance estimate of second order moment by nonlinear correlator in presence of additive amplitude and phase modulation and normal noise 07 p0939 A72-19021

Hybrid carrier and modulation tracking loops exploiting sideband coherency for phase coherent tracking, telemetry and command system performance improvements 07 p0939 A72-19066

Optimal continuous recording of amplitude-phase distributions on spatial carrier frequency for light wave modulation and optical antenna simulation 08 p1132 A72-21263

Spurious target generation due to hard limiting in pulse compression radars with three phase coded signals superposed at input, comparing with digital simulation 08 p1134 A72-21416

Time dependent phase modulation for high effective reference to object beam intensity ratio, noting linear recording of holograms 09 p310 A72-22649

Multimode ring laser gyro phase modulation theory based on oppositely directed traveling waves 09 p1324 A72-23084

Multimode ring laser gyro with intracavity phase modulation, discussing experimental results concerned with lock-in at low rotation rates 09 p1324 A72-23085

Holographic method for investigating piston type vibrations with phase modulated reference light beam 09 p317 A72-23682

Error probability and reception stability in synchronous detection of phase manipulated signals with additive Gaussian noise at multiplied carrier frequency 10 p1436 A72-24587

Spectral distribution of signal power in AM, FM and PM PCM systems with time division multiplexing 10 p1439 A72-24909

Uncertainty functions side maxima for phase manipulated signals with low sidelobe levels in autocorrelation functions, noting Doppler frequency shift effect 10 p1440 A72-24916

Interference polarization filter by modulation and phase detection for passband narrowing and secondary maxima attenuation, discussing application to photoelectric recording system 11 p1632 A72-25708

Laser emission spectrum broadening due to saturable dye filter bleaching, discussing amplitude and phase modulation contributions 11 p1649 A72-26341

Communication systems design with error control, applying algebraic codes to biphasic and multiphase modulation systems 12 p1782 A72-27488

AM/PM conversion and transfer in nonlinear signal transmission systems, calculating coefficients as function of multicarrier powers for intelligible crosstalk 12 p1782 A72-27554

Q switched carbon dioxide laser based on PM by rotating mirror in one arm of Michelson interferometer, establishing phase relationships 13 p1968 A72-29287

Destabilizing factors effect on parameters of transistorized single circuit phase modulator with varicap control 13 p1932 A72-29455

Atmospheric turbulence induced wave front distortion effects on fast-tracking laser antenna performance, considering infinite plane wave random complex phase modulation 14 p2110 A72-30550

Mechanical oscillator model for experimental investigation of multistage electrical frequency multipliers subharmonic transient oscillations, considering energy flow under constant and/or phase modulated excitation 14 p2131 A72-30719

SSB signal generation without Nyquist filter or auxiliary equipment for PM modems in data transmission 15 p2195 A72-31620

Design data of guided wave structures for electrooptical modulation, evaluating propagation wave numbers, attenuation rate, phase modulation rate and dispersion characteristic 15 p2246 A72-31667

Mode locked lasers, investigating effect of grating-induced phase and spatial modulations by multiple transverse modes on pulse compression across beam cross section 16 p2403 A72-33840

Signal detection by receivers with modulus processing 17 p2515 A72-34836

Differentially coherent detection scheme with error-correcting capability by means of decision patterns. 17 p2766 A72-38605

Harmonic mode locking of the Nd:YAG laser. 19 p2813 A72-38688

Phase modulated data transmission with partial pilot signals, interpolating reference demodulation signals at receiving end by maximum cross correlation 23 p3264 A72-43771

Frequency conversion and limiter action for an angle-modulated wave with amplitude fluctuation in a half-wave linear mixer.

23 p3265 A72-44179

PHASE SHIFT

Electrostatic waves in longitudinally magnetized plasmas with random electron charge distribution and applied magnetic field, finding phase characteristics

01 p0106 A72-10128

Plane electromagnetic wave scattering by imperfectly conducting cylinder with radially inhomogeneous dielectric coating, using phase shift method for evaluation

01 p0024 A72-10130

Differential phase shift and absorption measurements of partially reflected radio waves, providing electron density and collision frequency data from 70-90 km

01 p0030 A72-10836

Phase difference measurement between magnetoelectric components returned from lower ionosphere due to pulsed radio signal, obtaining electron density profiles

01 p0063 A72-10914

Spatial distribution of plasma density from phase shift measurement in millimeter waves based on microwave multichannel probes

02 p0263 A72-11412

FM homodyne phase meter with klystron oscillator for measuring plasma electron concentration, presenting block diagrams of meter, detector and oscillator

02 p0223 A72-11414

Direct phase measuring and measured phase compensating microwave devices designed for plasma diagnostics applications

02 p0223 A72-11416

Phase measurements at if in microwave plasma diagnostics, examining phase stabilization processes

02 p0223 A72-11417

Diurnal and seasonal changes in occurrence frequency of rapid phase fluctuations in vlf received at Franz Josef Land correlated with geophysical observations

02 p0172 A72-11922

Spectral characteristics of ionospheric signal by phase lags introduced in multichannel field recorder

02 p0172 A72-11926

Propagation modes attenuation and phase shift of electromagnetic plane wave in superconducting coaxial cylindrical waveguide

03 p0321 A72-13170

Low energy phase shifts for elastic scattering of electrons by Li and Na

03 p0391 A72-13745

Molecular collision model, comparing generalized phase shift approximation method with classical trajectory calculations for rotational inelasticity

03 p0391 A72-13857

Heuristic theory of positron-helium elastic scattering phase shifts and cross sections

03 p0393 A72-14399

Vlf phase regressions at sunrise related to variations of reflection coefficient in D region, using IENGf data

04 p0485 A72-14465

Intermolecular potentials determination by inverting phase shifts obtained from high resolution measurements of protons differential elastic scattering by rare gas atoms

04 p0552 A72-14577

Wideband microwave acoustic delay line design featuring superior bandwidth, phase linearity, spurious echo and insertion loss characteristics

04 p0521 A72-14720

X ray stars atmospheric ionization effects by vlf phase tracking relative to Omega navigation accuracy, diurnal shift variations and astrophysical data

04 p0486 A72-14877

Linearly polarized wave excitation with specified phase shift and predetermined amplitude ratio by waveguide slots, giving slot configuration design formulas

04 p0487 A72-15243

Diurnal phase and amplitude variations of long radio waves at great distances, explaining sunrise and sunset fadings

04 p0492 A72-15443

Mechanical impedance and phase angle time variation in restrained primate during prolonged sinusoidal vibration

[ASME PAPER 71-WA/BHF-8] 05 p0616 A72-15946

Low cost automated digitized measurement for microwave antenna feed power gain and relative phase, using computer facilities

05 p0637 A72-16420

Coherence function and phase shift dependence of free ocean surface on angular energy distribution in two dimensional wind induced wave spectrum

06 p0841 A72-17625

Radiation polarization from Jovian disk center as function of phase angle from polarimetric observations

06 p0884 A72-18033

Harmonically modulated reflected light signals phase shift and demodulation, assuming single scattering

06 p0848 A72-18047

Radome checkout ensuring reproducibility by insertion phase delay measurement

06 p0822 A72-18195

Microwave dispersive line structures with nonlinear phase characteristics, considering use of empty waveguide segment near cut-off

06 p0785 A72-18312

Optimal receiver synthesis for radio signals with differentiable components of continuous Markov processes masked by phase interference and white noise

07 p0937 A72-18847

Antenna radiation pattern synthesis, discussing current phase and amplitude distribution determination by iterative and quadratures solutions respectively

07 p0953 A72-19004

Spectrometers for phase audible frequencies, discussing linearization theory and application to spectrum analyzer calculation

07 p0983 A72-19186

Second order mode locked GaAs junction laser, observing mode frequencies and phases configurations during self pulsing

07 p1001 A72-19200

Phase shifts of circadian rhythm of optic nerve potentials from isolated eye of sea hare in darkness

07 p0919 A72-19534

Spectral photosensitivities for phase shifting of circadian body temperature rhythms in pocket mice

07 p0919 A72-19535

Phase shifting effect of light on circadian rhythm and photoreceptive pigment location in *Drosophila* in postpupation stages

07 p0919 A72-19536

Slip effect in diurnal phase and amplitude cycles of vlf signals in lower ionosphere due to wave interference at transmitting point

08 p1130 A72-20710

Quasi-stationary three dimensional array excitation by large phase shift calculated for circular conducting elements

08 p1140 A72-21262

Brightness distribution and phase dependence measured for spheres with different colors and roughness for Mars surface optical parameters model validity

08 p1238 A72-21830

Photoelectric measurements of brightness of Galilean satellites of Jupiter as function of solar phase angle

08 p1238 A72-21831

Probabilistic characteristics of radiation pattern for multielement antenna with nonpolar phase front

09 p1285 A72-22575

Phase angle measurements of frequency-oxygen atom lifetime relationship in pulsating auroras

09 p1298 A72-22589

Elastic singlet p wave phase shift calculation for electron scattering by H atom and He cation, using time dependent Hartree-Fock perturbation theory

09 p1355 A72-22786

Effective photoionization sections of neutral atoms, discussing photon energy effects, subshell periodicity and continuum functions phase shift

09 p1356 A72-22828

Information theory and ambiguity concept generalization for signal distinction by phase displacement in time and frequency

09 p1281 A72-23470

Ionospheric inhomogeneity studies from angle of arrival recordings of satellite beacon transmissions, using phase radiometer interferometry

09 p1305 A72-23576

Atmospheric refractive index inhomogeneity statistics from interferometer measurements of distance-dependent phase fluctuations in near-ground horizontal optical propagation paths under turbulence conditions

09 p1354 A72-23696

Phase shift methods for data transmission vestigial sideband signal generation, providing shaping functions by shift registers, weighting resistors, summing amplifiers and low pass filters

11 p1592 A72-25890

Radiation polarization from Jovian disk center as function of phase angle from polarimetric observations

11 p1719 A72-25969

Dynamic range errors and noise bands for phase comparison radio range finders with mutual automatic frequency control in interrogator and transponder

11 p1596 A72-26302

Statistical analysis of errors in altitude readings of phase comparison AM radio altimeters

11 p1633 A72-26303

Probability distribution density of phase difference between noise and signal-noise sum for radar system efficiency estimation, using Bessel and Whittaker functions

11 p1596 A72-26308

Three centimeter balanced ring modulator with carrier and sideband suppression using amplitude and phase relations

11 p1605 A72-26321

Phase metering information converters with digital analog computation, discussing analysis of prototype semiconductor model with ten-digit binary codes

11 p1602 A72-26449

VLF phase changes due to particle precipitation into geomagnetic anomaly during solar proton events explained by exponential ionospheric models with effective reflecting height

11 p1599 A72-26765

Ni powder artificial dielectric in waveguide transverse magnetic field, noting nonreciprocal nature of microwave attenuation and phase shift

11 p1607 A72-26786

Fourier phase angle models of intermittent atmospheric turbulence

12 p1838 A72-27025

Blue filter polarimeter observations of Deimos and Phobos, discussing polarization-phase angle curve for Deimos dust surface layer

12 p1865 A72-27097

Many electron pseudopotential method for electron-atom scattering, calculating singlet s wave and p wave phase shifts

12 p1848 A72-27429

Gage for solids and liquids moisture content measurement based on phase shift of UHF electromagnetic wave propagating through tested material, noting specimen thickness optimization

12 p1807 A72-27466

Chebyshev phase and time delay approximations existence and characterization

12 p1836 A72-27572

Polarization method for measuring small phase difference variations in microwave range, developing rules for optimum selection of multiplication factor

13 p1928 A72-28790

Phase error magnitudes due to individual microwave elements imperfections and multiple reflections in phase difference measurements by polarization method in microwave range

13 p1928 A72-28791

Forward loop signal attenuation and phase shift diagrams for design of feedback amplifier and compensation network for dc flyback converter

13 p1899 A72-29110

OMEGA phase shifts in auroral region due to solar phenomena, discussing methods eliminating PCA induced errors

13 p1997 A72-29185

Diurnal and seasonal changes in occurrence frequency of rapid phase fluctuations in VLF received at Franz Josef Land correlated with geophysical observations

13 p1920 A72-29234

Spectral characteristics of ionospheric signal by phase lags introduced in multichannel field recorder

13 p1920 A72-29238

Q switched carbon dioxide laser based on PM by rotating mirror in one arm of Michelson interferometer, establishing phase relationships

13 p1968 A72-29287

E region drift velocity estimates from amplitude and phase measurements of pulsed radio waves reflected from lower ionosphere

13 p1923 A72-29664

Jupiter electropolarimetric observations, showing polar regions polarization dependence on phase angle

13 p2050 A72-30069

Microwave device phase and amplitude frequency response measuring equipment with wide range test pulse generation, discussing design and performance

13 p1934 A72-30091

Lightly doped InP and vapor epitaxial GaAs laser, observing long wavelength shift in photoemission spectra peak

14 p2108 A72-31082

Van der Pol oscillator acted upon by weak random noise, evaluating oscillations envelope dispersion from probability density function and phase derivation

14 p2132 A72-31123

Model Martian atmosphere, investigating effects of departures from electron density profile spherical symmetry on radio wave phase shift in bistatic radar occultation experiment

15 p2194 A72-31440

Antarctic D region reflection heights from relative phase measurements on VLF transmissions at several phase locked frequencies, interpreting results by waveguide mode theory

15 p2200 A72-32105

Harmonics, intermodulation noise and small signal effects in discrete image points holographic recording on photopolymer material characterized by linear phase shift vs exposure

15 p2238 A72-32158

Random vibration optimal control by transfer function estimation, using relative phase information in cross spectral density functions to sort out self noise

15 p2215 A72-32629

Phase distribution randomization in switched antenna array, noting radiation pattern sidelobe compensation application 15 p2209 A72-32666

Interference measurement techniques for small phase difference changes, noting diffraction and noise effects as limiting factors 15 p2243 A72-32769

Phase and gain response of wideband coaxial X band microwave avalanche diode amplifiers 16 p2368 A72-33073

Polarization modes and phase shifts of normal oscillation modes in anisotropic optical traveling wave resonator with Brewster winders half wave plate and Faraday rotation cell 16 p2403 A72-33979

Pulse length evaluation from frequency domain phase function, applying to mode locked laser theory 17 p2562 A72-34292

Hue shifts accompany phase induced modulation enhancement of sinusoidally flickering lights 18 p2651 A72-36613

A nomogram for determining the phase difference of an elliptically polarized wave 18 p2663 A72-37219

Choice of parameters for measuring devices in a closed-loop linear control system 19 p2777 A72-37319

P-i-n variable attenuator with low phase shift 19 p2773 A72-38294

Slip effect in diurnal phase and amplitude cycles of VLF signals in lower ionosphere due to wave interference at transmitting point 19 p2765 A72-38338

Transmission and phase coefficient logarithmic decrements for wave propagation in random discrete scatterers 19 p2767 A72-38614

Representation of real narrowband signals through nonuniformly displaced basal functions with positive coefficients 19 p2768 A72-38668

Effect of a temporal shift in the min II of eclipsing binaries 20 p2975 A72-40072

Interferometric method for measuring electro-optic coefficients in crystals 21 p3095 A72-40138

The effect of amplitude and phase tolerances on the phase characteristics of dipole arrays 21 p3028 A72-40512

Signal transmission and detection in differentially encoded coherent multiple phase shift keyed digital communication systems, discussing carrier suppression-induced resolution ambiguity 21 p3017 A72-40861

The phase difference between coupled laser oscillations 22 p3184 A72-42109

On the comparison of phase and multi-layer techniques for numerical solution of the scattering problems 22 p3154 A72-42305

Wideband pulsed-RF phase measurement 23 p3270 A72-43575

Ultrasonic diffraction loss and phase change for broad-band pulses 23 p3313 A72-44115

Probabilistic characteristics of radiation pattern for multielement antenna with nonpolar phase front 24 p3384 A72-44754

Constrained proportional controller dynamic equation solution on analog computer, determining limit cycle phase shift and nonlinearity effects on self oscillation parameters 24 p3403 A72-45322

PHASE SHIFT CIRCUITS

NT CIRCULATORS [PHASE SHIFT CIRCUITS]

REDAP 31 network analysis program for design of S-band phase shifter with P-I-N diodes for phase array antennas 01 p0040 A72-10689

Radio wave polarization orthogonality recovery by using differential phase shifter and attenuator in radio communication systems 02 p0183 A72-12799

Active all-pass circuits transfer function and synthesis, including delay lines, phase correctors and wide-band phase shifter applications 03 p0338 A72-13169

Low cost ferrite remanence microwave phase shifter design using periodic loading structures 04 p0497 A72-14716

Reciprocal dual mode millimeter wavelength phase shifter design for use in phased array antennas, calculating phase shift and insertion loss vs frequency 04 p0498 A72-14719

Synthesis method for optimized single-stage reflection type phase shifters, determining transformation coefficient 05 p0634 A72-15831

Longitudinally magnetized fully filled square waveguide reciprocal ferrite phase shifter, predicting frequency characteristics by rotational error analysis 06 p0786 A72-18370

Digital loaded-line phase shifters for phased array antennas, discussing lossy microstrips effects and P-I-N diode switching shortcomings in design requirements 07 p0954 A72-19048

X band high power ferrite phase shifter design and performance 10 p1451 A72-24595

YIG tuned Gunn oscillator phase locking and shifting over 3 GHz range in X band, using feedback control 10 p1451 A72-24596

Broadband diode phase shifter design, discussing switched and loaded line, reflection and lumped element high pass and low pass circuits 11 p1607 A72-26992

Self excited oscillator using emitter follower circuit and distributed active RC phase shifter network 13 p1927 A72-28404

Nonideal component parts effect on behavior of digital microstrip closed circuit X band phase shifter, presenting detailed network analysis 15 p2201 A72-32471

Ferrite and dielectric element waveguide phase shifters with rectangular hysteresis loop, deriving differential phase and attenuation constants for wave propagation 15 p2202 A72-32662

The absolute calibration of periodic microwave phase shifters without a standard phase shifter 17 p2531 A72-35470

X- and Ku-band microelectronic phase shifters 17 p2531 A72-35767

Spatial diversity technique based on predetector equal-gain combining for fast fading reduction of AM radio receiver, using phase shifter 18 p2661 A72-36845

Nature of losses introduced into a ring resonator by a nonreciprocal phase-shifting device that employs the Faraday effect 19 p2814 A72-38788

Phase shifter number reduction effects on phased radar array radiation pattern distortion and sidelobe reduction 20 p2907 A72-39268

New active all-pass network with linear group delay 20 p2910 A72-39431

Faraday rotation dual-mode ferrite reciprocal phaser with performance and cost advantages over toroidal type for microwave phased array applications 20 p2909 A72-39733

A simple reference generator for lock-in amplifiers 21 p3025 A72-40206

Synthesis method for phase and loss optimized single-stage reflection type phase shifters, determining transformation coefficient 23 p3268 A72-43439

Recent advances in diode and ferrite phaser technology for phased-array radars. I. 23 p3270 A72-43572

A solid-state 'flux-drive' control circuit for latching-ferrite-phaser applications 23 p3275 A72-43574

Microwave phase shifting with gain using IMPATT diodes 24 p3385 A72-44963

PHASE SHIFT KEYING

Convolutional coding, Viterbi decoding and binary phase shift keyed modulation for reliable communication on power limited satellite and space channels 01 p0026 A72-10342

Multichannel space station communications using PCM-PSK-PM interplex modulation for reducing cross modulation loss 02 p0174 A72-12131

Binary differentially coherent phase shift keyed system, evaluating error probability performance in presence of thermal noise and intersymbol interference 06 p0772 A72-17408

Recovered carrier phase ambiguity resolution in four-phase PSK digital satellite communications system 06 p0772 A72-17409

Signal coding for discrete information in multichannel systems using multiple differential phase shift keying 06 p0773 A72-17500

Optimal PSK signals selection and synthesis from random sequences ensuring minimum value of maximum side peak of autocorrelation function 07 p0943 A72-19564

Pulse overlapping effects on phase jittering in carrier regeneration with quaternary phase shift keying 07 p0945 A72-19662

Synthesizing antenna arrays perpendicular to conducting screen by PSK signal theory, discussing optimal binary phasing and radiation patterns numerical data 10 p1450 A72-24507

Nonlinear filtering synthesis of optimal receiver for pseudorandom phase shift keyed signal with arbitrary modulation angle and white noise background 10 p1436 A72-24510

Bandpass filter harmonic signal phase shift distortion effect on transient response in PSK of multichannel transmission 12 p1783 A72-27630

Binary PSK signals optimized on minimax and quadratic criteria, noting design of coders and decoders on shift registers with external logic 13 p1914 A72-28415

Transistorized electronic equipment with delay line for optimal filtration of PSK signals 13 p1930 A72-29047

PSK signal cross-correlated receiver output SNR in presence of random misalignments with respect to carrier frequency and arrival signal time 13 p1921 A72-29283

Statistical analysis of random mismatched tapped delay line filters effect on binary phase shift keying pulse compression codes peak-to-sidelobe and SNR 15 p2196 A72-31792

Error rate of phase-shift keying in the presence of discrete multipath interference 17 p2516 A72-35334

Marcum Q function parameters approximations for error probabilities computation in multilevel frequency shift keying and differentially coherent phase shift keying systems 20 p2903 A72-39426

Susceptibility measurements on PCM-FM and four phase differential PSK digital receivers simulated on analog computer 21 p3016 A72-40852

Phase noise types in digital satellite communication links, discussing continuous binary phase shift keyed modulation systems with coherent detection 21 p3020 A72-40896

Optimal PSK signals selection and synthesis from random sequences, ensuring minimum value of maximum side peak of autocorrelation function 22 p3153 A72-42082

On the performance of digital communication systems with bandpass limiters. I - One-link system. II - Two-link system. 23 p3265 A72-44181

Spacing limitations of geostationary satellites using multilevel coherent PSK signals 23 p3265 A72-44183

Effects of bandlimiting on the coherent detection of PSK, ASK and FSK signals 24 p3380 A72-44900

PHASE TRANSFORMATIONS

NT ARC MELTING

NT BOILING

NT EVAPORATION

NT FILM BOILING

NT FREEZING

NT FUSION (MELTING)

NT LEIDENFROST PHENOMENON

NT LIQUEFACTION

NT MELTING

NT NUCLEATE BOILING

NT PROPELLANT EVAPORATION

NT SUBLIMATION

NT TRANSPIRATION

NT VACUUM MELTING

NT VAPORIZING

NT VIBRATIONAL FREEZING

NT ZONE MELTING

Ti alloys omega phase transformations by cryogenic cooling of bcc beta phase, interpreting electron diffraction pattern change in terms of displacement type reactions 01 p0082 A72-10204

Stress effects on TiNi compound martensitic transformation, investigating deformation as function of composition and heat treatment 01 p0087 A72-11023

Al-Mn system constitution, discussing metastable phase, high and room temperature modifications and transformation equilibrium 01 p0088 A72-11045

Phase oriented precipitation patterns of Ti in Ti-C-O system, discussing composition independence and dislocation networks 01 p0089 A72-11184

Equation of state for porous metals at high temperatures under strong shock compression, considering phase transitions 02 p0258 A72-11469

Allotropic transformations and recrystallization by precipitation hardening in pure Ti crystals, using field emission microscopy 02 p0242 A72-12007

Anodic polarization curves of Ni-Fe alloys relating reaction to attack at controlled voltage of gamma joints and Ni content, using electron microprobe 02 p0243 A72-12168

VT22 high strength Ti alloy beta phase decomposition kinetics studies under heat treatment, noting omega and alpha phases role for low plasticity 02 p0244 A72-12247

Ti-Cr alloys omega phase formation by measurements of hardness, Young modulus and internal friction 02 p0246 A72-12672

Gamma prime precipitate hardened Ni base alloys, attributing strengthening mechanism to coherency strains and precipitates antiphase boundary energy
02 p0247 A72-12817

Single crystal Si defect accumulation and transition to amorphous state under Xe, Ar, Ne, O and P ion irradiation, using EPR
02 p0269 A72-12884

Thermodynamic equilibrium variational theory for multiphase systems subject to nonhydrostatic stress, considering diffusion and phase transformations
03 p0455 A72-12908

Ultrasonic cavitation effects on martensitic specimens, observing plastic deformation, softening, phase transformations and decay
03 p0370 A72-13187

Residual stress formation mechanism in two phase Ti alloys under cutting and plastic deformation, showing phase transformation composition and structure effects
03 p0363 A72-13467

Argon plasma electromagnetic wave transformation and absorption measurements under various gas pressures
03 p0395 A72-13571

Beta structure effect on cyclic fatigue strength in Ti alloy under various heat treatments
03 p0372 A72-13595

Shock waves in solids, investigating Hugoniot curve for condensed and porous media and phase transformation effects in polycrystals
03 p0446 A72-13689

Sigma phase formation in chromous ferrite, investigating vacuum diffusion, hot and cold working, welding and additives effects
03 p0375 A72-13940

Mo and C additives effects on austenite susceptibility to deformation martensite formation and steel resistance to hydroerosion
03 p0375 A72-13941

Heat transfer coefficients to both sides of finite one dimensional slab subject to phase-change coating technique boundary conditions, deriving thin wing correction factors
03 p0457 A72-13956

Dilatometric investigation of martensitic transformation in TiNi compound, observing plastic memory effect
03 p0377 A72-14021

Heat and mass transfer processes in systems of bodies with variable phase boundaries, proposing difference scheme
03 p0458 A72-14159

Kinetic energy losses due to liquid-to-solid phase transformation in heated two-component flow ascending in tube
03 p0342 A72-14161

Low temperatures and deformation rates effect on martensitic phase formation in Cr-Ni austenitic stainless steel under compression and tension
03 p0379 A72-14378

Cholesterol esters polymorphic and mesomorphic behavior, using differential scanning calorimetry, X ray powder diffractometry and positron annihilation techniques
04 p0484 A72-15262

Ni-based metal graphite materials, investigating sintering process control variables effects on structure and phase composition responses
05 p0665 A72-16090

Transformations of Ti alloy in isothermal conditions, observing hardening and loss of ductility
05 p0673 A72-16149

Fe-Co alloy athermal transformation to bcc martensite at industrial cooling rates, investigating effects on mechanical properties
06 p0829 A72-17830

Anelasticity effects due to defects and phase transformations in solids - Conference, Lausanne, Switzerland, June 1970
06 p0830 A72-18291

Internal friction and plastic microstrains in martensitic transformation of Fe-Ni, Co-Ni, and Fe-Cr-Ni alloys
06 p0830 A72-18294

Phase composition and electrical and mechanical properties of compacted zirconium diboride/tungsten alloys after sintering in argon, carbonaceous medium and vacuum
06 p0832 A72-18428

Austenitizing conditions effects on hardness and microstructure of tempered steel, emphasizing martensite structure and grain size changes produced by controlled heat treatment
07 p0995 A72-19486

Ti, Fe, Co, Ni, Pt and steels phase transformation and thermal defect effects on high temperature thermal conductivity
07 p0102 A72-19548

Hardenability and pearlite stage isothermal transformation properties of direct-quenching low Cr case-hardening steels, discussing Mn, Mo and Ni alloying effects on machinability
07 p0995 A72-19571

Cu contents effect on Ti-Cu alloys physical and mechanical properties, discussing beta phase decomposition during annealing
07 p0102 A72-19574

Phase and microstructure changes during nitriding process of Fe-Ti alloys, stressing Ti concentration effect
07 p0103 A72-19749

Deformable thermally work hardenable Al-Mg-Li alloy, detailing phase composition changes during aging
07 p0104 A72-19838

Martensitic transformations induced by plastic deformation in Fe-Ni-Cr-C system, noting stacking fault energy dependence on temperature
07 p0105 A72-19928

Adiabatic reversion of Ni martensitic steel to austenite under shear in orthogonal cutting
07 p0996 A72-19934

Plasma spraying process effects on carbon steel coatings structure and bonding, considering optimal parameters, properties control and phase transformations
07 p0996 A72-19966

Alloying additives effects on Ti and Zr resistivity, thermal expansion, crystal lattice parameters and polymorphous transformations temperatures
07 p0107 A72-19990

Phase composition changes, crater formation and metal ejection during erosion by pulsed laser beam
07 p0109 A72-20610

Gamma irradiation effects on temperature of reversible solid-to-liquid phase transformation in Al
08 p1185 A72-21075

Biot variational principle for phase change problem with constant heat flux boundary condition and without melt removal, noting linear temperature profile choice
08 p1254 A72-21611

Free convection effect on plane crystallization front instability under conditions of phase transition, using method of small perturbations
08 p1151 A72-21661

Soviet papers on phase transformations covering supersaturated solid solutions decomposition, Nb-Al-Ge system phase diagram, martensite decomposition, etc
08 p1186 A72-21776

Cr-Tb alloys monotectic, eutectic and eutectoidal phase transformations study with differential thermal, metallographic, X ray structural and durometric analysis
08 p1187 A72-21781

Ni-Cr-Nb alloys structure and phase composition changes from W-Mo additions and hardening by intermetallic Ni-Nb precipitated from supersaturated solid solution
08 p1187 A72-21782

Ti-Co intermediate phase transformations discussing lattice formation, intermetallics melting points and stoichiometric composition
08 p1187 A72-21783

Helium cryostat for X ray studies of phase transformations and structural changes in single metal crystals
08 p1169 A72-21792

Ti, Zr and Hf hcp-bcc phase transformation isochromat spectroscopic investigation, noting fine structures to confirm electron state density
09 p1371 A72-22849

Microstructural transformations in preaged Ti alloys with unstable beta phase under external tensile stresses
09 p1328 A72-23032

Polymorphism in Ta vacuum condensates, observing beta-alpha phase transformation in films
09 p1329 A72-23041

Quenched and tempered Ni carbon steel retained austenite transformation and crack observation by X ray diffraction under low cycle fatigue testing
09 p1329 A72-23149

Micrograin superplasticity in eutectoid steel, discussing effect of transformation to austenite
09 p1330 A72-23380

Nonanalytic equation of state formulation at critical point of fluid phase transformation
09 p1413 A72-23690

Carbon effects on internal friction of low temperature Fe-Ni alloy during martensitic transformation
10 p1495 A72-24083

Equilibrium thermodynamics of critical points, discussing phase transition theory and scaling hypothesis for single component systems
10 p1562 A72-24400

Small scale flow and surface effects in multiphase media hydromechanics, obtaining entropy production in mixture for interphase transformations characterization
10 p1468 A72-24430

Enthalpy measurements of allotropic transformation of Co alloys during hcp-fcc transition with additive elements
10 p1498 A72-24850

Fracture strength relation to austenite stability in steels with plastic deformation caused by strain induced austenite-martensite transformation
10 p1499 A72-24894

Phase transformations and recrystallization study of Ti-steel bimetal with emission microscope, observing high temperature formation of titanium and vanadium carbides
11 p1654 A72-25493

Iron emission spectrum in phase transformations and recrystallization study of austenitic and carbon steels under high temperature hardening
11 p1655 A72-25496

Austenitizing condition effect on lower bainite transformation in eutectoid carbon steel
11 p1656 A72-25515

Transitional ferrite phase formation in Fe-Cr-Ni alloy evidenced on electron micrographs and diffraction patterns
11 p1657 A72-25760

Transition series oxides metal-insulator phase transition based on electron phonon interaction model
11 p1701 A72-26024

VT22 high strength Ti alloy beta phase decomposition kinetics under heat treatment, noting omega and alpha phases formation effect on ductility
11 p1660 A72-26133

Hugoniot equation of state measurements on iron-silicate garnet, showing shock induced transition to high pressure phase
11 p1627 A72-26524

Interference between recrystallization and allotropic transformation of cold rolled and annealed Co investigated by internal damping measurements
11 p1661 A72-26649

Austenite formation kinetics in Fe-C ferritic-pearlitic structure at 855 C, comparing experimental data with theoretical calculations
11 p1662 A72-26744

Metal silicide phase formation for Nb, Ta, Mo and W, examining Si diffusion and transport processes
11 p1664 A72-26859

W-Ni-Mo alloys obtained by powdered metals sintering, investigating mechanical properties, phase distribution and composition
11 p1666 A72-26876

Coherent phases transformations in alloys, investigating mechanical properties dependence on microstructural features
11 p1667 A72-26929

Multiphase Al alloys strengthening by dislocation substructures in repeated rolling and recovery cycles at elevated temperature
11 p1667 A72-26930

Grain boundary network of allotropic phase change for ductility enhancement in Fe-Ta alloys
11 p1668 A72-26941

Low temperature solid state phase transformations in 2H silicon carbide single crystals, noting time and temperature dependence
12 p1854 A72-27276

High purity Al single crystal orientation explained by Rowland transformation model, observing recrystallization grains
12 p1828 A72-27300

Isothermal profiles for Nb-Zr-C and Nb-Ti-C alloys from microstructural and X ray analyses, noting Widmanstam structure, and second phase formation
12 p1829 A72-27643

Metal surface layers structural changes under external friction, noting hardening, softening and phase transformations of active layer material
12 p1818 A72-28190

Time-temperature-precipitation (TTP) diagrams and phase instabilities of high temperature exposed Mo containing austenitic stainless steels
13 p1974 A72-28658

Mo influence on gamma prime phase precipitate in wrought Ni-base superalloys, considering solvus temperature, weight fraction and lattice parameters
13 p1975 A72-28669

Ordering in fcc lattice ternary alloys with allowance for atoms interactions, noting phase transformation critical temperature and superlattices existence
13 p1976 A72-28691

Ni-Mn alloy phase transformation characteristics from neutron diffraction and small angle scattering studies, showing ordered nearly stoichiometric metastable phase for entire temperature range
13 p1976 A72-28903

Co-Cu alloy phase formation and separation morphology changes with temperature and anomalous diffusive X ray scattering in solid solutions
13 p1976 A72-28905

Martensitic transformation in Cu-Al-Ni alloy thin film, investigating gamma-prime phase substructure formation and crystal growth pattern
13 p1976 A72-28907

Fcc lattice ferronickel alloys para-process susceptibility anomalous increase explanation by phase transition thermodynamic theory
13 p1977 A72-28911

Cu-Al-Ni alloys single crystals internal friction temperature dependence during martensitic transformations
13 p1977 A72-28912

Ni, Si and Mn alloying effect on structural transformations, phase composition and mechanical properties of cast Cr-Ni steels
14 p2114 A72-30273

Ti alloy volume reduction during decomposition of metastable alpha-prime, alpha-two and beta phases after cooling from beta range
14 p2114 A72-30401

U-Zr-Nb and U-Nb-Mo alloys gamma solid solution phase isothermal transformation kinetics at 500-600 C from dilatometric, microstructural and X ray analyses, noting decomposition
14 p2114 A72-30403

Maraging Fe-Ni-Co-Mo alloy ordered metastable omega phase formation during martensite aging from electron microscopic investigation, noting Co addition effects and precipitation
14 p2115 A72-30404

X ray and metallographic analyses of Ni-Mo, Ni-Ta, Ni-Nb, Ni-Zr and Ni-Ti alloys crystallized at high cooling rates, observing metastable phases
14 p2115 A72-30405

Gamma-prime phase crystal structure in Cu-Al-Ni alloy from electron microscopic study, noting twinning and substructure during formation
14 p2115 A72-30406

Martensitic transformation athermal kinetics and accompanied martensite morphology change in Fe-Ni and Fe-Ni-Cr alloys
14 p2115 A72-30407

Surface phase transformation during cavitation erosion in Co and Fe alloys, suggesting stacking fault energy effect on erosion resistance
14 p2119 A72-30603

Si phase identification in super alpha Ti alloys, using electron transmission microscopy and diffraction analyses
14 p2120 A72-30616

Minimum weight phase change thermal control device for planetary descent probes, discussing test over various heat loads
14 p2121 A72-30826

[AIAA PAPER 72-287] Shock heating caused material phase transformation effects on bumper shield performance, studying thin metal sheets response to like-material spheres impact
14 p2128 A72-30921

Zr-Cu-Mo system phase diagram from microscopy, X ray analysis and mechanical tests, noting beta solid solution transformation into alpha, omega and beta phase mixtures
14 p2122 A72-30978

Thermal and microstructural analysis of phase interactions in Mg alloys of Mg-Nd-Y system
14 p2124 A72-31028

Alloying effect on structural transformations and strain hardening during aging of two phase /alpha-beta/ Mg-Li-Zn alloys
14 p2124 A72-31031

Vacancy annealing effect on beta phase transformation during tempering of Ti alloy with Mo, showing strain hardening and contraction increase
14 p2124 A72-31032

Al-Mu-Li alloys phases mechanical and thermal properties under tensile and fatigue tests at room and elevated temperatures
14 p2124 A72-31037

Mn, Zr and Cr alloying effects on grain size and solid solution decomposition of cast Al-Zn-Mg alloy bars
14 p2125 A72-31039

Tensile strength and martensitic transformation effect on stainless steel plastic deformation at cryogenic temperatures
15 p2253 A72-31521

Diffusion layer formation on metallic surfaces, discussing saturation, crystallization, phase structure, chemical reactions, thermal and contact conditions
15 p2255 A72-31571

Solution kinetics of secondary phases in cast dendritic and nondendritic Mg-Zn and Mg-Zn-Zr alloys, using cylindrical and spherical diffusion models
15 p2257 A72-32119

Phase transitions effect on dc electrical resistance of barium titanate investigated for yttrium-doped polycrystals and for reduced single crystals
15 p2294 A72-32483

Crystallographic structure, phase transformations, Curie temperature and Faraday rotation of Ti-substituted MnBi films
15 p2294 A72-32522

Premartensitic beta phase instability, lattice vibration and shape memory effect in noble metal base and Ti alloys
15 p2259 A72-32641

Nb-Mo alloys elastic constants anomalous temperature dependence, proposing phase changes role and relationship to neutron diffraction and specific heat
16 p2405 A72-33167

Alpha to beta transformation of rhombohedral B, investigating lattice structure on heating stage in electron microscope
16 p2405 A72-33204

Time-temperature correlated phase transformations in zirconia nucleated magnesium-aluminum-silicon oxide glass ceramics for isothermal heat treatment
16 p2413 A72-33205

Quenching produced martensitic transformations from equilibrium beta phase region for Ti alloys with Ta
16 p2408 A72-33618

Precipitation reactions during tempering of Ti-Ta alloys, studying hcp and orthorhombic martensitic phases from electron microscope observations
16 p2408 A72-33619

Composition effect on strain-transformation and precipitation hardening of beta Ti alloys at 800-1100 F
16 p2410 A72-33813

Transformation induced plasticity /trip/ Ni-C steel strengthening by thermal cycling between martensite and reverted austenite
16 p2399 A72-33815

Russian book on metal alloys structure and properties covering structural changes in solid bodies, metals atomic structure, diffusion, phase transformations and composite materials
17 p2568 A72-35446

Cluster variation method for boundary free energy solution in lattice model applied to Ising phase and gas-liquid interface and longer range interaction
18 p2711 A72-36565

Thermodynamics and phase relations in refractory metal solid solutions containing carbon, nitrogen, and oxygen.
18 p2699 A72-36576

Phase stability and mechanical properties of carbide and boride strengthened chromium-base alloys.
18 p2700 A72-36579

Phase structure and solution kinetics of cast and wrought Al alloys after plastic deformation by rolling
18 p2700 A72-36585

Behavior of Fe-21.6 Ni, Fe-18.4 Ni-15.0 Co, Fe-16.8 Ni-5.0 Mo subjected to cumulative thermal cycling at 300 C/hr
18 p2701 A72-36701

The effect of Mo, Al, and C on phase transformations in Ni alloys
19 p2814 A72-37417

Some problems concerning microplastic deformation and isothermal transformation of Fe-Ni-C alloy. III - Effect of aging in the temperature range from 203 to 304 K on microplastic deformation at 77 K
19 p2814 A72-37419

Some problems concerning microplastic deformation and isothermal transformation of Fe-Ni-C alloy. IV - Effect of transformation plasticity on microplastic deformation at 77 K
19 p2815 A72-37420

Solid-state phase transformations.
19 p2815 A72-37442

Zr and V alpha and beta stabilizing element effects on phase boundaries in arc fused Ti-Al alloy studied by diffusion layer method
19 p2817 A72-37754

Alpha aluminum oxide whiskers growth in presence of lead by vapor/liquid/solid phase mechanism in moist hydrogen at 1200-1400 C
19 p2823 A72-38279

Aging characteristics of Ti-Mo base beta alloys.
19 p2820 A72-38371

Time spectrum and angular distribution for positron annihilation studies of electron structure and phase transformations of materials
19 p2845 A72-38401

Role of an electric field in the diffusion mechanism of the graphite-to-diamond phase transformation
19 p2823 A72-38405

X-ray analysis of iron-chrome solid solutions
19 p2821 A72-38572

The effect of plastic deformation on the martensite-to-austenite transition in an iron-nickel alloy.
20 p2938 A72-39298

Fine structure in quenched Fe-Al-C steels.
20 p2938 A72-39300

X ray diffraction study of crystal structure of metastable phase in rapidly solidified Al-Zr alloys
20 p2939 A72-39307

Decomposition, solubility and coherent phase stability of modulated structure Co-Ni-Ti system at high nucleation temperatures
20 p2939 A72-39312

Pressure pulsations relationship to fixed boundary of turbulent flow with kinematic structure, considering phase transitions effect
20 p2912 A72-39361

Phase transformations and exsolution in lunar and terrestrial calcic plagioclases.
20 p2970 A72-39480

A study of the liquid-vapor phase change of mercury based on irreversible thermodynamics.
20 p2983 A72-39481

[ASME PAPER 72-HT-A] Habit plane interpretations of surface martensite transformation and orientation measurements compared with invariant plane strain /IPS/ theory
21 p3065 A72-40088

Single and double shear invariant plane crystallographic theories for martensitic transformations, calculating lattice deformations by combined Bain and complementary shear strains
21 p3065 A72-40089

Fe-Ni sheet with austenitic cube texture by rolling and annealing, investigating plastic deformation during martensitic transformation
21 p3065 A72-40090

Stress induced martensitic transformation relationship to shape memory effect compared with su-

perelasticity, transformation plasticity and reversible linear change
21 p3065 A72-40091

Beta to omega phase transformation and structure in Zr and Ti alloys bcc solid solutions by dark field electron microscopy, diffraction and ultrasonic technique
21 p3065 A72-40092

Arc furnace for thermal analysis of ultra-refractory materials
21 p3039 A72-40208

Formation of deformation martensite in Fe-Ni-C alloys which do not undergo transformation on cooling.
21 p3066 A72-40270

Deformation-induced martensitic transformation in isothermal and athermal Fe-Ni-C alloys.
21 p3066 A72-40272

Phase transition between solid hydrate and saturated solution of lithium chloride electrically detected on a lithium chloride heated hygrometer.
21 p3054 A72-40689

Phase precipitation structure of superconducting Nb-Ti alloys after cold working and low temperature annealing
21 p3067 A72-40951

Dilatometric studies of volume compression effect during aging of nimonic alloy showing linear dependence of matrix lattice constant on gamma prime phase
21 p3068 A72-40957

On the growth kinetics of Laves phase precipitates in Fe-Ti alloys at elevated temperatures.
21 p3069 A72-41011

Holographic technique for investigation of critical phenomena in aniline-cyclohexane and triethylamine-water binary critical mixtures, noting phase transition visualization
21 p3056 A72-41219

Detection of crystals in CO2 jet plumes.
21 p3046 A72-41306

Changes in the phase composition of metal-glass materials depending on the sintering temperature
21 p3073 A72-41370

Martensite formation temperature decrease and grain size reduction caused by martensite crystals interaction with barriers in Fe alloy containing austenite beta phase particles
21 p3070 A72-41679

Alpha stabilizing Al and Sn suppression effect on beta-omega transformation during Ti alloy hardening
22 p3189 A72-42278

Dielectric dispersion of irradiated BaTiO3 near the phase transition.
22 p3215 A72-42934

X-ray structural examination of phase transformations in the VT14 titanium alloy during heating
22 p3192 A72-43015

Martensitic transformation in filamentary cobalt crystals
22 p3192 A72-43017

Carbide phases in nickel-based heat-resistant alloys
22 p3192 A72-43018

Fe-Ni-C martensite reverse transformation to austenite during large and rapid applied shear, evaluating shear zone neighboring partially pierced hole
22 p3193 A72-43031

Pure Co single crystals allotropic transformation effects on deformation behavior, noting flow stress and work hardening rate relationship to history
22 p3193 A72-43034

Enhanced strengthening of a spinodal Fe-Ni-Cu alloy by martensitic transformation.
22 p3194 A72-43040

Model of degenerate semiconductor near segnetoelectric phase transformation, noting superconducting state at low temperatures with corresponding impurity concentrations
23 p3323 A72-43317

Mechanical properties of titanium alloys with isomorphous beta-stabilizing elements
23 p3300 A72-43590

Martensitic transformation during deformation in titanium alloys with a metastable beta phase
23 p3300 A72-43591

Phase diagrams from X ray analysis of rapidly crystallized Ni-Sn alloys, noting crystal lattices and phase transformation
23 p3300 A72-43648

Peritectic solid phase transformations in cast homogenized Al-Cu-Li-Mn-Cd alloy, noting Li strengthening effect
23 p3303 A72-44093

Structure of the 01420 alloy with zirconium
23 p3303 A72-44094

Alpha aluminum whiskers growth in mullite ceramic composition following vapor-liquid-solid phase
23 p3303 A72-44152

Phase transformations in chromium-titanium compounds.
24 p3413 A72-44922

Residual stress formation mechanism in two phase Ti alloys under cutting and plastic deformation, showing phase transformation composition and structure effects
24 p3407 A72-44942

Non-steady shock waves in metals with phase transitions and hardening by explosion. 24 p3414 A72-45025

Factors affecting phase-change paint heat-transfer data reduction with emphasis on wall temperatures approaching adiabatic conditions. [AIAA PAPER 72-1030] 24 p3389 A72-45407

Transition of the oxide film on a molybdenum surface from the two-dimensional to the three-dimensional phase 24 p3432 A72-45503

Gas dynamics and shock wave physics of supersonic flow in two phase media, noting evaporation, condensation and phase transformations 24 p3364 A72-45525

PHASE VELOCITY

Propagating waves characteristics measurement on Yagi-Uda array, obtaining k-beta diagrams and phase velocities 01 p0043 A72-11244

Plasma oscillations stabilization, considering nonlinear effects in phase velocity of plasma waves 05 p0695 A72-16416

Vlf propagation and D region aeronomy model for vlf phase behavior predictions and observations during two solar eclipses 05 p0630 A72-16618

Phase and group velocity of electromagnetic waves in drifting uniaxial magnetoplasma, obtaining dispersion relation from Maxwell and plasma equations 06 p0853 A72-17349

Phase velocity of first order mode of vlf waves propagating in earth ionosphere 06 p0773 A72-17598

Resonant frequency, phase velocities and dispersion curves for wave propagation in isotropic elastic cylinders 06 p0895 A72-17854

Fast electron-cyclotron wave excitation with infinite phase velocity along magnetic field in nonequilibrium electron plasma 06 p0862 A72-18402

Drift waves propagation in ionized plasma, considering drift rate, ion sound phase velocity and effect of impurities 07 p1045 A72-20444

Long distance atmospheric propagation in earth-ionosphere waveguide, obtaining phase velocities and damping factors 08 p1131 A72-20802

Ar/He plasma acoustic wave properties, expressing phase velocity and damping as function of ion-electron temperature ratio and relative species densities 10 p1520 A72-24300

Phase velocity and Landau damping of ion acoustic waves propagating through plasma boundary layer at conducting sphere or cylinder based on two fluid model 10 p1523 A72-24746

Fast and slow ion acoustic free streaming wave propagation in drifting plasma, showing phase velocity and damping in agreement with Maxwellian distribution 11 p1692 A72-25518

Cylindrical waveguide proper modes instability regions boundary calculation, determining dispersion characteristics and waves phase and group velocities 12 p1791 A72-27537

Signal propagation along homogeneous drifting electron beam focused by strong magnetic field, obtaining phase velocity and space charge density 13 p1914 A72-28373

Frequency equation for torsional wave phase velocity in solid circular rod under initial tension, plotted for various propagation modes 13 p2002 A72-28620

Wave channel type antenna design with modulated phase velocity and multiple use of antenna array 13 p1929 A72-28895

VLF and LF electromagnetic waves amplitude and phase velocity in spherical earth-ionosphere waveguide, discussing wave hop method 13 p1923 A72-29661

Equations of motion for incompressible viscous fluid thin layer on cylinder outer side under gravity, calculating wave number, phase velocity and film thickness 14 p2094 A72-30699

Variable amplitude and phase velocity electromagnetic traveling wave field distribution in diverging MHD induction machine channel with liquid metal flow 16 p2435 A72-33282

Sea surface wind-caused waves spectral component phase velocity measurement method based on statistical treatment of synchronous continuous records of surface elevation 16 p2417 A72-33291

Electromagnetic waves attenuation and phase velocity correction in polycrystals with anisotropic crystal distribution 16 p2365 A72-34013

Fast electron cyclotron wave excitation with infinite phase velocity along magnetic field in nonequilibrium electron plasma 17 p2588 A72-34853

Measurements of ultrasonic velocities using a digital averaging technique. 18 p2691 A72-36401

WKB approximation to suggest vertical phase velocity measurement at turning points of acoustic-gravity wave propagation in thermosphere 18 p2686 A72-36411

Large-signal analysis of efficiency and nonlinear phase distortion in a phase velocity tapered traveling-wave tube. 24 p3385 A72-45283

PHASE-SPACE INTEGRAL

Optimization programs for linear control systems with nonconvex constraints on phase coordinates applied to material point transfer 04 p0504 A72-14624

Vlasov equation phase space boundary integration for evolution of one dimensional self gravitating collisionless stellar systems with constant density 05 p0714 A72-16056

Small scale phase space density granulations/clumps/ in turbulent plasma due to fluctuating electric field 07 p1041 A72-19510

Control synthesis equations for aircraft motion on phase space surface 09 p1261 A72-22208

PHASED ARRAYS

Phased array antennas design and performance characteristics, examining feeding and electronic scanning problems with special attention to all-solid-state designs 01 p0038 A72-10659

Microwave module circuit design for airborne phased array radar with distributed power generation, reception and phase shift functions, considering performance, reliability and cost 01 p0028 A72-10660

X-band linear phased array tracking antenna with digital phase shifters and beam steering, evaluating beamwidth, gain and direction error 01 p0028 A72-10663

Low sidelobe pencil beam thinned phased arrays design involving element position selection 01 p0039 A72-10664

Far field patterns of hourglass reflector phased array for electronic despin of communications antenna on spin stabilized satellite 01 p0029 A72-10666

Characteristic equation of surface wave propagation on two dimensional corrugated structures for phased array applications 01 p0030 A72-10845

Phased scanning array for ATC radar beacon systems, airport or air route surveillance radars and ground landing systems 01 p0098 A72-10962

Boundary value problem solution for multiple interleaved phased arrays of waveguide radiators operating at different frequencies, investigating transmission characteristics 01 p0042 A72-11234

Large reflector and phased array antennas, discussing synthesis and analysis, active impedance and blind spots, matching, beam steering and implementation 02 p0191 A72-11686

Radiation pattern and reflected field analysis for incident plane wave on phased arrays of thick wall rectangular waveguides 03 p0330 A72-13168

Planar phased array antennas with uniform current amplitudes, calculating beam-pointing error dependence on array geometry, phase errors and scan angle 03 p0325 A72-14179

Phased antenna array blind spot detection and elimination, describing aperture match with inductive irises 04 p0486 A72-14493

Waveguide radiators linear phased array impedance matching during E-plane wide angle scanning improved by reflection coefficient variation compensation 04 p0499 A72-15239

Random phasing algorithms to reduce phase quantization lobes for radiation patterns of commutated phased array antennas 05 p0634 A72-15820

Computer controlled production test system for airborne phased array modules, describing various measurement capabilities 05 p0637 A72-16417

Small array technique for active impedance amplitude and phase measurement of large phased arrays 06 p0782 A72-17361

Electronic scanning steerable phased array radar beam pointing capability improvement for moving target detection probability 06 p0772 A72-17423

S band module with Gunn diode oscillators in series connection used as phased array radar 250 W power sources with efficient heat sink 06 p0789 A72-18476

Digital loaded-line phase shifters for phased array antennas, discussing lossy microstrips effects and P-I-N diode switching shortcomings in design requirements 07 p0954 A72-19048

Element position design of pencil beam thin phased arrays with low sidelobes 07 p0941 A72-19256

Computer simulated phased arrays with randomly located elements, deriving peak sidelobe level for comparison with measurement 07 p0945 A72-19783

Anomalous wave nulls and relation to endfire surface wave radiation on phased arrays of TEM waveguides with metallic fences perpendicular to ground plane 07 p0945 A72-19788

Gain function for planar phased array far field pattern, deriving calculation method for excitation pattern for prescribed radiated beam behavior 08 p1132 A72-21328

Targets discovery in predetermined direction by phased array radar, using sequential analysis 09 p1278 A72-22896

Phased array radar systems synthesis based on life cycle cost minimization, taking into account high-speed digital data processing 09 p1280 A72-23374

Agile beam electronically scanned multitarget phased array tracking radar, dwell allocation strategy and trajectory extrapolation algorithm effects on target handling capacity 10 p1437 A72-24685

Single engine aircraft-borne weather radar with electronically scanned steerable phased array antenna [SAE PAPER 720315] 11 p1591 A72-25579

Finite and infinite number element phased array antennas, deriving active impedance, element pattern and power gain 11 p1593 A72-26096

Radiation pattern forming circuit with compensated mutual coupling in phased antenna arrays, noting synthesis by matched multipoles 11 p1598 A72-26712

Parasitic sidelobe suppression in radiation patterns of phase switching linear antenna array without gain loss 11 p1598 A72-26717

Communication and data relay satellites multibeam antennas characteristics, discussing multiple feed reflectors, bootlace lens configuration and phased arrays [AIAA PAPER 72-530] 12 p1789 A72-27355

Electro-optical processing of phased array signal reception, using electron beam addressing system with potassium dideuterium phosphate target crystal 12 p1785 A72-27954

Optimal parameters of electro-optical signal processor for phased array antennas, noting optical subsystem correspondence to optoacoustical spectrum analyzer 13 p1926 A72-28374

Mutual coupling in phased arrays of randomly spaced antennas, investigating probabilistic properties of main beam amplitude fluctuations 13 p1916 A72-28532

Two dimensional optical phased array beam steering based on membrane light modulation and high speed digital techniques 15 p2248 A72-32053

Airborne ground mapping and meteorological radar with steerable phased array antenna without mechanical scanners 15 p2200 A72-32216

Properties of a nonisosceles triangular grid planar phased array. 17 p2524 A72-34352

A broad-band wide-angle scan matching technique for large environmentally restricted phased arrays. 17 p2513 A72-34353

Computer aided impedance matching of an interleaved waveguide phased array. 17 p2525 A72-34373

Quadratic phase feed for phased arrays as method of preventing degradation of sidelobe level of patterns due to quantization 17 p2526 A72-34384

Book - Theory and analysis of phased array antennas 17 p2515 A72-34621

Broadband high power L-band phased array amplifier chain. 17 p2528 A72-34710

Statistical estimate of the attainable sidelobe level in phase-switched antenna arrays with a nonlinear initial phase lead 17 p2529 A72-34833

Solid state phased arrays for ECM applications. 17 p2531 A72-35569

Airborne waveguide element reliable advanced solid state radar /RASSR/ phased array radiation patterns and design 17 p2531 A72-35571

SHF airborne distributed phased array antenna system. 17 p2531 A72-35572

Cylindrical phased arrays - Beam scanning and sidelobe control. 17 p2531 A72-35573

Multifunction microwave apertures - Concepts and potential. 17 p2531 A72-35574

Digital tracking with phased arrays. 19 p2765 A72-38261

Methods for monitoring the parameters of phased antenna arrays. 19 p2767 A72-38622

Antenna pattern analysis for compatibility prediction. 20 p2902 A72-39000

Phase shifter number reduction effects on phased radar array radiation pattern distortion and sidelobe reduction 20 p2907 A72-39268

Faraday rotation dual-mode ferrite reciprocal phaser with performance and cost advantages over toroidal type for microwave phased array applications 20 p2909 A72-39733

A flat-feed technique for phased arrays. 21 p3026 A72-40356

On the removal of blindness in phased antenna arrays by element positioning errors. 21 p3027 A72-40363

Mutual coupling of infinite periodic phased arrays of arbitrarily oriented dipoles, investigating dipole length, orientation and phase effects on current distribution 21 p3027 A72-40368

Wave equation for infinitely long slotted screen in elliptic cylindric coordinates, noting radiation pattern for phased antenna array of metallized hyperbolic striplines 21 p3028 A72-40507

Design and investigations regarding a phase-controlled dipole group with radiation input 21 p3028 A72-40508

Numerical integration of integral equation for phased array radiation modeled by impedance filaments in conductive plane, noting excitation by magnetic flux 22 p3159 A72-42663

Random phasing algorithms to reduce phase quantization sidelobes for radiation patterns of commutated phased array antennas 23 p3268 A72-43428

Design of radiating elements for large planar arrays - Accomplishments and remaining challenges. 23 p3269 A72-43571

Recent advances in diode and ferrite phaser technology for phased-array radars. 1. 23 p3270 A72-43572

Influence of modulating /multiplicative/ noise on signal processing in a phased-array-antenna/receiver system 23 p3265 A72-44205

Butler-matrix fed arrays, discussing phase differences, scan steps and sectors, sidelobe structure and attenuation 23 p3273 A72-44363

PHASES

Phase extraction and analysis in superalloys - Summary of investigations by ASTM Committee E-4 Task Group 1. 23 p3304 A72-44257

PHENOLIC RESINS

Phenolic-novolak prepolymer molecular structure and pyrolysis reactions thermokinetic parameters, presenting statistical methods for estimating char yield 01 p0023 A72-11261

Fire resistant fibrous materials for potential military and transportation applications, considering aromatic polyamide polybenzimidazole, fluorocarbon resin polymer, phenolic and glass fibers and fabrics 08 p1191 A72-21586

Gruneisen tensor relationship to elastic and thermal properties of anisotropic quartz fiber-phenolic composite 10 p1500 A72-24251

Two dimensionally reinforced quartz-phenolic composite material dynamic fracture behavior under stress wave loading in uniaxial strain, noting spallation threshold time dependence 11 p1669 A72-25291

Carbon-phenolic composite ablation and expansion in thermal environment during reentry shielding, using flight and simulation tests [AIAA PAPER 72-363] 11 p1669 A72-25390

Mechanical behavior of three dimensional reinforced ablative composites, including carbon-phenolic, quartz-phenolic and quartz-carbon materials 11 p1670 A72-25459

Stress pulse attenuation in cloth-laminate quartz phenolic. 17 p2571 A72-35284

PHENOLS

NT BISPHENOLS

Mechanical and thermochemical erosion during ablation of silicophenolic material 04 p0597 A72-15554

PHENOMENOLOGY

Generalized Navier-Stokes equations for incompressible turbulent flow time mean values, using non-linear phenomenological theory 07 p0972 A72-20109

PHENYLS

NT POLYPHENYLS

Methyl phenyl polysiloxane bonded solid film lubricants, discussing air curing at ambient temperatures and performance tests 06 p0836 A72-18592

Electron impact induced fragmentation of alkyl-N-/1-phenylethyl/-carbamates of primary, secondary and tertiary alcohols, using deuterium labeling and high resolution mass spectrometry 07 p0936 A72-19500

PHILOSOPHY

NT PARADOXES

Human biology, including evolution, organism structure, organizations of people, degeneracy, interactions with environment and philosophical concepts 06 p0765 A72-18315

PHOBOS

Mars observation by Mariner 9, discussing TV pictures of surface, UV and IR spectroscopy of atmosphere, S band experiment and Phobos and Deimos studies 10 p1538 A72-24309

Blue filter polarimeter observations of Deimos and Phobos, discussing polarization-phase angle curve for Deimos dust surface layer 12 p1865 A72-27097

Phobos and Deimos orbital characteristics, noting related Martian physical properties determination 15 p2302 A72-31277

Mars and its satellites as viewed by Mariner 9 17 p2607 A72-34752

Viewing Phobos and Deimos for navigating Mariner 9. [AIAA PAPER 72-927] 24 p3423 A72-45433

PHONEMICS

Interhemispheric effects on choice reaction times to single and multiple letter displays, analyzing cerebral dominance and visual information transmission compared with verbal response 12 p1768 A72-27075

PHONOCARDIOGRAMS

U PHONOCARDIOGRAPHY

PHONOCARDIOGRAPHY

Lf subaudible chest wall vibration recordings, discussing external, epicardial surface and intraventricular pressure precordial displacement tracings 01 p0017 A72-10120

Right heart ventricle intracardiac phonocardiograms, recording pulmonary early diastolic click simultaneous with artery pressure curve diastolic wave 01 p0010 A72-10121

Doppler ultrasonic probe phonocardiography for human cardiovascular velocity measurement, showing normal tracings and aging effects 05 p0617 A72-16154

Doppler cardiometry determination of human cardiovascular velocities in patients with heart diseases, discussing impaired left ventricular function detection 05 p0617 A72-16155

Hot thermistor and hot-wire anemometer principles for phonocardiographic transducer design, using theory of hydraulic amplification with high SNR 10 p1430 A72-24374

Computer assisted monitoring of ECG waveforms and heart sounds frequency spectra to detect bubble laden blood during decompression sickness 11 p1587 A72-26626

Heart and circulatory system functional diagnostics, discussing ECG, blood pressure, X ray, phonocardiographical and pulmonary examinations 12 p1760 A72-27271

Temporal relation of the second heart sound to aortic flow in various conditions. 19 p2759 A72-38818

PHONON BEAMS

Noise characteristics of a digital system of light-beam deflection 24 p3410 A72-45323

PHONONS

NT PHONON BEAMS

Viscous friction effects on phonon-electron interactions and dislocation velocity by deformation measurement of metallic crystals under pulsating magnetic fields 02 p0243 A72-12169

Electroacoustic magnetic and Hall effects in semiconductors in strong electric field involving phonon production by supersonic electron drift 03 p0401 A72-13088

Background phonon X ray and gamma quanta intensities dependence on solar activity from Geiger counter recordings in deep space 05 p0711 A72-17046

PHOSPHATES

Multiphonon capture of charge carriers by deep impurity centers in homopolar semiconductors from generalized Lucovsky model 08 p1216 A72-21094

X ray diffuse scattering from Al crystal at 100-500 V, considering phonon modes effects on anharmonicity and atomic deformation 08 p1186 A72-21591

Phonon limited mean free path in Cd by limiting point method, proposing model with elastic anisotropy 08 p1217 A72-21592

Free and stressed polymer molecules nonlinear vibrations, estimating three- and four-phonon processes contribution to linear chain vibration bands half width by numerical methods 08 p1195 A72-21851

Ferroelectrics with strong hydrogen bonds, deriving self consistent optical phonon frequency and coupled proton-phonon vibration spectrum 09 p1366 A72-22221

Phonon dispersion curves from inelastic neutron scattering for actinide and transition metals carbides, noting superconducting properties 09 p1369 A72-22564

NbN family high transition temperature values application to phonon spectrum prediction based on superconductivity microscopic theory 09 p1369 A72-22565

Phonon dispersion curves of bcc transition metals for normal lattice vibration modes 09 p1369 A72-22680

Metal welded joints formation as diffusion intensification from atom jumps stimulation by phonons from atomic thermal vibrations or crystal defects generation 09 p1319 A72-22867

Franck-Condon phonon displacement effects on mobility edge and energy gap in disordered materials 09 p1357 A72-22986

Ion crystal plasma wave echoes from conduction electrons interaction with phonons in self consistent field 10 p1527 A72-24926

Phonon scattering and induced energy levels in electron irradiated Sb doped Ge in n to p-type conversion region, measuring thermal conductivity and Hall effect 12 p1857 A72-28057

Electroacoustomagnetic and Hall effects in semiconductors within strong electric field involving phonon production by supersonic electron drift 13 p2022 A72-29437

Steady motion of dense electron beam in rarefied phonon plasma along magnetic field, analyzing polarization effects 14 p2136 A72-30305

Strong LF electromagnetic wave propagation in semiconductors with inelastic scattering of current carriers by optical phonons, calculating harmonics reflection coefficients 14 p2142 A72-30361

Surface phonon appearance criteria associated with crystal surface gas adsorption, discussing entropy variation and colliding particle-crystal energy exchange 15 p2280 A72-31858

Electron contribution to phonon damping in anharmonic metal for collision-free regime, evaluating relaxation times 15 p2277 A72-31890

Angular force models with electron-ion interaction applied to bcc and fcc metals, calculating phonon dispersion curves for V, Nb and Ta 15 p2258 A72-32226

X ray Brillouin scattering investigation of phonon phenomena for small momentum transfers with Bragg condition nearly satisfied 15 p2250 A72-32308

Quantum crystals in the single-particle picture. 19 p2844 A72-37943

Solid state physics experiment for conduction electrons effective mass determination in ultrapur n-type InSb by means of magnetophonon effect 21 p3096 A72-40203

Steady motion of dense electron beam in rarefied phonon plasma along magnetic field, analyzing polarization effects 23 p3317 A72-43207

Phonon dispersion relations and Debye characteristic temperature for Ti, Hf and Y hcp lattices 24 p3415 A72-45629

PHOSPHATES

NT ADENINES

NT ADENOSINE DIPHOSPHATE [ADP]

NT ADENOSINE TRIPHOSPHATE [ATP]

NT ADENOSINES

NT AMMONIUM PHOSPHATES

NT CALCIUM PHOSPHATES

NT NUCLEOTIDES

NT POTASSIUM PHOSPHATES

Amino acid-phosphate anhydrides polymerization in presence of clay minerals, noting reactions superposition and monomer diffusion 04 p0483 A72-14774

Neural tissues excitability relationship to precellular organization, considering polyphosphate distribution in vertebrate tissues

04 p0470 A72-14789

Inorganic polyphosphates effect on phosphorus metabolism evolution in primary living organisms, noting polyphosphate glucokinase distribution in various microorganisms

04 p0470 A72-14797

Biological energy transformation origin and evolution, discussing inorganic pyrophosphates precursor to adenosine phosphates as energy carriers

04 p0470 A72-14798

Biological phosphate origin through atmosphere-hydrosphere interrelations, discussing concentrative processes, dehydration mechanics and evaporation

05 p0617 A72-16129

Trimethylphosphite interaction with acetyl- and benzoyl-p-quinone in dry nitrogen atmosphere, noting phosphate formation through intermediate bipolar ion

06 p0770 A72-17986

Lubricating mixtures of mineral oil with inorganic phosphates, hydroxides and sulfides, discussing lubrication mechanism and physical properties

06 p0837 A72-18603

Energy transfer rates and spectral line inhomogeneity of narrow band oscillation phosphate glass and inorganic liquid lasers with Nd

07 p1004 A72-19227

Zinc dithiophosphate and bisphenol effects on surface activation of additive compositions with succinimide base in lubricant applications

07 p1023 A72-19903

Synthetic fire resistant hydraulic fluids, comparing chlorinated hydrocarbons and phosphate esters chemical properties with water based products

08 p1197 A72-22160

Amorphous chromate and phosphate conversion coatings of Al, providing inert surface for painting

09 p1317 A72-22480

Thermolabile triose phosphate isomerase in psychrophilic *Clostridium* at moderate temperatures

10 p1426 A72-24750

Changes in energy stores in the hypoxic heart.

17 p2501 A72-34985

Rat pulmonary lipid metabolism during feeding and fasting from studies of lung lecithin half life after C-14/1/palmitate and H-3/U/glucose injection

18 p2651 A72-36573

Structure-property relationships in flame retardant systems - Relative effects of alkyl phosphates, phosphonates and phosphites on cellulose flammability.

20 p2987 A72-39698

PHOSPHIDES

NT GALLIUM PHOSPHIDES

NT INDIUM PHOSPHIDES

Peritectic interaction and phase diagrams of quasi-binary semiconductor CdAs-CdTe and CdP-CdSe systems

19 p2845 A72-38404

Structure and properties of nickel-phosphorus coatings as a function of the temperature and annealing time

20 p2929 A72-39583

PHOSPHINES

Vibrational IR and Raman spectra of dimethylaminodichlorophosphine, determining molecular structure symmetry in liquid and solid phases

04 p0481 A72-14444

Investigation of certain complex compounds of triaryl phosphines /phosphites/ in optically sensitized photographic emulsions

21 p3052 A72-40390

PHOSPHORESCENCE

Cameron bands phosphorescent yield of carbon monoxide from carbon dioxide photodissociation in helium buffer

11 p1590 A72-26013

Development of phosphorescence during ruby irradiation

23 p3323 A72-43412

A thermal mapping technique for shock tunnels and a practical data reduction procedure.

[ALAA PAPER 72-1031] 24 p3389 A72-45408

PHOSPHORIC ACID

Sorption properties of anodic aluminum oxides prepared in orthophosphoric and chromic acid solutions, determining dependence on pH by isotopic labeling method

05 p0624 A72-17055

Antioxidative and antiwear action of S-containing and S-free phosphoric acid ester additives in lubricating oils

12 p1835 A72-28201

Allyl esters of phosphoric acid preparation and application as substitutes for heavy metal sulfides and silver compounds in single operation photographic process

16 p2392 A72-33363

Mass and energy balance in air cooled matrix type phosphoric acid cell, noting operational reliability and construction

16 p2351 A72-33889

PHOSPHORS

Near field characteristics of solid state laser frequency converters emission, determining medium transluence during single pulse excitation of organic phosphors

10 p1490 A72-24052

Electron beam excited P-15 phosphor 3900 A spectral component fast decay time measurement by delayed coincidence technique

13 p2000 A72-29762

Mechanism and controlling factors of infrared-to-visible conversion process in Er³⁺/ and Yb³⁺/doped phosphors.

21 p3096 A72-40186

Optical quenching of the Gudden-Pohl effect in zinc sulfide luminophors and IR photography

21 p3057 A72-41680

Recombinational luminescence of NaI-Tl single crystals excited in the A-band of activation absorption

23 p3323 A72-43342

PHOSPHORUS

Thermoluminescent phosphorus films irradiation by electrons with energies up to 15 keV in vacuum chamber

01 p0114 A72-10372

Phosphorus absolute transition probabilities determination from P I and P II lines strength measurement, using gas-driven shock tube

01 p0104 A72-11111

Powdered chromium carbide-nickel alloys phosphorus addition effects on sintering temperature, shrinkage, density and hardness

03 p0372 A72-13546

Phosphorus-containing austenitic stainless steel, investigating quenching defects and precipitation from microstructure by transmission electron microscopy

03 p0379 A72-14260

Potassium chlorate/red phosphorus mixtures sensitivity tests for initiation by electrostatic discharge, heating and impact

08 p1221 A72-20776

Nonstabilized Ni-P thin films electrical conductivity at 50-280 C, using mass spectrographic, thermal differential, X ray diffraction and electron microdiffraction analyses

10 p1495 A72-24076

Zn, Ge and P based semiconductor alloy specimens chemical composition determination via ac polarograms

12 p1854 A72-27443

Significance of Apollo 11 and 12 lunar rock fragments of norite rich in K, rare earth elements and P /KREEP/ for lunar evolution assessment

13 p2037 A72-28990

PHOSPHORUS COMPOUNDS

NT ADENINES

NT ADENOSINE DIPHOSPHATE [ADP]

NT ADENOSINE TRIPHOSPHATE [ATP]

NT ADENOSINES

NT AMMONIUM PHOSPHATES

NT CALCIUM PHOSPHATES

NT GALLIUM PHOSPHIDES

NT INDIUM PHOSPHIDES

NT NUCLEOTIDES

NT ORGANIC PHOSPHORUS COMPOUNDS

NT PHOSPHATES

NT PHOSPHIDES

NT PHOSPHINES

NT PHOSPHORIC ACID

NT POTASSIUM PHOSPHATES

Phosphorus compounds incorporation in polyurethane foams and polyesters for flame retardancy

[PI PAPER 12] 03 p0380 A72-13246

Phosphorus effect on Widmanstatten pattern in iron meteorites, using Fe-Ni-P phase diagram and cooling experiments

06 p0878 A72-17792

Stimulated emission cross section, loss coefficient and terminal level lifetime of high power Nd-phosphorus oxychloride liquid lasers

07 p1004 A72-19226

Phosphorus hydride electron affinity determination by electron photodetachment cross section measurement, using ion cyclotron resonance spectrometer

07 p0935 A72-19432

Antiwear properties of mixed anhydrides of alkyl xanthogene and phosphorus containing acids for use as oil lubricant additives

09 p1336 A72-22499

Giant pulse amplification with neodymium-phosphorus oxychloride liquid laser amplifier

09 p1323 A72-22655

Optical Kerr constant measurement in liquid phosphoryl chloride and toluene and glasses, noting nonlinear refractivity

12 p1823 A72-27756

Laser effect in solution of neodymium oxide in mixture of phosphorus oxychloride and heavy water, presenting preparation procedure

15 p2246 A72-31680

Effect of neurohomologous phospholipids associated with other substances on experimental intoxication by asymmetrical dimethylhydrazine. II -

Biochemical aspects of the pyridoxine-phospholipid association

21 p3009 A72-41195

PHOSPHORUS METABOLISM

Biochemical processes and structures interrelation, using nucleoprotein coacervate models and ribonuclease and polynucleotide phosphorylase enzymes

04 p0469 A72-14783

Inorganic polyphosphates effect on phosphorus metabolism evolution in primary living organisms, noting polyphosphate glucokinase distribution in various microorganisms

04 p0470 A72-14797

Biological energy transformation origin and evolution, discussing inorganic pyrophosphates precursor to adenosine phosphates as energy carriers

04 p0470 A72-14798

Potassium cyanide effect on phospholipid exchange in rat brain and liver during histotoxic hypoxia as function of body temperature

05 p0618 A72-16357

Isolation stress effect on excretory products in unrestrained chimpanzee, suggesting Ca to P excretion ratio as physiological stress indicator

07 p0921 A72-20179

Calcium and phosphorus excretion relation to bone density changes in immobilized Macaca nemestrina monkeys

12 p1760 A72-27473

Chlorella population age structure and cell requirements correlation with nutrient medium nitrogen and phosphorus absorption

13 p1909 A72-29311

PHOSPHORYLATION

Energy transfer conditions of transdehydration reactions on primeval earth leading to transphosphorylation, transacylation and peptide synthesis

04 p0468 A72-14768

Inorganic phosphates-nucleoside hypohydrous thermal reaction mechanism, discussing thermal polymerization of orthophosphates for phosphorylation and condensing agents in primordial synthesis

04 p0483 A72-14770

Cyanogen induced phosphorylation of sugars in aqueous solution, discussing system prebiotic plausibility

04 p0483 A72-14771

Bacterial respiration through oxidative phosphorylation origin hypotheses, discussing photosynthesis and sulfate respiration in anoxygenic atmosphere and thiobacillus and aerobic evolution in oxygen at mesophere

04 p0470 A72-14798

Cold adaptation effects on rat skeletal muscle tissue Vant-Hoff coefficient, considering phosphorylation and oxidation rate, P/O and mitochondrial ATP-ase activity

13 p1902 A72-28639

Prebiotic thymidine phosphorylation at 65 C by urea-phosphate mixtures in simulated desert conditions

15 p2185 A72-31629

PHOTOABSORPTION

Electron and population densities in inhomogeneous nonequilibrium plasmas with photoabsorption, using radiative transport equation

02 p0266 A72-12441

Photoabsorption and simple and multiple excitations of rare gases internal atomic layers under X ray action, relating electron transition and relaxed core energies

09 p1357 A72-22836

Total absorption cross sections of several gases of aeronomic interest at 584 A.

22 p3152 A72-42419

Light absorption by visual pigment in photoreceptor, noting Airy disk diameter effect

23 p3259 A72-44388

Calculation of photoabsorption processes in helium.

24 p3426 A72-45012

Photoionization and photoabsorption cross sections for ionospheric calculations.

24 p3400 A72-45590

PHOTOCATHODES

Fabry lens application in stellar photometry, describing technique of image construction on photomultiplier tube cathode

07 p0985 A72-19419

Alkali antimonide photocathodes photoelectric yield /quantum efficiency/ relation to reversible variation of surface potential, noting critical current density temperature dependence

08 p1171 A72-21968

Low light level small intensifier/vidicon camera tube using bombardment induced conductivity target, and planar photocathode, detailing design and performance

08 p1171 A72-21969

III-V metal photocathodes for near IR and shorter wavelengths, noting performance improvements over conventional cathodes

11 p1630 A72-25683

- Photocathode relative sensitivity spatial distribution as function of wavelength, noting maximum shift from photoeffect contribution to photomultiplier current 19 p2800 A72-37821
- Effect of pulsed voltages fed into the external modulating electrode on the threshold sensitivity of a photomultiplier 19 p2774 A72-38415
- Richardson and effective work functions measurements for thermionic emission from alkali and extended red-sensitive trialkali photocathodes, discussing error minimization 20 p2890 A72-39646
- I-V, spectral and temperature characteristics of autophotocathode emission in p-type silicon cathodes with varying acceptor concentrations 21 p3098 A72-41692
- PHOTOCELLS**
- U PHOTOELECTRIC CELLS**
- PHOTOCHEMICAL REACTIONS**
- NT PHOTOCROMISM**
- NT PHOTODECOMPOSITION**
- NT PHOTOLYSIS**
- NT PHOTOSYNTHESIS**
- NT RADIOLYSIS**
- Photochemical ion-molecule reactions in ionosphere by air exhaust device and RF mass spectrometer observation in geophysical rocket experiment 01 p0068 A72-10591
- Mesosphere and lower thermosphere photochemical composition, allowing for molecular and eddy diffusion 03 p0345 A72-12980
- Photochemical models of aeronomic formation and dissociation of hydrogen and ozone in mesosphere and stratosphere 03 p0346 A72-13377
- Quantum yield observations for photochemistry of ozone and singlet molecular oxygen in atmosphere 03 p0347 A72-13393
- Photochemical reactions in pyrimidine base of DNA after UV irradiation, relating mutagenic and lethal effect to dimerization 04 p0467 A72-14608
- Photochemical electron transfer evolution models, noting titanium and zinc oxides as photosensitizers 04 p0484 A72-14777
- Pigments participation in lipid systems formation, considering chlorophyll photochemical activity in surface active agents 04 p0469 A72-14785
- Interstellar formaldehyde, ammonia, water, methane and carbon dioxide photochemistry, discussing decomposition and lifetime 04 p0578 A72-15311
- Molecular oxygen evolution Mn catalyst photoactivation as two-quantum process, discussing kinetic model computer simulation 04 p0484 A72-15740
- Jupiter atmosphere chemical and photochemical analysis, using solar-composition adiabatic equilibrium model for coloration, electric discharge and UV irradiation studies 05 p0714 A72-16132
- Martian atmosphere evolution, stressing photochemical production of oxygen, carbon and nitrogen 06 p0889 A72-18275
- Atmospheric ozone photochemistry, discussing pure oxygen and moist atmospheres, NO mechanism, tracer applications, stratospheric dynamics and Umkehr observations 07 p0979 A72-20228
- Organic dyes molecular photodecay effect on output and power losses of laser activated by flash pump white light 08 p1184 A72-22029
- Planetary scale circulation systems effects on photochemistry and transport processes of minor neutral constituents in mesosphere and lower thermosphere 09 p1274 A72-22353
- Stratospheric ozone photochemistry through nitrogen oxides and hydrogen compounds reactions, noting controlling effect of water vapor 09 p1298 A72-22674
- Photochemical models to simulate composition and reactions of upper atmosphere, noting transport importance 10 p1474 A72-24713
- Mesosphere and lower thermosphere heating and associated solar UV radiation absorption calculation based on diurnally varying photochemical diffusive model 10 p1475 A72-24943
- UV light production of free radicals in proteins and model compounds in vacuum and low temperatures, using EPR techniques 12 p1778 A72-27223
- Abiogenic formation of nucleic acid bases and nucleosides in photochemically synthesized self sustaining coacervates 12 p1761 A72-27657
- Equatorial F region photoionization and chemical loss rates for electrons from simultaneous observations of vertical drift velocity and electron concentration, deriving plasma transport 13 p1949 A72-29336
- Photochemical model of N and NO distribution based on E region ion composition 15 p2226 A72-31916
- Rhodamine 6G photodegradation resistance improvement in cooled solid matrices of polymethylmethacrylate, investigating time and temperature dependence of bleaching by linearly polarized lasers 16 p2401 A72-33386
- Photochemistry of the lower troposphere. 17 p2511 A72-34635
- Utilization of photorecombination of radicals and atoms in continuous-wave lasers. 20 p2932 A72-39508
- Photoanodic engraving process produced high bit density surface relief holograms on semiconductor crystals for data storage, retrieval and replication applications 21 p3054 A72-40614
- Photochemistry of the airglow continuum. 22 p3153 A72-42889
- Formation of urea and guanidine by irradiation of ammonium cyanide. 23 p3262 A72-43569
- Supersonic combustion photochemical initiation feasibility, measuring quantum yields and induction times in hydrogen, oxygen and chlorine mixtures 24 p3464 A72-45058
- Photochemistry of unsaturated polymers. 24 p3378 A72-45280
- Formulation of diurnal D-region models using a photochemical computer code and current reaction rates. 24 p3399 A72-45583
- PHOTOCHEMISTRY**
- U PHOTOCHEMICAL REACTIONS**
- PHOTOCROMISM**
- Absorption and exposure characteristics of silver halide photochromic glasses for hologram recording 01 p0068 A72-10622
- Inorganic photochromic and cathodochromic recording materials in single crystal and powder forms, considering color change properties during light or electron beam exposures 06 p0866 A72-17950
- Reversible photodimerization of polycyclic aromatic hydrocarbons as basis for optical information storage, discussing monomer and photodimer photosensitivity, thermal stability and refractive index specifications 09 p1314 A72-23331
- Photochromic crystal materials erase mode recording characteristics measurement, using Ar laser for optical recording and readout 15 p2240 A72-32361
- High contrast and sensitivity thermal erase cathodochromic sodalite for storage and display applications, measuring contrast ratio versus electron beam flux 15 p2240 A72-32362
- Recording holographic interferograms in a lanthanum-doped fluoride crystal 21 p3053 A72-40476
- PHOTOCONDUCTIVITY**
- Transverse photoconductivity and dark I-V characteristics of n-GaAs compensated with Cr in high electric field at room temperature 03 p0401 A72-13586
- Light wave electric field Franz-Keldysh effect on GaAs absorption edge, using electroabsorption, electroreflectance and photoconductivity spectrum and internal photoeffect analysis 04 p0561 A72-14621
- Microwave photoconductivity and photodielectric effect in organic semiconductors 04 p0561 A72-15083
- Photoconductive detection and generation of far IR radiation in high purity epitaxial GaAs 04 p0563 A72-15605
- IR luminescence and photoconductivity in p-type GaSe single crystals alloyed with Sn and Ge impurities 08 p1216 A72-21069
- Low light level small intensifier/vidicon camera tube using bombardment induced conductivity target, and planar photocathode, detailing design and performance 08 p1171 A72-21969
- Radiation induced extrinsic photoconductivity in Li doped Si, examining localized energy levels in forbidden gap 09 p1372 A72-23238
- Zinc oxide as refractory material, discussing optical, elastic and electro- and photoconductivity properties 10 p1501 A72-24732
- Developers evaluation for processing of photoresist used in hologram recording 12 p1812 A72-27956
- Li dopant radiation damage inhibiting effect on electron irradiated n-type silicon, discussing EPR and photoconductivity experimental results 12 p1856 A72-28023
- Optical interband transition energies in Ni and Ni based alloys, measuring light conductivity at various spectral energies 13 p1976 A72-28904
- Negative photoconductivity effect in high resistance n-type indium phosphide single crystals, noting photocurrent spectral distribution and I-V characteristics 13 p2022 A72-29647
- Memory and photoconductivity in CdSe polycrystals at 77 and 300 K, plotting photocurrent vs illumination levels 13 p2024 A72-30046
- Free carrier mobility dependence on excitation light intensity in CdSe single crystals with negative photoconductivity 14 p2141 A72-30169
- Room temperature negative photoconductivity of p-type ZnTe-CdTe solid solutions mixed crystals within model with electron and hole capture levels 14 p2141 A72-30173
- High resistance n-type InP crystals electrical conductivity and photoconductivity characteristics at 80 K, discussing photosensitivity spectral distribution and temperature dependence 15 p2290 A72-31371
- Surface treatment effects on light and X ray irradiated surface photoconductivity of InSb semiconductor single crystals at liquid nitrogen temperature 15 p2292 A72-31866
- Photoconductivity in depleted surface layer of quasi-monopolar semiconductors with arbitrary diffusion to Debye lengths ratio, noting n-type low resistance gallium arsenide 15 p2296 A72-32694
- Transient behaviour of laser generated carrier mobility in n-Ge. 18 p2697 A72-36351
- Photoluminescence and photoconductivity of hole-type cadmium telluride single crystal films 19 p2845 A72-38403
- Photoconductivity and electroconductivity spectral distributions in glassy cadmium silicon germanium arsenide semiconductors at 300 K related to quantum mechanism 19 p2847 A72-38682
- The field strength conditions for measuring the carrier lifetime in semiconductor crystals by the light flash method 21 p3098 A72-41487
- Cd Se polycrystal memory and photoconductivity at 77 and 300 K, plotting photocurrent vs illumination levels 22 p3214 A72-42734
- Note on the experimental determination of photoconductive response characteristics of amorphous semiconductors. 24 p3431 A72-44716
- Determination of electron and hole capture rates in nickel-doped germanium using photomagnetolectric and photoconductive methods. 24 p3432 A72-45388
- PHOTOCONDUCTORS**
- G-r noise in intrinsic photoconductors for Auger band-to-band radiative recombination 06 p0865 A72-17365
- Vibration simulation of elastohysterical systems on analog computers using photocurrent-voltage relationship of polycrystalline photoresistors 06 p0900 A72-18674
- IR radiation detection by microwave biased photoconductor, lead-tin telluride photovoltaic detector and thermal imaging pyroelectric detector and array system 07 p1034 A72-19425
- Computer simulation for performance of carbon dioxide laser heterodyne communication system with photoconductive n-type mercury-cadmium telluride detector/mixer 15 p2198 A72-32062
- Thermoplastic photoconductor media for holographic recording, discussing structure fabrication techniques and performance 15 p2239 A72-32359
- Dosimetric characteristics of CdS semiconductor detectors and photoresistors for gamma rays recording 16 p3390 A72-33076
- Mercury-cadmium telluride photoconductive detectors array for S-192 multispectral scanner for Skylab earth scanning experiments 23 p3288 A72-43879
- Mercury-cadmium telluride multispectral photoconductive detectors, discussing fabrication techniques and performance characteristics 23 p3288 A72-43880

Heterodyne, microwave bias and pyroelectric photon infrared detectors, noting mixed crystal photoconductive and photovoltaic detectors
23 p3291 A72-44392

PHOTOCURRENTS

U ELECTRIC CURRENT
U PHOTOELECTRIC EMISSION

PHOTODECOMPOSITION

Interstellar formaldehyde, ammonia, water, methane and carbon dioxide photochemistry, discussing decomposition and lifetime
04 p0578 A72-15311

Explosive p-process nucleosynthesis limiting conditions in supernova envelopes, using proton capture and neutron photodisintegration rates
04 p0579 A72-15318

Flashlamp pumped cryptocyanine Q switched high peak power ruby lasers, noting UV radiation responsible for methanolic solution photochemical decomposition
15 p2249 A72-32156

PHOTODETACHMENT

Meteors radio echo duration dependence on electron attachment, photodetachment and turbulent and ambipolar diffusion deionization processes
09 p1383 A72-22502

Meteor method for determining errors in rate measurement of electron attachment to neutral air particles based on nonexistent recombination, turbulent diffusion and photodetachment
09 p1383 A72-22503

Electron attachment, photodetachment and turbulent diffusion deionization effects on duration distribution of Geminid meteor radio echoes
09 p1384 A72-22512

Relative cross sections for gas phase photodetachment of electrons from amide and arsenide ions using ion cyclotron resonance spectrometer
13 p1914 A72-30064

Gas phase photodetachment of electron from selenide ion, determining affinity and spin-orbit coupling constant for SeH negative ion
16 p2360 A72-33580

An investigation of the ionospheric D region at sunrise. I - Time variations of ozone, metastable molecular oxygen, and atomic oxygen. II - Estimation of some photodetachment rates. III - Time variations of negative-ion and electron densities.
18 p2656 A72-36295

Photodetachment of electrons from major negative ions in the lower D region.
18 p2686 A72-36622

PHOTODIODES

Si monolithic multispectral image photosensor array for satellite application, presenting fabrication and spectral response data
04 p0500 A72-15304

Silicon Schottky barrier photodiodes development for photographic, photometric and analytical instrumentation, comparing sensitivity, time response and fatigue characteristics with classical photodetectors
06 p0813 A72-17428

Pulsed dye lasers logarithmic detector circuit with two ultrafast photodiodes, eliminating intensity variations problem
07 p1005 A72-19415

Physical and operational characteristics of Si and Ge photoelectric semiconductor devices with p-n junctions, discussing photodiodes, phototransistors, mosaic arrays and coordinate sensitive structures
08 p1139 A72-21055

Photogrammetric measurement with photodiode sensor arrays substitution for film in cameras and yielding real time readout of stellar and satellite coordinates
08 p1169 A72-21700

Optoelectronic elements for information system applications, discussing photomultipliers, photodiodes, photoresistors, avalanche and photoparametric diodes response and bandwidth characteristics
08 p1169 A72-21844

Image dissector, silicon photodiode and vidicon behavior comparison for medium resolution star mappers design for three axis stabilized vehicles
08 p1172 A72-21975

Lead tin telluride photovoltaic p-n junction diode and lasers, discussing n-type layer fabrication by proton bombardment
10 p1450 A72-24552

Avalanche photodiode optical detector noise amplitude distribution as function of operating conditions
13 p1971 A72-29924

Instrumental errors estimation in photomultipliers and photodiodes during measurement of short time phase fluctuations in quasi-harmonic signals
15 p2246 A72-31424

Light emitting diodes, photodiodes and photon coupled pair temperature compensation schemes, including uses of n-p-n transistors, operational amplifier and thermistor-resistor network
15 p2247 A72-32034

Avalanche photodiodes for Nd and injection lasers radiation detection, reducing noise equivalent power
15 p2247 A72-32035

Avalanche photodiode with n-p-p-i double diffused reach-through structure for visible and near-IR regions, noting high efficiency, low noise and gain stability
15 p2248 A72-32036

Unmodulated solar radiation effect on electro-optical photoreceptors voltage sensitivity, noting photomultipliers and silicon photodiodes
15 p2237 A72-32121

Photodiode assembly for fast laser pulses and optical signal detection, utilizing Hewlett-Packard 5082-4220 diode in impedance matched holder
15 p2208 A72-32432

Photodiode-operational amplifier circuit for pulsed laser systems energy variations monitoring, noting insensitivity to ambient light conditions
16 p2402 A72-33607

High-speed image scanning devices using acoustic surface waves and photodiode array.
18 p2658 A72-36267

Solid state laser sources, light modulators and silicon avalanche photodiode detectors for fiber optical communication, discussing performance and limitations from system design viewpoint
21 p3018 A72-40866

Low capacitance high speed lead tin telluride photodiodes via liquid phase epitaxial growth, discussing frequency response to Nd-YAG and carbon dioxide lasers
22 p3159 A72-42620

Mercury-cadmium telluride photodiode detectors for near IR laser receivers, discussing time response and I-V characteristics as function of temperature
23 p3296 A72-43881

PHOTODISSOCIATION

Molecular continuity relationship relating discrete absorption oscillator strengths to photodissociation cross sections
01 p0104 A72-11115

Kinetic model and analysis of elementary characteristics of carbon trifluoride photodissociation laser
03 p0366 A72-13078

Oxygen and hydrogen atoms production in atmosphere by photodissociation, investigating terrestrial hydrogen escape efficiency
03 p0346 A72-13381

Molecular oxygen photodissociation in Schumann-Runge bands, discussing determination of solar radiation penetration depth into chemosphere
03 p0412 A72-13386

Atmospheric model for mesosphere odd-nitrogen concentration relation to NO dissociation rate and downward flux through mesopause
03 p0350 A72-13526

Atomic selective two step photoionization and molecular photodissociation by tunable laser radiation, experimenting on Rb vapor and HCl respectively [CLEA PAPER 12,4]
07 p1005 A72-19395

Photodissociation cross sections of methyl chloride and nitrous oxide cations, using ion cyclotron resonance technique
07 p0936 A72-19492

Neutral species chemical reactions in D and E regions, taking into account effects of photodissociation and transport by horizontal and vertical flow and molecular diffusion
07 p0936 A72-20039

Nitrogen dioxide photodissociation by pulsed ruby laser at 6943 Å, noting single photon energy relationship to dissociation energy
07 p0937 A72-20676

Fluorescence and absorption spectra from oxygen sulfur dichloride photodissociation in vacuum UV, discussing SO formation
11 p1590 A72-26012

Cameron bands phosphorescent yield of carbon monoxide from carbon dioxide photodissociation in helium buffer
11 p1590 A72-26013

Zeeman effects in hyperfine structure of atomic iodine photodissociation laser emission, noting magnetic fields effect on time behavior
11 p1692 A72-26558

Time estimate criterion of lasing breakdown in photodissociative iodine-alkyl lasers with iodine molecule buildup
12 p1819 A72-27053

Kinetic model and analysis of time characteristics of trifluoriodomethane photodissociation laser
13 p1968 A72-29428

Carbon origin in comets associated with propyne photodissociation by solar 1216 Å Lyman alpha radiation
13 p2050 A72-29995

Bond dissociation energy calculation for carbon disulfide in vacuum UV from fluorescence threshold energy of incident photons, measuring absorption coefficient at 1200-1400 Å
13 p1914 A72-30060

Molecular iodine photolysis in photodissociative laser due to selective pumping, noting recombination-like storage mechanism
14 p2110 A72-30354

Solar radiation induced molecular oxygen photodissociation rate as function of column density and temperature in mesosphere and lower thermosphere
16 p2383 A72-32967

French monograph - Determination of the absolute value of the absorption in the bands of the Schumann-Runge system of molecular oxygen
19 p2836 A72-37476

Isotopic effect in photodissociation processes of triplet excited molecules
19 p2838 A72-38779

Two-step photodissociation of ammonia molecules excited by laser radiation.
21 p3013 A72-40724

Generation spectrum kinetics of a photodissociative iodine laser
23 p3297 A72-44480

Multiphoton dissociation, predissociation, and autoionization of the hydrogen molecule.
24 p3427 A72-45476

Analytic criteria for laser quenching moment, generation power and stimulated emission energy for photodissociative iodine-alkyl lasers with iodine molecule buildup
24 p3412 A72-45706

PHOTOELASTIC ANALYSIS

Elastic incompressible isotropic transparent media, deriving photoelastic effect relationship to stress function
01 p0089 A72-10123

Clearance, friction and load effects on turbine blade root fastening stress distribution, comparing finite element method with photoelastic experimental results
01 p0141 A72-11048

Polycarbonate yield locus from strain rate, creep, isotropy, isoclinic and reloading tests on perforated plates [SESA PAPER 1819]
02 p0248 A72-11501

Electromagnetic plane stress wave generation by capacitor bank for transient loading of photoelastic models along straight and curved boundaries [SESA PAPER 1907A]
02 p0199 A72-11503

Air holography interferometry for acrylic model materials inspection and selection for optical flatness, comparing with photoelasticity [SESA PAPER 1941]
02 p0224 A72-11516

Stress distribution analysis of femoral neck, using three dimensional photoelastic model
03 p0318 A72-12957

TV time lapse interferometry and contouring for photoelastic nondestructive testing, comparing with photographic techniques
03 p0358 A72-13436

Stress-strain state determination for plane orthotropic bodies by optical polarization method, discussing numerical methods for stress and strain tensor components
03 p0445 A72-13580

Griffith crack propagation in polymethyl methacrylate, examining stress changes by photoelastic method
03 p0380 A72-13719

Longitudinal and transverse wave diffraction on cavities, investigating field pattern by dynamic photoelasticity method with flat models
03 p0452 A72-14131

Photothermoelastic analysis of shrinkage stresses near discontinuity in fiber composite material, relating matrix cracking to fiber packing
06 p0835 A72-17800

Residual stress measurements in metals by annular photoelastic gages, obtaining relationship to fringe orders
06 p0818 A72-18317

Elastic-plastic strain measurement on flat steel surfaces by moiré gratings, using electroluminescent source and crossing jig
06 p0818 A72-18323

Interferometric holography application to photoelastic stress analysis of opaque anisotropic composite plates under static and dynamic transverse and in-plane loads
06 p0898 A72-18349

Photoelastic analysis of cylindrical shells of revolution with one hemispheric closed end and reinforcing flanges at opposite end rim, examining boundary conditions effects
06 p0899 A72-18640

Transient high speed deformations analysis of annealed Al under impact loads by three dimensional moiré fringe techniques
07 p0983 A72-19131

Two- and three dimensional photoelastic experiments evaluation to obtain principal stresses differences
07 p1088 A72-19171

Physical analysis of photoelastic interferometry and holography, considering retardation, isochromic and isopachic fringe systems and model materials
08 p1166 A72-21330

Photoelastic measurement of stress concentration in three dimensional fiber reinforced brittle plastic matrix under uniaxial tension [PI PAPER 1]
09 p1398 A72-22538

Photothermoelasticity method for determining thermal stresses
09 p1402 A72-22737

Photoelastic studies of plane stress fields in plate induced by moving loads at subsonic, transonic and supersonic speeds
10 p1553 A72-23746

Photoelastic analysis of piezooptical and rheological properties of anisotropic composite glass plastics
10 p1557 A72-24626

Photothermoelastic analysis of temperature and rupture stress in cryogenic tanker structures, using steel and plastic ship models
[AIAA PAPER 72-344]
11 p1728 A72-25373

Infinite elastic thick plate with loads symmetrical to axis of revolution and middle plane, analyzing stress functions, Fourier-Bessel expansion and photoelastic experiment
11 p1626 A72-26427

Three dimensional photothermoelastic method of refrigeration with composite model to study transient thermal stresses in wing rib
14 p2168 A72-30907

Real time focused image holographic interferometry for deformation recording in diffusively reflecting plate under compression
15 p2233 A72-31415

Holography application to photoelastic stress analysis, showing information content correspondence to angles of incidence for different model regions
16 p2389 A72-32905

Differential stress-holo-interferometry.
[SESA PAPER 1989A]
17 p2554 A72-34816

Photoelasticity, holography, moiré and strain gage methods in European experimental mechanics research
18 p2733 A72-36357

Polarization offset angle effect on isochromatic fringe visibility of holographic photoelasticity recordings, noting reference beam ellipticity adjustment
18 p2733 A72-36360

Techniques in photoelastic analysis of pressure vessels.
18 p2690 A72-36363

Three dimensional photoelastic analysis of edge loaded ring reinforced rotating shells with zero bending, assuming pure membrane stress field
18 p2733 A72-36365

An optical method for the determination of constrained zones at crack-tips.
18 p2733 A72-36368

Mechanical component acceleration-induced stress and transient phenomena analysis by dynamic photoelasticity and interferometry, applying to elastic birefringent and other materials
18 p2734 A72-36373

Photoelastic investigation of a Hertzian contact with shallow grooves in the contact area.
18 p2734 A72-36374

Photoelastic study of stress concentration in rectangular panels with inserts.
18 p2734 A72-36376

Effect of fiber end, fiber orientation and spacing in composite materials.
18 p2738 A72-37086

An improved Cranz-Schardin high-speed camera for two-dimensional photomechanics.
19 p2795 A72-37516

A general theory of polarization holography and its application to photoelastic analysis.
19 p2799 A72-37627

Photoelastic determination of mixed mode stress intensity factors.
20 p2981 A72-39963

The gamma-ray-irradiation method applied to three-dimensional thermal photoelasticity.
21 p3051 A72-40230

Edge effect improved fringe definition on high contrast film by pseudo-solarization for polariscopes in photoelastic stress analysis
21 p3052 A72-40232

Three-dimensional photoelastic and finite-element analysis of a propellant grain.
21 p3052 A72-40237

Determination of stresses along the symmetry axis in the isometric problem on the basis of an elastooptical image of isochromes
21 p3122 A72-41347

Stress differentiation procedure for screen technique studies in dynamic photoelasticity, giving expressions for elastic modulus and Poisson coefficient
21 p3123 A72-41363

Dynamic photoelasticity application to periodic/vibrating and pulse/stress wave fields, considering loading rate effect on material fringe value
22 p3237 A72-42767

Photoelastic analysis of cardiovascular-magnitude stress pattern produced by flow through gelatin-agar walled channels for analysis of mechanical stresses on blood vessel walls
23 p3260 A72-43936

Photoelastic analysis with Stokes vector and new methods for the determination of characteristic parameters in three dimensional photoelasticity.
23 p3354 A72-44255

Mapping of large dynamic deflections of structures.
24 p3454 A72-44606

Photoelastic verification of a mechanical model for the flow of a granular material.
24 p3460 A72-45697

PHOTOELASTIC MATERIALS

Local heating effect of electrical resistance gages measuring strain across thickness of plane photoelastic Araldite models
12 p1807 A72-27316

Materials selection for models used in thermal stress studies by restrained shrinkage method with emphasis on polyurethanes
12 p1813 A72-27460

Composite materials stress analysis techniques, discussing strain gages, photoelastic coatings moiré and holographic applications
[ASME PAPER 72-DE-6]
14 p2167 A72-30861

A photoelastic material with variable modulus of elasticity.
19 p2822 A72-37731

Comparison of experimental and numerical results concerning a hollow photoelastic bar with a slot subjected to torsion
21 p3122 A72-41337

PHOTOELASTIC STRESS MEASUREMENT

U PHOTOELASTIC ANALYSIS

PHOTOELASTICITY

NT PHOTOVISCOELASTICITY

Dislocations forces during sintering of loose and cold-pressed metal powders, using photoelasticity for stress estimation and electron microscopy for defects structure
02 p0232 A72-11430

Nonlinear photoelasticity, elastoplasticity and creep problems studies by optical polarization methods, comparing transparent model and photoelastic coating techniques
02 p0289 A72-11613

Photoelastic investigation of star shaped models for loading direction influence on shear stress distribution at notch tip region in uniform tensile field
10 p1559 A72-24897

Photoelasticity with stress induced optical activity analysis using Stokes parameters, discussing rotational effects in scattered light problems
15 p2277 A72-32235

Direct and indirect creep modelling technique in photoelasticity.
18 p2734 A72-36379

Stress wave propagation observation in rigid high modulus epoxy polymer by slow motion photography, noting photoelastic properties and viscosity effect
18 p2734 A72-36380

Poincare sphere application to polarimetry and two- and three-dimensional photoelasticity by scatter light
18 p2691 A72-36381

Application of matricial formalisms to the specification of light polarization changing systems.
20 p2928 A72-40025

Photoelastic study of stress concentration in perforated composite pipes under external pressure
22 p3233 A72-42064

Pulse modulation of a laser during the tuning of an auxiliary passive resonator with the aid of ultrasound
22 p3186 A72-42666

A neoteric interferometer for use in holographic photoelasticity.
23 p3290 A72-43985

Photothermoelastic study of stress concentrations in a plate with internal heating.
23 p3349 A72-43986

Orthotropic photoelasticity methods application to concentrated force on half plane edge and to stress distribution on elliptical hole boundary in tensile strip
24 p3455 A72-44790

PHOTOELECTRIC CELLS

NT PHOTOVOLTAIC CELLS

Electric and photoelectric properties of CdTe films, describing solar cells preparation
04 p0465 A72-14593

Photometers with CdS cells, discussing calibration difficulties
07 p0992 A72-20584

Low temperature Si photoconverters transparent in IR solar spectrum tested on Cosmos satellites
07 p0915 A72-20616

Polarization effect on sensitivity of photocells and photomultipliers with/without cover glass
09 p1289 A72-23670

Electronic fringe counter with CdS cell photosensors, dc bridge and strip recorder for interferometric applications
12 p1792 A72-27762

Digital theodolite for automatic angle measurement with photoelectric sensor and magnetic data recorder for computer use
16 p2394 A72-33800

PHOTOELECTRIC EMISSION

Measurement of surface leakage currents in a semiconductor photoelectric converter
22 p3140 A72-43188

Influence of nonuniformities of the built-in field on the collection efficiency of a semiconductor photocell
22 p3140 A72-43190

PHOTOELECTRIC EFFECT

NT PHOTOIONIZATION

Lateral photoelectric effect in junction FET under homogeneous illumination, detailing current-voltage characteristics
01 p0114 A72-10859

Light wave electric field Franz-Keldysh effect on GaAs absorption edge, using electroabsorption, electroreflectance and photoconductivity spectrum and internal photoeffect analysis
04 p0561 A72-14621

Microwave photoconductivity and photodiodelectric effect in organic semiconductors
04 p0561 A72-15083

Zero crossing photoelectric autoreflector pickoffs for readout gyro systems with suspended spherical rotors, classifying systems according to modulation type
05 p0661 A72-16036

Photoelectric transducer with electric pulses as measure of rotating disk angle of turn, discussing design and measurement accuracy
05 p0662 A72-16124

Photoelectrically excited electrons diffusion and dc effect in ZnO single crystals, calculating drift mobility and lifetime product
05 p0667 A72-16158

Solar cells with improved photoelectric efficiency, describing use of noncorroding Ti-Pd-Ag contacts, titanium oxide antireflection layer and welded cell joints
06 p0760 A72-17751

Photoelectric temperature measurements in contact zone during grinding of aluminum oxide ceramic materials by synthetic diamond disks
07 p0997 A72-20252

Alkali antimonide photocathodes photoelectric yield /quantum efficiency/ relation to reversible variation of surface potential, noting critical current density temperature dependence
08 p1171 A72-21968

Scanning photoelectric image conversion /photoanalyzing/ systems for data telemetry from remote optical sensors
11 p1634 A72-26461

High temperature gaseous disperse flow radiation spectra photoelectric recording by DFS-8 spectrograph
12 p1812 A72-28116

Spectral line width measurement accuracy based on digital autocorrelation of photon counting fluctuations, noting light field and photoelectric process limiting effects
16 p2357 A72-32949

Photocathode relative sensitivity spatial distribution as function of wavelength, noting maximum shift from photoeffect contribution to photomultiplier current
19 p2800 A72-37821

Quenching of fluorescence and the photoeffect in anthracene crystals
19 p2847 A72-38782

PHOTOELECTRIC EMISSION

G and K giants atmospheric parameters determination by photoelectric indices, considering effective temperature, chemical composition and surface gravity
01 p0132 A72-11013

Lunar occultation light curve model for photoelectric data analysis, using least squares method
03 p0421 A72-13133

Photoemission from polyethylene, Kapton, Teflon and polyvinyl chloride under photon irradiation
03 p0403 A72-14084

Photoemission electron microscopy application to refractory metals and nonmetallic materials, discussing image formation and contrast enhancement problems
10 p1493 A72-23823

Photoemission from tetracene organic semiconductors due to electron capture defect ionization by excitons
11 p1700 A72-25785

Satellite surface coating materials photoemission properties, discussing reflectance, work function, photoyield and photoelectron energy distributions
12 p1844 A72-27280

Transparent dielectric surface photoelectric emission current under laser pulse illumination, noting correlation to surface treatment and damage threshold
12 p1822 A72-27613

Negative photoconductivity effect in high resistance n-type indium phosphide single crystals, noting photocurrent spectral distribution and I-V characteristics
13 p2022 A72-29647

Lightly doped InP and vapor epitaxial GaAs laser, observing long wavelength shift in photoemission spectra peak
14 p2108 A72-30182

Jupiter decametric radiation modulation by photoelectron emission by satellite Io, describing future probe experimental test

14 p2156 A72-30558

Photoelectric emission usefulness for investigation of energy parameters and optical transitions of semiconductor surfaces

15 p2276 A72-31865

Optical field emission effects on photoelectron emission nonlinearity from metal cathode using ultrashort mode locked laser pulses

15 p2250 A72-32303

Report on photo-sheath calculations for the satellite GEOS.

17 p2553 A72-34629

Photoemissive properties of bismuth-cesium films

17 p2595 A72-34754

Undamped photocurrent fluctuations in CdSe single crystals

18 p2718 A72-36348

Quantitative microstructural measurements by room temperature photoemission electron microscopy, discussing relief contrast, edge effect, resolution and information depth

18 p2719 A72-36831

Angular distribution measurements of photoemitted electrons for InAs by means of magnetic field.

19 p2843 A72-37406

Low light level optics for image forming photoemissive sensors, discussing refractive and catadioptric lenses and reflective systems with magnetic focusing

20 p2921 A72-39029

Photoemissive method of recording Mertz shadowgrams and vibrating electrode technique for reading out images in reconstruction of X ray sources original distribution

21 p3051 A72-40219

I-V, spectral and temperature characteristics of autophotoelectron emission in p-type silicon cathodes with varying acceptor concentrations

21 p3098 A72-41692

Photoelectron energy distributions from clean polycrystalline W, observing surface state

22 p3190 A72-42477

Photoemission from surface states on tungsten.

22 p3190 A72-42478

Investigation of the nature of photostimulated exoelectronic emission during the friction of precision contacts

22 p3183 A72-43158

Photoemission studies of wurtzite zinc oxide.

24 p3432 A72-45387

PHOTOELECTRIC GENERATORS

Au film optical refractivity, absorptivity and transmittance in visible and UV ranges of Au-GaAs and Au-GaP photoelectric converters

14 p2141 A72-30224

Determination of the quality of the reflective properties of mirrors used in photoelectric converter assemblies

17 p2498 A72-35510

Investigation of the dependence of the electrical characteristics of a 'Fotovolta'-type high-voltage matrix photoconverter on the radiation intensity and temperature

17 p2498 A72-35511

PHOTOELECTRIC MATERIALS

Preparation and properties of nonheat-treated single crystal Cu₂S-CdS heterojunctions.

17 p2595 A72-35331

PHOTOELECTRIC PHOTOMETRY

U ELECTROPHOTOMETERS

PHOTOELECTRICITY

Interference polarization filter by modulation and phase detection for passband narrowing and secondary maxima attenuation, discussing application to photoelectric recording system

03 p0356 A72-13096

Interference polarization filter by modulation and phase detection for passband narrowing and secondary maxima attenuation, discussing application to photoelectric recording system

11 p1632 A72-25708

Weak signals detection at visible wavelengths with background noise, examining photoelectric recording and optimal detection characteristics of receiver

11 p1596 A72-26314

Photoelectric properties of cadmium telluride thin film solar cells, discussing energy gap temperature dependence, work function and current variations anomalies

12 p1756 A72-28018

High resolution angular velocity measurement by high speed digital transducer feeding photosensor pick-up pulses into pulse shaping circuit

14 p2103 A72-30199

Procedure for the calibration of photoelectric components in the IR spectral range

18 p2693 A72-37005

A photoelectric method for measuring the temperature pulsations of solids

19 p2799 A72-37664

Rational selection of structures and parameters for photoelectric meters and follow-up systems

19 p2801 A72-37964

Influence of a surface space charge on certain photoelectric properties of p-type gallium arsenide

21 p3098 A72-41684

Electroconductivity anisotropy effect on transverse Demer effect angular dependence and spectral distribution in p-type CdSb lattice

21 p3098 A72-41693

Effect of the video signal shaping mechanism in a photosensitive scanistor sensor on the optical data processing accuracy

21 p3058 A72-41735

Automatic coaxial alignment system with photoelectric positioning sensors, discussing alignment errors as function of light source distance and components spacing

21 p3059 A72-41817

PHOTOELECTROMAGNETIC DETECTORS

U RADIATION MEASURING INSTRUMENTS

PHOTOELECTRONICS

U ELECTRONICS

U PHOTOELECTRICITY

PHOTOELECTRONS

Ionspheric photoelectron fluxes and motions simulated by Monte Carlo technique, including transport effects, elastic and inelastic collisions and energy losses

03 p0412 A72-13517

Energy transfer rate from photoelectrons to thermal electrons, presenting function of three independent variables

03 p0413 A72-13532

Molecular oxygen photoelectron spectra at autoionizing resonance frequencies, comparing with Franck-Condon calculations

04 p0552 A72-14892

Height profiles for volume emission rate and intensity of second positive band of nitrogen molecule excited by photoelectron impact, noting solar activity effects

04 p0518 A72-14962

Intensity-height profiles for molecular oxygen first and second negative bands in F region, using equilibrium velocity distribution of photoelectrons

04 p0518 A72-14963

Windowless ultrahigh vacuum photoelectron spectrometer for high resolution studies of gas-metal surface reactions, measuring electron energy levels

04 p0523 A72-15489

Molecular nitrogen photoelectron impact excitation of Herman-Kaplan upper electronic state, considering cascade contribution to low lying states in electron auroras and dayglow

06 p0806 A72-17647

Statistical model of signal amplitude distribution and thermoelectron noise of photoelectron multiplier

06 p0816 A72-17837

Photoelectron flux measurement of intensities of plasma lines in radar incoherent scatter spectrum by uhf radar

06 p0874 A72-18732

Phosphorus hydride electron affinity determination by electron photodetachment cross section measurement, using ion cyclotron resonance spectrometer

07 p0935 A72-19432

Thermostimulated autophotoelectron emission from Cr-alloyed p-type GaAs electrode, determining spectral distribution and light and electric field effects on current

08 p1216 A72-21071

Molecular X ray emission spectra interpretation based on singly ionized states observation by photoelectron spectroscopy and transition probability calculation

09 p1357 A72-22838

Rare earth elements outer electrons X ray and UV photoemission spectra interpretation by multiplet splitting of final state

09 p1371 A72-22844

Differential photoelectron flux in lower ionosphere during 7 March 1970 solar eclipse observed by Nike-Apache rockets

09 p1378 A72-23012

Differential photoelectron fluxes at 560 km altitude observed by OVI-18 satellite on 22 March 1969, noting latitudinal variation

09 p1378 A72-23013

Receivers for PPM optical communication and pulsed signal detection in background light, evaluating upper bounds on error probability based on photoelectron Poisson statistics

11 p1591 A72-25311

Conjugate point photoelectron flux measurements in ionosphere during 7 March 1970 solar eclipse, using retarding potential analyzer onboard Nike-Tomahawk rocket

12 p1801 A72-27153

Resonance scattering and direct photoelectron excitation contribution to molecular nitrogen first positive bands emission in day airglow from rocket measurements

13 p1953 A72-29808

Predawn airglow enhancement project, discussing magnetically conjugate photoelectron impact excitation observation and geophysical interpretation

14 p2098 A72-30147

Incoherent scatter and filter photometer search for 6300 A predawn enhancement by magnetically conjugate photoelectron impact excitation, comparing with ionospheric electron density

14 p2098 A72-30148

Solar UV Lyman alpha radiation intensity measurements, using Vertikal-1 rocket-borne photometer and photoelectron analyzer

14 p2128 A72-30465

Photoelectron precipitation induced dissociation of atmospheric nitrogen molecules during moderate solar activity

14 p2102 A72-30659

Radiative transfer equation application to ionospheric photoelectrons transport, predicting photoelectrons angular distribution and escape flux

16 p2444 A72-32963

Electrons angular distribution effect on photoionization branching ratio measurement by photoelectron spectroscopy

17 p2552 A72-34288

Report on photo-sheath calculations for the satellite GEOS.

17 p2553 A72-34629

Use of X-ray photoelectron spectroscopy to study bonding in Cr, Mn, Fe, and Co compounds.

18 p2657 A72-36568

Signal-to-noise ratio of a photodetector with a virtual cathode

21 p3055 A72-40802

Photoelectron energy distributions from clean polycrystalline W, observing surface state

22 p3190 A72-42477

Threshold characteristics of receivers with optical quantum amplifiers.

24 p3412 A72-45617

PHOTOEMISSION

U PHOTOELECTRIC EMISSION

PHOTOEMISSION

U EMISSION

PHOTOELECTRIC EMISSION

PHOTOEMITTERS

U PHOTOELECTRIC MATERIALS

PHOTO GEOLOGY

Photogeological remote sensing of high voltage dc power transmission system induced ground current paths, discussing X-15 near IR photographic recordings

02 p0212 A72-11826

Satellite photographs of Himalayan-Indian Ocean tectonic patterns, showing major left and right lateral shear belts as evidence of wrench movements

05 p0655 A72-16046

Photointerpretation methods for earth resources and geological studies, discussing quantitative photogrammetric techniques, automation and digital evaluation methods

09 p1302 A72-23292

Black and white vs color photography application to photogeological interpretation of West Greenland Precambrian terrain

09 p1303 A72-23294

Photogeologic evidence of differentiation and deposition of lunar highland volcanic rocks at Apollo 16 landing site

12 p1866 A72-27115

The accuracy of the intermittent photographic film advance in the camera of an airborne thermal scanner.

18 p2692 A72-36697

PHOTOGRAMMETRY

Photogrammetry - Conference, San Francisco, September 1971

01 p0065 A72-10448

ERTS satellite return beam vidicon TV system and multispectral scanner images, describing photogrammetric and cartographic evaluations

01 p0065 A72-10449

Precision photogrammetric techniques coordinated with classical geodetic surveys for moderate cost control surveys, discussing error sources

01 p0065 A72-10455

Aerial triangulation for optimum photogrammetric project parameters, discussing flight altitude, bridging distance and control points for computerized optimization

01 p0066 A72-10462

Photogrammetric techniques for Tranquillity base experiment locations map based on surface and spacecraft photographs

02 p0280 A72-12198

Astronomical method of satellite photograph reduction in geodesy using photogrammetric technique

02 p0231 A72-12602

Urban area aerial photography survey for large scale photomaps, discussing building feature examination and universal stereophotogrammetric instruments utilization

03 p0362 A72-14311

Photogrammetric coordinate relation of points on lunar surface and stereo panoramas of scanning photographs by Luna 9 and 13 orbiters

05 p0660 A72-15832

Buffalo photographic aircraft for oil slick remote sensing, using aerial cameras and thermal IR scanner

05 p0658 A72-16600

A-7 D/E navigation/weapon delivery system flight testing, using photogrammetric technique
05 p0663 A72-16656

Lunar configuration, limb relief and coordinates of western hemisphere and far side from Zond 6 photograph reduction
05 p0721 A72-17040

Computerized photogrammetric terrain analysis and representation in three dimensional coordinates, discussing construction of digital terrain model
06 p0813 A72-17429

Interpolation in numerical photogrammetry by least squares method
06 p0815 A72-17752

Planiacart stereoplotter for map compilation and revision in photogrammetry
06 p0815 A72-17756

Satellite-borne multispectral photographic line-scan system with direct optoelectrical signal conversion for photogrammetric and cartographic applications
06 p0815 A72-17757

Film flatness in airborne cameras, reducing large area and short period photogrammetric deviations
06 p0815 A72-17758

Apollo 6 photogrammetric, photometric and neutron activation analysis of smoke plume, determining eddy diffusivity
06 p0819 A72-18439

Lunar center of mass position with respect to visible hemisphere physical surface calculated from photogrammetric analysis and Lunar Orbiter 1 data
08 p1232 A72-21158

Photogrammetric light beam refraction during aerial surveys, considering air pressure, temperature and humidity gradients in and out of camera carrier
08 p1165 A72-21161

Photogrammetric measurement with photodiode sensor arrays substitution for film in cameras and yielding real time readout of stellar and satellite coordinates
08 p1169 A72-21700

Terrestrial altitude differences effects on photogrammetric data accuracy in two step compensation with models
09 p1311 A72-22966

Rectification process for transformation of single photograph orientation into setting value, noting reduced accidental residual errors
09 p1311 A72-22967

Mean coordinate and distance errors in photogrammetric measurements of two neighboring models carried out by two image scales and four aerial cameras
09 p1311 A72-22969

Object reconstruction procedure in two- and multimedia photogrammetry involving image distortion by refraction on interfaces
09 p1311 A72-22970

Mitogenic and IR radiation and plant bioelectricity in photogrammetry, using metabolic energy-photoemulsion relation
09 p1312 A72-23283

Measurement accuracy and reliability of photogrammetric methods in stereoscopic height determinations of wooded areas
09 p1312 A72-23284

Photointerpretation methods for earth resources and geological studies, discussing quantitative photogrammetric techniques, automation and digital evaluation methods
09 p1302 A72-23292

Aerial photography and photogrammetry objectives and requirements for natural resources surveys
09 p1304 A72-23312

Mathematical model of block adjustment and star coordinate accuracy in photographic astrometry
09 p1392 A72-23541

Apollo mapping camera system synchronized laser altimetry utilization in astro-photogrammetric triangulation
12 p1872 A72-27816

Film flatness in airborne cameras, reducing large area and short period photogrammetric deviations
12 p1809 A72-27818

Photogrammetric camera system imaging characteristics comparison with aerial reconnaissance, multispectral and return beam vidicon systems, noting economic benefits due to smaller scale imagery
12 p1805 A72-27819

Large scale mapping by photogrammetric method based on contour points of outdated small scale aerial survey photographs, noting root-mean-square errors
13 p1959 A72-29633

Algorithms for photogrammetric model coordinates variance and covariance estimation, considering convergence properties
16 p2384 A72-33029

Three dimensional transformation for continental scale geodetic grids photogrammetry by satellite method, noting scale alteration and Euler angles determination
16 p2387 A72-33799

Photogrammetric light beam refraction during aerial surveys, considering air pressure, temperature and humidity gradients in an out of camera carrier
17 p2552 A72-34452

Holographic photogrammetry and cartography
17 p2555 A72-35184

Epipolar scanning to convert image correlation from two dimensional to one dimensional task for application to photogrammetric automation
18 p2691 A72-36492

Nonholographic coherent optical correlation for automatic stereoperception.
18 p2691 A72-36493

The precision-processing subsystem for the Earth Resources Technology Satellite.
18 p2674 A72-36497

A new computer-assisted stereocomparator.
18 p2664 A72-36499

Russian book - Refraction of light rays in the atmosphere
19 p2834 A72-37448

Holography application in photogrammetric contour mapping, discussing topographic data acquisition, storage, retrieval and display problems
19 p2797 A72-37609

Lunar center of mass position with respect to visible hemisphere physical surface calculated from photogrammetric analysis and Lunar Orbiter 1 data
20 p2969 A72-39263

Aerotriangulation by simultaneous adjustment of photogrammetric and geodetic observations /SAPGO/ incorporating geodetic distances, horizontal angles, Laplace azimuths, longitudes, latitudes and elevation differences
20 p2927 A72-39738

Photogrammetric refraction equation and integral interpretation for actual atmosphere, climate and weather conditions suitable for photographic flights
20 p2927 A72-39739

The measurement of three-dimensional body movements by the use of photogrammetry.
20 p2898 A72-39806

Photogrammetric method for determining the deflection of light beams by spacecraft windows during flight
21 p3052 A72-40305

Russian book - Stereophotogrammetric processing methods for photographs made from a mobile basis.
22 p3175 A72-40205

Investigations regarding the condition of normal equations in the case of block triangulation according to the bundle method. I
23 p3284 A72-43632

Coordinates of features on the Mariner 6 and 7 pictures of Mars.
24 p3436 A72-44695

Improvement of an algorithm for the rejection of points in the solution of a mutual orientation problem on a digital computer
24 p3401 A72-44861

Determination of the covariance matrix of the spatial coordinates of points of a geometrical model
24 p3397 A72-44867

PHOTOGRAPH INTERPRETATION
U PHOTINTERPRETATION
PHOTOGRAPHIC DEVELOPERS
Astronomical photographic emulsions and phenidonehydroquinone developer relative detective quantum efficiency measurements
03 p0352 A72-13007

Developers evaluation for processing of photoresist used in hologram recording
12 p1812 A72-27956

PHOTOGRAPHIC EMULSIONS
NT NUCLEAR EMULSIONS
Astronomical photographic emulsions and phenidonehydroquinone developer relative detective quantum efficiency measurements
03 p0352 A72-13007

Surface phase holograms recorded on materials with depth removal effect on exposure, noting emulsion thickness effect on image quality
03 p0359 A72-13449

Amplitude holograms diffraction effectiveness increase by conversion to phase holograms through photoemulsion bleaching, evaluating various bleaching agents effectiveness
05 p0663 A72-16614

Holographic measurement for optical transfer function of lenses, considering negative black and white photographic indicator emulsion effect
05 p0663 A72-16728

Scanned reference beam holography techniques with limited exposure time, noting use of hypersensitized photographic plates
07 p0985 A72-19418

Latent image formation in radiographic emulsion of AgBr crystals dispersed in gelatin layer, considering crystal structure and X and gamma rays energy recording
07 p0991 A72-20424

Two point analysis of phase, coherence and emulsion response effects on holographic image resolution
08 p1168 A72-21698

Hologram diffraction efficiency for bleached high resolution photoemulsions for blue line of He-Cd laser
09 p1311 A72-22964

PHOTOGRAPHIC FILM
Ecological study of damp wasteland according to seasons and with various photographic emulsions
09 p1303 A72-23293

Photopolymers formulations and processing for holography applications, discussing sensitivity, keeping and reciprocity properties
10 p1482 A72-24566

Impurity centers formation and development in AgBr/I₁ photographic emulsion under ultrasonic irradiation
11 p1636 A72-26794

Crowded photographic emulsions, predicting granularity of multilayer sandwich as function of layers number
12 p1808 A72-27676

Photoemulsion diffraction efficiency from latent holographic image signal formed during beam incidence on one or both photoplate sides
13 p1959 A72-29685

Aerial survey camera with automatic exposure control, discussing film emulsions sensitivity characteristics, object light intensity range and measuring methods
14 p2105 A72-30839

Emulsion response and phase effects on two point resolution in coherent holographic imaging systems, using Rayleigh criterion
15 p2237 A72-32058

Harmonics, intermodulation noise and small signal effects in discrete image points holographic recording on photopolymer material characterized by linear phase shift vs exposure
15 p2238 A72-32158

Resultant modulation transmission function of projection photometry photographic materials, discussing techniques for resolution and sharpness
16 p2392 A72-33364

Holographic image reconstruction using He-Ne laser as coherent light source and black-white and color photographic emulsions
17 p2554 A72-34930

Holographic interferometry application to weak inhomogeneities visualization in gas flows, using photographic emulsion nonlinear properties
17 p2558 A72-35893

Image forming mechanism in photographic silver halide emulsions due to incident optical signals, considering latent image amplification process efficiency
19 p2800 A72-37857

Investigation of certain complex compounds of triaryl phosphines /phosphites/ in optically sensitized photographic emulsions
21 p3052 A72-40390

Characteristics of the low temperature effect of an electric field on the sensitivity of photographic emulsions
21 p3053 A72-40391

PHOTOGRAPHIC EQUIPMENT
NT BALLISTIC CAMERAS
NT CAMERAS
NT FRAMING CAMERAS
NT HIGH SPEED CAMERAS
NT LALLEMAND CAMERAS
NT PANORAMIC CAMERAS
NT PHOTOGRAPHIC PROCESSING EQUIPMENT
NT PHOTOGRAPHIC RECTIFIERS
NT SCHMIDT CAMERAS
NT TELEVISION CAMERAS

Camera slit lamp apparatus design for anterior eye diagnosis in two dimensional and stereoscopic photography and ophthalmic application
04 p0478 A72-14725

Photo-optical instrumentation - Conference, Tokyo, June 1970
06 p0812 A72-17426

The laser - A source of light in high speed photography
17 p2563 A72-35182

Optimum diopter value for a view-finder of photographic camera.
21 p3054 A72-40729

Measurement of the optical transfer function of an onboard objective in the space environment
24 p3403 A72-45225

PHOTOGRAPHIC FILM
NT MICROFILMS
Remote sensing photointerpretation tests, discussing film-filter combinations, image acquisition time, scale and detection accuracy
01 p0065 A72-10450

Photosensitive magneto-optic films for large capacity computer memories
01 p0035 A72-11316

Crimped films for object reconstruction and image storage, comparing performance to holographic films
01 p0073 A72-11318

Digital picture processing techniques for increased detail resolution, applying equidensity film methods [DFVLR-SONDDR-170]
02 p0229 A72-12018

Apodized Fresnel zone plate construction for solar X-ray image formation
03 p0354 A72-13047

High resolution CRT application to UV film recording and radar and X ray scanning

03 p0360 A72-13712

Visual film, TV and optical data systems unified classification for performance criteria based on equation similar to ideal imaging system description by Rose

03 p0329 A72-14188

Film flatness in airborne cameras, reducing large area and short period photogrammetric deviations

06 p0815 A72-17758

Real time hologram photosensitive materials, determining power requirements and resolution for diffraction gratings in saturable absorbers and absorbing liquids

[CLEA PAPER 15.4] 07 p0984 A72-19397

Automatic photoelectric device for measuring internal stresses and deformations of photographic films

07 p0988 A72-19861

Electron photon cascade energy measurement by photometering blackened spots on X ray films

07 p0988 A72-19870

Commercial radiographic system with data enhancement based on monochromatic blue film, noting image quality and exposure range

07 p0991 A72-20425

TV tube type image sensors to replace photographic film for space telescope, discussing design and performance

08 p1169 A72-21956

Multiband aerial photography application to vegetal cover determination, evaluating film types, seasons and scales

09 p1302 A72-23287

Terrain evaluation by aerial imagery, discussing various film types for conventional visible and IR black and white and color photography, thermal IR and/or radar

09 p1303 A72-23303

Pulsed laser sensitometer using multiple imaging technique to retrieve average energy distribution from photographic plate optical density

09 p1325 A72-23346

Diffraction efficiency of phase holograms formed by surface deformation of light sensitive dichromated gelatin films

12 p1808 A72-27600

Film flatness in airborne cameras, reducing large area and short period photogrammetric deviations

12 p1809 A72-27818

Radiation transfer equations solved in isotropic light scattering approximation, relating transfer function to motion picture film optical properties

13 p1955 A72-28519

Photographic observation of satellites to sixth magnitude with K-24 aerial camera on Polaroid 3000 and 10,000 ASA film, recording time signals on magnetic tape

14 p2084 A72-30235

Modulated laser beam record wideband signals on photographic film, discussing noise sources and compensation methods for SNR improvement

15 p2248 A72-32039

Dynamic particle field in-line holographic recordings using IR film and p-n junction GaAs lasers

15 p2237 A72-32056

Thick phase holograms in dichromated gelatin, discussing physical properties requirements and reliable processing procedures

15 p2239 A72-32355

Thermoplastic photoconductor media for holographic recording, discussing structure fabrication techniques and performance

15 p2239 A72-32359

Recyclable holographic recording media performance parameters comparison to develop tradeoffs for storage and imaging applications

15 p2239 A72-32360

Photographic characteristics of high resolution film for Orion spaceborne astronomical observatory spectrograms, discussing aerospace environment effect on sensitivity and physicochemical properties

15 p2243 A72-32745

Off-axis hologram recording on thin bismuth film with picosecond pulse train from mode-locked Nd-glass laser

17 p2558 A72-35817

Digital image processing and interpretation of photographic film data

18 p2690 A72-36319

The accuracy of the intermittent photographic film advance in the camera of an airborne thermal scanner

18 p2692 A72-36697

Laser beam scanning and recording in two dimensional pattern on silver halide, evaluating systems performance based on signal response, granularity and noise characteristics

20 p2930 A72-39040

Production of holograms developed on a film by white light

21 p3053 A72-40392

Compensation of Fabry-Perot surface defects. II - Silicon oxide compensating layers

21 p3053 A72-40608

PHOTOGRAPHIC MEASUREMENT NT PHOTOGRAMMETRY

Forestry and agricultural applications of multiband photography, considering photointerpretation of black and white, color and IR photographs

01 p0057 A72-10459

Noncoherent moire contour-sum contour-difference and vibration analysis of three dimensional objects using grid projection and offset camera

03 p0358 A72-13438

Velocity measurement of glass particles emerging from plasma flame by high speed cine-streak photography

03 p0361 A72-13992

Meteor passage time determination by optical shutter with wedge-shaped blades for light flux periodic intersection and production of two discontinuous lines for identification

06 p0816 A72-17930

Brightness profiles of earth daytime horizon from Soyuz spacecraft photographic photometry, deriving atmospheric scattering coefficient relation to optical thickness vertical distribution

06 p0808 A72-18040

Photorecorder for burning rate measurements, consisting of electric motor driven film carrying rotating drum in slitted housing and flame front imaging optical system

06 p0817 A72-18215

Electron photon cascade energy measurement by photometering blackened spots on X ray films

07 p0988 A72-19870

High speed photographic pyrometer for surface temperature measurements on aerodynamic models during free flight in aeroballistic range

15 p2237 A72-32050

Slope angle determination with respect to photograph surface from visible horizon line configuration

15 p2238 A72-32123

High and medium energy molecular beam detection for large dispersion angle collision cross sections determination, using photographic plates

16 p2389 A72-33060

Displacement measurement from double-exposure laser photographs

17 p2564 A72-35751

Meteor passage time determination by optical shutter with wedge-shaped blades for light flux periodic intersection and production of two discontinuous lines for identification

18 p2693 A72-37155

Hering's law of equal innervation and the position of the binoculars

19 p2756 A72-37828

Exact positions of Mars as determined by the photographic method at Pulkovo in 1966 and 1967

19 p2859 A72-37914

Exact positions of Uranus for 1919 through 1969 according to photographic observations at Pulkovo and Tashkent

19 p2859 A72-37915

Catalog of individual motions of stars in the open star cluster NGC 6866 and vicinity

19 p2860 A72-37918

Computer processed Mars photographic positional measurements with Pulkovo normal astrophotograph in 1965

19 p2861 A72-37985

Surface tilt and vibration measurements by laser speckle pattern photography, comparing with moire fringes in strain analysis

20 p2930 A72-39032

Determination of corneal configuration by the measurement of its derivatives

21 p3055 A72-40745

Optical method for measuring the concentrations of axisymmetric gas jets

21 p3055 A72-40990

Comet integral brightness estimation by mathematical analysis of photometric characteristics

21 p3110 A72-41449

Ground observation for outer planets natural satellites ephemeris, using astronomic telescopes, photographic and plate reduction techniques

[ALAA PAPER 72-904] 24 p3443 A72-45426

PHOTOGRAPHIC PROCESSING

Drobyshev stereograph corrector operation for aerial photographs processing with transformed beam of stereoprojector

09 p1308 A72-22483

High efficiency low noise volume /Lippmann-Bragg/ holograms recorded on photographic plate, using bleaching-darkening procedure

11 p1629 A72-25316

Exposure conditions and film processing parameters effects on sensitivity, diffraction efficiency and SNR of holograms recorded with continuous and pulsed radiation sources

11 p1637 A72-26796

Allyl esters of phosphoric acid preparation and application as substitutes for heavy metal sulfides and silver compounds in single operation photographic process

16 p2392 A72-33363

Remotely sensed data processing by scanner/printer designed for photograph scanning, geometric correction and photographic printing of corrected image

18 p2691 A72-36495

Edge effect improved fringe definition on high contrast film by pseudo-solarization for polariscopes in photoelastic stress analysis

21 p3052 A72-40232

Separation and detection of signals in the presence of nonadditive noise

21 p3023 A72-41746

Photographic processing method for solar activity macrostructural distributions determination, suppressing minor and sporadic formations by defocusing technique

23 p3340 A72-44231

PHOTOGRAPHIC PROCESSING EQUIPMENT

Plateholder for on site wet processing of holograms in real time holographic interferometry, obtaining undistorted reconstructed image by liquid gate immersion

07 p0992 A72-20581

PHOTOGRAPHIC RECORDING

Absorption and exposure characteristics of silver halide photochromic glasses for hologram recording

01 p0068 A72-10622

Coronal events in 5303 A wavelength, discussing loops and arches and slow and fast events from photographic recordings

03 p0422 A72-13209

Target motion simulator with photographic recording of image velocity and motion compensation in cameras, discussing errors

03 p0356 A72-13226

Solar spectra photographic recording technique, using spectra-spectroheliography method with data reduction

03 p0429 A72-13313

Surface phase holograms recorded on materials with depth removal effect on exposure, noting emulsion thickness effect on image quality

03 p0359 A72-13449

Liquid breakdown and subsequent propagation by focused high power laser irradiation, presenting short term photography of event sequence

[AD-736005] 03 p0368 A72-13606

High resolution CRT application to UV film recording and radar and X ray scanning

03 p0360 A72-13712

Photomaterial nonlinear effects on contour distortion in holographic recording of Fourier image slit for graphic memory use

04 p0522 A72-15151

High speed photography and radiography applications to high explosives research, discussing shock wave visualization, illumination techniques for rapid processes time resolution, etc

06 p0813 A72-17436

Photo-optical techniques in biomedical data acquisition, discussing cineangiography and X ray tomography applications in cardiological research work

06 p0766 A72-17437

Self calibration of surveying cameras for three dimensional object photography without control points, using homologous ray method

06 p0815 A72-17754

Pulsed and hf electric field effects on ionizing particle recording in nuclear and photographic emulsions

06 p0816 A72-17833

Photorecorder for burning rate measurements, consisting of electric motor driven film carrying rotating drum in slitted housing and flame front imaging optical system

06 p0817 A72-18215

Photographic observations of W particle cluster high velocity impact against polystyrene, paraffin and W targets for energy dissipation in meteorite impact simulations

08 p1232 A72-21152

Three dimensional hologram recording and reconstruction, discussing image geometry, reference beam intensity, size finiteness, transition limits and photosensitive materials

08 p1166 A72-21399

Multibeam indicator with block diagram description for meteor ranging radar and photofilm based recording system

09 p1308 A72-22508

Time dependent phase modulation for high effective reference to object beam intensity ratio, noting linear recording of holograms

09 p1310 A72-22649

Vesicular films in electron and laser beam recording suitable for computer output microfilm duplication and graphic arts

10 p1488 A72-23930

Recording holographic networks in polycrystalline transparent ferroelectric ceramics of lead and lanthanum titanate-zirconate system

10 p1480 A72-24111

Ultrahigh strain rate measurement via diffraction gratings directly impressed into test material surface, recording outputs by high speed cameras or photoelectric techniques

10 p1487 A72-24573

Image dissector system fabrication for two dimensional area scanning, applying to photograph digitization
11 p1631 A72-25688

Holographic recording systems stabilization with intermittent exposure control for interference patterns fidelity
12 p1806 A72-27263

Multiple exposure hologram recording on photosensitive plate for extended reference-beam source
12 p1808 A72-27601

Photosensitive polymeric films for hologram recording with high diffraction efficiency, requiring low laser powers
12 p1808 A72-27602

Holographic interferometry for impact loaded object transient impulse response recording with double-pulse Q switched laser
12 p1809 A72-27761

Image deformation sources correction in space photography, discussing stationary and moving cameras and panoramic and complex sensing systems
12 p1809 A72-27817

Optical feedback exposure control mechanism of high resolution CRT film recorder intended for tactical military usage
12 p1810 A72-27932

Developers evaluation for processing of photoresist used in hologram recording
12 p1812 A72-27956

Involuntary head movement and helmet motion displacements during human centrifuge runs to 6 Gz from photographic recordings
12 p1766 A72-28288

Solar flare induced vortex ring formation, describing photographic observations by Okayama Astrophysical Observatory solar telescope on 30 October 1970
13 p2048 A72-29741

Noise suppression by time exposure oscilloscope photography to enhance repetitive electric signals obscured by noise of equal amplitude
13 p1959 A72-29754

Automatic digitizing and recording of analog information from oscilloscope photographs
13 p1959 A72-29755

Holographic diffraction grating production by impressing interference fringes with photographic procedure, using two laser beams
14 p2105 A72-30579

Three dimensional medium recording of multicolor holographic interferometry, comparing scale factor, spatial frequency and optical distortions with two dimensional medium
15 p2233 A72-31412

Two beam high speed frame holographic recording of dynamic processes, using passive shutter ruby laser with diaphragmed resonator
15 p2233 A72-31417

Time-average holography with thin phase recording materials, obtaining characteristic function solution for sinusoidal vibration and constant velocity motion
15 p2235 A72-31614

Modulated laser beam record wideband signals on photographic film, discussing noise sources and compensation methods for SNR improvement
15 p2248 A72-32039

Dynamic particle field in-line holographic recordings using IR film and p-n junction GaAs lasers
15 p2237 A72-32056

Harmonics, intermodulation noise and small signal effects in discrete image points holographic recording on photopolymer material characterized by linear phase shift vs exposure
15 p2238 A72-32158

Holographic information storage survey, discussing hologram classification, characteristics, physical recording processes, and capacity-limiting factors
15 p2239 A72-32351

Undoped lithium niobate for holographic storage applications, reviewing physics and recording performance
15 p2239 A72-32353

Off-axis phase holograms of photographic transparencies recording, comparing Fresnel, Fraunhofer and lensless Fourier transform holograms
15 p2239 A72-32358

Comet Tago-Sato-Kosaka /1969/ L alpha emission image recorded by f/2 objective-grating spectrograph aboard Aerobee rocket, discussing ice sublimation in nucleus
16 p2455 A72-33466

Stabilizing techniques for holographic recording.
17 p2556 A72-35416

Effect of photographic factors on the line intensities in the Fraunhofer spectrum of the sun
19 p2860 A72-37960

Optical design and production of low cost oscilloscope camera incorporating reliable setting for correct exposure and focus
20 p2921 A72-39031

Photographic observations of W particle clusters high velocity impact against polystyrene, paraffin and W targets for energy dissipation in meteorite impact simulations
20 p2969 A72-39257

Electronic circuit for linearizing the transfer function of a photographic plate used in mass-spectrometry.
20 p2925 A72-39428

Comparison of information takeoff from a shadow-indication instrument by television and photographic techniques
20 p2928 A72-40049

Production of holograms developed on a film by white light
21 p3053 A72-40392

Experimental investigation of a holographic system that records front surface detail from a scene moving at high velocities.
21 p3053 A72-40612

Dry photopolymer holographic recording film with ability to form images in near real time by exposure without processing
21 p3054 A72-40620

A large viewfield laser photographic system for in-flight model contour measurements in an aeroballistic range.
22 p3179 A72-42679

Scanning electron microscope stereophotographic picture synthesis from sequential holographic recording of three dimensional objects
23 p3290 A72-43904

Metallic solid material transient displacement field measurement by moire fringe photographic recording technique with computer program for data analysis
24 p3401 A72-44611

Studying hologram imagery by a ray-tracing method.
24 p3401 A72-44773

A new method for linear recording in holography retaining the reconstruction efficiency.
24 p3401 A72-44775

Simplified, low-noise processing technique for photographic phase holograms.
24 p3401 A72-44804

PHOTOGRAPHIC RECORDING INSTRUMENTS
U OPTICAL MEASURING INSTRUMENTS
U PHOTOGRAPHIC RECORDING
U RECORDING INSTRUMENTS

PHOTOGRAPHIC RECTIFIERS
A digital portable line-drawing rectifier.
18 p2692 A72-36500

PHOTOGRAPHIC TRACKING
WINDCO interactive man-computer system for automated cloud motion tracking using precisely aligned digital ATS satellite pictures
01 p0070 A72-10872

Systematic errors in scan-and-measure devices for tracking cameras photographs analysis, discussing correction during measurements
08 p1209 A72-21913

Pallada, Vesta, Irida and Harmony asteroids positions computed from observations with 400 mm photographic telescope
09 p1389 A72-23066

Camera shake under stress of tracking moving targets viewed briefly in poor light, considering blur in horizontal and vertical dimension
10 p1483 A72-24986

Photographic observation of satellites to sixth magnitude with K-24 aerial camera on Polaroid 3000 and 10,000 ASA film, recording time signals on magnetic tape
14 p2084 A72-30235

Radio meteor orbit inclination angle dispersions for semimajor axis intervals compared with photographic meteors
16 p2456 A72-33514

Error analysis of East European triangulation network photographic observations of Echo and Pagueos satellites from ground stations
16 p2387 A72-33798

Automated cloud tracking using precisely aligned digital ATS pictures.
17 p2521 A72-34411

Photographic observation of artificial earth satellites without the aid of time recording devices. II
17 p2517 A72-35384

The track method and its application in studies of atomized-fuel combustion kinetics
18 p2720 A72-36243

Accuracy of the determination of the positions of stars and artificial satellites from an aircraft
19 p2861 A72-37973

Triaxial mount for electrophotometric observations of satellites during their transit into the shadow of the earth
23 p3290 A72-44040

PHOTOGRAPHS
NT CLOUD PHOTOGRAPHS
NT LUNAR PHOTOGRAPHS
NT MOTION PICTURES

PHOTOGRAPHY
NT AERIAL PHOTOGRAPHY
NT ALL SKY PHOTOGRAPHY
NT ASTRONOMICAL PHOTOGRAPHY
NT BLACK AND WHITE PHOTOGRAPHY
NT CHRONOPHOTOGRAPHY
NT CINEMATOGRAHY
NT CLOUD PHOTOGRAPHY
NT COLOR PHOTOGRAPHY

NT ELECTRO-OPTICAL PHOTOGRAPHY
NT FRACTOGRAPHY
NT FRAME PHOTOGRAPHY
NT HOLOGRAPHY
NT INFRARED IMAGERY
NT INFRARED PHOTOGRAPHY
NT LUNAR PHOTOGRAPHY
NT MICROWAVE PHOTOGRAPHY
NT MULTISPECTRAL PHOTOGRAPHY
NT ORTHOPHOTOGRAPHY
NT PHOTOMICROGRAPHY
NT RADAR PHOTOGRAPHY
NT ROCKET-BORNE PHOTOGRAPHY
NT SATELLITE-BORNE PHOTOGRAPHY
NT SCHLIEREN PHOTOGRAPHY
NT SHADOWGRAPH PHOTOGRAPHY
NT SPACEBORNE PHOTOGRAPHY
NT SPECTROPHOTOGRAPHY
NT STEREOPHOTOGRAPHY
NT ULTRAVIOLET PHOTOGRAPHY
NT ULTRAVIOLET PHOTOMETRY

Silicon Schottky barrier photodiodes development for photographic, photometric and analytical instrumentation, comparing sensitivity, time response and fatigue characteristics with classical photodetectors
06 p0813 A72-17428

Holography applications and processes, discussing holographic microscopy, particle analysis, high speed photography, data storage and retrieval, interferometry, nondestructive testing, etc
07 p0989 A72-20221

New technique of image multiplexing using random diffuser.
21 p3050 A72-40145

Photographic material characteristics for adequate diffraction efficiency and contrast and noise levels and acceptable nonlinear distortions of holograms, noting optical transfer function optimization
21 p3052 A72-40389

PHOTOINTERPRETATION
Remote sensing photointerpretation texts, discussing film-filter combinations, image acquisition time, scale and detection accuracy
01 p0065 A72-10450

Agricultural land use analysis by remote sensing, discussing side-looking airborne radar systems and image interpretation for local needs
01 p0056 A72-10456

Forestry and agricultural applications of multiband photography, considering photointerpretation of black and white, color and IR photographs
01 p0057 A72-10459

Interpretation model for aircraft and spacecraft remote sensing of tropical agricultural systems
02 p0210 A72-11798

Sea waves energy spectra from optical Fourier analysis of ocean photographs under particular skylight irradiance
02 p0211 A72-11809

Southern corn leaf blight detectability by remote sensing based on pattern recognition technique application to multispectral color and IR photographic and scanner data
02 p0212 A72-11814

Small scale aerial photography use in regional agricultural survey, discussing equipment used, sampling techniques and data collection and interpretation
02 p0213 A72-11835

Spectral texture effects on remotely sensed high altitude automatic IR image interpretation, using Bayesian probability techniques
02 p0228 A72-11873

Land pattern mapping from monoisimagery analysis, using coordinate digitizer system with planimetric computer input
02 p0187 A72-11874

Crop, soil and geological mapping from digitized multispectral satellite photography, discussing data processing requirements and surface features distinguishable from satellite altitudes
02 p0214 A72-11876

Thermal modeling for IR images geologic interpretation, discussing physical parameters role in materials natural environmental diurnal temperature behavior
02 p0214 A72-11877

Natural formation interpretation from spectrophotometric measurements of underlying earth surface from manned spacecraft Soyuz 7 and Soyuz 9
02 p0228 A72-11887

Hyperaltitude photography evaluation for geological mapping, comparing Gemini 4 and aerial photographs
02 p0216 A72-11891

Urban geographic social-spatial pattern determination with aerial photographic interpretation
02 p0229 A72-12019

Quantitative reliability criteria for aerial photo decoding, noting dependence on observation time
02 p0229 A72-12172

Satellite photograph interpretations, discussing wind direction indication, cloud structure, automatic mapping and hydrographic exploration
03 p0351 A72-14306

Book on aerial photoecology covering aerial survey images interpretation, processing and printing operations and economic considerations

04 p0514 A72-14572

Panoramic aerial cameras with revolving objective or mirror, presenting formulas for photoimage plots geometric characteristics

09 p1308 A72-22487

Photointerpretation - Conference, Dresden, Germany, September 1970, Parts 1 and 2

09 p1301 A72-23276

Aerial photography interpretation for studies of natural environment and resources

09 p1312 A72-23277

Multifactor landscape synthesis of aerial imagery for regional surveys

09 p1301 A72-23278

Aerial photointerpretation for landscape analysis with respect to agricultural land use, considering geomorphologic, hydrographic, soil and microclimatic conditions

09 p1301 A72-23280

Urban geography of U.S. cities on vertical aerial photography, considering site, location, street orientation, expansion, business districts and transportation networks

09 p1301 A72-23281

False color aerial photographs interpretation for cultivated wooded area inventory

09 p1302 A72-23282

Multiband color aerial photography interpretation for forest appraisal in U.S.S.R.

09 p1302 A72-23285

Color aerial photographs interpretation for forest tree type composition determination, comparing to IR sensitive black and white films

09 p1302 A72-23286

Multiband photointerpretation of forested land units, using aerial black and white photographs and film-filter combinations

09 p1302 A72-23288

Aerial photointerpretation in forest administration, discussing electronic data processing methods

09 p1302 A72-23291

Photointerpretation methods for earth resources and geological studies, discussing quantitative photogrammetric techniques, automation and digital evaluation methods

09 p1302 A72-23292

Ecological study of damp wasteland according to seasons and with various photographic emulsions

09 p1303 A72-23293

Black and white vs color photography application to photogeological interpretation of West Greenland Precambrian terrain

09 p1303 A72-23294

Education and training of personnel for photointerpretation, discussing psychological, physiological and methodological aspects of aerial photointerpretation

09 p1272 A72-23298

Psychological aspects in aerial photointerpretation, discussing importance of perception of image contrast, contours and areal distribution

09 p1272 A72-23299

Internal and integral aerial photointerpretation, discussing enhancement of information quality, quantity and reliability through participation of experts in various specialized fields

09 p1303 A72-23300

Spatial filtering techniques and numerical classification methods for pattern recognition in automated photointerpretation

09 p1312 A72-23305

Sea depth determination in coastal waters based on solar reflection aerial photographs interpretation, presenting formula as function of swell parameters

09 p1303 A72-23307

Automation of aerial photointerpretation based on application of photometric, microdensitometric and digital computer technology

09 p1313 A72-23308

Topographical stereo map plotting apparatus with auxiliary device for orthophoto production, describing design for combined photointerpretation-cartographic applications

09 p1313 A72-23309

Optical image filtering to simplify and facilitate automatic aerial photointerpretation processes

09 p1313 A72-23310

Color interpretation of pedological factors from aerial photographs in relation to agricultural seasons and use of panchromatic and false color emulsions

09 p1304 A72-23313

Terrain evaluation for engineering purposes through aerial photointerpretation in terms of physiography, geology, soil and vegetation

09 p1304 A72-23314

Three stage retinal model for visual monitoring method applied to computerized photointerpretation of aerial photographs

09 p1284 A72-23624

Atmospheric vertical shear at visible cloud level in Jupiter equatorial zone from blue and red wavelength photographs

10 p1531 A72-23712

Remotely sensed imagery data photointerpretation by gray tone texture context feature extraction, noting identification accuracy

10 p1442 A72-23812

Analog computer for practical evaluation of hologram interference fringes, analyzing errors

12 p1811 A72-27940

High speed photographic analysis of spot welding galvanized steel, observing three stage process

13 p1958 A72-29421

Photointerpretation and computerized radiometric analysis of ERTS multispectral TV and scanner imagery of Israel

15 p2221 A72-31242

Geographical interpretations of ESSA and Nimbus weather satellite pictures for earth resources applications, noting ERTS project

15 p2221 A72-31248

Exposure calibration, orientation and point coordinate distortions in aerial photographs from one or two camera stations

15 p2240 A72-32378

Texture measurements in earth resources data management system by automatic photointerpretation with analog and digital techniques, discussing data processing rate requirements

17 p2520 A72-34409

Screen equidensities in aerial photograph interpretation

17 p2555 A72-35337

Texture synthesis by image processing equipment consisting of digital computer and input/output unit, noting image signatures of constant parameter areas

17 p2555 A72-35338

Psychophysical information content evaluation of aerial photographic images by human viewer for photointerpretation and search in reference library

20 p2894 A72-39042

Investigation of the structural content and the determination of the optimal image of focus series in light and electron microscopy with the aid of Fraunhofer diffraction /structure spectroscopy/

21 p3055 A72-40747

Waterways outfall detection from color and IR color aerial photography, describing photointerpretation technique

22 p3181 A72-43197

Earth resources technology satellites /ERTS/ program requirements, considering coverage, spectral characteristics, system performance, photographic interpretation and information extraction

24 p3398 A72-45115

Detection of waste water effluents and of their surface spread in the English channel, the North sea and the Baltic sea, through determination of the surface temperature of the sea by means of infrared air pictures taken by satellites

24 p3398 A72-45223

PHOTOIONIZATION

Eta Carinae model with IR spectrum details described by compact H II region photoionized by hot massive star radiation

02 p0277 A72-11668

Altitude, photon wavelength and solar activity effects on photoionization yield of ionospheric monatomic and diatomic oxygen and nitrogen via Monte Carlo simulation

03 p0345 A72-12983

Series summations for perturbation theory of multiple photon ionization probabilities of atoms applied to hydrogen and helium

03 p0391 A72-13080

Formaldehyde photoionization and absorption spectrum measurements in vacuum UV region, using single configuration self consistent field procedure for Rydberg states and model

03 p0321 A72-13856

Fe group transition metal impurities in semiconductors, calculating ground state wave functions and photoionization cross section dependence on wavelength

04 p0563 A72-15473

Quasar photoionization and emission line spectra, determining radiation/gas density

05 p0720 A72-16713

Molecular Cs role in multiphoton ionization process during interaction with low intensity Q switched Nd-glass laser radiation

05 p0670 A72-17082

Ar core polarizability effect on photoionization cross section calculation for ground state configuration

05 p0693 A72-17173

Fast ionization fronts ahead of laser produced plasma expansion into low density gas, noting Langmuir probe and microwave diagnostics indication of photoionization density augmentation

06 p0864 A72-18532

Atomic selective two step photoionization and molecular photodissociation by tunable laser radiation, experimenting on Rb vapor and HCl respectively [CLEA PAPER 12,4]

07 p1005 A72-19395

Vibrationally excited nitrogen photoionization spectrum obtained with quadrupole mass spectrometer in flowing nitrogen afterglow

07 p1037 A72-19434

Methanol and formaldehyde photoionization by UV irradiation, determining ion yields as function of wavelength by mass spectrometric analysis

07 p1038 A72-20498

Diatomic oxygen and carbon dioxide density profiles effects on photoionization rates in D region [AD-741091]

09 p1274 A72-22356

Model calculation for electron production rates due to photoionization and particle precipitation below 100 km at midlatitude during solar minimum and maximum years

09 p1375 A72-22357

Ultrasoft X ray absorption spectra features of inner atomic shell photoionization in molecules

09 p1356 A72-22827

Effective photoionization sections of neutral atoms, discussing photon energy effects, subshell periodicity and continuum functions phase shift

09 p1356 A72-22828

Molecular gases absorption coefficients measurement in extreme UV, analyzing photoionization curves in energy range far beyond threshold

09 p1356 A72-22829

Absorption by Nd laser generated ionized Al plasma of extreme UV radiation due to inverse bremsstrahlung and photoionization

09 p1360 A72-22831

Excitation accompanying photoionization in atoms and molecules and relationship to electron correlation observed from rare gases inner and valence shell satellite lines measurements

09 p1356 A72-22835

Ultrasoft X ray region photoionization absorption spectra features of inert gases, solids, rare earth elements and transition metals

09 p1357 A72-22845

Photoionization cross sections for atoms and ions of Al, Si and Ar on basis of Hartree-Fock bound-electron and close coupling approximation free-electron wave functions

10 p1516 A72-24669

Critical shock wave velocity for ionization front propagation with photoionization of hydrogen by radiation, using pinch discharge tube measurements [ATA PAPER 72-410]

11 p1706 A72-26161

Population inversion through metastable ion formation by atomic inner shell electrons photoionization, determining effectiveness relationship to emission source plasma composition

11 p1648 A72-26332

Equatorial F region photoionization and chemical loss rates for electrons from simultaneous observations of vertical drift velocity and electron concentration, deriving plasma transport

13 p1949 A72-29336

Perturbation theory of hydrogen and helium atoms multiphoton ionization probabilities, proposing series summation method

13 p2007 A72-29430

Ionospheric oxygen ions loss rate in charge exchange reactions with hydrogen, molecular nitrogen and oxygen and atomic oxygen photoionization rate

13 p1953 A72-29811

Vertical distribution of atomic nitrogen ions in F region produced by dissociative photoionization and charge transfer, suggesting undiscovered source at 300 km altitude

13 p1954 A72-29815

Absorption coefficient of H-He plasma measured in temperature and electron density range of inverse bremsstrahlung and photoionization absorption

15 p2284 A72-31522

Precursor photoionization production of ionization onset point equivalent electron number densities, calculating phenomenon occurrence Mach number

15 p2281 A72-32407

Hydrogen direct photoionization and photoexcited autoionization cross sections calculation for radiation in 600-800 A region

16 p2431 A72-33579

Oscillator strength and ground state photoionization cross sections computation for Na, K, Rb and Cs atoms, including core polarization correction to dipole moment

16 p2431 A72-33724

Electrons angular distribution effect on photoionization branching ratio measurement by photoelectron spectroscopy

17 p2552 A72-34288

Photoionization models for the emission-line regions of quasi-stellar and related objects.

17 p2605 A72-34527

Cs vapor photoionization by sequential method via thermally tunable Ga-As laser and arc-lamp monochromator radiation

17 p2585 A72-34614

Photoionization of a gas by far ultraviolet radiation of a laser-created plasma 17 p2588 A72-34872

Brueckner-Goldstone many-body perturbation calculation of helium photoionization. 17 p2586 A72-35773

Excited-state cesium photoionization cross sections. 19 p2837 A72-37838

Effect of spatio-temporal laser light structure on multiphoton ionization. 20 p2934 A72-39814

Absorption spectra in the far ultraviolet of Be, B, C, N, Mg, Al, and Si 21 p3013 A72-40818

Coulomb approximation method for photoionization cross sections of hydrogen molecule singly excited states 22 p3208 A72-42718

Drift velocities, diffusion coefficients, and temperatures of photoions in argon, nitrogen, and oxygen 22 p3209 A72-42926

The ionization of caesium vapour by the method of space charge amplification. 23 p3316 A72-44344

Photoionization and photoabsorption cross sections of CO₂ at 584 Å. 23 p3317 A72-44519

Model potential calculations of lithium transitions. 24 p3426 A72-44808

Calculation of photoabsorption processes in helium. 24 p3426 A72-45012

Initiation of a detonation by a laser beam focused in a gaseous medium 24 p3410 A72-45026

Photoionization of N₂, O₂, NO, CO, and CO₂ by soft X rays. 24 p3426 A72-45302

Multiphoton dissociation, predissociation, and autoionization of the hydrogen molecule. 24 p3427 A72-45476

Photoionization and photoabsorption cross sections for ionospheric calculations. 24 p3400 A72-45590

PHOTOLUMINESCENCE

NT X RAY FLUORESCENCE

Photoluminescence of Er cations in CdS, observing group I co-dopants sensitizing behavior and broad-band emission spectra 04 p0563 A72-15472

IR luminescence and photoconductivity in p-type GaSe single crystals alloyed with Sn and Ge impurities 08 p1216 A72-21069

Radio luminescence of an yttrium-aluminum garnet activated by rare-earth elements 19 p2845 A72-38181

Photoluminescence and photoconductivity of hole-type cadmium telluride single crystal films 19 p2845 A72-38403

Low-temperature photoluminescence of GaAs under conditions of strong interaction of the non-equilibrium carriers. 19 p2847 A72-38821

PHOTOLUMINESCENT BANDS

Annealing behavior of electrical properties and photoluminescence spectra in electron irradiated n-type GaAs semiconductors 12 p1859 A72-28068

Quantum efficiency and radiative lifetime of the band-to-band recombination in heavily doped n-type GaAs. 19 p2844 A72-37947

PHOTOLYSIS

NT RADIOLYSIS

Hydrogen iodide flash photolysis in presence of nitrous oxide, carbon dioxide and water investigated by kinetic spectroscopy, observing imidogen as intermediate reaction product 01 p0023 A72-11114

Micrometer particle formation by water vapor photolysis at 1500-1700 Å, noting particle production rate and implications to planetary atmosphere physics 02 p0220 A72-12207

Ozone photolysis in UV region, determining primary products from oxygen optical emission detection using time-resolved flow system 03 p0320 A72-13394

Flash photolysis HF chemical laser pulse delay measurements, showing pressure, flash lamp intensity and optical cavity loss dependence 05 p0668 A72-16606

Sunlight irradiated atmosphere formaldehyde photolysis as hydrogen atom source, estimating photodecomposition rates from extinction rates and photochemical results 08 p1230 A72-20981

Chemistry and performance characteristics of flash photolysis and microwave discharge initiated CW carbon disulfide/oxygen lasers 09 p1325 A72-23236

Fast coaxial flash lamp pumped liquid dye laser /LDL/ for photolysis and biophysical and biochemical applications 09 p1326 A72-23406

Molecular process and pressure effects on hydrogen formation in methyl acetylene photolysis at 1236 Å 11 p1590 A72-26011

Carbon monoxide quantum yield measurements of carbon dioxide photolysis by radiation at 1470 and 1500-1670 Å 11 p1590 A72-26423

Ozone photochemical reactions measurements for quantum yield of UV photolysis in strong Hartley band with water vapor chain decomposition effects 14 p2083 A72-30134

Molecular iodine photolysis in photodissociative laser due to selective pumping, noting recombination-like storage mechanism 14 p2110 A72-30354

Absolute rate constant for the reaction H + H₂CO. 17 p2511 A72-34739

Nitrous oxide production from ozone photolysis reaction with molecular nitrogen 19 p2762 A72-38753

Ammonia photolysis and the role of ammonia in chemical revolution. 20 p2898 A72-39375

Pulsed photoexcitation /flash photolysis/ spectrophotometers in terms of light sources, recording sensitivity enhancement, data processing, laser use and performance requirements 21 p3058 A72-41726

PHOTOMAGNETIC EFFECTS

Carrier mobility measurement in inhomogeneous semiconductors based on bulk photovoltaic and photomagnetolectric effects 03 p0402 A72-13862

Determination of electron and hole capture rates in nickel-doped germanium using photomagnetolectric and photoconductive methods. 24 p3432 A72-45388

PHOTOMECHANICAL EFFECT

Electromechanical, photomechanical and concentration effects of impurities in semiconductors 21 p3098 A72-41677

PHOTOMECHANICS

U PHOTOGRAPHY

U PRINTING

PHOTOMETERS

NT ELECTROPHOTOMETERS

NT ULTRAVIOLET SPECTROMETERS

NT ULTRAVIOLET SPECTROPHOTOMETERS

Absolute UV calibration of rocket photometers used to update OAO calibration for determining energy distribution of reference stars 03 p0355 A72-13065

Real time analog video magnetogram, describing differential photometer for electronic subtraction technique 03 p0357 A72-13286

Light distribution photometry in Japan, discussing photometers, luminous flux integration and source distribution and positioning errors 03 p0358 A72-13426

Radiation thermometry trends, considering photodetectors, optical pyrometers and filters [ASME PAPER 71-WA/TEMP-3] 05 p0661 A72-15909

Incoherent optical system model with photodetectors governed by Laguerre counting statistics obtaining error probabilities for comparison with Poisson counting 06 p0776 A72-18394

Photometer using rotating wedge interference filter as wavelength scanning element near 6300 Å for high altitude sounding rocket application 07 p0985 A72-19403

Intercosmos 4 solar radiation equipment, including Lyman, optical and X ray photometers, spectroheliographs, polarimeters and optical orientation system 07 p0986 A72-19643

Spherical scatterers extinction efficiency effect on photometer optical systems transmittances, using Mie equation and numerical methods 07 p0987 A72-19831

Photometers with CdS cells, discussing calibration difficulties 07 p0992 A72-20584

Sensitivity threshold of optical heterodyne receiver as function of laser radiation amplitude spectrum, using photodetector output noise 08 p1181 A72-20794

Integrating two dimensional silicon diode array vidicon astronomical photometer for telescope use 09 p1313 A72-23330

Integrating silicon target vidicon photometer for two dimensional photometric images of planets and stars 11 p1631 A72-25686

Helios solar probe-borne zodiacal light photometer for diffuse light measurements in interplanetary space 11 p1632 A72-25805

Image tube /TV/ and scanning photometer sensor comparison for outer planet mission onboard navigation 15 p2270 A72-32192

Spectrophotometers and photometers calibration and standardization, emphasizing necessity for periodic control of instrument parameters 16 p2394 A72-33872

Book on Soviet astronomical reflecting telescopes, paraboloid mirrors, computer control, microphotometers and image converters 17 p2553 A72-34623

Performance of a modified Askania iris photometer. 18 p2692 A72-36768

Low temperature interference filter design for atmospheric windows far IR photometers based on selective restrahlen reflection of crystals 19 p2796 A72-37586

A system for programmed control of the motion of the carrier of a microphotometer along two coordinates 19 p2801 A72-37966

Airglow observations with a Hadamard photometer. 22 p3169 A72-42023

PHOTOMETRY

NT ASTRONOMICAL PHOTOMETRY

NT ELECTROPHOTOMETRY

NT SPECTROPHOTOMETRY

NT STELLAR SPECTROPHOTOMETRY

NT TELEPHOTOMETRY

NT ULTRAVIOLET PHOTOMETRY

NT VISUAL PHOTOMETRY

Silicon Schottky barrier photodiodes development for photographic, photometric and analytical instrumentation, comparing sensitivity, time response and fatigue characteristics with classical photodetectors 06 p0813 A72-17428

Apollo 6 photogrammetric, photometric and neutron activation analysis of smoke plume, determining eddy diffusivity 06 p0819 A72-18439

Nondestructive tests of welded joint heterogeneities and corrosion cavities by densitometric photometric differentiation of radiographs 07 p0995 A72-19674

Photometric monitoring of film thickness of stacked structures for high strength and laser flux resistance 07 p1049 A72-20126

Light emitting diodes for efficient conversion of electrical energy into electromagnetic radiation, discussing photometry, electrical injection, electroluminescence, design and applications 08 p1141 A72-21430

Automation of aerial photointerpretation based on application of photometric, microdensitometric and digital computer technology 09 p1313 A72-23308

Visual and automatic stereometric image analysis, citing minimum measurable contrast thresholds for various devices 10 p1478 A72-23826

Flame photometric detection of small concentrations of sulfur compounds in ambient air, describing spectrum scanning detector, rotating interference filter and correlation detector 10 p1480 A72-24101

Photometric determination of Mo in Ni based steels and alloys in molybdenum-unithiol complex form, noting temperature and aqueous solution pH effects 12 p1828 A72-27445

Disturbance-induced lunar surface darkening due to soil photometric function changes resulting from particle rearrangement 13 p2037 A72-28994

Operating conditions of photometers for optimum photomultiplier photon counting photometry, considering measurement precision dependence on experimental parameters 14 p2105 A72-30733

Whole blood flow dependence on optical density from light transmission measurement, showing photometric effects of red cell aggregation, deformation and orientation 15 p2185 A72-31639

Nike-Apache rocket-borne particle collection and photometry of noctilucent clouds, obtaining single-shadowed particle size distributions and inflight shadowing surface data 15 p2226 A72-31923

Daytime zodiacal light intensity and polarization measurement at elongation angles between 15-30 degrees from Skylark rocket photometric observations 15 p2227 A72-31951

Report to COSPAR on Netherlands space research covering solar and stellar radiation, cosmic gamma and X rays, photometry and satellite geodesy 15 p2338 A72-32010

Resultant modulation transmission function of projection photometry photographic materials, discussing techniques for resolution and sharpness 16 p2392 A72-33364

Microphotometric chemiluminescence measurement for analysis of turbulent flame fine structure for homogeneous air-fuel mixtures at high Reynolds numbers 16 p2479 A72-34005

Photocolorimetric determination of boron in nickel and titanium borides via Magnezone I in alkaline medium, determining solution pH, reaction time, light absorption, etc 18 p2655 A72-36099

Luminance profiles photometry for axisymmetrical propagation in propane-air turbulent flow combustion with turbulence level control in jet core

19 p2879 A72-37366

German monograph - A photometric method for measuring the concentration distribution in turbulent boundary layers

19 p2799 A72-37652

Photometric observations from sounding rockets - Selection of horizontal sightings

19 p2789 A72-37784

Auroral photometric observations at geomagnetically conjugate points.

22 p3169 A72-42020

Objective-prism plates photometric computerized calibration method based on continuum energy distribution of standard stars within photographic plate field

22 p3177 A72-42376

German monograph - A hologram interferometer for the determination of amplitude and phase of optical excitation in diffraction patterns.

22 p3181 A72-43056

PHOTOMICROGRAPHY

Micrographic evaluation of inclusions in austenitic stainless steel tubes ensuring surface quality control

07 p0994 A72-18972

Photomicroscopy of sintered refractory alloys and nonmetallics of B-Si-C-N system, discussing microstructural interactions between binder metal and refractory component

10 p1493 A72-23824

Graphite morphology in metallic materials from scanning electron micrographs, discussing sulfur contents effect in tempered cast iron

10 p1500 A72-23825

Interval scanning photomicrography for recording growth of microbial cell populations during incubation

13 p1911 A72-29749

Investigation of the structural content and the determination of the optimal image of focus series in light and electron microscopy with the aid of Fraunhofer diffraction/structure spectroscopy/

21 p3055 A72-40747

PHOTOMULTIPLIER TUBES

Rocket-borne photomultipliers housing, recommending fiber reinforced epoxy resin structure with metal flanges

03 p0440 A72-13062

Photomultiplier signal for water axial velocity in glass pipe, providing turbulent liquid flow information and laser Doppler velocimeter evaluation

04 p0520 A72-14438

Cu-Be electron multipliers SNR restoration by removing surface contamination on dynodes by chemical etching and cleaning

04 p0524 A72-15500

Channel electron multiplier efficiency for protons of 0.2-10 keV from aurora rocket sounding

04 p0524 A72-15501

Photomultiplier operation pulsed control in semiconductor circuit for background cosmic radiation noise error minimization in atmospheric shower station

06 p0811 A72-17294

Ultrahigh speed electro-optical cameras with exposure times of several picoseconds, using biplanar image converter, electron multiplier and Kerr cell

06 p0812 A72-17415

Statistical model of signal amplitude distribution and thermoelectron noise of photoelectron multiplier

06 p0816 A72-17837

Gain variations in channel electron multipliers, investigating total radiation exposure effect

07 p0984 A72-19324

Fabry lens application in stellar photometry, describing technique of image construction on photomultiplier tube cathode

07 p0985 A72-19419

Optoelectronic elements for information system applications, discussing photomultipliers, photodiodes, photoresistors, avalanche and photopotametric diodes response and bandwidth characteristics

08 p1169 A72-21844

Channel electron multiplier arrays for double proximity focusing image intensifier design

08 p1171 A72-21973

Polarization effect on sensitivity of photocells and photomultipliers with/without cover glass

09 p1289 A72-23670

Ultramicromanometer based on photomultiplier for low pressure Penning discharge light flux emission measurement

10 p1480 A72-24208

Multichannel photomultiplier matrix anode design for various tube types fabrication

11 p1631 A72-25687

Compact photomultiplier housing with controlled cooling, discussing temperature control and measurement

12 p1806 A72-27265

Low energy particles spectrometer channels calibration for satellite auroral observation, discussing photomultiplier detector properties

13 p1960 A72-29843

Molnaya 1 satellite slow neutron monitor with photomultiplier scanned scintillator, noting limiting effect of geomagnetic perturbations

14 p2105 A72-30628

Operating conditions of photometers for optimum photomultiplier photon counting photometry, considering measurement precision dependence on experimental parameters

14 p2105 A72-30733

Instrumental errors estimation in photomultipliers and photodiodes during measurement of short time phase fluctuations in quasi-harmonic signals

15 p2246 A72-31424

Photomultiplier negative electron affinity emitter materials photosensitivity performance, considering Cs-activated GaP and applications for low light level detection

15 p2291 A72-31531

Electron-optical parameters effect on GaP/Cs/dynode photomultipliers time response characteristics, describing computer simulation and pulse response measurement techniques

15 p2234 A72-31532

Ceramic envelope electron multiplier design with hemispherically shaped dynodes, discussing electron optics, photosensitivity and applications

15 p2234 A72-31533

Miniature high gain photomultiplier for pulse counting applications in close-packed arrays and mosaics for scintillation imaging and spectrum analyzing

15 p2234 A72-31534

Cerenkov counter for astronomical observatory high energy cosmic ray experiments, discussing UV-reflecting paint, radiator and photomultiplier positioning improvements

15 p2234 A72-31536

EUV open channel photomultipliers satellite-borne long term performance degradation, attributing sensitivity loss to grating contamination

15 p2235 A72-31645

Unmodulated solar radiation effect on electro-optical photoreceptors voltage sensitivity, noting photomultipliers and silicon photodiodes

15 p2237 A72-32121

Excess white noise source in photomultiplier as function of temperature from voltage, intensity and ion pulse measurements, noting effect on photon counting statistics

15 p2207 A72-32238

Scintillation telescopes for muon angular distribution, designing test device for photomultiplier tubes selection

17 p2556 A72-35437

Use of a loaded silicon elastomer for insulation of channel multipliers of onboard electrons

18 p2670 A72-37140

Photon count circuit conjugation with photomultiplier for spectrometric measurement of lines emitted by atomic barium jet excited by slow electron beam

19 p2799 A72-37671

Photocathode relative sensitivity spatial distribution as function of wavelength, noting maximum shift from photoeffect contribution to photomultiplier current

19 p2800 A72-37821

Effect of pulsed voltages fed into the external modulating electrode on the threshold sensitivity of a photomultiplier

19 p2774 A72-38415

The employment of a novel Quantacon photomultiplier for increasing the sensitivity of older flame photometers in the near IR

20 p2927 A72-39697

PHOTON ABSORPTION

U ELECTROMAGNETIC ABSORPTION

PHOTON BEAMS

NT LIGHT BEAMS

Two photon absorption of ruby laser emission in mixed zinc cadmium sulfide crystals, plotting laser light damping vs beam power density

09 p1322 A72-22212

Pulsed carbon dioxide laser output monitor with Ge cylinder using photon drag effect to measure radiation pulse profile

09 p1326 A72-23389

Superradiant laser stationary behavior and photon statistics, solving Fokker-Planck equation for quantum mechanical distribution function in Hilbert space of atomic system

10 p1514 A72-24247

Multiphoton ionization of atomic hydrogen in the presence of an intense electromagnetic field.

17 p2586 A72-35827

German monograph - A method for the determination of the differential albedo for photons in the range from 1-17 MeV

19 p2836 A72-37484

Photon count circuit conjugation with photomultiplier for spectrometric measurement of lines emitted by atomic barium jet excited by slow electron beam

19 p2799 A72-37671

Investigation of laser light spatial correlation by the photon coincidence method

21 p3064 A72-41691

PHOTON DENSITY

Monte Carlo calculations of lunar photon albedo from galactic and solar proton bombardment for lunar soil composition information

07 p1070 A72-19139

Relativistic beaming from periodically orbiting light point source in terms of photon fluxes, relating to pulsar radiation theory

19 p2835 A72-38697

Investigation by the photon count method of the statistical properties of the emission of a laser operating in the mode of several axial oscillations

21 p3063 A72-40784

PHOTON-ELECTRON INTERACTION

Soviet monograph on electron flux nonlinear interaction with slow electromagnetic waves in TWT, discussing output power and efficiency increase

03 p0333 A72-13949

Intraband multiphoton conduction-electron transfer probability in semiconductor under electromagnetic wave action in uniform magnetic field

08 p1216 A72-21066

Shock wave structure in radiation spectrum of photon-electron interaction via induced Compton effect

12 p1848 A72-27056

Photon trapping in photosystem II of photosynthesis - The fluorescence rise curve in the presence of 3-/3,4-dichlorophenyl/-1,1-dimethylurea.

17 p2505 A72-35761

Equations for electron and high-energy photon transfers in magnetic fields

19 p2837 A72-38059

Shock wave structure in radiation spectrum of photon-electron interaction via induced Compton effect

24 p3431 A72-45709

PHOTONIC PROPULSION

Interstellar flight conditions in photon vehicle

05 p0713 A72-15979

PHOTONS

NT LIGHT BEAMS

Optical radar target range estimation, determining suboptimum post detection signal processing algorithms in photon counting mode

01 p0024 A72-10047

Series summations for perturbation theory of multiple photon ionization probabilities of atoms applied to hydrogen and helium

03 p0391 A72-13080

Fluctuation theory for single mode laser detuning effect on photon intensity and spectral line width

03 p0368 A72-13671

Two photon method of measuring ultrashort pulses and nonlinear optical effectiveness of lasers in synchronized mode

03 p0369 A72-14063

Two-photon time distribution in mixture of light from He-Ne laser and Gaussian source of same central frequency

05 p0669 A72-16691

Multilayer X ray chamber for gamma quanta energy spectrum determination by primary photon impact and absorber calorimetric methods

06 p0869 A72-17266

Black radiation kinetics of photon thermalization in body cavity in static thermodynamic equilibrium

06 p0847 A72-17732

Photon radiative exit from scattering isothermal atmosphere containing atoms with two energy levels

06 p0848 A72-18051

Quantum optics analysis of light propagation and photon flux fluctuations in medium with random dielectric constant inhomogeneities

07 p0938 A72-18912

Photon counting system for low level radiation measurement in UV visible region, discussing simplifications

07 p0983 A72-19133

Lattice and photon components of thermal conductivity of cerium dioxide at high temperatures

07 p1044 A72-19881

Nitrogen dioxide photodissociation by pulsed ruby laser at 6943 A, noting single photon energy relationship to dissociation energy

07 p0937 A72-20676

Image photon counting technique using digital accumulation of individual events registered by high gain image intensifier and TV camera and stored in on-line computer

08 p1170 A72-21960

Finite rest masses of wave quanta in material media, discussing dispersion and Einstein formulas equivalence, Doppler effect, gravitational red shift and radio photon trajectories

10 p1512 A72-24790

Black radiation kinetics of photon thermalization in body cavity in static thermodynamic equilibrium

11 p1685 A72-25336

Image tube scanner photon loss probability, considering effects of system gain, aperture time and sweep rate via computer simulation

11 p1631 A72-25694

Evanescent photons absorption and emission in light excited molecules fluorescence
11 p1691 A72-26745

Angular annihilation photon distribution curves from positron-electron annihilation method for metallic phase interaction with crystal lattice in synthetic diamonds
12 p1833 A72-27764

Combined photon and particle diffusion of two level system with ground and excited atomic states and photon emission-formed radiation field
13 p2001 A72-28509

Perturbation theory of hydrogen and helium atoms multiphoton ionization probabilities, proposing series summation method
13 p2007 A72-29430

Photon correlation spectrometer for laboratory wind tunnel measurement of laser Doppler signals backscattered from dust particles
14 p2111 A72-30854

Joint photon-count probability distribution measurement of electric field amplitude correlation function for random-Gaussian light fields produced by laser beam scattering
15 p2280 A72-31378

Lunar laser ranging experiment single photon detection and nanosecond timing precision
15 p2233 A72-31530

Photon loss coefficients and gain measurement in CdS electron beam pumped lasers, noting absorption mechanism and efficiency
15 p2246 A72-31668

Nonionizing component of underground high energy cosmic radiation investigated with anticoincidence screen and counters, noting bremsstrahlung as photons source
15 p2301 A72-32232

Circularly polarized photon echo decay measurement as function of Cr concentration in ruby, noting relationships to temperature, pulse separation and external magnetic field
15 p2295 A72-32545

Born approximation for resonance bremsstrahlung emission and photon absorption cross sections at electron-ion scattering, solving multiparticle problem
15 p2279 A72-32697

Astronomical objects spectral lines red shift interpretation in terms of noncosmological origin and photon-photon interactions
16 p2450 A72-32863

Spectral line width measurement accuracy based on digital autocorrelation of photon counting fluctuations, noting light field and photoelectric process limiting effects
16 p2357 A72-32949

Q switched laser operation with electro-optic switch mechanism, measuring initial photon number per mode of Nd-glass and Nd-YAG lasers
16 p2399 A72-33014

A photon rest mass and the dispersion of longitudinal electric waves in interstellar space.
18 p2728 A72-36923

Two quantum induced photon-plasmon transition probability for hydrogen atom in processes of nebulae and stellar chromospheres
19 p2837 A72-38058

Macroscopic photon echo polarization and radiation intensity in Cr ion doped ruby laser stimulated by coherent light pulses
19 p2814 A72-38780

High energy particle and photon orbital and vortical motions in Kerr metric outside equatorial plane in gravitational field
20 p2953 A72-39341

Longitudinal electric waves absorption in interstellar space due to electron-heavy particle collisions, considering photon rest mass
20 p2969 A72-39348

Quantum optics analysis of light propagation and photon flux fluctuations in medium with random dielectric constant inhomogeneities
20 p2932 A72-39378

Effect of spatio-temporal laser light structure on multiphoton ionization.
20 p2934 A72-39814

Group theory for spontaneous coherent radiation of multilevel sources, noting angular distribution of photon echo effects
23 p3295 A72-43306

Theory of dispersion in relation to light shifts.
24 p3409 A72-44921

PHOTONUCLEAR REACTIONS
Device for studying the photonuclear interaction of superhigh-energy muons
23 p3291 A72-44440

Multiphoton dissociation, predissociation, and autoionization of the hydrogen molecule.
24 p3427 A72-45476

PHOTOOXIDATION
Linear four step model for photosynthetic molecular oxygen evolution, discussing oxidation states, flash yield oscillation damping and deactivation
06 p0770 A72-18424

Vehicle components oxidation in thermal control coatings, investigating resistance to oxidation by UV photoproducted ZnO electronic holes
[AIAA PAPER 72-264] 11 p1699 A72-25207

PHOTOPEAK
Numerical integration of gamma ray photopeak digital data from nondestructive activation analysis
20 p2899 A72-39834

PHOTOPIEZOELECTRICITY
U PHOTOELECTRICITY
U PIEZOELECTRICITY
PHOTOPLASTICITY
CdTe single crystals photoplastic characteristics, detailing illumination effect on yield stress and resistivity
15 p2294 A72-32501

Stress analysis in two dimensional bending process using the photo-rheological stress analysis.
22 p3183 A72-42483

PHOTOPRODUCTION
Charge carrier photoproduction and energy structure of trans-bis-indonylene (TBB)/ semiconductor thin films
11 p1700 A72-25784

PHOTORECEPTORS
Nonmammalian vertebrate retinal receptor rods and cones birefringence as function of fixation, temperature and immersing medium
01 p0014 A72-10862

Flavin photoreceptor participation in contemporary organism metabolic systems
04 p0469 A72-14781

Optical image transfer functions characteristics and modulation in isolated retinas and retinal receptors, noting similarity to optical fiber bundles
07 p0916 A72-19027

Coincidence model tests of photoperiodic time measurement relation to circadian system in moth *Pectinophora gossypiella*, using induction by skeleton photoperiods and light cycles
07 p0919 A72-19533

Phase shifting effect of light on circadian rhythm and photoreceptive pigment location in *Drosophila* in postpupation stages
07 p0919 A72-19536

Selective chromatic adaptation in cone photoreceptors of cynomolgous macaque monkeys, using late receptor potential as response index
13 p1907 A72-29967

Unmodulated solar radiation effect on electro-optical photoreceptors voltage sensitivity, noting photomultipliers and silicon photodiodes
15 p2237 A72-32121

Lamellar structure and rhodopsin location in bleached and unbleached rod photoreceptor membranes of dark adapted frog retinas by X ray diffraction study
15 p2186 A72-32199

Semiconductor quadrupole optical links consisting of electroluminescent diode and photoreceptor, discussing operation and design principles
17 p2594 A72-34333

The distribution of the long wave photoreceptors in the compound eye of the honey bee as revealed by selective osmic staining.
17 p2500 A72-34877

Electroretinographic evidence for a photopic system in the rat.
17 p2500 A72-34878

Fly colour vision.
18 p2651 A72-36609

Reliability of semiconductor optoelectronic components - Analysis of the long-term behavior
18 p2670 A72-37138

Isolated retina receptor potential amplitude relation to visual pigment bleaching kinetics, indicating excitation-inhibition receptor response generation mechanism
19 p2756 A72-37830

Threshold excitation, temporal summation, and impulse response function in the retina of the cat - Temporal receptive fields of retinal ganglion cells
19 p2758 A72-38648

The photopigment bleaching hypothesis of complementary after-images - A psychophysical test.
23 p3258 A72-44376

Component analysis of electroretinogram in dark and light adapted sheep eye, noting rod and cone receptor potentials and transient and dc responses
23 p3261 A72-44382

Light absorption by visual pigment in photoreceptor, noting Airy disk diameter effect
23 p3259 A72-44388

Small field tritanopia of central fovea in terms of dichromatic area color response mechanism and adaptation speed
23 p3259 A72-44390

Optical directionality of retinal receptors and corresponding points. I - Nasal-temporal asymmetry of retinal spatial values and orientation of receptors: Are the corresponding points cones. II - Variation of form of the experimental horoptera, and possibility of reorganization of the retinal correspondence according to the orientation of the eyes
24 p3371 A72-44907

PHOTOSENSITIVITY
Functional organization of the periphery effect in retinal ganglion cells.
24 p3371 A72-44908

PHOTORECONNAISSANCE
Computer image processing for photoreconnaissance, enhancement and calibration applications
01 p0070 A72-10870

Microwave and IR radiometer surveillance of oil spills, discussing sources tracking, sea surface oil volume and flow rate determination and terminal location prediction
05 p0658 A72-16599

Geomorphological and thermographic reconnaissance of Central Sahara, using orbital photographs
09 p1303 A72-23297

Computer processed image enhancement applications to spacecraft returned photoreconnaissance, discussing data transmission and resolution vs recognition and color quality
17 p2520 A72-34408

Photomorphic units for regional analysis from hyperaltitude and spacecraft remote sensing data
18 p2690 A72-36321

PHOTOREDUCTION
U PHOTOCHEMICAL REACTIONS
U REDUCTION [CHEMISTRY]
PHOTOSENSITIVITY
U PHOTOCONDUCTIVITY
PHOTORESISTORS
U PHOTOCONDUCTORS
PHOTOSENSITIVITY
NT LIGHT ADAPTATION
NT PHOTOTROPISM
Photosensitive MOS devices array as converters performing optical image data analysis, considering sensor sensitivity regulation
02 p0193 A72-12342

Photochemical electron transfer evolution models, noting titanium and zinc oxides as photosensitizers
04 p0484 A72-14777

Pulsed ruby laser and photopolymer materials applications to holography, considering research programs for surmounting difficulties
06 p0813 A72-17427

Silicon Schottky barrier photodiodes development for photographic, photometric and analytical instrumentation, comparing sensitivity, time response and fatigue characteristics with classical photodetectors
06 p0813 A72-17428

Real time hologram photosensitive materials, determining power requirements and resolution for diffraction gratings in saturable absorbers and absorbing liquids
07 p0984 A72-19397

Scanned reference beam holography techniques with limited exposure time, noting use of hypersensitized photographic plates
07 p0985 A72-19418

Spectral photosensitivities for phase shifting of circadian body temperature rhythms in pocket mice
07 p0919 A72-19535

Semiconductor structure investigation by measuring photoresponses to optical probe motion
07 p1049 A72-19963

Multipole network characteristics of optical link assemblies [optons/ using photosensitive element and light source
08 p1139 A72-21057

Photosensitive MOS devices array as converters performing optical image data analysis, considering sensor sensitivity regulation
08 p1143 A72-21948

Sintered cadmium sulfide films microstructure analyzed by X rays, discussing structural changes effects on dark resistance and photosensitivity
09 p1366 A72-22414

Absorption spectra and detection sensitivity enhancement by organic dye laser quenching with broadband cavity
09 p1323 A72-22601

Incoherently light radiating object and background light focusing on photosensitive mosaic, observing linear restoration by comparison of mean square error with Wiener filter theory
09 p1350 A72-22611

Polarization effect on sensitivity of photocells and photomultipliers with/without cover glass
09 p1289 A72-23670

Photopolymers formulations and processing for holography applications, discussing sensitivity, keeping and reciprocity properties
10 p1482 A72-24566

Photostimulated potentials of human visual cortex, determining retinal macular area involvement
10 p1426 A72-24786

Multiple exposure hologram recording on photosensitive plate for extended reference-beam source
12 p1808 A72-27601

Photosensitive polymeric films for hologram recording with high diffraction efficiency, requiring low laser powers
12 p1808 A72-27602

Color discrimination threshold determination for spectral sensitivity in subjects with congenital color vision disorders
13 p1903 A72-28763

Solar photosensitive elements prepared p-type GaAs liquid epitaxy on n-type GaAs substrate, measuring dark and light I-V characteristics and spectral response

14 p2142 A72-30225

High resistance n-type InP crystals electrical conductivity and photoconductivity characteristics at 80 K, discussing photosensitivity spectral distribution and temperature dependence

15 p2290 A72-31371

Photomultiplier negative electron affinity emitter materials photosensitivity performance, considering Cs-activated GaP and applications for low light level detection

15 p2291 A72-31531

Ceramic envelope electron multiplier design with hemispherically shaped dynodes, discussing electron optics, photosensitivity and applications

15 p2234 A72-31533

Celestial Thomson-scattering X ray polarimeter design for OSO-1, optimizing sensitivity in 4-24 keV energy range by Monte Carlo simulation computer program

15 p2234 A72-31540

EUV open channel photomultipliers satellite-borne long term performance degradation, attributing sensitivity loss to grating contamination

15 p2235 A72-31645

High contrast and sensitivity thermal erase cathodochromic sodalite for storage and display applications, measuring contrast ratio versus electron beam flux

15 p2240 A72-32362

Holograms on bismuth and paraffin thin films with pulsed high power TEA carbon dioxide IR laser, discussing photosensitivity and capability for interferometric measurement

16 p2392 A72-33390

Blue green algae *Anacystis nidulans* UV light-sensitive mutants photorecovery capacity following irradiation

16 p2356 A72-33673

Semiconductor optoelectronic devices, discussing light emitting indicator diodes, data display systems, photosensitive arrays and optical data transmission links

17 p2594 A72-34332

Colorimetric photometric matching tests, showing subject differences in parafoveal spectral sensitivity indicated by photopic curve peaks

17 p2508 A72-34882

Pyroelectric radiation detector with ferroelectric crystals, discussing operation mode, construction, sensitivity and IR applications

17 p2530 A72-35445

Photocathode relative sensitivity spectral distribution as function of wavelength, noting maximum shift from photoeffect contribution to photomultiplier current

19 p2800 A72-37821

Temperature dependence of electroconductivity and photosensitivity in CdS films

20 p2959 A72-39223

The employment of a novel Quantacount photomultiplier for increasing the sensitivity of older flame photometers in the near IR

20 p2927 A72-39697

Investigation of certain complex compounds of triaryl phosphines/phosphites/ in optically sensitized photographic emulsions

21 p3052 A72-40390

Characteristics of the low temperature effect of an electric field on the sensitivity of photographic emulsions

21 p3053 A72-40391

Spectral sensitivity after prolonged intense spectral light exposure of rhesus monkey corneas, demonstrating long term loss of cone photopigment response

21 p3000 A72-40739

Electronic superregeneration in semiconductor photosensitive structures with negative resistance

23 p3268 A72-43345

Sensitivity of the human ERG and VECP to sinusoidally modulated light

23 p3258 A72-44385

Visual sensitivity measurement in retinal areas with stepwise change from one monochromatic light to another, discussing eye movements effects and perception thresholds

23 p3258 A72-44385

PHOTOSENSORS

U PHOTOELECTRICITY

U RADIATION MEASURING INSTRUMENTS

PHOTOSPHERE

Brightness correlation and mapping of weak photospheric magnetic fields and faculae using CN 3883-A spectroheliograms

03 p0414 A72-12927

Prominent Zeeman multiplets in photosphere, penumbra, umbra and sunspot spectra, presenting ratios for temperature sensitivity measurements

03 p0415 A72-12933

Solar coronal magnetic field large scale structure relation to photospheric and interplanetary sector patterns

[AD-734628]

03 p0422 A72-13207

Kitt Peak 40 channel magnetograph using fiber optic probe for spectral and spatial resolution in weak photospheric field detection

03 p0356 A72-13282

Solar magnetic field configuration evolution in active region of photosphere, using solar magnetograph

03 p0428 A72-13305

Magnetic field fine structure in undisturbed photosphere for high latitude solar regions, constructing model to explain magnetograph response

03 p0428 A72-13306

Magnetograph scans of solar disk center supergranulation, showing downdrafts relation to magnetic field strength and chromosphere and photosphere brightness

03 p0429 A72-13307

High resolution magnetographic and spectrographic observations of plage fields and photospheric effects in weakly active regions

03 p0429 A72-13308

Zeeman spectroheliograms of photospheric magnetic fields in Ca I 6102.7 Å line

03 p0430 A72-13317

Five-minute plasma oscillations in solar photospheric and low chromospheric magnetic fields, discussing evidence, properties and production mechanism

03 p0430 A72-13319

H alpha solar flare association with photospheric magnetic field patterns, discussing flare insertion and relation to magnetic structure evolution

03 p0410 A72-13320

Corona X ray emitting structures comparison to photospheric magnetic field distribution

03 p0410 A72-13324

Photospheric vortex motions effect on flare productive magnetic patterns in solar active regions

03 p0411 A72-13330

Solar magnetic field distribution in sunspots surface layers, considering photospheric three dimensional magnetohydrostatic model

03 p0431 A72-13337

Solar magnetic field origin in fine structure elements of photosphere and sunspots

03 p0431 A72-13340

Solar magnetic field sector boundaries, discussing photospheric field direction, activity regions, flares, coronal enhancements, faculae and geomagnetic response

03 p0433 A72-13359

Solar photospheric facula blue light limb photographs, determining spatial variation in contrast levels

03 p0434 A72-13494

Solar magnetic fields small scale structure with emphasis on photospheric measurements, discussing sunspots fields

03 p0437 A72-13869

Rotating dipole sector structure of interplanetary and solar photospheric magnetic fields from spacecraft observations

03 p0437 A72-13871

Missing solar UV opacity from band adsorption coefficient comparison between photospheric diatomic molecules and metals and hydrogen

04 p0579 A72-15327

Goldberg-Unno method accuracy for solar photospheric microturbulent velocities, discussing correction for damping effect and LTE deviation

05 p0718 A72-16503

Intensity variations of CN photospheric and K line chromospheric network with time

05 p0718 A72-16505

Temperature variation with latitude in upper solar photosphere from photoelectric meridional and equatorial limb-darkening scans

05 p0719 A72-16710

Temperature and density fluctuations in photosphere from Fe and Mg line intensities, noting variations due to granulation in solar atmosphere model

06 p0876 A72-17579

Solar magnetic field filamentary structure based on analysis of photospheric photographs and presumptive spectrograms obtained during Soviet stratospheric observatory flight

06 p0886 A72-18100

Solar photosphere active regions and large scale flow patterns from Greenwich sunspot statistics

07 p1068 A72-18886

Sunspot umbra spectrophotometric scans with spatial cancellation techniques, finding 4200 K umbral temperature with 0.60 photosphere contrast

07 p1069 A72-19081

Solar MgH isotopic abundance ratios and photospheric lines, correcting previous overestimation for sunspot spectra analyses

07 p1071 A72-19179

Turbulent micro and macromotion velocities in solar photosphere from CN molecule vibrational band line contours

07 p1077 A72-19810

Solar energy sources and dissipation and emission mechanisms, considering radiant flux of convection zone and photosphere and solar variabilities

07 p1078 A72-20005

Electroconductivity distribution and vertical gradients in photospheric layers of solar active region, using approximate model

07 p1082 A72-20293

Three dimensional structure of interplanetary magnetic field from observed line of sight field component in solar photosphere

07 p1082 A72-20379

Solar corona structure during 22 September 1968 total eclipse noting N-S asymmetry and correspondence of large details to formations in photosphere and chromosphere

08 p1228 A72-20825

Solar rotation as function of heliographic altitude from measurements of Fe and H lines, sunspots and magnetic field in photosphere

10 p1541 A72-24569

Active chromosphere coupling to magnetic field determined by subphotospheric motions, discussing active regions rotation period

11 p1720 A72-26117

New and old sunspot groups proper motions in large scale flow of solar photosphere investigated as function of age, noting angular momentum transport direction

13 p2036 A72-28834

Outer corona and interplanetary space magnetic fields calculated from photosphere magnetic fields measured during 7 March 1970 solar eclipse

13 p2041 A72-29528

Spectral line variations in transition region from photosphere to chromosphere during March 1970 solar eclipse

13 p2041 A72-29530

Photospheric network, magnetic fields, Ca emission and continuum faculae from multichannel magnetograph observations

13 p2045 A72-29705

Observed continuous solar spectrum intensity comparison with photospheric models, noting bend-off due to veiled line haze

13 p2047 A72-29734

Solar photosphere velocity field photoelectric measurements, emphasizing long periods and low spatial wave numbers in deep layers

13 p2048 A72-29927

Solar photospheric fluctuations, applying fast Fourier transform to power coherence and phase spectra calculations

13 p2049 A72-29928

Undisturbed and active solar photospheric turbulent velocity determination by comparing half widths of observed weak Fraunhofer line profiles with model calculation

13 p2049 A72-29929

Solar magnetogram recorded mean photospheric magnetic field cross correlation with interplanetary magnetic field

13 p2049 A72-29935

Pleiades slow flareup in photosphere, comparing with Orion flare stars

15 p2304 A72-31329

Solar instruments and methods for photosphere magnetic field measurement, noting spectroheliographic mapping in violet spectral region

15 p2306 A72-31647

Photoelectric measurement of solar photosphere pole-equator temperature differences, analyzing statistical and systematic errors

15 p2317 A72-32770

Solar photosphere and low chromosphere spectral lines non-LTE empirical analysis, relating coefficients of departure from LTE to elemental state temperatures

15 p2317 A72-32771

High time resolution observations of photospheric velocity field, interpreting short period oscillations origin as result of combined image motion and Doppler velocity gradients

15 p2317 A72-32776

Solar photospheric resonance oscillation power spectrum observation, noting statistical significance

15 p2317 A72-32777

Solar rotational properties in photosphere, solar wind and magnetic fields, including long lived sunspots and magnetic dipole observations

16 p2459 A72-33917

Spectral analyses of solar photospheric fluctuations.

II.

17 p2608 A72-35081

A physical mechanism for the production of solar flares.

17 p2608 A72-35088

Photographic magnetograms comparison with H alpha filtergrams, investigating chromospheric features relationship to photospheric magnetic fields

17 p2616 A72-35702

Doppler shift of solar photospheric spectral lines related to downward motions over plages

17 p2617 A72-35705

Turbulent micro and macromotion velocities in solar photosphere from CN molecule vibrational band line contours

17 p2617 A72-35735

New measurements of the polarization of photo-spheric light near the solar limb
18 p2727 A72-36739

Photospheric faculae brightness influence on solar gravitational oblateness determination, considering criticism of Dicke-Goldenberg argument on Mercury excess perihelion motion
19 p2855 A72-37239

Radial velocities and brightness distribution in active and quiet solar atmosphere from magnetograph measurements, discussing motion directions in photosphere and chromosphere
19 p2858 A72-37818

Initial phase in the development of activity centers in the photosphere
19 p2860 A72-37951

Correlation of polarization in type III solar radio bursts at frequencies of 23.5 and 30 MHz
19 p2851 A72-38065

Energy spectrum of small scale solar magnetic fields.
20 p2971 A72-39765

Investigation of physical conditions in the solar photosphere by a curve of growth technique
21 p3102 A72-40097

Thermal oscillations in the high solar photosphere.
21 p3107 A72-41275

A method to calculate electric currents in quiescent prominences.
21 p3108 A72-41282

Behavior of carbon monoxide in the upper photosphere
21 p3114 A72-41777

Solar photospheric fluctuations measured from time sequence of Sacramento Peak Observatory spectrograms, using power, coherence and phase spectra computed by fast Fourier transform
22 p3221 A72-42029

Micro- and macroturbulent motions and the velocity spectrum of the solar photosphere.
22 p3221 A72-42030

Low abundance of solar photosphere iron from Fe I excitation and ionization computations, showing LTE departure effects on spectral lines
22 p3228 A72-42569

Free oscillations of the sun and their possible stimulation by solar flares.
22 p3219 A72-42570

PHOTOSYNTHESIS
Chlorella growth rate model, presenting specific photosynthetic and urea and carbon dioxide utilization rates
02 p0160 A72-12038

Acid base equilibrium effects on chlorophyll primary photosynthetic regulating mechanism, considering electron transfer to NADP and ATP formation
04 p0468 A72-14778

Pigment system and primary photosynthesis evolution, using comparative analysis of bacteriochlorophyll, bacterioviridin and chlorophyll
04 p0469 A72-14780

Bacterial respiration through oxidative phosphorylation origin hypotheses, discussing photosynthesis and sulfate respiration in anoxygenic atmosphere and thiobacillus and aerobe evolution in oxygen atmosphere
04 p0470 A72-14795

Biochemical functions of organisms in evolution of biosphere, presenting redox reactions, elementary compositions and metal compounds role in photosynthesis
04 p0470 A72-14796

Manganese catalyst photoactivation process for oxygen photosynthetic evolution investigated in Mn-deficient Anacystis nidulans cells
05 p0624 A72-15811

Linear four step model for photosynthetic molecular oxygen evolution, discussing oxidation states, flash yield oscillation damping and deactivation
06 p0770 A72-18424

Photon trapping in photosystem II of photosynthesis - The fluorescence rise curve in the presence of 3-/3,4-dichlorophenyl/-1,1-dimethylurea.
17 p2505 A72-35761

Thermodynamic properties and mathematical modeling of complex biological systems, considering energy and mass exchange in photosynthesizing organisms for exobiological life support
20 p2891 A72-38960

The presence of P700 in chloroplast fragments prepared by short time incubation with Triton X-100.
23 p3258 A72-44325

PHOTOTHERMOTROPISM
U ANISOTROPY
U PHOTOTROPISM
U TEMPERATURE EFFECTS

PHOTOTRANSISTORS
Physical and operational characteristics of Si and Ge photoelectric semiconductor devices with p-n junctions, discussing photodiodes, phototransistors, mosaic arrays and coordinate sensitive structures
08 p1139 A72-21055

Solid state array camera based on diffused junction phototransistors, discussing sensor technology and fabrication
12 p1810 A72-27931

The field-effect modified transistor - A high-responsivity photosensor.
23 p3273 A72-44455

PHOTOTROPISM
Phototropic substance effect on spatial structure of passive Q switched ruby laser emission, considering gallium phthalocyanine solution
02 p0239 A72-12568

Phototropic borosilicate glass optical density variation by exposure to UV or blue light, considering utilization for digital data storage and/or cathode ray tubes
22 p3180 A72-42941

PHOTOTUBES
NT PHOTOMULTIPLIER TUBES

PHOTOVISCOELASTICITY
Slow viscous flow shear stress and velocity field analysis, using photoviscosity and bubble technique [SESA PAPER 1902]
02 p0201 A72-11508

PHOTOVOLTAGES
Surface energy states of CdS basal plane based on photovoltage inversion effect model
03 p0400 A72-12991

PHOTOVOLTAIC CELLS
Copper sulfide-cadmium sulfide single crystal photovoltaic heterojunctions, showing optically induced and thermal effects on short circuit current degradation
03 p0389 A72-13603

Cadmium mercury telluride photovoltaic cell features, noting gigahertz range frequency response, heterodyne sensitivity, operating temperature and nonstoichiometric p-n junction preparation
07 p1003 A72-19224

IR radiation detection by microwave biased photoconductor, lead-tin telluride photovoltaic detector and thermal imaging pyroelectric detector and array system
07 p1034 A72-19425

French R and D programs on Si and various thin film photovoltaic solar cells, considering efficiency, reliability, and weight and cost reduction problems
12 p1756 A72-28002

Organic semiconductors for photovoltaic cell applications, discussing structural characteristics, improved charge transfer and crystallographic conductivity mechanisms
12 p1856 A72-28015

Determination of the parameters of minority carriers in semiconductor photocells from a spectral sensitivity curve
17 p2498 A72-35512

Reliability of HgTe-CdTe photovoltaic detectors
18 p2670 A72-37139

Effects of impurities on gamma-irradiated silicon crystal examined by photovoltaic effect of p-n junction diode.
21 p3097 A72-40693

Photovoltaic properties of single-crystal CdS-Cu2S cells.
22 p3214 A72-42457

PHOTOVOLTAIC EFFECT
Carrier mobility measurement in inhomogeneous semiconductors based on bulk photovoltaic and photomagnetolectric effects
03 p0402 A72-13862

Heterojunction p-GaAs-n-ZnSe diodes electrical and photovoltaic properties, showing space charge limited current effects
11 p1606 A72-26624

Photovoltaic effects in solar cell p-n homojunctions and heterojunctions at low and high excitation levels
12 p1855 A72-28006

Photovoltaic effect and energy band model of solar cell cadmium-sulfide-copper-disulfide heterojunctions
12 p1855 A72-28007

Low photon IR photovoltaic response of CdS-metal junction, noting energy conversion efficiency
12 p1855 A72-28009

Photovoltaic effects in CdS films evaporated onto barium titanate single crystal and ceramic ferroelectric substrates
12 p1856 A72-28014

Proton and electron radiation effects on silicon solar cells electric and photovoltaic properties, determining damage coefficients via minority carriers diffusion length measurement
12 p1759 A72-28045

Trapped charge effect on photovoltaic properties of copper sulfide-cadmium sulfide single crystal heterojunction in terms of tunneling by photocapacitance technique
15 p2294 A72-32520

Interpretation of steady-state surface photovoltage measurements in epitaxial semiconductor layers.
22 p3215 A72-43087

Heterodyne, microwave bias and pyroelectric photon infrared detectors, noting mixed crystal photoconductive and photovoltaic detectors
23 p3291 A72-44392

PHTHALATES
Shear modulus of liquids at elastohydrodynamic lubrication pressures.
21 p3059 A72-40688

PHTHALOCYANIN
Phototropic substance effect on spatial structure of passive Q switched ruby laser emission, considering gallium phthalocyanine solution
02 p0239 A72-12568

Organic catalysts for oxygen reduction, discussing phthalocyanines, Pfeiffer complexes and porphyrins
16 p2361 A72-33884

Investigation of the lubricant properties of molybdenum disulfide, graphite, and phthalocyanine
19 p2823 A72-38094

PHUGOID OSCILLATIONS
U OSCILLATIONS
U OSCILLATORS
U PITCH (INCLINATION)

PHYSICAL CHEMISTRY
Mercury vapor physicochemical processes kinematics in shock tube, determining electron gas energy balance equations
03 p0395 A72-13572

Fog modification at all temperatures with physicochemical techniques, discussing blowing hygroscopic salts and use of alginates of sodium and marine algae extracts
04 p0543 A72-14696

Irreversible thermodynamics applications to physicochemical and biological stability, including allosteric activation model
04 p0482 A72-14754

Glass network physical properties model, using physical chemistry description of crystal structure without regularly repeating lattice
10 p1502 A72-24735

Physicochemical processes in metal surface layers subjected to contact friction with aircraft fuels presence, noting secondary compounds and thermal oxidation acceleration
12 p1817 A72-28183

Liquid crystals synthesis, physical chemistry and material parameters effects on mesomorphic and electro-optical behavior
15 p2240 A72-32363

General analysis and synthesis of alloys and materials with inhomogeneous physical properties, noting thermal physicochemical methods for laminates and metal powders
16 p2405 A72-33095

Stress-strain state induced by local physicochemical transformations in a layer
22 p3242 A72-43164

PHYSICAL CONSTANTS TESTING REACTOR
U WATER COOLED REACTORS

PHYSICAL ENDURANCE
U PHYSICAL FITNESS

PHYSICAL EXAMINATIONS
Functional diagnostics of teeth condition as pilot health factor in stomatological aviation medicine, discussing caries, parodontosis and aerodontalgia
07 p0922 A72-20374

Physiological evaluation of crew piloting qualities, considering nervous/emotional stress, ECG, arterial pressure and breathing frequency recorded on simulator
07 p0934 A72-20375

Asthmatics evolution and treatments in armed forces aircrews, noting acetylcholine test
08 p1125 A72-21270

Clinical and laboratory examinations of workers exposed to trichlorotrifluoroethane vapor for long range health effects study
10 p1431 A72-24590

Potential coronary heart disease susceptibility indicators in ATC population, using Framingham age/obesity parameters
12 p1764 A72-28265

Diagnostic errors in draft age patients, noting doctor, examination methods, disease type and patient factors and psychosomatic disturbance detection
16 p2359 A72-34149

A model corporate pilot physical program.
20 p2897 A72-39746

PHYSICAL EXERCISE
Acute, short and long term and life long high altitude hypoxia exposure effects on pulmonary gas exchange control and efficiency during physical exercise
01 p0014 A72-10848

Ventricular ectopic arrhythmias from treadmill exercise in patients observed during ECG monitoring
02 p0156 A72-11424

Radiotelemetric cardiorespiratory determinations during submaximal dynamic exercise
02 p0168 A72-12134

Physical exercise effect on ECG atrial recovery wave duration and magnitude in humans with A-V blocks
02 p0166 A72-12891

Exercise ECG correlation to morphological patterns of selective cinecoronary arteriography and ventriculography, revealing significant information on occlusion and stenosis
03 p0314 A72-13178

Xenon 133 method for coronary blood flow measurement during exercise, noting unsuitability for patients with coronary disease

03 p0319 A72-13180

Training effect on oxygen consumption in negative muscular work, considering connective tissue strengthening and muscle viscosity changes

03 p0315 A72-13676

Free oxygen content and diffusion coefficient in adrenalectomized rat skeletal muscles after physical strain

03 p0317 A72-13991

Heat acclimatization, work habituation and exercise effects on body thermoregulation, measuring tympanic temperature, sweat rate and oxygen intake

04 p0472 A72-14896

Serum enzyme activity changes response to constant test exercise, discussing relation to maximum oxygen uptake

04 p0472 A72-14897

Physical conditioning effect on central and peripheral circulatory responses to arm work, measuring cardiac output at 80 percent maximum aerobic power

04 p0473 A72-14900

Peripheral modifications to exercise induced central drive for sweating, determining rates as functions of internal temperature

04 p0479 A72-15212

Daily prolonged exercises effects on human muscle glycogen utilization, noting reduced lactate accumulation and increased free fatty acid levels

04 p0480 A72-15213

Plasma renin activity during supine physical exercise as function of salt loading

04 p0480 A72-15214

Hypertrophic effects of chronic exercise on plasma corticosterone and adrenal cortex in rat

04 p0473 A72-15219

Exercise effects on pulmonary circulation in dogs, measuring pulsatile arterial flow and pressure and vascular input impedance, resistance and hydraulic power

04 p0475 A72-15464

Airline pilot postexercise electrocardiograms, showing S-T segment depression correlation to subsequent coronary heart disease

06 p0768 A72-17881

Electrophysiological responses to maximum exercise in healthy humans from polarcardiographic display of heart vector changes

07 p0916 A72-18891

Maximum aerobic power response and oxygen consumption to training stimulus intensity, duration and frequency, using bicycle ergometer exercise

07 p0916 A72-18965

Maximal oxygen intake prediction in acute moderate hypoxia during exercise, showing heart rate linearity with work load

07 p0916 A72-18966

Hemodynamic response to running exercise stress for aeronautics personnel selection, determining systolic ejection variation measurement and cardiac frequency increase

07 p0927 A72-19242

Acid base balance in arterialized capillary blood in men after maximal short duration exercise

07 p0929 A72-19441

Maximum oxygen intake during exercise on treadmill compared with bicycle ergometer, analyzing circulatory dynamic factors and cardiac output relation to oxygen transport capacity

07 p0922 A72-20251

Human performance and exhaustion predictive model from responses to exercise and environmental stresses, considering circulation, thermal regulation, work load and oxygen pressure effects

07 p0934 A72-20358

Autonomic blockade effects on reflex bradycardia due to phenylephrine induced arterial pressure in man during rest and supine exercise

07 p0925 A72-20688

Rebreathing technique to estimate human mixed venous oxygen and carbon dioxide tension changes at start of exercise under respiratory stress and natural conditions

08 p1122 A72-20883

Environmental chamber tests for ozone exposure effects on human pulmonary function at rest and during bicycle exercise

08 p1122 A72-20884

Oxygen intake and cardiac output measurements during various treadmill and bicycle ergometer exercises, relating exercise type to heart rate and arteriovenous oxygen differences

08 p1123 A72-20885

Acceleration tolerance increase by static forearm muscular contraction exercise comparison to g-suit protection during human centrifuge tests

08 p1114 A72-20887

Muscle blood flow relation to oxygen consumption from measurements during bicycle ergometer exercises, using Xe 133 clearance method

08 p1123 A72-20888

CO hypoxia effect on oxygen transport during exercise, discussing changes in cardiac and respiratory functions and work capacity

08 p1114 A72-20893

Hypoxic and normoxic gas mixture breathing during intense muscular activity, relating oxygen consumption and carbon dioxide elimination magnitudes and motor performance

08 p1121 A72-22081

Human blood serum 11-oxy corticosteroid content after maximum stress exercise, noting heart rate and blood pressure changes

09 p1266 A72-22878

Ventricular and supraventricular arrhythmias incidence during maximal treadmill exercise in normal man, noting age factor and cardiovascular disease presence effects

09 p1266 A72-23272

ECG, physical exercise and drug use in diagnosis and aeromedical evaluation of supraventricular arrhythmias, presenting case histories of pilots with wandering cardiac pacemakers

[AD-740987] 10 p1428 A72-23741

Continuous and intermittent maximal exercise effects on human muscle intracellular and capillary blood pH

10 p1425 A72-24477

Tachycardia role in coronary vascular bed hemodynamic response to severe exercise in dogs

10 p1426 A72-24483

Beta-adrenergic blocking effect on canine coronary and systemic hemodynamic adaptation during treadmill exercise

11 p1579 A72-25802

Bicycle ergometer measurements of thermoregulation input and output under wide range of work load and climatic conditions, deriving correlation equation

11 p1579 A72-25874

Maximal oxygen uptake and heart rate during ladder climbing, inclined treadmill running and cycling ergometer tests

11 p1586 A72-26612

Weight loss due to respiratory tract evaporative water loss during exercise, from humidity change, ventilatory exchange and oxygen uptake data

11 p1586 A72-26613

Speed and mechanical work measurements during knee bending and immediate or delayed leg extension exercise, showing muscle elastic potential energy utilization

11 p1587 A72-26615

Hemodynamic variables relation to coronary blood flow and myocardial oxygen consumption during upright bicycle exercise

11 p1587 A72-26618

Water filled volume and strain gage phethysmography for forearm blood flow measurement during isometric exercise

11 p1587 A72-26622

Physical training effect on rat cardiac function and metabolic response to hypoxia

11 p1581 A72-26701

Exercise role in ventilatory acclimatization to graded hypoxia in goats from carbon dioxide response curve measurements

12 p1762 A72-27727

Hemodynamic response to physical exercise stress in dogs with angiotensin-induced acute arterial hypertension

12 p1764 A72-28216

Stress vectorcardiography quantitative analysis of ECG response to treadmill exercise test to establish diagnosis criteria for coronary heart disease

12 p1775 A72-28282

Plasma protein concentration, volume and hematocrit changes during exercise, bed rest and high forward acceleration

12 p1766 A72-28296

Cardiorespiratory response to breathing dense sulfur fluoride-oxygen mixture under physical exercise conditions

12 p1767 A72-28314

Gas mask-caused air flow resistance effects on respiratory and circulatory response to exercise, assessing maximal oxygen uptake

13 p1906 A72-29818

Red blood cell reserve mobilization in healthy and chronically irradiated dogs after treadmill exercise

14 p2074 A72-30379

Cardiac stroke volume measurements during supine bicycle exercise and recovery period, using indicator-dilution technique

14 p2079 A72-30701

Sweating relation to body temperature after exhaustive exercise for various oxygen uptakes and ambient temperatures

14 p2079 A72-30702

Muscle cell ATP, creatine phosphate and lactate concentration changes relation to oxygen uptake during and after exercise

14 p2080 A72-30705

Exercise cardiometer with heart rate display on beat to beat basis, R wave recognition circuit and noise linear filtering efficiency

14 p2082 A72-31092

Cardiac output and body temperature response to prolonged intermittent exercise

15 p2185 A72-31448

Water loss replacement effect during rest and exercise in high temperature environment thermoregulation experiment

15 p2185 A72-31449

Two compartment analog model of thermoregulation during rest and exercise, considering temperature, heat conductance, sweat rate and oxygen uptake

15 p2185 A72-31450

Cardiac cycle length /RR interval/ and QT interval mathematical relationship from ECG obtained during exercise and recovery periods

15 p2187 A72-32747

Unconditioned /muscular load stimulus/ and conditioned /metronome stimulus/ cardiac reflexes in hypnotic and alert states

16 p2353 A72-32991

Ventilatory peripheral chemoreflex response to hypoxia during physical exercise in native highlanders and altitude-acclimated lowlanders

17 p2499 A72-34345

Myocardial lipid and carbohydrate metabolism in fasting men during prolonged exercise

17 p2499 A72-34347

Exercise capacity in a population of domestic fowl - Effects of selection and training

17 p2499 A72-34726

Work capacity and physiological responses to maximum exercise in 54 year old men in relation to heart disease and cardiovascular hazard studies

17 p2505 A72-35822

Hemodynamic thermoregulatory and sympathoadrenal responses to heat acclimatization in man during supine and upright position exercise

17 p2506 A72-35963

Bradycardia diving reflex to apneic face immersion related to physical exercise

17 p2506 A72-35964

Disproportional changes in hematocrit, plasma volume, and proteins during exercise and bed rest

17 p2506 A72-35966

Effect of nicotinic acid on myocardial metabolism in man at rest and during exercise

17 p2506 A72-35968

Correlation between ergometry, ballistocardiography and coronary angiography in 267 patients

18 p2649 A72-36034

Fluid transfer between blood and tissues during exercise

18 p2650 A72-36560

Left ventricular dynamics during handgrip

19 p2755 A72-37243

Systemic haemodynamics in borderline arterial hypertension - Responses to static exercise before and under the influence of propranolol

19 p2756 A72-37773

Changes of the catecholamine content in the brain of albino rats under overstrain caused by running in a rotating drum

19 p2757 A72-38034

Significance of the nature of an increase in physical strain as it affects the adaptation of an organism to intense muscular activity

20 p2891 A72-38933

Variation of the acetylcholine content and of the cholinesterase activity in the blood under muscular strain

20 p2891 A72-38934

A modified acetylene method for the determination of cardiac output during muscular exercise

20 p2898 A72-39807

Muscle metabolism of ATP, CP, glycogen and lactates at rest and during submaximal and maximal exercise

21 p3005 A72-40421

Muscle metabolism during isometric exercise performed at constant force

21 p3005 A72-40425

Chemical energy transformation to mechanical energy and heat in muscles during exercise, considering energy sources for contraction, oxidations, glycolysis and alactic anaerobic mechanism

21 p3003 A72-41470

Effect of hypoxia and physical activity on plasma enzyme levels in man

21 p3003 A72-41522

Effects of physical exercise on spinal reflectivity in man

21 p3003 A72-41524

Effects of externally imposed mechanical resistance on breathing dense gas at exercise - Mechanics of breathing

22 p3150 A72-42489

Heat strain in hot and humid environments

22 p3150 A72-42492

Speech intelligibility during exercise at normal and increased atmospheric pressures

22 p3150 A72-42496

Heat acclimatization by exercise-induced elevation of body temperature

22 p3151 A72-42741

Analysis of femoral venous blood during maximum muscular exercise

22 p3145 A72-42742

Yield of ischaemic exercise electrocardiograms in relation to exercise intensity in a normal population. 22 p3151 A72-42900

Lung volume changes of people in antihistostatic position in hospital beds for control, exercising and muscle electric-stimulated groups 23 p3256 A72-43918

Physical training as a prophylactic measure against the hypodynamic syndrome 23 p3260 A72-43920

Metabolic changes in healthy humans caused by prolonged bed rest in horizontal position, noting prevention by physical exercises and electric muscle stimulation 23 p3260 A72-43921

Animal studies of effect of chronic exercise on the heart and atherosclerosis - A review. 24 p3370 A72-44563

Changes in certain hemodynamic indices during muscular strain in people with differing capacity to perform work 24 p3370 A72-44591

Changes in the pituitary-thyroid and in the pituitary-gonad systems under conditions of functional loading and of physiological immobilization. 24 p3371 A72-44823

Longevity and cardiovascular mortality among former college athletes. 24 p3374 A72-45689

PHYSICAL FACTORS

Human functional level performance characteristics, noting relationship between spontaneous rhythm diurnal variations in psychic and physical performance 11 p1589 A72-26691

PHYSICAL FITNESS

Screening test for physical fitness on bicycle ergometer, comparing endurance indices derived from heart rate, oxygen consumption, oxygen debt and work rate measurements 01 p0010 A72-10212

Pilots oxygen uptake vs flight time and altitude as indicator of physical condition, noting large fluctuations and differences for individual pilots and different flights 05 p0623 A72-16748

Human tilt tolerance relation to aerobic capacity, weight, height and physical fitness, determining correlation coefficient between heart rate and orthostatic response 10 p1428 A72-23733

Hemodynamic criteria for physical fitness in air-men, discussing age dependent variations in heart beat, arterial pressure and body temperature 11 p1590 A72-26987

Physiological and subjective responses of physically fit young men to combined exercise-carbon dioxide stress tests 12 p1767 A72-28311

Exercise capacity in a population of domestic fowl - Effects of selection and training. 17 p2499 A72-34726

PHYSICAL OPTICS

Book - Introduction to optical electronics. 23 p3295 A72-43650

Exact solution of the equations of molecular optics for refraction and reflection of an electromagnetic wave on a semi-infinite dielectric. 23 p3313 A72-43803

PHYSICAL PROPERTIES

Interstellar medium physical properties and distribution, discussing ionization heating by starlight, cosmic X rays and subcosmic rays 01 p0128 A72-10413

Melting atmosphere, atomizing media and consolidation techniques effects on Co base alloy powder products physical properties 02 p0240 A72-11436

Physical properties of transition metals nitrides, carbonitrides and nitride-based cemented hard alloys, discussing carbides stability in presence of high pressure nitrogen 02 p0241 A72-11450

Physical properties of monocarbides of Zr, Nb and alloys in homogeneity range, explaining electronic structure relationship to composition changes 02 p0241 A72-11453

High speed jet noise source physical properties interpretation by theory and scale-model experiments for supersonic transport aircraft noise suppression problem 02 p0154 A72-11973

Critique of self similar solutions for physical property models of laminar boundary layer separation due to adverse pressure gradients, noting viscosity-enthalpy relation 02 p0204 A72-12265

Space environment simulator with ultrahigh vacuum chamber and UV and corpuscular radiation for material samples physical properties in-situ measurement 02 p0201 A72-12701

Titanium melting, casting and molding techniques, discussing shapes, sizes and physical properties 03 p0370 A72-13100

High strength Ti alloys for aircraft accessories structural materials, comparing room temperature physical properties of ultrahigh tensile steels and other alloys 03 p0373 A72-13617

Physicomechanical properties of metals at crystallization temperatures, considering density, viscosity, strength, hardness, elasticity and creep 03 p0378 A72-14219

Aerodynamic noise measurement, discussing physical units, spectral analysis, conversion and correction formulas 05 p0614 A72-17195

Mechanical, technological and physical properties of steel with and without molybdenum 05 p0679 A72-17204

Co and carbide containing alloys, investigating milling and sintering temperature effects on technological and physical properties 06 p0829 A72-17831

Radio galaxy spectra determination from measurements over various frequencies, noting correlation with physical parameters 06 p0879 A72-17859

Cu contents effect on Ti-Cu alloys physical and mechanical properties, discussing beta phase decomposition during annealing 07 p1012 A72-19574

Liquid polysulfide rubber, discussing fabrication method and physical properties 07 p1024 A72-20603

Physicomechanical properties of steel with oxide, sulfide, silicon, phosphorus and mixed metal-non-metal inclusions 07 p1022 A72-20618

Aluminum plated pyrotechnics physical properties and performance for electroexplosive device applications, describing particle size distribution and loading pressure dependence of density 08 p1221 A72-20772

Physical properties, combustion characteristics and applications of pyrotechnic castable composition for smoke generation 08 p1222 A72-20785

Furan resins and chemically resistant furan-fiberglass composites flame resistance, heat distortion and physical properties at high temperatures 08 p1192 A72-21678

Alicyclic dicarboxylic anhydride structure effects on cured epoxidized novalac resin physical and chemical properties 08 p1193 A72-21695

Soviet papers on imperfections of crystalline structure effects on physical and mechanical properties of metals and alloys, covering radiation damage, microdeformations, X ray investigations, etc 08 p1187 A72-21785

Material properties nonuniformities effect on wound fiber glass reinforced plastic rings and cylinders thermoelastic residual stresses 08 p1196 A72-21858

Fiber orientation effects on physical properties of carbon fiber-epoxy resin composites [PI PAPER 3] 09 p1337 A72-22540

Vacuum and inert gas TOR-1 device for studying physical properties of lunar soil and terrestrial analogs 10 p1478 A72-23754

Hot-stage optical microscopes for microhardness measurements at elevated temperatures, describing techniques to determine heat resistant alloys mechanical and physical properties temperature dependence 10 p1478 A72-23827

General dimensional analysis as extension of conventional/restricted/ dimensional analysis of physical phenomena, using progressive homogeneity law and fundamental magnitudes 10 p1503 A72-23918

Pi-theorem alternative formulation, defining independent dimensionless products in terms of universal constants, governing equations and initially and additionally specified physical quantities 10 p1503 A72-23920

Viking Lander physical properties experiments for Martian soil, studying bearing strength, cohesion, adhesion, grain size, porosity, thermal properties and internal friction 10 p1540 A72-24390

Glass network physical properties model, using physical chemistry description of crystal structure without regularly repeating lattice 10 p1502 A72-24735

Carbohydrate based gelling agent for gas turbine fuel, describing development and chemical and physical properties [ASME PAPER 72-GT-9] 11 p1702 A72-25612

Crash safe turbine fuel to reduce fire probability and severity during aircraft ground crash, investigating physical and chemical properties [ASME PAPER 72-GT-28] 11 p1702 A72-25624

Numerical calculation of temperature distribution and tempering depth for inductive hardening process with automatic material feed, taking into account temperature dependent material properties 11 p1639 A72-25898

Stellar atmospheric structure physical parameters from model atmosphere calculations, applying method to G and K stars 11 p1717 A72-25904

Luna 16 automatic probe drilling experiment, obtaining lunar rocks physicochemical properties for comparison with terrestrial rocks 11 p1613 A72-25938

Mechanical, technological and physical properties of steel with and without molybdenum 11 p1660 A72-26139

Organic and metal matrix composites physical and mechanical properties and application to spacecraft and missile components, considering cost effectiveness 11 p1674 A72-26233

Impact glass-like objects as evidence of meteoritic origin of Lunar Crater /India/, discussing physical, chemical and optical properties 11 p1723 A72-26521

Chemical composition, physical properties, microstructure and production of 1300 kg powder metallurgy forged billets 11 p1644 A72-26845

IMPATT diode and transferred electron Gunn devices for systems applications, comparing thermal noise and physical properties 12 p1788 A72-27295

GaAs semiconductor devices role in microwave communications, discussing physical properties and potential applications 12 p1792 A72-27736

Crystal growth, physical and spectroscopic properties and laser performance of Nd and Ho doped crystals with apatite structure 12 p1825 A72-27927

Fabrication, and physical, mechanical and ablation properties of three dimensional carbon-carbon cylinder composite materials 12 p1834 A72-28086

Ethylene-vinyl acetate-asphalt thermoplastic material properties, filler effects, application methods and commercial uses 12 p1835 A72-28094

Haynes high strength heat resistant Ni-Cr-W alloy metallurgical and structural relationship, mechanical and physical properties, oxidation and corrosion behavior and fabrication processes 13 p1973 A72-28649

Stratospheric aerosols physical properties and chemical composition, discussing various measuring techniques and results 13 p1991 A72-28839

Coastal and inland fog microphysical features, discussing visibility, liquid water content, drop size distributions and haze droplet concentrations 13 p1991 A72-28842

Combined thermal, vibrational and dimensional treatments effect on WC-Co alloy physical and mechanical properties, noting tensile and impact strength increase 13 p1979 A72-29480

Effect on physical and mechanical properties of hard metals due to gas sorption by metallic films spray-coated on surfaces, describing vacuum apparatus 13 p1939 A72-29488

High strength carbon fiber reinforced plastics, discussing fabrication techniques, fiber structural, physical and mechanical properties and potential technological applications 13 p1984 A72-30075

Cobalt-base superalloys powder-metallurgical fabrication techniques and related effects on physical and mechanical properties 13 p1982 A72-30126

Superplastic alloys based on Al, Cu, Zn, Mg, Ti and carbon or stainless steels, discussing macroscopic properties and manufacturing cost reduction 14 p2120 A72-30622

Explosives life limitation due to aging phenomena, discussing chemical and physical processes and environmental effects 14 p2143 A72-30752

Russian papers on light and nonferrous alloys structure and properties covering phase diagrams, alloying effects, reduction, crystallization and recrystallization, solid solutions decomposition, etc 14 p2123 A72-31027

Russian papers on rare earth metals and alloys covering physical properties, phase diagrams and industrial applications 15 p2252 A72-31183

Russian papers on intermetallic compounds covering structure, properties and applications of carbides, nitrides, oxides, phosphides, aluminides, antimonides, arsenides and chalcogenides 15 p2252 A72-31192

Physicochemical properties and composition diagrams of antimonides and arsenides of Zn, Cd, Al, In and Ga 15 p2290 A72-31194

- Epoxide resins for application in composite materials, discussing crosslinking reactions, temperature effects on cure, and electrical and physical properties 15 p2260 A72-31441
- Ultrasonic sound influence on metal physical and mechanical characteristics, utilizing in testing and manufacturing procedures 15 p2275 A72-31832
- General analysis and synthesis of alloys and materials with inhomogeneous physical properties, noting thermal physicochemical methods for laminates and metal powders 16 p2405 A72-33095
- Manufacturing process for glass fiber chopped strand mats, discussing physical and electrical properties and applications to filament winding 16 p2414 A72-33303
- Ionized gas-solid suspension thermal physical properties verification by micro-sized MgO dispersion in AR plasma [AIAA PAPER 72-688] 16 p2439 A72-34054
- Re applications technology, discussing production methods, mechanical and physical properties, plasma spraying, annealing and alloying techniques 17 p2567 A72-34825
- Physical property measurements at high temperatures. 17 p2554 A72-34934
- Composite materials sum and product physical properties, considering magnetostrictive and piezoelectric interactions 18 p2717 A72-35996
- Physical-mechanical properties of beryllium oxide and investigation of its electrical resistance under irradiation in a reactor 18 p2703 A72-36147
- Studies of physical-mechanical properties of monocrystall molybdenum and tungsten and electrical characteristics of TIC /thermionic converter/ 18 p2698 A72-36154
- Transition metals physical and mechanical properties, production, refining and vacuum processing techniques 18 p2696 A72-36840
- Properties of lithium greases as a function of the saturation level of commercial 12-oxytetrastearic acid 19 p2823 A72-38093
- A method of improving the physicochemical properties of filled epoxy compounds by treatment in an ultrasonic field 19 p2823 A72-38184
- Super-alpha Ti alloy development, measuring physical and mechanical properties 20 p2936 A72-39205
- Laminar composite materials with special physical properties 20 p2940 A72-39451
- Constitution and property relations regarding ceramics and other multiphase materials 20 p2940 A72-39453
- Physical properties of interstellar matter surrounding binary stars from astronomical spectroscopy, discussing eruptions and photometric changes 20 p2975 A72-40069
- Russian book on electron configuration model of condensed matter based on Hubbard model covering physicochemical properties of transition metals, alloys and compounds 21 p3066 A72-40348
- Russian book - Handbook of aircraft materials. 21 p3072 A72-40459
- Void lattice model for Mo physical properties and equilibrium lattice spacing determination, calculating defect Green function 21 p3066 A72-40623
- Certain physical properties of the borides of cobalt and nickel 21 p3068 A72-40953
- Russian book - Physical chemistry of rare metals. 22 p3190 A72-42802
- Physicochemical properties of rare earth metals for alloying Al, Mg, Cu and Ti, noting getter and permanent magnet materials 22 p3191 A72-42806
- Effect of rare earth metals on the structure and properties of aluminum and its alloys 22 p3192 A72-42818
- Physical properties and electronic structure of $V_{1-x}Cr_x/3Si$ ternary alloys 22 p3192 A72-43014
- Physicochemical properties of fiber carbides 23 p3299 A72-43291
- Physical and chemical properties and stratification of neutral matter in comet atmospheres, discussing neutral gas dynamics and surface brightness distribution in comet images 23 p3335 A72-43299
- Making a product from composites. II. 24 p3412 A72-44556
- Physical parameters of asteroids and interrelations with comets. 24 p3445 A72-45460

PHYSICAL SCIENCES

Physical and biological sciences approaches to attainment of knowledge, noting indeterminateness in organic realm 07 p0934 A72-20394

PHYSICAL WORK

- Age and physique effects on human continuous work capacity, monitoring heart rates during task performance 01 p0018 A72-10568
- Physical training effect on subjective rating of perceived exertion, investigating correlation with heart rate and blood lactate concentration 03 p0319 A72-13678
- Prolonged muscular work effects on erythrocyte 2,3-DPG generation relation to oxyhemoglobin affinity 04 p0472 A72-14898
- Quotient of arrhythmia relation to physical work load, noting heart rate amplitude and frequency variations 04 p0472 A72-14899
- Short and long term mental and physical work effects on central nervous system and motor apparatus in young people 04 p0474 A72-15230
- Optimum duration of human circadian cycle with respect to energy cost during work hours, relating normal cycle change to prolonged space mission stresses 05 p0619 A72-16639
- Rapid ventilatory response in man at work on set for different standard starting commands, discussing relation to work load and conditioning process 05 p0619 A72-16788
- Heart pacemaker activity during muscular exertion, developing mathematical model based on system dynamics transient processes analysis 06 p0764 A72-18059
- Acid-base balance shift during muscular exertion, determining pH and bicarbonate content variation by Astrup micromethod 06 p0765 A72-18062
- Human oxygen intake and blood lactic acid removal kinetics during recovery from mild steady work on bicycle ergometer 10 p1426 A72-24989
- Safe exposure times for men working in high temperature environments, showing hyperbolic heat collapse relationship to environmental severity 10 p1432 A72-24990
- Physical work capacity comparison during bicycle ergometry and treadmill walking tests, measuring oxygen uptake, ventilatory parameters and excess carbon dioxide production 11 p1579 A72-26095
- Simulated gravity environment tests of vertical jump features, recording work performed, body center of gravity upward velocity, potential and kinetic energy changes 12 p1770 A72-27479
- Rigid body model for nonholonomic kinematic linkages of tangentially sliding nonrolling bearings, noting virtual displacements and mechanical work 12 p1845 A72-27539
- Human visual accommodation biorhythm and reactions under hard physical work and visual stress 13 p1909 A72-28749
- Possibilities and dangers during long working periods in space rescue. 17 p2507 A72-34436
- Natural acclimatization to work in severe heat. 17 p2508 A72-34550
- Thermoregulation during positive and negative work at different environmental temperatures. 18 p2650 A72-36559
- Self-paced ergometer performance - Effects of pedal resistance, motivational contingency and inspired oxygen concentration. 18 p2653 A72-36911
- Relationships among isometric forces measured in aircraft control locations. 19 p2761 A72-38706
- The silent period in man during muscle lengthening produced by loading 20 p2892 A72-39590
- Metabolic energy requirements for pushing loaded handcarts, measuring expenditure during treadmill and outdoor asphalt circuit walking 21 p3005 A72-40419
- Hypercapnia with relief of hypoxia in normal individuals with increased work of breathing. 21 p3005 A72-40420
- Evaluation of cardiopulmonary function and work performance in man during caloric restriction. 21 p3005 A72-40423
- Mental and physical workload measure and differentiation in man machine systems 21 p3012 A72-41427
- Oxygen uptake kinetics for various intensities of constant-load work. 22 p3145 A72-42743

PHYSICIANS

- Civil aviation physician duties for airline personnel and passenger benefit, discussing medical advice, health precautions, first aid training, etc 08 p1125 A72-21269

PHYSICS

- Physics - Conference, Bratislava, Czechoslovakia, May 1968 08 p1205 A72-20936
- Physics - Conference, Evian, Haute-Savoie, France, May 1971 11 p1692 A72-26430

PHYSIOGRAPHY

U GEOMORPHOLOGY

PHYSIOLOGICAL ACCELERATION

- Cardiac acceleration by voluntary muscle contractions of minimal duration in men due to vagal tone inhibition 07 p0929 A72-19442
- Human leg muscle reflex excitability changes during angular acceleration, suggesting vestibular apparatus as coordination means in quasi-static and dynamic movement control 14 p2075 A72-30388
- Alcohol ingestion effect on vestibular responses to angular acceleration and Coriolis stimulation, discussing nystagmus and subjective responses 14 p2082 A72-31090
- Airline pilot rotation perception during angular acceleration tests, noting power law description of subjective motion for three major body axes 16 p2358 A72-33649
- Synchronous and asynchronous BASH /body acceleration synchronous with heart beat/ effects on hemodynamics and ventilation in dogs and humans 18 p2648 A72-36033

PHYSIOLOGICAL EFFECTS

- NT HEMODYNAMIC RESPONSES
- NT PHYSIOLOGICAL RESPONSES
- Environmental noise induced human fatigue, considering physiological and psychological effects 01 p0016 A72-10050
- Biochemical and physiological effects of Apollo flight diet, noting no significant variations in serum electrolytes, endocrine values, body fluids and hematologic parameters 02 p0167 A72-11707
- Physiological effects of localized ventilation, noting human comfort improvement association with reductions in average skin temperature and sweat rate 02 p0159 A72-11955
- Physiological effects of transfusing 2,3-diphosphoglycerate (DPG) depleted red cells with high oxygen affinity in anemic hypoxic patients 04 p0473 A72-15211
- Metrology and technology for sounds intense enough for physiological distress and mechanical structure damage, discussing accompanying high temperature and vibration [ONERA, TP NO. 1009] 05 p0661 A72-16024
- Adrenocortical steroids during acute exposure to environmental stresses, noting effects of injected cortisol removal, uptake and release 06 p0763 A72-17874
- Erythrocytes catalase activity and number content relationship in human and albino rats blood, discussing compensatory effects 06 p0764 A72-18060
- Tranquilizers effect on pilot in-flight performance, discussing flight safety, alcohol potentiating effect, student pilot stress reactions and airsickness treatment 06 p0768 A72-18158
- Harmful influence of random vibrations on human organism, discussing Fokker-Planck analysis and amplitude and frequency variation effects 06 p0770 A72-18720
- Ultrasonic transducer monitoring of decompression-caused gas bubbles in rat thigh muscle tissue for decompression sickness time course development studies 07 p0921 A72-20183
- Rhythmiasis as fundamental life characteristic analogous to homeostasis, discussing human circadian rhythm and cycle desynchrony during air travel 07 p0923 A72-20445
- Environmental chamber tests for ozone exposure effects on human pulmonary function at rest and during bicycle exercise 08 p1122 A72-20884
- Physiological evaluation of modified jet transport passenger oxygen mask from altitude chamber experiments 08 p1126 A72-21571
- Diurnal and beat-to-beat variation factors in vectorcardiograms, noting respiratory movements, electrode location shift, skin-electrode impedance and heart electrical center mobility 08 p1127 A72-21849
- Sonic booms effects on domestic and wild animals, discussing field and laboratory findings 09 p1267 A72-23322
- Medicobiological investigations of prolonged weightlessness effects on astronaut physiological system based on Soyuz flight program 10 p1425 A72-24409
- High altitude acclimatization effects on human lung diffusing capacity for carbon monoxide at different oxygen tensions 10 p1425 A72-24476

- Cardiovascular changes produced by whole body vibration of dogs and pigs, obtaining resonant frequencies of organ systems 10 p1426 A72-24484
- Clinical and laboratory examinations of workers exposed to trichlorotrifluoroethane vapor for long range health effects study 10 p1431 A72-24590
- Food deprivation stress effects on urinary excretion values in unrestrained chimpanzees 10 p1426 A72-24822
- Medical and physiological hazards for SST passengers and crews, discussing cumulative cosmic radiation and high altitude decompression risks 11 p1583 A72-25816
- Case report of rapid decompression in supersonic trainer aircraft pressurized cabin, discussing physical and blast effects, pressurization safety, decompression sickness and hypoxia 11 p1584 A72-26020
- Medical evaluation of manned space flight physiological effects, considering Mercury, Gemini and Apollo programs 11 p1585 A72-26100
- Time displacement effects on human physiological and psychological functions, discussing circadian rhythm phase shift and performance deficits 11 p1580 A72-26681
- Time zone transition induced circadian physical disturbance effect on military personnel mental and physiological performance 11 p1589 A72-26696
- Weightlessness effects on human organism, discussing physiological changes, artificial gravity by spacecraft rotation and exercise to counter adverse reactions 11 p1589 A72-26891
- Multihour immersion effects on blood plasma protein and electrolyte concentration in trained and untrained subjects 12 p1770 A72-27480
- Physiological and clinical effects of long distance flight in pressurized commercial planes with simulated altitudes over 15000 meters 12 p1771 A72-27486
- Magnetic storm strength ELF electromagnetic field effects on rabbits, dogs and bacteria, discussing changes in EEG, ECG and blood characteristics 12 p1763 A72-28214
- Ascorbic acid influence on blood coagulation and anticoagulation systems in dogs with acute hypoxia, discussing plasma recalcification time and heparin tolerance 12 p1764 A72-28217
- Plasma protein concentration, volume and hematocrit changes during exercise, bed rest and high forward acceleration 12 p1766 A72-28296
- Physiological effects of intense anticollision flash light backscatter pulses on instrument rated pilots 12 p1775 A72-28303
- Physiological effects on anesthetized and conscious dogs during exposure at 80,000 ft for different decompression rates, discussing cardiovascular, biochemical and pathological effects 12 p1768 A72-28322
- Effects of long periods of clinical death from drowning or lethal blood loss on higher nervous activity in reanimated dogs 13 p1902 A72-28642
- Radioprotectants /mexamine and cystamine/ effects on radio-hematic barrier permeability in rats under hypokinetic conditions 13 p1904 A72-29308
- Hermetic chamber medico-engineering experiment for long term isolation effects on human intestinal microflora, showing reduction and disappearance of certain microbe populations 13 p1904 A72-29323
- Human physiological function variations dependence on hyperthermia levels in high temperature environment 14 p2074 A72-30257
- Lower body decompression effects on ECG, showing heart rate increase, R and T amplitude changes and heart electric axis displacement 14 p2074 A72-30383
- Stepwise altitude acclimatization and subsequent reanimation after blood loss caused clinical death effects on dog peripheral blood erythrocytes, reticulocytes, hemoglobin and hematocrit 14 p2076 A72-30671
- Astronauts physiological and psychological reliability, discussing Apollo flights and prolonged missions to other planets 14 p2079 A72-30677
- Physiological and psychological effects of noise noting vulnerability of circulatory apparatus, neurovegetative system and stomach 14 p2079 A72-30696
- Russian book on functional morphology under extremal space flight conditions covering overloads, hypoxia and hyperoxia effects on organism and cellular structure and metabolism 14 p2077 A72-30996
- Medical factors in air racing accidents, investigating drug, fatigue and gastrointestinal symptoms effects on pilot reaction to emergency 14 p2081 A72-31089
- Technology R and D program to qualify man for long term weightlessness, assessing space flight stress effects on physiology and psychology 16 p2358 A72-33544
- Prolonged weightlessness effects on cardiovascular, digestive, musculoskeletal and nervous systems, blood and metabolism, noting compensatory reactions 16 p2354 A72-33546
- Physiological effects on prolonged weightlessness in dogs aboard Cosmos 110 biosatellite, emphasizing body weight loss and enzyme activity and bone tissue mineral concentration changes 16 p2354 A72-33547
- Weightlessness effects on animal voluntary motor activity and wakefulness from brain and muscle area electrical activity recordings during ballistic flight 16 p2355 A72-33548
- Space environment weightlessness induced perceptual deprivation, considering hand-eye coordination, visual judgments and motion and time perception 16 p2355 A72-33549
- Long term space flight weightlessness and hypodynamic effects on orthostatic and vestibular tolerances, infection susceptibility and drug reactivity 16 p2355 A72-33550
- Weightlessness effects on calcium and electrolyte metabolism from measurements during Gemini 7 flight, using dietary control and excreta collection techniques 16 p2355 A72-33552
- Hypothermia, asphyxia and ionizing radiation effects on rat immunological defense mechanisms against particulate antigens 16 p2355 A72-33555
- Astronauts red cell mass changes associated with space flight due to space and earth environment differences 16 p2356 A72-33564
- Aqueous formaldehyde effects on *Bacillus subtilis* spores, showing sporostasis due to germination inhibition and sporocidic due to temperature dependent inactivation 16 p2357 A72-33772
- Blood coagulation changes at high altitude predisposing to pulmonary hypertension. 17 p2498 A72-34222
- Effects of nitrogen and helium upon pulmonary damage after rapid decompression to 2 torr. [AD-746093] 17 p2508 A72-34544
- Effects of combined O-G simulation and hypergravity on eggs of the nematode, *Ascaris suum*. (DFVLR-SONDDR-225) 17 p2499 A72-34547
- Cell proliferation in lungs of mice exposed to elevated concentrations of oxygen. 17 p2499 A72-34548
- Exercise capacity in a population of domestic fowl - Effects of selection and training. 17 p2499 A72-34726
- Influence of hyperosmolality on left ventricular stiffness. 17 p2499 A72-34727
- Thermal neutral temperature of rats in helium-oxygen, argon-oxygen, and air. 17 p2500 A72-34728
- The effect of target contrast variation on dynamic visual acuity and eye movements. 17 p2508 A72-34876
- Light induced alterations in growth pattern of the avian eye. 17 p2500 A72-34880
- The effects of acute hypoxia on lipid synthesis in the rat heart. 17 p2501 A72-34979
- Effect of chronic hypoxia on the kinetics of energy transformation in heart mitochondria. 17 p2502 A72-34993
- Effects of hypoxia and ischemia on myocardial contraction - Alterations in the time course of force and ischemia-dependent inhomogeneity of contractility. 17 p2502 A72-34996
- Physical phenomena occurring in living objects under the action of constant magnetic fields 17 p2502 A72-35002
- The magnetic field, infection and immunity 17 p2503 A72-35009
- Effect of a magnetic field on the nervous system 17 p2503 A72-35010
- Pharmacological effects on the central adrenergic regulation mechanisms of blood circulation 17 p2504 A72-35019
- Bioelectric activity of the medulla oblongata during hypothermia and bloodletting 17 p2504 A72-35024
- Increased tolerance of leukemic mice to arabinosyl cytosine with schedule adjusted to circadian system. 17 p2505 A72-35397
- The effect of chloridazepoxide on visual field, extraocular muscle balance, colour matching ability and hand-eye co-ordination in man. 17 p2505 A72-35915
- Effects of vagotomy and increased blood pressure on the incidence of decompression-induced pulmonary hemorrhage. 18 p2650 A72-36446
- Body weight decreases in some proton exposed primates. 18 p2650 A72-36447
- Observations on microwave hazards to USAF personnel. 18 p2653 A72-36522
- Coronary collateral circulation and myocardial blood flow reserve. 19 p2755 A72-37500
- The effect of chronic erythrocytic polycythemia and high altitude upon plasma and blood volumes. 19 p2757 A72-38028
- Helium effect on cardiac mitochondria of mice. 19 p2759 A72-38712
- RNA content in the cortex neurons in connection with the change in its function during the emergence of an animal from hypothermia 20 p2890 A72-38928
- Changes in the overall electrical activity of the mesencephalic reticular formation, the hippocampus, and the cerebral cortex under the influence of hydrocortisone and DOCA 20 p2890 A72-38929
- Significance of the nature of an increase in physical strain as it affects the adaptation of an organism to intense muscular activity 20 p2891 A72-38933
- motion. 20 p2891 A72-38935
- The silent period in man during muscle lengthening produced by loading 20 p2892 A72-39590
- Circadian rhythms in physiological and psychological functions related to jet travel, studying body temperature variations and psychomotor performance during isolation and varying light-dark cycle conditions 20 p2897 A72-39723
- Comparison of irregular vibrations of a limited frequency range with sinusoidal vibrations in regard to their effect on man 20 p2897 A72-39804
- Effect of hypoxia on the condition of skeleton muscles in rats under hypokinesia 21 p2998 A72-40433
- Morpho-functional changes in the endocrine system during oxygen starvation 21 p2998 A72-40447
- Separation of central effects of CO2 and nicotine on ventilation and blood pressure. 21 p3001 A72-40918
- Blood serum enzymes activity changes in polytraumatized humans injured in automobile accidents 21 p3002 A72-41188
- Hematological modifications due to acute exposure to heat 21 p3002 A72-41191
- Effect of hypoxia and physical activity on plasma enzyme levels in man. 21 p3003 A72-41522
- Neurophysiological mechanisms of the extinction of the orienting reflex 22 p3142 A72-42280
- Effects of externally imposed mechanical resistance on breathing dense gas at exercise - Mechanics of breathing. 22 p3150 A72-42489
- Effects of the space flight environment on man's immune system. I - Serum proteins and immunoglobulins. 22 p3150 A72-42493
- Adaptive processes responsible for natural acclimatization of human organism to low ambient pressures at high altitudes 22 p3143 A72-42584
- Morphometric evaluation of changes in lung structure due to high altitude. 22 p3143 A72-42585
- Succinic and lactic dehydrogenases activities in homogenates from myocardial tissues of guinea pigs, rabbits and dogs in high altitude environments 22 p3144 A72-42592
- Coronary blood flow and myocardial metabolism in man at high altitude. 22 p3144 A72-42593
- Anatomy of the coronary circulation at high altitude. 22 p3144 A72-42594
- Effects of weightlessness on astronauts - A summary. 23 p3253 A72-43385
- Effects of an 18-day flight on the human body. 23 p3253 A72-43386
- Physiological and hematological effects of chronic irradiation. 23 p3254 A72-43392
- Influence of a preliminary exposure to carbon monoxide on the development of hypokinetic disturbances in albino rats 23 p3255 A72-43909

- Features of a speech signal during cumulative action of Coriolis accelerations 23 p3257 A72-44154
- Physiologic effects of passive hyperventilation on oxygen delivery and consumption. 23 p3258 A72-44365
- Animal studies of effect of chronic exercise on the heart and atherosclerosis - A review. 24 p3370 A72-44563

PHYSIOLOGICAL FACTORS

NT PHYSICAL FACTORS

- Book on physiological approach to ergonomics covering muscular system, performance, work and fatigue, working efficiency and environment, man machine systems, etc 07 p0930 A72-19875
- Flight personnel statistical survey of clinical, physical and psychic causes of temporary and permanent flight service unfitness 07 p0923 A72-20447
- Education and training of personnel for photointerpretation, discussing psychological, physiological and methodological aspects of aerial photointerpretation 09 p1272 A72-23298
- Human performance dependence on time of day, discussing circadian and physiological rhythms relation and environmental change effects 11 p1580 A72-26677
- Transzonal air travel as cause of psychological and physiological rhythm change effects on pilot performance 11 p1589 A72-26694
- Aircraft and other vehicle simulators for training crews, discussing evolution of needs, digital techniques, and visual and physiological experiences 14 p2092 A72-30844
- Visual stimulus orientation effect on movement perception, relating physiological and psychological factors 15 p2184 A72-31368
- Airline management and flight crew role in prevention, detection and dealing with airline pilot incapacitation in flight, noting physiological and psychological factor recognition 17 p2508 A72-34555
- Habitability factors in a rotating space station. 18 p2652 A72-36436
- Mutual relations between different physiological functions in circadian rhythms in man. 22 p3147 A72-42979

PHYSIOLOGICAL INDEXES

U PHYSIOLOGICAL TESTS

PHYSIOLOGICAL RESPONSES

NT HEMODYNAMIC RESPONSES

- Frog Rana temporaria striated muscle tension response recording during sudden fiber length alteration, suggesting force generation mechanism 01 p0009 A72-10017
- Vibration space analysis for human voice characteristics change during unintended speech under experimental psychological stresses and actual emergency situations 01 p0017 A72-10213
- Hypothermia induced by hypoxia in rats, discussing colonic temperature during high altitude exposures and seasonal variations 01 p0011 A72-10214
- Physiological response to affective visual stimuli, observing signal value change effect on forehead pulse amplitude and galvanic skin response 01 p0014 A72-10854
- Mice tolerance to long term accelerations or supergravities, detailing physiological consequences 01 p0014 A72-10934
- Short term response of insulin, glucose, growth hormone and corticosterone to acute vibration stress in rats 01 p0015 A72-11289
- Receptor activity control from clinical physiological and electrophysiological observation data analysis, noting central nervous system role and feedback and self adaption capabilities 02 p0157 A72-11543
- Inert gas narcosis under hyperbaric conditions relationship to mental performance and auditory and visual evoked responses in man 02 p0166 A72-11705
- Heart and respiration rates response to free fall parachuting, using FM/FM telemetry 02 p0167 A72-11709
- Pyramidal tract neuron reactions to antidromic and afferent stimuli in cats, determining somatosensor cortical neurons responses by intra- and extracellular potential outlets 02 p0159 A72-11768
- Bats auditory cortex electrical responses to ultrasonic stimuli, determining maximum sensitivity frequency range 02 p0159 A72-11769
- Ventilatory and metabolic responses of unanesthetized dogs exposed to various carbon dioxide concentrations at 2 and 18 C, discussing oxygen uptake relation to cold 02 p0159 A72-11954

Physical interpretations of physiological control, covering history, biochemical oscillator viewpoint of life and conferences 02 p0160 A72-12039

Alpha-L-fucosidase, beta- and alpha-D-galactosidases and alpha-D-mannosidase activity changes in human placenta at various embryogenesis phases 02 p0163 A72-12294

Retinomotor light/darkness responses phylogenetic variations, discussing retinal elements structural and functional development in fishes and amphibians 02 p0164 A72-12484

Visual response to monocularly and dichoptically presented flashed patterns, discussing physiological mechanism based on cortical visual field concept 02 p0164 A72-12485

Heat exposure effect on Sidman avoidance performance in rats, discussing organism thermoregulatory capacity disruption and shock and body temperature regulation 02 p0169 A72-12525

Physical exercise effect on ECG atrial recovery wave duration and magnitude in humans with A-V blocks 02 p0166 A72-12891

Astronaut zero gravity adaptive responses in performance, locomotion, orientation, sleep and physiological and functional characteristics 03 p0319 A72-13867

Operant conditioning for producing gross motor responses, discussing application to physical medicine and rehabilitation with mentally retarded Downs syndrome children 04 p0478 A72-14706

Daily prolonged exercises effects on human muscle glycogen utilization, noting reduced lactate accumulation and increased free fatty acid levels 04 p0480 A72-15213

Human coagulating and anticoagulating blood system changes due to emotional stress during parachute jumps, noting plasma recalcification time increase 04 p0474 A72-15233

Human vestibulo-ocular responses to oscillatory rotational stimulation during various sleep and arousal stages, discussing Sugie-Jones reflex system mathematical model 04 p0474 A72-15249

Cats cochlea and cochlear nucleus neural responses in auditory masking of low frequency tones, showing phase locked cells progressive desynchronization with intensity 04 p0475 A72-15251

External biodynamic models for human mechanical response to various environmental forces, emphasizing injury mechanisms [AD-736985] 04 p0481 A72-15266

High and low pass filtered clicks lateralization tests, suggesting lateral position discrimination dependence on lf content and cochlear partition apical end 04 p0550 A72-15297

Exercise effects on pulmonary circulation in dogs, measuring pulsatile arterial flow and pressure and vascular input impedance, resistance and hydraulic power 04 p0475 A72-15464

Single olfactory bulb units under cyclic stimulation, observing activity related to inhalation cycle and odor quality 05 p0617 A72-16162

Hypoxia effect on diurnal mitotic activity rhythm of marrow erythropoiesis system of guinea pigs in pressure chamber 05 p0618 A72-16631

Human craniocerebral trauma dependence on impact conditions, giving case histories 05 p0619 A72-16643

Rapid ventilatory response in man at work on set for different standard starting commands, discussing relation to work load and conditioning process 05 p0619 A72-16788

Human taste papillae sensitivity to chemical stimuli, showing stable quality and intensity response patterns 05 p0620 A72-17129

Occipital and vertex visual evoked response relation to sensory information, perception and stimulation 06 p0763 A72-17723

Electromyogram study of antagonist muscles reactions to Achilles tendon percussion or whole body sudden motion via test stand jerking 07 p0915 A72-18864

Electrophysiological responses to maximum exercise in healthy humans from polarcardiographic display of heart vector changes 07 p0916 A72-18891

Suppression of visual evoked responses to low intensity light flashes and shifting stripe patterns during saccadic eye movements 07 p0926 A72-19025

Extraretinal inflow eye position information awareness from experimental load application to eyes in total darkness 07 p0926 A72-19026

Computerized simulation from model of human pupillary motor behavioral response to light, accommodation and fusional inputs 07 p0928 A72-19310

Acid base balance in arterialized capillary blood in men after maximal short duration exercise 07 p0929 A72-19441

Eastbound and westbound transmeridian flights effect on body temperature and psychomotor and visual performance circadian rhythms, discussing readjustment times [AMRL-TR-71-89] 07 p0921 A72-20176

Cardiovascular and respiratory responses to intraarterial injection of K and Na ions in dogs for peripheral receptor site determination 07 p0921 A72-20177

Hyperbaric oxygen exposure effect on cardiovascular system in rats, discussing pulmonary edema relation to hypertensive left ventricular failure 07 p0921 A72-20182

Galvanic skin response techniques for palmar and dorsal sweat detection during motion sickness by vestibular stimulation, comparing arousal and thermal sweat response 07 p0933 A72-20185

Human performance and exhaustion predictive model from responses to exercise and environmental stresses, considering circulation, thermal regulation, work load and oxygen pressure effects 07 p0934 A72-20358

Inhaled oxygen pressure variation effects on adenosines, glucose, lactate and pyruvate levels in rat brains, noting anoxic limit value relation to age 07 p0924 A72-20658

Light-dark cycles and physiological stress stimuli effects on circadian rhythm in rat blood serum serotonin levels 08 p1115 A72-21081

Endurance exercise effect on respiratory capacity in white, red and intermediate muscles in rats, relating fiber type to oxidative capacity 08 p1115 A72-21083

Animal response to sonic booms, considering mink reactions in detail 08 p1119 A72-21909

Respiration in altered gas environment for spontaneous breathing and voluntarily maintained pulmonary ventilation level conditions 08 p1120 A72-22077

Arterial chemoreceptor deafferentation influence on rat respiratory response to hypoxic and hypercapnic gas mixture breathing 08 p1120 A72-22078

Human reactions to sonic boom acoustic stimuli noting startle reflex responses 09 p1267 A72-23320

Calorimetric study of sweating man response to drinking hot saline solution as function of temperature, volume and salinity of ingested liquid 09 p1267 A72-23441

Isolated specific color dependent waveforms of visual evoked response to strong colored lights relating luminance and wave amplitude changes 09 p1267 A72-23500

Sympathetic responses in human skin nerves with accompanying vasomotor reactions induced by emotional, thermal and respiratory stimuli 10 p1424 A72-24241

Single lateral geniculate neuron recording during receptive field-centered flashing spot variations for intensity response function comparison with optic neurons in cats 10 p1427 A72-25177

Lenticular conditioning-shock stimulation effect on cat visual cortex response to light stimuli, noting lateral gyrus photically evoked potential amplitude increase 11 p1578 A72-25801

Cardiovascular responses to positive pressure oxygen breathing from blood pressure and heart and respiratory rate measurements 11 p1584 A72-26017

Electromyogram and myogram responses in phasic stretch reflex under prestrain conditions as index of fusimotor activity level in normal humans 11 p1588 A72-26632

Mountain sickness relation to ventilation response to hypoxia, noting response intensity dependence on peripheral chemoreceptor sensitivity 12 p1771 A72-27481

Cat and rat cardiac and cardiovascular reflexes response to electric pulse stimulation of sensorimotor cerebral cortex 12 p1761 A72-27647

Cat auditory cortex neurons response to auditory and medial geniculate body electrical stimulation 12 p1761 A72-27651

Cerebrospinal fluid pH change effects on cat respiratory response before and after vagotomy, showing vagal activity relation to central chemical control of respiration 12 p1762 A72-27825

Metabolic and hormonal response adaptation to prolonged hypodynamics in water immersion/head out, 12 p1762 A72-27825

noting diurnal and nocturnal differences in circadian rhythms

12 p1765 A72-28267
Parachutist biomedical responses in aerial tow at 110-175 knots, determining heart and respiration rates and urinary catecholamines

12 p1774 A72-28272
Acceleration stress effects on splanchnic blood flow due to organ displacement and neurogenic vasoconstriction in vascular beds

12 p1765 A72-28285
Periodic, continuous and aperiodic white noise effects on human serial decoding performance, relating subjective and autonomic responses

12 p1775 A72-28289
Physiological and biochemical responses of Paramere caudatum to hypo- and hyperbaric stresses, discussing protoplasmic inactivation by high oxygen pressure

12 p1766 A72-28299
Thermoregulation changes during simulated weightlessness of prolonged bed rest, noting lower sweating threshold and decreased vasodilation /autonomic dysfunction/

12 p1767 A72-28301
Circadian rhythms of visual accommodation responses and physiological correlations during target tracking, recording monocular focus state by IR optometer

12 p1767 A72-28306
Physiological and subjective responses of physically fit young men to combined exercise-carbon dioxide stress tests

12 p1767 A72-28311
EEG recording and analysis by analog technique as means of studying human responses to hyperventilation

12 p1767 A72-28312
Cardiorespiratory response to breathing dense sulfur fluoride-oxygen mixture under physical exercise conditions

12 p1767 A72-28314
Pilot and back-seat man physiological responses during high-g aerial combat maneuvers in F-4E aircraft, discussing ECG, respiratory rate and minute volume

12 p1767 A72-28317
Neuroendocrine responses in microwave radiation exposed rats, correlating thyroid and thyrotropic activity

12 p1767 A72-28321
Miniature swine as human analog to investigate physiological response to high positive acceleration, comparing human and animal tolerances

12 p1768 A72-28329
Physiological evaluation of diastole mechanism in rat hypertrophied myocardium as function of heart rate, Ca ion concentrations and temperature

13 p1901 A72-28521
Disposable emergency oxygen mask for air passengers based on continuous flow, phase dilution principle, describing altitude chamber tests with human subjects to study physiological responses

13 p1908 A72-28702
Rat adrenal cortex morphology after 24 hour transverse exercise stress, studying changes in lipid, ascorbic acid and RNA content and acid phosphatase activity

13 p1904 A72-29310
Quantitative model to describe vestibular detection of body sway motion in postural response mode

13 p1905 A72-29374
Mechanical vibration induced physiological changes in rats, determining plasma Ca, Mg and inorganic phosphate concentration and xanthine oxidase activity response to frequency and g-levels

13 p1910 A72-29560
Gas mask-caused air flow resistance effects on respiratory and circulatory response to exercise, assessing maximal oxygen uptake

13 p1906 A72-29818
Alveolar carbon dioxide pressure-ventilation response curve measurement by Campbell rebreathing method in consecutive daily trials

13 p1906 A72-29846
Five-component cyclic model of retinal photopigment kinetics for photochemical changes corresponding to rod adaptation in rat and man in dark

13 p1906 A72-29966
Consensual photopupil responses to light flashes recorded in full dark adaptation, noting bleaching and backgrounds effects

13 p1907 A72-29969
Foveal and nonfoveal afterimages effects on saccadic behavior of eye movement

13 p1907 A72-29971
Cat visual cortex receptive field responses to light bands of variable widths and intervals

14 p2074 A72-30256
Delayed growth of rats carcasses and skeletal muscles during prolonged hypokinesia, comparing effects on flexor muscles to ankle joint extensors

14 p2074 A72-30378

Red blood cell reserve mobilization in healthy and chronically irradiated dogs after treadmill exercise

14 p2074 A72-30379
Visual cortex repetitive stimulation effect on primary response habituation in young normal rabbits and adults with septum pellucidum lesion

14 p2076 A72-30596
Cat cerebellum cortex evoked response impulses interaction during stimulation of hypothalamus and peripheral nerves

14 p2076 A72-30669
Human diaphoretic system physiology, discussing skin surface sweat excretion intensity relation to optimal balancing process in thermoregulation

14 p2076 A72-30672
Human organism readaptation after prolonged hypokinesia and weightlessness, discussing coordination disturbances, vegetative and vascular system instabilities, reduced orthostatic stability and asthenia

14 p2076 A72-30745
Platelet electrophoretic mobility response to adenosine diphosphate /ADP/ in patients with coronary artery disease

15 p2183 A72-31283
Human cerebral hemodynamic changes during arousal and orienting reactions to auditory stimuli

16 p2353 A72-32993
Long term weightlessness-induced physiological response normalization by muscle bioelectrostimulation, muscular tissue energy load increase and mineral metabolism stabilization

16 p2354 A72-33543
Organism response to extreme overload factors, discussing centrifuging and vibration stress effects on mean swimming time and post-irradiation survival time in mice

16 p2355 A72-33554
Psychological and physiological parameters correlation for astronaut functional state relation to emotional tension level during ground and flight tests

16 p2356 A72-33563
Simulation of the human cardiovascular system - A model with normal responses to change of posture, blood loss, transfusion, and autonomic blockade.

17 p2507 A72-34445
Vestibular behavior of fish during diminished g-force and weightlessness.

17 p2499 A72-34549
Natural acclimatization to work in severe heat.

17 p2508 A72-34550
Heat, noise and vibration stress combined effects on skin and rectal temperature, heart rate, weight loss and biochemical urinalysis

[AD-746083] 17 p2508 A72-34551
Stress and adaptation responses to repeated acute acceleration.

17 p2500 A72-34729
Linear-nonlinear-linear transition as a function of frequency in the retinal response to light.

17 p2508 A72-34885
Changes of intracellular myocardial electrolytes in experimental hypertension.

17 p2501 A72-34984
Ion alterations during myocardial ischemia.

17 p2502 A72-34994
Influence of thermal, osmotic, and chemical stimulations on food and water intake

17 p2504 A72-35016
New data on physiological adaptations to arid zones

17 p2504 A72-35021
Russian book - Intracranial blood circulation under conditions of accelerations and weightlessness

17 p2509 A72-35460
Work capacity and physiological responses to maximum exercise in 54 year old men in relation to heart disease and cardiovascular hazard studies

17 p2505 A72-35822
Functional development of the altitude convulsion mechanism in mice and rabbits /Research note/.

18 p2650 A72-36445
Role of the autonomic nervous system in the hypoxic response of the pulmonary vascular bed.

18 p2650 A72-36572
Optokinetic thresholds in the normal monkey.

18 p2651 A72-36610
Electrical stimulation of vestibular nuclei - Effects on light-evoked activity of lateral geniculate nucleus neurones.

19 p2758 A72-38220
Frequency response studies of human and avian respiratory regulation.

19 p2761 A72-38229
Receptive fields of units in the visual cortex of the cat in the presence and absence of bodily tilt.

19 p2758 A72-38646
Influence of rhythmic photostimulation on lower-order monkeys with hyperkinesia of post-encephalitic origin

20 p2890 A72-38930
Myogenic and eardrum evoked auditory potentials and cortical responses to 0.2 millisecond voltage pulse acoustic stimuli

20 p2891 A72-38932

Hemopoiesis in the pig-tailed monkey Macaca nemestrina during chronic altitude exposure.

20 p2892 A72-39344
Hematologic responses to hypobaric hypoxia.

20 p2892 A72-39345
Effects of chloralose-urethan anesthesia on temperature regulation in dogs.

21 p2997 A72-40426
A possible anatomical basis for descending control of impulse transmission through the dorsal horn.

21 p2998 A72-40578
Blood vessel reactions to natural defense and conditioned reflexes from plethysmography and blood pressure measurements, discussing cortical effects mechanisms

21 p3000 A72-40758
Tilt table tests for orthostatic tolerance, measuring heart rate, blood pressure and responses of fainters and nonfainters

21 p3008 A72-41020
Adrenaline and noradrenaline metabolic stages and production mechanism under various physiological and pathological conditions, noting application to flight emotional stress detection

21 p3002 A72-41196
Visual experience as a determinant of the response characteristics of cortical receptive fields in cats.

21 p3003 A72-41461
The prediction of the condition of man during a space flight

22 p3149 A72-42067
Effect of fasting on tolerance to moderate hypoxia.

22 p3150 A72-42487
New mechanical device for producing traumatic shock in dogs - Circulatory and respiratory responses.

22 p3142 A72-42490
Heart rate variability in a binary choice reaction task - An evaluation of some scoring methods.

22 p3143 A72-42550
The carotid body in animals at high altitude.

22 p3143 A72-42589
Suprapontine influences on hypoxic ventilatory control.

22 p3143 A72-42590
Histological analysis of hypoxia exposure effects on mouse skin homograft reaction due to lymphatic organ function changes

22 p3144 A72-42675
Time series analysis of meteoropathological disturbances of human regulation mechanisms, investigating annual variations of diurnal rhythms

22 p3147 A72-42977
Electrophysiological investigation of the excitation and inhibition processes in the auditory cortex

22 p3148 A72-43165
Limbic-neocortical, cardiovascular and hormonal system vegetative shifts associated with emotional behavior response, presenting neurogenic stress model for animals

22 p3148 A72-43166
Nervous mechanisms of the acoustic stress reaction

22 p3148 A72-43169
Calcium metabolism under stress and in repose.

23 p3254 A72-43389
Pyrogenal injection test for hematopoietic tissue function in dogs, describing response as transient leukopenia followed by pronounced leukocytosis due to bone marrow granulocyte ejection

23 p3255 A72-43911
Otorhinolaryngological organ response during hypokinetic antiothostatic bed rest for control, exercising and muscular electric-stimulated groups

23 p3256 A72-43917
The simultaneous action of stimulants and tranquilizers on the efficiency of a human operator

23 p3260 A72-43923
Electrophysiological analysis of limbic-reticular interaction during the orientating reflex

23 p3257 A72-44081
Responses of anterior suprasylvian gyrus neurons to peripheral stimuli of different modalities

23 p3257 A72-44090
Sensitivity of the human ERG and VECP to sinusoidally modulated light.

23 p3258 A72-44383
Techniques for analysing differences in VERs: Colored and patterned stimuli.

23 p3258 A72-44387
Ensemble characteristics of the human visual evoked response - Periodic and random stimulation.

24 p3374 A72-44575
Analysis of changes in thermal regulation after destruction of the medial preoptic area of the hypothalamus

24 p3371 A72-44593
Eye movements evoked by collicular stimulation in the alert monkey.

24 p3371 A72-44906
First-breath response of medullary inspiratory neurones to the mechanical loading of inspiration.

24 p3372 A72-44959
Comparison of three methods for quantitating respiratory response to hypoxia in man.

24 p3372 A72-44960

Response to daily lower body negative pressure /LBNP/ exposure /-70mm Hg/, with emphasis on plasma renin activity, sodium and potassium excretion. 24 p3377 A72-45658

Human physiological responses to high magnitude short duration positive accelerations, considering peripheral vision loss as function of time 24 p3377 A72-45660

PHYSIOLOGICAL TELEMETRY

U BIOTELEMETRY

PHYSIOLOGICAL TESTS

NT BODY SWAY TEST
NT CARBOXYHEMOGLOBIN TEST
NT EAR PRESSURE TEST
NT VESTIBULAR TESTS

Screening test for physical fitness on bicycle ergometer, comparing endurance indices derived from heart rate, oxygen consumption, oxygen debt and work rate measurements 01 p0010 A72-10212

Optimum muscle work conditions experiments with rabbits, correlating total work performance and power output with muscle temperature variations 02 p0160 A72-12013

Femoral arterial blood pressure third order waves onset mechanism in narcotized dogs, noting changed blood and respiration dynamics 02 p0160 A72-12014

Acute hypercapnia neurotropic effect in rabbits, describing carbon dioxide inhalation period, preanesthetic and narcotic stages and recovery phase 02 p0160 A72-12015

Monotonous auditory stimulation frequency effects on human orienting reaction habituation and sleep onset 02 p0169 A72-12494

Auto- and cross correlation functions for neuron reactions in vasomotorial center to adequate stimulation of cats vestibular apparatus 06 p0762 A72-17673

Organism blood volume and losses determination by measuring human body electrical resistance, noting unsatisfactory results 06 p0768 A72-17994

Visual acuity measurement methods, comparing angular acuity by Beyne optometer and morphoscopic acuity by Mercier optometric scale 07 p0927 A72-19246

ECG evidence of myocardial ischemia in patients without arteriographic evidence of coronary artery disease, studying myocardial oxygen supply 07 p0920 A72-19995

Asthmatics evolution and treatments in armed forces aircrews, noting acetylcholine test 08 p1125 A72-21270

Temporal summation function form change during dark adaptation, noting relationship to change under other stimulus manipulations 09 p1269 A72-22616

Respiration function testing device using spirometers and gas analyzers 09 p1272 A72-23256

Physiological index changes in parachutists of various ages, considering plasma recalcification, blood prothrombin, heparin time, fibrinolytic activity, pressure and heart beat 11 p1590 A72-26988

Visual acuity measurement by dynamic and static tests as function of target velocity and exposure time 13 p1911 A72-30042

Standardization of microwave irradiation experiments on animals, discussing power density level evaluations and local vs whole-body irradiation effects 14 p2080 A72-30746

Annual clinical and physiological evaluation of test pilots physical performance over ten year period from body composition, pulmonary function and work capacity measurements 14 p2082 A72-31093

Effects of instructions on measures of state and trait anxiety in flight students. 17 p2507 A72-34464

Rhesus monkey retinas ultrastructural alteration and damage in rods and cones produced by Q switched ruby laser coherent radiation 17 p2509 A72-35396

Study of bilateral cortical nerve connections between the preoral gyrus and various cortical regions 20 p2891 A72-39323

Problem of artificial gravitation in terms of experimental physiology 21 p3006 A72-40441

Separation of central effects of CO2 and nicotine on ventilation and blood pressure. 21 p3001 A72-40918

Body orientation under vertical sinusoidal vibration. 21 p3008 A72-41019

The Macruz index and its clinical evaluation in electrocardiography with regard to the selection and control of air crews 21 p3009 A72-41193

Potassium chloride test for electrocardiogram evaluation in flight personnel medical appraisal 21 p3012 A72-41747

Prediction of vegetative reactions in the case of stress and extreme effects upon the organism 22 p3149 A72-42069

Thirty day experiment for assessment of weightlessness simulation test methods and evaluation of applicable prophylactics 23 p3259 A72-43912

Health condition changes in test subjects during strict bed rest in hypokinetic recumbent and antiorthostatic position subject to lower body negative pressure 23 p3259 A72-43913

Changes in the impulse activity of cortical neurons during selective reinforcement of a chosen range of their interpulse intervals 23 p3257 A72-44087

Post-synaptic potentials of motor neurons of the facial nerve nucleus evoked by afferent and corticofugal pulse stimulation 23 p3257 A72-44091

Classification of neurons in the lumbosacral section of the spinal cord according to their discharge during evoked locomotion 23 p3257 A72-44092

Biochemical and physiological evaluation of nourishment of subjects feeding on dehydrated products in test chamber with regenerative life support system, discussing metabolic data and hormone function 24 p3375 A72-45128

PHYSIOLOGY

NT AUDIOLOGY
NT BODY COMPOSITION [BIOLOGY]
NT ELECTROPHYSIOLOGY
NT HEMATOPOIETIC SYSTEM
NT NEUROPHYSIOLOGY
NT PSYCHOPHYSIOLOGY
NT RESPIRATORY PHYSIOLOGY

Foresight, forecast and prognosis concepts in physiology, discussing intuition role and relation between molecular and cellular processes and organism activity 02 p0163 A72-12346

Energetic motor activity rule hypothesis for physiological mechanisms of certain ontogenesis patterns, suggesting motor activity as excess anabolism induction factor 09 p1264 A72-22225

Russian book - Mechanisms regulating physiological functions 17 p2503 A72-35014

Clinical observations as a research method in physiology 17 p2504 A72-35017

PIASECKI MILITARY AIRCRAFT

U MILITARY AIRCRAFT

PICKLING

U CHEMICAL CLEANING

PICKOFFS

U SENSORS

PICTURE TUBES

Color TV tube design without difference current generator, describing scanning unit saddle coils fabrication technique 18 p2667 A72-36678

PIERCING

Metal barrier maximum puncturable thickness dependence on high velocity meteorite particle impact parameters 22 p3234 A72-42217

PIEZOELECTRIC CRYSTALS

Piezoelectric interaction between Lamb waves and charge carriers in piezoelectric plate inserted into semiconductor 06 p0865 A72-17388

Lamb waves interaction with conduction electrons in piezosemiconductor, deriving dispersion equation for CdS wafers 06 p0865 A72-17393

Piezoresonance modulation of IR amplitude in GaAs crystal by electric field at single, doubled and quadrupled frequencies 06 p0866 A72-17843

Thin films thickness control by piezoelectric quartz crystal, discussing electrically excited oscillations wavelength and damping characteristics 07 p0990 A72-20285

Piezoelectric quartz crystal microbalance for material outgassing and optical element contaminant film measurements 12 p1806 A72-27043

Torsional crystal measurements of viscosity for He 4 and He 3-He 4 mixture at lambda points 12 p1888 A72-27388

Surface piezoelectric effects of mechanical bending of noncentrosymmetric CdS semiconductor wafers 13 p2020 A72-28524

Radiation coherence enhancement in pulsed semiconductor injection laser by voltage controlled barium zirconite piezoceramic element 15 p2245 A72-31416

Nondispersive guidance structure for acoustic surface waves due to velocity reduction of thin conducting strip on piezoelectric substrate 15 p2278 A72-32506

Piezosemiconductor crystals acoustoelectric surface domain waveguide effect for classical and transverse surface waves 16 p2441 A72-33596

Rayleigh wave propagation on a piezodielectric-semiconductor boundary 17 p2596 A72-35541

PIEZOELECTRIC GAGES

Variable torque determination in precision work technology, discussing electronic measurements of length, shaft deformation, torsion angle and force 14 p2104 A72-30485

PIEZOELECTRIC TRANSDUCERS

NT PIEZOELECTRIC GAGES

Multi-electrode piezoelectric chip ultrasonic transducer, sampling and readout techniques for radioisotope encapsulation testing 01 p0069 A72-10810

Gas turbine rotor disk and blade vibrations piezoelectric measurement, describing capacitive transmitter system devoid of rotor mounted power supplies 02 p0232 A72-12735

Ultrasonic resonance thickness gage sensitivity and accuracy, noting damper, piezoelectric plate, protector and frequency band influence 03 p0361 A72-13986

Acoustic emission systems application to materials nondestructive testing, discussing single and multiple piezoelectric transducer arrays with on-line computer analysis [SAE PAPER 720175] 06 p0819 A72-17323

Acoustic wave detection in strain transducer consisting of silicon insulated gate field effect transistor with piezoelectric film incorporated in insulator region 08 p1168 A72-21556

Statistical analysis of piezoelectric transducer voltage-displacement characteristic, determining linearity deviations magnitude 09 p1317 A72-23676

Transducers for piezoelectric detection of torsional waves for wire chambers 10 p1480 A72-24212

Electromechanical coupling and acoustic impedance response in piezoelectric transducer with diffusion under fixed charge 11 p1636 A72-26590

Piezoelectric transducer for indirect on-wrist blood pressure measurements for clinical environment 12 p1772 A72-27961

Laplace transformation for mechanical response of piezoelectric composite transducer under action of thermal field and electric potential, noting time dependent modulus of elasticity 13 p1955 A72-28621

Frequency method of mechanical impedance monitoring of natural frequency of transducer-article system under load in defectoscopy 13 p1956 A72-28923

Physical operation principles of semiconductor sensors using deformation potential for mechanical stress detection and measurement 14 p2104 A72-30445

Acoustic surface wave chirp filters application in pulse compression radar system, considering various piezoelectric substrate materials characteristics 14 p2089 A72-31045

Embedded piezoelectric quartz crystal transducer with Hopkinson pressure bar to measure internal dynamic stress 15 p2240 A72-32433

Piezoelectric shock transducers system performance tests, assessing previously recorded shock signatures 16 p2393 A72-33636

Piezoelectric waveguide generalized treatment via field representation by sum of normal mode waves, using modified orthogonality relation 16 p2369 A72-33761

High-frequency ultrasonic devices. 17 p2526 A72-34564

Theory for the excitation of SHF elastic waves by multiple-film transducers /Allowance for the influence of metallic and dielectric layers/ 17 p2529 A72-34843

Some uncommon electric transducers for the measurement of mechanical quantities. 18 p2690 A72-36369

Effect of electrode thickness on the frequency response of a piezoelectric transducer 18 p2693 A72-37218

A technique for position sensing and improved momentum evaluation of microparticle impacts in space. 19 p2795 A72-37518

Room temperature operation of microwave acoustic delay lines with magnesium aluminate spinel, discussing acoustic mode conversion and shear wave piezoelectric transducers 19 p2800 A72-37875

Analysis of piezoelectric thin-film transducers for elastic surface waves. 19 p2804 A72-38607

Pulsed operation mode of acoustic system of damper-piezovibrator-layer load connected into electrical circuit of thyatron generator
19 p2805 A72-38764

Acoustic emission experiments design based on piezoelectric transducer, discussing signal detection and data acquisition methods
20 p2924 A72-39278

Response of the average pressure acting on the surface of an emitting circular transducer due to different reflecting objects.
21 p3055 A72-40948

Pressure dependence of electrical characteristics of semiconductor sensors using deformation potential for mechanical stress detection and measurement
21 p3056 A72-41109

Application of piezoelectric transducers for the measurement of static pressures
21 p3035 A72-41811

Allowance for the striking angle of a meteoric body with penetration-depth and piezoelectric sensors in the evaluation of the spatial density of meteoric matter
22 p3234 A72-42219

Miniaturized piezoelectric transducer electronics versus charge amplifiers - A comparison of the two systems in vibration and pressure applications.
22 p3159 A72-42702

A preamplifier with high input impedance for use with piezoelectric sensors
22 p3160 A72-42923

On mechanical response of a non-uniform piezoelectric transducer under the influence of a body-force.
23 p3291 A72-44316

PIEZOELECTRICITY

Transverse acoustoelectric surface wave domain in piezo-semiconducting body, obtaining gain coefficient and generation threshold criterion
05 p0702 A72-16283

Two terminal semiconductor strain tensor based on evaporated piezoelectric layer for modulation of forward I-V characteristics of thin film diode
08 p1164 A72-20925

Piezoresistance magnitude and temperature dependence changes of electron irradiated n-type silicon due to oxygen vacancy complex /A center/
09 p1372 A72-23239

Telecommunications ultrasonic resonators, electromechanical and piezoelectric filters and microacoustic surface elastic wave devices
09 p1281 A72-23468

Coupled electroelastic vibrations of piezoceramic cylinders from polycrystalline electrostriction theory, taking into account mechanical and dielectric losses
14 p2132 A72-31117

Piezoelectric substrate covered with semiconductor layers, calculating sound amplification characteristics at microwave frequencies
15 p2197 A72-31893

Be doped p-type Si piezoresistance and hole transport properties dependence on temperature, crystal orientation and doping concentration
16 p2442 A72-33834

Composite materials sum and product physical properties, considering magnetostrictive and piezoelectric interactions
18 p2717 A72-35996

Acousto-optic modulation with coupled Gunn oscillator-piezoelectric structure.
20 p2960 A72-39702

Amplification of acoustic surface waves under transverse magnetic field in coupled intrinsic semiconductor-piezodielectric systems.
20 p2960 A72-39703

Method of eigenfunctions in problems of thermoelasticity and electroelasticity
21 p3122 A72-41348

Electromagnetic waves interaction with transverse waves of thin piezoelectric plate in waveguide, noting transformation into acoustic waves
23 p3312 A72-43407

PIEZOMETERS

State of gas parameters measurement apparatus at high temperatures and pressures involving constant volume piezometer with internal heating
06 p0814 A72-17616

PIEZORESISTIVE TRANSDUCERS

NT PIEZOELECTRIC GAGES
Viscously damped miniature piezoresistive biaxial accelerometer for operation in single cavity to 250 F
22 p3179 A72-42701

PIGEONS

Component duration and relative response rates in multiple schedules of pigeon training
08 p1128 A72-22175

PIGMENTS

NT CHLOROPHYLLS
NT CYTOCHROMES
Porphyrin exobiology, discussing organic and random biosynthesis and extraterrestrial existence based on interstellar spectral evidence
05 p0617 A72-16130

Phase shifting effect of light on circadian rhythm and photoreceptive pigment location in Drosophila in postupation stages
07 p0919 A72-19536

Zirconium dioxide white pigment coatings for spacecraft thermal control, discussing impurities effects on optical absorption properties
07 p1023 A72-19692

High purity fine particle pigment materials preparation for spacecraft thermal control coatings, discussing hydrothermal, cryochemical and vapor phase processes
10 p1500 A72-24145

Apollo 12 material effect on tobacco tissue cultures, noting pigment increase
12 p1761 A72-27626

Five-component cyclic model of retinal photopigment kinetics for photochemical changes corresponding to rod adaptation in rat and man in dark
13 p1906 A72-29966

Nitriles, nitrogen bases and prophyrin-like pigments catalytic synthesis products analysis by mass spectroscopy gas and other chromatographies
14 p2157 A72-30583

Human retinal rod rhodopsin bleaching and regeneration measurements, tracing dark adaptation curves
15 p2184 A72-31364

Dark adaptation studies of bleach-induced visual threshold rise and subsequent return to rhodopsin level
15 p2184 A72-31365

Lamellar structure and rhodopsin location in bleached and unbleached rod photoreceptor membranes of dark adapted frog retinas by X ray diffraction study
15 p2186 A72-32199

The distribution of the long wave photoreceptors in the compound eye of the honey bee as revealed by selective osmic staining.
17 p2500 A72-34877

Electroretinographic evidence for a photopic system in the rat.
17 p2500 A72-34878

Fly colour vision.
18 p2651 A72-36609

Isolated retina receptor potential amplitude relation to visual pigment bleaching kinetics, indicating excitation-inhibition receptor response generation mechanism
19 p2756 A72-37830

Spectral sensitivity after prolonged intense spectral light exposure of rhesus monkey corneas, demonstrating long term loss of cone photopigment response
21 p3000 A72-40739

The presence of P700 in chloroplast fragments prepared by short time incubation with Triton X-100.
23 p3258 A72-44325

The photopigment bleaching hypothesis of complementary after-images - A psychophysical test.
23 p3258 A72-44376

Light absorption by visual pigment in photoreceptor, noting Airy disk diameter effect
23 p3259 A72-44388

PIGS [SWINE]

U SWINE

PILOT ERROR

Aircraft accident statistical projections from human error review, analyzing situational circumstance limitations
14 p2081 A72-31086

Airplane attitude display motion relationship to external world as factor in pilot error due to visual frame of reference shift
14 p2083 A72-31151

Grouping of the causative factors in investigation of aircraft accidents attributed to pilot errors.
17 p2508 A72-34557

Relation between a pilot's sensory perception of linear accelerations and the aircraft motion.
24 p3377 A72-45654

PILOT PERFORMANCE

Foot forces exerted at various aircraft brake-pedal angles, observing 20 degree zone with maximum effectiveness
[AD-733551] 01 p0018 A72-10567

Soyuz 9 flight crew physiological data, discussing mental and physical performance and adaptation and readaptation to space-earth environments
01 p0020 A72-10933

Navigators, pilots and airman trainees response to Coriolis accelerations, investigating nystagmus sensitivity coefficient relationship to motion sickness resistance
01 p0021 A72-11286

Disorientation and related experiences reported by pilots flying several aircraft types, comparing with previous reports
01 p0021 A72-11288

Pilots in aircraft systems management involving machine and air traffic environment
03 p0309 A72-13419

Moving display visibility effect on pilot tracking performance, discussing dependence on illumination intensity and color
04 p0477 A72-14445

Collision avoidance systems and pilot warning instruments, minimizing cost by pilot detection, evaluation and avoidance execution
04 p0545 A72-14823

Pilot in-flight incapacitation probability from airline reports, career termination studies and questionnaire responses
04 p0479 A72-14870

Feedback gains for STOL aircraft display pilot interactive flight director design, using computerized approach-touchdown simulation and optimal control theory
[ASME PAPER 71-WA/AUT-9] 05 p0684 A72-15956

Pilot perception tests on estimating flight path inclination, ground image and touchdown time under poor visibility
05 p0684 A72-16180

Pilots oxygen uptake vs flight time and altitude as indicator of physical condition, noting large fluctuations and differences for individual pilots and different flights
05 p0623 A72-16748

General aviation type light airplanes pilot workload during steep landing approach, comparing flight tested control response parameters with handling qualities criteria
[AIAA PAPER 72-125] 05 p0613 A72-16941

Pilot evaluation of Boeing 747 handling, directional stability, stall, rudder feel forces, landing, inertial navigation and reliability
05 p0614 A72-16992

Emotional aspects of pilot performance under high stress in emergency situations, discussing psychophysiological training methods
05 p0623 A72-17098

Airline pilot performance in automated ATC system involving use of surveillance data and instantaneous discrete communications
06 p0844 A72-17331

Pilot role in automated ATC system using onboard situation display with navigation and collision avoidance devices
06 p0844 A72-17332

Airline pilot postexercise electrocardiograms, showing S-T segment depression correlation to subsequent coronary heart disease
06 p0768 A72-17881

Tranquilizers effect on pilot in-flight performance, discussing flight safety, alcohol potentiating effect, student pilot stress reactions and airsickness treatment
06 p0768 A72-18158

Psychophysiological potentials of pilots in simulated emergency situations, investigating motor reaction time, signal selection time, error number and type and processed information amount and rate
06 p0769 A72-18199

Aircraft pilot performance during instrument approach in low visibility conditions
07 p0925 A72-18832

Selective attention dichotic listening test as flying proficiency prediction criteria, discussing omission and intrusion errors
07 p0929 A72-19351

Sleep pattern relation to duty hours of aircrew operating worldwide east-west routes
07 p0932 A72-20178

Hypoxia effect on aircraft pilot performance during altitude and flight simulation, testing instrument landing approaches
[AMRL-TR-71-97] 07 p0933 A72-20186

Hypnotic drug use effect on pilot performance and flight safety, using glutethimide, flurazepam and placebo in double blind study
07 p0933 A72-20188

Physiological evaluation of crew piloting qualities, considering nervous/emotional stress, ECG, arterial pressure and breathing frequency recorded on simulator
07 p0934 A72-20375

Kalman filter estimator for nonlinear human pilot model parameters including time delay
08 p1145 A72-20861

Pilot and ATC radar controller workload variations relation, discussing distraction stress effects
09 p1271 A72-23132

Pilot warning systems for visual midair collision avoidance, noting reaction to imminent threats, scanning patterns and display sector size effects
[SAE PAPER 720312] 11 p1583 A72-25576

Case report of fighter pilot disorientation episode during night flying exercise, suggesting psychological stress factor
11 p1584 A72-26019

Transnational air travel as cause of psychological and physiological rhythm change effects on pilot performance
11 p1589 A72-26694

Factor analysis of grades for successful performance skill identification during undergraduate and graduate jet pilot training
12 p1769 A72-27472

Computer analysis of helicopter pilots eye movement patterns dependence on visual task skill and performance time

12 p1770 A72-27475

Vestibular, auditory, acceleration and altitude decompression testing of pilot following endolymphatic shunt surgery for Menieres disease

12 p1771 A72-27485

Flight tests of stability augmentation system for light airplane improving pilot control during IFR encounter

12 p1754 A72-27513

Project pilot criteria for preparation and execution of flight test specifications

12 p1754 A72-27517

Pilot evaluation of C-5 automatic landing system in Category III weather environment

12 p1842 A72-27521

Russian book on pathophysiological principles of air and space pharmacology covering stress and fatigue reduction and pilots and astronauts performance improvement

12 p1772 A72-27926

Pilot-aircraft system model for relationship between weapons delivery accuracy and manual flight control system design, noting display, computation and control aids to pilot

12 p1773 A72-28121

Arterial blood gas tensions, using sequential phased dilution for pilot oxygen delivery

12 p1764 A72-28255

Motion sickness experience correlations to vestibular tests in pilots and nonpilots

12 p1764 A72-28257

Semicircular canal function correlation to thresholds, aftereffects and power functions in pilot vestibular tests

12 p1764 A72-28259

Pilot glide slope and localized tracking performance during successive in-flight simulated ILS approaches

12 p1773 A72-28260

Biothermal response of increased core temperature in rhesus monkey to mechanical vibration, noting implications for pilot performance during prolonged buffeting

12 p1774 A72-28268

Angular oscillation in yaw effect of pilot visual performance, showing vestibulo-ocular compensation and frequency response

12 p1774 A72-28269

Mathematical expression for pilot incapacitation applied to data from high stress/short duration encounters with environmental problems

12 p1775 A72-28284

Workload modification effects on pilot neurological changes during Boeing 707 letdown, approach and landing

12 p1775 A72-28290

Physiological effects of intense anticollision flash light backscatter pulses on instrument rated pilots

12 p1775 A72-28303

Hypoxia effect on aircraft pilot performance, using Link GAT 1 trainer and controlled composition atmosphere under varied altitude conditions for simulated ILS landing approaches

12 p1776 A72-28310

Pilot pursuit tracking performance under acceleration stress, simulating high performance aircraft dynamics via human centrifuge equipped with simulated head-up predictive gunsight

12 p1776 A72-28320

FAA program for revision of aviation aircraft maximum allowable control forces specifications, taking into account female pilots capabilities

12 p1777 A72-28325

Medication effects on pilot performance, covering tranquilizers, sedatives, antibiotics, stimulants, anticholinergics and hypotension drugs

13 p1909 A72-28750

Pilot landing performance prediction criteria based on day and night carrier qualification trials and flight training

14 p2081 A72-31084

Medical factors in air racing accidents, investigating drug, fatigue and gastrointestinal symptoms effects on pilot reaction to emergency

14 p2081 A72-31089

Annual clinical and physiological evaluation of test pilots physical performance over ten year period from body composition, pulmonary function and work capacity measurements

14 p2082 A72-31093

Stapedectomy postoperative complications as flying hazard, discussing pilot reaction to middle ear pressure changes

14 p2082 A72-31094

General aircraft accident investigation approach, using subsequent psychosocial reconstruction of pilot lifestyle to explain accident-producing behavior

14 p2082 A72-31095

Pupil reflex loss /pupillotonia/ diagnosis in pilots, testing sensitivity to methacholine chloride [AD-744368]

14 p2082 A72-31096

ECG heart rate recording of helicopter instructor pilots during flight training tasks, administrative work, automobile driving and eating

14 p2082 A72-31097

Airplane attitude display motion relationship to external world as factor in pilot error due to visual frame of reference shift

14 p2083 A72-31151

Aircraft pilot reaction capability for switch activation in response to voice countdown, tone initiation and termination, noting standard deviation

15 p2188 A72-31787

Airline pilot rotation perception during angular acceleration tests, noting power law description of subjective motion for three major body axes

16 p2358 A72-33649

Airline management and flight crew role in prevention, detection and dealing with airline pilot incapacitation in flight, noting physiological and psychological factor recognition

17 p2508 A72-34555

Performance measurement in helicopter training and operations.

17 p2509 A72-35550

Pilot-fighter aircraft system mathematical model relating pilot performance to air to ground weapon delivery accuracy

17 p2493 A72-35564

Congruent and spurious motion in the learning and performance of a compensatory tracking task.

17 p2510 A72-35692

Human factors engineering techniques in pilot-aircraft-environment adaptation to ease workload and in performance efficiency improvement

17 p2493 A72-35792

Midair collision causes and prevention, considering pilot responsibilities, anticollision devices and procedures

19 p2831 A72-37800

Resumption of flight after retinal surgery

19 p2760 A72-37879

Active leisure effect on pilot work efficiency, health maintenance and job longevity

19 p2760 A72-38148

Studies in pilot training - The anatomy of transfer.

20 p2897 A72-39718

Instruments installation effect on soviet passenger aircraft pilot performance, discussing Tupolev aircraft control systems

21 p2994 A72-40173

Application of the head-up display /HUD/ to a commercial jet transport.

21 p3060 A72-41256

Improved qualitative flight data rating scales.

21 p2996 A72-41257

Results of the investigation of different extrapolation displays.

21 p3012 A72-41431

Influence of prolonged longitudinal accelerations on control habits

21 p3004 A72-41750

Biological rhythms origin and mechanisms, discussing 24-hour cycle, subcellular biological clock and rhythm disruption effects in speologists, astronauts and pilots

22 p3141 A72-41985

An analysis of aircraft lateral-directional handling qualities using pilot models.

22 p3137 A72-42347

Agricultural aircraft flight loads - Typical spectra and some observations on airworthiness.

24 p3366 A72-44734

Pilot workload assessment technique during transport aircraft approach and landing, correlating with aircraft serviceability, crew efficiency, navigation aids, meteorological conditions and control procedure factors

24 p3377 A72-45657

Intoxicating liquor and the general aviation pilot in 1971.

24 p3377 A72-45662

PILOT SELECTION

Long term prognosis of transient hypertension in young male adults, evaluating importance in pilot selection

01 p0022 A72-11295

Student naval aviator selection by multiple correlation technique using noncognitive college and flight background questionnaire to reduce attrition rate

02 p0166 A72-11704

Hazard rate of recurrence in patients with malignant melanoma, investigating survival

02 p0167 A72-11713

Hemodynamic response to running exercise stress for aeronautics personnel selection, determining systolic ejection variation measurement and cardiac frequency increase

07 p0927 A72-19242

Pilot selection criterion for replacement air group /RAG/, using scored maneuver item correlations for flight crew and pilot training

12 p1774 A72-28262

IR pupillography for screening narcoleptics and fatigue prone individuals from driver and pilot training applicants

12 p1777 A72-28323

Anthropometric data utilization for military pilot/aircraft compatibility evaluation, discussing cockpit exclusion code development and implementation

12 p1777 A72-28324

Piloting aptitude evaluation from ECG during hypoxia, considering right intraventricular conduction and ventricular repolarization anomalies

13 p1906 A72-29857

Prophylactic otolaryngological investigation of vestibular analyzer function in aviation medicine

15 p2186 A72-31769

California psychological inventory as a predictor of success in the Naval flight program.

24 p3377 A72-45655

PILOT TRAINING

Hypoxia tolerance among pupil pilots during aeromedical instruction in decompression chamber, obtaining EEG and cardiac rhythm recordings

04 p0466 A72-14567

Medicopsychological surveillance of aircrew in fighter pilot school, stressing time factor in pilot training

04 p0467 A72-14569

Fighter pilots training by simulators, determining learning effectiveness by mathematical model based on renewal theory

[AIAA PAPER 72-161]

05 p0644 A72-16827

Student pilot syncope during altitude chamber training, discussing physiological mechanism from cardiovascular studies and psychiatric evaluation

06 p0767 A72-17879

Night Carrier Landing Trainer flight and carrier environment simulator for A-7 aircraft pilot training, discussing performance predictions from computer data analysis

07 p0927 A72-19137

Disorientation in naval aircraft accidents from psychophysiological and environmental factors, suggesting flight scheduling and training improvements

08 p1126 A72-21574

Pilot survival probabilities under various conditions of high performance aircraft takeoff and landing accidents, suggesting emergency action guidelines for pilot training

10 p1428 A72-23732

Interactive computer graphics with three dimensional real time CRT display of air combat maneuvers for fighter pilot training

11 p1613 A72-26299

Factor analysis of grades for successful performance skill identification during undergraduate and graduate jet pilot training

12 p1769 A72-27472

Flight stress and performance of training in general aviation simulator compared with actual flight

12 p1774 A72-28261

Pilot selection criterion for replacement air group /RAG/, using scored maneuver item correlations for flight crew and pilot training

12 p1774 A72-28262

Anxiety relation to success or failure in naval flight training program

12 p1774 A72-28263

Pilot trainer transfer function identification for man-machine and on-line adaptive control system using analog/hybrid computer

14 p2091 A72-30721

Aircraft and other vehicle simulators for training crews, discussing evolution of needs, digital techniques, and visual and physiological experiences

14 p2092 A72-30844

Low cost flight simulator for general aviation pilot training, containing IFB instrumentation and turbulence injection device

15 p2214 A72-32211

Simulated blind approach trainer for general aviation aircraft pilot training, discussing design concept and instrumentation with emphasis on components simplicity and economy

17 p2536 A72-35325

Performance measurement in helicopter training and operations.

[PP-10-72]

17 p2509 A72-35550

Congruent and spurious motion in the learning and performance of a compensatory tracking task.

17 p2510 A72-35692

How United trains DC-10 pilots.

19 p2760 A72-37898

Studies in pilot training - The anatomy of transfer.

20 p2897 A72-39718

Future aspects of business aviation, discussing pilot training and aircraft reliability and maintenance in context of flight safety

20 p2988 A72-39741

Visual simulation - A proven training method.

20 p2897 A72-39749

PILOTTED CENTRIFUGES

U HUMAN CENTRIFUGES

PILOTLESS AIRCRAFT

NT TARGET DRONE AIRCRAFT

Unified single rf channel tracking, telemetry and command control systems for guidance of unmanned vehicles, including pilotless aircraft and satellites
05 p0685 A72-16556

Remotely manned vehicles (RMV) application in aerial warfare, considering anti-aircraft defenses lethality increase, equipment costs and role of man during combat mission
13 p1896 A72-28451

PILOTS (PERSONNEL)
NT AIRCRAFT PILOTS
NT TEST PILOTS
Sudden pilot incapacitation and death due to sub-arachnoid hemorrhage secondary to ruptured intracranial aneurysm
10 p1429 A72-23742

PINCH EFFECT
NT PLASMA PINCH
NT THETA PINCH
Multivalley semiconductors electrical pinch effect during electron heating, considering Sasaki effect and sample depletion
02 p0269 A72-12886

Dash phenomenon in eruptive loop prominences representing solar flare process at all levels of atmosphere, discussing pinch effect instability
03 p0411 A72-13332

Pinch-in effect due to emitter current distribution instability in transistors with emitter-stripe geometry
04 p0499 A72-15209

Magnetospheric quasi-stationary pinch effect and filamentary structure due to electron streams parallel to geomagnetic field lines
14 p2103 A72-30664

Barium cloud striations deformation in ionosphere explained by equations of motion for plasma cloud thin bar model, discussing pinch effect
16 p2387 A72-33907

Earth magnetosphere pinch effect related to geomagnetic field pulsations and polar aurora luminosity fluctuations
18 p2688 A72-36867

Time dependence of the divergence of the radiation emitted by a rhodamine laser pumped by a pinched discharge.
24 p3411 A72-45612

PINHOLES
Pinhole, fly-eye and holographic stereogram methods, examining resolution relationships, horizontal and vertical parallax and aberrations
05 p0663 A72-16673

X and gamma ray astronomy with multiple pinhole cameras and a posteriori image synthesis, obtaining SNR gain
11 p1629 A72-25313

PINTLES
Pintle-controlled rocket engine design with gimbaled supersonic splittine thrust vector control, featuring variable thrust, attitude controls and high propulsion efficiency
[SAE PAPER 710763] 01 p0115 A72-10260

PION BEAMS
Linear energy transfer distribution for negative pions beams in human tissue, calculating relative biological efficiency and oxygen enhancement ratio
[CERN-71-16] 02 p0162 A72-12064

Analysis of pion-helium scattering for the pion charge form factor.
19 p2837 A72-37922

PIONEER SPACE PROBES
Electrical power subsystem design in Pioneer F/G spacecraft, using SNAP 19 deployable radioactive thermoelectric generators supplemented by Ag-Cd battery
01 p0008 A72-11065

Pioneer F and G space probe EMC specification limits, comparing computer analysis prediction and system test data
03 p0329 A72-14048

Distributions and average values for proton speed, azimuthal and polar flow directions and proton temperature and density in solar wind from Pioneer data
07 p1063 A72-20380

Jupiter investigation by Pioneer F and G after asteroid belt traversal, discussing Jovian physical characteristics, spacecraft systems and experiments
08 p1230 A72-20979

Astronomical interpretation of dust particle data recorded by Pioneer spacecraft, suggesting sensor surface orientation role for error correction
08 p1232 A72-21149

Engraved message on Au anodized Al plate aboard Pioneer 10 spacecraft for extraterrestrials after exiting solar system via momentum exchange with Jupiter
08 p1236 A72-21459

Pioneer 10 probe survival hazards during passage through asteroids belt and intense Jupiter radiation fields
10 p1551 A72-24272

Conical scanning system for Pioneer Jupiter spacecraft pointing control, discussing signal processor, spacecraft dynamic behavior, system stability and error budget
15 p2320 A72-31791

Pioneer spacecraft intermittent solar wind streams data temporal variations analysis to account for anomalous type 3 bursts
15 p2299 A72-31964

Scientific problem resolution during Jupiter missions, discussing Pioneer probes, trapped particle belts, Red Spot, atmosphere, biological activity, internal heat sources and radio emission
19 p2864 A72-38381

Astronomical interpretation of dust particle data recorded by Pioneer spacecraft, suggesting sensor surface orientation role for error correction
20 p2968 A72-39254

Attitude perturbations of a spinning Jupiter Orbiter spacecraft.
[AIAA PAPER 72-920] 21 p3115 A72-41565

Explorer satellites and Pioneer space probes development program, discussing launching rockets, reentry tests, payloads, radio communication, Van Allen belts discovery, etc
23 p3358 A72-44353

PIONEER 6 SPACE PROBE
Solar wind reverse and forward oblique slow shocks, examining discontinuities from Pioneer 6 plasma and magnetic field data
01 p0120 A72-10882

PIONEER 7 SPACE PROBE
Pioneer 7 observations of the August 29, 1966, interplanetary shock-wave ensemble.
21 p3104 A72-40481

PIONEER 8 SPACE PROBE
Pioneer 8 plasma wave measurements at distant bow shock crossings, considering solar wind-magnetosheath interaction
01 p0062 A72-10903

Change in the eleven-year modulation at the time of the June 8, 1969, Forbush decrease.
22 p3172 A72-42424

PIONS
Absorbed doses at various depths in water target exposed to charged pions, muons and electron beams, using Monte Carlo program
[CERN-71-16] 02 p0162 A72-12063

Neutron energy spectrum of radiative pion captured by carbon 12, using gamma and neutron counters
05 p0692 A72-16688

Nuclear-electron cascades longitudinal evolution calculation in ionization calorimeter for primary nucleons and pions, using Monte Carlo method
06 p0811 A72-17260

Cosmic ray hadrons inelastic collision cross sections and partial K-neutral pion inelasticity factor in ionization calorimeter
06 p0868 A72-17262

High energy cosmic ray pions and nucleons interactions with atomic nuclei, using ionization calorimeter and spark chambers system
06 p0869 A72-17267

K-neutral pion inelasticity factor measurement for nucleon interactions in carbon corresponding to primary neutron energy transferred to pions
06 p0869 A72-17269

Secondary particles in pion-nucleon and coherent interactions, measuring momentum from multiple Coulomb scattering
06 p0870 A72-17272

Nuclear photoemulsions under bombardment by pion beam of 60 GeV/c momentum, investigating pion-nucleon interactions involving recoil protons
06 p0851 A72-17273

Pion-nucleon high energy interactions, determining inelasticity coefficient distribution
06 p0851 A72-17274

Spark calorimeter calibration by particle accelerator induced high energy pions, noting neutral and charged particles track detectors high geometric resolution
06 p0811 A72-17292

K-neutral pion energy fractions and inelasticity coefficients at primary energies of 100-1500 Gev during hadron-target interaction
06 p0872 A72-17295

Meteorological effects on cosmic rays, deriving muon and pion intensity and meteorological coefficient formulas and computer calculation scheme
07 p1066 A72-20654

Pion generation during collective interactions between nucleons of heavy cosmic ray nuclei, using Proton 4 satellite data
08 p1228 A72-22179

Pionic X ray fields and transitions in Li 6, Be 9, C 12 and O 16, obtaining 2p level absorption broadening
10 p1515 A72-24418

Scintillation TICI /Li,Be/ crystal response to 8 GeV ionizing negative pions, noting pulse shape and resolution characteristics
15 p2291 A72-31535

Meson exchange effects on solar pion-production process, using low energy Adler theorem with cross section correction factor
16 p2456 A72-33476

Pion-electron conjugation and twist angles determination in biphenyls via Raman intensity, comparing with hypsochromic UV shift of Suzuki method
16 p2431 A72-33585

Underground delayed shower particles small pulse events interaction analysis for muons and pions compared with quark behavior
16 p2450 A72-34140

Test of scale invariance in pion production at high energies using cosmic ray primary nucleon and sea level muon intensities.
17 p2599 A72-34875

Pion generation during collective interactions between nucleons in heavy cosmic ray nuclei, using Proton 4 satellite data
18 p2721 A72-36235

Pion exchange and the cosmic-ray nucleon cascade.
19 p2851 A72-37923

High altitude cosmic ray pion and nucleon interaction characteristics at high energies, using spark chamber, Cerenkov absorption spectrometer and ionization calorimeter measurements
23 p3329 A72-44402

Ionization calorimeter for neutral pion production investigation in high energy hadrons interaction, noting energy transfer identity for nucleon and pion interactions
23 p3330 A72-44409

Approximation for Monte Carlo method modeling of pion-nucleon and nucleon-nucleon inelastic collisions at high energies
23 p3317 A72-44414

High energy inelastic collisions of pions and protons with nuclear emulsion nucleons, noting pion pulse spectra
23 p3317 A72-44417

Characteristics of pion and nucleon interaction with carbon and aluminum nuclei over the energy range from 30 to 300 GeV
23 p3331 A72-44435

Study of the angular distribution of charged and neutral pions during inelastic interactions in the energy region above 1 TeV
23 p3291 A72-44443

Angular and impulse characteristics of negative-pion interactions at an energy of 60 GeV in the emulsion
23 p3292 A72-44446

PIPE FLOW
Laser anemometer system for instantaneous velocity measurement in turbulent pipe flow, determining two point velocity correlation coefficients
01 p0071 A72-11169

Hydraulic analogy application to heat conduction problems, considering seepage and network pipe flow models for complex heat flux phenomena representation
01 p0145 A72-11174

Pressure drop relation to entropy production in viscous low velocity adiabatic pipe flow, showing analogy with Oswatitch theorem
01 p0051 A72-11255

Equivalence laws and approximate equations for incompressible and compressible viscous flows in pipes with variable cross sections
01 p0051 A72-11256

Velocity and temperature effects on momentum and temperature equalization in coaxial turbulent jet mixing in pipe inlet section
[DFVLR-SONDDR-183] 01 p0051 A72-11257

Finite difference technique for heat transfer rate in laminar flow in tube with step change in cross section, discussing velocity profiles
02 p0301 A72-11273

Cross flow through in-line tube bank, investigating surface roughness effects on behavior by pressure drop, static pressure and skin friction distributions measurements
02 p0203 A72-12102

Thin liquid layer linear hydrodynamic stability in vertical rotating tube with core gas flow
02 p0303 A72-12353

Rarefied gases pressure flow and self diffusion through cylindrical tubes, presenting kinetic model with velocity independent mean free path
02 p0205 A72-12357

Heat transfer of nonequilibrium dissociating nitrogen dioxide in round tube, allowing for finite reaction velocity
02 p0303 A72-12861

Acoustic attenuation calculation for turbulent flow in rigid tubes, determining critical flow velocity dependence on wall roughness and sound wave frequency
03 p0340 A72-12954

Conducting fluid steady MHD pipe flow under transverse magnetic field, obtaining mass flow rate
03 p0394 A72-13241

Dynamic and electromagnetic characteristics of MHD flow in square tube with walls differing in electroconductivity within oblique transverse magnetic field
03 p0398 A72-14007

Kinetic energy losses due to liquid-to-solid phase transformation in heated two-component flow ascending in tube
03 p0342 A72-14161

Turbulent mixing length formulation and velocity profiles for non-Newtonian power law fluids, deter-

mining friction factor for pipe flow at high Reynolds numbers

03 p0343 A72-14318

Start-up flow of viscous incompressible fluid under constant head in entrance region of circular tube

03 p0344 A72-14343

Numerical solutions of integral equation for transition and turbulent flows through pipes and channels, discussing computer simulations

04 p0510 A72-14469

Pressure distribution and compressible gas critical flow rate in constant cross sectioned circular pipe with impermeable adiabatic wall from Frossel equations

04 p0511 A72-14640

Soviet book on hydraulics, hydraulic machines and hydraulic drives covering fluid dynamics, pipe flows, jet pumps, turbines, bladed transmissions, etc

04 p0466 A72-15247

Weakly ionized turbulent gas flow in pipe, comparing neutral and plasma fluctuations with laser beam scintillations

04 p0558 A72-15331

Conducting incompressible fluid in laminar pipe flow under traveling magnetic field, investigating friction coefficient and energy balance

04 p0558 A72-15341

High velocity unsteady flow calculations in metal pipes by numerical methods for boundary conditions, including turbomachinery, column separation and gas accumulator

[ASME PAPER 71-WA/FE-13] 05 p0646 A72-15931
Turbulent flow in smooth and rough pipes at Reynolds numbers 30,000-480,000, presenting velocity mean and fluctuating components rms and cross correlation values

[ASME PAPER 71-WA/FE-7] 05 p0647 A72-15935
Nonlinear disturbances of viscous flow in pipes and between rotating cylinders, considering Couette and Poiseuille flows

05 p0648 A72-16027

German book on turbulent flow theory and applications covering isotropic and homogeneous nonisotropic fields, shear flows, pipe flows, free turbulence, boundary layers, etc

05 p0649 A72-16286

Noncoagulating polydisperse aerosol deposition from two dimensional turbulent boundary layer and fully developed turbulent pipe flows

[ALAA PAPER 72-81] 05 p0650 A72-16806

Unsteady axisymmetric incompressible pipe flow solution near piston, using Navier-Stokes equations solution with finite difference forms

05 p0653 A72-17006

Uniformly curved fluid conveying tube free vibration and stability, showing flow velocity, fluid pressure and Coriolis force effects on natural frequency

06 p0821 A72-17853

Reynolds analogy based correlation method for Stanton number prediction for turbulent heat and mass transfer in smooth tubes

06 p0903 A72-18186

Heat transfer and drag during air laminar flow in circular pipe with constant heat flux density at wall

07 p0966 A72-18938

Temperature pulsation spectra of turbulent mercury flow in horizontal pipe at various Reynolds numbers, showing dependence on magnetic field

07 p1100 A72-19882

Heat and mass transfer in initial section of circular pipe under stabilized laminar flow, using modified Leveque method

07 p0968 A72-19883

Inviscid relaxing gas flow through tube with variable cross sectional area, deriving governing equation for weak discontinuity amplitude evolution

07 p0970 A72-20073

Turbulent friction coefficients and velocity distribution in channel and pipe flow, using eddy viscosity model

08 p1150 A72-21623

Unsteady uniform turbulent flow of incompressible liquid in circular pipe, verifying mathematical model with velocity distribution calculations

08 p1151 A72-21666

Hydrodynamics of dispersed annular two phase flow in cylindrical channels characterized by concurrent motion of flow core and liquid film at wall

08 p1151 A72-21667

Turbulence measurements in shear flow systems including pipe, tank and multijet reactor configurations

09 p1292 A72-22306

Visual observations of wall in turbulent pipe flow, using suspending solid MgO particles

09 p1306 A72-22310

German monograph on heat transfer in chemically reacting gases covering laminar and turbulent tube flows for dissociated dinitrogen tetroxide

09 p1274 A72-22339

Steady turbulent flow and heat transfer downstream of circular pipe sudden enlargement, computing streamline and temperature profiles and wall fluxes

09 p1412 A72-23687

Adiabatic velocity profiles and pressure variations of developing laminar flow in circular tube, using finite difference computation in FORTRAN IV

10 p1463 A72-23863

Steady compressible fluid flow and plane shock wave propagation in pipe bends, discussing parameter effects and boundary conditions

10 p1464 A72-23878

Solute dispersion distribution over tube cross section with flowing solvent, comparing with Gaussian distribution

10 p1466 A72-24330

Laminar flow dispersion coefficient for curved tubes and channels determined by mathematical model, permitting concentration distribution computation

10 p1468 A72-24371

Second order fluids plane Poiseuille flow instability to finite amplitude disturbances, noting implications to Toms friction pressure reduction phenomenon in pipe flow

10 p1470 A72-25065

Axial pressure variations in incompressible laminar tube flow with uniform suction, noting application to heat pipes

[AIAA PAPER 72-257] 11 p1614 A72-25202
Real time hologram-moire interferometry for visualization of turbulence phenomena in liquid flow through cylindrical pipe

11 p1629 A72-25317

Non-Newtonian pipe flow turbulence measurements by laser anemometer, describing optical system and signal processing instrumentation

11 p1646 A72-25554

Thermodynamic coupling effects on temperature distribution, Nusselt number and cooling requirements in laminar nonisothermal pipe flow with coolant injection

11 p1745 A72-25734

Fluid compressibility effect on nonstationary laminar flow within infinite cylindrical pipe

11 p1618 A72-26502

Turbulent pipe flow laminarization by fluid injection, measuring axial turbulence intensity field and streamwise velocity distribution by hot-film anemometer

11 p1619 A72-26636

Reynolds analogy for twisted liquid flow in tube with swirl vanes

11 p1619 A72-26968

Viscoplastic media flow rate in noncircular tube from Newtonian fluid velocity profile, using Green formula

12 p1799 A72-27981

Swirling flow in round pipe with sudden expansion, discussing separation and reversal characteristics

13 p1942 A72-29640

Hydraulic fluids flow measurement in pipes by ultrasonic waves convection method, discussing transducers performance and mounting

13 p1959 A72-29668

Turbulent friction relation to averaged velocity profile of liquid flow in pipes and channels

14 p2096 A72-31019

Heat and mass transfer in steady viscous flow through curved circular tubes, investigating velocity and temperature profiles

14 p2173 A72-31064

Tangential and radial eddy diffusivity effects on nonsymmetric turbulent diffusion in plain impervious tube as function of Schmidt number

14 p2096 A72-31069

Steady state temperature field and heat flux at wall for metallic coolant flow in thin walled axisymmetric pipe with nonhomogeneous Neumann boundary condition

16 p2477 A72-33413

Energy and momentum losses of high temperature gas flow through externally cooled tube, solving laminar flow differential equations numerically on digital computer

16 p2378 A72-33430

Heat transfer and friction coefficients for turbulent flow in rough tubes as function of Reynolds and Prandtl number, using von Karman method

16 p2478 A72-33513

Drag reducing polymers influence on velocity gradients at wall for turbulent pipe flow, observing viscous sublayer thickening

16 p2379 A72-33574

Negative pressure gradients effects on turbulent viscosity profiles for gas flow through tubes, comparing dependence on transverse coordinates to incompressible flow case

16 p2380 A72-33860

The effect of axial boundary motion on pressure surge generation

[ASME PAPER 71-WA/FE-15] 17 p2539 A72-34969

Heat and mass transfer in initial section of circular pipe under stabilized laminar flow, using modified Leveque method

17 p2637 A72-35131

On the flutter of thin cylindrical shells conveying fluid.

17 p2634 A72-35415

Some specific characteristics of turbulent wall pressure fluctuations in a flow in a tube

17 p2541 A72-35545

Flow problems solutions estimation by variational principles application, exemplifying by plane Couette and Poiseuille and axisymmetric pipe flow

18 p2679 A72-36391

The stability of Poiseuille flow in a pipe of circular cross-section.

18 p2681 A72-36480

Poiseuille flow linear spatial stability in rigid pipe under infinitesimal disturbances, obtaining propagation modes eigenvalues

18 p2681 A72-36481

Closed system of differential equations derived for kinematic characteristics of nonstationary turbulent flow in pressurized smooth pipe

19 p2785 A72-37473

Linearized problem of one-dimensional periodic gas flow in a pipe

19 p2786 A72-37666

The friction drag factor for an unsteady motion in tubes

20 p2913 A72-39392

An analysis of heat transfer in turbulent pipe flow with variable properties.

[ASME PAPER 72-HT-59] 20 p2985 A72-39657

Non-isothermal laminar flow of gases through cooled tubes.

[ASME PAPER 72-HT-45] 20 p2985 A72-39665

The linear stability of flow in a circular pipe in the presence of a strong transverse magnetic field.

20 p2958 A72-40018

Turbulent mixing of fluids of different density moving in a tube

21 p3044 A72-40129

Flow of a non-Newtonian fluid in a tube with sinusoidal deformation.

21 p3044 A72-40192

Perturbation analysis of aerodynamic test flow in Ludwig tubes, investigating nonsteady coupling effects on nozzle turbulent boundary layer

[AIAA PAPER 72-994] 21 p2993 A72-41580

Experimental friction factors for turbulent flow with suction in a porous tube.

21 p3047 A72-41618

Unsteady laminar flow in a tube with arbitrary variation of the flow rate in time

22 p3164 A72-41892

Extremal bounds for mass flow rate of laminar MHD flow in circular and thin walled conducting pipes at high Hartmann number

22 p3210 A72-42315

Reverse flow sensing hot wire anemometer.

22 p3177 A72-42392

Unsteady convective heat transfer in the initial section of a pipe with a smooth inlet

23 p3356 A72-43670

Approximation for boundary value problem of homogeneous stationary combustion in laminar gas flow through cylindrical tube

23 p3356 A72-43798

Experimental study of heat transfer during cooling of a high-temperature gas flow in a pipe.

23 p3357 A72-44539

Periodic solutions of a nonlinear mixed problem for the Navier-Stokes equations

24 p3418 A72-44780

Decay of swirl in a straight pipe flow /with hub at the entrance/.

24 p3394 A72-45367

PIPELINES

Creep deformation upper bounds for smooth pipe bends under constant external bending moments, using energy method analysis

16 p2473 A72-34123

Rocket body longitudinal autooscillation modes, taking into account pipeline fluid discontinuous cavitation oscillations

17 p2620 A72-34469

Rational utilization of the strength capabilities of thermal-expansion compensators

21 p3127 A72-41702

PIPER AIRCRAFT

Design and development program for air conditioning system of twin engine unpressurized Piper Navajo, noting flight test results

[SAE PAPER 720328] 11 p1577 A72-25590

PIPES (TUBES)

NT U BENDS

Torsional stiffness /shear modulus/ of glass fiber reinforced plastic tubes as function of filament winding angle

01 p0141 A72-10999

Strain anisotropy effect on thin walled tubular steel samples with combined bending and torsion, constructing matrix and stress vectors

03 p0445 A72-13578

Small parameter method solutions to linear viscoelasticity problems with nonhomogeneous temperature field applied to reinforced tube under internal pressure

03 p0454 A72-14217

Two dimensional stationary temperature fields determination in ribs, cylinders and pipes with temperature independent heat conductivity

05 p0746 A72-16188

Axisymmetric stress analysis in various weld configurations of stub end high pressure pipe connections, using finite element method

06 p0820 A72-17709

Combined stress wave propagation in thin welded prestressed tube under longitudinal and torsional impact loading

06 p0898 A72-18321

Micrographic evaluation of inclusions in austenitic stainless steel tubes ensuring surface quality control

07 p0994 A72-18972

End holes effects on dielectric constant measurement of long glass tubes by cylindrical microwave resonant cavity

08 p1164 A72-20940

Pipe joint flexible metal seal development and testing for Concorde Olympus 593 under thermal and pressure cycling

08 p1178 A72-21938

Metric swaged pipe coupling design and development for aircraft hydraulic systems, presenting fatigue test results

08 p1179 A72-21940

Secondary normal stresses in fixed flange zone of thin welded nonlinearly elastic pipe under bending moment and torsion

08 p1249 A72-22096

Low thermal flux glass fiber composite over-wrapped tubing with metallic liners for leak free cryogenic propulsion plumbing systems

11 p1637 A72-25364

Uniaxial, biaxial and shear loading tests on filament wound carbon-carbon composite tubes and rings

11 p1670 A72-25458

Thin walled tubular carbon steel specimen deformation pattern under biaxial tension and internal pressure at normal and low temperatures

12 p1830 A72-28227

Statistical energy analysis of sound-structural interaction, considering sound transmission through complex walls and piping systems and fluid filled container vibrations

13 p2005 A72-29556

Dispersion hardening /aging/ effect on embrittlement of Ni base alloys in cold worked pipes during heat treatment

15 p2255 A72-31569

A method of calculating acoustic resonance phenomena generated by the unsteadiness of singular pressure losses in the pipes

17 p2580 A72-34279

Brazed-welded lightweight high pressure aerospace tube-fittings.

17 p2560 A72-34939

Stress criterion for creep rupture in tubes under combined axial load and internal pressure, deriving stress concentration from high temperature tests

19 p2874 A72-37715

Reduction of temperature difference in shielding pipes for light-beam transmission.

20 p2903 A72-39267

On the radiation from an open-ended corrugated pipe carrying the HE sub 11 mode.

21 p3015 A72-40366

Photoelastic study of stress concentration in perforated composite pipes under external pressure

22 p3233 A72-42064

Theory of thin elastic shells applied to pipe bends subjected to bending and internal pressure.

24 p3456 A72-44795

PISTON ENGINES

NT DIESEL ENGINES

Uranium hexafluoride pulsed plasma core reactor with artificial neutron source for spark plug and enclosed by cylinder and piston analogous to internal combustion engine

01 p0100 A72-11361

Vibration of reciprocating engine crankshafts and steam turbine, alternator and gas turbine rotor shafts supported on hydrodynamic sleeve bearings

08 p1225 A72-22133

Russian book - The ASH-62IR engine /4th enlarged edition/.

21 p3098 A72-40463

PISTON THEORY

Ballistic piston fissioning plasma production involving compression of uranium hexafluoride

01 p0111 A72-11333

Poincare-Lighthill-Kuo perturbation method and method of characteristics equivalence in one dimensional fluid motion due to ideal piston periodic oscillation

03 p0341 A72-13239

Flying machine using reaction forces on body moving in compressible fluids within piston device equivalent to air pressure pump

08 p1108 A72-21798

Piston exerting pressure on liquid filled cylinder, determining deformation state based on thin elastic orthotropic plate theory

10 p1556 A72-24266

Two and three dimensional pistons motion in stationary gas, calculating potential flow characteristics near weak discontinuities as function of piston geometry and acceleration

10 p1468 A72-24431

Spherical, cylindrical or plane piston motion in nonuniform medium with radiative energy transfer, obtaining approximate analytic solutions and temperature profile behind shock front

15 p2336 A72-32394

Piston generated magnetosonic shocks, investigating ion and electron pressure effects on formation

15 p2281 A72-32415

Self-similar unsteady magnetogasdynamic flows of a radiating gas produced by the motion of a piston

18 p2716 A72-36897

Experimental investigation of finite-amplitude acoustic oscillations in a closed tube.

23 p3314 A72-44124

PITCH

Pitch shift of pure tone by masking tones and band limited noise

01 p0101 A72-10159

Multiple pure tone noise generation from turbofan blade to blade nonuniformities in rotor geometry, using two dimensional inviscid flow model

04 p0565 A72-15568

An aspect of the problem of pitch dependence on the duration of short sinusoidal signals.

20 p2897 A72-39217

Tone noise from rotor/stator interactions in high speed fans.

24 p3433 A72-44917

PITCH [INCLINATION]

Drift shells and pitch angle evolution of energetic particle motion in magnetospheric model including convection electric field

01 p0117 A72-10077

Aircraft pitching and yawing cross couplings compensation at high speed

01 p0005 A72-10506

Self organizing adaptive aircraft control system with C criterion pitch axis performance and failure compensation

03 p0337 A72-12920

Pitch angle distributions of energetic protons for different geomagnetic activity levels as function of invariant latitude and magnetic local time from ESRO IB satellite measurements

07 p1057 A72-19141

Pitch angle and radial diffusions relationship in presence of drift shell splitting at arbitrary equatorial pitch angle

07 p1057 A72-19147

Strong pitch angle scattering of energetic electrons in presence of electrostatic waves due to ion cyclotron instability above midlatitude ionospheric trough region

11 p1714 A72-26398

Anisotropic electron pitch angle distributions at synchronous altitude due to wave-particle scattering and ionospheric acceleration along field lines

15 p2299 A72-31961

Geomagnetically trapped protons pitch angle distribution from ESRO 2 semiconductor telescope measurements

15 p2300 A72-31991

Pitch-angle diffusion of radiation belt electrons within the plasmasphere.

17 p2602 A72-35597

A method of calculating the pitch angle distributions of particle fluxes based on rocket and satellite data.

17 p2558 A72-35840

PITCH ANGLES

U PITCH [INCLINATION]

PITCH ATTITUDE CONTROL

U LONGITUDINAL CONTROL

PITCHING MOMENTS

Wind tunnel stability tests of aerodynamic pitch damping of aircraft model oscillating in two degrees of freedom

03 p0307 A72-13539

Nonspinning satellite earth-pointing attitude control for elliptic orbits using active regulation of pitch moment of inertia

08 p1204 A72-21605

Pitching moments effect on phugoid and height mode stability of aircraft in supersonic flight

09 p1263 A72-23622

Nose bluntness effect on bodies of revolution pitching moment characteristics in incompressible flow at various angles of attack

11 p1573 A72-26576

Effect of lagging pitching moment on re-entry vehicle dynamic stability.

17 p2619 A72-34202

PITOT STATIC TUBES

U PITOT TUBES

U SPEED INDICATORS

PITOT TUBES

Flight test procedures for subsonic transport aircraft pitot static pressure system, recommending trailing cone calibration method

01 p0064 A72-10389

Hypersonic two component gas mixture nozzle flow with condensation or evaporation discontinuity, determining Pitot pressure limits

02 p0230 A72-12255

Spatial boundary layer variations in low speed wind tunnel working section due to settling chamber screens, discussing mesh variations effects on Preston tube measured pressure coefficient distributions

07 p0966 A72-19061

Yaw calibrations of Preston tubes for wall shear stress measurements in two and three dimensional turbulent boundary layers

08 p1254 A72-21627

Pitot tube pressure measurements in supersonic gas flow, calculating free molecular conditions limits

10 p1419 A72-24548

Velocity calculation from pitot tube pressure measurements in compressible two phase flow, taking into account droplet momentum loss

14 p2104 A72-30252

Viscosity, velocity gradient and wall effects on pitot tube measurement of gas flow velocity measurement in turbulent boundary sublayer

14 p2094 A72-30294

Cylindrical pitot tube displacement effects on stagnation point and static pressure angle in impeller nonuniform peripheral flow

14 p2094 A72-30720

Turbulent friction values diminished by reading errors in pitot tube flow measurement of solid particles suspensions and polymer solutions caused by viscoelastic associations

14 p2106 A72-31007

On the use of the Preston tube in elliptical ducts.

18 p2676 A72-37094

A new stagnation pressure probe having a high pressure recovery in supersonic flow.

22 p3179 A72-42687

A comparison of disturbance levels measured in hypersonic tunnels using a hot-wire anemometer and a pitot pressure probe.

24 p3388 A72-45402

PITTING

Titanium sulfide initiation of pitting corrosion of Ti stabilized corrosion resistant Cr-Ni-Ti steels

03 p0379 A72-14367

Potential change under pitting corrosion and repassivation on Cr-Ni steels alloyed with V, Si, Mo and Re

04 p0535 A72-15730

Pitting potential and intergranular corrosion of anodically polarized Al and Al alloys in electrolytes

04 p0536 A72-15736

Etch pit technique for titanium and zirconium crystal orientation determination, discussing etch pit locations and polycrystalline specimen goniomicroscopic observation

05 p0679 A72-17124

Pitting and film deposits with organic fluid by electrolysis and fluid flow, discussing electrokinetically produced corrosion

07 p1010 A72-18802

Corrosion effects evaluation from electrode potentials, noting copper pitting and weathering

08 p1189 A72-22108

Metal single crystals use for corrosion tests, noting anisotropy, adsorption, oxidation and pitting

08 p1189 A72-22111

Liquid flow cavitation impact on rotating disk surfaces, showing pitting characteristics dependence on physicochemical properties of specimens

09 p1327 A72-22297

Stainless steels sensitivity to pitting corrosion under sulfides action, measuring rupture potential

11 p1661 A72-26648

Active corrosion in aqueous solutions, discussing reactions, adsorption, intergranular attack, pitting, crevice corrosion and stress corrosion cracking

19 p2815 A72-37446

Electrochemical protection potential of metals and alloys in pitting, intergranular corrosion and stress corrosion cracking in presence of chlorides

21 p3065 A72-40087

Influence of prior electrochemical history on the propagation of localized corrosion.

22 p3195 A72-43129

PITUITARY GLAND

Hypophysectomy in rats, resulting in prolonged red blood cell survival due to oxygen consumption decrease and altered erythrocyte enzymatic processes

01 p0010 A72-10075

PITUITARY HORMONES

Shock-induced fighting effect on pituitary adrenocorticotrophic hormone ACTH and adrenocortical steroids plasma concentration in rats, relating psychological stress to physiological function

05 p0617 A72-16080

Human male gonadotropin secretion relation to sleep stages, using electrophysiologic recordings and radioimmunoassay techniques

05 p0620 A72-17128

Human prolactin - 24-hour pattern with increased release during sleep.

23 p3316 A72-43977

Changes in the pituitary-thyroid and in the pituitary-gonad systems under conditions of functional loading and of physiological immobilization.

24 p3371 A72-44823

PIVOTS

Impulse excited spatial systems of rigid bodies linked by pivot joints with arbitrary kinematics, applying Maxwell-Betti theorem

15 p2323 A72-31461

PLAGES [FACULAE]

U FACULAE

PLAN POSITION INDICATORS

Peak reading and thresholding in radar weather data processing, describing PPI map

06 p0843 A72-18440

PLANAR STRUCTURES

Planar Gunn effect devices for microwave oscillators, discussing impedance matching and diode conductivity profile effect on output power

01 p0028 A72-10628

MHD boundary waves properties, noting application to traveling wave nonreciprocal devices and planar structures based on microwave integrated circuits

01 p0029 A72-10703

Isoplanatic instrument wave aberration determination, using longitudinal defocusing

03 p0360 A72-13563

Stress-strain state determination for plane orthotropic bodies by optical polarization method, discussing numerical methods for stress and strain tensor components

03 p0445 A72-13580

Si planar unijunction transistor fabrication, operation principles, parameter measurements and applications

05 p0635 A72-16196

Critique on condition for planar antennas physical reliability, concerning smoothness of aperture edges

06 p0782 A72-17362

Gain function for planar phased array far field pattern, deriving calculation method for excitation pattern for prescribed radiated beam behavior

08 p1132 A72-21328

Nonlinear mathematical dc models of planar transistors for computerized IC design and analysis obtained by continuity equation approximate solution

12 p1789 A72-27313

Pulse generation in planar Gunn devices of epitaxially grown GaAs layers, measuring current reduction by domain nucleation

12 p1791 A72-27671

Forward voltage vs temperature characteristics for Si planar p-n junction diodes, determining zero temperature energy gaps for silicon, germanium and GaAs

13 p1933 A72-29824

Thermal resistance of planar semiconductor structures.

17 p2594 A72-34296

Properties of a nonisosceles triangular grid planar phased array.

17 p2524 A72-34352

Pattern synthesis of hexagonal planar arrays.

17 p2525 A72-34363

Comparison of computer-acquired performance data from several fixed spaced planar diodes.

17 p2496 A72-34605

Controlled self heating effect in semiconductor barium titanate positive temperature coefficient resistor substrate heater for planar Si devices

17 p2527 A72-34680

Monoplastic solid encapsulant for n-p-n and p-n-p silicon planar passivated signal transistors

17 p2528 A72-34715

Application of the moving-slit X-ray automonochromatization method in structural studies of planar diodes and an attempt to correlate electrical properties with lattice defects.

17 p2595 A72-34749

Calculation of two-dimensional cascades in isentropic flow

17 p2484 A72-34893

Design of radiating elements for large planar arrays - Accomplishments and remaining challenges.

23 p3269 A72-43571

Hypersonic flow around plane and axisymmetric bodies of arbitrary shape with inviscid radiating gas.

24 p3360 A72-45110

PLANE WAVES

Stepped reflector image region fields at plane wave incidence angle to reflector axis, determining field components as Fourier series

01 p0035 A72-10115

Plane electromagnetic wave scattering by imperfectly conducting cylinder with radially inhomogeneous dielectric coating, using phase shift method for evaluation

01 p0024 A72-10130

Asymptotic intensity fluctuations of plane light wave propagating in turbulent medium, using parabolic equation and Markov model

01 p0050 A72-10348

Transient electromagnetic plane wave ionospheric transmission and reflection, considering impulsive and step modulated sine wave excitations

01 p0031 A72-11102

Far field diffraction due to annular apertures of plane wave light rendered partially coherent by atmospheric turbulence

01 p0103 A72-11166

Numerical-integral equation approach to plane wave scattering from nonplanar conducting surface with sinusoidal height profile for magnetic field parallel to surface ridges

[AD-735574] 01 p0032 A72-11237

Radar target thin rectangular plate model backscattering from incident and reflected waves, noting front and trailing edge phenomena with emphasis on side edge contribution

01 p0032 A72-11250

Electromagnetic plane stress wave generation by capacitor bank for transient loading of photoelastic models along straight and curved boundaries [SESA PAPER 1907A]

02 p0199 A72-11503

Explosion induced plane shock wave propagation in gas medium with exponential density distribution, determining gas flow behavior by difference approximation method

02 p0201 A72-11578

Iterative truncation error estimates in solution for plane wave diffraction by grating

02 p0171 A72-11738

One dimensional plane magnetoacoustic wave stability from synchronous flow in narrow flow gap MHD induction machine

02 p0265 A72-12263

Einstein gravitational field equations plane-front parallel ray wave exact solutions generalization to f-g gravity theory equations exact solutions

02 p0260 A72-12375

Plane wave intensity fluctuations behind random phase screen, discussing phase structural function relation to field statistical properties and fluctuation dispersion

02 p0181 A72-12590

Diffraction of plane electromagnetic waves of arbitrary orientation and incidence on triangular grid of cylindrical conductors

02 p0183 A72-12753

Plane electromagnetic wave diffraction on magnetoactive plasma cylinder, using energy method and particle scattering model

02 p0183 A72-12754

Plane electromagnetic wave reflection and transmission at moving boundary between two dielectric media

03 p0321 A72-13091

Radiation pattern and reflected field analysis for incident plane wave on phased arrays of thick wall rectangular waveguides

03 p0330 A72-13168

Plane and conical shock waves, presenting graphs and tables for numerical applications

03 p0341 A72-13684

Simple wave interaction solutions for nonlinear plane k-waves of nonelliptic quasi-linear differential equations using Riemann invariants

03 p0389 A72-13885

Stress concentration at circular holes in polyurethane plates under plane compression wave, obtaining interference fringes

03 p0451 A72-14121

Relativistic equations of motion of charged particle interacting with plane electromagnetic wave propagating at arbitrary angle to uniform magnetic field for magnetosphere model

04 p0554 A72-14406

Plane shock wave and blunt body interaction in supersonic gas flow in two-diaphragm shock tube

04 p0461 A72-14639

Long wave propagation in curved ducts and pipes, considering plane wave transition and distortion

04 p0548 A72-14698

Frequency characteristics of selectively reflecting screens in multichannel parabolic mirror antennas and determination of Fresnel coefficients dependence on polarized plane wave incidence angle

04 p0499 A72-15241

Conformal transformations applications to plane electromagnetic wave diffraction by infinitely conducting network, discussing energy distribution

04 p0490 A72-15410

Plane wave diffraction by infinite strip grating, providing closed form solution by boundary value problem reduction to singular integral equation

04 p0490 A72-15411

Plane electromagnetic wave diffraction on two cylinders with different radii, assuming infinite length and ideal conductivity

04 p0491 A72-15413

Plane electromagnetic wave diffraction by periodic lattice of long finite conductivity cylinders with arbitrary electric radius

04 p0491 A72-15414

Electromagnetic traveling plane wave diffraction from arbitrary angled dielectric wedge, investigating surface currents on walls

04 p0491 A72-15420

Plane harmonic electromagnetic wave diffraction by conducting parallel half planes in uniaxially anisotropic media

04 p0492 A72-15447

Hf backscattering of plane electromagnetic wave at oblique incidence on conducting circular metallic disk, noting polarization dependence on angle

04 p0493 A72-15524

Nonstationary plane shock wave propagation in inelastic medium with soil properties, discussing boundary problem solution and numerical analysis

05 p0689 A72-16284

Plane electromagnetic wave diffraction by infinite cylinder with unsteady impedance boundary conditions

05 p0627 A72-16409

High frequency electric field backscattering by plane electromagnetic wave incident on perfectly conducting sphere with radially inhomogeneous dielectric coating

05 p0630 A72-16621

Multifrequency plane, spherical and beam waves propagation, calculating temporal frequency spectra in turbulent atmosphere

06 p0771 A72-17339

Electromagnetic plane wave diffraction by infinite slit in screen with surface impedance, deriving field and transmission coefficient by asymptotic numerical solution

06 p0771 A72-17352

Plane supersonic ionizing shock wave in magnetic field under small wave plane perturbation from equilibrium position, calculating stability from linearized equations

06 p0798 A72-17678

Differential equations describing dynamic behavior of unsteady plane exothermic reaction front in gasless system

06 p0903 A72-18204

Transient plane wave reflection and scattering by periodic grating of thin conducting cylinders

06 p0777 A72-18736

Ring-plane type slow wave structure hot tested near 3 cm for scale modeling in mm range

07 p0938 A72-18854

Test facility for thermal diffusivity measurements in solids by method of plane temperature waves using periodic optical heating at 1500 K

07 p0982 A72-18942

Plane harmonic waves propagation in stressed polycrystalline bodies with slight orthotropy in unstressed state, substantiating theory for initial stress determination by ultrasonic technique

07 p1090 A72-19753

Current distribution in cylindrical parasitic antenna immersed in arbitrarily directed and polarized incident plane electromagnetic wave

07 p0957 A72-19787

Gas motion behind plane detonation wave orthogonal to free surface, solving Goursat problem for perturbed region

07 p0969 A72-19979

Plane oblique shock wave diffraction on wedge moving in homogeneous gas flow at supersonic speed, reducing boundary value problem to Hilbert problem

07 p0910 A72-20317

Transverse hydromagnetic plane waves existence in uniformly heated electrically conducting fluid under temperature gradient and magnetic field

07 p1045 A72-20442

Plane electromagnetic wave reflection from conducting convex cylinder in radially inhomogeneous absorbing medium, deriving equations for beam trajectories calculation

08 p1131 A72-20742

Kirchhoff method application to asymptotic solution of plane wave diffraction on dielectric conical shells, calculating electromagnetic field vector

08 p1131 A72-20931

Microwave transmission loss prediction formula for obliquely incident plane wave leakage through perforated flat metal plate

08 p1135 A72-21559

Plane wave propagation in laminated reinforced elastic plates with difference-differential equations analysis

08 p1247 A72-21809

Horizontally polarized impulsive plane electromagnetic wave reflection from perturbed linear ionosphere model, obtaining transient response as inverse Fourier transform

08 p1136 A72-21979

Electromagnetic field radiation from linearly and sinusoidally variable thickness layered structures under plane wave and concentrated source excitations

08 p1137 A72-21986

Random gravitational plane wave metric effect on electromagnetic wave mean value, noting light dispersion and attenuation

09 p1351 A72-22682

Uniform plane wave theory of internal upconversion and frequency doubling in optical parametric oscillators

09 p1324 A72-23079

- Steady state plane wave theory of intracavity coupled parametric oscillator/unconverter, obtaining efficiency, pump power transmission and optimum output coupling
09 p1325 A72-23086
- Plane shock wave propagation in polytropic plastic body with elastic unloading properties, deriving closed form solution for time dependent stepwise decreasing load
09 p1353 A72-23554
- Dipole moment expression for Rayleigh scattering field from finite closed perfectly conducting body irradiated by LF plane electromagnetic wave
[AD-742573] 10 p1434 A72-23720
- Acoustic waves generation in liquids by Q-switched ruby laser, noting transition from plane to spherical waves with dye concentration and focusing configuration variations
10 p1490 A72-23954
- Plane harmonic compression waves scattering by circular holes in thin elastic plate, calculating dynamic stresses concentration
10 p1554 A72-24179
- Ionization kinetics influence on light absorption zone behind plane stationary shock wave in hydrogen
10 p1467 A72-24358
- Plane ionizing shock wave stability in MHD channel within magnetic field
10 p1522 A72-24542
- Plane electromagnetic wave diffraction on ideally conducting convex body of large electrical dimensions, obtaining Maxwell equations asymptotic solution
10 p1436 A72-24577
- Plane wave solutions to atmospheric gravity waves, including effects of nonlinearity, instability, molecular dissipation, temperature, wind and diurnal tides
10 p1473 A72-24705
- Laser conductive heating of plasma with accounted nuclear fusion energy, assuming plane thermal wave
10 p1522 A72-24722
- Plane and uniform heterogeneous electromagnetic waves reflection, observing Goos-Hanchen and Imbert effects
11 p1597 A72-26482
- Slow and fast plane magnetoacoustic waves mutual transformation and reflection at plasma and magnetic field inhomogeneities
11 p1698 A72-26643
- Submillimeter plane waves formation by quasi-optical line and diverging lens with phase front adjustment
11 p1598 A72-26719
- Colliding plane gravitational waves equations for linear polarization
12 p1845 A72-27409
- Reflection and transmission of plane E wave incident on moving conducting medium, discussing growing wave excitation
12 p1782 A72-27490
- Two dimensional wave motion generated in prestressed body by crack extension, noting consistency with fracture criterion related to cohesive traction zones near crack tip
12 p1883 A72-27560
- Plane monochromatic electromagnetic wave scattering by rotating metallic cylinder, noting frequency shift dependence on cylinder translational motion velocity
13 p1914 A72-28370
- Plane sound wave scattering by acoustically soft sphere at constant subsonic velocity
13 p2003 A72-28797
- Plane longitudinal displacement wave reflection from fixed surface in micropolar elastic half space, presenting reflection laws and amplitude ratios for specific cases
13 p2056 A72-29001
- Diagnostic procedures for nonhomogeneous plasma based on geometrical optics approximation, irradiating plasma by plane wave at oblique incidence
13 p2013 A72-29295
- High latitude ionospheric transmission and reflection properties for oblique hydromagnetic plane waves at micropulsation frequencies for daytime and nighttime conditions
13 p1951 A72-29390
- Fiberglass performance as duct liner in presence of spinning modes from free field measurements, noting ineffectiveness for plane wave attenuation
13 p2028 A72-29573
- Small amplitude plane wave speed variation with pressure for Na and K at absolute zero temperature, using crystal strain energy formulation
13 p2006 A72-29675
- Quasi-longitudinal and quasi-transverse plane wave propagation in anisotropic elastic-plastic solids, approximating Be single crystal behavior
14 p2163 A72-30176
- Wire antenna half-space problem analysis by Sommerfeld integral approach and plane wave reflection coefficient approximation
14 p2085 A72-30338
- Diffraction of plane waves scattered by impedance structures in anisotropic medium, noting wedge shaped region with cold plasma under external magnetic field
14 p2086 A72-30809
- Plane nonlinear wave propagation in transonic region of two dimensional and axisymmetric steady flows, considering disturbance at arbitrary point
14 p2095 A72-31000
- Submillimeter plane monochromatic waves propagation in ground layer of turbulent atmosphere, deriving received signals levels fluctuations
15 p2195 A72-31653
- Dispersion equations and resonant absorption of plane and cylindrical surface waves in transition layer between plasmas, noting Langmuir oscillations
15 p2286 A72-32385
- Plane wave dispersion and nonlocal elasticity equations linearization, demonstrating continuum treatment of lattice dynamics
15 p2330 A72-32445
- Nonlinear anisotropic elastic constitutive equations for micromorphic and micropolar mixtures, investigating plane wave propagation via field equations with restricted coupling
15 p2278 A72-32446
- Exact solutions for plane thermoelastic and magnetothermoelastic wave frequency equations, determining specific loss extremum values
15 p2336 A72-32447
- Plane electromagnetic wave diffraction on periodic arbitrary profile array, presenting near and far field asymptotic characteristics
15 p2202 A72-32660
- Radial vibrations and plane wave propagation in elastic deforming sphere with superimposed time dependent displacement field
16 p2467 A72-33117
- Nonlinearity effects on finite amplitude, plane uniform oblique shock wave reflection, using inviscid gas analogous solution techniques
16 p2426 A72-33661
- Constitutive equations for plane harmonic waves propagation in composite fiber reinforced elastic material
17 p2625 A72-34321
- Scattering of electromagnetic waves from an inhomogeneous magnetoplasma column moving in the axial direction
17 p2587 A72-34359
- Invariant imbedding in time-varying homogeneous nondispersive media
17 p2513 A72-34366
- Diffraction of electromagnetic waves by a two-dimensional aperture with arbitrary cross-sectional shape
17 p2514 A72-34385
- Diffraction of a plane electromagnetic wave on an anisotropic half-plane in free space and in a plane waveguide
17 p2515 A72-34828
- Ionization kinetics influence on light absorption zone behind plane stationary shock wave in hydrogen
17 p2539 A72-34957
- On the behavior of the electromagnetic field with crests
17 p2584 A72-35913
- Scattering of elastic waves by moving objects
18 p2709 A72-36403
- Elementary plane waves in a Signorini-Cattaneo's thermoelastic solid
18 p2735 A72-36512
- Electromagnetic radiation and scattering from loaded bodies of revolution of arbitrary shape, calculating plane wave scattering from apertures in cylinders and hemispheres
18 p2662 A72-36927
- Fourth moment of a wave propagating in a random medium
18 p2712 A72-37025
- Near sidelobes in Cassegrain antenna systems
18 p2668 A72-37039
- Approximate representation of a type of transcendental polynomials describing wave systems with fractional rational functions
19 p2834 A72-37751
- Scattering resonances of electromagnetic wave by an infinite plane grating with reflector
19 p2767 A72-38612
- Plane and cylindrical electromagnetic waves diffraction on infinitely long cylindrical bodies, calculating induced currents, diffraction patterns and near fields
19 p2767 A72-38634
- Plane wave diffraction in a plane waveguide array with protruding dielectric plates
19 p2768 A72-38655
- Plane TE polarized electromagnetic wave diffraction on infinite conducting cylinder in nonhomogeneous medium, calculating far field diffraction patterns
19 p2768 A72-38656
- Short-wave asymptotic representation of the solution to the problem of diffraction by a circular disk
19 p2769 A72-38849
- Plane electromagnetic wave diffraction on thin ribbons grating, discussing scattered field singularities for E polarized waves
19 p2769 A72-38850
- Plane electromagnetic waves diffraction at arbitrary orientation and incidence on triangular grid of cylindrical conductors
20 p2902 A72-39059
- Plane electromagnetic wave diffraction on magnetoactive plasma cylinder, using energy method and particle scattering model
20 p2902 A72-39060
- Reflection coefficient method of remote probing for inhomogeneous media, using plane wave incidence angle dependence
20 p2927 A72-39719
- Minkowski space-times for impulsive gravitational waves, considering idealized plane fronted wave form and limiting case of Robinson-Trautman null spherically fronted wave
20 p2955 A72-40007
- Gas motion behind plane detonation wave orthogonal to free surface, solving Goursat problem for perturbed region
20 p2915 A72-40035
- Plane acoustic pressure wave effect on motion of thin elastic truncated conical shell fastened in rigid screen, using Timoshenko theory
21 p3116 A72-40263
- A charged particle in the field of a transverse electromagnetic plane wave - A group-theoretical analysis
21 p3084 A72-40722
- Asymptotic solution of the wave equation with variable velocity and boundary conditions
21 p3075 A72-40838
- Diffraction of plane waves by a strip - Exact and asymptotic solutions
21 p3016 A72-40839
- Partial differential equation solution for plane electromagnetic wave diffraction by infinite dielectric cylinder of arbitrary cross section
21 p3085 A72-41199
- Combined tension-torsion elastic-plastic waves as propagating singular surfaces
21 p3121 A72-41244
- Diffraction of electromagnetic plane waves by infinite slit perforated in a conducting screen with finite thickness
21 p3022 A72-41267
- Averaged equations of simultaneous hydrodynamic expansion and thermal heating of two-temperature plasma, taking the recovery of thermonuclear fusion into account. I - The plane problem. II - The spherical problem.
21 p3093 A72-41476
- Book - Terrestrial propagation of long electromagnetic waves.
21 p3023 A72-41532
- Holographic system resolving capacity increase by oblique illumination of object, analyzing plane monochromatic wave transmission through one dimensional semitransparent body
21 p3058 A72-41791
- A problem of electromagnetic wave propagation in a moving plane stratified medium
22 p3155 A72-42653
- Diffraction of plane electromagnetic wave at a corrugated dielectric surface
22 p3155 A72-42662
- Bessel series solution to electromagnetic field and pulse function of cylindrical conducting screen located in monochromatic plane wave
22 p3155 A72-42667
- Plane waves in a new theory of thermoelasticity
22 p3239 A72-42856
- Diffraction of a plane wave by a ribbon grating in the case of short wavelengths
23 p3264 A72-43527
- Scattering of acoustical waves by a prolate spheroidal obstacle.
23 p3313 A72-44118
- One dimensional steady conducting gas flow in nonaccelerating coordinate system under magnetic field, calculating pressure, density and temperature variations with boundary shock wave
23 p3281 A72-44265
- Acoustic transmission and reflection by a shear discontinuity separating hot and cold regions.
23 p3315 A72-44373
- Use of the three-dimensional covariance matrix in analyzing the polarization properties of plane waves.
23 p3315 A72-44518
- Electromagnetic-wave propagation in a random nonlinear dispersive medium.
24 p3379 A72-44784
- Plane thermoelastic one-dimensional waves in an inhomogeneous medium with allowance for connectedness
24 p3459 A72-45266
- Reflection and transmission of electromagnetic waves by a moving inhomogeneous medium.
24 p3381 A72-45644

PLANET EPHEMERIDES

Minor planet Eros photographic observations by long-focus refracting telescopes and Ross cameras at various Yale observatories, tabulating ephemerides
[AD-737017] 02 p0286 A72-12894

Planetary mass determination tables, presenting mass inverse value in constants system with international ephemerides

04 p0575 A72-15032

Meridian circle planet and asteroid positions and deviations from ephemerides during 1950 to 1955

05 p0723 A72-17158

Outer planets masses and ephemerides, noting guidance system and fuel quantity for orbit corrections on interplanetary flight

15 p2312 A72-32181

Accuracy of outer-planet ephemerides.

19 p2857 A72-37683

Exact positions of Uranus for 1919 through 1969 according to photographic observations at Pulkovo and Tashkent

19 p2859 A72-37915

Results of observations of the minor planet Icarus by the Maksutov meniscus astrograph in Chile

19 p2859 A72-37916

Right ascensions of the sun, Mercury, and Venus observed with the transit instrument at Nikolaev during 1966-1967

19 p2861 A72-37982

Declinations of the sun, Mercury, and Venus in the FK4 system as deduced from observations with the vertical circle of the Nikolaev Observatory during 1966-1967

19 p2861 A72-37983

Attempt at determining the exact positions of Venus from photographic observations on the short-focus double astrograph and the 26-in. refractor of the Pulkovo observatory

19 p2861 A72-37984

Computer processed Mars photographic positional measurements with Pulkovo normal astrograph in 1965

19 p2861 A72-37985

Determination of major planet coordinates by an expeditionary astrograph

19 p2861 A72-37986

Photoelectric transit observations of Saturn and Mars, showing culmination in universal ephemerides time

19 p2862 A72-37987

New method of calculating disturbed ephemeris of minor planets

21 p3102 A72-40095

Recent developments in the theory of the motion of the moon.

21 p3102 A72-40124

Accurate positions of the planet Pluto in the years 1969-1970.

21 p3105 A72-40576

Ephemerides and improved orbital elements of minor planets, noting general theory of relativity verification from astronomical observations of Icarus

24 p3437 A72-44758

Poorly founded systems of equations in astronomical practice and methods for their solution

24 p3437 A72-44760

Correction of the orbits of 161 minor planets

24 p3437 A72-44763

Observations of minor planets at the Crimean Astrophysical Observatory AN SSSR, XVIII

24 p3437 A72-44764

Ground observation for outer planets natural satellites ephemeris, using astrometric telescopes, photographic and plate reduction techniques

24 p3443 A72-45426

Accuracy of the determination of the zero points of a fundamental catalog from observations of major and minor planets

24 p3447 A72-45676

Photographic observations of Mars at the Main Astronomical Observatory, AN USSR during 1963-1967

24 p3448 A72-45686

PLANET ORIGINS

U PLANETARY EVOLUTION

PLANETARY ATMOSPHERES

NT JUPITER ATMOSPHERE

NT MARS ATMOSPHERE

NT VENUS ATMOSPHERE

Planetary atmosphere IR radiative transfer model using matched asymptotic expansions method

01 p0125 A72-10099

Transfer from high elliptical to circular orbit, using successive spacecraft braking maneuvers in planetary atmosphere with incomplete information

01 p0130 A72-10927

Micrometer particle formation by water vapor photolysis at 1500-1700 Å, noting particle production rate and implications to planetary atmosphere physics

02 p0220 A72-12207

Solar wind induced atmospheric mass loss from magnetic field-free planets, using mass, momentum and energy conservation laws

02 p0275 A72-12465

Spherical planetary atmosphere tendency equation of pressure variation for horizontal stratification, using static and continuity equation in spherical harmonics

03 p0351 A72-14356

Rotating and nonuniform planetary exosphere model, examining density profiles

04 p0579 A72-15333

Radio absorption spectra sounding for planetary atmospheric impurities calculating water vapor content in Venus cloud level

05 p0715 A72-16169

Thermodynamic parameters correlation of planetary atmosphere with planetary probe parachute descent rate applied to Venera 5 and 6 data

05 p0721 A72-16769

Radiative heat transfer damping rates of turbulent temperature pulsations in upper planetary atmospheres, assuming Kirchhoff radiation law validity

06 p0882 A72-17935

Atmospheric freestream pressure profiles determination from base pressure and flow phenomena of Mars, Venus or Jupiter entry probes

[AIAA PAPER 72-202]

07 p0982 A72-18959

Planetary atmosphere diffuse radiation from limb side, applying to Mars atmospheric emission

08 p1238 A72-21832

Methane contribution to thermal opacity in Uranus and Neptune atmospheres for atmospheric model synthesis

09 p1383 A72-22293

German monograph on optimal planetary atmosphere effects for increasing hyperbolic velocity at flyby for Venus and Earth

09 p1383 A72-22322

Spectral line formation in cloudy planetary atmospheres, applying to Venus

09 p1386 A72-22669

Exospheric temperatures in hydrogen dominated planetary atmospheres for evaporative loss rates estimation, noting two component diffusive equilibrium model

09 p1393 A72-23661

Mars and Venus probes entry into planetary atmospheres, discussing aerodynamics of trajectory control and soft landing

09 p1394 A72-23673

Photographic measurements of Saturn, observing atmospheric belt latitudes, ring dimensions and southern hemisphere bright spot rotation

10 p1531 A72-23711

Spacecraft-based observations of gamma and X radiation resulting from planetary surface and atmosphere processes to obtain source medium chemical composition

10 p1530 A72-25060

Time dependent geopotential as function of position weighted atmospheric density from Poisson equation, noting satellite orbit perturbations due to mass shifts in planetary atmospheres

12 p1838 A72-27022

Diving operations medical aspects significance for manned planetary surface exploration in high density atmospheres, considering protective clothing, breathing apparatus and gas mixtures, etc

12 p1769 A72-27415

Mars and Venus instrumented spacecraft flight results, describing planetary topographies, atmospheres and magnetic fields

12 p1877 A72-27650

Laboratory simulation of diffuse reflectivity from plane parallel cloudy planetary atmosphere, comparing to theory

12 p1796 A72-27947

Radio absorption spectra sounding for planetary atmospheric impurities calculating water vapor content in Venus cloud level

14 p2149 A72-30238

Saturn thermal radio emission brightness temperature calculations for subcloud atmosphere ammonia abundance evaluation

14 p2152 A72-30490

Saturn rings gas-dust atmosphere, thickness and motion, considering planetary radio emission and brightness temperature

14 p2161 A72-31073

Light rays total, astronomical and photogrammetric refraction in planetary atmospheres with arbitrary composition

15 p2224 A72-31602

Planetary cloudy atmosphere synthetic spectral line profile computation, using analytic scattering diagrams

15 p2192 A72-31649

Solar wind and planetary atmosphere interaction observation by simulation of ionization mechanism in comet, using gun produced plasma stream and gas cloud

15 p2301 A72-32341

Hydrogen to helium mixing ratio in giant planets from far IR spectroscopy for atmospheric thermal models and greenhouse effect calculations

15 p2315 A72-32727

Stellar and planetary atmosphere dynamics, deriving balance equations for variance analysis of angular momentum

16 p2453 A72-33247

Planetary atmospheres and interiors in terms of dynamics, rotation, magnetic fields, Jupiter features, geomagnetism, earth baroclinic waves, global circulation and gravitation, etc

16 p2384 A72-33339

Solar radiation anisotropic nonconservative scattering in semiinfinite atmosphere, calculating plane and spherical albedo by exponential kernel approximation

16 p2446 A72-33463

Radiative heat transfer damping rates of turbulent temperature pulsations in upper planetary atmospheres, assuming Kirchhoff radiation law validity

16 p2459 A72-33776

Longitudinal dynamic stability of hypersonic shuttle vehicle designed for operation to planetary atmosphere rim

16 p2462 A72-34019

Planetary atmosphere thermodynamic parameters correlation between spacecraft parachute descent rate and measured data, noting Venera spacecraft example

17 p2610 A72-35272

Radiation transfer in planetary atmospheres with a three-term scattering indicatrix

17 p2618 A72-35810

The influence of line shape and band structure on temperatures in planetary atmospheres.

18 p2726 A72-36640

Titan and its atmosphere.

18 p2729 A72-36989

Similarity theory of planetary atmosphere circulations applied to solar atmosphere in terms of radius and rotatory Mach number

19 p2863 A72-38066

Absorption line profile and equivalent line width derivation for planetary atmosphere with low and high optical thicknesses, assuming arbitrary scattering coefficients

19 p2863 A72-38071

Saturn thermal radio emission brightness temperature calculations for subcloud atmosphere ammonia abundance evaluation

19 p2864 A72-38319

Rayleigh and Raman scattering by H₂ in a planetary atmosphere.

20 p2966 A72-38914

Russian book - Large-scale motions in the convective zones of stars and large planets.

21 p3104 A72-40462

New observations on the Kuiper bands of Uranus.

21 p3106 A72-41043

Temperature range estimation method for planetary atmospheric component generating spectral lines, applying to Venus observations at 7820 Å carbon dioxide band

21 p3106 A72-41045

Minor constituents in planetary atmospheres - Ultraviolet spectroscopy from the Orbiting Astronomical Observatory.

21 p3111 A72-41459

Integrals of the motion for optimal trajectories in atmospheric flight.

[AIAA PAPER 72-931]

21 p3112 A72-41570

The total pulsation-frequency spectrum of a polytropic atmosphere

21 p3114 A72-41779

A calculated hydrogen distribution in the exosphere.

22 p3168 A72-42004

Theory of radiative heat transfer in polytropic atmospheres

22 p3229 A72-42962

Absorption profile of a planetary atmosphere - A proposal for a scattering independent determination.

23 p3289 A72-43889

Jupiter - Its Red Spot and disturbances in 1970-1971.

24 p3435 A72-44690

On required guidance for transfer from hyperbolic trajectory to the planetary satellite orbit by aerodynamic drag in atmosphere.

24 p3450 A72-45176

Radiation gasdynamics of planetary entry - Concepts and recent advances.

24 p3361 A72-45188

Optimization of spacecraft reentry into a planetary atmosphere

24 p3453 A72-45597

Approximate formulas for the intensity of diffuse reflected emission from a semiinfinite atmosphere

24 p3448 A72-45685

PLANETARY BASES

Mars and Venus automatic station data transmission systems for surface and atmosphere studies, discussing relay and direct transmission modes

15 p2203 A72-31823

PLANETARY COMPOSITION

Outer planets satellites physics and chemistry, discussing steady state thermal models based on energy equilibrium between internal radioactivity decay and surface radiation

04 p0568 A72-14495

Mars Hellas area surface features, relating crater absence to surface age and white spot phenomena to water reservoir under permafrost layer

06 p0881 A72-17929

Mariner 9 experiments, discussing IR interferometric spectroscopy observations of Mars dust composition and pole flattening

06 p0889 A72-18340

Oxygen isotopic abundances and equilibrium temperatures of meteoritic minerals, chondrules, meteorites and planets

07 p0985 A72-19589

Earth and moon chemical composition differences based on model of lunar formation from circumterrestrial swarm of particles and larger objects

07 p1077 A72-19820

Mars internal structure models with chondrite as potential core-forming material, discussing absence of internal origin magnetic field

07 p1084 A72-20518

Viking Lander seismic investigations for Martian tectonic activity, internal structure and composition, core size and conditions of formation

10 p1540 A72-24389

Viking Lander magnetic properties investigation of Martian surface with implications for planetary composition and differentiation and atmospheric interaction

10 p1541 A72-24391

Extraterrestrial environment utilization, describing space power plants, manufacturing operations in earth orbit and planetary mineral resources

12 p1871 A72-27625

Chemical equilibrium models of low temperature condensation from solar nebula relating to planetary composition

15 p2311 A72-32083

Planetary atmospheres and interiors in terms of dynamics, rotation, magnetic fields, Jupiter features, geomagnetism, earth baroclinic waves, global circulation and gravitation, etc

16 p2384 A72-33339

Earth and moon chemical composition differences based on model of lunar formation, from circumterrestrial swarm of particles and larger objects

17 p2618 A72-35745

General relativistic planetary structures comparison with Newton gravitational theory, deriving field equations for spherically symmetric planets with explicit pressure and density distributions

18 p2728 A72-36751

Mars Hellas region surface features, relating crater absence to surface age and atmospheric condensation-produced white spot phenomena to sub-permafrost water reservoir

18 p2730 A72-37154

Statistical mechanics of light elements at high pressure. II - Hydrogen and helium alloys.

21 p3106 A72-41044

Thin ice crust, chondritic composition and ionospheric considerations for Io electrical conductivity and decametric radio emission modulation in unipolar inductor model

24 p3437 A72-44704

PLANETARY ENTRY

U ATMOSPHERIC ENTRY

PLANETARY ENVIRONMENTS

NT JUPITER ATMOSPHERE

NT MARS ATMOSPHERE

NT MARS ENVIRONMENT

NT PLANETARY ATMOSPHERES

NT VENUS ATMOSPHERE

Solar flare, galactic and magnetically trapped (Van Allen) nuclear particle radiation environments calculation for three outer planet Grand Tour missions

03 p0413 A72-14095

Astrogenic and planetogenic environments characteristics examination for stellar spectral classes effect on intelligent life evolutionary pace and existence probability

04 p0573 A72-14887

PLANETARY EVOLUTION

Rotation production in giant planets by gaseous impact, discussing Jupiter and Saturn formation

02 p0282 A72-12331

Terrestrial planets internal constitution and thermal history model, emphasizing iron fractionation in structure

03 p0418 A72-13110

Early catastrophic degassing of earth, considering mechanisms and times from volatiles abundances and distribution in atmosphere, hydrosphere and crust

03 p0350 A72-13744

Toroidal oscillations of spherical planetary models, presenting regular eigenfunction form near center

03 p0352 A72-14381

Jupiter outer satellite group formation theory, suggesting asteroid-larger satellite collision

04 p0569 A72-14496

Martian atmospheric volatiles history, noting initial chemical conditions favorable to abiotic organic synthesis

04 p0569 A72-14503

Protoplanetary bodies mass distribution by coagulation theory, using inverse power law

06 p0884 A72-18030

Martian atmosphere evolution, stressing photochemical production of oxygen, carbon and nitrogen

06 p0889 A72-18275

Planetary bodies mass and energy losses as indications of eruptive evolution, discussing mean densities, geological processes scale and volcanic activities

08 p1228 A72-20829

Lunar evolution theory, discussing terrestrial cluster dynamics during earth accumulation

08 p1231 A72-21129

Origin of life as chemical evolution product, tracing juvenile carbon history through planetary and geological phases

08 p1162 A72-22004

Planetary atmospheres composition diversity, discussing evolution of Mars, Venus, earth and Jupiter from primitive solar nebula

08 p1119 A72-22012

Life beyond solar system, discussing planetary formation and prebiological organic chemistry developments and interstellar communication

08 p1120 A72-22016

Adsorption role in planetary primordial rare gas origin based on adsorptivity pattern of pulverized Alende meteoritic samples at 113 K

09 p1385 A72-22597

Martian cratering by asteroid impact, discussing Palomar-Leiden asteroid statistics, Opik capture theory and evolutionary extrapolation limitations

10 p1531 A72-23705

Protoplanetary bodies mass distribution by coagulation theory, using inverse power law

11 p1719 A72-25966

Rotation production in giant planets by gaseous impact, discussing Jupiter and Saturn formation

13 p2039 A72-29215

Protoplanet cloud model of solar system as flat gas-dust disk, discussing density profile, gravitational stability and mass loss

14 p2148 A72-30206

Book on astronomy covering optical and radio telescopes properties and atmospheres of inner and outer planets, stellar lifetimes and evolution, galaxies, cosmology, etc

15 p2306 A72-31516

Earth and Mars - Evolution of atmospheres and surface temperatures.

17 p2613 A72-35395

Astronomical model for primitive solar nebula showing planetary evolution in hot initial state under centrifugal forces

17 p2614 A72-35677

Lunar composition as a clue to the early history of the solar system.

17 p2614 A72-35678

Planetary volcanic activity and matter disintegration as source of development in solar system, using density and rotational energy data

18 p2725 A72-36521

Space science advances and NASA Planetary Program, noting solar system evolution, life origin and Skylab and Space Shuttle programs

19 p2855 A72-37274

Chronology of first phases of formation of solar system solid objects, meteorites and primitive lunar rocks, describing models

19 p2867 A72-38548

Metal/silicate fractionation in the solar system.

20 p2967 A72-39177

Ammonia photolysis and the role of ammonia in chemical revolution.

20 p2898 A72-39375

Russian book - Hydrodynamic evolution model of the earth.

21 p3103 A72-40461

Role of the swarm of satellite-particles on the origination of the earth's rotation

22 p3220 A72-41916

Earth geophysical effects due to tidal capture of moon from direct orbit, discussing volcanism, atmosphere and hydrosphere origins and biological evolution

22 p3226 A72-42539

Origin and evolution of the earth-moon system.

22 p3227 A72-42540

Book on moons and planets covering celestial mechanics, solar system origin, stellar formation, comets, asteroids, meteorites, planetary interiors, surfaces, atmospheres, etc

22 p3228 A72-42750

Shmidt cosmological hypothesis impact on geophysics, geochemistry and geology, discussing planetary evolution, initial earth temperature and gravitational differentiation

22 p3230 A72-43154

Protoplanet cloud model of solar system as flat gas-dust disk, discussing density profile, gravitational stability and mass loss

23 p3333 A72-43236

Production of light elements in the solar system.

23 p3335 A72-43487

Lunar composition in terms of evolutionary mode based on inhomogeneous planetary accretion and high temperature condensation

24 p3439 A72-44977

Early stage condensation in planetary formation, discussing atomic and molecular reactions in interstellar space and earth outer atmosphere properties

24 p3444 A72-45452

Origin of the planetary systems astronomical evidence in other stars.

24 p3444 A72-45453

A gasdynamical view on the motion, heating and accretion of solid bodies in the solar system.

24 p3444 A72-45456

Conditions in the early solar system, as inferred from meteorites.

24 p3445 A72-45458

On certain aerodynamic processes for asteroids and comets.

24 p3445 A72-45463

Investigation of solar system evolution by automatic vehicles on the moon.

24 p3445 A72-45466

PLANETARY EXPLORATION

U SPACE EXPLORATION

PLANETARY EXPLORER

U OUTER PLANETS EXPLORERS

PLANETARY GRAVITATION

Gravitational fields of giant planets in hydrostatic equilibrium, solving equations for linear and quadratic density distributions

03 p0436 A72-13818

Conditionally periodic motions of particle in gravitational field of axisymmetric oblate planet, describing canonical transformations for Hamiltonian function reduction to normal form

04 p0572 A72-14638

Perturbed satellite motion in gravitational field of aspherical rotating planet

06 p0892 A72-18036

Statistical and probabilistic analyses of comet groups existence with similar orbital elements, considering gravitational capture by trans-Neptunian planets

07 p1075 A72-19559

Short period comets orbital evolution and major planets gravitational effects, discussing cometary cloud formation, diffusion, motion and discovery

07 p1078 A72-19981

Planetary perturbation of orbits of long period comets with large perihelion distances

07 p1081 A72-20236

Perturbed satellite motion in gravitational field of aspherical rotating planet

11 p1727 A72-25972

Jupiter and Saturn gravitational moments from available models, taking into account rotation, density and radius

12 p1871 A72-27744

Mars doublet cratering by impacting meteoroid breakup due to stresses in gravitational field, using Monte Carlo simulation

14 p2149 A72-30317

Trajectory analysis for swingby technique using Jovian gravitational field for leaving ecliptic plane along heliocentric orbit and for solar flyby at specified distance

14 p2150 A72-30452

Error sources in numerical integration of spacecraft equations of motion in solar and planetary gravitational fields, suggesting methods for improving accuracy

14 p2151 A72-30453

Stability analysis of satellite motions in Newton planetary field by Liapunov method, considering ellipsoid of revolution under gravitation of sphere

14 p2162 A72-31081

Preflight and real time gravity sensing for Mariner 9 satellite orbit determination during Mars 1971 mission

15 p2270 A72-32186

Gravitational fields of Jupiter and Saturn

19 p2857 A72-37734

Cometary parent bodies transfer to short period orbits by Jupiter caused gravitational disturbances, noting qualitative analysis of orbits evolution

22 p3219 A72-41913

Saturn-Jupiter rebound - A method of high-speed spacecraft ejection from the solar system.

23 p3340 A72-44323

Russian book - Space research 1970: Investigation of the gravitational fields and shapes of the earth, other planets, and the moon on the basis of spacecraft observations.

24 p3443 A72-45399

PLANETARY LANDING

Digital computer investigation of radio signals transmitted by Vener 7 during Venus soft landing, describing spectral analysis and telemetric data detection methods

05 p0630 A72-16770

Static and dynamic analysis of legged planetary instrument landers, taking into account structural flexibility, elastic-plastic gear load characteristics and soil properties

11 p1725 A72-25396

Digital computer investigation of radio signals transmitted by Venera 7 during Venus soft landing, describing

ing spectral analysis and telemetric data detection methods

17 p2516 A72-35273

Experimental and simulation study results on the development of a planetary landing site selection system.

[AIAA PAPER 72-868] 20 p2951 A72-39131

Space Shuttle landing navigation using precision distance measuring equipment.

24 p3421 A72-44637

The results of Soviet research into Mars.

24 p3447 A72-45559

PLANETARY LONGITUDE

U PLANET EPHEMERIDES

PLANETARY MAGNETIC FIELDS

Solar wind induced atmospheric mass loss from magnetic field-free planets, using mass, momentum and energy conservation laws

02 p0275 A72-12465

Planetary magnetic activity effects on hf cosmic noise absorption measurements at low and temperature latitudes

04 p0516 A72-14941

Geophysical applications of high resolution magnetometers to geomagnetic measurements, archaeological investigations and satellite sounding of planetary magnetic fields

06 p0812 A72-17374

Mariner 9 radio tracking measurements of Mars gravity field and pole direction, comparing to moon and earth

06 p0890 A72-18346

Mars and Venus instrumented spacecraft flight results, describing planetary topographies, atmospheres and magnetic fields

12 p1877 A72-27650

Planetary atmospheres and interiors in terms of dynamics, rotation, magnetic fields, Jupiter features, geomagnetism, earth baroclinic waves, global circulation and gravitation, etc

16 p2384 A72-33339

Extensive air showers and the sporadic decimeter radio emission of Jupiter

19 p2863 A72-38073

PLANETARY MASS

Planetary mass estimation from radar and optical observation data analysis of sun and planets [AD-737167]

01 p0127 A72-10292

Planetary mass distribution in solar system from gravitational contraction of nebula formed by accretion of ring shaped particle cloud

02 p0282 A72-12311

Jupiter mass from motion of /76/ Freia, plotting residuals in right ascension and declination

02 p0286 A72-12893

Planetary mass determination tables, presenting mass inverse value in constants system with international ephemerides

04 p0575 A72-15032

Outer planets mass determination noting anomalous latitude residuals of Uranus

04 p0575 A72-15033

Solar system data processing system /SSDPS/ computer solution for major planetary masses from optical, radar and radio tracking data

04 p0575 A72-15034

Planetary mass errors effects on orbit determinations, discussing Ceres mass from influence on Pallas orbit

04 p0575 A72-15035

Jupiter mass correction from minor planets /153/ Hilda, /279/ Thule and /334/ Chicago observations

04 p0576 A72-15036

Principal planets mass derivation using fundamental and independent determinations in table form

04 p0576 A72-15037

Jupiter mass from discrete time observations of JIX satellite positions and velocities, using sequential Kalman-Bucy filter

06 p0876 A72-17580

Protoplanetary bodies mass distribution by coagulation theory, using inverse power law

06 p0884 A72-18030

Planetary bodies mass and energy losses as indications of eruptive evolution, discussing mean densities, geological processes scale and volcanic activities

08 p1228 A72-20829

Disturbing parameters effect on spacecraft trajectory X coordinate values estimation, including planetary masses and coordinates, astronomical unit and light speed

08 p1232 A72-21151

Outer planet mass determination limitations from mutual motion perturbations

08 p1236 A72-21636

Protoplanetary bodies mass distribution by coagulation theory, using inverse power law

11 p1719 A72-25966

Lunar mass, gravitational field and moments of inertia from Lunar Orbiter spacecraft Doppler tracking data

13 p2037 A72-28989

Mars and moon cores elastic properties inferred from hydrostatic equilibrium based on observed data for total mass, radius and moment of inertia

13 p2048 A72-29809

Earth-moon system mass from ratio of solar mass to sum of terrestrial and lunar masses, discussing solar attraction effects and radar distance measurements

15 p2306 A72-31598

Outer planets masses and ephemerides, noting guidance system and fuel quantity for orbit corrections on interplanetary flight

15 p2312 A72-32181

The Laplace plane and the masses of the planets

17 p2618 A72-35813

The masses, densities and moments of inertia of Uranus and Neptune.

20 p2967 A72-39184

Disturbing parameters effect on spacecraft trajectory X coordinate values estimation, including planetary masses and coordinates, astronomical unit and light speed

20 p2969 A72-39256

A determination of the motion of the ecliptic.

23 p3337 A72-43833

Determination of parameters related to the interior of Mercury.

24 p3436 A72-44696

PLANETARY MOTION

U SOLAR ORBITS

PLANETARY NEBULAE

Planetary nebulae dynamic models, incorporating expanding shell thermal histories and thermal stability in terms of high temperature evolutionary phase

02 p0276 A72-11667

Planetary nebula IC 418 reddening constant from Paschen line intensities of IR spectrum

04 p0570 A72-14554

Orion and planetary gaseous nebula helium atoms metastable triplet states population calculations

04 p0578 A72-15314

Planetary nebulae NGC 2392, 6210, 6826, 6720 and 6853 observations, presenting monochromatic photographs and isophotic contours

05 p0713 A72-16021

Model computations for population I stars of 0.6, 0.8 and 1.2 solar masses, considering evolutionary sequences correspondence to planetary nebulae evolution

06 p0882 A72-17999

Faint planetary nebulae classification and measurement in northern Milky Way between Cygnus and Perseus from Schmidt camera survey

07 p1070 A72-19084

Planetary nebula IR continuum and line radiation from spectrophotometric observation relation to visual and radio wave data

08 p1235 A72-21387

Hyades member star BD plus 16.516 deg described as late evolution product of binary system with mass exchange and loss through planetary nebula phase

10 p1543 A72-24618

Luminous filaments model of density condensations optically thick to ionizing radiation in planetary nebulae

10 p1550 A72-25197

Planetary nebula classification based on forbidden line ratios and morphology, discussing galactic plane distribution, radial velocities and evolution

12 p1867 A72-27209

Planetary nebulae RF observations comparison with optically determined H-beta intensity for extinction coefficients

15 p2307 A72-31797

Planetary nebulae nuclei evolution, describing shell ejection mechanism with dependence on progenitor star luminosity

16 p2451 A72-33032

Planetary nebula M2-9 spectrum analysis, discussing IR excess, internal motions and Fe II emission lines

16 p2455 A72-33459

Energy level population and emission spectrum of C IV ion in planetary nebula with radiative excitation

16 p2458 A72-33688

Emission line polarization prediction for planetary nebula C IV ion emitted spectrum via theory for energy level population

16 p2458 A72-33689

Theoretical He-triplet line strengths compared with astronomical observations of planetary nebulae and H II regions

17 p2614 A72-35646

Observations of planetary nebulae at 1.65 to 3.4 microns.

19 p2854 A72-37233

Statistical investigations of motions and distances of planetary nebulae

19 p2860 A72-37969

Photometric study of the NGC 3587 planetary nebula /the Owl/ observed in H sub alpha light - Structure of hydrogen in the nebula

20 p2973 A72-39890

Numerical model of NGC 7662 consistent with line strengths and ratios, considering double shell structure and central star flux deviation from black body

21 p3105 A72-41033

Ionization structure and coarse and fine analyses in planetary nebulae spatial spectroscopic diagnostics based on line profile monochromatic intensity integral equation inversion

23 p3339 A72-44236

PLANETARY ORBITS

Jupiter outer satellite origin, considering capture orbit dimensions based on three body elliptical problem

02 p0275 A72-11594

Meridian circle planet and asteroid positions and deviations from ephemerides during 1950 to 1955

05 p0723 A72-17158

Relative motion of two mass points linked by flexible weightless tether in orbit around planet

06 p0891 A72-18695

Trojan deep space communications systems, maintaining powerful relay satellites in equilibrium at Lagrangian points of earth, Mars and Venus orbits

10 p1548 A72-24975

Three body problem study of satellite capture by planets in elliptical orbits, deriving orbital elements in terms of mass ratio and planetary orbit eccentricity

12 p1865 A72-27096

Phobos and Deimos orbital characteristics, noting related Martian physical properties determination

15 p2302 A72-31277

Orbital correction problems for vehicle around spherical planet, considering velocity, fuel consumption and trajectory optimization

15 p2308 A72-31819

Computational method for determining numerical values of relativity by two-way Doppler radio tracking and ranging data from planetary orbiting spacecraft

15 p2310 A72-31978

Existence proof and boundary regions for multiple solutions in minor planets circular orbits determination

18 p2723 A72-36085

Representation of the coordinates of a satellite of a spheroidal planet with the aid of series expansions

21 p3102 A72-40099

Least squares method for satellite motion parameters determination in orbital plane, using altimeter distance to planet surface measurements

22 p3223 A72-42202

Ephemerides and improved orbital elements of minor planets, noting general theory of relativity verification from astronomical observations of Icarus

24 p3437 A72-44758

Search for trans-Plutonian planets with the aid of periodic comets

24 p3437 A72-44759

Correction of the orbits of 161 minor planets

24 p3437 A72-44763

Maneuver design and implementation for the Mariner 9 mission.

24 p3443 A72-45429

[AIAA PAPER 72-913] Mariner 9 Mars orbital trajectory analysis from earth based radio data, considering gravity field, n-body perturbation and solar radiation pressure effects [AIAA PAPER 72-928]

24 p3443 A72-45434

PLANETARY QUARANTINE

Papers on planetary quarantine covering microbial survival in deep space, contamination by nonsterile flight hardware and sterilization

01 p0019 A72-10817

Planetary quarantine microbiological and engineering problems, discussing cost, international policies, contamination and sterilization

01 p0019 A72-10818

Planetary quarantine cost and mission success constraints, formulating mathematical models for international goals and implementation systems

01 p0019 A72-10819

Planetary quarantine microbial contamination control, considering clean room concept and microbiological barrier techniques

01 p0019 A72-10821

Nonsterile space flight hardware effects on planetary quarantine, evaluating contamination sources, design and mission parameters, cleanliness conditions and bioload

01 p0020 A72-10824

Optimum aim point biasing in case of a planetary quarantine constraint.

20 p2968 A72-39196

Development of planetary quarantine in the United States.

23 p3259 A72-43382

Effects of aeolian erosion on microbial release from solids.

23 p3253 A72-43384

Application of planetary quarantine methodology and spacecraft sterilization technology to improved health care delivery.

24 p3375 A72-45148

PLANETARY RADIATION

To modulation of Jupiter decametric emissions, using cyclotron magnetosphere model and coupling by whistler mode electromagnetic waves

Jupiter decameter radio burst possibility as indicator of high velocity fluxes and shock waves in solar wind

Martian radio emission at 8.57 mm during 1971 approach, comparing brightness temperature to Jupiter

Grating spectra of Jupiter North Equatorial Belt, noting absorption feature at 4.73 microns

Giant planets internal constitution models, discussing Jupiter visual magnitude variability, Saturn ring system, cold matter equations of state and He abundances

Real time complete Stokes vector scanning photoelectric polarimeter with 16 cm aperture for measuring visible radiation of solar disk, corona, moon and planets

Mars short wave line spectra from measurement with reflector, estimating nitrogen dioxide content in atmosphere

Jovian planets methane and ammonium absorption bands spectrophotometric investigation, noting Saturn spectral variations

Jupiter decametric radio emission relation to solar wind, geomagnetic activity and shock waves causing Forbush decreases

Saturn radio emission and brightness temperature measurements, determining rings optical thickness upper limit

Extrasolar planets UVB color indices calculation, noting relative reflectivity and primary star color

Jovian decametric radiation observations, showing satellite Io relative position correlated to highest frequency

Venus, M17 and M82 observation on ground through 345 micron atmospheric window, discussing IR fluxes

Bright O, C and carbon dioxide emissions in Martian airglow from temperature profile models based on Mariner UV spectrometry

Venus 8.2 mm radio emission dependence on sun-light phase angle, considering implications regarding day/night atmospheric temperature variations

Radiation polarization from Jovian disk center as function of phase angle from polarimetric observations

Astronomical model for Jovian decametric radio emission control by Io satellite based on two surface sources on planet and particle interaction with plasma

Maximum cut-off frequency of Io controlled Jovian decametric radiation as function of lambda coordinates

Cyclotron magnetoacoustic wave generation by planets and binary stars in circular orbits, deriving interstellar gas density variations

UV absorption levels in different areas of Jupiter disk from spectrophotometric studies at 3300-4800 A, noting temporal variations in reflectance

Venus, Mars, Jupiter and Saturn UV spectra from OAO-2 objective grating spectrophotometry, obtaining planetary albedos from G-type stars observations

Saturn radio emission detection and measurement at 49.5 cm, determining equivalent disk brightness temperature

Narrow band frequency drifts of polarized Jovian L bursts from simultaneous radio observations

Spacecraft-based observations of gamma and X radiation resulting from planetary surface and atmosphere processes to obtain source medium chemical composition

Venus 8.2 mm radio emission dependence on sun-light phase angle, considering implications for day/night atmospheric temperature variations

Radiation polarization from Jovian disk center as function of phase angle from polarimetric observations

Three station interferometer observations of Jovian decametric burst at 18 MHz, discussing possible solar wind interference

Jupiter decameter radio bursts as indicator of high velocity fluxes and shock waves in solar wind

Mars surface normal albedo distribution function from red light photometry data

Monochromatic brightness coefficient measurements for Jupiter and Saturn disk centers and Uranus geometric albedo

Jupiter decametric radiation modulation by photoelectron emission by satellite Io, describing future probe experimental test

Saturn rings gas-dust atmosphere, thickness and motion, considering planetary radio emission and brightness temperature

Venus long wave radiation spectral composition, angular distribution and carbon dioxide transmission from thermal, structure and vertical radiation absorption profile

Jovian synchrotron emission measurements by radioheliograph at 80 MHz, passing square low detector outputs through RC integrators

Mars violet haze and blue clearing for Syrtis Major-Arabia from photographic and photoelectric data

Venus brightness temperature and phase dependence at 2.7 cm wavelength during 1968-1970

Photometric search for Venus halo effect during 1970 inferior conjunction in relation to brightness maximum and ice in cloud tops

Hydrogen to helium mixing ratio in giant planets from far IR spectroscopy for atmospheric thermal models and greenhouse effect calculations

Mars integrated radio temperature relation to blanket electrical properties for 1971 opposition, assuming Martian soil properties independence from depth and temperature

Fourier analysis of Pluto light curve in terms of geometrical model consisting of bright and dark areas

The plasma physics of the Jovian decameter radiation.

Strong beaming of Jupiter's non-Io-related radio emission.

Brief survey of the problems of space radiobiology and radiation safety in space flights.

Some photometric parameters of the minor planet 2 Pallas.

Extensive air showers and the sporadic decameter radio emission of Jupiter

Saturn ring thickness estimates according to observations in 1966

Measurement of Jovian radio emission at a wavelength of 2.94 m

Mars surface normal albedo distribution function from red light photometry data

Monochromatic brightness coefficient measurements for Jupiter and Saturn disk centers and Uranus geometric albedo

Mars atmosphere temperature profiles inference from outgoing radiation spectral characteristics, constructing atmospheric model

Electrodynamic effects of Jupiter's satellite Io.

Jupiter - New evidence of long-term variations of its decimeter flux density.

Uranus methane brightening at limb and south pole explained by Rayleigh scattering and haze in upper atmosphere

Sunlight scattering by double reflection on rough and absorbing surfaces, deriving fractional circular polarization from models for comparison with observation

Structure of Jupiter's decametric radio sources - Two-dimensional probability and flux studies, 1957-1970.

PLANETARY SURFACES

PLANETARY ROTATION

Limited three body problem applied to planetary angular momentum increment due to accretion of particles in heliocentric orbits, discussing planet rotation laws

Rotation production in giant planets by gaseous impact, discussing Jupiter and Saturn formation

Linearized continuous baroclinic atmospheric model, discussing stability for planetary vorticity gradient

Perturbed satellite motion in gravitational field of aspherical rotating planet

Jovian belts, zones, great red spot, white ovals and atmospheric rotation and circulation from methane photographs analysis, comparing to earth atmosphere

Mariner 9 radio tracking measurements of Mars gravity field and pole direction, comparing to moon and earth

Numerical simulation of atmospheric turbulence in planetary boundary layer due to wind shear and/or unstable thermal stratification, noting buoyancy and planetary rotation effects

Perturbed satellite motion in gravitational field of aspherical rotating planet

Cosmic spherical rotating bodies angular velocity zonal distribution determination, noting application to Jupiter and Saturn

Limited three body problem applied to planetary angular momentum increment due to accretion of particles in heliocentric orbits, discussing planet rotation laws

Rotation production in giant planets by gaseous impact, discussing Jupiter and Saturn formation

Solar activity long term effects on Jupiter cloud structure rotational periods, using Chree superposition analysis

Earth based Mars photographic observations with direct image transmission via TV system, determining rotation period

Saturn rotation period latitudinal difference, presenting graphic plots derived from various visual observations

Russian book - Large-scale motions in the convective zones of stars and large planets.

The role of eruptive centers of the atmosphere of Jupiter in the determination of the rotation velocity of the core

Jupiter - Its Red Spot and disturbances in 1970-1971.

PLANETARY SATELLITES

U NATURAL SATELLITES

PLANETARY SPACE FLIGHT

U INTERPLANETARY FLIGHT

PLANETARY SPACECRAFT

U INTERPLANETARY SPACECRAFT

PLANETARY SURFACES

NT MARS SURFACE

Organic materials detection on planetary surfaces with in situ gas chromatography and mass spectrometry

Automatic craft for planet surface exploration, classifying propulsion gear

Planetary and lunar surface relief reconstruction from photographic imagery, discussing statistical morphological characteristics determination from relief

Jupiter evolution from summer 1969 to autumn 1970, noting north equatorial and south temperate bands and Red Spot intensity and surroundings

Photographic measurements of Saturn, observing atmospheric belt latitudes, ring dimensions and southern hemisphere bright spot rotation

Steady state exact solutions of MHD equations for perfectly conducting self gravitating incompressible fluid, showing solutions existence for rotating planetary ellipsoid free liquid surface

Topography of swath around Venus equator from wavelength dependence of radar cross section

Spacecraft-based observations of gamma and X radiation resulting from planetary surface and at-

mosphere processes to obtain source medium chemical composition 10 p1530 A72-25060

Circularly polarized ultrashort radio wave reflection from lunar and planetary surfaces, determining angular scattering spectrum 11 p1599 A72-26908

Mercury topography and scattering characteristics from 3.8 cm radar observations, comparing to Mars and Venus 12 p1865 A72-27098

Diving operations medical aspects significance for manned planetary surface exploration in high density atmospheres, considering protective clothing, breathing apparatus and gas mixtures, etc 12 p1769 A72-27415

Mars and Venus instrumented spacecraft flight results, describing planetary topographies, atmospheres and magnetic fields 12 p1877 A72-27650

Venus atmospheric parameters below critical refraction and surface refractive index from signal amplitude measurement by radio holographic occultation techniques 14 p2151 A72-30467

Wind velocity and some Venusian surface characteristics monitored by the "Venera-7" automatic interplanetary station 17 p2610 A72-35210

How to measure surface and atmospheric conditions on Venus by microwave interferometry 17 p2611 A72-35321

Russian book - Physics of the earth and planets: Figures and internal structure 19 p2856 A72-37474

Methods of radar studies of the moon and planets from spacecraft 21 p3103 A72-40307

Albedo and surface illuminance of a planet having a nonhomogeneous purely scattering atmosphere 21 p3050 A72-41796

Jupiter surface maps for 1965-70 from drawings obtained with astrophotograph, noting high activity and eruptive changes after 1961-63 outburst 22 p3220 A72-41920

Jupiter surface maps from synoptic observations with refracting telescope, considering white cloud formations and atmosphere motions 22 p3220 A72-41921

Effects of aeolian erosion on microbial release from solids 23 p3253 A72-43384

PLANETARY TEMPERATURE

Titan and Galilean satellites effective temperatures from broadband observations, suggesting low surface emissivity or high opacity for Titan 13 p2041 A72-29417

Mars upper cover temperature, representing diurnal variations at different areographic latitudes as harmonic series 14 p2148 A72-30207

Unipolar steady electromagnetic bow shock interaction of Mercury with solar wind, calculating planetary surface temperature 15 p2303 A72-31305

Jupiter cloud models, observational characteristics and temperature error at 5 micron wavelength 15 p2312 A72-32095

Jupiter atmospheric greenhouse effect modeled by two layer emission, deriving temperatures from non-gray step function approximation of IR absorption 15 p2312 A72-32096

Uranus, Neptune and Pluto disk temperature observations via National Radio Astronomy Observatory interferometer 16 p2455 A72-33464

The spectrum of Mars between 8 and 13 microns 17 p2606 A72-34575

Earth and Mars - Evolution of atmospheres and surface temperatures 17 p2613 A72-35395

Gas-liquid hydrogen mixture and helium adiabatic model of Jupiter temperature and pressure distribution, estimating planet center temperature 19 p2863 A72-38074

Martian surface relief and atmospheric properties from Mars probe observations, considering soil, dust storms, temperature distribution and life possibility 22 p3222 A72-42139

Mars upper cover temperature, representing diurnal variations at different areographic latitudes as harmonic series 23 p3333 A72-43237

PLANETOCENTRIC COORDINATES

NT GEOCENTRIC COORDINATES

Representation of the coordinates of a satellite of a spheroidal planet with the aid of series expansions 21 p3102 A72-40099

PLANETOLOGY

Review of papers on planetology given at Brighton symposium, covering moon, Venus, Mars and Jupiter 01 p0132 A72-11071

Martian internal structure, investigating oxidation rate of chondritic material 02 p0277 A72-11752

Terrestrial planets internal constitution and thermal history model, emphasizing iron fractionation in structure 03 p0418 A72-13110

Mariner Venus/Mercury 1973 flyby mission imaging experiment, discussing mission constraints, objectives and use of real time transmission vidicon camera and high resolution UV photography 04 p0568 A72-14494

Mars carbon dioxide distribution map determination of surface topography from spectrophotometric observations of equatorial region 04 p0569 A72-14499

Earth mantle and core density using Monte Carlo models compared with lunar structure from crust and seismology data, noting planetological contrast 04 p0571 A72-14616

Outer planets mass determination noting anomalous latitude residuals of Uranus 04 p0575 A72-15033

Principal planets mass derivation using fundamental and independent determinations in table form 04 p0576 A72-15037

Nearby spherical planet with two irrotational force fields, comparing identical frequency along latitude and meridian circles 05 p0656 A72-16185

Distant stellar satellites existence possibility based on maximum distance estimation for material particle motion stability with respect to sun or another star 08 p1231 A72-21133

Soviet papers on physics of moon and planets covering Martian violet clouds, UV absorption levels in Jupiter and Saturn disks, etc 08 p1237 A72-21826

Martian crater obliteration theory, suggesting filling by dust deposition 10 p1531 A72-23706

Book on stellar astronomy covering H-R diagram, solar system, nuclear energy sources, Milky Way Galaxy, quasars, cosmology, planetology, etc 16 p2453 A72-33275

Internal structure dynamics of earth, moon and planets, showing density variation and bulk modulus as function of pressure with correction of Bullen hypothesis 16 p2461 A72-34176

International Geological Congress, 24th, Montreal, Canada, August 21-30, 1972, Proceedings. Section 15 - Planetology. 17 p2614 A72-35676

Russian book - Physics of the earth and planets: Figures and internal structure 19 p2856 A72-37474

Book on moons and planets covering celestial mechanics, solar system origin, stellar formation, comets, asteroids, meteorites, planetary interiors, surfaces, atmospheres, etc 22 p3228 A72-42750

Solar system thin disk form planet formation in equatorial plane from nebula dust component, discussing gravitational effects and mass increase rate 23 p3335 A72-43261

Russian book - Space research 1970: Investigation of the gravitational fields and shapes of the earth, other planets, and the moon on the basis of spacecraft observations. 24 p3443 A72-45399

PLANETS

NT EARTH (PLANET)

NT EXTRASOLAR PLANETS

NT JUPITER (PLANET)

NT MARS (PLANET)

NT MERCURY (PLANET)

NT NEPTUNE (PLANET)

NT PLUTO (PLANET)

NT SATURN (PLANET)

NT URANUS (PLANET)

NT VENUS (PLANET)

Book on earth, moon and planet space photography, discussing synoptic meteorological data, mapping, surface detail inspection and planetary exploration 03 p0438 A72-14099

Outer planets satellites physics and chemistry, discussing steady state thermal models based on energy equilibrium between internal radioactive decay and surface radiation 04 p0568 A72-14495

Telescope observations of occultations of stars by outer planets, natural satellites and asteroids 09 p1387 A72-22977

Disk diameter errors due to wire thickness in reduction of visual planetary observations 09 p1311 A72-23062

Trans-Plutonian planet effect on Halley comet, considering perihelion errors and comet residuals 13 p2038 A72-29012

Sub-Mercurial planet Vulcan observation data, calculating orbital elements, angular size and velocity radial distance and object diameter 14 p2149 A72-30234

New orbital elements for moon and planets. 17 p2609 A72-35106

A possible mechanism for the capture of micrometeoritic particles by the earth and other planets of the solar system. 17 p2619 A72-35939

Positions of the major planets and the moon observed at the 0.33 M photographic equatorial 19 p2858 A72-37856

Data link design for planetary video data transmission back to earth based on rate distortion theory generalization of information theory 21 p3019 A72-40891

Search for trans-Plutonian planets with the aid of periodic comets 24 p3437 A72-44759

Biological aspects of communications with extraterrestrial intelligence, discussing life existence possibility on wandering planets 24 p3372 A72-45127

Critical inclinations and eccentricities concepts for N planet problem, applying results to general three body problem 24 p3442 A72-45239

From plasma to planet; Proceedings of the Twenty-First Nobel Symposium, Saltsjobaden, Sweden, September 6-10, 1971. 24 p3444 A72-45451

PLANFORMS

NT ARROW WINGS

NT CARET WINGS

NT DELTA WINGS

NT RECTANGULAR PANELS

NT RECTANGULAR PLANFORMS

NT RECTANGULAR PLATES

NT RECTANGULAR WINGS

NT SWEPTBACK WINGS

NT TRAPEZOIDAL TAIL SURFACES

NT VARIABLE SWEEP WINGS

NT WING PLANFORMS

PLANIMETRY

U DIMENSIONAL MEASUREMENT

PLANNING

Arc-air method application to groove planing, cutting and beveling, describing manual, semiautomatic and full-automatic units 07 p0994 A72-18932

PLANKTON

Monograph on Jurassic and Cretaceous Hagias-tridae from Blake-Bahama Basin and Great Valley Sequence in California 04 p0519 A72-15258

Paleomicrobiological analysis of northwest Scotland Stoor Formation black shale pre-Paleozoic spheroidal unicellular fossils as probable form of marine phytoplankton 05 p0655 A72-16042

PLANKTON BLOOM

U PLANKTON

PLANNING

NT AIRPORT PLANNING

NT MANAGEMENT PLANNING

NT MISSION PLANNING

NT PRODUCTION PLANNING

NT PROJECT PLANNING

NT URBAN PLANNING

PLANOTRONS

NT CATHODE RAY TUBES

NT CELESTIALS

NT THERMIONIC DIODES

Amplifier stability in optimal frequency regime, relating cut-off voltage and plate current as function of magnetic field, input power and geometrical parameters 07 p0953 A72-19014

PLANT ROOTS

Remote sensing investigation of root wilt disease in coconut plants in Kerala state /India/ 01 p0020 A72-10951

Gravity effects on plant organ orientation with respect to force direction from Chara rhizoid cell statoliths 15 p2189 A72-31932

PLANTS (BOTANY)

NT ALGAE

NT BACILLUS

NT BACTERIA

NT BLUE GREEN ALGAE

NT CHLORELLA

NT CLOSTRIDIUM BOTULINUM

NT ESCHERICHIA

NT EUGLENA

NT FOLIAGE

NT GIBBERELLINS

NT GRASSES

NT HYDROGENOMONAS

NT LEAVES

NT PSEUDOMONAS

NT SPORES

NT TOBACCO

NT TRADESCANTIA

NT TREES (PLANTS)

NT YEAST

Plant leaves light reflectance, transmittance and absorptance characteristics relationship to leaf

mesophyll arrangement, considering interpretation of aircraft/spacecraft remotely sensed data

02 p0213 A72-11856

Origin and development of plasma membrane derived invaginations in *Vinca rosea*, observing endocytosis in plant cells

05 p0616 A72-15810

Manganese catalyst photoactivation process for oxygen photosynthetic evolution investigated in Mn-deficient *Anacystis nidulans* cells

05 p0624 A72-15811

Illumination effect on proton and gamma irradiated cabbage plant growth, height and foliage, indicating radiation protective effect for certain light intensities

05 p0622 A72-16649

Radiative transfer equation for solar irradiance penetration of turbid atmosphere and plant canopy, using four point quadrature method

09 p1297 A72-22442

Mitogenic and IR radiation and plant bioelectricity in photogrammetry, using metabolic energy-photoemulsion relation

09 p1312 A72-23283

Biological experiments on plants, animals and bacteria aboard Zond 5, 6 and 7 space probes, noting flight conditions effect on physiological functions and hereditary structures

11 p1579 A72-25941

Plant leaves biochemical activities study by light scattering techniques, discussing photometric, spectroscopic and bionics methods

13 p1955 A72-28518

Hermetic chamber medico-engineering experiment for long term isolation effects on human intestinal microflora, showing reduction and disappearance of certain microbe populations

13 p1904 A72-29323

Dose response curves for pink somatic mutations in *Tradescantia* after neutron and X ray irradiation

15 p2186 A72-31723

Man, chlorella and wheat plant in life-supporting biological system, showing compatibility relative to gas and water exchange

15 p2189 A72-31826

Cytological, genetic and physiological analyses of space flight factors effects on seeds and plants aboard Zond 5 probe

15 p2186 A72-31828

Gravity effects on plant organ orientation with respect to force direction from Chara rhizoid cell statoliths

15 p2189 A72-31932

Action of a constant magnetic field on plant growth

17 p2503 A72-35006

Instrumental neutron-activation determination of cobalt and certain other elements in plant materials

22 p1383 A72-42471

Determination of copper, iron, cobalt, nickel, and manganese in biological samples of vegetable origin

23 p3260 A72-43924

PLANTS [INDUSTRIES]

U INDUSTRIAL PLANTS

PLASMA ACCELERATION

Plasma jet formation within high pressure discharges in air at atmospheric pressure, discussing electrode configuration, current density and accelerating magnetic field strength

03 p0396 A72-13662

Acceleration equations for plasma injectors with capacitive and inductive energy storage elements

05 p0697 A72-16985

Electric eddy currents formation during thermal acceleration of inviscid quasi-linear plasma in profiled channel

08 p1215 A72-21654

Snow-plough model of plasma acceleration for determining time dependence, gas density distribution and energy transfer

09 p1359 A72-22819

Solid body model for electric arc acceleration in thermionic cathode rail accelerator, discussing plasma mass effects

[AIAA PAPER 72-412]

11 p1706 A72-26162

Parallel rail solid fuel pulsed electric microthruster performance, noting mathematical model for mass ablation and plasma acceleration mechanism

[AIAA PAPER 72-458]

11 p1708 A72-26194

Shock-induced flow acceleration in Ar plasma, studying shock front behavior from high-speed photographs

11 p1696 A72-26374

Linear electron acceleration mechanism in plasma, showing polarization fluctuations in diode under strong electric field

11 p1699 A72-26761

Acceleration equations for plasma injectors with capacitive and inductive energy storage elements

12 p1850 A72-27129

Russian book on electrodynamic plasma acceleration covering charged particles motion in electromagnetic field and pulsed, MHD, steady and Hall accelerators

12 p1853 A72-28341

Some comments on the generation of electromagnetic traveling and standing waves for inductive acceleration of plasmas

[DFVLR-SONDDR-209]

17 p2589 A72-34895

Electron and plasma particle acceleration by moving pulsed laser, noting appearance of fast particles, hard radiation and neutrons

23 p3295 A72-43312

Calculation of the parameters of a plasma accelerated in a high-frequency electric field and a static magnetic field

23 p3320 A72-43660

PLASMA ACCELERATORS

NT COAXIAL PLASMA ACCELERATORS

High velocity plasma generation in induction hydrodynamic shock tube and flow into rail type plasma accelerator, investigating possible T layer formation

01 p0110 A72-11203

Passive electric microwave probe with balancing capacitance for studying waveguide fields at high microwave power levels in radiative plasma accelerators

02 p0223 A72-11418

Compressible turbulent boundary layer equations for flow on B wall of MHD accelerator, including electron thermal nonequilibrium and finite rate ionization

03 p0397 A72-13923

One dimensional continuous electrode shock tube driven MHD accelerator, analyzing unsteady flow behind ionizing shock wave by method of characteristics [AIAA PAPER 72-102]

05 p0697 A72-16973

Pulsed flat electrode erosion plasma accelerator, determining electric and magnetic fields distribution, current density and electron concentration

05 p0697 A72-16987

Unipolar pulsed plasma accelerator, describing trigatron circuit design for generation of 100 kA unipolar current pulses of 35 microsec duration

07 p1040 A72-19316

Electromagnetic plasma accelerator with electron drift and diffusion towards anodes, neutral gas ionization and extended ion acceleration zone

09 p1361 A72-22955

Steady state plasma interactions with electromagnetic force field in plasma accelerators, showing shock wave formation

[AIAA PAPER 72-413]

11 p1706 A72-26163

Magnetic fields effect on anode heat losses in MPD accelerator arcs, noting minimal charge current density

[AIAA PAPER 72-502]

11 p1711 A72-26225

Pulsed flat electrode erosion plasma accelerator, determining electric and magnetic fields distribution, current density and electron concentration

12 p1850 A72-27131

Pulse plasma injector accelerating circuit resistance dependence on time and current amplitude calculated from current oscillograms

13 p2010 A72-28733

Supersonic dense low temperature plasma jet generation by pulse mode accelerator based on dielectric erosion and electrically exploded conductor

13 p2011 A72-29007

High speed frame photography application in spectroscopic studies of plasma jet in cylindrical pulsed accelerator with dielectric

15 p2283 A72-31418

Fine structure similarities between solar flares and current sheath in laboratory hot plasma coaxial accelerator, noting X ray and high energy particles production mechanism

16 p2438 A72-33919

Electromagnetic plasma accelerator with electron drift and diffusion towards anodes, neutral gas ionization and extended ion acceleration zone

17 p2593 A72-35884

Production of intense ion beams by high-frequency electric fields

19 p2839 A72-37331

Measurement of electron concentration in the plasma of a pulsed erosion-type accelerator

19 p2843 A72-38535

Estimation of the mass composition and energy spectrum of a plasma jet from a conical pulsed accelerator

21 p3089 A72-40134

PLASMA ARC SPRAYING

U ARC SPRAYING

U PLASMA SPRAYING

PLASMA ARC WELDING

Plasma generator with Ar as ionizing medium for metal cutting and welding, discussing protection against secondary arc formation

08 p1176 A72-21048

Ar-H microplasma welding of thin Cr steel sheets with narrow seams for aircraft engines and precision equipment casings

09 p1318 A72-22548

Pulsed microplasma and intermediate current plasma welding of AL, comparing with tungsten arc and electron beam welding

09 p1320 A72-23628

Pulse shaping, arc plasma jets and torch movement indexing for high precision pulsed tungsten inert gas (TIG) welding

09 p1321 A72-23635

Prototype fine wire feed unit and microplasma welding torch and equipment for butt welding of Ni maraging steel, testing welds mechanically

09 p1321 A72-23636

Plasma arc and MIG /metal inert gas/ welding combination with filler wire, obtaining high melting rates and penetration control

09 p1322 A72-23645

Automatically controlled plasma arc welding for uniform cross section weld seams production under fluctuating electric current conditions, describing electronic control system

15 p2244 A72-31773

Magnetic control of arc plasma and its application for welding

24 p3406 A72-44777

PLASMA ARCS

U PLASMA JETS

PLASMA CHEMISTRY

Chemical reaction rates for dissociation and exchange in nonisothermal plasma from molecular energy level occupation investigation

20 p2957 A72-39018

Formation and loss of O₂+/ and O₄+/ ions in krypton-oxygen afterglow plasmas

23 p3316 A72-44345

Kinetic equations for a chemically reacting plasma

24 p3430 A72-45566

PLASMA CLOUDS

Plasma inhomogeneities effect on radio wave absorption in interstellar clouds of ionized hydrogen, analyzing cosmic radio emission spectrum

08 p1231 A72-21120

Geomagnetic field effects on initially spherically symmetric ion cloud diffusive motion in earth upper atmosphere

09 p1297 A72-22577

Spectrum of hot hydrogen plasma continuum radiation, discussing models for Scorpius X-1 source and inhomogeneous clouds

09 p1391 A72-23536

Deionization mechanism of expanding plasma cloud produced by arc burning in vacuum, discussing charged particle concentration and ion thermal velocity

10 p1521 A72-24356

Rocket released artificial Cs plasma clouds in upper atmosphere, measuring electron density by HF radar observation

15 p2231 A72-32330

Geomagnetic field line tracing by plasma clouds produced by Ba vapor release, noting different ion drift rates and directions

16 p2384 A72-32977

Barium cloud striations deformation in ionosphere explained by equations of motion for plasma cloud thin bar model, discussing pinch effect

16 p2387 A72-33907

Deionization mechanism of expanding plasma cloud produced by arc burning in vacuum, discussing charged particle concentration and ion thermal velocity

17 p2589 A72-34956

Motion of ion-cloud in the ionosphere, field-aligned cloud with Gaussian distribution of ionization density

17 p2546 A72-35060

Superposition principle in test particle method for reducing plasma cloud kinetic theory to determination of conditional probability function involving Vlasov equation

17 p2591 A72-35163

Study of the motion of ionized artificial clouds in the upper atmosphere

18 p2688 A72-36864

Effect of Thomson scattering on the emission spectrum of an optically semitransparent plasma

21 p3102 A72-41774

Transfer effects on X-ray lines in optically thick celestial sources

24 p3435 A72-44843

Microwave observations of a partially ionized interstellar cloud

24 p3447 A72-45551

PLASMA COMPOSITION

Ion charge composition in plasma-electron beam system in strong longitudinal magnetic field, noting multiply charged ions production under high temperature conditions

05 p0701 A72-17235

Satellite and ground station observed ionospheric plasma parameters comparison, considering electron density and temperature and ion temperature and composition

12 p1804 A72-27785

Nature of ion generation during the action of laser emission on a solid body

19 p2811 A72-38193

Estimation of the mass composition and energy spectrum of a plasma jet from a conical pulsed accelerator

21 p3089 A72-40134

PLASMA CONDUCTIVITY

Plasma hydrodynamic Buneman current instability under strong electric field, considering nonlinear stage in one dimensional case

01 p0105 A72-10024

Acoustic instability of plasma with current under equilibrium ionization and moderate neutral gas pressures

01 p0109 A72-10485

MHD instabilities of plasma with current, using two fluid model in crossed magnetic-electric fields

01 p0109 A72-10486

Kubo bulk electrical conductivity of two dimensional guiding center plasma in strong dc magnetic field

02 p0263 A72-11966

Free hf discharge plasma column generator, discussing equipment and current and resistance measurements

03 p0393 A72-13083

Plasma conductivity frequencies, including electromagnetic wave propagation in alternating field and scattered light intensities

03 p0396 A72-13653

Intense pulsed electron beam production by current flow through narrow gap filled with plasma

03 p0396 A72-13656

Immersion-type electroconductivity probe for anisotropic plasmas, calculating Hall coefficient

03 p0397 A72-13922

Rotationally symmetric static incompressible infinite conducting plasma elliptic differential equation reduction to boundary value problem

03 p0400 A72-14353

Nonideality effects on Coulomb gas conductivity by finding conductivity due to electron scattering at atoms, solving kinetic equation of three component plasma model

05 p0694 A72-15850

Poloidal Hall current calculation in hydrodynamic approximation for stationary weakly interacting and conducting cylindrical plasma flow with uniform transverse flow parameter distribution

05 p0701 A72-17240

Plasma conductivity dependence on electron velocity distribution function in distorted Maxwellian form

06 p0860 A72-17690

Thermal conductivity of stationary toroidal plasma in form of Pfirsch-Schluter diffusion factor, using ion heat balance equation

07 p1042 A72-19616

External circuit coupling effects on dc anomalous resistivity in electron plasma oscillation

07 p1043 A72-19666

Combustion product plasma electrical conductivity dependence on neutral component density fluctuation

07 p1044 A72-19888

Dense low temperature Ar and Hg plasmas, observing correlation between electrical conductivity and optical emission

10 p1517 A72-23835

Nonlinear conductivity of plasma with FM electromagnetic wave propagation, proposing electronic current density calculation method

10 p1519 A72-24130

Electrical conductivity of two dimensional strongly magnetized guiding center plasma, using Liouville equation

11 p1693 A72-25563

Magnetosphere neutral layer plasma conductivity determination from model of linear magnetic dipole in conducting fluid flow

11 p1622 A72-25945

Plasma interchange instability and convection in gravitational field, showing viscosity and resistivity stabilization and critical Reynolds number

11 p1697 A72-26584

Nonequilibrium ionization phenomena effects on electric conductivity of combustion gas-particle plasma generated by aluminized fuel seeded with potassium nitrate

13 p2013 A72-29363

Nonlinear model of ionization instability of MHD generators, assuming discharge stability with alternating layers of high and low electrical conductivity

13 p2014 A72-29371

Magnetosheath electron precipitation effect on dayside auroral-oval plasma density and conductivity, relating precipitation heat flux to solar wind energy density

13 p1950 A72-29381

Free HF discharge plasma column generator, discussing equipment and current and resistance measurements

13 p2015 A72-29433

Electron-ion collision frequency and conductivity of non-Debye plasma formed in high pressure discharge from Ar, Kr and Xe tubes

13 p2018 A72-29891

Low temperature homogeneous plasma electric conductivity in magnetic field, noting monotonic decrease

13 p2018 A72-29892

Ion-acoustic oscillations effect on turbulent plasma electric conductivity within weak external electric field

13 p2019 A72-29990

Isotropic conducting plasma dynamic behavior near rotating magnetized sphere, showing electric field-produced meridional convective currents

14 p2138 A72-30630

Hydromagnetic waves excited by transverse magnetic dipole in finite-conductivity plasma

14 p2102 A72-30662

Nonideality effects on Coulomb gas conductivity by finding conductivity due to electron scattering at atoms, solving kinetic equation of three component plasma model

15 p2283 A72-31269

Electrical conductivity of shock wave produced Xe plasma measured by probe, noting dependence on Mach number

15 p2284 A72-31583

Anisothermal magnetoplasma with non-Maxwellian particle distribution function, calculating electrical conductivity collisional factor from convergent classical kinetic equation

15 p2287 A72-32410

Multispecies magnetoplasma as electrical conductivity tensor collision factor from quantum mechanical convergent kinetic equation

15 p2287 A72-32411

Microscopic theory of weakly ionized plasma conductivity, showing particle diffusion function or transition probability description by linear Boltzmann equation

15 p2287 A72-32412

Auroral electrojet polarization model, considering ionospheric Hall and Pedersen conductance maximum due to precipitation from electron plasma sheet inner edge

[AD-745672] 16 p2444 A72-32961

Heat conductivity effect on structure and critical Mach number of shock wave propagation across magnetic field in cold rarefied plasma

16 p2435 A72-33152

Nitrogen plasma jet flow, attributing discrepancies in electrical conductivity and velocity to shock effects on probe measurements

[AIAA PAPER 72-671] 16 p2440 A72-34069

Combustion product plasma electrical conductivity dependence on neutral component density fluctuation

17 p2590 A72-35136

Transverse diffusion and conductivity coefficients for a three-dimensional magnetized equilibrium plasma.

17 p2592 A72-35379

Soft collision plasma scattering function, conductivity and particle energy loss from simplified Fokker-Planck collision model

17 p2592 A72-35621

Electric fields in MHD channels in the case of anisotropic and nonuniform conductivity

18 p2716 A72-36817

Temperature dependence of the electron thermal conductivity in rare gas plasmas.

18 p2716 A72-36958

Wave propagation in plasmas with fluctuations.

19 p2842 A72-38525

Stability of a plasma conductor with axial current, surrounded by cold gas with a pressure gradient

19 p2842 A72-38533

Observation of superheat instability in a fully ionized current-carrying plasma.

20 p2958 A72-39854

Nonlinear magnetosonic waves in a plasma with a finite conductivity.

21 p3090 A72-40485

Impedance of a partially ionized cesium plasma.

21 p3091 A72-40694

Boundary fluctuations of a plasma column with a current

22 p3211 A72-42655

Disequilibria created by an electric field in a nitrogen plasma

23 p3321 A72-43695

Role of nonlinear effects in the problem of the anomalous resistance of a plasma

23 p3322 A72-44481

PLASMA CONFINEMENT

U PLASMA CONTROL

PLASMA CONTROL

Nonlocal theory of electrostatic trapped particle instability in collisionless toroidal plasma, estimating particle mode nonlinear diffusion coefficient

01 p0108 A72-10239

Nonlocal behavior of ion sound instability in collisionless nonuniform confined plasma shock wave

01 p0108 A72-10240

Electrostatic potential fluctuations spectrum in turbulent hot ion plasma confined between magnetic mirrors, investigating mode coupling, energy cascading and electron concentration

01 p0108 A72-10242

Ideally conducting plasma confined in vacuum by circularly polarized magnetic field, investigating MHD

instabilities suppression by distributed automatic control system

01 p0109 A72-10503

Electrical and nuclear propulsion plasma containment problems, discussing simulation experiments and scaling devices feasibility

01 p0117 A72-10938

Quasi-static surface waves at Maxwellian plasma boundary with diffuse electron scattering, considering plasma electromagnetic oscillations

02 p0266 A72-12577

Equilibrium state linear theta pinch plasma confinement dependence on nonuniform magnetic force lines curvature radius

03 p0396 A72-13659

Moving plasma beam capture by transverse magnetic field due to polarization space charges electrostatic separation

03 p0396 A72-13657

Plasma density profiles by microwave interferometry technique in Sirius stellarator diverter for two magnetic field configurations and injection methods

04 p0555 A72-14619

Electron beam interaction with bounded solid state plasma, deriving slow wave dispersion relations

04 p0561 A72-15080

Toroidal plasma column in Tokamak systems, discussing field inhomogeneity role in maintaining equilibrium with conducting casing, confirming magnetic field and transformer iron core

04 p0557 A72-15171

Flutelike microinstabilities in mirror-confined homogeneous magnetized one-species plasma with broad perpendicular velocity distribution

04 p0559 A72-15354

Plasma ion collision transport analogy with turbulent velocity space momentum transfer, explaining confined plasma runaway electron absence in strong electric fields

04 p0560 A72-15469

Magnetic multipole confinement of magnetic field-free He and Ar plasmas in vacuum chamber, observing decay

06 p0854 A72-17505

Ion distribution function oscillations in first order ionic waves of single ended Q device, noting plasma confinement in static magnetic field

06 p0855 A72-17507

Closed line magnetic confinement device filled with laser produced hydrogen plasma, discussing laser beam high speed numerical control for injected pellet interception

[CLEA PAPER 12.1] 07 p1040 A72-19392

Field free constricted plasma discharge stability between electrodes, obtaining critical current

07 p1042 A72-19608

High frequency heating of dense toroidal plasma by nonaxisymmetric ion cyclotron waves resonant excitation in closed magnetic trap

07 p1043 A72-19638

Stability conditions of dissipative trapped ion mode in axisymmetric toroidal confinement systems, in vestigating collisional damping rate

07 p1045 A72-20476

Design equations for transpiration radiometer applicable to radiation measurement from confined Ar plasma

08 p1163 A72-20919

Two dimensional model for plasma without magnetic field trapped near current sheet end in dipole magnetic field resembling geomagnetic tail

08 p1157 A72-21108

Electron beam interaction with bounded homogeneous plasma layer natural oscillations, using collisionless kinetic equation

08 p1215 A72-21720

Propagation time of charge diffusion across magnetic field in bounded plasma

08 p1215 A72-21879

Soviet book on plasma physics and controlled thermonuclear synthesis covering plasma-electromagnetic interactions, magnetic traps and plasma cryogenic technology

09 p1361 A72-23201

Colliding plasma flows motion and capture in transverse magnetic field with mirror configuration, noting polarization effect

09 p1362 A72-23209

Plasma injected into closed multipole magnetic trap, investigating plasma wave locking time and characteristic life

09 p1362 A72-23213

Plasma injection in magnetic trap along curvilinear inhomogeneous magnetic field, showing long plasmasoids polarization and drift reduction by depolarization currents

09 p1363 A72-23218

Star stellarator model for hot electron plasma production by steady electron beam injection in closed magnetic traps

09 p1363 A72-23219

Crossed fields effect on plasma injection in magnetic trap

09 p1363 A72-23220

Multipole magnetic field configuration effectiveness in electromagnetic plasma trap, discussing electron losses critical angle and captured ions maximum density
09 p1363 A72-23221

Target jet density variations effect on vacuum in neutral atom beam ionization region of fast neutral particle magnetic trap
09 p1363 A72-23223

Charged to neutral particle transformation capacity of wide aperture recharge target formed by supersonic gas jets in magnetic trap with annular nozzle
09 p1363 A72-23224

Bounded plasma ionization instability inhomogeneity scale evaluation, assuming negligible electron energy losses due to heat conduction
10 p1517 A72-23844

Rotating low density plasma in magnetic mirror trap with Penning discharge, determining conditions for oscillations damping and plasma lifetime
10 p1521 A72-24354

Superconducting levitron machine for trapped hot plasma stability and confinement studies in vacuum, discussing construction and coil performance
10 p1460 A72-24758

Collective self fields generated from intense electron beams for high energy positive particle acceleration and Astron hot plasma confinement for fusion control
10 p1523 A72-24788

Parallel viscous modification of resistive tearing instability in Cartesian model of hard core pinch plasma confinement
10 p1523 A72-24795

Ion and electron temperature ratios in hot plasma, discussing energy relaxation, heating and cooling effects and electrostatic confinement by ambipolar diffusion
10 p1524 A72-25032

Plasma equilibrium configurations, considering magnetically contained focus in external magnetic field
11 p1694 A72-25788

Collisional distributions in mirror plasmas, using successive approximation technique for Fokker-Planck equation lowest eigenvalue and eigenmode
11 p1694 A72-25792

Laser pulse form effect on confined plasma heating, taking into account inverse electron-ion bremsstrahlung and stimulated Compton scattering
11 p1651 A72-26672

Nature and requirements of electrostatic inertial plasma confinement, deriving potential and particle densities as function of radius, grid voltage and current
12 p1850 A72-27281

Ionization stabilization in MHD generators by sensing electron density perturbation with linear feedback into nonequilibrium plasma
13 p2014 A72-29369

Nd laser irradiation of LiH particles in magnetic trap, investigating resultant plasma expansion and diffusion
13 p2015 A72-29431

Plasma diffusion coefficient in crossed electric and magnetic fields, discussing lifetime in magnetic trap and expression for ion mobility
13 p2019 A72-29942

Plasma capture by stellarator diverter magnetic field, noting stream length controllability by field pulse duration
14 p2135 A72-30168

Plasma heating in Tuman 2 toroidal magnetic trap by microwave injection at upper hybrid frequencies
14 p2137 A72-30311

Plasma containment by superposed fields/sustained field/ technique application to theta pinch, studying hydrogen and helium discharge behavior
14 p2138 A72-30400

Plasma containment in toroidal systems investigated on basis of fluid model containing inertia, momentum transfer, ionic collisions and thermal conductivity effects
15 p2285 A72-32273

Magnetic field profile optimization for beta-limitation in minimum-B mirror confined plasma in nuclear reactor
16 p2432 A72-32805

Skin effect in large hot tokamaks predicted by computer studies based on empirical transport coefficients, discussing suppression by moving limiter
16 p2433 A72-32812

Magnetic configuration for plasma confinement in torsatron with helical windings and no toroidal field coils
16 p2433 A72-32816

High latitude trapping boundary for 20 KeV electrons and 100 KeV protons during intense geomagnetic substorms, observing field-line motion
16 p2444 A72-32958

Nuclear composition telescope measurements on-board OGO 5 satellite, observing presence of geomagnetically trapped carbon, nitrogen and oxygen nuclei
16 p2382 A72-32959

Particle and energy fluxes across magnetic field in axisymmetric toroidal magnetic traps and plasmas with weak collisions, calculating radial electric field
16 p2440 A72-34153

RF discharge gap in cascaded plasma limiters, using tritium igniter as reliable electron priming source
18 p2715 A72-36451

Magnetic surface equation and collisional diffusion of finite beta tokamak plasma in low density regime
19 p2838 A72-37330

Electron-plasma-wave shocks in a bounded plasma.
19 p2840 A72-37719

Parametric coupling of large amplitude pump wave to E layer plasma mode to explain auroral electrojet irregularities external production and control
19 p2793 A72-38746

Pulsed IR laser for heating superdense plasma to high temperature, featuring inertial confinement by use of short duration energy and strong magnetic field
19 p2843 A72-38823

Determination of the magnetic field B in vacuum for general two-dimensional MHD-equilibria.
20 p2957 A72-39352

Plasma equilibrium in configurations with a helical magnetic axis with allowance for toroidality.
20 p2957 A72-39353

Low beta model of collision dominated plasma flow effect on toroidal confinement, simulating Stellarator, Levitron and Tokamak
20 p2957 A72-39356

Computer simulation of RF-confinement of plasmas in an open-ended toroidal quadrupole.
21 p3089 A72-40191

Resonant scattering of trapped particles by toroidal plasma modes.
21 p3092 A72-41217

Transverse velocity shear instabilities within a magnetically confined plasma.
21 p3093 A72-41628

External high-frequency modulation of an electron beam and heating of plasma ions in the case of beam-plasma instability in the magnetic trap
21 p3095 A72-41678

Pressure dependent microwave cavity breakdown field relationship to steady state plasma luminosity interpretation as evidence of RF confinement of low density plasma
22 p3212 A72-42897

Confinement time of plasma injected in magnetic field of racetrack with diverter, noting plasma equilibrium in toroidal magnetic field
22 p3213 A72-43106

Plasma heating in Tuman 2 toroidal magnetic trap by microwave injection at upper hybrid frequencies
23 p3318 A72-43213

Landau dispersion equations for oscillations damping of bounded electron plasma, noting application to plasma cylinder in conducting tube
23 p3319 A72-43410

Apparent constant wavelength oscillations in a bounded plasma.
23 p3320 A72-43577

High frequency heating of dense toroidal plasma by nonaxisymmetric cyclotron waves resonant excitation in closed magnetic trap
24 p3427 A72-44568

Magnetic control of arc plasma and its application for welding.
24 p3406 A72-44777

Kinetic approximation for confined electron beam stability in plasma situated in magnetic field, deriving instability increments and dispersion relations
24 p3428 A72-45078

Instability of a magnetically active plasma in the presence of a specified transverse velocity of the ions
24 p3429 A72-45488

Transformation of trapped charged particles to transit particles under the influence of a high-frequency electric field
24 p3429 A72-45494

PLASMA CYLINDERS

Plasma column equilibrium position feedback control based on combination principle, analyzing system stability
01 p0109 A72-10502

Traveling wave antenna for exciting ion cyclotron waves in cylindrical anisotropic magnetoplasma
02 p0188 A72-11468

Plane electromagnetic wave diffraction on magnetoactive plasma cylinder, using energy method and particle scattering model
02 p0183 A72-12754

Free hf discharge plasma column generator, discussing equipment and current and resistance measurements
03 p0393 A72-13083

Vacuum UV spectra of free plasma column in microwave field at high pressures for discharge in helium-deuterium mixture
03 p0394 A72-13084

Wall double layer temperature and plasma oscillations effect on electron energy distribution in low discharge plasma column
03 p0394 A72-13192

Nonlinear ionization wave equation, calculating nonlinear response of unstable positive plasma column to weak pulse disturbance
03 p0399 A72-14346

Nonuniform radial electric field effects on low beta magnetized plasma column stability from numerical analysis for weakly collisional regime
04 p0557 A72-15023

Plasma column interaction with counter rotating hf magnetic fields of multipole configurations, calculating angular velocity
04 p0557 A72-15169

Nonlinear surface wave propagation on pinched cylindrical plasma, developing asymptotic approach from L undquist equations
04 p0559 A72-15348

Geomagnetic tail natural oscillations, applying model of plasma cylinder with free boundary immersed in interplanetary medium
05 p0659 A72-17044

Poloideal Hall current calculation in hydrodynamic approximation for stationary weakly interacting and conducting cylindrical plasma flow with uniform transverse flow parameter distribution
05 p0701 A72-17240

Cylindrical alkali metal plasma column structure in single ended Q device under axial magnetic field
06 p0854 A72-17503

Cylindrical plasma ion-acoustic resonance measurements from various excitation methods for noise component identification
06 p0856 A72-17523

Q-machine plasma column drift instability passive feedback control, regulating feedback drive current phase and amplitude by varying resonance circuit characteristics
06 p0857 A72-17532

Electrostatic energy analyzer for local ion velocity distribution function measurement in double ended Q machine plasma column
06 p0814 A72-17551

Force-free magnetic fields effects on plasma column stability
06 p0860 A72-17744

Anisotropic equilibrium solution to Vlasov equation for high beta theta pinch plasma column
07 p1045 A72-20478

Dynamic stabilization of MHD instabilities in plasma column by multipole hf fields, analyzing dispersion equation
07 p1045 A72-20479

Refraction of electromagnetic wave with electric field perpendicular to applied magnetic field in anisotropic plasma cylinder cross section
07 p1046 A72-20507

Weakly damped Alfvén ion-cyclotron waves and fast magnetoacoustic waves in infinite plasma cylinder inserted into current bearing finite coil
07 p1046 A72-20516

Slow and fast longitudinal ion acoustic waves in plasma cylinder under axial magnetic field
08 p1215 A72-21873

Plasma flows interaction with plasma cylinder in diverter magnetic field, investigating plasma dynamics with electric probes, plasmascope and mass spectrograph
09 p1362 A72-23210

Charged and neutral particles radial distribution across positive isothermal plasma column in high current discharges
10 p1521 A72-24355

Positive plasma column theory for longitudinal cylindrical discharge problem in ambipolar conditions, stressing surface and bulk temperature effects
10 p1521 A72-24357

Magnetic diffusion into moving cylindrical incompressible plasma with radial divergence
10 p1521 A72-24413

Combined plasma and magnetic field cumulation due to heavy conducting liner implosion, noting compression parameters for plane and cylindrical bodies
10 p1523 A72-24723

Electron densities and drift velocities dependence on macroscopic discharge parameters in positive column of He-Cd laser
10 p1493 A72-25048

Plasma column stabilization by constant longitudinal inhomogeneous magnetic and rotating HF electromagnetic fields, noting application to plasma convective instabilities
11 p1694 A72-25786

Finite element method application to hydromagnetic plasma stability analysis, considering cylindrical plasma immersed in axial magnetic field and bounded by conducting shell
11 p1695 A72-25794

Plasma layer effect on natural oscillations of magnetosphere tail, using infinite plasma cylinder model immersed in interplanetary plasma
11 p1622 A72-25944

Geomagnetic tail model with plasma cylinder immersed into solar wind, obtaining dispersion equation for oscillations
11 p1627 A72-26532

Bounded systems dispersion relations interpretation for plasma waves and instabilities on finite cylinders, with emphasis on end plate damping and axial current effects on Q machines

11 p1697 A72-26597

Electromagnetic wave propagation in cylindrical plasma column of electrons and ions with and without applied uniform magnetic field in absence of collisions

13 p2010 A72-28681

Free HF discharge plasma column generator, discussing equipment and current and resistance measurements

13 p2015 A72-29433

Vacuum UV spectra of free plasma column in microwave high pressure discharge in helium-deuterium mixture

13 p2015 A72-29434

Homogeneous plasma column generation by HF generator, probing for electron temperature and charged particle concentration

13 p2015 A72-29507

Dispersion characteristics of ion-acoustic waves in positive gas discharge plasma column

13 p2019 A72-29912

Experimental investigation of electrostatic cyclotron harmonic waves excited in inhomogeneous plasma column with axial magnetic field by RF capacitor field

14 p2138 A72-30398

Magnetized plasma discharge steady state problem of finite cylinder positive column in magnetic field, detailing radial and axial solutions

15 p2288 A72-32508

Ion acoustic and guided electron plasma waves excitation by grid antenna produced LF signals in cylindrical plasma column

15 p2289 A72-32650

Plasma column formation by interaction with rotating HF electromagnetic field and longitudinal constant magnetic field

16 p2433 A72-32815

Magnetic field distribution measurement in axisymmetric plasma column inside Tokamak device by alpha particle beam from radioisotope

16 p2434 A72-32818

Nonlinear electromagnetic wave interaction in rarefied plasma cylinder subject to constant magnetic field in hydrodynamic approximation

16 p2363 A72-33479

Low pressure He and Ne discharge generated positive plasma column potential, determining electron concentration from electron energy distribution functions

16 p2437 A72-33746

Probe temperature, shape and size effects on electron energy distribution measurements for positive plasma column of low pressure He and Ne discharges

16 p2437 A72-33750

Electron-ion heating in high beta perpendicular collisionless shock waves by plasma cylinder magnetic compression using theta pinch

16 p2439 A72-33936

Scattering of electromagnetic waves from an inhomogeneous magnetoplasma column moving in the axial direction.

17 p2587 A72-34359

Charged and neutral particles radial distribution across positive isothermal plasma column in high current discharges

17 p2589 A72-34955

The propagation of non-axisymmetric Alfvén waves in an argon plasma.

17 p2591 A72-35371

Two fluid MHD model to study cylindrical plasma condenser resonance properties in crossed axial magnetic and alternating electric fields

17 p2593 A72-35881

Excitation of nanosecond waves on positive columns.

19 p2838 A72-37328

Kinetic theory of surface waves in a cylindrical plasma waveguide

19 p2842 A72-38531

Plane electromagnetic wave diffraction on magnetoactive plasma cylinder, using energy method and particle scattering model

20 p2902 A72-39060

Identification of transverse Kelvin-Helmholtz turbulence in a magnetoplasma column.

21 p3091 A72-40768

Method of calculation of the emission coefficient of a cylindrical plasma starting from the experimental profile of the intensity

21 p3092 A72-41198

Electronically scannable plasma leaky wave antenna system.

21 p3022 A72-41325

Eigenvalue numerical solution for dispersion relation and propagation characteristics of nonlocal drift waves in cylindrical plasma based on two fluid model

21 p3093 A72-41495

Transverse velocity shear instabilities within a magnetically confined plasma.

21 p3093 A72-41628

Helical field experiments on a three-meter theta pinch.

21 p3094 A72-41636

Comet tail wave motion explanation via consideration as plasma cylinder with free boundary tangential discontinuity surface immersed in interplanetary plasma

22 p3221 A72-42011

Boundary fluctuations of a plasma column with a current

22 p3211 A72-42655

Pulse discharge plasma in Ar with gas ionization level near unity, noting plasma cylinder parameters, electron temperature and I-V characteristics

22 p3212 A72-43103

Landau dispersion equations for oscillations damping of bounded electron plasma, noting application to plasma cylinder in conducting tube

23 p3319 A72-43410

Apparent constant wavelength oscillations in a bounded plasma.

23 p3320 A72-43577

Study of microwave scattering in a plasma-beam discharge

23 p3321 A72-44212

Nonlinear effects in the dynamic behavior of the positive column from a low-voltage low-pressure discharge

24 p3428 A72-44965

PLASMA DECAY

High resolution apparatus to record time dependent light flux variations at 380-700 nm, discussing He plasma decay investigation

01 p0064 A72-10375

Photoresonance cesium plasma development and decay, determining density spatial-temporal behavior and recombination and polar diffusion coefficients by probe measurements

03 p0396 A72-13664

Collisional radiative recombination applicability to time dependent electron density decay in helium afterglow before reaching quasi-steady state

04 p0555 A72-14579

Submillimeter wave sulfur dioxide molecular laser, investigating lasing lines, plasma decay and relaxation, line interactions and signal temporal behavior

04 p0532 A72-15595

Magnetic multipole confinement of magnetic field-free He and Ar plasmas in vacuum chamber, observing decay

06 p0854 A72-17505

Weakly ionized decaying afterglow plasma potential fluctuation and instability in magnetic field, using electrostatic probes

06 p0860 A72-17692

Radial distribution of charged particle concentration fluctuation during decaying plasma instability development magnetic field

06 p0863 A72-18416

Plasma decay instabilities in finite amplitude Alfvén wave field, discussing critical wave amplitude

11 p1694 A72-25790

Parametric decay instability of Langmuir and acoustic plasma waves induced by incident electromagnetic wave near plasma frequency, noting application to ionospheric instabilities

13 p2012 A72-29126

Weakly ionized plasma decay within cylinder with electrically conducting walls in presence of longitudinal magnetic field, determining electric current dependence on cylinder length

13 p2016 A72-29603

Mass spectrometric techniques for collision processes in decaying nitrogen-helium and nitrogen-neon plasmas, obtaining ambipolar diffusion coefficients and reaction rate constants

15 p2283 A72-31299

Anomalous diffusion coefficient of axially decaying RF discharge collisional plasma under instability mode suppressed by feedback technique

16 p2437 A72-33657

Radial distribution of charged particle concentration fluctuation during decaying plasma instability development in magnetic field

17 p2588 A72-34865

Thermal decay of an infrared-laser-heated arc plasma.

21 p3090 A72-40341

Weakly ionized plasma decay within cylinder with electrically conducting walls in presence of longitudinal magnetic field, determining electric current dependence on cylinder length

21 p3091 A72-40657

Measurements of enhanced absorption of electromagnetic waves and effective collision frequency due to parametric decay instability.

21 p3092 A72-40829

PLASMA DENSITY

Electron layer precession under magnetic field in background plasma, noting density effect on instability

01 p0107 A72-10144

Double Langmuir probe, microwave cavity and upper hybrid frequency measurements of plasma density in hydrogen, helium, neon and argon

01 p0110 A72-11190

Electron density microwave measurements in helium-neon laser plasma, discussing population inversion during glow discharge

01 p0081 A72-11216

Strong linearly polarized electromagnetic wave propagation in overdense plasmas, considering relativistic electron velocities and nonlinear penetration effect

01 p0111 A72-11226

High speed streak cameras applicability to low density theta pinch studies, describing image converters design, operation and block diagrams

02 p0263 A72-11410

Spatial distribution of plasma density from phase shift measurement in millimeter waves based on microwave multichannel probes

02 p0263 A72-11412

Multifrequency interferometer for inhomogeneous plasma density soundings, determining time dependence, spatial distribution and plasma layer size

02 p0263 A72-11413

Low temperature plasma electron density measurements using ruby laser light scattering method

02 p0264 A72-12210

Signal modification of microwaves propagating transversely in underdense turbulent plasma jet

02 p0265 A72-12365

Electron and population densities in inhomogeneous nonequilibrium plasmas with photoabsorption, using radiative transport equation

02 p0266 A72-12441

Excited Hg atom and electron concentration measurement behind shock front in nonstationary plasma by continuous displacement recording of interference bands

03 p0357 A72-13374

Plasmoid transport in quadrupole and octupole magnetic fields, measuring plasma amounts in axial region charged particle densities and flux densities at vacuum chamber wall

03 p0395 A72-13568

Photoresonance cesium plasma development and decay, determining density spatial-temporal behavior and recombination and polar diffusion coefficients by probe measurements

03 p0396 A72-13664

High temperature dense plasma formation by laser heating of gas target, noting fusion reaction in deuterium-tritium mixture

03 p0399 A72-14066

Electron-ion recombination and ambipolar diffusion disruption of electron density in cryogenic helium plasma, using cavity resonator measurements

03 p0399 A72-14067

Force free high beta plasma stability in homogeneous magnetic field and with inhomogeneous temperature and density

04 p0554 A72-14408

Plasma electron density profiles from Tonks-Dattner resonance frequencies for plane parallel and cylindrical columns

04 p0554 A72-14530

Direct display plasma density and temperature meter, using floating double probe method

04 p0520 A72-14533

Plasma density profiles by microwave interferometry technique in Sirius stellarator diverter for two magnetic field configurations and injection methods

04 p0555 A72-14619

Argon and nitrogen plasma viscosity measurements, using pressure difference probe

04 p0558 A72-15344

Plasma satellite linewidth broadening due to density inhomogeneity, considering evidence based on light scattering from Ar plasma jet

04 p0559 A72-15355

German monograph on spectroscopic investigation of Cs plasma electron density and temperature and excited atom density in various operational states of thermionic converter

04 p0560 A72-15699

Electron temperature measurement error elimination with radio frequency Langmuir probe in low density plasma, measuring floating potential

05 p0694 A72-16049

Interplanetary media plasma density fluctuations and power law spectra effects on radio wave scintillation

05 p0695 A72-16068

Hf electromagnetic field spectrum in one dimensional plasma cavity in pressure balance for arbitrary density

05 p0696 A72-16604

Electromagnetic wave scattering by underdense plasma layer, considering perturbation calculation for Gaussian, sech squared and parabolic density distribution

06 p0853 A72-17350

- Ion-acoustic collisionless shock generation by initial plasma density discontinuity in Q machine, correlating experimental results with numerical simulation
06 p0856 A72-17520
- Hf fluctuations in density gradient of alkali plasma within Q device
06 p0858 A72-17536
- Interplanetary plasma electron and proton density fluctuation measurements by space probes and from radio sources scintillation spectra, noting agreement with power-law irregularity spectrum
06 p0881 A72-17901
- Radial distribution of charged particle concentration fluctuation during decaying plasma instability development magnetic field
06 p0863 A72-18416
- Plasma density inhomogeneity effects on beam-plasma instability and Landau damping from digital simulation using charge sheet model
06 p0865 A72-18541
- Electrical conductivity of nonideal low temperature plasma as function of metallization densities, applying to semiconductors and mercury vapor systems
07 p1043 A72-19880
- Combustion product plasma electrical conductivity dependence on neutral component density fluctuation
07 p1044 A72-19888
- Collisionless ion beam plasma simulation of ionospheric plasma with Langmuir interpretation of density and frequency agreement
07 p1044 A72-20367
- Rf excitation produced plasma instability, considering density fluctuation and drive frequency introduction by amplitude modulation
07 p1045 A72-20441
- Hf potential effect on high amplitude waves propagation in magnetoactive plasma plane layer, noting particle density distribution
08 p1212 A72-21211
- High energy electron beam interaction with dense plasma, investigating unstable waves growth by numerical methods
08 p1213 A72-21259
- Laser plasma density and velocity distributions and mass flow from surface and plasma pressure in target heating process based on interferometric measurements
08 p1215 A72-21719
- Hollow cylindrical cathode discharge sustaining potential reduction and recombination probability increase from transverse magnetic field and rising pressure and plasma density
09 p1361 A72-22957
- Moving plasma interaction with oblique magnetic field, establishing magnetization ranges for plasma density and velocity
09 p1362 A72-23208
- Reference electrode area and floating potential influence in Langmuir probe measurements of plasma density and temperature
09 p1311 A72-23229
- Coulomb interactions within dense Boltzmann plasma in transition from ideal to nonideal state, proposing effective Coulomb pair cross section concept
10 p1517 A72-23834
- Quiescent steady state plasma production by beam-plasma discharges in uniform magnetic fields, showing plasma density fluctuation relation to Penning effect
10 p1519 A72-24022
- Relativistic electron beam injection into dense plasma, analyzing perturbed electric and magnetic fields and charge and current densities
10 p1521 A72-24353
- Density fluctuations and ion acoustic two stream instability characteristics of RF generated plasma derived from electromagnetic scattering at 24 GHz
10 p1523 A72-24800
- Low temperature plasma electron density measurements using ruby laser light scattering method
11 p1693 A72-25706
- Nonideal dense plasma properties, discussing electrostatic shielding, many particle clusters, phase transitions, metallization and electrical conductivity [AIAA PAPER 72-414]
11 p1695 A72-26164
- Interplanetary plasma microinstabilities within framework of underlying electron-proton solar exosphere, discussing solar wind high beta effects
11 p1714 A72-26529
- Plasmoid transport in quadrupole and octupole magnetic fields, measuring axial charged particle and flux densities at vacuum chamber wall
11 p1699 A72-26755
- Electromagnetic wave transformation and absorption in Ar plasma with nonmonotonic longitudinal density distribution
11 p1699 A72-26758
- Electrical conductivity measurement of dense nonideal Cs plasma at high pressure and temperatures
12 p1849 A72-27057
- Statistical Coulomb potential and thermodynamic, kinetic and optical properties of nonideal dense plasma
12 p1853 A72-28173
- Input impedances and current distributions of cylindrical monopole antennas of various lengths in hot lossy plasma as function of plasma density
13 p2009 A72-28538
- Low energy Cs ion beam energy loss during traverse through near-thermal equilibrium Cs plasma as function of plasma density, comparing measurements with theoretical predictions
13 p2011 A72-29000
- Magnetosheath electron precipitation effect on dayside auroral-oval plasma density and conductivity, relating precipitation heat flux to solar wind energy density
13 p1950 A72-29381
- Magnetic apex coordinate system for plasma density organization in low and middle latitude F2 region
13 p1951 A72-29395
- Electromagnetic waves scattering by underdense plasmas, examining intermittency phenomenon due to mixing between turbulent inner and outer inviscid wake
13 p1922 A72-29473
- Positively and negatively charged plasma components thermodynamic density fluctuations effect on ionospheric and magnetospheric slowly varying electric fields measurement
13 p1953 A72-29810
- Discharge tube geometry effects on sensitivity of plasma electron density measurement by cylindrical cavity resonators
13 p2018 A72-29822
- Enhanced damping of electrostatic wave primary mode due to combination scattering from plasma electron density oscillations
13 p2018 A72-29854
- Dense isothermal plasma heating due to electron and ion scattering on turbulent pulsations of electric field oscillations
13 p2019 A72-29916
- Density and electric field oscillations of plasma in stellarator, considering magnetic field strength effect, stabilization by ionic collisions and energy pumping mechanism
13 p2019 A72-29985
- Millimeter wave scattering at turbulent density discontinuities in plasma from electrodeless inductive discharge
14 p2136 A72-30174
- Microwave interferometry as plasma diagnostic technique to measure electron densities in partially ionized dense gases
14 p2103 A72-30177
- Pulsed Ar plasma temperature and charged particle concentration obtained as functions of elapsed discharge time by spectroscopic observation
14 p2139 A72-30780
- Magnetosphere thermal plasma densities determination from hydromagnetic whistler digital sonograms and modified normalized dispersion curves
15 p2283 A72-31430
- Thermodynamic plasma density fluctuation induced electric noise field measurement as means to determine plasma density and electron and ion temperatures
15 p2284 A72-31943
- High power carbon dioxide laser produced dense He plasma, comparing experimental and theoretical Stark profile of forbidden and allowed transitions
15 p2285 A72-32223
- Direct display plasma density and temperature meter with Langmuir probe for ionospheric observation
15 p2231 A72-32338
- Glow mode electron plasma source for space chamber, measuring electron density and temperature for comparison with back diffusion sources
15 p2286 A72-32339
- Dense helium theta pinch plasma heating by TEA carbon dioxide laser, studying temperature and density with high speed photography and spectrography
15 p2251 A72-32530
- Spectroscopic analysis of condensations density and intensity variations in solar eruptive prominences, discussing hypothetical magnetic field effects
15 p2318 A72-32781
- Langmuir wave coupling in inhomogeneous plasma due to combined density gradient and external HF electric field
16 p2436 A72-33654
- Plasma electron density profile reflection coefficient frequency-dependent amplitude and phase determination by measuring time response to fast-rising voltage pulse
16 p2437 A72-33767
- Microwave absorption by longitudinally inhomogeneous plasma, noting waveguide excitation in critical density region
17 p2588 A72-34859
- Radial distribution of charged particle concentration fluctuation during decaying plasma instability development in magnetic field
17 p2588 A72-34865
- Relativistic electron beam injection into dense plasma, analyzing perturbed electric and magnetic fields and charge and current densities
17 p2589 A72-34954
- Electrical conductivity of nonideal low temperature plasma as function of metallization densities, applying to semiconductors and mercury vapor systems
17 p2590 A72-35129
- Combustion product plasma electrical conductivity dependence on neutral component density fluctuation
17 p2590 A72-35136
- Toroidal plasma spectroscopic investigation from current pulse start to afterglow, noting electron temperature and density radial distributions and energy balance
17 p2591 A72-35373
- Investigation of transient pressures in the plasma of a thermionic emission converter
18 p2647 A72-36214
- Determination of the plasma density in a collisionless plasma.
18 p2717 A72-37041
- Nonlinear theory of density fluctuations in turbulent plasmas.
19 p2841 A72-38443
- Mathematical model for perfectly absorbing spherical Langmuir probe in collisionless plasma, obtaining plasma density and ion temperature
19 p2842 A72-38524
- Wave propagation in plasmas with fluctuations.
19 p2842 A72-38525
- Exact solution of the problem of measuring the parameters of a dense plasma with the aid of a spherical probe
19 p2842 A72-38534
- Kinetic theory of density fluctuations in a magnetized collision-dominated plasma in an electric field.
19 p2792 A72-38745
- Double-beam interferometry method for investigating axisymmetric configurations of dense plasma.
20 p2958 A72-39505
- Parametric excitation of Bernstein waves in inhomogeneous magneto-plasmas.
21 p3089 A72-40187
- Plasma low density regions caused by Langmuir turbulence, discussing energy dissipation of long wave oscillations and wave collapse
21 p3090 A72-40410
- Identification of transverse Kelvin-Helmholtz turbulence in a magnetoplasma column.
21 p3091 A72-40768
- The measurement of the local electron density by means of direct reading microwave interferometer.
21 p3056 A72-41220
- Calibration procedure to correct for the effects of dielectric containers in microwave plasma density measurements.
21 p3056 A72-41377
- Measurement of the electron density distribution in plasmas from the bending of a gas laser beam.
22 p3211 A72-42396
- Self-consistent description of the magnetotail current system.
22 p3172 A72-42429
- Lyman alpha resonance line asymmetry calculation in dense hydrogen plasma, noting disagreement between theory and experiment
22 p3212 A72-42917
- Method of solving boundary-value problems for a Langmuir probe in a dense plasma
22 p3213 A72-43119
- Possibility of determining the three-dimensional distribution of a plasma with the aid of an SHF resonator
22 p3214 A72-43122
- Ray structures of polar auroras and their association with drift-current instability in a plasmoid
23 p3282 A72-43358
- Longitudinal magnetic field effect on the characteristics of a high frequency ion source
24 p3428 A72-45015
- Electrical conductivity measurement of dense nonideal Cs plasma at high pressure and temperatures
24 p3431 A72-45710

PLASMA DIAGNOSTICS

- Strong ionizing shock waves production in hydrogen and deuterium gases, measuring plasma electron temperature, axial electric field and density and magnetic field compression
[AD-734469]
01 p0108 A72-10237
- Nonisothermal theory of electrostatic probe in weakly ionized plasma, giving I-V characteristics
01 p0108 A72-10238
- Neutron production mechanism and energy spectrum in thermal plasma focus by time of flight spectrometry
01 p0109 A72-10243
- Mass spectrometric investigation of high power laser beam plasma on solid target, determining multicharged ion yield, energy, angular distribution and recombination effect
01 p0079 A72-10349
- Plasma source with arc stabilized by supersonic air stream, measuring enthalpy, heat flux and potential distribution
01 p0048 A72-10491

Carbon dioxide laser electrical plasma properties from probe and techniques, discussing effects of electron energy distributions, dissociation and N, He and Xe additions

01 p0079 A72-10514

Magnetospheric diagnostics from ground stations data, considering dimensions, cusp, ring current, tail flux, electric fields, radiation zone, solar wind and interplanetary field

01 p0132 A72-11072

Microwave measurements of plasma parameters in medium pressure gas discharges in absence of constant magnetic field and in weak electromagnetic field

01 p0072 A72-11215

Argon-hydrogen plasma seeded with submicron tungsten particles, measuring composition, temperature, radiant heat output and opacity

01 p0112 A72-11343

Papers on plasma diagnostics, Volume 1, Optical techniques

02 p0263 A72-11401

Michelson interferometers with large interference fields for plasma diagnostics emphasizing structural rigidity, monochromatic light pulse power, instrument vibrations resistance, etc

02 p0223 A72-11402

Fabry-Perot interferometer for studying spatial distribution of plasma electron concentration, discussing resolution using solid state gas laser light source

02 p0223 A72-11403

Laser spark plasma initial development phase showing high electron temperature and concentration, continuous spectrum emission, line broadening and shock wave formation

02 p0237 A72-11405

Plasma diagnostics facilities design, circuit diagrams and operation based on Q switched ruby laser and optical recording system

02 p0237 A72-11407

High speed photographs of plasma emission spectra in UV and soft X radiation spectrum regions, discussing theory, design and operation of facilities

02 p0223 A72-11408

Millimeter and submillimeter microwave spectrometric studies of high temperature plasmas and noise emission, discussing instrumentation and absolute measurements

02 p0223 A72-11409

Direct phase measuring and measured phase compensating microwave devices designed for plasma diagnostics applications

02 p0223 A72-11416

Phase measurements at if in microwave plasma diagnostics, examining phase stabilization processes

02 p0223 A72-11417

Time of flight mass spectrometers for plasmoids generated by theta pinch and discharge over organic glass, showing ion and electron currents oscillograms

02 p0223 A72-11420

Plasma state variables diagnosis using laser light scattering

02 p0263 A72-11697

Plasma electron density depletion by electron attaching gas introduction, deriving electrostatic probe technique

02 p0264 A72-12261

Induction heated low density supersonic free plasma jet diagnosis, determining velocities and heavy particle temperatures

02 p0265 A72-12361

Ion and electron temperatures difference relaxation rate in uniform plasma, noting relationship to Debye length

02 p0267 A72-12769

Space potential determination in plasma diagnostics, comparing second harmonic analysis with experimental results

02 p0268 A72-12868

Plasma physical characteristics, considering experiments with Ba and Sr atom clouds introduced into ionosphere

03 p0394 A72-13196

Plasma diagnostic technique using three-mirror He-Ne laser interferometer for electron concentration measurement

04 p0555 A72-14654

Rectangular pulse propagation through inhomogeneous medium as plasma diagnostics, investigating electron collisions effect on signal distortion

04 p0556 A72-14946

Ultrarapid holographic camera for plasma diagnostics, noting exposure time and reconstructed image resolution

04 p0521 A72-14972

Numerical method for cylindrical microwave cavities calibration for plasma diagnostics, noting computer programs applicability for arbitrary electron density radial distributions

05 p0662 A72-16418

Metastable He atoms concentration in plasma from absorption characteristics at temperatures 4-300 K and pressures 1-70 mm Hg

05 p0696 A72-16612

Nonlinear wave coupling, scattering and radiation in plasmas for diagnostics application

05 p0699 A72-17221

Heated lithium ion system (HELIOS) facility for quiescent steady state plasma studies, noting MHD instabilities minimization

06 p0854 A72-17502

Density and flux measurements by Langmuir probes in uranium plasma produced in single ended Q device, noting application to isotope separation

06 p0855 A72-17506

Electron temperature fluctuations associated with drift-type instability in Q device, discussing plasma diagnostic techniques

06 p0857 A72-17530

Exact linear dielectric operator for stratified plasma streams with velocity gradients for diagnostics with electromagnetic waves

06 p0861 A72-17748

Linear Z plasma pinch in Ar as spectroscopic source, investigating effects on shock-piston separation

06 p0865 A72-18544

Subtractive microwave holography application to plasma discharge diagnostics

07 p0981 A72-18889

Schlieren cinematographic and holographic diagnostic of giant pulse ruby laser produced plasma in Xe [CLEA PAPER 12,2]

07 p1040 A72-19393

Comparative IR schlieren and interferometry techniques for measuring electron density profiles from refractive index effects of rotationally symmetric plasmas

07 p0986 A72-19613

Plasmasphere structure as outermost ionospheric region from direct measurements by particle traps, ion mass spectrometers and Langmuir probes on satellites

07 p0978 A72-20044

Transient plasma diagnostics using carbon dioxide laser interferometry and absorption for electron density and temperature determination

07 p1008 A72-20557

Plasma diagnostics using carbon dioxide laser absorption and interferometry, comparing electron densities with shock data

07 p1008 A72-20565

Multiple charge Al and C ions X-UV spectra use for studying laser produced plasmas build up and expansion regions

09 p1359 A72-22830

Gas discharge plasma detection characteristics, examining electron and ion densities and collision rates dependence on electromagnetic field frequency and amplitude

09 p1361 A72-22956

Plasma flows interaction with plasma cylinder in diverter magnetic field, investigating plasma dynamics with electric probes, plasmascope and mass spectrograph

09 p1362 A72-23210

Coulomb interactions within dense Boltzmann plasma in transition from ideal to nonideal state, proposing effective Coulomb pair cross section concept

10 p1517 A72-23834

Electra method of plasma diagnosis around reentry vehicle head, describing onboard antennas impedance measurements and use of triple Langmuir probe mounted on telescopic mast

10 p1552 A72-24659

Quadrupole probe theory for hot collisionless isotropic plasma, noting impedance dependence on electron temperature at resonance and optimum dimension relationship to Debye length

10 p1523 A72-24798

Langmuir probe techniques for plasma measurement in ion thruster hollow cathode discharge configurations

[AIAA PAPER 72-416]

11 p1706 A72-26166

Plasma diagnostics of inductively coupled RF Hg discharge in RIT-10 ion thruster

[AIAA PAPER 72-472]

11 p1709 A72-26203

MPD thruster diagnostics and interpretation of electric current distribution, applying integral form of Maxwell equation for moving Hall probe

[AIAA PAPER 72-498]

11 p1711 A72-26221

Electron temperature determination from rate of ionization due to collisions between electrons and neutral particles in plasma

11 p1697 A72-26586

Spherical probe impedance characteristics in isotropic plasma predicted by hydrodynamic theory compared to experimental results

11 p1699 A72-26768

High temperature heating of plasma by ultrashort laser pulses focused onto lithium deuteride, noting various diagnostic methods

12 p1851 A72-27581

Diagnostic procedures for nonhomogeneous plasma based on geometrical optics approximation, irradiating plasma by plane wave at oblique incidence

13 p2013 A72-29295

Homogeneous plasma column generation by HF generator, probing for electron temperature and charged particle concentration

13 p2015 A72-29507

Electron density and temperature measurement from scattering of laser radiation in plasma within axisymmetric toroidal magnetic mirror machine

13 p2017 A72-29609

Discharge tube geometry effects on sensitivity of plasma electron density measurement by cylindrical cavity resonators

13 p2018 A72-29822

Microwave interferometry as plasma diagnostic technique to measure electron densities in partially ionized dense gases

14 p2103 A72-30177

Multiply charged ions motion velocity measurement for pulsed discharge plasma in nitrogen, krypton and xenon

14 p2139 A72-30777

Soft X ray emission for plasma temperature determination in laser induced gas breakdown for air and He

14 p2139 A72-30805

Electronic density measurement in ionized Cs vapor by observation of fundamental series lines mixture, comparing to Stark widening theory based profiles

14 p2134 A72-30852

Spoke and disk mode for rotating plasma production in hydrogen, using high speed photographic, electrical and magnetic diagnostic techniques

14 p2139 A72-30855

Hydrogen plasma ion density determination from atomic beam attenuation by resonant charge exchange with protons

15 p2284 A72-31582

Electrical conductivity of shock wave produced Xe plasma measured by probe, noting dependence on Mach number

15 p2284 A72-31583

Thermodynamic plasma density fluctuation induced electric noise field measurement as means to determine plasma density and electron and ion temperatures

15 p2284 A72-31943

Direct display plasma density and temperature meter with Langmuir probe for ionospheric observation

15 p2231 A72-32338

Symmetrical and asymmetrical electrostatic probes for RF plasma discharge data, describing feedback network, stabilization, generation and electron temperature profiles

15 p2288 A72-32509

Thermal induction plasmas phase measurements using dual magnetic probe system

15 p2289 A72-32511

Magnetic field distribution measurement in axisymmetric plasma column inside Tokamak device by alpha particle beam from radioisotope

16 p2434 A72-32818

Visible and UV stimulated emission in plasma of direct pinch discharge on Ar II and III ions, discussing application possibility to plasma diagnostics

16 p2400 A72-33297

Book on plasma production, diagnostics and thermodynamics for equilibrium and stationary ionization states covering magnetic containment, toroidal and adiabatic traps, MHD flow, etc

16 p2435 A72-33450

Continuously burning optical discharge in Ar and Xe at atmospheric pressures, evaluating laser beam energy absorption, electron density and plasma temperature

16 p2402 A72-33691

Plasma electron density profile reflection coefficient frequency-dependent amplitude and phase determination by measuring time response to fast-rising voltage pulse

16 p2437 A72-33767

Low density and pressure air plasma electron density simultaneous measurements by Langmuir and RF capacitance probes

16 p2438 A72-33836

Russian monograph on ionospheric measurements covering plasma parameters, wave propagation, absorption sounding methods and radio communication applications

16 p2387 A72-33875

Blunt nose cone flow field characteristics microwave measurement at stagnation point during atmospheric reentry, using plasma diagnostic sensors with antennas and electrostatic probes

[AIAA PAPER 72-693]

16 p2345 A72-34049

Material injection RF blackout alleviation and plasma diagnostic measurement with electrostatic probes and S-band reflectometer during RAM C-III reentry flight

[AIAA PAPER 72-690]

16 p2365 A72-34052

Ionized gas-solid suspension thermal physical properties verification by micro-sized MgO dispersion in Ar plasma

[AIAA PAPER 72-688]

16 p2439 A72-34054

Plasma electron density measurements using flat plate and semifocal millimeter wave Fabry-Perot interferometers

[AIAA PAPER 72-672]

16 p2440 A72-34067

- Nitrogen plasma jet flow, attributing discrepancies in electrical conductivity and velocity to shock effects on probe measurements
[ALAA PAPER 72-671] 16 p2440 A72-34069
- Optically thick plasma temperature profile determination by extended brightness emissivity method
16 p2440 A72-34100
- Theory of a coaxial gas-discharge generator loaded by a spiral line
17 p2529 A72-34841
- Spectral measurements of atomic level populations in a plasma
17 p2591 A72-35307
- Runaway electrons in toroidal plasma investigation by thick target bremsstrahlung measurement, noting energy distribution and runaway rate estimates
17 p2591 A72-35370
- An analysis of Pioneer 9 low-frequency wave observations near interplanetary discontinuities.
17 p2614 A72-35585
- Explorer 33 and 35 plasma observations of magnetosheath flow.
17 p2548 A72-35587
- Ion temperature diagnostic using a high power alternating current probe.
17 p2557 A72-35617
- Gas discharge plasma detection characteristics, examining electron and ion densities and collision rates dependence on electromagnetic field frequency and amplitude
17 p2593 A72-35885
- Investigation of physical processes and optimization of thermionic converters with a Cs-Ba filling
18 p2647 A72-36203
- Probe measurements of a cesium plasma in a simulated thermionic energy converter.
18 p2647 A72-36206
- Hybrid and pyrotechnic IR flare generated plasma effects on dual frequency Doppler range measurement system, discussing diagnostics and contamination concentration analysis
18 p2660 A72-36339
- Transition from sheath-convection to saturation-current behaviour of a Langmuir probe in a flowing plasma.
18 p2715 A72-36688
- Time-resolved diagnostic method for hydrogen plasmas.
18 p2716 A72-36949
- Electron density measurements in early stage of the high current pulsed discharge.
18 p2716 A72-36957
- Determination of the plasma density in a collisionless plasma.
18 p2717 A72-37041
- An appraisal of the single Langmuir probe technique in the study of afterglow plasmas.
19 p2840 A72-37456
- Interferometric holography of laser-produced gas breakdown.
19 p2798 A72-37623
- Potential created by a point charge oscillating in an inhomogeneous plasma
19 p2842 A72-38522
- Mathematical model for perfectly absorbing spherical Langmuir probe in collisionless plasma, obtaining plasma density and ion temperature
19 p2842 A72-38524
- Exact solution of the problem of measuring the parameters of a dense plasma with the aid of a spherical probe
19 p2842 A72-38534
- Purification of hydrogen plasmoids by the magnetic field of an injector-diverter device
19 p2843 A72-38539
- Fixed-bias floating double-probe technique with simple Langmuir-probe characteristics.
19 p2804 A72-38592
- Effect of plasma resistance on electron temperature measurement by means of an electrostatic probe.
19 p2804 A72-38593
- A new method for in situ electron temperature determinations from plasma wave phenomena.
19 p2793 A72-38758
- Heat-pipe plasma oven for microwave and spectroscopic measurements.
20 p2912 A72-39433
- Double-beam interferometry method for investigating axisymmetric configurations of dense plasma.
20 p2958 A72-39505
- Measurements of plasma velocity distributions in free-burning dc arcs up to 2160 A.
20 p2958 A72-39644
- Interferometric study of a TEA-CO₂ laser produced plasma.
20 p2958 A72-39816
- A technique for recording Langmuir probe characteristics in afterglow plasmas.
21 p3051 A72-40212
- A system of disc-stabilized dc arc and solution nebulization device for the investigation of multicomponent plasmas.
21 p3039 A72-40213
- Electron density and temperature measurement from laser radiation scattering in plasma within axisymmetric toroidal magnetic mirror machine
21 p3091 A72-40663
- Impedance of a partially ionized cesium plasma.
21 p3091 A72-40694
- Coulomb-collision corrected ion-acoustic line profiles.
21 p3092 A72-40819
- An apparatus to investigate plasmas at very high pressure.
21 p3056 A72-41004
- The measurement of the local electron density by means of direct reading microwave interferometer.
21 p3056 A72-41220
- Polarization interaction between plasma flows in a transverse magnetic field
21 p3095 A72-41689
- Reflector-analyzers for studies of rarefied low-energy plasmas
21 p3058 A72-41731
- Ar plasma diagnostics from stabilized arc emission spectra, noting thermodynamic equilibrium in central zone of arc channel
22 p3209 A72-41880
- Uniform low temperature gas discharge plasma diagnostics in shielded volume, noting application of stable plasma generation effect for isotope analysis
22 p3210 A72-42152
- Simultaneous solar-wind plasma and magnetic-field measurements in the expected region of the extended geomagnetic tail.
22 p3170 A72-42405
- High energy electron spatial distribution in plasma sheet from Ogo 5 magnetometer experiments
22 p3211 A72-42406
- An optical magnetic probe with pulsed detector voltage.
22 p3177 A72-42447
- Recent progress regarding the measurement techniques in the hypersonic area [ONERA, TP NO. 1055]
22 p3178 A72-42581
- Direct measurement of diffusion cooling in an afterglow plasma.
22 p3212 A72-42918
- Plasma diagnostics by means of microwave cavity resonators
22 p3212 A72-42950
- Electronic density and temperature deduced from the observation of the cone of resonance of an antenna in a magnetoplasma
22 p3212 A72-43049
- Spectroscopic study of the parameters of a turbulent plasma
22 p3213 A72-43107
- Method of solving boundary-value problems for a Langmuir probe in a dense plasma
22 p3213 A72-43119
- Possibility of determining the three-dimensional distribution of a plasma with the aid of an SHF resonator
22 p3214 A72-43122
- Monochromatic plasma waves linear and nonlinear coupling, discussing LF modulation partial transfer /Luxembourg effect/ and application to ionospheric diagnostics
23 p3319 A72-43517
- Damping of finite-amplitude electron plasma waves in a collisionless plasma.
23 p3321 A72-44075
- Measurements of magnetotail plasma flow made with Vela 4B.
23 p3342 A72-44514
- A Lecher wire microwave interferometer for measurements of electron density and electron temperature in a flowing transient plasma.
23 p3292 A72-44543
- Some infrared diagnostic techniques in high temperature gasdynamics.
24 p3402 A72-45043
- Sharp focused short pulse X ray source with laser flash synchronization for radiographic plasma diagnostics
24 p3429 A72-45495
- Determination by the scattering method of the parameters of a plasma produced by a laser spark in air
24 p3429 A72-45496
- PLASMA DIFFUSION**
- Meteor trail forms diversity explanation from magnetic pressure and Reynolds number and plasma diffusion in magnetic fields, discussing geomagnetic effect on trail shape
02 p0282 A72-12336
- Neodymium laser plasma dispersion and diffusion in magnetic field, using electrostatic injection of LiH particles
03 p0393 A72-13081
- Fluctuations and diffusion correlation analysis in linear octupole magnetic confinement, determining dispersion relation for interchange instability
03 p0396 A72-13660
- LF oscillations due to drift diffusion of current free weakly ionized inhomogeneous plasma in magnetic field
05 p0697 A72-16984
- Parallel and perpendicular magnetic field effects on optically injected electron-hole plasma diffusion in Ge from density measurement by infrared beam absorption technique
05 p0702 A72-17167
- Equilibrium diffusion of rotating plasma in toroidal systems, deriving two fluid hydrodynamic equations with allowance for ion temperature perturbation
05 p0701 A72-17242
- Cross-field current driven ion acoustic instability in two plasma devices, causing neutral sheet phenomena, anomalous dispersion and ion heating
[AD-740261] 06 p0858 A72-17541
- Cyclotron resonance interaction between electromagnetic waves and nonthermal plasmas for Cauchy velocity distributions yielding algebraic dispersion equations
06 p0860 A72-17745
- Plasma ambipolar diffusion coefficient and electron density determination from thermal density fluctuations cross spectrum based on Langmuir probe measurements
06 p0864 A72-18536
- Critical magnetic flux indications of microanomalous plasma diffusion in electron bombardment ion engines
07 p1054 A72-19614
- Ionization change induced stratiion instability of low temperature plasma with ambipolar diffusion in transverse magnetic field
07 p1043 A72-19878
- Dynamic stabilization of MHD instabilities in plasma column by multipole hf fields, analyzing dispersion equation
07 p1045 A72-20479
- Hydrogen plasma generation by microwave field in magnetic-mirror device due to electron cyclotron resonance, measuring transverse diffusion coefficient dependence on magnetic field
07 p1046 A72-20506
- Ambipolar diffusion in weakly ionized unstable plasma afterglow in presence of uniform axial magnetic field
07 p1047 A72-20558
- Propagation time of charge diffusion across magnetic field in bounded plasma
08 p1215 A72-21879
- Plasma turbulent diffusion effects on particle trajectories in phase space as Weiner process
09 p1358 A72-22294
- Collisionless plasmas numerical simulation with weighted particles and periodically reconstructed distribution function, estimating diffusion rates
09 p1358 A72-22462
- Geomagnetic field effects on initially spherically symmetric ion cloud diffusive motion in earth upper atmosphere
09 p1297 A72-22577
- Deionization mechanism of expanding plasma cloud produced by arc burning in vacuum, discussing charged particle concentration and ion thermal velocity
10 p1521 A72-24356
- Time dependent solutions of Tokamak equilibrium equations for plasma diffusive processes
11 p1694 A72-25787
- Charge carrier density, neutral gas density, electric potential and electron temperature profiles in cylindrical diffusion column, considering electron pressure
11 p1698 A72-26646
- LF oscillations due to drift-diffusion of current free weakly ionized inhomogeneous plasma in magnetic field
12 p1850 A72-27128
- Thermal equilibrium coefficient of ionized plasma spatial diffusion transverse to strong uniform dc magnetic field, extending Taylor-McNamara calculation scheme to three dimensions
13 p2011 A72-29120
- Meteor trail forms diversity explanation from magnetic pressure and Reynolds number and plasma diffusion in magnetic fields, discussing geomagnetic effect on trail shape
13 p2039 A72-29220
- Nd laser irradiation of LiH particles in magnetic trap, investigating resultant plasma expansion and diffusion
13 p2015 A72-29431
- Kinetic equation of repeatedly ionized plasma from hyperbolic diffusion method, calculating direct transitions between excited ion states
13 p2008 A72-29895
- Plasma diffusion coefficient in crossed electric and magnetic fields, discussing lifetime in magnetic trap and expression for ion mobility
13 p2019 A72-29942
- F region plasma one dimensional nonisothermal diffusion for positive ions with allowance for ionization and recombinations and gravitational forces
15 p2232 A72-32731
- Anomalous diffusion coefficient of axially decaying RF discharge collisional plasma under instability mode suppressed by feedback technique
16 p2437 A72-33657

Resonant diffusion in strongly turbulent plasmas, deriving equations for evolution of macroscopic properties including temperature and flow speed

16 p2439 A72-33934

Deionization mechanism of expanding plasma cloud produced by arc burning in vacuum, discussing charged particle concentration and ion thermal velocity

17 p2589 A72-34956

Ionization change induced striation instability of low temperature plasma with ambipolar diffusion in transverse magnetic field

17 p2590 A72-35128

Theory of magnetically conjugate transport of cold plasma in the outer low-latitude ionosphere

17 p2548 A72-35218

VLF wave propagation and its interaction with the magnetoplasma.

17 p2516 A72-35357

Spectral dependence of diffusion in a magnetized plasma.

17 p2592 A72-35623

The determination of diffusion coefficient for Na in dc arc plasma by measurements of intensity distribution of emitted light.

18 p2716 A72-36959

Magnetic surface equation and collisional diffusion of finite beta tokamak plasma in low density regime

19 p2838 A72-37330

Computer simulation of RF-confinement of plasmas in an open-ended toroidal quadrupole.

21 p3089 A72-40191

Integral equation for electromagnetic field in diffuse boundary plasma, noting anomalous skin effect

21 p3090 A72-40409

Direct measurement of diffusion cooling in an after-glow plasma.

22 p3212 A72-42918

Determination of the duration of the diffusional motion of charges in a plasma with allowance for bulk ionization

22 p3213 A72-43116

Calculation of transport coefficients of a non-Lorentzian plasma

23 p3321 A72-43821

PLASMA DIODES

Linear electron acceleration mechanism in plasma, showing polarization fluctuations in diode under strong electric field

03 p0395 A72-13573

Linear electron acceleration mechanism in plasma, showing polarization fluctuations in diode under strong electric field

11 p1699 A72-26761

Boundary conditions and equations of plasma arc discharge in cylindrical diode with azimuthal magnetic field

12 p1850 A72-27132

I-V-characteristics of a plane parallel cesium diode with tantalum and tungsten emitter.

18 p2646 A72-36196

Nonlinear current oscillations in a plasma diode

18 p2714 A72-36205

Short cesium plasma discharge diode as physical model for thermionic converter, studying ionization, recombination and microwave radiation

18 p2714 A72-36212

PLASMA DISCHARGES

U PLASMA JETS

PLASMA DISPERSION

U PLASMA DIFFUSION

PLASMA DYNAMICS

Plasma hydrodynamic Buneman current instability under strong electric field, considering nonlinear stage in one dimensional case

01 p0105 A72-10024

Linear theory of transverse electromagnetic waves and instabilities in uniform plasma during propagation along magnetic field, considering multifluid and kinetic description

01 p0108 A72-10189

Plasma electron and proton motion in equatorial plane of magnetosphere under geomagnetic disturbance generated electric field

01 p0058 A72-10586

German monograph on toroidal electric arc plasma with allowance for induced flow, covering tube wall heat transfer, electric field, MHD vortex development, mathematical model, etc

02 p0263 A72-11650

Solar wind plasma spherically symmetrical outflow allowing for equations of motion of velocity components, discussing interplanetary field and single fluid MHD

02 p0278 A72-11914

Coulomb logarithm for hot plasma viscosity coefficient in magnetic field by quantum mechanical unified theory

02 p0267 A72-12770

Macroscopic geometry and velocity spaces of plasma collective modes involving long range force interaction between particles

02 p0267 A72-12841

Plasma interchange instability in quadrupole and octupole magnetic fields determination by disturbance wavelength ratio to ion cyclotron radius

03 p0396 A72-13659

Self consistent theory of waves in fluctuating plasma, discussing Klimontovich-Maxwell electromagnetic field equations uniqueness solution and kinetic equation

04 p0493 A72-15449

Computerized simulation techniques for plasmas, discussing electrostatic particle model properties and implications

05 p0694 A72-16058

Dynamic stabilization of transverse Kelvin-Helmholtz instability driven by nonuniform plasma motion, using ac electric field near ion cyclotron frequency

06 p0857 A72-17531

Moving isotropic plasma half space effect on magnetic or electric line source radiation patterns

07 p1044 A72-20192

Reverse deflection and contraction of collisionless plasma beam during motion along curved magnetic field lines

07 p0979 A72-20378

Atmospherical model for plasma motion along surface of geomagnetic tail under action of interplanetary, magnetic lines of forces

08 p1153 A72-20722

MGD equations for ideal plasma steady plane adiabatic flow in magnetic field, considering analogy to Chaplygin equations

08 p1214 A72-21645

Supersonic plasma flow in narrow rectangular channel and free incompressible inviscid conducting liquid jet motion within pulsating transverse magnetic field

08 p1214 A72-21652

Plasma jet dynamics in axially symmetric magnetic field, obtaining magnetic field generated by conduction currents as function of plasma macroparameters

09 p1362 A72-23206

Moving plasma interaction with oblique magnetic field, establishing magnetization ranges for plasma density and velocity

09 p1362 A72-23208

Colliding plasma flows motion and capture in transverse magnetic field with mirror configuration, noting polarization effect

09 p1362 A72-23209

Plasma flows interaction with plasma cylinder in diverter magnetic field, investigating plasma dynamics with electric probes, plasmoscope and mass spectrograph

09 p1362 A72-23210

Plasma injection in magnetic trap along curvilinear inhomogeneous magnetic field, showing long plasmoids polarization and drift reduction by depolarization currents

09 p1363 A72-23218

Magnetic diffusion into moving cylindrical incompressible plasma with radial divergence

10 p1521 A72-24413

Ionized plasma electron velocity distribution function relaxation numerical calculation to validate local Maxwellian form during transport process

11 p1693 A72-25523

Plasma equilibrium configurations, considering magnetically contained focus in external magnetic field

11 p1694 A72-25788

Ionospheric physics, attributing anomalies to plasma motions

11 p1621 A72-25835

Optimization criteria for electric feeding in quasi-steady MPD thruster, discussing energy storage bank characteristics determination

[AIAA PAPER 72-462]

11 p1709 A72-26197

Dense hydrogen plasmoids injection with linear pinch gun into biconical cusp field, observing axial reciprocating motion

11 p1697 A72-26575

Spark interferometry of plasma filaments in gases from self focused single mode ruby laser beam

12 p1852 A72-27869

Explicit numerical modeling method for dynamics of dense high temperature laser-produced plasmas, discussing time scale for energy transfer from electrons to ions

13 p2009 A72-28424

Solar wind plasma spherically symmetrical outflow allowing for equations of motion of velocity components, discussing interplanetary field and single fluid MHD

13 p2039 A72-29226

Plasma inhomogeneity in crossed electromagnetic field, comparing motion velocity to ion component transverse drift rate in polarized electric field

13 p2019 A72-29893

Ion viscosity tensor and ion thermal flux derived for microinstabilities of inhomogeneous collisional high pressure plasma, noting second derivatives of temperature

14 p2137 A72-30395

Isotropic conducting plasma dynamic behavior near rotating magnetized sphere, showing electric field-produced meridional convective currents

14 p2138 A72-30630

Magnetosphere tail internal plasma boundary layer dynamics during substorms based on aurora data

14 p2103 A72-30663

Signal spectrum sidebands asymmetry of LF waves in plasma with electric current and ion stream, suggesting amplitude and frequency modulation

15 p2284 A72-31650

Finite beta plasma drift cone instability relationship to mirror ratio and plasma temperature changes

15 p2288 A72-32422

Plasma accumulation in electrostatic potential well produced by electron space charges, determining diocotron instability as function of electron plasma and gyrofrequency ratio

16 p2434 A72-32819

Soft X-ray spectral studies of plasma dynamics in solar flares from Bragg crystal spectrometer OSO 6 recordings

16 p2449 A72-33918

Plasma motion relation to magnetic field line motion for imperfect electroconductivity, noting comparison with total particle drift distance

16 p2439 A72-33931

Spark interferometry of plasma filaments in gases from self focused single mode-locked ruby laser pulses

16 p2439 A72-33978

Thermomagnetic effect in a plasma placed in a non-homogeneous magnetic field

17 p2588 A72-34838

Papers on kinetic equations covering axiomatics, quantum and relativistics, plasma kinetic theory role in spectral line width, etc

17 p2590 A72-35151

The self-consistent test particle approach to relativistic kinetic theory.

17 p2590 A72-35156

Constants of the linearized motion of Vlasov-plasmas.

17 p2590 A72-35158

Solar flare initial, explosive and decay phases related to plasma motion, soft X-rays and radio emission

17 p2600 A72-35348

Auroral absorption and magnetospheric plasma dynamics pattern from arctic stations atmospheric opacity data

18 p2688 A72-36859

Study of the mechanism of motion of nonequilibrium plasma inhomogeneities in a magnetic field

18 p2717 A72-37176

Electromagnetic and space charge disturbance transmission and reflection at plasma boundary and oblique incidence, discussing isotropic Vlasov plasma

19 p2839 A72-37336

Relation between the plasma ion current and the surface defects produced by ruby and neodymium laser emission

19 p2812 A72-38210

Atmospherical model for plasma motion along surface of geomagnetic tail under action of interplanetary magnetic lines of force

19 p2791 A72-38350

Influence of plasma kinetic processes on electrically excited CO₂ laser performance.

19 p2812 A72-38598

Laser output power increase with plasma dynamic carbon dioxide laser configuration, noting steady population inversion in pure hydrogen atoms

20 p2934 A72-39932

Reductive perturbation method application to Vlasov equation governing one dimensional motion of collisionless plasmas, investigating nonlinear modulation of plasma waves

21 p3089 A72-40188

Boltzmann kinetic equation for nonideal plasma with allowance for polarization effects, noting collision integral convergence

21 p3090 A72-40412

Rayleigh-Taylor instability in a composite medium.

21 p3104 A72-40478

Low frequency electrostatic waves in a turbulent plasma.

21 p3092 A72-41221

Hamiltonian analysis of charged particle motion in the pulsar rotating magnetic field.

21 p3111 A72-41472

Polarization interaction between plasma flows in a transverse magnetic field

21 p3095 A72-41689

On the physical mechanism of the magnetospheric substorm development.

22 p3169 A72-42012

Polarizational interaction of opposed plasma flows in a linear octupolar magnetic field

22 p3214 A72-43121

Methods of solving one-dimensional problems of radiative gasdynamics

23 p3320 A72-43528

Circularly polarized waves in magnetoplasmas containing negative ions.

23 p3323 A72-44533

Nonlinear effects in the dynamic behavior of the positive column from a low-voltage low-pressure discharge

24 p3428 A72-44965
From plasma to planet; Proceedings of the Twenty-First Nobel Symposium, Saltsjbaden, Sweden, September 6-10, 1971.

24 p3444 A72-45451
Chemical effects in plasma condensation.

24 p3429 A72-45457
Rapid radial displacement of a toroidal plasma filament by a transverse magnetic field

PLASMA ELECTRODES

Low density plasma flute oscillations stabilization by feedback system with potential sensors and electrodes, deriving dispersion equation

05 p0697 A72-16983
Pulsed flat electrode erosion plasma accelerator, determining electric and magnetic fields distribution, current density and electron concentration

05 p0697 A72-16987
Self regenerating molten seed electrodes for open cycle MHD power generators longevity, regulating combustion chamber and gas flow seeding

06 p0862 A72-18336
Performance characteristics and limitations of electrode and insulation materials for open and closed cycle MHD generators, noting ceramic compositions for channel

AD-737019 09 p1335 A72-22401
Electric discharge plasma generator consisting of concentric or parallel electrodes mounted on titanium hydride coated heat resistant ceramic disk

10 p1521 A72-24365
Current sheet velocity limitation in magnetically driven shock tube with plasma electrodes, examining wall ablation and friction and Hall current effects

ALAA PAPER 72-409 11 p1695 A72-26160
Low density plasma flute oscillations stabilization by feedback system with potential sensors and electrodes, deriving dispersion equation

12 p1850 A72-27127
Pulsed flat electrode erosion plasma accelerator, determining electric and magnetic fields distribution, current density and electron concentration

12 p1850 A72-27131
Current distribution over coaxial plasma gun outer electrode, attributing current concentration at electrode edge to accelerator cavity conductivity anisotropy

13 p2012 A72-29140
Nonequilibrium MHD generator with electrode walls slanted away from magnetic field direction, predicting electrical performance for comparison with flat wall generator

13 p1899 A72-29352
Linear nonequilibrium Faraday type MHD generator, predicting electrode configuration effects on voltage drops, axial leakages and current distribution

13 p1900 A72-29353
Low voltage arc plasma in low pressure Cs vapors, determining charged particle concentration and potential distribution in interelectrode gap

17 p2588 A72-34861
Electric discharge plasma generator consisting of concentric or parallel electrodes mounted on titanium hydride coated heat resistant ceramic disk

17 p2589 A72-34964
On the discharge instability in thermionic converters with long electrodes

18 p2647 A72-36217
Anode heat transfer for a flowing argon plasma at elevated electron temperature.

22 p3210 A72-41952
Potential drops near electrodes in a pulsed plasma accelerator

22 p3213 A72-43108
Plasma diagnostics for electron-ion oscillation discharge in alternating positive-negative electrodes under axial magnetic field, noting electrons drift

PLASMA ENGINES

Uranium hexafluoride pulsed plasma core reactor with artificial neutron source for spark plug and enclosed by cylinder and piston analogous to internal combustion engine

01 p0100 A72-11361
Electron density and temperature fluctuations coupled through Ohm law for ionizable medium, applying to MHD generators and MPD arc thrusters

ALAA PAPER 72-101 05 p0706 A72-16813
Electron density and temperature temporal and radial profiles in megawatt MPD-arc thruster exhaust, using Thomson scattering technique

ALAA PAPER 72-209 05 p0707 A72-16887
Overall characteristics of optimal quasi-steady plasma thruster system, discussing mass, burning time and thrust variations as function of power supply and pulse duration

ALAA PAPER 72-456 11 p1708 A72-26192
System tradeoffs for high performance pulsed MPD thruster in space mission application

ALAA PAPER 72-457 11 p1708 A72-26193

Solid teflon pulsed plasma thruster quasi-steady and short pulse discharge operations, discussing propulsion system performance and erosion behavior

ALAA PAPER 72-459 11 p1709 A72-26195
Quasi-steady MPD thruster system, discussing gas injection, electronic synchronization and electrolytic pulse forming network

ALAA PAPER 72-461 11 p1613 A72-26196
Electric propulsion systems assessment for military spacecraft, discussing ion, colloid, pulsed and quasi-steady plasma thrusters

ALAA PAPER 72-493 11 p1711 A72-26217
Near field megawatt single shot exhaust flow and propulsion characteristics of pulsed MPD arc thruster

ALAA PAPER 72-500 11 p1711 A72-26223
Mass flow and current distribution in magnetic MPD accelerator thruster plumes calculated from meridional flow stream function equation

ALAA PAPER 72-501 11 p1696 A72-26224
Solid propellant pulsed plasma microthruster performance tests, describing engine design and operation

ALAA PAPER 72-460 13 p2026 A72-28945
Laser pulse produced high temperature plasma engine propulsion system, noting thrust/power ratio and requirements for orbital applications

ALAA PAPER 72-719 16 p2443 A72-34029
Effects of heat addition in divergent nozzles with application to MPD thrusters.

17 p2635 A72-34213

PLASMA FLOW

U MAGNETOHYDRODYNAMIC FLOW

PLASMA FLUX MEASUREMENTS

Plasma flux interaction with axially symmetric magnetic field, investigating electrical polarization behavior

03 p0395 A72-13569
Reference electrode area and floating potential influence in Langmuir probe measurements of plasma density and temperature

09 p1311 A72-23229
Plasma flux interaction with axially symmetric magnetic field, investigating electrical polarization behavior

11 p1699 A72-26756

PLASMA FREQUENCIES

Electron cyclotron harmonics emission as function of electron plasma frequency in He reflex discharge, measuring electron densities

01 p0105 A72-10026
Plasma waves maximum radiation temperatures near fundamental and second harmonic electron frequency

02 p0265 A72-12308
Frequency spectrum analysis of electromagnetic self radiation from plasma interacting with high energy electron beam

03 p0393 A72-13082
Parametric excitation of hf and lf plasma oscillations by modulated shf field dependent on field strength at carrier frequency

03 p0394 A72-13086
Magnetospheric electron cyclotron and Langmuir plasma frequencies ratio determination from satellite observed electron and ion density data

05 p0659 A72-16765
Hot plasma transverse and longitudinal wave parametric excitation by intense laser light near plasma frequency, noting instability role in resonant coupling mechanism

05 p0699 A72-17172
Self-excited lf oscillations in inhomogeneous rf collisional plasma, determining frequency as function of tube length, axial magnetic field and gas neutral pressure

06 p0857 A72-17533
Ion sound waves decay instability induced by large amplitude Bernstein mode in plasma

06 p0859 A72-17546
Nonlinear microwave absorption by plasma between cyclotron and hybrid frequencies for critical magnetic field

06 p0776 A72-18408
Hf instability on whistler branch of finite pressure plasma with nonmonotonic ion distribution function under Landau damping effect

07 p1042 A72-19615
Collisionless ion beam plasma simulation of ionospheric plasma with Langmuir interpretation of density and frequency agreement

07 p1044 A72-20367
Charged conductors in homogeneous collisionless magnetoactive plasma at hybrid frequencies, investigating antenna array quasi-electrostatic field one dimensional structure

08 p1138 A72-20746
Sporadic E layer structure model from radiosonde observation, noting peak plasma frequency variation and total reflection by blobs

10 p1441 A72-25153
Midlatitude sporadic E layer observed by rocket and radio sounding, deriving plasma frequency from peak electron density

10 p1477 A72-25156

Anomalous plasma heating by laser irradiation with superimposed electric field oscillating near plasma frequency

11 p1696 A72-26326
Moving striations in tapered gaseous discharge tube, noting frequency dependence on tube radius

11 p1698 A72-26644
Electron density profiles calculation from ionograms, obtaining equivalent delay caused by ionization below minimum plasma frequency

12 p1802 A72-27307
Computerized calculation of wave dispersion curves for hot Maxwellian electron magnetoplasma, applying to upper hybrid and cyclotron frequencies

13 p2013 A72-29340
Frequency spectrum analysis of electromagnetic self radiation from plasma interacting with high energy electron beam

13 p2015 A72-29432
Parametric excitation of HF and LF plasma oscillations by AM SHF field, noting dependence on field strength at carrier frequency

13 p2015 A72-29436
Contaminated Langmuir probes LF admittance measurements in mercury vapor plasma, considering dielectric relaxation in insulating layers

15 p2241 A72-32516
Nonlinear microwave absorption by plasma between cyclotron and hybrid frequencies for critical magnetic field

17 p2588 A72-34858
Magnetospheric electron cyclotron and Langmuir plasma frequencies ratio determination from satellite observed electron and ion density data

17 p2548 A72-35268
HF electrostatic wave instability induced in plasma by electron beam, noting resonant frequency Doppler shift

17 p2591 A72-35369
Detection of solar-wind electron plasma frequency fluctuations in an oblique nonlinear magnetohydrodynamic wave.

17 p2602 A72-35610
Subharmonic frequency division for neon discharge plasma oscillations under resonance due to nonuniform electric field

18 p2714 A72-36111
The electromagnetic radiation near the ion plasma frequency emitted by a turbulently heated plasma.

18 p2715 A72-36598
Drude theory of electromagnetic waves in an inclined magnetic field. I - One-band model of charge carriers.

19 p2840 A72-37510
Plasma heating by nonlinear damping of resonantly excited longitudinal oscillations produced by two parallel laser beams with difference frequency equal to plasma frequency

21 p3090 A72-40342
Plasma heating by large-amplitude, low-frequency electric fields.

21 p3094 A72-41630
Measurement of nonthermal oscillations at the plasma frequency and its harmonics in a magnetized arc plasma, using the high-frequency Stark effect.

22 p3212 A72-42916
Plasma frequency, hybrid frequency and harmonic gyrofrequency electron resonances due to electrostatic waves in ionosphere observed with topside sounders aboard rockets and satellites

23 p3263 A72-43513
Crossover frequencies in multicomponent plasmas with negative ions.

23 p3323 A72-44525
Investigation wave transformation and absorption by a plasma in the upper hybrid frequency range

24 p3429 A72-45491

PLASMA GENERATION

U PLASMA GENERATORS

PLASMA GENERATORS

NT DUOPLASMATRONS

NT PLASMA GUNS

NT PLASMATRONS

Plasma generation and continuous sustainment by laser beam and optical plasmatron

01 p0109 A72-11073
High velocity plasma generation in induction hydrodynamic shock tube and flow into rail type plasma accelerator, investigating possible T layer formation

01 p0110 A72-11203
Ballistic piston fissioning plasma production involving compression of uranium hexafluoride

01 p0111 A72-11333
Excited state and electron densities in noble and atmospheric gas plasmas created by alpha particle induced ion irradiation, discussing plasma kinetic processes and superimposed electric field effects

01 p0112 A72-11335
High temperature U plasma generation at near gas core reactor conditions by sliding spark discharge into capillary channel lined with sintered uranium dioxide

01 p0112 A72-11338

Time of flight mass spectrometers for plasmoids generated by theta pinch and discharge over organic glass, showing ion and electron currents oscillograms
02 p0223 A72-11420

Thermal flux model of lithium plasma source at various temperatures and pressures, using arc channel model with conducting cross section
02 p0268 A72-12859

Free hf discharge plasma column generator, discussing equipment and current and resistance measurements
03 p0393 A72-13083

Plasma beam production with Penning type discharge, demonstrating anisotropic electron temperature
03 p0395 A72-13566

Power and gas consumption for inductive plasma formed in Ar atmosphere, measuring radial distribution of magnetic field axial component
03 p0395 A72-13652

High temperature dense plasma formation by laser heating of gas target, noting fusion reaction in deuterium-tritium mixture
03 p0399 A72-14066

He plasma generation by transversely excited carbon dioxide laser, determining density and temperature profiles of luminous fireball
04 p0558 A72-15345

Laser produced spark plasma, calculating threshold conditions for onset of stimulated scattering process and self focusing
04 p0559 A72-15346

Laser induced gas breakdown in chemical reactions and explosions during plasma creation, using time resolved spectroscopy and titanium oxide probes
05 p0624 A72-16666

Molecular Cs role in multiphoton ionization process during interaction with low intensity Q switched Nd-glass laser radiation
05 p0670 A72-17082

Nonequilibrium plasma production by induced electric field in helium and argon streams in magnetic field
05 p0700 A72-17229

Low voltage arc discharge development in cesium vapor with glowing spherical plasma cluster formation in electrode gap
05 p0701 A72-17238

Quiescent large volume collisionless He and Ar plasma generation via hf electric fields, noting low cost
06 p0854 A72-17504

Density and flux measurements by Langmuir probes in uranium plasma produced in single ended Q device, noting application to isotope separation
06 p0855 A72-17506

Initial development period of low voltage arc discharge in cesium vapor leading to quasi-neutral plasma formation
06 p0860 A72-17696

Fast ionization fronts ahead of laser produced plasma expansion into low density gas, noting Langmuir probe and microwave diagnostics indication of photoionization density augmentation
06 p0864 A72-18532

Spectral analysis of light reflected from Nd laser produced deuterium plasma, observing Doppler shift
07 p1039 A72-18888

Schlieren cinematographic and holographic diagnostic of giant pulse ruby laser produced plasma in Xe [CLEA PAPER 12,2]
07 p1040 A72-19393

X ray spectrum and D-D neutrons emission from high temperature plasma produced by two pulsed Nd-glass laser systems [CLEA PAPER 12,3]
07 p1041 A72-19394

Faraday rotators acting as optical isolators for high power giant pulse lasers used for plasma production
07 p1008 A72-20368

Langmuir electron oscillation excitation by ion beam at velocity exceeding average electron thermal velocity in plasma formed by residual gas ionization
07 p1046 A72-20505

Hydrogen plasma generation by microwave field in magnetic-mirror device due to electron cyclotron resonance, measuring transverse diffusion coefficient dependence on magnetic field
07 p1046 A72-20506

Plasma generator with Ar as ionizing medium for metal cutting and welding, discussing protection against secondary arc formation
08 p1176 A72-21048

Laser systems for lunar ranging and high temperature plasma generation
08 p1182 A72-21336

Population inversion development and breakdown in active medium produced by plasma generation during pulsed discharge in molecular nitrogen laser
08 p1183 A72-21716

Plasma emitter shape determination in accelerating electric field for charged particle flux production
09 p1358 A72-22490

Early phase time development of far UV line radiation from plasma production by focusing Q switched ruby laser onto solid Mg target
09 p1325 A72-23232

Plasma production from hydrogen solid targets by pulsed carbon dioxide TEA laser, noting diagnostic methods
09 p1325 A72-23237

Xenon plasma produced in cascaded arcs, investigating spectral line widths, temperature and electron density profiles, transition probabilities and I-V characteristics
09 p1364 A72-23392

Spectroscopic techniques for high temperature materials research program, studying light emission from plasmas generated by intense electron beam
10 p1518 A72-23937

Intense relativistic electron beam-plasma interactions in finite cavities, calculating neutral gas charge production and gas breakdown times
10 p1518 A72-23960

Quiescent steady state plasma production by beam-plasma discharges in uniform magnetic fields, showing plasma density fluctuation relation to Penning effect
10 p1519 A72-24022

Electric discharge plasma generator consisting of concentric or parallel electrodes mounted on titanium hydride coated heat resistant ceramic disk
10 p1521 A72-24365

Density fluctuations and ion acoustic two stream instability characteristics of RF generated plasma derived from electromagnetic scattering at 24 GHz
10 p1523 A72-24800

Higher harmonics intensities dependence on fundamental of electron oscillation in beam generated plasma
10 p1524 A72-24920

Multiply charged ion plasmas production in heavy ion accelerator by laser beam interaction with vaporized target material
10 p1516 A72-25033

Heavy ion acceleration from strong electron beam in metallic plasma obtained with ruby laser and positive voltage pulses
10 p1524 A72-25034

Plasma beam production with Penning type discharge, demonstrating anisotropic electron temperature
11 p1699 A72-26753

Quiescent plasma production with axially homogeneous density distribution in skipping magnetic fields by electron cyclotron resonance discharge, noting high electron temperatures
12 p1851 A72-27400

Magnetic field effect on ruby laser generated plasma in solid target, measuring thermal ion energy increase
12 p1852 A72-27879

Quasi-stationary supersonic plasma flare generation by lamp-pumped rhodamine laser, studying shock wave structure by high speed cinematography
12 p1825 A72-27882

Hydrogen plasma production, using linearly polarized microwaves with superimposed magnetic field
13 p2010 A72-28683

Heating mechanisms in laser pulse produced plasma from electron temperature and reflectivity measurements
13 p2011 A72-28999

Supersonic dense low temperature plasma jet generation by pulse mode accelerator based on dielectric erosion and electrically exploded conductor
13 p2011 A72-29007

Nonequilibrium ionization phenomena effects on electric conductivity of combustion gas-particle plasma generated by aluminized fuel seeded with potassium nitrate
13 p2013 A72-29363

Free HF discharge plasma column generator, discussing equipment and current and resistance measurements
13 p2015 A72-29433

Homogeneous plasma column generation by HF generator, probing for electron temperature and charged particle concentration
13 p2015 A72-29507

Spoke and disk mode for rotating plasma production in hydrogen, using high speed photographic, electrical and magnetic diagnostic techniques
14 p2139 A72-30855

Plasma source efficiency with active element positioned between two plane parallel pumping elements
15 p2246 A72-31423

Glow mode electron plasma source for space chamber, measuring electron density and temperature for comparison with back diffusion sources
15 p2286 A72-32339

Book on plasma production, diagnostics and thermodynamics for equilibrium and stationary ionization states covering magnetic containment, toroidal and adiabatic traps, MHD flow, etc
16 p2435 A72-33450

Conditions defined for recombination induced inversion of populations of resonance and fundamental levels in laser beam produced plasma
16 p2438 A72-33835

Magnetic field effect on ruby laser generated plasma in solid target, measuring thermal ion energy increase
16 p2439 A72-33988

Plasma emitter shape determination in accelerating electric field for charged particle flux production
17 p2588 A72-34653

Electric discharge plasma generator consisting of concentric or parallel electrodes mounted on titanium hydride coated heat resistant ceramic disk
17 p2589 A72-34964

Quiescent large-volume collisionless HF discharge plasma generator with zero magnetic field, noting low noise level due to self-stabilizing feature
17 p2592 A72-35814

Pulsed power - A new technology for controlled thermonuclear fusion.
18 p2715 A72-36332

Momentum transfer and plasma formation above a surface with a high-power CO₂ laser.
19 p2811 A72-37864

Plasma formation on Al target surface by ruby laser beam irradiation, discussing electron and ion velocities as functions of beam power density
19 p2811 A72-38197

Pulsed metallic-plasma generators.
20 p2958 A72-39781

Interferometric study of a TEA-CO₂ laser produced plasma.
20 p2958 A72-39816

Neutron production in exploding-wire discharges.
21 p3089 A72-40338

The possibility of producing plasma regions at thermonuclear fusion conditions in a supersonic flow by means of high power electron beam.
21 p3092 A72-41224

Far UV radiating hot dense microplasma production by laser heating for measuring by resonant absorption small quantities of gaseous element
21 p3093 A72-41341

High-intensity X-ray spectra and stimulated emission from laser plasmas.
22 p3210 A72-41990

Uniform low temperature gas discharge plasma diagnostics in shielded volume, noting application of stable plasma generation effect for isotope analysis
22 p3210 A72-42152

Caloric state equation for isentropes and temperature calculation of nonideal Cs plasma produced in high density vapors by shock wave compression
23 p3318 A72-43320

Pulsed laser produced high temperature plasma for electric power generation by controlled nuclear fusion, discussing gas dynamic model
23 p3321 A72-43723

Nanosecond and picosecond laser-produced CD₂ plasmas.
24 p3427 A72-44709

Electron-ion recombination in a helium plasma produced by laser.
24 p3428 A72-44799

Determination by the scattering method of the parameters of a plasma produced by a laser spark in air
24 p3429 A72-45496

Plasma produced by laser irradiation of solid targets as a source of highly stripped ions.
24 p3430 A72-45603

High temperature deuterium plasma production by laser heating of gas filled cylindrical tube, optimizing pulse duration and tube configuration
24 p3431 A72-45712

PLASMA GUNS

Magnetoplasmadynamic supersonic ring duct as electromagnetic shock tube or plasma gun, emphasizing plasma flow-magnetic field interaction
01 p0110 A72-11204

Microwave, X ray and corpuscular emission by gas discharges in coaxial plasma gun, measuring pressure and current distribution
09 p1362 A72-23212

Velocity and temperature attenuation of argon and nitrogen jets expelled from plasma spray guns into physically identical ambient medium
13 p2011 A72-28920

Current distribution over coaxial plasma gun outer electrode, attributing current concentration at electrode edge to accelerator cavity conductivity anisotropy
13 p2012 A72-29140

Optical measurements of electric fields turbulence level in gun plasma, noting compatibility with spatial Landau damping
15 p2287 A72-32409

High-speed photography of a plasma focus.
18 p2716 A72-36946

PLASMA HEATING

Induction plasma heating simulation of open cycle gas core nuclear rocket engine, describing plasma forming material feed, permeable walls and propellant seeding
01 p0112 A72-11346

Intracavity radiation induced arc breakdown in TEA carbon dioxide laser for application in plasma heating
02 p0238 A72-12205

Flame propagation and overdense heating in laser beam created plasma, calculating density and temperature profiles by one dimensional continuum hydrodynamic theory
02 p0238 A72-12363

High temperature dense plasma formation by laser heating of gas target, noting fusion reaction in deuterium-tritium mixture 03 p0399 A72-14066

Mathematical model for two-stream instability induced anomalous resistivity and heating in plasma with equal initial electron and ion temperatures in static electric field 04 p0554 A72-14402

High power Q switched ruby laser beam one dimensional penetration depth into metal as function of time, emphasizing ionization and plasma heating 04 p0528 A72-14536

Nuclear fusion by laser radiation, discussing plasma heating mechanisms and limitations in DD reaction production 04 p0557 A72-15172

Electromagnetic absorption heating in cold randomly inhomogeneous plasma, discussing consequences of thermal particle motion neglect 04 p0489 A72-15393

Cumulation-laser heating of D-T plasma for cylindrical wave, investigating pulse energy increase for critical temperature attainment from average value mathematical model 05 p0695 A72-16279

Nuclear microfusion energy recovery threshold increase during laser pulse heating process of D-T plasma 05 p0695 A72-16280

Quasi-monochromatic radio signal propagation for arbitrary amplitude and phase envelopes in nonlinear medium with nonlinearity caused by plasma heating 05 p0627 A72-16404

Turbulent heating in computer simulation of modified plasma two stream instability driven by relative electron-ion drifts across magnetic field 05 p0696 A72-16687

Argon plasma transient axial flow and heating characteristics in pinched column of linear z-pinch device with collapsing current sheets conversion to axial streaming velocity [AIAA PAPER 72-208] 05 p0696 A72-16886

Electron heating model in perpendicular collisionless plasma shock waves based on electron trapping by turbulent electric field 05 p0697 A72-17014

Plasma heating and compression with nonadiabatic charged particle motion in uniform magnetic field 05 p0701 A72-17239

Parametric excitation of ion-acoustic waves in Q machine plasma, controlling electron temperature by amplitude modulated rf heating 06 p0855 A72-17513

Energy absorption measurements of ion heating by ion-acoustic waves in ion streaming plasma 06 p0856 A72-17518

Statistical hf electron heating at oscillating plasma boundary with acceleration of double Langmuir layer 06 p0860 A72-17691

Ion heating caused by ion acoustic waves in ion streaming argon plasma 06 p0860 A72-17746

Soviet book on turbulent plasma theory covering stationary-turbulence spectra, instabilities, electromagnetic properties and wave propagation, particle stochastic acceleration, turbulent heating, etc 06 p0863 A72-18522

Plasma turbulent heating effectiveness by longitudinal ion current in mirror machine, determining hot ion lifetime and energy distribution function 07 p1039 A72-18913

Thermal conductivity of stationary toroidal plasma in form of Pfirsch-Schluter diffusion factor, using ion heat balance equation 07 p1042 A72-19616

High frequency heating of dense toroidal plasma by nonaxisymmetric ion cyclotron waves resonant excitation in closed magnetic trap 07 p1043 A72-19636

Ion heating in high Mach number oblique collisionless shock waves, noting role of two-ion beam instability from digital simulation 07 p1043 A72-19665

Radio wave alternating electric field heating of ionospheric plasma electrons with density increase below 200 km and decrease at F layer maximum 08 p1152 A72-20703

Moving plasma heating by fast large amplitude hf magnetoacoustic wave, noting Doppler effect resonance splitting 08 p1212 A72-21070

Charged particles nonlinear oscillations in nonhomogeneous plasma, noting amplitude limitation and heating by external hf field energy absorption 08 p1212 A72-21210

Laser heating of plasma based on thermal conductivity mechanism, considering nuclear microfusion energy recovery 08 p1213 A72-21303

Laser plasma density and velocity distributions and mass flow from surface and plasma pressure in target heating process based on interferometric measurements 08 p1215 A72-21719

Magnetized large volume plasma heating by hf ring field at ion cyclotron frequency 08 p1215 A72-21727

Powder materials heating and melting temperatures calculation in free turbulent nitrogen and argon plasma jets 08 p1181 A72-22098

German monograph on wall stabilized Ar arc column displacement by pulsed HF radiation heating covering power absorption determination based on theoretical model 09 p1358 A72-22341

Plasma filament equilibrium in Sirius stellarator during heating by fast magnetosonic wave 09 p1363 A72-23214

Pulsed carbon dioxide laser heating of theta pinch plasma by inverse bremsstrahlung and induced Compton processes 09 p1364 A72-23233

Short laser pulses for plasma heating, considering turbulent heating mechanisms, neutron yield and electromagnetic radiation 09 p1364 A72-23444

Laser heating of plasma based on heat conduction mechanism of spherical thermal wave, taking into account nuclear fusion heat generation 09 p1365 A72-23551

Laser heating and fusion energy recovery of D-T plasma by mechanical-magnetic cumulation, considering cylindrical wave system 09 p1365 A72-23553

Diaphragmless electrothermal shock tube for collision in preheated Ar, using RF plasma heater 10 p1459 A72-24410

Closed form solution for spherical and cylindrical wave propagation in laser conductively heated plasma, considering account of nuclear fusion energy recovery 10 p1522 A72-24721

Laser conductive heating of plasma with accounted nuclear fusion energy, assuming plane thermal wave 10 p1522 A72-24722

Anomalous heating due to nonlinear parametric interaction between plasma and laser radiation, calculating laser power thresholds for nonlinear instability effects 11 p1695 A72-25857

Anomalous plasma heating by laser irradiation with superimposed electric field oscillating near plasma frequency 11 p1696 A72-26326

Laser light intensity relationship to temperature distribution in completely ionized plasma, defining optimal heating conditions 11 p1696 A72-26342

Toroidal plasmas heating by neutral injection, discussing ion acceleration, charge exchange and fast ion trajectories 11 p1697 A72-26582

Laser pulse form effect on confined plasma heating, taking into account inverse electron-ion bremsstrahlung and stimulated Compton scattering 11 p1651 A72-26672

Pulsed RF hydrogen plasma heating in mirror machine near ion cyclotron frequency and harmonics 11 p1699 A72-26703

High power Nd glass laser with stepwise pulse amplification for intensive heating of solid target plasmas 12 p1849 A72-27061

Electron heating in weakly ionized collisionless beam plasma discharge as function of neutral gas pressure and plasma column length 12 p1850 A72-27130

Holographic Fourier spectroscopy for microwave radiation spectra of toroidal plasma with turbulent heating 12 p1850 A72-27135

Averaged equations for laser heating of two temperature plasma with allowance for nuclear fusion energy, noting inequality of ion and electron temperature 12 p1851 A72-27395

High temperature heating of plasma by ultrashort laser pulses focused onto lithium deuteride, noting various diagnostic methods 12 p1851 A72-27581

Laser pulse heating of plasma, predicting efficiency enhancement by addition of heavy element impurities or deuterides to solid target surface 12 p1852 A72-27621

Heat conduction heating of plasma by high power ultrashort laser pulse incident on solid target, noting focusing and energy absorption role 12 p1852 A72-27622

Quasi-linear approximation equations for relativistic charged particles beam dissipative instability in collisional plasma, noting electrons heating at high collision frequencies 12 p1852 A72-27860

High brightness picosecond light pulses generation by laser with multiple internal reflection amplifier for plasma heating 12 p1824 A72-27872

Theta pinch plasma heating by carbon dioxide laser transverse pulses, substantiating theoretical considerations by experimental observations 12 p1852 A72-27880

Plasma heating by HF electrostatic instabilities excitation with current across external magnetic field, estimating turbulence, ion collision frequencies and ion heating rates 13 p2009 A72-28426

Self stabilization, measurement of two-ion beam instability generated by microturbulent ion heating in plasma with variable temperature ratio 13 p2007 A72-28428

Hg fed hollow cathode ion thruster thermal and plasma heating characteristics, using Wiener-Kalman filtered temperature measurements [AIAA PAPER 72-476] 13 p2027 A72-28947

Heating mechanisms in laser pulse produced plasma from electron temperature and reflectivity measurements 13 p2011 A72-28999

Experimental investigation of toroidal discharge electrostatic potential fluctuations in turbulently heated plasma, discussing correlation with effective conductivity 13 p2012 A72-29122

High energy electron heating of solar flare plasma with X-ray emission due to thermal and nonthermal bremsstrahlung 13 p1033 A72-29745

Plasma ion heating by magnetoacoustic waves, presenting resonance peak-magnetic field intensity relations for various densities and ion energy 13 p2019 A72-29913

Dense isothermal plasma heating due to electron and ion scattering on turbulent pulsations of electric field oscillations 13 p2019 A72-29916

Kinetic instability bursts during heating of electron plasma in cylindrical resonator with standing electromagnetic waves 14 p2136 A72-30308

Kinetic instabilities during electron plasma heating in HF field of cylindrical resonator, discussing electron energy distribution function effect 14 p2137 A72-30309

Plasma heating in Tuman 2 toroidal magnetic trap by microwave injection at upper hybrid frequencies 14 p2137 A72-30311

Artificial meteor ablation on iron oxides by arc heated air plasma stream for product and environment identification studies 14 p2150 A72-30319

Spectral changes of light reflected back from plasma during heating by mode locked Nd laser, noting equidistant lines presence 14 p2138 A72-30447

Ionospheric electron density changes caused by strong radio waves induced plasma heating 14 p2102 A72-30657

Radial transport instability during intense microbeam heating of thin plasma column, noting maximum temperatures and phase coherence cut-off effect 15 p2286 A72-32306

Turbulent heating and resistivity in cool electron theta pinches due to IF long wavelength modified two stream and drift instabilities 15 p2288 A72-32426

Thermal induction plasmas phase measurements, using dual magnetic probe system 15 p2289 A72-32511

Dense helium theta pinch plasma heating by TEA carbon dioxide laser, studying temperature and density with high speed photography and spectrography 15 p2251 A72-32530

Quasi-linear approximation of absorption of oscillations excited by electron beam in nonuniform plasma, noting electron distribution change with heating under magnetic field 16 p2432 A72-32807

Plasma corona electron temperature decoupling from core of solid deuterium pellet heated in vacuum by convergent laser beams 16 p2433 A72-32810

Ion acoustic, electron plasma and cyclotron harmonic waves parametric instabilities in magnetic field and applications to plasma heating 16 p2433 A72-32811

Laser heating of two temperature plasma based on conductive heat transfer, taking into account nuclear fusion energy 16 p2434 A72-32876

High brightness picosecond light pulses generation by laser with multiple internal reflection amplifier for plasma heating 16 p2403 A72-33981

Theta pinch plasma heating by carbon dioxide laser transverse pulses, substantiating theoretical considerations by experimental observations 16 p2439 A72-33989

Plasma-ion beam nonlinear interaction for beam velocity exceeding electrons thermal velocity, noting plasma heating and beam energy dissipation 16 p2440 A72-34154

Ion heating via turbulent ion acoustic waves.
17 p2588 A72-34873

The electromagnetic radiation near the ion plasma frequency emitted by a turbulently heated plasma.
18 p2715 A72-36598

Nature of sound dispersion in a plasma
18 p2717 A72-37178

Periodic heating mechanism in solar flares.
19 p2851 A72-37888

Plasma heating by fast electrons, and nonthermal X rays during solar flares
19 p2851 A72-38063

Averaged equations of the combined process of hydrodynamic expansion and conduction heating of plasma, the recovered energy of nuclear fusion being taken into consideration. I - The plane problem.
19 p2841 A72-38095

Alternative description of the conduction-type laser heating process of two-temperature plasma in the spherically symmetric case, the nuclear fusion energy being taken into consideration.
19 p2841 A72-38096

Radio wave alternating electric field heating of ionospheric plasma electrons with density increase below 200 km and decrease at F layer maximum
19 p2790 A72-38331

Influence of different types of oscillations on ion heating in plasma-beam discharges.
19 p2843 A72-38820

Pulsed IR laser for heating superdense plasma to high temperature, featuring inertial confinement by use of short duration energy and strong magnetic field.
19 p2843 A72-38823

Plasma turbulent heating effectiveness by longitudinal ion current in mirror machine, determining hot ion lifetime and energy distribution function
20 p2957 A72-39379

Inverse bremsstrahlung caused fast cascade of electrons with Boltzmann energy distribution to explain laser induced gas breakdown via plasma heating
20 p2934 A72-39645

Thermal decay of an infrared-laser-heated arc plasma.
21 p3090 A72-40341

Plasma heating by nonlinear damping of resonantly excited longitudinal oscillations produced by two parallel laser beams with difference frequency equal to plasma frequency
21 p3090 A72-40342

Solar wind models of energy transport mechanisms and nonthermal heating requirements, comparing predictions with spacecraft observation
21 p3100 A72-40484

The study of turbulence in theta-pinch plasma with azimuthal magnetic field.
21 p3091 A72-40571

Transit time heating in stochastic electromagnetic fields.
21 p3092 A72-41222

Averaged equations of simultaneous hydrodynamic expansion and thermal heating of two-temperature plasma, taking the recovery of thermonuclear fusion into account. I - The plane problem. II - The spherical problem.
21 p3093 A72-41476

The problem of conductivity-type laser heating of two-temperature plasma, the nuclear fusion energy being taken into consideration, in the spherically symmetric case.
21 p3093 A72-41480

Averaged equations of laser heating of Z-pinch plasma the nuclear fusion energy being taken into consideration.
21 p3093 A72-41481

Plasma heating by large-amplitude, low-frequency electric fields.
21 p3094 A72-41630

Resonances in the collisionless heating of a plasma by transit time magnetic pumping.
21 p3094 A72-41631

Deuterium-tritium heating to thermonuclear temperatures by means of ion-ion collisions in the presence of intense laser radiation.
21 p3094 A72-41632

External high-frequency modulation of an electron beam and heating of plasma ions in the case of beam-plasma instability in the magnetic trap
21 p3095 A72-41678

Possible mechanisms of turbulent heating of a plasma by ultrashort laser emission pulses
21 p3095 A72-41823

Magnetic-field-enhanced heating of plasmas with CO₂ lasers.
22 p3210 A72-41969

The heating of the solar plasma due to microwave phenomena correlated with type II meter bursts.
22 p3222 A72-42041

Influence of single-pulse emission from a ruby laser on the plasma of a mercury vapor lamp
22 p3184 A72-42105

Alternative description of laser plasma heating for spherical thermal wave, the fusion energy being taken into account.
22 p3211 A72-42629

Averaged equations for joint treatment of hydrodynamic expansion and conduction-type heating of plasma, the energy of nuclear fusion being taken into consideration. II - Spherical problem.
22 p3211 A72-42630

Transport of RF energy to the lower hybrid resonance in an inhomogeneous plasma.
22 p3212 A72-42898

Kinetic instability bursts during heating of electron plasma in cylindrical resonator with standing electromagnetic waves
23 p3317 A72-43210

Kinetic instabilities during electron plasma heating in HF field of cylindrical resonator, discussing electron energy distribution function effect
23 p3317 A72-43211

Plasma heating in Tuman 2 toroidal magnetic trap by microwave injection at upper hybrid frequencies
23 p3318 A72-43213

Investigation of the heating of the plasma ion component by a collisionless shock wave
23 p3318 A72-43310

Particle distribution function evolution effect on turbulent plasma heating by wave interaction, considering stochastic heating of ions
23 p3318 A72-43314

Collisionless heating of plasma ions by an ion beam
23 p3318 A72-43321

Averaged equations of laser heating of plasma in a focus-type system taking into account the heat of nuclear fusion.
23 p3322 A72-44223

Averaged equations of laser heating of two-temperature plasma in a focus-type system taking into account the heat of nuclear fusion.
23 p3322 A72-44224

Spectroscopic measurements for atmospheric nitrogen and helium arcs.
23 p3322 A72-44326

Stimulated emission in vacuum far ultraviolet during rapid heating of the plasma electrons by ultrashort light pulses
23 p3322 A72-44466

Role of nonlinear effects in the problem of the anomalous resistance of a plasma
23 p3322 A72-44481

Parametric instabilities and anomalous heating of plasmas near the lower hybrid frequency.
23 p3323 A72-44545

High frequency heating of dense toroidal plasma by nonaxisymmetric cyclotron waves resonant excitation in closed magnetic trap
24 p3427 A72-44568

Anode sheath plasma current instabilities, examining electron and ion turbulent heating, plasma particle limiting energies and unsteady oscillation spectra
24 p3429 A72-45490

Superhigh-frequency heating of a plasma and longitudinal electron heat conductivity in a magnetic field
24 p3429 A72-45492

Current induced drift rate of plasma electrons in electric and magnetic fields, noting electron velocities in turbulent heating of plasma
24 p3429 A72-45507

Nonlinear instability of Bernstein modes pumped by an electromagnetic wave.
24 p3430 A72-45571

High power Nd glass laser with stepwise pulse amplification for intensive heating of solid target plasmas
24 p3431 A72-45714

PLASMA INSTABILITY

U MAGNETOHYDRODYNAMIC STABILITY

PLASMA INTERACTIONS

NT PLASMA-ELECTROMAGNETIC INTERACTION

Transient shock produced plasma flow interactions with transverse magnetic field
01 p0105 A72-10020

Tago-Sato-Kosaka and Bennett comets plasma tails interaction with interplanetary magnetic field, demonstrating cometary events correlatability with solar wind data
01 p0128 A72-10419

Interplanetary magnetic field angular gradient and sectorial effects on solar wind, discussing wind velocity
01 p0118 A72-10583

Pioneer 8 plasma wave measurements at distant bow shock crossings, considering solar wind-magnetosheath interaction
01 p0062 A72-10903

Galactic cosmic ray-solar wind nonlinear interaction effects on solar wind geometry near and far from sun
02 p0272 A72-11917

Pseudowave front spreading at leading edge of plasma slab during injection at high velocity into denser background plasma
02 p0265 A72-12364

Plasma flux interaction with axially symmetric magnetic field, investigating electrical polarization behavior
03 p0395 A72-13569

Plasma beams injection into toroidal magnetic field along gradient or radius, using polarizational interaction
03 p0396 A72-13658

Electron beam interaction with bounded solid state plasma, deriving slow wave dispersion relations
04 p0561 A72-15080

Dispersion properties of drift waves in low-beta weakly collisional plasma in presence of ion acoustic or Langmuir waves parallel to magnetic lines
05 p0698 A72-17019

Perturbation theory, saturation and relaxation effects in electron and ion plasma wave echoes
05 p0699 A72-17220

Stationary plasma flow interaction with axisymmetric spatially periodic magnetic field in presence of Hall effect, determining electric currents structure
05 p0701 A72-17241

Worldwide magnetic storm due to solar wind interaction with geomagnetic field, discussing field deformation
06 p0803 A72-17368

Solar wind stream-stream interactions, studying time profiles, velocity variations, corotating spiral, increased pressure due to radial compression and zonal flow directions
06 p0872 A72-17443

Wave exciting grid-plasma interaction in single ended Q device, determining ion velocity distribution function
06 p0855 A72-17510

Plasma wave growth from large diameter electron beam interaction with quiet collisionless unmagnetized discharge plasma, measuring linear dispersion properties
06 p0858 A72-17539

Langmuir wave-caused electron plasma distribution function deformation, discussing particle trapping effects
06 p0858 A72-17542

Colliding plasmas transverse instabilities, investigating ion dynamic and electron beam induced return currents effects
07 p1041 A72-19508

Solar wind and geomagnetic tail interaction with moon, discussing lunar Mach cone evidence for anisotropic wave propagation in magnetized collisionless warm plasma
07 p1061 A72-20025

Apollo 15 lunar subsatellite particle experiment subsystem design for studying magnetosphere dynamics, plasmas-moon interaction and solar flare physics
08 p1168 A72-21519

Mariner 4 trajectory relation to proposed location of bow wave caused by solar wind interaction with Mars ionosphere, noting planet orbit aberration effects
09 p1385 A72-22581

Comet gas production and interaction with solar wind, discussing visible plasma tail within flow pattern
09 p1387 A72-22755

Dielectric permeability tensor operator for surface wave-electron beam interaction in relativistic nonuniform plasma stream with cylindrical geometry
09 p1359 A72-22769

Plasmoids interaction in diverter magnetic field, investigating integral electron capture intensity
09 p1362 A72-23205

Interacting viscous conducting media flow in inclined channel in presence of transverse magnetic field, using Moiseev asymptotic method for steady flows with wavy interface
10 p1522 A72-24546

Interaction solutions of steady crossed field MHD channel flows for perfect, singly ionizing monatomic and thermodynamically unspecified gases
10 p1523 A72-24789

Geomagnetic field and magnetosphere variations due to solar wind interactions, using rocket, satellite and indirect measurements
11 p1621 A72-25841

Astronomical models of solar wind interaction with interstellar medium, determining magnetic field effects on shock wave
11 p1713 A72-25946

Boundary layer turbulence development by gas flow interaction with arc plasma in supersonic nozzle, causing light emission fluctuations
[AIAA PAPER 72-415]
11 p1617 A72-26165

Slow and fast plane magnetoacoustic waves mutual transformation and reflection at plasma and magnetic field inhomogeneities
11 p1698 A72-26643

Plasma flux interaction with axially symmetric magnetic field, investigating electrical polarization behavior
11 p1699 A72-26756

Nonlinear interactions between synthesized plasma positive and negative ion beams, discussing effect on individual velocity distribution functions
12 p1849 A72-27058

Transient current density in plasma subjected to pulsed electric field derived from Boltzmann transfer equation
12 p1850 A72-27278

Localized magnetic field for wind tunnel wall-plasma heat transfer minimization, preserving flow characteristics
12 p1852 A72-27684

Theoretical and computer simulation of laminar interactions of plasmas with different mass and density, discussing piston-ion dynamics solutions
13 p2009 A72-28427

Book on nonlinear coherent and turbulent collisionless plasma theory covering collective /wave-particle and wave-wave/ interactions and mathematical methods
13 p2011 A72-29099

Computerized simulation of single large amplitude whistler wave propagation in plasma, noting collisionless damping, oscillations and equilibrium
13 p2012 A72-29128

Galactic cosmic ray-solar wind nonlinear interaction effects on solar wind geometry near and far from sun
13 p2030 A72-29229

Comet-like interaction of Venus atmosphere with solar wind from Venus probe data, noting absence of bow shock wave and ionospheric tail
13 p2050 A72-29956

Electron beam-helicons interaction in semiconductor plasma, determining instabilities onset conditions for unbounded system
14 p2141 A72-30172

Nonlinear interaction between oscillations produced by monoenergetic particles beam passing through plasma
14 p2136 A72-30306

Nonlinear interaction of resonant plasma oscillations with nonresonant wave pulse, using water bag model of electron plasma
14 p2140 A72-30936

Comets Tago-Sato-Kosaka and Bennet UV observational data interpretation for origin, constitution and interaction with solar wind, emphasizing total gas production
16 p2459 A72-33914

Venus comet-like interaction with solar wind explained via He outer atmosphere with preferential heating by wind
16 p2459 A72-33915

Observations of the region of interaction between the solar-wind plasma and Mars
17 p2600 A72-35219

Detection of solar-wind electron plasma frequency fluctuations in an oblique nonlinear magnetohydrodynamic wave.
17 p2602 A72-35610

Magnetic dipole field interaction with plasma flow ions, noting qualitative model of solar wind flow past magnetosphere
17 p2593 A72-35905

Laser-induced damage in transparent dielectrics - The relationship between surface damage and surface plasmas.
21 p3062 A72-40241

Collisionless momentum transfer interactions in laser produced plasma on solid target, refuting Wright model
21 p3090 A72-40339

About the interaction between a satellite and its environmental ionospheric plasma.
21 p3090 A72-40454

Interaction of a streaming plasma with a magnetic mirror.
21 p3094 A72-41635

Magnetohydrodynamic theory for the interaction of an interplanetary double-shock ensemble with the earth's bow shock.
22 p3170 A72-42404

Upper limit of the torque of the solar wind on the earth.
22 p3219 A72-42427

Polarizational interaction of opposed plasma flows in a linear octupolar magnetic field
22 p3214 A72-43121

Nonlinear interaction between oscillations produced by monoenergetic particles beam passing through plasma
23 p3317 A72-43208

The critical velocity of gas-plasma interaction and its possible hetegonic relevance.
24 p3429 A72-45468

Nonlinear interactions between synthesized plasma positive and negative ion beams, discussing effect on individual velocity distribution functions
24 p3431 A72-45711

PLASMA JET SYNTHESIS
Plasma jet formation within high pressure discharges in air at atmospheric pressure, discussing electrode configuration, current density and accelerating magnetic field strength
03 p0396 A72-13662

PLASMA JET WIND TUNNELS
Localized magnetic field for wind tunnel wall-plasma heat transfer minimization, preserving flow characteristics
12 p1852 A72-27684

Simulation in plasma wind tunnels of the environmental conditions for sounding rocket experiments
20 p2912 A72-39928

Helium-cooled mass spectrograph and frigen-cooled radiometer in a plasma wind tunnel
20 p2928 A72-39929

PLASMA JETS
Plane and spherical geometry anisotropic plasma jet stability, considering uniform velocity streaming immersed in magnetic field surrounded by nonconducting medium
01 p0106 A72-10131

Plasma source with arc stabilized by supersonic air stream, measuring enthalpy, heat flux and potential distribution
01 p0048 A72-10491

Nonlinear skin effects in gas discharge and semiconductor plasmas during electromagnetic wave propagation and dissipation, obtaining wave amplitude and carrier temperature dependence on reflection parameters
01 p0102 A72-10974

Pulsed hf discharge in hydrogen based on laser light scattering on plasma electrons, noting position of satellites in spectra
02 p0237 A72-11406

Light emission intensity correlation functions associated with If oscillations in beam plasma discharge
02 p0263 A72-11421

Wall stabilized Ar arc plasma, investigating Boltzmann equilibrium existence between spectral energy levels
02 p0264 A72-12025

Heat transfer from augmented flames and plasma jets based on magnetically rotated arcs, measuring transfer rate as function of electromagnetic torque
02 p0301 A72-12031

Induction heated low density supersonic free plasma jet diagnosis, determining velocities and heavy particle temperatures
02 p0265 A72-12361

Signal modification of microwaves propagating transversely in underdense turbulent plasma jet
02 p0265 A72-12365

Directly heated cathode effect on He-Ne laser power output and relaxation oscillations in discharge gap
02 p0239 A72-12763

Steel coatings produced by plasma jets on experimental machine parts, determining friction wear resistance by successive tests
03 p0363 A72-13548

Coaxial plasma source energetic characteristics, establishing plasmoid energy linear dependence on battery stored energy
03 p0395 A72-13567

Electron impact Stark broadening of ionized chlorine lines in pulsed arc plasma using laser interferometric and spectroscopic measurements
03 p0396 A72-13748

Cross flow blown two dimensional stationary plasma arc deflection and temperature distribution as function of collisional drift velocity and electric field
03 p0397 A72-13921

Velocity measurement of glass particles emerging from plasma flame by high speed cine-streak photography
03 p0361 A72-13992

Heat transfer from nitrogen plasma jet mixed with cold gas to cooled reactor channel walls at various channel expansion degree values
04 p0555 A72-14645

Ar gas dc discharge plasma characteristics in crossed electric and magnetic fields, examining equivalent pressure concept
04 p0556 A72-14945

Plasma jet technique for self lubricating antifriction Ni, Sn or Cu coatings for MoS2 particle oxidation protection
04 p0527 A72-15664

Plasma discharge instability in air in polyethylene and organic glass capillaries with evaporating walls, using time lapse filming
05 p0693 A72-15840

Electric field strength, radiated power and radial temperature distribution measurements in high pressure Ar cascade arc
05 p0695 A72-16156

Radiation transport mechanism and transport coefficients in high pressure Ar cascade arc, measuring electric field strength, radiated power and radial temperature distribution
05 p0695 A72-16157

Optical radiation from plasma discharge of electron bombardment mercury ion thruster, discussing electron temperature and primary electron fraction [AIAA PAPER 72-205]
05 p0706 A72-16851

Electron heating in weakly ionized collisionless beam plasma discharge as function of neutral gas pressure and plasma column length
05 p0697 A72-16986

Boundary conditions and equations of plasma arc discharge in cylindrical diode with azimuthal magnetic field
05 p0697 A72-16988

Plasma jet injection stoppage and reflection in strong transverse magnetic field, considering instability due to flow interactions
06 p0860 A72-17694

Dimensionless parameter for thermodynamic state prediction in atmospheric pressure plasma jets, using conservation equations
06 p0862 A72-18188

Ionization mechanism for low voltage neon plasma arcs, determining non-Maxwellian energy distribution effects and excited atoms collisions role
06 p0862 A72-18333

Cathode temperature measurement in erosion and heat transport reduction by cesium seeding of Ar plasma arc
06 p0862 A72-18334

Negative hydrogen ion production during charge exchange between protons in thick Li, Na, K and Mg vapor jets
06 p0863 A72-18410

Low voltage arc plasma in low pressure Cs vapors, determining charged particle concentration and potential distribution in interelectrode gap
06 p0863 A72-18413

Subtractive microwave holography application to plasma discharge diagnostics
07 p0981 A72-18889

Field free constricted plasma discharge stability between electrodes, obtaining critical current
07 p1042 A72-19606

Wall stabilized dc arc channel for plasma viscosity and flow characteristics studies, using pressure probe
07 p1043 A72-19877

Reverse deflection and contraction of collisionless plasma beam during motion along curved magnetic field lines
07 p0979 A72-20378

Turbulent heating arc plasma voltage and current digital measurement recording, computing time dependent resistivity
07 p1045 A72-20400

Secondary gas flow effect on energy transfer distributions from plasma torches, obtaining radial distributions of current and energy flux
07 p1046 A72-20546

Optical and electrical characteristics of gas discharge plasma in pulsed radiation sources as function of power dissipation
07 p1047 A72-20611

Metal working by plasma beam in turning machine, applying to high strength alloys
08 p1175 A72-21045

Plasma beam cutting of Al sheets, discussing heat effect on surface oxides and microstructure and plasmagenic gas influence
08 p1176 A72-21047

Coalescence /collapse/ of overlapping spectral lines due to nonadiabatic broadening for Stark structure of hydrogen and helium lines in discharge plasma
08 p1211 A72-21717

Powder materials heating and melting temperatures calculation in free turbulent nitrogen and argon plasma jets
08 p1181 A72-22098

German monograph on plasma arc machining and cutting of metallic materials on lathe as function of electric power and torch performance
09 p1317 A72-22327

Cs diode discharge current oscillations in Knudsen plasma containing electron and positive ion fluxes from thermionic emission and surface Cs ionization
09 p1361 A72-22960

Convective heat transfer between jets produced by plasmatoms and heated substrate, showing independence of plasma flow rate
09 p1319 A72-23189

Short plasmoids production in hydrogen plasma jets by applying pulsed multipole magnetic field generated in linear quadrupole system
09 p1362 A72-23203

Plasma jet dynamics in axially symmetric magnetic field, obtaining magnetic field generated by conduction currents as function of plasma macroparameters
09 p1362 A72-23206

Radial temperature distribution in Ar plasma jet, assuming local thermodynamic equilibrium
09 p1364 A72-23387

Radial temperature distribution determination in nitrogen plasma jet from continuous spectral background intensity measurement
10 p1519 A72-24131

Argon plasma jet mean flow velocity radial distribution measurement method
10 p1520 A72-24205

Positive plasma column theory for longitudinal cylindrical discharge problem in ambipolar conditions, stressing surface and bulk temperature effects
10 p1521 A72-24357

Plasma beam cyclotron instability theory based on computer simulation, noting stabilizing effect due to Landau damping
11 p1693 A72-25562

Boundary layer turbulence development by gas flow interaction with arc plasma in supersonic nozzle, causing light emission fluctuations [AIAA PAPER 72-415]
11 p1617 A72-26165

Pulsed plasma thruster arc electron density measurement by Mach-Zehnder interferometer and He-Ne

laser, determining exhaust ion temperature and total charge
[AIAA PAPER 72-463] 11 p1709 A72-26198

Quasi-steady operation establishment in pulsed MPD arc jet, investigating ion density radial distribution and initial tank pressure and magnetic field effects on plasma front arrival
[AIAA PAPER 72-496] 11 p1696 A72-26219

Mass, momentum and energy distribution measurement in quasi-steady MPD discharge, obtaining velocity vector profiles
[AIAA PAPER 72-497] 11 p1696 A72-26220

Quasi-steady Ar MPD arc exhaust plume structure from spectroscopic and photographic investigation, noting dependence on arc current and mass flow rate
[AIAA PAPER 72-499] 11 p1696 A72-26222

Coaxial plasma source energetic characteristics, establishing plasmoid energy linear dependence on battery stored energy
11 p1699 A72-26754

Spacecraft propulsion based on electric energy extraction from solar wind or energy transfer from ground via plasma arcs
11 p1712 A72-26779

Electron heating in weakly ionized collisionless beam plasma discharge as function of neutral gas pressure and plasma column length
12 p1850 A72-27130

Boundary conditions and equations of plasma arc discharge in cylindrical diode with azimuthal magnetic field
12 p1850 A72-27132

Plasma sheath from plane negatively biased electrode immersed in low pressure discharge investigated by ion acoustic waves and hot probe
12 p1850 A72-27279

Probe triggered audio frequency plasma oscillation period dependence on applied magnetic field and discharge current
13 p2010 A72-28544

Pulse plasma injector accelerating circuit resistance dependence on time and current amplitude calculated from current oscillograms
13 p2010 A72-28733

Velocity and temperature attenuation of argon and nitrogen jets expelled from plasma spray guns into physically identical ambient medium
13 p2011 A72-28920

Supersonic dense low temperature plasma jet generation by pulse mode accelerator based on dielectric erosion and electrically exploded conductor
13 p2011 A72-29007

Energy distribution in plasma jet as function of capacitance and energy of storage elements and storage circuit inductance
13 p2015 A72-29452

Coaxial source accelerating circuit resistance, capacitance and inductance effect on velocity imparted to plasma jet
13 p2015 A72-29453

Drift dissipative instability in bounded gas discharge plasma within magnetic field, investigating oscillations dependence on gas pressure and field strength
13 p2016 A72-29605

Resonant irradiation effect on cesium discharge plasma, charge density, electron temperature and electric field strength
13 p2017 A72-29610

Transverse magnetic field effect on electron temperature and energy distribution and spectral lines of gas discharge plasma
13 p2017 A72-29635

Detonation wave generation in gas discharge plasma by pulsed electrical discharge
14 p2137 A72-30313

Electron-ion modes parametric coupling in low pressure RF self sustained plasma discharge, noting plasma frequency emissions
14 p2138 A72-30399

Anomalous excitation of nitrogen positive bands in seeded Ar free plasma jet, measuring oscillator strengths of atoms
14 p2140 A72-30899

Heat transfer distribution in supersonic arc plasma constrictor of variable cross sectional area ducts, including pressure and compression shock front effects
14 p2141 A72-31071

Economics of material cutting and removal by plasma torches, presenting cutting rates as function of plate thickness for different materials
15 p2243 A72-31321

High speed frame photography application in spectroscopic studies of plasma jet in cylindrical pulsed accelerator with dielectric
15 p2283 A72-31418

Rotatory gas temperature determination in carbon dioxide laser discharge plasma, plotting dependence on discharge current
15 p2245 A72-31419

Hollow cathode plasma discharge model, calculating variation of pressure upstream from active zone in terms of discharge current
15 p2286 A72-32275

Magnetized plasma discharge steady state problem of finite cylinder positive column in magnetic field, detailing radial and axial solutions
15 p2288 A72-32508

Symmetrical and asymmetrical electrostatic probes for RF plasma discharge data, describing feedback network, stabilization, generation and electron temperature profiles
15 p2288 A72-32509

Experimental methods for studying interactions between plasma streams and three dimensional magnetic dipole fields
16 p2454 A72-33384

Energy transfer of thermal coupled radiation with turbulent convection in electric arcs in atmospheric air plasma
[AIAA PAPER 72-685] 16 p2480 A72-34057

Statistical correlation of X-band microwave scattering by overdense intermittently turbulent ionized Ar jet with flux fluctuations from electrostatic probe observations
[AIAA PAPER 72-674] 16 p2440 A72-34065

Nitrogen plasma jet flow, attributing discrepancies in electrical conductivity and velocity to shock effects on probe measurements
[AIAA PAPER 72-671] 16 p2440 A72-34069

Thermionic Cs arc theory applicability evaluation, considering collision dominated transport equations for plasma
17 p2587 A72-34616

Low voltage arc plasma in low pressure Cs vapors, determining charged particle concentration and potential distribution in interelectrode gap
17 p2588 A72-34861

Wall stabilized dc arc channel for plasma viscosity and flow characteristics studies, using pressure probe
17 p2590 A72-35127

Beam-generated collisionless ion-acoustic shocks.
17 p2592 A72-35626

Cs diode discharge current oscillations in collisionless Knudsen plasma containing electron and positive ion fluxes from thermionic emission and surface Cs ionization
17 p2593 A72-35889

Variables influencing the characteristics of plasma-sprayed coatings.
17 p2561 A72-35920

The Maxwellization of electrons in Cs-plasma of a low-voltage arc discharge
18 p2715 A72-36215

On the discharge instability in thermionic converters with long electrodes
18 p2647 A72-36217

Transition from sheath-convection to saturation-current behaviour of a Langmuir probe in a flowing plasma.
18 p2715 A72-36688

Directly heated cathode effect on He-Ne laser power output and relaxation oscillations in discharge gap
20 p2931 A72-39069

Multi-cycle plasma arc evaluation of oxidation inhibited carbon-carbon material for shuttle leading edges.
[ASME PAPER 72-ENAV-26] 20 p2894 A72-39151

Measurements of plasma velocity distributions in free-burning dc arcs up to 2160 A.
20 p2958 A72-39644

Pulsed metallic-plasma generators.
20 p2958 A72-39781

HF absorption of electromagnetic field in ionized oxygen plasma as function of dc discharge current
20 p2958 A72-39969

Estimation of the mass composition and energy spectrum of a plasma jet from a conical pulsed accelerator
21 p3089 A72-40134

A system of disc-stabilized dc arc and solution nebulization device for the investigation of multicomponent plasmas.
21 p3039 A72-40213

Laser action on unclassified xenon transitions in a highly ionized plasma.
21 p3089 A72-40242

Thermal decay of an infrared-laser-heated arc plasma.
21 p3090 A72-40341

The beam-plasma discharge laser
21 p3062 A72-40406

Drift dissipative instability in bounded gas discharge plasma within magnetic field, investigating oscillations dependence on gas pressure and field strength
21 p3091 A72-40659

Resonant irradiation effect on Cs discharge plasma charge density, electron temperature and electric field strength
21 p3091 A72-40664

Carbon dioxide laser excitation by injection of plasma jets produced by capillary plasmotrons
21 p3063 A72-40835

Influence of boundaries on the ionization instability of a plasma in a discharge of coaxial geometry
22 p3209 A72-41876

Measurement of nonthermal oscillations at the plasma frequency and its harmonics in a magnetized arc plasma, using the high-frequency Stark effect.
22 p3212 A72-42916

Detonation wave generation in gas discharge plasma by pulsed electrical discharge
23 p3318 A72-43215

Stimulated emission with pumping by a pulsed electron beam formed in a direct discharge
23 p3295 A72-43319

Special features of photoresonance perturbation relaxation in a low-temperature discharge plasma
23 p3319 A72-43409

Plane parallel nonuniform velocity plasma streams instability in absence and presence of magnetic field, comparing with ideal conductive fluid flows
23 p3320 A72-43518

Study of microwave scattering in a plasma-beam discharge
23 p3321 A72-44212

Glow discharge in rare-gas and metal vapour mixture. I - Distribution functions and kinetic coefficients in He-Cd mixture discharge.
23 p3322 A72-44320

PLASMA LAYERS

NT PLASMA SHEATHS

Plasma sheet structures, dynamics and role in magnetospheric substorm onset as function of near earth and distant merging regions
01 p0052 A72-10082

Geomagnetic storm field recovery near synchronous satellite ATS 1 in terms of ring current belt and plasma sheet variations
01 p0053 A72-10088

Magnetic field and plasma sheet variations observation by IMP 3 satellite in distant magnetotail during magnetospheric substorms
01 p0060 A72-10888

Plasma sheet positive ions flux enhancement detection at lunar distance during lunar eclipse and geomagnetic storm
02 p0283 A72-12452

Second harmonic emission from plasma hybrid resonance region during electromagnetic wave normal incidence on nonhomogeneous magnetoactive plasma layer
02 p0180 A72-12578

Decay interactions among plasma wave and two opposed electromagnetic waves in homogeneous layer of isotropic collisionless plasma, observing stimulated Raman scattering
02 p0180 A72-12579

Plasma sheet thinning in substorms correlated to auroral oval poleward expansion and associated phenomena in magnetotail
03 p0348 A72-13514

Plasma layer implosion in theta pinch, deriving modified snow plow equations from MHD equations
04 p0556 A72-14855

Spherical antenna covered by lossy hot plasma layer, calculating radiation fields by transmission line theory
04 p0493 A72-15525

Weak D type ionization waves stable in optically thick plasma layer behind front of interstellar gas
05 p0715 A72-16210

Diffusion equations of ion components of plane stratified plasma /ionosphere/, taking into account wind effect and vertical temperature distribution
05 p0658 A72-16402

Slant incident electromagnetic wave absorption in linear plasma layers due to field swelling in resonance region
05 p0627 A72-16403

Self action penetration of electromagnetic wave through dense collisionless plasma layer in high vacuum, using antenna microwave probes
05 p0695 A72-16601

Plane magnetized plasma layer interaction with hf electromagnetic field, showing electric field strength and direction dependence on ion acoustic-Alfven velocity ratio
05 p0697 A72-16982

Half wavelength antenna radiation admittance into warm lossy two layer plasma half space, using effects of slot width and electron collision frequency
06 p0781 A72-17348

Electromagnetic wave scattering by underdense plasma layer, considering perturbation calculation for Gaussian, sech squared and parabolic density distribution
06 p0853 A72-17350

Statistical hf electron heating at oscillating plasma boundary with acceleration of double Langmuir layer
06 p0860 A72-17691

Radio wave beam trajectories in laminar isotropic plasma layer, using dynamic systems theory
06 p0774 A72-17731

Electrostatic field excitation in plasma layer by plane transverse electromagnetic wave as function of incident angle
06 p0862 A72-18339

Parallel plate waveguide radiation into dielectric or plasma layer, using Hilbert formulation
06 p0791 A72-18734

Plasma layer growth and equilibrium magnetic fields for astron configurations, solving stream function by finite difference methods

07 p1042 A72-19512

Anisotropic grounded dielectric or plasma layer motion effects on magnetic or electric current line source radiation patterns

07 p0946 A72-19802

Plasma sheet distribution in magnetosphere from low energy particle observations in equatorial region of magnetotail

07 p0977 A72-20031

Geomagnetic tail role in magnetospheric substorms, discussing solar wind energy storage, magnetic merging process and plasma sheet origin

07 p0977 A72-20032

X band microwave attenuation measurements in high density air plasma layer at aperture antenna in rectangular shock tube

07 p0949 A72-20560

Correlation functions describing fluctuation of slow electromagnetic waves in plasma layer

08 p1212 A72-21065

Radio signal attenuation by thin overdense plasma boundary layer on reentry body as function of incident power

08 p1135 A72-21624

Fluctuating signal propagation in plane laminar medium acting as spatial frequency filter, determining electron density distribution curvature radius in plasma layers

08 p1135 A72-21732

Phase velocity and Landau damping of ion acoustic waves propagating through plasma boundary layer at conducting sphere or cylinder based on two fluid model

10 p1523 A72-24746

Electromagnetic wave propagation and absorption in weakly inhomogeneous plasma layer, calculating conditions for transformation into plasma wave

10 p1523 A72-24799

Apollo 14 charged particle lunar environment experiment data analysis, noting earth plasma sheet absence at lunar distance during geomagnetically quiet times

10 p1476 A72-24961

Radio wave beam trajectories in laminar isotropic plasma layer, using dynamic systems theory

11 p1591 A72-25335

Plasma layer effect on natural oscillations of magnetosphere tail, using infinite plasma cylinder model immersed in interplanetary plasma

11 p1622 A72-25944

Current flow across double layer plasma in SERT 2 type hollow cathode ion thruster, using Langmuir probes

11 p1706 A72-26168

Average plasma sheet configuration in geomagnetic tail at lunar orbit, presenting seasonal dependence and variations with geomagnetic activity

11 p1624 A72-26396

Plane magnetized plasma layer interaction with HF electromagnetic field, showing electric field strength and direction dependence on ion acoustic-Alfven velocity ratio

12 p1850 A72-27126

High frequency potential effect on fast transverse magnetic waves along plasma layer bounded by two conducting plates

12 p1785 A72-27855

Multilayer plasma model for MHD pulse propagation in ionospheric waveguide, noting approximation of Alfven velocity distribution by plasma layers

13 p1946 A72-28585

Convective hydromagnetic stability of hot conducting fluid layer in magnetic field by Liapunov method

13 p2011 A72-28891

Nonlinear model of ionization instability of MHD generators, assuming discharge structure with alternating layers of high and low electrical conductivity

13 p2014 A72-29371

Plasma current layer formation due to electric field directed along magnetic field neutral line

13 p2017 A72-29699

Two dimensional equilibrium solution of plasma sheet, applying to tail magnetosphere problem

13 p1954 A72-29959

Isolated finite amplitude electrostatic oscillations production in thin plasma layer between two parallel metallic surfaces in magnetic field

14 p2136 A72-30302

Magnetosphere tail internal plasma boundary layer dynamics during substorms based on aurora data

14 p2103 A72-30663

Variable circular polarization of X ray star SCO X-1 optical radiation due to Thomson scattering in magnetoactive plasma shell

15 p2304 A72-31328

Field distribution and absorption coefficient calculations for normal incidence of extraordinary electromagnetic wave on linear plasma layer in hybrid resonance region

16 p2363 A72-33480

Critical layer equations of plasma resistive instabilities, using sheet pinch model

16 p2436 A72-33577

Consequences of an isotropic static plasma sheet in models of the geomagnetic tail.

17 p2545 A72-34636

Dipole antenna radiation in homogeneous plasma layer magnetized by normal uniform magnetic field, calculating radiation pattern

19 p2768 A72-38661

Explorer 35 observation of geomagnetic tail low energy electrons, noting plasma sheet extension to lunar distance and correlation with solar wind

19 p2853 A72-38737

High energy electron spatial distribution in plasma sheet from Ogo 5 magnetometer experiments

22 p3211 A72-42406

Plasma sheet characteristics of geomagnetic tail at 60 earth radii, inferring spatial distribution of magnetic field magnitude and plasma energy density

22 p3211 A72-42407

Magnetic tension induced stress balance in plasma sheet, considering pressure gradient along geomagnetic tail axis, plasma flow kinetic energy and pressure anisotropy

22 p3211 A72-42408

Multilayer plasma model for MHD pulse propagation in ionospheric waveguide, noting approximation of Alfven velocity distribution by plasma layers

24 p3397 A72-45085

PLASMA LIFETIME

High speed photography in high temperature short duration plasmas, using Kerr cell, image converter, framing and streak cameras

06 p0813 A72-17435

Longitudinal ambipolar acoustic instability effect on duration of plasma particle motion to wall across magnetic field, using phase method

06 p0860 A72-17693

Rotating low density plasma in magnetic mirror trap with Penning discharge, determining conditions for oscillations damping and plasma lifetime

10 p1521 A72-24354

Plasma diffusion coefficient in crossed electric and magnetic fields, discussing lifetime in magnetic trap and expression for ion mobility

13 p2019 A72-29942

Confinement time of plasma injected in magnetic field of racetrack with diverter, noting plasma equilibrium in toroidal magnetic field

22 p3213 A72-43106

PLASMA LOSS

Wave induced Q machine cesium plasma loss produced by current-driven collisional drift instability

06 p0857 A72-17527

Stable mirror plasma machine, determining particle distribution near loss cone by asymptotic analysis based on transit to mean collision times ratio

16 p2432 A72-32808

Particle scattering due to Rosenbluth-Post convective plasma loss-cone instability distribution function

17 p2587 A72-34189

Experimental and two-dimensional computational study of end losses from a theta pinch.

17 p2592 A72-35628

PLASMA OSCILLATIONS

Warm inhomogeneous plasma models perturbation analysis, computing high frequency oscillation and eigenfrequencies and eigenfunctions formulas

01 p0106 A72-10134

Periodic inhomogeneous plasma electrostatic waves, considering dispersion relation and longitudinal oscillations

01 p0107 A72-10141

Phase measurements at if in microwave plasma diagnostics, examining phase stabilization processes

02 p0223 A72-11417

Light emission intensity correlation functions associated with If oscillations in beam plasma discharge

02 p0263 A72-11421

Solar prominence oscillatory motion on 26 March 1964 association with plasmoids generated by pinch tube plasma

02 p0278 A72-12044

Lf drift-type and ion-acoustic oscillations in weakly ionized currentless plasma at low gas pressures in longitudinal magnetic field

02 p0265 A72-12291

Quasi-static surface waves at Maxwellian plasma boundary with diffuse electron scattering, considering plasma electromagnetic oscillations

02 p0266 A72-12577

Parametric excitation of hf and lf plasma oscillations by modulated shf field dependent on field strength at carrier frequency

03 p0394 A72-13086

Wall double layer temperature and plasma oscillations effect on electron energy distribution in low discharge plasma column

03 p0394 A72-13192

Five-minute plasma oscillations in solar photospheric and low chromospheric magnetic fields, discussing evidence, properties and production mechanism

03 p0430 A72-13319

Fluctuations and diffusion correlation analysis in linear octupole magnetic confinement, determining dispersion relation for interchange instability

03 p0396 A72-13660

Plasma shock wave oscillation profile dependence on ion and electron friction and viscosity

04 p0555 A72-14620

Stark contours of hydrogen spectral lines in turbulent plasma with high noise level due to hf Langmuir oscillations

04 p0557 A72-14986

Time dependent hydromagnetic oscillations in contained rotating conducting fluid under magnetic field, using interior boundary layer expansion

04 p0549 A72-15115

Weakly ionized turbulent gas flow in pipe, comparing neutral and plasma fluctuations with laser beam scintillations

04 p0558 A72-15331

High beta plasma lf wave parallel propagation to equilibrium magnetic field, deriving large scale length perturbations from coupled nonlinear partial differential equations

04 p0559 A72-15349

Ion-acoustic instability in ionosphere in presence of fast particles inhomogeneity, estimating ions and electrons drift velocities

05 p0656 A72-16245

Plasma oscillations stabilization, considering nonlinear effects in phase velocity of plasma waves

05 p0695 A72-16416

Low density plasma flute oscillations stabilization by feedback system with potential sensors and electrodes, deriving dispersion equation

05 p0697 A72-16983

Lf oscillations due to drift diffusion of current free weakly ionized inhomogeneous plasma in magnetic field

05 p0697 A72-16984

Parametric plasma instability in hf electric field and constant magnetic field, noting longitudinal plasma oscillations growth

05 p0700 A72-17234

Longitudinal hf oscillations in homogeneous magnetoactive plasma by fast monoenergetic electron excitation

06 p0853 A72-17389

Nonlinear oscillation amplitude of ion beam due to phase bunching in interaction with plasma electrons

06 p0853 A72-17395

Self-excited lf oscillations in inhomogeneous rf collisional plasma, determining frequency as function of tube length, axial magnetic field and gas neutral pressure

06 p0857 A72-17533

Plasma perturbations and destabilization in curved magnetic field due to electronic electrical conductivity finiteness

06 p0860 A72-17684

Statistical hf electron heating at oscillating plasma boundary with acceleration of double Langmuir layer

06 p0860 A72-17691

Conversion effectiveness of oscillations induced by electron beam in bounded anisotropic plasma into electromagnetic emission

06 p0860 A72-17700

Collisionless plasma oscillations in external uniform magnetic field, described by initial value problem for nonrelativistic linearized Vlasov-Maxwell equations

06 p0862 A72-18251

Fast electron-cyclotron wave excitation with infinite phase velocity along magnetic field in nonequilibrium electron plasma

06 p0862 A72-18402

Weakly ionized plasma instability in strong nonuniform magnetic field with convective flow and steadily oscillating final state

06 p0865 A72-18543

Low frequency drift instability in local electron cyclotron resonance produced plasma, discussing oscillation fundamental frequency characteristics, wave propagation, density and potential waves, etc

07 p1039 A72-18799

Book on unmagnetized plasma theory covering Vlasov and Klimontovich models, electrostatic solutions, plasma oscillations, nonlinear phenomena, statistical descriptions, BBGKY correlations, etc

07 p1041 A72-19449

Electrostatically driven oscillations near lower hybrid resonance frequency in linear plasma device, measuring refractivity during wave propagation

07 p1043 A72-19664

External circuit coupling effects on dc anomalous resistivity in electron plasma oscillation

07 p1043 A72-19666

Vibration modes and stability of nonequilibrium low density He-Cs plasma in magnetic field

07 p1043 A72-19876

Electrostatic oscillations of multiveLOCITY electron streams in hot inhomogeneous plasma

07 p1046 A72-20502

Stepwise ionization effects on ionic wave propagation and oscillation stability in inert gas dc discharges

07 p1046 A72-20503

Spark source generated electron beam interaction with plasma in uniform magnetic field, estimating HF longitudinal oscillation power

07 p1046 A72-20504

Optical transmission, reflection and absorption of thin rubidium films for parallel and perpendicularly polarized monochromatic radiation, investigating volume and surface plasma oscillations

07 p1050 A72-20523

Electrostatic oscillations enhancement in magnetized plasma by hf electromagnetic waves, noting detection by light scattering

07 p1046 A72-20539

Nonlinear ion acoustic instability in plasma for subharmonic and harmonic forcing oscillations similar to Van der Pol effect

07 p1046 A72-20541

Microwave signal attenuation in LF oscillation plasma beam discharge, comparing to braking cyclotron absorption effect

08 p1212 A72-20792

Charged particles nonlinear oscillations in nonhomogeneous plasma, noting amplitude limitation and heating by external hf field energy absorption

08 p1212 A72-21210

Electron beam interaction with bounded homogeneous plasma layer natural oscillations, using collisionless kinetic equation

08 p1215 A72-21720

Electron plasma fluctuations in semiconductor with nonparabolic conduction band under external electric and magnetic fields

08 p1218 A72-21877

Electron plasma oscillations distribution upstream from earth bow shock, evaluating OGO-E plasma wave detector data

09 p1300 A72-23019

Electron beam and plasma nonlinear interactions, noting scattering zone, amplitude oscillation maximum, longitudinal velocity and relaxation patterns

10 p1517 A72-23760

LF drift-type and ion-acoustic oscillations in weakly ionized currentless plasma at low gas pressures in longitudinal magnetic field

10 p1517 A72-23765

Strong magnetic fields and electric current densities effects on acoustic oscillations and instability in stationary inhomogeneous low temperature plasma flow in crossed fields

10 p1517 A72-23838

Grid produced LF electrostatic perturbations propagation and damping in near isothermal plasma, discussing ion ballistic contributions to ion acoustic waves

11 p1692 A72-25520

Longitudinal plasma oscillations nonlinear instability due to energy transformation into harmonics and subharmonics

11 p1695 A72-25795

Plasma layer effect on natural oscillations of magnetosphere tail, using infinite plasma cylinder model immersed in interplanetary plasma

11 p1622 A72-25944

Anomalous plasma heating by laser irradiation with superimposed electric field oscillating near plasma frequency

11 p1696 A72-26326

Geomagnetic tail model with plasma cylinder immersed into solar wind, obtaining dispersion equation for oscillations

11 p1627 A72-26532

Mathematical model of weak coupling influence on damped harmonic oscillators with different eigenfrequencies applied to bounded plasma oscillations

11 p1698 A72-26600

Larmor frequency influence on Rayleigh-Taylor instability of viscous Hall plasma with magnetic field

11 p1698 A72-26604

Moving striations in tapered gaseous discharge tube, noting frequency dependence on tube radius

11 p1698 A72-26644

Plasma-ion beam system drift beam instability in longitudinal magnetic field, noting oscillations frequencies dependence

12 p1849 A72-27060

Electromagnetic wave field effects on cold magnetoactive plasma potential oscillations, solving dispersion equation for sub-ion gyroscopic frequencies

12 p1849 A72-27066

Low density plasma flute oscillations stabilization by feedback system with potential sensors and electrodes, deriving dispersion equation

12 p1850 A72-27127

LF oscillations due to drift-diffusion of current free weakly ionized inhomogeneous plasma in magnetic field

12 p1850 A72-27128

Probe triggered audio frequency plasma oscillation period dependence on applied magnetic field and discharge current

13 p2010 A72-28544

LF oscillations and electron drift in frozen plasma under strong electromagnetic radiation, deriving formulas for coupled Alfvén and spiral waves

13 p2035 A72-28593

Local perturbation generated waves in homogeneous plasma at rest subjected to uniform magnetic field

13 p2010 A72-28680

Mathematical model for ionized plasma response to sinusoidal perturbations, calculating dispersive waves in MHD generators with working fluid of potassium seeded argon

13 p2014 A72-29372

Parametric excitation of HF and LF plasma oscillations by AM SHF field, noting dependence on field strength at carrier frequency

13 p2015 A72-29436

Parametric instability of magnetoactive plasma relative to nonpotential oscillations excitation, deriving threshold value of HF field strength

13 p2016 A72-29601

Drift dissipative instability in bounded gas discharge plasma within magnetic field, investigating oscillations dependence on gas pressure and field strength

13 p2016 A72-29605

MHD stability in Hg vapor discharge plasma excited by standing microwave near electron cyclotron resonance, discussing electron energy anisotropy effect on LF oscillations

13 p2017 A72-29618

Nonradial oscillations and energy transport in nonmagnetic stationary rotating stellar wind in local theory limit

13 p2033 A72-29725

Enhanced damping of electrostatic wave primary mode due to combination scattering from plasma electron density oscillations

13 p2018 A72-29854

Dense isothermal plasma heating due to electron and ion scattering on turbulent pulsations of electric field oscillations

13 p2019 A72-29916

Density and electric field oscillations of plasma in stellarator, considering magnetic field strength effect, stabilization by ionic collisions and energy pumping mechanism

13 p2019 A72-29985

Stationary nonlinear ion acoustic oscillations in dense weakly ionized current carrying plasma, considering wave propagation velocity and instability process

13 p2019 A72-29988

Ion-acoustic oscillations effect on turbulent plasma electric conductivity within weak external electric field

13 p2019 A72-29990

Dispersion equation derivation for HF electromagnetic waves in weakly ionized plasma in crossed fields, noting oscillation spectrum

13 p2020 A72-30048

Current instability of electron-ion plasma in magnetic field produced by moving resonance charges

14 p2136 A72-30301

Dynamic behavior of long-period oscillations of surface wave type in system of inhomogeneous ion beams moving in dense plasma along magnetic field

14 p2136 A72-30307

LF and HF oscillations in plasma-electron beam system, investigating instability control

14 p2137 A72-30310

Ultrasonic wave excitation in potassium seeded flame, showing amplitude proportional to harmonic perturbation frequency imposed on plasma

14 p2170 A72-30417

Nonlinear interaction of resonant plasma oscillations with nonresonant wave pulse, using water bag model of electron plasma

14 p2140 A72-30936

Nonlinear plasma oscillations effect on electron bunching in microwave devices, noting space charge waves of finite amplitude

14 p2089 A72-31106

Flow-plasma system described by hydrodynamic equations, comparing self oscillatory process features with other systems

14 p2141 A72-31129

Numerical analysis of steady one dimensional quasi-shock waves in collisionless plasma within longitudinal uniform magnetic field, noting oscillations behind wave front

15 p2284 A72-31584

Dispersion equations and resonant absorption of plane and cylindrical surface waves in transition layer between plasmas, noting Langmuir oscillations

15 p2286 A72-32385

Electron beam-plasma system oscillation spectrum control through modulation by external HF signal, discussing theory and experimental verification

15 p2289 A72-32671

Quasi-linear approximation of absorption of oscillations excited by electron beam in nonuniform plasma, noting electron distribution change with heating under magnetic field

16 p2432 A72-32807

Ultrarelativistic electrons beam steady injection into plasma filled half space, using weak turbulence theory for assumed beam excited oscillations interaction

16 p2440 A72-34156

Application of the floating-potential probe for studies of low-frequency oscillations in a plasma

17 p2588 A72-34755

Fast electron cyclotron wave excitation with infinite phase velocity along magnetic field in nonequilibrium electron plasma

17 p2588 A72-34853

Coupled mode equations derivation for wave interactions in plasmas, considering oscillations production and cold magnetized plasma

17 p2589 A72-34923

Vibration modes and stability of nonequilibrium low density He-Cs plasma in magnetic field

17 p2589 A72-35126

Cs diode discharge current oscillations in collisionless Knudsen plasma containing electron and positive ion fluxes from thermionic emission and surface Cs ionization

17 p2593 A72-35885

Nonlinear current oscillations in a plasma diode

18 p2714 A72-36205

Nature of sound dispersion in a plasma

18 p2717 A72-37178

Natural oscillations of type-I comet tails

19 p2864 A72-38081

Wave propagation in plasmas with fluctuations

19 p2842 A72-38525

Low-frequency vibrations in a rarefied bounded plasma

19 p2842 A72-38530

Discontinuous generation of ultrahigh frequency oscillations during a plasma-beam interaction

19 p2768 A72-38664

Influence of different types of oscillations on ion heating in plasma-beam discharges

19 p2843 A72-38820

Possible uses of plasma oscillations in thin metal films

20 p2959 A72-39053

Drift instabilities in an inhomogeneous collisionless plasma

20 p2957 A72-39355

Plasma heating by nonlinear damping of resonantly excited longitudinal oscillations produced by two parallel laser beams with difference frequency equal to plasma frequency

21 p3090 A72-40342

Plasma low density regions caused by Langmuir turbulence, discussing energy dissipation of long wave oscillations and wave collapse

21 p3090 A72-40410

Nonlinear ion sound in a fully ionized current-carrying plasma

21 p3090 A72-40411

The study of turbulence in theta-pinch plasma with azimuthal magnetic field

21 p3091 A72-40577

Parametric instability of magnetoactive plasma relative to nonpotential oscillations excitation, deriving threshold value of HF field strength

21 p3091 A72-40655

Drift dissipative instability in bounded gas discharge plasma within magnetic field, investigating oscillations dependence on gas pressure and field strength

21 p3091 A72-40659

MHD stability in Hg vapor discharge plasma excited by standing microwave near electron cyclotron resonance, discussing electron energy anisotropy effect on LF oscillations

21 p3091 A72-40671

Excitation of volume ion-acoustic oscillations in an inhomogeneous dense plasma by the field of an electromagnetic wave

21 p3092 A72-40836

Amplitude and phase space potential oscillations measurements with hot electron probe in collisional Cs plasma compared with linear drift wave theory

21 p3093 A72-41376

Plasma heating by large-amplitude, low-frequency electric fields

21 p3094 A72-41630

Suppression of oscillations in a plasma-beam system by modulation of low frequency signals

21 p3095 A72-41681

Low-frequency oscillations in a Penning-discharge plasma under conditions of a cyclotron ion source

21 p3095 A72-41682

External high-frequency modulation of an ion beam and the absorption of beam-plasma instability oscillations in a plasma situated in a magnetic field of mirror configuration

21 p3095 A72-41683

Plasma echo-type oscillations in n-type InSb semiconductor, noting conduction band nonparabolicity effects

21 p3098 A72-41687

Development of nonlinear oscillations in the interaction between a modulated electron beam and a plasma

22 p3211 A72-42651

Measurement of nonthermal oscillations at the plasma frequency and its harmonics in a magnetized arc plasma, using the high-frequency Stark effect

22 p3212 A72-42916

Electromagnetic disturbances within a degenerate electron plasma in a quizzing magnetic field

22 p3212 A72-43010

Surface drift vibrations of a weakly ionized plasma

22 p3212 A72-43102

- Instability of a weakly ionized plasma with respect to vibrations with wavelengths of the order of the Debye radius 22 p3213 A72-43104
 - An ion-cyclotron instability of a plasma produced by a fast-ion beam 22 p3213 A72-43113
 - Noncoherent excitation of plasma vibrations by an almost monoenergetic relativistic beam 22 p3213 A72-43114
 - Current instability of electron-ion plasma in magnetic field produced by moving resonance charges 23 p3317 A72-43203
 - Dynamic behavior of long-period oscillations of surface wave type in system of inhomogeneous ion beams moving in dense plasma along magnetic field 23 p3317 A72-43209
 - LF and HF oscillations in plasma-electron beam system, investigating instability control 23 p3317 A72-43212
 - Interaction between a plasma and an electron-beam modulated by low-frequency oscillations 23 p3318 A72-43309
 - Collisionless heating of plasma ions by an ion beam 23 p3318 A72-43321
 - Long wave oscillations attenuation by charged particle collisions in one- and two-component hot and cold Boltzmann plasma, using kinetic and polarization vector equations 23 p3318 A72-43325
 - Excitation of potential oscillations in a plasma by a flow of phased oscillators 23 p3319 A72-43401
 - Plasma diagnostics for electron-ion oscillation discharge in alternating positive-negative electrodes under axial magnetic field, noting electrons drift 23 p3319 A72-43403
 - Special features of photoresonance perturbation relaxation in a low-temperature discharge plasma 23 p3319 A72-43409
 - Landau dispersion equations for oscillations damping of bounded electron plasma, noting application to plasma cylinder in conducting tube 23 p3319 A72-43410
 - Low frequency oscillations of cesium and mercury vapor plasmas, noting intensity distribution, radiation pattern and polarization characteristics of microwave emission 23 p3319 A72-43411
 - Physical processes of weak, single wave and strong plasma turbulence and instabilities driven by oscillating fields 23 p3319 A72-43514
 - On the instability of nonlinear longitudinal oscillations of magnetoactive plasma. 23 p3320 A72-43524
 - Strictional nonrelativistic effect on uniform non-relativistic monoenergetic beam interaction with isotropic bounded plasma, investigating plasma oscillations and stability 23 p3320 A72-43576
 - Apparent constant wavelength oscillations in a bounded plasma. 23 p3320 A72-43577
 - Role of nonlinear effects in the problem of the anomalous resistance of a plasma 23 p3322 A72-44481
 - LF oscillations and electron drift in frozen plasma under strong electromagnetic radiation, deriving formulas for coupled Alfvén and spiral waves 24 p3440 A72-45093
 - Anode sheath plasma current instabilities, examining electron and ion turbulent heating, plasma particle limiting energies and unsteady oscillation spectra 24 p3429 A72-45490
 - Generation of plasma oscillation by beam-plasma interaction. 24 p3430 A72-45574
 - Plasma-ion beam system drift beam instability in longitudinal magnetic field, noting oscillations frequencies dependence 24 p3431 A72-45713
 - Electromagnetic wave field effects on cold magnetoactive plasma potential oscillations, solving dispersion equation for sub-ion gyroscopic frequencies 24 p3431 A72-45719
- PLASMA PERTURBATION**
U PLASMA OSCILLATIONS
PLASMA PHYSICS
- Internal electrostatic field effect on ion separation in expanding pulsed laser produced plasmas 01 p0105 A72-10021
 - MHD equations for plasma of arbitrary collision frequency in weakly inhomogeneous magnetic field, considering collisional and resonant particle effects 01 p0108 A72-10241
 - Ion electromagnetic cyclotron modes growth rates in multicomponent magnetospheric plasmas, discussing instabilities enhancement 01 p0062 A72-10906
 - Electrically ionized striated plasma flow in annular channel, noting application to synchronous induction MHD generator 01 p0111 A72-11209
 - Plasma physics computer simulation of double stream and beam instabilities, wavelength nonlinearities and velocity distribution, using superparticle and Vlasov equation models 02 p0263 A72-11691
 - Papers on plasma physics, covering ionospheric plasma resonances, fusion research, electrostatic precipitator, two stream instability, adiabatic motion and relativistic beam equilibria 02 p0267 A72-12837
 - Solid state colloidal plasma physics, discussing statistical ionization mechanics, electron emission and recombination, rocket exhausts, MHD generation, metal vapors electrostatic precipitation, etc 02 p0267 A72-12842
 - Plasma physical characteristics, considering experiments with Ba and Sr atom clouds introduced into ionosphere 03 p0394 A72-13196
 - Solar corona MHD and plasma physical structure, considering macroscopic and microscopic properties 03 p0422 A72-13204
 - Solar wind 10-9900 eV electron flux, evaluating energy transport in plasma rest frame 03 p0412 A72-13507
 - Linear electron acceleration mechanism in plasma, showing polarization fluctuations in diode under strong electric field 03 p0395 A72-13573
 - Ions acceleration during current passage through plasma, discussing maximum energies, threshold current and electron beam flux density 03 p0396 A72-13661
 - Theta pinch plasma electron density with high time resolution by side-on interferometry at 10.6 microns 03 p0396 A72-13670
 - Rotationally symmetric static incompressible infinite conducting plasma elliptic differential equation reduction to boundary value problem 03 p0400 A72-14353
 - Electron heating by oscillating electric field in presence of steady magnetic field, solving Boltzmann transport equation for electron velocity distribution in plasma 04 p0556 A72-14947
 - Finite Larmor radius effect on Rayleigh-Taylor plasma instability in vertical magnetic field, characterizing solution by variational principle 04 p0557 A72-15022
 - Nonideality effects on Coulomb gas conductivity by finding conductivity due to electron scattering at atoms, solving kinetic equation of three component plasma model 05 p0694 A72-15850
 - Plasma physics collective phenomena enhancing effect on relaxation processes, emphasizing relevance to stellar dynamics [AD-739801] 05 p0714 A72-16059
 - Cosmic plasma phenomena in astrophysics, discussing distribution, ionospheric disturbances, magnetospheric waves, solar wind, etc 05 p0723 A72-17217
 - Thermodynamic equilibrium relations in optically thin plasma models for hydrogen and argon systems 05 p0699 A72-17218
 - Thermodynamic equilibrium, transport and optical properties and quantum effects in nonideal plasmas, using Monte Carlo method 05 p0700 A72-17223
 - Ion accelerating system for minimum angular ion beam divergence with plasma ions ejection from source through slits in electrodes 05 p0701 A72-17236
 - Quiescent plasmas - Conference, Elsinore, Denmark, September 1971 06 p0854 A72-17501
 - Ion acoustic waves instability from electron-ion temperature difference in homogeneous collisional ionized plasma, using fluid equations perturbation analysis 06 p0856 A72-17524
 - Boltzmann integrals for inelastic collisions and radiative processes in stationary monatomic plasma, using Grad 8-moment approximation of particles momentum distribution functions 06 p0861 A72-18174
 - Single species one dimensional Vlasov plasma linearized analysis as initial value problem with periodic boundary conditions, using Hamilton variational principle 06 p0864 A72-18537
 - Infinite uniform Vlasov plasma response to steady state transverse excitation, considering spatial electron cyclotron damping 06 p0864 A72-18539
 - [AD-737564] Plasma Dory-Guest-Harris type instability nonlinear evolution from numerical integration of Vlasov equation, using particle simulation and Fourier-Hermite transform methods 06 p0865 A72-18542
 - Discrete wave packets observed in solar wind, discussing mechanism similar to echo phenomenon in plasma physics 07 p1057 A72-19143
 - Radiative cooling induced thermal instability mechanism for condensation in astrophysical plasma 07 p1040 A72-19348
 - Book on unmagnetized plasma theory covering Vlasov and Klimontovich models, electrostatic solutions, plasma oscillations, nonlinear phenomena, statistical descriptions, BBGKY correlations, etc 07 p1041 A72-19449
 - Transverse electromagnetic instabilities in anisotropic plasmas, confirming by computer simulation energy constants derived from nonlinear Vlasov-Maxwell equations 07 p1041 A72-19509
 - Shock wave collision induced population inversion in electromagnetic shock tubes, measuring plasma absorption coefficient 07 p1044 A72-20074
 - Solar wind plasma parameter spatial perturbation problem solution by method of characteristics 08 p1225 A72-20721
 - Plasma rotation during theta pinch collapse, determining ion azimuthal velocity from fields and pressure gradient measurements via Ohms law 08 p1213 A72-21255
 - Hydrogen line broadening in plasma theory with limitations of Stark component intensity distribution by quasi-static and impact approximations 09 p1358 A72-22493
 - Two fluid MHD model for flat plasma condenser in crossed magnetic and alternating electric fields, calculating impedance and disturbed plasma parameters 09 p1360 A72-22953
 - Alfvén waves development and high pressure plasma hydrodynamic and kinetic instabilities dependence on magnetic field to temperature gradients ratio 09 p1360 A72-22954
 - Soviet book on plasma physics and controlled thermonuclear synthesis covering plasma-electromagnetic interactions, magnetic traps and plasma cryogenic technology 09 p1361 A72-23201
 - Single helix magnetic field with axial current, discussing field lines rotatory transformation and magnetic well and shear effect on plasma behavior 09 p1363 A72-23216
 - Homogeneous plasma internal feedback mechanism and structure, discussing instabilities control by external feedback 09 p1365 A72-23474
 - High pressure CO and N plasmas production by uncoupling electron temperature from number density, measuring electron-ion recombination rates 10 p1518 A72-23962
 - Fourier transform and angular distribution of light diffraction by plasma with strong correlations 10 p1519 A72-24129
 - Nonideal dense plasma properties, discussing electrostatic shielding, many particle clusters, phase transitions, metallization and electrical conductivity [AIAA PAPER 72-414] 11 p1695 A72-26164
 - Chemical ionizing mass spectrometry with electron bombardment of reactant gas, discussing plasma chromatography 11 p1590 A72-26389
 - Computer simulation of plasmas by following actual orbits of particles interacting through electrostatic forces 12 p1852 A72-27914
 - Relaxation processes enhancement by collective particle collisions effects in plasma, stressing application to stellar dynamics 12 p1853 A72-27915
 - Book on theory of fully ionized plasmas covering Coulomb systems equilibrium and nonequilibrium states, charged particle radiation and interactions with EM fields 13 p2011 A72-29098
 - Two point correlation description of MHD plasma properties subject to electrothermal instability, calculating electron number density and temperature fluctuations 13 p2015 A72-29373
 - Electron-ion collision frequency and conductivity of non-Debye plasma formed in high pressure discharge from Ar, Kr and Xe tubes 13 p2018 A72-29891
 - Kinetic model for electromagnetic field fluctuations in bounded isotropic plasma half space with specular reflection of electrons at boundary 14 p2135 A72-30170
 - Maximum ion energy dependence on radiation density in laser plasma 14 p2137 A72-30315
 - High momentum transfer collisions importance for anisotropic part of distribution function in Lorentz and single component plasmas 14 p2134 A72-30802
 - Nonideality effects on Coulomb gas conductivity by finding conductivity due to electron scattering at atoms, solving kinetic equation of three component plasma model 15 p2283 A72-31269

Bremsstrahlung photon emission rate from Maxwellian plasma, determining soft X ray diagnostic techniques applicability for laser produced plasmas

15 p2285 A72-32271

Analytical solution of dispersion equation for ionization instability threshold in unbounded low temperature plasma, noting independence of relaxation rates

15 p2286 A72-32277

Rotating plasmas steady MHD equilibria without PS factor enhancement, considering cases of vanishing and nonvanishing toroidal current

16 p2433 A72-32817

Electric and magnetic field effects on auroras formation, noting similarity with thermonuclear reactor plasma

16 p2456 A72-33518

Russian book on magnetogasdynamic flow theory and calculations covering plasma flows and energy conversion in MHD channels of dc generator

16 p2438 A72-33873

Cosmic plasma physics - Conference, Frascati, Italy, September 1971

16 p2459 A72-33901

Cosmic plasma relations with laboratory plasmas within astrophysics, considering inhomogeneity, electrostatic double layers, filamentary structures and non-Maxwellian effects

16 p2438 A72-33902

The plasma physics of the Jovian decameter radiation.

17 p2605 A72-34539

Hydrogen line broadening in plasma theory with limitations of Stark component intensity distribution by quasi-static and impact approximations

17 p2588 A72-34657

The electromagnetic field generated by an electric dipole in a spherical cavity immersed in a nonlinear plasma

17 p2588 A72-34746

Solution of the Boltzmann equation for a fully ionized plasma in an oscillatory electric field and a steady magnetic field. V - Explicit solution for a homogeneous plasma in a high-frequency electric field.

17 p2589 A72-35057

Statistical mechanics of magneto-active plasma.

17 p2590 A72-35144

A review of the unified theory of relaxations in plasmas.

17 p2590 A72-35159

Verification of theory for plasma of finite-size particles.

17 p2592 A72-35618

Soft collision plasma scattering function, conductivity and particle energy loss from simplified Fokker-Planck collision model

17 p2592 A72-35621

Two fluid MHD model for flat plasma condenser in crossed magnetic and alternating electric fields, calculating impedance and disturbed plasma parameters

17 p2593 A72-35882

Alfven waves development and high pressure plasma hydrodynamic and kinetic instabilities dependence on magnetic field to temperature gradients ratio

17 p2593 A72-35883

Laboratory model information relating to modeled geophysical phenomena, noting magnetosphere study from plasma physics experiments

17 p2551 A72-35904

Energy spectrum of interplanetary-plasma discontinuities

18 p2715 A72-36653

Simple inexpensive laboratory-quality Rogowski TEA laser.

19 p2810 A72-37514

Inertial plasma effect in a glow discharge - A new principle of oscillation measurement

19 p2800 A72-37756

Solar wind plasma parameter spatial perturbation problem solution by method of characteristics

19 p2852 A72-38349

Diffusion cooling in neon, argon, and krypton afterglow plasmas.

19 p2841 A72-38378

Effect of a cooling gas layer on the geometrical dimensions of an induction plasma

20 p2957 A72-39219

Balescu-Guernsey-Lenard kinetic equation for homogeneous dilute electron gas extended to higher densities, specifying conditions for BBGKY hierarchy correlation functions solution

20 p2958 A72-39815

Shock front radius of subsonic radiation front driven by plasma fireball during final stages of decaying laser spark

20 p2934 A72-39844

Short distance behaviour of the pair correlation function for classical plasmas.

21 p3091 A72-40570

Formation of intense charged particle beams in a current-carrying plasma.

21 p3092 A72-40834

Electric field intensity distribution function for thermoelectronic emission from hot cathodes in low temperature plasma, using Richardson formula

21 p3094 A72-41656

Maximum ion energy dependence on radiation density in laser plasma

23 p3318 A72-43218

Electrical characteristics of a CO laser discharge plasma

24 p3411 A72-45500

PLASMA PINCH

NT THETA PINCH

Two dimensional collisionless plasmas instability with neutral points, discussing sheet pinch with periodic structure

01 p0105 A72-10022

Solar prominence oscillatory motion on 26 March 1964 association with plasmoids generated by pinch tube plasma

02 p0278 A72-12044

Bulk recombination effects on nonstationary pinching and collapse of electron-hole plasma by magnetic field in crystal

03 p0401 A72-13581

Nonlinear surface wave propagation on pinched cylindrical plasma, developing asymptotic approach from L undquist equations

04 p0559 A72-15348

X ray pulse spectra measurement from Z-pinch plasma focus devices, describing Ross filter system with silicon diode detector capable of nanosecond time resolution

04 p0524 A72-15537

Argon plasma transient axial flow and heating characteristics in pinched column of linear z-pinch device with collapsing current sheets conversion to axial streaming velocity

[ALAA PAPER 72-208]

05 p0696 A72-16886

Linear Z plasma pinch in Ar as spectroscopic source, investigating effects on shock-piston separation

06 p0865 A72-18544

Interferometric measurements of time dependent electron density in Xe pinched plasma laser, showing laser lines due to transitions in triply ionized species

09 p1366 A72-23700

MHD sheet pinch model time dependent nonequilibria stability determined by equations of incompressible viscous resistive magnetofluid

[AD-739661]

10 p1523 A72-24795

Parallel viscous modification of resistive tearing instability in Cartesian model of hard core pinch plasma confinement

10 p1523 A72-24795

Neutron flux and energy spectra from crossed field acceleration model of plasma focus and z-pinch discharges

11 p1693 A72-25565

Dense hydrogen plasmoids injection with linear pinch gun into biconical cusp field, observing axial reciprocating motion

11 p1697 A72-26575

MHD instabilities growth rates from diffuse linear pinch equations of motion solution

15 p2287 A72-32416

Two dimensional unsteady solutions to MHD equations, describing matter compression near zero line of magnetic field for solar flares and z pinch studies

16 p2435 A72-33151

Russian papers on physical processes in lasers covering mode locking regime, pinch discharge, electronic transitions in diatomic molecules and laser control

16 p2400 A72-33295

Visible and UV stimulated emission in plasma of direct pinch discharge on Ar II and III ions, discussing application possibility to plasma diagnostics

16 p2400 A72-33297

Critical layer equations of plasma resistive instabilities, using sheet pinch model

16 p2436 A72-33577

Plasma velocity, ion density and electrical conductivity from electron density and temperature and electromagnetic field profile measurements in Ar plasma inverse pinch

19 p2841 A72-38437

Pinch effect in a germanium electron-hole plasma

21 p3096 A72-40414

Averaged equations of laser heating of Z-pinch plasma the nuclear fusion energy being taken into consideration.

21 p3093 A72-41481

Hydrodynamic instability of a plasma boundary with a magnetic field, taking viscosity into account

22 p3210 A72-42277

Ray structures of polar auroras and their association with drift-current instability in a plasmoid

23 p3282 A72-43358

Averaged equations of laser heating of plasma in a focus-type system taking into account the heat of nuclear fusion.

23 p3322 A72-44223

PLASMA POTENTIALS

Plasma potentials spatial distribution measurement, describing switching circuit and probe design

01 p0109 A72-10580

Space potential determination in plasma diagnostics, comparing second harmonic analysis with experimental results

02 p0268 A72-12868

Collision integral for classical electron plasma, concerning Born-Bogoliubov-Green-Kirkwood-Yvon equations for long range interaction potential and motions of multiple particles

03 p0399 A72-14069

Electron temperature measurement error elimination with radio frequency Langmuir probe in low density plasma, measuring floating potential

05 p0694 A72-16041

Low density plasma flute oscillations stabilization by feedback system with potential sensors and electrodes, deriving dispersion equation

05 p0697 A72-16983

Pseudowaves and ion acoustic waves simulation, calculating time evolution of ion distribution for oscillating negative plasma potentials applied at grid

06 p0855 A72-17512

Potential around moving test particle in quiescent plasma, discussing energy loss, transport properties and gravitational analog

06 p0859 A72-17549

Single ended Q machine Ba plasma probe measurements of ion temperatures perpendicular to magnetic field, electron temperatures and plasma densities and potentials

06 p0859 A72-17550

Pulsating point charge potential in cold homogeneous boundless magnetoplasma with complex permittivity tensor coefficients for quadrupole probes theory

06 p0859 A72-17638

Weakly ionized decaying afterglow plasma potential fluctuation and instability in magnetic field, using electrostatic probes

06 p0860 A72-17692

Saha equation for plasma ionization energy lowering, using three particle distribution function and BBGKY hierarchy

08 p1212 A72-20939

Potential distribution in positive ion sheath around plane Langmuir probe immersed in plasma

08 p1215 A72-22074

Second derivative measurement of Langmuir probe characteristics for electron energy distribution functions in nonstationary plasmas by sample and hold technique

09 p1359 A72-22654

Plasma potential determination near probe by space charge layer reactance observation

09 p1361 A72-22962

Reference electrode area and floating potential in fluence in Langmuir probe measurements of plasma density and temperature

09 p1311 A72-23229

Electromagnetic wave field effects on cold magnetoactive plasma potential oscillations, solving dispersion equation for sub-ion gyroscopic frequencies

12 p1849 A72-27066

Low density plasma flute oscillations stabilization by feedback system with potential sensors and electrodes, deriving dispersion equation

12 p1850 A72-27127

Low pressure He and Ne discharge generated positive plasma column potential, determining electron concentration from electron energy distribution functions

16 p2437 A72-33746

Hot probe determination of space potential in low pressure He and Ne discharge plasmas via probe characteristics second derivative

16 p2437 A72-33748

Application of the floating-potential probe for studies of low-frequency oscillations in a plasma

17 p2588 A72-34755

Effect of a transverse magnetic field on the operation of a thermionic converter under undercompensated Knudsen conditions.

17 p2497 A72-34862

Plasma potential determination near probe by space charge layer reactance observation

17 p2593 A72-35892

Sinusoidal potential distributions and volt-ampere characteristics of Knudsen-mode thermionic emission converters

18 p2646 A72-36198

The influence of a nonequilibrium electron distribution function near the cathode and fractional coverage on the characteristics of a thermionic emission converter in the arc mode

18 p2647 A72-36220

Potential created by a point charge oscillating in an inhomogeneous plasma

19 p2842 A72-38522

A comparison of some particle-in-cell plasma simulation methods.

21 p3089 A72-40105

Identification of transverse Kelvin-Helmholtz turbulence in a magnetoplasma column.

21 p3091 A72-40768

Amplitude and phase space potential oscillations measurements with hot electron probe in collisional Cs plasma compared with linear drift wave theory

21 p3093 A72-41376

Potential drops near electrodes in a pulsed plasma accelerator

22 p3213 A72-43108

Plasma diagnostics for electron-ion oscillation discharge in alternating positive-negative electrodes under axial magnetic field, noting electrons drift

23 p3319 A72-43403

Electromagnetic wave field effects on cold magnetoactive plasma potential oscillations, solving dispersion equation for sub-ion gyroscopic frequencies

24 p3431 A72-45719

PLASMA POWER SOURCES

NT PLASMA ENGINES

PLASMA PROBES

NT ELECTROSTATIC PROBES

Plasma potentials spatial distribution measurement, describing switching circuit and probe design

01 p0109 A72-10580

Flowing plasma ionization density measurement by stagnation probe, comparing measured with calculated plasma sheath convection current values [AD-738692]

01 p0110 A72-11189

Electron and ion drift rate effect on floating double probe characteristics in Maxwellian plasmas

02 p0266 A72-12768

Immersion-type electroconductivity probe for anisotropic plasmas, calculating Hall coefficient

03 p0397 A72-13922

Direct display plasma density and temperature meter, using floating double probe method

04 p0520 A72-14533

Cylindrical positive probe behavior in high speed collisionless mesothermal plasma flow

[ONERA, TP NO. 1000]

05 p0660 A72-15860

Current drainage from dilute plasma to high voltage probe via holes in Kapton H polyimide film, quartz and fluorinated ethylene propylene type C

[AIAA PAPER 72-105]

05 p0696 A72-16815

Electromagnetic and electroacoustic near zone fields of linear antenna in plasma measured by diagnostic probe

05 p0700 A72-17232

Static high pressure spherical plasma probe theories verification, showing saturation currents and I-V characteristics agreement with calculated values

[AD-740015]

06 p0853 A72-17416

Single ended Q machine Ba plasma probe measurements of ion temperatures perpendicular to magnetic field, electron temperatures and plasma densities and potentials

06 p0859 A72-17550

Dipolar rf probe admittance measurements in simulated ionosphere for satellite plasma experiments

06 p0811 A72-18733

Electric field measurements in ionosphere and magnetosphere by double probe and electron and ion drift techniques

07 p0978 A72-20042

Plasma potential determination near probe by space charge layer reactance observation

09 p1361 A72-22962

Collisionless plasma spherical probe RF sheath model based on quasi-static approximation and electrostatic theory

09 p1365 A72-23520

Ionospheric and magnetospheric electric field measurements by rocket, satellite or balloon-borne electrostatic probes or by plasma drift methods

10 p1473 A72-24529

Quadrupole probe theory for hot collisionless isotropic plasma, noting impedance dependence on electron temperature at resonance and optimum dimension relationship to Debye length

10 p1523 A72-24798

Spherical probe impedance characteristics in isotropic plasma predicted by hydrodynamic theory compared to experimental results

11 p1699 A72-26768

Plasma sheath from plane negatively biased electrode immersed in low pressure discharge investigated by ion acoustic waves and hot probe

12 p1850 A72-27279

Nanosecond response magnetic probes to measure fast disturbances in oblique shock waves within collisionless plasma, describing experimental technique

15 p2235 A72-31646

Boundary layer ionization on flat plate and cylindrical plasma probes in high speed flow, considering ionized continuum flow and collisionless plasma

16 p2374 A72-32831

Hot probe determination of space potential in low pressure He and Ne discharge plasmas via probe characteristics second derivative

16 p2437 A72-33748

Probe temperature, shape and size effects on electron energy distribution measurements for positive plasma column of low pressure He and Ne discharges

16 p2437 A72-33750

Ion temperature diagnostic using a high power alternating current probe.

17 p2557 A72-35617

Plasma potential determination near probe by space charge layer reactance observation

17 p2593 A72-35892

Plasma immersion probe measurements of electron work function.

18 p2690 A72-36127

Design considerations in the measurement of electron temperature in the ionosphere.

19 p2801 A72-37926

Pioneer 7 observations of the August 29, 1966, interplanetary shock-wave ensemble.

21 p3104 A72-40481

Measurement of ionic parameters of a cesium plasma with the help of a grid probe with a cooled collector

22 p3211 A72-42645

PLASMA PROPULSION

High temperature gaseous U fission plasma core reactor engine concepts for space propulsion

01 p0099 A72-11327

Nozzle and cavity wall cooling limitations on uranium plasma nuclear rocket specific impulse, discussing wall heat flux and transpirational cooling by propellant flow

03 p0387 A72-14383

Quasi-steady MPD propulsion systems for astronautical applications, describing electric energy storage bank, mass supply system, accelerator and operation principle

09 p1374 A72-22934

Pulsed plasma thruster arc electron density measurement by Mach-Zehnder interferometer and He-Ne laser, determining exhaust ion temperature and total charge

[AIAA PAPER 72-463]

11 p1709 A72-26198

PLASMA RADIATION

Electron energy equation and recombination radiation loss for atomic radiating optically thin plasmas, using Kramers-Unsold approximation

01 p0106 A72-10097

Line radiation from theta pinch with oscillatory ion and electron density applied to solar spectral studies

01 p0106 A72-10098

Hot magnetoplasmas cyclotron radiation, investigating thermal particle motion effects

01 p0107 A72-10142

Spectral distribution of total continuous emission coefficient for LTE hydrogen plasma over 8000-16,000 K and 400-15,000 A ranges, observing Stark broadening

01 p0108 A72-10175

Uranium arc plasma visible and near UV emission coefficients as function of U partial pressure and corresponding temperatures

01 p0112 A72-11337

Uranium and tungsten plasmas emission and absorption properties at shock tube generated pressures of 3-48 atm and temperatures of 7,000-12,000 K

01 p0112 A72-11339

Photometric calibration of long wavelength vacuum UV standards by synchrotron and plasma black body radiation

01 p0073 A72-11399

Stabilized hydrogen plasma arc spectral radiation as light source for vacuum UV radiometry, comparing output with W strip and carbon sources

01 p0073 A72-11400

Radiative heat transfer within nonisothermal air plasma, presenting centerline temperature data for various boundary pressures and temperatures

[ASME PAPER 71-HT-G]

02 p0302 A72-12316

Frequency spectrum analysis of electromagnetic self radiation from plasma interacting with high energy electron beam

03 p0393 A72-13082

Cold plasma flow rate determination from emission inhomogeneities, using time of flight method and high speed streak photography for instantaneous velocity measurements

03 p0396 A72-13663

Halos around black holes, showing luminosities caused by synchrotron radiation of magnetized plasma

03 p0435 A72-13803

Ambipolar diffusion influence on MHD generator electrical conductivity, discussing plasma radiation, electron escape generator geometry and efficiency and ignition temperature range

04 p0554 A72-14404

Radiation intensity and losses in dense high temperature hydrogen plasma containing bare nuclei and hydrogen-, helium-, lithium- and beryllium-like ions as impurities

04 p0557 A72-15170

Plasma satellite linewidth broadening due to density inhomogeneity, considering evidence based on light scattering from Ar plasma jet

04 p0559 A72-15355

Moving type 4 radio burst observation with radioheliograph, suggesting isolated self contained synchrotron emitting plasmoid and relation to coronal magnetic field

05 p0710 A72-16521

Fiber optics system for H beta line shape measurement in transient high temperature plasma, using narrow slits at spectrograph exit plane

[AIAA PAPER 72-106]

05 p0663 A72-16816

Nonlinear wave coupling, scattering and radiation in plasmas for diagnostics application

05 p0699 A72-17221

Phase and group velocity of electromagnetic waves in drifting uniaxial magnetoplasma, obtaining dispersion relation from Maxwell and plasma equations

06 p0853 A72-17349

Photoelectron flux measurement of intensities of plasma lines in radar incoherent scatter spectrum by uhf radar

06 p0874 A72-18732

Two channel high resolution spectrometric measurements of plasma velocity from intrinsic radiation in optical range by Doppler effect

07 p1044 A72-19885

Microwave radiation intensity and spectral frequencies of Knudsen discharge in cesium plasma

07 p1046 A72-20515

Design equations for transpiration radiometer applicable to radiation measurement from confined Ar plasma

08 p1163 A72-20919

Solar coronal plasma radiative capacity and temperature structure from cooling function in thermal balance equation

08 p1231 A72-21124

Optical and inner shell X ray transitions in highly ionized Cu, Fe and Ti observed from point plasma source generated in linear vacuum discharge

09 p1360 A72-22833

Early phase time development of far UV line radiation from plasma production by focusing Q switched ruby laser onto solid Mg target

09 p1325 A72-23232

Plasma interpretation of solar type 3 and spike bursts associations from high time resolution radioastrigraphic observations

09 p1392 A72-23540

Dense low temperature Ar and Hg plasmas, observing correlation between electrical conductivity and optical emission

10 p1517 A72-23835

Time dependent light emission from mesoplasmas in Si p-n junctions in pulse mode, showing carrier heating effect

11 p1700 A72-25780

Holographic Fourier spectroscopy for microwave radiation spectra of toroidal plasma with turbulent heating

12 p1850 A72-27135

Perturbation theory for electromagnetic radiation in weakly anisotropic magnetoplasma, calculating Green function for delta function source oriented parallel to static magnetic field

12 p1783 A72-27668

Frequency spectrum analysis of electromagnetic self radiation from plasma interacting with high energy electron beam

13 p2015 A72-29432

Carbon dioxide arc plasma emissivity in visible range at atmospheric pressure and 6500-9500 K, discussing diatomic carbon concentration

13 p2016 A72-29520

Spectral changes of light reflected back from plasma during heating by mode locked Nd laser, noting equidistant lines presence

14 p2138 A72-30447

Plasma radiation from collisionless MHD shock waves, discussing waves generation and angular distribution

14 p2138 A72-30555

Ar plasma spectral lines, calculating temperature functions of excitation to fourth ionization multiple at atmospheric pressure

14 p2139 A72-30782

Spectrochemical trace analyses in electric arc plasma, examining external magnetic field effects on spectral line intensity variation

14 p2139 A72-30784

High power carbon dioxide laser produced dense He plasma, comparing experimental and theoretical Stark profile of forbidden and allowed transitions

15 p2285 A72-32223

Algorithms for incorporating electromagnetic field into plasma numerical simulation to explain unwanted noise generation rates

15 p2288 A72-32421

Theory for plasma radiation from collisionless MHD shock waves applied to Type 2 solar radio bursts, comparing to type 4 bursts

16 p2446 A72-33461

Nonlinear wave interaction in anisotropic plasmas, discussing helicon decay with acoustic wave emission and quasi-longitudinal waves with magnetoacoustic wave emission

16 p2436 A72-33748

- Monochromatic radiation pulse transfer in absorbing plasma, deriving heat wave propagation velocity 16 p2437 A72-33692
- Photoionization of a gas by far ultraviolet radiation of a laser-created plasma 17 p2588 A72-34872
- Two channel high resolution spectrometric measurements of plasma velocity from intrinsic radiation in optical range by Doppler effect 17 p2590 A72-35133
- The electromagnetic radiation near the ion plasma frequency emitted by a turbulently heated plasma 18 p2715 A72-36598
- Self-similar unsteady magnetogasdynamic flows of a radiating gas produced by the motion of a piston 18 p2716 A72-36897
- Spectral intensity measurements from high-pressure nitrogen plasmas 19 p2840 A72-37836
- Plasma electron velocity distributions determined from the polarization of free-free bremsstrahlung 19 p2841 A72-38439
- The incoherent scattering of radiation from a high temperature plasma 19 p2842 A72-38523
- Finite sized optically thin radiating plasma stability analysis, deriving luminosity function for metastable state existence from mathematical model 20 p2958 A72-39456
- Nonthermal emission of a magnetoactive plasma in the field of super-high-frequency pumping wave 21 p3090 A72-40407
- Excitation of electromagnetic waves in a plasma by a relativistic electron beam 21 p3092 A72-40787
- Method of calculation of the emission coefficient of a cylindrical plasma starting from the experimental profile of the intensity 21 p3092 A72-41198
- Electronically scannable plasma leaky wave antenna system 21 p3022 A72-41325
- Influence of the lowering of the ionization energy on the continuous radiation of an argon plasma 21 p3093 A72-41343
- Charged particle uniform motion in sinusoidally space-time periodic medium, determining Cerenkov and transition radiation field spectrum from Brillouin diagram 21 p3088 A72-41378
- Electron processes in nonrelativistic electron streams against stationary ion background as wave packet envelope deformation in space and time 21 p3094 A72-41652
- Effect of Thomson scattering on the emission spectrum of an optically semitransparent plasma 21 p3102 A72-41774
- High-intensity X-ray spectra and stimulated emission from laser plasmas 22 p3210 A72-41990
- A transpiration radiometer for measurement of total thermal radiation from a flowing plasma 22 p3179 A72-42691
- Analytical model of the flash produced in aluminum-aluminum hypervelocity impacts 22 p3207 A72-42867
- Electromagnetic emission during the development of a hydrodynamic beam instability in a bounded plasma 22 p3213 A72-43115
- Low frequency oscillations of cesium and mercury vapor plasmas, noting intensity distribution, radiation pattern and polarization characteristics of microwave emission 23 p3319 A72-43411
- Method for solving the problem of radiation in an anisotropic plasma 23 p3321 A72-44220
- PLASMA RESONANCE**
- HF capacitive discharge plasma resonance under weak transverse magnetic field in vacuum 01 p0106 A72-10041
- Diffuse plasma resonances in space interpreted by wave-particle nonlinear interaction in weakly turbulent plasma, considering electrostatic electron cyclotron wave instability 02 p0265 A72-12366
- Second harmonic emission from plasma hybrid resonance region during electromagnetic wave normal incidence on nonhomogeneous magnetoactive plasma layer 02 p0180 A72-12578
- Papers on plasma physics, covering ionospheric plasma resonances, fusion research, electrostatic precipitator, two stream instability, adiabatic motion and relativistic beam equilibria 02 p0267 A72-12837
- Plasma resonances due to satellite antenna from ionospheric topside sounder observations 02 p0222 A72-12838
- Photoresonance cesium plasma development and decay, determining density spatial-temporal behavior and recombination and polar diffusion coefficients by probe measurements 03 p0396 A72-13664
- Plasma electron density profiles from Tonks-Dattner resonance frequencies for plane parallel and cylindrical columns 04 p0554 A72-14530
- Nonlinear phenomena in transition region through resonance of dense inhomogeneous plasma in alternating electromagnetic field 04 p0489 A72-15390
- Collision resonance effects on transverse wave propagation direction in collisionless plasma for upper ionospheric sounding 04 p0490 A72-15403
- Slant incident electromagnetic wave absorption in linear plasma layers due to field swelling in resonance region 05 p0627 A72-16403
- Electrostatic shift and broadening of Landau resonance by particle-wave interaction in turbulent plasmas 05 p0700 A72-17231
- Nonlinear amplitude distribution of electromagnetic wave propagating in plasma near hybrid resonance frequencies 06 p0771 A72-17390
- Cylindrical plasma ion-acoustic resonance measurements from various excitation methods for noise component identification 06 p0856 A72-17523
- Electrostatic hf wave propagation in one dimensional collisionless plasma, describing electron trapping and oscillations and resonance-produced sidebands 06 p0858 A72-17544
- Rf transmission between two parallel whip antennas in warm plasma, noting received signal increase at probe resonant frequency 06 p0860 A72-17747
- Electrostatically driven oscillations near lower hybrid resonance frequency in linear plasma device, measuring refractivity during wave propagation 07 p1043 A72-19664
- Moving plasma heating by fast large amplitude hf magnetoacoustic wave, noting Doppler effect resonance splitting 08 p1212 A72-21070
- Two fluid MHD model to study cylindrical plasma condenser resonance properties in axial magnetic and alternating electric fields 09 p1360 A72-22952
- Electromagnetic waves penetration through magnetized plasma into lower hybrid resonance region examined in geometrical optics approximation 10 p1521 A72-24352
- Quadrupole probe theory for hot collisionless isotropic plasma, noting impedance dependence on electron temperature at resonance and optimum dimension relationship to Debye length 10 p1523 A72-24798
- Wave particle interaction around lower hybrid resonance frequency, deriving whistler mode wave growth rate during propagation in magnetoactive plasma penetrated by nonthermal particles 10 p1476 A72-24959
- Resonant three wave interaction in magnetized spatially uniform plasma under constant magnetic field 11 p1698 A72-26603
- Plasma ion heating by magnetoacoustic waves, presenting resonance peak-magnetic field intensity relations for various densities and ion energy 13 p2019 A72-29913
- Electric multipole moments calculation by quasi-static method for homogeneous quasi-neutral oblate plasmoid during resonance 13 p2020 A72-30014
- Nonlinear interaction of resonant plasma oscillations with nonresonant wave pulse, using water bag model of electron plasma 14 p2140 A72-30936
- Ionospheric plasma resonance time duration variation with latitude, altitude and ratio of electron plasma frequency to electron cyclotron frequency 15 p2223 A72-31429
- Cs plasma electron density radial distributions from resonance absorption in discharge tube 15 p2286 A72-32302
- Dispersion equations and resonant absorption of plane and cylindrical surface waves in transition layer between plasmas, noting Langmuir oscillations 15 p2286 A72-32385
- Singly ionized Ca and Mg electron impact broadened resonance lines from rapid scanning Fabry-Perot spectrometer measurements in shock tube generated high temperature plasma 15 p2282 A72-32643
- Field distribution and absorption coefficient calculations for normal incidence of extraordinary electromagnetic wave on linear plasma layer in hybrid resonance region 16 p2363 A72-33480
- Alouette 2 plasma resonances observation near ionospheric electron cyclotron frequency harmonics, interpreting frequency shift as wave dispersion effects 17 p2546 A72-34692
- The surface plasmon resonance effect in holography 17 p2553 A72-34723
- Electromagnetic waves penetration through magnetized plasma into lower hybrid resonance region examined in geometrical optics approximation 17 p2589 A72-34953
- Two fluid MHD model to study cylindrical plasma condenser resonance properties in crossed axial magnetic and alternating electric fields 17 p2593 A72-35881
- Amplitude limits to the theory of resonant absorption in cold plasmas 18 p2716 A72-36960
- Nonlinear saturation of the ion-acoustic instability 19 p2840 A72-37931
- VLF emission artificial triggering by whistler Morse pulses in magnetosphere, explained in terms of resonant trapped particle current and wave field behavior 20 p2903 A72-39549
- Resonances in the collisionless heating of a plasma by transit time magnetic pumping 21 p3094 A72-41631
- Absorption of an obliquely incident extraordinary wave in a weakly inhomogeneous plasma in the hybrid resonance region 21 p3095 A72-41694
- Electron density and temperature in microwave plasmas at higher pressures 22 p3211 A72-42479
- Electric multipole moments calculation by quasi-static method for homogeneous quasi-neutral oblate plasma spheroid during electromagnetic interaction under resonance conditions 22 p3212 A72-42729
- Transport of RF energy to the lower hybrid resonance in an inhomogeneous plasma 22 p3212 A72-42898
- Electronic density and temperature deduced from the observation of the cone of resonance of an antenna in a magnetoplasma 22 p3212 A72-43049
- Nonlinear evolution of a quasi-monochromatic packet of spiral waves in a plasma 23 p3318 A72-43324
- Symposium on Waves and Resonances in Plasmas, St. John's, Newfoundland, Canada, July 5-9, 1971, Proceedings 23 p3319 A72-43511
- Frequency dependent antenna impedance characteristics in ionospheric plasma, discussing anisotropic and isotropic electron plasmas, loop antennas resonance rectification and ion effects 23 p3319 A72-43512
- Plasma frequency, hybrid frequency and harmonized frequency electron resonances due to electrostatic waves in ionosphere observed with topside-sounders aboard rockets and satellites 23 p3263 A72-43513
- Midlatitude VLF emissions in magnetosphere due to plasma resonance instability near plasmopause, using ground, rocket and satellite observations, estimating electron energy 23 p3263 A72-43515
- Rocket observation of topside resonances 23 p3286 A72-44517
- Resonant diffusion in the presence of strong plasma turbulence 24 p3430 A72-45567
- PLASMA RINGS**
- U TOROIDAL PLASMAS**
- PLASMA ROCKETS**
- U PLASMA ENGINES**
- PLASMA SHEATHS**
- Flowing plasma ionization density measurement by stagnation probe, comparing measured with calculated plasma sheath convection current values [AD-738692] 01 p0110 A72-11189
- Ion transit time effects on plasma sheath RF admittance, using equivalent circuits for representation in low and high frequency ranges 03 p0394 A72-13150
- Filamentary magnetic structure production on plasma current sheath of coaxial deuterium operated accelerator for laboratory observations of solar flare processes 03 p0411 A72-13338
- Transient response of negatively biased Langmuir probes for planar and cylindrical plasma sheaths under large amplitude pulsed potentials [AD-739787] 03 p0361 A72-13924
- Rectangular slot antennas radiation through inhomogeneous plasma layer with dielectric window, obtaining input admittances by fields modal expansion 04 p0554 A72-14412
- Plasma sheath drift origin of hot ions in modified Penning discharge 04 p0551 A72-14439
- Spacecraft reentry communications, discussing plasma sheaths, blackout alleviation and flight experiments 05 p0628 A72-16562
- Parallel current and sheath effects on collisional drift waves normal mode structure in Q machines with

- end plates, using slab plasma model with uniform magnetic field 07 p1042 A72-19511
- X ray spectrum analysis of Sco XR-1 sources, showing plasma sheath with high electron temperature 07 p1076 A72-19804
- Far field radiation pattern from magnetic line source covered with moving uniaxial or isotropic nondispersive dielectric or cold plasma sheaths 08 p1137 A72-21985
- Potential distribution in positive ion sheath around plane Langmuir probe immersed in plasma 08 p1215 A72-22074
- Collisionless plasma spherical probe RF sheath model based on quasi-static approximation and electrostatic theory 09 p1365 A72-23520
- Input impedance of plane antenna immersed in plasma within magnetic field and propagating sheath waves 10 p1520 A72-24132
- Nonlinear sheath admittance, currents and charges associated with high peak voltage drive on VLF-ELF dipole antenna moving in ionosphere 11 p1599 A72-26769
- Plasma sheath from plane negatively biased electrode immersed in low pressure discharge investigated by ion acoustic waves and hot probe 12 p1850 A72-27279
- Theory of magnetotail elongation based on magnetosphere neutral layer drift notion due to electric current from trapped charge carriers inside surrounding plasma sheath 12 p1802 A72-27770
- Viscous shock layer analysis application to blunt nosed reentry vehicle plasma layer nonequilibrium flow species distribution, considering electron density [AIAA PAPER 72-689] 16 p2346 A72-34053
- Report on photo-sheath calculations for the satellite GEOS. 17 p2553 A72-34629
- Sheath effects and related charged-particle acceleration by Jupiter's satellite Io. 17 p2611 A72-35320
- X ray spectrum analysis of Sco X-1 type sources, showing plasma sheath with high electron temperature 17 p2617 A72-35727
- Measurements of the plasma sheath capacitance using a simple tunnel diode oscillator. 17 p2558 A72-35847
- High-voltage thermionic reactor using double-sheath fuel elements. 18 p2644 A72-36171
- Prediction of electron concentration reductions in re-entry flow fields due to electrophilic liquid and water injection. 18 p2730 A72-36537
- About the interaction between a satellite and its environmental ionospheric plasma. 21 p3090 A72-40454
- Admittance measurements of a 36-m dipole antenna in the topside ionosphere. 22 p3153 A72-42007
- Theoretical study and wind tunnel simulation of the electrical phenomena of reentry 22 p3231 A72-43092
- Isolated finite amplitude electrostatic oscillations production in thin plasma layer between two parallel metallic surfaces in magnetic field 23 p3317 A72-43204
- Plasma sheet variations during substorms. 24 p3396 A72-44851
- Anode sheath plasma current instabilities, examining electron and ion turbulent heating, plasma particle limiting energies and unsteady oscillation spectra 24 p3429 A72-45490
- ## PLASMA SLABS
- Pseudowave front spreading at leading edge of plasma slab during injection at high velocity into denser background plasma 02 p0265 A72-12364
- Circularly polarized electromagnetic wave propagation through afterglow helium slab plasma near electron cyclotron frequency 02 p0266 A72-12653
- Electromagnetic impulse wave impingement on semiinfinite isotropic plasma slabs with arbitrary incidence angle and polarization, calculating signal reflection in terms of Bessel functions 08 p1137 A72-21990
- Obliquely incident electromagnetic waves reflection and transmission by moving compressible plasma slab, applying field and wave-four vectors Lorentz transformations to wave equations 13 p2010 A72-28543
- Electrostatic cyclotron harmonic waves propagation in inhomogeneous electron plasma slab, deriving RF electric field 14 p2138 A72-30397
- Infinite cross section electron beam interaction with infinite turbulent plasma slab with finite thickness 16 p2438 A72-33837
- Radiation from a magnetic line source covered with an anisotropic warm plasma slab. 17 p2587 A72-34386
- Amplitude limits to the theory of resonant absorption in cold plasmas. 18 p2716 A72-36960
- Equilibrium configurations of Vlasov plasmas carrying a current component along an external magnetic field. 19 p2839 A72-37332
- Electromagnetic wave propagation in a moving sinusoidal stratified turbulent plasma medium. 21 p3093 A72-41323
- Effects of parallel wavelength on the collisional drift instability. 21 p3093 A72-41627
- ## PLASMA SOUND WAVES
- ## U MAGNETOHYDRODYNAMIC WAVES
- ## U PLASMA WAVES
- ## PLASMA SPECTRA
- Laser spark plasma initial development phase showing high electron temperature and concentration, continuous spectrum emission, line broadening and shock wave formation 02 p0237 A72-11405
- High speed photographs of plasma emission spectra in UV and soft X radiation spectrum regions, discussing theory, design and operation of facilities 02 p0223 A72-11408
- Electron impact broadening of ionized Be and Ba lines in electric shock tube plasma, measuring electron density and temperatures 03 p0393 A72-13020
- Three frequency radar spectral measurements of two stream and gradient plasma instabilities in equatorial electrojet as function of wavelength 03 p0349 A72-13521
- Plasma line enhancement variabilities in ionospheric modification experiments due to radar wave scattering, number density gradient and diagnostic beam temperature and orientation 06 p0805 A72-17470
- Soviet book on turbulent plasma theory covering stationary-turbulence spectra, instabilities, electromagnetic properties and wave propagation, particle stochastic acceleration, turbulent heating, etc 06 p0863 A72-18522
- Far UV Al line spectra from laser produced plasma in 35-50 A range 07 p1038 A72-19835
- Plasma lf waves nonlinear spectral broadening in magnetic field based on degeneracy splitting 07 p1045 A72-20443
- Spectrum of hot hydrogen plasma continuum radiation, discussing models for Scorpius X-1 source and inhomogeneous clouds 09 p1391 A72-23536
- Plasma spectral absorption coefficients determination by organic dye laser with tunable radiation frequency 13 p2015 A72-29504
- Adiabatic characteristics of impact to quasi-static transition during electron induced Stark hydrogen line broadening in plasmas 13 p2016 A72-29516
- Carbon dioxide arc plasma emissivity in visible range at atmospheric pressure and 6500-9500 K, discussing diatomic carbon concentration 13 p2016 A72-29520
- Solar plasmas intensity ratios of He-like ion line emission, showing dependence on atomic number and electron temperature 13 p2018 A72-29737
- Ion sound turbulence in dense plasma within magnetic field, representing global equilibrium spectrum 14 p2137 A72-30356
- Plasma emission spectrum of circulating and sealed carbon dioxide molecular laser, discussing concentration dependencies 14 p2110 A72-30786
- Ionized plasma line widths and intensities due to Landau and collisional damping, observing effects by light scattering techniques 14 p2140 A72-30901
- Ar plasma radiation dispersion by plane grating, measuring ionic spectral lines and continuous spectrum intensity time variation 15 p2286 A72-32340
- Electron beam-plasma system oscillation spectrum control through modulation by external HF signal, discussing theory and experimental verification 15 p2289 A72-32671
- Toroidal plasma spectroscopic investigation from current pulse start to afterglow, noting electron temperature and density radial distributions and energy balance 17 p2591 A72-35373
- Spectral intensity measurements from high-pressure nitrogen plasmas. 19 p2840 A72-37836
- Heat-pipe plasma oven for microwave and spectroscopic measurements. 20 p2912 A72-39433
- Estimation of the mass composition and energy spectrum of a plasma jet from a conical pulsed accelerator 21 p3089 A72-40134
- Electron impact effects on Ba I, Ba II and Sr I selected spectral line Doppler widths calculated for laser-generated plasmas for chemical release simulation 21 p3092 A72-40821
- Application of holographic Fourier spectroscopy to the analysis of the microwave radiation spectrum 21 p3058 A72-41733
- Recombination continuum in a lithium plasma spectrum 22 p3210 A72-42171
- Spectroscopic study of the parameters of a turbulent plasma 22 p3213 A72-43107
- Determination of magnetic fields in plasmas from hydrogen spectral line profiles 23 p3318 A72-43313
- New lines of neon ions in the range 50-200 A. 23 p3315 A72-43802
- Magnetic pulsation spectra in a nonisothermal plasma 23 p3323 A72-44483
- Excitation mechanisms in the argon-ion spectrum at near laser conditions and temperatures and densities in a hollow cathode argon-arc discharge. 24 p3428 A72-44807
- Determination by the scattering method of the parameters of a plasma produced by a laser spark in air 24 p3429 A72-45496
- ## PLASMA SPRAYING
- Metal matrix fabrication processes, considering plasma sprayed and diffusion bonded tapes and consolidated sheet material 01 p0074 A72-10733
- Plasma arc testing of space shuttle Nb and Co alloys thermal protection materials, using IR radiometric and photographic techniques 01 p0048 A72-10977
- Plasma sprayed tungsten and zirconium dioxide coatings porosity on chromium bronze, Ti and Al alloys and steel 03 p0363 A72-13550
- Low cost metal matrix composition fabrication techniques, considering plasma spraying and continuous casting 03 p0364 A72-14236
- Sputtering sources fabrication by plasma spraying for nitride films deposition with Ta-Hf mixtures 04 p0527 A72-15494
- Composite plasma sprayed coatings of Cu, Ni and boron nitride, noting antifriction and wear characteristics 06 p0822 A72-18429
- Plasma spraying process effects on carbon steel coatings structure and bonding, considering optimal parameters, properties control and phase transformations 07 p0996 A72-19966
- Plasma spraying of high temperature resistant powder materials, investigating feed rate effect on particles adhesion and deposition layer properties 08 p1175 A72-21046
- Plasma coating formation mechanisms and parameters, studying metal surface and deposited particles temperatures, spraying time effects, etc 10 p1487 A72-24488
- Semiconductor materials etching and surface coating with protective silicon dioxide film in low temperature oxygen plasma 11 p1700 A72-25777
- Velocity and temperature attenuation of argon and nitrogen jets expelled from plasma spray guns into physically identical ambient medium 13 p2011 A72-28920
- Re applications technology, discussing production methods, mechanical and physical properties, plasma spraying, annealing and alloying techniques 17 p2567 A72-34825
- Variables influencing the characteristics of plasma-sprayed coatings. 17 p2561 A72-35920
- Effect of structural parameters and temperature on the effective thermal conductivity of plasma-sputtered aluminum oxide 18 p2696 A72-37188
- Structural features of plasma and gas-flame deposited aluminum oxide coatings 19 p2810 A72-38680
- Fabricating aluminum matrix composites. I - A survey of aluminum matrix composites. 22 p3182 A72-41996
- Feeder for the supply of powder materials to spraying setups 23 p3278 A72-43293
- ## PLASMA STABILITY
- ## U MAGNETOHYDRODYNAMIC STABILITY
- ## PLASMA TEMPERATURE
- Warm inhomogeneous plasma models perturbation analysis, computing high frequency oscillation and eigenfrequencies and eigenfunctions formulas 01 p0106 A72-10134

Two dimensional plasma under dc magnetic field, investigating thermal equilibrium with Liouville equation and BBGKY hierarchy

01 p0107 A72-10145

Collisionless plasma shock wave measurements in magnetic field, determining plasma temperature and free electron densities

01 p0108 A72-10236

Optimal conditions for energy conversion in MHD generator, observing ion seeding effect on plasma temperature

01 p0009 A72-11207

Plasma temperature and seed atom concentration in MHD generator ducts and combustion chambers by optical measurements, discussing boundary layer thickness, optical density, etc

01 p0072 A72-12118

Plasma ion temperature and neutral collision frequency determination by Langmuir probes [AD-739452]

02 p0264 A72-12262

Plasma waves maximum radiation temperatures near fundamental and second harmonic electron frequency

02 p0265 A72-12308

Radiative heat transfer within nonisothermal air plasma, presenting centerline temperature data for various boundary pressures and temperatures [ASME PAPER 71-HT-G]

02 p0302 A72-12316

Electron temperature measurements in ionospheric isotropic nonequilibrium plasma by electrostatic probes and radar backscatter

03 p0349 A72-13520

Mathematical model for two-stream instability induced anomalous resistivity and heating in plasma with equal initial electron and ion temperatures in static electric field

04 p0554 A72-14402

Force free high beta plasma stability in homogeneous magnetic field and with inhomogeneous temperature and density

04 p0554 A72-14408

Direct display plasma density and temperature meter, using floating double probe method

04 p0520 A72-14533

Continuously burning optical discharge in Ar and Xe at atmospheric pressures, evaluating laser beam energy absorption, electron density and plasma temperature

05 p0669 A72-16679

Temperature inhomogeneity effect on plasma column microwave resonant behavior in presence of axial magnetic field, ascribing spectral shifts to electron density and temperature profiles changes

06 p0854 A72-17417

Electrostatic wave instabilities at harmonics of electron cyclotron frequency in hot and cold anisotropic plasma with Maxwellian temperature distribution

07 p1039 A72-18824

Structural interactions between magnetosphere and ionosphere in terms of electrostatic field associated with plasma temperature difference

07 p0979 A72-20046

Solar coronal plasma radiative capacity and temperature structure from cooling function in thermal balance equation

08 p1231 A72-21124

Steady flow of dual temperature plasma into vacuum from widening nozzle, taking into account electron thermal conductivity and heat exchange between components

08 p1214 A72-21653

Reference electrode area and floating potential influence in Langmuir probe measurements of plasma density and temperature

09 p1311 A72-23229

Flat plate Langmuir probe measurement of electron temperature in plasma with elliptically anisotropic velocity distribution, discussing probe orientation effects

09 p1366 A72-23578

Zero temperature relativistic plasma ground state energy calculation using Fermi momentum and Green function

11 p1694 A72-25715

Temperature anisotropy quasi-linear relaxation thermodynamics in collisionless plasma, analyzing system free energy

11 p1698 A72-26599

Electrical conductivity measurement of dense nonideal Cs plasma at high pressure and temperatures

12 p1849 A72-27057

Statistical analysis of spectrographic plasma temperature measurements, obtaining numerical solution to Abel integral equation

12 p1852 A72-27685

Growth rates of unstable electromagnetic waves propagating perpendicularly to symmetric counterstreaming finite temperature plasmas

13 p2012 A72-29129

One dimensional unsteady flow of dense magnetized plasma, investigating time evolution of temperature profile in wall layer and thermal conductivity

13 p2018 A72-29876

Pulsed laser plasma temperature determination by radiation measurements in X ray and visible spectral regions using foil method

13 p2018 A72-29887

Electric arc plasma, predicting elements addition and electron density alteration effects on radial temperature distribution

14 p2139 A72-30778

Electric arc plasma, investigating reaction energy effects on radial temperature distribution

14 p2139 A72-30779

Pulsed Ar plasma temperature and charged particle concentration obtained as functions of elapsed discharge time by spectroscopic observation

14 p2139 A72-30780

Ar plasma spectral lines, calculating temperature functions of excitation to fourth ionization multiple at atmospheric pressure

14 p2139 A72-30782

Soft X ray emission for plasma temperature determination in laser induced gas breakdown for air and He

14 p2139 A72-30805

Two counter streaming plasmas with anisotropic temperatures, deriving instability condition for ordinary mode electromagnetic propagation perpendicular to external magnetic field

14 p2140 A72-30935

Direct display plasma density and temperature meter with Langmuir probe for ionospheric observation

15 p2231 A72-32338

Glow mode electron plasma source for space chamber, measuring electron density and temperature for comparison with back diffusion sources

15 p2286 A72-32339

Finite beta plasma drift cone instability relationship to mirror ratio and plasma temperature changes

15 p2288 A72-32422

Laser heating of two temperature plasma based on conductive heat transfer, taking into account nuclear fusion energy

16 p2434 A72-32876

Alfven wave firehose instability relaxation calculation to include nonlinear terms for explanation of solar wind temperature anisotropies by collisionless mechanism

16 p2449 A72-33933

Resonant diffusion in strongly turbulent plasmas, deriving equations for evolution of macroscopic properties including temperature and flow speed

16 p2439 A72-33934

Steady state magnetically balanced cross flow arc, calculating flow and temperature fields and boundary shape under assumption of two independent variables [AIAA PAPER 72-687]

16 p2439 A72-34055

Optically thick plasma temperature profile determination by extended brightness emissivity method

16 p2440 A72-34100

Flare-time temperature in soft X-ray sources

17 p2598 A72-34537

Effect of ionic viscosity on the stability of a finite-pressure plasma

19 p2842 A72-38529

On the physical nature of cosmic electromagnetic absorption. V - The Einstein-de Sitter cosmology with plasma coupled to radiation at non-relativistic temperature

20 p2967 A72-39185

On the physical nature of cosmic electromagnetic absorption. VI - The Einstein-de Sitter cosmology with plasma coupled to radiation at relativistic temperature

20 p2967 A72-39186

Caloric state equation for isentropes and temperature calculation of nonideal Cs plasma produced in high density vapors by shock wave compression

23 p3318 A72-43320

A current instability in the neutral layer of the tail of the earth's magnetosphere

23 p3283 A72-43368

Spatial and temporal temperature distribution in plasma from a low-voltage aperiodic spark discharge in an atmosphere of argon

23 p3320 A72-43677

Averaged equations of laser heating of two-temperature plasma in a focus-type system taking into account the heat of nuclear fusion

23 p3322 A72-44224

Temperature of a free plasma filament in a high-frequency field at high pressures

23 p3322 A72-44464

Pressure, temperature, current density, and potential difference fluctuations in subsonic flow of combustion products plasma, noting steadiness, ergodicity and distribution functions

24 p3429 A72-45502

Electrical conductivity measurement of dense nonideal Cs plasma at high pressure and temperatures

24 p3431 A72-45710

PLASMA THEORY
U PLASMA PHYSICS

PLASMA TURBULENCE

LF large scale oblique Alfven wave propagation in turbulent ion acoustic plasma, investigating dispersion relation, Landau damping and interactions

01 p0107 A72-10137

Electrostatic potential fluctuations spectrum in turbulent hot ion plasma confined between magnetic mirrors, investigating mode coupling, energy cascading and electron concentration

01 p0108 A72-10242

Propagators in strong plasma turbulence, considering characteristic trajectories of Vlasov equation

01 p0109 A72-10244

Modified Born approximation for electromagnetic backscattering cross section from turbulent plasmas noting attenuation leading to saturation and cross polarization

01 p0031 A72-10846

Signal modification of microwaves propagating transversely in underdense turbulent plasma jet

02 p0265 A72-12365

Diffuse plasma resonances in space interpreted by wave-particle nonlinear interaction in weakly turbulent plasma, considering electrostatic electron cyclotron wave instability

02 p0265 A72-12366

Weakly turbulent plasma wave system, obtaining drift solution for stationary distribution stability

03 p0394 A72-13274

Hf plasma turbulence in solar flares due to nonlinear conversion of ion-acoustic plasmons to Langmuir plasmons

03 p0413 A72-13812

Transverse shock waves fine structure and saturation of ion-acoustic turbulence in collisionless plasma, using magnetic field probe and MHD equations

03 p0399 A72-14068

H beta satellites observation in presence of oscillating electric field associated with plasma turbulence [AD-741085]

04 p0555 A72-14576

Stark contours of hydrogen spectral lines in turbulent plasma with high noise level due to hf Langmuir oscillations

04 p0557 A72-14986

Plasma ion collision transport analogy with turbulent velocity space momentum transfer, explaining confined plasma runaway electron absence in strong electric fields

04 p0560 A72-15469

Relativistic electron pitch-angle diffusion driven by oblique lf whistler-mode turbulence in collisionless plasma immersed in static magnetic field

05 p0699 A72-17024

Electrostatic shift and broadening of Landau resonance by particle-wave interaction in turbulent plasmas

05 p0700 A72-17231

Soviet book on turbulent plasma theory covering stationary-turbulence spectra, instabilities, electromagnetic properties and wave propagation, particle stochastic acceleration, turbulent heating, etc

06 p0863 A72-18522

Plasma turbulent heating effectiveness by longitudinal ion current in mirror machine, determining hot ion lifetime and energy distribution function

07 p1039 A72-18913

Continuum plasma turbulent boundary layer structure in shear flow, showing electron to ion saturation currents ratio decrease from laminar case

07 p1040 A72-18953

Small scale phase space density granulations/clumps in turbulent plasma due to fluctuating electric field

07 p1041 A72-19510

Supraluminous wave instability in weakly turbulent plasmas, using Vlasov equations

07 p1043 A72-19619

Turbulent heating arc plasma voltage and current digital measurement recording, computing time dependent resistivity

07 p1045 A72-20400

Ion-sound plasma turbulence theory, considering collisionless shock waves data and anomalous resistivity calculations

07 p1045 A72-20480

Quasi-linear theory validity for turbulent collisionless plasmas, considering bump-in-tail and weak symmetric two-stream instabilities

07 p1045 A72-20481

Growth rate estimation of negative energy Bernstein and ion acoustic waves explosive interaction, noting collisionless shock turbulence

08 p1212 A72-21248

Turbulized combustion product plasma electrical conductivity, noting temperature dependent variation

08 p1214 A72-21649

Self consistent collisionless theory of turbulent low Mach number ion-acoustic shocks, noting resistive heating

09 p1360 A72-22872

Turbulent plasma electric field energy density spectrum from statistical mechanics investigation based on canonical formalism for electron plasma

12 p1851 A72-27387

Book on nonlinear coherent and turbulent collisionless plasma theory covering collective /wave-particle and wave-wave/ interactions and mathematical methods
13 p2011 A72-29099

Experimental investigation of toroidal discharge electrostatic potential fluctuations in turbulently heated plasma, discussing correlation with effective conductivity
13 p2012 A72-29122

Electron density effect on microwave scattering from turbulent plasma, observing change from volume to surface scattering at critical density value
13 p2012 A72-29130

Ionization turbulence effect on nonequilibrium plasma MHD generator performance, using I-V characteristics equation
13 p1900 A72-29354

Random phase approximation for nonlinear theory of MHD nonequilibrium plasma steady turbulent regime, noting ionization level rise by energy dissipation
13 p2013 A72-29359

Large amplitude interplanetary solar wind discontinuities observed by OGO-5 plasma spectrometer and magnetometers, considering magnetic drift waves mechanism for plasma turbulence generation
13 p2031 A72-29378

Carbon dioxide laser light scattering measurements of turbulence in high beta collisionless plasma shock wave
13 p2018 A72-29853

Ion-acoustic oscillations effect on turbulent plasma electric conductivity within weak external electric field
13 p2019 A72-29990

Ion sound turbulence in dense plasma within magnetic field, representing global equilibrium spectrum
14 p2137 A72-30356

Helicon /whistler/ turbulence spectra in collisionless plasma due to ion scattering, considering self trapping and stability along magnetic field with Landau absorption decay
14 p2137 A72-30357

Waves and particles interaction in weakly turbulent collision-free Vlasov plasma under pure Coulomb interaction and zero magnetic field
14 p2140 A72-30937

Kinetic equations for turbulent magnetized plasma, considering wave-wave interactions and wave energy in terms of second order Markov differential equation
14 p2141 A72-30940

Turbulent plasma dynamo mechanisms of magnetic field origin in astrophysics, noting Steenbeck and Parker theories
14 p2162 A72-31150

Langmuir waves scattering by denser plasma ions as dominant turbulent process momentum exchange between dynamic plasmas, applying to galaxies expansion into intergalactic media
15 p2285 A72-32269

Singly scattered radiation in weakly inhomogeneous turbulent plasma for incidence angles greater than critical angle, calculating backscattered wave depolarization from radiative transport equation
15 p2288 A72-32425

Turbulent heating and resistivity in cool electron theta pinches due to IF long wavelength modified two stream and drift instabilities
15 p2288 A72-32426

Infinite cross section electron beam interaction with infinite turbulent plasma slab with finite thickness
16 p2438 A72-33837

Conservation equations for wave and/or turbulence momentum and energy flux in interplanetary space shock vicinity, developing modifications for electron temperature calculations
16 p2459 A72-33913

MHD fluid model for collisionless shock waves in turbulent plasma with enhanced transport coefficients, noting laboratory experiments and satellite and radio observations
16 p2439 A72-33932

Resonant diffusion in strongly turbulent plasmas, deriving equations for evolution of macroscopic properties including temperature and flow speed
16 p2439 A72-33934

Wave propagation in a stratified turbulent magnetized plasma. I.
17 p2587 A72-34516

Flow conditioning in electric discharge convection lasers.
17 p2562 A72-34638

Combustion product plasma electrical conductivity dependence on neutral component density fluctuation
17 p2590 A72-35136

Plasma turbulence in solar atmosphere upper layers related to chromospheric flares and radio bursts
17 p2612 A72-35349

Turbulence of electrostatic electron cyclotron harmonic waves observed by Ogo 5.
17 p2549 A72-35599

Phenomenological model for incoherent microwave scatter attenuation from turbulent plasma, establishing

relation between plasma parameters and attenuation coefficient
17 p2517 A72-35622

Structure of the power-law spectra of relativistic electrons in a turbulent plasma
17 p2593 A72-35907

Two dimensional turbulence model for charge fluctuations statistical mechanics of nonlinear guiding center plasma
18 p2714 A72-36014

Turbulent heating of electrons and ions in a collisionless shock wave.
18 p2715 A72-36599

Study of the mechanism of motion of nonequilibrium plasma inhomogeneities in a magnetic field
18 p2717 A72-37176

High power pulsed HCN laser.
19 p2811 A72-37583

Decay of pregalactic vortex motions
19 p2862 A72-38057

Markovian plasma turbulence model to obtain convergent perturbation series for diffusion coefficient via trajectories in particle propagator
19 p2841 A72-38442

Nonlinear theory of density fluctuations in turbulent plasmas.
19 p2841 A72-38443

Plasma turbulent heating effectiveness by longitudinal ion current in mirror machine, determining hot ion lifetime and energy distribution function
20 p2957 A72-39379

Plasma low density regions caused by Langmuir turbulence, discussing energy dissipation of long wave oscillations and wave collapse
21 p3090 A72-40410

Nonlinear magnetosonic waves in a plasma with a finite conductivity.
21 p3090 A72-40485

The study of turbulence in theta-pinch plasma with azimuthal magnetic field.
21 p3091 A72-40571

Identification of transverse Kelvin-Helmholtz turbulence in a magnetoplasma column.
21 p3091 A72-40768

Low frequency electrostatic waves in a turbulent plasma.
21 p3092 A72-41221

Electromagnetic wave propagation in a moving sinusoidal stratified turbulent plasma medium.
21 p3093 A72-41323

Radiative transport analysis of electromagnetic propagation in isotropic plasma turbulence.
21 p3094 A72-41634

Turbulent plasma 'caldrons' in galactic nuclei
21 p3114 A72-41772

Application of multiple-scattering theory to the derivation of kinetic equations for waves in a weakly turbulent plasma
22 p3212 A72-42665

Spectroscopic study of the parameters of a turbulent plasma
22 p3213 A72-43107

Particle distribution function evolution effect on turbulent plasma heating by wave interaction, considering stochastic heating of ions
23 p3318 A72-43314

Ray structures of polar auroras and their association with drift-current instability in a plasmoid
23 p3282 A72-43358

Generation threshold of anomalous resistance for longitudinal currents in the magnetosphere
23 p3284 A72-43379

Physical processes of weak, single wave and strong plasma turbulence and instabilities driven by oscillating fields
23 p3319 A72-43514

Direct and cross polarized backscatter power from a turbulent plasma.
23 p3320 A72-43521

Weak electrostatic turbulence observation in earth bow shock magnetic field gradient, suggesting cyclotron drift instability role
23 p3342 A72-44523

Steady-state distribution of the charged and neutral particle concentration in a bounded high-temperature turbulent plasma
24 p3429 A72-45493

Resonant diffusion in the presence of strong plasma turbulence.
24 p3430 A72-45567

Wave growth in a strongly turbulent plasma.
24 p3430 A72-45568

PLASMA WAVES

NT ELECTROSTATIC WAVES

Collisionless plasma shock wave measurements in magnetic field, determining plasma temperature and free electron densities
01 p0108 A72-10236

Energy and momentum transfer between fields and particles in plasma crossed by transverse electromagnetic wave, investigating MHD stability
01 p0109 A72-10884

Pioneer 8 plasma wave measurements at distant bow shock crossings, considering solar wind-magnetosheath interaction
01 p0062 A72-10903

Electromagnetic waves diffusion by space-time fluctuations in plasma electron density [ONERA, TP NO. 1043]
01 p0110 A72-11180

Antenna If impedance measurements of lower terrestrial plasma wave characteristics, using equivalent impedance probe circuit
02 p0172 A72-11946

Nonuniform plasmas resonant wave-particle interactions, using linearized Vlasov equation
02 p0264 A72-12119

Plasma waves maximum radiation temperatures near fundamental and second harmonic electron frequency
02 p0265 A72-12308

Pseudowave front spreading at leading edge of plasma slab during injection at high velocity into denser background plasma
02 p0265 A72-12364

Decay interactions among plasma wave and two opposed electromagnetic waves in homogeneous layer of isotropic collisionless plasma, observing stimulated Raman scattering
02 p0180 A72-12579

Gyroresonance plasma wave absorption in corona, investigating solar radio bursts fine structure
03 p0415 A72-12935

Rain type periodic solar radio bursts interpreted on basis of stream instability pulsating regime, considering plasma waves excitation
03 p0406 A72-12936

Weakly turbulent plasma wave system, obtaining drift solution for stationary distribution stability
03 p0394 A72-13274

Argon plasma electromagnetic wave transformation and absorption measurements under various gas pressures
03 p0395 A72-13571

Self consistent kinetic equations for evolution of particle distribution functions and wave intensity spectra of relativistic spatially homogeneous multisppecies plasma in ambient magnetic field
04 p0553 A72-14401

Plasma shock wave oscillation profile dependence on ion and electron friction and viscosity
04 p0555 A72-14620

Density waves propagation and amplification in p-InSb electron-hole plasmas, investigating dependence on frequency and injection level
04 p0561 A72-14851

Dispersion relation for MHD wave propagation through partially ionized magnetoplasma, discussing collision frequencies effects
04 p0556 A72-14943

Coulomb collisions nonlinear effects on Landau damping of weakly damped plasma electron wave
04 p0559 A72-15347

High beta plasma If wave parallel propagation to equilibrium magnetic field, deriving large scale length perturbations from coupled nonlinear partial differential equations
04 p0559 A72-15349

Self focusing of electromagnetic waves in isotropic plasma, investigating nonlinear relaxation processes
04 p0489 A72-15391

Self consistent theory of waves in fluctuating plasma, discussing Klimontovich-Maxwell electromagnetic field equations uniqueness solution and kinetic equation
04 p0493 A72-15449

Plasma oscillations stabilization, considering nonlinear effects in phase velocity of plasma waves
05 p0695 A72-16416

Electron heating model in perpendicular collisionless plasma shock waves based on electron trapping by turbulent electric field
05 p0697 A72-17014

Nonlinear MHD wave trains in cold collisionless plasma investigated by numerical and analytical methods
05 p0698 A72-17018

Dispersion properties of drift waves in low-beta weakly collisional plasma in presence of ion acoustic or Langmuir waves parallel to magnetic lines
05 p0698 A72-17019

Dispersion relations for frequencies near first two harmonics of perpendicular magnetosonic waves in relativistic anisotropic plasmas
05 p0698 A72-17020

Longitudinal electrostatic waves in perpendicular collisionless plasma shock, investigating stability
05 p0698 A72-17021

Dispersion relation for electrostatic plasma waves propagation at frequencies near electron cyclotron harmonics in warm magnetoplasma, determining refractive index curves
05 p0698 A72-17023

Acoustic waves generation in afterglow of weakly ionized low pressure He plasma, using electrostatic probe
05 p0699 A72-17083

Hot plasma transverse and longitudinal wave parametric excitation by intense laser light near plasma frequency, noting instability role in resonant coupling mechanism

05 p0699 A72-17172

Perturbation theory, saturation and relaxation effects in electron and ion plasma wave echoes

05 p0699 A72-17220

Ion-acoustic waves and ionization waves instabilities in gas discharge plasmas

05 p0699 A72-17222

Coupled longitudinal and transverse plasma waves propagating normal to applied magnetic field, using three fluid model

05 p0700 A72-17230

Electrostatic waves perturbed distribution function behavior in presence of forced oscillations, considering Maxwellian ion and electron plasma waves excited by dipole

06 p0855 A72-17508

Non-Maxwellian plasma response to acoustic wave propagation in single ended Q device, investigating ion distribution function

06 p0855 A72-17509

Single-ended Q machine grid-excited density perturbation and ion wave propagation properties from linearized Vlasov equations

06 p0855 A72-17514

Ion density perturbations propagation through plasma with double-humped Maxwellian ion velocity distribution in single-ended Q machine

06 p0855 A72-17515

Ion acoustic wave excitation in plasma by modulated energetic electron beam, compared with grid excitation

06 p0856 A72-17519

Wake behind body moving in plasma parallel to magnetic field, observing coupling with parallel ion acoustic waves and with perpendicular Bernstein modes

06 p0875 A72-17525

Wave induced Q machine cesium plasma loss produced by current-driven collisional drift instability

06 p0857 A72-17527

Linear dispersion relation for pressure gradient driven drift waves instabilities from ion and electron thermal conductivity effects in collisional plasma

06 p0857 A72-17529

Spontaneous collisionless drift waves due to pressure gradient in hydrogen plasma column, studying magnetic field and reflecting conditions effects

06 p0857 A72-17534

Collisionless drift waves in thermally ionized Li plasma column under variable shear magnetic field

06 p0857 A72-17535

Normal mode solutions for bounded systems from linear dispersion roots, discussing plasma waves and instabilities and damping effects in Q machines

06 p0858 A72-17537

Electron plasma wave echoes experimental investigation, discussing amplitude decay under plasma and random noise influence

06 p0858 A72-17538

Plasma wave growth from large diameter electron beam interaction with quiet collisionless unmagnetized discharge plasma, measuring linear dispersion properties

06 p0858 A72-17539

Acquisition and processing of plasma fluctuation data using fast Fourier transform analog-digital spectral analysis technique

06 p0859 A72-17548

Stratified anisotropic multifluid plasma wave propagation from transverse field equations, using Green function and Fourier transform method

06 p0773 A72-17597

Ion heating caused by ion acoustic waves in ion streaming argon plasma

06 p0860 A72-17746

Ion acoustic and cyclotron harmonic plasma waves parametric excitation by hf electric field, measuring thresholds and growth rates agreeable with theory

06 p0861 A72-17827

Two fluid plasma longitudinal ion and electron waves nonlinear interactions excitation of type 2 bursts, considering radiation flux density

06 p0862 A72-18175

Soviet book on turbulent plasma theory covering stationary-turbulence spectra, instabilities, electromagnetic properties and wave propagation, particle stochastic acceleration, turbulent heating, etc

06 p0863 A72-18522

Fast ionization fronts ahead of laser produced plasma expansion into low density gas, noting Langmuir probe and microwave diagnostics indication of photoionization density augmentation

06 p0864 A72-18532

Low frequency drift instability in local electron cyclotron resonance produced plasma, discussing oscillation fundamental frequency characteristics, wave propagation, density and potential waves, etc

07 p1039 A72-18799

Nonlinear monochromatic Alfvén wave propagation parallel to magnetic field in anisotropic plasma with long wavelength beam instability

07 p1039 A72-18915

Nonlinear Landau damping of longitudinal plasma waves in dc magnetic field, obtaining wave-particle interactions from Vlasov equation by perturbation theory and method of characteristics

07 p1041 A72-19505

Nonlinear Landau damping and growth of finite amplitude cyclotron harmonic plasma waves in magnetic field, measuring coupling coefficients by calibrated interferometer

07 p1041 A72-19506

Ion-acoustic solitary waves formation and interaction in collisionless warm plasma, using Vlasov equation for ions and Boltzmann distribution for electrons

07 p1041 A72-19507

Parallel current and sheath effects on collisional drift waves normal mode structure in Q machines with end plates, using slab plasma model with uniform magnetic field

07 p1042 A72-19511

Dispersion relation for uhf drift waves in nonuniform plasma with cold electrons drift through stationary ions, deriving plasma stability conditions

07 p1042 A72-19612

Stationary high beta plasma shock waves generated in plasma wind tunnel by impinging on magnetic field, comparing with earth bow shock

07 p1042 A72-19617

Supraluminous wave instability in weakly turbulent plasmas, using Vlasov equations

07 p1043 A72-19619

Electrostatically driven oscillations near lower hybrid resonance frequency in linear plasma device, measuring refractivity during wave propagation

07 p1043 A72-19664

Collisionless plasma electronic shock waves /stationary heat discontinuity/ observation, proving stationary shock wave existence

07 p1043 A72-19874

Solar radio bursts classification, discussing normal and magnetic bremsstrahlung and plasma waves conversion

07 p1079 A72-20012

Solar wind and geomagnetic tail interaction with moon, discussing lunar Mach cone evidence for anisotropic wave propagation in magnetized collisionless warm plasma

07 p1061 A72-20025

Plasma lf waves nonlinear spectral broadening in magnetic field based on degeneracy splitting

07 p1045 A72-20443

Drift waves propagation in ionized plasma, considering drift rate, ion sound phase velocity and effect of impurities

07 p1045 A72-20444

Reactive mechanism of nonlinear mixing in resonant excitation of ion plasma waves by vlf and whistler waves

07 p1046 A72-20540

Electronic correlator for plasma wave induced coherent signals cross correlation measurement, producing 1 microsecond time delays by automatically switching lumped circuit delay line

07 p0958 A72-20582

Hf potential effect on high amplitude waves propagation in magnetoactive plasma plane layer, noting particle density distribution

08 p1212 A72-21211

Electromagnetic wave polarization effect on linear transformation of waves in inhomogeneous magnetoactive plasma in magnetic field

08 p1212 A72-21245

Charge separation effects on plasma shock wave profile in perpendicular propagation to magnetic field, using moment equations derived from Boltzmann equations for electrons and ions [AD-742533]

08 p1213 A72-21254

Sound wave propagation in plasma, attributing acoustic cavity resonance curve sharpening to collisional energy transfer from electrons to neutrals

08 p1213 A72-21256

High energy electron beam interaction with dense plasma, investigating unstable waves growth by numerical methods

08 p1213 A72-21259

Population inversion in plasma via colliding waves generated by symmetric electrodeless electromagnetic shock tube

08 p1147 A72-21304

Slow and fast longitudinal ion acoustic waves in plasma cylinder under axial magnetic field

08 p1215 A72-21873

Electron Larmor radius effect on hf hose and mirror instabilities of fast magnetoacoustic and ion acoustic waves in nonisothermal plasma

08 p1215 A72-21874

Electrostatic plasma wave conversion into electromagnetic waves, calculating dispersion relation at all wavelengths for perpendicular propagation mode

08 p1137 A72-21989

Chemionization in oxyhydrogen plasma detonation waves

08 p1129 A72-22045

Effective transmission coefficient increase for Langmuir and electromagnetic waves passing through density barrier via perturbation transport by resonant electrons

08 p1216 A72-22090

Electron plasma oscillations distribution upstream from earth bow shock, evaluating OGO-E plasma wave detector data

09 p1300 A72-23019

Plasma injected into closed multipole magnetic trap, investigating plasma wave locking time and characteristic life

09 p1362 A72-23213

Electromagnetic and plasma wave reflection at interface between moving dielectric medium and compressible plasma

09 p1364 A72-23243

Inhomogeneous plasma effect on helical slow wave systems approximated by anisotropically conducting plane

10 p1522 A72-24518

Electromagnetic wave propagation and absorption in weakly inhomogeneous plasma layer, calculating conditions for transformation into plasma wave

10 p1523 A72-24799

Ion crystal plasma wave echoes from conduction electrons interaction with phonons in self consistent field

10 p1527 A72-24926

Linear wave dispersion in homogeneous beam plasma system, considering pressure anisotropies generated by external magnetic field

10 p1524 A72-24927

Vlasov perturbation theory of nonlinear plasma wave with Landau damping based on Korteweg-de Vries equation

11 p1692 A72-25517

Fast and slow ion acoustic free streaming wave propagation in drifting plasma, showing phase velocity and damping in agreement with Maxwellian distribution

11 p1692 A72-25518

Perturbation technique application to nonlinear behavior of ion waves produced by two-beam instability in plasma

11 p1692 A72-25519

Spatial distribution of electron beam excited plasma wave spectrum, determining wavenumber, amplitude and frequency by incoherent microwave scattering

11 p1693 A72-25564

Magnetoacoustic wave propagation and reflection in equilibrium inhomogeneous plasma under nonuniform magnetic field

11 p1695 A72-26094

Shock-induced flow acceleration in Ar plasma, studying shock front behavior from high-speed photographs

11 p1696 A72-26374

One dimensional time independent solution to Vlasov-Poisson system of nonlinear electrostatic plasma waves, noting Maxwell distributions for free and trapped particles

11 p1697 A72-26596

Bounded systems dispersion relations interpretation for plasma waves and instabilities on finite cylinders, with emphasis on end plate damping and axial current effects on Q machines

11 p1697 A72-26597

Nonlinear waves in nonuniform plasma, extending Butler and Gribbon formulation for Vlasov-Poisson equations

11 p1697 A72-26598

Resonant three wave interaction in magnetized spatially uniform plasma under constant magnetic field

11 p1698 A72-26603

Electromagnetic wave transformation and absorption in Ar plasma with nonmonotonic longitudinal density distribution

11 p1699 A72-26758

Nonlinear wave interaction in plasma with random inhomogeneities, using quasi-hydrodynamic approximation

12 p1849 A72-27062

Electron wave sideband frequencies and wave-trapped electron oscillations as cause of plasma instability

12 p1851 A72-27430

Compressible anisotropic magnetoplasma filled cylindrical waveguide excitation by electric dipole, plotting electric field patterns as function of electron temperature and density

12 p1782 A72-27489

Radiation patterns of circular loop antenna in isotropic compressible plasma, discussing far fields for electromagnetic and electron plasma waves

12 p1790 A72-27491

Plasma ionization traveling disturbances velocity and spatial structure in strong electromagnetic waves field

13 p1915 A72-28469

- Local perturbation generated waves in homogeneous plasma at rest subjected to uniform magnetic field 13 p2010 A72-28680
- Electromagnetic wave propagation in cylindrical plasma column of electrons and ions with and without applied uniform magnetic field in absence of collisions 13 p2010 A72-28681
- Book on nonlinear coherent and turbulent collisionless plasma theory covering collective /wave-particle and wave-wave/ interactions and mathematical methods 13 p2011 A72-29099
- Collisional plasma shock waves structure in electromagnetic shock tube with strong transverse bias magnetic field, using two fluid Navier-Stokes equations 13 p2011 A72-29119
- Nonlinearity effect on electron plasma wave dispersion relation, using numerical simulation and theoretical analysis by perturbation expansion and Hamilton variational principle 13 p2011 A72-29121
- Unsteady state propagation of weak nonlinear plasma waves in magnetic field, discussing shock wave formation and compression pulse evolution 13 p2012 A72-29124
- Parametric decay instability of Langmuir and acoustic plasma waves induced by incident electromagnetic wave near plasma frequency, noting application to ionospheric instabilities 13 p2012 A72-29126
- Antenna LF impedance measurements of lower terrestrial plasma wave characteristics, using equivalent impedance probe circuit 13 p1920 A72-29258
- Plasma wave measurements during OGO-5 dayside magnetosphere polar cusp encounters, discussing ULF magnetic field wave levels and VLF electric field amplitude ranges 13 p1950 A72-29380
- Dispersion equations for electron and ion cyclotron waves propagating perpendicularly to magnetic field in plasma 13 p2016 A72-29602
- Carbon dioxide laser light scattering measurements of turbulence in high beta collisionless plasma shock wave 13 p2018 A72-29853
- Shock wave and isentropic compression/expansion in plasma with anomalous thermodynamic properties due to strong particle interactions, discussing phase transitions types 13 p2019 A72-29904
- Quasi-hydrodynamic equations for transverse waves in inhomogeneous plasma, using geometric optics approximation 13 p2019 A72-29986
- Stationary nonlinear ion acoustic oscillations in dense weakly ionized current carrying plasma, considering wave propagation velocity and instability process 13 p2019 A72-29988
- Nonequilibrium plasma wave scattering cross section dependence on energy bands shape and field orientation in semiconductors 13 p2023 A72-29992
- Dispersion of polyhelical nonrelativistic electron flow interacting with slow waves of magnetized cold plasma, observing instability in presence of Doppler effects 14 p2136 A72-30304
- Alfven waves parametric amplification in magnetized plasma, showing dependence on wave frequency and phase and perturbation field strength 14 p2137 A72-30396
- Plasma radiation from collisionless MHD shock waves, discussing waves generation and angular distribution 14 p2138 A72-30555
- Wave pattern of three dimensional hydromagnetic perturbations produced by harmonic magnetic dipole in anisotropic plasma 14 p2102 A72-30661
- Electromagnetic waves propagation in inhomogeneous moving cold electron plasma without external magnetic field and collisions, investigating dynamo-optical effects 14 p2086 A72-30790
- Magnetized nonuniform plasmas, discussing description to all orders in electron and ion temperatures of waves by operator method 14 p2139 A72-30879
- Two counter streaming plasmas with anisotropic temperatures, studying instability condition for ordinary mode electromagnetic propagation perpendicular to external magnetic field 14 p2140 A72-30935
- Waves and particles interaction in highly turbulent collision-free Vlasov plasma under pure Coulomb interaction and zero magnetic field 14 p2140 A72-30937
- Anisotropic homogeneous plasmas, deriving computer model to predict effects of circularly polarized parallel plasma waves in external uniform magnetic field direction on instabilities 14 p2140 A72-30938
- Kinetic equations for turbulent magnetized plasma, considering wave-wave interactions and wave energy in terms of second order Markov differential equation 14 p2141 A72-30940
- Ionosphere radio wave propagation from fluid plasma wave and magnetically nonpermeable medium electrodynamics studies 15 p2193 A72-31281
- Signal spectrum sidebands asymmetry of LF waves in plasma with electric current and ion stream, suggesting amplitude and frequency modulation 15 p2284 A72-31650
- Collisions role in nonlinear mode coupling and harmonic generation associated with electromagnetic wave in plasma, describing plasma electron distribution function by kinetic equation 15 p2195 A72-31679
- Steepest descent path of integral describing transient plane wave propagation in anisotropic cold plasma, relating to evanescent wave arrival 15 p2285 A72-32109
- Langmuir waves scattering by denser plasma ions as dominant turbulent process momentum exchange between dynamic plasmas, applying to galaxies expansion into intergalactic media 15 p2285 A72-32269
- Monochromatic plasma wave excitation by cold electron beam, obtaining instability maximum amplitude and oscillation period 15 p2285 A72-32270
- Kinetic energy and momentum of longitudinal waves in plasmas, deriving Landau dispersion equation from conservation laws 15 p2285 A72-32272
- Solitons propagation in two ion streams plasma for cold and finite temperature ions, noting periodic waves condition 15 p2286 A72-32276
- Sounding rocket experiment on nonlinear interaction between two electron plasma waves and ion acoustic wave in ionosphere to investigate artificial realization feasibility 15 p2231 A72-32333
- Small-amplitude near-steady oblique shock waves in cold collisionless plasma, considering magnetoacoustic and Alfven waves 15 p2287 A72-32414
- Ionic collision effects on spatial ion wave echoes in single-ended Q machine plasma, noting echo peak amplitude damping 15 p2288 A72-32423
- Ion acoustic and guided electron plasma waves excitation by grid antenna produced LF signals in cylindrical plasma column 15 p2289 A72-32650
- Magnetoactive plasma transverse waves propagation near electron gyrofrequency harmonics, taking into account electron collisions and relativistic effects 15 p2289 A72-32734
- Ion acoustic, electron plasma and cyclotron harmonic waves parametric instabilities in magnetic field and applications to plasma heating 16 p2433 A72-32811
- Plasma wave excitation by monoenergetic relativistic electron beam, investigating beam-plasma wave synchronism during instability development 16 p2434 A72-32912
- Nonlinear wave interaction in anisotropic plasmas, discussing helicon decay with acoustic wave emission and quasi-longitudinal waves with magnetoacoustic wave emission 16 p2436 A72-33478
- Plasmapause and geomagnetic micropulsations correlation from universal magnetospheric instability model, noting drift waves conversion to sound or Alfven waves 16 p2387 A72-33906
- MHD fluid model for collisionless shock waves in turbulent plasma with enhanced transport coefficients, noting laboratory experiments and satellite and radio observations 16 p2439 A72-33932
- Q switched laser produced hemispherical shock waves in Ar and He plasmas, determining primary and secondary wave trajectories [AIAA PAPER 72-720] 16 p2439 A72-34028
- Effective transmission coefficient increase for Langmuir and electromagnetic waves passing through density barrier via perturbation transport by resonant electrons 17 p2588 A72-34661
- Coupled mode equations derivation for wave interactions in plasmas, considering oscillations production and cold magnetized plasma 17 p2589 A72-34923
- Charged particle stream neutralization and stabilization in solar corona, noting plasma wave and relation to type 3 radio bursts 17 p2608 A72-35093
- Linear transformation and absorption of electromagnetic waves in plasma 17 p2591 A72-35165
- Nonlinear collisional excitation of plasma waves. 17 p2591 A72-35372
- Carbon dioxide laser light scattering from cyclotron-harmonic waves in steady state rarefied collisionless plasma, noting associated electron density fluctuations 17 p2591 A72-35378
- An analysis of Pioneer 9 low-frequency wave observations near interplanetary discontinuities. 17 p2614 A72-35585
- Observation of very-low-frequency whistler-mode waves in the region of the radiation-belt slot. 17 p2517 A72-35598
- A model for drift pair and hook burst emission from the solar corona. 17 p2617 A72-35712
- Instability of electromagnetic cyclotron harmonic waves in plasmas. 17 p2592 A72-35775
- Observation of satellite modes in a beam-plasma instability. 18 p2715 A72-36600
- Growth rate and frequency dispersion characteristics of drift waves in an RF collisional plasma. 18 p2716 A72-36924
- Vlasov and Maxwell equations solution for surface waves dispersion in semiinfinite hot plasma 18 p2716 A72-36925
- Nonlinear equations for explosive instabilities of three plasma waves interaction with mutually different linear damping 19 p2838 A72-37326
- Sideband growth in nonlinear Landau wave-particle interaction. 19 p2838 A72-37327
- Longitudinal waves in a perpendicular collisionless plasma shock. IV - Gradient B. 19 p2838 A72-37329
- Green function for temporal electromagnetic plasma wave echoes oblique to external magnetic field, calculating current density and damping term 19 p2839 A72-37333
- Scattering of Langmuir waves produced by a beam with finite transverse dimensions. 19 p2839 A72-37337
- Drude theory of electromagnetic waves in an inclined magnetic field. I - One-band model of charge carriers. 19 p2840 A72-37510
- Electron-plasma-wave shocks in a bounded plasma. 19 p2840 A72-37719
- Solitary waves properties and propagation at right angles to magnetic field in two ion beam magnetized plasma 19 p2841 A72-38441
- Wave propagation in plasmas with fluctuations. 19 p2842 A72-38525
- Unsteady weakly nonlinear waves in a multicomponent plasma with allowance for weak dissipation 19 p2842 A72-38528
- Parametric coupling of large amplitude pump wave to E layer plasma mode to explain auroral electrojet irregularities external production and control 19 p2793 A72-38746
- Pulse propagation in a magnetoplasma. I - Longitudinal propagation. 19 p2843 A72-38751
- Nonlinear monochromatic Alfven wave propagation along magnetic field in anisotropic rarefied plasma with firehose instability 20 p2957 A72-39381
- Parametric excitation of Bernstein waves in inhomogeneous magneto-plasmas. 21 p3089 A72-40187
- Reductive perturbation method application to Vlasov equation governing one dimensional motion of collisionless plasmas, investigating nonlinear modulation of plasma waves 21 p3089 A72-40188
- Effects of Landau damping on nonlinear wave modulation in plasma. 21 p3089 A72-40189
- Fresnel-like interference on an ion-wave decay in a plasma. 21 p3089 A72-40200
- Magnetoplasma surface waves in polar semiconductors: Retardation effects. 21 p3096 A72-40344
- Contribution to nonlinear theory of electron-beam kinetic instability in a plasma 21 p3090 A72-40408
- Plasma low density regions caused by Langmuir turbulence, discussing energy dissipation of long wave oscillations and wave collapse 21 p3090 A72-40410
- Nonlinear magnetosonic waves in a plasma with a finite conductivity. 21 p3090 A72-40485
- Dispersion equations solved for electron and ion cyclotron waves propagating perpendicularly to magnetic field in plasma 21 p3091 A72-40656
- Dispersive waves in a slightly ionized nonequilibrium plasma. 21 p3092 A72-41223

Spontaneous emission of plasma waves in the presence of a finite amplitude wave
21 p3093 A72-41494

Eigenvalue numerical solution for dispersion relation and propagation characteristics of nonlocal drift waves in cylindrical plasma based on two fluid model
21 p3093 A72-41495

Effects of parallel wavelength on the collisional drift instability.
21 p3093 A72-41627

Coupled fields in inhomogeneous warm plasmas with static pressure gradients. I.
22 p3210 A72-42313

Nonlinearity and inhomogeneity effects on plasma wave excitation by beating two laser beams, taking into account Lorentz force modulation by large amplitude plasma wave
22 p3185 A72-42475

Development of nonlinear oscillations in the interaction between a modulated electron beam and a plasma
22 p3211 A72-42651

Application of multiple-scattering theory to the derivation of kinetic equations for waves in a weakly turbulent plasma
22 p3212 A72-42665

Wave propagation in plasma modulated by external electric field, noting dispersion equation for coupled waves and instability conditions
22 p3212 A72-43101

Surface drift vibrations of a weakly ionized plasma
22 p3212 A72-43102

Instability of a weakly ionized plasma with respect to vibrations with wavelengths of the order of the Debye radius
22 p3213 A72-43104

Electromagnetic emission during the development of a hydrodynamic beam instability in a bounded plasma
22 p3213 A72-43115

Dispersion of polyhelical nonrelativistic electron flow interacting with slow waves of magnetized cold plasma, observing instability in presence of Doppler effects
23 p3317 A72-43206

Conditions for magnetoactive plasma longitudinal waves with phase velocity near light velocity existence, investigating increments during synchrotron instability due to relativistic particles
23 p3262 A72-43311

Surface wave parametric excitation by weak HF electric field in semibounded plasma, calculating near threshold instability by dispersion equation
23 p3318 A72-43322

Nonlinear evolution of a quasi-monochromatic packet of spiral waves in a plasma
23 p3318 A72-43324

Symposium on Waves and Resonances in Plasmas, St. John's, Newfoundland, Canada, July 5-9, 1971, Proceedings.
23 p3319 A72-43511

Physical processes of weak, single wave and strong plasma turbulence and instabilities driven by oscillating fields
23 p3319 A72-43514

Ray tracing in ionosphere and magnetoionic theory application to coupling in cold plasma waves, considering linear waves, electrodes, particles and echoes as exciters
23 p3319 A72-43516

Monochromatic plasma waves linear and nonlinear coupling, discussing LF modulation partial transfer /Luxembourg effect/ and application to ionospheric diagnostics
23 p3319 A72-43517

Damping of finite-amplitude electron plasma waves in a collisionless plasma.
23 p3321 A72-44075

Multicomponent plasmas with static magnetic field, deriving dielectric tensor and dispersion relation for wave propagation by linearization technique
24 p3428 A72-44967

High-frequency instabilities in a plasma with a nonlinear ion-acoustic wave
24 p3429 A72-45489

Investigation wave transformation and absorption by a plasma in the upper hybrid frequency range
24 p3429 A72-45491

Current-driven drift wave instability in a sheared magnetic field.
24 p3430 A72-45570

Nonlinear wave interaction in plasma with random inhomogeneities, using quasi-hydrodynamic approximation
24 p3431 A72-45715

PLASMA-ELECTROMAGNETIC INTERACTION
Scattering cross section of electromagnetic wave by collisionless plasma perpendicular to applied magnetic field
01 p0105 A72-10025

Monochromatic waves propagating in uniform magnetoplasma, considering resonant interaction with electrostatic approximation
01 p0107 A72-10138

Ordinary electromagnetic waves propagating in plasma, calculating thermal and particle collisional corrections with moment approach
01 p0107 A72-10140

Linear theory of transverse electromagnetic waves and instabilities in uniform plasma during propagation along magnetic field, considering multifluid and kinetic description
01 p0108 A72-10189

Energy and momentum transfer between fields and particles in plasma crossed by transverse electromagnetic wave, investigating MHD stability
01 p0109 A72-10884

Electromagnetic instability of linearly polarized mode propagation perpendicular to magnetic field in two colliding plasma streams
01 p0110 A72-11112

Magnetoplasmodynamic supersonic ring duct as electromagnetic shock tube or plasma gun, emphasizing plasma flow-magnetic field interaction
01 p0110 A72-11204

Microwave measurements of plasma parameters in medium pressure gas discharges in absence of constant magnetic field and in weak electromagnetic field
01 p0072 A72-11215

Strong linearly polarized electromagnetic wave propagation in overdense plasmas, considering relativistic electron velocities and nonlinear penetration effect
01 p0111 A72-11226

Passive electric microwave probe with balancing capacitance for studying waveguide fields at high microwave power levels in radiative plasma accelerators
02 p0223 A72-11418

Shf electromagnetic radiation interaction with solid body plasma, explaining wave propagation in solid state plasma waveguides
02 p0170 A72-11561

Magnetosonic perturbations caused by ideally conducting sphere expansion in cold plasma, determining electric field and magnetic induction time dependences
02 p0217 A72-11939

Electromagnetic wave propagation perpendicular to applied uniform magnetic field in relativistic plasma, deriving dispersion relation for stability criterion
02 p0264 A72-12024

Heat transfer from augmented flames and plasma jets based on magnetically rotated arcs, measuring transfer rate as function of electromagnetic torque
02 p0301 A72-12031

Lf drift-type and ion-acoustic oscillations in weakly ionized currentless plasma at low gas pressures in longitudinal magnetic field
02 p0265 A72-12291

Decay interactions among plasma wave and two opposed electromagnetic waves in homogeneous layer of isotropic collisionless plasma, observing stimulated Raman scattering
02 p0180 A72-12579

Electromagnetic wave reflection and transmission by stratified multilayered parallelly moving plasma media, using propagation matrices
02 p0182 A72-12652

Plane electromagnetic wave diffraction on magnetoactive plasma cylinder, using energy method and particle scattering model
02 p0183 A72-12754

Right handed circularly polarized electromagnetic wave propagation in hot inhomogeneous plasma, deriving local dispersion equation by WKB methods
03 p0393 A72-12949

Strong circularly polarized electromagnetic wave scattering by plasma electron as function of amplitude and magnetic field with radiation reaction
03 p0321 A72-13077

Penetration depth of hf electromagnetic waves in weakly ionized plasma, considering nonlinearity effect on ionization balance
03 p0394 A72-13085

Parametric excitation of hf and lf plasma oscillations by modulated shf field dependent on field strength at carrier frequency
03 p0394 A72-13086

Helmet streamer interaction of coronal material with magnetic fields, considering inertial, pressure, gravitational and magnetic forces
03 p0431 A72-13339

Relativistic plasma with particles interacting through electromagnetic field, constructing statistical description by reduced distribution functions and correlation patterns
03 p0395 A72-13626

Plasma conductivity frequencies, including electromagnetic wave propagation in alternating field and scattered light intensities
03 p0396 A72-13653

Neutral current sheets in slow moving plasma with frozen-in magnetic field with null force line
03 p0438 A72-14070

Current source generated electromagnetic and electroacoustic wave propagation through homogeneous,

isotropic compressible electron-ion plasma, using two fluid continuum theory
04 p0554 A72-14510

Current density nonlinear transient response and energy absorption of weakly ionized plasma under pulsed electric field
04 p0555 A72-14532

Trapped particles induced by fluctuating magnetospheric electric and magnetic fields, calculating radial diffusion and energy distribution and time variations
04 p0566 A72-14723

Hydromagnetic whistler traveling wave tube amplification in magnetosphere, deriving temporal growth rate dependence on plasma parameters
04 p0517 A72-14950

Electron-ion-plasmon-photon interactions and energy exchange mechanism in plasma-field /laser pulse/ systems
04 p0557 A72-15155

Plasma column interaction with counter rotating hf magnetic fields of multipole configurations, calculating angular velocity
04 p0557 A72-15169

MHD stability of plasma boundary in transverse constant magnetic and hf circularly polarized fields
04 p0558 A72-15174

Cylindrical grid-like antenna in anisotropic compressible homogeneous plasma, obtaining magnetic field effects on wave dispersion by numerical solution
04 p0488 A72-15306

Network formulations of electromagnetic fields in moving dispersive plasma media by equivalent parameter representation
04 p0490 A72-15400

Electromagnetic wave propagation and stability in inhomogeneous collisionless plasma under static magnetic field
04 p0490 A72-15401

Transient signal propagation in unbounded time-spatial dispersive hot plasmas, using convolution integral equations
04 p0490 A72-15402

Electromagnetic wave reflection from region with variable drift velocity and polarization of waves propagating in nonuniformly moving medium, applying to isotropic plasma
04 p0491 A72-15421

Spherical antenna covered by lossy hot plasma layer, calculating radiation fields by transmission line theory
04 p0493 A72-15525

Organic dye lasers radiation nonlinear interaction with alkali metals spark discharge plasma, showing angular and spectral broadening
04 p0532 A72-15573

Nonlinear ponderomotive forces in intense laser light interaction with plasma
04 p0560 A72-15618

Book on electromagnetic waves in moving magnetoplasmas covering propagation in infinite and bounded plasmas subject to magnetic fields for nonrelativistic and relativistic velocities
05 p0695 A72-16396

Slant incident electromagnetic wave absorption in linear plasma layers due to field swelling in resonance region
05 p0627 A72-16403

Quasi-monochromatic radio signal propagation for arbitrary amplitude and phase envelopes in nonlinear medium with nonlinearity caused by plasma heating
05 p0627 A72-16404

Laser radiation amplification, investigating opposing laser pulses interaction in plasma
05 p0668 A72-16414

Self action penetration of electromagnetic wave through dense collisionless plasma layer in high vacuum, using antenna microwave probes
05 p0695 A72-16601

Hf electromagnetic field spectrum in one dimensional plasma cavity in pressure balance for arbitrary density
05 p0696 A72-16604

Periodic quasi-noise spectrum and amplitude modulation of lf pulsed signals from earth in magnetosphere plasma
05 p0696 A72-16605

Electromagnetic wave transmission and reflection by semiinfinite moving anisotropic plasma with parallel static magnetic field, considering incident H wave
05 p0696 A72-16623

Monochromatic radiation pulse transfer in absorbing plasma, deriving heat wave propagation velocity
05 p0696 A72-16680

Plane magnetized plasma layer interaction with hf electromagnetic field, showing electric field strength and direction dependence on ion acoustic-Alfven velocity ratio
05 p0697 A72-16982

Electromagnetic wave scattering by underdense plasma layer, considering perturbation calculation for Gaussian, sech squared and parabolic density distribution
06 p0853 A72-17350

Polarization electric field and depolarization current measurements in plasma flows along toroidal solenoid with diverter

06 p0853 A72-17387

Nonlinear amplitude distribution of electromagnetic wave propagating in plasma near hybrid resonance frequencies

06 p0771 A72-17390

Electromagnetic wave propagation and thermal spread in uniform magnetoplasma at electron-cyclotron resonance frequencies, discussing kinetic and multifluid theory

06 p0854 A72-17489

Nonlinear scattering of microwave signals incident on unmagnetized cold plasma column

06 p0859 A72-17547

Magneto-viscous interactions in combustion plasma, measuring velocity distributions for ordinary hydrodynamic and MHD flow with transverse magnetic field

06 p0859 A72-17618

Plasma jet injection stoppage and reflection in strong transverse magnetic field, considering instability due to flow interactions

06 p0860 A72-17694

Cyclotron resonance interaction between electromagnetic waves and nonthermal plasmas for Cauchy velocity distributions yielding algebraic dispersion equations

06 p0860 A72-17745

Rf transmission between two parallel whip antennas in warm plasma, noting received signal increase at probe resonant frequency

06 p0860 A72-17747

Waveform distortion of strong field amplitude modulated plane electromagnetic wave propagating in anisotropic plasma

06 p0862 A72-18338

Electrostatic field excitation in plasma layer by plane transverse electromagnetic wave as function of incident angle

06 p0862 A72-18339

Nonlinear microwave absorption by plasma between cyclotron and hybrid frequencies for critical magnetic field

06 p0776 A72-18408

Microwave absorption by longitudinally inhomogeneous plasma, noting waveguide excitation in critical concentration region

06 p0776 A72-18409

Magnetic effects on Lorentz plasma collision processes, calculating electron distribution function in presence of strong arbitrarily oriented magnetic and weak electric fields

06 p0864 A72-18535

Elf/vlf radiation resistance of finite electric dipole oriented at arbitrary angle in cold uniform magnetoplasma, deriving general integral expression

07 p1039 A72-18823

Cylindrical antenna radiation resistance and total radiated power in weakly ionized plasma, considering electron collisional effects

07 p0944 A72-19592

Ground plane absorption coefficient effects on admittance of slot antenna radiating into warm lossy plasma

07 p0957 A72-19797

Refraction of electromagnetic wave with electric field perpendicular to applied magnetic field in anisotropic plasma cylinder cross section

07 p1046 A72-20507

Electrostatic oscillations enhancement in magnetized plasma by hf electromagnetic waves, noting detection by light scattering

07 p1046 A72-20539

Reactive mechanism of nonlinear mixing in resonant excitation of ion plasma waves by vlf and whistler waves

07 p1046 A72-20540

Microwave signal attenuation in lf oscillation plasma beam discharge, comparing to braking cyclotron absorption effect

08 p1212 A72-20792

Correlation functions describing fluctuation of slow electromagnetic waves in plasma layer

08 p1212 A72-21065

Far field radiation pattern from magnetic line source covered with moving uniaxial or isotropic nondispersive dielectric or cold plasma sheaths

08 p1137 A72-21985

Electromagnetic impulse wave impingement on semiinfinite isotropic plasma slabs with arbitrary incidence angle and polarization, calculating signal reflection in terms of Bessel functions

08 p1137 A72-21990

Electron temperature effects on radiation fields and resistance of short electric dipole antenna embedded in hot uniaxial plasma

08 p1215 A72-21991

Large amplitude electrostatic ion acoustic shock production by superposing pulsed photoionized plasma slab on dc background

09 p1360 A72-22871

Soviet book on plasma physics and controlled thermonuclear synthesis covering plasma-electromagnetic interactions, magnetic traps and plasma cryogenic technology

09 p1361 A72-23201

Contractible current loop model for radius variations, induction current, temperature and inertia center velocity in plasmoid interacting with axially symmetric magnetic field

09 p1361 A72-23202

Short plasmoids production in hydrogen plasma jets by applying pulsed multiple magnetic field generated in linear quadrupole system

09 p1362 A72-23203

Pulsed plasma flow interaction with spatially periodic magnetic field generated by coaxial coils with alternating currents, noting MHD stability

09 p1362 A72-23207

Moving plasma interaction with oblique magnetic field, establishing magnetization ranges for plasma density and velocity

09 p1362 A72-23208

Colliding plasma flows motion and capture in transverse magnetic field with mirror configuration, noting polarization effect

09 p1362 A72-23209

Electromagnetic wave propagation obliquely incident on thermal inhomogeneous plasma at frequencies near second electron cyclotron harmonic

09 p1365 A72-23521

LF drift-type and ion-acoustic oscillations in weakly ionized currentless plasma at low gas pressures in longitudinal magnetic field

10 p1517 A72-23765

Intense relativistic electron beam-plasma interactions in finite cavities, calculating neutral gas charge production and gas breakdown times

10 p1518 A72-23960

High intensity laser radiation absorption in plasma produced from thick metal targets and thin Au foil

10 p1490 A72-23967

FM electromagnetic wave propagation in Lorentzian plasma, taking into account harmonic generations effect

10 p1520 A72-24209

Microwave amplitude modulation during propagation through RF plasma under perpendicular low intensity time dependent magnetic field

10 p1520 A72-24345

Electromagnetic wave propagation perpendicular to magnetic field in two-component warm plasma, obtaining dispersion relations for transverse waves

10 p1520 A72-24350

Electromagnetic waves penetration through magnetized plasma into lower hybrid resonance region examined in geometrical optics approximation

10 p1521 A72-24352

Inhomogeneous plasma effect on helical slow wave systems approximated by anisotropically conducting plane

10 p1522 A72-24518

Induced Compton scattering and nonlinear electromagnetic wave propagation in laser beam focused plasma

10 p1522 A72-24605

Electromagnetic wave propagation in weakly nonstationary plasma, determining variations of wave amplitudes and polarization characteristics

10 p1523 A72-24782

Inhomogeneous rarefied plasma, investigating nonlocal, linear and nonlinear effects on electromagnetic wave reflection and transmission

11 p1694 A72-25717

Plasma column stabilization by constant longitudinal inhomogeneous magnetic and rotating HF electromagnetic fields, noting application to plasma convective instabilities

11 p1694 A72-25786

Thomson scattering of electromagnetic wave in plasma and ionosphere for studying electron and ion temperatures

11 p1621 A72-25838

Linear antenna in anisotropic plasma with ion depletion, calculating reactance change due to surrounding dielectric layer thickness

11 p1593 A72-25949

Steady state plasma interactions with electromagnetic force field in plasma accelerators, showing shock wave formation

11 p1706 A72-26163

Anomalous plasma heating by laser irradiation with superimposed electric field oscillating near plasma frequency

11 p1696 A72-26326

Third harmonic current density excitation by HF electric field in Lorentz plasma, calculating electron distribution function with unnormalized spherical harmonics and Fourier series

11 p1697 A72-26553

Auroral plasma particle discharge during motion in strong inhomogeneous magnetic field, magnetospheric instability due to temperature anisotropy

11 p1715 A72-26904

Radio wave propagation characteristics in Venusian atmosphere and interplanetary plasma from Venera 7 probe data

11 p1599 A72-26907

Stimulated monochromatic electromagnetic wave scattering derived from analysis of nonlinear interactions in magnetoactive plasma

12 p1849 A72-27063

Longitudinal electromagnetic wave excitation in restricted plasma by relativistic electron beam injection, determining increments, frequency distribution and width of spectra

12 p1849 A72-27064

Energy spectra of multiply charged ions formed in laser beam interaction with plasma, noting recombination process role

12 p1849 A72-27065

Electromagnetic wave field effects on cold magnetoactive plasma potential oscillations, solving dispersion equation for sub-ion gyroscopic frequencies

12 p1849 A72-27066

Plane magnetized plasma layer interaction with HF electromagnetic field, showing electric field strength and direction dependence on ion acoustic-Alfven velocity ratio

12 p1850 A72-27126

Radar backscattering cross section and power of conducting cylindrical spacecraft in compressible electron-ion plasma environment

12 p1779 A72-27173

Variational and statistical methods for adiabatic electron plasma with self consistent field interaction in terms of Lagrange, Hamilton and Liouville formalization

12 p1850 A72-27185

Thermal electron relativistic streaming effects on electromagnetic instability in magnetoplasmas

12 p1851 A72-27389

ATS F Environmental Measurements Experiment package for synchronous altitude space environment and electromagnetic-ionospheric interactions studies

12 p1795 A72-27525

VLF and LF electromagnetic ground wave propagation between points on smooth curved lunar surface surrounded by free space or cold isotropic plasma

12 p1783 A72-27635

Wave equations for electromagnetic wave propagation in electron-ion-neutral particle magnetoplasma, using macroscopic approach

12 p1852 A72-27850

High frequency potential effect on fast transverse magnetic waves along plasma layer bounded by two conducting plates

12 p1785 A72-27855

Strong field electromagnetic wave interactions with anisotropic plasmas, considering electron velocity distribution function

13 p2009 A72-28449

LF oscillations and electron drift in frozen plasma under strong electromagnetic radiation, deriving formulas for coupled Alfven and spiral waves

13 p2035 A72-28593

Book on theory of fully ionized plasmas covering Coulomb systems equilibrium and nonequilibrium states, charged particle radiation and interactions with EM fields

13 p2011 A72-29098

Electromagnetic wave absorption in warm homogeneous plasma under static magnetic field parallel to surface, taking into account plasma-vacuum boundary conditions

13 p2012 A72-29123

Magnetosonic perturbations caused by ideally conducting sphere expansion in cold plasma, determining electric field and magnetic induction time dependences

13 p1949 A72-29251

Strong circularly polarized electromagnetic wave scattering by plasma electron with radiation reaction, determining cross section as function of amplitude and magnetic field strength

13 p2015 A72-29427

Penetration depth of HF electromagnetic waves in weakly ionized plasma, considering nonlinearity effect on ionization balance

13 p2015 A72-29435

Parametric excitation of HF and LF plasma oscillations by AM SHF field, noting dependence on field strength at carrier frequency

13 p2015 A72-29436

Electromagnetic waves scattering by underdense plasmas, examining intermittency phenomenon due to mixing between turbulent inner and outer inviscid wake

13 p1922 A72-29473

High power Q switched ruby laser radiation transmission through optically dense plasma, noting bleaching and increased absorptivity

13 p2016 A72-29521

Plasma current layer formation due to electric field directed along magnetic field neutral line

13 p2017 A72-29699

Nonlinear damping of potential monochromatic waves in inhomogeneous plasma, obtaining resonance particle distribution function

13 p1923 A72-29984

Dispersion equation derivation for HF electromagnetic waves in weakly ionized plasma in crossed fields, noting oscillation spectrum

13 p2020 A72-30048

Plasma instability theories for radio auroras, reviewing radar and radio observation systems and ion acoustic and drift gradient predictions

14 p2098 A72-30140

Electromagnetic wave propagation in weakly nonstationary plasma, determining variation with time and polarization plane rotation

14 p2136 A72-30219

Nonlinear AM and FM due to bonded nature of quasi-monochromatic whistler packets in magnetosphere

14 p2085 A72-30448

Isotropic conducting plasma dynamic behavior near rotating magnetized sphere, showing electric field-produced meridional convective currents

14 p2138 A72-30630

Electromagnetic waves backscattering in magnetoactive plasma containing random inhomogeneities of electron density, calculating field spatial-time and cross correlation functions

14 p2086 A72-30789

Unipolar steady electromagnetic bow shock interaction of Mercury with solar wind, calculating planetary surface temperature

15 p2303 A72-31305

Stationary plasma flow interaction with dipole magnetic field to study geophysical phenomena in upper atmosphere

15 p2286 A72-32343

Singly scattered radiation in weakly inhomogeneous turbulent plasma for incidence angles greater than critical angle, calculating backscattered wave depolarization from radiative transport equation

15 p2288 A72-32425

Monochromatic radio wave propagation in interplanetary plasma, deriving frequency spectrum and phase and amplitude fluctuations

15 p2202 A72-32656

Electron beam modulation by SHF noise signal in plasma-beam system

15 p2289 A72-32698

Plasma column formation by interaction with rotating HF electromagnetic field and longitudinal constant magnetic field

16 p2433 A72-32815

Electromagnetic gain mechanisms with required energy supplied by static currents and magnetic fields in homogeneous plasmas

16 p2434 A72-32853

Cylindrical antenna immersed in weakly ionized magnetoplasma, calculating steady magnetic field effect on electromagnetic and electroacoustic radiation resistances

16 p2434 A72-32860

Tropical sporadic E reflections and vertical plasma instabilities as function of equatorial electrojet and electron drift ratio based on ionogram observations

16 p2382 A72-32867

Experimental methods for studying interactions between plasma streams and three dimensional magnetic dipole fields

16 p2454 A72-33384

Free electrons-laser interaction induced electron forward drift and dc current generation, deriving drift velocity by nonrelativistic classical and quantum mechanical theories

16 p2402 A72-33397

German monograph on solar wind-coronal magnetic field interactions, presenting numerical calculation of time dependent coronal states

16 p2445 A72-33425

Longitudinal and transverse electromagnetic wave penetration into semiinfinite collisional plasma with fractionally accommodating boundary, obtaining reflection coefficient and surface impedance

16 p2435 A72-33449

Nonlinear electromagnetic wave interaction in rarefied plasma cylinder subject to constant magnetic field in hydrodynamic approximation

16 p2363 A72-33479

Monochromatic electromagnetic wave reflection and transmission at oblique incidence on sharp plasma boundary of moving ionization source

16 p2363 A72-33481

Plasma magnetoresistance in variable magnetic field measured on n-type InSb sample for SHF inertialess power sensor development

16 p2436 A72-33482

Langmuir wave coupling in inhomogeneous plasma due to combined density gradient and external HF electric field

16 p2436 A72-33654

Electromagnetic wave propagation in uniform and nonuniform plasmas with enough strength to cause relativistic electron velocities, considering linear polarization and nonlinear penetration effects

16 p2438 A72-33926

Conducting fluid flow near neutral sheet in magnetic field, assuming cold polar wind plasma geomagnetic tail

16 p2438 A72-33930

Nonlinear theory of crossed field and two stream instabilities of nonthermal plasma motions in equatorial electrojet

16 p2387 A72-33937

Material injection RF blackout alleviation and plasma diagnostic measurement with electrostatic probes and S-band reflectometer during RAM C-III reentry flight [AIAA PAPER 72-690]

16 p2365 A72-34052

Scattering of electromagnetic waves from an inhomogeneous magnetoplasma column moving in the axial direction.

17 p2587 A72-34359

Wave propagation in a stratified turbulent magnetized plasma. I.

17 p2587 A72-34516

Nonlinear microwave absorption by plasma between cyclotron and hybrid frequencies for critical magnetic field

17 p2588 A72-34858

Microwave absorption by longitudinally inhomogeneous plasma, noting waveguide excitation in critical density region

17 p2588 A72-34859

Electromagnetic waves penetration through magnetized plasma into lower hybrid resonance region examined in geometrical optics approximation

17 p2589 A72-34953

Linear transformation and absorption of electromagnetic waves in plasma

17 p2591 A72-35165

Carbon dioxide laser light scattering from cyclotron-harmonic waves in steady state rarefied collisionless plasma, noting associated electron density fluctuations

17 p2591 A72-35378

Instability of electromagnetic cyclotron harmonic waves in plasmas.

17 p2592 A72-35775

Gas discharge plasma detection characteristics, examining electron and ion densities and collision rates dependence on electromagnetic field frequency and amplitude

17 p2593 A72-35885

Subharmonic frequency division for neon discharge plasma oscillations under resonance due to nonuniform electric field

18 p2714 A72-36111

Hybrid and pyrotechnic IR flare generated plasma effects on dual frequency Doppler range measurement system, discussing diagnostics and contamination concentration analysis

18 p2660 A72-36339

Influence of an interface on the spectrum of incoherently reflected waves

18 p2661 A72-36657

Hall phenomena in a plasma flow situated in a traveling magnetic field

18 p2716 A72-36816

Reflection of microwave through laboratory plasma.

18 p2716 A72-36947

On the influence of excited ions and crossed electric and magnetic fields on ionisation cross-sections.

18 p2714 A72-36956

Propagation of electromagnetic waves in a rarefied plasma situated in an alternating magnetic field

18 p2717 A72-37177

Excitation of nanosecond waves on positive columns.

19 p2838 A72-37328

Transmission and reflection of an electromagnetic wave incident normally on a plasma half-space.

19 p2840 A72-37726

Propagation of surface waves along a plane boundary between two magnetoactive plasmas

19 p2842 A72-38532

Numerical solution to the problem of propagation of ELF electromagnetic waves in the lower ionosphere

19 p2767 A72-38651

Kinetic theory of density fluctuations in a magnetized collision-dominated plasma in an electric field.

19 p2792 A72-38745

A general method for integrating the Schrodinger equation with a singular right-hand side in a homogeneous and constant electromagnetic field

19 p2843 A72-38855

Plane electromagnetic wave diffraction on magnetoactive plasma cylinder, using energy method and particle scattering model

20 p2902 A72-39060

Radial penetration of a hot plasma associated with a large-scale electric field in the magnetosphere, and some related problems.

20 p2916 A72-39228

The effect of asymmetry on toroidal hydromagnetic waves in a dipole field.

20 p2957 A72-39230

Relationship of interplanetary magnetic field structure with development of substorm and storm main phase.

20 p2968 A72-39232

Nonthermal emission of a magnetoactive plasma in the field of super-high-frequency pumping wave

21 p3090 A72-40407

Integral equation for electromagnetic field in diffuse boundary plasma, noting anomalous skin effect

21 p3090 A72-40409

Rayleigh-Taylor instability in a composite medium.

21 p3104 A72-40478

Higher harmonics and transport coefficients of plasmas in circularly polarized magnetic fields and additional electromagnetic fields.

21 p3091 A72-40489

Impedance of a partially ionized cesium plasma.

21 p3091 A72-40694

Scattering of a spherical wave at a spherical discontinuity with an arbitrary radial distribution of the refractive index

21 p3016 A72-40793

Measurements of enhanced absorption of electromagnetic waves and effective collision frequency due to parametric decay instability.

21 p3092 A72-40829

Excitation of volume ion-acoustic oscillations in an inhomogeneous dense plasma by the field of an electromagnetic wave.

21 p3092 A72-40836

Propagation constants of electromagnetic waves along an infinitely long conducting wire in a general magnetoplasma.

21 p3092 A72-41266

Electromagnetic wave propagation in a moving sinusoidal stratified turbulent plasma medium.

21 p3093 A72-41323

Radiative transport analysis of electromagnetic propagation in isotropic plasma turbulence.

21 p3094 A72-41634

Investigation of the interaction between a plasma flow and an axisymmetric magnetic field

21 p3094 A72-41655

Polarization interaction between plasma flows in a transverse magnetic field

21 p3095 A72-41689

Absorption of an obliquely incident extraordinary wave in a weakly inhomogeneous plasma in the hybrid resonance region

21 p3095 A72-41694

Study of the thermal self-focusing of electromagnetic waves in a plasma

22 p3211 A72-42652

Application of multiple-scattering theory to the derivation of kinetic equations for waves in a weakly turbulent plasma

22 p3212 A72-42665

Electric multipole moments calculation by quasi-static method for homogeneous quasi-neutral oblate plasma spheroid during electromagnetic interaction under resonance conditions

22 p3212 A72-42729

Pressure dependent microwave cavity breakdown field relationship to steady state plasma luminosity interpretation as evidence of RF confinement of low density plasma

22 p3212 A72-42897

Electromagnetic disturbances within a degenerate electron plasma in a quantizing magnetic field

22 p3212 A72-43010

Plasma-electromagnetic interaction with surface wave propagation along boundary, obtaining boundary conditions for longitudinal and transverse wave amplitudes with allowance for particles interaction

22 p3213 A72-43117

Surface wave parametric excitation by weak HF electric field in semibounded plasma, calculating near threshold instability by dispersion equation

23 p3318 A72-43322

Nonlinear evolution of a quasi-monochromatic packet of spiral waves in a plasma

23 p3318 A72-43324

Use of the simulation method for the solution of a dispersion problem for the propagation of symmetrical magnetic waves in a rectangular waveguide filled with a nonhomogeneous plasma

23 p3263 A72-43450

Wave attenuation during plasma propagation, discussing particle collisions, absorption effect on geometric optics and linear mode coupling in cold magnetized plasma

23 p3320 A72-43519

Field components of coupled electromagnetic and electron acoustic waves in warm stratified plasmas, using first order wave equations and Heading embedded form

23 p3322 A72-44319

Spectral composition and phase function of plane monochromatic light wave scattering by electrons in high temperature plasma

23 p3322 A72-44465

Magnetic pulsation spectra in a nonisothermal plasma

23 p3323 A72-44483

Crossover frequencies in multicomponent plasmas with negative ions.

23 p3323 A72-44525

Parametric instabilities and anomalous heating of plasmas near the lower hybrid frequency.
23 p3323 A72-44545

Radiation from an electric dipole in anisotropic media.
24 p3424 A72-44706

LF oscillations and electron drift in frozen plasma under strong electromagnetic radiation, deriving formulas for coupled Alfvén and spiral waves
24 p3440 A72-45093

Investigation wave transformation and absorption by a plasma in the upper hybrid frequency range
24 p3429 A72-45491

Rapid radial displacement of a toroidal plasma filament by a transverse magnetic field
24 p3429 A72-45506

Self-consistent electromagnetic waves in relativistic Vlasov plasmas.
24 p3430 A72-45569

Nonlinear instability of Bernstein modes pumped by an electromagnetic wave.
24 p3430 A72-45571

Generation of plasma oscillation by beam-plasma interaction.
24 p3430 A72-45574

Stimulated monochromatic electromagnetic wave scattering derived from analysis of nonlinear interactions in magnetoactive plasma
24 p3431 A72-45716

Longitudinal electromagnetic wave excitation in restricted plasma by relativistic electron beam injection, determining increments frequency distribution and width of spectra
24 p3431 A72-45717

Energy spectra of multiply charged ions formed in laser beam interaction with plasma, noting recombination process role
24 p3431 A72-45718

Electromagnetic wave field effects on cold magnetoactive plasma potential oscillations, solving dispersion equation for sub-ion gyroscopic frequencies
24 p3431 A72-45719

PLASMA-PARTICLE INTERACTIONS

Electrostatic wave-particle interactions in inhomogeneous collisionless plasma, calculating resonant distribution function, charge densities and trapping periods
01 p0107 A72-10136

Electron layer precession under magnetic field in background plasma, noting density effect on instability
01 p0107 A72-10144

Charged particles magnetic scattering on cyclotron instability waves of radiation belt plasma, estimating proton relaxation time
01 p0119 A72-10608

Nonuniform plasmas resonant wave-particle interactions, using linearized Vlasov equation
02 p0264 A72-12119

Diffuse plasma resonances in space interpreted by wave-particle nonlinear interaction in weakly turbulent plasma, considering electrostatic electron cyclotron wave instability
02 p0265 A72-12366

Two stream instabilities of low density beam-plasma interaction in finite and zero magnetic fields
02 p0267 A72-12839

Relativistic beam equilibria above 10,000 amps, considering axial, diffuse, sharp boundary and azimuthal current models
02 p0267 A72-12840

Frequency spectrum analysis of electromagnetic self radiation from plasma interacting with high energy electron beam
03 p0393 A72-13082

Cross flow blown two dimensional stationary plasma arc deflection and temperature distribution as function of collisional drift velocity and electric field
03 p0397 A72-13921

Collision integral for classical electron plasma, concerning Born-Bogoliubov-Green-Kirkwood-Yvon equations for long range interaction potential and motions of multiple particles
03 p0399 A72-14069

Quasi-linear relaxation of fast ion beam in cold plasma moving transverse to magnetic field
04 p0554 A72-14403

One dimensional collisionless plasma instability driven by cold electron beam, determining limits from beam trapping
04 p0559 A72-15353

Electron heating in weakly ionized collisionless beam plasma discharge as function of neutral gas pressure and plasma column length
05 p0697 A72-16986

Longitudinal hf oscillations in homogeneous magnetoactive plasma by fast monoenergetic electron excitation
06 p0853 A72-17389

Collisionless relaxation of interpenetrating ion beams in Ar plasma, showing velocity spectrum broadening during Langmuir frequency periods
06 p0853 A72-17394

Nonlinear oscillation amplitude of ion beam due to phase bunching in interaction with plasma electrons
06 p0853 A72-17395

Electron beam interaction with collisionless plasma, obtaining beam spatial distribution function from velocity diffusion coefficient measurement
06 p0858 A72-17540

Longitudinal electron plasma waves interaction with electron distribution, investigating energy transfer
06 p0858 A72-17543

Conversion effectiveness of oscillations induced by electron beam in bounded anisotropic plasma into electromagnetic emission
06 p0860 A72-17700

Astronomical model for Jovian decametric radio emission control by Io satellite based on two surface sources on planet and particle interaction with plasma
06 p0891 A72-18504

Nonlinear Landau damping of longitudinal plasma waves in dc magnetic field, obtaining wave-particle interactions from Vlasov equation by perturbation theory and method of characteristics
07 p1041 A72-19505

Stability of electron beam injected into magnetospheric plasma at small and high altitudes
07 p0979 A72-20377

Spark source generated electron beam interaction with plasma in uniform magnetic field, estimating HF longitudinal oscillation power
07 p1046 A72-20504

Langmuir electron oscillation excitation by ion beam at velocity exceeding average electron thermal velocity in plasma formed by residual gas ionization
07 p1046 A72-20505

Artificial magnetosphere interaction with 8 keV electrons in hydrogen plasma beam simulating solar wind, noting penetration caused by boundary instability
08 p1156 A72-20823

High energy electron beam interaction with dense plasma, investigating unstable waves growth by numerical methods
08 p1213 A72-21259

Electron beam interaction with bounded homogeneous plasma layer natural oscillations, using collisionless kinetic equation
08 p1215 A72-21720

Asymptotic expressions for electromagnetic field and currents induced in unbounded dense plasma by relativistic electron beam passage
08 p1215 A72-21721

Fine structure of energy distribution function for electron beam interacting with plasma
08 p1215 A72-21722

Low energy ions and negative particle fluxes simultaneous enhancements due to Apollo 14 lunar module impact, suggesting solar wind and gas cloud interaction as acceleration mechanism
09 p1388 A72-23018

Star stellator model for hot electron plasma production by steady electron beam injection in closed magnetic traps
09 p1363 A72-23219

Electron beam and plasma nonlinear interactions, noting scattering zone, amplitude oscillation maximum, longitudinal velocity and relaxation patterns
10 p1517 A72-23760

Relativistic electron beam and ring phenomena calculation using plasma simulation program CYLRAD
10 p1518 A72-23958

Relativistic heavy ion in plasma, calculating energy loss based on electron scattering and momentum transfers
10 p1515 A72-24344

Relativistic electron beam injection into dense plasma, analyzing perturbed electric and magnetic fields and charge and current densities
10 p1521 A72-24353

Collisionless thermalization of ion beam by interaction with plasma, noting acoustic instability growth
10 p1524 A72-24921

Wave particle interaction around lower hybrid resonance frequency, deriving whistler mode wave growth rate during propagation in magnetoactive plasma penetrated by nonthermal particles
10 p1476 A72-24959

Ion sources for high temperature operation based on electron bombardment and beam-plasma interactions
10 p1516 A72-25031

Spatial distribution of electron beam excited plasma wave spectrum, determining wavenumber, amplitude and frequency by incoherent microwave scattering
11 p1693 A72-25564

Charged particles effect on plasma negative ions, examining Stark effect in energy level
11 p1693 A72-25714

Electron energy, mobility and bremsstrahlung in weakly ionized nonisothermal plasmas, using Kogan approximation
11 p1698 A72-26647

Plasma-ion beam system drift beam instability in longitudinal magnetic field, noting oscillations frequencies dependence
12 p1849 A72-27060

Longitudinal electromagnetic wave excitation in restricted plasma by relativistic electron beam injection, determining increments, frequency distribution and width of spectra
12 p1849 A72-27064

Electron heating in weakly ionized collisionless beam plasma discharge as function of neutral gas pressure and plasma column length
12 p1850 A72-27130

Electron beam velocity distribution function fine structure for plasma-beam discharge in hydrogen within longitudinal magnetic field
12 p1850 A72-27261

Quasi-linear approximation equations for relativistic charged particles beam dissipative instability in collisional plasma, noting electrons heating at high collision frequencies
12 p1852 A72-27860

Kinetic approximation for bounded electron beam stability in plasma situated in magnetic field, deriving instability increments and dispersion relations
13 p2010 A72-28578

Magnetosonic waves interactions with energy particles in plasmasphere, demonstrating magnetosonic waveguide channel existence around earth below plasmasphere
13 p1947 A72-28605

Low energy Cs ion beam energy loss during traverse through near-thermal equilibrium Cs plasma as function of plasma density, comparing measurements with theoretical predictions
13 p2011 A72-29000

Frequency spectrum analysis of electromagnetic self radiation from plasma interacting with high energy electron beam
13 p2015 A72-29432

Shock wave and isentropic compression/expansion in plasma with anomalous thermodynamic properties due to strong particle interactions, discussing phase transitions types
13 p2019 A72-29904

Nonlinear theory of interaction between restricted relativistic particle beam and plasma, determining field amplitudes and beam radii
13 p2019 A72-29989

Microscopic processes within high energy ion acceleration in laser-produced plasmas, discussing transient electric field role
14 p2136 A72-30178

Gyrosynchrotron radiation fields from mildly relativistic electrons in magnetoactive plasma, studying radiative transfer problem
14 p2138 A72-30556

Waves and particles interaction in weakly turbulent collision-free Vlasov plasma under pure Coulomb interaction and zero magnetic field
14 p2140 A72-30937

Solar wind and planetary atmosphere interaction observation by simulation of ionization mechanism in comet, using gun produced plasma stream and gas cloud
15 p2301 A72-32341

Electron beam-plasma system oscillation spectrum control through modulation by external HF signal, discussing theory and experimental verification
15 p2289 A72-32671

Magnetic field distribution measurement in axisymmetric plasma column inside Tokamak device by alpha particle beam from radioisotope
16 p2434 A72-32818

Plasma wave excitation by monoenergetic relativistic electron beam, investigating beam-plasma wave synchronism during instability development
16 p2434 A72-32912

Infinite cross section electron beam interaction with infinite turbulent plasma slab with finite thickness
16 p2438 A72-33837

Rotating plasma-neutral gas collision interaction studies, determining particle energy and velocity in partially ionized plasmas
16 p2438 A72-33916

Plasma-ion beam nonlinear interaction for beam velocity exceeding electrons thermal velocity, noting plasma heating and beam energy dissipation
16 p2440 A72-34154

Ultrarelativistic electrons beam steady injection into plasma filled half space, using weak turbulence theory for assumed beam excited oscillations interaction
16 p2440 A72-34156

Relativistic electron beam injection into dense plasma, analyzing perturbed electric and magnetic fields and charge and current densities
17 p2589 A72-34954

Particle interactions in real and numerically simulated plasmas, considering effects of macroparticles formation via idealized clustering
17 p2590 A72-35143

Kinetic theory of waves in hot, low density plasma.
17 p2591 A72-35161

Wave-wave interactions due to scattering by electrons.
17 p2591 A72-35162

Pitch-angle diffusion of radiation belt electrons within the plasmasphere.

17 p2602 A72-35597

Nonthermal solar X-ray bursts origin in non-Maxwellian electron fluxes interactions with surrounding plasma, reviewing energy spectra

18 p2721 A72-36093

Model improvements for thermionic diode plasmas.

18 p2715 A72-36218

Observation of satellite modes in a beam-plasma instability.

18 p2715 A72-36600

Scattering of Langmuir waves produced by a beam with finite transverse dimensions.

19 p2839 A72-37337

Energy loss of fast electrons and positrons in a plasma.

19 p2840 A72-37727

Effects of collisions on perpendicular longitudinal ion wave propagation in a magnetized plasma.

19 p2841 A72-38438

Structure of ion acoustic solitons and shock waves in a two-component plasma.

19 p2841 A72-38440

Nonlinear interaction of a small cold beam and a plasma. II.

19 p2841 A72-38444

Radiation of charged particle moving uniformly in a nonstationary magnetoactive plasma

19 p2843 A72-38570

Discontinuous generation of ultrahigh frequency oscillations during a plasma-beam interaction

19 p2768 A72-38664

Influence of different types of oscillations on ion heating in plasma-beam discharges.

19 p2843 A72-38820

A comparison of some particle-in-cell plasma simulation methods.

21 p3089 A72-40105

The beam-plasma discharge laser

21 p3062 A72-40406

Contribution to nonlinear theory of electron-beam kinetic instability in a plasma

21 p3090 A72-40408

Nonlinear theory of the monochromatic circularly polarized VLF and ULF waves in the magnetosphere.

21 p3015 A72-40480

Excitation of electromagnetic waves in a plasma by a relativistic electron beam

21 p3092 A72-40787

Three-dimensional pattern of instability development during the interaction between a modulated electron beam and a plasma

21 p3092 A72-40800

Frictional effects with neutrals and the gravitational instability of a plasma.

21 p3093 A72-41332

Spontaneous emission of plasma waves in the presence of a finite amplitude wave.

21 p3093 A72-41494

External high-frequency modulation of an electron beam and heating of plasma ions in the case of beam-plasma instability in the magnetic trap

21 p3095 A72-41678

External high-frequency modulation of an ion beam and the absorption of beam-plasma instability oscillations in a plasma situated in a magnetic field of mirror configuration

21 p3095 A72-41683

Development of nonlinear oscillations in the interaction between a modulated electron beam and a plasma

22 p3211 A72-42651

Injection of an electron beam into a plasma bounded by a conducting casing

22 p3213 A72-43105

An ion-cyclotron instability of a plasma produced by a fast-ion beam

22 p3213 A72-43113

Noncoherent excitation of plasma vibrations by an almost monoenergetic relativistic beam

22 p3213 A72-43114

Electromagnetic emission during the development of a hydrodynamic beam instability in a bounded plasma

22 p3213 A72-43115

Plasma-electromagnetic interaction with surface wave propagation along boundary, obtaining boundary conditions for longitudinal and transverse wave amplitudes with allowance for particles interaction

22 p3213 A72-43117

Kinetics of impact-radiative ionization and recombination

23 p3318 A72-43296

Interaction between a plasma and an electron-beam modulated by low-frequency oscillations

23 p3318 A72-43309

Stimulated emission with pumping by a pulsed electron beam formed in a direct discharge

23 p3295 A72-43319

Collisionless heating of plasma ions by an ion beam

23 p3318 A72-43321

Nonlinear evolution of a quasi-monoenergetic packet of spiral waves in a plasma

23 p3318 A72-43324

Long wave oscillations attenuation by charged particle collisions in one- and two-component hot and cold Boltzmann plasma, using kinetic and polarization vector equations

23 p3318 A72-43325

Excitation of potential oscillations in a plasma by a flow of phased oscillators

23 p3319 A72-43401

Strictional nonlinearity effect on uniform non-relativistic monoenergetic beam interaction with isotropic bounded plasma, investigating plasma oscillations and stability

23 p3320 A72-43576

Plasma-beam interaction in limited geometry: Temperature effects

23 p3321 A72-43700

Ion acceleration during expansion of a rarefied plasma

23 p3322 A72-44482

Electromagnetic instabilities produced by neutral-particle ionization in interplanetary space.

23 p3332 A72-44506

Interaction of the solar wind with the neutral component of the interstellar gas.

23 p3332 A72-44507

Kinetic approximation for confined electron beam stability in plasma situated in magnetic field, deriving instability increments and dispersion relations

24 p3428 A72-45078

Magnetosonic waves interactions with energy particles in plasmasphere, demonstrating magnetosonic waveguide channel existence around earth below plasmasphere

24 p3398 A72-45105

Impacting polar plasma thermalization during comet close approach to sun, considering solar wind-comet interaction role

24 p3445 A72-45470

Wave growth in a strongly turbulent plasma.

24 p3430 A72-45568

Plasma-ion beam system drift beam instability in longitudinal magnetic field, noting oscillations frequencies dependence

24 p3431 A72-45713

Longitudinal electromagnetic wave excitation in restricted plasma by relativistic electron beam injection, determining increments frequency distribution and width of spectra

24 p3431 A72-45717

PLASMAGUIDES

Microwave absorption by longitudinally inhomogeneous plasma, noting waveguide excitation in critical concentration region

06 p0776 A72-18409

Ionization wave propagation in inert gas due to microwave resonance quanta diffusion, explaining plasmaguide phenomena

07 p1040 A72-18916

Microwaves propagation through circular waveguide partially filled with lossless cold electron plasma dielectric, presenting computed dispersion curves for waveguide and plasmaguide modes

10 p1522 A72-24677

Multilayer plasma model for MHD pulse propagation in ionospheric waveguide, noting approximation of Alfvén velocity distribution by plasma layers

13 p1946 A72-28585

Theory of a coaxial gas-discharge generator loaded by a spiral line

17 p2529 A72-34841

Microwave absorption by longitudinally inhomogeneous plasma, noting waveguide excitation in critical density region

17 p2588 A72-34859

Two dimensional turbulence model for charge fluctuations statistical mechanics of nonlinear guiding center plasma

18 p2714 A72-36014

Properties of plane asymmetric plasma waveguides in applications to the propagation of short radio waves along inhomogeneities in the outer ionosphere

18 p2662 A72-36855

Kinetic theory of surface waves in a cylindrical plasma waveguide

19 p2842 A72-38531

Propagation of ionization wave in rarefied noble gases due to microwave resonance quanta diffusion, explaining plasmaguide phenomena

20 p2957 A72-39382

Use of the simulation method for the solution of a dispersion problem for the propagation of symmetrical magnetic waves in a rectangular waveguide filled with a nonhomogeneous plasma

23 p3263 A72-43450

Plasma-beam interaction in limited geometry: Temperature effects

23 p3321 A72-43700

Multilayer plasma model for MHD pulse propagation in ionospheric waveguide, noting approximation of Alfvén velocity distribution by plasma layers

24 p3397 A72-45085

PLASMAPAUSE

Hydrogen ions concentration in dayside region of plasmasphere from OGO 5 satellite mass spec-

trometry, noting plasmopause position as function of magnetic activity

01 p0061 A72-10892

Nonducted vlf wave propagation near plasmopause during whistlers based on diffusive equilibrium and collisionless models for magnetospheric electron density distribution

02 p0222 A72-12873

Plasmasphere size changes from K indices of geomagnetic activity, comparing with Binsack formula

03 p0344 A72-12909

Bremsstrahlung X rays from electron precipitation associated with discrete vlf emissions, recording wave-particle experiment near plasmopause with balloon-borne counters in Antarctica

03 p0413 A72-13536

Nighttime plasmopause and thermal ion plasma structures relationship to micropulsations, considering excitation in post storm recovery and diurnal plasma bulge regions

06 p0804 A72-17453

Colliding ion streams thermalization beyond plasmopause via unstable ion waves excitation or Coulomb collisions

06 p0805 A72-17464

Plasmasphere structure as outermost ionospheric region from direct measurements by particle traps, ion mass spectrometers and Langmuir probes on satellites

07 p0978 A72-20044

Large scale structure of plasmopause in equatorial plane based on whistler and upper ionosphere sounding data

07 p0978 A72-20045

Duskside magnetic activity relationship with bulge detection by whistler method, investigating plasmopause deformation

07 p0979 A72-20381

OGO-E plasmopause crossing correlation with ground observations of Pi geomagnetic micropulsations

08 p1159 A72-21223

Thermal positive ion densities measurement in outer ionosphere and magnetosphere by OGO 1 satellite, relating plasmopause distribution and magnetic activity level

[AD-742186] 09 p1300 A72-23011

Ogo-5 observation of lower hybrid resonance noise, bursts, VLF hiss and whistlers near plasmopause during large magnetic storm

11 p1624 A72-26399

Midlatitude stable auroral arc observation from OVI-10, showing generation at plasmopause due to turbulent dissipation of ring current energy

11 p1624 A72-26401

Magnetospheric equator plane electron density profiles determination from plasmopause whistlers observed in UK

11 p1626 A72-26421

Plasmopause and geomagnetic micropulsations correlation from universal magnetospheric instability model, noting drift waves conversion to sound or Alfvén waves

16 p2387 A72-33906

Cerenkov instability and VLF emissions generated outside the plasmopause.

17 p2547 A72-35063

Ring current effect on magnetospheric electron density profiles derived from plasmopause whistlers.

17 p2600 A72-35368

Radiation belt electron lifetimes and removal through pitch angle diffusion by plasmaspheric whistler waves in cyclotron harmonics

20 p2918 A72-39532

Magnetospheric interactions with topside ionosphere in terms of polar wind ion flows and density related to plasma temperature, F 2 region and cusp observations

20 p2918 A72-39537

Plasmopause nightside, daytime and bulge positive ion concentration measurements with OGO 5 mass spectrometer compared with magnetospheric convection model

20 p2919 A72-39544

Radiation belt protons and ion-cyclotron wave interactions accounting for magnetospheric ring current instabilities during storm at plasmopause

20 p2919 A72-39545

Stationary adiabatic plasma flow in the magnetosphere.

20 p2919 A72-39547

Relative movements of mid-latitude trough and scintillation boundary.

23 p3282 A72-43267

Midlatitude VLF emissions in magnetosphere due to plasma resonance instability near plasmopause, using ground, rocket and satellite observations, estimating electron energy

23 p3263 A72-43515

PLASMAS [PHYSICS]

NT ARGON PLASMA

NT BETA PARTICLES

NT CESIUM PLASMA

NT COLD PLASMAS

NT COLLISIONLESS PLASMAS

NT COSMIC PLASMA

NT DEUTERIUM PLASMA
 NT ELECTRON PLASMA
 NT HELIUM PLASMA
 NT HIGH TEMPERATURE PLASMAS
 NT HYDROGEN PLASMA
 NT METALLIC PLASMAS
 NT MICROPLASMAS
 NT NITROGEN PLASMA
 NT NONEQUILIBRIUM PLASMAS
 NT NONUNIFORM PLASMAS
 NT OXYGEN PLASMA
 NT RAREFIED PLASMAS
 NT RELATIVISTIC PLASMAS
 NT ROTATING PLASMAS
 NT SOLAR WIND
 NT STELLAR WINDS
 NT THERMAL PLASMAS
 NT URANIUM PLASMAS
 Relativistic electron beams in plasma, considering electrostatic instability conditions and critical currents
 01 p0109 A72-10975
 Fabry-Perot interferometer employing gas laser for plasma bursts electron concentrations measurements at 3.39 micron wavelength
 02 p0223 A72-11404
 Solar prominence oscillatory motion on 26 March 1964 association with plasmoids generated by pinch tube plasma
 02 p0278 A72-12044
 Electromagnetic wave scattering by electron charge density fluctuations in plane waveguide with magnetoactive plasma, showing cross section spectrum function of plasma properties
 02 p0183 A72-12766
 Statistical model of small scale discrete structure of magnetoplasma in solar active regions
 03 p0430 A72-13335
 Coaxial plasma source energetic characteristics, establishing plasmoid energy linear dependence on battery stored energy
 03 p0395 A72-13567
 Angular and linear velocities of plasmoid in coaxial accelerator under axisymmetric magnetic field
 03 p0398 A72-14002
 Anisotropic effects use in passive semiconductor magnetoplasma for submillimeter isolators and circulators development, describing transmission devices based on Faraday rotation
 04 p0563 A72-15600
 Anisotropic plasma rotational discontinuity theory, considering parallel and perpendicular components of plasma pressure and magnetic induction
 05 p0695 A72-16074
 Stability of weakly ionized homogeneous plasma placed in weak microwave field and in constant magnetic field, expressing growth increments of longitudinal waves
 06 p0861 A72-17902
 Numerical model for ion beam instability in nonisothermal plasma with electron temperature much greater than ion temperature
 06 p0861 A72-17915
 Weakly ionized plasma instability in strong nonuniform magnetic field with convective flow and steadily oscillating final state
 06 p0865 A72-18543
 Ion-electron collisions effect on ion cloud motion in magnetoactive plasma immersed in uniform external electric field
 07 p1055 A72-18894
 Pulsed IR carbon dioxide TEA laser for two dimensional interferometry of theta pinch plasma during discharge
 07 p1005 A72-19416
 Boltzmann equation solution in terms of irreducible spherical tensors and Talmi coefficients, calculating stress tensor for fully ionized plasma in strong magnetic field
 09 p1341 A72-22681
 Ellipsoidal plasmoid equilibrium revolution frequency and potential energy and stability in external hf fields
 09 p1362 A72-23204
 Plasma flow interaction with magnetic pulse field barrier from magnetic coil for short plasmoids formation
 09 p1362 A72-23211
 German monograph on electric arc behavior in narrow channel with plasma cooling by channel wall and continuously decreasing current for switching applications
 10 p1517 A72-23773
 Ionization equilibrium description by quantum statistical fugacity expansion of pressure for partially ionized plasmas
 10 p1524 A72-24929
 Coaxial plasma source energetic characteristics, establishing plasmoid energy linear dependence on battery stored energy
 11 p1699 A72-26754
 Burgers binary and Shkarofsky multiple collision theory numerical application to electrical conductivity in partially ionized solar magnetoplasma
 13 p2018 A72-29714

Fast pressure gage with protection against magnetized plasma parasitic effects to measure neutral pressure
 15 p2241 A72-32439
 Numerical analysis of boundary value problem for finite cylindrical dipole antenna of arbitrary orientation in magnetized plasma approximated by uniaxial medium
 16 p2366 A72-34107
 Stimulated effects in the radiative recombination from electron-hole liquid in semiconductors.
 19 p2844 A72-37932
 Electromagnetic wave scattering by electron charge density fluctuations in plane waveguide with magnetoactive plasma, showing cross section spectrum function of plasma properties
 20 p2903 A72-39072
PLASMATRONS
 NT DUOPLASMATRONS
 Plasma generation and continuous sustainment by laser beam and optical plasmatron
 01 p0109 A72-11073
 Thermal and I-V characteristics of dc plasmatron with vortex stabilized arc, interelectrode insert and diverging arc channel for various nozzle diameters
 05 p0694 A72-15854
 Thermal and electrical characteristics of plasmatrons with interelectrode partition and distributed air supply, determining efficiency dependence on current
 07 p1040 A72-18996
 PIG discharge system with plasma feed from duoplasmatron ion source for steady state operation with ion energies 1.5-5 keV
 08 p1214 A72-21435
 Coaxial plasmatron with central electrode composed of cylindrical Cu and W thermionic cathodes, noting thermal efficiency
 08 p1214 A72-21455
 Turbulent mixing of high temperature Ar jet injected into ring slipstream of air in dc plasmatron with coaxial nozzle and fixed arc
 09 p1410 A72-22677
 Convective heat transfer between jets produced by plasmatrons and heated substrate, showing independence of plasma flow rate
 09 p1319 A72-23189
 Trioplasmatron using crossed field hydrogen discharge between cold cathode and disk anode, noting pulse modulation applications
 13 p1927 A72-28380
 Thermal flux distribution in sectioned plasmatron channel with supersonic Ar plasma injection, discussing energy dissipation
 13 p2017 A72-29634
 Thermal and I-V characteristics of dc plasmatron with vortex stabilized arc, interelectrode insert and diverging arc channel for various nozzle diameters
 15 p2283 A72-31271
 Carbon dioxide laser excitation by injection of plasma jets produced by capillary plasmatrons
 21 p3063 A72-40835
 Approximate calculation of a laminar arc discharge in a cylindrical channel
 22 p3210 A72-42285
PLASMOIDS
 U PLASMAS [PHYSICS]
PLASMONS
 Hf plasma turbulence in solar flares due to nonlinear conversion of ion-acoustic plasmons to Langmuir plasmons
 03 p0413 A72-13812
 The surface plasmon resonance effect in holography.
 17 p2553 A72-34723
 Two quantum induced photon-plasmon transition probability for hydrogen atom in processes of nebulae and stellar chromospheres
 19 p2837 A72-38058
 Degenerate electron gas self energy approximation by dielectric function, calculating quasi-particle and plasmon properties
 24 p3428 A72-44797
PLASTIC AIRCRAFT STRUCTURES
 Lightweight low pressure plastic hose assemblies in aircraft and missile petroleum base fuel and synthetic lubricating oil systems at 395-710 R and up to 200 psi [SAE ARP 1180]
 01 p0006 A72-10388
 Price/demand/cost economic aspects of carbon fiber reinforced plastics composites in aero-engine applications
 04 p0536 A72-14743
 Carbon fiber resin composite characteristics for airframe component design, comparing with metal materials
 04 p0537 A72-14746
 Low cost 300 gallon fiber reinforced plastic aircraft wing fuel tank manufacturing technology
 08 p1177 A72-21693
 Titanium-boron-epoxy composite materials selection and fracture mechanics criteria for B-1 bomber structural design
 09 p1317 A72-22477

Boron-epoxy composite design for aircraft structures, discussing materials variations, strength prediction inadequacies and full scale tests
 11 p1670 A72-25454
 Structural requirements for normal category plastic aircraft civil certification, noting compliance with Federal Aviation Regulations
 [SAE PAPER 720304]
 11 p1575 A72-25568
 Dynamic properties of thermosetting plastic composites unidirectionally reinforced by high elastic moduli boron and carbon fiber for aircraft structural applications
 12 p1882 A72-27343
 Fiberglass reinforced plastic fuselage production for AN-2m aircraft, noting plastic-plastic and metal-plastic joints
 13 p1897 A72-29462
 Lightning current tests of aircraft glass/carbon fiber reinforced plastics materials
 13 p1898 A72-30040
 Data generation for engineering design with advanced composites.
 17 p2571 A72-35653
PLASTIC ANISOTROPY
 NT ELASTIC ANISOTROPY
 Subgrain rotation induced angular anisotropy of plastic deformation of oriented Mo single crystals during rolling
 05 p0674 A72-16354
 Stainless steels with improved formability developed through assessment of stress-strain curve slope and plastic strain ratio
 07 p1011 A72-19477
 Plastic stress-strain anisotropy of metals under forming for mild steel, austenitic stainless steel and Mg, showing nonconformability with Hill criterion
 07 p1020 A72-20432
 Anisotropy effect on glass fiber reinforced plastics cyclic deformability and heating kinetics under cyclic tension compression loads
 08 p1191 A72-21501
 Cicala formulas generalization and plasticity theory for deformation strain anisotropy, sliding and elastic strains influence on shear stress
 08 p1246 A72-21806
 Equivalent stress and plastic strain rates, based on shear stress hypothesis for theory of anisotropic plasticity of plastic materials under combined stress
 10 p1553 A72-23745
 Subgrain rotation induced angular anisotropy of plastic deformation of oriented Mo single crystals during rolling
 11 p1652 A72-25339
 Quasi-longitudinal and quasi-transverse plane wave propagation in anisotropic elastic-plastic solids, approximating Be single crystal behavior
 14 p2163 A72-30176
 Hot rolled steel bar strain history effect on isotropic and anisotropic plastic behavior, considering additional tension and torsion data
 15 p3235 A72-31527
 Plastic anisotropy quantitative calculation formula verified on Cu, Ni and Al, discussing physical sense of coefficients
 18 p2735 A72-36475
 Anisotropy and hydrostatic stress effects on yield criteria of nonwork-hardening plastic material under plane strain conditions
 21 p3117 A72-40674
PLASTIC COATINGS
 Transparent rain repellent polymer coatings, discussing water repellency theory, polymer chemical structures, adhesion to glass surfaces and evaluation methods
 03 p0381 A72-14237
 Stress-strain characteristics of nylon-polyurethane coated fabric under biaxial tension and shear forces
 05 p0736 A72-16108
 Plastic encapsulated transistors and IC moisture resistance tests for reliability under laboratory and field conditions
 06 p0782 A72-17363
 Aircraft fuselage acrylic glazing design, covering passenger cabin window, cockpit windscreen and various surface coatings
 12 p1753 A72-27008
 Al alloy welded seams corrosion fatigue strength increase by epoxy polymer coatings under cyclic tensile stresses
 16 p2397 A72-33268
 The detection of unreliable contacts by noise measurements.
 18 p2720 A72-37111
 On the measurement of mechanical tension in plastic encapsulated devices by means of piezo-resistance.
 18 p2669 A72-37112
 Reliability of integrated circuits with plastic encapsulation
 18 p2669 A72-37114
 Reversible changes in polyethylene coating adhesion due to thermo-oxidative destruction of polyethylene
 21 p3072 A72-40082

- Asbestos-textolite coating required thickness calculation with allowance for aerodynamic heating, discussing softening mechanisms
21 p3074 A72-41709
- Testing of plastic lubricants in ball bearings with rocking motion on the TSKB 16-T test stand
23 p3307 A72-43975
- PLASTIC DEFORMATION**
- Cobalt and lanthanum with face and body centered lattices, studying plastic deformation during allotropic transformations under sliding friction and gripping
01 p0074 A72-10579
- Metals mechanical behavior, considering plastic deformability, strain hardening, cohesion and engineering performance prediction
01 p0086 A72-10985
- Nonlinear effects due to crack front plastic yield and slow crack extension in energy release rate and fracture toughness calculations
01 p0140 A72-10993
- Macrosonic metal crystal plastic deformation applications to aircraft and spacecraft materials production, considering internal friction and energy conversion into strain energy and heat
01 p0071 A72-11020
- Soviet papers on deformation of metals and alloys covering rolling, mechanical properties and plastic deformation of W, Mo and Ni alloys
01 p0077 A72-11076
- Physical inconsistencies of mechanical-mathematical concepts of metal deformation, considering friction forces, lubricant action and plastic tensors and deviators
01 p0102 A72-11077
- Deformation and compression characteristics of W wire rolled from flattened vacuum melts
01 p0077 A72-11084
- Plastic deformation, heat treatment and grinding of set blank W casts for strip and foil production
01 p0088 A72-11085
- Plate buckling elastoplastic process derivation allowing for secondary plastic deformation onset, examining stress discontinuity at overloading and unloading zones boundary
02 p0289 A72-11614
- Elastoplastic deformation in medium with initial dislocations and temperature field, expressing kinetic stress and distortion tensors by Hamiltonian derivatives
02 p0290 A72-11630
- Thermoplasticity problems of materials with time dependent mechanical properties, obtaining approximate plastic deformation under cyclic loading
02 p0291 A72-11638
- Lower bound deformation theorem for rigid plastic continua under impulsive loads, emphasizing kinematically admissible velocity field
02 p0259 A72-12237
- Eutectic Ni-Cr alloy temperature effects on deformation rate on plasticity, noting superplasticity point
02 p0244 A72-12243
- Rigid plastic circular plate dynamic model with yield time delay, discussing residual deflection as function of load duration
02 p0293 A72-12426
- Inhomogeneous microstructure elastoplastic medium, examining strain and work in plastic deformation
02 p0293 A72-12427
- Metal fatigue mechanisms in subcreep temperature range, discussing response to cyclic loading including hardening, softening and inhomogeneous plastic strain development
02 p0295 A72-12496
- Yield relationship to coupling of plastic waves, obtaining stress-strain diagrams
02 p0297 A72-12613
- Empirical power law application to secondary creep, steady state hot working and high temperature tensile or compressive yielding, discussing activation parameters interrelations
02 p0247 A72-12814
- Secondary slip in impact loaded Al single crystal disks, interpreting face deformation bands
02 p0247 A72-12819
- Ultrasonic cavitation effects on martensitic specimens, observing plastic deformation, softening, phase transformations and decay
03 p0370 A72-13187
- Deformation kinetics relationship to scale effect in notched samples during elastoplastic loading phase
03 p0443 A72-13455
- Residual stress formation mechanism in two phase Ti alloys under cutting and plastic deformation, showing phase transformation composition and structure effects
03 p0363 A72-13467
- Cyclic deformation and energy dissipation during fatigue breakdown in steels under tension-compression and torsion
03 p0372 A72-13590
- Optimal cyclic fatigue strength of low C steel from critical deformation rate during thermomechanical treatment
03 p0372 A72-13597

- Rigid/plastic media plane and axially symmetric deformations determination, using principal and slip line numerical analysis methods
03 p0446 A72-13704
- Thick walled rigid plastic cylinders under pressure, obtaining uniqueness and stability of finite deformation
03 p0446 A72-13706
- Plastic torsion of prismatic and anisotropic rods, emphasizing inhomogeneity problems numerical solution
03 p0447 A72-13853
- Thermodynamic theory of rheological materials with internal changes accounting for higher gradients of deformation and temperature
03 p0448 A72-13888
- Tungsten wire deformation structure from swaging or rolling and drawing processes, noting cylindrical texture superimposed on fiber texture
03 p0375 A72-13933
- Substructure variations and crystal lattice periods dependence on compression stress in beryllium single crystals during plastic deformation due to base slip
03 p0376 A72-14018
- Ti-Al-V room temperature creep, considering tensile and torsional loading, plastic deformation, stress relief and design limitations
03 p0377 A72-14171
- Anisotropic media elastoplastic behavior, developing plastic deformation theory from stress-strain relationships for linearly elastic media
03 p0454 A72-14216
- Elastoplastic body random vibration analysis by statistical linearization, obtaining free elastic vibration mode shapes and damping constants
04 p0586 A72-15005
- Cylindrical shell stability and load capacity at large plastic deformations under internal pressure
04 p0587 A72-15019
- Nonlinear elastoplastic deformations of flexible shells of revolution, calculating stress concentration at circular hole in spherical shell
04 p0588 A72-15049
- Plastic strain and rupture characteristics of thin walled tubular Ni samples under complex loading and biaxial tension
04 p0588 A72-15058
- Effective plastic strain for Tresca and von Mises materials, investigating hot rolled mild steel specimens
04 p0590 A72-15187
- Strain hardening for steel strength increase to 300 kg/sq mm by sequentially combined mechanical and thermal processing, involving plastic deformation, quenching and aging
04 p0527 A72-15454
- Dislocation splitting and stacking fault energy variation during plastic deformation of TaC at 2200 C, using bending tests and microscope observations
05 p0670 A72-15861
- Local plastic deformation relation to tangential shear stresses, deriving expressions to determine critical levels
05 p0734 A72-15982
- X ray topography of natural diamond, showing impurity platelet distribution, slip depth, temperature and stress conditions after plastic deformation
05 p0702 A72-16020
- Internal friction changes in aluminum single crystal after uniaxial plastic deformation and irradiation
05 p0673 A72-16148
- Plastic stress and strain intensity factors for cracked plates in tensile fields
05 p0737 A72-16323
- Plastic zone formation and fatigue crack propagation rate during high cyclic bending of metals
05 p0674 A72-16326
- Subgrain rotation induced angular anisotropy of plastic deformation of oriented Mo single crystals during rolling
05 p0674 A72-16354
- Smooth curved metal surfaces thermal conductance at high vacuum, verifying contacting surfaces plastic deformation
05 p0666 A72-16868
- [AIAA PAPER 72-20]
Aging effect on duraluminum electrical resistivity alteration at low temperature plastic deformation
05 p0679 A72-17181
- Plastic deformation of solid body in terms of slip dislocations displacement rate
06 p0894 A72-17687
- Green-Naghdi nonlinear thermodynamics of elastoplastic deformation at finite strain, discussing relationship to nonisothermal theory
06 p0896 A72-17921
- Physical theory of plasticity, considering mathematical hypotheses and assumptions, single crystals dislocations and plastic deformation, polycrystals homogeneous strain analysis, slip theories, etc
06 p0896 A72-17962
- Viscoplasticity theory thermodynamic foundations, considering stress/strain states time and deformation path dependence
06 p0896 A72-17963

- Internal friction and plastic microstrains in martensitic transformation of Fe-Ni, Co-Ni, and Fe-Cr-Ni alloys
06 p0830 A72-18294
- Deformation stresses and strains in quasi-static low cycle fracture of stabilizing, softening and strain hardening materials
06 p0831 A72-18352
- Plasticity onset and brittle fracture of annealed steel as function of preceding strains
06 p0831 A72-18354
- Maximum temperature-holding time effects on plastic deformation and fracture of steel under thermal cyclic loads
06 p0831 A72-18359
- Plastic deformation and elastic stiffness of refractory metals, discussing impurities, alloying, temperature, work hardening, strain rate and texture effects
06 p0822 A72-18519
- Refractory and structural steels and Al alloys, obtaining low cyclic plastic deformation and breaking stress curves
06 p0898 A72-18549
- Steel sheet creep, plastic deformation and service life under temperature and stress cycles
06 p0899 A72-18558
- Deformability and strength of soft fiber reinforced plastics under biaxial tension, determining low temperature critical tensile stresses and elongation ratios
06 p0836 A72-18562
- Deformation kinetics and failure of refractory Nb and Mo base alloys in plastic state under low cyclic fatigue
06 p0833 A72-18631
- High temperature tests of short time strength, hardness and moduli of elasticity of W-MO alloys subject to plastic deformation and annealing
06 p0833 A72-18633
- Cyclic loading failure criteria based on plastic deformation energy concepts, considering material load carrying capacity
06 p0899 A72-18650
- Plastic deformation fatigue theory extended to tests at stresses below elastic limit, explaining cyclic loading frequency effect on fatigue life
06 p0899 A72-18652
- Stress distribution during plastic deformation of steel turbine disk from hardness measurements
06 p0900 A72-18670
- Plastic deformation, creep rupture strength, endurance limit and service life of prestressed strain hardenable material
06 p0900 A72-18681
- Idealized model for anisotropy of metals inelastic characteristics due to plastic deformation, demonstrating applicability to polycrystalline materials
06 p0900 A72-18688
- Plastic strain and fracture of metals by specific internal energy change method, investigating mechanical work and heat release
06 p0900 A72-18691
- Hardening phases effect on plastic deformation resistance of Ti and Ti alloys
06 p0835 A72-18746
- Creep and plastic deformation analysis of riveted joint elements using elastoplastic theory
07 p1087 A72-18982
- Transient high speed deformations analysis of annealed Al under impact loads by three dimensional moire fringe techniques
07 p0983 A72-19131
- Managing steel embrittlement by titanium carbide lattices separation during cooling, suggesting rapid quenching and plastic deformation temperature reduction
07 p1012 A72-19677
- Computerized estimation of deformation parameters for Sellars-Tegart equation relating stress, strain rate and temperature in creep and hot torsion testing of metals
07 p1090 A72-19736
- Increased microplastic deformation resistance, relaxation stability and aging of beryllium by cyclic heat treatment
07 p1013 A72-19740
- Material anisotropy effect on stress-strain state and limiting load in plane plastic deformation
07 p1091 A72-19764
- Automatic photoelectric device for measuring internal stresses and deformations of photographic films
07 p0988 A72-19861
- Martensitic transformations induced by plastic deformation in Fe-Ni-Cr-C system, noting stacking fault energy dependence on temperature
07 p1015 A72-19928
- Hardening mechanisms during plastic deformation of pure bcc metals, discussing stresses relation to fine structure and crystal dislocation paths
07 p1018 A72-20142
- Cold brittleness of transition metal alloys with bcc lattices, discussing elastic characteristics, packing defects energy, plastic deformation and rhenium admixture
07 p1018 A72-20143

Nb and Nb alloys mechanical properties during plastic deformation and heat treatment, discussing grain size, dislocation structure and substructural changes effects 07 p1018 A72-20144

Metals and alloys breakdown toughness and mechanical properties predictions under various loading conditions, discussing interatomic bonds and plastic deformation zone size 07 p1019 A72-20146

Computerized dynamic simulation with graphic display of crystal plastic dislocation movement among random obstacles, emphasizing stress-strain, strain rate and thermal activation mechanisms 07 p1095 A72-20338

Magnetic domain structure of Ni single crystals after plastic deformation as function of stress induced anisotropy of layer-like dislocations 07 p1020 A72-20411

Strain rate effects on strain hardening of duralumin, copper and lead, noting yield stress sensitivity to deformation induced temperature changes 07 p0998 A72-20527

Alpha Ti plastic deformation behavior below 700 K, determining activation area and enthalpy as functions of stress and temperature 08 p1186 A72-21247

Elastic-plastic deformation of thin membrane shells 08 p1244 A72-21290

Metal cold working mechanics, discussing model based on equality of internal and external forces needed for plastic deformation 08 p1176 A72-21439

Anisotropy effect on glass fiber reinforced plastics cyclic deformability and heating kinetics under cyclic tension compression loads 08 p1191 A72-21501

Plastics optimal reinforcement in given stressed state by determining shortest path from stress point to strength region 08 p1244 A72-21502

Friction and bending effect on unidirectional glass fiber reinforced plastic ring deformation distribution 08 p1191 A72-21504

Critique of paper on lower bounds on deformations of dynamically loaded rigid plastic continua 08 p1245 A72-21630

Strength analysis of thin elatoplastic shell with allowance for compressibility, relating loads and moments to deformation of middle surface 08 p1246 A72-21712

X ray study of martensite fine structure produced by plastic deformation in Fe-Ni alloy 08 p1188 A72-21788

Plastic deformation characteristics of Fe-Cr-Ni alloy single crystals at low temperatures 08 p1188 A72-21790

Cicala formulas generalization and plasticity theory for deformation strain anisotropy, sliding and elastic strains influence on shear stress 08 p1246 A72-21806

Thin shell theory analysis of thin walled cylindrical shell necking phenomenon as tensile deformation nonuniformity 08 p1248 A72-21821

Biaxial tension and combined tension-torsion induced initial yield surfaces and plastic deformation onset, using localized strain theory 08 p1195 A72-21852

Viscoplasticity techniques application to deforming portion strain and strain rate fields of axisymmetric Al alloy extrusion with various flow patterns 08 p1250 A72-22194

Al alloy and brass deformation compression tests inadequacy for friction determination and boundary analysis, EP additives and hydrodynamic and solid lubricants evaluation 08 p1181 A72-22195

Plastic deformation friction fracturing, stress concentration, free surface changes and load displacement analysis with upper bound, slip line and finite element methods 08 p1250 A72-22197

Workability tests from material deformation stress determination and fracture strain rate relation for forging, extrusion and rolling limits predictions 08 p1190 A72-22198

High temperature alloy deformation superplasticity and formability relation with microstructure, fine structure and load requirements for hot working with high strain rate 08 p1250 A72-22200

Thermomechanical and plastic deformation behavior of polycrystalline alumina at elevated temperatures 09 p1335 A72-22394

Cryostat for high resolution tensile measurements of thermally activated processes during plastic deformation 09 p1398 A72-22657

Stress-strain state of circular conical shell of linearly variable thickness within small elastoplastic deformation theory, assuming specific convective heat transfer at surface 09 p1401 A72-22722

Sign-variable nonisothermal plastic deformation and creep behavior of polycrystalline construction materials, taking into account Bauschinger effect 09 p1401 A72-22726

Creep properties in turbine disks of heat resistant alloy under plastic deformation due to nonstationary thermal conditions 09 p1401 A72-22730

Fatigue strength of heat resistant materials under thermal cyclic loads leading to sign variable plasticity and creep 09 p1402 A72-22732

Plastic slip in notched half plane undergoing antiplane deformation, using screw dislocation continuous distribution theory 09 p1403 A72-22747

Mathematical thermodynamic theory for plastic deformation induced internal structure changes in rheological material, describing homogeneous response by temperature and deformation gradients 09 p1403 A72-22761

Al alloys degree of deformation dependence on pulse energy during extrusion by pulsed magnetic field, showing hardening effect 09 p1319 A72-22865

Energy balance criterion application to crack growth under cyclic fatigue loading, considering stress-strain behavior of plastic deformation energy 09 p1404 A72-22911

Optical simulation of plastic strain distribution with models prepared from organic glass, investigating birefringence effect 09 p1406 A72-23182

Plastic compression of short cylinders prepared from incompressible rigid-plastic material with variable vertical yield point distribution, deriving variational equation of plastic flow 09 p1406 A72-23183

Plastic deformation effect on structure and properties of steel sheet under biaxial tension at liquid nitrogen temperature 09 p1330 A72-23187

Elastic and plastic buckling analysis of uniformly compressed rectangular plates, using Kantorovich method 09 p1408 A72-23556

Equivalent stress and plastic strain rates, based on shear stress hypothesis for theory of anisotropic plasticity of plastic materials under combined stress 10 p1553 A72-23745

Elastoplastic deformation of Zn single crystals under uniaxial tensile loads, noting critical stresses relationship to current pulses 10 p1553 A72-23766

Optical and electron microscopic study of Inconel 625 precipitation and recrystallization behavior over temperature range under plastic deformation 10 p1494 A72-23829

Fracture toughness expressions including nonlinear effects due to crack front plastic yield and possible crack extension prior to fracture instability [SMRT PAPER L 1/4] 10 p1497 A72-24396

Transmission electron microscope examination of deformation microstructures adjacent to fatigue cracks in Al alloys 10 p1497 A72-24823

Fracture energy and deformation of unidirectionally and randomly oriented lamellar Al-Cu eutectics from surface microstructure studies 10 p1499 A72-24893

Fracture strength relation to austenite stability in steels with plastic deformation caused by strain induced austenite-martensite transformation 10 p1499 A72-24894

Subgrain rotation induced angular anisotropy of plastic deformation of oriented Mo single crystals during rolling 11 p1652 A72-25339

Plastic behavior of laterally loaded beams and rectangular plates, formulating upper and lower bound theorems 11 p1728 A72-25372

[AIAA PAPER 72-343] Ni and Ni alloys microstructure under tensile stress, determining Cr and Ti effects on plastic deformation at high temperature 11 p1654 A72-25494

High temperature metallographic methods in microstructure study of austenitic heat resistant steel under plastic deformation and heat treatment 11 p1654 A72-25495

Perforated plates plastic deformation, stresses and strains near holes, using strain gage data in biaxial tensile tests 11 p1733 A72-25540

Creep and low cycle fatigue dynamic behavior, noting stress concentration time dependence, strain hardening and local plastic deformations in dead annealed Al thin walled tubes 11 p1658 A72-25829

Temperature and strain rate effects on superplasticity of Ni-Cr eutectic alloy 11 p1659 A72-26129

Dislocation velocity-stress relationship in plastically deformed Al at room temperature, noting entropy term in Gibbs free energy equation 11 p1661 A72-26652

Plastic percentage reduction of area and elongation for circular cylindrical sample in tensile deformation, proposing stress analysis method for metallic sleeves under low cycle loads 11 p1738 A72-26810

Deformation drawing textures of bcc metals, including W 11 p1644 A72-26838

Zone refined prism slip oriented Be single crystals deformation substructure analysis by synergetic method combining transmission electron microscopy, X ray topography and X ray diffraction profile analysis 11 p1666 A72-26928

Deformation characteristics and mechanical properties of superplastic alloys, stressing metallographic techniques 11 p1739 A72-26936

Boundary surfaces during plastic buckling of hollow cylindrical shell under combined loading by external pressure and axial force 12 p1880 A72-27231

Quenched beryllium bronze alloy plastic deformation effects on anomalous and ordinary stress relaxation processes 12 p1828 A72-27292

Plastic deformation resistance nonuniformity in Al alloys, determining stresses 12 p1829 A72-27457

Tensile plastic deformation effect on structural evolution of Ti-Ni alloy under anisothermic heat treatment 12 p1830 A72-27738

Elastoplastic deformation effects on load bearing capacity of samples with stress concentrators under alternating cyclic loading, obtaining nomograms by digital computer 12 p1887 A72-28228

Low carbon steel prior plastic deformation effects on mechanical hysteresis loop shape 12 p1887 A72-28234

Cyclic nonisothermal plastic deformation of ductile disk, verifying experimentally with turbine disk of heat resistant alloys 13 p2053 A72-28398

High strength low alloy steel and stainless steel recrystallization after hot working at plastic deformation temperature 13 p1973 A72-28654

Strain rate controlling mechanisms of superplastic deformation at various stresses and temperatures, considering vacancy and dislocation creep and grain boundary sliding 13 p1974 A72-28657

Deformation limits in thin and thick walled metal blanks axisymmetric drawing process, determining stress-strain state based on prescribed velocity field 13 p1963 A72-28743

High temperature contact creep tests in vacuum and in metal melts, noting adsorption effect on surfaces plastic deformation 13 p1963 A72-28768

Austenite deformation effect on thermal stability and hardness of Ni steels at various C and Ni concentrations 13 p1977 A72-29019

Plane plastic deformation during single pass rolling of corrugated metal sheet, determining stress-strain fields for first and second phases 13 p1964 A72-29148

Al and AlMg single crystals static recovery and stacking fault energy at 77-500 K in plastic deformation, noting cross slip onset at 500 K 13 p1978 A72-29222

Dislocations with Burgers vector during Zr single crystals deformation at different temperatures, examining shear plane foils by electron microscope 13 p1978 A72-29223

Plastic deformation in bcc metal single crystals, discussing glide and work hardening, dislocations, core structure and atomic calculations 13 p2061 A72-29874

Electron shell structure in annealed and plastically deformed W-Re alloys from positron annihilation angular distributions 13 p1981 A72-29908

Elastic effects in metal hardness testing with blunt indenter, considering indentation in rigid plastic manner 14 p2113 A72-30268

Electric current pulses effect on Zn monocrystals plastic deformation before brittle rupture, noting critical normal stresses increase 14 p2115 A72-30411

Metal creep activation energy determination during plastic deformation process, using temperature differential method 14 p2115 A72-30412

Temperature effects on critical crack opening as fracture toughness criterion for medium strength steel, taking into account local plasticity and propagation resistance 14 p2118 A72-30590

Fatigue crack growth rate in precracked steel samples observed at 100 C by etching technique, noting flow stress and yield in plastic zone

14 p2119 A72-30608

Transverse strain coefficient for steel box-section beam under tension, presenting test values for deformations before and beyond elastic limit

14 p2166 A72-30692

Creep deformation transition theory in spherical shells, using generalized strain measure for asymptotic solution

14 p2169 A72-30999

Material constants for strain hardened polycrystalline metals calculated from mathematical model for plastic deformation

15 p2322 A72-31361

Viscoplastic flow of inhomogeneous shells of revolution obeying Tresca condition, noting plastic deformation velocity relation to stresses

15 p2325 A72-31605

Plastic deformations accumulation and breakdown initiation in notched steel specimens, discussing effects of mechanical properties, geometry and heat treatment

15 p2256 A72-31607

Metal fatigue tests at various frequencies to observe surface structure, dislocations in crack vicinity, plastic deformation and ultrasonic resonance techniques

15 p2257 A72-31839

Plastic deformation in metals and highly crystalline polymers as function of shear strain, strain rate, frequency and vibrational amplitude

15 p2328 A72-31840

High amplitude ultrasonic stress waves effect on metals elastic and plastic deformation characteristics, verifying model for sound waves-lattice structure interactions

15 p2328 A72-31842

Electron microscopic investigation of slip processes during plastic deformation of WC-Co based cermets, observing WC grain boundary sliding and Co phase crystal lattice transformations

15 p2257 A72-32117

Mobile dislocation density and strain rate sensitivity of bcc Fe-Ni alloys from deformation onset to high temperature plateau

15 p2258 A72-32639

Stress-strain relations for inelastic deformation of anisotropic strain hardenable shells of revolution under arbitrary plasticity conditions

15 p2332 A72-32678

Plastic deformation and limiting strain curves of Ti alloys in plane stressed state, comparing with yield and rupture conditions

15 p2259 A72-32684

Deformation modes for deep drawing of extramild steel sheets, noting susceptibility and rupture criteria

16 p2396 A72-32872

Work hardening and anisotropy coefficients effects on deep drawing limit curves for extramild steel, noting rupture strain and deformation trajectories

16 p2396 A72-32873

Finite element method application to nonlinear dynamic problems exemplified by study of plastic deformation behavior of cylindrical billet under impact of heavy rigid body

16 p2466 A72-33019

Edge-loaded rectangular plate buckling behavior in elastoplastic range between proportional limit and yield point

16 p2466 A72-33020

Yield conditions formulation restrictions for large elastoplastic deformations, discussing isotropic and anisotropic hardening

16 p2396 A72-33024

Aluminum oxide reproducible layers plastic deformability or microhardness from molecular beam scattering distribution

16 p2430 A72-33064

Al-Cu-Mg alloys room temperature age hardening, determining effects of tension load up to plastic deformation from measurements of mechanical properties and electrical resistance [DFVLR-SONDDR-188]

16 p2408 A72-33674

Material thoutin in deformed metal sheet specimens under explosive forming, using air cell effect

16 p2399 A72-33775

Composite cylinder of helically wound fiber laminates, calculating torsional fracture strength with allowance for plastic deformation due to matrix distortion

16 p2472 A72-33949

Error analysis of dynamic yield point measurements based on residual deformation from impact tests of Al alloy and steel specimens

16 p2472 A72-34016

Unified description of structures behavior subject to elastic, creep and plastic deformations

16 p2473 A72-34117

Three dimensional elastoviscoplastic theory for complex structures static-dynamic creep deformation under time varying stress and temperature fields, generalizing Odqvist-Hoff law

16 p2473 A72-34211

Creep deformation upper bounds for smooth pipe bends under constant external bending moments, using energy method analysis

16 p2473 A72-34123

Uncontained plastic flow onset speeds for cylinders rotating about longitudinal axes, investigating relation to bursting speed

16 p2475 A72-34172

Plastic deformation at a stably growing crack tip.

17 p2569 A72-34252

Geometric instabilities in isotropic plastic solids under increasing uniaxial compression.

[ASME PAPER 72-APM-28] 17 p2624 A72-34310

Thermodynamic basis for plasticity theory in case of small deformations, considering elastic region isotropic representation and linear relation as response to pure expansion

17 p2627 A72-34770

Elastoplastic bending of rectangular plates with large deflection.

[ASME PAPER 72-APM-34] 17 p2628 A72-34785

On uniqueness in ideally elastoplastic problems in case of nonassociated flow rules.

[ASME PAPER 72-APM-33] 17 p2628 A72-34786

Spatial and temporal load pulse parameters for circular cylindrical shells /tubes/ dynamic plastic deformation

[ASME PAPER 72-APM-29] 17 p2628 A72-34790

Dynamically loaded elastic, viscous, plastic and rigid, viscoplastic structures instantaneous mode responses definitions and characterization by variational criteria with isometric constraints

[ASME PAPER 72-APM-17] 17 p2628 A72-34799

Strain history effect on isotropic and anisotropic plastic behavior.

[SESA PAPER 1940] 17 p2631 A72-34820

Mathematical models for metallic plastic strain hardening under cyclic loads, introducing internal state parameters

17 p2632 A72-35111

Thermodynamic infinitesimal theory of viscoplasticity

17 p2632 A72-35112

Elastoplastic structural analysis from design viewpoint, discussing load limits and stability estimates based on large deformation assumption

17 p2632 A72-35113

Russian book - Plastic deformation of high-alloy steels and alloys

17 p2568 A72-35454

Russian book - Determination of stresses in the plastic region from the hardness distribution

18 p2732 A72-36300

An approach to the analysis of the nonlinear deformation and fatigue response of components subjected to complex service load histories.

18 p2733 A72-36355

Strain measure determined plastic stress concentrations around discontinuities in flat plates compared with incremental theory

18 p2733 A72-36359

Application of an analog computer to the calculation of partially plasticized rotating circular disks prepared from strain-hardenable materials

18 p2735 A72-36421

Phase structure and solution kinetics of cast and wrought Al alloys after plastic deformation by rolling

18 p2700 A72-36585

Effects of combined high and low temperature deformation processing of beta III titanium.

18 p2701 A72-36590

A non-linear integral-type theory of inelasticity for transversely isotropic materials.

18 p2738 A72-37075

Some problems concerning microplastic deformation and isothermal transformation of Fe-Ni-C alloy. III - Effect of aging in the temperature range from 203 to 304 K on microplastic deformation at 77 K

19 p2814 A72-37419

Some problems concerning microplastic deformation and isothermal transformation of Fe-Ni-C alloy. IV - Effect of transformation plasticity on microplastic deformation at 77 K

19 p2815 A72-37420

Physics of strengthening mechanisms in crystalline solids.

19 p2843 A72-37444

The plastic deformation behavior of Mo single crystals under compression.

19 p2816 A72-37689

Structures and materials performance under creep and plastic deformation, discussing energy theorems implications

19 p2874 A72-37705

A new morphological element on the viscous breakdown microsurface of hypoeutectoid steels

19 p2817 A72-37737

Aluminum. II - A review of deformation properties of high purity aluminium and dilute aluminium alloys.

19 p2818 A72-37832

Regularities in the deformation and failure of commercial iron in a complex stress state under low-temperature conditions

19 p2818 A72-38005

Plasticity and rupture of heat-resistant materials subjected to a small number of cycles of simultaneous variation of temperature and load

19 p2818 A72-38006

Plane stress rupture criterion for age hardening materials during plastic deformation, calculating resistance to shear and torsion of solid and hollow round bars

19 p2818 A72-38009

Theory for transverse vibrations of beams during elastoplastic deformations

19 p2877 A72-38179

The effect of hydrostatic pressure on plastic deformation and creep of polycrystalline metals at elevated temperatures.

20 p2977 A72-38871

Elastoplastic axisymmetric bending of a clamped circular plate under the action of a conically-distributed variable load

20 p2978 A72-39022

The effect of plastic deformation on the martensite-to-austenite transition in an iron-nickel alloy.

20 p2938 A72-39298

Deformation and failure characteristics of joints in a Ni-Al system under the action of high thermal pulses

20 p2942 A72-39822

Fe-Ni sheet with austenitic cube texture by rolling and annealing, investigating plastic deformation during martensitic transformation

21 p3065 A72-40090

Anisotropy and hydrostatic stress effects on yield criteria of nonwork-hardening plastic material under plane strain conditions

21 p3117 A72-40674

Plastic deformation in annealed aluminium bar containing circumferential semicircular notch.

21 p3118 A72-40719

On basic principles of the slip theory of plasticity.

21 p3121 A72-41241

Hysteresis curve equation for calculation of elastoplastic deformations caused by forced vibrations, taking into account medium compressibility and inertial forces

21 p3123 A72-41359

Perfectly plastic media under the action of multiparameter loads

21 p3123 A72-41393

Constitutive equations of generalized Brandt-Reuss theory of elastoplastic deformation, noting second order effects

21 p3124 A72-41506

Buckling of inelastic cylindrical shells under axial impact.

21 p3124 A72-41507

Theory of slow elastic-plastic deformation of polycrystalline metals with micro-stresses as latent variables descriptive of the state of the material.

21 p3124 A72-41508

Theoretical and experimental investigation of the relationship between plastic and creep deformation of structures.

21 p3124 A72-41509

Line integral expressions along line singularity loop for elastic strain and curvature, observing plastic dislocations, distortions and rotations

21 p3125 A72-41511

Calculation of sandwich shells of revolution at large elastic-plastic deflections.

21 p3125 A72-41512

Disclinations theory described by plastic and elastic distortions, considering line singularity and dislocation loop

21 p3125 A72-41513

Investigation of fatigue-failure mechanisms and inelastic deformation of metals in torsion

21 p3071 A72-41703

Convergence of the homogeneous linear approximation method in problems of plasticity theory of inhomogeneous bodies

22 p3232 A72-41911

Matthiessen rule on binary alloy electrical resistivity temperature derivative, discussing data deviations in substitutional alloys after quenching, radiation damage and plastic deformation

22 p3189 A72-42298

Measurement of the stacking-fault energy of gold using the weak-beam technique of electron microscopy.

22 p3177 A72-42320

Kinetic aspects of plastic strain induced martensite in polycrystalline Fe-Ni-C alloy from tensile tests on austenitic specimens

22 p3189 A72-42437

Cyclic hardening of Al-Zn single crystals at constant plastic strain amplitude, observing similarity between fatigue hardening and work hardening

22 p3189 A72-42439

Clamped circular rigid-plastic plates subjected to central blast loading.

22 p3235 A72-42601

On the formation of plastic adiabatic bands in a thin tube subjected to a dynamic torsion

22 p3236 A72-42638

Investigation of the drop forging process applied to magnesium alloys 22 p3183 A72-42816

The application of the finite element displacement method to problems of elastoplastic deformation. 22 p3238 A72-42832

Deformation mechanism of aluminum and zinc single crystals during low-temperature cavitation 22 p3192 A72-43019

Mathematical model for plastic deformation of polycrystalline materials with Hooke's law elastic strains 22 p3242 A72-43135

Study of the process of powder knurling to articles 23 p3292 A72-43279

Continual theory of dislocations and the theory of small elastoplastic deformations 23 p3345 A72-43584

Equilibrium equations and deformation of elastoplastic thin isotropic cylindrical shell with circular hole, noting nonlinear partial differential equations for plate displacements 23 p3345 A72-43587

Martensitic transformation during deformation in titanium alloys with a metastable beta phase 23 p3300 A72-43591

Crack opening displacement relationship to notch root contraction from fracture toughness tests, describing plastic deformation mechanism at notch tip 23 p3346 A72-43704

Lutetium strength and plastic deformation characteristics under tension, presenting temperature and strain rate effects 23 p3301 A72-43754

Limiting equilibrium of shells of revolution and circular plates with allowance for shear stresses 23 p3348 A72-43789

Elastic and plastic deformations in torsional moment loaded rod, noting successive approximation for stress functions 23 p3348 A72-43794

Determination of the stressed state in a welded joint in plastic deformation 23 p3293 A72-44019

Non-linear free vibration of a beam with time-dependent material properties. 23 p3355 A72-44374

Field-ion microscopic study of the interstitial plasticity of tungsten single crystals 23 p3304 A72-44484

The difference in the plastic deformation of the surface and bulk layers of polycrystalline iron under fatigue loading 23 p3304 A72-44490

Characterization of four polymeric materials at strain rates from 0.0001 to 1000 per sec. 24 p3417 A72-44612

The cyclic plastic strain and cumulative fatigue damage - Fatigue damage caused by the stress below the fatigue limit. 24 p3454 A72-44628

Stress-strain diagrams from high and low temperature tests of Y alloy rods, noting temperature effects on plastic deformation 24 p3413 A72-44724

Computation of post-yield behaviour in notch-bend and tension testpieces. 24 p3456 A72-44796

Fatigue crack closure at positive stresses. 24 p3457 A72-44819

Elasto-plastic stress analysis - A generalization for various constitutive relations including strain softening. 24 p3457 A72-44880

Deformation kinetics relationship to scale effect in notched samples during elastoplastic loading phase 24 p3458 A72-44930

Residual stress formation mechanism in two phase Ti alloys under cutting and plastic deformation, showing phase transformation composition and structure effects 24 p3407 A72-44942

Some extremal properties and energy theorems for inelastic materials and their relationship to the deformation theory of plasticity. 24 p3460 A72-45692

On dual energy theorems for a class of elastic-plastic problems due to G. Maier. 24 p3460 A72-45693

Local plastic deformation relation to tangential shear stresses, deriving expressions to determine critical levels 24 p3460 A72-45724

Deformation stresses and strains in quasi-static low cycle fracture of stabilizing, softening and strain hardening materials 24 p3460 A72-45739

Plasticity onset and brittle fracture of annealed steel as function of preceding strains 24 p3416 A72-45741

Maximum temperature-holding time effects on plastic deformation and fracture of steel under thermal cyclic loads 24 p3416 A72-45746

PLASTIC FILMS
U POLYMERIC FILMS
PLASTIC FLOW
NT TRESCA FLOW

Two component flow and optimal strength ratios between core and shell materials during extrusion of composite bimetallic specimens into circular tubes 01 p0077 A72-11078

Plastic flow material transport during sintering, considering dislocation nucleation mechanism 02 p0232 A72-11429

Incompressible power law pseudo-plastic material plane flow in converging channel and axially symmetric converging flow in circular cone 04 p0513 A72-15287

Fracture theory application to rotating cylinder velocity field determination, emphasizing plastic equilibrium and flow behavior 05 p0738 A72-16424

Alloying elements effects upon iron mechanical properties, investigating lattice parameters, temperature dependence of yielding and plastic flow, solid solution strengthening and softening, etc 05 p0676 A72-17101

Ferritic stainless steel roping/buckling/morphology and texture explanation by anisotropic plastic flow 05 p0677 A72-17105

Plastic flow stress around dislocations on Ni-Al intermetallic cube and octahedral cross slip systems 05 p0678 A72-17118

Book on plasticity theory covering stress and strain as basic concepts of continuum mechanics, differential equations of motion, plastic flow, yield criteria, elastic-plastic equilibrium, plane strain, etc 08 p1244 A72-21477

Plastic flow properties and stress measurement for metal working conditions with flat ring compression specimens and interfacial friction consideration 08 p1250 A72-22196

Rotationally symmetrical cylindrical shell loaded by uniform pressure distribution along length, calculating quasi-steady viscoplastic flow under Huber-Mises condition 09 p1399 A72-22696

Computer algorithm for thermoplastic stress-strain state of thin shells of revolution based on plastic flow theory, taking into account loading history 09 p1401 A72-22724

Spatial plastic flow in arbitrary incompressible continuous medium with instantaneously inextensible family of planes, deriving velocity field formulas 09 p1403 A72-22758

Riemann invariants method for plasticity theory application to first order quasi-linear systems, considering plastic flow in arbitrary die 09 p1403 A72-22760

Anisotropic plate theory for perfectly plastic flow, expressing yield condition in terms of mixed stress-anisotropy tensors 09 p1403 A72-22765

Carbon fiber reinforced plastic toughness from strain concentration and plastic flow observation near crack tip by moire technique 09 p1339 A72-23170

Plastic compression of short cylinders prepared from incompressible rigid-plastic material with variable vertical yield point distribution, deriving variational equation of plastic flow 09 p1406 A72-23183

Tensile plastic flow and fracture behavior of PdSi based alloys in glassy microcrystalline and crystalline states, noting shear deformation bands 09 p1339 A72-23382

Metallographic study of denuded zones from diffusional flow in hydrided Mg superplastic alloy with Zn and Zr 09 p1331 A72-23383

Low carbon ultrafine grain steel tensile behavior, noting critical grain size for stable/unstable plastic flow transition 11 p1661 A72-26651

Reversible stress effects in theory of plastic flow in strain hardened metals at high temperatures 12 p1879 A72-27159

Fiber composites plastic flow and fracture, using plane strain model for analysis 12 p1884 A72-27730

Strain release method for investigating thermally activated microflow mechanisms in solids, discussing technique for activation energy and relaxation strength measurements 16 p2372 A72-32822

Riemann invariants method for nonelliptic first order systems with two independent variables, presenting application to perfectly plastic material flow in die without friction 16 p2467 A72-33140

Plastic flow, yield strength and fracture of unidirectional A1-B fiber composite sheet under biaxial tension 16 p2411 A72-33821

Uncontained plastic flow onset speeds for cylinders rotating about longitudinal axes, investigating relation to bursting speed 16 p2475 A72-34172

Flow and fracture criteria for powder forging. 19 p2815 A72-37597

Thermal and athermal components of the flow stress in zone-refined titanium. 19 p2820 A72-38298

Plastic flow and strain hardening theories for short time tensile creep in high temperature metal formation, applying to Al alloys 21 p3125 A72-41510

Shear-strain-rate effects in a high-strength aluminum alloy. 23 p3302 A72-43983

Temperature change direct measurement and annealing experiment via differential power analysis to determine stored energy release in metal plastic flow during compression 24 p3405 A72-44613

Plastic flow around an expanding crack. 24 p3456 A72-44812

PLASTIC MATERIALS
U PLASTICS
PLASTIC MEMORY

Anelastic solid energy dissipation linear memory models based on viscoelasticity theory, applied to earth and metals experimental data and dynamic loading problems 02 p0294 A72-12447

Dilatometric investigation of martensitic transformation in TiNi compound, observing plastic memory effect 03 p0377 A72-14021

Elastoplastic stability of structural rods in unloadable systems, considering load carrying capacity increase by critical state onset delay 03 p0454 A72-14214

Plastic strains and crack growth in Al alloy under static and repeated static loading 13 p1977 A72-28915

Constitutive equations for multipolar solid with memory, deriving boundary conditions and free energy equation from first and second thermodynamics laws respectively 15 p2273 A72-31363

Hot rolled steel bar strain history effect on isotropic and anisotropic plastic behavior, considering additional tension and torsion data 15 p2325 A72-31527

Thermodynamic theory of materials with memory depending on temperature gradient summed history 16 p2425 A72-33587

Interdependence of the commutation and memorization effects and the thermal behavior in a series of chalcogenide glasses 18 p2718 A72-36344

A model of a nonlinear viscoelastic medium allowing for the effects of cumulative damage 19 p2871 A72-37528

Stress induced martensitic transformation relationship to shape memory effect compared with superelasticity, transformation plasticity and reversible linear change 21 p3065 A72-40091

Thermoelastic martensite caused elastic vibration damping in Cu-Al-Ni alloy, observing shape memory effect 22 p3190 A72-42442

PLASTIC PROPERTIES
NT ELASTOPLASTICITY
NT PHOTOPLASTICITY
NT THERMOPLASTICITY
NT VISCOPLASTICITY
NT YIELD POINT

Differential equations derived for elastic-plastic behavior of rotationally symmetric shells, approximating in finite difference forms and solved by elimination method 01 p0138 A72-10394

Recrystallization and rolling temperature effects on W strength and plasticity 01 p0088 A72-11083

Turbine blades adaptability limits to temperature variations, considering rectangular cross section plastic rod under programmed thermal and tensile load cycles 01 p0143 A72-11372

Finite plasticity incremental and total strain theories for nonproportionate loading of circular steel and Al alloy torsion-tension members assuming von Mises yield [SESA PAPER 1901] 02 p0288 A72-11519

Three dimensional problems in stability, elasticity and plasticity theory for isotropic, anisotropic and inhomogeneous bodies, noting applications to machine construction, civil engineering, geophysics, etc 02 p0288 A72-11602

Thin shell creep and plasticity analyses reduced to linear programming problem by functionals and finite difference equations 02 p0290 A72-11622

Dynamic and plastic behavior of mild steel and Al wide beams and rectangular flat plates 02 p0291 A72-11964

VT22 high strength Ti alloy beta phase decomposition kinetics studies under heat treatment, noting omega and alpha phases role for low plasticity 02 p0244 A72-12247

Ductility relationship to plasticity characteristics in cylindrical steel samples with short notch under tension

03 p0443 A72-13458

Approximate S-N fatigue testing/digital computer method for quasi-static boundary value problems in plasticity theory, applying to continuum models

03 p0453 A72-14210

Mathematical plasticity theory of stress-strain relations under complex loading, including broken line trajectories

03 p0453 A72-14211

Rheological relations of moment-stress plasticity for steady and cyclic loads, using small elastoplastic strains

03 p0453 A72-14212

Yield point elongated and strain hardened rectangular plates, calculating plastic coefficients in geometrically nonlinear bending problem

04 p0588 A72-15057

Cyclic strain accumulation induced creep behavior prediction via plasticity model, considering non-homogeneous stress states

[ASME PAPER 71-APM-NN] 04 p0589 A72-15179

Dimpling behavior of metal plate with mode I edge crack, relating flaw depth, applied stress level and crack tip plastic zone

05 p0673 A72-16305

Zircaloy plastic properties and fatigue fracture modes under strain controlled push-pull cyclic loads, noting plastic anisotropy changes for warm cross rolled and recrystallized materials

05 p0678 A72-17120

Low temperature tensile strength and plasticity of Ti alloys containing zirconium

05 p0679 A72-17203

Superplasticity relation to heat resistance in metal systems Ni-Cr, Ni-Cr-W-Ti-Al and Ti-Si

05 p0680 A72-17212

Split Hopkinson pressure bar for studying material plastic behavior under impact, discussing principles, equipment and test results

06 p0814 A72-17742

Physical theory of plasticity, considering mathematical hypotheses and assumptions, single crystals dislocations and plastic deformation, polycrystals homogeneous strain analysis, slip theories, etc

06 p0896 A72-17962

Plasticity of Al alloy thin walled tubular specimens under axial tension and internal pressure at 293, 173 and 93 K

06 p0833 A72-18561

Metal strip with circular hole under tension, calculating plastic strain and stress concentration coefficients

06 p0899 A72-18567

Carbon effects on strength, ductility, brittle transition and plastic strains of tungsten at high temperatures

06 p0833 A72-18634

Cast electron-beam remelted Mo, investigating carbon and zirconium carbide additions effects on cold shortness and low temperature plasticity

06 p0833 A72-18645

Idealized model for anisotropy of metals inelastic characteristics due to plastic deformation, demonstrating applicability to polycrystalline materials

06 p0900 A72-18685

Strength and plasticity characteristics of hardened multilayer structural steels, investigating layer thickness effect

07 p1013 A72-19746

Semimomentless theory of closed cylindrical plastic shells subject to random gust loads, obtaining normal circumferential force, shear, transverse bending moment and shell thickness

07 p1092 A72-19851

Cold working effects on plasticity of hardened Al at 20-400 C

07 p1015 A72-19902

Transverse anisotropy effect on collapse loads of plastic rotating disks and circular plates

07 p1093 A72-19946

Bounds for impulsively loaded plastic structures, considering fixed end beam with uniform velocity distribution

07 p1093 A72-19947

Finite element method for elastic plastic sandwich plates analysis, presenting Lagrange multipliers interpretation

07 p1093 A72-19951

Crack initiation and propagation microscopic and phenomenological characteristics, discussing breakdown, plasticity and microcrack convergence

07 p1094 A72-20147

Strength and strain theory statistical analysis for perfectly brittle and plastic materials, assuming ultimate or elastic limit strain as governing factor

07 p1097 A72-20536

Plasticity conditions of monocrystals of higher symmetry tetragonal system, using energy density and deformation relations

08 p1242 A72-20938

Book on plasticity theory covering stress and strain as basic concepts of continuum mechanics, differential

ferential equations of motion, plastic flow, yield criteria, elastic-plastic equilibrium, plane strain, etc

08 p1244 A72-21477

Strain hardening law for rigid incompressible material with plastic properties independent of mean normal stress

08 p1248 A72-21820

C and Re effects on brittleness threshold temperature and plasticity of Mo-Re alloy

09 p1326 A72-22227

Impurities effect on Mo plastic properties and toughness, suggesting lower vacuum arc welding rates and increased electron beam zone refining runs

09 p1326 A72-22228

Cast Nb alloys plasticity enhancement by heat treatment, discussing solid solution decay kinetics and carbides composition of Nb-Mo-Zr-C system

09 p1327 A72-22229

Crystalline ceramics compressive fracture strength and microhardness tests at room temperature, suggesting microplasticity role in failure mechanisms

09 p1334 A72-22388

Alumina microstructure, grain size and impurities effects on ballistic performance, discussing results in terms of microplasticity

09 p1334 A72-22390

Riemann invariants method for plasticity theory application to first order quasi-linear systems, considering plastic flow in arbitrary die

09 p1403 A72-22760

Constitutive equations for materials with time dependent and time independent plasticity, applying to impact of identical bars

09 p1328 A72-22996

Safety factor distribution function for plastic collapse of structure with random resistance members, discussing variance-expected value ratio

09 p1406 A72-23075

Metal creep fatigue analysis and life prediction by inelastic strain ranges partitioning into reversed tensile and compressive plasticity and creep components

09 p1406 A72-23198

Micrograin superplasticity in eutectoid steel, discussing effect of transformation to austenite

09 p1330 A72-23380

One dimensional nonviscous dynamic plasticity theory applicability to impacting rod problems tested experimentally using results from three dimensional and viscous similarity considerations

09 p1408 A72-23557

Book on plastic analysis and plate, shell and disk theories and design covering stress-strain concepts, laws and theorems

10 p1553 A72-23749

Fatigue crack propagation theory based on linear accumulation of metallurgical damage in plastic region

10 p1553 A72-24098

Fatigue crack propagation relation to plasticized zone formation at crack tip in ferritic carbon steels and in Cr-Ni austenitic stainless steels

10 p1558 A72-24855

Variational methods for approximate solutions to Fredholm integral equations describing stress intensity factors and plastic regions of Dugdale cracks [AD-744365]

10 p1558 A72-24892

Crack shape and plastic energy dissipation rate relation to plate thickness and applied stress for penny-shaped crack in elastic plate

10 p1559 A72-24896

Superplasticity relation to heat resistance in metal systems Ni-Cr, Ni-Cr-W-Ti-Al and Ti-Si

11 p1727 A72-25338

High strength quenched steel with high ductility at cryogenic temperatures and negligible cooling rate effects on plasticity during welding

11 p1660 A72-26136

Fe effect on plasticity and ductility of dispersion hardened Ni alloys with various quantities of Nb and Ti at cryogenic temperature

11 p1660 A72-26137

Low temperature tensile strength and plasticity of Ti alloys with zirconium, investigating sensitivity to stress concentrations

11 p1660 A72-26138

IC plastic encapsulation reliability problems related to die stability, wire bond and package moisture integrity

11 p1606 A72-26546

Tensile strength, plastic properties and notch sensitivity from low temperature tests of binary Ti alloys, noting effects of Sn content and temperature

12 p1831 A72-28239

Perfect and imperfect plastic column buckling, describing bifurcation and stability theory for elastic-plastic and rigid-plastic bodies

13 p2054 A72-28480

Internal pressure induced stresses, displacements and time-variable plasticity radii for thick walled fiber reinforced cylinder with hereditary elastic binder interlayers

13 p2055 A72-28557

Plastic properties of locally heated refractory metals in hot pressing calculated from temperature distribution

13 p1966 A72-29465

Phase composition, structure and strength properties of aluminizing coatings on Ni-Al alloys, noting plasticity increase due to Ta addition

13 p1980 A72-29485

Sn alloying effect on heat resistant Ni-Cr alloys plastic strain resistance and strength at room and high temperatures

14 p2114 A72-30274

Superplastic alloys based on Al, Cu, Zn, Mg, Ti and carbon or stainless steels, discussing macroscopic properties and manufacturing cost reduction

14 p2120 A72-30622

Composition, strength and plasticity of ultralight Mn-Li alloys with two-phase alpha-beta base

14 p2125 A72-31040

Optimal plastic design of doubly symmetric closed ring and frame structures of idealized sandwich section under uniform internal pressure

15 p2322 A72-31346

Plasticity, elastic relaxation and stress-strain relation characterization for Schofield-Scott Blair media, using nonequilibrium thermodynamics method

15 p2331 A72-32482

Aluminum oxide reproducible layers plastic deformability or microhardness from molecular beam scattering distribution

16 p2430 A72-33064

Superplasticity in two phase compositions based on refractory metal alloys, noting creep rate dependence on concentration and electroconductivity

16 p2405 A72-33094

Elastoplastic torsion of homogeneous and inhomogeneous torus segments of arbitrary cross section, noting plastic bands propagation with increasing torque

16 p2467 A72-33119

Inverse transformations in mathematical models of elasticity and plasticity problems reducible to biharmonic equation

16 p2468 A72-33163

Transformation induced plasticity (triple) Ni-C steel strengthening by thermal cycling between martensite and reverted austenite

16 p2399 A72-33815

Elastic-plastic-viscous model for creep analysis of rheo-mobile materials, taking into account cracks and other defects

16 p2412 A72-34116

Plastic buckling theory, presenting yield surfaces in tension-torsion stress space for pure aluminum

17 p2632 A72-35245

Nonequilibrium thermodynamics with rate equations as nonlinear solid mechanics foundation, noting viscoelastic, viscoplastic and plastic behavior

18 p2732 A72-36076

An approximate theoretical study of the dynamic plastic behavior of shells

18 p2732 A72-36077

A finite element approach to optimal design of plastic structures in plane stress

18 p2739 A72-37165

Computer method for plasticity theory boundary value problem for medium with unknown equations of state, using complex load simulating device

19 p2870 A72-37387

Internal stresses in a superplastic Mg alloy

20 p2935 A72-39002

The plastic behavior of pure and dispersion-hardened nickel in the temperature range from 20 to 600 C

20 p2940 A72-39455

Stress induced martensitic transformation relationship to shape memory effect compared with superelasticity, transformation plasticity and reversible linear change

21 p3065 A72-40091

Deformation microstructure of fine grained and plate-like structure two phase Ti alloys, noting plasticity decrease in beta phase presence

21 p3068 A72-40963

A quadratic programming approach to the impulsive loading analysis of rigid plastic structures

21 p3120 A72-41205

Certain class of solutions of the three-dimensional problem for a rigid perfectly plastic material with a family of momentarily inextensible planes

21 p3123 A72-41392

Symposium on Foundations of Plasticity, Warsaw, Poland, August 29-September 2, 1972, Proceedings

21 p3124 A72-41501

On the plastic behaviour of time dependent materials - Theoretical and experimental investigation

21 p3124 A72-41504

Extremum principles for a class of dynamic rigid-plastic problems

22 p3235 A72-42522

Limit analysis and plastic design of structural elements of complex shape

22 p3235 A72-42577

The dynamic plastic behavior of shells

22 p3236 A72-42756

Impulsive loading in structural plasticity, obtaining displacement bounds via deformation theory based on extremum paths

22 p3237 A72-42759

Cast heterophase Mo and alloys fracture strength and plastic characteristics, investigating crystal growth texture, orientation and substructure 23 p3301 A72-43741

Inelastic transverse strain coefficient and Poisson ratio dependences on plastic and brittle properties 23 p3348 A72-43752

Width/thickness ratio effect on steel, brass and molybdenum sheet specimens plasticity and deformation under tension at room temperature 23 p3301 A72-43758

Statistical strength and plasticity criterion for materials in a complex stress-strain state 23 p3349 A72-43953

Investigation of the strength of construction materials for various principal-stress relations 23 p3349 A72-43955

Ultrasonic treatment of the MA2-1 alloy during recrystallization 23 p3303 A72-44096

Experimental characterization of yield induced by surface flaws 23 p3353 A72-44230

Plastic design of regular orthotropic grids with two adjacent edges fixed, free, or hinged 24 p3456 A72-44794

Ductility relationship to plasticity characteristics in cylindrical steel samples with short notch under tension 24 p3458 A72-44933

PLASTIC YIELDING

U PLASTIC DEFORMATION

PLASTICITY

U PLASTIC PROPERTIES

PLASTICIZERS

Plasticizers and modifiers effect on epoxy polymers structure from electron microscopy and IR spectroscopy, observing chemical reactions between aliphatic resin and hardening agent 13 p1983 A72-28689

Microfiber extrusion of plasticized mixtures based on titanium and silicon carbides, showing optimum extrusion rate dependent on deformation and strengthening 13 p1967 A72-30102

Thermosetting polybutadienes as co-curing plasticizers for thermoplastics reinforcement, noting oxidation resistance at room and moderately elevated temperatures 16 p2415 A72-33416

PLASTICS

NT ACRYLIC RESINS

NT EPOXY RESINS

NT FURAN RESINS

NT NYLON (TRADEMARK)

NT PHENOLIC RESINS

NT POLYAMIDE RESINS

NT POLYBUTADIENE

NT POLYESTER RESINS

NT POLYETHYLENE TEREPHTHALATE

NT POLYETHYLENES

NT POLYMETHYL METHACRYLATE

NT POLYPROPYLENE

NT POLYSTYRENE

NT POLYTETRAFLUOROETHYLENE

NT POLYVINYL CHLORIDE

NT REINFORCED PLASTICS

NT SYNTHETIC RESINS

NT TEFLON (TRADEMARK)

NT THERMOPLASTIC RESINS

NT THERMOSETTING RESINS

NT VINYL COPOLYMERS

Gas bubble damage centers in organic glass produced by quasi-steady ruby laser pulse induced high temperature heating, using high speed photography 01 p0079 A72-10373

High performance aerospace vehicles transparent materials, discussing glasses, plastics and optical coatings, solar properties, refractive index, UV transmittance and radiation damage susceptibility 01 p0091 A72-10765

Carrying capacity solutions for perforated circular plates of rigid plastic material by kinematic method 01 p0143 A72-11366

Adhesives and techniques for bonding plastics with plastics and nonplastic materials 02 p0236 A72-12610

Flammability smoke hazards and combustion product toxicity tests of plastics [PI PAPER 2] 03 p0379 A72-13243

Ductile plastics solid phase forming, discussing forging, extrusion deep drawing and rubber cushion forming techniques 04 p0538 A72-15451

Minimum weight design of perfectly plastic continuous sandwich beams with two equal spans for movable loads 04 p0593 A72-15647

Failure analysis of plastic materials susceptible to cyclic strain hardening under thermal load, considering residual stress concentration 06 p0898 A72-18547

Filler particles orientation effects on plastic bearing materials friction and wear properties, discussing experimental testing methods 06 p0836 A72-18595

Plastics cutting and drilling with carbon dioxide IR laser beam, discussing economics and commercially available equipment 07 p0999 A72-20554

Plastics - Conference, Washington, D.C., February 1972 08 p1192 A72-21676

Plane shock wave propagation in polyotropic plastic body with elastic unloading properties, deriving closed form solution for time dependent stepwise decreasing load 09 p1353 A72-23554

Loading process behind reflected and refracted shock waves in plastic layered media with linear elastic unloading 09 p1353 A72-23555

Failure mode control in plastic packaged IC for screening and quality assurance 10 p1447 A72-24010

Automated microdynamometer for thin plastic specimens microtension tests with continuous microscopic observation and automatic diagram plotting 11 p1633 A72-26288

Plastic materials adaptability to solid and hollow turbine blades, deriving thermally and mechanically induced stresses 11 p1738 A72-26799

Testing machine for synthetic plastic cylindrical specimens cyclic cophasal compression-torsion load tests, describing mechanical and hydraulic subsystems and testing techniques 13 p1938 A72-28559

Coating materials for metal surface wear inhibition by adhesive and abrasive interactions minimization, discussing laminar solids, plastics, ceramics and soft metals [ASME PAPER 72-DE-48] 14 p2108 A72-30874

Load cycle frequency and time characteristic effects on plastics fatigue behavior, considering relaxation, retardation and internal damping induced heating effects 16 p2416 A72-34145

Time and temperature independent permissible deformation limits as basis for dimensioning of cyclically and multiaxially stressed plastics structural components 16 p2416 A72-34147

Shaping the future with plastics; Proceedings of the Thirtieth Annual Technical Conference, Chicago, Ill., May 15-18, 1972. Part 1. 17 p2570 A72-34712

Evaluation of plastic materials for semiconductor encapsulation. 17 p2570 A72-34716

Smoke development of plastics under various fire parameters. 17 p2570 A72-34718

Plastics in very-high and ultrahigh frequency applications 17 p2571 A72-35068

Influence of the polarity of the dispersive medium on the structure and properties of plastic lubricants 17 p2571 A72-35176

Mechanical structure and component stress measurement by reinforced concrete, microconcrete, elastic and plastic models 18 p2733 A72-36370

Experimental determination of ultrasonic wave velocities in plastics, elastomers, and syntactic foam as a function of temperature. 18 p2703 A72-36415

A mechanical pulsator for testing plastics with the capacity for adjusting cyclic and mean load during test 18 p2676 A72-37097

Constitutive equations and optical yielding of anisotropic perfectly plastic dielectrics. 19 p2878 A72-38799

Constitutive equations and wave propagation of anisotropic perfectly plastic materials. 19 p2878 A72-38800

Bending vibration test of glass-textolites, noting temperature effect on vibration damping properties 21 p3073 A72-41357

Perfectly plastic media under the action of multiparameter loads 21 p3123 A72-41393

Fabrication of shaping cermet elements of die-casting molds for plastics by the hydrostatic pressing method 22 p3182 A72-42199

The modulus of elasticity of plastic materials at stress times between .001 and 10,000,000 seconds 22 p3197 A72-42859

Hermetic sealing of electronic subsystems with plastics 23 p3294 A72-44142

Characterization of four polymeric materials at strain rates from 0.0001 to 1000 per sec. 24 p3417 A72-44612

PLASTISOLS
NT SMOKE

PLATE [METAL]
U METAL PLATES
PLATE THEORY

Buckling of boron/aluminum and graphite/resin fiber composite anisotropic plates, giving load vs fiber orientation angle for various plate aspect ratios 01 p0139 A72-10739

Unidirectional and bidirectional composite laminates subjected to cylindrical bending under uniformly distributed and concentrated loads 02 p0292 A72-11989

Vibration and buckling analysis of doubly curved composite monocoque plates and shells of positive and negative Gaussian curvature, examining stacking sequence effect 02 p0292 A72-11990

Static solution for circular plates of cylindrically monoclinic materials 02 p0293 A72-12277

Bending moments in transversely isotropic rectangular cantilever plate of low shear rigidity 02 p0299 A72-12684

Two dimensional viscoelastic fluid flow past infinite plate with time dependent suction and constant and periodic free stream velocity 03 p0341 A72-13630

Two dimensional boundary value problems for rectangular plates in bending with rigidity variation, using Kantorovich, trigonometric and Horvay functions 03 p0449 A72-13907

Stress concentration problems in two and three dimensional elastoplasticity, using Ilyushin small deformation theory 03 p0453 A72-14213

Circumferential undulations of flanges from theory of nonsymmetrical bending of circular plates 04 p0584 A72-14472

Free vibration and buckling of orthotropic skew plates with different edge conditions, using Ritz variational method 04 p0584 A72-14508

Forced and free transverse vibrations of flat rectangular plates with attached concentrated masses 04 p0584 A72-14521

Three dimensional analysis for free vibrations of simply supported viscoelastic rectangular plates 04 p0585 A72-14841

Conforming rectangular and triangular finite elements for plate free vibrations analysis in bending 04 p0585 A72-14846

Variable thickness plate under cylindrical bending, considering stress concentration around circular hole 04 p0586 A72-14991

Fundamental frequency calculation method for bars and plates with arbitrary fixity of rotations, discussing buckling and vibration with realistic boundary conditions 04 p0591 A72-15275

Magnitude and distribution of stresses produced by external energy sources in thick plate 04 p0593 A72-15657

Three dimensional temperature distribution at thermally insulated crack in plate 04 p0593 A72-15658

Disturbances in infinite plate of viscoelastic material due to impulsive radial forces and twist on inner surface of circular hole, using Laplace transformation 04 p0594 A72-15709

Boundary collocation method for estimating stress intensity factors for through-thickness interior crack in finite rectangular plate [ASME PAPER 71-MET-L] 05 p0732 A72-15794

Piecewise linear approximation of inverse nonstationary conductive heat transfer through unbounded plate with arbitrary temperature distribution and asymmetric boundary conditions 05 p0742 A72-15847

Vibration and stability of rectangular plates with mixed edge conditions, reducing dual series equations to homogeneous Fredholm integral equations [ASME PAPER 71-WA/APM-21] 05 p0733 A72-15959

Theoretical and experimental heat transfer at plate in longitudinal jet flow with strong transverse inhomogeneity 05 p0649 A72-16228

Plastic stress and strain intensity factors for cracked plates in tensile fields 05 p0737 A72-16323

Concentration profile equations for finite length flat vertical plate moving in viscous incompressible fluid 05 p0650 A72-16783

Iterative solution for non-Lévy rectangular plates with corner supports, assuming small deflection theory 06 p0896 A72-17966

Temperature stress distribution in infinite plate with time varying heat transfer coefficient 06 p0899 A72-18565

Collocation least square solutions of boundary value problems, applying to prismatic bar torsion and plate bending 07 p1025 A72-18790

Mean square error and bound on relative error for Reissner plate theory, including shear deformation effect

07 p1087 A72-18812

Sound pressure in liquid layer, bounded by oscillating plate under bending as function of boundary acoustic impedance

07 p1034 A72-18923

Shallow spherical shell equations solution for vibration mode and natural frequencies from analogous vibrating plate solution

07 p1089 A72-18489

Symmetrical bending of variable thickness circular plate solved by classical method and Reissner and Vekua equations

07 p1092 A72-19852

Stressed state of isotropic nonlinear plate with doubly periodic system of curvilinear holes

07 p1094 A72-20208

Analytical model for surface fatigue crack configuration during propagation into thick plate under cyclic loading

[AD-741575] 07 p1095 A72-20242

Laminar natural convection heat transfer from leading edge of isothermal plate under nonuniform gravity [ASME PAPER 71-HT-CC]

08 p1250 A72-20875

Elastic rectangular plate instability in pure bending along two perpendicular directions solved by Karman nonlinear equation reduction to partial differential equations integration

08 p1247 A72-21817

Quadrilateral four node nonconforming plate bending finite elements for structural vibration and stability analysis

08 p1250 A72-22142

Anisotropic plate theory for perfectly plastic flow, expressing yield condition in terms of mixed stress-anisotropy tensors

09 p1403 A72-22765

Book on plastic analysis and plate, shell and disk theories and design covering stress-strain concepts, laws and theorems

10 p1553 A72-23749

Simply supported skew plates stability under combined loading, noting wing and tail design applications for high speed aircraft and missiles

10 p1555 A72-24196

Existence and uniqueness theorem for weak solution of clamped elastic plate equilibrium problem, using micropolar flat plate bending theory

10 p1555 A72-24202

Plate and thin and thick walled shells treated as three dimensional solids, noting finite element method limitation

10 p1559 A72-24925

Finite element generalization of plate displacement functions to shell analysis, using strain energy tensor concept

10 p1560 A72-25187

Linear contingency method for elasticity theory of anisotropic plate with elliptic hole, deriving boundary value problems solutions

11 p1733 A72-25543

Flexural vibration of rectangular orthotropic plates with clamped, simply supported and/or free edges, presenting solution method for coupled characteristic equation pairs

11 p1735 A72-25737

Annular plate with supporting edge beams and concentrated load, showing deflection decrease with stiffness

11 p1736 A72-25990

Proper vibration frequencies of thin imbedded plate obtained by layer potentials method

11 p1737 A72-26477

Finite difference equations for plate and shell calculations with various boundary conditions

12 p1878 A72-27089

Convergence of plate bending eigenvalue solutions from conforming displacement finite elements based on thick plate free vibration conversion to isoperimetric variational problem

12 p1879 A72-27194

Periodic liquid heating through infinite plate, taking into account temperature induced variation in heat capacity and conductivity

12 p1888 A72-27227

Stress-strain state approximation for isotropic strip with circular hole, noting method adaptability to computer computations

12 p1880 A72-27232

Third approximation solution to elastic bending equilibrium equations of Vekua plate theory in form of holomorphic functions

12 p1880 A72-27237

Closed form solution for dynamic response of infinite plate with elastic foundation and damping under arbitrary initial conditions and load distribution

12 p1883 A72-27559

Lagrange multiplier method derivation of variational functional for finite element method and applications to plate and shell problems

13 p2055 A72-28623

Thick rectangular plate stress functions under linear tensile forces application to longitudinal edges and resultant forces application to transverse edges

13 p2055 A72-28735

Heated three layer plate with load-carrying layers of different materials, thicknesses and temperatures, calculating stability under uniaxial tension

13 p2055 A72-28736

Thermal stress distribution determination in isotropic plate with rigid circular insert, using small parameter technique

13 p2056 A72-28913

Computer algorithm for plates and shells internal forces and moments and stress-strain state determination from strain gage data

13 p2058 A72-29144

Two dimensional boundary value problems of elasticity for simply connected noncanonical domains, using small parameter method

13 p2062 A72-29952

Point heat source induced thermal stresses in elliptic plate with circular holes, determining stress-strain field by two dimensional elasticity theory

14 p2166 A72-30689

Optical anisotropy effects in birefringent materials by reflected shadow method and extension of theory for constrained zones around cracked plates under plane stress

14 p2167 A72-30903

Thin elastic plates finite displacement flexure behavior, using piecewise linear finite element incremental stiffness technique

14 p2168 A72-30933

Experimental setup and flow patterns for natural convective heat transfer from plate with arbitrary inclination

14 p2173 A72-31060

Laminated plate continuum theory with microstructure, studying one dimensional harmonic wave propagation in infinite laminate

14 p2169 A72-31147

Variational principle based Pian hybrid finite element procedure for static cylindrical shell analysis extended to plate and shell vibration

14 p2169 A72-31149

Berger equation inconsistencies for large deflections of thin elastic plates with freely moveable edges

14 p2169 A72-31173

Piecewise linear approximation of inverse nonstationary conductive heat transfer through unbounded plate with arbitrary temperature distribution and asymmetric boundary conditions

15 p2334 A72-31266

Finite element analysis of circular and elliptical plates with curved boundaries, discussing high precision triangular plate bending element modification for accuracy improvement

15 p2326 A72-31715

Mixed triangular finite element model for plate bending problems including shear deformation effects, discussing error analysis and convergence

15 p2326 A72-31716

Finite element method application to thin plate bending problem to illustrate efficiency of sector elements for sectorial and annular plates

15 p2326 A72-31720

Poisson ratio changes effect on equilibrium problems solutions in thin plate theory via invariant imbedding technique, using Cauchy system formulation

15 p2330 A72-32444

Equilibrium equations for boundary value problems in Vekua theory with moments allowance for plate with circular hole under bending and torsion

15 p2333 A72-32682

Transverse shear deformations in laminated anisotropic plates from generalized treatment for isotropic and sandwich plates with homogeneous cores

[AD-745613] 16 p2375 A72-32846

Homogeneous differential equations of elastic rectangular plates with linear thickness variation, using Gran Olsson solution

16 p2471 A72-33682

Coupled thermoelastic theory for thin plates, using perturbation method to find free vibration frequencies of plates under various boundary conditions

16 p2471 A72-33785

Optimal design of static laterally loaded fiber reinforced plates, determining optimum load-path directions at all plate points

16 p2475 A72-34174

Large amplitude vibration of a circular plate with concentric rigid mass.

[ASME PAPER 71-APMW-11] 17 p2625 A72-34319

Anisotropic laminated plates theories reliability comparison, noting applications to thin and sandwich plates

17 p2625 A72-34326

On the analysis of unsymmetrical cross-ply rectangular plates.

17 p2626 A72-34328

Bending of skew plates of variable rigidity.

17 p2626 A72-34329

Nonlinear flexural vibrations of a clamped circular plate.

[ASME PAPER 72-APM-18] 17 p2628 A72-34798

Plate surface temperature during aerodynamic heating in supersonic gas flow, using linearized Pohlhausen method

17 p2485 A72-35139

Elastic behavior of multilayered bidirectional composites.

17 p2632 A72-35234

Finite element solutions for laminated thick plates.

17 p2633 A72-35292

Monograph - The finite-element method in plate bending analysis

17 p2634 A72-35547

Plate vibrations and layer potentials

18 p2736 A72-37001

Variational principle based three dimensional elasticity theory of micropolar anisotropic sandwich plates, considering transverse shear and strains and rotary inertia

18 p2737 A72-37057

Infinite plate with a supported reinforced circular hole.

18 p2738 A72-37071

Classical plate theory for variable-thickness isotropic elastic axisymmetric circular plates in partial contact with each other and with rigid smooth surfaces of revolution

18 p2738 A72-37072

Analysis of an inclined crack centrally placed in an orthotropic rectangular plate.

19 p2870 A72-37221

Mathematical analogies in a theory of shallow spherical shells and plates allowing for transverse shear

19 p2872 A72-37540

Limit analysis for plates - A simple loading problem involving a complex exact solution.

19 p2872 A72-37599

Bubnov-Vlasov variational method for thin parallelogram plates bending under complex loads, calculating edge skew and side length effects

19 p2877 A72-38160

Application of the Bubnov-Galerkin method to the approximate integration of a Timoshenko-type equation

19 p2877 A72-38188

Convergence of a simple iteration scheme in equilibrium problems of flexible plates

19 p2877 A72-38201

Hall field occurrence conditions in small semiconductor plates, discussing Hall generator design and layer temperature as function of time

19 p2776 A72-38725

Fiberglass reinforced plastics tensile test specimens aspect ratio effect on tensile properties, considering deformation of orthotropic rectangular plate with uniform forced displacement

20 p2943 A72-38889

Plate bending analysis with hybrid triangular and rectangular finite elements, deriving stiffness matrix via optimized stress functions

20 p2979 A72-39556

Strongly coupled stress waves in heterogeneous plates.

20 p2980 A72-39616

The influence of finite-deformations upon the creep behavior of circular plates.

20 p2980 A72-39693

Stress intensity factors for transversely loaded elastic plates and their application to predictions of crack arrest.

20 p2981 A72-39956

Maximum deflection and bending moments of simply supported anisotropic rectangular plate under uniform transverse load, using double Fourier series

20 p2981 A72-39973

The influence of end plate and bulkhead on the shell of variable rectangular profile subjected to simultaneous torsion and bending at middle planes.

20 p2982 A72-40065

The effect of couple-stresses on stress concentration of a ring inclusion.

21 p3117 A72-40681

Vibration of trapezoidal cantilever plates with partial root chord support.

21 p3121 A72-41225

Bent plates and shells equations and rupture modes, characterizing cracks and stress intensity

21 p3122 A72-41338

Boundary value problems of lattice plates statics for transversally loaded homogeneous strip, noting elastically supported continuous plates

21 p3123 A72-41394

Mixed finite element analysis of elasto-plastic plates in bending.

21 p3124 A72-41502

Book - Analysis of plates.

21 p3125 A72-41530

Simple thickness modes for laminated composite materials.

22 p3235 A72-42465

Optimum design of circular sandwich plates.

22 p3239 A72-42843

- Vibrations of circular plates of variable thickness under an inplane force. 22 p3240 A72-42908
- German monograph - Heat stresses in circular plates subject to finite deflections. 22 p3241 A72-43058
- Steady thermoelastic state in an infinite plate with a moving parabolic cut 23 p3345 A72-43586
- Numerical solution of a boundary-value bending problem for rectangular plates with free and freely supported opposite edges 23 p3345 A72-43645
- A nonlinear problem of pure bending of a three-layer plate with a corrugated sheet filler 23 p3346 A72-43655
- A finite element stress analysis of a crack in a bi-material plate. 23 p3346 A72-43707
- Elastodynamic theory of natural symmetrical vibrations of sandwich plates, assuming filler motion and layer displacements governed by Lamé and Kirchhoff equations 23 p3348 A72-43790
- Nonlinear thin elastic plate deformation differential relations and static boundary conditions along contour, verifying theory by bending experiment on rectangular plate 23 p3348 A72-43791
- Photothermoelastic study of stress concentrations in a plate with internal heating. 23 p3349 A72-43986
- Large deflection of rectangular orthotropic plates. 23 p3352 A72-44111
- Line spring analysis model for long part-through surface cracks in walls of plate or shell structures, formulating constitutive laws 23 p3353 A72-44234
- Dynamic response of circular plates to pulse loads. 23 p3354 A72-44254
- Stress distributions in a semi-infinite plate with a row of circular holes. 23 p3355 A72-44398
- Laminated thick plate and shell analysis by the assumed stress hybrid model. 24 p3453 A72-44601
- Dynamic blast loads on preheated and prestressed thin plates. 24 p3454 A72-44607
- Post-buckling of axially compressed plates. 24 p3455 A72-44632
- Vibration frequencies and modes determination for clamped rectangular plates of orthotropic material, using weighted residual technique and polynomial approximation 24 p3455 A72-44683
- Buckling and lateral vibration of rectangular plates subject to inplane loads - A Ritz approach. 24 p3458 A72-44887
- A method of determining the eigenfrequencies of closed circular conical plates in the Vlasov-Mustari hypothesis 24 p3459 A72-45441

PLATELETS

- Magnetite forms in Orgueil meteorite, observing platelets, stackings and framboids by scanning electron microscope 04 p0569 A72-14506
- Human epicardial arterial circulation platelet aggregates role in sudden coronary death, discussing relation to atherosclerotic stenosis and acute thrombi 05 p0616 A72-16013
- Dietary lipid effect on platelet adhesion and aggregation, blood coagulation and fibrinolysis and relation to atherosclerosis and thrombosis 08 p1117 A72-21543
- Crowding phenomenon effect on blood cell oxygen consumption, using Cartesian diver technique for polymorphonuclear leukocyte, lymphocyte and platelet measurements 12 p1763 A72-27842
- Platelet electrophoretic mobility response to adenosine diphosphate /ADP/ in patients with coronary artery disease 15 p2183 A72-31283
- Platelet aggregates role in intramyocardial vessel circulation impedance in patients dying suddenly of coronary artery disease 15 p2186 A72-31770

PLATENS

- Plane-strain compression of rigid plastic material between flat platens, approximating frictional boundary conditions by entrapped viscous fluid lubricant 16 p2428 A72-34171

PLATES

- Flexural vibrating free edge plate transducer with stepped thickness for high directional ultrasonic radiation generation in fluids 11 p1687 A72-26060
- Calculation of sum-frequency electromagnetic waves emitted by a multilayer nonlinear plate 17 p2516 A72-35168
- Small forced oscillations produced by infinite plate vibrations in stratified and rotating viscous fluids, investigating resonance effects on propagation 20 p2912 A72-39330

PLATES (STRUCTURAL MEMBERS)

- NT ANISOTROPIC PLATES
- NT ANNULAR PLATES
- NT CANTILEVER PLATES
- NT CIRCULAR PLATES
- NT CORRUGATED PLATES
- NT ELASTIC PLATES
- NT ORTHOTROPIC PLATES
- NT PERFORATED PLATES
- NT POROUS PLATES
- NT REINFORCED PLATES
- Stress intensity factors for circular crack near surface of semiinfinite solid, considering pure beam bending and approximate thickness effect for plate deep surface flaw 01 p0140 A72-10991
- Plate buckling elastoplastic process derivation allowing for secondary plastic deformation onset, examining stress discontinuity at overloading and unloading zones boundary 02 p0289 A72-11614
- Beams and plates resting on elastic base with loads moving along line or strip, calculating wave processes based on half space dynamic model 02 p0290 A72-11629
- Newtonian quasi-static crack propagation theory application to nonlinear structures, considering slender beams, plates and circular cylindrical shells 02 p0292 A72-12029
- Fourier series terms number effect on sandwich plate critical shear stress calculation accuracy 02 p0294 A72-12438
- Three layer plates elastoplastic stability, describing breakdown conditions by five differential equations with five unknown variables 02 p0299 A72-12690
- Complex geometry inhomogeneous sandwich plate, calculating temperature field with R functions 03 p0456 A72-13738
- Plate under projectile impact, calculating motion response due to random initial velocity distribution over surface by stochastic model 03 p0447 A72-13852
- Three layer plates stability with light fillers, noting filler thickness effect on approximate solutions accuracy 03 p0454 A72-14377
- Skew plates buckling with different edge support conditions, presenting Rayleigh-Ritz method results for various combinations of side ratio, skew angle and loadings 04 p0584 A72-14509
- Plates in uniaxial compression with various support conditions at unloaded boundaries, predicting behavior after buckling 04 p0591 A72-15288
- Natural frequencies and vibration mode shapes of simply supported symmetric trapezoidal plates 04 p0592 A72-15564
- Scaling laws for vibrating beams and plates, stressing shear and rotatory inertia effects 06 p0894 A72-17769
- Postbuckling collapse, end shortening, stiffness and ultimate load for geometrically imperfect simply supported plates with stress free edges 06 p0896 A72-17964
- Forced nonlinear oscillations of finite plate in plane supersonic gas flow, considering elastic forces and resonant characteristics deformation 06 p0901 A72-18708
- Error analysis of finite element solutions for elastic-plastic sandwich plates 07 p1086 A72-18779
- Natural frequencies and vibration modes of simply supported tapered skew rhombic plates, considering thickness and skew angle effects 07 p1088 A72-19116
- Vibration characteristics of simply supported unsymmetric trapezoidal plates 07 p1089 A72-19644
- Stress analysis of infinite plate with parallel cracks under symmetrical edge loads 07 p1092 A72-19781
- Quasi-static stability of sandwich plates hinged over edge in finite difference formulation 07 p1094 A72-20213
- Nonlinear modal response analysis of plate structures under random acoustic excitation, using finite element method and perturbation technique 08 p1245 A72-21607
- Nonlinear beam and plate analysis, obtaining smooth elastic-plastic transition through modified Richard moment-rotation equation application 08 p1249 A72-21923
- Axisymmetric grid plate bending and torsion under normal forces and moment vectors loads, determining stress-strain state from finite difference equations 09 p1398 A72-22692
- Grid plates of complex structure, determining stress-strain state by asymptotic solution of boundary value problem for sixth order differential equations 09 p1398 A72-22693
- Thermal buckling of parallelogram shaped plate under stationary temperature field and uniformly distributed forces, deriving critical load 09 p1402 A72-22733

PLATES (STRUCTURAL MEMBERS)

- Vibration of infinite thin plate coupled with acoustic field in surrounding fluid, using Fourier transformation 10 p1511 A72-24223
- Nonuniform vortex flow of compressible gas past cascade of plates, noting monochromatic pressure waves at harmonics of plate vibration frequency 10 p1418 A72-24538
- Gradient iterative techniques application to finite element vibration and stability analysis of skew plates 10 p1558 A72-24878
- Beryllium sheet and foil application to lightweight space structures, discussing mechanical properties [AIAA PAPER 72-404] 11 p1726 A72-25425
- Damping additions for plates using constrained thin viscoelastic sheets and metallic layers 11 p1688 A72-26063
- Transverse bending theory for sandwich plates, considering core and face equilibrium and compatibility equations 11 p1737 A72-26587
- Bending of unbounded plate coupled to elastic isotropic half space with vertical and horizontal springs, calculating contact stresses by double Fourier transforms 12 p1878 A72-27082
- Computer calculation of minimum weight ribbed plates under axial compression by random search method and linear programming 12 p1878 A72-27083
- Tensile strength of fiber glass reinforced plastic elements joined by cover plates and nonlinearly elastic adhesives 13 p1962 A72-28737
- Acoustic shock wave diffraction at moving or static plate immersed in ideal gas 13 p1943 A72-30011
- Stress concentration in symmetrical U-notched plates, comparing data with Baratta, Neal, Neuber and Heywood formulas 14 p2167 A72-30904
- Acoustic wave diffraction at fixed plate boundary, determining velocity field by inverting Volterra-type integral equations 14 p2070 A72-31016
- Supersonic ideal gas flow in corner formed by intersecting plates, using direct computation method for nonequilibrium flows with detached shock waves 14 p2071 A72-31021
- Shock wave interaction with supersonic moving plate, calculating plate lift as function of time 14 p2071 A72-31024
- Optimal geometrical and physical properties of sandwich plates with rigid cores under compressive load, discussing critical stress and structural stability 15 p2322 A72-31359
- Bending of clamped skew plate under uniform loading, using Gaydon-Shephard eigenfunction expansion method 16 p2463 A72-32836
- Two dimensional fibrous medium model for strain and stress analysis of structural plate formed by three dimensional grid of rods 16 p2467 A72-33115
- Resonant vibration of thin walled rods and stiffened plates and cylindrical shells, noting aircraft and rocket structures 16 p2471 A72-33679
- Heat transfer by free convection from a longitudinally vibrating vertical plate. 17 p2637 A72-35045
- Bending and vibration of multilayered sandwich plates, presenting static and dynamic analysis method 17 p2635 A72-35976
- Symmetrical and antisymmetrical wrinkling of sandwich panels. 18 p2736 A72-37056
- Elastic stability of folded plate structures of triangular cross-section. 18 p2738 A72-37073
- FORTAN subroutines for plate bending and plane stress elements stiffness and geometric matrices generation, taking into account anisotropic properties and linear thickness variations 18 p2739 A72-37166
- Thermal stability of skewed plates 19 p2871 A72-37430
- Elastic stability theory of compressible and incompressible composite media 19 p2871 A72-37530
- Free vibrations of multilayer sandwich plates in the presence of in-plane loads. 19 p2876 A72-38020
- Observation and analysis of simulated ultrasonic acoustic emission waves in plates and complex structures. 20 p2925 A72-39284
- Laminar free convection from a rotating radial plate. [ASME PAPER 72-HT-46] 20 p2985 A72-39664
- An equivalent grid framework for skew plates in flexure. 20 p2980 A72-39689
- Buckling of plates and cylindrical panels under the action of axial dynamic compression 22 p3232 A72-41923

- Chladni's patterns for random vibration of a plate.
22 p3236 A72-42758
- Combined mode crack extension in adhesive joints.
23 p3305 A72-43493
- Experimental analysis of the stress distribution in the vicinity of a nonwelded rigid circular inclusion in the interior of a plate stressed in monoaxial tension
23 p3446 A72-43691
- Thermoviscoelastic problem for semiinfinite plate, determining temperature field and stresses permitting heat propagation
23 p3347 A72-43749
- Stress function for thermal shock in plate with cylindrical heat source, noting thermal stress concentration in optical materials under electromagnetic radiation
23 p3348 A72-43792
- Triangular element for multilayer sandwich plates.
23 p3351 A72-44108
- Stress-strain characterization of part-through crack in plate under tension in terms of stress intensity factor
23 p3352 A72-44227
- Stress intensity factors for embedded elliptical crack in semiinfinite solid and for semielliptical surface crack in plate under tension and/or bending
23 p3353 A72-44231
- Fatigue crack propagation in A514 base plate and welded joints.
23 p3354 A72-44309
- The use of bar buckling eigenfunctions in the stability analysis of clamped skew plates.
23 p3355 A72-44456
- Plastic flow around an expanding crack.
24 p3456 A72-44812
- The damping properties of elastically supported sandwich plates.
24 p3458 A72-44915
- Diffraction of an acoustic wave by a stationary plate
24 p3360 A72-44987

PLATFORMS

- High speed accelerometers to determine test platform tilt and translational motion displacements, discussing instrument configurations without gyroscopes
[AIAA PAPER 72-818] 20 p2923 A72-39105

PLATING

- NT ELECTROPLATING
NT NICKEL PLATE
Hydrogen generation mechanism during cadmium plating of steel, describing porosity testing technique
04 p0527 A72-15548
- Storage characteristics of plated magnetic wire for nondestructive read and write
16 p2369 A72-33672

PLATINUM

- Square wave source gated detector bridge for precise resistance measurement, discussing design and performance, and application in Pt resistance thermometry
06 p0785 A72-18244
- Impurities effect on platinum resistance thermometers temperature reading accuracy, presenting empirical formula for approximate error estimate as function of operational conditions
13 p1960 A72-29906
- Hydrocarbon oxidation and catalysis on Pt fuel cell electrodes, using electrochemical methods with isotopic exchange and gas chromatography
16 p2361 A72-33878
- Cubic sodium tungsten bronze electrocatalytic activity increase for oxygen reduction by traces of Pt
16 p2361 A72-33883
- Diffusion limitation avoidance at high current densities by fuel cell preparation via Pt thin film sputtering on porous vycol substrates
16 p2352 A72-33893
- Calibration and application techniques for platinum resistance thermometers.
[ASME PAPER 71-WA/TEMP-2] 17 p2554 A72-34965
- Platinum and gold in chondritic meteorites.
17 p2610 A72-35149
- Rheological properties of molybdenum and platinum of bamboo structure under bending loads
21 p3071 A72-41712
- Current noise and conductance-temperature characteristics of thin discontinuous Pt films on glass substrate interpreted by quantum mechanical electron tunneling model
22 p3214 A72-42453

PLATINUM ALLOYS

- Alloying component effect on Pt catalytic activity in anodic oxidation of methanol for fuel cells
16 p2361 A72-33881
- Phase diagrams, solubility and alloying of Pt, Pd, Ru, Ir and Rh with noble, alkali earth, rare earth and transition metals
22 p3191 A72-42810

PLENUM CHAMBERS

- Spatial boundary layer variations in low speed wind tunnel working section due to settling chamber screens, discussing mesh variations effects on Preston tube measured pressure coefficient distributions
07 p0966 A72-19061

- Effect on supersonic jet noise of nozzle plenum pressure fluctuations.
17 p2597 A72-35243

PLETHYSMOGRAPHY

- Respiratory flow resistance measurements in man, comparing esophageal catheter, pletismographic, forced pressure oscillations and airway interrupter methods
04 p0481 A72-15222
- Combined photoelectric-photographic and pletismographic technique for continuous measurement of rabbit ear vein diameter and tissue volume changes
09 p1273 A72-23443
- Pletismographic and laryngoscopic investigation of glottis opening and airway resistance relation to lung volume during panting and continuous slow expiration
11 p1586 A72-26611
- Water filled volume and strain gage pletismography for forearm blood flow measurement during isometric exercise
11 p1587 A72-26622

PLEXIGLASS (TRADEMARK)

- U POLYMETHYL METHACRYLATE
PLOTTERS

- NT X-Y PLOTTERS
Planicart stereoplotter for map compilation and revision in photogrammetry
06 p0815 A72-17756
- Topographical stereo map plotting apparatus with auxiliary device for orthophoto production, describing design for combined photointerpretation-cartographic applications
09 p1313 A72-23309
- Automated microdynamometer for thin plastic specimens microtension tests with continuous microscopic observation and automatic diagram plotting
11 p1633 A72-26288
- Automatic device for plotting antenna polar diagrams
17 p2529 A72-34766
- Stereoplotting instrument concept based on image data selection independence from object space model reconstruction
18 p2691 A72-36498
- A digital portable line-drawing rectifier.
18 p2692 A72-36500

PLOTTING

- Field and test data analysis with time share computer, using Weibull probability plotting, hazard rates and least squares regression
02 p0185 A72-11555
- Generalized root locus graphical plotting by method of normals, comparing to Rimsii method while applying to third order systems
06 p0840 A72-18664
- Photomaps plotting from high altitude photographs, presenting expressions for segment areas selection
13 p1954 A72-28496

PLOTTING INSTRUMENTS

- U PLOTTERS
PLUG NOZZLES
Jet engine silencing plug nozzle suppressor configurations acoustic and thrust performance measurements
[AIAA PAPER 72-160] 05 p0706 A72-16826
- PLUGS
Boron-epoxy structure repair technology based on titanium plugs and fiberglass, discussing equipment, graphical design and nondestructive tests
08 p1193 A72-21691

PLUMBANE

- U METAL HYDRIDES
PLUMES
NT ROCKET EXHAUST
Chapman-Korst model for prediction of flow characteristics within plume induced boundary layer separation in rocket propelled vehicles during power-on maneuvers
01 p0050 A72-10376

- Two dimensional underexpanded jet plumes flow distribution determination using time dependent finite difference method
02 p0301 A72-12257
- Rocket plume contamination effect on transmitting and reflecting materials optical properties, noting predominant absorption and scattering effects
[AIAA PAPER 72-56] 05 p0750 A72-16967
- Convective plumes model with heat flux, layer depth and surface turbulence intensity as parameters
[AD-745511] 09 p1347 A72-23655
- Wet and dry bent over plumes comparison, constructing plume paths for various atmospheric stability conditions
11 p1681 A72-26082
- Quasi-steady Ar MPD arc exhaust plume structure from spectroscopic and photographic investigation, noting dependence on arc current and mass flow rate
[AIAA PAPER 72-499] 11 p1696 A72-26222

- Mass flow and current distribution in magnetic MPD accelerator thruster plumes calculated from meridional flow stream function equation
[AIAA PAPER 72-501] 11 p1696 A72-26224

- Aitken condensation nuclei clouds microstructure and area contamination profiles, discussing small sources pollution and plumes polyfurfuration
[AIAA PAPER 71-1125] 11 p1628 A72-26989
- Detection of crystals in CO₂ jet plumes.
21 p3046 A72-41306

- Simulation of the interaction of high altitude plumes and a high-speed free-stream flow.
[AIAA PAPER 72-1019] 21 p3042 A72-41598
- Plume impingement force during tandem stage separation at high altitudes.
22 p3231 A72-42872

PLUTO (PLANET)

- Jupiter, Saturn, Uranus, Neptune and Pluto state of knowledge, noting angular momentum fraction, red spot, albedos, densities, atmospheric compositions, natural satellites, etc
12 p1870 A72-27345
- Fourier analysis of Pluto light curve in terms of geometrical model consisting of bright and dark areas
16 p2452 A72-33131
- Uranus, Neptune and Pluto disk temperature observations via National Radio Astronomy Observatory interferometer
16 p2455 A72-33464
- Accurate positions of the planet Pluto in the years 1969-1970.
21 p3105 A72-40576

PLUTONIUM

PLUTONIUM ISOTOPES

- PLUTONIUM ISOTOPES
Pu-244 fission Xe isotopic composition parameters in achondrite meteorites, using lunar spallation systematics
01 p0124 A72-10058
- Pu 244/U 238 fission track retention age of whitlockite crystal in lunar breccia 14321 from Fra Mauro formation
15 p2307 A72-31722
- Thermal release Xe analysis of neutron irradiated white inclusion samples from Allende carbonaceous meteorite, noting iodine and plutonium isotopes abundance
18 p2728 A72-36971
- Xenon isotope fission component due to extinct Pu-244 in lunar breccia, noting storage details in terms of crustal material dating
20 p2967 A72-39182

PLUVIOGRAPHS

- U RAIN GAGES
U RECORDING INSTRUMENTS

PNEUMATIC CIRCUITS

- German book on fluidics covering pneumatic logic elements and systems with and without moving parts and applications in sensors, transducers, power amplifiers, analog-to-digital converters, decoders, etc
01 p0072 A72-11276
- Temperature, flow, end conditions and branching on small signal sinusoidal amplitude frequency response of pneumatic lines, investigating transfer functions
[ASME PAPER 71-WA/AUT-5 (FLCS)] 05 p0615 A72-15958
- Pneumatic fluid power valve flow rate derivation in terms of flow passage effective area and critical pressure ratio
08 p1113 A72-22158
- Pneumatic amplifiers with controlled pressure during subcritical and supercritical flow, considering jet-resonant choke, conical and membrane systems
11 p1578 A72-26783
- Output impedance of a jet element
19 p2754 A72-37994
- Multivariable static /combination/ switching characteristics of TRIMELOG pneumatic logic elements
19 p2754 A72-38644
- Realization of static /combination/ logic switches with the aid of TRIMELOG pneumatic elements. II
20 p2890 A72-39423

PNEUMATIC CONTROL

- Turbine aerodynamics research trends, covering engine cooling, high work factor turbines, pneumatic variable geometry and computer analysis
11 p1572 A72-26036
- Water table study of monostable fluidic amplifiers with allowance for geometrical similarity and Reynolds number for air operated models
16 p2353 A72-34139
- Gas bearing gyroscope for fluidic guidance and control system, satisfying missile and recoverable booster requirements
18 p2648 A72-36557
- Pneumatically isolated test platform local gravity vector active control to investigate seismic level disturbance effects on precision inertial components evaluation
[AIAA PAPER 72-843] 20 p2923 A72-39086
- Investigation of the dynamic characteristics of the speed governor of a hydropneumatic feed drive
23 p3253 A72-44022

PNEUMATIC EQUIPMENT

- NT GAS VALVES
NT PNEUMATIC CIRCUITS

Aircraft high pressure oxygen cylinder system filler valve optimum standards, discussing automatic fill rate and pressure sensitive closing control, design, construction and performance
[SAE AS 1225] 01 p0006 A72-10385

Electropneumatic converter for pneumatic pulse transformation into dc or ac signal, using corona discharge current 03 p0311 A72-13556

Stainless steel circular tubes size and fittings effects on pneumatic pulse wave distortion and attenuation in fluidic pulse generation system 08 p1111 A72-20928

Pneumatic machine for microfriction stud welding of dissimilar metals 09 p1320 A72-23631

Pneumatically assisted parachute deployment at high altitudes with low accelerations 10 p1421 A72-24273

Pneumatic fluidic logic elements design based on Coanda effect to realize conjunction, equivalence, nonequivalence, alternative and implication functions 10 p1423 A72-25112

German monograph on small variable-speed motors with high impulse performance, considering asynchronous cage type, dc shunt type and pneumatic motors 15 p2182 A72-31325

Space shuttle umbilical systems for mating, connection and checkout of carrier assemblies and couplings for cryogenic, electrical, pneumatic and hydraulic services 15 p2213 A72-31695

Russian book - Assembly and testing of hydraulic and pneumatic systems of flight vehicles 19 p2753 A72-37300

Mathematical model of seismic isolation block and pneumatic suspension for inertial guidance component tests to describe design factors effects on vibration behavior [AIAA PAPER 72-844] 20 p2950 A72-39085

The problem of the minimum frequency of natural pressure oscillations in pneumo-hydraulic systems 23 p3252 A72-43652

Method of calculating pneumatic spray nozzles 23 p3325 A72-44015

PNEUMATIC PROBES
Cooled miniature pneumometric probes for high temperature gases dynamic or stagnation pressure and velocity measurement 01 p0072 A72-11213

Point density measurement and crack detection in P/M green compacts with interconnected porosity by pneumatic tests, noting application to quality control 02 p0233 A72-11458

Pneumatic thermistor transducer to measure steam ejection time interval between cardiac volume pulse upstroke start and maximum rise rate occurrence 11 p1588 A72-26633

Lagrange interpolation formula to determine flow elements shape in pneumatic sensor head with extended measurement range 14 p2104 A72-30372

PNEUMATIC RESET
U PNEUMATIC CONTROL

PNEUMOGRAPHICS
U PNEUMOGRAPHY

PNEUMOGRAPHY
Electrical thermometer mounted on breathing mask for electropneumograms, measuring temperature change in respiration air flow 02 p0169 A72-12518

EEG phase asymmetry fluctuations relation to respiration rhythm in subjects from pneumograms during rest, mental activity, hypnosis and sleep 05 p0620 A72-17214

Respiration rate transmitter with miniature pressure transducer for measuring pneumograph variations in animals over FM-FM telemetry system 08 p1124 A72-20898

Cotton wick probe-transducer assembly for pneumograph recording of rabbit respiratory rate 11 p1587 A72-26619

POCKELS EFFECT
U BIREFRINGENCE

POGO EFFECTS
Control system for stabilization of liquid propellant rockets Pogo oscillations, discussing structure, fuel tank and feed system, combustion chamber, control gain and accelerometer installations 10 p1551 A72-24027

The calculation of elastic tanks partially filled with liquids for prediction of the Pogo effect 24 p3392 A72-45152

POHLHAUSEN METHOD
Pohlhausen type integral method for dissociative binary mixture nonequilibrium laminar boundary layer on flat plate, using Crocco relationship between enthalpy and velocity profile 16 p2378 A72-33436

POHLHAUSEN SOLUTION
U POHLHAUSEN METHOD

POIKILOTHERMIA
NT FROGS
NT SNAKES

POINCARÉ PROBLEM

Poincaré noninvariance of Stigma equation as alternative to Dirac equation for spin one-half finite mass particles 15 p2280 A72-31519

Direct periodic orbits in planar restricted barycentric three body problem, using Poincaré variables and Hamiltonian function 15 p2307 A72-31763

Poincaré, Lorentz and Einstein contributions to relativity theory construction according to Whittaker, discussing influence on contemporary scientists 20 p2954 A72-40003

POINCARÉ SPHERES
Relativistic counterpart of Poincaré condition for angular velocity of rigidly rotating star, discussing equilibrium disturbance effects 10 p1549 A72-25058

Poincaré sphere application to polarimetry and two- and three-dimensional photoelasticity by scatter light photoelasticity 18 p2691 A72-36381

Infinitely distant points of a differential equation 23 p3309 A72-43846

POINT DEFECTS

NT FRENKEL DEFECTS
NT VACANCIES [CRYSTAL DEFECTS]
Fatigue cracks nucleation in steel bearings subjected to cyclic contact stresses 03 p0377 A72-14020

Se and Zn doped n and p type gallium arsenide point defects, considering thermal conductivity, relaxation time and phonon scattering cross section effects 03 p0404 A72-14239

High purity polycrystalline Al hf low strain fatigue measurements by piezoelectrically driven exponential horn, estimating critical point defect concentration 06 p0893 A72-17420

Hardening mechanisms of interaction between superlattice dislocations and point defects in Ni-Al intermetallic compound mechanical properties strain rate and temperature dependence 06 p0832 A72-18420

Two electrical transducer techniques for dilatometric study of quenched-in point defects 07 p0993 A72-20589

Ceramic materials stress-strain behavior dependence on microstructural factors, discussing point defects, pore size and grain boundaries 09 p1334 A72-22392

Stoichiometry effect on high temperature creep in oxides, relating impurities, point defects concentration and diffusion 09 p1335 A72-22397

Dielectric and semiconductor crystals surface defects, considering electric polarization structures 10 p1525 A72-23761

Electrical resistivity restoration in Van Arke type Zr deformed by lamination at 78 K attributed to point defects elimination 10 p1495 A72-24085

Dislocation damping by point defects entrapment, calculating internal friction force rate dependence based on weak interactions continuum model 10 p1527 A72-24979

Book on binary metal oxides covering nonstoichiometry, electrical conductivity, diffusion theory, point defects, high temperature creep and electrochemical transport properties 10 p1527 A72-25075

Elastic constants of dilute Mo-Re alloys with bcc structure, determining randomly distributed point defects low concentration effects with T-matrix method 11 p1656 A72-25724

Point defects investigation in Si and Ge by diffusion techniques, precipitation from supersaturated solid solutions, quenching from high temperatures and plastic deformation 12 p1856 A72-28053

EPR for point defects produced in Si by fast neutron irradiation, emphasizing damage cluster model 12 p1858 A72-28060

Mobile point defects interaction with moving dislocation in inelastic solid bodies, considering energy dissipation due to impurity relaxation 14 p2169 A72-30954

Energy losses due to hysteresis friction during oscillations of dislocations in elastic field of point defect in solids, discussing temperature and amplitude effects 14 p2121 A72-30955

Study of point defects produced in aluminum by tempering and irradiation with electrons 18 p2702 A72-36705

The interaction of lattice defects and grain boundaries. 20 p2962 A72-39996

POINT MATCHING METHOD [MATHEMATICS]
U BOUNDARY VALUE PROBLEMS

POINT SOURCES
Fluid dynamical study of accretion process with gravitating point source motion through adiabatic gas, applying to galaxies 01 p0126 A72-10289

Kr 85 clouds released by instantaneous point sources, measuring speed, height, short period concentrations, crosswind and downwind concentration integrations and dimensions 01 p0095 A72-10828

Fast hyperbolic MHD flow past point source, considering geometry and disturbances singularities of MHD Mach cones 02 p0266 A72-12369

Diffuse reflection of point source /flare/ light emission for cold dwarf star semifinite plane parallel atmosphere, calculating polarization 02 p0285 A72-12831

Short wave asymptotic formulas for shadow zone of plane diffraction, discussing asymptotic solutions for field from point source 04 p0489 A72-15386

Faust project history, scientific objectives and present status, discussing stars, nebulae, quasars point sources and galactic photometry 04 p0583 A72-15691

Varying energy and gamma /quasi-steady/ models for point source blast waves from high speed solids impact, comparing 1100-0-aluminum shock decay data 05 p0736 A72-16101

Thermal signal propagation in flowing fluid, plane, line and point sources of varying heat, calculating temperature distribution with conduction and convection heat transfer equation 05 p0746 A72-16295

Rocket orbit in mass point gravitational field, studying KS variables separability, elliptic functions and equivalent problems 06 p0877 A72-17656

Light field in cloud and fog plane layers from stationary collimated point source propagation 06 p0848 A72-17937

Loop structure of Monoceros supernova remnant, predicting thermal soft X ray point source as cooling neutron star 07 p1073 A72-19421

Point explosion in cosmic spheroid with exponential density distribution, observing shock wave propagation along symmetry axis direction 07 p1075 A72-19583

Cosmos satellite measurements of high energy gamma quanta from Crab Nebula region, indicating excess flux association with Taurus constellation point source 07 p1064 A72-20636

Ray trace of sound refraction by point source on jet flow axis, numerically calculating directivity pattern 08 p1152 A72-21893

Sound refraction by sinusoidal point source in subsonic jet flow, obtaining solution by finite difference method for comparison with ray tracing results 08 p1152 A72-21894

Russian papers on mathematical problems of wave propagation and diffraction theory, covering elastic and short waves and point sources 11 p1688 A72-26377

Waveguide point source field, analyzing short wave asymptotic properties of Helmholtz equation Green function in inhomogeneous medium 11 p1689 A72-26382

Point source wave field diffraction on nontransparent circular cone, using steepest descent method and integral transformations 11 p1597 A72-26385

Point heat source induced thermal stresses in elliptic plate with circular holes, determining stress-strain field by two dimensional elasticity theory 14 p2166 A72-30689

Spectral image formation and aberration by spherical concave grating for point light source, using geometric optics method 15 p2278 A72-32337

Quasi-static thermal stresses in circular disk due to rotating point heat source on surface 16 p2470 A72-33594

Light field in cloud and fog plane layers from stationary collimated point source propagation 16 p2426 A72-33778

Shadowing function calculation as rough surface point illumination probability by point source radiation, assuming surface elevation as random process 18 p2710 A72-36407

High energy gamma radiation from the galactic centre region. 18 p2722 A72-36998

Wave-front singularities for two-dimensional anisotropic elastic waves. 18 p2739 A72-37175

Relativistic beaming from periodically orbiting light point source in terms of photon fluxes, relating to pulsar radiation theory 19 p2835 A72-38697

Distribution of illumination in a point image in the presence of birefringence in the optical system /case of axial symmetry/ 19 p2836 A72-38789

Some features of instantaneous point source diffusion within a turbulent boundary layer. 21 p3078 A72-40467

Diffusion from a continuous source in relation to the Eulerian properties of turbulence. 21 p3046 A72-41248

Astrophysical equipment for Cerenkov radiation measurement from atmospheric showers, discussing source of high energy gamma rays in galactic equator direction

23 p3328 A72-43226

High energy gamma ray point sources in Cassiopeia and Cygnus regions, using extensive air shower Cerenkov flashes detection technique

23 p3329 A72-43941

Scattering of acoustical waves by a prolate spheroidal obstacle.

23 p3313 A72-44118

Steady two-dimensional viscous flow in a jet.

23 p3282 A72-44303

Small disturbances propagation effect on self similar flow due to point explosion in medium with density varying according to distance from center

24 p3390 A72-44786

POINT TO POINT COMMUNICATIONS

Analytical optimization of point to point communication above spherical ground, obtaining frequency minimizing transmission losses

03 p0325 A72-14193

Point-to-point national data communication geostationary satellite system associated with computers, discussing organization, earth station equipment and technical and economical feasibility

24 p3380 A72-44975

POINTING CONTROL SYSTEMS

Satellite attitude estimation on elliptic orbits by Kalman filters with periodic coefficients, demonstrating efficiency by earth pointing satellite using different instrumentation noise models

05 p0685 A72-16442

OAQ space telescope of 120 inches aperture, discussing structural design, geometric configuration and stabilization and pointing control system

05 p0663 A72-16800

Satellite launch vehicles guidance and control systems, discussing control parameters for minimum injection error

07 p1033 A72-20604

Nonspinning satellite earth-pointing attitude control for elliptic orbits using active regulation of pitch moment of inertia

08 p1204 A72-21605

Astronomical pointing of radio telescopes using on-line computer

12 p1793 A72-27813

Conical scanning system for Pioneer Jupiter spacecraft pointing control, discussing signal processor, spacecraft dynamic behavior, system stability and error budget

15 p2320 A72-31791

Application of the Volterra series to the analysis and design of an angle track loop.

19 p2830 A72-37283

Colorimetric and spectrophotometric gradient systems comparison for bright stars used in automatic telescope pointing control, discussing interstellar absorption

19 p2860 A72-37955

Fine guidance pointing stability of a 120-inch /3 meter/ large space telescope /LST/.

[AIAA PAPER 72-853]

20 p2949 A72-39076

Description and in-orbit performance of the Orbiting Solar Observatory control system.

[AIAA PAPER 72-852]

20 p2975 A72-39077

Error analyses of Euler angle transformations arising in design of precision pointing systems, guidance sensors and instruments with gimbals

[AIAA PAPER 72-851]

20 p2949 A72-39078

Astronomical telescope hybrid pointing control system with double gimbal control moment gyros and orthogonally mounted reaction wheels to achieve extreme accuracy and stability

[AIAA PAPER 72-854]

20 p2924 A72-39138

An automatic mass-trim system for spinning spacecraft.

20 p2977 A72-39603

Attitude perturbations of a spinning Jupiter Orbiter spacecraft.

[AIAA PAPER 72-920]

21 p3115 A72-41565

Performance optimization of satellite semipassive aerodynamic attitude controller for near-earth orbits, considering damping time and pointing error

[AIAA PAPER 72-923]

21 p3082 A72-41567

Automatic coaxial alignment system with photoelectric positioning sensors, discussing alignment errors as function of light source distance and components spacing

21 p3059 A72-41817

An inertially balanced servo.

23 p3311 A72-43866

OSO pointing accuracy improvement through dual spin stabilization, discussing OSO design evolution 1962-72

24 p3449 A72-45145

POINTS [MATHEMATICS]

NT FIXED POINTS [MATHEMATICS]

Point estimate calculation of underlying distribution function for probability plot, developing confidence coefficient for Weibull model

02 p0252 A72-11557

Chebyshev polynomials best approximation with respect to linear space spanned by odd degree polynomials, obtaining extreme point sets

04 p0539 A72-14729

Shooting and imbedding methods for theoretical analysis and approximate numerical solution of two-point boundary value problems involving n-vector-valued functions

[AD-743615]

04 p0539 A72-15043

Approximations and bifurcations in flight dynamic system, investigating singular point motion over trajectory during partition process

05 p0611 A72-16582

Existence and bifurcation conditions of singular point consisting of spliced focus spliced out of ordinary trajectories, investigating stability

05 p0690 A72-16593

Program system for computation of surface from set of data points, using piecewise polynomial functions

06 p0815 A72-17753

Boundary points regularity for second order elliptic equation with continuous coefficients

08 p1198 A72-21165

Functional analysis techniques for existence of holonomic solutions to linear differential equation systems with singular points

09 p1342 A72-23254

Flight mechanics of point with limited power propulsion system and energy storage unit, investigating variational maximum payload problem with singular control optimization

11 p1727 A72-25932

Lower and upper bounds for number of lattice points in simplex, using linear programming algorithm for generating feasible cutting patterns for paper reels

11 p1678 A72-26157

Nonlinear algebraic transformation to determine straight line and second order curve intersection point in aircraft lofting problem

13 p1986 A72-28742

Existence and bifurcation conditions of singular point consisting of focus fused from ordinary trajectories, investigating dynamic system stability

19 p2834 A72-37565

Introduction of time and space into a point system endowed with a signal

20 p2946 A72-39574

POISEUILLE FLOW

U LAMINAR FLOW

POISONS

NT CARBAMATES [TRADENAME]

NT INSECTICIDES

NT URETHANES

Photon trapping in photosystem II of photosynthesis - The fluorescence rise curve in the presence of 3-/3,4-dichlorophenyl/-1,1-dimethylurea.

17 p2505 A72-35761

POISSON DENSITY FUNCTIONS

Random processes models based on Poisson sequences extended to simultaneous asymmetry and probability density function excess, establishing asymptotic relationships

02 p0216 A72-11919

Moving object trajectory determination by a posteriori Poisson signal transmission analysis with random parameters

05 p0626 A72-16205

Failure analysis probability for structures excited by randomly varying dynamic loads, comparing Gaussian and filtered Poisson processes

07 p1093 A72-19948

Algorithm for asymptotic power series for Poisson process residence time function generation in band with delaying screen

08 p1198 A72-20998

Bayes estimators for Poisson distribution random parameters and reliability function, using Monte Carlo method and maximum likelihood estimation

08 p1200 A72-21590

Convergence of random number sums of independent infinitesimal multidimensional stochastic step processes to generalized Poisson processes

09 p1340 A72-22423

Energetic particle flux measurement on spacecraft based on statistics of overflowing register counting Poisson process

09 p1312 A72-23261

Markovian characteristics of time dependent excursions and independent incursions processes provided with limits to left and continuous to right, noting Poisson punctual process and Borel sets

10 p1505 A72-24114

Statistical analysis for single airport ATC digital simulation using Poisson distribution law, calculating optimal number of channels

13 p1996 A72-29179

Random processes models based on Poisson sequences extended to simultaneous asymmetry and probability density function excess, establishing asymptotic relationships

13 p1948 A72-29231

Book - Elements of applied stochastic processes

17 p2575 A72-34624

Optimal search in the presence of Poisson-distributed false targets.

21 p3075 A72-40837

Receiver processing for direct-detection optical communication systems.

21 p3017 A72-40859

Sequential analysis algorithm for data channel detection of received signal represented by Poisson sequence of quantum transitions under large SNR

23 p3266 A72-44206

Cumulants of multidimensional response of linear and nonlinear systems to Poisson distributed impulses, estimating joint probability distribution and evaluating threshold statistics

23 p3314 A72-44368

Charts for confidence limits and tests for failure rates.

23 p3294 A72-44395

POISSON EQUATION

Difference schemes for first and third order Poisson equation in polar, cylindrical and spherical coordinates

02 p0252 A72-11735

Cauchy-Poisson problem of infinitely deep fluid wave motion resulting from initial particle velocities and horizontal equilibrium surface change

04 p0511 A72-14648

Computing techniques for finite Fourier transform, applying to Poisson equation, interpolation and quadrature and data smoothing

07 p1025 A72-18784

First boundary value problem solution of nonlinear Poisson equation in rectangular region by finite difference equations approximation

08 p1198 A72-20902

Poisson equation boundary value problems summary representation formulas for three layer annular sector with Dirichlet or Neumann conditions

08 p1205 A72-20963

Conjugate solution for Poisson equation of heat transfer in laminar flow with developed velocity profile in flat channel with internal constant heat sources

08 p1252 A72-21314

Poisson heat transfer equation for complex boundary three dimensional region, solving by constant sign functions with aid of R conjunctions

08 p1253 A72-21456

Moving and inertial trihedron orientation determination from absolute angular velocity vector, solving Poisson equations system

08 p1205 A72-21802

Trapezoidal plate thermoelasticity problem for various thermal load distributions, solving Poisson equation for sectorial annular region

09 p1400 A72-22711

One dimensional time independent solution to Vlasov-Poisson system of nonlinear electrostatic plasma waves, noting Maxwell distributions for free and trapped particles

11 p1697 A72-26596

Nonlinear waves in nonuniform plasma, extending Butler and Gribbon formulation for Vlasov-Poisson equations

11 p1697 A72-26598

Boundary value problems of Poisson equation for rectangle having side with mixed boundary conditions, discussing solution by summary representations and successive approximations methods

13 p1986 A72-29071

Vectorial differential equations in potential theory, discussing Fredholm alternative in normalized spaces, generalized harmonic vector fields, Poisson equation and Robins-Praeger problem

15 p2261 A72-31452

Poisson equations solution in orthogonal curvilinear coordinate systems to allow Laplace and Helmholtz equations separability, applying to hydrodynamic, electrostatic, electromagnetic and MHD problems

15 p2278 A72-32249

The Dirichlet problem of the Poisson integrodifferential equation

19 p2825 A72-38208

Modified Ritz method to find optimum boundaries to elliptic systems governed by Laplace or Poisson equation

19 p2826 A72-38246

Calculation of a plane stationary temperature field in the presence of a heat source

20 p2987 A72-39915

Book - The method of fractional steps: The solution of problems of mathematical physics in several variables

22 p3208 A72-43200

POISSON PROCESS

U POISSON DENSITY FUNCTIONS

U STOCHASTIC PROCESSES

POISSON RATIO

Preferred orientation effects on X ray stress measurement of Young modulus and Poisson ratio of Al alloy

06 p0829 A72-17793

Al wrought alloys dynamic elasticity modulus and Poisson ratio dependence on temperature, using ultrasonic measurement method

07 p1019 A72-20239
Volume averages of stress and strain changes induced by Poisson ratio variation in boundary value problems of three dimensional classical elastostatics

12 p1884 A72-27566
Poisson ratio changes effect on equilibrium problems solutions in thin plate theory via invariant imbedding technique, using Cauchy system formulation

15 p2330 A72-32444
The transverse Poisson's ratio of composites.

17 p2571 A72-35289
Dependence of linear elasticity solutions on the elastic constants. II - Dependence on the shear modulus in elastostatics.

21 p3119 A72-41106
Connexions between the moduli for anisotropic elastic materials.

21 p3119 A72-41107
Inelastic transverse strain coefficient and Poisson ratio dependences on plastic and brittle properties

23 p3348 A72-43752

POLAR AURORAS

U AURORAS

POLAR CAP ABSORPTION

Vlf electromagnetic wave perturbations in transpolar propagation, noting time dependent behavior of polar cap absorption effects

01 p0056 A72-10441
Solar cosmic ray cutoff rigidity increase during polar cap absorption related to geomagnetic perturbation onset

02 p0273 A72-11938
Polar cap absorption event, investigating solar high energy protons precipitation effects

05 p0709 A72-16239
Solar cosmic ray flare of 11-18 April 1969, investigating effect on polar cap absorption in lower ionosphere

07 p1066 A72-20650
Polar orbiting satellite observations of energetic solar proton entrance into polar cap during March 1970 solar event

09 p1376 A72-22588
Laboratory simulation of VLF/ELF radio waves transpolar ionospheric propagation, taking into account polar cap absorption

09 p1279 A72-23016
Day, night and sunset mesospheric nitric oxide concentrations during polar cap absorption from rocket measurements of cation composition and charged particle densities
[AD-741709]

09 p1300 A72-23026
Ionospheric disturbances and prediction dependence on solar and geophysical activities, discussing SID, pca, auroral absorption and F 2 region

11 p1623 A72-26267
OMEGA phase shifts in auroral region due to solar phenomena, discussing methods eliminating PCA induced errors

13 p1997 A72-29185
Solar cosmic ray cut-off rigidity increase during PCA related to geomagnetic perturbation onset

13 p2030 A72-29250
Daytime 30 MHz PCA from satellite and riometer measurements, noting linear relationship to square root of integral and differential solar proton fluxes

13 p2030 A72-29339
Low altitude electron-ion dissociative recombination and ion-ion neutralization coefficients during PCA event from ESRO rocket flights data

13 p2032 A72-29653
Magnetospheric geometry derivation from ISIS-1 observations of soft particles penetration into polar cap and auroral regions, discussing entry and energization mechanisms

15 p2227 A72-31953
Satellite charged particle observations and polar cap riometer absorption measurements during solar cosmic ray events, noting electrons and protons contributions

15 p2300 A72-31965
Note on the characteristics of sunspot groups which produce solar proton flares.

17 p2608 A72-35087
Ionospheric magnetic disturbances during March 1970 related to solar flare corpuscular and proton fluxes, generating ring current and PCA absorption

18 p2688 A72-36857
D region ion compositions model during quiet and intense PCA conditions associated with dissociative recombination and ion-ion neutralization

POLAR CAPS

Solar proton entry observations over polar caps in relation to magnetosphere, magnetotail and magnetopause models

02 p0275 A72-12463
Polar cap region solar particle fluxes from Esro 1/Aurorae satellite recordings, noting north-south asymmetry

03 p0348 A72-13506

Midday oval, cusp region and polar cap auroral electron precipitation at low magnetic activity, presenting intensity vs altitude profiles for nitrogen ion line emissions

03 p0350 A72-13531
Annual heat balance in Martian northern polar cap, considering atmospheric, ground and solar heat flux absorbed by snow

03 p0436 A72-13817
Southern Martian polar cap seasonal change, describing variation at vernal equinox and dry ice hypothesis

04 p0581 A72-15621
Carbon dioxide frost identification on Martian polar caps by Fourier spectroscopy

06 p0881 A72-17900
Solar electrons and protons measurements in interplanetary space and in magnetotail, noting access to north polar cap
[AD-744404]

07 p1058 A72-19156
VLF signals Antarctic ice cap attenuation determined at Byrd station from relative phase and amplitude observations over short and long great circle paths

09 p1281 A72-23511
Mars south polar cap surface roughness and photometric function from Mariner 7 UV spectrometric experiment

10 p1531 A72-23708
Mars biology likelihood from long winter model, suggesting north polar cap summer remnant vaporization as atmosphere, liquid water and greenhouse effect source

10 p1424 A72-23717
Jupiter polar caps, Red Spot and equatorial belts visual observations during 1970 opposition

10 p1542 A72-24570
Simultaneous Esro satellites observation of spatial and temporal particle flux variations over polar caps

11 p1714 A72-26418
Polar cap magnetic field induced by currents along magnetospheric lines of force during polar substorm

13 p1946 A72-28587
Polar thermospheric wind calculation from convection electric field measurements in polar cap ionosphere, using simple ionospheric model

13 p1950 A72-29385
Magnetospheric particles and interplanetary magnetic field measurements for solar proton event of March 1970, noting polar cap structures

16 p2444 A72-32956
Critical component of the interplanetary magnetic field responsible for large geomagnetic effects in the polar cap.

17 p2548 A72-35590
Observed seasonal change of the Martian polar cap.

17 p2615 A72-35679
Spatial distribution and temporal nature of the entry of solar cosmic rays into the polar cap

17 p2603 A72-35870
Mars polar caps formation at aerographic latitudes, assuming water vapor condensation on ground and water presence in carbon dioxide snow

19 p2863 A72-38072
Secular and seasonal modifications of Mars surface, considering southern polar cap and 1971 dust storm

19 p2865 A72-38475
Reconnection of the geomagnetic tail deduced from solar-particle observations.

19 p2792 A72-38730
Magnetospheric interactions with topside ionosphere in terms of polar wind ion flows and density related to plasma temperature, F 2 region and cusp observations

20 p2918 A72-39537
Ionospheric and magnetospheric electric field strength measurements in auroral and polar cap regions by Ba ion cloud and double floating probe techniques

20 p2918 A72-39543
Midday auroras and polar cap auroras.

20 p2920 A72-39978
On the classification of high-latitude auroras.

20 p2920 A72-39979
DP-2 mode daily magnetic variation in polar cap based on magnetic and auroral records, noting relationship to magnetospheric substorms

22 p3168 A72-42005
Polar-cap measurements of solar-flare protons with energies down to 12.4 keV.

22 p3218 A72-42425
Polar-cap electric field distributions related to the interplanetary magnetic field direction.

22 p3172 A72-42432
Different conductivities effect in ionospheric E layer of polar cap regions, noting electric current along high latitude magnetic field force lines

23 p3283 A72-43370
Model for the uneven illumination of polar caps by solar protons.

23 p3286 A72-44502
Electron polar cap and the boundary of open geomagnetic field lines.

23 p3286 A72-44522

POLAR COORDINATES

Difference schemes for first and third order Poisson equation in polar, cylindrical and spherical coordinates

02 p0252 A72-11735
VOR, Direct Measuring Equipment and TACAN polar coordinate radio navigation systems history, improvements and future development

02 p0257 A72-12646
Axisymmetric Reissner-Sagoci problem in linear micropolar elasticity for stress and displacement under load applied by rigid circular disk

03 p0448 A72-13890
Electrophysiological responses to maximum exercise in healthy humans from polarcardiographic display of heart vector changes

07 p0916 A72-18891
Dipolar coordinate system for geomagnetic field dipole approximation in studies of diffusion and heat conduction in F region and outer ionosphere

14 p2102 A72-30652
Straightforward difference scheme for nonlinear parabolic equations in polar coordinates

24 p3420 A72-45649

POLAR IONOSPHERE BEACON

U BEACON SATELLITES

POLAR METEOROLOGY

Nighttime polar atmospheric structure and temperature variations due to gas kinetic and electron energy changes

05 p0656 A72-16240
Polar night jet idealized model with zero tropospheric and constant vertical stratospheric shear, considering instability due to small wave disturbances

07 p1030 A72-19103

POLAR NAVIGATION

Polar navigation with transverse mercator technique for aircraft using secant geared ground position indicators

01 p0097 A72-10181
Polar region performance of OMEGA navigation system, noting addition of selectable grid reference, multiple parallel DR system, manual celestial computation and bearing resolver

13 p1999 A72-29200

POLAR ORBITS

ESRO polar orbiting meteorological satellite, discussing design features and operational instruments

01 p0126 A72-10186
Geomagnetic survey by polar-orbiting OGO 2 and 4, discussing data acquisition and reduction results and accuracy

02 p0219 A72-12081
Heos-A2 satellite polar orbit mission to study electron, proton and alpha particle population outside magnetosphere and in neutral point region

19 p2857 A72-37783
Polar orbiting operational weather satellites.

24 p3451 A72-45197

POLAR REGIONS

NT ANTARCTIC REGIONS

NT ARCTIC REGIONS

High latitude magnetotail highly directed nearly monoenergetic positive ions population observation during geomagnetic storms, using Vela satellites electrostatic analyzers

01 p0060 A72-10887
Daytime bottomside polar F layer latitudinal cross section construction from ionograms recorded in aircraft
[AD-738278]

01 p0061 A72-10900
Diurnal and seasonal changes in occurrence frequency of rapid phase fluctuations in vlf received at Franz Josef Land correlated with geophysical observations

02 p0172 A72-11922
Geomagnetic field and AU/AL index variations with UT during international quiet days at high latitudes interpreted as electrojet diurnal redistribution

02 p0217 A72-11930
Energy conversions and mean vertical motions in high latitude summer mesosphere and lower thermosphere, observing reaction kinetics

03 p0346 A72-13380
Venusian polar tropopause and cloud layer from IR spectral recording in carbon dioxide band near inferior conjunction for crescent regions

03 p0436 A72-13814
Time variation of mean values for magnetic field elements strength and size in solar polar regions, noting solar activity maximum effect

03 p0436 A72-13830
High latitude scintillation effects on vhf and S band polar orbiting satellite transmissions, examining ionospheric irregularities

04 p0487 A72-14952
Circumpolar region object position autonomous determination from arbitrarily zenith-oriented moving horizontal platform position coordinates

04 p0545 A72-15002
Azur satellite for investigating polar regions, inner radiation belt and solar particle emission

05 p0715 A72-16135

Azur satellite ground station network with polar stations for telemetry reception 05 p0643 A72-16140

Magnetic perturbations in near polar region and morning-night sectors of auroral oval as function of current sources and modulation by universal time 05 p0657 A72-16276

Proton measurements in ring current by OGO-3 satellite compared with geomagnetic field data at low and high latitudes 05 p0711 A72-17034

Auroral zone vlf hiss and associated low energy electron precipitation in polar magnetosphere [AD-736327] 06 p0804 A72-17456

Off-ecliptic north-south anisotropies in cosmic radiation intensity during polar storm events 06 p0873 A72-17467

Latitude dependent discrepancy between low latitude satellite drag deduced densities at high latitudes and Jacchia model 07 p0976 A72-19167

Interplanetary origin of magnetospheric electric fields responsible for polar magnetic disturbances 07 p0979 A72-20382

Polar latitude sporadic E layer diurnal variations with appearance dependence on cutoff frequency 08 p1130 A72-20727

Lower ionospheric electron density profile determination at high latitudes from riometric observations, discussing cosmic radio emission absorption representation 08 p1225 A72-20730

Eastern and western polar electrojets intensity diurnal variations with respect to universal time 08 p1154 A72-20740

Geophysical data analysis for high latitude negative geomagnetic disturbances revealing geomagnetic pulsations during auroral arcs passage 08 p1155 A72-20809

Pulsating polar auroral line emission spectra observation at 3914 and 5577 Å by rocket-borne photometers 09 p1301 A72-23262

Short period terms in earth rotation rate and polar motion, considering data truncation effects on periodograms 10 p1475 A72-24872

Anomalous F region ionization in darkened high latitudes during solar activity growth and abatement 11 p1623 A72-26270

Electrostatic resonances associated with maximum frequencies of cyclotron-harmonic waves at high and low latitudes, presenting dispersion curves and ray paths 11 p1624 A72-26400

Interplanetary magnetic field direction and high latitude ionospheric currents in dayside auroral regions, showing plasma drift induced magnetic disturbances 11 p1626 A72-26419

Polar region performance of OMEGA navigation system, noting addition of selectable grid reference, multiple parallel DR system, manual celestial computation and bearing resolver 13 p1999 A72-29200

Diurnal and seasonal changes in occurrence frequency of rapid phase fluctuations in VLF received at Franz Josef Land correlated with geophysical observations 13 p1920 A72-29234

AU and AL indices variations effect on geomagnetic field during international quiet days at high latitudes interpreted as electrojet diurnal redistribution 13 p1948 A72-29242

Plasma wave measurements during OGO-5 dayside magnetosphere polar cusp encounters, discussing ULF magnetic field wave levels and VLF electric field amplitude ranges 13 p1950 A72-29380

High latitude ionospheric transmission and reflection properties for oblique hydromagnetic plane waves at micropulsation frequencies for daytime and nighttime conditions 13 p1951 A72-29390

Polar zone thermospheric temperature variations due to atmospheric cooling, H component variations and discrete perturbation 14 p2097 A72-30133

Mars observations during 1971 opposition, noting south pole phenomena relation to Martian atmosphere changes 15 p2306 A72-31600

Temperature and density data deviation from stratosphere and mesosphere mean season model values at high latitudes 15 p2225 A72-31907

Solar proton flux density angular and latitude distribution in polar regions magnetosphere from satellite observation 15 p2299 A72-31921

Geomagnetic field aligned electron anisotropies at high latitudes for energies 1 and 6 keV observed by

ESRO satellite, noting two regions of maximum occurrence frequency 15 p2226 A72-31928

Aerodynamic drag at high latitudes observed from Molniya satellites orbit analysis, suggesting upper atmosphere density change 15 p2229 A72-31989

Polar/midlatitude model of atmospheric density variations from LOGACS low altitude satellite accelerometer experiment 15 p2229 A72-32000

Review of symposium on D region, upper polar ionosphere, magnetosphere and wave-particle interactions 15 p2229 A72-32251

Summer upper mesosphere and lower thermosphere positive ion composition at high latitudes from Nike Cajun rocket soundings 16 p2383 A72-32966

Some aspects of survival and rescue of astronauts in polar regions. 17 p2507 A72-34435

Ion concentration inhomogeneities in the ionosphere at an altitude of 600 km 17 p2547 A72-35207

High latitude observation of precipitating electron spikes by polar orbiter OGO 4 satellite, noting population dependence on local trapping limit 17 p2601 A72-35591

Russian book - Morphology and physics of the polar ionosphere 17 p2550 A72-35851

Auroral electron energy spectra at high latitudes from polar auroral arcs luminosity profile examination 17 p2550 A72-35853

Models for F region and topside ionospheric storms morphology, discussing electric current disturbance at polar region 18 p2685 A72-35994

Dependence of sporadic ionization in the high-latitude ionospheric E-region on magnetic activity 18 p2688 A72-36860

Polar latitude sporadic E layer diurnal variations with appearance dependence on cut-off frequency 19 p2766 A72-38355

Lower ionospheric electron density profile determination at high latitudes from riometric observations, proposing cosmic radio emission absorption representation 19 p2791 A72-38358

Easterly and westerly polar electrojets intensity diurnal variations with respect to universal time and geo- and heliophysical phenomena 19 p2791 A72-38368

Coordinate system for use with high-latitude energetic-particle phenomena. 19 p2853 A72-38729

A satellite survey of vector electric fields in the ionosphere at frequencies of 10 to 500 hertz. I - Isotropic, high-latitude electrostatic emissions. 19 p2768 A72-38742

Polar upper ionosphere morphology above E layer, discussing effects of winds, field aligned currents and electron precipitation 20 p2918 A72-39534

High latitude variations of F-region electron temperature. 20 p2918 A72-39535

The anomaly of the neutral wind at a height of approximately 200 km at high latitudes. 20 p2918 A72-39536

Polar ionosphere ELF/VLF noise distribution from Alouette 2 electric dipole observations 20 p2903 A72-39538

Aircraft and spacecraft high latitude optical measurements of magnetosphere-related emissions, discussing red arcs, IR auroras, X ray pulsations, conjugate effects, etc 20 p2918 A72-39539

Properties of low energy particle impacts in the polar domain in the dawn and dayside hours. 20 p2964 A72-39541

High latitude particle precipitation and source regions in the magnetosphere. 20 p2964 A72-39542

An orthographic photomap of the South Pole of Mars from Mariner 7. 21 p3110 A72-41455

The location of the Mountains of Mitchel and evidence for their nature in Mariner 7 pictures. 21 p3110 A72-41456

Mariner 7 ultraviolet spectrometer experiment - Topographic slopes of Mars' polar region. 21 p3110 A72-41457

A measurement of ionospheric electric fields at high latitude. 22 p3169 A72-42015

Solar polar regions magnetic fields polarity and strength during 1960-1971 22 p3221 A72-42026

Occurrence of Pc 4, 5 micropulsation activity at the polar cusp. 22 p3171 A72-42411

Annual height and temperature distribution charts of polar and tropical tropopause over Northern Hemisphere 23 p3310 A72-43534

O-plus/ H-plus/ and He-plus/ ion distributions in a new polar wind model. 24 p3400 A72-45587

POLAR SUBSTORMS

Magnetospheric substorm model for auroral activity sudden increase and ionospheric current development explanation by shock wave excitation in magnetospheric tail neutral layer 02 p0217 A72-11927

Magnetosphere and adjacent regions magnetic surveys by OGO 1 and 3 satellites, discussing magnetopause, bow shock, magnetosheath, geomagnetic tail, ring current and polar substorms 02 p0220 A72-12084

Magnetic flux determination in magnetosphere tail during substorm from auroral oval boundary and center location observation 06 p0807 A72-17985

Magnetospheric and polar substorms model for auroral particles acceleration and geomagnetic tail current diversion to auroral oval night side 07 p0977 A72-20029

Auroral forms dynamics dependence on solar wind and DP intensity in magnetosphere 07 p0977 A72-20030

Pulsating auroras morphology in polar substorm, recording poleward expansion and eastward drifting patches with all sky cameras 08 p1157 A72-21117

Polar magnetic substorm generation through ionospheric current intensification in westward electrojet localized region, noting interplanetary magnetic field role 08 p1159 A72-21494

Infrasound pressure disturbance generation during 31 October 1968 polar substorms growth and decay from North American stations observations 10 p1475 A72-24953

Fast auroral hydromagnetic wave occurrence relation to substorm activity, suggesting role of enhanced particle population in magnetospheric region 10 p1476 A72-24962

Auroral conjugate points relative motion during substorms, showing existence of equatorward and poleward auroral arc systems 11 p1625 A72-26404

Negative auroral arc infrasonic wave observations during substorm poleward expansions at Inuvik, Canada 11 p1627 A72-26516

Peak electron energy spectra during auroral substorm from high energy resolution balloon X ray measurements 12 p1804 A72-27787

Polar cap magnetic field induced by currents along magnetospheric lines of force during polar substorm 13 p1946 A72-28587

Magnetospheric substorm model for auroral activity sudden increase and ionospheric current development explanation by shock wave excitation in magnetospheric tail neutral layer 13 p1948 A72-29239

Magnetospheric ring current relation to polar magnetic substorm from charged particle measurements by satellites and magnetic field measurements at ground 13 p1952 A72-29658

Magnetosphere tail internal plasma boundary layer dynamics during substorms based on aurora data 14 p2103 A72-30663

Correlated particle flux, magnetic field, electron intensity and riometer absorption measurements during recovery phase of polar magnetic substorm on 6 March 1970 15 p2226 A72-31946

Interplanetary magnetic field variations and auroral zone substorm activity observation, noting time delay between IMF southward turning and negative magnetic bay 16 p2451 A72-32974

VLF emissions during post breakup phase of polar substorm. 17 p2547 A72-35064

Observations of the auroral oval by the Alaskan meridian chain of stations. 17 p2548 A72-35594

Auroral motion analysis based on baylike disturbances against quiet field background during polar substorm 17 p2550 A72-35858

Electron and proton acceleration in the outer magnetosphere regions during polar substorms 18 p2688 A72-36866

Measurements of MeV-electrons during the recovery-phase of a polar magnetic substorm on March 6, 1970. 19 p2789 A72-37409

Shock wave excitation by moving solar wind discontinuity in geomagnetic tail as cause of active phase of magnetospheric substorm 19 p2791 A72-38344

- Relationship of interplanetary magnetic field structure with development of substorm and storm main phase. 20 p2968 A72-39232
- Signatures for substorm development of the growth phase and expansion phase. 20 p2916 A72-39237
- Formation of auroral patches in the midday sector during a substorm. 20 p2916 A72-39239
- Auroral space-time regularities relationship to magnetospheric variations, precipitating electron fluxes, magnetic tail formation and substorms. 20 p2920 A72-39977
- Positive geomagnetic bays in evening high-latitudes and their possible connection with partial ring current. 21 p3049 A72-41387
- DP-2 mode daily magnetic variation in polar cap based on magnetic and auroral records, noting relationship to magnetospheric substorms. 22 p3168 A72-42005
- Quadruple conjugate pair observations of the sudden commencement absorption event on June 17, 1965. 23 p3286 A72-44526
- Preconditions for the triggering of polar magnetic substorms by storm sudden commencements. 23 p3286 A72-44531
- Behavior of outer radiation zone and a new model of magnetospheric substorm. 24 p3396 A72-44850
- Ionospheric current relation to magnetospheric field-aligned and ring currents, noting effect of magnetospheric tail electric field on polar magnetic substorms. 24 p3396 A72-44852
- Micropulsations and VLF emissions during substorms. 24 p3396 A72-44855
- Substorm related changes in the geomagnetic tail - The growth phase. 24 p3397 A72-44856
- Polar cap magnetic field induced by currents along magnetospheric lines of force during polar substorm. 24 p3397 A72-45087
- POLARIMETERS**
- X ray astronomy techniques survey, covering image forming telescopes, detectors, nondispersive spectrometers and polarimeters. 03 p0353 A72-13037
- Stellar X ray emission polarization measurement using Thomson scattering polarimeter [AD-736550]. 03 p0353 A72-13041
- Real time complete Stokes vector scanning photoelectric polarimeter with 16 cm aperture for measuring visible radiation of solar disk, corona, moon and planets. 03 p0356 A72-13279
- Jones matrix representation of optical instruments applied to Fourier interferometers /spectrometers and spectropolarimeters/. 03 p0358 A72-13434
- Intercoms 4 solar radiation equipment, including Lyman, optical and X ray photometers, spectroheliographs, polarimeters and optical orientation system. 07 p0986 A72-19643
- Rotating analyzer astronomical photopolarimeter automation by on-line computer control system. 11 p1600 A72-25695
- Jupiter electropolarimetric observations, showing polar regions polarization dependence on phase angle. 13 p2050 A72-30069
- Celestial Thomson-scattering X ray polarimeter design for OSO-1, optimizing sensitivity in 4-24 keV energy range by Monte Carlo simulation computer program. 15 p2234 A72-31540
- Transient high voltage and electric field measurement with electro-optical fringe pattern method employing pulsed laser Kerr system polarimeter. 15 p2240 A72-32434
- A graphite crystal polarimeter for stellar X-ray astronomy. 17 p2553 A72-36637
- Polarimeter for recording of magneto-optical rotation dispersion and Kerr equatorial effect in visible, near UV and near IR spectral ranges. 22 p3176 A72-42108
- The techniques of present-day radioastronomy. 24 p3439 A72-44946
- POLARIMETRY**
- Calibration of polarimetric measurements in terms of magnetic fields, using Stokes parameters without line formation dependence. 03 p0427 A72-13280
- Lunar regolith top surface polarimetric properties of sunlight-exposed rocks and fines compared to terrestrial rocks and meteorites. 06 p0887 A72-18225
- Quasars and Seyfert and N-galaxies compact nuclei radiation polarization from polarimetric and photometric observations. 08 p1234 A72-21281
- Sun vicinity skylight polarization influence on polarimetric K corona observations, discussing inaccuracy sources. 09 p1392 A72-23544
- Photometric UVB and polarimetric observations of rotation period, polarization curves and phase coefficients of asteroid Flora, comparing with moon. 10 p1531 A72-23709
- R Coronae Borealis type variable stars spectral, IR and polarimetric studies, outlining common features and hypotheses for phenomenon explanation. 10 p1549 A72-25055
- Blue filter polarimeter observations of Deimos and Phobos, discussing polarization-phase angle curve for Deimos dust surface layer. 12 p1865 A72-27097
- Daytime sky polarimetry of scattered light in atmosphere during solar eclipses. 12 p1800 A72-27141
- Polarimetric determination of angle between polarization planes of emission and external radiation field in three level gas laser, noting resonator anisotropy properties. 13 p1970 A72-29687
- On polarimetry in solar active regions. V - The magnetic field immediately before and after a flare. 17 p2617 A72-35706
- Poincare sphere application to polarimetry and two- and three-dimensional photoelasticity by scatter light photoelastometry. 18 p2691 A72-36381
- Quartz and calcite spectral emission polarization calculation from Fresnel equation, comparing results with field measurements with broadband IR radiometer. 21 p3097 A72-40603
- Polarization measurements of the supernova in M101. 23 p3333 A72-43227
- Interferometric spectropolarimetry - Alternate experimental methods. 23 p3289 A72-43890
- POLARIS MISSILES**
- Polaris and Poseidon missile systems reliability assessment, discussing test programs, analytical techniques and data management. 10 p1551 A72-24013
- Polaris submarine-weapon system autonomous organization and management technique based on team combining Navy and civilian contractors in close working relationship. 23 p3358 A72-44358
- POLARITY**
- Solar magnetic field large scale patterns and apparent regularities, noting active longitude 27-day rotation periods and polarity differences. 03 p0432 A72-13354
- Identification of short polarity events by transforming marine magnetic profiles to the pole. 20 p2917 A72-39476
- Annual and solar-magnetic-cycle variations in the interplanetary magnetic field, 1926-1971. 23 p3286 A72-44504
- POLARIZATION**
- Interference polarization filter by modulation and phase detection for passband narrowing and secondary maxima attenuation, discussing application to photoelectric recording system. 03 p0356 A72-13096
- Interference polarization filter by modulation and phase detection for passband narrowing and secondary maxima attenuation, discussing application to photoelectric recording system. 11 p1632 A72-25708
- POLARIZATION [CHARGE SEPARATION]**
- NT DIELECTRIC POLARIZATION
- NT ELECTROLYTIC POLARIZATION
- Al-Mg alloy under reverse bending fatigue in aqueous sodium chloride with constant load and potentiostatic control, determining anodic polarization effects on fatigue life. 01 p0087 A72-11033
- Anodic polarization curves of Ni-Fe alloys relating reaction to attack at controlled voltage of gamma joints and Ni content, using electron microprobe. 02 p0243 A72-12168
- Two dimensional analysis of carrier circulation in MOS transistors for arbitrary polarization, including surface effects. 03 p0330 A72-13166
- Moving plasma beam capture by transverse magnetic field due to polarization space charges electrostatic separation. 03 p0396 A72-13657
- Plasma beams injection into toroidal magnetic field along gradient or radius, using polarizational interaction. 03 p0396 A72-13658
- Polarization and stress tensor characteristics as function of interaction between mechanical, thermal and electromagnetic processes in elastic isotropic dielectrics. 03 p0390 A72-14103
- Dielectric siphons, using weak polarization force density exerted on insulating dielectric liquids by nonuniform electric field. 04 p0520 A72-14416
- Rotational excitation of polyatomic molecule by electron collision attributed to polarization and electrostatic forces. 04 p0552 A72-14852
- Monograph on semiclassical gas laser theory covering electromagnetic fields, atomic polarization, multimode theory, traveling- and standing-wave laser principles, collision effects, etc. 05 p0668 A72-16398
- Ar core polarizability effect on photoionization cross section calculation for ground state configuration. 05 p0693 A72-17173
- Temperature effects on anodic polarization of Ti open surface and corrosion crevices, discussing critical potential relation to pitting. 06 p0829 A72-17946
- Hydrogen cracking of high strength steels during cathode polarization in acidic media, investigating time to cracking variation with current density. 07 p1013 A72-19770
- Charge separation effects on plasma shock wave profile in perpendicular propagation to magnetic field, using moment equations derived from Boltzmann equations for electrons and ions [AD-742533]. 08 p1213 A72-21254
- Plasma injection in magnetic trap along curvilinear inhomogeneous magnetic field, showing long plasmoids polarization and drift reduction by depolarization currents. 09 p1363 A72-23218
- Quasi-continuous charge carrier traps in molecular single crystals associated with polarization energy dissipation. 11 p1700 A72-25782
- Thunderstorms physical mechanisms of charge generation and separation, considering correlation between lightning and precipitation. 13 p1995 A72-29873
- Electron pressure effect on lunar wake shape and size, calculating electric field created by charge separation. 15 p2308 A72-31925
- Interstellar H I region strong polarization shock structure, obtaining charge separation field via beam continuum distribution and Mott-Smith approach. 16 p2453 A72-33168
- Propagation and instability characteristics of small signal electro-fluid-mechanical space charge and polarization waves in nonhomogeneous fluids. 17 p2542 A72-35612
- Effect of atomic polarizability on low-energy free-free radiative transitions. 19 p2837 A72-37839
- A new type of switching and memory effect by controlling the polarized field in semiconductor interface. 20 p2961 A72-39709
- Boltzmann kinetic equation for nonequilibrium plasma with allowance for polarization effects, noting collision integral convergence. 21 p0390 A72-40412
- Capacitance voltage characteristics instability of metal-aluminum oxide-silicon dioxide-silicon /MAOS/ structures, suggesting polarization effect in layer formed during deposition and annealing. 23 p3324 A72-44070
- Comparison of the vectors of the ventricular depolarization and repolarization of man during immersion in a standing position. 24 p3372 A72-44924
- Radar cross sections of conducting bodies of revolution, noting electric/magnetic polarizability tensors in LF Rayleigh scattering. 24 p3381 A72-45639
- POLARIZATION [SPIN ALIGNMENT]**
- Angular distributions of proton polarization during elastic scattering by V, Cr, Ni and Co nuclei in high energy region. 08 p1211 A72-21093
- Possibilities of determining complex form factors from experiments with polarized particles. 21 p3086 A72-40100
- POLARIZATION [WAVES]**
- NT CIRCULAR POLARIZATION
- NT ELLIPTICAL POLARIZATION
- Oblique electromagnetic wave propagation modes in anisotropic ionized stratified medium, investigating electric field and polarization components. 01 p1016 A72-10133
- Nonconservative radiative transfer in spherically symmetric system, calculating linearly polarized electron scattering atmosphere. 01 p1012 A72-11127
- Midlatitude ionospheric radio wave absorption measurements, using radio astronomical polarization method. 02 p0172 A72-11945
- Nighttime lower ionosphere electron density distribution models for vertically polarized radio wave propagation parameters. 02 p0173 A72-12112

Diffuse reflection of point source /flare/ light emission for cold dwarf star semiinfinite plane parallel atmosphere, calculating polarization

02 p0285 A72-12831

Polarization distribution and inversion of solar impulsive microwave bursts at 17 GHz

03 p0407 A72-12940

Linear polarization of pulsar PSR 22 18 plus 47 radio emission pulses, attributing periodic fine structure of spectrum to rotation of polarization plane in interstellar medium

03 p0436 A72-13824

Elastic wave velocities and polarization in planes of cubic crystals, plotting velocity curves

03 p0402 A72-13861

Self mode locked dual polarization carbon dioxide laser, obtaining simultaneous active stabilization and frequency modulation

04 p0529 A72-14604

Fluorescence polarization and intensities of nitric oxide vibrational bands from Cd line and continuum excitation for spectrometer calibration

04 p0552 A72-14893

Frequency characteristics of selectively reflecting screens in multichannel parabolic mirror antennas and determination of Fresnel coefficients dependence on polarized plane wave incidence angle

04 p0499 A72-15241

Linearly polarized wave excitation with specified phase shift and predetermined amplitude ratio by waveguide slots, giving slot configuration design formulas

04 p0487 A72-15243

Electromagnetic wave reflection from region with variable drift velocity and polarization of waves propagating in nonuniformly moving medium, applying to isotropic plasma

04 p0491 A72-15421

Astrophysics of interstellar medium, discussing direct and indirect observations including 21 cm H lines and starlight extinction and polarization

04 p0581 A72-15622

Extensive air showers radio emission polarization, spatial distribution and electric field strength, noting geomagnetic mechanism effect

06 p0870 A72-17278

Lunar regolith top surface polarimetric properties of sunlight-exposed rocks and fines compared to terrestrial rocks and meteorites

06 p0887 A72-18225

Wave-like ionospheric disturbance effect on phase polarization fading of vertical sounding signal, using numerical integration by computer

08 p1130 A72-20709

Electromagnetic wave polarization effect on linear transformation of waves in inhomogeneous magnetoactive plasma in magnetic field

08 p1212 A72-21245

Quasars and Seyfert and N-galaxies compact nuclei radiation polarization from polarimetric and photometric observations

08 p1234 A72-21281

Polarization corrections for normal electromagnetic waves passing from homogeneous to nonhomogeneous anisotropic medium

08 p1135 A72-21735

Geodetic optical distance measuring instruments with electro-optical polarization modulators, comparing characteristics of four possible configurations

09 p1314 A72-23336

Vertical angle estimation for HF sky wave multimode signals arrival, noting validity for arbitrary antenna elements polarization

09 p1281 A72-23513

Polarization maps of extended extragalactic and galactic radio sources at 6 cm wavelength

10 p1545 A72-24793

Magnetospheric equatorial compressional wave propagation to ground observed as transverse wave, noting plane of polarization

11 p1625 A72-26413

Colliding plane gravitational waves equations for linear polarization

12 p1845 A72-27409

VLF recorder for measurement of incident direction, polarization, phase and amplitude of 16 and 60 kHz transmitter signals

12 p1796 A72-27791

Hydrogen plasma production, using linearly polarized microwaves with superimposed magnetic field

13 p2010 A72-28683

Polarization method for measuring small phase difference variations in microwave range, developing rules for optimum selection of multiplication factor

13 p1928 A72-28790

Phase error magnitudes due to individual microwave elements imperfections and multiple reflections in phase difference measurements by polarization method in microwave range

13 p1928 A72-28791

Midlatitude ionospheric radio wave absorption measurements, using radio astronomical polarization method

13 p1920 A72-29257

Polarization-color effect in K corona during 7 March 1970 eclipse observation, using Wollaston prism and filter combination

13 p2043 A72-29544

Magnetic field effect on polarization plane rotation and emission frequency shift of He-Ne ring laser at 3.39 micron wavelength

16 p2402 A72-33485

Emission line polarization prediction for planetary nebula C IV ion emitted spectrum via theory for energy level population

16 p2458 A72-33689

Polarization measurements of radio sources at 9.55-mm wavelength

17 p2603 A72-34439

Tracking radar system rain clutter reduction by backscatter polarization technique for signal phase and magnitude adjustment

18 p2659 A72-36310

Wave-like ionospheric disturbance effect on phase polarization fading of vertical sounding signal, using numerical integration by computer

19 p2765 A72-38337

Propagation of horizontally polarized VLF waves - Systems implications

21 p3021 A72-40905

Electromagnetic induction in a half-space with a cylindrical inhomogeneity

23 p3284 A72-43423

POLARIZATION CHARACTERISTICS

Polarization diversity radar power law relations from measurements with size and shape distributed scatterers in comparison with linearly polarized system

01 p0030 A72-10832

Type 4 solar radio burst multiple magnetic loop structure and polarization observation by 80 MHz heliography

02 p0272 A72-11648

Venus cloud reflected radiation flux and polarization by Monte Carlo technique, using models with different particle size distributions

02 p0280 A72-12193

B and Be type stars intrinsic polarization, considering UVB spectra and effects on observed polarization

02 p0283 A72-12628

Radio wave polarization orthogonality recovery by using differential phase shifter and attenuator in radio communication systems

02 p0183 A72-12799

Semiconducting crystal superconductivity in laser field by interaction between electron conduction band and light induced polarization

02 p0269 A72-12883

Cosmic X ray sources polarization, spectra and locations measurement, describing Skylark experiments and UK-5 satellite-borne instruments

03 p0409 A72-13042

Pressure scanning Fabry-Perot magnetometer using KDP crystal and Glan-Thompson prism with echelle interferometer spectrograph for polarized Zeeman components

03 p0356 A72-13283

Telescopic phase retardation effect on Zeeman triplet Fe of polar sunspot umbrae in Stokes parameter measurements

03 p0357 A72-13288

Magnetic fields orientation in solar corona from polarization measurements in green line

03 p0431 A72-13343

Solar active region properties at millimeter wavelengths, suggesting chromospheric magnetic field measurement possibility from polarization

03 p0432 A72-13348

Solar corona observations during total eclipse of 22 September 1968, presenting photographs, polarization measurements, photometric data, structure and isophotes

03 p0434 A72-13492

Crab Nebula optical pulsar NP 0532 polarization minima delay mechanism, suggesting relativistic radiation from region orbiting relativistically around neutron star

03 p0434 A72-13553

Plasma flux interaction with axially symmetric magnetic field, investigating electrical polarization behavior

03 p0395 A72-13569

Linear electron acceleration mechanism in plasma, showing polarization fluctuations in diode under strong electric field

03 p0395 A72-13573

Pulsed Nd laser beam polarization components energy measurement by double reflecting plate calorimeter, checking accuracy against NBS liquid cell calorimeter

04 p0531 A72-15479

Pulsar PSR 0809 plus 74 observations indicating organized variation in polarization synchronized with drifting subpulses

04 p0581 A72-15513

Hf backscattering of plane electromagnetic wave at oblique incidence on conducting circular metallic disk, noting polarization dependence on angle

04 p0493 A72-15524

Microwave antennas, feed systems, strip transmission lines and test instrumentation, examining radiation patterns, design and polarization characteristics

05 p0635 A72-16330

Controlled polarization pattern of rectangular guide slots array as function of exciting wave parameters, presenting formulas for elliptical polarization distortion determination

05 p0635 A72-16331

Receiver arrangement for polarization selection based on multiplication of heterodyne-converted and amplified signals taken from dual-input antenna receiving elliptically polarized field

05 p0635 A72-16332

Reflection and transmission characteristics of circularly polarized horn antenna, discussing bandwidth properties, phase differences, polarization characteristics and voltage SWR

05 p0635 A72-16334

Polarization changes with distance from microwave antenna in near and intermediate zones for circularly and elliptically polarized fields in square and rectangular apertures

05 p0635 A72-16335

Polarization and energy characteristics of two mutually orthogonal slots cut in rectangular guide, allowing for reciprocal effects of slot arms

05 p0635 A72-16337

Polarization electric field and depolarization current measurements in plasma flows along toroidal solenoid with diverter

06 p0853 A72-17387

Structure, absolute photometry and polarization of corona from solar eclipse observation on 22 September 1968

06 p0883 A72-18026

Molybdenum disulfide and layer lattice materials lubricating mechanism and effectiveness from sulfur atoms strong polarization, using scanning electron microscope

06 p0822 A72-18157

Radially conducting cone wave spectrum calculation for noncophasal excitation, noting circularly polarized TEM and elliptically polarized TM wave amplitudes

07 p0938 A72-19003

Total flux and polarization of solar S-component at mm wavelengths, obtaining radio source optical depth by evaluation of QL propagation based on magnetoionic theory

07 p1069 A72-19080

Midlatitude geomagnetic micropulsations polarization and spectral characteristics, explaining behavior in terms of MHD wave propagation theories

07 p0975 A72-19152

Particle production and vacuum polarization, in anisotropic gravitational field, discussing energy momentum tensor values and collapse behavior

07 p1034 A72-19632

Circular and rectangular waveguide excited dielectric spheres as antenna feed, noting gain and polarization linearity

07 p0957 A72-19796

Type 3 bursts mean polarization level at 20-200 MHz, considering vertical spacing of radio waves emission levels

07 p1077 A72-19813

Pulsars radio observation for mean polarization parameters

07 p1079 A72-20049

Polarization distortion of partially polarized wave emission and reception by two channel horn antennas, noting radio astronomy, radar and optics applications

08 p1138 A72-20788

Venus clouds composition from spectral and polarization data, considering hydrochloric acid particles model

08 p1230 A72-20980

Reactions of aniline with isoamyl nitrite and phenyldiazonium borofluoride with caustic potash, investigating kinetics of chemical polarization of products nuclei

09 p1275 A72-22497

Transparency and polarization characteristics of three four-component Industrar-52 lenses with 1.5 aperture ratio and 50 cm focal length

09 p1309 A72-22516

Polarization fraction calculation for Lyman alpha radiation from excited H atom collisions, using Glauber, Born and Vainshtein approximations

09 p1355 A72-22790

Radio emission from pulsar CP 1133, comparing amplitude and polarization characteristics of two subpulses

09 p1387 A72-22987

Polarization characteristics measurement for PC 1 geomagnetic micropulsations propagated through ionospheric ducts, noting hydromagnetic emissions and whistlers relation to high latitude source region

09 p1299 A72-22989

Circular polarization measurements of Crab Nebula pulsar NP 0532, including main pulse leading and trailing edge components

09 p1394 A72-23675

Quasar and radio galaxy emission intensity and polarization variation models, comparing with observations

10 p1534 A72-23901

Traveling wave mode ring laser operation, obtaining active medium polarization changes through longitudinal magnetic field excitation by capacitor discharge through spiral pump lamps

10 p1492 A72-24363

Polarization characteristics and losses of anisotropic laser resonators composed of arbitrary number of mirrors

10 p1492 A72-24364

Electromagnetic wave propagation in weakly nonstationary plasma, determining variations of wave amplitudes and polarization characteristics

10 p1523 A72-24782

Receiving antennas polarization parameters selection in side-looking synthetic aperture radars

10 p1453 A72-24905

Optical and X ray pulsars, discussing Crab pulsar, emission behavior, pulse intensity, periodicity, polarization properties and antenna emission, plasma maser and Chiu models

10 p1547 A72-24919

Polarization characteristics of ferroelectric barium strontium titanates in solid solution at 4-100 K

10 p1527 A72-24984

Chloride ion concentration effect on polarization behavior of Fe-Ni alloy, noting cathodic curve parallel shift in noble potential direction

11 p1652 A72-25290

V 1057 Cyg photometry and polarimetry, considering model with two circumstellar shells stellar flux absorption and reradiation

11 p1716 A72-25678

Structure, absolute photometry and polarization of corona from solar eclipse observation on 22 September 1968

11 p1719 A72-25962

Jones matrix method for polarization natural states, frequencies and mode losses calculation in anisotropic optical resonators

11 p1688 A72-26347

Solenoid-produced local axial magnetic field influence on beat signal frequency characteristics in ring laser with nearly linearly polarized emission

11 p1650 A72-26357

Plasma flux interaction with axially symmetric magnetic field, investigating electrical polarization behavior

11 p1699 A72-26756

Linear electron acceleration mechanism in plasma, showing polarization fluctuations in diode under strong electric field

11 p1699 A72-26761

Interferometer investigations of Cassiopeia linear polarization at centimeter wavelengths, explaining results by source model incorporating Faraday depolarization

12 p1865 A72-27094

Geostationary satellites spacing dependence on quantifying factors, describing space environment experiments for satellite attitude stability and ground station antenna patterns and polarization effects

12 p1780 A72-27365

Linearly and circularly polarized electromagnetic field effective scattering areas relationships, considering radar reflection in reverse direction

12 p1783 A72-27629

Solar radio astronomy instrumental requirements for 20 meter wavelength interferometry, metric and decametric flux and polarization measurements

12 p1872 A72-27815

Probability and collisional relaxation in stellar systems, discussing gravitational polarization, collective interactions and spatial inhomogeneity

12 p1872 A72-27891

Polarization and dynamical friction drags on star in uniform infinite media and flat rotation sheet

12 p1872 A72-27892

Daytime sky brightness and scattered light polarization, emphasizing atmospheric radiation field characteristics

13 p1945 A72-28516

Parabolic, Cassegrain, spherical and horn-parabolic axisymmetric mirror antennas, calculating primary radiating element orientation effects on radiation polarization characteristics

13 p1931 A72-29277

Polarization and spatial and frequency characteristics of ground signal resulting from finite source Pc 1 micropulsation disturbance

13 p1922 A72-29391

Satellite photometric observatory for solar corona intensity and polarization measurements during 7 March 1970 total eclipse

13 p2043 A72-29546

Conversion efficiency and polarization behavior of Gunn diodes in resonant cavities, using I-V characteristics

13 p1937 A72-29866

Electromagnetic wave propagation in weakly nonstationary plasma, determining variation with time and polarization plane rotation

14 p2136 A72-30219

Steady motion of dense electron beam in rarefied phonon plasma along magnetic field, analyzing polarization effects

14 p2136 A72-30305

Cosmic ray anomalous absorption height dependence on zenith distance in midlatitude ionosphere during solar flare emission from polarization study

14 p2146 A72-30461

July 1952 polarization change in lunar crater Posidonius from polarimeter observations

14 p2152 A72-30488

Crab pulsar LF radiation polarization parameters and pulse shapes, showing highly polarized precursor component

14 p2156 A72-30567

Radio wave reflection from ionosphere, determining polarization and fluctuation characteristics via Stokes parameters

14 p2100 A72-30636

Radio phase interferometers for emitter position location, predicting polarization mismatch errors effects on accuracy

15 p2206 A72-31777

Diurnal variations of micropulsation activity polarization parameters in horizontal plane, describing experimental technique

15 p2230 A72-32258

Linear polarization and depolarization observation of quasar red shift explained as Faraday dispersion in or near source

15 p2313 A72-32365

Inner solar corona electron density distribution as function of heliographic latitude, longitude and radial distance from K-coronameter polarization-brightness data

15 p2318 A72-32786

Auroral electrojet polarization model, considering ionospheric Hall and Pedersen conductance maximum due to precipitation from electron plasma sheet inner edge

[AD-745672]

16 p2444 A72-32961

Quantitative evolution model for time variable flux densities and polarization characteristics of isolated moving type 4 events

16 p2444 A72-33041

Polarization observations of Saturnian satellite Iapetus leading and trailing hemispheres, showing albedo difference consistent with light curve amplitude

16 p2453 A72-33139

Diffuse galactic light polarization characteristics from OSO-5 observations, discussing model of starlight scattering by interstellar dust

16 p2446 A72-33468

Iterative procedure for Maxwell equations exact solution for anisotropic birefringent medium, applying result to limiting polarization problem

16 p2425 A72-33490

Solenoid-produced local axial magnetic field influence on beat signal frequency characteristics in ring laser with nearly linearly polarized emission

16 p2403 A72-33710

Pre-main-sequence stars. II - Stellar polarization in NGC 2264 and the nature of circumstellar shells.

17 p2605 A72-34531

Monte Carlo treatment of Lyman-alpha radiation in a plane-parallel atmosphere.

17 p2598 A72-34538

Traveling wave mode ring laser operation, obtaining active medium polarization changes through longitudinal magnetic field excitation by capacitor discharge through spiral pump lamps

17 p2563 A72-34962

Polarization characteristics and losses of anisotropic laser resonators composed of arbitrary number of mirrors

17 p2563 A72-34963

Solar corona emission line polarization numerical computation based on magnetic dipole transition scattering function for interpretation in terms of magnetic field direction

17 p2608 A72-35084

Type 3 bursts mean polarization level at 20-200 MHz, considering vertical spacing of radio waves emission levels

17 p2618 A72-35738

Polarization and interferometric investigations of discharge modes in thermionic energy converters

18 p2647 A72-36219

VLF hiss intensity, polarization, incidence angle and arriving direction observation at Antarctica station during magnetic disturbances

18 p2660 A72-36431

VLF-ELF hiss polarization and right/left component ratios recording at antarctic station, using sweep polarimeter

18 p2660 A72-36432

Polarization and velocity field in the galaxy M 82.

18 p2727 A72-36729

POLARIZATION CHARACTERISTICS

Latitudinal rotation direction daytime characteristics of pc 5 pulsation polarization based on global magnetic observations

18 p2689 A72-36870

Polarization effects during electron scattering in the gravitational field of a rotating source

18 p2712 A72-36967

The structure of the Crab Nebula at 2.7 and 5 GHz.

I. 19 p2855 A72-37340

July 1952 polarization change in lunar crater Posidonius from polarimeter observations

19 p2864 A72-38317

Plasma electron velocity distributions determined from the polarization of free-free bremsstrahlung.

19 p2841 A72-38439

Computer program for solar corona emission line polarization computation to interpret measurements in terms of coronal magnetic field direction

20 p2971 A72-39757

Line spectra and continuum polarization in magnetic white dwarfs.

20 p2971 A72-39760

Linear and circular polarization of synchro-compton radiation scattered by optically thin power law distribution of gyrating ultrarelativistic electrons

20 p2965 A72-39893

Application of matricial formalisms to the specification of light polarization changing systems.

20 p2928 A72-40025

A contribution to the numerical treatment of the electromagnetic field /H-polarization/ in horizontally non-homogeneous models of the earth.

21 p3048 A72-40498

Turnstile antennas polydirectional emission and polarization characteristics, discussing relationship formulation by Scott-Soo Hoo theorem

21 p3030 A72-40531

VHF-FM radio transmitting antenna for waves of circular, elliptical, and horizontally, vertically, or obliquely linear polarization

21 p3031 A72-40543

Horizontally polarized polydirectional or beam antenna, which is slightly out of round and consists of benn units, for television and FM radio

21 p3031 A72-40544

Coupled multiconfigurational self-consistent-field method of atomic dipole polarizabilities. I - Theory and application to carbon.

21 p3087 A72-40776

Linear cross polarization and attenuation measurements on terrestrial link at 11 GHz correlated with rainfall information

21 p3017 A72-40855

Polarization follower tracking linear vector transmitted by satellite with high precision, noting spacecraft attitude control and Faraday rotation measurements applications

21 p3021 A72-40907

Polarization characteristics of Schwarzschild black hole gravitational synchrotron radiation in terms of Stokes parameters

21 p3107 A72-41215

New measurements of the polarization of X-ray solar flares.

21 p3101 A72-41293

Observations of linear polarization of radio sources at 7.2 cm.

21 p3109 A72-41326

Polarization interaction between plasma flows in a transverse magnetic field

21 p3095 A72-41689

Pc 1 hydromagnetic whistlers and emissions polarization characteristics measured in plane of earth surface

22 p3169 A72-42019

Electromagnetic field, polarization and population inversion equations for spiked emission operation analysis in single mode laser

22 p3184 A72-42153

Brightness and polarization structure of four supernova remnants 3C58, IC443, W28, and W44 at 2.8 centimeter wavelength.

22 p3224 A72-42382

Effect of a polarizing current on the activity of neurons of the respiratory center

22 p3145 A72-42725

Polarized radio emission from five supernova remnants.

22 p3229 A72-42994

Polarizational interaction of opposed plasma flows in a linear octupolar magnetic field

22 p3214 A72-43121

Amplitude-time and polarization characteristics of the subpulses of the CP 1133 pulsar

22 p3230 A72-43136

Steady motion of dense electron beam in rarefied phonon plasma along magnetic field, analyzing polarization effects

23 p3317 A72-43207

Polarization measurements of the supernova in M101.

23 p3333 A72-43227

Polarization characteristics and wave vector direction effect on cross section of incident and diffuse light scattered in liquid, determining frequency shift functions

23 p3312 A72-43318

Temperature and polarization dependence of arsenic sulfide single crystals and thin films intrinsic absorption edge, determining forbidden bandwidth and transitions types

23 p3324 A72-43688

Interferometric spectropolarimetry - Alternate experimental methods.

23 p3289 A72-43890

Use of the three-dimensional covariance matrix in analyzing the polarization properties of plane waves.

23 p3315 A72-44518

Particle production and vacuum polarization in anisotropic gravitational field, discussing energy momentum tensor values and collapse behavior

24 p3424 A72-44564

Linear polarization survey for galactic background radiation at 1415 MHz in North Polar Spur, Cetus Arc and Loop III, noting continuous maxima shift

24 p3438 A72-44835

Wave and polarization equations for short coherent light pulses transmission in linear amplifying and absorbing media, noting single pulse formation in lasers

24 p3410 A72-45420

Analysis of the polarization properties of TW laser emission

24 p3411 A72-45497

Resonator polarization parameters effect on backwave attenuation in three and four mirror TW ring laser, noting colliding waves intensity dependence on polarization angle

24 p3411 A72-45505

POLARIZATION CHARTS

U GRAPHS [CHARTS]

U POLARIZATION [WAVES]

POLARIZED ELASTIC WAVES

Dynamic stress concentration around elliptical discontinuities in elastic medium, considering rigid and empty cavity scatterers for compression and vertically polarized shear incident waves

[ASME PAPER 72-APM-D] 10 p1554 A72-24180

POLARIZED ELECTROMAGNETIC RADIATION

NT POLARIZED LIGHT

NT SYNCHROTRON RADIATION

Strong linearly polarized electromagnetic wave propagation in overdense plasmas, considering relativistic electron velocities and nonlinear penetration effect

[AD-736322] 01 p0111 A72-11226

Book on microwave techniques covering Maxwell equations, electromagnetic wave propagation in conducting media, complex notation, plane polarized waves transmission and reflection, wave equations, etc

01 p0043 A72-11275

Vertically polarized logarithmically periodic monopole antenna for incoming wave front reception with low elevation angles in 1.5 to 30 MHz frequency range

02 p0195 A72-12697

Two finite conducting cylinders radial vibrations in E polarized electromagnetic wave, detailing pressure distribution and resonance effects

02 p0262 A72-12877

Right handed circularly polarized electromagnetic wave propagation in hot inhomogeneous plasma, deriving local dispersion equation by WKB methods

03 p0393 A72-12949

Solar flare associated magnetic field behavior and radio emission polarization in October 1968 active center, describing polarity flux variations

03 p0411 A72-13328

Parallel polarized electromagnetic waves scattering by radially inhomogeneous isotropic dielectric cylinders, computing scattered field coefficients by Fourier least squares fit technique

04 p0485 A72-14413

Structure, absolute photometry and polarization of corona from solar eclipse observation on 22 September 1968

06 p0883 A72-18026

Radiation polarization from Jovian disk center as function of phase angle from polarimetric observations

06 p0884 A72-18033

Pulse reflection of polarized plane electromagnetic wave from cold plasma ionosphere model with vertical magnetic field

06 p0777 A72-18729

Gas laser emission fluctuations of total radiation energy, polarized field components and line widths in longitudinal magnetic field

07 p0999 A72-18911

Radio emission of Lupus region believed to contain supernova of 1006 A.D., noting strong polarization

07 p1076 A72-19607

Optical transmission, reflection and absorption of thin rubidium films for parallel and perpendicularly polarized monochromatic radiation, investigating volume and surface plasma oscillations

07 p1050 A72-20523

Electromagnetic wave polarization effect on linear transformation of waves in inhomogeneous magnetoactive plasma in magnetic field

08 p1212 A72-21245

Horizontally polarized impulsive plane electromagnetic wave reflection from perturbed linear ionosphere model, obtaining transient response as inverse Fourier transform

08 p1136 A72-21979

Surface current density of perfectly conducting polygonal cylinders for axially polarized incident electromagnetic field

09 p1350 A72-22247

Time dependent parallel and cross polarized electromagnetic pulse propagation in magnetoionic medium for normal incidence

09 p1280 A72-23231

Structure, absolute photometry and polarization of corona from solar eclipse observation on 22 September 1968

11 p1719 A72-25962

Radiation polarization from Jovian disk center as function of phase angle from polarimetric observations

11 p1719 A72-25969

Isolation between two orthogonally polarized beams radiated by single paraboloidal reflector, discussing polarization coupling to earth receiving antenna

[AIAA PAPER 72-531] 12 p1789 A72-27356

Numerical calculation of electromagnetic scattering properties of two dimensional bodies with arbitrary cross section, considering TM polarization of excitation and fields mode matching

13 p1916 A72-28534

Jet aircraft photographic observation of solar corona polarization during March 1970 solar eclipse

13 p2043 A72-29547

Photographic polarimeter measurement of linear polarization of coronal emission lines during 7 March 1970 solar eclipse

13 p2043 A72-29547

Polarimetric determination of angle between polarization planes of emission and external radiation field in three level gas laser, noting resonator anisotropy properties

13 p1970 A72-29687

Jupiter electropolarimetric observations, showing polar regions polarization dependence on phase angle

13 p2050 A72-30069

July 1952 polarization change in lunar crater Posidonius from polarimeter observations

14 p2152 A72-30488

Crab pulsar LF radiation polarization parameters and pulse shapes, showing highly polarized precursor component

14 p2156 A72-30567

Diffraction analysis of Fabry-Perot interferometer with metal mirror gratings for oblique incident polarized plane electromagnetic wave reception

15 p2233 A72-31413

Diffuse galactic light polarization characteristics from OSO-5 observations, discussing model of starlight scattering by interstellar dust

16 p2446 A72-33468

Results of observation of spectra and polarization of meter solar radio emission with high time resolution - May-June, 1969.

17 p2602 A72-35714

VLF-ELF hiss polarization and right/left component ratios recording at antarctic station, using sweep polarimeter

18 p2660 A72-36432

Measurement of integral parameters of the nighttime ionosphere by observations of signals from the 'Intercomos 2' artificial earth satellite

18 p2689 A72-36877

Observation of linear polarization of solar microwave bursts.

18 p2722 A72-36997

The measurement of polarized 10-micron radiation from cool stars with circumstellar shells.

19 p2854 A72-37232

Transmission and reflection of an electromagnetic wave incident normally on a plasma half-space.

19 p2840 A72-37726

Polarization observations of solar radio emission at the 3.15-cm wavelength

19 p2858 A72-37801

July 1952 polarization change in lunar crater Posidonius from polarimeter observations

19 p2864 A72-38317

Cross-polarized radiation from convex spherical antennas with a phase-opposed field distribution

19 p2774 A72-38414

Plane electromagnetic wave diffraction on thin ribbons grating, discussing scattered field singularities for E polarized waves

19 p2769 A72-38850

Two dimensional linear polarization radio distribution maps of 3C 270 and 3C 452 radio galaxies, relating to source magnetic field structure

20 p2965 A72-38904

Gas laser emission fluctuations of total radiation energy, polarized field components and line widths in longitudinal magnetic field

20 p2931 A72-39377

Isotropically and anisotropically polarized He-Ne lasers output dependence on longitudinal magnetic fields, noting electron density radial redistribution in gas discharge plasma

20 p2932 A72-39411

The Mueller matrix for scattering - Including the effects of interference.

20 p2970 A72-39754

Cross polarizing effects of a water film on a parabolic reflector at microwave frequencies.

21 p3027 A72-40375

An antenna principle with universally polydirectional radiation for large spin-stabilized flight devices

21 p3030 A72-40532

VHF-FM radio transmitting antenna for waves of circular, elliptical, and horizontally, vertically, or obliquely linear polarization

21 p3031 A72-40543

New measurements of the polarization of X-ray solar flares.

21 p3101 A72-41293

Faraday rotation of linearly polarized radio waves from the Crab Nebula by the solar corona.

21 p3109 A72-41327

Effect of radiation polarization on hologram quality

22 p3176 A72-42107

Coupled fields in inhomogeneous warm plasmas with static pressure gradients. I.

22 p3210 A72-42313

Analytical model for a polarizable medium at radio and lower frequencies.

22 p3155 A72-42467

Polarized radio emission from five supernova remnants.

22 p3229 A72-42994

Polarization measurements of the supernova in M101.

23 p3333 A72-43227

Amplification of cylindrical electromagnetic waves reflected from a rotating body

23 p3262 A72-43307

Reflectivity dependence of triple polarization grid on elements spacing and wires orientation, noting bandwidth of ray guide matching transformer

23 p3269 A72-43446

Direct and cross polarized backscatter power from a turbulent plasma.

23 p3320 A72-43521

Evaluation of the reliability of diversity reception by antennas of different polarizations

23 p3271 A72-43777

Polarization of the central field of a wave reflected from the ionosphere

23 p3265 A72-44175

Circularly polarized waves in magnetoplasmas containing negative ions.

23 p3323 A72-44533

Influence of the polarization of incident radiation on the distribution of the energy absorbed in a particle

24 p3424 A72-44621

POLARIZED LIGHT

Goos-Hanchen nonpolarized light effect for laser beam separation into rectilinearly polarized beams during reflection

01 p0101 A72-10042

Sky light polarization, cloudiness and view angle effects on oil remote detection over water surface, describing passive radiometric techniques

[AIAA PAPER 71-1075] 01 p0057 A72-10536

Topmost soil layer moisture content measurement by reflected visible light polarization enhancement

02 p0209 A72-11794

Oblique rotator model for time dependent light polarization of red long period variables, considering dust particle alignment in outer atmospheric layers near magnetic poles

02 p0283 A72-12630

Collisional relaxation rate effects of atomic level polarization on spectral line formation in solar magnetic regions

03 p0427 A72-13294

Multiple scattering polarization of sunlight reflected by terrestrial water clouds as function of particle shape and size, using doubling method

03 p0384 A72-14145

Book on lasers and applications covering theories of light, polarization, coherence, resonators, mirrors, modes, electro-optical effect, communication, holography, etc

06 p0827 A72-18524

Anomalous Hall effect of polarized electrons spin-orbit interactions in semiconductors, involving emf appearance in electric field and polarized light

07 p1048 A72-19642

Light polarization in Honda comet head, discussing brightness distribution

08 p1229 A72-20833

Sun vicinity skylight polarization influence on polarimetric K corona observations, discussing inaccuracy sources

09 p1392 A72-23544

Polarization effect on sensitivity of photocells and photomultipliers with/without cover glass

09 p1289 A72-23670

- Current-optical effects of anisotropic absorption of polarized and unpolarized light in rarefied cosmic media 10 p1525 A72-23763
- Light polarization in anisotropic Zeeman laser under axial magnetic field 10 p1491 A72-24134
- Mu Cephei light polarization explanation, deriving spatial orientation of rotational axis and rotation period 10 p1546 A72-24832
- Anomalous refraction maxima in bidirectional plane polarized radiant flux transmittances of roughened dielectric surfaces [AIAA PAPER 72-302] 11 p1742 A72-25236
- Light polarization modes in gas ring laser with optically active isotopic cell, showing dependence on circular field coupling coefficient 13 p1968 A72-29512
- Light intensity and linear polarization for single scattering by ice clouds in visible and IR, approximating crystals with long circular cylinders 14 p2128 A72-30349
- Daytime zodiacal light intensity and polarization measurement at elongation angles between 15-30 degrees from Skylark rocket photometric observations 15 p2227 A72-31951
- Zodiacal light brightness and polarization measurement from OSO-5 with photometers at 4180 and 6820 Å 16 p2385 A72-33467
- Photographic technique to obtain isophotic contours of solar corona polarized light during total eclipse 16 p2393 A72-33624
- New measurements of the polarization of photospheric light near the solar limb 18 p2727 A72-36739
- Effect of fluidization on the polarization of reflected light from lunar dust layers 18 p2729 A72-36987
- Macroscopic photon echo polarization and radiation intensity in Cr ion doped ruby laser stimulated by coherent light pulses 19 p2814 A72-38780
- Interferometric spectropolarimetry - Alternate experimental methods. 23 p3289 A72-43890
- Polarization of emission in the IC 4592 and IC 4601 nebulae 23 p3338 A72-44032
- Anomalous Hall effect of polarized electrons spin-orbit interactions in semiconductors, involving emf appearance in electric field and polarized light 24 p3431 A72-44573
- Approximate formulae for mixed modulated coherent and partially polarized chaotic light. 24 p3425 A72-44769
- POLARIZED RADIATION**
- NT POLARIZED ELASTIC WAVES
- NT POLARIZED ELECTROMAGNETIC RADIATION
- NT POLARIZED LIGHT
- NT SYNCHROTRON RADIATION
- Feautrier numerical solutions to transfer equation of polarized continuum radiation from sunspot in chromosphere 01 p0101 A72-10096
- Pulsar PSR 0833-45 linear polarization measurements at 300 and 1420 MHz, showing frequency invariance with interstellar scattering and Faraday rotation allowance 01 p0133 A72-11119
- Crab Nebula pulsar NP 0532 model for interaction and polarization of radio radiation with surrounding media 02 p0277 A72-11772
- Rapidly varying radio source VRO 42.22.01 /BL Lac/ observations, presenting flux density and linear polarization variations 02 p0277 A72-11774
- Stellar X ray emission polarization measurement using Thomson scattering polarimeter [AD-736550] 03 p0353 A72-13041
- Short wavelength continuous solar X-radiation polarization and angular distribution measurements, revealing physical processes in solar flares 03 p0409 A72-13126
- Coherence properties of polarized radiation in weak magnetic fields, considering scattering redistribution for normal Zeeman triplet 03 p0427 A72-13292
- Homogeneous polarization diagrams synthesis for entire radiation pattern of single reflector pencil beam antenna, noting radiator aperture misalignment effect 08 p1138 A72-20933
- Pulsed GaAs injection laser active region anisotropy and radiation polarization under spontaneous and coherent emission conditions 08 p1183 A72-21772
- Gravitational wave antenna response to linear, mixed and randomly polarized sources, discussing Weber signals galactic nucleus source 11 p1717 A72-25882
- Combination antenna unit with vertical monopole and two perpendicular slots in horizontal plane to yield steerable cardioid-shaped pattern for vertically polarized waves 15 p2206 A72-31776
- Transfer of polarized radiation in a stellar atmosphere. 17 p2605 A72-34533
- Redistribution of resonance radiation. I - The effect of collisions. 17 p2605 A72-34534
- Effect of polarization on the apparent emittance of rectangular groove cavities. 20 p2954 A72-39629
- POLARIZERS**
- Polarizer circuit for reduction of output power fluctuations in He-Ne laser 06 p0825 A72-17842
- Grid polarisers for use in the near infrared. 20 p2922 A72-39046
- POLAROGRAPHS**
- U POLAROGRAPHY
- POLAROGRAPHY**
- Polarographic method for simultaneous measurement of wall gradients of velocity and of concentration in unsteady laminar or steady turbulent flow 06 p0797 A72-17558
- Zn, Ge and P based semiconductor alloy specimens chemical composition determination via ac polarograms 12 p1854 A72-27443
- Gravimetric and polarographic determination of W in binary W-Mo alloys, noting methods accuracy 18 p2655 A72-36098
- POLES**
- Multiplication operator unidimensional perturbation by independent variable, considering spectral function density poles and branch points 03 p0382 A72-13728
- Magnetic field and polar region geometry effects on hollow cathode thruster performance of Kaufman electric engine [AIAA PAPER 72-417] 11 p1706 A72-26167
- POLICIES**
- NT PROCUREMENT POLICY
- Public policy, regulatory controls, market strategies and systems economics considerations for future U.S. domestic communication satellite system 21 p3132 A72-40865
- Forecasting as a means for scientific and technological policy control. 23 p3358 A72-44350
- POLISHING**
- NT ELECTROPOLISHING
- NT VIBRATORY POLISHING
- Milling, band grinding, final manual polishing and tumbler polishing effects on fatigue life and surface finish of steel compressor blades 06 p0824 A72-18651
- Large astronomical telescopes construction, discussing aspherical surfaces control, grinding, polishing and optical testing procedures 15 p2234 A72-31612
- POLITICS**
- International criminal court for aircraft hijacking, examining political and jurisdictional aspects 05 p0752 A72-15837
- Short haul air transportation system economic and political problems, noting community acceptance and passenger service standards 16 p2481 A72-33310
- Book - Law and politics in outer space: A bibliography. 21 p3132 A72-41535
- POLLEN**
- Influence of temperature shocks on seed formation after irradiation of pollen from *Tradescantia paludosa*. 19 p2761 A72-38642
- POLLUTANTS**
- U CONTAMINANTS
- POLLUTION**
- NT AIR POLLUTION
- NT ENVIRONMENT POLLUTION
- NT NOISE POLLUTION
- NT THERMAL POLLUTION
- NT WATER POLLUTION
- POLYACRYLATES**
- U ACRYLIC RESINS
- POLYAMIDE RESINS**
- NT NYLON [TRADEMARK]
- Temperature effects on strength and deformability of randomly reinforced fiberglass polyamides 02 p0250 A72-12678
- Fire resistant fibrous materials for potential military and transportation applications, considering aromatic polyamide polybenzimidazole, fluorocarbon resin polymer, phenolic and glass fibers and fabrics 08 p1191 A72-21586
- Gamma radiation effect on cracking and tensile strength of polycapromide /capron/ film 08 p1196 A72-21870
- Molecular structure and thermomechanical properties of polyimide and polyamide resins used for precision parts 12 p1833 A72-27406
- POLYATOMIC GASES**
- NT DIATOMIC GASES
- Resonant transport properties of polyatomic gases in collinear static and oscillating magnetic fields, using microscopic kinetic equation 04 p0553 A72-15633
- Kinetic theory of wall temperature jump and near-wall temperature distribution in polyatomic gases, solving simultaneous singular linear integral equations by numerical methods 06 p0904 A72-18528
- Magnetic field influence on shear viscosity of polyatomic gases, measuring rectangular cross section capillary flow resistance for different field orientations 07 p1038 A72-20398
- Thermomagnetic slip produced by certain temperature gradient and magnetic field combinations in rarefied polyatomic gas channel flow 07 p0973 A72-20399
- Nonspherical and nonadditive interactions contribution to third virial coefficient of polyatomic gas, discussing anisotropy, shape factor, and intermolecular forces 08 p1211 A72-21292
- Kinetic model for polyatomic gas heat transfer between parallel plates, considering boundary value problem with arbitrary accommodation coefficients 11 p1744 A72-25559
- Burnett theory of thermal transpiration in capillary with wall accommodation for polyatomic gases, using Chapman-Enskog constitutive relations 11 p1746 A72-26010
- Combined translational and internal relaxation theory of sound propagation in polyatomic gases, using 17 moment approximation 11 p1687 A72-26054
- Waldman-Snyder equation application to sound absorption and dispersion in dilute polyatomic gases, presenting truncation procedure for perturbation function expansion in irreducible Cartesian tensors 14 p2131 A72-30673
- Light scattering by monatomic and polyatomic gases, superimposing effects due to rotational and translational molecular relaxation 16 p2428 A72-32944
- Dipole moment derivative of triatomic hydrogen ion electronic ground state, considering fundamental spectrum observation in hydrogen gas in local thermodynamic equilibrium 22 p3209 A72-42720
- POLYATOMIC MOLECULES**
- NT DIATOMIC MOLECULES
- NT TRIATOMIC MOLECULES
- Rotational excitation of polyatomic molecule by electron collision attributed to polarization and electrostatic forces 04 p0552 A72-14852
- Large diatomic and polyatomic molecules formation from big radicals in interstellar medium, noting association reaction role 06 p0891 A72-18506
- Polyatomic ions interaction with neutral molecules in gases, calculating ion mobility as function of temperature from core model representation 09 p1355 A72-22788
- Chemical lasers diatomic and triatomic molecules dissociation in nonequilibrium conditions, discussing vibrational energy exceeding gas temperature 11 p1646 A72-25713
- H I region molecular formation on interstellar dust grains, discussing nonequilibrium evaporation mechanism for adsorbed particles 16 p2452 A72-33128
- Rates of interaction of vibrationally excited hydroxyl $\nu = 9$ with diatomic and small polyatomic molecules. 17 p2511 A72-35648
- Strict allowance for the variation of the system of normal coordinates in the theory for the vibronic spectra of polyatomic molecules 19 p2838 A72-38777
- Intramolecular interactions and vibronic spectra of polyatomic molecules. IV - Electronic relaxations: Configurational and relaxational spectra - The four-level arrangement 19 p2838 A72-38778
- Measurement of thermal relaxation time of vibration of polyatomic molecules by the impact tube method 24 p3402 A72-45045
- Theoretical interpretation of the optical and electron scattering spectra of polyatomic molecules. III - N₂O and the discovery of resonant phenomena in the B region at 6.8 eV. 24 p3426 A72-45301
- POLYBENZIMIDAZOLE**
- Polybenzimidazole fabric treatment for flammability reduction in oxygen atmospheres 07 p1023 A72-19055
- POLYBUTADIENE**
- Thermosetting polybutadienes as co-curing plasticizers for thermoplastics reinforcement, noting oxidation resistance at room and moderately elevated temperatures 16 p2415 A72-33416

POLYCARBONATES

- Polycarbonate yield locus from strain rate, creep, isotropy, isoclinic and reloading tests on perforated plates [SESA PAPER 1819] 02 p0248 A72-11501
- Polycarbonate merits as visual solid detector in high energy radiation dosimetry [CERN-71-16] 02 p0162 A72-12066
- Polycarbonate yield dependence on temperature in uniaxial compression and tensile tests described by modification of Eyring theory of non-Newtonian viscosity 08 p1191 A72-21184
- Acrylics and polycarbonates properties in aircraft transparencies design, emphasizing cost and optical, mechanical, thermal and chemical properties 12 p1832 A72-27009
- Polycarbonates applications in aircraft transparencies, discussing chemical, heat, impact and abrasion resistance, toughness and weathering 12 p1832 A72-27010
- Transparent aircraft polycarbonate glazing systems shielding properties for projectile and bird impacts 12 p1832 A72-27015
- Tailoring the interface in graphite-reinforced polycarbonate. 17 p2570 A72-34713
- Use of the third-harmonic method for the selection of metal-bonded polycarbonate capacitors which are stable in time 18 p2669 A72-37115
- POLYCRYSTALS**
- Balance laws of micromorphic theory for polycrystalline mixtures, granular composites and fluid suspensions involving motions with wavelength comparable to intrinsic discontinuities in materials 01 p0102 A72-10320
- Polycrystalline Mo work function calculation from electron emission microscopy, determining crystallographic grain orientation effects 01 p0071 A72-11027
- Beryllium microstructure and hexagonal close packed polycrystal material residual thermal stresses, calculating thermal expansion coefficients 01 p0087 A72-11028
- Annealed pure Al polycrystals fatigue behavior data under elevated temperatures, using transmission electron microscopy 02 p0242 A72-11525
- Polycrystalline bodies thermoelastic behavior under random external forces, determining thermal microstress distribution parameters by statistical boundary value formulation 02 p0290 A72-11632
- Dielectric properties of high purity polycrystalline barium titanate, observing temperature effects as function of heat treatment [AD-737022] 02 p0269 A72-12417
- Polycrystalline materials wedge crack growth enhancement by vacancy diffusion under creep failure conditions, considering grain boundary sliding mechanism 03 p0442 A72-12998
- Superferromagnetism in thin polycrystalline Gd and Gd-Au films having Curie points near room temperature 03 p0401 A72-13583
- Shock waves in solids, investigating Hugoniot curve for condensed and porous media and phase transformation effects in polycrystals 03 p0446 A72-13689
- Stress measurement at surface of polycrystalline bodies by nondestructive X ray diffractometry method 04 p0525 A72-15553
- Mono- and polycrystalline Ni high temperature creep kinetics, investigating substructural changes 05 p0671 A72-16000
- High purity polycrystalline Al hf low strain fatigue measurements by piezoelectrically driven exponential horn, estimating critical point defect concentration 06 p0893 A72-17420
- Physical theory of plasticity, considering mathematical hypotheses and assumptions, single crystals dislocations and plastic deformation, polycrystals homogeneous strain analysis, slip theories, etc 06 p0896 A72-17962
- Microscopic-macroscopic transition in heterogeneous metal polycrystals and multiphase composites at finite strain 06 p0897 A72-18068
- Idealized model for anisotropy of metals inelastic characteristics due to plastic deformation, demonstrating applicability to polycrystalline materials 06 p0900 A72-18685
- Plane harmonic waves propagation in stressed polycrystalline bodies with slight orthotropy in unstressed state, substantiating theory for initial stress determination by ultrasonic technique 07 p1090 A72-19753
- Thermoelastic characteristics and crystal phase distribution effect on microstructural stresses and thermal expansion of polycrystalline refractory materials 07 p1018 A72-20133
- Monocrystals elastic anisotropy effects on polycrystalline sinter matrix minimum porosity, thermal conductivity, mechanical and elastic properties, thermal stress resistance and Hugoniot elastic limit 08 p1186 A72-21441
- Nonbasal deformation modes activation in Czochralski sapphire and fine grained alumina polycrystals deformation, noting water weakening 09 p1335 A72-22395
- Sign-variable nonisothermal plastic deformation and creep behavior of polycrystalline construction materials, taking into account Bauschinger effect 09 p1401 A72-22726
- Optical properties of Gd polycrystals in IR, explaining frequency dependence of complex permittivity 09 p1372 A72-23040
- Cooperative and sequential sensization effect on He emissive states population in polycrystalline barium and yttrium fluorides with trivalent Yb 10 p1525 A72-24044
- Recording holographic networks in polycrystalline transparent ferroelectric ceramics of lead and lanthanum titanate-zirconate system 10 p1480 A72-24111
- High temperature creep behavior of sintered polycrystalline strontium zirconate as function of temperature, stress, grain size and strain level, using pure bending test method 10 p1497 A72-24275
- Polycrystalline Mo fatigue behavior under cyclic stresses, discussing grain size effect on fatigue life and relationship between cycle dependent yield and French damage line 11 p1658 A72-25830
- Roller polycrystalline metal samples principal anisotropy direction determination by acoustic measurements at ultrasonic frequencies 12 p1806 A72-27086
- German Si and polycrystalline solar cells development survey, discussing interconnection techniques, module design and filter applications for performance improvements 12 p1756 A72-28003
- External magnetic field effect on two frequency quadrupole spin echo in polycrystalline specimen 13 p1915 A72-28473
- Polycrystalline alpha Ti work hardening at low temperatures and different purities, discussing plastic strain effects 13 p1975 A72-28671
- Polycrystalline microstructure changes of corundum during high temperature creep tests, using optical microscopy 13 p1983 A72-28775
- Hydrostatic pressure effect on tensile creep and creep rupture of polycrystalline metals at high temperatures 13 p2058 A72-29450
- Ruby laser emission second harmonic generation effectiveness in organic polycrystals from comparison to lithium niobate 13 p1970 A72-29689
- Increased volume fraction effect on transverse rupture strength and fracture toughness of hot pressed and annealed composites of polycrystalline magnesium oxide 13 p1980 A72-29828
- Memory and photoconductivity in CdSe polycrystals at 77 and 300 K, plotting photocurrent vs illumination levels 13 p2024 A72-30012
- Loading conditions effect on relaxation and creep in inhomogeneous hereditary elastoplastic polycrystalline materials 14 p2168 A72-30953
- Material constants for strain hardened polycrystalline metals calculated from mathematical model for plastic deformation 15 p2322 A72-31361
- Polycrystalline Mo-Re alloy under cold longitudinal, transverse, cross and pack rolling, noting twin and dislocation microstructures 15 p2256 A72-31669
- Current noise spectra in single crystals and polycrystals of transition metal compounds, discussing flicker noise origin 15 p2293 A72-32384
- Velocity distributions of molecular beams evaporating into vacuum from polycrystalline hexachlorobenzene and sulfur surfaces 16 p2429 A72-33058
- Multiple plastic and viscoplastic potentials for single crystal and polycrystal with mean densities and mean lengths of dislocations as internal variables 16 p2470 A72-33615
- Electromagnetic waves attenuation and phase velocity correction in polycrystals with anisotropic crystal distribution 16 p2365 A72-34013
- Effects of disorientation of grains on the viscoplastic behavior of fcc polycrystals 17 p2634 A72-35407
- The effect of hydrostatic pressure on plastic deformation and creep of polycrystalline metals at elevated temperatures. 20 p2977 A72-38878

- Self-diffusion of cobalt in coarse grained polycrystalline Ni-Co alloys at low temperature. 20 p2935 A72-39016
- Corundum polycrystalline microstructure changes during high temperature creep tests, using optical microscopy 21 p3072 A72-40269
- Theory of slow elastic-plastic deformation of polycrystalline metals with micro-stresses as latent variables descriptive of the state of the material. 21 p3124 A72-41508
- Influence of polycrystallinity on transconductance of thin-film transistor. 22 p3159 A72-42309
- Kinetic aspects of plastic strain induced martensite in polycrystalline Fe-Ni-C alloy from tensile tests on austenitic specimens 22 p3189 A72-42437
- Cd Se polycrystal memory and photoconductivity at 77 and 300 K, plotting photocurrent vs illumination levels 22 p3214 A72-42734
- Physicochemical investigation of the thermionic emission properties of metals and alloys 22 p3191 A72-42811
- Mathematical model for plastic deformation of polycrystalline materials with Hooke's law elastic strains 22 p3242 A72-43135
- Polycrystalline aluminum and magnesium oxide ceramics fracture strength, considering plastic deformation and twinning role in crack nucleation 23 p3305 A72-43505
- Determination of the regions of action of various creep mechanisms in ceramic materials 23 p3307 A72-43932
- Dislocation-substructure-strengthening and mechanical-thermal treatment of metals. 23 p3304 A72-44299
- High-temperature creep of polycrystalline chromium. 23 p3304 A72-44449
- A study of the effect of grain orientation misfit on the viscoplastic behavior of polycrystalline metals /fcc system/ 24 p3414 A72-45251
- Thermoelastic characteristics and crystal phase distribution effect on microstructural stresses and thermal expansion of polycrystalline refractory materials 24 p3416 A72-45759
- POLYCYTHEMIA**
- The effect of chronic erythrocytic polycythemia and high altitude upon plasma and blood volumes. 19 p2757 A72-38028
- POLYESTER RESINS**
- Chlorendic acid based Hetrion 92C fire retardant chemical resistant polyester for fiberglass reinforced structure applications 08 p1192 A72-21677
- Epoxy and polyester resin fatigue fracture tests for cyclic stress and moisture effects 08 p1192 A72-21680
- Creep test for microfailures of glass reinforced epoxy and polyester laminates immersed in water at ultimate flexural stress 09 p1336 A72-22537
- Water damage in glass fiber-polyester resin composites, discussing fiber debonding, crack propagation and water resistance 11 p1675 A72-26950
- Fracture toughness measurements of polyester composites reinforced with chopped steel wires compared with Cooper theory 16 p2413 A72-33203
- Resin selection for manufacture of chemically resistant glass fiber reinforced polyesters, considering structural factors of chain for susceptibility to alkaline hydrolysis 16 p2414 A72-33304
- The fracture energy of a glass fibre composite. 17 p2570 A72-34670
- Work of fracture of fibre-reinforced polymers. 23 p3306 A72-43561
- POLYESTERS**
- Phosphorus compounds incorporation in polyurethane foams and polyesters for flame retardancy [PI PAPER 12] 03 p0380 A72-13246
- Polyester bonded explosives mechanical and thermal properties, noting need for desensitizing against shock and friction effects 14 p2145 A72-30768
- Flame retardant glass reinforced thermoplastic polyester Celanex processing and performance, considering flammability, and electrical/mechanical properties 16 p2415 A72-33420
- POLYETHER RESINS**
- NT POLYMETHYL METHACRYLATE
- POLYETHYLENE TEREPHTHALATE**
- Nonlinear viscoelastic behavior of isotropic unoriented crystalline polyethylene terephthalate at 70-100 C, using creep, recovery and load tests 16 p2416 A72-33614
- POLYETHYLENES**
- NT POLYETHYLENE TEREPHTHALATE

Polyethylene-FLOX hybrid stage optimum combustion chamber pressure, representing pressure dependent factors by simple analytical models
01 p0117 A72-11221

Polyethylene and polypropylene combustion, investigating additives and surrounding gaseous composition effects on flammability and volatile products during thermal degradation
02 p0248 A72-11767

Photoemission from polyethylene, Kapton, Teflon and polyvinyl chloride under photon irradiation
03 p0403 A72-14084

Linear polyethylene irradiation, investigating chain scission processes importance, critical conditions for gelation and sol/gel partitioning
04 p0484 A72-15258

Polyethylene oxidative degradation study with gas chromatographic techniques, obtaining aliphatic and organic compounds at 75-200 C in varying oxygen concentrations
08 p1128 A72-21425

Chopped fiber glass reinforced high density thermoplastic polyethylene composite, determining critical fiber length, interfacial adhesion and fracture toughness
08 p1193 A72-21684

Radial and axial residual stress components in glass fiber reinforced polyethylene, comparing with adhesion strength obtained by shear method
08 p1196 A72-21862

Irradiation effects on linear polyethylene molecular weight fractions in molten and crystalline states, determining sol-gel partitioning to establish critical conditions for gelation
09 p1337 A72-22550

Radical concentrations in gamma irradiated poly(ethylene 2,6-naphthalene dicarboxylate)/ by ESR spectrum analysis
10 p1433 A72-23847

Crystal-morphology role in refraction of cold drawn polyethylene samples of varying lamellar thickness and density, relating elastic restoring force to crystal deformation
12 p1832 A72-27283

Ion bombardment and partial discharges effects on polyethylene sheet, observing structural changes by IR spectroscopy
13 p1984 A72-29788

Aluminum/plastic semifinished material - A new material for multiple applications
20 p2944 A72-39452

Reversible changes in polyethylene coating adhesion due to thermo-oxidative destruction of polyethylene
21 p3072 A72-40082

On the stress-strain curve of polyethylene filled with randomly oriented glass fibers.
21 p3073 A72-40721

Nanosecond and picosecond laser-produced CD2 plasmas.
24 p3427 A72-44709

POLYGONIZATION
Crystals deformation and orientation effects on Al polygonization process, noting dislocation densities dependence on stress axis orientation
13 p1972 A72-28464

Hollow elliptical waveguide numerical analysis by polygon approximation with computer program to obtain cutoff wavelength without Mathieu functions
14 p2087 A72-30943

POLYGONS
NT PARALLELOGRAMS
NT RECTANGLES
NT SQUARES [MATHEMATICS]
NT TETRAGONS
NT TRAPEZOIDS
NT TRIANGLES

POLYHEDRONS
NT PARALLELEPIPEDS
NT RHOMBOHEDRONS
NT TETRAHEDRONS

Radiative cooling system for nearly spherical or polyhedral bodies using radially attached diverging conical elements
02 p0304 A72-12863

Atmospheric motion equations numerical integration, presenting conservative finite difference approximation for quasi-uniform spherical grids derived from regular polyhedrons
13 p1985 A72-28445

POLYIMIDE RESINS
Polyimide prepolymer formulation for glass and graphite reinforced composites autoclave processing via increased melt phase duration and temperature range
01 p0090 A72-10729

Thermal and environmental exposure effects on high temperature mechanical properties of graphite/polyimide composites
01 p0090 A72-10730

Characterization of graphite/polyimide composites for space shuttle applications
01 p0092 A72-10784

Space shuttle oriented polyimide reinforced Ti matrix composites properties, noting weight saving
01 p0139 A72-10785

Epoxy- and polyimide-graphite composites electrical dissipation factor and capacitance measurements as guide to molding quality, describing equipment
02 p0250 A72-12609

Polyarylates, polyimides and thermosetting polymers role in sliding friction of self lubricating plastics, noting temperature effects
06 p0837 A72-18599

Molecular structure and thermomechanical properties of polyimide and polyamide resins used for precision parts
12 p1833 A72-27406

POLYIMIDES
NT KAPTON [TRADEMARK]
Self lubricating polytetrafluoroethylene and polyimide composites transfer film formation tests, studying film thickness and uniformity
06 p0824 A72-18596

Aromatic polyimide binder for compression moldable high performance composites preparation with thermal curing to obtain good thermal-oxidative stability and toughness
12 p1834 A72-28090

Addition type polyimide-graphite fiber composites fabrication from monomeric reactant solutions to improve mechanical properties and thermal stability
12 p1834 A72-28091

Thermomechanical and thermogravimetric analyses of systematic series of polyimides.
17 p2511 A72-34714

Boron polyimide composite development.
21 p3072 A72-40553

POLYMER CHEMISTRY
Thermally stable organic polymer fiber production methods and performance evaluation in high temperature environments, discussing structure types, flammability and tensile properties
02 p0248 A72-11771

Polymer adhesives chemistry and properties in 450 F air, discussing weight loss and strength values
03 p0381 A72-14233

Ordinary and macroporous structured polycondensation oxidation-reduction polymers synthesis, discussing application to organic impurities removal from atmospheric moisture condensates
05 p0622 A72-16645

Liquid polysulfide rubber, discussing fabrication method and physical properties
07 p1024 A72-20603

Model reactions between phthalic anhydride and o-phenylenediamine under polymerization-analogous conditions for polyimidazopyrrolone formation
19 p2762 A72-37647

Russian book - Macromolecules at the boundary between phases.
21 p3071 A72-40077

Synthesis of polymers with conjugate bonds on the basis of dilithium-derivative aromatic hydrocarbons
23 p3262 A72-43929

Photochemistry of unsaturated polymers.
24 p3378 A72-45280

POLYMER PHYSICS
Safe stressing of high strength and locally nonbrittle solid bodies, testing hard polymers at room temperature
04 p0593 A72-15656

Rheological model of reticular polymers and glass fiber reinforced plastics based on stress-strain relationship during damped creep elastic deformation
08 p1191 A72-21499

Morphology and physicomechanical properties of carbonized polyacrylonitrile fibers by scanning electron microscopy, discussing macro and microdefects effects on strength characteristics
08 p1195 A72-21762

Setup to determine sonic creep and acoustic fatigue in polymers under symmetrical and asymmetrical load cycles at sonic and ultrasonic oscillation frequencies
08 p1147 A72-21763

Free and stressed polymer molecules nonlinear vibrations, estimating three- and four-phonon processes contribution to linear chain vibration bands half width by numerical methods
08 p1195 A72-21851

Perforated flexible polymer plates stressed state problem with boundary conditions and viscoelastic and creep properties effects
08 p1248 A72-21861

Crystalline polymers behavior as multiphase composite solid, calculating supermolecular structures effects on stiffness properties
14 p2163 A72-30181

Nonlinear physical dependence of reticular polymers and glass fiber reinforced plastics under conditions of diminishing creep
19 p2822 A72-37527

Rheological characteristics of orthotropically reinforced polymer materials
19 p2822 A72-37531

Contractile and muscle-like fibers and autopsulation systems for polymer engine and spring action studies
19 p2760 A72-38200

Statistical failure characteristics and probability evaluation of the static strength of structural components made of composite polymer materials
20 p2943 A72-38942

Prediction of deformability and fracture processes for polymer materials
20 p2943 A72-38943

Influence of technological factors upon the mechanical reliability of composite-material structures
20 p2943 A72-38945

Electron spin resonance of gamma-irradiated poly(ethylene 2,6-naphthalene dicarboxylate).
20 p2898 A72-39400

Monte Carlo studies of the relaxation of vector end-to-end length in random-coil polymer chains.
20 p2898 A72-39599

Friction and molecular structure - The behaviour of some thermoplastics.
20 p2945 A72-39974

Calculation of the surface properties of elastic polymer molecules in athermal solutions by the Guggenheim method
21 p3095 A72-40078

Concentration dependence of surface tension in solutions of surface-inactive polymers
21 p3072 A72-40079

Application of statistical methods to studies of the surface properties of polymers
21 p3072 A72-40080

Changes in the wear resistance of polymer surface layers in aggressive and biologically active media
21 p3072 A72-40081

Polymer adsorption as a cause of changes in contact interaction intensity between two solid surfaces
21 p3059 A72-40083

Electron microscope investigation of the effect of fillers on the formation of supramolecular structures and on the type of breakdown in amorphous and crystalline polymers
21 p3072 A72-40084

Temperature-time effects on fracture failure mode and strength of polymeric glasses in terms of Ludwik brittle-ductile transition hypothesis and Griffith theory
23 p3305 A72-43503

Molecular mechanical aspects of the isothermal rupture of elastomers.
23 p3305 A72-43507

Characterization of four polymeric materials at strain rates from 0.0001 to 1000 per sec.
24 p3417 A72-44612

POLYMERIC FILMS
NT KAPTON [TRADEMARK]
NT MYLAR [TRADEMARK]
Crystal structure of alpha poly-p-xylylene films from electron microscopy and diffraction and X ray scattering
02 p0248 A72-11466

Polymer films friction properties under high pressure, discussing Amonton law failure and adhesion theory application
06 p0837 A72-18597

Stress relaxation measurement assembly for polymer film and fiber samples under tensile stresses at 213-573 K
07 p0986 A72-19779

Band averaged optical constants and IR characteristics of thin plastic films with/without metal substrate, using transmittance measurements [ASME PAPER 70-WA/HT-15]
08 p1205 A72-20874

Gamma radiation effect on cracking and tensile strength of polycapromide /capron/ film
08 p1196 A72-21870

Electron bombardment deposited polymer thin films electrical properties as function of formation current, noting increase in crosslinking and dangling bonds
12 p1788 A72-27277

Photosensitive polymeric films for hologram recording with high diffraction efficiency, requiring low laser powers
12 p1808 A72-27602

Thin polymer film bleachable dye switches for Q switched laser to achieve high power single pulse radiation
12 p1822 A72-27612

Metallic, ceramic, polymeric, composite and solid film lubricant friction and wear properties and testing [ASME PAPER 72-DE-28]
14 p2108 A72-30869

Al alloy welded seams corrosion fatigue strength increase by epoxy polymer coatings under cyclic tensile stresses
16 p2397 A72-33268

Heavy cosmic ray nuclei tracks in etched plastic sheets flown in satellites and balloons, discussing detector response as function of velocity
16 p2447 A72-33730

Adhesive joints strength and polymeric film breakdown dependence on substrate molecular forces at base interface
19 p2806 A72-37533

Reversible changes in polyethylene coating adhesion due to thermo-oxidative destruction of polyethylene
21 p3072 A72-40082

Dry photopolymer holographic recording film with ability to form images in near real time by exposure without processing

21 p3054 A72-40620

Thin film deposition of carbon on polypropylene, noting morphological templates role in enhancement of polymer nucleation during recrystallization

23 p3305 A72-43269

Determination of the optical thickness of polymer fracture surface layers from interference phenomena.

23 p3307 A72-44317

Thermal anomalies in stressed Teflon.

24 p3417 A72-44766

Photochemistry of unsaturated polymers.

24 p3378 A72-45280

Stress-strain state in tension of orthogonally stiffened fiberglass-reinforced plastic with cracks in transversely stiffened layers

24 p3460 A72-45754

POLYMERIZATION

NT COPOLYMERIZATION

NT DIMERIZATION

NT VINYL COPOLYMERS

Morphology of poly-p-xylylene crystallized during polymerization from X ray measurements, electron and optical microscopy and differential thermal analysis

02 p0247 A72-11465

Preferential polymerization and adsorption of L-optical isomers of amino acids on kaolinite, indicating role in prebiotic protein origin

03 p0321 A72-13743

Inorganic phosphates-nucleoside hypohydrous thermal reaction mechanism, discussing thermal polymerization of orthophosphates for phosphorylation and condensing agents in primordial synthesis

04 p0483 A72-14770

Amino acid-phosphate anhydrides polymerization in presence of clay minerals, noting reactions superposition and monomer diffusion

04 p0483 A72-14774

Cation polymerization of beta-propiolactone without initial kinetics dependence on monomers concentration, relating acyl ion bonding and electron donor groups

09 p1275 A72-22496

Adhesives polymerization and rapid ambient temperature curing, using Co 60 gamma rays and electron beams

12 p1833 A72-28079

Spectral intensity distribution of vibrational electron interaction with strong coupling during polymerization of monomer cyanine dye and dimer molecules

15 p2280 A72-31410

Polymerization characteristics of 4-ferrocenyl-1, 3-pentadiene monomer, discussing synthesis on molar scale

17 p2512 A72-35934

Model reactions between phthalic anhydride and o-phenylenediamine under polymerization-analogous conditions for polyimidazopyrrolone formation

19 p2762 A72-37647

Statistical mechanics of polymerized materials.

22 p3197 A72-42796

POLYMERS

Additives and reactive retardants flame inhibiting properties for polymers, discussing various testing techniques

01 p0090 A72-10286

Flammability tests for polymer materials used in computers and business machines, evaluating procedures in terms of reproducibility, difficulty and equipment requirements

01 p0145 A72-10287

High speed tensile impact test for polymers at large loading rate, describing equipment design and test technique

01 p0048 A72-10782

Nonmetallic material properties effects on structural design for reliability, considering molecular chain folding, polymer crystallization, entropic molecular segregation, adhesion and intermolecular forces

01 p0092 A72-10986

Organic semiconductor developments in chemistry and physicochemistry of multiconjugate systems and polymer complexes with charge transfer

01 p0114 A72-11074

Test equipment for glass and polymer fibers strength and lifetime in vacuum and inert bases under static loads

01 p0093 A72-11382

Low strength polymeric materials specimen geometry and lateral constraints effects on isothermal compressibility by compression tests

02 p0248 A72-11518

Flame spread rate over combustible polymer fuel specimens as function of surface, sample, composition, pressure and oxygen mole fraction

02 p0301 A72-11965

Linear viscoelasticity theory dynamic functions, deriving delay and relaxation times distribution functions in polymers

02 p0293 A72-12211

Boron-containing polymer heterogeneous combustion determination using hybrid regression rate with thermal degradation and surface temperature data

02 p0270 A72-12260

Flame retardant mechanism in hydrocarbon polymer combustion, discussing halogen adverse effect on thermal stability

[PI PAPER 10] 03 p0380 A72-13244

Fire retardant capabilities of bromine and chlorine compounds in polymers

[PI PAPER 13] 03 p0380 A72-13247

Amorphous polymer dielectric luminescence and destruction under Q switched laser radiation with subthreshold power and picosecond pulses

03 p0369 A72-14071

Transparent rain repellent polymer coatings, discussing water repellency theory, polymer chemical structures, adhesion to glass surfaces and evaluation methods

03 p0381 A72-14237

Diffusion rate of diluted drag reducing polymers in turbulent boundary layer

03 p0343 A72-14319

Suppressed turbulent diffusion of drag reducing polymer solution in turbulent boundary layer, measuring concentration with laser-phototransistor unit

[AD-737467] 03 p0343 A72-14321

Flat plate in turbulent shear flow polymer solution, predicting maximum drag reduction with interactive layer concept

03 p0343 A72-14322

Esters and amides participation in prebiotic polymers, discussing ribosome bonds and messenger RNA

04 p0468 A72-14767

Polymer fractionation in simulated Jovian atmosphere according to molecular weight, suggesting substance responsible for red color

04 p0572 A72-14773

Alpha amino acids proteinoids or thermal polymers enzyme activity, investigating hydrolytic activities and decarboxylation reactions

04 p0483 A72-14776

Ion selective accumulation model of carbohydrates diffusing through artificial polymer membranes, relating prebiological systems to catalytic microsystems

04 p0469 A72-14788

Kinetic rate theory extended to time dependent flow behavior of viscoelastic materials /polymers/ under constant stress and shear

04 p0512 A72-15263

Catalytic action in organic catalyst predecessors of contemporary enzymes, discussing polymers of alpha-amino acids and hydrogen cyanide

05 p0624 A72-16128

Metal polymer interface synthesis based on linearly cyclic organoelementary high molecule compounds, analyzing heat and thermal oxidation resistances

05 p0680 A72-16202

Combusting polymers gasification effective heat values determination from correlation of surface regression rate and oxygen impingement rate data

[AIAA PAPER 72-34] 05 p0749 A72-16898

Pulsed ruby laser and photopolymer materials applications to holography, considering research programs for surmounting difficulties

06 p0813 A72-17427

Combined tension-torsion creep testing of polymers, discussing equivalent stress and strain concept, testing apparatus and preliminary results for polythene

06 p0835 A72-17795

Polymers mechanical losses temperature-frequency dependence, using nonlinear viscoelastic theory

06 p0838 A72-18678

Fire resistant fibrous materials for potential military and transportation applications, considering aromatic polyamide polybenzimidazole, fluorocarbon resin polymer, phenolic and glass fibers and fabrics

08 p1191 A72-21586

Nonlinear viscoelastic body model for stress relaxation of amorphous linear polymers below vitrification temperature for various deformations, temperatures and deformation speeds

08 p1194 A72-21751

Test procedures and apparatus for short and long term creep of polymer monofilaments under radial compression

08 p1194 A72-21758

Composite viscous polymer cylindrical shells buckling modes under prolonged loading, taking into account initial imperfections

08 p1248 A72-21859

Polymers viscoelastic behavior during crosslinking reactions, deriving equations for creep response to step increase in crosslink density

09 p1336 A72-22521

Photopolymers formulations and processing for holography applications, discussing sensitivity, keeping and reciprocity properties

10 p1482 A72-24566

Linear viscoelasticity theory dynamic functions, deriving delay and relaxation times distribution functions in polymers

11 p1734 A72-25709

Polymers flammability tests for research, safety and acceptance purposes, noting ignition limits, decomposition and testing procedures

11 p1746 A72-26044

Longitudinal bending stability of hard polymer rods under compression load and creep

11 p1675 A72-26824

Polymer testing machine for simultaneous structural and mechanical properties measurement of specimens subjected to uniaxial tensile loads for broad temperature range

12 p1795 A72-27465

Tribochemical effects during friction of non-lubricated amorphous and crystalline polymer surfaces under mild and hard contacting conditions

12 p1835 A72-28200

Reliability tests on miniature ceramic capacitors encapsulated by epoxy-novolac block polymer compounds

13 p1919 A72-29061

Nonuniform concentration mechanism for observed drag reduction in flows with high molecular weight polymer additives, considering boundary layer with varying viscosity on sphere

13 p1942 A72-29113

Heat resistance of thermostable organic materials /amorphous glass and high polymers/, improving plastic stability by glass fibers addition, intermolecular arrangements modification and synthesis

[ONERA, TP NO. 1107] 14 p2125 A72-30529

Cooperative direction changing isomer movement on polymer chain lattice describing equations derivation procedure

14 p2125 A72-30962

Turbulent friction values diminished by reading errors in pitot tube flow measurement of solid particles suspensions and polymer solutions caused by viscoelastic associations

14 p2106 A72-31007

Plastic deformation in metals and highly crystalline polymers as function of shear strain, strain rate, frequency and vibrational amplitude

15 p2328 A72-31840

Friction and wear properties of carbon fiber reinforced polymers sliding against metals in pure and sea water and aqueous solutions

16 p2396 A72-33123

Carbon fibers reinforced polymer wear rate decrease in organic fluids associated with films development on steel counterface, noting application in lubricated systems

16 p2397 A72-33124

Polymeric structural adhesives thermal stability evaluation, recommending thermodifferential analysis and calorimetry to supplement thermogravimetric method

16 p2415 A72-33510

Drag reducing polymers influence on velocity gradients at wall for turbulent pipe flow, observing viscous sublayer thickening

16 p2379 A72-33574

Model with lamellae and tie molecules disordered alignments to explain relation between stress-strain behavior and bond fracture in highly oriented polymer fibers

17 p2569 A72-34258

Polymers ignition time measurement in cabinet with benzene flames and W filament lamps, noting black body radiation source absorbance and incident irradiance effects

17 p2636 A72-34719

Laser velocimeter measurement of Reynolds stress and turbulence in dilute polymer solutions.

17 p2541 A72-35252

Stress wave propagation observation in rigid high modulus epoxy polymer by slow motion photography, noting photoelastic properties and viscosity effect

18 p2734 A72-36380

On the fatigue crack propagation in polymeric materials.

20 p2943 A72-38886

Structure-property relationships in polymeric materials.

20 p2944 A72-39212

Review - Fatigue-crack propagation in metallic and polymeric materials.

20 p2980 A72-39793

Toxicological evaluation of some synthetic materials designed for airtight space equipment

21 p2998 A72-40434

The dynamic viscoelastic properties of some non-crystalline metals.

22 p3214 A72-42792

Relaxations in polymers at low temperatures.

22 p3196 A72-42793

Thermal properties of polymers below 4 K.

22 p3197 A72-42800

Filler quantity and type effects on mechanical energy losses in polymers, discussing molecular interaction and chemical bond influences

23 p3306 A72-43731

The molecular-kinetic theory of polymer adhesion 23 p3307 A72-43930

Nuclear and dipole relaxation at polymer-polymer interfaces 23 p3307 A72-43931

Polymer fatigue failure mechanism examination on constant deflection type testing machine, investigating applied stress and temperature effects on crack propagation rate 24 p3455 A72-44631

Book - A review of the science of fibre reinforced plastics. 24 p3417 A72-44674

Methods for determining thermal properties of anisotropic systems. 24 p3465 A72-45633

POLYMETHYL METHACRYLATE

Mechanical breakdown characteristics of polymethyl methacrylate and polystyrene samples exposed to picosecond pulses emitted by Q switched laser 02 p0250 A72-12680

Impurities effects on crack initiation and propagation in polymethyl methacrylate under laser pulsed radiation 02 p0250 A72-12689

Griffith crack propagation in polymethyl methacrylate, examining stress changes by photoelastic method 03 p0380 A72-13719

Polymethyl methacrylate fatigue strength at elevated temperatures, discussing sample preparation, test equipment and procedures 04 p0537 A72-14750

Low frequency biaxial load effect on stress concentration factors for circular and elliptical holes in Plexiglas plates 06 p0898 A72-18350

Notch length effect on stress concentration in polymethyl methacrylate sample from tensile, impact and bending tests 08 p1196 A72-21867

Fatigue fracture of polymethyl methacrylate at room temperature under uniaxial failure cycled loading 09 p1339 A72-23244

Light beams diffraction patterns of thin plexiglass plate for load induced thickness variations, noting crack opening and edge sliding modes stress intensity factors [ASME PAPER 71-APM-QQ] 10 p1553 A72-24178

Rapid laser heating induced stress generation in carbon fiber-polymethyl methacrylate composite 12 p1833 A72-27286

Microcuts as equivalent mechanical stress concentrators for breakdown energy estimation in flat polymethyl methacrylate glass specimens under impact bending loads 13 p1983 A72-28563

Rhodamine 6G photodegradation resistance improvement in cooled solid matrices of polymethylmethacrylate, investigating time and temperature dependence of bleaching by linearly polarized lasers 16 p2401 A72-33386

Iron-containing catalysts action mechanism during ammonium perchlorate-polymethyl methacrylate mixture burning in nitrogen atmosphere 19 p2847 A72-38456

Plexiglas spheres and cubes effect on circular and rectangular waveguide aperture antennas directive radiation patterns and sidelobe reduction 21 p3021 A72-40904

Relaxations in polymers at low temperatures. 22 p3196 A72-42793

Crack propagation speed measurements with wedge loaded double cantilever beam of PMMA, calculating stress intensity, strain energy release rate and kinetic energy 23 p3346 A72-43709

POLYMORPHISM

Crystal structure of alpha poly-p-xylylene films from electron microscopy and diffraction and X ray scattering 02 p0248 A72-11466

Cholesterol esters polymorphic and mesomorphic behavior, using differential scanning calorimetry, X ray powder diffractometry and positron annihilation techniques 04 p0484 A72-15262

Polymorphism in Ta vacuum condensates, observing beta-alpha phase transformation in films 09 p1329 A72-23041

Mica polymorph distribution among space groups from unit layer and stacking sequence characteristics 12 p1802 A72-27512

Metastable coesite crystal growth in highly strained quartz under 5-20 kb pressures and 450-900 C. 14 p2099 A72-30322

Organ cell lysosomes polymorphic properties and formation by Golgi complex, discussing role in neurocyte structure restitution following gamma irradiation 14 p2075 A72-30594

Hf binary systems phase diagrams, noting components effect on melting point, polymorphous transformations and mutual solubility 14 p2122 A72-30979

Crystal structures and transition temperatures of polymorphous metals, discussing mechanical properties, thermal conditions for deformation and metal working by pressure 22 p3190 A72-42803

POLYNOMIALS

NT DYADICS

NT HERMITIAN POLYNOMIAL

Computer generated Lamé functions of first kind definable by polynomial coefficients and eigenvalues 01 p0093 A72-10005

Survey and bibliography of extrapolation processes in numerical analysis based on polynomial or rational functions 02 p0252 A72-11546

Approximation of functions with diophantine conditions by polynomials with integral coefficients 03 p0382 A72-13948

Chebyshev polynomials best approximation with respect to linear space spanned by odd degree polynomials, obtaining extreme point sets 04 p0539 A72-14729

Orthogonal polynomials in several variables relation to approximate multiple integration, extending Stroud theorem for two-dimensional regions cubature formulas to n-dimension 04 p0539 A72-14731

Matrix representation of nonlinear equation iterations based on polynomial methods, considering convergence and application to parallel computation 04 p0540 A72-15373

Admittance calculation for vertical monopole antenna driven by coaxial line, approximating current distribution by polynomial with complex coefficients 04 p0501 A72-15429

Singular integral equation in radiative transfer theory with polynomial scattering indicatrices 04 p0597 A72-15643

Polynomial class random process realization based on statistical methods of processing spacecraft orbital measurement data, considering random and systematic errors 05 p0683 A72-16763

Lemma for determining relatively prime relationship between two multivariable polynomials, considering singularities of second kind 06 p0783 A72-17485

Hollow waveguide performance numerical solution review covering finite difference and element methods, polynomial approximation, point matching, integral equations and conformal transformation 06 p0784 A72-18237

Real rational function Cauchy index computed from integral functions of polynomial coefficients and signature of infinite class of matrices 07 p1026 A72-18817

Stability and local error of difference formulas derived from characteristic polynomial for first order ordinary differential equation solution 07 p1028 A72-20472

Class of homogeneous polynomial solutions to differential equations of motion of elastic body 08 p1242 A72-20912

Liapunov theorem for polynomial solution existence for first order inhomogeneous system of linear partial differential equations 08 p1205 A72-20958

Multiple completeness characteristics of eigenvectors and adjoint vectors of polynomial operator packets in separable Hilbert space 08 p1198 A72-21096

Polynomial solutions to integrodifferential equation of motion of solid body with fixed point for Lagrange conditions 08 p1207 A72-21342

Solutions existence for algebraic invariant relation to integrodifferential equation of motion of solid body about fixed point in trigonometric and exponential polynomials class 08 p1207 A72-21346

Sretenskii-Chaplygin integral in polynomial form for solution to gyrostat motion problem 08 p1208 A72-21356

Generalized polynomial operators for nonlinear systems analysis, presenting local invertibility theorem 09 p1341 A72-23092

Power series solutions to transition and matrix covariance differential equations, obtaining truncation error bounds and polynomial approximations 09 p1341 A72-23093

Partial differential equation for thin walled circular cylindrical shells, deriving solutions for displacement and stresses in terms of surface coordinates low degree polynomials 10 p1557 A72-24560

Polynomial theory problems, using Bezoutian matrix formed from polynomials a and b and matrix polynomial relating b to companion matrix of a 11 p1678 A72-26155

Random process quantization interval search algorithm based on signal approximation by n-th degree polynomial 11 p1602 A72-26439

Thermal stresses in homogeneous isotropic and composite curved beams for temperature distribution in polynomial form with coefficients representing functions of two remaining coordinates 11 p1737 A72-26665

Error bounds for finite element methods and approximation with piecewise polynomials for elliptical differential equations solution 11 p1679 A72-26956

Fourth order polynomial method and computational algorithm for direct integration of n body systems, discussing two body encounters and binary systems 12 p1875 A72-27917

Computer programmed algorithm for conducting smooth piecewise polynomial third order approximation in spline function determination 13 p1986 A72-29065

Polynomial surface approximation to OMEGA sky wave corrections for small computer compatible with automatic receiver 13 p1925 A72-29187

Transfer function of polynomial discrete linear pulse systems for differential equation solution 13 p1936 A72-29269

K-order differential equation solution obtained for system of polynomial functions for shallow spherical shell under uniform pressure, using Bubnov-Galerkin and collocation methods 13 p2062 A72-29947

System of equations derived for unsteady temperature field of arbitrary multilayer shell, using polynomial expression as temperature approximation for shell thickness 13 p2066 A72-29949

Modified finite element method application to plane elastic area elementary triangles strained and stressed state description by polynomial algebraic expressions and harmonic functions 14 p2163 A72-30188

Polynomial spline function for approximate solution of Cauchy problem for nonlinear differential equations of order n 14 p2126 A72-30716

Matrices and permutation rules for tetrahedral polynomial finite elements for Helmholtz equation, commenting on computer time and convergence rate 14 p2126 A72-30932

Parameter-dependent linear and nonlinear equation systems solution by approximation polynomials, developing numerical algorithms 15 p2261 A72-31496

Bairstow Method extension with restored convergence for multiple quadratic factors using interval arithmetic 15 p2262 A72-31631

Shape functions for finite element analysis in n-dimensional space, examining completeness of polynomial interpolation and computational efficiency 15 p2326 A72-31713

Polynomial approximation of measurement signals with variability, comparing Taylor, Abdulaev and Newton formulas 15 p2235 A72-31848

Global meteorological data analysis using Gram-Schmidt generated orthogonal polynomial base functions 15 p2266 A72-32719

Filtering polynomial technique to estimate wind, divergence and vertical motion profiles, suppressing random error effects 16 p2418 A72-33667

Polynomial class random process realization based on statistical methods of processing spacecraft orbital measurement data, considering random and systematic errors 17 p2576 A72-35266

Nonlinear dynamic feedback control systems modeling by parameter estimation scheme with polynomial representation for state variables 18 p2672 A72-36057

Approximate representation of a type of transcendental polynomials describing wave systems with fractional rational functions 19 p2834 A72-37751

Symmetric and innerwise matrices for the root-clustering and root-distribution of a polynomial. 19 p2825 A72-37851

Mathematical determination of decibel-loudness index, tables for various frequencies. 20 p2956 A72-40076

Computerized design for cylindrical cable antenna, using polynomial approximation of current to reduce computer size and time requirements 21 p3028 A72-40511

Determination of pulsed amplifier correction parameters with the aid of approximating polynomials 21 p3034 A72-41120

Mathematical spectra theory application to matrix eigenvalue problem, obtaining explicit form of determinant characteristic polynomial by numerical methods 21 p3076 A72-41781

Stability criterion and imaginary axis displacement for real roots determination of algebraic equations on analog computers

21 p3025 A72-41806

Asymptotic behavior of the eigenvalues and eigenfunctions of the Sturm-Liouville operator with a complex-valued polynomial potential. I

22 p3198 A72-41854

Polynomial operators for nonlinear systems analysis.

23 p3308 A72-43599

A direct method for computing optimal feedback control for linear systems.

23 p3275 A72-43613

Optimal design of indeterminate truss using geometric programming.

23 p3354 A72-44256

Approximation of continuous periodic functions by Faward sums

24 p3419 A72-45550

Approximation of analytic functions by trigonometric polynomials over an interval smaller than the period

24 p3419 A72-45550

POLYPHENYLS

Electron transfer frequencies and triplet-triplet transition spectra of polyphenyl compound molecule scintillators for UV lasers, using chaotic phase method

13 p1968 A72-29509

Pion-electron conjugation and twist angles determination in biphenyls via Raman intensity, comparing with hypsochromic UV shift of Suzuki method

16 p2431 A72-33585

POLYPROPYLENE

Parachute canopy fabrics and rigging lines cordage properties requirements, considering nylon, polypropylene, silk, cotton and nonwoven scrim-reinforced fabrics

01 p0005 A72-10314

Polyethylene and polypropylene combustion, investigating additives and surrounding gaseous composition effects on flammability and volatile products during thermal degradation

02 p0248 A72-11767

Thermoplastic polypropylene sandwich molds stiffness variation with time, noting three point bending and creep tests

11 p1673 A72-25550

Coupled glass-fibre/polypropylene composite - An initial evaluation.

18 p2703 A72-36269

Ultrasonic wave generation in solids using transducer composed of high rigidity dielectric /polypropylene/ between two electrodes

18 p2691 A72-36402

Thin film deposition of carbon on polypropylene, noting morphological templates role in enhancement of polymer nucleation during recrystallization

23 p3305 A72-43269

A comparison of single-integral non-linear viscoelasticity theories.

24 p3460 A72-45695

A power-law model for the multiple-integral theory of non-linear viscoelasticity.

24 p3460 A72-45696

POLYQUINOXALINES

Fiber reinforced plastic composite seals for liquid hydrogen and nuclear radiation environments, stressing polyquinoxaline fitness

01 p0075 A72-10773

POLYSACCHARIDES

NT CELLULOSE

NT GLYCOGENS

NT STARCHES

POLYSTYRENE

Mechanical breakdown characteristics of polymethyl methacrylate and polystyrene samples exposed to picosecond pulses emitted by Q switched laser

02 p0250 A72-12680

Horn lens antennas for millimeter wave radiometric applications, discussing medium gain polystyrene lens design to obtain low peak sidelobes

04 p0503 A72-15608

Dynamic shear modulus and damping of polystyrene composites filled with glass, salt and foam, including skin effect correction

10 p1500 A72-24260

Relaxations in polymers at low temperatures.

22 p3196 A72-42793

POLYSULFIDES

Liquid polysulfide rubber, discussing fabrication method and physical properties

07 p1024 A72-20603

POLYTETRAFLUOROETHYLENE

Ti surface oxide films ionic and electronic conductivity properties and correlation with crevice corrosion susceptibility in contact with polytetrafluoroethylene gaskets

04 p0535 A72-15732

Polyfluoroethylene-based composite materials mechanical properties, discussing strengthening mechanism of filler additions

05 p0682 A72-15989

Ground plane curvature effect on aperture admittance of waveguide fed axial slot on teflon coated metal cylinder for underdense plasma

06 p0771 A72-17354

Self lubricating polytetrafluoroethylene and polyimide composites transfer film formation tests, studying film thickness and uniformity

06 p0824 A72-18596

PTFE thin films interspersal with lumps and streaks from transfer to smooth surface during low speed sliding, discussing friction coefficient under various conditions

16 p2396 A72-32870

Fillers effect on polytetrafluoroethylene friction properties, electroconductivity and thermal conductivity, noting friction coefficient reduction by laminar filler structures

16 p2413 A72-33269

Adhesion and transfer of PTFE to metals studied by Auger Emission Spectroscopy.

19 p2807 A72-37646

Friction and molecular structure - The behaviour of some thermoplastics.

20 p2945 A72-39974

Thermal anomalies in stressed Teflon.

24 p3417 A72-44766

Polyfluoroethylene-based composite materials mechanical properties, discussing strengthening mechanism of filler additions

24 p3417 A72-45731

POLYTOPES

Polytropic masses oscillations under rapid uniform rotation, using variational principle

04 p0579 A72-15320

POLYTROPIC PROCESSES

Hydromagnetic cylindrical blast wave propagation in self gravitating polytropic gas, obtaining graphs for velocity, pressure, density and magnetic field distributions

02 p0264 A72-12181

Lf convective oscillations in polytropic atmospheres within strong magnetic field, considering stability of quasi-adiabatic and quasi-isothermal motions

07 p1082 A72-20376

Hypersonic polytropic transformation of ideal fluid under mechanical or geometrical conditions

11 p1572 A72-26092

Approximate calculation of correction to universal law of propagation of one dimensional shock waves in stationary polytropic gas

13 p1943 A72-29882

Mathematical model for magnetized solar wind with one fluid MHD and polytropic state equations, calculating magnetic field variables at earth

13 p2034 A72-29958

Compressor exergetic efficiency calculation from gas exergy losses caused by pressure drop and cooling, noting relations to isothermal, adiabatic and polytropic efficiencies

19 p2746 A72-37668

Negative index polytropic sphere gravitational collapse structure, noting application to interstellar gas clouds thermal equilibrium

19 p2857 A72-37794

Flow calculation for polytropic process with friction and heat transfer

20 p2913 A72-39371

Two phase stellar structure with polytropic equations of state for shell and core, calculating configuration mass, radius and energy

21 p3102 A72-40098

Closed form solution for the sonic boom in a polytropic atmosphere.

21 p2992 A72-41258

Differential rotation of polytropic stellar models by structural equilibrium equations, disproving Porfiriev theory

21 p3114 A72-41775

The total pulsation-frequency spectrum of a polytropic atmosphere

21 p3114 A72-41779

Theory of radiative heat transfer in polytropic atmospheres

22 p3229 A72-42962

Resonance effects on second order anharmonic pulsational amplitudes for polytropic main sequence evolutionary models, classifying Cepheid-type pulsators

24 p3437 A72-44832

POLYURETHANE FOAM

Discretely oriented thread reinforced polyurethane cryogenic foam insulation systems for liquid hydrogen fuel tanks

01 p0092 A72-10981

[MDAC-WD-1756] Phosphorus compounds incorporation in polyurethane foams and polyesters for flame retardancy

03 p0380 A72-13246

[PI PAPER 12] Testing machine for creep resistance of foam plastics under simultaneous static and vibration loads

14 p2092 A72-30591

Energy absorbing characteristics of rigid urethane foams.

20 p2943 A72-38885

POLYURETHANE RESINS

Stress concentration at circular holes in polyurethane plates under plane compression wave, obtaining interference fringes

03 p0451 A72-14121

Polyurethane O ring seals for high pressure applications, discussing stress relaxation /creep/ behavior, resilience and tear and abrasion resistance

08 p1173 A72-21023

Materials selection for models used in thermal stress studies by restrained shrinkage method with emphasis on polyurethanes

12 p1813 A72-27460

Adhesion effects on tensile and thermal expansion properties of aluminum oxide particles filled epoxy-urethane polymer at ambient and liquid nitrogen temperatures

16 p2415 A72-33415

A photoelastic material with variable modulus of elasticity.

19 p2822 A72-37731

The fracture energy and some mechanical properties of a polyurethane elastomer.

19 p2823 A72-38450

Development of a solid fuel on a polyurethane basis for a hybrid rocket propulsion system with 98% nitric acid as oxidizer

20 p2962 A72-39416

POLYVINYL CHLORIDE

Plasticized PVC compounds, investigating chlorine based fire retardants role in increasing flame resistance

03 p0380 A72-13248

[PI PAPER 14] Photoemission from polyethylene, Kapton, Teflon and polyvinyl chloride under photon irradiation

03 p0403 A72-14084

A comparison of single-integral non-linear viscoelasticity theories.

24 p3460 A72-45695

PONDEROMOTIVE FORCES

Nonlinear ponderomotive forces in intense laser light interaction with plasma

04 p0560 A72-15618

Trap magnetic system with coil generated field increasing towards periphery, showing radial dependence and acting ponderomotive forces

09 p1363 A72-23215

Deposition of dielectric films on the electrodes of an electrostatic gyroscope

21 p3059 A72-41814

PONTRYAGIN PRINCIPLE

Time optimal phase locked AFC system synthesis based on Pontryagin maximum principle, comparing computerized and experimental transient response

01 p0024 A72-10049

High order optimality conditions of singular controls, considering Pontryagin maximum principle Bellman dynamic programming and functional analysis

01 p0044 A72-10297

Linear plants time optimal control, deriving auxiliary equations system solution in accordance with Pontryagin maximum principle

07 p0959 A72-19127

Soviet book on optimal trajectory synthesis covering second order linear control systems analysis based on Pontryagin maximum principle and Boltyanski theory

08 p1197 A72-20750

Pontryagin maximum principle application to optimal linear filtration for multivariable systems with signal processing

08 p1133 A72-21374

Adjoint control transformations advantages in optimal trajectories determination by Pontryagin maximum principle

10 p1547 A72-24879

Pontryagin maximum principle application to minimum deflection of cantilever beam under own weight

10 p1558 A72-24880

Linear maximization of turbine disk natural vibration frequencies combination, solving optimal control problem via Pontryagin maximum principle

11 p1734 A72-25727

Pontryagin maximum principle for optimal terminal velocity control of automatic space probe descent in Mars atmosphere

14 p2162 A72-30456

The maximum principle and controllability of nonlinear equations.

17 p2533 A72-34951

Optimality conditions of second and higher orders for discrete systems, discussing functional minimization and Pontryagin maximum principle limitations

17 p2534 A72-35725

Minimum fuel control of second order system in n-dimensional Euclidean space, examining Pontryagin maximum principle applicability

18 p2673 A72-36696

Optimal control with partially specified input functions.

18 p2673 A72-36821

Pontryagin Minimum Principle application to stochastic optimal control problems formulated around linear systems with Gaussian noise and general cost criteria

19 p2779 A72-38234

Necessary conditions for optimality in a general class of non-linear mixed boundary value control problems.

21 p3037 A72-40644

Minimum weight design of circular plates with limited thickness.

21 p3125 A72-41515

Trajectory deviation conditions in second order linear differential escape game, using Pontryagin principle

22 p3204 A72-41903

Pontryagin maximum principle for fundamental frequency variation limits of longitudinal vibrations of variable cross section rod

22 p3234 A72-42148

Pontryagin equations for Markov process limits probability, solving problem of one dimensional steady random process limits for given initial probability density function

22 p3205 A72-42227

Linear vector formulation of pursuit problems with pursuer discrimination, using Mishchenko-Pontryagin curvature conditions

23 p3307 A72-43220

POPULATION INVERSION

Electron density microwave measurements in helium-neon laser plasma, discussing population inversion during glow discharge

01 p0081 A72-11216

Small signal gain and radiant power of carbon dioxide gas dynamic laser, presenting temperature distribution and population inversion

03 p0368 A72-13920

Pulsed Ar ion laser quantitative level population mechanism in gas discharges, discussing radiation trapping effects on 4s doublet based on spontaneous emission line data

04 p0529 A72-14602

Carbon dioxide-nitrogen-water or He mixtures expansion through supersonic nozzles, showing population inversion of vibrational energy levels

04 p0513 A72-15337

Rapid expansion nozzles for gas dynamic laser working gas vibrational energy freezing to obtain population inversion, considering size and shape effects on performance

05 p0669 A72-16965

Population inversion of carbon dioxide molecules in gas flow expanding from nozzle

06 p0852 A72-17904

Quasi-stationary carbon dioxide laser with pulse excitation, noting high population inversion values

06 p0826 A72-17916

Chemical lasers technology, considering population inversion, excited state molecules production, potential energy surfaces calculation and computer simulation

06 p0826 A72-18457

Population inversion production in sulfur dioxide molecular laser

06 p0827 A72-18459

Shock wave collision induced population inversion in electromagnetic shock tubes, measuring plasma absorption coefficient

07 p1044 A72-20074

Population inversion in plasma via colliding waves generated by symmetric electrodeless electromagnetic shock tube

08 p1147 A72-21304

Population inversion development and breakdown in active medium produced by plasma generation during pulsed discharge in molecular nitrogen laser

08 p1183 A72-21716

GaAs semiconductor injection lasers, discussing time characteristics of current carriers, population inversion and resonator Q factor modulation

08 p1184 A72-22032

Inversion spatial nonuniformity effects on spectrum and kinetics of ruby laser, using spherical mirrors

10 p1491 A72-24361

Population inversion through metastable ion formation by atomic inner shell electrons photoionization, determining effectiveness relationship to emission source plasma composition

11 p1648 A72-26332

Molecular energy levels population inversions calculated from vibrational temperatures in carbon dioxide laser discharge plasma

11 p1649 A72-26339

Ar laser levels population inversion dependence on current density, discharge tube pressure and magnetic flux

11 p1649 A72-26350

Populations modulation and spatial harmonics influence on gas and solid state laser radiation characteristics, discussing uniform and nonuniform line broadening

11 p1650 A72-26353

Q switched ruby laser radiation spatial coherence, considering modes relationship to permittivity inhomogeneities and changes due to holes burning in population inversion

12 p1821 A72-27591

Chemical laser dynamics review, discussing population inversion, molecular vibrational relaxation and reactions initiation methods

12 p1822 A72-27605

Nd-fiberglass laser intensity fluctuations due to fibers absorption centers, deriving population inversion threshold, pumping power and center formation rate from kinetic equations

12 p1825 A72-27884

Population inversion in exothermal decomposition reactions of multiatomic molecules for chemical and collision laser systems

13 p1912 A72-28778

Inversion population distribution during nonexcited carbon dioxide and excited nitrogen molecules plane jets interaction in diffusion carbon dioxide laser

14 p2109 A72-30314

Molecular nitrogen pulsed laser wavelength measurements, observing IR bands, stimulated emission lines and population inversion mechanisms

15 p2249 A72-32151

Ar laser levels population inversion dependence on current density, discharge tube pressure and magnetic flux

16 p2402 A72-33703

Populations modulation and spatial harmonics influence on gas and solid state laser radiation characteristics, discussing uniform and nonuniform line broadening

16 p2402 A72-33706

Conditions defined for recombination induced inversion of populations of resonance and fundamental levels in laser beam produced plasma

16 p2438 A72-33835

Nd-fiberglass laser intensity fluctuations due to fibers absorption centers, deriving population inversion threshold, pumping power and center formation rate

16 p2404 A72-33993

Experimental evidence for stationary population inversions of atomic levels in an expanding hydrogen plasma

17 p2589 A72-34898

Inversion spatial nonuniformity effects on spectrum and kinetics of ruby laser with spherical mirrors

17 p2563 A72-34960

Electrical CO mixing gas dynamic laser

17 p2564 A72-35483

CW optically pumped tunable dye laser wavelength ranges, linewidth, mode purity, polarization and power output characteristics

17 p2565 A72-35947

Laser output power increase with plasma dynamic carbon dioxide laser configuration, noting steady population inversion in pure hydrogen atoms

20 p2934 A72-39932

Electromagnetic field, polarization and population inversion equations for spiked emission operation analysis in single mode laser

22 p3184 A72-42153

Molecular vibration levels inversion ratios increase by vibrationally cold CO addition to CW CO chemical laser, observing R-branch emission lines

22 p3185 A72-42615

Inversion population distribution during nonexcited carbon dioxide and excited nitrogen molecules plane jets interaction in diffusion carbon dioxide laser

23 p3294 A72-43217

A new method of measuring temperature, inversion ratio, and pressure-broadened linewidth in a CW molecular laser.

23 p3297 A72-44188

Theory of pulsed internal optical parametric oscillators.

24 p3409 A72-44714

High speed mixing of nitrogen vibrationally excited with carbon dioxide

24 p3464 A72-45065

POPULATION THEORY

Lunar crater population and distribution time development under meteoroid and solar wind bombardment, developing model for absolute formation ages

01 p0124 A72-10056

Pulsed laser emission in carbon monoxide, calculating molecular excited state populations

02 p0237 A72-11471

Vibrational population of molecular nitrogen electronic states in normal auroras, examining electron impact and cascade contributions

03 p0349 A72-13524

Orion and planetary gaseous nebula helium atoms metastable triplet states population calculations

04 p0578 A72-15314

Collisional radiative model of population densities of metastable electron levels of orthohelium in low pressure rf helium plasma

05 p0694 A72-15998

Carbon dioxide-air-helium molecular systems population excitation rates with current, gas composition and partial pressures dependence

08 p1183 A72-22028

Cooperative and sequential sensitization effect on He emissive states population in polycrystalline barium and yttrium fluorides with trivalent Yb

10 p1525 A72-24044

CO-He laser vibrational population distribution and small signal gain measurements, comparing with prediction based on V-V anharmonic exchange relaxation

12 p1827 A72-28222

Multiple decision procedures, discussing location, scale parameters, discrete populations and multinomial and multivariate normal distributions in subset selection formulation

14 p2126 A72-30998

Radiative transfer in freely expanding gaseous Ba clouds, deriving atomic states level populations ratio

15 p2223 A72-31428

Mach 26 shock wave in nitrogen investigated by electron beam fluorescence technique, determining population distribution among rotational states

15 p2281 A72-32404

Emission line polarization prediction for planetary nebula C IV ion emitted spectrum via theory for energy level population

16 p2458 A72-33689

Transition probabilities and collision-induced transitions in excited levels of neon.

21 p3061 A72-40136

Populating excited states of incoherent atoms using coherent light.

21 p3088 A72-40778

Solar coronal F component separation from K component by utilizing elongation dependence differences in scattering populations, computing F for wide range of parameters

21 p3106 A72-41041

Recoil effect on inverted molecules changing pumping conditions and gain for interstellar, OH maser intensity and radial velocity variations

21 p3102 A72-41773

Electron distribution fluctuation in two level system of unstable electron gas, noting periodic time dependence of population

23 p3319 A72-43406

POPULATIONS

Interval scanning photomicrography for recording growth of microbial cell populations during incubation

13 p1911 A72-29749

Spectral measurements of atomic level populations in a plasma

17 p2591 A72-35307

PORES

NT MICROPOROSITY

Porosity and W inclusions effects on Al alloy weld strength, presenting radiographic and tensile test data

01 p0074 A72-10282

Mathematical model of porosity gas transport test for automated fusion welding operation using mass spectrometer

01 p0076 A72-10815

Fiberglass reinforced plastics heat conductivity as function of porosity, reinforcement factor and density

02 p0250 A72-12686

Plasma sprayed tungsten and zirconium dioxide coatings porosity on chromium bronze, Ti and Al alloys and steel

03 p0363 A72-13550

Carbon fiber reinforced material porosity source, applying equilibrium configurations of liquid films on parallel uniform cylindrical rod hexagonal and cubic arrays

04 p0537 A72-15087

Hydrogen generation mechanism during cadmium plating of steel, describing porosity testing technique

04 p0527 A72-15548

Ceramic materials stress-strain behavior dependence on microstructural factors, discussing point defects, pore size and grain boundaries

09 p1334 A72-22392

Mercury porosimetry for iron powders void and internal particle porosity change as function of compacting pressure, noting compressibility improvement by precompacting and annealing

11 p1639 A72-25288

Ductile fracture development in steel due to microcracks and pores formation

11 p1660 A72-26140

Powder metallurgy sintering process variables for dimensional control of bronze parts, discussing strength and porosity level specifications

11 p1640 A72-26243

Chemical composition, powder particle size, porosity and heat treatment effects on sulfurized iron graphite cermets durability

13 p1984 A72-30118

Sunspot formation due to magnetic flux concentration in active region and formation of invisible pores with suppressed granular motion

14 p2148 A72-30205

Porous cellular structure materials, investigating porosity effects on modulus of elasticity based on central monoporosity model

14 p2165 A72-30433

Porosity effect on mechanical properties, airtightness, corrosion resistance and moisture absorption of glass fiber reinforced plastics

16 p2414 A72-33270

Local vertical porosity and heat transfer coefficient relation to diluted fluidized bed relative height

16 p2479 A72-33851

Gas shielded arc welding of Ni, discussing current density, energy, arc length and preheating temperature effects on welds porosity

18 p2695 A72-36427

Ways of reducing porosity in argon-arc welding of thin titanium sheets.

18 p2695 A72-36428

Bounds for heat transport in a porous layer.

21 p3127 A72-40119

IR reflectance (or emittance) remote spectroscopy of mineral particulate surfaces, discussing particle size, surface roughness, porosity and mixing ratios effects

22 p3178 A72-42526

Sunspot formation due to magnetic flux concentration in active region and formation of invisible pores with suppressed granular motion

23 p3333 A72-43235

Brittle ceramic materials strength, showing porosity effect dependence on Weibull homogeneity parameter value

23 p3306 A72-43750

POROUS BOUNDARY LAYER CONTROL

Heat transfer in kinetic burning in turbulent boundary layer on porous surface for carbon dioxide blown in air stream with dissociated oxygen

05 p0746 A72-16223

Heat and mass exchange in laminar boundary layer in air-carbon dioxide binary mixture under free convection on porous heated vertical surface

08 p1255 A72-21664

Suction or injection interaction with rotation in three dimensional MHD flow between two porous nonconducting disks under magnetic field

10 p1524 A72-25039

Blowing and suction effects on pulsations of isothermal turbulent jets propagating along porous cylinder

12 p1752 A72-28169

Inversion of a laminar boundary layer during the injection of CO₂ through a vertical porous surface under natural convection conditions

19 p2881 A72-38191

Investigation of propeller vortex noise including the effects of boundary layer control.

24 p3359 A72-44680

Velocity profiles of plane turbulent flow of incompressible fluid on porous surface in presence of suction

24 p3390 A72-45007

POROUS MATERIALS

Porous stainless steels as filter medium, describing manufacturing techniques, properties and applications

02 p0233 A72-11449

Equation of state for porous metals at high temperatures under strong shock compression, considering phase transitions

02 p0258 A72-11469

Self sustained oscillations of mechanical system with infinite number of degrees of freedom, considering application to diffusion in porous medium

02 p0258 A72-11496

Differential pressure effects of gas-liquid configuration on porous electrode activity in oxygen cathodes

03 p0311 A72-12923

Shock waves in solids, investigating Hugoniot curve for condensed and porous media and phase transformation effects in polycrystals

03 p0446 A72-13689

McNamee-Gibson displacement potential functions generalization to problems for compressible pore fluid in theory of consolidation or thermoelasticity

03 p0455 A72-14389

Viscous fluid flow at small Reynolds numbers past porous permeable sphere, obtaining drag formula

04 p0511 A72-14858

Unsteady nonisothermal gas flow through semiminfinite porous medium, using linearized flow equations for small pressure variation

04 p0512 A72-15200

Metal oxide powder surface measurement using modified Kozeny-Karman formula, considering porous space, gas kinetic slip and air permeability effects

05 p0665 A72-16087

Steady and unsteady creep stages in porous body sintering and hot compacting, using three dimensional viscous flow theory

05 p0665 A72-16092

Compressible turbulent boundary layer properties on porous cone at Mach 8, examining Crocco theory for flows with mass addition

05 p0602 A72-16536

Mass transfer effects on hypersonic turbulent boundary layer properties from profile measurements on porous cone

[AIAA PAPER 72-184] 05 p0650 A72-16839

Transient compressible heat and mass transfer in porous media, solving coupled nonlinear partial differential equations in finite difference form by iterative technique

[AIAA PAPER 72-23] 05 p0749 A72-16914

One dimensional two phase flow transpiration cooling through porous metals

[AIAA PAPER 72-24] 05 p0749 A72-16915

Two phase heat transfer in porous metal transpiration cooling system, comparing measured with calculated temperature distribution

[AIAA PAPER 72-25] 05 p0749 A72-16916

Soviet book on superduity refractory porous ceramics covering preparation, structure and properties as thermal insulators, high temperature filters and catalyst carriers

06 p0836 A72-18520

Solid lubricant coatings adherence to porous materials, discussing porosity acquired by sulfuration treatment in melted salts bath on soft steel surface

06 p0823 A72-18590

Transient three dimensional natural convective modes in porous media as function of Rayleigh number

07 p1099 A72-19623

Porous materials fabrication from chromium carbide powders, considering compaction procedures involving sinusoidal and pulsating vibrations

07 p1017 A72-19968

Heat exchange extremum boundary value problems for flow direction reversal, considering thermal treatment of porous materials

08 p1253 A72-21457

Porous-tungsten mercury vaporizers design and tests for flow rate, liquid intrusion pressure level and mechanical strength

[AIAA PAPER 72-484] 11 p1710 A72-26210

Electrical and thermal conductivity, elastic properties and resistance to bending of porous tungsten in porosities region

11 p1665 A72-26868

Unsteady viscous incompressible electrically conducting fluid flow generated by porous disk rotation, investigating transverse magnetic field effect

12 p1851 A72-27305

Incompressible potential flow model of porous parachute canopy flow field, using Stokes stream function for axisymmetric vortex sheet in uniform steady stream

12 p1755 A72-28123

Flow characteristics in air injection through porous surface of blunt bodies, noting blowing parameter effect on boundary layer flow

12 p1752 A72-28143

High porosity nichrome fiber materials sintering at 1000-1350 C, considering size, electric conductivity, shear strength, interfibrillar contact and briquet quality

13 p1967 A72-30105

Porous Ti alloys production with Mo, Cr and Pd, considering optimum sintering temperatures and hydrogenation

13 p1981 A72-30106

Conditions for obtaining high porosity materials of complex carbides by combined reduction-carbideization of metal oxides with soot in vacuum

13 p1967 A72-30114

Elastic deformations of porous Cu, Mo and W fiber materials after pressing and sintering due to residual stress relaxation

14 p2106 A72-30151

Shock induction melting and vaporization in metals, investigating initial porosity effect

14 p2113 A72-30185

Porous cellular structure materials, investigating porosity effects on modulus of elasticity based on central monoporosity model

14 p2165 A72-30433

Recovery factors on porous surface within gas screen region in supersonic turbulent boundary layer for various air injection rates

14 p2070 A72-31017

Incompressible elastico-viscous liquid steady state laminar source flow between stationary infinite porous disks, noting Reynolds number effects

15 p2219 A72-32512

Reflection of weak shock waves from permeable materials.

17 p2581 A72-35250

Effect of pore pressure on the velocity of compressional waves in low-porosity rocks.

18 p2685 A72-36031

Nusselt number dependence on Rayleigh number for steady convection in porous medium, explaining heat transport abrupt change by breakdown of Darcy law

18 p2740 A72-36484

The dry wear behaviour of porous cobalt.

18 p2696 A72-36795

On the two-dimensional deformation of a semi-infinite porous elastic medium.

18 p2736 A72-36929

Creep of porous nickel in oxidizing and neutral media

19 p2819 A72-38287

Strength properties of highly porous materials made of metallic fibers

19 p2820 A72-38288

Theory of heat transfer in a two-dimensional porous cooled medium and application to an eccentric annular region.

[ASME PAPER 72-HT-47] 20 p2985 A72-39663

Russian book - Heat and mass transfer: A reference book.

21 p3128 A72-40350

Study of the properties of porous materials of nickel-molybdenum and nickel-chromium-molybdenum alloys

22 p3188 A72-42193

Gas permeability of high-porosity nickel cermet

22 p3188 A72-42196

Numerical analysis of the natural convection in a porous medium between two concentric cylinders

22 p3244 A72-42640

Study of the process of niobium carbide production in a fluidized bed

23 p3293 A72-43294

Thermophysical properties of highly porous thermochemically treated metal-ceramic iron

23 p3299 A72-43295

Magnetostriction of porous nickel films

23 p3299 A72-43340

Pores visualization in porous materials by liquid filling and subsequent solidification and basic material removal, observing porous samples of sintered W and nichrome powders

23 p3290 A72-44016

POROUS PLATES

Unsteady flow in laminar boundary layers along infinite porous flat plate with time dependent suction

02 p0206 A72-12620

Heat transfer characteristics of transpired and accelerated turbulent boundary layer on porous plate, comparing with prediction techniques

[ASME PAPER 71-HT-BB] 08 p1251 A72-20880

Laminar free convective flow of viscoelastic fluid past infinite porous plate

08 p1151 A72-21748

Permeable porous plate surface properties effect on boundary layer stability

09 p1293 A72-22408

Velocity slip effect on squeeze film between porous rectangular plates, calculating pressure, load carrying capacity, film thickness and response time

10 p1488 A72-24820

Thermal radiation shielding of porous surface on heated plate by absorbing gas transpiration, suggesting carbon dioxide, metal vapors and particulate mixture

[AIAA PAPER 72-277] 11 p1740 A72-25217

Surface temperature distribution for porous plate in supersonic flow with gas injection into turbulent boundary layer

13 p1893 A72-28917

Navier-Stokes equation for rotating liquid axial flow past porous plate, noting velocity distribution for suction and thinning effect for blowing

13 p1942 A72-29127

Wind tunnel measurement of intermittency in turbulent boundary layer on porous plate for alternating laminar and turbulent air flow

15 p2217 A72-31610

Pressure increase induced by heat release for laminar flame sheet in hypersonic stream, considering fuel injection through semiinfinite porous flat plate

15 p2337 A72-32590

Skin friction effects due to Hall currents in conducting unsteady slip flow over porous flat plate under transverse magnetic field

16 p2435 A72-33108

Viscous dissipation effects on unsteady free convective flow past an infinite, vertical porous plate with constant suction.

17 p2637 A72-35047

Flow near an accelerated porous flat plate.

17 p2540 A72-35054

Unsteady temperature distribution for laminar flow in a porous straight channel.

17 p2541 A72-35434

Experimental study of the structure of a turbulent boundary layer on a plate with helium injection

18 p2682 A72-36888

Velocity profile measurements in a turbulent boundary layer on a permeable plate

18 p2642 A72-37184

Turbulent boundary layer static pressure and heat exchange dependence on gas injection through porous surface

20 p2912 A72-39363

Thermal state of selectively absorbing plane gas layer blown from porous plate into stabilized turbulent high temperature gas flow, considering radiative and convective heat transfer

21 p3131 A72-41672

Magnetic field and suction effects on unsteady MHD free convection flow of conductive fluid around nonconductive porous flat plate

21 p3095 A72-41787

Fundamental studies of turbulent boundary layers with injection or suction through porous wall. III - Investigations on the separation of turbulent boundary layers in strong adverse pressure gradients with injection through porous flat plate.

22 p3165 A72-41945

POROUS WALLS

Velocity slip effect on porous walled squeeze fluid films, obtaining film load carrying capacity and thickness-time relation

[ASME PAPER 71-LUB-4] 02 p0234 A72-11526

Velocity profiles of turbulent boundary layers with injection or suction through porous walls as function of momentum thickness by Truelsenbrodt method

02 p0202 A72-11663

Elastico-viscous incompressible fluid laminar boundary layer flow past infinite plane porous wall, deriving velocity and temperature distributions by two-sided Laplace transform technique

03 p0340 A72-13024

Two dimensional elasto-viscous incompressible fluid flow past porous wall with variable suction, analyzing temperature field of laminar thermal boundary layers

03 p0341 A72-13500

Viscoelastic fluid flow past infinite plane porous wall with time dependent suction, investigating mean velocity profile and wall shear stress

04 p0514 A72-15704

Incompressible turbulent flow in parallel-plate channel with one porous bounding wall, using velocity slip model

[ASME PAPER 71-WA/FE-1] 05 p0647 A72-15939

Local or radiative-convective heat transfer coefficient determinatin at porous surface in presence of two dimensional temperature field, using temperature gradient method

05 p0751 A72-17070

Axisymmetric turbulent jets local entrainment rate as function of axial distance from nozzle exit, using Ricou-Spalding porous wall technique

10 p1481 A72-24425

Laminar boundary layer instability to longitudinal vortices onset due to homogeneous suction from slightly concave permeable wall, determining Goertler parameter and wavenumber critical values

10 p1470 A72-25064

Wind tunnel wall blockage and lift interference reduction by streamwise porosity distribution

11 p1613 A72-26001

Heat and momentum transfer of binary gas mixture flow in parallel plate channel with mass injection from porous wall, calculating velocity, pressure and temperature distributions

11 p1746 A72-26538

Heat transfer during gas injection through mesh packet porous wall, using gradient method

11 p1748 A72-26972

Free convection effect on vertical porous insulation layer thermal conductivity in high pressure gas environment

14 p2172 A72-31057

Thermal molecular jets mixing produced by Knudsen effusion from porous wall, obtaining Boltzmann equation approximate solution by moment method via assumed distribution function

16 p2429 A72-33055

Laminar flow in an annulus with porous outer wall.

18 p2683 A72-37054

Heat transfer in a channel with a porous wall for turbine cooling application.

[ASME PAPER 72-HT-39] 20 p2986 A72-39667

Wall interference effects on cone-cylinder pressure distribution in variable porosity trisonic wind tunnel as function of model blockage and Mach number

[AIAA PAPER 72-1010] 21 p3041 A72-41592

Wall porosity and angle of attack effects on jet stretcher flow field for supersonic engine inlet testing, using three dimensional method of characteristics

[AIAA PAPER 72-1025] 21 p3042 A72-41603

Experimental friction factors for turbulent flow with suction in a porous tube.

21 p3047 A72-41618

Two dimensional MHD fluctuating flow of incompressible electrically conducting rarefied gas past infinite porous wall for slip-flow regime with variable suction

21 p3095 A72-41784

An initial two-dimensional wall interference investigation in a transonic wind tunnel with variable porosity test section walls.

[AIAA PAPER 72-1011] 24 p3389 A72-45409

PORPHYRINS

Abiogenic formation and fluorescence spectra of porphrin, chlorin and bacteriochlorin during chemical evolution, using pyrrol-formaldehyde model

08 p1122 A72-22185

NT CHLOROPHYLLS

Porphyrin exobiology, discussing organic and random biosynthesis and extraterrestrial existence based on interstellar spectral evidence

05 p0617 A72-16130

Abiogenic formation and fluorescence spectra of porphrin, chlorin and bacteriochlorin during chemical evolution, using pyrrol-formaldehyde model

08 p1122 A72-22185

Nitriles, nitrogen bases and porphyrin-like pigments catalytic synthesis products analysis by mass spectroscopy gas and other chromatographies

14 p2157 A72-30583

Organic catalysts for oxygen reduction, discussing phthalocyanines, Pfeiffer complexes and porphyrins

16 p2361 A72-33884

PORTABLE EQUIPMENT

Portable detector-recorder for automobile, blast furnace, railroad car, engine room and helicopter infrasonic noise measurements, discussing peak frequencies and subjective effects

01 p0101 A72-10157

Portable self contained ultrasonic field inspection equipment for nondestructive crack detection in T53 gas turbine compressor disks

01 p0076 A72-10814

Portable electronic wattmeter for nonsinusoidal waveform low power factor circuit measurement, discussing design, calibration and applications

[IEEE PAPER 8,2] 03 p0332 A72-13757

Self contained portable data acquisition system for marine, environmental and ecology research, using multiple analog recording and digital telemetry transmitter

06 p0797 A72-18613

Transportable lunar ranging with neodymium glass laser and Coude optical system, noting geophysical applications

[CLEA PAPER 9,6] 07 p0943 A72-19388

High resolution portable hologram microscope based on pulsed ruby laser to avoid vibration degrading effects

[CLEA PAPER 15,7] 07 p0984 A72-19398

Absolute gravity measurement methods and instruments, noting portable laser interferometer and formula derived from satellite observations

07 p1034 A72-19595

Transportable radio telescope for atmospheric attenuation and solar activity observations

09 p1316 A72-23509

Lightweight man-portable uncooled semiconductor laser illuminator design for field use in night vision applications

15 p2248 A72-32047

Portable X ray calorimeter for simultaneous fluence and front surface dose measurement in Ta from pulsed electron accelerations

15 p2241 A72-32440

A portable coaxial collinear antenna.

17 p2526 A72-34377

A unitized and portable holographic interferometer. [ASME PAPER 72-HT-10]

20 p2927 A72-39681

Active transistorized directional dipole VHF receiving antennas for ATC and mobile applications and field intensity measurement

21 p3030 A72-40527

A portable self-contained gas chromatograph.

23 p3292 A72-44544

PORTS [OPENINGS]

Hydraulic servomechanism spool type control valve orifice flow characteristics, measuring mass flow for various spool determined port shapes

07 p0915 A72-20533

POSEIDON MISSILES

Polaris and Poseidon missile systems reliability assessment, discussing test programs, analytical techniques and data management

10 p1551 A72-24013

POSITION

Hf ballistocardiography in erect position, noting tracing quality in Starr table

03 p0318 A72-13146

POSITION [LOCATION]

NT SOLAR POSITION

Soviet book on space navigation covering dimensional spaces, navigation functions, relativistic phenomena, position finding, motion parameters, statistical methods, etc

02 p0256 A72-12297

Circumpolar region object position autonomous determination from arbitrarily zenith-oriented moving horizontal platform position coordinates

04 p0545 A72-15002

OMEGA system application to airborne long range navigation, describing aircraft position determination technique for extended flight over water without line-of-sight radio navigation aids

05 p0686 A72-16655

Synchronous satellite surveillance system for transoceanic ATC, using suboptimal/modified Kalman/ filter for aircraft position and velocity computation

08 p1204 A72-21091

Single Integrated Signal Device to aid in locating downed airmen awaiting rescue in dense jungle terrain by Search and Rescue aircraft

08 p1112 A72-21580

Delphinus Nova positions determination from plates obtained with photographic telescope with/without diffraction gratings

09 p1389 A72-23067

Tago-Sato-Kosako comet positions determination from plates obtained with photographic telescope, tabulating averaged spherical coordinates

09 p1389 A72-23068

Precise optical positions of nine compact radio sources in AGK 3 catalog

10 p1536 A72-24140

Asteroidal positions from plates from Zeiss astrophotograph at Turin Observatory, discussing reduction methods and error analysis

11 p1717 A72-25901

Selenodetic catalog centers mutual positions determination from lunar near side hypsometric charts

11 p1724 A72-26911

Photographic position of comet Ikeya-Seki, presenting data reduction procedure

12 p1868 A72-27220

Correlation technique for position location in surveillance and navigation by phase extraction from range tones using synchronous satellites

[AIAA PAPER 72-564] 12 p1842 A72-27375

Position information in lunar cartographic products evaluated by Apollo data, obtaining reliability factors

12 p1871 A72-27530

AN/ARN-99 OMEGA lane ambiguity resolution for receiver location, using multiple state vector Kalman filter approach

13 p1997 A72-29189

Program for orbital determination and prediction of satellite positions from observations at one station

15 p2268 A72-31941

Radio sources position determination by lunar occultation, noting observation technique and data analysis method

16 p2453 A72-33287

Jupiter Red Spot position determinations by East German observers tabulated

16 p2456 A72-33496

Satellites use for position determination and data acquisition systems application to earth sciences and industry

17 p2603 A72-34398

Log periodic dipole antenna systems for ILS localizers, noting reduced sensitivity to snow and ice

19 p2830 A72-37279

Positions of the major planets and the moon observed at the 0.33 M photographic equatorial

19 p2858 A72-37856

Determination of major planet coordinates by an expeditionary astrophotograph

19 p2861 A72-37986

Initial results of a PM study in the Hydra ring

19 p2866 A72-38493

Accurate positions of radio sources at 408 MHz.

19 p2868 A72-38698

Radio position accuracy of pulsar PSR 1749-28 from lunar occultations compared to time of arrival measurements

20 p2969 A72-39388

Location estimation for spacecraft landed on Mars surface via statistical techniques application to earth based radio tracking data, taking into account ephemeris biases

21 p3082 A72-41554

Applications of a technique for estimating aircraft states from recorded flight test data

[AIAA PAPER 72-965] 22 p3138 A72-42360

POSITION ERRORS

ATC separation minima and navigational errors on airways in general and long range oceanic environments

01 p0096 A72-10177

Geometry and latitude/longitude differentials approximations for position fixing by Doppler signals and earth satellites

01 p0097 A72-10182

Optimal stabilization law for ensuring gyroscopic equilibrium position asymptotic stability in rms error, aperiodicity and system transient response time

02 p0230 A72-12338

Light distribution photometry in Japan, discussing photometers, luminous flux integration and source distribution and positioning errors

03 p0358 A72-13426

Error covariance matrix evaluation at end of orbit extrapolation in terms of state vectors at measurement, discussing computation and interpretation

05 p0720 A72-16753

Satellite motion state vector accuracy estimate algorithm based on angular measurements of stellar positions relative to satellite sent probe

05 p0687 A72-16762

Methodical errors in spacecraft local vertical determination due to variability of physical effects, considering planet oblateness, atmospheric refraction, incident radiation fluctuations, etc

05 p0721 A72-16764

Double parasitic loop counterpoise antenna radiation properties comparison to VOR systems, noting siting error reduction

06 p0782 A72-17357

GEOS satellite orbit determination and prediction errors from optical tracking systems and gravity models, estimating resonant coefficients

06 p0877 A72-17653

Transit instrument system year-to-year stability in astronomical time determination, considering seasonal wave causes and star coordinate errors

06 p0885 A72-18037

Two-channel direction finding with point source emission and spaced antennas reception, investigating cross correlation and background noise interference effects on accuracy

07 p0938 A72-19007

Radar tracking pulse scheduling in dense target environment with position estimation error constraints to avoid false return with track correlations

08 p1134 A72-21407

Local level and space stable inertial navigation systems, comparing position error propagation

08 p1204 A72-21410

Optimal stabilization law for ensuring gyroscopic equilibrium position asymptotic stability in rms error, aperiodicity and system transient response time

08 p1168 A72-21553

Terrestrial altitude differences effects on photogrammetric data accuracy in two step compensation with models

09 p1311 A72-22966

Mean coordinate and distance errors in photogrammetric measurements of two neighboring models carried out by two image scales and four aerial cameras

09 p1311 A72-22969

Star catalogs comparison and stellar positional differences and motion studies using random field theory

09 p1388 A72-23052

Lunar objects position accuracy assessment based on pairwise comparison of current selenodetic reference catalogs

09 p1388 A72-23054

Disk diameter errors due to wire thickness in reduction of visual planetary observations

09 p1311 A72-23062

Astronomical identification of optical objects near SC2 radio sources position, noting probability parameters and measurement error

10 p1546 A72-24837

Transit instrument system year-to-year stability in astronomical time determination, considering seasonal wave causes and star coordinate errors

11 p1719 A72-25973

Azimuth-bearing error dispersion in surveillance radar measurements, using Markov chains

11 p1595 A72-26297

OMEGA phase shifts in auroral region due to solar phenomena, discussing methods eliminating PCA induced errors

13 p1997 A72-29185

Optimal optical measurement for two dimensional object position on plane in Gaussian background noise, calculating mean square error for false identification probability determination

13 p1920 A72-29280

High speed and resolution laser scanning by optomechanical methods, discussing theoretical bandwidth, resolution limits, position error correction measures and performance optimization

15 p2248 A72-32037

Relationship between static pressure error/position error/and measurable flight parameters for different aircraft weights and configurations

16 p2393 A72-33637

Coordinate and speed error dependence on instrumental errors of inertial navigation system using gyrohorizoncompass

16 p2420 A72-33960

Statistical analysis of position-fixing general theory for systems with Gaussian errors

17 p2578 A72-34294

The reduction of false tracks during automatic tracking

17 p2522 A72-34826

Satellite motion state vector accuracy estimate algorithm based on angular measurements of stellar positions relative to satellite launched probe

17 p2578 A72-35265

Methodical errors in spacecraft local vertical determination due to variability of physical effects, considering planet oblateness, atmospheric refraction, incident radiation fluctuations, etc

17 p2610 A72-35267

Error investigation for the location of the sources of atmospheric by radio direction finding

18 p2706 A72-36429

Analysis of the division-line errors of the Pulkovo meridian circle by observations of stars

19 p2801 A72-37912

Exact positions of Mars as determined by the photographic method at Pulkovo in 1966 and 1967

19 p2859 A72-37914

Exact positions of Uranus for 1919 through 1969 according to photographic observations at Pulkovo and Tashkent

19 p2859 A72-37915

The impact of gradiometer techniques on the performance of inertial navigation systems

[AIAA PAPER 72-850] 20 p2949 A72-39079

Design of a reduced-state suboptimal filter for self-calibration of a terrestrial inertial navigation system.

[AIAA PAPER 72-849] 20 p2949 A72-39080

A versatile Kalman technique for aircraft or missile state estimation and error analysis using radar tracking data.

[AIAA PAPER 72-838] 20 p2950 A72-39089

Enlarging the region of convergence of Kalman filters that encounter nonlinear elongation of measured range.

[AIAA PAPER 72-879] 20 p2907 A72-39121

Landing-site and orientation determination for a spacecraft on Mars

21 p3103 A72-40302

On the removal of blindness in phased antenna arrays by element positioning errors.

21 p3027 A72-40363

Accurate positions of the planet Pluto in the years 1969-1970.

21 p3105 A72-40576

A hybrid navigation concept using a spinning satellite-borne interferometer and self-contained equipment.

21 p3082 A72-41083

Influence of stick efficiency on tracking error applying two slightly different control elements.

21 p3012 A72-41429

Spacecraft local vertical estimation and error limits in meridional and equatorial planes based on terrestrial IR radiation measuring instruments

22 p3223 A72-42205

Analytical assessment of the accuracy of autonomous space navigation from measurements of the flight altitude and zenithal distance of one reference star

22 p3202 A72-42222

Theoretical and practical comparison between two minute Doppler and short Doppler satellite position fix accuracy.

22 p3203 A72-42947

The application of error control techniques in the design of an advanced augmented inertial surveying system.

24 p3421 A72-44641

Integrated navigation systems and Kalman filtering - A perspective.

24 p3386 A72-44642

Possible impact of area navigation upon MLS requirements for azimuth angular coverage and range.

24 p3422 A72-44643

Numerical analysis of global satellite triangulation grid projects

24 p3397 A72-44868

POSITION INDICATORS

NT PLAN POSITION INDICATORS

NT RADIO DIRECTION FINDERS

NT SPACECRAFT POSITION INDICATORS

Polar navigation with transverse mercator technique for aircraft using secant geared ground position indicators

01 p0097 A72-10181

Airborne pictorial navigation systems for visual indication of aircraft position in addition to digital readout

02 p0256 A72-12106

Doppler system with navigation radar device, computer unit and data transmitter for continuous recording of aircraft position and speed

02 p0258 A72-12749

Laser interferometers for displacement, length, gas refractivity, laser wavelength and relative object position measurements

[CLEA PAPER 15.1] 07 p1005 A72-19396

Astrolabe design and operation for reconnaissance and simultaneous determination of latitude and longitude

08 p1165 A72-21022

Wind tunnel model magnetic suspension system with remote position sensor based on optical contrasts scanning analysis

10 p1461 A72-24763

Optical TV scanning for wind tunnel model position detection in magnetic suspension system for sphere low density drag measurements

[ONERA, TP NO. 988] 10 p1461 A72-24764

Wind tunnel model remote position sensing and control systems, discussing drift reduction in magnetic suspension

10 p1461 A72-24768

Electromagnetic position sensor for magnetically supported model in wind tunnel, discussing design, operation principles and performance

10 p1462 A72-24773

Rotating mirror image position sensor for high angular resolution optical tracking, discussing performance improvement by computer generated variable density spatial filter

11 p1591 A72-25312

Position and minimum scattering algorithms for narrow band signal source received by spaced receivers forming antenna arrays with large separations

11 p1598 A72-26715

Pulse-sounding position finding device for light parachute probes conducting ionospheric studies, discussing design features

13 p1922 A72-29350

Airplane attitude display motion relationship to external world as factor in pilot error due to visual frame of reference shift

14 p2083 A72-31151

Radio phase interferometers for emitter position location, predicting polarization mismatch errors effects on accuracy

15 p2206 A72-31777

Radiation source position a posteriori probability density function determination with empirical prior knowledge to provide simple computational procedures

15 p2267 A72-31778

Roll angle detector for angular position measurement of two independent bodies, using optical-mechanical-electrical system

15 p2268 A72-32043

Accuracy of the determination of the positions of stars and artificial satellites from an aircraft

19 p2861 A72-37973

Choice of optimal geometrical relationships in a transformer-type angle converter

21 p3058 A72-41805

POSITIONING

High accuracy position determination from hyperbolic radio navigation time differences based on Sodano inverse solution of geodesics

11 p1684 A72-26498

Lens parameters selection and prisms position optimization in light beam to avoid premature damage

12 p1808 A72-27623

OMEGA receiver with digital solid state circuits for remote unmanned platform positioning, discussing ship to shore tests and design features

13 p1925 A72-29184

POSITIONING DEVICES [MACHINERY]

NT BOOMS [EQUIPMENT]

Ruby laser telemetry station operated at 0.7 microns, describing telescope pointing system

07 p0947 A72-20257

Aiming stabilization by gyroscopic system, discussing mechanical mirror-gyroscopic links, mirrors lightening and prism or lens anamorphosers

07 p0990 A72-20403

Electromagnetic remote model positioning sensing system for wind tunnels with magnetic suspension, using differential transformer action

10 p1461 A72-24762

Process control of the 100-m telescope - Digital control

19 p2803 A72-38486

Process control of the 100-m telescope - Communication of the observer with the computer-controlled telescope

19 p2804 A72-38487

Flight and centrifuge tested aircrew tilting supinating seats biomedical and technical adequacy as acceleration protective man machine system

19 p2761 A72-38707

POSITIVE FEEDBACK

Electroluminescent image converter with positive optical feedback, investigating steady state bistable operation mode stability

02 p0193 A72-12341

Superregenerative linear mode amplification in Q switched He-Xe laser as function of resonator phase, length and signal angle

04 p0531 A72-15147

Electroluminescent image converter with positive optical feedback, investigating steady state bistable operation mode stability

08 p1143 A72-21947

LF noise generator with Rice variable amplitude probability distribution law, using shielded vacuum tube superregenerative amplifier

09 p1285 A72-22345

Noise characteristics of regenerative amplifier with direct coupling to load

13 p1929 A72-28897

Selectivity evaluation for regenerative amplifiers of complex design

13 p1929 A72-28898

Electro-optical regenerative assembly with p-n-p structure, emphasizing positive feedback and I-V characteristics

13 p1933 A72-29976

Regenerative nonlinear RC amplifier oscillations due to series opposed varicap diode capacitance

18 p2665 A72-36109

Delay-lock repeater tracking system utilizing superregenerative interrogator.

21 p3082 A72-41084

SNR improvement by negative feedback and deterioration by positive feedback in amplifiers, discussing input circuit thermal noise

21 p3034 A72-41123

Regenerative optical link assembly for weak image amplification and spectral conversion, using photoreistor as light receiver

22 p3159 A72-42272

Electronic superregeneration in semiconductor photosensitive structures with negative resistance

23 p3268 A72-43345

POSITRON ANNIHILATION

Nonthermal ultrarelativistic plasmas covariant analysis with quantum electrodynamics and Green function theory of nonequilibrium statistical mechanics, discussing electron-positron pair production and annihilation

10 p1525 A72-25100

Russian book on transition metals and alloys electron structure and electronic properties covering paramagnetism, positron annihilation, magnetic transformations and electron heat capacity

11 p1659 A72-26069

Angular annihilation photon distribution curves from positron-electron annihilation method for metallic phase interaction with crystal lattice in synthetic diamonds

12 p1833 A72-27764

Electron shell structure in annealed and plastically deformed W-Re alloys from positron annihilation angular distributions

13 p1981 A72-29908

Positron annihilation lifetimes and trapping probabilities for vacancies and dislocations in Al single crystal

15 p2258 A72-32228

The imaging properties of the positron camera

18 p2652 A72-36424

Anisotropy of angular distribution of radiation due to positron annihilation on the surface of Mo single crystals.

19 p2844 A72-37691

Time spectrum and angular distribution for positron annihilation studies of electron structure and phase transformations of materials

19 p2845 A72-38401

Effect of voids on angular correlation of positron annihilation photons in molybdenum.

22 p3187 A72-41967

POSITRONS

Heuristic theory of positron-helium elastic scattering phase shifts and cross sections

03 p0393 A72-14399

Emission energy of positrons thermalized in moderators and coated with Au, suggesting Au negative work function existence

08 p1217 A72-21339

Solar atmosphere low energy positron production by solar particle fluxes demodulated according to cosmic ray transport equations

09 p1378 A72-23022

Interstellar cosmic ray electron component and isotopic composition relations from positron observations

16 p2448 A72-33741

Generalization of basic equations of aerodynamics and electrodynamics.

17 p2539 A72-35043

Energy loss of fast electrons and positrons in a plasma.

19 p2840 A72-37727

POST-BLAST NUCLEAR RADIATION

Stratospheric concentration of radioactive carbon from 1961-62 nuclear tests by balloon measurements over European U.S.S.R. territory during 1967-69

23 p3286 A72-44492

POSTFLIGHT ANALYSIS

Hybrid computer simulation for telemetry data collected during missile flight control system model post-flight verification and hardware performance analysis

07 p1085 A72-20332

Effects of an 18-day flight on the human body.

23 p3253 A72-43386

POSTULATES

U AXIOMS

POSTURE

Human postural control system dynamic model, discussing stick man pitch axis dynamics digital simulation and difficulties in linearizing equations of motion

03 p0318 A72-13163

Human muscular electrical activity in various body positions, noting potentials during natural and unaccustomed postures

03 p0317 A72-13990

Simulation of the human cardiovascular system - A model with normal responses to change of posture, blood loss, transfusion, and autonomic blockade.

17 p2507 A72-34445

The silent period in man during muscle lengthening produced by loading

20 p2892 A72-39590

Vestibular system functional relationship to postural reflex mechanism involving labyrinth and gravireceptors responses

22 p3147 A72-42788

Lung volume changes of people in antihydrostatic position in hospital beds for control, exercising and muscle electric-stimulated groups

23 p3256 A72-43918

POTASSIUM

NT LIQUID POTASSIUM

NT POTASSIUM ISOTOPES

Vapor bubble growth on heated surface with random temperature distribution and liquid microfilm for water and boiling potassium

02 p0303 A72-12862

Atmospheric Na, Li and K layers height, width, abundance and thickness from twilight glow measurements, using birefringent filter type photometers

08 p1159 A72-21224

Solar gravitational red shift measurement from solar and laboratory potassium absorption line comparison, using atomic beam resonance scattering technique

10 p1541 A72-24415

Significance of Apollo 11 and 12 lunar rock fragments of norite rich in K, rare earth elements and P /KREEP/ for lunar evolution assessment

13 p2037 A72-28990

Sleep deprivation effects on diurnal urine potassium excretion, showing individual circadian rhythm variations

13 p1904 A72-29320

Ar and K electron cross section determination for momentum transfer, using dc conductivity measurement of high pressure plasma

14 p2134 A72-30803

Potassium atomic beam aerodynamic acceleration by He-Ar free jet, determining beam intensity as function of nozzle-skimmer distance, carrier gas pressure and nozzle temperature

16 p2429 A72-33056

Oscillator strength and ground state photoionization cross sections computation for Na, K, Rb and Cs atoms, including core polarization correction to dipole moment

16 p2431 A72-33724

Exchangeable potassium in heart disease - Long-term effects of potassium supplements and amiloride.

17 p2500 A72-34932

Ion alterations during myocardial ischemia.

17 p2502 A72-34994

Respiratory effects of hypochloremic alkalosis and potassium depletion in the dog.

21 p2997 A72-40418

Electron attachment and compound formation in flames. V - Negative ion formation in flames containing chromium and potassium.

22 p3244 A72-42717

Excitation contraction correlates in true ischemia.

23 p3255 A72-43814

Intracellular potassium in cells of the distal tubule.

24 p3373 A72-45231

POTASSIUM CHLORIDES

Optical absorption in UV and IR of proton bombarded potassium chloride at liquid nitrogen temperature attributed to trapped protons

08 p1211 A72-21249

Determination, by X-ray photometry, of the frequencies of thermal oscillations which propagate themselves, following the axes of symmetry in a potassium chloride single crystal, at temperatures of 295, 80, and 5 K

19 p2844 A72-37791

Potassium chloride test for electrocardiogram evaluation in flight personnel medical appraisal

21 p3012 A72-41747

POTASSIUM CHROMATES

Heating effect on potassium bichromate-saturated anodic aluminum oxide electrical characteristics, discussing surface conductivity and capacity and solution pH

05 p0667 A72-17052

POTASSIUM COMPOUNDS

NT POTASSIUM CHLORIDES

NT POTASSIUM CHROMATES

NT POTASSIUM HYDROXIDES

NT POTASSIUM OXIDES

NT POTASSIUM PERCHLORATES

NT POTASSIUM PHOSPHATES

Potassium chlorate/red phosphorus mixtures sensitivity tests for initiation by electrostatic discharge, heating and impact

08 p1221 A72-20776

Boron/potassium nitrate parachute mortar design for aircraft and spacecraft applications, comparing with high-low propellant

08 p1221 A72-20783

Superconductivity observation in Na, K and Rb intercalates of molybdenum disulfide comparing transition temperatures

09 p1368 A72-22561

Spectroscopic and stimulated emissive properties of neodymium ions in potassium yttrium tungstate crystals at 77 and 300 K

11 p1701 A72-26362

Electro-optic KTN /potassium tantalate niobate/ crystals for modulators, deflectors, phase shifters and polarization rotator devices

20 p2922 A72-39047

Fourier transform C-13 nmr analysis of some free and potassium-ion complexed antibiotics.

20 p2898 A72-39399

POTASSIUM HYDROXIDES

Rechargeable oxygen electrode research program for hydrogen oxygen fuel cells and metal-oxygen batteries, discussing KOH solutions effects

04 p0466 A72-14675

POTASSIUM ISOTOPES

Apollo 12 and 14 lunar soils K, Rb and Sr isotopic composition evaluation, noting microbreccia as major nonbasaltic constituent

11 p1723 A72-26497

POTASSIUM OXIDES

Sealed cabin air regeneration by means of potassium superoxide, noting weight and space savings

11 p1586 A72-26594

Cation self diffusion coefficients in potassium oxide-strontium oxide-silicon dioxide glass, using radioactive tracers and sequential etching technique

13 p1912 A72-28625

Diffusion in the system K2O-SrO-SiO2. IV - Mobility model, electrostatic effects, and multicomponent diffusion.

21 p3097 A72-40935

POTASSIUM PERCHLORATES

Burning rate dependence on oxidizer particle size of ammonium or potassium perchlorate mixtures with organic fuels

09 p1373 A72-23146

Powdered Al additions effect on burning rates of three component mixture systems based on ammonium and potassium perchlorates

19 p2847 A72-37361

POTASSIUM PHOSPHATES

Electro-optical multiple transit laser beam deflection system using KDP crystals and quadrupole electrode arrangements

07 p1000 A72-19011

Intraresonator modulation of ruby laser with frequency near neighboring axial oscillations frequency difference, describing Q switch based on transverse electro-optical effect in KDP crystal

10 p1490 A72-24047

Mode selection in high coherence ruby laser using KDP Q switch

12 p1823 A72-27618

Angular spectrum of second harmonic generation during two frequency interactions in KDP laser

13 p1969 A72-29524

Light signal modulation by traveling wave in circular waveguide with coaxial KDP crystal

15 p2207 A72-31881

Fracture of nonlinear KDP and LiNbO3 crystals by ruby laser radiation

19 p2812 A72-38537

Stress induced birefringence in an isolated and a shortcircuited KH2PO4 crystal.

23 p3324 A72-44322

POTENTIAL

Homogeneous isotropic elastic medium thermomechanicity equations based on variational principles noting definite integrals solutions by means of delayed potentials

09 p1406 A72-23070

POTENTIAL ENERGY

NT BIOELECTRIC POTENTIAL

NT CONTACT POTENTIALS

NT COULOMB POTENTIAL

NT ELECTRIC POTENTIAL

NT GEOPOTENTIAL HEIGHT

NT IONIZATION POTENTIALS

NT LOW VOLTAGE

NT PHOTOVOLTAGES

NT PLASMA POTENTIALS

NT SPIKE POTENTIALS

Binary systems formation probability during triple encounters, observing dependence on system/potential energy ratio

03 p0435 A72-13809

Potential energy principle in equilibrium stability problems for flexible extendable thread, using Liapunov method

03 p0390 A72-14208

Different pair potentials for simulating vacancy in Al, discussing program planning for relaxations calculation around vacancy to effect computing time reduction

03 p0378 A72-14253

Electron tunneling probabilities through slowly varying potential energy barrier with potential holes evaluated by T scattering matrix interaction formalism

04 p0563 A72-15471

Nonlinear dynamic system mathematical model for unit mass particle escape trajectories from potential well, taking account of trapped motions and stable oscillations

07 p1025 A72-18807

Storm available potential energy generation and boundary layer frictional dissipation estimation in heat transfer from ocean to atmosphere within east coast cyclone

07 p0980 A72-20451

Quantum and classical gravitation theory Mercury perihelion motion dependence on fourth order potential in scalar and Dirac fields

07 p1084 A72-20689

Number of molecular hydrogen ion vibrational levels, using phase function method for scattering length and potential energy

08 p1211 A72-21293

Gravitational field potential energy-momentum pseudotensor component determination in general relativity theory

08 p1207 A72-21301

Particle motion in conformal spaces in general relativity, deriving gravitational potential and proper energy of mass point

08 p1209 A72-21369

Ellipsoidal plasmoid equilibrium revolution frequency and potential energy and stability in external hf fields

09 p1362 A72-23204

IR spectra and intermolecular potentials of nitrogen matrix-isolated protonated and deuterated nitromethane

10 p1434 A72-24339

Trajectory dynamics for fluorine atoms reaction with H molecules, predicting total available energy from energy release on potential energy surface

10 p1434 A72-24343

Solid body elastic deformation potential energy and structure calculation on computer by finite element method and calculus of variations

10 p1559 A72-24924

Target position information for radar energy potential calculation and detection quality, describing transmitter power reduction for normal range distribution density

11 p1596 A72-26313

Potential or gravitational energy in Newtonian physics based on Maxwell definition, noting energy transfer

12 p1843 A72-27187

Model potential method for calculating positively charged diatomic sodium molecular ions potential energy curves and resonance charge transfer cross sections

12 p1848 A72-28350

Quantum mechanical calculation of interaction potential energy surface role in vibrational excitation of diatomic molecules

14 p2134 A72-30750

Approximate values for elastic body stresses and displacements based on finite element method and virtual displacements and minimum potential energy principles equivalence

15 p2323 A72-31477

Langmuir probe susceptance- and conductance-voltage measurements via in-phase and quadrature component plots as function of applied dc potential

15 p2241 A72-32515

Potential energy curves for exothermic reaction between oxygen cations and nitrogen molecules to form nitric oxide and atomic nitrogen

16 p2360 A72-32921

Gravitational field potential energy-momentum pseudotensor component determination in general relativity theory

17 p2580 A72-34659

Determination of accurate potential strengths to yield specified eigenvalues of the radial Schrodinger equation.

21 p3086 A72-40109

The effect of target absorption on the attenuation characteristics of bremsstrahlung generated at constant medium potentials.

21 p3087 A72-40474

Scattering cross section glory undulations relationship to potential energy of interaction of two molecules with minimum containing one or more bound states

21 p3087 A72-40561

Mixed-displacement finite-element analysis with particular application using plane-stress triangles.

24 p3455 A72-44789

Theoretical interpretation of the optical and electron scattering spectra of polyatomic molecules. III - N₂O and the discovery of resonant phenomena in the B region at 6.8 eV.

24 p3426 A72-45301

POTENTIAL FIELDS

Multichannel topography of human scalp alpha EEG potential fields

01 p0016 A72-10072

Plasma source with arc stabilized by supersonic air stream, measuring enthalpy, heat flux and potential distribution

01 p0048 A72-10491

Cascade connected electrode scheme for MHD applications, noting potential and current distributions and Hall voltage buildup

02 p0265 A72-12276

Automatized graphic information input into computer, using electric potential distribution introduced into conducting underlay sheet by current carrying drawing pen

03 p0326 A72-13093

Tunneling current calculation for free electrons subject to arbitrary one-electron potential, using Keldysh perturbation theory

03 p0404 A72-14266

Surface potential effects on splitting of p- and d-orbitals of atoms and ions approaching bcc and fcc substrates

03 p0393 A72-14340

Low voltage arc plasma in low pressure Cs vapors, determining charged particle concentration and potential distribution in interelectrode gap

06 p0863 A72-18413

Nonlinear dynamic system mathematical model for unit mass particle escape trajectories from potential well, taking account of trapped motions and stable oscillations

07 p1025 A72-18807

Three element einzel and asymmetric voltage lenses for electron optics, calculating focal lengths and spherical aberrations based on potential distribution inside equidiameter coaxial cylinders

07 p0992 A72-20585

Diffused electron and ion currents through grid anode of cesium thermionic diode, determining electron temperature and potential distribution in electrode gap

08 p1113 A72-21747

Potential distribution in positive ion sheath around plane Langmuir probe immersed in plasma

08 p1215 A72-22074

Attractive well potential effects on vibrational transition probability during atom-diatom molecule collinear collision

10 p1514 A72-24335

Automatized graphic information input into computer, using electric potential distribution introduced into conducting underlay sheet by current carrying drawing pen

11 p1601 A72-25705

Retarding potential analyzer errors and performance degradation due to grid plane potential depressions

11 p1634 A72-26411

Nature and requirements of electrostatic inertial plasma confinement, deriving potential and particle densities as function of radius, grid voltage and current

12 p1850 A72-27281

Helmholtz equation numerical solution for potential field problems with arbitrary boundary conditions of wave propagation, diffusion and thermal conduction in mathematical physics

12 p1846 A72-27553

Time dependent and stationary two dimensional calculation of current and potential distributions in MHD generator preionizer and entrance region flow

13 p2013 A72-29358

Minimum magnetic field energy of two dimensional magnetosphere with neutral sheet for arbitrary dipole inclination to solar wind as function of potential difference on boundary points

14 p2101 A72-30643

Characteristic functions of potential distribution on sphere with longitude dependent conductivity for application to ionosphere electrodynamics

14 p2101 A72-30644

Earth surface layer potential density from gravity anomalies combined with satellite Doppler observations

16 p2382 A72-32888

Experimental investigation of the parameters of a statistical Gaussian field model for centimeter waves beyond the radio horizon

17 p2515 A72-34834

Low voltage arc plasma in low pressure Cs vapors, determining charged particle concentration and potential distribution in interelectrode gap

17 p2588 A72-34861

Effect of a transverse magnetic field on the operation of a thermionic converter under undercompensated Knudsen conditions.

17 p2497 A72-34862

Calculation of the dependence of the charge density on the distribution of the potential in crossed symmetric electric and magnetic fields

17 p2593 A72-35903

Third integral of equations of motion in axisymmetric potential field, noting Jeans theorem for phase density in star system

19 p2863 A72-38068

Calculation of electrostatic potential distribution in semiconductor's contact region during passage of injecting into blocking contact due to illumination.

19 p2846 A72-38626

Superposition method for potential distribution in plane tetrode field with unipotential and bipotential grids, noting electro-optical effect in cylindrical lenses

19 p2776 A72-38667

Representation of solenoidal vector fields in bounded domains by poloidal and toroidal scalar potentials, discussing applications in fluid mechanics, elastic vibrations and electromagnetic theory

23 p3313 A72-43716

POTENTIAL FLOW

NT EQUIPOTENTIALS

Harmonium reed self excited oscillation mechanism, describing flow visualization, jet instability potential flow and aerodynamic forces

01 p0002 A72-11232

Multicellular viscous vortex core embedded in unsteady outer potential swirling flow, obtaining numerical solution

02 p0253 A72-11971

Near pressure field within subsonic circular turbulent cold jet potential cone, noting peak in power spectra

02 p0150 A72-11974

Unsteady supersonic aerodynamic forces on oscillating circular cylindrical shell calculated using linearized equation of potential flow

02 p0151 A72-12256

Complex perturbation potential of constant vortex shear flows around airfoil activated by motion in presence of rectilinear wall

05 p0600 A72-16122

Nonlinear unsteady potential flow of incompressible fluid past slender wing, using linearized vortex distribution method

05 p0600 A72-16214

Zhukovskii potentials for ideal fluid motion in spherical or cylindrical cavity with arbitrary radial partitions

05 p0648 A72-16218

Vortical flow of incompressible fluid in finite region bounded by potential flow and with Bernoulli constant jump at boundary

05 p0649 A72-16581

Subsonic and transonic compressible potential flow over nonlifting hovering helicopter rotor blades, calculating flow field by three-dimensional nonlinear relaxation scheme

05 p0607 A72-16901

Nonuniform potential and dissipation flow structure of turbulent diffusion flame front at high Reynolds numbers

06 p0902 A72-18104

Steady subsonic potential gas flow in multiply connected regions, determining velocity field via boundary value problem solution for quasi-linear elliptic equations set

06 p0801 A72-18123

Rotational flow computation, using iteration methods for irrotational and solenoidal vector field components

07 p0966 A72-18811

Subsonic three dimensional potential flow computational method lifting aerodynamic configurations analysis and design

07 p0907 A72-18958

Hydrodynamic stability small perturbation theory, considering potential flow in contact with flexible membrane

07 p0969 A72-20067

Irrotational two dimensional transonic flow past symmetric profile with and without shock

07 p0909 A72-20068

Plane irrotational flow of fluid with arbitrary thermodynamic properties in throat of Laval nozzle, solving flow equations

07 p0972 A72-20111

Plane potential flow problem for laminar boundary layer on rotating infinite cylindrical blade, using conformal coordinate transformation

08 p1108 A72-21614

Frontogenesis models based on horizontal deformation field, noting uniform and nonuniform potential vorticity

09 p1347 A72-23652

Steady inviscid irrotational transonic flow in two dimensional symmetric and axially symmetric nozzle throats

10 p1417 A72-23875

Equation of isovolumetric fluid pulsed and potential flow in convergent duct solved by perturbation method

10 p1465 A72-24118

Cochlea enclosed two dimensional cavity potential flow model for fluid mechanical theory of hearing

10 p1430 A72-24295

Two and three dimensional pistons motion in stationary gas, calculating potential flow characteristics near weak discontinuities as function of piston geometry and acceleration

10 p1468 A72-24431

Smoke trail motions in winds with constant shear, considering potential, vorticity and stratified flows

10 p1475 A72-24748

Plane irrotational motion of ideal incompressible fluid perturbed by profile movement and deformation, obtaining aerodynamic forces power

10 p1420 A72-24853

Computerization of panel flutter boundary calculations with aerodynamic forces derived from linear three dimensional unsteady potential flow theory

11 p1731 A72-25424

Unsteady aerodynamic forces on flat plate in locally perturbed incompressible potential flow, investigating angle of attack frequency response to periodic local perturbations

11 p1573 A72-26579

Perturbation analysis of perfect gas unsteady transonic irrotational inviscid flow in two dimensional channel, presenting numerical computation of flow structure temporal change

11 p1618 A72-26635

Streamlines and fluid diffusion determination for axisymmetric irrotational and rotational flows in

ducted propellers, noting conformal mapping of arbitrarily shaped domain onto rectangle
12 p1751 A72-27168

Multiple scale asymptotic method for nonlinear theory of dispersive periodic waves with slowly varying parameters, noting equations for irrotational motion of perfect relativistic fluid
12 p1843 A72-27170

Velocity dominated singularities generalized to solutions of Einstein equations with irrotational perfect fluid sources within hydrodynamic cosmological models
12 p1870 A72-27410

Incompressible potential flow model of porous parachute canopy flow field, using Stokes stream function for axisymmetric vortex sheet in uniform steady stream
12 p1755 A72-28123

Plane potential flow stability with respect to bounded and free hollow vortices, using conformal mapping method
13 p1941 A72-28716

Plane unsteady potential isotropic gas flow equations solution interpreted as shallow water motion over horizontal bottom
13 p1893 A72-28717

Aerodynamic profiles lift coefficient determination by empirical formula based on potential flow lines obtained by conformal mapping
13 p1894 A72-29132

Analytical models for potential flow through smooth edged orifice, comparing acoustical inertance predicted and experimental values
13 p2006 A72-29770

Stream surfaces of three dimensional sub and supersonic irrotational gas flows in variable cross section channels and nozzles
13 p1895 A72-30004

Three dimensional potential flow with lift about solid body calculated by distribution of sink, source and vortex type singularities satisfying Laplace equation
16 p2342 A72-32896

Elliptic-hyperbolic relaxation algorithm for solution to three dimensional nonlinear transonic small disturbance potential equation for flow about swept wings
[AIAA PAPER 72-677] 16 p2346 A72-34063

Asymptotic character of turbulent boundary layer longitudinal velocity distribution along flat plate at low Reynolds number, using Hirsch theory for potential flow
17 p2539 A72-34908

Contribution to the study of flows with surface chemical reactions in the boundary layer
17 p2541 A72-35455

Inviscid perfect gas supersonic steady irrotational flow past wedge, investigating analytical solution validity in downstream region behind shock
17 p2544 A72-35900

Incompressible potential flow solution for axisymmetric body-duct configurations.
18 p2683 A72-36940

Vortical flow of incompressible fluid in finite region bounded by potential flow and with Bernoulli constant jump at boundary
19 p2785 A72-37552

Calculation of the plane potential flow past rotating radial blade cascades
19 p2746 A72-38547

Surface vorticity theory for axisymmetric potential flow past annular aerofoils and bodies of revolution with application to ducted propellers and cowl.
19 p2747 A72-38554

Solution of some boundary value problems in the theory of potential gas flows and weak shock wave propagation
20 p2913 A72-39404

Study of the flow of a heavy fluid with free surface from a symmetrical tank
20 p2913 A72-39417

Potential flow calculations to support two-dimensional wind tunnel tests on high-lift devices.
[ICAS PAPER 72-13] 21 p2991 A72-41138

Velocity distribution of quasi-steady and steady flow of ideal incompressible fluids with congruent streamlines, investigating conditions for vortex and irrotational flow
22 p3164 A72-41906

Plane potential flow stability with respect to small perturbation flow of bounded and free hollow vortices, using conformal mapping method
22 p3165 A72-42093

Plane unsteady potential isotropic gas flow equations solution interpreted as shallow water motion over horizontal bottom
22 p3165 A72-42094

Equations of plane potential electrohydrodynamic flow, noting jet and quasi-one dimensional flows of charged particles in curvilinear electrostatic field
22 p3210 A72-42269

Singular points in conical flow streamline patterns, considering rotational and irrotational flows
22 p3135 A72-42580

Stream surfaces of three dimensional sub and supersonic irrotational gas flows in variable cross section channels and nozzles
22 p3135 A72-42727

Calculation of potential flow about aerofoils using approximation by splines.
22 p3135 A72-42849

An improved solution of the two-dimensional jet-flapped airfoil problem.
23 p3247 A72-43329

Three dimensional supersonic flow past bodies with a smooth generatrix
23 p3248 A72-43651

Computation of the potential-theoretical flow around wing-fuselage combinations and a comparison with measurements
23 p3249 A72-44298

Steady two-dimensional viscous flow in a jet.
23 p3282 A72-44303

Resistance in potential flows with no wakes and with steady closed wake, calculating normal and tangential thrusts contributions for sphere and circular cylinder
24 p3390 A72-44986

The determination of a general relation between the aerodynamic properties of a single airfoil and those of the same airfoil arranged in an arbitrary cascade.
24 p3363 A72-45363

Some experiences with the solution of potential flow in the plane cascade on the computer.
24 p3393 A72-45365

POTENTIAL GRADIENTS

Electrode potential gradients during dimensional electrochemical treatment of Ni and Ni based alloys
08 p1175 A72-21041

Point discharge current and precipitation effect on atmospheric potential gradient vertical profile
12 p1839 A72-27501

Solar activity effects on atmospheric electricity during favorable weather conditions, discussing troposphere potential gradient and earth air current
13 p2029 A72-28622

Classical flow problem solution by fixed point approach, using quasi-Lipschitz conditions for Newtonian potential gradients
15 p2216 A72-31468

Potential drops near electrodes in a pulsed plasma accelerator
22 p3213 A72-43108

POTENTIAL PROBLEMS

U POTENTIAL THEORY

POTENTIAL THEORY

Stokes and Love integral representations for elastodynamic displacement fields in elastic solid deduced by potential theory method
01 p0138 A72-10513

Direct method for dual and triple integral equations involving inverse Mellin transforms in potential mixed boundary value problems
01 p0094 A72-11390

Micropolar elastic theory axial symmetric problems, deriving differential equations for elastic potential and half space
02 p0260 A72-12239

Curve and surface fitting with Schmidt potential functions, including polynomial and straight line fit
02 p0252 A72-12601

Rigid boundary effect on thin panel flutter speed, determining aerodynamic forces via linearized potential theory
03 p0443 A72-13402

Double forces distribution over elastic body surface from Lamé equation describing static defects, discussing Kupradse potential and sources corresponding to plane dislocations and cracks
03 p0444 A72-13501

Lifting surface linearized potential theory for unsteady aerodynamic forces on wing and horizontal tail surfaces, using computer program
03 p0308 A72-13541

Biharmonic stress and displacement potentials for two dimensional boundary problems in elasticity theory, using Galerkin method
03 p0453 A72-14207

Validity hypothesis for total creep rate potential in strain-hardenable materials, discussing carbon steel torsion and tensile tests
04 p0586 A72-15006

Nonlinear hereditary elasticity theory boundary value problem solution using complex potentials in successive approximation algorithm for stress concentration and nonlinear creep analysis
04 p0588 A72-15059

Circular arc blades two dimensional cascade performance test data for various cambers comparison with potential theory data
05 p0602 A72-16485

Potential parameters determination from collision integrals in thermodynamic properties calculation for combustion products at moderate and low temperatures
05 p0751 A72-17067

Complex potentials for nonlinear elasticity, creep and small elastoplastic deformations, applying to

stress concentration at curvilinear hole in infinite plane
05 p0742 A72-17183

Layer potentials continuity in theory of vibrations of elastic medium
06 p0894 A72-17556

Classical elasticity displacement problem solution by integral equation method based on Betti tensor counterpart of Green procedure in potential theory
07 p1026 A72-18813

Boundary value problem related to iteration equation of generalized axisymmetrical potential theory, obtaining exact solution via Jacobi polynomials and difference scheme
07 p1036 A72-20219

Elasticity and potential theory axisymmetric problems solution for sphere and spherical cavity, constructing x-analytic functions for boundary surfaces
08 p1242 A72-20908

Axisymmetric potential theory boundary value problems for iterative elliptic differential equation in rectangle and half strip
08 p1198 A72-20961

Integral relations derivation for stationary and nonstationary potential motions in cases of zero and infinite conductivity, applying to wave expansion in cylindrical waveguide
08 p1212 A72-20966

Lattice type structures as discrete elasticity problem, determining potential of thin rods connecting rigid nodes pairs from equations of motion and constitutive equations
08 p1244 A72-21302

Potential equations and singularities methods comparison for two dimensional flow field cascades and stress distribution elasticity theories
09 p1260 A72-22627

Micropolar elasticity plane problem singular solution based on stress equations and elastic potentials methods, discussing thermal stress concentration
09 p1402 A72-22743

Potential function criterion for feature selection in pattern recognition, obtaining upperbound estimate of misrecognition probability
09 p1342 A72-23419

Shock wave profile equation derivation based on minimal entropy rate variational principle for stationary irreversible processes, using local potential for Boltzmann type equation
09 p1295 A72-23473

Ion acceleration by relativistic electron-beam-formed plasma, explaining ion energy dependence on neutral gas pressure by potential well model
10 p1518 A72-23961

Velocity and magnetic field expressed by six scalar potentials from MHD equations system, noting compressible fluids flow
10 p1520 A72-24219

Generalized thermodynamic potentials and universal criteria for direction of evolution of irreversible processes from Gibbs function stability analysis
10 p1562 A72-24250

Many electron pseudopotential method for electron-atom scattering, calculating singlet s wave and p wave phase shifts
12 p1848 A72-27429

Elastodynamics three dimensional problems formulation using displacement potential functions
12 p1883 A72-27544

Harmonically oscillating rectangular wing in unsteady transonic flow, obtaining two part boundary value problem for linear potential equation
12 p1751 A72-27545

Stokes-Helmholtz decomposition role in displacement potentials derivation in elasticity
12 p1884 A72-27569

Boundary layer approach to local potential solution of diffusion equations, applying to transpiration cooled half space and heat conduction in melting solid
13 p2064 A72-28885

Vectorial differential equations in potential theory, discussing Fredholm alternative in normalized spaces, generalized harmonic vector fields, Poisson equation and Robins-Praeger problem
15 p2261 A72-31452

Diatomic molecules partition functions derivation by classical and quantum mechanical theories for simple harmonic oscillator and square-well potential
15 p2280 A72-31693

On the introduction of potential functions in linear elasticity
17 p2627 A72-34773

Local potential concept based variational method for eigenvalue problems of disturbance damping or amplification in stability analysis
17 p2583 A72-35641

Hulthen and Schwarzschild potentials in the Klein-Gordon equation.
18 p2711 A72-36515

Phase-plane solution for the electrostatic field of an ionospheric satellite.
18 p2728 A72-36950

Diffraction and potentials of multilayers
18 p2736 A72-37003

The superharmonic functions in the axiomatics of M. Brelot associated with a degenerate elliptical operator

24 p3418 A72-44825

Thermoelastic waves propagation in homogeneous isotropic medium, considering potential functions

24 p3460 A72-45598

POTENTIOMETERS [INSTRUMENTS]

Hydraulic test facility for dynamic characteristics of potentiometric pressure sensors with connecting lines of various geometries, shaping pressure pulse signal by electromagnetic valve

13 p1957 A72-29135

Single automatic potentiometer based maximum-minimum temperature control unit, noting elimination of dual temperature regulators

14 p2104 A72-30444

Book - Electromechanical system components.

20 p2890 A72-39811

POTENTIOMETERS [RESISTORS]

Low resistance thermometry with transformer coupled potentiometer circuit to obtain size reduction and ability for direct exposure to fluid

10 p1482 A72-24806

POTENTIOMETRIC ANALYSIS

Aeros satellite mass spectrometer, retarding potential analyzer and neutral gas thermograph onboard experiments, noting measurements and data transmission triggering by flight direction sensor [DGLR PAPER 71-093]

02 p0284 A72-12727

Al-Zn-Mg alloy intergranular corrosion in un-stressed condition, detecting anodic paths at grain boundaries by potentiostatic technique

04 p0535 A72-15731

POTENTIOMETRY

U POTENTIOMETRIC ANALYSIS

POWDER [PARTICLES]

NT FINES

NT METAL POWDER

NT POWDERED ALUMINUM

Thermal conductivity cell for dielectric materials powdered samples and thermal diffusivity and conductivity measurements, using line heat source principle

04 p0523 A72-15493

Composite propellant powder combustion velocities as function of pressure, discussing powder sensitivity, limiting kinetic stage changes and surface monovariant equilibrium

06 p0867 A72-17568

Nonsteady powder combustion under harmonically varying pressure

06 p0902 A72-17907

Powder combustion rate dependence on light irradiation intensity

06 p0902 A72-17908

Erosion burning in cylindrical ballistite powder N specimens under 50-80 kg/sq cm in simulated constant pressure combustion chamber with supersonic and subsonic nozzles

06 p0903 A72-18208

Porous materials fabrication from chromium carbide powders, considering compaction procedures involving sinusoidal and pulsating vibrations

07 p1017 A72-19968

Plasma spraying of high temperature resistant powder materials, investigating feed rate effect on particles adhesion and deposition layer properties

08 p1175 A72-21046

Equations derived for powder burning in semiclosed chamber from phenomenological theory of unsteady burning, solving equations for variations in critical nozzle diameter

08 p1254 A72-21658

Gas temperature variation effects on powder burning stability in rocket combustion chamber from unsteady powder burning theory

08 p1255 A72-21659

Powder materials heating and melting temperatures calculation in free turbulent nitrogen and argon plasma jets

08 p1181 A72-22098

LF self oscillation processes associated with burning powders, showing origin in thermal relaxation instability in heated condensed phase layer

09 p1411 A72-22883

High purity fine particle pigment materials preparation for spacecraft thermal control coatings, discussing hydrothermal, cryochemical and vapor phase processes

10 p1500 A72-24145

Ball milling effects on alumina and tungsten carbide powder sinterability due to particle comminution and microstrains

11 p1642 A72-26827

Thermoplastic materials casting procedures to mold high melting point metal compound powders

11 p1645 A72-26861

Slag powdery material moisture content determination by absolute pyridine adsorption method of moisture extraction

12 p1813 A72-27450

Device for comparing powders friability to ascertain quality of compacts fabricated on automatic sintering

presses, noting applications in ceramic, chemical and pharmaceutical industry

12 p1795 A72-27468

Nd laser second harmonic generation by organic crystalline powders, noting suitability of benzophenone, xanthone, benzimidazol and resorcin

12 p1823 A72-27854

Powder combustion on metal plate at constant pressure based on two-phase model of condensed system thermal decomposition

13 p0265 A72-29879

Titanium nitride powder obtained by hydrogen reduction of titanium tetrachloride in nitrogen flow heated in microwave electrodeless discharge

13 p1967 A72-30111

Chemical composition, powder particle size, porosity and heat treatment effects on sulfurized iron graphite cermets durability

13 p1984 A72-30118

Ferrite powder relative density as function of temperature, sintering time and pressure during hot pressing, noting creep activation energy and vacancy motion

14 p2107 A72-30775

Brightness matrix of a flat powdered layer with opaque particles in the single-scattering approximation

19 p2836 A72-38783

A nonacoustic wave instability of processes in a solid-fuel engine

22 p3217 A72-43182

Feeder for the supply of powder materials to spraying setups

23 p3278 A72-43293

Influence of the oxidation of finely dispersed graphite powders on their compactibility

23 p3307 A72-44018

POWDER METALLURGY

Powder metallurgy - Conference, New York, July 1970, Volume 4, Processes, Volume 5, Materials and properties

02 p0239 A72-11426

Chloride process produced tungsten powder for tungsten carbides production, discussing impurities, particle shape and size distribution, carburization behavior and applications

02 p0239 A72-11427

High energy rate compacting methods in powder metallurgy, considering use of high explosives in water or air and impulse pressing of metal powders

02 p0233 A72-11438

Al alloy powder metallurgy part production, discussing sintering procedures in nitrogen and dissociated ammonia in vacuum

02 p0233 A72-11440

Forged Inconel alloy 718 metal powder preforms for dense aircraft engine compressor rotor blades

02 p0233 A72-11441

Ni base superalloy powder with refractory oxide particle dispersion, presenting high temperature creep, stress rupture, microstructure activation energy and processing history

02 p0240 A72-11442

Powder metallurgy advantages for Ni-based superalloys, presenting thermomechanical process results

02 p0240 A72-11443

Thorium oxide dispersion strengthened Ni powder metallurgy alloys, noting thermomechanical processing effects on tensile strength

02 p0241 A72-11447

Powder metallurgy processed Mo alloy, investigating destructive and nondestructive tests, structural grain size and hardness, wedge density and metallography

02 p0241 A72-11454

Corrosion effect on mechanical properties of sintered powder iron and bronze parts, describing test procedure for corrosion resistance determination

02 p0241 A72-11459

Material characteristics effect on compaction behavior of metal powders, stressing density and pressure measurements

02 p0242 A72-11460

Press and sinter production of Ni maraging steel powder metallurgy parts

02 p0234 A72-11464

Transition metal oxides hot extrusion sintering, discussing temperature and pressure effects on compacting density

02 p0244 A72-12349

Superalloy compositions prealloyed powders strengthening by secondary gamma phase precipitation, noting high temperature strength without ductility loss after thermomechanical treatment and aging

02 p0247 A72-12856

Powder metallurgical tungsten fine wire creep behavior at 2100-3000 C, determining activation energy and stress dependence

03 p0370 A72-12996

Powdered chromium carbide-nickel alloys phosphorus addition effects on sintering temperature, shrinkage, density and hardness

03 p0372 A72-13546

Steels gas-powder facing with boron carbide, testing microhardness and wear resistance

03 p0363 A72-13547

Heat treated single-phase Pr-Co powder compacts, measuring coercivity as function of annealing or sintering temperature

[IEEE PAPER 7,3] 03 p0402 A72-13756

NDT for detecting density variation, local anomalies regions and completeness of copper-infiltrated W powder rocket nozzle inserts

03 p0364 A72-14025

Metal oxide powder surface measurement using modified Kozeny-Karman formula, considering porous space, gas kinetic slip and air permeability effects

05 p0665 A72-16087

Titanium powder metallurgy in ordnance applications, discussing hardware, weight economies and market development

06 p0822 A72-18071

Hot pressing of sintered refractory metal oxide powders of Ti, Zr, U, Nb and Cr, showing improved compacting by raising temperature

06 p0822 A72-18427

Extruded superalloy powder structural shapes preparation by filled billet technique for improved chemical and mechanical properties

07 p0994 A72-19483

Optimum exposure time for sintering in Ar flow of porous rolled product of Ti powders determined from physicomechanical properties changes

07 p0996 A72-19964

WC powder milling and sintering, investigating strain and dislocation density effects on behavior by scanning electron microscope

08 p1176 A72-21440

Powder metallurgy Ni-Cr thoria cleaning by reduction with atmosphere of hydrogen plus HCl or HBr

10 p1488 A72-24697

Metal forming techniques for gas turbine engines, considering isothermal, radial and powder metallurgy preform forgings, contoured cross and form rolling, and squeeze casting

[ASME PAPER 72-GT-58] 11 p1638 A72-25649

Russian book on powdered metals toxicity covering industrial dust, physiological effects, safety standards, electron configurations and crystalline structure

11 p1584 A72-26067

Iron base powders material requirements and forging processes, discussing powder composition, inclusions effect and preform densification

11 p1639 A72-26241

Powder metallurgy sintering process variables for dimensional control of bronze parts, discussing strength and porosity level specifications

11 p1640 A72-26242

Refractory powder metallurgy - Conference, Reutte, Austria, June 1971, Volumes 1, 2, 3 and 4

11 p1642 A72-26826

Metal powder mixing, examining friction effects and optimal particle sizes, shapes and amounts

11 p1642 A72-26828

Continuous hot pressing of high density reactive ceramic and metal powder materials in alumina die

11 p1643 A72-26832

Ni additive effects on tungsten trioxide reduction with hydrogen and W powder sinterability

11 p1643 A72-26835

Chemical composition, physical properties, microstructure and production of 1300 kg powder metallurgy forged billets

11 p1644 A72-26845

Solid state reactions in powder metallurgical production and working of Mo alloy, considering sintering process

11 p1644 A72-26846

Microstructural properties of Ni-Al powder synthetic material from transmission and photoemission electron microscopy, discussing low and high temperature strength characteristics

11 p1645 A72-26855

High melting point alloy and metal powder production by vacuum atomization, using rotary vane and electron beam melting techniques

11 p1645 A72-26860

Chemical and physical activation mechanisms of sintering metal powder compacts

11 p1645 A72-26862

High temperature materials powder metallurgy for space applications, discussing melting points

11 p1665 A72-26866

Powder metallurgy versus melting and casting of high temperature alloys, tool steels and specialty alloys

11 p1646 A72-26869

Superalloy powder metallurgy process based on inert gas atomization of molten metal to low interstitial content powders and densification by extrusion

11 p1665 A72-26870

Cermets technology applications, discussing powder metallurgy role and sintering mechanism

11 p1665 A72-26871

Electronic structure of technological processes in powder metallurgy of high temperature materials

11 p1646 A72-26872

Composite powders preparation by metals deposition from aqueous solution onto core materials by gaseous hydrogen at high temperature and pressure, noting coating application

11 p1646 A72-26875

W-Ni-Mo alloys obtained by powdered metals sintering, investigating mechanical properties, phase distribution and composition

11 p1666 A72-26876

Fracture micromechanism in liquid-phase sintered W-Fe-Ni powder composites, using scanning electron microscopy

11 p1668 A72-26942

Quenched powder metallurgy of high strength-high conductivity wrought Cu-Zr and Cu-Zr-Cr alloys, using nitrogen atomization

13 p1974 A72-28659

High temperature constant load creep tests on pure powder metallurgy W and tungsten-thoria alloy, discussing stress dependence

13 p1975 A72-28665

Iron powder specific surface and particle size effect on shrinkage during sintering

13 p1966 A72-29800

Pressed and sintered preforms of Ti and alloys for forge and extrusion operations, noting processing time reduction and smooth surface

13 p1982 A72-30120

Cobalt-base superalloys powder-metallurgical fabrication techniques and related effects on physical and mechanical properties

13 p1982 A72-30126

Welded Al alloys at temperatures above 100 C, discussing traditional and powder metallurgy and mechanical properties dependence on time, temperature and creep

14 p2116 A72-30528

Variables influencing the characteristics of plasma-sprayed coatings.

17 p2561 A72-35920

Inhomogeneity of high melting temperature elements in titanium alloys.

18 p2701 A72-36693

Fall Powder Metallurgy Conference, Detroit, Mich., October 19-21, 1971, Proceedings.

19 p2815 A72-37591

Deformation, densification and material fracture characteristics for powder preform design for hot forging

19 p2806 A72-37593

Precision forging technology for Al sintered powder metal preforms for prototype fabrication

19 p2806 A72-37594

Characterization of commercial titanium powders.

19 p2815 A72-37595

Fabrication of Hastelloy B sheet by powder metallurgy using blends of elemental powders and homogenization/deformation processing.

19 p2815 A72-37596

Flow and fracture criteria for powder forging.

19 p2815 A72-37597

Fabrication and properties of carbon-containing iron fibers and fiber sinter bodies

20 p2939 A72-39439

Powder-metallurgical production of dispersion-hardened nickel and cobalt alloys

20 p2929 A72-39454

Mg-Al powder mixtures sintering and coining, describing fabrication procedure, microstructure and mechanical properties

21 p3067 A72-40832

Strengthening of tungsten by powder metallurgical internal oxidation.

21 p3067 A72-40833

Effect of inertial loading on the compression of powdered materials by a vibration process

21 p3061 A72-41369

Solid-state reactions during the production of TZM molybdenum alloy by powder metallurgical methods

22 p3187 A72-41972

The effect of mixed milling on the sintering of WC-Co hardmetals.

22 p3188 A72-41975

Fine grained WC phase structure, physicochemical and cutting properties of Ti-Co alloy, using W powder prepared by tungsten oxide reduction in single stage muffle furnace

22 p3188 A72-42192

German monograph - Contribution to the investigation of the fatigue strength of sintered iron.

22 p3194 A72-43066

Iron-nickel-molybdenum carbonyl powders

23 p3298 A72-43276

Solid powder metallurgy tungsten alloys, determining scale factor effect on bending strength and fatigue limit

23 p3301 A72-43751

Metalceramic alloy of the B2Zn type

23 p3302 A72-44010

Boundary layer stability and turbulence observation by flow visualization using dense Al flake suspension

09 p1292 A72-22304

Magnetic-explosive welding /magneweld/ process using capacitor discharge through wire coil, noting sintered Al powder and Zircaloy 2 applications

09 p1321 A72-23638

Aluminizing process improvement by CaAl and ammonium chloride contents increase in powder

13 p1964 A72-29020

Multicomponent system combustion of Al suspensions in kerosene, determining ignition temperature as function of metal particle size and concentration

16 p2476 A72-33256

Powdered Al additions effect on burning rates of three component mixture systems based on ammonium and potassium perchlorates

19 p2847 A72-37361

Influence of pressure on the combustion process of aluminum powders

19 p2847 A72-37368

Precision forging technology for Al sintered powder metal preforms for prototype fabrication

19 p2806 A72-37594

Flow and fracture criteria for powder forging.

19 p2815 A72-37597

Mg-Al powder mixtures sintering and coining, describing fabrication procedure, microstructure and mechanical properties

21 p3067 A72-40832

Inflammation and burning of powdered aluminum in high-temperature gaseous media and in heterogeneous condensed systems

22 p3245 A72-43178

Al powder bonding during compaction by explosively driven plates, measuring shock wave amplitudes, pressure drop, layer separation and critical pressures in spall plane

22 p3184 A72-43183

POWDERED METALS

U METAL POWDER

POWER AMPLIFIERS

S band transistor power amplifier design and performance, noting application for 960 telephone channel radio relay system

01 p0038 A72-10657

Large signal nonlinear modeling and digital simulation of microwave transistor power amplifier and GaAs Gunn relaxation oscillator

01 p0041 A72-10691

Balanced negative feedback circuits for reducing nonlinear distortions in distributed gain power amplifiers

02 p0193 A72-12223

Narrow band medium power X, Ku and C band solid state amplifiers, demonstrating TWT replacement with GaAs and avalanche diodes

03 p0334 A72-14072

High power reflection-type pulsed microwave amplifier using high efficiency antiparallel avalanche diode pair connected at transmission line ends

04 p0497 A72-14714

Microstrip configuration for microwave GaAs IMPATT diode oscillators and power amplifiers

05 p0633 A72-15782

Microwave IC power amplifiers for radio relay, telemetry, phased array radar and TWT replacement

05 p0634 A72-15784

High power L-band microminiaturized hybrid type integrated transistor amplifier design and realization by computer

06 p0785 A72-18314

High power negative resistance amplifiers, calculating relationship among output, gain, gain compression and efficiency for comparison with GaAs avalanche diode amplifier experiment

07 p0958 A72-19920

Waveguide cavity Gunn microwave power amplifiers, predicting maximum small signal gain and FM and AM noise performance

07 p0958 A72-19921

Transistor power amplifier for 2.5 GHz range directional transmitters, noting cooling problems elimination

08 p1140 A72-21306

Multichannel junction gate FET /Gridistor/ for microwave power amplifier, discussing design, fabrication and performance

08 p1141 A72-21429

Solid state microwave power amplifier with unidirectional transmission line loaded by negative resistance diode series, calculating large signal characteristics

08 p1142 A72-21558

Secondary breakdown effects on hf power transistor amplifier electrical characteristics, describing operation limits

09 p1288 A72-23364

Nonlinear microwave power amplifiers with IMPATT diodes in stable and injection locked modes, predicting behavior for comparison with experiment

10 p1451 A72-24592

Power supply for magnetic suspension system, using controlled rectifier and dc power amplifier circuits

10 p1461 A72-24767

VHF and UHF radio transmitters with strip transmission lines, discussing transistor power amplifier design

10 p1441 A72-25116

Wideband push-pull transistorized power amplifier free of nonlinear distortions due to scattering inductance of load transformer

13 p1926 A72-28378

Electron beam amplifier based on fast cyclotron wave interaction with slow synchronous wave in axisymmetrical electrostatic field, discussing power efficiency increase

15 p2210 A72-32737

Ac voltage squaring with semiconductor power amplifier based on electronic servo principle and feedback circuit

16 p2370 A72-33958

Modular I-band solid-state microwave amplifier.

17 p2528 A72-34711

Comments on thermal cycles of silicon power transistors

18 p2667 A72-36794

Physical parameters and structure of microwave power transistors, noting scanning electron microscope analysis of fine structure

18 p2671 A72-37144

Dynamic behavior of nonlinear power amplifiers in stable and injection-locked modes.

19 p2773 A72-38293

High-power microwave amplifier using IMPATT diodes.

20 p2909 A72-39776

Master oscillator/power amplifier laser systems output beam divergence and far field brightness, comparing to Gaussian plane waves

23 p3296 A72-43901

POWER CONDITIONING

Power conditioning - IEEE Conference, California Institute of Technology, Pasadena, April 1971

01 p0007 A72-11051

Power conditioning requirements and tradeoff considerations for space shuttle, warning against central power conversion use on orbiter and booster vehicles

01 p0007 A72-11052

Power processing requirements for solar electric propulsion in deep space mission, noting use of electron bombardment ion thruster with hollow cathode

01 p0007 A72-11055

Vhf dc-dc conversion and regulation in low MHz range, discussing power loss reduction

01 p0007 A72-11057

Dc-dc converter input filter requirements and design for spacecraft power processing equipment

01 p0007 A72-11058

Power conditioners operating frequencies determination by series resonant circuits, noting frequency stability and reliability

01 p0008 A72-11061

Multiphase, 2 kw, high voltage, regulated, conditioned power supply for space application, discussing efficiency, weight, design and performance

01 p0008 A72-11063

One millipound colloid thruster power conditioning and control system design, presenting circuit diagrams, fault protection efficiency and high voltage transformer

01 p0009 A72-11070

ALSEP central station data subsystem, discussing power conditioning unit and electric power subsystem

04 p0508 A72-15094

Transistorized automatic feedback power level control for centimeter band reflex klystron oscillator for electron paramagnetic resonance studies

06 p0784 A72-18166

Electrostatic rf ion thruster development, including power conditioning and control units

07 p1054 A72-19600

Transcendental Si power rectifier with high current and power dissipation capacity, discussing design, fabrication and performance tests

08 p1111 A72-21413

Computerized design and weight estimation of high voltage power conditioner for communication spacecraft

08 p1112 A72-21417

Solar cells in satellite power supplies, discussing design, environment effects, reconditioning, microwave performance and testing

10 p1422 A72-24150

Power-combining methods for synchronous detuned solid state microwave oscillators with stable large signal locking characteristics, noting feasibility

10 p1449 A72-24306

ATS F ion thruster system for north-south station-keeping, discussing specific impulse, thrust vectoring, propellant system and power conditioning circuitry

11 p1707 A72-26180

Prime 30 cm ion thruster power conditioning and control system development, integration and testing

12 p1860 A72-27424

POWDERED ALUMINUM

Al powder burning in flame jets produced by ballistite powder N, using scanning spectrographic system for combustion temperatures, products and dynamics

06 p0903 A72-18209

Tactical satellite communication system and ground terminal design options for efficiency improvement, considering power sharing, priority system frequency allocation and system control concepts

12 p1785 A72-27844

Structural evaluations and dynamic testing of solar electric propulsion components, surveying power conditioning panel modal frequencies by holographic interferometry technique

[AIAA PAPER 72-442] 13 p1899 A72-28941

High voltage solar array technology, studying power conditioning control system design and array-space plasma interactions

[AIAA PAPER 72-443] 13 p1899 A72-28942

Characteristics of nonredundant auxiliary and prime propulsion power processors for electron bombardment ion thruster in communication satellites, discussing modular transistorized and SCR systems

[AIAA PAPER 72-518] 13 p2027 A72-28980

Pulsed IMPATT diode oscillators, pulse power capabilities, considering microwave circuit, dc and pulse biasing, power limitation and circuit anomalies

13 p1931 A72-29109

Solid state dc power controller design functional requirements, considering system overcurrent protection, power control by low voltage signals, power output to load status, etc

15 p2182 A72-31219

Thermionic reactor power conditioner design for nuclear electric propulsion.

17 p2495 A72-34582

A study of the heat flow and thermal instabilities in high power hybrid integrated circuits.

17 p2527 A72-34678

Voltage-conversion for incore-thermionic-reactors.

18 p2645 A72-36182

Multimesa versus annular construction for high average power in semiconductor devices.

18 p2666 A72-36455

Power regulation in the Symphonie satellite

18 p2648 A72-36682

The effect of junction temperature on the output power of a silicon IMPATT diode.

19 p2773 A72-38145

The relative merits of thyristors and power transistors for fast power-switching applications.

22 p3159 A72-42306

Metal-oxide varistor - A new way to suppress transients.

23 p3272 A72-44100

POWER CONVERSION

U ELECTRIC GENERATORS

POWER DENSITY

U FLUX DENSITY

POWER EFFICIENCY

P-I-N diodes power handling characteristics in high power solid state TR switches

01 p0042 A72-10708

Thermocouple efficiency with respect to Thomson effect and electric resistivity temperature dependence

03 p0360 A72-13651

EMC improvement with least sacrifice of power efficiency in designing dc/dc converters and switching voltage regulators

03 p0312 A72-14049

Nuclear Brayton space power systems, discussing efficiency, isotope decay and reactor design

04 p0546 A72-14423

Antenna arrays performance optimization, emphasizing directivity and signal to noise power ratio

04 p0499 A72-15301

Gyroresonance devices efficiency increase, discussing magnetostatic field distribution optimization in interaction space

04 p0502 A72-15575

Ten-stage electrostatic depressed collector designed with analog computer for improving klystron power conversion efficiency

05 p0637 A72-16365

Vapor-grown GaAs transfer electron microwave oscillator, discussing design, fabrication and CW power conversion efficiency

05 p0637 A72-16366

Microwave antenna efficiency measurement by integrated isotropic levels comparison, featuring elimination of error due to specular ground reflections

05 p0637 A72-16421

Harmonic power extraction from series-stacked high efficiency avalanche diodes at superhigh frequencies on simple microstrip circuits

06 p0788 A72-18468

GaAs IMPATT diodes performance improvement, describing fabrication methods to achieve 6.7 watts output at 15 percent efficiency

06 p0789 A72-18474

High power efficiency CW Gunn devices design and fabrication, discussing GaAs preparation techniques and device physics

06 p0789 A72-18478

Spacecraft power system with Maximum Power Point Tracker, discussing German Aeros satellite and orbit simulation program

07 p0914 A72-19090

High power negative resistance amplifiers, calculating relationship among output, gain, gain compression and efficiency for comparison with GaAs avalanche diode amplifier experiment

07 p0958 A72-19920

Gunn diode microwave oscillator thermal resistance reduction for increased output power and efficiency

07 p0958 A72-20685

He-Ne laser resonator misalignment effect on output power, determining mirror arrangement precision tolerance for set fluctuation levels

08 p1181 A72-21163

Atomic, ion and electron transition pulsed gas discharge lasers, considering power efficiency factors, vacuum UV region and gas density

08 p1182 A72-21644

Broadband electrostatically focused klystron for airborne radar application, discussing focusing cell design, amplification and efficiency

10 p1446 A72-23821

Coupled line microstrip circuit for high power and efficiency L and S band TRAPATT diode oscillators

10 p1450 A72-24307

GaAs abrupt junction IMPATT diode large signal operation analysis, noting oscillation efficiency HF fall-off characteristics

10 p1450 A72-24557

Computer simulation for TRAPATT circuit response to periodic current impulse, noting avalanche diode microwave oscillation efficiency

10 p1458 A72-24935

Hydrothermodynamic foundations of hydrofoil engines employing gas-water mixtures and gas turbine generators, analyzing thrust coefficient and power efficiency

10 p1528 A72-25128

Low voltage transversely excited gas transport CW carbon dioxide laser, discussing construction and power output, gain and efficiency

11 p1646 A72-25304

Axial flow compressor and turbine loss coefficients, correlating blade rows geometric and aerodynamic variables effects

[ASME PAPER 72-GT-18] 11 p1703 A72-25617

Four stage gas turbine, measuring blade surface roughness and profile changes effects on flow characteristics and efficiency

[ASME PAPER 72-GT-34] 11 p1704 A72-25630

High efficiency CW performance of InP transferred electron microwave oscillator with anomalous I-V characteristics temperature dependence

11 p1604 A72-25750

Hydrogen resistojets design and testing with Re heat exchangers, noting appropriate power efficiency and exhaust velocity for synchronous communication satellites orbital transfer

[AIAA PAPER 72-449] 11 p1708 A72-26186

Semiconductor injection laser with distributed radiative loss, calculating radiation line shape and width and quantum efficiency

11 p1648 A72-26329

Vortex discharge in Ar as optical pumping source for ionic crystal CW lasers, comparing efficiency with YAG-Nd crystal pumping

11 p1648 A72-26331

Epitaxial InP diode for high efficiency circuit controlled microwave oscillator, discussing solution growth technique, layers electrical properties and I-V performance

12 p1854 A72-27162

K band Read avalanche diodes fabricated by epitaxial deposition and diffusion processes, measuring capacitance-voltage characteristics and oscillator power efficiency

12 p1790 A72-27441

Light power coupling efficiency from GaAs injection laser into single- and multimode fibers

12 p1820 A72-27507

Laser with unstable telescopic resonator and large radiation loss, calculating energy characteristics and power efficiency

12 p1821 A72-27590

High order optical harmonic generation and many-quantum processes efficiency in multimode laser radiation field

12 p1821 A72-27593

Optical interaction of inhomogeneously excited semiconductor injection laser diodes, noting power efficiency increase with inhomogeneity

12 p1822 A72-27606

C and X band CW GaAs Schottky barrier IMPATT oscillators with nichrome as barrier metal, noting high power efficiency and low noise performance

12 p1793 A72-27966

Silicon solar cells IR reflectance improvement by reflecting back electrode, obtaining 10 percent efficiency increase

12 p1758 A72-28032

Simulation model test for effects of cooling air exhaust into gas flow area on turbine blading efficiency, obtaining dimensionless expression for experimental data generalization

12 p1862 A72-28148

Picosecond pulse efficient second harmonic generation by crystals inside high power dye mode locked Nd-glass laser folded cavity

12 p1826 A72-28220

MHD power generators analytical modeling by digital technique for prediction of performance and efficiency as function of size and operating conditions

[AD-741173] 13 p1900 A72-29355

Thermal-to-electric power conversion efficiency of nonequilibrium MHD generator with Cs seeded noble gases, considering electrode configuration and gas dynamic effects

13 p1900 A72-29356

Conditions derived for reactive two-terminal-pair matching transformer networks operation at maximum power transfer efficiency

14 p2087 A72-30334

Efficiency of pulsed tubular pumping lamps made of quartz glass investigated by active element luminescence measurement, noting dependence on current density

15 p2246 A72-31425

High efficiency X band pulse operation of transferred electron oscillator in hybrid mode, noting high material quality and optimum impedance match

15 p2206 A72-31548

High power CW Nd-YAG laser efficiency improvement by optical pump wavelength, power coupling and balance factors, noting krypton arc lamp contribution

15 p2247 A72-32029

Room temperature GaAlAs single-heterojunction diode lasers structure, fabrication, threshold current density and quantum efficiency dependence on wavelength and temperature

15 p2247 A72-32032

Avalanche photodiode with n-p-pi-p double diffused reach-through structure for visible and near-IR regions, noting high efficiency, low noise and gain stability

15 p2248 A72-32036

Input match conditions for broadband mixer conversion loss minimization, comparing optimization procedures

15 p2208 A72-32392

Gunn diode elements design, operation, performance, efficiency, heat dissipation, lifetime and applications as microwave oscillators

15 p2208 A72-32500

Electron beam amplifier based on fast cyclotron wave interaction with slow synchronous wave in axisymmetrical electrostatic field, discussing power efficiency increase

15 p2210 A72-32737

High efficiency and power S-band pulsed oscillator using avalanche diode and microstrip circuit

16 p2369 A72-33759

Si p-n junction solar cell fill factor for electric power available to load, noting discrepancy between calculated and measured values due to recombination

17 p2494 A72-34264

He-Ne laser resonator misalignment effect on output power, determining mirror arrangement precision tolerance for set fluctuation levels

17 p2562 A72-34454

Avalanche diode oscillators.

17 p2526 A72-34563

Output performance of a thermionic converter with an oriented tungsten /110/ emitter and a polycrystalline tungsten collector.

17 p2496 A72-34604

Laser beam power transmission to lunar bases or spacecraft from nuclear fueled satellite power station, discussing achievable ranges and efficiencies

17 p2611 A72-35328

Military jet engines centrifugal fuel pumps power requirements for throttled operation, noting pressure stability improvement at low flow rates

18 p2694 A72-36041

Hydraulic pump design for efficiency increase, weight reduction and service life and reliability improvement

18 p2694 A72-36045

Si solar cell design for high power/weight ratio and extreme environmental operating conditions, describing technological innovations for reliability and efficiency enhancement

19 p2754 A72-37780

A solid-state transponder source using high-efficiency silicon avalanche oscillators.

19 p2774 A72-38400

Approximate calculation of the maximum efficiency of an O-type oscillator with a resonance delay system in the presence of losses

19 p2774 A72-38412

Influence of gas pressure in arc lamps on the pumping efficiency of CW garnet lasers.

20 p2933 A72-39513

HF chemical lasers pumped by atomic fluorine with molecular hydrogen, calculating intensity and efficiency by reaction kinetics analysis for comparison with computer solutions

21 p3062 A72-40617

- Atomic, ion and electron transition pulsed gas discharge lasers, considering power efficiency factors, vacuum UV region and gas density
21 p3064 A72-41301
- Experimental procedure for determining the strength losses in the individual elements of wave-type toothed gears
22 p3182 A72-41866
- Push-pull transistor amplifier fed from two different voltage power supplies, noting power efficiency improvement
22 p3158 A72-42115
- Determination of the efficiency and range of application of turbines with velocity stages with the aid of the complex power coefficient
23 p3325 A72-43666
- X-band silicon double-drift IMPATT diodes using multiple epitaxy.
23 p3273 A72-44334
- Pulsed carbon dioxide laser medium composition, pressure and electrical parameters effects on output power, energy and efficiency from mathematical model solution of kinetic equations
24 p3409 A72-44966
- Metal vapor plasma as working medium in MHD generator, discussing hydrodynamic relations, power efficiency and thermodynamic cycle
24 p3428 A72-45169
- Large-signal analysis of efficiency and nonlinear phase distortion in a phase velocity tapered traveling-wave tube.
24 p3385 A72-45283
- Investigation of a partial admission double-vane-ring stage with bypass of the second ring
24 p3364 A72-45621
- ## POWER GAIN
- Transistorized pulse amplifier stage, showing gain as function of resistor parameters in collector circuit.
01 p0035 A72-10200
- Doping profile effects on reflection-type IMPATT diode microwave amplifiers, presenting power-gain vs frequency curves
01 p0037 A72-10643
- Synchronized multiple microwave oscillators power and noise characteristics at microwave and millimeter frequencies, discussing magic T configuration
01 p0037 A72-10648
- CW power of single cavity multiple IMPATT diode oscillator at 9.1 GHz, comparing with moding of multiple device oscillators
01 p0038 A72-10649
- Short backfire antenna gain increase, considering construction case, reflector arrangement and circular polarization
01 p0040 A72-10684
- Moderate gain superdirective antenna arrays design based on backfire principle, using parasitic elements
01 p0040 A72-10685
- Static I-V characteristics and gain properties of lateral p-n-p transistors, using multijunction analysis
02 p0189 A72-11522
- Dual gate GaAs microwave FET, measuring second gate voltage effects on power gain and noise
02 p0191 A72-11893
- TWT small parameters measurement for gain calculation, using equivalent transmission line model
02 p0193 A72-12229
- Center fed full wave dipole antenna with feed points displaced transverse to dipole axis, considering radiation patterns, electrical properties and power gain
02 p0177 A72-12325
- Saturation effect on power gain-bandwidth product of carbon dioxide regenerative ring laser amplifiers operating below threshold
03 p0366 A72-12964
- Spectroscopic characteristics of continuous wave neutral argon laser using helium and chlorine for power enhancement
03 p0367 A72-13432
- Superradiative properties of high gain flashlamp-pumped dye laser amplifier, determining small signal amplification as function of pumping power and frequency
03 p0369 A72-14393
- Active loop-dipole antennas with height reduction properties at resonance, deriving input impedance power gain and radiation patterns
04 p0502 A72-15519
- Frequency response of passive dipole antennas fed by transistor circuit, investigating power gain, bandwidth and voltage SWR
04 p0503 A72-15670
- Electrical properties of unbalanced center-fed non-planar dipole antenna, discussing radiation patterns and resistance, power gain, aperture and efficiency
04 p0503 A72-15674
- N-channel Si MOS microwave transistor, discussing fabrication, design, power gain, stability, noise figure, equivalent circuit and applications
05 p0636 A72-16361
- Low cost automated digitized measurement for microwave antenna feed power gain and relative phase, using computer facilities
05 p0637 A72-16420
- Optimal hf triode oscillation tripler with allowance for power limitation by thermal losses on plate and grid electrodes
05 p0638 A72-17184
- Four uhf antennas buried beneath refractory concrete, discussing design, fabrication and power gain and azimuthal pattern measurements
06 p0771 A72-17345
- Electronically scanned steerable antenna array design with interelement coupling, considering maximum gain and radiation pattern control
06 p0773 A72-17497
- Yagi antenna radiation pattern parameters optimization for maximum directional gain, minimum sidelobe and optimal slope curvature
07 p0952 A72-18852
- Statistical characteristics of antenna gain threshold as function of link trajectory during radiation pattern shift with respect to fixed orientation
07 p0953 A72-19006
- Frequency and power characteristics of transistorized generators of harmonic oscillations
07 p0956 A72-19569
- Cylindrical antenna radiation resistance and total radiated power in weakly ionized plasma, considering electron collisional effects
07 p0944 A72-19592
- Circular semiinfinite dielectric rod antenna, determining near- and far-zone fields, gain and beamwidth under excitation by HE/sub 11/hybrid mode
07 p0956 A72-19782
- K and Ka bands standard electromagnetic horn gain measurement and error analysis at different wavelengths by two-antenna method
07 p0957 A72-19784
- Balun-fed open sleeve dipole in front of metallic reflector for 225-400 MHz band operation, investigating radiation pattern and gain
07 p0957 A72-19794
- Circular and rectangular waveguide excited dielectric spheres as antenna feed, noting gain and polarization linearity
07 p0957 A72-19796
- Waveguide cavity Gunn microwave power amplifiers, predicting maximum small signal gain and FM and AM noise performance
07 p0958 A72-19921
- Gain saturation measurements in carbon dioxide TEA pulsed amplifiers at 330 torr
07 p1009 A72-20569
- Hf and shf power transistor gain, efficiency and electrical characteristics for wideband linear amplifiers
08 p1139 A72-21051
- Gain function for planar phased array far field pattern, deriving calculation method for excitation pattern for prescribed radiated beam behavior
08 p1132 A72-21328
- Optimal output power of avalanche transit time diode oscillator in millimeter band as function of electric field and diode geometry
08 p1141 A72-21378
- Pulse duration reduction with power gain during second harmonic generation by nonlinear crystal in Q switched buildup resonator
08 p1183 A72-21729
- Small signal microwave transistors design with arsenic and phosphorus diffused emitters, comparing performance in terms of power gain-bandwidth product, maximum frequency and noise figure
08 p1142 A72-21743
- Nd smooth pulsed laser action with narrow spectral line and emission amplification from Nd doped phosphate and silicate glass rods
08 p1183 A72-22027
- Magnetic field effect on gain saturation in CW Ar laser associated with Zeeman splitting
08 p1184 A72-22036
- Broadband electrostatically focused klystron for airborne radar application, discussing focusing cell design, amplification and efficiency
10 p1446 A72-23821
- Supercritical CW GaAs transferred electron broadband reflection amplifier power gain and noise figure at 34 GHz
10 p1449 A72-24301
- CW circuit stabilized InP microwave reflection amplifiers in Q band, determining power gain and noise figure
10 p1450 A72-24308
- Molecular diffusion laser gain determination from interaction kinetics between diatomic and cold working gases, examining annihilation processes
10 p1491 A72-24360
- Carbon dioxide laser output power enhancement methods, discussing gas transport, atmospheric pressure and gas dynamic lasers
10 p1492 A72-24849
- Matched acoustic generator for sweep frequency testing of power gain of fluoric amplifiers [ASME PAPER 71-WA/FLCS-2]
10 p1423 A72-25051
- Time resolved gain in water and water-gas mixtures as function of composition and excitation current, considering relaxation rate in pulsed water vapor laser
11 p1691 A72-25302
- Low voltage transversely excited gas transport CW carbon dioxide laser, discussing construction and power output, gain and efficiency
11 p1646 A72-25304
- Fluidic proportional and digital amplifiers environmental effects on sensitivity of gain, noise and null shift based on dependence on Reynolds number [ASME PAPER 72-GT-84]
11 p1577 A72-25660
- Expected value of two dimensional Gaussian random array gain, assuming two dimensional isotropic noise field of single frequency
11 p1604 A72-26040
- Finite and infinite number element phased array antennas, deriving active impedance, element pattern and power gain
11 p1593 A72-26096
- Transversely excited pulsed carbon dioxide laser, measuring spatial resolution of gain
11 p1647 A72-26323
- IC lateral p-n-p multijunction transistor frequency characteristics analysis, noting parasitic effects, cutoff frequencies and power gain
12 p1788 A72-27311
- TWT amplifiers electronic reflections and gain ripple
12 p1790 A72-27435
- Nd-glass amplifier gain saturation by 1.06 micron light pulses determined by two laser states lifetimes and degeneracies and thermalization rates
12 p1792 A72-27752
- Carbon monoxide laser output power variation as function of oxygen tension
12 p1823 A72-27755
- Laser resonator transverse and longitudinal mode selection techniques, considering single frequency stabilization, gain saturation theory and applications
12 p1826 A72-27964
- TEA pulsed carbon dioxide laser with continuous shaped electrodes, investigating hydrogen addition effects on power output and gain
12 p1827 A72-28224
- Nonequilibrium carrier distribution in drift junction transistor, considering base region hindering field effect on transit time, current gain cut-off and frequency response
13 p1926 A72-28371
- Spatially resolved gain measurements in carbon dioxide laser amplifier, considering gas mixture, flow rate, temperature, pressure and current effects
13 p1967 A72-28448
- Large signal four-pole parameters and optimum conditions determination for RF high gain amplifiers with class C operated transistors
13 p1921 A72-29344
- Carbon dioxide laser vibrational-rotational band small signal gain factor dependence on time elapsing after breakdown of equilibrium distribution
13 p2008 A72-29503
- CW tunable semiconductor laser measurement of CO laser amplifier gain line shape for several vibration-rotation lines
15 p2245 A72-31382
- Transistorized pulse amplifier stage, showing gain as function of resistor parameters in collector circuit.
15 p2206 A72-31624
- Log periodic dipole antenna input impedance and gain characteristics derivation via periodically loaded line theory and Poynting vector method, discussing separation angle effect
15 p2208 A72-32473
- GaAs laser properties determination by gallium arsenide-aluminum gallium arsenide double heterostructure junction diode laser, noting gain and loss at room temperature
15 p2250 A72-32519
- Transversely excited pulsed carbon dioxide laser with and without hydrogen addition, observing gain spatial and temporal dependence
15 p2251 A72-32529
- Optically pumped pulsed hydrogen fluoride gas laser, observing anisotropic ultrahigh gain emission in rotational transitions
15 p2251 A72-32531
- Electromagnetic gain mechanisms with required energy supplied by static currents and magnetic fields in homogeneous plasmas
16 p2434 A72-32853
- Phase and gain response of wideband coaxial X band microwave avalanche diode amplifiers
16 p2368 A72-33073
- Active medium spontaneous radiation level effect on traveling wave amplifier gain factor, supporting theoretical results by experiments with superluminescent Ne-He active medium
16 p2400 A72-33277
- Effect of nozzle throat radius of curvature on gasdynamic laser gain.
17 p2561 A72-34210
- Phase optimization of antenna array gain with constrained amplitude excitation.
17 p2513 A72-34355

The fabrication and evaluation of a micropower transistor and hybrid RF amplifier.

17 p2528 A72-34688

Molecular diffusion laser gain determination from interaction kinetics between diatomic and cold working gases, examining annihilation processes

17 p2563 A72-34959

Gain and relaxation studies in transversely excited HF lasers.

17 p2564 A72-35344

Multicomponent structure of Nd-glass laser radiation, observing active medium gain band portions interrelationships in free running and stimulated emission operation modes

17 p2564 A72-35507

Mixing process at the emitter-base junction of a high-frequency transistor.

18 p2667 A72-36948

18 GHz paramps with both liquid helium and room temperature operations and with triple-tuned gain characteristics.

19 p2770 A72-37254

Gain and visualization of the modes of a thermally stabilized HCN laser.

19 p2810 A72-37455

Yagi-Uda helical antenna array with moderate gain and compact mechanical design, determining electrical characteristics

19 p2773 A72-37941

Transverse mode selection in injection lasers with widely spaced heterojunctions.

19 p2812 A72-38595

High power microwave nanosecond pulse generator with waveguide standing wave resonator, noting power gain and pulse shape

19 p2776 A72-38672

The effect of cross relaxation on the behavior of gas laser oscillators.

19 p2813 A72-38691

Calculations of gain and power output for a gas-dynamic laser.

19 p2813 A72-38693

Gain averages as criteria for antenna EMC-performance.

20 p2902 A72-39001

Metal-insulator-semiconductor-insulator-metal structure light pulse amplification investigating power gain and photocurrent dependences on applied voltage and applicability as radiation detector

20 p2960 A72-39517

Amplification of mode-locked trains with a liquid laser amplifier, Nd³⁺/POCl₃:ZrCl₄.

20 p2934 A72-39642

High-power microwave amplifier using IMPATT diodes.

20 p2909 A72-39776

Gain of arrays of dipoles with a ground plane.

21 p3027 A72-40364

Constrained optimization of the gain of an array of thin wire antennas.

21 p3027 A72-40374

Reflector optimization of backfire antennas with the aid of the theory of the Fresnel zones

21 p3031 A72-40541

Diagram and gain measurements regarding antennas conducted with a helicopter for the range from 0.5 to 800 MHz

21 p3031 A72-40545

Dielectric slab surrounding medium gain effects on bound modes amplification via estimation of evanescent surface wave interactions in optical waveguide by perturbation theory

21 p3062 A72-40605

Certain features of the use of controllable-gain transistors

21 p3033 A72-40944

Frequency and power characteristics of transistorized generators of harmonic oscillations

22 p3158 A72-42087

Absorption coefficient and gain of a GaAs injection laser

22 p3184 A72-42104

Gain measurements of matrix-type TEA CO₂ laser.

23 p3296 A72-44072

A wide-band Gunn-effect CW waveguide amplifier.

23 p3272 A72-44193

Effect of capacitance on gain in a transversely pulsed CO₂ discharge.

23 p3298 A72-44534

Gain and line width in stimulated Brillouin scattering in gases.

24 p3412 A72-45616

POWER GENERATORS

U ELECTRIC GENERATORS

POWER LIMITED SPACECRAFT

Optimal dynamic system design for maneuvers with complete statistical information applied to limited power space flight

05 p0641 A72-16313

Optimal dynamic system design for maneuvers with complete statistical information applied to limited power space flight

11 p1610 A72-25796

Space communications period forecasting algorithm for limited power ground based transmitters and spacecraft in earth orbit

11 p1598 A72-26735

POWER LIMITERS

Semiconductor diodes for microwave power control

21 p3033 A72-40939

Mathematical description and calculation of the steady-state regime of a microwave power stabilizer with a semiconductor attenuator

23 p3270 A72-43766

POWER PLANTS

Satellite solar power stations, considering energy conversion, microwave generators and beam transfer to earth

02 p0155 A72-11770

Soviet wind tunnel for power plant-environment interactions studies, discussing working sections velocity distributions calibration

13 p1939 A72-29644

Russian papers on cooled high temperature gas turbines covering engine theory and design, power plants development, heat transfer and air cooling systems

13 p2029 A72-29925

Russian book - Optimization of thermal circuits of complex gas-turbine power plants

19 p2848 A72-37450

POWER REACTORS

Split-core heat pipe reactor for out-of-core thermionic power systems, using center gap for fuel reactivity control

04 p0546 A72-14425

Angular quadrature effects on two dimensional space power reactor radiation shield calculation for manned space station application

04 p0546 A72-14426

POWER SERIES

NT TAYLOR SERIES

Solution of N planets equations of motion around sun with recurrent power series in time

01 p0123 A72-10014

Jacobian matrix partial derivatives for orbital motion representation by time step power series

06 p0877 A72-17651

Convergent power series solution in powers of time for unsteady viscous flow near stagnation after impulsive motion of bluff body from vorticity distribution viewpoint

06 p0757 A72-18135

Power series method with Cauchy formula for non-linear partial differential equations solution in unsteady periodic temperature oscillations

06 p0905 A72-18727

Algorithm for asymptotic power series for Poisson process residence time function generation in band with delaying screen

08 p1198 A72-20998

Ordinary linear differential equation boundary value problem solution in form of asymptotic series in powers of small parameter

08 p1199 A72-21462

Sundman power series convergence enhancement in three body problem by Poincare transformation

09 p1350 A72-22482

Power series solutions to transition and matrix covariance differential equations, obtaining truncation error bounds and polynomial approximations

09 p1341 A72-23093

Pade table for formal power series with notation for extension to Laurent series, relating algebraic theory to bigradient determinants and numerical analysis algorithms

11 p1676 A72-25501

Square matrix inverse computation by convergent power series method

11 p1678 A72-26368

Wall-impedance waveguide propagation constant determination from Rayleigh-Schrodinger power expansion of perturbed eigenvalues

15 p2194 A72-31549

Independent variable transformations for stepwise solution of differential equations of motion power series expansions, considering convergence radius

17 p2609 A72-35105

The linearized solutions as applied to the half-jet mixing.

18 p2683 A72-36928

Numerical integration method with recurrent power series for motion and variational equations of elliptic restricted three body problem

19 p2862 A72-38019

Solution of nonlinear integro-differential Volterra equations and their systems with the aid of power series

19 p2825 A72-38196

Asymptotic series solution of optimal systems with small time-delay.

19 p2826 A72-38268

Finite difference calculus development of method to express thermodynamic limit of statistical-mechanical average as power series in number density, noting advantages and applicability

21 p3087 A72-40562

Investigation of the convergence region boundary in a power series of functions of two complex variables

21 p3075 A72-41090

A method for solving Cauchy problems for systems of differential equations with rational coefficients

21 p3075 A72-41093

Infinite rectangular elastic bar surface mass distribution effects on harmonic wave propagation modes, obtaining approximate solution by expanding displacement as power series

23 p3352 A72-44123

A power-law model for the multiple-integral theory of non-linear viscoelasticity.

24 p3460 A72-45696

POWER SPECTRA

Near pressure field within subsonic circular turbulent cold jet potential cone, noting peak in power spectra

02 p0150 A72-11974

Periodicities from power spectrum analysis of light curve of RR Tauri variable

02 p0281 A72-12302

Power spectrum analysis of multilevel digital signals phased modulated by arbitrary pulse shapes, giving examples for rectangular and raised-cosine pulses

02 p0183 A72-12797

Ionospheric small scale electron density irregularity structure from power spectral analysis of radio source scintillation observations

03 p0345 A72-12985

Pulsars CP 0329, 0950, 1133 and 1919 pulse height fluctuations at 408 MHz, showing period features in power spectrum with integrated pulse amplitudes

04 p0581 A72-15512

Power spectra of ionospheric electron content fluctuations from 6 year continuous records, noting gravity wave and seasonal daily variations

05 p0655 A72-16066

Interplanetary media plasma density fluctuations and power law spectra effects on radio wave scintillation

05 p0695 A72-16068

Solar self oscillation interference from magnetographic observation, noting power concentration in space and frequency

05 p0718 A72-16502

Mercury radar scattering properties, producing Fourier power spectrum from echo signals

06 p0880 A72-17864

Pattern recognition through atmospheric turbulence by reflected coherent light power spectrum recording technique, using Wiener-Khinchin theorem

07 p0982 A72-19054

Spontaneous emission from driven Doppler broadened gas of two level atoms radiating into free space, predicting power spectrum

07 p0940 A72-19194

X ray power density spectrum observation of pulsars, detecting Crab Nebulae pulsar radiation

07 p1080 A72-20051

Earth and interplanetary magnetic fields spectral power density characteristics at 0.0001-1 Hz

08 p1153 A72-20718

Stationary statistical model for microwave oscillator flicker frequency noise, leading to power spectral density and time domain frequency instability

08 p1141 A72-21431

Aperture filtering effects on amplitude scintillation power spectra of paraboloid radio telescope over millimeter wave propagation path

08 p1136 A72-21982

Microwave induced dc voltages across unbiased Josephson tunnel junctions, showing power spectra dependence on magnetic field

09 p1367 A72-22458

Fresnel diffraction integrals for irradiance and power distribution calculations of Gaussian beams focused through annular apertures

09 p1352 A72-23334

Nonlinear longitudinal aerodynamic characteristics effect on rigid aircraft response to normal acceleration due to atmospheric turbulence, using power spectral technique

09 p1263 A72-23461

Time dependent power spectral density function for first passage probabilities in nonstationary random processes in civil engineering involving earthquakes and wind

10 p1514 A72-25188

Power spectral density function parameters with random vibration applications, considering response spectra of multidegree of freedom linear systems

10 p1560 A72-25189

Auditory sensation overall loudness prediction for steady broad-band noise from summation of weighted intensities of power spectrum sub-bands

11 p1686 A72-25800

Continuous He-Ne laser radiation power interferometry using Michelson interferometer with frequency doubler

12 p1819 A72-27051

Random vibration of two multimodal mechanical systems with point coupling, obtaining power flow spectral density by statistical energy analysis

13 p2005 A72-29563

Solar photospheric fluctuations, applying fast Fourier transform to power coherence and phase spectra calculations 13 p2049 A72-29928

Nonlinear resonating correlator with orthogonal filters, considering cut-off frequency of ergodic random process with constant power spectral density 14 p2090 A72-31125

Filtering and hard-limiting effects on digital FM signals power spectra, using Postl direct method 15 p2194 A72-31543

Acoustic mode propagation and interaction in hard walled cylindrical ducts, determining pressure and power spectral densities from pressure cross spectrum measurements 15 p2277 A72-32018

Electron density fluctuation measurements in hypervelocity projectile hypersonic turbulent wakes, showing power spectra 15 p2242 A72-32584

Solar photospheric resonance oscillation power spectrum observation, noting statistical significance 15 p2317 A72-32777

Power spectrum of light scattered from surface waves thermally excited on carbon dioxide liquid-vapor interface near critical point 16 p2423 A72-32948

Radio source power spectra modulation dependence on distance and thickness of solar wind scattering region and on wind velocity component multiplicity 16 p2451 A72-33034

Electromagnetic radiation frequency spectrum and mean power from accelerated magnetic dipoles in circular and Keplerian orbits, noting implications for pulsars 16 p2453 A72-33285

Quasars and emission line objects red shift distribution using power spectrum analysis method 16 p2457 A72-33625

Charged particle energy dissipation in cold collisional plasma, discussing collisions effect on power spectrum 16 p2436 A72-33651

Satellite measurement of ground-based CW Ar laser source scintillation, deriving log amplitude variance, probability distribution and power spectral density from telemetered data 17 p2513 A72-34289

Spectral analyses of solar photospheric fluctuations. II. 17 p2608 A72-35081

Correlation functions and reconstruction error for quantized Gaussian signals transmitted over discrete memoryless channels. 17 p2516 A72-35333

Image autocorrelation function models and power spectra, obtaining probability distribution, variance and correlation coefficients of image orthogonal transformations 17 p2518 A72-35672

Sonic jet noise pressure source model for radiated sound power and jet pressure frequency spectra ratio derivation with application to noise suppression 18 p2680 A72-36414

Study of the solar wind using the power spectrum of interplanetary scintillation of radio sources. 18 p2722 A72-36730

Earth and interplanetary magnetic fields spectral power density characteristics at 0.0001-1 Hz, noting ambiguities due to variable investigation conditions 19 p2791 A72-38346

Harmonic mode locking of the Nd:YAG laser. 19 p2813 A72-38688

Photometric and power spectrum observation of peculiar blue variable star, showing low amplitude high frequency luminosity oscillations, hydrogen deficiency and degeneracy 20 p2966 A72-38921

Multimode dielectric waveguide with random coupling, discussing pulse dispersion improvement and loss penalty from power spectrum derivation 20 p2901 A72-38923

Spectral characteristics of a single-frequency argon laser with an absorbing film. 20 p2932 A72-39509

Spectra of a frequency-shift-keyed signal amplitude-modulated by a sinusoidal wave. 20 p2904 A72-39771

Techniques for power spectrum moment estimation. 21 p3021 A72-40911

Solar photospheric fluctuations measured from time sequence of Sacramento Peak Observatory spectrograms, using power, coherence and phase spectra computed by fast Fourier transform 22 p3221 A72-42029

Radar auroral echo VHF power spectrum analysis of ionospheric irregularities, using range-time-intensity film strips 22 p3171 A72-42415

Aircraft structural design loads definition by mission analysis criteria, taking into account gust loads via power spectral density method 22 p3138 A72-42828

Light beam modulated by uniformly spaced circular apertures, calculating Fourier power spectrum for

homogeneous and bivariate normal intensity distributions 23 p3289 A72-43900

The EAS power spectrum at sea level for N = 10 million to 1 billion particles 23 p3330 A72-44418

Saturn systems holddown acoustic efficiency and normalized acoustic power spectrum. 24 p3433 A72-44681

POWER SUPPLIES

Series inverter silicon controlled rectifier 2800 watt dc power supply, noting high efficiency, low weight and stable voltage regulation 01 p0008 A72-11064

Aircraft hybrid electrical power systems, describing variable frequency generation and high voltage dc distribution 01 p0009 A72-11068

Optimum power allocation in design of phase-coherent receiver having bandpass limiter, extending technique from single channel to two channel system 02 p0174 A72-12136

Concorde aircraft electrical power systems design, noting dc and emergency supplies and installation 03 p0311 A72-12910

Temperature gradients and dynamics of transient heating and cooling processes in metallic thermistors connected in series to power supplies 08 p1252 A72-21307

Overall characteristics of optimal quasi-steady plasma thruster system, discussing mass, burning time and thrust variations as function of power supply and pulse duration 11 p1708 A72-26192

[AIAA PAPER 72-456] Optimized 100 We multicell thermionic power supply design with high reliability, noting isomite converter performance characteristics 17 p2495 A72-34583

Dc power supply for military electronics applications, describing circuit design for well regulated and filtered output dc voltage from various ac or dc sources 17 p2497 A72-34708

Airborne equipment electric power supply standards to provide characteristics limits for compatibility with ground support systems [SAE AS 1212] 18 p2648 A72-36535

German monograph - Investigations concerning a new frequency changer with 'forced' commutation for supplying power to one- or multiple phase consumers 19 p2753 A72-37482

Realisation of a high-efficiency electrodischarge-machining power supply. 19 p2807 A72-37846

A digital computer simulation model for an SCR dc to dc voltage converter. 19 p2754 A72-38267

TV-radio satellite receiver equipment, considering power requirements, antenna, energy supply and placing into 24-hour orbit 23 p3262 A72-43300

System design of a near-self-supporting lunar colony. 24 p3388 A72-45192

Airport power supply system to meet increased load terminal demands, describing main and emergency standby network layout and equipment 24 p3388 A72-45272

POWER SUPPLY CIRCUITS

Pulse width modulated transistor series inverter with inductor transformer in low power applications, noting short circuit and no-load protection 01 p0007 A72-11060

High power series voltage regulators, discussing power hybrid microelectronic design techniques 08 p1112 A72-21415

Metal inert gas (MIG)/welding of thin sheets, using Si controlled rectifier power source 09 p1320 A72-23627

Power transistor thermal cycling ratings and fatigue testing under operating conditions 10 p1447 A72-24011

Power supply for magnetic suspension system, using controlled rectifier and dc power amplifier circuits 10 p1461 A72-24767

Supervisory circuits in electronic data processing power supplies, describing inadmissible line voltages indication networks 10 p1445 A72-24818

Microwave power transistors and active two terminal devices performance, describing representative applications 11 p1607 A72-26983

Voltage controlled low power current sources characteristics, discussing circuits, transistor and emitter resistance and operational amplifiers 13 p1900 A72-30052

Polyphase ac power systems I-V characteristics determination via application of symmetrical sequence components principle, examining system protection and reliability aspects 15 p2204 A72-31216

Mobile X ray apparatus for radiographic flaw detection, describing tuned transformer high voltage source as power supply to sealed sectionalized X ray tube 19 p2805 A72-38766

Control circuit for a power supply of a laser pump lamp. 20 p2933 A72-39524

POWER TRANSMISSION

Photogeological remote sensing of high voltage dc power transmission system induced ground current paths, discussing X-15 near IR photographic recordings 02 p0212 A72-11826

Gear transmission systems statistical characteristics under dynamic loads, noting normal Gaussian curve for operating conditions 04 p0585 A72-14614

Pollution free electrical power generation from solar energy, discussing microwave transmission to earth, power shortages, thermal pollution and solar cell manufacture cost [ASME PAPER 71-WA/SOL-2] 05 p0614 A72-15892

Point contact realization between helical transmission wheels teeth 05 p0667 A72-17058

Laboratory evaluation of engine oils, transmission lubricants and hydraulic fluids utilization in hydraulic power transmission systems 08 p1192 A72-21635

Transmission locked differentials and variable ratio drive improvement effect on engine driven machine high speed performance and stability 08 p1113 A72-22097

Spectrometric oil analysis program [SOAP] method for turbopet and helicopter transmissions damage monitoring and flight safety 09 p1319 A72-22933

Power transfer in optical fiber with nonuniform refractivity in mode propagation direction, using coupled mode theory 12 p1779 A72-27164

Hydraulic transmission for driving helicopter tail rotor, noting compensatory system for engine failure 12 p1755 A72-27862

High voltage dc arc interrupter for use in high power pulse generators and switching application in high voltage dc power transmission system 15 p2201 A72-32569

Laser beam power transmission to lunar bases or spacecraft from nuclear fueled satellite power station, discussing achievable ranges and efficiencies 17 p2611 A72-35328

POYNTING THEOREM

Rod antenna near field energy flow direction and intensity characterization by time independent and dependent components of Poynting vector 13 p1932 A72-29398

Log periodic dipole antenna input impedance and gain characteristics derivation via periodically loaded line theory and Poynting vector method, discussing separation angle effect 15 p2208 A72-32473

POYNTING-ROBERTSON EFFECT

Magnetoelastic coupling existence between shearing stresses and linear deformation, noting influence on Poynting effect experimental results 13 p1980 A72-29782

PPI [POSITION INDICATORS]

U PLAN POSITION INDICATORS

PPM [MODULATION]

U PULSE POSITION MODULATION

PRANDTL NUMBER

Linear spin-down of stratified rotating Boussinesq fluid in circular cylinder as function of Prandtl number, noting solar interior problem 01 p0051 A72-11231

Chapman-Enskog method modification for gas flow Prandtl boundary layer zero approximation distribution function construction, applying Mises transform to Boltzmann equation 05 p0653 A72-17209

Correlation for Prandtl number effect on laminar forced convective heat transfer with secondary flow 07 p1100 A72-19629

Binary gas mixtures calculation for Schmidt, Prandtl and Lewis number dependence on pressure, temperature and chemical composition 07 p1101 A72-20600

Identification method applicability to Prandtl number determination in turbulent flow 08 p1149 A72-21312

Chapman-Enskog method modification for gas flow Prandtl boundary layer zero approximation distribution function construction, applying Mises transform to Boltzmann equation 11 p1614 A72-25332

Magnetic structure of ionizing oblique shock waves with transverse and normal components in zero magnetic Prandtl number limit 11 p1618 A72-26606

Three dimensional free convection boundary layer equations solution at two dimensional isothermal stagnation point with various Prandtl numbers 11 p1747 A72-26662

Prandtl number effect on stratified free shear layer stability, comparing critical Richardson number to linear inviscid theory result

13 p1942 A72-29111

Heat transfer in MHD boundary layer flow of conducting incompressible fluid with aligned magnetic field on flat plate at high Prandtl number

14 p2141 A72-31068

A comparison of the solutions of Prandtl's and Navier-Stokes equations in a superposed fluctuating flow.

18 p2684 A72-37084

Hypersonic unsteady compressible boundary layer dependence on Prandtl number.

19 p2787 A72-38429

Nonisothermal surface cooling for arbitrary temperature distribution and Prandtl number approaching zero, solving thermal boundary layer equations by series expansion

21 p13129 A72-41061

Buoyancy effects on laminar heat transfer in the thermal entrance region of horizontal rectangular channels with uniform wall heat flux for large Prandtl number fluid.

22 p3243 A72-41956

PRANDTL-MEYER EXPANSION

NT THERMAL BUCKLING

Two dimensional Prandtl-Meyer flow anisotropy of ideal gas expanding into vacuum, using free path probe-molecule technique

12 p1799 A72-28178

The shock-combustion /expansion-combustion/ polar with allowance for variation of the specific heat ratio of a gas passing through a flame front

24 p3465 A72-45446

PRASEODYMIUM

Heat treated single-phase Pr-Co powder compacts, measuring coercivity as function of annealing or sintering temperature

[IEEE PAPER 7.3] 03 p0402 A72-13756

PREAMPLIFIERS

Double beam spectrophotometer with automatic gain controlled preamplifier to achieve insensitivity to signal strength change in noise at low cost

07 p0992 A72-20579

Radio pulse synchronous detection with wideband preamplifier, evaluating frequency mismatch effects on signal distortion by transient response analysis

12 p1783 A72-27631

Compensation of nonlinear selectivity distortions in radio receivers with broadband preamplification stages, noting circuit diagrams for preselector correctors

13 p1927 A72-28412

Thermal imaging with pyroelectric IR detector arrays, discussing signal processing by digital technique to eliminate voltage offset variations effects in preamplifiers

20 p2928 A72-39968

Optical communication channel optimization with binary signals preamplified in optical parametric amplifier, noting amplifier gain and SNR

21 p3016 A72-40783

A preamplifier with high input impedance for use with piezoelectric sensors

22 p3160 A72-42923

Parametric preamplifiers for transistorized nuclear-emission detectors and their capabilities

24 p3402 A72-44894

PRECAMBRIAN PERIOD

Artificial microfossil permineralization of blue green algae in silica, simulating Precambrian geochemical preservation

04 p0514 A72-14415

Hereditary endosymbiotic model of microbial evolution of Precambrian prokaryotic and eukaryotic cells

04 p0471 A72-14800

Fluid inclusions in quartz crystals from calcite in Precambrian metasedimentary rocks in South-West Africa

07 p0975 A72-18907

Precambrian paleobiological history from fossil records, discussing heterotrophic living systems and eucaryote emergence in evolutionary organization development

08 p1162 A72-22003

Carbon isotopic studies of organic matter in Precambrian rocks

09 p1304 A72-23496

PRECAUTIONS

U ACCIDENT PREVENTION

PRECESSION

NT LARMOR PRECESSION

NT PROTON PRECESSION

Electron layer precession under magnetic field in background plasma, noting density effect on instability

01 p0107 A72-10144

Gyroscope precession in earth gravitational field, considering impulse energy vector and angular momentum tensor

02 p0229 A72-11970

Thomas precession description with Lorentz transformation

03 p0388 A72-12989

Precessing elliptical orbits stability in Schwarzschild field

04 p0571 A72-14559

Gyroscope precession equations over infinite time interval from conditions based on solutions to differential equations with small parameters at derivatives

04 p0521 A72-15001

Lunisolar precession and equinox motion, discussing determination methods based on proper motions referred to fundamental systems

04 p0575 A72-15026

Precession from proper motions of stars with respect to galaxies, discussing correction for systematic errors

04 p0575 A72-15027

Astronomical coordinate system, examining equinox proper motion and precession corrections

04 p0575 A72-15029

Earth nutation tables, comparing precession-nutations and tidal potential

04 p0575 A72-15031

Lunisolar precession and equinox motion from Cepheids proper motion, using recently determined distance values

04 p0576 A72-15038

Earth precession constant correction, considering Fricke catalogs

04 p0576 A72-15039

Dynamic analysis of vertical rotor rotating in elastic sliding bearings, analyzing precession stability and self oscillation zone

04 p0594 A72-15748

Terrestrial pole motion components, discussing variations in Chandler wobble period and sidereal motion direction and average annual motion along ellipse

07 p0976 A72-19815

Coupled motions of rotating free solid body and elastic rod torsional bending vibrations with precession and forced vibrations from energy exchange

08 p1205 A72-20959

Optimal nomographic determination of surface gyrocompass parameters ensuring minimum period of undamped precession oscillations

09 p1307 A72-22346

Precessional corrections, solar motion and galactic rotation determination from proper motions by maximum likelihood method, taking into account stars visual magnitude

09 p1391 A72-23535

Earth precession as origin of geomagnetic field, discussing dynamo theory and core electroconductivity

10 p1472 A72-24524

Chandlerian wobble period correlation to damping coefficient of earth polar motion for 10 yr intervals during 1900-1970

10 p1475 A72-24871

Axisymmetric satellite rotation about center of mass in circular orbit under Newtonian gravitational field, considering precessional stability

13 p2052 A72-30002

Precession theory for transient response of gyroscope to rotation by Hook sphere using supplementary rotor

15 p2235 A72-31897

Precessional torque of conducting fluid as source of geodynamo action, noting oblate spheroidal experiment

16 p2385 A72-33341

Terrestrial pole motion components, discussing variations in Chandler wobble period and sidereal motion direction and average annual motion along ellipse

17 p2549 A72-35740

The Chandlerian wobble from 1900 to 1970.

18 p2727 A72-36731

Relativity gyroscope experiment at arbitrary orbit inclinations.

20 p2972 A72-39870

The stability of a uniaxial gyro stabilizer under conditions of dry friction in the stabilization and precession axes

21 p3059 A72-41813

Axisymmetric satellite rotation about center of mass in circular orbit under Newtonian gravitational field, considering precessional stability

22 p3231 A72-42730

A determination of the motion of the ecliptic.

23 p3337 A72-43833

Earth precession, nutation, polar axis displacement and rotation period reduction, discussing solid core existence within liquid core, elasticity and polar displacement

23 p3341 A72-44462

Spin stabilization dispersive effect on marginally stable bodies due to precession rate, comparing analytical results with aeroballistic range measurements

24 p3362 A72-45340

PRECIPITATION

Fan shaped precipitate formation during supersaturated Al-Zr solid solution decomposition, discussing interpretation as grain boundary migration

02 p0247 A72-12820

Heat resistant Ni alloys grain boundaries precipitates as function of composition and heat treatment, noting effects on mechanical properties

14 p2118 A72-30589

PRECIPITATION [CHEMISTRY]

Silicide precipitation in Ti-Zr-Al-Si system, discussing microstructure correlation with mechanical properties

03 p0374 A72-13927

Electron microscopic examination of molybdenum alloy thin plates aging at 700 C observing nucleation and precipitated phase

05 p0673 A72-16147

Vacancy supersaturation effect on enhanced precipitation by high flux electron irradiation in stainless steel

07 p1033 A72-20410

Electron microscopic, area diffraction and spectral analyses of carbide precipitates in Cr-Mo steels with different heat treatments and microstructures

10 p1494 A72-23828

Optical and electron microscopic study of Inconel 625 precipitation and recrystallization behavior over temperature range under plastic deformation

10 p1494 A72-23829

Neutron irradiation effects on GP zones and precipitates in ternary Al alloy, measuring X ray small angle scattering and electrical resistivity

11 p1655 A72-25514

Metallographic examination of stainless steel specimens exposed to long term creep rupture tests, noting carbides precipitation and stress induced grain boundary migration

11 p1658 A72-25832

Cold working effect on precipitation-recrystallization interaction in Cu-Ni-Zn alloy, discussing superposed strengthening mechanism during annealing

11 p1641 A72-26738

Mo-Hf alloys high temperature mechanical properties improvement by internal diffusion nitriding, noting precipitates effects

11 p1644 A72-26843

Carbide precipitation effect on structure and high temperature strength of Co based alloys

11 p1667 A72-26932

X ray diffraction patterns of aging nimonin alloys, noting effects of atomic volume difference between precipitation phase and matrix

13 p1976 A72-28766

Electron microscopic investigation of Al-Mn alloy precipitate structure and morphology after annealing induced decomposition

15 p2257 A72-32114

Volumetric analysis of Th, Zr and Li hydrides precipitation in Mg alloys, determining rate equation and activation energy

15 p2257 A72-32118

Nitride precipitate platelets and dislocation loops formation in Nb-N alloys during aging at 535 C from electron microscope observations of structural changes

16 p2405 A72-32999

Separation of iron and annealing-out of lattice defects in rapidly-solidified aluminum-iron alloys. I - Microstructure and properties of quenched samples. II - Tempering behavior

17 p2567 A72-35174

Phase transformations and exsolution in lunar and terrestrial calcic plagioclases.

20 p2970 A72-39480

X ray diffraction patterns of aging nimonin alloys, noting effects of atomic volume difference between precipitation phase and matrix

21 p3065 A72-40267

Stainless steels high temperature creep rupture strength relationship to carbide precipitation morphology

21 p3069 A72-41013

German monograph - Gas-phase precipitation and high-temperature oxidation of titanium carbide.

22 p3194 A72-43053

PRECIPITATION [METEOROLOGY]

NT HAIL

NT RAIN

NT SNOW

NT SNOW COVER

Rain, snow and hail precipitation effects on radio link signal attenuation, scattering and fading along various transmission paths at millimeter and centimeter wavelengths

01 p0027 A72-10407

Remote sensing applications to operational weather forecasting including ground optical measurement of cloud base height and radar observation of precipitation

02 p0253 A72-11825

Meteorological precipitation and earth surface under cloud characteristics from airborne microwave

radiation measurements using millimeter and centimeter waves
02 p0216 A72-11889
Radar accuracy for precipitation measurements, discussing error sources
02 p0254 A72-12784
Wind velocity spatial derivative determination by radar observation of signal reflection from atmospheric water particles
03 p0383 A72-13483
METROMEX field project to investigate inadvertent weather modification by urban-industrial effects and man-made precipitation changes
03 p0384 A72-13636
Precipitation effects on optical transfer function of turbulent atmosphere at 1.2 km, comparing to clear, overcast and cloudy skies
05 p0656 A72-16176
Oxygen and hydrogen stable isotopes utilization for studying water vapor in precipitations, constructing meteorological model
05 p0684 A72-16793
Atmospheric attenuation due to rain based on links experiment and statistical study of equivalent precipitation for given path length and time percentage
07 p0939 A72-19188
Radio attenuation above 10 GHz based on theoretical model of equivalent precipitation on path using intensity spatial distribution function within rain cell
07 p0940 A72-19189
Rain attenuation determination at 15 and 35 GHz under precipitation condition from emission measurement and correlation to regression line, using portable radiometric system
[AD-741093] 07 p0946 A72-19791
Extraterrestrial magnetic spheroid concentrations observed in October 1967 and 1969 proposing relationship to rainfall frequency
08 p1226 A72-21109
Wind shear, turbulence, precipitation, temperature, visibility and ceiling effects on airport capacity, suggesting weather data integration into ATC system for pilots information
08 p1147 A72-21521
Numerical forecasting model with precipitation as function of vertical velocity and humidity distribution, noting orographic influence and atmosphere static stability
08 p1200 A72-21796
Soviet papers on cloud seeding effects and meteorological radar studies covering precipitation formation, atmospheric model and reflected signal statistical characteristics
08 p1201 A72-21992
Discriminant analysis application to data on precipitation formation in convective cumulus clouds to relate process to surrounding atmosphere and cloud characteristics
08 p1201 A72-21993
Intense precipitation contour zone distinguishing methods error estimation in seeding experiments on frontal clouds
08 p1201 A72-21994
Cloud and precipitation dynamic processes effects on reflected radar signal statistical characteristics
08 p1137 A72-21996
Cloud and precipitation elementary processes effects on reflected radar signal fluctuation spectrum during hydrometeor formation
08 p1201 A72-21997
Primitive equation multilayer model for winter precipitation prediction in U.S. northeast coastal region, noting correlation with observational data
09 p1344 A72-22428
Methyl alcohol-ethylene glycol self mixing antifreeze solution for precipitation gages
11 p1682 A72-26088
Wind velocity spatial derivative determination by radar observation of signal reflection from atmospheric water particles
11 p1682 A72-26253
Point discharge current and precipitation effect on atmospheric potential gradient vertical profile
12 p1839 A72-27501
Tropical thunderstorm precipitation current variations due to lightning produced atmospheric electric field changes, considering charged raindrops turbulent diffusion
12 p1839 A72-27502
Cosmogenic radionuclides pickup by cloud water and deposition in precipitation described by model
12 p1863 A72-27503
Precipitation exceedance rates charts for various risks, using statistical models
13 p1989 A72-28811
Total precipitable water in atmosphere vertical column relation to surface humidity from measurements at desert, coastal and maritime sites
13 p1989 A72-28812
Shower precipitation amounts forecasting by layer method, showing inadequacy from viewpoint of physical principles
13 p1995 A72-29594

Thunderstorms physical mechanisms of charge generation and separation, considering correlation between lightning and precipitation
13 p1995 A72-29873
Weather radar observations of Alps foothill region convective precipitation development and lifetime
13 p1996 A72-30088
Precipitation effects on optical transfer function of turbulent atmosphere at 1.2 km, comparing to clear, overcast and cloudy skies
14 p2099 A72-30245
Laser optical and IR radiation attenuation in atmospheric precipitation, considering snow, rain and drizzle
18 p2697 A72-36103
Theoretical model, laboratory experiments and in situ measurements by instrumented sailplane for investigating cloud and precipitation formation physics relationship to atmospheric pollutants cleansing
23 p3311 A72-44263
Liquid and solid precipitation on aircraft structure surfaces, discussing potential hazards to engine components and aircraft controls due to ice formation
23 p3252 A72-44339

PRECIPITATION HARDENING
NT MARAGING
High temperature carbide dispersion strengthened Nb alloys, using heat and thermomechanical treatments
01 p0085 A72-10863
Extruded AlMgSi alloy manufacturing conditions effect on strength, surface finish and anodized appearance, discussing evenly distributed fine hardening precipitates, metal purity, etc
01 p0077 A72-11043
Precipitation hardened Al-Cu alloy microstructure relation to fatigue and tensile properties, emphasizing particle size and distribution, moving dislocations and grain boundary effects
01 p0088 A72-11044
Phase oriented precipitation patterns of Ti in Ti-C-O system, discussing composition independence and dislocation networks
01 p0089 A72-11184
Holes dispersion hardening in sintered metal powder, discussing dispersed particle effects
02 p0233 A72-11446
Thorium oxide dispersion strengthened Ni powder metallurgy alloys, noting thermomechanical processing effects on tensile strength
02 p0241 A72-11447
Aluminum oxide dispersion hardened ferritic heat resisting Cr steel, describing liquid phase sintering effects on high temperature tensile strength
02 p0241 A72-11448
Matrix hardening in dispersion strengthened powder products, discussing dispersion, grain boundary and solid solution hardening
02 p0241 A72-11457
Allotropic transformations and recrystallization by precipitation hardening in pure Ti crystals, using field emission microscopy
02 p0242 A72-12007
Microstructure and mechanical properties of iron base superalloys, examining precipitation hardening by gamma prime and secondary intermetallic compounds formation
02 p0245 A72-12505
Fabricable high strength Inconel 706 precipitation hardening superalloy, noting savings in Ni, Nb and Mo content
02 p0245 A72-12507
Gamma prime precipitate hardened Ni base alloys, attributing strengthening mechanism to coherency strains and precipitates antiphase boundary energy
02 p0247 A72-12817
Superalloy compositions prealloyed powders strengthening by secondary gamma phase precipitation, noting high temperature strength without ductility loss after thermomechanical treatment and aging
02 p0247 A72-12856
Tubular and rod extruded age hardenable Al alloys, determining mechanical anisotropic properties from yield loci and r values
03 p0369 A72-12957
Grain size effect on age hardened Mg-Zn alloy yield and flow stress, using tensile test and electron and optical microscopy at various temperatures
03 p0374 A72-13716
Mg-Zn alloys precipitation hardening mechanism at various aging stages, considering yield strength increase due to interface dislocations
03 p0374 A72-13717
Phosphorus-containing austenitic stainless steel, investigating quenching defects and precipitation from microstructure by transmission electron microscopy
03 p0379 A72-14260
Grain size and precipitate parameters effect on creep properties of Ni-Cr alloys
03 p0379 A72-14339
Substitutional dynamic strain aging effects on Fe-Nb alloys mechanical properties, attributing ductility reduction to work hardening and strain rate effects
04 p0534 A72-15576

Ta-W-Hf alloy ultrahigh vacuum high temperature creep tests, showing deoxidation effect on creep behavior and early test stage oxygen-associated dynamic strain aging
05 p0674 A72-16392
Age hardened Al-Cu single crystal anisotropy from stress-strain curves, using plane strain compression tests
[AD-743602] 05 p0677 A72-17106
Mo- and Ta-base refractory alloys creep tests, determining interactions between creep strength, fatigue life and strain aging by fatigue vibration application
05 p0677 A72-17111
Fe effect on dispersion hardened Ni alloys with various quantities of Nb and Ti during cryogenic operation
05 p0679 A72-17202
Gas turbine superalloys high temperature oxidation resistance by fiber strengthening, rare earth alloying, precipitation hardening and intermetallic compounds
06 p0828 A72-17611
Dynamic strain aging significance in titanium, observing reduction of temperature and strain rate effects on stress-strain curves shapes
06 p0830 A72-18054
Mg dispersion hardening techniques, exploring internal oxidation of alloys containing rare earths
07 p1011 A72-19481
Ti-Al-V alloy biaxial yield strength improvement by combined texture and age hardening, using hydroburst tests
07 p1011 A72-19482
Heat resistant weldable precipitation hardened Ni base alloy, discussing intermetallic phase hardening
07 p1014 A72-19842
Age hardening of Mo alloys with titanium and zirconium carbides at high temperatures after quenching
07 p1014 A72-19844
Tensile strength enhancement of dislocated martensites in Fe alloys by precipitate dispersion in austenite prior to transformation
07 p1016 A72-19936
Carbide precipitation effect on strength of austroformed hardenable hypoeutectoid and hypereutectoid stainless steels
07 p1016 A72-19943
Precipitation hardening of quenched superconducting Nb-Al alloys, examining polycrystalline and single crystal samples and intermetallic phases
07 p1050 A72-20155
Tungsten dispersion strengthening by hafnium nitride covapor deposition, discussing effects of matrix microstructure and dispersoids number, size and spacing variations
07 p1019 A72-20366
Precipitates dispersion and fluxoid pinning /critical current density/ in superconducting Nb-Hf alloy during aging, using transmission electron microscopy
07 p1020 A72-20409
Precipitation hardened Ni-Al alloy mechanical properties, relating ductility and strength to precipitate caused inhibition of microcrack initiation and propagation
07 p1021 A72-20438
Dispersion strengthening of electrolytically deposited nickel-aluminum oxide alloys, comparing tensile tests to theoretical values
08 p1186 A72-21442
Precipitation effect on microstructure, coercive force, resistivity and cell formation changes in heterogeneous decomposition of supersaturated solid solutions and aging alloys
08 p1218 A72-21777
Ni-Cr-Nb alloys structure and phase composition changes from W-Mo additions and hardening by intermetallic Ni-Nb precipitated from supersaturated solid solution
08 p1187 A72-21782
Transmission electron microscope investigation of Al-Mg-Si alloy precipitation, showing Guinier-Preston zone visibility due to matrix elastic strain introduction
09 p1328 A72-22983
Extruded dispersion strengthened Mg-MgO alloys microstructure, discussing high temperature creep effect on dislocation structure changes
09 p1328 A72-22984
Recrystallization of dispersion strengthened alloys with bcc lattice, deriving equations for grain size changes
09 p1328 A72-23031
Thermomechanical strengthening of gamma prime precipitation hardened nickel base superalloy, emphasizing working operation and dislocation substructure
09 p1330 A72-23777
Fe effect on plasticity and ductility of dispersion hardened Ni alloys with various quantities of Nb and Ti at cryogenic temperature
11 p1660 A72-26137
Alpha Zr tensile properties tests noting strain aging effects on strain rate, work hardening and ductility anomalies
11 p1661 A72-26595

- Cold working effect on Cu-Ni-Si-Mg and Cu-Ni-Si-Cr alloys age hardening behavior, presenting hardness and tensile strength vs aging time at 350 and 400 C
11 p1662 A72-26743
- Dispersed phase nickel-thoria alloy production method based on organometallic compounds, avoiding high temperature and solvent elimination difficulties
11 p1664 A72-26849
- Dispersion strengthened nickel-chromium-thoria alloy production methods, noting halogen gas phase diffusion process
11 p1645 A72-26850
- Microstructure and mechanical properties of dispersion strengthened Co alloys, investigating heat treatment effects
11 p1664 A72-26851
- High temperature creep properties of W-Re alloy under vacuum for thoria dispersion hardening from electron microscope and activation energy studies
11 p1665 A72-26863
- Coherent precipitate structure in Fe-Ni-Co-Mo maraging alloys, using electron microscopy
11 p1668 A72-26940
- Plane titanium and niobium carbide precipitation in microalloyed steels during heat treatment above 1300 C, noting eutectic sulfide effect
12 p1827 A72-27102
- Electron microscope study of commercial Ni superalloys, discussing intermetallic compound and carbide precipitation hardening
12 p1827 A72-27137
- Time-temperature-precipitation (TTP) diagrams and phase instabilities of high temperature exposed Mo containing austenitic stainless steels
13 p1974 A72-28658
- Mo influence on gamma prime phase precipitate in wrought Ni-base superalloys, considering solvus temperature, weight fraction and lattice parameters
13 p1975 A72-28669
- Precipitated carbide role in Cr-Ni stainless steels high temperature properties and creep rupture strength
13 p1979 A72-29447
- Dispersion hardening of Nb, Cr, Mo and W by inserting dispersed particles of refractory compounds into metal matrix
14 p2112 A72-30152
- Phase precipitated helicoidal dislocations and vacancy-type stacking faults in aged austenite Fe-Ni-Ti alloy, using electron microscope diffraction contrast analysis
14 p2112 A72-30162
- Microstructure effects on thermomechanically processed dispersion strengthened Ni alloys yield strength at various temperatures
14 p2114 A72-30368
- Co, Mo, Ti and Al alloying effects on aging and hardening processes in Ni steel from hardness, thermal emf and electrical resistance measurements
14 p2115 A72-30408
- Accelerated intergranular corrosion and grain boundary precipitation mechanisms in stainless steel Fe-Ni-Cr alloy, using Huey, acid and Strauss tests
14 p2118 A72-30548
- Uniformly distributed precipitates effect on hardness increase in aging of ferritic matrix Fe-Co-Ti and Fe-Co-Al alloys
14 p2119 A72-30605
- Slip band blocking effect of disperse particles on crack suppression and creep rupture strength of intermetallic Al-Fe-Ni alloy
14 p2124 A72-31033
- Russian papers on alloying and properties of heat resistant alloys covering creep, solid solution and dispersion hardening, chemical interactions and protective coatings
15 p2254 A72-31557
- Heat resistance improvement by interface dislocation, dispersion hardening and reinforcement of Mo, Fe, Ni and Al metals and alloys
15 p2254 A72-31560
- Dispersion hardening of Nb-Zr-O and Nb-Hf-O alloys, discussing composition and heat treatment effects on aging, recrystallization temperature and grain growth
15 p2255 A72-31567
- Dispersion hardening Ni base alloys for gas turbine blades, considering composition, structure, gamma phase and embrittlement avoidance
15 p2255 A72-31568
- Dispersion hardening /aging/ effect on embrittlement of Ni base alloys in cold worked pipes during heat treatment
15 p2255 A72-31569
- Mg base alloys precipitation processes studied by electron microscopy, emphasizing Mn precipitation in Mg-Th alloy
16 p2405 A72-32998
- Co-Cr-C system carbon activity and solubility at 950-1200 C, deriving equation for temperature dependence and solid solution-carbide precipitation zone boundaries
16 p2407 A72-33441
- Cold rotatory forging and subsequent heating effects on microstructure, texture and mechanical properties of dispersion hardened Ni specimens obtained by hot extrusion
16 p2407 A72-33530
- Precipitation reactions during tempering of Ti-Ta alloys, studying hcp and orthorhombic martensitic phases from electron microscope observations
16 p2408 A72-33619
- Al-Cu-Mg alloys room temperature age hardening, determining effects of tension load up to plastic deformation from measurements of mechanical properties and electrical resistance
16 p2408 A72-33674
- Precipitation hardening effects on yield strength, toughness and ductile to brittle transition temperature of low alloy steels containing Nb
16 p2409 A72-33809
- Discontinuous precipitation and site nucleation in quenched and aged Al based Zn alloys as function of temperature
16 p2410 A72-33812
- Composition effect on strain-transformation and precipitation hardening of beta Ti alloys at 800-1100 F
16 p2410 A72-33813
- Temperature and stress dependence of steady state creep rate for dispersion strengthened Ag-gallium oxide alloys, noting grain size effect on activation energy
16 p2411 A72-34094
- New observations of preprecipitation phenomena in Al-Mg and Al-Mg-Zn alloys
17 p2566 A72-34286
- Precipitation caused surface defects on Al-Mg-Si alloy extrusions, considering segregation streaks, cooling induced microstructural stains and cold working-annealing produced heterogeneous zones
18 p2699 A72-36225
- Interstitial and substitutional dynamic strain aging of Fe-Nb alloy and Al-Nb bearing steel at 295-950 K
18 p2699 A72-36342
- An electron microscopy study of carbide precipitation in vanadium.
18 p2699 A72-36577
- Phase stability and mechanical properties of carbide and boride strengthened chromium-base alloys.
18 p2700 A72-36579
- The structure of the metastable precipitates formed during ageing of an Al-Mg-Si alloy.
18 p2702 A72-36743
- The effect of Mo, Al, and C on phase transformations in Ni alloys
19 p2814 A72-37417
- Solid-state phase transformations.
19 p2815 A72-37442
- German monograph - Effect of molybdenum and degree of age hardening on the corrosion properties of maraging chromium steels
19 p2816 A72-37654
- Dispersion hardening fabrication of hollow cooled blades of thin cermet layer and embedded plastic metal core, using aluminum oxynitrate in water-alcohol solution
19 p2809 A72-38282
- Aging characteristics of Ti-Mo base beta alloys.
19 p2820 A72-38371
- Deformation and fracture of dispersion-strengthened nickel charged with hydrogen.
20 p2935 A72-39004
- A review of the science, technology, and applications of dispersion strengthened Ni-Cr- and Co-Cr-base alloys.
20 p2936 A72-39209
- Tensile and compressive stress coarsening effects on coherent gamma prime precipitate yield strength of Ni-base superalloy single crystals
20 p2938 A72-39299
- The effects of composition and annealing conditions on the stability of columbium /niobium/-treated low-carbon steels.
20 p2938 A72-39301
- Elevated temperature ductility minimum in Hastelloy alloy X.
20 p2938 A72-39304
- Powder-metallurgical production of dispersion-hardened nickel and cobalt alloys
20 p2929 A72-39454
- The plastic behavior of pure and dispersion-hardened nickel in the temperature range from 20 to 600 C
20 p2940 A72-39455
- Structure and properties of nickel-phosphorus coatings as a function of the temperature and annealing time
20 p2929 A72-39583
- Precipitation thermodynamics of unstable and metastable solid solutions, discussing interfaces, vacancies, spinodal decomposition, nucleation, reversion and macroscopic diffusion
20 p2943 A72-40000
- Strengthening of tungsten by powder metallurgical internal oxidation.
21 p3067 A72-40833
- Oxidation of TD nickel at 1050 and 1200 C as compared to three grades of nickel of different purity.
21 p3067 A72-40915
- Phase precipitation structure of superconducting Nb-Ti alloys after cold working and low temperature annealing
21 p3067 A72-40951
- Strain aging of pure aluminum annealed from pre-melting temperature
21 p3060 A72-40954
- Precipitation of aluminum nitride in low-alloy steel
21 p3068 A72-40956
- Nickel-titanium intermetallic phase effect on recrystallization of dispersion hardening high melting point steel during furnace and induction heating
21 p3071 A72-41789
- Precipitation rate characteristics in age hardenable quenched alloys explained by transient analysis of vacancy annealing kinetics
22 p3189 A72-42441
- Thermomechanical manipulation of precipitate shape in a titanium-base alloy.
22 p3194 A72-43044
- Influence of the nature of the particle distribution of the hardening phase in powders on the thermal stability of dispersion-strengthened nickel
23 p3302 A72-44011
- Thermal diffusion annealing improved Ni-B composite electrolytic coatings with uniform B distribution over bulk matrix
23 p3303 A72-44012
- The creep of dispersion-strengthened Ni-Co alloys.
24 p3413 A72-44923
- Co-V solid solution decomposition by equilibrium phase precipitation at aging temperatures, using electron microscopic and X ray analysis
24 p3414 A72-45382
- Growth kinetics of dispersed thoria in Ni and Ni-Cr alloys.
24 p3415 A72-45480
- ### PRECIPITATION PARTICLE MEASUREMENT
- Cumulus and stratumcumulus ice crystal and nuclei concentrations, drop size distributions, glaciation differences and enhancement mechanisms
07 p1030 A72-19101
- Cumulus cloud microstructure measurement by single particle optical spectrometer, inferring transition from water to ice phase regions from droplet size and number distributions
09 p1307 A72-22444
- Airborne electrostatic probe for cloud droplet size measurement, calculating flow distribution and particle trajectories
16 p2390 A72-33150
- Studies of vertical motions in cloud systems by using a coherent pulse radar in the decimeter wavelength range
19 p2829 A72-38773
- Theoretical model, laboratory experiments and in situ measurements by instrumented sailplane for investigating cloud and precipitation formation physics relationship to atmospheric pollutants cleansing
23 p3311 A72-44263
- ### PRECIPITATORS
- #### NT ELECTROSTATIC PRECIPITATORS
- #### PRECISION
- Cloud height measurement with rotating beam ceilometers, discussing precision and representativeness
13 p1992 A72-28849
- Variable torque determination in precision work technology, discussing electronic measurements of length, shaft deformation, torsion angle and force
14 p2104 A72-30485
- ### PRECONDITIONING
- Stellar multilevel spectral line formation solution by preconditioning procedure based on core frequency transfer determination by local saturation approximation
20 p2954 A72-39758
- ### PREDICTION ANALYSIS TECHNIQUES
- Integral method for predicting streamline development of plane turbulent jets and wall jets in uniform streaming flow
01 p0051 A72-11393
- Satellite tracking by combined optimal estimation and control techniques with Kalman filter, considering radio antenna and optical tracking systems
02 p0285 A72-12812
- Mathematical modeling methodology for communication receiver life cycle EMC decisions, considering analysis and prediction problems with emphasis on nonlinear circuits and systems
03 p0324 A72-14034
- Bias and variance prediction efficiency in two stage sampling designs
03 p0383 A72-14368
- Nonlinear plant and observation models with white Gaussian noise and continuous data, obtaining state vector a posteriori probability density for optimal prediction
04 p0506 A72-15112
- Adaptive control algorithm with disturbance prediction for solution of deterministic and stochastic op-

timization problems of linear equation of state and quadratic performance criteria

05 p0639 A72-15759

Complex systems stochastic survivability estimates dependence on delay depth and initial conditions of interaction

05 p0640 A72-16204

Satellite motion state vector accuracy estimate algorithm based on angular measurements of stellar positions relative to satellite sent probe

05 p0687 A72-16762

Stochastic dynamic equations for atmospheric prediction and numerical weather forecasting, using barotropic model

06 p0841 A72-17633

Coupled detection-estimation of Gauss-Markov processes in white Gaussian noise, deriving Bayes optimal recursive rules

06 p0775 A72-18388

Forecasting technique for accumulated particulate contamination on spacecraft assemblies, discussing cleanliness optimization and test procedures

07 p0915 A72-18763

Range rate prediction algorithm for pulse Doppler ambiguity resolution by invariant imbedding method

07 p0941 A72-19303

Deterministic model for new product innovation adoption rate in commercial aircraft jet engine market

07 p1105 A72-20269

Computer simulation prediction program for attitude disturbance torques for Tiros series spacecraft rotational motion control

07 p1086 A72-20361

Turbopump rotating assembly bearing parameters and inertia products estimation and identification by extended Kalman filtering

08 p1173 A72-20844

Compensated Kalman filter as suboptimal state estimator to eliminate steady state bias errors in use with mismatched asymptotic time-invariant case

08 p1144 A72-20845

Dynamic system time varying parameters on-line estimation using adaptive extended Kalman filter based on predicted error covariance matrix alteration

08 p1144 A72-20847

Real time recursive algorithms for estimating coefficients of fixed knot spline approximation to trajectory

08 p1197 A72-20849

Biased estimator as alternative to linear unbiased estimator for dynamic system model states and parameters optimization and regulation, noting squared errors sum

08 p1144 A72-20852

Combined signal detection and trajectory estimation functions optimization application to Monte Carlo simulation for trajectory moving across two dimensional grid

08 p1144 A72-20858

Standard linear estimation and control problem with quadratic loss, optimizing information rate by minimizing total measurements number through Riccati equation singular solution

08 p1144 A72-20859

Optimal filtering for state estimation of nonlinear dynamic models observed with discrete noisy observations by retaining second order terms in series approximation

08 p1145 A72-20863

Orbit determination using Kalman-Bucy filter to estimate state and unmodeled acceleration approximated as first order stationary Gauss-Markov process

08 p1145 A72-20867

Conditional mean state estimate approximation for nonlinear systems by parallel computation to reduce computer time

08 p1145 A72-20868

Spectral density estimates for discrete time models of steady nonGaussian random processes, noting dispersion in asymptotic expression

08 p1198 A72-20996

Best approximation estimates for function of many variables by sums of two functions of smaller number of variables

08 p1199 A72-21299

Soviet book on determinate, stationary, nonstationary and industrial random processes prediction, covering adaptive filters and algorithms

08 p1146 A72-21675

Controlled plants operation efficiency change prediction by analytic and probabilistic methods with data processing

08 p1180 A72-22064

Radio system failure prediction based on parameter variation a priori or a posteriori data, determining reliability and optimal preventive maintenance intervals

08 p1143 A72-22070

Probability weather forecasts reliability, considering utility and spherical and logarithmic validities

08 p1203 A72-22124

Optimal probing signals design for state vector parameter estimation, considering Fisher information matrix function as optimality criterion

10 p1454 A72-23786

Compression of data from measurements in real time nonlinear estimation to reduce data processing requirements without performance deterioration, applying to reentry vehicle tracking

10 p1442 A72-23802

Optimal nonlinear estimation problem with nonlinear plant and observation models obtaining state vector a posteriori probabilities for prediction and smoothing via partition theorem

[AD-736521] 10 p1455 A72-23803

Mathematical model as basis for equipment design-sensitive maintainability prediction technique, using information theory concepts of design interpretation

10 p1503 A72-23979

Reliability and time to failure prediction for degradation-prone systems via Markov processes theory

10 p1504 A72-23988

Theorem proved for pattern classification system effectiveness for system reliability prediction

10 p1504 A72-23996

Dormant aerospace electronic system sedentary or nonoperating failure rate analysis by prediction technique

10 p1447 A72-24008

Self learning estimator for tracking, using heuristic technique for time-varying estimates sequence determination

10 p1457 A72-24500

Observation errors effects on satellite attitude best least squares estimate based on direction measurements, using Monte Carlo method computer simulation

10 p1438 A72-24692

Mean square error and functional state prediction algorithm for plants controlled by automatic system containing digital computer

11 p1600 A72-25439

Fatigue life cumulative damage prediction procedure for engineering metals subjected to complicated stress-strain histories, noting errors in average mean stress method

11 p1658 A72-25831

Radiation source position a posteriori probability density function determination with empirical prior knowledge to provide simple computational procedures

15 p2267 A72-31778

Random vibration optimal control by transfer function estimation, using relative phase information in cross spectral density functions to sort out self noise

15 p2215 A72-32629

Electronic circuit reliability prediction model with statistical dependence for detailed failure modes

16 p2371 A72-33345

Random scale parameter of Weibull distribution with known shape parameter obtained via empirical Bayes estimation

16 p2398 A72-33346

Weibull distribution parameters estimation for general device class from limited failure data through regression models, using least squares method

16 p2398 A72-33349

Monthly mean air temperature anomalies annual forecasts based on Fourier analysis of 1900-1970 statistical data

16 p2418 A72-33381

Baysian recursive linear Kalman filtering technique for image estimation with noise background elimination, proposing time invariant dynamic model to provide stationary statistics

17 p2520 A72-34403

Techniques for control of long-term reliability of complex integrated circuits. II - A technique for the prediction of failure rates for MSI and LSI devices.

17 p2528 A72-34687

Long-term prediction of artificial satellite motion along almost circular orbits allowing for a random number of zonal harmonics

17 p2607 A72-35033

Nonlinear dynamic feedback control systems modeling by parameter estimation scheme with polynomial representation for state variables

18 p2672 A72-36057

Generalized dynamic systems and process prediction

19 p2833 A72-37378

Local and regional weather forecasting based on multilinear regression technique

21 p3078 A72-40765

Prediction error growth computation by test-field model for inertial range atmospheric turbulent flows in three and two dimensions

22 p3167 A72-42501

Book - EMI prediction and analysis techniques.

22 p3156 A72-43198

Lifetime estimation, optimal experimental design and stress level severity prediction in parametric and nonparametric accelerated life tests

24 p3406 A72-44671

Life prediction of expulsion bladders through fatigue test and fold strain analysis.

24 p3455 A72-44672

PREDICTIONS NT FLOOD PREDICTIONS

NT IMPACT PREDICTION

NT LINEAR PREDICTION

NT PERFORMANCE PREDICTION

Predictive filtering of multi-channel time series records with application to Doppler radar data.

19 p2781 A72-38272

Prediction role in execution of manual control with display device to aid human operator adaptation

21 p3010 A72-41406

Prediction displays based on the extrapolation method.

21 p3010 A72-41409

Estimation and prediction of Gumbel and Frechet distribution parameters, noting statistical decision in tests, sequential analysis and graphical procedures

22 p3199 A72-42968

PREDICTORS

U PREDICTIONS

PRELIGHT OPERATIONS

NT COUNTDOWN

PREFORMS

Forged Inconel alloy 718 metal powder preforms for dense aircraft engine compressor rotor blades

02 p0233 A72-11441

Fe powder preform hot rolling, investigating mechanical properties, microstructure and internal oxidation resistance as function of final density

10 p1488 A72-24695

Iron base powders material requirements and forging processes, discussing powder composition, inclusions effect and preform densification

11 p1639 A72-26241

Pressed and sintered preforms of Ti and alloys for forge and extrusion operations, noting processing time reduction and smooth surface

13 p1982 A72-30120

Deformation, densification and material fracture characteristics for powder preform design for hot forging

19 p2806 A72-37593

Precision forging technology for Al sintered powder metal preforms for prototype fabrication

19 p2806 A72-37594

PREGNANCY

Tentorium cerebelli microstructure and leaflets strength in study of chronic and acute hypoxia injury to fetus during pregnancy and labor

09 p1266 A72-23193

PREHEATERS

U HEATING EQUIPMENT

PREHEATING

U HEATING

PRELAUNCH TESTS

Digital computer automated test equipment and procedures for remote sensors and electronics for scanning celestial sphere for X rays prior to spacecraft launch

02 p0200 A72-12479

Minuteman HERO /hazards of electromagnetic radiation to ordnance/ preflight testing, describing ordnance monitoring system based on fiber optic data links

08 p1220 A72-20767

PRELOADING

U PRESTRESSING

PREMIXED FLAMES

Premixed combustible system in laminar axisymmetric stagnation flow, considering steady state and transient response of state variables, blow off extinction, ignition and heat flux

[AD-743387] 03 p0458 A72-14222

Combustion reactions of water catalyzed gas-phase oxidation of carbon monoxide in premixed stagnation flow at atmospheric pressure

[AD-743563] 03 p0459 A72-14223

Reaction kinetics of NO and CO formation in lean premixed hydrocarbon-air flames

04 p0594 A72-14409

CW CO laser by discharging premixed carbon disulfide-oxygen flame, suggesting chemical pumping mechanism and flame laser possibility

04 p0529 A72-14589

Directionality and far field structure of combustion generated noise, using premixed turbulent flame models

[AIAA PAPER 72-198] 05 p0748 A72-16875

Optical anemometers for mean and fluctuating velocities in premixed flame of town gas-air combustion system, noting velocity probability density distribution

13 p1955 A72-28546

Discussion of the thermal state of an open air premixed methane-oxygen flame.

19 p2883 A72-38871

Comparison of homogeneous gas-phase reaction kinetics for complete segregation and complete micromixing.

[WSCI PAPER 72-6] 20 p2982 A72-38972

German monograph - The transfer behavior of premixed flames.

22 p3244 A72-43076

Flame structure and flame reaction kinetics. VI - Structure, mechanism and properties of rich hydrogen + nitrogen + oxygen flames.

24 p3461 A72-44919

- Flame structure and flame reaction kinetics. VII - Reactions of traces of heavy water, deuterium and carbon dioxide added to rich hydrogen + nitrogen + oxygen flames. 24 p3378 A72-44920
- Two-dimensional supersonic flow with flame sheets. 24 p3360 A72-44988
- PREPARATION**
 NT PRECONDITIONING
 NT PRESTRESSING
PREPOLYMERS
 NT DIMERS
 Polyimide prepolymer formulation for glass and graphite reinforced composites autoclave processing via increased melt phase duration and temperature range 01 p0090 A72-10729
 Phenolic-novolac prepolymer molecular structure and pyrolysis reactions thermokinetic parameters, presenting statistical methods for estimating char yield 01 p0023 A72-11261
- PRESELECTORS**
 U PREAMPLIFIERS
- PRESINTERING**
 U SINTERING
- PRESESSES**
 Press for air sensitive materials preparation for IR spectroscopic examination 07 p0965 A72-20577
- PRESSING**
 Additional deformation work for splines forming in splined circular profiles pressing, deriving characteristic displacement velocity distribution equations 13 p1963 A72-28744
- PRESSING [FORMING]**
 NT COINING
 NT STAMPING
 Ti powder technology, discussing pressed and sintered parts, forging and extrusion preforms and composites 02 p0233 A72-11437
 High energy rate compacting methods in powder metallurgy, considering use of high explosives in water or air and impulse pressing of metal powders 02 p0233 A72-11438
 Press and sinter production of Ni maraging steel powder metallurgy parts 02 p0234 A72-11464
 Press forged ceramic crystals deformation, recrystallization, strength and fracture properties, comparing sapphires, rubies and spindels 08 p1196 A72-21917
 Strain work per unit time for static and dynamic pressing processes, taking into account inertial forces 13 p1966 A72-29466
 Fabrication of shaping cermet elements of die-casting molds for plastics by the hydrostatic pressing method 22 p3182 A72-42199
- PRESSORS**
 U VASOCONSTRICTOR DRUGS
- PRESSURE**
 NT ATMOSPHERIC PRESSURE
 NT BASE PRESSURE
 NT BLOOD PRESSURE
 NT CRITICAL PRESSURE
 NT DENSIFICATION
 NT DIFFERENTIAL PRESSURE
 NT DYNAMIC PRESSURE
 NT ELECTRON PRESSURE
 NT GAS PRESSURE
 NT HIGH ALTITUDE PRESSURE
 NT HIGH PRESSURE
 NT HIGH VACUUM
 NT HYDROSTATIC PRESSURE
 NT HYPERTENSION
 NT HYPOXEMIA
 NT ILLUMINANCE
 NT IMPACT LOADS
 NT INLET PRESSURE
 NT INTERNAL PRESSURE
 NT INTRACRANIAL PRESSURE
 NT INTRAOCULAR PRESSURE
 NT ISOSTATIC PRESSURE
 NT LOW PRESSURE
 NT LUMINANCE
 NT LUMINOUS INTENSITY
 NT OVERPRESSURE
 NT OXYGEN TENSION
 NT PARTIAL PRESSURE
 NT RADIATION PRESSURE
 NT SOUND PRESSURE
 NT STAGNATION PRESSURE
 NT STATIC PRESSURE
 NT SUPERCRITICAL PRESSURES
 NT SYSTOLIC PRESSURE
 NT TRANSIENT PRESSURES
 NT ULTRAHIGH VACUUM
 NT VACUUM
 NT VAPOR PRESSURE
 NT WALL PRESSURE
 NT WATER PRESSURE
 NT WIND PRESSURE

PRESSURE BREATHING

- High pressure gas mixture breathing effects on intercostales externi muscles electrical activity and respiratory cycle time in rats 08 p1121 A72-22082
- Vasopressin [antidiuretic hormone] role in central vascular volume and fluid balance maintenance during continuous positive pressure breathing in dogs 17 p2505 A72-35917

PRESSURE BROADENING

- Carbon dioxide laser modulation by molecular Stark effect in deuterated ammonia, observing pressure broadening coefficient 04 p0528 A72-14585
- Microwave spectrum of compressed O₂-foreign gas mixtures in the 48-81 GHz region. 24 p3378 A72-44871

PRESSURE CABINS**U PRESSURIZED CABINS****PRESSURE CHAMBERS**
 NT HYPERBARIC CHAMBERS
 NT VACUUM CHAMBERS

- Pressure chamber training effects on rats chain motor reflexes hypoxia adaptation, noting sinocarotid receptors importance in compensatory-adaptive reactions 13 p1902 A72-28641

- Ultrahigh tensile strength steel pressure chamber fracture behavior in high stress concentration fields 15 p2330 A72-32345

- Shock wave propagation velocity increase in combustion shock tubes through intermediate pressure chamber, using streak camera and microwave Doppler technique for velocity measurements 16 p2375 A72-32839

- Two chamber adiabatic test compression system design with controlled throttle for high temperature nitrogen and nitrous oxide-type gases with exothermal reactions 18 p2676 A72-37189

- Prediction of vegetative reactions to extremal actions on the organism 22 p3141 A72-42168

PRESSURE COEFFICIENT**U AERODYNAMIC COEFFICIENTS****PRESSURE DISTRIBUTION**

- Parachute inflation loads and times, presenting calculation method based on unsteady pressure distribution on decelerating inflating parabolic shell of revolution with unsteady starting vortex 01 p0004 A72-10311

- Estimation method for surface pressure distribution on cascade airfoil in retarded flow, applying to axial flow turbomachines design with suction performance and efficiency 01 p0001 A72-10396

- Sonic boom pressure signatures during F-104 overflights at Mach 1.3 and 30,000 ft, explaining variations by atmospheric turbulence 01 p0006 A72-11158

- Digital simulation of general atmospheric circulation via spatial finite difference dense grid, considering surface properties and pressure distribution maps 02 p0252 A72-11652

- Near pressure field within subsonic circular turbulent cold jet potential cone, noting peak in power spectra 02 p0150 A72-11974

- Cross flow through in-line tube bank, investigating surface roughness effects on behavior by pressure drop, static pressure and skin friction distributions measurements 02 p0203 A72-12102

- Wideband acoustic pressure field sensing by moving receivers and sensors, calculating motion effects on response including directional pattern and gain 02 p0259 A72-12176

- Aerodynamic forces and pressure distribution measurement on wing-body combination model, investigating boundary layer on wing upper surface 02 p0151 A72-12228

- Force and pressure distribution measurements on delta wing-body combination in compressible flow, investigating Reynolds number effect [DGLR PAPER 71-118] 02 p0152 A72-12707

- Blade cascades pressure distribution for plane incompressible flow with boundary layer separation near trailing edges, replacing blade profiles by vortex fields [DGLR PAPER 71-097] 02 p0153 A72-12728

- Unsteady pressure distribution on harmonically oscillating circular cylindrical fuselage body with conical nose and delta wing with straight, cubic or sinusoidal leading edges [DGLR PAPER 71-080] 02 p0153 A72-12730

- Unsteady flow theory for radial gas lubricated bearing, deriving velocity and pressure distribution expressions 03 p0363 A72-13577

- Two dimensional airfoil pressure distribution measurements at high subsonic speeds, comparing normal force coefficients corrected for wind tunnel interference effects with theoretical calculations [DFVLR-SONDDR-168] 03 p0308 A72-13609

- Spherical planetary atmosphere tendency equation of pressure variation for horizontal stratification, using static and continuity equation in spherical harmonics 03 p0351 A72-14356

- Pressure distribution and compressible gas critical flow rate in constant cross sectioned circular pipe with impermeable adiabatic wall from Frossel equations 04 p0511 A72-14640

- Pressure and convective heat transfer distribution at air inlet central body surface, reducing Navier-Stokes equations to partial differential equations with similar solutions 04 p0596 A72-14971

- Pressure field calculations for random vibrations in wide class of elastic shells containing acoustic medium, discussing turbulent boundary layer-caused pulsations 04 p0586 A72-15010

- Nearly free molecular slit flow of gas from reservoir at finite pressure and temperature ratios 04 p0512 A72-15120

- Radiated pressure field in unbounded acoustic medium produced by pulsed elastic cylindrical circular shell 04 p0590 A72-15188

- Radial pressure distribution in laminar flow of compressible fluid between two coaxial disks from analog computer study 04 p0514 A72-15702

- Tangential blowing and wall cooling effects on axisymmetric models flow separation at Mach 6, comparing pressure distribution with Busemann formula 05 p0601 A72-16227

- Rectangular variable thickness plate deflection under uniform lateral pressure, solving nonlinear partial differential equations with variable coefficients by iterative procedure 05 p0738 A72-16533

- Leaning vanes for fan noise reduction, discussing rotor-stator plane fluctuating pressure amplitude decrease and radial distribution modification [AIAA PAPER 72-126] 05 p0706 A72-16823

- Finite periodic beam response to turbulent boundary layer pressure field fluctuation, using transfer matrix technique [AIAA PAPER 72-171] 05 p0650 A72-16832

- Axisymmetric bodies with discontinuous curvature in transonic flow, calculating surface pressure distribution [AIAA PAPER 72-137] 05 p0606 A72-16891

- Neutral atoms pressure distribution along capillary and pressure compensating channel during discharge in argon ion laser 05 p0670 A72-16990

- Laminar flow airfoils for gliders, optimizing profiles for favorable velocity and pressure distribution 05 p0610 A72-17194

- Critical review on data accuracy of maximum principal elastic stresses and deflections of thin initially-flat square isotropic plates under uniform normal pressure 06 p0894 A72-17796

- Narrow groove theory of spiral grooved gas bearings, obtaining pressure distribution and small perturbation stiffness performance 06 p0821 A72-17807

- Spatial boundary layer variations in low speed wind tunnel working section due to settling chamber screens, discussing mesh variations effects on Preston tube measured pressure coefficient distributions 07 p0966 A72-19061

- Computerized simulation of two dimensional turbulent flow in Fourier space with random initial conditions on coefficients, discussing velocity, pressure and vorticity fields 07 p0971 A72-20084

- Numerical determination of particle number and mass flux density in monatomic rarefied gas flow through circular orifice at finite pressure ratio 07 p0972 A72-20107

- Viscous interaction effects on pressure distributions and heat transfer rate on two dimensional surface under high altitude hypersonic flight conditions 07 p0910 A72-20110

- Side force and shock wave induced by obstacle on rocket engine nozzle wall, investigating pressure distribution 07 p1055 A72-20250

- Sealing pressure and optimal groove form for concentric running screw viscosity seals in laminar flow 08 p1178 A72-21931

- Atmospheric boundary layer pressure field expansion into dual series of natural time dependent components to separate fluctuations within monthly period for weather forecasts 08 p1203 A72-22125

- Acoustic approximation of pressure step discontinuity sound propagation in attenuating and dispersive ionosphere 08 p1162 A72-22139

- Rotationally symmetrical cylindrical shell loaded by uniform pressure distribution along length, calculating

quasi-steady viscoplastic flow under Huber-Mises condition

09 p1399 A72-22696

Pressure distribution around circular cylinder with shrouds of various geometry for suppressing flow induced vibrations at subcritical and transition Reynolds number

09 p1261 A72-23315

Adiabatic velocity profiles and pressure variations of developing laminar flow in circular tube, using finite difference computation in FORTRAN IV

10 p1463 A72-23863

Pressure distribution and force coefficients for cones at angles of incidence as function of Mach number, using extended method of equivalent axisymmetric bodies

10 p1417 A72-24028

Numerical solution for super-Alfvénic supersonic aligned MGD flow over cone with attached shock wave, obtaining surface pressure coefficients, current and vorticity distributions

10 p1418 A72-24463

Elastic lung shaped model for distribution analysis of weight induced stresses, strains and surface pressures in lung

10 p1425 A72-24479

Rectangular and D-shaped cylinders pressure distribution and aerodynamic force measurements in two dimensional flow as function of cross sectional height/width ratio

10 p1419 A72-24840

Linear wave dispersion in homogeneous beam plasma system, considering pressure anisotropies generated by external magnetic field

10 p1524 A72-24927

Fluctuating turbulent stresses effects on flow over wavy boundary, comparing calculated with measured pressure distributions

[AD-724545]

10 p1470 A72-25066

Axial pressure variations in incompressible laminar tube flow with uniform suction, noting application to heat pipes

[AIAA PAPER 72-257]

11 p1614 A72-25202

Bolted joint thermal conductance, considering interfacial pressure distribution and surface roughness effects

[AIAA PAPER 72-282]

11 p1741 A72-25222

Base pressure distribution measurement for free flying sharp cone at hypersonic speeds and high angles of attack

[AIAA PAPER 72-316]

11 p1567 A72-25250

Jet flaps for high turning compressor cascades in incompressible axial flow, calculating blade pressure and jet slope distributions

[ASME PAPER 72-GT-16]

11 p1569 A72-25615

Secondary flow measurements in rotating ducts, obtaining pressure distributions and cross-flow velocities

[ASME PAPER 72-GT-17]

11 p1569 A72-25616

Supersonic turbine cascade flow properties and pressure distributions on blades, comparing calculated results with experimental data

[ASME PAPER 72-GT-47]

11 p1570 A72-25639

Turbocompressor deceleration cascades blades surface roughness effects on boundary layer, noting pressure and velocity distributions

[ASME PAPER 72-GT-48]

11 p1570 A72-25640

Radial turbine flow analysis, comparing calculated shroud static pressure distribution and outlet velocity profile with measured data

[ASME PAPER 72-GT-50]

11 p1570 A72-25642

Gas-particle flow trajectories, velocities and pressure distribution in axial flow turbine stage, using cascade tunnel and high speed photographic techniques

[ASME PAPER 72-GT-57]

11 p1571 A72-25648

Pressure and temperature fields expansion in natural orthogonal components, considering application to long range forecasts construction

11 p1683 A72-26889

Bubnov-Galerkin method for dynamic stability of closed thin walled orthotropic cylindrical shell loaded by variable external pressure

11 p1739 A72-26977

Neutral atoms pressure distribution along capillary and pressure compensating channel during discharge in argon ion laser

12 p1819 A72-27133

Boussinesq solution for elastic surface deflection due to continuous pressure with polynomial distribution over triangular area

12 p1884 A72-27568

Shadowgraph photography method for supersonic air flow pattern around porous cone in uniform injection, noting pressure distribution dependence

12 p1752 A72-27986

Nonuniform gas pressure distribution near circular multiple inlet of inherently compensated thrust bearing, considering inward-outward radial flow resistance differential

13 p1963 A72-28748

Surface pressure and vector wind fields computerized analysis from satellite radar radiometer simulation and conventional data

13 p1995 A72-29619

Wind tunnel investigation of pressure perturbations on plane surface due to gas jet injected from surface into subsonic air drift flow

13 p1894 A72-29637

Shock waves amplification by interaction with burning gas-liquid mixture, noting triangular profile of pressure variations behind wave front

13 p2065 A72-29888

Cs vapors thermal conductivity at various temperatures and pressures, using low emissivity Ni cylinders

13 p2065 A72-29896

French monograph on flow near rotor blade tips, discussing three dimensional circulation and boundary layer effects, energy losses, velocity and pressure distributions, etc

14 p2069 A72-30950

Pressure distribution and heat transfer in flow separation zone of cone tipped cylindrical body, using shadowgraph photography for flow visualization

14 p2070 A72-31005

Turbulent boundary layer separation zone subsonic flow before two dimensional rectangular step, examining flow pattern and static pressure distribution

14 p2096 A72-31020

Pressure distribution over delta wing with blunted edges at small angles of attack in hypersonic wind tunnel tests

14 p2071 A72-31022

Iterative numerical solution of linear differential equations system for wind vertical velocity and local pressure variation along vertical line

15 p2265 A72-31344

Deflection and energy dissipation of thin cascade profiles in transonic flow for given pressure distribution, noting boundary layers and separated flow

15 p2178 A72-31501

Orbiting satellite environment and self contamination, calculating pressure, density and condensation rates and adsorption layers on critical surfaces

15 p2321 A72-31870

Contracting or diverging stream flow mean velocity change effects on airfoil pressure distribution, circulation and lift, deriving vortex distribution expression

15 p2179 A72-32023

Large amplitude deflections and induced stresses in uniformly pressure loaded circular plate on elastic foundation, using von Karman coupled nonlinear partial differential equations

15 p2331 A72-32558

Subsonic and supersonic steady two dimensional compressible turbulent boundary layer flow past wavy wall, presenting wall pressure and temperature distributions

16 p2341 A72-32828

Forced vibrations of thick homogeneous anisotropic elastic sphere, studying dynamic response to uniformly distributed internal and external pressure

16 p2424 A72-33147

Vapor pressure and velocity distributions in rarefied gas flows through narrow slits under vacuum conditions with ice sublimation

16 p2380 A72-33854

Flow area computerized prediction for multicompartiment series-parallel spacecraft venting satisfying pressure differential requirements

[AIAA PAPER 72-707]

16 p2462 A72-34038

Transonic airfoil section design to given surface pressure distribution, applying finite difference procedures to transonic small disturbance equations

[AIAA PAPER 72-679]

16 p2346 A72-34062

Velocity-pressure correlations in a homogeneous turbulence associated with a plane pure deformation

17 p2537 A72-34280

Unsteady flow at the junction of a branched duct

17 p2539 A72-34971

Pressure distribution on a yawed wedge interacted by an oblique shock

17 p2485 A72-35239

Study of flow in a passage in the presence of transverse alternating pressure gradients

19 p2785 A72-37467

Gas-liquid hydrogen mixture and helium adiabatic model of Jupiter temperature and pressure distribution, estimating planet center temperature

19 p2863 A72-38074

An experimental study of the sensitivity to freestream turbulence of heat transfer in wakes of cylinders in crossflow

19 p2787 A72-38396

Post-critical deformations of a cylindrical shell subject to the action of external pressure and a temperature field

19 p2878 A72-38472

Pressure pulsation measurements at nose of well-streamlined body of revolution at high Reynolds numbers, noting turbulent pressure field intensity growth and decay

20 p2912 A72-39362

Pressure jump across normal ionizing shock waves

21 p3045 A72-40566

Experimental investigation of pressure profiles in a helical shock wave irregularly reflected in plexiglass cylinders

21 p3045 A72-40988

Calculation of rib-reinforced minimum-weight cylindrical shells under external pressure by the random search method

21 p3119 A72-41099

Engine inlet total pressure distortion effects on multistage axial compressor and turbojet/turbofan engine performance and stability, considering inlet-engine compatibility

[ICAS PAPER 72-19]

21 p2991 A72-41144

Theoretical and experimental study of the pressure and heat-flux distributions on a control surface in the presence of a thick hypersonic turbulent boundary layer

[ICAS PAPER 72-23]

21 p2991 A72-41148

Integral equation for pressure distribution by rigid punch contact with elastic half space, solving by Mathieu function expansion in Fourier series

21 p3126 A72-41541

Wall interference effects on cone-cylinder pressure distribution in variable porosity trisonic wind tunnel as function of model blockage and Mach number

[AIAA PAPER 72-1010]

21 p3041 A72-41592

Photoelastic study of stress concentration in perforated composite pipes under external pressure

22 p3233 A72-42064

Self-consistent description of the magnetotail current system

22 p3172 A72-42429

Fluid sphere of uniform density and vanishing pressure at periphery, expressing internal motion in terms of Schwarzschild mass and radius and central pressure

22 p3205 A72-42451

Sea level tropospheric pressure distribution persistence correlation to solar corpuscular radiation measured by planetary scale geomagnetic disturbance

22 p3219 A72-42517

German monograph - Pressure variation along a plane slender wedge and along a slender cone of revolution at decelerated flight in the supersonic range near sonic velocity

22 p3136 A72-43074

Flutter analysis and unsteady pressure fields induced by pitching motions of wall mounted sweptback wing, verifying experimentally lifting surface theory in high subsonic range

22 p3241 A72-43094

Calculation of radial pressures in metal-fiber-reinforced materials during compacting

23 p3298 A72-43277

Pressure at the trailing edge and losses in turbine bladings with air injection into the blade wake

23 p3248 A72-43661

Frequency response of ducts in the shape of a truncated cone

23 p3279 A72-43697

Asymmetric imperfections effect on spherical elastic shell buckling strength under uniform external pressure

23 p3351 A72-44104

Computation of the potential-theoretical flow around wing-fuselage combinations and a comparison with measurements

23 p3249 A72-44298

Viscous interaction over concave and convex surfaces at hypersonic speeds

23 p3249 A72-44308

Pressure and temperature change on the wall surface in strong shock wave diffraction

24 p3391 A72-45047

Performance and flow properties change through a rocket turbine by presence of solid particles

24 p3361 A72-45206

Trailing vortex effects on wing pressure distribution from low speed wind tunnel tests, discussing effect of wing-vortex distance

24 p3362 A72-45331

An experimental investigation of a jet issuing from a wing in crossflow

24 p3362 A72-45332

The wedge probe - A review

24 p3404 A72-45355

Experimental research on the wave resistance of a thin spindle with an annular shield in a supersonic axial flow

24 p3364 A72-45393

Average circumferential pressure on inclined bodies of revolution at hypersonic speed

24 p3365 A72-45788

PRESSURE DRAG

NT INTERFERENCE DRAG

NT SUPERSONIC DRAG

NT WAVE DRAG

Wake outflow concept application to flow separation phenomena, enabling determination of base pressure for drag calculations

[DFVLR-SONDDR-176]

05 p0603 A72-16702

Navier-Stokes equation solution for laminar incompressible flow past parabolic cylinder, investigating skin friction and pressure drag

06 p0798 A72-17782

Base pressure drag reduction on rectangular wings with blunt trailing edges from low speed wind tunnel measurements

[DFVLR-SONDDR-219]

10 p1419 A72-24842

Subsonic powered nacelle wind tunnel model for investigation of geometric variables effect on pressure drag
[ASME PAPER 72-GT-14] 11 p1568 A72-25613

PRESSURE DROP

Pressure drop relation to entropy production in viscous low velocity adiabatic pipe flow, showing analogy with Oswatitsch theorem
01 p0051 A72-11255

Kinetic energy correction in capillary viscometry, observing pressure drops and mass flow rates
02 p0202 A72-11724

MHD flow development in parallel plate channel entrance region, obtaining numerical solution for velocity distribution, pressure drop and length at different Hartmann numbers
02 p0266 A72-12493

Rectangular and triangular duct entrance region laminar flow pressure losses from velocity profiles and integral energy equation
04 p0512 A72-15194

Pressure drop of homogeneous and annular wick heat pipes using hydrogen, nitrogen and oxygen working fluids, discussing heat transfer capacity
[ASME PAPER 71-WA/HT-13] 05 p0744 A72-15873

Navier-Stokes equations solution by finite difference methods for steady incompressible laminar vapor flow in symmetrical and unsymmetrical heat pipes, calculating pressure losses
[ASME PAPER 71-WA/HT-15] 05 p0744 A72-15874

Boundary layer growth measurements in optimum annular diffusers, discussing pressure recovery and mean total pressure loss
[AIAA PAPER 72-86] 05 p0604 A72-16807

Shocked flow and pressure loss computation for axial flow compressor cascades, using time dependent finite difference technique
[ASME PAPER 72-GT-31] 11 p1569 A72-25627

Screw type axial flow pump impellers pressure losses generalization by dimensionless coefficient in Euler number form
12 p1752 A72-28139

Impulse liquid jet pressure reduction in closed vessel under adiabatic conditions and evaporation intensity dependence on jet velocity
16 p2476 A72-33259

German monograph on pressure loss and heat transfer in heat exchangers, taking into account hydrodynamic and thermal inflow velocity and temperature distribution
16 p2478 A72-33504

German monograph on surface roughness effects on pressure loss and heat transfer in high temperature turbulent flow, deriving universal laws
16 p2478 A72-33506

Prediction of tank pressure history in a blowdown propellant feed system.
17 p2537 A72-34211

A method of calculating acoustic resonance phenomena generated by the unsteadiness of singular pressure losses in the pipes
17 p2580 A72-34279

Determination of the parameters associated with a singular pressure loss permitting the calculation of acoustic resonance phenomena and the role of these parameters
18 p2680 A72-36465

Vapor pressure decrease rate during cooling agent introduction in semiclosed volume, determining pressure drop from energy and mass conservation equations
19 p2879 A72-37355

Study of flow in a passage in the presence of transverse alternating pressure gradients.
19 p2785 A72-37467

Compressor exergetic efficiency calculation from gas exergy losses caused by pressure drop and cooling, noting relations to isothermal, adiabatic and polytropic efficiencies
19 p2746 A72-37668

Pressure loss and heat transmission in cylindrical ducts
[ONERA, TP NO. 1057] 19 p2880 A72-37768

A theoretical solution of the Lockhart and Martinelli flow model for calculating two-phase flow pressure drop and hold-up.
19 p2787 A72-38392

Determination of pressure losses in turbomachines.
24 p3393 A72-45353

Investigations on the stability of the characteristic of radial flow fans.
24 p3363 A72-45356

A study of loss of radial equilibrium solution in axial-flow blade row design calculations.
24 p3393 A72-45358

PRESSURE EFFECTS

Impurity, surrounding gas and pressure effects on organic semiconducting material electrical conductivity, discussing carrier origin and number, and measurement techniques
01 p0113 A72-10125

Acoustic power radiated by jet aircraft fuselage structure exposed to turbulent boundary layer pressure field, evaluating noise reduction treatments
01 p0002 A72-10216

Heat transfer in turbulent flow of equilibrium dissociating nitrogen tetroxide within round tube, considering pressure, temperature and mass flow rate effects
01 p0145 A72-10490

Impact sensitivity of space shuttle materials in liquid and gaseous oxygen at high pressures
01 p0102 A72-10772

Superpressure balloons (tetrans)/ performance characteristics, determining ascent rates and superpressure, stress and volume perturbations due to forced change in height
01 p0005 A72-10829

Polyethylene-FLOX hybrid stage optimum combustion chamber pressure, representing pressure dependent factors by simple analytical models
01 p0117 A72-11221

Human mental and psychomotor performance measurements in compressed oxygen-helium atmosphere pressure chamber for dive between 100 and 1500 feet
02 p0166 A72-11701

Thermal conductivity measurement of dissociating nitrogen dioxide over 548-792 K and 1-30 atm
02 p0170 A72-12091

Hypersonic boundary layer transition in presence of wind tunnel noise, indicating rms sound pressure relationship to transition Reynolds number
02 p0151 A72-12278

Active ingredient oxidizing potential and pressure effects on burning rate of explosive substances
02 p0302 A72-12292

Dust grain existence at large distances from galactic plane by computing interstellar radiation field pressure effects on grains
02 p0283 A72-12629

Bending stresses in composite shell at conical interface between metal and fiberglass reinforced plastic portions under internal pressure
02 p0298 A72-12683

Differential pressure effects of gas-liquid configuration on porous electrode activity in oxygen cathodes
03 p0311 A72-12923

Pressure induced band deformation effect on magnetic susceptibility of Ti-V and V-Cr alloys
03 p0370 A72-13087

Lunar induced and permanent magnetism, discussing solar wind dynamic pressure effects and Apollo data
03 p0418 A72-13109

High velocity impact reduced temperature increase due to shock compression in metals, discussing pressure and charge effects
03 p0442 A72-13240

Creep buckling of cylindrical finite two-layer shell under external hydrostatic pressure, considering rigidly clamped and hinged end conditions
03 p0444 A72-13574

Thick walled rigid plastic cylinders under pressure, obtaining uniqueness and stability of finite deformation
03 p0446 A72-13706

Critical load and stability analysis for three layer orthotropic cylindrical shell with filler under nonuniform external pressure
03 p0448 A72-13906

Long period perturbations arising in orbits of artificial satellites with large surface to mass ratio under solar radiation pressure and earth oblateness effects
04 p0572 A72-14637

Carbon dioxide gas dynamic laser mixture at high pressure, investigating gain and vibrational kinetics
04 p0531 A72-15336

Weak magnetic moments measurement under pressure and over wide temperature range by Faraday method, discussing magnetometer and cryogenic equipment modifications
[AD-740076] 04 p0522 A72-15478

Rate constant for quenching of B⁺/super 2/Sigma⁺ state of CN radical as function of quenching collision relative velocity and total pressure in fluorescence cell
04 p0553 A72-15635

Quasi-stationary pulsed discharge characteristics of nitrogen plasma as function of current density and pressure
05 p0693 A72-15839

Temperature, pressure and crystallization time effects on artificial diamond crystal growth of various morphological shapes
05 p0681 A72-16355

Meridional curvature effect on thin walled cylindrical shell buckling under external constant directional lateral pressure
05 p0739 A72-16546

Metastable He atoms concentration in plasma from absorption characteristics at temperatures 4-300 K and pressures 1-70 mm Hg
05 p0696 A72-16612

Mass addition distribution and gas injectant effects on heat transfer rates, transition locations and surface pressures of sharp cone
[AIAA PAPER 72-183] 05 p0748 A72-16838

SST operational maneuver effects on sonic boom, discussing steady flight and acceleration-to-cruise pressure signatures
[AIAA PAPER 72-196] 05 p0613 A72-16981

Hydraulic fluids behavior under extreme temperature, pressure and filtration conditions, considering viscosity, wear and corrosion resistance
05 p0681 A72-17084

Supercritical deformation, bulging and instability of spherical edge clamped shell under external pressure, applying variational principle
05 p0742 A72-17210

Solar wind stream-stream interactions, studying time profiles, velocity variations, corotating spiral, increased pressure due to radial compression and zonal flow directions
06 p0872 A72-17443

Hydrostatic pressure effects on I-V characteristics of amorphous semiconductor germanium telluride sulfide arsenide
06 p0865 A72-17493

Composite propellant powder combustion velocities as function of pressure, discussing powder sensitivity, limiting kinetic stage changes and surface monovariant equilibrium
06 p0867 A72-17568

Spin stabilized axisymmetric probe altitude deviation due to solar pressure in elliptic orbits
06 p0892 A72-17655

Condenser microphones sensitivity and frequency response characteristics measurement at normal and elevated atmospheric pressures in hyperbaric chamber air and He-air environments
06 p0766 A72-17808

Finite amplitude fluctuations evolution in extended self-gravitating media for initial disturbances, taking into account pressure effects
06 p0880 A72-17888

Nonsteady powder combustion under harmonically varying pressure
06 p0902 A72-17907

Output power dependence on pressure and magnetic field strength in Kr ion laser for green, yellow and red lines
06 p0826 A72-18010

Mathematical-physical model for laser pulsed radiation-induced pressure wave transmission through surface and internal biological tissues
06 p0768 A72-18150

Operational stability of rocket engine with combustion chamber having charge of two propellant types with different burning rate dependences on pressure
06 p0867 A72-18206

Erosion burning in cylindrical ballistite powder N specimens under 50-80 kg/sq cm in simulated constant pressure combustion chamber with supersonic and subsonic nozzles
06 p0903 A72-18208

Burning rates dependence on pressure in mixtures of ammonium perchlorate with succinic, glutaric, adipic, azelaic, sebacic, fumaric and aminosuccinic acids
06 p0867 A72-18210

High energy chemical propellant combustion under adiabatic and nonadiabatic conditions, calculating product equilibrium state as functions of temperature and pressure with computer program
06 p0903 A72-18212

Recombination coefficient, ionization rates and average lifetime of ions in rarefied carbon-air flames, investigating pressure and additives effects
06 p0904 A72-18213

Polymer films friction properties under high pressure, discussing Amontons law failure and adhesion theory application
06 p0837 A72-18597

Solar radiation pressure effects on gravity oriented satellites librational dynamics, using digital computer aided numerical analysis and analog simulation
07 p1067 A72-18789

External pressure effects on stability of closed toroidal shell with circular cross section
07 p1087 A72-18993

Extraretinal inflow eye position information awareness from experimental load application to eyes in total darkness
07 p0926 A72-19026

Axisymmetric deformation of infinite cylindrical shell under stress-strain state arising from internal pressure in statistically inhomogeneous Winklerian medium
07 p1088 A72-19258

Classical path theory of pressure broadening in radiating atomic system perturbed by other atoms
07 p1037 A72-19497

Nitrogen interaction with liquid binary Ni alloys, investigating solubility as function of temperature and pressure and titanium nitrides existence conditions
07 p1011 A72-19547

Pure and doped ammonium perchlorate deflagration rate sensitivity due to sample temperature and environmental pressure changes
07 p1051 A72-19729

Aircraft noise protective earplug design, employing perforated and slit modifications for additional protection without tympanic membrane pressure excess risk
07 p0933 A72-20187

- Pressure effects on molten metals reactions with ambient atmosphere during purification by distillation, obtaining impurities concentration ratio via Langmuir relative volatility rule
07 p0997 A72-20287
- Inhomogeneous high-collision finite pressure plasma stability, finding thermal instability development under uniform temperature and arbitrary pressure
07 p1046 A72-20514
- External pressure effects on cantilever rotating shaft vibration, determining critical whirling speed as function of pressure and area distribution by energy method
07 p1096 A72-20528
- Secondary explosive spark detonators design and performance, determining ambient pressure variations effects on firing characteristics
08 p1219 A72-20758
- Splanchnic vascular bed role in human blood pressure regulation from lower body negative pressure tests, measuring blood flow from hepatic dye removal rates
08 p1123 A72-20889
- Electrical erosion efficiency of metal working under increased pressure in discharge gap in air and water
08 p1174 A72-21029
- Compression cycles effects on alveolar volumes of sea lions and dogs excised lungs, noting decompression sickness prevention by airways cartilaginous reinforcement
08 p1116 A72-21186
- Multimode cavity for simultaneous oxygen/argon plasma excitation and electron density measurements, noting gas pressure effect
08 p1213 A72-21323
- Heat transfer in shield-vacuum thermal insulation layers at various temperatures and pressures, noting conductivity anisotropy
08 p1253 A72-21451
- Evaporation and combustion of liquids injected into high temperature supersonic flow, considering interrelation with pressure variations
08 p1253 A72-21454
- Time varying external pressure effect on creep collapse of long thin walled quasielliptical cylindrical shell, taking into account elastic deformation
08 p1245 A72-21612
- Mathematical model of solar radiation pressure effects on earth satellite orbit
08 p1237 A72-21643
- Orthotropic hinged cylindrical shell stability under uniform external pressure, deriving linearized three dimensional differential equations
08 p1246 A72-21711
- Deformability and carrying capacity of glass fiber-polymer composite thick walled rings under internal or external pressure
08 p1195 A72-21764
- Building structures response to transient pressures caused by sonic booms, discussing three dimensional loading effects, air cavity coupling and nonlinearities influence
08 p1249 A72-21908
- Stress-deformation effects on gasket joint of metal seals at high pressures
08 p1178 A72-21933
- Bushing seal with pressure dependent clearance for reciprocating piston rod or rotating shaft, presenting laminar and turbulent axial flow theory
08 p1178 A72-21936
- Pressure gradient relations for viscous fluid flow in clearance seals at high pressures
08 p1178 A72-21937
- Pipe joint flexible metal seal development and testing for Concorde Olympus 593 under thermal and pressure cycling
08 p1178 A72-21938
- Reduced air pressure effect on He-Ne laser output power via self heating
08 p1184 A72-22033
- Solar magnetic fields forced latitudinal drift rate due to differential rotation, taking into account turbulent friction and pressure forces
09 p1382 A72-22286
- La superconductivity pressure dependence based on valency considerations, noting actinides metals and alloys localized magnetism explanation by simple model
09 p1368 A72-22557
- Pressure effects on transition temperature and electronic structure of narrow band superconductors
09 p1368 A72-22562
- Transition temperature pressure dependence determination for d- and f-band superconductor metals, alloys and compounds
09 p1368 A72-22563
- Chinchilla and guinea pig tolerances to hypoxia and hyperoxia in pressure chamber tests, suggesting relation to red blood cell size and number
09 p1265 A72-22647
- Pressure broadened atomic line shapes calculation for Cs resonance line pressurized by Ar, using Lennard-Jones potentials
09 p1354 A72-22663
- Temperature and internal pressure effects on circular cylindrical shell stability under tension and compression, deriving critical temperature and loads
09 p1402 A72-22736
- Optimum pressure and field conditions for intense relativistic electron beam transport in longitudinal magnetic field
09 p1360 A72-22870
- Pressure effect on combustion rate of Mg particles in water vapors
09 p1411 A72-22887
- Pulsed carbon dioxide laser operation, measuring pulse energy variation with gas pressure, expansion nozzle shape and output mirror transmission
09 p1323 A72-22980
- Samaria distribution effect on Ni-Cr alloy oxidation rate for various oxygen pressures, discussing behavior of electroplated and bulk specimens
09 p1332 A72-23585
- Increased atmospheric pressure influence on blood coagulation in rabbits, showing post-decompression hypercoagulation followed by hypocoagulation
09 p1268 A72-23597
- Pressure sensitivity of Na-K-Mg ATPase activity from rat intestine, investigating inhibiting effects of oxygen, nitrogen and helium tension increases
10 p1424 A72-23731
- Active ingredient oxidizing potential and pressure effects on burning rate of explosive substances
10 p1561 A72-23767
- Ion acceleration by relativistic electron-beam-formed plasma, explaining ion energy dependence on neutral gas pressure by potential well model
10 p1518 A72-23961
- Chest strapping-induced increased lung recoil pressure effects on maximal expiratory flow relation to lung surface compliance decrease
10 p1425 A72-24478
- Modular carbon dioxide laser design and operational features, reporting measured data on plasma tube current, pressure and gas mixture flow rate effects on power output
10 p1492 A72-24565
- Pressure dependence of gas laser intensity, taking into account velocity changing collisions with foreign gas atoms
10 p1492 A72-24604
- Rb87 vapor laser with optical pumping, measuring nitrogen or nitrogen argon mixture buffer gas partial pressure effect on power output
10 p1493 A72-24911
- Supercritical deformation, bulging and instability of spherical edge clamped shell under external pressure, applying variational principle
11 p1727 A72-25341
- Dynamic nonlinear elastic response of buckling sensitive cylindrical shells to lateral pressure loading, using numerical and computerized analysis
11 p1729 A72-25386
- Rectangular skin panel vibration modes aerodynamic damping dependence on Mach number, dynamic pressure, mode shape and turbulent boundary layer thickness
11 p1568 A72-25423
- Design considerations in selecting geometries for high pressure ratio single stage centrifugal compressors
11 p1571 A72-25665
- Molecular process and pressure effects on hydrogen formation in methyl acetylene photolysis at 1236 Å
11 p1590 A72-26011
- Cardiovascular responses to positive pressure oxygen breathing from blood pressure and heart and respiratory rate measurements
11 p1584 A72-26017
- Effective atmospheric emissivity for clear skies, showing dependence on surface vapor pressure
11 p1681 A72-26084
- Quasi-steady operation establishment in pulsed MPD arc jet, investigating ion density radial distribution and initial tank pressure and magnetic field effects on plasma front arrival
11 p1696 A72-26219
- Ar laser levels population inversion dependence on current density, discharge tube pressure and magnetic flux
11 p1649 A72-26350
- Pure metals bulk modulus pressure dependence from detonation generated shock wave data, using empirical relations between propagation velocity and material flow rate
11 p1662 A72-26741
- Test device for reinforced plastics mechanical properties under heating and pressure with allowance for gas permeability
11 p1613 A72-26813
- Thermodynamic description of metal rich side of Nb-Mo-N solid solution, determining equilibrium nitrogen solubility as function of pressure and temperature
11 p1664 A72-26842
- Nonregular oceanic level fluctuations dependence on atmospheric pressure and tangential wind stress, deriving fluctuation spectrum from linear hydrodynamic model
11 p1682 A72-26882
- Hydraulic vortex amplifiers with and without diffusers, discussing supply pressure and liquid viscosity effects on system performance
11 p1578 A72-26980
- Quadrupole ion pump performance characteristics, presenting pumping speed as function of pressure at different peak voltages
12 p1805 A72-27040
- Electrical conductivity measurement of dense nonideal Cs plasma at high pressure and temperatures
12 p1849 A72-27057
- Dynamic deflection of elastic rectangular plate hinged to rigid base moving under sinusoidal pressure impulse action, noting base inertia effect
12 p1879 A72-27091
- Newton-Busemann pressure law derived for hypersonic rotationally symmetric flow from momentum theory considerations and plane flows
12 p1751 A72-27120
- Fourier transform approximate inversion solution for transient pulse propagation from spherical cavity with surface under impulsive pressure in viscoelastic medium
12 p1844 A72-27196
- Boron doped n-type Si planar diode and n-p-n epitaxial planar Si transistor junctions investigating hydrostatic pressure effects on static characteristics and breakdown voltage
12 p1789 A72-27314
- Hydrostatic pressure effect on itinerant antiferromagnetic ordering in Cr-Fe alloys with Ru and Mn additions
12 p1828 A72-27432
- Pathological significance of high oxygen tension exposure effects on acid soluble collagen extracted from mouse skin
12 p1760 A72-27483
- Pressure effects on resonance fluorescence lifetimes in sulfur hexafluoride-air mixtures exposed to carbon dioxide laser radiation
12 p1826 A72-27929
- Closed thin circular cylindrical shells external pressure pulse and structural parameters effects on stability under dynamic loading
12 p1886 A72-28129
- Thin surface film lamination in antifriction carbon-graphite materials under critical specific pressure, discussing crystalline phase in wear products
12 p1818 A72-28192
- Gas turbine engine compressor blade and materials fatigue strength dependence on pressure under contact friction corrosion
12 p1831 A72-28244
- USAF V-51R noise protector earplugs modification to allow for pressure equalization during aircraft climb and descent
12 p1774 A72-28276
- Axisymmetric stability of spherical cap rigidly clamped at contour of shells of revolution, using variational difference method for uniformly distributed external pressure
13 p2053 A72-28393
- Spatially resolved gain measurements in carbon dioxide laser amplifier, considering gas mixture, flow rate, temperature, pressure and current effects
13 p1967 A72-28448
- Uniaxial elastic deformation pressure effects on electronic conduction in tetrahedrally bonded amorphous semiconducting thin films as function of temperature
13 p2021 A72-28574
- Finite circular cylindrical shell under uniform pressure on outer rim, comparing stresses and displacements
13 p2055 A72-28624
- Pressure law for flow between two parallel plates describing medium action on plates, noting plate flutter analogy to buckling
13 p2056 A72-29002
- Vacuum induction melting process for high temperature steels and superalloys fabrication, emphasizing control over temperature, pressure, beneficial trace elements and harmful impurities
13 p1964 A72-29100
- Catalytic effects on ammonium perchlorate combustion pressure limits, noting distribution, concentration and particle size effects
13 p2025 A72-29303
- Solid propellants burning rate dynamic response to rapid pressure changes, discussing equations applicability to combustion extinction prediction as function of pressure decay rate
13 p2065 A72-29304
- Time history model of transient ignition to self sustained propellant burning, taking into account pressure effects and igniter heat flux
13 p2065 A72-29305
- Hydrostatic pressure effect on tensile creep and creep rupture of polycrystalline metals at high temperatures
13 p2058 A72-29450
- Combustion products thermodynamic parameters for natural gas burning in oxygen atmosphere, plotting gas temperature and flow rates against pressure and excess oxidant ratio
13 p2065 A72-29451

Cryogenic liquids cavitation erosion of plastic and cold-short metals at 77 K, determining vapor pressure effect

13 p1979 A72-29479

Ammonium perchlorate burning rate temperature dependence as function of pressure and oxidizer particle size, noting low pressure deflagration limit [ONERA, TP NO. 1079]

13 p2025 A72-29669

Small amplitude plane wave speed variation with pressure for Na and K at absolute zero temperature, using crystal strain energy formulation

13 p2006 A72-29675

K-order differential equation solution obtained for system of polynomial functions for shallow spherical shell under uniform pressure, using Bubnov-Galerkin and collocation methods

13 p2062 A72-29947

Concentration profile derivation for fluid flow near rotating disk with chemical reactions, considering concentration gradient and barodiffusion effects

13 p1944 A72-30049

Nitrous oxide band intensities, half widths and pressure broadening coefficients

13 p2008 A72-30059

Hydrated iron silicon fluoride internal motion pressure dependence examined by wide-line and NMR techniques, noting corrections of second moments for bulk paramagnetic effects

13 p1914 A72-30061

Magnesium particle combustion in rarefied air during pressure changes, discussing combustion time decrease with pressure increase

14 p2170 A72-30236

Free stream turbulence and pressure gradient effects on boundary layer transition, correlating theoretical prediction methods and experimental results

14 p2093 A72-30253

Tubular materials plane stress-strain test facility for combined axial load and internal pressure effects, describing principal components

14 p2092 A72-30442

Co-Cr alloy oxidation as function of temperature and oxygen partial pressure, discussing solid state diffusion

14 p2118 A72-30544

Octahedral TiC single crystals oxidation at high temperature in oxygen, carbon dioxide and mixtures, investigating oxygen partial pressure effects on kinetics

14 p2121 A72-30772

Ferrite powder relative density as function of temperature, sintering time and pressure during hot pressing, noting creep activation energy and vacancy motion

14 p2107 A72-30775

Pressure effects of Ar and He mixtures on Cs atomic line shapes calculated assuming additivity of perturber interactions

14 p2134 A72-30838

Free convection effect on vertical porous insulation layer thermal conductivity in high pressure gas environment

14 p2172 A72-31057

Stapedectomy postoperative complications as flying hazard, discussing pilot reaction to middle ear pressure changes

14 p2082 A72-31094

Free electrons in condensed matter under high pressure, calculating number with Thomas-Fermi statistical model

15 p2305 A72-31338

Relaxation oscillations in He gas discharge tubes with cold Mo cathode as function of pressure and discharge length

15 p2245 A72-31408

Carbon dioxide TEA high output pulsed laser, testing wide range of carbon dioxide-nitrogen-helium mixtures at various pressures

15 p2246 A72-31638

Optimization of heat pipe with wick and annulus liquid flow, investigating effect of pressure loss and recovery in vapor passage

15 p2335 A72-31767

Piston generated magnetosonic shocks, investigating ion and electron pressure effects on formation

15 p2281 A72-32415

Surface electrode distance, area and pressure effects on electromyogram recording of large skeletal muscle electrical activity during defined muscular tensions

15 p2190 A72-32490

Air pressure effects on absorption dependence at IR wavelengths, using water vapor transmittance windows

15 p2202 A72-32657

Temperature and pressure requirements for producing superfluid liquid molecular hydrogen, noting use of solid deuterium or Ne walls to prevent hydrogen solidification

16 p2422 A72-32911

Nonlinear stress-strain-curvature problem applied to noncircular cylindrical membrane shell under lateral pressure

16 p2464 A72-32917

Unsteady Falkner-Skan flow solution by finite difference method for pressure gradient effect on transient response of laminar boundary layer

16 p2376 A72-33015

Small disturbance behavior in laminar boundary layer on elastic surface experiencing deformation under perturbing pressure, noting surface resilience effect

16 p2377 A72-33164

Ar laser levels population inversion dependence on current density, discharge tube pressure and magnetic flux

16 p2402 A72-33703

Hydrogen solubility in Zr-Nb-H systems as function of composition, temperature and hydrogen equilibrium pressure

16 p2410 A72-33816

Pressure effects on heat transfer from heated surface to fluidized bed at 150-1000 C, noting carrier gas heat conductivity effects

16 p2479 A72-33852

Negative pressure gradients effects on turbulent viscosity profiles for gas flow through tubes, comparing dependence on transverse coordinates to incompressible flow case

16 p2380 A72-33860

Lateral pressure gradient and suction effects on laminar incompressible boundary layer separation on curved surfaces predicted by generalized tow-layer flow model

[AIAA PAPER 72-698]

16 p2380 A72-34045

Flowing air glow discharge near IR emission spectrum as function of pressure, noting atomic lines

16 p2427 A72-34097

Pressurized crack behavior in two-dimensional rocket motor geometries.

17 p2596 A72-34203

Stresses in a welded diaphragm due to boundary contraction and normal uniform pressure.

[SESA PAPER 1811]

17 p2631 A72-34821

The effect of axial boundary motion on pressure surge generation.

[ASME PAPER 71-WA/EE-15]

17 p2539 A72-34969

Austenitic steel stress corrosion prevention at high temperatures and pressures, investigating inhibitor adsorption properties from capacitance measurements and polarization curves

17 p2568 A72-35474

Sudden freeze approximation for fluid flow systems relaxation time at constant enthalpy and pressure

17 p2542 A72-35633

Stability of a dome rigidly clamped over its edge under uniform external pressure

17 p2635 A72-35806

Mathematical model for flow limitation in collapsible tube in relation to pressure in pulmonary and circulatory system

17 p2510 A72-35972

Effect of pore pressure on the velocity of compressional waves in low-porosity rocks.

18 p2685 A72-36031

Investigation of transient pressures in the plasma of a thermionic emission converter

18 p2647 A72-36214

Arc mode thermionic converter at low cesium vapor pressures

18 p2647 A72-36216

Theoretical model for plane turbulent wakes subject to adverse, favorable and mixed pressure gradients based on Reynolds stress equation, describing experimental verification

18 p2680 A72-36477

Electric contact between metal and n-type semiconductor, investigating contact pressure effects on electron tunneling and phonon conductance to provide band structure

18 p2718 A72-36488

Influence of pressure on the combustion process of aluminum powders

19 p2847 A72-37368

Influence of pressure, mass flow rate, and nozzle angle on the chemical relaxation in nozzles

19 p2880 A72-37494

Behavior of glass fiber reinforced plastic cylindrical shells under the action of external pressure pulses

19 p2872 A72-37538

Importance of nozzle geometry to high-pressure gas-dynamic lasers.

19 p2811 A72-37867

Pressure shift of the magnetic resonance line of neon in a He-Ne laser.

19 p2811 A72-37930

Effect of chemical reaction reversibility on the temperature and pressure dependence of burning rates

19 p2882 A72-38455

Characteristics of a closed-type aerostatic slider bearing

19 p2809 A72-38565

The effect of cross relaxation on the behavior of gas laser oscillators.

19 p2813 A72-38691

Radio-frequency preionization in a supersonic transverse electrical discharge laser.

19 p2813 A72-38694

Neurologic oxygen toxicity - Effects of switch of inert gas and change of pressure.

19 p2758 A72-38704

Experimental investigation of the detonation properties of hydrogen-oxygen and hydrogen-nitric oxide mixtures at initial pressures up to 40 atmospheres.

19 p2883 A72-38875

The effect of hydrostatic pressure on plastic deformation and creep of polycrystalline metals at elevated temperatures.

20 p2977 A72-38878

Testing of hydrogen pressure or stress concentration induced crack propagation theory for steels based on decohesion mechanism

20 p2935 A72-39003

Influence of gas pressure in arc lamps on the pumping efficiency of CW garnet lasers.

20 p2933 A72-39513

Effect of uniaxial pressure on the threshold current of double-heterostructure GaAs lasers.

20 p2933 A72-39559

Nonperiodic oceanic level fluctuations dependence on atmospheric pressure and tangential wind stress, deriving fluctuation spectrum from linear hydrodynamic model

20 p2948 A72-39569

HCN laser mechanical, pressure, temperature and voltage environmental factors effects on output power stability

20 p2934 A72-39967

HF absorption of electromagnetic field in ionized oxygen plasma as function of dc discharge current

20 p2958 A72-39969

Steady capillary-gravitational waves of finite amplitude generated by pressure periodically distributed along the flow surface of a fluid of finite depth.

21 p3044 A72-40261

Transverse CO2 laser action at several atmospheres.

21 p3062 A72-40572

Shear modulus of liquids at elastohydrodynamic lubrication pressures.

21 p3059 A72-40688

Pressure dependence of electrical characteristics of semiconductor sensors using deformation potential for mechanical stress detection and measurement

21 p3056 A72-41109

Engine inlet total pressure distortion effects on multistage axial compressor and turbojet/turbofan engine performance and stability, considering inlet-engine compatibility

21 p2991 A72-41144

Behavior of viscoelastic shallow spherical shells subjected to dynamic pressure.

21 p3122 A72-41245

Forced vibration solution and wind tunnel investigation of shallow cylindrical shells under moving pulsating pressure discontinuities, noting compression shock effects

21 p3122 A72-41352

Reynolds number and drive power variation with Mach number, pressure and temperature in cryogenic wind tunnel

21 p3040 A72-41581

Heat transfer performance of stationary two phase closed thermosiphon with water and Freon as working fluids, discussing effects of operating pressure and heat flux

21 p3131 A72-41621

Hydrostatic pressure effects on atomic configuration based on principle of equivalence related to Einstein gravitational equations

22 p3205 A72-42459

Equimolar oxyhydrogen detonation wave behavior near pressure limit, considering unsteadiness caused by tube length

22 p3244 A72-42485

Oxygen consumption in liquid breathing mice.

22 p3142 A72-42488

Speech intelligibility during exercise at normal and increased atmospheric pressures.

22 p3150 A72-42496

Case report on dive decompression induced maxillary sinus barotrauma due to sinus pressure buildup caused by ostium blockage

22 p3150 A72-42497

Influence of a sinusoidal pressure variation on contact thermal resistances

22 p3244 A72-42644

Attitude control of satellites using the solar radiation pressure.

22 p3231 A72-42871

Pressure dependent microwave cavity breakdown field relationship to steady state plasma luminosity interpretation as evidence of RF confinement of low density plasma

22 p3212 A72-42897

Effect of the process of crystallization of the liquid phase under pressure on the properties of Silumin

22 p3192 A72-42959

Study of the variation of the intensity of vibration-rotation spectra of hydrogen halide molecules under the action of compressed foreign gases

22 p3209 A72-43047

Pressure effect at arbitrary Knudsen numbers.

23 p3279 A72-43216

- Laser compression of matter to super-high densities - Thermonuclear (CTR) applications 23 p3294 A72-43262
- Lower-body negative pressure as a method of preventing shifts associated with changes in the hydrostatic pressure of blood 23 p3256 A72-43919
- Gain measurements of matrix-type TEA CO₂ laser. 23 p3296 A72-44072
- Quartz and feldspar glasses produced by natural and experimental shock. 23 p3285 A72-44136
- A new method of measuring temperature, inversion ratio, and pressure-broadened linewidth in a CW molecular laser. 23 p3297 A72-44188
- The pressure dependence of the E2 reflectivity peak and of the dielectric constant in III-V semiconductors. 23 p3324 A72-44321
- Influence of elevated partial oxygen pressure on the sympathetic-adrenal and acetylcholine systems 24 p3371 A72-44595
- Development of a push-pull fatigue testing machine under high pressure, and the results of preliminary fatigue tests. 24 p3401 A72-44630
- The influence of the atmosphere on the wavelength of the He-Ne laser and the solution of corrections of the laser interferometer. 24 p3409 A72-44771
- Investigation of radiation paramagnetic defects in alkaline-silicate glass subjected to the action of high quasi-hydrostatic pressures - Structure of hole defects 24 p3417 A72-45421
- Unconjugated urinary corticosterone excretion in laboratory rats exposed to high pressure helium-oxygen environments. 24 p3374 A72-45656
- Electrical conductivity measurement of dense nonideal Cs plasma at high pressure and temperatures 24 p3431 A72-45710
- PRESSURE FIELDS**
U PRESSURE DISTRIBUTION
PRESSURE GAGES
 NT BAYARD-ALPERT IONIZATION GAGES
 NT IONIZATION GAGES
 NT KNUDSEN GAGES
 NT MANOMETERS
 NT PENNING GAGES
 NT PIEZOELECTRIC GAGES
 NT PIEZOMETERS
 NT VACUUM GAGES
- Strain gage and manganin pressure gage instrumentation for magnetic driven flyer plate facility [MDAC-WD-1700] 02 p0223 A72-11502
- Nuclear transducer for atmospheric pressure measurements based on alpha radiation detection, discussing accuracy, linearity and possible error sources 07 p1033 A72-20307
- Static pressure tube calibration for surface pressure measurements in flow over flat plate and airfoil 09 p1261 A72-22937
- Fast response pressure gage for short duration shock reflection measurements in shock tubes, using dual capacitive sensing elements with signal differencing for ionized gases 09 p1315 A72-23401
- Oscillating membrane pressure gage for direct electrical measurements of fast and large pressure variations, noting insensitivity to interference 11 p1636 A72-26700
- Partial pressure gage to measure water vapor-produced hydrogen content in metal samples, using reference gas evolution curves 12 p1807 A72-27451
- Differential error of fused quartz Bourdon tube precision pressure gages as function of absolute pressure level tested for nitrogen 13 p1959 A72-29764
- Fast pressure gage with protection against magnetized plasma parasitic effects to measure neutral pressure 15 p2241 A72-32439
- Effect of surface heterogeneity on the adsorptive behavior of orbiting pressure gages. 19 p2869 A72-38752
- Relative safety afforded operator by various hydrogen pressure gage case designs, recommending specific features and mounting requirements 19 p2755 A72-38833
- Instrumentation for measuring static pressure fluctuations within the atmospheric boundary layer. 20 p2927 A72-39799
- PRESSURE GAUGES**
U PRESSURE GAGES
PRESSURE GRADIENTS
 Three dimensional boundary layer gas flow in large pressure gradient region, using two dimensional boundary layer equations 02 p0201 A72-11580
- Turbulent boundary layer flow past surface with arbitrary temperature distribution, presenting approximate heat transfer solution with allowance for pressure gradient and Reynolds number 02 p0201 A72-11582
- Critique of self similar solutions for physical property models of laminar boundary layer separation due to adverse pressure gradients, noting viscosity-enthalpy relation 02 p0204 A72-12265
- Skirt friction measurement in nonisobaric subsonic flow with pressure gradient over airfoil section by surface impact probes 02 p0151 A72-12275
- Intermittency factor of diffuser flow boundary layer with positive pressure gradient, using hot wire anemometers and multichannel analyzer 04 p0461 A72-14411
- Rectangular channel flow of two immiscible viscoelastic Maxwell fluids with transient pressure gradient, deriving interface velocity, flow rate and wall resistance components 04 p0514 A72-15705
- Velocity profile shapes computation in supersonic compressible turbulent boundary layers with adverse pressure gradients, discussing data and theory discrepancy, curvature, and three dimensional effects 05 p0649 A72-16544
- Boundary layer of gas-particle flows with pressure gradient, numerically integrating momentum equation for cascade particulate flow [AIAA PAPER 72-87] 05 p0604 A72-16808
- Three dimensional hypersonic turbulent boundary layer under normal and longitudinal pressure gradients and cross flow along windward symmetry plane of body of revolution [AIAA PAPER 72-186] 05 p0605 A72-16841
- Pressure gradient effect on mixing length for equilibrium turbulent boundary layers, calculating eddy viscosity [AIAA PAPER 72-213] 05 p0651 A72-16855
- Viscous incompressible flow in straight duct, relating duct wall drag, axial pressure gradient, flux rate and cross sectional area 05 p0653 A72-17002
- Linear dispersion relation for pressure gradient driven drift waves instabilities from ion and electron thermal conductivity effects in collisional plasma 06 p0857 A72-17529
- Spontaneous collisionless drift waves due to pressure gradient in hydrogen plasma column, studying magnetic field and reflecting conditions effects 06 p0857 A72-17534
- Low turbulence wind tunnel with closed circuit design and pressure gradient adjustment capability for turbulent boundary layer studies 06 p0795 A72-17713
- Similitude solutions for turbulent boundary layers in compressible flow with pressure gradient and heat transfer at wall, obtaining velocity and enthalpy profiles 06 p0798 A72-17845
- Pressure gradient effects on hypersonic turbulent skin friction and boundary layer temperature, velocity and Mach number distributions and shape factors [AIAA PAPER 72-215] 06 p0799 A72-17923
- Thermomolecular pressure gradients and temperatures in flow between parallel plates for statistical gas models at arbitrary Knudsen numbers 07 p1101 A72-20513
- Two phase boundary layer flow for laminar two dimensional steady forced film condensation with pressure gradients for fluids of small Prandtl numbers [ASME PAPER 71-HT-Y] 08 p1251 A72-20878
- Plasma rotation during theta pinch collapse, determining ion azimuthal velocity from fields and pressure gradient measurements via Ohms law 08 p1213 A72-21255
- Pressure gradient relations for viscous fluid flow in clearance seals at high pressures 08 p1178 A72-21937
- Wall law for axisymmetric turbulent boundary layers in zero pressure gradient fluid flow through circular cylinders, noting negative and positive wake regions [ASME PAPER 71-APM-VV] 10 p1465 A72-24177
- Wind tunnel investigation of adiabatic compressible turbulent boundary layer in adverse and favorable pressure gradients at supersonic speed 10 p1468 A72-24421
- Pressure jumps lower bounds across supersonic transports induced shock waves in homogeneous atmosphere, using Whitham function in terms of Riemann integral 10 p1420 A72-24846
- Second order fluids plane Poiseuille flow instability to finite amplitude disturbances, noting implications to Toms friction pressure reduction phenomenon in pipe flow 10 p1470 A72-25065
- Adverse pressure gradients effect on two dimensional supersonic turbulent boundary layer, measuring axial distribution of pressure, temperature, mass flow, turbulence intensity and wall shear 11 p1614 A72-25245
- Temperature distributions in constant viscosity incompressible Couette flow with additional pressure gradients 11 p1743 A72-25262
- Turbojet simulator for supersonic wind tunnel models, simulating inlet mass flow ratio and exhaust nozzle pressure ratio [ASME PAPER 72-GT-89] 11 p1705 A72-25664
- Compressible turbulent boundary layer with arbitrary pressure gradients on solid or permeable surfaces, using extended mixing length theory 11 p1616 A72-25917
- Dynamic response of MHD flow under impulsive pressure gradient, obtaining approximate analytic solutions for conduits of arbitrary cross sections by complex variable approach 11 p1695 A72-26039
- Morning glory, showing squall formation by atmospheric hydraulic jump favored by slack pressure gradients, cloudless skies and low latitudes 11 p1681 A72-26080
- Single linear measure of systolic pressure gradient for calculation of aortic valve area in stenosis severity assessment 12 p1762 A72-27734
- Constant pressure gradient valves static characteristics, describing approximate procedures for flow rate determination without allowance for hydrodynamic effects 13 p1899 A72-29134
- Large scale motion of turbulent boundary layer during relaminarization under strong pressure gradient, obtaining fluctuating velocity components and tangential Reynolds stress 13 p1944 A72-30028
- Laminar mixing zone calculated for two homogeneous compressible gas flows with pressure gradient, noting coincidence of velocity distribution for identical gas dynamic parameters 14 p2070 A72-31009
- Two dimensional incompressible turbulent boundary layer in arbitrary pressure gradient, obtaining mathematical model for solution by implicit finite difference method 15 p2217 A72-31718
- Perfect gas unsteady compressible homentropic flow with zero spatial pressure gradient, deriving characteristic equations 15 p2218 A72-32324
- Pressure increase induced by heat release for laminar flame sheet in hypersonic stream, considering fuel injection through semiinfinite porous flat plate 15 p2337 A72-32590
- Velocity and temperature distribution for viscous incompressible fluid unsteady flow between two parallel plates with pressure gradient linearly varying with time 15 p2219 A72-32599
- Flow equations for corner boundary layer with favorable pressure gradients, indicating separation type main velocity profile 16 p2378 A72-33406
- Heat transfer through laminar boundary layer with allowance for streamwise pressure gradient effect on velocity field, using Lighthill method 16 p2477 A72-33427
- Steam-condensate mixture boundary layer flow along curved body surface with arbitrary pressure gradient at low Mach number and constant physical properties 16 p2378 A72-33437
- Lateral pressure gradient and suction effects on laminar incompressible boundary layer separation on curved surfaces predicted by generalized tow-layer flow model [AIAA PAPER 72-698] 16 p2380 A72-34045
- Compressible boundary layer with normal pressure gradients, investigating quasi-similar, nonlinear integro-differential equations properties at wall and sharp and blunt leading edges 16 p2345 A72-34048
- Effect of rotation on laminar compressible fluid flow in a vertical cylinder. 17 p2539 A72-34972
- Stability of spiral flow and of the flow in a curved channel. 17 p2540 A72-35051
- Contribution to the study of flows with surface chemical reactions in the boundary layer 17 p2541 A72-35455
- Shear stresses distribution in isothermal incompressible turbulent boundary layer with positive pressure gradient by diffusers in open jet wind tunnel 17 p2544 A72-35931
- Eddies memory in turbulent shear flow from experiments on plane turbulent wakes undergoing equilibrium transition under impulsive pressure gradient effect 18 p2680 A72-36476
- Theoretical model for plane turbulent wakes subject to adverse, favorable and mixed pressure gradients based on Reynolds stress equation, describing experimental verification 18 p2680 A72-36477
- A note on the effects of pressure gradients on fluid flow with atmospheric applications. 18 p2706 A72-36644
- The forces on a flat plate in a Couette flow. 18 p2683 A72-36996

Study of flow in a passage in the presence of transverse alternating pressure gradients.

19 p2785 A72-37467

Stability of a plasma conductor with axial current, surrounded by cold gas with a pressure gradient

19 p2842 A72-38533

Dynamic pressure, downwash and pressure gradient corrections of wind tunnel model measurements, discussing displacement limit for adequate accuracy [DFVLR-SONDDR-214]

19 p2747 A72-38687

Turbulent boundary layer calculation, investigating surface roughness, pressure gradient and surface temperature effects

20 p2912 A72-39365

Prediction of turbulent boundary layer heat transfer with pressure gradient and mass transfer.

[ASME PAPER 72-HT-16]

20 p2987 A72-39686

An inverse problem in boundary-layer flows - Numerical determination of pressure gradient for a given wall shear.

21 p3043 A72-40108

Behavior of a laminar boundary layer in the presence of a positive pressure gradient

[ICAS PAPER 72-17]

21 p3045 A72-41142

Experimental friction factors for turbulent flow with suction in a porous tube.

21 p3047 A72-41618

Fundamental studies of turbulent boundary layers with injection or suction through porous wall. III - Investigations on the separation of turbulent boundary layers in strong adverse pressure gradients with injection through porous flat plate.

22 p3165 A72-41945

Coupled fields in inhomogeneous warm plasmas with static pressure gradients. I.

22 p3210 A72-42313

Magnetic tension induced stress balance in plasma sheet, considering pressure gradient along geomagnetic tail axis, plasma flow kinetic energy and pressure anisotropy

22 p3211 A72-42408

German monograph - Contribution to the experimental investigation of the heat transfer in a turbulent wall boundary layer in the region of a strong pressure rise.

22 p3167 A72-43064

Influence of wall injection on the turbulent tensions in the exterior regions of a boundary layer

23 p3279 A72-43698

Water tunnel study of turbulent boundary layers structure in incompressible fluid with longitudinal pressure gradient at inlet section of converging and diverging nozzles

24 p3390 A72-45006

PRESSURE HEADS

Start-up flow of viscous incompressible fluid under constant head in entrance region of circular tube

03 p0344 A72-14343

Lagrange interpolation formula to determine flow elements shape in pneumatic sensor head with extended measurement range

14 p2104 A72-30372

PRESSURE MEASUREMENTS

Unsteady flow about two dimensional airfoils, determining surface pressure fluctuations induced by turbulent boundary layers

01 p0001 A72-10217

Pressure altimeter system minimum safe performance standards for subsonic aircraft operation, describing test procedures

[SAE AS 942]

01 p0064 A72-10386

Turbulent supersonic separated flow field analysis and pressure measurements for two dimensional and axisymmetric internal and external flow models

[DGLR PAPER 71-076]

02 p0152 A72-12710

Two dimensional airfoil pressure distribution measurements at high subsonic speeds, comparing normal force coefficients corrected for wind tunnel interference effects with theoretical calculations

[DFVLR-SONDDR-168]

03 p0308 A72-13609

Base pressure determination for subsonic isothermal central and peripheral jets of incompressible fluid discharging into subsonic slipstream

03 p0342 A72-13912

Pressure measuring method with piston manometers for absolute vacuum gage calibration

04 p0507 A72-14440

Argon and nitrogen plasma viscosity measurements, using pressure difference probe

[AD-739835]

04 p0558 A72-15344

Small pressure difference measurement in gas flow, using transducer based on liquid electrical conductivity measurement

04 p0523 A72-15483

Periodic pressure fluctuations measurements on fixed blades of high power axial compressor, describing calibration and data acquisition methods

[ONERA, TP NO. 967]

04 p0463 A72-15555

Combination flow-pressure measuring instrument based on rotating Flösdorf manometer with switching relay system

04 p0525 A72-15665

Average stagnation pressure measurement in low velocity ducted gas flow with nonuniform velocity

profiles, discussing mathematical technique and computer program

[ASME PAPER 71-WA/PUR-1]

Approximate numerical method for calculating flow profiles in arteries from local pressure measurements, taking into account Navier-Stokes equations nonlinear terms

[ASME PAPER 71-WA/BHF-3]

Hydrogen fueled supersonic burning combustor testing, determining wall static pressure, hydrogen radial distribution, Pitot pressure and Mach number at combustor exit

05 p0704 A72-16107

Jet interaction induced supersonic turbulent boundary layer separation, obtaining flat plate pressure measurements and jet plume shadowgraphs

05 p0602 A72-16537

Surface pressure approximation formula for inclined circular cone in supersonic flow

05 p0603 A72-16547

Shock interference heating in hypersonic flows, measuring pressure and heat transfer in wind tunnels

[AIAA PAPER 72-78]

05 p0604 A72-16805

Surface heat transfer and pressure measurements for downstream effects of transpiration cooled nose tip, using nitrogen as injectant fluid

[AIAA PAPER 72-185]

05 p0605 A72-16840

Subsonic wind tunnel investigation of aircraft wake far field structure, measuring trailing vortex decay by yawhead pressure probe

[AIAA PAPER 72-40]

05 p0607 A72-16902

Pressure determination in kinematic pairs of spatial landing gear mechanism, describing rotatory and spherical pairs reactions to various combinations of momenta

05 p0614 A72-17057

Convective heat flow pressure and density measurements at surface of central body of air inlet with live point and axial symmetry

06 p0755 A72-17560

Shock tube experimental techniques for studying fast processes coupled to shock wave propagation in reactive gases, describing pressure, density and temperature measurement methods

06 p0800 A72-18120

Nuclear transducer for atmospheric pressure measurements based on alpha radiation detection, discussing accuracy, linearity and possible error sources

07 p1033 A72-20307

Mean sound pressure level measurement with mobile microphone carriers, noting difference from mean energy density measurement

08 p1165 A72-21297

Interlaboratory comparison of piston-cylinder pressure calibration based on albite breakdown to jadeite and quartz under pressure

08 p1165 A72-21298

Pressure sensor measurements of fluctuating aerodynamic forces on rotor blades related to compressor noise generation

[ASA PAPER H 6]

08 p1107 A72-21486

Test apparatus and measurement of sealing pressure and temperature in threads of concentric running screw viscosity seals in laminar flow

08 p1178 A72-21932

Static pressure tube calibration for surface pressure measurements in flow over flat plate and airfoil

09 p1261 A72-22937

Temperature effects on low pressure calibration in vacuum gage metrology

09 p1312 A72-23249

Direct single electrode measurement of carbon dioxide partial pressure in liquids and gases, using pH changes due to gas diffusion

09 p1317 A72-23671

Measuring instrument for minute pressure differences, noting accuracy

09 p1317 A72-23692

Reference transfer method for in situ calibration of ionization gages, determining pressure ratio of molecular gas flow through fixed orifices

10 p1480 A72-24147

Turbulent flow velocity and pressure fluctuations mean square values measurement by electrokinetic probe based on electrical properties of double metal-fluid interface layer

10 p1480 A72-24204

Pitot tube pressure measurements in supersonic gas flow, calculating free molecular conditions limits

10 p1419 A72-24548

Hypersonic gun tunnel balance and pressure measurements on sharp leading edge delta wings, comparing experimental coefficients and shock angles with predicted values

11 p1571 A72-25735

Venera 7 satellite data during descent through Venus atmosphere and activity after soft landing on 25 December 1970, noting temperature and pressure measurements

11 p1718 A72-25937

Measurement of light pressure-force on Echo 1 satellite based on satellite surface reflection and stellar magnitude as function of phase angle

11 p1718 A72-25939

Electrolyte hydrostatic pressure measurement in limited volume biological compartments by fluid filled glass micropipette used in microtransducer capacity

11 p1587 A72-26623

Vacuum gage calibration standardization by piston manometer method of pressure determination from direct force-area measurement

12 p1805 A72-27037

Lunar surface neutral gas pressure measurement by Apollo 14 cold cathode ionization gage, determining day and night temperature effects on vacuum quality

12 p1805 A72-27041

Surface pressure via satellite-borne measurements of atmospheric transmission near absorption band

12 p1802 A72-27710

Gas compressibility measurements at high pressure and temperature using externally heated pressure vessels

12 p1889 A72-28106

Near ground pressure differentials caused by large transport aircraft induced wake vortices, comparing measured data with Bernoulli formula theoretical values

12 p1752 A72-28122

Airborne gravimetry experiment yielding high resolution pressure and altitude measurements, describing equipment

13 p1994 A72-28877

Pressure measurement between compressor impeller blades during steady and transient operation, discussing system circuit diagram

13 p1957 A72-29139

Wind tunnel investigation of wake pressure and vortex shedding characteristics of flow past spheres as function of Reynolds number

13 p1896 A72-30099

Velocity calculation from pitot tube pressure measurements in compressible two phase flow, taking into account droplet momentum loss

14 p2104 A72-30252

Lagrange interpolation formula to determine flow elements shape in pneumatic sensor head with extended measurement range

14 p2104 A72-30372

Aileron vibration pressure measurement in plane-parallel transonic flow, evaluating damping characteristics with allowance for shock motion caused nonlinear effects

14 p2071 A72-31026

Microscale static pressure fluctuation measurements in lower atmospheric boundary layer turbulent flow using Eulerian measurements

15 p2265 A72-31618

Fast pressure gage with protection against magnetized plasma parasitic effects to measure neutral pressure

15 p2241 A72-32439

Pressure measuring instruments design, considering fluid, piston, spring, electrical and ultrasonic manometers

16 p2391 A72-33240

Pressure, shear stress and yaw angle measurements in flow through aircraft intake S-shaped ducts with turbulent boundary layer at entry, noting vortex generation

16 p2377 A72-33403

Turbulence induced sound pressure level measurement for noise generated by grill in air flow, using streamlined probe microphone

16 p2344 A72-34001

Liquid propellant rocket engines three dimensional nozzle admittance determination by impedance tube method from pressure distribution measurement, taking into account nozzle geometry effect

[AIAA PAPER 72-666]

16 p2443 A72-34071

Automated constant cuff-pressure system to measure average systolic and diastolic blood pressure in man.

17 p2507 A72-34298

Contact pressure between an elastic spherical shell and a rigid plate.

[ASME PAPER 72-APM-31]

17 p2628 A72-34788

Measurement of pressure fluctuations within subsonic turbulent jets.

18 p2681 A72-36575

Measuring instruments for gas pressure determination in vacuum systems, noting application of thermal conductivity or ionization characteristics of gas molecules

18 p2692 A72-36835

The measurement of partial pressure in vacuum technology and vacuum physics

18 p2692 A72-36836

Study of cesium vapor pressure by the boiling point method

18 p2713 A72-37179

Gauges for ultrahigh vacuum.

19 p2803 A72-38390

Boundary-layer effects on pressure variations in Ludwig tubes.

20 p2914 A72-39620

Errors in static pressure measurements due to protruding pressure taps.

21 p3050 A72-40117

Pressure jump across normal ionizing shock waves.

21 p3045 A72-40566

- Electro-osmotic energy conversion in the glass/n-propanol system. 21 p2997 A72-41384
- Hydrodynamic test tunnel for unsteady pressure and force measurements and hydrogen bubble flow visualization data acquisition [AIAA PAPER 72-999] 21 p3041 A72-41585
- Evaluation of transonic and supersonic wind-tunnel background noise and effects of surface pressure fluctuation measurements. [AIAA PAPER 72-1004] 21 p3041 A72-41588
- Application of piezoelectric transducers for the measurement of static pressures 21 p3035 A72-41811
- Recent progress regarding the measurement techniques in the hypersonic area [ONERA, TP NO. 1055] 22 p3178 A72-42581
- An improved pressure-sphere anemometer. 22 p3178 A72-42596
- High response two-transducer pressure measurement for evaluating nonuniform and unsteady inlet air-flow distortion effects on supersonic jet engine stability and performance 22 p3216 A72-42683
- Experimental investigation of finite-amplitude acoustic oscillations in a closed tube. 23 p3314 A72-44124
- Pressure fluctuations resulting from the interaction between a shock wave and a turbulent boundary layer. 24 p3359 A72-44682
- Pressure and magnetic field probe measurements in transverse shock waves in ionizing hydromagnetic regimes, investigating bow shock effects on accuracy 24 p3390 A72-44708
- ## PRESSURE MICROPHONES
- ### U MICROPHONES
- #### PRESSURE OSCILLATIONS
- Supersonic wind tunnel study of flow induced pressure oscillations in shallow rectangular cavity, investigating resonant frequencies and pressure mode shapes 01 p0049 A72-10221
- Wind resonance in ionosphere under pressure fluctuations, noting turbulent friction factor above 110 km 01 p0058 A72-10589
- Holographic investigation of acoustical fields, describing shadowgraph recording apparatus for sound pressure amplitude distribution 03 p0352 A72-12918
- Surface pressure fluctuations near axisymmetric stagnation point in flow over simple impinged body, showing fluid strain suppression of turbulence 06 p0757 A72-18133
- Incipient wing stall detection by unsteady pressure monitoring via flush-mounted microphones, discussing flow patterns on models 07 p0908 A72-19093
- Cross correlation analysis of turbulent jet flow noise with pressure fluctuation as acoustic source [ASA PAPER H 12] 08 p1150 A72-21488
- Solar five minute oscillations in isothermal atmosphere by base pressure fluctuations 09 p1382 A72-22287
- Turbulent flow velocity and pressure fluctuations mean square values measurement by electrokinetic probe based on electrical properties of double metal-fluid interface layer 10 p1480 A72-24204
- Infrasonic pressure disturbance generation during 31 October 1968 polar substorms growth and decay from North American stations observations 10 p1475 A72-24953
- Acoustic dipole radiation by wall pressure fluctuations in turbulent boundary layer flow over rigid and plane surface at low Mach number 13 p1894 A72-29583
- Entropy waves effect on gas pressure oscillations during powder combustion in semiclosed volume, noting resonant frequencies equation 16 p2475 A72-33096
- Temperature and stress fields generated by pulsating internal pressure in viscoelastic hollow sphere with temperature dependent material properties, using iterative numerical procedure 16 p2473 A72-34122
- Effect on supersonic jet noise of nozzle plenum pressure fluctuations. 17 p2597 A72-35243
- Experimental determination of the aeroacoustic environmental about a slender cone. [AIAA PAPER 72-706] 17 p2486 A72-35482
- Some specific characteristics of turbulent wall pressure fluctuations in a flow in a tube 17 p2541 A72-35545
- Combustion noise generation by burning fuel-air mixtures induced pressure fluctuations as result of time variable heat release rate due to turbulence 18 p2741 A72-36505
- Measurement of pressure fluctuations within subsonic turbulent jets. 18 p2681 A72-36575
- Statistical characteristics of surface pressure pulsations in turbulent boundary layer of incompressible fluid, discussing effects near smooth flat wall 19 p2785 A72-37472
- Space correlations of the fluctuating pressure in subsonic turbulent jets. 20 p2913 A72-39555
- Instrumentation for measuring static pressure fluctuations within the atmospheric boundary layer. 20 p2927 A72-39799
- Description of global-scale circulation cells in the tropics with a 40-50 day period. 22 p3201 A72-42506
- Atmospheric waves observed in the planetary boundary layer using an acoustic sounder and a microbarograph array. 22 p3202 A72-42599
- Analysis and correlation of data on pressure fluctuations in separated flow. 23 p3247 A72-43331
- The problem of the minimum frequency of natural pressure oscillations in pneumatic-hydraulic systems 23 p3252 A72-43652
- Frequency dependence of axially oscillated nozzles admittance real and imaginary parts for different Mach numbers, convergence angles and curvature radii, comparing theory and experiment 24 p3433 A72-45144
- ## PRESSURE PROBES
- ### U PRESSURE SENSORS
- #### PRESSURE PULSES
- Shell bending and Timoshenko-type theory to solve stresses of semiinfinite elastic circular cylindrical shells produced by radial pressure pulses [ASME PAPER 71-WA/APM-16] 05 p0733 A72-15964
- Plane symmetrical exothermic reaction center dynamic behavior, deriving system nonlinear transfer function-pressure pulse and unit mass heat release relationships [AIAA PAPER 72-67] 05 p0750 A72-16934
- Thermodynamic function error influence on rocket engine combustion product characteristics including combustion chamber temperature and specific pressure pulse 05 p0751 A72-17069
- Dynamic response predictions of fluidically controlled pulsatile hydraulic flow and pressure generator for biomedical systems 07 p0914 A72-18820
- Damping measurements of hydrodynamic vibrations of cylinder excited by random pressure field of liquid flow 10 p1465 A72-24073
- Wind tunnel inlet effect on pulsed flow, relating velocity and pressure pulses 10 p1417 A72-24216
- Hydraulic test facility for dynamic characteristics of potentiometric pressure sensors with connecting lines of various geometries, shaping pressure pulse signal by electromagnetic valve 13 p1957 A72-29135
- Effect of a distributed sand roughness on the spectrum of wall pressure pulsations in a turbulent flow in a tube 17 p2541 A72-35542
- Behavior of glass fiber reinforced plastic cylindrical shells under the action of external pressure pulses 19 p2872 A72-37538
- Influence of a trailing vortex on friction pulsations in the near-wall region of the leading stagnation point of a cylinder in transverse flow 19 p2786 A72-38041
- Pressure pulsations relationship to fixed boundary of turbulent flow with kinematic structure, considering phase transitions effect 20 p2912 A72-39362
- Pressure pulsation measurements at nose of well-streamlined body of revolution at high Reynolds numbers, noting turbulent pressure field intensity growth and decay 20 p2912 A72-39362
- Carrying capacity of thin-walled shells subjected to impulsive radial pressure loads 22 p3233 A72-42052
- Clamped circular rigid-plastic plates subjected to central blast loading. 22 p3235 A72-42601
- Evaluation of the pulse-contour method of determining stroke volume in man. 23 p3256 A72-43934
- ## PRESSURE RECOVERY
- Boundary layer growth measurements in optimum annular diffusers, discussing pressure recovery and mean total pressure loss 05 p0604 A72-16807
- Pressure recovery calculation for subsonic adiabatic air flow through diffusers with tail pipes, assuming turbulent inlet boundary layer 10 p1415 A72-23855
- Diffuser performance and idling characteristics in shock tube at Mach 8, discussing pressure recovery factor laminar and transition flows in boundary layer 10 p1419 A72-24545
- Discharge and pressure recovery coefficients of blocked gas flow in curvilinear channel with guide vanes, minimizing losses and separation at convex wall 11 p1574 A72-26971
- Pressure recovery and control characteristics of turbulence amplifiers with jet of rectangular section, using large scale water model 16 p2350 A72-33178
- A new stagnation pressure probe having a high pressure recovery in supersonic flow. 22 p3179 A72-42687
- Influence of tangential fluid injection on the performance of two-dimensional diffusers. [ASME PAPER 72-FE-16] 23 p3280 A72-44064
- Supersonic aircraft engine inlet performance in terms of pressure recovery, discussing oblique shock wave formation ahead of entrance to improve efficiency 24 p3360 A72-44991
- ## PRESSURE REDUCTION
- ### NT EXPLOSIVE DECOMPRESSION
- Nonuniform flow along axial turbomachine blades, presenting pressure loss evaluation method under boundary layer effect on external walls 01 p0002 A72-11271
- Boeing 707 rapid decompression at 25,000 feet, noting rivet hole fatigue damage 02 p0167 A72-11715
- Stator blade design to shield turbofan from pressure disturbances arising in downstream subsonic duct [AIAA PAPER 72-84] 05 p0707 A72-16883
- Embryogenesis of fertile chicken eggs in pure oxygen at reduced pressure 09 p1265 A72-22642
- Increased atmospheric pressure influence on blood coagulation in rabbits, showing post-decompression hypercoagulation followed by hypocoagulation 09 p1268 A72-23597
- Hydrogen chloride addition effect on hydrocarbon flammability under reduced pressure, studying flame stability limits of methane, ethylene, acetylene and n-butane in oxygen 10 p1562 A72-24236
- Vestibular, auditory, acceleration and altitude decompression testing of pilot following endolymphatic shunt surgery for Menieres disease 12 p1771 A72-27485
- Physiological effects on anesthetized and conscious dogs during exposure at 80,000 ft for different decompression rates, discussing cardiovascular, biochemical and pathological effects 12 p1768 A72-28322
- Lower body decompression effects on ECG, showing heart rate increase, R and T amplitude changes and heart electric axis displacement 14 p2074 A72-30383
- Hyperbaric environment decompression effects on human blood and urine chemistry and hemostatic system, showing physiological parameter alteration in presence and absence of bends symptoms 14 p2081 A72-31087
- Supersonic molecular jet improvement via expansion chamber residual gas pressure reduction and nozzle stagnation pressure increase 16 p2429 A72-33053
- Inflation pressure caused deformations of thin toroidal shells, discussing wrinkle development due to pressure reduction [ASME PAPER 72-APM-32] 17 p2628 A72-34787
- Peripheral venous renin activity during 70 deg tilt and lower body negative pressure. 19 p2758 A72-38703
- Environmental, medical and acoustic investigations with underwater laboratory, discussing cabin atmosphere control, depressurization, health conditions and sonar operation 20 p2898 A72-39938
- Study of hemodynamics during the action of decompression and accelerations 21 p3006 A72-40444
- ## PRESSURE REGULATORS
- Pneumatic amplifiers with controlled pressure during subcritical and supercritical flow, considering jet-resonant choke, conical and membrane systems 11 p1578 A72-26783
- Analog simulation of direct acting gas pressure regulators in terms of spring, flow and friction forces 13 p1956 A72-28703
- Constant pressure gradient valves static characteristics, describing approximate procedures for flow rate determination without allowance for hydrodynamic effects 13 p1899 A72-29134
- Investigation of the damping features of a pressure regulator 17 p2559 A72-34916
- ## PRESSURE SENSORS
- ### NT BOURDON TUBES
- Aircraft high pressure oxygen cylinder system filler valve optimum standards, discussing automatic fill rate and pressure sensitive closing control, design, construction and performance [SAE A1225] 01 p0006 A72-10385
- Book on pressure probe methods for wind speed and direction covering incompressible and subsonic compressible flow pressures, temperature, etc 01 p0072 A72-11273

Wideband acoustic pressure field sensing by moving receivers and sensors, calculating motion effects on response including directional pattern and gain

02 p0259 A72-12176

Small pressure difference measurement in gas flow, using transducer based on liquid electrical conductivity measurement

04 p0523 A72-15483

Sensitivity predictions of boundary layer pressure fluctuations for round, square and rectangular transducers

07 p0986 A72-19596

Cerebro-spinal fluid pressure remote monitoring by intracranially implanted radio pressure transducers, describing receiver-detector-recorder system

07 p0930 A72-19911

Respiration rate transmitter with miniature pressure transducer for measuring pneumograph variations in animals over FM-FM telemetry system

08 p1124 A72-20898

Miniature three-position pressure valve for on-board calibration of pressure transducers in wind tunnel models, noting time lag reduction

08 p1164 A72-20923

Multiplex electrohydraulic system for aircraft fly by wire actuators with majority voting and pressure logic, discussing frequency response and environmental tests

08 p1113 A72-22152

German monograph on shaft and wall effect in aerodynamic measurements with three orifice pressure probes in wind tunnels

09 p1259 A72-22320

Capacitive electret pressure sensors calibration for interior measurements in turbine engines, jets and exhaust nozzles

[ONERA, TP NO. 982] 09 p1310 A72-22815

Turbulent flow velocity and pressure fluctuations mean square values measurement by electrokinetic probe based on electrical properties of double metal-fluid interface layer

10 p1480 A72-24204

Fluidic wind sensor measurements from low threshold to high velocities, noting wind angle resolution from output differential pressure signal

10 p1484 A72-25083

Flow measurement instrumentation for turbomachine rotors, noting telemetry type data transmission system with strain gage pressure transducers for turbocompressor

[ASME PAPER 72-GT-55] 11 p1630 A72-25646

Impact probe displacement effects in supersonic turbulent boundary layer in terms of Mach number profiles

11 p1572 A72-26005

Thermistor vacuum gage with interchangeable sensing heads, providing improved pressure response and direct interchanging without recalibration

11 p1636 A72-26776

Piezoelectric transducer for indirect on-wrist blood pressure measurements for clinical environment

12 p1772 A72-27961

Hydraulic test facility for dynamic characteristics of potentiometric pressure sensors with connecting lines of various geometries, shaping pressure pulse signal by electromagnetic valve

13 p1957 A72-29135

Test equipment for high strain rates in shear with torsional split Hopkins pressure bar

16 p2373 A72-33196

High precision electrostatic feedback transducer for very low differential pressure measurement in gas media, suggesting low pressure standard role

[RAE-TR-71022] 16 p2394 A72-33638

Some uncommon electric transducers for the measurement of mechanical quantities.

18 p2690 A72-36369

Optimal vascular pressure measurements with transducers located outside body with rigid and elastic tube couplings

19 p2760 A72-37757

A fluidic sensor for closed loop engine acceleration control.

19 p2849 A72-38049

Pressure transmitter for flow parameter measurements of aerodynamic nozzles and static pressure taps rotating on turbine rotor blades

22 p3176 A72-42250

High response two-transducer pressure measurement for evaluating nonuniform and unsteady inlet air-flow distortion effects on supersonic jet engine stability and performance

22 p3216 A72-42683

Engine compressor face rake for flight test instrumentation F-14A/TF-30.

22 p3216 A72-42686

A new stagnation pressure probe having a high pressure recovery in supersonic flow.

22 p3179 A72-42687

Miniaturized piezoelectric transducer electronics versus charge amplifiers - A comparison of the two systems in vibration and pressure applications.

22 p3159 A72-42702

A comparison of disturbance levels measured in hypersonic tunnels using a hot-wire anemometer and a pitot pressure probe.

[AIAA PAPER 72-1003] 24 p3388 A72-45402

PRESSURE SUITS

NT SPACE SUITS

Pressure suit effects on psychomotor skills, testing manual dexterity, tracking skills, hand strength, steadiness and coordination for pressurized, unpressurized and shirtsleeve conditions

10 p1431 A72-24796

Life support equipment and pressure suit operational requirements from viewpoint of flight crews and test pilots

12 p1771 A72-27516

Valsalva and M-1 maneuvers acceleration tolerance protective effects during high-g centrifuging with and without anti-g suits

12 p1767 A72-28318

Acceleration protection properties of modified partial pressure suit, determining tolerance limits by vision impairment criteria during centrifuge tests

12 p1776 A72-28319

PRESSURE SWITCHES

Miniature three-position pressure valve for on-board calibration of pressure transducers in wind tunnel models, noting time lag reduction

08 p1164 A72-20923

PRESSURE TRANSDUCERS

U PRESSURE SENSORS

PRESSURE VESSELS

Fiber reinforced filament wound composites for pressure vessel applications, investigating mechanical properties

01 p0090 A72-10741

Cryogenically formed prestressed stainless steel glass fiber reinforced vessels, demonstrating structural performance for space shuttle life support oxygen/nitrogen high pressure gas tanks

01 p0139 A72-10770

Acoustic emission tests of nuclear pressure vessels and piping, detecting weld slag, porosity, fatigue microcracking and stress corrosion cracking

01 p0048 A72-10802

Fragment velocity for bursting gas containers in vacuum

[ASME PAPER 71-PVP-14] 02 p0295 A72-12473

Pressure vessels with cracks, formulating stress analysis for safety factors

03 p0443 A72-13452

Pressurized vessel bottoms weakened by central hole with edge stiffened by elastic ring, determining stress-strain state and stress concentration

03 p0451 A72-14120

Mean and fluctuating temperature dependence of gas discharging from orifice to atmosphere on pressure vessel wall heat transfer

[ASME PAPER 71-WA/HT-32] 05 p0745 A72-15884

Elastoplastic creep analysis for cylindrical pressure vessel structural response during cyclic thermal shock, internal pressure and extended high temperature loading

[ASME PAPER 71-WA/PVP-12] 05 p0732 A72-15911

Arc cast vacuum melted Mo base alloy properties, production and applications to heat pipes, aerospace structures and pressure vessels

11 p1644 A72-26844

High pressure oxygen control for synthesis and vapor phase equilibria, discussing tensiometric measurements and cold seal pressure vessel techniques

12 p1778 A72-28105

Gas compressibility measurements at high pressure and temperature using externally heated pressure vessels

12 p1889 A72-28106

Crack propagation in biaxially stressed and heat treated cylindrical pressure vessel observed by strain gage displacement measurement, noting effects of initial surface cracks

14 p2169 A72-31176

Deformation and stress in shells with discontinuous wall thickness variations, noting cylinder with ribs under internal pressure

15 p2326 A72-31705

Hot water rocket engine design and operation principles, discussing high pressure tank and nozzle characteristics

15 p2297 A72-31830

Impulse liquid jet pressure reduction in closed vessel under adiabatic conditions and evaporation intensity dependence on jet velocity

16 p2476 A72-33259

Stable bifurcation mode prior to instability in thick walled cylindrical viscoplastic pressure vessel under internal hydrostatic pressure

16 p2474 A72-34129

Effects of yielding and size upon fracture of plates and pressure cylinders.

17 p2565 A72-34251

Shape factors for nozzle corner cracks evaluated from epoxy-model pressure vessels.

17 p2630 A72-34814

Techniques in photoelastic analysis of pressure vessels.

18 p2690 A72-36369

Applications of holographic nondestructive testing techniques in engineering.

19 p2806 A72-37604

Filament wound cylindrical pressure vessel design and development for operation under cyclic-loaded high hydraulic pressure in underwater environment

19 p2877 A72-38164

Zero-gravity thermal performance of the Apollo cryogenic gas storage system.

19 p2869 A72-38836

Static and dynamic fatigue behavior of glass filament-wound pressure vessels at ambient and cryogenic temperatures.

19 p2823 A72-38881

Effect of residual elements on radiation strengthening in iron alloys, pressure vessel steels, and welds.

20 p2937 A72-39285

Determination of the optimal parameters of high pressure cryogenic fluid storage systems.

20 p2962 A72-39358

Influence of discontinuity stresses on main propellant tankage of a space shuttle orbiter.

[ICAS PAPER 72-10] 21 p3120 A72-41135

Filament wound pressure vessel isotensoid theory, considering composite material as macroscopically homogeneous anisotropic continuum

22 p3238 A72-42838

Pressure vessels with cracks, formulating stress analysis for safety factors

24 p3458 A72-44927

PRESSURE WAVES

U ELASTIC WAVES

PRESSURE WELDING

NT DIFFUSION WELDING

NT EXPLOSIVE WELDING

NT ULTRASONIC WELDING

Pneumatic machine for microfriction stud welding of dissimilar metals

09 p1320 A72-23631

Tensile and fatigue tests of dissimilar metal joints made by friction pressure welding

09 p1321 A72-23640

Microstructure and mechanical properties of heat treated friction welds at high temperatures

11 p1641 A72-26489

Continuous drive friction welding of mild steel, noting burn-off rate relationship to tensile strength

11 p1641 A72-26492

Conduction electron phonon scattering effect on electrical resistance of metallic contacts during pressure welding

16 p2370 A72-33951

A preliminary investigation of joining methods for aluminum-graphite composites.

17 p2561 A72-35661

PRESSURIZED CABINS

Human factors relation to pressurized cabin development, discussing aircraft safety, high altitude tests, pressure loss predictions and cabin altitude selection

04 p0479 A72-14868

Hypoxia incidents in Strategic Air Command due to cabin pressurization malfunction

08 p1126 A72-21566

Case report of rapid decompression in supersonic trainer aircraft pressurized cabin, discussing physical and blast effects, pressurization safety, decompression sickness and hypoxia

11 p1584 A72-26020

Physiological and clinical effects of long distance flight in pressurized commercial planes with simulated altitudes over 1500 meters

12 p1771 A72-27486

Leak detection in pressurized installations via NDT, discussing uses of fluid tracers, thermal and acoustic sensors, halogen detectors, He mass spectrometers and radioactive tracers

14 p2104 A72-30374

PRESSURIZING

NT FUEL TANK PRESSURIZATION

Stress analysis of pressurized ribbed cylindrical shell with intersecting reinforced circular hole under internal pressure

[ASME PAPER 71-PVP-8] 02 p0294 A72-12470

Water radiolysis within sealed Al capsules in nuclear reactor, calculating pressure rise due to water decomposition via predictive models derived by multiple regression analysis

04 p0546 A72-14425

Bend tests for minimum radius/thickness ratio of Ti and Be alloy sheets in pressurized fluid

[ASME PAPER 71-WA/PT-8] 05 p0671 A72-15913

Eddy current extensometer for monitoring long term creep in diameter of pressurized tubular stainless steel specimens

11 p1613 A72-25821

PRESTON TUBES

U PITOT TUBES

U SPEED INDICATORS

PRETRAINING

U PRESTRESSING

- PRESTRESSING**
Initial strains effect on propagation rate of elastic waves, applying finite deformation theory 01 p0138 A72-10581
Torsional prestrain effects on 1100-F Al alloy thin walled tubes yield locus, calculating distortion degree by statistical characteristics 01 p0086 A72-11000
Previous loading effect on contact area and prints number and size distribution and thermal conductance for two nominally flat surfaces in contact [ASME PAPER 71-LUB-M] 02 p0234 A72-11528
Pretwisted tapered cantilever beam torsional vibration natural frequencies determination by Galerkin method for solution of differential equation of motion 02 p0297 A72-12533
Steels modulus of elasticity dependence on prestressing level produced by transverse and longitudinal tension 03 p0371 A72-13462
Shock precompression effect on dynamic fracture strength of steel and Al alloy, investigating crack initiation and growth 04 p0533 A72-14541
Creep damage mechanics, considering fracture initiation and propagation and prior loadings effect [ASME PAPER 71-WA/MET-1] 05 p0732 A72-15908
Combined stress wave propagation in thin walled prestressed tube under longitudinal and torsional impact loading 06 p0898 A72-18321
Plastic deformation, creep rupture strength, endurance limit and service life of prestressed strain hardenable material 06 p0900 A72-18681
Prestressing effect on stress corrosion resistance of fatigue precracked high strength steels 07 p1016 A72-19941
Prestressed glass reinforced composites mechanical behavior, taking into account manufacture induced residual stress concentrations 08 p1192 A72-21674
Various restrain dislocation distributions effect on mechanical twinning behavior in purified Nb single crystals 10 p1497 A72-24824
Static loading and monoharmonic excitation influence on transverse vibrations of eccentrically prestressed metallic beam 11 p1732 A72-25535
Prestressed circular ring snap-through under continuously distributed or discrete torsional loads, determining critical torque by asymptotic solution 11 p1734 A72-25721
Two dimensional wave motion generated in prestressed body by crack extension, noting consistency with fracture criterion related to cohesive traction zones near crack tip 12 p1883 A72-27560
Velocity behavior of shear waves propagating in uniaxially prestressed isotropic elastic body 12 p1886 A72-27982
Dynamic response and buckling mode of elastically supported circular plates with initial tension under arbitrary surface load 15 p2332 A72-32578
Prestraining effect on metal fatigue strength, showing increase relation to yield strength and ultimate strength 16 p2463 A72-32903
Prestrained and annealed elastic materials stress-strain relationship calculation in plastic range, compared with tensile and compression load tests results 16 p2472 A72-33948
Governing equation derivation for coupled extension, flexure and torsion in pretwisted curved beams of thin walled open section, using three dimensional elasticity [ASME PAPER 72-APM-5] 17 p2630 A72-34809
Axial-symmetric deformations of a rubber-like cylinder under initial stress 18 p2738 A72-37081
Linear physical and nonlinear geometric formulation of design problem for prestressed rubber parts based on elasticity theory in terms of assembly requirements 19 p2871 A72-37428
Experimental technique for determination of roller bearing preload to optimize dynamic characteristics and minimize operating temperature 19 p2810 A72-38650
Optimal compression of constant-thickness media in a plane stress state 21 p3123 A72-41391
Optimization of the range of elastic behavior of unidirectional composites by prestraining 22 p3194 A72-43041
Recovery of high temperature deformed Ni-Al alloys 23 p3300 A72-43564
Dynamic blast loads on preheated and prestressed thin plates 24 p3454 A72-44607
- The effect of pre-strain on the yield behavior of vanadium 24 p3413 A72-44721
Steels modulus of elasticity dependence on prestressing level produced by transverse and longitudinal tension 24 p3413 A72-44937
Welding airframe structures in titanium using tensile loading to overcome distortion 24 p3407 A72-45000
- PRETREATMENT**
NT PRESTRESSING
PRETWISTING
U PRESTRESSING
U TWISTING
PREVENTION
NT ACCIDENT PREVENTION
NT CORROSION PREVENTION
NT FIRE PREVENTION
NT ICE PREVENTION
Markov model random variation optimal periodicity in preventive maintenance operations, estimating distribution density and moments 04 p0527 A72-15574
- PRIMARY BATTERIES**
NT ALKALINE BATTERIES
NT METAL AIR BATTERIES
NT ZINC-OXYGEN BATTERIES
PRIMARY COSMIC RAYS
NT SOLAR COSMIC RAYS
Model with large Lorentz factor and relativistic relations violations to explain theoretical estimate disparity with experimental data for high energy primary cosmic rays 01 p0118 A72-10156
Primary cosmic ray nuclear component, discussing Cosmos 163 measurements 01 p0119 A72-10603
Atmospheric primary and secondary cosmic ray propagation with close reference to two-fire-ball, H-quantum and excited baryon models of multiple meson production 01 p0121 A72-11122
Ultrahigh energy cosmic ray models indication of galactic origin and composition, based on energy spectrum flattening data 02 p0272 A72-11901
Nuclear emulsion and solid track threshold dosimetry for ion spectrum division of heavy relativistic particles in primary cosmic rays [CERN-71-16] 02 p0162 A72-12065
Thin-down intensities for heavy primaries at SST flight levels, using plastic stacks measurements [CERN-71-16] 02 p0274 A72-12077
Primary cosmic ray interaction with tissues, emphasizing biological effects and nuclear reactions induced radioactivity in astronaut body 03 p0313 A72-12911
Antiprotons abundance in primary cosmic radiation near geomagnetic equator from asymmetrical flux balloon measurements 03 p0407 A72-12992
High energy primary cosmic ray particle evidence from energetic air shower observation data analysis 03 p0413 A72-14097
High energy cosmic ray track angular azimuthal distribution in lunar silicate rocks 04 p0577 A72-15154
Primary cosmic ray electrons energy spectrum measurements, using balloon-borne absorption spectrometer 04 p0568 A72-15509
High energy cosmic ray electrons anisotropy, considering diffusion from discrete source model 04 p0568 A72-15510
Primary cosmic ray proton energy spectrum in 50 Ge V to 300 Te V range, using Proton 1, 2 and 3 satellite-borne counters 05 p0709 A72-16231
Inelastic nuclear interactions between 200-GeV cosmic ray particles and polyethylene targets, correlating similarity property, angular momentum spectra and secondary particle pairs 06 p0868 A72-17258
Heavy nonrelativistic single charge particle recording in cosmic rays at sea level, using scintillation and anticoincidence Cerenkov counters 06 p0870 A72-17276
Energy spectrum, composition and anisotropy study of cosmic radiation from extensive air showers, using scintillation and Cerenkov detectors 06 p0870 A72-17277
Primary cosmic radiation energy spectrum approximation from air showers, high-energy hadrons and Proton 4 data 06 p0870 A72-17281
Extensive air shower characteristics and muon counts at different level observations relative to particle number and primary energy spectra 06 p0871 A72-17284
K-neutral pion energy fractions and inelasticity coefficients at primary energies of 100-1500 Gev during hadron-target interaction 06 p0872 A72-17295
- Light generator aided autonomous calibration of Cerenkov spectrometer for continuous primary cosmic nuclear flux measurements 06 p0815 A72-17832
Short and long term spectral modulation of primary cosmic rays above 2 GV during solar cycle 19 descending phase, presenting neutron monitors calibration procedure 06 p0874 A72-18160
Cosmic ray showers age distribution, assuming composite nature of horizontal showers due to initiation by several primary showers 07 p1056 A72-18908
Energy spectrum of primary cosmic ray electrons at 2-200 GeV, using balloon-borne counter telescope with gas Cerenkov counter 07 p1059 A72-19578
Primary cosmic radiation nucleonic component composition comparison with elements natural abundance, discussing mechanism of matter injection into cosmic ray accelerator 07 p1059 A72-19586
Papers on high energy cosmic ray and nuclear interactions covering extensive air showers, cloud chamber data, electron-photon cascades, solar activity effects, etc 07 p1060 A72-19863
Mathematical model for superheavy cosmic ray production by spallation on interstellar hydrogen, assuming single source for particle injection with given charge spectrum 07 p1062 A72-20197
Primary cosmic rays energy spectrum at 100-1000 TeV from Proton 4 satellite data 07 p1064 A72-20629
Primary cosmic ray particles disappearance and proton spectrum slope rise in 1 TeV energy region from Proton satellites data 07 p1064 A72-20630
Primary cosmic rays alpha particles and protons energy spectra similarity and intensity difference at .05 to 1.6 TeV, using Proton satellites data 07 p1064 A72-20631
Primary cosmic radiation antiproton flux, finding .005 ratio upper limit to proton flux with balloon-borne magnetic spectrometer 07 p1064 A72-20633
Probabilistic integral multiplicity of generation of primary cosmic ray particles from count rate and primary spectrum relationship, using definition for neutron component calculations 07 p1067 A72-20656
Primary cosmic ray high energy gamma quanta flux measurements on Cosmos 208 satellite-borne instruments 08 p1225 A72-20798
Excess radiation and primary cosmic ray intensity variations at 200-350 km during 1965-1969 solar cycle from Cosmos satellite data 08 p1227 A72-21156
Nucleonic cascade model analysis of underground vertical muon curve for primary cosmic ray nucleon spectrum below 40 TeV 10 p1529 A72-24417
Antimatter search in primary cosmic rays by balloon-borne superconducting magnetic spectrometer capable of direct matter-antimatter separation 12 p1863 A72-27296
High energy solar and galactic cosmic ray chemical composition, considering electron component abundances and beryllium-boron ratio 12 p1863 A72-27426
Composition of radiation excess over primary cosmic ray background recorded by Cosmos satellites below midlatitude belt region 14 p2147 A72-30626
Primary cosmic rays antineutrino content upper limit from emulsions investigations with balloons and satellites 14 p2148 A72-30885
Light flashes observed by astronauts on exposure to primary cosmic radiation during translunar flights, investigating effect upon retina in man and animal 15 p2189 A72-31917
Lateral distribution, radiation spectra and pulse shapes calculated from mathematical models of cosmic ray showers radio emission, noting chemical composition of primary particle 15 p2230 A72-32262
Light elements production from primary cosmic rays spallation in interstellar gas, noting diffusion coefficient of relativistic particles in galaxy 15 p2301 A72-32754
Satellite-borne semiconductor particle detector telescope for C and Mn isotopes identification in heavy primary cosmic rays, considering scintillation counter and mass resolutions 16 p2389 A72-32883
Primary cosmic rays extragalactic origin, considering high energy electrons, background X and gamma rays and cosmic protons 16 p2445 A72-33126
Isotopic composition of primary cosmic radiation - Conference, Lyngby, Denmark, March 1971 16 p2446 A72-33726

- Isotopic abundance analysis of primary cosmic radiation with nuclear emulsion technique, discussing mass measurements in Be, C, O, Ne, Mg and Fe tracks
16 p2447 A72-33731
- HEAO experiment proposal for Be to Sn flux and energy spectra and Be to Fe isotopic composition of galactic primary cosmic rays
16 p2447 A72-33733
- Electron showers of high primary energy in lead.
17 p2585 A72-35472
- Excess radiation and primary cosmic ray intensity variations at 200-350 km during 1965-1969 solar cycle from Cosmos satellite data
20 p2964 A72-39261
- Test of hadronic scaling at cosmic-ray energies.
21 p3100 A72-40831
- Particle trajectory and time of flight measurement in search for anti-alpha particles in primary cosmic radiation, using magnetic spectrometer with spark chambers
22 p3219 A72-42568
- Collective interactions of the nucleons of heavy nuclei in high-energy cosmic rays
23 p3330 A72-44408
- EAS Cerenkov glow and the relation of shower strength to the primary-particle energy
23 p3330 A72-44419
- Energy spectrum and composition of primary cosmic radiation at energies from 50 to 5000 TeV
23 p3330 A72-44422
- Certain characteristics of the muon and electron components of extensive air showers at mountain level
23 p3331 A72-44425
- S-system motion effect on angular distribution of secondary high energy particle cluster in showers formed by primary and neutral particles, considering nucleon collision line
23 p3331 A72-44436
- Recording high-energy particle interactions by the method of the controlled emulsion stack of large volume
23 p3291 A72-44438
- Primary cosmic ray nucleon spectrum from sea-level muon spectrum and scaling hypothesis parameters.
23 p3332 A72-44458
- The cosmic-ray spectral modulation above 2 GV. IV - The influence on the attenuation coefficient of the nucleonic component.
24 p3434 A72-44783
- PRIMATES**
NT CHIMPANZEES
NT HUMAN BEINGS
NT MONKEYS
Medical primatology - Conference, New York, September 1969
03 p0313 A72-13068
- Anatomical-physiological, optical and behavioral-similarities of nonhuman and human primates
03 p0313 A72-13069
- Mechanical impedance and phase angle time variation in restrained primate during prolonged sinusoidal vibration
[ASME PAPER 71-WA/BHF-8] 05 p0616 A72-15946
- Skeletal bones ash content in man and primates, implying differences due to adaptive physiological function
10 p1424 A72-23736
- PRIMERS [COATINGS]**
Amorphous chromate and phosphate conversion coatings of Al, providing inert surface for painting
09 p1317 A72-22480
- PRIMERS [EXPLOSIVES]**
Detonating cut-off pyrotechnic chain of explosive devices for stage separation involving primers, relays and fuses
08 p1221 A72-20777
- PRINCETON SAILWINGS**
U SAILWINGS
- PRINTED CIRCUITS**
NT LARGE SCALE INTEGRATION
NT MEDIUM SCALE INTEGRATION
Analog matrix, input data and procedure for Al frame and Cu-clad printed circuit board module thermal resistance analysis using ECAP program
01 p0035 A72-10380
- Circuit boards contact assembly by special type rivets, discussing technical and economic advantages for prototype or small series fabrication of printed circuit devices
06 p0784 A72-18192
- Multilayer thin film microcircuits and printed circuits partial capacitance and potential coefficient approximate calculation by matrix method
07 p0953 A72-19016
- Printed circuit boards and RC elements soldered connections reliability under high temperature and excessive current conditions, discussing test procedure and evaluation criteria
07 p0994 A72-19247
- Adhesives use for assembly of mechanical, optical, nucleonic and electronic instruments including printed and integrated circuits
07 p0992 A72-20576
- Electron-optical system with electro- and magneto-static lenses, ensuring large image reduction for producing printed microcircuits
10 p1482 A72-24589
- Screen printed large thick film multilayer interconnection board assemblies for electronic packaging, discussing fabrication and feasibility
16 p2368 A72-33194
- Computers and automatic drafting machines as aids in artwork production for printed circuits
19 p2809 A72-38307
- Regeneration metering methods and equipment for acidic and alkaline etching of normal plated circuit boards.
20 p2929 A72-39491
- Recent developments in silicone elastomers for macroencapsulation.
20 p2944 A72-39492
- Antenna with printed elements for a VOR-S navigation installation
21 p3031 A72-40536
- Automation of high reliability multilayer printed circuit board fabrication.
22 p3184 A72-43173
- PRINTED RESISTORS**
High value thin-film-on-silicon resistors for hybrid applications.
22 p3160 A72-42825
- Accelerated life testing of thick film resistors.
24 p3384 A72-44668
- PRINTERS**
NT PRINTERS [DATA PROCESSING]
Remotely sensed data processing by scanner/printer designed for photograph scanning, geometric correction and photographic printing of corrected image
18 p2691 A72-36495
- PRINTERS [DATA PROCESSING]**
Electronic deflection printer with holographic memory, using photosensitive device for textual recording
01 p0073 A72-11320
- High speed material transfer recording equipment for alphanumeric printers, toned image graphic and microimage computer printer applications
10 p1489 A72-23934
- PRINTING**
NT LITHOGRAPHY
Anhyseretic contact printing magnetization simulation by computer with Preisach diagram modified by Onsager field effect
[IEEE PAPER 14,2] 03 p0327 A72-13768
- The use of satellites to meet future press requirements.
18 p2743 A72-37012
- An improved Cranz-Schardin high-speed camera for two-dimensional photomechanics.
19 p2795 A72-37516
- PRISMATIC BARS**
Plastic torsion of prismatic and anisotropic rods, emphasizing inhomogeneity problems numerical solution
03 p0447 A72-13853
- Two dimensional boundary value problem in elasticity for rectangular prism vibrations, considering dynamic stress and frequency characteristics
03 p0449 A72-13908
- Collocation least square solutions of boundary value problems, applying to prismatic bar torsion and plate bending
07 p1025 A72-18790
- Longitudinal vibrations of composite rod under concentrated impact forces at junctions between prismatic sections
10 p1557 A72-24627
- Tangential stresses, rigidity characteristics and stress functions of prismatic grooved circular shafts, showing summary representations and integral transformations methods interrelationship
13 p2057 A72-29062
- Torsional behavior of prismatic rods with polygonal cross section, using method of summary representations
13 p2057 A72-29080
- Bending vibrations of finite length prismatic bar moved in longitudinal direction through tubelike supports, using variational technique
20 p2979 A72-39332
- Constitutive equations and boundary value problems in discrete theory of elasticity, noting linear systems of prismatic rods and lattice type shells
21 p3123 A72-41390
- Nonlinear elastic torsion analysis for aerospace materials.
23 p3354 A72-44251
- Torsion analysis of prismatic bars of different cross sections based on dipolar stress theory, applying to anisotropic media
24 p3457 A72-44872
- PRISMS**
NT PRISMATIC BARS
Thin walled prismatic structural members under uneven axial moment distribution, formulating force deflection equations for torsional-flexural behavior
01 p0141 A72-11049
- Telescope construction for solar prominences observation, discussing reflection prisms effect on light rays path and image displacement
08 p1165 A72-21088
- Mode locked ruby laser having triangular ring cavity with four prisms to obtain reliable single-transverse-mode Q switched and normal operation
11 p1647 A72-26150
- Lens parameters selection and prisms position optimization in light beam to avoid premature damage
12 p1808 A72-27623
- Determination of the angular divergence of laser radiation by a transforming system of prisms.
20 p2933 A72-39523
- Continuously tunable dye laser to obtain output wavelength variation by changing pump laser beam incidence angle on prism lateral face
20 p2933 A72-39563
- Optical devices to produce transmitted image rotation about axis, comparing derotation systems and roll and high-speed prisms
20 p2927 A72-39849
- Improvements in electro-optic circular-scan deflectors.
21 p3050 A72-40146
- Objective-prism plates photometric computerized calibration method based on continuum energy distribution of standard stars within photographic plate field
22 p3177 A72-42376
- Self-aligning comparison beam methods for one-, two- and three-dimensional optical velocity measurements.
22 p3177 A72-42395
- Astrospectrography with a mirror telescope. II - One-prism spectrograph with 60 deg flint prism
22 p3178 A72-42545
- A laser beam divider with continuous adjustment of the intensity ratio
23 p3294 A72-43225
- IR spectroscopy techniques based on Pfund triple-pass absorption cell, image slicer and achromatic doublet lenses, presenting graphs for prism dispersion design parameters
23 p3289 A72-43895
- PRIVATE AIRCRAFT**
U GENERAL AVIATION AIRCRAFT
- PRIVATE AVIATION**
U CIVIL AVIATION
U GENERAL AVIATION AIRCRAFT
- PROBABILITY**
U PROBABILITY THEORY
- PROBABILITY DENSITY FUNCTIONS**
NT NORMAL DENSITY FUNCTIONS
NT PEARSON DISTRIBUTIONS
NT RAYLEIGH DISTRIBUTION
NT WEIBULL DENSITY FUNCTIONS
- Random processes models based on Poisson sequences extended to simultaneous asymmetry and probability density function excess, establishing asymptotic relationships
02 p0216 A72-11919
- Nonlinear theory of cascaded two-way coherent spacecraft tracking system model, obtaining steady state probability density functions of phase and Doppler error
02 p0174 A72-12137
- Suboptimal nonlinear filter performance evaluation methods based on Kolmogorov equations for Markov process transition density function
04 p0505 A72-15040
- Nonlinear plant and observation models with white Gaussian noise and continuous data, obtaining state vector a posteriori probability density for optimal prediction
04 p0506 A72-15112
- First passage time boundary value problem for first order phase locked loop systems, determining probability density function of time to cycle-slip
07 p0959 A72-19273
- Probability density and distribution functions of first arrival time at boundary by steady normal random process
09 p1289 A72-22217
- Molecular beam velocity distribution measurement from integral quantity, obtaining precise results in noisy environment and probability density function by numerical deconvolution
09 p1356 A72-22793
- Multivariable probability density determination of random vibration systems with n degrees of freedom by Fokker-Planck equation
09 p1353 A72-23609
- Probability density functions shape estimation by deterministic heuristic and entropy maximization algorithms
10 p1442 A72-23798
- Optimal nonlinear estimation problem with nonlinear plant and observation models obtaining state vector a posteriori probabilities for prediction and smoothing via partition theorem
[AD-736521] 10 p1455 A72-23803
- Noncoherent detection of sinusoidal signal imbedded in clutter and Gaussian noise, obtaining proba-

bility density as function of SNR and clutter-to-noise ratio
10 p1437 A72-24691

Time dependent power spectral density function for first passage probabilities in nonstationary random processes in civil engineering involving earthquakes and wind
10 p1514 A72-25188

Probability density distributions for distance from arbitrary point to randomly distributed weather stations
11 p1592 A72-25767

Combined probability density of amplitude and phase difference distribution of signal and noise sum in moving target selection radar systems
11 p1596 A72-26307

Probability distribution density of phase difference between noise and signal-noise sum for radar system efficiency estimation, using Bessel and Whittaker functions
11 p1596 A72-26308

Probability distribution density of amplitude difference of target signal and correlated noise sum for radar efficiency estimation
11 p1596 A72-26309

Associative impulse analyzer for measurement of probability density functions in electronic memories
11 p1602 A72-26446

Probability density function of hologram exposure irradiation in terms of Bessel function, adding uniform beam coherently to random speckle pattern
11 p1636 A72-26749

Random vibratory processes and envelopes distributions interrelationship, tabulating probability density functions and moments
12 p1846 A72-27725

Probability density functions for output process in frequency discriminator under action of additive mixture of fluctuating radio signal and random noise
13 p1914 A72-28411

Density function for lower troposphere vertical turbulence diffusion coefficient derived from atmosphere radiometric probe data
13 p2029 A72-28456

Optical anemometers for mean and fluctuating velocities in premixed flame of town gas-air combustion system, noting velocity probability density distribution
13 p1955 A72-28546

Random processes models based on Poisson sequences extended to simultaneous asymmetry and probability density function excess, establishing asymptotic relationships
13 p1948 A72-29231

Sinusoidal signal and stationary quasi-white Gaussian noise mixture effects on stochastic phase locked AFC system operation, noting phase error probability density function
13 p1921 A72-29285

Van der Pol oscillator acted upon by weak random noise, evaluating oscillations envelope dispersion from probability density function and phase derivation
14 p2132 A72-31123

Earth satellite orbit motion in terms of probability densities and distributions for large populations and single satellites
15 p2307 A72-31692

Radiation source position a posteriori probability density function determination with empirical prior knowledge to provide simple computational procedures
15 p2267 A72-31778

Sea clutter measurement at low grazing angles by high resolution radar, noting non-Rayleigh probability density and variation with frequency, pulsewidth and polarization
15 p2196 A72-31786

Higher moments of Reynolds stress fluctuations and velocity components in turbulent boundary layer, obtaining probability density distributions
15 p2218 A72-32401

Probability density for interplanetary scintillation at 74 MHz, noting log normal distribution
16 p2450 A72-32953

Nonparametric probability density function modeling algorithms comparison for convergence rate and limit cycle stability relative to implementation ease
16 p2367 A72-33867

Search density function optimality for randomly moving target in n dimensional space with location probability density function satisfying given partial differential equation
17 p2574 A72-34340

Structural system response to white noise excitation, deriving integral equation for first passage time density function via Markov process model [ASME PAPER 72-APM-11]
17 p2629 A72-34805

Master equations for finite systems
17 p2576 A72-35153

Error rate of phase-shift keying in the presence of discrete multipath interference.
17 p2516 A72-35334

Non-analytic character of the shear-tensor distribution function in incompressible turbulence.
18 p2678 A72-36012

Statistical self-similarity and inertial subrange turbulence.
18 p2678 A72-36021

Probability density - A new approach to system electromagnetic compatibility testing of digital circuits.
20 p2906 A72-38980

Interference performance degradation to digital systems.
20 p2901 A72-38984

Error incidence probability for system control reliability determination, assuming Markov process
22 p3162 A72-42183

Pontryagin equations for Markov process limits probability, solving problem of one dimensional steady random process limits for given initial probability density function
22 p3205 A72-42227

Response of linear and nonlinear continuous structures subject to random excitation and the problem of high-level excursions.
22 p3241 A72-42970

Suitability of the normal density assumption for processing multispectral scanner data.
22 p3157 A72-43025

The intermittent small-scale structure of turbulence - Data-processing hazards.
23 p3282 A72-44305

Interplanetary scintillation of radio sources observed through solar corona, deriving higher central moments from skewness coefficient of probability density function
24 p3437 A72-44831

Statistical analysis of the turbulence near a wall by conditional sampling
24 p3392 A72-45066

Intermittent character of the viscous sublayer and interpretation of probability density measurements
24 p3392 A72-45072

On the S/N-characteristics in PCM systems for a class of signals with representative amplitude distributions.
24 p3380 A72-45282

Classical calculations of H₂O rotational excitation in energetic atom-molecule collisions.
24 p3427 A72-45309

Autocorrelation function of smooth steady random signal determination from consecutive derivative dispersions by MacLaurin, least squares and Taylor methods
24 p3380 A72-45317

PROBABILITY DISTRIBUTION FUNCTIONS

Error probability distributions in navigational statistics involving single or identical and diverse instruments or operators
01 p0096 A72-10176

Cyanide and carbon molecules and isotopes electronic systems opacity probability distribution functions for stellar equilibrium model atmospheres calculations
03 p0416 A72-13012

Continuity of probability distribution functions obtained by superposition
04 p0540 A72-15260

Subjective probability distributions for random device-generated Bernoulli process unknowns, discussing distribution median and quartiles and hypothetical sample impact assessment techniques
05 p0616 A72-15812

Combined delay and loss common-control queueing system, obtaining stationary state loss and waiting probabilities and waiting time distribution function
06 p0794 A72-18243

Stochastic differential equations for a posteriori probability distribution in problems of Markov process parameter estimation, adaptive filtering and signal detection
06 p0794 A72-18301

Phase lock loop receiving system digital simulation for estimating mean time to indicate lock and probability distribution function for wide SNR range
07 p0939 A72-19065

Objects visual detection probability distribution as function of angular size, contrast and search time, comparing binocular and monocular searches effectiveness
07 p0931 A72-19919

Random antenna radiation patterns probability distribution law and Dolph-Chebyshev array design, calculating minimum statistical sidelobe level
08 p1138 A72-20930

Lower confidence bound for reliability and specifications for nonnormally distributed stress corrosion test data, using Weibull statistical distribution
08 p1189 A72-22102

Hydrometeorological parameters spatial-temporal variations analysis and forecasting based on association functions and conditional probability distribution functions
08 p1202 A72-22116

Probability density and distribution functions of first arrival time at boundary by steady normal random process
09 p1289 A72-22217

Long distance communications multimode waveguides and probability distributions on symplectic group in extension of mathematical model with random inhomogeneities
09 p1277 A72-22474

Error probability estimates in two channel diversity reception systems with allowance for fading correlation and incomplete signal separation
09 p1278 A72-22572

Computerized and analytic techniques for estimating multiplexed systems output probability distribution, considering system effectiveness, reliability and survivability
10 p1486 A72-23977

Retrieval model based on probability distribution defined on set of all admissible arrays of elements in loci set
10 p1446 A72-25191

Probabilistic analysis of technological systems precision, estimating distribution functions of random output parameters
11 p1609 A72-25430

Strike aircraft reliability prediction in cost effectiveness analyses, showing failure probability distribution with time
13 p1896 A72-28360

Signal detection sequential procedure duration probability distribution at frequency discriminator output for arbitrarily shaped background noise energy spectrum
13 p1915 A72-28474

Optimal level of recording defects in ultrasonic flaw detection, taking into account inspection conditions and defect size probability distribution
13 p1956 A72-28924

Amplitude probability distribution of radio waves reflected from traveling ionospheric disturbances superimposed on small scale irregularities
13 p1921 A72-29338

Stochastic differential equations for a posteriori probability distribution in problems of Markov process parameter estimation, adaptive filtering and signal detection
13 p1937 A72-29441

Earth satellite orbit motion in terms of probability densities and distributions for large populations and single satellites
15 p2307 A72-31692

Pulse and monochromatic short wave signals phase/amplitude autocorrelation functions and probability distributions during oblique incidence reflection from ionosphere
15 p2197 A72-31876

Structural failure probability distribution for threshold stress crossings in random vibration, using Poisson approximation
16 p2468 A72-33227

Error probability distribution of digital data magnetic recording in computer drum memory
16 p2367 A72-33262

Satellite measurement of ground-based CW Ar laser source scintillation, deriving log amplitude variance, probability distribution and power spectral density from telemetered data
17 p2513 A72-34289

Superposition principle in test particle method for reducing plasma cloud kinetic theory to determination of conditional probability function involving Vlasov equation
17 p2591 A72-35163

Three point distribution function related to lower order functions for closure of hierarchy of equations for turbulent probability distribution functions
18 p2677 A72-36005

Possible refinement of the lognormal hypothesis concerning the distribution of energy dissipation in intermittent turbulence.
18 p2678 A72-36018

Some observed properties of atmospheric turbulence.
18 p2705 A72-36019

Stochastic optimal path selection via N discrete points set, discussing probability distributions and computer requirements
18 p2672 A72-36055

On discrete-time Kalman filter in singular case and a kind of pseudo-inverse of a matrix.
18 p2672 A72-36059

Video data transmission minimum channel capacity requirement calculation from rate distortion function of source with known probability distribution
18 p2657 A72-36253

Condition for the equivalence of two important adaptation algorithms and its relationship to effective estimates of probability-distribution parameters
19 p2825 A72-37439

Book - Bayesian statistics: A review.
20 p2946 A72-39728

Characteristic properties and estimation of reliability functions for redundant systems
21 p3038 A72-40713

Ultrasonic sound beam measurement of flow circulation variations in circular cylinder wake, evaluating probability distribution of beam phase fluctuations
21 p2990 A72-40947

Determination of the probability for passage of molecules through the working rotor of a turbomolecular vacuum pump with nonparallel walls of the channel between vanes

22 p1319 A72-41862

Probability distribution of velocities and temperatures near a wall

23 p3279 A72-43696

Optimal search with uncertain sweep width.

23 p3308 A72-43805

Probability distribution of vertical longitudinal shear fluctuations.

23 p3281 A72-44146

Estimates of unknown parameter from quantized observations given as sequence of evenly distributed random values, noting optimal grouping equations for general distribution function

23 p3266 A72-44218

Fluctuations of the spatial distribution of the number of particles in showers generated by muons in heavy material

23 p3331 A72-44431

Statistical techniques for severely censored random samples with known and unknown probability distribution functions

24 p3418 A72-44665

Point and confidence interval estimates for acceleration and aging component probability distribution functions in accelerated life tests and reliability prediction

24 p3406 A72-44669

Error probability estimates in two channel diversity reception systems of digital data transmission with allowance for fading correlation and incomplete signal separation

24 p3379 A72-44751

PROBABILITY THEORY

Kennedy Space Center thunderstorm forecasting system, discussing data processing with conditional and exposure period probabilities and nonlinear predictors multiple regression equations

01 p0094 A72-10826

Statistical model for communication probability estimate based on signal-to-interference and SNR criteria

01 p0031 A72-10997

Point estimate calculation of underlying distribution function for probability plot, developing confidence coefficient for Weibull model

02 p0252 A72-11557

Signals detection under unknown direction and arrival time conditions, developing performance evaluation method based on detection probability-false alarm curves

02 p0180 A72-12573

Aircraft trajectory optimization for maximum profit as decisional problem under risk conditions, determining probabilities by Monte Carlo method

02 p0257 A72-12747

Binary systems formation probability during triple encounters, observing dependence on system/potential energy ratio

03 p0435 A72-13809

Finite memory uncertain stochastic controller, developing optimal and suboptimal algorithms

03 p0329 A72-14181

PCM/NRZ signal band limiting effect on bit error probability, presenting SNR degradation as function of bandwidth-bit duration product and bit patterns

03 p0325 A72-14192

Near optimum limiting and blanking levels /error probability/ selection for binary signal matched filter reception in Gaussian and impulse noise, discussing performance simulation

04 p0486 A72-14485

Probability amplitude analysis of statistical behavior of fading signal envelope

04 p0493 A72-15457

Electron tunneling probabilities through slowly varying potential energy barrier with potential holes evaluated by T scattering matrix interaction formalism

04 p0563 A72-15471

German monograph on thermionic power supply equipment converter network reliability covering I-V characteristics and failure probability calculation

04 p0466 A72-15696

Mixtures, periods and factors of tau-regular probability laws in topological group or half group

05 p0682 A72-16121

Probabilistic output analysis of dynamic nonlinear system with random characteristics by functional Volterra series

05 p0641 A72-16315

Trapping probability in gas-surface interactions from empirical accommodation coefficients, using simple model based on assumed attractive square well and impulsive-repulsive potential

05 p0624 A72-16394

Book on random functions and turbulence covering probability theory, random processes and fields, statistical correlation and spectral methods, numerical weather forecasting, etc

05 p0649 A72-16397

Probability formula for pulse coincidence frequency from different independent radars

05 p0629 A72-16579

Acquisition probability equation for navigation systems terrain correlation devices, using two different correlation algorithms

[AIAA PAPER 72-122] 05 p0688 A72-16974

Binary differentially coherent phase shift keyed system, evaluating error probability performance in presence of thermal noise and intersymbol interference

06 p0772 A72-17408

Continuous linear probability functions characterization, applying to p-radonizing operators

06 p0838 A72-17554

Conditional expectation and integral of random closed convexity in probability space

06 p0839 A72-17555

Combined delay and loss common-control queueing system, obtaining stationary state loss and waiting probabilities and waiting time distribution function

06 p0794 A72-18243

Block orthogonal M-ary communication over fading dispersive channel with intermittent on-off noiseless feedback, calculating upper and lower bounds on error probability

06 p0776 A72-18389

Variable length codes using Fano metric for minimum error probability sequential decoding

06 p0776 A72-18393

Incoherent optical system model with photodetectors governed by Laguerre counting statistics obtaining error probabilities for comparison with Poisson counting

06 p0776 A72-18394

Binary detector with dual gating function between first and second quantization processes, estimating false alarm and rejection probabilities

07 p0937 A72-18851

Complex sampling with cascaded triple input majority logic redundant systems, deriving failure probability

07 p0949 A72-19173

Statistical and probabilistic analyses of comet groups existence with similar orbital elements, considering gravitational capture by trans-Neptunian planets

07 p1075 A72-19559

Failure analysis probability for structures excited by randomly varying dynamic loads, comparing Gaussian and filtered Poisson processes

07 p1093 A72-19948

Probability estimates for aircraft encounters with heavy rain

07 p1031 A72-20365

Probabilistic logic method, concepts and elementary operations in combining Boolean algebra and probability theory

08 p1197 A72-20869

Random vibration theory and Markov processes in nonlinear stochastic systems with probability and asymptotic methods application

08 p1205 A72-20965

Quantitative and qualitative reliability estimates for electronic and mechanical products, obtaining conditional probabilities of flawless operation

08 p1179 A72-22052

Reliability analysis of redundant and nonredundant systems with different component failures, using probability theory

08 p1180 A72-22053

Reliability equivalence systems with excessive and deficient group redundancy, noting replacement conditions and flawless operation probability

08 p1143 A72-22060

Controlled plants operation efficiency change prediction by analytic and probabilistic methods with data processing

08 p1180 A72-22064

Probabilistic-statistical method for recognition and short term forecasting of convective clouds, spring floods, hail, thunderstorms and showers

08 p1202 A72-22115

Probability weather forecasts reliability, considering utility and spherical and logarithmic validities

08 p1203 A72-22124

Probabilistic characteristics of radiation pattern for multielement antenna with nonpolar phase front

09 p1285 A72-22575

Laser induced surface damage probability as function of power density, suggesting electron avalanche breakdown as cause

09 p1324 A72-23083

Potential function criterion for feature selection in pattern recognition, obtaining upperbound estimate of misrecognition probability

09 p1342 A72-23419

N fail-safe logics for circuit fault restoration, comparing with failure probability of majority voting scheme and quadded logic

09 p1283 A72-23420

Probability estimates of aircraft encounters with hail, discussing variations with locality, hailstone size and height and supersonic transport experience

09 p1346 A72-23423

Membership probabilities for open cluster IC 4665 based on relative proper motions

09 p1391 A72-23531

Optimal tracking filter for processing sensor data of imprecisely determined origin in surveillance system by minimizing effects of correlation uncertainties

10 p1455 A72-23787

Probabilistic methods application to software reliability analysis, deriving expressions for hazard, density, failure and reliability functions

10 p1486 A72-23983

Confidence level determination in terms of reliability index /MTBF/ for MIL-STD-781 truncated sequential probability ratio tests

10 p1444 A72-23989

Prediction method for computing maintenance technician reliability as probability of equipment repair completion within given time

10 p1486 A72-24000

Probability model of statistical independence relationships among two events and environmental event, examining all combinations of definition statements for reliability analysis

10 p1504 A72-24015

Complex system represented by fault-free with independent components, calculating confidence interval for failure probability by moment method

10 p1444 A72-24018

Commercial aircraft reliability program development from informal continuous product improvement to formalized methods based on reliability logic diagrams and probability calculations

10 p1421 A72-24019

Probabilistic derivation of quantum mechanics wave equations for Brownian motion and spatial-temporal diffusion

10 p1505 A72-24071

Linear processes coupling and cylindrical probability imaging through nonlinear mappings, noting relationship to Ito theory of stochastic integrals

10 p1505 A72-24072

Binary split phase FSK signal noncoherent detection by multiple predetection filtering, noting probability of error per bit

10 p1437 A72-24686

Radar sequential detector for digital processing of signal masked by noise, determining false alarm and detection probabilities and mean test duration

10 p1439 A72-24908

Statistical analysis of entire set based on subsets, discussing problem formulation in probabilistic language

10 p1506 A72-25117

Model for I/O channel traffic in computer systems, obtaining closed solution for stationary probabilities of state

10 p1446 A72-25148

Receivers for PPM optical communication and pulsed signal detection in background light, evaluating upper bounds on error probability based on photoelectron Poisson statistics

11 p1591 A72-25311

Servo systems operational reliability analysis for variable intensity of fluctuating interference, discussing Markov process probability determination and Kolmogoroff equations solution

11 p1609 A72-25441

Probabilistic output analysis of dynamic nonlinear system with random characteristics by functional Volterra series

11 p1610 A72-25798

Accumulator type radar detector analysis by Markov chains method, discussing false alarm and detection probabilities

11 p1592 A72-25807

Narrow pulse optical communication digital systems with PPM and on-off keying, investigating timing error effects on bit error probabilities

11 p1592 A72-25885

Upper bound on probability of specified errors pattern occurrence for amplitude modulated digital communications systems subject to intersymbol interference and random noise

11 p1592 A72-25889

Russian book on approximate solutions of boundary value problems covering elliptic differential equations and Ritz, moment, straight lines and probability modeling methods

11 p1677 A72-26065

Scalar and vector partitions of forecasts probability score in two state situation

11 p1681 A72-26078

McShane belated stochastic integral existence theorem with quasi-martingale process for sample continuity assumption

11 p1678 A72-26156

Measurable multiapplications and convex integrals properties in complete probability and Banach spaces

11 p1678 A72-26476

Noise immunity and code sequence rejection probability in real multifrequency communications systems with multipositional frequency shift keying

11 p1598 A72-26729

Near circular orbit elements determination as functions of satellite initial speed and coordinates deviation by mathematical expectation procedure

11 p1724 A72-26912

Carbon monoxide and hydrogen adsorption on graphite, measuring sticking probabilities
12 p1777 A72-27039

Probability and collisional relaxation in stellar systems, discussing gravitational polarization, collective interactions and spatial inhomogeneity
12 p1872 A72-27891

Russian papers on adaptive control systems covering automata and game theory, learning models, Markov processes and probability theory
12 p1787 A72-27921

Detection probability for moving small targets embedded in random white noise on TV display, comparing machine processed pattern recognition techniques and human performances
12 p1843 A72-27933

Recombination parameters in low resistivity gamma irradiated n-type Ge, obtaining energy levels and temperature dependence of electron and hole capture probabilities
12 p1857 A72-28056

Russian book on random processes theory covering random sequences and functions and probability measures in functional spaces, limit theorems, etc
12 p1837 A72-28339

Mathematical model for digital systems reliability, determining probability of success and of various failure modes
13 p1923 A72-28356

Finite time element method for failure probability prediction in multiple load-path system with random loads, noting flow chart for suggested computer program
13 p2052 A72-28369

Mutual coupling in phased arrays of randomly spaced antennas, investigating probabilistic properties of main beam amplitude fluctuations
13 p1916 A72-28532

Error probabilities estimates for communication systems using orthogonal multiposition signals in information transmission, noting techniques applicability to diversity reception systems with self selection
13 p1918 A72-28893

Optimal multistep sampling procedures for production quality control, discussing methods for minimization of error probabilities and total sampling volume
13 p1965 A72-29167

Perturbation theory of hydrogen and helium atoms multiphoton ionization probabilities, proposing series summation method
13 p2007 A72-29430

Digital FM signal receiver with postdetector integration, determining error probability as function of input SNR and noise stability
14 p2084 A72-30332

Statistical inferences on two parameter Weibull reliability function from classical, Bayesian and structural probability viewpoint
15 p2264 A72-31800

Probabilistic information model of adaptive predictor filters (APF) with latent memory simulated on digital and analog computers
15 p2211 A72-31896

Incoherent receiver noise stability in multichannel system with channel frequency separation, deriving formula for receiver error probability
15 p2209 A72-32668

Probabilistic analysis of aircraft crash-caused structural damage to nuclear power plant, using Monte Carlo method and yield line theory for perforation and collapse modes
16 p2421 A72-33600

Error probabilities in digital communication systems subject to mixture of man made or natural impulsive and Gaussian noise
16 p2365 A72-34106

Book - An introduction to applied probability and random processes
17 p2575 A72-34625

On the first-exursion probability in stationary narrow-band random vibration. II.
[ASME PAPER 72-APM-16]
17 p2628 A72-34800

A probabilistic model of a control computer complex for estimating the efficiency of communication of a computer with data sources and receivers
17 p2522 A72-35029

Variational and probabilistic methods for multiphase media, noting applications in electrodynamics, nonlinear plasticity and mechanics
17 p2632 A72-35110

Evaluating alternate paths in R & D project planning.
17 p2639 A72-35340

Real and definite processes in complete probabilized space, showing Markov process as solution of stochastic differential equation
17 p2576 A72-35420

Numerical solution of an optimal control problem with a probability criterion.
17 p2534 A72-35531

Central probability limit theorems and asymptotic normality in fluid mechanics for random stationary processes with uniform ergodicity and strong mixing
18 p2677 A72-36003

Structure, analysis and synthesis of time series models, discussing kernel Hilbert space, spectral estimation, moving averages, identification, etc
18 p2678 A72-36023

Octal Reed-Solomon code to obtain decoding error probability approximation improvement over minimum distance bound
18 p2658 A72-36266

Shadowing function calculation as rough surface point illumination probability by point source radiation, assuming surface elevation as random process
18 p2710 A72-36407

Reliability of simulations of asymptotically steady and strictly ergodic stochastic processes
18 p2704 A72-36467

Theory of optimum M-ary laser detection.
18 p2661 A72-36683

Probability threshold of data element similarity as separation criterion for automatic multiparameter biomedical data classification
20 p2893 A72-38937

Photogrammetrically determined cloud-free line-of-sight through the atmosphere.
20 p2947 A72-38963

Probability theory central limit theorem application to dynamic system generated by billiard scattering motion
20 p2945 A72-39403

Marcum Q function parameters approximations for error probabilities computation in multilevel frequency shift keying and differentially coherent phase shift keying systems
20 p2903 A72-39426

Book - Weak convergence of measures: Applications in probability.
20 p2946 A72-39730

Probability model and causal approach to failure mechanisms and reliability of control systems applied to IC
21 p3024 A72-40711

Liminal stimuli binoptic detection variation with ratio of left eye to right eye detection probabilities
21 p3007 A72-40734

Error probability for multilevel PAM transmission with intersymbol interference, Gaussian and impulsive noise.
21 p3019 A72-40888

Kullback-Leibler information function and the sequential selection of experiments to discriminate among several linear models.
21 p3075 A72-41187

Probabilistic approach to design of control systems.
21 p3038 A72-41232

Machine vibration diagnostics and damping, emphasizing filter lattice foundation structures, probability analysis and Bayes formula application
22 p3182 A72-42127

Pontryagin equations for Markov process limits probability, solving problem of one dimensional steady random process limits for given initial probability density function
22 p3205 A72-42227

Noncoherent scattering probabilistic formulation in terms of mean intensity averaged over absorption profile and mean scatterings number required for photon escape
22 p3206 A72-42559

Aircraft structural safety criteria based on acceptable failure probability, determining critical load levels
22 p3138 A72-42829

Uniform estimate of the residual term in a multidimensional limiting theorem for homogeneous Markov chains on the basis of a class of all measurable convex sets. I
23 p3307 A72-43344

Probabilistic model for tensile strength of brittle fibers, discussing clamping effects at various gage lengths and Weibull flaw structure
23 p3305 A72-43490

CAT probabilities relationship to temperature radiation gradients determined by IR spectrometers onboard Nimbus satellites
23 p3310 A72-43614

Flawless operation probability for information transmission reliability of electronic logic circuits with binary data inputs
23 p3271 A72-43784

Probability of digital-data reception with a given confidence level under conditions of random radio noise
23 p3266 A72-44208

Probabilistic characteristics of radiation pattern for multielement antenna with nonpolar phase front
24 p3384 A72-44754

Development and present-day state of the fatigue-damage theories.
24 p3457 A72-44873

PROBES

The characteristics of a cylindrical probe at high subsonic speeds. I - The case of zero inclination angle.
22 p3135 A72-42484

PROBLEM SOLVING

NT ASYMPTOTIC METHODS
NT ITERATIVE SOLUTION
NT THEOREM PROVING

Problem solving research, discussing trouble shooting, logic, light pattern, search, fire control, code transformation, perceptual maze and computer administered tasks
01 p0020 A72-11192

Holographic technique development review, discussing current and future applications and unsolved problems
09 p1315 A72-23375

Cost effective innovations in space programs management, discussing communication, problem solving and reward and punishment
[AIAA PAPER 72-246]
10 p1564 A72-24451

Automated problem solving in continuous stochastic processes, using nonergodic representation of Gaussian process with continuous spectral density
15 p2204 A72-32588

Atmospheric optics inverse problem solution, comparing orthogonal functions series expansion and statistical regularization method algorithms
22 p3202 A72-43006

Learning and solving complex problems of reasoning - A test-theoretical investigation of the complexity of compound problems of predictive logic
24 p3373 A72-45244

PROCEDURES

NT FINITE ELEMENT METHOD
NT OPTICAL CORRECTION PROCEDURE
PROCESSORS (COMPUTERS)
U CENTRAL PROCESSING UNITS
U COMPUTERS

PROCUREMENT

NT GOVERNMENT PROCUREMENT
Gas turbine procurement standard rating and performance indicators, noting dependence on ambient conditions
[ASME PAPER 71-WA/GT-1]
05 p0703 A72-15894

Proposed ASME procurement standards for gas turbines and generators, with compilation and definitions of specification terms
[ASME PAPER 71-WA/GT-2]
05 p0703 A72-15895

Proposed gas turbine procurement standards for gaseous and liquid fuel specifications emphasizing fuel contaminants
[ASME PAPER 71-WA/GT-3]
05 p0703 A72-15896

Proposed gas turbine procurement standards for shipment and installation preparation
[ASME PAPER 71-WA/GT-4]
05 p0703 A72-15897

PROCUREMENT MANAGEMENT

Parametric cost estimating aids DOD in systems acquisition decisions.
17 p2639 A72-34461

Cost-to-produce estimation consideration as design parameter in defense material contractual arrangement
17 p2639 A72-34462

Defense system procurement evaluation before documentation release to industry, discussing improved specifications, competition, planning and data requirements
17 p2639 A72-34463

French aerospace industry difficulties in procuring parts, suggesting purchasing centralization or setting up of parts stocks
17 p2639 A72-35951

Competitive prototype strategy to reduce weapon system development risks and uncertainties with emphasis on simplified management and procurement
18 p2742 A72-36074

Reliable component procurement for Symphonie satellite, discussing parts list, specifications and sub-contract monitoring and inspection
18 p2670 A72-37124

Problems encountered in aerospace material components procurement, considering purchase centralization and inventories creation policies
18 p2743 A72-37125

Problems confronting the engineer in charge of procurement of components intended for electronic aerospace systems
18 p2743 A72-37126

Time ratio models of equipment availability for using and procuring agencies, considering performance effectiveness criterion and suboptimization risk
24 p3467 A72-44659

PROCUREMENT POLICY

Problems encountered in aerospace material components procurement, considering purchase centralization and inventories creation policies
18 p2743 A72-37125

Successful engineering design teams characteristics in development of complex defense systems, discussing organization size, experience, documentation and procurement practices
21 p3132 A72-40972

PRODUCT DESIGN

U PRODUCT DEVELOPMENT
PRODUCT DEVELOPMENT

NT WEAPONS DEVELOPMENT
Aircraft producibility considerations in preliminary design and production planning phases
[SAE PAPER 710746]
01 p0074 A72-10245

Dispersion strengthened Ni-Cr alloys processing technique and mill products development, noting increased strength at elevated temperatures

01 p0075 A72-10744

Joint venture and international collaboration in guided weapon systems design, development and production, discussing cost sharing coordination between governments and contractors

01 p0147 A72-11156

Space vehicles development and fabrication cost estimation, deriving statistical-analytical formulas with allowance for technical complexity and learning factor

01 p0147 A72-11219

Product support functional organization, discussing support systems analysis and engineering, trainer design, technical proposals and publications, customer training, field service, etc

04 p0597 A72-15224

Aircraft gas turbine engine and components post-war development in Japan

05 p0705 A72-16499

Materials selection problems due to wide variety of new products, discussing technologically and economically optimal decisions on product design, development and future substitutions

06 p0906 A72-18255

Deterministic model for new product innovation adoption rate in commercial aircraft jet engine market

07 p1105 A72-20269

Reliability growth curves for product assessment as technical management forecasting technique

10 p1564 A72-24004

Commercial aircraft reliability program development from informal continuous product improvement to formalized methods based on reliability logic diagrams and probability calculations

10 p1421 A72-24019

Hybrid neuristor transmission lines with planar p-n-p semiconductor structures, discussing development, testing and electrical parameters

10 p1448 A72-24281

Product assurance cost aspects on high reliability space programs, discussing design, packaging, failure trends, acceptance testing and Apollo project

10 p1551 A72-24452

Design and development program for air conditioning system of twin engine unpressurized Piper Navajo, noting flight test results

[SAE PAPER 720328]

11 p1577 A72-25590

High bypass ratio JT15D-1 turbofan engine design and development testing

[SAE PAPER 720352]

11 p1703 A72-25603

Specification requirements for quality assurance of automated data processing systems based on hardware development procedures

11 p1602 A72-26791

Dynamic systems as models for electronic measuring instruments computerized development and design

12 p1791 A72-27579

High electric power output Si solar cell development, discussing increased energy conversion efficiency

12 p1757 A72-28026

Incentive contracts with price differential acceptance test plans to motivate producer to product improvement, defining admissible strategies in terms of risk limitation

13 p2066 A72-28354

Product reliability prediction from failure mode analysis, examining component design, quality control, engineering analysis configuration selection and product testing

[ASME PAPER 72-DE-17]

14 p2108 A72-30863

Aerospace technology transfer to and utilization by industry for product development and improvement, discussing NASA structural analysis computer program (NASTRAN)

[ASME PAPER 72-DE-60]

14 p2175 A72-30875

Semiconductor devices quality assurance based on electrical and mechanical performance tests at every stage of product manufacture from initial design

14 p2091 A72-31164

NASA/General Electric joint development of low noise propulsion technology, describing demonstrator engine A design, components development and aerodynamic/acoustic performance evaluation

[AIAA PAPER 72-657]

16 p2443 A72-34077

Microwave technology - A five year prospective.

17 p2528 A72-34709

Helicopters technical and marketing projections for 1980s, emphasizing reliability, maintainability and maneuverability in design philosophy

17 p2491 A72-34926

NASA technology transfer from information dissemination and service to product development, noting firemen breathing system

17 p2639 A72-35506

Hydrogen oxygen fuel cell development for spacecraft power supply systems, emphasizing service life and reliability under elevated temperature and high current density

19 p2754 A72-37643

Human engineering requirements in aircraft system development.

21 p3011 A72-41423

Integration of safety engineering into a cost optimized development program.

[SAWE PAPER 945]

23 p3358 A72-43485

Plastic balloons development for high altitude research, discussing construction technology, launch methods and scientific achievements

24 p3368 A72-45141

PRODUCTION ENGINEERING

NT PRODUCTION PLANNING

Book on vacuum brazing covering dissimilar metals joining, stress cracking, corrosion resistance, joint design, heat treatment and production engineering problems

01 p0073 A72-10165

Monograph on electron beam welding covering space charge effect, equipment, metallurgical and mechanical aspects, production engineering, economics and applications

01 p0073 A72-10167

Aircraft producibility considerations in preliminary design and production planning phases

[SAE PAPER 710746]

01 p0074 A72-10245

Production cost control and tracking, discussing design decision effects

[SAE PAPER 710747]

01 p0146 A72-10246

Aircraft design producibility to reduce production cost and enhance product profitability, using joint engineering and manufacturing team

[SAE PAPER 710748]

01 p0074 A72-10247

Plastic deformation, heat treatment and grinding of set blank W casts for strip and foil production

01 p0088 A72-11085

Electrodischarge and electrochemical machining applications in continuous repetitive production of aircraft jet engine components

01 p0078 A72-11150

Navy uhf telemetry transmitter production system, discussing test program contribution to quality control

02 p0177 A72-12322

Hybrid circuit production, considering face down assembly of flip chip and beam lead semiconductor devices

02 p0195 A72-12608

Large length-to-diameter ratio two layer blank bimetallic hard alloy product manufacture by extrusion die method, noting mechanical properties

05 p0666 A72-16098

MOS components technology with low threshold voltage, noting wafer surface planarity and smallness of parasitic capacitances and layer resistivity

05 p0702 A72-16181

Quality control of powdered metal parts, considering chemical, atomization, electrolytic and mechanical production stages, tool inspection and test patterns

06 p0822 A72-18070

Semifinished product production technology influence on heat resistant alloys mechanical properties, considering forging, rolling, casting, melting, diffusion welding and powder metallurgy

06 p0834 A72-18647

Nd-YAG laser system generating gold conductor patterns on ceramic substrates, using numerical control system for Si production

07 p1002 A72-19213

Automated detonator production facility features, describing modernization program

08 p1221 A72-20780

Soviet book on control system technology for flight vehicles covering production of mechanical, hydraulic, pneumatic, electric and electronic elements

08 p1179 A72-22024

Reliability tests improvement by ergodic processes failure prediction and data storage for high reliability products manufactured in small numbers

08 p1180 A72-22067

Sequential reliability control and analysis in low run production with plan optimization and tests number reduction

08 p1181 A72-22069

Computer aided administrative control systems development for industrial enterprises management, covering product manufacture

08 p1256 A72-22146

Measured quantity distribution effect on measurement errors, noting application in mass production process control

09 p1316 A72-23662

Constituents, processing, fabrication and structure effects on artificial graphitic materials ablation performance in sublimation regime from high temperature tests

[AIAA PAPER 72-298]

11 p1742 A72-25235

Production manufacturing processes improvements for composite materials

11 p1674 A72-26232

Metrological techniques reliability for industrial production processes, plotting quality control curves

11 p1637 A72-26823

Design and production related cost reduction factors in universal digital computers fabrication

11 p1603 A72-26825

Arc cast vacuum melted Mo base alloy properties, production and applications to heat pipes, aerospace structures and pressure vessels

11 p1644 A72-26844

Solid state reactions in powder metallurgical production and working of Mo alloy, considering sintering process

11 p1644 A72-26846

Surface integrity machining practices application to jet engines production, noting cost reduction and process selection and quality control improvement

[ASM PAPER W 72-27.2]

12 p1862 A72-28163

Algorithm and computer program to calculate low run multiple nomenclature production process optimal parameters

13 p1962 A72-28741

Semiconductor devices series production process control and analysis by statistical procedures, noting computer controlled data acquisition system for silicon diodes production

13 p1965 A72-29166

Computer method of link formation in multiple nomenclature aircraft production lines, minimizing idle time

13 p1966 A72-29464

Soft and out-of-vacuum electron beam welding system for high productivity, describing characteristics

16 p2397 A72-33224

Automatic control for selective precision joint assembly of fuel pump equipment, reducing unfinished product volume

16 p2397 A72-33261

Technical and economic aspects of explosive metal fabrication, considering requirements for close tolerances, nonsymmetrical shapes, large size workpieces and unusual material properties

16 p2398 A72-33354

Russian book on aircraft turbine and spacecraft rocket engine assembly covering process schedules, work organization, precision, joints and couplings, quality control, etc

16 p2399 A72-33373

B-1 production planning and engineering, discussing manpower, tooling, structural components tests, schedules and cost estimates

17 p2559 A72-34389

Northrop A-9A attack aircraft production planning, discussing design features and management/engineering organizational changes in anticipation of USAF production contract

17 p2488 A72-34391

A-10 prototype designed for production.

17 p2488 A72-34392

Price adjusted single sampling with linear indifference.

17 p2560 A72-34943

Russian book on radio component design covering radio equipment component properties, effects of geometry and materials, technological processes and microelectronics

17 p2531 A72-35496

Diogenes development program to obtain information on converters mass production, selling price and service life under irradiation, noting application to thermoelectronic reactor construction

18 p2709 A72-36188

Installation of a production line for high-reliability silicon diodes - Results obtained: Application of the underlying principles to more complex components

18 p2670 A72-37121

Industrial production of high-quality active semiconductor components

18 p2670 A72-37123

Qualification procedure for high reliability electronic part requirements for noncontinuous production

18 p2744 A72-37134

Production measuring equipment and techniques for quality control, emphasizing measurement accuracy, speed and cost effectiveness maximization

19 p2802 A72-38304

Control center relation to process control computers in production engineering, discussing information flow and communication in man machine systems

19 p2761 A72-38310

Industrial work study methods application to aerospace manufacturing for establishment of efficient work methods, facilities utilization and productivity controls

21 p3132 A72-41643

Precision forged turbine and compressor blades.

22 p3183 A72-42518

National Electronic Packaging and Production Conference, Anaheim, Calif., February 8-10, 1972 and New York, N.Y., June 13-15, 1972, Proceedings of the Technical Program.

22 p3161 A72-43171

Material properties, metallurgy, production technology and operational factors effects on machinery structural strength

23 p3347 A72-43733

Equipment assembly design optimization by operational versions determination and criteria evaluation for optimal conditions, noting rotary wing design
23 p3294 A72-44024

Automatic complex control systems with digital computer application for optimal control of production systems, selecting optimality criterion from hierarchically distributed local criteria
24 p3387 A72-45513

PRODUCTION MANAGEMENT

Configuration management on small production contracts for U.S. Government, including identification, control and accounting
03 p0460 A72-14204

Resource analyses for R & D programs.
17 p2639 A72-35339

Maintenance processes planning in air transportation, discussing aircraft availability, cost analysis and production management
17 p2560 A72-35441

Organization of fabrication to obtain high-reliability hybrid circuits
18 p2669 A72-37118

Technical and economic processes representation of radioelectronic equipment synthesis optimization using elementary random magnitudes involving output parameters deterioration rates and fabrication tolerances
23 p3269 A72-43442

PRODUCTION METHODS

U PRODUCTION ENGINEERING

Algorithm for optimal strategy in statistical plant control for machine parts production and assembly, discussing measuring equipment errors effects
13 p1965 A72-29168

B-1 production planning and engineering, discussing manpower, tooling, structural components tests, schedules and cost estimates
17 p2559 A72-34389

Northrop A-9A attack aircraft production planning, discussing design features and management/engineering organizational changes in anticipation of USAF production contract
17 p2488 A72-34391

Algorithm for solving the schedule planning problem in mass production
[AD-742589] 21 p3132 A72-41790

PRODUCTIVITY

Soviet air traffic service productivity increase and manpower saving by introduction of new airliner types
05 p0612 A72-16779

Optimization for maximum productivity of electric spark machining with vibrating electrode, noting erosion product removal difficulties
08 p1174 A72-21033

Industrial enterprise training expense planning in terms of staff productivity and work time
11 p1748 A72-26543

Military R and D organization questionnaires data analysis to obtain relationship between job productivity, satisfaction, ability, age and salary
12 p1891 A72-27655

Industrial work study methods application to aerospace manufacturing for establishment of efficient work methods, facilities utilization and productivity controls
21 p3132 A72-41643

PROFICIENCY

U ABILITIES

PROFICIENCY MEASUREMENT

U HUMAN PERFORMANCE

U PERFORMANCE TESTS

PROFILES

Calculation of a profile or of a cascade of profiles for a velocity distribution given as a function of potential
22 p3136 A72-43096

Suction side velocity distribution parameter characteristic relationship to profile geometrical parameters in turbine blade cascade system
24 p3394 A72-45366

PROFILOMETERS

Diffraction optical dimensional measurement, discussing profile determination from diffraction patterns
[CLEA PAPER 11.5] 07 p0984 A72-19391

Stress-strain curve correction for triaxial stress state and strain rate at arbitrary temperatures, describing instrument for continuous test specimen profile measurement
16 p2469 A72-33232

PROGNOSIS

Foresight, forecast and prognosis concepts in physiology, discussing intuition role and relation between molecular and cellular processes and organism activity
02 p0163 A72-12346

Prognosis algorithm to infer vector predictor by analogy as basis for statistical weather forecasting
08 p1203 A72-22126

Prognostic value of an electrocardiographic sign in acute myocardial infarction.
19 p2756 A72-37871

PROGRAM MANAGEMENT

U PROJECT MANAGEMENT

PROGRAMMED INSTRUCTION

Computer programmed instruction checklist for reliability and maintainability engineers requirements
10 p1443 A72-23981

PROGRAMMING

NT QUADRATIC PROGRAMMING

PROGRAMMING [SCHEDULING]

NT THRUST PROGRAMMING

Project management mathematical models for task scheduling, resource allocation, information planning and decision making
06 p0905 A72-18067

Schedule analysis computer program algorithms for waterfall bar chart display and commodity flow processing and graphing through network
15 p2203 A72-31696

A system for programmed control of the motion of the carriage of a microphotometer along two coordinates
19 p2801 A72-37966

PROGRAMMING LANGUAGES

NT ALGOL

NT CONTEXT FREE LANGUAGES

NT FORTRAN

NT MACHINE ORIENTED LANGUAGES

General purpose simulation system /GPSS/ to program discrete time dependent mathematical models related to transport and queueing processes
17 p2521 A72-34471

Computer programming languages, discussing system dependent and problem-oriented languages, ALGOL, FORTRAN and applicability ranges
17 p2523 A72-35444

Long-term orbit prediction using two-variable asymptotic expansions and the automated manipulation capabilities of the FORMAC language.
[ALAA PAPER 72-938] 21 p3113 A72-41576

Programming for discrete events simulation models, discussing languages construction from general programming language building blocks
23 p3268 A72-44144

An interactive approach for the generation and verification of test sequences in a logic system
24 p3382 A72-44662

Precompiler to simplify programming of celestial mechanics problems in TRIGMAN formula manipulation system, introducing data tube SERIES into FORTRAN program
24 p3442 A72-45242

PROGRAMS

NT APOLLO PROJECT

NT COMSAT PROGRAM

NT DEFENSE PROGRAM

NT EARTH RESOURCES PROGRAM

NT EUROPEAN SPACE PROGRAMS

NT LUNAR PROGRAMS

NT MACHINE-INDEPENDENT PROGRAMS

NT MARINER PROGRAM

NT NASA PROGRAMS

NT RAND PROJECT

NT ROVER PROJECT

NT SKYLAB PROGRAM

NT SPACE PROGRAMS

NT U.S.S.R. SPACE PROGRAM

NT UNIVERSITY PROGRAM

PROJECT MANAGEMENT

Organization, management, contract placement and financing of CECELES/ELDO European multinational program for launcher development
01 p0146 A72-10947

Quality control function in configuration management, discussing hardware and software validity for decision formulation
02 p0304 A72-11553

European Space Research and Technology Center satellite project control system, describing critical path network analysis, work package cost control and project planning
02 p0304 A72-12035

Mathematical model for research payoff estimation by internal rate of return method used by large corporations for project evaluation
02 p0305 A72-12695

Helios solar probe mission, describing project management, data reception system, trajectory monitoring and international cooperation
[DGLR PAPER 71-052] 02 p0284 A72-12720

Systems analysis for equipment performance and data management in aerospace programs
03 p0460 A72-14199

Industrial R and D data collection to relate idea dispositions by management to subjective evaluation, considering urgency, predictability and expected time horizon roles
04 p0598 A72-15455

DELTA flow chart and network method for R and D projects planning and scheduling
04 p0598 A72-15456

Europa 3 booster rocket development for future European space programs, discussing performance characteristics, project management and international cooperation aspects
05 p0724 A72-16310

Project management mathematical models for task scheduling, resource allocation, information planning and decision making
06 p0905 A72-18067

Remote sensing for earth resources data, discussing sensors equipment and project organization and management
06 p0810 A72-18615

Cost effective innovations in space programs management, discussing communication, problem solving and reward and punishment
[ALAA PAPER 72-246] 10 p1564 A72-24451

Product assurance cost aspects on high reliability space programs, discussing design, packaging, failure trends, acceptance testing and Apollo project
[ALAA PAPER 72-247] 10 p1551 A72-24452

Electromagnetic compatibility system design checklist, noting usefulness to project personnel
[SAE AIR 1221] 11 p1604 A72-26026

Lunar roving vehicle qualification program to meet performance specifications under lunar conditions, describing testing procedures and project management techniques
15 p2214 A72-32613

Diogenes development program to obtain information on converters mass production, selling price and service life under irradiation, noting application to thermoelectronic reactor construction
18 p2709 A72-36188

Quantitative evaluation for R and D resource allocation in terms of funding project priorities
19 p2884 A72-38024

Systems management in major projects exemplified by the German Satellite Control Center
19 p2783 A72-38303

French space program management planning, discussing orientation, operation and control of activities
19 p2884 A72-38566

Recent advances in R & D value measurement and project selection methods.
20 p2988 A72-39397

Integration of safety engineering into a cost optimized development program.
[SAWE PAPER 945] 23 p3358 A72-43485

NASA ICBM/IRBM space program major management decisions and highlights concerning Atlas, Titan and Thor
23 p3358 A72-44356

Three solid stage Minuteman ICBM, discussing all-inertial guidance system, ablative reentry vehicle and management arrangements
23 p3358 A72-44357

NASA's management concept for the Space Shuttle Program.
24 p3468 A72-45194

PROJECT PLANNING

Azur satellite project definition organizational structure and time schedule, noting management and implementation problems
05 p0752 A72-16136

NASA programs phased planning and quality assurance techniques, noting cost effectiveness
07 p1102 A72-19126

Project pilot criteria for preparation and execution of flight test specifications
12 p1754 A72-27517

Reliability role in commercial and military telecommunication satellite system planning, discussing economic factors, earth station redundancies and maintenance, spare levels and control systems
13 p2051 A72-28352

Technological forecasting in venture analysis and planning for long-term growth objectives, engineering project selection and resource allocation
[ASME PAPER 72-DE-26] 14 p2174 A72-30868

Evaluating alternate paths in R & D project planning.
17 p2639 A72-35340

Development of planetary quarantine in the United States.
23 p3259 A72-43382

PROJECTED AREAS

U PROJECTIVE GEOMETRY

PROJECTILE CRATERING

Basalt plates craters produced by steel balls, noting profiles at normal and oblique impacts
08 p1232 A72-21153

Craters produced by high speed hardened spherical particles, investigating depth and diameter relationship to impact speed
11 p1738 A72-26919

Impact crater formation at intermediate velocities.
[ASME PAPER 72-MAT-C] 17 p2631 A72-34967

Profile and depth of microcraters formed in glass.
18 p2736 A72-36972

The forces for projectile penetration of aluminum.
19 p2871 A72-37461

Basalt plates craters produced by high velocity impact of steel spheres, noting profiles at normal and oblique angles
20 p2978 A72-39258

PROJECTILE PENETRATION

U TERMINAL BALLISTICS

PROJECTILES

NT HYPERVELOCITY PROJECTILES

Coriolis acceleration effects on flight of projectiles fired from earth surface, discussing horizontal and vertical velocities

01 p0132 A72-11050

Shock hardened delayed transmission pulse code modulated system for artillery projectile instrumentation with in-barrel and in-flight monitoring capability

02 p0175 A72-12155

Slender projectile supersonic flight in fluid with nonequilibrium transformations, comparing theoretical shock decay angle with Wegener-Klikoff measurements

03 p0307 A72-13158

Low-drag artillery projectile aerodynamic characteristics and dynamic flight behavior from wind tunnel, spark range and instrumented flight tests, describing mathematical trajectory simulation

[AIAA PAPER 72-979] 22 p1314 A72-42334

Free-flight projectiles aerodynamic characteristics and trajectories from yawsonde and radar track data, obtaining best fit coefficients by equations of motion numerical integration

[AIAA PAPER 72-978] 22 p1314 A72-42335

Effects of rifling and N-vanes on the Magnus characteristics of bodies of revolution.

[AIAA PAPER 72-970] 22 p1315 A72-42341

Heat addition to supersonic flow by shock induced combustion studied by spherical and conical projectiles shot into explosive gas mixtures

24 p3362 A72-45338

Determination of aerodynamic drag from radar data.

24 p3362 A72-45337

PROJECTION

Multiple projection assembly for topographic maps preparation by satellite photographs optical projection onto model surfaces, exemplifying by reverse lunar hemisphere

08 p1165 A72-21155

Multiple projection assembly for topographic maps preparation by satellite photographs optical projection onto model surfaces, exemplifying by reverse lunar hemisphere

20 p2924 A72-39260

PROJECTIVE DIFFERENTIAL GEOMETRY

U DIFFERENTIAL GEOMETRY

U PROJECTIVE GEOMETRY

PROJECTIVE GEOMETRY

NT MERCATOR PROJECTION

Geometric central projection properties of optical illusions, including Muller-Lyer, Zollner and Hering configurations

05 p0689 A72-16194

Projective geometry method for elastic curve shape of equilibrium-state thin rod subject to end forces

08 p1209 A72-21365

Computerized reconstruction of orthogonal representations from cylindrical and conical mapped projections with known parameters and base

13 p1956 A72-28738

Resultant modulation transmission function of projection photometry photographic materials, discussing techniques for resolution and sharpness

16 p2392 A72-33364

Projective properties of holographic imaging.

24 p3401 A72-44767

PROJECTORS

Synchronization system for remote control and performance checking of motion picture projectors with running film, discussing recording equipment and stroboscopic pulsed illuminator operations

04 p0521 A72-14711

Zeiss /Jena/ stereoplanigraph design and operation to obtain purely optical projection for object reconstruction, discussing human operator replacement by objective electro-optical system

16 p2394 A72-33870

PROJECTS

NT APOLLO PROJECT

NT ORBITER PROJECT

NT RAND PROJECT

NT ROVER PROJECT

PROLATE SPHEROIDS

Prolate spheroidal functions application to optical system performance characteristics, discussing laser modes, signals maximal concentration, image data extrapolation, etc

04 p0548 A72-14741

Prolate and oblate spheroids flow field generated by axial translatory oscillations in still incompressible viscous fluid from Stokes linearized equations, deriving formulas for drag

10 p1418 A72-24462

Scattering of acoustical waves by a prolate spheroidal obstacle.

23 p3313 A72-44118

PROMETHIUM

Pm existence evidence for HR 465 from analysis of Pm II spectral line data

18 p2727 A72-36738

PROMINENCES

NT SOLAR PROMINENCES

Red interference filter design for high performance prominence telescope for H alpha line observation

01 p0064 A72-10203

PROPAGATION

Finite particle propagator constructed by path integral method, deriving infinitesimal propagator in relativistic quantum mechanics from mass nature consideration in Machian cosmological sense

13 p2001 A72-28499

PROPAGATION [EXTENSION]

NT CRACK PROPAGATION

NT FLAME PROPAGATION

PROPAGATION MODES

Oblique electromagnetic wave propagation modes in anisotropic ionized stratified medium, investigating electric field and polarization components

01 p0106 A72-10133

Propagators in strong plasma turbulence, considering characteristic trajectories of Vlasov equation

01 p0109 A72-10244

Atmospheric wave propagation mode parameters frequency dependence analysis from duct model, calculating received signal time behavior by waveguide transfer function

01 p0027 A72-10408

Multimode feeds development for offset Cassegrain tracking antennas

01 p0040 A72-10678

Radiation patterns from rectangular guide horns with impedance walls, analyzing hybrid modes

01 p0040 A72-10681

Ferrite-loaded waveguide Y-junction field mode identification by eigenvalue phase-frequency characteristics measurement, applying to millimeter wave circulator synthesis

01 p0041 A72-10697

Electromagnetic instability of linearly polarized mode propagation perpendicular to magnetic field in two colliding plasma streams

01 p0110 A72-11112

Tropospheric layer structures effect on long range vhf radio communication, calculating wave modes attenuation rate and electric field patterns

01 p0032 A72-11238

Vlf propagation across discontinuous daytime-nighttime transitions in anisotropic terrestrial waveguide, developing dominant mode approximations of transmission and reflection coefficients

01 p0032 A72-11239

Galaxy source of ultrahigh energy cosmic rays, interpreting energy spectrum kinks as galactic to metagalactic radiation transition

01 p0122 A72-11270

Power flow approximation for long distance long wave propagation of ground source between earth and ionosphere, comparing mode theory to heuristic approach

01 p0033 A72-11310

Magnetosphere model for low energy cosmic ray proton propagation mode to synchronous orbit satellite, calculating geomagnetic cutoffs and penetration regions

[AD-741079] 02 p0274 A72-12453

Electromagnetic fields calculation in one dimensional resonator with moving boundaries, considering orthogonal dynamic modes

02 p0195 A72-12591

Cylindrical gravitational waves propagation modes in hot plasma subject to axial magnetic field, investigating instability conditions

03 p0388 A72-13025

Propagation modes attenuation and phase shift of electromagnetic plane wave in superconducting coaxial cylindrical waveguide

03 p0321 A72-13170

Thin film optical waveguides using magneto-optic GdIG as substrate, discussing computerized design for propagation mode converter efficiency

[IEEE PAPER 3,6] 03 p0332 A72-13755

Minority carriers localized surface distribution effect on helicon propagation modes reflectivity in semiconductor

03 p0402 A72-13797

Reciprocal dual mode millimeter wavelength phase shifter design for use in phased array antennas, calculating phase shift and insertion loss vs frequency

04 p0498 A72-14719

Air-filled elliptical waveguide with nonmagnetic metal wall, determining dominant TE mode attenuation by perturbation method with Bessel function

04 p0491 A72-15426

Modes propagating inside tubular microwave antenna, studying canonical problems by asymptotic and modal techniques

04 p0501 A72-15430

Ricocheting mechanism in short radio wave propagation in ionosphere, using ray trajectories and field intensities equations

04 p0492 A72-15439

Cut-off frequencies of degenerate LSE and LSM modes in rectangular waveguides containing dielectric layers in H plane

04 p0502 A72-15526

Inverse scattering by ray optics for conducting wedge, considering TE and TM edge diffracted fields

04 p0551 A72-15671

Waveguide with slanted aperture, determining propagation mode and wave amplitude from radiation level at Brillouin angle

05 p0625 A72-15828

TEM modes characteristics in shielded stripline with four internal strips, tabulating characteristic impedances at different line parameters

05 p0636 A72-16339

Inverse electromagnetic field problem for one dimensional resonator, determining size change from intrinsic mode

05 p0627 A72-16408

Ray-optical calculation of modes scattered by obstacle in two dimensional waveguide or duct with weakly inhomogeneous medium and nonvanishing surface impedance walls

05 p0630 A72-16622

Sound propagation within and radiated from annular duct flow, measuring acoustic distributions for single and multimode excitations

[AIAA PAPER 72-197] 05 p0691 A72-16924

Attenuation characteristics of corrugated rectangular waveguides propagating dominant hybrid mode

05 p0638 A72-17076

Ion sound waves decay instability induced by large amplitude Bernstein mode in plasma

06 p0859 A72-17546

Phase velocity of first order mode of vlf waves propagating in earth ionosphere

06 p0773 A72-17598

Surface roughness effect on TEM mode propagation, discussing perturbation and Bessel series methods

06 p0774 A72-17738

Wave propagation in single mode clad glass fiber light waveguide, discussing fiber core minimum diameter and various loss mechanisms

06 p0825 A72-17773

Hollow and dielectric loaded waveguide modes solution, comparing finite element and finite difference methods based on coefficient matrices and computing time considerations

07 p0952 A72-18793

Thin film optical waveguide with crystal quartz as substrate, observing reversible TE to TM mode conversion due to anisotropy

[AD-738761] 07 p0953 A72-18878

Ogo 6 ionospheric measurement of proton whistlers wave-normal vector, investigating propagation modes

07 p1057 A72-19148

Metal clad dielectric slab waveguide for integrated optics, obtaining dispersion equation solution and propagation modes from simplified model

07 p0940 A72-19220

Parallel current and sheath effects on collisionless drift waves normal mode structure in Q machines with end plates, using slab plasma model with uniform magnetic field

07 p1042 A72-19511

Anomalous wave nulls and relation to endfire surface wave radiation on phased arrays of TEM waveguides with metallic fences perpendicular to ground plane

07 p0945 A72-19788

Group and symmetry theory application to degenerate mode splitting in magnetron cavity systems with electromagnetic fields disturbances

08 p1142 A72-21740

Electrostatic plasma wave conversion into electromagnetic waves, calculating dispersion relation at all wavelengths for perpendicular propagation mode

08 p1137 A72-21989

Laser pulse propagation measurements on multimode glass fibers to evaluate communication potential

09 p1323 A72-22868

Alternative TEM and waveguide type equivalent circuits for rectangular resonator loaded by lumped capacitance

09 p1289 A72-23365

Mode theory of long distance VLF propagation, deriving equation for flat earth-ionosphere waveguides

09 p1282 A72-23570

Microwave attenuation factor of TE and TM modes in hollow conducting elliptical waveguides, using first order perturbation formula for calculation

10 p1451 A72-24594

Book on continuous transitions in open waveguides covering plane directive surface, single wire transmission line and layered waveguide surface wave propagation modes

10 p1436 A72-24675

Ground wave propagation over spherical earth, considering land-sea and homogeneous paths

10 p1438 A72-24740

Nonlinear HF ionospheric instabilities classification on unified basis by coupled mode theory

10 p1440 A72-24936

Multimode dielectric slab waveguide power coupling due to core-cladding interface irregularities, obtaining power distribution and radiation losses

11 p1603 A72-25270

Microwave resonators excited in coupled and E sub zero modes, determining equivalent circuit and Sommerfeld resonator Q factor and guide wavelength
11 p1605 A72-26369

Ionospheric scattered wave propagation mode and weak echo delay explained by analysis-derived model
11 p1597 A72-26570

Mode coupling effects on radio wave partial reflection from lower ionosphere at vertical incidence, using matrix perturbation analysis
11 p1599 A72-26764

Equivalent network for symmetric inductive irises, investigating simultaneous effect of finite thickness and higher order mode interaction by variational approach
11 p1607 A72-26993

Power transfer in optical fiber with nonuniform refractivity in mode propagation direction, using coupled mode theory
12 p1779 A72-27164

Microstrip transmission lines analysis by integral equations approach, assuming TEM mode
12 p1782 A72-27492

Cylindrical waveguide proper modes instability regions boundary calculation, determining dispersion characteristics and waves phase and group velocities
12 p1791 A72-27537

Susceptance inductive loaded evanescent mode waveguide filters with reduced length, using quartz tuned elements
12 p1792 A72-27697

ELF wave propagation velocities in earth-ionosphere waveguide, studying fast and slow modes
12 p1784 A72-27789

TE mode propagation properties in circular waveguide, determining communication link transmitting and receiving equipment requirements
12 p1784 A72-27795

Directional and mode characteristics of coaxial exciter for high area utilization and low halation paraboloid antennas
12 p1793 A72-27812

Measurement of spatially coherent and incoherent structure of axial compressor-generated noise modes propagating in duct
[ONERA, TP NO. 1045] 12 p1861 A72-28049

Frequency equation for torsional wave phase velocity in solid circular rod under initial tension, plotted for various propagation modes
13 p2002 A72-28620

Scattering matrix derivation for parallel plate waveguide array terminated in infinite plane, determining neighboring guides TEM modes mutual coupling
13 p1921 A72-29345

Whistler mode signals observation in conjugate region of 200 kHz broadcast station by satellite-borne narrow band receiver, considering field-aligned ducted and nonducted propagation
13 p1950 A72-29384

Fiberglass performance as duct liner in presence of spinning modes from free field measurements, noting ineffectiveness for plane wave attenuation
13 p2028 A72-29573

Ionospheric absorption measurement by IF mode field strength recording with A3 circuit at 6 MHz, noting diurnal and seasonal variations
13 p1952 A72-29660

Two counter streaming plasmas with anisotropic temperatures, deriving instability condition for ordinary mode electromagnetic propagation perpendicular to external magnetic field
14 p2140 A72-30935

Multimode millimeter waveguides and optical fibers, deriving signal transmission distortion from transfer function and corresponding impulse response statistics
15 p2193 A72-31351

Rectangular, elliptical and parabolic waveguides TM and TE modes relation and cutoff wavelength analysis by finite element method, suggesting mode classifying system
15 p2205 A72-31354

Multiple port waveguide circulators bandwidth performance calculation to include higher order cylindrical and evanescent modes
15 p2205 A72-31356

Multimode optical fiber waveguide theoretical model to predict pulse propagation dispersion for comparison with measurements
15 p2194 A72-31546

Dispersion equation determining periodic structures natural modes propagation constants, using induced electromotive and magnetomotive forces method
15 p2195 A72-31655

Microwave measurements on high permittivity materials with slotted waveguides excited in E mode
15 p2207 A72-31894

Acoustic mode propagation and interaction in hard walled cylindrical ducts, determining pressure and power spectral densities from pressure cross spectrum measurements
15 p2277 A72-32018

Attenuation rate of electromagnetic waves for dominant ELF and VLF modes of earth crust waveguide
15 p2200 A72-32110

Epitaxial YIG film separated from conductive plane by thin dielectric layer, considering magnetostatic propagation dispersion and insertion loss
15 p2294 A72-32502

First mode calculations for VLF atmospherics parameters of group delay time and spectral amplitude ratio based on Wait-Walters model
16 p2362 A72-32890

Earth crust waveguide three layer model for electromagnetic wave propagation, showing mode relation to absorption conditions
16 p2362 A72-33074

Millimeter band open cavity resonator using trihedral reflector diffraction grating and inclination control for mode selection
16 p2364 A72-33491

Piezoelectric waveguide generalized treatment via field representation by sum of normal mode waves, using modified orthogonality relation
16 p2369 A72-33761

A mode-averaging diversity combiner.
17 p2513 A72-34360

Calculation of the critical frequencies of higher-order modes in a hollow elliptic waveguide
17 p2516 A72-34846

Wave interference effect in whistler mode reflection coefficients for model lower ionospheres.
17 p2548 A72-35465

Circular waveguides lined with artificial anisotropic dielectrics.
17 p2530 A72-35468

Propagation mode and scattering loss of a two-dimensional dielectric waveguide with gradual distribution of refractive index.
17 p2530 A72-35469

Stability of the dynamic parameters of a transistor in a small signal mode superimposed on a static injection mode
17 p2596 A72-35801

Propagation mechanism of tensor wave in solid elastic body due to impact.
18 p2734 A72-36377

On the reflection of whistler mode waves from model lower ionospheres.
18 p2660 A72-36430

Poiseuille flow linear spatial stability in rigid pipe under infinitesimal disturbances, obtaining propagation modes eigenvalues
18 p2681 A72-36481

Scattering characteristics of a cross-junction of oversized waveguides.
18 p2660 A72-36486

Dual amplitude construction possibility from general field theory couplings and propagators, considering factorization on multiperipheral configuration in translational and rotational modes
18 p2713 A72-36516

Dispersion curves of mixing mode between electrostatic and electromagnetic waves propagating perpendicularly to ambient magnetic field for hydrogen plasma with Maxwellian velocity profile
19 p2839 A72-37335

Electric dipole radiation at VLF in a uniform warm magneto-plasma.
19 p2840 A72-37833

Transverse mode selection in injection lasers with widely spaced heterojunctions.
19 p2812 A72-38595

Multimode dielectric waveguide with random coupling, discussing pulse dispersion improvement and loss penalty from power spectrum derivation
20 p2901 A72-38923

Vector wave solution of light beam propagating along lenslike medium.
20 p2903 A72-39266

Radiation heat transfer between closely spaced metal surfaces at low temperature - The impact of discrete modes of the radiation field.
20 p2983 A72-39483

[ASME PAPER 72-HT-O]

Optical propagation in space-time-modulated media using many-space-scale perturbation theory.
21 p3014 A72-40142

Wave propagation on helical antennas.
21 p3015 A72-40352

Analysis and design of TEM-line antennas.
21 p3026 A72-40353

On the radiation from an open-ended corrugated pipe carrying the HE sub 11 mode.
21 p3015 A72-40366

Magnetospheric propagation of auroral hiss with whistler mode dispersive properties, suggesting burst source locations and mechanisms
21 p3048 A72-40399

Partial derivatives of dispersion curves for higher modes of Love waves in a single-layered medium.
21 p3084 A72-40496

Two-hybrid mode feed design procedure and performance for small and large f/D ratio reflectors of microwave telescope
21 p3029 A72-40515

Correcting effects of corrugated boundaries on coaxial radiators asymmetry and sidelobes, investigating waveguide hybrid modes induced transverse fields
21 p3029 A72-40516

Dielectric slab surrounding medium gain effects on bound modes amplification via estimation of evanescent surface wave interactions in optical waveguide by perturbation theory
21 p3062 A72-40605

Application of the transmission-line-matrix method to homogeneous waveguides of arbitrary cross-section.
21 p3032 A72-40629

Eigenvalues associated with balanced hybrid modes expressed in closed form to derive conical scalar horn antenna far field radiation patterns
21 p3032 A72-40630

Electromagnetic-wave propagation along a horizontal wire above ground.
21 p3015 A72-40633

D-region measurements with the differential-absorption, differential-phase partial-reflection experiments.
22 p3172 A72-42423

Fundamental transverse electric field (TE-sub 0/ mode selection for thin-film asymmetric light guides.
22 p3186 A72-42622

Waveguide with slanted aperture, determining propagation mode and wave amplitude from radiation level at Brillouin angle
23 p3263 A72-43436

Investigation of stepped irregularities in coaxial lines with allowance for higher-order modes
23 p3263 A72-43447

Stationary solitary, snoidal and sinusoidal ion acoustic waves.
23 p3320 A72-43520

Perpendicular collisionless shock wave instability.
23 p3320 A72-43523

Multimoded components wavefront arrival angle from measurements of signal induced in linear array, discussing numerical calculation from linear equation solution and polynomial roots
23 p3264 A72-43601

Infinite rectangular elastic bar surface mass distribution effects on harmonic wave propagation modes, obtaining approximate solution by expanding displacement as power series
23 p3352 A72-44123

Mean stress effects on fatigue crack propagation rate from tests at various temperatures, assuming initial, tensile and shear modes and final propagation stages
24 p3454 A72-44627

PROPAGATION VELOCITY

Initial strains effect on propagation rate of elastic waves, applying finite deformation theory
01 p0138 A72-10581

Sound wave propagation velocity in partially dissociated and ionized gas, discussing attenuation coefficient, chemical process relaxation time and high temperature oxygen and nitrogen calculations
01 p0051 A72-11212

High strength steels stress corrosion crack propagation velocity relationship to crack tip stress intensity
02 p0295 A72-12482

Human pulse wave propagation velocity measurement, using biotelemetry system of photoresistance sensors and endoscopic bulbs connected to electrocardiograph
02 p0169 A72-12519

Straight beams and rectangular frames stress-strain calculation under pulsed loading, taking into account shock waves finite propagation velocity and internal damping
02 p0300 A72-12855

Radio wave scattering observation in turbulent lower ionosphere, determining vertical propagation velocity dispersion by statistical analysis
03 p0322 A72-13476

Functional based measurements of propagating devices based on cylindrical domains in orthoferrites and garnets, noting storage capability
03 p0333 A72-13783

[IEEE PAPER 28,2]

Elastic wave velocities and polarization in planes of cubic crystals, plotting velocity curves
03 p0402 A72-13861

Tunguska explosion of 30 June 1908, determining air waves propagation velocity
03 p0438 A72-13981

Fatigue crack propagation rates for aluminum alloy plates under mode I extensional loads and transverse mode II bending loads
05 p0732 A72-15793

[ASME PAPER 71-MET-1]

Electrical analog to determine potential field distribution for crack growth monitoring of edge notched and compact tension specimens for current input and probe positions optimization
05 p0666 A72-16303

Plastic zone formation and fatigue crack propagation rate during high cyclic bending of metals
05 p0674 A72-16326

Interplanetary magnetic field effect on flare-generated weak shock wave propagation speed and transit time

06 p0875 A72-17461

Velocity ratio /1.468/ of light received from quasar PKS 2134 plus 004 to light propagation velocity in vacuum

07 p1073 A72-19412

Conductive heat flux propagation rate in gases as function of absolute temperature

08 p1253 A72-21447

Propagation time of charge diffusion across magnetic field in bounded plasma

08 p1215 A72-21879

Thin plates heated by heat sources, solving two dimensional problem in thermoelasticity via Fourier and Laplace transformations with allowance for heat propagation rate

09 p1400 A72-22718

Bromine additions effect on normal laminar flame propagation velocity of methane-air mixture at high pressures

09 p1411 A72-22889

Strong shock wave acceleration during passage through decreasing density region observed in experiments with explosions in Ar-H mixture

09 p1295 A72-22961

Apollo 14 explosion seismic shock waves and compressional wave velocity

09 p1390 A72-23495

Cylindrical tube geometry and electrode separation effects on normal ionizing shock waves, showing speed proportional to azimuthal drive and axial magnetic fields

10 p1470 A72-24794

Electron beam fluorescence method for normal shock wave velocity distribution in Ar-He mixtures

11 p1615 A72-25556

Metal stress corrosion crack propagation rate theory based on film rupture mechanism

11 p1735 A72-25852

Wave equation for sound velocity propagation in suspensions based on mass and momentum balances

11 p1687 A72-26056

Radio wave scattering observation in turbulent lower ionosphere, determining vertical propagation velocity dispersion by statistical analysis

11 p1593 A72-26246

Characteristic shocks propagation velocity, showing exceptionality of hyperbolic conservative system multiple waves

11 p1689 A72-26479

Cyclic loads frequency and environmental effects on fatigue crack propagation rate, comparing theoretical results with Al alloy thin plates experimental data

11 p1663 A72-26802

Microstrip propagation and loss filling factor design formulas for magnetic substrates

11 p1599 A72-26991

Heat and momentum transfer properties and storm propagation speed under steady convective overturning in shear, considering cumulonimbus convection scale of atmospheric motion

12 p1840 A72-27704

Wave packet group velocity concept interpretation and application, considering propagation in dissipative media

12 p1783 A72-27719

ELF wave propagation velocities in earth-ionosphere waveguide, studying fast and slow modes

12 p1784 A72-27789

Self similar blast waves propagation, studying flow field in terms of shock front velocity and ambient atmospheric density variation ahead of front [AD-745816]

12 p1889 A72-27832

Velocity behavior of shear waves propagating in uniaxially prestressed isotropic elastic body

12 p1886 A72-27982

Plasma ionization traveling disturbances velocity and spatial structure in strong electromagnetic waves field

13 p1915 A72-28469

Small amplitude plane wave speed variation with pressure for Na and K at absolute zero temperature, using crystal strain energy formulation

13 p2006 A72-29675

One dimensional wave equation for stress wave propagating at variable velocity for case of monotone decreasing rate

15 p2327 A72-31738

Constant stress effect on propagation velocity of elastic waves in three dimensional body, considering earth crust and earthquake prediction applications

15 p2329 A72-32284

Shock wave propagation velocity increase in combustion shock tubes through intermediate pressure chamber, using streak camera and microwave Doppler technique for velocity measurements

16 p2375 A72-32839

Monochromatic radiation pulse transfer in absorbing plasma, deriving heat wave propagation velocity

16 p2437 A72-33692

Transient thermal waves in the general theory of heat conduction with finite wave speeds.

[ASME PAPER 72-APM-23] 17 p2636 A72-34794

Use of special gauges for determining crack growth rate in fatigue in the AU4G1 aluminium alloy

17 p2567 A72-34890

Strong shock wave acceleration during passage through decreasing density region observed in experiments with gas discharges and Ar-H mixture explosions

17 p2544 A72-35890

Rotary shocks and waves of relativistic magnetohydrodynamics

17 p2593 A72-35908

Experimental determination of ultrasonic wave velocities in plastics, elastomers, and syntactic foam as a function of temperature.

18 p2703 A72-36415

Determination of shock wave velocity in the interplanetary medium

18 p2728 A72-36875

A study of thermoelastic waves by the method of characteristics.

18 p2737 A72-37068

A universal connexion for waves in anisotropic media.

19 p2875 A72-37840

Pressure propagation rate relation to local sound speed in unsteady anisotropic gas flow with particle-varying specific entropy

19 p2788 A72-38564

Earth density, surface wave velocity and other properties calculation from model consistent with physical and petrological mantle theories

20 p2917 A72-39475

Spin wave theory and sublattice magnetization of Cr obtaining wave velocity

21 p3097 A72-40626

Asymptotic solution of the wave equation with variable velocity and boundary conditions.

21 p3075 A72-40838

Wave propagation in thermal rate dependent thermoelastic materials.

21 p3107 A72-41278

Propagation rate and the existence range of turbulent flame

21 p3131 A72-41660

Numerical analysis of wave processes in a three-layer strip with rigid filler

22 p3232 A72-41872

Sudden impulses in the geomagnetotail and the vicinity.

22 p3168 A72-42002

Modified Gilman equation relating dislocation velocity to applied effective stress shown in agreement with stress relaxation experiments on Ti

22 p3189 A72-42436

Measurements of the local velocity of shock and detonation waves by schlieren interferometry of Doppler-shifted laser light.

22 p3178 A72-42455

Equimolar oxyhydrogen detonation wave behavior near pressure limit, considering unsteadiness caused by tube length

22 p3244 A72-42485

Thermal properties of polymers below 4 K.

22 p3197 A72-42800

Crack propagation speed measurements with wedge loaded double cantilever beam of PMMA, calculating stress intensity, strain energy release rate and kinetic energy

23 p3346 A72-43709

Fatigue crack propagation in A514 base plate and welded joints.

23 p3354 A72-44309

Mean stress effects on fatigue crack propagation rate from tests at various temperatures, assuming initial, tensile and shear modes and final propagation stages

24 p3454 A72-44627

Plastic flow around an expanding crack.

24 p3456 A72-44812

Determination of the detonation velocity of isotomic mixtures

24 p3462 A72-45032

Divergent cylindrical detonation of nitromethane

24 p3463 A72-45037

PROPAGATORS

U PROPAGATION

PROPANE

Airport cold fog attenuation by propane atomization technique, discussing application at Orly

04 p0508 A72-14686

Kinetic model for propane pyrolysis based on most important free radical reaction steps

06 p0770 A72-17777

Nitric oxide formation rate in combustion products of propane-air and hydrogen-air diluent flames

07 p0935 A72-19361

Flat flame deflagration tube measurements of laminar flame velocities for propane-ammonia-air mixtures in fuel rich region

16 p2480 A72-34006

A mathematical model of cold propane flames

18 p2741 A72-37016

Luminance profiles photometry for axisymmetrical propagation in propane-air turbulent flow combustion with turbulence level control in jet core

19 p2879 A72-37366

PROPELLANT ADDITIVES

NT PROPELLANT BINDERS

Double base propellant nitroglycerin interactions with inhibition materials cellulose acetate and ethyl cellulose, noting time and temperature effects

14 p2145 A72-30767

PROPELLANT BINDERS

Combustion of composite solid propellants with ammonium perchlorate base and pyrolyzable binder, investigating perchlorate grain size, binder concentration and catalyst effects

06 p0867 A72-17574

Quench combustion studies with two dimensional propellant sandwiches with ammonium perchlorate oxidizer and various binders, using high pressure combustion vessel for deflagration characteristics determination

07 p1051 A72-19727

Gamma radiation effects on composite propellants stability, investigating polyurethane, polybutadiene, silicone and polyisoprene binders mechanical properties

14 p2144 A72-30760

Insulation and bonding materials effects on double base solid propellants stability, using vacuum reactivity testing technique

14 p2145 A72-30766

Polyester bonded explosives mechanical and thermal properties, noting need for desensitizing against shock and friction effects

14 p2145 A72-30768

Ignition of a mixture of ammonium perchlorate and starch by incandescent wires

19 p2847 A72-37367

PROPELLANT CHEMISTRY

Analysis of reaction products of nitrogen tetroxide with hydrazines under nonignition conditions.

20 p2898 A72-39610

PROPELLANT COMBUSTION

NT SOLID PROPELLANT IGNITION

Aluminized solid propellant transient burning rate augmentation as function of acceleration vector magnitude and orientation, applying centrifugal accelerations of zero to 140 g

01 p0114 A72-10378

Pure solid and composite propellants combustion theory based on laminarized solutions to energy and flow conservation equations

02 p0270 A72-11766

Linear law and catalyst modification of ammonium nitrate combustion, using ammonium perchlorate-base propergols theory

02 p0270 A72-12165

Burner design for solid propellants burning properties dynamic testing, using broadband tuned Helmholtz resonator for instability onset delay

04 p0509 A72-15497

Solid propellant flame spectral and temporal details during unstable and stable combustion, using middle infrared spectrometer

05 p0703 A72-16896

Wall thermal radiation influence on solid propellants burning rate in electrically heated tube furnace, noting correlation with laminar flame theory

05 p0703 A72-16938

Boron containing solid propellant combustion efficiency and fuel-air ratio determination from particle laden plume nonequilibrium effects in ducted subsonic flow

05 p0750 A72-16972

Burning gunpowder surface reactions relative to temperature, chemical enthalpy and acoustic waves of pressure, velocity and density

05 p0751 A72-17211

Combustion of composite solid propellants with ammonium perchlorate base and pyrolyzable binder, investigating perchlorate grain size, binder concentration and catalyst effects

06 p0867 A72-17574

Gunpowder burning stability in semiclosed volume from automatic control theory methods application to temperature and pressure dynamics

06 p0903 A72-18205

Operational stability of rocket engine with combustion chamber having charge of two propellant types with different burning rate dependences on pressure

06 p0867 A72-18206

Plane two dimensional flow in channel of rocket engine with solid propellant combustion, obtaining burning rates

06 p0867 A72-18207

High energy chemical propellant combustion under adiabatic and nonadiabatic conditions, calculating product equilibrium state as functions of temperature and pressure with computer program

06 p0903 A72-18212

Quench combustion studies with two dimensional propellant sandwiches with ammonium perchlorate

oxidizer and various binders, using high pressure combustion vessel for deflagration characteristics determination 07 p1051 A72-19727

Dissolved gases effect on liquid surface state during high pressure liquid monopropellant strand combustion 08 p1222 A72-22046

Burning rate of composite solid propellant charges, noting application in solid propellant pressure accumulators 09 p1411 A72-22893

Surface ignition behavior of M2 double base propellant, analyzing reaction kinetics 10 p1528 A72-25142

Burning gunpowder surface reactions relative to temperature, chemical enthalpy and acoustic waves of pressure, velocity and density 11 p1744 A72-25337

Combustion surface acoustic admittance model of blended solid propellant with allowance for foam zone inertia and solid/gas interface reactions 12 p1889 A72-27980

Mathematical model of reactive fluid flows during postignition transients in hybrid propellant rocket system 13 p2025 A72-28416

Solid rocket propellant combustion instability research, discussing data acquisition and reduction, motor instrumentation, motors and burning rate measurements 13 p2024 A72-28929

Solid propellants oscillatory burning with gas phase time lag, solving nonsteady governing differential equations by numerical integration 13 p2065 A72-29301

Time history model of transient ignition to self sustained propellant burning, taking into account pressure effects and igniter heat flux 13 p2065 A72-29305

Carboxy-terminated polybutadiene/ammonium perchlorate base solid propellants aging properties under long time storage conditions at 243-353 K, considering mechanical, dimensional and combustion properties 14 p2145 A72-30763

Combustion of liquid propellants under supercritical conditions 17 p2637 A72-34946

Investigation of the resonant combustion of a rocket charge with longitudinal slots 18 p2720 A72-36241

Nonlinear equations solutions for interior ballistics parameters of solid rocket propellants combustion during rocket engine nozzle opening 19 p2878 A72-37352

Acceleration effects on burning velocity of aluminumized condensed rocket propellant systems, calculating particle size and slag mass 19 p2847 A72-37360

Mechanism and characteristics of condensed system ignition by a dispersed flow 19 p2882 A72-38451

Iron-containing catalysts action mechanism during ammonium perchlorate-polyethyl methacrylate mixture burning in nitrogen atmosphere 19 p2847 A72-38456

Physical model of the onset of turbulent burning of compacted systems in a half-closed volume 21 p3131 A72-41699

Ionization mechanism and condensed and gas phase kinetics of oxidizer burning during ammonium perchlorate combustion 22 p3215 A72-43140

Ionization zone formation and condensed and gaseous phase kinetics during ammonium perchlorate burning in nitrogen atmosphere 22 p3215 A72-43179

Burn-up rate of a solid-propellant slab in contact with a solid-oxidizer layer 22 p3245 A72-43180

Microscopic and electron-microscopic investigation of the catalysis of ammonium perchlorate combustion 22 p3216 A72-43186

Development of a rocket propulsion system with 500 kgf vacuum thrust for liquid hydrogen/liquid fluorine 23 p3325 A72-43620

Ideal high energy liquid rocket propellants combinations for high propulsive efficiencies, considering hydrogen, hydrazine, diborane and ammonia and various oxidizers 23 p3358 A72-44355

The transient processes in hybrid solid propellant combustion chamber throttled by supersonic nozzle. 24 p3434 A72-45198

PROPELLANT DECOMPOSITION

Thermal decomposition of perchloric acid vapor in Pyrex reaction vessels at 279-471 C, using flow technique 09 p1276 A72-23143

Thermochemical methods for plasticized/stabilized cellulose nitrate kinetic constants determination for

lifetime estimation, presenting isothermal decomposition curves 14 p2144 A72-30753

Effective stabilizer content measurement in smokeless powder propellants, discussing nitrogen dioxide generation by cellulose nitrate and glycerin trinitrate decomposition 14 p2144 A72-30755

PROPELLANT EVAPORATION

Spacecraft propulsion into orbit by ground based high-power lasers via thrust generation by material evaporation, emphasizing advantages in launching small payloads 13 p2025 A72-28454

Jets breakup, liquid propellant evaporation and cross sectional area variation in rocket motor combustion chambers 24 p3433 A72-44998

PROPELLANT GRAINS

Algot 3 solid propellant rocket motor design for Scout D and E launch vehicles first stage, considering high total impulse, payload/mass capability and propellant grains [SAE PAPER 710765] 01 p0115 A72-10261

Fracture analysis of two dimensional thermal loaded solid propellant rocket grain models under cooldown [SESA PAPER 1927A] 02 p0270 A72-11513

Optimal design criteria for multigrain solid propellant rockets, considering powder weight, burning time and combustion chamber length 05 p0704 A72-16351

Solid charge design for hybrid rocket engine with constant liquid propellant component consumption, deriving differential equation for perforated grain burning rate 07 p1053 A72-18994

Solid propellant gas generators, discussing propellant processing, grain, ignition, insulation and restrictions 09 p1263 A72-23600

Effective stabilizer content measurement in smokeless powder propellants, discussing nitrogen dioxide generation by cellulose nitrate and glycerin trinitrate decomposition 14 p2144 A72-30755

Propellant powders safe life prediction based on short-time tests, discussing aging effects on chemical stability after 7-11 years air conditioned storage 14 p2144 A72-30756

Pressurized crack behavior in two-dimensional rocket motor geometries. 17 p2596 A72-34203

Swept frequency resolution and optical processing in propellant grain flaw detection by microwave holography, using Vander Lugt filter imaging 19 p2798 A72-37626

Three-dimensional photoelastic and finite-element analysis of a propellant grain. 21 p3052 A72-40237

PROPELLANT MASS RATIO

Multimission capability of solar electric propulsion [SEP] spacecraft, analyzing payload variations, propellant requirements, thrusting time limitations and throttling range [AIAA PAPER 72-51] 10 p1552 A72-25125

PROPELLANT OXIDIZERS

U ROCKET OXIDIZERS

PROPELLANT PROPERTIES

NT PROPELLANT SENSITIVITY

Liquid nitrate ester sensitivity and dissolved water desensitization, using thermal initiation and drop weight impact tests 09 p1373 A72-23145

PROPELLANT SPRAYS

Popping phenomena with the hydrazine nitrogen-tetroxide propellant system. 22 p3215 A72-42866

PROPELLANT STORAGE

Nitrate ester propellants self ignition hazard and ballistic stability, describing heat generation test at various temperatures for long term storage 14 p2144 A72-30754

Propellant powders safe life prediction based on short-time tests, discussing aging effects on chemical stability after 7-11 years air conditioned storage 14 p2144 A72-30756

Cast double base propellant rocket motors safe storage and service life assessment, examining environmental storage conditions and accelerated temperature effects 14 p2144 A72-30758

Composite and double base solid propellant rocket motors storage, considering ingredients and materials compatibility and ignition temperatures effects on spontaneous inflammation potential 14 p2144 A72-30761

Solid rocket propellants storage life analysis and prediction by mathematical modeling of physical-chemical failure generating processes 14 p2145 A72-30762

Carboxy-terminated polybutadiene/ammonium perchlorate base solid propellants aging properties under long time storage conditions at 243-353 K, con-

sidering mechanical, dimensional and combustion properties 14 p2145 A72-30763

Long term storage and propellant transfer capabilities of propellant depot system design to act in earth orbit as resupply station for cargo/personnel shuttles 19 p2870 A72-38831

PROPELLANT TANKS

Fiberglass overwrapped Al alloy for space shuttle cryogenic hydrogen and oxygen tanks, noting weight reduction and impeding effect on cyclic loading induced crack growth rate 01 p0139 A72-10738

Symphonic satellite stability during perigee, apogee and orbital transfer, considering propellant motion in tank and spinning top containing liquid 02 p0287 A72-12717

Finite element analysis of hydroelastic properties of Saturn 5 full scale S-2 LOX tank, comparing with water tests [AIAA PAPER 72-173] 05 p0740 A72-16833

Rotor components vibration destabilizing effects on dual spin spacecraft dynamics, considering turbulent liquid sloshing in Intelsat 4 propellant tank 07 p0973 A72-20488

Space tug design constraints, configurational alternatives, subsystem arrangements, docking system, propellant tank pressurization system, main engine and power supply, etc 13 p2051 A72-28933

Combined spot weld-adhesive bonding to join sheet metal parts with applications to propellant tanks and spacecraft and aircraft structures [SME PAPER AD 72-710] 18 p2695 A72-36526

Dual spin spacecraft simulation on three axis air bearing ball in atmosphere testing propellant tank dissipation and spacecraft stability in autotrack mode [AIAA PAPER 72-860] 20 p2911 A72-39108

Influence of discontinuity stresses on main propellant tankage of a space shuttle orbiter [ICAS PAPER 72-10] 21 p3120 A72-41135

The calculation of elastic tanks partially filled with liquids for prediction of the Pogo effect 24 p3392 A72-45152

PROPELLANT TESTS

Burner design for solid propellants burning properties dynamic testing, using broadband tuned Helmholtz resonator for instability onset delay 04 p0509 A72-15497

Automated mechanical system for solid propellant sheet stretch tests in two directions as function of time 08 p1147 A72-21331

PROPELLANT TRANSFER

A 10,000-gpm liquid hydrogen transfer system for the Saturn/Apollo program. 19 p2784 A72-38829

Long term storage and propellant transfer capabilities of propellant depot system design to act in earth orbit as resupply station for cargo/personnel shuttles 19 p2870 A72-38831

The Scout launch vehicle system. 24 p3450 A72-45165

PROPELLANTS

- NT AEROZINE
- NT CASE BONDED PROPELLANTS
- NT COLLOIDAL PROPELLANTS
- NT COMPOSITE PROPELLANTS
- NT CRYOGENIC ROCKET PROPELLANTS
- NT DOUBLE BASE PROPELLANTS
- NT DOUBLE BASE ROCKET PROPELLANTS
- NT GASEOUS ROCKET PROPELLANTS
- NT GELLED PROPELLANTS
- NT GUN PROPELLANTS
- NT HIGH ENERGY PROPELLANTS
- NT HIGH TEMPERATURE PROPELLANTS
- NT HYBRID PROPELLANTS
- NT HYPERGOLIC ROCKET PROPELLANTS
- NT LIQUID ROCKET PROPELLANTS
- NT METAL PROPELLANTS
- NT MONOPROPELLANTS
- NT RDX
- NT ROCKET PROPELLANTS
- NT SOLID PROPELLANTS
- NT SOLID ROCKET PROPELLANTS
- NT TETRYL

Russian book on combustion products thermodynamic and thermophysical properties covering fuels and propellants characteristics, equilibrium fuel compositions, gas phase transfer and expansion processes, etc 12 p1890 A72-28336

PROPELLER BLADES

Bending stress analysis of rectangular plate with variable stiffness applied to marine propeller blade 02 p0298 A72-12673

Composite propeller blades with carbon fiber reinforced plastics spar for hovercraft, presenting mechanical properties test data for different composite configurations 07 p0912 A72-19062

Plane potential flow problem for laminar boundary layer on rotating infinite cylindrical blade, using conformal coordinate transformation 08 p1108 A72-21614

- Simple Doppler radar using the CL8630 Gunn effect oscillator for the observation of small rotating objects. 17 p2524 A72-34245
- Comparison of two types of blade profile for axial-flow fans 18 p2720 A72-36000
- Complex vortex core fine structure around propeller tip observed via smoke and stroboscopic lighting, presenting photographs 19 p2786 A72-37747
- Investigation of the stability of the tip vortex generated by hovering propellers and rotors. 24 p3361 A72-45327

PROPELLER DRIVE

NT HELICOPTER PROPELLER DRIVE

PROPELLER EFFICIENCY

- Altitude-velocity dependence of turboprop engine equivalent horse power, propeller output and specific fuel consumption, discussing performance characteristics relation to ambient air temperature 05 p0708 A72-17100

- Leading edge serrations effect on rotor noise and aerodynamic characteristics, noting vortex and rotational noise reduction and overall efficiency decrease [AIAA PAPER 72-655] 16 p2349 A72-34079

- Rotary wings lift and efficiency increase by circulation control via tangential blowing about bluff trailing edge airfoils [AHS PREPRINT 603] 17 p2489 A72-34492

PROPELLER FANS

- Prop-fan engine for quiet STOL propulsion, discussing noise characteristics, weight advantage, response and reduced fuel consumption 03 p0406 A72-13697

- Variable pitch fans for STOL aircraft thrust/shaft engine, noting short field capability and quietness 09 p1374 A72-23447

- Low pressure ratio Q-FAN propulsor noise reduction tests on wind tunnel model, discussing source components and design configurations [ASME PAPER 72-GT-40] 11 p1569 A72-25634

- Comparison of two types of blade profile for axial-flow fans 18 p2720 A72-36000

- Variable pitch fans - Successors to the aircraft propeller. 22 p3216 A72-42927

PROPELLER SLIPSTREAMS

- Nonuniform propeller streams effects on aerodynamic characteristics of high aspect ratio wing, using airfoil theory [AD-745477] 07 p0908 A72-19092

PROPELLER SYNCHRONIZERS

U PROPELLERS

U SYNCHRONIZERS

PROPELLERS

NT PROPELLER FANS

NT SHROUDED PROPELLERS

NT TILTED PROPELLERS

NT VARIABLE PITCH PROPELLERS

- Paired Gill propeller anemometer response function in generalized wind vector sensor application, proposing algorithm for magnitude and direction errors reduction in output analyses 09 p1307 A72-22434

- Critique of general momentum theory of propeller actuator disk model, showing flow field determination from nonlinear elliptic differential equation solution 11 p1572 A72-25998

- Acoustic measurements for STOL turboprop transport aircraft propeller configurations under static, taxi and flyover conditions, discussing quiet propeller noise signature 13 p1897 A72-29571

- Investigation of propeller vortex noise including the effects of boundary layer control. 24 p3359 A72-44680

PROPHYLAXIS

- Isoniazid tuberculosis chemoprophylaxis safety in aviation personnel, discussing renal function, serum transaminase activity, hematology, electrocardiograms and neurological examinations 04 p0479 A72-14872

- Automatic ECG recording and analysis by electronic data processing equipment, discussing methods of data acquisition and transmission for routine diagnosis and prophylactic mass examinations 12 p1772 A72-27821

- Thirty day experiment for assessment of weightlessness simulation test methods and evaluation of applicable prophylactics 23 p3259 A72-43912

- Physical training as a prophylactic measure against the hypodynamic syndrome 23 p3260 A72-43920

- A special vitamin complex for prophylaxis of atherosclerosis in aviation personnel 23 p3261 A72-44153

PROPORTIONAL CONTROL

- Directional selector valves with proportional flow control under varying load conditions, discussing hydraulic spool valves design 03 p0312 A72-13963

- Logical synthesis of hybrid off-on control systems with proportional and binary variables, presenting example of fluid power, electronic and fluidic implementation [ASME PAPER 71-WA/FLCS-1] 05 p0640 A72-15919

- Linear single and multiloop control system synthesis for sensitivity reduction by introducing signals proportional to sensitivity functions with analyzer 05 p0640 A72-16207

- Stability degree analysis of linear feedback control systems with dead time, presenting proportional and integral compensation diagrams produced with digital computer program 09 p1291 A72-23370

- Fluid amplification principles, discussing bistable and proportional amplification, signal transmission and transduction to and from fluid signals [ASME PAPER 72-DE-20] 14 p2073 A72-30864

- Dynamic motion analysis of digital servo system with proportional bang-bang control by trajectory mapping on phase plane 15 p2211 A72-31895

- Jet turbulence interaction and velocity effects on noise level of proportional fluid amplifiers 16 p2350 A72-33177

- Proportional navigation with a maneuvering target. 19 p2830 A72-37290

- Proportional control of space vehicles with the aid of auxiliary jet engines 20 p2977 A72-39593

- Constrained proportional controller dynamic equation solution on analog computer, determining limit cycle phase shift and nonlinearity effects on self oscillation parameters 24 p3403 A72-45322

PROPORTIONAL COUNTERS

- NASA spacecraft instrumentation for high energy phenomena measurements, discussing collimated proportional counters, wire grid digitized spark chambers and modulation and slit collimators 03 p0353 A72-13038

- Low power X ray diffractometer with multiwire proportional counter detector array for remote mineralogical analysis of lunar, planetary or asteroid soils detector array 08 p1167 A72-21507

- Circuits for pulse rise time discrimination in proportional counters with different gas mixtures 08 p1167 A72-21511

- X ray observatory with gas filled proportional counters, discussing pulse height analyzer, command system, calibration and power distribution 08 p1167 A72-21512

- Oxygen ionization and ion mobility measurements in air by open proportional counting chamber with electron counter and exoelectron emitter 09 p1305 A72-22203

- Low energy X ray measurements with sealed Ti window proportional counter, applying to rocket observation of Sco X-1 15 p2240 A72-32438

- The solar X-ray spectrum deduced from a proportional counter experiment and the resultant production of ionization in the mesosphere. 22 p3170 A72-42368

- Stopping rate of negative cosmic-ray muons near sea level. 23 p3332 A72-44501

PROPORTIONAL LIMIT

- Strength and strain theory statistical analysis for perfectly brittle and plastic materials, assuming ultimate or elastic limit strain as governing factor 07 p1097 A72-20536

- Calculation of a thin-walled small-aspect-ratio wing beyond the limit of proportionality 23 p3346 A72-43654

PROPRIOCEPTION

NT AUTOKINESIS

- Extraretinal inflow eye position information awareness from experimental load application to eyes in total darkness 07 p0926 A72-19026

- Neck proprioception effects and otolith organ activity in perceived visual target elevation under centrifuging stress 12 p1776 A72-28305

- Human brain sensorimotor region EEG dependence on proprioceptive influence, instruction for active movement and preparation passive movement of hand 16 p2353 A72-32992

- The design of a nonlinear multi-parameter model for the human operator. 21 p3011 A72-41421

PROPRIOCEPTORS

- Sensorimotor mechanism of proprioceptors in muscles and tendons, considering reflexive control of position and motion 22 p3146 A72-42781

- The reflex and mechanical response of the inspiratory muscles to an increased airflow resistance. 24 p3372 A72-44958

PROPULSION

NT AUXILIARY PROPULSION

NT CHEMICAL PROPULSION

- NT ELECTRIC PROPULSION**
- NT ELECTROMAGNETIC PROPULSION**
- NT ELECTROSTATIC PROPULSION**
- NT HYBRID PROPULSION**
- NT ION PROPULSION**
- NT JET PROPULSION**
- NT LOW THRUST PROPULSION**
- NT MARINE PROPULSION**
- NT NUCLEAR ELECTRIC PROPULSION**
- NT NUCLEAR PROPULSION**
- NT PHOTONIC PROPULSION**
- NT PLASMA PROPULSION**
- NT SOLAR PROPULSION**
- NT SPACECRAFT PROPULSION**
- NT UNDERWATER PROPULSION**

- Blast wave techniques for exothermic processes in relation to propulsion systems, using shock or detonation tubes, point explosions, reflected shocks and implosion vessels [AD-737415] 01 p0117 A72-10939

PROPULSION CALCULATIONS

U MATHEMATICAL MODELS

U PROPULSION

PROPULSION SYSTEM CONFIGURATIONS

- Propulsion system optimization for commercial transport aircraft design under Advanced Transport Technology study, considering impact on aircraft gross weight [SAE PAPER 710760] 01 p0115 A72-10257

- Propulsion system optimization in transonic transport aircraft design, considering nacelle integration, engine choice, noise attenuation and technology utilization [SAE PAPER 710762] 01 p0115 A72-10259

- Europa 3 candidate propulsion modules system analysis, considering payload, mission flexibility, orbital injection precision, synchronous satellite design influence, satellite-booster interfaces and costs 02 p0287 A72-12731

- Aircraft power plant management, discussing integration of intake, engine and exhaust system from control standpoint 03 p0405 A72-13418

- Propulsion twin spool power plant design and dimensioning with selective high pressure cut-off for supersonic aircraft with part of flight in subsonic range [DFVLR-SONDR-169] 03 p0406 A72-13608

- Prop-fan engine for quiet STOL propulsion, discussing noise characteristics, weight advantage, response and reduced fuel consumption 03 p0406 A72-13697

- Ramjet engine propulsion systems for large aircraft above Mach number 2.5 04 p0565 A72-14450

- Aircraft and reusable spacecraft propulsion systems current status and future development, discussing noise and exhaust emission problems, V/STOL bypass and fan engines, ramjets, etc 05 p0705 A72-16735

- Earthbound missile propulsion systems, reviewing turbojet and ramjet engines, liquid, solid and hybrid propellant rocket engines and composite propulsion systems for special applications 05 p0705 A72-16741

- Current and future rocket and spacecraft propulsion systems based on chemical propellants, nuclear thermoelectric, electrostatic and electromagnetic power generators 05 p0705 A72-16743

- VJ-101A and B V/STOL weapon system design, describing various propulsion system configurations 07 p0912 A72-19250

- High specific impulse-medium thrust propulsion device based on gas acceleration by traveling conduction waves 07 p1054 A72-19694

- Mitsubishi T-2 two-place supersonic trainer, describing prototype airframe and propulsion system design and operational features 07 p0913 A72-20306

- Commercially available aircraft turbofan engines specifications, describing design features and performance characteristics 07 p1055 A72-20625

- Propulsion system/airframe matching in hybrid V/STOL airplanes, stressing thrust vector management, lift engine bypass ratio and power plant packaging design [ASME PAPER 72-GT-106] 11 p1576 A72-25671

- Propulsion system based on ion tunneling through preferentially oriented metal crystal lattice [AIAA PAPER 72-480] 11 p1710 A72-26208

- Tu-154 aerodynamic design, discussing arrow wing and propulsion unit characteristics 12 p1753 A72-27268

- Ion thruster module design for primary electric propulsion systems, discussing optical configurations, discharge chamber, control and performance tests [AIAA PAPER 72-508] 12 p1860 A72-27423

- Characteristic thrust concept introduced to classify propulsion system tasks related to geosynchronous communications spacecraft, developing approximate analytical models [AIAA PAPER 72-514] 13 p2052 A72-28977

Propulsion modes compared for communication satellites design optimization, discussing attitude and longitude control, orbit inclination control, station change and orbit raising
[AIAA PAPER 72-517] 13 p2052 A72-28979

Characteristics of nonredundant auxiliary and prime propulsion power processors for electron bombardment ion thruster in communication satellites, discussing modular transistorized and SCR systems
[AIAA PAPER 72-518] 13 p2027 A72-28980

L-1011 propulsion, fuel, flight control, navigation, avionics, communication, electrical, environmental control and auxiliary power systems, discussing structure and high lift devices
15 p2181 A72-32427

Pressurized crack behavior in two-dimensional rocket motor geometries.
17 p2596 A72-34203

Mixed-mode propulsion - Optimum burn profile for two-mode systems.
17 p2596 A72-34203

Propulsion technology advance factors, stressing noise and exhaust emissions reduction, economic considerations and aircraft performance
19 p2848 A72-37679

High subsonic transport aircraft design development based on supercritical aerodynamic configuration and advanced structural, flight control and propulsion system technologies
[AIAA PAPER 72-756] 20 p2889 A72-40056

Analysis of a lateral-directional airframe/propulsion system interaction of a Mach 3 cruise aircraft.
[AIAA PAPER 72-961] 22 p3137 A72-42348

Configuration analysis as applied to aerospace vehicle design synthesis.
[SAWE PAPER 91.1] 23 p3342 A72-43458

IL-62 aircraft propulsion system design and installation details, operational surveillance system and maintenance operations
23 p3325 A72-43639

Application of quadratic optimization to supersonic inlet control.
23 p3251 A72-44195

Aircraft gas turbine engines environmental effects, considering thermal radiation, acoustic emissions and exhaust gases in relation to propulsion system design parameters
23 p3328 A72-44296

The development of GH2/GO2-pulse mode rocket engines in the thrust range of 6,660-9,340 N /1,500-2,100 lbs/.
24 p3434 A72-45207

On the utilization of thermonuclear propulsion for an upper stage of the Europa III launcher
24 p3424 A72-45227

PROPULSION SYSTEM PERFORMANCE

Advanced technology air transports propulsion system requirements, considering design, engine performance and reliability, maintenance, airline problems, noise and pollution control
[SAE PAPER 710761] 01 p0115 A72-10258

Ten mlb concentric tubes biowaste resistojet thrust performance for hydrogen, water, methane, carbon dioxide and biopropellant mixtures, discussing vibration, shock and acceleration tests
[SAE PAPER 710769] 01 p0116 A72-10263

Aerospike rocket engine system for orbit-to-orbit space shuttle, discussing light-weight regeneratively cooled thrust chamber performance tests
[SAE PAPER 710770] 01 p0116 A72-10264

Jet noise reduction technology, hardware and tests for NASA Quiet Engine Program to develop low noise subsonic civil transport aircraft propulsion system
[SAE PAPER 710774] 01 p0116 A72-10266

Airline Propulsion Team approach to DC-10 aircraft power plant design for maximum operational effectiveness
[SAE PAPER 710778] 01 p0116 A72-10270

Nuclear gas core and fusion rocket engines performance potential for various space missions, comparing capabilities in terms of payload ratio
01 p0099 A72-11328

Nuclear light bulb rocket engine design and performance, presenting start-up, steady state operation, shutdown, dynamic response and control
01 p0100 A72-11354

Ramjet engine propulsion systems for large aircraft above Mach number 2.5
04 p0565 A72-14450

Europa 3 booster rocket development for future European space programs, discussing performance characteristics, project management and international cooperation aspects
05 p0724 A72-16310

Pulsed electric microthruster with solid fuel feed system, noting electrode geometry effects on performance and ablation patterns
[AIAA PAPER 72-210] 05 p0705 A72-16799

Ion engine performance optimization by power sharing with secondary batteries on synchronous equatorial satellites
[AIAA PAPER 72-206] 05 p0706 A72-16852

Gas generator performance shifts involving military trim level variations by TF-30 engines in high relative

humidity environment caused by condensation in inlet duct
07 p1052 A72-18759

Commercially available aircraft turbofan engines specifications, describing design features and performance characteristics
07 p1055 A72-20625

High performance sounding rockets design, discussing Skylark propulsion system improvement and new rocket vehicle design for 200 kg payload capability with existing motor hardware
08 p1241 A72-21172

Soviet civil gas turbine engines construction and performance, noting relatively high specific fuel consumption
08 p1223 A72-21275

Electrodynamic thrusters for flight vehicle propulsion, reviewing design, efficiency and performance
08 p1224 A72-21669

Controllable high energy hydrogen-oxygen rocket propulsion systems performance and combustion characteristics, considering mixture ratio, pressure, chamber geometric characteristics, injection area and velocity ratios
11 p1703 A72-25298

Air lubricated bearings for high performance aircraft gas turbines, studying design and performance in turboshaft engine
[ASME PAPER 72-GT-38] 11 p1638 A72-25632

Propulsion system design for military VTOL aircraft, emphasizing subsonic cruise to maximum thrust ratio and exhaust downwash characteristics
[ASME PAPER 72-GT-73] 11 p1704 A72-25655

Propulsion control systems design for military and commercial V/STOL aircraft, considering power management performance with minimum weight and maximum reliability and maintainability
[ASME PAPER 72-GT-79] 11 p1705 A72-25659

Propulsion system flexibility in V/STOL aircraft with one lift-cruise engine, discussing takeoff thrust requirements and cruise fuel consumption efficiency
[ASME PAPER 72-GT-105] 11 p1576 A72-25670

Flight mechanics of point with limited power propulsion system and energy storage unit, investigating variational maximum payload problem with singular control optimization
11 p1727 A72-25932

Magnetic field and polar region geometry effects on hollow cathode thruster performance of Kaufman electric engine
[AIAA PAPER 72-417] 11 p1706 A72-26167

Hollow cathode discharge effects on throttled electron bombardment ion thruster performance, considering discharge region diameter and length and baffle aperture area
[AIAA PAPER 72-421] 11 p1706 A72-26169

Resistojet performance models for investigating energy losses in hydrogen, ammonia, methane and carbon dioxide nozzle flows
[AIAA PAPER 72-455] 11 p1708 A72-26191

System tradeoffs for high performance pulsed MPD thruster in space mission application
[AIAA PAPER 72-457] 11 p1708 A72-26193

Parallel rail solid fuel pulsed electric microthruster performance, noting mathematical model for mass ablation and plasma acceleration mechanism
[AIAA PAPER 72-458] 11 p1708 A72-26194

Solid teflon pulsed plasma thruster quasi-steady and short pulse discharge operations, discussing propulsion system performance and erosion behavior
[AIAA PAPER 72-459] 11 p1709 A72-26195

RF ion thruster flight prototype development, describing test facilities, design and performance
[AIAA PAPER 72-471] 11 p1709 A72-26202

Duration test and performance of annular colloid thruster, noting specific impulse increase and electrostatic vectoring
[AIAA PAPER 72-483] 11 p1710 A72-26209

Electron bombardment ion thruster performance characteristics with variable magnetic baffle and hollow cathode
[AIAA PAPER 72-489] 11 p1710 A72-26214

Capillary fed annular colloid thruster operating characteristics, considering I-V relationship, thrust and exhaust velocities and propulsive efficiency
[AIAA PAPER 72-490] 11 p1710 A72-26215

Spacecraft nuclear electric propulsion system multimission performance evaluation, discussing launch mode and vehicle capability factors in system size selection
[AIAA PAPER 72-503] 11 p1685 A72-26226

Solar electric propulsion subsystem performance tested on breadboard model, noting electrical power conversion, command, thrust vector control and propellant supply
[AIAA PAPER 72-507] 11 p1711 A72-26227

Multimission and engine performance requirements for solar electric spacecraft propulsion stage configurations, considering launch vehicle compatibility integration payload and environmental extreme effects
[AIAA PAPER 72-465] 11 p1712 A72-26325

Ion thruster module design for primary electric propulsion systems, discussing optical configurations, discharge chamber, control and performance tests
[AIAA PAPER 72-508] 12 p1860 A72-27423

Nuclear rocket for space tug, comparing performance and operational costs with chemical propulsion
13 p2000 A72-28926

Argon and mercury ion engines operation, performance and control, evaluating safety and ease of handling from laboratory test data
13 p2026 A72-28931

Solid propellant pulsed plasma microthruster performance tests, describing engine design and operation
[AIAA PAPER 72-460] 13 p2026 A72-28945

Structurally integrated ion thruster /SIT-5/ for synchronous satellites attitude control and station-keeping, presenting design and performance data
[AIAA PAPER 72-492] 13 p2027 A72-28950

Two stream ejector propulsion performance, measuring nozzle geometry effect on discharge coefficient for 2-90 deg convergence angles
[ONERA, TP NO. 1050] 15 p2177 A72-31208

Flexible launch vehicle optimal and constrained-optimal control for performance index minimization, using sensors and constant feedback gains
15 p2321 A72-32585

Aero engines and propulsion systems development contribution to air transport economics and regularity, considering environmental factors
16 p2443 A72-33313

Nuclear electric propulsion systems performance evaluation for various escape missions
17 p2606 A72-34577

A capillary-fed annular colloid thruster.
17 p2598 A72-35491

Thermonuclear fusion spacecraft propulsion systems operation principles, interplanetary orbit-to-orbit mission capabilities and environmental safeguard problems
17 p2598 A72-35953

Propulsive performance of a 30 kW arc-jet thruster stabilized by vortex and magnetic forces.
19 p2848 A72-37925

Engine inlet total pressure distortion effects on multistage axial compressor and turbojet/turbofan engine performance and stability, considering inlet-engine compatibility
[ICAS PAPER 72-19] 21 p2991 A72-41144

Elements of the theory of gas-turbine-unit designs
21 p3100 A72-41700

Variable pitch fans - Successors to the aircraft propeller.
22 p3216 A72-42927

Development of a rocket propulsion system with 500 kgf vacuum thrust for liquid hydrogen/liquid fluorine
23 p3325 A72-43620

Experience with the NRC 10 ft. x 20 ft. V/STOL propulsion tunnel - Some practical aspects of V/STOL engine model testing.
23 p3278 A72-44247

Thermodynamic cycle parameter effects on bypass turbofan jet engine fuel consumption and performance under various flight conditions and engine ratings
23 p3326 A72-44281

Supersonic aircraft engine inlet performance in terms of pressure recovery, discussing oblique shock wave formation ahead of entrance to improve efficiency
24 p3360 A72-44991

Linear theory of a solid propellant rocket motor with modulated exhaust
24 p3433 A72-45116

Contribution to the discussion of mixed-mode propulsion and reusable one-stage-to-orbit vehicles.
24 p3450 A72-45191

The development of GH2/GO2-pulse mode rocket engines in the thrust range of 6,660-9,340 N /1,500-2,100 lbs/.
24 p3434 A72-45207

Test facilities for aeroropulsion systems, emphasizing utilization, cost and technical advantages, aircraft inlet-engine systems compatibility and test types
[AIAA PAPER 72-1034] 24 p3388 A72-45401

PROPULSIVE EFFICIENCY

NT PROPELLER EFFICIENCY

Pinle-controlled rocket engine design with gimbaled supersonic splittine thrust vector control, featuring variable thrust, attitude controls and high propulsion efficiency
[SAE PAPER 710763] 01 p0115 A72-10260

Small three spool, reverse and mixed flow turbofan engine for business jets, discussing fuel consumption reduction, thermodynamic performance, efficiency and maintainability
[SAE PAPER 710776] 01 p0116 A72-10268

Minimum propellant impulsive optimal spacecraft guidance and trajectory problem, developing deterministic theory in discrete linear quadratic form with second order perturbation analysis
01 p0130 A72-10929

Space vehicle with solid-liquid propulsion system, determining optimal initial mixing ratio for cylindrical configuration [DGLR PAPER 71-101] 02 p0271 A72-12706

Convergent conical nozzle shape effect on propulsive performance and compressible flow field internal characteristics [ASME PAPER 71-WA/FE-3] 05 p0647 A72-15937

Electrostatic surface and bulk ionization on thrusters current densities for propulsive and working fluid utilization efficiency 05 p0705 A72-16772

Specific impulse, mass and propellant efficiency characteristics of miniature motors using cryogenic fuels for auxiliary rocket thrusters 07 p0914 A72-18983

Electrogasdynamic thrusters for flight vehicle propulsion, reviewing design, efficiency and performance 08 p1224 A72-21669

High energy rocket propellants for space probe propulsion systems, evaluating various propellant combinations in terms of specific impulse, toxicity, corrosiveness, cost and availability 11 p1702 A72-25299

Capillary fed annular colloid thruster operating characteristics, considering I-V relationship, thrust and exhaust velocities and propulsive efficiency [AIAA PAPER 72-490] 11 p1710 A72-26215

Electrostatic surface ionization and electron bombardment on thrusters current densities for propulsive and working fluid utilization efficiency 17 p2597 A72-35275

Ion-thruster propellant utilization. 17 p2597 A72-35490

Generalized relations for determining specific impulse losses in nonequilibrium two-phase nozzle flows 20 p2914 A72-39909

Gasdynamic investigation of a turbine with evaporative air cooling of the nozzle guide vanes 23 p3325 A72-43662

Ideal high energy liquid rocket propellants combinations for high propulsive efficiencies, considering hydrogen, hydrazine, diborane and ammonia and various oxidizers 23 p3358 A72-44355

PROPYLENE

Ultralow sliding friction during bombardment of polypropylene, molybdenum disulfide and graphite surfaces with charged helium atoms at room temperature in vacuum chamber 02 p0249 A72-12282

Ultralow sliding friction during bombardment of polypropylene, molybdenum disulfide and graphite surfaces with charged helium atoms at room temperature in vacuum chamber 11 p1639 A72-25707

PROTECTING

U EXPLORATION

PROSTHETIC DEVICES

Hydrodynamic model of human systemic arterial circulation to test artificial heart pumps [ASME PAPER 71-WA/AUT-13] 05 p0621 A72-15954

Medical equipment advancements through NASA sponsored aerospace research program, describing prosthetic urethral valve, air oximeter, radiation dosimeter and electromyographic muscle trainer 06 p0765 A72-18616

Wear resistance and friction coefficients in physiologic solution of thermoplastic materials for prosthetic application in hip joints 08 p1194 A72-21760

Artificial heart-lungs model with contractile polymer membrane as synthetic muscles to react with gases and liquids, discussing design features 10 p1431 A72-24640

Pure biocarbons for skeletal fixation of limb prosthetic devices, noting load bearing applications dependence on brittle characteristics 12 p1773 A72-28095

Non-invasive assessment of prosthetic mitral paravalvular and intravalvular regurgitation. 17 p2498 A72-34221

PROTECTION

NT ACCELERATION PROTECTION

NT CIRCUIT PROTECTION

NT CORROSION PREVENTION

NT EYE PROTECTION

NT RADIATION PROTECTION

NT RADIATION SHIELDING

NT SOLAR RADIATION SHIELDING

NT THERMAL PROTECTION

Impact tests on anthropomorphic dummies for protection effectiveness evaluation of lap belt, Air Force shoulder harness-lap belt and airbag-lap belt restraints [AD-741530] 12 p1769 A72-27471

PROTECTIVE CLOTHING

NT HELMETS

NT PRESSURE SUITS

NT SPACE SUITS

Food ration effect on metabolite elimination rate in humans wearing isolation garment at rest or performing physical labor 05 p0622 A72-16644

Flame resistant materials for aircraft fire fighter protective clothing from systems approach tests 08 p1126 A72-21585

Water cooled suits efficiency and effectiveness for heat removal, noting importance of head area 14 p2081 A72-31085

Thermally protective life rafts and clothing evaluation for cold sea survival potential assessment and tolerance limit determination 14 p2081 A72-31088

Monograph on hot environments stress covering heat exchange at skin surface, clothing effect, body temperature regulation and sweating control 15 p2185 A72-31515

Human tolerance to high, sustained +Gz acceleration. 19 p2758 A72-38702

Comparison of physical, biophysical and physiological methods of evaluating the thermal stress associated with wearing protective clothing. 20 p2898 A72-39808

PROTECTIVE COATINGS

NT ANODIC COATINGS

NT CERAMIC COATINGS

NT PRIMERS [COATINGS]

Nb alloy silicide coating thickness data correlation by thermoelectric, metallographic and pointed micrometer techniques, discussing state of art in thickness control, penalties and substrate independence 01 p0075 A72-10750

Coated Nb alloys as reradiative thermal protection system skin materials for space shuttle, investigating flaw growth 01 p0085 A72-10757

Field repair of Nb alloy panels with protective coatings designed as part of space shuttle thermal protection system 01 p0091 A72-10758

Field repair of fused slurry silicide coating for oxidation protection of Nb alloys in space shuttle environment 01 p0075 A72-10759

Lightning protective coatings for boron/epoxy composite materials, discussing high current damage mechanisms, simulation facility and test results on aluminum foils, meshes, etc 01 p0092 A72-10783

Diffusion aluminide protective coating formation mechanisms on Ni-base superalloys observed from microstructures and compositions in Ni-Al intermetallics 01 p0089 A72-11165

Steels gas-powder facing with boron carbide, testing microhardness and wear resistance 03 p0363 A72-13547

Transparent rain repellent polymer coatings, discussing water repellency theory, polymer chemical structures, adhesion to glass surfaces and evaluation methods 03 p0381 A72-14237

Elastomeric protective coating requirements from existing electrochemical metallic corrosion theories 03 p0364 A72-14238

Ni-Cr-Al-Si and Fe-Cr-Al-Y oxidation resistant claddings for superalloys, comparing to commercial aluminide coatings by cyclic furnace and high velocity burner rig tests 04 p0533 A72-14700

Vacuum diffused Cr, Si, Ti and combined coatings effect on heat resistance of Nb and Nb alloys 04 p0534 A72-15660

Plasma jet technique for self lubricating antifriction Ni, Sn or Cu coatings for MoS₂ particle oxidation protection 04 p0527 A72-15664

Filiform corrosion of steel, magnesium and aluminum coated and uncoated surfaces in humid and corrosive atmospheres 04 p0536 A72-15735

Oxidation and hot corrosion tests of coated Ta and Ta based alloys between 800 and 1500 C in still air and in oxidizing gas stream 06 p0828 A72-17614

Solid lubricant coatings adherence to porous materials, discussing porosity acquired by sulfuration treatment in melted salts bath on soft steel surface 06 p0823 A72-18590

Zirconium dioxide white pigment coatings for spacecraft thermal control, discussing impurities effects on optical absorption properties 07 p1023 A72-19692

Formation kinetics, phase composition and structure of oxide films in binary and ternary iron-base chromium aluminum alloys, studying hydrogen penetration characteristics 07 p1013 A72-19771

Transition metal superconducting thin films and rf cavity surface protective coverings, investigating properties by low energy electron diffraction and Auger spectroscopy 09 p1368 A72-22560

Laser damage resistance properties of thin film multilayer antireflection coatings for quartz optics 09 p1326 A72-23348

Protective aluminum oxide scale development on Ni-Cr-Al alloy, describing transient oxidation stage 09 p1332 A72-23584

High purity fine particle pigment materials preparation for spacecraft thermal control coatings, discussing hydrothermal, cryochemical and vapor phase processes 10 p1500 A72-24145

Pyrolytic graphite coated rocket nozzle design, discussing substrate properties, coating thickness, erosion rates and rocket tests 10 p1500 A72-24199

Physicochemical principles of inorganic materials production, considering heat resistant alloys, oxygen free and oxide cermets, glasses, glass ceramics and protective coatings 10 p1501 A72-24408

Semiconductor materials etching and surface coating with protective silicon dioxide film in low temperature oxygen plasma 11 p1700 A72-25777

Superalloys and refractory materials high temperature protective coatings, noting lack of uniformity in testing methods 11 p1674 A72-26286

NDT of diffusion formed coatings on refractory alloys and superalloys, stressing eddy current technique 11 p1641 A72-26287

Antioxidation coatings of Ta and Ta alloys for high temperature long term operation, emphasizing sintered molybdenum disilicide 11 p1663 A72-26840

Satellite surface coating materials photoemission properties, discussing reflectance, work function, photoyield and photoelectron energy distributions 12 p1844 A72-27280

Anodic oxide film protective properties for Al and Al alloys, evaluating via film dissolution time observation in chromic and phosphoric acids mixture 12 p1828 A72-27453

Protective coatings for corrosion prevention of high strength steels under environmental conditions of humidity, salt fog, tap and salt water immersion 12 p1835 A72-28157

Fusion silicide protective coatings performance for Ta alloys under simulated reentry conditions, noting oxidation rate, ductile brittle bend transition temperature and mechanical properties 12 p1835 A72-28162

Vibratory effects of disturbances transmitted from vehicle to viscoelastic vibroprotective damping coating in presence and absence of resonance 13 p2055 A72-28558

Paint coatings aging effect on D167 type alloy corrosion fatigue in NaCl solution, noting protective efficiency decrease 13 p1984 A72-29486

Thin oxidation resistant alloy claddings for superalloys, comparing performance with aluminide coatings by cyclic furnace and high velocity burner rig tests 14 p2113 A72-30271

Environmental effects on aircraft structure operational reliability, discussing failure removal and protective coating lifetime 14 p2072 A72-30285

Disilicide coated Ta-W alloy system oxidation behavior at 927-1482 C, using thermogravimetric, X ray diffraction and electron microprobe analyses 14 p2121 A72-30771

Coating materials for metal surface wear inhibition by adhesive and abrasive interactions minimization, discussing laminar solids, plastics, ceramics and soft metals [ASME PAPER 72-DE-48] 14 p2108 A72-30874

Niobium carbide coatings for carbon steels and cermets, comparing with titanium carbide coatings 17 p2567 A72-35124

Investigation of the optical and pyrometric behavior of surface coatings for the Helios probe 19 p2880 A72-37493

Estimation of the accuracy of the method of measuring the bending of strips in order to determine residual stresses. 19 p2806 A72-37574

Exploratory investigation of Y, La, and Hf coatings for nitridation protection of chromium alloys. 20 p2944 A72-39290

Electrolytic and nonelectrolytic diffusion methods for protective coatings production from gas, liquid or solid phase, discussing wear resistance enhancement in boridized steels 20 p2929 A72-39449

Recent developments in silicone elastomers for macroencapsulation. 20 p2944 A72-39492

Influence of a protective coating on the frequency characteristics of hot-film anemometer sensors 21 p3050 A72-40131

Influence of the structure on the emissivity of aluminum-chromium-phosphate coatings at high temperatures 21 p3072 A72-40383

Recent development on thermal design of spacecraft. 21 p3115 A72-41125

Light transmission, reflection and environment problems of hydrophilic coatings for fog and frost protection in aviation instrument window design
22 p3196 A72-42519

Formation of defects in reflecting coatings under the action of high temperatures
22 p3197 A72-43193

PROTECTORS
NT EAR PROTECTORS
PROTEIN METABOLISM
NT LIPID METABOLISM
Biochemical processes and structures interrelation, using nucleoprotein coacervate models and ribonuclease and polynucleotide phosphorylase enzymes
04 p0469 A72-14783

Conversion of angiotensin to angiotensin 2 in dog pulmonary circulation, studying peptide synthesis, radioimmunoassay and in vivo and plasma in vitro metabolism
04 p0475 A72-15465

Pathogenesis of in-flight illusory acceleration sensations, discussing amino acid level, protein metabolism rate and pyridoxin metabolism
05 p0619 A72-16642

Protein biosynthesis inhibitors retardation of noradrenaline and serotonin induced hyperpolarization of neuron membranes in cortical sensomotor region of rabbits
08 p1122 A72-22192

Urine and plasma protein and creatinine measurements in acclimatized and unacclimatized men before, during and after high altitude ascent
10 p1426 A72-24482

Multihour immersion effects on blood plasma protein and electrolyte concentration in trained and untrained subjects
12 p1770 A72-27480

Plasma protein concentration, volume and hematocrit changes during exercise, bed rest and high forward acceleration
12 p1766 A72-28296

Myocardial protein synthesis in acute myocardial hypoxia and ischemia.
17 p2501 A72-34980

Disproportional changes in hematocrit, plasma volume, and proteins during exercise and bed rest.
17 p2506 A72-35966

Hypoxic theory for atherosclerosis formation, noting blood plasma protein concentration effects on oxygen diffusion
18 p2651 A72-37030

Protein synthesis in the cell-free system of the human thyroid gland
19 p2757 A72-38212

Effects of free amino acid doses and of amino acid metabolism cofactors on the distribution of regional free amino acid resources in the brain and blood of animals
20 p2891 A72-39324

Thyroglobulin content and variations in the proteolytic activity of the thyroid gland tissue in animals under hypoxic conditions
20 p2893 A72-39727

Human tryptophan and tyrosine metabolism - Effects of acute exposure to cold stress.
21 p2997 A72-40417

Incorporation of methionine-S 35 in the proteins of the digestive organs of rabbits under the action of radiation and vibration
21 p2998 A72-40440

Nitrogen excretion as a measure of protein metabolism in man under different conditions of renal function.
21 p3003 A72-41523

Changes in blood serum proteins under the effect of hyperoxia in intact rats with thyroid gland dysfunction
22 p3142 A72-42283

PROTEINOIDS
Alpha amino acids proteinoids or thermal polymers enzyme activity, in investigating hydrolytic activities and decarboxylation reactions
04 p0483 A72-14776

Enzymically synthesized homopolynucleotide and lysine-rich proteinoid microparticles effect on aminoacyl adenylate condensation as basis for genetic code origin
06 p0770 A72-17724

PROTEINS
NT ADENINES
NT ADENOSINE DIPHOSPHATE [ADP]
NT ADENOSINE TRIPHOSPHATE [ATP]
NT ADENOSINES
NT CARBOXYHEMOGLOBIN
NT COENZYMES
NT FIBRIN
NT GLOBULINS
NT GLUTATHIONE
NT GUANINES
NT LIPOPROTEINS
NT NUCLEOTIDES
NT OXIDASE
NT OXYHEMOGLOBIN
NT PEPTIDES
NT PROTEINOIDS
NT PROTOPROTEINS

Molecular evolutionary changes in amino acids of proteins due to mutant random fixation, comparing human and fish hemoglobin chains
02 p0158 A72-11761

Free radicals participation in cell membrane biopotential generation mechanism, comparing properties of protein molecules with semiconductors
02 p0169 A72-12348

Stabilized human plasma protein solution analysis, noting albumin presence
03 p0316 A72-13855

Molecular paleontology of fossil organic remnants in Molluscan shell proteins
04 p0467 A72-14753

Nucleic acid, protein and cell primordial sequence, ribosomes and genetic code for life origin, discussing experiments on homopolyamine acids reaction with mononucleotides
04 p0468 A72-14775

Molecular evolution of biological membrane from lipid film to lipoprotein particle assembly, using bacterial biochemistry
04 p0469 A72-14786

Protein evolution, discussing biological group amino and nucleic acid structure variations from phylogenetic tree of cytochrome c data
04 p0470 A72-14791

Ribosomes origin and rRNA evolution, considering biogenesis from coacervate to protocell and protein biosynthesis
04 p0470 A72-14793

Protein-rich food substitute from microalgae cultures for human nutrition, describing experimental production, protein value determination, special diets and food shortage relief
06 p0768 A72-18159

Molecular aspects of structural and functional circadian rhythms in chloroplasts of unicellular alga Acetabularia, emphasizing protein synthesis role
07 p0919 A72-19540

Thermal stability variations in blood serum protein after electrical stimulation of rabbit hypothalamic structures
07 p0920 A72-19649

Thyroid glands iodine concentrations, blood proteins and morphological changes in rats with acute hypoxic hypoxia and pulmonary edema
07 p0924 A72-20620

Gaseous nitrogen production in humans under steady-state conditions, relating expired nitrogen minute volume increase after protein consumption to possible gastrointestinal and metabolic effects
08 p1122 A72-20882

Radial diffusion and convection capillary model for analysis of tissue protein concentration and colloidal osmotic pressure changes during transcappillary fluid movement
08 p1114 A72-20896

Amino acid sequences of proteins from living organisms, considering evolutionary process
08 p1119 A72-22009

Genetic organization emergence, considering pretranslational evolution in nontranslational protein synthesis, nucleic acid evolution and gene origin
08 p1119 A72-22010

Blood serum proteins thermal stability in patients with vegetative vascular and neuroendocrine syndromes, discussing ATP effects
09 p1266 A72-22877

Parenterally introduced protein hydrolyzates and aminoacids influence on human pancreas enzyme secretion activity
09 p1268 A72-23595

UV light production of free radicals in proteins and model compounds in vacuum and low temperatures, using EPR techniques
12 p1778 A72-27223

Nonprotein amino acids detection in presence of protein amino acids by amino acid analyzer, noting separation of chemically similar compounds
13 p1913 A72-29774

Protein biosynthesis R and D, discussing rate control, structure and medical and nutritional applications
14 p2076 A72-30600

Role of the synthesis of nucleic acids and proteins in the adaptation of the organism to altitude hypoxia.
17 p2502 A72-34990

Adaptability limits on protein-nuclein-water life under exobiological extremal conditions, considering macromolecules, extraterrestrial life search and origin
20 p2891 A72-38958

PROTOBIOLOGY
Life origin in space from point of hydrocarbons, cyanides, abiogenic organic synthesis and protobionts evolution
04 p0467 A72-14752

Ribosomes origin and rRNA evolution, considering biogenesis from coacervate to protocell and protein biosynthesis
04 p0470 A72-14793

PROTON BEAMS
Approximate expression for charge exchange spreading of proton beam precipitating into atmosphere, showing dependence on atmospheric structure, collision data and primary particle energy
09 p1377 A72-22591

PROTON ENERGY
Frequency distribution changes of energy deposited in short pathlengths as function of energy degradation of primary proton beam
13 p2004 A72-29425

Proton beam effect on carbon dioxide laser discharge I-V characteristics and emission power
14 p2109 A72-30352

Fast metastable hydrogen atom beam production by proton beam-Cs vapor charge exchanges
16 p2429 A72-33057

PROTON BELTS
Quasi-steady spectrum of hydromagnetic noise in proton belt, using random excited broad wave fields in nonisothermal magnetosphere
01 p0118 A72-10367

Solar wind proton penetration through earth magnetosphere, taking into account drift, force lines curvature and nonstationary plasma boundary
05 p0709 A72-16255

Secular geomagnetic dipole moment decrease effect on inner proton belt proton energy distribution, comparing with radial diffusion influences
07 p1058 A72-19159

Van Allen proton belt model, considering ionosphere particle acceleration by stochastic interaction with hydromagnetic waves due to solar wind at magnetosphere shock front
10 p1529 A72-24245

Geomagnetically trapped protons pitch angle distribution from ESRO 2 semiconductor telescope measurements
15 p2300 A72-31991

Low-energy proton observations in July and August, 1970, on the 'Molniia-1' satellite
17 p2600 A72-35208

PROTON DAMAGE
Si solar cells nonpenetrating proton damage model in satellite radiation environment, showing open and short circuit current dependence on proton energy
07 p0914 A72-20492

Solar cells testing and array performance evaluation for communications satellites at Comsat laboratories, noting electron irradiation and proton damage studies
12 p1759 A72-28044

PROTON DENSITY [CONCENTRATION]
NT MAGNETOSPHERIC PROTON DENSITY
Interplanetary plasma electron and proton density fluctuation measurements by space probes and from radio sources scintillation spectra, noting agreement with power-law irregularity spectrum
06 p0881 A72-17901

Distributions and average values for proton speed, azimuthal and polar flow directions and proton temperature and density in solar wind from Pioneer data
07 p1063 A72-20380

Nonadiabatic and atmosphere induced energy losses as causes of proton capture in geomagnetic field
11 p1715 A72-26915

Low-energy proton observations in July and August, 1970, on the 'Molniia-1' satellite
17 p2600 A72-35208

Compressions and rarefactions in the solar wind - Vela 3.
23 p3332 A72-44509

PROTON ENERGY
Balloons measurements for differential energy spectra of cosmic ray protons and He over half solar cycle 1965-1969, using Geiger tube hodoscope
01 p0119 A72-10876

Trapped protons low energy differential spectra from polar orbiting Injun 5 satellite measurements, suggesting radiation belts impulsive acceleration mechanism
01 p0120 A72-10891

Rocket-borne measurement of particle fluxes and currents in auroral arc, determining pitch-angle distribution of electron and proton energies
01 p0120 A72-10897

Incomplete ring current decay during magnetic storm development, discussing field asymmetry based on global network synchronous observations and generation mechanism by protons
02 p0218 A72-11949

Magnetosphere model for low energy cosmic ray proton propagation mode to synchronous orbit satellite, calculating geomagnetic cutoffs and penetration regions
02 p0274 A72-12453

Electric field aligned sheet currents of low energy electrons and protons near auroral arc, obtaining magnetic signatures
03 p0349 A72-13516

Channel electron multiplier efficiency for protons of 0.2-10 keV from aurora rocket sounding
04 p0524 A72-15501

Solar wind protons adiabatic spatial cooling related to temperature anisotropy
05 p0709 A72-16067

Primary cosmic ray proton energy spectrum in 50 Ge V to 300 Te V range, using Proton 1, 2 and 3 satellite-borne counters
05 p0709 A72-16231

Long time variations of proton energy spectra in inner radiation belt during solar cycle
05 p0710 A72-16767

Geomagnetically trapped low energy proton flux distribution due to 17 April 1965 magnetic storm, noting adiabatic effects
[AD-736383] 06 p0803 A72-17452

Vacuum chamber sputtering techniques for CsI/Tl and NaI/Tl thin films for soft proton scintillation detector
06 p0816 A72-17834

Secular geomagnetic dipole moment decrease effect on inner proton belt proton energy distribution, comparing with radial diffusion influences
07 p1058 A72-19159

Multichannel modular spectrometer with electrostatic analyzers for low energy electron and proton flux measurement
07 p0988 A72-19954

Distributions and average values for proton speed, azimuthal and polar flow directions and proton temperature and density in solar wind from Pioneer data
07 p1063 A72-20380

Si solar cells nonpenetrating proton damage model in satellite radiation environment, showing open and short circuit current dependence on proton energy
07 p0914 A72-20492

Primary cosmic ray particles disappearance and proton spectrum slope rise in 1 TeV energy region from Proton satellites data
07 p1064 A72-20630

Primary cosmic rays alpha particles and protons energy spectra similarity and intensity difference at .05 to 1.6 TeV, using Proton satellites data
07 p1064 A72-20631

High resolution multiple particle spectrometer for measuring energetic protons, electrons and alpha particles during solar particle events
08 p1167 A72-21509

Polar orbiting satellite observations of energetic solar proton entrance into polar cap during March 1970 solar event
09 p1376 A72-22588

Cosmic ray proton and He nuclei differential energy spectra measurements by balloon-borne ionization spectrometer
11 p1712 A72-25881

Incomplete ring current decay during magnetic storm development, discussing field asymmetry based on global network synchronous observations and generation mechanism by protons
13 p1949 A72-29261

Inner Van Allen zone proton energy spectrum at 30-300 MeV from ESRO 2 satellite measurements
13 p2031 A72-29383

Energetic electron and proton trapping in lower solar atmosphere magnetic field, discussing particle injection, bremsstrahlung and gyro synchrotron radiation
13 p2046 A72-29719

Satellite-borne low energy electron and proton spectrometer for measuring auroral electron and proton spectra
13 p1960 A72-29841

Solar proton events end prediction from flux decay rates observation, noting particle energy effect on accuracy
15 p2301 A72-31999

A two-fluid solar wind model with anisotropic proton temperature.
17 p2599 A72-35097

Long term variations of proton flux and energy spectra in inner radiation belt during solar cycle
17 p2600 A72-35270

Cosmic ray electron spectrum and its modulation near solar maximum.
17 p2601 A72-35583

Entry of high-energy solar protons into the distant geomagnetic tail.
17 p2601 A72-35588

Auroral electron acceleration by longitudinal electric field due to protons defreezing above ionosphere.
17 p2550 A72-35852

Auroral proton energy time behavior estimation based on magnetic and ionospheric data from ground observations
17 p2550 A72-35855

Azimuthal propagation of low-energy solar-flare protons as observed from spacecraft very widely separated in solar azimuth.
19 p2852 A72-38726

Several observations of low-energy solar-proton spectra and possible interpretations.
19 p2852 A72-38727

Geomagnetic cutoffs for cosmic-ray protons for seven energy intervals between 1.2 and 39 Mev.
19 p2852 A72-38728

Studies of outer belt and slot region protons at low altitudes.
19 p2853 A72-38740

PROTON FLUX DENSITY
Solar proton flux and energy spectra from 1968-1969 ESRO 2 satellite measurements, detailing 18 November 1968 event
[CERN-71-16] 02 p0273 A72-12073

Cosmic proton and neutron produced recoil proton energy spectra measurements along earth-moon-earth trajectory with nuclear emulsions aboard Zond 5 and 7 [CERN-71-16] 02 p0273 A72-12074

Apollo 11 and 12 rock samples depth profiles for Al, Na, Mn, S, V, Ca, P, Co, Fe, Cu and Sc isotopic contents, estimating solar proton flux
02 p0282 A72-12327

Hydrogen density and proton flux in topside ionosphere over Arecibo from incoherent scatter observations
02 p0274 A72-12455

Antiproton flux energy spectrum in Galactic interstellar space, discussing flux peak
03 p0408 A72-13005

Inner radiation belt proton source and loss processes, obtaining flux intensities, energy spectrums and radial distributions
03 p0412 A72-13513

Inner solar system particle propagation model solved for radial gradient of galactic protons, comparing to Mariner 4 measurements
03 p0412 A72-13527

Proton measurements in ring current by OGO-3 satellite compared with geomagnetic field data at low and high latitudes
05 p0711 A72-17034

Geomagnetically trapped low energy proton flux distribution due to 17 April 1965 magnetic storm, noting adiabatic effects
[AD-736383] 06 p0803 A72-17452

Galactic cosmic ray particle intensity decrease relationship to low energy proton flux increase based on interplanetary Zond 3 and Venera probes measurements
07 p1063 A72-20626

Primary cosmic radiation antiproton flux, finding .005 ratio upper limit to proton flux with balloon-borne magnetic spectrometer
07 p1064 A72-20633

Ionospheric disturbances relation to interplanetary positive ion and proton fluxes intensity and velocity from Mariner 2, Venus 3 and Vela 2 observations, discussing F2 region
11 p1713 A72-26268

Radial profiles of ionized He flux and protons in magnetosphere, taking into account charge exchange processes and fluctuating electrostatic fields
11 p1624 A72-26397

Solar proton event classification system with index of three digits representing proton flux, absorption and sea level neutron monitor response measurements
11 p1714 A72-26425

Apollo 11 and 12 rock samples depth profiles for cosmogenic Al, Na, Mn, S, V, Ca, P, Co, Fe, Cu and Sc isotopic contents, estimating solar proton flux
13 p2039 A72-29211

Proton and electron fluxes limits in synchronous orbit, investigating local time dependence
13 p2031 A72-29393

Low energy proton flux increases associated with geomagnetic storms due to interplanetary shock waves occurring during solar cosmic ray flare event decay
13 p2032 A72-29724

Solar proton flux density angular and latitude distribution in polar regions magnetosphere from satellite observation
15 p2299 A72-31921

Solar proton events end prediction from flux decay rates observation, noting particle energy effect on accuracy
15 p2301 A72-31999

Long term variations of proton flux and energy spectra in inner radiation belt during solar cycle
17 p2600 A72-35270

Azimuthal propagation of low-energy solar-flare protons as observed from spacecraft very widely separated in solar azimuth.
19 p2852 A72-38726

Limits to energetic proton fluxes trapped in Jupiter's magnetosphere.
22 p3221 A72-42021

Results of cosmic ray intensity measurements on the Venus-7 automatic station
22 p3218 A72-42213

Daily variation of electron and proton geomagnetic cutoffs calculated for Fort Churchill, Canada.
22 p3170 A72-42401

Polar-cap measurements of solar-flare protons with energies down to 12.4 keV.
22 p3218 A72-42425

Pioneer 8 observation of diffuse magnetosphere-magnetopause boundary, noting proton flux intensity and flow angle
23 p3341 A72-44512

Detection of earthward flow of keV protons in the geomagnetic tail at lunar distances.
23 p3333 A72-44532

PROTON IMPACT
Excitation and ionization cross sections and rate coefficients of hydrogen-like ions by electron and proton impact in Bethe-Born approximation
06 p0852 A72-18052

Differential and total ionization cross sections of multielectron atoms by electron and proton impact
10 p1515 A72-24602

Positive ions excitation cross sections calculated for proton impact induced transitions among fine structure states
10 p1543 A72-24619

Electron production cross section during He atom ionization by proton impact, noting peak existence for electrons near incident proton velocities
15 p2281 A72-32220

Upper limit of the mean interaction path of cosmic protons generating extensive air showers
17 p2598 A72-34287

Electronic excitation of N2 and dissociative excitation of O2 by proton impact.
23 p3317 A72-44520

Full-range solution for the measurement of thin-film surface densities with proton-excited X rays.
24 p3431 A72-44715

PROTON IRRADIATION
Relative biological effectiveness of energetic protons for somatic effects induction in mice during whole body irradiation, using mean energy of solar event protons
[CERN-71-16] 02 p0161 A72-12054

Mitotic index and aberrant mitose frequency in mice corneal and intestinal epithelial cells exposed to 50-630 MeV protons, estimating relative biological efficiency coefficients
[CERN-71-16] 02 p0161 A72-12055

High energy proton irradiation late pathological effects on rabbit brains, discussing brain lesions and radiation dosages
[CERN-71-16] 02 p0161 A72-12056

Biological efficiency of secondary radiations from 70 GeV protons interaction with target, discussing dose dependences and restoration process relative rates
[CERN-71-16] 02 p0161 A72-12057

Nonuniform high energy proton irradiation of dogs, evaluating and predicting biological effects
[CERN-71-16] 02 p0161 A72-12061

Average radiation Q factor and dose radiation spectrum measurement in phantoms irradiation by proton beams
[CERN-71-16] 02 p0162 A72-12069

N-p silicon solar cells damage at room temperature by proton and deuteron irradiation, considering particle mass and energy functions and illuminating light wavelength effects
04 p0561 A72-14574

Cosmic ray induced radioactivity effects on diffuse gamma ray background measurement from 600 MeV proton irradiation experiment
04 p0567 A72-15324

Illumination effect on proton and gamma irradiated cabbage plant growth, height and foliage, indicating radiation protective effect for certain light intensities
05 p0622 A72-16649

Biological damage inflicted to rats by protons, X rays and gamma rays
06 p0762 A72-17675

Proton bombarded CsI crystal spallation-caused radioactive decay products contribution to background rate in satellite X ray telescope detector
06 p0853 A72-18084

Quasi-nucleonic interactions of high energy protons in nuclear emulsion irradiated within pulsed magnetic field
07 p1038 A72-19869

Energy spectrum of radiation defects in proton bombarded n-type Si crystals from Hall effect and electroconductivity measurements
07 p1049 A72-19901

Optical absorption in UV and IR of proton bombarded potassium chloride at liquid nitrogen temperature attributed to trapped protons
08 p1211 A72-21249

Lead tin telluride photovoltaic p-n junction diode and lasers, discussing n-type layer fabrication by proton bombardment
10 p1450 A72-24552

Semi-insulated gate GaAs FET fabrication by proton bombardment
12 p1790 A72-27438

Laboratory irradiation tests with van de Graaff generator for simulation of spacecraft components radiation damage due to high energy space protons and electrons
12 p1863 A72-27552

Proton and electron radiation effects on silicon solar cells electric and photovoltaic properties, determining damage coefficients via minority carriers diffusion length measurement
12 p1759 A72-28045

Monoenergetic electrons and low energy protons radiation damage effect on Si solar cell electrical and optical properties
12 p1759 A72-28046

Proton irradiation effects on monkey central nervous system, showing inflammatory reaction and neuroglial astrocyte glycogen accumulation
13 p1906 A72-29833

Radiation effects measurement on neutron, proton and electron irradiated Li-drifted Si detectors by IR response technique, comparing characteristics with photovoltage effect 15 p2234 A72-31538

Radiation damage effects in Li compensated Si nuclear particle detectors induced by irradiation with electrons, protons and fast neutrons 15 p2291 A72-31539

Spacecraft bacteria population resistance to simulated Jovian trapped radiation belt electrons and solar wind protons, noting dependence on isolate, dose and electron energy 15 p2186 A72-31993

Simulated Nimbus orbital electron, proton and UV radiation effects on wide bandpass glass and narrow bandpass thin film interference filters and fused silicas 15 p2277 A72-32157

Target anion effect on radioactive Sb and Te distribution formed by high energy proton irradiation of cesium salts containing oxygen 15 p2282 A72-32485

Cross section measurement for low energy proton reactions with N 14 and O 16 targets observing Be 7 and C 11 in N 14 16 p2447 A72-33735

Proton bombarded stripe geometry heterojunction lasers for 300 K CW operation compared with oxide insulated lasers 16 p2403 A72-33757

Brain tumors in irradiated monkeys. 17 p2505 A72-35647

Body weight decreases in some proton exposed primates. 18 p2650 A72-36447

Non-destructive activation analysis of some elements in stony meteorites by proton- and bremsstrahlen-irradiation. 20 p2899 A72-39833

Electron abundance equilibrium as factor in biological effectiveness of proton beam irradiation of animals 21 p2998 A72-40450

Summary of latent effects in long term survivors of whole body irradiations in primates. 23 p3254 A72-43393

The effects of irradiation with protons on the crystallographic order of the compound Bi₂Te₂Se. 24 p3432 A72-45200

PROTON MAGNETIC RESONANCE

The state of water in muscle tissue as determined by proton nuclear magnetic resonance. 24 p3371 A72-44774

PROTON PRECESSION

Magnetic anomalies in New Guinea-New Zealand region from geomagnetic measurements with proton magnetometer, noting effects of andesite-basalt volcanic processes and nuclear precession signal 23 p3284 A72-43380

PROTON PRECIPITATION

Low energy solar proton propagation and interplanetary magnetic field measurements, comparing with population in solar wind 03 p0407 A72-12943

Polar cap absorption event, investigating solar high energy protons precipitation effects 05 p0709 A72-16239

Magnetospheric current effects on geomagnetic field structure, noting electron and proton precipitation into auroral zone 05 p0657 A72-16275

Fitch angle distributions of energetic protons for different geomagnetic activity levels as function of invariant latitude and magnetic local time from ESR0 IB satellite measurements 07 p1057 A72-19141

Approximate expression for charge exchange spreading of proton beam precipitating into atmosphere, showing dependence on atmospheric structure, collision data and primary particle energy 09 p1377 A72-22591

VLF phase changes due to particle precipitation into geomagnetic anomaly during solar proton events explained by exponential ionospheric models with effective reflecting height 11 p1599 A72-26765

Auroral particle precipitation /keV electrons and protons/ morphology from ESR0 IA particle spectrometer measurement, discussing particle populations in day and night magnetospheres 12 p1864 A72-27786

ESR0 IA satellite observations of trapped and precipitated proton energy spectrum as function of invariant latitude on 8 March 1970 14 p2146 A72-30141

Auroral substorm and proton auroras during moderate geomagnetic disturbances 17 p2550 A72-35857

Local-time survey of plasma at low altitudes over the auroral zones. 19 p2792 A72-38739

High latitude particle precipitation and source regions in the magnetosphere. 20 p2964 A72-39542

Auroral electron and proton distribution in magnetosphere and precipitation pattern from satellite, rocket and ground based observations 20 p2920 A72-39976

PROTON RESONANCE

Measurement of longitudinal relaxation times for spin-decoupled protons. 24 p3427 A72-45400

PROTON SATELLITES

Primary cosmic ray particles disappearance and proton spectrum slope rise in 1 TeV energy region from Proton satellites data 07 p1064 A72-20630

Proton 2 and 4 and Cosmos 196 orientation by quick response algorithm from onboard three component magnetometer readings 08 p1240 A72-21138

Proton 2 and 4 and Cosmos 196 orientation by high speed algorithm from onboard three component magnetometer readings 20 p2976 A72-39243

PROTON SCATTERING

Charged particles magnetic scattering on cyclotron instability waves of radiation belt plasma, estimating proton relaxation time 01 p0119 A72-10608

Water absorber lateral scattering effect on absorbed dose from 400 MeV neutron and proton beams [CERN-71-16] 02 p0162 A72-12062

Proton elastic scattering by deuterons in backward hemisphere, examining normal and center of mass scattering angle and differential cross section 04 p0551 A72-14437

Intermolecular potentials determination by inverting phase shifts obtained from high resolution measurements of protons differential elastic scattering by rare gas atoms 04 p0552 A72-14577

Solar protons propagation from instantaneous injection source and inhomogeneities interaction description by mean free path and scattering angle specification 07 p1063 A72-20627

Angular distributions of proton polarization during elastic scattering by V, Cr, Ni and Co nuclei in high energy region 08 p1211 A72-21093

Particle-proton total cross section from cosmic ray data on proton-air inelastic cross sections 11 p1712 A72-25884

Charged particles propagation in magnetic field and scattering medium with constant and variable transport paths, applying to proton propagation for solar flares 13 p2029 A72-28576

Elastic scattering of 600-MeV protons from H, D, He-3, and He-4. 19 p2837 A72-38025

Coherent cross section effects on primary particle energy in inelastic proton interaction with carbon nuclei at 20-600 GeV 23 p3332 A72-44439

Parasitic pitch angle diffusion of radiation belt particles by ion cyclotron waves. 23 p3333 A72-44527

Charged particles propagation in magnetic field and scattering medium with constant and variable transport mean free path, applying to proton propagation for solar flares 24 p3435 A72-45076

PROTON TELESCOPES

U PARTICLE TELESCOPES

PROTON 2 SATELLITE

Rarefied gas interaction with spacecraft surface, calculating aerodynamic forces and accommodation coefficient for Proton 2 satellite 14 p2162 A72-30474

PROTON 4 SATELLITE

Primary cosmic rays energy spectrum at 100-1000 TeV from Proton 4 satellite data 07 p1064 A72-20629

PROTON-PROTON REACTIONS

Energy dependence of solar proton-proton reaction, generating p-p wave function from Schroedinger equation 05 p0718 A72-16501

Elemental synthesis and energy sources in stellar evolution, hydrogen, helium and advanced burning stages, p-p cycle, e process and nuclear equilibrium 06 p0876 A72-17585

Antiproton energy spectrum in cosmic rays from primary proton-interstellar hydrogen collision in two fireball model 12 p1863 A72-27186

The evolution of the solar inner rotation by the Eddington-Sweet type circulation under the influence of the solar wind torque. 17 p2613 A72-35497

PROTONS

NT RECOIL PROTONS

NT SOLAR PROTONS

Geomagnetic PDP pulsations oscillation frequency drift, considering proton motion characteristics in magnetospheric equatorial plane 02 p0217 A72-11931

Inner radiation belt proton source and loss processes, obtaining flux intensities, energy spectrums and radial distributions 03 p0412 A72-13513

Explosive p-process nucleosynthesis limiting conditions in supernova envelopes, using proton capture and neutron photodisintegration rates 04 p0579 A72-15318

Proton recording equipment onboard automatic interplanetary stations Zond 4 and 5 at 1.5-50 MeV using silicon drift counters 06 p0814 A72-17699

Ogo 6 ionospheric measurement of proton whistlers wave-normal vector, investigating propagation modes 07 p1057 A72-19148

Solar cosmic ray diffusion in interplanetary medium, describing solar flare proton and heavy nuclei propagation in terms of time of arrival measurements 08 p1227 A72-21157

Ferroelectrics with strong hydrogen bonds, deriving self consistent optical phonon frequency and coupled proton-phonon vibration spectrum 09 p1366 A72-22221

Geomagnetic PDP pulsations oscillation frequency drift, considering proton motion characteristics in magnetospheric equatorial plane 13 p1949 A72-29243

Proton accretion effect on circumstellar dust grains mass, noting impossibility of grain formation in H II region 13 p2048 A72-29790

Cross section determination of proton production in collisions of electrons and hydrogen ions 14 p2134 A72-30801

Cross sections for dissociative excitation of hydrogen ions by electrons determined by coincident detection of protons and H atoms 14 p2134 A72-30804

Hydrogen plasma ion density determination from atomic beam attenuation by resonant charge exchange with protons 15 p2284 A72-31582

Solar wind model dividing interplanetary space in one fluid and two fluid collisionless regions, discussing proton thermal anisotropy 15 p2300 A72-31996

Time constancy of physical constants in expanding universe, discussing light speed, Planck constant and electron and proton mass in context of Dirac hypothesis 16 p2425 A72-33517

Proton capture mean lifetimes in fast C-N cycle, presenting nitrogen/carbon abundance ratio variation with temperature 18 p2721 A72-36650

Electron and proton acceleration in the outer magnetosphere regions during polar substorms 18 p2688 A72-36866

Recombination of protons and negative hydrogen ions in slow collisions. 18 p2713 A72-36953

Radiation belt protons and ion-cyclotron wave interactions accounting for magnetospheric ring current instabilities during storm at plasmapause 20 p2919 A72-39545

Universe evolution study from contemporary chemical composition of cosmic matter, noting concentration changes of protons, neutrons and He 4 22 p3222 A72-42140

PROTOPLASM

Physiological and biochemical responses of *Paramecium caudatum* to hypo- and hyperbaric stresses, discussing protoplasmic inactivation by high oxygen pressure 12 p1766 A72-28299

PROTOPROTEINS

Protobionts formation by random aggregation and reproduction from proteins and nucleic acids macromolecules 04 p0469 A72-14782

PROTOSTARS

NT T TAURI STARS

Dense cloud and protostar molecules from molecular line emission, considering mass effects in stellar evolution 03 p0419 A72-13120

Cosmic and solar wind abundance analysis for D and He-3 in protosolar gas, noting chemical equilibrium reaction role in D enrichment 12 p1868 A72-27216

Collapse calculations for 0.25-10 solar mass spherical protostars, discussing stellar core evolution and temperature distribution in infalling cloud 17 p2606 A72-34674

Protostars formation through interstellar atomic hydrogen clouds gravitational collapse, deriving critical mass, surface temperatures and luminosities 19 p2865 A72-38478

The influence of local conditions in the interstellar medium upon star formation. 19 p2868 A72-38699

Computer-aided numerical experiment of cluster mass increase by accretion in protostar evolution 21 p3113 A72-41754

PROTOTYPES

Reliability data collection methods, considering equipment initial design, breadboard models, prototype, production, acceptance, qualification, field installation and operation

10 p1443 A72-23975

Weapon systems reliability assessment based on limited prototype flight test results

13 p1962 A72-28359

A-10 prototype designed for production

17 p2488 A72-34392

Competitive prototype strategy to reduce weapon system development risks and uncertainties with emphasis on simplified management and procurement

18 p2742 A72-36074

Production of prototype hybrid micro-electronic modules using thin film substrates

20 p2908 A72-39493

Improving R & D management through prototyping

21 p3132 A72-40970

Defense systems development based on balance between theoretical studies and hardware prototyping for uncertainty reduction in performance and cost

21 p3132 A72-40971

PROTOZOA

NT AMOEBA

NT FLAGELLATA

DNA-RNA molecular hybridization testing of chronon theory of circadian timekeeping in protozoa cells

07 p0920 A72-19542

Physiological and biochemical responses of Paramécie caudatum to hypo- and hyperbaric stresses, discussing protoplasmic inactivation by high oxygen pressure

12 p1766 A72-28299

PROTUBERANCES

Boundary layer transition effect on three dimensional shock interactions due to blunt protuberances and axial compression corner

[AD-743741]

08 p1150 A72-21629

The effects of protuberances and scaling parameters on the aerodynamic characteristics of an air-to-air cruciform missile

[AIAA PAPER 72-969]

22 p3231 A72-42342

PROUSTITE

Image conversion from 10.6 to 0.65 micron wavelength by nonlinear optical method in proustite crystal

12 p1821 A72-27604

Vibration spectra of the isomorphous proustite-pyrrargyrite series

20 p2932 A72-39506

PROVING

NT THEOREM PROVING

PSEUDOMONAS

Fine structure of Pseudomonas saccharophila at early and late log phase of growth, using electron microscopy and various culture techniques

07 p0922 A72-20238

PSEUDONOISE

Weak signal turnaround transponder design for pseudonoise coded ranging systems, discussing bandwidth optimization and performance comparison between various receiver configurations

10 p1452 A72-24688

Optimal quantization parameters for pseudonoise signals at radio receiver output, estimating static error in correlation function measurement

13 p1919 A72-29048

PSEUDORANDOM SEQUENCES

Digital system for wideband Gaussian noise generation using simultaneously generated PN-sequence with analog summation of independent binary waveforms

07 p0941 A72-19284

Cross correlation identification of linear time varying processes based on pseudorandom sequences, presenting digital simulation results

07 p0948 A72-20390

Antisymmetric pseudorandom signal performance in measurement of second order kernels in Volterra series representation of nonlinear system by cross correlation

10 p1439 A72-24805

Auto and cross correlation functions of combined binary pseudorandom sequences in digital space communication systems

10 p1439 A72-24907

Russian book on random signal generation covering ultralow and audio frequency spectra, random number and pseudorandom signals simulation and automatic control

12 p1786 A72-28347

Efficient computer decoding of pseudorandom radar signal codes

22 p3153 A72-41978

Moire screens coded with pseudo-random sequences

23 p3289 A72-43892

PSYCHIATRY

NT SOCIAL PSYCHIATRY

Civil aeronautics environment relation to psychiatrists and medical psychologists treatment of air navigation personnel, discussing chemotherapeutic

and psychotherapeutic treatment administration problems

07 p0927 A72-19243

Psychiatric preventive intervention in emotional crisis situations during patients aeromedical evacuation and transportation, discussing personnel shortage

10 p1429 A72-23743

Flight psychiatry in NATO countries, discussing organization and facilities with respect to military and civil aviation

13 p1911 A72-29858

PSYCHOACOUSTICS

Standard procedures development for perceived noisiness or noise annoyance evaluation, taking into account spectral complexity, spectra weighting, time integration and onset duration

07 p0932 A72-20166

Acoustic tests of jet aircraft noise and sonic boom effects on sleep pattern and human performance, using EEG analysis

[ASA PAPER W 11]

08 p1125 A72-21487

Biologist view of behavioristic approach to psychoacoustics, criticizing mechanical concept of living organism as inadequate for understanding human sensory system

11 p1583 A72-25732

Monograph on perceptual analysis of sound covering peripheral auditory system functions, subjective pitch perception, periodic pulse and white noise harmonic audibility, masking behavior, etc

15 p2188 A72-31514

Individual functions and intersubject differences of noise annoyance susceptibility, noting relationship to Rorschach test

16 p2357 A72-32987

Noise pollution measurements parameter selection based on human reactions and attitudes, discussing psychoacoustic experiments, ratings and acoustic instruments

16 p2390 A72-33165

Lateral inhibition in auditory perception proved by psychophysical study of nervous activity stimuli patterns, noting erroneous measurement of pure tone masked threshold

16 p2357 A72-33970

Sonic boom startle - A field study in Meppen, West Germany

24 p3374 A72-44916

PSYCHOLOGICAL EFFECTS

NT ILLUSIONS

NT MOON ILLUSION

NT OCULOGRAPHIC ILLUSIONS

Environmental noise induced human fatigue, considering physiological and psychological effects

01 p0016 A72-10050

Visual masking effect due to light offset, investigating human identification response to tachistoscopic test stimuli on lighted background with simultaneous shut-off

02 p0166 A72-11550

Medicopsychological surveillance of aircrew in fighter pilot school, stressing time factor in pilot training

04 p0467 A72-14569

Aircraft and other transient noise levels temporal characteristics effect on noise assessment

04 p0464 A72-14843

Differential neurophysiological and psychological effects of subanesthetic concentrations of cyclopropane, diethyl ether, methoxyflurane and ethrane in conscious man

04 p0480 A72-15220

Human trace responses generation and storage under light stimulus reinforcement of sound conditioning from galvanic skin reactions observation

04 p0475 A72-15581

Transmeridian flight psychological effects on aircrews, discussing anxiety, stress, circadian rhythm disruption and sleep loss effects on performance deterioration

06 p0766 A72-17816

Standard procedures development for perceived noisiness or noise annoyance evaluation, taking into account spectral complexity, spectra weighting, time integration and onset duration

07 p0932 A72-20166

Psychophysical comparison methods for evaluating noisiness or annoyance values of sounds

07 p0932 A72-20168

Community response prediction to noise based on laboratory tests of individual acceptability judgments

07 p0932 A72-20172

Hyperventilation relationship with spasmodic, noting psychoemotional cause and neuromuscular excitability

07 p0922 A72-20384

Improperly controlled learning processes relationship to hypertonic blood pressure irregularities pathogenesis in rats, investigating negative emotional reactions effects

07 p0925 A72-20659

Noise effects on human attention and work efficiency in extroverted and introverted individuals

08 p1128 A72-22137

Psychiatric preventive intervention in emotional crisis situations during patients aeromedical evacuation and transportation, discussing personnel shortage

10 p1429 A72-23743

Menu selection for SKYLAB astronauts by computer technique based on mixed integer programming code, using measure of pleasure lists

12 p1769 A72-27442

Meteorological-astronomical diurnal and seasonal environmental rhythm simulation for psychological stresses alleviation in long term space missions

13 p1910 A72-29322

Relationship of visibility fluctuations in set of luminous circles to verbal response learned for each circle, showing word association influence on stimuli perception

13 p1911 A72-29851

Divided attention effect localization, using choice tracking task reaction times in sequential stage model for human information processing

13 p1911 A72-29852

Electric stimulation of rabbit brain limbic formations /claustrum, amygdala, hippocampus/, showing effect on emotional response motor and vegetative components

14 p2076 A72-30668

Astronauts physiological and psychological reliability, discussing Apollo flights and prolonged missions to other planets

14 p2079 A72-30677

Physiological and psychological effects of noise noting vulnerability of circulatory apparatus, neurovegetative system and stomach

14 p2079 A72-30696

Technology R and D program to qualify man for long term weightlessness, assessing space flight stress effects on physiology and psychology

16 p2358 A72-33544

Vicarious influence effect on eliciting pain in individuals subjected to previously reported nonpainful electric shocks

18 p2654 A72-36916

Psychic adaptation of man to a long-duration stay in space

22 p3149 A72-41988

Development of a defensive conditioned reflex to a light stimulus after previous visual deprivation

23 p3257 A72-44078

PSYCHOLOGICAL FACTORS

Sensory psychological invariance formation for perceptual functions in human visual system

01 p0011 A72-10468

Soviet book on astronaut activity psychological features covering space flight living conditions, space and time perception psychophysiological mechanism changes and weightlessness effects

03 p0317 A72-14246

Flight personnel statistical survey of clinical, physical and psychic causes of temporary and permanent flight service unfitness

07 p0923 A72-20447

High gravity environment exposure effects on gravity preference in chronically centrifuged rats, showing dependence on reference level

08 p1122 A72-20787

Electrophysiological, neurophysiological, metabolic, vegetative, psychological, chemical and pathological aspects of sleep, noting disturbance and wakefulness mechanisms for various clinical disorders

09 p1264 A72-22223

ATC operator stress factor evaluation from information theory analysis of radio telecommunication information content

09 p1271 A72-23134

ATC task analysis by subjective rating of work load, discussing information processing measures, scoring method and observer rating procedure

09 p1271 A72-23135

Education and training of personnel for photointerpretation, discussing psychological, physiological and methodological aspects of aerial photointerpretation

09 p1272 A72-23298

Psychological aspects in aerial photointerpretation, discussing importance of perception of image contrast, contours and areal distribution

09 p1272 A72-23299

Soviet space crews selection and training based on professional and scientific background, emphasizing psychological qualities for working compatibility in space environment

09 p1274 A72-23672

Human biodynamic and behavioral response to whole body vibration, discussing subjective judgment of vibration intensity and effects on performance

10 p1431 A72-24797

Case report of fighter pilot disorientation episode during night flying exercise, suggesting psychological stress factor

11 p1584 A72-26019

Time displacement effects on human physiological and psychological functions, discussing circadian rhythm phase shift and performance deficits

11 p1580 A72-26681

- Human functional level performance characteristics, noting relationship between spontaneous rhythm diurnal variations in psychic and physical performance
11 p1589 A72-26691
- Sleep deprivation effect on circadian rhythms in human performance, psychological fatigue ratings, catecholamine excretion and urine flow
11 p1581 A72-26692
- Transzonal air travel as cause of psychological and physiological rhythm change effects on pilot performance
11 p1589 A72-26694
- Periodic, continuous and aperiodic white noise effects on human serial decoding performance, relating subjective and autonomic responses
12 p1775 A72-28289
- Workload modification effects on pilot neurological changes during Boeing 707 letdown, approach and landing
12 p1775 A72-28290
- Time perception distortion level in simulated and real flight due to task complexity-related pilot emotional stress
14 p2078 A72-30392
- Psychological criteria for flying personnel selection in civil aviation, noting performance prediction based on maximum likelihood estimates
14 p2080 A72-30816
- General aircraft accident investigation approach, using subsequent psychosocial reconstruction of pilot lifestyle to explain accident-producing behavior
14 p2082 A72-31095
- Visual stimulus orientation effect on movement perception, relating physiological and psychological factors
15 p2184 A72-31368
- Preferences for signaled over unsignaled noise from subjectively rated noise intensity experiments, discussing preparatory response vs information cognitive control interpretations
15 p2187 A72-32763
- Noise pollution measurements parameter selection based on human reactions and attitudes, discussing psychoacoustic experiments, ratings and acoustic instruments
16 p2390 A72-33165
- Psychological and physiological parameters correlation for astronaut functional state relation to emotional tension level during ground and flight tests
16 p2356 A72-33563
- Response-dependent electric shock punishment schedule preference during response sequence in food-deprived pigeons
16 p2357 A72-33773
- Effects of instructions on measures of state and trait anxiety in flight students.
17 p2507 A72-34464
- Airline management and flight crew role in prevention, detection and dealing with airline pilot incapacitation in flight, noting physiological and psychological factor recognition
17 p2508 A72-34555
- Helicopters and turboprops as space conserving alternatives for automobile urban transportation, emphasizing comfort and convenience
17 p2639 A72-35505
- Obedience to rotation-indicating visual displays as a function of confidence in the displays.
17 p2510 A72-35943
- Extraversion, neuroticism, and color preferences.
18 p2653 A72-36903
- Experimental tests of Voth-Mayman hypothesis of autokinesia mediation by attention distribution mechanism
18 p2653 A72-36904
- Personality correlates of lateral eye movement and handedness.
18 p2653 A72-36905
- Error arising from experimenter influence on subject behavior and performance, discussing expectancy effects on stimulus presentation and IQ and success-failure judgments
18 p2653 A72-36907
- Repression-sensitization and duration of visual attention.
18 p2654 A72-36917
- Manipulation of projected afterimages by means of the physiological theory imposed on the observer.
18 p2654 A72-36920
- STOL ride quality criteria - Passenger acceptance. [AIAA PAPER 72-790]
19 p2749 A72-38107
- General principles and detail similarities in visual pattern analysis by single neuron operation, computer programs and psychological perception
20 p2891 A72-39275
- Circadian rhythms in physiological and psychological functions related to jet travel, studying body temperature variations and psychomotor performance during isolation and varying light-dark cycle conditions
20 p2897 A72-39723
- Professional capabilities activation of flying personnel, discussing psychological training for flight fitness
21 p3004 A72-40172
- Effect of psychotropic substances on human resistance to acceleration
21 p3006 A72-40443
- Psychological principles of active rest during long space flights
21 p3006 A72-40446
- Effects of weightlessness on astronauts - A summary.
23 p3253 A72-43385
- Effects of an 18-day flight on the human body.
23 p3253 A72-43386
- ## PSYCHOLOGICAL INDEXES
- ### U PSYCHOLOGICAL TESTS
- ### PSYCHOLOGICAL TESTS
- #### NT RORSCHACH TESTS
- Psychological threshold for successiveness, tabulating probabilities for correct guesses of stimuli order
01 p0013 A72-10713
- Contrast reversal or distance paradox in temperature perception aftereffect
01 p0013 A72-10716
- Position constancy and motion perception tests of head movement feedback calibration of perceived direction of optical motions
01 p0013 A72-10719
- Psychological tests of airmen with performance error histories, considering psychic characteristics for limited assignment readjustment
03 p0316 A72-13723
- Universal perception meter for measurements in work psychology laboratories, discussing characteristics and operation
03 p0320 A72-13884
- Exploratory test of extrasensory perception to identify random order of symbols in space during Apollo 14 flight with four subjects on earth
04 p0565 A72-14888
- Subjective probability distributions for random device-generated Bernoulli process unknowns, discussing distribution median and quartiles and hypothetical sample impact assessment techniques
05 p0616 A72-15812
- Pilot perception tests on estimating flight path inclination, ground image and touchdown time under poor visibility
05 p0684 A72-16180
- Aeromedical diagnostics for aircraft pilot hearing sense tests, considering cockpit environment and stress-produced impairments in central nervous system
05 p0623 A72-16781
- Chlorpromazine tranquilizer influence on squirrel monkeys in electric shock tests, shifting postevent aggressivity to pre event anticipation
07 p0916 A72-18975
- Selective attention dichotic listening test as flying proficiency prediction criteria, discussing omission and intrusion errors
07 p0929 A72-19351
- Sonic boom exposure effect on humans based on visual performance and tracking tests
08 p1127 A72-21912
- Operator independence test for human performance reliability modelling based on symptom detection and fault location of sonar system failure
10 p1429 A72-24002
- Aptitude screening test of ATC training applicants, using directional heading determination under aural distraction
12 p1773 A72-28252
- Frequency-specific color aftereffects as result of alternate exposure of subject to inspection gratings of different spatial frequencies
13 p1901 A72-28615
- Ideas of individual on group members majority behavior in various situations, noting norm concept confirmation from psychological tests on reference groups
13 p1903 A72-28796
- Response bias and sensitivity variations in psychophysical test of rats discrimination between standard and attenuated auditory signal intensities
16 p2356 A72-33648
- Altitude effects on decision making performance of cognitive, psychomotor and complex card sorting tasks
16 p2357 A72-34096
- Visual-tactile senses conflict experimental examination, discussing vision as dominant modality
17 p2507 A72-34249
- Developmental relationships between field independence and fixity-mobility.
18 p2651 A72-36906
- Psychological tests to judge maximum and minimum nonphysical subjective attraction forces between two parallel bars
18 p2654 A72-36919
- Mach band measurement by psychological compensation technique, causing band disappearance by changes in stimulus pattern luminance and brightness distribution relations
19 p2760 A72-37827
- Psychological tests for diurnal variations of human visual discrimination threshold by varying test object illumination level
20 p2891 A72-38931
- A psychologist's laboratory approach to a human factors problem.
21 p3012 A72-41430
- Moving spot detection threshold measurement for varying exposures, noting product of stimulus duration and velocity for comparison with Bloch law
22 p3151 A72-42930
- Complete assimilation of briefly presented lines.
23 p3261 A72-44150
- Learning and solving complex problems of reasoning - A test-theoretical investigation of the complexity of compound problems of predictive logic
24 p3373 A72-45244
- California psychological inventory as a predictor of success in the Naval flight program.
24 p3377 A72-45655
- ## PSYCHOLOGY
- ### NT MILITARY PSYCHOLOGY
- ### NT PSYCHOACOUSTICS
- ### NT PSYCHOPHYSICS
- ## PSYCHOMETRICS
- Sleep, lack of sleep and circadian rhythm effects on psychometric test performance
11 p1581 A72-26684
- Psychometric test for auditory stimulus duration difference estimation, noting Weber fraction for temporal gaps marker condition
21 p3004 A72-40345
- Subjective and objective sensory physiology, discussing transformation processes in sensory receptors and nerves, psychophysical scaling methods, chemoreceptors and peripheral adaptation
22 p3146 A72-42777
- ## PSYCHOMOTOR PERFORMANCE
- ### NT PSYCHOSOMATICS
- Optimal psychomotor performance in relation to thermal comfort conditions in man, using complex dual tests and subjective rating scales
01 p0016 A72-10117
- Human mental and psychomotor performance measurements in compressed oxygen-helium atmosphere pressure chamber for dive between 100 and 1500 feet
02 p0166 A72-11701
- Concurrent and terminal display exposure effects on perceptual adaptation for localizing movements with displacing prism
03 p0319 A72-13878
- Operant conditioning for producing gross motor responses, discussing application to physical medicine and rehabilitation with mentally retarded Downs syndrome children
04 p0478 A72-14706
- Short and long term mental and physical work effects on central nervous system and motor apparatus in young people
04 p0474 A72-15230
- Bioelectric activity study of cat and dog cerebral inter-central relations during various motor activities and poses
04 p0474 A72-15231
- Frontal lobe damage effect on conditional motor reflexes, communication capability and emotional behavior in baboon apes
04 p0476 A72-15583
- Simulated sonic boom effect on tracking performance and autonomic response, noting heart rates, skin conductance and startle reflex
06 p0767 A72-17868
- Mental rehearsal and physical practice relation to learning rate for rotary pursuit tracking skill acquisition
07 p0925 A72-18801
- Natural visual capture result of vision and touch conflict in bilateral comparisons of object length
10 p1430 A72-24270
- Pressure suit effects on psychomotor skills, testing manual dexterity, tracking skills, hand strength, steadiness and coordination for pressurized, unpressurized and shirtsleeve conditions
10 p1431 A72-24796
- Choice reaction task times for responses to signals by middle, little and index fingers
10 p1432 A72-24985
- Camera shake under stress of tracking moving targets viewed briefly in poor light, considering blur in horizontal and vertical dimension
10 p1483 A72-24986
- Sleep loss and work-rest cycle effects on combat efficiency, considering psychomotor reactivity, vigilance and decision making capacity
11 p1588 A72-26688
- Inspiration, expiration and hand muscle control comparison in psychophysical category production method for human voluntary breathing regulation investigation
12 p1763 A72-27843
- Statistical evaluation of feedback role in simple movements in terms of Index of Preprogramming
15 p2187 A72-32761
- Weightlessness effects on animal voluntary motor activity and wakefulness from brain and muscle area electrical activity recordings during ballistic flight
16 p2355 A72-33548

Altitude effects on decision making performance of cognitive, psychomotor and complex card sorting tasks

16 p2357 A72-34096

Vestibular behavior of fish during diminished g-force and weightlessness.

17 p2499 A72-34549

Increase in skeletal muscle performance during emotional stress in man.

17 p2500 A72-34942

Circadian rhythms in physiological and psychological functions related to jet travel, studying body temperature variations and psychomotor performance during isolation and varying light-dark cycle conditions

20 p2897 A72-39723

Influence of prolonged longitudinal accelerations on control habits

21 p3004 A72-41750

German monograph - Control performance as a function of the transmission ratio and the Coulomb friction in the operational element.

22 p3152 A72-43052

Involuntary eye movements during the performance of mental tasks

23 p3260 A72-44077

Behavior concept formulation for visceral systems, considering digestive system data and extension from motor function concepts

24 p3370 A72-44586

PSYCHOPHYSICS

NT PSYCHOACOUSTICS

Psychology of visual form perception in relation to neurophysiological principles of lateral interaction and organization, considering retinal images, aftereffects, binocular vision, etc

01 p0011 A72-10469

Psycho-physical theory of human mind, discussing molecular biological processes of neuron recording in terms of quantum mechanics

06 p0769 A72-18191

Psychophysical comparison methods for evaluating noisiness or annoyance values of sounds

07 p0932 A72-20168

Inspiration, expiration and hand muscle control comparison in psychophysical category production method for human voluntary breathing regulation investigation

12 p1763 A72-27843

Experimental testing of theory of signal detectability derived psychophysical models application to two-pulse visual stimuli temporal discrimination

15 p2184 A72-31379

Response bias and sensitivity variations in psychophysical test of rats discrimination between standard and attenuated auditory signal intensities

16 p2356 A72-33648

Evidence for the role of the transient neural 'off-response' in perception of light decrement - A psychophysical test derived from neuronal data in the cat.

17 p2500 A72-34884

Determining the detectability range of camouflaged targets.

17 p2510 A72-35690

Psychophysical procedures to investigate selective visual adaptation to light of different wavelengths from test gratings with various orientations and spatial frequencies

19 p2756 A72-37829

Psychophysical information content evaluation of aerial photographic images by human viewer for photointerpretation and search in reference library

20 p2894 A72-39042

Measurement of specific mechanical impedance of the skin - Effects of static force, site of stimulation, area of probe, and presence of a surround.

21 p3005 A72-40347

1971 Rayleigh Gold Medal Address - Calculating the perceived level of light and sound.

22 p3205 A72-42462

Subjective and objective sensory physiology, discussing transformation processes in sensory receptors and nerves, psychophysical scaling methods, chemoreceptors and peripheral adaptation

22 p3146 A72-42777

PSYCHOPHYSIOLOGY

Environmental noise induced human fatigue, considering physiological and psychological effects

01 p0016 A72-10050

Psychophysiological potentials of pilots in simulated emergency situations, investigating motor reaction time, signal selection time, error number and type and processed information amount and rate

06 p0769 A72-18199

Disorientation in naval aircraft accidents from psychophysiological and environmental factors, suggesting flight scheduling and training improvements

08 p1126 A72-21574

Physiology of sleep phases and dreams, discussing data on highly organized and interacting neurohumoral mechanisms exhibiting alternating forms of brain bioelectric activity

08 p1118 A72-21838

Soviet book on psychic phenomena and brain, covering cybernetics, dialectical materialist implications, consciousness, psychophysiology and cerebral neurodynamic structures

08 p1121 A72-22164

Self estimated distractibility in subjects related to attention lapses during perceptual motor performance, indicating psychophysiological changes

12 p1776 A72-28307

Future spacecraft habitable compartment layout from psychophysiological viewpoint, considering human visual and motor field parameters and crew members social needs

13 p1910 A72-29321

Low-altitude flight imposed psychophysiological stresses due to air turbulence discomfort, instrument dial vibration and ground-based navigational objects recognition difficulty

14 p2080 A72-30747

Psychological principles of active rest during long space flights

21 p3006 A72-40446

Critique of Pavlov conditioned reflex role in higher nervous activity and association principle role in psychic activity

21 p3001 A72-40811

PSYCHOSOMATICS

Case history of student aviator with psychosomatic Lymphogranuloma venereum related to vestibular apparatus

02 p0167 A72-11712

Diagnostic errors in draft age patients, noting doctor, examination methods, disease type and patient factors and psychosomatic disturbance detection

16 p2359 A72-34149

German book - Somatic sensitivity, smell and taste.

22 p3145 A72-42776

PSYCHOTHERAPY

Civil aeronautics environment relation to psychiatrists and medical psychologists treatment of air navigation personnel, discussing chemotherapeutic and psychotherapeutic treatment administration problems

07 p0927 A72-19243

PSYCHROMETERS

LICI dew point hygrometer operation investigated by double ventilation psychrometers, noting measurement error dependence on relative humidity and temperature

10 p1483 A72-25015

PSYCHROPHILES

Hydrostatic pressure and temperature effects on growth of psychrophilic marine bacterium, emphasizing inhibited amino acid transport and respiration

01 p0011 A72-10322

PTM [MODULATION]

U PULSE TIME MODULATION

PUBLIC RELATIONS

Optical and electronic imaging systems optimization for solar system exploration, discussing effects on public support for national funding

12 p1807 A72-27346

PULLEYS

Approximate stress calculation in friction pulley shells of multipulley hoisting machines, using method of initial parameters

07 p1094 A72-20134

PULLING

Van der Pol oscillator periodic pulling behavior under weak perturbation near natural frequency, analyzing Fourier frequency spectrum

14 p2132 A72-31122

PULMONARY CIRCULATION

Computer controlled scintiscanning for pulmonary blood flow distribution, discussing real time data monitoring, contour plots and three dimensional and wall reflection maps

01 p0020 A72-11038

Hemodynamics, pulmonary gas exchange and circulatory responses to high altitude in subjects with previous history of high altitude pulmonary edema

02 p0156 A72-11422

Exercise effects on pulmonary circulation in dogs, measuring pulsatile arterial flow and pressure and vascular input impedance, resistance and hydraulic power

04 p0475 A72-15464

Conversion of angiotensin to angiotensin 2 in dog pulmonary circulation, studying peptide synthesis, radioimmunoassay and in vivo and plasma in vitro metabolism

04 p0475 A72-15465

Wien intravascular effect on plasma carbon dioxide gradients near pulmonary capillary wall, discussing free energy requirements

08 p1114 A72-20890

Digital computer simulation of circulatory and respiratory systems interaction model for oxygen and carbon dioxide gas exchange between pulmonary blood and alveolar air

09 p1268 A72-22456

Vasomotor efferent effects on rabbit lung posterior lobe blood content in response to electrical stimulation of vagus nerve peripheral ends

09 p1268 A72-23693

Pulmonary capillary bed filling as function of arterial pressure in perfused frozen dog lungs

10 p1425 A72-24480

Blood flow stratification effect on alveolar gas exchange in liquid filled lungs in dogs from Xe 133 concentration measurements

10 p1425 A72-24481

Open capillaries control mechanism of pulmonary diffusion capacity, presenting mathematical interpretation of humoral and hydraulic blood pressure control

10 p1426 A72-24787

Sheet flow theory for pulmonary alveolar blood flow, discussing blood pressure effects, membrane tension, blood volume and transit time distribution

11 p1589 A72-26702

Tilt table test for gravitational stress effects on human pulmonary capillary blood flow

12 p1765 A72-28286

Blood coagulation changes at high altitude predisposing to pulmonary hypertension.

17 p2498 A72-34222

Effects of diffusion impairment on O2 and CO2 time courses in pulmonary capillaries.

17 p2506 A72-35967

Mathematical model for flow limitation in collapsible tube in relation to pressure in pulmonary and circulatory system

17 p2510 A72-35972

A model of fluctuating alveolar gas exchange during the respiratory cycle.

18 p2650 A72-36571

Role of the autonomic nervous system in the hypoxic response of the pulmonary vascular bed.

18 p2650 A72-36572

Relationship of pulmonary artery to left ventricular diastolic pressures in acute myocardial infarction.

20 p2892 A72-39461

Heart function and pulmonary circulation in humans suffering from chronic mountain sickness

22 p3143 A72-42587

Hypothalamic control of the systemic and lung circulation and functional significance of this control

22 p3148 A72-43168

Rheographic investigation of cerebral, pulmonary and peripheral circulation during bed rest in antithrostatic position

23 p3255 A72-43914

Possibility of determining the lung ventilation volume by the mathematical modeling method

24 p3374 A72-44597

Comparative study of regional hemodynamics during tilt test and lower body negative pressure exposure.

24 p3373 A72-45131

PULMONARY FUNCTIONS

Right heart ventricle intracardiac phonocardiograms, recording pulmonary early diastolic click simultaneous with artery pressure curve dirotic wave

01 p0010 A72-10121

Pulmonary functional inhomogeneities effects on steady state oxygen and CO diffusing capacity estimates in gas transfer resistances terms

01 p0014 A72-10847

Acute, short and long term and life long high altitude hypoxia exposure effects on pulmonary gas exchange control and efficiency during physical exercise

01 p0014 A72-10848

Inspiration time correction factor for pulmonary diffusing capacity measurement by single breath method.

01 p0015 A72-11259

Altitude hypoxia human pulmonary compliance relation between static transpulmonary pressure and inspired volume

02 p0159 A72-11958

Lung ventilation nonuniformity determination by single calm breath method, showing nitrogen concentration in alveolar phases

02 p0165 A72-12515

Pulmonary RC network and multiple breath nitrogen washout time constants mathematical relationship for breathing mechanics measurement, discussing lung compliance and resistance

04 p0478 A72-14862

Respiratory flow resistance measurements in man, comparing esophageal catheter, plethysmographic, forced pressure oscillations and airway interrupter methods

04 p0481 A72-15222

Single breath method for pulmonary diffusing capacity measurement with respect to total lung capacity and inspiration time

05 p0620 A72-17174

Hypoxia pretreatment for decreased pulmonary oxygen toxicity during high pressure oxygen breathing in rats

07 p0917 A72-19328

Cardiovascular and respiratory responses to intraarterial injection of K and Na ions in dogs for peripheral receptor site determination

07 p0921 A72-20177

Hyperbaric oxygen exposure effect on cardiovascular system in rats, discussing pulmonary edema relation to hypertensive left ventricular failure

07 p0921 A72-20182

Environmental chamber tests for ozone exposure effects on human pulmonary function at rest and during bicycle exercise

08 p1122 A72-20884

Cardiorespiratory functions in child swimmers and nonathletes during growth, relating training to oxygen transport system dimensions

08 p1123 A72-20894

Respiration in altered gas environment for spontaneous breathing and voluntarily maintained pulmonary ventilation level conditions

08 p1120 A72-22077

Laryngeal motoneuron activity during Hering-Breuer reflexes, noting inspiratory fibers firing inhibition and activation during lung inflation

09 p1266 A72-22975

Aerobic work capacity indices of gas exchange pulse rate, pulmonary ventilation and acid base balance in runners, determining maximum oxygen utilization

09 p1268 A72-23596

High altitude acclimatization effects on human lung diffusing capacity for carbon monoxide at different oxygen tensions

10 p1425 A72-24476

Chest strapping-induced increased lung recoil pressure effects on maximal expiratory flow relation to lung surface compliance decrease

10 p1425 A72-24478

Elastic lung shaped model for distribution analysis of weight induced stresses, strains and surface pressures in lung

10 p1425 A72-24479

Pulmonary atelectasis and arterial-venous shunting and heart displacement prevention during centrifuging of dogs breathing oxygenated liquid fluorocarbon in water immersion respirator

11 p1579 A72-26609

Plethysmographic and laryngoscopic investigation of glottis opening and airway resistance relation to lung volume during panting and continuous slow expiration

11 p1586 A72-26611

Digital computer technique for computation of pulmonary mechanics parameters, using phasor method and Fourier series analysis of respiratory flow signals

11 p1587 A72-26620

Native highlander and lowlander chemoreflex ventilatory response to transient carbon dioxide inhalation at low and high altitudes

12 p1762 A72-27728

Pulmonary oxygen transport dynamic model representing lung gas-side airway and alveolar regions and blood-side capillary bed

13 p1909 A72-28996

Four-parallel-compartment lung model for emptying pattern study, using expired nitrogen concentration data to calculate alveolar dilution ratio and emptying rate

14 p2079 A72-30703

Annual clinical and physiological evaluation of test pilots physical performance over ten year period from body composition, pulmonary function and work capacity measurements

14 p2082 A72-31093

Nonlinear theory of pulmonary ventilation distribution in two compartment model of human lungs

16 p2358 A72-33025

Rebreathing studies of carbon dioxide pressure level effect on carbon dioxide content difference in arterial blood and alveolar gas during exercise and rest

17 p2499 A72-34346

Respiratory frequency and alveolar oxygen and carbon dioxide tension relationship to hypercapnia in man

17 p2506 A72-35965

Gas induced osmosis as factor in pulmonary homeostasis, showing differential water retention in lungs ventilated with normoxic nitrous oxide compared with air

17 p2506 A72-35970

Pulmonary gas exchange in Andean natives at high altitude.

18 p2650 A72-36570

Rat pulmonary lipid metabolism during feeding and fasting from studies of lung lecithin half life after C-14/1palmate and H-3/U/glucose injection

18 p2651 A72-36573

Regional lung function in man during immersion with the head above water.

19 p2758 A72-38701

Pulmonary air-trapping induced by water immersion.

19 p2759 A72-38711

Evaluation of cardiopulmonary function and work performance in man during caloric restriction.

21 p3005 A72-40423

Regional lung function during early acclimatization to 3,100 m altitude.

21 p3005 A72-40424

A method for spiographic display of functional residual capacity and other lung volumes.

21 p3005 A72-40427

Electrically sensed changes in chest and abdomen diameter for tidal volume, respiratory frequency and minute ventilation measurements

21 p3006 A72-40428

Hypoxic pulmonary steady-state diffusing capacity for CO and alveolar-arterial O2 pressure differences in growing rats after adaptation to a simulated altitude of 3500 m.

21 p3003 A72-41622

Control of the circulating blood mass in the case of a functional detachment of various amounts of pulmonary tissue

21 p3012 A72-41825

Effects of externally imposed mechanical resistance on breathing dense gas at exercise - Mechanics of breathing.

22 p3150 A72-42489

Transarterial leakage - A possible mechanism of high altitude pulmonary oedema.

22 p3143 A72-42588

Lung volume changes of people in antihypostatic position in hospital beds for control, exercising and muscle electric-stimulated groups

23 p3256 A72-43918

Possibility of determining the lung ventilation volume by the mathematical modeling method

24 p3374 A72-44597

Determination of the diffusional capability of lungs by the method of delayed respiration

24 p3374 A72-44598

PULMONARY LESIONS

Effects of nitrogen and helium upon pulmonary damage after rapid decompression to 2 torr.

17 p2508 A72-34544

Influence of prolonged starvation on the frequency of occurrence of decompression-induced pulmonary hemorrhage.

17 p2508 A72-34545

PULSARS

Pulsar nature and radiation mechanism, examining rotating neutron stars structure and atmospheric dynamics

01 p0131 A72-10973

Pulsar PSR 0833-45 linear polarization measurements at 300 and 1420 MHz, showing frequency invariance with interstellar scattering and Faraday rotation allowance

01 p0133 A72-11119

Pulse widths formed by relativistic beaming pulsars effect on emission spectra

01 p0133 A72-11130

Quasar model proposal as giant pulsar rejected discussing mass, radius, magnetic field strength, luminosity and gamma radiation

01 p0134 A72-11144

Pulsar magnetosphere axisymmetric and vacuum oblique rotator models, emphasizing electromagnetic field properties

01 p0134 A72-11159

Pulsar NP 0532 pulsed hard X ray energy spectrum measurement, using balloon sounding data

01 p0134 A72-11160

Radio variable sources PKS 0727-11 and 1514-24 observation at 2295 MHz, presenting flux measurements and drift curves

01 p0134 A72-11161

Crab Nebula pulsar NP 0532 model for interaction and polarization of radio radiation with surrounding media

02 p0277 A72-11772

Extended Thomas-Fermi isolated atom model for pulsar outermost crust magnetic field effects, using pressure-density equations of state

02 p0277 A72-11903

Second decrease in Vela Pulsar period, noting time span between discontinuities and supernova remnant Vela X

02 p0277 A72-11904

Interferometric observations of pulsars at 2.7 and 8.1 GHz, determining radiant flux densities

02 p0278 A72-11906

Nonthermal radio source G 55.7 plus 3.4 structure in pulsar CP 1919 direction, presenting intensity contours and integrated flux density spectrum

02 p0278 A72-11907

Pulsar distances and energy from assumed interstellar electron density, considering nonplausibility of associations with supernovae

02 p0278 A72-12047

High velocity interstellar Ca II near Vela pulsar 0833-45, discussing absorption line association with Vela X, Y, Z supernova remnant complex

02 p0279 A72-12191

Nonlinear discrete radio source spectra deviations from power law at 10-5000 MHz, considering low energy relativistic electron excess

02 p0281 A72-12305

Source motion effects on Doppler period variations of high velocity pulsars, considering first and second time derivatives

02 p0281 A72-12309

Weak dipole magnetic field effect on oscillation frequencies of conducting gaseous polytrope stars, using variational equation

02 p0260 A72-12310

Electromagnetic emission from pulsar with magnetic force tube on surface of magnetosphere treated as rotating magnetic multipole

02 p0285 A72-12833

Pulsar observation data, presenting period histogram, intensity, shape and polarization variations, position distribution, physical nature and spectra

03 p0417 A72-13102

Pulsar theory, discussing rotating neutron star principle, kinetic energy, structure, atmosphere, radiation mechanics and supernovae remnants

03 p0417 A72-13103

Pulsars formation rate and connection with supernovae and cosmic rays, discussing stellar magnetic field strength

03 p0421 A72-13134

Pulsar origin of cosmic rays, considering accelerated charged particles maximum energy

03 p0421 A72-13135

Neutron star surface structure and cooling calculations for pulsar cosmic ray production through surface material acceleration

03 p0421 A72-13136

Crab Nebula optical pulsar NP 0532 polarization minima delay mechanism, suggesting relativistic radiation from region orbiting relativistically around neutron star

03 p0434 A72-13553

Gas heating by If radiation due to Compton scattering near quasars, Seyfert galaxies nuclei and pulsars

03 p0435 A72-13801

Linear polarization of pulsar PSR 22 18 plus 47 radio emission pulses, attributing periodic fine structure of spectrum to rotation of polarization plane in interstellar medium

03 p0436 A72-13824

Electromagnetic pulsar models features and predictions, using rotating neutron stars with strong dipolar magnetic fields

03 p0437 A72-13873

Charged particle motion in pulsar electromagnetic fields, discussing coherent synchrotron radiation and charge bunching

03 p0438 A72-13874

Coherent synchrotron radiation from model with charge distribution moving on ring, applying to pulsars

04 p0566 A72-14555

Relaxation time estimation for electron velocity relative to dilute vortex core array in rotating neutron superfluid, applying to pulsar slowdown rate

04 p0571 A72-14590

Pulsar model, discussing polar radiation diagram formation with source motion around neutron star

04 p0573 A72-14903

Universal steady X ray background theory, examining superposition of radiation from pulsars in various galaxies

04 p0566 A72-14909

Declination, average pulse energy and pulse shape of weak pulsars, determining barycentric period

04 p0574 A72-14981

Pulsar radiation scattering in interstellar medium, using Gaussian spatial autocorrelation function

04 p0577 A72-15281

Pulsar CP 0328 wideband rf spectrum long term periodicity, considering origin during propagation through interstellar medium

04 p0580 A72-15369

Pulsars CP 0329, 0950, 1133 and 1919 pulse height fluctuations at 408 MHz, showing period features in power spectrum with integrated pulse amplitudes

04 p0581 A72-15512

Pulsar PSR 0809 plus 74 observations indicating organized variation in polarization synchronized with drifting subpulses

04 p0581 A72-15513

Pulsar PP 0943 radio emission, showing short time intensity increases

04 p0581 A72-15514

X ray and gamma astronomy, discussing old and blue stars, supernova remnants, radio galaxies, quasars and pulsars

04 p0582 A72-15687

Pulsar planetary systems observation from perturbation of pulse arrival time

05 p0712 A72-15771

Gamma ray absorption near Crab Nebula pulsar NP 0532 within beam model, discussing pair production in photon field

05 p0711 A72-17161

Pulsar long term intensity variations due to intrinsic structure or propagation effects

06 p0878 A72-17670

Crab Nebula and Vela pulsar constant elastic energy density contours, discussing micro and macroquakes

06 p0886 A72-18095

Pulsar produced cosmic rays energy spectrum, investigating light elements origin

06 p0874 A72-18161

Isolated pulsar or neutron star upper mass limit based on consideration of rotational energy by ejection of low energy cosmic rays or photons

06 p0891 A72-18508

Cosmological red shift and galactic evolution effects on line features in X ray background due to young pulsars in supernova remnants

06 p0891 A72-18509

Pulsar dynamics and electrodynamics for power derivation from rotational energy, discussing toroidal magnetic field induced nonhydrostatic stress in neutron star

07 p1068 A72-19001

Interplanetary scintillation of two pulsars, discussing scattering and amplitude modulation of incident radiation propagated through interstellar medium

07 p1069 A72-19073

X ray pulsar observed near Crab Nebula by balloon-borne telescope, discussing identification with NP 0532 or NP 0532

07 p1070 A72-19122

Crab Nebula pulsed X radiation from balloon flights, extracting pulsar profile

07 p1056 A72-19135

Pulsar rotation and dispersion from polarization and pulse arrival time observations, calculating magnetic field components in path to pulsars

07 p1072 A72-19343

Field approach to gravitation accounting for energy release and nonthermal radiation occurrence in pulsars and quasars

07 p1075 A72-19576

Papers on pulsar physics covering interstellar cloud properties, optical and X ray observations, rotating neutron stars, cosmic rays, etc

07 p1079 A72-20048

Pulsars radio observation for mean polarization parameters

07 p1079 A72-20049

Pulsars optical counterpart observation, noting Crab Nebula pulsar visual magnitude

07 p1080 A72-20050

X ray power density spectrum observation of pulsars, detecting Crab Nebulae pulsar radiation

07 p1080 A72-20051

Pulsar periods measurement with pulse arrival time calculation based on source position

07 p1080 A72-20052

Interstellar cloud properties based on electron concentration integral along line of sight from pulsar radiation measurements

07 p1080 A72-20053

Pulsar distance determination from electron density distribution in line of sight estimated from frequency dispersion measures

07 p1080 A72-20054

Pulsars suggested as rotating neutron stars based on collapsed star magnetic field strength, mass-radius relation and radio flux emission

07 p1080 A72-20055

Pulsar model based on neutron star rotation with skew magnetic field, considering radiated particle acceleration responsible for high energy activity in supernova remnants

07 p1080 A72-20057

Magnetosphere theory of pulsar electrodynamics, discussing unipolar inductor with iron sphere having uniform magnetization parallel to rotation axis

07 p1080 A72-20058

Pulsar production rate relationship to high energy cosmic ray origin and number density

07 p1081 A72-20059

Pulsed gamma ray emission measurement above 50 MeV from Crab Nebula pulsar with balloon-borne spark chamber

07 p1063 A72-20235

Ultrarelativistic cosmic plasma analysis of high density electron beams transport across strong magnetic fields with application to pulsar NP 0532 spectrum

07 p1064 A72-20634

High energy gamma quanta point sources from extensive air showers Cerenkov flares records, finding flux limits of radio galaxy and pulsars

07 p1064 A72-20635

Steady state problem of energy spectrum of variable magnetic field accelerated electrons, considering synchrotron X ray emission of Crab pulsar and nebula

08 p1231 A72-21119

Observational parameters of 61 pulsars, tabulating names, right ascension and declination, galactic longitude and latitude and period and dispersion measures

08 p1233 A72-21179

Pulsar and supernova remnant relative space position based on runaway pulsar hypothesis, discussing pulsar period-luminosity relation from evolutionary standpoint

08 p1233 A72-21180

Pulsar and quasar energy sources, discussing Crab nebula, rotating neutron stars and gravitational collapse role

08 p1233 A72-21208

Pulsar braking index and period-pulse width distribution calculations within proposed model leading to neutron star surface magnetic field strength estimates

08 p1235 A72-21389

Crab pulsar optical pulse stability comparison to radio frequency output, noting negative results in search for polar precession

08 p1235 A72-21396

Quasar rotation and pulsation periods within pulsar models, postulating supermassive stars /one million-one billion solar masses/ as energy sources

09 p1385 A72-22536

Pulsars CP 0328 and NP 0531 (twinkling explained by interstellar electron density fluctuations due to Alfvén wave passage and coupling of cosmic rays to interstellar gas

09 p1377 A72-22753

Radio emission from pulsar CP 1133, comparing amplitude and polarization characteristics of two subpulses

09 p1387 A72-22987

Long time behavior of neutron star magnetic fields, noting pulsar evidence for large internal fields in main sequence stars

09 p1389 A72-23393

Circular polarization measurements of Crab Nebula pulsar NP 0532, including main pulse leading and trailing edge components

[AD-736711]

09 p1394 A72-23675

Main sequence star evolution relation to pulsar formation, discussing stellar core density at carbon ignition with respect to critical density limit

09 p1394 A72-23698

Pulsar electrodynamic properties, radiation mechanism, galactic distribution and pulse shape, period distribution and propagation characteristics, reviewing Crab Nebula pulsar features

10 p1533 A72-23888

Pulsar radiation mechanism study from magnetosphere structure model, taking into account neutron star evaporated gas accumulation in gravitation-centrifugal force balance region

10 p1544 A72-24672

Optical and X ray pulsars, discussing Crab pulsar, emission behavior, pulse intensity, periodicity, polarization properties and antenna emission, plasma maser and Chiu models

10 p1547 A72-24919

Pulsar rotational models, considering white dwarves, neutron stars, oblique rotators, etc

11 p1718 A72-25907

Crab pulsar period speedup observed by optical timing on 26 October 1971, noting similarity to September 1969 event

11 p1724 A72-26573

Pulsar speed increase mechanism as metastable flow state transition in neutron star superfluid core

11 p1724 A72-26705

Arecibo observatory research, discussing pulsars, radio source scintillation and ionospheric heating

12 p1795 A72-27427

Pulsar 21 cm pulse profile measurement, discussing installation design and operational principles

12 p1872 A72-27809

Crab Nebula pulsar X ray radiation pulses at 100-400 keV searched for via balloon flights with NaI detector

13 p2034 A72-29965

Pulsar PSR 1154-62 association with nearby galactic radio source having supernova remnant shell structure and spectrum characteristics

14 p2150 A72-30369

Trillion electron volt pulsed gamma rays from Crab Nebula pulsar NP 0532

14 p2156 A72-30566

Crab pulsar LF radiation polarization parameters and pulse shapes, showing highly polarized precursor component

14 p2156 A72-30567

Near field effects on pulsar particle acceleration, relating electric and magnetic field magnitudes

14 p2156 A72-30568

Pulsars distance computation, considering period-luminosity relationship and uncertainties inherent in dispersion measure /DM/ method

14 p2159 A72-30738

Interstellar medium physical conditions from 21 cm hydrogen emission line observations in direction of pulsars, using 25 meter Dwingeloo radiotelescope

14 p2159 A72-30744

Magnetic neutron stars /pulsars/ atmosphere, questioning vacuum approximation method applicability

14 p2160 A72-30887

Radio emission due to relativistic electrons spiral orbit motion in rotating pulsating neutron star

15 p2304 A72-31333

Rotating neutron stars stability and radial pulsations by energy method, allowing for relativistic effects

15 p2304 A72-31335

Rotating white dwarfs and neutron stars quasi-radial pulsations frequencies, discussing central densities critical values

15 p2304 A72-31336

Variable cosmic X ray source location determination, noting Crab pulsar as radio, optical, X ray and gamma source

15 p2298 A72-31599

Flare mechanism of pulsar radiation near magnetic poles of rotating neutron stars

15 p2298 A72-31627

Time transfer measurement between two locations using nearly simultaneous reception times from optical pulsar signal transmission

15 p2199 A72-32076

Pulsar rotating electromagnetic field vectors classification for magnetosphere models

16 p2450 A72-32866

Vela pulsar speedup explanation by corequake release of elastic energy stored within solid neutron lattice

16 p2450 A72-32869

Pulsars 0950 plus 08 and 1133 plus 16 flux density spectra measurements at 1.4-5.0 GHz, noting equivalent continuum break

16 p2456 A72-33477

Pulsar pulse broadening due to multiple scattering by interstellar medium, finding exponential decay time constant relation to rms broadening of angular size

16 p2457 A72-33686

Pulsars MP 1055, PSR 1556-44 and MP 1700 discovery in search within radio source survey at Molonglo Radio Observatory

16 p2459 A72-33723

Pulsar radio and optical observations, discussing periods, pulse shapes at various frequencies and marching subpulses

16 p2460 A72-33925

Mathematical model for magnetosphere surrounding rotating neutron star, noting computer programs for Maxwell and plasma equations solution

16 p2460 A72-33927

Pulsars radiation mechanism relationship to magnetospheric conditions, considering optical, X ray and gamma radiation

16 p2460 A72-33928

Equations of state and equilibrium for electron gas in strong magnetic field, discussing effects in pulsar crusts and atmospheres

16 p2460 A72-33929

Fermi lectures by Dyson on neutron stars and pulsars origin and structure, using perfect gas and realistic models

16 p2460 A72-33974

NP 0532 precursor pulse as radiation scattered from main pulse beam by ring of material centered on pulsar

17 p2603 A72-34192

Optical timing of the Crab pulsar, NP 0532.

17 p2605 A72-34535

Russian book - Theory of gravitation and the evolution of stars

17 p2613 A72-35452

Formation of neutron star spots and its connection with pulsars. I.

17 p2613 A72-35502

Gamma radiation production through interaction between high energy particles emitted by pulsar originating in supernova core and gas in supernova envelope

18 p2721 A72-36088

Electron and nuclear components and transformations of matter under extreme conditions of pressure and temperature exemplified in stellar /pulsar/ evolution

18 p2725 A72-36520

Influence of interstellar discontinuities on the shape of radio pulses from pulsars

18 p2726 A72-36652

Anomalous motion of radiating particles in strong fields.

18 p2713 A72-36712

Binary, rotatory and oscillatory theories on pulsar existence, considering energy emission and Maxwell equations

18 p2728 A72-36765

Book on quasars and pulsars covering nature, origin, life span, universe concept with motion as fundamental unit and space-time reciprocal relationship

18 p2729 A72-37023

Density of the solar corona from occultations of NP 0532.

19 p2855 A72-37242

Detection of high-energy gamma rays from the Crab Nebula.

19 p2850 A72-37503

The primary spectrum of the eclipsing binary LR Centauri.

19 p2856 A72-37505

On the optical search for Centaurus X-3.

19 p2856 A72-37506

Preliminary results of observations of the pulsar CP 1133 with the aid of a device for recording Cerenkov flares of extensive atmospheric showers

19 p2850 A72-37806

Pulsar properties correlation with radially oscillating coherent plasma of electron-positron pair production by strong electric field around central object

19 p2859 A72-37892

Short-period pulsar intensity variations at 70 to 115 MHz

19 p2862 A72-38056

Neutron-rich nuclei in a Fermi gas

19 p2837 A72-38060

Pulsars as stellar population, considering physical models, pulse emission radiation mechanism and use in galaxy studies 19 p2865 A72-38476

Relativistic beaming from periodically orbiting light point source in terms of photon fluxes, relating to pulsar radiation theory 19 p2835 A72-38697

Energy spectrum and composition of pulsar-accelerated cosmic rays. 20 p2964 A72-39343

Radio position accuracy of pulsar PSR 1749-28 from lunar occultations compared to time of arrival measurements 20 p2969 A72-39388

A tabulation of pulsar observations. 20 p2969 A72-39390

Neutron star detection based on nearby pulsar soft thermal X ray flux observations 21 p3107 A72-41218

Hamiltonian analysis of charged particle motion in the pulsar rotating magnetic field. 21 p3111 A72-41472

VLF electromagnetic radiation frequency observation for pulsar pulsation or rotation period 21 p3111 A72-41485

Frequency correlation measurement of pulsar spectral fine structure due to radio emission scattering by interstellar plasma 21 p3101 A72-41752

Sodium to calcium ion abundances ratio variation model in interstellar clouds, comparing with pulsar dispersion and LF radio absorption measurements 22 p3224 A72-42383

Neutron star model for magnetic field and superfluidity effects on cooling during pulsar stage 22 p3228 A72-42565

Amplitude-time and polarization characteristics of the subpulses of the CP 1133 pulsar 22 p3230 A72-43136

Cross correlated interstellar scintillation patterns of circumpolar pulsar PSR 0329+54 at 408 MHz, interpreting transverse velocities in Galaxy 23 p3334 A72-43253

A study of galactic supernova remnants. II - Supernova rate, galactic radio emission and pulsars. 23 p3337 A72-43829

Upper limit on the gravitational flux reaching the earth from the Crab pulsar. 23 p3337 A72-43874

Centaurus X-3 - Possible reactivation of an old neutron star by mass exchange in a close binary. 24 p3439 A72-44976

PULSATING FLOW

UNSTEADY FLOW

PULSE AMPLITUDE

Physiological response to affective visual stimuli, observing signal value change effect on forehead pulse amplitude and galvanic skin response 01 p0014 A72-10854

Longitudinal stress pulse amplification during propagation along tapered elastic bars in direction of decreasing cross section 02 p0287 A72-11504

[SESA PAPER 1894] Pulsars CP 0329, 0950, 1133 and 1919 pulse height fluctuations at 408 MHz, showing period features in power spectrum with integrated pulse amplitudes 04 p0581 A72-15512

Light amplifier steady state pi pulse local instability against amplitude perturbations in absence of relaxation or inhomogeneous broadening 07 p1002 A72-19204

Low induction 500-kV 1-microsecond 5-kJ pulsed voltage generator, discussing design features 07 p0946 A72-19958

Nanosecond solid dielectric discharger fired by Q switched ruby laser for commutation of coaxial line forming high amplitude voltage pulses 07 p1008 A72-20509

Giant pulse amplification with neodymium-phosphorus oxychloride liquid laser amplifier 09 p1323 A72-22655

Pulse amplitude system with finite data recording time, deriving transfer function for signal shaper 11 p1609 A72-25444

E region drift velocity estimates from amplitude and phase measurements of pulsed radio waves reflected from lower ionosphere 13 p1923 A72-29664

Microwave device phase and amplitude frequency response measuring equipment with wide range test pulse generation, discussing design and performance 13 p1934 A72-30091

Steady state laser mode locking with saturable absorber, describing pulse shape and amplitude as function of quantity of absorbing medium 14 p2111 A72-30793

Calibrated LF acceleration vibrocardiography to examine hemodynamics indices relation to main wave amplitudes 15 p2188 A72-31313

Effect of pulsed voltages fed into the external modulating electrode on the threshold sensitivity of a photomultiplier 19 p2774 A72-38415

Amplification cascade designs for harmonic and pulsed signals with a high frequency emitter correction 21 p3033 A72-40946

Determination of pulsed amplifier correction parameters with the aid of approximating polynomials 21 p3034 A72-41120

A meter giving the number of overshoots of the realization of a steady random process 21 p3058 A72-41732

Effects of bandlimiting on the coherent detection of PSK, ASK and FSK signals. 24 p3380 A72-44900

PULSE AMPLITUDE MODULATION

Radio signals information capability estimation during propagation through electromagnetic fields, using pulse amplitude modulation 01 p0065 A72-10446

Pulse amplitude modulated tester with shift register generated sequence and conventional data /PCM/ bit synchronizer and detector 02 p0192 A72-12148

Amplitude and phase modulated radar pulse train representation by complex number sequences, discussing generation, processing, and Z transform application to combination codes 06 p0773 A72-17495

PCM systems low pass filter characteristics from PAM off-band signals noise attenuation calculations 07 p0943 A72-19435

Russian papers on discrete control systems covering inertialess Markov objects, pulse amplitude and frequency modulation and statistical analysis 11 p1609 A72-25442

Absolute stability conditions of zero solution for PAM automatic control systems equations in terms of transfer function 11 p1609 A72-25446

PAM time division multiplex crosspoint circuit with scanning filters, discussing applications to PBX, ground station and terminal exchanges with PCM transmission link 11 p1604 A72-25909

Absolute instability of nonlinear pulse-amplitude modulated control systems - Frequency criteria 21 p3038 A72-40707

Error probability for multilevel PAM transmission with intersymbol interference, Gaussian and impulsive noise. 21 p3019 A72-40888

Increasing the linearity of the time scale of a time-amplitude-code converter 21 p3035 A72-41728

PULSE CODE MODULATION

NT DELTA MODULATION

Incoherent optical communications fixed receiver passband, determining SNR for pulse time and code modulation with discrete time 01 p0024 A72-10198

Multichannel space station communications using PCM-PSK-PM interplex modulation for reducing cross modulation loss 02 p0174 A72-12131

Pulse amplitude modulated tester with shift register generated sequence and conventional data /PCM/ bit synchronizer and detector 02 p0192 A72-12148

Shock hardened delayed transmission pulse code modulated system for artillery projectile instrumentation with in-barrel and in-flight monitoring capability 02 p0175 A72-12155

Pulse coded processing system EMC performance measurement, considering CW and pulsed interference effects and application to ATC radar beacon system transponders 03 p0324 A72-14033

PCM/NRZ signal band limiting effect on bit error probability, presenting SNR degradation as function of bandwidth-bit duration product and bit patterns 03 p0325 A72-14192

Computerized PCM data presentation and real-time monitoring system, presenting functional flow diagrams for computer program 05 p0633 A72-16677

Fast frequency switching for shift keying pulse code modulation with two cavity modes for Gunn oscillator frequency states 05 p0631 A72-17072

PCM systems low pass filter characteristics from PAM off-band signals noise attenuation calculations 07 p0943 A72-19435

Spectral distribution of signal power in AM, FM and PM PCM systems with time division multiplexing 10 p1439 A72-24909

Noise threshold improvement of PCM signals for satellite transmission, using quality detector and error detecting codes 10 p1441 A72-25102

PAM time division multiplex crosspoint circuit with scanning filters, discussing applications to PBX, ground station and terminal exchanges with PCM transmission link 11 p1604 A72-25909

PCM and FDM/FM systems noise and signal distortion analysis by digital simulation with FORTRAN language based on fast Fourier transform 11 p1601 A72-26043

Soviet book on radio receiver design covering military applications, bandwidth requirements, network synthesis and AM, FM, SSB, Doppler, phase metering, PCM and radar equipment 11 p1604 A72-26045

Mutually coupled continuous time orthogonal binary random processes, illustrating transition from discrete to exponential interval distribution 11 p1611 A72-26298

Spectral correlation and transition probabilities of mutually dependent orthogonal binary random signals 11 p1595 A72-26299

Message distortions analysis in PCM communications systems due to phase fluctuations of synchronization signal 11 p1598 A72-26728

Voice digital data rate reduction technique by exploiting zero and one bits imbalance in PCM TDM bit stream output encoding, discussing hardware implementation 12 p1785 A72-27845

Spectrum analysis of PCM/AM-FM and PCM/FM-FM telemetry signals, using approximation technique to Fourier transform time signal to frequency domain 13 p1919 A72-29025

Pulse signal transmission through bandpass error free wideband PCM communications systems 13 p1919 A72-29055

PCM speech transmission systems, comparing pseudorandomly dithered quantization with fixed level method by intelligibility and subjective appreciation tests and statistical analysis 14 p2087 A72-30942

Data transmission developments, considering computer improvements, networks, routes and frequency multiplexed PCM system 15 p2195 A72-31619

Incoherent optical communications fixed receiver passband, determining SNR for pulse time and code modulation with discrete time 15 p2195 A72-31622

Optical PCM communication system with megabits/sec information rate based on dye laser with combined frequency-time division multiplexing 15 p2198 A72-32060

Time division demultiplexing technique using two channel simulation of twenty-four channel digital optical PCM communication system 15 p2200 A72-32163

Serial PCM system for flight test data acquisition and reduction compared with Harrier system 16 p2364 A72-33644

Millimeter-wave solid-state exciter-modulator-amplifier module for gigabit data-rate. 19 p2771 A72-37267

Susceptibility measurements on PCM-FM and four phase differential PSK digital receivers simulated on analog computer 21 p3016 A72-40852

Feedback quantization noise effects on differential PCM systems, showing SNR relation to noise optimized prediction 21 p3017 A72-40860

Decision directed phase locked loops acquisition properties improvement technique for PCM bit synchronizer of random nonreturn to zero data 21 p3038 A72-40872

Increasing the linearity of the time scale of a time-amplitude-code converter 21 p3035 A72-41728

Dual mode - An efficient encoding method of nonsynchronous data signals on PCM. 21 p3023 A72-41827

Binary symmetric channel error effects on PCM color image transmission. 22 p3153 A72-41977

Application of digital techniques to the measurement of PCM signal power. 22 p3155 A72-42705

Symbol synchronization advances impact on PCM bit synchronizers design, discussing symbol detection and timing extraction circuits 22 p3155 A72-42706

A new optical PCM communication system 22 p3186 A72-42939

Computer-aided binary code sequence selection for data acquisition system in PCM-TDMA satellite communication, evaluating performance and reliability 24 p3379 A72-44779

On the S/N-characteristics in PCM systems for a class of signals with representative amplitude distributions. 24 p3380 A72-45282

PULSE COMMUNICATION

PM communication systems with Gaussian and clipped noise carriers, calculating SNR 01 p0024 A72-10129

Bit error rate estimation for narrow band digital communication in presence of atmospheric radio noise bursts 01 p0025 A72-10334

Digital telemetry/communication laser link system design for operation at 1 gigabit/sec

02 p0174 A72-12143

Wideband spectrum utilization above 10 GHz for high speed digital communications and ecological monitoring

02 p0176 A72-12182

Receiver detection characteristics for multiplicative processing of coherent signal pulses with unknown initial phase and slowly fluctuating amplitude

02 p0176 A72-12215

Power spectrum analysis of multilevel digital signals phased modulated by arbitrary pulse shapes, giving examples for rectangular and raised-cosine pulses

02 p0183 A72-12797

Correlation functions of signal and noise at output of discrete channel, determining SNR or speech intelligibility

03 p0323 A72-13891

Code performance evaluation over real digital channels, characterizing channel error process by multigap statistics

03 p0325 A72-14183

High speed digital communication over space to earth satellite links by quadriphase modulation, discussing modulator, receiver and system technology for maximizing data transfer

04 p0485 A72-14477

High speed digital communication at millimeter wavelengths, discussing system requirements, digital computer use, transmission data rate and equipment development

04 p0485 A72-14481

Nonrecursive and recursive adaptive equalizers for digital communication, discussing computerized simulation of performance

04 p0493 A72-15520

Pulse overlapping effects on phase jittering in carrier regeneration with quaternary phase shift keying

07 p0945 A72-19662

Digital simulation for predicting performance of data communication networks with computerized switching centers, detailing space shuttle interior communication system

07 p0952 A72-20364

On-line equalization of digital communication channels, discussing extended discrete Kalman filter use as adaptive equalizer

08 p1131 A72-20855

Laser pulse propagation measurements on multimode glass fibers to evaluate communication potential

09 p1323 A72-22868

Time dependent parallel and cross polarized electromagnetic pulse propagation in magnetoelectric medium for normal incidence

09 p1280 A72-23231

Auto and cross correlation functions of combined binary pseudorandom sequences in digital space communication systems

10 p1439 A72-24907

Narrow pulse optical communication digital systems with PPM and on-off keying, investigating timing error effects on bit error probabilities

11 p1592 A72-25885

Upper bound on probability of specified errors pattern occurrence for amplitude modulated digital communications systems subject to intersymbol interference and random noise

11 p1592 A72-25889

Alternating period compensation system velocity characteristics shaping problems, determining pulse repetition periods parameters by graph-analytical method

11 p1596 A72-26311

Message distortions analysis in PCM communications systems due to phase fluctuations of synchronization signal

11 p1598 A72-26728

Capacitive memory storage for filtration of repetitive pulse radio signals mixed with additive noise

11 p1598 A72-26734

Radio pulse synchronous detection with wideband preamplifier, evaluating frequency mismatch effects on signal distortion by transient response analysis

12 p1783 A72-27631

HF backscatter pulse signal incidence elevation angle measurements based on amplitude ratio of two antennas with different vertical patterns

12 p1783 A72-27779

Local FM radio pulse scattering by cylinder and linear cylinder array in Kirchhoff approximation

13 p1914 A72-28407

Pulse signal transmission through bandpass error free wideband PCM communications systems

13 p1919 A72-29055

Digital communication system for analog signal transmission by digital modulation techniques, presenting detection schemes

15 p2201 A72-32565

Correlation functions of signal and noise at output of discrete channel, determining SNR or speech intelligibility

15 p2202 A72-32702

TDM and FDM digital communication systems performance comparison, noting equivalence in theoretical efficiency and generated waveforms

16 p2363 A72-33216

Carrier synchronization and polyphase signal detection in digital communication network for high speed data transmission, deriving reconstructed noisy signal error probability

16 p2363 A72-33218

Error probabilities in digital communication systems subject to mixture of man made or natural impulsive and Gaussian noise

16 p2365 A72-34106

Propagation of pulsed-carrier signals in random media

17 p2514 A72-34380

Longitudinal pulses propagation in straight hollow circular elastic tubes, presenting strain-time records [ASME PAPER 72-APM-10]

17 p2629 A72-34806

A 5-kW peak transmitter for the 7-m wavelength

17 p2519 A72-35960

Optimal signal design for digital center of gravity feedback communications over white noise channels, using energy ratio functions

18 p2659 A72-36316

Air/ground digital communications in airline operations

18 p2660 A72-36561

Design of band-limited signal with no intersymbol interference - An extension of sampling function

19 p2767 A72-38606

Calculation of pulsed signal amplitudes at linear filter output in optical communication systems

19 p2768 A72-38671

Pulsed operation mode of acoustic system of damper-piezovibrator-layer load connected into electrical circuit of thyatron generator

19 p2805 A72-38764

Multimode dielectric waveguide with random coupling, discussing pulse dispersion improvement and loss penalty from power spectrum derivation

20 p2901 A72-38923

Electromagnetic compatibility enhancement during functional integration and operation of transmitters and receivers in digital communication systems

20 p2901 A72-38983

Interference performance degradation to digital systems

20 p2901 A72-38984

Automatic position reporting, ATC communication, weather information and message identification via digital ground-air-ground data link, discussing operational and maintenance requirements

21 p3080 A72-40286

Computer simulation of a digital satellite communications link

21 p3024 A72-40854

Signal transmission and detection in differentially encoded coherent multiple phase shift keyed digital communication systems, discussing carrier suppression-induced resolution ambiguity

21 p3017 A72-40861

Hybrid digital transmission systems based on optical fiber waveguides and analog repeaters, noting YAG laser light modulation by phase shift keyed sub-carrier

21 p3018 A72-40868

Injection laser and light emitting diode techniques to transmit digital data in local distribution

21 p3018 A72-40869

Reliability aspects of fading in microwave line of sight using digital transmission

21 p3019 A72-40887

Computer simulation of a digital satellite communications system utilizing TDMA and coherent quadriphase signalling

21 p3020 A72-40895

Phase noise types in digital satellite communication links, discussing continuous binary phase shift keyed modulation systems with coherent detection

21 p3020 A72-40896

Bandwidth economy for multiplexed digital signals

21 p3020 A72-40897

An irregular signal phase discriminator

21 p3033 A72-40943

Shaping circuit for complex RF pulse consisting of simultaneous equilength square pulses with different frequencies, discussing carrier frequencies selection

21 p3022 A72-41118

On a feedback communication system having iteration control in the forward channel

21 p3039 A72-41826

Characteristics of filtering the Rayleigh parameter of pulse signals in the presence of noise

22 p3154 A72-42228

Characteristics of an optimal algorithm for detecting Gaussian signals against a pulse noise background for receivers with a logarithmic amplifier

22 p3154 A72-42238

Wideband pulsed-RF phase measurement

23 p3270 A72-43575

On the performance of digital communication systems with bandpass limiters. I - One-link system. II - Two-link system

23 p3265 A72-44181

SECANT midair collision avoidance system based on nonsynchronous microsec pulse transmission and receiving via randomly selected frequency, describing modular components and operating principles

24 p3422 A72-44647

PULSE COMPRESSION

Pulse compression of radar signals by ultrasonic liquid delay line, stressing wideband damped electroacoustic transducers construction

01 p0044 A72-11321

Satellite-borne radar altimetry pulse compression, discussing signal return statistics, receiver models and detected waveshape relation to altitude, attitude and antenna beamwidth errors

02 p0172 A72-11870

Mean value, repetition and discontinuity errors of spectral transposition method involving memory storage and compressed signal processing

03 p0338 A72-13892

Short duration high peak power laser pulses generation and measurement, examining active and passive mode locking, chirping, pulse compression and optical pumping

04 p0530 A72-14735

Frequency domain representation of Doppler invariant FM signal defining matched pulse compression filter

04 p0507 A72-15693

Q switched high power laser pulse compression based on optical polarization change on passing through Kerr-active medium

07 p1000 A72-19038

Range sidelobe suppression technique for Barker type phase reversal codes in digital processor for pulse compression

08 p1133 A72-21404

Ultrasonic imaging technique based on optical pulse compression, noting image forming and range discriminating capability

12 p1808 A72-27677

Acoustic surface wave chirp filters application in pulse compression radar system, considering various piezoelectric substrate materials characteristics

14 p2089 A72-31045

Statistical analysis of random mismatched tapped delay line filters effect on binary phase shift keying pulse compression codes peak-to-sidelobe and SNR

15 p2196 A72-31792

Mean value, repetition and discontinuity errors of spectral-transposition method involving memory storage and compressed signal processing

15 p2212 A72-32703

Mode locked lasers, investigating effect of grating-induced phase and spatial modulations by multiple transverse modes on pulse compression across beam cross section

16 p2403 A72-33840

Incoherent scatter observations at Arecibo using compressed pulses

18 p2659 A72-36299

Cross-ambiguity function for a linear FM pulse compression radar

19 p2764 A72-37868

Correction of diffraction errors in acoustic-surface-wave pulse-compression filters

21 p3034 A72-41464

Variable-bandwidth frequency-modulation chirp pulse compression using a longitudinal acoustic-wave convolver at 1.3 GHz

21 p3023 A72-41468

Effect of envelope limiting in pulse-compression moving-target-indicator radar systems

24 p3380 A72-45575

GaAs semiconductor injection laser and amplifier-absorber emission and light pulse transmission characteristics determination, noting nonlinear absorptivity, bleaching threshold and pulse compression factor

24 p3412 A72-45619

PULSE DIFFRACTION

Ultrasonic diffraction loss and phase change for broad-band pulses

23 p3313 A72-44115

High power monopulse laser with a stabilized spectrum and radiation directivity close to that of diffraction

24 p3410 A72-45422

PULSE DOPPLER RADAR

NT MONOPULSE RADAR

NT PULSE RADAR

Pulsed Doppler radar loss of detection probability due to echo signal misalignment, discussing distance measurement refinement by interpolation

02 p0179 A72-12571

Real time coherent optical processor of pulse Doppler radar signals with Fresnel diffraction masks for PCW target range rate determination

03 p0322 A72-13437

Range rate prediction algorithm for pulse Doppler ambiguity resolution by invariant imbedding method

07 p0941 A72-19303

PULSE DURATION

Burst and quasi-continuous forms atmospheric radio noise short term characteristics above different thresholds, considering pulse duration and spacing

01 p0031 A72-10998

Pulse widths formed by relativistic beaming pulsars effect on emission spectra 01 p0133 A72-11130

Picosecond pulse production and measurement from mode locked Nd glass laser 02 p0238 A72-12492

Radio telescope variable profile antenna autocollimation adjustment for separating transmitted and received signals pulse-time characteristics 02 p0231 A72-12521

Acoustic wave excitation in water droplet with giant pulse radiation from Q switched laser, noting diffraction effects on laser power density requirement 03 p0367 A72-13372

Intense pulsed electron beam production by current flow through narrow gap filled with plasma 03 p0396 A72-13656

Pulsed injection laser current pulse height, width and rise time controls, comparing use of tube, transistor and SCR discharge circuits 04 p0528 A72-14420

Mode-locked transversely excited atmospheric pressure carbon dioxide laser pulse duration dependence on cavity modulation frequency and loss 04 p0529 A72-14588

Short duration high peak power laser pulses generation and measurement, examining active and passive mode locking, chirping, pulse compression and optical pumping 04 p0530 A72-14735

Declination, average pulse energy and pulse shape of weak pulsars, determining barycentric period 04 p0574 A72-14981

Ultrashort light pulse emission during mode locking in ruby lasers in free emission operation, examining first spike radiation 05 p0668 A72-16413

Flash photolysis HF chemical laser pulse delay measurements, showing pressure, flash lamp intensity and optical cavity loss dependence 05 p0668 A72-16606

Cracks interactions with transversal and surface elastic waves, relating crack propagation threshold conditions to critical pulse duration 06 p0893 A72-17419

Dye laser system with narrow linewidth oscillator, transverse mode selector, power amplifier and nitrogen pumping, noting 50 kw and 5 nsec pulse generation capability 07 p1002 A72-19209

Unipolar pulsed plasma accelerator, describing trigatron circuit design for generation of 100 kA unipolar current pulses of 35 microsec duration 07 p1040 A72-19316

Pulsed voltage oscillator for nanosecond range operation under pressure in nitrogen-filled tank as conducting shield 07 p0946 A72-19957

Low induction 500-kV 1-microsecond 5-kJ pulsed voltage generator, discussing design features 07 p0946 A72-19958

Optimum pulse duration for ionospheric oblique backscatter sounding, determining receiver signal power input dependence on pulse duration 08 p1131 A72-20820

Pulse duration reduction with power gain during second harmonic generation by nonlinear crystal in Q switched buildup resonator 08 p1183 A72-21729

Subnanosecond light pulse generation by Ne laser at 5401 Å by amplified spontaneous emission 09 p1323 A72-22869

Pulse shaping, arc plasma jets and torch movement indexing for high precision pulsed tungsten inert gas/TIG/welding 09 p1321 A72-23635

Carbon dioxide-helium-nitrogen laser with non-linearly absorbing cell, presenting emission pulse duration and rate 11 p1646 A72-25712

Semiconductor laser thermal resistance and time constant evaluation, obtaining operating temperature range and maximum attainable pulse width 11 p1647 A72-25808

Pulse width relationship to frequency broadening during self phase modulation of propagating short laser pulse 11 p1647 A72-26151

Ultrashort pulse lasing techniques, covering mode formation, secondary effects and two photon recording of emission structures 11 p1652 A72-26792

High power light pulse generation with steep leading edges in Nd-glass laser, noting duration change based on transparency increase under light transmission 12 p1820 A72-27583

High power pulse generation by ruby laser under free oscillation, using resonator with dielectric mirrors 12 p1821 A72-27597

Heat conduction heating of plasma by high power ultrashort laser pulse incident on solid target, noting focusing and energy absorption role 12 p1852 A72-27622

Pulsar 21 cm pulse profile measurement, discussing installation design and operational principles 12 p1872 A72-27809

Resonant interaction and self transparency effect of coherent ultrashort light pulse passing through semiconductor 12 p1824 A72-27868

High brightness picosecond light pulses generation by laser with multiple internal reflection amplifier for plasma heating 12 p1824 A72-27872

Pumping current pulse duration effect on lasing threshold of injection lasers with diffusion junctions and heterojunctions in GaAs-AlAs system 12 p1824 A72-27877

Picosecond pulse efficient second harmonic generation by crystals inside high power dye mode locked Nd-glass laser folded cavity 12 p1826 A72-28220

Pulse energy and temporal width produced in self locking operation of laser with homogeneous gain line 13 p1968 A72-28686

Electroexplosive devices firing energy parameters determination by capacitor discharge system providing exponential pulses terminated at adjustable width 14 p2143 A72-30200

Laser radiation time characteristics measurement based on multiphoton processes in opposite light beams, estimating accuracy necessary for registration of ultrashort pulses 14 p2111 A72-30794

Short signal pulse shaping based on phase and amplitude selective properties of distributed parametric amplifiers operating under nonlinear conditions 14 p2090 A72-31112

Foveal light pulse duration effects on reaction time, showing stimulus intensity-time reciprocity 15 p2188 A72-31509

Dye-induced saturated frequency sweeping effects on mode-locked laser pulse broadening and substructures 15 p2250 A72-32523

High speed photography ultrafast shutter based on polymethine cyanide dyes saturability for measuring mode locked ruby laser pulse duration 15 p2241 A72-32535

Electro-optical Q switch synchronized by laser radiation for nanosecond light pulse shaping with energy dependent triggering 16 p2400 A72-33082

Hybrid low power consumption magnetic/fluidic pulse shortener for fluid logic control circuits consisting of short cylindrical chamber with input and output port 16 p2350 A72-33179

Pulsar pulse broadening due to multiple scattering by interstellar medium, finding exponential decay time constant relation to rms broadening of angular size 16 p2457 A72-33686

Time variable pulse front fluctuations effect on random error in digital pulse duration measurements 16 p2395 A72-33953

Resonant interaction and self transparency effect of coherent ultrashort light pulse passing through semiconductor 16 p2403 A72-33977

Pumping current pulse duration effect on lasing threshold of injection lasers with diffusion junctions and heterojunctions in GaAs-AlAs systems 16 p2404 A72-33986

Oriental Kerr effect direct observation via birefringence relaxation time measurement in self focusing region of mode locked Q switched laser picosecond pulses 17 p2561 A72-34190

Pulse length evaluation from frequency domain phase function, applying to mode locked laser theory 17 p2562 A72-34292

Radio pulse shaping network synthesis composed of lumped elements, noting pulse duration limitation by network efficiency 17 p2533 A72-34837

Excitation of a long-pulse CO2 laser with a short-pulse longitudinal electron beam 17 p2565 A72-35815

Off-axis hologram recording on thin bismuth film with picosecond pulse train from mode-locked Nd-glass laser 17 p2558 A72-35817

Doppler Q switching in a single-mode CO2 laser by a rotating mirror 19 p2812 A72-38594

An aspect of the problem of pitch dependence on the duration of short sinusoidal signals 20 p2897 A72-39217

Single-mode laser with a continuously variable pulse duration 20 p2933 A72-39511

Q switched Nd-YAG laser with lithium niobate crystal cut at Brewster angle for reproducible and controllable giant pulse generation 20 p2933 A72-39562

One-to-one telescope with pressurized Ar gas for nanosecond and picosecond laser output pulse sensitive detection via gas breakdown and energy absorption 21 p3062 A72-40618

Low cost design of linear pulse stretcher circuit for short duration pulse time measurement in nuclear instrumentation and computing counters 21 p3033 A72-40997

Q-switched CO2 lasers with variable pulse delay 21 p3064 A72-41006

The detectability of a brief gap in a pulse of light as a function of its temporal location within the pulse 21 p3002 A72-41023

Linear analog to pulsewidth converter insertion into control loop in dc/dc regulators for space applications to permit high sampling frequencies 21 p2997 A72-41081

Observation of transient behavior of picosecond laser pulses 21 p3064 A72-41380

A threshold device for establishing the time of pulsed signals 21 p3035 A72-41727

Influence of instantaneous and prolonged pulses on the oscillations of timing-device oscillators 21 p3059 A72-41815

Investigation of the shape of the radiation pulse of a self-mode-locked laser 23 p2394 A72-43303

Fluctuation mechanism of ultrashort pulse generation by laser with saturable absorber 23 p2397 A72-44184

Interferometric measurement of the elongation of a pulsed diode laser 23 p2397 A72-44185

Experiment for studying the pulse shape of Cerenkov emission at large distances from an extensive air shower 23 p3330 A72-44420

A new method of optical coupling of two laser cavities which permits stable generation of ultrashort optical pulses 24 p3410 A72-45075

Control of laser pulse duration by nonlinear absorption in semiconductors 24 p3411 A72-45605

PULSE DURATION MODULATION

Pulse width modulated transistor series inverter with inductor transformer in low power applications, noting short circuit and no-load protection 01 p0007 A72-11060

Noise reduction in pulse width modulated converters with rms voltage values digital readout, using active or passive filters methods 03 p0331 A72-13557

Analytical design of pulse width modulated systems with time constant and delay for electronic control, using Z transform 10 p1457 A72-24458

Pulse width modulated regulating dc-to-dc converter with small number of transistors to improve circuit reliability 10 p1452 A72-24680

Output voltage characteristics of single phase thyristor inverter based on pulse duration modulation with direct shaping of control pulses, considering harmonic coefficients 11 p1603 A72-25277

Period modulation of HF oscillation by symmetrical and asymmetrical signals applied to detection in noise 11 p1597 A72-26318

Suppressed clock pulse duration modulation for noisy voice communication channels with hard limiting satellite repeaters, discussing system design and test data 21 p3020 A72-40898

A generator with a pulse-width modulator, producing arbitrarily shaped high voltage 21 p3058 A72-41734

Global asymptotic stability of two classes of control system with pulse-width and pulse-frequency modulation 22 p3162 A72-42184

PULSE FREQUENCY MODULATION

Integrated PFM feedback control system, investigating stable periodic oscillation based on nonlinear discrete equivalence 04 p0506 A72-15114

Optimal detection of Markov radio signals with intrapulse FM using nonlinear filtration theory 04 p0487 A72-15146

Russian papers on discrete control systems covering inertialess Markov objects, pulse amplitude and frequency modulation and statistical analysis 11 p1609 A72-25442

Approximate statistical analysis of PFM and combined modulation systems, proposing linearization method 11 p1609 A72-25447

Extremal feedback control system operation with integral PFM in extremum drift mode, determining equations of motion and steady state regime 11 p1610 A72-25449

Asymptotic stability of astatic pulse frequency modulated feedback control systems with discrete correction, obtaining sufficient conditions in closed form with Liapunov method 11 p1610 A72-25450

Data processing in isolated crab biological strain receptor formed by muscle, transducer and encoder, noting pulse frequency modulation in encoding process

12 p1771 A72-27577

Evaluation of the basis parameters of a frequency-code receiver with a generalized differential circuit

19 p2771 A72-37304

Determination of the spectra of modulated pulse trains by the spectral function method

22 p3154 A72-42122

Global asymptotic stability of two classes of control system with pulse-width and pulse-frequency modulation

22 p3162 A72-42184

PULSE FREQUENCY MODULATION TELEMETRY
Europa 2 launch vehicle standardized PCM/FM and FM/PM telemetry system compared with Europa 1

05 p0630 A72-16751

PULSE GENERATORS

Avalanche pulse generator with pretrigger output for reflection coefficient and step function response measurements

02 p0195 A72-12605

Solid state tunnel diode amplifier-rectifier expander for microwave pulse regenerators

03 p0335 A72-14184

Gaussian envelope microwave pulse generation using absorption p-i-n diode modulator, predicting performance by digital simulation

04 p0498 A72-14718

Electromagnetic solitary waves /solitons/, noting medium macroscopic motion absence and parametric pulse generation

04 p0489 A72-15387

Pulsed cylindrical converging shock wave generation in decreasing density medium by axial explosion-implosion discharge

05 p0700 A72-17233

Unipolar pulsed plasma accelerator, describing trigger circuit design for generation of 100 kA unipolar current pulses of 35 microsec duration

07 p1040 A72-19316

Pulsed voltage oscillator for nanosecond range operation under pressure in nitrogen-filled tank as conducting shield

07 p0946 A72-19957

Low induction 500-kV 1-microsecond 5-kJ pulsed voltage generator, discussing design features

07 p0946 A72-19958

Oscillatory shock pulse reproduction with specified spectrum for performing shock testing with electrodynamic or electrohydraulic shaker-amplifier-equalizer system

07 p0965 A72-20199

Stainless steel circular tubes size and fittings effects on pneumatic pulse wave distortion and attenuation in fluidic pulse generation system

08 p1111 A72-20928

Transistorized static pulse generators for spark erosion machining, discussing operating principle, design, applications, automatic control system and maintenance procedures

08 p1146 A72-21038

TEA atmospheric pressure carbon dioxide laser driven by 200 kV Marx generator pulse

08 p1183 A72-21800

Subnanosecond light pulse generation by Ne laser at 5401 A by amplified spontaneous emission

09 p1323 A72-22869

Digital pulse programmer with saturation burst sequence for pulsed nuclear magnetic resonance spectroscopy

12 p1806 A72-27125

Receptor membrane pulse generation electronic model with tunnel diode negative resistance circuit

12 p1771 A72-27578

Giant pulses generation by ruby laser under self Q switching conditions

12 p1821 A72-27592

Pulse generation in planar Gunn devices of epitaxially grown GaAs layers, measuring current reduction by domain nucleation

12 p1791 A72-27671

Coaxial integrated pulse generator and gas laser with double transmission line for energy storage, noting design parameters selection

12 p1823 A72-27700

Picosecond pulse efficient second harmonic generation by crystals inside high power dye mode locked Nd-glass laser folded cavity

12 p1826 A72-28220

Microwave device phase and amplitude frequency response measuring equipment with wide range test pulse generation, discussing design and performance

13 p1934 A72-30091

Dc X ray timing pulse generator for light gas gun triggering based on projectile interruption technique

15 p2241 A72-32441

Generator for data transmission lines stochastic noise bursts simulation with statistically independent burst durations and intervals

15 p2201 A72-32475

High voltage dc arc interrupter for use in high power pulse generators and switching application in high voltage dc power transmission system

15 p2201 A72-32569

Shift register implemented binary transversal filter type digital pulse waveform generators truncation and approximation error spectrum analysis via inverse Fourier transform

16 p2362 A72-32854

High voltage single nanosecond pulse generator for variable load using commutator with shaping line charging circuit

16 p2368 A72-33077

High voltage nanosecond pulse generator triggered by laser radiation from transmission stripline discharger for multichannel synchronous operation

16 p2404 A72-33083

Room temperature vibrational relaxation measurements in gases subsequent to laser pumping by picosecond pulse generated transient stimulated Raman scattering

16 p2401 A72-33389

High brightness picosecond light pulses generation by laser with multiple internal reflection amplifier for plasma heating

16 p2403 A72-33981

Active elements for high power Nd-glass laser facility to generate short and ultrashort pulses

16 p2404 A72-33990

Pulsed power - A new technology for controlled thermonuclear fusion.

18 p2715 A72-36332

A solid-state transponder source using high-efficiency silicon avalanche oscillators.

19 p2774 A72-38400

High power microwave nanosecond pulse generator with waveguide standing wave resonator, noting power gain and pulse shape

19 p2776 A72-38672

A fast, high repetition rate avalanche transistors pulser for capacitive loads.

20 p2907 A72-39435

Pulse generator for modulation of a low-voltage Pockels cell.

20 p2933 A72-39525

Q switched Nd-YAG laser with lithium niobate crystal cut at Brewster angle for reproducible and controllable giant pulse generation

20 p2933 A72-39562

A simple reference generator for lock-in amplifiers.

21 p3025 A72-40206

Neutron production in exploding-wire discharges.

21 p3089 A72-40338

Snap-off diodes for avalanche generators step pulse output rise time steepening, describing circuit diagram and time-volt-ampere characteristics

21 p3035 A72-41650

A generator with a pulse-width modulator, producing arbitrarily shaped high voltage

21 p3058 A72-41734

Fluctuation mechanism of ultrashort pulse generation by laser with saturable absorber.

23 p3297 A72-44184

A new method of optical coupling of two laser cavities which permits stable generation of ultrashort optical pulses

24 p3410 A72-45075

PULSE HEATING

Laser pulse heating inability to quench in disorder in Fe-Al alloy

05 p0669 A72-16796

Pulsed arc TIG welding with modulation of current from standard power source, comparing performance with steady dc method

09 p1320 A72-23632

High temperature gradients in pulsed heated Mo specimen under vacuum, using photomicrographic technique

11 p1629 A72-25267

Laser pulse form effect on confined plasma heating, taking into account inverse electron-ion bremsstrahlung and stimulated Compton scattering

11 p1651 A72-26672

Theta pinch plasma heating by carbon dioxide laser transverse pulses, substantiating theoretical considerations by experimental observations

16 p2439 A72-33989

Measurement of melting point and electrical resistivity /above 3600 K/ of tungsten by a pulse heating method.

20 p2941 A72-39722

Measurement of the thermal diffusivity of semiconductors by the light pulse technique

21 p3095 A72-40133

Effect of the rate of pulsed heating of a bar on the magnitude of the thermoelastic stresses

21 p3126 A72-41548

Possible mechanisms of turbulent heating of a plasma by ultrashort laser emission pulses

21 p3095 A72-41823

Electric resistance and enthalpy of molybdenum and tungsten

23 p3272 A72-44167

PULSE HEIGHT

U PULSE AMPLITUDE

PULSE MODULATION

NT DELTA MODULATION

NT PULSE AMPLITUDE MODULATION

NT PULSE CODE MODULATION

NT PULSE DURATION MODULATION

NT PULSE FREQUENCY MODULATION

NT PULSE FREQUENCY MODULATION

TELEMETRY

NT PULSE POSITION MODULATION

NT PULSE TIME MODULATION

PM communication systems with Gaussian and clipped noise carriers, calculating SNR

01 p0024 A72-10129

Modulation/demodulation techniques for optical one-gigabit/sec intersatellite data transmission link system, comparing per-unit data costs for system selection

02 p0174 A72-12142

Pulse modulator thyristor circuit design and optimum operating conditions for driving high peak power radar magnetron

02 p0195 A72-12694

Millimeter wave pulse signal transmission path length modulator with P-I-N diode switch, discussing system design and experimental results

02 p0196 A72-12798

Spatial pulse modulation of optical signals for use in picture transmission, cinematography and holography

03 p0358 A72-13440

Time-optimal mathematical models operating with low-frequency pulse-frequency-modulated input information converted to an intermediate digital code

17 p2524 A72-35786

Stability of nonlinear automatic systems with double pulse modulation, discussing systems with linear and nonlinear pulse elements

19 p2777 A72-37435

An optical communication system using envelope modulation.

19 p2766 A72-38604

Saturation protection of a maser amplifier by the pulse-modulated pumping method

21 p3063 A72-40785

Pulse modulation of a laser during the tuning of an auxiliary passive resonator with the aid of ultrasound

22 p3186 A72-42666

PULSE POSITION MODULATION

Imperfect timing degradation of direct detection /noncoherent/ optical system using pulse position modulation bits

02 p0174 A72-12141

Pulse position modulation system for minimizing rf blackout during 2 kW S band reentry telemetry transmission

02 p0175 A72-12158

Pulsed coherent radar with pulse position random modulation, discussing subclutter visibility, target attenuation and blind speeds cancellation and radial speed measurement without range ambiguities

06 p0775 A72-18184

Receivers for PPM optical communication and pulsed signal detection in background light, evaluating upper bounds on error probability based on photoelectron Poisson statistics

11 p1591 A72-25311

Dual threshold temporal fixation of pulse signal from two points on leading edge

13 p1914 A72-28410

Energy spectra of mixed discrete random processes in statistical multiplexing systems with pulse position, delta and pulse code modulation

13 p1919 A72-29054

PULSE RADAR

NT MONOPULSE RADAR

Clutter suppression by amplitude weighted pulse trains in coherent radar, obtaining optimum weights and signal-to-clutter gain as function of Doppler frequency

01 p0030 A72-10789

Approximate signal-clutter ratio formulas for airborne pulse radar system, eliminating computer calculations

02 p0176 A72-12216

Optimal synthesis of pulse repetition frequency control and filtering circuits of radar range finder in Gaussian approximation

02 p0183 A72-12759

Detection characteristics of optimal interperiod processing radar pulse systems for arbitrary correlation of signal and noise fluctuations

04 p0487 A72-15145

Pulse and Doppler microwave radars comparison with respect to accuracy of moving targets velocity measurements and power characteristics

05 p0661 A72-16034

Probability formula for pulse coincidence frequency from different independent radars

05 p0629 A72-16579

Amplitude and phase modulated radar pulse train representation by complex number sequences, discussing generation, processing, and Z transform application to combination codes

06 p0773 A72-17495

Pulsed coherent radar with pulse position random modulation, discussing subclutter visibility, target at-

tenation and blind speeds cancellation and radial speed measurement without range ambiguities

06 p0775 A72-18184

Microwave instrument landing systems based on continuous radar scanning technique, using pulse format for data transmission

06 p0846 A72-18399

Coherent radar pulse train clutter performance prediction for targets with range acceleration effects on Doppler response

08 p1133 A72-21405

Radar tracking pulse scheduling in dense target environment with position estimation error constraints to avoid false return with track correlations

08 p1134 A72-21407

Spurious target generation due to hard limiting in pulse compression radars with three phase coded signals superposed at input, comparing with digital simulation

08 p1134 A72-21416

C-band pulse beacon ranging system for collision avoidance, detailing interrogation, response and system test modes

09 p1349 A72-22908

Pulse radar radio altimeter for balloon atmospheric sounding

10 p1484 A72-25088

Amplitude-time quantization of radar pulse signals in analog-digital converter, improving noise threshold and ranging accuracy

11 p1595 A72-26294

Operation analysis of automatic range finders in pulse radars regarding target search and lock-on functions

11 p1595 A72-26300

Pulse-pulse frequency agility influence on radar detection in sea and rain clutter with decorrelation, eliminating multiple-time-around echoes

13 p1917 A72-28695

Pulse radar equipment for meteor height measurement from nonsaturated trails by phase difference method

13 p1929 A72-29028

Passive clutter region and reflecting area calculation for ground surface illuminated by pulse radar antenna

13 p1919 A72-29053

Acoustic surface wave chirp filters application in pulse compression radar system, considering various piezoelectric substrate materials characteristics

14 p2089 A72-31045

Monostatic radar measurement for incoherent scatter correlation function in lower ionosphere, using spaced short pulses transmission to obtain adequate height resolution

15 p2200 A72-32106

RF time domain nonreal time reflectometer operating as nanosecond radar with pulse spectrum lines reflections measured and stored for echo computation

19 p2770 A72-37256

Postdetection integration loss for logarithmic detectors.

19 p2763 A72-37295

Cross-ambiguity function for a linear FM pulse compression radar.

19 p2764 A72-37868

Studies of vertical motions in cloud systems by using a coherent pulse radar in the decimeter wavelength range

19 p2829 A72-38773

Optimal synthesis of pulse repetition frequency control and filtering circuits of radar range finder in Gaussian approximation

20 p2902 A72-39065

Weighting factor and transmission time optimization in video MTI radar.

21 p3022 A72-41082

Optimal receivers for measuring time lags of pulse signals in the presence of fading

22 p3154 A72-42123

Faraday effect of incoherently scattered radar signals

23 p3263 A72-43365

Wideband pulsed-RF phase measurement.

23 p3270 A72-43575

Effect of envelope limiting in pulse-compression moving-target-indicator radar systems.

24 p3380 A72-45575

PULSE RATE

Human pulse wave propagation velocity measurement, using biotelemetry system of photoresistance sensors and endoscopic bulbs connected to electrocardiograph

02 p0169 A72-12519

Self pulsed electrically initiated HF and DF chemical laser with high pulse repetition frequency gain switched operation

06 p0826 A72-18458

Transversely excited atmospheric (TEA) carbon dioxide laser in single pulse and high repetition rate operation

07 p1003 A72-19220

Picosecond pulse distortion under multimode conditions in optical fiber communication systems

07 p0940 A72-19231

Uncooled GaAs injection laser with high pulse repetition rate, discussing structural features and current-power characteristics

08 p1181 A72-20748

Pulse rate and pumping power effects on emission spectra and I-V characteristics of multielement GaAs injection lasers

08 p1181 A72-20796

Carbon dioxide-helium-nitrogen laser with nonlinearly absorbing cell, presenting emission pulse duration and rate

11 p1646 A72-25712

Alternating period compensation system velocity characteristics shaping problems, determining pulse repetition periods parameters by graph-analytical method

11 p1596 A72-26311

Pneumatic thermistor transducer to measure steep ejection time interval between cardiac volume pulse upstroke start and maximum rise rate occurrence

11 p1588 A72-26633

Second, third and fourth optical harmonics generation of Nd-doped YAG laser radiation under Q switching fast repetition pulse conditions

12 p1821 A72-27594

TEA carbon dioxide laser time dependent gain and cavity losses analysis, using lasing onset delay with current pulse

14 p2109 A72-30184

Pulse nitrogen laser at high repetition rate.

19 p2813 A72-38696

Changes in the impulse activity of cortical neurons during selective reinforcement of a chosen range of their interpulse intervals

23 p3257 A72-44087

PULSE RECORDERS

U COUNTERS

PULSE TIME MODULATION

NT PULSE DURATION MODULATION

NT PULSE POSITION MODULATION

Incoherent optical communications fixed receiver passband, determining SNR for pulse time and code modulation with discrete time

01 p0024 A72-10198

Decoder for delay-modulated digital data conversion to nonreturn to zero data, discussing time-phase ambiguity resolution capability in real time

01 p0025 A72-10331

Incoherent optical communications fixed receiver passband, determining SNR for pulse time and code modulation with discrete time

15 p2195 A72-31622

Increasing the linearity of the time scale of a time-amplitude-code converter

21 p3035 A72-41728

Analysis of the basic metrological characteristics of Vernier time-pulse converters

21 p3035 A72-41729

PULSE WIDTH

U PULSE DURATION

PULSE WIDTH AMPLITUDE CONVERTERS

Noise reduction in pulse width modulated converters with rms voltage values digital readout, using active or passive filters methods

03 p0331 A72-13557

A differential-integral amplitude-time converter of nanosecond-range pulses

19 p2771 A72-37305

PULSE WIDTH MODULATION

U PULSE DURATION MODULATION

PULSED JET ENGINES

System tradeoffs for high performance pulsed MPD thruster in space mission application

[AIAA PAPER 72-457] 11 p1708 A72-26193

Quasi-steady MPD thruster system, discussing gas injection, electronic synchronization and electrolytic pulse forming network

[AIAA PAPER 72-461] 11 p1613 A72-26196

Near field megawatt single shot exhaust flow and propulsion characteristics of pulsed MPD arc thruster

[AIAA PAPER 72-500] 11 p1711 A72-26223

Solid propellant pulsed plasma microthruster performance tests, describing engine design and operation

[AIAA PAPER 72-460] 13 p2026 A72-28945

One dimensional theory of electric discharge detonation effects in flame propagation within square duct with combustible gas mixture, applying to electrochemical pulse jet engine

24 p3464 A72-45064

PULSED LASERS

NT Q SWITCHED LASERS

Internal electrostatic field effect on ion separation in expanding pulsed laser produced plasmas

01 p0105 A72-10021

Parametric amplification of laser waves with amplitude and phase modulation under exponential signal growth applied to Raman scattering picosecond pulse field

01 p0079 A72-10346

Gas bubble damage centers in organic glass produced by quasi-steady ruby laser pulse induced high temperature heating, using high speed photography

01 p0079 A72-10373

Pin electrode transversely excited atmospheric pressure carbon dioxide laser construction and pulse power outputs up to 60 kW

[AD-738684] 01 p0079 A72-10516

Airborne and spaceborne remote measurement and mapping of atmospheric nitric oxide, describing system configuration with mono or bistatic and pulsed or CW laser

[AIAA PAPER 71-1112] 01 p0068 A72-10556

Precision phase indicating pulsed optical range finder, using uncooled semiconductor laser

01 p0080 A72-10621

Clad-to-core bond testing in radioisotope irradiation strips by pulsed laser ultrasonic schlieren system

01 p0080 A72-10811

Acousto-optical extraction of energy stored in pulsed He-Ne laser cavity, using modulator with piezoelectric transducer at light-ultrasound interaction region

01 p0081 A72-11322

Nuclear radiation enhancement of carbon dioxide laser performance, discussing low pressure CW and high pressure pulsed discharges

01 p0082 A72-11330

Pulsed laser emission in carbon monoxide, calculating molecular excited state populations

02 p0237 A72-11471

Mode locked He-Ne laser for optical communication, investigating steady state pulse behavior from injection locking theory

02 p0237 A72-11559

Pulsed ruby laser with complex mirror resonator including optical delay line, observing mode locking effects in emission dynamics

02 p0238 A72-12290

Picosecond pulse production and measurement from mode locked Nd glass laser

02 p0238 A72-12492

Sequential dielectric breakdown of air by focused radiation from mode locked pulsed carbon dioxide TEA laser

03 p0366 A72-12966

Laser pumping pulse shape effects on second harmonic emission waveform during nonlinear crystal excitation by ultrashort light pulse

03 p0366 A72-13368

Two photon method of measuring ultrashort pulses and nonlinear optical effectiveness of lasers in synchronized mode

03 p0369 A72-14063

Pulsed injection laser current pulse height, width and rise time controls, comparing use of tube, transistor and SCR discharge circuits

04 p0528 A72-14420

Atmospheric pressure pulsed carbon dioxide laser using preionization by injected high energy electrons from surrounding glow discharge, obtaining highest output from gas mixture

[AD-746376] 04 p0529 A72-14586

Mode-locked transversely excited atmospheric pressure carbon dioxide laser pulse duration dependence on cavity modulation frequency and loss

04 p0529 A72-14588

Pulsed nitrous oxide molecular laser upper energy level relaxation time measurement by afterglow pulse-gain technique

04 p0529 A72-14601

Pulsed Ar ion laser quantitative level population mechanism in gas discharges, discussing radiation trapping effects on 4s doublet based on spontaneous emission line data

04 p0529 A72-14602

Book on optics covering gas lasers, power output vs frequency, picosecond laser pulses, Q switching principles, mode locking, optical propagation through turbulent atmosphere, etc

04 p0548 A72-14733

Short duration high peak power laser pulses generation and measurement, examining active and passive mode locking, chirping, pulse compression and optical pumping

04 p0530 A72-14735

Digital measurement of pulsed laser energy, using planar vacuum photodiode detector with photocurrent capacitive integration and voltmeter display

04 p0530 A72-14921

Pulsed chemical laser started by transverse electrical discharge, observing output energy dependence on fluorine compound used

04 p0530 A72-14974

Pulsed Nd laser beam polarization components energy measurement by double reflecting plate calorimeter, checking accuracy against NBS liquid cell calorimeter

04 p0531 A72-15479

Visual display IR spectrometer for pulsed transversely excited carbon dioxide laser, tabulating observed wavelengths

[AD-740011] 04 p0524 A72-15540

Pyroelectric detector noise equivalent power limitation factors, discussing heterodyne systems and pulsed submillimeter lasers detection

04 p0551 A72-15602

Giant pulse ruby laser operated at 6 Hz, describing shutter, shutter control unit, cooling system and electrical power supply and control circuits

05 p0667 A72-16035

Laser radiation amplification, investigating opposing laser pulses interaction in plasma

05 p0668 A72-16414

Laser pulse induced stimulated Raman scattering /SRS/ in linearly dispersionless medium measuring delay between laser and Stokes pulse maxima by photon absorption fluorescence technique

05 p0693 A72-17170

Passive nonlinear output coupler for mode-locked high power picosecond pulse laser, using optical Kerr effect

05 p0670 A72-17190

Pulsed ruby laser and photopolymer materials applications to holography, considering research programs for surmounting difficulties

06 p0813 A72-17427

Heating dynamics of transparent dielectrics exposed to pulsed laser beam operating in free laser mode

06 p0825 A72-17697

Single pulse Nd laser with KDP cascade multipliers and tunable frequency converter using organic dye solution

06 p0825 A72-17841

Low energy per pulse high repetition rate laser radar capabilities for atmospheric density measurement above 30 km

06 p0775 A72-18093

Laser beam welding by solid state pulsed lasers, discussing heat conduction relation to power density utilization

06 p0822 A72-18254

Self pulsed electrically initiated HF and DF chemical laser with high pulse repetition frequency gain switched operation

06 p0826 A72-18458

Atmospheric pressure pulsed chemical laser based on reaction between fluorine and hydrogen or deuterium

07 p0999 A72-18877

Laser triggered avalanche transistor voltage generator for picosecond streak camera used in laser pulse diagnostics

07 p0999 A72-18881

Kinetic model for gas dynamic laser energy extraction from carbon dioxide-nitrogen-helium mixture, predicting gain, saturation and pulse length

07 p1001 A72-19195

Pulsed ruby laser mode structure effects on quartz damage, noting dependence on propagation and polarization directions with crystal

07 p1001 A72-19196

High voltage axially pulsed carbon dioxide laser performance test, determining output energy dependence on tube parameters

07 p1001 A72-19197

GaAs junction laser, determining second order dispersion in mode locking and self pulsing from output field amplitude correlation measurement

07 p1001 A72-19198

Second order mode locked GaAs junction laser, observing mode frequencies and phases configurations during self pulsing

07 p1001 A72-19200

High power UV light pulse generation using Nd-YAG laser with frequency doubling

07 p1002 A72-19202

Dye laser system with narrow linewidth oscillator, transverse mode selector, power amplifier and nitrogen pumping, noting 50 kw and 5 nsec pulse generation capability

07 p1002 A72-19209

High intensity pulsed laser beam heating of solid transparent materials

07 p1002 A72-19212

Single mode high power pulsed nitrogen/carbon dioxide laser with unstable resonator coupling and diffraction limited focusing

07 p1002 A72-19215

Pulsed combustion heated gas dynamic carbon dioxide laser, comparing with continuous version

07 p1003 A72-19219

Transversely excited atmospheric /TEA/ carbon dioxide laser in single pulse and high repetition rate operation

07 p1003 A72-19220

High repetition rate pulsed IR xenon laser using transversely excited discharge

07 p1003 A72-19221

Pulsed and CW laser beam propagation through atmosphere

07 p0942 A72-19380

Military pulsed range finder design involving modularity, cooling, optical system and solid state receiver

07 p0942 A72-19384

Control optimization of pulsed laser automatic tracking system, analyzing angular and temporal distribution of signals

07 p0942 A72-19386

X ray spectrum and D-D neutrons emission from high temperature plasma produced by two pulsed Nd-glass laser systems

[CLEA PAPER 12,3] 07 p1041 A72-19394

Pulsed dye lasers logarithmic detector circuit with two ultrafast photodiodes, eliminating intensity variations problem

07 p1005 A72-19415

Pulsed IR carbon dioxide TEA laser for two dimensional interferometry of theta pinch plasma during discharge

07 p1005 A72-19416

Pulsed laser beam effect on residual stresses behavior in transverse weld on cylindrical shell

07 p0996 A72-19776

Dynamics of flare formation by pulsed laser beam at surface of alkali halide crystals

07 p1007 A72-20124

Faraday rotators acting as optical isolators for high power giant pulse lasers used for plasma production

07 p1008 A72-20368

Liquid pulsed laser active element lens parameters effects on output radiation divergence

07 p1008 A72-20511

Laser triggered spark gaps characteristics initiated by switched out picosecond pulse from mode locked Nd-glass laser, investigating breakdown formation time delay

07 p1008 A72-20547

Gain saturation measurements in carbon dioxide TEA pulsed amplifiers at 330 torr

07 p1009 A72-20569

Wavelength tunable dye laser pumped by dual pulse lamps with Fabry-Perot interferometer in resonator

07 p1009 A72-20614

Nitrogen dioxide photodissociation by pulsed ruby laser at 6943 Å, noting single photon energy relationship to dissociation energy

07 p0937 A72-20676

Uncooled GaAs injection laser with high pulse repetition rate, discussing structural features and current-power characteristics

08 p1181 A72-20748

Pulsed carbon dioxide laser welding of miniature explosive detonators

08 p1221 A72-20778

Emission dynamics of pulsed laser with optical delay line in resonator

08 p1181 A72-20797

Narrow-band pulsed laser radar photocount distribution statistics in thermal background radiation, noting detection performance dependence on signal and noise absolute level and SNR

08 p1134 A72-21420

Atomic, ion and electron transition pulsed gas discharge lasers, considering power efficiency factors, vacuum UV region and gas density

08 p1182 A72-21644

Pulsed GaAs injection laser active region anisotropy and radiation polarization under spontaneous and coherent emission conditions

08 p1183 A72-21772

Nd smooth pulsed laser action with narrow spectral line and emission amplification from Nd doped phosphate and silicate glass rods

08 p1183 A72-22027

Thermal self disturbance effect on second harmonic generation in crystals and CW and pulsed lasers

08 p1184 A72-22034

Rhodium solution laser emission pulse characteristics relation to pumping energy distribution over container end surface

08 p1184 A72-22048

Self mode locking operation of transversely excited atmospheric pressure carbon dioxide pulsed laser with helical pumping

08 p1184 A72-22075

Spectroscopy model design using ruby laser highly monochromatic light pulses, electro-optical scanning and high speed photography to study atmospheric gases absorption spectra

09 p1322 A72-22205

Hollow sphere calorimeter for high power pulsed laser energy measurements in broad spectral range, comparing with liquid calorimeter

09 p1323 A72-22656

Modal behavior and temperature tuning of pulsed room temperature GaAs laser, using hyperfine energy level separation

09 p1323 A72-22768

Pulsed carbon dioxide laser operation, measuring pulse energy variation with gas pressure, expansion nozzle shape and output mirror transmission

09 p1323 A72-22980

Laser pulse description by Fourier analysis, showing broadened spectral line widths relationship to cavity modes

09 p1324 A72-23078

Single picosecond light pulses from mode locked Nd-glass laser, discussing temporal structure, spectral energy distribution and pulse shape measurements

09 p1324 A72-23082

FM mode locked Nd-YAG pulsed laser controlled bistable phase position operation, using modulator cut as Brewster angle prism

[AD-741511] 09 p1325 A72-23089

German monograph on pulsed laser induced spherical unsteady blast waves in stationary and flowing gases

09 p1325 A72-23161

Pulsed carbon dioxide laser heating of theta pinch plasma by inverse bremsstrahlung and induced Compton processes

09 p1364 A72-23233

Plasma production from hydrogen solid targets by pulsed carbon dioxide TEA laser, noting diagnostic methods

09 p1325 A72-23237

Pulsed laser sensitometer using multiple imaging technique to retrieve average energy distribution from photographic plate optical density

09 p1325 A72-23346

Short laser pulses for plasma heating, considering turbulent heating mechanisms, neutron yield and electromagnetic radiation

09 p1364 A72-23444

Pulsed ruby laser with complex mirror resonator with optical delay line, observing mode locking effects in emission dynamics

10 p1488 A72-23764

Time resolved gain in water and water-gas mixtures as function of composition and excitation current, considering relaxation rate in pulsed water vapor laser

11 p1691 A72-25302

Atmospheric water vapor measurements by Raman backscatter from pulsed laser radar, comparing with meteorological tower data

11 p1680 A72-25347

Pulse width relationship to frequency broadening during self phase modulation of propagating short laser pulse

11 p1647 A72-26151

Transversely excited pulsed carbon dioxide laser, measuring spatial resolution of gain

11 p1647 A72-26323

Pumping conditions relationship to tube filling in Nd-YAG pulsed laser

11 p1649 A72-26344

Injection laser pulsed emission mode effect on spectral characteristics

11 p1650 A72-26359

Multichannel monopulse Nd glass laser design characteristics, describing input generator, preamplifier and amplifier channel beam distribution

11 p1651 A72-26363

Total emitted power calculated for transversely pumped pulsed molecular nitrogen laser at 3371 Å

11 p1651 A72-26504

Ultrashort pulse lasing techniques, covering mode formation, secondary effects and two photon recording of emission structures

11 p1652 A72-26792

High power Nd glass laser with stepwise pulse amplification for intensive heating of solid target plasmas

12 p1849 A72-27061

Transparent dielectrics destruction by mode-locked laser ultrashort pulses, discussing filamentary defect presence indication of radiation self focusing

12 p1853 A72-27068

Kinetics and cavity intensity models for output characteristics of pulsed electric discharge carbon dioxide lasers

12 p1820 A72-27287

High power light pulse generation with steep leading edges in Nd-glass laser, noting duration change based on transparency increase under light transmission

12 p1820 A72-27583

High power pulse generation by ruby laser under free oscillation, using resonator with dielectric mirrors

12 p1821 A72-27597

Radiation distribution and power output characteristics of Nd in phosphorus oxychloride solution circulating liquid pulsed laser for various flow velocities

12 p1821 A72-27599

Nd-glass amplifier gain saturation by 1.06 micron light pulses determined by two laser states lifetimes and degeneracies and thermalization rates

12 p1792 A72-27752

Light pulse propagation in ring laser model employing homogeneously broadened gain line and discrete loss

12 p1823 A72-27754

Spectral output of pulsed discharge initiated hydrogen fluoride chemical laser as function of pressure and gas composition

12 p1823 A72-27839

High brightness picosecond light pulses generation by laser with multiple internal reflection amplifier for plasma heating

12 p1824 A72-27872

Temperature distribution and heat dissipation calculations for CW and pulsed laser optical elements

12 p1824 A72-27873

Theta pinch plasma heating by carbon dioxide laser transverse pulses, substantiating theoretical considerations by experimental observations

12 p1852 A72-27880

Active elements for high power Nd-glass laser facility to generate short and ultrashort pulses 12 p1825 A72-27881

Computer simulation of pulsed hydrofluoric acid laser pumped by chain reaction, investigating cavity and chemical parameters effects on laser pulse 12 p1826 A72-27938

TEA pulsed carbon dioxide laser with continuous shaped electrodes, investigating hydrogen addition effects on power output and gain 12 p1827 A72-28224

Destructive changes in rabbit brain and eyes under pulsed laser beam irradiation 13 p1910 A72-29333

Steels structural and microhardness changes by pulsed laser beam induced local heat treatment, noting needleshaped grain refinement 13 p1979 A72-29482

Stimulated luminescence in activated Nd glass by pulsed laser radiation at 1060 nm wavelength 13 p1969 A72-29519

Pulsed chemical high pressure laser efficiency and output energy increase due to carbon dioxide introduction into deuterium-fluorine mixture 13 p1970 A72-29698

Pulsed laser plasma temperature determination by radiation measurements in X ray and visible spectral regions using foil method 13 p2018 A72-29887

High power monopulse Nd laser, obtaining single longitudinal frequency stabilized mode with anisotropic spar or quartz plates 13 p1971 A72-29922

Xenon filled coaxial pulse tube for pumping organic dye solutions, obtaining intensive light flashes 13 p1971 A72-29923

TEA carbon dioxide laser time dependent gain and cavity losses analysis, using lasing onset delay with current pulse 14 p2109 A72-30184

Transverse flow transverse pulsed chemical CO laser, describing Q switching, pulse duration power efficiency and chemical deactivation processes 14 p2109 A72-30187

Steady state laser mode locking with saturable absorber, describing pulse shape and amplitude as function of quantity of absorbing medium 14 p2111 A72-30793

Difference-frequency mixing of pulsed carbon dioxide lasers with non-phase-matched GaAs for submillimeter wave generation 15 p2290 A72-31384

Laser emission from pulsed transverse electric discharge in supersonic nozzle downstream region gas dynamic cooled mixture 15 p2245 A72-31385

Radiation coherence enhancement in pulsed semiconductor injection laser by voltage controlled barium zirconite piezoceramic element 15 p2245 A72-31416

Carbon dioxide TEA high output pulsed laser, testing wide range of carbon dioxide-nitrogen-helium mixtures at various pressures 15 p2246 A72-31638

Pulsed solid state lasers with large area Si photodiode for output measurement in feedback control system to compensate flash lamp aging 15 p2247 A72-32027

Nd glass laser drilling and welding applications and tests on materials to evaluate feasibility and operational advantages, identifying optimal pulse energies and durations 15 p2244 A72-32028

Moderate power GaAs single heterojunction injection laser diodes fabrication and operation characteristics in pulsed mode at 250-400 K 15 p2247 A72-32033

Molecular nitrogen pulsed laser wavelength measurements, observing IR bands, stimulated emission lines and population inversion mechanisms 15 p2249 A72-32151

Laser interference fringe jitter due to wavelength instability, suggesting pulse shape blurring intensity variation control by flat or large-angle wedge beam splitter 15 p2249 A72-32166

Transversely excited pulsed carbon dioxide-nitrogen-helium laser with electrical discharge determined optimum partial pressure 15 p2249 A72-32236

Transient high voltage and electric field measurement with electro-optical fringe pattern method employing pulsed laser Kerr system polarimeter 15 p2240 A72-32434

Dye-induced saturated frequency sweeping effects on mode-locked laser pulse broadening and substructures 15 p2250 A72-32523

Transversely excited pulsed carbon dioxide laser with and without hydrogen addition, observing gain spatial and temporal dependence 15 p2251 A72-32529

Optically pumped pulsed hydrogen fluoride gas laser, observing anisotropic ultrahigh gain emission in rotational transitions 15 p2251 A72-32531

High speed photography ultrafast shutter based on polymethine cyanide dyes saturability for measuring mode locked ruby laser pulse duration 15 p2241 A72-32535

Transverse electric discharge pulsed carbon dioxide laser, measuring refractivity time history by interferometry for comparison with prediction 15 p2251 A72-32537

Microwaves interaction with ultrashort laser pulse generated traveling refractive index changes in liquids with orientational Kerr effect 15 p2252 A72-32652

Passive shutter power absorption effect on periodically triggered pulsed ruby laser output instability, showing optical inhomogeneity interferograms 16 p2400 A72-33189

Pulsed emission at pulse front in molecular hydrogen, deuterium and nitrogen at near IR electronic transitions, analyzing spectral, temporal and energy characteristics 16 p2401 A72-33298

Intense emission from high pressure pulsed carbon dioxide chemical transfer laser by flash photolysis initiated deuterium-fluorine exothermic chain reactions 16 p2401 A72-33392

Photodiode-operational amplifier circuit for pulsed laser systems energy variations monitoring, noting insensitivity to ambient light conditions 16 p2402 A72-33607

Injection laser pulsed emission mode effect on spectral characteristics 16 p2403 A72-33712

Multichannel monopulse Nd glass laser design characteristics, describing input generator, preamplifier and amplifier channel beam distribution 16 p2403 A72-33715

Mode locked lasers, investigating effect of grating-induced phase and spatial modulations by multiple transverse modes on pulse compression across beam cross section 16 p2403 A72-33840

High brightness picosecond light pulses generation by laser with multiple internal reflection amplifier for plasma heating 16 p2403 A72-33981

Active elements for high power Nd-glass laser facility to generate short and ultrashort pulses 16 p2404 A72-33990

Laser pulse produced high temperature plasma engine propulsion system, noting thrust/power ratio and requirements for orbital applications [ALAA PAPER 72-719] 16 p2443 A72-34029

Study of transient phenomena by a TEA CO2 laser associated with a liquid-crystal detector 17 p2562 A72-34285

Spectroscopy of pulsed HF chemical lasers using an infrared vidicon camera tube. 17 p2562 A72-34641

Certain characteristics of an electron-pumped pulsed laser of small dimensions 17 p2562 A72-34839

Gain and relaxation studies in transversely excited HF lasers. 17 p2564 A72-35344

Breakdown in argon and nitrogen under the influence of a 0.35-micron picosecond laser pulse. 17 p2564 A72-35508

Excitation of a long-pulse CO2 laser with a short-pulse longitudinal electron beam. 17 p2565 A72-35815

Atmospheric pressure carbon dioxide pulsed IR laser to obtain 80 w peak power by optical pumping with TEA HBr laser and filter 17 p2565 A72-35816

Frequency dependent loss in self-pulsing ring laser. 18 p2697 A72-36337

Simple inexpensive laboratory-quality Rogowski TEA laser. 19 p2810 A72-37514

High power pulsed HCN laser. 19 p2811 A72-37583

A holographic method for optical adjustment of pulsed laser beams 19 p2811 A72-37674

Experimental evidence of an X-ray laser /Coherent radiation/copper/II/ gel target/neodymium-glass pump/. 19 p2811 A72-37774

Nonlinear optics with picosecond laser pulses. 19 p2812 A72-38379

Electric discharge concept to uncouple electron density from temperature for production of stable uniform electric laser discharges 19 p2812 A72-38596

Harmonic mode locking of the Nd:YAG laser. 19 p2813 A72-38688

Theory of spontaneous mode locking in lasers using a circuit model. 19 p2813 A72-38690

Radio-frequency preionization in a supersonic transverse electrical discharge laser. 19 p2813 A72-38694

Pulse nitrogen laser at high repetition rate. 19 p2813 A72-38696

Pulsed IR laser for heating superdense plasma to high temperature, featuring inertial confinement by use of short duration energy and strong magnetic field 19 p2843 A72-38823

Pulsed and repetitively Q switched ruby and Nd laser design characteristics for optical applications and holography 20 p2930 A72-39027

Investigation of radiation field distribution in a ruby laser with a SFR high speed camera 20 p2931 A72-39318

Laser action with coupled types of oscillations 20 p2931 A72-39319

Laser power and pulse duration requirements for hot plasma production by flame propagation in solid DT targets for controlled thermonuclear fusion 20 p2931 A72-39354

Generation of controllable light pulses in an electron-beam-pumped laser. 20 p2933 A72-39514

Determination of the angular divergence of laser radiation by a transforming system of prisms. 20 p2933 A72-39523

Frequency-tunable stimulated IR parametric fluorescence produced by barium sodium niobate crystal pumped with picosecond pulses from frequency-doubled mode locked Nd-glass laser 20 p2933 A72-39560

Gas breakdown in the laser as the limitation of pulsed high-pressure CO2 lasers. 20 p2934 A72-39565

Amplification of mode-locked trains with a liquid laser amplifier, Nd/3+/-POCl3:ZrCl4. 20 p2934 A72-39642

As-Te-Ge amorphous semiconductor film optical memory effect due to crystallization and reversion during exposure to pulsed laser beam, noting writing and erasing characteristics 20 p2961 A72-39708

Self-induced pulsations in the light output from double-heterostructure injection lasers. 20 p2934 A72-39710

Pump laser design for an infrared upconverter. 20 p2934 A72-39873

Mode locked carbon dioxide with transverse pulse pumping, using Ge ultrasonic diffraction cell as active loss modulator 20 p2934 A72-39965

Flash lamp optimal operating parameters determination by impedance matching to driving circuit and spectral matching to material of optically pumped solid state pulsed lasers 21 p3061 A72-40204

Laser action on unclassified xenon transitions in a highly ionized plasma. 21 p3089 A72-40242

Explanation of limiting diameters of the self-focusing of light. 21 p3062 A72-40337

A new method of exciting uniform discharges for high pressure lasers. 21 p3062 A72-40568

Transverse CO2 laser action at several atmospheres. 21 p3062 A72-40572

High power pulsed ruby laser and sapphire rods optical contacting technique 21 p3063 A72-40622

Stimulated thermal scattering of picosecond laser pulses. 21 p3063 A72-40779

Light pulse structure and bandwidth bounds in ruby laser with delay line inside variable effective length resonator 21 p3066 A72-40799

Single transverse mode operation of a pulsed volume excited atmospheric pressure CO2 laser using an unstable resonator. 21 p3064 A72-41197

Atomic, ion and electron transition pulsed gas discharge lasers, considering power efficiency factors, vacuum UV region and gas density 21 p3064 A72-41301

The problem of conductivity-type laser heating of two-temperature plasma, the nuclear fusion energy being taken into consideration, in the spherically symmetric case. 21 p3093 A72-41480

Pulsed monochromatic laser with toluene, xylene, ethanol, isoamyl alcohol and dimethylformamide solutions of organic dyes, discussing wavelength variations and power outputs 21 p3064 A72-41736

Emission synchronization in pulsed lasers 21 p3064 A72-41741

Possible mechanisms of turbulent heating of a plasma by ultrashort laser emission pulses 21 p3095 A72-41823

Pulse energy and temporal/spatial distribution of carbon dioxide laser pumped by energy transfer from vibrationally excited DF produced by deuterium-fluorine chain reaction 22 p3185 A72-42617

- Spontaneous self mode locking in transversely excited nitrogen laser operation in first positive system 22 p3186 A72-42618
- Pulsed room temperature laser action of Si-doped double heterostructure GaAs p type diodes within 9100-9500 Å wavelengths, discussing threshold current densities and power efficiency 22 p3186 A72-42621
- Superradiant laser excitation at 3371 Å in molecular nitrogen second positive band system by high energy electron beam, noting 6 nsec pulse outputs to 24 MW 22 p3186 A72-42623
- Electro-optical design and performance parameters of polluted air liquid droplet size distribution measurement by pulsed junction diode laser light external scattering 22 p3179 A72-42680
- Pulsed atmospheric-pressure carbon-dioxide laser initiated by a cold-cathode glow-discharge electron gun. 22 p3186 A72-42753
- The photochemical iodine laser - A high-power laser 22 p3186 A72-42940
- Holograms of spark discharges excited by nanosecond electric pulses 22 p3181 A72-43112
- Electron and plasma particle acceleration by moving pulsed laser, noting appearance of fast particles, hard radiation and neutrons 23 p3295 A72-43312
- Pulsed laser produced high temperature plasma for electric power generation by controlled nuclear fusion, discussing gas dynamic model 23 p3321 A72-43723
- Influence of steric effects and compressibility on nonlinear response to laser pulses and the diameters of self-trapped filaments. 23 p3296 A72-43873
- Interferometric measurement of the elongation of a pulsed diode laser. 23 p3297 A72-44185
- Alkali metal vapor Q switches for synchronizing mode-locked laser pulse trains with external events. 23 p3297 A72-44189
- Nanosecond and picosecond laser-produced CD2 plasmas. 24 p3427 A72-44709
- Pulsed carbon dioxide laser medium composition, pressure and electrical parameters effects on output power, energy and efficiency from mathematical model solution of kinetic equations 24 p3409 A72-44966
- Wave and polarization equations for short coherent light pulses transmission in linear amplifying and absorbing media, noting single pulse formation in lasers. 24 p3410 A72-45420
- High power monople laser with a stabilized spectrum and radiation directivity close to that of diffraction 24 p3410 A72-45422
- Sharp focused short pulse X ray source with laser flash synchronization for radiographic plasma diagnostics 24 p3429 A72-45495
- Pulsed laser employing a rhodamine 6G solution in ethyl alcohol with an output energy of 110 J 24 p3411 A72-45498
- Plasma produced by laser irradiation of solid targets as a source of highly stripped ions. 24 p3430 A72-45603
- Control of laser pulse duration by nonlinear absorption in semiconductors. 24 p3411 A72-45605
- Increase in the ratio of the energy of ultrashort laser pulses to the energy of the background radiation. 24 p3411 A72-45613
- High power Nd glass laser with stepwise pulse amplification for intensive heating of solid target plasmas 24 p3431 A72-45714
- Transparent dielectrics destruction by mode-locked laser ultrashort pulses, discussing filamentary defect presence indication of radiation self focusing 24 p3432 A72-45721
- PULSED RADIATION**
- NT ELECTROMAGNETIC PULSES**
- Cepheid variables mass discrepancy from evolution and pulsation theories, emphasizing opacity changes, luminosity values and effective temperature 01 p0133 A72-11128
- Pulsar NP 0532 pulsed hard X ray energy spectrum measurement, using balloon sounding data 01 p0134 A72-11160
- Acoustic pulse generation and transmission loss characteristics measurement by single pulse method with simple shape to facilitate Fourier analysis 03 p0388 A72-12955
- Radio-astronomical evidence for magnetohydrodynamical pulsations in corona, considering solar radio burst model of pulsating structure due to synchrotron radiation 03 p0432 A72-13349

- Acoustic wave excitation in water droplet with giant pulse radiation from Q switched laser, noting diffraction effects on laser power density requirement 03 p0367 A72-13372
- Critique of quasar model of independent random pulse emitting sources conglomeration, noting brightness fluctuations incompatibility 03 p0435 A72-13802
- Emission spectrum and intensity variation of organic dye solutions excited by nitrogen laser pulsed radiation 04 p0529 A72-14655
- Pulsar radiation scattering in interstellar medium, using Gaussian spatial autocorrelation function 04 p0577 A72-15281
- Pulsar PSR 0809 plus 74 observations indicating organized variation in polarization synchronized with drifting subpulses 04 p0581 A72-15513
- X ray pulse spectra measurement from Z-pinch plasma focus devices, describing Ross filter system with silicon diode detector capable of nanosecond time resolution 04 p0524 A72-15537
- Short narrow light pulse reflection from thick turbid medium with strong anisotropic scattering, obtaining backscattering signal power from unsteady transport equation solution 05 p0690 A72-16292
- Monochromatic radiation pulse transfer in absorbing plasma, deriving heat wave propagation velocity 05 p0696 A72-16680
- Self induced transparency effect in ruby laser, investigating light transmission and pulse delay and broadening as function of input energy 05 p0670 A72-17171
- Pulsed FM radio pulse signal reflection from inhomogeneous plasma or ionosphere calculating electron collision loss effects on distortion 06 p0854 A72-17487
- Pulsed and CW solid state microwave oscillator EM noise as function of power level and locking parameters 06 p0788 A72-18465
- Light amplifier steady state pi pulse local instability against amplitude perturbations in absence of relaxation or inhomogeneous broadening 07 p1002 A72-19204
- Scorpius X-1 and Cygnus X-1 pulsed radio emission search by sensitive de-dispersing technique 07 p1073 A72-19422
- Electromagnetic scattering of square pulse from lossy dielectric slab mounted on perfectly conducting planar ground surface 07 p0945 A72-19660
- Multichannel frequency spectrum analyzer for single radio pulse component frequency measurement 07 p0988 A72-19960
- Pulsed gamma ray emission measurement above 50 MeV from Crab Nebula pulsar with balloon-borne spark chamber 07 p1063 A72-20235
- Optical and electrical characteristics of gas discharge plasma in pulsed radiation sources as function of power dissipation 07 p1047 A72-20611
- Pulsating auroras morphology in polar substorm, recording poleward expansion and eastward drifting patches with all sky cameras 08 p1157 A72-21117
- Mathematical model of gravitational wave zone for ring emanated smooth axisymmetric toroidal pulse 08 p1158 A72-21177
- Electromagnetic impulse wave impingement on semiinfinite isotropic plasma slabs with arbitrary incidence angle and polarization, calculating signal reflection in terms of Bessel functions 08 p1137 A72-21990
- Radio emission from pulsar CP 1133, comparing amplitude and polarization characteristics of two subpulses 09 p1387 A72-22987
- Radio receiver-transmitter system for synchronous heterodyne signal detection of 6 GHz band electromagnetic channel pulsed response, discussing operational principles and accuracy 09 p1280 A72-23353
- Pulsed carbon dioxide laser output monitor with Ge cylinder using photon drag effect to measure radiation pulse profile 09 p1326 A72-23389
- Radiant heat flux measurement during pulsed processes from surface in high temperature emitting gas, using thin film sensor with small time constant 10 p1561 A72-23843
- Dielectrics breakdown under ultrashort neodymium laser pulses at fundamental and second harmonic frequencies 11 p1647 A72-25719
- Radiation efficiency of electric power-energy conversion during pulsed discharge in Xe tube 11 p1651 A72-26364

- Spectropyrometric device for pulsed light or plasma source temperature measurement, noting operation in 2000-40000 C range 11 p1635 A72-26465
- Exposure conditions and film processing parameters effects on sensitivity, diffraction efficiency and SNR of holograms recorded with continuous and pulsed radiation sources 11 p1637 A72-26796
- Singly and doubly resonant pulsed optical parametric oscillators driven by time-dependent pump, deriving output power rise time by steady state analysis 12 p1792 A72-27751
- Instantaneous and averaged emission spectra of injection laser under spontaneous pulsation as function of operation mode and photon distribution 12 p1824 A72-27875
- Pulsed IMPATT diode oscillators, pulse power capabilities, considering microwave circuit, dc and pulse biasing, power limitation and circuit anomalies 13 p1931 A72-29109
- Error analysis of ionospheric parameter measurement by satellite transmitted or reflected multiple frequency pulsed radiation signal, using perturbation method 13 p1920 A72-29276
- Pulse-sounding position finding device for light parachute probes conducting ionospheric studies, discussing design features 13 p1922 A72-29350
- Single pulses and random samplings signal spectrum analysis on real time scale by ultrasonic dispersion waveguide 13 p1934 A72-30018
- X ray source Cygnus X-1 pulsation periodicity analysis, showing random shot noise characteristics 14 p2156 A72-30571
- Geomagnetic field perturbation by gamma quanta pulsating source, studying accompanying radio emission behavior 14 p2101 A72-30645
- Color photoelectric light pulsations curve of RU Cam variable star during October 1969-August 1970, noting constant mean luminosity and color 14 p2158 A72-30729
- Laser radiation time characteristics measurement based on multiphoton processes in opposite light beams, estimating accuracy necessary for registration of ultrashort pulses 14 p2111 A72-30794
- Extensive air showers at zenith, measuring associated UHF radio pulses with optical Cerenkov emission receiver as trigger source 14 p2147 A72-30858
- Nonlinear interaction of resonant plasma oscillations with nonresonant wave pulse, using water bag model of electron plasma 14 p2140 A72-30936
- Giant pulse radiation in Q factor modulated Nd glass laser frequency stabilization by molecular Cs vapor 15 p2245 A72-31411
- Efficiency of pulsed tubular pumping lamps made of quartz glass investigated by active element luminescence measurement, noting dependence on current density 15 p2246 A72-31425
- Multimode optical fiber waveguide theoretical model to predict pulse propagation dispersion for comparison with measurements 15 p2194 A72-31546
- High efficiency X band pulse operation of transferred electron oscillator in hybrid mode, noting high material quality and optimum impedance match 15 p2206 A72-31548
- Pulse and monochromatic short wave signals phase/amplitude autocorrelation functions and probability distributions during oblique incidence reflection from ionosphere 15 p2197 A72-31876
- Discrete frequency modulated signals with frequency shifted identical envelope pulses, discussing transmission, construction and correlation functions 15 p2197 A72-31878
- Optical pulse wave field longitudinal and transverse statistical correlations during propagation in turbulent atmosphere 15 p2198 A72-32061
- Supernovae produced fluorescence pulses search in upper atmosphere by automatic coincident light receivers 15 p2313 A72-32233
- Quasi-optical transmission line stability improvement, investigating pulsating light beam concept 15 p2202 A72-32663
- Train synchronism of second harmonic excitation/pumping/ by periodic sequence of ultrashort light pulses 16 p2402 A72-33493
- Monochromatic radiation pulse transfer in absorbing plasma, deriving heat wave propagation velocity 16 p2437 A72-33692
- Radiation efficiency of electric power-energy conversion during pulsed discharge in Xe tube 16 p2403 A72-33716

- High efficiency and power S-band pulsed oscillator using avalanche diode and microstrip circuit
16 p2369 A72-33759
- Radio spectrographic measurements of type 4 solar radio bursts harmonic and pulsation structures
16 p2459 A72-33921
- NP 0532 precursor pulse as radiation scattered from main pulse beam by ring of material centered on pulsar
17 p2603 A72-34192
- Pulsating X ray sources with 1 sec periods as stars with central densities between neutron stars and white dwarfs
17 p2599 A72-35074
- Temporal distribution of Cerenkov light from extensive air showers, discussing experimental setup and pulse shape
17 p2599 A72-35140
- The shielding effect of metallic spherical envelopes with respect to very short EM waves and pulses
17 p2530 A72-35223
- Influence of interstellar discontinuities on the shape of radio pulses from pulsars
18 p2726 A72-36652
- Spectral densities of radio emission fluxes from discrete radio sources at the 3.5-cm /8550 MHz/ wavelength
19 p2850 A72-37804
- Weber coincidence experiments in terms of cosmological gravitational waves, noting inconsistency in radiated pulse energy estimate
19 p2866 A72-38491
- Measurement of electron concentration in the plasma of a pulsed erosion-type accelerator
19 p2843 A72-38535
- Discontinuous generation of ultrahigh frequency oscillations during a plasma-beam interaction
19 p2768 A72-38664
- Organic dye laser molecular sublevel relaxation effects on steady state pi pulse behavior and spectral hole burning from resonance radiation propagation analysis
20 p2932 A72-39503
- Injection laser under self-Q-switching conditions.
20 p2933 A72-39515
- Morphologic maps of pulsating aurora for late afternoon and evening geomagnetic sector near Tromsø during 1967-1969
20 p2918 A72-39540
- Pulsed photoexcitation /flash photolysis/ spectrophotometers in terms of light sources, recording sensitivity enhancement, data processing, laser use and performance requirements
21 p3058 A72-41726
- Quasi-periodic solar radio pulsations at decimetric wavelengths.
22 p3222 A72-42045
- Influence of single-pulse emission from a ruby laser on the plasma of a mercury vapor lamp
22 p3184 A72-42105
- Bessel series solution to electromagnetic field and pulse function of cylindrical conducting screen located in monochromatic plane wave
22 p3155 A72-42667
- Stimulated emission with pumping by a pulsed electron beam formed in a direct discharge
23 p3295 A72-43319
- Temperature calculation in a multilayered wall acted on by a thermal pulse.
23 p3357 A72-44537
- Note on the experimental determination of photoconductive response characteristics of amorphous semiconductors.
24 p3431 A72-44716
- PULSEJET ENGINES**
Influence of an electrical discharge in a flame on the propagation of the flame
18 p2740 A72-36244
- Development of a GH2/GO2 pulsejet engine with 6.7 kN thrust for the attitude control system of the space shuttle
19 p2848 A72-37495
- Pulsed-jet engine of Messerschmitt-Boelkow-Blohm without valve flaps
19 p2849 A72-38031
- PULSES**
NT ELECTRIC PULSES
NT ELECTROMAGNETIC PULSES
NT GEOMAGNETIC MICROPULSATIONS
NT GEOMAGNETIC MICROPULSATIONS
NT MICROPULSATIONS
NT PRESSURE PULSES
Initially sharp cylindrical pressure pulse propagation and stress wave attenuation in linear elastic fiber reinforced composites
11 p1730 A72-25415
- Limited energy source operational time comparison for continuous and pulse mode operations
15 p2196 A72-31785
- Influence of molecular laser parameters on the pulse shape in Q-switched operation
17 p2563 A72-35301
- Absolute accuracy of the pulse-echo overlap method and the pulse-superposition method for ultrasonic velocity.
23 p3313 A72-44114
- PULVERIZING**
U GRINDING [COMMINUTION]
- PUMP IMPELLERS**
Screw type axial flow pump impellers pressure losses generalization by dimensionless coefficient in Euler number form
12 p1752 A72-28139
- Cavitation study of pump with semiopen impeller, obtaining hydraulic performance, flow photographs and noise level
17 p2561 A72-35899
- Deterioration of shaft bearings of electromotor driving aircraft centrifugal fuel pump, determining lateral force acting on impeller
23 p3252 A72-43663
- PUMPING**
Many element GaAs and CdS semiconductor laser achieving high power output by electron beam pumping
12 p1822 A72-27616
- Stellar OH radical emission amplification by maser effect raising low energy molecules to high energy by pumping
14 p2110 A72-30578
- CdS crystals lasing in air at atmospheric pressure and room temperature by low voltage electron beam pumping through Ni film
15 p2245 A72-31319
- Electrical pumping discharge confined by liquid wall of vortex channel in dye laser solution
15 p2251 A72-32528
- Train synchronism of second harmonic excitation /pumping/ by periodic sequence of ultrashort light pulses
16 p2402 A72-33493
- Certain characteristics of an electron-pumped pulsed laser of small dimensions
17 p2562 A72-34839
- Energy characteristics of the laser action in rhodamine 6G pumped by a pinched discharge.
20 p2933 A72-39512
- Generation of controllable light pulses in an electron-beam-pumped laser.
20 p2933 A72-39514
- Mode locked carbon dioxide with transverse pulse pumping, using Ge ultrasonic diffraction cell as active loss modulator
20 p2934 A72-39965
- HF chemical lasers pumped by atomic fluorine with molecular hydrogen, calculating intensity and efficiency by reaction kinetics analysis for comparison with computer solutions
21 p3062 A72-40617
- Carbon dioxide laser excitation by injection of plasma jets produced by capillary plasmatrons
21 p3063 A72-40835
- Time variations in the far-field diffraction patterns of spatial modes from electron-beam-pumped semiconductor lasers.
24 p3409 A72-44712
- PUMPS**
NT CENTRIFUGAL PUMPS
NT CONDENSATION PUMPS
NT DIFFUSION PUMPS
NT ELECTROMAGNETIC PUMPS
NT FUEL PUMPS
NT ION PUMPS
NT JET PUMPS
NT MOLECULAR PUMPS
NT TURBINE PUMPS
NT VACUUM PUMPS
NT VISCOPUMPS
Springs fracture and vibration in injection pumps by analog model
02 p0236 A72-12437
- Disk pump driven fluid layer device for density stratified water channel flow measurements, using hydrogen bubble technique
04 p0509 A72-15118
- German monograph on losses in gear pumps, discussing leakage, mechanical and hydraulic losses, measurement techniques and equipment, etc
10 p1422 A72-23774
- Cavitation failure of aircraft hydraulic plunger pump elements from microscopic and metallographic analysis
13 p1899 A72-28732
- Hydraulic pump design for efficiency increase, weight reduction and service life and reliability improvement
18 p2694 A72-36045
- Hydrodynamic pivoting-pad vane tips for high-speed vane pumps.
18 p2694 A72-36046
- Low inlet pressure performance of gerotor lube and scavenge pumps.
18 p2694 A72-36047
- PUNCHES**
Thickness-punch size ratio effects on stress state response of elastic plates and beams in flat contact under symmetric loads due to rigid punches
18 p2734 A72-36378
- Contact interactions of smooth rigid punch impressing into thin laminar anisotropic reinforced plastic plate
19 p2872 A72-37541
- Integral equation for pressure distribution by rigid punch contact with elastic half space, solving by Mathieu function expansion in Fourier series
21 p3126 A72-41541
- PUNCTURING**
U PIERCING
- PUPA**
Phase resetting behavior of circadian rhythm of pupal eclosion in fruitfly populations
07 p0918 A72-19529
- PUPIL SIZE**
Pupil size spontaneous oscillation /Hippus/, discussing development by repeated light step and accommodation and disappearance due to mental activity
02 p0164 A72-12490
- Computerized simulation from model of human pupillary motor behavioral response to light, accommodation and fusional inputs
07 p0928 A72-19310
- Optic disk drusen and Marcus Gunn pupillary phenomenon relation to visual field defects, discussing need for calibrated perimetry and binocular field testing
07 p0933 A72-20190
- Age dependence of changes in pupil diameter in the dark.
21 p3007 A72-40732
- PUPILLOMETRY**
IR pupillography for screening narcoleptics and fatigue prone individuals from driver and pilot training applicants
12 p1777 A72-28323
- PUPILS**
Consensual photopupil responses to light flashes recorded in full dark adaptation, noting bleaching and backgrounds effects
13 p1907 A72-29969
- Pupil reflex loss /pupilloptosis/ diagnosis in pilots, testing sensitivity to methacholine chloride
14 p2082 A72-31096
- Analysis and synthesis of visual phenomena in microscopic vision - with particular reference to visual acuity.
21 p3084 A72-40748
- PURIFICATION**
NT AIR PURIFICATION
Blood self purification enteral mechanism in dogs, determining leukocyte population changes before and after feeding and intravenous interferon injections
07 p0915 A72-18867
- Pressure effects on molten metals reactions with ambient atmosphere during purification by distillation, obtaining impurities concentration ratio via Langmuir relative volatility rule
07 p0997 A72-20287
- PURIFIERS**
U PURIFICATION
- PURINES**
NT ADENINES
NT GUANINES
NT URIC ACID
NT XANTHINES
Studies in prebiotic synthesis. VII - Solid-state synthesis of purine nucleosides.
23 p3262 A72-43567
- PURSUIT TRACKING**
Impulse motion convergence in game theory, considering control problems of pursuit involving escape and capture
05 p0690 A72-16583
- Optimality conditions for safe time in linear pursuit problems within n-dimensional Euclidean space
05 p0683 A72-16584
- Suboptimal security solution of linear quadratic pursuit evasion game with state dependent, control dependent and additive noises, deriving equations for state estimation
06 p0794 A72-18151
- Mental rehearsal and physical practice relation to learning rate for rotary pursuit tracking skill acquisition
07 p0925 A72-18801
- Optimal thrust reversing in pursuit evasion games between two aircraft in horizontal plane, considering cost functions and termination criteria
07 p0912 A72-19282
- Minimax terminal state estimator existence and structure for linear discrete system, applying to stochastic pursuit evasion games of LQG variety
07 p1027 A72-19283
- Theorem of pursuit game with curvature constraints during two points motion in Euclidean space
11 p1675 A72-25320
- Antagonistic pursuit games of prescribed duration in abstract topological space with defined distance function
11 p1676 A72-25326
- Multistage pursuit-evasion game on circle, constructing player optimal strategies via measure theory
12 p1836 A72-27511
- Pilot pursuit tracking performance under acceleration stress, simulating high performance aircraft dynamics via human centrifuge equipped with simulated head-up predictive gunsight
12 p1776 A72-28320

Tracker recovery strategy during temporary target obscuration in pursuit tracking task, analyzing control stick movements

13 p1911 A72-29820

Eye movement pattern monitoring to investigate retinal afterimage role in release of pursuit movements

17 p2508 A72-34886

Rotary pursuit task practice effects on transfer of motor skill from slower to faster speeds

18 p2654 A72-36915

Impulse motion encounter in game theory, considering control problems of pursuit involving escape and capture

19 p2825 A72-37554

Optimality conditions for safe time in linear pursuit problems within n-dimensional Euclidean space

19 p2825 A72-37555

The dynamic modeling technique for obtaining closed-loop control laws for aircraft/aircraft pursuit-evasion problems.

19 p2753 A72-38276

Linear vector formulation of pursuit problems with pursuer discrimination, using Mishchenko-Pontyagin curvature conditions

23 p3307 A72-43220

Trajectory bundles in metric space for objects motion study in dynamic pursuit games, noting Pontryagin and Pshenichnii methods for differential games solution

23 p3308 A72-43415

Differential pursuit games with nonlinear evading player and linear pursuer, considering determination of initial states

23 p3277 A72-44001

Differential games problem of pursuit tracking solved by invariants theory, noting explicit laws of pursuer activity control

24 p3387 A72-45518

Experimental determination of the distribution rule for the time of failure-free operator action in the tracking mode [with pursuit]

24 p3377 A72-45521

Aircraft interception avoidance problem solved by differential game theory, discussing human operator decision making for random pursuit tracking

24 p3377 A72-45523

PUSH-PULL AMPLIFIERS

Push-pull magnetic amplifier circuit operation as variable polarity dc source for electroplating applications

11 p1603 A72-25279

Wideband push-pull transistorized power amplifier free of nonlinear distortions due to scattering inductance of load transformer

13 p1926 A72-28378

Optimal design of broad passband in unilateral parametric balance amplifier

13 p1928 A72-28789

Circuits for electromagnetic interference reduction in broadband solid state radio transmitters, discussing balanced transistor amplifier

15 p2209 A72-32564

Push-pull transistor amplifier fed from two different voltage power supplies, noting power efficiency improvement

22 p3158 A72-42115

PWM [MODULATION]

U PULSE DURATION MODULATION

PYLONS

The application of non-planar lifting surface theory to the calculation of external-store loads.

[AIAA PAPER 72-971] 22 p3135 A72-42340

PYRAMIDAL BODIES

Pyramidal horn antenna with mesh conducting surface comparing response with geometrically similar horn with continuous walls

06 p0783 A72-17600

PYRANOMETERS

International comparison of standard solar radiation measurement pyranometers

06 p0816 A72-17925

Annual variations of calibration factors of star pyranometers for copper-constantan and nichrome-constantan thermocouples

07 p0991 A72-20450

Integration sphere facility with water cooled long arc xenon sources for pyranometer calibration, discussing operation theory and system design

22 p3163 A72-42692

PYREX [TRADEMARK]

U BOROSILICATE GLASS

PYRIDINES

NT NICOTINIC ACID

Slag powdery material moisture content determination by absolute pyridine adsorption method of moisture extraction

12 p1813 A72-27450

PYRIDOXINE

Pathogenesis of in-flight illusory acceleration sensations, discussing amino acid level, protein metabolism rate and pyridoxin metabolism

05 p0619 A72-16642

Effect of neurohomologous phospholipids associated with other substances on experimental intoxication by asymmetrical dimethylhydrazine. II -

Biochemical aspects of the pyridoxine-phospholipid association

21 p3009 A72-41195

PYRIMIDINES

NT MITOCHONDRIA

NT THYMIDINE

Photochemical reactions in pyrimidine base of DNA after UV irradiation, relating mutagenic and lethal effect to dimerization

04 p0467 A72-14608

PYRO CERAM [TRADEMARK]

Industrial pyroceramic materials usable under friction without lubrication

21 p3061 A72-41374

PYROELECTRICITY

Gallium-doped Ge bolometers and triglycine sulfate pyroelectric far IR detector, testing performance as functions of frequency and temperature

04 p0525 A72-15601

Pyroelectric detector noise equivalent power limitation factors, discussing heterodyne systems and pulsed submillimeter lasers detection

04 p0551 A72-15602

Pyroelectric IR detectors hf performance in direct and heterodyne modes, including thermal expansion effects

04 p0563 A72-15603

Pyroelectric laser power meter with built-in calibration based on reference heating by IF current, describing operation, design and testing

05 p0662 A72-16347

IR radiation detection by microwave biased photoconductor, lead-tin telluride photovoltaic detector and thermal imaging pyroelectric detector and array system

07 p1034 A72-19425

IR image tube with electronic scanning and pyroelectric target for uncooled operation at ambient temperature, noting wideband spectral sensitivity

08 p1171 A72-21966

Pyroelectric radiation detector with ferroelectric crystals, discussing operation mode, construction, sensitivity and IR applications

17 p2530 A72-35445

Thermal imaging with pyroelectric IR detector arrays, discussing signal processing by digital technique to eliminate voltage offset variations effects in preamplifiers

20 p2928 A72-39968

Heterodyne, microwave bias and pyroelectric photon infrared detectors, noting mixed crystal photoconductive and photovoltaic detectors

23 p3291 A72-44392

PYROGEN

Electric pulse initiated pyrogen jet squid igniter consisting of magnesium-fluorocarbon coated bridgwire and pellet enclosed in Mk 1 or 2 gilding metal cup

08 p1221 A72-20774

Pyrogenal injection test for hematopoietic tissue function in dogs, describing response as transient leukopenia followed by pronounced leukocytosis due to bone marrow granulocyte ejection

23 p3255 A72-43911

PYROGRAPHALLOY

U COMPOSITE MATERIALS

U PYROLYTIC GRAPHITE

U REFRACTORY MATERIALS

PYROHELIOMETERS

Precision radiometric techniques in meteorology and geostrophysics, discussing references, pyroheliometric scale, transfer calibrations and solar radiation measurements

10 p1485 A72-25097

Experimental comparisons of the international pyroheliometric scale with the absolute radiation scale.

23 p3290 A72-44274

PYROLYSIS

Iron meteorite formation model based on metal carbonyls low temperature thermal decomposition in comets

01 p0124 A72-10061

Phenolic-novolac prepolymer molecular structure and pyrolysis reactions thermokinetic parameters, presenting statistical methods for estimating char yield

01 p0023 A72-11261

Kinetics of shock wave pyrolysis of pentafluoroethane dilute mixture in Ar at 1180-1470 K

02 p0170 A72-11520

High temperature CIF reaction kinetics in thermal decomposition shock tube study, using chlorine atom two-body emission

04 p0484 A72-15463

Kinetic model for propane pyrolysis based on most important free radical reaction steps

06 p0770 A72-17777

Barium perchlorate thermal decomposition mechanism, presenting pressure-time and weight-loss curves

07 p1051 A72-19360

Particle formation rates in thermal decomposition of acetylene in diffusion flame, noting activation energy

07 p1099 A72-19373

Ethyl radicals reactions in shock tube produced pyrolysis of azoethane, using time of flight mass spectrometer

07 p0935 A72-19433

Methane pyrolysis in glow discharges /cold plasmas/, discussing chemical reactions initiated by high energy electrons inelastic collisions with gas molecules

07 p0937 A72-20286

Thermal decomposition kinetics of tetramethylene tetranitramine beta HMX from differential thermal analysis and activation energy calculation

08 p1219 A72-20755

Thermal decomposition of perchloric acid vapor in Pyrex reaction vessels at 279-471 C, using flow technique

09 p1276 A72-23143

Chromatographic analysis of reaction products of HCl-accelerated neopentane pyrolysis, showing tert-butyl chloride formation

10 p1434 A72-24235

Electrically heated thermal decomposition hydrazine thrusters, discussing propellant supply pressures compatibility and thrust levels

[AIAA PAPER 72-451] 11 p1708 A72-26188

Thermal vacuum tests of rhenium disulfide decomposition as function of temperature at 800-1200 C, using thermogravimetric method

13 p2023 A72-29649

Powder combustion on metal plate at constant pressure based on two-phase model of condensed system thermal decomposition

13 p2065 A72-29879

Destructive effect of combustion and pyrolysis products in intake air on fire extinguishers foam production

14 p2084 A72-30339

Thermocatalytic pyrolysis for hydrogen generation from liquid hydrocarbon fuels with absolute cracking reaction efficiency

16 p2361 A72-33890

Studies on flame-resistant epoxy resin - Pyrolysis of tetra-brominated epoxy resin and flame-resistant mechanism.

18 p2704 A72-36519

Formation of hydrogen from amine oxidation and pyrolysis.

19 p2883 A72-38874

Vacuum thermal decompositions of the nitrate salts of hydrazine.

19 p2848 A72-38876

Vapor deposition effects on high density Mo, W and Nb obtained by carbonyls pyrolysis or chlorides and fluorides reduction

20 p2941 A72-39821

Physical, mechanical and thermal characteristics of reimpregnated pyrolyzed carbon-carbon and graphite-graphite composites

[ICAS PAPER 72-29] 21 p3073 A72-41154

Supersonic jet engine fuels production by gasoline vapor pyrolysis, discussing physico-chemical characteristics and combustion properties

24 p3432 A72-44625

PYROLYTIC GRAPHITE

Pyrolytic graphite heat conductivity coefficients in direction perpendicular to deposition surface at high temperatures

01 p0090 A72-10488

Quantum oscillations of minority Fermi surface carriers as function of magnetic field in Hall effect and thermoelectric power in pressure-annealed pyrolytic graphite

02 p0268 A72-11673

Electrical conductivity of pyrographite at high temperatures along and across deposition plane, using optical pyrometer measurements

02 p0251 A72-12860

Supramolecular structure artificial defects influence on mechanical strength of pyrographite

07 p1024 A72-20136

Surface active medium effect on free surface energy and strength of pyrographite in ethyl alcohol solution, using crack kinetics experiment

08 p1197 A72-22182

Pyrolytic graphite coated rocket nozzle design, discussing substrate properties, coating thickness, erosion rates and rocket tests

10 p1500 A72-24199

Directional dependence of the high-temperature thermal diffusivity of crystal-oriented pyrolytic graphite

18 p2704 A72-37180

Quantum limit studies in single crystal and pyrolytic graphite.

21 p3097 A72-41186

Thermal and electrical conductivities, thermal expansion and specific heat of commercial graphite obtained by precipitation of methane pyrolysis products on hot surface

23 p3306 A72-43689

Nonlinear theory for static analysis of moderately thick circular cylindrical shells under axisymmetric loads applied to pyrolytic graphite

24 p3454 A72-44603

Supramolecular structure artificial defects and bond strength influence on mechanical strength of pyrographite 24 p3418 A72-45761

PYROLYTIC MATERIALS

NT PYROLYTIC GRAPHITE

Combustion chamber and nozzle materials for fluorine and/or metal combustng high energy propellant rocket engines, considering cooled and uncooled nozzles and spoiler plates 01 p0117 A72-10941

Minority carriers similarity in graphite natural single crystals and pyrolytic samples 01 p0114 A72-11035

UV radiation effects on pyrolytic boron nitride lattice imperfections, using space environment simulator 09 p1336 A72-22404

Properties of pyrolytic oil hydrogenated aromatic fraction, noting suitability for jet fuels applications 14 p2145 A72-31075

PYROMETERS

NT RADIATION PYROMETERS

Spectrophotometric device for pulsed light or plasma source temperature measurement, noting operation in 2000-40000 C range 11 p1635 A72-26465

Pyrometric obturation devices effect on sample temperature level during high temperature tests with radiant heating 13 p1960 A72-29903

High speed photographic pyrometer for surface temperature measurements on aerodynamic models during free flight in aeroballistic range 15 p2237 A72-32050

PYROMETRY

U TEMPERATURE MEASUREMENT

PYROPHYLLITE

The effect of firing temperature on properties of natural steatite and pyrophyllite. 17 p2569 A72-34666

PYROTECHNICS

Explosives and pyrotechnics - Conference, Philadelphia, September 1971 08 p1218 A72-20751

Explosive/pyrotechnics performance monitoring for acceptance, lot qualification, comparison testing and system design guidelines 08 p1219 A72-20760

Pyrotechnic hazard classification for property and personnel protection in event of accidental explosion 08 p1220 A72-20768

Aluminum plated pyrotechnics physical properties and performance for electroexplosive device applications, describing particle size distribution and loading pressure dependence of density 08 p1221 A72-20772

Safety evaluation for pyrotechnic devices during life cycle including R and D, production, loading, handling, shipment, storage, maintenance and disposal 08 p1221 A72-20773

Detonating cut-off pyrotechnic chain of explosive devices for stage separation involving primers, relays and fuses 08 p1221 A72-20777

Physical properties, combustion characteristics and applications of pyrotechnic castable composition for smoke generation 08 p1222 A72-20785

PYROXENES

NT ENSTATITE

Apollo 14 lunar soil sample 14163 orthopyroxene composition, determining K, P and rare earth elements 01 p0125 A72-10066

Cation distribution observation over nonequivalent lattice sites in shocked orthopyroxene, noting Mg and Fe order-disorder 01 p0053 A72-10293

Apollo 14 basaltic rocks cooling deduced from divalent Mg and Fe ionic distribution in pyroxene, noting process interruption below 840 C 11 p1724 A72-26574

Lunar and terrestrial pyroxenes phase structure electron microscopic investigation, using ion-thinned samples 11 p1725 A72-26952

Apollo 14 breccia sample inverted pigeonites /pyroxenes/ as evidence of lunar plutonic rocks, using optical, electron probe and X ray diffraction techniques 12 p1865 A72-27112

Microprobe analysis of Timmersoi hypersthene chondrite from Niger Republic, noting equilibrium between olivine and orthopyroxene at 850 C 13 p2035 A72-28751

Fe and Ti ion bands in lunar pyroxenes and olivines single crystals polarized absorption spectra 14 p2154 A72-30510

Lunar rock 12052 euhedral clinopyroxenes composed of honey yellow pigeonite cores overgrown by dark brown augite 16 p2454 A72-33448

Lithology of Apollo 14 lunar clastic rocks from Fra Mauro region, noting different makeups of glassy

matrix and particles, plagioclase, pyroxene and lithic clasts 16 p2457 A72-33675

A re-examination of relationships among pyroxene-plagioclase achondrites. 20 p2900 A72-39840

Phenocryst fabric in lunar basalt sample 12052 from the Ocean of Storms. 21 p3106 A72-41115

PYROXYLIN

U CELLULOSE NITRATE

PYRRHOTITE

NT TROILITE

PYRROLES

NT INDOLES

NT TRYPTOPHAN

Model reactions between phthalic anhydride and o-phenylenediamine under polymerization-analogous conditions for polyimidazopyrrolone formation 19 p2762 A72-37647

PYRUVATES

Acute and chronic hypercapnia effect on lactate, pyruvate, alpha-ketoglutarate, glutamate and phosphocreatine contents of rat brain 03 p0316 A72-13677

Q

Q DEVICES

Characteristic scale lengths of stationary ionic collisional shocks in Q device perpendicular to magnetic field, presenting shock thickness variation with Mach number and density 01 p0105 A72-10028

Cylindrical alkali metal plasma column structure in single ended Q device under axial magnetic field 06 p0854 A72-17503

Density and flux measurements by Langmuir probes in uranium plasma produced in single ended Q device, noting application to isotope separation 06 p0855 A72-17506

Ion distribution function oscillations in first order ionic waves of single ended Q device, noting plasma confinement in static magnetic field 06 p0855 A72-17507

Non-Maxwellian plasma response to acoustic wave propagation in single ended Q device, investigating ion distribution function 06 p0855 A72-17509

Wave exciting grid-plasma interaction in single ended Q device, determining ion velocity distribution function 06 p0855 A72-17510

Perturbed density and ion velocity distribution functions of grid-excited ion acoustic waves in collisionless plasma in single ended Q device 06 p0855 A72-17511

Single-ended Q machine grid-excited density perturbation and ion wave propagation properties from linearized Vlasov equations 06 p0855 A72-17514

Ion density perturbations propagation through plasma with double-humped Maxwellian ion velocity distribution in single-ended Q machine 06 p0855 A72-17515

Plasma microinstabilities due to ion acoustic waves propagation with double-humped ion velocity distribution function in Q machine 06 p0855 A72-17516

Thermal noise and ion-acoustic waves excitation in Q machine two beam plasma with high temperature ratio in presence of inhomogeneous B-field, observing instability 06 p0856 A72-17517

Ion-acoustic collisionless shock generation by initial plasma density discontinuity in Q machine, correlating experimental results with numerical simulation 06 p0856 A72-17520

Wake behind obstacle immersed in plasma flow of single ended Q-machine, using experiment as diagnostic of ion distribution function 06 p0856 A72-17526

Wave induced Q machine cesium plasma loss produced by current-driven collisional drift instability 06 p0857 A72-17527

Collisional drift instability dependence on parallel wavelength in potassium Q device plasma 06 p0857 A72-17528

Electron temperature fluctuations associated with drift-type instability in Q device, discussing plasma diagnostic techniques 06 p0857 A72-17530

Q-machine plasma column drift instability passive feedback control, regulating feedback drive current phase and amplitude by varying resonance circuit characteristics 06 p0857 A72-17532

Hf fluctuations in density gradient of alkali plasma within Q device 06 p0858 A72-17536

Normal mode solutions for bounded systems from linear dispersion roots, discussing plasma waves and instabilities and damping effects in Q machines 06 p0858 A72-17537

Single ended Q machine Ba plasma probe measurements of ion temperatures perpendicular to magnetic field, electron temperatures and plasma densities and potentials 06 p0859 A72-17550

Electrostatic energy analyzer for local ion velocity distribution function measurement in double ended Q machine plasma column 06 p0814 A72-17551

Resonance charge exchange cross section measurements for Cs at 2 eV within Q machine, discussing ion energy resolution improvement 06 p0859 A72-17552

Parallel current and sheath effects on collisional drift waves normal mode structure in Q machines with end plates, using slab plasma model with uniform magnetic field 07 p1042 A72-19511

Electrostatic ion wave Landau damping in magnetic field of Ar plasma QP machine 08 p1213 A72-21250

Bounded systems dispersion relations interpretation for plasma waves and instabilities on finite cylinders, with emphasis on end plate damping and axial current effects on Q machines 11 p1697 A72-26597

Ionic collision effects on spatial ion wave echoes in single-ended Q machine plasma, noting echo peak amplitude damping 15 p2288 A72-32423

Nonexistence of ion acoustic waves and Landau damping driven electrostatically in an ideal Q machine. 21 p3090 A72-40340

Measurements of enhanced absorption of electromagnetic waves and effective collision frequency due to parametric decay instability. 21 p3092 A72-40829

Effects of parallel wavelength on the collisional drift instability. 21 p3093 A72-41627

Transverse velocity shear instabilities within a magnetically confined plasma. 21 p3093 A72-41628

Q FACTORS

High Q oscillator with simulated inductor circuit consisting of negative immittance converter and RC elements 01 p0035 A72-10127

Average radiation Q factor and dose radiation spectrum measurement in phantoms irradiation by proton beams [CERN-71-16] 02 p0162 A72-12069

Linear energy transfer response of polyvinyltoluene plastic scintillator, presenting data on quality factor and radiation dose equivalent determinations in mixed radiation field [CERN-71-16] 02 p0168 A72-12071

Microwave lumped element impedance measurements from 1 to 12 GHz by resonant transmission line frequency and Q perturbation technique 05 p0637 A72-16419

Quartz oscillator short term frequency instability lower limit estimation by calculating Q values and non-linearity and resonator parameter fluctuation effects 07 p0953 A72-19009

Shf resonator small resonant frequency shift and Q factor changes measurement based on FM signal envelope shape analysis 07 p1046 A72-20508

GaAs semiconductor injection lasers, discussing time characteristics of current carriers, population inversion and resonator Q factor modulation 08 p1184 A72-22032

Q factor over temperature range of microwave resonator coupled with drifting indium antimonide plasma 09 p1285 A72-22895

Wideband microwave device with diode and single component correction circuits Q factors measurement from frequency dependence of input traveling wave coefficients 10 p1453 A72-24918

Pulsed perturbation and Q coupled extremal control systems with noise distortion, obtaining optimal transfer functions with Kolmogoroff-Wiener method 11 p1610 A72-25448

Passive Q factor modulation in carbon dioxide laser by resonance absorption saturation in osmium tetroxide vapors, noting vapor pressure effects 11 p1650 A72-26355

Microwave resonators excited in coupled and E sub zero modes, determining equivalent circuit and Sommerfeld resonator Q factor and guide wavelength 11 p1605 A72-26369

Mode chart and unloaded quality factor of elliptic microstrip resonator operating in inverse or radial TM modes 11 p1607 A72-26996

- Solid state laser resonator inhomogeneous dielectric and mirror elements matching effects on Q factor and output power
12 p1822 A72-27609
- Strip and line source antennas quality factor, examining relationship to superconductivity ratio
13 p1916 A72-28535
- Machine oil wear degree and Fe content determination by placing sample into induction coil and measuring coil Q at RF
13 p1957 A72-29142
- Two cavity self exciting SHF microwave oscillator with resistance coupling through low Q-factor resonant diaphragm, noting frequency stability
14 p2090 A72-31121
- Open terminations of cylindrical waveguide periodically loaded by metallic irises, investigating cavity resonator size effects on resonant frequency, mode and quality factor
15 p2194 A72-31547
- Passive Q factor modulation in carbon dioxide laser by resonance absorption saturation in osmium tetroxide vapors, noting vapor pressure effects
16 p2402 A72-33708
- A fast numerical method for determining the optimum SNR of an array subject to a Q factor constraint.
17 p2514 A72-34372
- Pulsed Impatt diode oscillator circuit design and operation frequency prediction for high Q coaxial structures from equivalent circuit
17 p2526 A72-34466
- Superconducting-cavity-stabilised oscillator of high stability.
17 p2530 A72-35386
- Excitation of a confocal spherical laser resonator.
19 p2810 A72-37403
- A comparison of manufacturing techniques for hybrid microwave circuits.
20 p2908 A72-39496
- Calculation of two- and three-stage broadband amplifiers with parallel correction from the standpoint of a maximum quality factor with an optimally flat amplitude characteristic
21 p3027 A72-40477
- Automatic measurement of microwave-cavity parameters using stable sampled control loops.
21 p3034 A72-41465
- Miniature modular wideband parametric amplifier for centimeter range, using Q optimal coupled circuit with passband dependent on diode time constant
22 p3158 A72-42088
- Q SWITCHED LASERS**
- Multimode Q switched ruby laser temporal coherence, comparing theoretical with experimental results from Michelson two-beam interferometer measurements
01 p0080 A72-10849
- Oscillation transient in molecular Q switched ammonia beam maser following Stark voltage pulse in resonant cavity
01 p0081 A72-11186
- Instabilities in dye switched ruby lasers emission distribution, investigating filament modes
01 p0081 A72-11314
- Plasma diagnostics facilities design, circuit diagrams and operation based on Q switched ruby laser and optical recording system
02 p0237 A72-11407
- Double 45 degree z cut KD P electro-optic Q switch simulation with programmable desk top computer, deriving extinction ratio dependence plot graphs
02 p0224 A72-11746
- Solid state Q switched laser emission frequency drift from Fabry-Perot rings interferograms
02 p0237 A72-12108
- Phototropic substance effect on spatial structure of passive Q switched ruby laser emission, considering gallium phenylcyanine solution
02 p0239 A72-12568
- Mechanical breakdown characteristics of polymethyl methacrylate and polystyrene samples exposed to picosecond pulses emitted by Q switched laser
02 p0250 A72-12680
- Cross-excited carbon-dioxide-nitrogen laser with pulse sharpening effect due to self-Q-switching, finding optimal nitrogen mixing ratio for peak power
02 p0239 A72-12827
- Single mode solid state laser periodic Q switching effects on spike pulse shape and synchronization by harmonic analysis with convergent series
03 p0366 A72-13371
- Acoustic wave excitation in water droplet with giant pulse radiation from Q switched laser, noting diffraction effects on laser power density requirement
03 p0367 A72-13372
- Multiphotonic ionization of atomic cesium jet by Q switched ruby laser beam
03 p0392 A72-14061
- Self focusing effect of Q switched single mode ruby laser emission in CdS crystal, noting 60 kw minimum threshold power
03 p0369 A72-14064

- Amorphous polymer dielectric luminescence and destruction under Q switched laser radiation with subthreshold power and picosecond pulses
03 p0369 A72-14071
- High power Q switched ruby laser beam one dimensional penetration depth into metal as function of time, emphasizing ionization and plasma heating
04 p0528 A72-14536
- Internal Q switching in CdS laser activated by exciton recombination, observing lag in emission onset after input pulses delivery
04 p0528 A72-14575
- Relaxation processes in Michelson interferometer as integral part of carbon dioxide laser cavity in phase Q switching regime
04 p0530 A72-14990
- Superregenerative linear mode amplification in Q switched He-Xe laser as function of resonator phase, length and signal angle
04 p0531 A72-15147
- Amplitude characteristics of Q switched He-Xe laser at 3.5 microns, using rotating reflection prism and velocity equations
04 p0531 A72-15149
- Tunable optical and IR radiation source by rotating lithium niobate crystal in front of Q switched ruby laser
04 p0550 A72-15599
- Carbon dioxide laser Q switching by molecular gases intracavity Stark modulation with sine or square wave electric field, using methyl chloride and difluoroethane
05 p0669 A72-16609
- Mathematical-physical model for laser pulsed radiation-induced pressure wave transmission through surface and internal biological tissues
06 p0768 A72-18150
- Q switched high power laser pulse compression based on optical polarization change on passing through Kerr-active medium
07 p1000 A72-19038
- Continuously pumped repetitively Q switched Nd-yttrium-aluminum trioxide laser, discussing mode selection technique based on gain excess over hold-off loss
07 p1000 A72-19045
- Ho doped YLF and YAG laser threshold and slope characteristics at room temperature, considering Q-switched operation lifetime
07 p1004 A72-19233
- Neodymium-glass laser emission spectral and temporal correlations during Q switching by rotating prisms and passive shutter
07 p1006 A72-19633
- Nanosecond solid dielectric discharger fired by Q switched ruby laser for commutation of coaxial line forming high amplitude voltage pulses
07 p1008 A72-20509
- Output characteristics of Q switched liquid laser as function of pumping pulse, cavity mirror reflectivity and cavity length
07 p1008 A72-20544
- Direct detonation of insensitive PETN, RDX and tetryl explosives with Q switched ruby laser radiation
08 p1220 A72-20771
- Pulse duration reduction with power gain during second harmonic generation by nonlinear crystal in Q switched buildup resonator
08 p1183 A72-21729
- Early phase time development of far UV line radiation from plasma production by focusing Q switched ruby laser onto solid Mg target
09 p1325 A72-23232
- Electro-optical Q switching of solid state laser sources without linear energy polarization in optical resonator
09 p1326 A72-23422
- Internal Q switching and long time delay emission in electron beam excited p-type and n-type GaAs lasers, indicating optical absorption traps
10 p1489 A72-23947
- Acoustic waves generation in liquids by Q-switched ruby laser, noting transition from plane to spherical waves with dye concentration and focusing configuration variations
10 p1490 A72-23954
- Intracavity modulation of ruby laser with frequency near neighboring axial oscillations frequency difference, describing Q switch based on transverse electro-optical effect in KDP crystal
10 p1490 A72-24047
- Defocused confocal Fabry-Perot spherical interferometer for analysis of Q switched visible and near IR lasers longitudinal mode outputs
10 p1481 A72-24564
- IR radiation generation by Raman scattering and difference frequency mixing with Q switched Nd-YAG laser, noting peak power and photon conversion efficiency
11 p1647 A72-26149
- Mode locked ruby laser having triangular ring cavity with four prisms to obtain reliable single-transverse-mode Q switched and normal operation
11 p1647 A72-26150

- Q switched laser system emitting light pulses for high speed cinematography synchronized illumination
11 p1649 A72-26343
- Q switched ruby laser radiation spatial coherence, considering modes relationship to permittivity inhomogeneities and changes due to holes burning in population inversion
12 p1821 A72-27591
- Giant pulses generation by ruby laser under self Q switching conditions
12 p1821 A72-27592
- Second, third and fourth optical harmonics generation of Nd-doped YAG laser radiation under Q switching fast repetition pulse conditions
12 p1821 A72-27594
- Thin polymer film bleachable dye switches for Q switched laser to achieve high power single pulse radiation
12 p1822 A72-27612
- Mode selection in high coherence ruby laser using KDP Q switch
12 p1823 A72-27618
- Holographic interferometry for impact loaded object transient impulse response recording with double-pulse Q switched laser
12 p1809 A72-27761
- Q switched YAG-Nd laser implementation into target designators and range finders, stressing temperature insensitive design with electronic compensation and thermal equalization
12 p1825 A72-27928
- Q switched carbon dioxide laser based on PM by rotating mirror in one arm of Michelson interferometer, establishing phase relationships
13 p1968 A72-29287
- High power Q switched ruby laser radiation transmission through optically dense plasma, noting bleaching and increased absorptivity
13 p2016 A72-29521
- Transverse flow transverse pulsed chemical CO laser, describing Q switching, pulse duration power efficiency and chemical deactivation processes
14 p2109 A72-30187
- Giant pulse radiation in Q factor modulated Nd glass laser frequency stabilization by molecular Cs vapor
15 p2245 A72-31411
- Flashlamp pumped cryptocyanine Q switched high peak power ruby lasers, noting UV radiation responsible for methanolic solution photochemical decomposition
15 p2249 A72-32156
- Stimulated emission in molecular iodine vapor phase laser optically pumped by Q switched Nd-YAG laser second harmonics
15 p2251 A72-32538
- High power carbon dioxide lasers review covering CW, Q switched and pulsed atmospheric pressure lasers and various excitation techniques
16 p2399 A72-32848
- Q switched laser operation with electro-optic switch mechanism, measuring initial photon number per mode of Nd-glass and Nd-YAG lasers
16 p2399 A72-33014
- Electro-optical Q switch synchronized by laser radiation for nanosecond light pulse shaping with energy dependent triggering
16 p2400 A72-33082
- Q switched and free emission mode locking of neodymium glass and ruby lasers via liquid bleachable dye filter
16 p2400 A72-33296
- Oriental Kerr effect direct observation via birefringence relaxation time measurement in self focusing region of mode locked Q switched laser picosecond pulses
17 p2561 A72-34190
- Simple technique for sequential Q-switching of molecular lasers.
17 p2563 A72-35193
- Influence of molecular laser parameters on the pulse shape in Q-switched operation
17 p2563 A72-35301
- A periodic laser in high-frequency Q-switched operation
17 p2563 A72-35305
- Passive Q switching extension of carbon dioxide laser output frequency range using dichloro-difluoro methane as saturable absorber
17 p2564 A72-35347
- Experimental analysis of the vibrational-rotational line content of a Q-switched CO₂ laser.
18 p2697 A72-36501
- Laser machining of thin films. I - Irradiation characteristics of a focused Q-switched YAG laser beam.
18 p2695 A72-36518
- Single-crystal, electro-optic shutter for Q-switching lasers emitting unpolarized radiation.
18 p2698 A72-36698
- Passive mode-locking and Q-switching of high power lasers by means of the optical Kerr effect.
19 p2811 A72-37844
- Active Q switching technique for producing high laser power in a single longitudinal mode.
19 p2811 A72-37845

Fracture of nonlinear KDP and LiNbO₃ crystals by ruby laser radiation 19 p2812 A72-38537

Doppler Q switching in a single-mode CO₂ laser by a rotating mirror. 19 p2812 A72-38594

Coherent optical signal superregenerative amplification in Q switched gas laser, calculating sensitivity of He-Ne laser light amplifier 19 p2813 A72-38663

Multipulsing behavior of electrooptically Q-switched lasers. 19 p2813 A72-38692

Pulsed and repetitively Q switched ruby and Nd laser design characteristics for optical applications and holography 20 p2930 A72-39027

Influence of the refractive index nonlinearity on the dynamics of emission from semiconductor lasers. 20 p2932 A72-39504

Single-mode laser with a continuously variable pulse duration. 20 p2933 A72-39511

Injection laser under self-Q-switching conditions. 20 p2933 A72-39515

Shock waves resulting from interaction of laser radiation with transparent solids. 20 p2933 A72-39522

Pulse generator for modulation of a low-voltage Pockels cell. 20 p2933 A72-39525

Q switched Nd-YAG laser with lithium niobate crystal cut at Brewster angle for reproducible and controllable giant pulse generation 20 p2933 A72-39562

Transition metal complex organic dye solution for Nd-glass laser Q-switching and mode locking, noting high photochemical stability 21 p3062 A72-40244

Q-switched CO₂ lasers with variable pulse delay. 21 p3064 A72-41006

Observation of transient behavior of picosecond laser pulses. 21 p3064 A72-41380

Electro-, magneto- and acousto-optical methods for laser Q-switching, discussing physical and operational principles 22 p3186 A72-42942

Investigation of the shape of the radiation pulse of a self-mode-locked laser 23 p3294 A72-43303

Alkali metal vapor Q switches for synchronizing mode-locked laser pulse trains with external events. 23 p3297 A72-44189

Neodymium-glass laser emission spectral and temporal correlations during Q switching by rotating prisms and passive shutter 24 p3408 A72-44565

Theory of pulsed internal optical parametric oscillators. 24 p3409 A72-44714

A new method of optical coupling of two laser cavities which permits stable generation of ultrashort optical pulses 24 p3410 A72-45075

Control of laser pulse duration by nonlinear absorption in semiconductors. 24 p3411 A72-45605

Periodic control of the emission from a ruby laser achieved by a Q switch utilizing the transverse electrooptical effect. 24 p3412 A72-45618

Q VALUES

Q values contradiction between lunar and earth rocks, discussing internal friction 04 p0580 A72-15450

Amplitude and frequency characteristics of avalanche diode microwave oscillator loaded with resonant circuits, noting Q value effect on self oscillations 14 p2089 A72-31109

Q values from lunar seismic record measurements indicating separation of scattering and real loss parameters effects on energy propagation, discussing geophysical models 18 p2724 A72-36288

RC gyrator filters frequency characteristics stability analysis, noting elements sensitivity as function of frequency and Q value 19 p2774 A72-38421

Nonlinear molecular absorption cell for frequency stabilization of carbon dioxide laser radiation, discussing stability limit dependence on amplification, absorptivity and Q value 22 p3184 A72-42102

QSO (RADIO SOURCES)

U QUASARS

QUADRANT METEOROIDS

Quadrant meteoritic shower upper atmosphere contamination effects on twilight and night sky brightness 02 p0283 A72-12467

Radio echo observation of Quadrant meteor showers right ascension and declination, observing

mean range and influx rate as function of universal time 10 p1545 A72-24808

Quadrant underdense and overdense meteors observations during sunrise on 16.67 MHz pulsed radar 15 p2312 A72-32197

QUADRANTS

Disk stretching under tensile stresses, determining stress at arbitrary point in half band form connected with quadrant 05 p0737 A72-16294

Comets heliographic coordinates and angles quadrants from orbital elements 08 p1229 A72-20832

QUADRATIC EQUATIONS

State space technique application to discrete linear control systems synthesis, discussing time-optimal and quadratic-cost problems, and pole assignment method 17 p2532 A72-34246

QUADRATIC PROGRAMMING

Linear and quadratic programming procedures in optimal control problems of stochastic and deterministic system design 02 p0198 A72-12807

Two parameter trajectory measurement optimal planning reduced to quadratic programming based on linear programming generalization for continuous case 05 p0721 A72-16758

Nonlinear filter dynamics for stochastic optimal control for quadratic cost functional, evaluating performance 08 p1145 A72-20866

Missile tracking laws for inhomogeneous linear-quadratic performance optimization 11 p1593 A72-25992

Data processing method for optimal prediction of spacecraft orbital elements, using dynamic and quadratic programming 14 p2151 A72-30455

Two parameter trajectory measurement optimal planning reduced to quadratic programming based on linear programming generalization for continuous case 17 p2610 A72-35261

Computation of optimal controls by a method combining quasi-linearization and quadratic programming. 18 p2673 A72-36824

A quadratic programming approach to the impulsive loading analysis of rigid plastic structures. 21 p3120 A72-41205

Mathematical formulation of linear programming problem, reducing vector value optimal management plan determination to quadratic programming problem 22 p3198 A72-42179

QUADRATURE APPROXIMATION

U QUADRATURES

QUADRATURES

Linear stochastic-parameter output channel, examining signal quadrature components statistical characteristics 01 p0024 A72-10199

Nth order linear differential inequalities reduction to first order, permitting Chaplygin theorem infinite applicability limit and solution by quadratures 03 p0382 A72-14313

Angular quadrature effects on two dimensional space power reactor radiation shield calculation for manned space station application 04 p0546 A72-14426

Wilf-type quadrature formulas with preassigned nodes, featuring existence of error bound without derivatives 05 p0632 A72-15816

Computing techniques for finite Fourier transform, applying to Poisson equation, interpolation and quadrature and data smoothing 07 p1025 A72-18784

Sensitivity loss from approximation to radar and sonar signal square law detectors in quadrature systems with postdetection integration 10 p1437 A72-24690

Poised and nonpoised Hermite-Birkhoff interpolation problems application to quadratic formulas and expansions and completely convex functions 11 p1732 A72-25504

Quadrature solution for variable mass point motion under perturbing force in trajectory plane normal to velocity vector 13 p2003 A72-28725

Linear stochastic-parameter output channel, examining signal quadrature components statistical characteristics 15 p2195 A72-31623

Bairstow Method extension with restored convergence for multiple quadratic factors using interval arithmetic 15 p2262 A72-31631

Damping perturbation of high order nonlinear autonomous Liapunov system, reducing system equations integration to quadratures via transformation to lower order quasi-linear nonautonomous system 16 p2422 A72-32938

Relationship between finite differences and quadratures of a Green's function for a second-order ordinary differential operator 17 p2577 A72-35803

Quadrature solution for variable mass point motion under perturbing force in trajectory plane normal to velocity vector 22 p3205 A72-42101

A simple quadrature method for computing laminar boundary layers. 22 p3165 A72-42110

Application of the method of mechanical quadratures to the approximate solution of nonlinear singular integral equations 24 p3419 A72-45646

QUADRUPOLE LENSES

U MAGNETIC LENSES

QUADRUPOLE NETWORKS

Staged corrector, transformer and low pass filter two terminal pair matching network for resonant circuits using semiconductor elements 03 p0333 A72-13897

Computerized filter design, discussing frequency analysis and synthesis programs for quadrupole eigenmodes and transfer function 11 p1604 A72-26089

Three section stepped structure to satisfy requirements for multifunction matching four-pole in signal network with active semiconductor component 15 p2210 A72-32708

Synthesis of passive matching two-ports with given apparent resistances. III 20 p2907 A72-39424

Possibility of developing combination method for calculating, with a controlled quantization step, the response of a nonlinear network 21 p3074 A72-40184

Complex amplitude four-pole network nonlinear conversion of sum of sinusoidal oscillations 22 p3158 A72-42083

Determination of the spectra of modulated pulse trains by the spectral function method 22 p3154 A72-42122

Calculation of the nonlinear dynamic regime of a two-terminal pair network with a weak nonlinearity 23 p3270 A72-43772

QUADRUPOLES

Electric quadrupole to magnetic dipole f-values for CO fourth positive and nitrogen Lyman-Birge-Hopfield systems, using curve of growth method 01 p1013 A72-10092

Plasmoid transport in quadrupole and octupole magnetic fields, measuring plasma amounts in axial region charged particle densities and flux densities at vacuum chamber wall 03 p0395 A72-13568

Quadrupole mass spectrometer ultimate characteristics concerning resolution, range, recording speed, working pressure and sensitivity 03 p0360 A72-13665

Hyperfine interactions of Fe cations in ilmenite determined by Mossbauer spectroscopy, noting internal magnetic field and quadrupole coupling constant 09 p1367 A72-22457

Ion quadrupole effects in ion-molecule collisions, calculating capture cross sections and ion trajectories 09 p1354 A72-22658

Optical hyperfine structure of Ne 21 excited states and quadrupole moment obtained by laser induced line narrowing techniques 10 p1515 A72-24601

Gravitational quadrupole radiation derivation from Einstein equations integration by successive approximation and variable separation procedures 10 p1513 A72-25167

Plasmoid transport in quadrupole and octupole magnetic fields, measuring axial charged particle and flux densities at vacuum chamber wall 11 p1699 A72-26755

Quadrupole ion pump performance characteristics, presenting pumping speed as function of pressure at different peak voltages 12 p1805 A72-27040

Solar magnetic field variation during solar rotation from sunspot observations, noting similarity to magnetic stars and behavior as quadrupole magnetic rotor 12 p1871 A72-27746

External magnetic field effect on two frequency quadrupole spin echo in polycrystalline specimen 13 p1915 A72-28473

Human torso surface mathematical model to determine equivalent heart dipole and quadrupole locations for ECG measurements 13 p1908 A72-28571

Relaxation methods of magnetic and acoustic spectroscopy for studies of gravitational and inertial dipoles and quadrupoles in molecules and nuclei of solid bodies 14 p2143 A72-30963

Semiconductor quadrupole optical links consisting of electroluminescent diode and photoreceptor, discussing operation and design principles 17 p2594 A72-34333

Differential equations for digital model of linear quadrupole, discussing digital simulation of analog radio equipment circuits

19 p2775 A72-38659

A long line as a limit of an infinite quadrupole chain

20 p2904 A72-39592

Computer simulation of RF-confinement of plasmas in an open-ended toroidal quadrupole.

21 p3089 A72-40191

QUALITATIVE ANALYSIS

Binary systems phase diagrams qualitative and quantitative analysis based on free atoms electron state energy ratios, formulating solid solubility criterion

14 p2123 A72-30994

Qualitative determination of organometallic substances in solid propellants by thin layer chromatography

23 p3262 A72-43598

QUALITY CONTROL

Hat section stiffened compression panel of graphite/epoxy composite for space shuttle, discussing quality control procedures

01 p0139 A72-10736

Integrity control procedures for machining, drilling and grinding of steel and Ti alloy aircraft parts, discussing nondestructive inspection method

[SME PAPER IQ 71-238] 01 p0076 A72-10969

Point density measurement and crack detection in P/M green compacts with interconnected porosity by pneumatic tests, noting application to quality control

02 p0233 A72-11458

Quality control - Conference, Chicago, May 1971

02 p0304 A72-11551

NERVA fuel quality control, discussing planning, nondestructive tests, computer data acquisition and certification systems

02 p0258 A72-11552

Quality control function in configuration management, discussing hardware and software validity for decision formulation

02 p0304 A72-11553

NASA quality assurance program, discussing management planning, assessment, failure prevention and cost effectiveness

02 p0304 A72-11554

Navy uhf telemetry transmitter production system, discussing test program contribution to quality control

02 p0177 A72-12322

Thermography capabilities and limitations for design analysis and quality control in nondestructive testing of material test vehicle carbon-carbon composite cones

03 p0364 A72-14026

Boron/aluminum composite sheet quality evaluation by radiography, ultrasonic C-scanning and micro-ohm resistance measurement, correlating with resistance weld strength

04 p0526 A72-14839

Hydrogen generation mechanism during cadmium plating of steel, describing porosity testing technique

04 p0527 A72-15548

Foundry Al alloys elasticity limit estimation via regression formulas, discussing application to quality control

04 p0534 A72-15560

Metallurgical treatment control reliability in machine part mechanical properties quality evaluation

05 p0671 A72-15993

Turbojet aircraft engine overhauling planning and execution, discussing dismantling, washing, galvanic treatments, acceptance checks and quality controls

05 p0643 A72-16014

Laser interferometer for quality control of optical parts and instruments

05 p0668 A72-16191

Quality control of powdered metal parts, considering chemical, atomization, electrolytic and mechanical production stages, tool inspection and test patterns

06 p0822 A72-18070

Radome checkout ensuring reproducibility by insertion phase delay measurement

06 p0822 A72-18195

Micrographic evaluation of inclusions in austenitic stainless steel tubes ensuring surface quality control

07 p0994 A72-18972

Turboprop electric igniter climatic test problems and equipment for assessing quality control

07 p0954 A72-19112

NASA programs phased planning and quality assurance techniques, noting cost effectiveness

07 p1102 A72-19126

Quartz crystal oscillator device for continuous monitoring and controlling thin film thickness in optical and electronic applications, noting temperature effects on crystal oscillating frequency

07 p0990 A72-20284

Optimal test conditions in magnetoscopic control by electrical system for subsurface defects detection, obtaining tangential magnetic field on carbon steel plates

07 p0991 A72-20421

IR ray thermography, discussing application to tires testing and rubber manufacture

07 p0991 A72-20422

Utility function construction for engineering plants quality criteria

09 p1413 A72-22216

Measured quantity distribution effect on measurement errors, noting application in mass production process control

09 p1316 A72-23662

Complete reliability program major activity areas identification, discussing various components interrelations

10 p1485 A72-23973

Statistical test plans with improved flexibility, application ease and efficiency for maintainability demonstration

10 p1504 A72-23998

Design review as management tool for complex systems quality and reliability assurance, discussing Skylab program

10 p1486 A72-24005

Failure mode control in plastic packaged IC for screening and quality assurance

10 p1447 A72-24010

Delayed pulse echo and through-transmission ultrasonic techniques for nondestructive inspection and quality control of braze bonds in high current electric contact assemblies

10 p1487 A72-24173

Reference radiosondes for quality control of global high altitude temperature, pressure and humidity measurements, discussing dual soundings and synoptic comparison

10 p1484 A72-25077

Visual image indicator used beside and behind objects for neutron radiography quality determination and radiographs series grading

11 p1632 A72-25822

Powder metallurgy sintering process variables for dimensional control of bronze parts, discussing strength and porosity level specifications

11 p1640 A72-26243

Tolerance intervals in multiple type acceptance sampling plans with attribute-based inspection

11 p1749 A72-26790

Specification requirements for quality assurance of automated data processing systems based on hardware development procedures

11 p1602 A72-26791

Metrological techniques reliability for industrial production processes, plotting quality control curves

11 p1637 A72-26823

Optical quality requirements for aircraft transparencies, considering resolution, haze, halation, light transmission, distortion, binocular deviation, double images, scratches and inclusions

12 p1832 A72-27003

Device for comparing powders friability to ascertain quality of compacts fabricated on automatic sintering presses, noting applications in ceramic, chemical and pharmaceutical industry

12 p1795 A72-27468

Reliability, quality and testing assurance in ATS F and G system, discussing computerized handling of spacecraft parts information

12 p1814 A72-27524

Lens evaluation procedure based on optical transfer function data, discussing computer displays and merit parameters

12 p1810 A72-27936

NASA reliability and quality assurance methodology to improve hospital biomedical equipment, using space electric rocket test example

12 p1814 A72-27960

Numerically controlled composite tape laying machine, discussing production run simulation, raw material quality effect and control corrective devices

12 p1815 A72-28078

Surface integrity machining practices application to jet engines production, noting cost reduction and process selection and quality control improvement

[ASM PAPER W 72-27.2] 12 p1862 A72-28163

Parametric approaches to statistical burn-in or debugging problems in aircraft reliability analysis

13 p1985 A72-28363

Optimal multistep sampling procedures for production quality control, discussing methods for minimization of error probabilities and total sampling volume

13 p1965 A72-29167

Indirect statistical quality control procedure for piece goods in batch based on image recognition technique for data classification

13 p1965 A72-29175

Reliability of nondestructive ultrasonic testing methods of quality control, discussing defect size distribution and detectability coefficient

14 p2106 A72-30149

Hot worked Al alloy machine elements mechanical properties scattering, discussing quality control procedures

14 p2114 A72-30275

French quality assurance of electronic components, discussing organizational links with international bodies

14 p2174 A72-30848

Product reliability prediction from failure mode analysis, examining component design, quality control, engineering analysis configuration selection and product testing

[ASME PAPER 72-DE-17] 14 p2108 A72-30863

Semiconductor devices quality assurance based on electrical and mechanical performance tests at every stage of product manufacture from initial design

14 p2091 A72-31164

Internal reflection IR spectroscopy application to composite and double base propellants study, discussing merits as quality control technique

15 p2296 A72-32312

Surface crack detection in ferrous and nonferrous metals, glass, ceramics and plastics by water-washable dye penetrants process

16 p2397 A72-33239

Computerized calculation of electronic circuit and equipment reliability and quality control, presenting task examples and printout form

16 p2368 A72-33347

Russian book on aircraft turbine and spacecraft rocket engine assembly covering process schedules, work organization, precision, joints and couplings, quality control, etc

16 p2399 A72-33373

Principle of control of aspherical surfaces by holography and moires

17 p2554 A72-34912

A recognition method for technical diagnosis of analog electronic circuits

17 p2522 A72-34913

Price adjusted single sampling with linear indifference.

17 p2560 A72-34943

Acoustic emission technique as NDT method for quality control of brazed metal-ceramic bonding

18 p2695 A72-36458

The AEG 60-50 process computer in special research field 55 at the Rhein-Westphalian Technische Hochschule at Aachen

18 p2664 A72-36680

Quality assurance of transistor chips for the user

18 p2669 A72-37120

Microwave varactors for communications satellites

18 p2670 A72-37122

Reliability assurance of space equipment components, discussing drift and failure modes, computerized simulation and thermal maps

18 p2743 A72-37127

Standardization and quality assurance of electronic devices on the national and European levels

18 p2743 A72-37129

Components analysis laboratory with curve tracers, third harmonic index equipment, noise meters, TV X ray system and metallographic microscopes

18 p2676 A72-37132

Production and test facilities availability effect on costs involved in obtaining item at required quality level, examining component rejects and defectives

18 p2670 A72-37133

Qualification procedure for high reliability electronic part requirements for noncontinuous production

18 p2744 A72-37134

Quality and reliability evaluation method for integrated circuits using MOS transistors - Option: Circuits on request

18 p2671 A72-37141

Test structures - Powerful technique for quality evaluation and reliability assessment of MSI and LSI /medium and large scale integrated circuits/.

18 p2671 A72-37143

Surface evaluation of airfoils via contouring.

19 p2806 A72-37605

A stand for quality control of the vibrational characteristics of 'ultraquiet' radial ball bearings

19 p2807 A72-37663

Production measuring equipment and techniques for quality control, emphasizing measurement accuracy, speed and cost effectiveness maximization

19 p2802 A72-38304

An automated instrument for monitoring the quality of recovered water.

[ASME PAPER 72-ENAV-16] 20 p2895 A72-39161

Al-B and Al-Ti-B alloys fabrication, discussing quality control and grain refinement

20 p2936 A72-39207

Variation analysis and design of experiments as an aid to design quality assurance.

20 p2930 A72-39856

Microelectronic component reliability prediction technique with near Weibull method accuracy in absence of detailed sampling life test results

20 p2930 A72-39857

Information criterion for optimal planning of reliability acceptance tests maximizing average effect

21 p3038 A72-40714

Single and double sample Dodge-Romig lot tolerance percent defective /LTPD/ rectifying inspection plans, using standard tables

21 p3059 A72-40827

Holographic interference as a means for quality determination of adhesive bonded metal joints.

[ICAS PAPER 72-06] 21 p3060 A72-41131

An immersion interferometer for monitoring the quality of second-order aspherical surfaces
21 p3058 A72-41808

Precision forged turbine and compressor blades.
22 p3183 A72-42518

Methods for the quality control of the reflecting surfaces of solar energy condensers /Survey/
22 p3140 A72-43187

Information theory application for structural complexity measure of microelectronic logic circuits for digital computers, noting elements standardization for design quality criteria
23 p3269 A72-43441

Non-destructive testing of adhesive bonded metal-to-metal joints. I.
24 p3408 A72-45289

NDT application and development in industry, considering confidence in inspection techniques, framework and management resistance
24 p3408 A72-45295

Metallurgical treatment control reliability in machine part mechanical properties quality evaluation
24 p3416 A72-45735

QUALITY FACTORS

U Q FACTORS

QUANTITATIVE ANALYSIS

Resonance neutron transmission for nondestructive absorption spectroscopic evaluation of quantitative chemical or isotopic composition at depth in large samples
01 p0069 A72-10806

Specific quantitative trace analysis technique for solids using spark source mass spectrometry
03 p0361 A72-13849

Thin layer chromatography technique for rapid quantification of bacterial cell adenosine triphosphate, using microscope ultraviolet photometer
06 p0763 A72-17872

Diastereomeric S-prolyl dipeptide derivatives adaptation to gas chromatographic quantitative estimation of R- and S-leucine enantiomers
11 p1590 A72-26366

Partial pressure gage to measure water vapor-produced hydrogen content in metal samples, using reference gas evolution curves
12 p1807 A72-27451

Binary systems phase diagrams qualitative and quantitative analysis based on free atoms electron state energy ratios, formulating solid solubility criterion
14 p2123 A72-30994

Red blood cell metabolite 1,3 diphosphoglycerate determination method by rapid deproteination, concentration by precipitation and enzymatic reaction
15 p2190 A72-32488

Improved techniques for separation and determination of rare-earth elements in extraterrestrial material.
20 p2900 A72-39836

Rapid determination of total carbon content in titanium carbide
22 p3176 A72-42200

QUANTIZATION

U MEASUREMENT

QUANTIZER

U COUNTERS

QUANTUM AMPLIFIERS

Optimal location of nonreciprocal disk shaped YIG element traveling wave quantum ruby paramagnetic amplifier for weak magnetic levels
08 p1138 A72-20795

Signal detection in ruby element quantum paramagnetic amplifier operating at liquid nitrogen temperature
08 p1141 A72-21377

Ruby use for submillimeter range optically pumped quantum paramagnetic amplifier
08 p1183 A72-21770

Saturation protection of a maser amplifier by the pulse-modulated pumping method
21 p3063 A72-40785

QUANTUM COUNTERS

Superconducting quantum flux sensors for measuring magnetic fields and susceptibility, voltage and resistance
09 p1308 A72-22466

Solar X ray burst analysis from individual quantum/energy and time recordings by Lunokhod 1 spectrometer
13 p2032 A72-29700

Investigation by the photon count method of the statistical properties of the emission of a laser operating in the mode of several axial oscillations
21 p3063 A72-40784

QUANTUM ELECTRODYNAMICS

Electron emission in strong electromagnetic waves within quantum electrodynamics, discussing energy losses and electron pair production
03 p0415 A72-13003

Hf solid state and quantum electronic devices - Conference, Cornell University, August 1971
06 p0787 A72-18453

Pulsar dynamics and electrodynamics for power derivation from rotational energy, discussing toroidal magnetic field induced nonhydrostatic stress in neutron star
07 p1068 A72-19001

Nonthermal ultrarelativistic plasmas covariant analysis with quantum electrodynamics and Green function theory of nonequilibrium statistical mechanics, discussing electron-positron pair production and annihilation
10 p1525 A72-25100

Propagation theory and quantum electrodynamics for light transmission in scattering media
13 p2002 A72-28511

Book - Topics in solid state and quantum electronics
17 p2594 A72-34560

QUANTUM GENERATORS

U STIMULATED EMISSION DEVICES

QUANTUM MECHANICS

NT QUANTUM ELECTRODYNAMICS

Inertial-gravitational mass ratio in classical and quantum case, proving equivalence principle non-validity for Brans-Dicke gravitation theory compared to Einstein theory
01 p0102 A72-10861

Noninteracting Fermi gas in finite square-well potential, obtaining quantum mechanical solution of Schroedinger equation
02 p0262 A72-11671

Quantum oscillations of minority Fermi surface carriers as function of magnetic field in Hall effect and thermoelectric power in pressure-annealed pyrolytic graphite
02 p0268 A72-11673

Three dimensional angle dependent model for three body problem, considering exact quantum mechanical reactive scattering cross sections
02 p0262 A72-11911

Coulomb logarithm for hot plasma viscosity coefficient in magnetic field by quantum mechanical unified theory
02 p0267 A72-12770

Quantum mechanical calculations of autoionization structure in ionization of Ba positive ions by electron impact
03 p0391 A72-13746

Quantum mechanical analysis of detuning in cascaded cavity molecular beam masers
03 p0368 A72-13747

Quantum mechanical electron motion problem in binary alloy crystal lattice, discussing Bloch approximation, energy spectra, and third element admixture conductivity effects
07 p1049 A72-20150

Atom interactions with rf field, using quantum mechanical interpretation in terms of photons
07 p1038 A72-20433

Quantum mechanical transport equation for radiation interactions with molecules subject to perturber atom collisions, describing macroscopic density matrix evolution
07 p1039 A72-20683

Probabilistic derivation of quantum mechanics wave equations for Brownian motion and spatial-temporal diffusion
10 p1505 A72-24071

Nonrelativistic quantum concept of electromagnetic field interaction with charged microparticles
11 p1692 A72-26093

Interstellar anomalous 6 centimeter formaldehyde absorption in diffuse dark nebulae, discussing quantum mechanics of collisional pumping process
11 p1720 A72-26112

Book on density matrix theory application to lasers and masers, covering quantum mechanics, perturbation theory, magnetism and magnetic resonance, statistical ensembles, etc
12 p1826 A72-28203

Finite particle propagator constructed by path integral method, deriving infinitesimal propagator in relativistic quantum mechanics from mass nature consideration in Machian cosmological sense
13 p2001 A72-28499

Quantum kinetic equation for monatomic and molecular gases optical characteristics calculation, considering spontaneous emission spectrum of atoms
14 p2110 A72-30358

Quantum mechanical calculation of interaction potential energy surface role in vibrational excitation of diatomic molecules
14 p2134 A72-30750

Rare earth metals and alloys technology assessment and utilization covering quantum mechanics concepts application to Fermi surface
15 p2289 A72-31184

Diatomic molecules partition functions derivation by classical and quantum mechanical theories for simple harmonic oscillator and square-well potential
15 p2280 A72-31693

Expansion formulas for Kampe de Fériet and radial wave functions application to heat conduction and quantum mechanics problems
15 p2336 A72-32398

Multispecies magnetoplasma ac electrical conductivity tensor collision factor from quantum mechanical convergent kinetic equation
15 p2287 A72-32411

Quantum mechanics framework for electron movement perpendicular to intense magnetic field, predict-

ing energy broadening with time for initially monoenergetic electron beam
16 p2422 A72-32881

Quantum mechanics variational methods reformulation for turbulent diffusion of marked particles
16 p2379 A72-33570

Acoustic tunnel effect in elastic waveguide, noting penetration coefficient and quantum mechanics potential barrier
16 p2364 A72-33588

A one-dimensional harmonic oscillator in quantum mechanics with a nonnegative distribution function in the phase space
17 p2579 A72-34198

New demonstration of the adiabatic theorem for conservative systems in wave mechanics
18 p2711 A72-36473

On the algebraic structure of a class of solvable quantum problems.
18 p2711 A72-36514

Quantum fields interaction with classical sources on Schwarzschild background, noting mass, charge and angular momentum as sole measurable quantum numbers of black hole
18 p2726 A72-36716

Measurements of the laser linewidth due to quantum phase and quantum amplitude noise above and below threshold. I.
19 p2811 A72-38084

Observation of quantum-phase and quantum-amplitude noise for a laser below and above threshold.
20 p2934 A72-39813

Hydrodynamic and Wiener-Siegel hidden parameter models incapability for quantum mechanics reduction to classical mechanics, obtaining proofs to von Neumann theorem
23 p3312 A72-43298

QUANTUM NUMBERS

Magnetic mirror system to study Lorentz ionization of highly excited hydrogen atoms with quantum numbers 6-7 in strong magnetic fields
09 p1363 A72-23222

Na atoms D line radiation excited in collisions with molecular gases, noting transfer cross section dependence on kinetic energy for given quantum number change
13 p2009 A72-30063

Tabulation of diatomic molecular lines observed in sunspot spectra with rotation branch, quantum number and vibration band
15 p2316 A72-32750

Quantum fields interaction with classical sources on Schwarzschild background, noting mass, charge and angular momentum as sole measurable quantum numbers of black hole
18 p2726 A72-36716

QUANTUM STATISTICS

Topological structure of anharmonically coupled many body problem, describing generalized Bose operators formulation
02 p0262 A72-12049

Thermodynamic equilibrium, transport and optical properties and quantum effects in nonideal plasmas, using Monte Carlo method
05 p0700 A72-17223

Superradiant laser stationary behavior and photon statistics, solving Fokker-Planck equation for quantum mechanical distribution function in Hilbert space of atomic system
10 p1514 A72-24247

Quantum condensation in finite volume boson gas, using Bogoliubov quasi-expectation value method
10 p1563 A72-24676

Ionization equilibrium description by quantum statistical fugacity expansion of pressure for partially ionized plasmas
10 p1524 A72-24929

Papers on kinetic equations covering axiomatics, quantum and relativistics, plasma kinetic theory role in spectral line width, etc
17 p2590 A72-35151

QUANTUM THEORY

Stimulated Raman scattering effect on two quantum absorption during RF radiation first and third harmonics interaction
02 p0180 A72-12582

Nonstationary radiation transfer with one dimensional anisotropic scattering, deriving Bessel function expressions for quantum exit from semiinfinite medium
02 p0262 A72-12830

Astronomical photographic emulsions and phenidonehydroquinone developer relative detective quantum efficiency measurements
03 p0352 A72-13007

Molecular oxygen evolution Mn catalyst photoactivation as two-quantum process, discussing kinetic model computer simulation
04 p0484 A72-15740

Monograph on semiclassical gas laser theory covering electromagnetic fields, atomic polarization, multimode theory, traveling- and standing-wave laser principles, collision effects, etc
05 p0668 A72-16398

Laser quantum theory for single mode steady state emission fluctuations and instability region with high density of excited atoms

07 p0999 A72-18910

Quantum optics analysis of light propagation and photon flux fluctuations in medium with random dielectric constant inhomogeneities

07 p0938 A72-18912

Electrons and ionized impurities interaction in thin quantizing layers, discussing donor activation energy and kinetic characteristics

07 p1048 A72-19640

Density matrix equation solution in Liouville space, using variational procedure for laser mode equation and separable interaction method

07 p1006 A72-19670

Redundancy of Hamiltonian constraints in classical and Dirac quantum theories of gravitation, suggesting replacement by single integral-form condition

07 p1035 A72-20195

Wightman field theory generalization for application to gravitational field quantization, describing curved space-time by strongly geodesically complete manifolds

07 p1036 A72-20198

Quantum and classical gravitation theory Mercury perihelion motion dependence on fourth order potential in scalar and Dirac fields

07 p1084 A72-20689

Quantum gravitation theory and Mercury perihelion motion, calculating three body potentials from treatment of celestial bodies as nucleon assemblies

07 p1084 A72-20690

Electronic factors role in intermolecular interactions and biochemical evolution, applying quantum biochemistry

08 p1128 A72-22006

Molecular hydrogen dissociation by He, observing molecule initial quantum states effect on temperature dependent reaction cross section

09 p1357 A72-22855

Finite rest masses of wave quanta in material media, discussing dispersion and Einstein formulas equivalence, Doppler effect, gravitational red shift and radio photon trajectories

10 p1512 A72-24790

Quantum beats in transitions from levels subject to optical cascades

12 p1847 A72-27184

High order optical harmonic generation and many-quantum processes efficiency in multimode laser radiation field

12 p1821 A72-27593

Russian monograph on laser kinetic theory covering quanta dissipative systems, lasing equations, steady state, semiconductor emission, giant pulses, magnetic quantization, etc

12 p1827 A72-28338

Electron distribution near semiconductor-metal contact, discussing current carriers quantum properties effects

13 p2021 A72-28679

Atomic hydrogen viscosity and thermal conductivity coefficients for 1-100,000 K, using quantum theory for low temperatures and classical mechanics for high temperatures

13 p2065 A72-29299

Geomagnetic field perturbation by gamma quanta pulsating source, studying accompanying radio emission behavior

14 p2101 A72-30645

Quantum models for the lowest-order velocity-dominated solutions of irrotational dust cosmologies.

17 p2613 A72-35392

The classification of transitions between levels of principal quantum numbers 3 and 4 in Fe IX to XVI and Mn VIII to XV.

17 p2586 A72-35834

Quantum noise in semiconductor lasers.

18 p2697 A72-36345

Optical polarization effects in a gas laser.

18 p2697 A72-36487

On the adiabatic invariants of a quantified system perturbed by a coherent wave

19 p2834 A72-37789

Quantum crystals in the single-particle picture.

19 p2844 A72-37943

Laser quantum theory for single mode emission fluctuations and instability region with high density of excited atoms, noting self consistent field effects

20 p2931 A72-39376

Quantum optics analysis of light propagation and photon flux fluctuations in medium with random dielectric constant inhomogeneities

20 p2932 A72-39378

Quantum limit studies in single crystal and pyrolytic graphite.

21 p3097 A72-41186

Quantum-chemical model of organic ring-shaped molecule with persistent magnetization at microscopic level

22 p3150 A72-42318

Molecular crystals stationary Raman oscillators quantum model, deriving coupled nonlinear equations for excited modes polariton operators

24 p3409 A72-44912

Supersonic combustion photochemical initiation feasibility, measuring quantum yields and induction times in hydrogen, oxygen and chlorine mixtures

24 p3464 A72-45058

QUARKS

Relativistic quark search by flash tube chamber in extensive air showers at ground level

03 p0410 A72-13149

German monograph on experimental search for quarks in cosmic ultraradiation, describing hodoscope for particle ionization measurement

09 p1378 A72-23100

Underground delayed shower particles small pulse events interaction analysis for muons and pions compared with quark behavior

16 p2450 A72-34140

Liquid scintillation counters application in search for relativistic quarks in cosmic rays, setting upper confidence limits on particle intensity

17 p2601 A72-35471

Upper limits on vertical fluxes of $1/3$ e and $2/3$ e charged quarks in cosmic rays from observations with scintillation counter telescope

21 p3101 A72-41450

QUARRIES

U MINES (EXCAVATIONS)

QUARTZ

NT COESITE

Impurity-related color centers and electron-hole traps in quartz by electron spin resonance and thermoluminescence observations

02 p0207 A72-11598

Anharmonic thickness shear oscillations in hf quartz resonators with round coaxial electrodes, using Mindlin approximation to wave equation

02 p0191 A72-12032

Tunnel diode quartz oscillator frequency stability improvement and dc power requirement reduction using nonlinear feed circuits

03 p0331 A72-13555

Possible origin of dissymmetry of life, excluding synthesis under influence of optically active quartz

04 p0468 A72-14758

Normal diathermancy coefficient determination from quartz and distilled water spectral transmittance data, applying to diathermic cooling system design

05 p0751 A72-17071

Thin film optical waveguide with crystal quartz as substrate, observing reversible TE to TM mode conversion due to anisotropy

07 p0953 A72-18878

Fluid inclusions in quartz crystals from calcite in Cambrian metasedimentary rocks in South-West Africa

07 p0975 A72-18907

Quartz oscillator short term frequency instability lower limit estimation by calculating Q values and non-linearity and resonator parameter fluctuation effects

07 p0953 A72-19009

Phase locking loop synchronized quartz oscillator for integral frequency multiplication in wideband carrier frequency systems

07 p0954 A72-19174

Pulsed ruby laser mode structure effects on quartz damage, noting dependence on propagation and polarization directions with crystal

07 p1001 A72-19196

Carbon dioxide laser radiation interaction with solids, applying to fused quartz drilling

09 p1323 A72-22904

Gruneisen tensor relationship to elastic and thermal properties of anisotropic quartz fiber-phenolic composite

10 p1500 A72-24251

Two dimensionally reinforced quartz-phenolic composite material dynamic fracture behavior under stress wave loading in uniaxial strain, noting spallation threshold time dependence

11 p1669 A72-25291

Mechanical behavior of three dimensional reinforced ablative composites, including carbon-phenolic, quartz-phenolic and quartz-carbon materials

11 p1670 A72-25459

Relaxation oscillator synchronized by quartz crystal between emitter and base of unijunction transistor, obtaining sinusoidal output by series-connected RC load

13 p1926 A72-28377

Ablation rate growth phenomenon in meltable material with increasing thermal flux, discussing quartz glass characteristics

13 p2066 A72-30007

Eruptive center location and flow direction measurements for andesite and quartz latite lava flows in Mogollon Mountains

15 p2223 A72-31579

Linear and rotational quartz fiber accelerometers suitable for geophysical and inertial use.

20 p2923 A72-39103

[AIAA PAPER 72-822]

Quartz and calcite spectral emission polarization calculation from Fresnel equation, comparing results with field measurements with broadband IR radiometer

21 p3097 A72-40603

Kinetics of carbothermal reduction of quartz under vacuum.

21 p3073 A72-40934

Ablation rate growth phenomenon in fusible material with diminished thermal flux, discussing quartz glass characteristics

22 p3244 A72-42728

Quartz and feldspar glasses produced by natural and experimental shock.

23 p3285 A72-44136

QUARTZ CRYSTALS

Cosmic and X ray irradiated quartz particles as contributor to interstellar extinction, discussing grain radiation damage measurements and absorption spectra in wavelengths of approximately 1600 A to 20 micrometers

01 p0134 A72-11163

Electronic chronometer design problems, describing quartz clock components and temperature and voltage variation effect on accuracy

04 p0525 A72-15572

Quartz crystal oscillator device for continuous monitoring and controlling thin film thickness in optical and electronic applications, noting temperature effects on crystal oscillating frequency

07 p0990 A72-20284

Thin films thickness control by piezoelectric quartz crystal, discussing electrically excited oscillations wavelength and damping characteristics

07 p0990 A72-20285

Interatomic force model for elastic properties of alpha quartz and alkali halides generalized for specified structure under arbitrary pressure

07 p0980 A72-20519

Quartz crystals ultrasonic vibrations produced by laser beam, noting light modulation depth dependence on effective cross section and amplitude

09 p1322 A72-22415

Laser damage resistance properties of thin film multilayer antireflection coatings for quartz optics

09 p1326 A72-23348

Stopfenheim Kuppel area as part of meteorite crating event forming Reis Kessel and Steinheim Basin from quartz grain shock feature analysis

10 p1537 A72-24159

Piezoelectric quartz crystal microbalance for material outgassing and optical element contaminant film measurements

12 p1806 A72-27047

Susceptance inductive loaded evanescent mode waveguide filters with reduced length, using quartz tuned elements

12 p1792 A72-27697

Metastable coesite crystal growth in highly strained quartz under 5-20 kb pressures and 450-900 C

14 p2099 A72-30322

Embedded piezoelectric quartz crystal transducer with Hopkinson pressure bar to measure internal dynamic stress

15 p2240 A72-32433

Minimum values estimation of amplitude fluctuations dispersion and spectral line width for conventional and quartz crystal controlled oscillators

15 p2210 A72-32735

Quartz microbalance studies of an adsorbed helium film.

18 p2719 A72-36677

High-sensitivity resonant-quartz scales operating in high vacuum at very low temperature - Application to the study of gas-solid interactions

19 p2800 A72-37834

Magnitude of the attenuation troughs of a two-branch filter with multiple-frequency quartz resonators

23 p3272 A72-44170

QUARTZ LAMPS

Cartridge system for substrate heating to 500 C in vacuum chamber during metals or semiconductor vapor deposition, describing carbon block-high intensity quartz lamp assembly

07 p0984 A72-19325

QUARTZ TRANSDUCERS

Differential error of fused quartz Bourdon tube precision pressure gages as function of absolute pressure level tested for nitrogen

13 p1959 A72-29764

Improvements in the wide-band vertical quartz torsion accelerometer.

18 p2689 A72-36030

On mechanical response of a non-uniform piezoelectric transducer under the influence of a body-force.

23 p3291 A72-44316

Monolithic quartz and ceramic bandpass filters for narrow band analog data transmission systems

23 p3273 A72-44347

QUASARS

Radio sources structure in astronomical catalog, noting no difference between quasars and radio galaxies

01 p0127 A72-10291

Astronomical research, discussing Venus exploration, stellar evolution quasar structure, Maffei galaxies, black holes, dwarfs and neutron star model

01 p0133 A72-11099

Critique on luminosity volume test for quasars, considering space distribution and luminosity function

01 p0133 A72-11126

Quasar model proposal as giant pulsar rejected discussing mass, radius, magnetic field strength, luminosity and gamma radiation

01 p0134 A72-11144

Radio galaxy and quasar structure from 3.8 cm observations, fitting models to data

02 p0279 A72-12186

Quasar evolution models statistics suggesting relationship to radio galaxies, discussing continuity equation for density and luminosity changes

02 p0279 A72-12187

Bright galaxies and quasars associations based on spatial distribution and red shift considerations, discussing probability analysis

02 p0279 A72-12188

Astrophysical cosmology, discussing universe expansion, Robertson-Walker models, radio sources, quasars, cosmic X ray background, intergalactic media, etc

03 p0426 A72-13268

General relativity and cosmology of quasi-stellar objects, covering distances, red shifts and gravitational fields

03 p0426 A72-13270

Gas heating by If radiation due to Compton scattering near quasars, Seyfert galaxies nuclei and pulsars

03 p0435 A72-13801

Critique of quasar model of independent random pulse emitting sources conglomeration, noting brightness fluctuations incompatibility

03 p0435 A72-13802

Quasar radio and optical luminosity evolution, criticizing Arakelian method

03 p0439 A72-14297

Electromagnetic radiation in universe, discussing relict radio emission, energy density, hot model isotropic extragalactic component isolation, intergalactic gas, radio sources and quasars

03 p0414 A72-14317

Extragalactic astronomy observational paradoxes, discussing quasar red shifts and clumpings in directions of bright galaxies

04 p0568 A72-14414

Abundance ratios in quasar PKS 0237-23 from absorption spectrum measurements and explosive nucleosynthesis calculations

04 p0570 A72-14526

Optical search for Ryle-Neville radio sources, discussing cosmological model constraints and quasar and radio galaxies optical and radio luminosity functions

04 p0570 A72-14549

Expanding source model for quasars and Seyfert galaxy nuclei radio outbursts from extension of radio galaxy evolution models

04 p0573 A72-14874

Quasar red shift origin in terms of cosmological, gravitational and Doppler hypothesis, comparing with Seyfert galaxies

04 p0577 A72-15165

Numerical fluctuations minimization during luminosity functions and density evolution derivations from data subject to observational selection, applying to 3CR quasars

04 p0577 A72-15284

N galaxies and quasars properties comparison, suggesting continuous distribution and luminosity function

04 p0578 A72-15285

Optical object identified with radio source 3C 455 as quasar, noting relationship to SO galaxy NGC 7413

04 p0580 A72-15371

Quasar red shifts and spatial density with statistical approach, confirming cosmological distances and uniform distribution in accompanying space

04 p0580 A72-15452

X ray and gamma astronomy, discussing old and blue stars, supernova remnants, radio galaxies, quasars and pulsars

04 p0582 A72-15687

Faust project history, scientific objectives and present status, discussing stars, nebulae, quasars point sources and galactic photometry

04 p0583 A72-15691

External galaxies and quasars - IAU Conference, University of Uppsala, Sweden, August 1970

05 p0716 A72-16369

Optical spectra of compact objects, reviewing emission line spectra of quasars

05 p0716 A72-16372

Spectral energy distributions of peculiar galaxies and quasars by photoelectric spectrometry, observing emission lines strength

05 p0716 A72-16373

Radiation transfer by resonant scattering in expanding nebula with applications to quasars having blueward absorption wings

05 p0716 A72-16374

Light fluctuations of quasars in Harvard historical plate collection

05 p0716 A72-16375

Radio emission from compact extragalactic objects, including quasars and nuclei of compact, Seyfert and N type galaxies

05 p0716 A72-16376

Quasar radio structure, investigating morphology, statistical characteristics, angular size of spectra and red shift correlations from interferometer measurements

05 p0716 A72-16377

Spectral and time variations at radio frequencies of QSO and radio galaxies from Parkes catalog

05 p0717 A72-16378

Repeated explosions mechanism in nuclei of galaxies and quasars due to instability in twisted magnetic fields, noting clouds and relativistic plasma ejection

05 p0717 A72-16379

Cosmological evidence from radio galaxies and optical object counts, quasar red shifts and evolutionary properties

05 p0717 A72-16383

Quasar primordial He content prediction from primordial temperature fluctuations necessary for galaxy formation

05 p0717 A72-16384

Quasar photoionization and emission line spectra, determining radiation/gas density

05 p0720 A72-16713

Radio quiet quasar PHL 957 absorption line spectra obtained at telescope with Cassegrain image tube and multichannel spectrometer and integrating TV camera

05 p0720 A72-16714

Quasar mass determination, attributing absorption line red shift to radially moving gas clouds

05 p0723 A72-17157

Terrestrial atmospheric effects on quasar red shift measurements, considering night sky emission lines and atmospheric window size limits

05 p0723 A72-17159

Quasar luminosity due to unique big bang in specific space-time region, considering Minkowski geometry

06 p0878 A72-17669

Red shift determination for two galaxies near PSK 2251 plus 11 quasar from Ca II H and K absorption line measurements

06 p0881 A72-17898

Quasars red shift distribution apparent maximum for Z near 2.0, investigating possible sources of observational selection

06 p0882 A72-18000

Galactic nuclei and quasars as IR source, noting critical accretion of gas at neutron stars

06 p0883 A72-18015

Extragalactic radio sources, discussing galactic radiation, quasars, nonthermal emissions, energy dissipation and spectrum analysis

06 p0886 A72-18172

Radio sources and quasar structure angular resolution determination with distant radio telescope interferometry and microwave relay links

06 p0886 A72-18177

Hubble diagram history, present status, extension and improvement, considering quasars, galactic red shifts and other extragalactic radio sources

07 p1068 A72-18999

UBV photometry for stars near quasars and N and Seyfert galaxies, noting suitability as secondary photoelectric standards or photographic sequences for monitoring programs

07 p1071 A72-19336

Velocity ratio 1/468/ of light received from quasar PKS 2134 plus 004 to light propagation velocity in vacuum

07 p1073 A72-19412

Quasar 3C 273 light variation periodicities search, noting confidence level concerning resonance periods

07 p1073 A72-19424

Field approach to gravitation accounting for energy release and nonthermal radiation occurrence in pulsars and quasars

07 p1075 A72-19576

Structure and evolution of radio galaxies and quasars, considering luminosity-sustaining energy source, emission mechanism, variability and mean activity time

07 p1083 A72-20469

Astrophysical study of cosmological evolution, discussing evidence from radio source counts and quasar spatial distribution

07 p1084 A72-20471

Pulsar and quasar energy sources, discussing Crab nebula, rotating neutron stars and gravitational collapse role

08 p1233 A72-21208

Quasars and Seyfert and N-galaxies compact nuclei radiation polarization from polarimetric and photometric observations

08 p1234 A72-21281

Quasars and optical quasi-stellar galaxies comparisons for red shifts and luminosities distributions

08 p1234 A72-21283

Radio galaxy and quasar evolution models derived by formalism for number of sources in universe at any instant of cosmic time

08 p1234 A72-21382

Quasars and Seyfert galaxies radiation, discussing dust clouds, synchrotron and unstable plasma models

08 p1234 A72-21383

Quasi-stellar radio sources spectroscopic and photometric observations, determining spatial distribution and bivariate radio and optical luminosity function

09 p1382 A72-22279

Quasi-stellar objects hydrogen L-alpha lines computation via cloud collapse and ionizing radiation flux model, comparing computed distribution with PHL 957 and 4C 05.34 observations

09 p1382 A72-22280

Quasar rotation and pulsation periods within pulsar models, postulating supermassive stars /one million-one billion solar masses/ as energy sources

09 p1385 A72-22536

Intergalactic matter infall in galaxies, discussing quasar absorption spectra, hydrogen clouds, accretion rate and relations to spiral structure

09 p1386 A72-22660

Quasar 3C279 flux density variation measurement as evidence for alternate model to explain apparent expansion rate of 10c

09 p1387 A72-22976

Radio source observational identification as radio and normal galaxies and quasars, examining models for compact and large double radio source features and mechanisms

10 p1533 A72-23886

Radio-emitting and radio-quiet quasar optical emission and absorption line spectra

10 p1534 A72-23897

Quasar and galactic nuclei emission line spectral data corrected for interstellar extinction

10 p1534 A72-23898

Compact radio sources in galactic nuclei, discussing similarity to quasars in repetitive generation of relativistic particles

10 p1534 A72-23900

Quasar and radio galaxy emission intensity and polarization variation models, comparing with observations

10 p1534 A72-23901

Optical properties of nuclei of normal, Seyfert and N-type galaxies and quasars from spectrographic and photometric observations

10 p1534 A72-23902

Quasar redshift distribution and optical and radio luminosity functions analysis

10 p1534 A72-23904

Space densities and time scales of Seyfert galaxies, radio galaxies and quasi-stellar objects

10 p1534 A72-23905

Massive rotating objects with magnetic fields in galactic nuclei, considering similarities between Crab Nebula and quasars

10 p1535 A72-23908

Bright black holes from quasars condensation toward Schwarzschild radius, investigating primeval galaxies angular momentum increase and core concentration due to frictional effects

10 p1535 A72-23909

Quasars as cosmological and local objects, considering red shift origin and optical and radio luminosities comparison with galaxies

10 p1541 A72-24522

Quasars energy source and structure in terms of kinetic energy conversion to radiation in shock fronts of colliding gas clouds

10 p1544 A72-24671

Positions, flux densities and identifications for weak sources in Parkes catalog at 2700 MHz, including galaxies and quasars

10 p1545 A72-24792

Optical and physical properties and energy content of extragalactic radio sources, discussing radio galaxies and quasars

10 p1547 A72-24941

Galactic nuclei and quasars as IR sources, noting critical accretion of gas at neutron stars

11 p1718 A72-25951

Fowler quasars and exploding galaxies model tested by hydrodynamic equations numerical solution for premain sequence contraction and relativistic collapse of nonrotating supermassive star

12 p1866 A72-27202

Elliptical radio galaxies and quasars intrinsic emitted radio power correlation to spectral indices interpreted as evolutionary track in terms of model

12 p1867 A72-27210

Radio source and radio quiet quasars identifications for statistical correlation with bright galaxies positions

12 p1871 A72-27742

Quasars interpreted as active stage in galactic evolution with successive explosions in nucleus condensations

13 p2039 A72-29089

Circular polarization disputed for Seyfert galaxy NGC 1068, quasar 3C 273 and X ray source Sco X-1

13 p2041 A72-29414

Quasar color indices and redshift correlation, using catalog data on U, B and V colors

14 p2150 A72-30371

Radiation pressure on quasar outer envelope material as cause of mass outflow for masses less than gravitational force-determined critical value

14 p2155 A72-30552

List of galaxies with UV continuum, noting emission lines, Seyferts, quasars and spectral energy distribution

15 p2304 A72-31326

Quasar electromagnetic radiation emission in terms of general relativistic coupling between gravitational field and charged particle radiation field

15 p2306 A72-31592

Linear polarization and depolarization observation of quasar red shift explained as Faraday dispersion in or near source

15 p2313 A72-32365

Spectral index-luminosity relation for radio galaxies and quasi-stellar sources with power law spectra

15 p2315 A72-32714

Quasars 3C273 and 3C279 superlight velocity and distances from interferometer pattern changes in 1970-1971

16 p2450 A72-32865

Quasars spectroscopic observations, noting red shift and line spectra errors and corrections

16 p2452 A72-33133

Sounding rocket observations of quasar 3C 273 X ray spectrum for upper limits to absolute abundance of He in intergalactic medium

16 p2446 A72-33451

Critique of papers on quasars covering theory of gravitational lens intensified bright compact objects

16 p2454 A72-33452

Optical circular polarization search in quasars, Seyfert galaxies nuclei, BL Lac and OJ 287

16 p2456 A72-33472

Quasars and emission line objects red shift distribution using power spectrum analysis method

16 p2457 A72-33625

Compact extragalactic nonthermal sources.

17 p2604 A72-34519

Heavy element enrichment of protogalactic primordial gas by quasars matter ejection into intergalactic medium

17 p2604 A72-34526

Photoionization models for the emission-line regions of quasi-stellar and related objects.

17 p2605 A72-34527

Slope-gradient diagram of galaxies and quasars

17 p2607 A72-34919

Book on quasars and pulsars covering nature, origin, life span, universe concept with motion as fundamental unit and space-time reciprocal relationship

18 p2729 A72-37023

On the ability of the luminosity-volume test to reveal the statistical evolution of the luminosity of quasi-stellar sources.

19 p2854 A72-37226

Physical associations between quasi-stellar objects and galaxies.

19 p2854 A72-37227

Single body and stellar cluster models of quasars and galactic nuclei stability, noting neutron and collapsing star lifetimes

19 p2862 A72-38052

Galactic X rays investigation with X ray telescope on Lunokhod 1, noting observed singularities connection with statistical distribution of quasars and radio galaxies

19 p2802 A72-38090

Hydrodynamic model calculations for dynamically unstable supermassive stars.

19 p2866 A72-38490

Electromagnetic background radiation in universe, discussing relic radio emission, energy density, hot model isotropic extragalactic component isolation, intergalactic gas, radio sources and quasars

19 p2854 A72-38815

Differentially rotating magnetoid model for quasar and radio galaxies matter ejection and luminosity mechanisms in terms of magnetic field evolution and current sheet generation

20 p2965 A72-38903

Statistical studies of the evolution of extra-galactic radio sources. I, II, & III.

21 p3105 A72-41026

Quasar 3C 323.1 in rich compact galactic cluster Zw Cl 1545.1+2104, considering red shift, energy distribution and luminosity

21 p3107 A72-41268

Observations of linear polarization of radio sources at 7.2 cm.

21 p3109 A72-41326

Hubble constant, Friedmann time and expanding universe limits from measurements of distances to furthest galaxies, considering quasar red shift cut-off

22 p3222 A72-42138

Interferometric observations of lunar occultations of radio sources, showing positions, brightness distributions, spectral index variations and quasar coincidence

23 p3334 A72-43260

Faraday depolarization of extragalactic radio sources.

23 p3335 A72-43268

Quasars as images of Seyfert nuclei.

23 p3336 A72-43559

Quasar red shift relationship to cosmological distance, considering explanation in terms of gravitational and Doppler effects and unknown processes

23 p3338 A72-43993

Radio galaxies and quasars observations cosmological interpretation, discussing radio source counts, spectral index and angular size relations to distance and expanding sources apparent motions

23 p3340 A72-44245

Energy sources for extragalactic explosive phenomena in galactic nuclei and quasars, considering gravitation and double radio sources

24 p3439 A72-45018

QUASI-PARTICLES

U ELEMENTARY EXCITATIONS

QUASI-STEADY STATES

Overall characteristics of optimal quasi-steady plasma thruster system, discussing mass, burning time and thrust variations as function of power supply and pulse duration

[AIAA PAPER 72-456] 11 p1708 A72-26192

Dynamic and thermal laminar compressible boundary layers on flat plate, noting interaction of two quasi-steady flows

[ONERA, TP NO. 1068] 12 p1797 A72-27167

Quasi-steady state combustion theories compared with observations of hydrocarbon fuel droplet and flame zone diameters, noting underestimation of burning rate

13 p2063 A72-28545

Hingeless elastic helicopter blades coupled flap-lag motion under quasi-steady aerodynamic loads, reducing equations of motion to coupled nonlinear differential equations

15 p2180 A72-31211

QUASI-STELLAR RADIO SOURCES

U QUASARS

QUASILINEARITY

U NONLINEARITY

QUATERNARY ALLOYS

Zincblende ternary and quaternary alloy systems, calculating charge distribution in space by pseudopotential approach

03 p0404 A72-14261

Mixed zincblende ternary and quaternary alloys, comparing empirical pseudopotential and dielectric model methods for energy gap calculation

03 p0404 A72-14262

Quaternary Mo-Zr-Cr-C system, investigating fcc phase liquidation from phase diagram by chemical, metallographic and X ray analyses

05 p0666 A72-16099

Cr-Ti-V-B alloys rod specimens grain size and brittleness-viscosity transition temperature after heat treatment, cooling and bending tests

07 p1023 A72-20668

Nb-Ti-Zr-Hf system phase diagram from X ray analysis, observing beta solid solution below solid curve

14 p2122 A72-30977

Phase diagram of quaternary W-Mo-Nb-Ta alloy system, noting dependence of hardness on composition and temperature

14 p2122 A72-30982

QUATERNIONS

Digital differential analyzers number comparison in realization of direction cosine, Euler angle and quaternion attitude algorithms

07 p0949 A72-19296

QUENCHING

Optical quenching of the Gudden-Pohl effect in zinc sulfide luminophors and IR photography

21 p3057 A72-41680

Analytic criteria for laser quenching moment, generation power and stimulated emission energy for photodissociative iodine-alkyl lasers with iodine molecule buildup

24 p3412 A72-45706

QUENCHING (COOLING)

Quenching effects on thoriated-dispersed Ni sheet plastic stress relaxation and room temperature mechanical properties

02 p0247 A72-12822

Phosphorus-containing austenitic stainless steel, investigating quenching defects and precipitation from microstructure by transmission electron microscopy

03 p0379 A72-14260

Quenched and tempered Ni-Cr-Nb-Co alloy, describing cellular precipitation mechanism

04 p0533 A72-14977

Strain hardening for steel strength increase to 300 kg/sq mm by sequentially combined mechanical and thermal processing, involving plastic deformation, quenching and aging

04 p0527 A72-15454

Rate constant for quenching of B⁺/super 2/Sigma-plus state of CN radical as function of quenching collision relative velocity and total pressure in fluorescence cell

04 p0553 A72-15635

Laser pulse heating inability to quench in disorder in Fe-Al alloy

05 p0669 A72-16796

Electron transmission microscope study of quenched Mo-N alloys supersaturated solid solution low temperature aging behavior, investigating recovery processes

06 p0830 A72-18056

Phase diagrams of yttrium, erbium and ytterbium oxides at 1500-2400 C, using annealing and quenching method with differential thermal analysis

07 p1047 A72-18858

Flame quenching limits in narrow channels, considering effect of gas expansion during combustion on flame arresters use possibility

07 p1099 A72-19369

Managing steel embrittlement by titanium carbonitrides lattices separation during cooling, suggesting rapid quenching and plastic deformation temperature reduction

07 p1012 A72-19677

Internal friction measurements of tempered martensitic Cr steel quenched from 1100 C, connecting friction peaks with precipitation phenomena

07 p1021 A72-20486

Two electrical transducer techniques for dilatometric study of quenched-in point defects

07 p0993 A72-20589

Temperature dependence of electrical resistance and thermal conductivity in duralumin quenched at 77 K

07 p1022 A72-20663

Electrical resistance and thermal conductivity dependence on temperatures in duralumin quenched at 77 K

07 p1022 A72-20666

Heat treatment, water quenching and aging effects on Ti-V alloys hardening and structural properties, discussing omega phase formation

07 p1023 A72-20667

Niobium nitride neutronographic structural study with diffractometer after foil nitriding and rapid cooling

07 p1023 A72-20670

Quenched aluminum oxide rod residual stress profile from strain and heat transfer rates measurements and temperature distribution calculation

08 p1196 A72-21918

Quenched specimen anisotropic surface heating effect in liquid vaporization characteristics determination

10 p1561 A72-24207

High strength quenched steel with high ductility at cryogenic temperatures and negligible cooling rate effects on plasticity during welding

11 p1660 A72-26136

Austenizing temperature relationship to quenching rate in ultrahigh strength steels with high fracture toughness, recommending two step quench technique

12 p1829 A72-27695

Liquid quenched Sb-transition metal binary alloy constitution, finding metastable phases in quenched Cr-Sb and Mn-Sb alloys

13 p1975 A72-28672

Quenching rate and alloying element content effects on precipitation extent and corrosion resistance of Al-Cu alloys, discussing microstructure, chemical composition and mechanical properties

14 p2119 A72-30604

Mutual solid solubilities of rare earth metals with Zr extended by splat quenching, noting metastable low temperature allotropic forms of solid solutions

14 p2119 A72-30609

Amorphous structure analysis of splat quenched Cu-Zr noncrystalline phase, using electron microscopy

16 p2410 A72-33814

As-quenched and aged form of omega phase in Ti-Nb alloys investigated by electron microscopy and X ray diffraction

16 p2410 A72-33818

Separation of iron and annealing-out of lattice defects in rapidly-solidified aluminum-iron alloys. I - Microstructure and properties of quenched samples. II - Tempering behavior

17 p2567 A72-35174

Determination of the quenching of O(1D) by molecular nitrogen using the ionospheric modification experiment.

18 p2685 A72-35991

Metallurgical aspects in the development of AlMgSi alloys with a low sensitivity to quenching

18 p2699 A72-36224

Vapor pressure decrease rate during cooling agent introduction in semiclosed volume, determining pressure drop from energy and mass conservation equations

19 p2879 A72-37355

Quench-ageing behaviour of 40Co-38Ni-17Cr-5Ti alloy.

20 p2935 A72-39141

Matthiessen rule on binary alloy electrical resistivity temperature derivative, discussing data deviations in substitutional alloys after quenching, radiation damage and plastic deformation

22 p3189 A72-42298

Precipitation rate characteristics in age hardenable quenched alloys explained by transient analysis of vacancy annealing kinetics

22 p3189 A72-42441

Different forms of elimination of quenching lacunae in supersaturation in the case of aging of two alloys, Al-Cu and Al-Mg-Si

22 p3190 A72-42444

Structure of the 01420 alloy with zirconium

23 p3303 A72-44094

Investigation of the process of D16-alloy quenching in liquid nitrogen

23 p3294 A72-44095

QUEUEING THEORY

Combined delay and loss common-control queueing system, obtaining stationary state loss and waiting probabilities and waiting time distribution function

06 p0794 A72-18243

Stochastic simulation model for space shuttle fleet operations, using closed loop queueing system approach

07 p0965 A72-20330

Monotonicity theorems for functionals and transformations in stochastic models of queueing, reliability and optimality problems

09 p1343 A72-23565

Reliability design for airborne ecological system for jumbo jets, discussing toilet flushing and multiple server queueing model

10 p1429 A72-23999

General purpose simulation system /GPSS/ to program discrete time dependent mathematical models related to transport and queueing processes

17 p2521 A72-34471

Analysis of a control computer complex as a multiphase queueing system

17 p2522 A72-35030

Computer-controlled queueing system with service interruptions.

23 p3275 A72-43605

R

RABBITS

High energy proton irradiation late pathological effects on rabbit brains, discussing brain lesions and radiation dosages

02 p0161 A72-12056

RACE FACTORS

Age dependence of changes in pupil diameter in the dark.

21 p3007 A72-40732

RACETRACKS [PARTICLE ACCELERATORS]

Confinement time of plasma injected in magnetic field of racetrack with diverter, noting plasma equilibrium in toroidal magnetic field

22 p3213 A72-43106

RACON BEACONS

U RADAR BEACONS

RADAR

NT COHERENT RADAR
NT CONTINUOUS WAVE RADAR
NT DOPPLER RADAR
NT LANDING RADAR
NT METEOROLOGICAL RADAR
NT MONOPULSE RADAR
NT MOVING TARGET INDICATORS
NT OPTICAL RADAR
NT PULSE DOPPLER RADAR
NT PULSE RADAR
NT RADAR MEASUREMENT
NT RANGE AND RANGE RATE TRACKING
NT SATELLITE-BORNE RADAR
NT SEARCH RADAR
NT SECONDARY RADAR
NT SIDE-LOOKING RADAR
NT SURVEILLANCE RADAR
NT TRACKING RADAR

Fast Fourier transforms for digital matched filters in wideband radars, using computer simulation for word size and dynamic range relationship determination

02 p0188 A72-12398

Russian papers on radar theory and techniques covering signal measurement, MTI, clutter suppression, false alarm, bearing errors, automatic ranging and tracking, etc

11 p1595 A72-26293

RADAR ALTIMETERS

U RADIO ALTIMETERS

RADAR ANTENNAS

Tubular traveling wave antenna array for radar applications and microwave television transmitters, describing computer program for design

01 p0039 A72-10668

Broadband beam scanned linear waveguide antenna array design with FMCW short range high resolution radar for airport navigational aid in fog

01 p0039 A72-10669

French book on antenna application to radars and space techniques covering UHF techniques, mathematical theories and apparatus development

05 p0626 A72-16287

Vertical dipole antenna design for CW Doppler radar midair collision avoidance system

05 p0629 A72-16571

Optimal design of directive dielectric loaded circular waveguide antenna for parabolic reflectors and radar detection

06 p0782 A72-17356

Electronic scanning steerable phased array radar beam pointing capability improvement for moving target detection probability

06 p0772 A72-17423

S band module with Gunn diode oscillators in series connection used as phased array radar 250 W power sources with efficient heat sink

06 p0789 A72-18476

Antenna near field correction for backscatter gain in two-beam incoherent scatter radar measurements at Arecibo Observatory

08 p1137 A72-21983

Phased array radar systems synthesis based on life cycle cost minimization, taking into account high-speed digital data processing

09 p1280 A72-23374

Arecibo Observatory radio-radar telescope design and operation, discussing reflector wire mesh surface, computer control and data acquisition, ionosphere and pulsar studies and interferometry

10 p1459 A72-24310

Single engine aircraft-borne weather radar with electronically scanned steerable phased array antenna [SAE PAPER 720315]

11 p1591 A72-25579

Pulse excitation of traveling wave antenna array, describing spectral method of solving high resolution side-looking radar limitation

13 p1915 A72-28526

Aircraft measurements of radiation pattern of radar antenna system used for meteor height observation

13 p1919 A72-29027

Passive clutter region and reflecting area calculation for ground surface illuminated by pulse radar antenna

13 p1919 A72-29053

Airborne ground mapping and meteorological radar with steerable phased array antenna without mechanical scanners

15 p2200 A72-32216

Computer aided impedance matching of an interleaved waveguide phased array.

17 p2525 A72-34373

Airborne waveguide element reliable advanced solid state radar /RASSR/ phased array radiation patterns and design

17 p2531 A72-35571

Gain averages as criteria for antenna EMC-performance.

20 p2902 A72-39001

Phase shifter number reduction effects on phased radar array radiation pattern distortion and sidelobe reduction

20 p2907 A72-39268

Reliable advanced solid state radar /RASSR/ array design featuring transmit-receive elements arranged in triangular grid and built-in test equipment

20 p2904 A72-39732

A proposed approach for increasing the azimuthal resolution in HF radar.

21 p3015 A72-40360

Radar double beam dielectric radiator antenna design for ATC in 1250-1350 MHz range

21 p3030 A72-40530

Linear HF radar antenna array aperture synthesis for ionospherically propagated signal reception in airplane for achievement of ideal directivity without ionospheric compensation

21 p3022 A72-41080

Recent advances in diode and ferrite phaser technology for phased-array radars. I.

23 p3270 A72-43572

Wideband limitations of waveguide arrays.

23 p3270 A72-43573

Optimisation of slope of difference-mode radiation pattern in sum-and-difference-comparison monopulse radar.

23 p3264 A72-43606

Electromagnetic thickness measurement on the AWACS radome.

24 p3384 A72-44901

RADAR APPROACH CONTROL

Terrain clearance during descent and approach of aircraft under radar control, discussing optimum profile, ATC, nav aids and rules

01 p0097 A72-10183

Airfield Vehicle Obstacle Indication Device short range high-definition radar system for aircraft navigation aid

02 p0173 A72-12042

Limited scan antenna system for precision approach radar, detailing design for reflector, aperture gain and phased array

02 p0193 A72-12393

Tactical ATC display system for airport surveillance, precision approach and landing and operator/aircraft/machine operations by using terminal Area Surveillance Radar

02 p0230 A72-12421

Low cost vertical crossed beam radar systems for nonprecision approach in small airports, reducing track error

04 p0545 A72-14829

ILS development, discussing four course radio ranges, autoland and radar systems

09 p1349 A72-23449

RADAR ASTRONOMY

Solar corona research, discussing radio and radar astronomy and UV spectrum observations

03 p0422 A72-13202

Minor planets radar measurements contribution to astrometric corrections, obtaining solutions for conditional equations systems representative of Cerera observations

04 p0572 A72-14635

Radar observations of Martian craters and scarp during 1971 opposition

04 p0579 A72-15359

Radar observation of Mars surface, noting rugged terrain and craters

04 p0579 A72-15360

Venus equatorial region surface height variations from interplanetary radar echo delay measurements, discussing resolution, repeatability and radius

07 p1073 A72-19352

Mercury topography and scattering characteristics from 3.8 cm radar observations, comparing to Mars and Venus

12 p1865 A72-27098

Microwave radiometry for celestial body emitted or reflected radiation observation, discussing radar cartography with emphasis on side-looking and synthetic aperture radars advantages

15 p2232 A72-31251

RADAR ATTENUATION

Azimuth display of attenuation instrument used with weather radar to measure rain induced attenuation over slant paths

15 p2207 A72-32101

Slant path radar attenuation events due to rain during summers at 10 GHz, obtaining statistics on frequency of occurrence, extent in azimuth and duration

15 p2200 A72-32103

Gain averages as criteria for antenna EMC-performance.

20 p2902 A72-39001

Direct and cross polarized backscatter power from a turbulent plasma.

23 p3320 A72-43521

RADAR BACKSCATTER

U BACKSCATTERING

U RADAR BACKSCATTERING

RADAR BEACONS

Phased scanning array for ATC radar beacon systems, airport or air route surveillance radars and ground landing systems

01 p0098 A72-10962

Discrete address ATC radar beacon system operation and design

02 p0256 A72-12378

Pulse coded processing system EMC performance measurement, considering CW and pulsed interference effects and application to ATC radar beacon system transponders

03 p0324 A72-14033

ATC radar beacon system developments, considering diversity transponders, interrogator environment control, electronic scan cylindrical array antenna design and discrete address mode

04 p0508 A72-14832

FORTAN digital simulation of ATC radar beacon system making possible computer generated movie display

07 p0950 A72-19301

C-band pulse beacon ranging system for collision avoidance, detailing interrogation, response and system test modes

09 p1349 A72-22908

Bearing azimuth measurement accuracy improvement by ATC beacon system/secondary surveillance radar using monopulse technique

18 p2662 A72-37047

Potential value of turn-rate telemetry in tracking of aircraft equipped with discrete address beacon system /DABS/ for ATC, discussing tracking algorithms design

19 p2830 A72-37282

RADAR BEAMS

Microwave Doppler scanning landing guidance system with radar beam comparison and signal format simplification suggestion

06 p0846 A72-18398

Microwave instrument landing systems based on continuous radar scanning technique, using pulse format for data transmission

06 p0846 A72-18399

Target azimuth and elevation estimation by four beam cluster, analyzing angle estimation accuracy as function of SNR by computerized Monte Carlo simulation

07 p0941 A72-19304

First and second order backscattering, beam divergence, angular field of view, field size and receiver distance of water clouds illuminated by continuous lidar beam

15 p2200 A72-32154

Error analysis for digital avionics system involving Doppler navigation by intermittent scanning of single beam multimode radar, noting optimum statistical data processing

15 p2271 A72-32204

RADAR CLUTTER MAPS

Biological radar clutter control by adaptive systems techniques, developing computer simulation for angel tolerance from bird electromagnetic characteristics

07 p0942 A72-19305

Passive clutter region and reflecting area calculation for ground surface illuminated by pulse radar antenna

13 p1919 A72-29053

RADAR CORNER REFLECTORS

Luneburg lens spherical antenna microwave radiation pattern, computing Maxwell equations via Tai method

21 p3030 A72-40529

RADAR CROSS SECTIONS

Radar target thin rectangular plate model backscattering from incident and reflected waves, noting front and trailing edge phenomena with emphasis on side edge contribution

01 p0032 A72-11250

Resonance rail line scattering range using flat parallel conductor transmission line for radar cross section measurement

01 p0032 A72-11251

Radar target cross section parameters statistical analysis, discussing real target categories and relative measuring methods

02 p0181 A72-12641

Bistatic radar scatter communication effective coverage analysis, considering dependence on equipment and target locations and properties

03 p0321 A72-13092

Radar cross section computation and contours map for thin straight wire, noting resonant peak and interference null variations with frequency and aspect ratio

06 p0771 A72-17351

Topography of swath around Venus equator from wavelength dependence of radar cross section

10 p1548 A72-24972

X band radar target cross section representation by discrete point reflector models, deriving boresight error mean and variance in presence of n-target sources

15 p2201 A72-32474

Conducting body radar scattering control by reactive loading, discussing field pattern synthesis for real current with least mean-square approximation

17 p2513 A72-34358

Radar cross section fluctuation statistics description by generalized chi-square distribution, discussing target detection probabilities maximum likelihood estimates

19 p2763 A72-37293

Radar as a diagnostic tool for lightning.

20 p2948 A72-39350

Radar cross sections of conducting bodies of revolution, noting electric/magnetic polarizability tensors in L.F Rayleigh scattering

24 p3381 A72-45639

Axial-radar cross section of finite cones by the equivalent-current concept with higher-order diffraction.

24 p3381 A72-45640

RADAR DATA

Radar signal and data processing with digital techniques, using pipeline fast Fourier transform methods

02 p0188 A72-12397

Radar data automatic extraction, discussing azimuth quantization methods, moving window detection, coordinate measurement and ATCAS extractor

02 p0181 A72-12650

Peak reading and thresholding in radar weather data processing, describing PPI map

06 p0843 A72-18440

Radar observed apparent land breeze front off Wallops Island, giving temperature and wind profiles

06 p0843 A72-18441

Reduced data storage requirement of synthetic aperture radar for target classification by fast Fourier transform

08 p1134 A72-21422

Digital filter synthesis for radar signal processing applications, discussing frequency sampling method extension with advantage of known waveform and reduced computations

08 p1146 A72-21916

Radar data statistical evaluation, emphasizing mean Doppler shift for aircraft radial velocity calculation

09 p1278 A72-22897

Viking Mars Orbiter and Lander radio and radar science experiments, noting surface tracking, dual frequency S and X band data and communications system

10 p1539 A72-24380

Meteor trail radar data processing for upper atmosphere research, proposing dissemination for dynamosphere synoptic exploration

10 p1438 A72-24716

Parallel digital computer application to radar tracking data processing, discussing system design for efficiency maximization and performance, desensitization in traffic level fluctuation

15 p2203 A72-31781

Synthetic aperture radar data processing via tilted plane optical system, explaining technique in terms of holographic analogy

19 p2796 A72-37584

Automatic air targets recognition via digital radar data processing, discussing methods for noise signals suppression

21 p3081 A72-40547

Efficient computer decoding of pseudorandom radar signal codes.

22 p3153 A72-41978

Determination of aerodynamic drag from radar data.

24 p3362 A72-45337

Parallel Element Processing Ensemble (PEPE)/digital computer for real time radar data processing and control, discussing system design and applications

24 p3383 A72-45666

Parallel processing of ballistic missile defense radar data with PEPE.

24 p3383 A72-45667

RADAR DETECTION

Synthetic aperture radar application to oil spill detection and monitoring for ocean surface, demonstrating feasibility

[ALAA PAPER 71-1072] 01 p0057 A72-10534

Noisy radar signal processing by spectral analysis method

02 p0177 A72-12225

Splash detection radar digital signal processing by off-line computer using wideband video recorder

02 p0178 A72-12399

Pulsed Doppler radar loss of detection probability due to echo signal misalignment, discussing distance measurement refinement by interpolation

02 p0179 A72-12571

Narrow-band radar/sonar signal optimal detection under known direction and uncertain phase/arrival time conditions, considering statistical signal sampling

02 p0180 A72-12572

Sequential analysis of statistical hypotheses applied to radar detection and coded communications systems

02 p0181 A72-12643

Radar detection and resolution, discussing computer analysis of interval modulated signal ambiguity properties and synthesis method

02 p0181 A72-12648

CAT detection by airborne laser Doppler radar and ground based ultrasensitive microwave Doppler radar methods

04 p0543 A72-14822

Detection characteristics of optimal interperiod processing radar pulse systems for arbitrary correlation of signal and noise fluctuations

04 p0487 A72-15145

Radar and radiometric millimeter wave signal systems in near earth environment for remote detection purposes

04 p0494 A72-15610

Range resolution effect on distributed radar target detection in white noise and clutter, using square law envelope detector with linear integrator

05 p0628 A72-16567

Nonparametric constant false alarm rate (CFAR)/radar extractor for target detection in background noise, using sign test

05 p0629 A72-16570

Clear air atmospheric target detection, comparing bistatic and monostatic radar techniques

05 p0630 A72-16835

Decision error estimates applied to detection problem with digital radar, computing upper and lower bounds for error probability

05 p0632 A72-17093

Electronic scanning steerable phased array radar beam pointing capability improvement for moving target detection probability

06 p0772 A72-17423

Suboptimum linear quadratic algorithm for optical radar signals postdetection processing and target range estimation

07 p0943 A72-19522

Relation for detector-aperture size for spatially coherent detection with dependent scattering applied to realistic laser radar signal signatures

09 p1278 A72-22618

Sequential analysis of statistical hypotheses in radar target detection and in communications systems

09 p1282 A72-23680

Optimal correlating detector of fluctuating two frequency radar signals in unknown random noise

10 p1436 A72-24515

Constant false alarm rate signal processors for several electromagnetic interference types, using distribution-free methods and maximum likelihood estimation in radar target detection

10 p1437 A72-24683

Radar detection performance calculation with post-detection integration using single valued loss and ideal curves in terms of SNR

10 p1437 A72-24689

Sensitivity loss from approximation to radar and sonar signal square law detectors in quadrature systems with postdetection integration

10 p1437 A72-24690

Radar IF voltage in-phase and quadrature components detection thresholds, evaluating square and octagonal approximations to circle for false alarm probabilities

10 p1438 A72-24693

Radar sequential detector for digital processing of signal masked by noise, determining false alarm and detection probabilities and mean test duration

10 p1439 A72-24908

Tuned laser radar detection and ranging of high altitude Ba ion cloud by photon counting, discussing SNR requirement

10 p1440 A72-24963

Accumulator type radar detector analysis by Markov chains method, discussing false alarm and detection probabilities

11 p1592 A72-25807

Target position information for radar energy potential calculation and detection quality, describing transmitter power reduction for normal range distribution density

11 p1596 A72-26313

Passive detection radar system for bombers, calculating target distance during horizontal flight

11 p1597 A72-26316

Pulse-pulse frequency agility influence on radar detection in sea and rain clutter with decorrelation, eliminating multiple-time-around echoes

13 p1917 A72-28695

Frequency agile radar techniques for improving detection and range resolution and reducing interference and sea and ground clutter

13 p1917 A72-28696

Sonar techniques application to radar, stressing utilization of preformed channels in rapid and distant detection of satellites and ballistic missiles

15 p2197 A72-31874

Time-compressed displays for target detection.

17 p2510 A72-35945

Overall detection probability for fluctuating and nonfluctuating target models.

19 p2763 A72-37294

Postdetection integration loss for logarithmic detectors.

19 p2763 A72-37295

Radar observations of equatorial spread F in a region of electrostatic turbulence.

23 p3286 A72-44528

RADAR DIRECTION FINDERS

U RADIO DIRECTION FINDERS

RADAR DISPLAYS

U RADARSCOPES

RADAR ECHOES

NT ANGELS

NT CLUTTER

NT LUNAR RADAR ECHOES

NT VENUS RADAR ECHOES

Search radar performance environmental model using clutter and interference returns

02 p0178 A72-12389

Target detection in sea clutter, showing non-Rayleigh distributed high resolution radar envelope return

02 p0178 A72-12400

Pulsed Doppler radar loss of detection probability due to echo signal misalignment, discussing distance measurement refinement by interpolation

02 p0179 A72-12571

Microwave propagation anomalies due to meteorological factors, discussing superrefractive atmospheric layers effects on radar data reliability and undesirable echoes appearance on display screen

02 p0182 A72-12746

Geomagnetic field effect on radar echoes from meteor trains during Geminid shower

03 p0345 A72-12982

Optimal discrimination rule for dual frequency radar targets with inadequate echo signal and background noise level parameters

05 p0625 A72-15821

Radar instrument for measuring snow density, water content, layer depth and inhomogeneity based

on snow cover electrical properties effects on echo characteristics 06 p0805 A72-17591

Mercury radar scattering properties, producing Fourier power spectrum from echo signals 06 p0880 A72-17864

Small radar equivalent surface measurements by Doppler differentiation between signal in target and parasitic echoes 06 p0775 A72-18193

Spectrum shape of Doppler radar return from two dimensional random rough surface model using helmholtz integral approach and Kirchhoff approximation 09 p1277 A72-22314

Supercell, multicell and sheared severe hailstorms structure and motion observation by radar echoes, noting propagation characteristics 09 p1345 A72-22447

Rainfall rate estimation by radar reflectivity measurements based on atmospheric parameters obtained from radiosonde data 09 p1345 A72-22449

Visual and radar echo location of organized updraft on thunderstorms and hailstorms 09 p1346 A72-22452

Orionid meteor head echoes variations with diurnal radiant motion compared to Perseid meteors 09 p1389 A72-23395

Doppler spectral width of radar signal reflected from sea surface as function of illuminated region dimensions, waviness scale and emission factors 10 p1439 A72-24904

Radar echo maximum intensity display by digital comparator with shift register video signals storage in National Severe Storms Laboratory 11 p1591 A72-25762

Atmospheric constituents dimension, composition and dynamics from optical radar echo observation of laser light scattering 11 p1592 A72-25849

Linearly and circularly polarized electromagnetic field effective scattering areas relationships, considering radar reflection in reverse direction 12 p1783 A72-27629

Automatic real time processing of meteor radar echoes, using digital computers 13 p1924 A72-29033

Radar clutter models and comparison with measurements, discussing parameters for description and main functions for suppression 13 p1922 A72-29396

Persistent intense CAT in upper level frontal zone, discussing synoptic features, vertical wind shears, radar echoes and turbulence intensity 13 p1995 A72-29622

Mercury perihelion advance determination from radar echo delays measurement 16 p2453 A72-33190

Design of nonrecursive digital moving-target-indicator radar filters. 18 p2667 A72-36687

Radar meteorology in the Soviet Union - 1970. 18 p2707 A72-36719

RF time domain nonreal time reflectometer operating as nanosecond radar with pulse spectrum lines reflections measured and stored for echo computation 19 p2770 A72-37256

German monograph - A proposal for a radar device with two simultaneously emitted radar frequencies which has a reduced susceptibility to disturbances produced by sea echoes 19 p2764 A72-37481

The occurrence of radio aurora at high latitudes - The IGY period, 1957-1959. 20 p2904 A72-39982

Radar auroral echo VHF power spectrum analysis of ionospheric irregularities, using range-time-intensity film strips 22 p3171 A72-42415

Optimal discrimination rule for dual frequency radar targets with inadequate echo signal and background noise level parameters 23 p3263 A72-43429

Equatorial spread F - Recent observations and a new interpretation. 23 p3286 A72-44530

RADAR EQUIPMENT

NT PLAN POSITION INDICATORS

NT RADAR ANTENNAS

NT RADAR BEACONS

NT RADAR CORNER REFLECTORS

NT RADAR FILTERS

NT RADAR RECEIVERS

NT RADAR REFLECTORS

NT RADAR TRANSMITTERS

NT RADARSCOPEs

Microwave module circuit design for airborne phased array radar with distributed power generation, reception and phase shift functions, considering performance, reliability and cost 01 p0028 A72-10660

Radar signal digital processing for replacing analog circuitry, discussing rf signal representation, sidelobe reduction, coherent processors and filter design 02 p0178 A72-12396

Pulse modulator thyristor circuit design and optimum operating conditions for driving high peak power radar magnetron 02 p0195 A72-12694

Bistatic radar scatter communication effective coverage analysis, considering dependence on equipment and target locations and properties 03 p0321 A72-13092

Time shared performance test monitor function, operation and self repair of corporate fed array radars with computer control for long time internal reliability 03 p0321 A72-13165

Microwave IC power amplifiers for radio relay, telemetry, phased array radar and TWT replacement 05 p0634 A72-15784

L- and X-band Y junction waveguide circulators for medium and peak high powers in radar applications, discussing operation principle and design 06 p0785 A72-18311

Solid state Ku-band local Gunn oscillator for airborne radar applications, discussing design and batch process fabrication 06 p0789 A72-18480

ATC radar performance monitoring, considering advances in radar signal processing and digital display techniques 08 p1134 A72-21525

Radar equipment complex in Dushanbe for upper atmosphere wind measurements in meteor physics studies 09 p1308 A72-22506

Multibeam indicator with block diagram description for meteor ranging radar and photofilm based recording system 09 p1308 A72-22508

Cumulative index of papers on radar systems published in IRE/IEEE journals since World War II 10 p1438 A72-24694

Airport meteorological instrumentation, discussing ground wind, visibility, cloud height, air temperature and humidity detectors and radar equipment 10 p1484 A72-25093

Secondary surveillance radar systems design and planning for ATC application 13 p1917 A72-28698

Radar facility for weak meteor observation, describing antennas, transmitters, receivers, filters, calibration techniques and recording instruments 13 p1919 A72-29026

Pulse radar equipment for meteor height measurement from nonsaturated trails by phase difference method 13 p1929 A72-29028

Optimal radar recording systems for meteor trail observations providing signal detection, processing and storage triggering and echo discrimination 13 p1929 A72-29030

High reliability long life grid pulsed L band traveling wave tube with integral solenoid focusing for high power radar use 14 p2089 A72-31046

Surveillance radar for clutter rejection and signal loss reduction at airports, discussing system design features 18 p2662 A72-37046

Microwave hologram radar imagery. 19 p2764 A72-37602

Radar EMI to voice communication receivers. 20 p2902 A72-38991

Pulse time positioning under background noise in radar and radar navigation range finders, noting root-mean-square errors and transient response 22 p3153 A72-42117

RADAR FILTERS

Radar signal digital processing for replacing analog circuitry, discussing rf signal representation, sidelobe reduction, coherent processors and filter design 02 p0178 A72-12396

Acoustic surface wave chip filters application in pulse compression radar system, considering various piezoelectric substrate materials characteristics 14 p2089 A72-31045

Jointly optimal filters for fixed range radar filter-sampler-filter system, determining impulse response function forms 15 p2207 A72-31793

Recursive digital MTT radar filter design in z plane, detailing spectrum rolloff and flat passband in amplitude response 16 p2369 A72-33758

Design of nonrecursive digital moving-target-indicator radar filters. 18 p2667 A72-36687

RADAR IMAGERY

Crop discrimination with manual and automatic computerized side-looking radar imagery analysis for microtexture pattern recognition 01 p0065 A72-10451

Agriculture and natural vegetation remote sensing programs, discussing dichotomous keys for side-looking airborne radar imagery analysis 01 p0056 A72-10457

Spatial alignment for low noise difference picture detection in side-looking radar imagery 01 p0129 A72-10874

Remote sensor viewing angle effect on detectability of geological faults in side-looking airborne radar image data by optical spatial frequency analysis 02 p0209 A72-11791

Lake ice surveillance via airborne radar, presenting images of ice forms and land features 02 p0211 A72-11805

Side-looking airborne radar imagery for sea ice drift size, shape and surface characteristics determination [AD-733605] 02 p0215 A72-11882

RADAM /Radar Amazon/ side-looking radar imagery and multiband aerial photography for mineral, vegetation, soil and water resources mapping in Brazil 02 p0216 A72-11890

Side-looking airborne radar /SLAR/ images comparison with small-scale low-sun black and white aerial photographs 05 p0661 A72-16041

Multispectral remote sensing techniques, equipment and applications, discussing color and IR camera, line scanning and radar systems and automated interpretation devices 09 p1312 A72-23304

Airborne microwave hologram radar system, discussing along- and cross-track direction resolution realization by synthetic aperture technique and phased receiving array respectively 15 p2196 A72-31788

Computerized analytical system for side-looking radar imagery interpretation by isodensitracer scanned density data multivariate analysis applied to environmental discrimination 15 p2198 A72-32064

Radar imaging systems application to cartography, geology, hydrology, biogeography, oceanography and geography, emphasizing remote sensing in cloudy environments 16 p2364 A72-33634

Flight test evaluation of a forward looking radar system for search and rescue applications. [AHS PREPRINT 633] 17 p2490 A72-34499

Transformation of points from sidelooking radar images into the map system. 17 p2555 A72-35336

Digital technique for automatic change detection in aerial reconnaissance side-looking radar imagery, discussing image correlators 17 p2557 A72-35554

Infrared and radar maps of the lunar equatorial region. 18 p2725 A72-36289

Recent research applicable to the design of electronic displays. 18 p2653 A72-36902

Microwave hologram radar imagery. 19 p2764 A72-37602

Digital processing for motion compensation in high resolution airborne synthetic aperture radar imagery in presence of simultaneous longitudinal, lateral and vertical maneuvers 21 p3022 A72-41076

RADAR MAPS

NT RADAR IMAGERY

AS-11A stereoplotter computerized adaptation to stereo-modeling of SLAR terrain mapping 06 p0818 A72-18330

Source distribution estimate in radar mapping, comparing prolate spherical wave functions inverse versus truncated Fourier transform methods 07 p0946 A72-19792

Papers on thermal characteristics of moon covering earth based and in situ surface temperature measurements, radar mapping, heat flow experiments, etc 12 p1869 A72-27326

Lunar surface roughness mapping by combined IR and radar measurements 12 p1869 A72-27328

Microwave radiometry for celestial body emitted or reflected radiation observation, discussing radar cartography with emphasis on side-looking and synthetic aperture radars advantages 15 p2232 A72-31251

Topographic mapping from airborne radar geodetic measurements, evaluating photogrammetric accuracy 15 p2224 A72-31603

Aircraft radar for weather data, ground mapping, avoidance modes and independent landing monitor function, presenting straight and slant approach simulation data 21 p3080 A72-40290

RADAR MEASUREMENT

Planetary mass estimation from radar and optical observation data analysis of sun and planets [AD-737167] 01 p0127 A72-10292

Wind profile determinations at 90-100 km from meteor trail drift and ionosphere inhomogeneity radar data, noting semidiurnal harmonics in wind components 01 p0058 A72-10563

Ocean wave height measurements with nanosecond radar, using ground truths to relate radar measurements to actual sea conditions 02 p0172 A72-11869

Radar measurement accuracy in log-normal clutter of fluctuating targets in random noise or intentional interference

02 p0178 A72-12401

Sporadic meteor orbital parameters measurement by continuous radar, determining out-of-atmosphere rate

02 p0283 A72-12524

Radar target cross section parameters statistical analysis, discussing real target categories and relative measuring methods

02 p0181 A72-12641

Radar meteorology, discussing equipment design, radar observation station net need, aeronautical applications and laser devices utilization

02 p0254 A72-12783

Radar accuracy for precipitation measurements, discussing error sources

02 p0254 A72-12784

Wind velocity spatial derivative determination by radar observation of signal reflection from atmospheric water particles

03 p0383 A72-13483

Three frequency radar spectral measurements of two stream and gradient plasma instabilities in equatorial electrojet as function of wavelength

03 p0349 A72-13521

Minor planets radar measurements contribution to astrometric corrections, obtaining solutions for conditional equations systems representative of Cerera observations

04 p0572 A72-14635

Atmospheric turbulence detection sensors, reviewing microwave radar, acoustic, Doppler lidar, laser fringe anemometry and passive IR techniques

04 p0530 A72-14833

Jimsonde high resolution temperature sensor for FPS-16 Radar/Jimsphere wind system, analyzing rms errors

04 p0522 A72-15157

Angular coordinates and slope determination from monopulse radar measurements of two unresolved targets

05 p0629 A72-16578

Holographic Ice Survey System for down looking radar probing and measurement of sea ice and glaciers, discussing ice electrical properties and system design

06 p0814 A72-17590

Radar instrument for measuring snow density, water content, layer depth and inhomogeneity based on snow cover electrical properties effects on echo characteristics

06 p0805 A72-17591

Turbulent energy dissipation rate statistical characteristics above 1000 m from radar measurements, discussing atmospheric boundary layer quantities

06 p0841 A72-17940

Small radar equivalent surface measurements by Doppler differentiation between signal in target and parasitic echoes

06 p0775 A72-18193

Geodetic and oceanographic applications of radar equipped satellites in polar orbits for measuring heights along geoid

06 p0809 A72-18259

Atmospheric lee waves three dimensional structures through high sensitivity Doppler radar measurements based on backscatter from refractive index inhomogeneities

07 p0129 A72-19100

Wind measurements in lower troposphere by meteor radar method, presenting models of prevailing circulation in meteor zone over Eurasia and Arctic

08 p1161 A72-21538

Optimal variant of meteor wind patrol radar station for atmospheric circulation study

08 p1147 A72-21886

Sectoral radio measurement of meteor trail drifts with IF radar signals, determining Doppler shift sign and period

08 p1238 A72-21887

Radar measurement of meteor bodies mass distribution parameter

08 p1239 A72-21889

Meteorological radar measurements, noting missile tracking radio interferometer noise due to stochastic refractive ray bending and associated multipath conditions

08 p1136 A72-21978

Antenna near field correction for backscatter gain in two-beam incoherent scatter radar measurements at Arecibo Observatory

08 p1137 A72-21983

Soviet papers on cloud seeding effects and meteorological radar studies covering precipitation formation, atmospheric model and reflected signal statistical characteristics

08 p1201 A72-21992

Airborne radar measurement of 2.25 cm backscatter from sea surface, obtaining wind speed by computerized clustering data analysis techniques

09 p1296 A72-22312

E region ion density and composition determination by incoherent scatter radar measurement [AD-742618]

09 p1375 A72-22365

Nighttime radar method of meteor radio echo observation to determine electron attachment rate to neutral air particles

09 p1383 A72-22504

Leonid meteor trail drift measurements in upper atmosphere, comparing radar system with precise goniometric capabilities to photographic methods

09 p1383 A72-22509

Noncontacting measurements by miniature CW Doppler radar with semiconductor microwave generator

09 p1285 A72-22691

Meteor trail winds over Europe, discussing continuous wave radar observations and measurement errors with respect to height and time

10 p1474 A72-24708

Radio meteor winds determination in Southern Hemisphere from vertically emitted continuous wave radiation, considering diurnal variations and wind and turbulence effects

10 p1474 A72-24709

Meteor trail wind radar measurements over Illinois, discussing scattering properties and monostatic vs multistatic coherent systems

10 p1474 A72-24710

Stanford pulse Doppler radar and digital data acquisition system for meteor trail wind measurements

10 p1438 A72-24711

Wind velocity spatial derivative determination by radar observation of signal reflection from atmospheric water particles

11 p1682 A72-26253

Target angular position measurement by surveillance radar on background of correlated interference

11 p1595 A72-26296

Azimuth-bearing error dispersion in surveillance radar measurements, using Markov chains

11 p1595 A72-26297

Artificial heating of lower ionosphere in controlled experiment, measuring electron temperature increase by radar backscatter system

11 p1625 A72-26412

Ambiguity of radar phase measurement above sea within radio horizon, noting optimal relation between wavelength and optical paths difference of direct and reflected ray

12 p1784 A72-27799

Small scale atmospheric turbulent motions sensing by FPS-16 Radar/Jimsphere meteorological balloon system, analyzing wind velocity data from dual radar measurements

13 p1990 A72-28818

Frequency discriminator use for range measurements with FM radar systems, deriving reflecting target distance relationship to output voltage

13 p1918 A72-28892

Radar clutter models and comparison with measurements, discussing parameters for description and main functions for suppression

13 p1922 A72-29396

Planetary distance and velocity measurement with radar signal frequency modulation, describing Venus observations

14 p2148 A72-30209

Lunar surface profile, subsurface features and electrical properties measurement for Apollo 17 coherent radar and optical recording system

14 p2085 A72-30512

Model Martian atmosphere, investigating effects of departures from electron density profile spherical symmetry on radio wave phase shift in bistatic radar occultation experiment

15 p2194 A72-31440

Topographic mapping from airborne radar geodetic measurements, evaluating photogrammetric accuracy

15 p2224 A72-31603

Sea clutter measurement at low grazing angles by high resolution radar, noting non-Rayleigh probability density and variation with frequency, pulsewidth and polarization

15 p2196 A72-31786

Rocket and radar-meteor wind observations of zonal flow, noting annual and semiannual components for northern latitudes at 60-130 km

15 p2229 A72-31985

Lunar radar measurement for remotely located clock time synchronization, discussing applications to deep space tracking, computer technique for time delay correction and accuracy

15 p2199 A72-32069

Monostatic radar measurement for incoherent scatter correlation function in lower ionosphere, using spaced short pulses transmission to obtain adequate height resolution

15 p2200 A72-32106

Rocket released artificial Cs plasma clouds in upper atmosphere, measuring electron density by HF radar observation

15 p2231 A72-32330

Rocket-borne laser radar for aerosol observation in upper atmosphere, noting light scattering layer relation to noctilucent cloud appearance

15 p2231 A72-32331

Mars topography variations from earth based surface height radar ranging and Mariner spectrophotometric observation of Mars atmosphere

15 p2313 A72-32346

Dust influx into upper atmosphere above 30 km determined from laser radar measurement

16 p2386 A72-33610

Turbulent energy dissipation rate statistical characteristics above 1000 m from radar measurements, discussing atmospheric boundary layer quantities

16 p2418 A72-33781

Remote measurements of the atmosphere using Raman scattering.

17 p2547 A72-35195

Auroral radio reflection regions spatial distribution from radar measurement, noting backscattering indicatrix independence on geographical latitudes

17 p2519 A72-35873

A new, earth-based radar technique for the measurement of lunar topography.

18 p2659 A72-36277

Chatanika, Alaska, auroral-zone incoherent-scatter facility.

18 p2674 A72-36297

Incoherent scatter observations at Arecibo using compressed pulses.

18 p2659 A72-36299

Complex index of refraction of airborne fly ash determined by laser radar and collection of particles at 13 km.

18 p2661 A72-36637

Measurement of aerosol motion and wind velocity in the lower troposphere by Doppler optical radar.

18 p2706 A72-36638

Radar as a diagnostic tool for lightning.

20 p2948 A72-39350

Investigation of moisture content in the atmosphere by the method of ground radar thermal measurements

20 p2949 A72-39945

Methods of radar studies of the moon and planets from spacecraft

21 p3103 A72-40307

Bistatic radar measurements of the surface of Mars with Mariner 1969.

21 p3110 A72-41453

Martian topography according to ground-based radar measurements and the CO₂ absorption observed from the earth and from the Mariner 6 and 7 spacecraft

21 p3114 A72-41766

Determination of radio-meteor velocity with a minimum rms error

22 p3220 A72-41918

Results of a comparison between radar meteor wind measurements and simultaneous lower ionosphere drift measurements in the same area.

22 p3154 A72-42361

Planetary distance and velocity measurement with radar signal frequency modulation, describing Venus observations

23 p3333 A72-43239

Clear air turbulence detection possibility by optical laser radar and turbulent fluctuation correlations

23 p3264 A72-43898

Rocket-borne GaAs laser radar system with scatter light detector and data processor for upper atmosphere aerosol and pollution measurements

24 p3409 A72-44778

Determination of aerodynamic drag from radar data.

24 p3362 A72-45337

RADAR NAVIGATION
Mathematical analysis of separation standards and aircraft navigational collision risk for parallel tracks in radar monitored systems

01 p0096 A72-10178

Stellar attitude reference and navigation associative processor with high computational speed for radar approach control in ATC

02 p0256 A72-12033

Proposed microwave ILS, discussing continuous step and Doppler scanned radar scanning beams

06 p0846 A72-18396

Pilot and ATC radar controller workload variations relation, discussing distraction stress effects

09 p1271 A72-23132

Tactical approach landing radar tests for low lift drag ratio aircraft in unpowered flight, using F-104D as test aircraft

15 p2267 A72-31694

Ranging signals for aeronautical satellite systems

17 p2516 A72-35220

Collision avoidance system electromagnetic compatibility with radar altimeters designed for 1600 MHz aeronavigation band

21 p3018 A72-40881

CW radar system for tactical aircraft real time command, control and positioning, using combination of frequency and time multiplexing for range measurement

22 p3203 A72-42946

RADAR OBSERVATION
U RADAR TRACKING

RADAR PHOTOGRAPHY

Electron attachment rate determination by combined photographic and radar observation of meteors
01 p0128 A72-10601

Small meteor bodies fragmentation, using radar diffraction patterns
03 p0438 A72-13982

Terrain evaluation by aerial imagery, discussing various film types for conventional visible and IR black and white and color photography, thermal IR and/or radar
09 p1303 A72-23303

Shower structure in sporadic meteor background from statistical analysis of radar range-time photographs, noting unidentified radiant activity
15 p2313 A72-32366

Two dimensional images from remote sensors, discussing geometrical properties and imaging equations for aerial, IR and radar photographs
17 p2555 A72-35335

RADAR RANGE

Automated radar terminal system /ARTS/ for monitoring and tracking all aircraft within radar range, displaying identification, altitude and ground speed information to air traffic controller
01 p0098 A72-10960

Airfield Vehicle Obstacle Indication Device short range high-definition radar system for aircraft navigation aid
02 p0173 A72-12042

Range resolution effect on distributed radar target detection in white noise and clutter, using square law envelope detector with linear integrator
05 p0628 A72-16567

FM-CW radar range measurement by carbon dioxide laser, considering laser output nonlinear variation due to frequency pulling/pushing and refractivity changes
07 p0940 A72-19205

Meteor trails radar ranging system with circular vernier scanning and brightness indication with high accuracy
09 p1308 A72-22507

Multibeam indicator with block diagram description for meteor ranging radar and photofilm based recording system
09 p1308 A72-22508

Amplitude-time quantization of radar pulse signals in analog-digital converter, improving noise threshold and ranging accuracy
11 p1595 A72-26294

Target position information for radar energy potential calculation and detection quality, describing transmitter power reduction for normal range distribution density
11 p1596 A72-26313

Frequency agile radar techniques for improving detection and range resolution and reducing interference and sea and ground clutter
13 p1917 A72-28696

Radar range reduction by snowfall, considering path attenuation and clutter power backscattered from near target precipitation
13 p1917 A72-28699

Aircraft geodetic coordinates computation from radar range measurements and flight altitude over earth ellipsoid
15 p2224 A72-31601

CW radar system for tactical aircraft real time command, control and positioning, using combination of frequency and time multiplexing for range measurement
22 p3203 A72-42946

RADAR RECEIVERS

Satellite-borne radar altimetry pulse compression, discussing signal return statistics, receiver models and detected waveshape relation to altitude, attitude and antenna beamwidth errors
02 p0172 A72-11870

X band gallium arsenide field effect transistor, noting applications for radar receivers, microwave communication links and electronic countermeasures
02 p0193 A72-12184

Optimal sequential multiple decision procedures for radar receiver using Monte Carlo method
05 p0628 A72-16565

GaAs Schottky barrier diodes design, manufacture and characteristics, discussing radar receiver and communication equipment applications
05 p0638 A72-16595

Angle tracking radar receiver signal analysis simplification by use of complex variables
10 p1437 A72-24684

Soviet book on radio receiver design covering military applications, bandwidth requirements, network synthesis and AM, FM, SSB, Doppler, phase metering, PCM and radar equipment
11 p1604 A72-26045

Search radar constant false alarm rate receiver circuit for background noise and clutter compensation, using matched dispersive delay lines flanking hard limiter
16 p2365 A72-33762

The use of semiconductor diodes to protect a radar receiver
18 p2663 A72-37217

High burnout gallium arsenide Schottky barrier diodes.
19 p2770 A72-37259

Microwave low noise amplifiers for use in radar systems.
20 p2907 A72-39220

Detection of Doppler radio signals on a receiver with an additive noise blip number counter
21 p3022 A72-41116

Optimal receivers for measuring time lags of pulse signals in the presence of fading
22 p3154 A72-42123

RADAR RECEPTION

Pulse compression of radar signals by ultrasonic liquid delay line, stressing wideband damped electroacoustic transducers construction
01 p0044 A72-11321

Search radar performance environmental model using clutter and interference returns
02 p0178 A72-12389

Wideband high power radars alignment and testing, including range sidelobes reduction
02 p0178 A72-12392

Receiving antennas polarization parameters selection in side-looking synthetic aperture radars
10 p1453 A72-24905

Dyadic correlation function method for structured radar signal sidelobe suppression during reception, noting Walsh function role
21 p3020 A72-40901

RADAR REFLECTIONS

U RADAR ECHOES

RADAR REFLECTORS

NT RADAR CORNER REFLECTORS

Vertical air motion three dimensional field measurement near mobile fronts by high precision tracking of air-dropped radar reflectors, noting quantitative rainfall prediction
07 p1029 A72-19098

Aerospace systems radar target computer simulation model based on simple multiple reflector geometrical configuration
07 p0948 A72-20345

RADAR RESOLUTION

MTI radar system design philosophy for target detection in land clutter environment
02 p0178 A72-12390

Target detection in sea clutter, showing non-Rayleigh distributed high resolution radar envelope return
02 p0178 A72-12400

Radar detection and resolution, discussing computer analysis of interval modulated signal ambiguity properties and synthesis method
02 p0181 A72-12648

Range rate prediction algorithm for pulse Doppler ambiguity resolution by invariant imbedding method
07 p0941 A72-19303

Optimal synthesis of four radar waveform classes with distinct resolution properties based on target environment analysis
08 p1133 A72-21403

Criterion for estimating radar capability to resolve two targets with differential motion, noting application to synthetic aperture radars and Doppler filters
08 p1134 A72-21424

Airborne microwave hologram radar system, discussing along- and cross-track direction resolution realization by synthetic aperture technique and phased receiving array respectively
15 p2196 A72-31788

A proposed approach for increasing the azimuthal resolution in HF radar.
21 p3015 A72-40360

Analysis of optimal space-time signal discrimination
23 p3266 A72-44217

RADAR SCANNING

Phased array antennas design and performance characteristics, examining feeding and electronic scanning problems with special attention to all-solid-state designs
01 p0038 A72-10659

Broadband beam scanned linear waveguide antenna array design with FMCW short range high resolution radar for airport navigational aid in fog
01 p0039 A72-10669

Phased scanning array for ATC radar beacon systems, airport or air route surveillance radars and ground landing systems
01 p0098 A72-10962

Limited scan antenna system for precision approach radar, detailing design for reflector, aperture gain and phased array
02 p0193 A72-12393

High resolution CRT application to UV film recording and radar and X ray scanning
03 p0360 A72-13712

Proposed microwave ILS, discussing continuous step and Doppler scanned radar scanning beams
06 p0846 A72-18396

Microwave Doppler scanning landing guidance system with radar beam comparison and signal format simplification suggestion
06 p0846 A72-18398

Microwave instrument landing systems based on continuous radar scanning technique, using pulse format for data transmission
06 p0846 A72-18399

Meteor trails radar ranging system with circular vernier scanning and brightness indication with high accuracy
09 p1308 A72-22507

Computerized analytical system for side-looking radar imagery interpretation by isodensitracer scanned density data multivariate analysis applied to environmental discrimination
15 p2198 A72-32064

Error analysis for digital avionics system involving Doppler navigation by intermittent scanning of single beam multimode radar, noting optimum statistical data processing
15 p2271 A72-32204

Directivity pattern accuracy effects on angular coordinate determination by scanning active optical radars
16 p2362 A72-33188

German monograph - A search procedure for electronic radar.
22 p3156 A72-43054

RADAR SCATTERING

Polarization diversity radar power law relations from measurements with size and shape distributed scatterers in comparison with linearly polarized system
01 p0030 A72-10832

Radar backscatter time response waveforms for cube from If data and diffraction analysis
01 p0030 A72-10843

Air pollution measurements by laser radar, using coherence properties to discriminate between backscatter due to molecular atmospheric constituents and pollutant particulates
02 p0212 A72-11816

NASA/MSC earth observation aircraft program radar scatterometers, presenting system evaluation
02 p0172 A72-11849

Composite scattering theory mathematical model for radar backscattering cross section relation to ocean surface conditions and wind velocity
02 p0172 A72-11868

Bistatic radar scatter communication effective coverage analysis, considering dependence on equipment and target locations and properties
03 p0321 A72-13092

Electron temperature measurements in ionospheric isotropic nonequilibrium plasma by electrostatic probes and radar backscatter
03 p0349 A72-13520

Covariance matrix of coordinate fluctuations of instantaneous radar center of reflection from set of scatterers
04 p0487 A72-15144

Oxygen ions vertical flux altitude distribution in F layer from incoherent scatter radar measurements, noting existence in protonosphere during daytime [AD-737929]
05 p0629 A72-16616

Plasma line enhancement variabilities in ionospheric modification experiments due to radar wave scattering, number density gradient and diagnostic beam temperature and orientation
06 p0805 A72-17470

Mercury radar scattering properties, producing Fourier power spectrum from echo signals
06 p0880 A72-17864

Photoelectron flux measurement of intensities of plasma lines in radar incoherent scatter spectrum by uhf radar
06 p0874 A72-18732

Antenna near field correction for backscatter gain in two-beam incoherent scatter radar measurements at Arecibo Observatory
08 p1137 A72-21983

Meteor trail wind radar measurements over Illinois, discussing scattering properties and monostatic vs multistatic coherent systems
10 p1474 A72-24710

Artificial heating of lower ionosphere in controlled experiment, measuring electron temperature increase by radar backscatter system
11 p1625 A72-26412

Mercury topography and scattering characteristics from 3.8 cm radar observations, comparing to Mars and Venus
12 p1865 A72-27098

Radar backscattering cross section and power of conducting cylindrical spacecraft in compressible electron-ion plasma environment
12 p1779 A72-27173

Spaceborne scatterometer measurement standard deviation derivation, noting integration time, signal bandwidth and SNR effects on accuracy
12 p1783 A72-27636

Wavelength choice for ground based operational weather radar systems as function of reflectivity dependence on scattering hydrometeors /raindrops, hailstones/
13 p1917 A72-28694

Rocket-borne inflatable sphere for radar signal backscatter calibrations at reentry altitudes and for simultaneous atmospheric density determination

13 p1918 A72-28819

E and F regions plasma horizontal drift measurements by oblique incidence incoherent scatter radar system, suggesting solar semidiurnal tidal oscillation dynamo action

13 p2031 A72-29386

First and second order backscattering, beam divergence, angular field of view, field size and receiver distance of water clouds illuminated by continuous lidar beam

15 p2200 A72-32154

Spread F association with ionospheric tilts due to total electron content drift, using incoherent scatter radar

15 p2230 A72-32261

Conducting body radar scattering control by reactive loading, discussing field pattern synthesis for real current with least mean-square approximation

17 p2513 A72-34358

Tracking radar system rain clutter reduction by backscatter polarization technique for signal phase and magnitude adjustment

18 p2659 A72-36310

German monograph - A proposal for a radar device with two simultaneously emitted radar frequencies which has a reduced susceptibility to disturbances produced by sea echoes

19 p2764 A72-37481

Lunar radar backscattering measurement of 0.86 cm circularly polarized radiation, noting echo polarization ratio and depolarization variations with incidence angle

19 p2868 A72-38735

Direct measurements of plasma drift velocities at high magnetic latitudes.

19 p2793 A72-38757

A proposed approach for increasing the azimuthal resolution in HF radar.

21 p3015 A72-40360

Backscatter from gated fluctuating regions - A Bremner series approach.

21 p3015 A72-40361

Faraday effect of incoherently scattered radar signals

23 p3263 A72-43365

Direct and cross polarized backscatter power from a turbulent plasma.

23 p3320 A72-43521

RADAR SIGNATURES

Backscatter hf radar signature analysis in relation to medium scale traveling ionospheric disturbances, using computer ray tracing technique

01 p0030 A72-10837

Combined FM CW radar and radiometer at millimeter wavelengths, investigating objects signatures measurement

04 p0494 A72-15611

Relation for detector-aperture size for spatially coherent detection with dependent scattering applied to realistic laser radar signal signatures

09 p1278 A72-22618

RADAR TARGETS

Radar target thin rectangular plate model backscattering from incident and reflected waves, noting front and trailing edge phenomena with emphasis on side edge contribution

01 p0032 A72-11250

Radar target cross section parameters statistical analysis, discussing real target categories and relative measuring methods

02 p0181 A72-12641

Bistatic radar scatter communication effective coverage analysis, considering dependence on equipment and target locations and properties

03 p0321 A72-13092

Target trajectory detector optimization, using data and Markovian chain apparatus

03 p0323 A72-13831

Radar signal processing by digital computer modeling, presenting apparent target splitting probability and azimuth estimate distribution for shifting window target detectors

03 p0326 A72-14361

Optimal discrimination rule for dual frequency radar targets with inadequate echo signal and background noise level parameters

05 p0625 A72-15821

Range resolution effect on distributed radar target detection in white noise and clutter, using square law envelope detector with linear integrator

05 p0628 A72-16567

Computational model of post mixer spectra of periodic FM altimeters with area target returns, using radar scattering coefficient

05 p0637 A72-16568

Nonparametric constant false alarm rate /CFAR/ radar extractor for target detection in background noise, using sign test

05 p0629 A72-16569

Angular coordinates and slope determination from monopulse radar measurements of two unresolved targets

05 p0629 A72-16578

Quasi-specular and Lambert reflection of short radio waves from lunar surface dependent on central portion of near side

05 p0631 A72-17039

Pulsed coherent radar with pulse position random modulation, discussing subclutter visibility, target attenuation and blind speed cancellation and radial speed measurement without range ambiguities

06 p0775 A72-18184

Small radar equivalent surface measurements by Doppler differentiation between signal in target and parasitic echoes

06 p0775 A72-18193

Target azimuth and elevation estimation by four beam cluster, analyzing angle estimation accuracy as function of SNR by computerized Monte Carlo simulation

07 p0941 A72-19304

Aerospace systems radar target computer simulation model based on simple multiple reflector geometrical configuration

07 p0948 A72-20345

Radar tracking pulse scheduling in dense target environment with position estimation error constraints to avoid false return with track correlations

08 p1134 A72-21407

Multipath angle error reduction using multiple radar target signal processor with angle tracking of wave fronts

08 p1134 A72-21408

Targets discovery in predetermined direction by phased array radar, using sequential analysis

09 p1278 A72-22896

Adaptive optimal antenna array detection of unknown spatial location radar targets, noting tradeoff between array size and signal energy with respect to performance

10 p1434 A72-23809

Instantaneous frequency statistical characteristics of passive noise spectra and fluctuating signals reflected from nonpoint moving radar targets

10 p1436 A72-24514

Operation analysis of automatic range finders in pulse radars regarding target search and lock-on functions

11 p1595 A72-26300

Radar systems of effectiveness for moving target selection with alternating period compensation devices, allowing for signals and noise statistical properties

11 p1596 A72-26306

Combined probability density of amplitude and phase difference distribution of signal and noise sum in moving target selection radar systems

11 p1596 A72-26307

Probability distribution density of amplitude difference of target signal and correlated noise sum for radar efficiency estimation

11 p1596 A72-26309

X band radar target cross section representation by discrete point reflector models, deriving boresight error mean and variance in presence of n-target sources

15 p2201 A72-32474

Generalized radar equations derivation to obtain Doppler frequency shift and variance in Fresnel zone due to target movement

16 p2365 A72-33765

Automatic air targets recognition via digital radar data processing, discussing methods for noise signals suppression

21 p3081 A72-40547

Optimal discrimination rule for dual frequency radar targets with inadequate echo signal and background noise level parameters

23 p3263 A72-43429

RADAR TRACKING

Optical radar target range estimation, determining suboptimum post detection signal processing algorithms in photon counting mode

01 p0024 A72-10047

Electron attachment rate determination by combined photographic and radar observation of meteors

01 p0128 A72-10601

Automated radar terminal system /ARTS/ for monitoring and tracking all aircraft within radar range, displaying identification, altitude and ground speed information to air traffic controller

01 p0098 A72-10960

Remote sensing applications to operational weather forecasting including ground optical measurement of cloud base height and radar observation of precipitation

02 p0253 A72-18255

Low angle monopulse radar tracking errors due to multipath, considering amplitude variation across antenna aperture and reduction by target-image resolution

02 p0178 A72-12391

Antenna azimuthal radiation patterns and meteor radiant distribution effects on wind velocity measurement by radar observation of meteor trains

05 p0715 A72-16251

Vertical air motion three dimensional field measurement near mobile fronts by high precision tracking of air-dropped radar reflectors, noting quantitative rainfall prediction

07 p1029 A72-19098

Radar verification of sporadic E layer formation from meteoritic atoms and ions production by meteoric ablation

08 p1154 A72-20728

Radar tracking pulse scheduling in dense target environment with position estimation error constraints to avoid false return with track correlations

08 p1134 A72-21407

Multipath angle error reduction using multiple radar target signal processor with angle tracking of wave fronts

08 p1134 A72-21408

Air masses circulation in atmospheric upper layers during IQSY from meteor trail drifts observation by radar tracking method

08 p1161 A72-21882

German monograph on models for automatic radar tracking methods covering error probabilities, reliability and false information reception

09 p1348 A72-22321

Electron attachment rate relation to altitude in radar observation of meteor trails

09 p1384 A72-22513

Radio transmitter characteristics for radar sounding of upper atmosphere and meteor trails

09 p1278 A72-22874

Upper atmospheric dynamics and electrodynamic processes for evaluation of meteor trail radar observations in synoptic meteorology

10 p1473 A72-24702

Radio echo observation of Quadrantid meteor showers right ascension and declination, observing mean range and influx rate as function of universal time

10 p1545 A72-24808

Russian book on radar studies of moon covering lunar motion, dimensions, mass, density and surface layer thermal and optical properties

11 p1720 A72-26047

Tropical depression analysis based on radar data, observing large divergence in maximum vorticity areas

11 p1681 A72-26079

Probability distribution density of phase difference between noise and signal-noise sum for radar system efficiency estimation, using Bessel and Whittaker functions

11 p1596 A72-26308

Atmospheric density annual and diurnal variations in lower ionosphere, from satellite radar tracking data, considering drag coefficient modeling and orbit determination techniques

11 p1625 A72-26410

Upper wind measurement by balloon-borne targets or radiosondes tracking by primary and secondary radars and radio theodolites

13 p1917 A72-28697

Meteorological rising balloon systems accuracy limitation, noting response to wind field changes, aerodynamic self oscillations and radar tracking errors

13 p1990 A72-28817

Space center trajectory and telemetry systems, including radar stations, interferometric equipment, optical methods and interlinked computers

13 p1938 A72-28961

Radar facility for weak meteor observation, describing antennas, transmitters, receivers, filters, calibration techniques and recording instruments

13 p1919 A72-29026

Aircraft measurements of radiation pattern of radar antenna system used for meteor height observation

13 p1919 A72-29027

Pulse radar equipment for meteor height measurement from nonsaturated trails by phase difference method

13 p1929 A72-29028

Instrument errors of RF phase comparison altimeter for meteor height measurements, using radar tracked aircraft flights calibration

13 p1957 A72-29029

Optimal selectivity digital recorders for meteor trails radar observations, considering input process quantization rate and spectral width selection

13 p1929 A72-29031

Radar observation of meteor geocentric velocity dependence on radiant elongation angle

13 p2038 A72-29035

Atmospheric turbulence anisotropy from meteor trails radar observations statistics, presenting plots of velocity field transverse structure

13 p2038 A72-29036

Adaptive radar tracking processes in presence of clutter, comparing efficiencies via mathematical models

15 p2196 A72-31747

Parallel digital computer application to radar tracking data processing, discussing system design for efficiency maximization and performance, desensitization in traffic level fluctuation
15 p2203 A72-31781

ATC procedures training by digital radar simulators, taking into account geographic terrain, radar, wind and aircraft characteristics and flight plans
15 p2214 A72-32098

Quadrant underdense and overdense meteor observations during sunrise on 16.67 MHz pulsed radar
15 p2312 A72-32197

Shower structure in sporadic meteor background from statistical analysis of radar range-time photographs, noting unidentified radiant activity
15 p2313 A72-32366

Mathematical models for radio attenuation in ice by electromagnetic absorption and reflection from interfaces, noting radar tracking
16 p2363 A72-33290

The reduction of false tracks during automatic tracking
17 p2522 A72-34826

Signal generator designed for calibration and control of interferometric radar station to observe and study radio echoes induced by meteor trails
17 p2519 A72-35959

Refraction correction of rocket tracking radar inputs in near real time.
18 p2661 A72-36636

Determination of upper atmosphere parameters by measuring the ambipolar diffusion coefficient by the method of meteor trail radar observations
18 p2688 A72-36862

Optimal minimal-order observers for discrete-time systems - A unified theory.
18 p2674 A72-37099

Potential value of turn-rate telemetry in tracking of aircraft equipped with discrete address beacon system /DABS/ for ATC, discussing tracking algorithms design
19 p2830 A72-37282

Application of the Volterra series to the analysis and design of an angle track loop.
19 p2830 A72-37283

Target tracking based on the Kalman-Bucy filter
19 p2778 A72-37750

Digital tracking with phased arrays.
19 p2765 A72-38261

Radar verification of sporadic E layer formation from meteoric atoms and ions produced by meteoroid ablation
19 p2791 A72-38356

A versatile Kalman technique for aircraft or missile state estimation and error analysis using radar tracking data.
20 p2950 A72-39089

Investigations on the use of a Kalman filtering method in tracking systems for air traffic control.
21 p3082 A72-41168

Experimental determination of fall rate of 'N5' chaff on the heights 50-90 km.
21 p3049 A72-41498

Free-flight projectiles aerodynamic characteristics and trajectories from yawsonde and radar track data, obtaining best fit coefficients by equations of motion numerical integration
22 p3134 A72-42335

RADAR TRANSMISSION

Optimal synthesis of four radar waveform classes with distinct resolution properties based on target environment analysis
08 p1133 A72-21403

Coherent IR heterodyne receivers with quantum noise threshold sensitivity for laser communications and radar transmission
15 p2198 A72-32063

A 5-kW peak transmitter for the 7-m wavelength
17 p2519 A72-35960

Weighting factor and transmission time optimization in video MTI radar.
21 p3022 A72-41082

RADAR TRANSMITTERS

Transistor power amplifier for 2.5 GHz range directional transmitters, noting cooling problems elimination
08 p1140 A72-21306

Radiosonde balloon tracking errors in upper atmosphere wind measurement with Loran C, Omega and radar transmitters
10 p1441 A72-25092

Computer program to simulate electromagnetic signal densities, data rates and power from land based radar transmitters as functions of time and location
20 p2902 A72-38992

RADARSCOPES

NT PLAN POSITION INDICATORS

Double ended scan converters for multisensor data display in radar, sonar and TV applications
02 p0193 A72-12394

Time-compressed displays for target detection.
17 p2510 A72-35945

RADIAL DISTRIBUTION

Inner radiation belt proton source and loss processes, obtaining flux intensities, energy spectrums and radial distributions
03 p0412 A72-13513

Power and gas consumption for inductive plasma formed in Ar atmosphere, measuring radial distribution of magnetic field axial component
03 p0395 A72-13652

WKB type solution for electromagnetic wave propagation in circularly cylindrical coordinate system with rho-dependent refractivity, using Bessel function
04 p0488 A72-15384

Radial pressure distribution in laminar flow of compressible fluid between two coaxial disks from analog computer study
04 p0514 A72-15702

Electric field strength, radiated power and radial temperature distribution measurements in high pressure Ar cascade arc
05 p0695 A72-16156

Radial distribution of charged particle concentration fluctuation during decaying plasma instability development magnetic field
06 p0863 A72-18416

Solar modulated galactic cosmic rays radial gradient idealized model for comparable deceleration and convection effects
07 p1057 A72-19138

Secondary gas flow effect on energy transfer distributions from plasma torches, obtaining radial distributions of current and energy flux
07 p1046 A72-20546

Trap magnetic system with coil generated field increasing towards periphery, showing radial dependence and acting ponderomotive forces
09 p1363 A72-23215

Radial temperature distribution in Ar plasma jet, assuming local thermodynamic equilibrium
09 p1364 A72-23387

Radial temperature distribution determination in nitrogen plasma jet from continuous spectral background intensity measurement
10 p1519 A72-24131

Argon plasma jet mean flow velocity radial distribution measurement method
10 p1520 A72-24205

Charged and neutral particles radial distribution across positive isothermal plasma column in high current discharges
10 p1521 A72-24355

Apollo 14 charged particle lunar environment experiment data analysis, noting earth plasma sheet absence at lunar distance during geomagnetically quiet times
10 p1476 A72-24961

Radial density profiles and emittance for nitrogen ion beams from Penning-type cyclotron ion source with hot filament
10 p1516 A72-25028

Radial small-signal gain profile measurement in carbon dioxide laser discharge tube explained by axial gas temperature increase with discharge current
11 p1647 A72-26145

Radial profiles of ionized He flux and protons in magnetosphere, taking into account charge exchange processes and fluctuating electrostatic fields
11 p1624 A72-26397

Temperature gradient and thermoelastic stresses in Nd-YAG laser active elements under continuous pumping conditions, noting refractivity radial distribution
12 p1822 A72-27614

Radial temperature and water vapor concentration profiles of radiating combustion source from optical method, using IR band model
12 p1811 A72-27945

Radial magnetic field geometry for total ion utilization in Kaufman thrusters, noting uniform current density and plasma generation and high electrical efficiency
13 p2027 A72-28948

Solar radial brightness distribution, using mm observations during 7 March 1970 solar eclipse for improved angular resolution
13 p2042 A72-29531

Charged particle inertial-electrostatic containment in spherical diode gas discharge gap, measuring flux radial and energy distributions
13 p1933 A72-29915

Electron temperature radial dependence in two fluid models of solar wind, noting unrealistic assumption of heat conduction dominated electron gas energy equation
13 p2034 A72-29961

Lunar gravitational field expansion coefficients C20 and C22 calculation, using Cassini equator inclination and radial bulk density distribution
14 p2149 A72-30213

Earth electrical conductivity radial distribution effect on solar quiet day geomagnetic field variations
14 p2103 A72-30666

RADIAL FLOW

Electric arc plasma, predicting elements addition and electron density alteration effects on radial temperature distribution
14 p2139 A72-30778

Electric arc plasma, investigating reaction energy effects on radial temperature distribution
14 p2139 A72-30779

Cs plasma electron density radial distributions from resonance absorption in discharge tube
15 p2286 A72-32302

Radial transport instability during intense microbeam heating of thin plasma column, noting maximum temperatures and phase coherence cut-off effect
15 p2286 A72-32306

Galactic ridge of discrete diffuse X ray sources, calculating intensity in terms of scale height and radial gradient
17 p2598 A72-34523

Radial distribution of charged particle concentration fluctuation during decaying plasma instability development in magnetic field
17 p2588 A72-34865

Charged and neutral particles radial distribution across positive isothermal plasma column in high current discharges
17 p2589 A72-34955

Monte Carlo calculation of radial and time dependence of isophote diagrams for Cerenkov light in 0.1 to 1 TeV extensive air shower
17 p2599 A72-35142

The interference function of molten metals
17 p2568 A72-35175

Radial density distribution and luminosity functions for stars in alpha Persei cluster
19 p2863 A72-38070

Observations of the radial gradient of galactic cosmic radiation over a solar cycle.
20 p2964 A72-39337

X-ray diffraction studies on liquids at very high pressures along the melting curve. I, II.
21 p3084 A72-40558

Pressure jump across normal ionizing shock waves.
21 p3045 A72-40566

Gross properties of five Scd galaxies as determined from 21-centimeter observations.
21 p3105 A72-41027

Method of calculation of the emission coefficient of a cylindrical plasma starting from the experimental profile of the intensity
21 p3092 A72-41198

Stresses and strains in the plastic range in an annular disk due to steady-state radial temperature variation.
21 p3121 A72-41210

Interaction of a steady plasma flow with a dipole magnetic field in the presence of a radial electric field.
21 p3093 A72-41388

Circular cracks in tension and torsion.
21 p3123 A72-41395

Lunar gravitational field expansion coefficients C20 and C22 calculation, using Cassini equator inclination and radial bulk density distribution
23 p3334 A72-43243

Determination of parameters related to the interior of Mercury.
24 p3436 A72-44696

RADIAL FLOW

Compressible viscous flow between concentric fixed and rotating disks, comparing analog computer calculation with experiment on radial flow
02 p0203 A72-12099

Navier-Stokes equation analysis of three dimensional steady radial expansion of viscous heat-conducting compressible fluid from spherical sonic source into vacuum
03 p0343 A72-14247

Unsteady radial flow between fixed and oscillating walls, obtaining flow equations and air bearings stability conditions
04 p0511 A72-14970

Radial heat propagation in cylindrical rarefied gas column from impulsive axial line source input, obtaining perturbed gas temperature by summation procedure
05 p0743 A72-15867

Radial inflow gas turbine rotating blades aerodynamic characteristics, noting exducer shape effect on turbine performance
05 p0601 A72-16484

Stress analysis of radial flow impeller disk due to centrifugal force in steady state of high speed rotation by matrix finite element method
05 p0741 A72-16996

Landau instability effect on density waves propagation in self gravitating disk of differentially rotating and nonrotating stars populations, noting radial flow of matter
09 p1384 A72-22518

Compressible flow measurement and loss prediction in radial vaneless diffuser in centrifugal compressor, using hot-wire anemometers
10 p1416 A72-23861

- Small radial inflow turbines for space applications, considering blade-shroud clearance, blade loading and exit diffuser design [ASME PAPER 72-GT-42] 11 p1704 A72-25636
- Radial turbine flow analysis, comparing calculated shroud static pressure distribution and outlet velocity profile with measured data [ASME PAPER 72-GT-50] 11 p1570 A72-25642
- Radial inflow compressor feasibility, discussing blade loadings for various pressure ratios and efficiency of rotor and diffuser [ASME PAPER 72-GT-52] 11 p1570 A72-25644
- Inward radial flow turbines under unsteady flow conditions with full and partial admission, predicting performance by method of characteristics 12 p1751 A72-27349
- Nonuniform gas pressure distribution near circular multiple inlet of inherently compensated thrust bearing, considering inward-outward radial flow resistance differential 13 p1963 A72-28748
- N-dimensional traveling waves in nonviscous polytropic gas with prescribed flow variable boundary conditions on arbitrarily shaped hypersurface, discussing application to radial flow 15 p2216 A72-31310
- Flow theory improvement for laminar radial flow between parallel plates, considering inertial effects 15 p2219 A72-32479
- Calculation of the plane potential flow past rotating radial blade cascades 19 p2746 A72-38547
- Inviscid non-monatomic interstellar gas radial flow, considering gravitational and heat conducting effects in stellar winds 20 p2967 A72-39193
- Investigations on the stability of the characteristic of radial flow fans. 24 p3363 A72-45356
- RADIAL VELOCITY**
- CH Cygni spectrum analysis in activity phase, discussing blue continuum, emission and UV absorption lines, radial velocity and stratification effects 01 p0131 A72-11008
- Stellar radial velocities observation with photoelectric spectrometer, discussing catalog errors 04 p0577 A72-15280
- Virgo cluster galaxies evolutionary sequence in radial velocity-nuclear magnitude diagram in terms of morphology, radial color variations, nuclear size and radio emission 05 p0717 A72-16382
- Peculiar interacting extragalactic system NGC 6438, noting same red shift velocity of irregular and SO components 05 p0720 A72-16715
- Radial velocity effects on diameter and luminosity functions of dwarf galaxies 06 p0883 A72-18019
- High radial velocity neutral hydrogen outside galactic plane, noting inability to correlate with radio spurs, absorption and emission regions 07 p1069 A72-19082
- Orbital elements from radial velocity measurements for single line K giant binary star 4 Ursae Minoris 07 p1071 A72-19337
- Solar wind radial velocity variations effects on interplanetary magnetic field spiral structure 07 p1079 A72-20019
- Radial velocity distribution at supersonic compressor inlet from duct-cowl and wall pressure measurements [ONERA, TP NO. 975] 09 p1260 A72-22812
- Radar data statistical evaluation, emphasizing mean Doppler shift for aircraft radial velocity calculation 09 p1278 A72-22897
- Cassiopeia region galactic structure study via objective prism, cataloging stars radial velocities and distances 09 p1391 A72-23539
- Large Magellanic Cloud star membership, comparing Sanduleak catalog based on objective-prism spectroscopy with Fehrenbach-Duflo catalog based on radial velocities 09 p1392 A72-23547
- Geomagnetic field inflation during magnetic storm main phase, considering energy sources and injected proton plasma radial velocity 10 p1472 A72-24274
- Southern Hemisphere interstellar clouds radial velocities from optical and radio observations 10 p1542 A72-24612
- Radial velocities of galaxies derived from spectrograms, describing reduction procedure 10 p1548 A72-24965
- Steady state radial inlet pressure distortion index for axial flow compressor, examining radial velocity, continuity equation and mathematical model [ASME PAPER 72-GT-109] 11 p1571 A72-25673
- Radial velocity effects on diameter and luminosity functions of dwarf galaxies 11 p1718 A72-25955

- Planetary nebula classification based on forbidden line ratios and morphology, discussing galactic plane distribution, radial velocities and evolution 12 p1867 A72-27209
- Interstellar atomic hydrogen observations in radio nebula W 3 direction, noting 21-cm absorption line profile coincidence with Cn alpha recombination line in radial velocity 12 p1868 A72-27219
- Spectroheliograph study of fine structure of Evershed effect, determining radial velocity in penumbra along dark filaments and interfilamentary space 13 p2047 A72-29739
- H II regions radial velocities in Carina arms from Fabry-Perot interferometric H alpha measurements, determining early stars distances from spectroscopic and photoelectric observations 14 p2159 A72-30740
- Polarization and velocity field in the galaxy M 82. 18 p2727 A72-36729
- Changes in the spectrum of the star Be HD 217050 18 p2727 A72-36733
- The structure of the Coma cluster of galaxies. 19 p2854 A72-37229
- Least squares method for Y Cyg spectroscopic elements improvement based on radial velocity measurements, noting nonexistence of gamma velocity variability 19 p2858 A72-37809
- Double system HD 175514. III - Analysis of 1968 observations 19 p2858 A72-37810
- Solar chromospheric flare details motion differences from spectrum analysis and H alpha line frame photography, noting radial velocities difference 19 p2851 A72-37816
- Radial velocities and brightness distribution in active and quiet solar atmosphere from magnetograph measurements, discussing motion directions in photosphere and chromosphere 19 p2858 A72-37818
- Table for reduction of stellar radial velocities to the center of the sun 19 p2859 A72-37909
- Standard iron wavelengths for determining the radial velocities of stars 19 p2859 A72-37910
- Statistical investigations of motions and distances of planetary nebulae 19 p2860 A72-37969
- Density wave detection by local hydrogen gas and young stars radial velocities comparison with Lin theory of galactic spiral structure 19 p2866 A72-38494
- Coude spectra, abundance ratios and radial and rotational velocities of He rich stars, using microphotometer equivalent width tracings 19 p2866 A72-38502
- Stellar-statistical formulation of the problem of setting up an astronomical radial velocity system. 21 p3109 A72-41439
- The kinematics of semi-regular red variables in the solar neighborhood. 21 p3111 A72-41473
- Recoil effect on inverted molecules changing pumping conditions and gain for interstellar, OH maser intensity and radial velocity variations 21 p3102 A72-41773
- Investigation of several nebulae in Cassiopeia with a Fabry-Perot interferometer. 23 p3333 A72-43233
- Radial velocity periodic variability determination from shell star 88 Herculis hydrogen lines, obtaining hypothetical spectroscopic binary elements 23 p3340 A72-44237
- On the possible existence of different interstellar extinction laws in the spiral arms and in the field regions. 24 p3438 A72-44836
- An H I velocity-longitude diagram for the Southern Milky Way. 24 p3438 A72-44845
- Rapid radial displacement of a toroidal plasma filament by a transverse magnetic field 24 p3429 A72-45506
- RADIANCE**
- Earth upper atmosphere outgoing thermal radiation radiance calculation in near IR spectrum 06 p0808 A72-18041
- Satellite radiance data for altitude and amplitude monitoring of stratospheric warming, comparing with rocketsonde and radiosonde observations 13 p1991 A72-28823
- Ballistic density and wind determination from radiances observed by satellite IR spectrometer /SIRS/ onboard Nimbus 3 13 p1991 A72-28825
- Selective chopper radiometer /SCR/ radiances comparison to rocketsonde data, showing vertical resolution of stratosphere and mesosphere temperature changes during midwinter disturbance 15 p2228 A72-31976
- Effect of aerosol variation on radiance in the earth's atmosphere-ocean system. 17 p2547 A72-35194

- Regression technique for determining temperature profiles in the upper stratosphere from satellite-measured radiances. 21 p3052 A72-40249
- Seasonal, nonseasonal and synoptic global variations in stratosphere temperature from satellite-measured radiances, discussing latitudinal warming-cooling relationships 21 p3048 A72-40253
- RADIANT COOLING**
- Radiative cooling system for nearly spherical or polyhedral bodies using radially attached diverging conical elements 02 p0304 A72-12863
- Radiator fins for cooling electronic equipment elements, calculating design parameters effects on heat transfer efficiency 05 p0746 A72-16198
- Radiative cooling effect on enthalpy distribution in air behind incident shock waves produced in explosively driven shock tubes 06 p0904 A72-18529
- Radiative cooling induced thermal instability mechanism for condensation in astrophysical plasma 07 p1040 A72-19348
- Radiative cooling effects in absorbing-emitting gas behind reflected shock waves, using expansion procedure in small density ratio across shock front [AD-738781] 07 p0967 A72-19503
- Spatial layer cooling during surface emission according to Stefan-Boltzmann law, assuming heat source inside body 08 p1253 A72-21445
- Radiational cooling and heating rates for ice and water clouds based on radiative divergence measurements with allowance for latent load 09 p1348 A72-23660
- Thermal radiative cooling system characteristics determination, taking into account surface material thermal conductivity and blackness degree dependence on temperature 10 p1561 A72-23840
- Thermodynamic analysis and parameter optimization of a solar thermoelectric power plant with heat removal by radiation 17 p2497 A72-35509
- Formation of clouds in a cooling interstellar medium. 19 p2854 A72-37231
- German monograph - Cooling of geometrically simple bodies /flat plate, cylinder, sphere/ by convection and radiation. 22 p3244 A72-43062
- RADIANT FLUX DENSITY**
- NT ELECTRON FLUX DENSITY
- NT ILLUMINANCE
- NT IRRADIANCE
- NT LUMINANCE
- NT LUMINOUS INTENSITY
- NT NEUTRON FLUX DENSITY
- NT PARTICLE FLUX DENSITY
- NT PROTON FLUX DENSITY
- NT RADIANCE
- NT SOLAR CONSTANT
- NT SOLAR FLUX DENSITY
- High resolution apparatus to record time dependent light flux variations at 380-700 nm, discussing He plasma decay investigation 01 p0064 A72-10375
- Cosmic ray density distribution inside cosmic ray modulating spherical cone in solar wind, noting modulation depth quasi-periodic variation 01 p0119 A72-10606
- F 2 layer critical frequency variations relation to solar radio flux intensity, using mathematical approximations 01 p0059 A72-10613
- Luminosity function at 400 and 2700 MHz of radio galaxies in Parkes Catalog, discussing optical and radio flux densities 01 p0131 A72-11004
- Irregular, spiral and elliptical galaxies radio continuum measurements at 1420 MHz, presenting positions flux densities and brightness distributions 01 p0131 A72-11005
- Extraterrestrial gamma ray flux contribution to total 0.7-4.5 MeV radiation at various altitudes by balloon sounding 01 p0120 A72-11007
- NGC 5128 nucleus radio emission flux density measurement, noting angular size 01 p0132 A72-11090
- Temporal behavior, intensity fluctuations and energy spectrum of pulsating X ray source Cygnus X-1 from Uhuru observations 01 p0121 A72-11092
- Critique on luminosity volume test for quasars, considering space distribution and luminous function 01 p0133 A72-11126
- Neutrino flux from solar models differing in opacity, equations of state and nuclear cross section factors 01 p0122 A72-11146
- Radio variable sources PKS 0727-11 and 1514-24 observation at 2295 MHz, presenting flux measurements and drift curves 01 p0134 A72-11161

Rapidly varying radio source VRO 42.22.01 /BL Lac/ observations, presenting flux density and linear polarization variations 02 p0277 A72-11774

Compact extragalactic radio source spectrum analysis, discussing successive uncorrelated outburst models 02 p0277 A72-11775

Earth surface and atmosphere remote sensing by airborne microwave measurements, noting ocean surface emittance dependence on temperature, surface conditions and pollution 02 p0207 A72-11779

Interferometric observations of pulsars at 2.7 and 8.1 GHz, determining radiant flux densities 02 p0278 A72-11906

Nonthermal radio source G 55.7 plus 3.4 structure in pulsar CP 1919 direction, presenting intensity contours and integrated flux density spectrum 02 p0278 A72-11907

Venus cloud reflected radiation flux and polarization by Monte Carlo technique, using models with different particle size distributions 02 p0280 A72-12193

Current dependent intensity of spontaneous emission of GaAs injection laser operated at 300 K 02 p0238 A72-12204

Cosmic ray intensity long term modulation and 27 day recurrence relationship to solar activity 03 p0407 A72-12945

High energy solar and celestial X ray experiment with OSO 5, measuring spectrum as function of time, intensity and spatial distribution 03 p0353 A72-13044

Solar spectral radiation intensity calibration methods in 10-4000 A range, including black body source, tungsten lamp, carbon arc, detectors, synchrotron radiation, etc 03 p0355 A72-13064

Giant planets internal constitution models, discussing Jupiter visual magnitude variability, Saturn ring system, cold matter equations of state and He abundances 03 p0418 A72-13111

Eclipsing variable star EQ Taurus photoelectric brightness variation observations in B and V light 03 p0433 A72-13488

Solar limb flare observations on 4 November 1968, presenting photographs and intensive green coronal luminescence 03 p0434 A72-13493

Single channel photometer measurement possibility in UVB magnitudes of variable stars 03 p0359 A72-13497

Eclipsing variable system AW Peg spectrophotometric data, examining spectral line geometries and intensities and atmospheric conditions 03 p0439 A72-14244

Quasar band and optical luminosity evolution, criticizing Arakelian method 03 p0439 A72-14297

Electromagnetic radiation in universe, discussing relic radio emission, energy density, hot model isotropic extragalactic component isolation, intergalactic gas, radio sources and quasars 03 p0414 A72-14317

Emission spectrum and intensity variation of organic dye solutions excited by nitrogen laser pulsed radiation 04 p0529 A72-14655

Radiation intensity of CW argon ion laser with nonlinearly absorbing argon cell in cavity, showing pressure relation to amplification and absorption 04 p0530 A72-14658

Thin amplitude dynamic holograms diffraction efficiency, showing dependence on interference pattern, modulation depth, radiation intensity and material properties 04 p0521 A72-14659

Solar radiation characteristics, calculating concentration and spectral energy distribution 04 p0572 A72-14701

Solar K corona intensity and electron density determination from photographs without eclipse 04 p0574 A72-14924

Van Rhijn height and intensity variations of 5577 A emission in night E layer airglow 04 p0518 A72-14960

Declination, average pulse energy and pulse shape of weak pulsars, determining barycentric period 04 p0574 A72-14981

Radiation intensity and losses in dense high temperature hydrogen plasma containing bare nuclei and hydrogen-, helium-, lithium- and beryllium-like ions as impurities 04 p0557 A72-15170

Numerical fluctuations minimization during luminosity functions and density evolution derivations from data subject to observational selection, applying to 3CR quasars 04 p0577 A72-15284

Markarian galaxies photometric observations, presenting emission line intensities and UVB magnitudes 04 p0578 A72-15309

Galactic center region, Virgo and Crab Nebula gamma ray observations, measuring intensity and energy spectra 04 p0578 A72-15312

Cas A, Tau A, Cyg A and Orion Nebula absolute flux density measurements at centimeter wavelengths 04 p0578 A72-15313

Pulsar PP 0943 radio emission, showing short time intensity increases 04 p0581 A72-15514

Emitting-absorbing flames diagnostics, measuring spectrally resolved radiant energy with fiber optic probe data [ASME PAPER 71-WA/FU-1] 05 p0661 A72-15915

Earth radiation flux spectral intensity measurements in winter, noting latitudinal distributions, day and night variations and oceanic and continental curves 05 p0656 A72-16234

Active solar regions effects on galactic cosmic ray intensity 05 p0710 A72-16526

Venus, M17 and M82 observation on ground through 345 micron atmospheric window, discussing IR fluxes 05 p0710 A72-16709

Upper atmosphere atomic hydrogen H alpha emission, correlating intensity and hydroxyl vibration temperature 05 p0659 A72-17036

Ionospheric geocoronal L alpha emission intensity related to solar activity level from Cosmos 215 satellite data 05 p0659 A72-17038

Background phonon X ray and gamma quanta intensities dependence on solar activity from Geiger counter recordings in deep space 05 p0711 A72-17046

Constant cosmic spherule influx rate measured on quaternary deep sea sediments 05 p0722 A72-17153

Extragalactic radio sources luminosity function and luminosity density function from radio index surface brightness, discussing evolution and agreement with models 05 p0722 A72-17156

Energy spectrum of muon formed electromagnetic cascades in vertical cosmic radiation flux 06 p0871 A72-17287

Off-ecliptic north-south anisotropies in cosmic radiation intensity during polar storm events 06 p0873 A72-17467

Atomic hydrogen 6300 A forbidden line emission altitude and intensity during predawn enhancement, using rotating photometer 06 p0806 A72-17644

Laser radiation intensity modulation by time varying magnetic field 06 p0825 A72-17685

Radiation intensity angular distribution from optically thick plane cloud layer reflection, relating photon survival probability and scattering functions 06 p0807 A72-17939

Auroral zone electron precipitation events before and at negative magnetic bays onset, presenting balloon recordings of bremsstrahlung X-rays intensity 06 p0808 A72-18092

Balloon measurement of low energy cosmic gamma ray flux, obtaining energy spectrum 07 p1059 A72-19585

Energetic gamma quantum flux recording from extragalactic source 3C 120 by Cosmos 251 and 264 satellites 07 p1076 A72-19803

Solar energy sources and dissipation and emission mechanisms, considering radiant flux of convection zone and photosphere and solar variabilities 07 p1078 A72-20005

Thin films thickness and refraction index calculation from curves of specularly reflected X ray intensity vs grazing angle, obtaining surface roughness variance 07 p1050 A72-20405

Magneto-optical effect on CW radiation intensity of Ar laser with cell in magnetic field for various gain conditions 07 p1009 A72-20615

High energy gamma quanta point sources from extensive air showers Cerenkov flares records, finding flux limits of radio galaxy and pulsars 07 p1064 A72-20635

High energy electrons and gamma quantum flux in upper atmospheric layers from high altitude balloon measurements 07 p1065 A72-20639

Solar modulation of cosmic ray intensity in stratosphere, examining relationship to sunspots group number and heliographic latitudes over 11 year period 07 p1065 A72-20641

Three dimensional cosmic ray anisotropy and density distribution at earth orbit and in interplanetary space with allowance for primary particle and nucleon energy spectrum 07 p1065 A72-20645

Stratospheric cosmic ray short period variations at 30 km by spectral density method 07 p1066 A72-20653

Excess radiation and primary cosmic ray intensity variations at 200-350 km during 1965-1969 solar cycle from Cosmos satellite data 08 p1227 A72-21156

High energy gamma radiation intensity from galactic plane in Cygnus-Cassiopeia region, using balloon-borne telescope 08 p1227 A72-21215

Global radiation flux and energy sum calculation from turbidity factor and cloud cover parameters, comparing with measurements in tropics and polar region 08 p1201 A72-21797

Geocoronal hydrogen Lyman alpha glow intensity and zenith angle dependence from observations by rocket-borne extreme UV photometers 09 p1298 A72-22593

Hollow sphere calorimeter for high power pulsed laser energy measurements in broad spectral range, comparing with liquid calorimeter 09 p1323 A72-22656

Tabulation of calculated rotational line intensities relative to integrated vibration-rotation band intensity for various electron transitions of nitrous oxide 09 p1276 A72-22665

Quasar 3C279 flux density variation measurement as evidence for alternate model to explain apparent expansion rate of 10c 09 p1387 A72-22976

Line intensity variation simulation in Raman spectrum of oxygen with allowance for spin splitting of rotational levels 09 p1358 A72-23049

Electromagnetic wave scattering by arbitrarily oriented circular ice cylinders, deriving far field intensities for linearly polarized incident waves 09 p1280 A72-23341

Cassiopeia A secular flux density decrease relative to Cygnus A and Taurus A at 1.4 and 3 GHz, discussing application to antennas and radio telescopes calibration 09 p1390 A72-23529

Relative intensity of solar XUV emission lines of Li isoelectronic sequence ions, taking into account transitional collision strengths 09 p1391 A72-23532

UV radiation intensity altitude dependence and absorption by ozone, considering diurnal and annual variations and biological effects 09 p1268 A72-23625

Radiant flux from finite cylindrical volume to coaxial screen calculated under quasi-homogeneous medium and arbitrary optical thickness assumptions 10 p1561 A72-23841

Galactic center radio, IR, X ray, gamma ray and molecular spectral features, considering models for source component emission mechanisms and energy densities 10 p1533 A72-23887

Quasar and radio galaxy emission intensity and polarization variation models, comparing with observations 10 p1534 A72-23901

Methane absorption line profile, intensity and width studied with magnetically tuned He-Ne laser 10 p1490 A72-24041

CO Cameron system band intensity from measurements of equivalent widths of resolved rotational lines, using Doppler growth curve for line strength conversion 10 p1514 A72-24095

Radial temperature distribution determination in nitrogen plasma jet from continuous spectral background intensity measurement 10 p1519 A72-24131

Extragalactic supernovae X ray luminosity upper limits from OSO 3 data, estimating total energies 10 p1544 A72-24667

Average electric field and power density of electromagnetic wave scattered from rough layer with plane interface, calculating scattering cross sections 10 p1512 A72-24744

Airborne IR radiometric measurements of upward vertical radiance from tropical sea surface at 10-12 microns, noting absorption coefficient dependence on water vapor 10 p1474 A72-24747

Positions, flux densities and identifications for weak sources in Parkes catalog at 2700 MHz, including galaxies and quasars 10 p1545 A72-24792

Spectral indices of extragalactic radio sources at 1.4 GHz independent on flux density 10 p1545 A72-24807

Coma constellation hard X ray intensity sky map at 20-150 keV from balloon observations 10 p1530 A72-24948

Optical method based on spectral line center intensity recording to measure plasma temperature in MHD generators channels and combustion chambers 10 p1525 A72-25111

Fan beam surveys of radio sources with Cambridge telescope, presenting catalogs of galactic coordinates and flux density measurements

10 p1549 A72-25194

Anomalous refraction maxima in bidirectional plane polarized radiant flux transmittances of roughened dielectric surfaces

[AIAA PAPER 72-302]

11 p1742 A72-25236

Model atmosphere with n homogeneous layers and ground surface for solar radiation flux calculation

[AD-744410]

11 p1620 A72-25307

X ray diffraction by alpha Ti, calculating reflections relative intensity and position to identify peaks

11 p1658 A72-25826

Outer space and earth surface galactic cosmic ray intensity data correlation analysis for studying interplanetary magnetic field structure

11 p1713 A72-25936

Spectral components of thermal reflectance as function of directional incident intensity variations

11 p1746 A72-25993

Solar X-rays absorption profiles and residual fluxes in D and E layers during 7 March 1970 eclipse from rocket measurements

12 p1863 A72-27146

Solar Lyman alpha radiation flux over disk during solar eclipse from rocket measurements

12 p1863 A72-27147

Laser emission intensity enhancement based on stimulated Brillouin scattering effect by raising pumping level, energy density and pulse duration

12 p1821 A72-27587

Sco X-1 2-14 keV X ray flux variations from Skylark 901 and S55 observations

12 p1864 A72-27694

Solar cell array tests for high intensity application up to 0.3 AU from sun under simulated space environment

12 p1758 A72-28035

Anisotropic light scattering layer radiation intensity dependence on optical coordinate, obtaining integral equations for semiinfinite and finitely thick layers

13 p2001 A72-28502

Light propagation patterns in absorbing and scattering medium with radiation density dependent optical properties

13 p2002 A72-28510

Meteor-induced magnetic effect on cosmic ray intensity for meteor streams with orbits normal or parallel to interplanetary magnetic field lines of force

13 p2029 A72-28592

Corpuscular radiation intensity relationship to midlatitude mesosphere temperature from rocket and balloon sounding and ground measurements

13 p2029 A72-28603

Satellite photometric observatory for solar corona intensity and polarization measurements during 7 March 1970 total eclipse

13 p2043 A72-29546

Bright point intensity distribution on CN spectroheliogram of sunspot penumbra on 4 July 1970

13 p2045 A72-29710

Brightenings and surglelike spikes associated with low amplitude soft solar X-ray background flux in H alpha above limb, assessing energy budget

13 p2032 A72-29718

Electron temperature and emission measures during solar X-ray flares, studying effects of gradual and rapid radiation flux increases

13 p2032 A72-29722

Solar plasmas temperature ratios of He-like ion line emission, showing dependence on atomic number and electron temperature

13 p2018 A72-29737

Galactic cosmic rays density distribution normal to solar equatorial plane and resultant semidiurnal anisotropy, comparing different methods results with experimental observations

13 p1033 A72-29807

Flux density variations incidence among extragalactic sources found by 3.8 cm sky survey

13 p2048 A72-29830

Energy flux intensity in selectively radiating gas nonisothermal layer from radiant transfer equation and mathematical model

13 p2066 A72-29898

Hydrogen and hydrogen-helium isothermal radiative intensity at various temperatures, density ratios and path lengths, accounting for reabsorption due to overlapping lines

13 p2008 A72-30056

Collisional relaxation and rotational intensity distributions in aeronomic spectra, including radiative losses effects from weak interaction model

13 p2008 A72-30057

Nitrous oxide band intensities, half widths and pressure broadening coefficients

13 p2008 A72-30059

X ray flux associated with gravitational radiation pulses, determining upper limit with balloon-borne apparatus

13 p2007 A72-30121

Nocturnal low intensity auroral red arcs observations by meridian scanning photometer, comparing with green emission

14 p2097 A72-30136

Auroral emission spectrum intensity ratios for IBC 2 system observed via aircraft flown digital multichannel photometer

14 p2097 A72-30137

Nightglow small scale intensity fluctuations of 5777 A atomic oxygen emission due to turbulent transport of horizontal wind observed with photometers

14 p2098 A72-30143

Nightglow ground based spectrophotometric observations of hydroxyl emission intensity and rotational temperature variations related with solar and geophysical activity

14 p2098 A72-30144

Maximum ion energy dependence on radiation density in laser plasma

14 p2137 A72-30315

Solar cyclic intensity variation of excessive radiation with respect to galactic radiation background at low altitudes from satellite data analysis

14 p2146 A72-30475

Uhuru satellite observation of transient X ray source in constellation Lupus, discussing five month period intensity variation

14 p2157 A72-30572

Galactic supernova remnants radio frequency absorption line observations, deriving distances, radio luminosity function and distribution

14 p2158 A72-30726

Ionized plasma line widths and intensities due to Landau and collisional damping, observing effects by light scattering techniques

14 p2140 A72-30901

Solar X-ray flux daily changes before and after proton flare, using zero-epoch superposition method

14 p2148 A72-30911

Transient North-South anisotropies in cosmic radiation intensity, noting occurrence during Forbush decreases

15 p2298 A72-31432

Cosmic ray density gradient perpendicular to ecliptic plane, noting component introduction into diurnal variation depending on sense and direction of interplanetary magnetic field

15 p2298 A72-31436

Diffuse cosmic gamma ray flux density and energy spectrum observation at equatorial balloon altitude, discussing photon count, flux and spectra

15 p2299 A72-31924

V/Vm insensitivity to red shift random shuffling based on luminosity function in Einstein-de Sitter cosmological model

15 p2314 A72-32375

IR radiant energy emission from conical jet exhaust of turbojet aircraft

15 p2298 A72-32399

Solar O VI, Ne VIII and Mg X spectral lines intensity ratios from XUV rocket measurements, comparing data with Jordan-Allen-Dupree ionization equilibrium calculations [AD-745811]

15 p2318 A72-32783

Face centered solid crystal cell spatial distribution effect on body surface-reflected molecular beam intensity distribution

16 p2430 A72-33066

Critique of papers on quasars covering theory of gravitational lens intensified bright compact objects

16 p2454 A72-33452

Centaurus region hard X ray flux temporal variations from OSO-3 X ray telescope observations

16 p2446 A72-33458

Pulsars 0950 plus 08 and 1133 plus 16 flux density spectra measurements at 1.4-5.0 GHz, noting equivalent continuum break

16 p2456 A72-33477

Radiation intensity angular distribution from optically thick plane cloud layer reflection, relating photon survival probability and scattering functions

16 p2426 A72-33780

X ray flux anomalous minima observations in Cen X-3 with rocket-borne argon-methane proportional counter

16 p2461 A72-34162

Origin of the low energy diffuse cosmic X-ray flux.

17 p2599 A72-35071

Fraunhofer lines emergent intensity fluctuation caused by temperature and pressure perturbation in solar atmosphere

17 p2608 A72-35080

Extragalactic radio source 3C 1202 microwave flux density variations suggesting superrelativistic expansion

17 p2611 A72-35295

Radio observations of two supernova remnants, HB21 and IC443, at 4170 MHz.

17 p2613 A72-35500

Investigation of the dependence of the electrical characteristics of a 'Fotovolt'-type high-voltage matrix photoconverter on the radiation intensity and temperature

17 p2498 A72-35511

Calculation of solar radiation incident on a cylindrical surface

17 p2498 A72-35515

Theoretical He-triplet line strengths compared with astronomical observations of planetary nebulae and H II regions

17 p2614 A72-35646

Periodic intensity oscillations in center of H alpha supergranulation network, in rosette centers and in plage granules

17 p2616 A72-35701

Energetic gamma quantum flux recording from radio galaxy 3C 120 by Cosmos 251 and 264 satellites

17 p2617 A72-35726

Calibration of the flux density of Cassiopeia A and Cygnus A in the range 300-9375 MHz.

17 p2617 A72-35728

Focused irradiance fluctuations beyond a layer of turbulent atmosphere.

17 p2518 A72-35754

Auroral zone splitting into various radiation intensity regions, discussing DR currents influence on particle motion in magnetosphere and structural relationship

17 p2550 A72-35856

Radio galaxies monochromatic luminosity-spectral index relationship from 3CR spectra studied at 10 MHz to 10,700 MHz

18 p2726 A72-36621

Galactic and metagalactic background radiation

18 p2722 A72-36723

North-south asymmetry in cosmic ray intensity increases before magnetic storms

18 p2722 A72-36851

Relationship between X-ray luminosity and velocity dispersion in clusters of galaxies.

19 p2856 A72-37501

Measurements of radiation flux at the moment of ignition of a solid propellant [ONERA, TP NO. 1067]

19 p2800 A72-37759

Forbidden line intensities in cesium plasmas.

19 p2840 A72-37776

Spectral densities of radio emission fluxes from discrete radio sources at the 3.5-cm /8550 MHz/ wavelength

19 p2850 A72-37804

Periodic heating mechanism in solar flares.

19 p2851 A72-37888

Short-period pulsar intensity variations at 70 to 115 MHz

19 p2862 A72-38056

Accurate positions of radio sources at 408 MHz.

19 p2868 A72-38698

Optimum generation conditions for a neon-helium laser operating in the axial TEM/sub 00/ mode

19 p2814 A72-38784

Observations at 408 MHz of radio sources from the 4C catalogue. IV - Declination range 20 to 0 deg.

19 p2869 A72-38825

Accurate flux densities at 5009 MHz of 1007 radio sources.

20 p2967 A72-39190

Microradiometer for studying the structures of highly intensive radiation fields

20 p2924 A72-39224

Excess radiation and primary cosmic ray intensity variations at 200-350 km during 1965-1969 solar cycle from Cosmos satellite data

20 p2964 A72-39261

Flux densities, positions, and structures for a complete sample of intense radio sources at 1400 MHz.

21 p3105 A72-40575

Method of calculation of the emission coefficient of a cylindrical plasma starting from the experimental profile of the intensity

21 p3092 A72-41198

Variable radio objects BL Lac, OJ 287, AP Lib, B2 1212+30 and ON 231 observed in IR spectral range, noting variations in flux

21 p3107 A72-41270

Jupiter - New evidence of long-term variations of its decimeter flux density.

21 p3107 A72-41274

Radiative transfer equations solution for stellar spherical atmosphere by Grant-Hunt method, approximating intensity derivative over angular variable with Legendre polynomials

21 p3109 A72-41433

Quantitative spectroscopy of the aurora. I - The spectrum of bright aurora between 7000 and 9000 A at 7.5 A resolution.

21 p3049 A72-41724

Radiometer with protective mica window for radiant flux densities measurement of near IR sources, noting reading independence of sources spectra characteristics

21 p3059 A72-41821

Simultaneous measurements of H alpha and H beta Balmer lines and He D3 line in faint prominences, showing emission intensity ratios dependence on layer total optical thickness

22 p3221 A72-42034

Radiation intensity of a steady flame above a burning fluid
22 p3243 A72-42166

Spatial distribution of excess-radiation intensity at low altitudes
22 p3218 A72-42212

Atmospheric effects on the surface cosmic ray meson intensity recorded in London.
22 p3218 A72-42369

Noncoherent scattering probabilistic formulation in terms of mean intensity averaged over absorption profile and mean scatterings number required for photon escape
22 p3206 A72-42559

Multisectional CW gas dynamic laser output radiation density distribution control via transmitting mirror with variable reflection coefficient
22 p3186 A72-42632

Satellite measurements of solar X-ray flux and their use for interpretation of sudden ionospheric disturbances.
22 p3219 A72-42884

Maximum ion energy dependence on radiation density in laser plasma
23 p3318 A72-43218

Statistical analysis of Forbush decreases and the preceding increases in cosmic-ray intensity
23 p3328 A72-43354

Methods of solving one-dimensional problems of radiative gasdynamics
23 p3320 A72-43528

Laser radiation geometric divergence and variation of transmitted intensity with mirror transmissivity at centerline for unstable cavity viewed as oscillator-amplifier
23 p3296 A72-43902

Galactic submillimeter background radiation energy density limit, taking into account recalibrated gamma ray flux measurements agreement with cosmic ray-interstellar matter interactions
23 p3329 A72-43942

The occultation of beta Sco by Jupiter.
24 p3436 A72-44699

Diffusion processes of cosmic rays with energies between 2 and 20 GV during Forbush decreases - The diurnal effect.
24 p3434 A72-44785

Interplanetary scintillation of radio sources observed through solar corona, deriving higher central moments from skewness coefficient of probability density function
24 p3437 A72-44831

Meteor-induced magnetic effect on cosmic ray intensity for meteor streams with orbits normal or parallel to interplanetary magnetic field lines of force
24 p3435 A72-45092

Corpuscular radiation intensity relationship to midlatitude mesosphere temperature from rocket and balloon soundings and ground measurements
24 p3435 A72-45103

Approximate formulas for the intensity of diffuse reflected emission from a semiinfinite atmosphere
24 p3448 A72-45685

Continuous He-He laser radiation intensity correlation function measurement, using Michelson interferometer and frequency doubler
24 p3412 A72-45704

RADIANT HEATING

Simulation of nuclear light bulb engine propellant radiative heating, using argon seeded with micronized carbon particles and 500 kw dc arc as radiant energy source
01 p0099 A72-11344

Heavy elements gamma heating, using LiF thermoluminescent dosimeters and computer programmed photon transport calculations
04 p0546 A72-14427

Ablation performance of dielectric heat shields for planetary entry, testing diffuse reflectance by convective and radiative heating
05 p0747 A72-16809 [AIAA PAPER 72-89]

Unsteady thermal conductivity and heat transfer in solid bodies heated by radiation, using cascade linearization method
07 p1100 A72-19884

Conical foil radiation detectors sensitivity and time response, formulating time dependent thermal equations
08 p1166 A72-21433

Radiational cooling and heating rates for ice and water clouds based on radiative divergence measurements with allowance for latent load
09 p1348 A72-23660

Vaporization characteristics of carbon heat shields under radiative heating, presenting estimates of vaporization heat from energy balance
11 p1741 A72-25234 [AIAA PAPER 72-296]

Ear site body temperature measurement relation to radiant heating of scalp and upper face
12 p1768 A72-28333

Pyrometric obturation devices effect on sample temperature level during high temperature tests with radiant heating
13 p1960 A72-29903

Unsteady thermal conductivity and heat transfer in solid bodies heated by radiation, using cascade linearization method
17 p2637 A72-35132

Hematological modifications due to acute exposure to heat
21 p3002 A72-41191

RADIANT INTENSITY

U RADIANT FLUX DENSITY

RADIATION ABSORPTION

NT ATMOSPHERIC ATTENUATION

NT AURORAL ABSORPTION

NT ELECTROMAGNETIC ABSORPTION

NT MOLECULAR ABSORPTION

NT PHOTOABSORPTION

NT POLAR CAP ABSORPTION

NT SELF ABSORPTION

NT ULTRAVIOLET ABSORPTION

NT X RAY ABSORPTION

Energy-momentum tensor for radiation and radiative viscosity in optically thick matter having Thomson scattering with photon absorption and emission processes
01 p0129 A72-10798

Fused silica optical transmittance at elevated temperatures during high energy electron bombardment, noting optical absorption at short wavelengths
01 p0103 A72-11357

Atmospheric scattering and absorption effects on target/background discrimination in environmental remote sensing at 0.4-3.0 microns spectral region
02 p0213 A72-11858

Absorbed doses at various depths in water target exposed to charged pions, muons and electron beams, using Monte Carlo program [CERN-71-16]
02 p0162 A72-12063

Acoustic absorption materials weak shock wave reflection and attenuation determination by shadow-graph-schlieren photography and pressure transducers
02 p0259 A72-12177

Magnetic atomic beam absorption filter for high resolution solar field observations
03 p0357 A72-13290

Ruby laser radiation nonlinear absorption by azulene solutions derived by taking into account two-photon transitions for comparison with measurement
03 p0366 A72-13367

Relaxation and heating rate due to solar radiation absorption by 2.7 and 4.3 micron vibration-rotation bands of carbon dioxide
03 p0347 A72-13387

Stellar field structure in NGC 2129 cluster direction, discussing interstellar radiation absorption and star distribution
03 p0433 A72-13491

Excited IR fluorescence in gas compounds with negligible absorption, using CW carbon dioxide laser
03 p0367 A72-13554

Optical excitation of divergent alkali atomic beam by radiation absorption, deriving absorption coefficient for line broadening and/or Doppler effect
03 p0393 A72-14062

Temperature reduction produced by partial cloud cover effect on radiation received by Nimbus 3 IR radiometer
03 p0385 A72-14226

Time variations of zonal averages of albedo and absorbed solar radiation derived from brightness data of digitized satellite pictures
03 p0385 A72-14228

Planetary nebula IC 418 reddening constant from Paschen line intensities of IR spectrum
04 p0570 A72-14554

Gas lasers application to precise length measurements via absorbing medium resonance determined wavelength
04 p0530 A72-14734

Air pollutant detection by multiple slit correlation spectrometry and laser absorption technique, noting sensitivity enhancement by laser output increase
04 p0530 A72-14894

Radiation intensity and losses in dense high temperature hydrogen plasma containing bare nuclei and hydrogen-, helium-, lithium- and beryllium-like ions as impurities
04 p0557 A72-15170

Flow distribution behind shock wave with intense laser radiation absorption and laser-triggered thermonuclear reactions
04 p0559 A72-15351 [AD-736299]

Hydrogen plasma absorption coefficients at laser frequencies over 0.3371-10.6 microns
05 p0694 A72-15997

Refraction theory applied to isotropic absorbing media, noting spatial distribution of incoherent components according to polarization states
05 p0689 A72-16173

Monochromatic radiation pulse transfer in absorbing plasma, deriving heat wave propagation velocity
05 p0696 A72-16680

Gamma ray absorption near Crab Nebula pulsar NP 0532 within beam model, discussing pair production in photon field
05 p0711 A72-17161

Laser pulse induced stimulated Raman scattering /SRS/ in linearly dispersionless medium measuring delay between laser and Stokes pulse maxima by photon absorption fluorescence technique
05 p0693 A72-17170

Total atmospheric water vapor content from solar radiation absorption observation at millimeter wavelengths
06 p0817 A72-18091

Microwave biased millimeter and submillimeter wave detector with n-type InSb, using down conversion process and free carrier absorption for detection
06 p0866 A72-18384

Gas kinetic cooling by absorption of carbon dioxide laser radiation, explaining by vibrational energy transfer and relaxation rates
07 p1000 A72-19046

Radiative cooling effects in absorbing-emitting gas behind reflected shock waves, using expansion procedure in small density ratio across shock front [AD-738781]
07 p0967 A72-19503

Zirconium dioxide white pigment coatings for spacecraft thermal control, discussing impurities effects on optical absorption properties
07 p1023 A72-19692

Two photon absorption of ruby laser emission in mixed zinc cadmium sulfide crystals, plotting laser light damping vs beam power density
09 p1322 A72-22212

German monograph on wall stabilized Ar arc column displacement by pulsed HF radiation heating covering power absorption determination based on theoretical model
09 p1358 A72-22341

Book on heat transfer by thermal radiation, covering black body radiation, electromagnetic theory, energy exchange, Monte Carlo solution, and absorbing and emitting media
09 p1411 A72-23046

UV radiation intensity altitude dependence and absorption by ozone, considering diurnal and annual variations and biological effects
09 p1268 A72-23625

Monochromatic absorption coefficients determination for Ar heated in wall-stabilized arc at high temperatures and pressures
10 p1517 A72-23836

IR absorption spectrum of gaseous ozone, obtaining mechanical anharmonicity coefficients and zero order wave numbers
10 p1511 A72-24226

Electromagnetic wave propagation and absorption in weakly inhomogeneous plasma layer, calculating conditions for transformation into plasma wave
10 p1523 A72-24799

Mesosphere and lower thermosphere heating and associated solar UV radiation absorption calculation based on diurnally varying photochemical diffusive model
10 p1475 A72-24943

Thermal neutrons anomalous absorption by indium antimonide crystals, determining absorption coefficient by integral reflectivity measurements
10 p1527 A72-24980

Multidimensional formulation of surfaces configuration factor in radiative semidiathermanous absorbing media by change of variable method [AIAA PAPER 72-275]
11 p1685 A72-25215

Spherically specularly reflecting nonresonant cavities for use as absorption cells in far IR spectroscopy, predicting performance
11 p1629 A72-25301

Passive Q factor modulation in carbon dioxide laser by resonance absorption saturation in osmium tetroxide vapors, noting vapor pressure effects
11 p1650 A72-26355

Solar proton event classification system with index of three digits representing proton flux, absorption and sea level neutron monitor response measurements
11 p1714 A72-26425

Inclination and absorption effects on galaxies apparent diameters, optical luminosities and neutral atomic hydrogen radiation
11 p1724 A72-26725

Single mode gas laser with internal absorption cell, emphasizing frequency standard application
12 p1819 A72-27285

Effect of pumping radiation absorption by electron-excited molecules on organic compounds lasing efficiency
12 p1825 A72-27883

Nd-fiberglass laser intensity fluctuations due to fibers absorption centers, deriving population inversion threshold, pumping power and center formation rate from kinetic equations
12 p1825 A72-27884

Atmospheric nitric acid vapor radiation absorption measurements at various partial pressures
12 p1805 A72-27993

Efficiency response of covered Si detectors to monoenergetic gamma rays, considering Lucite, Al, Cu and Pb absorbers
13 p1954 A72-28429

Refraction theory applied to isotropic absorbing media, noting spatial distribution of incoherent components according to polarization states

14 p2130 A72-30242

Nonlinear radiation absorption and resonance molecular fluorescence of saturated diatomic Rb vapors excited by Q switched ruby laser

14 p2109 A72-30353

Thermal defocusing of high intensity continuous Ar laser radiation in absorbing medium with allowance for spherical aberrations

14 p2110 A72-30355

Cosmic ray anomalous absorption height dependence on zenith distance in midlatitude ionosphere during solar flare emission from polarization study

14 p2146 A72-30461

Black holes due to gravitational collapses, including radiation emission/absorption, pulsars and binary stars

14 p2151 A72-30478

Model for hot stars mass outflow due to gas acceleration by radiation absorption in UV resonance lines

15 p2305 A72-31341

Molecular oxygen concentrations from solar Lyman alpha radiation absorption profile in mesosphere, using rocket-borne nitric oxide filled ion chamber

15 p2230 A72-32264

Gravitational absorption investigation from lunisolar attraction observed by tracking high flying satellite in eccentric polar orbit

16 p2382 A72-32892

Solar radiation absorption measurements in 2150 A region as function of altitude to obtain oxygen and ozone densities

16 p2384 A72-32975

Precursor ionization upstream from shock wave due to shock emitted radiation absorption by easily ionizable impurity species

16 p2379 A72-33512

Monochromatic radiation pulse transfer in absorbing plasma, deriving heat wave propagation velocity

16 p2437 A72-33692

Passive Q factor modulation in carbon dioxide laser by resonance absorption saturation in osmium tetroxide vapors, noting vapor pressure effects

16 p2402 A72-33708

Temperature field in flat plate with selective radiation absorption coefficient, using asymptotic representations for internal heat flux radiation component

16 p2479 A72-33858

Effect of pumping radiation absorption by electron-excited molecules on organic compounds lasing efficiency

16 p2404 A72-33992

Nd-fiberglass laser intensity fluctuations due to fibers absorption centers, deriving population inversion threshold, pumping power and center formation rate

16 p2404 A72-33993

Theory of photon-induced hopping on acceptors in p-type germanium.

17 p2595 A72-34750

Electrons and photons interaction with relict radiation, establishing high energy gamma rays energy and intensity attenuation length

17 p2600 A72-35145

Auroral cosmic radio emission absorption mechanisms, considering ionization rate, recombination coefficient and collision frequency effects

17 p2602 A72-35865

Radiation absorption and emission in atmosphere IR spectrum influenced by water droplets around atmosphere contamination particles

17 p2552 A72-35942

Source function for radiative fields produced by uniform parallel irradiation of scattering absorbing medium of finite optical thickness, using radiative transfer linearity

19 p2834 A72-37837

Ionospheric D region, a sensitive detector of hard X-rays of solar subflares.

19 p2852 A72-38628

The use of infrared absorption to determine density of liquid hydrogen.

19 p2805 A72-38836

The effect of target absorption on the attenuation characteristics of bremsstrahlung generated at constant medium potentials.

21 p3087 A72-40474

Absorption spectra in the far ultraviolet of Be, B, C, N, Mg, Al, and Si

21 p3013 A72-40818

Influence of the lowering of the ionization energy on the continuous radiation of an argon plasma

21 p3093 A72-41343

Radiation absorption calculation for nonisothermal gas containing combustion products, noting approximation for water vapor radiation

22 p3243 A72-41885

Atmospheric nitric acid vapor radiation absorption measurements at various partial pressures

22 p3174 A72-43007

Indirect transitions and absorption in the mid-IR region of the spectrum in SSBBr crystals

23 p3323 A72-43337

Recombinational luminescence of NaI-Tl single crystals excited in the A-band of activation absorption

23 p3323 A72-43342

On the physical nature of cosmic neutrino absorption. I - Cosmological models with continuous creation. II - Cosmological models without continuous creation.

24 p3439 A72-44974

RADIATION BELTS

NT ARTIFICIAL RADIATION BELTS

NT INNER RADIATION BELT

NT OUTER RADIATION BELT

NT PROTON BELTS

Charged particles magnetic scattering on cyclotron instability waves of radiation belt plasma, estimating proton relaxation time

01 p0119 A72-10608

Trapped protons low energy differential spectra from polar orbiting Injun 5 satellite measurements, suggesting radiation belts impulsive acceleration mechanism

01 p0120 A72-10891

Solar flare, galactic and magnetically trapped /Van Allen/ nuclear particle radiation environments calculation for three outer planet Grand Tour missions

03 p0413 A72-14095

Solar wind effects on storms and structure of magnetosphere and radiation belt maintenance

03 p0350 A72-14304

Electron lifetime in earth radiation belt due to resonant scattering with hiss vlf radiation

05 p0711 A72-17045

Geomagnetically trapped low energy proton flux distribution due to 17 April 1965 magnetic storm, noting adiabatic effects

[AD-736383] 06 p0803 A72-17452

Statistical hypothesis of Van Allen radiation belts, using Vlasov equations for self consistent plasma fields

07 p1055 A72-18805

Magnetospheric trapped particle diffusion coefficients and acceleration in earth radiation belts

07 p1062 A72-20035

Magnetosphere If electric fields influence on trapped radiation region particle behavior, considering magnetic drift rates

07 p1062 A72-20036

Satellite, space probe and observatory data impact on space physics, considering solar wind, interplanetary magnetic field, Van Allen belt and Chapman-Ferraro theory

10 p1538 A72-24268

Book on earth environment covering atmospheric structure, terrestrial magnetic field, solar radiation, micrometeorites, ionosphere and van Allen belts

10 p1478 A72-25173

Natural oscillations of magnetosphere and trapped radiation transport by electromagnetic pulses as possible mechanism for disturbances from thermonuclear explosion reaction on particles in natural radiation belt

11 p1712 A72-25935

Dayside magnetosphere stably trapped radiation zone high latitude boundary determination from energetic electron intensity spatial distribution observation by Imp 3 satellite

11 p1713 A72-26106

DR ring current belt formation due to electron and proton gradient drift in inhomogeneous geomagnetic field, calculating charged particles trajectories

14 p2101 A72-30646

Geomagnetic field multipoles effects on radiation belt particle motion for analysis of true anomalies

15 p2222 A72-31280

Energetic electrons generation and relaxation in narrow belt near 2.8 L measured with Cosmos 137 Cerenkov counter

15 p2299 A72-31909

Spacecraft bacteria population resistance to simulated Jovian trapped radiation belt electrons and solar wind protons, noting dependence on isolate, dose and electron energy

15 p2186 A72-31993

Interplanetary radiation types in terms of possible space flight hazards, discussing electromagnetic and corpuscular radiation, cosmic rays and radiation belts

16 p2446 A72-33553

Pitch-angle diffusion of radiation belt electrons within the plasmasphere.

17 p2602 A72-35597

Observation of very-low-frequency whistler-mode waves in the region of the radiation-belt slot.

17 p2517 A72-35598

Scientific problem resolution during Jupiter missions, discussing Pioneer probes, trapped particle belts, Red Spot, atmosphere, biological activity, internal heat sources and radio emission

19 p2864 A72-38381

Radiation belt electron lifetimes and removal through pitch angle diffusion by plasmaspheric whistler waves in cyclotron harmonics

20 p2918 A72-39532

Mid-latitude D-region ionization associated with the 'slot' in radiation belt electrons.

20 p2964 A72-39533

Radiation belt protons and ion-cyclotron wave interactions accounting for magnetospheric ring current instabilities during storm at plasmaopause

20 p2919 A72-39545

Parasitic pitch angle diffusion of radiation belt particles by ion cyclotron waves.

23 p3333 A72-44527

RADIATION CONTROL

U RADIATION PROTECTION

RADIATION COUNTERS

NT CERENKOV COUNTERS

NT ELECTRON COUNTERS

NT NEUTRON COUNTERS

NT NEUTRON SPECTROMETERS

NT PARTICLE TELESCOPES

NT PROPORTIONAL COUNTERS

NT QUANTUM COUNTERS

NT SCINTILLATION COUNTERS

NT SPARK CHAMBERS

Tissue equivalent plastic counter for radiation dose equivalent measurement in mixed radiation field, discussing data processing

[CERN-71-16] 02 p0163 A72-12070

Long wavelength focusing collector for X ray astronomy with effective bandpass of 100-280 eV determined by low energy transmitting counter windows and paraboloid mirror reflectivity

[AD-736551] 03 p0353 A72-13040

Heavy nonrelativistic single charge particle recording in cosmic rays at sea level, using scintillation and anticoincidence Cerenkov counters

06 p0870 A72-17276

Photon counting system for low level radiation measurement in UV visible region, discussing simplifications

07 p0983 A72-19133

Laser Doppler velocimeter signals statistical properties, examining bandwidth, counting time and input SNR effects on zero crossing counter output fluctuations rms value

07 p0990 A72-20370

Narrow-band pulsed laser radar photocount distribution statistics in thermal background radiation, noting detection performance dependence on signal and noise absolute level and SNR

08 p1134 A72-21420

Energetic particle flux measurement on spacecraft based on statistics of overflowing register counting Poisson process

09 p1312 A72-23261

VLF atmospherics count comparability in broadband and narrow-band operation, presenting amplitude frequency response

09 p1301 A72-23268

Operating conditions of photometers for optimum photomultiplier photon counting photometry, considering measurement precision dependence on experimental parameters

14 p2105 A72-30733

Cross sections for dissociative excitation of hydrogen ions by electrons determined by coincident detection of protons and H atoms

14 p2134 A72-30804

Lunar laser ranging experiment single photon detection and nanosecond timing precision

15 p2233 A72-31530

Miniature high gain photomultiplier for pulse counting applications in close-packed arrays and mosaics for scintillation imaging and spectrum analyzing

15 p2234 A72-31534

Radiation damage effects in Li compensated Si nuclear particle detectors induced by irradiation with electrons, protons and fast neutrons

15 p2291 A72-31539

Apollo lunar surface experiments package suprathermal ion detector measurements in lunar environment

15 p2309 A72-31957

Satellite Prospero onboard micrometeoroid detector data analysis for near earth flux

15 p2310 A72-31987

Relativistic electron characteristics in interplanetary space from onboard satellite detector measurements beyond magnetospheric influence

[IGPP-UCR-72-11] 15 p2300 A72-31998

Nonionizing component of underground high energy cosmic radiation investigated with anticoincidence screen and counters, noting bremsstrahlung as photons source

15 p2301 A72-32232

Satellite-borne semiconductor particle detector telescope for C and Mn isotopes identification in heavy primary cosmic rays, considering scintillation counter and mass resolutions

16 p2389 A72-32883

Galactic X and gamma ray astronomical observations from balloons, rockets and satellites, discussing radiation counters

16 p2445 A72-33075

Cosmic ray isotopic data extraction via geomagnetic field, discussing magnetic effects on particle flux and finite resolution limitations of counters

16 p2447 A72-33728

The geometric factor of a cylindrical plate electrostatic analyzer. 17 p2553 A72-34639

Investigation of Freon fire-extinguishing systems with a nucleonic gage. 18 p2648 A72-36674

Photon count circuit conjugation with photomultiplier for spectrometric measurement of lines emitted by atomic barium jet excited by slow electron beam. 19 p2799 A72-37671

Anomalous increase in the total X-ray background at balloon altitude. 19 p2853 A72-38755

Coincidence counting applied to the activation analysis of meteorites and rocks. 20 p2900 A72-39841

Lunar shadowing of charged particles with arbitrary gyroradii and steady drift transverse to magnetic field applied to detector in low lunar orbit. 21 p3104 A72-40482

The solar X-ray spectrum deduced from a proportional counter experiment and the resultant production of ionization in the mesosphere. 22 p3170 A72-42368

Determination of characteristic magnitudes of toroidal electrostatic analyzers - Application to the optimization of analyzers used in space physics. 22 p3180 A72-42935

RADIATION DAMAGE

Inhaled ozone effect on chromosome aberrations break frequencies in circulating blood lymphocytes of irradiated Chinese hamsters. 01 p0015 A72-11149

Cosmic and X ray irradiated quartz particles as contributor to interstellar extinction, discussing grain radiation damage measurements and absorption spectra in wavelengths of approximately 1600 Å to 20 micrometers. 01 p0134 A72-11163

High peak power LSA epitaxial GaAs diode relaxation oscillator breakdown under neutron irradiation. 01 p0404 A72-11309

Mathematical model for radiation damage cross section linear energy transfer dependence, explaining experimental values of relative biological effectiveness [CERN-71-16]. 02 p0160 A72-12052

Focused laser beam interaction with liquid metal particles, discussing fluid phase light screening effect, droplet evaporation and mass expulsion characteristics. 03 p0368 A72-13668

Amorphous polymer dielectric luminescence and destruction under Q switched laser radiation with subthreshold power and picosecond pulses. 03 p0369 A72-14071

Li-diffused Si compared to conventionally doped materials under neutron irradiation, considering carrier removal. 03 p0403 A72-14078

Nuclear radiation interference and damage effects in galactic and solar cosmic ray measurements during charged particle experiments by deep space missions. 03 p0438 A72-14085

Radiation damage in MgO, ZnO and magnesium difluoride, considering energy dependence and roles of radiolysis and elastic collisions. 03 p0404 A72-14088

Li-containing solar cell damage and recovery characteristics measurement under 1-MeV electron irradiation, deriving diffusion-length damage coefficient. 03 p0312 A72-14092

MIS semiconductors radiation-hardening mechanisms and radiation effects on electrical properties and degradation. 03 p0405 A72-14281

N-p silicon solar cells damage at room temperature by proton and deuteron irradiation, considering particle mass and energy functions and illuminating light wavelength effects. 04 p0561 A72-14574

Photochemical reactions in pyrimidine base of DNA after UV irradiation, relating mutagenic and lethal effect to dimerization. 04 p0467 A72-14608

Mathematical model for blood leucocyte population changes after radiation exposure within Blair model leucocytes hemopoietic to cardiovascular systems transport. 05 p0618 A72-16635

Biological damage inflicted to rats by protons, X rays and gamma rays. 06 p0762 A72-17675

Neutron irradiation induced material degradation and circuit failure in high power GaAs Gunn diode oscillator operating in LSA relaxation mode. 06 p0788 A72-18472

Neutron damage effects on red and green output of GaP light emitting diodes at 300 K. 07 p1047 A72-19043

Pulsed ruby laser mode structure effects on quartz damage, noting dependence on propagation and polarization directions with crystal. 07 p1001 A72-19196

Energy spectrum of radiation defects in proton bombarded n-type Si crystals from Hall effect and electroconductivity measurements. 07 p1049 A72-19901

Neutron irradiation produced lattice disorder in Li doped float zone melted n-p type Si solar cells. 08 p1216 A72-21182

Biological hazards of high intensity light sources, considering physiological factors involved in threshold eye damage values determination. 08 p1125 A72-21333

Primary and secondary radiation damage to metals and alloys crystal lattices. 08 p1187 A72-21786

Radiation damage by heavy solar particles in soil grains from Lunik 16 and landing Apollo sites. 09 p1381 A72-22269

German monograph on Frenkel defect structures in thin gold wire at high electron irradiation dose, using electrical resistance measurements. 09 p1354 A72-22325

Ceramic laser materials failure due to optically induced damage, estimating stresses and changes in refractive indices under thermal effects. 09 p1336 A72-22403

Fast neutron radiation damage to glass ceramics and amorphous semiconductors electrical properties. 09 p1336 A72-22405

Laser induced surface damage probability as function of power density, suggesting electron avalanche breakdown as cause. 09 p1324 A72-23083

Radiation induced extrinsic photoconductivity in Li doped Si, examining localized energy levels in forbidden gap. 09 p1372 A72-23238

Laser damage resistance properties of thin film multilayer antireflection coatings for quartz optics. 09 p1326 A72-23348

Radiation damage in bcc metal Mo and W foils under energetic Au ion irradiation, noting vacancy dislocation loops. 09 p1331 A72-23506

Ribonuclease molecule damage and enzyme activity under UV irradiation and repeated freezing and thawing. 09 p1274 A72-23594

Spacecraft thermal control coating damage by energetic Hg ion bombardment, using absorbance measurements [AIAA PAPER 72-445]. 11 p1746 A72-26183

Transparent dielectrics destruction by mode-locked laser ultrashort pulses, discussing filamentary defect presence indication of radiation self focusing. 12 p1853 A72-27068

Temperature dependence of destruction threshold of lithium niobate surface under laser irradiation, noting ferroelectric properties effects. 12 p1853 A72-27069

Laboratory irradiation tests with van de Graaff generator for simulation of spacecraft components radiation damage due to high energy space protons and electrons. 12 p1863 A72-27552

Transparent dielectric surface photoelectric emission current under laser pulse illumination, noting correlation to surface treatment and damage threshold. 12 p1822 A72-27613

Industrial safety rules recommendations for lasers based on radiation biological effects and eye optical and physiological properties. 12 p1771 A72-27615

Lens parameters selection and prisms position optimization in light beam to avoid premature damage. 12 p1808 A72-27623

Pathophysiology of exposure to UV, IR, coherent, microwave and RF radiations, discussing potential hazards, damage, human tolerance threshold, protection guides and safety standards. 12 p1772 A72-27963

Electron bombardment effects on transport properties and carrier lifetime degradation of Li doped Si solar cells. 12 p1856 A72-28024

Proton and electron radiation effects on silicon solar cells electric and photovoltaic properties, determining damage coefficients via minority carriers diffusion length measurement. 12 p1759 A72-28045

Monoenergetic electrons and low energy protons radiation damage effect on Si solar cell electrical and optical properties. 12 p1759 A72-28046

ESRO satellites solar array performance under orbital environmental conditions, discussing radiation damage and earth albedo effects. 12 p1759 A72-28047

Irradiation produced defects and electrical properties of n and p-type Si, discussing radiation damage due to neutron and ion implantation. 12 p1857 A72-28058

Radiation damage in carbon doped silicon irradiated at low temperatures by 2 MeV electrons, noting isotope shifts. 12 p1857 A72-28059

Li defect interactions in electron irradiated n-type single crystal Si from electron paramagnetic resonance measurements. 12 p1858 A72-28063

Radiation effects in InSb, GaSb and GaAs, stressing orientation dependence of damage production at electron energies near threshold and recovery data. 12 p1858 A72-28066

Electron energy threshold measurements in irradiated II-VI compounds interpreted in terms of damage on metal and chalcogenide sublattices. 12 p1859 A72-28070

Electron radiation damage and edge emission of cadmium telluride, presenting cathodoluminescence spectra. 12 p1859 A72-28071

Lattice damage measurement of Cd ion implanted GaAs semiconductors by optical reflection and scanning electron microscope. 12 p1859 A72-28075

Surface damage equations for heavy ion irradiated Si and GaAs single crystals in terms of incident fluence. 13 p2020 A72-28430

Permanent operational characteristics changes of Si and Ge transistors bombarded by gamma and neutron radiation. 13 p1928 A72-28700

Energetic Hg ion bombardment erosive and chemical effects on spacecraft surfaces downstream of electrostatic rockets [AIAA PAPER 72-446]. 13 p1983 A72-28944

Destructive changes in rabbit brain and eyes under pulsed laser beam irradiation. 13 p1910 A72-29333

Proton irradiation effects on monkey central nervous system, showing inflammatory reaction and neuroglial astrocyte glycogen accumulation. 13 p1906 A72-29833

Radiation damage effects in Li compensated Si nuclear particle detectors induced by irradiation with electrons, protons and fast neutrons. 15 p2291 A72-31539

Light flashes observed by astronauts on exposure to primary cosmic radiation during translunar flights, investigating effect upon retina in man and animal. 15 p2189 A72-31917

Neutron irradiation effects on structural materials brittle fracture initiation and propagation mechanisms, discussing residual elements influence on radiation defect stabilization. 15 p2258 A72-32486

Neutronically generated He irradiation effects on high temperature fracture of fcc, bcc and hcp structural metals and alloys. 15 p2258 A72-32487

Rhodamine laser radiation effects on absorbing materials investigated by high speed cinematography and shock wave structure. 16 p2404 A72-33991

Effects of junction depth on the radiation damage of silicon solar cells. 17 p2594 A72-34388

Implications of ceramic-insulator irradiation results for thermionic reactor design. 17 p2496 A72-34592

Radiation damage to refractory metals as related to thermionic applications. 17 p2566 A72-34595

Russian book - Characteristics of radiation damage caused by high energy particles in semiconductors. 17 p2595 A72-34700

Electron paramagnetic resonance of radiation damage in a lunar rock. 17 p2609 A72-35098

Effect of lunar ground on radiation damage in mice. 17 p2504 A72-35214

Rhesus monkey retinas ultrastructural alteration and damage in rods and cones produced by Q switched ruby laser coherent radiation. 17 p2509 A72-35396

Brain tumors in irradiated monkeys. 17 p2505 A72-35647

French monograph - Experimental characterization and analysis of the effect of ionizing radiation on the electrical properties of MOS transistors. 17 p2531 A72-35650

A field-ion microscope study of ion-implantation in iridium. I, II. 18 p2719 A72-36747

Properties of 1 MeV electron-irradiated defect centers in p-type silicon. 19 p2844 A72-37687

Relation between the plasma ion current and the surface defects produced by ruby and neodymium laser emission. 19 p2812 A72-38210

Fracture of nonlinear KDP and LiNbO3 crystals by ruby laser radiation. 19 p2812 A72-38537

Analogy in the evolution of surface and bulk damage features produced by laser radiation in transparent glasses. 19 p2812 A72-38541

- Relation between diffusion and defect formation rates in silicon detectors exposed to gamma radiation 20 p2959 A72-38956
- Effect of residual elements on radiation strengthening in iron alloys, pressure vessel steels, and welds. 20 p2937 A72-39289
- An interpretation of radiation effects on mechanical properties of carbon fibres based on a 'sheath' and 'core' model of fibre structure. 20 p2944 A72-39794
- Laser-induced damage in transparent dielectrics - The relationship between surface damage and surface plasmas. 21 p3062 A72-40241
- Anatomy and thermal history of laser self-focusing damage tracks in glass. 21 p3062 A72-40245
- Effect of prolonged gamma irradiation on the functional capacity of leukocytes 21 p3103 A72-40438
- The effects of X-ray irradiation on MAS diodes. 21 p3032 A72-40695
- Correlation of irradiation data using activation fluences and irradiation temperature. 21 p3083 A72-40763
- Hematological modifications due to acute exposure to heat 21 p3002 A72-41191
- Changes produced in the nerve structures of the stellate ganglion by total X-ray irradiation 22 p3140 A72-41925
- Ionizing radiation effects on mitosis and nucleic acid synthesis, noting protective chemical agents and hematological evaluation of radiation damage and marrow regeneration 22 p3141 A72-41986
- Nature of radiation defects formed by ruby laser emission on the surface of solids 22 p3185 A72-42273
- Matthiessen rule on binary alloy electrical resistivity temperature derivative, discussing data deviations in substitutional alloys after quenching, radiation damage and plastic deformation 22 p3189 A72-42298
- Investigation of radiation paramagnetic defects in alkaline-silicate glass subjected to the action of high quasi-hydrostatic pressures - Structure of hole defects 24 p3417 A72-45421
- Transparent dielectrics destruction by mode-locked laser ultrashort pulses, discussing filamentary defect presence indication of radiation self focusing 24 p3432 A72-45721
- Temperature dependence of destruction threshold of lithium niobate surface under laser irradiation, noting ferroelectric properties effects 24 p3432 A72-45722

RADIATION DETECTORS

- NT DOSIMETERS
- NT SILICON RADIATION DETECTORS
- NT THRESHOLD DETECTORS [DOSIMETERS]
- Magnetosphere model for low energy cosmic ray proton propagation mode to synchronous orbit satellite, calculating geomagnetic cutoffs and penetration regions [AD-71079] 02 p0274 A72-12453
- Gamma ray detection system using scintillation counter and active anticoincidence shield 03 p0352 A72-13028
- Major sources of background counts for collimation gamma ray detector, measuring radiation direction and energy spectrum from balloon altitudes 03 p0352 A72-13032
- Pyroelectric detector noise equivalent power limitation factors, discussing heterodyne systems and pulsed submillimeter lasers detection 04 p0551 A72-15602
- Gravitational radiation short bursts detector, treating SNR by fluctuations method 05 p0715 A72-16183
- Gravitational radiation detector angular dependence, obtaining directivity pattern 05 p0656 A72-16184
- Energy spectrum, composition and anisotropy study of cosmic radiation from extensive air showers, using scintillation and Cerenkov detectors 06 p0870 A72-17277
- Dumbbell and Weber cylindrical gravitational wave detectors sensitivity comparison 06 p0848 A72-17828
- Microwave biased millimeter and submillimeter wave detector with n-type InSb, using down conversion process and free carrier absorption for detection 06 p0866 A72-18384
- Nuclear transducer for atmospheric pressure measurements based on alpha radiation detection, discussing accuracy, linearity and possible error sources 07 p1033 A72-20307
- Upper atmosphere temperature measurement by homodyne detection of excited atoms and molecules radiation, using photodiode beat frequencies produced by spectral line emission 08 p1154 A72-20739

- Multiple-wire spark counter characteristics for alpha particle detection, discussing electrodes surface finish and gas filling 08 p1164 A72-20941
- Conical foil radiation detectors sensitivity and time response, formulating time dependent thermal equations 08 p1166 A72-21433
- Particle detector assembly for low energy heavy mass cosmic ray nuclei identification 08 p1167 A72-21508
- UK-5 satellite all sky X ray monitor consisting of pinhole camera, position sensitive proportional counter and data processing electronics 08 p1228 A72-21513
- Surface contamination effect on alpha particle resolution of surface barrier detector/preamplifier combination for use in space environment 08 p1168 A72-21517
- Alternating Josephson effect and junctions applications to radiation generators and detectors, electromotive force regulators, oscillators, mixers and noise thermometers 09 p1370 A72-22799
- Flame photometric detection of small concentrations of sulfur compounds in ambient air, describing spectrum scanning detector, rotating interference filter and correlation detector 10 p1480 A72-24101
- Transducers for piezoelectric detection of torsional waves for wire chambers 10 p1480 A72-24212
- Maximum likelihood receiver performance for optical detection of multimode laser or scattered radiation, considering photocounting distribution, decision threshold and error probability 10 p1452 A72-24681
- Ionospheric detection of cosmic X rays by VLF links using nova sources 11 p1714 A72-26417
- Book on information theory of atmospheric visibility covering vision threshold conditions, eye as radiation detector and short waves field near ground 11 p1691 A72-26697
- Linear detectors for broadband and high intermediate frequency measurements in radio astronomy 12 p1793 A72-27810
- Crystal characteristics of optical detectors for direct measurement of high power laser radiation 12 p1824 A72-27874
- Semiconductor gamma ray detectors development, using cadmium dichlorides, dibromides, diiodides and difluorides as doping agents in CdTe crystal growth 14 p2142 A72-30549
- Trillion electron volt pulsed gamma rays from Crab Nebula pulsar NP 0532 14 p2156 A72-30566
- Gravitational radiation generation and detection, discussing Weber detector, interaction with electric and magnetic fields and gravitational astronomy 15 p2273 A72-31287
- Radioisotope camera based on electron avalanche in liquid Xe, noting spatial and energy resolution advantages over existing gamma ray cameras 15 p2234 A72-31537
- Optical communications photodetector sensitivity assessed from input power ratio of ideal and actual detector, noting amplitude modulated systems 15 p2235 A72-31621
- Semiconductor devices application to gamma ray, X ray and nuclear radiations detection and analysis 15 p2235 A72-31644
- Frequency modulated laser radiation detection, studying photomultiplier current harmonics, phase/amplitude detector nonlinearities and noise-resonator coupling effects 15 p2246 A72-31882
- Suprathermal ion detector measurements on lunar surface by Apollo 12 and 14 astronauts to provide search for lunar exosphere phenomena 15 p2301 A72-32092
- Solar and geocoronal hydrogen Lyman alpha radiation detector, discussing ion chamber with magnesium difluoride window and nitric oxide gas 15 p2239 A72-32336
- Nomogram for heat detector size determination from thermal inertia index and Biot number 16 p2395 A72-33968
- Crystal characteristics of optical detectors for direct measurement of high power laser radiation 16 p2403 A72-33983
- Atomic, molecular and ionic species detection in upper atmosphere by measurement of resonance fluorescence radiation excited by tunable laser radiation [AIAA PAPER 72-661] 16 p2388 A72-34073
- Semiconductor low-energy X-ray spectrometry 17 p2552 A72-34335
- A search for high energy gamma-rays from solar active regions. 17 p2599 A72-35092
- Analysis of geometry effects in the detection of Cerenkov light from extensive air showers. 17 p2599 A72-35141

- Pyroelectric radiation detector with ferroelectric crystals, discussing operation mode, construction, sensitivity and IR applications 17 p2530 A72-35445
- Mathematical methods for improving the significance of scintigrams 18 p2652 A72-36425
- German monograph - A method for the determination of the differential albedo for photons in the range from 1-17 MeV 19 p2836 A72-37484
- Upper atmosphere temperature measurement by homodyne detection of excited atoms and molecules radiation, using photodiode beat frequencies produced by spectral line emission 19 p2791 A72-38367
- Anomalous increase in the total X-ray background at balloon altitude. 19 p2853 A72-38755
- Measurements of electron detection efficiencies in solid state detectors. 20 p2925 A72-39401
- The detection of gravitational waves by electromagnetic oscillators. 20 p2974 A72-40024
- Radiometry error analysis for diffraction at radiation beam limiting screens, calculating corrections for circular source and detector 21 p3050 A72-40149
- One-to-one telescope with pressurized Ar gas for nanosecond and picosecond laser output pulse sensitive detection via gas breakdown and energy absorption 21 p3062 A72-40618
- Construction and operation of a Weber-type gravitational-wave detector and of a divided-bar prototype. 21 p3057 A72-41486
- Particle, plasma and field detectors for rocket investigations in and above atmosphere, considering PCM telemetry system and balloon-borne X ray telescope system 21 p3057 A72-41617
- Gravitational wave detector design based on fine components of scattered light spectrum 21 p3086 A72-41696
- Geometric factor of a cosmic ray detector - Equivalence of alternative analytical derivations. 22 p3178 A72-42647
- Esro 1 /Aurora/ satellite electron intensity measurements, explaining disparities between different experiments by detectors low-energy thresholds difference 22 p3173 A72-42648
- Mercury-cadmium telluride photoconductive detectors array for S-192 multispectral scanner for Skylab earth scanning experiments 23 p3288 A72-43879
- Mercury-cadmium telluride multispectral photoconductive detectors, discussing fabrication techniques and performance characteristics 23 p3288 A72-43880
- Effect of fluorescence observation geometry on lifetime measurement, including the development of an approximation to the detector collection efficiency integral. 23 p3288 A72-43884
- Calculation of middle ultraviolet radiation detector response to solar radiation as a function of altitude. 23 p3289 A72-43897
- Controlled secondary electron emission and some possibilities for its application in particle detectors 23 p3316 A72-44159
- Signal-to-energy conversion function in the photometry of solar soft X-radiation with broad-band detectors. 23 p3329 A72-44238
- Electronic detection of ionizing-particle tracks in liquid argon 23 p3291 A72-44442
- Parametric preamplifiers for transistorized nuclear-emission detectors and their capabilities 24 p3402 A72-44894

RADIATION DISTRIBUTION

- NT ANTENNA RADIATION PATTERNS
- NT DIFFRACTION PATTERNS
- NT SIDELOBES
- Redistribution function of line radiation during scattering without atom velocity restriction 01 p0104 A72-10093
- Atomic models of velocity noncorrelated radiation line scattering with frequency redistribution at large distance from atmosphere 01 p0104 A72-10094
- Fraunhofer hologram for recording square of modulus of far field radiation pattern due to mixture of known and unknown source distributions 02 p0224 A72-11548
- Tissue equivalent plastic counter for radiation dose equivalent measurement in mixed radiation field, discussing data processing [CERN-71-16] 02 p0163 A72-12070
- Linear energy transfer response of polyvinyltoluene plastic scintillator, presenting data on quality factor

- and radiation dose equivalent determinations in mixed radiation field
[CERN-71-16] 02 p0168 A72-12071
- Angular dependence of radiation emitted by earth-atmosphere system and reflected by space, noting application to radiation balance mean value computation 02 p0255 A72-12790
- Radiation pattern from open ended parallel plate waveguide with arbitrary electric or magnetic aperture field distribution, using Wiener Hopf technique 03 p0331 A72-13409
- High power CW gas dynamic laser mode-control experiment with unstable resonator at high Fresnel number, obtaining near and far field intensity distribution 04 p0529 A72-14605
- Van Rijn height and intensity variations of S577 A emission in night E layer airglow 04 p0518 A72-14960
- Waveguide structures partially filled with bulk negative differential conductivity media, describing wave propagation characteristics and power distributions 04 p0501 A72-15427
- Waveguide with slanted aperture, determining propagation mode and wave amplitude from radiation level at Brillouin angle 05 p0625 A72-15828
- Two dimensional time dependent nonlinear radiative transfer and nonequilibrium diffusion in arbitrary geometry by synthesis method 05 p0746 A72-15996
- Atmospheric optics and geophysics problems modeling arrangement reproducing radiation field within light scattering medium 05 p0658 A72-16293
- Sound propagation within and radiated from annular duct flow, measuring acoustic distributions for single and multimode excitations [AIAA PAPER 72-197] 05 p0691 A72-16924
- Scaling hypothesis testing by angular distributions from cosmic ray experiments 05 p0711 A72-17125
- Injection laser threshold current density, radiation pattern and electric field distribution relation to layer thickness and dielectric constants, using waveguide theory 06 p0825 A72-17772
- Azimuthal IR radiation distribution of atmospheric brightness cross sections at various zenith angles from balloon programmed-control radiometer data 06 p0808 A72-18042
- Parallel plate waveguide radiation into dielectric or plasma layer, using Hilbert formulation 06 p0791 A72-18734
- Forbush decreases in cosmic radiation, discussing cosmic ray flow pattern deduction from anisotropies, modulation dependence on rigidity and theoretical models 07 p1058 A72-19355
- Open ended parallel plate waveguide, calculating radiation pattern variation with diaphragm dimension 07 p0945 A72-19663
- Magnetic bremsstrahlung energy straggling and radiation reaction, calculating particle and emitted photon distribution 07 p1037 A72-19668
- Approximate solution to Elenbass-Geller equation of arc electric and radiation characteristics as function of thermal conductivity by Galerkin method 07 p1043 A72-19879
- Cosmic ray muons integral energy spectrum and angular distribution at sea level represented by power law, using primary interaction model 07 p1063 A72-20475
- Liquid pulsed laser active element lens parameters effects on output radiation divergence 07 p1008 A72-20511
- Solar active regions effects on galactic cosmic ray distribution and interplanetary magnetic field structure 07 p1065 A72-20646
- High energy charged particles angular distribution measurements in equatorial region cosmic radiation above atmosphere by Proton 2 satellite 08 p1226 A72-20799
- Solar modulation process for galactic cosmic ray particle time variation, discussing interplanetary magnetic fields and plasma, energy losses from solar wind deceleration, etc 08 p1227 A72-21188
- Narrow-band pulsed laser radar photocount distribution statistics in thermal background radiation, noting detection performance dependence on signal and noise absolute level and SNR 08 p1134 A72-21420
- Nd-glass laser time characteristics and radiation ordering from cavity lengthening 08 p1183 A72-21771
- Ray trace of sound refraction by point source on jet flow axis, numerically calculating directivity pattern 08 p1152 A72-21893
- Holographic image reconstruction for individual transverse laser modes radiation intensity distribution 08 p1169 A72-21915
- Far field radiation pattern from magnetic line source covered with moving uniaxial or isotropic nondispersive dielectric or cold plasma sheaths 08 p1137 A72-21985
- Nonuniform non-Lambertian diffusely scattering surface optical transfer characteristics and initial irradiance distribution inside sphere, discussing spherical harmonic moment measurement 09 p1309 A72-22610
- Interplanetary space three dimensional cosmic ray variations from harmonic components of diurnal variations 09 p1377 A72-22926
- Expression for annual modulation of diurnal variation from generalized cosmic ray anisotropy in space, applying to earth revolution induced modulation 09 p1377 A72-22927
- Semidiurnal cosmic ray anisotropy, eliminating atmospheric effects and global isotropic variations in cosmic ray telescope 09 p1377 A72-22928
- Space anisotropy responsible for solar semidiurnal variation of cosmic ray intensity studied with data from worldwide network of neutron monitor stations 09 p1377 A72-22929
- German monograph on radiation characteristics of planar systems in aperture plane of parallel plate waveguide, obtaining relationship between electric and magnetic fields 10 p1434 A72-23775
- Apollo 14 charged particle lunar environment experiment data analysis, noting earth plasma sheet absence at lunar distance during geomagnetically quiet times 10 p1476 A72-24961
- Multimode dielectric slab waveguide power coupling due to core-cladding interface irregularities, obtaining power distribution and radiation losses 11 p1603 A72-25270
- Radiation resistance for natural modes of rectangular panel from far field acoustic radiation energy distribution 11 p1687 A72-26059
- Video information transmission over planar and rectangular multimode waveguides under excitation by coherent light, calculating field distribution by geometrical optics approximation 11 p1633 A72-26330
- X ray diffusion by thin films under grazing incidence, using reciprocity theorem 11 p1689 A72-26484
- Two dimensional characteristic and distribution functions of monomode laser radiation random processes with nonlinear optics application 11 p1651 A72-26716
- High order optical harmonic generation and many-quantum processes efficiency in multimode laser radiation field 12 p1821 A72-27593
- Radiation distribution and power output characteristics of Nd in phosphorus oxychloride solution circulating liquid pulsed laser for various flow velocities 12 p1821 A72-27599
- Hydromagnetic wave scattering of high energy cosmic rays in highly ionized interstellar gas to confine cosmic rays to Milky Way 12 p1864 A72-27745
- Sea level absolute vertical cosmic ray muon intensity from range spectrometer measurements within tropic zone 12 p1864 A72-28225
- Laplace transform method in unsteady radiation field theory, discussing generalization from steady luminescence to inhomogeneous media and forbidden band frequency radiative transport 13 p2001 A72-28506
- Approximate solution to spectral line frequency resonance radiation transport equation, assuming total radiation redistribution with respect to frequencies 13 p2001 A72-28508
- Combined photon and particle diffusion of two level system with ground and excited atomic states and photon emission-formed radiation field 13 p2001 A72-28509
- Numerical description of electromagnetic radiation from open-ended flanged waveguides, giving truncation corrected expressions for field behavior in aperture perimeter vicinity 13 p1915 A72-28520
- MHD laser discharge characteristics under generator conditions, emphasizing interaction of gas ionization instabilities and lasing radiation field 13 p2014 A72-29367
- Sound generation by finite rectangular plate vibrations, deriving radiated power as function of aspect ratio and vibration pattern 13 p2005 A72-29564
- Polarimetric determination of angle between polarization planes of emission and external radiation field in three level gas laser, noting resonator anisotropy properties 13 p1970 A72-29687
- Radiation defectoscopy methods based on calculating perturbations in gamma radiation field due to inhomogeneities 14 p2106 A72-30150
- Vertical propagation of large scale disturbances in long wave radiation field into upper atmosphere, using linearized hydrothermodynamic equations 14 p2127 A72-30262
- Mars surface normal albedo distribution function from red light photometry data 14 p2152 A72-30489
- Visual observation of continuous hydrocarbon acid laser modes and beam energy distribution, using cholesteric liquid crystal image converter 14 p2111 A72-30851
- Beam divergence prediction for multiple transverse laser modes, proposing tables and graphs to determine angular spread in far field 15 p2247 A72-32031
- Solar radiation angular field structure from upper atmospheric boundary scattering, taking into account underlying surface albedo fluctuations 16 p2386 A72-33783
- Gaussian electromagnetic radiation beam propagation in turbulent medium, calculating broadening dependence on outer scale by modified Karman spectrum characterization 17 p2580 A72-34291
- High-radiance room-temperature GaAs laser with controlled radiation in a single transverse mode 17 p2563 A72-35342
- Displacement measurement from double-exposure laser photographs 17 p2564 A72-35751
- Laser and mercury lamp outputs spatial coherence measurement by speckle patterns produced with ground glass as random inhomogeneous medium 17 p2565 A72-35752
- Cosmic ray anisotropy and conditions in the interplanetary medium during a solar cycle 17 p2603 A72-35871
- Studies on radiation balance at a tropical station 18 p2722 A72-36759
- Series solution for electromagnetic wave propagation in radially and axially nonuniform media - Geometrical-optics approximation 18 p2712 A72-37024
- Anisotropy of angular distribution of radiation due to positron annihilation on the surface of Mo single crystals 19 p2844 A72-37691
- Source function for radiative fields produced by uniform parallel irradiation of scattering absorbing medium of finite optical thickness, using radiative transfer linearity 19 p2834 A72-37837
- Mars surface normal albedo distribution function from red light photometry data 19 p2864 A72-38318
- Cosmic-ray diffusion coefficient in interplanetary space 19 p2853 A72-38756
- A sealed, sectionalized million-V X-ray tube 19 p2776 A72-38767
- Two dimensional linear polarization radio distribution maps of 3C 270 and 3C 452 radio galaxies, relating to source magnetic field structure 20 p2965 A72-38904
- Dynamic electromagnetic scattering pattern of flying object, constructing quasi-ergodicity condition to compute standard statistical descriptions for recognition 20 p2903 A72-39071
- Investigation of radiation field distribution in a ruby laser with a SFR high speed camera 20 p2931 A72-39318
- Estimation of the turbulent diffusion coefficient and of the vertical wind velocity component from the distribution of natural radioactivity 20 p2964 A72-39320
- Radiation from a particle in static electric and magnetic fields 20 p2956 A72-39459
- Determination of the angular divergence of laser radiation by a transforming system of prisms 20 p2933 A72-39523
- Effect of spatio-temporal laser light structure on multiphoton ionization 20 p2934 A72-39814
- Optical diffractometer with laser beam having approximately uniform transverse intensity distribution 21 p3051 A72-40210
- Electronically scannable plasma leaky wave antenna system 21 p3022 A72-41325
- Radiation of an oscillating charge in a three-dimensional periodically inhomogeneous medium 21 p3023 A72-41844
- Effects of thermo-optical distortion on the radiation loss magnitude and spatial-angular radiation characteristics for a lamp-pumped rhodamine-6G laser 22 p3185 A72-42173
- Spatial distribution of excess-radiation intensity at low altitudes 22 p3218 A72-42212

- On the comparison of phase and multi-layer techniques for numerical solution of the scattering problems. 22 p3154 A72-42305
- Approximate theory of the CW gasdynamic laser with an unstable resonator. 22 p3186 A72-42631
- East-west asymmetry of cosmic rays at the sea level in the range of geomagnetic latitudes from 50°N to 20°S. 23 p3328 A72-43355
- Second positive system of nitrogen bands in the day airglow from Cosmos-224 data. 23 p3282 A72-43356
- Waveguide with slanted aperture, determining propagation mode and wave amplitude from radiation level at Brillouin angle. 23 p3263 A72-43436
- Laser beam periodic coupler design based on radiation property reciprocity theorem, suggesting use of reflecting layers and long wavelength gratings. 23 p3288 A72-43888
- Light beam modulated by uniformly spaced circular apertures, calculating Fourier power spectrum for homogeneous and bivariate normal intensity distributions. 23 p3289 A72-43900
- Angular distribution of extensive air showers in a range of large zenith angles. 23 p3330 A72-44421
- Investigation of EAS characteristics at sea level with the aid of the classical method and by the method of recording radio emission. 23 p3330 A72-44423
- Density distribution of the radiation passing through a scattering medium from a bounded source. 24 p3424 A72-44634
- Radiation from an electric dipole in anisotropic media. 24 p3424 A72-44706
- Approximate temperature distribution for a diffuse, highly reflecting material. 24 p3465 A72-45790
- RADIATION DOSAGE**
- Space crew radiation dosage calculation from Mars mission high impulse gas core nuclear rocket engine exhaust plume fission fragments. 01 p0022 A72-11353
- Radiation induced disease development related to dose, dose rate and radiation quality, discussing different models. [CERN-71-16] 02 p0161 A72-12053
- High energy proton irradiation late pathological effects on rabbit brains, discussing brain lesions and radiation dosages. [CERN-71-16] 02 p0161 A72-12056
- Relative biological effectiveness of high energy radiations, noting dependence on radiation quality, system, dose and dose rate. [CERN-71-16] 02 p0161 A72-12058
- Effective dose change after repeated radiation exposures as function of time intervals between fractions, evaluating space flight radiation hazards. [CERN-71-16] 02 p0161 A72-12059
- Polycarbonate merits as visual solid detector in high energy radiation dosimetry. [CERN-71-16] 02 p0162 A72-12066
- High energy nucleon tissue doses calculation based on averaged characteristics of nuclear interactions. [CERN-71-16] 02 p0162 A72-12067
- Depth-dose experiments with monoenergetic 14 MeV neutrons in low scatter environment, describing test facility. [CERN-71-16] 02 p0162 A72-12068
- Average radiation Q factor and dose radiation spectrum measurement in phantoms irradiation by proton beams. [CERN-71-16] 02 p0162 A72-12069
- Linear energy transfer response of polyvinyltoluene plastic scintillator, presenting data on quality factor and radiation dose equivalent determinations in mixed radiation field. [CERN-71-16] 02 p0168 A72-12071
- Ionization chamber for direct measurement of radiation dose equivalent, describing high voltage switching circuit. [CERN-71-16] 02 p0168 A72-12072
- Radiation doses received by cosmonauts in manned Soyuz 3-9 from mission retrieved thermoluminescent glass dosimeters. [CERN-71-16] 02 p0168 A72-12075
- Cosmic ray exposure thindown tracks in human tissue from solar minimum to maximum at SST flight level. [CERN-71-16] 02 p0163 A72-12079
- Radiation exposure during high altitude flights, considering normal radiation levels due to galactic radiation and short term increases due to solar flares. 03 p0315 A72-13234
- Biological dosimetry in acute human irradiation from cytogenic study of peripheral blood and bone marrow. 04 p0467 A72-14606
- Blue green algae *Anacystis nidulans* photorecovery after Co 60 gamma radiation exposures, using white and red light. 04 p0475 A72-15516

- Bacteriophage synergistic inactivation by heat and ionizing radiation from kinetic model describing dose rate and temperature dependences. 06 p0768 A72-18185
- Relative biological effectiveness of high X ray doses given to radish seeds, studying irradiation rate effect on germination probability. 09 p1265 A72-22524
- High dose rate electron beam irradiation using telescoping drift tube for flash X ray machine. 10 p1509 A72-23935
- Three year varied dose and acute exposure gamma irradiation of dogs, noting radiobiological effects from hematological, cytological and physiological examinations. 13 p1903 A72-29307
- Dose response curves for pink somatic mutations in *Tradescantia* after neutron and X ray irradiation. 15 p2186 A72-31723
- Irradiation system for animal and human subjects exposure to controlled microwave radiation in environmental tests. 15 p2191 A72-32573
- Book on radiation protection measurement covering dose determination, activity and contamination measurement, radionuclide determination, semiconductor detectors, etc. 16 p2421 A72-33276
- A new model for estimating space proton dose to body organs. 17 p2508 A72-35354
- Neuropathological evaluation of monkeys exposed to body-alone X-radiation. 18 p2649 A72-36439
- The use of a scintillation counter to measure diagnostic X-ray tube kilovoltage, radiation exposure rates and contamination by low energy gamma emitters. 18 p2655 A72-37197
- Radiobiological problems caused by supersonic transport /With a survey of the first results established by tests performed on board the Concorde prototype/. 19 p2762 A72-38713
- New cancer therapy treatment techniques using space dosimetric concepts. 24 p3374 A72-45112

RADIATION EFFECTS

- NT RADIATION DAMAGE**
- NT RADIATION INJURIES**
- NT RADIOLYSIS**
- Acoustic emission characteristics from nuclear reactor irradiated steels during tensile and wedge opening load tests. 01 p0068 A72-10803
- Primeval fireball cosmic background radiation spectrum in homogeneous axisymmetric anisotropic world model including electron neutrino effects on expansion dynamics. 01 p0121 A72-11139
- Nuclear radiation enhancement of carbon dioxide laser performance, discussing low pressure CW and high pressure pulsed discharges. 01 p0082 A72-11330
- Transparent fused silica wall irradiation induced optical absorption and heat deposition in nuclear light bulb engine. 01 p0103 A72-11356
- Chronic microwave irradiation effects on experimental animal blood forming systems, examining peripheral blood count changes and nuclei and mitosis abnormalities in erythroblastic and lymphoid cells. 02 p0158 A72-11708
- Mitotic index and aberrant mitose frequency in mice corneal and intestinal epithelial cells exposed to 50-630 MeV protons, estimating relative biological efficiency coefficients. [CERN-71-16] 02 p0161 A72-12055
- Biological efficiency of secondary radiations from 70 GeV protons interaction with target, discussing dose dependences and restoration process relative rates. [CERN-71-16] 02 p0161 A72-12057
- Relative biological effectiveness of high energy radiations, noting dependence on radiation quality, system, dose and dose rate. [CERN-71-16] 02 p0161 A72-12058
- Radiobiological effects of nonuniform body irradiation, discussing regeneration process stimulation by partially shielded bone marrow. [CERN-71-16] 02 p0161 A72-12060
- Nonuniform high energy proton irradiation of dogs, evaluating and predicting biological effects. [CERN-71-16] 02 p0161 A72-12061
- Intracavity radiation induced air breakdown in TEA carbon dioxide laser for application in plasma heating. 02 p0238 A72-12205
- Ultralow sliding friction during bombardment of polypropylene, molybdenum disulfide and graphite surfaces with charged helium atoms at room temperature in vacuum chamber. 02 p0249 A72-12282
- Optically thin radiation effects on local heat transfer in gas flow narrow duct thermal entrance region, presenting Nusselt number variations terms for uniform and parabolic velocity profiles. 02 p0303 A72-13231

- Impurities effects on crack initiation and propagation in polymethyl methacrylate under laser pulsed radiation. 02 p0250 A72-12689
- Primary cosmic ray interaction with tissues, emphasizing biological effects and nuclear reactions induced radioactivity in astronaut body. 03 p0313 A72-12911
- Sequential dielectric breakdown of air by focused radiation from mode locked pulsed carbon dioxide TEA laser. 03 p0366 A72-12966
- Strong circularly polarized electromagnetic wave scattering by plasma electron as function of amplitude and magnetic field with radiation reaction. 03 p0321 A72-13077
- Liquid breakdown and subsequent propagation by focused high power laser irradiation, presenting short term photography of event sequence. [AD-736005] 03 p0368 A72-13606
- Solar radiation effects on planar librational motion and attitude of gravity oriented satellites at high altitudes. 03 p0434 A72-13613
- Gas heating by If radiation due to Compton scattering near quasars, Seyfert galaxies nuclei and pulsars. 03 p0435 A72-13801
- Low energy electron beam irradiation of aluminum-silicon nitride-silicon structures for elimination of bias polarization effects on I-V characteristics. 03 p0402 A72-13865
- Nuclear and space radiation effects - Conference, University of New Hampshire, Durham, July 1971. 03 p0402 A72-14076
- Vacuum UV irradiation of silicon dioxide, discussing positive charging for photon energies above threshold for electron-hole pair creation. 03 p0403 A72-14080
- Vitreous silica and silicon-silicon dioxide interface defect structure and behavior during ionizing or particle irradiation. 03 p0403 A72-14081
- Air ionization, secondary electron emission and Compton currents at W-Be interfaces under Co 60 gamma radiation. 03 p0403 A72-14083
- Photoemission from polyethylene, Kapton, Teflon and polyvinyl chloride under photon irradiation. 03 p0403 A72-14084
- Nuclear radiation interference and damage effects in galactic and solar cosmic ray measurements during charged particle experiments by deep space missions. 03 p0438 A72-14085
- LSI/MOS logic circuits radiation effects prediction from modeling studies of individual devices on test chip. 03 p0334 A72-14087
- High intensity ionizing gamma ray pulsed radiation effects on Gunn diode microwave oscillator failure modes. 03 p0334 A72-14089
- Transient radiation effects on silicon diodes in avalanche breakdown, considering voltage regulating diode response and temperature compensating junction effects. 03 p0334 A72-14090
- Gamma and neutron radiation effects on bipolar transistor current gain response predicted from multiple linear regression analysis. 03 p0335 A72-14091
- Matched Si junction FET under neutron burst and pulsed gamma radiation, investigating device parameters degradation. 03 p0335 A72-14093
- Ionizing radiation effects in cavities of microwave Gunn oscillators, noting large dose rate effects on circuit performance. 03 p0335 A72-14094
- Ni-C solid solution, determining room temperature neutron irradiation effects on C distribution during decomposition. 03 p0378 A72-14251
- MIS semiconductors radiation-hardening mechanisms and radiation effects on electrical properties and degradation. 03 p0405 A72-14281
- Pulsed Ar ion laser quantitative level population mechanism in gas discharges, discussing radiation trapping effects on 4s doublet based on spontaneous emission line data. 04 p0529 A72-14602
- Carbohydrate metabolism, glycolytic ferment activities and leukocyte size under ionizing radiation, showing compensatory bone marrow cell formation with leukopenia. 04 p0467 A72-14609
- Biological effects of unfocused laser radiation on DNA and RNA synthesis and cell activities in thymine dependent *E. coli* strain. 04 p0477 A72-14610
- Temperature variations in 30-100 km region of atmosphere, investigating solar radiation effects. 04 p0516 A72-14935

Ultrasonically produced cavitation events correlation to amoeba cells number decrease under 1 MHz irradiation

Cosmic ray induced radioactivity effects on diffuse gamma ray background measurement from 600 MeV proton irradiation experiment

Solar radiation effects on earth atmosphere with MR-12 and M-100 meteorological rockets launched at onset of chromospheric flare, noting atmospheric parameters measurements

Sublethal X radiation effects on rat erythropoietic system during altitude hypoxia acclimatization

Space environment weightlessness and radiation effects on leeches biorhythm, metabolism, reproduction and growth from rocket biological experiments

N-channel MOS FET, measuring X ray irradiation effects on drain current and transfer characteristics at room temperature

Internal friction changes in aluminum single crystal after uniaxial plastic deformation and irradiation

Vacuum chamber simulation of solar radiation effects on space satellites and components at 300-400 miles, using short arc xenon lamps

Illumination effect on proton and gamma irradiated cabbage plant growth, height and foliage, indicating radiation protective effect for certain light intensities

Neutron energy spectrum of radiative pion captured by carbon 12, using gamma and neutron counters

Equilibrium temperature distribution on radiatively adiabatic smooth and rough planes uniformly irradiated by collimated solar flux

Direct earth radiation, albedo and shadow effects on attitude dynamics of gravity orientated satellites

Shock wave shape and strength alteration by radioisotope emissions from body surface in supersonic airstream

Electron irradiation effects on MOS structures at vfi, considering inversion layer cut-off frequency and surface state density

Visual discrimination task-trained monkeys performance and physiology after pulsed mixed gamma-neutron irradiation, noting blood pressure and respiratory and heart rate changes

Shielding of solid surface vaporizing under laser radiation effect in presence of thermal and ionizational nonequilibrium, investigating absorption flare onset mechanism

Powder combustion rate dependence on light irradiation intensity

Inorganic photochromic and cathodochromic recording materials in single crystal and powder forms, considering color change properties during light or electron beam exposures

Lunar surface rocks, soil and breccia chemical composition, discussing element concentration, radiation effects on surface chemistry and volcanism

Neutron irradiation effect on grain boundary relaxation in Al and Al-Li alloy by internal friction investigation

Endurance limit of construction materials under fast and thermal neutron irradiation in reactor channel

Cosmic radiation effects in Concorde prototype cabin, using photographic dosimeters for neutron dose measurement and nuclear emulsions for all charged particle recordings

Gain variations in channel electron multipliers, investigating total radiation exposure effect

Atomic selective two step photoionization and molecular photodissociation by tunable laser radiation, experimenting on Rb vapor and HCl respectively

Pulsed and continuous rf irradiation effects on mitotic activity and chromosomal aberrations in regenerating rat liver tissue

Vacancy supersaturation effect on enhanced precipitation by high flux electron irradiation in stainless steel

Nb-Nb point-contact Josephson junctions response to submillimeter radiation from HCN and DCN lasers

Microwave temperature sensor for radiation environment use, discussing cavity resonator design and operation, thermal cycling tests and comparative radiometer technique

Nuclear radiation effects on ceramic cemented strain gages and polyimide encapsulated epoxy bonded gages

Gamma irradiation effects on temperature of reversible solid-to-liquid phase transformation in Al

Laser radiation effects on optical glass volume and surface, discussing failure characteristics

Stagnation conditions of magnetoradiative supersonic flow through shock waves for temperature dependent specific heat parameter

Gamma radiation effect on cracking and tensile strength of polycapromide /capron/ film

Transparent and opaque materials fracture mechanism analogies under laser beam action, determining dislocation structure

High energy particle and ionizing radiation effects on glasses in aerospace environment

UV radiation effects on pyrolytic boron nitride lattice imperfections, using space environment simulator

Microwave induced dc voltages across unbiased Josephson tunnel junctions, showing power spectra dependence on magnetic field

Cosmos 243 microwave radiation analysis over cultivated terrain, showing radio brightness temperature dependence on soil temperature and humidity effect on emissivity

Relative biological effectiveness of high X ray doses given to radish seeds, studying irradiation rate effect on germination probability

Irradiation effects on linear polyethylene molecular weight fractions in molten and crystalline states, determining sol-gel partitioning to establish critical conditions for gelation

Homogeneous linear approximations in uncoupled problems of thermoradiative elasticity and plasticity of solid body under nonuniform heating and radioactive radiation

Neutron irradiation effect on submicroporosity formation and redistribution in structural graphite

Dislocation loops in thin W foil due to ion irradiation, using electron microscopic analysis

Cosmic radiation effects and damage on solar cells, discussing shielding, stability improvement, space environments, minority carrier lifetime and photosensitivity spectral distribution

LF radiation effect on angular momentum distribution of interstellar grains with permanent dipole moments

Cosmic ray ionization rate for hydrogen calculated for ambipolar diffusion efficiency in decoupling magnetic flux from gas during cloud collapse with angular momentum

Gamma ray radiation effects on epoxy resin electric properties, studying electric insulation and arc resistances and dielectric breakdown strength

Rhesus monkey retinal image diameter estimation during exposure to Ar and He-Ne laser irradiation, using microphotometer scans

Metal matrix composites, testing neutron irradiation effects on mechanical properties for nuclear application feasibility

Neutron irradiation effects on GP zones and precipitates in ternary Al alloy, measuring X ray small angle scattering and electrical resistivity

Linear impulsive spin down from rigid body rotational equilibrium of radiation penetrated opaque compressible fluid in circular cylinder

Ultralow sliding friction during bombardment of polypropylene, molybdenum disulfide and graphite surfaces with charged helium atoms at room temperature in vacuum chamber

Natural oscillations of magnetosphere and trapped radiation transport by electromagnetic pulses as possible mechanism for disturbances from thermonuclear explosion reaction on particles in natural radiation belt

Critical shock wave velocity for ionization front propagation with photoionization of hydrogen by radiation, using pinch discharge tube measurements

Laser induced transparent dielectrics surface fracture mechanism determination based on electron microscopic photograph analysis and disturbed specular reflection under predischage conditions study

Impurity centers formation and development in AgBr// photographic emulsion under ultrasonic irradiation

Be foil electrical resistance change during and after pulsed laser irradiation and annealing

UV light production of free radicals in proteins and model compounds in vacuum and low temperatures, using EPR techniques

Coincidence effects of subionospheric extraterrestrial radiation focusing on ionospheric changes and stratospheric warmings

Electron irradiation effects on Li doped silicon solar cells, noting changes in donor concentration and defects formation

Radiation effects in semiconductors - Conference, State University of New York, Albany, August 1970

Irradiated semiconductors defects theory, considering electronic structure in rigid lattice and lattice distortion near defects

Low temperature irradiation and annealing effects in germanium, calculating charge states for donor and acceptor centers

Recombination luminescence in irradiated Si, investigating uniaxial stress and temperature variations effects

Recombination luminescence in irradiated Si, investigating thermal annealing and Li impurity effects

Annealing effects on gamma ray irradiated Li compensated p-type B doped Si semiconductor

Electron irradiation of n-type Si or Te doped GaAs, determining carrier removal rate, mobility changes and annealing characteristics

Carrier concentration Hall mobility and photoconductivity in n- and p-type CdTe after neutron and electron bombardment

Te single crystal electrical resistivity and Hall coefficient effects of electron irradiation, suggesting point defects and dislocations interaction

Solar activity effects on biosphere processes, discussing radiation-induced molecular activation mechanisms in water and biological plasma calcium ion concentration changes

Neuroendocrine responses in microwave radiation exposed rats, correlating thyroid and thyrotropic activity

Russian book on penetrating radiation effect on radio components covering resistors and capacitors electrophysical characteristics and parameters changes under gamma and neutron radiation

Light propagation patterns in absorbing and scattering medium with radiation density dependent optical properties

Diamond powder lattice parameter changes during fast electron irradiation at various temperatures, discussing crystal defect stability and neutron irradiation comparison

Three year varied dose and acute exposure gamma irradiation of dogs, noting radiobiological effects from hematological, cytological and physiological examinations

D region chemistry based on earth albedo effects from airborne radio sounding experiments, suggesting visible light energy flux role

Strong circularly polarized electromagnetic wave scattering by plasma electron with radiation reaction, determining cross section as function of amplitude and magnetic field strength

Gamma irradiation effects on epoxy-diane resin creep and stress relaxation properties indicated by loaded specimens birefringence patterns

Material removal nature during focused laser radiation action on substances with different thermal diffusivity coefficients

13 p1968 A72-29508

Resonant irradiation effect on cesium discharge plasma, charge density, electron temperature and electric field strength

13 p2017 A72-29610

Electron impact induced aureole epoxides fragmentation, discussing ion formation, intermediates, thermal rearrangement and mass spectra

13 p1913 A72-29775

Co 60 gamma radiation effect on stimulated ruby laser emission delay time, pulse duration, energy curve and intensity

13 p1972 A72-30005

Collisional relaxation and rotational intensity distributions in aeronomic spectra, including radiative losses effects from weak interaction model

13 p2008 A72-30057

Spontaneous radiative dissociation in molecular hydrogen vibrational levels as function of emission wavelength, discussing fluorescent spectra, radiation lifetimes and centrifugal distortion

13 p2008 A72-30058

Red blood cell reserve mobilization in healthy and chronically irradiated dogs after treadmill exercise

14 p2074 A72-30379

Amitetravite /biological protectant/ effect on natural immunity state of dogs exposed to chronic gamma irradiation simulating space flight environment

14 p2074 A72-30380

Ar-39/Ar-38 cosmic ray exposure age calculation from Sikhote-Alin meteorite fall fragment content of Ar-39, Ar-38, Ne-21 and He-3

14 p2157 A72-30584

Organ cell lysosomes polymorphic properties and formation by Golgi complex, discussing role in neurocyte structure restitution following gamma irradiation

14 p2075 A72-30594

Stellar radiation and gravitational effects on neutral atoms and dust grains at large distances for various spectral type stars in schematical evolutionary galaxy

14 p2158 A72-30735

Standardization of microwave irradiation experiments on animals, discussing power density level evaluations and local vs whole-body irradiation effects

14 p2080 A72-30746

Gamma radiation effects on composite propellants stability, investigating polyurethane, polybutadiene, silicone and polyisoprene binders mechanical properties

14 p2144 A72-30760

Cosmic ray irradiations study of gas rich meteoroid auribles by track method, comparing with lunar soils

15 p2303 A72-31308

Microwave induced cutaneous heat and pain perception thresholds, noting usefulness as possible radiation hazard warning

15 p2188 A72-31506

Scintillation TlCl /I,Be/ crystal response to 8 GeV ionizing negative pions, noting pulse shape and resolution characteristics

15 p2291 A72-31535

Radiation effects measurement on neutron, proton and electron irradiated Li-drifted Si detectors by IR response technique, comparing characteristics with photovoltage effect

15 p2234 A72-31538

Spacecraft bacteria population resistance to simulated Jovian trapped radiation belt electrons and solar wind protons, noting dependence on isolate, dose and electron energy

15 p2186 A72-31993

Radiation effect on isothermal discontinuity amplitude for stationary shock wave structure with heat transfer and dissipation

15 p2335 A72-32099

Unmodulated solar radiation effect on electro-optical photoreceptors voltage sensitivity, noting photomultipliers and silicon photodiodes

15 p2237 A72-32121

Si solar cell efficiency in synchronous orbit radiation field increase via improvement in diffusion profile, low resistivity material and diode characteristics

15 p2183 A72-32131

Simulated Nimbus orbital electron, proton and UV radiation effects on wide bandpass glass and narrow bandpass thin film interference filters and fused silicas

15 p2277 A72-32157

Supernovae produced fluorescence pulses search in upper atmosphere by automatic coincident light receivers

15 p2313 A72-32233

Active medium spontaneous radiation level effect on traveling wave amplifier gain factor, supporting theoretical results by experiments with superluminescent Ne-He active medium

16 p2400 A72-33277

Induced electron emission dependence on polarization, frequency and intensity of second wave incident on electron with anomalous magnetic moment

16 p2424 A72-33365

N-type GaAs absorption spectra construction from transmission spectra, considering effects of irradiation by fast protons, electrons, neutrons and alpha particles

16 p2441 A72-33368

Laser irradiation induced refractive index change in evaporated chalcogenide glass films of As-S-Ge system

16 p2401 A72-33395

Organism response to extreme overload factors, discussing centrifuging and vibration stress effects on mean swimming time and post-irradiation survival time in mice

16 p2355 A72-33554

Li, Be and B nuclei production via nuclear spallation reactions generated by Galactic cosmic ray bombardment of interstellar gas

16 p2448 A72-33737

Nonionizing electromagnetic radiation effects in biological systems, discussing microwave penetration, therapeutic warming, light scattering in tissues and medical instrument applications

16 p2359 A72-33754

Transient 10 MeV electron radiation effects on RF power and recovery time of GaAs Schottky barrier IMPATT diodes

16 p2370 A72-33766

Mathematical model for deuterium slab solid and plasma under laser pulses irradiation, noting shock wave propagation and slab acceleration

[ALAA PAPER 72-721] 16 p2439 A72-34027

Effect of fast-neutron irradiation on ceramics and ceramic-metal seals.

17 p2559 A72-34591

Cythere capsule for irradiation of experimental fuel elements under geometric and thermal conditions representative of thermionic converters

17 p2579 A72-34619

Transparent and opaque crystal surface fracture mechanism analogies under laser beam action, determining dislocation structure

17 p2562 A72-34664

Polymers ignition time measurement in cabinet with benzene flames and W filament lamps, noting black body radiation source absorbance and incident irradiance effects

17 p2636 A72-34719

Influence of a magnetic field on radiation-induced chromosome aberrations in plants

17 p2503 A72-35007

Sonic discontinuities in a radiative gas.

17 p2582 A72-35435

The radiative transfer equation and environmental effects in the upper atmosphere.

[ALAA PAPER 72-663] 17 p2583 A72-35485

Neutron irradiation effects on thermionic converter materials, performance and service life

18 p2707 A72-36140

Thermionic converters fuel tests by uranium dioxide-Mo cermet irradiation, noting fission gas retention and metallic matrix deformation

18 p2708 A72-36141

Physical-mechanical properties of beryllium oxide and investigation of its electrical resistance under irradiation in a reactor

18 p2703 A72-36147

The stability of structure of physical mechanical properties of molybdenum and tungsten after irradiation and thermal influence

18 p2698 A72-36153

Room temperature ductility of different types of molybdenum after differing annealing

18 p2698 A72-36155

Radiation-hardened components, circuits and systems.

18 p2665 A72-36308

The effects of electron bombardment on the noise properties of field effect transistors.

18 p2666 A72-36322

Shadowing function calculation as rough surface point illumination probability by point source radiation, assuming surface elevation as random process

18 p2710 A72-36407

Body weight decreases in some proton exposed primates.

18 p2650 A72-36447

Interaction energy and force between screw dislocation and spherical inhomogeneity, discussing voids growth in irradiated materials

18 p2718 A72-36510

Study of point defects produced in aluminum by tempering and irradiation with electrons

18 p2702 A72-36705

Classification of shock waves in a radiating gas

18 p2682 A72-36806

Space environment simulation and testing techniques, considering vacuum systems, low temperature, solar radiation and motion simulation

18 p2676 A72-36833

Viscoelastic analysis of graphite under neutron irradiation and temperature distribution.

18 p2704 A72-37088

Breakdown of some transparent dielectrics under the action of neodymium and ruby lasers in free light emission modes

19 p2810 A72-37542

Short-circuit current in silicon solar cells - Dependence on cell parameters.

19 p2753 A72-37567

Radio luminescence of a yttrium-aluminum garnet activated by rare-earth elements

19 p2845 A72-38181

Influence of temperature shocks on seed formation after irradiation of pollen from *Tradescantia paludosa*.

19 p2761 A72-38642

Cytologic aspect of RF radiation in the monkey.

19 p2758 A72-38709

Radiobiological problems caused by supersonic transport /With a survey of the first results established by tests performed on board the Concorde prototype/.

19 p2762 A72-38713

Russian book - Radiation effect method in the investigation of the structure and properties of solids.

20 p2958 A72-38951

Diffusion effects in solids caused by radiation exposure, calculating diffusion coefficients of additions and defects

20 p2958 A72-38952

Subthreshold radiation effect in silicon

20 p2959 A72-38953

Experimental determination of the coefficients of radiantly stimulated diffusion of sulphur in cadmium sulfide

20 p2959 A72-38954

Electron spin resonance of gamma-irradiated poly(ethylene 2,6-naphthalene dicarboxylate).

20 p2898 A72-39400

Shock waves resulting from interaction of laser radiation with transparent solids.

20 p2933 A72-39522

As-Te-Ge amorphous semiconductor film optical memory effect due to crystallization and reversion during exposure to pulsed laser beam, noting writing and erasing characteristics

20 p2961 A72-39708

Effect of spatio-temporal laser light structure on multiphoton ionization.

20 p2934 A72-39814

Relaxation oscillations induced in semi-insulating CdS with helium neon laser irradiation.

20 p2934 A72-39817

Radiation effects on isothermal discontinuity amplitude for stationary shock wave structure with heat transfer and dissipation

21 p3128 A72-40266

Vestibular labyrinth reactions and nystagmus thresholds in dogs during negative angular accelerations and simulated chronic galactic radiation from Co 60 gamma source

21 p2998 A72-40439

Incorporation of methionine-S 35 in the proteins of the digestive organs of rabbits under the action of radiation and vibration

21 p2998 A72-40440

Electron abundance equilibrium as factor in biological effectiveness of proton beam irradiation of animals

21 p2998 A72-40450

Resonant irradiation effect on Cs discharge plasma charge density, electron temperature and electric field strength

21 p3091 A72-40664

Temporal, energy and spectral properties of Cr laser output, considering ruby absorption before/after Co 60 gamma irradiation and radiation density distribution during pumping flashes

21 p3063 A72-40666

Local necrosis, parenchyma incisions and vascularization of rabbit liver tissue under pulsed and continuous laser beams

21 p3002 A72-40991

Influence of irradiation by 1.2-MeV electrons on the electrophysical properties of p-Si single crystals grown in a hydrogen atmosphere

21 p3098 A72-41686

The density of H2 molecules in dark interstellar clouds.

22 p3224 A72-42385

Collisional excitation of carbon monoxide in interstellar clouds.

22 p3227 A72-42553

Radiation, evaporation and the maintenance of turbulence under stable conditions in the lower atmosphere.

22 p3201 A72-42597

Co 60 gamma radiation effect on stimulated ruby laser emission delay time, pulse duration, energy curve and intensity

22 p3186 A72-42731

Depth distributions of cosmic ray produced radionuclides in chondrites and achondrites, determining apheia from Al 26 activities

22 p3228 A72-42861

Dielectric dispersion of irradiated BaTiO3 near the phase transition.

22 p3215 A72-42934

Variation of the output of radioluminescence of organic scintillators with energy loss and the number of charges of ionizing particles

22 p3180 A72-42938

Influence of Cosmos 368 space flight conditions on radiation effects in yeasts, hydrogen bacteria and seeds of lettuce and pea.

23 p3254 A72-43390

Physiological and hematological effects of chronic irradiation.

23 p3254 A72-43392

Summary of latent effects in long term survivors of whole body irradiations in primates.

23 p3254 A72-43393

Analysis of survival and cause of death statistics for mice under single and duration-of-life gamma irradiation.

23 p3254 A72-43394

Formation of urea and guanidine by irradiation of ammonium cyanide.

23 p3262 A72-43569

Influence of X-ray irradiation in 25- and 250-r doses on the transplant immunity in mice differing by weak and strong histoincompatibility systems

23 p3255 A72-43910

Visual perception of accelerated nitrogen nuclei interacting with the human retina.

23 p3256 A72-43940

Estimates of creep-fatigue interaction in irradiated and unirradiated austenitic stainless steels.

24 p3412 A72-44554

Radiation influences on a white-coated thermistor temperature sensor in a radiosonde.

24 p3401 A72-44620

Hall generator operation characteristics under load, power, temperature and nuclear radiation conditions

24 p3385 A72-45270

Natural aging and radiation-induced life shortening in *Drosophila melanogaster*.

24 p3373 A72-45279

Photochemistry of unsaturated polymers.

24 p3378 A72-45280

Pulsating conditions in the evaporation of optical materials under the influence of CO₂ laser radiation.

24 p3411 A72-45610

Be foil electrical resistance change during and after pulsed laser irradiation and annealing

24 p3432 A72-45720

RADIATION EXPOSURE

U RADIATION DOSAGE

RADIATION FIELDS

U RADIATION DISTRIBUTION

RADIATION HARDENING

Radiation-hardened components, circuits and systems.

18 p2665 A72-36308

Polyacrylonitrile based carbon fiber strengthening by fast neutron irradiation at high temperatures

22 p3196 A72-41965

RADIATION HAZARDS

Effective dose change after repeated radiation exposures as function of time intervals between fractions, evaluating space flight radiation hazards

[CERN-71-16] 02 p0161 A72-12059

Rabbit and monkey corneal damage following CW carbon dioxide laser irradiation, discussing hazard level derivation

[FPRC/1314] 02 p0163 A72-12413

Semiconductor devices potential interference and biological exposure hazards in microwave leakage field, considering shielding and filtering methods for reducing susceptibility

03 p0320 A72-14032

Cataractogenesis from microwave radiation exposure, discussing protection, legislation and Western and Soviet literature review

06 p0767 A72-17877

Minuteman HERO /hazards of electromagnetic radiation to ordnance/ preflight testing, describing ordnance monitoring system based on fiber optic data links

08 p1220 A72-20767

Inexpensive solid state microwave sources development and applications considering spectrum allocations, health hazards and reliability problems

09 p1285 A72-22595

Pioneer 10 probe survival hazards during passage through asteroids belt and intense Jupiter radiation fields

10 p1551 A72-24272

Medical and physiological hazards for SST passengers and crews, discussing cumulative cosmic radiation and high altitude decompression risks

11 p1583 A72-25816

Soviet book on radiation hazards and protection in space covering detection, radiobiology and effects on human organism

11 p1713 A72-26050

Pathophysiology of exposure to UV, IR, coherent, microwave and RF radiations, discussing potential hazards, damage, human tolerance threshold, protection guides and safety standards

12 p1772 A72-27963

Electromagnetic pulsed radiation fields effects on monkeys and dogs behavior and blood chemistry, noting biological hazard absence

14 p2078 A72-30423

Ultrabroadband probe design for microwave radiation intensity measurement in harmful exposure study

15 p2191 A72-32574

Interplanetary radiation types in terms of possible space flight hazards, discussing electromagnetic and corpuscular radiation, cosmic rays and radiation belts

16 p2446 A72-33553

Radiation hazards in space with respect to galactic radiation shielding, solar flare prediction and conventional terrestrial safety standards

16 p2358 A72-33556

Microwave radiation - Biophysical considerations and standards criteria.

17 p2507 A72-34299

Observations on microwave hazards to USAF personnel.

18 p2653 A72-36522

High level E-field susceptibility measurement problems and techniques.

20 p2906 A72-38981

RADIATION HEATING

U RADIANT HEATING

RADIATION INDICATORS

U DOSIMETERS

U INDICATING INSTRUMENTS

RADIATION INJURIES

Rabbit and monkey corneal damage following CW carbon dioxide laser irradiation, discussing hazard level derivation

[FPRC/1314] 02 p0163 A72-12413

Mathematical-physical model for laser pulsed radiation-induced pressure wave transmission through surface and internal biological tissues

06 p0768 A72-18150

Viruslike particles in salivary glands, muscles and nerves of normal and gamma irradiated *Drosophila melanogaster*, showing age dependent infection

08 p1116 A72-21198

High energy UV solar radiation transfer by stratospheric aerosols to biosphere, considering radiation injury to human lung

09 p1298 A72-22662

Visible and invisible nonionizing radiation produced human injuries, considering visual and retinal effects and induced thermal stresses

17 p2499 A72-34300

Neuropathological evaluation of monkeys exposed to body-alone X-radiation.

18 p2649 A72-36439

RADIATION INTENSITY

U RADIANT FLUX DENSITY

RADIATION LAWS

NT KIRCHHOFF LAW OF RADIATION

NT STEFAN-BOLTZMANN LAW

RADIATION MEASUREMENT

Cosmic gamma rays at 0.3-3.7 MeV measured by Na/Tl crystal detector 64-channel spectrometer on-board Cosmos 135 and 163

01 p0118 A72-10153

Primary component corrections for global cosmic ray variations from latitudinal expeditions, discussing adaptation to computer

01 p0118 A72-10584

Cosmic ray neutron leakage flux and energy spectrum measurements in 0.01-10 MeV range by OGO 6 satellite-borne neutron detector

01 p0119 A72-10877

Remote sensing of surface radiation temperature topographic variations by precision radiation thermometer equipped aircraft, calibrating for atmospheric attenuation

02 p0210 A72-11803

Terrestrial radiation emission mapping from imagery produced by scanning radiometer, discussing remote sensors used to study surface energy phenomena

02 p0210 A72-11804

Aerial Radiological Measuring System for environmental radiation detection and tracking, emphasizing snow mass prediction by terrain radiation attenuation measurement

02 p0215 A72-11884

Neutron albedo flux recording instrument with composite scintillation crystal and photomultiplier scanning to monitor near space

02 p0273 A72-11934

Thin-down intensities for heavy primaries at SST flight levels, using plastic stacks measurements

02 p0274 A72-12077

Graphite, Mo, Ta and W thermal radiation total emittance measurement in 1200-2400 K range, evaluating recorded data by computer program

02 p0243 A72-12101

Upper cloud boundary height determination using Cosmos 320 satellite combined reflected solar and intrinsic radiation measurements

02 p0253 A72-12213

Long wavelength focusing collector for X ray astronomy with effective bandpass of 100-280 eV determined by low energy transmitting counter windows and paraboloid mirror reflectivity

[AD-736511] 03 p0353 A72-13040

Earth limb radiance measurements inversion, yielding temperature distribution as function of altitude in real atmospheres

03 p0384 A72-14146

Passive airborne mapping of radiation sources, using fixed side-looking multilobed and scanning fan beam antenna pattern with coherent optical processing of film records

04 p0495 A72-14491

Dicke-type microwave radiometer for daily measurements of 2800 MHz solar flux, discussing antenna system and dynamic range

04 p0522 A72-15163

Cosmic ray induced radioactivity effects on diffuse gamma ray background measurement from 600 MeV proton irradiation experiment

04 p0567 A72-15324

Nuclear charge composition and energy spectra measurement for hydrogen, helium and medium nuclei in 12 April 1969 solar particle event

04 p0567 A72-15325

Holographic methods of antenna radiation pattern measurement, noting applications to radio astronomy and radar

06 p0816 A72-17920

International comparison of standard solar radiation measurement pyranometers

06 p0816 A72-17925

Thermal emittance measuring methods for solids at temperatures above 1500 K, discussing emittance dependence on surface characteristics

06 p0818 A72-18253

Photon counting system for low level radiation measurement in UV visible region, discussing simplifications

07 p0983 A72-19133

Spurious physical effects in penetrating cosmic ray showers resulting from momentum measurement errors

07 p1060 A72-19853

Interstellar cloud properties based on electron concentration integral along line of sight from pulsar radiation measurements

07 p1080 A72-20053

Primary cosmic ray high energy gamma quanta flux measurements on Cosmos 208 satellite-borne instruments

08 p1225 A72-20798

Temperature effects elimination from underground muon intensity measurements

08 p1226 A72-20813

Atmospheric water vapor submillimeter absorption lines in high resolution radiation transmission measurements with Froome type plasma metal junction device

10 p1472 A72-24175

Global sea surface temperature distribution determination with ITOS 1 radiation measurements and composite histogram, discussing RMS errors

11 p1620 A72-25763

Neutron albedo flux recording instrument with composite scintillation crystal and photomultiplier scanning to monitor near space

13 p2030 A72-29246

Pulsed laser plasma temperature determination by radiation measurements in X ray and visible spectral regions using foil method

13 p2018 A72-29887

Outgoing 15 micron carbon dioxide band radiation measurement optimization for atmospheric thermal sounding by satellite

14 p2099 A72-30243

Composition of radiation excess over primary cosmic ray background recorded by Cosmos satellites below midlatitude belt region

14 p2147 A72-30626

Energetic electrons generation and relaxation in narrow belt near 2.8 L measured with Cosmos 137 Cerenkov counter

15 p2299 A72-31909

Circumsolar radiation measurement discrepancy explanation based on comparison with results obtained by international pyrheliometer scale

15 p2238 A72-32169

Portable X ray calorimeter for simultaneous fluence and front surface dose measurement in Ta from pulsed electron accelerations

15 p2241 A72-32440

Vertical temperature profile retrieval from satellite radiance measurements for insertion into numerical atmospheric circulation model, discussing sensitivity test

15 p2267 A72-32728

Spectral line width measurement accuracy based on digital autocorrelation of photon counting fluctuations, noting light field and photoelectric process limiting effects

16 p2357 A72-32949

Book on radiation protection measurement covering dose determination, activity and contamination mea-

surement, radionuclide determination, semiconductor detectors, etc

16 p2421 A72-33276

Atmospheric absorption height determination from orbital elements during solar radiation satellite observation

16 p2386 A72-33603

Atomic, molecular and ionic species detection in upper atmosphere by measurement of resonance fluorescence radiation excited by tunable laser radiation

[AIAA PAPER 72-661] 16 p2388 A72-34073

Rigidity dependence of cosmic ray modulation function at 2-13 Gv from C-130 aircraft survey flights data

17 p2602 A72-35606

VLF hiss intensity, polarization, incidence angle and arriving direction observation at Antarctica station during magnetic disturbances

18 p2660 A72-36431

Some aspects of cosmic ray differential spectrum measurements

18 p2722 A72-36852

New method for determining the integral radiative capacity of partially transparent materials at high temperatures

18 p2704 A72-37190

High energy gamma ray sources search by Cerenkov radiation recording from extensive air showers, noting atmospheric transparency effects

19 p2850 A72-37805

Spectral intensity measurements from high-pressure nitrogen plasmas.

19 p2840 A72-37836

Evaluating the light from the sun.

19 p2790 A72-37933

Radiative properties of upper and middle level clouds and of vertically developing clouds

20 p2949 A72-39948

Description and use of a method for characterizing noise sources in jets

[ICAS PAPER 72-35] 21 p3046 A72-41160

Cosmogenic radionuclides in the Allende and Murchison carbonaceous chondrites.

22 p3225 A72-42466

Cloud structure and cover determination from actinometric short wave solar radiation and IR cloud radiation measurements

23 p3311 A72-43627

Statistics of the radiation from astronomical masers.

23 p3337 A72-43872

Investigation of the angular distribution of particles on the basis of Cosmos-219 satellite data

23 p3343 A72-44174

Experimental comparisons of the international pyrheliometric scale with the absolute radiation scale.

23 p3290 A72-44274

High altitude cosmic ray pion and nucleon interaction characteristics at high energies, using spark chamber, Cerenkov absorption spectrometer and ionization calorimeter measurements

23 p3329 A72-44402

Ultrahigh energy gamma quanta families detection by airborne emulsion chamber at 500-2500 m altitude, calculating energy distribution distortion by Monte Carlo method

23 p3329 A72-44403

Experiment for studying the pulse shape of Cerenkov emission at large distances from an extensive air shower

23 p3330 A72-44420

Angular distribution of extensive air showers in a range of large zenith angles

23 p3330 A72-44421

Investigation of EAS characteristics at sea level with the aid of the classical method and by the method of recording radio emission

23 p3330 A72-44423

Muon component near the axis of an extensive air shower

23 p3331 A72-44426

RADIATION MEASURING INSTRUMENTS

NT ACTINOMETERS

NT BOLOMETERS

NT CERENKOV COUNTERS

NT DICKE RADIOMETERS

NT DOSIMETERS

NT EBERT SPECTROMETERS

NT ELECTRON COUNTERS

NT ELECTROPHOTOMETERS

NT ELECTROSTATIC PROBES

NT FABRY-PEROT SPECTROMETERS

NT HODOSCOPES

NT INFRARED DETECTORS

NT INFRARED INSTRUMENTS

NT INFRARED SCANNERS

NT INFRARED SPECTROMETERS

NT INFRARED SPECTROPHOTOMETERS

NT MICROWAVE RADIOMETERS

NT NEUTRON COUNTERS

NT NEUTRON SPECTROMETERS

NT PARTICLE TELESCOPES

NT PHOTOMETERS

NT PROPORTIONAL COUNTERS

NT PYRANOMETERS

NT QUANTUM COUNTERS

NT RADIATION COUNTERS

NT RADIATION DETECTORS

NT RADIOMETERS

NT RIOMETERS

NT SCINTILLATION COUNTERS

NT SILICON RADIATION DETECTORS

NT SOLAR SPECTROMETERS

NT SPARK CHAMBERS

NT SPECTROHELIOGRAPHS

NT SPECTROPHOTOMETERS

NT SPECTRORADIOMETERS

NT THRESHOLD DETECTORS [DOSIMETERS]

NT ULTRAVIOLET SPECTROMETERS

NT ULTRAVIOLET SPECTROPHOTOMETERS

Rocket-borne apparatus for X ray measurement in 25 to 200 keV range, noting primary diffuse component and earth albedo spectral analyses

02 p0231 A72-12448

Astronomical Netherlands Satellite automatic stabilized detection system for soft celestial X rays measurement, describing various modes of operation

03 p0554 A72-13048

Real time complete Stokes vector scanning photoelectric polarimeter with 16 cm aperture for measuring visible radiation of solar disk, corona, moon and planets

03 p0356 A72-13279

Radiation measuring instruments assembly for extensive air showers and cosmic ray particle nuclear interactions at high energies

07 p0988 A72-19868

Multichannel modular spectrometer with electrostatic analyzers for low energy electron and proton flux measurement

07 p0988 A72-19954

Measuring equipment for charged particles spatial distribution in cosmic ray showers, considering multiaxial and secondary young showers

08 p1226 A72-21077

OSO-H solar X ray instrument for solar flares energy release investigation via thermal and nonthermal electrons X ray emission

08 p1167 A72-21514

Pulsed carbon dioxide laser output monitor with Ge cylinder using photon drag effect to measure radiation pulse profile

09 p1326 A72-23389

Interferometric photoelectric scans of interstellar Ca K lines in stellar spectra, noting interstellar Na lines presence

10 p1544 A72-24663

Photosensor aperture shape and line scan spacing effect in reducing facsimile camera aliasing

12 p1807 A72-27408

Upper atmospheric measurement of incident solar UV radiation penetration to lower levels, discussing measuring instruments

13 p2030 A72-28826

Astrophysical equipment for Cerenkov radiation measurement from atmospheric showers, discussing source of high energy gamma rays in galactic equator direction

14 p2146 A72-30201

Radiation measurements and thermal IR and photographic imaging techniques in meteorology and earth resources survey applications

15 p2221 A72-31241

Ultrabroadband probe design for microwave radiation intensity measurement in harmful exposure study

15 p2191 A72-32574

Preliminary results of observations of the pulsar CP 1133 with the aid of a device for recording Cerenkov flares of extensive atmospheric showers

19 p2850 A72-37806

Automated data processing and display capabilities of radiation measuring systems for surveillance, protection and control in nuclear research, medicine and power production

19 p2802 A72-38306

Microradiometer for studying the structures of highly intensive radiation fields

20 p2924 A72-39224

The universal high temperature emissometer.

[ASME PAPER 72-HT-1] 20 p2926 A72-39675

Gamma quanta recording efficiency and energy determination by gamma telescopes, calculating root-mean-square error of real gamma spectra

21 p3026 A72-40323

Astrophysical equipment for Cerenkov radiation measurement from atmospheric showers, discussing source of high energy gamma rays in galactic equator direction

23 p3328 A72-43226

Recording high-energy particle interactions by the method of the controlled emulsion stack of large volume

23 p3291 A72-44438

The field-effect modified transistor - A high-responsivity photosensor.

23 p3273 A72-44455

Extraterrestrial electromagnetic radiation and particle flux characteristics of low and medium energy, considering onboard spacecraft measuring instruments and data processing systems

24 p3404 A72-45398

RADIATION MEDICINE

NT RADIOBIOLOGY

Automated data processing and display capabilities of radiation measuring systems for surveillance, protection and control in nuclear research, medicine and power production

19 p2802 A72-38306

RADIATION METERS

U RADIATION MEASURING INSTRUMENTS

RADIATION NOISE

U ELECTROMAGNETIC NOISE

RADIATION PRESSURE

NT ELECTRON PRESSURE

NT ILLUMINANCE

NT LUMINANCE

NT LUMINOUS INTENSITY

NT SOUND PRESSURE

Satellite attitude and libration control by solar radiation pressure

01 p0135 A72-10928

Closed rectangular cavity resonator with conducting walls, calculating differences of electromagnetic zero point fluctuation radiation pressure

02 p0260 A72-12434

Dust grain existence at large distances from galactic plane by computing interstellar radiation field pressure effects on grains

02 p0283 A72-12629

Long period perturbations arising in orbits of artificial satellites with large surface to mass ratio under solar radiation pressure and earth oblateness effects

04 p0572 A72-14637

Nonstationary hydroacoustic wave diffraction at curvilinear rigid surface, deriving transfer function and radiation pressure

04 p0589 A72-15062

Acoustic radiation pressure of small radius spherical obstacle in high level harmonic plane field for application to microphone calibration

[ONERA, TP NO. 1008] 05 p0661 A72-16023

Spherical ice and graphite particles absorption, scattering and radiation pressure coefficients and albedo, noting application to interstellar extinction

06 p0875 A72-17296

Mathematical-physical model for laser pulsed radiation-induced pressure wave transmission through surface and internal biological tissues

06 p0768 A72-18150

Laser radiation pressure applications to isotope and particle separation, optical levitation, high velocity acceleration and atomic beam analysis

06 p0826 A72-18176

Solar radiation pressure effects on gravity oriented satellites librational dynamics, using digital computer aided numerical analysis and analog simulation

07 p1067 A72-18789

Environmental forces effects on gravity oriented satellites attitude dynamics, considering earth atmosphere aerodynamic and solar radiation forces effects

07 p1085 A72-19060

Mathematical model of solar radiation pressure effects on earth satellite orbit

08 p1237 A72-21643

Solar radiation pressure effects on orbital evolutions of light artificial earth satellites

10 p1543 A72-24632

Measurement of light pressure-force on Echo 1 satellite based on satellite surface reflection and stellar magnitude as function of phase angle

11 p1718 A72-25939

Radiation pressure on quasar outer envelope material as cause of mass outflow for masses less than gravitational force-determined critical value

14 p2155 A72-30552

Pageos balloon satellite orbital perturbations due to erratic solar radiation pressure induced accelerations, comparing modified Smith perturbation model calculations with photometric observations

15 p2228 A72-31975

Solar radiation pressure effects on balloon satellite behavior, noting orbital eccentricity variations

16 p2463 A72-34182

Spherically symmetric system of radiating body surrounded by absorbing dust zone, investigating relativistic radiation pressure effects

19 p2859 A72-37893

Cosmological model radiation pressure and density calculation by red shift-stellar magnitude ratios from galactic observations

21 p3109 A72-41441

Solar pressure control of a spinning satellite with a stabilized platform.

[AIAA PAPER 72-918] 21 p3115 A72-41563

Attitude control of satellites using the solar radiation pressure.

22 p3231 A72-42871

Theoretical interpretation of emf generation between noncompressed parts of bimetallic junction traversed by shock wave, taking into account radiation pressure of phonon gas

22 p3207 A72-43050

To the problem of satellite's perturbed motion under the influence of solar radiation pressure.

24 p3442 A72-45237

RADIATION PROTECTION

NT RADIATION SHIELDING
NT SOLAR RADIATION SHIELDING
Integrated electronics digital-analog solar cell array control unit, discussing circuit design and radiation hardening
01 p0042 A72-11059
Protection against accelerator and space radiation Conference, Geneva, April 1971, Volume 1, Health physics
[CERN-71-16] 02 p0160 A72-12051
In-flight warning meter for solar and cosmic radiation dose equivalent measurements for radiological protection in SST aircraft
[CERN-71-16] 02 p0274 A72-12078
MIS semiconductors radiation-hardening mechanisms and radiation effects on electrical properties and degradation
03 p0405 A72-14281
Soviet book on radiation hazards and protection in space covering detection, radiobiology and effects on human organism
11 p1713 A72-26050
Pathophysiology of exposure to UV, IR, coherent, microwave and RF radiations, discussing potential hazards, damage, human tolerance threshold, protection guides and safety standards
12 p1772 A72-27963
Shielding metallic interlayer technique to protect MIS device against degradation due to ionizing radiation effects
13 p2023 A72-29836
P channel MOS transistors hardening against ionizing radiation based on positive space charge density and electrode injection efficiency
13 p2023 A72-29837
Book on radiation protection measurement covering dose determination, activity and contamination measurement, radionuclide determination, semiconductor detectors, etc
16 p2421 A72-33276
Brief survey of the problems of space radiobiology and radiation safety in space flights
17 p2509 A72-35376
The use of a scintillation counter to measure diagnostic X-ray tube kilovoltage, radiation exposure rates and contamination by low energy gamma emitters
18 p2655 A72-37197
Automated data processing and display capabilities of radiation measuring systems for surveillance, protection and control in nuclear research, medicine and power production
19 p2802 A72-38306
Missile guidance electronic packaging and module design for circuit protection against X rays, gamma radiation and nuclear blast damages
20 p2909 A72-39766
RADIATION PYROMETERS
Gas turbine blade temperature measurement by radiation pyrometer, discussing thermal radiation sensing and fiber optics transmission, signal processing and real time temperature characteristic display
[SAE PAPER 7201 59] 06 p0812 A72-17321
Optical pyrometers with dual spectral ratios to eliminate instrument error due to selective radiation
22 p3175 A72-41887
Experimental setup for the investigation of the spectral radiative capability of metals
22 p3175 A72-41893
RADIATION RESISTANCE
U RADIATION TOLERANCE
RADIATION SHIELDING
NT SOLAR RADIATION SHIELDING
Aerospace radioisotope power systems, discussing heat source technology, shielding, safety and thermoelectric integration
[SAE AIR 1213] 01 p0098 A72-10387
Multilayer insulation materials for reusable space vehicles thermal protection and radiation shielding, tabulating thermal conductivity values for various materials
01 p0092 A72-10780
Active shielding against radiation in space using charged particle deflection by electric and magnetic fields
[CERN-71-16] 02 p0258 A72-12076
Angular quadrature effects on two dimensional space power reactor radiation shield calculation for manned space station application
04 p0546 A72-14426
Curved-wall annular exhaust diffusers for hot engine parts IR shielding, evaluating performance tests for swirl flow and ejector secondary flow effects on pressure recovery
[ASME PAPER 71-WA/FE-35] 05 p0646 A72-15922
Shielding of solid surface vaporizing under laser radiation effect in presence of thermal and ionizational nonequilibrium, investigating absorption flare onset mechanism
06 p0825 A72-17905
Tranquillity Base rocks irradiation depths and cosmic rays exposure ages from rare gases in samples, noting correlated variations in He 3/Ne 21 and Ar 38/Ne 21 due to shielding differences
09 p1377 A72-22596

Cosmic radiation effects and damage on solar cells, discussing shielding, stability improvement, space environments, minority carrier lifetime and photosensitivity spectral distribution
10 p1422 A72-24312
Thermal radiation shielding of porous surface on heated plate by absorbing gas transpiration, suggesting carbon dioxide, metal vapors and particulate mixture
[AIAA PAPER 72-277] 11 p1740 A72-25217
Low cost radiation shield for thermistor deployment in atmospheric boundary layer, noting measurement accuracy relationship to data acquisition system
11 p1682 A72-26087
Shielding metallic interlayer technique to protect MIS device against degradation due to ionizing radiation effects
13 p2023 A72-29836
Radiation hazards in space with respect to galactic radiation shielding, solar flare prediction and conventional terrestrial safety standards
16 p2358 A72-33556
NASA-Lewis experiences with multigroup cross sections and shielding calculations.
19 p2833 A72-37633
RADIATION SICKNESS
Radiation induced disease development related to dose, dose rate and radiation quality, discussing different models
[CERN-71-16] 02 p0161 A72-12053
Relative biological effectiveness of energetic protons for somatic effects induction in mice during whole body irradiation, using mean energy of solar event protons
[CERN-71-16] 02 p0161 A72-12054
Influence of ionizing radiation on the tooth organ
22 p3141 A72-41987
RADIATION SOURCES
NT MONOCHROMATORS
NT POINT SOURCES
Supernova Vela X and local remnants as origin of below 1000 GeV cosmic electrons, deducing existence at 10 to 15 GeV from moon positron showers
01 p0119 A72-10853
Cygnus X-6 soft X ray source location, presenting polycarbonate pulse-height spectrum and counter response to different model source energy spectra
01 p0121 A72-11096
Cosmic soft X ray and UV radiation sources, discussing transition radiation emission in interstellar space
01 p0121 A72-11121
Spacecraft attitude determination with single-axis sensor and single natural radiation source with relative mutual motion, deriving error equations
01 p0032 A72-11224
Extragalactic cosmic ray hypothesis plausibility from viewpoints of energy supply, acceleration process efficiency, galactic nucleus activity and intergalactic space
01 p0122 A72-11268
Galaxy source of ultrahigh energy cosmic rays, interpreting energy spectrum kinks as galactic to metagalactic radiation transition
01 p0122 A72-11270
Fraunhofer hologram for recording square of modulus of far field radiation pattern due to mixture of known and unknown source distributions
02 p0224 A72-11548
Ultrahigh energy cosmic ray models indication of galactic origin and composition, based on energy spectrum flattening data
02 p0272 A72-11901
Frequency variations from uniformly moving source in homogeneous and inhomogeneous isotropic plasmas, calculating source-to-transmitted-wave group velocity ratio from Doppler curves slopes
02 p0264 A72-12120
Magellanic Clouds X ray sources from Uhuru satellite observations, discussing time variability
02 p0280 A72-12195
X ray astronomy observations, discussing Sco X-1 and Tau X-1 sources
03 p0408 A72-13036
Image blurring effects due to atmospheric boundary layer refractivity turbulent fluctuations during remote optical radiation source observations
03 p0359 A72-13482
Pulsar model, discussing polar radiation diagram formation with source motion around neutron star
04 p0573 A72-14903
Universal steady X ray background theory, examining superposition of radiation from pulsars in various galaxies
04 p0566 A72-14909
Nighttime radio absorption from lower ionospheric ionization by Sco X-1 and Tau X-1 X rays, using full wave admittance method
04 p0519 A72-15161
Cosmic gamma radiation theoretical and experimental investigations, discussing sources, interactions with interstellar and intergalactic media, atmospheric backgrounds, balloon and satellite measurements, etc
05 p0709 A72-16328
Variable circular polarization in optical emission of X ray source Sco X-1, noting oscillations amplitude
06 p0878 A72-17785

Jet noise simple-source theory experimental verification, determining relation of measured sound power and jet pressure levels of turbojet engine
06 p0867 A72-17856
Soft X ray survey of galactic plane from Sagittarius to Vela by proportional counter, observing radiation sources
06 p0873 A72-17890
Galactic nuclei and quasars as IR source, noting critical accretion of gas at neutron stars
06 p0883 A72-18015
High energy particle sources, taking into account cosmic ray sources, sun, artificial plasmas, interplanetary and planetary sources, interstellar space, supernovae, radio galaxies and quasars
07 p1059 A72-19428
Anisotropic grounded dielectric or plasma layer motion effects on magnetic or electric current line source radiation patterns
07 p0946 A72-19802
X ray spectrum analysis of Sco XR-1 sources, showing plasma sheath with high electron temperature
07 p1076 A72-19804
Moving isotropic plasma half space effect on magnetic or electric line source radiation patterns
07 p1044 A72-20192
Scorpius X-1 linear optical polarization, comparing intrinsic to interstellar theories
08 p1235 A72-21390
Upper soft X ray limits to Virgo sources from Aerobee 170 rocket sounding
08 p1227 A72-21394
Balloon observations of low energy Scorpius X-1 gamma ray spectrum
08 p1227 A72-21395
High resolution rocket-borne X ray spectrometer with cooled lithium drifted semiconductor detectors for measuring differential X ray energy spectrum of SCO XR-1
08 p1168 A72-21518
Models of galactic diffuse sources of soft cosmic X rays, estimating spectrum and intensity
08 p1228 A72-21650
Narrow band signal envelope analysis of astronomically observed quasi-monochromatic emission sources
08 p1135 A72-21731
Gamma radiation source energy and activity determination for radiometric flaw detection in steel
08 p1177 A72-21775
Black body X ray sources creation due to neutron stars rotational energy dissipation by strain hysteresis in crust
09 p1382 A72-22284
Periodic intensity and period variations of X ray pulsating source Cen X-3 caused by occulting binary system from Uhuru satellite observation
09 p1382 A72-22289
Hard X radiation source in Vela X supernova remnant direction detected during balloon flight on 25 November 1970
09 p1383 A72-22290
Simulated superposed coherent and chaotic /thermal/ radiation of arbitrary spectral shape, using laser beam modulation and photocount statistics
09 p1352 A72-23240
Gravitational radiation from isolated material source in terms of van der Burg solution to Einstein field equations
09 p1352 A72-23359
Galactic and universal theories of cosmic ray source mechanisms, energy requirements, particle composition, propagation through interstellar matter and acceleration in supernovae remnants
10 p1533 A72-23889
Quasars energy source and structure in terms of kinetic energy conversion to radiation in shock fronts of colliding gas clouds
10 p1544 A72-24671
Airglow intensities and upper atmosphere physical processes relationship, discussing spectral features, emission brightness and excitation sources
10 p1474 A72-24714
Gravitational wave antenna response to linear, mixed and randomly polarized sources, discussing Weber signals galactic nucleus source
11 p1717 A72-25882
Gravitational wave observation interpretations, discussing Weber theory of galactic nucleus isotropic radiation and synchrotron radiation sources in terms of black hole existence
11 p1717 A72-25883
Galactic nuclei and quasars as IR sources, noting critical accretion of gas at neutron stars
11 p1718 A72-25951
Image blurring effects due to atmospheric boundary layer refractivity turbulent fluctuations during remote optical radiation source observations
11 p1633 A72-26252
Grain heating model of H II region to explain 100 micron emission predominance in IR sources
12 p1871 A72-27693
Sco X-1 2-14 keV X ray flux variations from Skylark 901 and S55 observations
12 p1864 A72-27694

Statistical analysis of solar microwave bursts, examining radiation source development and emission mechanism

12 p1872 A72-27814

Bright stars X Per and HD 77581 as candidates for X ray sources 2U 0352plus30 and 2U 0900minus40 respectively

13 p2041 A72-29413

E region ionosonde observations to reconstruct ionizing X ray and far UV radiation source distribution over solar disk during March 1970 total solar eclipse

13 p2044 A72-29552

Moving sound sources spectral analysis techniques, discussing computer controlled one-third octave band and narrowband analysis

13 p2005 A72-29566

Interaction between generating lines in coupled channels with arbitrary line broadening, studying radiation generation regimes in cascade circuit

13 p1970 A72-29680

Coronal condensation X ray sources from heliograms, discussing relation to active region evolution

14 p2146 A72-30204

Celestial sources investigation for high energy cosmic gamma rays with particular attention to Crab Nebula

14 p2147 A72-30560

Random variations in interferometer complex visibility function magnitude and phase, refractive index and source angular size

14 p2156 A72-30561

X ray source Cygnus X-1 pulsation periodicity analysis, showing random shot noise characteristics

14 p2156 A72-30571

Uhuru satellite observation of transient X ray source in constellation Lupus, discussing five month period intensity variation

14 p2157 A72-30572

Geomagnetic field perturbation by gamma quanta pulsating source, studying accompanying radio emission behavior

14 p2101 A72-30645

Variable cosmic X ray source location determination, noting Crab pulsar as radio, optical, X ray and gamma source

15 p2298 A72-31599

Radiation source position a posteriori probability density function determination with empirical prior knowledge to provide simple computational procedures

15 p2267 A72-31778

Nonionizing component of underground high energy cosmic radiation investigated with anticoincidence screen and counters, noting bremsstrahlung as photons source

15 p2301 A72-32232

Hydroxyl emission sources classification from observed main line polarization and satellite lines

15 p2315 A72-32710

IR photometry of IR-OH sources, showing IR colors correlation with velocity separation of OH emission peaks

15 p2315 A72-32711

Relativistic charged particles produced transition radiation as diffuse cosmic X rays source, discussing validity based on interstellar space energy density consideration

15 p2301 A72-32716

Expanding loops of H alpha filaments in peculiar galaxy M 82 investigated by microwave radio map, suggesting thermal and nonthermal radiation sources

15 p2317 A72-32757

Radiation source motion at superluminal speed in vacuum, defining conditions for Vavilov-Cerenkov and Doppler effects

15 p2279 A72-32767

Heliograph and interferometer observations of type 3 bursts, plotting relative positions of fundamental and second harmonic radiation sources

16 p2445 A72-33043

Primary cosmic rays extragalactic origin, considering high energy electrons, background X and gamma rays and cosmic protons

16 p2445 A72-33126

Galaxy M87 X ray source origin, suggesting hot plasma thermal emission or ejected relativistic electrons interacting with intergalactic magnetic or radiation fields

16 p2452 A72-33135

Diffuse X ray emission from galaxy interarm region, suggesting population of unresolvable low luminosity sources as emission model

16 p2445 A72-33138

Galactic X ray sources from June 1969 rocket flight in Brazil, comparing spectra to bremsstrahlung, black body and power law models

16 p2446 A72-33457

Planetary nebula M2-9 spectrum analysis, discussing IR excess, internal motions and Fe II emission lines

16 p2455 A72-33459

Uhuru satellite data on periodic pulsating X ray source in Hercules, interpreting intensity variations as occulting binary star system effect

16 p2446 A72-33475

Cen X-3 system X ray flux amplitude periodic variations, proposing model composed of source orbiting around massive body with ionized gas cloud in between

16 p2446 A72-33611

Computer simulation of airborne gamma ray spectrometer with prescribed photopeak windows from flight over surfaces with arbitrary-dimension radiation sources

16 p2392 A72-33617

Quasars and emission line objects red shift distribution using power spectrum analysis method

16 p2457 A72-33625

Diffusion propagation and source distribution effects on cosmic ray charge composition and anisotropy in galactic disk, considering nuclear fragmentation

16 p2448 A72-33742

Galactic ridge of discrete diffuse X ray sources, calculating intensity in terms of scale height and radial gradient

17 p2598 A72-34523

Pulsating X ray sources with 1 sec periods as stars with central densities between neutron stars and white dwarfs

17 p2599 A72-35074

X ray astronomy observational procedures, discussing source location and models, X ray detectors, satellite-borne equipment, correlation maps and diffuse X ray background studies

17 p2612 A72-35377

The estimation of nonstationary spectra from moving acoustic source distributions.

[AIAA PAPER 72-667]

17 p2583 A72-35486

Elastic cylindrical antenna detection relationship to gravitational radiation sources

17 p2584 A72-35914

Solar flares and radio bursts significance for chromosphere and corona studies, considering radiation frequency-source location relations

17 p2603 A72-35957

On the radiation of discontinuous gold films by electric current transmission.

18 p2718 A72-36349

Error investigation for the location of the sources of atmospherics by radio direction finding.

18 p2706 A72-36429

Classification of shock waves in a radiating gas

18 p2682 A72-36806

High energy gamma radiation from the galactic centre region.

18 p2722 A72-36998

X ray observation inadequacy in detection of background radiation surface brightness fluctuations due to irregular distribution within galactic cluster sources

18 p2729 A72-37006

High energy gamma ray sources search by Cerenkov radiation recording from extensive air showers, noting atmospheric transparency effects

19 p2850 A72-37805

Statistical analysis for best fit of compact X ray object spectra to black body, bremsstrahlung and power law models

20 p2969 A72-39387

Design of a specular aspheric surface to uniformly radiate a flat surface using a nonuniform collimated radiation source.

[ASME PAPER 72-HT-J]

20 p2984 A72-39653

Photoemissive method of recording Mertz shadowgrams and vibrating electrode technique for reading out images in reconstruction of X ray sources original distribution

21 p3051 A72-40219

On a galactic origin for the soft X-ray background.

21 p3100 A72-41029

Photometric analysis of X-ray photographs of sun obtained with rocket-borne zone plate camera in XUV region

21 p3108 A72-41289

Solar soft X-rays and solar activity. II - Observational assessment of the role of the type III acceleration mechanism in establishment of the soft X-ray source volume.

21 p3101 A72-41294

Bremsstrahlung from cylindrical beta sources.

21 p3088 A72-41383

Balloon techniques in X ray astronomy, considering emission mechanisms of discrete cosmic sources

21 p2996 A72-41616

Radiometer with protective mica window for radiant flux densities measurement of near IR sources, noting reading independence of sources spectra characteristics

21 p3059 A72-41821

The interaction of Sco X-1 with its environment.

22 p3218 A72-42387

Observation of several X-ray sources in 1970 September.

22 p3219 A72-42554

Integration sphere facility with water cooled long arc xenon sources for pyranometer calibration, discussing operation theory and system design

22 p3163 A72-42692

Compton scattering by thermal electrons in X-ray sources.

23 p3328 A72-43230

Coronal condensation X ray sources from heliograms, discussing relation to active region evolution

23 p3328 A72-43234

Gamma radiation of Magellanic Clouds and metagalactic origin of cosmic rays.

23 p3328 A72-43264

Group theory for spontaneous coherent radiation of multilevel sources, noting angular distribution of photon echo effects

23 p3295 A72-43306

High energy gamma ray point sources in Cassiopeia and Cygnus regions, using extensive air shower Cerenkov flashes detection technique

23 p3329 A72-43941

Sharp focused short pulse X ray source with laser flash synchronization for radiographic plasma diagnostics

24 p3429 A72-45495

RADIATION SPECTRA

NT ABSORPTION SPECTRA

NT BALMER SERIES

NT D LINES

NT ELECTROMAGNETIC SPECTRA

NT ELECTRONIC SPECTRA

NT EMISSION SPECTRA

NT FRAUNHOFER LINES

NT H ALPHA LINE

NT H BETA LINE

NT H GAMMA LINE

NT H LINES

NT HERZBERG BANDS

NT INFRARED SPECTRA

NT K LINES

NT LINE SPECTRA

NT LYMAN SPECTRA

NT MICROWAVE SPECTRA

NT PASCHEN SERIES

NT RADIO SPECTRA

NT RAMAN SPECTRA

NT RYDBERG SERIES

NT SOLAR SPECTRA

NT STELLAR SPECTRA

NT TELLURIC LINES

NT ULTRAVIOLET SPECTRA

NT VIBRATIONAL SPECTRA

Radiation spectral properties in mode locking region of He-Ne 20 laser at 0.63 microns, generating three axial modes

01 p0078 A72-10154

Action kinetics and radiation spectra of multiruby lasers, determining effect of crystal C axes angular orientation relative to ruby pairs geometrical axes

01 p0079 A72-10374

Primeval fireball cosmic background radiation spectrum in homogeneous axisymmetric anisotropic world model including electron neutrino effects on expansion dynamics

01 p0121 A72-11139

Galaxy source of ultrahigh energy cosmic rays, interpreting energy spectrum kinks as galactic to metagalactic radiation transition

01 p0122 A72-11270

Pulsed hf discharge in hydrogen based on laser light scattering on plasma electrons, noting position of satellites in spectra

02 p0237 A72-11406

Average radiation Q factor and dose radiation spectrum measurement in phantoms irradiation by proton beams

[CERN-71-16]

02 p0162 A72-12069

Ionospheric effects of X ray flare on 8 July 1968, estimating ionizing radiation spectral characteristics from SID observation

03 p0407 A72-12986

Spectral distribution of radiation arising from nonlinear Thomson scattering of strong electromagnetic wave by ultrarelativistic electrons

03 p0390 A72-13017

Spectral and energetic characteristics of ruby laser radiation with two types of three-level radiation centers

03 p0367 A72-13582

Spectrum of low modulation frequencies of He-Ne laser radiation produced by motion of external reflector of matched and unmatched three-mirror resonators

03 p0368 A72-13666

Fast particle interaction with intergalactic matter, discussing relaxation of power law cosmic ray spectra

04 p0570 A72-14553

Planetary wave spectrum calculation by Galerkin method, discussing angular velocity of longest Rossby waves distortable by zonal flow

05 p0655 A72-16170

Earth radiation flux spectral intensity measurements in winter, noting latitudinal distributions, day and night variations and oceanic and continental curves

05 p0656 A72-16234

Cosmic ray spectrum at nonrelativistic energy region, noting ionization loss effects

05 p0709 A72-16238

- Extensive air shower spectra based on electron and muon number 06 p0871 A72-17283
- Altitude effects on high energy neutrons and galactic gamma rays flux and spectrum variations from balloon flight studies 06 p0873 A72-17639
- Short and long term spectral modulation of primary cosmic rays above 2 GV during solar cycle 19 descending phase, presenting neutron monitors calibration procedure 06 p0874 A72-18160
- Pulsar produced cosmic rays energy spectrum, investigating light elements origin 06 p0874 A72-18161
- Radiation temperature of carbon monoxide molecules in solar atmosphere from vibratory-rotatory spectral measurements 07 p1077 A72-19811
- Spectral distribution of electromagnetic radiation emitted by charge moving in gravitational field of spherically symmetric black holes 07 p1081 A72-20226
- Solar cosmic ray spectra at time of ejection from flare region and arrival near earth 08 p1226 A72-20812
- Mars atmosphere temperature profiles inference from outgoing radiation spectral characteristics, constructing atmospheric model 08 p1232 A72-21147
- Nucleonic cascade model analysis of underground vertical muon curve for primary cosmic ray nucleon spectrum below 40 TeV 10 p1529 A72-24417
- Shock wave structure in radiation spectrum of photon-electron interaction via induced Compton effect 12 p1848 A72-27056
- Global ground stations for lower VLF atmospherics arrival directions and spectral parameters observation 12 p1804 A72-27792
- Self consistent model for cosmic ray propagation from sources in Galaxy toward earth, using H and He isotope interstellar spectra 13 p2031 A72-29409
- Planetary wave spectrum calculation by Galerkin method, discussing discrete modes of longest Rossby waves distortable by zonal flow 14 p2099 A72-30239
- Lateral distribution, radiation spectra and pulse shapes calculated from mathematical models of cosmic ray showers radio emission, noting chemical composition of primary particle 15 p2230 A72-32262
- Cosmic ray electron search and study, comparing near earth to interstellar spectrum 16 p2448 A72-33869
- Radiation temperature of carbon monoxide molecules in solar atmosphere from vibratory-rotatory spectral measurements 17 p2618 A72-35736
- Mars atmosphere temperature profiles inference from outgoing radiation spectral characteristics, constructing atmospheric model 20 p2968 A72-39252
- Charged particle uniform motion in sinusoidally space-time periodic medium, determining Cerenkov and transition radiation field spectrum from Brillouin diagram 21 p3088 A72-41378
- Optical pyrometers with dual spectral ratios to eliminate instrument error due to selective radiation 22 p3175 A72-41887
- Experimental setup for the investigation of the spectral radiative capability of metals 22 p3175 A72-41893
- Russian book - Radiation characteristics of gases at high temperatures. 22 p3243 A72-42075
- Investigation of the shape of the radiation pulse of a self-mode-locked laser 23 p3294 A72-43303
- Gas absorption lines detection based on multiple light passage through absorbing medium during generation process, noting radiation spectra of neodymium glass laser 23 p3295 A72-43305
- Steady-state lasing spectrum of a CO₂ laser at reduced working-mixture pressures 23 p3295 A72-43681
- Cylindrical waveguide with density modulated electron beam pumped by external electromagnetic field, considering Doppler effect conditions in beam radiation spectrum 23 p3265 A72-44157
- Utilization of a composite resonator for improving the monochromaticity of a semiconductor laser with electron-beam excitation 23 p3297 A72-44468
- The cosmic-ray spectral modulation above 2 GV. IV - The influence on the attenuation coefficient of the nucleonic component. 24 p3434 A72-44783
- High power monopulse laser with a stabilized spectrum and radiation directivity close to that of diffraction 24 p3410 A72-45422
- Shock wave structure in radiation spectrum of photon-electron interaction via induced Compton effect 24 p3431 A72-45709
- RADIATION THERAPY**
New cancer therapy treatment techniques using space dosimetric concepts. 24 p3374 A72-45112
- RADIATION TOLERANCE**
Al, Mo and Cr radiation resistance as gate electrodes and corresponding MOS devices, discussing radiation behavior model revision 03 p0403 A72-14079
- P-channel MOS devices radiation hardening by thermal silicon dioxide gate insulator optimization, applying to circuit fabrication 03 p0403 A72-14082
- P-channel MOS/silicon-on-sapphire transistor logic circuits for aerospace systems, investigating radiation hardness and performance potential 03 p0334 A72-14086
- Elf/vlf radiation resistance of finite electric dipole oriented at arbitrary angle in cold uniform magnetoplasma, deriving general integral expression 07 p1039 A72-18823
- Circadian periodicity of resistance to ionizing radiation in pocket mouse at high and low metabolic rate 07 p0918 A72-19532
- Radiation resistance of Si photodetectors for star sensors in satellites, using electrical and optical tests 09 p1369 A72-22653
- Electric dipole radiation at VLF in a uniform warm magneto-plasma. 19 p2840 A72-37833
- RADIATIVE HEAT TRANSFER**
High temperature nongray kernel functions application to radiative heat transfer for bounded hydrogen plasma 01 p0145 A72-10100
- Venusian atmosphere heat transfer processes, calculating radiant fluxes and convective motion model 01 p0127 A72-10364
- Venus subcloud layer, investigating radiant heat transfer in convective lower atmosphere 01 p0128 A72-10370
- Radiative heat transfer equilibrium in Earth, Venus and Mars atmospheres, taking into account interaction with ground 01 p0058 A72-10561
- Venus lower atmosphere from Venera 4, 5 and 6 and Mariner 5 data, evaluating greenhouse effect by microwave absorption and by nongray radiative model 01 p0129 A72-10795
- Nuclear light bulb engine concept, detailing radiant heat transfer calculations in fuel and buffer gas regions 01 p0099 A72-11345
- Transparent fused silica wall irradiation induced optical absorption and heat deposition in nuclear light bulb engine 01 p0103 A72-11356
- Radiative heat transfer between gas flow and axisymmetric ablating body near stagnation point, considering ablation products effects under boundary layer chemical equilibrium conditions 02 p0300 A72-11577
- Radiative heat transfer across vacuum gap between two closely spaced metal bodies with arbitrary dielectric properties, solving Maxwell equations 02 p0300 A72-11672
- Radiative heat transfer within nonisothermal air plasma, presenting centerline temperature data for various boundary pressures and temperatures [ASME PAPER 71-HT-G] 02 p0302 A72-12316
- Optically thin radiation effects on local heat transfer in gas flow narrow duct thermal entrance region, presenting Nusselt number variations terms for uniform and parabolic velocity profiles 02 p0303 A72-12321
- Optimal radiative capacity of star shaped radiator with mirror reflecting surfaces for vacuum cooling of elongated finned bodies 02 p0304 A72-12867
- Stellar secular stability during complex roots onset in model evolution, discussing radiative heat transport coefficient effects 03 p0416 A72-13004
- Heat transfer through fabrics by convection, conduction, radiation and vaporization related to skin temperature and thermal injury 03 p0319 A72-13700
- Radiative cooling effects on flow field and heat transfer behind reflected shock wave [AD-737423] 04 p0597 A72-15338
- Radiator fins for cooling electronic equipment elements, calculating design parameters effects on heat transfer efficiency 05 p0746 A72-16198
- Radiative transfer in gray medium with prescribed spatial temperature distribution in rectangular enclosures with nonisothermal walls, deriving exact solutions by radiation transport theory [AIAA PAPER 72-21] 05 p0748 A72-16869
- Graphite ablation in combined convective and radiative heating, considering mass and energy transfer effects [AIAA PAPER 72-88] 05 p0750 A72-16954
- Local or radiative-convective heat transfer coefficient determination at porous surface in presence of two dimensional temperature field, using temperature gradient method 05 p0751 A72-17070
- Radiative heat transfer damping rates of turbulent temperature pulsations in upper planetary atmospheres, assuming Kirchhoff radiation law validity 06 p0882 A72-17935
- Conductive and radiative energy transfer in absorbing, emitting and conducting medium bounded by two black plates, using Milne-Eddington type absorption coefficient 06 p0903 A72-18187
- Nonlinearly radiating semifinite heat conducting solid surface temperature, expressing heating rate as nonnegative integrable function of time [AD-743533] 07 p1098 A72-18814
- Convective conductance meter for continuous measurement of outdoor exposed surface convection coefficient, using electrically heated plaques with known surface radiation properties 07 p0981 A72-18821
- Radiative heat transfer characteristics of optimal geometry radiating stainless steel fin 07 p1098 A72-18997
- Solar coronal plasma radiative capacity and temperature structure from cooling function in thermal balance equation 08 p1231 A72-21124
- Energy transfer from radiative heat source near summer pole to radiative heat sink near winter pole, investigating large scale eddies and gravity waves 08 p1161 A72-21536
- Calorimetric gage for convective and radiative wall heat flux measurements in Ar arc plasma 08 p1254 A72-21628
- Book on heat transfer by thermal radiation, covering black body radiation, electromagnetic theory, energy exchange, Monte Carlo solution, and absorbing and emitting media 09 p1411 A72-23046
- One dimensional conductive and radiative heat transfer through gray medium bounded by two diffuse surfaces, noting solutions existence and uniqueness 09 p1412 A72-23586
- Thermal stratification of mesosphere and lower thermosphere at low latitudes with allowance for turbulent mixing, showing molecular oxygen and ozone radiative heating prevalence 09 p1347 A72-23589
- Jupiter atmosphere thermospheric temperature profile from heat conduction equation, noting radiative and convective transfer 09 p1393 A72-23658
- Nonstationary radiative heat transfer between cylindrical body and ambient medium, determining regular heating condition region 10 p1561 A72-23842
- Radiant heat flux measurement during pulsed processes from surface in high temperature emitting gas, using thin film sensor with small time constant 10 p1561 A72-23843
- IR radiative energy transfer to laminar flow of nongray absorbing emitting gases through circular tube 10 p1563 A72-25038
- Energy transfer in thermally developing laminar gas flows with radiative interaction, using total band absorptance model [AD-745475] 10 p1563 A72-25043
- Finite element method for boundary value radiative and convective heat transfer problems [AIAA PAPER 72-274] 11 p1740 A72-25214
- Free convection-radiative heat transfer interaction of real gases in laminar boundary layer on vertical plate, using exponential wideband model for total band absorptance [AIAA PAPER 72-278] 11 p1740 A72-25218
- Nonisothermal hydrogen plasma channel flow and radiative heat transfer combined with convective and conductive transfer between isothermal black parallel boundaries [AIAA PAPER 72-279] 11 p1692 A72-25219
- Configuration factors for radiative heat transfer analysis with partially occluded surfaces, defining areas by computer technique 11 p1742 A72-25238
- Roughness effects on radiant heat transfer between interacting surfaces based on Beckman reflectance model [AIAA PAPER 72-305] 11 p1742 A72-25239
- Radiative heat transfer spectral, temperature and directional dependence on interacting opaque surfaces system properties, noting models with accounted nongray character [AIAA PAPER 72-306] 11 p1742 A72-25240

Space shuttle orbiter reentry heat shield materials, considering hot structures and hot radiative metallic, ceramic insulative and ablative heat shields

11 p1660 A72-26245

Stress rupture strength, short term strength, creep and heat resistance measurement arrangement for coated refractory materials at 1500-1700 C in air with radiative heating

12 p1796 A72-28248

Combined radiation-convection interaction for slow speed gas flow over flat plate, comparing with two dimensional and axisymmetric stagnation point geometries

13 p2064 A72-28631

Iterative-zonal method for radiative heat transfer calculations with capability to numerically determine radiation characteristics of optically and energetically homogeneous zones

13 p2065 A72-29643

Radiative-dynamic model for static stability of rotating atmospheres, deriving mean equilibrium value of Richardson number in troposphere

14 p2127 A72-30341

Temperature difference between steadily flowing fluid and solid sphere due to viscous dissipation determined for simultaneous conduction and radiation [DFVLR-SONDDR-220]

14 p2105 A72-30710

Mass entrainment products effect on radiative and convective heat transfer during decomposition of graphite blunt body in steady hypersonic flow of radiating air

14 p2174 A72-31158

Non-spherical thermal wave propagation, considering two dimensional structure wave front radiative diffusion problem

15 p2336 A72-32513

Convective and radiative heat transfer in compressible gas boundary layer

16 p2343 A72-32995

Two layer model for diurnal temperature variations analysis for radiative heat transfer between lower atmosphere and underlying layer

16 p2417 A72-33293

Normal-mode expansion technique for unsteady radiative and conductive heat transfer in absorbing emitting isotropically scattering slab with reflective boundaries

16 p2478 A72-33438

Radiative heat transfer damping rates of turbulent temperature pulsations in upper planetary atmospheres, assuming Kirchhoff radiation law validity

16 p2459 A72-33776

Radiative and convective heat transfer for stagnation point flow of emitting carbon dioxide and nitrogen gas mixture, assuming thermodynamic equilibrium in shock layer

17 p2636 A72-34470

Radiation with free convection in an absorbing, emitting and scattering medium

17 p2637 A72-35046

Lateral heat exchange in a thermocouple

17 p2498 A72-35513

Analytical solutions for straight oblique shock waves in radiating gases

17 p2542 A72-35616

Radiant interchange among suspended particles and its effect on thermal relaxation in gas-particle mixtures

17 p2638 A72-35643

Transient radiative heat transfer in a non-gray medium

19 p2880 A72-37835

A critical examination of the validity of simplified models for radiant heat transfer analysis

19 p2882 A72-38399

The effect of changing CO₂ concentration on radiative heating rates - Further comments

20 p2947 A72-38969

Radiation heat transfer between closely spaced metal surfaces at low temperature - The impact of discrete modes of the radiation field

20 p2983 A72-39483

Efficient computation of radiant-interchange configuration factors within the enclosure

20 p2983 A72-39488

Effect of polarization on the apparent emittance of rectangular groove cavities

20 p2954 A72-39629

Mathematical models for radiative heat transfer prediction in real enclosures, noting directional characteristics of heat exchanging surfaces

20 p2984 A72-39652

Design of a specular aspheric surface to uniformly radiate a flat surface using a nonuniform collimated radiation source

20 p2984 A72-39653

Numerical experiment of radiative-convective equilibrium of the Martian atmosphere

21 p3105 A72-40772

Shadow shields for minimizing radiant heat transfer into cryogenic propellant tanks on interplanetary missions, predicting performance for comparison with scale model experiment

21 p3130 A72-41181

Diffusive and radiative effects on vaporization times of drops in film boiling

21 p3130 A72-41185

Steady radiating gas flow past a semi-infinite flat plate at a constant temperature for an optically thick case

21 p3131 A72-41497

Thermal state of selectively absorbing plane gas layer blown from porous plate into stabilized turbulent high temperature gas flow, considering radiative and convective heat transfer

21 p3131 A72-41672

Heat transfer by radiation in a glass fiber insulator

22 p3243 A72-41891

Radiant conduction heat transfer in semitransparent solid materials

22 p3243 A72-41955

Theory of radiative heat transfer in polytropic atmospheres

22 p3229 A72-42962

Generalized integral equations of radiative heat exchange

23 p3357 A72-44536

Temperature calculation in a multilayered wall acted on by a thermal pulse

23 p3357 A72-44537

Radiation gasdynamics of planetary entry - Concepts and recent advances

24 p3361 A72-45188

Approximate temperature distribution for a diffuse, highly reflecting material

24 p3465 A72-45790

RADIATIVE LIFETIME

Neutral Cr beam excited states radiative lifetime measurement by beam foil method

03 p0390 A72-13016

SiO transitions radiative lifetimes and absolute oscillator strengths from RKR Franck-Condon factors

13 p2008 A72-30054

Quantum efficiency and radiative lifetime of the band-to-band recombination in heavily doped n-type GaAs

19 p2844 A72-37947

Radiative lifetimes for some resonance transitions of Fe I and Fe II in the region between 2300 A and 3050 A, and the application to iron abundance determinations in the sun and in the QSO PHL 938

20 p2966 A72-38915

Oscillator strength for sulfur monoxide transition band systems calculated from radiative lifetime with Franck-Condon factors

20 p2966 A72-38916

RADIATIVE RECOMBINATION

Electron energy equation and recombination radiation loss for atomic radiating optically thin plasmas, using Kramers-Unsold approximation

01 p0106 A72-10097

Interstellar molecules formation by radiative association and chemical reactions

03 p0320 A72-13121

Solar corona atomic states radiative and collisional transitions, inferring radiative recombination cross section from bound-free absorption coefficient

03 p0422 A72-13203

Rf diagnostic technique for carbon and hydrogen /H I/ cloud recombination lines in cool interstellar medium

04 p0570 A72-14525

Collisional radiative recombination applicability to time dependent electron density decay in helium afterglow before reaching quasi-steady state

04 p0555 A72-14579

G-r noise in intrinsic photoconductors for Auger band-to-band radiative recombination

06 p0865 A72-17365

Radiative transition probabilities and recombination coefficients of ion C IV

09 p1354 A72-22664

Radio recombination lines broadening in hydrogen by electron collisions, using Baranger impact theory

10 p1435 A72-24142

Numerical and shock tube experiments for variation of bound electron temperature and nonequilibrium chemical and radiative relaxation behind normal shock waves in air, using atom-molecule collision model

18 p2681 A72-36564

Study of the mechanism of radiative recombination in vitreous and monocrystalline arsenic selenide

19 p2844 A72-37684

Excited-state cesium photoionization cross sections

19 p2837 A72-37838

Stimulated effects in the radiative recombination from electron-hole liquid in semiconductors

19 p2844 A72-37932

Quantum efficiency and radiative lifetime of the band-to-band recombination in heavily doped n-type GaAs

19 p2844 A72-37947

Radiative recombination of atoms as a resonance scattering process

21 p3087 A72-40560

Kinetics of impact-radiative ionization and recombination

23 p3318 A72-43296

Evidence for radiative electron capture by fast, highly stripped heavy ions

23 p3316 A72-44073

Influence of atom-atom collisions on the collisional-radiative ionization and recombination coefficients of helium plasmas

24 p3428 A72-44798

Model potential calculations of lithium transitions

24 p3426 A72-44808

RADIATIVE TRANSFER

NT RADIATIVE HEAT TRANSFER

Feautrier numerical solutions to transfer equation of polarized continuum radiation from sunspot in chromosphere

01 p0101 A72-10096

Planetary atmosphere IR radiative transfer model using matched asymptotic expansions method

01 p0125 A72-10099

Water quality monitoring by radiative transport equation for reflectance measurements of laser light scattered from turbid water polluted with absorber and scatterer particles

[AIAA PAPER 71-1098]

01 p0058 A72-10547

Nonconservative radiative transfer in spherically symmetric system, calculating linearly polarized electron scattering atmosphere

01 p0102 A72-11127

Energy release and accelerating inner stream effects on flow field near fuel injection in gas core reactor, basing Euler equations energy diffusion term on radial radiative transport

01 p0100 A72-13151

Half range diff. rental approximation for spherically symmetric radiative transfer in concentric spheres with and without internal heat sources

02 p0302 A72-12259

Nonstationary radiation transfer with one dimensional anisotropic scattering, deriving Bessel function expressions for quantum exit from semiinfinite medium

02 p0262 A72-12830

Polarization and atmospheric inhomogeneity effects on solar radiative transfer in turbid atmospheres, using diffused reflection and transmission matrices

02 p0222 A72-12836

Spherical harmonics method utilization in radiative transfer calculations, describing characteristic equations roots determination technique

03 p0389 A72-13795

Measurement techniques for electrically heated temperature probes in flames, considering wire sensor diameter and radiative transfer

03 p0456 A72-13925

Grad moment method application to radiative transfer in medium with relativistic differential motions, obtaining Eddington approximation and Thomas radiative-viscosity terms

04 p0579 A72-15322

Singular integral equation in radiative transfer theory with polynomial scattering indicatrices

04 p0597 A72-15643

Rarefied gases thermal energy diffusion model, using radiative transfer electrical network analog

[ASME PAPER 71-WA/HT-4]

05 p0743 A72-15865

Two dimensional time dependent nonlinear radiative transfer and nonequilibrium diffusion in arbitrary geometry by synthesis method

05 p0746 A72-15996

Radiation transport mechanism and transport coefficients in high pressure Ar cascade arc, measuring electric field strength, radiated power and radial temperature distribution

05 p0746 A72-16157

Radiation transfer by resonant scattering in expanding nebula with applications to quasars having blueward absorption wings

05 p0716 A72-16374

Radiative transfer and chemical nonequilibrium phenomena for radiating flow field predictions behind high altitude hypervelocity normal shock waves

05 p0603 A72-16545

Mathematical model for radiative transfer properties of high albedo carbon dioxide and water cryodeposits on opaque substrate

[AIAA PAPER 72-58]

05 p0749 A72-16929

Photon radiative exit from scattering isothermal atmosphere containing atoms with two energy levels

06 p0848 A72-18051

Homogeneous isotropically scattering spherical media atmospheric model for radiative transfer problem, using combined operational method

06 p0842 A72-18083

Boltzmann integrals for inelastic collisions and radiative processes in stationary monatomic plasma, using Grad 8-moment approximation of particles momentum distribution functions

06 p0861 A72-18174

Surface relief effect on radiative properties of solid body with random surface roughness distribution

07 p1098 A72-18934

Solar chromosphere radiative transfer and thermal conduction coupling, applying singular perturbation method to Frisch analysis

07 p1070 A72-19087

Homogeneous isotropic Newtonian and Robertson-Walker cosmological models, discussing radiative transfer and optics
07 p1074 A72-19431

High temperature radiative transfer and hydrodynamics, discussing radiant heat transfer dominant equation, diffusion descriptions, scattering kernel, dispersive media and heavy electron model of scattering
07 p1101 A72-19923

Energy transport within stellar structure, discussing radiative transfer and opacity relationship to mean free path of radiation
07 p1078 A72-19924

Transfer characteristics of solar radio radiation in scattering corona
07 p1062 A72-20230

IR radiation radiative transfer calculation for selected spectral intervals due to various model cloud droplet size distribution
07 p0980 A72-20456

Radiative thermal flux model of Venus atmosphere, using Venera data and greenhouse effect
08 p1233 A72-21193

Self-similar adiabatic expansion of gas behind shock wave front sustained by radiation, describing gas pressure, density and velocity profiles
08 p1152 A72-22049

Radiative transfer equation for solar irradiance penetration of turbid atmosphere and plant canopy, using four point quadrature method
09 p1297 A72-22442

Nongray treatment of nonisothermal IR radiative transfer problem in terms of mean absorption coefficient
09 p1354 A72-22668

Pseudo-hemispherical properties applied to radiative transfer in absorbing-emitting medium involving specular directional surfaces
09 p1351 A72-22671

Phase plane method for one dimensional stationary problem solution in radiative gas dynamics, calculating temperature behind shock wave front
10 p1469 A72-24544

Gas role in radiative transfer and free convection between concentric spheres, noting gray gas assumption validity
[AIAA PAPER 72-280] 11 p1740 A72-25220

Radiative transfer theory for passage wall surface roughness effects on light transmission and reflection
[AIAA PAPER 72-303] 11 p1742 A72-25237

Heat conduction and radiative transfer equations of IR cooling by atomic O in thermosphere
11 p1622 A72-25848

Radiative properties of charged particles moving in attractive Coulomb fields related to repulsive fields by symmetry relationships
12 p1848 A72-28155

Asymptotic and exact methods for light scattering problems in radiative transport theory, discussing finitely thick plane layer luminescence
13 p2001 A72-28503

Numerical methods to solve boundary value problems of monochromatic transport equations in light scattering media optics
13 p2001 A72-28504

Monte Carlo method for radiative transport theory problems, considering mathematical models of light scattering media and photon trajectory random elements
13 p2001 A72-28505

Laplace transform method in unsteady radiation field theory, discussing generalization from steady luminescence to inhomogeneous media and forbidden band frequency radiative transport
13 p2001 A72-28506

Light propagation from unsteady source through homogeneous turbid light scattering media, using analytic and numerical methods for unsteady radiative transport equation solution
13 p2031 A72-28507

Approximate solution to spectral line frequency resonance radiation transport equation, assuming total radiation redistribution with respect to frequencies
13 p2001 A72-28508

Statistical physics multiple wave scattering-phenomenological radiation transfer equation relations, using Green function
13 p2002 A72-28512

Radiation transfer equations solved in isotropic light scattering approximation, relating transfer function to motion picture film optical properties
13 p1955 A72-28519

Nonlinear differential energy equation of static state stellar atmospheres with radiation and heat conduction terms
13 p2036 A72-28890

Sunspot energy deficit relation to model depth, deriving facular model with two dimensional radiative transfer analysis
13 p2045 A72-29712

Energy flux intensity in selectively radiating gas nonisothermal layer from radiant transfer equation and mathematical model
13 p2066 A72-29898

Solar H alpha profile formation from non-LTE radiative transfer solutions through model atmosphere by integro-differential equation technique
13 p2049 A72-29931

Radiative energy transfer through gray gas layer between black concentric spheres at different temperatures
13 p2066 A72-30055

Adiabatic density perturbations damping by radiative viscosity and heat conductivity, taking into account plasma recombination in hot expanding Universe
14 p2148 A72-30202

Gyrosynchrotron radiation fields from mildly relativistic electrons in magnetoactive plasma, studying radiative transfer problem
14 p2138 A72-30556

Atomic hydrogen collisional and radiative transition rates, computing excitation and ionization cross sections
14 p2133 A72-30564

Molecular band model for inhomogeneous radiating gases nonuniform transfer paths based on single collision broadened spectral line growth
14 p2135 A72-30891

Radiative transfer in Mars and above-cloud Venus carbon dioxide atmospheres, studying diurnal variations in temperature profile
14 p2160 A72-30897

Book on extended surface thermal transfer covering heat exchanger design, convective transfer, radiation and computer programs
14 p2172 A72-30975

Radiative transfer in freely expanding gaseous Ba clouds, deriving atomic states level populations ratio
15 p2223 A72-31428

Upward and downward radiative transfer in atmosphere-ocean system model calculated by Monte Carlo method, noting turbidity effect on radiance
15 p2224 A72-31673

Spherical, cylindrical or plane piston motion in nonuniform medium with radiative energy transfer, obtaining approximate analytic solutions and temperature profile behind shock front
15 p2336 A72-32394

Earth atmosphere water vapor mixing ratio profiles from relaxation method for full radiative transfer equation inverse solution
15 p2266 A72-32724

Radiative transfer equation application to ionospheric photoelectrons transport, predicting photoelectrons angular distribution and escape flux
16 p2444 A72-32963

Energy level population and emission spectrum of C IV ion in planetary nebula with radiative excitation
16 p2458 A72-33688

Monochromatic radiation pulse transfer in absorbing plasma, deriving heat wave propagation velocity
16 p2437 A72-33692

Radiant energy transfer in dispersive medium of low optical density under LTE and radiant equilibrium
16 p2427 A72-33859

Transfer of polarized radiation in a stellar atmosphere.
17 p2605 A72-34533

Monte Carlo treatment of Lyman-alpha radiation in a plane-parallel atmosphere.
17 p2598 A72-34538

Eigenvalues and eigenvectors for solutions to the radiative transport equation.
17 p2576 A72-35259

The radiative transfer equation and environmental effects in the upper atmosphere.
[AIAA PAPER 72-663] 17 p2583 A72-35485

Chromospheric structure, magnetic field configuration, radiative transfer and energy balance relationship to solar prominences formation from corona
17 p2616 A72-35693

On the choice of boundary conditions for integration of transfer equations.
17 p2577 A72-35695

Radiation transfer in planetary atmospheres with a three-term scattering indicatrix
17 p2618 A72-35810

General theory of spherically symmetric boundary-value problems of the linear transport theory.
17 p2583 A72-35825

Anomalous motion of radiating particles in strong fields.
18 p2713 A72-36712

Radiation scattering matrix derivation with allowance for phase correlation, deriving method of radiation transfer equations solution for magnetic field
19 p2834 A72-37819

Source function for radiative fields produced by uniform parallel irradiation of scattering absorbing medium of finite optical thickness, using radiative transfer linearity
19 p2834 A72-37837

Effect of atomic polarizability on low-energy free-free radiative transitions.
19 p2837 A72-37839

Stellar emission and absorption line spectra formation in presence of magnetic field interpreted by radiative transfer equation solution, considering dwarf stars observation
20 p2956 A72-39753

Stellar multilevel spectral line formation solution by preconditioning procedure based on core frequency transfer determination by local saturation approximation
20 p2954 A72-39758

Transfer of resonance-line radiation in differentially expanding atmospheres. I - General considerations and Monte Carlo calculations.
21 p3106 A72-41037

Transfer of resonance-line radiation in differentially expanding atmospheres. II - Analytic solution for the case of coherence in the frame of the fluid.
21 p3106 A72-41038

Probability interpretation of radiative transfer to calculate magnetic field-originating spectral line formation dependence on solar atmosphere mean optical depth
21 p3107 A72-41276

Radiative transfer equations solution for stellar spherical atmosphere by Grant-Hunt method, approximating intensity derivative over angular variable with Legendre polynomials
21 p3109 A72-41433

Chou-Tien nonplane-parallel solution to transfer equation for radiation scattering by free electrons in stellar spherical atmosphere by regional averaging procedure
21 p3109 A72-41434

Radiative transport analysis of electromagnetic propagation in isotropic plasma turbulence.
21 p3094 A72-41634

Russian book - Radiation characteristics of gases at high temperatures.
22 p3243 A72-42075

Internal dust effects on nebulae structure and spectrum, solving radiation transfer equation for spherical models with nonisotropic scattering
22 p3227 A72-42558

Unsteady phenomena in the world of stars and galaxies
22 p3230 A72-43153

Adiabatic density perturbations damping by radiative viscosity and heat conductivity, taking into account plasma recombination in hot expanding universe
23 p3333 A72-43231

Methods of solving one-dimensional problems of radiative gasdynamics
23 p3320 A72-43528

Semigray approximation to nongray radiative transfer, taking into account mean absorption coefficient variation with spatial position and photon propagation direction
23 p3314 A72-44328

Radiative transfer in a gray isothermal spherical layer.
24 p3461 A72-44805

Necessary conditions for steady state in radiation-Matter interaction and the role of entropy.
24 p3461 A72-44806

An experimental investigation of radiative properties of aluminum oxide particles.
24 p3461 A72-44809

Radiation properties of the semi-infinite vortex sheet.
24 p3359 A72-44918

Hypersonic flow around plane and axisymmetric bodies of arbitrary shape with inviscid radiating gas.
24 p3360 A72-45110

Influence of a temperature dependent spectral absorption coefficient on radiative flux.
24 p3466 A72-45791

RADIATORS

Electric field distribution in waveguide-slot radiator, describing measurement technique
05 p0635 A72-16333

Reciprocal effects of rectangular guide-slot radiators with circular polarization, analyzing field ellipticity factor change for cross-cut slot under neighboring array slots influence
05 p0635 A72-16336

RADICALS

Radical concentrations in gamma irradiated poly(ethylene 2,6-naphthalene dicarboxylate)/ by ESR spectrum analysis
10 p1433 A72-23847

Utilization of photorecombination of radicals and atoms in continuous-wave lasers.
20 p2932 A72-39508

RADIO ALTIMETERS

Satellite-borne radar altimetry pulse compression, discussing signal return statistics, receiver models and detected waveshape relation to altitude, attitude and antenna beamwidth errors
02 p0172 A72-11870

Computational model of post mixer spectra of periodic FM altimeters with area target returns, using radar scattering coefficient
05 p0637 A72-16568

Geodetic and oceanographic applications of radar equipped satellites in polar orbits for measuring heights along geoid
06 p0809 A72-18259

FM/CW varactor Gunn diode oscillator powered subminiature IC radar altimeter design on homodyne principle for ultralight reliable minimum chance detection 06 p0819 A72-18473

Pulse radar radio altimeter for balloon atmospheric sounding 10 p1484 A72-25088

Statistical analysis of errors in altitude readings of phase comparison AM radio altimeters 11 p1633 A72-26303

Synchronous detector technique for statistical properties improvement in phase comparison AM radio altimeter signal 11 p1633 A72-26304

Statistical error analysis of phase comparison FM radio altimeter during signal processing, investigating range finding strength distribution of echo reflectance 11 p1633 A72-26305

Satellite altimetry based on ocean backscattering, analyzing received signal model and altitude errors 13 p1955 A72-28533

Airborne gravimetry experiment yielding high resolution pressure and altitude measurements, describing equipment 13 p1994 A72-28877

Instrument errors of RF phase comparison altimeter for meteor height measurements, using radar tracked aircraft flights calibration 13 p1957 A72-29029

Skylab radar altimeter for earth surface features remote sensing with high range resolution mode for ocean wave height determination 15 p2236 A72-31995

Collision avoidance system electromagnetic compatibility with radar altimeters designed for 1600 MHz aeronavigation band 21 p3018 A72-40881

RADIO ANTENNAS

Radio astronomy technology developments, discussing antennas, receivers and data processing 01 p0047 A72-10417

Large steerable radio reflectors profile measurement with laser system, describing instrument design, accuracy and modifications 02 p0238 A72-12113

Radio telescope variable profile antenna autocollimation adjustment for separating transmitted and received signals pulse-time characteristics 02 p0231 A72-12521

Circular polarization parasitical signal reduction in variable profile antennas by curved wire grating, noting application to solar magnetic field studies by radio methods 03 p0331 A72-13289

Isolated antenna system for shielded enclosure measurements at 20-200 MHz, discussing associated circuits design and performance tests 03 p0333 A72-14037

Metrology and radio performance of steerable antenna paraboloidal reflector, considering profile measurements by optical range finder and laser methods 04 p0493 A72-15518

Noise parameters of space communication systems ground receiving antennas, considering noise effects on gain and radiation patterns 06 p0783 A72-17499

Radio direction finding with discrete antenna scanning and multilevel beacon signal quantization, investigating accuracy 07 p0943 A72-19523

Balun-fed open sleeve dipole in front of metallic reflector for 225-400 MHz band operation, investigating radiation pattern and gain 07 p0957 A72-19794

Electromagnetic field around thin linear receiving antenna by superposition of incident wave with antenna scattered field, deriving differential equations solution for field lines 08 p1132 A72-21327

Iterative algorithm for digital adaptive null steering of RF antenna arrays, demonstrating feasibility by computer simulation 09 p1289 A72-23416

Vertical angle estimation for HF sky wave multimode signals arrival, noting validity for arbitrary antenna elements polarization 09 p1281 A72-23513

Linear antenna in anisotropic plasma with ion depletion, calculating reactance change due to surrounding dielectric layer thickness 11 p1593 A72-25949

Microwave antenna radiation patterns from far field measurements by radio holograms with probe 11 p1598 A72-26718

Noise factor formula of antenna matched multiple loop radio receiver input network with series connected coupled stages 11 p1598 A72-26732

HF backscatter pulse signal incidence elevation angle measurements based on amplitude ratio of two antennas with different vertical patterns 12 p1783 A72-27779

Airborne OMEGA navigation system performance, discussing transmission facilities, three frequency

receiver, flight tests and optimization of receiving antenna 13 p1998 A72-29191

Correlation between two base-station antennas affected by local scatterers and directions of incoming mobile radio waves. 18 p2661 A72-36846

Switches for high-frequency channels 21 p3026 A72-40317

Determination of the form of the capture area of a receiving antenna on the basis of energy streamlines 21 p3030 A72-40525

Broad-band transistorized receiving antennas in the frequency range between 10 kHz and 10 MHz 21 p3030 A72-40526

Active transistorized directional dipole VHF receiving antennas for ATC and mobile applications and field intensity measurement 21 p3030 A72-40527

Antenna with printed elements for a VOR-S navigation installation 21 p3031 A72-40536

Self-tuning and self-programming antenna matching devices for the frequency range 1.5-30 MHz and their application 21 p3031 A72-40538

VHF-FM radio transmitting antenna for waves of circular, elliptical, and horizontally, vertically, or obliquely linear polarization 21 p3031 A72-40543

Horizontally polarized polydirectional or beam antenna, which is slightly out of round and consists of beam units, for television and FM radio 21 p3031 A72-40544

Propagation constants of electromagnetic waves along an infinitely long conducting wire in a general magnetoplasma. 21 p3092 A72-41266

Evaluation of the reliability of diversity reception by antennas of different polarizations 23 p3271 A72-43777

Thermal energy dissipation in artificial antennas of large broadcasting transmitters studying cooling systems 23 p3278 A72-44311

Wideband antenna test facility. 24 p3389 A72-45554

RADIO ASTRONOMY

Molecular processes in interstellar space and life origin, discussing radio astronomy observations, catalytic action and hydroxyl radicals in galaxies 01 p0128 A72-10398

Radio astronomy technology developments, discussing antennas, receivers and data processing 01 p0047 A72-10417

Sizes, shapes and temporal characteristics of small scale inhomogeneities in F region, using vertical sounding, space diversity reception and radio astronomy 01 p0059 A72-10610

Core sources in Seyfert and normal galaxies, analyzing radio observations by Westerbork synthesis radio telescope at 1415 MHz 01 p0132 A72-11012

Radio source counts at 6 cm by National Radio Astronomy Observatory 140 and 300 foot telescopes 01 p0132 A72-11089

Radome enclosed Haystack parabolic antenna characteristics as radio astronomical instrument, discussing gain, polarization, interference susceptibility and noise temperature 01 p0032 A72-11233

Midlatitude ionospheric radio wave absorption measurements, using radio astronomical polarization method 02 p0172 A72-11945

Radio galaxy and quasar structure from 3.8 cm observations, fitting models to data 02 p0279 A72-12186

Frequency allocation for space research, radio astronomy, time signal and earth resources exploration, reviewing allowable power flux density and emitter power 02 p0177 A72-12386

Emission nebulae in Magellanic Clouds observed at 408 MHz, calculating electron density and total mass 02 p0285 A72-12796

Milky Way Galaxy spiral structure determination, presenting arms anatomy, gas and star kinetics and radio astronomy data 03 p0417 A72-13104

Solar corona research, discussing radio and radar astronomy and UV spectrum observations 03 p0422 A72-13202

Solar outer corona steamer density and temperature data from type 3 solar radio burst observation by space radio astronomy 03 p0424 A72-13223

Large-scale solar coronal magnetic field from optical and radio observations for corpuscular propagation in corona and interplanetary medium 03 p0432 A72-13346

Monochromatic radio emission from decilight years distant stars, discussing search experiment by low noise multichannel receivers 03 p0436 A72-13827

Rf diagnostic technique for carbon and hydrogen /H I/ cloud recombination lines in cool interstellar medium 04 p0570 A72-14525

Cas A, Tau A, Cyg A and Orion Nebula absolute flux density measurements at centimeter wavelengths 04 p0578 A72-15313

Long base radio interferometry at centimeter wavelength for angular measurement accuracy improvement in astronomy and geophysics 04 p0495 A72-15728

Partial solar eclipse observation at 9 mm wavelength on 25 February 1971, noting limb brightening 05 p0718 A72-16509

Maffei 2 galaxy radio maps and H line studies, discussing distances, intrinsic luminosity, flux density and apparent size 06 p0886 A72-18097

Neutral interstellar hydrogen atoms mean volume density from Lyman alpha absorption and radio measurements in solar region 06 p0886 A72-18098

RAE-1 measurements of H radio phenomena in magnetosphere, solar corona and Galaxy, discussing design, calibration and performance 08 p1137 A72-21984

Microwave absorption in high pressure hydrogen based on radio astronomical measurements of Uranus brightness temperature 08 p1239 A72-22088

Cassiopeia A secular flux density decrease relative to Cygnus A and Taurus A at 1.4 and 3 GHz, discussing application to antennas and radio telescopes calibration 09 p1390 A72-23529

Galaxy NGC 253 mass and distance from neutral hydrogen spectral line observations with radio telescope 09 p1391 A72-23533

Radio source observational identification as radio and normal galaxies and quasars, examining models for compact and large double radio source features and mechanisms 10 p1533 A72-23886

Fixed base two element interferometer for radio astronomy, obtaining beavertail radiation pattern by use of earth rotation 10 p1482 A72-24578

Radio continuum survey of spiral galaxies M51 and NGC 5195 for study of galactic magnetic field and cosmic rays origin and distribution 10 p1543 A72-24623

Astronomical identification of optical objects near 5C2 radio sources position, noting probability parameters and measurement error 10 p1546 A72-24837

Radio methods for cosmological model testing, discussing radio telescope requirements, source sampling procedures and counts as basic cosmological data 10 p1549 A72-25054

Radio observation of neutral hydrogen near galactic center, noting expanding and rotating ring of gas from kinematic model 12 p1867 A72-27211

Low noise receivers in radio astronomy, discussing accuracy requirements for line measurements and very long baseline interferometry 12 p1792 A72-27806

Pulsar 21 cm pulse profile measurement, discussing installation design and operational principles 12 p1872 A72-27809

Linear detectors for broadband and high intermediate frequency measurements in radio astronomy 12 p1793 A72-27810

Solar radio astronomy instrumental requirements for 20 meter wavelength interferometry, metric and decametric flux and polarization measurements 12 p1872 A72-27815

Midlatitude ionospheric radio wave absorption measurements, using radio astronomical polarization method 13 p1920 A72-29257

Solar maps from quiet sun center limb microwave radio telescope observations during cycle maximum 13 p2048 A72-29742

Saturn thermal radio emission brightness temperature calculations for subcloud atmosphere ammonia abundance evaluation 14 p2152 A72-30490

Crab pulsar LF radiation polarization parameters and pulse shapes, showing highly polarized precursor component 14 p2156 A72-30567

Venus and earth atmospheres dissimilarity from radio astronomy and space probes observations 14 p2158 A72-30695

Planetary nebulae RF observations comparison with optically determined H-beta intensity for extinction coefficients 15 p2307 A72-31797

- Ku band radio interferometer for discrete radio sources mapping, discussing construction and incorporated PDP-8 computer for pointing, tracking, delay compensation and data analysis 15 p2207 A72-32107
- High resolution radio observation of H II region W 51, noting compact components with emission measures agreement with recombination line data non-LTE analysis 16 p2457 A72-33684
- Galactic radio feature Loop III extension south of galactic plane from Jodrell Bank Mk I radio telescope observations at 38 MHz 16 p2458 A72-33690
- Radio maps of extragalactic sources at 2.7 and 5.0 GHz presented with physical data for various components 16 p2458 A72-33718
- Pulsars MP 1055, PSR 1556-44 and MP 1700 discovery in search within radio source survey at Molongui Radio Observatory 16 p2459 A72-33723
- Pulsars radiation mechanism relationship to magnetospheric conditions, considering optical, X ray and gamma radiation 16 p2460 A72-33928
- Decametric radio identification of an extragalactic X-ray source. 17 p2604 A72-34520
- Microwave absorption in high pressure hydrogen based on radio astronomical measurements of Uranus brightness temperature 17 p2606 A72-34651
- Radio detection of Cygnus X-3. 17 p2612 A72-35366
- Radio observations of Cygnus X-3. 17 p2612 A72-35367
- The structure of the Crab Nebula at 2.7 and 5 GHz. 19 p2855 A72-37340
- Saturn thermal radio emission brightness temperature calculations for subcloud atmosphere ammonia abundance evaluation 19 p2864 A72-38319
- Magellanic clouds structure and dynamics from optical and radio observations, discussing interconnecting magnetic field existence 19 p2865 A72-38481
- 1400-MHz survey of bright galaxies. 19 p2866 A72-38501
- Accurate positions of radio sources at 408 MHz. 19 p2868 A72-38698
- Radio position accuracy of pulsar PSR 1749-28 from lunar occultations compared to time of arrival measurements 20 p2969 A72-39388
- A tabulation of pulsar observations. 20 p2969 A72-39390
- Radio astronomical event visible image generation by electro-optical processing comparing SNR performance and electronic complexity with conventional technique 20 p2904 A72-39787
- The type IIIb burst - A precursor of decametre type III radio-burst. 20 p2965 A72-39882
- Low-noise parametric amplifiers for radio astronomical observations at 18 to 21 cm wavelengths 21 p3025 A72-40303
- Multiple-frequency operation of the Culgoora radioheliograph. 21 p3053 A72-40397
- Spherical reflector as possible antenna for millimeter wave astronomy, discussing feed design for spherical aberration corrections 21 p3029 A72-40519
- Flux densities, positions, and structures for a complete sample of intense radio sources at 1400 MHz. 21 p3105 A72-40575
- A two-element telescope of high collecting efficiency for sub-millimetre astronomy. 21 p3055 A72-40825
- Observations of linear polarization of radio sources at 7.2 cm. 21 p3109 A72-41326
- A dual frequency, dual polarized feed for radioastronomical applications. 21 p3034 A72-41400
- A longitude survey of radio recombination lines from the diffuse interstellar medium. 22 p3227 A72-42552
- 21 cm observations of NGC45. 22 p3229 A72-42995
- Amplitude-time and polarization characteristics of the subpulses of the CP 1133 pulsar 22 p3230 A72-43136
- A study of galactic supernova remnants. II - Supernova rate, galactic radio emission and pulsars. 23 p3337 A72-43829
- The techniques of present-day radioastronomy. 24 p3439 A72-49466
- RADIO ASTRONOMY EXPLORER SATELLITE**
Radio Astronomy Explorer Satellite data on solar bursts, interstellar medium ionized component distribution, cosmic rays and galactic halo magnetic fields 03 p0330 A72-13067
- RADIO ATTENUATION**
Electron density profile determination in D region based on frequency dependence of radio waves absorption, discussing lower ionosphere anomalous ionization 01 p0059 A72-10595
- Aerial Radiological Measuring System for environmental radiation detection and tracking, emphasizing snow mass prediction by terrain radiation attenuation measurement 02 p0215 A72-11884
- Radio wave polarization orthogonality recovery by using differential phase shifter and attenuator in radio communication systems 02 p0183 A72-12799
- Hf radio wave reflection at vertical incidence from ionosphere, calculating distance attenuation by ray-tracing techniques 04 p0487 A72-14886
- Ionospheric absorption measurements at 2.2 MHz by vertical incidence pulse sounding method, observing diurnal and seasonal variations 04 p0518 A72-14965
- Ionospheric radio absorption, observing diurnal and seasonal variations and sunspot numbers and solar flares effects 04 p0518 A72-14966
- Anomalous changes in ionospheric radio absorption during winter at midlatitudes, investigating diurnal and seasonal variations and stratospheric warming 04 p0518 A72-14967
- Nighttime radio absorption from lower ionospheric ionization by Sco X-1 and Tau X-1 X rays, using full wave admittance method 04 p0519 A72-15161
- Atmospheric molecular and aerosol absorption effects on submillimeter radio wave propagation using laser, BWT and liquid He receiver-transmitter devices 04 p0551 A72-15607
- D region ionization by electron fluxes as explanation for latitudinal radio wave absorption 05 p0656 A72-16249
- Radio wave absorption during oblique propagation through ionosphere from vertical measurements, using rhombic antenna at 25 MHz 05 p0657 A72-16267
- N/h/ electron concentration profile in ionospheric D layer by exponent of frequency dependence of radio wave absorption 05 p0627 A72-16401
- Radio attenuation above 10 GHz based on theoretical model of equivalent precipitation on path using intensity spatial distribution function within rain cell 07 p0940 A72-19189
- Round-the-world short wave signals propagation and waveguides effective volume and attenuation characteristics, relating ionospheric effects and nonlinear beam defocusing 08 p1130 A72-20704
- Radio absorption in lower ionosphere obtained from vertical distribution of electron density and production rates from solar protons energy spectrum 08 p1226 A72-20816
- Magnetic field effect on ELF radio wave attenuation during propagation under six ionospheres, showing dependence of minimum on propagation path geomagnetic latitude 08 p1131 A72-21103
- Plasma inhomogeneities effect on radio wave absorption in interstellar clouds of ionized hydrogen, analyzing cosmic radio emission spectrum 08 p1231 A72-21120
- Atmospheric vertical humidity profile from ground measurements of radio wave absorption at 1.35 cm water vapor line 08 p1158 A72-21192
- Wind and density measurements by small sounding rockets, comparing results with ground observed radio wave absorption diurnal variations 08 p1160 A72-21531
- D region neutral gas winds, density changes and short wave radio absorption correlation, determining air mass flow rates from chaff fall rate measurements 08 p1160 A72-21532
- Radio signal attenuation by thin overdense plasma boundary layer on reentry body as function of incident power 08 p1135 A72-21624
- Radio absorption and scattering cross sections of thin cylinder with arbitrary electron density distribution in ionosphere, observing resonance effects 08 p1239 A72-21890
- VLF signals Antarctic ice cap attenuation determined at Byrd station from relative phase and amplitude observations over short and long great circle paths 09 p1281 A72-23511
- Venusian atmosphere RF refractive attenuation height dependence, field strength measurements comparison, inversion layer influence and surface echoes effects 10 p1541 A72-24501
- Radio attenuation by rain at 37 GHz using sun as source compared with sky emission observations, noting apparent absorber temperature effect 12 p1783 A72-27665
- Ionospheric radio adsorption measuring device with readout data convenient for visual and computer processing, discussing block and circuit diagrams 13 p1955 A72-28602
- E region electron collision frequency vertical distribution by ground measurement of radio wave absorption, using electron concentration data obtained by rocket-borne interferometer 14 p2100 A72-30462
- Ionospheric attenuation of 3-100 MHz radio waves, interpreting scatter mode propagation mechanism as total reflection from lower ionizational irregularities 14 p2086 A72-30658
- Mathematical models for radio attenuation in ice by electromagnetic absorption and reflection from interfaces, noting radar tracking 16 p2363 A72-33290
- Material injection RF blackout alleviation and plasma diagnostic measurement with electrostatic probes and S-band reflectometer during RAM C-III reentry flight [AIAA PAPER 72-690] 16 p2365 A72-34052
- Collisional losses in a very-low-frequency duct associated with the lower-hybrid-resonance frequency. 17 p2517 A72-35608
- Signal reflection height seasonal variations effect on radio waves absorption estimation from vertical ionospheric sounding 18 p2662 A72-36881
- Circumterrestrial short wave signals propagation and waveguides effective volume and attenuation characteristics, relating ionospheric effects and nonlinear beam defocusing 19 p2765 A72-38332
- An improved design and measurement of attenuation characteristics of RF suppressors. 20 p2902 A72-38997
- Linear cross polarization and attenuation measurements on terrestrial link at 11 GHz correlated with rainfall information 21 p3017 A72-40855
- Extending the range of attenuation measurements. 21 p3022 A72-40999
- A presumptive formula for snowfall attenuation of radio waves. 21 p3023 A72-41829
- Propagation loss of centimeter and millimeter waves in rainfall. 21 p3023 A72-41833
- Sodium to calcium ion abundances ratio variation model in interstellar clouds, comparing with pulsar dispersion and LF radio absorption measurements 22 p3224 A72-42383
- Magnitude of the attenuation troughs of a two-branch filter with multiple-frequency quartz resonators 23 p3272 A72-44170
- Ionospheric radio absorption measuring device with readout data convenient for visual and computer processing, discussing block and circuit diagrams 24 p3402 A72-45102
- RADIO AURORAS**
Optical aurora relationship to radio counterpart, showing backscattered signal peak amplitude close correlation to magnetic bay peaks 01 p0056 A72-10440
- Radio auroral electrojet aspect sensitivity and Farley two stream instability, discussing magnetic field distortion and orthogonal deviation as function of current strength and direction 07 p0976 A72-19163
- Vertical density gradients as source of two stream instability irregularities in radio aurora theory 07 p0976 A72-19164
- B type discrete radio aurora theoretical prediction based on drift gradient instability, comparing with observations 13 p1951 A72-29651
- Radio aurora ion-acoustic wave propagation direction divergence due to magnetic field distortion by large ionospheric horizontal sheet current [AD-746367] 13 p1923 A72-29662
- Plasma instability theories for radio auroras, reviewing radar and radio observation systems and ion acoustic and drift gradient predictions 14 p2098 A72-30140
- The occurrence of radio aurora at high latitudes - The IGY period, 1957-1959. 20 p2904 A72-39982
- RADIO BEACONS**
Radio aids for air navigation and traffic control in Italy, discussing facilities development 02 p0257 A72-12748
- Radio direction finding with discrete antenna scanning and multilevel beacon signal quantization, investigating accuracy 07 p0943 A72-19523
- ILS development, discussing four course radio ranges, autoland and radar systems 09 p1349 A72-23449

- ATS F/G radio beacon experiments for study of exosphere and ionosphere integrated electron content, spatial structure and time dependent behavior
12 p1782 A72-27526
- Ground station-observed balloon-borne radio beacon method for Finnish stellar triangulation network measurement
15 p2226 A72-31929
- Computational method for determining numerical values of relativity by two-way Doppler radio tracking and ranging data from planetary orbiting spacecraft
15 p2310 A72-31978
- Observations of scintillations of two satellite beacons near the boundary of the irregularity region.
20 p2916 A72-39227

RADIO BLACKOUT

U BLACKOUT (PROPAGATION)

RADIO BROADCASTING

U BROADCASTING

RADIO BURSTS

NT SOLAR RADIO BURSTS

Bit error rate estimation for narrow band digital communication in presence of atmospheric radio noise bursts

Burst and quasi-continuous forms atmospheric radio noise short term time characteristics above different thresholds, considering pulse duration and spacing
01 p0025 A72-10334

Jupiter decameter radio burst possibility as indicator of high velocity fluxes and shock waves in solar wind
01 p0031 A72-10998

Expanding source model for quasars and Seyfert galaxy nuclei radio outbursts from extension of radio galaxy evolution models
02 p0273 A72-11935

Aerospace type electroexplosive devices gross sensitivity to short damped rf energy burst
04 p0573 A72-14874

Velocity space instability in hot electron plasma created by adiabatic compression in pulsed magnetic mirror, observing radiation bursts below electron cyclotron frequency during compression
08 p1213 A72-21257

Narrow band frequency drifts of polarized Jovian L bursts from simultaneous radio observations
10 p1532 A72-23713

Three station interferometer observations of Jovian decametric burst at 18 MHz, discussing possible solar wind interference
12 p1871 A72-27743

Jupiter decameter radio bursts as indicator of high velocity fluxes and shock waves in solar wind
13 p2030 A72-29247

Io effects on Jupiter decametric radio bursts, discussing ionosphere vs solid surface for required conductivity
16 p2455 A72-33465

Solar wind velocity near Jupiter correlated to Io geocentric phase during radio bursts, noting plasma-sphere models
16 p2459 A72-33904

Correlation studies of solar X-ray and radio bursts.
17 p2600 A72-35318

Extensive air showers and the sporadic decameter radio emission of Jupiter
19 p2863 A72-38073

RADIO COMMUNICATION

NT PULSE FREQUENCY MODULATION

TELEMETRY

NT RADIO RELAY SYSTEMS

NT RADIO TELEGRAPHY

NT RADIO TELEMETRY

NT TELEPHONY

NT TELEPHOTOMETRY

Radio communication accuracy characteristics in calculation of maximum frequency, skip distance and emission angle by transmission curves for midlatitude ionosphere
01 p0028 A72-10600

Tropospheric layer structures effect on long range vhf radio communication, calculating wave modes attenuation rate and electric field patterns
01 p0032 A72-11238

Italian monograph on ionospheric radio propagation, covering weather forecasts and radio communications
03 p0323 A72-13844

Electromagnetic-thermal properties of lunar surface layers for radio communication around moon
04 p0577 A72-15121

Optimal two stage signal search in frequency vs arrival time indeterminacy plane of communication system
04 p0487 A72-15148

Communication satellites for European radio and TV broadcasts, discussing use of American, CETS-C and Symphonie satellites
04 p0494 A72-15677

Symphonic communication satellite applications in radio and TV broadcasting, discussing Retelsat network, Socrate and Memini projects, educational TV, etc
04 p0494 A72-15680

Airline air/ground radio communications and data link service implementation for San Francisco-Hawaii center
06 p0770 A72-17337

AM/PM distortion intermodulation in FM/FDM radio systems during two-path propagation, using Fourier series method for noise power spectra calculation
06 p0775 A72-18239

Communication satellites rf assignment by ITU for prevention of jamming, discussing radio communication conferences regulatory actions
07 p1104 A72-19469

Radio communication system optimization from viewpoints of global synthesis, including economics and partial synthesis based on noise stability, precision and reliability
08 p1136 A72-21845

Optimal answer-back communications systems using feedback channel for error checking
09 p1277 A72-22568

Russian papers on ionospheric perturbations and effects on radio communication covering vertical ionization profiles, F 2 critical frequencies, short wave propagation, etc
11 p1593 A72-26266

AMSAT-OSCAR-B series of radio communication satellite for worldwide use with low cost terminals in amateur and education services
12 p1779 A72-27351

Aircraft antennas design for radio links to satellites for aeronautical communication and ATC, proposing use of beam steering system
13 p1932 A72-29347

Data system in Eole satellites program, discussing balloon localization, UHF information transmission and reception, distance measurement and data acquisition
15 p2268 A72-31981

Time sharing radio communication system analysis with amplitude modulated carrier, noting power reduction, sideband content and multiplexing
15 p2201 A72-32566

Russian monograph on ionospheric measurements covering plasma parameters, wave propagation, absorption sounding methods and radio communication applications
16 p2387 A72-33875

A comparison of voice communication techniques for aeronautical and marine applications.
17 p2512 A72-34267

Shaping circuit for complex RF pulse consisting of simultaneous equilength square pulses with different frequencies, discussing carrier frequencies selection
21 p3022 A72-41118

Optimum reception algorithms in communication systems with decision feedback in presence of noise in forward and return channel
24 p3379 A72-44747

Potential of the navy navigation satellite system in predicting ionospheric characteristics.
24 p3447 A72-45555

RADIO CONTROL

Unified single rf channel tracking, telemetry and command control systems for guidance of unmanned vehicles, including pilotless aircraft and satellites
05 p0685 A72-16556

RF augmentation in CO2 closed-cycle dc electric-discharge convection lasers.
17 p2565 A72-35818

Spacecraft antenna feeder channel parameter control in flight
21 p3026 A72-40319

Pressure dependent microwave cavity breakdown field relationship to steady state plasma luminosity interpretation as evidence of RF confinement of low density plasma
22 p3212 A72-42897

Noise resistance of optical communication links with radio and optical AGC systems
23 p3264 A72-43770

RADIO DIRECTION FINDERS

Phase comparison direction finder with successive signals comparison using commutation of two antenna elements for target acquisition and tracking operations
02 p0176 A72-12219

Covariance matrix of coordinate fluctuations of instantaneous radar center of reflection from set of scatterers
04 p0487 A72-15144

Radio direction finding techniques using amplitude-trigonometric interpolation between signals received at circular antenna array
05 p0628 A72-16555

Two-channel direction finding with point source emission and spaced antennas reception, investigating cross correlation and background noise interference effects on accuracy
07 p0938 A72-19007

Radio direction finding with discrete antenna scanning and multilevel beacon signal quantization, investigating accuracy
07 p0943 A72-19523

FM/CW interferometric ionosonde used for interferometric direction finding, computing incident

azimuth and elevation from baseline array phase differences
09 p1281 A72-23514

Amplitude comparison direction finding systems, calculating error due to clutter from incident signal and noise angular distribution relationship to measured arrival angle
10 p1439 A72-24803

Minimum sidelobe radiation level of circular aperture antennas as function of gain and direction finding characteristics
11 p1597 A72-26709

Adcock direction finder errors due to diurnal and sporadic ionospheric variations and tilting layers effects on reflected signal
12 p1804 A72-27780

Arrival angles of radio wave reflected from ionosphere for remote short wave transmitter direction finding
13 p1917 A72-28601

Error investigation for the location of the sources of atmospherics by radio direction finding.
18 p2706 A72-36429

A high-accuracy radio direction finder with a moving antenna
23 p3270 A72-43769

Arrival angles of radio wave reflected from ionosphere for remote short wave transmitter direction finding
24 p3380 A72-45101

Utilization of a satellite system for navigation and control of shipping
24 p3422 A72-45224

RADIO ECHOES

Lindauer electron density profile for maximum F layer over sunspot cycle using frequency dependent radio ground echo in satellite ionograms
01 p0054 A72-10421

Differential phase shift and absorption measurements of partially reflected radio waves, providing electron density and collision frequency data from 70-90 km
01 p0030 A72-10836

Numerical analysis of radio echoes decay rate from randomly ionized meteor trails
01 p0130 A72-10913

Reflection and transmission coefficients for radio waves incident upon thin highly ionized layers, comparing with sporadic E reflections
03 p0344 A72-12976

Wideband microwave acoustic delay line design featuring superior bandwidth, phase linearity, spurious echo and insertion loss characteristics
04 p0521 A72-14720

Hf radio wave reflection at vertical incidence from ionosphere, calculating distance attenuation by ray-tracing techniques
04 p0487 A72-14886

Elliptical polarization and depolarization coefficients for monochromatic radio waves reflected from F 2 ionosphere using Stokes parameters
05 p0656 A72-16241

Electron concentration and collisions number fluctuations effect on D region profiles based on radio waves partial reflection data
05 p0656 A72-16244

Geomagnetic pulsations correlation with h type ionospheric sporadic echoes, considering effects on electromagnetic disturbances transmission
05 p0659 A72-16725

Midlatitude F region wavelike disturbances detection by hf radio echo techniques, discussing correlation with jet stream associated tropopause wind patterns
07 p0974 A72-18885

Ionospheric drift characteristics from vertical and oblique radio soundings, discussing instrumental effects
08 p1156 A72-20818

Diurnal fluctuations in radio echo producing ionospheric region horizontal scale and height, discussing dependence on solar position
08 p1131 A72-20819

Meteors radio echo duration dependence on electron attachment, photodetachment and turbulent and ambipolar diffusion deionization processes
09 p1383 A72-22502

Nighttime radar method of meteor radio echo observation to determine electron attachment rate to neutral air particles
09 p1383 A72-22504

Radio echo determination of meteor body distribution by mass with allowance for electron attachment and overestimated nighttime values
09 p1383 A72-22505

Electron attachment, photodetachment and turbulent diffusion deionization effects on duration distribution of Geminid meteor radio echoes
09 p1384 A72-22512

Radio echo observation of Quadrantid meteor showers right ascension and declination, observing mean range and influx rate as function of universal time
10 p1545 A72-24808

Small scale wind shear effects on overdense and underdense radio meteor echoes, noting premature decay and scatter in decay time

10 p1440 A72-24952
Single pulse radio echo fading dependence on sporadic E layer critical and screening frequencies

11 p1595 A72-26282
Statistical error analysis of phase comparison FM radio altimeter during signal processing, investigating range finding strength distribution of echo reflectance

11 p1633 A72-26305
Ionospheric scattered wave propagation mode and weak echo delay explained by analysis-derived model

11 p1597 A72-26570
Mode coupling effects on radio wave partial reflection from lower ionosphere at vertical incidence, using matrix perturbation analysis

11 p1599 A72-26764
Circularly polarized ultrashort radio wave reflection from lunar and planetary surfaces, determining angular scattering spectrum

11 p1599 A72-26908
Automatic statistical analyzer for radio meteor echo multiplicity recording in three coordinate /multivariable/ space, including instrument error allowance

13 p1929 A72-29032
Amplitude probability distribution of radio waves reflected from traveling ionospheric disturbances superimposed on small scale irregularities

13 p1921 A72-29338
Upper atmosphere horizontal wind velocity from meteor trails radio echoes, noting structural function anisotropy

14 p2127 A72-30263
Radio wave reflection from ionosphere, determining polarization and fluctuation characteristics via Stokes parameters

14 p2100 A72-30636
Meter and decimeter wave reflected signals distribution and surface backscattering patterns effective bandwidth investigation by method based on Doppler effect

14 p2086 A72-30792
Lunik 14 spacecraft radio signal reflection from lunar surface, showing energy spectrum dependence on surface roughness

15 p2202 A72-32655
D region electron concentration and collision frequency with neutral molecules from radio waves backscattered by inhomogeneities in propagation medium

16 p2385 A72-33484
Auroral radio reflection regions spatial distribution from radar measurement, noting backscattering indicatrix independence on geographical latitudes

17 p2519 A72-35873
Results of simultaneous measurements of the spectrum of auroral radio echoes at two frequencies

17 p2519 A72-35874
Influence of ionospheric currents on the geometry of auroral radio echoes

17 p2519 A72-35875
Relationship between auroral radio echoes and other geophysical phenomena

17 p2519 A72-35876
Signal generator designed for calibration and control of interferometric radar station to observe and study radar echoes induced by meteor trails

17 p2519 A72-35959
The interpretation of ionospheric radio drift measurements. V - Demonstration of the point effect in time-averaged correlations and drift calculations.

19 p2794 A72-38862
Recent work on ionospheric irregularities and drifts.

20 p2920 A72-39981
Lateral deviation of radio waves reflected from ionosphere.

21 p3022 A72-41321
Reflection and refraction of radio waves from the ionosphere in presence of time-varying irregularities.

22 p3154 A72-42302
An investigation of the ground diffraction pattern of radio waves reflected by the ionosphere.

22 p3154 A72-42362
The effect of meteoric ion processes on radio studies of meteoroids.

23 p3336 A72-43558
Characteristics of nonuniform regions responsible for microwave signals auroral scattering, noting observations with two sidelobes radio interferometer

24 p3397 A72-45084
Arrival angles of radio wave reflected from ionosphere for remote short wave transmitter direction finding

24 p3380 A72-45101

RADIO ELECTRONICS
Progress in radio science 1966-1969 - Conference, Ottawa, August 1969, Volume 3, radio waves and circuits and radio electronics

02 p0190 A72-11676
Russian book on penetrating radiation effect on radio components covering resistors and capacitors electrophysical characteristics and parameters changes under gamma and neutron radiation

12 p1793 A72-28342

RADIO EMISSION

NT RADIO BURSTS
NT SOLAR RADIO BURSTS
NT SOLAR RADIO EMISSION

Earth surface thermal radio emission measurements by UHF radiometry onboard Cosmos 243 satellite, showing brightness profiles of water, ice and land areas

01 p0053 A72-10363
NGC 5128 nucleus radio emission flux density measurement, noting angular size

01 p0132 A72-11090
Martian radio emission at 8.57 mm during 1971 approach, comparing brightness temperature to Jupiter

02 p0280 A72-12196
Synchrotron and thermal H II region radio emission in Magellanic Clouds

03 p0425 A72-13259
Monochromatic radio emission from decilight years distant stars, discussing search experiment by low noise multichannel receivers

03 p0436 A72-13827
Saturn radio emission and brightness temperature measurements, determining rings optical thickness upper limit

03 p0438 A72-13977
Quasar radio and optical luminosity evolution, criticizing Arakelian method

03 p0439 A72-14297
Gum Nebula size, emission features and expansion dynamics, discussing Zeta Puppis UV spectrum and Vela X radio emission

03 p0440 A72-14364
Pulsar PP 0943 radio emission, showing short time intensity increases

04 p0581 A72-15514
Radio emission from compact extragalactic objects, including quasars and nuclei of compact, Seyfert and N type galaxies

05 p0716 A72-16376
Quasar radio structure, investigating morphology, statistical characteristics, angular size of spectra and red shift correlations from interferometer measurements

05 p0716 A72-16377
Extensive air showers radio emission polarization, spatial distribution and electric field strength, noting geomagnetic mechanism effect

06 p0870 A72-17278
Radio emitting giant loops in the Galaxy, considering supernova radiation induced nebulae model to explain spectral and polarization properties

06 p0876 A72-17649
Venus 8.2 mm radio emission dependence on sun-light phase angle, considering implications regarding day/night atmospheric temperature variations

06 p0884 A72-18031
Astronomical model for Jovian decametric radio emission control by Io satellite based on two surface sources on planet and particle interaction with plasma

06 p0891 A72-18504
Scorpius X-1 and Cygnus X-1 pulsed radio emission search by sensitive de-dispersing technique

07 p1073 A72-19422
Radio emission of galactic clusters at 1.4 and 2.7 GHz, computing mean electron density and hydrogen gas mass

07 p1075 A72-19577
Radio emission of Lupus region believed to contain supernova of 1006 A.D., noting strong polarization

07 p1076 A72-19607
Radio telescope for cosmic radio emission reception at 50-2 cm wavelengths, describing parabolic and auxiliary reflectors

07 p0965 A72-20299
Auroral ionosphere radio self emission at supercritical frequencies from accelerated protons charge exchange effects, comprising radio bursts, storms and amplifications

08 p1153 A72-20713
Interferometer detection of variable radio emission associated with X ray source GX9 plus 1, observing also GX349 plus 2 and GX350 plus 0

08 p1232 A72-21176
Radio emission from pulsar CP 1133, comparing amplitude and polarization characteristics of two subpulses

09 p1387 A72-22987
Saturn radio emission detection and measurement at 49.5 cm, determining equivalent disk brightness temperature

10 p1531 A72-23710
Galactic center radio, IR, X ray, gamma ray and molecular spectral features, considering models for source component emission mechanisms and energy densities

10 p1533 A72-23887
Pulsar electrodynamic properties, radiation mechanism, galactic distribution and pulse shape, period distribution and propagation characteristics, reviewing Crab Nebula pulsar features

10 p1533 A72-23888
Quasars as cosmological and local objects, considering red shift origin and optical and radio luminosities comparison with galaxies

10 p1541 A72-24522

Radio emission variations of eclipsing binary stars beta Persei and beta Lyrae tabulated

10 p1547 A72-24946
Ionospheric total electron content measurement by satellite radio emissions

11 p1632 A72-25840
Venus 8.2 mm radio emission dependence on sun-light phase angle, considering implications for day/night atmospheric temperature variations

11 p1719 A72-25967
Galactic H II regions with radio emission at 1400 MHz, using National Radio Astronomy Observatory 300 ft telescope

11 p1724 A72-26785
Elliptical radio galaxies and quasars intrinsic emitted radio power correlation to spectral indices interpreted as evolutionary track in terms of model

12 p1867 A72-27210
Lunar microwave emission, constructing thermophysical models for radio observations and brightness temperature variations

12 p1869 A72-27327
Geomagnetic field perturbation by gamma quanta pulsating source, studying accompanying radio emission behavior

14 p2101 A72-30645
Saturn rings gas-dust atmosphere, thickness and motion, considering planetary radio emission and brightness temperature

14 p2161 A72-31073
Radio emission due to relativistic electrons spiral orbit motion in rotating pulsating neutron star

15 p2304 A72-31333
Callisto radio emission analysis by ice body model, noting brightness temperature calculation of ice surface

15 p2308 A72-31904
Lateral distribution, radiation spectra and pulse shapes calculated from mathematical models of cosmic ray showers radio emission, noting chemical composition of primary particle

15 p2230 A72-32262
Model for VLF emissions triggered by whistlers and man-made radio signals, noting effects of wave packet and second order resonance

16 p2365 A72-33905
NP 0532 precursor pulse as radiation scattered from main pulse beam by ring of material centered on pulsar

17 p2603 A72-34192
Association between quasi-periodic VLF emission and micropulsation.

17 p2516 A72-35065
Investigation of energetic charged particles and VLF emissions on the 'Interkosmos-3' satellite

17 p2600 A72-35209
Strong beaming of Jupiter's non-lo-related radio emission.

17 p2610 A72-35224
Arch prominence outside west limb on 24 April 1971, noting H alpha monochromatic image, internal motion of matter and radio emission

17 p2614 A72-35503
Auroral cosmic radio emission absorption mechanisms, considering ionization rate, recombination coefficient and collision frequency effects

17 p2602 A72-35865
Bremsstrahlung as a possible source of UHF emissions from lightning.

19 p2828 A72-37894
Measurement of Jovian radio emission at a wavelength of 2.94 m

19 p2864 A72-38080
Radio luminescence of an yttrium-aluminum garnet activated by rare-earth elements

19 p2845 A72-38181
Auroral ionosphere radio self emission at supercritical frequencies from accelerated protons charge exchange effects, comprising radio noise bursts, storms and amplifications

19 p2790 A72-38341
Pulsars as stellar population, considering physical models, pulse emission radiation mechanism and use in galaxy studies

19 p2865 A72-38476
VLF emission artificial triggering by whistler morse pulses in magnetosphere, explained in terms of resonant trapped particle current and wave field behavior

20 p2903 A72-39549
Electrodynamic effects of Jupiter's satellite Io.

21 p3104 A72-40483
Observations of sources of maser radio emission with an angular resolution of 0.0002 sec

21 p3101 A72-41751
Polarized radio emission from five supernova remnants.

22 p3229 A72-42994
Investigation of EAS characteristics at sea level with the aid of the classical method and by the method of recording radio emission

23 p3330 A72-44423
Thin ice crust, chondritic composition and ionosphere considerations for Io electrical conductivity and decametric radio emission modulation in unipolar inductor model

24 p3437 A72-44704

Micropulsations and VLF emissions during substorms.
24 p3396 A72-44855

RADIO ENERGY

U RADIANT FLUX DENSITY
U RADIO WAVES

RADIO EQUIPMENT

NT IONOSONDES
NT RADIO ANTENNAS
NT RADIO BEACONS
NT RADIO FILTERS
NT RADIO RECEIVERS
NT RADIO TELESCOPES
NT RADIO TRANSMITTERS
NT RADIOSONDES
NT RADIOTELEPHONES
NT RAWINSONDES
NT RECEPTION DIVERSITY
NT SPACECRAFT ANTENNAS
NT SUPERHETERODYNE RECEIVERS
NT TRANSMITTER RECEIVERS
NT TRANSPONDERS
NT VERY HIGH FREQUENCY RADIO EQUIPMENT
NT WHISTLER RECORDERS

Soviet book on aircraft radio equipment covering transmission and reception, velocity and coordinates measurements, siting and navigation, flying target interception, reconnaissance, landing systems, etc
05 p0637 A72-16530

Radio system operational reliability analysis by mathematical methods with use of digital computer, discussing statistical modeling algorithm
08 p1143 A72-22065

Economic factors influence on reliability optimization of complex radio systems and elements
08 p1143 A72-22066

Radio system failure prediction based on parameter variation a priori or a posteriori data, determining reliability and optimal preventive maintenance intervals
08 p1143 A72-22070

Radio electronic equipment IC and microelectronics development trends, considering bipolar and MOS transistors applications in digital and analog computers and telemetry
10 p1454 A72-25176

Russian book on radio component design covering radio equipment component properties, effects of geometry and materials, technological processes and microelectronics
17 p2531 A72-35496

Reliability estimation for actively redundant radio electronic systems
19 p2774 A72-38424

Differential equations for digital model of linear quadrupole, discussing digital simulation of analog radio equipment circuits
19 p2775 A72-38659

Technical and economic processes representation of radioelectronic equipment synthesis optimization using elementary random magnitudes involving output parameters deterioration rates and fabrication tolerances
23 p3269 A72-43442

Allowance for correlation in the prediction of reliability parameters for radio equipment
23 p3270 A72-43767

Linear theory of a microwave distributed amplifier based on an avalanche transit-time diode
23 p3271 A72-43776

Calculation of the temperature field in a ventilated cassette-type radio electronic device
24 p3386 A72-45324

RADIO FILTERS

Optimal filter and polarity coincidence correlator signal detection efficiency for arbitrary noise distribution
02 p0176 A72-12217

Transient characteristics of phase lock automatic frequency control system with integrating filter, using nonlinear phase-plane method
02 p0176 A72-12224

Stability conditions and effective bandwidths of first and second degree pulsed phase locked AFC systems with proportionately integrating filter, using Z transform method
05 p0625 A72-15825

Frequency characteristics effect to determine voltage and current smoothing coefficients and resistances of transistor ripple filter with emitter circuit load
05 p0634 A72-16168

Passive radio interference filtration analysis, obtaining SNR maximization by ambiguity function partial volume minimization
07 p0937 A72-18848

Nonorthogonality noise at matched radio filter output between stations operating simultaneously in same frequency band in discrete address wideband communication system, defining minimum SNR conditions
07 p0937 A72-18849

Capture range and acquisition time analysis of phase locked loop with active filter
10 p1458 A72-24934

Capacitive memory storage for filtration of repetitive pulse radio signals mixed with additive noise
11 p1598 A72-26734

Preliminary frequency selection during matched signal filtering
21 p3021 A72-40941

Characteristics of filtering the Rayleigh parameter of pulse signals in the presence of noise
22 p3154 A72-42228

Stability conditions and effective bandwidths of first and second degree pulsed phase locked AFC systems with proportionately integrating filter, using Z transform method
23 p3263 A72-43433

Use of selective RC amplifiers in the radio-frequency amplifier stages of superheterodyne radio receivers
23 p3271 A72-43775

Magnitude of the attenuation troughs of a two-branch filter with multiple-frequency quartz resonators
23 p3272 A72-44170

RADIO FREQUENCIES

NT C BAND
NT EXTREMELY HIGH FREQUENCIES
NT EXTREMELY LOW RADIO FREQUENCIES
NT HIGH FREQUENCIES
NT LOW FREQUENCIES
NT LOW FREQUENCY BANDS
NT MICROWAVE FREQUENCIES
NT SUPERHIGH FREQUENCIES
NT ULTRAHIGH FREQUENCIES
NT VERY HIGH FREQUENCIES
NT VERY LOW FREQUENCIES

High resolution RF linear mass spectrometer for separation of ions formed by electron impact on organic molecules
01 p0064 A72-10043

RF intrinsic and up or down-converted modulation noise mutual relationship with application to IMPATT diode oscillators
01 p0035 A72-10114

Ferrite rod antennas calibration for radio frequency measurements up to 1 MHz
02 p0195 A72-12606

Ion transit time effects on plasma sheath RF admittance, using equivalent circuits for representation in low and high frequency ranges
03 p0394 A72-13150

Abnormal rf hysteresis and bias voltage effect in resonant cavity Gunn devices
03 p0331 A72-13646

Starlight intensity modulation at discrete radio frequencies due to enhanced ionospheric electron density fluctuations
03 p0438 A72-14096

Electronic collision frequency relationship with radio frequency in F region, investigating height, diurnal and seasonal variations
04 p0516 A72-14933

Ionospheric scintillation fading observations by NASA satellite tracking and data acquisition networks, noting frequency dependence in auroral regions
05 p0631 A72-16858

Gaussian rf noise effect on optical detection signal fluctuations in optically pumped frequency standards
07 p0938 A72-19013

Pulsed and continuous rf irradiation effects on mitotic activity and chromosomal aberrations in regenerating rat liver tissue
07 p0917 A72-19443

Communication satellites rf assignment by ITU for prevention of jamming, discussing radio communication conferences regulatory actions
07 p1104 A72-19469

Atom interactions with rf field, using quantum mechanical interpretation in terms of photons
07 p1038 A72-20433

Rf excitation produced plasma instability, considering density fluctuation and drive frequency introduction by amplitude modulation
07 p1045 A72-20441

Venusian atmosphere RF refractive attenuation height dependence, field strength measurements comparison, inversion layer influence and surface echoes effects
10 p1541 A72-24501

Radiative displacement of molecular beam sidebands by spatiotemporal modulation of irradiating RF field
10 p1492 A72-24858

RF ion thruster flight prototype development, describing test facilities, design and performance
11 p1709 A72-26202

Plasma diagnostics of inductively coupled RF Hg discharge in RIT-10 ion thruster
11 p1709 A72-26203

RF ion microthruster discharge vessel and plasma holder material investigation, considering quartz, boron nitride and aluminum oxide
11 p1709 A72-26204

RF ion thruster for spacecraft propulsion, discussing tests and digital computer calculations to optimize design parameter
11 p1709 A72-26205

F 2 region critical radio frequencies forecasts from solar cycles, ionospheric disturbances data, latitude and annual and diurnal variations
11 p1594 A72-26272

Gas laser oscillation frequency stabilization by comparing mode separation with RF standard
12 p1822 A72-27608

Large signal four-pole parameters and optimum conditions determination for RF high gain amplifiers with class C operated transistors
13 p1921 A72-29344

Single point thunderstorm ranging method based on two radio frequencies field intensity spectral components ratio
14 p2129 A72-30639

Optically pumped magnetometer error, predicting atomic g-factor modification by nonresonant RF field
15 p2239 A72-32335

The fabrication and evaluation of a micropower transistor and hybrid RF amplifier.
17 p2528 A72-34688

Influence of horizontal electron-concentration gradients on the magnitude of the maximum usable frequency and the trajectory of radio wave propagation in the ionosphere
17 p2519 A72-35878

An adaptive processor for RF antenna arrays.
18 p2659 A72-36329

Cytologic aspect of RF radiation in the monkey.
19 p2758 A72-38709

Analytical model for a polarizable medium at radio and lower frequencies.
22 p3155 A72-42467

RADIO FREQUENCY DISCHARGE

HF capacitive discharge plasma resonance under weak transverse magnetic field in vacuum
01 p0106 A72-10041

Free hf discharge plasma column generator, discussing equipment and current and resistance measurements
03 p0393 A72-13083

Free atoms and radicals elementary reactions, passing parent molecules through electrodeless rf or microwave discharge at various pressures and temperatures
03 p0320 A72-13392

Free HF discharge plasma column generator, discussing equipment and current and resistance measurements
13 p2015 A72-29433

Electron-ion modes parametric coupling in low pressure RF self sustained plasma discharge, noting plasma frequency emissions
14 p2138 A72-30399

Symmetrical and asymmetrical electrostatic probes for RF plasma discharge data, describing feedback network, stabilization, generation and electron temperature profiles
15 p2288 A72-32506

Anomalous diffusion coefficient of axially decaying RF discharge collisional plasma under instability mode suppressed by feedback technique
16 p2437 A72-33657

Quiescent large-volume collisionless HF discharge plasma generator with zero magnetic field, noting low noise level due to self-stabilizing feature
17 p2592 A72-35814

RF discharge gap in cascaded plasma limiters, using tritium igniter as reliable electron priming source
18 p2715 A72-36451

Radio-frequency preionization in a superconic transverse electrical discharge laser.
19 p2813 A72-38694

Effect of a cooling gas layer on the geometrical dimensions of an induction plasma
20 p2957 A72-39219

Spectroscopic study of the parameters of a turbulent plasma
22 p3213 A72-43107

RADIO FREQUENCY HEATING

Parametric excitation of ion-acoustic waves in Q machine plasma, controlling electron temperature by amplitude modulated rf heating
06 p0855 A72-17513

German monograph on wall stabilized Ar arc column displacement by pulsed HF radiation heating covering power absorption determination based on theoretical model
09 p1358 A72-22341

Diaphragmless electrothermal shock tube for collision in preheated Ar, using RF plasma heater
10 p1459 A72-24410

Pulsed RF hydrogen plasma heating in mirror machine near ion cyclotron frequency and harmonics
11 p1699 A72-26703

Fusion reactor RF heating below 100 MHz, discussing coil structures and arcing and cooling problems in main fusion region
16 p2433 A72-32813

Numerical analysis of microwave heat generation in disc-shaped Luneberg lenses.
21 p3032 A72-40627

Transport of RF energy to the lower hybrid resonance in an inhomogeneous plasma.
22 p3212 A72-42898

Superhigh-frequency heating of a plasma and longitudinal electron heat conductivity in a magnetic field
24 p3429 A72-45492

RADIO FREQUENCY IMPEDANCE PROBES
Antenna lf impedance measurements of lower terrestrial plasma wave characteristics, using equivalent impedance probe circuit
02 p0172 A72-11946

Electron temperature measurement error elimination with radio frequency Langmuir probe in low density plasma, measuring floating potentials
05 p0694 A72-16049

Dipolar rf probe admittance measurements in simulated ionosphere for satellite plasma experiments
06 p0811 A72-18733

Antenna LF impedance measurements of lower terrestrial plasma wave characteristics, using equivalent impedance probe circuit
13 p1920 A72-29258

Linear ICs application to RF probe for ionospheric electron density measurements from rockets or satellites
15 p2240 A72-32389

Low density and pressure air plasma electron density simultaneous measurements by Langmuir and RF capacitance probes
16 p2438 A72-33836

Electron temperature and density determination from RF impedance probe measurements in the lower ionosphere.
20 p2916 A72-39229

RADIO FREQUENCY INTERFERENCE
NT ATMOSPHERICS
NT BLACKOUT [PROPAGATION]
NT CHIRP SIGNALS
NT COSMIC NOISE
NT DAWN CHORUS
NT ELECTROMAGNETIC NOISE
NT HISS
NT IONOSPHERIC CROSS MODULATION
NT IONOSPHERIC NOISE
NT IONOSPHERICS
NT SHOT NOISE
NT SUDDEN ENHANCEMENT OF ATMOSPHERICS
NT THERMAL NOISE
NT WHISTLERS

RF interference in angle-modulated system with predetection linear bandpass filter, calculating output power spectral density in baseband
01 p0045 A72-10332

Centimeter waves fading due to interference from tropospheric multipath propagation
01 p0027 A72-10412

Phase error in 136 MHz interferometer due to galactic nucleus passage, obtaining lower bound
02 p0175 A72-12160

Fluctuating white and narrow band noise and interference pulse effects on monopulse goniometer
02 p0176 A72-12220

Frequency sharing criteria for terrestrial and space services, showing improved radio spectrum utilization and permissible interference
02 p0178 A72-12388

Search radar performance environmental model using clutter and interference returns
02 p0178 A72-12389

Semiconductor devices potential interference and biological exposure hazards in microwave leakage field, considering shielding and filtering methods for reducing susceptibility
03 p0320 A72-14032

Computerized simulation for AM radio receiver waveform performance degradation under pulsed interference
03 p0324 A72-14035

Composite incidental man-made radio noise data correlation to envelope statistic transformation hypothesis based on vlf airborne measurements of metropolitan area noise
03 p0324 A72-14042

RF interference measurements on guided hf ionospheric propagation in OV-41 dual satellite experiment
03 p0324 A72-14042

Economics in electromagnetic field measurement surveys for siting of earth stations operating in shared frequency bands at 4 and 6 GHz, considering interference detection
03 p0324 A72-14044

Graphical and tubular methods for frequency assignment to avoid intermodulation interference in channelized bands
03 p0325 A72-14046

Ground secondary radar interrogator system using monopulse technique for bearing measurement, accuracy and interference reduction
04 p0493 A72-15523

Multifrequency array antenna of interlaced open ended waveguide elements for L, S and C bands, reducing mutual interaction by cross polarization
06 p0782 A72-17360

Interference above ionosphere of lf radio waves emitted by multiple lightning discharges concluded

from spectrographic observation of whistler received onboard Injun 5 satellite
06 p0773 A72-17567

Optimal receiver synthesis for radio signals with differentiable components of continuous Markov processes masked by phase interference and white noise
07 p0937 A72-18847

Passive radio interference filtration analysis, obtaining SNR maximization by ambiguity function partial volume minimization
07 p0937 A72-18848

Nonorthogonality noise at matched radio filter output between stations operating simultaneously in same frequency band in discrete address wideband communication system, defining minimum SNR conditions
07 p0937 A72-18849

Optimal radio signal processing system on background of correlated interference, calculating detection characteristics
07 p0937 A72-18850

Geostationary communication satellites and terrestrial radio relays frequency sharing, controlling interference by flux density and transmitter power limitation
07 p0948 A72-20490

Reflected signal and receiver noise interference error in antenna temperature and calibration measurements by artificial moon method in centimeter and decimeter bands
08 p1142 A72-21726

Linear analysis and synthesis of three dimensional interference system stationary in space and time domains
09 p1278 A72-22573

Visual aurora and Explorer 40 satellite simultaneous observations of VLF radio noise, noting hiss associated with light emissions and associated charged particle flux
09 p1299 A72-23006

Estimate of effectiveness of utilization of composite signals to combat external interference with available a priori data
10 p1436 A72-24580

Optimal reception system synthesized for FM signal with phase fluctuation masked by narrow band AM and white noise
13 p1914 A72-28414

NASA program for acquisition, analysis and dissemination of space propagation and interference data for space systems designers, operators and regulatory agencies [AIAA PAPER 72-577]
13 p1918 A72-28985

Monte Carlo simulation for imperfect second order hybrid phase locked loop in radio frequency interference and Gaussian noise backgrounds, employing digital computer simulation model
13 p1935 A72-29104

Operation of information satellites in an interference environment.
17 p2515 A72-34518

Wave interference effect in whistler mode reflection coefficients for model lower ionospheres.
17 p2548 A72-35465

Digital simulation for radio frequency interference and specular multipath effects on FM spread spectrum demodulation with feedback and phase lock loops
18 p2659 A72-36317

Fluctuation frequency correlation for radio waves reflected from the ionosphere
18 p2662 A72-36879

Digital simulations of effects of two-antenna interference on space vehicle guidance.
19 p2830 A72-37292

Man-made electromagnetic noise in southern California and southern Nevada.
19 p2764 A72-37869

On the source of sunrise effects in the low ionosphere.
19 p2792 A72-38627

Electromagnetic compatibility and interference problems of radar altimeters, collision avoidance systems and air and marine mobile satellite communication equipment in 1600 MHz region
20 p2901 A72-38977

Analog computer simulation for PCM-FM and four-phase DPSK digital radio receivers susceptibility to interference sources
20 p2905 A72-38985

Frequency assignment for collocated transmitters using the branch-and-bound technique.
20 p2901 A72-38986

Electromagnetic compatibility problem of RF oscillators and switching operations in power network as interference source, discussing transmission line shielding and coupling impedance
20 p2901 A72-38988

Microwave emission from geological materials - Observations of interference effects.
20 p2917 A72-39477

ATS F and G radio link with ground stations, discussing telemetry and command functions with redundancy for RF interference minimization
21 p3019 A72-40883

Statistical tests for spectral correlation analysis of continuum VHF radio emission fluctuations from noise storms
21 p3102 A72-41778

Linear analysis and synthesis of three dimensional interference system stationary in space and time domains
24 p3379 A72-44752

RADIO FREQUENCY NOISE
U ELECTROMAGNETIC NOISE
RADIO FREQUENCY RADIATION
U RADIO WAVES
RADIO FREQUENCY SHIELDING
Isolated antenna system for shielded enclosure measurements at 20-200 MHz, discussing associated circuits design and performance tests
03 p0333 A72-14037

Pit shielded antenna measurements for communications satellite earth stations in 4 and 6 GHz bands, considering position range and erosion effects
15 p2196 A72-31794

Electromagnetic compatibility problem of RF oscillators and switching operations in power network as interference source, discussing transmission line shielding and coupling impedance
20 p2901 A72-38988

RADIO GALAXIES
Interacting radio galaxies, considering dynamics of streaming through intergalactic medium and secondary radio structures origin
01 p0126 A72-10288

Radio sources structure in astronomical catalog, noting no difference between quasars and radio galaxies
01 p0127 A72-10291

Luminosity function at 400 and 2700 MHz of radio galaxies in Parkes Catalog, discussing optical and radio flux densities
01 p0131 A72-11004

Irregular, spiral and elliptical galaxies radio continuum measurements at 1420 MHz, presenting positions flux densities and brightness distributions
01 p0131 A72-11005

Core sources in Seyfert and normal galaxies, analyzing radio observations by Westerbork synthesis radio telescope at 1415 MHz
01 p0132 A72-11012

Radio galaxy and quasar structure from 3.8 cm observations, fitting models to data
02 p0279 A72-12186

Quasar evolution models statistics suggesting relationship to radio galaxies, discussing continuity equation for density and luminosity changes
02 p0279 A72-12187

Optical search for Ryle-Neville radio sources, discussing cosmological model constraints and quasar and radio galaxies optical and radio luminosity functions
04 p0570 A72-14549

Expanding source model for quasars and Seyfert galaxy nuclei radio outbursts from extension of radio galaxy evolution models
04 p0573 A72-14874

Spectral and time variations at radio frequencies of QSO and radio galaxies from Parkes catalog
05 p0717 A72-16378

Cosmological evidence from radio galaxies and optical object counts, quasar red shifts and evolutionary properties
05 p0717 A72-16383

Radio galaxy spectra determination from measurements over various frequencies, noting correlation with physical parameters
06 p0879 A72-17859

Ejection behavior of relativistic particle magnetized clouds in radio galaxies central parts, noting interaction with interstellar medium
06 p0891 A72-18503

Optical observation of southern radio sources with 60 inch telescope at Cerro Tololo (Chile), measuring red shifts for radio galaxies
07 p1072 A72-19342

Structure and evolution of radio galaxies and quasars, considering luminosity-sustaining energy source, emission mechanism, variability and mean activity time
07 p1083 A72-20469

Astrophysical study of cosmological evolution, discussing evidence from radio source counts and quasar spatial distribution
07 p1084 A72-20471

High energy gamma quanta point sources from extensive air showers Cerenkov flares records, finding flux limits of radio galaxy and pulsars
07 p1064 A72-20635

Radio galaxy and quasar evolution models derived by formalism for number of sources in universe at any instant of cosmic time
08 p1234 A72-21382

Radio galaxies spectra and red shifts observed with Lick 120 inch telescope
08 p1235 A72-21393

MHD stability problems in radio galaxy structure and cosmic ray interaction with magnetic fields
09 p1386 A72-22751

- Weak extragalactic X ray sources radio identification, suggesting production by inverse Compton losses of electrons from radio galaxies 09 p1377 A72-22988
- Radio source observational identification as radio and normal galaxies and quasars, examining models for compact and large double radio source features and mechanisms 10 p1533 A72-23886
- Quasar and radio galaxy emission intensity and polarization variation models, comparing with observations 10 p1534 A72-23901
- Space densities and time scales of Seyfert galaxies, radio galaxies and quasi-stellar objects 10 p1534 A72-23905
- Positions, flux densities and identifications for weak sources in Parkes catalog at 2700 MHz, including galaxies and quasars 10 p1545 A72-24792
- Optical and physical properties and energy content of extragalactic radio sources, discussing radio galaxies and quasars 10 p1547 A72-24941
- Elliptical radio galaxies and quasars intrinsic emitted radio power correlation to spectral indices interpreted as evolutionary track in terms of model 12 p1867 A72-27210
- Heavily obscured galaxy IC 10 21-cm line observation with radio telescope and neutral hydrogen diameter measurement for distance estimation 12 p1868 A72-27215
- Visibility function change of low red shift radio galaxy 3C 120 from interferometer observations, noting high speed expansion 13 p2041 A72-29418
- Spectral index-luminosity relation for radio galaxies and quasi-stellar sources with power law spectra 15 p2315 A72-32714
- Expanding loops of H alpha filaments in peculiar galaxy M 82 investigated by microwave radio map, suggesting thermal and nonthermal radiation sources 15 p2317 A72-32757
- Double radio extensions in galactic cluster members, rejecting interacting galaxy hypothesis in favor of independent nonoptical radio galaxies in cluster intergalactic media 16 p2451 A72-32989
- Energetic gamma quantum flux recording from radio galaxy 3C 120 by Cosmos 251 and 264 satellites 17 p2617 A72-35726
- Calibration of the flux density of Cassiopeia A and Cygnus A in the range 300-9375 MHz 17 p2617 A72-35728
- Radio galaxies monochromatic luminosity-spectral index relationship from 3CR spectra studied at 10 MHz to 10,700 MHz 18 p2726 A72-36621
- Gas ejections in NGC 4486 and activity problems of galactic nuclei 19 p2862 A72-38051
- Galactic X rays investigation with X ray telescope on Lunokhod 1, noting observed singularities connection with statistical distribution of quasars and radio galaxies 19 p2802 A72-38090
- 1400-MHz survey of bright galaxies 19 p2866 A72-38501
- Differentially rotating magnetoid model for quasar and radio galaxies matter ejection and luminosity mechanisms in terms of magnetic field evolution and current sheet generation 20 p2965 A72-38903
- Two dimensional linear polarization radio distribution maps of 3C 270 and 3C 452 radio galaxies, relating to source magnetic field structure 20 p2965 A72-38904
- Emission lines and optical continuum of Seyfert radio galaxy 3C 120 from spectrophotometric scans 20 p2965 A72-38905
- Statistical studies of the evolution of extra-galactic radio sources. I, II, & III. 21 p3105 A72-41026
- Observations of linear polarization of radio sources at 7.2 cm. 21 p3109 A72-41326
- The emission-line spectrum of Cygnus A. 23 p3334 A72-43251
- Faraday depolarization of extragalactic radio sources. 23 p3335 A72-43268
- Radio galaxies and quasars observations cosmological interpretation, discussing radio source counts, spectral index and angular size relations to distance and expanding sources apparent motions 23 p3340 A72-44245
- RADIO HORIZONS**
- Tropospheric transhorizon meter, decimeter and centimeter wave propagation mechanisms, suggesting model for scattering and partial reflection effects 01 p0054 A72-10402
- Atmospheric water vapor role in waveguide effects above sea on millimeter and centimeter propagation along transhorizon and beyond horizon paths 01 p0026 A72-10403
- Ambiguity of radar phase measurement above sea within radio horizon, noting optimal relation between wavelength and optical paths difference of direct and reflected ray 12 p1784 A72-27799
- Experimental investigation of the parameters of a statistical Gaussian field model for centimeter waves beyond the radio horizon 17 p2515 A72-34834
- RADIO INTERFERENCE**
- U RADIO FREQUENCY INTERFERENCE**
- RADIO INTERFEROMETERS**
- Electronic equipment and calibration procedures for 86 MHz radio interferometer providing synchronized astronomical observations 02 p0194 A72-12576
- Distance effects on radio interferometric measurement accuracy, discussing single error source influence on total error 02 p0182 A72-12708
- German vhf ground telemetry satellite tracking system radio interferometer, discussing specifications and performance 02 p0182 A72-12732
- Satellite tracking radio interferometer with 1 deg sec directional accuracy, discussing low noise level and precise time allocation requirements 02 p0182 A72-12738
- [DGLR PAPER 71-124] 02 p0182 A72-12738
- Satellite orbit determination accuracy from radio interferometer tracking data containing systematic errors, using digital computer techniques on Symphonie transfer orbit 02 p0182 A72-12744
- [DFVLR-SONDDR-212] 04 p0495 A72-15728
- Long base radio interferometry at centimeter wavelength for angular measurement accuracy improvement in astronomy and geophysics 05 p0660 A72-15829
- Two channel radio interferometry, determining limiting accuracy characteristics under arbitrary phase error 05 p0660 A72-15830
- Radio interferometer sensitivity dependence on interrogation frequency for amplitude and time quantization of input signal spectra 05 p0660 A72-15830
- Interferometric measurement at 1415 MHz of radio telescope paraboloidal antenna radiation pattern, using cosmic radio sources with known flux density as signal source 07 p0945 A72-19789
- Interferometer detection of variable radio emission associated with X ray source GX9 plus 1, observing also GX349 plus 2 and GX350 plus 0 08 p1232 A72-21176
- Tracking interferometer observations for compact radio source structure investigation with simple models constructed for several individual sources 08 p1235 A72-21384
- Meteorological radar measurements, noting missile tracking radio interferometer noise due to stochastic refractive ray bending and associated multipath conditions 08 p1136 A72-21978
- Fixed base two element interferometer for radio astronomy, obtaining beavertail radiation pattern by use of earth rotation 10 p1482 A72-24578
- Solar radio astronomy instrumental requirements for 20 meter wavelength interferometry, metric and decametric flux and polarization measurements 12 p1872 A72-27815
- Characteristics of nonuniform regions responsible for microwave signals auroral scattering, noting observations with two sidelobe radio interferometer 13 p1946 A72-28584
- Visibility function change of low red shift radio galaxy 3C 120 from interferometer observations, noting high speed expansion 13 p2041 A72-29418
- Radio phase interferometers for emitter position location, predicting polarization mismatch errors effects on accuracy 15 p2206 A72-31777
- Long baseline radio interferometry with independent frequency standards for geodetic and astrometric applications 15 p2199 A72-32074
- Extra-atmospheric astronomical studies and instruments, discussing spaceborne, X ray and heavy orbiting telescopes and ground-space radio interferometer designs 16 p2462 A72-33516
- Small amplitude libration stability and damping system for gravitationally stabilized tethered orbiting radio interferometer satellite system 16 p2462 A72-34020
- Steerable directional VHF antenna design for radio interferometric tracking and ranging of Symphonie satellite 17 p2536 A72-35432
- [DFVLR-SONDDR-222] A hybrid navigation concept using a spinning satellite-borne interferometer and self-contained equipment. 21 p3082 A72-41083
- Broadband continua temporal behavior at type IV initial stages, recording by radio interferometers 21 p3101 A72-41296
- Observations of sources of maser radio emission with an angular resolution of 0.0002 sec 21 p3101 A72-41751
- Two channel radio interferometry, determining limiting accuracy characteristics under arbitrary phase error 23 p3287 A72-43437
- Radio interferometer sensitivity dependence on interrogation frequency for amplitude and time quantization of input signal spectra 23 p3287 A72-43438
- The techniques of present-day radioastronomy. 24 p3439 A72-44946
- RADIO METEOROLOGY**
- Radar meteorology, discussing equipment design, radar observation station net need, aeronautical applications and laser devices utilization 02 p0254 A72-12783
- Indirect measurement of the atmospheric refraction index with the aid of radiosonde data 19 p2789 A72-37744
- Conceptual possibilities of studies of moisture content in the atmosphere from thermal radio emission in the submillimeter wavelength range 21 p3078 A72-41798
- RADIO METEORS**
- Interplanetary medium spherical solid component model from radio meteor orbit catalog, discussing density of interplanetary dust, meteor matter and cosmic fallout on sun 02 p0282 A72-12332
- Upper atmosphere Na abundance compared to radio meteor rate after diurnal effects elimination 06 p0876 A72-17645
- Radio meteors observability and wave reflection from trails, discussing velocities, deceleration and vertical distribution 08 p1130 A72-20712
- Multicomponent meteoritic composition effects on meteor trails radio wave reflections, obtaining ionospheric electron concentration distribution 08 p1131 A72-20805
- Radio meteor observations of upper atmosphere long period wind variations, determining oscillation spectra peaks by harmonic analysis 08 p1161 A72-21537
- Radio meteor measurements of ionospheric drifts by two separated stations, obtaining wind velocities mean hourly values correlation coefficient 08 p1238 A72-21883
- Sectorial radio measurement of meteor trail drifts with lf radar signals, determining Doppler shift sign and period 08 p1238 A72-21887
- Graphic determination of reflecting points location on active curve of given point meteor radiant based on stereographic projection and radio transmission properties 08 p1239 A72-21892
- Meteors radio echo duration dependence on electron attachment, photodetachment and turbulent and ambipolar diffusion ionization processes 09 p1383 A72-22502
- Orionid meteor head echoes variations with diurnal radiant motion compared to Perseid meteors 09 p1389 A72-23395
- Meteor trail winds over Europe, discussing continuous wave radar observations and measurement errors with respect to height and time 10 p1474 A72-24708
- Radio meteor winds determination in Southern Hemisphere from vertically emitted continuous wave radiation, considering diurnal variations and wind and turbulence effects 10 p1474 A72-24709
- Radio echo observation of Quadrantid meteor showers right ascension and declination, observing mean range and influx rate as function of universal time 10 p1545 A72-24808
- Small scale wind shear effects on overdense and underdense radio meteor echoes, noting premature decay and scatter in decay time 10 p1440 A72-24952
- Radar facility for weak meteor observation, describing antennas, transmitters, receivers, filters, calibration techniques and recording instruments 13 p1919 A72-29026
- Aircraft measurements of radiation pattern of radar antenna system used for meteor height observation 13 p1919 A72-29027
- Pulse radar equipment for meteor height measurement from nonsaturated trails by phase difference method 13 p1929 A72-29028
- Instrument errors of RF phase comparison altimeter for meteor height measurements, using radar tracked aircraft flights calibration 13 p1957 A72-29029

- Optimal radar recording systems for meteor trail observations providing signal detection, processing and storage triggering and echo discrimination
13 p1929 A72-29030
- Optimal selectivity digital recordings for meteor trails radar observations, considering input process quantization rate and spectral width selection
13 p1929 A72-29031
- Automatic statistical analyzer for radio meteor echo multiplicity recording in three coordinate /multivariable/ space, including instrument error allowance
13 p1929 A72-29032
- Automatic real time processing of meteor radar echoes, using digital computers
13 p1924 A72-29033
- Algorithm for meteor velocity calculation from radio observation data, noting symmetrical error distribution function of velocities
13 p1924 A72-29034
- Radar observation of meteor geocentric velocity dependence on radiant elongation angle
13 p2038 A72-29035
- Interplanetary medium spherical solid component model from radio meteor orbit catalog, discussing density of interplanetary dust, meteor matter and cosmic fallout on sun
13 p2039 A72-29216
- Midlatitude upper atmosphere wind, tide and turbulence measurements, using radar observations of meteor trails
14 p2099 A72-30248
- Upper atmosphere horizontal wind velocity from meteor trails radio echoes, noting structural function anisotropy
14 p2127 A72-30263
- Meteor trail drifts at 95 km over Turkmenistan from November 1969-August 1970 radar observations, comparing to Frunze, Dushanbe and Kharkov wind data
15 p2305 A72-31372
- Quadrant underdense and overdense meteor observations during sunrise on 16.67 MHz pulsed radar
15 p2312 A72-32197
- Radio meteor orbit inclination angle dispersions for semimajor axis intervals compared with photographic meteors
16 p2456 A72-33514
- Relative orbit inclination dispersions of minor planets, fireballs and photographic and radio meteors, indicating common origin
16 p2456 A72-33515
- The effect of wind shear gradients on underdense radio meteor decay times.
17 p2517 A72-35398
- Radio meteors observability and wave reflection from trails, discussing velocities, deceleration and vertical distribution
19 p2765 A72-38340
- Determination of radio-meteor velocity with a minimum rms error
22 p3220 A72-41918
- Determination of the coefficient of electron attachment to particles of meteor material
23 p3339 A72-44169
- RADIO NAVIGATION**
NT DECCA NAVIGATION
NT HYPERBOLIC NAVIGATION
NT LORAN
NT LORAN C
NT LORAN D
NT SHORAN
NT TACAN
NT VHF OMNIRANGE NAVIGATION
Radio aids to maritime and aerial navigation - Conference, Trieste, June 1971
02 p0257 A72-12640
- L band in satellite system for aerial navigation aid, discussing position accuracy, data transmission and voice communication and modulation methods
02 p0257 A72-12642
- VOR, Direct Measuring Equipment and TACAN polar coordinate radio navigation systems history, improvements and future development
02 p0257 A72-12646
- Maritime and aerial navigation radio aids, discussing recent technological advances
02 p0258 A72-12750
- Radiative coupling of fed and unfed adjacent antennas in navigation systems rotating beam circular arrays, deriving equivalent circuit via quadrupole theory
05 p0635 A72-16300
- Soviet book on aircraft radio equipment covering transmission and reception, velocity and coordinates measurements, siting and navigation, flying target interception, reconnaissance, landing systems, etc
05 p0637 A72-16530
- Adaptive maximum likelihood receiver for direct ranging navigation, comparing with phase locked receivers
05 p0686 A72-16560
- Radio technical capabilities and limitations of ATC systems - Conference, Washington, D.C., November 1971
06 p0844 A72-17326
- Combined inertial/radio navigation systems for cost reduction, noting superior accuracy of VOR and DME
06 p0846 A72-18286
- Outer planets Grand Tour trajectory correction requirements, examining combined radio/onboard navigation system and delta V estimates [AIAA PAPER 72-54]
07 p1068 A72-18947
- Omega radio navigation system laning problem, discussing ambiguity resolution by multiple state vector Kalman filter
08 p1144 A72-20860
- High accuracy position determination from hyperbolic radio navigation time differences based on Sodano inverse solution of geodesics
11 p1684 A72-26498
- Russian book on flight navigation cybernetics covering Doppler, astro and radio inertial schemes and satellite systems
12 p1843 A72-28344
- Radio navigation satellite systems for ship and aircraft location determination, using time-frequency measurements
15 p2199 A72-32071
- The Omega navigation system - Its history, application and versatility.
17 p2578 A72-35559
- A historical survey of the application of the Doppler principle for radio navigation.
19 p2830 A72-37276
- A hybrid navigation concept using a spinning satellite-borne interferometer and self-contained equipment.
21 p3082 A72-41083
- Pulse time positioning under background noise in radar and radio navigation range finders, noting root-mean-square errors and transient response
22 p3153 A72-42117
- Space Shuttle landing navigation using precision distance measuring equipment.
24 p3421 A72-44637
- RADIO OBSERVATION**
Radio observations of filaments in absorption against solar disk during 11 September 1969 and 7 March 1970 eclipses
03 p0415 A72-12939
- He abundances in gaseous nebulae by optical and radio observation, discussing hydrogen and helium recombination spectra interpretation
03 p0419 A72-13115
- Mariner 9 radio occultation measurements of Mars day side atmosphere, indicating isothermal temperature, surface pressures and ionosphere properties
06 p0890 A72-18345
- Rain attenuation determination at 15 and 35 GHz under precipitation condition from emission measurement and correlation to regression line, using portable radiometric system [AD-741093]
07 p0946 A72-19791
- Pulsars radio observation for mean polarization parameters
07 p1079 A72-20049
- Solar active regions temperature measurements from 2 cm radioheliograms, using high resolution radio telescope
07 p1082 A72-20296
- Radio meteors observability and wave reflection from trails, discussing velocities, deceleration and vertical distribution
08 p1130 A72-20712
- Ionospheric integral electron concentration data from measurements of Elektron 1 and 3 satellites coherent radio wave emission
08 p1155 A72-20800
- Radio observation of flare sources and emission areas above coronal condensations during 22 September 1968 solar eclipse
08 p1228 A72-20828
- Southern Hemisphere interstellar clouds radial velocities from optical and radio observations
10 p1542 A72-24612
- Radio telescope observation of galaxy NGC 5253 in 21 cm line, noting centrally condensed emission complex of ionized gas
10 p1543 A72-24620
- Sporadic E layer variations monitoring in 50 MHz band, examining diurnal, seasonal, magnetic and meteoroid showers relationships of oblique incidence paths
10 p1441 A72-25152
- Midlatitude sporadic E layer observed by rocket and radio sounding, deriving plasma frequency from peak electron density
10 p1477 A72-25156
- Traveling ionospheric disturbance radio sounding during 7 March 1970 solar eclipse time, noting wave front orientation
12 p1801 A72-27158
- Outer Planet Grand Tours Missions radio science experiments for planetary and satellite atmospheres and surfaces, celestial mechanics, relativity, interplanetary medium and solar corona
12 p1870 A72-27347
- Characteristics of nonuniform regions responsible for microwave signals auroral scattering, noting observations with two sidelobes radio interferometer
13 p1946 A72-28584
- D region chemistry based on earth albedo effects from airborne radio sounding experiments, suggesting visible light energy flux role
13 p1950 A72-29342
- Spectral radio observations of 7 March 1970 solar eclipse, noting McMath plages intense activity source flux characteristics and weaker source bremsstrahlung emission
13 p2044 A72-29551
- Predicting electron density for type 3 solar burst excitation by LF satellite radio observations
13 p2032 A72-29723
- Narrow antenna radiation beam used for size and location determination of solar microwave radio burst observed with radio telescope
13 p2048 A72-29743
- Equatorial quiet solar atmosphere model for chromosphere-corona transition region based on cm radio observation and hydrodynamical conservation equations
13 p2049 A72-29933
- Radio waves field strength measurement and recording for D region behavior during partial solar eclipse of 25 February 1971
13 p1961 A72-30050
- Venus atmospheric parameters below critical refraction and surface refractive index from signal amplitude measurement by radio holographic occultation techniques
14 p2151 A72-30467
- Pulsar radio and optical observations, discussing periods, pulse shapes at various frequencies and marching subpulses
16 p2460 A72-33925
- MHD fluid model for collisionless shock waves in turbulent plasma with enhanced transport coefficients, noting laboratory experiments and satellite and radio observations
16 p2439 A72-33932
- Fluctuations of water vapour content in the troposphere as derived from interferometric observations of celestial radio sources.
17 p2545 A72-34690
- Radio observations of two supernova remnants, HB21 and IC443, at 4170 MHz.
17 p2613 A72-35500
- Whistler activity in central Europe during the period of increasing solar activity from 1964 to 1968.
18 p2657 A72-36230
- On an anomaly in long-range short-wave propagation from the equatorial region to central Europe.
18 p2657 A72-36232
- Study of the motion of ionized artificial clouds in the upper atmosphere
18 p2688 A72-36864
- Measurement of integral parameters of the nighttime ionosphere by observations of signals from the 'Intercosmos 2' artificial earth satellite
18 p2689 A72-36877
- Determination of the predominant wind vector from meteor radar observations
19 p2857 A72-37740
- Polarization observations of solar radio emission at the 3.15-cm wavelength
19 p2858 A72-37801
- Radio meteors observability and wave reflection from trails, discussing velocities, deceleration and vertical distribution
19 p2765 A72-38340
- The generation and propagation of VLF emissions.
20 p2904 A72-39984
- Radio galaxies and quasars observations cosmological interpretation, discussing radio source counts, spectral index and angular size relations to distance and expanding sources apparent motions
23 p3340 A72-44245
- Characteristics of nonuniform regions responsible for microwave signals auroral scattering, noting observations with two sidelobes radio interferometer
24 p3397 A72-45084
- RADIO OCCULTATION**
Mars atmospheric temperature, pressure and electron density from radio occultation measurement with Mariner 6 and 7, noting frozen carbon dioxide in middle atmosphere
13 p2039 A72-29335
- RADIO PROBING**
Lunar crust exploration by vlf electromagnetic surface waves, discussing frequency dependent depth penetration, conducting layers detection and communication or navigation use
03 p0436 A72-13821
- Machine oil wear degree and Fe content determination by placing sample into induction coil and measuring coil Q at RF
13 p1957 A72-29142
- A new method for in situ electron temperature determinations from plasma wave phenomena.
19 p2793 A72-38758

- An ultra-broadband probe for RF radiation measurements. 20 p2921 A72-38993
- A small ELF electric field probe. 20 p2921 A72-38994
- Reflection coefficient method of remote probing for inhomogeneous media, using plane wave incidence angle dependence 20 p2927 A72-39719

RADIO PROPAGATION

U RADIO TRANSMISSION RADIO RANGE

- Short wave skip distance calculation as function of path inclination to ionospheric layer for linear and parabolic ionization distributions 01 p0028 A72-10612
- Supermode F range spreading and evening type transequatorial propagation, considering single scattering in east-west plane 03 p0321 A72-12994
- Auroral absorption prediction during disturbed conditions in communications as function of frequencies and radio ranges at different geomagnetic time and coordinates 05 p0626 A72-16009
- Onboard orbital navigation system analysis on space shuttle radio range and range rate measurement data relative to ground beacon, using Kalman filter 08 p1203 A72-20856
- Dynamic range errors and noise bands for phase comparison radio range finders with mutual automatic frequency control in interrogator and transponder 11 p1596 A72-26302

RADIO RANGES

U RADIO BEACONS

RADIO RECEIVERS

- NT SUPERHETERODYNE RECEIVERS
- NT TRANSMITTER RECEIVERS
- NT WHISTLER RECORDERS
- Wideband FSK receiver for space telemetry, calculating error probability in multipath signal fading due to planetary surface reflections 01 p0025 A72-10329
- Radio astronomy technology developments, discussing antennas, receivers and data processing 01 p0047 A72-10417
- Receiver performance characteristics and failure mechanism in presence of interference, discussing measurement methods for interference susceptibility 02 p0192 A72-12150
- Receiver detection characteristics for multiplicative processing of coherent signal pulses with unknown initial phase and slowly fluctuating amplitude 02 p0176 A72-12215
- Nighttime hf radio wave field intensity measurement and absorption observation by narrow band receiver 02 p0184 A72-12874
- Receiving equipment in 23 cm band for Krakow 15 m radio telescope 03 p0339 A72-13173
- Linear radio receiver circuit synthesis for output signal structure and rotational choice, using reduction algorithm 03 p0323 A72-13894
- Mathematical modeling methodology for communication receiver life cycle EMC decisions, considering analysis and prediction problems with emphasis on nonlinear circuits and systems 03 p0324 A72-14034
- Computerized simulation for AM radio receiver waveform performance degradation under pulsed interference 03 p0324 A72-14035
- Microstrip double down-converter receiver in civil satellite earth stations for reduced interface problems, increased reliability and minimum initial cost 03 p0334 A72-14074
- Radio pulse signal fixed source location estimate with nondirectional space diversity receivers in arbitrary configuration antenna array 05 p0625 A72-15822
- Receiver arrangement for polarization selection based on multiplication of heterodyne-converted and amplified signals taken from dual-input antenna receiving elliptically polarized field 05 p0635 A72-16332
- Adaptive maximum likelihood receiver for direct ranging navigation, comparing with phase locked receivers 05 p0686 A72-16560
- Microwave receiver double diffused MOS transistor /D-MOST/ device advantages over bipolar device 06 p0790 A72-18485
- Optimal receiver synthesis for radio signals with differentiable components of continuous Markov processes masked by phase interference and white noise 07 p0937 A72-18847
- Microwave IC front end receiver synthesis for radio relay system, considering low noise figure achievement by Si Schottky barrier diodes 07 p0955 A72-19356

- Ionospheric drifts measurement by small base diversity reception method, investigating dependence on receiving antennas orientation 08 p1154 A72-20731
- Nonlinear filtering synthesis of optimal receiver for pseudorandom phase shift keyed signal with arbitrary modulation angle and white noise background 10 p1436 A72-24510
- Estimate of effectiveness of utilization of composite signals to combat external interference with available a priori data 10 p1436 A72-24580
- Modulating /multiplicative/ noise effects on output signal characteristics of receiver designed for optimal reception on background of Gaussian noise 10 p1439 A72-24906
- Soviet book on radio receiver design covering military applications, bandwidth requirements, network synthesis and AM, FM, SSB, Doppler, phase metering, PCM and radar equipment 11 p1604 A72-26045
- Monolithic micropower command receiver to extend lifetime of implanted biotelemetry system 11 p1586 A72-26564
- Noise factor formula of antenna matched multiple loop radio receiver input network with series connected coupled stages 11 p1598 A72-26732
- Aircraft distance measuring equipment with VOR radio receivers and ground station transponder for pulse interrogation 12 p1842 A72-27105
- Low noise receivers in radio astronomy, discussing accuracy requirements for line measurements and very long baseline interferometry 12 p1792 A72-27806
- Four-phase radio continuum receiver with digital demodulation and signal integration for transfer into on-line computer, discussing calibration 12 p1793 A72-27808
- Compensation of nonlinear selectivity distortions in radio receivers with broadband preamplification stages, noting circuit diagrams for preselector correctors 13 p1927 A72-28412
- Optimal quantization parameters for pseudonoise signals at radio receiver output, estimating static error in correlation function measurement 13 p1919 A72-29048
- Design characteristics and in-flight performance tests of computerized airborne OMEGA receiver, noting time independent one mile accuracy 13 p1997 A72-29188
- AN/ARN-99 OMEGA lane ambiguity resolution for receiver location, using multiple state vector Kalman filter approach 13 p1997 A72-29189
- Airborne OMEGA navigation system performance, discussing transmission facilities, three frequency receiver, flight tests and optimization of receiving antenna 13 p1998 A72-29191
- Preproduction OMEGA aircraft receivers and antennas development and flight testing, noting signal loss problems in high noise or precipitation static environments 13 p1998 A72-29198
- Subtraction circuit design for impulse noise elimination at front end of aircraft oriented OMEGA navigation system receiver 13 p1999 A72-29204
- Hardware and software integration of OMEGA and LORAN C and D receivers based on hyperbolic navigation systems compatibility 13 p1999 A72-29205
- RF receiver predetection SNR measurement from average postdetection signal-plus-noise and noise-only voltages, tabulating computed results 15 p2196 A72-31782
- Estimation-correlation principle application to harmonic signal receiver with unknown carrier frequency, using searching phase locked AFC circuit as estimation unit 15 p2202 A72-32667
- Incoherent receiver noise stability in multichannel system with channel frequency separation, deriving formula for receiver error probability 15 p2209 A72-32668
- Linear radio receiver circuit synthesis for output signal structure and rational selection, using reduction algorithm 15 p2202 A72-32705
- Solid state modular ground based distance measuring equipment /DME/ receiver for en route aircraft navigation and landing 16 p2420 A72-33521
- Signal detection by receivers with modulus processing 17 p2515 A72-34836
- Conference on Radio Receivers and Associated Systems, University College of Swansea, Swansea, Wales, July 4-6, 1972, Proceedings. 18 p2661 A72-36842

- Spatial diversity technique based on predetector equal-gain combining for fast fading reduction of AM radio receiver, using phase shifter 18 p2661 A72-36845
 - Geostationary or orbital satellite tracking radio receiver with steerable antenna for beacon signal detection and locking, discussing system design and performance 18 p2661 A72-36847
 - Earth station receivers for global and domestic FM systems. 18 p2662 A72-36848
 - Evaluation of the basis parameters of a frequency-code receiver with a generalized differential circuit 19 p2771 A72-37304
 - Radio astronomical observations in the 0.9 to 1.5 mm band using a 22-m radio telescope with an n-InSb receiver 19 p2858 A72-37803
 - Ionospheric drifts measurement by small base diversity reception method, investigating dependence on receiving antennas orientation 19 p2791 A72-38359
 - Theoretical and experimental investigations of a second-order phase-coordinate receiver 19 p2775 A72-38658
 - Ionosonde receiver with automatic noise suppression and digital-analogue recording of the first ionospheric reflection. 19 p2805 A72-38867
 - Analog computer simulation for PCM-FM and four-phase DPSK digital radio receivers susceptibility to interference sources 20 p2905 A72-38985
 - Radar EMI to voice communication receivers. 20 p2902 A72-38991
 - Low noise microwave parametric amplifier design for space communication receivers, using inverted diode balanced mixers 21 p3025 A72-40304
 - Low noise receiver for satellite broadcasting. 21 p3019 A72-40886
 - Threshold noise of an FM receiver at small signal-to-noise ratios 22 p3154 A72-42236
 - FM receiver noise figure measurement - A simplified method. 22 p3155 A72-42704
 - Radio pulse signal fixed source location estimate with nondirectional space diversity receivers in arbitrary configuration antenna array 23 p3263 A72-43430
 - Influence of modulating /multiplicative/ noise on signal processing in a phased-array-antenna/receiver system 23 p3265 A72-44205
- ### RADIO RECEPTION
- Short wave radio reception and signal path at magnetically conjugate point in Southern Hemisphere, using 40-110 msec delay times 01 p0028 A72-10592
 - Vertically polarized logarithmically periodic monopole antenna for incoming wave front reception with low elevation angles in 1.5 to 30 MHz frequency range 02 p0195 A72-12697
 - Radio signal parameters with unknown envelope approximated by orthonormal function series during white noise background reception 05 p0625 A72-15823
 - Reciprocity theorems in electromagnetic theory concerned with radio transmitting and receiving point interchange for electric dipole sources 05 p0625 A72-16008
 - Satellite broadcasting for direct individual and community reception as mass communication means, discussing UN role and international juridical problems 07 p1104 A72-19472
 - Diversity reception during radio wave scattering on statistically uneven surface, using geometrical optics method 07 p0944 A72-19566
 - Gating duration influence in reception channel on singular signal detection in normal noise 09 p1278 A72-22571
 - Error probability estimates in two channel diversity reception systems with allowance for fading correlation and incomplete signal separation 09 p1278 A72-22572
 - Radio receiver-transmitter system for synchronous heterodyne signal detection of 6 GHz band electromagnetic channel pulsed response, discussing operational principles and accuracy 09 p1280 A72-23353
 - Multiplicative noise envelope distribution for ionospheric scatter channel from single and diversity radio reception, noting meteor trails effects on electromagnetic wave propagation 12 p1782 A72-27627
 - HF radio signal reception behavior near maximum usable frequency during evening and at midnight, noting SNR 14 p2085 A72-30656

Signal parameter estimation accuracy in nonoptimal reception on noise background with random uniformly distributed initial phase
15 p2195 A72-31665

Additive fluctuation noise rejection during the quasi-coherent reception of phase-manipulated signals
20 p2900 A72-38896

Determination of the form of the capture area of a receiving antenna on the basis of energy streamlines
21 p3030 A72-40525

Broad-band transistorized receiving antennas in the frequency range between 10 kHz and 10 MHz
21 p3030 A72-40526

Diversity reception during radio wave scattering on statistically uneven surface, using geometrical optics method
22 p3153 A72-42084

Radio signal parameters with unknown envelope approximated by orthonormal function series during white noise background reception
23 p3263 A72-43431

Evaluation of the reliability of diversity reception by antennas of different polarizations
23 p3271 A72-43777

Probability of digital-data reception with a given confidence level under conditions of random radio noise
23 p3266 A72-44208

Gating duration influence in reception channel on singular signal detection in normal noise
24 p3379 A72-44750

Error probability estimates in two channel diversity reception systems of digital data transmission with allowance for fading correlation and incomplete signal separation
24 p3379 A72-44751

Interplanetary scintillation of radio sources observed through solar corona, deriving higher central moments from skewness coefficient of probability density function
24 p3437 A72-44831

RADIO REFLECTION
U RADIO ECHOES

RADIO RELAY SYSTEMS
S band transistor power amplifier design and performance, noting application for 960 telephone channel radio relay system
01 p0038 A72-10657

Waveguide channel microwave bandpass filters for radio relay systems, discussing methods of improving group delay in passband and attenuation at harmonic frequencies
01 p0041 A72-10694

EMC criteria for sharing frequency bands between communication satellite and terrestrial microwave radio relay systems
03 p0324 A72-14045

Radio sources and quasar structure angular resolution determination with distant radio telescope interferometry and microwave relay links
06 p0886 A72-18177

Microwave IC front end receiver synthesis for radio relay system, considering low noise figure achievement by Si Schottky barrier diodes
07 p0955 A72-19356

Geostationary communication satellites and terrestrial radio relays frequency sharing, controlling interference by flux density and transmitter power limitation
07 p0948 A72-20490

Feasibility of collocating a radio relay station with a sharing earth station.
17 p2512 A72-34268

Comparison of circuit call capacity of demand-assignment and preassignment operation.
17 p2512 A72-34270

Radiation patterns of wideband horn antenna loaded by dielectric belt, noting satellite and terrestrial radio relay applications
21 p3036 A72-41832

RADIO SCATTERING
Nighttime radio satellite scintillation from ionospheric irregularities heights associated with magnetic activity at subauroral latitudes
02 p0221 A72-12468

Radio wave scattering observation in turbulent lower ionosphere, determining vertical propagation velocity dispersion by statistical analysis
03 p0322 A72-13476

Mf/hf/vhf scattering from sea, deriving received power and spectral energy density dependence on grazing angle, frequency, range and surface impedance
06 p0770 A72-17338

Radio waves arrival angles distribution function in Fraunhofer diffraction zone upon plane wave normal incidence on inhomogeneous scattering layer
07 p0938 A72-19017

Diversity reception during radio wave scattering on statistically uneven surface, using geometrical optics method
07 p0944 A72-19566

Scattering and scintillations of rf radiation from distant discrete astronomical sources as measure of interplanetary plasma irregularities
07 p1079 A72-20020

Transfer characteristics of solar radio radiation in scattering corona
07 p1062 A72-20230

Scattered signal power approximation during ionospheric oblique backscatter sounding, using geometrical optics method
08 p1130 A72-20733

Radio absorption and scattering cross sections of thin cylinder with arbitrary electron density distribution in ionosphere, observing resonance effects
08 p1239 A72-21890

Geometric optics approximation for rf wave forward and backscatter characteristics by spherical overdense clouds for several electron density distributions
08 p1136 A72-21980

Backscattering properties of ground observed with HF high resolution oblique sounding equipment
09 p1281 A72-23512

HF radio waves scattering by spherical electron cloud with Gaussian density distribution
09 p1282 A72-23515

HF radio wave backscatter from sea surface to obtain gravity wave structure information
10 p1438 A72-24739

Electromagnetic theory of HF radio ground wave backscattering from gently rippled sea surfaces, discussing approximations for separated transmitting and receiving antennas case
10 p1438 A72-24742

Radio wave scattering observation in turbulent lower ionosphere, determining vertical propagation velocity dispersion by statistical analysis
11 p1593 A72-26246

Simultaneous measurements of ionospheric electrons number vertical distribution by incoherent ground radio wave scattering and coherent signals from Intercosmos 2 and Cosmos 321 satellites
11 p1628 A72-26918

HF backscatter pulse signal incidence elevation angle measurements based on amplitude ratio of two antennas with different vertical patterns
12 p1783 A72-27779

Local FM radio pulse scattering by cylinder and linear cylinder array in Kirchhoff approximation
13 p1914 A72-28407

Signal level fluctuations line spectra energy characteristics comparison for oblique and oblique-backscatter sounding, noting changes in harmonics intensity and period
14 p2085 A72-30638

Meter and decimeter wave reflected signals distribution and surface backscattering patterns effective beamwidth investigation by method based on Doppler effect
14 p2086 A72-30792

Coronal randomly distributed anisotropic density inhomogeneities induced refraction and scattering effects on solar radio sources at 80 MHz
16 p2452 A72-33042

NP 0532 precursor pulse as radiation scattered from main pulse beam by ring of material centered on pulsar
17 p2603 A72-34192

Scattered signal power approximation during ionospheric oblique backscatter sounding, using geometrical optics method
19 p2766 A72-38361

On the source of sunrise effects in the low ionosphere.
19 p2792 A72-38627

Energy characteristics of radio signals scattered by statistically uneven surface, proposing statistical variables substitution
20 p2900 A72-38892

Frequency correlation measurement of pulsar spectral fine structure due to radio emission scattering by interstellar plasma
21 p3101 A72-41752

Diversity reception during radio wave scattering on statistically uneven surface, using geometrical optics method
22 p3153 A72-42084

Specific effective scattering area of the lunar, Martian, and Venusian surfaces in the radio range
22 p3223 A72-42214

The scintillation of extended radio sources when the receiver has a finite bandwidth. III - Further methods.
23 p3341 A72-44396

RADIO SIGNAL ABSORPTION
U ELECTROMAGNETIC ABSORPTION

RADIO SIGNAL PROPAGATION
U RADIO TRANSMISSION

RADIO SIGNALS
Phase difference measurement between magnetoionic components returned from lower ionosphere due to pulsed radio signal, obtaining electron density profiles
01 p0063 A72-10914

Estimation algorithm for arbitrary parameter of narrow band radio signal with unknown amplitude and phase during reception on additive normal noise background
02 p0176 A72-12218

Random errors in arrival time measurements of sinusoidal radio signal under noise and pulse interference
03 p0323 A72-13893

Optimal detection of Markov radio signals with intrapulse FM using nonlinear filtration theory
04 p0487 A72-15146

Radio pulse signal fixed source location estimate with nondirectional space diversity receivers in arbitrary configuration antenna array
05 p0625 A72-15822

Radio signal parameters with unknown envelope approximated by orthonormal function series during white noise background reception
05 p0625 A72-15823

Integral equations derived for single and composite radio signals with maximum energy concentration in given time interval or frequency band
05 p0625 A72-15824

Radio signal group trajectory in ionosphere expressed as series expansion in terms of increasing power of beam reflection height
05 p0626 A72-16250

Radio signal electron-phonon detector design and experimental realization, considering requirements for minimum transduction and surface wave propagation loss
05 p0626 A72-16281

Ionospheric electron content from Faraday rotation observed on satellite radio signals at various frequencies
05 p0659 A72-17095

Pulsed FM radio pulse signal reflection from inhomogeneous plasma or ionosphere calculating electron collision loss effects on distortion
06 p0854 A72-17487

Multichannel frequency spectrum analyzer for single radio pulse component frequency measurement
07 p0988 A72-19960

Maximum likelihood estimate of carrier frequency and arrival direction of radio signals in background noise for large aperture antennas
08 p1133 A72-21373

VLF signals Antarctic ice cap attenuation determined at Byrd station from relative phase and amplitude observations over short and long great circle paths
09 p1281 A72-23511

Vertical angle estimation for HF sky wave multimode signals arrival, noting validity for arbitrary antenna elements polarization
09 p1281 A72-23513

Synchronous detector technique for statistical properties improvement in phase comparison AM radio altimeter signal
11 p1633 A72-26304

Holographic method of correlation and spectral analysis of radio signals applied to stable oscillator, randomly inhomogeneous media fields and stereophonic transmission measurements
11 p1636 A72-26726

Radio pulse synchronous detection with wideband preamplifier, evaluating frequency mismatch effects on signal distortion by transient response analysis
12 p1783 A72-27631

Probability density functions for output process in frequency discriminator under action of additive mixture of fluctuating radio signal and random noise
13 p1914 A72-28411

Aircraft applications of composite signal OMEGA configuration with phase data combined at separate carrier with weighting coefficients, discussing advantages over uncompensated navigation systems
13 p1998 A72-29192

Ionospheric radio signal reflection fields verified via quantitative statistical reliability criterion
14 p2100 A72-30634

Extrasolar civilization search via possibly used electromagnetic signal types, discussing frequency and time domains
15 p2302 A72-31292

Bayesian estimation for nonlinear filtration of nonstationary non-Gaussian radio signals, deriving second central moments and parameter estimate errors
15 p2195 A72-31656

Signal parameter estimation accuracy in nonoptimal reception on noise background with random uniformly distributed initial phase
15 p2195 A72-31665

Random errors in arrival time measurements of sinusoidal radio signal under noise and pulse interference
15 p2202 A72-32704

Rayleigh distribution of radio signals partially reflected from D region, noting amplitude fluctuations dependence on antenna radiation pattern
15 p2202 A72-32733

Model for VLF emissions triggered by whistlers and man-made radio signals, noting effects of wave packet and second order nonresonance

16 p2365 A72-33905

The interpretation of ionospheric radio drift measurements. IV - The effects of signal coupling among spaced sensor channels.

17 p2515 A72-34699

Radio pulse shaping network synthesis composed of lumped elements, noting pulse duration limitation by network efficiency

17 p2533 A72-34837

Optimal predistortion efficiency for multiplicative disturbances in radio signal transmitting channel, noting Rayleigh distribution of signal fluctuations

17 p2518 A72-35778

Study of unsteady processes in the ionosphere and outer space by using quantum frequency stabilizers

18 p2687 A72-36853

Measurement of integral parameters of the nighttime ionosphere by observations of signals from the 'Intercoms 2' artificial earth satellite

18 p2689 A72-36877

Method and equipment for checking chronometers by one-second timing radio signals under field conditions

19 p2795 A72-37346

SHF signal power influence on detector current, noting signal dependence on virtual cathode potential and signal power

19 p2774 A72-38410

Transmission of two partially time coincident linearly frequency modulated signals through limiter-filter system, noting distortion and satellite signals generation

19 p2766 A72-38419

Theoretical and experimental investigations of a second-order phase-coordinate receiver

19 p2775 A72-38658

Correlation and indeterminate functions of signals with discrete frequency-time structure, noting linear frequency modulation of signal element

19 p2768 A72-38669

Energy characteristics of radio signals scattered by statistically uneven surface, proposing statistical variables substitution

20 p2900 A72-38892

Additive fluctuation noise rejection during the quasi-coherent reception of phase-manipulated signals

20 p2900 A72-38896

Bayes theorem for radio signals parameter estimation on random noise background, using rectangular function of losses

21 p3016 A72-40797

Detection of Doppler radio signals on a receiver with an additive noise blip number counter

21 p3022 A72-41116

Measurement of a radio signal nonenergetic parameter at high additive and modulation noise levels

21 p3022 A72-41117

Statistical characteristics of an optimal detector of randomly fading pulse signals

22 p3154 A72-42229

Radio pulse signal fixed source location estimate with nondirectional space diversity receivers in arbitrary configuration antenna array

23 p3263 A72-43430

Radio signal parameters with unknown envelope approximated by orthonormal function series during white noise background reception

23 p3263 A72-43431

Integral equations derived for single and composite radio signals with maximum energy concentration band in given time interval or frequency

23 p3263 A72-43432

Influence of a nonlinearity in a coherent accumulator of pulse signals on the gain in the signal-to-noise ratio

23 p3264 A72-43762

Relation between satellite radio signal scintillations and magnetic activity

23 p3264 A72-43850

RADIO SOURCES [ASTRONOMY]

NT CASSIOPEIA A

NT EXTRAGALACTIC RADIO SOURCES

NT PULSARS

NT QUASARS

NT RADIO GALAXIES

NT RADIO STARS

Radio sources structure in astronomical catalog, noting no difference between quasars and radio galaxies

01 p0127 A72-10291

Radio source counts, cosmology and evolution in uniform model universes

01 p0127 A72-10323

Core sources in Seyfert and normal galaxies, analyzing radio observations by Westerbork synthesis radio telescope at 1415 MHz

01 p0132 A72-11012

Radio source counts at 6 cm by National Radio Astronomy Observatory 140 and 300 foot telescopes

01 p0132 A72-11089

NGC 5128 nucleus radio emission flux density measurement, noting angular size

01 p0132 A72-11090

Radio variable sources PKS 0727-11 and 1514-24 observation at 2295 MHz, presenting flux measurements and drift curves

01 p0134 A72-11161

Jet-like structure formation by close juxtaposition of 80 MHz sources observed in late phase of complex solar burst, presenting model for explanation

02 p0272 A72-11649

Rapidly varying radio source VRO 42.22.01 /BL Lac/ observations, presenting flux density and linear polarization variations

02 p0277 A72-11774

Compact extragalactic radio source spectrum analysis, discussing successive uncorrelated outburst models

02 p0277 A72-11775

Solar wind electron density variations, discussing radio source interplanetary scintillation and angular distribution measurements at various distances from sun

02 p0277 A72-11902

Lunar occultation observations of radio source PKS 1514-24, presenting brightness distributions

02 p0277 A72-11905

Nonthermal radio source G 55.7 plus 3.4 structure in pulsar CP 1919 direction, presenting intensity contours and integrated flux density spectrum

02 p0278 A72-11907

Southern radio sources optical identification by photography using fiber optics image tube

02 p0285 A72-12795

Ionospheric small scale electron density irregularity structure from power spectral analysis of radio source scintillation observations

03 p0345 A72-12985

Occultation curves for optical and radio lunar occultation analysis of radio sources, considering detection and measurement of binary systems

03 p0420 A72-13130

Solar decimeter and hectometer wavelength radio burst generation, examining dynamic spectra and source position as function of frequency and time

03 p0424 A72-13221

Astrophysical cosmology, discussing universe expansion, Robertson-Walker models, radio sources, quasars, cosmic X ray background, intergalactic media, etc

03 p0426 A72-13268

Electromagnetic radiation in universe, discussing relict radio emission, energy density, hot model isotropic extragalactic component isolation, intergalactic gas, radio sources and quasars

03 p0414 A72-14317

Galactic plane 100 micron survey, detecting continuum radio sources, bright and dark nebula and IR stars

04 p0570 A72-14524

Optical search for Ryle-Neville radio sources, discussing cosmological model constraints and quasar and radio galaxies optical and radio luminosity functions

04 p0570 A72-14549

Radio astronomical observation of two local sources associated with unipolar sunspot group 275 and bipolar group 282, investigating emission directivity and brightness temperature

04 p0572 A72-14636

Electronographic photography of 3C 173 radio source and stars in same field

04 p0574 A72-14975

Optical object identified with radio source 3C 455 as quasar, noting relationship to SO galaxy NGC 7413

04 p0580 A72-15371

Pulsar PP 0943 radio emission, showing short time intensity increases

04 p0581 A72-15514

Cosmological evolution theories, discussing big bang theory, galactic evolution, quasars, pulsars, gravitational collapse, stellar evolution, supernovae, black holes, etc

05 p0716 A72-16311

Radio emission from compact extragalactic objects, including quasars and nuclei of compact, Seyfert and N type galaxies

05 p0716 A72-16376

Extragalactic radio sources luminosity function and luminosity density function from radio index surface brightness, discussing evolution and agreement with models

05 p0722 A72-17156

Extragalactic radio sources, discussing galactic radiation, quasars, nonthermal emissions, energy dissipation and spectrum analysis

06 p0886 A72-18172

Radio sources and quasar structure angular resolution determination with distant radio telescope interferometry and microwave relay links

06 p0886 A72-18177

Interplanetary scintillation and angular dimensions of radio sources at 81.5 MHz, using diffraction theory

06 p0889 A72-18327

Radio sources sky survey with radio telescope, discussing 5C1 and 5C2 spectral distributions

07 p1069 A72-19074

Optical observation of southern radio sources with 60 inch telescope at Cerro Tololo /Chile/, measuring red shifts for radio galaxies

07 p1072 A72-19342

Radio emission of galactic clusters at 1.4 and 2.7 GHz, computing mean electron density and hydrogen gas mass

07 p1075 A72-19577

Synchrotron emission source identification from spectral index dependence on frequency

07 p1059 A72-19807

Scattering and scintillations of rf radiation from distant discrete astronomical sources as measure of interplanetary plasma irregularities

07 p1079 A72-20020

Radio sources fine structure survey at 81.5 MHz, finding angular diameters by interplanetary scintillation technique

07 p1081 A72-20231

Solar radio emission, considering sources of slowly varying waves, brightness temperature distribution, frequency spectra and fluctuations

08 p1228 A72-20827

Spectral characteristics of continuous radio emission of extragalactic binary objects, discussing model of binary radio source formation from dipole nucleus

08 p1231 A72-21118

Interferometer detection of variable radio emission associated with X ray source GX9 plus 1, observing also GX349 plus 2 and GX350 plus 0

08 p1232 A72-21176

Synchro-Compton theory for variable compact components in extragalactic radio sources, suggesting stellar mass object collapse as energy source

08 p1233 A72-21181

Intense discrete extragalactic radio source counts at 1400 MHz, noting number-flux density relation and separation dependence of surface brightness

08 p1233 A72-21213

Tracking interferometer observations for compact radio source structure investigation with simple models constructed for several individual sources

08 p1235 A72-21384

Weak extragalactic X ray sources radio identification, suggesting production by inverse Compton losses of electrons from radio galaxies

09 p1377 A72-22988

Book on astronomy and cosmology covering big bang, steady state and oscillating universe theories, radio sources, galaxies, interstellar meteor relativity and extraterrestrial life

09 p1389 A72-23248

Circular polarization measurements of extragalactic radio sources at 1.4 and 5 GHz

09 p1393 A72-23568

Uhuru satellite development history and preliminary X ray observation, analysis of radiation source emission characteristics, locations and identifications

10 p1533 A72-23892

Compact radio sources in galactic nuclei, discussing similarity to quasars in repetitive generation of relativistic particles

10 p1534 A72-23900

Nonthermal emission and ejection of matter from galactic nuclei, discussing radio, optical and IR synchrotron sources and background radiation

10 p1535 A72-23906

Cosmic epoch dependent evolution of radio sources with identified optical counterparts

10 p1535 A72-23912

Variable radio structure model using relativistic electron cloud outbursts in stationary magnetic field tubes for faster than light velocities

10 p1536 A72-24139

Precise optical positions of nine compact radio sources in AGK 3 catalog

10 p1536 A72-24140

Relative orientation of major axes of double radio sources, comparing with Brown ordering of galaxies on megaparsec scale

10 p1541 A72-24472

Spectral indications of activity in galactic center, discussing radio source Sagittarius A and expanding hydrogen clouds

10 p1541 A72-24568

OH emission characteristics of IR stars from model with asymmetrical expansion outward of circumstellar OH clouds

10 p1542 A72-24613

Coma galaxy cluster X ray and radio source region magnetic field origin as primordial metagalactic flux or strong radio source remnant

10 p1542 A72-24617

Radio telescope observation of galaxy NGC 5253 in 21 cm line, noting centrally condensed emission complex of ionized gas

10 p1543 A72-24620

Intergalactic medium presence in clusters of galaxies from investigation of separation and size-separation ratio of double radio sources located inside and outside clusters

10 p1544 A72-24670

- Positions, flux densities and identifications for weak sources in Parkes catalog at 2700 MHz, including galaxies and quasars 10 p1545 A72-24792
- Polarization maps of extended extragalactic and galactic radio sources at 6 cm wavelength 10 p1545 A72-24793
- Spectral indices of extragalactic radio sources at 1.4 GHz independent on flux density 10 p1545 A72-24807
- Astronomical identification of optical objects near 5C2 radio sources position, noting probability parameters and measurement error 10 p1546 A72-24837
- Radio methods for cosmological model testing, discussing radio telescope requirements, source sampling procedures and counts as basic cosmological data 10 p1549 A72-25054
- Fan beam surveys of radio sources with Cambridge telescope, presenting catalogs of galactic coordinates and flux density measurements 10 p1549 A72-25194
- Fluid dynamics stability of double radio sources in intergalactic medium, discussing evolution, ram pressure mechanism and Rayleigh-Taylor and Kelvin-Helmholtz effects 10 p1550 A72-25196
- Galactic H II regions with radio emission at 1400 MHz, using National Radio Astronomy Observatory 300 ft telescope 11 p1724 A72-26785
- Arecibo observatory research, discussing pulsars, radio source scintillation and ionospheric heating 12 p1795 A72-27427
- Radio source and radio quiet quasars identifications for statistical correlation with bright galaxies positions 12 p1871 A72-27742
- Metagalactic magnetic field contributions to observed Faraday rotation measurements for distant extragalactic radio sources 13 p2039 A72-29088
- Galactic structure, ionized gas distribution and radio source diameter studies from interstellar scattering at 81.5 MHz, comparing with pulsars 13 p2050 A72-29962
- Spectral variability of radio sources in cm excess category, including quasi-stellar, Seyfert galaxy, optical variable and compact sources 13 p2050 A72-29964
- Pulsar PSR 1154-62 association with nearby galactic radio source having supernova remnant shell structure and spectrum characteristics 14 p2150 A72-30369
- Galactic supernova remnants radio frequency absorption line observations, deriving distances, radio luminosity function and distribution 14 p2158 A72-30726
- Relict radio fluctuation observations, investigating adiabatic density perturbations related to formation of galaxies and galactic clusters 14 p2159 A72-30788
- Optical identification of two radio source samples from astronomical B2 catalog, providing finding charts and reference star positions for investigated fields 15 p2316 A72-32749
- Coronal scattering effects on type 3 solar bursts, using radio sources scintillation model and Monte Carlo ray tracing technique 15 p2316 A72-32752
- HF radiation in type 3 burst sources, discussing amplification by proton and electron streams 15 p2316 A72-32753
- Radio source power spectra modulation dependence on distance and thickness of solar wind scattering region and on wind velocity component multiplicity 16 p2451 A72-33034
- Radio source scintillation observations by arms of one mile radio telescope at Molonglo Observatory 16 p2451 A72-33035
- Coronal randomly distributed anisotropic density inhomogeneities induced refraction and scattering effects on solar radio sources at 80 MHz 16 p2452 A72-33042
- Compact radio sources observation by long coherence intercontinental interferometry in trans-Pacific experiments 16 p2452 A72-33047
- Radio source Oj 287 photometric and polarimetric observations, noting optical intensity and plane polarization variability 16 p2452 A72-33134
- Radio sources position determination by lunar occultation, noting observation technique and data analysis method 16 p2453 A72-33287
- Radio source concentration mapping near NGC 7331 and Stephan quintet group 16 p2455 A72-33469
- High resolution radio observation of H II region W 51, noting compact components with emission measures agreement with recombination line data non-LTE analysis 16 p2457 A72-33684
- Radio sources with straight spectra and spectral index of 0.3, noting relationship to self absorption, electron energy distribution and cosmological evolution 16 p2457 A72-33685
- Radio sources reidentification in field of Coma Cluster of galaxies by Schmidt telescope 16 p2458 A72-33719
- Polarization measurements of radio sources at 9.55-mm wavelength. 17 p2603 A72-34439
- Observations of some small-diameter radio sources at 408 MHz. 17 p2603 A72-34440
- Fluctuations of water vapour content in the troposphere as derived from interferometric observations of celestial radio sources. 17 p2545 A72-34690
- Sheath effects and related charged-particle acceleration by Jupiter's satellite Io. 17 p2611 A72-35320
- Radio observations of two supernova remnants, HB21 and IC443, at 4170 MHz. 17 p2613 A72-35500
- Synchrotron emission source identification from spectral index dependence on frequency 17 p2602 A72-35731
- Energy spectrum of interplanetary-plasma discontinuities 18 p2715 A72-36653
- Study of the solar wind using the power spectrum of interplanetary scintillation of radio sources. 18 p2722 A72-36730
- Microwave celestial water-vapor sources. 18 p2729 A72-36990
- Spectral densities of radio emission fluxes from discrete radio sources at the 3.5-cm /8550 MHz/ wavelength 19 p2850 A72-37804
- Study of a faint nebula identified as the HB-21 radio source 19 p2862 A72-38054
- Hydrodynamic model calculations for dynamically unstable supermassive stars. 19 p2866 A72-38490
- 1400-MHz survey of bright galaxies. 19 p2866 A72-38501
- Accurate positions of radio sources at 408 MHz. 49 p2868 A72-38698
- Electromagnetic background radiation in universe, discussing relict radio emission, energy density, hot model isotropic extragalactic component isolation, intergalactic gas, radio sources and quasars 19 p2854 A72-38815
- Observations at 408 MHz of radio sources from the 4C catalogue. IV - Declination range 20 to 0 deg. 19 p2869 A72-38825
- Interferometer detection of radio sources near pulsing extar Hercules X-1 during low X ray luminosity period 20 p2963 A72-38918
- Accurate flux densities at 5009 MHz of 1007 radio sources. 20 p2967 A72-39190
- Hydroxyl and water radio sources scale and geometry constraints placed by interstellar maser gain saturation relation to emission solid angle 21 p3062 A72-40565
- Variable radio objects BL Lac, OJ 287, AP Lib, B2 1212+30 and ON 231 observed in IR spectral range, noting variations in flux 21 p3107 A72-41270
- Observations of sources of maser radio emission with an angular resolution of 0.0002 sec 21 p3101 A72-41751
- H 157 alpha recombination line from H I region before NGC 2024 radio source, considering average electron concentration and line origin 21 p3102 A72-41776
- The Cygnus X-region. VII - Radio continuum search for a ring of filaments around the area. 22 p3225 A72-42390
- Identification and removal of phase errors in interferometry. 23 p3287 A72-43259
- Interferometric observations of lunar occultations of radio sources, showing positions, brightness distributions, spectral index variations and quasar coincidence 23 p3334 A72-43260
- The cosmological evolution of radio sources of large angular extent. 23 p3336 A72-43554
- Statistics of the radiation from astronomical masers. 23 p3337 A72-43872
- Solar wind velocity determination from radio sources interplanetary scintillation observations, noting magnitude and direction variations with time 23 p3333 A72-44529
- Structure of Jupiter's decametric radio sources - Two-dimensional probability and flux studies, 1957-1970. 24 p3436 A72-44691
- Observations of the interplanetary medium and of the structure of radio sources using higher moments of interplanetary scintillations. 24 p3437 A72-44830
- Possible explanation of non-power-law radio spectra of cosmic radio sources. 24 p3446 A72-45477
- ### RADIO SPECTRA
- #### NT MICROWAVE SPECTRA
- Orion A and M17 radio recombination line width increases, discussing Stark broadening functional dependence on principal quantum number 01 p0131 A72-11010
- Nonlinear discrete radio source spectra deviations from power law at 10-5000 MHz, considering low energy relativistic electron excess 02 p0281 A72-12305
- Frequency sharing criteria for terrestrial and space services, showing improved radio spectrum utilization and permissible interference 02 p0178 A72-12388
- Pulsar CP 0328 wideband rf spectrum long term periodicity, considering origin during propagation through interstellar medium 04 p0580 A72-15369
- Low velocity neutral hydrogen spur coincidence with radio continuum Loop IV, discussing average excess surface density and total mass 05 p0711 A72-15765
- Radio absorption spectra sounding for planetary atmospheric impurities calculating water vapor content in Venus cloud level 05 p0715 A72-16169
- Spectral and time variations at radio frequencies of QSO and radio galaxies from Parkes catalog 05 p0717 A72-16378
- Radio galaxy spectra determination from measurements over various frequencies, noting correlation with physical parameters 06 p0879 A72-17859
- Plasma inhomogeneities effect on radio wave absorption in interstellar clouds of ionized hydrogen, analyzing cosmic radio emission spectrum 08 p1231 A72-21120
- Radio recombination lines broadening in hydrogen by electron collisions, using Baranger impact theory 10 p1435 A72-24142
- Spectral indications of activity in galactic center, discussing radio source Sagittarius A and expanding hydrogen clouds 10 p1541 A72-24568
- Elliptical radio galaxies and quasars intrinsic emitted radio power correlation to spectral indices interpreted as evolutionary track in terms of model 12 p1867 A72-27210
- Surface wave devices signal processing for space communication, developing fast lock up spread spectrum communication link broadband 13 p1920 A72-29106
- Spectral variability of radio sources in cm excess category, including quasi-stellar, Seyfert galaxy, optical variable and compact sources 13 p2050 A72-29964
- Spiral galaxies radio sources spectral components, noting relativistic electrons radiation and luminosity-surface brightness diagram 14 p2148 A72-30203
- Radio absorption spectra sounding for planetary atmospheric impurities calculating water vapor content in Venus cloud level 14 p2149 A72-30238
- Interstellar medium physical conditions from 21 cm hydrogen emission line observations in direction of pulsars, using 25 meter Dwingeloo radiotelescope 14 p2159 A72-30744
- Jovian synchrotron emission measurements by radioheliograph at 80 MHz, passing square low detector outputs through RC integrators 15 p2307 A72-31799
- First mode calculations for VLF atmospherics parameters of group delay time and spectral amplitude ratio based on Wait-Walters model 16 p2362 A72-32890
- Radio sources with straight spectra and spectral index of 0.3, noting relationship to self absorption, electron energy distribution and cosmological evolution 16 p2457 A72-33685
- Results of simultaneous measurements of the spectrum of auroral radio echoes at two frequencies 17 p2519 A72-35874
- Short-period pulsar intensity variations at 70 to 115 MHz 19 p2862 A72-38056
- Galactic radio emission spectrum analysis via horn antennas with wavelength proportional apertures, calculating full beam antenna temperatures for selected radio frequencies 19 p2852 A72-38484
- Observations at 408 MHz of radio sources from the 4C catalogue. IV - Declination range 20 to 0 deg. 19 p2869 A72-38825

- X-ray and HF microwave bursts correspondence shown in observations of 24 October 1969 impulsive solar flare and of XUV and radio emissions 21 p3108 A72-41290
- Millimeter absorption features corresponding with H alpha dark filaments on disk and emissive regions in solar prominences, discussing electron temperatures and densities 22 p3221 A72-42035
- Quasi-periodic solar radio pulsations at decimetric wavelengths. 22 p3222 A72-42045
- Power-law wavenumber spectrum deduced from ionospheric scintillation observations. 22 p3171 A72-42416
- Extragalactic object categorization according to IR luminosities, considering radiation mechanism models and IR spectra relation to radio spectrum 22 p3228 A72-42571
- Spiral galaxies radio sources spectral components, noting relativistic electrons radiation and luminosity-surface brightness diagram 23 p3333 A72-43232
- Interferometric observations of lunar occultations of radio sources, showing positions, brightness distributions, spectral index variations and quasar coincidence 23 p3334 A72-43260
- Possible explanation of non-power-law radio spectra of cosmic radio sources. 23 p3446 A72-45477
- RADIO SPECTROSCOPY**
- Solar type 3 bursts from high resolution radio spectrographs, deriving coronal temperatures from decay times 06 p0876 A72-17576
- Plasma interpretation of solar type 3 and spike bursts associations from high time resolution radiospectrographic observations 09 p1392 A72-23540
- Self oscillations of microwave autodyne oscillator loaded by two resonant cavities, noting radio spectroscopic applications 14 p2089 A72-31110
- Frequency marker measurement of nuclear quadrupole resonance (NQR) signal in pulsed radio spectrometer compared with zero beat method 16 p2390 A72-33078
- Dispersion signal recording for klystron AFC radio spectrometer by low frequency magnetic field modulation 22 p3175 A72-41900
- RADIO STARS**
- NT PULSARS**
- Radio stars wave amplitude scintillation during passage through ionosphere observed by interferometer, noting association with geomagnetic field fluctuation 04 p0567 A72-14953
- Interferometric observations of emission of radio eclipsing binaries beta Persei and beta Lyrae at 2965 and 8085 MHz 07 p1082 A72-20289
- Turbulent LF electric field fluctuations relationship with disturbed F region, spread F and scintillations of radio stars and satellites 09 p1300 A72-23025
- Simultaneous observations of radio flares from beta Persei on 25-25 January 1972 at 2.8, 3.7 and 11.1 cm, noting spectral characteristics difference from quasi-steady component 10 p1547 A72-24945
- Earth station parabolic antenna gain-noise temperature ratio measurement using radio star and Applications Technology Satellite technique [AIAA PAPER 72-528] 12 p1779 A72-27354
- Radio detection of Cygnus X-3. 17 p2612 A72-35366
- Radio observations of Cygnus X-3. 17 p2612 A72-35367
- Eclipsing and spectroscopic binary beta Persei radio star, suggesting X ray source nature 19 p2851 A72-37889
- The scintillation of extended radio sources when the receiver has a finite bandwidth. III - Further methods. 23 p3341 A72-44396
- RADIO TELEGRAPHY**
- Potential response of maritime services to craft and persons in distress at sea. 17 p2488 A72-34431
- RADIO TELEMETRY**
- NT PULSE FREQUENCY MODULATION TELEMETRY**
- Geomagnetic storms and anomaly observation by Satellite 1964 83C telemetry data transmission to ground stations network 02 p0219 A72-12083
- Radiotelemetric cardiorespiratory determinations during submaximal dynamic exercise 02 p0168 A72-12134
- Intermodulation noise in multichannel frequency division multiplex telemetry systems due to nonlinearities in transmitter-receiver links and tape recorder 02 p0175 A72-12145

- Telemetry receiver signal data quality in terms of RF, if AGC, AFC and AM rejection circuitry requirements 02 p0192 A72-12149
- Prototype compact ruggedized crystal-controlled L-band artillery telemetry transmitter design and performance 02 p0192 A72-12156
- Dielectric loaded cavity or waveguide slot antennas for telemetry applications, describing design and fabrication 02 p0192 A72-12157
- Pulse position modulation system for minimizing RF blackout during 2 kW S band reentry telemetry transmission 02 p0175 A72-12158
- Navy uhf telemetry transmitter production system, discussing test program contribution to quality control 02 p0177 A72-12322
- Digital telemetry data transmitter featuring triangular wave generator and signal mixer for reducing sensitivity to transmission path characteristics variations 02 p0179 A72-12415
- Time discrimination utilization in EMC, considering automatic position telemetering system using time division technique 03 p0325 A72-14047
- Telemetry systems with discrete compression-expansion function, calculating noise stability improvement as compared to linear and nonlinear signal conversion operations 04 p0487 A72-15000
- Exercise ECG multichannel radio telemetry equipment, discussing sources of malfunction and unreliability and remedial procedures 05 p0621 A72-16610
- Biomedical telemetry instrumentation for radio sensing and transmitting biological information from animals and man, including location by satellite-borne receivers 07 p0931 A72-19915
- Hybrid computer simulation for telemetry data collected during missile flight control system model post-flight verification and hardware performance analysis 07 p1085 A72-20332
- ATC operator stress factor evaluation from information theory analysis of radio telecommunication information content 09 p1271 A72-23134
- Digital data transition tracking loop as practical implementation of optimum self bit synchronizer in Mariner spacecraft telemetry demodulators 10 p1437 A72-24687
- Low cost real time computerized C 14 radiorespirometry telemetering system for monitoring human metabolism data during space missions 12 p1774 A72-28277
- Telemetry equipment of network tracking stations for CNES Symphonie satellites at 136-138 and 148 MHz [DGLR PAPER 72-015] 13 p1939 A72-28966
- Dielectric waveguide X band telemetry system for remote power and multiplexing applications in noisy electromagnetic pulse environment 14 p2087 A72-31047
- Integrated airborne-ground based instrumentation system for variable stability X-22A aircraft flying qualities research, discussing telemetry, mobile van, landing aids and airplane design 16 p2348 A72-33628
- Aircraft FDM and TDM systems, considering signal processing, cable requirements and applications to aircraft weapon systems and telemetry 18 p2692 A72-36529
- Investigation of the redundancy of telemetry information from the automatic lunar stations Luna 9 and Luna 13 21 p3014 A72-40312
- Simulation of the process of reducing the redundancy of multichannel telemetry information on a digital computer by the method of adaptive break down into discrete elements and associative sorting 21 p3014 A72-40313
- Reduction of redundant multichannel telemetry information by the method of adaptive break down into discrete elements and associative sorting 21 p3014 A72-40315
- Applicability of associative computers to parallel adaptive break down of telemetry information into discrete elements 21 p3014 A72-40316
- Telemetric frame compression coefficient and shaping algorithm for spacecraft data processing systems for arbitrary number of active channels 21 p3014 A72-40326
- ATS F and G radio link with ground stations, discussing telemetry and command functions with redundancy for RF interference minimization 21 p3019 A72-40883
- Possibility of employing a transistorized self-excited oscillator with a thermistor as radio sensor of temperature 21 p3058 A72-41792
- Radiorespirometry in the case of work and sports activities 22 p3149 A72-42071

- Telemetry acquisition of aerodynamic heat rates to conical, free-flight models at Mach 6 in an aeroballistic range. 22 p3155 A72-42703
- Broadband magnetic tape predetection recording of data modulated carrier MHz radio telemetry signals, applying to Aris, Mercury and Gemini programs 24 p3385 A72-45269
- RADIO TELESCOPES**
- Radio telescopes quality criteria, noting performance dependence on antennas dimensions and distribution 01 p0047 A72-10194
- Feed requirements and design of Effelsberg radio telescope with parabolic reflector operating down to 1 cm wavelengths 01 p0040 A72-10676
- Hybrid mode secondary focus feed realization for Effelsberg radio telescope, giving antenna radiation patterns 01 p0040 A72-10677
- Radio telescope variable profile antenna autocollimation adjustment for separating transmitted and received signals pulse-time characteristics 02 p0231 A72-12521
- Receiving equipment in 23 cm band for Krakow 15 m radio telescope 03 p0339 A72-13173
- Radiation pattern of radio astronomical paraboloidal reflector antenna in Dwingeloo, Netherlands, determining directivity and beam efficiency 04 p0501 A72-15423
- Radio sources and quasar structure angular resolution determination with distant radio telescope interferometry and microwave relay links 06 p0886 A72-18177
- Radio sources sky survey with radio telescope, discussing 5C1 and 5C2 spectral distributions 07 p1069 A72-19074
- Interferometric measurement at 1415 MHz of radio telescope paraboloidal antenna radiation pattern, using cosmic radio sources with known flux density as signal source 07 p0945 A72-19789
- Radio telescope for cosmic radio emission reception at 50-2 cm wavelengths, describing parabolic and auxiliary reflectors 07 p0965 A72-20299
- Transportable radio telescope for atmospheric attenuation and solar activity observations 09 p1316 A72-23509
- Arecibo Observatory radio-radar telescope design and operation, discussing reflector wire mesh surface, computer control and data acquisition, ionosphere and pulsar studies and interferometry 10 p1459 A72-24310
- Radio telescope observation of galaxy NGC 5253 in 21 cm line, noting centrally condensed emission complex of ionized gas 10 p1543 A72-24620
- Radiation pattern determination parabolic Cassegrain radio telescope reflector antennas from Fresnel zone emission source, using holographic technique 10 p1482 A72-24783
- Radio methods for cosmological model testing, discussing radio telescope requirements, source sampling procedures and counts as basic cosmological data 10 p1549 A72-25054
- Computer control data acquisition system for 46 meter radio telescope at Algonquin Observatory 11 p1631 A72-25697
- Dicke radiometer for 100 meter radio telescope, discussing demodulator design with dc coupling for difference signal and individual switching phases 12 p1792 A72-27807
- Waveguides for primary and hybrid mode horns for secondary feeders of deep paraboloid reflector radio telescope in Effelsberg, West Germany 12 p1793 A72-27811
- Astronomical pointing of radio telescopes using on-line computer 12 p1793 A72-27813
- Paraboloid and elliptical mirrors in 100 m radio telescope for Helios space probe signals reception, noting device compatibility for data exchange with NASA [DGLR PAPER 72-019] 13 p1939 A72-28964
- Solar radio emission map at 1.2 mm wavelength obtained with He cooled Ge bolometer connected radio telescope 13 p2046 A72-29716
- Narrow antenna radiation beam used for size and location determination of solar microwave radio burst observed with radio telescope 13 p2048 A72-29743
- Radio source scintillation observations by arms of one mile radio telescope at Molonglo Observatory 16 p2451 A72-33035
- Radio pulses from extensive air showers detected by antenna array with east-west oriented dipoles connected in parallel 16 p2444 A72-33036

Calibration of the flux density of Cassiopeia A and Cygnus A in the range 300-9375 MHz.
17 p2617 A72-35728

Radio astronomical observations in the 0.9 to 1.5 mm band using a 22-m radio telescope with an n-InSb receiver
19 p2858 A72-37803

Process control of the 100-meter telescope - Astronomical concept
19 p2803 A72-38485

Process control of the 100-m telescope - Digital control
19 p2803 A72-38486

Process control of the 100-m telescope - Communication of the observer with the computer-controlled telescope
19 p2804 A72-38487

A development study for a 65-m radio telescope for the mm wave range
19 p2804 A72-38510

Two-hybrid mode feed design procedure and performance for small and large f/D ratio reflectors of microwave telescope
21 p3029 A72-40515

Double-dipole exciter for the primary focus of the 100-m radio telescope Effelsberg
21 p3029 A72-40518

Emission and absorption spectral behavior observation by millimeter radio telescopes for molecules in interstellar space of Milky Way galaxy spiral arms
24 p3439 A72-44905

The techniques of present-day radioastronomy.
24 p3439 A72-44946

RADIO TRACKING
NT WILDLIFE RADIOLOCATION
Pulse IMPATT diode Ka band microwave rf head mechanically steered antenna array for airborne monopulse tracker applications
01 p0039 A72-10661

Aerial Radiological Measuring System for environmental radiation detection and tracking, emphasizing snow mass prediction by terrain radiation attenuation measurement
02 p0215 A72-11884

Phase comparison direction finder with successive signals comparison using commutation of two antenna elements for target acquisition and tracking operations
02 p0176 A72-12219

Satellite tracking by combined optimal estimation and control techniques with Kalman filter, considering radio antenna and optical tracking systems
02 p0285 A72-12812

Lunar gravity measurements via Apollo 14 Doppler radio tracking over 100 kilometer band during low periapsis altitude orbits, relating to surface features
05 p0722 A72-17126

Mariner 9 radio tracking measurements of Mars gravity field and pole direction, comparing to moon and earth
06 p0890 A72-18346

Sounding rocket radio tracking systems with real time trajectory plotting, developing computer program for exoatmospheric trajectory determination
07 p0939 A72-19089

Viking Mars Orbiter and Lander radio and radar science experiments, noting surface tracking, dual frequency S and X band data and communications system
10 p1539 A72-24380

Digital data transition tracking loop as practical implementation of optimum self bit synchronizer in Mariner spacecraft telemetry demodulators
10 p1437 A72-24687

Upper wind measurement by balloon-borne targets or radiosondes tracking by primary and secondary radars and radio theodolites
13 p1917 A72-28697

Loran/OMEGA course and track equipment (ILO-CATE) for remote object tracking by retransmission technique, eliminating search from search and rescue missions
13 p1997 A72-29182

Computational method for determining numerical values of relativity by two-way Doppler radio tracking and ranging data from planetary orbiting spacecraft
15 p2310 A72-31978

Solar tracking via automatic 5-GHz radiometer with paraboloid antenna, using continuous polar axis rotation in one direction
18 p2691 A72-36433

Geostationary or orbital satellite tracking radio receiver with steerable antenna for beacon signal detection and locking, discussing system design and performance
18 p2661 A72-36847

Delay-lock repeater tracking system utilizing super-regenerative interrogator.
21 p3082 A72-41084

Location estimation for spacecraft landed on Mars surface via statistical techniques application to earth based radio tracking data, taking into account ephemeris biases
21 p3082 A72-41554

Earth-based navigation capabilities for outer planet missions.
[AIAA PAPER 72-925] 24 p3423 A72-45430

RADIO TRANSMISSION
NT DOUBLE SIDEBAND TRANSMISSION
NT IONOSPHERIC F-SCATTER PROPAGATION
NT IONOSPHERIC PROPAGATION
NT MICROWAVE ATTENUATION
NT MICROWAVE TRANSMISSION
NT MULTIPATH TRANSMISSION
NT SHORT WAVE RADIO TRANSMISSION
NT SINGLE SIDEBAND TRANSMISSION
NT TRANSEQUATORIAL PROPAGATION
NT TRANSHORIZON RADIO PROPAGATION
Atmospheric waveforms in relation to source location, source vicinity electric field properties, VLF radio wave propagation, frequency spectra and lightning discharges
01 p0024 A72-10124

Tropospheric transhorizon meter, decimeter and centimeter wave propagation mechanisms, suggesting model for scattering and partial reflection effects
01 p0054 A72-10402

Atmospheric water vapor role in waveguide effects above sea on millimeter and centimeter propagation along transhorizon and beyond horizon paths
01 p0026 A72-10403

Atmospheric wave propagation mode parameters frequency dependence analysis from duct model, calculating received signal time behavior by waveguide transfer function
01 p0027 A72-10408

Tropospheric effects on vhf satellite signal transmission noted from time lags between observed and calculated satellite rise time
01 p0027 A72-10409

Daily, annual and long term ionosscatter and sporadic E variations above Europe, using hf propagation measurements
01 p0055 A72-10432

Radio signals information capability estimation during propagation through electromagnetic fields, using pulse amplitude modulation
01 p0065 A72-10446

Smith method for radio wave propagation time lag calculation, assessing maximum error by comparing calculated with measured distance/frequency characteristics
01 p0028 A72-10617

Midlatitude vhf phase detection of magnetic field aligned ionospheric irregularities
01 p0031 A72-10916

VLF propagation across discontinuous daytime-nighttime transitions in anisotropic terrestrial waveguide, developing dominant mode approximations of transmission and reflection coefficients
01 p0032 A72-11239

Spatial correlation coefficients measurements on one-hop hf radio waves obliquely reflected from ionosphere for various antenna spacings
01 p0032 A72-11252

Approximate height formula for radio ray propagating through spherically stratified smoothly varying troposphere, evaluating exponential model atmosphere
01 p0032 A72-11253

Power flow approximation for long distance long wave propagation of ground source between earth and ionosphere, comparing mode theory to heuristic approach
01 p0033 A72-11310

Radio signal fading analysis by ray tracing for transmission in spherically stratified atmosphere, assuming refractivity linear variation with height
02 p0179 A72-12414

Long distance monitoring method for short wavelength radio transmission to remote countries
02 p0182 A72-12671

Reflection and transmission coefficients for radio waves incident upon thin highly ionized layers, comparing with sporadic E reflections
03 p0344 A72-12976

Periodic microimpulsations in amplitude and bandwidth observed in long duration vhf whistler mode signals from ground stations, considering explanations
03 p0322 A72-13530

Soviet book on ground wave radio propagation at medium and long wavelengths covering field strength calculations over plane and spherical earth, soil conductivity, etc
03 p0323 A72-13950

Book on radio wave propagation covering ground, tropospheric and ionospheric waves, atmospheric and cosmic noise, reflection, attenuation, signal distortion, space communication, etc
04 p0487 A72-15269

Full wave solution for vertically polarized radio wave propagation over rough variable impedance surface by Fourier transform
04 p0492 A72-15437

Tethered flying rotor platform for reconnaissance, fire control and radio transmission assignments in naval missions, discussing system characteristics
04 p0465 A72-15652

Reciprocity theorems in electromagnetic theory concerned with radio transmitting and receiving point interchange for electric dipole sources
05 p0625 A72-16008

Quasi-monochromatic radio signal propagation for arbitrary amplitude and phase envelopes in nonlinear medium with nonlinearity caused by plasma heating
05 p0627 A72-16404

Digital computer investigation of radio signals transmitted by Vener 7 during Venus soft landing, describing spectral analysis and telemetric data detection methods
05 p0630 A72-16770

Rf transmission between two parallel whip antennas in warm plasma, noting received signal increase at probe resonant frequency
06 p0860 A72-17747

Magnetoguided whistler propagation, observing longitudinal current in ionospheric plasma
06 p0808 A72-18064

Refractive index structural constant relationship to atmosphere mean meteorological parameters, observing phase difference fluctuations of radio propagation in atmospheric surface layer
06 p0778 A72-18750

Anik communications satellite for Canadian domestic television and radio broadcasting networks
07 p0944 A72-19655

Ionospheric heating effects of vlf radio wave transmitters, relating changes in electron density and collision frequencies, reflection coefficients and wave fields
08 p1132 A72-21104

Mountains located on meteor propagation path of radio waves, investigating effect on transmission region size
08 p1239 A72-21891

Graphic determination of reflecting points location on active curve of given point meteor radiant based on stereographic projection and radio transmission properties
08 p1239 A72-21892

Optimal detection of rectangular radio signal pulse envelope distortions by multiplex fluctuations over white noise background
10 p1436 A72-24516

Radio propagation over slightly roughened curved earth surface, using perturbation method and Taylor series in model calculation
10 p1439 A72-24743

Radio wave beam trajectories in laminar isotropic plasma layer, using dynamic systems theory
11 p1591 A72-25335

Clock synchronization of multichannel radio communications systems using orthogonal signals with overlapping transmission spectra
11 p1598 A72-26727

Analytic ray path solutions for HF radio wave transmission through plane stratified isotropic ionospheric model
11 p1599 A72-26763

Radio wave propagation characteristics in Venusian atmosphere and interplanetary plasma from Venera 7 probe data
11 p1599 A72-26907

VLF recorder for measurement of incident direction, polarization, phase and amplitude of 16 and 60 kHz transmitter signals
12 p1796 A72-27791

Cross loop antenna for apparent azimuthal direction of incidence of VLF transmitter, showing night time bearing direction changes
12 p1784 A72-27794

Radio wave propagation control by superrefraction layers, investigating daily weather forecast technology improvement
12 p1784 A72-27797

Millimeter to meter waves propagation conditions prediction in horizontally inhomogeneous coastal foreground by meteorological parameters, considering wind effects on refractivity
12 p1784 A72-27798

Full wave analysis of radio wave propagation over rough surfaces characterized by variable impedance and height parameters
13 p1916 A72-28539

Relations between normal mode radio propagation parameters and properties of earth-low ionosphere isotropic waveguide, allowing for geomagnetic field
13 p1945 A72-28583

NASA program for acquisition, analysis and dissemination of space propagation and interference data for space systems designers, operators and regulatory agencies
[AIAA PAPER 72-577] 13 p1918 A72-28985

Airborne OMEGA navigation system performance, discussing transmission facilities, three frequency receiver, flight tests and optimization of receiving antenna
13 p1998 A72-29191

Whistler mode signals observation in conjugate region of 200 kHz broadcast station by satellite-borne narrow band receiver, considering field-aligned ducted and nonducted propagation
13 p1950 A72-29384

Oblique radio wave propagation through horizontally stratified ionosphere, considering electron collisions effects, reflection behavior and coupling levels
13 p1923 A72-29657

Aeronautical communication satellite technical and economic survey, considering wave propagation, noise, aircraft antennas and VHF and UHF links
15 p2193 A72-31180

Whistler propagation in magnetosphere disturbed by ring current, explaining electron density decrease
15 p2194 A72-31433

Ionospheric electron density measurement by radio propagation method, recording traveling ionospheric disturbance effect and sporadic E strata thicknesses
15 p2223 A72-31438

Time-frequency dissemination system design, discussing radio propagation, time signals, noise effects, synchronous satellite transponders and TV use, accuracy, geographical coverage and costs
15 p2198 A72-32065

Precise time and frequency dissemination via Loran C navigation system, discussing user techniques, economics and radio propagation mode and terrain effects on accuracy
15 p2268 A72-32067

Monochromatic radio wave propagation in interplanetary plasma, deriving frequency spectrum and phase and amplitude fluctuations
15 p2202 A72-32656

A mode-averaging diversity combiner.
17 p2513 A72-34360

Digital computer investigation of radio signals transmitted by Venera 7 during Venus soft landing, describing spectral analysis and telemetric data detection methods
17 p2516 A72-35273

Influence of horizontal electron-concentration gradients on the magnitude of the maximum usable frequency and the trajectory of radio wave propagation in the ionosphere
17 p2519 A72-35878

Investigation of radio-wave propagation by the oblique sounding method /Survey/
17 p2519 A72-35879

Satellite communications in Japan.
19 p2766 A72-38603

VHF-FM radio transmitting antenna for waves of circular, elliptical, and horizontally, vertically, or obliquely linear polarization
21 p3031 A72-40543

Planning of a broadcast-satellite service.
21 p3016 A72-40771

Complex detection - A waveform preserving technique for single-sideband demodulation.
21 p3017 A72-40862

FM signal distortion during passage through two-element antenna array to determine usable bandwidth from transmission characteristics viewpoint
21 p3022 A72-41265

International space telecommunication law and UN resolution concerning geostationary satellite orbit use for radio transmission
21 p3132 A72-41319

A presumptive formula for snowfall attenuation of radio waves.
21 p3023 A72-41829

Very-high-frequency wave propagation by the temperate-latitude sporadic-E layer.
22 p3154 A72-42367

Radiation field of a plane aperture in an inhomogeneous stratified medium over a large-radius sphere
22 p3155 A72-42654

A comparison of field-strengths of 164 kHz radio waves transmitted from Tashkent and received at Ahmedabad with flare-time solar X-ray emissions measured in satellites.
23 p3262 A72-43275

TV-radio satellite receiver equipment, considering power requirements, antenna, energy supply and placing into 24-hour orbit
23 p3262 A72-43300

Relations between normal mode radio propagation parameters and properties of earth-lower ionosphere isotropic waveguides, taking into account geomagnetic field
24 p3397 A72-45083

RADIO TRANSMITTERS

NT IONOSONDES

NT RADIO BEACONS

NT RADIOSONDES

NT RADIOTELEPHONES

NT RAWINSONDES

NT TRANSMITTER RECEIVERS

Grid controlled 100 W microwave transmitter power triode for space applications, noting high reliability and stability through use of metal dispenser cathode
01 p0009 A72-11223

Radio propagation from transmitter moving through irregular stationary ionospheric plasma, obtaining fluctuation dispersions for Faraday rotation angle and rate, phase, Doppler shift and refractions
04 p0489 A72-15395

Respiration rate transmitter with miniature pressure transducer for measuring pneumograph variations in animals over FM-FM telemetry system
08 p1124 A72-20898

Radio transmitter characteristics for radar sounding of upper atmosphere and meteor trails
09 p1278 A72-22874

VHF and UHF radio transmitters with strip transmission lines, discussing transistor power amplifier design
10 p1441 A72-25116

Space communications period forecasting algorithm for limited power ground based transmitters and spacecraft in earth orbit
11 p1598 A72-26735

Navigation accuracy of corrected OMEGA close to transmitter, using aircraft flight test at 500 nm range
13 p1997 A72-29186

Circuits for electromagnetic interference reduction in broadband solid state radio transmitters, discussing balanced transistor amplifier
15 p2209 A72-32564

Frequency assignment for collocated transmitters using the branch-and-bound technique.
20 p2901 A72-38986

The effects of transmitter source and load impedance on harmonic output spectrum - A new measurement method.
20 p2921 A72-38996

Temperature transmission from biopotential radiotelemetry transmitters.
22 p3151 A72-42745

High power radio transmitter for structural investigation of ionospheric D and E regions by signal reflection and electron concentration profiles
23 p3263 A72-43378

RADIO WAVE REFRACTION

Atmospheric radio refractive index computation errors derived from monthly averages of pressure, dry bulb temperature and vapor pressure
01 p0095 A72-10835

Orbiting lunar spacecraft Endeavor radio transmission postoccultation reception, considering surface wave propagation and mountain formation prismatic refraction
02 p0171 A72-11753

Scintillation effects on synchronous satellite communications systems at 250 MHz in equatorial region, discussing diversity techniques and composite diffraction refraction theory
05 p0631 A72-16906

Radio wave propagation control by superrefraction layers, investigating daily weather forecast technology improvement
12 p1784 A72-27797

UHF radio signals refraction angles and group delay times for biexponential model of ionospheric electron density profile
18 p2657 A72-36101

Influence of interstellar discontinuities on the shape of radio pulses from pulsars
18 p2726 A72-36652

Determination of the refractive index of air by a dispersion method based on the use of radio waves
22 p3155 A72-42722

RADIO WAVES

NT DECA-METRIC WAVES

NT DECIMETER WAVES

NT EXTRATERRESTRIAL RADIO WAVES

NT GALACTIC RADIO WAVES

NT IONOSPHERIC NOISE

NT LONG WAVE RADIATION

NT MICROWAVES

NT MILLIMETER WAVES

NT RADIO BURSTS

NT RADIO EMISSION

NT SHORT WAVE RADIATION

NT SKY WAVES

NT SOLAR RADIO BURSTS

NT SOLAR RADIO EMISSION

NT SUBMILLIMETER WAVES

NT WHISTLERS

Electron concentration profiles in D region from radio wave partial reflection coefficients
01 p0028 A72-10614

Spatial correlation coefficients measurements on one-hop hf radio waves obliquely reflected from ionosphere for various antenna spacings
01 p0032 A72-11252

Nighttime ionospheric radio wave propagation, determining geomagnetic latitude variations effects on absorption and reflection
02 p0218 A72-11944

Nighttime lower ionosphere electron density distribution models for vertically polarized radio wave propagation parameters
02 p0173 A72-12112

Stimulated Raman scattering effect on two quantum absorption during RF radiation first and third harmonics interaction
02 p0180 A72-12582

Radio wave polarization orthogonality recovery by using differential phase shifter and attenuator in radio communication systems
02 p0183 A72-12799

Nighttime hf radio wave field intensity measurement and absorption observation by narrow band receiver
02 p0184 A72-12874

Ray path and absorption calculation for mf and hf radio wave oblique propagation through model ionosphere in nighttime, noting E region ionization role
02 p0184 A72-12875

Radio propagation from transmitter moving through irregular stationary ionospheric plasma, obtaining fluctuation dispersions for Faraday rotation angle and rate, phase, Doppler shift and refractions
04 p0489 A72-15395

Interplanetary media plasma density fluctuations and power law spectra effects on radio wave scintillation
05 p0695 A72-16068

Radio wave beam trajectories in laminar isotropic plasma layer, using dynamic systems theory
06 p0774 A72-17731

Radio wave alternating electric field heating of ionospheric plasma electrons with density increase below 200 km and decrease at F layer maximum
08 p1152 A72-20703

Long radio waves slant incidence on isotropic inhomogeneous ionospheric plasma
08 p1131 A72-20737

Earth location effect in Fresnel diffraction zone on comparator performance, measuring phase difference fluctuations in turbulent atmospheric boundary layer radio waves
09 p1284 A72-22232

Phase errors in range finding measurements with radio waves reflection from underlying surface
09 p1277 A72-22481

HF radio waves induced incoherent scatter spectrum enhancement, noting parametric instabilities in ionosphere
09 p1279 A72-23014

Laboratory simulation of VLF/ELF radio waves transpolar ionospheric propagation, taking into account polar cap absorption
09 p1279 A72-23016

Nighttime E region electron density variation effects on MF and HF radio wave propagation, discussing ionospheric absorption detection experiments
11 p1593 A72-26070

Angles of arrival and skip distances prediction of radio waves near MUF, using monthly forecasts of quiet and perturbed ionospheric parameters and N/h profiles
11 p1594 A72-26276

Ionospheric radio wave absorption and intensity calculation, using vertical sounding data and riometric measurements
11 p1594 A72-26278

Plasma parametric instabilities excitation by radio waves in ionosphere, noting LF ionic and HF electrostatic wave growth
11 p1628 A72-26767

Cascade ionization of air by RF electric fields and intense laser pulses, solving Boltzmann equation for electron distribution
12 p1848 A72-27390

Beamed radio waves interaction in E and F1 regions propagation, noting beam width and field amplitude changes caused by defocusing
13 p1945 A72-28579

D region electron density profiles calculated as function of solar zenith angles, noting LF radio wave propagation
13 p1945 A72-28582

Virtual height dependence of ionospheric F region parameters including angular divergence of reflected radio waves, heterogeneity coefficient and random and drift motions velocity
13 p1948 A72-29038

Nighttime ionospheric radio wave propagation, determining geomagnetic latitude variations effects on absorption and reflection
13 p1949 A72-29256

Ionospheric electron density changes caused by strong radio waves induced plasma heating
14 p2102 A72-30657

Ionospheric models with constant electron density contours axially symmetrical to earth centered dipole magnetic field, discussing radio ray paths
15 p2230 A72-32263

Model for VLF emissions triggered by whistlers and man-made radio signals, noting effects of wave packet and second order resonance
16 p2365 A72-33905

Dispersion and random changes in the ground pattern of radio waves reflected from the ionosphere.
18 p2660 A72-36459

Radio wave alternating electric field heating of ionospheric plasma electrons with density increase below 200 km and decrease at F layer maximum
19 p2790 A72-38331

Long radio waves oblique incidence on isotropic inhomogeneous ionospheric plasma
19 p2766 A72-38365

- Ionospheric heating and electron density modification by high powered radio waves, describing research facility
20 p2919 A72-39724
- Isothermal ionization of the lower ionosphere under the action of radio waves
23 p3283 A72-43362
- Analytic ray trajectory model of radio wave lateral incidence on traveling large scale ionospheric inhomogeneities as function of location and azimuthal angle departure
23 p3263 A72-43377
- Polarization of the central field of a wave reflected from the ionosphere
23 p3265 A72-44173
- Beamed radio waves interaction in E and F I regions propagation, noting beam width and field amplitude changes caused by defocusing
24 p3397 A72-45079
- D region electron density profiles calculated as function of solar zenith angles, noting LF radio wave propagation
24 p3397 A72-45082
- RADIOACTIVE AGE DETERMINATION**
Apollo 14 crystalline rocks and fragments Rb/Sr, Ar 40/Ar 39 or cosmic ray exposure ages from electron microprobe and petrographic microscope examination
01 p0123 A72-10051
- Apollo 14 rocks, breccia fragments and soil samples ages from Ar 40/Ar 39 and cosmic ray dating, discussing basalt Ar release patterns
01 p0117 A72-10052
- Apollo 14 Fra Mauro site basaltic rocks and breccia clast internal Rb-Sr isochrons, comparing to Tranquility Sea basalts
01 p0123 A72-10053
- Radiometric upper limit to Fra Mauro Formation pebble age by Rb-Sr isotopic dating method
01 p0124 A72-10055
- Apollo 12 lunar samples exoelectrons of thermally stimulated emission, noting concentration of traps for radiation history measurement
01 p0124 A72-10063
- Sphene U-Pb age resistance to thermal metamorphism, discussing zircon U-Pb and biotite and hornblende K-Ar ages within thermal aureole
01 p0052 A72-10069
- Whole rock Rb-Sr measurements of hypersthene /including black/ chondrites for shock and reheating effects, noting data conformance to 4.5-4.6 giga-year isochron
04 p0571 A72-14566
- Cosmic ray exposure age of australites and far-east tektites, using C14 content as indication of terrestrial age
06 p0878 A72-17761
- Uranium content and radiogenic ages by fission track analysis in hypersthene, bronzite, amphibole and carbonaceous chondrites
06 p0878 A72-17791
- Apollo 15 rock 15555 age by argon-40-argon-39 dating
06 p0888 A72-18265
- Lunar mare basalt 15555 age by Rb-Sr and K-Ar techniques
06 p0888 A72-18266
- Gas retention and cosmic ray exposure ages of lunar rock from Hadley Rille, using isotopic dilution method
06 p0888 A72-18268
- Rb-Sr internal isochron determination of Luna 16 maria basalt age, discussing major lunar magmatic activity time interval
09 p1380 A72-22263
- Gas retention and cosmic ray exposure ages of Luna 16 basalt fragment from Mare Fecunditatis
09 p1380 A72-22264
- Tranquility Base rocks irradiation depths and cosmic rays exposure ages from rare gases in samples, noting correlated variations in He 3/Ne 21 and Ar 38/Ne 21 due to shielding differences
09 p1377 A72-22596
- Terrestrial stony meteorites age determination from C 14 content
09 p1386 A72-22661
- Lunar crust and mantle evolution from Rb-Sr ages of Apollo 15 mare basalt samples
10 p1537 A72-24161
- Rb-Sr isotopic age determination on density and size fractions of Apollo 11 fine soil and basaltic materials
10 p1538 A72-24165
- Radiogenic Ar 40/Ar 39 age and cosmic ray irradiation history of Apollo 15 anorthosite sample 15415, indicating Imbrian impact heating
12 p1862 A72-27111
- U, Th, Pb and rare earth elements abundances and Pb 207/Pb 206 ages of Apollo lunar minerals by ion microprobe mass analysis
12 p1866 A72-27114
- U-Th-Pb ages in Apollo 14 basalts and initial radiogenic Pb in lunar rocks, comparing with Rb-Sr and K-Ar isotopic method
15 p2303 A72-31301
- Pu 244/U 238 fission track retention age of whitlockite crystal in lunar breccia 14321 from Fra Mauro formation
15 p2307 A72-31722
- The exposure time of the Kiffa meteorite
17 p2603 A72-34200
- Apollo 14 Rb-Sr isotope rock sample data, relating isochron age to igneous crystallization time
17 p2607 A72-35073
- Gas retention chronology of Petersburg and other meteorites.
18 p2723 A72-36062
- Irradiation history of grain aggregates in ordinary chondrites - Possible clues to the advanced stages of accretion.
24 p3444 A72-45455
- RADIOACTIVE CONTAMINANTS**
The use of a scintillation counter to measure diagnostic X-ray tube kilovoltage, radiation exposure rates and contamination by low energy gamma emitters.
18 p2655 A72-37197
- RADIOACTIVE DATING**
U RADIOACTIVE AGE DETERMINATION
RADIOACTIVE DECAY
NT NEUTRON EMISSION
Proton bombarded CsI crystal spallation-caused radioactive decay products contribution to background rate in satellite X ray telescope detector
06 p0853 A72-18084
- Cosmological implications of radioactive decays study by Rutherford, suggesting evolving nonstatic universe
09 p1386 A72-22688
- Apollo 15 lunar heat flow experiment, discussing temperature data from probes and long lived radioisotopes decay effects
12 p1869 A72-27332
- Adiabatic effect of slow rotational molecular diffusion on perturbed angular correlations of gamma radiation for radioactive studies in viscous media
13 p2008 A72-29863
- Time invariance violation in charge asymmetry experiment, showing K-meson decay rate difference reversal from world to antiworld with particle unchanged
14 p2130 A72-30265
- Be 7 destruction via nuclear decay instigated by atomic electron capture in interstellar medium, considering Ar 37, Ca 41, Ti 44, V 49, Cr 51, Mn 53 and Fe 54
16 p2447 A72-33736
- Th 228 decay from short and long term simulation tests of thorium dioxide heat source in thermionic energy converter with W capsule
18 p2709 A72-36162
- RADIOACTIVE ELEMENTS**
U RADIOACTIVE ISOTOPES
RADIOACTIVE FALLOUT PARTICLES
U PARTICLES
RADIOACTIVE ISOTOPES
NT PLUTONIUM ISOTOPES
NT TRANSURANIUM ELEMENTS
NT TRITIUM
Nondestructive identification of alloy elements by nondispersive X ray fluorescence spectroscopy using Si/Li detectors and radioisotope sources for mobile applications
01 p0069 A72-10805
- Multielectrode piezoelectric chip ultrasonic transducer, sampling and readout techniques for radioisotope encapsulation testing
01 p0069 A72-10810
- Clad-to-core bond testing in radioisotope irradiation strips by pulsed laser ultrasonic schlieren system
01 p0080 A72-10811
- Nondestructive radioactive gas penetrant tests for porosity and fatigue damage in jet engine castings
01 p0069 A72-10813
- Al 26 production rates from Al, Si, S, Mg and Ca in Bruderheim chondrite by weighted least squares analysis
03 p0435 A72-13691
- Shock wave shape and strength alteration by radioisotope emissions from body surface in supersonic airstream
05 p0654 A72-17226
- Primordial radioelements and cosmogenic radionuclides in Apollo 15 basalt, breccia and soil samples
06 p0889 A72-18274
- Radionuclides formation rate as function of depth in moon for bombardments by galactic cosmic ray particles and by solar protons
07 p1057 A72-19140
- Isotope radiometric density measurement errors for thin material sections, presenting mathematical analysis for measurement procedures optimization
07 p0995 A72-19651
- Radioactive molybdenum disulfide lubrication films distribution on nitrated steel and on magnesium pig iron
07 p0996 A72-19775
- Cosmogenic radionuclides pickup by cloud water and deposition in precipitation described by model
12 p1863 A72-27503
- Radiovoltaic generator energy conversion by thin film solar cells, noting performance dependence on semiconductor band gap and radioisotope characteristics
12 p1757 A72-28021
- Lunar origin and evolution, considering gravitational energy, radioactive isotopes and tidal deformations as heat sources
14 p2161 A72-30997
- Radioisotope camera based on electron avalanche in liquid Xe, noting spatial and energy resolution advantages over existing gamma ray cameras
15 p2234 A72-31537
- Thermal history and early magmatism for lunar models, considering high near-surface temperatures and radionuclides upward transport during melting
15 p2311 A72-32082
- The exposure time of the Kiffa meteorite
17 p2603 A72-34200
- German monograph - Studies of high-temperature corrosion of cobalt and cobalt alloys with radioactive isotopes
19 p2816 A72-37657
- Neutron activation analysis of tin in geochemical and cosmochemical material, using 40 minute Sn-123.
20 p2900 A72-39843
- Nuclear particle fluxes and radioactive isotopes production rate distribution from cosmic rays data along orbits, calculating iron meteorite dimensions prior to atmosphere entry
22 p3220 A72-41919
- An isotopic criterion for estimating the length of meteorite orbits
22 p3223 A72-42160
- Cosmogenic radionuclides in the Allende and Murchison carbonaceous chondrites.
22 p3225 A72-42466
- Depth distributions of cosmic ray produced radionuclides in chondrites and achondrites, determining aphelia from Al 26 activities
22 p3228 A72-42861
- Charged and neutral cosmic rays radioactive isotope and momentum distribution measuring techniques in high energy particle astronomy observatories /HEAO/
24 p3404 A72-45540
- RADIOACTIVE MATERIALS**
Internal strain measurement in solid elastomeric materials by radioactive implant method using pinhole camera or multichannel collimator
07 p0992 A72-20583
- Viking Lander detection of metabolically produced radioactive labeled gas in Mars surface samples
10 p1540 A72-24386
- Target anion effect on radioactive Sb and Te distribution formed by high energy proton irradiation of cesium salts containing oxygen
15 p2282 A72-32485
- RADIOACTIVE NUCLIDES**
U RADIOACTIVE ISOTOPES
RADIOACTIVE WASTES
Space and atmosphere contamination by industrial wastes, aircraft and spacecraft exhaust and radioactive waste disposal, considering legal safeguards
07 p1104 A72-19466
- Transportation of radioactive waste-materials into the sun.
24 p3450 A72-45184
- RADIOACTIVITY**
Relief effects on atmospheric natural radioactivity vertical distribution
02 p0275 A72-12879
- Primary cosmic ray interaction with tissues, emphasizing biological effects and nuclear reactions induced radioactivity in astronaut body
03 p0313 A72-12911
- Cosmic ray induced radioactivity effects on diffuse gamma ray background measurement from 600 MeV proton irradiation experiment
04 p0567 A72-15324
- Lunar thermal history and radioactivity upper limits determination consistent with proposed temperature distribution and Apollo chondrite data, implying low uranium content
04 p0581 A72-15579
- Low radioactivity of surface exposed lunar rock from alpha spectrometry, indicating absence of radon outgassing
15 p2303 A72-31304
- Argon 37/argon 39 activity ratios in meteorites and the spatial constancy of the cosmic radiation
18 p2723 A72-36027
- Estimation of the turbulent diffusion coefficient and of the vertical wind velocity component from the distribution of natural radioactivity
20 p2964 A72-39320
- RADIOBIOLOGY**
Biological dosimetry in acute human irradiation from cytogenic study of peripheral blood and bone marrow
04 p0467 A72-14606
- Proliferative blood forming tissue activity under chronic gamma ray irradiation in guinea pigs by quantitative methods, showing myeloid and reticular disturbances of bone marrow
04 p0467 A72-14607

Electrocardiography telemetry system for intense radiation environment, describing electrode and transmitter implantation in monkey and heart signal transmission and reception

05 p0623 A72-16678

Soviet book on radiation hazards and protection in space covering detection, radiobiology and effects on human organism

11 p1713 A72-26050

Three year varied dose and acute exposure gamma irradiation of dogs, noting radiobiological effects from hematological, cytological and physiological examinations

13 p1903 A72-29307

Brief survey of the problems of space radiobiology and radiation safety in space flights.

17 p2509 A72-35376

Some aspects of the use of small needle-shaped semiconductor detectors in the determination of regional distribution and transport of labelled compounds.

18 p2655 A72-37195

Radiobiological problems caused by supersonic transport /With a survey of the first results established by tests performed on board the Concorde prototype/.

19 p2762 A72-38713

Ionizing radiation effects on mitosis and nucleic acid synthesis, noting protective chemical agents and hematological evaluation of radiation damage and marrow regeneration

22 p3141 A72-41986

Instrumental neutron-activation determination of cobalt and certain other elements in plant materials

22 p3183 A72-42471

Simultaneous neutron-activation analyses of scandium, cobalt, iron, and zinc in biological objects with the aid of a total-absorption gamma spectrometer

23 p3259 A72-43347

Physiological and hematological effects of chronic irradiation.

23 p3254 A72-43392

Summary of latent effects in long term survivors of whole body irradiations in primates.

23 p3254 A72-43393

The precise simulation of image transfer systems with the aid of an optical convolution obtained with a rotating slit of prescribed form

23 p3261 A72-44361

RADIOCHEMICAL SEPARATION

Multielement neutron activation analysis of geological and lunar material using chemical group separations and high resolution gamma spectrometry.

20 p2899 A72-39830

Improved techniques for separation and determination of rare-earth elements in extraterrestrial material.

20 p2900 A72-39836

RADIOCHEMISTRY

NT RADIOCHEMICAL SEPARATION

Conversion of angiotensin to angiotensin 2 in dog pulmonary circulation, studying peptide synthesis, radioimmunoassay and in vivo and plasma in vitro metabolism

04 p0475 A72-15465

RADIOGENIC MATERIALS

Lunar soil radiogenic U-Th-Pb analyses of Lunik 16 samples from Sea of Fertility

09 p1381 A72-22278

RADIOGONIOMETERS

Fluctuating white and narrow band noise and interference pulse effects on monopulse goniometer

02 p0176 A72-12220

Leonid meteor trail drift measurements in upper atmosphere, comparing radar system with precise goniometric capabilities to photographic methods

09 p1383 A72-22509

Radiogoniometer error analysis for receiver internal noise and external interference sources, noting sources angular distribution effect on instrument error

22 p3158 A72-42233

RADIOGRAPHY

NT ANGIOGRAPHY

Reactor source neutron radiography for nondestructive testing, noting hydrogen detection, boron fiber imaging and photographic or electronic color enhancement

01 p0069 A72-10807

Radiographic detection of small flaws in bulk graphite and carbon/carbon composites, improving image quality and sensitivity by contrasting liquid impregnation

01 p0069 A72-10808

Nondestructive radiographic tests for void and unbond detection in Scout solid propellant rocket motors

01 p0114 A72-10812

Solar coronal MHD disturbance off eastern limb correlation with complex radio event observed simultaneously with white light coronameter and Culgoora radioheliograph

02 p0276 A72-11647

Single scan TV-radiography system for providing A-D converter analog signal for digital data acquisition, obtaining transfer functions

04 p0522 A72-15226

High speed photography and radiography applications to high explosives research, discussing shock wave visualization, illumination techniques for rapid processes time resolution, etc

06 p0813 A72-17436

Aseptic bone necrosis pathology from radiographic studies in dogs with decompression sickness noting articular cartilage erosion and joint dysplasia and exostosis

06 p0764 A72-17876

Neutron radiography visual examination method, using uniform intensity neutron beam from nuclear reactor source

06 p0816 A72-17998

Nondestructive tests of welded joint heterogeneities and corrosion cavities by densitometric photometric differentiation of radiographs

07 p0995 A72-19674

Pulsed radiography of X ray absorption by plasma behind incident shock wave in Cs vapors, noting mirror behind shock front and wave reflection

07 p1044 A72-19887

Electron beam welding induced secondary X rays observation with pinhole X ray movie camera to determine beam-metal interactions during penetration

07 p0997 A72-20003

Latent image formation in radiographic emulsion of AgBr crystals dispersed in gelatin layer, considering crystal structure and X and gamma rays energy recording

07 p0991 A72-20424

Commercial radiographic system with data enhancement based on monochromatic blue film, noting image quality and exposure range

07 p0991 A72-20425

High neutron absorption doping material selection for enhancing explosive mixtures neutron radiographic image without interference with chemical reaction

08 p1220 A72-20769

High temperature radiographic techniques for measurements of molten ceramics density, melting point, phase transitions, surface tension and viscosity up to 3000 C

09 p1333 A72-22378

Thermal neutron radiography industrial applications, describing nondestructive testing techniques

10 p1485 A72-23813

Radiographic image enhancement based on mathematical concepts of image convolution, Fourier transformation and spatial frequency filtering, discussing hardware and computer needs

10 p1481 A72-24322

Visual image indicator used beside and behind objects for neutron radiography quality determination and radiographs series grading

11 p1632 A72-25822

Radiographs electronic image contrast enhancement by video signal generation with amplitude proportional to density rate of change, discussing system dynamic response and resolution

11 p1633 A72-26034

Hemodynamic assessment of arterial blood flow from radiograph measurements of aorta branching points

11 p1582 A72-26774

Metal matrix composites radiography in NDT, discussing parameters optimization and uses of microfilm, densitometers and high resolution vidicon tubes

12 p1813 A72-27199

Hemodynamic effects of angiographic contrast medium in patients with and without heart disease, discussing myocardial performance during first ten beats

12 p1762 A72-27732

Composite materials evaluation methods, discussing high quality photographs, radiography, laser holographic interferometry, thermographic fluorescent phosphors, liquid crystals and acoustic techniques

12 p1815 A72-28101

Radiographic measurement of gas turbine components during response to thrust changes, using linear accelerator for X ray generation

14 p2092 A72-30620

Pulsed radiography of X ray absorption by plasma behind incident shock wave in Cs vapors, noting mirror behind shock front and wave reflection

17 p2590 A72-35135

The imaging properties of the positron camera

18 p2652 A72-36424

Thermal neutron radiography as NDT technique for industrial inspection, noting advantages for low atomic number and radioactive materials

18 p2695 A72-36457

Operation and performance characteristics of flying spot scanning X ray imaging systems for rapid film safe parcel inspection

18 p2692 A72-36671

Factors governing radiographic crack detectability in steel weld specimens.

18 p2695 A72-36673

Two new methods to increase the contrast of track-etch neutron radiographs.

19 p2833 A72-37636

Nondestructive testing of advanced composites.

19 p2799 A72-37669

Selection of characteristics for automatic classification of welding defects in radiographic testing.

19 p2805 A72-38763

Mobile X ray apparatus for radiographic flaw detection, describing tuned transformer high voltage source as power supply to sealed sectionalized X ray tube

19 p2805 A72-38766

Determination of the elastic modulus of the left-ventricle myocardium with the aid of X-ray kymography

20 p2893 A72-38940

A radiographic technique using an electron beam welder.

20 p2929 A72-39340

The gamma-ray-irradiation method applied to three-dimensional thermal photoelasticity.

21 p3051 A72-40230

Effects of coronary arteriography on myocardial blood flow.

23 p3256 A72-43933

Sharp focused short pulse X ray source with laser flash synchronization for radiographic plasma diagnostics

24 p3429 A72-45495

RADIOISOTOPE BATTERIES

Aerospace radioisotope power systems, discussing heat source technology, shielding, safety and thermoelectric integration

01 p0098 A72-10387

Unitized bellow radioisotope thermoelectric generator concept for long term stability, using standardized design, fabrication and qualification

05 p0615 A72-15940

Geometry comparisons for weight and safety of multiwatt radioisotope heaters.

17 p2579 A72-35352

Nuclear rocket reactor and radioisotope power technology for propulsion and electricity requirements in spacecraft and space stations

24 p3423 A72-45166

United States Space Nuclear Electric Power Program.

24 p3424 A72-45179

RADIOLOGY

Aerial Radiological Measuring System for environmental radiation detection and tracking, emphasizing snow mass prediction by terrain radiation attenuation measurement

02 p0215 A72-11884

New cancer therapy treatment techniques using space dosimetric concepts.

24 p3374 A72-45112

RADIOLYSIS

Radiation damage in MgO, ZnO and magnesium difluoride, considering energy dependence and roles of radiolysis and elastic collisions

03 p0404 A72-14088

Water radiolysis within sealed Al capsules in nuclear reactor, calculating pressure rise due to water decomposition via predictive models derived by multiple regression analysis

04 p0546 A72-14429

Hydrazine thrusters for space application.

21 p3098 A72-40123

RADIOMETERS

NT DICKE RADIOMETERS

NT INFRARED DETECTORS

NT INFRARED SCANNERS

NT MICROWAVE RADIOMETERS

NT SPECTRORADIOMETERS

Monostatic and bistatic lidar and solar radiometer sensing techniques for remote measuring of aerosol size distributions

01 p0066 A72-10528

Phase stable locked local oscillators for K band radiometers for long baseline interferometric measurements, emphasizing construction technique

01 p0044 A72-11307

Calorimetric and radiometric methods for thermal radiation properties of solids, considering reflectance, absorbance, transmittance and spectral emittance

02 p0223 A72-11499

Millimeter wave sky noise temperature measurement with 16 and 35 GHz radiometers, including antenna loss and rain and cloud effects

02 p0171 A72-11665

Terrestrial radiation emission mapping from imagery produced by scanning radiometer, discussing remote sensors used to study surface energy phenomena

02 p0210 A72-11804

ERTS-A satellite geometric and radiometric received image errors, presenting detection and correction with digital algorithms

02 p0171 A72-11847

Airborne remote CAT detection equipment, examining pulsed Doppler laser and IR radiometry

04 p0521 A72-14831

Horn lens antennas for millimeter wave radiometric applications, discussing medium gain polystyrene lens design to obtain low peak sidelobes

04 p0503 A72-15608

Pressure modulated carbon dioxide radiometer for remote temperature sounding in upper atmosphere
05 p0663 A72-16692

Nighttime ground surface temperature prediction by net flux radiometer
05 p0684 A72-16792

Narrow beam radiometer design and performance for atmospheric radiation studies including water vapor continuum absorption and high layer clouds emissivity
06 p0819 A72-18447

Balloon-borne radiometer-sonde measurement of stratospheric downward emission in absorption spectral region of water vapor rotational band
07 p0982 A72-19105

Isotope radiometric density measurement errors for thin material sections, presenting mathematical analysis for measurement procedures optimization
07 p0995 A72-19651

Multicarrier communications satellite signal power, center frequency and rms deviation computer controlled monitoring system with frequency shift radiometer principle
07 p0948 A72-20491

Design equations for transpiration radiometer applicable to radiation measurement from confined Ar plasma
08 p1163 A72-20919

Gamma radiation source energy and activity determination for radiometric flaw detection in steel
08 p1177 A72-21775

Nimbus 4 satellite-borne selective chopper radiometer design characteristics, obtaining maps of stratospheric warmings in both hemispheres
08 p1173 A72-22168

Radiometric method for atmospheric moisture data retrieval above radiosonde hygistor cut-off or during malfunction, inferring average moisture decrease through radiative transfer equation
09 p1307 A72-22441

Successful operational satellite sounding probabilities with normal global cloud cover by vertical temperature profile radiometer
10 p1508 A72-25082

Precision radiometric techniques in meteorology and geostrophysics, discussing references, pyrohelimetric scale, transfer calibrations and solar radiation measurements
10 p1485 A72-25097

Far IR filters for rocket-borne radiometer, discussing Ulrich theory and characteristic impedance determination
11 p1629 A72-25310

Ground based radiometric measurements of vertical temperature profiles in planetary boundary layer, describing data reduction technique
11 p1681 A72-26083

Surface pressure and vector wind fields computerized analysis from satellite radar radiometer simulation and conventional data
13 p1995 A72-29619

Adaptive radiometer dynamic properties and parameters optimization based on minimum mean square error criterion
14 p2088 A72-30373

Sea surface temperature determination on Nimbus 2 satellite, using three channels in medium resolution IR radiometer
15 p2224 A72-31674

Selective chopper radiometer /SCR/ radiances comparison to rocketsonde data, showing vertical resolution of stratosphere and mesosphere temperature changes during mid winter disturbance
15 p2228 A72-31976

IR heterodyne radiometer SNR and spectral resolution, noting application to solar physics and air pollution detection
17 p2555 A72-35196

Russian monograph on heat measurement covering methods and instruments for heat flux determination, radiometers, thermal conductivity gages and electrical calorimeters
17 p2556 A72-35495

A new project of 8-cm radioheliograph
18 p2691 A72-36434

Meteorological applications of the Nimbus 4 temperature-humidity infrared radiometer, 6.7 micron channel data
18 p2707 A72-36718

Microradiometer for studying the structures of highly intensive radiation fields
20 p2924 A72-39224

Mathematical model for moving radiometer system for reflected solar radiation measurement, discussing instrument time constant effect on surface emittance variations reproduction
20 p2927 A72-39795

Helium-cooled mass spectrograph and frigen-cooled radiometer in a plasma wind tunnel
20 p2928 A72-39929

Radiometry error analysis for diffraction at radiation beam limiting screens, calculating corrections for circular source and detector
21 p3050 A72-40149

Radiometer with protective mica window for radiant flux densities measurement of near IR sources, noting reading independence of sources spectra characteristics
21 p3059 A72-41821

A transpiration radiometer for measurement of total thermal radiation from a flowing plasma
22 p3179 A72-42691

Experimental comparisons of the international pyrohelimetric scale with the absolute radiation scale
23 p3290 A72-44274

RADIOISOTOPES
U RADIOACTIVE ISOTOPES

RADIOPATHOLOGY
Changes produced in the nerve structures of the stellate ganglion by total X-ray irradiation
22 p3140 A72-41925

RADIOPROTECTIVE AGENTS
U ANTIRADIATION DRUGS

RADIOSENSITIVITY
U RADIATION TOLERANCE

RADIOSONDES
NT IONOSONDES
NT RAWINSONDES
Kinematic vertical motions computation from radiosonde wind observations, correlating with synoptic features
01 p0095 A72-10855

APZ-2 daytime actinometric radiosonde measuring long wave radiation balance in presence of short wave solar radiation
06 p0814 A72-17626

Balloon-borne radiometer-sonde measurement of stratospheric downward emission in absorption spectral region of water vapor rotational band
07 p0982 A72-19105

Radiometric method for atmospheric moisture data retrieval above radiosonde hygistor cut-off or during malfunction, inferring average moisture decrease through radiative transfer equation
09 p1307 A72-22441

Rainfall rate estimation by radar reflectivity measurements based on atmospheric parameters obtained from radiosonde data
09 p1345 A72-22449

Hair hygrometer for FM radiosonde in-flight air humidity measurements, discussing design, operation and accuracy test in extreme weather conditions
10 p1483 A72-25005

Reference radiosondes for quality control of global high altitude temperature, pressure and humidity measurements, discussing dual soundings and synoptic comparison
10 p1484 A72-25077

Loran-Omega course and track equipment /LO-CATE/ of integrated upper air meteorological sounding systems, describing radiosonde navigational aids
10 p1484 A72-25086

Radiosonde balloon tracking errors in upper atmosphere wind measurement with Loran C, Omega and radar transmitters
10 p1441 A72-25092

Sporadic E layer structure model from radiosonde observation, noting peak plasma frequency variation and total reflection by blobs
10 p1441 A72-25153

Similarity method to compute ionosphere drift velocity and direction from radio sounding data
19 p2792 A72-38640

Radiation influences on a white-coated thermistor temperature sensor in a radiosonde
24 p3401 A72-44620

RADIOTELEPHONES
Two way telephone communication to individual subscribers and thin route exchange terminals via satellites, discussing cost, performance and capacity [AIAA PAPER 72-541]
12 p1780 A72-27364

RADIOTHERAPY
U RADIATION THERAPY

RADOME MATERIALS
Dielectric materials for antenna system radomes, discussing electromagnetic wave propagation and climatic factors effects
03 p0381 A72-14362

Electromagnetic thickness measurement on the AWACS radome
24 p3384 A72-44901

X-ray inspection of the AWACS radome attachment locations
24 p3406 A72-44902

RADOMES
Radome enclosed Haystack parabolic antenna characteristics as radio astronomical instrument, discussing gain, polarization, interference susceptibility and noise temperature [AD-737166]
01 p0032 A72-11233

Radome checkout ensuring reproducibility by insertion phase delay measurement
06 p0822 A72-18195

Geometrical optics approximation for angular error calculation of microwave antenna radome, noting boresight error proportionality to walls electrical thickness
23 p3271 A72-43837

RADON
NT RADON ISOTOPES
Low radioactivity of surface exposed lunar rock from alpha spectrometry, indicating absence of radon outgassing
15 p2303 A72-31304

RADON ISOTOPES
Random walk atomic migration model for radon diffusion through lunar regolith into atmosphere
13 p2038 A72-28995

Measurements of radon emanation from Apollo 11, 12, and 14 fines.
18 p2728 A72-36970

Equilibrium lunar atmospheric content of radon-222, noting earth based diffusion constants inapplicability in moon vacuum conditions
20 p2972 A72-39861

RAFTS
NT LIFE RAFTS

RAIL TRANSPORTATION
Air transport vs other travel, discussing time, costs, popularity and technology
03 p0459 A72-13485

Computerized man machine systems human factors research simulator, discussing application to railroad train operations
06 p0795 A72-17434

Prediction models for dynamic environment experienced by cargo during air and rail transportation
15 p2339 A72-32610

RAILROADS
U RAIL TRANSPORTATION

RAILS
Continuously supported railroad track under axial compression forces and moving load, noting critical velocity for high speed trains
09 p1409 A72-23558

RAIN
Rain droplet size distribution effects on microwave attenuation at millimeter wavelengths, comparing calculation with measurement
01 p0027 A72-10406

Transparent rain repellent polymer coatings, discussing water repellency theory, polymer chemical structures, adhesion to glass surfaces and evaluation methods
03 p0381 A72-14237

Rain amount forecasting based on five level atmosphere model and hydrothermodynamics equations, calculating vertical currents under uniform atmospheric boundary layer stratification conditions
07 p1029 A72-18859

Rain induced flood mathematical model, optimizing parameters and applying to hydrological forecasts
07 p1029 A72-18862

Vertical air motion three dimensional field measurement near mobile fronts by high precision tracking of air-dropped radar reflectors, noting quantitative rainfall prediction
07 p1029 A72-19098

Atmospheric attenuation due to rain based on links experiment and statistical study of equivalent precipitation for given path length and time percentage
07 p0939 A72-19188

Radio attenuation above 10 GHz based on theoretical model of equivalent precipitation on path using intensity spatial distribution function within rain cell
07 p0940 A72-19189

Rain attenuation determination at 15 and 35 GHz under precipitation condition from emission measurement and correlation to regression line, using portable radiometric system [AD-741093]
07 p0946 A72-19791

Probability estimates for aircraft encounters with heavy rain
07 p1031 A72-20365

Rainfall rate estimation by radar reflectivity measurements based on atmospheric parameters obtained from radiosonde data
09 p1345 A72-22449

Turbulent jets effectiveness in protection of aircraft surfaces from rain, describing wind tunnel simulation of takeoff and landing
10 p1463 A72-25137

Radio attenuation by rain at 37 GHz using sun as source compared with sky emission observations, noting apparent absorber temperature effect
12 p1783 A72-27665

Azimuth display of attenuation instrument used with weather radar to measure rain induced attenuation over slant paths
15 p2207 A72-32101

Slant path radar attenuation events due to rain during frequencies at 10 GHz, obtaining statistics on frequency of occurrence, extent in azimuth and duration
15 p2200 A72-32103

Fog, cloud, rain and snow detection by acoustic echo sounding, noting effects of energy scattered from atmospheric boundary layer velocity and temperature fluctuations
15 p2267 A72-32725

- Tracking radar system rain clutter reduction by backscatter polarization technique for signal phase and magnitude adjustment 18 p2659 A72-36310
- Linear cross polarization and attenuation measurements on terrestrial link at 11 GHz correlated with rainfall information 21 p3017 A72-40855
- Propagation loss of centimeter and millimeter waves in rainfall. 21 p3023 A72-41833
- Thermodynamic conditions for the development of convective clouds and a method of forecasting the quantity of rainfall 22 p3202 A72-42953
- RAIN GAGES**
- Sensors measurement accuracy for rainfall amount and duration determination by automatic remote transmitting meteorological station 10 p1483 A72-25017
- RAIN IMPACT DAMAGE**
- Thunderstorm flight testing for evaluation of rain, ice, lightning and turbulence effects on aircraft, engine and systems operating characteristics 06 p0760 A72-18500
- Raindrop breakup in the shock layer of a high-speed vehicle. 24 p3395 A72-45780
- RAINDROPS**
- Positive corona streamers interactions with cloud droplets atomized from water and glycerin solution, discussing atmospheric significance 06 p0841 A72-17823
- Rain droplets growth by collision and coalescence during fall through sheared air flow, discussing discrepancies between calculated and experimental collision efficiencies 11 p1619 A72-26642
- Theoretical and measured rainfall attenuation of millimeter waves, correlating attenuation coefficients, rain rate and drop size distributions 12 p1785 A72-27803
- Mathematical model for flow field inside raindrop under aerodynamic transient stresses before impingement at stagnation point of blunt body in supersonic flight 13 p1942 A72-29224
- Raindrop breakup in the shock layer of a high-speed vehicle. 24 p3395 A72-45780
- RAINSTORMS**
- NT THUNDERSTORMS**
- Ground terminals spatial diversity for earth satellite mm wave communication systems to avoid attenuations by rainfall 13 p1989 A72-28810
- Shower precipitation amounts forecasting by layer method, showing inadequacy from viewpoint of physical principles 13 p1995 A72-29594
- RAKES**
- Engine compressor face rake for flight test instrumentation F-14A/TF-30. 22 p3216 A72-42686
- RAMAN EFFECT**
- U RAMAN SPECTRA**
- RAMAN LASERS**
- Remote air pollution detection by laser methods, comparing Raman backscattering, resonance backscattering and resonance absorption 04 p0531 A72-15300
- Tunable semiconductor and spin-flip Raman lasers for IR applications [AD-738713] 05 p0667 A72-15788
- Air pollutant monitoring and remote analysis by Raman, fluorescence and resonance backscattering, Rayleigh scattering and absorption laser radar techniques 06 p0827 A72-18460
- Tunable monochromatic IR laser based on magneto-Raman scattering from conduction electrons in n-type InSb, discussing physical processes and experimental techniques 15 p2250 A72-32393
- RAMAN SCATTERING**
- U RAMAN SPECTRA**
- RAMAN SPECTRA**
- Parametric amplification of laser waves with amplitude and phase modulation under exponential signal growth applied to Raman scattering picosecond pulse field 01 p0079 A72-10346
- Laser radar application to air pollution measurement, discussing techniques and instrumentation utilizing elastic, Raman and fluorescence scattering [AIAA PAPER 71-1056] 01 p0028 A72-10527
- Fabry-Perot interferometer application as filter with transmission windows at regular intervals in wave numbers to detect Raman scattered radiation from atmospheric gases [AIAA PAPER 71-1078] 01 p0067 A72-10537
- Environmental pollution sensing by vibrational laser Raman scattering probe measuring species constituents

- cy and temperature, discussing fluorescence, scattering cross sections and band shape [AIAA PAPER 71-1084] 01 p0067 A72-10541
- Raman scattering from water vapor for Ar laser wavelengths in remote atmospheric humidity measurements [AIAA PAPER 71-1085] 01 p0104 A72-10542
- Raman scattering cross sections and depolarization ratios of atmospheric gaseous pollutants as function of incident photon energy [AIAA PAPER 71-1086] 01 p0104 A72-10543
- Decay interactions among plasma wave and two opposed electromagnetic waves in homogeneous layer of isotropic collisionless plasma, observing stimulated Raman scattering 02 p0180 A72-12579
- Stimulated Raman scattering effect on two quantum absorption during RF radiation first and third harmonics interaction 02 p0180 A72-12582
- Ruby and Nd lasers fundamental emission effects on excitation of stimulated Raman scattering in liquid and crystalline media by second harmonics 03 p0366 A72-13364
- Ground based atmospheric vertical temperature profiles measurement by Raman backscatter from molecular nitrogen 03 p0348 A72-13430
- Raman scattering cross section measurement for atmospheric nitrogen tetroxide, using Q switched ruby laser excitation source 03 p0367 A72-13601
- Coherence of excitations produced in crystal by Raman effect via two beam method 03 p0368 A72-13796
- Vibrational IR and Raman spectra of dimethylaminodichlorophosphine, determining molecular structure symmetry in liquid and solid phases 04 p0481 A72-14444
- Laser pulse induced stimulated Raman scattering /SRS/ in linearly dispersionless medium measuring delay between laser and Stokes pulse maxima by photon absorption fluorescence technique 05 p0693 A72-17170
- Stimulated Raman emission in glass fiber optical waveguides with low threshold broadband gain, permitting construction of wideband amplifiers and oscillators 07 p0953 A72-18876
- Stokes Q branch fundamental vibrational Raman light scattering cross sections and depolarization ratio measurement for molecular gases 07 p1038 A72-20292
- Ground based Raman laser backscatter measurement of stratospheric water vapor content, noting 1 ppm accuracy 08 p1161 A72-21825
- Air pollution monitoring with tunable lasers employing Raman scattering, resonantly excited or hot gases emission and resonant absorption 09 p1322 A72-22313
- Atmospheric temperature vertical profiles by laser Raman backscatter measurements 09 p1307 A72-22439
- Vibrational laser Raman scattering from flame gases for nitrogen, oxygen and water vapor 09 p1276 A72-22978
- Line intensity variation simulation in Raman spectrum of oxygen with allowance for spin splitting of rotational levels 09 p1358 A72-23049
- Raman band rotational structure computer simulation, noting application to gaseous chlorine spectrum analysis 09 p1358 A72-23050
- Thin GaP film composition and structure determination by laser Raman scattering 09 p1314 A72-23345
- Laser radar technique for invisible air pollutants remote sensing systems, comparing Raman backscattering resonance scattering and absorption schemes 10 p1489 A72-23952
- Raman spectra of azoanisole and anizaladiazin in liquid crystal states excited by Ar laser, revealing lattice vibrations attenuation near transition point 10 p1490 A72-24042
- Preresonance Raman scattering tensor in Born-Oppenheimer approximation of molecular wave functions 10 p1491 A72-24110
- Atmospheric water vapor measurements by Raman backscatter from pulsed laser radar, comparing with meteorological tower data 11 p1680 A72-25347
- Laser stimulated Raman scattering and IR absorption on crystal defects leading to atomic migration in solids 11 p1647 A72-26144
- IR radiation generation by Raman scattering and difference frequency mixing with Q switched Nd-YAG laser, noting peak power and photon conversion efficiency 11 p1647 A72-26149

- Raman effect application to study of gas vibration relaxation downstream of shock wave 12 p1888 A72-27180
- Remote measurement of cloud ice and water content from Raman scattering of ground based laser signal 12 p1840 A72-27547
- Energy and time characteristics of Raman scattering by benzene in laser cavity as function of medium thickness and cavity length 13 p1969 A72-29523
- Point density measurement in gas jets by flow visualization based on Raman spectrum lines proportionality [ONERA, TP NO. 1080] 13 p1959 A72-29670
- Gas temperature from Raman rotational line intensities generated by lidar techniques applied to inelastic Raman scattering 15 p2232 A72-31373
- Two-magnon Raman scattering in antiferromagnets, obtaining amplitude-renormalization factor by extended Dyson-Maleev graphical approach to include corrections in transition operator M 15 p2295 A72-32548
- Azomethane and azomethane-d6 IR and Raman spectra, discussing fundamental modes vibrational assignment based on band contours, isotopic shift ratios and group frequency correlations 16 p2360 A72-32923
- Computerized analysis of overlapping Raman and IR spectral lines, describing routine for resolving complex spectrum into component lines via operator intervention 16 p2366 A72-33027
- Room temperature vibrational relaxation measurements in gases subsequent to laser pumping by picosecond pulse generated transient stimulated Raman scattering 16 p2401 A72-33389
- Pion-electron conjugation and twist angles determination in biphenyls via Raman intensity, comparing with hypsochromic UV shift of Suzuki method 16 p2431 A72-33585
- Remote measurements of the atmosphere using Raman scattering. 17 p2547 A72-35195
- Tunable Raman excitation and vibrational relaxation in diatomic molecules. 17 p2586 A72-35802
- Nd-glass laser interaction with singly stimulated two-photon emission and anti-Stokes Raman scattering from metastable state He, calculating cross sections 17 p2565 A72-35831
- Infrared and Raman spectra of lunar samples from Apollo 11, 12 and 14. 18 p2724 A72-36279
- Rayleigh and Raman scattering by H2 in a planetary atmosphere. 20 p2966 A72-38914
- Vibration spectra of the isomorphous proustite-pyrrargyrite series. 20 p2932 A72-39506
- Stimulated thermal and Mandelstam-Brillouin scattering of light in liquid nitrogen and oxygen. 20 p2933 A72-39520
- Anisotropy of Raman scattering by optical phonons in cubic zinc blende crystals, describing experimental arrangements 21 p3061 A72-40141
- Explanation of limiting diameters of the self-focusing of light. 21 p3062 A72-40337
- Raman scattering techniques applied to problems in solid state physics. 21 p3096 A72-40602
- An experimental study in the application of the Raman scattering technique as a remote sensor of gas temperature and number density in hypersonic CF4 flow. [AIAA PAPER 72-1018] 21 p3057 A72-41597
- Fundamental infrared lattice vibration spectrum and the laser-excited Raman spectrum of MoSe2. 22 p3185 A72-42321
- Coriolis constants for prolate symmetric top molecules from gas phase Raman band contours observation, noting comparison with IR spectroscopy 22 p3209 A72-42719
- On the use of a Fabry-Perot interferometer for the study of Raman spectra of gases under high resolution. 24 p3426 A72-44904
- Molecular crystals stationary Raman oscillators quantum model, deriving coupled nonlinear equations for excited modes polariton operators 24 p3409 A72-44912
- RAMAN SPECTROSCOPY**
- Light source fluctuations compensation in Raman spectroscopy, describing ratio recording system for photon counters 04 p0523 A72-15491
- Precision frequency calibrator for Raman spectrometers, using Fabry-Perot etalon 07 p0983 A72-19318

High resolution Raman spectroscopy of low pressure gases, using single mode Ar laser
09 p1323 A72-22613

Spectroscopic moments of molecular collision induced far IR and Raman spectra, stressing gas dimers contribution
09 p1276 A72-22859

Tunable dye laser system with narrow band filter for Raman spectroscopy of gases
09 p1326 A72-23351

Active spectroscopy of Raman scattering of light with the aid of a quasicontinuously tunable parametric generator.
20 p2934 A72-39852

RAMJET ENGINES
NT PULSEJET ENGINES
NT SUPERSONIC COMBUSTION RAMJET ENGINES
Ramjet engine propulsion systems for large aircraft above Mach number 2.5
04 p0565 A72-14450

Future interstellar ramjet concepts, considering interstellar hydrogen fuel use for thermonuclear reactor and problems of fuel energy losses, plasma containment and structural limitations
09 p1374 A72-23250

Russian book on theory of ramjet and rocket ramjet engines covering supersonic diffuser operational principles and design, nozzle, combustion chamber and ejector
12 p1862 A72-28346

Axisymmetric jet stretcher diffuser performance for ramjet engine inlet configurations, testing at angles of attack and supersonic flow velocities
[AIAA PAPER 72-1024]
21 p2993 A72-41602

Various efficiencies of fluid flows and application to the hypersonic ramjet
24 p3360 A72-44993

RAMJET MISSILES
Structural limitations of interstellar ramjet, investigating operation during travel in high matter number density space
07 p1054 A72-20249

RAMSAUER EFFECT
Collisional cyclotron instability nature in ionized gases in presence of Ramsauer effect
10 p1520 A72-24224

Elastic electron-neutral interaction in argon in the vicinity of the Ramsauer minimum
22 p3211 A72-42642

RAND PROJECT
U.S. reconnaissance satellites development, discussing RAND project, Agena, Discoverer, Samos and Midas
12 p1876 A72-27109

RANDOM ACCESS MEMORY
NT CORE STORAGE
Digital holographic memory with acousto-optical deflection random access and automatic inscription
01 p0073 A72-11319

Magnetic bubble repertory dialer memory design, noting bit storage capacity and random access
[IEEE PAPER 28,1]
03 p0328 A72-13782

Random access memory based on multichip array with MOS-bipolar device combinations by hybrid techniques, bypassing handling and cost limitations
03 p0329 A72-14185

Operational ternary computer random access memory, describing capacity and access and conversion times
08 p1138 A72-20872

Random access memory with single error correction circuitry, predicting failure, card and module removal rates by computer simulation
10 p1443 A72-23980

High performance low power complementary MOS memories based on silicon-on-sapphire technology, noting quiescent power dissipation
11 p1606 A72-26565

Diffraction theory for large storage capacity holographic random access memory design, discussing geometric optimization of detector array and storage plate
15 p2238 A72-32159

Electronically restored holographic data recording process for analog shape visualization with random access computer storage, discussing system design and capabilities
18 p2659 A72-36271

RANDOM DISTRIBUTIONS
U STATISTICAL DISTRIBUTIONS
RANDOM ERRORS
Gyro drift random error dispersion reduction in compensated closed loop multirotor gyroscopic systems by cross couplings
02 p0231 A72-12566

Random errors in arrival time measurements of sinusoidal radio signal under noise and pulse interference
03 p0323 A72-13893

Polynomial class random process realization based on statistical methods of processing spacecraft orbital measurement data, considering random and systematic errors
05 p0683 A72-16763

Optimal averaging of discontinuous processes with distributed parameters, taking into account random disturbances and measurement errors
05 p0683 A72-17130

Lunar limb charts comparison, computing corrections to orbital elements and systematic and random errors
09 p1388 A72-23056

Standard deviation in ghost lines size due to random sampling position errors of monochromatic spectral line in Fourier transform spectroscopy
09 p1314 A72-23344

Point motion in random error region applied to synchronous satellite trajectory control by single impulse correction
11 p1684 A72-26902

Antenna synthesis and inverse problems solution by regularization methods, considering radiation patterns and random error effects
13 p1928 A72-28529

Statistical analysis of random mismatched tapped delay line filters effect on binary phase shift keying pulse compression codes peak-to-sidelobe and SNR
15 p2196 A72-31792

Random errors in arrival time measurements of sinusoidal radio signal under noise and pulse interference
15 p2202 A72-32704

Time variable pulse front fluctuations effect on random error in digital pulse duration measurements
16 p2395 A72-33953

Problem of antenna parameter optimization in the presence of random errors
17 p2529 A72-34831

Polynomial class random process realization based on statistical methods of processing spacecraft orbital measurement data, considering random and systematic errors
17 p2576 A72-35266

Gas turbine engine performance measurement via parameters averaging method, noting integration time determination for given error limits
23 p3325 A72-43669

RANDOM LOADS
NT GUST LOADS
Nonlinear boundary value problem of creep for isotropic bodies with random mechanical properties under random loads, calculating structural component reliability and service life
02 p0289 A72-11619

Polycrystalline bodies thermoelastic behavior under random external forces, determining thermal microstress distribution parameters by statistical boundary value formulation
02 p0290 A72-11632

Minimum weight beams and frames calculation for random loads taking into account material carrying capacity
02 p0291 A72-11727

Statistical methods of stress and reliability analyses of elastic systems under random external loads
03 p0453 A72-14206

Helicopter rotor blade response to random loads treated by theory of linear dynamic systems with time-varying coefficients
05 p0613 A72-16940

Beams and square plates nonlinear vibration response to random concentrated driving force solved numerically on digital computer
06 p0901 A72-18718

Semimomentless theory of closed cylindrical plastic shells subject to random gust loads, obtaining normal circumferential force, shear, transverse bending moment and shell thickness
07 p1092 A72-19851

Nonlinear modal response analysis of plate structures under random acoustic excitation, using finite element method and perturbation technique
08 p1245 A72-21607

Asymptotic dynamic response of infinite beam on elastic foundation to randomly moving load
11 p1727 A72-25292

Finite time element method for failure probability prediction in multiple load-path system with random loads, noting flow chart for suggested computer program
13 p2052 A72-28369

Minimum weight reliable beams and frames calculation for random loads, using one degree of freedom system to obtain closed form solution
14 p2164 A72-30237

Welded steel airframe residual fatigue life tests by nonstationary random loading, applying to jet trainer aircraft landing gear
14 p2107 A72-30277

Random deflection function for taut string on elastic foundation subject to random loads, using invariant imbedding method and Fokker-Planck equations
15 p2273 A72-31311

Dynamic stability of elastic systems under broadband random excitation, presenting solution for straight rod under axial pulsating forces via perturbation method
15 p2274 A72-31460

Single degree of freedom system displacement response exceedance of given level under nonstationary random excitation, considering aircraft flight through turbulent region with variable intensity
15 p2279 A72-32592

Calculation of correlation matrices for linear systems subjected to nonwhite excitation.
[ASME PAPER 71-APMW-10]
17 p2625 A72-34316

Numerical solution for the mean first-passage-time for snap-through of shells.
18 p2737 A72-37061

Method of measuring modal characteristics of a structure subjected to a random excitation
22 p3242 A72-43095

RANDOM NOISE
NT RANDOM SIGNALS
Random background noise effect on nonlinear self oscillation envelope passage time moments, discussing relationship between amplitude and frequency stabilities
01 p0035 A72-10032

PM communication systems with Gaussian and clipped noise carriers, calculating SNR
01 p0024 A72-10129

Data compression and random noise effects on pattern recognition and picture quality of multispectral scanner data
02 p0227 A72-11840

Optimal filter and polarity coincidence correlator signal detection efficiency for arbitrary noise distribution
02 p0176 A72-12217

Radars measurement accuracy in log-normal clutter of fluctuating targets in random noise or intentional interference
07 p0178 A72-12401

Frequency fluctuations in nonlinear self oscillating system in presence of periodic nonstationary random noise effects
02 p0195 A72-12586

Near optimum limiting and blanking levels (error probability) selection for binary signal matched filter reception in Gaussian and impulse noise, discussing performance simulation
04 p0486 A72-14485

Optimal control synthesis for linear systems with quadratic functional under random white noise
05 p0641 A72-16314

Recurrent algorithms for optimal signal detection on background of random noise, using Markov processes
05 p0627 A72-16406

Electron plasma wave echoes experimental investigation, discussing amplitude decay under plasma and random noise influence
06 p0858 A72-17538

Noise, delay and interruption caused communication degradation effects on feedback control system performance, considering air navigation and computer aided command and control on battlefield
06 p0794 A72-18242

IMPATT diode microwave oscillators and amplifiers calculating noise sideband correlation factor at randomly large signal frequencies
06 p0788 A72-18464

Gaussian rf noise effect on optical detection signal fluctuations in optically pumped frequency standards
07 p0938 A72-19013

Optimal signal detection relative to Neumann-Pearson criterion invariant with respect to amplitude and random noise intensity in radio location
07 p0938 A72-19019

Mathematical expectation of angularly modulated signal in unsteady linear random noise, using Marchenko formula
07 p0939 A72-19020

Digital system for wideband Gaussian noise generation using simultaneously generated PN-sequence with analog summation of independent binary waveforms
07 p0941 A72-19284

Bayesian estimate of signal parameters in random noise background under mutually exclusive hypotheses about statistical properties
07 p0943 A72-19515

Weak signal detection in additive mixture on non-Gaussian random-correlated noise, deriving algorithms for discrete- and continuous-time and coherent detection problems
07 p0943 A72-19521

Automatic digital detection of fluctuating Rice-distributed signals in presence of Gaussian noise, using M-out-of-N threshold detection criteria
07 p0947 A72-20194

Computer simulation of empirical confidence limits for variance spectra, applying to Gaussian random noise data stochastic model
07 p0951 A72-20360

Gaussian noise quasi-optimal filtering in optical communication system, evaluating signal timing accuracy in detector-amplifier circuits
08 p1136 A72-21914

Random frequency FM noise model for microwave Gunn effect oscillators
09 p1288 A72-23122

Optimal correlating detector of fluctuating two frequency radar signals in unknown random noise

10 p1436 A72-24515

Error probability and reception stability in synchronous detection of phase manipulated signals with additive Gaussian noise at multiplied carrier frequency

10 p1436 A72-24587

Modulating /multiplicative/ noise effects on output signal characteristics of receiver designed for optimal reception on background of Gaussian noise

10 p1439 A72-24906

Optimal distribution of resources in automatic systems for detection and measurement of random concentrated noises number in assigned frequency range

10 p1440 A72-24917

Optimal control synthesis for linear systems with quadratic functional under random white noise

11 p1610 A72-25797

Phase noise and transient times for binary quantized digital phase locked loops in white Gaussian noise

11 p1592 A72-25886

Upper bound on probability of specified errors pattern occurrence for amplitude modulated digital communications systems subject to intersymbol interference and random noise

11 p1592 A72-25889

Probability density functions for output process in frequency discriminator under action of additive mixture of fluctuating radio signal and random noise

13 p1914 A72-28411

Least squares method algorithm for estimating unsteady harmonic signal parameter in presence of normally distributed additive noise

13 p1915 A72-28435

Monte Carlo simulation for imperfect second order hybrid phase locked loop in radio frequency interference and Gaussian noise backgrounds, employing digital computer simulation model

13 p1935 A72-29104

X ray source Cygnus X-1 pulsation periodicity analysis, showing random shot noise characteristics

14 p2156 A72-30571

Correlation measurements of LF current noise and frequency fluctuations in Gunn oscillators, emphasizing generation-recombination noise component

14 p2088 A72-30916

Van der Pol oscillator acted upon by weak random noise, evaluating oscillations envelope dispersion from probability density function and phase derivation

14 p2132 A72-31123

Van der Pol and nonlinear parametric oscillators fluctuations due to random noises analyzed by averaging method and discrete Markov processes

14 p2133 A72-31134

Current noise spectra in single crystals and polycrystals of transition metal compounds, discussing flicker noise origin

15 p2293 A72-32384

Generator for data transmission lines stochastic noise bursts simulation with statistically independent burst durations and intervals

15 p2201 A72-32475

Fluctuation analysis of parametric frequency multipliers and dividers, discussing short time instabilities caused by system noise

15 p2212 A72-32736

Optimization of noise impeding observation of dynamic system subjected to random perturbations, discussing optimal control based on least square estimate

16 p2371 A72-33090

Error probabilities in digital communication systems subject to mixture of man made or natural impulsive and Gaussian noise

16 p2365 A72-34106

Propagation of pulsed-carrier signals in random media

17 p2514 A72-34380

Bayesian recursive estimation by Kalman filtering for enhancement of image corrupted by additive random noise

17 p2557 A72-35539

Time-compressed displays for target detection

17 p2510 A72-35945

Exponentially weighted noncoherent integration of pulsed signals in the presence of Gaussian noise and random impulse noise

19 p2767 A72-38623

Minimax technique for direct synthesis of Kalman-like filter under large uncertainties in a priority statistics of plant and measurement noises

20 p2907 A72-39120

Mean value of noisy signal quantized by analog/digital converter, noting input noise level relation to estimate accuracy

20 p2904 A72-39785

Effect of fringe on masking-level difference when gating from uncorrelated to correlated noise

21 p2997 A72-40346

Optimal risk equation and solution existence and uniqueness of dual control problems with unknown parameter and additive disturbances

21 p3038 A72-40706

Bayes theorem for radio signals parameter estimation on random noise background, using rectangular function of losses

21 p3016 A72-40797

Error probability for multilevel PAM transmission with intersymbol interference, Gaussian and impulsive noise

21 p3019 A72-40888

Statistical estimation of the signal-to-noise ratio beyond a linear detector

21 p3022 A72-41073

Detection of Doppler radio signals on a receiver with an additive noise blip number counter

21 p3022 A72-41116

Measurement of a radio signal nonenergetic parameter at high additive and modulation noise levels

21 p3022 A72-41117

Characteristics of filtering the Rayleigh parameter of pulse signals in the presence of noise

22 p3154 A72-42228

Statistical synthesis of navigation aids systems with unsteady random interferences, obtaining optimization criterion by least squares method

22 p3202 A72-42232

Influence of noise on the accuracy of microwave phase meters

23 p3272 A72-43845

Linearizing compensation for nonlinear control system transformation into linear system without approximation, discussing differential operator matrix definition and random noise effects

23 p3277 A72-43945

Probability of digital-data reception with a given confidence level under conditions of random radio noise

23 p3266 A72-44208

Cumulants of multidimensional response of linear and nonlinear systems to Poisson distributed impulses, estimating joint probability distribution and evaluating threshold statistics

23 p3314 A72-44368

RANDOM NUMBERS

Book on discrete event computer simulation for complex systems synthesis and analysis covering random numbers use, languages, and interactive man machine applications

06 p0779 A72-17812

Convergence of random number sums of independent infinitesimal multidimensional stochastic step processes to generalized Poisson processes

09 p1340 A72-22423

Russian book on random signal generation covering ultralow and audio frequency spectra, random number and pseudorandom signals simulation and automatic control

12 p1786 A72-28347

Random number method for particle motion in homogeneous turbulence field, using Brownian motion Markov process for turbulence approximation

13 p1940 A72-28421

Computerized Monte Carlo techniques for nonlinear error analysis of system behavior, using random number generators for input distribution simulation

15 p2264 A72-32184

Circuit synthesis for random numbers probabilistic digital transducers reduced to synthesis of random binary signal converters, noting method description with Boolean functions

16 p2372 A72-34012

Stochastic coder electronic circuit for random numbers conversion into electrical voltages and vice versa, noting compactness and low cost

23 p3273 A72-44460

RANDOM PROCESSES

NT RANDOM WALK

Kalman filtering process digital simulation by numerical integration of matrix differential equations describing linear system random process model and optimal filter

01 p0024 A72-10225

Power flow approximation for long distance long wave propagation of ground source between earth and ionosphere, comparing mode theory to heuristic approach

01 p0033 A72-11310

Random processes models based on Poisson sequences extended to simultaneous asymmetry and probability density function excess, establishing asymptotic relationships

02 p0216 A72-11919

Feedback control dynamic system described by linear differential equation with random coefficients, calculating parameters distribution effect on behavior precision

02 p0197 A72-12339

Markov chain successive approximation method for electromagnetic wave propagation in medium with random large discontinuities, using scalar parabolic equation

02 p0181 A72-12588

Random method to solve basic rarefied gas/Boltzmann/ equation, applying to elastic collisions

04 p0551 A72-14518

Random method solution of Boltzmann equation for pseudoshock /relaxation mixing/, applying to random collisions of molecular beams

04 p0551 A72-14519

Statistical properties of random-phase modulated laser beams, calculating coherence functions of optical fields

04 p0528 A72-14580

Proteobionts formation by random aggregation and reproduction from proteins and nucleic acids macromolecules

04 p0469 A72-14782

Economically optimal operation of protection circuit for plant subject to stationary random process, determining failure rate of plant

04 p0496 A72-14995

Light transmission in medium with random inhomogeneities in Markov random process approximation, obtaining short wave field statistical characteristics

04 p0488 A72-15380

Antenna design and performance in random fields, using statistical description of fields

04 p0500 A72-15394

Multidimensional random hypersurfaces generation with given statistical properties on digital computer, using linear filter theory

04 p0540 A72-15628

Upper and lower bounds for expected value and variance of minimum material weight necessary for random resistance structure able to support assigned loads

04 p0593 A72-15648

Subjective probability distributions for random device-generated Bernoulli process unknowns, discussing distribution median and quartiles and hypothetical sample impact assessment techniques

05 p0616 A72-15812

Random phasing algorithms to reduce phase quantization lobes for radiation patterns of commutated phased array antennas

05 p0634 A72-15820

Statistical description of Brownian particle motion in turbulent flow, using theory of canonical correlations

05 p0648 A72-16171

Model reference adaptive control system synthesis in presence of random perturbations, considering error signal derivative use to form parameter adjustment algorithm

05 p0640 A72-16200

Probabilistic output analysis of dynamic nonlinear system with random characteristics by functional Volterra series

05 p0641 A72-16314

Fixed level intersection by two stationary ergodic independent random processes in observation time function dynamic control sampling and reliability estimation

05 p0641 A72-16314

Book on random functions and turbulence covering probability theory, random processes and fields, statistical correlation and spectral methods, numerical weather forecasting, etc

05 p0649 A72-16397

Polynomial class random process realization based on statistical methods of processing spacecraft orbital measurement data, considering random and systematic errors

05 p0683 A72-16763

Characteristic functional for random delayed events and cluster processes, using Blanc-Lapierre statistical model

05 p0693 A72-17079

Low deviation FM wave spectral density estimation as infinite series by low pass Gaussian random process

06 p0772 A72-17407

Digital computer techniques for randomly excited n-degrees of freedom structural system response by discrete time series with output covariance

06 p0895 A72-17857

Fiberglass reinforced plastics under constant strain rate, deriving failure models as random process for microscopic crack propagation

06 p0898 A72-18548

Selective summation techniques for coherent Green function in random isotropic turbulent media, comparing Dyson, Keller and renormalization methods

06 p0777 A72-18739

System parameters random step changes effect on nonlinear system steady vibration stability

07 p1088 A72-19172

Smoothed randomized functionals and algorithms in adaptation and learning theory, accounting for constraints by generalized penalty function method

07 p0960 A72-19653

Axially compressed cylindrical shells with axisymmetric imperfections, analyzing random buckling behavior and failure probability by statistical methods

07 p1089 A72-19689

Spectral density estimates for discrete time models of steady nonGaussian random processes, noting dispersion in asymptotic expression

08 p1198 A72-20990

Tropospheric scatter path characteristics as communication channel with random fluctuations, deriving signal autocorrelation function from mean power pulse response
08 p1132 A72-21329

Feedback control dynamic system described by linear differential equation with random coefficients, calculating parameters distribution effect on behavior precision
08 p1146 A72-21554

Soviet book on determinate, stationary, nonstationary and industrial random processes prediction, covering adaptive filters and algorithms
08 p1146 A72-21675

Linear system oscillations and stability under random disturbances, using Laplace transform and Sh-tokalo method
08 p1146 A72-21730

Consistent finite element method to analyze random response of complex structures based on standard modal approach
08 p1248 A72-28123

Probability density and distribution functions of first arrival time at boundary by steady normal random process
09 p1289 A72-22217

Seyfert galactic nuclei structure, discussing thermal X rays indication of significant random motions and difficulty of energy source determination
09 p1386 A72-22686

Fourier transform plane irradiance distribution for random phase data masks in holographic data recording, discussing phase quantization level change effects
09 p1314 A72-23335

Stationary Kalman-Bucy filter synthesis from filter coefficients and correlation matrix of filtration errors, discussing random process estimation application
09 p1289 A72-23434

Filtration and extrapolation of multivariable random processes described by linear differential equations system, examining adaptive filter synthesis
09 p1283 A72-23436

Dynamic systems stability problems, differential equations linearization and random processes
09 p1343 A72-23603

One degree of freedom mechanical system with jump-like variable mass, determining displacement and velocity statistical characteristics under random excitation and mass addition
09 p1353 A72-23608

Time optimal control of distributed systems with random properties, considering n integral relations and flying wing vehicle torsional vibration problems
10 p1421 A72-24427

Time dependent power spectral density function for first passage probabilities in nonstationary random processes in civil engineering involving earthquakes and wind
10 p1514 A72-25188

Computer approximate computation of multidimensional normal distribution, examining error measure, random processes and correlation coefficient
11 p1676 A72-25429

Probabilistic analysis of technological systems precision, estimating distribution functions of random output parameters
11 p1609 A72-25430

Digital computer simulation of random processes specified by canonical expansion, discussing quantization steps for storage requirements reduction
11 p1600 A72-25432

Transfer functions algebraic determination for stationary object from random processes realizations, proposing algorithm
11 p1610 A72-25451

Stationary and nonstationary random envelope processes digital simulation, presenting application to crack propagation under random loadings
11 p1686 A72-25730

Probabilistic output analysis of dynamic nonlinear system with random characteristics by functional Volterra series
11 p1610 A72-25798

Fixed level intersection by two stationary ergodic independent random processes in observation time for dynamic control sampling and reliability estimation
11 p1610 A72-25799

Mutually coupled continuous time orthogonal binary random processes, illustrating transition from discrete to exponential interval distribution
11 p1611 A72-26298

Switch detector output random process energy spectrum and autocorrelation function, noting distortion reduction by proper parameter choice
11 p1605 A72-26317

Random process quantization interval search algorithm based on signal approximation by n -th degree polynomial
11 p1602 A72-26439

Two dimensional characteristic and distribution functions of monomode laser radiation random processes with nonlinear optics application
11 p1651 A72-26716

Probability density function of hologram exposure irradiation in terms of Bessel function, adding uniform beam coherently to random speckle pattern
11 p1636 A72-26749

Multiple function stochastic automata performance in environment with random control processes, showing improved learning rate
12 p1787 A72-27922

Airplane sideslip and yaw rate perturbations by continuous random vertical and side gusts, using low pass filtered white noise representation for mathematical modeling
12 p1755 A72-28125

Russian book on random processes theory covering random sequences and functions and probability measures in functional spaces, limit theorems, etc
12 p1837 A72-28339

Random retrieval algorithms in finite set of preset movement directions, considering quadratic function minimization
13 p1924 A72-28610

Energy spectra of mixed discrete random processes in statistical multiplexing systems with pulse position, delta and pulse code modulation
13 p1919 A72-29054

Mathematical random fluctuation models for noise and energy spectra of pulsed processes during current passage through semiconductor
13 p2021 A72-29064

Redundant and nonredundant self adaptive systems reliability, discussing statistical random process characteristics
13 p1936 A72-29170

Statistical homogeneity criteria for automatic equipment operation reliability, using Poisson flow model with random fluctuations
13 p1965 A72-29173

Random processes models based on Poisson sequences extended to simultaneous asymmetry and probability density function excess, establishing asymptotic relationships
13 p1948 A72-29231

Star escape and accumulation in halo from stellar random gravitational encounters in spherical system dense central core
13 p2040 A72-29402

Random homogeneous turbulence generation of rms weak magnetic field fluctuation in infinite medium with short correlation time
13 p2015 A72-29403

Digital computer estimates of random processes spectral density by statistical correlation method, calculating errors in numerical integration techniques
13 p1937 A72-29495

Microinhomogeneous solid bodies elastic fields and effective moduli calculation method within framework of random field theory, using singular approximation
13 p2062 A72-29884

Minimum phase systems application for linear estimation of steady random sequences of signals, obtaining transfer function for optimal frequency filter
13 p1937 A72-29999

Randomized electromagnetic field propagation through uniform medium, deriving autocorrelation and intensity fluctuation spectrum expressions
13 p2007 A72-30124

Statistical description of Brownian particle velocity in turbulent flow, using theory of canonical correlations
14 p2093 A72-30240

Stability conditions for damped single degree of freedom oscillator system under stationary narrow-band random excitation, obtaining approximate solution by perturbation method
14 p2131 A72-30718

Nonlinear autooscillatory systems forced vibration under random perturbations, calculating dynamic processes by statistical linearization
14 p2132 A72-31114

Nonlinear resonating correlator with orthogonal filters, considering cut-off frequency of ergodic random process with constant power spectral density
14 p2090 A72-31125

Reflection and transmission coefficients of long lossy single mode waveguide line with random inhomogeneities
15 p2195 A72-31654

Signal with bounded spectrum, obtaining higher derivatives by reduction to stationary random process filtering problem solvable with Kolmogorov-Wiener and Kalman-Bucy techniques
15 p2207 A72-32171

Magnetic probe measurement of random fluctuations in transverse magnetic field caused by He plasma produced in arc discharge
15 p2287 A72-32408

Random matrix spectra of eigenvalues in terms of Wigner set for statistical description of heavy nuclei energy levels
15 p2282 A72-32449

Heat conduction in infinite incompressible fluid with turbulent velocity field, deriving physically impossible growth in time of long-wavelength modes of average temperature
16 p2424 A72-33127

Optimal invariant control system synthesis for inertial plants with nonminimal phases and random perturbation compensation
16 p2371 A72-33263

Steady state creep of composite material with discontinuous fibers, determining random function mean and variance for fiber stress distribution
16 p2412 A72-34115

Generalized random systems with complete connections
17 p2573 A72-34276

Book - An introduction to applied probability and random processes
17 p2575 A72-34625

Free vibrations analysis of linear aerodynamic conservative structures in elastic range by finite element method, applying to transient or random forced responses calculation
17 p2626 A72-34742

Polynomial class random process realization based on statistical methods of processing spacecraft orbital measurement data, considering random and systematic errors
17 p2576 A72-35266

Counting theorems for random processes discretization in linear systems described by finite spectrum functions
17 p2534 A72-35776

Stochastic model for unsteady rhythmic processes based on periodical correlation of random processes
17 p2534 A72-35777

Spectral properties of periodically correlated random processes
17 p2535 A72-35784

Central probability limit theorems and asymptotic normality in fluid mechanics for random stationary processes with uniform ergodicity and strong mixing
18 p2677 A72-36003

Cameron-Martin-Wiener /C-M-W/ representations of nonlinear random process tested on Burger turbulence for real fluid problem
18 p2677 A72-36010

Maximum likelihood identification of time varying and random system parameters.
18 p2673 A72-36822

Recursive stochastic approximation of autocorrelation function for stationary random process based on mean-square error and maximum likelihood methods
19 p2824 A72-37285

Some problems concerning stability in the presence of small random disturbances
19 p2833 A72-37324

Linear partial differential equations with random forcing.
19 p2825 A72-37573

Optimization of control and observation processes in a dynamic system at random disturbances
19 p2778 A72-37991

Stellar rings and stellar cavities as random phenomena
19 p2866 A72-38492

Stationary Kalman-Bucy filter synthesis from filter coefficients and correlation matrix of filtration errors, discussing random process estimation application
19 p2782 A72-38517

Filtration and extrapolation of multidimensional random processes described by linear differential equations system, examining adaptive filter synthesis
19 p2770 A72-38519

Transmission and phase coefficient logarithmic decrements for wave propagation in random discrete scatterers
19 p2767 A72-38614

Response of linear periodically time varying systems to random excitation.
20 p2946 A72-39636

Selection of an optimal control law for time-lag control systems subjected to random load disturbances
21 p3038 A72-40705

Statistical continuous random process theory of homogeneous and isotropic turbulence in terms of energy transfer in wave number space based on Kolmogoroff hypothesis
21 p3045 A72-41025

Comparison of design procedures of vibration absorbers for systems with random excitations.
21 p3121 A72-41230

A meter giving the number of overshoots of the realization of a steady random process
21 p3058 A72-41732

A design procedure for intermediate-order observer-estimators for linear discrete-time dynamical systems.
22 p3161 A72-41994

Pontryagin equations for Markov process limits probability, solving problem of one dimensional steady random process limits for given initial probability density function
22 p3205 A72-42227

Statistical characteristics of an optimal detector of randomly fading pulse signals
22 p3154 A72-42229

On the ergodic coefficients concerning generalized random systems with complete bonds
22 p3199 A72-42637

Optimal random disturbance intensity control of dynamic systems, minimizing error with respect to observed and controlled plant coordinates

23 p3274 A72-43221

Functional method investigations of imbedding theorems for random weight spaces of high order irregular elliptic equations with uniform boundary conditions

23 p3307 A72-43222

Random phasing algorithms to reduce phase quantization sidelobes for radiation patterns of commutated phased array antennas

23 p3268 A72-43428

Achievement of given motion by impulse correction under arbitrary disturbances/difference models

23 p3313 A72-44044

Column buckling under random initial deformations influence, determining mean square nonstationary deflection by Green function technique

23 p3351 A72-44106

Optimal equalization of discrete signals passed through a random channel.

23 p3265 A72-44178

Robert Bruce's spider problem extended - Reliability of adaptive experimental systems.

24 p3406 A72-44666

RANDOM SAMPLING

Narrow-band radar/sonar signal optimal detection under known direction and uncertain phase/arrival time conditions, considering statistical signal sampling

02 p0180 A72-12572

Interrogation frequency effects in random access analog multiplexers operating on flying capacitor at very high sampling frequencies

02 p0195 A72-12692

Bias and variance prediction efficiency in two stage sampling designs

03 p0383 A72-14368

Standard deviation in ghost lines size due to random sampling position errors of monochromatic spectral line in Fourier transform spectroscopy

09 p1314 A72-23344

System diagnosis based on ordered statistical samples, discussing Kolmogoroff-Smirnoff detector use for on-line computers in testing noisy systems

10 p1482 A72-24597

Random process quantization interval search algorithm based on signal approximation by n -th degree polynomial

11 p1602 A72-26439

Single pulses and random samplings signal spectrum analysis on real time scale by ultrasonic dispersion waveguide

13 p1934 A72-30018

Best linear invariant estimation of Weibull parameters - Samples censored by time and truncated distributions.

22 p3199 A72-42969

The random-sampling procedure in oscilloscope technology

23 p3273 A72-44348

Statistical techniques for severely censored random samples with known and unknown probability distribution functions

24 p3418 A72-44665

RANDOM SIGNALS

Random and algorithmic procedures employing three-valued logic system for sequential circuits fault detection test sequence generation

02 p0185 A72-11486

Ultrasonic defectoscope sensitivity, discussing statistical character of random signal level distribution and test conditions

03 p0364 A72-13988

Amplitude, time and frequency domain analysis of random signals, measuring probability density, cross correlation and cross spectral density functions

05 p0629 A72-16598

Stability analysis of steady control systems acted upon by random signal in single valued one dimensional nonlinearity form, using statistical linearization

07 p0959 A72-18989

Optimal PSK signals selection and synthesis from random sequences ensuring minimum value of maximum side peak of autocorrelation function

07 p0943 A72-19564

Estimation-correlation principle and optimal detector for incomplete a priori information signal reception on random and white noise background

08 p1131 A72-20790

Nonlinear filtering synthesis of optimal receiver for pseudorandom phase shift keyed signal with arbitrary modulation angle and white noise background

10 p1436 A72-24510

Data window for digital spectrum estimation of random data by fast Fourier transform techniques, noting bandwidth increase by various data smoothing sequences

10 p1439 A72-24804

Nonlinear filtering for random signals in statistically unknown noise, noting application to satellite orbit determination, aircraft navigation and missile tracking

11 p1611 A72-25986

Spectral correlation and transition probabilities of mutually dependent orthogonal binary random signals

11 p1595 A72-26299

Russian book on random signal generation covering ultralow and audio frequency spectra, random number and pseudorandom signals simulation and automatic control

12 p1786 A72-28347

Spatial-temporal coherent processing technique application to thermal radio emission random signal reception, deriving ambiguity function

13 p1920 A72-29282

PSK signal cross-correlated receiver output SNR in presence of random misalignments with respect to carrier frequency and arrival signal time

13 p1921 A72-29283

Probability functional formulas for quasi-determinate signal on unsteady normal noise background for use in false alarm and correct detection

15 p2195 A72-31664

Circuit synthesis for random numbers probabilistic digital transducers reduced to synthesis of random binary signal converters, noting method description with Boolean functions

16 p2372 A72-34012

Radiation pattern determination for an antenna receiving random signals

17 p2517 A72-35540

Woodward ambiguity function extension to random signals, noting Gaussian signal in white noise with given autocorrelation function

19 p2766 A72-38418

Signal recognizing algorithms for class of large number of normal distributions with unknown probabilities, using statistical complex hypothesis verification

19 p2770 A72-38466

Optimal PSK signals selection and synthesis from random sequences, ensuring minimum value of maximum side peak of autocorrelation function

22 p3153 A72-42082

Characteristics of an optimal algorithm for detecting Gaussian signals against a pulse noise background for receivers with a logarithmic amplifier

22 p3154 A72-42238

Linear filtration of random signals based on the criterion of maximum signal-to-noise ratio

23 p3273 A72-44215

Determination of the energy spectrum of the initial process in an amplitude gate subjected to the action of a random signal

24 p3380 A72-44897

Autocorrelation function of smooth steady random signal determination from consecutive derivative dispersions by MacLaurin, least squares and Taylor methods

24 p3380 A72-45317

RANDOM VARIABLES

Coded multiple FSK in presence of random variable phase, predicting optimum reception performance relationship to phase distribution and SNR

01 p0025 A72-10330

Linear interpolation for homogeneous isotropic random field observed on denumerable system of spheres, deriving explicit formula analogous to Kotelnikov-Shannon

01 p0094 A72-11266

Book on random data analysis and measurement procedures covering physical systems dynamic response properties, random processes, statistical sampling, data acquisition and processing, etc

03 p0327 A72-13175

Local theorem in strengthened form for independent integral-valued lattice random variables

04 p0539 A72-15256

Average ray direction and mean square deviation formula for electromagnetic wave propagation in random inhomogeneous medium suited for calculation by ray tracing program

04 p0488 A72-15382

Markov model random variation optimal periodicity in preventive maintenance operations, estimating distribution density and moments

04 p0527 A72-15574

Moving object trajectory determination by a posteriori Poisson signal transmission analysis with random parameters

05 p0626 A72-16205

Optimal averaging of control in distributed random parameter system described by hyperbolic partial differential equations, considering boundary values on characteristics as control functions

05 p0683 A72-17133

Wiener-Hermite random variable expansion technique with time dependent base for turbulence applied to Burger equation

07 p0967 A72-19502

Clutter correlated lognormal random variables generation from statistically independent Gaussian random variables for radar simulations

08 p1134 A72-21423

Bayes estimators for Poisson distribution random parameters and reliability function, using Monte Carlo method and maximum likelihood estimation

08 p1200 A72-21590

Wiener generalized harmonic analysis relationship to steady random functions, emphasizing higher order properties and ergodic process conditions

10 p1504 A72-24063

Local limit theorems for sequence of nonidentically distributed independent integral-valued lattice random variables

11 p1676 A72-25356

Random Fredholm and Volterra integral equations applied to stochastic systems, investigating absolute stability concept

11 p1679 A72-26780

Atmospheric model for random density variations effects on space shuttle reentry parameters, using Monte Carlo trajectories for delta wing orbiter

13 p1990 A72-28814

Random variations in interferometer complex visibility function magnitude and phase, refractive index and source angular size

14 p2156 A72-30561

Random deflection function for taut string on elastic foundation subject to random loads, using invariant imbedding method and Fokker-Planck equations

15 p2273 A72-31311

Complex structures dynamic analysis by component mode technique, treating modal characteristics as random variables

15 p2331 A72-32555

Random scale parameter of Weibull distribution with known shape parameter obtained via empirical Bayes estimation

16 p2398 A72-33346

First and second moment of an optical wave propagating in a random medium - Equivalence of the solution of the Dyson and Bethe-Salpeter equation to that obtained by the Huygens-Fresnel principle.

17 p2580 A72-34290

Book - Weak convergence of measures: Applications in probability.

20 p2946 A72-39730

Performance of antennas in random fields.

21 p3026 A72-40355

Independent cascaded multicomponent random variable system gain statistics relationship to individual component based on moment derivation, obtaining curves from variance equation

21 p3022 A72-41087

Convergence rate estimates for the sums of random values determined in a Markov chain with absorption

21 p3075 A72-41094

Random function theory method for estimation of tensile, compressive and shear strength and elastic constants of monodirectional fiberglass reinforced plastics

21 p3073 A72-41708

Stochastic and deterministic relationships between random variables, noting correlation coefficient as measure of regression lines representation accuracy

22 p3178 A72-42449

Optimal control of stochastic systems with continuous and discontinuous random disturbances, obtaining problem solution conditions for linear system via dynamic programming

23 p3276 A72-43782

Reliability estimation in life testing in the presence of an outlier observation.

23 p3309 A72-43807

Estimates of unknown parameter from quantized observations given as sequence of evenly distributed random values, noting optimal grouping equations for general distribution function

23 p3266 A72-44218

RANDOM VIBRATION

Statistical variance of eigenvalues and eigenvectors in random structure dynamic analysis by component mode synthesis

[SAE PAPER 710786]

01 p0137 A72-10277

Error fluctuation component spectral density determination in closed automatic nonlinear system for controlling random vibration spectrum

01 p0045 A72-10505

Stochastic differential equations vector solution by two-time method, applying to random harmonic oscillators and wave propagation in random media

[AD-733125]

01 p0093 A72-10510

Factorial design model of materials fatigue failure under narrow band random vibrations

01 p0140 A72-10942

Equivalent harmonic solutions for systematic drift of astatic gyroscope about outer gimbal axis with base under random angular vibrations

02 p0231 A72-12564

Statistical linearization approach to determine approximate instantaneous correlation matrices of nonlinear structure response to nonwhite excitation

02 p0298 A72-12663

Elastoplastic body random vibration analysis by statistical linearization, obtaining free elastic vibration mode shapes and damping constants

04 p0586 A72-15005

Pressure field calculations for random vibrations in wide class of elastic shells containing acoustic medium, discussing turbulent boundary layer-caused pulsations

04 p0586 A72-15010

Plane physical pendulum motion stability under randomly oscillating suspension point with allowance for viscous friction

04 p0549 A72-15055
Statistical distribution of maximum response for reliability-based optimum spacecraft structural design for random excitations from booster shutdown

05 p0724 A72-16103
Random vibrations nonlinear theory, investigating nonlinear systems response to random excitation via Markov processes modeling

06 p0896 A72-17961
Lightly damped nonlinear mechanical oscillators under random excitation, calculating stationary response frequency and autocorrelation by heuristic procedures

06 p0849 A72-18693
Nonlinear elastic systems with distributed parameters, obtaining single frequency mode random oscillations solution of boundary value problem by asymptotic method and Markov process

06 p0850 A72-18700
Random vibrations in rectangular plate clamped on opposite sides by load, determining natural oscillation frequencies by Ritz technique

06 p0901 A72-18719
Harmful influence of random vibrations on human organism, discussing Fokker-Planck analysis and amplitude and frequency variation effects

06 p0770 A72-18720
Random vibrations and antitorque moments of rigid shaft with precision bearings, considering effects of geometrical fabrication defects and nonuniform film thickness

06 p0824 A72-18722
Gyro-pendulum accelerometers, calculating moving base oscillation effect on performance by random function representation through canonical expansions

06 p0819 A72-18723
Dynamic response and functional state of human operator subjected to harmonic and random vibrational excitations, discussing biodynamic nonlinear oscillatory system model construction

06 p0770 A72-18728
Random vibrational stress and displacement spectra for linear complex mechanical dissipative systems with strong resistance and finite degrees of freedom

07 p1091 A72-19763
Random vibration theory and Markov processes in nonlinear stochastic systems with probability and asymptotic methods application

08 p1205 A72-20965
Two reflector Cassegrain antenna secondary reflector random fluctuations effects on drift in main lobe direction

08 p1143 A72-21846
Random vibration of linearly elastic lumped mass systems containing, nonlinear damping to ideal stationary Gaussian white noise excitation

09 p1408 A72-23460
Nonlinear vibrations under random excitation, discussing equivalent linearization and small parameter perturbation methods and Fokker-Planck equation

09 p1353 A72-23604
Nonlinearity effects on random vibration displacement and frequency characteristics of one degree of freedom system, using Fokker-Planck equation

09 p1353 A72-23605
Nonlinear random radial vibration of elastic cylindrical shell under load, using stochastic linearization and correlation analysis

09 p1409 A72-23606
Zaidenberg correlation method for nonlinear systems dynamic properties under random excitation, determining statistically equivalent linearized terms for equations of motion

09 p1353 A72-23607
Multivariable probability density determination of random vibration systems with n degrees of freedom by Fokker-Planck equation

09 p1353 A72-23609
Damping measurements of hydrodynamic vibrations of cylinder excited by random pressure field of liquid flow

10 p1465 A72-24073
Steady state operation of automatic control system to stabilize random vibration spectra, noting maximum control accuracy at optimum loop gain

10 p1457 A72-24635
Power spectral density function parameters with random vibration applications, considering response spectra of multidegree of freedom linear systems [ASCE PREPRINT 1375]

10 p1560 A72-25189
Flight vehicle structures optimum design for random vibration environment, presenting formulation as nonlinear programming problem

11 p1736 A72-26003
Shear stress and traveling wave response of plate bonded to randomly vibrating viscoelastic half space for soil vibration studies

11 p1688 A72-26062
Random vibratory processes and envelopes distributions interrelationship, tabulating probability density functions and moments

12 p1846 A72-27725

Random vibration statistics of lifting rotors with feedback controls, solving response variance matrix by random inputs shaping filters

13 p2057 A72-29096
Random vibration of two multimodal mechanical systems with point coupling, obtaining power flow spectral density by statistical energy analysis

13 p2005 A72-29563
Second order moments of system with parametric excitation by filtered white noise calculated with Fokker-Planck equation, giving condition for mean-square-stability

14 p2131 A72-30711
Instability regions of vibratory system with two degrees of freedom under random parametric effect, calculating bounds by numerical and analytical methods

15 p2275 A72-31608
Multidegree of freedom linear systems mean-square response to nonstationary random vibratory excitation, using staircase approximation to continuous intensity functions

15 p2331 A72-32552
Transfer function estimates in random vibration test control, using digital techniques for rapid reduction of statistical errors

15 p2215 A72-32626
Random vibration optimal control by transfer function estimation, using relative phase information in cross spectral density functions to sort out self noise

15 p2215 A72-32629
Natural frequency distribution theory of thin elastic shells under random vibrations in wideband field

15 p2332 A72-32677
Structural failure probability distribution for threshold stress crossings in random vibration, using Poisson approximation

16 p2468 A72-33227
Random ionization waves convective instability in glow discharge positive column, calculating fluctuations spectrum as function of position along column for localized white noise source

16 p2437 A72-33747
On the first-excursion probability in stationary narrow-band random vibration. II. [ASME PAPER 72-APM-16]

17 p2628 A72-34800
Structural system response to white noise excitation, deriving integral equation for first passage time-density function via Markov process model [ASME PAPER 72-APM-11]

17 p2629 A72-34805
Non-stationary random vibration of non-linear structures.

21 p3125 A72-41517
Chladni's patterns for random vibration of a plate.

22 p3236 A72-42758
Response of linear and nonlinear continuous structures subject to random excitation and the problem of high-level excursions.

22 p3241 A72-42970
Forced harmonic and random vibrations of concentric cylindrical shells immersed in acoustic fluids.

23 p3352 A72-44117
Analysing vibration and shock data. I - Data acquisition and pre-processing.

24 p3382 A72-45287
Evaluation of the danger of damage to mechanical systems exposed to random vibrations

24 p3459 A72-45449

RANDOM WALK

Elliptic and parabolic partial differential difference equations solution using modified random walk Monte Carlo technique

01 p0093 A72-10858
Turbulent particle diffusion statistical mechanical model, using random walk

03 p0344 A72-14331
Hybrid Monte Carlo techniques with digital and analog computers and minimal interface, simulating random walks for partial differential equations solution

08 p1138 A72-21602
Random walk models replacing Fokker-Planck equation for many particle systems with Coulomb interactions

10 p1513 A72-25041
Monte Carlo random walk methods for directional emittance of one dimensional absorbing-scattering slab with reflecting boundaries, considering refractive index, optical thickness and albedo

11 p1743 A72-25243
Discrete random walk heat conduction equation for thin layer with stepwise temperature change, comparing with parabolic and hyperbolic solutions

11 p1744 A72-25266
Random walk atomic migration model for radon diffusion through lunar regolith into atmosphere

13 p2038 A72-28995
Low storage numerical solution of waveguide problem based on impulse analysis, using random walk technique to eliminate large matrix processing

15 p2194 A72-31542
Focused light beam intensity fluctuations measurement during passage through turbulent atmosphere, discussing random walks effects on dispersion

16 p2364 A72-33494

Random geometric problems suggested by turbulence.

18 p2678 A72-36016
High order terms diffusion equation derivation for strong fluctuating flows by random walk method, discussing phenomenological analogy with equations of motion

24 p3390 A72-44994

RANEY NICKEL U CATALYSTS U NICKEL

RANGE [EXTREMES] NT FREQUENCY RANGES NT PROPORTIONAL LIMIT NT RADIO RANGE NT ROCHE LIMIT

Phase error in 136 MHz interferometer due to galactic nucleus passage, obtaining lower bound

02 p0175 A72-12160
Dynamic structural analysis by finite element method, describing error bounds for eigenvalue analysis by elimination of variables

03 p0442 A72-13401
Nonthermal electron spectra hardness limit during flash phase of solar flares from OGO-5 observation

04 p0566 A72-14561
Upper and lower bounds for expected value and variance of minimum material weight necessary for random resistance structure able to support assigned loads

04 p0593 A72-15648
Continuous linear elastic systems characteristic vibrations differential operator eigenvalues lower bounds calculation, obtaining Green integral operator first invariant upper bound via stress function

04 p0540 A72-15706
Error bounds on elastic-plastic strain wave measurements, considering one dimensional wave propagation in semiinfinite bar [ASME PAPER 71-MET-7]

05 p0731 A72-15789
Bounds on condition number for irregular meshes of finite elements expressed in terms of extremal eigenvalues of element matrices

05 p0682 A72-16540
Dynamic buckling of elastic shallow structures under periodic loading, determining critical load upper and lower bounds by energy method

07 p1090 A72-19731
Bounds for impulsively loaded plastic structures, considering fixed end beam with uniform velocity distribution

07 p1093 A72-19947
Iteration procedure for approximate integration of nonlinear system of partial differential equations with time lag, presenting upper and lower estimates

07 p1028 A72-20209
Upper soft X ray limits to Virgo sources from Aerobee 170 rocket sounding

08 p1227 A72-21394
Critique of paper on lower bounds on deformations of dynamically loaded rigid plastic continua

08 p1245 A72-21630
Upper bounds on lumped and continuous dynamic systems motion under loads and perturbations, discussing structure stability conditions [ASME PAPER 71-APMW-3]

10 p1554 A72-24188
Finite element method for approximate solution of elliptic partial differential equations on unbounded domains, proving error bounds

11 p1675 A72-25271
Lower bound estimates of error distributions for analog computer solutions of linear algebraic equations

11 p1600 A72-25433
Primary cosmic rays antineutrino content upper limit from emulsions investigations with balloons and satellites

14 p2148 A72-30885
A posteriori error bounds for approximate solutions of linear second-order ordinary differential equations.

19 p2824 A72-37372
Digital simulation for selection of extremal and lengthwise admissible paths on unidirectional computer graph

22 p3156 A72-42146
Extremal bounds for mass flow rate of laminar MHD flow in circular and thin walled conducting pipes at high Hartmann number

22 p3210 A72-42315
Navier-Stokes evolution inequality bounded solution existence and uniqueness theorems for two dimensional space

22 p3200 A72-43201

RANGE AND RANGE RATE TRACKING

Real time coherent optical processor of pulse Doppler radar signals with Fresnel diffraction masks for PCW target range rate determination

03 p0322 A72-13437
Range rate prediction algorithm for pulse Doppler ambiguity resolution by invariant imbedding method

07 p0941 A72-19303
Onboard orbital navigation system analysis on space shuttle radio range and range rate measurement data relative to ground beacon, using Kalman filter

08 p1203 A72-20856

White Sands Missile Range and Range-Rate system design and verification to meet midcourse tracking requirements under severe target dynamics
08 p1133 A72-21402

A test of the effect of satellite spin on two-way Doppler range-rate measurements.
19 p2830 A72-37278

RANGE CONTROL U TRAJECTORY CONTROL

RANGE ERRORS
Elevation angle and range error correction equations for satellite tracking data processing with assumed spherical tropospheric refractivity
09 p1281 A72-23510

Dynamic range errors and noise bands for phase comparison radio range finders with mutual automatic frequency control in interrogator and transponder
11 p1596 A72-26302

RANGE FINDERS NT LASER RANGE FINDERS NT OPTICAL RANGE FINDERS

Optimal synthesis of pulse repetition frequency control and filtering circuits of radar range finder in Gaussian approximation
02 p0183 A72-12759

Adaptive maximum likelihood receiver for direct ranging navigation, comparing with phase locked receivers
05 p0686 A72-16560

Phase errors in range finding measurements with radio waves reflection from underlying surface
09 p1277 A72-22481

C-band pulse beacon ranging system for collision avoidance, detailing interrogation, response and system test modes
09 p1349 A72-22908

Operation analysis of automatic range finders in pulse radars regarding target search and lock-on functions
11 p1595 A72-26300

Dynamic range errors and noise bands for phase comparison radio range finders with mutual automatic frequency control in interrogator and transponder
11 p1596 A72-26302

Statistical error analysis of phase comparison FM radio altimeter during signal processing, investigating range finding strength distribution of echo reflectance
11 p1633 A72-26305

Passive detection radar system for bombers, calculating target distance during horizontal flight
11 p1597 A72-26316

Frequency discriminator use for range measurements with FM radar systems, deriving reflecting target distance relationship to output voltage
13 p1918 A72-28892

Hybrid and pyrotechnic IR flare generated plasma effects on dual frequency Doppler range measurement system, discussing diagnostics and contamination concentration analysis
18 p2660 A72-36339

Optimal synthesis of pulse repetition frequency control and filtering circuits of radar range finder in Gaussian approximation
20 p2902 A72-39065

Pulse time positioning under background noise in radar and radio navigation range finders, noting root-mean-square errors and transient response
22 p3153 A72-42117

RANGE INDICATORS U INDICATING INSTRUMENTS U RANGE FINDERS

RANGE MEASUREMENT
U RANGE FINDING
RANGE FINDING

Propagation delays for clock synchronization from synchronous satellite tracking by range measurements
05 p0628 A72-16563

Suboptimum linear quadratic algorithm for optical radar signals postdetection processing and target range estimation
07 p0943 A72-19522

Meteor trails radar ranging system with circular vernier scanning and brightness indication with high accuracy
09 p1308 A72-22507

Multibeam indicator with block diagram description for meteor ranging radar and photofilm based recording system
09 p1308 A72-22508

Weak signal turnaround transponder design for pseudonoise coded ranging systems, discussing bandwidth optimization and performance comparison between various receiver configurations
10 p1452 A72-24688

Correlation technique for position location in surveillance and navigation by phase extraction from range tones using synchronous satellites
12 p1842 A72-27375

Planetary distance and velocity measurement with radar signal frequency modulation, describing Venus observations
14 p2148 A72-30209

Single point thunderstorm ranging method based on two radio frequencies field intensity spectral components ratio
14 p2129 A72-30639

Time synchronized ranging system /TSRS/ providing high-speed real-time two-way data link between community members
19 p2764 A72-37904

Planetary distance and velocity measurement with radar signal frequency modulation, describing Venus observations
23 p3333 A72-43239

RANGER LUNAR PROBES

Recent moon exploration, discussing Ranger and Lunar Orbiter photographs for crater and volcano studies and landing site mapping and Apollo program rock studies
06 p0887 A72-18217

RANGER SATELLITES U RANGER LUNAR PROBES

RANGES [FACILITIES]
NT BALLISTIC RANGES
NT MISSILE RANGES

RANK TESTS
Nonrandomized distribution-free ranking and selection procedures under subset selection formulation, considering application to reliability problems
13 p1962 A72-28366

Effectiveness of certain easily realized rank detection algorithms for noise-masked signals
23 p3266 A72-44216

RANKINE CYCLE
Heat pipe radiator with 50 kW heat rejection capability for potassium working fluid of Rankine cycle space power system, discussing design, fabrication and testing
05 p0744 A72-15875

Design of high-temperature liquid-metal systems.
[ASME PAPER 72-AERO-13] 22 p3204 A72-43149

RANKINE TEMPERATURE SCALE
U TEMPERATURE SCALES
RANKINE-HUGONIOT RELATION

Numerical analysis of three dimensional inviscid supersonic flow field about complex vehicle geometry, using finite difference technique and Rankine-Hugoniot relations
05 p0606 A72-16847

Curvature and thickness corrective terms in Rankine-Hugoniot relation for shock wave propagation of ideal gases binary mixture
10 p1417 A72-24117

Solar wind thermal anisotropy effects on least squares estimates of interplanetary shock parameters and associated normals from Rankine-Hugoniot equations
16 p2444 A72-32973

Modification of the Rankine-Hugoniot relations for shocks in space.
23 p3341 A72-44510

RAOULT LAW
Vapor pressure and partial thermodynamic functions of Co-Ni alloys, observing negative deviations from Raoult law
03 p0374 A72-13928

RAPCON [CONTROL]
U RADAR APPROACH CONTROL
RAPID EYE MOVEMENT STATE

EEG and electrooculogram recording of chimpanzee sleep, noting rapid eye movement stages
01 p0009 A72-10074

Rapid eye movement sleep deprivation and hyperventilation oxygenation influence on gamma-aminobutyric acid levels in mice brains, suggesting protective mechanism against nerve cell oxygen intoxication
07 p0922 A72-20191

Day/night workers sleep patterns in terms of intrasleep REM-NREM ultradian cycle, noting sleep temporal instability for night workers
10 p1428 A72-23730

Mental performance tests in sleep deprived subjects for indication of recuperative function of slow wave and REM sleep stages
11 p1580 A72-26682

Nocturnal primate Aotus trivirgatus wakefulness-sleep cycles during dark/light periods expressed in REM/non-REM percentages
13 p1903 A72-29300

Latent desynchronization caused by disturbances in circadian rhythms, noting rapid eye movement state
13 p1904 A72-29314

REM period functional maintenance of coordinated eye movement facilitation and binocular depth perception accuracy following sleep
17 p2509 A72-35462

RAPID TRANSIT SYSTEMS
The design and operation of a large tube-vehicle aerodynamic testing facility.
[AIAA PAPER 72-1001] 21 p3041 A72-41586

RARE EARTH ALLOYS
NT ERBIUM ALLOYS
NT NEODYMIUM ALLOYS

Cobalt-rare earth single particles hysteresis loops interpretation, considering coercive force relationship to particle size
03 p0402 A72-13781

Gas turbine superalloys high temperature oxidation resistance by fiber strengthening, rare earth alloying, precipitation hardening and intermetallic compounds
06 p0828 A72-17611

Mg dispersion hardening techniques, exploring intermetal oxidation of alloys containing rare earths
07 p1011 A72-19481

Rare earth metals microadditions influence on Ni grain boundaries free energy and compounds formation
07 p1012 A72-19676

Rare earth metals effects on chromium brittle transition temperature, showing maximum plasticity with lanthanum addition
07 p1019 A72-20151

Magnetic phenomena effects on superconductivity in simple and transition metals and dilute rare earth alloys
11 p1701 A72-26025

Russian papers on rare earth metals and alloys covering physical properties, phase diagrams and industrial applications
15 p2252 A72-31183

Rare earth metals and alloys technology assessment and utilization covering quantum mechanics concepts application to Fermi surface
15 p2289 A72-31184

Phase diagrams of rare earth ternary alloys with transition metals and Si, noting semiconductor properties
15 p2289 A72-31189

Rare earth metals interactions with V, Nb and Mo alloys, describing procedures for interstitial impurities removal
15 p2252 A72-31190

Russian book - Physical chemistry of rare metals.
22 p3190 A72-42802

Physicochemical properties of rare earth metals for alloying Al, Mg, Cu and Ti, noting getter and permanent magnet materials
22 p3191 A72-42806

Physical metallurgy of single crystals of high-melting and rare metals and alloys
22 p3191 A72-42807

Magnesium alloys containing rare-earth metals as materials with special physical properties
22 p3192 A72-42817

Heat-resistant copper-base alloys containing rare-earth and high-melting metals, characterized by high electrical conductivity
22 p3192 A72-42819

RARE EARTH COMPOUNDS
NT CERIUM OXIDES
NT ERBIUM COMPOUNDS
NT NEODYMIUM COMPOUNDS
NT SAMARIUM COMPOUNDS
NT SCANDIUM COMPOUNDS
NT YTTERBIUM COMPOUNDS

Rare earth tungstate refractory ceramics, determining mechanical properties, crystalline structure and electrical/chemical parameters
05 p0675 A72-16700

X ray and differential thermal analysis for phase diagrams of binary alloys of samarium oxides and gadolinium oxides with calcium oxides, noting solid solutions formation
23 p3304 A72-43250

A differential spectrophotometric extraction method of determining yttrium-subgroup rare-earth elements /REE/ in complex objects
23 p3324 A72-44164

RARE EARTH ELEMENTS
NT CERIUM
NT DYSPROSIUM
NT ERBIUM
NT EUROPIUM
NT GADOLINIUM
NT HOLMIUM
NT LANTHANUM
NT LUTETIUM
NT NEODYMIUM
NT PRASEODYMIUM
NT PROMETHIUM
NT SAMARIUM
NT SCANDIUM
NT TERBIUM
NT YTTERBIUM
NT YTTRIUM

Japanese lava geochemical analysis, determining K, Rb, Sr, Ba and rare earth concentrations with mass spectrometric stable isotope dilution
01 p0051 A72-10059

Apollo 14 lunar soil sample 14163 orthopyroxene composition, determining K, P and rare earth elements
01 p0125 A72-10066

Horizontally averaged nonthermal velocities determination in lower solar chromosphere, observing Doppler widths of weak rare earth emission lines in H and K wings
05 p0718 A72-16504

Chondrite normalized rare earth abundances in lunar silicate liquid-type materials from Mare Tranquillitatis and Oceanus Procellarum associated with evolution
08 p1233 A72-21218

Rare earth and trace elements in Lunik 16 soil, comparing abundances with chondrites and Apollo samples
09 p1381 A72-22274

Bulk and rare earth abundances in Luna 16 soil levels A and D by sequential instrumental neutron activation analysis
09 p1381 A72-22275

Electronic transition between energy bands as explanation for two optical absorption maxima in rare earth metals
09 p1369 A72-22609

Rare earth elements outer electrons X ray and UV photoemission spectra interpretation by multiplet splitting of final state
09 p1371 A72-22844

Ultrasoft X ray region photoionization absorption spectra features of inert gases, solids, rare earth elements and transition metals
09 p1357 A72-22845

Symmetric fission of superheavy nuclei, observing overabundance of rare earth elements
10 p1515 A72-24526

Rare earth metals addition effect on mechanical properties of electrolytic hydrogen-refined Cr, noting low temperature ductility
12 p1831 A72-28241

Significance of Apollo 11 and 12 lunar rock fragments of norite rich in K, rare earth elements and P /KREEP/ for lunar evolution assessment
13 p2037 A72-28990

Mutual solid solubilities of rare earth metals with Zr extended by splat quenching, noting metastable low temperature allotropic forms of solid solutions
14 p2119 A72-30609

Lunar rock 14310 whitlockite richness in rare earth elements relative to associated apatite
16 p2454 A72-33446

Enstatite chondrite Abee isotopic ratios of Gd, Sm and Eu comparison with terrestrial samples
16 p2457 A72-33566

Radio luminescence of an yttrium-aluminum garnet activated by rare-earth elements
19 p2845 A72-38181

Neutron activation and mass spectrometry methods for geochemical analysis of rare earth elements in meteoritic, lunar and terrestrial materials
20 p2899 A72-39835

Improved techniques for separation and determination of rare-earth elements in extraterrestrial material.
20 p2900 A72-39836

Mutual interactions of thorium, lanthanides, and bismuth in Th-Ln-Bi solutions - Evidence for the formation of ThLnBi₃/y compounds.
20 p2942 A72-39986

Direct fitting of spin wave energies to interatomic exchange parameters in the ferromagnetic rare earth metals.
21 p3097 A72-40625

Stratospheric balloons role in galactic cosmic radiation research with detection techniques for study of rate and heavy elements abundances and isotopic composition analysis
21 p3101 A72-41615

Physicochemical properties of rare earth metals for alloying Al, Mg, Cu and Ti, noting getter and permanent magnet materials
22 p3191 A72-42806

Effect of rare earth metals on the structure and properties of aluminum and its alloys
22 p3192 A72-42818

Lasing properties of yttrium orthoaluminate doped with rare-earth metals
22 p3187 A72-42943

Rare earth and other abundances in the Murchison carbonaceous meteorite.
23 p3262 A72-44131

RARE GASES

NT ARGON
NT ARGON ISOTOPES
NT HELIUM
NT HELIUM ATOMS
NT HELIUM FILM
NT HELIUM ISOTOPES
NT LIQUID HELIUM
NT NEON
NT NEON ISOTOPES
NT RADON
NT RADON ISOTOPES
NT XENON
NT XENON ISOTOPES

Double Langmuir probe, microwave cavity and upper hybrid frequency measurements of plasma density in hydrogen, helium, neon and argon
01 p0110 A72-11190

Inert gas narcosis under hyperbaric conditions relationship to mental performance and auditory and visual evoked responses in man
[AD-736736] 02 p0166 A72-11705

Apollo 12 lunar soil samples solar wind noble gas analysis of KREEP fragments, estimating Surveyor Crater age
03 p0414 A72-12902

Ionization waves linear theory for low pressure noble gas strong current column, showing self excitation limit and temperature dependence of energy loss rate
03 p0400 A72-14351

Elastic scattering without dissociation of nitrogen molecular ions by noble gas targets in 0.3-3 keV range, analyzing energy loss
03 p0393 A72-14357

Intermolecular potentials determination by inverting phase shifts obtained from high resolution measurements of protons differential elastic scattering by rare gas atoms
04 p0552 A72-14577

Steady normal shock wave analysis in binary inert monatomic gas mixtures using kinetic theory moment method
04 p0513 A72-15340

Velocity dependence of ionization cross section of Ar, Kr and Xe during thermal energy metastable neon atoms impact, obtaining secondary electron ejection efficiency
04 p0553 A72-15640

Hydrogen 2p and 2s states formation during 1-25 keV atomic collisions with rare gases from Lyman alpha radiation cross section measurement
05 p0693 A72-17168

Largest Apollo 15 lunar rock mass spectrometry analyses of noble gases with gas retention age estimation and spallation Kr data
06 p0888 A72-18267

Thermal conductivities of gaseous binary mixtures of methyl nitrate with helium, neon, argon and nitrogen
07 p1051 A72-19365

Thermal conductivity of argon, helium, hydrogen, nitrogen, carbon dioxide, methane and ethane gases at high temperature and pressure
07 p1099 A72-19620

Stepwise ionization effects on ionic wave propagation and oscillation stability in inert gas dc discharges
07 p1046 A72-20503

Noble and molecular gases addition in reactions induced in ethylene by carbon dioxide-nitrogen-helium laser
07 p1009 A72-20693

Rare gas concentrations in Luna 16 fines, using stepwise heating technique
09 p1380 A72-22266

Mass spectroscopic measurement of inert gases in Lunik 16 fragments and dust samples
09 p1380 A72-22267

Tranquility Base rocks irradiation depths and cosmic rays exposure ages from rare gases in samples, noting correlated variations in He 3/Ne 21 and Ar 38/Ne 21 due to shielding differences
09 p1377 A72-22596

Adsorption role in planetary primordial rare gas origin based on adsorptivity pattern of pulverized Allende meteoritic samples at 113 K
09 p1385 A72-22597

Trapped He, Ne and Ar isotopic variations presence in meteorites due to rare gas ions implantation by solar wind and flares
09 p1385 A72-22599

Thermodynamic formulation of noble gases equilibrium and transport properties at low and moderate densities, proposing corresponding states law
09 p1410 A72-22767

Resonance theory of three body ion-atom association reactions in rare gases, estimating quasi-bound electron state population and deactivation cross section
09 p1356 A72-22792

Excitation accompanying photoionization in atoms and molecules and relationship to electron correlation observed from rare gases inner and valence shell satellite lines measurements
09 p1356 A72-22835

Photoabsorption and simple and multiple excitations of rare gases internal atomic layers under X ray action, relating electron transition and relaxed core energies
09 p1357 A72-22836

Ultrasoft X ray region photoionization absorption spectra features of inert gases, solids, rare earth elements and transition metals
09 p1357 A72-22845

Pressure, temperature and nozzle size effects on molecular cluster formation in expanding supersonic jets of rare gases, nitrogen and carbon dioxide
09 p1294 A72-22853

Pulsed arc TIG welding with modulation of current from standard power source, comparing performance with steady dc method
09 p1320 A72-23632

Mass and energy balance for electrode wire fusion in pulsed current MIG /metal inert gas/ welding, discussing pulse duration and amplitude requirements and shielding gas composition effect
09 p1321 A72-23644

Rb 87 line shift produced by rare buffer gases and molecular nitrogen measured from applied magnetic field magnitude and hyperfine structure of D lines
10 p1490 A72-24040

Rare gases concentrations and isotope ratios in Haverø ureilite meteorite, including He, Ar, Ne, Kr and Xe
10 p1538 A72-24167

Nonequilibrium ionization theories for high pressure discharge in inert gas-alkali metal vapor
10 p1515 A72-24414

Electron beam fluorescence method for normal shock wave velocity distribution in Ar-He mixtures
11 p1615 A72-25556

Gas rich meteorites and lunar materials solar rare gases component observed and predicted relative abundance agreement indicating absence of fractionation in solar nebula formation
11 p1721 A72-26118

Filler wires developing for inert gas welding of stainless maraging steel
11 p1660 A72-26488

Rare gas ion laser excited by electrodeless microwave discharges, noting external magnetic field effects on output
11 p1651 A72-26571

Thermal release patterns and activation energies of spallogenic He, Ne and Ar from Carbo iron meteorite
12 p1866 A72-27116

Inert gas-oxygen mixtures fire retardant properties under atmospheric and hypobaric pressures, measuring effectiveness by standard fabric burning rate
12 p1890 A72-28309

Thermal-to-electric power conversion efficiency of nonequilibrium MHD generator with Cs seeded noble gases, considering electrode configuration and gas dynamic effects
13 p1900 A72-29356

Dc and RF sputter deposition in ionized inert gas of thin film coatings solid state microelectronics, solid lubricants and corrosion resistance applications [ASME PAPER 72-DE-37] 14 p2108 A72-30871

Energy and angular distribution of hydrogen and rare gas ions backscattered from polycrystalline metal surfaces
15 p2276 A72-31852

Oxygen chemisorption effect on rare gas beams reflection from refractory metals polycrystalline surfaces, interpreting experimental results by simple correlation model
16 p2431 A72-33068

Effects of nitrogen and helium upon pulmonary damage after rapid decompression to 2 torr. [AD-746093] 17 p2508 A72-34544

Gas retention chronology of Petersburg and other meteorites.
18 p2723 A72-36062

On the influence of excited ions and crossed electric and magnetic fields on ionisation cross-sections.
18 p2714 A72-36956

Temperature dependence of the electron thermal conductivity in rare gas plasmas.
18 p2716 A72-36958

Propagation of ionization wave in rarefied noble gases due to microwave resonance quanta diffusion, explaining plasmaguide phenomena
20 p2957 A72-39382

Free fall column theory allowing for 'neutral gas reduction' by ionization processes, and application of this theory to noble gas ion lasers
21 p3090 A72-40488

Inert gas effects on embryonic development.
22 p3145 A72-42744

Solar wind noble gases and solar flare emitted Fe group nuclei energetic tracks in chondrite Weston, considering galactic cosmic ray generated tracks
22 p3228 A72-42863

Isotopic compositions of rare gases in the carbonaceous chondrites Mokoia and Allende.
22 p3229 A72-42899

Electronic energy transfer phenomena in rare gases.
24 p3429 A72-45310

RAREFACTION

High altitude rocket plume rarefaction effects, predicting inviscid, merged, transition, first collision and free molecular flow regimes
08 p1128 A72-21610

RAREFACTION WAVES

U ELASTIC WAVES

RAREFIED GAS DYNAMICS

Narrow groove theory for spiral groove viscous pump gas bearings generalized to include rarefied gas and turbulence effects
02 p0234 A72-11531

Rarefied gases pressure flow and self diffusion through cylindrical tubes, presenting kinetic model with velocity independent mean free path
02 p0205 A72-12357

Heat transfer in rarefied Couette gas flow, obtaining reduced distribution function, macroscopic temperature profile and heat flux
03 p0456 A72-13242

Random method to solve basic rarefied gas /Boltzmann/ equation, applying to elastic collisions
04 p0551 A72-14518

Asymptotic integration method solution of heat transfer equation with constant wall temperature for low speed slip flow regime
05 p0599 A72-15866

[ASME PAPER 71-WA/HT-5] 05 p0599 A72-15866

Book on heat and mass transfer, covering research results over 1953-1969 on supersonic aircraft and mis-

siles cooling problems, rarefied gas dynamics boundary layer flow, etc

05 p0747 A72-16399

Environmental analysis of gas particle/probe aeroshell interaction in rarefied flow of high altitude Jupiter entry

05 p0721 A72-16844

Axial structure of free air jet in rarefied atmosphere, measuring pressure and density

06 p0797 A72-17561

Nonequilibrium thermodynamics description of rarefied gas relaxation phenomena for very fast flow processes with translational temperatures

06 p0902 A72-18137

Neutral unexcited gas atoms or molecules scattering at solid surfaces, interpreting molecular beam experimental results in terms of classical dynamics

07 p0969 A72-20065

Numerical determination of particle number and mass flux density in monatomic rarefied gas flow through circular orifice at finite pressure ratio

07 p0972 A72-20107

Direct simulation Monte Carlo method for rarefied gas dynamics, discussing computer display units use for flow visualization

07 p0973 A72-20344

Thermomagnetic slip produced by certain temperature gradient and magnetic field combinations in rarefied polyatomic gas channel flow

07 p0973 A72-20399

Molecular rotation stimulation and deactivation of diatomic molecule addition to monatomic gas, discussing energy exchange in rarefied gas flow

08 p1211 A72-21656

Vibrating membrane generated acoustic pressure wave propagation in rarefied gas, applying to solid surface-gas interaction models

09 p1294 A72-22762

Flat face cylinders in rarefied supersonic gas flow, investigating perturbed region evolution based on pitot tube method

10 p1415 A72-23751

Kinetic equations derivation for rarefied chemically reacting monatomic or stable molecular gases

10 p1514 A72-23845

Steady two dimensional flow of monatomic rarefied gas past semiinfinite beam

10 p1418 A72-24543

Steady rarefied gas flow around sphere with radial reflection of particles along normals, calculating gas dynamics variables of conservation equation

10 p1419 A72-24628

Rarefied flow fields and heating rates for space shuttle orbiter reentry at high angles of attack, using Monte Carlo simulation technique

11 p1567 A72-25248

Third order constitutive equations for transport coefficients in rarefied gases, using Chapman-Enskog theory

11 p1617 A72-26009

Turbulence microcharacteristics of rarefied suspension gas flow, using Topler schlieren-diffusion technique

12 p1752 A72-28172

Internal rarefied gas flow, taking into account molecular backscattering due to wall surface roughness

13 p1942 A72-29117

Rarefied gas flows effect on metals creep properties, examining molecular flow density distribution as function of specimen surface distance from nozzle

13 p1979 A72-29483

Convective heat transfer of sphere in rarefied gas subsonic flow, comparing calculation with measurement

14 p2071 A72-31023

Hydrodynamic and molecular velocity characteristics of rarefied gas motion between infinite plane parallel emitting and absorbing surfaces, using Boltzmann equation

14 p2096 A72-31025

Ionized and neutral specie concentration in rarefied hypersonic wake flow behind cone, using electrostatic and electron density probes

15 p2177 A72-31209

Rarefied gas flow problems, discussing mean free path effects on sharp nosed conical and bluff bodies drag and heat transfer coefficients

15 p2218 A72-32314

Monte Carlo simulation method for flow field around two dimensional or axisymmetric body immersed in hypersonic rarefied gas flow

16 p2342 A72-32882

Atomic and molecular beams fluid dynamic applications in rarefied gas flows exemplified by satellite drag coefficient measurement

16 p2429 A72-33052

Hydrodynamic equations for low speed steady external rarefied gas flows past circular cylinder, noting drag and heat transfer coefficients

16 p2344 A72-33568

Vapor pressure and velocity distributions in rarefied gas flows through narrow slits under vacuum conditions with ice sublimation

16 p2380 A72-33854

Operation and calibration of three blade rotating vane anemometer for rarefied gas flow velocity measurement

16 p2395 A72-33966

Electron-optical methods of investigating inhomogeneities in rarefied gases.

17 p2552 A72-34515

Triple collision effects in the transport properties for a gas of hard spheres.

17 p2585 A72-35157

Rarefied hypersonic flow characteristics of delta wings and trailing edge spoilers.

17 p2485 A72-35229

Book - Introduction to the kinetic theory of gas flows

17 p2541 A72-35450

Spectroscopic determination of the rotational temperature in a rarefied supersonic flow in glowing-discharge excited nitrogen.

17 p2544 A72-35928

Estimation of the conductance of channels for rarefied gas flow by means of an optical analogue.

19 p2795 A72-37466

A flow induced by thermal stress in rarefied gas.

21 p2989 A72-40193

Limiting properties of solutions of the Boltzmann equation.

21 p3086 A72-40264

Formation of a shock wave around a blunt conical body placed in a rarefied hypersonic flow

21 p2993 A72-41340

Simulation of the interaction of high altitude plumes and a high-speed free-stream flow.

[AIAA PAPER 72-1019] 21 p3042 A72-41598

Two dimensional MHD fluctuating flow of incompressible electrically conducting rarefied gas past infinite porous wall for slip-flow regime with variable suction

21 p3095 A72-41784

Rarefied gas flow through a slit.

24 p3395 A72-45572

RAREFIED GASES

NT COSMIC GASES

NT INTERPLANETARY GAS

NT INTERSTELLAR GAS

Digital computer simulation of rarefied gas molecular beam-rough metal surface interaction

03 p0392 A72-14057

Rarefied gas heat transfer problem between two parallel plates of different temperatures, evaluating nonlinear Boltzmann equation with Monte Carlo techniques

04 p0595 A72-14599

Rarefied gases thermal energy diffusion model, using radiative transfer electrical network analog

[ASME PAPER 71-WA/HT-4] 05 p0743 A72-15865

Radial heat propagation in cylindrical rarefied gas column from impulsive axial line source input, obtaining perturbed gas temperature by summation procedure

[ASME PAPER 71-WA/HT-7] 05 p0743 A72-15867

Recombination coefficient, ionization rates and average lifetime of ions in rarefied carbon-air flames, investigating pressure and additives effects

06 p0904 A72-18213

Neutral monatomic rarefied gas-surface interaction at energy levels 0.1-10 eV, using Boltzmann equation

07 p0969 A72-20061

Steady state and temperature relaxation of rarefied gas between two plane parallel plates

08 p1211 A72-21871

Rarefied gas sealant viscoelastic performance prediction by analytical models, comparing results with experiments on multiple grooved samples

08 p1177 A72-21929

Thirteen moment closed system of approximate integral equations for rarefied gases density, velocity, temperature, stress tensor and thermal flux vector

09 p1259 A72-22425

Thermodynamic formulation of noble gases equilibrium and transport properties at low and moderate densities, proposing corresponding states law

09 p1410 A72-22767

Current-optical effects of anisotropic absorption of polarized and unpolarized light in rarefied cosmic media

10 p1525 A72-23763

Heat transfer between alternating hot and cold parallel plates of constant temperature situated in low density gas

10 p1562 A72-24537

Nonlinear heat conduction in rarefied gases between concentric cylinders and spheres, using series expansion in terms of temperature difference for closed-form solution

13 p2064 A72-29118

Steady barotropic inviscid flows of rarefied gas plasmas as free jet and within cylindrical channel in axisymmetric external magnetic field with Hall effect

13 p2018 A72-29823

Magnesium particle combustion in rarefied air during pressure changes, discussing combustion time decrease with pressure increase

14 p2170 A72-30236

Rarefied gas interaction with spacecraft surface, calculating aerodynamic forces and accommodation coefficient for Proton 2 satellite

14 p2162 A72-30474

Temperature-slip problem in rarefied gases, obtaining exact solution by generalized BGK scattering model and Wiener Hopf technique

14 p2095 A72-30882

Thermal force exerted on spherical particle between two flat plates in stagnant monatomic rarefied gas, using moment solution to Boltzmann equation

15 p2336 A72-32403

Gas mixtures separation in Kantrowitz-Grey underexpanded molecular jet background as function of rarefaction degree, using electron beam fluorescence technique for concentration measurements

16 p2429 A72-33054

Quantum Boltzmann equation for a laser.

17 p2563 A72-35160

Solution to a relaxation problem by the discrete velocity method with the aid of the Boltzmann equation

17 p2586 A72-35809

High vacuum and rarefied atmosphere creep apparatus.

17 p2536 A72-35846

Thermal stress induced flow around constant temperature solid sphere in rarefied gas with uniform temperature gradient, using asymptotic theory

19 p2788 A72-38433

Hot rarefied neutral gas existence in interstellar space on basis of data collected in 21 cm hydrogen line

19 p2865 A72-38480

Variance reduction in Monte Carlo analysis of rarefied gas diffusion.

21 p3046 A72-41183

RAREFIED PLASMAS

Discrete ionospheric model of supersonic two dimensional low density plasma flow past large bodies, using quasi-neutrality condition

01 p0001 A72-10588

Rarefied plasma hydrodynamic equations for rotational discontinuities in solar wind, discussing magnetic field modulus jumpwise changes

02 p0272 A72-11915

Circularly polarized microwave damping at electron cyclotron frequency in low density magneto cesium plasma, investigating power absorption coefficient and refractive index

04 p0555 A72-14853

Electron temperature measurement error elimination with radio frequency Langmuir probe in low density plasma, measuring floating potential

05 p0694 A72-16046

Current drainage from dilute plasma to high voltage probe via holes in Kapton H polyimide film, quartz and fluorinated ethylene propylene type C

[AIAA PAPER 72-105] 05 p0696 A72-16815

Low density plasma flute oscillations stabilization by feedback system with potential sensors and electrodes, deriving dispersion equation

05 p0697 A72-16983

Ground plane curvature effect on aperture admittance of waveguide fed axial slot on teflon coated metal cylinder for underdense plasma

06 p0771 A72-17354

Rotating low density plasma in magnetic mirror trap with Penning discharge, determining conditions for oscillations damping and plasma lifetime

10 p1521 A72-24354

Inhomogeneous rarefied plasma, investigating non-local, linear and nonlinear effects on electromagnetic wave reflection and transmission

11 p1694 A72-25717

Low density plasma flute oscillations stabilization by feedback system with potential sensors and electrodes, deriving dispersion equation

12 p1850 A72-27127

Rarefied plasma hydrodynamic equations for rotational discontinuities in solar wind, discussing magnetic field modulus jumpwise changes

13 p2030 A72-29227

Steady motion of dense electron beam in rarefied phonon plasma along magnetic field, analyzing polarization effects

14 p2136 A72-30305

Electron-ion modes parametric coupling in low pressure RF self sustained plasma discharge, noting plasma frequency emissions

14 p2138 A72-30399

Heat conductivity effect on structure and critical Mach number of shock wave propagation across magnetic field in cold rarefied plasma

16 p2435 A72-33152

Nonlinear electromagnetic wave interaction in rarefied plasma cylinder subject to constant magnetic field in hydrodynamic approximation

16 p2363 A72-33479

Low density and pressure air plasma electron density simultaneous measurements by Langmuir and RF capacitance probes

16 p2438 A72-33836

Magnetogasdynamic heat transfer to hemispherical body in supersonic low density plasma, noting magnetic field effects on heat flux
[AIAA PAPER 72-686] 16 p2346 A72-34056

Vibration modes and stability of nonequilibrium low density He-Cs plasma in magnetic field
17 p2589 A72-35126

Carbon dioxide laser light scattering from cyclotron-harmonic waves in steady state rarefied collisionless plasma, noting associated electron density fluctuations
17 p2591 A72-35378

Statistical model of chemical reactions in nonisothermal low pressure plasma.
18 p2715 A72-36567

Propagation of electromagnetic waves in a rarefied plasma situated in an alternating magnetic field
18 p2717 A72-37177

Low-frequency vibrations in a rarefied bounded plasma
19 p2842 A72-38530

Nonlinear monochromatic Alfvén wave propagation along magnetic field in anisotropic rarefied plasma with firehose instability
20 p2957 A72-39381

Effect of angle of incidence on the response of cylindrical electrostatic probes at supersonic speeds.
20 p2926 A72-39602

Reflector-analyzers for studies of rarefied low-energy plasmas
21 p3058 A72-41731

Pressure dependent microwave cavity breakdown field relationship to steady state plasma luminosity interpretation as evidence of RF confinement of low density plasma
22 p3212 A72-42897

Steady motion of dense electron beam in rarefied phonon plasma along magnetic field, analyzing polarization effects
23 p3317 A72-43207

Ion acceleration during expansion of a rarefied plasma
23 p3322 A72-44482

RASERS
U MASERS

RATE METERS
U MEASURING INSTRUMENTS

RATE OF CLIMB INDICATORS
Variometer system for sailplanes sinking or climbing rates direct readout, describing pressure difference measuring concept based on reservoir-capillary system
21 p3051 A72-40225

Variometer system for sailplanes sinking or climbing rates direct readout, describing pressure difference measuring concept based on reservoir-capillary system
23 p3292 A72-44451

RATES (PER TIME)
NT ACCELERATION [PHYSICS]
NT ACOUSTIC VELOCITY
NT AIRSPEED
NT ANGULAR ACCELERATION
NT ANGULAR VELOCITY
NT ARRHYTHMIA
NT BRADYCARDIA
NT BURNING RATE
NT COLLISION PARAMETERS
NT COLLISION RATES
NT CRITICAL VELOCITY
NT CURRENT DENSITY
NT DECAY RATES
NT DECELERATION
NT DRIFT RATE
NT ELECTRON DECAY RATE
NT ELECTRON FLUX DENSITY
NT ESCAPE VELOCITY
NT EVAPORATION RATE
NT EXHAUST VELOCITY
NT FLOW VELOCITY
NT FLUX [RATE]
NT FLUX DENSITY
NT GROUP VELOCITY
NT HEART RATE
NT HEAT FLUX
NT HIGH ACCELERATION
NT HIGH GRAVITY ENVIRONMENTS
NT HIGH SPEED
NT HYPERSONIC SPEED
NT ILLUMINANCE
NT IMPACT ACCELERATION
NT ION PRODUCTION RATES
NT IRRADIANCE
NT LIGHT SPEED
NT LOADING RATE
NT LUMINANCE
NT LUMINOUS INTENSITY
NT MAGNETIC FLUX
NT MASS FLOW RATE
NT NEUTRON FLUX DENSITY
NT ORBITAL VELOCITY
NT PARTICLE ACCELERATION
NT PARTICLE FLUX DENSITY
NT PHASE VELOCITY
NT PHOTON DENSITY

NT PHYSIOLOGICAL ACCELERATION
NT PLASMA ACCELERATION
NT PROPAGATION VELOCITY
NT PROTON FLUX DENSITY
NT PULSE RATE
NT RADIAL VELOCITY
NT RADIANCE
NT RADIANT FLUX DENSITY
NT RECOMBINATION COEFFICIENT
NT RELATIVISTIC VELOCITY
NT RESPIRATORY RATE
NT ROTOR SPEED
NT SOLAR CONSTANT
NT SOLAR FLUX
NT SOLAR FLUX DENSITY
NT SOLAR VELOCITY
NT SOUND INTENSITY
NT SPIN REDUCTION
NT STRAIN RATE
NT SUBSONIC SPEED
NT SUPERSONIC SPEEDS
NT SYSTOLE
NT TACHYCARDIA
NT TERMINAL VELOCITY
NT TIP SPEED
NT TRANSONIC SPEED
NT WIND VELOCITY

Linear airspeed and runway rate field displays, measuring initial response latencies, control reversals and root mean square tracking errors
06 p0845 A72-17717

Stopping rate of negative cosmic-ray muons near sea level.
23 p3332 A72-44501

RATINGS
Gas turbine procurement standard rating and performance indicators, noting dependence on ambient conditions
[ASME PAPER 71-WA/GT-1] 05 p0703 A72-15894

Improved qualitative flight data rating scales.
21 p2996 A72-41257

RATIOMETERS
Double beam scanning vacuum UV spectrometer and logarithmic ratiometer for reflectivity and transmission measurements on solids, liquids and gases
[AD-745497] 09 p1313 A72-23329

RATIONAL FUNCTIONS
Survey and bibliography of extrapolation processes in numerical analysis based on polynomial or rational functions
02 p0252 A72-11546

Real rational function Cauchy index computed from integral functions of polynomial coefficients and signature of infinite class of matrices
07 p1026 A72-18817

Holomorphic rational functions involving error bounds without derivatives solution by numerical differentiation procedure
14 p2126 A72-30709

Open circuit voltage transfer function synthesis to realize arbitrary real rational function in complex variable, using generalized positive impedance converter
15 p2211 A72-31847

Approximate representation of a type of transcendental polynomials describing wave systems with fractional rational functions
19 p2834 A72-37751

Reinforcement method algorithm for inversion of matrix with rational function terms
21 p3075 A72-41313

Multidimensional asynchronous FM sampled data systems stability, considering continuous linear part transfer matrix poles located on imaginary axis
22 p3162 A72-42080

Infinitely distant points of a differential equation
23 p3309 A72-43846

RATIOS
NT ASPECT RATIO
NT DIMENSIONLESS NUMBERS
NT FINENESS RATIO
NT FUEL-AIR RATIO
NT GRASHOF NUMBER
NT HARTMANN NUMBER
NT HIGH ASPECT RATIO
NT INDEXES [RATIOS]
NT LEWIS NUMBERS
NT LIFT DRAG RATIO
NT LOW ASPECT RATIO
NT MACH NUMBER
NT MASS RATIOS
NT NUSSELT NUMBER
NT OPTICAL REFLECTION
NT PAYLOAD MASS RATIO
NT PECLET NUMBER
NT POISSON RATIO
NT PRANDTL NUMBER
NT PROPELLANT MASS RATIO
NT RAYLEIGH NUMBER
NT REYNOLDS NUMBER
NT RICHARDSON NUMBER
NT SCALE [RATIO]
NT SCHMIDT NUMBER
NT SIGNAL TO NOISE RATIOS
NT SIMILARITY NUMBERS
NT STANDING WAVE RATIOS
NT STANTON NUMBER

NT STRESS RATIO
NT THICKNESS RATIO
NT THRUST-WEIGHT RATIO
NT VOID RATIO

Automatic computation of exponentials, logarithms, ratios and square roots.
18 p2705 A72-37021

The automatic computation of exponentials, logarithms, ratios, and square roots.
24 p3383 A72-45668

RAWINSONDES
Extrapolation procedure for determining small-scale wind shear definition from Rawinsonde vertical wind profiles statistical data for aerospace vehicle design
07 p1085 A72-19687

Upper troposphere-lower stratosphere geostrophic wind deviation from rawinsonde and pressure-height data in El Paso-White Sands area, using finite difference method
13 p1988 A72-28447

RAY TRACING
Approximate height formula for radio ray propagating through spherically stratified smoothly varying troposphere, evaluating exponential model atmosphere
01 p0032 A72-11253

Radio signal fading analysis by ray tracing for transmission in spherically stratified atmosphere, assuming refractivity linear variation with height
02 p0179 A72-12414

Manual reduction of Faraday rotation observations of ionospheric electron density at low latitudes, comparing with computer ray trace analysis
02 p0221 A72-12462

Ray path and absorption calculation for mf and hf radio wave oblique propagation through model ionosphere in nighttime, noting E region ionization role
02 p0184 A72-12875

Computer based analysis of holography using ray tracing and wave front matching aberrations
03 p0358 A72-13433

Hf radio wave reflection at vertical incidence from ionosphere, calculating distance attenuation by ray-tracing techniques
04 p0487 A72-14886

Average ray direction and mean square deviation formula for electromagnetic wave propagation in random inhomogeneous medium suited for calculation by ray tracing program
04 p0488 A72-15382

Asymptotic theory of diffraction at waveguide open end, using generalization by ray and parabolic equation methods
04 p0489 A72-15385

Geomagnetic field-hf sky wave orthogonality conditions, discussing ray tracing for signals reflected in ionosphere
05 p0630 A72-16619

Ray-optical calculation of modes scattered by obstacle in two dimensional waveguide or duct with weakly inhomogeneous medium and nonvanishing surface impedance walls
05 p0630 A72-16622

Optical properties of paraboloid-hyperboloid mirror X ray telescopes evaluated by ray tracing method, noting resolution and focal plane curvature approximation
07 p0985 A72-19405

Ray trace of sound refraction by point source on jet flow axis, numerically calculating directivity pattern
08 p1152 A72-21893

First order imagery in neighborhood of base ray transversing arbitrary optical system, discussing relationships among anamorphic nature, astigmatism and image rotation
09 p1309 A72-22606

Radio wave beam trajectories in laminar isotropic plasma layer, using dynamic systems theory
11 p1591 A72-25335

Electrostatic resonances associated with maximum frequencies of cyclotron-harmonic waves at high and low latitudes, presenting dispersion curves and ray paths
11 p1624 A72-26400

Acoustic ray tracing of long range infrasonic signals from launch and reentry of Saturn 5 rockets
11 p1690 A72-26512

Analytic ray path solutions for HF radio wave transmission through plane stratified isotropic ionospheric model
11 p1599 A72-26763

Luminosity distribution in plane of image produced by radiation from plane parallel plate, taking into account rays real path
13 p1955 A72-28498

Acoustic ray path method for computing atmospheric conditions effect on aircraft noise propagation, using digital computer
13 p1897 A72-28840

Correction formulas for aerial photograph distortions due to internal refraction of light rays in separation of gas media by lateral surface of circular cylinder
15 p2277 A72-32124

Ray geometry, travel time and spreading loss derivation for refracted/bottom-reflected ray propagation

tion in channel with horizontal and vertical sound speed gradients 18 p2710 A72-36413

Acoustic ray deflection by aircraft wake vortices with viscous core, observing maximum deflection angles during large aircraft landing 18 p2641 A72-36417

Analysis of multiple hologram optical elements with low dispersion and low aberrations. 19 p2796 A72-37578

Propagation of internal acoustic-gravity waves around a spherical earth. 19 p2793 A72-38748

Ray tracing in ionosphere and magnetoionic theory application to coupling in cold plasma waves, considering linear waves, electrodes, particles and echoes as exciters 23 p3319 A72-43516

Ray optics applications to electromagnetics and other disciplines, discussing matrix representation for wavefront curvature and field computation simplification via transformations 23 p3314 A72-44331

Optical alignment of planes and straight lines in space by reflecting prism systems and double ray bundles with mirror symmetry 24 p3424 A72-44768

Studying hologram imagery by a ray-tracing method. 24 p3401 A72-44773

RAYLEIGH DISTRIBUTION

Target detection in sea clutter, showing non-Rayleigh distributed high resolution radar envelope return 02 p0178 A72-12400

Error distribution computation for combined Rayleigh-Gaussian statistics data, applying to antenna radiation beam-pointing example 04 p0500 A72-15303

Microwave radio link transmission loss Rayleigh-like long term distribution explained by two-path propagation model 12 p1784 A72-27796

Statistical methods for friction and wear processes, noting Rayleigh distribution of wear particles, surface dispersion velocity, energy dissipation and friction force 12 p1818 A72-28186

Rayleigh distribution of radio signals partially reflected from D region, noting amplitude fluctuations dependence on antenna radiation pattern 15 p2202 A72-32733

Optimal predistortion efficiency for multiplicative disturbances in radio signal transmitting channel, noting Rayleigh distribution of signal fluctuations 17 p2518 A72-35778

Characteristics of filtering the Rayleigh parameter of pulse signals in the presence of noise 22 p3154 A72-42228

RAYLEIGH NUMBER

Transient three dimensional natural convective modes in porous media as function of Rayleigh number 07 p1099 A72-19623

Turbulent gas flow induced by laser heating, emphasizing Rayleigh number as stability criterion 09 p1295 A72-23492

Thermal convective instability in semiinfinite constant temperature viscous fluid with lower boundary suddenly heated, calculating neutral stability curve and critical Rayleigh number 16 p2478 A72-33656

Nusselt number dependence on Rayleigh number for steady convection in porous medium, explaining heat transport abrupt change by breakdown of Darcy law 18 p2740 A72-36484

RAYLEIGH SCATTERING

Rayleigh distance for reflection from curved surfaces in Cassegrain subreflector geometrical optics design 04 p0499 A72-15207

Air pollutant monitoring and remote analysis by Raman, fluorescence and resonance backscattering, Rayleigh scattering and absorption laser radar techniques 06 p0827 A72-18460

Thermal equilibrium fluctuations and Rayleigh light scattering in isotropic gyrotropic continuous medium with internal rotational degrees of freedom 07 p1034 A72-18909

Dipole moment expression for Rayleigh scattering field from finite closed perfectly conducting body irradiated by LF plane electromagnetic wave [AD-742573] 10 p1434 A72-23720

Binary gas mixture density correlation functions from initial value problem based on linearized Boltzmann equation for analysis of Rayleigh-Brillouin scattering 16 p2428 A72-32942

Rayleigh-Brillouin light scattering in He-Xe gas mixtures, noting thermal fluctuations effect 16 p2422 A72-32943

Elastic longitudinal or shear wave scattering by movable rigid sphere embedded in elastic solid, showing inverse Rayleigh limit dependence 16 p2423 A72-32988

Rayleigh and Raman scattering by H2 in a planetary atmosphere. 20 p2966 A72-38914

Flashlamp-pumped dye lasers for investigations of the upper atmosphere. 24 p3409 A72-44948

Determination by the scattering method of the parameters of a plasma produced by a laser spark in air 24 p3429 A72-45496

Radar cross sections of conducting bodies of revolution, noting electric/magnetic polarizability tensors in LF Rayleigh scattering 24 p3381 A72-45639

RAYLEIGH WAVES

Rayleigh type transverse surface wave existence in continuous elastic body with nonlocal interaction 09 p1403 A72-22748

Plane stratified earth crust parameters determination from dispersion curve of Rayleigh surface waves fundamental tone 09 p1304 A72-23488

Stationary HF Rayleigh waves in surface waveguide, considering transverse and longitudinal wave velocities in half space with elastic medium 11 p1688 A72-26378

Guided elastic wave propagation near curved surfaces and in nonconstant thickness layers, discussing asymptotic solution and applications to Love, Rayleigh and Lamb waves [ASME PAPER 72-APM-OO] 17 p2580 A72-34306

Rayleigh wave propagation on a piezoelectric-semiconductor boundary 17 p2596 A72-35541

Rayleigh wave effects in an elastic half-space. 20 p2980 A72-39615

Propagation of Rayleigh waves on visco-elastic cylindrical surfaces placed in a magnetic field. 22 p3207 A72-42876

Electronic devices with Rayleigh ultrasonic acoustic surface wave excitation for storage, recognition and separation of electrical signals usually requiring computerized operation 23 p3314 A72-44148

RAYLEIGH-RITZ METHOD

Skew plates buckling with different edge support conditions, presenting Rayleigh-Ritz method results for various combinations of side ratio, skew angle and loadings 04 p0584 A72-14509

Rayleigh method convergence in ideal fluids axisymmetric flow stability with free boundaries and perturbations without mass forces 08 p1148 A72-20909

Rayleigh-Ritz method supplement for optimal evaluation of eigenvalue bounds for semibounded self adjoint operators 09 p1353 A72-23484

Modified Rayleigh-Ritz method to obtain lower bounds of eigenvalues, applying to uniform cantilever column buckling 15 p2275 A72-31710

A method for selection of significant terms in the assumed solution in a Rayleigh-Ritz analysis. 17 p2634 A72-35408

Free vibrations of an arbitrary structure in terms of component modes. [ASME PAPER 72-APM-T] 23 p3350 A72-44054

Bounds to bending frequencies of a rotating beam. 23 p3354 A72-44249

RBE

U RELATIVE BIOLOGICAL EFFECTIVENESS (RBE)

RC CIRCUITS

High Q oscillator with simulated inductor circuit consisting of negative immittance converter and RC elements 01 p0035 A72-10127

Affined RC or RL networks, investigating real and equal or imaginary, conjugate and inverse voltage and current transmittances 02 p0197 A72-12240

Active RC circuit with grounded capacitors capable of functioning as differentiator, bridge, inductance simulator, bandpass filter and oscillator 03 p0337 A72-14354

RC network synthesis technique using grounded gyrator and summing amplifier, applying to thin film RC networks and IC operational amplifiers 04 p0504 A72-14570

Pulmonary RC network and multiple breath nitrogen washout time constants mathematical relationship for breathing mechanics measurement, discussing lung compliance and resistance 04 p0478 A72-14862

Printed circuit boards and RC elements soldered connections reliability under high temperature and excessive current conditions, discussing test procedure and evaluation criteria 07 p0994 A72-19247

Automatic assembly machines for IC batch production, involving terminal cutting and bending and RC element insertion 09 p1292 A72-23255

Polynomial filter design with three layer RC distributed elements and operational amplifiers, investigating active elements effects on response 09 p1290 A72-23354

FM measurement system with linear resistance-to-frequency converter realized in RC oscillator form, discussing design problems 10 p1482 A72-24598

Network synthesis for various second and third order sinusoidal oscillators consisting of linear passive or active RC circuits and amplifier 10 p1452 A72-24802

Linear constant systems synthesis with structural constraints in state space form, applying to RC filter circuit 10 p1453 A72-25101

Lumped parameter nonlinear RC circuit lung model for positive pressure respirator design 11 p1588 A72-26631

Solid state RC network for single sideband frequency converter using phase difference carrier suppression 11 p1598 A72-26731

RC network synthesis for accurate realization of complex transmission zeros without capacitor adjustment 12 p1794 A72-27696

Relaxation oscillator synchronized by quartz crystal between emitter and base of unijunction transistor, obtaining sinusoidal output by series-connected RC load 13 p1926 A72-28377

Active transistorized low pass RC filter providing fourth-order transfer function and uniform frequency response 13 p1927 A72-28381

Self excited oscillator using emitter follower circuit and distributed active RC phase shifter network 13 p1927 A72-28404

Forced oscillations in RC amplifier with negative feedback through nonlinear bandpass filter with varicaps 13 p1931 A72-29266

Lumped approximation to distributed RC notch networks for linear IC, deriving open circuit voltage transfer functions and root locus graphs 14 p2092 A72-31170

Active RC circuit synthesis by state model method, minimizing capacitances of admittance matrix for microelectronic circuit technology 15 p2210 A72-31595

Calculation of steady modes of operation of RC circuits with jumpwise varying parameters 17 p2533 A72-34761

Optimization of the functions of a circuit with lumped and distributed RC parameters 17 p2535 A72-35785

Regenerative nonlinear RC amplifier oscillations due to series opposed varicap diode capacitance 18 p2665 A72-36109

Synthesis of networks containing three-layer rectangular distributed RC elements and nonideal operational amplifiers 18 p2673 A72-36791

Analysis of the performance of a single-half-period synchronous relay detector with an active-capacitance load 19 p2801 A72-37963

Amplitude and harmonic oscillation characteristics of quaternary RC parametron using tunnel diodes 19 p2773 A72-38211

Nonlinear double T-shaped RC filter 19 p2774 A72-38417

RC gyrator filters frequency characteristics stability analysis, noting elements sensitivity as function of frequency and Q value 19 p2774 A72-38421

A frequency transformation chart for RC-active band-pass filters. 20 p2907 A72-39432

Network analysis and frequency response of LF filter with distributed RC structure and voltage converter 22 p3158 A72-42120

Voltage generalized-impedance converter synthesis with RC circuits for obtaining current transfer function proportional to square of s with application to filter design 22 p3140 A72-42303

Use of selective RC amplifiers in the radio-frequency amplifier stages of superheterodyne radio receivers 23 p3271 A72-43775

An approach for generation of second order RC-active filters. 23 p3276 A72-43863

RC, RL and RLC networks associated tunnel diode circuits normalized graphs, design method and stability consideration 23 p3272 A72-43988

RDX

Al alloys welding with Pb sheathed linear ribbon
RDX explosives by parallel plate process, achieving
high weld strength

08 p1173 A72-20779

Method of measuring the fine structure of detonation
fronts in solid explosives.

24 p3463 A72-45039

REACTANCE

Impedance strip synthesis on symmetric cylindrical
antenna excited by phased magnetic flux ring, determining
radiation pattern for pure reactance conditions

08 p1131 A72-20932

Plasma potential determination near probe by space
charge layer reactance observation

09 p1361 A72-22962

Circuit of two parallel connected vacuum pentodes
with different reactances to provide exact voltage division
of ac signals by another

13 p1930 A72-29045

Conditions derived for reactive two-terminal-pair
matching transformer networks operation at maximum
power transfer efficiency

14 p2087 A72-30334

Conducting body radar scattering control by reactive
loading, discussing field pattern synthesis for real
current with least mean-square approximation

17 p2513 A72-34358

Plasma potential determination near probe by space
charge layer reactance observation

17 p2593 A72-35892

REACTION CONTROL

Proportional-integral control of reactants supply for
hydrazine-oxygen fuel cells with pulse controlled solenoids

06 p0867 A72-18290

Analog fluidics systems status, exemplifying attitude
reaction control for solar observation rocket
and air gauging in textile industry

08 p1111 A72-20927

REACTION JET ATTITUDE CONTROL

U ATTITUDE CONTROL

U JET THRUST

REACTION JETS

U JET FLOW

U JET THRUST

REACTION KINETICS

Ionospheric ion formation and neutralization reaction
rate coefficients determination by fitting measured
electron concentration profiles with computer
generated profiles

01 p0059 A72-10616

Thoriated Ni-Cr alloys oxidation kinetics at high
temperatures, discussing oxide formations as function
of CR content

01 p0089 A72-11664

Phenolic-novolak prepolymer molecular structure
and pyrolysis reactions thermokinetic parameters,
presenting statistical methods for estimating char yield

01 p0023 A72-11261

Kinetics of shock wave pyrolysis of pentafluoroethane
dilute mixture in Ar at 1180-1470 K

02 p0170 A72-11520

Rotation and mass inclusion into study of energy
barriers location effects on thermonuclear reaction
dynamics

02 p0262 A72-11981

Resistometric investigation of Ge addition effect on
Al-Zn alloy clustering kinetics, determining Ge atom-
vacancy binding energy

02 p0247 A72-12821

Heat transfer of nonequilibrium dissociating
nitrogen dioxide in round tube, allowing for finite
reaction velocity

02 p0303 A72-12861

Kinetic model and analysis of elementary characteristics
of carbon trifluoriodide photodissociation laser

03 p0366 A72-13078

Tungsten, molybdenum and tantalum disulfides oxidation
rate determination by fluidized bed technique,
calculating kinetic and diffusive processes activation
energy

03 p0370 A72-13184

Energy conversions and mean vertical motions in
high latitude summer mesosphere and lower thermosphere,
observing reaction kinetics

03 p0346 A72-13380

Positive ion composition in equatorial D region,
investigating reaction kinetics

03 p0412 A72-13522

Carbon-oxygen reaction kinetic limitations on carbon
ablation rate, discounting diffusional transport
limits above 1650 K

03 p0457 A72-13955

Reaction kinetics of NO and CO formation in lean
premixed hydrocarbon-air flames

04 p0594 A72-14409

Kinetic-analytical models for nitric oxide formation
in combustion processes, evaluating heterogeneous effects

04 p0482 A72-14581

Computer program for construction and integration
of chemical reaction rate equations, applying to nitric
oxide formation and decomposition

[WSCI PAPER 71-27] 04 p0482 A72-14583

Vibrations effect on corrosion rate by experimental
method, comparing reaction kinetics on two
specimens with and without alternating stresses

04 p0591 A72-15237

High temperature ClF reaction kinetics in thermal
decomposition shock tube study, using chlorine atom
two-body emission

04 p0484 A72-15463

Mass spectroscopic rate constants for reactions of
negative ions of rhenium and tungsten oxides with
chlorine and nitrogen dioxide

04 p0484 A72-15639

Carbon dioxide-carbon monoxide vibrational energy
transfer rate at 730-2325 K from measurements following
heating in shock tube

04 p0553 A72-15641

Crack corrosion in metals and metal alloys, considering
electrochemical reaction kinetics as function
of oxygen concentration and pH

04 p0536 A72-15738

Molecular oxygen evolution Mn catalyst photoactivation
as two-quantum process, discussing kinetic
model computer simulation

04 p0484 A72-15740

Gas turbine combustors performance model, using
reaction rate equation from elementary mass balance
equation

[ASME PAPER 71-WA/GT-5] 05 p0704 A72-15898

Soot oxidation rate from diffusion flame measurements
extrapolated for gas turbine combustion chambers

05 p0747 A72-16368

Self ignition in hydrogen oxidation kinetics, considering
convection, molecular diffusion, mixing and pressure

05 p0625 A72-17213

Molecular oxygen dissociation rate constant determination
during interaction with He atoms in cylindrical
shock tube

06 p0852 A72-17686

Kinetic model for propane pyrolysis based on most
important free radical reaction steps

06 p0770 A72-17777

Reactive solid or fuel combustion, deriving equations
for movement and deformation of reaction front
during oxidant diffusion through ash mantle

06 p0902 A72-18155

Solid propellant reaction kinetics at gaseous fuel
and catalyst-containing ammonium perchlorate interface,
studying ignition and deflagration

07 p1051 A72-19367

Surface and thermal effects on hydrogen oxidation,
calculating explosion limits and slow reaction rates

07 p0935 A72-19370

Rate controlled partial thermodynamic equilibrium
method for treating reacting gas mixtures, applying to
freezing reactions in internal combustion engine

07 p1099 A72-19371

Particle formation rates in thermal decomposition of
acetylene in diffusion flame, noting activation energy

07 p1099 A72-19373

Product of net branching factor and induction
period in hydrocarbon oxidation at low temperatures,
tabulating results

07 p1051 A72-19374

Temperature dependence of carbon monoxide reaction
rate with hydroxyl, noting activation energy

07 p0935 A72-19376

Kinetic data analysis of internal oxidation in dilute
Ni-Be alloys, deriving activation energy and diffusivity
of oxygen in Ni

07 p1021 A72-20435

Thermal decomposition kinetics of tetramethylene
tetranitramine beta HMX from differential thermal
analysis and activation energy calculation

08 p1219 A72-20755

Start reaction effect on burning time sequence of
hydrogen combustion in air

08 p1129 A72-22171

D and E region ion chemistry reaction rate measurements,
noting hydration, charge exchange and ion-atom
interchanges

09 p1275 A72-22366

Room temperature reactions involving ionospheric
cluster ions, discussing rate constants measurement
by stationary afterglow and drift tube facilities

09 p1275 A72-22367

Cation polymerization of beta-propiolactone
without initial kinetics dependence on monomers
concentration, relating acyl ion bonding and electron
donor groups

09 p1275 A72-22496

Reactions of aniline with isomyl nitrite and phenyldiazonium
borofluoride with caustic potash, investigating
kinetics of chemical polarization of products nuclei

09 p1275 A72-22497

D region negative ion reaction schemes, discussing
reaction rates of nitrogen dioxide with hydrogen

09 p1275 A72-22592

Nitrogen adsorption kinetics on bulk W targets investigated
by ultrahigh vacuum, molecular beam,
reflexion detector method

09 p1276 A72-22806

Carburization kinetics of Nb in acetylene or
methane at high temperatures and low pressure

09 p1319 A72-22985

Parabolic oxidation kinetics of Ni-Ti alloy compound
at elevated temperatures

09 p1330 A72-23358

Cyclic oxidation kinetics of Hastelloy X sheet and
wire specimens for high temperature alloy evaluation
in transpiration cooled engine components manufacture

09 p1331 A72-23476

Temperature effects on kinetics of methane decomposition
on carbon fiber at high temperatures, showing
characteristics relationship to carbon gasification
reactions

10 p1433 A72-24086

Thermal energy reaction rates determination for
partial charge transfer chemical reactions, comparing
with electron transfer efficiencies

10 p1514 A72-24336

Molecular diffusion laser gain determination from
interaction kinetics between diatomic and cold working
gases, examining annihilation processes

10 p1491 A72-24360

Ionization equilibrium description by quantum
statistical fugacity expansion of pressure for partially
ionized plasmas

10 p1524 A72-24929

Inhomogeneous sink distribution effect on vacancy
annealing kinetics and activation energy in metals

10 p1499 A72-24983

Surface ignition behavior of M2 double base propellant,
analyzing reaction kinetics

10 p1528 A72-25142

Atmospheric metal ion chemistry, tabulating thermal
energy binary and three body reaction rate data

10 p1434 A72-25160

One dimensional pulsating detonations calculation
with induction zone kinetics, obtaining Chapman-Jouguet
steady solution profiles

11 p1745 A72-25983

Austenite formation kinetics in Fe-C ferritic-pearlitic
structure at 855 C, comparing experimental data
with theoretical calculations

11 p1662 A72-26744

High temperature low pressure reaction kinetics of
nitrogen sorption by titanium foil, using ultrahigh
vacuum microbalance

12 p1777 A72-27045

Low pressure hydrogen and titanium thin film reaction
rate measurement, using flow technique

12 p1778 A72-27046

Shock heated methane-oxygen-argon mixtures ignition
delay time from reaction kinetics calculations

12 p1778 A72-27852

Dimensionless heat transfer equations of reacting
media in chemical equilibrium, using Lewis-Semenov
criterion

12 p1889 A72-28140

Statistical adsorption kinetics model with electron
desorption of oxygen on polycrystalline W, noting
sticking coefficients

13 p1912 A72-28523

Coupling between chemical kinetics and sound
propagation, discussing conditions for amplification
and attenuation of acoustic wave

13 p1912 A72-28547

Reclaimed surface, ground and sewage water oxidizability
measurement, studying oxidation kinetics of
potassium bichromate distilled urine condensate
admixtures

13 p1910 A72-29313

Kinetic model and analysis of time characteristics of
trifluoriodomethane photodissociation laser

13 p1968 A72-29428

Zr oxidation kinetics at 440-850 C for 3 min maximum
exposure time, observing type oxide change
relationship to activation energy

14 p2113 A72-30247

U-Zr-Nb and U-Nb-Mo alloys gamma solid solution
phase isothermal transformation kinetics at 500-600 C
from dilatometric, microstructural and X ray analyses,
noting decomposition

14 p2114 A72-30403

Co-Cr alloy high temperature oxidation kinetics
reduction by Y addition, presenting metallographic
study

14 p2118 A72-30543

Protein biosynthesis R and D, discussing rate control,
structure and medical and nutritional applications

14 p2076 A72-30600

Disturbed ionospheric electron and ion kinetics,
detailing dissociative recombination as regulating
process for temporal evolution

14 p2102 A72-30654

Thermochemical methods for plasticized/stabilized
cellulose nitrate kinetic constants determination for
lifetime estimation, presenting isothermal decomposition
curves

14 p2144 A72-30753

Octahedral TiC single crystals oxidation at high temperature in oxygen, carbon dioxide and mixtures, investigating oxygen partial pressure effects on kinetics
14 p2121 A72-30772

Formation mechanism of sodium sulfate from gas turbine fuel combustion, discussing thermodynamic equilibria and reaction kinetics
15 p2297 A72-31294

IR internal reflection spectroscopy application to dynamic chemical changes study on ammonium perchlorate surface during thermal decomposition, observing crystal lattice transformation
15 p2296 A72-32313

Reaction rate coefficient evaluation for charge transfer from doubly positive carbon ion to helium at 100-100,000 K, discussing effect on interstellar medium
16 p2360 A72-33455

Solid phase reaction kinetics in zirconium beryllide alloys with Ta and Nb at 900-1400 K, noting Be diffusion effect
16 p2408 A72-33535

Decay rate coefficients at 250-370 K for three-body recombination kinetics of O and CO, considering CO, carbon dioxide and nitrogen as third body
17 p2511 A72-34736

Absolute rate constant for the reaction $H + H_2CO$.
17 p2511 A72-34739

Comments upon shock-initiated oxidations by nitrous oxide.
17 p2511 A72-34905

Molecular diffusion laser gain determination from interaction kinetics between diatomic and cold working gases, examining annihilation processes
17 p2563 A72-34959

Rates of interaction of vibrationally excited hydroxyl $\nu = 9$ with diatomic and small polyatomic molecules.
17 p2511 A72-35648

Equilibrium distribution of chemical species in a reacting gas mixture
17 p2512 A72-35808

Perturbation method in inelastic interaction model for transport processes in reacting gases described by Boltzmann kinetic equation
18 p2713 A72-36807

Two component reaction kinetics model for numerical analysis of combustion during two- and three dimensional supersonic steady flow of hydrogen-air fuel mixtures
19 p2880 A72-37389

Ion mobilities and ion-molecule reaction rates in oxygen.
19 p2836 A72-37457

Atomic oxygen-ozone gas phase reaction rate constant direct measurement in steady state flow system at 269-409 K under excess ozone conditions
19 p2762 A72-38221

Burning of carbon particles in a supersonic chemically active gas flow
19 p2882 A72-38454

IR chemiluminescence technique [method of arrested relaxation/ to measure spectral energy distribution among Cl and HI and DI reaction products
19 p2763 A72-38802

Rate constant determination for reaction product molecule in vibrational and rotational quantum states, obtaining spectral energy distribution
19 p2763 A72-38803

Energy distribution among reaction products. VI - F + H₂, D₂.
19 p2763 A72-38804

Relaxation of a reacting gas described by the Boltzmann kinetic equation
19 p2838 A72-38856

Comparison of homogeneous gas-phase reaction kinetics for complete segregation and complete micromixing.
[WSCIPAPER 72-6]
20 p2982 A72-38972

Chemical reaction rates for dissociation and exchange in nonisothermal plasma from molecular energy level occupation investigation
20 p2957 A72-39018

Study of titanium and titanium oxide structures corresponding to different kinetics of oxidation obtained at 850 C
20 p2936 A72-39206

HF chemical lasers pumped by atomic fluorine with molecular hydrogen, calculating intensity and efficiency by reaction kinetics analysis for comparison with computer solutions
21 p3062 A72-40617

The reduction of chlorine on carbon in AlCl₃-KCl-NaCl melts.
21 p3013 A72-40843

Effects of scale porosity, second-phase oxides, and doping in the high-temperature oxidation of cobalt and dilute cobalt-chromium alloys.
21 p3067 A72-40845

Kinetics of carbothermal reduction of quartz under vacuum.
21 p3073 A72-40934

Thermodynamic parameters and reacting multicomponent mixture composition, using state equations and energy conservation equations for reaction kinetics
21 p3013 A72-40989

Propagation rate and the existence range of turbulent flame
21 p3131 A72-41660

Structural and reaction kinetic characteristics of W, Ti and Ta/C-Co systems, considering solubility, surface energy, diffusion, segregation and grain growth
21 p3071 A72-41849

The density of H₂ molecules in dark interstellar clouds.
22 p3224 A72-42385

Kinetic aspects of plastic strain induced martensite in polycrystalline Fe-Ni-C alloy from tensile tests on austenitic specimens
22 p3189 A72-42437

Precipitation rate characteristics in age hardenable quenched alloys explained by transient analysis of vacancy annealing kinetics
22 p3189 A72-42441

Oxidation rate anisotropy investigation on coupon specimen of Ta-Mo alloy at 950 C
22 p3190 A72-42770

A study of the rates of carbon-carbon dioxide reaction in the temperature range 839 to 1050 C.
22 p3153 A72-43037

Decarburization kinetics of low alloy ferritic steels in sodium.
22 p3194 A72-43042

Propagation of the front of an exothermic reaction in condensed mixtures whose components interact through a high-melting layer
22 p3245 A72-43177

Quantitative evaluation of the kinetics of free-radical processes in animal organs under hypoxic conditions
24 p3371 A72-44596

Flame structure and flame reaction kinetics. VI - Structure, mechanism and properties of rich hydrogen + nitrogen + oxygen flames.
24 p3461 A72-44919

Flame structure and flame reaction kinetics. VII - Reactions of traces of heavy water, deuterium and carbon dioxide added to rich hydrogen + nitrogen + oxygen flames.
24 p3378 A72-44920

The kinetics of the reaction between oxygen and sulfur on a Ni(111) surface.
24 p3378 A72-44951

Theoretical analysis of a rotating two-phase detonation in liquid rocket motors.
24 p3433 A72-45053

Kinetic equations solution approximation for two species isothermal reactions in homogeneous turbulent mixing
24 p3392 A72-45059

Developing laminar and turbulent duct flow with chemical reaction.
24 p3378 A72-45061

Formulation of diurnal D-region models using a photochemical computer code and current reaction rates.
24 p3399 A72-45583

REACTION TIME

NT CHRONAXY

Body cooling effect on human vigilance in hot environments, testing reaction time to visual stimuli and auditory signal detection rate
01 p0021 A72-11290

Reactions choice limiting cueing signals effect on reaction time, considering dependence on time interval between cueing and start signals
02 p0165 A72-12852

Visceral afferentation role in vestibular system activity from experiments on rabbit stomach and rectum mechanoreceptor stimulation effects on vestibulo-oculomotor reflexes
05 p0618 A72-16630

Human immediate memory adaptation to speed stress, discussing response time and performance accuracy relationship to stimuli complexity and input speed
06 p0766 A72-17716

Reaction time to visual orientation change, obtaining aftereffects as function of orientation specific adaptation duration and separation angle between inspection and test lines
08 p1124 A72-20986

Cat middle ear muscles motor units twitch tension and contraction time in response to motor neuron threshold stimulation
08 p1116 A72-21137

Vibrotactile warning device effectiveness under auditory and visual loadings, investigating reaction time and errors number
08 p1126 A72-21569

Component duration and relative response rates in multiple schedules of pigeon training
08 p1128 A72-22175

Choice reaction task times for responses to signals by middle, little and index fingers
10 p1432 A72-24985

Sleep loss effect on reaction and movement times during information processing in step tracking task
11 p1580 A72-26680

Sleep-wakefulness cycle variations effect on reaction time and spontaneous tempo during time isolation experiment, showing tendency toward circadian rhythm
11 p1581 A72-26687

Cumulative sleep deficit, preceding sleep or wakefulness period duration and body temperature effects on reaction time in multiple choice visual task
11 p1581 A72-26690

Interhemispheric effects on choice reaction times to single and multiple letter displays, analyzing cerebral dominance and visual information transmission compared with verbal response
12 p1768 A72-27075

Bed rest and positive radial acceleration effect on peripheral visual response time, considering blackout or grayout prediction possibilities
12 p1766 A72-28297

Divided attention effect localization, using choice tracking task reaction times in sequential stage model for human information processing
13 p1911 A72-29852

Matched luminance chromatic stimuli wavelength effects on human visual latency
14 p2074 A72-30267

Heat chamber treadmill work-induced thermal stress effects on reaction time to foveally and peripherally presented visual stimuli
14 p2078 A72-31154

Foveal light pulse duration effects on reaction time, showing stimulus intensity-time reciprocity
15 p2188 A72-31509

Aircraft pilot reaction capability for switch activation in response to voice countdown, tone initiation and termination, noting standard deviation
15 p2188 A72-31787

Size scaling rate from retinal image size comparison judgment time during observation of briefly presented concentric rectangles of varying size and orientation
15 p2187 A72-32762

Predictive model for human operator performance in short term visual information processing based on psychological research to obtain decision accuracy and response time
16 p2359 A72-33865

Detection and recognition of colored signal lights.
17 p2510 A72-35691

Effect of set size, age, and mode of stimulus presentation on information-processing speed.
18 p2654 A72-36922

Theoretical models for speed-accuracy tradeoff during difficult visual discrimination tasks under time pressure
18 p2655 A72-37220

Operative memory mechanism as visual system neuron chain storage of stimuli from image recognition time measurements
20 p2891 A72-38936

Perceptual differentiation of sequential visual patterns.
21 p3008 A72-41021

Temporal and spatial characteristics of selective encoding from visual displays.
21 p3009 A72-41255

Reaction time to the second of two shortly spaced auditory signals both varying in intensity.
22 p3142 A72-42549

Dependence of inhibitory areas of inferior colliculus neurons on the time characteristics of acoustic stimuli
22 p3145 A72-42724

Perceptual latency as a function of stimulus onset and offset and retinal location.
23 p3258 A72-44386

REACTION WHEELS

SAS-A satellite attitude control and determination systems, discussing momentum wheel development, nutation damper and magnetic torquing
03 p0442 A72-14398

Satellite attitude control with gimbaled reaction wheel digital system, discussing logic and computerized design, implementation, fabrication and performance tests
05 p0726 A72-16458

Synchronous communication satellites body stabilized three axis attitude control superiority over dual spin techniques, emphasizing single large pitch momentum wheel configuration with magnetic torquing [AIAA PAPER 72-572]
12 p1876 A72-27380

REACTIVITY

Reactive and nonreactive channels full particle scattering amplitudes using coupled integral equations
02 p0262 A72-11910

REACTOR CHEMISTRY

U RADIOCHEMISTRY

REACTOR CORES

Radiant heat attenuation of W seeded hydrogen aerosol at high pressure and temperature for gas core nuclear rocket propellant application
01 p0112 A72-11340

Shock tube technique for opacity measurement at high pressures in seeded hydrogen for gas core nuclear rockets
01 p0099 A72-11342

Induction plasma heating simulation of open cycle gas core nuclear rocket engine, describing plasma forming material feed, permeable walls and propellant seeding
01 p0112 A72-11346

Design of 6000 Mw open cycle gas core nuclear rocket engine with hydrogen as propellant, considering critical U 235 mass, major reactor components and specific impulse
01 p0099 A72-11347

Open cycle gas core nuclear rocket engine, determining scaling laws for buoyancy force effect on fuel containment at various flow parameters
01 p0099 A72-11348

Flow characteristics of colloid core reactor rocket engine, studying two component vortex flows with solid to gas mass density ratios over 100
[AD-735527] 01 p0100 A72-11359

Liquid containment in gas driven vortex with air-water mixture densities above 100 times gas flow, discussing applicability to colloidal core nuclear reactor performance estimation
01 p0100 A72-11360

Split core heat pipe nuclear reactor dynamics, describing shutdown mechanisms, ramp reactivity inputs fuel melting temperature and wall heat flux
04 p0546 A72-14421

Mini-cavity gas core reactor concept for low thrust high impulse probe propulsion, using U 233 or 235 fuel
04 p0546 A72-14422

Split-core heat pipe reactor for out-of-core thermionic power systems, using center gap for fuel reactivity control
04 p0546 A72-14425

Critical spherical symmetry benchmark experiment on gas core nuclear reactor using uranium hexafluoride
05 p0688 A72-16387

Reactor core length, externally configured thermionic converter.
17 p2495 A72-34589

State of development of diodes for incore thermionic fuel elements.
18 p2708 A72-36150

Investigations concerning metal-hydride technology and hydrogen transport in the incore thermionic reactor /ITR/-core.
18 p2699 A72-36157

Dynamics and control of an incore-thermionic-reactor in the power region.
18 p2644 A72-36174

Critical experiment ITR - Methods of nuclear design calculation and theoretical interpretation of experimental data.
18 p2709 A72-36185

Results of a preliminary experimental investigation of a vapor transport fuel pin.
19 p2832 A72-37631

REACTOR DESIGN
Design of 6000 Mw open cycle gas core nuclear rocket engine with hydrogen as propellant, considering critical U 235 mass, major reactor components and specific impulse
01 p0099 A72-11347

Angular quadrature effects on two dimensional space power reactor radiation shield calculation for manned space station application
04 p0546 A72-14426

Thermionic reactors design based on flashlight and external fuel concepts for nuclear electric propulsion
17 p2494 A72-34580

Implications of ceramic-insulator irradiation results for thermionic reactor design.
17 p2496 A72-34592

Fabrication and testing of tungsten heat pipes for heat pipe cooled reactors.
17 p2636 A72-34596

Effect of neutron spectra on the swelling of ceramic insulators and implications for thermionic reactor design.
18 p2703 A72-36146

Thermionic fuel cladding development, compatibility, stability and performance for uranium carbide-tungsten and uranium oxide-tungsten systems at high temperatures under irradiation
18 p2709 A72-36164

Aspects on the modular lay-out of incore thermionic reactors.
18 p2645 A72-36175

Significance of the results of the ITR critical experiments for the calculation of an incore-thermionic reactor.
18 p2645 A72-36180

Voltage-conversion for incore-thermionic-reactors.
18 p2645 A72-36182

A comparison of thermionic reactor designs employing a common thermionic fuel element.
18 p2645 A72-36183

The 20 kW_e thermoelectronic reactor project
18 p2645 A72-36184

Critical experiment ITR - Methods of nuclear design calculation and theoretical interpretation of experimental data.
18 p2709 A72-36185

An out-of-core thermionic-converter system for nuclear space power.
18 p2645 A72-36187

A small, 1400 K, reactor for Brayton space power systems.
19 p2833 A72-37635

REACTOR FUELS
U NUCLEAR FUELS
REACTOR MATERIALS
Endurance limit of construction materials under fast and thermal neutron irradiation in reactor channel
06 p0834 A72-18682

High temperature Co-base alloy for nuclear, chemical and reentry vehicle applications
09 p1327 A72-22478

Charpy impact tests of neutron irradiated nuclear reactor component steels to determine ductile/brittle transition temperature, describing setup and gas heating and cooling procedures
16 p2373 A72-33222

Neutron irradiation effects on thermionic converter materials, performance and service life
18 p2707 A72-36140

Investigations concerning metal-hydride technology and hydrogen transport in the incore thermionic reactor /ITR/-core.
18 p2699 A72-36157

Breeder reactor testing of fast neutron irradiation effect on alumina and yttria cylinders for thermionic fuel rod designs
18 p2708 A72-36161

REACTOR PHYSICS
Sizing an external-fueled in-core thermionic reactor.
17 p2495 A72-34588

REACTOR SAFETY
Nuclear safety in nuclear power and propulsion devices for space.
24 p3424 A72-45180

REACTOR TECHNOLOGY
Structural mechanics in reactor technology - Conference, Berlin, Germany, September 1971
10 p1556 A72-24392

NASA-Lewis experiences with multigroup cross sections and shielding calculations.
19 p2833 A72-37633

READING
Cortical responses to visually displayed word and nonsense syllable stimuli, using EEG and computer techniques
04 p0474 A72-15248

Discrete automatic monitoring and measuring systems with discrete random sequence and continuous process reconstructed output signals, deriving probability criteria for reading frequency determination
11 p1611 A72-26438

READOUT
Noise reduction in pulse width modulated converters with rms voltage values digital readout, using active or passive filters methods
03 p0331 A72-13557

Nondestructive readout in computer storage of plated wires on Permalloy film deposited substrates, testing design parameters effects on performance
[IEEE PAPER 11,2] 03 p0332 A72-13762

Plated-wire computer memory using thin Permalloy film on W wire substrate, testing nondestructive and destructive readout characteristics
[IEEE PAPER 11,3] 03 p0327 A72-13763

High speed easy rewrite read-only memory using plated wire with multilayered nondestructive readout magnetic thin film, testing performance
[IEEE PAPER 11,4] 03 p0332 A72-13764

Destructive readout computer memory of wire substrate electrodeposited with two thin Permalloy layers separated by Cu
[IEEE PAPER 11,5] 03 p0332 A72-13765

Magneto-optic storage density and read-write rate, discussing transducer cost, solid state injection lasers, holographic techniques and high activity data base applications
[IEEE PAPER 19,1] 03 p0361 A72-13774

Zero crossing photoelectric autoreflector pickoffs for readout gyro systems with suspended spherical rotors, classifying systems according to modulation type
05 p0661 A72-16036

Time range extension methods for rapid readout dual wavelength spectrophotometers
07 p0983 A72-19319

Broadband 100 MHz multichannel laser recorder and automatic data readout system using digital signal processing
10 p1488 A72-23932

High accuracy relative attitude readout mechanization, discussing analog and digital design, closed loop analysis and simulation
15 p2270 A72-32191

Reading of holograms by a semiconductor injection laser.
20 p2933 A72-39518

Elimination of an ambiguity in the reading of digital computational devices
21 p3035 A72-41810

Optimal linear inertia-free processing of meter readouts with allowance for control-equipment signals
24 p3403 A72-45316

REAL GASES
Real gas effects in atmosphere to make sonic bang shock wave full dispersion and thickness wide variations
02 p0154 A72-11972

Real gas tailored shock tube Mach numbers by analytical method, investigating driver temperature effect
02 p0205 A72-12269

Nonideality effects on Coulomb gas conductivity by finding conductivity due to electron scattering at atoms, solving kinetic equation of three component plasma model
05 p0694 A72-15850

Nonadiabatic real gas nozzle flow with friction and heat transfer to wall, obtaining solution by Runge-Kutta method
05 p0610 A72-17066

Stellar structure calculation by real gas equation of state, considering He abundances and solar lines of ionizable metal atoms
07 p1078 A72-19925

Nonideality effects on Coulomb gas conductivity by finding conductivity due to electron scattering at atoms, solving kinetic equation of three component plasma model
15 p2283 A72-31269

Flow of a real gas in annular channels with curvilinear walls at large MHD-interaction parameters
17 p2587 A72-34457

Numerical calculation of third virial coefficient in equation of state of real gases eliminating errors associated with substitution of integration infinite integral
19 p2838 A72-38462

The behavior of two-phase systems during adiabatic expansion
20 p2953 A72-39595

Analysis of real-gas and matrix-conduction effects in cyclic cryogenic regenerators.
[ASME PAPER 72-HT-27] 20 p2986 A72-39672

The cooling problem in the case of laminar boundary layers of real gases
[DFVLR-SONDDR-223] 21 p3131 A72-41619

REAL NUMBERS
NT INTEGERS
Dense convexes class characterization in real seminormalized space on basis of decomposition family concept
13 p1987 A72-29779

Introduction of time and space into a point system endowed with a signal
20 p2946 A72-39574

REAL TIME OPERATION
Acoustic echo sounder as real time monitor of airport environmental meteorological parameters
01 p0103 A72-11137

Three-failure-tolerant digital computer system design using adaptive majority voting in hardware and software for real time control application
02 p0185 A72-11488

Flight training simulator programming, noting operation under real time executive
02 p0199 A72-11653

Aerodynamic multivariable function generation in real time simulation of high performance missile
02 p0186 A72-11656

Pohlman cell for ultrasonic hologram production, describing construction, resolution and real time reconstruction
02 p0225 A72-11751

Real time programmable video data compression system for microwave transmission of ATS satellite pictures between acquisition station and central computer processing
02 p0173 A72-12128

Digital computer memory system for real time processing of air and naval traffic data, discussing logic design, time comparisons and optimum use
02 p0188 A72-12647

Wind tunnels measuring equipment and procedures and data acquisition and processing systems electronics, describing computerized real time data processing system
[DFVLR-SONDDR-156] 02 p0201 A72-12898

Real time ground control optimization of data acquisition of solar spectra scans from OSO 6
03 p0417 A72-13060

Digital videomagnetograph providing real time display of line of sight component of solar magnetic fields
03 p0356 A72-13281

Real time analog video magnetogram, describing differential photometer for electronic subtraction technique
03 p0357 A72-13286

Two dimensional time resolved and real time IR interferograms obtained with pulsed Nd doped glass laser illuminated Michelson interferometer
03 p0362 A72-14200

Far IR Fourier spectrometer with built-in real time digital computer for routine physical and chemical spectroscopy 04 p0520 A72-14523

Space real time data links during processing of French D2 scientific satellite for hydrogen frequency bands investigation 05 p0628 A72-16447

Computerized PCM data presentation and real-time monitoring system, presenting functional flow diagrams for computer program 05 p0633 A72-16677

Time optimal trajectory graphical construction procedure from energy state approximation as basis of computational algorithm for real time onboard flight optimization [AIAA PAPER 72-123] 05 p0688 A72-16968

Ultrasonic acoustic holography for real time non-destructive testing of cracks, voids, nonbonds and other defects in metals, ceramics and plastics [SAE PAPER 720173] 06 p0811 A72-17319

Nematic liquid crystals application to real time optical data processing 06 p0847 A72-17565

GPSS/360 interactive simulation program with report generator, selective output display and HELP blocks for model manipulation and real time viewing 06 p0780 A72-17980

Nationwide real time automated ATC system interconnected by data transmission links, discussing radar signal acquisition/transfer and computer complex 06 p0845 A72-18283

Sounding rocket radio tracking systems with real time trajectory plotting, developing computer program for exoatmospheric trajectory determination 07 p0939 A72-19089

Real time near optimal closed loop control solution to fixed time nonlinear differential game by periodically updating to two point boundary value problem 07 p1027 A72-19278

On-line digital computer system for real time interpretation and report generation of electrocardiograms from remote locations over switched telephone network 07 p0928 A72-19311

Real time hologram photosensitive materials, determining power requirements and resolution for diffraction gratings in saturable absorbers and absorbing liquids [CLEA PAPER 15.4] 07 p0984 A72-19397

Real time computer aided mechanical testing and data analysis system for composites, confirming computer analysis by motion pictures of thin walled graphite/epoxy composite fracture 07 p0965 A72-19734

Apollo manned mission real time ground support computer simulation for NASA flight controller training to maximize flight crew safety 07 p0933 A72-20329

Hybrid computer and graphics terminals for real time dynamic man machine interaction, discussing AM communication system simulation 07 p0951 A72-20335

Real time computer simulation of command and control in transportation systems, detailing models, and programming technique and ATC controller effectiveness evaluation 07 p0952 A72-20363

Placeholder for on site wet processing of holograms in real time holographic interferometry, obtaining undistorted reconstructed image by liquid gate immersion 07 p0992 A72-20581

Real time recursive algorithms for estimating coefficients of fixed knot spline approximation to trajectory 08 p1197 A72-20849

Recursive and nonrecursive real time spline methods for nonlinear estimation of independent trajectory parameters for vehicle entering earth atmosphere 08 p1197 A72-20862

Sliding friction and normal force adhesion under ultrahigh vacuum environment, describing test apparatus for real time analysis via contact resistance measurement 08 p1176 A72-21436

Atmospheric temperature profiles real time retrieval from Nimbus 4 satellite IR spectrometric observation, describing method used in dynamical weather forecasting 09 p1345 A72-22440

ATC systems analysis by computerized real time environmental simulation, taking into account new aircraft types, navigation and supervision aids 09 p1348 A72-22782

Multichannel oscillograph for real time biomedical studies of LF physiological processes 09 p1270 A72-22881

Fixed frequency or wideband real time measurements of microwave reflection and transmission coefficients and fields in open or closed structures 09 p1289 A72-23425

Suboptimal decision algorithm to correlate sensor data with stored tracks in real time track-while-scan surveillance system 10 p1441 A72-23780

Compression of data from measurements in real time nonlinear estimation to reduce data processing requirements without performance deterioration, applying to reentry vehicle tracking 10 p1442 A72-23802

Executive job handling program for operation with fault tolerant multiprocessor in real time control environment 10 p1442 A72-23816

Hardware monitor and associated analysis programs to evaluate real time satellite command and control digital computer system performance 10 p1442 A72-23817

Laser recording real time imagery for use in tactical reconnaissance aircraft 10 p1488 A72-23928

Classification of automatic meteorological ground stations networks in populated areas, discussing required equipment, data transmission, real time operation and costs 10 p1507 A72-25021

Real time pilot reports via digital ground-air-ground data link, discussing encoding and processing equipment, meteorological codes and automatic real time weather forecasts 10 p1440 A72-25079

Real time measurements of ground level and airborne particle concentrations and diffusion in 10-100 km range 11 p1681 A72-26081

Hybrid computers application to digital communication systems design, using real time simulation 12 p1786 A72-27324

Real time depth gated acoustic image holography, using scanning laser beam pulse echo technique 12 p1809 A72-27840

Holograph generation, electric signal conversion and transmission and remote location simultaneous Lumatron reconstruction 12 p1811 A72-27951

Holographic system stability tested by diffraction efficiency-exposure curves obtained in real time from probing holograms sequence, emphasizing temperature effects 13 p1956 A72-28685

Automatic real time processing of meteor radar echoes, using digital computers 13 p1924 A72-29033

Real time interferential spectrum analysis of deterministic signals in form of partially summed Fourier series 13 p1919 A72-29041

Dispersion method for real time spectral analysis of signals by Fourier transform for class of integrable functions with finite energy 13 p1919 A72-29042

Sky wave correction /Swanson/ model and computer program for real time propagation prediction for airborne OMEGA system 13 p1997 A72-29190

Real time focused image holographic interferometry for deformation recording in diffusively reflecting plate under compression 15 p2233 A72-31415

Mariner 9 TV experiment image data display, processing and production for real time analysis, noting computer algorithms 15 p2236 A72-31982

Real time holographic quasi-dynamic 3-D image display, discussing computerized synthetic hologram generator concept and system block diagram 15 p2237 A72-32054

Programmable digital differential analyzer for connection to digital computer, discussing dynamical problem solution and real time systems simulation capability 15 p2204 A72-32387

Signal analyzer for LF real time measurement of mechanical impedance by Fourier integral analysis 15 p2215 A72-32628

Speckle pattern method of laser holography for structural vibration and surface strain study, noting real time operation 16 p2388 A72-32821

Materials characteristics relevance for USAF technology, discussing processing conditions, environment simulation, real time techniques, ultrasonic and X ray inspection methods, etc 16 p2404 A72-32823

STRADA landing trajectory recording system for real time flight path restitution during approach and landing, using computer and lidar techniques 16 p2420 A72-32895

Performance characteristics and design options for software controlled I/O processor for aerospace computer applications with high speed real time responses 17 p2521 A72-34702

Numerical integration of ordinary differential equations in a real-time modeling procedure 17 p2576 A72-35041

Real-time vibration analysis of rib-stiffened plates by holographic interferometry. 18 p2690 A72-36361

Refraction correction of rocket tracking radar inputs in near real time. 18 p2661 A72-36636

Real time holographic contouring and coherent light interferometry of gear tooth surfaces. 19 p2797 A72-37606

The non-stroboscopic visualisation of vibrational patterns by real-time/time averaged hologram interferometry. 19 p2873 A72-37618

Microwave holographic imaging techniques for aircraft landing aids and airport security applications, discussing real time operation 19 p2798 A72-37625

Time synchronized ranging system (TSRS) providing high-speed real-time two-way data link between community members 19 p2764 A72-37904

Real time telemetry processing systems, describing display features and limitations [AIAA PAPER 72-783] 19 p2752 A72-38142

Nonlinear programming in computerized electronic circuits design, discussing optimization methods and real time operation 19 p2782 A72-38578

A holographic memory recording matrix permitting real-time data modification. 20 p2922 A72-39037

Real time estimation of trajectory for lifting reentry vehicle of shuttle orbiter type, discussing iterated nonlinear filter and adaptive filter [AIAA PAPER 72-874] 20 p2966 A72-39126

Experimental and simulation study results on the development of a planetary landing site selection system. [AIAA PAPER 72-868] 20 p2951 A72-39131

The study of vibration patterns using real-time hologram interferometry. 20 p2927 A72-39848

Real-time launch vehicle steering program selection. [AIAA PAPER 72-830] 20 p2977 A72-40058

Dry photopolymer holographic recording film with ability to form images in near real time by exposure without processing 21 p3054 A72-40620

Optimal single stage control law applicable to linear multivariable systems based on discrete-time analysis, discussing real time simulation on hybrid computer 21 p3037 A72-40637

Automated area navigation with real time track computation, discussing information processing by on-board computer for immediate pilot instruction 21 p3081 A72-40683

Optimum damping for accelerometers. 22 p3175 A72-41930

Real time correlator design and operation with signal delay at 40 Hz-20 kHz, using Stieltjes principle 22 p3176 A72-42244

Analysis of the structure of the flow downstream of a sudden widening 22 p3167 A72-42643

Engine compressor face rake for flight test instrumentation F-14A/TF-30. 22 p3216 A72-42686

Digital data system with real time displays and multiprocessor capability for multistep of aircraft structure with operational manpower reduction, assessing performance 22 p3163 A72-42696

A near real time data acquisition/reduction facility for the Boeing wind tunnels. 22 p3164 A72-42699

Real time analog computation at light speed and rapid access data storage in optical data processing systems, considering coherent electro-optical instrumentation 22 p3180 A72-42713

CW radar system for tactical aircraft real time command, control and positioning, using combination of frequency and time multiplexing for range measurement 22 p3203 A72-42946

The optimal control of merging aircraft - Implementation of the hybrid air traffic controller. 23 p3277 A72-43868

Multipoint real time all-day computerized noise monitoring system for diagnostic evaluation of airport, discussing design and applications 24 p3387 A72-44684

Parallel Element Processing Ensemble /PEPE/ digital computer for real time radar data processing and control, discussing system design and applications 24 p3383 A72-45666

REAL VARIABLES

- NT ABEL FUNCTION
- NT ASYMPTOTES
- NT ASYMPTOTIC SERIES
- NT BESSEL FUNCTIONS
- NT BETHE-SALPETER EQUATION
- NT BIHARMONIC EQUATIONS
- NT BLASIUS EQUATION
- NT BOREL SETS

NT BURGER EQUATION
 NT CALCULUS OF VARIATIONS
 NT CHANDRASEKHAR EQUATION
 NT COLLINEARITY
 NT DELTA FUNCTION
 NT DIFFERENTIAL EQUATIONS
 NT DUFFING DIFFERENTIAL EQUATION
 NT EINSTEIN EQUATIONS
 NT ELLIPTIC DIFFERENTIAL EQUATIONS
 NT EXISTENCE THEOREMS
 NT EXTREMUM VALUES
 NT FALKNER-SKAN EQUATION
 NT FOKKER-PLANCK EQUATION
 NT FOURIER SERIES
 NT FOURIER-BESSEL TRANSFORMATIONS
 NT FUNCTIONAL INTEGRATION
 NT GAUSS EQUATION
 NT GREEN FUNCTION
 NT HANKEL FUNCTIONS
 NT HYPERBOLIC FUNCTIONS
 NT INTEGRAL CALCULUS
 NT JACOBI INTEGRAL
 NT JACOBI MATRIX METHOD
 NT KERNEL FUNCTIONS
 NT LAME WAVE EQUATIONS
 NT LEBESGUE THEOREM
 NT LIAPUNOV FUNCTIONS
 NT LIMITS [MATHEMATICS]
 NT LINEAR EQUATIONS
 NT LIOUVILLE EQUATIONS
 NT LIPSCHITZ CONDITION
 NT MEASURE AND INTEGRATION
 NT MINIMA
 NT NEUMANN PROBLEM
 NT NONLINEAR EQUATIONS
 NT NUMERICAL INTEGRATION
 NT PADE APPROXIMATION
 NT PARABOLIC DIFFERENTIAL EQUATIONS
 NT PARTIAL DIFFERENTIAL EQUATIONS
 NT PERIODIC FUNCTIONS
 NT POISSON EQUATION
 NT POWER SERIES
 NT QUADRATIC EQUATIONS
 NT RUNGE-KUTTA METHOD
 NT SERIES [MATHEMATICS]
 NT STURM-LIOUVILLE THEORY
 NT TANGENTS
 NT TAYLOR SERIES
 NT TRIGONOMETRIC FUNCTIONS
 NT VECTOR ANALYSIS
 NT VLASOV EQUATIONS
 NT VORTICITY
 NT WEIERSTRASS FUNCTIONS
 NT WEIGHTING FUNCTIONS
 NT WHITTAKER FUNCTIONS

REATTACHED FLOW
 Nozzle boundary layers effect on reattachment position of two dimensional jet to adjacent flat plate, noting Reynolds number influence 02 p0150 A72-11729
 Two dimensional flow attachment to flat plates, investigating Coanda effect 06 p0798 A72-17776
 Attached and separated turbulent viscous regions resulting from shock wave-boundary layer interactions in hypersonic flow 07 p0966 A72-18949 [AIAA PAPER 72-74]
 Flow field model of convective heat transfer along reattachment surface in planar supersonic turbulent flow [ASME PAPER 71-HT-W] 08 p1251 A72-20876
 Hot gas heat transfer measurements in separation, reattachment and redevelopment regions downstream of abrupt circular channel expansion [ASME PAPER 71-HT-DD] 08 p1251 A72-20881
 Turbulent shear layer flow in reattachment region downstream of backward facing step and non-monotonic return to ordinary boundary layer state, noting eddy length scale decrease 10 p1468 A72-24467
 Turbulent separating and reattaching supersonic boundary layer flows in two dimensional compression corner, noting Reynolds number effect on separated shear layer length 11 p1618 A72-26634
 Leading edge boundary layer flow separation and reattachment processes in airfoil dynamic stall, considering effect of angle of attack rate of change 15 p2179 A72-32024
 Attachment length as stability criterion for bluff-body stabilized electrodeless arc, showing linear dependence on flow velocity ratio to power density 15 p2336 A72-32406
 Reattachment heat transfer for laminar or turbulent separated shear layers, comparing predictions with measurements for cavities, ramps, spiked-nose bodies and forward facing step [AIAA PAPER 72-717] 16 p2344 A72-34031
 Shear-layer flow regimes and wave instabilities and reattachment lengths downstream of an abrupt circular channel expansion. [ASME PAPER 72-APM-2] 17 p2538 A72-34811
 Integral and correlation methods for separation and reattachment phenomena in aerodynamics, applying to turbulent boundary layer [ONERA, TP NO. 1072] 19 p2786 A72-37762

Re-developing turbulent boundary layers behind yawed separation bubbles. 19 p2747 A72-38812
 Heat transfer at reattachment of a compressible flow over a backward facing step with a suction slot. 20 p2885 A72-39626
 Analysis and correlation of data on pressure fluctuations in separated flow. 23 p3247 A72-43331

REATTACHMENT
U ATTACHMENT
REBREATHING
 Human blood carboxyhemoglobin saturation relation to inspired air oxygen and CO concentrations from small closed rebreathing system tests [AD-740929] 04 p0472 A72-14863
 Rebreathing technique to estimate human mixed venous oxygen and carbon dioxide tension changes at start of exercise under respiratory stress and natural conditions 08 p1122 A72-20883
 Added elastic load tests for thoracic elastance change effects on human response to carbon dioxide inhalation, using rebreathing technique 12 p1762 A72-27726
 Alveolar carbon dioxide pressure-ventilation response curve measurement by Campbell rebreathing method in consecutive daily trials 13 p1906 A72-29846
 Rebreathing studies of carbon dioxide pressure level effect on carbon dioxide content difference in arterial blood and alveolar gas during exercise and rest 17 p2499 A72-34346
 Pulmonary air-trapping induced by water immersion. 19 p2759 A72-38711
 A modified acetylene method for the determination of cardiac output during muscular exercise. 20 p2898 A72-39807

RECEIVERS
 NT LINEAR RECEIVERS
 NT LOGARITHMIC RECEIVERS
 NT RADAR RECEIVERS
 NT RADIO RECEIVERS
 NT RADIOTELEPHONES
 NT SUPERHETERODYNE RECEIVERS
 NT TELEVISION RECEIVERS
 Spectral characteristics of ionospheric signal by phase lags introduced in multichannel field recorder 02 p0172 A72-1926
 Optimum power allocation in design of phase-coherent receiver having bandpass limiter, extending technique from single channel to two channel system 02 p0174 A72-12136
 Technical characteristics of vhf/AM receiving transmitter, noting MTBF improvement 02 p0182 A72-12651
 Wireless electronic time distributing system, investigating integrable digital receiver circuit and frequency bandwidths 02 p0197 A72-12696
 Conversion coefficients of optical heterodyne receiver mixer for various amplitude-phase distributions of interfering signal 07 p1000 A72-19012
 Sensitivity of optical autodyne quantum receiver in presence of output noise, using photomultiplier signal model 07 p1000 A72-19022
 Digital decision directed suboptimal receiver design for random multipath channel communication with intersymbol interference, predicting performance for steady state probability of correct decision 07 p0941 A72-19272
 Minimum frequency separation between avionics receivers and transmitters for acceptable interference level 08 p1131 A72-20929
 TE mode propagation properties in circular waveguide, determining communication link transmitting and receiving equipment requirements 12 p1784 A72-27795
 Spectral characteristics of ionospheric signal by phase lags introduced in multichannel field recorder 13 p1920 A72-29238
 Asymptotic receiver characteristics, discussing signal detection in spherically invariant noise 15 p2196 A72-31871
 Susceptibility measurements on PCM-FM and four phase differential PSK digital receivers simulated on analog computer 21 p3016 A72-40852
 Direct-detection optical receivers for angle-modulated signals. 21 p3017 A72-40858
 Communication receivers interference modeling - Nonlinear transfer functions from circuit analysis - Mild excitations. 21 p3019 A72-40890
 Book - EMI prediction and analysis techniques. 22 p3156 A72-43198
 Optimal signal processing in systems with multiple reception elements/channels/ 23 p3266 A72-44219

Coupled active parallel doublets network within external electromagnetic field at receiving station, investigating decoupling function between radiating elements 24 p3382 A72-45771

RECEIVING SYSTEMS
U RECEIVERS
RECEPTACLES [CONTAINERS]
U CONTAINERS
RECEPTION DIVERSITY
 Correlation between two base-station antennas affected by local scatterers and directions of incoming mobile radio waves. 18 p2661 A72-36846
 Fluctuation frequency correlation for radio waves reflected from the ionosphere 18 p2662 A72-36879

RECEPTORS [PHYSIOLOGY]
NT PROPRIOCEPTORS
 Lateral spatial interactions of sensory receptors, discussing mathematical theory for monocular visual inputs described by real valued functions on continuum 01 p0021 A72-11196
 Receptor activity control from clinical physiological and electrophysiological observation data analysis, noting central nervous system role and feedback and self adaption capabilities 02 p0157 A72-11543
 Fish electroreceptor system morphology, physiology and evolution, considering electric current action, peripheral coding activity and central subsystems 02 p0157 A72-11545
 Visceral afferentation role in vestibular system activity from experiments on rabbit stomach and rectum mechanoreceptor stimulation effects on vestibular-oculomotor reflexes 05 p0618 A72-16630
 Formulas derived for forces on receptor formation of vestibular apparatus from mathematical analysis of natural human head movements, discussing otoliths and semicircular canals 05 p0622 A72-16641
 Retinal cell adaptation as result of receptor membrane response range saturation, considering dark adaptation and increment threshold 06 p0761 A72-17604
 Vestibulometric swing to obtain measured doses of receptor stimulation in otolith apparatus and semicircular labyrinth ducts with simultaneous physiological data recording 06 p0769 A72-18200
 Cardiovascular and respiratory responses to intraarterial injection of K and Na ions in dogs for peripheral receptor site determination 07 p0921 A72-20177
 Bulbar respiratory neuron discharge pattern response to nasal and tracheal receptor stimulation in cats, relating changes in neuronal activity and intratracheal pressure 08 p1117 A72-21473
 Propranolol as adrenergic beta receptor inhibiting agent for hyperthyroidism symptom amelioration 08 p1118 A72-21550
 Data processing in isolated crab biological strain receptor formed by muscle, transducer and encoder, noting pulse frequency modulation in encoding process 12 p1771 A72-27577
 Receptor membrane pulse generation electronic model with tunnel diode negative resistance circuit 12 p1771 A72-27578
 Quantitative model to describe vestibular detection of body sway motion in postural response mode 13 p1905 A72-29374
 Interrelation of interoceptors and exteroceptors in the process of urination and defecation reflex act maturation in ontogeny 17 p2504 A72-35022
 Morphological and electrophysiological analysis of afferent receptor connections in cerebellar cortex, discussing fast conducting, diffuse reticular and inferior olive fiber paths 21 p3004 A72-41674
 Subjective and objective sensory physiology, discussing transformation processes in sensory receptors and nerves, psychophysical scaling methods, chemoreceptors and peripheral adaptation 22 p3146 A72-42777
 Olfactory perception neurophysiological mechanism, discussing receptor cells sensory thresholds and time, temperature and humidity effects 22 p3146 A72-42782

RECESSES
 Analytical and graphical calculations of stress concentration coefficients and stress gradients in machine parts with recesses and finite depth cuts 01 p0144 A72-11377

RECIPROCAL THEOREMS
 Reciprocity relations for electromagnetic waves scattered by isolated, stratified and composite anisotropic obstacles 04 p0547 A72-14535

Magnetoionic mode reciprocity for oblique incident electromagnetic wave propagation through birefringent stratified media 04 p0492 A72-15445

Reciprocity theorems in electromagnetic theory concerned with radio transmitting and receiving point interchange for electric dipole sources 05 p0625 A72-16008

Reciprocity theorem for antenna directivity pattern measurement of optical superheterodyne receiver for carbon dioxide laser radiation 08 p1140 A72-21376

Thermal diffusion in solids subject to deformation, using classical elasticity theory body force analogy for variational and reciprocal theorems 09 p1403 A72-22757

Laser beam periodic coupler design based on radiation property reciprocity theorem, suggesting use of reflecting layers and long wavelength gratings 23 p3288 A72-43888

RECIPROCATING ENGINES

U PISTON ENGINES

RECIRCULATIVE FLUID FLOW

Equilibrium shear flow of stratified brine in cyclically continuous rectangular tank, discussing stable density region erosion by turbulent layers, Richardson numbers, transition layer and entrainment 01 p0051 A72-11228

Residence time of foreign gas introduced within wake recirculation region behind slender body in axisymmetric supersonic laminar/turbulent flow [AD-733525] 03 p0308 A72-13633

Anticavitation properties improvement of volute centrifugal pumps during low flow rate operation by reducing back currents with truncated cone 07 p0914 A72-18984

Recirculation criteria for confined jet flames in cylindrical combustion chamber, using Thring-Newby number 09 p1411 A72-23144

Numerical prediction of inert and reacting steady internal two dimensional recirculating flows by finite difference method, including turbulence and combustion models 10 p1561 A72-23868

Numerical solution of turbulent recirculating flow, using energy equation to estimate eddy viscosity distribution 10 p1464 A72-23869

Photographic flow visualization of steady recirculating wakes behind sphere and oblate spheroids for low Reynolds numbers 15 p2180 A72-32419

Circulating toroidal vortex pattern in initial region of turbulent coaxial jet stream mixing obtained with hot-wire anemometer, static pressure probes and shadowgraphy [ASME PAPER 72-APM-30] 17 p2538 A72-34789

Mixing of slipstreams in a channel of constant cross section in the presence of a recirculation zone 21 p3129 A72-40982

Calculation of the recirculation flow of VTOL lift engines. [ICAS PAPER 72-42] 21 p3099 A72-41167

Reacting and nonreacting swirl recirculation bubble gasdynamic structure in fuel combustion systems, noting anisotropic turbulence from hot-wire anemometer measurements 24 p3461 A72-45024

The damping of precessing vortex cores by combustion in swirl generators. 24 p3464 A72-45060

RECLAMATION

NT MATERIALS RECOVERY

NT WATER RECLAMATION

RECOGNITION

NT CHARACTER RECOGNITION

NT PATTERN RECOGNITION

NT SPEECH RECOGNITION

NT TARGET RECOGNITION

NT TIMBER IDENTIFICATION

Hologram data treatment comparison to human brain function, discussing recognition signals, Pavlovian qualities and intelligence function 06 p0768 A72-17997

Simultaneous detection and recognition of chromatic flashes. 22 p3152 A72-42933

RECOIL PROTONS

Cosmic proton and neutron produced recoil proton energy spectra measurements along earth-moon-earth trajectory with nuclear emulsions aboard Zond 5 and 7 [CERN-71-16] 02 p0273 A72-12074

Nuclear photoemulsions under bombardment by pion beam of 60 GeV/c momentum, investigating pion-nucleon interactions involving recoil protons 06 p0851 A72-17273

RECOILINGS

Recoil effect on inverted molecules changing pumping conditions and gain for interstellar, OH maser intensity and radial velocity variations 21 p3102 A72-41773

RECOMBINATION COEFFICIENT

Ionized argon recombination rate constant determination as function of temperature, using dual frequency laser interferometry measurement of corner expansion flow 01 p0050 A72-10851

Dissociative recombination coefficients of water vapor and nitric oxide in determining D region electron densities 03 p0347 A72-13389

Photoresonance cesium plasma development and decay, determining density spatial-temporal behavior and recombination and polar diffusion coefficients by probe measurements 03 p0396 A72-13664

Solar coronal total dielectronic recombination coefficient simple relationships for isoelectronic sequences of H, He, Ne, K-Ni and Li-F, Na-A and Cu-Kr 05 p0718 A72-16510

Electron-ion recombination rate measurements in flowing afterglow, using sampling mass spectrometer and floating double probe 06 p0851 A72-17318

Ionspheric electron density profiles and time variation of electron production rate for X-ray flare of 30 January 1968, observing decrease in effective recombination coefficient 06 p0874 A72-18088

Recombination coefficient, ionization rates and average lifetime of ions in rarefied carbon-air flames, investigating pressure and additives effects 06 p0904 A72-18213

Radiative transition probabilities and recombination coefficients of ion C IV 09 p1354 A72-22664

E layer effective recombination coefficient determination from solar flare enhanced electron density and solar X-ray flux measurements and ionspheric relaxation time constant evaluation 11 p1627 A72-26766

Secondary autoionization reduction of recombination coefficient during dielectronic recombination process, considering importance in Fe ions 12 p1864 A72-27747

Recombination parameters in low resistivity gamma irradiated n-type Ge, obtaining energy levels and temperature dependence of electron and hole capture probabilities 12 p1857 A72-28056

Solar flare flux effects on D region effective ion recombination coefficient decrease, discussing electron and negative ion densities 13 p1913 A72-29654

Seasonal features of nocturnal 6300 A emission variation and decay coefficient in nightglow related to recombination coefficient for F layer ionization 14 p2097 A72-30132

Singly and doubly ionized He plasma recombination and ionization coefficients due to electronic collisions and radiative absorption 19 p2841 A72-38083

Radiative recombination of atoms as a resonance scattering process. 21 p3087 A72-40560

Electron and positive ion density altitude distributions in the equatorial D-region. 22 p3170 A72-42366

The effective recombination coefficient in the ionspheric D region 23 p3283 A72-43364

Theoretical estimate of the effective recombination coefficient in the D region. 23 p3284 A72-43818

Measurement of the rate coefficient for the recombination of He+ with electrons. 23 p3315 A72-43869

On the determination of minority carrier lifetime and surface recombination velocity from the transient response of MOS capacitors. 23 p3324 A72-44071

Formation and loss of O₂⁺/+ and O₄⁺/+ ions in krypton-oxygen afterglow plasmas. 23 p3316 A72-44345

Dissociative recombination at elevated temperatures. I - Experimental measurements in krypton afterglows. 23 p3316 A72-44346

Influence of atom-atom collisions on the collisional-radiative ionization and recombination coefficients of helium plasmas. 24 p3428 A72-44798

RECOMBINATION REACTIONS

NT ATOMIC RECOMBINATION

NT ELECTRON RECOMBINATION

NT ELECTRON-ION RECOMBINATION

NT HYDROGEN RECOMBINATIONS

NT ION RECOMBINATION

NT OXYGEN RECOMBINATION

NT RADIATIVE RECOMBINATION

Orion A and M17 radio recombination line width increases, discussing Stark broadening functional dependence on principal quantum number 01 p0131 A72-11010

Nitrogen dioxide producing chemiluminescent radiative and three-body recombination reaction at low pressures, determining airflow and oxygen atoms decay time by resonance fluorescence method 03 p0347 A72-13395

Carrier transport effects in semiconductors for carrier recombination time approaching relaxation time 03 p0333 A72-13863

Space charge recombination in forward biased diffused p-n junction silicon diodes 04 p0562 A72-15127

Quantum efficiency at 6300 and 6364 A of recombination mechanism in nighttime F layer, obtaining ionspheric electron density profiles 07 p0974 A72-18893

Silicon-silicon dioxide system, investigating effect of heating in dry and moist He on capture-center and recombination parameters by thermal and pyrolytic techniques 08 p1216 A72-21068

Nonlinear initial boundary value problem for time dependent convection-diffusion equation with ionization and recombination reactions 09 p1341 A72-22472

Recombination diffusion length of minority carriers in thin layer cuprous sulfide solar cells 12 p1856 A72-28011

Recombination luminescence in irradiated Si, investigating uniaxial stress and temperature variations effects 12 p1858 A72-28061

Recombination luminescence in irradiated Si, investigating thermal annealing and Li impurity effects 12 p1858 A72-28062

Microwave recombination lines from emitters with mass greater than 12 amu in Orion B and W3A regions. 13 p2041 A72-29415

Disturbed ionspheric electron and ion kinetics, detailing dissociative recombination as regulating process for temporal evolution 14 p2102 A72-30654

Electric field and volume charge density distribution in bipolar conductivity semiconductor with recombination instability 15 p2291 A72-31392

Conditions defined for recombination induced inversion of populations of resonance and fundamental levels in laser beam produced plasma 16 p2438 A72-33835

Decay rate coefficients at 250-370 K for three-body recombination kinetics of O and CO, considering CO, carbon dioxide and nitrogen as third body 17 p2511 A72-34736

Utilization of photorecombination of radicals and atoms in continuous-wave lasers. 20 p2932 A72-39508

Interstellar gas electron temperature determination from recombination line spectra observations along galactic ridge 20 p2971 A72-39858

H 157 alpha recombination line from H I region before NGC 2024 radio source, considering average electron concentration and line origin 21 p3102 A72-41776

Recombination continuum in a lithium plasma spectrum 22 p3210 A72-42171

A longitude survey of radio recombination lines from the diffuse interstellar medium. 22 p3227 A72-42552

Investigation of the fast recombination channel in InSe during excitation by neodymium laser light 23 p3295 A72-43339

Recombinational luminescence of NaI-Tl single crystals excited in the A-band of activation absorption 23 p3323 A72-43342

Static and dynamic characteristics of double-injection currents in p'-n-n' diode structures with deep impurities and nonideally injecting junctions 23 p3268 A72-43346

Impedance of a unipolar semiconductor diode under conditions of space-charge limited current with allowance for recombination 23 p3270 A72-43630

A kinetic-theory description of a chemically reacting gas. 23 p3357 A72-44272

Instabilities in the reaction zones of detonation waves. 24 p3462 A72-45029

Determination of electron and hole capture rates in nickel-doped germanium using photomagnetolectric and photoconductive methods. 24 p3432 A72-45388

Mean dissociative and effective recombination coefficients of E region, discussing charged particle reactions effect on model formation 24 p3399 A72-45584

RECOMPRESSION

U COMPRESSING

RECONNAISSANCE

NT AERIAL RECONNAISSANCE

NT PHOTORECONNAISSANCE

NT SPECTRAL RECONNAISSANCE

Tethered flying rotor platform for reconnaissance, fire control and radio transmission assignments in naval missions, discussing system characteristics 04 p0465 A72-15652

RECONNAISSANCE AIRCRAFT
NT EARTH RESOURCES SURVEY AIRCRAFT
S-3A Viking land based antisubmarine warfare maritime and reconnaissance aircraft, describing flight controls, structural design, underslung podded engines and operational equipment 06 p0758 A72-17583

VAK 191 B V/STOL reconnaissance fighter prototype test program, describing simulations, bench, ground, static, hovering and flight tests 07 p0912 A72-19249

SR-71 aircraft ejection seat, obtaining ejection survival rate from case histories 08 p1112 A72-21562

Laser recording real time imagery for use in tactical reconnaissance aircraft 10 p1488 A72-23928

The VAK 191 B VTOL fighter and reconnaissance aircraft 19 p2748 A72-37825

RECONNAISSANCE DRONE AIRCRAFT
U RECONNAISSANCE SPACECRAFT
NT MIDAS SATELLITES

RECONSTRUCTION
NT WAVE FRONT RECONSTRUCTION
Object reconstruction procedure in two- and multimedia photogrammetry involving image distortion by refraction on interfaces 09 p1311 A72-22970

Stereoplotting instrument concept based on image data selection independence from object space model reconstruction 18 p2691 A72-36498

RECORDING
NT DATA RECORDING
NT DATA SMOOTHING
NT MAGNETIC RECORDING
NT PHOTOGRAPHIC RECORDING

RECORDING HEADS
Magnetic recording head designs, covering information density, head-tape subsystems and head materials electrical and mechanical suitability 16 p2394 A72-33643

RECORDING INSTRUMENTS
NT FLIGHT LOAD RECORDERS
NT FLIGHT RECORDERS
NT LUNAR SEISMOGRAPHS
NT OSCILLOGRAPHS
NT PLOTTERS
NT SEISMOGRAPHS
NT WEATHER DATA RECORDERS
NT WHISTLER RECORDERS
NT X-Y PLOTTERS

High resolution apparatus to record time dependent light flux variations at 380-700 nm, discussing He plasma decay investigation 01 p0064 A72-10375

Thermovisors /recording IR detectors/ development, discussing application to biomedical investigations and disease diagnostics 01 p0022 A72-11293

Neutron albedo flux recording instrument with composite scintillation crystal and photomultiplier scanning to monitor near space 02 p0273 A72-11934

Multichannel high-speed high-density digital recorder, describing tape transport and signal system 02 p0187 A72-12151

Doppler system with navigation radar device, computer unit and data transmitter for continuous recording of aircraft position and speed 02 p0258 A72-12749

Interference polarization filter by modulation and phase detection for passband narrowing and secondary maxima attenuation, discussing application to photoelectric recording system 03 p0356 A72-13096

Cathode ray tube recorder for remote airborne photographic mission 03 p0360 A72-13711

Synchronization system for remote control and performance checking of motion picture projectors with running film, discussing recording equipment and stroboscopic pulsed illuminator operations 04 p0521 A72-14711

Intense noise measurement device for heat flow environments, discussing applications to jet engines, nozzle exits, turbine exhausts and volcanic craters [ONERA, TP NO. 1010] 05 p0661 A72-16025

Five component electromagnetic field station to record geomagnetic field magnetic and electric components variations 05 p0643 A72-16253

Proton recording equipment onboard automatic interplanetary stations Zond 4 and 5 at 1.5-50 MeV using silicon drift counters 06 p0814 A72-17699

IR ray thermography, discussing application to tires testing and rubber manufacture 07 p0991 A72-20422

Multibeam indicator with block diagram description for meteor ranging radar and photofilm based recording system 09 p1308 A72-22508

Cardiac cycle intervals measurement with multibeam cathode oscilloscope synchronized with multichannel polycardiographic automatic recording machine 09 p1272 A72-23192

Differential thermal analysis for electrical insulation thermal degradation and thermogram shape, combining equations for required life line 09 p1339 A72-23271

Criterion for signals records legibility obtained by analog recorders, deriving relationship between normalized root-mean-square error and apparent frequency 09 p1316 A72-23663

Laser recording real time imagery for use in tactical reconnaissance aircraft 10 p1488 A72-23928

Wide bandwidth electron beam analog recorder and reproducer, using signal processing electronics and silver halide film 10 p1479 A72-23931

Broadband 100 MHz multichannel laser recorder and automatic data readout system using digital signal processing 10 p1488 A72-23932

High speed material transfer recording equipment for alphanumeric printers, toned image graphic and microimage computer printer applications 10 p1489 A72-23934

Interference polarization filter by modulation and phase detection for passband narrowing and secondary maxima attenuation, discussing application to photoelectric recording system 11 p1632 A72-25708

Crack initiation detecting and recording instrument with optical strain gages for double shear fatigue tests of aircraft fasteners 11 p1632 A72-25823

Two coordinate oscillograph recording device with automatic reversing for stress-strain tests under static and cyclic loads 11 p1637 A72-26814

ELF wideband noise receiver for atmospherics waveshape magnetic tape recording, computer processing and system simulation 12 p1791 A72-27637

Optical feedback exposure control mechanism of high resolution CRT film recorder intended for tactical military usage 12 p1810 A72-27932

Surface charge density in thermoplastic recording, showing potential-relief modulation dependence on frequency, scanning rate and electron beam properties 13 p1954 A72-28402

Optimal radar recording systems for meteor trail observations providing signal detection, processing and storage triggering and echo discrimination 13 p1929 A72-29030

Optimal selectivity digital recorders for meteor trails radar observations, considering input process quantization rate and spectral width selection 13 p1929 A72-29031

Automatic statistical analyzer for radio meteor echo multiplicity recording in three coordinate /multivariable/ space, including instrument error allowance 13 p1929 A72-29032

Neutron albedo flux recording instrument with composite scintillation crystal and photomultiplier scanning to monitor near space 13 p2030 A72-29246

Photospheric network, magnetic fields, Ca emission and continuum faculae from multichannel magnetograph observations 13 p2045 A72-29705

Thickness gage for continuous autographic record in nondestructive testing of irregular cross section specimens 13 p1959 A72-29759

Nondestructive technique for continuous recording of thickness or contour profiles, using mechanical probes 13 p2000 A72-29760

Ti-Si system phase diagram and equilibrium states, noting crystal lattices and thermograms 14 p2123 A72-30986

Two dimensional acousto-optical light beam deflection system for laser recorder error correction 15 p2248 A72-32038

Five channel recording instrument for energy dissipation evaluation in electric machines from thermal emf measurements 16 p2392 A72-33284

Two beam optical recording instrument for atmospheric IR transmissivity, discussing spectrophotometers with changeable NaCl, KBr and LiF prisms 16 p2392 A72-33294

Automatic recording instrument for crack initiation time and breakdown curve for low carbon and stain-

less steel corrosion-fatigue tests under bending and tensile loads 16 p2394 A72-33849

Evaluation of the possibilities of IR diffraction spectrometers 19 p2801 A72-37965

A device for recording acoustic signals of crack formation in brittle materials 19 p2802 A72-38018

Automated airborne recording system to obtain data on aircraft engines, subsystems and operational performance, considering cost and economic benefits [AIAA PAPER 72-752] 19 p2802 A72-38126

Apparatus for measurement and automatic graphical recording of variations of electrical characteristics of a metal-insulator-semiconducting structure 21 p3051 A72-40209

Polarimeter for recording of magnetooptical rotation dispersion and Kerr equatorial effect in visible, near UV and near IR spectral ranges 22 p3176 A72-42108

Electronic analyzer of structural vibration frequency characteristics and mutual spectra, considering bandpass filter and automatic frequency spectra recorder 22 p3176 A72-42134

An advanced strain level counter for monitoring aircraft fatigue. 22 p3179 A72-42688

Instrumentation systems design for extended bandwidth data acquisition, discussing problem areas in transducers, amplifiers and signal conditioning, data recording and playback 22 p3157 A72-42712

A transmitting television tube for collecting information from streamer spark chambers 23 p3290 A72-44160

RECOVERABILITY
Soviet papers on digital computers application to reliability problems solution for recoverable, failing, controlled, redundant and electronic systems 08 p1179 A72-22051

Reliability estimates for continuously inspected recoverable systems, determining readiness factor for periodic checkout 08 p1180 A72-22054

Functional readiness of periodically inspected recoverable systems with different failure causes 08 p1180 A72-22055

Reliability of recoverable information systems with temporal redundancy 08 p1180 A72-22058

RECOVERABLE LAUNCH VEHICLES
German monograph on liquid air fractionation during flight of recoverable spacecraft carrier propelled by air breathing propulsion systems 09 p1374 A72-23160

RECOVERABLE SATELLITES
U RECOVERABLE SPACECRAFT
RECOVERABLE SPACECRAFT
NT APOLLO SPACECRAFT
NT MERCURY SPACECRAFT
NT REUSABLE SPACECRAFT
NT SPACE SHUTTLES
NT VOSKHOZ MANNED SPACECRAFT
NT VOSTOK SPACECRAFT

Recoverable-observation Cosmos satellites, discussing launch frequency, recovery beacons, binary coded Morse code transmissions and flight duration relation to resolution 12 p1877 A72-27689

Space tug for recoverable reusable system with winged manned boost-glide vehicle, discussing feasibility in economics and engineering 13 p2051 A72-28930

RECOVERY
Recovery factors on porous surface within gas screen region in supersonic turbulent boundary layer for various air injection rates 14 p2070 A72-31017

RECOVERY PARACHUTES
Parachute based recovery system for experimental lifting body LB-21 developed and flight tested 12 p1877 A72-27411

Equipment for ground and sea recovery of sounding rocket payloads, discussing airbrakes, buoy and parachute assemblies 15 p2319 A72-31690

Parachute systems and flotation gear used to recover sounding rocket payloads and components after water landings 15 p2320 A72-31691

RECOVERY ZONES
Splash detection radar digital signal processing by off-line computer using wideband video recorder 02 p0178 A72-12399

Equipment for ground and sea recovery of sounding rocket payloads, discussing airbrakes, buoy and parachute assemblies 15 p2319 A72-31690

RECRYSTALLIZATION
Recrystallization and rolling temperature effects on W strength and plasticity 01 p0088 A72-11083

Allotropic transformations and recrystallization by precipitation hardening in pure Ti crystals, using field emission microscopy

02 p0242 A72-12007

Melting effect on recrystallization of overheated tempered steel, discussing rectification under conditions favoring formation of silicon-oxygen compounds

03 p0376 A72-14017

Annealing effects in plated-wire memory elements, discussing recrystallization in Permalloy films from grain size and magnetic dispersion observations

04 p0504 A72-15716

Dissolved oxygen effect on structure and toughness of nonalloyed extruded steels, observing austenite recrystallization kinetics retardation after hot plastic deformation

05 p0672 A72-16143

X ray study of structural changes in Ni single crystals during recrystallization process after uniaxial deformation under compression loads with high loading rates

06 p0834 A72-18744

Recrystallized and unrecrystallized deformed semifinished wrought Al alloy under cyclic and static loads, investigating macrofracture kinetics

07 p1014 A72-19840

Press forged ceramic crystals deformation, recrystallization, strength and fracture properties, comparing sapphires, rubies and spinels

08 p1196 A72-21917

Recrystallization effects on thin ZnTe film structure, electrical and optical properties

09 p1367 A72-22421

Recrystallization of dispersion strengthened alloys with bcc lattice, deriving equations for grain size changes

09 p1328 A72-23031

Optical and electron microscopic study of Inconel 625 precipitation and recrystallization behavior over temperature range under plastic deformation

10 p1494 A72-23829

Dislocations distribution in Al single crystals observed by X ray topography, noting effects of critical work hardening with annealing and secondary recrystallization

10 p1495 A72-24068

Phase transformations and recrystallization study of Ti-steel bimetal with emission microscope, observing high temperature formation of titanium and vanadium carbides

11 p1654 A72-25493

Iron emission spectrum in phase transformations and recrystallization study of austenitic and carbon steels under high temperature hardening

11 p1655 A72-25496

Interference between recrystallization and allotropic transformation of cold rolled and annealed Co investigated by internal damping measurements

11 p1661 A72-26649

Cold working effect on precipitation-recrystallization interaction in Cu-Ni-Zn alloy, discussing superposed strengthening mechanism during annealing

11 p1641 A72-26738

Work hardening and recrystallization grain structure of sintered and electron bombardment melted Ta after annealing

11 p1644 A72-26839

High purity Al single crystal orientation explained by Rowland transformation model, observing recrystallization grains

12 p1828 A72-27300

High strength low alloy steel and stainless steel recrystallization after hot working at plastic deformation temperature

13 p1973 A72-28654

Tempered or recrystallized chromium steels tensile behavior at 0 to 700 C, showing strength dependence on martensite transformation induced dislocation structure

13 p1975 A72-28667

Hardened coarse-grained steels recrystallization during fast heating, investigating martensite phase macro- and microstructural changes by X ray analysis

13 p1977 A72-28908

Primary recrystallization in TD-nickel bars on sublight optical level identified by transmission electron microscopy examination of deformation and annealing substructures

14 p2119 A72-30601

Dispersion hardening of Nb-Zr-O and Nb-Hf-O alloys, discussing composition and heat treatment effects on aging, recrystallization temperature and grain growth

15 p2255 A72-31567

Micropores pinning effect on grain boundaries mobility during drawn tungsten wire recrystallization, determining pores induced repulsive force

15 p2257 A72-32116

Forming techniques and heat treatment effects on recrystallization characteristics of heat resistant Cr alloy, noting high temperature influence on crystal structure

16 p2407 A72-33531

Techniques to curb static austenite recrystallization rate in martensitic sheet steel through high temperature thermomechanical treatment through minute Ti or Zr additions

18 p2701 A72-36702

Secondary recrystallization of nickel 270 work-hardened by tension

18 p2702 A72-36704

Grain size distribution in recrystallized alpha-titanium.

19 p2820 A72-38297

Dynamic recrystallization occurrence during deformation at elevated temperatures, examining subgrain structure role in austenitic stainless steels

20 p2942 A72-39990

Nucleation of new grains in recrystallization of cold-worked metals.

20 p2930 A72-39995

Recrystallized Al monocrystals applications to optics and X ray spectroscopy, describing preparation methods

21 p3065 A72-40085

Recrystallization and polygonization conditions in high purity metals, noting critical temperature and additives effect

21 p3065 A72-40093

Changes in the structure of nickel-beryllium alloys during deformation, recrystallization, and aging

21 p3068 A72-40959

Nickel-titanium intermetallic phase effect on recrystallization of dispersion hardening high melting point steel during furnace and induction heating

21 p3071 A72-41789

Alloying and impurity effects on mechanical and recrystallization properties of Ta obtained by arc, electron beam and zone melting

22 p3191 A72-42809

Recrystallization and grain growth in titanium. I - Characterization of the structure.

22 p3193 A72-43032

Thin film deposition of carbon on polypropylene, noting morphological templates role in enhancement of polymer nucleation during recrystallization

23 p3305 A72-43269

Ultrasonic treatment of the MA2-1 alloy during recrystallization

23 p3303 A72-44096

Electron-microscope study on the recrystallization in technically pure aluminium.

24 p3412 A72-44719

RECTANGLES

Boundary value problems of Poisson equation for rectangle having side with mixed boundary conditions, discussing solution by summary representations and successive approximations methods

13 p1986 A72-29071

RECTANGULAR BEAMS

Solid rectangular beams under bending tests, obtaining tension-compression stress-strain curves

01 p0141 A72-11002

Finite periodic beam response to turbulent boundary layer pressure field fluctuation, using transfer matrix technique

05 p0650 A72-16832

Thermoelastic coupling effect in thermal shock problem on surface of simply supported rectangular beam

09 p1401 A72-22719

Variational equations of motion for three layered laminated sandwich beam vibrations, assuming small elastic deformations and axial and bending motion

11 p1731 A72-25420

Torsional stress analysis of rectangular beam composed of two elastic materials, using complex variable and conformal mapping

11 p1733 A72-25544

Optimal cross section selection of rectangular beams in oblique bending by nonlinear programming and learning algorithm

13 p2056 A72-28914

Infinite rectangular elastic bar surface mass distribution effects on harmonic wave propagation modes, obtaining approximate solution by expanding displacement as power series

23 p3352 A72-44123

RECTANGULAR GUIDES

Radiation patterns from rectangular guide horns with impedance walls, analyzing hybrid modes

01 p0040 A72-10681

Thick overlay elastic rectangular microwave guides, investigating layer thickness effect, energy partition and higher modes

01 p0042 A72-10706

Low loss reactive wall rectangular and circular waveguides with periodic dielectric structures for millimeter wave and high power applications

02 p0190 A72-11678

Parallel longitudinal resonant slots in rectangular waveguide broad wall, determining mutual impedance from magnetic field reaction

02 p0173 A72-12109

Closed rectangular cavity resonator with conducting walls, calculating differences of electromagnetic zero point fluctuation radiation pressure

02 p0260 A72-12434

Radiation pattern and reflected field analysis for incident plane wave on phased arrays of thick wall rectangular waveguides

03 p0330 A72-13168

Computer solution to vector variational formulation of electromagnetic Maxwell equations for dielectrically loaded rectangular waveguide

03 p0335 A72-14249

Rectangular slot antennas radiation through inhomogeneous plasma layer with dielectric window, obtaining input admittances by fields modal expansion

04 p0554 A72-14412

Infinitely long rectangular waveguide discontinuity problem, calculating reflection and transmission coefficients of wave propagation

04 p0491 A72-15428

Cut-off frequencies of degenerate LSE and LSM modes in rectangular waveguides containing dielectric layers in H plane

04 p0502 A72-15526

Controlled polarization pattern of rectangular guide slots array as function of exciting wave parameters, presenting formulas for elliptical polarization distortion determination

05 p0635 A72-16331

Reciprocal effects of rectangular guide-slot radiators with circular polarization, analyzing field ellipticity factor change for cross-cut slot under neighboring array slots influence

05 p0635 A72-16336

Polarization and energy characteristics of two mutually orthogonal slots cut in rectangular guide, allowing for reciprocal effects of slot arms

05 p0635 A72-16337

Electromagnetic wave propagation in rectangular waveguide with periodic ferrite structure, presenting computer graphics for stop bandwidth vs magnetic field strength

05 p0627 A72-16342

Characteristic impedance formulas for rectangular waveguides with dielectric slab, discussing interference filter design application

05 p0627 A72-16343

Attenuation characteristics of corrugated rectangular waveguides propagating dominant hybrid mode

05 p0638 A72-17076

Rectangular and orthogonal circular waveguides hybrid junction with magnetized ferrite resonators along axes, discussing design and applications

07 p0952 A72-18844

Scattering properties of conducting cylindrical obstacle in rectangular waveguide, deriving scattered field integral representation via Green function

07 p0944 A72-19593

Circular and rectangular waveguide excited dielectric spheres as antenna feed, noting gain and polarization linearity

07 p0957 A72-19796

Phased directional surface wave splitters and microwave and integrated optics elements based on single mode, dielectric and rectangular waveguides

08 p1131 A72-20935

Electromagnetic wave propagation along open rectangular dielectric waveguide, deriving dispersion equations for surface waves propagation constants

08 p1136 A72-21739

Wide rectangular low loss metal waveguide with dielectric layer on opposite walls, noting attenuation based on eigenwaves

10 p1451 A72-24585

Dyadic Green functions for cylindrical circular or rectangular waveguides with moving isotropic homogeneous media

10 p1440 A72-25046

Video information transmission over planar and rectangular multimode waveguides under excitation by coherent light, calculating field distribution by geometrical optics approximation

11 p1633 A72-26330

Lossless distributed rectangular microwave structure with dielectrics interposed between two conductive metallic layers, noting existence of transmission zeros and filter properties

11 p1607 A72-26990

Eigenfunctions, eigenvalues and microwave attenuation constants in square and rectangular waveguides with rounded corners

11 p1607 A72-26994

Mechanical fabrication of rectangular to cylindrical waveguide transitions for X band

13 p1932 A72-29475

Simplified equivalent circuit analysis for Gunn diode coupling to rectangular waveguide by inductive post, using perturbation approximation

15 p2205 A72-31353

Electromagnetic boundary value problem of two rectangular waveguides coupled by aperture radiating into free space, solving integral equation by moments method

15 p2205 A72-31357

Book - Theory and analysis of phased array antennas

17 p2515 A72-34621

Application of the impedance treatment to diffraction problems for a rectangular waveguide

17 p2529 A72-34848

Wave reflection and transmission characteristics of angled rectangular waveguide, deriving scattering matrix 19 p2764 A72-37938

A quasi-optical directional coupler. 20 p2907 A72-39222

A rectangular beam waveguide resonator and antenna. 21 p3026 A72-40358

Stationary expressions for scattering coefficients of rectangular waveguides with dielectric plugs constituting a finite planar array. 21 p3027 A72-40371

Experimental investigation of the propagation of electromagnetic waves in a rectangular waveguide partially filled with n-InSb in the presence of a transverse magnetic field 21 p3016 A72-40796

Scattering by a cylindrical semiconductor rod of anisotropic permittivity perpendicular to the electric field in a rectangular waveguide. 21 p3023 A72-41836

Coupling by slots in rectangular waveguides with arbitrary wall thickness. 22 p3159 A72-42752

Wideband limitations of waveguide arrays. 23 p3270 A72-43573

Analysis of the electric field distribution in a rectangular waveguide with a flat transverse inhomogeneity. 23 p3272 A72-44141

Radiation from an open-ended waveguide with extended dielectric loading. 24 p3381 A72-45643

RECTANGULAR PANELS

Snapping process dynamics of shallow elastic hinged cylindrical panel of rectangular planform under gaseous, liquid and solid loads 08 p1242 A72-21228

Orthotropic point-supported rectangular panel vibration and flutter analysis for natural frequencies and flutter boundaries, applying to space shuttle design [AIAA PAPER 72-350] 11 p1728 A72-25379

Rectangular skin panel vibration modes aerodynamic damping depend on Mach number, dynamic pressure, mode shape and turbulent boundary layer thickness [AIAA PAPER 72-402] 11 p1568 A72-25423

Radiation resistance for natural modes of rectangular panel from far field acoustic radiation energy distribution 11 p1687 A72-26059

Photoelastic study of stress concentration in rectangular panels with inserts. 18 p2734 A72-36376

RECTANGULAR PLANFORMS

NT RECTANGULAR PANELS

NT RECTANGULAR PLATES

NT RECTANGULAR WINGS

Evaluation of the downwash integral for rectangular planforms by the BAC subsonic lifting-surface method. 19 p2747 A72-38810

RECTANGULAR PLATES

Radar target thin rectangular plate model backscattering from incident and reflected waves, noting front and trailing edge phenomena with emphasis on side edge contribution 01 p0032 A72-11250

Dynamic and plastic behavior of mild steel and Al wide beams and rectangular flat plates 02 p0291 A72-11964

Postshear buckling, diagonal tension behavior of rectangular laminated boron-epoxy plates clamped on each side, observing stacking sequence effect 02 p0249 A72-11995

Circular cylindrical sandwich panel and rectangular sandwich plates dynamic stability under periodic external loads derived from mathematical model 02 p0298 A72-12664

Bending stress analysis of rectangular plate with variable stiffness applied to marine propeller blade 02 p0298 A72-12673

Bending moments in transversely isotropic rectangular cantilever plate of low shear rigidity 02 p0299 A72-12684

Square orthotropic and isotropic plates stability with square hole under uniformly distributed load 02 p0299 A72-12685

Chordwise bending vibrations and flutter of thin isotropic rectangular plates, considering static and dynamic responses 03 p0443 A72-13404

Two dimensional boundary value problems for rectangular plates in bending with rigidity variation, using Kantorovich, trigonometric and Horvay functions 03 p0449 A72-13907

Cracked rectangular plates vibration and stability, computing eigenvalues, natural frequencies and moment distribution 04 p0583 A72-14448

Forced and free transverse vibrations of flat rectangular plates with attached concentrated masses 04 p0584 A72-14521

Three dimensional analysis for free vibrations of simply supported viscoelastic rectangular plates 04 p0585 A72-14841

Conforming rectangular and triangular finite elements for plate free vibrations analysis in bending 04 p0585 A72-14846

Yield point elongated and strain hardened rectangular plates, calculating plastic coefficients in geometrically nonlinear bending problem 04 p0588 A72-15057

Rectangular plates nonlinear vibrations under combined static and vibrational loads, using Bubnov-Galerkin method on Karman type nonlinear differential equations 04 p0588 A72-15061

Boundary collocation method for estimating stress intensity factors for through-thickness interior crack in finite rectangular plate [ASME PAPER 71-MET-L] 05 p0732 A72-15794

Vibration and stability of rectangular plates with mixed edge conditions, reducing dual series equations to homogeneous Fredholm integral equations [ASME PAPER 71-WA/APM-21] 05 p0733 A72-15959

Bimetallic rectangular plate with two interconnected layers of anisotropic and isotropic materials and large deflections in nonuniform pressure and temperature field 05 p0735 A72-16016

Rectangular variable thickness plate deflection under uniform lateral pressure, solving nonlinear partial differential equations with variable coefficients by iterative procedure 05 p0738 A72-16533

Critical review on data accuracy of maximum principal elastic stresses and deflections of thin initially-flat square isotropic plates under uniform normal pressure 06 p0894 A72-17796

Large deflection of rectangular thin elastic plates with unsupported edges, using finite difference technique based on dynamic relaxation methods 06 p0895 A72-17799

Iterative solution for non-Levy rectangular plates with corner supports, assuming small deflection theory 06 p0896 A72-17966

Temperature induced bending of thin freely supported rectangular plate, obtaining stress-strain state 06 p0899 A72-18564

Beams and square plates nonlinear vibration response to random concentrated driving force solved numerically on digital computer 06 p0901 A72-18718

Random vibrations in rectangular plate clamped on opposite sides by load, determining natural oscillation frequencies by Ritz technique 06 p0901 A72-18719

Moment stresses and deflections of rigidly clamped hinged and simply supported square elastic plates beyond elastic limit, deriving equilibrium and strain compatibility equations 07 p1091 A72-19759

Free vibration determination method for thin rectangular plate with arbitrary boundary conditions and thickness variations 07 p1092 A72-19857

Frequency analysis of tapered rectangular orthotropic plates, determining bounds 07 p1092 A72-19945

Method of images solution for stress systems in rectangular plate under general self equilibrant edge tractions 07 p1095 A72-20244

Elastic rectangular plate instability in pure bending along two perpendicular directions solved by Karman nonlinear equation reduction to partial differential equations integration 08 p1247 A72-21817

Resonant frequencies of rectangular plate with two sides subject to mixed boundary conditions, expressing vibration modes in terms of Fourier series 08 p1249 A72-21946

Necking instability in rectangular elastoplastic plate under biaxial tension, obtaining condition for equilibrium bifurcation by variational method 09 p1398 A72-22532

Stress analysis of isotropic linearly elastic square plate of constant thickness loaded by concentrated forces at edges 09 p1399 A72-22698

Central crack in plane orthotropic rectangular sheet under tension, showing stress intensity factors dependence on geometric and elastic constants 09 p1404 A72-22915

Parametric instability of flat rectangular plates under periodic or shear sinusoidal in-plane boundary loads 09 p1408 A72-23463

Elastic and plastic buckling analysis of uniformly compressed rectangular plates, using Kantorovich method 09 p1408 A72-23556

Numerical computation of bilateral bounds for arbitrary vectorial and tensorial field quantities of elastic bodies eigenvibration states, applying to thin rectangular plate 09 p1409 A72-23566

Static deflections determination of thin rectangular plates with point clamped restraints, using Ritz method with Lagrange multipliers 10 p1555 A72-24193

Velocity slip effect on squeeze film between porous rectangular plates, calculating pressure, load carrying capacity, film thickness and response time 10 p1488 A72-24820

Freely supported rectangular plate flexure under arbitrarily distributed load, obtaining differential equations solution in trigonometric polynomials 10 p1559 A72-24996

Plastic behavior of laterally loaded beams and rectangular plates, formulating upper and lower bound theorems [AIAA PAPER 72-343] 11 p1728 A72-25372

Elastic body transverse impact against vibrating rectangular plate with allowance for rotatory inertia and shearing forces, using wave equation 11 p1732 A72-25532

Rigidly connected rectangular plates stress-strain calculation with finite difference method 11 p1733 A72-25538

Computerized analysis of prismatic rectangular plate assemblies natural frequencies and initial buckling stresses 11 p1734 A72-25731

Flexural vibration of rectangular orthotropic plates with clamped, simply supported and/or free edges, presenting solution method for coupled characteristic equation pairs 11 p1735 A72-25737

Vibration of simply supported rectangular plate with unidirectional linear thickness variation, using perturbation technique for eigenvalue problem derived by Galerkin method 11 p1735 A72-25739

Bending of simply supported thin square plate clamped around central circular hole and under uniformly distributed transverse load 11 p1736 A72-25985

Finite element method for buckling coefficients of isotropic rectangular plate subject to linearly varying axial compression, using general linear geometric matrix 11 p1736 A72-25999

Large deflection of variable thickness square plate under uniform load, using strain energy method 11 p1737 A72-26588

Dynamic deflection of elastic rectangular plate hinged to rigid base moving under sinusoidal pressure impulse action, noting base inertia effect 12 p1879 A72-27091

Analytical solution to difference stability equations, evaluating adequacy of difference scheme for circular cylindrical shell and rectangular hinged plate under compression 13 p2053 A72-28389

Finite element method for calculating vibrations of thin rectangular plate with four degrees of freedom 13 p2000 A72-28466

Thick rectangular plate stress functions under linear tensile forces application to longitudinal edges and resultant forces application to transverse edges 13 p2055 A72-28735

Thermoelastic vibrations of simply supported rectangular plate produced by temperatures prescribed on faces, obtaining solution in trigonometric series form 13 p2056 A72-28888

Plane stressed state of elastic rectangular plate solved by method of summary representations 13 p2057 A72-29067

Bending of rectangular plates clamped at three edges, establishing sufficient conditions for application of simple iterations to linear algebraic equations solution 13 p2057 A72-29077

Finite element method for in-plane free vibrations of shear wall type structures, noting rectangular plate elements with six degrees of freedom per node 13 p2057 A72-29092

Stress-strain state of elastic rectangular plate under arbitrary edge forces on displacements 13 p2058 A72-29458

Sound generation by finite rectangular plate vibrations, deriving radiated power as function of aspect ratio and vibration pattern 13 p2005 A72-29564

Critical force instability analysis for rectangular plates with mixed boundary conditions, using deflection forms in Fourier series 14 p2165 A72-30575

Bending deflections of rectangular plates with laminated orthotropic layers analysis by finite element displacement, comparing with carbon fiber reinforced plastic structures 14 p2167 A72-30905

Rectangular plate nonlinear lumped-parameter model for large displacement amplitudes, deriving differential equations of motion via Hamilton principle and Euler equations

14 p2169 A72-31148

Stress analysis and deflection equation for uniformly loaded and heated two layer clamped rectangular plate

15 p2322 A72-31362

Thermal shock induced thermoelastic vibrations of rectangular plate calculated by Ritz averaging method

15 p2333 A72-32689

Edge-loaded rectangular plate buckling behavior in elastoplastic range between proportional limit and yield point

16 p2466 A72-33020

Elastic bending of rectangular continuous orthotropic plate with variable rigidities and elastic foundation coefficients for discontinuous boundary conditions along one edge

16 p2467 A72-33118

Sudden heating-induced deflection of rectangular plate fitted into equal sized excavation in elastic foundation with relatively very low thermal conductivity

16 p2475 A72-33148

Analytical solution of stress distribution and load endurance of perforated square plate supported at corners, comparing with photoelastic observations

16 p2470 A72-33410

Homogeneous differential equations of elastic rectangular plates with linear thickness variation, using Gran Olsson solution

16 p2471 A72-33682

Instantaneous and time dependent solutions for thin rectangular plates nonlinear creep bending within framework of Karman theory

16 p2473 A72-34126

On the analysis of unsymmetrical cross-ply rectangular plates.

17 p2626 A72-34328

Approximate solutions of problems involving simultaneous multifunctional nonlinear partial differential equations, noting rectangular plate deflection under lateral pressure

[ASME PAPER 72-APM-47] 17 p2627 A72-34780

Elastoplastic bending of rectangular plates with large deflection.

[ASME PAPER 72-APM-34] 17 p2628 A72-34785

Anisotropic rectangular plate free flexural vibration improved solution via Fourier analysis

18 p2734 A72-36419

Bending of rectangular plates of linearly varying thickness

18 p2736 A72-36991

Reflection and refraction of elastic waves in edge-impacted rectangular plates.

18 p2737 A72-37065

The effect of an elastic edge restraint on the forced vibration of a rectangular plate.

18 p2737 A72-37066

The dynamic characteristics of clamped rectangular plates of orthotropic material.

18 p2737 A72-37067

Analysis of an inclined crack centrally placed in an orthotropic rectangular plate.

19 p2870 A72-37221

Limit analysis for plates - A simple loading problem involving a complex exact solution.

19 p2872 A72-37599

Creep-buckling of flat rectangular plates when the creep exponent ranges from 3 to 7.

19 p2875 A72-37717

Experimental investigation of flexural vibration damping in supported square plates with coatings

19 p2876 A72-38004

Fiberglass reinforced plastics tensile test specimens aspect ratio effect on tensile properties, considering deformation of orthotropic rectangular plate with uniform forced displacement

20 p2943 A72-38889

A plane contact problem of thermoelasticity for a composite rectangle

20 p2978 A72-39019

Pure bending of a rectangular plate made of heteromodulus material

20 p2978 A72-39020

Maximum deflection and bending moments of simply supported anisotropic rectangular plate under uniform transverse load, using double Fourier series

20 p2981 A72-39973

Book - Analysis of plates.

21 p3125 A72-41530

Temperature distribution and heat flux in infinite length rectangular and finite length cylindrical fins, examining validity of one dimensional approximation

22 p3243 A72-41961

Bending of a rectangular plate with a clamped edge and an internal symmetric cut

22 p3234 A72-42291

Nonlinear natural vibrations of rectangular plates and cylindrical panels

22 p3242 A72-43134

Numerical solution of a boundary-value bending problem for rectangular plates with free and freely supported opposite edges

23 p3345 A72-43645

Longitudinal compression of a three-layer plate with initial deflection and a physical nonlinearity of the middle layer /the filler/

23 p3346 A72-43673

Plane elastostatic analysis of V grooved rectangular plates notch angle and specimen geometry effects on stress intensity factors and fracture toughness measurements

23 p3346 A72-43703

Nonlinear thin elastic plate deformation differential relations and static boundary conditions along contour, verifying theory by bending experiment on rectangular plate

23 p3348 A72-43791

Large deflection of rectangular orthotropic plates.

23 p3352 A72-44111

Vibration frequencies and modes determination for clamped rectangular plates of orthotropic material, using weighted residual technique and polynomial approximation

24 p3455 A72-44683

Buckling and lateral vibration of rectangular plates subject to inplane loads - A Ritz approach.

24 p3458 A72-44887

Partial differential heat conduction equation for temperature distribution in rectangular plate, comparing with finite difference solution

24 p3465 A72-45268

RECTANGULAR WIND TUNNELS

Rectangular wind tunnel study of suction effect on velocity profiles and characteristics of turbulent boundary layer

24 p3390 A72-45005

RECTANGULAR WINGS

Drag and lift experimental determination for low aspect ratio rectangular wings with blunt trailing edges at Mach numbers 0.5-2.2

[DGLR PAPER 71-114] 02 p0152 A72-12712

Wind tunnel investigation of unswept rectangular wing with externally blown single slotted flap, determining optimum slot width as function of momentum coefficient and flap deflection

04 p0462 A72-15461

Wind tunnel measurements for near flow field velocity distribution in rectangular wing wake turbulence, comparing with flight measurements

[AIAA PAPER 72-41] 05 p0609 A72-16948

Base pressure drag reduction on rectangular wings with blunt trailing edges from low speed wind tunnel measurements

[DFVLR-SONDDR-219] 10 p1419 A72-24842

Harmonically oscillating rectangular wing in unsteady transonic flow, obtaining two part boundary value problem for linear potential equation

12 p1751 A72-27545

Downwash distribution at surface of rectangular planform wings with prescribed subsonic aerodynamic loading for various aspect ratios

19 p2747 A72-38809

Application of the finite element method to torsional flutter analysis on an analog computer

20 p2980 A72-39907

RECTIFICATION

Rectification process for transformation of single photograph orientation into setting value, noting reduced accidental residual errors

09 p1311 A72-22967

RECTIFIERS

NT AVALANCHE DIODES
NT GERMANIUM DIODES
NT THYRISTORS

Efficiency/reliability design requirements of driven transistor synchronous rectifiers in low output voltage applications

01 p0042 A72-11053

Five layer resonant transparent semiconductor device structures for microwave amplifiers, reactive elements, low current rectifiers and filters

08 p1139 A72-21059

Diode half wave rectifier for ac-to-dc signal conversion in electronic voltmeter

09 p1306 A72-22343

Power supply for magnetic suspension system, using controlled rectifier and dc power amplifier circuits

10 p1461 A72-24767

Silicon carbide rotating rectifier alternator with solid lubricated bearings for high altitude environments, noting applicability to supersonic aircraft

17 p2498 A72-35565

A six-phase bridge rectifier circuit with a reduced number of controlled rectifiers and a rigid external characteristic during high-level regulation

19 p2774 A72-38585

RECUPERATORS

U REGENERATORS
RECURSION FORMULAS

U RECURSIVE FUNCTIONS

RECURSIVE FUNCTIONS

Dynamic model for estimating Bayesian recursive images by linear Kalman filtering

01 p0046 A72-10866

Real time recursive algorithms for estimating coefficients of fixed knot spline approximation to trajectory

08 p1197 A72-20849

Maxwell equations solution for electromagnetic field in circular cylindrical tubes, deriving recursion formulas for computer processing

16 p2364 A72-33668

Recursive filtering techniques in space navigation, describing initialization procedure to account for state vector errors correlation

17 p2532 A72-34214

On structures for nonrecursive digital filters.

17 p2516 A72-35221

Recursive bootstrap maximum likelihood estimators algorithms for identification of process modeled by stable linear difference equation under additive output measurement noise

18 p2672 A72-36056

Role of recursive estimation in statistical image enhancement.

18 p2658 A72-36260

A numerical method for coupled differential equations.

18 p2705 A72-37174

Recursive stochastic approximation of autocorrelation function for stationary random process based on mean-square error and maximum likelihood methods

19 p2824 A72-37285

Recursive updating of smoothing and filtering algorithms for discretely observed continuous dynamic linear systems

19 p2826 A72-38274

RED ARCS

Stable red arc 6300 A emission calculation from satellite electron temperature and density data during geomagnetic storms

01 p0061 A72-10893

DR-current belt dynamics during magnetic storms based on ground observation data on midlatitude red arcs

02 p0217 A72-11929

Electrodynamics of ionosphere and magnetosphere, discussing irregularities, red arc and auroral thermosphere density and temperature changes

06 p0809 A72-18279

Auroral F region electron density enhancement relation to sporadic F2 and red oxygen emission

08 p1226 A72-21111

Midlatitude stable auroral red arcs observation from OV1-10, showing generation at plasmopause due to turbulent dissipation of ring current energy

11 p1624 A72-26401

DR-current belt dynamics during magnetic storms based on ground observation data on midlatitude red arcs

13 p1948 A72-29241

Subauroral red arcs formation mechanism involving magnetosphere-ionosphere energy conduction and lower atmosphere neutral composition changes due to turbulent mixing

13 p1952 A72-29802

Electric field excited stable auroral red arc time dependent behavior, noting inconsistency with satellite and ground observation of 6300 A emission for electron energy

13 p1953 A72-29812

Photometric all sky observations of stable auroral red arcs on 8-9 March 1970, determining altitudes of 6300 A, 5577 A and 4278 A emissions

16 p2384 A72-32978

Certain characteristics of ionospheric disturbances in the F region during type A red colored polar auroras

17 p2551 A72-35866

Midlatitude red arc observations by satellite and ground station, suggesting thermal conduction theory of formation from ionospheric electron and ion temperatures and densities

18 p2685 A72-35985

Rocket measurements of electron influx during a major magnetic storm with type A aurora.

23 p3332 A72-44515

RED BLOOD CELLS

U ERYTHROCYTES

RED SHIFT

Electromagnetic cylindrical wave group aging properties, describing extragalactic red shift production mechanism

01 p0135 A72-11325

Galactic clusters red shifts and absolute spectral energy distributions, inferring evolutionary effects by comparison with giant elliptical galaxies light energy distribution

02 p0279 A72-12185

Bright galaxies and quasars associations based on spatial distribution and red shift considerations, discussing probability analysis

02 p0279 A72-12188

Rotating relativistic stellar models, covering coordinate systems injection energy, convection, red shift, external gravitational waves and black holes

03 p0426 A72-13269

General relativity and cosmology of quasi-stellar objects, covering distances, red shifts and gravitational fields 03 p0426 A72-13270

Extragalactic astronomy observational paradoxes, discussing quasar red shifts and clumpings in directions of bright galaxies 04 p0568 A72-14414

Quasar red shift origin in terms of cosmological, gravitational and Doppler hypothesis, comparing with Seyfert galaxies 04 p0577 A72-15165

Quasar red shifts and spatial density with statistical approach, confirming cosmological distances and uniform distribution in accompanying space 04 p0580 A72-15452

Red shift data for galaxies in clusters, groups and pairs, discussing type, magnitude, diameter, color and inclination 05 p0714 A72-16077

Quasar radio structure, investigating morphology, statistical characteristics, angular size of spectra and red shift correlations from interferometer measurements 05 p0716 A72-16377

Hubble parameter derivation for regions beyond local anisotropy, discussing cluster galaxies magnitude-red shift diagram 05 p0717 A72-16380

Cosmological evidence from radio galaxies and optical object counts, quasar red shifts and evolutionary properties 05 p0717 A72-16383

Freundlich red shift of wavelengths in solar spectrum, deriving scattering cross section 05 p0719 A72-16527

Peculiar interacting extragalactic system NGC 6438, noting same red shift velocity of irregular and SO components 05 p0720 A72-16715

Quasar mass determination, attributing absorption line red shift to radially moving gas clouds 05 p0723 A72-17157

Terrestrial atmospheric effects on quasar red shift measurements, considering night sky emission lines and atmospheric window size limits 05 p0723 A72-17159

Red shift determination for two galaxies near PSK 2251 plus 11 quasar from Ca II H and K absorption line measurements 06 p0881 A72-17898

Quasars red shift distribution apparent maximum for Z near 2.0, investigating possible sources of observational selection 06 p0882 A72-18000

Red shift and spectral line broadening model based on emitting and absorbing atom effects 06 p0883 A72-18023

Cosmological red shift and galactic evolution effects on line features in X ray background due to young pulsars in supernova remnants 06 p0891 A72-18509

Hubble diagram history, present status, extension and improvement, considering quasars, galactic red shifts and other extragalactic radio sources 07 p1068 A72-18999

Optical observation of southern radio sources with 60 inch telescope at Cerro Tololo /Chile/, measuring red shifts for radio galaxies 07 p1072 A72-19342

Galactic clusters size determination from known red shift relation, discussing distribution inhomogeneities, evolution, universe expansion and Hubble constant correction 08 p1234 A72-21282

Quasars and optical quasi-stellar galaxies comparisons for red shifts and luminosities distributions 08 p1234 A72-21283

Radio galaxies spectra and red shifts observed with Lick 120 inch telescope 08 p1235 A72-21393

Cosmological model with negative and positive mass particles, discussing cosmological term, gravitation shielding, red shift and interacting Vorontsov Veliaminov galaxies 09 p1379 A72-22202

Redshifted L alpha flux upper limit restricting hot ionized gas models for gravitational binding of Coma galactic cluster 09 p1383 A72-22292

Gravitational red shift due to three body effect as relativity test 10 p1532 A72-23850

Velocity dispersions and discrepant red shifts in groups of galaxies, using virial theorem for galaxy mass calculations 10 p1534 A72-23903

Quasar redshift distribution and optical and radio luminosity functions analysis 10 p1534 A72-23904

Solar gravitational red shift measurement from solar and laboratory potassium absorption line comparison, using atomic beam resonance scattering technique 10 p1541 A72-24415

Quasars as cosmological and local objects, considering red shift origin and optical and radio luminosities comparison with galaxies 10 p1541 A72-24522

Zero-pressure universe model parameters from red shift and apparent magnitude data for clusters of galaxies 10 p1545 A72-24809

Red shift-absolute magnitude relation for uniform time-dependent universe expansion rate suggesting large scale clustering modifications based on light propagation model 10 p1545 A72-24810

Red shift and spectral line broadening model based on emitting and absorbing atom effects 11 p1718 A72-25959

Cosmological origin of red shift in spectral lines of astromonic bodies, suggesting interpretation based on inelastic interactions between photons of essentially nonzero mass 11 p1723 A72-26507

Space-time model locally identical with Minkowski space in geometrical and causality features, implying non-Doppler red shift and cosmology 12 p1868 A72-27218

Visibility function change of low red shift radio galaxy 3C 120 from interferometer observations, noting high speed expansion 13 p2041 A72-29418

Quasar color indices and redshift correlation, using catalog data on U, B and V colors 14 p2150 A72-30371

Expanding universe postulate vs tired light effect for cosmological red shift explanation, discussing possible tests 14 p2155 A72-30551

Linear polarization and depolarization observation of quasar red shift explained as Faraday dispersion in or near source 15 p2313 A72-32365

V/Vm insensitivity to red shift random shuffling based on luminosity function in Einstein-de Sitter cosmological model 15 p2314 A72-32375

Astronomical objects spectral lines red shift interpretation in terms of noncosmological origin and photon-photon interactions 16 p2450 A72-32863

Quasars spectroscopic observations, noting red shift and line spectra errors and corrections 16 p2452 A72-33133

Negligible intergalactic matter model, deriving distance-red shift relation and comparing to acceleration parameter of homogeneous model 16 p2455 A72-33470

Magnitude redshift relation in flat Brans-Dicke cosmology, discussing gravitational constant effects on stellar evolution and galactic luminosity 16 p2455 A72-33471

Red shift observations for galactic studies, discussing Stephan Quintet in Pegasus, spiral galaxy expulsion evolutionary hypothesis and Andromeda velocity patterns 16 p2456 A72-33541

Quasars and emission line objects red shift distribution using power spectrum analysis method 16 p2457 A72-33625

Interpretation of rotation measures of radio sources. 17 p2606 A72-34573

Relativistic kinetic theory combined with surface layer theory in curved space-time to study counter-rotating disks with fine central red shift 17 p2582 A72-35389

Theoretical explanation of the solar limb effect. 17 p2618 A72-35895

On the ability of the luminosity-volume test to reveal the statistical evolution of the luminosity of quasi-stellar sources. 19 p2854 A72-37226

Physical associations between quasi-stellar objects and galaxies. 19 p2854 A72-37227

The correlation of redshift with magnitude and morphology in the coma cluster. 19 p2854 A72-37228

Cosmological model radiation pressure and density calculation by red shift-stellar magnitude ratios from galactic observations 21 p3109 A72-41441

Nonvelocity origin of excess red shift in companion galaxies from observation of H and K absorption lines of Ca II 22 p3220 A72-41962

Hubble constant, Friedmann time and expanding universe limits from measurements of distances to furthest galaxies, considering quasar red shift cut-off 22 p3222 A72-42138

Faraday depolarization of extragalactic radio sources. 23 p3335 A72-43268

Interpretation of rotation measures of radio sources. II. 23 p3337 A72-43828

Quasar red shift relationship to cosmological distance, considering explanation in terms of gravitational and Doppler effects and unknown process 23 p3338 A72-43993

REDUCED GRAVITY

Capillary forces effects on free surface liquid behavior in partial or total weightlessness, reviewing sloshing problem mathematical treatments 06 p0802 A72-18717

REDUCTION [CHEMISTRY]

NT DEOXIDIZING

NT HYDROGENATION

Oxygen determination in Nb with reduction fusion, determining metallic bath temperature, nature and composition effects on extraction efficiency 03 p0374 A72-13674

Water disinfection by Ag coated filters obtained by silver nitrate reduction with ascorbic acid, hydroquinone, formaldehyde and sodium tartrate activated carbon and ion exchange resin surfaces 05 p0622 A72-16637

Ordinary and macroporous structured polycondensation oxidation-reduction polymers synthesis, discussing application to organic impurities removal from atmospheric moisture condensates 05 p0622 A72-16645

Powder metallurgy Ni-Cr thoria cleaning by reduction with atmosphere of hydrogen plus HCl or HBr 10 p1488 A72-24697

High C 13 content in carbonaceous phases of carbonaceous chondrites accounted for by Rayleigh distillation with oxidized and reduced forms of carbon 10 p1547 A72-24951

Ni additive effects on tungsten trioxide reduction with hydrogen and W powder sinterability 11 p1643 A72-26835

Chemical vapor deposition of W and Mo by hydrogen reduction of hexafluorides, noting crystal structure and microporosity 11 p1644 A72-26837

Titanium nitride powder obtained by hydrogen reduction of titanium tetrachloride in nitrogen flow heated in microwave electrodeless discharge 13 p1967 A72-30111

Lower oxide mechanism in reduction-oxidation reactions during Ti steels electrosmelting with slag and gas phases 14 p2112 A72-30158

Chain reaction mechanisms of fuel combustion in presence of metal oxides for ores reduction application 15 p2335 A72-31850

Cubic sodium tungsten bronze electrocatalytic activity increase for oxygen reduction by traces of Pt 16 p2361 A72-33883

Organic catalysts for oxygen reduction, discussing phthalocyanines, Pfeiffer complexes and porphyrins 16 p2361 A72-33884

Quinones as reversible redox couples for rechargeable cathodes, noting air regeneration capacity in organic electrolytes 16 p2352 A72-33898

Bosch CO2 reduction unit research and development. [ASME PAPER 72-ENAV-10] 20 p2896 A72-39167

Bosch carbon dioxide reduction process for manned spacecraft oxygen recovery, analyzing carbon and water forming reactions with iron as catalyst [ASME PAPER 72-ENAV-9] 20 p2896 A72-39168

Low-temperature reduction of molybdenum and tungsten oxides 20 p2941 A72-39820

The reduction of chlorine on carbon in AlCl3-KCl-NaCl melts. 21 p3013 A72-40843

Fine grained WC phase structure, physicomachanical and cutting properties of Ti-Co alloy, using W powder prepared by tungsten oxide reduction in single stage muffle furnace 22 p3188 A72-42192

REDUNDANCY

Redundancy reduction method for multichannel spectrometer solar radio data processing, using least squares technique 01 p0128 A72-10418

Pattern recognition, invariance, redundancy and information reduction in computer aided image processing 01 p0034 A72-10475

Geophysical satellites high resolution imaging systems data redundancy reduction, using Apollo 9 photographs for computerized statistical analysis of picture structure 02 p0226 A72-11837

Redundancy of Hamiltonian constraints in classical and Dirac quantum theories of gravitation, suggesting replacement by single integral-form condition 07 p1035 A72-20195

Soviet papers on digital computers application to reliability problems solution for recoverable, failing, controlled, redundant and electronic systems 08 p1179 A72-22051

System reliability improvement by redundancy, noting independence of distribution law type 08 p1180 A72-22057

Reliability of recoverable information systems with temporal redundancy

08 p1180 A72-22058

Reliability of redundant schemes with quorum element, noting optimal parameters for known failure damages

08 p1180 A72-22059

Reliability equivalence systems with excessive and deficient group redundancy, noting replacement conditions and flawless operation probability

08 p1143 A72-22060

Holographic prerecorded TV system, discussing coherent light noise elimination and redundancy effects on image quality

15 p2239 A72-32356

An attitude reference system with discrete-correction capability.

22 p3203 A72-42864

Statistical method of failure analysis for redundancy forms selection, noting aircraft safety and reliability

22 p3139 A72-42973

REDUNDANCY ENCODING

Run length encoding for removing redundancy from video signals, determining upper bound on compression ratio based on first order Markov model

06 p0773 A72-17488

Data transmission interference protection under extreme noise, using tolerance detectors with redundancy coding

09 p1278 A72-22851

Investigation of the redundancy of telemetry information from the automatic lunar stations Luna 9 and Luna 13

21 p3014 A72-40312

Simulation of the process of reducing the redundancy of multichannel telemetry information on a digital computer by the method of adaptive break down into discrete elements and associative sorting

21 p3014 A72-40313

Reduction of redundant multichannel telemetry information by the method of adaptive break down into discrete elements and associative sorting

21 p3014 A72-40315

Error correcting codes applied to satellite channels.

21 p3018 A72-40874

Forward-error correction with decision feedback.

23 p3268 A72-44175

REDUNDANT COMPONENTS

Soviet book on reliable logic units design covering adaptive redundant and nonredundant control systems, threshold functions, optimal adaptation algorithms, restoring circuits, etc

01 p0033 A72-10296

Soviet progress and bibliography on fault tolerant digital computers design, emphasizing redundancy application to achieve high reliability

02 p0184 A72-11484

Ultrareliable fault-tolerant digital computer design with protective standby replacement and hybrid redundancy, presenting mathematical models for system reliability evaluation

02 p0185 A72-11487

Distributed fault-tolerant aerospace digital computer design with duplicated central multiprocessor, triplicated memory and conventional redundancy local processors for error detection and correction

02 p0185 A72-11489

Hardware and software parallel digital computer system described by flow table model, calculating output hazard for unbounded line delay effects

02 p0185 A72-11490

Redundancy with repair for system mean time to first failure, presenting differential equation coefficients for Markov process

02 p0236 A72-11556

Redundancy configuration effect on electronic system reliability, discussing MTBF and cost analysis

02 p0194 A72-12445

Reliability behavior of complex systems with standby redundancy under different failure and repair echelons

02 p0194 A72-12446

Fully redundant relay and data command system for SAS-A satellite, discussing operation and reliability tests

03 p0442 A72-14397

Time to failure statistics for communications satellites redundant systems with spares and negative exponential reliability function, discussing perfect and imperfect switching

05 p0731 A72-17250

Complex sampling with cascaded triple input majority logic redundant systems, deriving failure probability

07 p0949 A72-19173

Sequential behavior and inherent tolerance to memory faults in terms of minimum redundancy

07 p0950 A72-19300

Hydrazine and ammonia resisto-jet systems for satellites orbit and attitude control, discussing component redundancy and mass requirements in terms of system optimization

07 p1054 A72-19603

Fully redundant hermetically sealed cable cutter for application to electroexplosive devices in space

08 p1221 A72-20775

Reliability analysis of redundant and nonredundant systems with different component failures, using probability theory

08 p1180 A72-22053

Stochastic rule for optimum moment of preventive maintenance of redundant technological systems, predicting system reliability

08 p1180 A72-22056

Redundant polystable element designs with autonomous redundant state breakdown controls for reliability improvement in automatic control systems

09 p1290 A72-22547

Fault tolerant redundancy for manned spacecraft computers considered as long term desirable solution from cost analysis

10 p1443 A72-23819

Complex system mission worth optimization by redundancies discussing MISDGRAD computer program to evaluate cost-reliability for mission without maintenance

10 p1550 A72-23994

Design considerations and reliability analysis for long duration manned space missions, noting redundancy and inflight maintenance requirement

[AIAA PAPER 72-239] 10 p1487 A72-24446

Econometric approach to space shuttle design for optimum operational redundancy levels, using payload-cost effectiveness criterion

[AIAA PAPER 72-242] 10 p1551 A72-24448

Reliability analysis of repairable redundant systems with random replenishment of reserves, using discrete time Markov process theory

11 p1600 A72-25440

Terminology definitions for redundant flight control systems

[SAE ARP 1181] 11 p1684 A72-26031

German VAK 191B V/STOL fighter aircraft design, development and flight tests, noting redundant control systems

12 p1753 A72-27166

Redundant and nonredundant self adaptive systems reliability, discussing statistical random process characteristics

13 p1936 A72-29170

Electromechanical redundant activating mechanism for F-4 aircraft dual tandem hydraulic power servo, noting application to fly by wire control

14 p2072 A72-30422

Reliability-maximizing digital computer synthesis based on multiple redundant network design, discussing majority structure distribution optimization technique

15 p2203 A72-32174

Optimal algorithm for failure detection and identification in redundant gyro-accelerometer sensor systems, including Monte Carlo simulation

15 p2270 A72-32188

Failure detection techniques for Space Shuttle redundant multiple gimbaled inertial measurement units, using simulated boost and entry trajectories

15 p2270 A72-32189

Gyro drift detection and isolation for redundant inertial measuring unit configuration of Carousel V system

15 p2270 A72-32190

Analog simulation method for highly redundant structure optimization based on reproducing structure mechanical behavior in stabilized stress states

16 p2463 A72-32899

Mathematical model for reliability analysis of modularly redundant electronic systems with unequal failure rates for operating and standby units

16 p2398 A72-33344

Development of electronic part failure rates for long-duration space missions.

17 p2527 A72-34684

Functional equipment active and standby redundancy for flight safety and air traffic punctuality improvement, noting Boeing 747 aircraft redundant systems

17 p2492 A72-35476

Techniques for generating highly reliable redundant systems.

18 p2663 A72-36309

Integrity of flight control system design.

18 p2643 A72-37032

Error correction in redundant logic circuits without application of majority elements

19 p2769 A72-37758

Some effects of bias errors in redundant flight control systems.

19 p2779 A72-38237

Reliability estimation for actively redundant radio electronic systems

19 p2774 A72-38424

Quadruple-redundancy management for fly-by-wire control system reliability, discussing analog circuit and digital computer voter/monitor techniques

[AIAA PAPER 72-884] 20 p2910 A72-39117

Maximum likelihood failure detection for redundant inertial instruments.

[AIAA PAPER 72-864] 20 p2923 A72-39133

An adaptive technique for a redundant-sensor navigation system.

[AIAA PAPER 72-863] 20 p2952 A72-39134

Reliability prediction of a two-unit standby redundant system with standby failure.

20 p2929 A72-39855

Characteristic properties and estimation of reliability functions for redundant systems

21 p3038 A72-40713

ATS F and G radio link with ground stations, discussing telemetry and command functions with redundancy for RF interference minimization

21 p3019 A72-40883

Reliability-maximizing digital computer synthesis based on redundant network design, discussing majority structure optimal allocation technique

22 p3157 A72-43008

Fault-tolerance experiments with the JPL STAR computer.

24 p3383 A72-45671

A prognosis on fault-tolerant digital control systems.

24 p3383 A72-45672

REDUNDANT STRUCTURES

U REDUNDANT COMPONENTS

REENTRY

NT HYPERBOLIC REENTRY

NT HYPERSONIC REENTRY

NT MANNED REENTRY

NT SPACECRAFT REENTRY

REENTRY ANGLE

U ANGLES [GEOMETRY]

U REENTRY TRAJECTORIES

REENTRY BODIES

U REENTRY VEHICLES

REENTRY COMMUNICATION

Pulse position modulation system for minimizing rf blackout during 2 kW S band reentry telemetry transmission

02 p0175 A72-12158

Spacecraft reentry communications, discussing plasma sheaths, blackout alleviation and flight experiments

05 p0628 A72-16562

Radio signal attenuation by thin overdense plasma boundary layer on reentry body as function of incident power

08 p1135 A72-21624

REENTRY EFFECTS

Multiple reentry effects on space shuttle thermal protective superalloys mechanical properties, presenting cyclic simulation results for different temperatures, pressures and stresses

01 p0084 A72-10754

Microwave breakdown prediction models for antenna system in ionized reentry environment

04 p0486 A72-14530

Rectangular slots linear array and feed network performance in reentry plasma environment, obtaining self and mutual impedances, gain and radiation pattern

13 p1916 A72-28533

Onboard radiometric measurement of bow shock generated UV radiation during atmospheric reentry of experimental sphere

[AIAA PAPER 72-692] 16 p2462 A72-34050

Material injection RF blackout alleviation and plasma diagnostic measurement with electrostatic probes and S-band reflectometer during RAM C-III reentry flight

[AIAA PAPER 72-690] 16 p2365 A72-34052

Theoretical and experimental investigations on the problem of aerodynamic heating of re-entry vehicles.

[ICAS PAPER 72-39] 21 p3130 A72-41164

Total enthalpy measurement from blunt body gas cap emission in arc-heated wind tunnels - Results and application.

[AIAA PAPER 72-1021] 21 p2993 A72-41599

REENTRY GLIDERS

U LIFTING REENTRY VEHICLES

REENTRY GUIDANCE

Spacecraft banking control during reentry, deriving dynamic equations of angular motion

05 p0730 A72-17026

Two step spacecraft reentry guidance involving skip trajectory at parabolic speeds, proposing algorithm for running coordinate and speed vector components values

11 p1684 A72-26896

Perturbation method for two point boundary value problem for fluid flow applied to optimal reentry control problem

16 p2462 A72-34166

Synthesis of a nonlinear law for the control of spacecraft motion in the atmosphere of the earth

17 p2621 A72-35202

Thermally controlled entry guidance for shuttle.

[AIAA PAPER 72-831] 20 p2951 A72-39096

Optimal guidance for the space shuttle transition.

24 p3422 A72-45186

REENTRY PHYSICS

Roll control algorithm for parabolic velocity spacecraft reentry, using successive stepwise extrapolation of approach trajectory parameters

05 p0685 A72-16431

Spacecraft motion control algorithm for reentry at escape velocity based on object motion model

11 p1684 A72-26900

Electrostatic flush disk and cylindrical probe construction and electron density data during atmospheric reentry from beryllium sphere experiments
[AIAA PAPER 72-691] 16 p2346 A72-34051

Viscous shock layer analysis application to blunt nosed reentry vehicle plasma layer nonequilibrium flow species distribution, considering electron density
[AIAA PAPER 72-689] 16 p2346 A72-34053

Experimental determination of the aeroacoustic environmental about a slender cone.
[AIAA PAPER 72-706] 17 p2486 A72-35482

Prediction of electron concentration reductions in re-entry flow fields due to electrophilic liquid and water injection.
[AIAA PAPER 72-670] 18 p2730 A72-36537

Theoretical study and wind tunnel simulation of the electrical phenomena of reentry
22 p3231 A72-43092

REENTRY RANGE

Analytical evaluation of the spacecraft descent range for hyperbolic reentry trajectories
17 p2610 A72-35203

Investigation of the range of landing area distances for earth atmosphere reentries at hyperbolic velocities
17 p2622 A72-35204

REENTRY SHIELDING

Niobium alloy for reentry vehicle heat shields, describing slurry coating process reliability
01 p0077 A72-10982

Heat and mass transfer blowing correction correlations for graphite and charring ablator reentry nosetip and heat shield applications
[AIAA PAPER 72-91] 05 p0748 A72-16810

Material design for filament wound graphite-graphite fiber/matrix composite heat shields for improved performance during reentry
08 p1245 A72-21597

Delta wing configuration design with anheal heat shield for high lift reentry in 6-20 Mach number range.
[AIAA PAPER 72-132] 09 p1259 A72-22501

Thin liquid surface water film cooling tests for mass loss under simulated reentry heating and shear conditions
10 p1563 A72-24648

Carbon-phenolic composite ablation and expansion in thermal environment during reentry shielding, using flight and simulation tests
[AIAA PAPER 72-363] 11 p1669 A72-25390

Space shuttle orbiter reentry heat shield materials, considering hot structures and hot radiative metallic, ceramic insulative and ablative heat shields
11 p1660 A72-26245

Thermomechanical erosion prediction for ablative, composite material, reentry nosetip applications and model development for heating, pressure and shear forces
[AIAA PAPER 72-299] 14 p2171 A72-30827

Apollo heat shield silica reinforcement fiber and ablation char reactions in laboratory and actual reentry tests
14 p2172 A72-30922

Carbon-carbon composites for space shuttle reentry thermal protection.
17 p2572 A72-35667

The development of the Apollo entry thermal protection system.
21 p3115 A72-41124

REENTRY TRAJECTORIES

Orbital plane rotation and terminal impact ascending node and inclination of satellite during ballistic reentry
01 p0052 A72-10078

Reentry glider approximate optimal atmospheric entry trajectories, maximizing function of terminal velocity, altitude, flight path and heading angles subject to three terminal nonlinear constraints
01 p0128 A72-10377

Isotopic heat source unit multiple elliptical orbit reentry unperturbed by solar-lunar gravitational forces, deriving analytical model of grazing trajectories, aerodynamic heating and thermochemical ablation
03 p0457 A72-13959

Spacecraft reentry trajectory parameter selection and optimal control algorithm under random atmospheric density variation
05 p0685 A72-16429

Atmospheric reentry trajectory mechanics investigation method, considering flight path angle vs atmospheric density
05 p0728 A72-16704

Spacecraft trajectories for reentry at hyperbolic velocity, examining aerodynamic control loads and characteristics in atmospheric skip
11 p1718 A72-25929

Atmospheric model effects on space shuttle ascent and reentry trajectories and aerodynamic heating
13 p1990 A72-28813

Atmospheric model for random density variations effects on space shuttle reentry parameters, using Monte Carlo trajectories for delta wing orbiter
13 p1990 A72-28814

Analytical evaluation of the spacecraft descent range for hyperbolic reentry trajectories
17 p2610 A72-35203

Investigation of the range of landing area distances for earth atmosphere reentries at hyperbolic velocities
17 p2622 A72-35204

The optimum configuration and the optimum reentry trajectory of space shuttle vehicles.
[ICAS PAPER 72-27] 21 p2991 A72-41152

Application of plane fixed equations of motion to reentry vehicle flight analysis.
24 p3452 A72-45345

Space shuttle optimal entry trajectories for thermal protection system weight minimization, considering constant and variable angles of attack
[AIAA PAPER 72-977] 24 p3452 A72-45414

Lifting entry optimization equations for fixed angle of attack with path control for roll modulation of lift, considering space shuttle orbiter configuration
[AIAA PAPER 72-933] 24 p3443 A72-45435

Comparison of linear and Riccati equations used to solve optimal control problems.
24 p3420 A72-45776

REENTRY VEHICLES

NT APOLLO SPACECRAFT

NT LIFTING REENTRY VEHICLES

NT MERCURY SPACECRAFT

NT RECOVERABLE SPACECRAFT

NT REUSABLE SPACECRAFT

NT VOSKHOD MANNED SPACECRAFT

NT VOSTOK SPACECRAFT

Strain gage tests on three dimensional composites for reentry vehicle structural design evaluation
02 p0287 A72-11506

Aerodynamic design of atmospheric reentry vehicles forebody, considering maximum drag for hypersonic bodies
02 p0149 A72-11726

Dynamic damping coefficient extraction from reentry vehicle flight test telemetered lateral rate data
03 p0441 A72-13951

Newtonian theory for maximum lift drag ratio of blunt-cone cylinder bodies, optimizing rocket reentry nose shape
05 p0602 A72-16535

Telemetry system on board beryllium sphere reentry vehicle for hypersonic gas dynamics and wake chemistry experiments, using flush mounted antennas with isotropic radiation pattern
[AIAA PAPER 72-176] 05 p0631 A72-16836

Altitude chamber simulation of reentry bodies separation from ballistic missiles, examining body shape, nozzle dimensions, gas pressure and distance effects
[ONERA, TP NO. 1029] 05 p0645 A72-17198

Rocket powered air launched lifting body reentry vehicles testing, stressing performance, handling qualities and crew preparation
06 p0892 A72-18494

Closed loop covariances prediction in reentry vehicle tracking and data compression, presenting simulation results
08 p1144 A72-20846

Thermal stress measurement and thermoelastic behavior of carbon-carbon-materials for reentry nose cones, describing gage mounting, temperature compensation and data recording
08 p1164 A72-20921

High temperature Co-base alloy for nuclear, chemical and reentry vehicle applications
09 p1327 A72-22478

Emergency reentry manned spacecraft remedial concepts, mission constraints and system designs in terms of cost effectiveness
09 p1396 A72-23159

Adaptive filter techniques application to maneuvering reentry vehicle tracking, using Wald sequential test, decision theory and stochastic approximation
10 p1509 A72-23779

Lift variation effect on rolling reentry vehicle trajectory, calculating deviation from zero-lift impact point
10 p1552 A72-24651

Electra method of plasma diagnosis around reentry vehicle head, describing onboard antennas impedance measurements and use of triple Langmuir probe mounted on telescopic mast
10 p1552 A72-24659

Microwave breakdown calculation on symmetrically excited conical reentry vehicle based on variational technique, comparing with experimental data
13 p1916 A72-28536

Elastomeric silicone ablator heat shields thermal characteristics from NASA Planetary Atmosphere Experiments Test vehicle earth atmosphere entry measurements
[AIAA PAPER 72-326] 13 p2064 A72-28953

Blunt planetary entry vehicles thermal flux prediction, taking into account viscosity, conduction, dissociation, ionization, nongray radiation, surface emissivity and ablation effects
15 p2335 A72-31816

Aerothermochemical analysis of the thermosetting hydrocarbon plastic ablation rate under heat transfer at reentry vehicle hypersonic stagnation point, describing pyrolysis by chemical kinetic equation
15 p2335 A72-32149

Bumerang lifting body design for reentry vehicles, discussing optimal configurations and experimental flight testing
16 p2462 A72-33050

Low recession graphite nosetip design for ballistic reentry, considering blunt and sharp configurations in terms of thermally induced tensile strain survival
[AIAA PAPER 72-705] 16 p2472 A72-34039

Effect of lagging pitching moment on re-entry vehicle dynamic stability.
17 p2619 A72-34202

Exact solution for dynamic oscillations of re-entry bodies.
17 p2622 A72-35231

Reentry vehicle spiral descent terminal guidance, verifying concept feasibility through hybrid man-in-loop simulators
[AIAA PAPER 72-834] 20 p2950 A72-39093

Investigations concerning reentry bodies in the hypersonic tunnels of Goettingen
20 p2886 A72-39933

Turbulent base heating on a slender re-entry vehicle.
21 p2992 A72-41308

Ablative nose shape change effects on re-entry vehicle aerodynamic performance.
[AIAA PAPER 72-974] 22 p3230 A72-42337

Effect on entry vehicle dynamic stability of aerodynamic and mass asymmetry coupling.
[AIAA PAPER 72-973] 22 p3231 A72-42338

Measurement system decomposition for aerodynamic coefficient estimation.
[AIAA PAPER 72-964] 22 p3177 A72-42345

Heat transfer effects on reentry vehicle surfaces boundary layer stability and aerodynamic characteristics, noting stall angle reduction and drag increase from wind tunnel tests
[AIAA PAPER 72-960] 22 p3137 A72-42357

Evaluation of windward streamline effective cone boundary-layer analyses.
22 p3136 A72-42874

Roll dynamic behavior of a very slender reentry vehicle.
24 p3452 A72-45348

Flight test evaluation of a fluidically actuated monopropellant hydrazine roll control system.
[AIAA PAPER 72-975] 24 p3452 A72-45410

REFERENCE ATMOSPHERES

Meteorological reference level location without wind information for use in numerical weather prediction
12 p1838 A72-27024

Variations of the planetary values of the F2 layer thickness and the parameters of the neutral atmosphere
23 p3284 A72-43375

REFERENCE STARS

Stellar photometric classification by comparing color indices to indices of standard stars with UPX-YZVS system, outlining computer method
11 p1715 A72-25294

Satellite-star optical navigation data from Mariner program, describing objectives and performance of preflight and real time activities leading to successful performance
15 p2271 A72-32196

Analysis of the division-line errors of the Pulkovo meridian circle by observations of stars
19 p2801 A72-37912

Accurate positions of the planet Pluto in the years 1969-1970.
21 p3105 A72-40576

Analytical assessment of the accuracy of autonomous space navigation from measurements of the flight altitude and zenithal distance of one reference star
22 p3202 A72-42222

Objective-prism based photometric computerized calibration method based on continuum energy distribution of standard stars within photographic plate field
22 p3177 A72-42376

Photographic observations of Mars at the Main Astronomical Observatory, AN USSR during 1963-1967
24 p3448 A72-45686

REFERENCE SYSTEMS

Lunisolar precession and equinox motion, discussing determination methods based on proper motions referred to fundamental systems
04 p0575 A72-15026

Model reference adaptive control system synthesis in presence of random perturbations, considering error signal derivative use to form parameter adjustment algorithm
05 p0640 A72-16208

Three component airborne magnetometer design, discussing direction reference system and stabilized platform
06 p0812 A72-17372

Algorithmic procedure in compensator design for hyperstable discrete model reference adaptive systems /MRAS/

07 p1027 A72-19294

Reference grid construction for lunar craters in system with scale and orientation independent of other

- systems, discussing preliminary catalog compilation from lunar photographs 09 p1388 A72-23055
- Algorithm and formulas for lunar limb absolute heights determination in selenodetic reference points system from lunar photographs 09 p1388 A72-23057
- Magnetic apex coordinate system for plasma density organization in low and middle latitude F2 region 13 p1951 A72-29395
- Stress and heat flux constitutive equations dependence on observer reference frame, considering field equation for temperature of gas at rest 16 p2478 A72-33526
- Table for reduction of stellar radial velocities to the center of the sun 19 p2859 A72-37909
- An attitude reference system with discrete-correction capability. 22 p3203 A72-42864
- REFERENCES [STANDARDS]**
- U STANDARDS**
- REFINING**
- NT ELECTROSLAG REFINING**
- Al-B and Al-Ti-B alloys fabrication, discussing quality control and grain refinement 20 p2936 A72-39207
- REFLECTANCE**
- NT SPECTRAL REFLECTANCE**
- Water quality monitoring by radiative transport equation for reflectance measurements of laser light scattered from turbid water polluted with absorber and scatterer particles 01 p0058 A72-10547 [AIAA PAPER 71-1098]
- Electron concentration profiles in D region from radio wave partial reflection coefficients 01 p0028 A72-10614
- Coaxial connector standard interfaces for optimum microwave performance, discussing single connector reflection coefficient measurement equipment and procedures 01 p0041 A72-10693
- Vlf propagation across discontinuous daytime-nighttime transitions in anisotropic terrestrial waveguide, developing dominant mode approximations of transmission and reflection coefficients 01 p0032 A72-11239
- Water depth attenuation coefficients and bottom reflectance characteristics from large area multispectral scanner measurements for discharge and concentrations monitoring 02 p0211 A72-11812
- Multispectral scanner data training sets size effect on correlation between soil reflectance and organic matter content obtained from ground truth 02 p0227 A72-11845
- Plant leaves light reflectance, transmittance and absorbance characteristics relationship to leaf mesophyll arrangement, considering interpretation of aircraft/spacecraft remotely sensed data 02 p0213 A72-11856
- Green and blue-green algae reflectance and transmittance characteristics, selecting spectral bands for multispectrum scanning of algal suspensions in water bodies 02 p0213 A72-11857
- Short backfire antenna directivity determination from plane conduction reflection coefficient 02 p0192 A72-12111
- Avalanche pulse generator with pretigger output for reflection coefficient and step function response measurements 02 p0195 A72-12605
- Reflection and transmission coefficients for radio waves incident upon thin highly ionized layers, comparing with sporadic E reflections 03 p0344 A72-12976
- Au thin film effective optical constant calculation from measured reflection and transmission coefficients and thickness by approximate formulas 03 p0401 A72-13363
- Minority carriers localized surface distribution effect on helicon propagation modes reflectivity in semiconductor 03 p0402 A72-13797
- Statistical processing of phase dependence of Martian integral brightness at 0.3-1.1 microns, noting abrupt reflectivity decrease 03 p0436 A72-13816
- Vlf phase regressions at sunrise related to variations of reflection coefficient in D region, using IENGf data 04 p0485 A72-14465
- Waveguide radiators linear phased array impedance matching during E-plane wide angle scanning improved by reflection coefficient variation compensation 04 p0499 A72-15239
- Human skin thermal radiation properties, presenting data on reflection, emission, transmission and complex refraction [ASME PAPER 71-WA/HT-37] 05 p0620 A72-15888
- Long E-plane sectoral horn, deriving complex reflection coefficient from aperture by geometrical diffraction theory 06 p0781 A72-17346
- Thermostated integrating sphere for low temperature measurements of reflection and transmission coefficients of materials with arbitrary scattering functions 06 p0816 A72-17838
- Rough surfaces with orthogonal parallel V grooves, studying shadowing, interreflection and masking effects on bidirectional reflectance from He-Ne laser illumination [AIAA PAPER 72-55] 06 p0848 A72-17924
- Visual/graphical recording microwave reflectometer for measuring reflection coefficient along waveguide component, based on Fourier transform evaluation by real time analog method 06 p0786 A72-18369
- Longitudinal and transverse nonresonant slots on waveguide, calculating susceptance, conductance, reflectance and transmittance as function of wavenumber 07 p0952 A72-18843
- Stepped microwave bandpass filters with bypass and flattened reflection coefficient and delay, discussing design and implementation 07 p0954 A72-19175
- Modal matching method evaluating planar surface waveguide junction transmission and reflection coefficients, comparing to integral equation method 07 p0955 A72-19253
- Direct coupled waveguide cavity resonator equalizer networks, determining reflection coefficient, phase, amplitude and time delay characteristics by scattering matrix theory 07 p0955 A72-19327
- Ruby laser power output losses at 80 K with spectral line suppression dependence on surface reflection coefficient of plane parallel plate in resonator 08 p1183 A72-22026
- Scattering computations of albedo reflectance for model media as function of incidence angle 09 p1299 A72-22808
- GaAs lidar reflectance of fair weather cumulus clouds at 0.903 micron from aircraft observation 09 p1280 A72-23349
- Fixed frequency or wideband real time measurements of microwave reflection and transmission coefficients and fields in open or closed structures 09 p1289 A72-23425
- Electroreflectance study of mixed gallium and indium phosphides 10 p1525 A72-24228
- Microwave diagnostics of P doped Si semiconductor crystal prism determining relation between complex permittivity and reflection factor by variational method 10 p1450 A72-24404
- Sea foam emission and reflection characteristics at microwave frequencies from radiometric measurements, correlating data as functions of frequency and angle 10 p1475 A72-24749
- Bidirectional reflectance from randomly rough engineering surfaces, using photographic technique [AIAA PAPER 72-308] 11 p1742 A72-25242
- Microwave two port waveguide transmission efficiency determination by reflection coefficient measurements 11 p1599 A72-26997
- Laboratory simulation of diffuse reflectivity from plane parallel cloudy planetary atmosphere, comparing to theory 12 p1796 A72-27947
- Heating mechanisms in laser pulse produced plasma from electron temperature and reflectivity measurements 13 p2011 A72-28999
- Reflectivity of metals at high temperatures based on Drude theory and electron-phonon scattering, detailing temperature dependence and optical constants 14 p2129 A72-30183
- Wire antenna half-space problem analysis by Sommerfeld integral approach and plane wave reflection coefficient approximation 14 p2085 A72-30338
- Epitaxial film system parameters determination based on variational technique of computing electromagnetic waves reflectance and transmissivity in semiconductor structures 14 p2142 A72-30811
- Reflectivity-emissivity relationship for isothermal atmosphere with coherent scattering and continuous absorption, generalizing for noncoherent case with line opacity 14 p2131 A72-30890
- Reflection and transmission coefficients of long lossy single mode waveguide line with random inhomogeneities 15 p2195 A72-31654
- Lossless low pass ladder network synthesis in terms of reflection coefficient poles and zeros with application to bandpass matching problem 15 p2212 A72-32248
- Elastic wave scattering by moving slab, calculating reflection and transmission coefficients for various incidence angles, frequencies and motion velocities 15 p2219 A72-32476
- Plasma electron density profile reflection coefficient frequency-dependent amplitude and phase determination by measuring time response to fast-rising voltage pulse 16 p2437 A72-33767
- Infrared and Raman spectra of lunar samples from Apollo 11, 12 and 14. 18 p2724 A72-36279
- Reflection coefficient method of remote probing for inhomogeneous media, using plane wave incidence angle dependence 20 p2927 A72-39719
- Corrugated image screens advantages over flat screens, determining light intensity per corrugation, maximum viewing angle and reflection factor 21 p3055 A72-40743
- Partial reflections from a thin parabolic layer in the lower D-region. 22 p3170 A72-42374
- Multisectional CW gas dynamic laser output radiation density distribution control via transmitting mirror with variable reflection coefficient 22 p3186 A72-42632
- Reflectivity dependence of triple polarization grid on elements spacing and wires orientation, noting bandwidth of ray guide matching transformer 23 p3269 A72-43446
- The pressure dependence of the E2 reflectivity peak and of the dielectric constant in III-V semiconductors. 23 p3324 A72-44321
- Determination of the reflecting power of a hilly terrain, knowing the reflective power of a flat terrain of the same nature 24 p3381 A72-45769
- Approximate temperature distribution for a diffuse, highly reflecting material. 24 p3465 A72-45790
- REFLECTED RADIATION**
- U REFLECTED WAVES**
- REFLECTED RAYS**
- U REFLECTED WAVES**
- REFLECTED WAVES**
- Detonation waves collision in variable gas medium with plane, cylindrical or spherical obstruction, determining gas parameters behind reflected shock wave 02 p0201 A72-11579
- Contactless optical strain measurement based on speckle pattern change of diffusely reflected laser light 02 p0225 A72-11755
- Upper cloud boundary height determination using Cosmos 320 satellite combined reflected solar and intrinsic radiation measurements 02 p0253 A72-12213
- Radiative cooling effects on flow field and heat transfer behind reflected shock wave [AD-737423] 04 p0597 A72-15338
- Electric network scattering matrix and associated incident and reflected wave variables concepts applications in linear optimal control problem 04 p0507 A72-15528
- Electromagnetic wave transmission and reflection by semiinfinite moving anisotropic plasma with parallel static magnetic field, considering incident H wave 05 p0696 A72-16623
- Ablation performance of dielectric heat shields for planetary entry, testing diffuse reflectance by convective and radiative heating 05 p0747 A72-16809 [AIAA PAPER 72-89]
- Holographic recording of focused images using reference laser beam reflected from object in direction of diffraction maxima 06 p0817 A72-18012
- Light diffuse transmission and reflection by semiinfinite atmosphere with four term scattering indicatrix 06 p0884 A72-18029
- Macroscopic boundary conditions of gas-solid interface interaction as function of gas temperature and transport coefficients variation in shock reflection problems 06 p0902 A72-18107
- Galactic cepheid RS Puppis and surrounding ring-structured nebula luminous variations and evolution, using reflecting shell model 07 p1069 A72-19079
- Radiative cooling effects in absorbing-emitting gas behind reflected shock waves, using expansion procedure in small density ratio across shock front [AD-738781] 07 p0967 A72-19503
- Plane electromagnetic wave reflection from conducting convex cylinder in radially inhomogeneous absorbing medium, deriving equations for beam trajectories calculation 08 p1131 A72-20742
- Phase errors in range finding measurements with radio waves reflection from underlying surface 09 p1277 A72-22481
- Loading process behind reflected and refracted shock waves in plastic layered media with linear elastic unloading 09 p1353 A72-23555

Shock wave propagation in ducts with abrupt area expansion, discussing vortices generation and wave diffraction and reflection effects on ducted flow 10 p1464 A72-23880

Nonlinear diffraction of weak shock waves near rigid wall with sharp bend, obtaining approximate solution by matched asymptotic expansion method 10 p1468 A72-24432

Earth electrical parameters measurement by radio wave methods involving electromagnetic propagation along or reflection from surface, considering penetration depth, earth stratification and surface inhomogeneities 10 p1474 A72-24737

Wedge reflected shock profiles, comparing results for various Mach numbers and incidence angles with predictions based on Whitham theory 11 p1616 A72-25918

Light diffuse transmission and reflection by semi-infinite atmosphere with four term scattering indicatrix 11 p1719 A72-25965

Plane and uniform heterogeneous electromagnetic waves reflection, observing Goos-Hanchen and Imbert effects 11 p1597 A72-26482

TWT amplifiers electronic reflections and gain ripple 12 p1790 A72-27435

Reflection and transmission of plane E wave incident on moving conducting medium, discussing growing wave excitation 12 p1782 A72-27490

Statistical model for short wave radio signal fading at oblique signal reflection from ionosphere, determining pulse amplitude and duration distribution laws 13 p1915 A72-28468

Arrival angles of radio wave reflected from ionosphere for remote short wave transmitter direction finding 13 p1917 A72-28601

Virtual height dependence of ionospheric F region parameters including angular divergence of reflected radio waves, heterogeneity coefficient and random and drift motions velocity 13 p1948 A72-29038

Face centered solid crystal cell spatial distribution effect on body surface-reflected molecular beam intensity distribution 16 p2430 A72-33066

Autoignition behind reflected shock waves for hydrocarbon-oxygen mixtures, demonstrating two ignition modes via schlieren photographic records 16 p2479 A72-34002

Pressure distribution on a yawed wedge interacted by an oblique shock. 17 p2485 A72-35239

Shock tube investigation of low-density heated fluid element dynamic reaction to reflected shock wave passage, noting similarity to atmospheric thermals 17 p2542 A72-35615

Ray geometry, travel time and spreading loss derivation for refracted/bottom-reflected ray propagation in channel with horizontal and vertical sound speed gradients 18 p2710 A72-36413

Dispersion and random changes in the ground pattern of radio waves reflected from the ionosphere. 18 p2660 A72-36459

Influence of an interface on the spectrum of incoherently reflected waves 18 p2661 A72-36657

Transmission and reflection of an electromagnetic wave incident normally on a plasma half-space. 19 p2840 A72-37726

Energy variation curves for direct flare radiation and reflection from eruptive star atmosphere, discussing color variations 19 p2858 A72-37808

Experimental investigation of pressure profiles in a helical shock wave irregularly reflected in plexiglass cylinders 21 p3045 A72-40988

On the conditions for the appearance of the Mach effect in the reflection of an oblique shock wave in supersonic flow 21 p3046 A72-41339

Amplification of cylindrical electromagnetic waves reflected from a rotating body 23 p3262 A72-43307

Exact solution of the equations of molecular optics for refraction and reflection of an electromagnetic wave on a semi-infinite dielectric. 23 p3313 A72-43803

Reflection of pulses at the interface between an elastic rod and an elastic half-space. 23 p3314 A72-44119

Polarization of the central field of a wave reflected from the ionosphere 23 p3265 A72-44173

Venus high albedo, discussing compound reflecting layer and liquid Hg cloud models 24 p3436 A72-44692

Approximate formulas for the intensity of diffuse reflected emission from a semiinfinite atmosphere 24 p3448 A72-45685

Mach reflection from overexpanded nozzle flows. 24 p3365 A72-45794

REFLECTING TELESCOPES

Cassegrain type astronomical reflecting telescope design, describing auxiliary equipment 01 p0047 A72-10202

Cast telescope mirror design with light metallic structures, examining possibilities offered by composite high modulus fiber structures [ONERA, TP NO. 1022] 05 p0660 A72-15855

Small lunar based reflecting telescopes with Cassegrainian and catadioptric optical systems, discussing design and operation 08 p1164 A72-20976

Holographic correction of reflecting refracting telescope objective mirror deformation aberrations, noting interferometric attachment 10 p1479 A72-24049

Astronomical reflector telescope design, describing thermal effects on Al mirror and image intensification 12 p1807 A72-27428

Aplanatic mirror-lens telescope systems with spherical optics, discussing isochromatic corrective lens specifications 14 p2104 A72-30497

Book on Soviet astronomical reflecting telescopes, paraboloid mirrors, computer control, microphotometers and image converters 17 p2553 A72-34623

Adaptation of the Schupmann medial telescope to a large scale astronomical optical system. 19 p2797 A72-37587

Aplanatic mirror-lens telescope systems with spherical optics, discussing isochromatic corrective lens specifications 19 p2803 A72-38326

Astrospectrography with a mirror telescope. II - One-prism spectrograph with 60 deg flint prism 22 p3178 A72-42545

A large multiple mirror telescope /MMT/ project. 22 p3180 A72-42988

REFLECTION

NT INFRARED REFLECTION

NT RETROREFLECTION

NT SIGNAL REFLECTION

NT SPECULAR REFLECTION

NT ULTRAVIOLET REFLECTION

NT WAVE REFLECTION

REFLECTION COEFFICIENT

U REFLECTANCE

REFLECTIVITY

U REFLECTANCE

REFLECTOMETERS

NT MICROWAVE REFLECTOMETERS

Aqueous solutions specular reflectance measurement, using organic dye laser spectrophotometer at 360-650 nm and reflectometer equipped spectrophotometer at 0.2-20 micron wavelengths 02 p0226 A72-11831

Reflectometer based on quasi-optical transmission line using conversion of incident and reflected waves into opposed circularly polarized components 13 p1954 A72-28375

REFLECTOR SATELLITES

U PASSIVE SATELLITES

REFLECTORS

NT FRESNEL REFLECTORS

NT PARABOLIC REFLECTORS

NT PARABOLOID MIRRORS

NT RADAR CORNER REFLECTORS

NT RADAR REFLECTORS

NT SOLAR REFLECTORS

Stepped reflector image region fields at plane wave incidence angle to reflector axis, determining field components as Fourier series 01 p0035 A72-10115

High efficiency reflector antennas, discussing secondary subreflector for feed energy redistribution 01 p0039 A72-10671

Reflector antennas with very high front-to-back ratio - Theory and experiments on models. 01 p0029 A72-10673

Lunar laser ranging for orbital and rotational motion, continental drift and pole studies, discussing Lunokhod I roving vehicle mounted laser reflector 01 p0031 A72-11152

Microwave half blinder for sidelobe reduction in large horn reflector antennas in E plane radiation for horizontal polarization 01 p0043 A72-11243

Large reflector and phased array antennas, discussing synthesis and analysis, active impedance and blind spots, matching, beam steering and implementation 02 p0191 A72-11686

Large steerable radio reflectors profile measurement with laser system, describing instrument design, accuracy and modifications 02 p0238 A72-12113

High accuracy laser reflector telemetric measurement for earth-moon distance variation in time by correlation method 04 p0495 A72-15727

Nighttime laser ranging of French reflector for Soviet Lunokhod, discussing universal-ephemeris time difference determination 05 p0721 A72-16771

Spherical reflector antenna phase aberration correction by planar array feeds, discussing synthesis procedure for mean square error minimization 06 p0781 A72-17344

Balun-fed open sleeve dipole in front of metallic reflector for 225-400 MHz band operation, investigating radiation pattern and gain 07 p0957 A72-19794

Tracking efficiency of laser telemetry on reflector carrying satellites 07 p0947 A72-20259

Tracking efficiency calculation for laser telemetry with laser reflector on nonstabilized satellite 07 p0947 A72-20260

Lunar laser reflectors specifications and fabrication procedures, discussing lunar environment simulator and optical test equipment, techniques and results 07 p0947 A72-20261

Optical high precision surfaces correction method for laser based reflectors on vacuum vapor differential deposition 07 p1007 A72-20262

Double passed Michelson interferometer with polarizing beam splitter, quarter wave plates and cube corner reflectors to obtain immunity to mirror misalignment 11 p1635 A72-26500

Laser tracking measurements of distance to light reflector mounted on Lunokhod 1, describing equipment and procedure 12 p1825 A72-27888

Iterative method for synthesis of reflector antenna array of dipole elements to provide given radiation pattern, obtaining impedance matching values 13 p1926 A72-28372

Reflector networks analysis for optimal operation of electronic scanning antenna in illuminated grating 15 p2195 A72-31670

Laser tracking measurements of distance to light reflector mounted on Lunokhod 1, describing equipment and procedure 16 p2404 A72-33997

Nighttime laser ranging of French reflector for Soviet Lunokhod, discussing universal-ephemeris time difference determination 17 p2611 A72-35274

Control of the incore thermionic reactor /ITR/ by movable reflector elements. 18 p2645 A72-36189

Three axis angular deviations measurement by flexure monitor system for spacecraft, using pulsed light sources, autocollimator and porro reflectors [AIAA PAPER 72-855] 20 p2951 A72-39106

Reflector profiles for the pencil-beam Cassegrain antenna. 20 p2903 A72-39221

Two-hybrid mode feed design procedure and performance for small and large f/D ratio reflectors of microwave telescope 21 p3029 A72-40515

Series-dipole antenna design based on Ehrenspeck short backfire antenna mirror method, noting small dimensions and cost reduction 21 p3031 A72-40539

Radiation pattern and gain of reflector antenna with adjusting ring, discussing directivity and bandwidth 21 p3031 A72-40540

Reflector optimization of backfire antennas with the aid of the theory of the Fresnel zones 21 p3031 A72-40541

Multiple beam fixed reflector antenna configuration selection for reliable satellite communication earth stations, considering tradeoffs between gain, transmitter power and receiver noise temperature 21 p3032 A72-40879

Diffraction by an infinite corner reflector transversely loaded by concentric dielectric slabs. 22 p3159 A72-42301

REFLEXES

NT CAROTID SINUS REFLEX

NT RESPIRATORY REFLEXES

Soviet book on physiology of conditioned reflexes covering brain and nervous system, tonic reflexes, functional models, inhibition localization, etc 01 p0011 A72-10295

Human and monkey muscle tonic vibration reflex response to vibratory stimulation dependent on frequency range, electromyograph discharge interval length, etc 02 p0163 A72-12250

Bainbridge reflex mechanism, showing sinus ganglion role in tachycardia onset 02 p0165 A72-12514

Spinal reflexes through electric stimulation of gastrocnemius and soleus human leg muscles, attributing increased tendon reflex amplitudes to gamma motoneurons hyperactivation 04 p0467 A72-14704

Blink reflexes in man during sleep and wakefulness, discussing electromyographically recorded orbicularis

oculi mono- and polysynaptic responses to electrical stimuli 04 p0474 A72-15250

Conditioned reflex as component of artificial conditioned-natural unconditioned reflex system controlling adaptive behavioral patterns, noting contribution to complex nervous activity understanding 04 p0476 A72-15582

Frontal lobe damage effect on conditional motor reflexes, communication capability and emotional behavior in baboon apes 04 p0476 A72-15583

Human arm muscle motor neuron reflex response to rectangular pulse excitation of ulnar nerve 04 p0476 A72-15587

Cat mean renal nerve activity modification by hypothalamus stimulation and baroreceptor reflex interactions, discussing mean aortic pressure variation effects 04 p0477 A72-15722

Visceral afferentation role in vestibular system activity from experiments on rabbit stomach and rectum mechanoreceptor stimulation effects on vestibulo-oculomotor reflexes 05 p0618 A72-16630

Carbon monoxide induced hypoxia inhibition of reflex vasoconstriction in man in presence of normal arterial oxygen tension 07 p0929 A72-19438

Hypothalamic stimulation conditioned negative fear reflex in cats before/after neocortex isolation 07 p0920 A72-19859

Entropy effect in two dimensional conditional reflex decision situations upon rats central nervous analysis-synthesis processes 07 p0925 A72-20661

Central nervous plasticity and stereotypy intercorrelation in conditional reflex two dimensional decision situations 07 p0925 A72-20662

Digital simulation of human cardiovascular system, noting blood pressure control by physiological reflexes 08 p1125 A72-21475

Soviet papers on human higher nervous activity physiology covering conditioned reflexes and adaptive behavior, neurotropic substance effects, mathematical and structural modeling, etc 08 p1118 A72-21834

Neurophysiological mechanisms responsible for conditioned reflexes, considering cells, reaction relationship to animal behavior, neuronal stimuli interactions, internal inhibitions and trace process reproduction 08 p1118 A72-21835

Conditioned reflex mechanisms responsible for regulation of emotions in higher order animal and human neurophysiology 08 p1118 A72-21837

Conditioned reflex activity, discussing biological and nervous system, electric analog simulation and mathematical and structural modeling 08 p1127 A72-21842

Human reactions to sonic boom acoustic stimuli, noting startle reflex responses 09 p1267 A72-23320

Electromyogram and myogram responses in phasic stretch reflex under prestrain conditions as index of fusimotor activity level in normal humans 11 p1588 A72-26632

Cat and rat cardiac and cardiovascular reflexes response to electric pulse stimulation of sensorimotor cerebral cortex 12 p1761 A72-27647

Concentrated and extended learning effects on formation rate and retention degree of conditioned reflex during mice adaptation to high altitude hypoxia 13 p1903 A72-28770

Human spinal segment functional state before voluntary movement during water immersion, using H-reflex for spinal cord motoneuron excitability evaluation 14 p2073 A72-30255

Human leg muscle reflex excitability changes during angular acceleration, suggesting vestibular apparatus as coordination means in quasi-static and dynamic movement control 14 p2075 A72-30388

Unconditioned /muscular load stimulus/ and conditioned /metronome stimulus/ cardiac reflexes in hypnotic and alert states 16 p2353 A72-32991

Water immersion tests to study body fluid balance disturbances during weightlessness, observing diuretic reflex control of blood volume 16 p2355 A72-33551

Interrelation of interoceptors and exteroceptors in the process of urination and defecation reflex act maturation in ontogeny 17 p2504 A72-35022

New experimental data on the morpho-physiological analysis of the adaptation phenomenon in the somatic reflex arch 17 p2504 A72-35023

Vasomotor reflex locking level 17 p2504 A72-35025

Reflex and conditional movement observation of central nervous system function restitution in Macaca mulatta monkeys with cortical lesions, studying pathological forced grasping 18 p2651 A72-36977

Proteinase activity in different regions of the brain during development and inhibition of a conditioned passive-avoidance reflex 20 p2890 A72-38927

Role of efferent influences of temporo-rhinencephalic cerebral structures in pre-adjustment alterations of spinal motor neuron excitability 21 p2999 A72-40596

Vasomotor reflexes and the principle of descending control 21 p2999 A72-40597

Polysynaptic sympatho-reticular and somatic afferent visceral links between internal organs and cerebrum in interoceptive reflex fields 21 p3000 A72-40755

Blood vessel reactions to natural defense and conditioned reflexes from plethysmography and blood pressure measurements, discussing cortical effects mechanisms 21 p3000 A72-40758

Breathing rate response to oral instructions in relationship to nervous system, bronchial muscle tonus and gas metabolism rate reflex-type changes 21 p3001 A72-40761

Higher nervous activity of monkeys two years after the extirpation of the dorsolateral frontal cortex 21 p3001 A72-40803

Role of the reticular formation of the mid-brain in the storage and recreation of a system of conditioned reflexes 21 p3001 A72-40809

Critique of Pavlov conditioned reflex role in higher nervous activity and association principle role in psychic activity 21 p3001 A72-40811

A mathematical model of the chemoreflex control of ventilation. 21 p3008 A72-40917

Effects of physical exercise on spinal reflectivity in man 21 p3003 A72-41524

Electrophysiological analysis of defense reflex and unconditioned reaction and conditioned signal analyzers in nodal mechanisms of functional system /afferent synthesis, decision making, correction, etc/ 21 p3004 A72-41675

Neurophysiological mechanisms of the extinction of the orientating reflex 22 p3142 A72-42280

Sensorimotor mechanism of proprioceptors in muscles and tendons, considering reflexive control of position and motion 22 p3146 A72-42781

Vestibular system functional relationship to postural reflex mechanism involving labyrinth and graviceptors responses 22 p3147 A72-42788

Functional insufficiency of the neuromuscular system caused by weightlessness and hypokinesia. 23 p3253 A72-43387

Development of a defensive conditioned reflex to a light stimulus after previous visual deprivation 23 p3257 A72-44078

Age-induced long-term memory changes in animals 23 p3257 A72-44079

Characteristics of conditioned reflexes to an ecologically adequate stimulus in hens 23 p3257 A72-44080

Electrophysiological analysis of limbic-reticular interaction during the orientating reflex 23 p3257 A72-44081

Influence of the nervous system and its mediators on the spontaneous contractile activity of a smooth muscle 24 p3370 A72-44590

REFRACTED RADIATION

U REFRACTED WAVES

REFRACTED RAYS

U REFRACTED WAVES

REFRACTED WAVES

Normal electromagnetic wave propagation in randomly inhomogeneous medium in presence of superrefraction, deriving phase fluctuation spectra by perturbation method 02 p0180 A72-12587

Acoustic waves refraction, reflection and transmission from moving medium layer with space-dependent velocity, considering Poiseuille flow three sublayer approximation 06 p0848 A72-17852

Refraction of electromagnetic wave with electric field perpendicular to applied magnetic field in anisotropic plasma cylinder cross section 07 p1046 A72-20507

Ray trace of sound refraction by point source on jet flow axis, numerically calculating directivity pattern 08 p1152 A72-21893

Sound refraction by sinusoidal point source in subsonic jet flow, obtaining solution by finite difference method for comparison with ray tracing results 08 p1152 A72-21894

Loading process behind reflected and refracted shock waves in plastic layered media with linear elastic unloading 09 p1353 A72-23555

Venusian atmosphere RF refractive attenuation height dependence, field strength measurements comparison, inversion layer influence and surface echoes effects 10 p1541 A72-24501

Plane acoustic-gravity wave reflection, refraction and amplification at interface separating two fluids in relative motion, noting shear flow speed effect 16 p2383 A72-32968

Ray geometry, travel time and spreading loss derivation for refracted/bottom-reflected ray propagation in channel with horizontal and vertical sound speed gradients 18 p2710 A72-36413

Strong intensity fluctuations of a spherical wave propagating in a randomly refractive medium 18 p2661 A72-36659

Reflection and refraction of elastic waves in edge-impacted rectangular plates. 18 p2737 A72-37065

Propagation of internal acoustic-gravity waves around a spherical earth. 19 p2793 A72-38748

Reflection and refraction of radio waves from the ionosphere in presence of time-varying irregularities. 22 p3154 A72-42302

Exact solution of the equations of molecular optics for refraction and reflection of an electromagnetic wave on a semi-infinite dielectric. 23 p3313 A72-43803

REFRACTING TELESCOPES

Holographic correction of reflecting refracting telescope objective mirror deformation aberrations, noting interferometric attachment 10 p1479 A72-24049

Aplanatic mirror-lens telescope systems with spherical optics, discussing isochromatic corrective lens specifications 14 p2104 A72-30497

Mars observations in 1965, 1967 and 1969 by 150 mm and 400 mm refracting telescopes noting surface map and drawings 15 p2305 A72-31397

Aplanatic mirror-lens telescope systems with spherical optics, discussing isochromatic corrective lens specifications 19 p2803 A72-38326

Jupiter surface maps from synoptic observations with refracting telescope, considering white cloud formations and atmosphere motions 22 p3220 A72-41921

REFRACTION

NT ATMOSPHERIC REFRACTION

NT BIREFRINGENCE

NT RADIO WAVE REFRACTION

Lateral refraction dependence on earth rotation and correction formula for angle measurement errors in class I triangulation 09 p1299 A72-22946

Anomalous refraction maxima in bidirectional plane polarized radiant flux transmittances of roughened dielectric surfaces 11 p1742 A72-25236

Acoustic refraction and attenuation in cylindrical and annular ducts. 17 p2582 A72-35414

Human observation error effect on astronomical refraction calculation from time determination of solar limbs passages across optical instrument reticle 24 p3438 A72-44863

REFRACTIVE INDEX

U REFRACTIVITY

REFRACTIVITY

Narrow-band type 4 bursts behavior comparison with synchrotron radiation in media with refractive index less/equal unity, determining magnetic field and electron energy 01 p0118 A72-10415

Atmospheric radio refractive index computation errors derived from monthly averages of pressure, dry bulb temperature and vapor pressure 01 p0095 A72-10835

Atmospheric refractive index structure parameter variation with height and measurement near ground [AD-739059] 02 p0253 A72-12546

Lorentz polarization effects on complex refractive index and wave polarization of magnetoionic theory 04 p0548 A72-14944

WKB type solution for electromagnetic wave propagation in circularly cylindrical coordinate system with rho-dependent refractivity, using Bessel function 04 p0488 A72-15384

Short waves damping or increasing in bounded thick waveguide with real or complex refraction index 04 p0492 A72-15446

Human skin thermal radiation properties, presenting data on reflection, emission, transmission and complex refraction
[ASME PAPER 71-WA/HT-37] 05 p0620 A72-15888

Refraction theory applied to isotropic absorbing media, noting spatial distribution of incoherent components according to polarization states
05 p0689 A72-16173

Holographic measurements of dioptric powers and glass defects in thin transparent sheet under vertical or oblique parallel and divergent light
05 p0662 A72-16190

Ray statistics of electromagnetic wave scattering in homogeneous isotropic turbulent medium with ellipsoidal inhomogeneities of refractive index, using Fokker-Planck equation
05 p0626 A72-16243

Dispersion relation for electrostatic plasma waves propagation at frequencies near electron cyclotron harmonics in warm magnetoplasma, determining refractive index curves
05 p0698 A72-17023

Refractive index structural constant relationship to atmosphere mean meteorological parameters, observing phase difference fluctuations of radio propagation in atmospheric surface layer
06 p0778 A72-18750

Atmospheric lee waves three dimensional structures through high sensitivity Doppler radar measurements based on backscatter from refractive index inhomogeneities
07 p1029 A72-19100

Aging effect on visual acuity variations relation to refraction variations in flight deck personnel, noting eye functional value diminution
07 p0927 A72-19244

Electrostatically driven oscillations near lower hybrid resonance frequency in linear plasma device, measuring refractivity during wave propagation
07 p1043 A72-19664

Thin films thickness and refraction index calculation from curves of specularly reflected X ray intensity vs grazing angle, obtaining surface roughness variance
07 p1050 A72-20405

Ceramic laser materials failure due to optically induced damage, estimating stresses and changes in refractive indices under thermal effects
09 p1336 A72-22403

Refractivity measurement of pure hexagonal structure 2H SiC over visible range, determining birefringence from curve fitting of data to Cauchy dispersion equation
09 p1309 A72-22603

Power integral method for electric and magnetic dipole antennas vlf/elf radiation patterns in cold magnetoplasma, emphasizing focusing effects of refractive index surface
09 p1279 A72-23009

Elevation angle and range error correction equations for satellite tracking data processing with assumed spherical tropospheric refractivity
09 p1281 A72-23510

Atmospheric refractive index inhomogeneity statistics from interferometer measurements of distance-dependent phase fluctuations in near-ground horizontal optical propagation paths under turbulence conditions
09 p1354 A72-23696

Monte Carlo random walk methods for directional emittance of one dimensional absorbing-scattering slab with reflecting boundaries, considering refractive index, optical thickness and albedo
[ALAA PAPER 72-309] 11 p1743 A72-25243

IR refractivity measurement for atmospheric aerosol substances and sea salts
[AD-744397] 11 p1620 A72-25306

Ternary chalcopyrite semiconductors refractivity measurement over range of wavelengths and optical nonlinear coefficient for second harmonic generation from carbon dioxide laser
11 p1701 A72-26148

Lithium niobate crystal refractive index inhomogeneity influence on second harmonic generation from He-Ne laser
11 p1650 A72-26360

Discharge current effect on refractive index in carbon dioxide laser
11 p1650 A72-26361

Critical values for two surface optical systems of refracting imaginary case modules in coupling and lens design
11 p1691 A72-26746

Power transfer in optical fiber with nonuniform refractivity in mode propagation direction, using coupled mode theory
12 p1779 A72-27164

Temperature gradient and thermoelastic stresses in Nd-YAG laser active elements under continuous pumping conditions, noting refractivity radial distribution
12 p1822 A72-27614

Correction to nonlinear refractivity calculation for cubic lattice crystal with allowance for higher induced multipoles
12 p1855 A72-27620

Optical Kerr constant measurement in liquid phosphoryl chloride and toluene and glasses, noting nonlinear refractivity
12 p1823 A72-27756

Martian ionosphere electromagnetic wave propagation characteristics for E, F1 and F2 models, calculating refractive index for zero and nonzero collision frequencies
13 p1922 A72-29474

Refraction theory applied to isotropic absorbing media, noting spatial distribution of incoherent components according to polarization states
14 p2130 A72-30242

Random variations in interferometer complex visibility function magnitude and phase, refractive index and source angular size
14 p2156 A72-30561

Light rays total, astronomical and photogrammetric refraction in planetary atmospheres with arbitrary composition
15 p2224 A72-31602

Turbulence and nonlinear thermal blooming effects as cause of refractive attenuation of laser beam intensities
15 p2249 A72-32160

High energy storage laser material Nd-doped silicate oxyapatite refractivity temperature dependence characteristics measurement
15 p2249 A72-32167

Transverse electric discharge pulsed carbon dioxide laser, measuring refractivity time history by interferometry for comparison with prediction
15 p2251 A72-32537

Microwaves interaction with ultrashort laser pulse generated traveling refractive index changes in liquids with orientational Kerr effect
15 p2252 A72-32652

Electromagnetic single scattering near critical point in inhomogeneous optical medium with variable refractivity, discussing reflected light effect and Poynting vector reduction to Bragg conditions
15 p2279 A72-32693

Laser irradiation induced refractive index change in evaporated chalcogenide glass films of As-S-Ge system
16 p2401 A72-33395

Holographic virtual image formation and magnification by classical geometrical optics laws application, deriving equivalent law of refraction
16 p2392 A72-33599

Extraordinary wave instabilities in collision dominated plasma taking into account finite wave number, noting dispersion equation for refractive index larger than unity
16 p2436 A72-33653

Lithium niobate crystal refractive index inhomogeneity influence on second harmonic generation from He-Ne laser
16 p2403 A72-33713

Refractive index in carbon dioxide laser effect on discharge current
16 p2403 A72-33714

Propagation mode and scattering loss of a two-dimensional dielectric waveguide with gradual distribution of refractive index.
17 p2530 A72-35469

Complex index of refraction of airborne fly ash determined by laser radar and collection of particles at 13 km.
18 p2661 A72-36637

Quantitative schlieren techniques applied to high current arc investigations.
19 p2797 A72-37588

Measurement of three-dimensional refractive-index fields by holographic interferometry.
19 p2798 A72-37621

Indirect measurement of the atmospheric refraction index with the aid of radiosonde data
19 p2789 A72-37744

Atmospheric turbulence induced optical effects due to refractive index fluctuations, solving Maxwell equations for instantaneous intensity distribution function
20 p2948 A72-39055

Influence of the refractive index nonlinearity on the dynamics of emission from semiconductor lasers.
20 p2932 A72-39504

Balloon measurements of tropospheric turbulence vertical profiles, obtaining temperature and refractive index structure coefficients
21 p3077 A72-40144

Scattering from inhomogeneous cylindrically symmetric lenses with a line infinity in the index of refraction.
21 p3050 A72-40148

Temperature effects on water refractive index from normal incidence IR spectral reflectance measurements
21 p3012 A72-40150

Chemical composition, refractivity and temperature dependence of blackness levels of aluminum oxide-chromium oxide-phosphorus oxide ceramic coatings flame sprayed on steel
21 p3072 A72-40384

Transparent film thickness, refractivity and birefringence measurements by white light interferometric gage, noting performance insensitivity to chemical composition, film temperature and haze level
21 p3053 A72-40601

The use of high refractive index glasses of low dispersion for the correction of medium and high ametropia.
21 p3084 A72-40731

Scattering of a spherical wave at a spherical discontinuity with an arbitrary radial distribution of the refractive index
21 p3016 A72-40793

Ionospheric refractivity and attenuation surface deformation relationship to ion cyclotron whistlers near cross-over level between zero and critical coupling angles
22 p3168 A72-42006

Measurement of the electron density distribution in plasmas from the bending of a gas laser beam.
22 p3211 A72-42396

Determination of the refractive index of air by a dispersion method based on the use of radio waves
22 p3155 A72-42722

Determination of the refractive index by the X-ray interferometry method
23 p3287 A72-43414

Interstellar circular polarization.
23 p3336 A72-43556

Motion thresholds for fovea and peripheral retina with/without correction for peripheral refractive error
23 p3260 A72-43978

Quartz and feldspar glasses produced by natural and experimental shock.
23 p3285 A72-44136

Influence of a linear inhomogeneity of the refractive index of nonlinear crystals on second-harmonic generation.
24 p3411 A72-45604

Measurement of the angular divergence and of the refraction of a laser beam in the ground layer of the atmosphere.
24 p3380 A72-45611

REFRACTOMETERS

Refractometer design based on air dielectric constant dependence on humidity, comparing performance with Ly-alpha humidityometer
06 p0841 A72-17668

Fast response solid state phase lock refractometer for airborne measurement of atmospheric refractive index
19 p2802 A72-38225

REFRACTORY MATERIALS

NT CHROMIUM

NT IRIIDIUM

NT MOLYBDENUM

NT MOLYBDENUM ALLOYS

NT NIOBIUM

NT NIOBIUM ALLOYS

NT REFRACTORY METAL ALLOYS

NT REFRACTORY METALS

NT RHENIUM

NT RHENIUM ALLOYS

NT TANTALUM

NT TANTALUM ALLOYS

NT TUNGSTEN

NT TUNGSTEN ALLOYS

Refractory material development for space shuttle hydrogen tank reusable internal gas layer insulation
01 p0139 A72-10777

Ni base superalloy powder with refractory oxide particle dispersion, presenting high temperature creep, stress rupture, microstructure activation energy and processing history
02 p0240 A72-11442

Refractory materials strength testing equipment and techniques at high temperatures, covering creep, hardness, fatigue, ultrasonic, energy dissipation and loading tests
02 p0291 A72-11636

Refractory titanium oxide deposition by hot front method of chemical reaction in vapor phase
02 p0170 A72-12166

Refractory metal oxides hot microhardness and thermal stability over wide temperature range, noting softening rate variation with temperature
02 p0244 A72-12350

Materials stability testing in high temperature propane-butane combustion product flow, selecting compact silicon carbide for structural use in redox medium
02 p0251 A72-12866

German monograph on refractory materials elasticity modulus determination at elevated temperatures, describing device based on characteristic vibrations frequency relation to temperature
04 p0510 A72-15698

Rare earth tungstate refractory ceramics, determining mechanical properties, crystalline structure and electrical/chemical parameters

05 p0675 A72-16700

Refractory materials fabrication characteristics for aerospace technology, presenting listing of synergic agents for use with inhibitors

05 p0681 A72-16774

Refractory metallic and nonmetallic materials thermal conductivity above 1500 K, noting unreliable white oxides lattice conductivity results

06 p0828 A72-17612

Heat resistant reinforced plastics from glass and pyrolytic carbon fibers by silicoorganic polymer treatment

06 p0835 A72-17735

Fatigue life and creep tests of refractory materials under programmed thermal cycling for different stress levels

06 p0831 A72-18351

Niobium carbide thermodynamic properties tabulated for 0-3000 K, deriving equation for heat capacity from low temperature experiments

06 p0832 A72-18430

Soviet book on superduty refractory porous ceramics covering preparation, structure and properties as thermal insulators, high temperature filters and catalyst carriers

06 p0836 A72-18520

Thermoelastic characteristics and crystal phase distribution effect on microstructural stresses and thermal expansion of polycrystalline refractory materials

07 p1018 A72-20133

High temperature black body model based on induction heating of graphite crucible, noting application to stellar energy spectral distribution determination

07 p0991 A72-20404

Plasma spraying of high temperature resistant powder materials, investigating feed rate effect on particles adhesion and deposition layer properties

08 p1175 A72-21046

Compression creep mechanisms in ceramic materials at elevated temperatures by lattice dislocations, grain boundary sliding and stress directed diffusion

09 p1334 A72-22393

Photomicrography of sintered refractory alloys and nonmetallics of B-Si-C-N system, discussing microstructural interactions between binder metal and refractory component

10 p1493 A72-23824

Spectroscopic techniques for high temperature materials research program, studying light emission from plasmas generated by intense electron beam

10 p1518 A72-23937

High temperature sintering induced dislocations in refractory materials, studying material and diffusion transport processes

10 p1496 A72-24244

Papers on high temperature oxides covering refractory glasses, glass-ceramics, mullite, oxide spinels, glass networks theory and physical chemistry principles application

10 p1501 A72-24726

Refractory glass formulation principles, compositions and properties, discussing vitreous silica production

10 p1501 A72-24727

Refractory glass-ceramics forming systems characteristics and production, discussing crystallization factors

10 p1501 A72-24728

Mullite as part of aluminum oxide-silicon dioxide system, discussing formation, structure, physical chemistry, additives effects and high alumina refractories

10 p1501 A72-24729

Zinc oxide as refractory material, discussing optical, elastic and electro- and photoconductivity properties

10 p1501 A72-24732

Fusion cast zirconia-alumina-silica refractories manufacturing process, phase diagrams, chemical and physical properties and industrial applications

10 p1502 A72-24734

Space shuttle heat shield metallic refractory, superalloy and composite materials joining, discussing vacuum furnace brazing of Al/B matrix structures [AIAA PAPER 72-387]

11 p1638 A72-25408

Recrystallized silicon carbide and reaction bonded silicon nitride as construction materials for gas turbine engine components, describing thermal and mechanical properties

[ASME PAPER 72-GT-20]

11 p1673 A72-25619

High temperature metal fiber reinforced ceramic matrix composites for turbine vanes, showing strength toughness and crack depths dependence on interfacial bond

[ASME PAPER 72-GT-51]

11 p1704 A72-25643

Superalloys and refractory materials high temperature protective coatings, noting lack of uniformity in testing methods

11 p1674 A72-26286

Dislocation slip motions as densification kinetics mechanism in refractory materials sintering process,

discussing electron microscopic observations of partially sintered MgO and W compacts

11 p1643 A72-26834

NASA program to develop heat resistant materials for aerospace applications, discussing refractory carbides, nitrides and borides temperature dependent behavior and properties

11 p1664 A72-26857

High temperature materials powder metallurgy for space applications, discussing melting points

11 p1665 A72-26866

Electronic structure of technological processes in powder metallurgy of high temperature materials

11 p1646 A72-26872

Stress rupture strength, short term strength, creep and heat resistance measurement arrangement for coated refractory materials at 1500-1700 C in air with radiative heating

12 p1796 A72-28248

Structural design characteristics of low density fiber ceramic materials coated with refractory ceramics for space shuttle reusable surface insulation thermal protection systems

[AIAA PAPER 72-372]

13 p2056 A72-28957

Design and operation of experimental facility for thermal fatigue testing of heat resistant materials

13 p1939 A72-29145

High melting point transition metals carbides, nitrides, borides, silicides and oxides thermal conductivity as function of characteristic temperature

13 p1981 A72-29905

High refractory gadolinium oxide-strontium oxide system phase diagram and transition temperature by X ray and differential thermal analyses

13 p1984 A72-30109

Refractory compounds single crystals preparation, emphasizing hot pressing under high pressures

13 p1982 A72-30113

Dispersion hardening of Nb, Cr, Mo and W by inserting dispersed particles of refractory compounds into metal matrix

14 p2112 A72-30152

Refractory fiber metal reinforcement and matrix incorporation, considering SiC fiber reinforced Al

14 p2107 A72-30532

Vacuum vaporization of niobium, tantalum, zirconium and hafnium carbide phases, using Langmuir method

15 p2253 A72-31200

Microstructural damage effect on high temperature materials creep life, considering Robinson and Odqvist correlation laws

16 p2474 A72-34127

Physical property measurements at high temperatures.

17 p2554 A72-34934

Refractory materials fabrication characteristics for aerospace technology, presenting listing of synergic agents for use with halogenous inhibitors

17 p2571 A72-35277

Some data on interatomic interaction in solid high-melting compounds of titanium, vanadium, and chromium with light metals

17 p2569 A72-35520

Book - Chemical properties and analysis of refractory compounds

18 p2655 A72-36094

Oxidation resistance at high temperatures of refractory materials based on silicon nitride and carbide in various concentrations, showing time and temperature dependence

18 p2703 A72-36096

Investigation of the properties of electrode materials made on the basis of high-melting-point compounds and alloys

18 p2698 A72-36136

NASA research on refractory carbides, nitrides and borides, discussing electronic and defect structures, hot extrusion, uranium nitride, cermets for bearings and composite evaluation

18 p2701 A72-36594

Refractory materials cyclic elastoplastic tests under shear with holding creep, showing relationship between creep rate and recurrent static deformation

19 p2876 A72-38007

Prospects for the development of technically usable fiber-reinforced high-temperature materials

20 p2940 A72-39448

Arc furnace for thermal analysis of ultrarefractory materials

21 p3039 A72-40208

Interaction of nonmetallic refractory compounds with transition metals and ferroalloys

21 p3066 A72-40394

Processing of carbon/carbon composites - An overview.

21 p3072 A72-40552

A study on the correlation between thermal fatigue and low-cycle fatigue at elevated temperatures.

21 p3119 A72-41008

Self-propagating high-temperature synthesis of refractory inorganic compounds

22 p3188 A72-42165

Production and properties of materials of the Si3N4-Cr2O3 system

23 p3298 A72-43283

Growth rate of refractory oxide particles in nickel cermets

23 p3299 A72-43290

Investigation of the influence of the gas medium on the phase composition and certain properties of refractory materials containing zirconium

23 p3306 A72-43690

Refractory materials heat resistance criteria, taking into account hollow cylinder thermal stress distribution

23 p3306 A72-43738

Elastic stiffness and ductility of refractory materials of long service life, noting creep diagrams and tensile strength

23 p3301 A72-43959

Test equipment for heat resistance determination of brittle refractory material, noting data processing procedure and formulas for temperature distribution and thermal stress

23 p3278 A72-43962

Contribution to the study of some HfO2-MO systems

23 p3302 A72-43999

Contribution to the study of phenomena of ordering of defects in single crystals of alumina- or zirconia-base refractory materials

23 p3302 A72-44000

Some strength characteristics of graphite/zirconium carbide composites

23 p3307 A72-44013

Fatigue life and creep tests of refractory materials under programmed thermal cycling for different stress levels

24 p3416 A72-45738

Thermoelastic characteristics and crystal phase distribution effect on microstructural stresses and thermal expansion of polycrystalline refractory materials

24 p3416 A72-45759

REFRACTORY METAL ALLOYS

NT MOLYBDENUM ALLOYS

NT NIOBIUM ALLOYS

NT RHENIUM ALLOYS

NT TANTALUM ALLOYS

NT TUNGSTEN ALLOYS

Space shuttle mechanical fastener design, discussing drives, threads, manufacturing and refractory alloys

01 p0075 A72-10751

Refractory alloy weldability and brazing, discussing manual and automatic tungsten arc and electron beam processes and fillers

01 p0075 A72-10752

Multiple reentry effects on space shuttle thermal protective superalloys mechanical properties, presenting cyclic simulation results for different temperatures, pressures and stresses

01 p0084 A72-10754

Mo- and Ta-base refractory alloys creep tests, determining interactions between creep strength, fatigue life and strain aging by fatigue vibration application

05 p0677 A72-17111

Phase diagram of Ta-B system by thermal, X ray and microstructural analyses

06 p0833 A72-18434

Refractory and structural steels and Al alloys, obtaining low cyclic plastic deformation and breaking stress curves

06 p0898 A72-18549

Transition metals distribution of IV-VI and VIII a groups in metastable refractory nickel alloys gamma and gamma-prime phases

07 p1012 A72-19678

Refractory alloys softening under stress relaxation conditions at high temperatures, noting plastic strain hardening effect absence

07 p1018 A72-20138

Ni based superrefractory alloy high temperature fatigue tests, studying creep as function of stress load and frequency and temperature

07 p1022 A72-20487

Photomicrography of sintered refractory alloys and nonmetallics of B-Si-C-N system, discussing microstructural interactions between binder metal and refractory component

10 p1493 A72-23824

NDT of diffusion formed coatings on refractory alloys and superalloys, stressing eddy current technique

11 p1641 A72-26287

Force distribution in refractory Ti alloy cutting with circular self turning blades, noting effects of feeding speed, cut area and cutter angle

13 p1966 A72-29467

Unsteady loading effects in high temperature fatigue tests of refractory alloys for turbine blades, noting steady and programmed notch tests

13 p1980 A72-29494

Deep diffused layer sintering of metal-ceramic cutting alloys with variable Co content for increased wear resistance and tensile strength

13 p1982 A72-30112

Refractory material blade alloys fatigue life up to 950 C under nonstationary loading, noting log-normal law distribution

14 p2116 A72-30428

Superplasticity in two phase compositions based on refractory metal alloys, noting creep rate dependence on concentration and electroconductivity

16 p2405 A72-33094

Fabrication of refractory metals.

17 p2559 A72-34187

Work functions of some emitting and collecting refractory metal single crystals.

17 p2595 A72-34601

High-temperature resistant cobalt alloys

17 p2567 A72-35173

An electron microscopy study of carbide precipitation in vanadium.

18 p2699 A72-36577

Inhomogeneity of high melting temperature elements in titanium alloys.

18 p2701 A72-36693

Russian book - Physical chemistry of rare metals.

22 p3190 A72-42802

Physical metallurgy of single crystals of high-melting and rare metals and alloys

22 p3191 A72-42807

Microstructural aspects of the fracture of two-phase alloys.

23 p3299 A72-43510

Influence of the sintering medium on the quality of metallic ceramic hard alloys containing zirconium and hafnium carbides

23 p3303 A72-44017

Refractory alloys softening under stress relaxation conditions at high temperatures, noting plastic strain hardening effect absence

24 p3416 A72-45763

REFRACTORY METALS

NT CHROMIUM
NT IRIIDIUM
NT MOLYBDENUM
NT NIOBIUM
NT RHENIUM
NT TANTALUM
NT TUNGSTEN

Equation of state for porous metals at high temperatures under strong shock compression, considering phase transitions

02 p0258 A72-11469

Refractory metal thermocouple research program, describing design and performance of ultrahigh vacuum high temperature furnace system

04 p0524 A72-15550

Refractory metal multilevel interconnection systems, comparing materials fabrication, yield and circuit performance with diffused Si planar runs and polycrystalline Si films

05 p0636 A72-16362

Book on refractory metals creep rupture behavior to high temperatures covering test procedures and data analysis for W, Re, Ta, Mo and Nb and alloys

06 p0828 A72-17725

Hot pressing of sintered refractory metal oxide powders of Ti, Zr, U, Nb and Cr, showing improved compacting by raising temperature

06 p0822 A72-18427

Plastic deformation and elastic stiffness of refractory metals, discussing impurities, alloying, temperature, work hardening, strain rate and texture effects

06 p0822 A72-18519

Heat resistant metals long time creep prediction at low stresses or temperatures

06 p0834 A72-18668

Surface and interfacial energies measurement by multiphase equilibrium method for refractory metal monocarbides with liquid cobalt

07 p1010 A72-19136

Metals and alloys for aerospace applications, emphasizing creep and fatigue properties and oxidation resistance at high temperatures

08 p1185 A72-21171

Cold shortness of W and related refractory metals, noting oxide phases and impurities effects on mechanical properties temperature dependence

09 p1326 A72-22226

Photoemission electron microscopy application to refractory metals and nonmetallic materials, discussing image formation and contrast enhancement problems

10 p1493 A72-23823

Refractory powder metallurgy Conference, Reutte, Austria, June 1971, Volumes 1, 2, 3 and 4

11 p1642 A72-26826

Refractory metal powders spherical agglomerates growth and strength in rotating tumbler, noting particle size dependence on binder

11 p1643 A72-26829

Nitrogen solubility, degassing kinetics and diffusion coefficients for Mo-N, W-N and Re-N systems for 1300-3050 C

11 p1663 A72-26841

Metal silicide phase formation for Nb, Ta, Mo and W, examining Si diffusion and transport processes

11 p1664 A72-26859

Sliding dry friction of hard refractory metals and ceramics, discussing surface changes as function of load, sliding speed, temperature and mechanical properties

12 p1817 A72-28184

Friction characteristics of high melting point metal chalcogenides as function of load and temperature, noting friction coefficient variations

12 p1817 A72-28185

High temperature strength of low ductile refractory metals, describing test equipment

13 p1978 A72-29446

Plastic properties of locally heated refractory metals in hot pressing calculated from temperature distribution

13 p1966 A72-29465

Sintering and melting preparation effects on mechanical properties of refractory W-Re alloys, considering sigma phase in solid alpha solution

14 p2116 A72-30530

Refractory metals vacuum melting for ingot production and purification in arc and electron bombardment furnaces

14 p2107 A72-30531

High temperature forging apparatus for refractory metals under vacuum or inert atmosphere

15 p2241 A72-32443

Oxygen chemisorption effect on rare gas beams reflection from refractory metals polycrystalline surfaces, interpreting experimental results by simple correlation model

16 p2431 A72-33068

Liquid metals thermodynamic properties tabulation, including high melting transition metals, based on levitation data and periodic table correlations

16 p2479 A72-34000

Radiation damage to refractory metals as related to thermionic applications.

17 p2566 A72-34595

Compatibility of brazed joints with potassium and vacuum.

17 p2567 A72-34938

Vapor deposition of refractory metals applied to thermionic conversion - Performance of deposits obtained by reduction of fluorides at high temperature and low pressure

18 p2656 A72-36138

Thermodynamics and phase relations in refractory metal solid solutions containing carbon, nitrogen, and oxygen.

18 p2699 A72-36576

Equilibria and degassing kinetics in the systems Mo-N, W-N, and Re-N

18 p2701 A72-36596

High temperature and vacuum solar furnace processing of refractory metals in space or on moon

19 p2857 A72-37675

Extension Seminar on High Temperature Strength of Metals, Kyoto, Japan, August 21, 1971, Preprints.

21 p3068 A72-41007

Book - Metal matrix composites.

21 p3070 A72-41528

Gas adsorption by refractory metal single crystals.

22 p3187 A72-41940

Contact interaction between high-melting compounds and liquid metals. I - Interaction between subgroup IVA metals and metals of the iron family

23 p3299 A72-43287

Precise alignment and uniform distribution of fibres in a metal matrix.

24 p3413 A72-44898

Physicomechanical properties of titanium-tungsten solid alloys with deficiency of carbon in the carbide solid solution lattice

24 p3415 A72-45385

REFRASIL [TRADEMARK]

U FIBERS

U SILICON DIOXIDE

REFRIGERATING

Living organisms defense and preservation via refrigeration and vacuum combined use in lyophilization technique

12 p1769 A72-27293

Three dimensional photothermoelastic method of refrigeration with composite model to study transient thermal stresses in wing rib

14 p2168 A72-30907

Cryopump cooling requirements, refrigeration, design and vacuum application, considering Brayton, Claude, Stirling cycles and Joule-Thomson and regenerative processes

18 p2696 A72-36838

Book - Advances in cryogenic engineering, Volume 17

19 p2883 A72-38826

REFRIGERATING MACHINERY

NT REFRIGERATORS

REFRIGERATORS

Miniature refrigerators design for electronic devices, noting application to IR detectors cooling

03 p0313 A72-14366

Mathematical analysis of Vuilleumier refrigerator, calculating internal pressures, temperatures and gas flow rates via computer program

[ASME PAPER 71-WA/HT-33] 05 p0745 A72-15886

Mechanical seal for airborne Stirling cycle cryogenic refrigerator, noting He cross leaks and sealing faces galling and blistering

[ASLE PREPRINT 72AM 16] 13 p1964 A72-28973

REFUELING

NT AIR TO AIR REFUELING

Static electricity in fueling of supertanks.

21 p3040 A72-41375

REGENERATION [ENGINEERING]

Regenerative system reliability, examining oscillation mode selector

03 p0333 A72-13833

Closed loop life support systems, discussing manned ninety day test in space station simulator, Soviet experiments and water and oxygen regeneration

10 p1432 A72-24973

Skylab regenerative carbon dioxide removal system.

[ASME PAPER 72-ENAV-4] 20 p2896 A72-39173

A regenerative high multiplicity tunnel-diode frequency multiplier

21 p3034 A72-41122

The Space Station Prototype Program - The development of a regenerative life support system for extended-duration missions.

24 p3375 A72-45193

REGENERATION [PHYSIOLOGY]

Radiobiological effects of nonuniform body irradiation, discussing regeneration process stimulation by partially shielded bone marrow

[CERN-71-16] 02 p0161 A72-12060

Pulsed and continuous rf irradiation effects on mitotic activity and chromosomal aberrations in regenerating rat liver tissue

07 p0917 A72-19443

Supercellular regulators of triggering mechanism of regenerative reaction in sternum erythropoietic bone marrow tissue

13 p1901 A72-28636

Vagus nerve regeneration in humans after stomach cancer surgery

13 p1903 A72-28779

REGENERATIVE COOLING

Aerospike rocket engine system for orbit-to-orbit space shuttle, discussing light-weight regeneratively cooled thrust chamber performance tests

[SAE PAPER 710770] 01 p0116 A72-10264

Compressibility effects on straight through labyrinth seal performance in regenerative turbomachine

08 p1178 A72-21935

Heat transfer ratios in multifluid regenerative systems

20 p2984 A72-39650

REGENERATIVE CYCLES

U REGENERATION [ENGINEERING]

REGENERATIVE FEEDBACK

U POSITIVE FEEDBACK

REGENERATORS

NT THERMOSIPHONS

Gas turbine recuperator technology, discussing use of compact efficient heat transfer surfaces developed for aerospace heat exchangers

[ASME PAPER 72-GT-32] 11 p1703 A72-25628

Liquid metal regenerator design and test evaluation for gas turbine engine fuel consumption improvement

[ASME PAPER 72-GT-33] 11 p1704 A72-25629

Analysis of real-gas and matrix-conduction effects in cyclic cryogenic regenerators.

[ASME PAPER 72-HT-27] 20 p2986 A72-39672

REGGE POLES

Duality concept in elementary particle physics, discussing pion-nucleon scattering, amplitude exchange degeneracy, Regge poles and Veneziano models

05 p0692 A72-17077

Regge calculus representation existence for solutions of initial value problem for spaces with axial symmetry

16 p2422 A72-32879

REGIONAL PLANNING

NT URBAN PLANNING

REGIONS

NT ANTARCTIC REGIONS

NT ARCTIC REGIONS

NT AURORAL ZONES

NT D REGION

NT E REGION

NT F REGION

NT FRESNEL REGION

NT LUMBAR REGION

NT NULL ZONES

NT POLAR REGIONS

NT TEMPERATE REGIONS

NT TROPICAL REGIONS

REGISTERS [COMPUTERS]

NT SHIFT REGISTERS

Registers and digital circuits with FETs and integrated operational amplifiers to permit analog measurements storage for display on CRT oscilloscope

15 p2204 A72-32499

Effects of finite register length in digital filtering and the fast Fourier transform.

20 p2904 A72-39780

REGRESSION [STATISTICS]

U REGRESSION ANALYSIS

REGRESSION ANALYSIS

Kennedy Space Center thunderstorm forecasting system, discussing data processing with conditional and exposure period probabilities and nonlinear predictors multiple regression equations

01 p0094 A72-10826

Field and test data analysis with time share computer, using Weibull probability plotting, hazard rates and least squares regression

02 p0185 A72-11555

Stratospheric water vapor concentration annual variability from regression analysis of monthly measurements initiated as IQSY program

03 p0385 A72-14148

Foundry Al alloys elasticity limit estimation via regression formulas, discussing application to quality control

04 p0534 A72-15560

Stochastic approximation algorithm with nonstationary regression function for signal parameter estimation, considering convergence, mean square error bound and applications

07 p1027 A72-19291

Stochastic optimization of airborne laser seeker system design parameters to maximize target acquisition probability through regression analysis of data from computerized model

10 p1437 A72-24682

Parameter identification method for mathematical extremal control model of complex structure for static plants based on regression analysis

10 p1458 A72-25192

Statistical multiple regression equations for identification of artificial graphite properties effect on ablation performance

11 p1669 A72-25233

Kennedy Space Center area afternoon convective thunderstorm activity and associated weather phenomena prediction via multivariate regression analysis

13 p1989 A72-28803

Regression technique for determining temperature profiles in upper stratosphere from satellite measured radiances, noting accuracy

13 p1990 A72-28822

Satellite radiance data to determine stratospheric layer thickness, comparing empirical regression equations to mean weighted temperatures

13 p1991 A72-28824

Overestimation in optimization problems calculated by regressive equation, comparing with actual effect in static process

13 p1936 A72-29158

Linear statistical forecasting with noncorrelated predictors by multiple regression equations, showing degradation dependence on sampled cross covariances

13 p1995 A72-29591

Nonlinear regression method for nonlinear least squares problem compared to other solution techniques, discussing convergence theorems and computational results

15 p2262 A72-31632

Weibull distribution parameters estimation for general device class from limited failure data through regression models, using least squares method

16 p2398 A72-33349

Stepwise multiple regression techniques for Nimbus 3 IR interferometer-spectrometer /IRIS/ data inversion, obtaining radiation predictors of meteorological parameters

16 p2418 A72-33666

Welded Al joints fatigue resistance from iterative nonlinear regression analysis with multiparameter endurance curves

16 p2412 A72-34141

Regression analysis for steady state N2 inequality in O2 consumption calculations.

17 p2507 A72-34542

An operations research approach to solve complex and unstructured problems illustrated for the case of cost-plus-award fee contracts.

17 p2639 A72-35341

Certain properties of continuous stochastic approximation procedures

19 p2824 A72-37325

A biased filter for linear discrete dynamic systems.

19 p2781 A72-38273

Regression-line studies of E-region seasonal anomaly.

19 p2794 A72-38863

Regression technique for determining temperature profiles in the upper stratosphere from satellite-measured radiances.

21 p3052 A72-40249

Local and regional weather forecasting based on multilinear regression technique

21 p3078 A72-40765

A gradient method of expanding a group data handling method to new plants not studied by experiments

22 p3162 A72-42242

Stochastic and deterministic relationships between random variables, noting correlation coefficient as measure of regression lines representation accuracy

22 p3178 A72-42449

Fundamentals of multivariate analysis - Linear regression.

23 p3310 A72-44394

REGULATION
U CONTROL
REGULATIONS

German Federal Republic territorial air traffic regulations covering general, VFR and IFR rules, equipment and personnel examination and certification, safety, takeoff and landing, accidents, etc

02 p0305 A72-12621

Legal problems of aircraft hijacking, discussing jurisdiction, duty to prosecute, penalties, extradition, sanctions and international criminal tribunal

05 p0752 A72-15833

Federal Air Regulations procedures for civil transport aircraft flight testing under natural and/or simulated icing conditions

06 p0760 A72-18501

Federal regulation of airline mergers from viewpoint of history and current evaluating procedures in U.S.

07 p1106 A72-20675

Book on world airlines economic regulation, analyzing multilateral international agreements, national aviation interests and competitive situation

11 p1748 A72-25923

Charter air traffic regulations under German air law, discussing legal safeguards relative to economic, personnel, technical and organizational aspects

11 p1748 A72-26559

Book on air transportation, covering history, government agencies roles in economic and safety regulation of air carriers, accounting, financial and legal aspects, etc

12 p1891 A72-28205

Building soundproofing codes for airport zoning ordinances, emphasizing wider latitude in land use options

13 p2067 A72-29561

U.S.S.R. civil aviation regulations on takeoff and landing minimum conditions for cloud ceilings and visibility range for various aircraft characteristics and equipment

14 p2129 A72-30820

U.S. federal regulation on occupational noise exposure control for hearing loss prevention, discussing noise measurement, reduction and periodic tests

16 p2358 A72-33324

Government regulations effects on local service airlines cost performance and growth strategies

16 p2481 A72-33374

Planning of a broadcast-satellite service.

21 p3016 A72-40771

Public policy, regulatory controls, market strategies and systems economics considerations for future U.S. domestic communication satellite system

21 p3132 A72-40865

REGULATORS

NT AUTOMATIC FREQUENCY CONTROL

NT CURRENT REGULATORS

NT FLOW REGULATORS

NT FREQUENCY CONTROL

NT GIBBERELLINS

NT OXYGEN REGULATORS

NT PRESSURE REGULATORS

NT SPEED REGULATORS

NT THERMOSTATS

NT VOLTAGE REGULATORS

Distributed parameter state regulator system, investigating order of spatial discretization error in finite difference approximation to optimal response, control and performance cost

[AD-738401] 05 p0639 A72-15805

Minimax solution of linear regulator problem, presenting algorithm for numerical computation

05 p0682 A72-16451

External disturbance accommodation in optimal control, based on characterization of waveform modes, applying to linear-quadratic regulator problem

07 p0963 A72-20591

Optimal regulator inverse problem analysis for multiinput systems with integral type performance indices, using state variable canonical form

17 p2534 A72-35527

Regulator vector selection algorithm for largest estimate of exponential absolute control stability region based on Popov frequency condition reformulation

23 p3276 A72-43853

Analytical designing of regulators for second-order nonlinear systems

24 p3387 A72-45519

REHEATING

U HEATING

REIGNITION

U IGNITION

REINFORCED MATERIALS

U COMPOSITE MATERIALS

REINFORCED PLASTICS

High temperature strength degradation of graphite and boron reinforced epoxy composites after room temperature aging

01 p0090 A72-10728

Polyimide prepolymer formulation for glass and graphite reinforced composites autoclave processing via increased melt phase duration and temperature range

01 p0090 A72-10729

Thermal and environmental exposure effects on high temperature mechanical properties of graphite/polyimide composites

01 p0090 A72-10730

Boron-epoxy tubular struts for one third scale space shuttle booster thrust truss structure, discussing design, analysis, fabrication, weight, test and quality control

01 p0138 A72-10735

Hat section stiffened compression panel of graphite/epoxy composite for space shuttle, discussing quality control procedures

01 p0139 A72-10736

Aluminum stiffening structural sections selectively reinforced with boron/epoxy composite materials, discussing mechanical properties, cost effectiveness and stress distribution

01 p0139 A72-10737

Buckling of boron/aluminum and graphite/resin fiber composite anisotropic plates, giving load vs fiber orientation angle for various plate aspect ratios

01 p0139 A72-10739

Fiber reinforced plastic composite seals for liquid hydrogen and nuclear radiation environments, stressing polyquinoxaline fitness

01 p0075 A72-10773

Lightning protective coatings for boron/epoxy composite materials, discussing high current damage mechanisms, simulation facility and test results on aluminum foils, meshes, etc

01 p0092 A72-10783

Graphite filament reinforced plastics strength, performance properties, fabrication processes and tooling concepts

[SME PAPER EM 71-205] 01 p0076 A72-10968

Unidirectional glass/graphite fiber-epoxy resin composite, discussing fabrication and performance tests for mechanical properties

[SME PAPER EM 71-192] 01 p0092 A72-10971

Torsional stiffness /shear modulus/ of glass fiber reinforced plastic tubes as function of filament winding angle

01 p0141 A72-10999

Minimum weight web-core sandwich panels under axial compression loads, presenting numerical results for boron-epoxy and graphite-epoxy composites

01 p0142 A72-11131

Winding fiber reinforced plastics, investigating fiber curvature effects on elastic constants and tensile strength optimization

02 p0248 A72-11626

Acoustic emission monitoring of boron epoxy composite, showing crack extension characterization by emission bursts

02 p0249 A72-11993

Nonlinear creep of glass fabric-plastic composite under loading in uniaxial stressed state

02 p0250 A72-12676

Temperature effects on strength and deformability of randomly reinforced fiberglass polyamides

02 p0250 A72-12678

Mechanical breakdown prediction of loaded fiberglass reinforced plastic by seismoacoustic technique, investigating load effects on seismoacoustic emission

02 p0250 A72-12679

Reinforcing fibers length effect on cross breaking strength and rupture area size at surface for silicoorganic glass reinforced plastic

02 p0250 A72-12681

Fiberglass reinforced plastics heat conductivity as function of porosity, reinforcement factor and density

02 p0250 A72-12686

Glass fabric reinforced composite materials stress distribution under longitudinal loading, using finite element method with two dimensional model

03 p0381 A72-13720

Price/demand/cost economic aspects of carbon fiber reinforced plastics composites in aero-engine applications

04 p0536 A72-14743

Carbon fiber resin composite characteristics for airframe component design, comparing with metal materials

04 p0537 A72-14746

Sliding friction and wear behavior of carbon fiber reinforced composites with thermosetting resins, thermoplastic polymers and metal base materials

04 p0537 A72-14747

Carbon fiber reinforced thermoplastics tested for gears and bearings applications, including wear, static, dynamic, surface tension, stereoscan and microscopy effects

04 p0537 A72-14748

Glass fiber reinforced plastic composites design, strain limitation and creep fatigue properties for large structures

04 p0537 A72-14749

Glass variables effect on polypropylene, polystyrene and Nylon-6 glass filled thermoplastic

composites mechanical properties, discussing silane coupling agents and injection moulding machine conditions 04 p0537 A72-15085

Asbestos fiber reinforced plastics composites fabrication techniques, discussing possible applications 04 p0537 A72-15086

Carbon fiber-resin laminates ballistic impact resistance, discussing damage and interlaminar shear strength 04 p0537 A72-15089

Heat resistant reinforced plastics from glass and pyrolytic carbon fibers by silicoorganic polymer treatment 06 p0835 A72-17735

Soviet book on nonmetallic material strength during nonuniform heating covering, load endurance, bending phenomena and thermal stability of fiberglass, pyroceramics and reinforced plastics 06 p0796 A72-18521

Fiberglass reinforced plastics under constant strain rate, deriving failure models as random process for microscopic crack propagation 06 p0898 A72-18548

Deformability and strength of soft fiber reinforced plastics under biaxial tension, determining low temperature critical tensile stresses and elongation ratios 06 p0836 A72-18562

High temperature testing assembly for reinforced plastics and binders in oxidizing and inert media under tension, compression, bending and cleavage loads 06 p0797 A72-18569

Composite propeller blades with carbon fiber reinforced plastics spar for hovercraft, presenting mechanical properties test data for different composite configurations 07 p0912 A72-19062

Stress-strain state in tension of orthogonally stiffened fiberglass-reinforced plastic with cracks in transversely stiffened layers 07 p1094 A72-20128

Elastic properties of bonded orthotropic layer plates, finding good agreement with fiberglass reinforced plastic laminates 07 p1097 A72-20596

Stress concentration and elastohereditary values at curvilinear hole in fiberglass reinforced plastic plate under bending moment 08 p1243 A72-21237

Rheological model of reticular polymers and glass fiber reinforced plastics based on stress-strain relationship during damped creep elastic deformation 08 p1191 A72-21499

Glass fiber reinforced plastics irreversible cumulative damage under axial cyclic tension compression loads with heat production 08 p1191 A72-21500

Anisotropy effect on glass fiber reinforced plastics cyclic deformability and heating kinetics under cyclic tension compression loads 08 p1191 A72-21501

Plastics optimal reinforcement in given stressed state by determining shortest path from stress point to strength region 08 p1244 A72-21502

Elastic filler rigidity effect on cylindrical glass fiber reinforced plastic shells stability loss and critical load value under axial compression 08 p1245 A72-21503

Friction and bending effect on unidirectional glass fiber reinforced plastic ring deformation distribution 08 p1191 A72-21504

Prestressed glass reinforced composites mechanical behavior, taking into account manufacture induced residual stress concentrations 08 p1192 A72-21674

Chlorendic acid based Hetron 92C fire retardant chemical resistant polyester for fiberglass reinforced structure applications 08 p1192 A72-21677

Furan resins and chemically resistant furan-fiberglass composites flame resistance, heat distortion and physical properties at high temperatures 08 p1192 A72-21678

Glass fiber reinforced plastic composites fracture characteristics, considering fiber content, fiber-matrix bond strength, yarn geometry, orientation and ply stacking sequence effects 08 p1192 A72-21679

Thermal and mechanical properties of randomly reinforced fiber/resin composites including boron/epoxy, Thorne/epoxy and S glass/epoxy materials 08 p1192 A72-21682

Inorganic single crystal titanate whisker fibers with high modulus strength for plastic reinforcement, noting mechanical, thermal and physical properties 08 p1193 A72-21685

Carbon/epoxy composite reinforced plastic materials feasibility for application to aircraft landing gear wheel fabrication 08 p1193 A72-21686

Composite filament wound boron-epoxy rocket motor combustion chamber design, fabrication and hydrostatic tests 08 p1177 A72-21692

Low cost 300 gallon fiber reinforced plastic aircraft wing fuel tank manufacturing technology 08 p1177 A72-21693

Adverse environmental effects on epoxy composites resin-glass interface properties, investigating epoxy-compatible silanes contribution to composite performance 08 p1194 A72-21696

Oriented glass fiber reinforced plastics fatigue strength and creep under interlayer shear and compression 08 p1194 A72-21752

Glass fiber reinforced polymer composite model for tensile stress distribution in matrix and fibers and at bond interface 08 p1194 A72-21753

Residual temperature stresses and deformations during thermal treatment of thick walled glass fiber reinforced plastic wound cylinders and rings 08 p1194 A72-21755

Torsion test determination of interlayer and intralayer-plane shear moduli in annular specimens of glass fiber reinforced plastics 08 p1194 A72-21756

Deformability and carrying capacity of glass fiber-polymer composite thick walled rings under internal or external pressure 08 p1195 A72-21764

Climatic load effects on carrying capacity of thick walled glass reinforced polymer rings with residual stresses 08 p1195 A72-21765

Nondestructive determination of glass reinforced plastics normal elastic and shear moduli and strength characteristics by vibrational, pulsed and acoustic methods 08 p1195 A72-21773

Additional vibrational loading effect on thin tubular glass fabric reinforced plastic samples creep under shear in reinforcement plane at 20-50 C 08 p1195 A72-21854

Fiberglass reinforced plastics creep characteristics under high strain rate loading-unloading conditions 08 p1195 A72-21855

Fiberglass reinforced plastics fatigue failure prediction based on test demonstrated correlation between static and cyclic strainability 08 p1195 A72-21856

Boron and carbon fiber reinforced plastics anisotropic stress-strain properties, considering fiber misalignments curvature and low shear resistance effects 08 p1196 A72-21857

Material properties nonuniformities effect on wound fiber glass reinforced plastic rings and cylinders thermoelastic residual stresses 08 p1196 A72-21858

Radial and axial residual stress components in glass fiber reinforced polyethylene, comparing with adhesion strength obtained by shear method 08 p1196 A72-21862

Extremal mechanical properties directions in orthotropic glass fiber reinforced plastics symmetry planes 08 p1196 A72-21866

Creep characteristics of unidirectional plastics reinforced by hollow glass fibers with insignificant capillary effect 08 p1196 A72-21868

Carbon fiber reinforced epoxy resin composites, testing fracture behavior in flexural and shear modes under static, fatigue and creep loading 09 p1334 A72-22389

Deposition of Ni-B coatings with specified electrical resistance onto fiberglass cloth reinforced plastics 09 p1318 A72-22528

Creep test for microfailures of glass reinforced epoxy and polyester laminates immersed in water at ultimate flexural stress 09 p1336 A72-22537

Photoelastic measurement of stress concentration in three dimensional fiber reinforced brittle plastic matrix under uniaxial tension 09 p1398 A72-22538

[PI PAPER 1] Fatigue failure mechanism in short fiber reinforced plastics, determining crack growth rates under cyclic loading 09 p1336 A72-22539

[PI PAPER 2] Fiber orientation effects on physical properties of carbon fiber-epoxy resin composites 09 p1337 A72-22540

[PI PAPER 3] Fiber thermoplastics matrix breakdown and mechanical properties enhancement, examining lateral and longitudinal strain during uniaxial tensile creep and recovery 09 p1337 A72-22541

[PI PAPER 4] Unidirectional and orthogonally cross-ply carbon fiber reinforced plastics laminates, determining interlaminar shear strength and fatigue life 09 p1337 A72-22543

REINFORCED PLASTICS

Carbon fiber reinforced epoxy resin composites fracture toughness dependence on fiber strength, diameter, volume fraction, modulus, fiber/matrix interface strength and temperature 09 p1337 A72-22544

[PI PAPER 9] Pultrusion process for carbon fiber reinforced plastic, compared with wet lay up technique, noting mechanical properties 09 p1318 A72-22545

[PI PAPER 10] Temperature induced stresses and displacements in fiberglass reinforced plastic cylindrical shell 09 p1399 A72-22704

Short fiber reinforced thermoset composite materials for engineering construction, tabulating flexural properties and Charpy impact strengths 09 p1338 A72-23165

Tensile microstrain and cyclic loading behavior of carbon fiber reinforced plastic composites at elevated temperature 09 p1338 A72-23169

Carbon fiber reinforced plastic toughness from strain concentration and plastic flow observation near crack tip by moire technique 09 p1339 A72-23170

Hugoniot equation of state for impact shock wave propagation along fiber direction in Al epoxy matrix composites 09 p1407 A72-23235

Gruneisen tensor relationship to elastic and thermal properties of anisotropic quartz fiber-phenolic composite 10 p1500 A72-24251

Tensile strength of notched carbon and glass fiber reinforced epoxy resin composites as function of crack size 10 p1500 A72-24253

Stress wave surfaces in graphite fiber-epoxy matrix anisotropic plates under transverse impact forces, using Mindlin approximation theory 10 p1555 A72-24255

Fatigue crack propagation in epoxy resin matrix reinforced with discontinuous metal fibers 10 p1501 A72-24261

S glass/epoxy composites strength retention properties under long duration tensile load, proposing use of stress rupture data for reliable safe structural design 10 p1501 A72-24263

Photoelastic analysis of piezooptical and rheological properties of anisotropic composite glass plastics 10 p1557 A72-24626

Glass content and temperature effects on fabric reinforced plastic laminates static behavior, analyzing tensile and bending strength and elastic moduli 10 p1501 A72-24660

Two dimensionally reinforced quartz-phenolic composite material dynamic fracture behavior under stress wave loading in uniaxial strain, noting spallation threshold time dependence 11 p1669 A72-25291

Carbon-phenolic composite ablation and expansion in thermal environment during reentry shielding, using flight and simulation tests 11 p1669 A72-25390

[AIAA PAPER 72-363] Fiber reinforced plastics thermophysical properties, thermal conductivity and heat capacity, determining effects of reinforcement fiber type, resin amount and type 11 p1669 A72-25391

[AIAA PAPER 72-366] Colaminated boron-polyimide film effect on strength of graphite fiber-epoxy resin composite double lap bolted joints 11 p1730 A72-25405

[AIAA PAPER 72-382] Linear elastic fracture mechanics extension to fiber reinforced plastic composite laminates, noting dependence on homogeneous model validity 11 p1730 A72-25406

[AIAA PAPER 72-384] Boron-epoxy reinforced composite metal shear web design for space shuttle orbiter main engine thrust beam structure 11 p1726 A72-25416

[AIAA PAPER 72-395] Composite F-111 fuselage design, analysis and testing, considering graphite, boron and glass-epoxy and boron-aluminum systems 11 p1575 A72-25453

Boron-epoxy composite design for aircraft structures, discussing materials variations, strength prediction inadequacies and full scale tests 11 p1670 A72-25454

Tubular specimens for testing mechanical properties of fiber reinforced composites under axial loading, discussing design, fabrication and end attachment problems 11 p1670 A72-25456

Thermal expansion measurements on graphite reinforced plastics, using Leitz dilatometer 11 p1670 A72-25460

Two stress level cumulative fatigue damage prediction for glass fiber-epoxy laminates 11 p1670 A72-25462

Stress analysis of short beam bending of graphite fiber reinforced epoxy composites 11 p1671 A72-25464

Interlaminar shear properties of polymer matrix composites from dual element beam moment test 11 p1671 A72-25465

Failure modes effect on compressive strength of boron-epoxy composites tested on coupons, honeycomb sandwich columns and beams 11 p1671 A72-25466

Embedded strain gage technique for subsurface tensile testing of boron-epoxy composites 11 p1671 A72-25467

Vacuum mold preparation and flexural testing of miniature carbon fiber reinforced composite specimens 11 p1671 A72-25468

Acoustic emission analysis of deformation and fracture modes under straining of fiber glass-epoxy composite structures, including NOL rings and vessels 11 p1671 A72-25469

Charpy impact strength data for unidirectional graphite, boron and glass-resin composites tested in fiber direction, noting tensile stress-strain characteristics importance 11 p1672 A72-25471

Bolted connections strength in graphite fiber-epoxy resin composites reinforced by colaminated boron film 11 p1672 A72-25476

Vibration characteristics of unidirectional filamentary boron-epoxy composite panels, obtaining nodal patterns, natural frequencies and damping coefficients 11 p1732 A72-25477

Fiberglass-graphite reinforcement of unidirectional epoxy laminates, examining longitudinal composite fracture stress and strain and tensile and compressive stiffness 11 p1672 A72-25485

Asbestos reinforced plastics safe handling and manipulation ensured by regulations provided precautions 11 p1583 A72-25549

Fracture surface energy and acoustic emission of boron fiber-epoxy resin composite, using linear elastic fracture mechanics and compliance variation methods 11 p1674 A72-25858

Multilevel structural analysis for multilayered fiber-epoxy and metal matrix composites, using FORTRAN IV 11 p1601 A72-26033

Organic matrices in structural composites, considering mechanical behavior, processability and properties in adverse environments 11 p1674 A72-26230

Laminated reinforced plastics structural design criteria obtained by statistical and deterministic approach 11 p1737 A72-26235

Glass textolites and high strength oriented plastics fracture mechanism in tension and bending, noting equalizing effect through proper cohesion characteristics between layers 11 p1674 A72-26804

Test device for reinforced plastics mechanical properties under heating and pressure with allowance for gas permeability 11 p1613 A72-26813

Water damage in glass fiber-polyester resin composites, discussing fiber debonding, crack propagation and water resistance 11 p1675 A72-26950

Thin cylindrical shells prepared from fiberglass reinforced plastics under long term compression, investigating strain buildup nature during creep process 12 p1878 A72-27078

Prager-Shield theory for optimal plastic design extended to multicomponent cost functions and load conditions, applying to fiber reinforced plate 12 p1881 A72-27243

Rapid laser heating induced stress generation in carbon fiber-poly(methyl methacrylate) composite 12 p1833 A72-27286

Dynamic properties of thermosetting plastic composites unidirectionally reinforced by high elastic moduli boron and carbon fiber for aircraft structural applications 12 p1882 A72-27343

Fiberglass reinforced thermoplastics and thermosets for corrosive environments, noting composites performance increase by constituents change 12 p1833 A72-27404

Glass fiber reinforced thermoplastic resins chemical and hydrolytic resistance, noting composites and polymers long term performance prediction in aggressive environments 12 p1833 A72-27405

Plywrap process for low cost automated fabrication of fiber reinforced plastic composites, noting applications from missile interstages to modular housing 12 p1815 A72-28081

Continuous woven fabric or roving filament reinforced thermoplastics production, discussing polymer binder systems, coupling agents, impregnation technique, processing parameters and equipment 12 p1815 A72-28083

Graphite fiber-epoxy composite systems development for F-5 aircraft landing gear door, speed brake, leading and trailing edge flaps and horizontal stabilizer 12 p1835 A72-28097

Composite materials mechanical and thermal properties for ATS reflector supporting truss, noting gra-

phite fiber reinforced epoxy plastic design, fabrication and tests 12 p1886 A72-28158

Two dimensional reinforced plastic material anisotropic creep derivation from orthotropic plate time functions and stress tensor invariants 13 p2034 A72-28437

Boron and carbon reinforced fiberglass plastics tensile strength characteristics, presenting static fatigue curves vs Poisson coefficient and elastic modulus for various fiber contents 13 p1982 A72-28552

Boron and carbon fiber reinforced plastics applications in aircraft and engine structural components, discussing dynamic and impact damping properties compared to conventional materials 13 p1982 A72-28555

Stress-strain concentrations near circular holes in fiberglass reinforced plastic plates under various types of load as function of hole diameter/plate width ratio, anisotropy and load 13 p1983 A72-28560

Fatigue strength and cumulative damage in fiberglass-epoxy composite specimens under unsteady elastic bending loads, determining loading spectrum effect on service life 13 p1983 A72-28562

Tensile strength of fiber glass reinforced plastic elements joined by cover plates and nonlinearly elastic adhesives 13 p1962 A72-28737

Glass and carbon fiber reinforced plastic beam specimens dynamic moduli and loss factors determination from vibration frequency and decay rate measurements 13 p1984 A72-29095

Fiberglass reinforced plastic fuselage production for AN-2m aircraft, noting plastic-plastic and metal-plastic joints 13 p1897 A72-29462

Fiber glass reinforced plastic structure design based on anisotropy, calculating optimum angle between reinforcement and horizontal axis 13 p2058 A72-29463

Bolkow 105C 5-place helicopter with twin turbine engine driven rigid glass-reinforced plastic rotor blades, emphasizing design philosophy of easy maintainability 13 p1898 A72-29871

Lightning current tests of aircraft glass/carbon fiber reinforced plastics materials 13 p1898 A72-30040

High strength carbon fiber reinforced plastics, discussing fabrication techniques, fiber structural, physical and mechanical properties and potential technological applications 13 p1984 A72-30075

Compacting kinetics of fiber reinforced sandwich composites during hot pressing controlled by plastic matrix sliding velocity 13 p1967 A72-30103

Carbon fiber reinforced plastics nondestructive testing by ultrasonic compressional and shear wave resonance 14 p2107 A72-30856

Boundary layer temperature profile for ablating asbestos-plastic composite samples measured under combined convection and radiant heat fluxes 14 p2172 A72-31003

Ribbon glass effect on thermal expansion of reinforced thermoplastic composites, comparing with fiber reinforced materials 15 p2259 A72-31255

One dimensional wave pulse propagation, attenuation and dispersion in uniaxially reinforced steel-epoxy resin composites 15 p2325 A72-31528

Friction and wear properties of carbon fiber reinforced polymers sliding against metals in pure and sea water and aqueous solutions 16 p2396 A72-33123

Carbon fibers reinforced polymer wear rate decrease in organic fluids associated with films development on steel counterface, noting application in lubricated systems 16 p2397 A72-33124

Fracture toughness measurements of polyester composites reinforced with chopped steel wires compared with Cooper theory 16 p2413 A72-33203

Porosity effect on mechanical properties, airtightness, corrosion resistance and moisture absorption of glass fiber reinforced plastics 16 p2414 A72-33270

Reinforced plastics - Conference, Karlovy Vary, Czechoslovakia, May 1972 16 p2414 A72-33301

Resin selection for manufacture of chemically resistant glass fiber reinforced polyesters, considering structural factors of chain for susceptibility to alkaline hydrolysis 16 p2414 A72-33304

Nondestructive vibration tests of fatigue crack damage in composite structures, investigating glass reinforced epoxy and polyester laminates 16 p2414 A72-33318

Cyclic compressive fatigue cracking tests of prenotched fiber reinforced epoxy materials at low stress 16 p2414 A72-33319

Compressive strength and stiffness improvement for crystalline thermoplastic polymers via solid glass sphere reinforcement 16 p2414 A72-33370

Reinforced thermoplastics - Conference, El Segundo, California, March 1972 16 p2415 A72-33414

Design criteria for fiber reinforced thermoplastic resins performance optimization, discussing temperature, humidity and chemicals effects 16 p2415 A72-33417

Foam content effect on fiberglass reinforced thermoplastic foam tensile and impact strength, thermal distortion and mold shrinkage properties 16 p2415 A72-33418

Glass reinforced thermoplastic resins flammability resistance, discussing test methods and flame retardant additives 16 p2415 A72-33419

Flame retardant glass reinforced thermoplastic polyester Celanex processing and performance, considering flammability, and electrical/mechanical properties 16 p2415 A72-33420

Stress-strain diagrams for orthotropic glass fiber reinforced plastic plates with circular hole under uniaxial tensile load 16 p2471 A72-33681

The fracture energy of a glass fiber composite. 17 p2570 A72-34670

Transition metal-modified matrix resins for composite materials. 17 p2570 A72-34672

Tailoring the interface in graphite-reinforced polycarbonate. 17 p2570 A72-34713

Failure mechanism for carbon fibers in epoxy novolac matrices under tensile loads 17 p2633 A72-35286

Static and tension fatigue and free edge delamination damage induced by uniaxial tensile loads in flat graphite/epoxy laminate coupons 17 p2571 A72-35291

Fracture mechanics of a fiber composite. 17 p2633 A72-35293

Composites technology, costs and performance review covering metal matrix composites, ceramic reinforced plastics and whisker composites 17 p2571 A72-35652

Data generation for engineering design with advanced composites. 17 p2571 A72-35653

Boron- and graphite-epoxy and boron-aluminum composites forming, processing and costs for aircraft structural materials 17 p2560 A72-35663

Coupled glass-fibre/polypropylene composite - An initial evaluation. 18 p2703 A72-36269

Nonlinear physical dependence of reticular polymers and glass fiber reinforced plastics under conditions of diminishing creep 19 p2822 A72-37527

Rheological characteristics of orthotropically reinforced polymer materials 19 p2822 A72-37531

Synthesis of optimal cylindrical reinforced-plastic shells under external pressure and axial compression 19 p2872 A72-37534

Behavior of glass fiber reinforced plastic cylindrical shells under the action of external pressure pulses 19 p2872 A72-37538

Dynamic stability of axisymmetrically heated glass fiber reinforced cylindrical plastic shells which are coupled with elastic cylinders 19 p2872 A72-37539

Temperature-time superposition applied to the relaxation properties of a glass fiber reinforced plastic and its binder 19 p2822 A72-37543

Yielding of fiber reinforced Tresca material. 19 p2873 A72-37695

Properties of internally lubricated glass-fortified thermoplastics for gears and bearings. 19 p2822 A72-37896

Model filament wound epoxy composites. 19 p2808 A72-38164

Stress analysis of shell junctions fabricated by the filament-winding method. 19 p2877 A72-38169

Machining boron-epoxy composites. 19 p2809 A72-38386

Static and dynamic fatigue behavior of glass filament-wound pressure vessels at ambient and cryogenic temperatures. 19 p2823 A72-38832

The study on dynamical behavior of fiberglass reinforced plastics (FRP) by dynamical mechanical model. 20 p2943 A72-38887

On the cumulative fatigue damage of glass fiber reinforced plastics subjected to repeated tensile impact load. 20 p2943 A72-38888

Fiberglass reinforced plastics tensile test specimens aspect ratio effect on tensile properties, considering deformation of orthotropic rectangular plate with uniform forced displacement 20 p2943 A72-38889

Statistical failure characteristics and probability evaluation of the static strength of structural components made of composite polymer materials 20 p2943 A72-38942

Prediction of deformability and fracture processes for polymer materials 20 p2943 A72-38943

Device for fatigue testing of fiberglass-reinforced plastic samples in a symmetrical tension-compression regime at acoustic oscillation frequencies 20 p2920 A72-38944

Influence of technological factors upon the mechanical reliability of composite-material structures 20 p2943 A72-38945

Features of deformation and stress distribution in a laminated plastic 20 p2944 A72-38948

Reinforced metals - Mechanical property considerations. 20 p2936 A72-39210

The fiber and filament reinforcement of plastic and brittle matrix materials 20 p2944 A72-39438

Longitudinal tensile failure of unidirectional fibrous composites. 20 p2944 A72-39789

Fatigue behavior of glass filament-wound epoxy composites in water. 21 p3072 A72-40246

On the stress-strain curve of polyethylene filled with randomly oriented glass fibers. 21 p3073 A72-40721

Dynamic inelastic properties of materials. I - Damping characteristics of fiber composites. II - Representation of time dependent characteristics of metals. [ICAS PAPER 72-28] 21 p3069 A72-41153

Non-destructive examination of fibre reinforced polymers with special reference to continuous carbon fibre reinforcement. [ICAS PAPER 72-44] 21 p3073 A72-41169

Random function theory method for estimation of tensile, compressive and shear strength and elastic constants of monodirectional fiberglass reinforced plastics 21 p3073 A72-41708

Thermal expansion coefficients of some fiberglass-reinforced plastics and their components under conditions of low and high temperatures 21 p3074 A72-41715

Fiber glass reinforced plastics elastoplastic behavior due to microcrack propagating across matrix, using elastic index of work done 22 p3232 A72-41943

The accumulation of damage in a glass-reinforced plastic under tensile and fatigue loading. 22 p3196 A72-42456

German monograph - Contribution to the reinforcement of plastics with special allowance for the reinforcement and matrix materials. 22 p3197 A72-43078

Mechanical tests of laminated plastics in solar installations 22 p3197 A72-43192

PRD-49, a new composite material - Its characteristics and its application to the BO-105 helicopter. [SAWE PAPER 915] 23 p3305 A72-43462

Mechanics of failure of fibrous composites. 23 p3345 A72-43508

Fracture mechanics of composites. 23 p3345 A72-43509

Work of fracture of fibre-reinforced polymers. 23 p3306 A72-43561

The use of a torsion machine to measure the shear strength and modulus of unidirectional carbon fibre reinforced plastic composites. 23 p3306 A72-43562

Book - A review of the science of fibre reinforced plastics. 24 p3417 A72-44674

The fracture toughness of fibre composites. 24 p3417 A72-44899

Utilization of advanced composite materials for spacecraft and space shuttle applications. 24 p3417 A72-45153

Fiber and filament reinforcement of plastic and brittle matrix materials 24 p3414 A72-45276

Stress-strain state in tension of orthogonally stiffened fiberglass-reinforced plastic with cracks in transversely stiffened layers 24 p3460 A72-45754

REINFORCED PLATES

Stress-strain characteristics of stochastically reinforced materials of high rigidity orthotropic elastic layers alternating with isotropic elastic or viscoelastic layers 02 p0248 A72-11623

Variable cross section elastic stringer end loaded longitudinal force transmission to stiffened elastic plate 03 p0444 A72-13465

Stress concentration at circular, elliptical, square, rectangular and triangular holes in isotropic plates stiffened by discontinuous elements under uniaxial tension 03 p0452 A72-14133

Optimum variable thickness reinforcement around circular hole in flat elastic sheet under radial tension 04 p0583 A72-14463

Single fiber reinforced plate initial stress distribution due to linear expansion coefficients difference between matrix and fiber, using optical polarization 06 p0836 A72-18557

Buckling under uniaxial compressive load of structural sections and stiffened flat plates reinforced with laminated composites 07 p1090 A72-19732

Rational parameters and reinforcement of stiffened laminar plates with instability tendencies under compression loads 08 p1243 A72-21236

Plane wave propagation in laminated reinforced elastic plates with difference-differential equations analysis 08 p1247 A72-21809

Stiffened panels initial buckling under longitudinal compression, presenting results obtained by numerical methods 10 p1558 A72-24843

Heterogeneous shear deformation effect on dynamic response of laminated plates for various local elastic deformation and interface conditions 11 p1731 A72-25419

Prager-Shield theory for optimal plastic design extended to multicomponent cost functions and load conditions, applying to fiber reinforced plate 12 p1881 A72-27243

Stress analysis of boron fiber-reinforced and isotropic Al panels under identical loading conditions 15 p2323 A72-31479

Contact problems for elastic semiplane reinforced with symmetric and asymmetric loaded elastic stiffeners 15 p2329 A72-32281

Buckling behavior of simply supported elastic folded plate structures without and with transverse stiffeners under symmetrical and asymmetrical uniform vertical loads 15 p2332 A72-32562

Elastic buckling of simply supported sandwich panels with fiber reinforced laminated face plates and honeycomb cores subjected to uniform end loading 16 p2469 A72-33405

Stress-strain diagrams for orthotropic glass fiber reinforced plastic plates with circular hole under uniaxial tensile load 16 p2471 A72-33681

Optimal design of static laterally loaded fiber reinforced plates, determining optimum load-path directions at all plate points 16 p2475 A72-34174

Real-time vibration analysis of rib-stiffened plates by holographic interferometry. 18 p2690 A72-36361

Contact interactions of smooth rigid punch impressing into thin laminar anisotropic reinforced plastic plate 19 p2872 A72-37541

Plane strain bending of laminated fibre-reinforced plates. 20 p2982 A72-40021

Russian book - Plates strengthened by composite rings and elastic cover pieces. 21 p3116 A72-40385

Fatigue strength of overloaded stiffeners in cracked panels, evaluating stress intensity factor and overload coefficients for fatigue crack propagation via finite element method 21 p3120 A72-41165

Mechanical properties of titanium strengthened by monodirectional molybdenum wires 21 p3069 A72-41354

Fibers-matrix force interaction effects in metal composites, analyzing stress-strain state of reinforced plate 23 p3306 A72-43728

Stability of orthotropic stiffened composite plates. 23 p3352 A72-44109

A sandwich plate with a part-through and a debonding crack. 24 p3456 A72-44813

Variable cross section elastic stringer end loaded longitudinal force transmission to stiffened elastic plate 24 p3458 A72-44940

REINFORCED SHELLS

Natural vibrations of closed crosswise reinforced orthotropic circular cylindrical shells, using digital computer solution 01 p0142 A72-11363

Computer program for thermal stress and buckling analysis of nonuniformly heated segmented ring-stiffened cylindrical and conical shells 02 p0293 A72-12252

Stress analysis of pressurized ribbed cylindrical shell with intersecting reinforced circular hole under internal pressure 02 p0294 A72-12470

[ASME PAPER 71-PVP-8] Highly elastic cylindrical layer reinforced with anisotropic shell, deriving stress-strain state and nonlinear elastic stability 02 p0299 A72-12687

Computer program for buckling loads of shallow stiffened eccentrically orthotropic sandwich shells [DGLR PAPER 71-109] 02 p0299 A72-12703

Fluid filled fiber reinforced spherical shells extensional vibrations, evaluating equivalent elastic orthotropic compliance constants, natural frequencies and mode shapes 03 p0443 A72-13403

Axisymmetric load influence on stability of eccentrically reinforced shells of revolution, determining critical loads and linear and nonlinear relations for moment-subcritical states 04 p0587 A72-15014

Soft uniaxial crosswise reinforced shell stability under internal pressure, determining equilibrium state 04 p0587 A72-15015

Thermoviscoelastic stress analysis for hollow circular cylinder with reinforcing interlayer under pressure, axial tension and nonstationary temperature field 04 p0587 A72-15016

Stress-strain state of thin ellipsoidal shell with central stiffened hole, using small elastoplastic deformation theory 04 p0588 A72-15050

Composite multilayer fibrous shell structural design optimization, using nonlinear mathematical programming methods [ASME PAPER 71-WA/DE-12] 05 p0733 A72-15943

Small deflection theory for dynamic elastic buckling of stringer-stiffened cylindrical shells under axial impact, discussing optimum stiffener geometry 05 p0742 A72-17248

Photoelastic analysis of cylindrical shells of revolution with one hemispheric closed end and reinforcing flanges at opposite end rim, examining boundary conditions effects 06 p0899 A72-18640

Rib reinforced cylindrical shells deformation under local load, examining stress-strain distribution 06 p0899 A72-18641

Dynamic behavior of stiffened hollow viscoelastic cylinder and elastic shell-contained sphere, taking into account compressibility and internal pressure 07 p1090 A72-19751

Automated minimum weight design of ring and stringer stiffened conical shells, using membrane theory for prebuckling analysis 08 p1245 A72-21599

Elasticity theory method for nonlinear stress-strain relationships in thin anisotropic shells, discussing fiberglass reinforced cylindrical shell 08 p1247 A72-21810

Elastic shell geometry and rigidity effects on critical load in pure bending within structurally orthotropic theory, taking into account reinforcing rib eccentricity 08 p1247 A72-21816

Additional vibrational loading effect on thin tubular glass fabric reinforced plastic samples creep under shear in reinforcement plane at 20-50 C 08 p1195 A72-21854

Asymmetrically stiffened elastic cylindrical shells under axial compression, calculating critical loads for various end conditions 11 p1733 A72-25541

Pressure loaded shallow spherical shells with reinforced circular holes, noting stress concentration increase due to reinforcement bead eccentricity 11 p1734 A72-25736

Vibration of free and fluid loaded uniform or rib reinforced cylindrical shells, solving equations of motion for natural frequencies 12 p1882 A72-27341

Nonlinear stability and vibrations of shallow shells eccentrically stiffened by oblique angled ribs under critical loads 12 p1885 A72-27971

Nonuniform heating effect on stability of eccentrically stiffened smooth cylindrical shells under combined loading 12 p1885 A72-27973

Rib reinforced cylindrical shell supercritical post-buckling strains, allowing for geometrical surface deflection 12 p1885 A72-27976

Carrying capacity of rigidly hinged shell of revolution with concentric reinforcing rib, applying to shallow spherical shell under uniform external pressure 14 p2166 A72-30687

- Response of a ring-reinforced cylindrical shell, immersed in a fluid medium, to an axisymmetric step pulse.
[ASME PAPER 72-APM-8] 17 p2624 A72-34314
- Buckling and vibration analysis for stiffened orthotropic shells of revolution.
17 p2632 A72-35242
- Buckling of shells with cutouts - Experiment and analysis.
17 p2634 A72-35405
- Three dimensional photoelastic analysis of edge loaded ring reinforced rotating shells with zero bending, assuming pure membrane stress field.
18 p2733 A72-36365
- Synthesis of optimal cylindrical reinforced-plastic shells under external pressure and axial compression.
19 p2872 A72-37534
- Zero-moment reinforced axisymmetric shells.
19 p2876 A72-38155
- Selection of optimal parameters of waffle structures from the condition of minimum weight.
20 p2980 A72-39905
- Dynamics of non-circular stiffened cylindrical shells.
21 p3116 A72-40333
- Calculation of rib-reinforced minimum-weight cylindrical shells under external pressure by the random search method.
21 p3119 A72-41099
- Influence of elastic constants on the stability margins and weight characteristics of fiberglass-reinforced shells.
22 p3196 A72-41864
- Buckling of integrally stiffened cylindrical shells - A review of experiment and theory.
22 p3239 A72-42846
- Longitudinal rib reinforced cylindrical shell under axial compression loads, determining equilibrium stability with approximation of transcendental equations.
23 p3347 A72-43748
- Hydrodynamic fluid pressure on a shell during hydraulic impact.
23 p3280 A72-43788
- Dynamic buckling of axially stiffened imperfect cylinders under axial impulse.
24 p3453 A72-44602
- Vibration of simply supported cylindrical shells with longitudinal stiffeners.
24 p3457 A72-44882
- X-ray inspection of the AWACS radome attachment locations.
24 p3406 A72-44902
- Action of a moving load on a composite shell with elastic filler.
24 p3459 A72-45262
- Mechanical behavior of fiber reinforced cylindrical shells.
24 p3461 A72-45783
- REINFORCEMENT [PSYCHOLOGY]**
- Human trace responses generation and storage under light stimulus reinforcement of sound conditioning from galvanic skin reactions observation.
04 p0475 A72-15581
- Characteristics of certain parameters of memory for visual signals in lower monkeys.
21 p3001 A72-40804
- REINFORCEMENT [STRUCTURES]**
- Aluminum stiffening structural sections selectively reinforced with boron/epoxy composite materials, discussing mechanical properties, cost effectiveness and stress distribution.
01 p0139 A72-10737
- Stressed state of reinforced physically nonlinear rods under torsion, using theory of functions of complex variables.
03 p0447 A72-13731
- Compression strength theory for monodirectional reinforced homogeneous anisotropic and piecewise homogeneous composite materials, using microvolume stability loss failure mechanism.
06 p0838 A72-18655
- Compressive strength of Ti alloy airframe skin stringer panels reinforced with B-Al composite by brazing.
11 p1729 A72-25387
- Selective reinforcement with high strength boron filament to achieve cost effectiveness and weight savings for composite structures.
11 p1731 A72-25417
- Anisotropic graphite composite laminates cutouts stress analysis by finite element method, predicting structural reinforcement behavior.
11 p1672 A72-25475
- Bolted connections strength in graphite fiber-epoxy resin composites reinforced by colaminated boron film.
11 p1672 A72-25476
- Bending of rectangular cross section cantilever beam with cylinder reinforced circular opening, calculating interface stress distribution as function of thickness and elasticity moduli ratio.
11 p1733 A72-25545
- Deformation and stress in shells with discontinuous wall thickness variations, noting cylinder with ribs under internal pressure.
15 p2326 A72-31705

- Contact problems for elastic semiplane reinforced with symmetric and asymmetric loaded elastic stiffeners.
15 p2329 A72-32281
- Initial yield surface of a unidirectionally reinforced composite.
[ASME PAPER 71-APMW-19] 17 p2623 A72-34301
- One-dimensional wave pulses in steel-epoxy composites.
[SESA PAPER 1945] 17 p2631 A72-34823
- Fatigue strength of overloaded stiffeners in cracked panels, evaluating stress intensity factor and overload coefficients for fatigue crack propagation via finite element method.
[ICAS PAPER 72-40] 21 p3120 A72-41165
- Battened columns out-of-plane buckling under axial loads and/or moments, deriving relationship between applied loads and section characteristics.
21 p3121 A72-41211
- REINFORCEMENT RINGS**
- Stress concentration around reinforced curvilinear hole in elastic infinite plate, discussing ring reinforcement rigidity effects.
03 p0447 A72-13730
- Doubly symmetric oval ring with stiffeners pair parallel to major or minor axis, investigating stress behavior under radial load.
[ASME PAPER 71-WA/DE-14] 05 p0732 A72-15941
- Axially compressed semi-sandwich corrugated ring-stiffened cylindrical shell crippling local buckling and general instability prediction by finite difference energy method.
[AIAA PAPER 72-138] 05 p0740 A72-16892
- Plane stability of isotropic plate with straight line series of holes reinforced by complex elements or multicomponent rings, determining stress concentrations.
08 p1246 A72-21710
- Ring stiffened truncated cone shells vibration mode tests, describing air and electrodynamic shakers and mobile noncontacting displacement sensitive sensor system.
12 p1882 A72-27340
- Anisotropic plate with doubly periodic system of elastic ring stiffened elliptic holes, calculating stresses at holes due to tensile forces applied at infinity.
14 p2165 A72-30685
- Rigidity effect of reinforcing rings on stressed state of physically nonlinear perforated elastic plates.
15 p2333 A72-32683
- Response of a ring-reinforced cylindrical shell, immersed in a fluid medium, to an axisymmetric step pulse.
[ASME PAPER 72-APM-8] 17 p2624 A72-34314
- An experimental buckling study of skin-corrugated ring-stiffened curved panels.
[SESA PAPER 1993A] 17 p2630 A72-34818
- Vibrations of a concentrated mass on a ring coupled to a thin shell.
20 p2981 A72-39908
- Russian book - Plates strengthened by composite rings and elastic cover pieces.
21 p3116 A72-40385
- Stress distribution in a cylindrical shell with reinforced holes.
21 p3126 A72-41542
- REINFORCING FIBERS**
- NT CARBON FIBERS**
- Yield-fracture criterion for angle ply laminate cylinders wound with filament in biaxial tension.
01 p0090 A72-10521
- High temperature strength degradation of graphite and boron reinforced epoxy composites after room temperature aging.
01 p0090 A72-10728
- Continuous casting of metallic tubular structural elements reinforced with boron filaments, stressing application to space shuttle structures.
01 p0074 A72-10731
- Fiber reinforced filament wound composites for pressure vessel applications, investigating mechanical properties.
01 p0090 A72-10741
- Cryogenically formed prestressed stainless steel glass fiber reinforced vessels, demonstrating structural performance for space shuttle life support oxygen/nitrogen high pressure gas tanks.
01 p0139 A72-10770
- Space shuttle oriented polyimide reinforced Ti matrix composites properties, noting weight saving.
01 p0139 A72-10785
- Unidirectional fiber array reinforced composites with improved longitudinal tensile strength and stiffness compared with structural metals.
[SME PAPER EM 71-283] 01 p0092 A72-10966
- Discretely oriented thread reinforced polyurethane cryogenic foam insulation systems for liquid hydrogen fuel tanks.
[MDAC-WD-1756] 01 p0092 A72-10981
- Mechanical strength and performance of combined multicomponent bonded materials, including laminar, fiber, flake filled and metal matrix composites.
01 p0093 A72-11086

- Fiber reinforced composite rotating disks stressed-strain state calculation, discussing steady state closed solutions and approximate methods.
01 p0142 A72-11175
- Viscoelastic parameters calculation for orthotropic composite materials reinforced by unidirectional fibers, giving time dependence of relaxation functions.
01 p0142 A72-11177
- Winding fiber reinforced plastics, investigating fiber curvature effects on elastic constants and tensile strength optimization.
02 p0248 A72-11626
- Stress concentration factors for fiber and matrix in axially loaded unidirectional composite with discontinuous fiber, using linearly elastic finite element analysis.
02 p0292 A72-11987
- Stress analysis for transverse deformation of fiber reinforced composites.
02 p0249 A72-11991
- Surface damage effect on strength of c-axis sapphire filaments, assessing impact on sapphire reinforced metal technology.
02 p0249 A72-11992
- Reinforcing fibers length effect on cross breaking strength and rupture area size at surface for silicoorganic glass reinforced plastic.
02 p0250 A72-12681
- Fluid filled fiber reinforced spherical shells extensional vibrations, evaluating equivalent elastic orthotropic compliance constants, natural frequencies and mode shapes.
03 p0443 A72-13403
- Glass fabric reinforced composite materials stress distribution under longitudinal loading, using finite element method with two dimensional model.
03 p0381 A72-13720
- Static load transfer to discontinuous elastic filament in fiber reinforced composite, determining fiber force longitudinal distribution by approximation to Fredholm integral equation.
03 p0455 A72-14384
- Stress channelling in transversely isotropic elastic composites, comparing classical theory with ideal fiber reinforced composite plane deformation theory.
03 p0455 A72-14385
- Finite amplitude stress wave propagation behind shock in unidirectionally reinforced fiber matrix composites under impact loads.
04 p0585 A72-14534
- Carbon fiber reinforced composites properties and design limitations relative to elastic anisotropy in pump and fan applications.
04 p0536 A72-14744
- Asbestos fiber reinforced plastics composites fabrication techniques, discussing possible applications.
04 p0537 A72-15086
- Carbon fiber reinforced material porosity source, applying equilibrium configurations of liquid films on parallel uniform cylindrical rod hexagonal and cubic arrays.
04 p0537 A72-15087
- Ceramic whisker and fiber reinforcement of metals, discussing manufacturing and testing problems.
04 p0533 A72-15088
- Fiber reinforced composites with transversely isotropic constituents, discussing various mathematical models for elastic constants calculation.
04 p0590 A72-15189
- Cast telescope mirror design with light metallic structures, examining possibilities offered by composite high modulus fiber structures.
[ONERA, TP NO. 1022] 05 p0660 A72-15855
- Photothermoelastic analysis of shrinkage stresses near discontinuity in fiber composite material, relating matrix cracking to fiber packing.
06 p0835 A72-17800
- Fiber reinforced materials mechanical properties, showing strength dependence on stress-strain behavior of fibers and binders and fiber volumetric proportions.
06 p0835 A72-18252
- Tensile strength of tungsten reinforced nickel, determining temperature effect on fibers deformation after vacuum rolling simultaneously with plastic matrix.
06 p0832 A72-18362
- Compressive strength of Cu-W fiber metal matrix composite as function of temperature, comparing to cermets.
06 p0832 A72-18363
- Single fiber reinforced plate initial stress distribution due to linear expansion coefficients difference between matrix and fiber, using optical polarization.
06 p0836 A72-18557
- Fibrous composite materials experimental failure studies at high temperatures and cyclic loading.
06 p0838 A72-18654
- Scanning electron microscope for metal matrix composite materials structure examination, emphasizing matrix behavior, filament under load and interface.
07 p0101 A72-19485
- Mechanical properties of fiber reinforced heat resistant alloys.
07 p0103 A72-19743

Nichrome matrix composites with W and Mo reinforcing fibers 07 p1013 A72-19744

Tungsten alloy filaments as reinforcing agent of heat resistant composite chromium alloy, investigating long term high temperature effects 07 p1013 A72-19745

Heat resistant Nichrome composite alloy with tungsten filament reinforcement, discussing manufacture and mechanical properties at 1100 C 07 p1013 A72-19747

Mechanical strength and microstructural characterization of sapphire ribbons and continuous filaments for composite materials 07 p1023 A72-19929

Limit analysis of ductile fiber reinforced structures, obtaining critical load of composite sandwich ring 07 p1093 A72-19950

Stress-strain state in tension of orthogonally stiffened fiberglass-reinforced plastic with cracks in transversely stiffened layers 07 p1094 A72-20128

Metallic matrix stress-strain properties from phenomenological model based on idealized behavior of system components, noting dependence on fiber volume content 08 p1185 A72-21183

Tensile strength estimation for two dimensional composite with brittle matrix and randomly orientated discontinuous elastic fibrous reinforcement 08 p1244 A72-21324

Random filament misalignment effects on rigidity and tensile strength of unidirectional graphite composites under shear loading 08 p1192 A72-21681

Chopped fiber glass reinforced high density thermoplastic polyethylene composite, determining critical fiber length, interfacial adhesion and fracture toughness 08 p1193 A72-21684

Inorganic single crystal titanate whisker fibers with high modulus strength for plastic reinforcement, noting mechanical, thermal and physical properties 08 p1193 A72-21685

Graphite fiber reinforced composites with high mechanical strength and modulus at low weights, fatigue resistance, vibration damping and tailorable thermal expansion coefficient 08 p1193 A72-21689

Low cost 300 gallon fiber reinforced plastic aircraft wing fuel tank manufacturing technology 08 p1177 A72-21693

Graphite fiber reinforcement of glass composite structure for increased cost effectiveness as compared to laminates and sandwich structures 08 p1193 A72-21694

Reinforcing fiber frame incurvation influence on elasticity and thermal expansion coefficients of composite material 08 p1194 A72-21754

Heat stretching-induced changes effect on strength, sorption and structural properties of polyformaldehyde fibers, noting structural orientation enhancement and porosity growth 08 p1194 A72-21757

Carbon fiber reinforced epoxy resin composites, testing fracture behavior in flexural and shear modes under static, fatigue and creep loading 09 p1334 A72-22389

Ceramic fiber reinforced Ni base alloy for gas turbine blades, improving creep resistance at high temperatures 09 p1335 A72-22396

Fatigue failure mechanism in short fiber reinforced plastics, determining crack growth rates under cyclic loading [PI PAPER 2] 09 p1336 A72-22539

Fiber orientation effects on physical properties of carbon fiber-epoxy resin composites [PI PAPER 3] 09 p1337 A72-22540

Unidirectional and orthogonally cross-ply carbon fiber reinforced plastics laminates, determining interlaminar shear strength and fatigue life [PI PAPER 8] 09 p1337 A72-22543

Carbon fiber reinforced epoxy resin composites fracture toughness dependence on fiber strength, diameter, volume fraction, modulus, fiber/matrix interface strength and temperature [PI PAPER 9] 09 p1337 A72-22544

Fiber composites mechanical properties - Conference, Teddington, England, November 1971 09 p1338 A72-23162

Aligned fibrous composites microstructural parameters, showing fiber thickness effect on fracture, fabrication, matrix cracking, creep resistance and fatigue 09 p1338 A72-23163

Single and multiple fractures in brittle matrix fibrous composites, discussing fracture energetics, stress-strain curves and hysteresis effects 09 p1338 A72-23164

Short fiber reinforced thermoset composite materials for engineering construction, tabulating flexural properties and Charpy impact strengths 09 p1338 A72-23165

Core and tube duplex fiber reinforced composites with fracture toughness capable of high stress level operation 09 p1338 A72-23166

Discontinuous rigid or creeping fiber reinforced composite materials, predicting steady state creep behavior 09 p1338 A72-23167

Two dimensional creeping flow in fiber reinforced composite under uniform tension, discussing matrix shear stress and fiber direct stress distributions 09 p1338 A72-23168

Tensile microstrain and cyclic loading behavior of carbon fiber reinforced plastic composites at elevated temperature 09 p1338 A72-23169

Carbon fiber reinforced plastic toughness from strain concentration and plastic flow observation near crack tip by moire technique 09 p1339 A72-23170

Strength and fracture energies and toughness in fibre reinforced ceramics 09 p1339 A72-23171

Stress concentration in elastic composite reinforced by two dimensional continuous parallel fiber array with one broken fiber 09 p1339 A72-23172

Tractions at interface between fiber and matrix in fiber reinforced composites, considering axially symmetric deformations and stress fields 09 p1339 A72-23173

Hugoniot equation of state for impact shock wave propagation along fiber direction in Al epoxy matrix composites 09 p1407 A72-23235

Metastable austenitic steel fiber to increase Al matrix strength to density ratio and fracture toughness 09 p1331 A72-23385

Elastoplastic analysis of unidirectional filament reinforced boron/aluminum and boron/epoxy composites under longitudinal loading, using finite element techniques 10 p1555 A72-24254

Crack toughness tests of fiber composite laminates, using linear elastic fracture mechanics 10 p1500 A72-24258

Fatigue crack propagation in epoxy resin matrix reinforced with discontinuous metal fibers 10 p1501 A72-24261

Linear equations relating elastic compliance coefficients of anisotropic two-phase fiber reinforced composites 10 p1556 A72-24262

Fiber reinforced materials mechanical properties calculation, taking into account various fiber orientations and multiaxial loads 10 p1501 A72-24493

High strength steel strip reinforced aluminum, discussing fabrication techniques and mechanical properties 10 p1498 A72-24839

Statistical bounding approach to fracture analysis of fiber reinforced composite materials tensile strength 10 p1502 A72-24883

Fiber reinforced plastics thermophysical properties, thermal conductivity and heat capacity, determining effects of reinforcement fiber type, resin amount and type [AIAA PAPER 72-366] 11 p1669 A72-25391

Linear elastic fracture mechanics extension to fiber reinforced plastic composite laminates, noting dependence on homogeneous model validity [AIAA PAPER 72-384] 11 p1730 A72-25406

Initially sharp cylindrical pressure pulse propagation and stress wave attenuation in linear elastic fiber reinforced composites [AIAA PAPER 72-394] 11 p1730 A72-25415

Selective reinforcement with high strength boron filament to achieve cost effectiveness and weight savings for composite structures [AIAA PAPER 72-396] 11 p1731 A72-25417

Elastic constants and bond stress distribution for discontinuous fiber-reinforced three dimensional composite subjected to uniaxial tension [AIAA PAPER 72-397] 11 p1731 A72-25418

Tubular specimens for testing mechanical properties of fiber reinforced composites under axial loading, discussing design, fabrication and end attachment problems 11 p1670 A72-25456

Fiber toughening mechanisms in continuous filament unidirectionally reinforced composites with elastoplastic matrices, discussing tensile energy storage in debonded region 11 p1671 A72-25463

Fracture toughness of anisotropic heterogeneous filamentary boron/aluminum composites, correlating test results with acoustic emissions from filament breakage 11 p1672 A72-25470

Charpy impact strength data for unidirectional graphite, boron and glass-resin composites tested in fiber direction, noting tensile stress-strain characteristics importance 11 p1672 A72-25471

Micromechanical and impact test investigation of unidirectional fiber composites impact resistance properties, considering longitudinal, transverse and shear modes 11 p1672 A72-25472

Vibration characteristics of unidirectional filamentary boron-epoxy composite panels, obtaining nodal patterns, natural frequencies and damping coefficients 11 p1732 A72-25477

Off axis and transverse tensile properties of boron reinforced Al alloys, correlating metallurgical structures with stress-strain curves and fractographic studies 11 p1654 A72-25479

Elastic glass and Thormel fiber/epoxy matrix composite material creep tests, determining creep rate dependence on specimen geometry and stress state 11 p1672 A72-25481

Critical aspect ratio of W fiber in copper matrix for stress rupture applications 11 p1654 A72-25482

Random filament misalignment effect on reinforced composite strength, discussing bundle, tensile and shear strengths 11 p1673 A72-25486

Experimental weave pattern for three dimensional continuously woven fiber glass reinforced composite fabric impregnated with epoxy resin [SAE PAPER 720340] 11 p1673 A72-25597

Book on carbon fibers in composite materials covering fiber testing and mechanical properties 11 p1674 A72-25924

Multilevel structural analysis for multilayered fiber-epoxy and metal matrix composites, using FORTRAN IV 11 p1601 A72-26033

High performance continuous filament reinforcements for nonmetallic matrix composites, emphasizing boron and graphite fibers 11 p1674 A72-26229

Fiber-matrix composites overall strength optimization, emphasizing matrix and interface effects 11 p1674 A72-26231

Reinforcing fibers precise alignment and uniform distribution in metal matrix 11 p1645 A72-26854

Filament reinforced boron-aluminum composites multiple fracture behavior dependence on cross section geometry from tensile test 11 p1668 A72-26944

Prager-Shield theory for optimal plastic design extended to multicomponent cost functions and load conditions, applying to fiber reinforced plate 12 p1881 A72-27243

Elastic wave propagation and energy scattering in materials reinforced by inextensible fibers 12 p1881 A72-27252

Fiberglass reinforced thermoplastics and thermosets for corrosive environments, noting composites performance increase by constituents change 12 p1833 A72-27404

Fiber composites plastic flow and fracture, using plane strain model for analysis 12 p1884 A72-27730

Computer program to reduce automated multiaxial testing strain gage and applied loads data from tubular or flat specimens including fiber composites 12 p1787 A72-27999

High modulus fiber composite circular tube specimens multiaxial load testing, noting gripping methods to reduce transitional strains 12 p1886 A72-28000

Plywrap process for low cost automated fabrication of fiber reinforced plastic composites, noting applications from missile interstages to modular housing 12 p1815 A72-28081

Continuous woven fabric or roving filament reinforced thermoplastics production, discussing polymer binder systems, coupling agents, impregnation technique, processing parameters and equipment 12 p1815 A72-28083

Graphite fiber with high tensile strength and modulus and good elongation at low cost for aerospace applications 12 p1834 A72-28084

Fiber reinforced Mod 3 carbon-carbon composites mechanical and thermal properties comparison with polycrystalline bulk graphite 12 p1834 A72-28087

Boron nitride coated boron fibers for metal matrix composite reinforcement, discussing surface nitriding process by heating 12 p1815 A72-28088

Addition type polyimide-graphite fiber composites fabrication from monomeric reactant solutions to improve mechanical properties and thermal stability 12 p1834 A72-28091

Fiberglass replacement by organic fiber for L-1011 interior sandwich panels and laminates, considering Nomex fiber in woven fabric 12 p1835 A72-28099

Composite materials mechanical and thermal properties for ATS reflector supporting truss, noting graphite fiber reinforced epoxy plastic design, fabrication and tests 12 p1886 A72-28158

Boron and carbon fiber reinforced plastics applications in aircraft and engine structural components, discussing dynamic and impact damping properties compared to conventional materials

13 p1982 A72-28555

Internal pressure induced stresses, displacements and time-variable plasticity radii for thick walled fiber reinforced cylinder with hereditary elastic binder interlayers

13 p2055 A72-28557

Finite plane elastic buckling deformations of incompressible composite columns reinforced by straight parallel fibers

13 p2059 A72-29599

High strength carbon fiber reinforced plastics, discussing fabrication techniques, fiber structural, physical and mechanical properties and potential technological applications

13 p1984 A72-30075

Compacting kinetics of fiber reinforced sandwich composites during hot pressing controlled by plastic matrix sliding velocity

13 p1967 A72-30103

Aluminum-stainless steel and Ni-Mo composites prepared by dynamic hot pressing, determining bond strength between fibers and reinforced metal matrix

14 p2107 A72-30431

Refractory fiber metal reinforcement and matrix incorporation, considering SiC fiber reinforced Al

14 p2107 A72-30532

High temperature composite turbine blade materials, discussing service conditions and fiber/matrix selection, noting cast Ni and Mo based alloy fibers

14 p2125 A72-30533

Apollo heat shield silica reinforcement fiber and ablation char reactions in laboratory and actual reentry tests

14 p2172 A72-30922

Stress analysis of boron fiber-reinforced and isotropic Al panels under identical loading conditions

15 p2323 A72-31479

Tangential force distribution at fiber surface in composite material under tensile stress without displacement at fiber axis

15 p2260 A72-31743

Structural components design from fiber composites, noting computer programs for structural and stress analysis

15 p2328 A72-32128

Carbon and graphite fiber reinforced composites elastic constants derived from ultrasonic immersion technique

15 p2261 A72-32503

Fracture toughness measurements of polyester composites reinforced with chopped steel wires compared with Cooper theory

16 p2413 A72-33203

Temperature effect on bonding strength between ceramic whiskers or fibers and metal matrices attributed to thermal expansion coefficients disparity

16 p2413 A72-33206

Dynamic load tests for impact strength of ceramic composites with fiber reinforced alumina matrix, obtaining dynamic stress-strain curves

16 p2414 A72-33300

Physical and chemical surface characteristics investigation methods for fiberglass rovings to consider suitability as reinforcement for synthetic resins

16 p2414 A72-33302

Design criteria for fiber reinforced thermoplastic resins performance optimization, discussing temperature, humidity and chemicals effects

16 p2415 A72-33417

Steady state creep of composite material with discontinuous fibers, determining random function mean and variance for fiber stress distribution

16 p2412 A72-34115

Optimal design of static laterally loaded fiber reinforced plates, determining optimum load-path directions at all plate points

16 p2475 A72-34174

Carbon fibers for composite materials reinforcement, discussing mechanical properties and economic factors

17 p2569 A72-34188

Constitutive equations for plane harmonic waves propagation in composite fiber reinforced elastic material

17 p2625 A72-34321

Results of preliminary studies of a bearingless helicopter rotor concept.

[AHS PREPRINT 600] 17 p2489 A72-34490

Ballistic-damage-tolerant composite flight control components.

[AHS PREPRINT 674] 17 p2626 A72-34514

Carbon fiber composites with ceramic and glass matrices. I - Discontinuous fibres.

17 p2570 A72-34668

Carbon fibre composites with ceramic and glass matrices. II - Continuous fibres.

17 p2570 A72-34669

Transition metal-modified matrix resins for composite materials.

17 p2570 A72-34672

Effect of end attachment on the strength of fiber reinforced composite cylinders.

[SESA PAPER 1994A] 17 p2630 A72-34817

Experimental investigation of the interlaminar shear properties of composite materials.

[SESA PAPER 1985A] 17 p2631 A72-34824

Study of the surface reactivity of carbon fibers by gas chromatography

17 p2570 A72-34891

Tridimensional textiles for composites.

17 p2571 A72-34935

Elastic behavior of multilayered bidirectional composites.

17 p2632 A72-35234

The transverse Poisson's ratio of composites.

17 p2571 A72-35289

Fracture mechanics of a fiber composite.

17 p2633 A72-35293

Shear deformation in heterogeneous anisotropic plates.

17 p2633 A72-35294

Fractography of fiber reinforced metal composites.

17 p2560 A72-35654

High strength alumina, boron, silicon carbide and graphite reinforcing fibers for composite materials

17 p2572 A72-35656

Sapphire filament mechanical property considerations of importance to Al₂O₃ reinforced metals.

17 p2572 A72-35658

High performance graphite ribbon - An advanced reinforcement material.

17 p2572 A72-35659

Mechanical properties of carbon filament wound carbon matrix composite from tensile tests, noting reinforcement efficiency

17 p2573 A72-35669

The development of high strength three dimensionally reinforced graphite composites.

17 p2573 A72-35670

The strength of fibre composites.

18 p2703 A72-36268

New developments in the study of fiber superalloys obtained by directional solidification

18 p2702 A72-37015

Effect of fiber end, fiber orientation and spacing in composite materials.

18 p2738 A72-37086

The stress boundary value problem for plane strain deformations of an ideal fibre-reinforced material.

19 p2870 A72-37371

Nonlinear physical dependence of reticular polymers and glass fiber reinforced plastics under conditions of diminishing creep

19 p2822 A72-37527

Some results of an experimental study of stress distribution at monofilament tips

19 p2822 A72-37529

Behavior of glass fiber reinforced plastic cylindrical shells under the action of external pressure pulses

19 p2872 A72-37538

Dynamic stability of axisymmetrically heated glass fiber reinforced cylindrical plastic shells which are coupled with elastic cylinders

19 p2872 A72-37539

Temperature-time superposition applied to the relaxation properties of a glass fiber reinforced plastic and its binder

19 p2822 A72-37543

Yielding of fiber reinforced Tresca material.

19 p2873 A72-37695

Effectiveness of using composite materials directionally reinforced by hollow fibers

19 p2823 A72-38002

Investigations into the impregnating behaviour of various reinforcing materials in the filament winding process.

19 p2808 A72-38171

The study on dynamical behavior of fiberglass reinforced plastics (FRP) by dynamical mechanical model.

20 p2943 A72-38887

High modulus fiber composites development from viewpoint of reinforcement patterns and material properties

20 p2943 A72-38946

Strength factors of fiber reinforced composites under tension, compression, shear, bending and plane stress

20 p2944 A72-38947

RF shielding and electrical properties of boron and carbon fiber reinforced composites.

20 p2944 A72-38987

The matrix fatigue behaviour of fibre composites subjected to repeated tensile loads - Application to B/Al 6061 composites.

20 p2936 A72-39208

Reinforced metals - Mechanical property considerations.

20 p2936 A72-39210

Theoretical model for acoustic emission relationship to fiber cracking during rising load tensile test on fiber reinforced composites

20 p2925 A72-39285

The transverse tensile properties of boron fiber reinforced aluminum matrix composites.

20 p2938 A72-39302

Boron and carbon fibers fabrication and properties for composite materials reinforcing elements, noting strength and stiffness dependence on stress orientation

20 p2944 A72-39437

The fiber and filament reinforcement of plastic and brittle matrix materials

20 p2944 A72-39438

Fabrication and properties of carbon-containing iron fibers and fiber sinter bodies

20 p2939 A72-39439

Coating of fibers and the fabrication of fiber-reinforced composite materials

20 p2929 A72-39443

Problems and possibilities of the production of fiber-reinforced metallic components by thermal spraying

20 p2929 A72-39444

Fiber arrangements for one, two and three dimensional ideal composite materials, discussing fabrication processes

20 p2940 A72-39446

Mechanical properties of boron fiber reinforced aluminum matrix composite, describing experimental and control techniques

20 p2940 A72-39447

Prospects for the development of technically usable fiber-reinforced high-temperature materials

20 p2940 A72-39448

Dynamic characteristics of composite laminates.

20 p2979 A72-39558

Interfacial characteristics of silicon carbide-coated boron-reinforced aluminum matrix composites.

20 p2941 A72-39791

Plane strain bending of laminated fibre-reinforced plates.

20 p2982 A72-40021

Dynamic inelastic properties of materials. I - Damping characteristics of fiber composites. II - Representation of time dependent characteristics of metals.

[ICAS PAPER 72-28] 21 p3069 A72-41153

Boron fiber reinforced composites technology assessment and utilization, stressing cost reduction

[ICAS PAPER 72-30] 21 p2995 A72-41155

Non-destructive examination of fibre reinforced polymers with special reference to continuous carbon fibre reinforcement.

[ICAS PAPER 72-44] 21 p3073 A72-41169

Metal fiber composites electrical resistivity as function of fiber volume proportion, evaluating vacuum cast Cu/W

21 p3073 A72-41373

Random function theory method for estimation of tensile, compressive and shear strength and elastic constants of monodirectional fiberglass reinforced plastics

21 p3073 A72-41708

Reinforcement of structural materials by long strong fibres.

22 p3241 A72-43026

Fabrication and properties of graphite fiber reinforced magnesium.

22 p3193 A72-43035

German monograph - Contribution to the reinforcement of plastics with special allowance for the reinforcement and matrix materials.

22 p3197 A72-43078

Composite Al- and Ni-base alloys strengthened by B and W/Mo fibers respectively for reduced weight wing spars and high temperature applications

22 p3197 A72-43139

Calculation of radial pressures in metal-fibre-reinforced materials during compacting

23 p3298 A72-43277

PRD-49, a new composite material - Its characteristics and its application to the BO-105 helicopter.

[SAWE PAPER 915] 23 p3305 A72-43462

High strength boron and borsic fiber reinforced aluminum composites.

23 p3299 A72-43491

Fiber composite columns under compression.

23 p3344 A72-43494

Effects of hydrostatic stress on the yielding of cold rolled metals and fiber-reinforced composites.

23 p3299 A72-43496

Work of fracture of fibre-reinforced polymers.

23 p3306 A72-43561

The use of a torsion machine to measure the shear strength and modulus of unidirectional carbon fibre reinforced plastic composites.

23 p3306 A72-43562

Fiber reinforced metallic matrix composite under creep, discussing rigidity, stress distribution, rupture strength and failure time

23 p3306 A72-43727

Fibers-matrix force interaction effects in metal composites, analyzing stress-strain state of reinforced plate

23 p3306 A72-43728

Heat resistant Ni-base composite stiffened with W wires, investigating interaction between alloy and fibers from metallographic and X ray diffraction microscopy data

23 p3301 A72-43740

Modified Hellinger-Reissner variational method applicable to harmonic waves moving normal to fiber reinforced layered elastic composite, tabulating eigenfrequencies
23 p3351 A72-44061

Book - A review of the science of fibre reinforced plastics.
24 p3417 A72-44674

Precise alignment and uniform distribution of fibres in a metal matrix.
24 p3413 A72-44898

The fracture toughness of fibre composites.
24 p3417 A72-44899

The effect of annealing temperature on certain properties of molybdenum and tungsten fibers
24 p3415 A72-45396

Tensile strength of tungsten reinforced nickel, determining temperature effect on fibers deformation after vacuum rolling simultaneously with plastic matrix
24 p3416 A72-45749

Compressive strength of Cu-W fiber metal matrix composite as function of temperature, comparing to ceramics
24 p3416 A72-45750

Mechanical behavior of fiber reinforced cylindrical shells.
24 p3461 A72-45783

REISSNER THEORY

Edge loaded cylindrical shells of resolution nonlinear axisymmetric deformation determination from asymptotic solution of Reissner equations, using multiple scale perturbation technique
01 p0136 A72-10031

Finite element and finite difference formulations for solid continua by variational principles, including potential energy, complementary energy and Reissner principles
07 p1087 A72-18792

Mean square error and bound on relative error for Reissner plate theory, including shear deformation effect
07 p1087 A72-18812

Flexure analysis of isotropic Reissner flat plates bonded by adhesive layer, deriving stress distribution equations in general tensor form
[AIAA PAPER 71-148] 07 p1089 A72-19688

Stable equilibrium conditions for linear elastic body, using Reissner functional
08 p1248 A72-21819

Evaluation of Reissner's correction for finite span aerodynamic effects.
18 p2736 A72-36774

Stress concentration around curvilinear holes in plates according to Reissner's theory
21 p3126 A72-41543

Reissner nonlinear equations for stability analysis of shallow shells of revolution, noting critical loads range and error analysis
22 p3232 A72-41856

Reissner-Sagoci problem for semiinfinite elastic solid stress and displacement determination, discussing generalization to nonhomogeneous media with circular part under axisymmetric twisting
23 p3314 A72-44266

REJECTION

Monotypic signal rejection by connecting line insertion to sensor and central electrical measuring device input galvanic decoupling
11 p1611 A72-26440

RELATIVE BIOLOGICAL EFFECTIVENESS (RBE)

Mathematical model for radiation damage cross section linear energy transfer dependence, explaining experimental values of relative biological effectiveness
[CERN-71-16] 02 p0160 A72-12052

Relative biological effectiveness of energetic protons for somatic effects induction in mice during whole body irradiation, using mean energy of solar event protons
[CERN-71-16] 02 p0161 A72-12054

Mitotic index and aberrant mitose frequency in mice corneal and intestinal epithelial cells exposed to 50-630 MeV protons, estimating relative biological efficiency coefficients
[CERN-71-16] 02 p0161 A72-12055

Relative biological effectiveness of high energy radiations, noting dependence on radiation quality, system, dose and dose rate
[CERN-71-16] 02 p0161 A72-12058

Effective dose change after repeated radiation exposures as function of time intervals between fractions, evaluating space flight radiation hazards
[CERN-71-16] 02 p0161 A72-12059

Relative biological effectiveness of high X ray doses given to radish seeds, studying irradiation rate effect on germination probability
09 p1265 A72-22524

Electron abundance equilibrium as factor in biological effectiveness of proton beam irradiation of animals
21 p2998 A72-40450

RELATIVISTIC EFFECTS

Gravitational potential tensor and equations of motion of relativistic mechanics for isolated system of masses
01 p0127 A72-10345

Pulse widths formed by relativistic beaming pulsars effect on emission spectra
01 p0133 A72-11130

Combustion fronts in relativistic hydrodynamics, considering theorem of detonation and deflagration velocity distribution
01 p0145 A72-11179

Soviet book on space navigation covering dimensional spaces, navigation functions, relativistic phenomena, position finding, motion parameters, statistical methods, etc
02 p0256 A72-12297

Computerized series solution of relativistic motion of planet Mercury for Schwarzschild and isotropic coordinates
02 p0260 A72-12306

Einstein light deflection by galaxy cluster gravitational field effect on extragalactic observations, explaining uniform background inhomogeneities
02 p0286 A72-12892

Rotating relativistic stellar models, covering coordinate systems injection energy, convection, red shift, external gravitational waves and black holes
03 p0426 A72-13269

Crab Nebula optical pulsar NP 0532 polarization minima delay mechanism, suggesting relativistic radiation from region orbiting relativistically around neutron star
03 p0434 A72-13553

Relativistic flight of decreasing mass, increasing acceleration and constant thrust rocket description from earth and rocket observer viewpoints, noting light flash transmission and arrival times
03 p0441 A72-13836

Rotating rigid rod and disk relativistic rings, discussing inertial frames significance
04 p0574 A72-14917

Electromagnetic fields produced by quasi-stationary gravitational collapse of uniformly rotating current carrying relativistic thin disk
04 p0579 A72-15321

Grad moment method application to radiative transfer in medium with relativistic differential motions, obtaining Eddington approximation and Thomas radiative-viscosity terms
04 p0579 A72-15322

Mass concept for moving crack, relating stress concentrations of elastic field with crack inertia
05 p0673 A72-16306

Hard X ray emission by thermal plasma, applying relativistic corrections to photon bremsstrahlung Maxwell distribution and cross section
06 p0873 A72-18004

Earth rotational direction and speed effects on terrestrial circumnavigation relativistic time, suggesting clock paradox empirical proof
06 p0849 A72-18381

Exact cosmological solutions in Brans-Dicke scalar tensor theory, noting consequences for solar relativistic effects
07 p1075 A72-19584

Quantum and classical gravitation theory Mercury perihelion motion dependence on fourth order potential in scalar and Dirac fields
07 p1084 A72-20689

Quantum gravitation theory and Mercury perihelion motion, calculating three body potentials from treatment of celestial bodies as nucleon assemblies
07 p1084 A72-20690

Steady state charged cylindrical electron-ion beam with high current in kinetics model framework, discussing densities proportionality and relativistic factor
09 p1360 A72-22951

Magnetic field generation problem in rotating relativistic star for barotropic medium
09 p1391 A72-23537

Bent lever equilibrium and relativistic mass for point body in motion, introducing von Laue energy flow inertia into d'Alembert principle
10 p1505 A72-24074

Transport coefficients calculation in gas kinetic theory by relativistic generalization of Enskog-Chapman method
10 p1510 A72-24106

Relativistic Zeeman-Stark effect on molecular jet due to molecular translational motion in continuous magnetic field
10 p1514 A72-24135

LTE solutions of relativistic Boltzmann equation in presence of external electromagnetic field
10 p1513 A72-24856

Relativistic shock propagation and search for electromagnetic pulses from supernovae, plotting kinetic energy factor vs external mass fraction
11 p1721 A72-26126

Multiple scale asymptotic method for nonlinear theory of dispersive periodic waves with slowly varying parameters, noting equations for irrotational motion of perfect relativistic fluid
12 p1843 A72-27170

Thermal electron relativistic streaming effects on electromagnetic instability in magnetoplasmas
12 p1851 A72-27389

Relativistic analysis for synchrotron gravitational radiation emitted by particle in circular orbit around Schwarzschild black hole, noting astrophysical implications
13 p2007 A72-30123

Approximate periodic solution of satellite equation of motion based on Schwarzschild metric integration, noting relativistic effects
14 p2162 A72-31108

Shell formation during star collapse due to rotational instability, discussing relativistic effects
15 p2305 A72-31337

Magnetoactive plasma transverse waves propagation near electron gyrofrequency harmonics, taking into account electron collisions and relativistic effects
15 p2897 A72-32734

Extragalactic radio source 3C 1202 microwave flux density variations suggesting superrelativistic expansion
17 p2611 A72-35295

Gravitational radiation from relativistic systems.
17 p2582 A72-35394

Synchrotron radiation-like angular distribution of gravitational synchrotron radiation produced by ultrarelativistic geodesic particle orbits in Schwarzschild geometry
17 p2583 A72-35820

Around-the-world atomic clocks - Predicted relativistic time gains.
17 p2584 A72-35838

Rotary shocks and waves of relativistic magnetohydrodynamics
17 p2593 A72-35908

Pulses of gravitational radiation of a particle falling radially into a Schwarzschild black hole.
18 p2711 A72-36714

Spherically symmetric system of radiating body surrounded by absorbing dust zone, investigating relativistic radiation pressure effects
19 p2859 A72-37893

Relativistic beaming from periodically orbiting light point source in terms of photon fluxes, relating to pulsar radiation theory
19 p2835 A72-38697

Stability of nonradial vibrational modes of relativistic neutron stars.
20 p2972 A72-39869

Best-fit estimate of relativistic effects in time-delay experiments.
20 p2972 A72-39871

Book - Dimensional analysis and group theory in astrophysics.
23 p3341 A72-44500

RELATIVISTIC PARTICLES

Relativistic electron beams in plasma, considering electrostatic instability conditions and critical currents
01 p0109 A72-10975

Cerenkov radiation detection by human eye, discussing relativistic muons passage through vitreous humor and retina
02 p0272 A72-11754

Quasi-linear theory of relativistic particle acceleration by hydromagnetic turbulence for small gyration radius expansion, using Vlasov equation
02 p0265 A72-12301

Nonlinear discrete radio source spectra deviations from power law at 10-5000 MHz, considering low energy relativistic electron excess
02 p0281 A72-12305

Relativistic beam equilibria above 10,000 amps, considering axial, diffuse, sharp boundary and azimuthal current models
02 p0267 A72-12840

Acceleration phase of solar cosmic rays and relativistic electrons in solar flare of 7 July 1966, discussing MHD shock waves generation
03 p0407 A72-12942

Spectral distribution of radiation arising from nonlinear Thomson scattering of strong electromagnetic wave by ultrarelativistic electrons
03 p0390 A72-13017

Relativistic quark search by flash tube chamber in extensive air showers at ground level
03 p0410 A72-13149

Cosmological density fluctuations in hadron state, examining relativistic free particle and high temperature hadron gas models
03 p0426 A72-13273

Spontaneous and induced Compton scattering of high frequency waves by relativistic electrons in synchrotron sources
04 p0487 A72-14902

Ejection behavior of relativistic particle magnetized clouds in radio galaxies central parts, noting interaction with interstellar medium
06 p0891 A72-18503

Emission characteristics of relativistic charge in rectilinear motion within gravitational wave field
08 p1206 A72-21072

Asymptotic expressions for electromagnetic field and currents induced in unbounded dense plasma by relativistic electron beam passage
08 p1215 A72-21721

Optimum pressure and field conditions for intense relativistic electron beam transport in longitudinal magnetic field

09 p1360 A72-22870

Compact radio sources in galactic nuclei, discussing similarity to quasars in repetitive generation of relativistic particles

10 p1534 A72-23900

Gas laser excitation by relativistic electron beam pulse axial propagation through optical cavity, studying mechanism through timing and pressure dependence measurements

10 p1489 A72-23946

Relativistic electron beam and ring phenomena calculation using plasma simulation program CYLRAD

10 p1518 A72-23958

Intense relativistic electron beam-plasma interactions in finite cavities, calculating neutral gas charge production and gas breakdown times

10 p1518 A72-23960

Relativistic heavy ion in plasma, calculating energy loss based on electron scattering and momentum transfers

10 p1515 A72-24344

Relativistic electron beam injection into dense plasma, analyzing perturbed electric and magnetic fields and charge and current densities

10 p1521 A72-24353

Hydrogen, deuterium, helium, nitrogen and argon ion production and acceleration by intense pulsed relativistic electron beam

10 p1517 A72-25037

Longitudinal electromagnetic wave excitation in restricted plasma by relativistic electron beam injection, determining increments, frequency distribution and width of spectra

12 p1849 A72-27064

High current relativistic electron beam properties, noting application in thermonuclear synthesis and accelerators

12 p1788 A72-27250

Quasi-linear approximation equations for relativistic charged particles beam dissipative instability in collisional plasma, noting electrons heating at high collision frequencies

12 p1852 A72-27860

Covariant statistical mechanics equations system for distribution function of relativistic particles in steady external gravitational field, noting Vlasov equation as limiting case

13 p2035 A72-28465

Wave equations and photon absorption cross section of relativistic electron in magnetic field, taking into account relativistic energies

13 p2002 A72-28647

High X ray luminosity associated with richest galaxy clusters, noting inverse Compton effect by relativistic electrons and bremsstrahlung from hot gas

13 p2040 A72-29412

Solar relativistic electrons and particle events spectra during 1967-1969 from IMP-4 observations

13 p1033 A72-29746

Nonlinear theory of interaction between restricted relativistic particle beam and plasma, determining field amplitudes and beam radii

13 p2019 A72-29989

Spiral galaxies radio sources spectral components, noting relativistic electrons radiation and luminosity-surface brightness diagram

14 p2148 A72-30203

Gyrosynchrotron radiation fields from mildly relativistic electrons in magnetoactive plasma, studying radiative transfer problem

14 p2138 A72-30556

Radio emission due to relativistic electrons spiral orbit motion in rotating pulsating neutron star

15 p2304 A72-31333

Relativistic electron characteristics in interplanetary space from onboard satellite detector measurements beyond magnetospheric influence [JGPP-UCR-72-11]

15 p2300 A72-31998

Ionization energy loss of relativistic heavy nuclei for close collisions as function of charge, computing Born approximation corrections via Mott exact cross section

15 p2282 A72-32647

Relativistic charged particles produced transition radiation as diffuse cosmic X rays source, discussing validity based on interstellar space energy density consideration

15 p2301 A72-32716

Relativistic electron ring oscillations in circular waveguide with allowance for walls finite conductivity, noting radiative instability at subcritical frequencies

15 p2210 A72-32738

Light elements production from primary cosmic rays spallation in interstellar gas, noting diffusion coefficient of relativistic particles in galaxy

15 p2301 A72-32754

Plasma wave excitation by monoenergetic relativistic electron beam, investigating beam-plasma wave synchronism during instability development

16 p2434 A72-32912

Solar radio bursts time sequence and positions observation during 24 January 1971 proton event, noting relation to relativistic particles acceleration into interplanetary field

16 p2445 A72-33045

Galaxy M87 X ray source origin, suggesting hot plasma thermal emission or ejected relativistic electrons interacting with intergalactic magnetic or radiation fields

16 p2452 A72-33135

Balloon flight observation of charge composition fine details and gross effects of isotopic abundance in near relativistic cosmic rays

16 p2447 A72-33729

Solar wind structure from observations and mathematical models, discussing effects of relativistic protons, heat transfer from electrons to protons and magnetic fields

16 p2449 A72-33909

Electromagnetic wave propagation in uniform and nonuniform plasmas with enough strength to cause relativistic electron velocities, considering linear polarization and nonlinear penetration effects

16 p2438 A72-33926

Ultrarelativistic electrons beam steady injection into plasma filled half space, using weak turbulence theory for assumed beam excited oscillations interaction

16 p2440 A72-34156

Parametric emission of relativistic electron clusters in a waveguide with a layered dielectric filling

17 p2529 A72-34850

Emission of coherent microwave radiation from a relativistic electron beam propagating in a spatially modulated field

17 p2589 A72-34874

Relativistic electron beam injection into dense plasma, analyzing perturbed electric and magnetic fields and charge and current densities

17 p2589 A72-34954

X ray sources associated with galactic clusters resulting from relativistic electrons Compton scattering on microwave background radiation

17 p2599 A72-35072

Liquid scintillation counters application in search for relativistic quarks in cosmic rays, setting upper confidence limits on particle intensity

17 p2601 A72-35471

Synchrotron radiation-like angular distribution of gravitational synchrotron radiation produced by ultrarelativistic geodesic particle orbits in Schwarzschild geometry

17 p2583 A72-35820

Steady state charged cylindrical electron-ion beam with high current in kinetic model framework, discussing densities proportionality and relativistic factor

17 p2593 A72-35880

Structure of the power-law spectra of relativistic electrons in a turbulent plasma

17 p2593 A72-35907

Pulsed power - A new technology for controlled thermonuclear fusion

18 p2715 A72-36332

Equations for electron and high-energy photon transfers in magnetic fields

19 p2837 A72-38059

Excitation of electromagnetic waves in a plasma by a relativistic electron beam

21 p3092 A72-40787

Turbulent plasma 'caldrons' in galactic nuclei

21 p3114 A72-41772

Solar flare associated relativistic electron acceleration relationship to cosmic ray and type 4 radio burst production

22 p3217 A72-42010

Noncoherent excitation of plasma vibrations by an almost monoenergetic relativistic beam

22 p3213 A72-43114

Spiral galaxies radio sources spectral components, noting relativistic electrons radiation and luminosity-surface brightness diagram

23 p3333 A72-43232

Relativistic test particle escape from circular orbit around central mass due to mass loss, considering orbiting body corrections due to general relativity

23 p3335 A72-43265

Conditions for magnetoactive plasma longitudinal waves with phase velocity near light velocity existence, investigating increments during synchrotron instability due to relativistic particles

23 p3262 A72-43311

Compression of high current relativistic electron beams using converging magnetic fields

23 p3315 A72-43525

The concepts of mean force, mean velocity, and ensemble velocity for a particle ensemble

24 p3425 A72-45070

Longitudinal electromagnetic wave excitation in restricted plasma by relativistic electron beam injection, determining increments frequency distribution and width of spectra

24 p3431 A72-45717

RELATIVISTIC PLASMAS

Electromagnetic wave propagation perpendicular to applied uniform magnetic field in relativistic plasma, deriving dispersion relation for stability criterion

02 p0264 A72-12024

Relativistic plasma with particles interacting through electromagnetic field, constructing statistical description by reduced distribution functions and correlation patterns

03 p0395 A72-13626

Self consistent kinetic equations for evolution of particle distribution functions and wave intensity spectra of relativistic spatially homogeneous multispecies plasma in ambient magnetic field

04 p0553 A72-14401

Repeated explosions mechanism in nuclei of galaxies and quasars due to instability in twisted magnetic fields, noting clouds and relativistic plasma ejection

05 p0717 A72-16379

Book on electromagnetic waves in moving magnetoplasmas covering propagation in infinite and bounded plasmas subject to magnetic fields for nonrelativistic and relativistic velocities

05 p0695 A72-16396

Dispersion relations for frequencies near first two harmonics of perpendicular magnetosonic waves in relativistic anisotropic plasmas

05 p0698 A72-17020

Ultrarelativistic cosmic plasma analysis of high density electron beams transport across strong magnetic fields with application to pulsar NP 0532 spectrum

07 p1064 A72-20634

Dielectric permeability tensor operator for surface wave-electron beam interaction in relativistic nonuniform plasma stream with cylindrical geometry

09 p1359 A72-22769

Ion acceleration by relativistic electron-beam-formed plasma, explaining ion energy dependence on neutral gas pressure by potential well model

10 p1518 A72-23961

Stability of superluminous and subluminal waves propagating transversely to external uniform magnetic field in streaming relativistic plasmas

10 p1522 A72-24608

Nonthermal ultrarelativistic plasmas covariant analysis with quantum electrodynamics and Green function theory of nonequilibrium statistical mechanics, discussing electron-positron pair production and annihilation

10 p1525 A72-25100

Zero temperature relativistic plasma ground state energy calculation using Fermi momentum and Green function

11 p1694 A72-25715

Relativistic plasma particle correlation function based on transverse electromagnetic field energy density treatment by enlarged Bogoliubov hypothesis

10 p2140 A72-30881

Nonequilibrium relativistic plasma fluctuations with direct movement of particles, considering isotropic velocity distribution of particles

15 p2289 A72-32695

Kinetic equations with radiation effects

17 p2590 A72-35155

Constants of the linearized motion of Vlasov-plasmas

17 p2590 A72-35158

On the physical nature of cosmic electromagnetic absorption. VI - The Einstein-de Sitter cosmology with plasma coupled to radiation at relativistic temperature

20 p2967 A72-39186

The self-consistent test-particle approach to relativistic kinetic theory

20 p2955 A72-40013

Isometric motion in relativistic magnetohydrodynamics

21 p3091 A72-40567

Self-consistent electromagnetic waves in relativistic Vlasov plasmas

24 p3430 A72-45569

RELATIVISTIC THEORY

Model with large Lorentz factor and relativistic relations violations to explain theoretical estimate disparity with experimental data for high energy primary cosmic rays

01 p0118 A72-10156

Relativistic nonlinear gravitational instability theory for hydrodynamical system of equations applicable to early cosmic expansion, deriving density perturbations associated with rotational and gravitational waves

02 p0275 A72-11524

Gaseous general relativistic kinetic theory, detailing matter model, thermodynamics, cosmology and Einstein field equation completion with Liouville or Boltzmann equation

03 p0388 A72-13266

Transport coefficients of relativistic gas by method of moments, assuming constant differential cross section of particle interactions in center of mass system

04 p0547 A72-14630

Monograph on nonequilibrium relativistic kinetic theory covering heuristic approach, Boltzmann equation, H theorem, equilibrium distributions, relativistic

thermodynamics, phenomenological transport theory, heat conduction coefficients, etc

05 p0689 A72-16289
Relativistic fluid dynamics - Conference, Bressanone, Italy, June 1970

06 p0846 A72-17251
Relativistic hydrodynamics, considering Cauchy problem in fluid evolution, ideal isentropic fluids, electromagnetic field effect and viscous/heat conducting thermodynamic flow models

06 p0846 A72-17252
Magnetosonic, Alfvén, shock and infinitesimal waves and corresponding rays in relativistic hydrodynamics and magnetohydrodynamics, using tensor distributions

06 p0847 A72-17253
General relativistic kinetic theory of gases, discussing microscopic model, space-time, self-consistent Einstein-Maxwell-Liouville equations and irreversible processes

06 p0847 A72-17255
Relativistic heat propagation models, considering hyperbolic system of partial differential equations, momentum-energy tensor for ideal fluid and classical Fourier law

06 p0847 A72-17256
Perturbations in Gödel universe, considering Einstein equations in relativistic cosmology

06 p0876 A72-17564
Stationary stars rigid and differential rotation angular velocity limits, showing analogous conditions in general relativity

06 p0882 A72-18001
Unsolved fluid dynamic problems, considering viscous fluids, epiphydrodynamics, magnetohydrodynamics, relativistic fluid dynamics and interstellar gas dynamics

06 p0800 A72-18112
Wightman field theory generalization for application to gravitational field quantization, describing curved space-time by strongly geodesically complete manifolds

07 p1036 A72-20198
Soviet monograph on universal gravitation covering pre-relativistic theories, inverse square law, relativistic effects, celestial mechanics, stellar structures and evolution, etc

08 p1231 A72-21025
White dwarfs rotation parameters relation to angular velocity within general relativity compared to analogous calculations in Newtonian theory

08 p1234 A72-21284
Equations of state for ultrahigh densities, obtaining relativistic statistical thermodynamics description of hadronic interactions

10 p1533 A72-23891
General relativistic gravitational waves analogy with electromagnetic radiation, examining relation to collapsed astronomical objects from black hole properties

10 p1533 A72-23893
Clebsch transformation in relativistic MHD, considering Maxwell equations in vacuum and electromagnetic perfect fluid in isentropic flow

10 p1519 A72-24126
Cold static superdense model for white dwarf and neutron stars, using relativity theory and variational principles for stellar structure in hydrostatic equilibrium

11 p1715 A72-25528
Local and cosmological irreversibility and time anisotropy theories from thermodynamics, statistical mechanics, astrophysics and quantum-relativity viewpoints

11 p1716 A72-25775
General relativity equations solution for interaction of gravitational radiation and conducting fluids in magnetic field, noting energy absorption in specified depth surface layer

11 p1720 A72-26116
Relativistic fluids dynamic equations, using Banach type Lagrangians

11 p1689 A72-26503
Chernikov approximation for general relativistic thermodynamics nonstationary equations of heat transfer, thermal and viscous stresses and entropy balance

12 p1844 A72-27188
Relativistic statistical mechanics invariant formula for coherence degree of plane blackbody radiation beam in arbitrary Lorentz frame, noting transformation law of temperature

12 p1846 A72-27741
Finite particle propagator constructed by path integral method, deriving infinitesimal propagator in relativistic quantum mechanics from mass nature consideration in Machian cosmological sense

13 p2001 A72-28499
Gravitational theory strong discontinuity conditions, using basis variational equation for field and media model construction in general relativity theory

13 p2002 A72-28711
Relativistic and Newtonian theory compared for orbiting satellite matter release criteria and subreleasing

change effects during gravitational collapse of central dense core

13 p2040 A72-29407
Relativistic theory gravitational analogue to electromagnetic radiation, suggesting black hole collision as galactic center flux mechanism

15 p2273 A72-31286
Charge and mass densities relation for stationary charged dust distribution in general relativity, investigating Einstein-Maxwell equations for stationary gravitational field

15 p2275 A72-31591
Quasar electromagnetic radiation emission in terms of general relativistic coupling between gravitational field and charged particle radiation field

15 p2306 A72-31592
Computational method for determining numerical values of relativity by two-way Doppler radio tracking and ranging data from planetary orbiting spacecraft

15 p2310 A72-31978
Space charge electron flow between parallel conducting walls, developing relativistic method for potential and field distribution time variation

15 p2279 A72-32510
Anisotropic and isotropic descriptions of physical process speeds in special relativity theory space-time metric

15 p2279 A72-32768
Lorentz-covariant procedure for equations of structure and motion of particles represented by singularities in Einstein relativistic field theory

16 p2422 A72-32880
Combustion fronts velocity comparison with light speed in relativistic hydrodynamics and MHD

17 p2589 A72-34911
Papers on kinetic equations covering axiomatics, quantum and relativistics, plasma kinetic theory role in spectral line width, etc

17 p2590 A72-35151
The self-consistent test particle approach to relativistic kinetic theory.

17 p2590 A72-35156
Relativistic kinetic theory combined with surface layer theory in curved space-time to study counter-rotating disks with fine central red shift

17 p2582 A72-35389
Nonspherical perturbations of relativistic gravitational collapse. I - Scalar and gravitational perturbations. II - Integer-spin, zero-rest-mass fields.

17 p2612 A72-35390
Closed rotating cosmologies containing matter described by the kinetic theory - Entropy production in the collision time approximation.

17 p2618 A72-35823
Magnetized deformable media in general relativity.

17 p2584 A72-35911
General relativistic planetary structures comparison with Newton gravitational theory, deriving field equations for spherically symmetric planets with explicit pressure and density distributions

18 p2728 A72-36751
Relativistic thermodynamics development based on invariant entropy concept, considering frictionless heat conduction and Carnot cycles

19 p2835 A72-37928
German book - Relativistic astrophysics

19 p2868 A72-38721
The Robertson-Walker cosmology and the Friedmann cosmology

20 p2975 A72-40071
Lorentz contraction and transformation of equilibrium forces and moments in inertial reference systems transition, discussing special relativity theory

21 p3084 A72-40938
Relativistic quasi-linear equations solution in dynamic theory of type III solar radio bursts under initial conditions of local explosion

21 p3101 A72-41295
Causality in the relativistic theory of elastic media in the three-dimensional case.

22 p3206 A72-42626
Solar neutrino flux dependence on gravitational effects, discussing Brans-Dicke gravitation theory and general relativity equations

22 p3229 A72-42957
Approximate solutions of the relativistic gravitational field equations to describe clusters of galaxies.

RELATIVISTIC VELOCITY

Relativistic equations of motion of charged particle interacting with plane electromagnetic wave propagating at arbitrary angle to uniform magnetic field for magnetosphere model

04 p0554 A72-14406
Variable radio structure model using relativistic electron cloud outbursts in stationary magnetic field tubes for faster than light velocities

10 p1536 A72-24139
Relativistic counterpart of Poincaré condition for angular velocity of rigidly rotating star, discussing equilibrium disturbance effects

10 p1549 A72-25058
Electromagnetic plane field cumulation by heavy conducting shells implosion with quasi-relativistic

velocity, solving Maxwell equations by characteristics method

12 p1851 A72-27396
Electromagnetic and gravitational waves emission by superlight sources in vacuum, considering multiparticle and form factor cut-off effect

14 p2130 A72-30625
Requirements and techniques of interstellar navigation, discussing astronomical maps and observational phenomena at relativistic travel velocities

15 p2267 A72-31291
Slowly rotating relativistic stars. VI - Stability of the quasi-radial modes.

20 p2966 A72-38909

RELATIVITY

Gravitational biology theory problems, discussing possibility of applying relativistic phenomena to living organisms in inertial or inertialess systems

02 p0160 A72-12016
Null electromagnetic field propagation in general relativity, applying to Stokes parameters definitions for monochromatic light

02 p0259 A72-12178
Einstein gravitational field equations plane-front parallel ray wave exact solutions generalization to f-g gravity theory equations exact solutions

02 p0260 A72-12375
General theory of relativity, examining differences between singularities in stationary and nonstationary fields from gravitational equations solutions

02 p0261 A72-12675
Particle motion in uniform acceleration field via Schwarzschild line element of general relativity, applying to clock paradox

03 p0388 A72-13227
General relativity and cosmology - Conference, Varenna, Italy, June-July 1969

03 p0426 A72-13265
Relativistic cosmological model, showing relation to fluid dynamics in Newtonian theory and space-time dependence on causality condition

03 p0426 A72-13267
General relativity and cosmology of quasi-stellar objects, covering distances, red shifts and gravitational fields

03 p0426 A72-13270
Homogeneous isotropic elastic medium free vibration in unbounded space, obtaining relativistic relations in wave field from mathematical model

03 p0389 A72-13425
Cosmological gravity fourth-order equation system yielding geodesic lines, considering cylindrical and spherical universes

03 p0435 A72-13726
Symplectic structure of continuous system, constructing relativistic free vibrating cord without linearization

03 p0389 A72-13792
Equilibrium rotating superdense baryons in general relativity theory, determining integral parameters /mass semiaxes quadrupole moment/ in angular velocity approximation

03 p0435 A72-13805
Tensor-tensor theory of gravitation, introducing first effect of Mach principle

04 p0573 A72-14905
General relativistic generalized field equations for scalar dependent tetrad, noting identity with Brans-Dicke theory

04 p0549 A72-15021
Variational principles in general relativity, deriving Einstein field equations and equations of motion for charged and uncharged self gravitating fluids

06 p0847 A72-17254
Quasar luminosity due to unique big bang in specific space-time region, considering Minkowskian geometry

06 p0878 A72-17669
General theory of relativity for symmetric field, discussing DE Dönder incompressible fluid model and Tolman-Schwarzschild metrics

06 p0847 A72-17682
Lorentz transformation role in special to general relativity theory transition, noting neglect by Einstein and general covariance physical meaning exaggeration

06 p0848 A72-17991
Energy complex in general relativity in form of tetrahedral gravitational theory, including solutions to Einstein equations

06 p0849 A72-18419
Neutral rotating mass shell surrounding concentric stationary electrically charged insulation, calculating induced dipole-like magnetic field from coupled linearized general relativity field equations

06 p0853 A72-18423
Astrophysics and general relativity - Conference, Brandeis University, Waltham, Massachusetts, June-July 1968

07 p1073 A72-19426
Exact cosmological solutions in Brans-Dicke scalar tensor theory, noting consequences for solar relativistic effects

07 p1075 A72-19584

Gravitational field potential energy-momentum pseudotensor component determination in general relativity theory

08 p1207 A72-21301

Particle motion in conformal spaces in general relativity, deriving gravitational potential and proper energy of mass point

08 p1209 A72-21369

Hydrodynamic analogy for astrophysical effects of general relativity theory, analyzing Chaplygin gas motion in three dimensional curvilinear coordinate system

08 p1209 A72-21876

Toroidal gravitational waves in general relativity, considering analog to imploding-exploding cylindrical waves, linear field equations and symmetric metric

08 p1210 A72-21922

Book on astronomy and cosmology covering big bang, steady state and oscillating universe theories, radio sources, galaxies, interstellar meteor relativity and extraterrestrial life

09 p1389 A72-23248

Gravitational red shift due to three body effect as relativity test

10 p1532 A72-23850

Asymmetric Einstein equations with impulse-energy tensor in canonical form derived from variational principle, defining space-time continuum as pseudo-Riemann manifold

10 p1510 A72-24120

Stress distribution in general relativity on oriented compact Riemann manifold

10 p1511 A72-24206

Einstein field equation representing static fluids in general relativity, obtaining all solutions with degenerate Weyl tensor

10 p1511 A72-24349

German book on gravitation theory and equivalence principle, covering Lorentz invariance in Riemann space, relativity and Einstein effects

10 p1512 A72-24752

Relativistic explanation for excess motion of Mercury perihelion in terms of solar oblateness and interior rotation mechanism

[AD-745666]

11 p1715 A72-25350

Second order gravitational waves in Einstein-Riemann four dimensional space-time, using method of characteristics

11 p1685 A72-25529

Gravitational collapse in Brans-Dicke and Einstein theories of gravity

11 p1716 A72-25530

Relativistic homogeneous anisotropic models analogs construction in Newtonian cosmology

11 p1716 A72-25711

Restricted two body problem anomalistic and sidereal orbital periods in general relativistic coordinate and proper time, noting cosmological constant

11 p1719 A72-25971

Body of revolution /saucer/ with nongeodesic internal stresses under gravitational field in terms of general relativity theory

12 p1843 A72-27048

Black hole concept in general relativity and gravitational collapse, considering deviations from spherical symmetry and gravitational wave emanation from Galactic center

12 p1871 A72-27690

General relativity equation of motion for spherically symmetric surface layer of ideal gas under central gravitational field

13 p2035 A72-28646

Japanese cosmological studies covering evolutionary cosmology, astrophysics, relativity, nuclear physics and metagalactic phenomena

13 p2038 A72-29083

Relativistic treatment of Dirac-Hestenes and Maxwell equations

13 p1987 A72-29787

Local Lorentz transformation in chronometric invariants, demonstrating appropriate operation for general covariant tensors from tetrad formalism

14 p2130 A72-30218

Axisymmetric celestial bodies equilibrium shapes in post-Newtonian approximation of general relativity using integrodifferential equation

14 p2161 A72-31077

Regge calculus representation existence for solutions of initial value problem for spaces with axial symmetry

16 p2422 A72-32879

Gravitational field potential energy-momentum pseudotensor component determination in general relativity theory

17 p2580 A72-34659

Field variations of perfect fluid in axisymmetric stationary universe within general relativity theory concept, noting energy extremal properties for rotating stars

17 p2607 A72-34921

On the stability of axisymmetric systems to axisymmetric perturbations in general relativity. I - The equations governing nonstationary, stationary, and perturbed systems.

17 p2611 A72-35315

Relativistic hydrodynamics and gravitational instability.

17 p2581 A72-35356

Intermediate-range gravity - A generally covariant model.

17 p2581 A72-35380

Static black hole noninteraction with exterior world by meson fields, noting baryon number conservation in general relativity

17 p2612 A72-35388

Quantum models for the lowest-order velocity-dominated solutions of irrotational dust cosmologies.

17 p2613 A72-35392

Hamiltonian formulation of spherically symmetric gravitational fields.

17 p2582 A72-35393

WKB approximation and oscillatory behaviour of null geodesics in general relativity.

17 p2583 A72-35795

Around-the-world atomic clocks - Observed relativistic time gains.

17 p2584 A72-35839

The Cauchy problem for the nonlinear Boltzmann equation in general relativity

18 p2710 A72-36471

Isotropic, space-like, Maxwellian particles of real mass and of time-like velocity

18 p2710 A72-36472

Hulthén and Schwarzschild potentials in the Klein-Gordon equation.

18 p2711 A72-36515

Book on classical relativity theory covering relativistic kinematics and mechanics, tensor calculus, electrodynamics, gravitational fields and effects, elastic continua mechanics, thermomechanics and cosmology

18 p2712 A72-36850

Locally Lorentz covariant gravitational field theory of Pauli-Fierz type with massless symmetric spin-2 field having source term as matter stress-energy tensor

18 p2712 A72-37161

Einstein relativity principle incompatibility with conservation of angular momentum, discussing invariance of inertia reference systems and formulas for relative and absolute velocities

19 p2834 A72-37921

Gravitational spin interaction.

19 p2835 A72-38425

Harmonic frames of reference in Einstein's theory of gravitation

20 p2953 A72-39406

Relativity gyroscope experiment at arbitrary orbit inclinations.

20 p2972 A72-39870

Book - General relativity: Papers in honour of J. L. Synge.

20 p2954 A72-40001

Einstein theories of special and general relativity, taking into account physical concepts relation to mathematical formalism, equivalence principle, field equations and gravitational waves

20 p2954 A72-40002

Poincaré, Lorentz and Einstein contributions to relativity theory construction according to Whittaker, discussing influence on contemporary scientists

20 p2954 A72-40003

The geometry of free fall and light propagation.

20 p2954 A72-40005

Plane-symmetric similarity solutions for self-gravitating fluids.

20 p2955 A72-40009

Gravitational field of arbitrarily thick steadily rotating shell in general relativity, using successive approximation method

20 p2955 A72-40010

General relativity equations for hydrostatic equilibrium of spherical distribution of mass combined with equations of state for highly relativistic neutron star central regions

20 p2955 A72-40011

The relativistic Boltzmann equation.

20 p2955 A72-40012

Spatially homogeneous general relativistic Bianchi cosmological models with diagonal metrics, noting field equations simplicity

21 p3104 A72-40569

Classical physics treatment combined with constitutive equations for local relativistic equivalence and material indifference principles

21 p3085 A72-41201

A new test of the second postulate of special relativity sensitive to first-order effects.

21 p3085 A72-41214

Gravitational theory strong discontinuity conditions, using fundamental variational equation for field and media model construction in general relativity theory

22 p3204 A72-42089

Double star components light aberration dependence on relative velocity of source and observer, considering two reference systems

22 p3225 A72-42458

On the stability of axisymmetric systems to axisymmetric perturbations in general relativity. II - A criterion for the onset of instability in uniformly rotating

configurations and the frequency of the fundamental mode in case of slow rotation.

22 p3206 A72-42566

Exact expressions for the properties of the zero-pressure Friedmann models.

22 p3229 A72-42890

Book - Gravitation and cosmology: principles and applications of the general theory of relativity.

22 p3208 A72-43080

Relativistic test particle escape from circular orbit around central mass due to mass loss, considering orbiting body corrections due to general relativity

23 p3335 A72-43265

Chaplygin gas flow equation for analogy between hydrodynamic and electrodynamic equations, noting special theory of relativity

23 p3312 A72-43404

Joining of two semiclosed worlds and a cosmological model of matter-antimatter asymmetry.

23 p3336 A72-43489

Generalization of the Taub-Kazner cosmological metric in the scalar-tensor gravitation theory.

23 p3313 A72-43500

Natural rotation of bodies in Einstein's theory of gravitation

23 p3313 A72-44038

Theoretical framework for testing gravitation and general relativity theories, considering completeness, self consistency and agreement with Newtonian physics

23 p3314 A72-44262

Ephemerides and improved orbital elements of minor planets, noting general theory of relativity verification from astronomical observations of Icarus

24 p3437 A72-44758

Angular momentum conservation laws formulation for Einstein field equations solution in general relativity, applying to Kerr metric

24 p3425 A72-44787

Closed-path interferometric experiments on the speed of light from moving sources.

24 p3425 A72-44788

Hyperbolic space criterion for cosmological model based on axioms conforming to special and general theory of relativity, noting coordinate transformation

24 p3439 A72-44969

On the gauge groups of linear conservative gravitational theories.

24 p3447 A72-45630

Body of revolution /saucer/ with nongeodesic internal stresses under gravitational field in terms of general relativity theory

24 p3425 A72-45701

RELAXATION

Ionized plasma electron velocity distribution function relaxation numerical calculation to validate local Maxwellian form during transport process

11 p1693 A72-25523

RELAXATION [MECHANICS]

NT SPIN-LATTICE RELAXATION

NT STRESS RELAXATION

Kinetic theory application to initially nonuniform gas relaxation to equilibrium, obtaining macroscopic velocity, density and temperature solutions by multitime scale perturbation methods

03 p0340 A72-13155

Different pair potentials for simulating vacancy in Al, discussing program planning for relaxations calculation around vacancy to effect computing time reduction

03 p0378 A72-14253

Quasi-linear relaxation of fast ion beam in cold plasma moving transverse to magnetic field

04 p0554 A72-14403

Random method solution of Boltzmann equation for pseudoshock /relaxation mixing/, applying to random collisions of molecular beams

04 p0551 A72-14519

Fast particle interaction with intergalactic matter, discussing relaxation of power law cosmic ray spectra

04 p0570 A72-14553

Self focusing of electromagnetic waves in isotropic plasma, investigating nonlinear relaxation processes

04 p0489 A72-15391

Fatigue strength optimization of bonded double strap metal joints, attributing stress concentration to plastic relaxation

[ASME PAPER 71-MET-Q]

05 p0731 A72-15791

Lynden-Bell statistical mechanics predictions compared with most and least violently relaxed one dimensional self gravitating systems, using computer experiments

05 p0714 A72-16055

Collective relaxation of two phase space density collisionless one dimensional self gravitating stellar systems, following boundary curve motion

05 p0714 A72-16057

Micron sized particle velocity relaxation measurement in shock wave, using laser Doppler methods

[CLEA PAPER 11,3]

07 p1005 A72-19389

Steady state and temperature relaxation of rarefied gas between two plane parallel plates

08 p1211 A72-21871

Electron beam and plasma nonlinear interactions, noting scattering zone, amplitude oscillation maximum, longitudinal velocity and relaxation patterns 10 p1517 A72-23760

Sound waves radiative damping in isothermal atmosphere, discussing relaxation influence on model response to body force and chromosphere dissipation effect on oscillation 10 p1543 A72-24622

Soviet papers on vibrational combustion systems covering flames relaxation in annular combustion chambers 11 p1745 A72-25751

Oscillatory relaxation combustion in annular chamber, applying kinematic theory to combustion frequencies and regions calculation 11 p1745 A72-25752

Oscillatory relaxation combustion regions determination in high pressure gas injection tubes, noting flame propagation rate relationship with mixing concentration 11 p1745 A72-25754

Temperature anisotropy quasi-linear relaxation thermodynamics in collisionless plasma, analyzing system free energy 11 p1698 A72-26599

Probability and collisional relaxation in stellar systems, discussing gravitational polarization, collective interactions and spatial inhomogeneity 12 p1872 A72-27891

Boundary curves for collective relaxation in one dimensional collisionless two phase space density self gravitating stellar system evolution, noting velocity dispersions dependence 12 p1875 A72-27913

Relaxation processes enhancement by collective particle collisions effects in plasma, stressing application to stellar dynamics 12 p1853 A72-27915

Rheological stress-strain relations in nonlinear viscoelasticity theory, calculating relaxation parameters for isotropic viscoelastic circular cylinder 13 p2059 A72-29493

Vibrational relaxation mechanism in supersonic flows of chemically reacting carbon dioxide-nitrogen mixture, using numerical integration 13 p1913 A72-29502

Russian papers on relaxation mechanisms in solids covering microscopic theory, mechanical, electrical, chemical, thermal and magnetic processes, equipment and techniques 14 p2121 A72-30951

Temperature aftereffect in heating and cooling of metals with cubic and noncubic lattices in relation to relaxation and hereditary deformation 14 p2143 A72-30952

Loading conditions effect on relaxation and creep in inhomogeneous hereditary elastoplastic polycrystalline materials 14 p2168 A72-30953

Mobile point defects interaction with moving dislocation in inelastic solid bodies, considering energy dissipation due to impurity relaxation 14 p2169 A72-30954

Dislocation substructures effect on relaxation and internal friction peak in cold rolled Mo single crystals after annealing 14 p2122 A72-30956

Relaxation and internal friction characteristics of beta-rhombohedral B at 80-1000 K, using LF vacuum oscillator with inverted torsion pendulum 14 p2122 A72-30958

Internal friction and relaxation mechanisms in substructure hardened fcc alloys and bcc metals, presenting dislocation parameters for annealed and cold worked Fe alloys 14 p2122 A72-30960

Unsteady torsional creep of multiply connected cylindrical rod with arbitrary cross section, calculating elliptic rod relaxation 15 p2327 A72-31744

Relaxation oscillations in dynamic systems describing turbulence in fluid, rigid body and particle motions 15 p2263 A72-31755

Plasticity, elastic relaxation and stress-strain relation characterization for Schofield-Scott Blair media, using nonequilibrium thermodynamics method 15 p2331 A72-32482

Recovery-work hardening model of steady state creep for Al, assuming equal internal and applied stress 15 p2259 A72-32642

Grain-size dependence of Snoek peaks in niobium. 17 p2566 A72-34671

Radiant interchange among suspended particles and its effect on thermal relaxation in gas-particle mixtures. [DFVLR-SONDDR-210] 17 p2638 A72-35643

Solution to a relaxation problem by the discrete velocity method with the aid of the Boltzmann equation 17 p2586 A72-35809

Relaxation of a reacting gas described by the Boltzmann kinetic equation 19 p2838 A72-38856

Mechanism for relaxation of cavitation erosion based on small perturbations, eliminating theory-experiment contradictions 21 p3044 A72-40271

Tunneling generation, relaxation, and tunneling detection of hole-electron imbalance in superconductors. 21 p3097 A72-40774

Relaxation oscillations in the envelopes of luminous red giants. 21 p3105 A72-41034

A possible problem in measuring hydrogen diffusivity at low temperatures by the Gorsky effect. 22 p3190 A72-42443

Relaxations in polymers at low temperatures. 22 p3196 A72-42793

Weak shock wave propagation in a relaxing gas. 24 p3391 A72-45042

Dispersion relations of scalar hereditary theory of nonlinear viscoelasticity, representing integral operators as orthonormalized function series in Fourier space 24 p3459 A72-45264

RELAXATION (PHYSIOLOGY)

Myorelaxant 3,5-dimethyl-4-bromopyrazol injection effect on rabbit and dog heart during direct extracardiac nerve stimulation 05 p0618 A72-16358

Force-velocity relations in cat papillary muscles isotonic relaxation, discussing effects of preloads and afterloads, temperature and stimulation frequency 09 p1265 A72-22864

RELAXATION METHOD (MATHEMATICS)

General MHD duct flow problems solution using machine transformation and finite difference technique supplemented by successive overrelaxation [ASME PAPER 71-WA/APM-15] 05 p0694 A72-15965

Difference equations and relaxation method for three dimensional transonic flow field about wings in terms of velocity potential [AIAA PAPER 72-189] 05 p0605 A72-16843

Large deflection of rectangular thin elastic plates with unsupported edges, using finite difference technique based on dynamic relaxation methods 06 p0895 A72-17799

Relaxation analysis of discontinuities in axisymmetric rotating actuator disk flow 11 p1569 A72-25622

Relaxation method for thermal computation programs to solve nonlinear heat exchange equations for steady state temperature distribution, discussing numerical instability due to linearization 14 p2170 A72-30684

Earth atmosphere water vapor mixing ratio profiles from relaxation method for full radiative transfer equation inverse solution 15 p2266 A72-32724

Norms of the successive overrelaxation method. 17 p2574 A72-34448

Existence of a unique solution for a class of nonlinear systems of equations and its calculation by iterative methods 19 p2827 A72-38546

Computation of single-conductor and symmetric and asymmetric two-conductor stripline characteristics by the relaxation method. 21 p3036 A72-41831

Large deflections of flat arbitrary membranes. 22 p3235 A72-42604

RELAXATION OSCILLATORS

NT PHANTASTRONS

Transferred electron microwave oscillators /three-level and LSA relaxation types/ and amplifiers /reflection and traveling wave types/ fabrication, technology and performance capabilities 01 p0035 A72-10627

Large signal nonlinear modeling and digital simulation of microwave transistor power amplifier and GaAs Gunn relaxation oscillator 01 p0041 A72-10691

High peak power LSA epitaxial GaAs diode relaxation oscillator breakdown under neutron irradiation 01 p0044 A72-11309

Directly heated cathode effect on He-Ne laser power output and relaxation oscillations in discharge gap 02 p0239 A72-12763

Relaxation processes in Michelson interferometer as integral part of carbon dioxide laser cavity in phase Q switching regime 04 p0530 A72-14990

Neutron irradiation induced material degradation and circuit failure in high power GaAs Gunn diode oscillator operating in LSA relaxation mode 06 p0788 A72-18472

Time behavior and spectra of relaxation oscillations in high gain IR xenon laser 07 p1001 A72-19199

Relaxation oscillator synchronized by quartz crystal between emitter and base of unijunction transistor, obtaining sinusoidal output by series-connected RC load 13 p1926 A72-28377

Relaxation oscillations in He gas discharge tubes with cold Mo cathode as function of pressure and discharge length 15 p2245 A72-31408

Tunnel diode harmonic relaxation frequency divider, obtaining large division factors and wide synchronization bands with sinusoidal output signal 15 p2206 A72-31666

Electron-relaxation effects in transferred-electron devices revealed by new simulation method. 18 p2667 A72-36689

LSA diode relaxation oscillator loading effect on oscillation damping, calculating optimum loading as function of conductance 18 p2667 A72-36690

Classical nonlinear electronic relaxation oscillators as EPR and NMR signal detectors, reconstructing resonance lines from absorption induced oscillator waveform changes 18 p2662 A72-36993

Stabilization of relaxation oscillators with components having an S-shaped current-voltage characteristic 20 p2906 A72-38891

Directly heated cathode effect on He-Ne laser power output and relaxation oscillations in discharge gap 20 p2931 A72-39069

Relaxation oscillations induced in semi-insulating CdS with helium neon laser irradiation. 20 p2934 A72-39817

Influence of a magnetic field on the operation of an oscillator employing a two-base diode 21 p3032 A72-40791

Final stages of transistorized sweep generators 22 p3158 A72-42114

RELAXATION TIME

Charged particles magnetic scattering on cyclotron instability waves of radiation belt plasma, estimating proton relaxation time 01 p0119 A72-10608

Shock wave damping and droplet atomization function of relaxation zone in noncombustible two phase gas-liquid mixtures 02 p0202 A72-11592

Carbon dioxide and hydrogen mixtures in shock tube, noting rotational- and translational-vibrational energy transfer role from relaxation time measurement 02 p0203 A72-12028

Compressible gas subsonic or transonic flow in front of obstacle, determining stagnation pressure with thermal relaxation time by numerical and wind tunnel methods 02 p0151 A72-12097

Linear viscoelasticity theory dynamic functions, deriving delay and relaxation times distribution functions in polymers 02 p0293 A72-12211

Ion and electron temperatures difference relaxation rate in uniform plasma, noting relationship to Debye length 02 p0267 A72-12769

Collisional relaxation rate effects of atomic level polarization on spectral line formation in solar magnetic regions 03 p0427 A72-13294

Carrier transport effects in semiconductors for carrier recombination time approaching relaxation time 03 p0333 A72-13863

Se and Zn doped n and p type gallium arsenide point defects, considering thermal conductivity, relaxation time and phonon scattering cross section effects 03 p0404 A72-14239

Relaxation time estimation for electron velocity relative to dilute vortex core array in rotating neutron superfluid, applying to pulsar slowdown rate 04 p0571 A72-14590

Pulsed nitrous oxide molecular laser upper energy level relaxation time measurement by afterglow pulse-gain technique 04 p0529 A72-14601

Collisionless relaxation of interpenetrating ion beams in Ar plasma, showing velocity spectrum broadening during Langmuir frequency periods 06 p0853 A72-17394

Markov processes in stellar dynamics, discussing relaxation and evaporation times and star velocity distribution for galactic cluster models 09 p1390 A72-23504

Observation and ionization relaxation times of Ar plasma produced in shock tube at Mach 10-13, describing experimental arrangement 10 p1519 A72-24056

Microwave equipment for electron density profiles determination used in ionization relaxation start study of shock induced Ar plasma 10 p1519 A72-24067

Solid state laser with slow relaxation bleachable filter, calculating modes self synchronization probability statistics relationship to relaxation time 10 p1492 A72-24512

Time resolved gain in water and water-gas mixtures as function of composition and excitation current, considering relaxation rate in pulsed water vapor laser
11 p1691 A72-25302

Linear viscoelasticity theory dynamic functions, deriving delay and relaxation times distribution functions in polymers
11 p1734 A72-25709

Shock tube rotational relaxation time measurements in cryogenic hydrogen, using laser schlieren optical system
11 p1691 A72-26008

E layer effective recombination coefficient determination from solar flare enhanced electron density and solar X-ray flux measurements and ionospheric relaxation time constant evaluation
11 p1627 A72-26766

Fall time calculation and junction capacitance effect in diodes with nonuniform base doping switched off by voltage and current generators
11 p1607 A72-26963

Chandrasekhar statistical stellar dynamics assumption generality compared to Chandrasekhar diffusion process, discussing discontinuous model, relaxation time, escape probability and numerical results
12 p1872 A72-27893

Galactic disk systems relaxation time due to particle encounters, discussing validity of Boltzmann-Vlasov equation
12 p1872 A72-27894

Massless test star velocity vector deflection in stellar field from numerical integration on relaxation times
12 p1873 A72-27901

Conductive heat propagation with finite rate for semibond solid body under periodic surface temperature fluctuations dependent on relaxation time
12 p1890 A72-28174

Relaxation hypothesis of cavitation erosion based on small perturbations, eliminating theory-experiment contradictions
13 p1941 A72-28776

Electron contribution to phonon damping in anharmonic metal for collision-free regime, evaluating relaxation times
15 p2277 A72-31890

Microwave diode switch operating at 35 GHz for spin lattice relaxation time measurement, discussing insertion loss, and rise and decay times characteristics
16 p2369 A72-33623

A review of the unified theory of relaxations in plasmas.
17 p2590 A72-35159

Gain and relaxation studies in transversely excited HF lasers.
17 p2564 A72-35344

Monochromatic carbon dioxide TEA laser
17 p2564 A72-35424

Sudden freeze approximation for fluid flow systems relaxation time at constant enthalpy and pressure
17 p2542 A72-35633

Chemical reactions effects on gas dynamics, considering relaxation phenomena in fluid flow
18 p2679 A72-36384

Nonlinear time evolution of firehose unstable MHD waves, noting quasi-linear theory truncation error for low wave numbers relaxation time and energy growth
19 p2839 A72-37334

Mathematical model for dielectrics with time dependent polarization, noting relaxation time distribution function
21 p3085 A72-41074

Homogeneous stellar system with purely gravitational interactions, predicting oscillatory relaxation time
22 p3207 A72-42853

Numerical simulation of the relaxation of a beam of charged particles in a strong electric field
23 p3315 A72-43530

Linearization of relaxation-time control in a transistorized multivibrator
23 p3270 A72-43765

Sound absorption in atmosphere at 20 C, predicting relaxation times and strengths in 100 Hz to 1 MHz as functions of relative humidity
23 p3285 A72-44112

Measurement of thermal relaxation time of vibration of polyatomic molecules by the impact tube method
24 p3402 A72-45045

Equations of motion of a viscous fluid with relaxation properties
24 p3393 A72-45256

Catalytic efficiencies of H₂O, D₂O, NO, and HCl in the vibrational relaxation of HF and DF.
24 p3378 A72-45306

Transport properties of a gas of diatomic molecules. V - GPS calculation of the rotational relaxation time of the Ar-N₂ system.
24 p3427 A72-45307

Transport properties of a gas of diatomic molecules. VI - Classical trajectory calculations of the rotational relaxation time of the Ar-N₂ system.
24 p3427 A72-45308

Measurement of longitudinal relaxation times for spin-decoupled protons.
24 p3427 A72-45400

Critical-point anomalies in the electron-paramagnetic-resonance linewidth and in the zero-field relaxation time of antiferromagnets.
24 p3432 A72-45674

RELAY SATELLITES

Eole satellite relay system for weather balloon location and data collection and transmission to ground stations
09 p1394 A72-22600

Trojan deep space communications systems, maintaining powerful relay satellites in equilibrium at Lagrangian points of earth, Mars and Venus orbits
10 p1548 A72-24975

Communication and data relay satellites multibeam antennas characteristics, discussing multiple feed reflectors, bootlace lens configuration and phased arrays
12 p1789 A72-27355

Regional microwave ground distribution facility for TV service organized for satellite relay transmitted video signals accommodation
13 p1918 A72-28984

Lunar exploration integrated program for 1980s, discussing halo orbit lunar far side data relay satellite advantages vs lunar orbit space station
15 p2321 A72-32318

RELIABILITY

NT AIRCRAFT RELIABILITY

NT CIRCUIT RELIABILITY

NT COMPONENT RELIABILITY

NT SPACECRAFT RELIABILITY

NT STRUCTURAL RELIABILITY

Multichannel communication system reliability, considering channel repair time random distribution
01 p0033 A72-11263

Probability weather forecasts reliability, considering utility and spherical and logarithmic validities
08 p1203 A72-22124

Internal and integral aerial photointerpretation, discussing enhancement of information quality, quantity and reliability through participation of experts in various specialized fields
09 p1303 A72-23300

Reliability and maintainability - Conference, San Francisco, January 1972
10 p1485 A72-23972

Computerized and analytic techniques for estimating multiplexed systems output probability distribution, considering system effectiveness, reliability and survivability
10 p1486 A72-23977

Satellite supplement to domestic communication systems, discussing network management, system reliability, broadband capacity, earth station flexibility and market proposals
12 p1781 A72-27374

Silicon solar cell fabrication technology developments for long mission life performance reliability over wide temperature and radiation intensity ranges
12 p1757 A72-28029

Reliability and stochastic stability theory relationships for multidimensional and continuous systems
13 p1985 A72-28486

Accelerated reliability, life, fatigue and performance tests of automatic systems components, noting mathematical models for minimum time techniques
13 p1965 A72-29172

Mass and energy balance in air cooled matrix type phosphoric acid cell, noting operational reliability and construction
16 p2351 A72-33889

RELIABILITY ANALYSIS

Mathematical reliability modeling for fault tolerant digital computers, summarizing error masking and standby sparing reliability equations
02 p0184 A72-11481

Ultrareliable fault-tolerant digital computer design with protective standby replacement and hybrid redundancy, presenting mathematical models for system reliability evaluation
02 p0185 A72-11487

Hardware and software parallel digital computer system described by flow table model, calculating output hazard for unbounded line delay effects
02 p0185 A72-11490

Quantitative reliability criteria for aerial photo decoding, noting dependence on observation time
02 p0229 A72-12172

Uhf varactors reliability, establishing rejection criterion by statistical analysis
02 p0194 A72-12444

Reliability behavior of complex systems with standby redundancy under different failure and repair echelons
02 p0194 A72-12446

Fully redundant relay and data command system for SAS-A satellite, discussing operation and reliability tests
03 p0442 A72-14397

Complex systems stochastic survivability estimates dependence on delay depth and initial conditions of interaction
05 p0640 A72-16204

Kalman linear filtering technique for spinning satellite attitude restitution, evaluating reliability by model for simulation of measurements by sensors
05 p0724 A72-16436

Time to failure statistics for communications satellites redundant systems with spares and negative exponential reliability function, discussing perfect and imperfect switching
05 p0731 A72-17250

Critique on condition for planar antennas physical reliability, concerning smoothness of aperture edges
06 p0782 A72-17362

Reliability of electroencephalography as diagnostic method from specialists interpretation of curve morphological features, discussing normal and pathological record evaluation
08 p1124 A72-21000

Emergency and test ejections with Martin-Baker seats, discussing fatality and injury causes and seat reliability
08 p1112 A72-21565

Graphical analysis of accelerated life test data on insulating fluids, capacitors, bearings and electronic devices, using inverse power law model
08 p1176 A72-21587

Bayes estimators for Poisson distribution random parameters and reliability function, using Monte Carlo method and maximum likelihood estimation
08 p1200 A72-21590

Soviet papers on digital computers application to reliability problems solution for recoverable, failing, controlled, redundant and electronic systems
08 p1179 A72-22051

Quantitative and qualitative reliability estimates for electronic and mechanical products, obtaining conditional probabilities of flawless operation
08 p1179 A72-22052

Reliability analysis of redundant and nonredundant systems with different component failures, using probability theory
08 p1180 A72-22053

Reliability estimates for continuously inspected recoverable systems, determining readiness factor for periodic checkout
08 p1180 A72-22054

Functional readiness of periodically inspected recoverable systems with different failure causes
08 p1180 A72-22055

System reliability improvement by redundancy, noting independence of distribution law type
08 p1180 A72-22057

Reliability of recoverable information systems with temporal redundancy
08 p1180 A72-22058

Reliability of redundant schemes with quorum element, noting optimal parameters for known failure damages
08 p1180 A72-22059

Reliability equivalence systems with excessive and deficient group redundancy, noting replacement conditions and flawless operation probability
08 p1143 A72-22060

Reliability of complex systems performing function with time dependent quantity
08 p1180 A72-22061

Reliability theory distribution function construction for failure analysis in physical processes, considering mechanical system service life and living organisms life span
08 p1180 A72-22062

Radio system operational reliability analysis by mathematical methods with use of digital computer, discussing statistical modeling algorithm
08 p1143 A72-22065

Reliability tests improvement by ergodic processes failure prediction and data storage for high reliability products manufactured in small numbers
08 p1180 A72-22067

Radio system failure prediction based on parameter variation a priori or a posteriori data, determining reliability and optimal preventive maintenance intervals
08 p1143 A72-22070

Bayesian analysis application to reliability and life parameter estimation for Weibull failure model, using Monte Carlo simulation
10 p1503 A72-23978

Probabilistic methods application to software reliability analysis, deriving expressions for hazard, density, failure and reliability functions
10 p1486 A72-23983

Computer reliability in terms of design criteria to minimize faults incidence, discussing failures detection and correction, fault diagnosis and system maintenance
10 p1444 A72-23985

Reliability statistics of third generation computer systems failure causes, emphasizing cumulative effects of hardware and software
10 p1444 A72-23986

Bayes analysis application to Weibull distribution parameters estimation, using entropy concept for figure of merit to assess reliability analysis 10 p1444 A72-23987

Reliability and time to failure prediction for degradation-prone systems via Markov processes theory 10 p1504 A72-23988

Confidence level determination in terms of reliability index /MTBF/ for MIL-STD-781 truncated sequential probability ratio tests 10 p1444 A72-23989

Theorem proved for pattern classification system effectiveness for system reliability prediction 10 p1504 A72-23996

Prediction method for computing maintenance technician reliability as probability of equipment repair completion within given time 10 p1486 A72-24000

Stochastic models of human performance effectiveness functions reliability and correctability from error data generated by tracking and vigilance tasks 10 p1429 A72-24001

Reliability growth curves for product assessment as technical management forecasting technique 10 p1564 A72-24004

Decision making models application to systems configuration, reliability, repair level and spares optimization and availability analysis 10 p1486 A72-24006

Apollo program management decisions based on reliability analysis, discussing incentive fees, testing optimization, engineering changes approval and flight readiness certification 10 p1486 A72-24007

Reliability prediction for MOS/LSI devices based on chip circuit configurations evaluation, extrapolating bipolar IC failure rate model 10 p1447 A72-24009

Probability model of statistical independence relationships among two events and environmental event, examining all combinations of definition statements for reliability analysis 10 p1504 A72-24015

Maximum likelihood method of combining system and component data for reliability estimates 10 p1444 A72-24016

Complex system represented by fault-free with independent components, calculating confidence interval for failure probability by moment method 10 p1444 A72-24018

Design considerations and reliability analysis for long duration manned space missions, noting redundancy and inflight maintenance requirement [AIAA PAPER 72-239] 10 p1487 A72-24446

Reliability, operational safety and system concept interrelationship in automatic meteorological stations 10 p1463 A72-25011

Optimal control design for digital guidance system, conducting efficiency and reliability analyses 11 p1600 A72-25437

Error correlation technique to ensure reliability of discrete automatically controlled digital systems inputs, noting lower redundancy requirement 11 p1600 A72-25438

Reliability analysis of repairable redundant systems with random replenishment of reserves, using discrete time Markov process theory 11 p1600 A72-25440

Servo systems operational reliability analysis for variable intensity of fluctuating interference, discussing Markov process probability determination and Kolmogoroff equations solution 11 p1609 A72-25441

Statistical diagnosis of aeronautical systems reliability and maintenance, using Benzecri factorial analysis for data reduction 11 p1639 A72-25817

Theoretical fatigue test procedure for reliability analysis of machine parts, calculating fatigue probability in load carrying components 11 p1640 A72-26244

Effectiveness and reliability criteria for information and monitoring systems performance evaluation, suggesting use of revenue ratio 11 p1611 A72-26437

Aircraft windscreen reliability, discussing delamination, interface shear stress effects and analogy to metal fatigue 12 p1812 A72-27011

Concorde aircraft optical transparency components design characteristics and reliability tests, noting visor, pilot forward windshield, flight deck side windows and cabin windows 12 p1753 A72-27012

Position information in lunar cartographic products evaluated by Apollo data, obtaining reliability factors 12 p1871 A72-27530

Operations research and reliability - Conference, Turin, Italy, June-July 1969 13 p1961 A72-28351

Reliability role in commercial and military telecommunication satellite system planning, discussing

economic factors, earth station redundances and maintenance, spare levels and control systems 13 p2051 A72-28352

Reliability requirements and optimization for complex systems, discussing method to improve component reliability of aircraft weapon system 13 p1961 A72-28353

Cost effectiveness determination for different levels of reliability and maintainability of training aircraft, using computer simulation 13 p2067 A72-28355

Mathematical model for digital systems reliability, determining probability of success and of various failure modes 13 p1923 A72-28356

Reliability prediction of system with components having independent and constant rate failures 13 p1961 A72-28357

Weapon systems reliability assessment based on limited prototype flight test results 13 p1962 A72-28359

Statistical principles of reliability assessment and sequential testing of complex systems, considering confidence level, probability of acceptance and cost factors 13 p1984 A72-28361

Reliability lower confidence limit estimation for serial systems with failure in any subsystems resulting in overall failure 13 p1962 A72-28362

Parametric approaches to statistical burn-in or debugging problems in aircraft reliability analysis 13 p1985 A72-28363

Mathematical models for complex system debugging in initial life period, noting maximum likelihood estimates for failure rate functions 13 p1962 A72-28365

Nonrandomized distribution-free ranking and selection procedures under subset selection formulation, considering application to reliability problems 13 p1962 A72-28366

System reliability demonstration test cost minimization for one-shot electroexplosive device 13 p2024 A72-28367

Reliability tests on miniature ceramic capacitors encapsulated by epoxy-novolac block polymer compounds 13 p1919 A72-29061

Reliability analysis of automatic systems with structural changes accumulated during operation, noting service life determination and damage prevention 13 p1936 A72-29169

Redundant and nonredundant self adaptive systems reliability, discussing statistical random process characteristics 13 p1936 A72-29170

Early design phase reliability analysis of large adaptive systems in terms of domination and graph theories 13 p1965 A72-29171

Statistical homogeneity criteria for automatic equipment operation reliability, using Poisson flow model with random fluctuations 13 p1965 A72-29173

Reliability of nondestructive ultrasonic testing methods of quality control, discussing defect size distribution and detectability coefficient 14 p2106 A72-30149

Training cockpit TL-29 mean time of failure-free operation from measurement data during development tests and two year guarantee, calculating avionic devices reliability 14 p2092 A72-30281

Ionospheric radio signal reflection fields verified via quantitative statistical reliability criterion 14 p2100 A72-30634

Astronauts physiological and psychological reliability, discussing Apollo flights and prolonged missions to other planets 14 p2079 A72-30677

Mathematical model for computation of electronic circuit drift reliability and circuit production yields, discussing operational parameter allowance 14 p2091 A72-31165

IC reliability assessment based on defects and failure mechanisms analysis instead of MTBF estimations 14 p2091 A72-31166

Reliability modeling principles, concepts and implementation techniques for switching system design 14 p2091 A72-31167

Accessory reliability relation to on-time performance, discussing production route in terms of specification, design, development and manufacture 15 p2339 A72-32463

Multi-environment reliability test program for airborne electronic systems under simulated temperature, humidity, vibration and shock conditions 15 p2215 A72-32616

Mathematical model for reliability analysis of modularly redundant electronic systems with unequal failure rates for operating and standby units 16 p2398 A72-33344

Electronic circuit reliability prediction model with statistical dependence for detailed failure modes 16 p2371 A72-33345

Computerized calculation of electronic circuit and equipment reliability and quality control, presenting task examples and printout form 16 p2368 A72-33347

Weibull distribution parameters estimation for general device class from limited failure data through regression models, using least squares method 16 p2398 A72-33349

Aerospace computer software validation and verification methods application to complex systems, discussing code execution and analysis tools, program diagnostics, cost and schedules 17 p2524 A72-35582

Reliability analysis of an intermittently used system with N types of failure. 18 p2693 A72-36024

Reliability of simulations of asymptotically steady and strictly ergodic stochastic processes 18 p2704 A72-36467

Study of reliability of Al-Au thermocompressions by measurement of resistance 18 p2668 A72-37105

Correlation between the reliability of silicon bipolar transistors and their excess background noise 18 p2669 A72-37110

The detection of unreliable contacts by noise measurements. 18 p2720 A72-37111

Quality assurance of transistor chips for the user 18 p2669 A72-37120

Reliability assurance of space equipment components, discussing drift and failure modes, computerized simulation and thermal maps 18 p2743 A72-37127

Standardization and reliability assurance on the national and European levels 18 p2743 A72-37128

Standardization and quality assurance of electronic devices on the national and European levels 18 p2743 A72-37129

Department of Defense Reliability Analysis Center. 18 p2676 A72-37131

Production and test facilities availability effect on costs involved in obtaining item at required quality level, examining component rejects and defectives 18 p2670 A72-37133

CNET Reliability Center and its activities in the field of aerospace devices 18 p2676 A72-37135

Reliability of HgTe-CdTe photovoltaic detectors 18 p2670 A72-37139

Quality and reliability evaluation method for integrated circuits using MOS transistors - Option: Circuits on request 18 p2671 A72-37141

Development of a complementary MOS technology of high reliability 18 p2671 A72-37142

Linear programming application to the solution of some optimum problems of reliability theory 19 p2825 A72-37995

Combined reliability and durability estimation for machines and devices under working conditions with the use of indicators of service life consumption 19 p2808 A72-38219

Reliability estimation for actively redundant radio electronic systems 19 p2774 A72-38424

Reliability prediction of a two-unit standby redundant system with standby failure. 20 p2929 A72-39855

Microelectronic component reliability prediction technique with near Wiebull method accuracy in absence of detailed sampling life test results 20 p2930 A72-39857

Reliability aspects of fading in microwave line of sight using digital transmission. 21 p3019 A72-40887

Quantitative aspects of reliability in process-control systems. 21 p3038 A72-40922

Prior distributions fitted to observed reliability data. 22 p3182 A72-41980

Bayesian decision analysis of the hazard rate for a two-parameter Weibull process. 22 p3198 A72-41981

Determining optimum burn-in and replacement times using Bayesian decision theory. 22 p3182 A72-41982

Error incidence probability for system control reliability determination, assuming Markov process 22 p3162 A72-42183

Reliability analysis in the estimation of transport-type aircraft fatigue performance. 22 p3241 A72-42971

Life estimation and prediction of fighter aircraft. 22 p3139 A72-42972

Aerospace vehicles preliminary design computer program to include cost, reliability, maintainability and safety parameters in addition to weight as performance determining factors [SAWE PAPER 940] 23 p3342 A72-43480

Reliability estimation in life testing in the presence of an outlier observation. 23 p3309 A72-43807

Asymptotic reliability estimates of monotonically structured complex logic systems with low and high component failure rates equivalent with exponential or Weibull distributions

23 p3267 A72-44004

Reliability analysis of a jet engine fuel system with the aid of an analog computer using operational data

23 p3236 A72-44282

Book on complete technological system reliability assessment covering performance requirement and achievement, transfer characteristics, sampling, estimation, confidence, synthesis problem, etc

23 p3294 A72-44499

A survey and comparison of methods for determining confidence bounds on system reliability from subsystem data.

24 p3406 A72-44652

Optimal cost effective sequencing model for component reliability tests, applying to complex electronic equipment

24 p3467 A72-44654

Ranking the reliability of two designs by Monte Carlo techniques.

24 p3383 A72-44655

Field reporting system for reliability analysis on telecommunication equipment.

24 p3384 A72-44657

Evaluation of guided missile system in-service reliability.

24 p3448 A72-44658

Allocating optimum time for systems malfunction search.

24 p3406 A72-44661

Robert Bruce's spider problem extended - Reliability of adaptive experimental systems.

24 p3406 A72-44666

Point and confidence interval estimates for acceleration and aging component probability distribution functions in accelerated life tests and reliability prediction

24 p3406 A72-44669

The problems of reliability growth and demonstration with military electronics.

24 p3384 A72-44670

Lifetime estimation, optimal experimental design and stress level severity prediction in parametric and nonparametric accelerated life tests

24 p3406 A72-44671

Reliability analysis based on time to the first failure.

24 p3455 A72-44727

Computer-aided binary code sequence selection for data acquisition system in PCM-TDMA satellite communication, evaluating performance and reliability

24 p3379 A72-44779

RELIABILITY CONTROL

U QUALITY CONTROL

U RELIABILITY ENGINEERING

RELIABILITY ENGINEERING

Soviet book on reliable logic units design covering adaptive redundant and nonredundant control systems, threshold functions, optimal adaptation algorithms, restoring circuits, etc

01 p0033 A72-10296

Nonmetallic material properties effects on structural design for reliability, considering molecular chain folding, polymer crystallization, entropic molecular segregation, adhesion and intermolecular forces

01 p0092 A72-10986

Air transportation system design for safety and efficiency, discussing navigation facilities and surveillance systems employment for blunder prevention

01 p0098 A72-11117

Aircraft integrated data systems, discussing cost effectiveness, reliability and maintenance

03 p0327 A72-13417

Reliability physics - IEEE Conference, Las Vegas, March-April 1971

03 p0335 A72-14276

Charged transfer devices and IGFET bucket brigade structures, discussing design measures and fabrication procedures for increased reliability

03 p0336 A72-14280

Au-Al wire bond, discussing intermetallic phase formation under elevated temperature treatments and reliability design limitations

03 p0364 A72-14284

Aerospace reliability methods, discussing distribution functions, sampling, accelerated life testing and case histories of space electric rocket and microthruster power conditioner tests

04 p0526 A72-14441

Book on system safety engineering covering systems analysis and engineering, evolution of safety philosophy, product reliability and liability, etc

04 p0477 A72-14573

Fixed level intersection by two stationary ergodic independent random processes in observation time for dynamic control sampling and reliability estimation

05 p0641 A72-16316

Bleed air type gas turbine compressor development, presenting reliability improvement program

05 p0705 A72-16500

Optimal control systems synthesis with allowance for given reliability, finding extremal value of quality

function with constraint on probability of fail-safe operation

06 p0794 A72-18305

Stochastic rule for optimum moment of preventive maintenance of redundant technological systems, predicting system reliability

08 p1180 A72-22056

Economic factors influence on reliability optimization of complex radio systems and elements

08 p1143 A72-22066

Sequential reliability control and analysis in low run production with plan optimization and tests number reduction

08 p1181 A72-22069

Lower confidence bound for reliability and specifications for nonnormally distributed stress corrosion test data, using Weibull statistical distribution

08 p1189 A72-22102

Redundant polystable element designs with autonomous redundant state breakdown controls for reliability improvement in automatic control systems

09 p1290 A72-22547

Monotonicity theorems for functionals and transformations in stochastic models of queueing, reliability and optimality problems

09 p1343 A72-23565

Task oriented maintainability engineering relationship to systems engineering and logistics support requirements

10 p1564 A72-23852

Complete reliability program major activity areas identification, discussing various components interrelations

10 p1485 A72-23973

Reliability data collection methods, considering equipment initial design, breadboard models, prototype, production, acceptance, qualification, field installation and operation

10 p1443 A72-23975

Interactive remote terminal as forming tool for reliability engineer to free from computational labor and concentrate on conceptual problems

10 p1443 A72-23976

Computer programmed instruction checklist for reliability and maintainability engineers requirements

10 p1443 A72-23981

Reliability program for SAAB 37 Viggen airborne computer, discussing prototype and components operating tests and failure rates

10 p1443 A72-23984

Complex system mission worth optimization by redundancies discussing MISDGRAD computer program to evaluate cost-reliability for mission without maintenance

10 p1550 A72-23994

Reliability decision making under uncertainty between alternative design approaches, using dynamic programming

10 p1504 A72-23995

Reliability design for airborne ecological system for jumbo jets, discussing toilet flushing and multiple server queueing model

10 p1429 A72-23999

Operator independence test for human performance reliability modelling based on symptom detection and fault location of sonar system failure

10 p1429 A72-24002

Design review as management tool for complex systems quality and reliability assurance, discussing Skylab program

10 p1486 A72-24005

Reliable interconnections for U.S. Army avionics, determining best technique for terminating flat conductor cables with electrical connectors

10 p1447 A72-24012

Polaris and Poseidon missile systems reliability assessment, discussing test programs, analytical techniques and data management

10 p1551 A72-24013

Cost effective nonstatistical procurement of VHF power transistors with high degree of confidence in reliability

10 p1447 A72-24014

Long time mission spacecraft computer reliability economics based on failure and step improvement costs evaluation

10 p1444 A72-24017

Commercial aircraft reliability program development from informal continuous product improvement to formalized methods based on reliability logic diagrams and probability calculations

10 p1421 A72-24019

Software reliability engineering, emphasizing looping, deadlocks and difficulties due to imperfect logic, and error causes

10 p1486 A72-24020

System reliability improvement technique for identification and prevention of failures, using Experience Storage Program for design problem documentation collecting, storage and retrieval

10 p1486 A72-24021

Informational reliability of automatic control system comparators, considering tolerance field contraction effect

10 p1456 A72-24081

Human operator role in space systems reliability, suggesting approaches to system design and program planning to exploit human potential

[AIAA PAPER 72-228] 10 p1430 A72-24439

Lunar roving vehicle reliability program and design features of mobility, electrical power and navigation subsystems

[AIAA PAPER 72-233] 10 p1460 A72-24443

Product assurance cost aspects on high reliability space programs, discussing design, packaging, failure trends, acceptance testing and Apollo project

[AIAA PAPER 72-247] 10 p1551 A72-24452

Reliable, economical and easily operated read-only magnetic core storage devices for control computers, discussing design features

10 p1445 A72-24639

Russian papers on cybernetic systems accuracy and reliability covering error correction schemes, statistical analysis and computer design

11 p1599 A72-25426

Cybernetic equipment reliability and precision analysis from algorithmic, conversion and instrumental errors, surveying digital, analog and hybrid computers and converters

11 p1608 A72-25427

Accuracy and reliability in engineering design of discrete automata without memory /logic circuits/, using Boolean algebra for mathematical models

11 p1600 A72-25434

Fixed level intersection by two stationary ergodic independent random processes in observation time for dynamic control sampling and reliability estimation

11 p1610 A72-25799

Metrological techniques reliability for industrial production processes, plotting quality control curves

11 p1637 A72-26823

Reliability, quality and testing assurance in ATS F and G system, discussing computerized handling of spacecraft parts information

12 p1814 A72-27524

Model for supervised repairable system reliability, assuming system life and repair times as exponential probability distributions with deterministic supervisor active and inactive times

12 p1814 A72-27555

NASA reliability and quality assurance methodology to improve hospital biomedical equipment, using space electric rocket test example

12 p1814 A72-27960

Weapon system reliability improvement through integrated maintenance data collection and evaluation system, considering maintenance organization and operation

13 p2067 A72-28368

Permanent operational characteristics changes of Si and Ge transistors bombarded by gamma and neutron radiation

13 p1928 A72-28700

Hailstone size estimation to design exposed equipment for irreversible impact damage prevention

13 p1993 A72-28854

Decision diagrams used in logic analysis for aircraft maintenance schedule testing relative to operational reliability control

13 p1967 A72-30041

Optimal control systems synthesis with allowance for given reliability, finding extremal value of quality function with constraint on probability of fail-safe operation

13 p1937 A72-30073

Environmental effects on aircraft structure operational reliability, discussing failure removal and protective coating lifetime

14 p2072 A72-30285

U.S. Army missile systems rocket motors life cycle reliability programs based on propellant laboratory analyses, motors static tests and field firings statistical evaluation

14 p2146 A72-30759

Product reliability prediction from failure mode analysis, examining component design, quality control, engineering analysis configuration selection and product testing

[ASME PAPER 72-DE-17] 14 p2108 A72-30863

Thin film resistor manufacture and evaluation for stability and long-life characteristics

14 p2091 A72-31171

Statistical inferences on two parameter Weibull reliability function from classical, Bayesian and structural probability viewpoint

15 p2264 A72-31800

Astronautical digital computing hardware and software trends and implications, considering data rates, reliability, LSI, speed-storage tradeoff, etc

15 p2203 A72-31822

Reliability-maximizing digital computer synthesis based on multiple redundant network design, discussing majority structure distribution optimization technique

15 p2203 A72-32174

Thick phase holograms in dichromated gelatin, discussing physical properties requirements and reliable processing procedures

15 p2239 A72-32355

Concorde engines design for maintainability and reliability to reduce turnaround time, discussing diagnostic facilities and on-wing maintenance features
15 p2298 A72-32457

Aircraft design for operational reliability and maintainability, emphasizing working relations coordination between manufacturer and operator
15 p2181 A72-32459

Spacecraft boom deployment dynamics environmental simulation and testing for preflight system reliability evaluation
15 p2321 A72-32627

Stress and parametric change analysis for failure mode identification and reliability screen tests of LSI circuits, noting MOS inverter operation and RAM mechanization
17 p2528 A72-34706

Microwave power junction transistor design factors effects on long and short term reliability and MTBF
18 p2666 A72-36552

Microwave junction transistor geometric design factors effect on reliability and performance, comparing overlay, interdigitated, mesh and inverse overlay structures
18 p2666 A72-36553

Integrity of flight control system design
18 p2643 A72-37032

Installation of a production line for high-reliability silicon diodes - Results obtained: Application of the underlying principles to more complex components
18 p2670 A72-37121

Development and production of French high-reliability components: The Concerto Program - The CNES-Concerto certificate
18 p2744 A72-37136

Si solar cell design for high power/weight ratio and extreme environmental operating conditions, describing technological innovations for reliability and efficiency enhancement
19 p2754 A72-37780

Designing aircraft structure for resistance and tolerance to battle damage.
[AIAA PAPER 72-773] 19 p2752 A72-38133

Relation between the reliability and allowable stress amplitude in fatigue design.
20 p2977 A72-38879

Quadruple-redundancy management for fly-by-wire control system reliability, discussing analog circuit and digital computer voter/monitor techniques
[AIAA PAPER 72-884] 20 p2910 A72-39117

Compression distillation unit design and development for integrated water and waste management system onboard spacecraft, describing reliability and performance tests
[ASME PAPER 72-ENAV-1] 20 p2897 A72-39176

Bayesian statistical decision theory and reliability-based design.
22 p3240 A72-42967

Reliability-maximizing digital computer synthesis based on redundant network design, discussing majority structure optimal allocation technique
22 p3157 A72-43008

Man serviced spacecraft systems reliability and maintainability optimization methodology, developing parametric data based on failure modes analysis, components MTBF, duty cycles, redundancy and costs
[SAWE PAPER 943] 23 p3343 A72-43483

Integration of safety engineering into a cost optimized development program.
[SAWE PAPER 945] 23 p3358 A72-43485

Book on complete technological system reliability assessment covering performance requirement and achievement, transfer characteristics, sampling, estimation, confidence, synthesis problem, etc
23 p3294 A72-44499

A concept of service life for estimating the reliability of machines and devices
24 p3405 A72-44623

Conference on Reliability Testing and Reliability Evaluation, The Hague, Netherlands, September 4-8, 1972, Proceedings.
24 p3405 A72-44651

Reliability, safety, maintainability and system effectiveness disciplines acquisition, processing, dissemination and exchange via Government-Industry Data Exchange Program and Failure Rate Data Program
24 p3467 A72-44660

NDT application and development in industry, considering confidence in inspection techniques, framework and management resistance
24 p3408 A72-45295

Fault-tolerance experiments with the JPL STAR computer.
24 p3383 A72-45671

A prognosis on fault-tolerant digital control systems.
24 p3383 A72-45672

Reliability of modular computer systems with varying configuration and load requirements.
24 p3383 A72-45673

Semaphore channel signaling reliability, presenting error protection and correction system
24 p3381 A72-45770

RELIEF MAPS
Martian surface relief observation from earth distance, showing telescope resolution requirements above dense atmospheric layers
03 p0438 A72-13983

Mars topographic map study of high velocity relief winds, showing seasonal and secular changes
04 p0569 A72-14502

Topographical stereo map plotting apparatus with auxiliary device for orthophoto production, describing design for combined photointerpretation-cartographic applications
09 p1313 A72-23309

Isogram map of Mare Imbrium reddening coefficients, noting correlation between chromaticity and relief details
14 p2148 A72-30208

Coherent optical terrain-relief determination using a matched filter.
18 p2691 A72-36491

Mariner 7 ultraviolet spectrometer experiment - Topographic slopes of Mars' polar region.
21 p3110 A72-41457

Martian topography according to ground-based radar measurements and the CO2 absorption observed from the earth and from the Mariner 6 and 7 spacecraft
21 p3114 A72-41766

Isogram map of Mare Imbrium reddening coefficients, noting correlation between chromaticity and relief details
23 p3333 A72-43238

RELIEVING
NT STRESS RELIEVING
RELUCTANCE
Thermal zero signal instabilities and error reduction in devices using reluctance sensors
02 p0231 A72-12562

Electrical conductivity, reluctance and Hall effect of n-type semiconductors determined at extremely low temperatures
15 p2291 A72-31389

RELUCTIVITY
U RELUCTANCE
REMAGNETIZATION
U MAGNETIZATION
REMANENCE
Lunar remanent magnetism origin theory from Apollo and Explorer data, suggesting solar wind, earth magnetosphere and lunar dynamo sources
01 p0134 A72-11269

Low cost ferrite remanence microwave phase shifter design using periodic loading structures
04 p0497 A72-14716

Stable remanent magnetization components of lunar rock samples from Apollo 11 and 12 missions, indicating liquid core origin
10 p1536 A72-24155

Lunar breccia and crystalline rocks thermoremanent magnetization characteristics, presenting alternating field and thermal demagnetization curves
14 p2154 A72-30507

Natural remanent magnetism creation in meteorites via shock passage in collisional fragments
16 p2451 A72-32990

Thermal stability of lunar rock remanence, indicating magnetization components acquired after initial cooling
22 p3226 A72-42535

Magnetism of meteorites - A review of Russian studies.
23 p3339 A72-44129

Thermal cycling tests for natural remanent magnetism of lunar soil samples, proposing magnetization mechanism of material buried in regolith
24 p3443 A72-45373

REMELTING
U MELTING
REMOTE CONSOLES
Time shared electronically patched hybrid computer for design automation, discussing remote terminal graphics capabilities and simulation language compiler
06 p0778 A72-17476

On-line digital computer system for real time interpretation and report generation of electrocardiograms from remote locations over switched telephone network
07 p0928 A72-19311

Optimal operation assignment and data array storage allocation in data system consisting of central processing unit and peripheral computer controlling data flow
09 p1283 A72-23439

Interactive remote terminal as formatting tool for reliability engineer to free from computational labor and concentrate on conceptual problems
10 p1443 A72-23976

REMOTE CONTROL
NT RADIO CONTROL
Synchronization system for remote control and performance checking of motion picture projectors with running film, discussing recording equipment and stroboscopic pulsed illuminator operations
04 p0521 A72-14711

Remote ignition with noncoherent light from pyrotechnic, electric and explosive sources through fiber optics
08 p1219 A72-20757

Book on telemetry and remote control covering information theory, analog/digital techniques, signal transmission, data processing and coding, etc
10 p1436 A72-24550

Electromagnetic remote model positioning sensing system for wind tunnels with magnetic suspension, using differential transformer action
10 p1461 A72-24762

Wind tunnel model remote position sensing and control systems, discussing drift reduction in magnetic suspension
10 p1461 A72-24768

Remotely manned systems technology for military, industrial, scientific and civil applications for hostile or difficult environments
11 p1612 A72-25256

Remotely manned vehicles /RMV/ application in aerial warfare, considering anti-aircraft defenses lethality increase, equipment costs and role of man during combat mission
13 p1896 A72-28451

OMEGA receiver with digital solid state circuits for remote unmanned platform positioning, discussing ship to shore tests and design features
13 p1925 A72-29184

Solid state dc power controller design functional requirements, considering system overcurrent protection, power control by low voltage signals, power output to load status, etc
15 p2182 A72-31219

Unmanned remotely controlled planetary rovers for Mars surface exploration, discussing design concepts
15 p2214 A72-32316

Automatic remote mechanical system parameter control by electrical elements, introducing rigidity for mass sensitive measurement in dynamometry
16 p2370 A72-33956

Remote power control for aircraft generating and distribution systems.
18 p2648 A72-37034

Flight-test experience in digital control of a remotely piloted vehicle.
[AIAA PAPER 72-883] 20 p2889 A72-40059

Switches for high-frequency channels
21 p3026 A72-40317

Human or computer control role in teleoperator remote control mechanisms, discussing control modes, sensing and transmission time delay problems
21 p3011 A72-41416

Remote transmission of telescope coordinate readings by industrial television
21 p3056 A72-41448

Remote control and navigation tests for application to long-range lunar surface exploration.
22 p3203 A72-43131

Teleoperator technology development, discussing remote operators, mobile manipulators and autonomous robots for man capability extension and industrial application
[ASME PAPER 72-AERO-18] 22 p3245 A72-43150

A teleoperator system for space application.
24 p3407 A72-45174

Remotely controlled astronomical observatory telescope Cassegrain focus, evaluating computerized automated electronic system advantage over conventional instrument
24 p3405 A72-45543

REMOTE HANDLING
Remotely manned systems technology for military, industrial, scientific and civil applications for hostile or difficult environments
11 p1612 A72-25256

Teleoperator manipulator for payload handling in space shuttle, noting design features and simulations of master-slave remote control system
[AIAA PAPER 72-238] 13 p1909 A72-29075

REMOTE SENSORS
Remote sensing photointerpretation tests, discussing film-filter combinations, image acquisition time, scale and detection accuracy
01 p0065 A72-10450

Data correlation and annotation of earth resources remote survey pictorial records
01 p0065 A72-10453

Agricultural land use analysis by remote sensing, discussing side-looking airborne radar systems and image interpretation for local needs
01 p0056 A72-10456

Agriculture and natural vegetation remote sensing programs, discussing dichotomous keys for side-looking airborne radar imagery analysis
01 p0056 A72-10457

ERTS satellite image processing for multispectral scanning system, discussing distortion from geometrical properties
01 p0066 A72-10458

Land pollution remote sensing, discussing economic and political impact in terms of land use, transportation, energy supplies and recreational opportunities
[AIAA PAPER 71-1039] 01 p0057 A72-10523

Monostatic and bistatic lidar and solar radiometer sensing techniques for remote measuring of aerosol size distributions
[AIAA PAPER 71-1057] 01 p0066 A72-10528

Remote sensing of regional vertical air column pollutants, discussing sulfur dioxide and nitrogen dioxide measurements by correlation spectrometer
[AIAA PAPER 71-1060] 01 p0057 A72-10529

Quantitative interpretation of correlation mask remote sensors UV, visible and IR spectral data, discussing beam transmittance attenuation by absorption, scattering and emission
[AIAA PAPER 71-1061] 01 p0066 A72-10530

Remote airborne sensors for sea water oil pollution surveillance in near UV, thermal IR and microwave regions
[AIAA PAPER 71-1073] 01 p0057 A72-10535

Sky light polarization, cloudiness and view angle effects on oil remote detection over water surface, describing passive radiometric techniques
[AIAA PAPER 71-1075] 01 p0057 A72-10536

Gaseous pollutants remote detection by IR heterodyne radiometer with tunable lasers
[AIAA PAPER 71-1079] 01 p0080 A72-10538

Carbon dioxide laser IR heterodyne radiometer for remote sensing of atmospheric pollution
[AIAA PAPER 71-1083] 01 p0067 A72-10540

Environmental pollution sensing by vibrational laser Raman scattering probe measuring species constituency and temperature, discussing fluorescence, scattering cross sections and band shape
[AIAA PAPER 71-1084] 01 p0067 A72-10541

Air pollution circulation patterns remote sensing, describing multispectral stereo image pairs digital cross correlation
[AIAA PAPER 71-1106] 01 p0067 A72-10551

Spaceborne Fourier interference spectrometer for environmental pollutant sensor, discussing IR detection systems, instrument servo, data reduction and handling systems and optical tolerance
[AIAA PAPER 71-1108] 01 p0067 A72-10552

Remote sensing of atmospheric pollutants and trace contaminants, presenting high speed high resolution, Fourier interferometer breadboard model
[AIAA PAPER 71-1109] 01 p0068 A72-10553

Airborne and spaceborne remote measurement and mapping of atmospheric nitric oxide, describing system configuration with mono or bistatic and pulsed or CW laser
[AIAA PAPER 71-1112] 01 p0068 A72-10556

Atmospheric carbon monoxide pollution sources, sink mechanism and remote sensing requirement
[AIAA PAPER 71-1120] 01 p0068 A72-10557

Laser fluorosensor for remote environmental probing, considering applications to oil slick mapping, locating lignin sulphate pollution sources and hydrologic monitoring of tracer dye dispersal
[AIAA PAPER 71-1121] 01 p0080 A72-10559

Remote sensing investigation of root wilt disease in coconut plants in Kerala state /India/
01 p0020 A72-10951

Spacecraft attitude determination with single-axis sensor and single natural radiation source with relative mutual motion, deriving error equations
01 p0032 A72-11224

Remote sensing of environment - Conference, University of Michigan, May 1971
02 p0207 A72-11776

Artificial satellites for earth resources and environmental contamination control, discussing remote sensing physical problems and earth surface radiative characteristics
02 p0207 A72-11778

Earth surface and atmosphere remote sensing by airborne microwave measurements, noting ocean surface emittance dependence on temperature, surface conditions and pollution
02 p0207 A72-11779

IR remote scanning of natural resources, discussing thermal to optical image conversion on photographic film
02 p0208 A72-11781

Airborne remote sensing of earth surface physical properties, using panchromatic and IR black and white, true color and IR false color photography
02 p0208 A72-11782

World Weather Watch and Global Atmospheric Research Program remote sensing applications, considering weather prediction and modification, atmosphere pollution monitoring and global atmosphere mathematical modeling and simulation
02 p0208 A72-11784

Soyuz 6 multispectral aerogeophysical measurements of Usturt plateau and Caspian and Aral Seas, discussing remote sensing information yield on earth water/land and atmosphere properties
02 p0208 A72-11785

Thermal IR remote sensing of surface geothermal heat flow, presenting nighttime heat budget equation based on solar and geothermal energy
02 p0208 A72-11786

Sedimentary rocks remote multispectral analysis by aerial data covering UV to microwave spectral regions
02 p0209 A72-11788

Remote sensor viewing angle effect on detectability of geological faults in side-looking airborne radar image data by optical spatial frequency analysis
02 p0209 A72-11791

Remote sensing for land use soil limitations recognition and mapping, using color encoded density slicing analysis
02 p0209 A72-11793

Northern Alps geology, hydrology, lithology and tectonic survey, using aircraft-borne thermal IR scanner remote sensor
02 p0209 A72-11795

Phyto-ecological approach to remote sensing of man made ecosystems, comparing vegetation and landscapes in Old and New Worlds
02 p0210 A72-11797

Multistage resource inventory and analysis program combining remote sensing techniques and ecological principles in California Desert pilot area, discussing photointerpretation and ground truthing
02 p0210 A72-11802

Remote sensing of surface radiation temperature topographic variations by precision radiation thermometer equipped aircraft, calibrating for atmospheric attenuation
02 p0210 A72-11803

Terrestrial radiation emission mapping from imagery produced by scanning radiometer, discussing remote sensors used to study surface energy phenomena
02 p0210 A72-11804

Atmospheric pollutants time and spatial profiles monitoring by geosynchronous satellite remote sensors
02 p0211 A72-11806

Ground based passive remote sensing of low altitude vertical temperature profiles by microwave radiometry
02 p0211 A72-11807

Natural formations optical spectral reflectance optimal coding with speedy digital computer processing advantage for remote sensing of earth surface
02 p0187 A72-11811

Southern corn leaf blight detectability by remote sensing based on pattern recognition technique application to multispectral color and IR photographic and scanner data
02 p0212 A72-11814

Forest vegetation distributional and statistical parameters ecological analysis by multiband remote sensing in areas devoid of ground control
02 p0212 A72-11815

Materials remote active sensing from ground, air and space by UV and visible laser induced luminescence, using excitation and emission spectral specificity for species identification
02 p0225 A72-11822

NASA/MSC Earth Resources Research Data Facility for remote sensing of geology, geography, agriculture, forestry, hydrology and oceanography
02 p0200 A72-11824

Remote sensing applications to operational weather forecasting including ground optical measurement of cloud base height and radar observation of precipitation
02 p0253 A72-11825

Photogeological remote sensing of high voltage dc power transmission system induced ground current paths, discussing X-15 near IR photographic recordings
02 p0212 A72-11826

Pollution and environmental quality remote sensing, describing five dimensional sensor/applications matrix for decision guidance
02 p0212 A72-11827

Natural resources multispectral remote sensing for national emergencies, discussing various imaging techniques
02 p0212 A72-11828

Oil spills remote detection by multispectral photography, IR scanner imagery and microwave radiometry
02 p0226 A72-11830

Remote sensor data analysis using color TV display system and interactive graphics equipment on-line to IBM 360/44 computer
02 p0226 A72-11838

Airborne sensors terrain classification, considering sample points clustering approach and signature analysis
02 p0227 A72-11844

Pattern recognition of multispectral scanner remote sensor data, using table look-up approach for processing simplicity and time reduction
02 p0227 A72-11846

Remote sensing of Indian resources, investigating Englemann Spruce beetle infestation, topographic features and potential mineral areas
02 p0213 A72-11848

Extended wavelength field spectroradiometry for multispectral scanner data interpretation in airborne observations
02 p0228 A72-11853

Sounding rockets in remote sensing programs for agricultural census and crop yield estimates in Argentina
02 p0228 A72-11854

Plant leaves light reflectance, transmittance and absorptance characteristics relationship to leaf mesophyll arrangement, considering interpretation of aircraft/spacecraft remotely sensed data
02 p0213 A72-11856

Atmospheric scattering and absorption effects on target/background discrimination in environmental remote sensing at 0.4-3.0 microns spectral region
02 p0213 A72-11858

Microwave spectrometer remote sensing of atmospheric temperature and water vapor, discussing cloud, topography and sea state effects and multiple regression statistical method
02 p0228 A72-11859

Computer program for atmospheric effects on IR radiation, calculating transmission and radiance spectra for various remotely sensed atmospheric, path and target conditions
02 p0187 A72-11862

Remote passive microwave sensing of ocean surface wind fields, discussing sea microwave brightness temperature dependence on wind speed
02 p0214 A72-11864

Passive microwave remote sensing, discussing thermal imaging, radiometer tracking and image deterioration due to antenna imperfections
02 p0214 A72-11865

Soil surface moisture content and temperature profile determination by remote microwave sensing
02 p0214 A72-11871

Spectral texture effects on remotely sensed high altitude automatic IR image interpretation, using Bayesian probability techniques
02 p0228 A72-11873

Automatic classification over extended remote sensing test sites, examining causes of variation in multispectral scanner data response
02 p0228 A72-11875

Automatic soil type mapping, using multispectral remote sensing and computerized pattern recognition
02 p0215 A72-11881

Hybrid system to process multispectral photographic data from aircraft and spacecraft sensors, assessing data quality, cost effectiveness and delay reduction
02 p0228 A72-11883

Chesapeake Bay aquatic ecosystems observations, using satellite remote sensing multispectral photography and imagery
02 p0215 A72-11885

Automated photometric wetland mapping using aerial color film microdensitometric analysis and computer techniques
02 p0215 A72-11886

Soviet aerial survey techniques for natural resources data, discussing photograph interpretation, fast aerospotometers, data processing and multispectrum cameras
02 p0216 A72-11888

Earth surface remote sensing with thermal IR radiation, investigating uncovered soils with heat balance equations under various weather conditions and times of day
02 p0172 A72-12017

Digital computer automated test equipment and procedures for remote sensors and electronics for scanning celestial sphere for X rays prior to spacecraft launch
02 p0200 A72-12479

Cathode ray tube recorder for remote airborne photographic mission
03 p0360 A72-13711

Remote meteorological elements sensing in terminal area, discussing radar, ceilings, thunderstorm warning, slant range visibility, low level winds and wind shear
04 p0543 A72-14692

Airborne remote CAT detection equipment, examining pulsed Doppler laser and IR radiometry
04 p0521 A72-14831

Atmospheric turbulence detection sensors, reviewing microwave radar, acoustic, Doppler lidar, laser fringe anemometry and passive IR techniques
04 p0530 A72-14833

Remote air pollution detection by laser methods, comparing Raman backscattering, resonance backscattering and resonance absorption
04 p0531 A72-15300

Si monolithic multispectral image photosensor array for satellite application, presenting fabrication and spectral response data
04 p0500 A72-15304

Al finished and Au plated triple calibration sphere as multispectral optical sensor for testing Cook hypothesis concerning satellite drag dependence on surface material
04 p0500 A72-15305

Radar and radiometric millimeter wave signal systems in near earth environment for remote detection purposes
04 p0494 A72-15610

Remote sensing with sounding rockets and balloons, discussing cost, mineralogical surveys, land use and hydrological assessments 05 p0654 A72-15756

Buffalo photographic aircraft for oil slick remote sensing, using aerial cameras and thermal IR scanner 05 p0658 A72-16600

Pressure modulated carbon dioxide radiometer for remote temperature sounding in upper atmosphere 05 p0663 A72-16692

CNES airborne remote sensing of earth resources comparison with classical photodetection methods, discussing application to oceanography, geology, agriculture, hydrology and human activities 06 p0803 A72-17385

Supplementary Aviation Information Display for ATC, discussing remote sensing capability and cost savings 06 p0845 A72-17424

Earth resources applications of multispectral remote sensing techniques for airborne and satellite-borne imaging systems, discussing microwave radiometer augmentation of visual and IR data 06 p0813 A72-17430

Raman laser radar /LIDAR/ for remote probing, discussing design, construction, testing, atmospheric scattering, and intensity and polarization measurements 06 p0824 A72-17588

Holographic Ice Survey System for down looking radar probing and measurement of sea ice and glaciers, discussing ice electrical properties and system design 06 p0814 A72-17590

Radar instrument for measuring snow density, water content, layer depth and inhomogeneity based on snow cover electrical properties effects on echo characteristics 06 p0805 A72-17591

Microwave radiometer and scatterometer sensing for earth surface and subsurface measurements 06 p0815 A72-17784

Thermal IR imaging remote sensing device for aerial earth resource surveys, noting hydrogeology, volcanology, forest fire and geothermal region detection and ice sheet study applications 06 p0807 A72-17789

Remote sensing methods in geology, discussing air/satellite-borne black and white, color and multispectral photographic, TV, multispectral scanning, IR and radar techniques 06 p0809 A72-18228

Remote sensing methods applications to environmental protection, discussing microwave, radar, IR, optical and acoustical active and passive methods [DGLR PAPER 71-132] 06 p0809 A72-18229

Atmospheric effects on remotely sensed earth surface signature recognition, considering scattering, absorption and emission effects [DGLR PAPER 72-130] 06 p0809 A72-18233

Remote sensing possibilities by aerial photographic methods based on scanning, scatterometer, radiometer and vidicon systems, discussing ground resolution, data automation and satellite observation [DGLR PAPER 71-128] 06 p0818 A72-18234

Air pollutant monitoring and remote analysis by Raman, fluorescence and resonance backscattering, Rayleigh scattering and absorption laser radar techniques 06 p0827 A72-18460

Remote sensing for earth resources data, discussing sensors equipment and project organization and management 06 p0810 A72-18615

Remote sensing of oil pollution on water by laser induced fluorescence, using airborne spectroscopy [AIAA PAPER 71-1076] 07 p0981 A72-18822

Nimbus 4 satellite selective chopper IR radiometer atmospheric temperature measurements from earth surface to 50 km altitude, describing instrument design, operation and performance 07 p1029 A72-19097

Remote sensing history and techniques, describing ERTS instrumentation for earth science studies 07 p0976 A72-19177

ERTS A and B satellite systems for multispectral imaging of earth surface, discussing sensors, operational control and data processing requirements and implementation 07 p1085 A72-19276

Earth satellite legal aspects under space treaty, discussing orbiting military remote sensing devices, national obligations and security issues 07 p1105 A72-19476

Telemetric instrumentation for remote physiological and behavioral observations of free roaming animals 07 p0930 A72-19912

ERTS program, discussing orbit selection and sensor equipment 07 p1085 A72-20305

Low power X ray diffractometer with multiwire proportional counter detector array for remote mineralogical analysis of lunar, planetary or asteroid soils detector array 08 p1167 A72-21507

Skylab S-193 altimeter experimental mission objectives and spacecraft instrumentation, considering precision designs, oceanographic surface remote sensing and electromagnetic scattering measurement 09 p1306 A72-22317

Multispectral remote sensing techniques, equipment and applications, discussing color and IR camera, line scanning and radar systems and automated interpretation devices 09 p1312 A72-23304

Suboptimal decision algorithm to correlate sensor data with stored tracks in real time track-while-scan surveillance system 10 p1441 A72-23780

Remotely sensed imagery data photointerpretation by gray tone texture context feature extraction, noting identification accuracy 10 p1442 A72-23812

Laser radar technique for invisible air pollutants remote sensing systems, comparing Raman backscattering resonance scattering and absorption schemes 10 p1489 A72-23952

Air pollution monitoring by remote optical sensing techniques based on light scattering measurements, noting suitability of high power laser probes 10 p1480 A72-24100

Wind tunnel model magnetic suspension system with remote position sensor based on optical contrasts scanning analysis 10 p1461 A72-24763

Wind tunnel model remote position sensing and control systems, discussing drift reduction in magnetic suspension 10 p1461 A72-24768

Scanning photoelectric image conversion /photoanalyzing/ systems for data telemetry from remote optical sensors 11 p1634 A72-26461

Spacecraft orientation angle measurement by inertial sensors, analyzing equipment kinematic efficiency and limitations 11 p1684 A72-26913

Remote measurement of cloud ice and water content from Raman scattering of ground based laser signal 12 p1840 A72-27547

Language description of remotely sensed image data, noting application to artificial intelligence, linguistic analysis and retrieval 13 p1924 A72-28525

Laser Doppler-type remote sensor for wind velocity and atmospheric turbulence measurements 13 p1956 A72-28859

United Nations FAO interest in remote sensing techniques application to agricultural, forestry and fisheries resources survey and management 15 p2220 A72-31228

European space program for remote sensing techniques application, noting earth resources survey satellites 15 p2220 A72-31229

International programs for simultaneous ecological study via remote sensing techniques, discussing European and Italian space programs 15 p2220 A72-31230

Satellite observation of earth surface, discussing remote sensing techniques application in pollution control and ecology 15 p2319 A72-31232

Satellite IR telescensors in oceanography for data acquisition on ocean state, circulation, surface temperature, salinity, pollution, etc 15 p2221 A72-31238

Satellite sensor cooling systems, considering cryogenic heat pipes, sublimation, radiation cones and surface treatment 15 p2319 A72-31240

Spaceborne and airborne remote sensing methods and applications for earth resources observation 15 p2221 A72-31245

Computer controlled ground truth station for environmental agricultural aerial photographic remote sensors data processing, discussing system components, printout format and computer program 15 p2213 A72-31249

Airborne remote sensing missions and instrumentation to investigate Penobscot River water ecology for thermal, chemical and solid pollutants 15 p2221 A72-31252

Unitary and interdisciplinary information processing of remote satellite observations of earth resources, noting ground station requirement for Italy 15 p2222 A72-31253

Spectral brightness coefficient and photodensity measurements for remote vegetation productivity sensing in visible band 15 p2222 A72-31396

Magnetic dipole or small current loop over homogeneous flat earth, calculating transient electromagnetic field for airborne remote sensing 15 p2224 A72-31672

Vehicle orientation degrees of freedom remote measurement with mounted passive devices and polariza-

tion-modulated light, discussing data reduction and system accuracy 15 p2267 A72-31780

Skylab radar altimeter for earth surface features remote sensing with high range resolution mode for ocean wave height determination 15 p2236 A72-31995

Satellite earth resources remote sensing in visible, IR and microwave regions for plant disease and salinity evaluation 15 p2229 A72-32049

Flexible launch vehicle optimal and constrained-optimal control for performance index minimization, using sensors and constant feedback gains 15 p2321 A72-32585

Coastal environment remote sensing from satellite and aircraft imaging platforms for geological, oceanographic and ecological investigations 15 p2232 A72-32622

Oil spills remote sensing in marine environment, using laser excited fluorescence for detection, identification and quantification 15 p2251 A72-32623

Remote sensing system for oil pollution spectral signature properties, analyzing UV, IR, visible light, radar and microwave data 15 p2242 A72-32624

Optical sensors for spacecraft attitude determination, discussing operation principles based on solar radiation, albedo, IR contrast and stellar radiation detection 16 p2389 A72-32849

Airport runway fog dispersal in UK, discussing cost projection for chemical seeding system combined with lidar remote sensing 16 p2418 A72-33500

Computerized aircraft landing measurement system for civil airport, using optical, seismic and IR sensors 16 p2374 A72-33627

Gases and vapors spectral signatures application in correlation spectroscopy and interferometry for aerospace monitoring of earth resources and pollution 16 p2393 A72-33630

Electro-optical torque sensor based on slit aperture produced diffraction patterns [SESA PAPER 1925-II] 17 p2553 A72-34813

Two dimensional images from remote sensors, discussing geometrical properties and imaging equations for aerial, IR and radar photographs 17 p2555 A72-35335

Transformation of points from side-looking radar images into the map system. 17 p2555 A72-35336

A relative performance analysis of atmospheric laser Doppler velocimeter methods. 17 p2558 A72-35949

Digital image processing and interpretation of photographic film data. 18 p2690 A72-36319

Remotely sensed data processing by scanner/printer designed for photograph scanning, geometric correction and photographic printing of corrected image 18 p2691 A72-36495

Canadian program for global environmental and world resources monitoring system, discussing management, technology and user interface [AIAA PAPER 72-742] 18 p2742 A72-36548

S-band radiometer design for high absolute precision measurement. 19 p2794 A72-37252

ERTS-borne return beam vidicon camera using high resolution TV sensors coaligned to view identical scene in different spectral bands 19 p2795 A72-37576

Thermal remote sensing of temperature distribution in semitransparent solids - A numerical experiment. [ASME PAPER 72-HT-5] 20 p2986 A72-39676

Remote sensing of urban 'heat islands' from an environmental satellite. 20 p2919 A72-39717

An albedo horizon sensor using hybrid circuitry. 21 p3050 A72-40122

Statistical analysis of information from remote space vehicles 21 p3015 A72-40327

A priori estimation of the quality of a data-compression system from the statistical characteristics of the sensors employed 21 p3024 A72-40328

The cost-effectiveness of advanced remote sensing systems. 21 p3131 A72-40864

An experimental study in the application of the Raman scattering technique as a remote sensor of gas temperature and number density in hypersonic CF4 flow. [AIAA PAPER 72-1018] 21 p3057 A72-41597

IR reflectance [or emittance] remote spectroscopy of mineral particulate surfaces, discussing particle size, surface roughness, porosity and mixing ratios effects 22 p3178 A72-42526

Low flying aircraft wake vortices tracking, describing sensing techniques based on acoustic pulse deflection and velocity field measurements

22 p3179 A72-42709

Application of differential OMEGA to remote environmental sensing.

24 p3421 A72-44639

Remote sensing of earth resources by microwave radiometry.

24 p3402 A72-45107

The role of the United Nations in earth resources satellites.

24 p3468 A72-45185

Streamflow forecasting project to assess feasibility of air and spaceborne remote sensed data acquisition application to watershed hydrological behavior prediction

24 p3398 A72-45215

REMS

U RAPID EYE MOVEMENT STATE

RENAL FUNCTION

Antidiuretic effect of acute thoracic and abdominal inferior vena cava constriction on arterial pressure, renal hemodynamics and electrolyte excretion

02 p0157 A72-11660

Cardiac output and autonomic nervous system role in antidiuretic response to acute thoracic superior vena cava constriction

02 p0157 A72-11661

Immobilization hypercalciuria, discussing treatment by diet-induced extracellular volume depletion and possible pathophysiologic mechanism of intercompartmental fluid and electrolyte shift

04 p0479 A72-14871

Cat mean renal nerve activity modification by hypothalamus stimulation and baroreceptor reflex interactions, discussing mean aortic pressure variation effects

04 p0477 A72-15722

Aortic constriction and release effects on kidney glomerulotubular balance in saline- and water-loaded dogs, studying sodium reabsorption changes

08 p1115 A72-21084

Prolonged water immersion effects on renal function and plasma volume in trained and untrained subjects, noting deleterious effect on orthostatic tolerance and work capacity

10 p1428 A72-23738

Renal clearance studies of left atrial distention effect in dog, indicating antidiuretic hormone inhibition mechanism of diuresis

12 p1763 A72-27828

Interrelationship of hemodynamic alterations of valvular heart disease and renal function - Influences on renal sodium reabsorption.

19 p2756 A72-37872

Renal polycystoma - Incidence among flight personnel

19 p2756 A72-37877

Renin in differential diagnosis of hypertension.

19 p2757 A72-38144

Effects of simulated high altitude on renin-aldosterone and Na homeostasis in normal man.

21 p3005 A72-40422

Studies of renal and extrarenal production of erythropoietin in male and female rats

21 p3002 A72-41190

Nitrogen excretion as a measure of protein metabolism in man under different conditions of renal function.

21 p3003 A72-41523

The effect of space flight conditions and prolonged hypokinesia on the kidney function in man

22 p3149 A72-42068

Capillary circulation as a regulator of sodium reabsorption and excretion.

23 p3257 A72-43995

Increased fluid turnover and the activity of the renin-angiotensin system under various experimental conditions.

23 p3257 A72-43997

RENDEZVOUS

NT EARTH ORBITAL RENDEZVOUS

NT ORBITAL RENDEZVOUS

NT SPACE RENDEZVOUS

RENDEZVOUS SPACECRAFT

Atmospheric rendezvous concept to increase space transportation system efficiency and flexibility, discussing structural weight savings

[AIAA PAPER 72-134]

05 p0730 A72-16889

Spaceborne laser radar for target acquisition and tracking in spacecraft rendezvous and docking applications

[CLEA PAPER 9,5]

07 p0943 A72-19387

Elliptical orbiting spacecraft minimum fuel consumption rendezvous maneuver, formulating variational extremum problem with constraints

14 p2150 A72-30329

RENDEZVOUS TRAJECTORIES

Consecutive collision orbits characterized by particle ejection from mass along x axis in restricted three body problem

01 p0122 A72-10006

Optimal allocation and guidance for linear time varying interception and rendezvous problems of dynamic deterministic or stochastic systems

05 p0686 A72-16558

Programmed minimax target acquisition in rendezvous game between conflictingly controlled motion and given set of vectors

07 p1028 A72-19969

Minimum time duration rocket interception, calculating trajectory parameters and target orbits in Earth gravitational field

09 p1393 A72-23573

Two and three impulse trajectories for fixed time and angle rendezvous between vacant circular coplanar orbits, defining optimality domain

11 p1719 A72-25977

Encounter trajectory design for solar electric propulsion rendezvous with low mass celestial bodies, noting target characteristics

[AIAA PAPER 72-424]

13 p2036 A72-28939

Navigational aspects of two impulse transfer initiated rendezvous with Deimos using modified Viking Monte Carlo error analysis program

15 p2269 A72-32177

Orbital trim by velocity factoring for Viking Mars mission terminal rendezvous and intermediate timing constraints involving orbital operations

15 p2269 A72-32179

Game problem of impulse controlled soft rendezvous of two material particles under attractive forces

16 p2422 A72-32928

Programmed minimax target acquisition in rendezvous game between conflict controlled motion and given set of vectors

20 p2947 A72-40026

Spacecraft rendezvous trajectories and targeting maneuvers onboard sequential computation, taking into account maneuver constraints and state vector update information

24 p3450 A72-45172

Rendezvous at specified destinations through optimum transfer paths

24 p3442 A72-45281

RENE 41

Acoustic emission monitoring of postweld heat treatment cracking in Rene 41 weldments, correlating relative crack susceptibility of different microstructures

11 p1653 A72-25345

REPAIRING

U MAINTENANCE

REPEATERS

Numerical linear interpolator design with ICs, noting application to digital filters and sampled data systems

09 p1289 A72-23677

Aircraft and water vehicles mobile communications via stationary satellite, discussing optimum multiple access and repeater configuration

[AIAA PAPER 72-565]

12 p1781 A72-27376

Flight prototype satellite communications repeater with two transponder channels and dual beam antenna, discussing design parameters and advanced systems application

[AIAA PAPER 72-579]

12 p1789 A72-27381

Binary logic circuits with interconnected repeaters and inverters, discussing signal level selection to ensure maximum noise stability

12 p1786 A72-28120

Attitude instruments, pitch and roll. I - Minimum performance standard for equipment.

[SAE AS 1162]

18 p2692 A72-36534

Binary logic circuits with interconnected repeaters and inverters, discussing signal level selection to ensure maximum noise stability

19 p2767 A72-38621

Hybrid digital transmission systems based on optical fiber waveguides and analog repeaters, noting YAG laser light modulation by phase shift keyed subcarrier

21 p3018 A72-40868

Delay-lock repeater tracking system utilizing superregenerative interrogator.

21 p3082 A72-41084

REPETITION

Acoustic stimuli transients rise time and repetition rate effects on loudness, applying various steady state noise calculation methods to transients Fourier transforms

13 p2004 A72-29097

REPORT GENERATORS

GPSS/360 interactive simulation program with report generator, selective output display and HELP blocks for model manipulation and real time viewing

06 p0780 A72-17980

On-line digital computer system for real time interpretation and report generation of electrocardiograms from remote locations over switched telephone network

07 p0928 A72-19311

REPORTS

Field reporting system for reliability analysis on telecommunication equipment.

24 p3384 A72-44657

REPRODUCTIVE SYSTEMS

NT TESTES

Alpha-L-fucosidase, beta- and alpha-D-galactosidases and alpha-D-mannosidase activity changes in human placenta at various embryogenesis phases

02 p0163 A72-12294

REPUBLIC MILITARY AIRCRAFT

U MILITARY AIRCRAFT

RESCUE OPERATIONS

Subsurface electromagnetic fields of current carrying cable line source on flat earth conducting half space, considering mine rescue operations

01 p0060 A72-10840

HH-53 rescue helicopter automatic approach and hover coupler for automatic transition from forward flight at constant deceleration and rate of descent

05 p0686 A72-16653

Crashproof rotorcraft STOL aircraft for rescue operation, discussing orthodox rigid and special rotary wings design, air tunnel experiment and flight tests

06 p0760 A72-18582

Survival rates in USAF accidents during 1965-69, noting visual sighting as primary rescue factor

08 p1109 A72-21564

Single Integrated Signal Device to aid in locating downed airmen awaiting rescue in dense jungle terrain by Search and Rescue aircraft

08 p1112 A72-21580

Rescue signaling devices design and operation, discussing pinpoint markers, rocket boosted panel markers, strobe units, antennas and balloon marker

08 p1112 A72-21584

Space rescue - Conference, Konstanz, West Germany, October 1970

09 p1395 A72-23151

Manned space flight escape, rescue and survival systems based on onboard, prepositioned aid and earth launched concepts, considering earth orbit, lunar and interplanetary missions

09 p1395 A72-23152

International standardization of manned spacecraft components for rescue efforts and joint multinational space missions

09 p1395 A72-23154

Parameters affecting communication and rescue time constraints for emergency astronaut return from low earth orbits

09 p1395 A72-23155

Lunar orbiting rescue vehicle design for Apollo missions, discussing guidance, navigation and communications

09 p1396 A72-23156

Lunar landing mission escape and rescue concepts, considering emergencies during earth orbit, translunar, lunar orbit, surface and rendezvous, transearth and earth reentry phases

09 p1396 A72-23157

Terminal guidance systems and techniques application to manned space flight rescue operations, discussing emergency location and rescue spacecraft communication and guidance

09 p1396 A72-23158

Loran/OMEGA course and track equipment /LO-CATE/ for remote object tracking by retransmission technique, eliminating search from search and rescue missions

13 p1997 A72-29182

Structural design and electrical drive mechanism of helicopter hoist for rescue operations

13 p1912 A72-30097

International Space Rescue Symposium, 4th, Brussels, Belgium, September 21, 1971, Proceedings.

17 p2620 A72-34426

Preventive and remedial space flight safety engineering, discussing escape capsules and onboard and earth-launched rescue systems

17 p2620 A72-34427

Long range planning for the development of space flight emergency systems.

17 p2620 A72-34428

Spacecraft rescue and recovery capabilities assessment based on anticipated U.S. space programs, discussing mission design, recovery response, weather prediction and communications

17 p2620 A72-34429

The role of the International Civil Aviation Organization /ICAO/ in organizing Search and Rescue Services /SAR/.

17 p2638 A72-34430

Potential response of maritime services to craft and persons in distress at sea.

17 p2488 A72-34431

Worldwide weather data system as important factor for search and rescue operations implementation

17 p2488 A72-34432

Medical and technical aspects of rescue and survival of astronauts in high mountain and mountainous remote areas.

17 p2507 A72-34434

Some aspects of survival and rescue of astronauts in polar regions.

17 p2507 A72-34435

Possibilities and dangers during long working periods in space rescue.

17 p2507 A72-34436

The earth orbit shuttle as a space rescue vehicle. 17 p2620 A72-34437

Spacecrews rescue requirements, considering escape capsules earth-based and orbit-based rescue systems and flight hazards 17 p2620 A72-34438

Flight test evaluation of a forward looking radar system for search and rescue applications. [AHS PREPRINT 633] 17 p2490 A72-34499

International Space Rescue Symposium, 2nd, Mar del Plata, Argentina, October 9, 1969, Proceedings. 17 p2622 A72-35549

FAA implemented airport certification legislation covering minimum safety standards, operation manual, emergency plan, fire and rescue service and pavement requirements 18 p2675 A72-36785

Helicopter search, rescue and transportation of wounded and ill persons in Denmark, discussing accidental hypothermia treatment 19 p2759 A72-38714

International Space Rescue Symposium, 1st, New York, N.Y., October 14, 1968, Proceedings. 20 p2977 A72-39550

A study of USAF survival accidents 1 Jan. 1965-31 Dec. 1969. 23 p3259 A72-34425

Naval helicopters applications to search and rescue, ASW, ground support and other roles, considering reliability and maintenance 24 p3365 A72-44685

Space rescue operations planning requirements for 1980s manned satellite missions, discussing vehicles, equipment and various mission phases 24 p3449 A72-45129

Extending the utility of the Space Shuttle as a space rescue vehicle. 24 p3449 A72-45130

Rescue operation capability for Skylab, discussing mission requirements, response time and vehicle configuration 24 p3449 A72-45132

Satellite relay and Omega navigation system for distress signal transmission and reception in global rescue alarm network serving ships, aircraft and spacecraft 24 p3467 A72-45134

Spacecraft rescue/recovery capabilities, discussing in-flight escape, ground egress and descent systems, performance and technical and human factors 24 p3450 A72-45147

Despinning and detumbling satellites in rescue operations. 24 p3450 A72-45160

Flight mechanics aspects in space transportation system for international rescue, analyzing potential crises situations requiring emergency action 24 p3451 A72-45217

Human organism and space flight stress endurance limits and manned space mission rescue capabilities requirements, considering cabin decompression, anoxia, radiation, onboard illness, etc 24 p3376 A72-45218

RESEARCH

NT CRITICAL PATH METHOD

NT DYNAMIC PROGRAMMING

NT GAME THEORY

NT HIGH TEMPERATURE RESEARCH

NT LINEAR PROGRAMMING

NT LOW DENSITY RESEARCH

NT MARKET RESEARCH

NT MINIMAX TECHNIQUE

NT NONLINEAR PROGRAMMING

NT OPERATIONS RESEARCH

NT SADDLE POINTS [GAME THEORY]

Clinical observations as a research method in physiology 17 p2504 A72-35017

RESEARCH AIRCRAFT

Augmentor wing jet STOL research aircraft development progress report covering design, engine tests, performance prediction, control simulation and stability augmentation [SAE PAPER 710757] 01 p0003 A72-10254

Handling qualities simulation program for augmentor wing jet STOL research aircraft considering control devices design 02 p0154 A72-11654

Environmental research with instrumented aircraft, discussing application to operational forecasting and weather modification experiments in hurricanes and tropical convective clouds 04 p0542 A72-14682

HP-115 slender wing research aircraft linear motion and undamped Dutch roll oscillations at high angles of attack [AIAA PAPER 72-62] 05 p0613 A72-16932

RESEARCH AND DEVELOPMENT

Industrial parachute R and D in UK, discussing management, technical staff requirements and government/industry liaison 01 p0004 A72-10304

Astronautical research - IAF Conference, Konstanz, West Germany, October 1970 01 p0130 A72-10926

NASA earth resources satellite R and D program for acquiring data on agriculture, forestry, geography, geology, hydrology, mineralogy and marine resources 01 p0063 A72-10949

German Research and Test Institute for Aero- and Astronautics 1970 report covering flow mechanics, power conversion, aerospace medicine, atmospheric physics, etc 01 p0048 A72-11151

METROMEX field project to investigate inadvertent weather modification by urban-industrial effects and man-made precipitation changes 03 p0384 A72-13636

Battery separator materials requirements derived from in-cell environment and battery mission, evaluating present technology for R and D area concentration 03 p0313 A72-14235

Rechargeable oxygen electrode research program for hydrogen oxygen fuel cells and metal-oxygen batteries, discussing KOH solutions effects 04 p0466 A72-14675

R and D requirements for international standard vhf instrument landing system for Category I, II and III operations in next decade 04 p0545 A72-14827

Industrial R and D data collection to relate idea dispositions by management to subjective evaluation, considering urgency, predictability and expected time horizon roles 04 p0598 A72-15455

DELTA flow chart and network method for R and D projects planning and scheduling 04 p0598 A72-15456

Electronics research and engineering - IEEE Conference, Boston, November 1971 05 p0633 A72-15779

Civil aviation R and D policy study, showing priorities for aircraft noise and congestion abatement and short haul systems 05 p0611 A72-15780

Rocket propellants R and D toward higher specific impulse, discussing liquid, solid, hybrid and tribrid systems 05 p0702 A72-16744

Price and technical quality effectiveness in winning government R and D contracts 06 p0905 A72-17397

NASA sponsored medical R and D programs for space applications, stressing benefits to earthbound medical services 06 p0769 A72-18626

Concorde aerodynamic configuration R and D, discussing wing layout in terms of drag, stability, control and weight distribution characteristics 07 p0911 A72-19057

In-house R and D laboratory organization cost effectiveness evaluation methods, discussing supervisory, program and special appraisals, visiting committees and natural competition 07 p1105 A72-19551

R and D management policies choices with respect to Bayesian decision-theoretic model in simulated environments 07 p1105 A72-19553

Technological forecasting method evaluation for R and D planning, fitting trend curves to sets of technological data 07 p1105 A72-20268

ESRO electric propulsion systems R and D, discussing various concepts in terms of weight, cost, thrust level, efficiency, simplicity, exhaust velocity and development potential [AIAA PAPER 72-478] 11 p1710 A72-26207

Dynamic modeling application to technological forecasting, discussing mathematical simulation for R and D management planning in project selection and budget allocation 11 p1748 A72-26284

NASA program to develop heat resistant materials for aerospace applications, discussing refractory carbides, nitrides and borides temperature dependent behavior and properties 11 p1664 A72-26857

Individuals with high information potential in informal communications networks of government R and D organizations, discussing personal characteristics 12 p1891 A72-27654

Military R and D organization questionnaires data analysis to obtain relationship between job productivity, satisfaction, ability, age and salary 12 p1891 A72-27655

French R and D programs on Si and various thin film photovoltaic solar cells, considering efficiency, reliability, and weight and cost reduction problems 12 p1756 A72-28002

Measuring technique importance for aircraft R and D, emphasizing quartz tensometer, digital control and signal processing 14 p2092 A72-30286

Time parameter in military air operations, discussing weapon systems R and D, all-weather capability, communications, reliability and maintainability, manpower training, etc 15 p2339 A72-32453

European unity as prerequisite for technological and scientific progress with respect to U.S. and Soviet superiority 16 p2480 A72-32893

Technology R and D program to qualify man for long term weightlessness, assessing space flight stress effects on physiology and psychology 16 p2358 A72-33544

System models for R and D processes in terms of state variables and control vectors, deriving algorithm for optimization 16 p2482 A72-33864

NASA R and D for STOL short haul transportation systems, discussing propulsive lift, blown flap and augmentor wing concepts, noise reduction, etc 17 p2487 A72-34238

Resource analyses for R & D programs. 17 p2639 A72-35339

Evaluating alternate paths in R & D project planning. 17 p2639 A72-35340

Experimental mechanics in research and development; Proceedings of the International Symposium, University of Waterloo, Waterloo, Ontario, Canada, June 12-16, 1972. Volumes 1 & 2. 18 p2732 A72-36352

NASA R and D programs for quiet STOL aircraft and engines development 18 p2721 A72-36503

Quantitative evaluation for R and D resource allocation in terms of funding project priorities 18 p2884 A72-38024

Pulsed-jet engine of Messerschmitt-Boelkow-Blohm without valve flaps 19 p2849 A72-38031

Fluidics - A potential technology for aircraft engine control. 19 p2849 A72-38047

Aircraft noise problem in piston engine to turbofan jumbo jet transports, discussing need for noise reduction research [AIAA PAPER 72-815] 19 p2750 A72-38117

Recent advances in R & D value measurement and project selection methods. 20 p2988 A72-39397

Improving R & D management through prototyping. 21 p3132 A72-40970

Defense Documentation Center independent R and D data bank for evolution and maintenance of creative technology oriented defense industry 21 p3132 A72-40974

NASA Quiet Engine program R and D on conventional takeoff and landing subsonic cruise aircraft engine noise [ICAS PAPER 72-48] 21 p3100 A72-41173

National aerospace R and D facilities requirements, establishing priority order for V/STOL, aeropropulsion systems, high Reynolds number, large transonic and true-temperature hypersonic test facilities [AIAA PAPER 72-1033] 21 p3043 A72-41608

Experiment design - An organized approach to data collection. 22 p3245 A72-41935

Planning and management requirements for aircraft jet engine control system research and development 23 p3294 A72-44285

Forecasting as a means for scientific and technological policy control. 23 p3358 A72-44350

R and D on environmental and thermal control/life support system application to lunar base mission, discussing reliability and food regeneration 24 p3375 A72-45164

Forecasting costs and completion dates for defense research and development contracts. 24 p3468 A72-45479

RESEARCH FACILITIES

NASA/MSC Earth Resources Research Data Facility for remote sensing of geology, geography, agriculture, forestry, hydrology and oceanography 02 p0200 A72-11824

European Space Research and Technology Center /ESTEC/ results in cosmic rays, ionospheric physics and surface physics 05 p0644 A72-16754

Heated lithium ion system /HELIOS/ facility for quiescent steady state plasma studies, noting MHD instabilities minimization 06 p0854 A72-17502

Sonic boom research facilities and techniques, emphasizing applicability to other environmental problems 09 p1262 A72-23317

Dynamical motion simulation facility for Symphonie satellite, using sensors, attitude control electronics and analog computer in closed loop system [DFVLR-SONDDR-201] 12 p1795 A72-27659

Zero gravity earth orbital cloud physics facility requirements and design concepts, noting experiments feasibility relative to astronaut performance 13 p1990 A72-28815

Supersonic combustion research facility design for studying air-fuel mixing processes, shock wave in-

duced temperature and pressure increments and flame holding devices

15 p2335 A72-31815

High temperature turbulent jet facility for studying ionic species produced by high temperature air and ablation products interaction with cool ambient air [AIAA PAPER 72-676]

17 p2536 A72-35480

German book on vacuum technology covering theory, measurement techniques and applications in nuclear physics research facilities, electronic tubes, space environment simulation, mass transfer, etc

18 p2709 A72-36250

Development of a hypervelocity wind tunnel.

18 p2676 A72-37095

Ionospheric heating and electron density modification by high powered radio waves, describing research facility

20 p2919 A72-39724

Canadian sonic boom simulation facilities.

21 p3040 A72-41151

National aerospace R and D facilities requirements, establishing priority order for V/STOL, aeropropulsion systems, high Reynolds number, large transonic and true-temperature hypersonic test facilities [AIAA PAPER 72-1033]

21 p3043 A72-41608

Sounding balloon services for extraterrestrial, atmospheric and terrestrial studies, emphasizing NCAR Balloon Flight Station facilities at Palestine, Texas

21 p2996 A72-41610

Experience with the NRC 10 ft. x 20 ft. V/STOL propulsion tunnel. Some practical aspects of V/STOL engine model testing.

23 p3278 A72-44247

RESEARCH MANAGEMENT

Industrial parachute R and D in UK, discussing management, technical staff requirements and government/industry liaison

01 p0004 A72-10304

Management enhancement of researchers motivation in times of economic uncertainty, stressing security related aspects of employment

06 p0905 A72-17396

Systems approach to technological forecasting for short range research, considering consumer, market and organizational resources

09 p1413 A72-22950

Improving R & D management through prototyping.

21 p3132 A72-40970

Research planning in steady compressible flow aerodynamics, discussing projects on annular wings, shockless transonic airfoils and Smith panel method for three dimensional flow problems

21 p2990 A72-41126

Experiment design - An organized approach to data collection.

22 p3245 A72-41935

Planning and management requirements for aircraft jet engine control system research and development

23 p3294 A72-44285

RESEARCH PROJECTS

Cost effective ship-based research balloon fleet for scientific experiments meeting stringent space research budget requirements

01 p0048 A72-10954

Mathematical model for research payoff estimation by internal rate of return method used by large corporations for project evaluation

02 p0305 A72-12695

Industrial R and D data collection to relate idea dispositions by management to subjective evaluation, considering urgency, predictability and expected time horizon roles

04 p0598 A72-15455

Upper atmosphere research rockets missions, payloads and measurements, describing various international aeronomy research projects

13 p2052 A72-30081

Research planning in steady compressible flow aerodynamics, discussing projects on annular wings, shockless transonic airfoils and Smith panel method for three dimensional flow problems

21 p2990 A72-41126

RAM - A concept for reducing space payload costs. [SAWE PAPER 942]

23 p3343 A72-43482

RESEARCH VEHICLES

AEROS research satellite control program, describing system objectives, operational testing, error analysis and command verification

13 p1918 A72-28968

Plastic balloons development for high altitude research, discussing construction technology, launch methods and scientific achievements

24 p3368 A72-45141

RESEKINE

The effect of hypoxia on the coronary blood flow in reserpinized dogs.

24 p3370 A72-44562

RESERVOIRS

A gradient method of expanding a group data handling method to new plants not studied by experiments

22 p3162 A72-42242

RESIDUAL GAS

Zone melting high vacuum facility with cryogenic pumping and residual gas carbon-containing components exclusion for ultrapure metals production

06 p0796 A72-17992

Langmuir electron oscillation excitation by ion beam at velocity exceeding average electron thermal velocity in plasma formed by residual gas ionization

07 p1046 A72-20505

German monograph on electron beam focusing in partial pressure analyzer with two compartment ion source, eliminating residual gas-filament interaction

09 p1306 A72-22318

Transit tube manometric system with fast particle beam ionization of residual gas molecules for vacuum measurements

09 p1364 A72-23226

ESRO 1 satellite residual gas outgassing rate and composition measurements during thermal heat balance tests, using mass spectrometer

09 p1263 A72-23260

Supersonic molecular jet improvement via expansion chamber residual gas pressure reduction and nozzle stagnation pressure increase

16 p2429 A72-33053

Electron beam focusing by ions in transverse gas flows, considering air, argon and helium residuals

20 p2952 A72-39070

RESIDUAL STRESS

Stress relaxation resistance at elevated temperatures after reloading as function of internal and effective stress

01 p0138 A72-10520

Steel and Ti-Al-V alloy surface integrity during various machining methods, considering microstructures, residual stress profiles and fatigue characteristics [SME PAPER IQ 71-237]

01 p0076 A72-10972

Beryllium microstructure and hexagonal close packed polycrystal material residual thermal stresses, calculating thermal expansion coefficients

01 p0087 A72-11028

Residual buckling strength of Al alloy elastic column with fatigue crack [SESA PAPER 1914A]

02 p0288 A72-11511

Rigid plastic circular plate dynamic model with yield time delay, discussing residual deflection as function of load duration

02 p0293 A72-12426

Second order electro-optic effect in diamond, discussing birefringence due to dispersion and random residual strains

02 p0260 A72-12545

Residual stress formation mechanism in two phase Ti alloys under cutting and plastic deformation, showing phase transformation composition and structure effects

03 p0363 A72-13467

Thermodynamic solids theory generalized for internal strains in perfect non-Bravais crystals, applying to trigonal Se and Te structure

04 p0562 A72-15470

Finite element micromechanical analysis of porous and filled ceramic composites for internal stresses and deformations

05 p0738 A72-16423

Residual stress measurements in metals by annular photoelastic gages, obtaining relationship to fringe orders

06 p0818 A72-18317

Residual stresses and geometrical imperfections effects on compressive strength of thin welded box columns

07 p1088 A72-19114

Pulsed laser beam effect on residual stresses behavior in transverse weld on cylindrical shell

07 p0996 A72-19776

Automatic photoelectric device for measuring internal stresses and deformations of photographic films

07 p0988 A72-19861

Residual stresses effect on technical cohesive strength of welded cylindrical shell with surface defects, presenting plane strain fracture toughness determination method

07 p0997 A72-20131

Internal strain measurement in solid elastomeric materials by radioactive implant method using pinhole camera or multichannel collimator

07 p0992 A72-20583

X ray and resistance strain gage techniques for bar and metal plate simultaneous residual stress determination

07 p0993 A72-20606

Prestressed glass reinforced composites mechanical behavior, taking into account manufacture induced residual stress concentrations

08 p1192 A72-21674

Residual temperature stresses and deformations during thermal treatment of thick walled glass fiber reinforced plastic wound cylinders and rings

08 p1194 A72-21755

Climatic load effects on carrying capacity of thick walled glass reinforced polymer rings with residual stresses

08 p1195 A72-21765

Material properties nonuniformities effect on wound fiber glass reinforced plastic rings and cylinders thermoelastic residual stresses

08 p1196 A72-21858

Radial and axial residual stress components in glass fiber reinforced polyethylene, comparing with adhesion strength obtained by shear method

08 p1196 A72-21862

Residual shrinkage and thermal stresses in adhesion bond models of metal coatings and cemented seams

08 p1248 A72-21865

Quenched aluminum oxide rod residual stress profile from strain and heat transfer rates measurements and temperature distribution calculation

08 p1196 A72-21918

Metal matrix composites deformation and mechanical properties prediction from component phases information, examining interface role, residual stress effect and thermal degradation

10 p1553 A72-24176

Dimensional stability and micromechanical properties of materials for use in OAO, investigating residual stresses, creep properties and stress relaxation [AIAA PAPER 72-325]

11 p1653 A72-25362

Boron fibers tensile and transverse strengths, relating severe anisotropy to residual stress pattern from preexistent flaws

11 p1672 A72-25484

Axial, circumferential and radial residual stresses calculation in polymetallic coatings and cylindrical elements during surface layer removal by electrochemical processing

11 p1737 A72-26263

Residual stresses and stress relaxation determination in electrochemical galvanic coating with automatic strain curve plotter

11 p1613 A72-26264

Diamond burnishing effect on surface quality and fatigue strength of steel, noting work hardening increase and compressive residual stresses buildup in surface layer

11 p1642 A72-26811

Body of revolution/ saucer/ with nongeodesic internal stresses under gravitational field in terms of general relativity theory

12 p1843 A72-27048

Stressed state induced in compound thick walled cylinder for testing residual tensile stresses effect on machine parts wear resistance

12 p1814 A72-27461

Heat treated Al alloy forgings stress relief by cold deformation between quench and age, examining effect on tensile properties and residual stresses [ASM PAPER W 72-53,1]

12 p1817 A72-28165

Heating rate effects on residual stresses in thick walled cylinders produced by winding heated binder impregnated fiberglass tape on cold spool

13 p1982 A72-28553

Fatigue limit and Woehler curve determined from notch tests, noting relation between fatigue damage and residual stresses in notched parts [ONERA, TP NO. 1083]

13 p1980 A72-29673

Welded machine component service history effects on residual fatigue life from statistical evaluation of factor experiment

14 p2107 A72-30278

Mechanical properties and residual stresses in and adjacent to interface of explosively welded Al-Zn-Mg alloy with steel, noting microcracks effect on weld strength

15 p2257 A72-32111

Embedded piezoelectric quartz crystal transducer with Hopkinson pressure bar to measure internal dynamic stress

15 p2240 A72-32433

Internal buckling of a laminated medium.

18 p2377 A72-37059

Calculation of residual stresses in wound materials produced by a layer-on-layer solidification process

19 p2872 A72-37532

Estimation of the accuracy of the method of measuring the bending of strips in order to determine residual stresses.

19 p2806 A72-37574

Some considerations on the residual stresses in orthogonal cut surface of aluminum.

20 p2978 A72-38884

Internal stresses in a superplastic Mg alloy.

20 p2935 A72-39002

Form of the modified Orowan creep equation for a case in which the internal stress is due to dislocation-interactions.

20 p2978 A72-39008

Distortion and residual stresses in welded aluminum structures.

20 p2928 A72-39204

Dislocation pile-ups in periodic internal stresses.

22 p3214 A72-42316

Optimization of the range of elastic behavior of unidirectional composites by prestraining.

22 p3194 A72-43041

Chemical etchants and etching procedure for decorating areas of residual tensile elastic surface stresses in ultrahigh strength steels without aging

22 p3183 A72-43045

Flow-stress recovery of nickel-aluminium alloys.
23 p3299 A72-43563

Residual stress formation mechanism in two phase Ti alloys under cutting and plastic deformation, showing phase transformation composition and structure effects
24 p3407 A72-44942

Body of revolution /saucer/ with nongeodesic internal stresses under gravitational field in terms of general relativity theory
24 p3425 A72-45701

Residual stresses effect on technical cohesive strength of welded cylindrical shell with surface defects, presenting plane strain fracture toughness determination method
24 p3408 A72-45757

RESILIENCE

Polyurethane O ring seals for high pressure applications, discussing stress relaxation /creep/ behavior, resilience and tear and abrasion resistance
08 p1173 A72-21023

Small disturbance behavior in laminar boundary layer on elastic surface experiencing deformation under perturbing pressure, noting surface resilience effect
16 p2377 A72-33164

RESIN BONDING

Resin bonded solid lubricant film thickness optimization from statistical analysis of bench and machine element test data
06 p0823 A72-18591

Wear behavior of molybdenum disulfide and antimony trioxide bonded solid film lubricant with air curing silicone resin, noting temperature and pretreatment effects
06 p0823 A72-18593

Resin bonded B-Al composites, discussing fabrication techniques and mechanical properties
12 p1815 A72-28098

Heat resistant adhesives properties and selection, discussing thermosetting thermoplastic resins and ceramic materials for temperatures to 4400 F
16 p2415 A72-33597

RESINS

NT ACRYLIC RESINS
NT EPOXY RESINS
NT FURAN RESINS
NT ION EXCHANGE RESINS
NT NYLON [TRADEMARK]
NT PHENOLIC RESINS
NT POLYAMIDE RESINS
NT POLYESTER RESINS
NT POLYIMIDE RESINS
NT POLYMETHYL METHACRYLATE
NT POLYURETHANE RESINS
NT SILICONE RESINS
NT SYNTHETIC RESINS
NT THERMOPLASTIC RESINS
NT THERMOSETTING RESINS
NT VINYL COPOLYMERS

Synthesis of a resin-metal damper whose characteristic shows minimum deviation from a constant-frequency response
19 p2806 A72-37429

RESISTANCE COEFFICIENTS
U COEFFICIENTS

RESISTANCE HEATING

Electrode boundary layer electrical breakdown mechanism with allowance for steep temperature gradients at surface, considering Joule heating or electrostatic field effect as causes
13 p2013 A72-29361

Joule heating power density in NbZr superconductor hollow cylinder, estimating temperature changes and instability locations
13 p2033 A72-29855

High light transmission electrically conducting Hyviz and gold film laminates for aircraft windshields and window heating applications
13 p1898 A72-30038

Thermospheric density annual and semiannual variations due to solar heat input into ozone layer and Joule heating, discussing decomposition into Fourier terms
15 p2229 A72-32255

Controlled self heating effect in semiconducting barium titanate positive temperature coefficient resistor substrate heater for planar Si devices
17 p2527 A72-34680

Investigation of nonstationary heating processes in thermal resistors fed from functional sources
21 p3129 A72-41060

Technological aspects concerning the structural elements in the development of resistance furnaces under vacuum
22 p3163 A72-42636

RESISTANCE THERMOMETERS

Constant temperature hot-wire anemometer compensation for thermal lag of wire or film resistance thermometer
09 p1306 A72-22307

Low resistance thermometry with transformer coupled potentiometer circuit to obtain size reduction and ability for direct exposure to fluid
10 p1482 A72-24806

Resistance wires and wire thermocouple junctions temperature response in low pressure gases, taking into account wire mounting temperature effect
11 p1632 A72-26000

Copper resistance thermoanemometer for channel unsteady air flow rate measurement, discussing design, operation principles and maximum error
12 p1812 A72-28146

Impurities effect on platinum resistance thermometers temperature reading accuracy, presenting empirical formula for approximate error estimate as function of operational conditions
13 p1960 A72-29906

Carbon resistance thermometers time response and thermal diffusivity measurements in liquid helium temperature range
15 p2234 A72-31581

Mesospheric air density and temperature measurements from rocket-borne resistance thermometers based on free molecular flow
15 p2225 A72-31911

Calibration and application techniques for platinum resistance thermometers.
[ASME PAPER 71-WA/TEMP-2]
17 p2554 A72-34965

Temperature-time characteristics of pulse-loaded temperature-measuring resistors
20 p2926 A72-39571

Reverse flow sensing hot wire anemometer.
22 p3177 A72-42392

RESISTIVITY
U ELECTRICAL RESISTIVITY

RESISTOJET ENGINES

Ten mlb concentric tubes biowaste resistojet thrust performance for hydrogen, water, methane, carbon dioxide and biopropellant mixtures, discussing vibration, shock and acceleration tests
01 p0116 A72-10263

Nozzle boundary layer effects on resistojets performance, presenting conical design model in heater stagnation conditions
03 p0405 A72-12973

Hydrazine and ammonia resisto-jet systems for satellites orbit and attitude control, discussing component redundancy and mass requirements in terms of system optimization
07 p1054 A72-19603

Biowaste resistojet propulsion system development program, discussing design, propellant management and control subsystems
[AIAA PAPER 72-448]
11 p1707 A72-26185

Hydrogen resistojet design and testing with Re heat exchanges, noting appropriate power efficiency and exhaust velocity for synchronous communication satellites orbital transfer
[AIAA PAPER 72-449]
11 p1708 A72-26186

Computer program for biowaste resistojet nozzle performance prediction, taking into account viscous effect at low Reynolds number
[AIAA PAPER 72-450]
11 p1708 A72-26187

High temperature biowaste resistojets with electrically conducting ceramic heaters, discussing lifetime and space station power systems adaptability
[AIAA PAPER 72-454]
11 p1708 A72-26190

Resistojet performance models for investigating energy losses in hydrogen, ammonia, methane and carbon dioxide nozzle flows
[AIAA PAPER 72-455]
11 p1708 A72-26191

Thermal storage type resistojets design for satellite attitude control, discussing heat loss minimization
13 p2026 A72-28927

Construction of a high-performance resistojet for satellite propulsion.
23 p3328 A72-44324

RESISTOJETS
U RESISTOJET ENGINES

RESISTORS

NT POTENTIOMETERS [RESISTORS]
NT PRINTED RESISTORS
NT THERMISTORS

Transistorized pulse amplifier stage, showing gain as function of resistor parameters in collector circuit
01 p0035 A72-10200

Lumped capacitors, inductors, resistors and gyrators for use at microwave frequencies, discussing design and applications up to X band
04 p0497 A72-14717

Bulk type variable resistors with properties controlled by composition during fabrication, evaluating inorganic binders with optimal properties
05 p0701 A72-15754

Thin film resistors and capacitors design, considering stability, power, size, film thickness, parasitic inductance capacitance and resistance and dielectric loss properties
06 p0790 A72-18573

Thin film conductors, distributed film resistors and capacitors design and associated IC layout to form functional arrays
06 p0790 A72-18574

Monolithic Si IC design and fabrication including resistors, capacitors, diodes, n-p-n, p-n-p, p-n-p-n and field effect transistors and inductors
06 p0791 A72-18576

VS type 2-W carbon resistor electrical aging operation, investigating optimal ambient temperature and duration
08 p1143 A72-22068

Reactivity evaporated titanium nitride resistors for thin film microcircuits, discussing nitrogen gas pressure and substrate temperature effects on electrical properties during evaporation
09 p1286 A72-22902

Niobium carbide resistors properties, investigating temperature dependence of electrical resistance and thermal stability
09 p1331 A72-23483

Technological parameters effects on resistance values dispersion of thick film resistors, reviewing stability test performance
12 p1788 A72-27274

Russian book on penetrating radiation effect on radio components covering resistors and capacitors electrophysical characteristics and parameters changes under gamma and neutron radiation
12 p1793 A72-28342

Thin film resistor manufacture and evaluation for stability and long-life characteristics
14 p2091 A72-31171

Transistorized pulse amplifier stage, showing gain as function of resistor parameters in collector circuit
15 p2206 A72-31624

Reliability of nichrome film resistors deposited in vacuum by sublimation on a glass substrate
18 p2669 A72-37117

RESOLUTION

NT ANGULAR RESOLUTION
NT HIGH RESOLUTION
NT RADAR RESOLUTION
NT SPECTRAL RESOLUTION

Scanning Fabry-Perot interferometer for He-Ne laser spectral composition, discussing transmission coefficient, resolution, resonator dissipative losses, active medium saturation and light field spatial nonuniformity
03 p0356 A72-13190

Quadrupole mass spectrometer ultimate characteristics concerning resolution, range, recording speed, working pressure and sensitivity
03 p0360 A72-13665

Pinhole, fly-eye and holographic stereogram methods, examining resolution relationships, horizontal and vertical parallax and aberrations
05 p0663 A72-16673

Resolution dependence on coherent properties of light source for aberration free annular aperture operating in partially coherent light, presenting composite intensity curves
07 p1008 A72-20545

Surface contamination effect on alpha particle resolution of surface barrier detector/preamplifier combination for use in space environment
08 p1168 A72-21517

Two point analysis of phase, coherence and emulsion response effects on holographic image resolution
08 p1168 A72-21698

Sensor spatial resolution effects on satellite estimation of earth cloud cover, simulating cloud distribution and size
09 p1345 A72-22450

Angular distribution of electrons at output of specimen observed by electron microscope, examining resolution problem for thin objects
11 p1635 A72-26483

Emulsion response and phase effects on two point resolution in coherent holographic imaging systems, using Rayleigh criterion
15 p2237 A72-32058

Autocorrelation methods to obtain diffraction-limited resolution with large telescopes.
20 p2920 A72-38922

Holographic system resolving capacity increase by oblique illumination of object, analyzing plane monochromatic wave transmission through one dimensional semitransparent body
21 p3058 A72-41791

The observation of chemical releases in the upper atmosphere.
22 p3152 A72-42022

Study of target edge response viewed through atmospheric turbulence over water.
23 p3289 A72-43896

Structural characteristics of high resolution NMR spectra, noting interrelationships between line positions and intensities
23 p3290 A72-44171

RESOLUTION CELL

Surface temperature measurement by microwave radiometry, noting sensitivity reduction due to moisture effects for resolution cell size targets
02 p0214 A72-11867

RESOLVENTS
U PROBLEM SOLVING

RESOLVERS

Synchros as electromechanical function generators and receivers for analog computers, examining errors in standard resolvers operation
03 p0328 A72-13841

RESOLVING POWER

U RESOLUTION

RESONANCE

- NT CYCLOTRON RESONANCE
- NT ELECTRON PARAMAGNETIC RESONANCE
- NT FERROMAGNETIC RESONANCE
- NT MAGNETIC RESONANCE
- NT MAGNETOSONIC RESONANCE
- NT MICROWAVE RESONANCE
- NT NUCLEAR MAGNETIC RESONANCE
- NT NUCLEAR QUADRUPOLE RESONANCE
- NT OPTICAL RESONANCE
- NT PARAMAGNETIC RESONANCE
- NT PLASMA RESONANCE
- NT PROTON MAGNETIC RESONANCE
- NT PROTON RESONANCE
- NT RESONANT VIBRATION
- NT SPIN RESONANCE

Duffing type quasi-linear differential equation system, obtaining ultrasubharmonic resonance by small parameter and harmonic balance methods for comparison with analog computer solutions

01 p0101 A72-10034

Quasi-periodic solution of nonlinear differential system in case of resonance, concerning Duffing equation

05 p0682 A72-16120

Near resonance due to commensurability between Jupiter-Saturn mean motions, discussing effect on planetary system secular disturbing function

06 p0877 A72-17659

Particular solutions to inhomogeneous Bessel and Legendre equations in resonance case

08 p1198 A72-20973

Sound wave propagation in plasma, attributing acoustic cavity resonance curve sharpening to collisional energy transfer from electrons to neutrals

08 p1213 A72-21256

Second order libration solution of ideal resonance problem, using Lie series perturbation technique

08 p1236 A72-21637

Resonance occurrence in generation-recombination noise spectrum of Co 60 gamma irradiated Ge single crystals, investigating Hall effect

09 p1372 A72-23112

Preresonance Raman scattering tensor in Born-Oppenheimer approximation of molecular wave functions

10 p1491 A72-24110

Gravitational constant determination by resonance method, describing experimental setup and procedure

10 p1510 A72-24127

Nonstationary nonlinear multidegree-of-freedom systems resonant response analysis by asymptotic method, investigating gyroscopic system for combination differential resonances

[AIAA PAPER 72-401]

11 p1629 A72-25422

Daytime and nighttime electron temperatures from topside resonances, using oblique echo theory

11 p1625 A72-26409

Active loop dipole aerials with height reduction properties at resonance, investigating transistor configurations in loop monopole aerial

12 p1792 A72-27699

Pressure effects on resonance fluorescence lifetimes in sulfur hexafluoride-air mixtures exposed to carbon dioxide laser radiation

12 p1826 A72-27929

Frequency modulation and transient effects in resonant propagation of coherent light pulses

12 p1826 A72-27939

Coherent brain model for evolution mechanisms of biological resonance in neuron network signal flow

13 p1908 A72-28455

Linearized steady motion of gas with mass sources and sinks, determining resonance onset conditions

13 p1893 A72-28731

Single circuit amplifier design characterized by cascade connections of transistors to resonance network

13 p1929 A72-28900

He ions motion normal to magnetic field under induced electric field, analyzing resonance mechanism

13 p2016 A72-29606

Resonant irradiation effect on cesium discharge plasma, charge density, electron temperature and electric field strength

13 p2017 A72-29610

Ferroresonant circuit with inductor, resistor, nonlinear ferrocapacitor and voltage source, deriving oscillation stability condition

14 p2090 A72-31119

Born approximation for resonance bremsstrahlung emission and photon absorption cross sections at electron-ion scattering, solving multiparticle problem

15 p2279 A72-32697

A method of calculating acoustic resonance phenomena generated by the unsteadiness of singular pressure losses in the pipes

17 p2580 A72-34279

Electron transmission spectroscopy - Core-excited resonances in diatomic molecules.

17 p2586 A72-35771

Wave function and resonance parameters for autoionization and ground states of helium and hydrogen

17 p2586 A72-35774

Determination of the parameters associated with a singular pressure loss permitting the calculation of acoustic resonance phenomena and the role of these parameters

18 p2680 A72-36465

Regularized first order algorithm for ideal resonance problem in solar system, considering solution in terms of elliptic functions

20 p2968 A72-39199

He ions motion normal to magnetic field under induced electric field, analyzing resonance mechanism

21 p3091 A72-40660

Resonant irradiation effect on Cs discharge plasma charge density, electron temperature and electric field strength

21 p3091 A72-40664

Measurement of internal magnetic field distribution in axially magnetized YIG rods based on magnetoelastic resonance absorption.

21 p3097 A72-40692

Study of the Stark effect in the resonance lines of sodium by an atomic jet method

22 p3209 A72-43048

Theoretical interpretation of the optical and electron scattering spectra of polyatomic molecules. III - N₂O and the discovery of resonant phenomena in the B region at 6.8 eV.

24 p3426 A72-45301

On the existence of a resonance-captured 'quasi-satellite' of the earth.

24 p3446 A72-45471

RESONANCE CHARGE EXCHANGE

Resonance charge exchange cross section measurements for Cs at 2 eV within Q machine, discussing ion energy resolution improvement

06 p0859 A72-17552

Field dependence of gaseous-ion mobility - Theoretical tests of approximate formulas.

23 p3316 A72-43871

RESONANCE SCATTERING

Lyman alpha, Lyman beta and Balmer alpha hydrogen airglow emission simultaneous measurements compared with solar radiation resonant scattering models

01 p0061 A72-10899

Radiation transfer by resonant scattering in expanding nebula with applications to quasars having blueward absorption wings

05 p0716 A72-16374

Electron lifetime in earth radiation belt due to resonant scattering with hiss vlf radiation

05 p0711 A72-17045

Radio absorption and scattering cross sections of thin cylinder with arbitrary electron density distribution in ionosphere, observing resonance effects

08 p1239 A72-21890

Sunlight resonance scattering by spherically symmetric optically thick artificial Sr clouds, comparing photometric data with computed theoretical isophotes, line profiles and irradiances

09 p1297 A72-22579

EUV resonance radiation from He atoms and ions in geocorona, comparing model calculation based on solar radiation resonance scattering with rocket experiments

09 p1378 A72-23010

Laser radar technique for invisible air pollutants remote sensing systems, comparing Raman backscattering resonance scattering and absorption schemes

10 p1489 A72-23952

Transition probabilities and line shapes and widths of unimolecular problem computed using numerical methods for scattering processes

10 p1514 A72-24337

Quasi-projection operators for calculating electron resonances in multitarget scattering tested on He ion autoionization system

12 p1847 A72-27385

Resonance scattering and direct photoelectron excitation contribution to molecular nitrogen first positive bands emission in day airglow from rocket measurements

13 p1953 A72-29808

Resonant and semiweak process production cross sections for massive Lee-Wick spin-zero and spin-one bosons at high energies

15 p2280 A72-31290

Coherence narrowing during multiple scattering of resonance radiation in atomic vapor, treating polarization transfer in terms of classical tensors

15 p2281 A72-32221

Redistribution of resonance radiation. I - The effect of collisions.

17 p2605 A72-34534

Backscatter of solar resonance radiation. I.

17 p2598 A72-34626

The solar wind H and He⁺/content.

17 p2598 A72-34627

Scattering resonances of electromagnetic wave by an infinite plane grating with reflector.

19 p2767 A72-38612

An application of the concepts and methods of linear systems analysis to the scattering of resonance radiation by an atomic vapour.

21 p3084 A72-40470

Radiative recombination of atoms as a resonance scattering process.

21 p3087 A72-40560

Transfer of resonance-line radiation in differentially expanding atmospheres. I - General considerations and Monte Carlo calculations.

21 p3106 A72-41037

Transfer of resonance-line radiation in differentially expanding atmospheres. II - Analytic solution for the case of coherence in the frame of the fluid.

21 p3106 A72-41038

Resonant scattering of trapped particles by toroidal plasma modes.

21 p3092 A72-41217

Gamma ray scattering asymmetries of Fe 57 nucleus, discussing hyperfine structure and conjugate spin transition

22 p3209 A72-42924

RESONANCE TESTING

Dynamic calibration by sound wave of hot wire operated by constant resistance method, using open resonance tube in homogeneous incompressible air flow

03 p0356 A72-13235

Ultrasonic resonance thickness gage sensitivity and accuracy, noting damper, piezoelectric plate, protector and frequency band influence

03 p0361 A72-13986

Carbon fiber reinforced plastics nondestructive testing by ultrasonic compressional and shear wave resonance

14 p2107 A72-30856

Combustion driven resonance tubes.

17 p2597 A72-34974

RESONANT CAVITIES

U CAVITY RESONATORS

RESONANT FREQUENCIES

Monochromatic waves propagating in uniform magnetoplasma, considering resonant interaction with electrostatic approximation

01 p0107 A72-10138

Supersonic wind tunnel study of flow induced pressure oscillations in shallow rectangular cavity, investigating resonant frequencies and pressure mode shapes

01 p0049 A72-10221

Curved beam finite elements comparison for structural vibration problems, obtaining ring natural frequencies

01 p1336 A72-10222

Direct-iterative eigensolution technique for simultaneous determination of structural system lowest frequencies and modal patterns, using reduced generalized coordinates and Stodola-Vianello method [SAE PAPER 710784]

01 p0137 A72-10275

Ultrasonic bonding tip design for densely wired electronic circuit boards, analyzing standing wave phenomena and resonant frequency

[SAE PAPER 710789]

01 p0074 A72-10279

Flexural vibrations of arbitrary ring with axial symmetric cross section, noting validity for natural frequencies prediction

01 p0138 A72-10395

Output power, efficiency and fundamental frequency resistance of Gunn microwave self oscillator in single and multiresonant mode

01 p0037 A72-10638

Power conditioners operating frequencies determination by series resonant circuits, noting frequency stability and reliability

01 p0008 A72-11061

Static loads effect on natural vibrations of thin truncated conical shells by shallow shell theory, determining resonant frequency spectrum due to prestressing

01 p0142 A72-11362

Thick orthotropic off-axis laminated plates vibration equations solution, presenting natural frequencies spectra and modal functions

02 p0249 A72-11988

Nonuniform plasmas resonant wave-particle interactions, using linearized Vlasov equation

02 p0264 A72-12119

Rotating cable of high slenderness ratio and small flexural rigidity with end masses, deriving transverse vibration mode shapes and natural frequencies from asymptotic solution

02 p0293 A72-12253

Unstiffened cylinders natural frequency equations, determining modal density distribution and acoustic radiation efficiency

02 p0293 A72-12373

Resonant and nonresonant sound transmission through cylinder walls, using statistical analysis

02 p0260 A72-12374

Pretwisted tapered cantilever beam torsional vibration natural frequencies determination by Galerkin method for solution of differential equation of motion

02 p0297 A72-12533

Resonance type rotating bending fatigue testing machine using specimens with attached inertial mass, presenting test results with carbon steel specimens 02 p0201 A72-12823

Phase stabilization of synchronized tracking oscillator with resonant frequency regulated by output voltage 03 p0333 A72-13895

Staged corrector, transformer and low pass filter two terminal pair matching network for resonant circuits using semiconductor elements 03 p0333 A72-13897

Multistage multiply branched multistage elastic systems natural frequencies and oscillation modes, presenting algorithm and iterative calculation procedure 03 p0449 A72-13913

Cracked rectangular plates vibration and stability, computing eigenvalues, natural frequencies and moment distribution 04 p0583 A72-14448

Natural vibration frequencies calculation of straight bars with stepwise variable cross sections by iterative technique based on method of three unknowns 04 p0584 A72-14522

Plasma electron density profiles from Tonks-Dattner resonance frequencies for plane parallel and cylindrical columns 04 p0554 A72-14530

Dynamic analysis of shallow shells with doubly-curved triangular finite element, investigating natural frequencies, mode shapes and convergence 04 p0587 A72-14844

Molecular oxygen photoelectron spectra at autoionizing resonance frequencies, comparing with Franck-Condon calculations 04 p0552 A72-14892

Self oscillating system stability under parametric excitation and harmonic force for large and small natural frequency mismatch 04 p0549 A72-15046

Optimal design of solid and three layer rods with prescribed natural frequencies for longitudinal and transverse vibrations, using minimum mass criterion 04 p0587 A72-15047

Fundamental frequency calculation method for bars and plates with arbitrary fixity of rotations, discussing buckling and vibration with realistic boundary conditions 04 p0591 A72-15275

Fabry-Perot open resonators, determining eigenvectors, resonant frequencies and diffraction losses by asymptotic perturbation method 04 p0502 A72-15436

Resonance degeneration removal in earth-ionosphere spherical cavity resonator, calculating eigenfrequencies by perturbation method 04 p0492 A72-15444

Circular disks, rings and perforated plates steady state field components, evolving forced and free vibration natural frequency equations 04 p0592 A72-15505

Natural frequencies and vibration mode shapes of simply supported symmetric trapezoidal plates 04 p0592 A72-15564

Integral equation for lowest natural frequency of vibrating beams, using eigenfunction theory 04 p0593 A72-15565

Resonant transport properties of polyatomic gases in collinear static and oscillating magnetic fields, using microscopic kinetic equation 04 p0553 A72-15633

Mean-square approximate estimator for standard deviation of natural frequency of two degrees of freedom spring systems, comparing with Monte Carlo simulation [ASME PAPER 71-WA/APM-7] 05 p0734 A72-15971

System natural frequency standard deviation estimator, using Monte Carlo method [ASME PAPER 71-WA/APM-8] 05 p0734 A72-15972

Vibration mode shapes and frequencies determination by finite element method using consistent and lumped masses formulations in differential equation solution, considering convergence rate [AD-739820] 05 p0736 A72-16086

Conical cavity resonator design for submillimeter wave electron beam devices, investigating mode and resonant frequency dependence on cavity size 05 p0636 A72-16364

Natural fluctuations effect on beat frequency dependence of opposed waves in ring laser on rotation velocity 05 p0668 A72-16405

Microwave lumped element impedance measurements from 1 to 12 GHz by resonant transmission line frequency and Q perturbation technique 05 p0637 A72-16419

Radar cross section computation and contours map for thin straight wire, noting resonant peak and interference null variations with frequency and aspect ratio 06 p0771 A72-17351

Monopole antenna with lumped mutual coupling between driven and folded sections, noting staggered resonant frequencies and bandwidth broadening from input impedance analysis 06 p0782 A72-17355

Analytical model of Gunn diode oscillating in resonant mode with domain quenching, determining current harmonics 06 p0783 A72-17573

Rf transmission between two parallel whip antennas in warm plasma, noting received signal increase at probe resonant frequency 06 p0860 A72-17747

Free flexural wave propagation in doubly periodic structures, obtaining natural frequencies 06 p0894 A72-17764

Environment acoustic resonant frequencies effect on flat steel plate vibration under direct and air flow vortex shedding excitations 06 p0894 A72-17768

Uniformly curved fluid conveying tube free vibration and stability, showing flow velocity, fluid pressure and Coriolis force effects on natural frequency 06 p0821 A72-17853

Resonant frequency, phase velocities and dispersion curves for wave propagation in isotropic elastic cylinders 06 p0895 A72-17854

Aerospace structures harmonic vibration tests, discussing structures natural frequency spectrum, mode isolation, eigenmodes and inertial characteristics 06 p0896 A72-17948

Dynamic properties of turbine wheels under bending vibrations, classifying resonant frequencies on basis of vibration modes 06 p0899 A72-18644

Resonant systems frequency characteristics measurement by sinusoidal input signal, determining optimal law of change in frequency scanning rate for minimal scan time 06 p0795 A72-18663

Forced nonlinear oscillations of finite plate in plane supersonic gas flow, considering elastic forces and resonant characteristics deformation 06 p0901 A72-18708

Nonlinear solid body system rotating and oscillating parts effect on spatial vibration stability, deriving excitation-natural frequencies relationship 06 p0850 A72-18711

Random vibrations in rectangular plate clamped on opposite sides by load, determining natural oscillation frequencies by Ritz technique 06 p0901 A72-18719

Torsional oscillation damping in circular rods coated with viscoelastic material as function of resonant frequency 07 p1087 A72-18924

Natural frequencies and vibration modes of simply supported tapered skew rhombic plates, considering thickness and skew angle effects 07 p1088 A72-19116

Shallow spherical shell equations solution for vibration mode and natural frequencies from analogous vibrating plate solution 07 p1089 A72-19489

Symmetrically loaded uniform thin circular ring natural vibration frequencies in radial and axial flexural modes, comparing experimental data with values predicted by group theory 07 p1096 A72-20499

Shf resonator small resonant frequency shift and Q factor changes measurement based on FM signal envelope shape analysis 07 p1046 A72-20508

Signal injection through laser transmitting window, showing effects on resonant frequency and locking mode [AD-738988] 07 p1009 A72-20680

Natural oscillation frequencies of piecewise homogeneous L-shaped membranes, determining eigenvalues of second order elliptical differential operator 08 p1241 A72-20903

Ideal liquid small oscillations natural frequencies and mode shapes in shell of revolution under weak gravitational field 08 p1148 A72-20956

Elimination of spherical cavity resonators natural frequencies degeneration through symmetry disrupting disturbance, using group theory for fields and frequencies calculations 08 p1209 A72-21737

Resonant frequencies of rectangular plate with two sides subject to mixed boundary conditions, expressing vibration modes in terms of Fourier series 08 p1249 A72-21946

Twin spool jet engine system, predicting shaft speed effects on whirling frequencies due to gyroscopic action with computer model 08 p1224 A72-22130

Maximum superconducting transition temperature estimation, discussing optimum resonant frequency for attractive interaction, umklapp electron scattering and lattice instabilities 09 p1367 A72-22553

Cavity resonator frequency detuning effects on FM and AM noise in cavity stabilized Gunn microwave oscillator 09 p1285 A72-22651

Variable rigidity circular isotropic plate vibration and bending, determining flexure surface and natural frequencies in terms of Fourier-Bessel series 09 p1399 A72-22699

Resonant frequencies of viscous liquid in rectangular tank calculated from stream functions, assuming two dimensional oscillations and laminar flow 09 p1295 A72-23074

Circular plates free flexural vibrations with and without damping, calculating resonant frequencies from corresponding Bessel functions 10 p1555 A72-24194

Cardiovascular changes produced by whole body vibration of dogs and pigs, obtaining resonant frequencies of organ systems 10 p1426 A72-24484

External load effects on natural frequencies of free end and centrally loaded cantilever beams and supported or clamped circular plates 10 p1558 A72-24814

Wave particle interaction around lower hybrid resonance frequency, deriving whistler mode wave growth rate during propagation in magnetoactive plasma penetrated by nonthermal particles 10 p1476 A72-24959

Loaded hydraulic cylinder response to step inputs in on-off servos with three position valves, considering cavitation effect on system natural frequency [ASME PAPER 72-AUT-A] 10 p1423 A72-25052

Cylindrical shell vibrations in incompressible inviscid fluid near free interface, calculating natural frequencies with Fourier transforms 10 p1471 A72-25130

Free in-plane vibrations of hinged and fixed uniform circular arches, discussing natural frequencies and flexural and extensional vibration modes 10 p1560 A72-25186

Automated optimization for preliminary design of supersonic aircraft wings, noting flutter, stresses and resonant frequency as dynamic constraints [AIAA PAPER 72-333] 11 p1727 A72-25368

Orthotropic point-supported rectangular panel vibration and flutter analysis for natural frequencies land flutter boundaries, applying to space shuttle design [AIAA PAPER 72-350] 11 p1728 A72-25379

Vibration characteristics of unidirectional filamentary boron-epoxy composite panels, obtaining nodal patterns, natural frequencies and damping coefficients 11 p1732 A72-25477

Linear maximization of turbine disk natural vibration frequencies combination, solving optimal control problem via Pontryagin maximum principle 11 p1734 A72-25727

Computerized analysis of prismatic rectangular plate assemblies natural frequencies and initial buckling stresses 11 p1734 A72-25731

Helicopter rotor blades bending vibrations, examining scale effects, dynamic similarity and natural frequencies via series of Legendre polynomials [AD-745569] 11 p1734 A72-25733

Radiation resistance for natural modes of rectangular panel from far field acoustic radiation energy distribution 11 p1687 A72-26059

Nonlinear traveling string transverse oscillations frequency, using Panavko direct linearization method 11 p1688 A72-26324

Jones matrix method for polarization natural states, frequencies and mode losses calculation in anisotropic optical resonators 11 p1688 A72-26347

Laser apparatus for resonant frequencies and oscillation amplitudes measurement of semiconductor devices structural elements 11 p1649 A72-26348

Electrostatic resonances associated with maximum frequencies of cyclotron-harmonic waves at high and low latitudes, presenting dispersion curves and ray paths 11 p1624 A72-26400

Proper vibration frequencies of thin imbedded plate obtained by layer potentials method 11 p1737 A72-26477

Lowest natural vibration frequencies of conical shell for various boundary conditions, using finite difference scheme 12 p1878 A72-27081

Hybrid cylindrical shell finite element, determining natural frequencies from equilibrium equations, stress functions stress-strain relationships and boundary force transfer matrices 12 p1882 A72-27339

Vibration of free and fluid loaded uniform or rib reinforced cylindrical shells, solving equations of motion for natural frequencies 12 p1882 A72-27341

Resonant frequency and vibration modes of variable cross section bar in elastic medium under transversal

force, noting dynamic programming combined with optimization principle 12 p1845 A72-27538

Energy method based approximate calculation for natural frequencies of single layer compound shells of revolution 12 p1886 A72-28144

Material fatigue failure criterion during cyclic loading, noting energy dissipation and resonant frequency roles 12 p1888 A72-28250

Approximate solution to spectral line frequency resonance radiation transport equation, assuming total radiation redistribution with respect to frequencies 13 p2001 A72-28508

Frequency method of mechanical impedance monitoring of natural frequency of transducer-article system under load in defectoscopy 13 p1956 A72-28923

Numerical analytical determination of natural vibration frequencies for membrane elastically clamped along portion of contour, using method of summary representations 13 p2004 A72-29078

Resonant frequencies of two thin walled cylindrical panels connected by elastic filler, considering symmetric and asymmetric vibration modes 13 p2058 A72-29146

Torsional vibration damping in circular rods coated with viscoelastic material, noting technique effectiveness at certain resonant frequencies 13 p2058 A72-29209

Natural oscillation frequencies of cavity-contained liquid in weak gravitational field, using variational principles 13 p1943 A72-29791

Complex elastic systems natural frequencies computation from measured dynamic response to harmonic excitation, applying to helicopter and transport aircraft 14 p2164 A72-30326

Computerized optimal design by nonlinear programming for minimum weight elastic plates crossed with rigid ribs for vibrational loading to meet natural frequencies condition 14 p2165 A72-30576

Structural systems stability and natural frequency analysis eigenvalue problems solution by Sturm sequence method, using finite element technique 14 p2168 A72-30931

Van der Pol oscillator periodic pulling behavior under weak perturbation near natural frequency, analyzing Fourier frequency spectrum 14 p2132 A72-31122

Nonlinear resonating correlator with orthogonal filters, considering cut-off frequency of ergodic random process with constant power spectral density 14 p2090 A72-31125

Dynamic spin disorder effect on electrical and thermal conductivity, noting low resonant frequency in metal atom magnon spectrum 15 p2290 A72-31388

Natural frequencies of beams with stepwise variable cross sections, approximating deflection shape by sectionwise representation of inertia load 15 p2323 A72-31454

Open terminations of cylindrical waveguide periodically loaded by metallic irises, investigating cavity resonator size effects on resonant frequency, mode and quality factor 15 p2194 A72-31547

Velocity gradient induced by local wall deformation, investigating effect on unstable natural frequencies amplification in laminar boundary layer 15 p2217 A72-31683

Boundary conditions for resonant frequencies calculation of turbine blades with Z-shaped and combined coupling sections 15 p2326 A72-31704

Rocket-observed energetic electron flux association with ground recorded plasmasphere whistler in terms of gyroresonant wave-particle interaction 15 p2198 A72-31948

Flexural vibrations of ring with arbitrary cross section, proposing theory for natural frequencies prediction by Ritz method 15 p2329 A72-32141

Quantitative measure for sensitivities of natural frequencies to perturbations leaving modes invariant 15 p2278 A72-32279

Natural frequency distribution theory of thin elastic shells under random vibrations in wideband field 15 p2332 A72-32677

Phase stabilization of synchronized tracking oscillator with resonant frequency regulated by output voltage 15 p2209 A72-32706

Weight minimization for simple structures with single natural frequency constraint, solving nonlinear two point boundary value problem by variational and numerical methods 16 p2463 A72-32834

Natural frequency of free beam-like vibration of coupled fluid/structural system of cylindrical rod submerged in ideal fluid enclosed by cylindrical shell 16 p2465 A72-32985

Entropy waves effect on gas pressure oscillations during powder combustion in semiclosed volume, noting resonant frequencies equation 16 p2475 A72-33096

Natural frequencies and vibration modes of free glider, using symmetrical matrix to replace three dimensional structure by approximate model 16 p2348 A72-33409

Laser apparatus for natural resonant frequencies and oscillation amplitudes measurement of semiconductor devices structural elements 16 p2402 A72-33701

Periodic perturbation effect on oscillatory system behavior at frequencies approaching resonance 16 p2426 A72-33789

Large amplitude vibration of a circular plate with concentric rigid mass. [ASME PAPER 71-APMW-11] 17 p2625 A72-34319

Natural bending frequency comparable to rotational frequency in rotating cantilever beam. 17 p2625 A72-34324

Natural frequencies of a cylindrical microwave cavity containing a coaxial cylindrical dielectric sample 17 p2513 A72-34334

Characteristics of Gunn elements CGY 11 to 14 and their application as microwave oscillators. II 17 p2530 A72-35150

A comparison of approximate methods for solving non-conservative problems of elastic stability. 17 p2634 A72-35410

Day to day variation of Schumann resonance frequency and occurrence of Pc 1 in view of solar activity. 17 p2548 A72-35464

Collisional losses in a very-low-frequency duct associated with the lower-hybrid-resonance frequency. 17 p2517 A72-35608

Magnetosphere resonant oscillations space-time characteristics for arbitrary azimuthal number, noting frequency dependence on geomagnetic shell 17 p2551 A72-35859

The effects of damping on a non-linear system with two degrees of freedom. 18 p2709 A72-36080

The effect of an elastic edge restraint on the forced vibration of a rectangular plate. 18 p2737 A72-37066

Natural frequencies and dynamic response constraints in optimal structural design, considering mathematical programming aspects 18 p2739 A72-37167

Methods for measuring the HF oscillation frequency in ultrasound pulses of equipment for diagnostic ultrasonography. 19 p2759 A72-37399

Further results on the stability of a finitely deformed thin cylindrical shell. 19 p2871 A72-37415

Applications of holography to vibrations of segmented shells. 19 p2873 A72-37617

Determination of the natural frequencies and modes of oscillation of a spherical resinous shell 19 p2873 A72-37662

Reflectionless ionospheric propagation of non-guided VLF descending wave near low hybrid resonance maximum frequency, investigating energy trajectory 19 p2790 A72-37793

Free vibrations of multilayer sandwich plates in the presence of in-plane loads. 19 p2876 A72-38020

Low-frequency vibrations in a rarefied bounded plasma 19 p2842 A72-38530

The locking effect in an autooscillatory system with two degrees of freedom 19 p2783 A72-38580

Eigenfrequencies of monolithic filters. 19 p2774 A72-38608

Complex resonant frequencies calculation in external diffraction problems for arbitrary shaped bodies, noting Green function poles correspondence to eigenvalue zeros of integral equation 19 p2767 A72-38652

Oscillatory circuits synthesis by wave resistance determination of homogeneous line segments for given resonant frequencies spectrum 19 p2768 A72-38660

Nonlinear system described by three generalized coordinates, noting dynamic response stability equivalence to two degrees of freedom system 20 p2953 A72-39553

Determination of the natural frequencies of cylindrical shells of variable thickness 20 p2980 A72-39906

Vibrations of a concentrated mass on a ring coupled to a thin shell 20 p2981 A72-39908

The effects of discrete masses and elastic supports on continuous beam natural frequencies. 21 p3116 A72-40335

Plasma heating by nonlinear damping of resonantly excited longitudinal oscillations produced by two parallel laser beams with difference frequency equal to plasma frequency 21 p3090 A72-40342

Coulomb-collision corrected ion-acoustic line profiles. 21 p3092 A72-40819

Resonant attitude instabilities for a symmetric satellite in a circular orbit. 21 p3115 A72-41046

Comparison of the classical and the global solutions of the ideal resonance problem. 21 p3085 A72-41047

Resonant frequency, fatigue and energy dissipation relations for endurance limit determination in Al alloy specimens under vibrational loads 21 p3070 A72-41368

Transient response of threshold lowering circuit with frequency converter for single contour IF amplifier with resonant frequency equal to carrier frequency 22 p3153 A72-42121

Pontryagin maximum principle for fundamental frequency variation limits of longitudinal vibrations of variable cross section rod 22 p3234 A72-42148

Low temperature characteristics of the Gunn diode. 22 p3159 A72-42307

The use of simple three-dimensional acoustic finite elements for determining the natural modes and frequencies of complex shaped enclosures. 22 p3206 A72-42464

Vibrations of circular plates of variable thickness under an inplane force. 22 p3240 A72-42908

Method of measuring modal characteristics of a structure subjected to a random excitation 22 p3242 A72-43095

Subharmonic generation in plane-parallel plate for light wave propagation perpendicularly to plate, noting frequency division near multiplicative resonance 23 p2395 A72-43408

Approximate calculation of a cavity resonator for n given initial natural frequencies 23 p3269 A72-43449

The problem of the minimum frequency of natural pressure oscillations in pneumo-hydraulic systems 23 p3252 A72-43652

Bearing supports elasticity effect on pendulum vibration of rigid rotating shaft with disk, noting vibrational frequencies relation to resonant frequencies 23 p3293 A72-43668

Hysteresis in a gas laser when passing from a single-frequency emission mode to a two-frequency mode 23 p3295 A72-43680

Spline transformation of independent variable for free transverse vibration of elastic bars with piecewise constant rigidity, calculating resonant frequencies 23 p3348 A72-43793

Experimental investigation of finite-amplitude acoustic oscillations in a closed tube. 23 p3314 A72-44124

Vibration characteristics of cylindrical shells with several axially equipaced constraints. 23 p3355 A72-44371

Improved calculation of resonant frequencies of Helmholtz resonators. 23 p3315 A72-44372

Free vibration frequencies and critical buckling loads for thin walled shells of revolution constructed out of layered or heterogeneous anisotropic materials 24 p3455 A72-44676

Resonance effects on second order anharmonic pulsational amplitudes for polytropic main sequence evolutionary models, classifying Cepheid-type pulsators 24 p3437 A72-44832

On the use of a coordinate transformation for analysis of axisymmetric vibration of polar orthotropic annular plates. 24 p3457 A72-44883

The effect of a harmonic-oscillator velocity distribution on an ideal solid-state laser. 24 p3409 A72-44953

Numerical analysis of natural frequency spectrum of plastic plate free vibrations in compressible inviscid fluid 24 p3459 A72-45003

Explicit series solutions for the frequencies of motion around the Lagrangean points in the restricted problem of three bodies. 24 p3440 A72-45136

Celestial mechanics ideal resonance problem global solution via Bohlin-von Zeipel perturbation technique, modifying Hamiltonian expansion point and separatrix and libration region singularities suppression method 24 p3440 A72-45138

RESONANT VIBRATION

Mossbauer spectra measurement of metallic iron, sodium nitroprusside, sodium ferrocyanide and ferro-

cyanide absorbers at 78-293 K, fitting temperature dependences and resonant velocity to models
01 p0114 A72-10324

Turbomachine blade frequency disalignment effects on resonant vibrations and stress distribution, using wheel model and computer solution
01 p0143 A72-11367

Resonant vibration and stresses of dynamically nonuniform annular cascade under aerodynamic interaction of alternating different blades
01 p0143 A72-11368

Self oscillating system resonant vibrations excitation for fatigue tests, determining frequency and amplitude relationship
03 p0443 A72-13456

Shallow spherical shell natural vibration frequencies, deflection and stress function, discussing effects of internal pressure, dimensions and material properties
03 p0453 A72-14209

Natural torsional vibrations of curved shafts, discussing oscillating system with varying flywheels
04 p0584 A72-14470

Natural vibration frequencies calculation of straight bars with stepwise variable cross sections by iterative technique based on method of three unknowns
04 p0584 A72-14522

Extremal problems of natural vibration spectrum optimal control in mechanical systems with constraints, using mathematical programming methods
04 p0586 A72-15004

German monograph on refractory materials elasticity modulus determination at elevated temperatures, describing device based on characteristic vibrations frequency relation to temperature
04 p0510 A72-15698

Geomagnetic tail natural oscillations, applying model of plasma cylinder with free boundary immersed in interplanetary medium
05 p0659 A72-17044

Stationary small elastoplastic longitudinal forced vibrations of rods with internal resonance obtaining asymptotic solution of nonlinear partial differential equations
06 p0900 A72-18676

Nonlinear resonance oscillations of flexible rod and elastic cylindrical shell under potential and nonpotential forces, investigating motion instability
06 p0900 A72-18704

Third-order resonance during oscillations of Hamiltonian system of nonlinearly coupled oscillators, obtaining equations of motion and phase portraits
07 p1035 A72-19978

Effective transmission coefficient increase for Langmuir and electromagnetic waves passing through density barrier via perturbation transport by resonant electrons
08 p1216 A72-22090

Frictional stick-slip autooscillations suppression by resonance effect during forced vibration in normal direction
08 p1181 A72-22181

Fundamental vibrations of long circular cylinder made of micropolar elastic solid, discussing dispersion equations
09 p1398 A72-22620

General structure steady state response under harmonic forcing in internal resonance relation, noting inertial nonlinearity effects on autoparametric interactions and energy flow
09 p1408 A72-23462

Natural and associated transverse vibrations of elastic beam under uniformly distributed moving load
12 p1879 A72-27092

Elastic rod system stationary vibrations under combinational parametric resonance due to internal energy dissipation, using matrix method
12 p1885 A72-27969

Resonant contact vibrations of sliding element in direction normal to friction surface, noting lubrication damping effect
12 p1818 A72-28188

Fourth order normal modes and resonances of nonlinear vibrations, applying to gyro horizon compass sensitive element gimbal motion
13 p2000 A72-28382

Harmonic functions system for resonant vibrations of liquid in elastic circular cylindrical tank, calculating shells surface pressure from equations of motion
13 p1940 A72-28394

Vibratory effects of disturbances transmitted from vehicle to viscoelastic vibroprotective damping coating in presence and absence of resonance
13 p2055 A72-28558

Nonlinear transverse forced resonant oscillations in isotropic elastic body and ideally conducting compressible fluid flowing in external magnetic field
13 p2010 A72-28719

HF transverse resonant vibrations of annular Al plates with polychlorovinyl and polyamide base coatings, noting damping and strain relationship to energy dissipation
14 p2164 A72-30427

Parameter resonances influenced by nonlinear damping amplitude-limiting due to vibrating systems nonlinearities with periodic coefficients
14 p2131 A72-30712

Potential waves generation by transverse current in ionospheric electrojet region, discussing lower hybrid resonance domain
15 p2232 A72-32732

Solar photospheric resonance oscillation power spectrum observation, noting statistical significance
15 p2317 A72-32777

Averaging and Ritz methods for solution approximation of nonlinear periodic and combined resonances in vibrating systems with multiple degrees of freedom
16 p2424 A72-33145

German papers on crack propagation in metal sheets, resonant vibration of cylindrical shells and stress concentration in plastic plates
16 p2470 A72-33676

Resonant vibration of thin walled rods and stiffened plates and cylindrical shells, noting aircraft and rocket structures
16 p2471 A72-33679

Effective transmission coefficient increase for Langmuir and electromagnetic waves passing through density barrier via perturbation transport by resonant electrons
17 p2588 A72-34661

Parametric resonance in an oscillatory circuit with a nonlinear p-n junction capacitance
17 p2533 A72-34757

On natural vibrations and waves in laminated orthotropic plates
17 p2581 A72-34803

[ASME PAPER 72-APM-14] Magnetosphere resonant oscillations space-time characteristics for arbitrary azimuthal number, noting frequency dependence on geomagnetic shell
17 p2551 A72-35859

Frictional stick-slip autooscillations suppression by resonance effect during forced vibration in normal direction
18 p2695 A72-36238

Investigation of the resonant combustion of a rocket charge with longitudinal slots
18 p2720 A72-36241

Resonant mode sound field radiated by nonuniform slender circular cross section free-free beams, using dipole array modeling
18 p2710 A72-36410

Low-frequency vibrations in a rarefied bounded plasma
19 p2842 A72-38530

The resonance mechanism of the biological action of vibration
20 p2897 A72-39409

Dynamic models for hydraulic machine parts, discussing resonant properties of one degree of freedom system and dynamic characteristics of nonlinear parametric systems
20 p2953 A72-39421

Third-order resonance during oscillations of Hamiltonian system of nonlinearly coupled oscillators, obtaining equations of motion and phase portraits
20 p2956 A72-40034

Nonlinear transverse forced resonant oscillations in isotropic elastic body and ideally conducting compressible fluid flowing in external magnetic field
22 p3210 A72-42096

Elastodynamic theory of natural symmetrical vibrations of sandwich plates, assuming filler motion and layer displacements governed by Lamé and Kirchhoff equations
23 p3348 A72-43790

Properties of a pulsed LiIO₃ doubly resonant parametric oscillator
23 p3297 A72-44187

Self oscillating system resonant vibrations excitation for fatigue tests, determining frequency and amplitude relationship
24 p3458 A72-44931

RESONATORS
NT CAVITY RESONATORS
NT MULTIMODE RESONATORS
Anharmonic thickness shear oscillations in hf quartz resonators with round coaxial electrodes, using Mindlin approximation to wave equation
02 p0191 A72-12032

Electromagnetic fields calculation in one dimensional resonator with moving boundaries, considering orthogonal dynamic modes
02 p0195 A72-12591

One dimensional nonhomogeneous wave equations solution for linear and hyperbolic moving boundary conditions applied to resonator fields
05 p0627 A72-16407

Inverse electromagnetic field problem for one dimensional resonator, determining size change from intrinsic mode
05 p0627 A72-16408

Longitudinal instability of electron beams interacting with passive resonator, considering Landau damping influence by linear differential equations of motion solution
05 p0701 A72-17243

Soviet book on Riemann-Hilbert problem method in electromagnetic waves theory, covering wave diffraction, scattering and propagation, waveguides and open resonators
08 p1137 A72-22021

Frequency splitting by diffraction at resonator mirrors of gas ring laser, deriving opposed waves lasing equations
10 p1490 A72-24045

Jones matrix method for polarization natural states, frequencies and mode losses calculation in anisotropic optical resonators
11 p1688 A72-26347

ADP or KDP crystal induced second harmonic emission from Ar laser resonator, noting crystal temperature effects on primary/secondary radiation phase synchronism
16 p2400 A72-33281

Possible field expansions in open waveguides and resonators
17 p2515 A72-34829

High power microwave nanosecond pulse generator with waveguide standing wave resonator, noting power gain and pulse shape
19 p2776 A72-38672

Nature of losses introduced into a ring resonator by a nonreciprocal phase-shifting device that employs the Faraday effect
19 p2814 A72-38788

Spectrum of stimulated emission in a resonator with plane mirrors
22 p3184 A72-42154

Optimal gyroresonator control in electric oscillating field by HF magnetic Lorentz force in terms of relativistic electron trajectory drifts
23 p3290 A72-44200

RESOURCE ALLOCATION
Project management mathematical models for task scheduling, resource allocation, information planning and decision making
06 p0905 A72-18067

Optimal allocation of tasks and resources, using asymptotic properties of stochastic approximation method
12 p1837 A72-27823

Technological forecasting in venture analysis and planning for long-term growth objectives, engineering project selection and resource allocation
14 p2174 A72-30868

[ASME PAPER 72-DE-26] Management information system role in cost effective civil and military aircraft operations, discussing hardware modification and human resources and communication system adaptation
15 p2339 A72-32458

Management alternatives evaluation methodology for capital expenditures on large facilities in terms of competitive capability enhancement for aerospace contracts
15 p2340 A72-32615

Resource allocation for minimum cost launch vehicle assignment to space missions, using network and dynamic programming algorithm
16 p2482 A72-33498

Resource analyses for R & D programs
17 p2639 A72-35339

Certain problems of the theory of hierarchical control systems
19 p2824 A72-37379

Quantitative evaluation for R and D resource allocation in terms of funding project priorities
19 p2884 A72-38024

Recent advances in R & D value measurement and project selection methods.
20 p2988 A72-39397

RESOURCES
NT EARTH RESOURCES
NT EXTRATERRESTRIAL RESOURCES

RESPIRATION
NT HIGH ALTITUDE BREATHING
NT LIQUID BREATHING
NT PRESSURE BREATHING

Hydrostatic pressure and temperature effects on growth of psychrophilic marine bacterium, emphasizing inhibited amino acid transport and respiration
01 p0011 A72-10322

Ventilatory and metabolic responses of unanesthetized dogs exposed to various carbon dioxide concentrations at 2 and 18 C, discussing oxygen uptake relation to cold
02 p0159 A72-11954

Nervous respiratory disorder in patients with diencephalic and vegetative vascular syndromes, discussing arterial hypoxemia development and resulting oxygen insufficiency
02 p0160 A72-12012

Lung ventilation nonuniformity determination by single calm breath method, showing nitrogen concentration in alveolar phases
02 p0165 A72-12515

Bacterial respiration through oxidative phosphorylation origin hypotheses, discussing photosynthesis and sulfate respiration in anoxygenic atmosphere and thiobacillus and aerobic evolution in oxygen atmosphere
04 p0470 A72-14795

Pulmonary RC network and multiple breath nitrogen washout time constants mathematical relationship for breathing mechanics measurement, discussing lung compliance and resistance

04 p0478 A72-14862

Breathing control during speech, noting carbon dioxide response, hyperventilation and apnea

04 p0480 A72-15218

Single olfactory bulb units under cyclic stimulation, observing activity related to inhalation cycle and odor quality

05 p0617 A72-16162

Single breath method for pulmonary diffusing capacity measurement with respect to total lung capacity and inspiration time

05 p0620 A72-17174

Human breathing metabolic simulation device for evaluating respiratory diagnostic, monitoring, support and resuscitation equipment

06 p0769 A72-18618

Ultrastructural and morphometric studies of beryllium oxide-contaminated environment effect on monkey and dog lung tissue

07 p0925 A72-20686

Gaseous nitrogen production in humans under steady-state conditions, relating expired nitrogen minute volume increase after protein consumption to possible gastrointestinal and metabolic effects

08 p1122 A72-20882

CO hypoxia effect on oxygen transport during exercise, discussing changes in cardiac and respiratory functions and work capacity

08 p1114 A72-20893

Diurnal and beat-to-beat variation factors in vectorcardiograms, noting respiratory movements, electrode location shift, skin-electrode impedance and heart electrical center mobility

08 p1127 A72-21849

Arterial chemoreceptor deafferentation influence on rat respiratory response to hypoxic and hypercapnic gas mixture breathing

08 p1120 A72-22078

Hypoxic and normoxic gas mixture breathing during intense muscular activity, relating oxygen consumption and carbon dioxide elimination magnitudes and motor performance

08 p1121 A72-22081

Human external respiration characteristics changes during increasing hypercapnia, relating carbon dioxide concentration rate to compensatory mechanisms and endurance

08 p1121 A72-22084

Respiration function testing device using spiromographs and gas analyzers

09 p1272 A72-23256

Chest strapping-induced increased lung recoil pressure effects on maximal expiratory flow relation to lung surface compliance decrease

10 p1425 A72-24478

Physical work capacity comparison during bicycle ergometry and treadmill walking tests, measuring oxygen uptake, ventilatory parameters and excess carbon dioxide production

11 p1579 A72-26095

Plethysmographic and laryngoscopic investigation of glottis opening and airway resistance relation to lung volume during panting and continuous slow expiration

11 p1586 A72-26611

Mathematical model of extracellular pH in brain tissue from blood and cerebrospinal fluid acid-base parameters for respiration central chemosensitive mechanism study

11 p1579 A72-26660

Respiration control by extracellular pH in medullary tissue, studying chemoreceptor response to hydrogen ion concentration in cat cerebrospinal fluid

11 p1579 A72-26661

Added elastic load tests for thoracic elastance change effects on human response to carbon dioxide inhalation, using rebreathing technique

12 p1762 A72-27726

Exercise role in ventilatory acclimatization to graded hypoxia in goats from carbon dioxide response curve measurements

12 p1762 A72-27727

Inspiration, expiration and hand muscle control comparison in psychophysical category production method for human voluntary breathing regulation investigation

12 p1763 A72-27843

Six day bed rest effect on external respiration and subcutaneous tissue oxygen metabolism, noting oxygen consumption decline

13 p1905 A72-29324

High temperature environment effects on rat organ and muscle tissue respiration, discussing temperature homeostasis maintenance

13 p1905 A72-29331

Gas mask-caused air flow resistance effects on respiratory and circulatory response to exercise, assessing maximal oxygen uptake

13 p1906 A72-29818

Alveolar carbon dioxide pressure-ventilation response curve measurement by Campbell rebreathing method in consecutive daily trials

13 p1906 A72-29846

Cardiovascular and respiratory changes in dogs exposed to acute overheating, relating ECG changes to adrenergic and hypoxia effects

14 p2074 A72-30382

Ventilatory peripheral chemoreflex response to hypoxia during physical exercise in native highlanders and altitude-acclimated lowlanders

17 p2499 A72-34345

Effects of nitrogen and helium upon pulmonary damage after rapid decompression to 2 torr.

[AD-746093] 17 p2508 A72-34544

Magnetic field effects in enzymes, tissue respiration and some metabolism characteristics of an intact organism

17 p2503 A72-35003

Bradycardia diving reflex to apneic face immersion related to physical exercise

17 p2506 A72-35964

Pulmonary gas exchange in Andean natives at high altitude.

18 p2650 A72-36570

A model of fluctuating alveolar gas exchange during the respiratory cycle.

18 p2650 A72-36571

Myth of nitrogen equality in respiration - Its history and implications.

19 p2758 A72-38708

Hypercapnia with relief of hypoxia in normal individuals with increased work of breathing.

21 p3005 A72-40420

Determination of oxygen consumption by use of the paramagnetic oxygen analyzer.

21 p3006 A72-40429

A mathematical model of the chemoreflex control of ventilation.

21 p3008 A72-40917

Separation of central effects of CO₂ and nicotine on ventilation and blood pressure.

21 p3001 A72-40918

The function of external respiration in mental activity

22 p3150 A72-42284

Mechanism of adaptation to hypoxic hypoxia

23 p3255 A72-43907

Determination of the diffusional capability of lungs by the method of delayed respiration

24 p3374 A72-44598

Comparison of three methods for quantitating respiratory response to hypoxia in man.

24 p3372 A72-44960

RESPIRATORS

Lumped parameter nonlinear RC circuit lung model for positive pressure respirator design

11 p1588 A72-26631

RESPIRATORY DISEASES

NT AEROSINUSITIS

NT ASTHMA

NT TUBERCULOSIS

Vectorcardiographic and electrocardiographic differentiation between cor pulmonale and anterior wall myocardial infarction.

21 p3001 A72-40769

Transarterial leakage - A possible mechanism of high altitude pulmonary oedema.

22 p3143 A72-42588

RESPIRATORY IMPEDANCE

Effects of externally imposed mechanical resistance on breathing dense gas at exercise - Mechanics of breathing.

22 p3150 A72-42489

The reflex and mechanical response of the inspiratory muscles to an increased airflow resistance.

24 p3372 A72-44958

First-breath response of medullary inspiratory neurons to the mechanical loading of inspiration.

24 p3372 A72-44959

RESPIRATORY PHYSIOLOGY

Respiration effects on human heart rate deceleration and biphasic cardiac response in aversive shock conditioning situation

01 p0010 A72-10195

Femoral arterial blood pressure third order waves onset mechanism in narcotized dogs, noting changed blood and respiration dynamics

02 p0160 A72-12014

Respiratory system frequency response analysis for chemical regulation of breathing, using time domain method and step functions

02 p0168 A72-12040

External respiration gas metabolism and energy consumption measurements for test pilots during parabolic trajectory flights in weightlessness simulation experiments

02 p0163 A72-12347

Electrical thermometer mounted on breathing mask for electropneumograms, measuring temperature change in respiration air flow

02 p0169 A72-12518

Magnetometer and spirometer ventilation measurements from chest and abdomen movements during carbon dioxide inhalation

05 p0619 A72-16790

Unattenuated ventilatory hypoxic drive in ovine and bovine species native to high altitude

07 p0917 A72-19445

Vagal control of ventilation and respiratory muscles during elevated pressures in cats

07 p0917 A72-19446

Endurance exercise effect on respiratory capacity in white, red and intermediate muscles in rats, relating fiber type to oxidative capacity

08 p1115 A72-21083

Bulbar respiratory neuron discharge pattern response to nasal and tracheal receptor stimulation in cats, relating changes in neuronal activity and intratracheal pressure

08 p1117 A72-21473

High pressure gas mixture breathing effects on intercostales externi muscles electrical activity and respiratory cycle time in rats

08 p1121 A72-22082

Digital computer technique for computation of pulmonary mechanics parameters, using phasor method and Fourier series analysis of respiratory flow signals

11 p1587 A72-26620

Mountain sickness relation to ventilation response to hypoxia, noting response intensity dependence on peripheral chemoreceptor sensitivity

12 p1771 A72-27481

Cerebrospinal fluid pH change effects on cat respiratory response before and after vagotomy, showing vagal activity relation to central chemical control of respiration

12 p1762 A72-27825

Cardiorespiratory response to breathing dense sulfur fluoride-oxygen mixture under physical exercise conditions

12 p1767 A72-28314

Supraspinal effects on different work regimes of supplementary respiratory muscles, using interference electromyograms cross correlation analysis

13 p1905 A72-29328

Respiratory and vasculomotor autonomic centers functional state relation to vestibular system from labyrinth electrical stimulation and shaking experiments

14 p2075 A72-30387

Cat bulbar respiratory neuron discharge modification by single electric shock stimulation of cerebral cortex

14 p2077 A72-30843

Respiratory effects of hypochloremic alkalosis and potassium depletion in the dog.

21 p2997 A72-40418

Comparative studies of the respiratory functions of mammalian blood.

21 p3002 A72-40919

New mechanical device for producing traumatic shock in dogs - Circulatory and respiratory responses.

22 p3142 A72-42490

Suprapontine influences on hypoxic ventilatory control.

22 p3143 A72-42590

Effect of a polarizing current on the activity of neurons of the respiratory center

22 p3145 A72-42725

Determination of the diffusional capability of lungs by the method of delayed respiration

24 p3374 A72-44598

Gas exchange mechanism in lung alveoles and capillaries, discussing cell metabolism for oxygen uptake and carbon dioxide formation

24 p3371 A72-44599

Respiration control mechanism ensuring adaptation to power requirements and chemical environment maintenance in tissues, considering brain stem location

24 p3371 A72-44600

Relative position of the rib within the chest and its determination on living subjects with the aid of a computer program.

24 p3372 A72-44957

RESPIRATORY RATE

Inspiration time correction factor for pulmonary diffusing capacity measurement by single breath method

01 p0015 A72-11259

Heart and respiration rates response to free fall parachuting, using FM/FM telemetry

02 p0167 A72-11709

Rapid ventilatory response in man at work on set for different standard starting commands, discussing relation to work load and conditioning process

05 p0619 A72-16788

EEG phase asymmetry fluctuations relation to respiration rhythm in subjects from pneumograms during rest, mental activity, hypnosis and sleep

05 p0620 A72-17214

Respiration rate transmitter with miniature pressure transducer for measuring pneumograph variations in animals over FM-FM telemetry system

08 p1124 A72-20898

Respiration control during hyperoxia, discussing chemoreceptor significance in minute volume respiration rate reduction mechanism from Pamir mountain aborigines oxygen breathing reaction studies

08 p1120 A72-22076

High pressure gas mixture breathing effects on intercostals external muscles electrical activity and respiratory cycle time in rats

08 p1121 A72-22082

Living being inhalation flow rate measurement, discussing performance and characteristics of respiratory flowmeter

10 p1479 A72-23971

Cotton wick probe-transducer assembly for pneumograph recording of rabbit respiratory rate

11 p1587 A72-26619

Parachutist biomedical responses in aerial tow at 110-175 knots, determining heart and respiration rates and urinary catecholamines

12 p1774 A72-28272

Human respiratory rate diurnal rhythm adjustments during inverted work-rest cycles in isolation chamber with controlled comfortable atmospheres

14 p2075 A72-30390

Electrically sensed changes in chest and abdomen diameter for tidal volume, respiratory frequency and minute ventilation measurements

21 p3006 A72-40428

Breathing rate response to oral instructions in relationship to nervous system, bronchial muscle tonus and gas metabolism rate reflex-type changes

21 p3001 A72-40761

Spinal cord heating and cooling effects on body temperature, respiratory and heart rates and arterial blood pressure, investigating feeding and drinking behaviors

22 p3150 A72-42672

RESPIRATORY REFLEXES

Cat respiratory center activity phase relation to arterial chemoreceptor afferent discharge oscillations effect on lung ventilation frequency

05 p0619 A72-16789

Respiration in altered gas environment for spontaneous breathing and voluntarily maintained pulmonary ventilation level conditions

08 p1120 A72-22077

Breathing regulation characteristics showing reflex control of respiratory functions in normal environment and brain tissue receptor control under hypoxia

08 p1121 A72-22079

Respiratory function control and physiological adaptation mechanisms evolution during changing earth atmosphere oxygen content, noting hypoxia sensitivity development

08 p1121 A72-22080

Laryngeal motoneuron activity during Hering-Breuer reflexes, noting inspiratory fibers firing inhibition and activation during lung inflation

09 p1266 A72-22975

Native highlander and lowlander chemoreflex ventilatory response to transient carbon dioxide inhalation at low and high altitudes

12 p1762 A72-27728

Patterns of spontaneous and reflexly-induced activity in phrenic and intercostal motoneurons.

21 p3003 A72-41462

Reflexive cardiac rhythm changes and arterial tension during hypoxia, noting differences due to animals, controlled respiration and pharmacological effects

22 p3141 A72-41984

Electromyographic investigation of diaphragm cross contraction following spinal cord section in cats, noting diaphragm motoneurons excitation by breathing center pulses

22 p3142 A72-42281

Genetic aspects of the blunted chemoreflex ventilatory response to hypoxia in high altitude adaptation.

22 p3144 A72-42591

Respiration control mechanism ensuring adaptation to power requirements and chemical environment maintenance in tissues, considering brain stem location

24 p3371 A72-44600

The reflex and mechanical response of the inspiratory muscles to an increased airflow resistance.

24 p3372 A72-44958

First-breath response of medullary inspiratory neurons to the mechanical loading of inspiration.

24 p3372 A72-44959

RESPIRATORY SYSTEM

NT BRONCHI

NT BRONCHIAL TUBE

NT DIAPHRAGM [ANATOMY]

NT LUNGS

NT NOSE [ANATOMY]

Radiotelemetric cardiorespiratory determinations during submaximal dynamic exercise

02 p0168 A72-12134

Respiratory adaptation to pure oxygen excess pressure after cockpit depressurization from flight simulator tests with pressure-suited pilots, presenting ECG reactions

05 p0623 A72-16749

Digital computer simulation of circulatory and respiratory systems interaction model for oxygen and carbon dioxide gas exchange between pulmonary blood and alveolar air

09 p1268 A72-22456

Weight loss due to respiratory tract evaporative water loss during exercise, from humidity change, ventilatory exchange and oxygen uptake data

11 p1586 A72-26613

Hyperoxia effect on human airways resistance during high pressure oxygen breathing

11 p1586 A72-26614

Frequency response studies of human and avian respiratory regulation.

19 p2761 A72-38229

High altitude physiology: Cardiac and respiratory aspects; Proceedings of the Symposium, London, England, February 17, 18, 1971.

22 p3143 A72-42583

Respiratory chain components correlation to tension production at various oxygen pressures in guinea pig ductus arteriosus, investigating light absorption changes

22 p3144 A72-42670

Aortic regurgitation variation with respiratory sinus arrhythmia and respiratory cycle in dogs during tachycardia and bradycardia

22 p3151 A72-42674

Respiratory control system benchmark simulation on hybrid computer for Cheyne-Stokes breathing, emphasizing equations for arterial and venous carbon dioxide and oxygen stores

23 p3268 A72-44551

Respiration control mechanism ensuring adaptation to power requirements and chemical environment maintenance in tissues, considering brain stem location

24 p3371 A72-44600

RESPIROMETERS

System distortion error characteristics for carrier gas type radiorespirometers, considering relation to system time constant

01 p0017 A72-10399

Single breath diffusing capacity and alveolar dead space measurements for carbon 18 monoxide using respiratory mass spectrometer

04 p0480 A72-15215

Respiratory flow resistance measurements in man, comparing esophageal catheter, plethysmographic, forced pressure oscillations and airway interrupter methods

04 p0481 A72-15222

Nose installed thermistor device for in-flight monitoring of pilot respiration and pulse rate

12 p1769 A72-27417

Low cost real time computerized C 14 radiorespirometry telemetering system for monitoring human metabolism data during space missions

12 p1774 A72-28277

Radiorespirometry in the case of work and sports activities

22 p3149 A72-42071

RESPONDERS

U TRANSPONDERS

RESPONSE BIAS

Random bias holographic technique for imaging three dimensional objects, using laser, one mirror, one diffuser and photographic plate

07 p0982 A72-19036

Response bias and sensitivity variations in psychophysical test of rats discrimination between standard and attenuated auditory signal intensities

16 p2356 A72-33648

Some effects of bias errors in redundant flight control systems.

19 p2779 A72-38237

RESPONSE TIME [COMPUTERS]

Frequency response data identification technique using adaptive hybrid computer to improve quality and acquisition time

13 p1935 A72-29103

RESPONSES

NT DYNAMIC RESPONSE

NT FREQUENCY RESPONSE

NT GALVANIC SKIN RESPONSE

NT HEMODYNAMIC RESPONSES

NT MODAL RESPONSE

NT PHYSIOLOGICAL RESPONSES

NT TIME RESPONSE

NT TRANSIENT RESPONSE

Response-dependent electric shock punishment schedule preference during response sequence in food-deprived pigeons

16 p2357 A72-33773

REST

NT BED REST

Effect of nicotinic acid on myocardial metabolism in man at rest and during exercise.

17 p2506 A72-35968

Psychological principles of active rest during long space flights

21 p3006 A72-40446

RESTRAINTS

U CONSTRAINTS

RESTRICTIONS

U CONSTRICTIONS

RESULTANTS

Influence coefficients for circumferential stress resultants in long conical shell elements without edges interaction

10 p1555 A72-24192

RETENTION [PSYCHOLOGY]

Instrument flying skills retention, discussing initial training, discrete procedural and tracking responses

01 p0018 A72-10564

Brain structures role in fixation of temporal relationships in information memory function of central nervous system

08 p1118 A72-21836

Concentrated and extended learning effects on formation rate and retention degree of conditioned reflex during mice adaptation to high altitude hypoxia

13 p1903 A72-28770

Hippocampus morphology and physiology in relationship to emotion and memory mechanisms, time links, visceral activity and motivations and endocrine control

16 p2353 A72-33099

Characteristics of certain parameters of memory for visual signals in lower monkeys

21 p3001 A72-40804

Some data on the interrelations of conscious and unconscious reactions

23 p3257 A72-44076

Age-induced long-term memory changes in animals

23 p3257 A72-44079

Content and time aspects of short and long term memory operation theories, relating attention and memory spans

24 p3373 A72-45243

RETICLES

Oscillating slot-and-bar and sinusoidal reticle scanners for measuring optical image velocity

03 p0326 A72-14202

Positive acceleration force-produced displacements of helmet-attached reticle in front of left eye

12 p1777 A72-28330

Human observation error effect on astronomical refraction calculation from time determination of solar limbs passings across optical instrument reticle

24 p3438 A72-44863

RETICULOCYTES

Proliferative blood forming tissue activity under chronic gamma ray irradiation in guinea pigs by quantitative methods, showing myeloid and reticular disturbances of bone marrow

04 p0467 A72-14607

Stepwise altitude acclimatization and subsequent re-animation after blood loss caused clinical death effects on dog peripheral blood erythrocytes, reticulocytes, hemoglobin and hematocrit

14 p2076 A72-30671

Modulating effect of limbic brain formations on the blood system

22 p3142 A72-42282

RETINA

Nonmammalian vertebrate retinal receptor rods and cones birefringence as function of fixation, temperature and immersing medium

01 p0014 A72-10862

Optic nerve axon diameters in central and peripheral cat retina related to conduction velocity groups

03 p0315 A72-13622

Synaptic contacts in vertebrate retinas, reviewing bipolar terminals, ganglion cells and amacrine responses from electron microscopy

06 p0762 A72-17719

Retinal ganglion cell spikes timing in mammalian retina, using electroretinography and computer analysis

06 p0762 A72-17721

Glycogen content and distribution determination in frog retina by histochemical analysis with intravascular injection of mixture preventing decomposition

06 p0764 A72-17987

Retina, tectum opticum and Rostral brain structures role in analysis and processing of visual sensory stimuli in cat distinguishing between prey and enemies

07 p0915 A72-18775

Cat retina ganglion cell threshold and latent responses to separate stimulation of receptive field center and periphery

08 p1117 A72-21474

Proposed cone sensitivities relation to Wright color discrimination lines, tabulating optimum weighting factors and longest to shortest chromaticity steps ratios

09 p1269 A72-22619

Three stage retinal model for visual monitoring method applied to computerized photointerpretation of aerial photographs

09 p1284 A72-23624

In vitro measurements of oxygen tension effect on teleost and amphibian retinal lactate dehydrogenase activity, discussing acetazolamide produced hypoxia effects

10 p1424 A72-23729

Photostimulated potentials of human visual cortex, determining retinal macular area involvement

10 p1426 A72-24786

Intraelectroretinographic analysis of light signal spatial summation at different retinal nerve levels in frogs

11 p1585 A72-26454

Isotopic labeled microspheres for cat uveal and retinal blood flow and oxygen consumption determination, studying increased intraocular pressure and carbon dioxide tension effects

12 p1763 A72-27841

Retina visual acuity testing by zero and first order moire fringes, using square-wave amplitude gratings

12 p1772 A72-27953

Human retinal rod rhodopsin bleaching and regeneration measurements, tracing dark adaptation curves

15 p2184 A72-31364

Dark adaptation studies of bleach-induced visual threshold rise and subsequent return to rhodopsin level

15 p2184 A72-31365

Monkey retinal ganglion and lateral geniculate nucleus cell maintained discharge rate indication of receptive field organization for various light stimulus intensities

15 p2184 A72-31370

Light flashes observed by astronauts on exposure to primary cosmic radiation during transular flights, investigating effect upon retina in man and animal

15 p2189 A72-31917

Lamellar structure and rhodopsin location in bleached and unbleached rod photoreceptor membranes of dark adapted frog retinas by X ray diffraction study

15 p2186 A72-32199

Electroretinographic illumination potentials dependence on extracellular chloride ion concentration in isolated frog retina

15 p2186 A72-32491

Visible and invisible nonionizing radiation produced human injuries, considering visual and retinal effects and induced thermal stresses

17 p2499 A72-34300

Gain control and contrast sensitivity in the vertebrate retina.

17 p2507 A72-34418

The uptake, metabolism and release of C/14-taurine by rat retina in vitro.

17 p2500 A72-34881

Rhesus monkey retinas ultrastructural alteration and damage in rods and cones produced by Q switched ruby laser coherent radiation

17 p2509 A72-35396

Model to account for visual responses to light flashes of dark adapted eye, discussing perceived brightness variation with intensity

18 p2651 A72-36611

Isolated retina receptor potential amplitude relation to visual pigment bleaching kinetics, indicating excitation-inhibition receptor response generation mechanism

19 p2756 A72-37830

Resumption of flight after retinal surgery

19 p2760 A72-37879

Synaptic patterns in the superficial layers of the superior colliculus of the monkey, Macaca mulatta.

19 p2758 A72-38647

Threshold excitation, temporal summation, and impulse response function in the retina of the cat - Temporal receptive fields of retinal ganglion cells

19 p2758 A72-38648

Study of the diffusing properties of the retina - Application to the optical system of the eye

21 p3007 A72-40736

Spectral sensitivity after prolonged intense spectral light exposure of rhesus monkey corneas, demonstrating long term loss of cone photopigment response

21 p3000 A72-40739

Effect of selenium on the formation of the electrical potential in the retina

22 p3148 A72-41898

Visual information space-time dependent filtering by retinal and geniculate body neural nets

22 p3142 A72-42299

On threshold mechanisms for achromatic and chromatic vision.

22 p3142 A72-42547

The electrical activity of the isolated frog retina in buffered chloride-deficient Ringer's solution

22 p3147 A72-42987

Visual perception of accelerated nitrogen nuclei interacting with the human retina.

23 p3256 A72-43940

Motion thresholds for fovea and peripheral retina with/without correction for peripheral refractive error

23 p3260 A72-43978

Localization and dynamic changes of glycogen in frog retina adapted to darkness or light. I, II.

23 p3258 A72-44377

Phase correlation between two sources formed on a diffusing surface - Application to the human retina

23 p3261 A72-44379

Visual sensitivity measurement in retinal areas with stepwise change from one monochromatic light to another, discussing eye movements effects and perception thresholds

23 p3258 A72-44385

Perceptual latency as a function of stimulus onset and offset and retinal location.

23 p3258 A72-44386

Functional organization of the periphery effect in retinal ganglion cells.

24 p3371 A72-44908

RETINAL ADAPTATION

NT DARK ADAPTATION NT LIGHT ADAPTATION

Retinomotor light/darkness responses phylogenetic variations, discussing retinal elements structural and functional development in fishes and amphibians

02 p0164 A72-12484

Retinal annulus onset and offset thresholds, discussing neural signals delay characteristics

02 p0164 A72-12488

Human visual system multiple channels sensitivity to patterns at low luminance or high drift rates, noting retinal ganglion cells selective sensitivity

06 p0761 A72-17602

Human visual system selective adaptability to speed, size and orientation, suggesting motion analysis by visual cortex neural subsystems

06 p0761 A72-17603

Retinal cell adaptation as result of receptor membrane response range saturation, considering dark adaptation and increment threshold

06 p0761 A72-17604

Stereoscopic acuity for photometrically matched background wavelengths at scotopic and photopic levels, plotting variable depth error as function of retinal illuminance

10 p1425 A72-24269

Selective chromatic adaptation in cone photoreceptors of cynomolgus macaque monkeys, using late receptor potential as response index

13 p1907 A72-29967

Visual latencies measurement as function of stimulus luminance and adaptation state by stereoscopic null method, characterizing relationship by inverse power function

13 p1911 A72-29968

Stabilized retinal image techniques to examine functional relationships between nonstabilized grating pattern orientation adaptation and stabilized line stimuli fading rates

16 p2358 A72-33646

Electroretinographic evidence for a photopic system in the rat.

17 p2500 A72-34878

Linear-nonlinear-linear transition as a function of frequency in the retinal response to light.

17 p2508 A72-34885

Effect of selective adaptation on detection of simple and compound parafoveal stimuli.

18 p2651 A72-36607

Contour-contingent color aftereffects - Retinal area specificity.

19 p2755 A72-37273

Interactions between spatial and kinetic dimensions in movement aftereffect.

21 p3003 A72-41254

The photopigment bleaching hypothesis of complementary after-images - A psychophysical test.

23 p3258 A72-44376

RETINAL IMAGES

Neuron responses in cat visual system /retina, geniculate body, primary, secondary and tertiary visual cortex/ to simple visual stimulus pattern

01 p0011 A72-10466

Psychology of visual form perception in relation to neurophysiological principles of lateral interaction and organization, considering retinal images, aftereffects, binocular vision, etc

01 p0011 A72-10469

Electronic analog models of human retina and visual system, discussing optical character recognition, signal processing, photoreceptor stimulation, visual cortex excitation and further model development

01 p0017 A72-10471

Human pattern analysis by stabilized retinal image fragmentation as function of fade frequencies for angle and line stimuli in different orientations

01 p0014 A72-10721

Binocular depth perception based on two retinal images spatial frequency content

02 p0164 A72-12486

Conduction velocity groups in cat optic nerve from antidromic responses recorded in peripheral retina and area centralis

03 p0315 A72-13621

Visual persistence and perceptual moment hypotheses for time-dependent visual illusion from viewing moving stroboscopically illuminated object

05 p0621 A72-16150

Optical image transfer functions characteristics and modulation in isolated retinas and retinal receptors, noting similarity to optical fiber bundles

07 p0916 A72-19027

Moving target resolution threshold in retina, discussing visual acuity relation to target angular velocity during ocular pursuit

07 p0926 A72-19029

Dynamic visual acuity and eye movement data for moving targets, deriving retinal target image position and velocity errors during ocular pursuit

07 p0926 A72-19030

Human binocular visual system fusional information processing, evaluating compensatory eye movements role in overcoming retinal image disparity

07 p0929 A72-19314

Rod-cone interaction in human scotopic vision, presenting test flash threshold as function of conditioning flash interval

08 p1116 A72-21460

Rhesus monkey retinal image diameter estimation during exposure to Ar and He-Ne laser irradiation, using microphotometer scans

11 p1582 A72-25314

Visual evoked cortical responses in objective refraction related to retinal image clarity for clinical applications

11 p1582 A72-25349

Gain control of cat retina rapid light adaptation process to attenuate signals reaching retinal ganglion cells from photoreceptors

12 p1760 A72-27299

Contrast enhancement for switch-on and -off modes of bar patterns, noting spatial transients due to primary image interaction with negative afterimage

12 p1808 A72-27679

Spatial and temporal summation characteristics and relationship in human peripheral retina investigated for stimuli viewed at eccentricity against luminous background

13 p1907 A72-29970

Linear systems theory for mathematical model of retinal image and ganglion cell excitation, calculating receptor layer luminance distributions for several stimulus patterns

15 p2184 A72-31367

Eagle eye retinal image quality determination by ophthalmoscopic method, comparing to human visual acuity

15 p2186 A72-31724

Size scaling rate from retinal image size comparison judgment time during observation of briefly presented concentric rectangles of varying size and orientation

15 p2187 A72-32762

Stabilized retinal image techniques to examine functional relationships between nonstabilized grating pattern orientation adaptation and stabilized line stimuli fading rates

16 p2358 A72-33646

Occipital EEG activity during fluctuations of perception under stabilized image and simplified stimulus conditions.

17 p2506 A72-34247

The influence of the modulation transfer function of the dioptric apparatus on the acuity and contrast of the retinal image in Rana esculenta.

17 p2508 A72-34883

Eye movement pattern monitoring to investigate retinal afterimage role in release of pursuit movements

17 p2509 A72-34886

Peripheral contrast thresholds for moving images.

17 p2509 A72-35688

Manipulation of projected afterimages by means of the physiological theory imposed on the observer.

18 p2654 A72-36920

The neurophysiology of binocular vision.

19 p2755 A72-37250

Differential effects of refractive errors and receptive field organization of central and peripheral ganglion cells.

19 p2756 A72-37826

Mach band measurement by psychological compensation technique, causing band disappearance by changes in stimulus pattern luminance and brightness distribution relations

19 p2760 A72-37827

An electronic model of visual receptive fields.

20 p2897 A72-39271

Discrimination sensitivity and black light density in the mesopic range

21 p3007 A72-40735

Fixation eye movements and the processing of visual information.

21 p3007 A72-40740

Some structural and functional characteristics of a retina projection onto the visual cortex of cats

21 p3001 A72-40808

Apparent movement and change in perceived location of a stimulus produced by a change in accommodative vergence.

21 p3002 A72-41024

The effect of size, retinal locus, and orientation on the visibility of a single afterimage.

21 p3003 A72-41253

Interactions between spatial and kinetic dimensions in movement aftereffect.

21 p3003 A72-41254

Optical directionality of retinal receptors and corresponding points. I - Nasal-temporal asymmetry of retinal spatial values and orientation of receptors: Are the corresponding points cones. II - Variation of form of the experimental horoptera, and possibility of reor-

ganization of the retinal correspondence according to the orientation of the eyes
24 p3371 A72-44907

Perception smear suppression during saccadic eye movements in terms of metacontrast determined by post-saccadic accumulated luminance relation to stimuli masking
24 p3373 A72-45377

RETRACTABLE EQUIPMENT

European A300B airbus flying control hydraulic system and landing gear design for safety and reliability, fatigue life, weight and maintenance
01 p0005 A72-10724

Glass-vinyl retractable windshield visor development for Concorde aircraft, considering rain, hail and icing effects, strength and stiffness under aerodynamic loading and heating
09 p1261 A72-22900

RETRACTABLE LANDING GEAR

U LANDING GEAR
U RETRACTABLE EQUIPMENT

RETRIEVAL

NT DATA RETRIEVAL
NT INFORMATION RETRIEVAL

RETROREFLECTION

Automatically retrodirective performance from circular arrays and circularly continuous aperture antennas, applying method to cylindrical antennas
01 p0043 A72-11248

Laser ranging retroreflector deployed by Apollo missions, discussing array design, structural support and thermal control
04 p0509 A72-15099

Angle scintillation in laser radar return from retroreflector, comparing measurement with theoretical derivation in terms of phase fluctuation parameter [CLEA PAPER 2,1]
07 p0942 A72-19377

Automatic laser tracking and ranging system for cooperative retroflective aircraft targets, discussing design, performance, eyesafe distance and atmospheric attenuation
07 p0942 A72-19385

Earth-moon distance measurement by laser ranging methods, discussing retroreflectors, light collectors, time interval measuring devices and moon ranging stations
13 p2037 A72-28993

Lunar physical libration measurement from Apollo laser experiment with retroreflectors, assessing obtained data
14 p2154 A72-30516

RETROSEQUENCING

U SEQUENTIAL CONTROL

RETURN BEAM VIDICONS

ERTS return beam vidicon system geometric calibration for high resolution photoimage maps cartographic referencing and register, discussing optical and electronic distortion sources
02 p0225 A72-11818

ERTS return beam vidicon imagery simulation, predicting resolvability of ground targets as function of target size, contrast, spectral distribution and radiance level
02 p0226 A72-11833

Image resolutions for ERTS return beam vidicon TV, Skylab multispectral cameras and Gemini/Apollo photographs
06 p0818 A72-18328

Return beam vidicon multispectral camera system for ERTS A and B, describing camera system design and performance characteristics in terms of ERTS mission purpose
07 p0986 A72-19601

Performance tests of return beam vidicon multispectral television camera system for ERTS program
07 p0986 A72-19657

Photogrammetric camera system imaging characteristics comparison with aerial reconnaissance, multispectral and return beam vidicon systems, noting economic benefits due to smaller scale imagery
12 p1805 A72-27819

ERTS-borne return beam vidicon camera using high resolution TV sensors coaligned to view identical scene in different spectral bands
19 p2795 A72-37576

High resolution multispectral camera system for ERTS A & B.
24 p3402 A72-45182

RETURN TO EARTH SPACE FLIGHT

Thrust power optimization for spacecraft earth-planet round trip trajectories
01 p0127 A72-10357

Reusable space tug mission profile for interplanetary spacecraft recovery, using branched trajectory, steepest descent optimization and propellant minimization
05 p0730 A72-16949

REUSABLE LAUNCH VEHICLES

Supersonic transition flight mode of reusable two stage space shuttle booster for orbiter launching, comparing with subsonic and high lift to drag designs [AIAA PAPER 72-133]
07 p1084 A72-18963

Space shuttle cost savings from viewpoints of reusable system, launch rate, vehicle life and overall program
12 p1877 A72-27514

REUSABLE SPACECRAFT

NT SPACE SHUTTLES

Multilayer insulation materials for reusable space vehicles thermal protection and radiation shielding, tabulating thermal conductivity values for various materials
01 p0092 A72-10780

European reusable space tug, discussing computer controlled attitude stabilization and maneuvering system design for orbital rendezvous and docking
05 p0725 A72-16446

Aircraft and reusable spacecraft propulsion systems current status and future development, discussing noise and exhaust emission problems, V/STOL bypass and fan engines, ramjets, etc
05 p0705 A72-16735

Control system design computerized optimization technique based on high speed repetitive simulations and gradient minimization, considering application to reusable and expendable boost vehicles
05 p0729 A72-16812

Reusable space tug mission profile for interplanetary spacecraft recovery, using branched trajectory, steepest descent optimization and propellant minimization
05 p0730 A72-16949

Reusable shuttle for cost reduction, including reusability rate, expanded orbit capabilities and flight frequency
06 p0906 A72-18171

Space shuttle vehicle configurations with reusable booster and orbiter modules, discussing cargo capacity, maneuvering capability, mission duration, engine characteristics and acceleration constraints
07 p1085 A72-19058

Space tug for recoverable reusable system with winged manned boost-glide vehicle, discussing feasibility in economics and engineering
13 p2051 A72-28930

Reusable two-stage meteorological rocket vehicle, discussing design, performance, second stage recovery technique and cost
17 p2619 A72-34185

Space shuttle configuration, discussing payload accommodation requirements, accessories, mission operations and reusable tug [AIAA PAPER 72-737]
18 p2731 A72-36546

Contribution to the discussion of mixed-mode propulsion and reusable one-stage-to-orbit vehicles.
24 p3450 A72-45191

The space tug orbital operations.
24 p3451 A72-45196

REVERSE TIME

U REACTION TIME

REVERSED FLOW

Supersonic flow patterns near yawed obstacles around flat plate sharp leading edge with high pressure regions in reversed separated flow zone
06 p0756 A72-18122

Heat exchange extremum boundary value problems for flow direction reversal, considering thermal treatment of porous materials
08 p1253 A72-21457

Reversed flow solutions of Falkner-Skan equation in boundary layer theory
11 p1676 A72-25361

Swirling flow in round pipe with sudden expansion, discussing separation and reversal characteristics
13 p1942 A72-29640

Numerical integration of boundary layer equations through region of reverse flow past parallel flat plate with negative surface velocity
13 p1944 A72-30033

Numerical check on boundary layer equations asymptotic expansion solutions for Falkner-Skan reverse flow and unit Prandtl number compressible boundary layer with blowing
15 p2219 A72-32589

Calculation of axisymmetric swirling and non-swirling turbulent jets
18 p2682 A72-36890

Reverse flow sensing hot wire anemometer.
22 p3177 A72-42392

Plume impingement force during tandem stage separation at high altitudes.
22 p3231 A72-42872

Flow model for the determination of the heat transfer on the base of vehicles with clustered H2-O2 rocket engines.
24 p3434 A72-45201

A finite-difference method for boundary layers with reverse flow.
24 p3395 A72-45789

REYNOLDS EQUATION

Turbulent flow from rotating disk, calculating mean velocities, turbulent intensities and Reynolds stress component
04 p0513 A72-15332

Reynolds analogy based correlation method for Stanton number prediction for turbulent heat and mass transfer in smooth tubes
06 p0903 A72-18186

Aerodynamic radial bearing analysis based on Reynolds equation, emphasizing gas bearing nonlinear oscillation stability
06 p0824 A72-18702

Radial gas bearing air lubrication theory, proving existence and uniqueness theorems for Reynolds equation periodic solution
07 p0998 A72-20473

Large scale motion of turbulent boundary layer during relaminarization under strong pressure gradient, obtaining fluctuating velocity components and tangential Reynolds stress
13 p1944 A72-30028

The Reynolds tensor in a homogeneous turbulence associated with a pure deformation
17 p2539 A72-34909

Theoretical model for plane turbulent wakes subject to adverse, favorable and mixed pressure gradients based on Reynolds stress equation, describing experimental verification
18 p2680 A72-36477

Measurements of Reynolds shear stress fluctuations in a turbulent boundary layer.
21 p3047 A72-41638

Kinetic theory of turbulent flow,
24 p3394 A72-45563

REYNOLDS LAW

U REYNOLDS EQUATION

REYNOLDS NUMBER

Pt coated W hot-wire anemometers sensitivities in supersonic turbulent flow at low Reynolds numbers [ONERA, TP NO. 1024]
01 p0064 A72-10037

Flow in turbulent trailing vortex, considering circulation profiles and Reynolds stress distribution [AD-740436]
01 p0049 A72-10232

Split-film anemometer probe determination of convective heat transfer coefficient azimuthal dependence in low Reynolds number flow over cylinders, discussing axial heat losses
02 p0224 A72-11725

Hypersonic boundary layer transition in presence of wind tunnel noise, indicating rms sound pressure relationship to transition Reynolds number
02 p0151 A72-12278

Meteor trail forms diversity explanation from magnetic pressure and Reynolds number and plasma diffusion in magnetic fields, discussing geomagnetic effect on trail shape
02 p0282 A72-12336

Force and pressure distribution measurements on delta wing-body combination in compressible flow, investigating Reynolds number effect [DGLR PAPER 71-118]
02 p0152 A72-12707

Turbulence degree effects on aerodynamic properties of planar decelerating cascades at Reynolds numbers 50,000-250,000, discussing blade boundary layer characteristics [DGLR PAPER 71-096]
02 p0153 A72-12716

Turbulent flow internal intermittency and fine structure distribution as function of Reynolds number, using hot-wire anemometer for velocity field measurements
03 p0340 A72-13156

Variational problem of conducting fluid flow in MHD channel at large magnetic Reynolds numbers at induction saturation
03 p0397 A72-13999

Laminar turbulent transition Reynolds number increase at finite perturbations in longitudinal magnetic field
03 p0398 A72-14003

Annular MHD channel laminar flow generation at supercritical Reynolds numbers by strong magnetic fields
03 p0398 A72-14005

Magnetic field distribution in linear MHD channel for large Reynolds numbers, determining current density and longitudinal field component
03 p0398 A72-14010

Asymptotic theory of heat transfer in two dimensional turbulent boundary layers of incompressible fluid at large Reynolds numbers
03 p0459 A72-14390

Viscous fluid flow at small Reynolds numbers past porous permeable sphere, obtaining drag formula
04 p0511 A72-14858

Laminar viscous flow past finite flat plate at high Reynolds numbers, solving Navier-Stokes equations
04 p0511 A72-14859

Low Reynolds number nonequilibrium stagnation heat transfer with helium, argon and hydrogen injection into air boundary and thin viscous shock layers [ASME PAPER 71-WA/HT-19]
05 p0647 A72-15878

Turbulent flow in smooth and rough pipes at Reynolds numbers 30,000-480,000, presenting velocity mean and fluctuating components rms and cross correlation values [ASME PAPER 71-WA/FE-7]
05 p0647 A72-15935

Axial flow multistage compressor design, discussing high speed flow measurements and Reynolds number and blade airfoil shape effect on aerodynamic performance

05 p0601 A72-16483

High Reynolds number flow between two infinite rotating disks, investigating viscosity effects on flow velocity distribution type from analytic approximation

05 p0649 A72-16611

Cardiac murmur level dependence on blood stream Reynolds number, tracing cardiac noise origin to blood turbulence

06 p0762 A72-17676

Increased Reynolds number simulation with roughness set on aircraft model in transonic flow, investigating flow separation by parietal visualization technique

06 p0758 A72-17846

Nonuniform potential and dissipation flow structure of turbulent diffusion flame front at high Reynolds numbers

06 p0902 A72-18104

Viscous incompressible flow past circular cylinder at Reynolds numbers 20-100 by finite difference methods, taking into account wake region behind body

06 p0756 A72-18125

Boundary layer transition on slender cone in hypersonic flow as function of nose bluntness, free stream Reynolds number and angle of attack

[AIAA PAPER 72-216]

07 p0908 A72-18961

Convective heat transfer coefficient for particles of arbitrary shape in flow at low Reynolds number, using equivalent radius method

07 p1098 A72-18985

Iterative solution of differential equations for steady plane flow with heat and mass transfer at high Reynolds numbers

07 p0971 A72-20098

Steady viscous incompressible fluid flow in circular disk with prescribed velocity components at low Reynolds numbers, considering computer tested numerical method

07 p0972 A72-20102

Temperature effects on hot-wire anemometer calibrations, plotting Nusselt number variation with Reynolds number

07 p0990 A72-20369

Modified mixing length velocity distribution predictions for turbulent boundary layers with uniform mass transfer for low and high Reynolds numbers

08 p1150 A72-21622

Critical Reynolds numbers estimation for flows having velocity profile with point of inflection, discussing plane parallel flows stability energetic analysis

08 p1151 A72-21660

Laminar/turbulent boundary layer transition on parabolic wing profile in supersonic wind tunnel, noting critical Reynolds number increase with leading edge thickness

09 p1259 A72-22407

Reynolds number and cylindrical spacing effect on Karman vortex street formation from smoke visualizations of single and tandem cylinder wakes

09 p1261 A72-22939

Energy spectrum and decay of random two dimensional vorticity distributions at large Reynolds number

[AD-740486]

09 p1294 A72-22943

Pressure distribution around circular cylinder with shrouds of various geometry for suppressing flow induced vibrations at subcritical and transition Reynolds number

09 p1261 A72-23315

Viscous boundary layer equations for MHD flow near rear stagnation point at small Reynolds number

09 p1296 A72-23674

Reynolds number and mainstream turbulence effects on laminar separation bubbles behavior in boundary layers on turbine blades in cascade

10 p1416 A72-23873

Decelerating motion of identical and independent water drops succession, determining drag coefficient as function of Reynolds number

10 p1465 A72-24104

Evaluation of Collis-Williams and Davies-Fisher heat transfer formulas for flow past fine wires based on Nusselt vs Reynolds number relationship

10 p1562 A72-24294

Infinitesimal centered disturbance effect on plane Poiseuille flow at supercritical Reynolds number, determining modulated wave as function of position and time

10 p1562 A72-24423

Wind tunnel investigation of Reynolds number effects on boundary layer separation incidence and maximum lift coefficient of high-lift device equipped aircraft model

10 p1419 A72-24657

Heat transfer and laminarization prediction by two equation turbulence model for accelerated boundary layer flows at low Reynolds number

11 p1743 A72-25260

Uniform and parallel magnetic field effects on hydromagnetic instability of two dimensional jet at small magnetic Reynolds numbers

11 p1693 A72-25521

Fluidic proportional and digital amplifiers environmental effects on sensitivity of gain, noise and null shift based on dependence on Reynolds number

[ASME PAPER 72-GT-84]

11 p1577 A72-25660

Turbulent flow time averaged description by Navier-Stokes equations, determining Reynolds number dependent stress tensor coefficients

11 p1615 A72-25722

Single continuous algebraic correlation equation for convective heat transfer in cross flow for wide Reynolds number range, considering applications to hot-wire anemometry

11 p1747 A72-26541

Plasma interchange instability and convection in gravitational field, showing viscosity and resistivity stabilization and critical Reynolds number

11 p1697 A72-26584

Turbulent separating and reattaching supersonic boundary layer flows in two dimensional compression corner, noting Reynolds number effect on separated shear layer length

11 p1618 A72-26634

High intensity free stream turbulence effects on flow past circular cylinder at subcritical Reynolds numbers, measuring unsteady lift and drag

11 p1573 A72-26640

Incompressible viscoelastic isotropic fluid stability in Couette flow, discussing physical parameters effect on critical Reynolds number and cells shape of secondary flow

12 p1797 A72-27169

Steady bifurcating time periodic solutions stability for flows in bounded domain with complex conjugate simple eigenvalues at critical Reynolds number

12 p1837 A72-27712

Mean velocity distribution and Reynolds stresses in turbulent wake behind flat plate in uniform incompressible flow

12 p1798 A72-27718

Energy dissipation for turbulent flow in turbine blades guide vanes calculated with allowance for effects of Reynolds number and turbulence intensity

12 p1752 A72-28137

Laminar channel flow stability loss dependence on Reynolds number and wave number, discussing conditions for separated flow self oscillations

13 p1941 A72-28765

Meteor trail forms diversity explanation from magnetic pressure and Reynolds number and plasma diffusion in magnetic fields, discussing geomagnetic effect on trail shape

13 p2039 A72-29220

Incompressible boundary layer velocity profile on swept wings, comparing critical Reynolds number to straight wing value

13 p1894 A72-29639

Von Karman constant in low Reynolds number turbulent flows, observing shear stress gradients effects on viscous sublayer

13 p1944 A72-30027

Slow viscous incompressible conducting fluid MHD flow between two nonparallel walls, obtaining velocity profile solution in power series for small Reynolds numbers

13 p2020 A72-30047

Wind tunnel investigation of wake pressure and vortex shedding characteristics of flow past spheres as function of Reynolds number

13 p1896 A72-30099

Laminar to turbulent boundary layer transition in supersonic flow over flat plate investigated in supersonic wind tunnels, noting unit Reynolds number effect

14 p2069 A72-31004

Flow induction by cylinder performing transverse periodic vibrations in viscous fluid, noting jet flow with large streaming Reynolds number

15 p2217 A72-31617

Three dimensional structure of transverse uniform flow around motionless circular cylinder for Reynolds number 45,000, investigating correlations of velocities on parallels to generatrices

15 p2179 A72-31684

Unsteady viscous flow effects on aerodynamic forces exerted on oscillating elliptic airfoil for various Reynolds numbers, angles of attack and frequencies

15 p2180 A72-32344

Higher moments of Reynolds stress fluctuations and velocity components in turbulent boundary layer, obtaining probability density distributions

15 p2218 A72-32401

Photographic flow visualization of steady recirculating wakes behind sphere and oblate spheroids for low Reynolds numbers

15 p2180 A72-32419

Incompressible elastico-viscous liquid steady state laminar source flow between stationary infinite porous disks, noting Reynolds number effects

15 p2219 A72-32512

Supersonic interaction effects on boundary layer flow structure in intersecting wedge corner at high Reynolds numbers from surface pressure measurements and oil flow visualization

16 p2341 A72-32830

Spanwise correlation measurement of vortex shedding behind circular cylinder in subcritical Reynolds number region

16 p2379 A72-33658

Curved surface laminar flow turbulence front expansion rates measurement at high Reynolds number on experimental setup, considering centrifugal forces

16 p2379 A72-33792

Coriolis forces effect on bubbles trajectories in rotating containers, determining critical Reynolds number

17 p2537 A72-34209

Electromagnetic characteristics of MHD channels with nonconducting walls at finite magnetic Reynolds numbers

17 p2587 A72-34456

Asymptotic character of turbulent boundary layer longitudinal velocity distribution along flat plate at low Reynolds number, using Hirsch theory for potential flow

17 p2539 A72-34908

Hypersonic wake aerodynamics at high Reynolds numbers

[AIAA PAPER 72-701]

17 p2486 A72-35484

Some measurements of the fine structure of large Reynolds number turbulence

18 p2678 A72-36020

Flow of a viscous liquid round a cylinder for Reynolds numbers 60 and 80

18 p2679 A72-36233

Reynolds stress development in wall region of turbulent shear flow of oil investigated by hot film measurement technique and anemometer signal analysis

18 p2680 A72-36478

Recent extensions to Eulerian methods for numerical fluid dynamics

18 p2682 A72-36803

Alternate singular perturbation theory of high Reynolds number flow over flat plate to eliminate asymptotic matching and composite solution for accuracy improvement

18 p2684 A72-37083

A kinematic theory of large magnetic Reynolds number dynamos

19 p2833 A72-37248

Finite amplitude neutrally stable two dimensional disturbances in parallel flows for large Reynolds numbers, investigating phase shift across critical layer

19 p2786 A72-37572

Pressure loss and heat transmission in cylindrical ducts

[ONERA, TP NO. 1057]

19 p2880 A72-37768

Generating high Reynolds-number flows

19 p2787 A72-38222

Pressure pulsation measurements at nose of well-streamlined body of revolution at high Reynolds numbers, noting turbulent pressure field intensity growth and decay

20 p2912 A72-39362

The calculation of low-Reynolds-number phenomena with a two-equation model of turbulence

[ASME PAPER 72-HT-20]

20 p2914 A72-39688

High Reynolds number turbulence and vortices in journal bearings, discussing validity of flow field models based on mixing length and pipe flow theory

20 p2930 A72-39972

Stability loss in Poiseuille flow within two dimensional channel during Reynolds number passage through critical value

21 p3044 A72-40265

Some results from tests in the NAE high Reynolds number two-dimensional test facility on 'shockless' and other airfoils

[ICAS PAPER 72-33]

21 p2991 A72-41158

Lift on airfoils with separated boundary layers

21 p2992 A72-41264

Reynolds number and drive power variation with Mach number, pressure and temperature in cryogenic wind tunnel

[AIAA PAPER 72-995]

21 p3040 A72-41581

Refinements in high-Reynolds-number shock-tunnel technology

[AIAA PAPER 72-996]

21 p3040 A72-41582

High Reynolds number transonic wind tunnel facility /HIRT/ for improved aerodynamic testing of modern combat and commercial aircraft performance, maneuverability and handling qualities

[AIAA PAPER 72-1035]

21 p3043 A72-41609

Transverse mass flow past a sphere at small Reynolds numbers

21 p3047 A72-41664

Laminar to turbulent transition in axisymmetrical submerged jets and slipstream flows of air and He, discussing Reynolds number effect

22 p3166 A72-42270

Incompressible free shear layers instability, considering Reynolds number, velocity profile, disturbances and compressibility effects

22 p3167 A72-42579

Wind tunnel measurement for demonstrating similarity of atmospheric turbulent boundary layer mean velocity and shear stress at high Reynolds number

22 p3201 A72-42598

- A note on the laminar mixing of two uniform parallel semi-infinite streams. 23 p3281 A72-44301
- Unsteady flow field near wall and Reynolds stress measurement in turbulent boundary layer, using conditional sampling technique with digital computer 23 p3282 A72-44304
- The large Reynolds number - Asymptotic theory of turbulent boundary layers. 24 p3392 A72-45248
- RHENIUM**
- High temperature solubility and diffusion coefficient of nitrogen in rhenium 12 p1827 A72-27138
- Low energy electron diffraction structures due to CO and oxygen adsorption on clean Re surfaces produced by Ar ion bombardment at 20 to 920 C 13 p2020 A72-28522
- Re single crystal LEED diffraction pattern, showing surface carbon structure 13 p2021 A72-28800
- Vacuum UV reflectance dependence of Re and W vapor-deposited films on substrate temperature during deposition, film thickness and aging in air 15 p2274 A72-31377
- Re applications technology, discussing production methods, mechanical and physical properties, plasma spraying, annealing and alloying techniques 17 p2567 A72-34825
- RHENIUM ALLOYS**
- Ta-Ra-B ternary alloy, investigating phase equilibria and isothermal cross sections with X ray analysis 03 p0374 A72-13739
- Fine structure of Mo-Re alloys single crystals in solid solution region as function of Re content 03 p0377 A72-14019
- C 14 diffusion coefficients in W and W-Re alloys single crystals at 1500-1800 C, discussing tracer activation energy and frequency factor 05 p0676 A72-16731
- Rhenium carbide synthesis at high pressure and temperature, searching for superconducting properties 06 p0828 A72-17617
- Diffusive mobility of C in Mo single crystals and Mo-Re alloy, using autoradiography and electron microscopy 06 p0829 A72-17733
- Cold brittleness of transition metal alloys with bcc lattices, discussing elastic characteristics, packing defects energy, plastic deformation and rhenium admixture 07 p1018 A72-20143
- Martensite first stage decomposition mechanism and kinetics during tempering of quenched Re steels with varying carbon concentration 08 p1187 A72-21779
- C and Re effects on brittleness threshold temperature and plasticity of Mo-Re alloy 09 p1326 A72-22227
- Diffusive mobility of C in Mo single crystals and Mo-Re alloy, using autoradiography and electron microscopy 11 p1652 A72-25340
- Elastic constants of dilute Mo-Re alloys with bcc structure, determining randomly distributed point defects low concentration effects with T-matrix method 11 p1656 A72-25724
- High temperature creep properties of W-Re alloy under vacuum for thoria dispersion hardening from electron microscope and activation energy studies 11 p1665 A72-26863
- Two phase and three phase composition of ternary alloys Nb-C-Re at 2000 C from X ray, metallographic and chemical analysis 13 p1973 A72-28567
- Electron shell structure in annealed and plastically deformed W-Re alloys from positron annihilation angular distributions 13 p1981 A72-29908
- Tungsten-rhenium alloys and tungsten self diffusion coefficient temperature dependence investigation, noting Re addition effects 14 p2114 A72-30402
- Sintering and melting preparation effects on mechanical properties of refractory W-Re alloys, considering sigma phase in solid alpha solution 14 p2116 A72-30530
- Polycrystalline Mo-Re alloy under cold longitudinal, transverse, cross and pack rolling, noting twin and dislocation microstructures 15 p2256 A72-31669
- Thermionic characteristics of carburized tungsten-rhenium alloys. 18 p2656 A72-36131
- Radiographic examination of rhenium-aluminum-boron and rhenium-silicon-boron ternary systems 19 p2822 A72-38679
- Binary and multicomponent Re alloys with W, Mo, Ni, Co and Cr, noting elastic and strength properties for torsional suspension structures 22 p3191 A72-42805
- RHENIUM COMPOUNDS**
- Mass spectroscopic rate constants for reactions of negative ions of rhenium and tungsten oxides with chlorine and nitrogen dioxide 04 p0484 A72-15639
- Tungsten and rhenium oxides negative ions source, presenting mass analysis table 07 p1037 A72-19323
- Thermal vacuum tests of rhenium disulfide decomposition as function of temperature at 800-1200 C, using thermogravimetric method 13 p2023 A72-29649
- RHEOELECTRICAL SIMULATION**
- Rarefied gases thermal energy diffusion model, using radiative transfer electrical network analog [ASME PAPER 71-WA/HT-4] 05 p0743 A72-15865
- Pump and unloading valve hydraulic system model with waves processes allowance in connecting pipe, discussing liquid mass and leakage effects on stability 11 p1578 A72-25770
- The steepening of the wavefront due to nonlinearities /An electric model test regarding the origin of shock waves/ 17 p2582 A72-35428
- A general method for the analysis of compact multifluid heat exchangers. [ASME PAPER 72-HT-14] 20 p2986 A72-39684
- Solution of the general linear programming problem by electronic simulation using the regularization method 21 p3023 A72-40155
- A model of low-frequency sound propagation in a lined duct. 21 p3085 A72-41112
- RHEOENCEPHALOGRAPHY**
- Objective evaluation of main rheoencephalogram parameter for disturbed brain blood circulation 12 p1773 A72-28218
- RHEOGRAPHY**
- U RECORDING INSTRUMENTS**
- U RHEOMETERS**
- RHEOLOGY**
- Rheological properties and architecture of arterial walls, using stress relaxation and stress-strain hysteresis tests on dog aorta, iliac and femoral strips 01 p0010 A72-10184
- Rheological properties of Maxwell fluid-St Venant solid model for solids, noting slip lines direction during plastic flow 02 p0259 A72-12238
- Thermodynamic theory of rheological materials with internal changes accounting for higher gradients of deformation and temperature 03 p0448 A72-13888
- Self similar solutions for unsteady shear flows of conducting Newtonian fluids with rheological power law under transverse magnetic field 03 p0397 A72-13997
- Full lubrication characteristics, discussing pressure pump, viscosity, MHD, volume elasticity, centrifugal and rheodynamic techniques 03 p0365 A72-14299
- Unsteady approach to nonisothermal flow theory for Couette flow, making general assumptions concerning rheological law and temperature dependence of fluidity 04 p0512 A72-14985
- Rheomobility effects in creep instability of rods with initial deflection, determining critical load by Ritz method 04 p0594 A72-15708
- Rheological model of reticular polymers and glass fiber reinforced plastics based on stress-strain relationship during damped creep elastic deformation 08 p1191 A72-21499
- Mathematical thermodynamic theory for plastic deformation induced internal structure changes in rheological material, describing homogeneous response by temperature and deformation gradients 09 p1403 A72-22761
- Photoelastic analysis of piezooptical and rheological properties of anisotropic composite glass plastics 10 p1557 A72-24626
- Constitutive equations for bimodulus elastic materials, postulating rheological model based on anisotropy stress-strain laws 11 p1736 A72-25984
- Rheological stress-strain relations in nonlinear viscoelasticity theory, calculating relaxation parameters for isotropic viscoelastic circular cylinder 13 p2059 A72-29493
- Instrument to determine steady and unsteady stress state of elastic fluids in isometric flow, noting rheological measurements in solved polymers 14 p2094 A72-30421
- Maxwell rheological creep model verification by tensile tests on Mg alloy at 150 C under step loadings, treating thermodynamics of ideal creep 16 p2412 A72-34111
- Rheological model for creep under intermittent square wave stress pulses, taking into account time dependent dislocation density 16 p2412 A72-34113
- Elastic-plastic-viscous model for creep analysis of rheo-mobile materials, taking into account cracks and other defects 16 p2412 A72-34116
- Hydrodynamic stability of the gradient flow of a conducting fluid with a rheological power law in a transverse magnetic field 18 p2716 A72-36814
- Rheological characteristics of orthotropically reinforced polymer materials 19 p2822 A72-37531
- Rheological properties of molybdenum and platinum of bamboo structure under bending loads 21 p0371 A72-41712
- Stress analysis in two dimensional bending process using the photo-rheological stress analysis. 22 p3183 A72-42483
- Glassy materials rheological behavior description in terms of stress function, discussing molecular processes transformation range thermodynamics 22 p3196 A72-42791
- Isotropic materials nonlinear rheonomic behavior at small strains, deriving model structure deformation laws 23 p3345 A72-43623
- RHEOMETERS**
- Rheographic investigation of cerebral, pulmonary and peripheral circulation during bed rest in antiorthostatic position 23 p3255 A72-43914
- RHODIUM**
- Pyrochlore and perovskite preparation and structure in bismuth rhodium oxide system, discussing variable position parameter, occupancy factor and structure stability 13 p2022 A72-29375
- RHODIUM ALLOYS**
- Phase diagrams, solubility and alloying of Pt, Pd, Ru, Ir and Rh with noble, alkali earth, rare earth and transition metals 22 p3191 A72-42810
- RHOMBOHEDRONS**
- Alpha to beta transformation of rhombohedral B, investigating lattice structure on heating stage in electron microscope 16 p2405 A72-33204
- RHYTHM [BIOLOGY]**
- NT CIRCADIAN RHYTHMS**
- Book on hibernation and hypothalamus covering central nervous system regulating mechanisms, biologic rhythmicity, migration, thermoregulation, torpor, human implications, etc 01 p0010 A72-10169
- Hybrid computer study of phenomenological biorhythms, discussing regular information isolation from biological noise 02 p0169 A72-12662
- Hippocampus electric activity and cardiac rhythms variations responses to various intensity electric stimulation of central gray matter 02 p0165 A72-12881
- Regular sinus rhythm bundle branch block effect on ballistocardiogram dynamics 03 p0314 A72-13143
- EEG phase asymmetry fluctuations relation to respiration rhythm in subjects from pneumograms during rest, mental activity, hypnosis and sleep 05 p0620 A72-17214
- Uniform visual field influence on electroencephalographic alpha rhythm in man, discussing ocular fixation, visual attention and vigilance change effects 07 p0916 A72-19040
- Occipital electroencephalographic response to slowly repeated aperiodic light flashes, discussing alpha wave and rhythmic afteractivity amplitude changes 07 p0916 A72-19041
- Phase relations between alpha waves in EEG and automated rhythmic motoric activity as function of subject behavioral activity and thalamic pacemaker zones 07 p0916 A72-19109
- Biochronometry - NAS-NASA Conference, Friday Harbor, Washington, September 1969 07 p0918 A72-19526
- Yeast glycolytic pathway oscillations relation to concentration of diphosphopyridine nucleotide and other metabolites, noting analogy to behavioral and physiological rhythms 07 p0920 A72-19541
- Orienting response indication by EEG alpha rhythm desynchronization in relation to visual stimulation intensity 11 p1585 A72-26238
- Human visual accommodation biorhythm and reactions under hard physical work and visual stress 13 p1909 A72-28749
- Seasonal rhythms of endocrine system in hibernating mammals, discussing central and peripheral biological clocks in relation to hypothalamus and pancreas/thyroid gland 16 p2353 A72-33100
- Stochastic model for unsteady rhythmic processes based on periodical correlation of random processes 17 p2534 A72-35777

- Participation of supraspinal structures in the formation and control of a system of arbitrary cyclic motions of man 21 p2999 A72-40594
- RIBBON PARACHUTES**
Supersonic ribbon parachute testing by transonic wind tunnel, rocket sled and water channel simulator 01 p0004 A72-10305
Ribbon parachutes drop tests at Mach 0.57-1.70, measuring opening shock loads and functioning time sequence 01 p0004 A72-10312
- RIBBONS**
High performance graphite ribbon - An advanced reinforcement material. 17 p2572 A72-35659
- RIBONUCLEIC ACIDS**
Biological effects of unfocused laser radiation on DNA and RNA synthesis and cell activities in thymine dependent *E. coli* strain 04 p0477 A72-14610
Esters and amides participation in prebiotic polymers, discussing ribosome bonds and messenger RNA 04 p0468 A72-14767
Ribosomes origin and rRNA evolution, considering biogenesis from coacervate to protocell and protein biosynthesis 04 p0470 A72-14793
RNA content changes in ground squirrel brain during active and hibernation states 06 p0764 A72-18058
DNA-RNA molecular hybridization testing of chronon theory of circadian timekeeping in protozoa cells 07 p0920 A72-19542
Ribonuclease molecule damage and enzyme activity under UV irradiation and repeated freezing and thawing 09 p1274 A72-23594
EEG investigation of circadian variations in qualitative and quantitative RNA content in human leukocytes, noting changes during sleep 18 p2651 A72-36624
RNA content in the cortex neurons in connection with the change in its function during the emergence of an animal from hypothermia 20 p2890 A72-38928
Nucleic acid hybridization with RNA immobilized on filter paper. 24 p3379 A72-45773
- RIBS (SUPPORTS)**
Two dimensional stationary temperature fields determination in ribs, cylinders and pipes with temperature independent heat conductivity 05 p0746 A72-16188
Rib reinforced cylindrical shells deformation under local load, examining stress-strain distribution 06 p0899 A72-18641
Liquid sloshing in circular cylindrical cavity with ribs mounted radially to walls, calculating oscillation frequencies and virtual masses 08 p1148 A72-20968
Computerized optimal design by nonlinear programming for minimum weight elastic plates crossed with rigid ribs for vibrational loading to meet natural frequencies condition 14 p2165 A72-30576
Selection of optimal parameters of waffle structures from the condition of minimum weight 20 p2980 A72-39905
Ribbed cylindrical shells modeling method for stress-strain state and stability 23 p3347 A72-43745
Longitudinal rib reinforced cylindrical shell under axial compression loads, determining equilibrium stability with approximation of transcendental equations 23 p3347 A72-43748
- RICCATI EQUATION**
Optimal control problem formulation as nonlinear two point boundary value problems, comparing linear systems and Riccati equations for solution 05 p0726 A72-16455
Standard linear estimation and control problem with quadratic loss, optimizing information rate by minimizing total measurements number through Riccati equation singular solution 08 p1144 A72-20859
Control optimization avoiding stability problem by integrating matrix Riccati equation 13 p1937 A72-30074
Optimal filter synthesis for linear time varying parameter control systems, using computer-aided solution of multidimensional Riccati equations 14 p2090 A72-31120
Matrix Riccati equation solution method in optimal control theory, noting boundary conditions implementation 15 p2265 A72-32803
Book - Riccati differential equations 17 p2577 A72-35798
Riccati equation asymptotic theory, deriving a priori bound dependence on information and control energy rates and state dimensions 20 p2945 A72-39347

- Iterative method of computing the limiting solution of the matrix Riccati differential equation. 23 p3275 A72-43610
Comparison of linear and Riccati equations used to solve optimal control problems. 24 p3420 A72-45776
- RICHARDSON NUMBER**
Stratospheric CAT relationships to baroclinic zones and Richardson number examined from aircraft observed cross sections data 01 p0096 A72-11282
Atmospheric static stability effect on turbulence layer thickness under nonuniform temperature, using correction factor dependent on Richardson number 03 p0386 A72-14334
Turbulence effects in stratified shearing flow, determining relationship between measured mass flux and overall Richardson number 06 p0798 A72-17762
Atmospheric models for critical flux Richardson number prediction for turbulence maintenance in stratified flows 12 p1840 A72-27702
Baroclinic long wave dynamic instability in Kochin two layer frontal model, extending Richardson number range in absence of beta effect 12 p1841 A72-27987
Prandtl number effect on stratified free shear layer stability, comparing critical Richardson number to linear inviscid theory result 13 p1942 A72-29111
Radiation, evaporation and the maintenance of turbulence under stable conditions in the lower atmosphere. 22 p3201 A72-42597
- RICHARDSON-DUSHMAN EQUATION**
U TEMPERATURE EFFECTS
U THERMIONIC EMISSION
- RIDGES**
Ridge dimensions determination and causes of self oscillation in solid surface layers deformation under sliding friction 12 p1817 A72-28182
- RIEMANN INTEGRAL**
U MEASURE AND INTEGRATION
- RIEMANN MANIFOLD**
Modified Riemann geometry for scalar-tensor theory of gravitation, emphasizing scalar field role relation to vector length change during point-to-point transport 07 p1036 A72-20196
Riemann invariants method for plasticity theory application to first order quasi-linear systems, considering plastic flow in arbitrary die 09 p1403 A72-22760
Mixed boundary elasticity solutions for plane with cuts on real axis, using hyperelliptic Riemann surface 10 p1553 A72-23768
Asymmetric Einstein equations with impulse-energy tensor in canonical form derived from variational principle, defining space-time continuum as pseudo-Riemann manifold 10 p1510 A72-24120
Stress distribution in general relativity on oriented compact Riemann manifold 10 p1511 A72-24206
German book on gravitation theory and equivalence principle, covering Lorentz invariance in Riemann space, relativity and Einstein effects 10 p1512 A72-24752
Differential geometry extremal problem of holomorphic embedding of complex curves in Kähler manifold with constant holomorphic curvature, using Riemann surface moduli theory 10 p1506 A72-24862
Variables separability conditions within Riemann space for Schroedinger and Laplace equations 15 p2264 A72-32278
Riemann invariants method for nonelliptic first order systems with two independent variables, presenting application to perfectly plastic material flow in die without friction 16 p2467 A72-33140
Equations of motion in the linear approximation. 19 p2835 A72-38174
- RIEMANN PROBLEM**
U CAUCHY PROBLEM
- RIEMANN SPACE**
U RIEMANN MANIFOLD
- RIEMANN WAVES**
Simple wave interaction solutions for nonlinear plane k-waves of nonelliptic quasi-linear differential equations using Riemann invariants 03 p0389 A72-13885
- RIFT VALLEYS**
U VALLEYS
- RIFTS**
U GEOLOGICAL FAULTS
- RIGGING**
Parachute canopy fabrics and rigging lines cordage properties requirements, considering nylon, polypropylene, silk, cotton and nonwoven scrim-reinforced fabrics 01 p0005 A72-10314

- High speed rotating test rig development for vibration testing of turbine blades, describing design layout 08 p1147 A72-22131
- RIGID BODIES**
U RIGID STRUCTURES
- RIGID MOUNTING**
Eccentric circular ring elastic contact with rigid symmetric dies under equal diametrically opposite loads 05 p0738 A72-16329
Elastic deformation and rigidity of rectangular, circular and elliptic gimbals for gyroscope suspension 13 p1957 A72-29272
Astronomical telescope hybrid pointing control system with double gimbal control moment gyros and orthogonally mounted reaction wheels to achieve extreme accuracy and stability [AIAA PAPER 72-854] 20 p2924 A72-39138
- RIGID ROTOR HELICOPTERS**
Bolkow 105C 5-place helicopter with twin turbine engine driven rigid glass-reinforced plastic rotor blades, emphasizing design philosophy of easy maintainability 13 p1898 A72-29871
German Bo 105 five-six seat light utility helicopter with rigid glass-fiber reinforced plastic rotor blades, presenting design and performance 14 p2072 A72-30678
The fatigue and fail-safe program for the certification of the Lockheed Model 286 rigid rotor helicopter. 24 p3366 A72-44733
Helicopter development, discussing articulated, rigid, tilt and stowed rotors, compound helicopters, rotor drives, flight control and avionics systems 24 p3369 A72-45558
- RIGID ROTORS**
Hingeless rotor helicopter blade steady state response with nonuniform inflow and elastic blade bending [AIAA PAPER 72-65] 05 p0741 A72-16933
Dynamic stability of spinning bodies with elastic rods and rigid symmetric rotors parallel to axis 10 p1552 A72-24645
Hingeless blades flap-lag oscillations linear stability characteristics in hovering flight, examining precone, elastic and pitch-lag coupling and induced inflow aerodynamic effects 14 p2072 A72-30289
Hingeless elastic helicopter blades coupled flap-lag motion under quasi-steady aerodynamic loads, reducing equations of motion to coupled nonlinear differential equations 15 p2180 A72-31211
Exploration of aeroelastic stability boundaries with a soft-in-plane hingeless-rotor model. [AHS PREPRINT 610] 17 p2489 A72-34493
On the stability of rotor-and-bearing systems and on the calculation of sliding bearings. 18 p2696 A72-36708
- RIGID STRUCTURES**
NT RIGID ROTORS
Nonporous rigid parachute models three component measurements, using low speed wind tunnel for testing skirt length effects on aerodynamic characteristics 01 p0003 A72-10303
Controllable states insufficiency to characterize rigid heat conductors dependence on temperature fields in experimental materials measurements programs 01 p0146 A72-11389
Stress and velocity distributions in homogeneous viscoelastic rigid body, deriving uniqueness theorems and minimum principles for limits problem 02 p0297 A72-12596
Rigid/plastic media plane and axially symmetric deformations determination, using principal and slip line numerical analysis methods 03 p0446 A72-13704
Stress concentration around reinforced curvilinear hole in elastic infinite plate, discussing ring reinforcement rigidity effects 03 p0447 A72-13730
Rotating rigid rod and disk relativistic rings, discussing inertial frames significance 04 p0574 A72-14917
Invariant manifolds in rigid body motion about fixed point, considering Euler-Poincaré, Lagrange-Poisson and Kovalevskaya cases 04 p0549 A72-15197
Rigid body general motion dynamic effects due to acceleration of arbitrary order, using Samov-Mangeron recursive formulas 04 p0551 A72-15746
Rigid shaft rotating in hinged and elastic supports with nonlinear characteristics of restoring force, determining free and forced vibration characteristics 06 p0900 A72-18696
Motion of two symmetrical rigid bodies connected by frictionless spherical hinge positioned at dynamic symmetry axes intersection 08 p1206 A72-21168
Critique of paper on lower bounds on deformations of dynamically loaded rigid plastic continua 08 p1245 A72-21630

Strain hardening law for rigid incompressible material with plastic properties independent of mean normal stress 08 p1248 A72-21820

Dynamics of rigid rotor supported on squeeze oil film bearings 08 p1225 A72-22134

Thermal insulations in form of thin shells of revolution with rigid external and elastic internal layers resting on rigid core 09 p1400 A72-22713

Discrete elasticity concept based on analysis of material points, lines, surfaces or rigid bodies interconnected by hyperelastic continuous bodies 09 p1403 A72-22759

Rigidly connected rectangular plates stress-strain calculation with finite difference method 11 p1733 A72-25538

Numerical solution of two massive rigid bodies impact with variable slipping direction using Routh momentum change theorem 11 p1735 A72-25769

Spin stabilized satellites attitude dynamics during rigid booms extension, deriving equations of motion approximate solution 11 p1726 A72-25915

Slow drop of heavy rigid spheres through vertical tube filled with viscous liquid, noting minimization of errors due to temperature and trajectory path 11 p1617 A72-26501

Bending problem for circular three layer plate with rigid circular insert, studying deflection under bending moment 12 p1879 A72-27090

Dynamic deflection of elastic rectangular plate hinged to rigid base moving under sinusoidal pressure impulse action, noting base inertia effect 12 p1879 A72-27091

Finite element equations for hybrid coordinate dynamic analysis of interconnected rigid bodies with elastic flexible appendages for use in spacecraft simulation 12 p1876 A72-27257

Rigid body model for nonholonomic kinematic linkages of tangentially sliding nonrolling bearings, noting virtual displacements and mechanical work 12 p1845 A72-27539

Structural design, performance and costs of rigid or semirigid solar panels for geostationary satellites power supplies 12 p1758 A72-28034

Axiomatic development of mechanics from geometrically formulated kinematics to statics of rigid bodies and systems, using virtual rate of work and reaction principles 13 p2000 A72-28477

Rigidity of developable surfaces with cylindrical connections and without plane domains, subjected to infinitesimally small bendings 13 p2061 A72-29793

Static deformation of laminar orthotropic shells of revolution with variable rigidity, using integral correlation method 13 p2061 A72-29795

Rigid smooth body pressing into elastic plate surface subjected to cylindrical bending, discussing contact problem and transverse shear strain 13 p2062 A72-29950

Natural convection initiation in fluid confined above and below by rigid conducting surfaces and laterally by rigid insulating vertical walls 14 p2172 A72-31054

Optimal geometrical and physical properties of sandwich plates with rigid cores under compressive load, discussing critical stress and structural stability 15 p2322 A72-31359

Impulse excited spatial systems of rigid bodies linked by pivot joints with arbitrary kinematics, applying Maxwell-Betti theorem 15 p2323 A72-31461

Relaxation oscillations in dynamic systems describing turbulence in fluid, rigid body and particle motions 15 p2263 A72-31755

Contact problems for elastic semiplane reinforced with symmetric and asymmetric loaded elastic stiffeners 15 p2329 A72-32281

Lagrange equations of second kind for rigid systems, using balances of linear and angular momenta for mass point or rigid body 16 p2466 A72-33021

Improved bounds for buckling loads of tapered inelastic columns. 17 p2626 A72-34330

Contact pressure between an elastic spherical shell and a rigid plate. 17 p2628 A72-34788 [ASME PAPER 72-APM-31]

Conventional aircraft flight mechanics, reviewing vector analytical treatment of rigid body statics 17 p2493 A72-35794

Multipole expansion of sound radiation from moving rigid bodies. 18 p2710 A72-36404

Separation and analysis of the acoustic field scattered by a rigid sphere. 18 p2710 A72-36408

Solution of the impact problem of an elastic body and a rigid obstacle by the source-sink method 18 p2736 A72-36811

A non-linear integral-type theory of inelasticity for transversely isotropic materials. 18 p2738 A72-37075

Stability analysis of internal pressure loaded crack in adhesive layer bonding elastic plate to rigid base using energy and critical load intensity criteria 19 p2870 A72-37245

Interaction between attitude libration and orbital motion of a rigid body in a near Keplerian orbit of low eccentricity. 20 p2968 A72-39197

Flight-mechanical analysis of various flight conditions of conventional aircraft. V - Mechanical foundations /Dynamics of the rigid body/ 21 p2994 A72-40175

Stability of a twisted orthotropic cylindrical shell with a jump-wise variable wall rigidity 21 p3118 A72-40815

Rigid form airship for transportation, discussing applications for special loads and scientific and service purposes, and design and construction problems 21 p2996 A72-41200

A quadratic programming approach to the impulsive loading analysis of rigid plastic structures. 21 p3120 A72-41205

Force-time investigations for the elastic impact between a rigid sphere and a thin layer. 21 p3121 A72-41212

Stationary motions of a triaxial body and their stabilities. 21 p3109 A72-41334

Certain class of solutions of the three-dimensional problem for a rigid perfectly plastic material with a family of momentarily inextensible planes 21 p3123 A72-41392

Integral equation for pressure distribution by rigid punch contact with elastic half space, solving by Mathieu function expansion in Fourier series 21 p3126 A72-41541

Rigid aircraft longitudinal dynamic response to random atmospheric turbulence, defining spectral gust alleviation factors in terms of mass scale and damping ratio parameters 21 p2996 A72-41641

Orbital and rotational motion stability of rigid body containing elastic rods and fluid-filled cavity 22 p3204 A72-42092

Investigation of the stability and vibrations of beams of variable rigidity by the method of bilateral estimates 22 p3234 A72-42147

Extremum principles for a class of dynamic rigid-plastic problems. 22 p3235 A72-42522

Rigid-body motions and strain-displacement equations of curved shell finite elements. 22 p3240 A72-42892

Flight mechanics analysis of various flight conditions for conventional aircraft. V - Mechanical foundations /dynamics of rigid bodies/ 23 p3251 A72-43641

On the approximation of the thermal conductivity of rigid heat conductors as a Cauchy problem. 23 p3356 A72-43721

Spline transformation of independent variable for free transverse vibration of elastic bars with piecewise constant rigidity, calculating resonant frequencies 23 p3348 A72-43793

About the first integrals of the generalized problem of translatory-rotary motion of rigid bodies. 24 p3442 A72-45235

Analogy between body force and inelastic strain gradient in all crystal systems. 24 p3459 A72-45247

RIGIDITY

Rotating cable of high slenderness ratio and small flexural rigidity with end masses, deriving transverse vibration mode shapes and natural frequencies from asymptotic solution 02 p0293 A72-12253

Optimal temperature fields in locally heated orthotropic cylindrical shells, determining rigidities effect 04 p0593 A72-15655

Random filament misalignment effects on rigidity and tensile strength of unidirectional graphite composites under shear loading 08 p1192 A72-21681

Transverse shear effect during bending of cantilever plates with low shear rigidity 08 p1248 A72-21864

Angular rigidity of support shaft elastic suspension of dynamically adjustable gyroscope 09 p1307 A72-22348

Variable rigidity circular isotropic plate vibration and bending, determining flexure surface and natural frequencies in terms of Fourier-Bessel series 09 p1399 A72-22699

Bending deflection calculation for laminated beams with layers of different rigidity 11 p1733 A72-25546

Rigidity calculation of double raw radial thrust annular ball bearing loaded by axial and radial force and torque 11 p1646 A72-26978

Russian monograph on three dimensional deformable bodies stability covering linearized equations for subcritical deformations and strength analysis of low shear rigidity structures 12 p1888 A72-28337

Tangential stresses, rigidity characteristics and stress functions of prismatic grooved circular shafts, showing summary representations and integral transformations methods interrelationship 13 p2057 A72-29062

Torsion problem of solid rod with wing profile shaped cross section solved by conformal mapping and gamma function derivative, calculating maximum stresses and rigidities 15 p2327 A72-31741

Variable rigidity effects of ball bearings on axial loading stability and failure of gyromotor supports 15 p2235 A72-31898

Thin elastic isotropic plates and shells thickness variation for rigidity functional stationary value, reducing problem to stress-strain state equations simultaneous solution 15 p2333 A72-32688

Elastic bending of rectangular continuous orthotropic plate with variable rigidities and elastic foundation coefficients for discontinuous boundary conditions along one edge 16 p2467 A72-33118

Rigidity dependence of cosmic ray modulation function at 2-13 Gv from C-130 aircraft survey flights data 17 p2602 A72-35606

Finite element models with rigid displacement for nonrigid structure analysis, noting curved beam and shells 18 p2739 A72-37173

Connexions between the moduli for anisotropic elastic materials. 21 p3119 A72-41107

Fiber reinforced metallic matrix composite under creep, discussing rigidity, stress distribution, rupture strength and failure time 23 p3306 A72-43727

RILLS U VALLEYS

RING CURRENTS

Geomagnetic storm field recovery near synchronous satellite ATS 1 in terms of ring current belt and plasma sheet variations 01 p0053 A72-10088

Decreasing period micropulsations during elementary magnetospheric substorms, discussing relation to ring current asymmetry development 01 p0059 A72-10602

DR-current belt dynamics during magnetic storm based on ground observation data on midlatitude red arcs 02 p0217 A72-11929

Incomplete ring current decay during magnetic storm development, discussing field asymmetry based on global network synchronous observations and generation mechanism by protons 02 p0218 A72-11949

Magnetosphere and adjacent regions magnetic surveys by OGO 1 and 3 satellites, discussing magnetopause, bow shock, magnetosheath, geomagnetic tail, ring current and polar substorms 02 p0220 A72-12084

Proton measurements in ring current by OGO-3 satellite compared with geomagnetic field data at low and high latitudes 05 p0711 A72-17034

Geomagnetic storm associated quasi-sinusoidal magnetic field micropulsations due to Alfvén/drift instability or enhanced storm-time ring current 06 p0804 A72-17454

Closed magnetic fields of helical ring currents on concentric spheres surrounded by semiconductor /Tornado trap/ 06 p0863 A72-18405

Low latitude surface horizontal magnetic field intensity depression due to quiet time ring current in magnetosphere as function of solar wind velocity 07 p1055 A72-18884

Ring current growth effects on midlatitude F region electron density change during large magnetic disturbances 08 p1152 A72-20706

Magnetized large volume plasma heating by hf ring field at ion cyclotron frequency 08 p1215 A72-21727

Equatorial ring current relation to polar electrojet during magnetosphere geomagnetic storm, discussing magnetosphere-ionosphere current systems 09 p1298 A72-22580

Midlatitude stable auroral red arcs observation from OV1-10, showing generation at plasmopause due to turbulent dissipation of ring current energy 11 p1624 A72-26401

DR-current belt dynamics during magnetic storm based on ground observation data on midlatitude red arcs

13 p1948 A72-29241

Incomplete ring current decay during magnetic storm development, discussing field asymmetry based on global network synchronous observations and generation mechanism by protons

13 p1949 A72-29261

Magnetospheric ring current relation to polar magnetic substorm from charged particle measurements by satellites and magnetic field measurements at ground

13 p1952 A72-29658

Ring current and polar electrojet effects on proton auroras oval during magnetic disturbances from H alpha line observation

13 p1952 A72-29659

DR ring current belt formation due to electron and proton gradient drift in inhomogeneous geomagnetic field, calculating charged particles trajectories

14 p2101 A72-30646

Whistler propagation in magnetosphere disturbed by ring current, explaining electron density decrease

15 p2194 A72-31433

Faraday ring currents induction by radial magnetic field in low pressure plasma supersonic ring channel flow driven by inductive hydrodynamic shock tube

16 p2437 A72-33749

Closed magnetic fields of helical ring currents on concentric spheres surrounded by conductor/Tornado trap/

17 p2588 A72-34855

Ring current effect on magnetospheric electron density profiles derived from plasmopause whistlers

17 p2600 A72-35368

A new source for the large-scale electric fields in the magnetosphere

18 p2686 A72-36623

Ionospheric magnetic disturbances during March 1970 related to solar flare corpuscular and proton fluxes, generating ring current and PCA absorption

18 p2688 A72-36857

Ring current growth effects on midlatitude F region electron density change during large magnetic disturbances

19 p2790 A72-38334

Radiation belt protons and ion-cyclotron wave interactions accounting for magnetospheric ring current instabilities during storm at plasmopause

20 p2919 A72-39545

A numerical solution for the near and far fields of an annular ring of magnetic current

21 p3015 A72-40354

Positive geomagnetic bays in evening high-latitudes and their possible connection with partial ring current

21 p3049 A72-41387

Induction effect of slowly decaying ring current, estimating electric field strength by model consisting of earth dipole and symmetric ring

22 p3172 A72-42430

Different conductivities effect in ionospheric E layer of polar cap regions, noting electric current along high latitude magnetic field force lines

23 p3283 A72-43370

Ionospheric current relation to magnetospheric field-aligned and ring currents, noting effect of magnetospheric tail electric field on polar magnetic substorms

24 p3396 A72-44852

RING DISCHARGE

Mathematical model of gravitational wave zone for ring emanated smooth axisymmetric toroidal pulse

08 p1158 A72-21177

RING LASERS

Mode locked oscillation in ring cavity Nd glass laser, showing satellite pulse and spectral broadening due to self phase modulation

02 p0238 A72-12203

Saturation effect on power gain-bandwidth product of carbon dioxide regenerative ring laser amplifiers operating below threshold

03 p0366 A72-12964

Ruby ring laser single mode operation with Fabry-Perot etalons for selective feedback, discussing laser emission spectrograms

03 p0366 A72-13194

Natural fluctuations effect on beat frequency dependence of opposed waves in ring laser on rotation velocity

05 p0668 A72-16405

Algebraic prediction formalism for ring laser mode coupling by phase modulation

05 p0668 A72-16566

Single isotope He-Ne laser gyro comparison with multiisotope system, noting strong mode competition in ring laser

[CLEA PAPER 18,9]

07 p1005 A72-19402

Nonlinear mode relationship of gas ring laser due to light scattering in inhomogeneities in active medium

07 p1009 A72-20612

Multimode ring laser gyro phase modulation theory based on oppositely directed traveling waves

09 p1324 A72-23084

Multimode ring laser gyro with intracavity phase modulation, discussing experimental results concerned with lock-in at low rotation rates

09 p1324 A72-23085

Frequency splitting by diffraction at resonator mirrors of gas ring laser, deriving opposed waves lasing equations

10 p1490 A72-24045

Traveling wave mode ring laser operation, obtaining active medium polarization changes through longitudinal magnetic field excitation by capacitor discharge through spiral pump lamps

10 p1492 A72-24363

Solenoid-produced local axial magnetic field influence on beat signal frequency characteristics in ring laser with nearly linearly polarized emission

11 p1650 A72-26357

Emission characteristics of single mode ring ruby laser under free oscillation conditions, discussing mode selection difficulties

12 p1821 A72-27598

Light pulse propagation in ring laser model employing homogeneously broadened gain line and discrete loss

12 p1823 A72-27754

Parametric resonance suppression in annular laser by steady noise perturbation, discussing beat signal spectrum

13 p1968 A72-29505

Standing wave and colliding wave lasing and synchronization region in ring laser using active gas isotope mixture

13 p1968 A72-29511

Light polarization modes in gas ring laser with optically active isotopic cell, showing dependence on circular field coupling coefficient

13 p1968 A72-29512

Opposing wave generation in gas ring laser with allowance for diffraction by finite apertures of cavity mirrors

13 p1970 A72-29678

Flashlamp pumped tunable narrowband traveling wave dye ring laser, stabilizing emission frequency by intracavity Fabry-Perot etalon

14 p2110 A72-30675

Small parameter method for analysis of encounter waves nonlinear self oscillations in ring gas laser, noting periodic energy transfer

14 p2111 A72-31104

Magnetic field effect on polarization plane rotation and emission frequency shift of He-Ne ring laser at 3.39 micron wavelength

16 p2402 A72-33485

Solenoid-produced local axial magnetic field influence on beat signal frequency characteristics in ring laser with nearly linearly polarized emission

16 p2403 A72-33710

Traveling wave mode ring laser operation, obtaining active medium polarization changes through longitudinal magnetic field excitation by capacitor discharge through spiral pump lamps

17 p2563 A72-34962

Hybrid injection locking of higher power CO₂ lasers

17 p2564 A72-35343

Frequency dependent loss in self-pulsing ring laser

18 p2697 A72-36337

Using ring lasers as rate sensors

19 p2812 A72-38223

Nature of losses introduced into a ring resonator by a nonreciprocal phase-shifting device that employs the Faraday effect

19 p2814 A72-38788

Polarization effect of attenuation of opposed-wave competition in ring lasers

20 p2932 A72-39412

Rectangular aperture diaphragm dimension determination for ring laser resonator principal transverse mode selection and higher modes suppression

20 p2933 A72-39510

Measurements of a mode-competition discriminant in a single-frequency argon ion ring laser

21 p3062 A72-40240

The phase difference between coupled laser oscillations

22 p3184 A72-42109

Unidirectional single frequency traveling wave CW pumped Nd-YAG ring laser, noting spatial hole burning elimination

22 p3185 A72-42614

Effects of radiation trapping on mode competition and dispersion in the ring laser

23 p3296 A72-43878

Influence of the imperfection of resonator elements on the characteristics of a triangular ring laser with a 90-degree Faraday rotator

24 p3408 A72-44622

External noise effect on capture conditions in ring laser, noting capture bandwidth narrowing with noise spectral density increase

24 p3410 A72-45423

Analysis of the polarization properties of TW laser emission

24 p3411 A72-45505

Resonator polarization parameters effect on backwave attenuation in three and four mirror TW ring laser, noting colliding waves intensity dependence on polarization angle

24 p3411 A72-45505

RING STRUCTURES

NT REINFORCEMENT RINGS

NT RING WINGS

Curved beam finite elements comparison for structural vibration problems, obtaining ring natural frequencies

01 p0136 A72-10222

Flexural vibrations of arbitrary ring with axial symmetric cross section, noting validity for natural frequencies prediction

01 p0138 A72-10395

Natural vibrations and resonant stresses of turbomachine blade rings and elastic bodies with cyclic symmetry, noting paradoxical frequency decrease

01 p0143 A72-11369

Natural bending-torsional vibrations of turbine blades connected by ring junctions, using dynamic pliability principle

01 p0143 A72-11370

Surface subsidence in semiinfinite resilient elastic solid mass supporting annular load distributed over circular ring

02 p0297 A72-12616

Anisotropic plate with hole stiffened at edge by thin isotropic ring, calculating thermal stress distribution

03 p0450 A72-14113

Pressurized vessel bottoms weakened by central hole with edge stiffened by elastic ring, determining stress-strain state and stress concentration

03 p0451 A72-14120

Rotating rigid rod and disk relativistic rings, discussing inertial frames significance

04 p0574 A72-14917

Buckling of radially constrained imperfect circular ring loaded within perfect rigid circular boundary, obtaining numerical solution by discrete treatment

04 p0591 A72-15286

Circular disks, rings and perforated plates steady state field components, evolving forced and free vibration natural frequency equations

04 p0592 A72-15505

Ring finite elements use in analysis of shells of revolution under axisymmetric loads

[ASME PAPER 71-WA/HT-22]

05 p0732 A72-15880

Flow calculations for subsonic and transonic portions of ring nozzles and plane curvilinear channels

05 p0601 A72-16226

Eccentric circular ring elastic contact with rigid symmetric dies under equal diametrically opposite loads

05 p0738 A72-16329

Coaxial and stripline wideband microwave hybrid ring junctions equivalent to magic Tees with improved electrical properties

05 p0636 A72-16344

Elastic constants measurement using vibrating wire strain gages on diametrically loaded circular disk and ring specimens

06 p0818 A72-18325

Ring-plane type slow wave structure hot tested near 3 cm for scale modeling in mm range

07 p0938 A72-18854

Elastic rods and rings stability under compression beyond elasticity limit, determining equilibrium branching characteristics near bifurcation point

07 p1095 A72-20314

Symmetrically loaded uniform thin circular ring natural vibration frequencies in radial and axial flexural modes, comparing experimental data with values predicted by group theory

07 p1096 A72-20499

Friction and bending effect on unidirectional glass fiber reinforced plastic ring deformation distribution

08 p1191 A72-21504

Torsion test determination of interlayer and intralayer-plane shear moduli in annular specimens of glass fiber reinforced plastics

08 p1194 A72-21756

Deformability and carrying capacity of glass fiber-polymer composite thick walled rings under internal or external pressure

08 p1195 A72-21764

Climatic load effects on carrying capacity of thick walled glass reinforced polymer rings with residual stresses

08 p1195 A72-21765

German monograph on ring shaped continuous beams calculation, deriving optimum support under torsional stress

09 p1397 A72-22335

Helically bound wire reinforced sprayed Al tubes and rings, investigating failure mechanism dependence on fracture modes from tensile and bending tests

09 p1330 A72-23174

Rotating gas and dust clouds as basis of ring and disk structures in celestial bodies

10 p1539 A72-24311

Interdiffusion of tight contact welded ring Ti-W pairs at high temperature, using X ray analysis and electron beam techniques 10 p1497 A72-24785

Ring assembly with hinged cross section and uniform radial and transverse loads, determining deflection dependence on bulkheads and rigidity of supports [AIAA PAPER 72-355] 11 p1729 A72-25384

Uniaxial, biaxial and shear loading tests on filament wound carbon-carbon composite tubes and rings 11 p1670 A72-25458

Carbon-carbon composite ring structure tested for processing cycle, design properties and ablative performance in solid rocket nozzle environment 11 p1673 A72-25488

Prestressed circular ring snap-through under continuously distributed or discrete torsional loads, determining critical torque by asymptotic solution 11 p1734 A72-25721

Expanding elliptical H I ring with major and minor axes of 1300 and 560 pc from type III supernova in solar neighborhood 13 p2048 A72-29831

Optimal plastic design of doubly symmetric closed ring and frame structures of idealized sandwich section under uniform internal pressure 15 p2322 A72-31346

Structural rings impulsively loaded by magnetic pressure between two parallel current-carrying conductors 15 p2322 A72-31348

Elastic deformation of thin walled spherical and cylindrical shells and associated rings under external loads for small displacements 15 p2325 A72-31604

Filler influence on critical load and buckling zone size in circular elastic three layer ring under uniformly distributed lateral load in rigid cavity 15 p2328 A72-31745

Flexural vibrations of ring with arbitrary cross section, proposing theory for natural frequencies prediction by Ritz method 15 p2329 A72-32141

Elastic-viscoplastic solution for deformation of impulsively loaded strain rate sensitive steel rings 16 p2464 A72-32916

Metal creep tests in thin walled ring shaped specimens for geometrical constancy under variable weights 16 p2472 A72-33850

Response of a ring-reinforced cylindrical shell, immersed in a fluid medium, to an axisymmetric step pulse. [ASME PAPER 72-APM-8] 17 p2624 A72-34314

Integral equation for electromagnetic wave scattering by thin dielectric ring 17 p2526 A72-34379

Bifurcation of circular rings under normal concentrated loads. [ASME PAPER 72-APM-55] 17 p2627 A72-34776

Friction, wear and noise of slip ring and brush contacts for synchronous satellite use. 18 p2693 A72-35982

The testing of contact materials for slip rings and brushes for space application. 18 p2698 A72-36117

Vibration of a stiffened ring considered as a cyclic structure. 18 p2739 A72-37205

Vibrations of elastically connected ring systems. 19 p2873 A72-37692

Thin elastic rings subjected to radial load sets. [ASME PAPER 71-WA/DE-2] 20 p2980 A72-39812

Expanding ring in Galactic center from analysis of microwave spectroscopic data, measuring expansion and rotation velocities 20 p2972 A72-39860

Elastic analysis for a radial crack in a circular ring. 20 p2981 A72-39959

Heat exchange with external medium along boundary of region bounded by smooth contours with heat insulated lateral surfaces, noting thermoelastic confocal elliptic ring 21 p3126 A72-41544

Extensional vibration of a certain type of composite circular plate with a central hole. 22 p3240 A72-42879

Thermal and mechanical stresses concentration near peripheral notches on ring-shaped graphite, noting notch sensitivity relationship to tip curvature and graphite grain size 23 p3306 A72-43755

Equilibrium and stress resultant displacement equations of thin rings based on virtual work principle, stressing warping and twisting moments 23 p3351 A72-44101

RING WINGS

V-wings and diamond ring-wings of minimum induced drag. 21 p2992 A72-41263

RINGS

Deep drawing of circular mild steel and aluminum sheets with polyurethane or rubber rings, examining strain distribution, shape and surface roughness 15 p2244 A72-32145

RIOMETERS

Cosmic noise ionospheric absorption measurements with riometers, showing mid and low latitudinal variation 02 p0221 A72-12464

French monograph on riometer measurement of abnormal ionospheric absorption, noting nighttime events association with F region lacunae 10 p1472 A72-23848

Satellite charged particle observations and polar cap riometer absorption measurements during solar cosmic ray events, noting electrons and protons contributions 15 p2300 A72-31965

Meridional motion of a corpuscular entry region from observations of riometric absorption 17 p2551 A72-35864

RIOMETRY

U MEASUREMENT

RI RIOMETERS

RISK

Aircraft trajectory optimization for maximum profit as decisional problem under risk conditions, determining probabilities by Monte Carlo method 02 p0257 A72-12747

Coronary angiography findings in 263 patients of different age groups compared with history of angina pectoris, risk factors and ECG at rest 03 p0314 A72-13177

Control, prediction and risk optimization in scheduling problems with incomplete random information 06 p0793 A72-17729

Suboptimal security solution of linear quadratic pursuit evasion game with state dependent, control dependent and additive noises, deriving equations for state estimation 06 p0794 A72-18151

Decision making under determinateness, risk and indeterminateness conditions 06 p0781 A72-18302

Aviation insurance and claim servicing risks in aircraft accidents, discussing coverage, claims investigation, litigation and settlement 07 p1106 A72-20673

Technology forecasting and risk assessment in V/STOL transport area, examining mission issues and selection criteria 09 p1261 A72-22473

Cost reduction by integration of assurance technologies from complex systems development risk management model [AIAA PAPER 72-245] 10 p1487 A72-24450

Control, prediction and risk optimization in scheduling problems with incomplete random information 11 p1608 A72-25331

Precipitation exceedance rates charts for various risks, using statistical models 13 p1989 A72-28811

Evaluating alternate paths in R & D project planning. 17 p2639 A72-35340

RITZ AVERAGING METHOD

Overdetermined collocation method change into Ritz-Galerkin method for applications to boundary value problems with eigenvalues 01 p0093 A72-10122

Ritz approximation to two dimensional strain elasticity and heat flow boundary value problems, considering piecewise linear and cubic functions for complete triangulation 03 p0381 A72-13620

Free oscillations of liquid masses contained in tanks, analyzing variational and Ritz methods 04 p0513 A72-15557

Rheomobility effects in creep instability of rods with initial deflection, determining critical load by Ritz method 04 p0594 A72-15708

Ritz-Galerkin process applied to coupled differential equations of motion of pretwisted tapered cantilever turbine blade vibrating in flexure 08 p1244 A72-21483

Ritz-Galerkin procedure used for nonlinear boundary value problems solution, noting convergence of perturbed Galerkin method 09 p1343 A72-23561

Static deflections determination of thin rectangular plates with point clamped restraints, using Ritz method with Lagrange multipliers 10 p1555 A72-24193

Ritz method application to transformations and complementations of polygenetic force problems of mechanics 10 p1512 A72-24521

Russian book on approximate solutions of boundary value problems covering elliptic differential equations and Ritz, moment, straight lines and probability modeling methods 11 p1677 A72-26065

Flexural vibrations of ring with arbitrary cross section, proposing theory for natural frequencies prediction by Ritz method 15 p2329 A72-32141

Thermal shock induced thermoelastic vibrations of rectangular plate calculated by Ritz averaging method 15 p2333 A72-32689

Averaging and Ritz methods for solution approximation of nonlinear periodic and combined resonances in vibrating systems with multiple degrees of freedom 16 p2424 A72-33145

Ritz method for truncated conical shell vibrations investigation, assuming deflection expanded in exponential power series 18 p2735 A72-36694

Modified Ritz method to find optimum boundaries to elliptic systems governed by Laplace or Poisson equation 19 p2826 A72-38246

Buckling and lateral vibration of rectangular plates subject to inplane loads - A Ritz approach. 24 p3458 A72-44887

RIVERS

Hydrologic data collection via ATS 1 satellite for river and flood forecast of National Weather Service, planning geostationary operational environmental satellites /GOES/ 09 p1296 A72-22315

Airborne remote sensing missions and instrumentation to investigate Penobscot River water ecology for thermal, chemical and solid pollutants 15 p2221 A72-31252

RIVETED JOINTS

Creep and plastic deformation analysis of riveted joint elements using elastoplastic theory 07 p1087 A72-18982

Bolted joint thermal conductance, considering interfacial pressure distribution and surface roughness effects [AIAA PAPER 72-282] 11 p1741 A72-25222

RIVETING

Circuit boards contact assembly by special type rivets, discussing technical and economic advantages for prototype or small series fabrication of printed circuit devices 06 p0784 A72-18192

Automatic riveting machine for fuel tight aircraft structures, describing process technique and machine design details and features 09 p1319 A72-22906

RIVETS

High strength bimetallic rivets produced by inertia welding Al-Ti alloy shank with pure Ti tail, noting weight and cost reduction for aerospace vehicle production [SAWE PAPER 902] 23 p3293 A72-43452

RL CIRCUITS

NT LC CIRCUITS

NT RL CIRCUITS

RC, RL and RLC networks associated tunnel diode circuits normalized graphs, design method and stability consideration 23 p3272 A72-43988

RLC CIRCUITS

Affined RC or RL networks, investigating real and equal or imaginary, conjugate and inverse voltage and current transmittances 02 p0197 A72-12240

Frequency criteria for stability of nonlinear multivariable RLC networks with bounded solutions approaching equilibrium 03 p0338 A72-13411

Automatic electromagnetic suspensions using tuned RLC saturable reactor control 10 p1460 A72-24761

Reduced voltage relay operation in aircraft high voltage ac power systems, describing RLC circuit theory, laboratory test arrangement and performance measurements 15 p2204 A72-31215

Digital simulation of stiff linear dynamic systems. 18 p2663 A72-36315

Transformation of reactive ladders into digital circuits. 20 p2910 A72-39427

Optimization of planar transistor operation modes in cascades with inductive correction 21 p3034 A72-41121

RC, RL and RLC networks associated tunnel diode circuits normalized graphs, design method and stability consideration 23 p3272 A72-43988

RLC NETWORKS

U RLC CIRCUITS

RNA

U RIBONUCLEIC ACIDS

ROADS

False color aerial photographs for road quality classification in forests 09 p1302 A72-23290

ROBOTS

Self adaptive controlled robot velocipedist, discussing speed control and equations of motion 04 p0505 A72-14984

Anthropomorphic robots design and performance for space exploration

05 p0644 A72-16448

Robots /electromechanical systems with local computers and sensor controlling motors and effectors/ space application categories and operating and decision making requirements

10 p1458 A72-23777

NASA teleoperator-robot development program, discussing technology and design studies related to space shuttle and stations, satellites and planetary vehicles

15 p2190 A72-32315

Book - Industrial robots - A survey: Details of construction, performance, prices, and applications /Enlarged edition/

22 p3183 A72-43099

Teleoperator technology development, discussing remote operators, mobile manipulators and autonomous robots for man capability extension and industrial application

[ASME PAPER 72-AERO-18] 22 p3245 A72-43150

ROCKET LIMIT

Satellite in eccentric Keplerian orbit transgressing Roche limit about rigid sphere, considering time dependent evolution problem with various centrifugal and tidal forces

01 p0134 A72-11145

Close binary system average gravity and effective temperature at Roche limit for 90 deg phase and both conjunctions, taking into account mass ratios and orbital inclination

06 p0882 A72-18002

X ray emitting component Centaurus X-3 mass limit in close eclipsing binary system with regard to Roche lobe principle

14 p2156 A72-30569

ROCKET BOOSTERS

U BOOSTER ROCKET ENGINES

ROCKET CHAMBERS

U COMBUSTION CHAMBERS

U THRUST CHAMBERS

ROCKET COMBUSTORS

U COMBUSTION CHAMBERS

U THRUST CHAMBERS

ROCKET ENGINE CASES

Fracture toughness of high strength alloys, discussing rocket motor cases, nondestructive test standards and subcritical crack growth

12 p1829 A72-27656

Load tests in air to evaluate maraging steels weldments for rocket motor case applications

20 p2942 A72-39955

ROCKET ENGINE CONTROL

Pintle-controlled rocket engine design with gimbaled supersonic splitline thrust vector control, featuring variable thrust, attitude controls and high propulsion efficiency

[SAE PAPER 710763] 01 p0115 A72-10260

Solid rocket on-off and acceleration control, discussing motor concepts, thrust modulation and potential technology applications

[SAE PAPER 710767] 01 p0116 A72-10262

Optimal control for thrusting rocket guidance with controllable steering angle rate during insertion into circular orbit, using flat earth approximation

01 p0097 A72-10383

One millipound colloid thruster power conditioning and control system design, presenting circuit diagrams, fault protection efficiency and high voltage transformer

01 p0009 A72-11070

Nuclear rocket time optimal start-up using distributed parameter system model with linear control and nonlinear state

04 p0547 A72-14672

KS-transformation based regularization technique modification for minimal fuel consumption rocket trajectory control during space maneuver

05 p0726 A72-16454

Electrostatic rf ion thruster development, including power conditioning and control units

07 p1054 A72-19600

Analog fluidics systems status, exemplifying attitude reaction control for solar observation rocket and air gauging in textile industry

08 p1111 A72-20927

Solid propellant rocket engine thrust vector control by four movable exhaust nozzles, nozzle exit cone secondary injection and flexible bearing nozzle

13 p2026 A72-28928

Argon and mercury ion engines operation, performance and control, evaluating safety and ease of handling from laboratory test data

13 p2026 A72-28931

Digital controller for high pressure rocket engine.

18 p2721 A72-36335

Considerations regarding the choice of the number of stages in long-range or high-altitude rockets

20 p2977 A72-39596

Conditions for impulsive thrust-coast-thrust minimum-time, fixed-fuel transfers between coplanar orbits.

24 p3440 A72-45149

Examination of rocket control system by means of analog computer.

24 p3450 A72-45175

ROCKET ENGINE DESIGN

Pintle-controlled rocket engine design with gimbaled supersonic splitline thrust vector control, featuring variable thrust, attitude controls and high propulsion efficiency

[SAE PAPER 710763] 01 p0115 A72-10260

Algol 3 solid propellant rocket motor design for Scout D and E launch vehicles first stage, considering high total impulse, payload/mass capability and propellant grains

[SAE PAPER 710765] 01 p0115 A72-10261

Aerospike rocket engine system for orbit-to-orbit space shuttle, discussing light-weight regeneratively cooled thrust chamber performance tests

[SAE PAPER 710770] 01 p0116 A72-10264

Design of 6000 Mw open cycle gas core nuclear rocket engine with hydrogen as propellant, considering critical U 235 mass, major reactor components and specific impulse

01 p0099 A72-11347

Nuclear light bulb rocket engine design and performance, presenting start-up, steady state operation, shutdown, dynamic response and control

01 p0100 A72-11354

Post Apollo program, considering space shuttle design, operation, transportation and payload cost reduction, rocket developments and plans for Mars expedition

03 p0440 A72-13612

Low cost large solid rocket boosters technology, discussing propellant, case material, insulation, nozzle ablatives and thrust vector control

04 p0565 A72-14435

Optimal design criteria for multigrain solid propellant rockets, considering powder weight, burning time and combustion chamber length

05 p0704 A72-16351

Hydrazine and ammonia resisto-jet systems for satellites orbit and attitude control, discussing component redundancy and mass requirements in terms of system optimization

07 p1054 A72-19603

High performance sounding rockets design, discussing Skylark propulsion system improvement and new rocket vehicle design for 200 kg payload capability with existing motor hardware

08 p1241 A72-21172

Electrodynamic thrusters for flight vehicle propulsion, reviewing design, efficiency and performance

08 p1224 A72-21669

Boron-epoxy reinforced composite metal shear web design for space shuttle orbiter main engine thrust beam structure

[AIAA PAPER 72-395] 11 p1726 A72-25416

Plasma diagnostics of inductively coupled RF Hg discharge in RIT-10 ion thruster

[AIAA PAPER 72-472] 11 p1709 A72-26203

RF ion microthruster discharge vessel and plasma holder material investigation, considering quartz, boron nitride and aluminum oxide

[AIAA PAPER 72-473] 11 p1709 A72-26204

RF ion thruster for spacecraft propulsion, discussing tests and digital computer calculations to optimize design parameter

[AIAA PAPER 72-474] 11 p1709 A72-26205

Liquid fuel rocket engines design for space applications, describing combustion chambers, thrust and vector control systems and propellant mixtures physicochemical properties

12 p1861 A72-27861

Waxwing solid propellant rocket motor design for third stage propulsion of Black Arrow satellite launcher

13 p2026 A72-28932

Structurally integrated ion thruster /SIT-5/ for synchronous satellites attitude control and station-keeping, presenting design and performance data

[AIAA PAPER 72-492] 13 p2027 A72-28950

Two stage solid propellant sounding rocket, discussing engine design, operation and tests

13 p2052 A72-29859

Liquid propellant rocket performance, stability and compatibility prediction techniques, noting effect on design time and cost

14 p2146 A72-30919

Hot water rocket engine design and operation principles, discussing high pressure tank and nozzle characteristics

15 p2297 A72-31830

Reusable two-stage meteorological rocket vehicle, discussing design, performance, second stage recovery technique and cost

17 p2619 A72-34185

Pressurized crack behavior in two-dimensional rocket motor geometries.

17 p2596 A72-34203

German book - Solid-propellant rocket engines I: Introduction and fundamentals

17 p2597 A72-35453

Development of a GH2/GO2 pulsejet engine with 6.7 kN thrust for the attitude control system of the space shuttle

19 p2848 A72-37495

Viking 2 rocket engines for Europa 3 first stage propulsion, describing engine components design and functions and performance test results

22 p3216 A72-42649

Construction of a high-performance resistojet for satellite propulsion.

23 p3328 A72-44324

Development and testing of a radioisotope-fueled thruster for spacecraft propulsion.

24 p3434 A72-45178

ROCKET ENGINE NOISE

Shock wave generation and propagation from Apollo rockets at orbital altitudes

11 p1690 A72-26513

Infrasound observations of natural background and signals from Apollo 14 and aircraft, using thermistor flowmeter microphone array

11 p1690 A72-26515

Acoustic environmental prediction model for near, mid and far field rocket engine noise

13 p2028 A72-29582

Aeroacoustic, vibration and shock environments for the space shuttle orbiter.

24 p3448 A72-44679

Saturn systems holddown acoustic efficiency and normalized acoustic power spectrum.

24 p3433 A72-44681

ROCKET ENGINES

NT ALGOL ENGINE

NT BOOSTER ROCKET ENGINES

NT DUCTED ROCKET ENGINES

NT ELECTRIC ROCKET ENGINES

NT ELECTROSTATIC ENGINES

NT HOT WATER ROCKET ENGINES

NT HYBRID PROPELLANT ROCKET ENGINES

NT HYDRAZINE ENGINES

NT HYDROGEN OXYGEN ENGINES

NT LIQUID PROPELLANT ROCKET ENGINES

NT MICROROCKET ENGINES

NT NUCLEAR ENGINE FOR ROCKET VEHICLES

NT NUCLEAR ROCKET ENGINES

NT SOLID PROPELLANT ROCKET ENGINES

TD nickel as construction material for rocket thrust chambers, discussing spin-forming, welding, machining, electric discharge machining and electroforming operations

01 p0075 A72-10753

Combustion chamber and nozzle materials for fluorine and/or metal combustors high energy propellant rocket engines, considering cooled and uncooled nozzles and spoiler plates

01 p0117 A72-10941

Gas-liquid bipropellant rocket motor system instability boundaries under various operating and design conditions, interpreting experimental results via time lag model

[AD-733596] 03 p0406 A72-13632

Diamant B launcher first stage Valois rocket motor combustion I, acoustic mode and if instabilities

[ONERA, TP NO. 1027] 03 p0406 A72-13641

Electrical measurements on capillary-fed colloid thruster with Zener diode-like I-V characteristic and constant propellant mass flow rate

04 p0565 A72-15204

Diffuser for altitude simulation in rocket motor operation, featuring film cooling with water inflow by motor exhaust gas ejector action

05 p0704 A72-16004

Aerodynamic interference between parallel bodies for estimating aerodynamic characteristics of rocket engine with auxiliary boosters, obtaining flow field by slender body theory

05 p0600 A72-16005

L instability in rocket motors with heterogeneous propellants, investigating sideways sawtooth model

[AIAA PAPER 72-33] 05 p0703 A72-16897

Thermodynamic function error influence on rocket engine combustion product characteristics including combustion chamber temperature and specific pressure pulse

05 p0751 A72-17069

Operational stability of rocket engine with combustion chamber having charge of two propellant types with different burning rate dependences on pressure

06 p0867 A72-18206

Side force and shock wave induced by obstacle on rocket engine nozzle wall, investigating pressure distribution

07 p1055 A72-20250

Controllable high energy hydrogen-oxygen rocket propulsion systems performance and combustion characteristics, considering mixture ratio, pressure, chamber geometric characteristics, injection area and velocity ratios

11 p1703 A72-25298

Cesium contact ion thruster, investigating carburized thoriated tungsten filaments electron emission under ion bombardment
[AIAA PAPER 72-440] 11 p1707 A72-26181

Quasi-steady MPD thruster system, discussing gas injection, electronic synchronization and electrolytic pulse forming network
[AIAA PAPER 72-461] 11 p1613 A72-26196

Optimization criteria for electric feeding in quasi-steady MPD thruster, discussing energy storage bank characteristics determination
[AIAA PAPER 72-462] 11 p1709 A72-26197

Duration test and performance of annular colloid thruster, noting specific impulse increase and electrostatic vectoring
[AIAA PAPER 72-483] 11 p1710 A72-26209

Capillary fed annular colloid thruster operating characteristics, considering I-V relationship, thrust and exhaust velocities and propulsive efficiency
[AIAA PAPER 72-490] 11 p1710 A72-26215

MPD thruster diagnostics and interpretation of electric current distribution, applying integral form of Maxwell equation for moving Hall probe
[AIAA PAPER 72-498] 11 p1711 A72-26221

Rectifier tube cathode as colloid thruster electron gun type neutralizer, discussing efficiency and accelerated life tests
[AIAA PAPER 72-511] 11 p1711 A72-26228

Rocket engines simulated high altitude testing, using multiple stage ejector augmented supersonic diffuser system
13 p1938 A72-28692

U.S. Army missile systems rocket motors life cycle reliability programs based on propellant laboratory analyses, motors static tests and field firings statistical evaluation
14 p2146 A72-30759

Nonchemical space propulsion systems for lunar and planetary flights, discussing fission, fusion and electric rockets
15 p2297 A72-31810

Russian book on aircraft turbine and spacecraft rocket engine assembly covering process schedules, work organization, precision, joints and couplings, quality control, etc
16 p2399 A72-33373

Liquid propellant rocket engines three dimensional nozzle admittance determination by impedance tube method from pressure distribution measurement, taking into account nozzle geometry effect
[AIAA PAPER 72-666] 16 p2443 A72-34071

Combustion instability oscillations damping in rocket motors by short nozzles, calculating acoustic losses
17 p2635 A72-34233

A capillary-fed annular colloid thruster.
17 p2598 A72-35491

Nonlinear equations solutions for interior ballistics parameters of solid rocket propellants combustion during rocket engine nozzle opening
19 p2878 A72-37352

Erosion combustion effect on unsteady solid rocket propellant burning stability during engine nozzle opening, noting combustion velocity and surface temperature
19 p2879 A72-37353

French monograph - Optimal impulse corrections for near-circular orbits - Comparison of various thruster configurations
19 p2856 A72-37491

Optimal three dimensional maneuvering of a rocket powered hypervelocity vehicle.
24 p3450 A72-45151

Performance and flow properties change through a rocket turbine by presence of solid particles.
24 p3361 A72-45206

ROCKET EXHAUST
Space crew radiation dosage calculation from Mars mission high impulse gas core nuclear rocket engine exhaust plume fission fragments
01 p0022 A72-11353

Electron density and temperature temporal and radial profiles in megawatt MPD-arc thruster exhaust, using Thomson scattering technique
[AIAA PAPER 72-209] 05 p0707 A72-16887

Rocket plume contamination effect on transmitting and reflecting materials optical properties, noting predominant absorption and scattering effects
[AIAA PAPER 72-56] 05 p0750 A72-16967

Nonequilibrium chemistry effects on electrical properties of solid propellant rocket motors turbulent afterburning exhaust plumes, describing free electron sources
07 p0935 A72-19359

High altitude rocket plume rarefaction effects, predicting inviscid, merged, transition, first collision and free molecular flow regimes
08 p1128 A72-21610

Optical radiation from Hg bombardment ion thrusters downstream regions due to excited atoms radiative decay, examining exhaust interference with star tracker
[AIAA PAPER 72-441] 11 p1707 A72-26182

Electrostatic rocket exhaust materials deposits effects on solar cells optical, thermal and electrical performance characteristics, using optical thin film theory
[AIAA PAPER 72-447] 11 p1578 A72-26184

Solar absorbance and thermal emittance of thermal control coatings contaminated by thruster exhaust in vacuum environment
[AIAA PAPER 72-263] 12 p1846 A72-27865

Competition criteria for chemical reactions selection in nonequilibrium computer calculations on combustion systems properties, noting seeded flames and rocket exhausts
13 p1912 A72-28548

Low thrust propulsion system effects on communication satellites subsystems, discussing mercury, cesium and Teflon rocket placement and effects of exhaust
[AIAA PAPER 72-519] 13 p2027 A72-28981

Boron ignition and combustion in air-augmented rocket afterburners.
17 p2636 A72-34902

Observation of ultraviolet radiation from a rocket exhaust plume at high altitudes.
20 p2984 A72-39641

Equations of motion for the variable mass flow-variable exhaust velocity rocket.
[AIAA PAPER 72-912] 21 p3112 A72-41559

ROCKET FIRING
Computer program for the calculation of the thrust and of the firing data of internal cylindrical rocket burners with different profiles
17 p2523 A72-35417

The use of an expansion tube with cold gas to determine rocket engine starting transient pressures during silo launch.
[AIAA PAPER 72-997] 21 p3040 A72-41583

ROCKET FLIGHT
Soviet book on rocket dynamics covering history, variable mass point aerodynamics and ballistics, numerical and computer methods and trajectory analysis
02 p0286 A72-12123

Relativistic flight of decreasing mass, increasing acceleration and constant thrust rocket description from earth and rocket observer viewpoints, noting light flash transmission and arrival times
03 p0441 A72-13836

Rocket motion in general central force field, obtaining primer vector integration for optimal coasting arc during orbital transfer
[AD-741964] 06 p0890 A72-18386

Liquid fuel elastic rocket motion stability in supersonic flight, using vibration and thrust vector control equations for dynamic properties description
08 p1241 A72-21633

Soviet book on longitudinal vibrations of rocket with liquid propellant engine covering rocket element dynamic characteristics and free vibration mode shape and frequency calculations
08 p1241 A72-22025

Minimum time duration rocket interception, calculating trajectory parameters and target orbits in Earth gravitational field
09 p1393 A72-23573

German monograph on flight performance optimization of solid propellant rockets covering thrust values, burning time, rocket design and orbits within earth atmosphere
10 p1550 A72-23770

Stability criteria for limiting oscillatory motion of coasting sounding rocket exiting atmosphere
13 p2051 A72-28886

Iterative solution of boundary value problem in multiple burn rocket trajectory optimization
15 p2308 A72-31820

The orbit of Cosmos 307 rocket and its use in atmospheric research.
17 p2545 A72-34632

Refraction correction of rocket tracking radar inputs in near real time.
18 p2661 A72-36636

Integrals of the motion for optimal trajectories in atmospheric flight.
[AIAA PAPER 72-931] 21 p3112 A72-41570

The dynamics of the ascending flight of sounding rockets
[ONERA, TP NO. 1056] 22 p3231 A72-42582

Government, military safety, police permission and insurance regulations for European rocket activities
24 p3467 A72-45124

ROCKET FUEL TANKS
U PROPELLANT TANKS
ROCKET LAUNCHERS
Mobile launching facility for high altitude sounding rockets, describing telemetered data recording, radar and optical tracking, range safety and payload recovery equipment
[DGLR PAPER 72-012] 16 p2374 A72-33499

ROCKET LAUNCHING
NT ORBITAL LAUNCHING
Guiana Space Center launch complexes for Diamant B and Europa satellite launchers and rocket probes, discussing trajectory, telemetry and safety measures
03 p0339 A72-12912

Dynamic characteristics of buoyant low altitude clouds formed by solid rocket motor launches, determining initial temperature by motion pictures combined with conservation equations
[ASME PAPER 71-WA/FE-33] 05 p0724 A72-15923

Longitudinal vibrations stability of launching rocket body, allowing for propellant sloshing, body dynamic deformation and motor dynamics
05 p0731 A72-17186

Transverse vibrations stability of launching rocket body, allowing for propellant sloshing and body elastic deformation
05 p0731 A72-17187

ESRO sounding rockets program survey, discussing launchings in terms of number, vehicle types and sites, member participation, payload integration policy and success rate
10 p1551 A72-24197

Acoustic ray tracing of long range infrasonic signals from launch and reentry of Saturn 5 rockets
11 p1690 A72-26512

Long range air coupled seismic wave recording from Apollo launchings, using microphones and seismographs arrays
11 p1690 A72-26514

On application of Kalman filtering technique to on-line orbit estimation of a launching vehicle.
22 p3203 A72-43142

Explorer satellites and Pioneer space probes development program, discussing launching rockets, reentry tests, payloads, radio communication, Van Allen belts discovery, etc
23 p3358 A72-44353

ROCKET LININGS
Experimental hybrid rocket engine combustion chamber with solid oxidizer lining of ammonium nitrate and perchlorate eutectic mixture
05 p0708 A72-17249

ROCKET MOTOR CASES
U ROCKET ENGINE CASES
ROCKET NOSE CONES
Dynamic behavior of M-4S rocket devices for strap-on booster separation and nose cone and flare deployment
22 p3232 A72-43143

ROCKET NOZZLES
Combustion chamber and nozzle materials for fluorine and/or metal combustng high energy propellant rocket engines, considering cooled and uncooled nozzles and spoiler plates
01 p0117 A72-10941

Rocket acceleration effect on internal isotropic nozzle flow, giving formulas for thermodynamic variables
03 p0441 A72-13627

NDT for detecting density variation, local anomalies regions and completeness of copper-infiltrated W powder rocket nozzle inserts
03 p0364 A72-14025

Pyrolytic graphite coated rocket nozzle design, discussing substrate properties, coating thickness, erosion rates and rocket tests
10 p1500 A72-24199

Molded carbon technique-produced carbon fiber/carbon composites, discussing flexural strength, toughness, crack resistance and rocket nozzle application
10 p1500 A72-24200

Carbon-carbon composite ring structure tested for processing cycle, design properties and ablative performance in solid rocket nozzle environment
11 p1673 A72-25488

High acceleration effects on gas flow patterns in rocket nozzles, detailing stagnation condition in combustion chamber and gas velocity and pressure at exit
15 p2297 A72-31813

Russian book on solid propellant rocket engines covering combustion chamber and nozzle layouts, working cycle and thrust control
16 p2443 A72-33350

Effects of heat addition in divergent nozzles with application to MPD thrusters.
17 p2635 A72-34213

Combustion instability oscillations damping in rocket motors by short nozzles, calculating acoustic losses
17 p2635 A72-34233

Flow in an accelerated rocket nozzle - Effect of variation of total mass. II
17 p2621 A72-34918

Development of moldable carbonaceous materials for ablative rocket nozzles.
17 p2572 A72-35668

Nonsymmetric flow in Laval-type rocket nozzles, deriving formulae for optimum nozzle design with neutralized lateral forces and turning couples
24 p3359 A72-44675

Decay of swirl in a straight pipe flow /with hub at the entrance/.
24 p3394 A72-45367

Burning rate dependence on oxidizer particle size of ammonium or potassium perchlorate mixtures with organic fuels

09 p1373 A72-23146

Combustion of solid-propellant layer in contact with a solid-oxidizer layer

18 p2720 A72-36239

ROCKET PROPELLANT TANKS

U PROPELLANT TANKS

ROCKET PROPELLANTS

NT AEROZINE

NT CRYOGENIC ROCKET PROPELLANTS

NT DOUBLE BASE ROCKET PROPELLANTS

NT GASEOUS ROCKET PROPELLANTS

NT HYPERGOLIC ROCKET PROPELLANTS

NT LIQUID ROCKET PROPELLANTS

NT METAL PROPELLANTS

NT MONOPROPELLANTS

NT SOLID ROCKET PROPELLANTS

Rocket fuel combustion products composition and combustion chamber temperature determination

03 p0405 A72-13474

Gas-liquid bipropellant rocket motor system instability boundaries under various operating and design conditions, interpreting experimental results via time lag model

[AD-733596] 03 p0406 A72-13632

Air-augmented shrouded and ducted rocket secondary combustor performance parameter analysis based on one dimensional conservation equations

03 p0405 A72-13834

Maximum propellant utilization in electron bombardment ion thruster for space applications

04 p0564 A72-14432

Rocket propellants R and D toward higher specific impulse, discussing liquid, solid, hybrid and tribrid systems

05 p0702 A72-16744

L instability in rocket motors with heterogeneous propellants, investigating sideways sandwich model

[AIAA PAPER 72-33] 05 p0703 A72-16897

High energy rocket propellants for space probe propulsion systems, evaluating various propellant combinations in terms of specific impulse, toxicity, corrosiveness, cost and availability

11 p1702 A72-25299

Low thrust propulsion system effects on communication satellites subsystems, discussing mercury, cesium and Teflon rocket placement and effects of exhaust

[AIAA PAPER 72-519] 13 p2027 A72-28981

Rocket propellants, propulsive charges and explosives lifetime - Conference, Karlsruhe, Germany, September-October 1971

14 p2143 A72-30751

Two phase propellant flow rate through simulated rotating liquid core nuclear rocket fuel bed under high centrifugal acceleration

14 p2129 A72-30923

A computation method for the determination of thermodynamic values and performance data of rocket propellants, propellant charges for cannons, and ignition mixtures

17 p2596 A72-35418

Acceleration effects on burning velocity of aluminumized condensed rocket propellant systems, calculating particle size and slag mass

19 p2847 A72-37360

Toxicity of rocket fuels

24 p3433 A72-44781

ROCKET PROPELLED SLEDS

Wind tunnel and rocket sled results with ribbon parachutes for supersonic release, discussing aerodynamic, structural flutter and inflation time characteristics.

01 p0004 A72-10308

ROCKET SONDES

U SOUNDING ROCKETS

ROCKET SOUNDING

Skyllark rocket observations of sporadic E layer magnetic fields, winds and ionization indicating ion divergence region

01 p0052 A72-10086

Ionogram observations of F layer electron refraction wave disturbance during small rocket ascent

01 p0054 A72-10423

Ionospheric ion formation and neutralization reaction rate coefficients determination by fitting measured electron concentration profiles with computer generated profiles

01 p0059 A72-10616

Rocket-borne measurement of particle fluxes and currents in auroral arc, determining pitch-angle distribution of electron and proton energies

01 p0120 A72-10897

Rocket-borne measurement of Birkeland ionospheric current density associated with auroral arc and electrojet

01 p0061 A72-10898

Sounding rockets in remote sensing programs for agricultural census and crop yield estimates in Argentina

02 p0228 A72-11854

Ionospheric propagation, reflection and absorption of vlf hiss in aurora from rocket observation during quiet and substorm conditions

02 p0221 A72-12458

Solar observation survey, considering sounding rockets, OSO, balloons, orbiting observatories, spectral resolution, spectral features and solar flare

03 p0409 A72-13050

Ionospheric ion-molecule and ion-electron reaction rate constants determination from nighttime flight of rocket-borne ion mass spectrometer data least square fitting

03 p0347 A72-13396

D region ion and electron density rocket measurement during sunrise, discussing negative ion electron affinity and ion production functions

03 p0347 A72-13397

Rocket measurement of highly collimated short duration bursts of auroral electrons, comparing with existing auroral models

03 p0349 A72-13515

Late twilight airglow vacuum UV spectra from sounding rocket observation, noting conjugate-point electron excitation role in O I emissions

03 p0350 A72-13525

Solar radiation effects on earth atmosphere with MR-12 and M-100 meteorological rockets launched at onset of chromospheric flare, noting atmospheric parameters measurements

04 p0580 A72-15453

Faust project history, scientific objectives and present status, discussing stars, nebulae, quasars point sources and galactic photometry

04 p0583 A72-15691

Remote sensing with sounding rockets and balloons, discussing cost, mineralogical surveys, land use and hydrological assessments

05 p0654 A72-15756

Rocket cosmic radio noise measurements at 1.16-2.40 MHz and 1600 km, confirming spectrum flatness

05 p0711 A72-15763

Sounding rocket observations of magnetic field aligned electron pitch angle distributions coincident with auroral precipitation band northern boundary

06 p0804 A72-17457

Rocket-borne vector magnetometer measurements of midlatitude ionospheric currents near sporadic E, noting nearly uniform vertical distribution

06 p0804 A72-17459

Stratospheric rocket sounding on global scale for studies of atmospheric circulation in equatorial zone, polar regions and hemispheres

06 p0840 A72-17620

UV spectrophotometry of late-type giant star [Arcurus] from Aerobee rocket, identifying Mg II doublet resonance line for stellar chromosphere

06 p0881 A72-17893

GX3 plus 1 identification by sounding rocket during lunar occultations, discussing magnitude

07 p1070 A72-19123

Zeta Orionis spectra at 922-1453 A from rocket spectroscopy, matching lines with stellar atmosphere models

07 p1072 A72-19346

Rocket astronomy development, reviewing V-2, Aerobee rocket and balloon-rocket flights for solar X rays and flares and galactic and extragalactic experiments

07 p1076 A72-19675

Atmospheric turbulence, wind velocity, temperature and density measurements at 90-250 km, using explosive contaminants release from Skylark rockets

07 p0979 A72-20265

Ionospheric electron concentration and temperature as function of solar zenith angle from rocket sounding

08 p1154 A72-20734

Far UV view of Orion from Aerobee rocket-borne electronographic camera photographs of Orion-Monoceros-Canis Major region

08 p1164 A72-20994

Spectrophotographic recording of UV auroral emissions during rocket probe flight, noting excitation by electron impact on molecular nitrogen

08 p1159 A72-21225

Upper soft X ray limits to Virgo sources from Aerobee 170 rocket sounding

08 p1227 A72-21394

North Polar Spur soft X rays observed by Aerobee 150 rocket launched from Woomera for enhanced emission

08 p1227 A72-21398

Wind and density measurements by small sounding rockets, comparing results with ground observed radio wave absorption diurnal variations

08 p1160 A72-21531

Mesospheric temperature and wind profiles during stratospheric warming from rocket grenade experiments

08 p1160 A72-21533

Mesosphere region positively and negatively charged particles concentration and mobility measurements by sounding rocket experiments

09 p1375 A72-22361

Supersonic and subsonic measurements of mesospheric ionization at night, using Arcas rocket parachute borne nose-up and blunt probes

09 p1296 A72-22362

Rocket sounding of auroral zone F region low energy electron precipitation and excitation and ionization processes

09 p1298 A72-22585

Differential photoelectron flux in lower ionosphere during 7 March 1970 solar eclipse observed by Nike-Apache rockets

09 p1378 A72-23012

Thermospheric structure between 100 and 400 km from rocket soundings and ground observations, noting mass spectrometers chemical reactions influence on atmosphere model accuracy

09 p1300 A72-23015

Sounding rocket spectral measurements of low energy auroral ion composition during premidnight breakup

09 p1300 A72-23020

Pulsating polar auroral line emission spectra observation at 3914 and 5577 A by rocket-borne photometers

09 p1301 A72-23262

Simultaneous rocket observation of wind shear and electron density profile in lower ionosphere, noting sporadic E layer formation

10 p1477 A72-25154

Midlatitude sporadic E layer observed by rocket and radio sounding, deriving plasma frequency from peak electron density

10 p1477 A72-25156

Daytime electron density profile in E and D regions from rocket lower ionosphere sounding, noting winter electromagnetic absorption anomaly

11 p1622 A72-26101

Electrostatic and electron temperature probes compared during ionospheric rocket soundings, noting lower ionosphere discrepancies due to surface contamination

11 p1633 A72-26102

Upper atmospheric satellite and rocket soundings reliability and utility, covering ionospheric radio propagation, numerical weather prediction and gravity waves

11 p1623 A72-26390

Atmospheric density variations from meteorological rocket soundings, discussing data reduction methods and error sources for bead thermistor and inflatable falling sphere instruments

11 p1626 A72-26473

Ionospheric and neutral atmospheric temperature profile, composition and electron density and energy measurements by MR-12 rocket

11 p1628 A72-26905

Ionospheric electron and ion densities during 12 November 1966 solar eclipse from rocket probe measurements

[AD-744390] 12 p1863 A72-27151

Diurnal and annual temperature variations at 30-60 km from statistical analysis of rocketsonde data, obtaining solar radiation errors magnitude

13 p1947 A72-28829

Rocket sounding of ozone diurnal variations in upper stratosphere and lower mesosphere

13 p1947 A72-28831

Low altitude electron-ion dissociative recombination and ion-ion neutralization coefficients during PCA event from ESRO rocket flights data

13 p2032 A72-29653

Wind tunnel tests for correction of temperature profile data in stratosphere and lower mesosphere obtained from SKUA rocket sounding

14 p2105 A72-30807

Ionospheric rotational temperature and density measurement, using fluorescence produced by rocket-borne electron beam gun

14 p2106 A72-30974

Wind profiles, turbulence, and temperature and density distribution of neutral upper atmosphere obtained via sounding with Skylark rockets carrying chemical seeding payloads

15 p2223 A72-31435

Cosmic ray chemical composition from particle sampling by rockets and satellites, comparing galactic rays, solar rays and sun

15 p2299 A72-31648

Upper atmosphere temperature and wind variations over Antarctic from meteorological rocket sounding, noting winter cyclonic vortex level

15 p2225 A72-31906

Atmospheric ion composition analysis by RF mass spectrometer during rocket ionosphere sounding, discussing meteor ionization layers

15 p2225 A72-31915

Micrometeorite flux observed by rocket-borne electroacoustic transducers

15 p2308 A72-31931

Equatorial ionospheric vertical electron density profiles measurement by rocket-borne phase measuring swept RF probe with dc biased sensor, comparing data with ionograms

15 p2226 A72-31940

Lower thermospheric neutral gas density and composition rocketborne mass spectrometric measurements with liquid He cooled ion source

15 p2236 A72-31942
Extraterrestrial He I 584 A background radiation suggested from rocket and satellite observations, noting interstellar medium temperature determination from isophotes

15 p2309 A72-31945
Daytime zodiacal light intensity and polarization measurement at elongation angles between 15-30 degrees from Skylark rocket photometric observations

15 p2227 A72-31951
Atmospheric density and temperature measurements by rocket-borne spheres during 1972 winter, observing variability with altitude

15 p2227 A72-31959
Atmospheric stratification, wind profiles and vertical density distribution of ions and neutral particles determined by rocket sounding

15 p2228 A72-31968
Electrical conductivity in mesosphere and upper stratosphere from rocket sounding by blunt probe technique, suggesting electron density profiles dependence on dissociative recombination variations

15 p2228 A72-31972
Selective chopper radiometer (SCR) radiances comparison to rocketsonde data, showing vertical resolution of stratosphere and mesosphere temperature changes during midwinter disturbance

15 p2228 A72-31976
Rocket and radar-meteor wind observations of zonal flow, noting annual and semiannual components for northern latitudes at 60-130 km

15 p2229 A72-31985
Report to COSPAR on UK ground based, rocket and satellite-borne space research experiments and 1971-1972 programs

15 p2337 A72-32005
Geocorona and interplanetary He glow EUV emission altitude distribution measured by exospheric sounding rocket-borne thin film photon counters

15 p2231 A72-32327
Near IR airglow observation by sound rocket to determine layer height diurnal variation and rocket axis zenith angle

15 p2231 A72-32328
Sounding rocket observation for emission height of night airglow continuum near 6050 A, using photoelectric photometers

15 p2231 A72-32329
Rocket-borne laser radar for aerosol observation in upper atmosphere, noting light scattering layer relation to noctilucent cloud appearance

15 p2231 A72-32331
VLF wave normal direction measurement during propagation through ionosphere by Doppler technique, using rocket-borne receivers

15 p2201 A72-32332
Lower thermosphere neutral composition from February 1969 rocket-borne mass spectrometer measurements over Fort Churchill, Canada

16 p2383 A72-32965
Summer upper mesosphere and lower thermosphere positive ion composition at high latitudes from Nike Cajun rocket soundings

16 p2383 A72-32966
Sounding rocket observations of quasar 3C 273 X ray spectrum for upper limits to absolute abundance of He in intergalactic medium

16 p2446 A72-33451
Galactic X ray sources from June 1969 rocket flight in Brazil, comparing spectra to bremsstrahlung, black body and power law models

16 p2446 A72-33457
Noctilucent cloud research, discussing morphology, rocket studies and ice particle theory

16 p2386 A72-33605
Digital computer program for automatic processing of rocketsonde and radar digitized data, presenting graphical output from meteorological rocket soundings during 7 March 1970 solar eclipse

16 p2419 A72-33944
Experimental evidences for a transient ion layer formation in connection with sudden ionospheric disturbances in the height range 20-50 km.

17 p2545 A72-34630
The El Arenosillo launch base, a rocket test center in Huelva province

17 p2536 A72-34944
Photometric observations from sounding rockets - Selection of horizontal sightings

19 p2789 A72-37784
Ionospheric electron concentration and temperature as function of solar zenith angle from rocket sounding

19 p2791 A72-38362
Heavy metal particle detection in noctilucent clouds by rocket experiments, using Pandora inflight shadowing technique

20 p2964 A72-39373
Recent positive and negative ion composition measurements in the lower ionosphere by means of mass spectrometers.

20 p2917 A72-39528

Experimental determination of fall rate of 'N5' chaff on the heights 50-90 km.

21 p3049 A72-41498
Stratospheric winds over Leba rocket sounding station in spring and autumn, 1970.

21 p3049 A72-41500
Particle, plasma and field detectors for rocket investigations in and above atmosphere, considering PCM telemetry system and balloon-borne X ray telescope system

21 p3057 A72-41617
A measurement of ionospheric electric fields at high latitude.

22 p3169 A72-42015
Particle flux measurements from rockets during a solar cosmic-ray flare in April, 1969

22 p3218 A72-42226
Rocket radiometers measurement of oxygen IR atmospheric system altitude profile at night, noting auroral enhancement possibility

22 p3170 A72-42365
Auroral EUV flux observation by Javelin sounding rocket photometers, comparing with visible and X ray emissions

22 p3171 A72-42417
A possible connection between a barium cloud and electron intensity fluctuations observed on a rocket flight at Kiruna.

22 p3172 A72-42433
Rocket measurement after sunset for altitude distribution of 1.27 micron band nightglow emission from diatomic oxygen molecules

22 p3172 A72-42435
Ozone measurements in the mesosphere during the solar proton event of 2 November 1969.

22 p3173 A72-42509
Investigation of the parachute inflation aid utilizing liquid vapor pressure.

22 p3139 A72-43141
A rocket measurement of the vertical distribution of atmospheric ozone.

23 p3285 A72-44242
Rocket measurements of electron influx during a major magnetic storm with type A aurora.

23 p3332 A72-44515
Rocket observation of topside resonances.

23 p3286 A72-44517

ROCKET TEST FACILITIES

Design, development and operation of liquid hydrogen plant, using production for rocket thrust chamber tests and tank pressurization studies

06 p0867 A72-17593
Rocket engines simulated high altitude testing, using multiple stage ejector augmented supersonic diffuser system

13 p1938 A72-28692
The El Arenosillo launch base, a rocket test center in Huelva province

17 p2536 A72-34944
Development of a digital control system for a spacecraft propulsion test facility.

19 p2783 A72-37641
The use of an expansion tube with cold gas to determine rocket engine starting transient pressures during silo launch.

[AIAA PAPER 72-997] 21 p3040 A72-41583

ROCKET THRUST

Thrust power optimization for spacecraft earth-planet round trip trajectories

01 p0127 A72-10357
Relativistic flight of decreasing mass, increasing acceleration and constant thrust rocket description from earth and rocket observer viewpoints, noting light flash transmission and arrival times

03 p0441 A72-13836
Analytic solution for optimal control circular orbit escape with constant thrust rocket, using Euler-Lagrange equations and perturbation technique

03 p0437 A72-13839
German monograph on flight performance optimization of solid propellant rockets covering thrust values, burning time, rocket design and orbits within earth atmosphere

10 p1550 A72-23770
Minimum time thrust start-up of nuclear rocket as optimal control problem with integrodifferential constraints, using Pontryagin maximum principle and calculus of variations

11 p1685 A72-25870
Electrically heated thermal decomposition hydrazine thrusters, discussing propellant supply pressures compatibility and thrust levels

[AIAA PAPER 72-451] 11 p1708 A72-26188
Prediction of tank pressure history in a blowdown propellant feed system.

17 p2537 A72-34211
Computer program for the calculation of the thrust and of the firing data of internal cylindrical rocket burners with different profiles

17 p2523 A72-35417
Thrust-weight ratio optimization for spacecraft orbit inclination change maneuver, deriving motion kinematics via point mass gravitational model

24 p3440 A72-45167

The development of GH2/GO2-pulse mode rocket engines in the thrust range of 6,660-9,340 N /1,500-2,100 lbs/.

24 p3434 A72-45207

ROCKET VEHICLES

NT AGENA ROCKET VEHICLES
NT ATLAS CENTAUR LAUNCH VEHICLE
NT BLACK KNIGHT ROCKET VEHICLE
NT DIAMANT LAUNCH VEHICLE
NT ELDO LAUNCH VEHICLE
NT MULTISTAGE ROCKET VEHICLES
NT SATURN LAUNCH VEHICLES
NT SCOUT LAUNCH VEHICLE
NT SKUA ROCKET VEHICLES
NT SKYLARK ROCKET VEHICLE
NT SOUNDING ROCKETS
NT THOR AGENA LAUNCH VEHICLE
NT VIKING ROCKET VEHICLE

Chapman-Korst model for prediction of flow characteristics within plume induced boundary layer separation in rocket propelled vehicles during power-on maneuvers

01 p0050 A72-10376
Transfer matrix method application to rocket vehicles structural dynamics, incorporating axial and aerodynamic lift forces in vibrational analysis

09 p1397 A72-23499
Resonant vibration of thin walled rods and stiffened plates and cylindrical shells, noting aircraft and rocket structures

16 p2471 A72-33679
Rendezvous at specified destinations through optimum transfer paths

24 p3442 A72-45281
Equations for the general motion of a rocket in a resistant medium

24 p3452 A72-45448

ROCKET-BORNE INSTRUMENTS

Mesospheric OH volume density profile measurements by rocket-borne high resolution polarized Ebert-Fastie spectrometer

01 p0062 A72-10912
Rocket-borne apparatus for X ray measurement in 25 to 200 keV range, noting primary diffuse component and earth albedo spectral analyses

02 p0231 A72-12448
Bragg crystal spectrometer for Sco X-1 spectrum scanning, using Aerobee 170 rocket

03 p0353 A72-13039
Rocket-borne photomultipliers housing, recommending fiber reinforced epoxy resin structure with metal flanges

03 p0440 A72-13062
Absolute UV calibration of rocket photometers used to update OAO calibration for determining energy distribution of reference stars

03 p0355 A72-13065
Rocket-borne spectrometers calibration for observing absolute intensity and center-to-limb variations of sun in vacuum UV region

03 p0355 A72-13066
Rocket-borne mass spectrometer with helium cooled electron bombardment ion source to reduce gas-wall interactions effects

04 p0524 A72-15538
High resolution rocket-borne X ray spectrometer with cooled lithium drifted semiconductor detectors for measuring differential X ray energy spectrum of SCO XR-1

08 p1168 A72-21518
Rescue signaling devices design and operation, discussing pinpoint markers, rocket boosted panel markers, strobe units, antennas and balloon marker

08 p1112 A72-21584
Electronography in space astronomy, discussing use of Lallemand electronic camera as photon receptor onboard balloons or rockets

08 p1170 A72-21963
Skylark 904 sounding rocket cosmic X ray experiment, discussing detector and counter operation and data retrieval technique

10 p1529 A72-24198
Far IR filters for rocket-borne radiometer, discussing Ulrich theory and characteristic impedance determination

11 p1629 A72-25310
Image intensifier tube scanner replacement of slit and multiplier tube of spectrograph, discussing application to rockets

11 p1631 A72-25689
Rocket-borne mass spectrometric studies of composition of lower thermosphere

11 p1622 A72-25847
Rocket-borne mass spectrometer tested in high velocity molecular beam facility for thermospheric atomic oxygen density measurement

11 p1634 A72-26422
Extreme UV solar images televised in flight with rocket-borne SEC vidicon system, noting pictures reconstruction enhancement

12 p1810 A72-27930
Rocket-borne inflatable sphere for radar signal backscatter calibrations at reentry altitudes and for simultaneous atmospheric density determination

13 p1918 A72-28819

Solar spectrum measurements at 2100-3200 Å by Aerobee rocket mounted Ebert-Fastie spectrometer with LiF diffusion plates

13 p2040 A72-29408

Aerobee rocket far UV flash spectrum observations of chromosphere and corona during 7 March 1970 solar eclipse

13 p2042 A72-29539

UV solar spectrum recorded by rocket-borne spectrograph with diffraction grating echelle in Czerny-Turner arrangement

13 p2044 A72-29703

Cylindrical electrostatic analyzers in rocket and satellite instruments for space low energy charged particles measurements

13 p1960 A72-29842

Solar UV Lyman alpha radiation intensity measurements, using Vertikal-1 rocket-borne photometer and photoelectron analyzer

14 p2128 A72-30465

K-2 astrophysical rocket observatory for far UV and X ray solar radiation recording, discussing trajectory, orientation and stabilization, electric and spectrographic instrumentation

14 p2163 A72-30970

Mesosphere and lower thermosphere temperature measurement by rocket-borne manometer, relating temperature variations to corpuscular flux intensity and sun generated geomagnetic excitations

15 p2225 A72-31910

Mesospheric air density and temperature measurements from rocket-borne resistance thermometers based on free molecular flow

15 p2225 A72-31911

Nike-Apache rocket-borne particle collection and photometry of noctilucent clouds, obtaining single-shadowed particle size distributions and inflight shadowing surface data

15 p2226 A72-31923

Micrometeorite flux observed by rocket-borne electroacoustic transducers

15 p2308 A72-31931

Mesospheric and lower thermospheric composition from neutral atmospheric particles measurement by rocket-borne instrument consisting of RF quadrupole mass spectrometer

15 p2228 A72-31967

Linear ICs application to RF probe for ionospheric electron density measurements from rockets or satellites

15 p2240 A72-32389

X ray flux anomalous minima observations in Cen X-3 with rocket-borne argon-methane proportional counter

16 p2461 A72-34162

A compact grating spectroheliograph for the MgII resonance lines.

17 p2554 A72-35079

Rocket-borne Cassegrain optic stellar electrophotometer for early star observations in 1300-2000 Å region

19 p2796 A72-37585

Exit slit mirror system in rocket-borne scanning Ebert grating spectrometer, discussing imaging properties and required adjustments

21 p3053 A72-40606

Observation of several X-ray sources in 1970 September.

22 p3219 A72-42554

Sounding rockets for astronomical research, discussing rocket types, payloads, launch sites, advantages over satellites, economic factors and future prospects

22 p3231 A72-42983

Tilting-filter measurements in dayglow rocket photometry.

23 p3289 A72-43893

Rocket-borne GaAs laser radar system with scatter light detector and data processor for upper atmosphere aerosol and pollution measurements

24 p3409 A72-44778

High level cleanliness maintenance and contamination control for instrument unit ring guidance system in Saturn 5 launch vehicle

24 p3388 A72-45297

ROCKET-BORNE PHOTOGRAPHY

Solar disk active centers X ray emission, using rocket mounted pinhole cameras

04 p0567 A72-15164

Mesosphere ozone number densities from rocket photometric measurement of lunar UV radiation absorption

09 p1385 A72-22583

Rocket-borne photographic measurement of Lyman alpha corona brightness during 7 March 1970 eclipse, comparing limb white light variations

13 p2043 A72-29541

White light and XUV coronas on 7 March 1970 from rocket photographs, comparing with X ray, Lyman alpha, Fe XIV and IR eclipse photographs

13 p2031 A72-29542

Rocket-borne coronagraph photometry of solar corona during 7 March 1970 eclipse for streamer analysis

13 p2043 A72-29543

Rocket observation of Ar XII-XVI, Ca XIV-XVIII, and Fe XIV, XV, XXIV in the extreme-ultraviolet spectrum of a solar flare.

20 p2963 A72-38913

Photometric analysis of X-ray photographs of sun obtained with rocket-borne zone plate camera in XUV region

21 p3108 A72-41289

ROCKETRY

U ROCKETS

ROCKETS

Rocket body longitudinal autooscillation modes, taking into account pipeline fluid discontinuous cavitation oscillations

17 p2620 A72-34469

Rocketry and space age inauguration, considering technical, engineering, management and political problem areas

23 p3358 A72-44354

ROCKS

NT ANDESITE

NT ANORTHOSITE

NT BASALT

NT BRECCIA

NT CARBONACEOUS ROCKS

NT ECGLOGITE

NT GRANITE

NT IGNEOUS ROCKS

NT LUNAR ROCKS

NT MOLDAVITE

NT PERIDOTITE

NT SEDIMENTARY ROCKS

NT SHALES

Major and trace element abundances in orogenic area volcanic rocks, considering geographic and stratigraphic relations and composition

05 p0658 A72-16721

Rock type discrimination from ratioed airborne thermal IR scanner images of Pisgah Crater /California/

08 p1162 A72-22018

Broad scale remote mapping of spectral composition of silicate rocks from thermal IR scanner data

14 p2099 A72-30321

Effect of pore pressure on the velocity of compressional waves in low-porosity rocks.

18 p2685 A72-36031

Tectonic dewatering and strain in the Michigamme Slate, Michigan.

18 p2686 A72-36223

Analytical model for a polarizable medium at radio and lower frequencies.

22 p3155 A72-42467

RODENTS

NT GROUND SQUIRRELS

NT MICE

NT RABBITS

RODS

Turbine blades adaptability limits to temperature variations, considering rectangular cross section plastic rod under programmed thermal and tensile load cycles

01 p0143 A72-11372

Stress concentration coefficients calculation at sharp cracks and notches for rods in tension, compression and combined bending and torsion

03 p0443 A72-13457

Stressed state of reinforced physically nonlinear rods under torsion, using theory of functions of complex variables

03 p0447 A72-13731

Plastic torsion of prismatic and anisotropic rods, emphasizing inhomogeneity problems numerical solution

03 p0447 A72-13853

Elastoplastic stability of structural rods in unloadable systems, considering load carrying capacity increase by critical state onset delay

03 p0454 A72-14214

Mathematical models of elastic shells and rods, discussing virtual work, operator classifications, deformations and constitutive equations

03 p0454 A72-14344

Rotating rigid rod and disk relative viscous rings, discussing inertial frames significance

04 p0574 A72-14917

Torsion of hollow beam consisting of two homogeneous isotropic rods with different elastic properties and simply connected cross sections, solving by conformal mapping

04 p0586 A72-14992

Optimal design of solid and three layer rods with prescribed natural frequencies for longitudinal and transverse vibrations, using minimum mass criterion

04 p0587 A72-15047

Rheomobility effects in creep instability of rods with initial deflection, determining critical load by Ritz method

04 p0594 A72-15708

Cross section geometry and deformation effects on rods vibration damping, determining surface layer energy absorbing properties for longitudinal and torsional oscillations

05 p0735 A72-15988

Flexural, longitudinal and torsional vibration damping of various size rods, taking into account surface layer energy loss

06 p0900 A72-18675

Stationary small elastoplastic longitudinal forced vibrations of rods with internal resonance obtaining asymptotic solution of nonlinear partial differential equations

06 p0900 A72-18676

Mixed boundary value problem of partial differential equations describing nonlinear viscoelastic vibration of clamped rods, examining asymptotic solution stability

06 p0901 A72-18716

Torsional oscillation damping in circular rods coated with viscoelastic material as function of resonant frequency

07 p1087 A72-18924

Similarity solution for nonlinear viscoplastic semi-infinite rod under constant velocity impact

07 p1088 A72-19115

Critical stability and supercritical equilibrium behavior of compressed viscoelastic rod

07 p1091 A72-19761

Experimental determination of torsional stresses in rod from moire patterns, describing facility and procedure

07 p1091 A72-19762

Algorithm for solving boundary value problem of integrodifferential equations describing temperature field inside hollow thin walled rod within solar radiation field in vacuum

07 p1028 A72-20207

Free oscillations frequencies and mode shapes determination of two parallel elastically coupled rods of variable cross section, applying Bubnov-Galerkin iterative method

08 p1243 A72-21231

Lattice type structures as discrete elasticity problem, determining potential of thin rods connecting rigid nodes pairs from equations of motion and constitutive equations

08 p1244 A72-21302

Projective geometry method for elastic curve shape of equilibrium-state thin rod subject to end forces

08 p1209 A72-21365

Bending and torsion of thin isotropic rod with identical principal rigidities in bending, writing elastic curve equation in cylindrical coordinate system

08 p1209 A72-21367

One dimensional nonviscous dynamic plasticity theory applicability to impacting rod problems tested experimentally using results from three dimensional and viscous similarity considerations

09 p1408 A72-23557

Wave propagation in bonded discretely inhomogeneous elastic cylindrical rods, including longitudinal and radial motions

09 p1409 A72-23563

Chemical surface treatment effects on mechanically gripped fiberglass rods tensile strength

11 p1674 A72-25827

Dynamical torsion theory of rods deduced from linear elasticity equations, using averaging technique

11 p1736 A72-25987

Thermoelastic stress and displacement in thin finite rod due to distributed time dependent heat sources

11 p1736 A72-25991

Longitudinal bending stability of hard polymer rods under compression load and creep

11 p1675 A72-26824

Longitudinal elastic impact wave propagation along branched thin rods, using Timoshenko theory

12 p1881 A72-27256

Unloading wave propagation in semiinfinite elastoplastic cylindrical rod for concave stress-strain diagram with no initial linear segment

13 p2053 A72-28388

Shearing stresses in rod under torsion, using Prandtl membrane analogy and moire interference fringes

13 p2053 A72-28397

Rods resistance to thermal shock under coupled thermoelasticity conditions, calculating critical thermal flux during thermodynamic compression waves propagation

13 p2053 A72-28399

Frequency equation for torsional wave phase velocity in solid circular rod under initial tension, plotted for various propagation modes

13 p2002 A72-28620

Torsional behavior of prismatic rods with polygonal cross section, using method of summary representations

13 p2057 A72-29080

Torsional vibration damping in circular rods coated with viscoelastic material, noting technique effectiveness at certain resonant frequencies

13 p2058 A72-29209

Stress distribution variations and wave propagation in viscoelastic rod of finite length under impact

14 p2163 A72-30191

Human retinal rod rhodopsin bleaching and regeneration measurements, tracing dark adaptation curves

15 p2184 A72-31364

Tapered elastic rod transient behavior under end impact due to mass striking, computing fixed end stress, struck end velocity and impact time duration
15 p2323 A72-31404

Dynamic stability of elastic systems under broadband random excitation, presenting solution for straight rod under axial pulsating forces via perturbation method
15 p2274 A72-31460

Nonlinear creep failure of imperfect sandwich structures under time variable loading, considering rod and cylindrical shell
15 p2324 A72-31490

Variable cross section rod free longitudinal and torsional vibration frequencies and mode shapes determined by slowly varying parameters approximation method
15 p2327 A72-31740

Flow distribution, vibration, wear and rupturing of rods in vertical pipe for various inlet flows investigated with high speed cameras, photography and transducers
16 p2376 A72-32996

Two dimensional fibrous medium model for strain and stress analysis of structural plate formed by three dimensional grid of rods
16 p2467 A72-33115

Finite length inhomogeneous elastic rod free vibration, deriving asymptotic expressions for eigenvalues and eigenfunctions
17 p2625 A72-34320

On disturbances in a viscoelastic rod of variable cross-section/of Reiss type placed in a magnetic field
18 p2711 A72-36752

Asymptotic method application to wave propagation in nonlinearly elastic rods, describing displacement field by perturbation series
19 p2875 A72-37885

Propagation of bending-torsional waves in a thin curved rod with allowance for the shear effect
19 p2877 A72-38189

Elastic wave propagation in a rod of finite length with a variable cross section
20 p2978 A72-39321

Simulation of torsional vibrations of rods without concentrated masses
21 p3116 A72-40167

Simulation of flexural vibrations of rods without concentrated masses
21 p3116 A72-40168

Axissymmetric impact of compactible rods subjected to finite deformations.
21 p3117 A72-40455

High power pulsed ruby laser and sapphire rods optical contacting technique
21 p3063 A72-40622

Measurement of internal magnetic field distribution in axially magnetized YIG rods based on magnetoelastic resonance absorption.
21 p3097 A72-40692

Application of methods in perturbation theory to the calculation of the natural vibrations of rod systems
21 p3119 A72-41097

Certain class of solutions of the three-dimensional problem for a rigid perfectly plastic material with a family of momentarily inextensible planes
21 p3123 A72-41392

Application of a method using slowly changing parameters for the approximate calculation of transverse vibrations of rods
21 p3126 A72-41550

Asymptotic analysis of the behavior of an elastic rod under aperiodic intense loading
21 p3127 A72-41670

Pontryagin maximum principle for fundamental frequency variation limits of longitudinal vibrations of variable cross section rod
22 p3234 A72-42148

Stability of elastoplastic rod under external conservative and nonconservative forces, discussing non-conservative component effect and critical load magnitude
22 p3234 A72-42149

Internal to total energy relation dependence on deformation time in impulsive loading of homogeneous free rod, noting energy conversion efficiency
23 p3344 A72-43338

Elastic and plastic deformations in torsional moment loaded rod, noting successive approximation for stress functions
23 p3348 A72-43794

Experimental investigation of displacements and stresses in a rod during impact loading
23 p3348 A72-43795

Unsteady longitudinal viscoelastic vibrations of a rod of variable thickness at small values of time
24 p3459 A72-45265

Cross section geometry and deformation effects on rods vibration damping, determining surface layer energy absorbing properties for longitudinal and torsional oscillations
24 p3460 A72-45730

ROGALLO WINGS
U FLEXIBLE WINGS
U FOLDING STRUCTURES

ROLL
Roll control algorithm for parabolic velocity spacecraft reentry, using successive stepwise extrapolation of approach trajectory parameters
05 p0685 A72-16431

HP-115 slender wing research aircraft linear motion and undamped Dutch roll oscillations at high angles of attack
05 p0613 A72-16932

[AIAA PAPER 72-62]
Three stage linear damping of satellite roll and yaw oscillations, using slip motion procedure
05 p2319 A72-31492

Roll angle detector for angular position measurement of two independent bodies, using optical-mechanical-electrical system
15 p2268 A72-32043

Finned missiles nonlinear rolling motion characteristics at large angles of attack, solving differential equation of motion by global nonlinear least squares method
22 p3134 A72-42333

[AIAA PAPER 72-980]
Effect on entry vehicle dynamic stability of aerodynamic and mass asymmetry coupling.
22 p3231 A72-42338

[AIAA PAPER 72-973]
Roll dynamic behavior of a very slender reentry vehicle.
24 p3452 A72-45348

ROLL CONTROL
U LATERAL CONTROL

ROLL FORMING
Metal forming techniques for gas turbine engines, considering isothermal, radial and powder metallurgy preform forgings, contoured cross and form rolling, and squeeze casting
11 p1638 A72-25649

[ASME PAPER 72-GT-58]
Bending roller adjustment parameters for casing shaping in machining process
11 p1642 A72-26815

Normal and tangential force factors in casing shaping by bend roll method
11 p1642 A72-26817

Metal rolling speed effect on force and friction reduction by ultrasonic vibrations imposed on rollers, noting coefficient of friction dependence on deformation
12 p1814 A72-27645

Surface finishing effects on steel sensitivity to stress concentration under variable loads, emphasizing diamond smoothing and roller technique
12 p1831 A72-28246

ROLLER BEARINGS
Misalignment effect on load distribution and fatigue life of tapered roller bearings
02 p0234 A72-11532

[ASME PAPER 71-LUB-6]
Rolling element fatigue lives of through hardened bearing materials, noting alloying percentage effect
02 p0235 A72-11535

[ASME PAPER 71-LUB-13]
Asymmetrically loaded cylindrical roller bearings, describing hollow ended design for fatigue life improvement
02 p0235 A72-11536

[ASME PAPER 71-LUB-14]
Series hybrid fluid film-rolling element bearing analytical and test evaluation for high speed thrust load turbine applications
02 p0235 A72-11537

[ASME PAPER 71-LUB-15]
Oil pumping ability of tapered roller bearing, using boundary layer theory
02 p0236 A72-11541

[ASME PAPER 71-LUB-21]
He-Ne laser velocimeter for roller bearing elements rotational speed measurements, discussing instrument construction and spatial resolution
02 p0224 A72-11745

Stressed state of radial bearings hollow rollers under loads concentrated along generatrix, evaluating test results by statistical analysis
05 p0665 A72-15984

Thin solid film lubricants for use with roller bearings at ambient and elevated temperatures, discussing surface treatment
06 p0823 A72-18585

Lubrication system filtration effects on rolling element bearing life and extended mean time to failure of gas turbine engines
07 p1052 A72-18754

Mathematical model for derivation of asperity or metal-metal contact load sharing of lubricated machine components in journal and roller bearings
09 p1317 A72-22248

Heat generation sources in high speed cylindrical roller bearings for gas turbine oil cooler design
12 p1816 A72-28111

Rolling-element bearings life estimation based on ASME engineering design guide, taking into account materials properties and processing, misalignment, speed and lubrication characteristics
14 p2108 A72-30870

[ASME PAPER 72-DE-29]
Elastic vibrations in roller bearings. I - The rotating mass is balanced with respect to its own rotation axis
17 p2561 A72-35894

Experimental technique for determination of roller bearing preload to optimize dynamic characteristics and minimize operating temperature
19 p2810 A72-38650

Stressed state of radial bearings hollow rollers under loads concentrated along generatrix, evaluating test results by statistical analysis
24 p3408 A72-45726

ROLLERS
Bending roller adjustment parameters for casing shaping in machining process
11 p1642 A72-26815

ROLLING
Gas saturated surface layer deformation in rolled Ti alloys as function of specimen thickness reduction
01 p0077 A72-11080

Recrystallization and rolling temperature effects on W strength and plasticity
01 p0088 A72-11083

Deformation and compression characteristics of W wire rolled from flattened vacuum melts
01 p0077 A72-11084

Thermomechanical conditions of plasticity-to-brittleness transition temperature for optimal rolling of cermet W strips
01 p0078 A72-11088

Rolling workability of pure W single crystals grown by electron beam zone melting technique, discussing crack occurrence
03 p0374 A72-13718

Tungsten wire deformation structure from swaging or rolling and drawing processes, noting cylindrical texture superimposed on fiber texture
03 p0375 A72-13933

Wing tip shape effects on vortex sheet rolling calculation by Belotserkovskii method
06 p0755 A72-17850

Tensile strength of tungsten reinforced nickel, determining temperature effect on fibers deformation after vacuum rolling simultaneously with plastic matrix
06 p0832 A72-18362

Fe powder preform hot rolling, investigating mechanical properties, microstructure and internal oxidation resistance as function of final density
10 p1488 A72-24695

Surface textures in rolled Al sheets, investigating friction and reduction
11 p1638 A72-25509

Rolling operations in vacuum for protection of metallic materials underprocessing
11 p1645 A72-26867

Velocity field at strain center during steel channel rolling, deriving relations for center contour calculation
13 p1964 A72-29149

Texture of Ti-Sn and Ti-Mn alloy specimens observed by X ray reflection technique after hot rolling, annealing and cold rolling
16 p2407 A72-33529

Tensile strength of tungsten reinforced nickel, determining temperature effect on fibers deformation after vacuum rolling simultaneously with plastic matrix
24 p3416 A72-45749

ROLLING CONTACT BEARINGS
U ANTI-FRICTION BEARINGS

ROLLING CONTACT LOADS
Tensometric damage detection in rolling contact bearings from bending stress spectrum, using Si strain and wire strain gages
01 p0078 A72-11379

Ball bearings rolling and spinning friction coefficients determination as function of stress at contact point, race and ball diameter
03 p0363 A72-13561

Structural inhomogeneities effect on fatigue phenomenon in rolling motion, discussing stress cycles preceding active surface degradation
04 p0526 A72-14473

Stressed state of radial bearings hollow rollers under loads concentrated along generatrix, evaluating test results by statistical analysis
05 p0665 A72-15984

Power parameter determination in rotary swaging of thin conical shells, discussing radial contact stresses
05 p0666 A72-16628

Ball bearing rolling contact lubricating oil film thickness theoretical prediction compared with experiment
09 p1318 A72-22850

Electroslag and vacuum remelted maraging steel rolling contact, investigating fatigue life as function of lubricant film thickness/surface roughness ratio
12 p1816 A72-28109

Rolling radius of driven cylindrical wheel with solid rubber tire as function of normal load and tire dimensions
13 p2003 A72-28919

Jet fuel hydrocarbon group chemical composition effects on antiwear characteristics in sliding friction and rolling simulation experiments
13 p2024 A72-29073

Rolling tire frequency response for angular oscillations about vertical axis through axle in wheel plane, using point contact theory
16 p2426 A72-33696

- Photoelastic investigation of a Hertzian contact with shallow grooves in the contact area
18 p2734 A72-36374
- Stressed state of radial bearings hollow rollers under loads concentrated along generatrix, evaluating test results by statistical analysis
24 p3408 A72-45726
- ROLLING MOMENTS**
STOL aircraft roll moment control possibility for externally-blown jet flap due to engine failure
02 p0154 A72-11700
- Thermally expanding surface effects on aerodynamic roll torques on smoothly ablating spinning cones, comparing analytic study and hypersonic wind tunnel test results
[AIAA PAPER 72-30]
05 p0608 A72-16923
- ROLLUP SOLAR ARRAYS**
U SOLAR ARRAYS
ROOM TEMPERATURE
Completely sealed off room temperature CO laser system, discussing performance and continuous wave power
01 p0080 A72-10852
- Room temperature nonaqueous organic solvent electrochemical cell, producing open-circuit potential of 4.5 V
03 p0311 A72-12924
- N-channel MOS FET, measuring X ray irradiation effects on drain current and transfer characteristics at room temperature
05 p0634 A72-16033
- Semiconductor lasers at room temperature, discussing hetero structures and diffused and epitaxial homostructures from basic operation modes and GaAs laser CW operation
06 p0825 A72-17771
- Optically pumped indium-gallium-arsenides laser coherent emission at room temperature, measuring total power conversion efficiency
[AD-737941]
07 p0999 A72-18882
- Transition metals IR spectral absorptivity evaluation at room and liquid He temperatures from reflectivity measurement relative to vapor deposited Au mirror
09 p1309 A72-22604
- Semiconductor laser continuous emission conditions at room temperature, assuming output power drop with increasing current due to p-n junction heating
10 p1492 A72-24582
- Room temperature negative photoconductivity of p-type ZnTe-CdTe solid solutions mixed crystals within model with electron and hole capture levels
14 p2141 A72-30173
- Resonance type facility using dynamic hysteresis loop method to test metal fatigue and anelasticity in torsion at room and high temperatures
14 p2092 A72-30443
- Differences in the creep characteristics at room temperature of steels with and without distinct yield point
17 p2566 A72-34397
- Experimental studies of injection lasers - Spontaneous spectrum at room temperature.
24 p3409 A72-44713
- ROOMS**
NT CLEAN ROOMS
ROOT-MEAN-SQUARE ERRORS
Robust delta modulator configuration with minimal mean square error from signal statistics estimates, discussing design and performance by digital simulation
04 p0486 A72-14486
- Cyclic phenomena periodicity by expected mean square deviation statistical analysis of observational data samples, using null hypothesis and unequally spaced sample intervals
04 p0574 A72-14908
- SNR effect on rms bearing error by amplitude comparison for nonscanning nontracking receiving system with two antenna lobes of arbitrary shape
05 p0629 A72-16577
- Mean square error and bound on relative error for Reissner plate theory, including shear deformation effect
07 p1087 A72-18812
- Stochastic approximation algorithm with nonstationary regression function for signal parameter estimation, considering convergence, mean square error bound and applications
07 p1027 A72-19291
- Computational mean square error due to roundoff in digital filters implemented on fixed point computers
07 p1033 A72-20346
- Criterion for signals records legibility obtained by analog recorders, deriving relationship between normalized root-mean-square error and apparent frequency
09 p1316 A72-23663
- Steepest descent variable step-size algorithm with dynamic programming for mean square error adaptive equalizer, noting convergence
10 p1455 A72-23794

- Mean square error and functional state prediction algorithm for plants controlled by automatic system containing digital computer
11 p1600 A72-25439
- Global sea surface temperature distribution determination with ITOS I radiation measurements and composite histogram, discussing RMS errors
11 p1620 A72-25763
- Failure rate function nonparametric estimators comparison on basis of asymptotic and Monte Carlo mean square errors
13 p1985 A72-28364
- Mean linear velocity of rotation on solar equator to improve Hart rotatory velocity fluctuation values, giving expressions for statistical reestimation of mean square errors
13 p2035 A72-28441
- Optimal optical measurement for two dimensional object position on plane in Gaussian background noise, calculating mean square error for false identification probability determination
13 p1920 A72-29280
- Adaptive radiometer dynamic properties and parameters optimization based on minimum mean square error criterion
14 p2088 A72-30373
- A modified gradient technique for solving boundary and initial value problems.
20 p2946 A72-39618
- Gamma quanta recording efficiency and energy determination by gamma telescopes, calculating root-mean-square error of real gamma spectra
21 p3026 A72-40323
- Reciprocal of normalized mean square error [MSE] and output SNR as performance measures in optimal and suboptimal demodulators
21 p3017 A72-40863
- Determination of radio-meteor velocity with a minimum rms error
22 p3220 A72-41918
- Pulse time positioning under background noise in radar and radio navigation range finders, noting root-mean-square errors and transient response
22 p3153 A72-42117
- Numerical solution of integral equations of the first kind, using a priori information about the function to be restored
22 p3198 A72-42276
- Extension of analytical design techniques to multivariable feedback control systems.
23 p3274 A72-43539
- Reciprocal mean-square error and signal-to-noise ratio as distinct performance measures in below-threshold communication.
23 p3265 A72-44177
- ROOTS OF EQUATIONS**
Stellar secular stability during complex roots onset in model evolution, discussing radiative heat transport coefficient effects
03 p0416 A72-13004
- Spherical harmonics method utilization in radiative transfer calculations, describing characteristic equations roots determination technique
03 p0389 A72-13795
- Elastic equilibrium of circular conical orthotropic shells with linearly varying thickness, determining real and complex roots of stress state characteristic equation
04 p0594 A72-15710
- Error covariance matrix square root calculation in orbit determination from ground based observations
05 p0720 A72-16752
- Generalized root locus graphical plotting by method of normals, comparing to Rinskii method while applying to third order systems
06 p0840 A72-18664
- Linear equations with periodic coefficients in mathematical models for systems with rotating components, discussing methods for obtaining closed form solutions
07 p0913 A72-20204
- Particular solutions to inhomogeneous Bessel and Legendre equations in resonance case
08 p1198 A72-20973
- Motion of heavy solid body about fixed point for Hess conditions, analyzing Euler-Poisson equations solution properties
08 p1207 A72-21345
- Trajectory properties of roots of characteristic equations with complex coefficients for two dimensional systems with feedforward and feedback cross couplings
08 p1200 A72-21768
- Differentiation method for complex root calculation for system of nonlinear equations with analytic functions
13 p1985 A72-28710
- Multidimensional asynchronous FM pulse systems stability, considering continuous linear part transmission matrix poles located on imaginary axis
15 p2212 A72-32172
- Lossless low pass ladder network synthesis in terms of reflection coefficient poles and zeros with application to bandpass matching problem
15 p2212 A72-32248

- A method of solving partial differential equations for boundary layers
17 p2537 A72-34195
- Boundary minorizing of the solution of an equation connected with the Signorini problem
18 p2704 A72-36466
- Symmetric and innerwise matrices for the root-clustering and root-distribution of a polynomial.
19 p2825 A72-37851
- Limiting value of the lower indicator, and lower bounds for integral functions with positive zeros
20 p2947 A72-39863
- General solution of a system of differential equations with an irregular singular point
21 p3075 A72-41095
- Stability criterion and imaginary axis displacement for real roots determination of algebraic equations on analog computers
21 p3025 A72-41806
- Multidimensional asynchronous FM sampled data systems stability, considering continuous linear part transfer matrix poles located on imaginary axis
22 p3162 A72-42080
- Limitations on the synthesis of control systems in the case of incompletely accessible state variables
22 p3162 A72-42739
- Infinitely distant points of a differential equation
23 p3309 A72-43846
- The accuracy of Donnell's theory for very high harmonic loading on closed cylinders.
23 p3350 A72-44059
- On zeros of solutions of the second-order linear differential equation with retardation.
24 p3419 A72-45577
- The automatic computation of exponentials, logarithms, ratios, and square roots.
24 p3383 A72-45668
- RORSCHACH TESTS**
Individual functions and intersubject differences of noise annoyance susceptibility, noting relationship to Rorschach test
16 p2357 A72-32987
- ROSETTE SHAPES**
FORTRAN programs for calculating principal stresses, strains and directions from rosette readings
06 p0781 A72-18324
- ROSSBY REGIMES**
Forced barotropic Rossby waves in homogeneous fluid in rotating cylindrical annulus with differentially rotating source-sink distribution
03 p0340 A72-12974
- Planetary wave spectrum calculation by Galerkin method, discussing angular velocity of longest Rossby waves distortable by zonal flow
05 p0655 A72-16170
- Rossby similarity for barotropic planetary boundary layer flows in terms of nondimensional Reynolds stress and eddy viscosity
09 p1346 A72-22811
- Barotropic instability and vorticity equation of zonal flow with superposed Rossby waves limiting predictability of real atmosphere
12 p1838 A72-27021
- Numerical model of global scale propagating waves in equatorial stratosphere generated by tropospheric heat sources for Kelvin and Rossby-gravity modes
12 p1839 A72-27029
- Transient planetary Rossby waves dynamics in winter stratosphere forced from below, using quasi-geostrophic midlatitude beta plane approximations
13 p1988 A72-28550
- Planetary wave spectrum calculation by Galerkin method, discussing discrete modes of longest Rossby waves distortable by zonal flow
14 p2099 A72-30239
- Planetary wave description by linear difference equation for vorticity transport on hemisphere, considering Laplace operator error
14 p2099 A72-30260
- Planetary waves in terms of geomagnetic secular variation due to earth core fluid oscillation under MHD forces, using thick shell model
16 p2385 A72-33342
- Planetary wave interaction in two level baroclinic atmosphere, using quasi-geostrophic equations
16 p2418 A72-33602
- A three-dimensional model of thermosphere dynamics. I - Heat input and eigenfunctions. II - Tidal waves. III - Planetary waves.
24 p3400 A72-45594
- ROTARY DRIVES**
U MECHANICAL DRIVES
ROTARY GYROSCOPES
NT FLUID ROTOR GYROSCOPES
Elastic strain effects in ball bearing supports on motion of gyroscope Cardan suspension
02 p0231 A72-12565
- Gyro drift random error dispersion reduction in compensated closed loop multirator gyrosopic systems by cross couplings
02 p0231 A72-12566
- Hodograph geometrical analysis of heavy gyrostator motion for center of mass and gyrostatic moment located on first and third principal axes of rotation
08 p1208 A72-21352

Stationary motions, stability of satellite with rotary gyroscope and gimbals in circular orbit and central Newtonian force field
08 p1241 A72-21801

Stationary motions stability of four rotor vertical gyroscopic system on satellite in circular orbit in Newtonian central force field
08 p1205 A72-21804

Vibration measurements of gyromotors with aerodynamic spherical and ball bearings
09 p1263 A72-22347

Hove gyroscope on base uniformly rotating about axis perpendicular to drive axis, considering forced motion elimination possibility
13 p1961 A72-30023

Permanent rotation of force-free gyroscope characterized by outer framework constant angular velocity, defining permanent axes of rotation
15 p2275 A72-31493

Precession theory for transient response of gyroscope to rotation by Hook sphere using supplementary rotor
15 p2235 A72-31897

Gas bearing gyroscope for fluidic guidance and control system, satisfying missile and recoverable booster requirements
18 p2648 A72-36557

High angular velocity device design problems, considering gyroscopes, ultracentrifuges, yarn-spinning textile machinery and dental drill
19 p2809 A72-38544

Compass effect of a gyroscope with forced rotation of the Cardan suspension
24 p3403 A72-45321

ROTARY STABILITY
NT GYROSCOPIC STABILITY
Precessing elliptical orbits stability in Schwarzschild field
04 p0571 A72-14559

Stability control of rotating circular plates with edge slots and membrane stresses by finite element method [ASME PAPER 71-WA/AUT-2] 05 p0733 A72-15951

Aerodynamic radial bearing analysis based on Reynolds equation, emphasizing gas bearing nonlinear oscillation stability
06 p0824 A72-18702

External pressure effects on cantilever rotating shaft vibration, determining critical whirling speed as function of pressure and area distribution by energy method
07 p1096 A72-20528

Rotational perturbation of three bodies in space tied by flexible elastic ropes, relating physical parameters to stable motion regions boundaries
08 p1240 A72-21141

Vibrations causes and degrees of freedom relationship in rotor machines at critical velocities, determining rotor imbalance from amplitude characteristics
08 p1243 A72-21232

Model stability of globular star cluster with nonzero rotational moment, discussing gravitational effects
09 p1383 A72-22494

Motion and stable equilibrium position of horizontal rotor with nonlinear elastic and internal damping properties, discussing stress-strain-time relations of shaft filaments
09 p1409 A72-23613

Axisymmetric satellite rotation about center of mass in circular orbit under Newtonian gravitational field, considering precessional stability
13 p2052 A72-30002

Rotating machines self excited lateral vibration and instability avoidance and identification [ASME PAPER 72-DE-21] 14 p1267 A72-30865

Material damping effect on rotating system stability as function of critical angular velocity, using elastic continuum whirling shaft model
16 p2465 A72-32986

Model stability of globular star cluster with nonzero angular momentum, discussing gravitational effects
17 p2606 A72-34658

On the stability of rotor-and-bearing systems and on the calculation of sliding bearings.
18 p2696 A72-36708

Linear pulsations and stability of differentially rotating stellar models. I - Newtonian analysis. II - General relativistic analysis.
19 p2855 A72-37247

Analysis of effects of fluid energy dissipation on spinning satellite control dynamics.
20 p2976 A72-39115

Rotational perturbation of three bodies in space tied by flexible elastic ropes, relating physical parameters to stable motion regions boundaries
20 p2977 A72-39246

Tidal perturbation of the non-radial oscillations of a star.
20 p2974 A72-39895

Axisymmetric satellite rotation about center of mass in circular orbit under Newtonian gravitational field, considering precessional stability
22 p3231 A72-42730

The rotating noncircular shaft as stability problem of a linear periodic system
23 p3347 A72-43718

ROTARY WING AIRCRAFT
NT COMPOUND HELICOPTERS
NT HELICOPTERS
NT MILITARY HELICOPTERS
NT RIGID ROTOR HELICOPTERS
Earplugs effect on passenger speech reception and intelligibility in rotary wing aircraft, noting protection against noise annoyance, fatigue and deafening
01 p0022 A72-11294

Rotary wing aircraft design features and performance, discussing military and civilian helicopters and future developments
05 p0612 A72-16734

Rotary wing aircraft first flight and envelope expansion at design gross weight
06 p0759 A72-18493

Tethered autostabilized rotor platform for military surveillance, target location and communication, discussing flight vehicle, tethering cable, ground station and guidance-control system
13 p1898 A72-30078

Rotary wing and VTOL aircraft induced downwash effects on ground personnel, considering injuries, body heat loss, work capability impairment and sound pressure effects
14 p2072 A72-30425

A survey of rotary-wing aircraft crashworthiness.
22 p3138 A72-42763

ROTARY WINGS
NT LIFTING ROTORS
NT RIGID ROTORS
NT TILTING ROTORS
NT TIP DRIVEN ROTORS
Automatic ultrasonic testing equipment for NDT tests of helicopter rotor blades
01 p0071 A72-11021

Matrix method calculation for aerodynamic loads, transverse forces, bending moments, torques and twist of hinged main rotor blades in helicopter during forward flight
02 p0294 A72-12440

Helicopter rotor tip drag relief estimate based on two dimensional drag divergence with Mach number, airfoil parameters and flight conditions
02 p0154 A72-12882

High speed helicopter elastic rotor blade suboptimal motion controller decreasing flapping motion and bending loads despite small control angles and vertical gusts
04 p0465 A72-15504

Helicopter rotor boundary layer, comparing analytical shear stress and velocity distributions obtained by momentum integral techniques with hot wire probe experimental data [AIAA PAPER 72-38] 05 p0607 A72-16900

Papers on critical and exploratory flight testing covering rotary wings, lifting bodies and jet engine aircraft
06 p0758 A72-18487

Articulated rotor blade flapping at 0-0.24 advance ratios and constant lift, discussing effects of shaft tilt and collective pitch variations
07 p0910 A72-20205

Critical lift and flow separation on helicopter rotor under dynamic loading as function of flow and blade characteristics
11 p1568 A72-25285

Helicopter rotor blades bending vibrations, examining scale effects, dynamic similarity and natural frequencies via series of Legendre polynomials [AD-745569] 11 p1734 A72-25733

Helicopter rotor blade spars shot peening in centrifugal vibrator, optimizing Cr-Mo-Ni steel surfaces work hardening
11 p1642 A72-26820

Ice formation on helicopter rotor blades, discussing atmospheric moisture and temperature conditions, blade surface temperature, centrifugal and aerodynamic forces and preventive measures
12 p1754 A72-27414

Hydraulic transmission for driving helicopter tail rotor, noting compensatory system for engine failure
12 p1755 A72-27862

Rotating airfoil experimental test program for verification of Himmelskamp and Dwyer-McCroskey theoretical analysis, presenting graphs of lift coefficient vs angle of attack
12 p1752 A72-28124

Subsonic and supersonic heavily loaded axial flow rotors noise, discussing helicopter blade slap effect and compressor rotor-stator interaction
13 p1897 A72-29570

Hingeless blades flap-lag oscillations linear stability characteristics in hovering flight, examining precone, elastic and pitch-lag coupling and induced inflow aerodynamic effects
14 p2072 A72-30289

Hughes 500 and OH-6 helicopter tail rotor cambered blades, comparing thrust and stall characteristics with symmetrical blades
14 p2072 A72-30290

French monograph on flow near rotor blade tips, discussing three dimensional circulation and boundary layer effects, energy losses, velocity and pressure distributions, etc
14 p2069 A72-30950

Hingeless elastic helicopter blades coupled flap-lag motion under quasi-steady aerodynamic loads, reducing equations of motion to coupled nonlinear differential equations
15 p2180 A72-31211

Nonlinear analysis of helicopter rotor blade free transverse vibration under air and centrifugal loadings during forward flight, using matrix method
15 p3233 A72-31407

American Helicopter Society Noise Subcommittee report on physical characteristics and major controlling parameters of rotor induced aerodynamic noise [AHS PREPRINT 625] 17 p2483 A72-34476

Boundary layer velocity profiles on a helicopter rotor blade in hovering and forward flight. [AHS PREPRINT 622] 17 p2484 A72-34482

The controllable twist rotor performance and blade dynamics. [AHS PREPRINT 614] 17 p2488 A72-34483

Influence of airfoils on stall flutter boundaries of articulated helicopter rotors. [AHS PREPRINT 621] 17 p2484 A72-34489

Results of preliminary studies of a bearingless helicopter rotor concept. [AHS PREPRINT 600] 17 p2489 A72-34490

Rotary wings lift and efficiency increase by circulation control via tangential blowing about bluff trailing edge airfoils [AHS PREPRINT 603] 17 p2489 A72-34492

Determination of airfoil and rotor blade dynamic stall response. [AHS PREPRINT 613] 17 p2490 A72-34495

Parametric studies of instabilities associated with large, flexible rotor propellers. [AHS PREPRINT 615] 17 p2490 A72-34496

The wake geometry of a hovering helicopter rotor and its influence on rotor performance. [AHS PREPRINT 620] 17 p2484 A72-34497

Linear air mass flow injection at helicopter rotor blade tips, considering effects on trailing vortex circulation strength [AHS PREPRINT 624] 17 p2484 A72-34498

Achieving fail safe design in rotors. [AHS PREPRINT 673] 17 p2491 A72-34513

Hydraulic systems for driving helicopter tail rotors. II 18 p2642 A72-36524

A vortex model for the study of the flow at the rotor blade of a helicopter
18 p2642 A72-36975

Analytical investigation of the effects of blade flexibility, unsteady aerodynamics, and variable inflow on helicopter rotor stall characteristics.
20 p2887 A72-38950

Unsteady rotor aerodynamics at low inflow and its effect on flutter. [AIAA PAPER 72-959] 22 p3135 A72-42349

Unsteady wake effects on progressing/regressing forced rotor flapping modes. [AIAA PAPER 72-957] 22 p3137 A72-42350

Flap-lag induced nonlinear oscillations in torsionally rigid helicopter blade, solving nonlinear equations of motion by multiple time scales asymptotic expansion [AIAA PAPER 72-956] 22 p3137 A72-42356

Main results of nonlinear rotor theory
23 p3247 A72-43419

Rotary wing head weight estimation for helicopter preliminary design and parametric studies, deriving semiempirical trend formula [SAWE PAPER 914] 23 p3344 A72-43461

Equipment assembly design optimization by operational versions determination and criteria evaluation for optimal conditions, noting rotary wing design
23 p2994 A72-44024

Effects of projectile damage on critical helicopter components.
24 p3454 A72-44609

Investigation of the stability of the tip vortex generated by hovering propellers and rotors.
24 p3361 A72-45327

The use of complex coordinates in the study of rotor dynamics. [AIAA PAPER 72-954] 24 p3369 A72-45413

ROTATING
U ROTATION
ROTATING BODIES
NT COMPRESSOR ROTORS
NT FLYWHEELS
NT IMPELLERS
NT LIFTING ROTORS
NT PUMP IMPELLERS
NT RIGID ROTORS
NT ROTARY WINGS
NT ROTATING CYLINDERS
NT ROTATING DISKS
NT ROTATING SPHERES
NT ROTORS
NT TILTING ROTORS
NT TIP DRIVEN ROTORS
NT TURBINE WHEELS

Iterative solutions for three dimensional turbulent boundary layers on rotating nose-body, using stream-wise and cross flow momentum equations
01 p0002 A72-11397

Rotating cable of high slenderness ratio and small flexural rigidity with end masses, deriving transverse vibration mode shapes and natural frequencies from asymptotic solution

02 p0293 A72-12253

Optimal stabilization of permanent rotation of solid body with arbitrary mass distribution by controlled gyroscope

02 p0230 A72-12337

Finite element technique for stress analysis of rotating bodies under axially symmetric stresses

02 p0293 A72-12343

Equilibrium rotating superdense baryons in general relativity theory, determining integral parameters /mass semiaxes quadrupole moment/ in angular velocity approximation

03 p0435 A72-13805

Polytropic masses oscillations under rapid uniform rotation, using variational principle

04 p0579 A72-15320

Laminar incompressible flow over yawed spinning bodies of revolution by Navier-Stokes solutions, discussing flow fields and corresponding force coefficients

[AIAA PAPER 72-112] 05 p0605 A72-16820

Thermally expanding surface effects on aerodynamic roll torques on smoothly ablating spinning cones, comparing analytic study and hypersonic wind tunnel test results

[AIAA PAPER 72-30] 05 p0608 A72-16923

Numerical solution method for laminar, time dependent and three dimensional boundary layer equations, applying to rotating flat plate in forward flight

[AIAA PAPER 72-109] 05 p0652 A72-16944

Gravitational intensification due to focusing of massive rotating gravitational wave emitting oblate object in galactic center

06 p0880 A72-17887

Neutral rotating mass shell surrounding concentric stationary electrically charged insulation, calculating induced dipole-like magnetic field from coupled linearized general relativity field equations

06 p0853 A72-18423

Free solid body kinetic moment vector effects on long period motion in resonant state during transition from rotational to somersaulting mode

06 p0849 A72-18699

Combined rotational motions of free solid and coupled elastic bodies oscillations around center of mass with nutation passive dampers

06 p0850 A72-18707

Photometer using rotating wedge interference filter as wavelength scanning element near 6300 Å for high altitude sounding rocket application

07 p0985 A72-19403

Variational principle in equilibrium and stability theory of rotating bodies under magnetic and thermal fields, explaining spiral branch number in galaxies

07 p1077 A72-19806

Conical gas film between rotating and vibrating conical rotor and nonmoving bearing, determining gas film stiffness and optimum angle

07 p0971 A72-20093

Existence and branching of analytical solutions to equations describing oscillatory-rotatory motions of system of two pendulums with different masses

07 p1036 A72-20217

Turbopump rotating assembly bearing parameters and inertia products estimation and identification by extended Kalman filtering

08 p1173 A72-20844

Coupled motions of rotating free solid body and elastic rod torsional bending vibrations with precession and forced vibrations from energy exchange

08 p1205 A72-20959

Rotational perturbation of three bodies in space tied by flexible elastic ropes, relating physical parameters to stable motion regions boundaries

08 p1240 A72-21141

Periodic motion of gyroscope, using geometrical method of analysis

08 p1207 A72-21348

Fourth algebraic integral in Kovalevskaya solution of rotating body motion about fixed point regarding angular momentum components

08 p1208 A72-21357

Descriptive geometric method for distribution of axes of uniform rotation of body containing ideal homogeneous incompressible fluid in uniform turbulent motion

08 p1209 A72-21364

Integral contact temperatures and heat balance calculation for heat transfer between contacting bodies with rotational motions

08 p1252 A72-21444

Optimal stabilization of permanent rotation of solid body with arbitrary mass distribution by controlled gyroscope

08 p1168 A72-21552

Liquid filled spinning projectiles and satellites flight stability based on Stewartson gyroscope analysis method

08 p1168 A72-21600

Liapunov stability of circular equatorial motions of light bodies in Kerr gravitational field of massive rotating body, using geodesic lines equations

08 p1210 A72-22071

Vibrations in rotating systems - Conference, London, February 1972

08 p1224 A72-22127

Transfer matrix and dynamic stiffness techniques application to critical speed analysis in rotating machinery

08 p1224 A72-22128

Contactless induction multipoint current sensor design and operation principles for turbomachine rotating component temperature measurement

09 p1310 A72-22740

Perturbed motion of rotating solid body with viscous fluid filled cavity, linearizing motion and Navier-Stokes equations

09 p1295 A72-23487

Massive rotating objects with magnetic fields in galactic nuclei, considering similarities between Crab Nebula and quasars

10 p1535 A72-23908

Dynamic stability of spinning bodies with elastic rods and rigid symmetric rotors parallel to axis

10 p1552 A72-24645

Lift variation effect on rolling reentry vehicle trajectory, calculating deviation from zero-lift impact point

10 p1552 A72-24651

Coupled mode model for dynamic interaction between flexible rotary machines and elastic supporting structures

[AIAA PAPER 72-375] 11 p1730 A72-25399

Linear impulsive spin down from rigid body rotational equilibrium of radiation penetrated opaque compressible fluid in circular cylinder

11 p1680 A72-25555

Baroclinic wave field distributions and balances in rotating annulus with free surface in atmospheric circulation study, noting Ekman layer features

11 p1680 A72-25765

Galaxy formation process in expanding universe from study of hydrodynamic equations for rotating gaseous ellipsoid with uniform density

11 p1717 A72-25865

Cosmic spherical rotating bodies angular velocity zonal distribution determination, noting application to Jupiter and Saturn

11 p1723 A72-26481

Nonresonant mode and nutation damping of rotational-vibrational motion of free solid body with elastic elements

12 p1846 A72-27968

Turbulent Ekman boundary layer characteristics in laboratory rotating apparatus compared with atmospheric field observation data and theories, noting similarity relation validity

14 p2094 A72-30418

Rotating machines self excited lateral vibration and instability avoidance and identification

[ASME PAPER 72-DE-21] 14 p2167 A72-30865

Slender rotating body aeroelastic behavior under inertial, gravitational, thrust, servocontrol, elastic and aerodynamic forces, presenting equilibrium equations in matrix form

15 p2319 A72-31210

Simple Doppler radar using the CL8630 Gunn effect oscillator for the observation of small rotating objects.

17 p2524 A72-34245

Vibration perturbation of slender rotating beam with end masses, using method of matched asymptotic expansions

[ASME PAPER 72-APM-B] 17 p2625 A72-34318

Time evolution of a rotating black hole immersed in a static scalar field.

17 p2605 A72-34536

Rotating body linear dynamic control by complex transfer function approach with application to stability conditions for controlled gyro and homing missiles

17 p2583 A72-35528

Variational principle in equilibrium and stability theory of rotating bodies under magnetic and thermal fields, explaining spiral branch number in galaxies

17 p2617 A72-35730

Passive stability of a spinning Skylab.

18 p2730 A72-36314

Three dimensional photoelastic analysis of edge loaded ring reinforced rotating shells with zero bending, assuming pure membrane stress field

18 p2733 A72-36365

Polarization effects during electron scattering in the gravitational field of a rotating source

18 p2712 A72-36967

Black hole rotational energy extraction by super-radiant scattering with impinging wave amplification and by floating particle orbits with zero net radiation reaction

19 p2857 A72-37720

Differentially rotating magnetoid model for quasar and radio galaxies matter ejection and luminosity mechanisms in terms of magnetic field evolution and current sheet generation

20 p2965 A72-38903

Analysis of effects of fluid energy dissipation on spinning satellite control dynamics.

[AIAA PAPER 72-886] 20 p2976 A72-39115

Rotational perturbation of three bodies in space tied by flexible elastic ropes, relating physical parameters to stable motion regions boundaries

20 p2977 A72-39246

Laminar free convection from a rotating radial plate.

[ASME PAPER 72-HT-46] 20 p2985 A72-39664

Gravitational field of arbitrarily thick steadily rotating shell in general relativity, using successive approximation method

20 p2955 A72-40010

Energy balance equation for machine unit with rotating element, noting energy distribution in periodic and nonperiodic operation modes

22 p3181 A72-41857

A method and equipment for the investigation of spatial vibrations in rotating reductor unit components

22 p3182 A72-42129

Bi-planar wind tunnel free flight test and instrumentation for difference between nonplanar and planar dynamic stability of blunt and sharp half cones, providing angular documentation

[AIAA PAPER 72-983] 22 p3163 A72-42331

Generalized subharmonic response of a missile with slight configurational asymmetries.

[AIAA PAPER 72-972] 22 p3134 A72-42339

Spin induced boundary layer distortion on rotating cone at supersonic speeds via spark shadowgraphs, correlating Magnus and normal force measurements with boundary layer configurations

[AIAA PAPER 72-967] 22 p3135 A72-42343

On the stability of axisymmetric systems to axisymmetric perturbations in general relativity. II - A criterion for the onset of instability in uniformly rotating configurations and the frequency of the fundamental mode in case of slow rotation.

22 p3206 A72-42566

Amplification of cylindrical electromagnetic waves reflected from a rotating body

23 p3262 A72-43307

Balancing aerospace bodies on industrial balancing machines.

[SAWE PAPER 929] 23 p3293 A72-43469

Rotating aerospace vehicles dynamic balance error terms due to despun masses misalignment and aerodynamic effects

[SAWE PAPER 930] 23 p3342 A72-43470

Natural rotation of bodies in Einstein's theory of gravitation

23 p3313 A72-44038

Bounds to bending frequencies of a rotating beam.

23 p3354 A72-44249

Rotating black holes - Separable wave equations for gravitational and electromagnetic perturbations.

24 p3439 A72-45014

About the first integrals of the generalized problem of translatory-rotary motion of rigid bodies.

24 p3442 A72-45235

ROTATING CONES

U CONICAL BODIES

U ROTATING BODIES

ROTATING CYLINDERS

Thin liquid layer linear hydrodynamic stability in vertical rotating tube with core gas flow

02 p0303 A72-12353

Motion stability of sphere and homogeneous semi-infinite rotating cylinder in circular orbits and monoenergetic streams, integrating by trajectories

02 p0285 A72-12832

Displacement equations for rotating cylinder of revolution with stress on boundary corresponding to centrifugal force

03 p0445 A72-13625

Closed form solution of wave equation for sound wave scattering by rotating cylinders and spheres

04 p0550 A72-15567

Nonlinear disturbances of viscous flow in pipes and between rotating cylinders, considering Couette and Poiseuille flows

05 p0648 A72-16027

Hydroelastic vibrations of incompressible inviscid liquid with free surface in uniformly rotating infinitely long circular cylindrical container, investigating response to cylinder walls forced excitations

05 p0735 A72-16065

Fracture theory application to rotating cylinder velocity field determination, emphasizing plastic equilibrium and flow behavior

05 p0738 A72-16424

Numerical solution to Navier-Stokes equations for viscous annular flow between rotating long eccentric cylinders

05 p0605 A72-16821

Coolant flow and heat transfer in rotating cylindrical enclosure, solving Navier-Stokes and energy equations by finite difference formulation

06 p0802 A72-18189

Couette flow between eccentric cylinders with inner cylinder rotating, using least squares numerical method for partial differential equations solution

07 p0970 A72-20070

- Flow stability of viscous fluid in annular space between rotating inner and axially oscillating coaxial outer cylinder, using perturbation method
07 p0971 A72-20089
- Plane potential flow problem for laminar boundary layer on rotating infinite cylindrical blade, using conformal coordinate transformation
08 p1108 A72-21614
- Corrugated cylinder steady rotation in incompressible viscous fluid based on linear or Stokes approximation
09 p1293 A72-22411
- Spiral flow stability between rotating and sliding cylinders, using modified energy theory based on assumption of disturbance invariance along preferred spiral direction
10 p1466 A72-24298
- Helical turbulent flow through concentric annulus with rotating inner cylinder, examining axial and tangential velocity distribution and shear stresses
10 p1471 A72-25190
- Small gap approximation for axial magnetic field effects on stability of nonrotationally symmetric disturbances in inviscid flow between concentric rotating cylinders
11 p1694 A72-25773
- Viscous flow stability between two rotating nonconcentric cylinders, obtaining approximate solution to eigenvalue problem by perturbation method
12 p1799 A72-27846
- Three dimensional hydrodynamic and thermal boundary layers and heat transfer for forced convection flow in rotating cylinder system
12 p1890 A72-28167
- Plane monochromatic electromagnetic wave scattering by rotating metallic cylinder, noting frequency shift dependence on cylinder translational motion velocity
13 p1914 A72-28370
- Viscous incompressible flow between two coaxial rotating circular cylinders with small uniform injection at inner cylinder, obtaining solution of Navier-Stokes equations
13 p1941 A72-28883
- Temperature distribution in rotating cylinder with moving surface source, allowing for heat transfer to ambient medium
13 p2064 A72-28916
- Induced magnetic field effects on MHD flow between rotating coaxial/insulator/ cylinders, obtaining exact solution and graphical results
15 p2288 A72-32420
- Uncontained plastic flow onset speeds for cylinders rotating about longitudinal axes, investigating relation to bursting speed
16 p2475 A72-34172
- Effect of rotation on laminar compressible fluid flow in a vertical cylinder.
17 p2539 A72-34972
- Stability of spiral flow and of the flow in a curved channel.
17 p2540 A72-35051
- Rotation of a cylinder about an eccentric parallel axis in a viscous fluid.
18 p2680 A72-36479
- Flow between eccentric rotating cylinders.
[ASME PAPER 72-LUB-J] 19 p2786 A72-37699
- Spectral theory of Taylor vortices. I - Structure of unstable modes.
19 p2788 A72-38550
- Non-local effects in the stability of flow between eccentric rotating cylinders.
21 p3043 A72-40111
- Draining of a fluid from a rotating cylindrical tank.
21 p3046 A72-41307
- Finite radial oscillations of uniformly rotating gravitating magnetized fluid cylinder model of star formation dynamics
21 p3109 A72-41331
- Correlation of Magnus force data for slender spinning cylinders.
[AIAA PAPER 72-966] 22 p3135 A72-42344
- Effects of non-homogeneity on the stresses in a rotating cylinder.
22 p3240 A72-42877
- Viscous torque on sphere immersed in Newtonian and non-Newtonian fluids in rotating cylinder, comparing experimental results with Collins theory
23 p3280 A72-43714
- Spectral characteristics of the scattering field of a uniformly traveling and rotating impedance cylinder
23 p3265 A72-44202
- Thermal radial stresses in axial compressor disk-to-drum transition areas of operating AM-3 aircraft engine
01 p0143 A72-11374
- Aircraft gas turbine rotating disks thermal and mechanical stresses under variable thermal conditions, describing test assembly
02 p0199 A72-11637
- Laminar flow between stationary and rotating disk with mass flow through concentric circular opening by finite difference method
02 p0203 A72-12098
- Compressible viscous flow between concentric fixed and rotating disks, comparing analog computer calculation with experiment on radial flow
02 p0203 A72-12099
- Slit element flow in shear flow turbopump rotors, presenting solutions for laminar and turbulent flow between two parallel disks rotating with same angular velocity
02 p0204 A72-12227
- Differential nonstationary heat equations numerical solution for bladed gas turbine air cooled disk, taking into account cascade vertical temperature variation and coolant heating
02 p0301 A72-12251
- Unsteady boundary layer flow of viscous incompressible fluid between two rotating coaxial parallel disks
02 p0205 A72-12538
- Gas turbine rotor disk and blade vibrations piezoelectric measurement, describing capacitive transmitter system devoid of rotor mounted power supplies
[DGLR PAPER 71-113] 02 p0232 A72-12735
- MHD flow due to impulsive rotation of infinite disk, observing magnetic field strength effects on velocity components and boundary layer displacement thickness
02 p0267 A72-12772
- Stability of plane rotating galaxies in magnetic field parallel to axis of rotation, showing linearized MHD equations self conjugate for radial disturbance case
03 p0435 A72-13806
- Potentials, currents and velocity variation of rotating conducting disk system in liquid metal medium under uniform longitudinal magnetic field
03 p0397 A72-13996
- MHD boundary layer on rotating disk and on body of revolution in longitudinal flow at large Stewart numbers
03 p0399 A72-14013
- Stress concentration at eccentric holes and effect on strength of full size rotating turbine disks
03 p0450 A72-14108
- Stress concentration of isotropic rotating multiply connected circular and elliptic plates weakened by two circular holes
03 p0450 A72-14114
- Unitary stress state and deformations in rotating axisymmetric disk, using function applicable to axisymmetric pipes
04 p0584 A72-14471
- Rotating rigid rod and disk relativistic rings, discussing inertial frames significance
04 p0574 A72-14917
- Thickness function corresponding to constant velocity loading condition for orthotropic annular circular plate with uniform stress
04 p0591 A72-15279
- Electromagnetic fields produced by quasi-stationary gravitational collapse of uniformly rotating current carrying relativistic thin disk
04 p0579 A72-15321
- Turbulent flow from rotating disk, calculating mean velocities, turbulent intensities and Reynolds stress component
04 p0513 A72-15332
- Compounded rotating disks stress-strain analysis from equilibrium and compatibility equations and boundary condition, comparing results with photoelastic and finite difference approximation
05 p0732 A72-15804
- Stability control of rotating circular plates with edge slots and membrane stresses by finite element method.
[ASME PAPER 71-WA/AUT-2] 05 p0733 A72-15951
- Photoelectric transducer with electric pulses as measure of rotating disk angle of turn, discussing design and measurement accuracy
05 p0662 A72-16124
- High Reynolds number flow between two infinite rotating disks, investigating viscosity effects on flow velocity distribution type from analytic approximation
05 p0649 A72-16611
- Stress analysis of radial flow impeller disk due to centrifugal force in steady state of high speed rotation by matrix finite element method
05 p0741 A72-16996
- Turbine rotating disk hyperbolic thickness critical profile by radial displacement solution
06 p0894 A72-17794
- Isolated rotating disks of stars galactic evolution model for gravitational field studies, noting dynamic instabilities and final exponential mass distribution
06 p0885 A72-18077
- Nimonic 75 sliding pin and rotating disk frictional force, wear rate and surface temperature
06 p0830 A72-18156
- Navier-Stokes equations numerical solution for viscous incompressible fluid in circular cylinder with rotating top disk, computing secondary flow at Reynolds numbers to 400
06 p0802 A72-18526
- Transverse anisotropy effect on collapse loads of plastic rotating disks and circular plates
07 p1093 A72-19946
- Rotating disk background and speed effects on perception of verticality motion in clockwise or counterclockwise direction
08 p1124 A72-20987
- Liquid flow cavitation impact on rotating disk surfaces, showing pitting characteristics dependence on physicochemical properties of specimens
09 p1327 A72-22297
- Nonlinear creep characteristics of variably thick rotating disks under nonuniform heating conditions, determining critical rpm and temperature field and time to failure
09 p1402 A72-22731
- Electrically conducting viscous incompressible fluid rotating with oscillating disk in magnetic field
09 p1366 A72-23575
- Laser beams cross-sectional power distribution measurement by spinning disk scanner, using dual beam oscilloscope for laser beam profile display
10 p1489 A72-23949
- Rotating gas and dust clouds as basis of ring and disk structures in celestial bodies
10 p1539 A72-24311
- Conducting fluid laminar free convective flow over heated rotating horizontal plate in presence of strong magnetic field aligned with rotation vector
10 p1522 A72-24465
- Spiral galaxy density wave maintenance mechanism from rotating disk star-gas system model description of stellar birth and disintegration effects
10 p1547 A72-24869
- Suction or injection interaction with rotation in three dimensional MHD flow between two porous nonconducting disks under magnetic field
10 p1524 A72-25039
- Finite difference method for bending stresses calculation in rotating disks subjected to irregularly distributed temperature, deriving digital computer program algorithm
11 p1712 A72-26976
- Unsteady viscous incompressible electrically conducting fluid flow generated by porous disk rotation, investigating transverse magnetic field effect
12 p1851 A72-27305
- Computer model for evolution of isolated rotating disks of stars, noting gravitational two stream dynamic instability for infinite double periodic stellar systems
12 p1874 A72-27909
- Iterative solution of coupled nonlinear differential equations under boundary conditions for flow and heat transfer of Rivlin-Ericksen fluid between rotating parallel disks
13 p1986 A72-28881
- Concentration profile derivation for fluid flow near rotating disk with chemical reactions, considering concentration gradient and barodiffusion effects
13 p1944 A72-30049
- Thin liquid films on rotating horizontal disk, measuring flow, thickness and stability with asymptotic-expansion solution
15 p2334 A72-31616
- Turbulent diffusion limiting flux variation with angular rotation velocity of rough rotating disk
15 p2217 A72-31676
- Turbulent flow between rotating disk and turbine engine body calculated from equations of axisymmetric viscous incompressible fluid flow
15 p2217 A72-31702
- Computer method of optimal turbomachine disk design, using local search techniques to determine disk minimum weight
15 p2328 A72-31746
- Solution existence for singular boundary value problem involving swirling flow, corresponding to problem of axisymmetric flow above rotating disk
16 p2377 A72-33186
- Rotating disk with eccentric elliptic insert determining elastic field in inclusion by complex variable technique
16 p2427 A72-33790
- The equilibria and oscillations of a family of uniformly rotating stellar disks.
17 p2605 A72-34529
- An asymptotic solution for the laminar flow of a thin film on a rotating disk.
[ASME PAPER 72-APM-38] 17 p2538 A72-34783
- Relativistic kinetic theory combined with surface layer theory in curved space-time to study counter-rotating disks with fine central red shift
17 p2582 A72-35389
- Application of an analog computer to the calculation of partially plasticized rotating circular disks prepared from strain-hardenable materials
18 p2735 A72-36421

ROTATING DISKS

- Whirling elastic shaft-disk system, investigating interaction effects of external and linear/nonlinear material damping, elastic restoring forces and inertia forces
01 p0101 A72-10036
- Fiber reinforced composite rotating disks stress-strain state calculation, discussing steady state closed solutions and approximate methods
01 p0142 A72-11175

On the steady flow between a rotating and a stationary disk with a uniform suction at the stationary disk. 18 p2683 A72-36994

Numerical studies of flow between rotating coaxial disks. 19 p2784 A72-37374

Influence of the earth's outgoing radiation on the temperature of a rotating disk in space 19 p2856 A72-37496

Direction of trailing in spiral galaxies 19 p2863 A72-38067

Hydromagnetic flow between two rotating disks with noncoincident parallel axes of rotation. 19 p2841 A72-38436

Note on displacements in accelerating disks of variable thickness. 20 p2980 A72-39690

Jet streams development in rotating gaseous disk at discrete orbital distances in solar system 20 p2972 A72-39859

Comparison of the experimental characteristics of disk-type and rotodynamic centrifugal pumps 20 p2930 A72-39924

An asymptotic solution for steady flow above an infinite rotating disk with suction. 20 p2886 A72-40015

A study of stress around non-central holes in a rotating tapered disc. 21 p3118 A72-40775

V/STOL aircraft configurations with lifting counter-rotating disks, presenting aerodynamic coefficients from rotating water tank experiments 21 p2990 A72-41070

The stress intensity factors of a radial crack in a finite rotating elastic disc. 21 p3124 A72-41397

Method of calculating rotating disk of complex profile 21 p3127 A72-41701

Studies on the convective heat transfer from a rotating disk. VI - Experiment on the laminar mass transfer from a stepwise discontinuous naphthalene disk rotating in a uniform forced stream. 22 p3243 A72-41946

Flight mechanics of spin stabilized rotating disks for special ordnance delivery, considering aerodynamic parameters relation to dynamic stability and orientation [AIAA PAPER 72-982] 22 p3134 A72-42332

The bursting speed of a symmetrical conical disk with radial holes. 22 p3238 A72-42835

Rotating disks optimal design allowing for creep from additional coupling imposition and contour displacement 23 p3347 A72-43746

Noncoaxial rotations of a disk and a fluid at infinity 23 p3248 A72-43824

Low cycle fatigue under biaxial strain controlled conditions. 23 p3354 A72-44259

The precise simulation of image transfer systems with the aid of an optical convolution obtained with a rotating slit of prescribed form 23 p3261 A72-44361

The coupled transverse vibrations of a spinning membrane disk with a central hub. 23 p3355 A72-44367

Magnetohydrodynamic flow between parallel rotating disks. I - Influence of finite wall-conductance. 23 p3322 A72-44400

Dynamic programming and the optimum design of rotating disks. 23 p3356 A72-44550

ROTATING ELECTRICAL MACHINES

Electrostatic force for rotational torque production, applying to motor design 11 p1603 A72-25743

ROTATING ENVIRONMENTS

Expanding rotating shearing Bianchi type IX universe, investigating rotation effects on singularity 04 p0549 A72-15290

Herzberger fundamental optical invariant for rotationally symmetric systems, using partial differential equations [AD-738406] 05 p0690 A72-16672

Pilot and nonpilot vestibular sensitivity to rotation, determining oculogyral illusion and rotation perception thresholds 06 p0767 A72-17867

Satellite orbital inclination change due to rotating upper atmosphere with day-to-night density variation, deriving resonance conditions 08 p1241 A72-21640

Perturbation solution of deceleration trajectory in ballistic reentry through rotating atmosphere with winds, assuming constant gravitational field and square law drag force 09 p1395 A72-22924

Nystagmus and illusory phenomena in man under simultaneous rotation in two perpendicular planes as function of vestibular excitation 09 p1267 A72-23593

Efferent vestibular activity in response to horizontal plane rotary stimulation in frog, showing efferent relations between both ears 10 p1426 A72-25099

Weightlessness effects on human organism, discussing physiological changes, artificial gravity by spacecraft rotation and exercise to counter adverse reactions 11 p1589 A72-26891

Radiative-dynamic model for static stability of rotating atmospheres, deriving mean equilibrium value of Richardson number in troposphere 14 p2127 A72-30341

Experimental motion sickness studies in slow rotation room simulating rotating spacecraft conditions, noting relation between subject susceptibility and number of head motions 16 p2354 A72-33542

Airline pilot rotation perception during angular acceleration tests, noting power law description of subjective motion for three major body axes 16 p2358 A72-33649

Coriolis forces effect on bubbles trajectories in rotating containers, determining critical Reynolds number 17 p2537 A72-34209

Obedience to rotation-indicating visual displays as a function of confidence in the displays. 17 p2510 A72-35943

The influence of clinostat rotation on the fertilized amphibian egg. 18 p2649 A72-36435

Habitability factors in a rotating space station. 18 p2652 A72-36436

Vestibular and optical stimuli interaction in human orientation, testing via Barany chair on rotating platform surrounded by optokinetic drum 21 p3007 A72-40751

Conjugate and disjunctive optokinetic eye movements in the rabbit, evoked by rotatory and translatory motion. 23 p3257 A72-44243

ROTATING FLUIDS

NT ROTATING LIQUIDS

Rankine vortex conducting gas rotating about cylinder axis, investigating magnetic field effects on transverse waves 01 p0106 A72-10132

Linear spin-down of stratified rotating Boussinesq fluid in circular cylinder as function of Prandtl number, noting solar interior problem 01 p0051 A72-11231

Rotation effects on three dimensional infinitesimal wave stability in Blasius boundary layer 02 p0205 A72-12354

Forced barotropic Rossby waves in homogeneous fluid in rotating cylindrical annulus with differentially rotating source-sink distribution 03 p0340 A72-12974

Perturbation induced long waves boundary effects in ideal incompressible fluid in uniformly rotating basin with stepwise depth difference, using Schwarz symmetry principle 03 p0340 A72-13094

Axissymmetric rotational motion of electrically conducting fluid between dielectric disks in crossed electric and magnetic fields 03 p0399 A72-14012

Supercritical stationary states of dissipative hydromagnetic rotating Couette flow between electrically insulating cylinders within axial magnetic field 04 p0554 A72-14405

Stratified fluid motion between two parallel infinite disks rotating with different angular velocities 04 p0511 A72-14857

Time dependent hydromagnetic oscillations in contained rotating conducting fluid under magnetic field, using interior boundary layer expansion 04 p0549 A72-15115

Weak dissipation and damping of nonlinear long waves propagating in rotating fluids by Korteweg-deVries equation 04 p0513 A72-15329

Flow separation of turbulent boundary layer ahead of inward-projecting normal step predicted by rotational flow analysis via iterative solution [ASME PAPER 71-WA/FE-32] 05 p0599 A72-15924

Stator-rotor induced annular incompressible rotating flow, allowing for blade loading generated vorticity within actuator disk theory [ASME PAPER 71-WA/FE-18] 05 p0599 A72-15929

High Reynolds number flow between two infinite rotating disks, investigating viscosity effects on flow velocity distribution type from analytic approximation 05 p0649 A72-16611

Rotating homogeneous incompressible fluid flow field over step with interior geostrophic regions, horizontal surfaces Ekman layers and vertical shear layers 05 p0653 A72-17008

Coriolis force effect on axially symmetric body oscillating slowly along axis in rotating viscous fluid 05 p0610 A72-17081

Cylindrically symmetrical low viscosity fluid distortion and homogeneous spiral flow stability under rotational self excitation 06 p0799 A72-17981

Homogeneous turbulence with rotatory anisotropy, determining alternating tensor with moment equations 06 p0800 A72-17988

MHD convection in rotating electrically conducting viscous fluid layer within magnetic field, investigating linear stability 06 p0861 A72-18069

Coolant flow and heat transfer in rotating circular cylindrical enclosure, solving Navier-Stokes and energy equations by finite difference formulation 06 p0802 A72-18189

Cylindrically symmetric blast wave generated by infinitely long line explosion in cold and homogeneous gas rotating rigidly within self gravitational field 07 p1070 A72-19134

Rotating homogeneous incompressible fluid flow over various bottom topographies, comparing numerical and analytical solutions with water tunnel experimental results 07 p0970 A72-20071

Trapped modes structure of rotating fluid in thin spherical shell, noting constitution of free oscillation periods 07 p0973 A72-20455

Spiral density waves in galactic model with differentially rotating interstellar gas and stars, deriving dispersion equation by frequency to wave numbers relation 09 p1384 A72-22517

Electrically conducting viscous incompressible fluid rotating with oscillating disk in magnetic field 09 p1366 A72-23575

Rotational, centrifugal and Coriolis force effects on turbulent boundary layer development, discussing changes in structure and shear stress distribution 10 p1464 A72-23870

Steady state exact solutions of MHD equations for perfectly conducting self gravitating incompressible fluid, showing solutions existence for rotating planetary ellipsoid free liquid surface 10 p1539 A72-24328

Convective motions in rotating laterally heated annulus with contacting rigid lid, determining radial temperature difference for transition to vortex regime 10 p1506 A72-24420

Columnar disturbance strengths upstream of obstacle in uniformly stratified or rotating flows relative to validity of Long hypothesis 10 p1470 A72-25063

Secondary flow measurements in rotating ducts, obtaining pressure distributions and cross-flow velocities [ASME PAPER 72-GT-17] 11 p1569 A72-25616

Relaxation analysis of discontinuities in axisymmetric rotating actuator disk flow [ASME PAPER 72-GT-26] 11 p1569 A72-25622

Hydromagnetic stability of rotating nondissipative inviscid incompressible conducting fluid annulus permeated by radially varying magnetic field, considering axisymmetric and nonaxisymmetric disturbances 11 p1619 A72-26639

Streak photography for three dimensional structure of thermal convection in rotating fluid under horizontal temperature gradient, noting time variations of baroclinic waves 12 p1809 A72-27701

Homogeneous turbulence with rotatory anisotropy, determining alternating tensor with moment equations 14 p2093 A72-30214

Computation method for rotating and nonrotating viscous flows boundary vorticity iteration parameters for use with time centered or alternating direction implicit time differencing approximation 14 p2093 A72-30228

Uniform rotation and magnetic field effects on gravitational stability of interface between two semi-infinite homogeneous streams 15 p2284 A72-31593

Velocity distributions for slow steady rotational motion of non-Newtonian inelastic viscous fluid contained between two concentric spheres, using successive approximations 15 p2217 A72-31689

Solution existence for singular boundary value problem involving swirling flow, corresponding to problem of axisymmetric flow above rotating disk 16 p2377 A72-33186

Initial value problem for compressible viscous heat-conducting fluid flows with basic rotation and density stratification in gravitational field 16 p2377 A72-33337

Plane hydromagnetic wave propagation in rotating fluid permeated by variable magnitude and direction magnetic field, observing wave-associated critical level 16 p2436 A72-33567

MHD wave propagation and generation during spin-up of rotating viscous incompressible electrically conducting fluid 16 p2436 A72-33572

The flow caused by the differential rotation of a right circular cylindrical depression in one of two rapidly rotating parallel planes.

17 p2540 A72-35189
Axisymmetric rotating flow past a circular disk.

17 p2540 A72-35190
Motion of a sphere in an electrically conducting rotating fluid.

18 p2714 A72-36123
Finite amplitude disturbances in the flow 8019 of inviscid rotating and stratified fluids over obstacles.

18 p2679 A72-36383
On the steady flow between a rotating and a stationary disk with a uniform suction at the stationary disk.

18 p2683 A72-36994
Classification of the magnetohydrodynamic motions of a rotating fluid

19 p2839 A72-37392
Stability of the Couette rotatory motion of two-phase media

19 p2787 A72-38209
Coriolis force influence on convective stability in viscoelastic fluid layer heated from below, contrasting with rotation effects on ordinary viscous fluid

20 p2982 A72-39326
Small forced oscillations produced by infinite plate vibrations in stratified and rotating viscous fluids, investigating resonance effects on propagation

20 p2912 A72-39330
Transient and steady state vorticity generated by horizontal temperature gradients.

20 p2987 A72-40016
An application of the shooting method to the stability problem for a stratified, rotating boundary layer.

21 p3043 A72-40106
Further study of the severe storm with a rotating updraft configuration.

21 p3077 A72-40466
Rotating fluids density stratification effect on characteristic features of homogeneous Taylor column, noting flow patterns

21 p2989 A72-40652
Free and forced trapped oscillation properties in inviscid rotating fluid, considering modifications for viscosity

21 p3049 A72-40654
Viscous torque on sphere immersed in Newtonian and non-Newtonian fluids in rotating cylinder, comparing experimental results with Collins theory

23 p3280 A72-43714
Elementary considerations of the fluid mechanics of tornadoes and hurricanes.

24 p3421 A72-45021
Stability of coaxial rotating jet and vortex of different densities.

24 p3394 A72-45562

ROTATING GENERATORS

NT AC GENERATORS

NT DYNAMOMETERS

NT TURBOGENERATORS

Kilowatt rotary dc-dc power transformer in modular levels for spacecraft applications, discussing electrical and mechanical designs and characteristics

08 p1112 A72-21414
Magnetic field generation in presence of turbulent velocity distribution, considering gyrotropy parameter equation and nonlinearity

11 p1686 A72-25716
Silicon carbide rotating rectifier alternator with solid lubricated bearings for high altitude environments, noting applicability to supersonic aircraft

17 p2498 A72-35565

ROTATING LIQUIDS

Spiral geometry and distribution of global geomagnetic anomalies, discussing ideal liquid motion between concentric spherical surfaces of earth sub-core and core radii

02 p0218 A72-11952
Motion of asymmetric body of revolution in rotating liquid, calculating drag on ellipsoid

02 p0204 A72-12175
Symphonic satellite stability during perigee, apogee and orbital transfer, considering propellant motion in tank and spinning top containing liquid

02 p0287 A72-12717
Rotary self excitation of helical flows in incompressible liquids, using Navier-Stokes equation

06 p0798 A72-17730
Ideal incompressible fluid sloshing under centrifugal force in partially filled conical cavity rotating at constant angular velocity

08 p1149 A72-21244
Liquid filled spinning projectiles and satellites flight stability based on Stewartson gyroscopic analysis method

08 p1168 A72-21600
Rotary self excitation of helical flows in incompressible liquids, using Navier-Stokes equation

11 p1614 A72-25333
Oscillation periods of rotating perfectly conducting liquid column in presence of axial magnetic field and uniform current

12 p1851 A72-27534

Uniform vertical magnetic field effect on Ekman layer over horizontal plate at rest relative to rotating conducting liquid

13 p2011 A72-29006

Navier-Stokes equation for rotating liquid axial flow past porous plate, noting velocity distribution for suction and thinning effect for blowing

13 p1942 A72-29127
Spiral geometry and distribution of global geomagnetic anomalies, discussing ideal liquid motion between concentric spherical surfaces of earth sub-core and core radii

13 p1949 A72-29264
Two phase propellant flow rate through simulated rotating liquid core nuclear rocket fuel bed under high centrifugal acceleration

14 p2129 A72-30923
Unsteady boundary layer flow equations for arbitrarily smooth bodies moving relatively slowly through rotating liquid

[DFVLR-SONDDR-211] 16 p2376 A72-33007
Rotatory motions of a body with a liquid-containing cavity

19 p2787 A72-38151
Flow stability of ideal compressible and incompressible fluids, solving Navier-Stokes equation for rotating liquid with free boundary in gravitational field

22 p3165 A72-42151
Free oscillations of a liquid rotating in a cylindrical vessel under conditions of weightlessness

22 p3165 A72-42251
The equilibrium configuration of a slowly rotating mass of liquid in the presence of a poloidal magnetic field.

23 p3322 A72-44306
Motion of a rotationally symmetrical gyro with an arbitrary number of vessels containing liquid

24 p3395 A72-45578

ROTATING MATTER

Star cluster stability in form of Einstein model of rotating spherically symmetrical mass system, using Newton approximation

06 p0883 A72-18018

Star cluster stability in form of Einstein model of rotating spherically symmetrical mass system, using Newton approximation

11 p1718 A72-25954

Velocity field measurements from M82/NGC 3034/galaxy H alpha, forbidden N II and S II emission lines, suggesting expanding ejecta cloud rotating about axis normal to galactic plane

13 p2040 A72-29401

Lunar dumbbell shaped glass globules formation due to rotation and surface tension effects of ejecta from meteoric impacts

15 p2306 A72-31628

Numerical calculation for axisymmetric gas cloud rotation effects on collapse, noting implications for star formation and fragmentation

16 p2458 A72-33722

Rotatory perturbations in anisotropic cosmology

19 p2864 A72-38078

Gravitational instability of perturbed and unperturbed matter distribution in form of density and velocity fluctuations associated with continuity relationship between wavelength and rotation direction

23 p3338 A72-44036

ROTATING MIRRORS

High speed rotating mirror camera adapted to solid state laser radiation, noting continuous recording and simultaneous imaging

07 p0990 A72-20401

High speed rotating mirror camera, describing multiplier device for doubling beam scanning speed

07 p0990 A72-20402

Rotating mirror image position sensor for high angular resolution optical tracking, discussing performance improvement by computer generated variable density spatial filter

11 p1591 A72-25312

Q switched carbon dioxide laser based on PM by rotating mirror in one arm of Michelson interferometer, establishing phase relationships

13 p1968 A72-29287

Doppler Q switching in a single-mode CO2 laser by a rotating mirror.

19 p2812 A72-38594

ROTATING PLASMAS

Interelectrode gap position control of discharge in coaxial gas heater with arc rotated by magnetic field

02 p0201 A72-12865

Plasma column interaction with counter rotating hf magnetic fields of multipole configurations, calculating angular velocity

04 p0557 A72-15169

Monograph on design and characteristics of rotating plasma device under crossed electric and magnetic fields, covering dynamic behavior of hydrogen puff

05 p0642 A72-15798

Equilibrium diffusion of rotating plasma in toroidal systems, deriving two fluid hydrodynamic equations with allowance for ion temperature perturbation

05 p0701 A72-17242

Plasma rotation during theta pinch collapse, determining ion azimuthal velocity from fields and pressure gradient measurements via Ohms law

08 p1213 A72-21255

Diamagnetic energy measurements on rotating plasma in crossed static electric and magnetic fields with short circuiting metal wall

10 p1519 A72-24097

Rotating low density plasma in magnetic mirror trap with Penning discharge, determining conditions for oscillations damping and plasma lifetime

10 p1521 A72-24354

Ohmic and internal friction loss minimization in stationary rotating incompressible plasmas, assuming magnetic and velocity fields as Trkal fields

10 p1524 A72-24928

Nonradial oscillations and energy transport in non-magnetic stationary rotating stellar wind in local theory limit

13 p2033 A72-29725

Spoke and disk mode for rotating plasma production in hydrogen, using high speed photographic, electrical and magnetic diagnostic techniques

14 p2139 A72-30855

Rotating plasmas steady MHD equilibria without PS factor enhancement, considering cases of vanishing and nonvanishing toroidal current

16 p2433 A72-32817

Rotating plasma-neutral gas collision interaction studies, determining particle energy and velocity in partially ionized plasmas

16 p2438 A72-33916

Solar flares and prominences rotational motions from spectrographic observations of atomic Al absorption line periodic asymmetry

17 p2608 A72-35086

Isometric motion in relativistic magnetohydrodynamics.

21 p3091 A72-40567

Transverse velocity shear instabilities within a magnetically confined plasma.

21 p3093 A72-41628

On some plasma rotation phenomena on the sun.

24 p3445 A72-45469

ROTATING SHAFTS

NT SHAFTS [MACHINE ELEMENTS]

NT TURBOSHAFTS

Whirling elastic shaft-disk system, investigating interaction effects of external and linear/nonlinear material damping, elastic restoring forces and inertia forces

01 p0101 A72-10036

Hydrostatic pressurized gas seals for rotating shafts under extreme operating conditions, discussing design requirements for small clearances and avoidance of pneumatic instabilities

02 p0236 A72-12425

Rotating shaft fatigue under variable stress cycles, determining safety, bending and torque coefficients

04 p0594 A72-15750

Rigid shaft rotating in hinged and elastic supports with nonlinear characteristics of restoring force, determining free and forced vibration characteristics

06 p0900 A72-18696

External pressure effects on cantilever rotating shaft vibration, determining critical whirling speed as function of pressure and area distribution by energy method

07 p1096 A72-20528

Under-lip temperatures and thermal conductivity in rotary shaft seals, using heat transfer analysis

08 p1178 A72-21934

Twin spool jet engine system, predicting shaft speed effects on whirling frequencies due to gyroscopic action with computer model

08 p1224 A72-22130

Vibration of reciprocating engine crankshafts and steam turbine, alternator and gas turbine rotor shafts supported on hydrodynamic sleeve bearings

08 p1225 A72-22133

Noncontact rotating shaft horsepower measurement, using phase displacement technique [ASME PAPER 72-GT-29]

11 p1630 A72-25625

Variable torque determination in precision work technology, discussing electronic measurements of length, shaft deformation, torsion angle and force

14 p2104 A72-30485

Control design for dynamic (vibratory) loading of high speed rotating machinery, discussing rotor, bearing span and support stiffness and coupling centering [ASME PAPER 72-DE-39]

14 p2167 A72-30872

Axisymmetric ductile rotating shaft failure modes, considering fatigue, buckling and impact stress factors [ASME PAPER 72-DE-40]

14 p2167 A72-30873

Dynamic structural analysis of system formed by engine, variable ratio differential and working machine, calculating differential ratio for constant shaft rotation speed

15 p2182 A72-31609

Rotating shaft bending vibrations under harmonically varying transverse load and periodic parametrically exciting axial force, using linearized theory of small displacements

16 p2463 A72-32877

Material damping effect on rotating system stability as function of critical angular velocity, using elastic continuum whirling shaft model

16 p2465 A72-32986

German monograph on rotating nonround shafts stability under torsion, obtaining equations of motion solution via convergent double series expansion

16 p2469 A72-33399

Unbalanced shafts vibration and stability characteristics, considering elastic and damping properties of sliding bearings oil films

18 p2731 A72-36069

The rotating noncircular shaft as stability problem of a linear periodic system

23 p3347 A72-43718

Effects of projectile damage on critical helicopter components.

24 p3454 A72-44609

ROTATING SPHERES

Composite rotating sphere with concentric inhomogeneity of elastic constants and outer boundary free from tractions, calculating stress by digital computer

02 p0259 A72-12180

Closed form solution of wave equation for sound wave scattering by rotating cylinders and spheres

04 p0550 A72-15567

Viscous fluid steady nonaxisymmetric flow past rotating sphere, obtaining antitorque moment expressions and resisting force projections

10 p1469 A72-24547

Isotropic conducting plasma dynamic behavior near rotating magnetized sphere, showing electric field-produced meridional convective currents

14 p2138 A72-30630

Free molecular flow over rotating sphere satellite, deriving aerodynamic forces on differential surface to determine drag and lift coefficients

16 p2341 A72-32844

Composite sphere and cylinder vibrations, considering radial and rotatory/torsional vibrations

18 p2735 A72-36756

Unsteady motion of a compressible viscous fluid in a spherical layer

18 p2682 A72-36882

Residual drag torque on magnetically suspended rotating spheres.

23 p3315 A72-44540

ROTATING STALLS

Analytical investigation of the effects of blade flexibility, unsteady aerodynamics, and variable inflow on helicopter rotor stall characteristics.

20 p2887 A72-38950

Analysis by hydraulic analogy of rotating separation in compressors

22 p3167 A72-43091

Blade torsional tuning to manage rotor stall flutter. [AIAA PAPER 72-958]

24 p3369 A72-45412

ROTATING VEHICLES

U ROTATING BODIES
U VEHICLES

ROTATION

NT AUTOROTATION
NT EARTH ROTATION
NT MOLECULAR ROTATION
NT PLANETARY ROTATION
NT SATELLITE ROTATION
NT SOLAR ROTATION
NT STELLAR ROTATION

Spatially homogeneous rotating and expanding universe models, deriving Lagrangian function from Einstein field equations

01 p0103 A72-11260

Perspective effects on direction of rotation judgments, using figures with rectangular and trapezoidal contours

02 p0167 A72-11898

Gyrostatt translational rotational motion equations in canonical form without trigonometric expressions in Hamiltonian

05 p0724 A72-16164

Perceived common rotary motion of ambiguous stimuli as criterion of perceptual grouping

06 p0765 A72-17413

Singular integral representations of displacement and rotation vectors for homogeneous isotropic centrosymmetric body, using Nowacki couple stress theory of thermoelasticity

16 p2465 A72-32984

Nonlinear equations of discrete elastic Cosserat media from multipolar media equations, studying small rotation theory

16 p2425 A72-33591

Optical devices to produce transmitted image rotation about axis, comparing derotation systems and roll and high-speed prisms

20 p2927 A72-39849

Control simulation models of three dimensional joint angle motions, including circle, ellipse and straight line trajectories and orientations in space

22 p3162 A72-42187

Interpretation of rotation measures of radio sources. II.

23 p3337 A72-43828

Numerical models of elliptical galaxy based on rotational speed and integral equations for mass distribution

23 p3338 A72-44033

ROTATIONAL FLOW

U FLUID FLOW
U VORTICES

ROTOR AERODYNAMICS

Unbalance response of rotor supported in hydrodynamic gas lubricated journal bearings

[ASME PAPER 71-LUB-10] 02 p0235 A72-11534

High speed helicopter elastic rotor blade suboptimal motion controller decreasing flapping motion and bending loads despite small control angles and vertical gusts

04 p0465 A72-15504

Optimal fixed point hovering rotor design for improved static performance by pulse theory

05 p0601 A72-16350

Helicopter rotor boundary layer, comparing analytical shear stress and velocity distributions obtained by momentum integral techniques with hot wire probe experimental data

05 p0607 A72-16900

Sail rotors for hovering platform, calculating rotor performance based on ideal two-dimensional flexible airfoil section characteristics

05 p0612 A72-16925

High tip speed low loading transonic fan rotor design for weak oblique shocks with improved efficiency and stall margin

07 p0907 A72-18951

Mathematical model for dissipative dual-spin satellite analysis, making use of high speed rotor symmetry to permit quasi-holonomic transformation

07 p1085 A72-19280

Articulated rotor blade flapping at 0-0.24 advance ratios and constant lift, discussing effects of shaft tilt and collective pitch variations

07 p0910 A72-20205

Dynamics of rigid rotor supported on squeeze oil film bearings

08 p1225 A72-22134

General solution for thin airfoil rectilinear motion in ideal incompressible gas, applying to rotor blade lift calculation

09 p1260 A72-22860

Leading edge serrations effect on rotor noise and aerodynamic characteristics, noting vortex and rotational noise reduction and overall efficiency decrease

[AIAA PAPER 72-655] 16 p2349 A72-34079

Exploration of aeroelastic stability boundaries with a soft-in-plane hingeless-rotor model.

[AHS PREPRINT 610] 17 p2489 A72-34493

Hingeless rotor - Experimental frequency response and dynamic characteristics with hub moment feedback controls.

[AHS PREPRINT 612] 17 p2489 A72-34494

Parametric studies of instabilities associated with large, flexible rotor propellers.

17 p2490 A72-34496

Rotor and grid motions associated with holomorphic two dimensional fluid velocity, obtaining aerodynamic forces

19 p2746 A72-37787

State-feedback-controllers and state-estimators design for roll-pitch-horizontal motions of helicopter near hover, using rotor dynamics model

[AIAA PAPER 72-778] 19 p2752 A72-38137

Analytical investigation of the effects of blade flexibility, unsteady aerodynamics, and variable inflow on helicopter rotor stall characteristics.

20 p2887 A72-38950

Comparison of the experimental characteristics of disk-type and rotodynamic centrifugal pumps

20 p2930 A72-39924

Tilt-propeller VTOL aircraft design evaluation based on aerodynamic and aeroelastic model and full scale performance tests

[AIAA PAPER 72-803] 20 p2889 A72-40054

Statistical analysis of influence coefficients and unbalance forces measurement errors in balancing of rotors

21 p2996 A72-41229

Unsteady rotor aerodynamics at low inflow and its effect on flutter.

[AIAA PAPER 72-959] 22 p3135 A72-42349

Helicopter rotor blade flapping motion stability, applying perturbation technique to linear equations of motion for different advance ratios and Lock numbers

[AIAA PAPER 72-955] 22 p3137 A72-42351

Flap-lag induced nonlinear oscillations in torsionally rigid helicopter blade, solving nonlinear equations of motion by multiple time scales asymptotic expansion

[AIAA PAPER 72-956] 22 p3137 A72-42356

Investigation of the stability of the tip vortex generated by hovering propellers and rotors.

24 p3361 A72-45327

The dissipation of tip vortices by mass injection with application to rotor systems.

24 p3362 A72-45329

Decay of swirl in a straight pipe flow /with hub at the entrance/.

24 p3394 A72-45367

Blade torsional tuning to manage rotor stall flutter.

[AIAA PAPER 72-958] 24 p3369 A72-45412

The use of complex coordinates in the study of rotor dynamics.

[AIAA PAPER 72-954] 24 p3369 A72-45413

ROTOR BLADES

Automatic ultrasonic testing equipment for NDT tests of helicopter rotor blades

01 p0071 A72-11021

Gas turbine rotor disk and blade vibrations piezoelectric measurement, describing capacitive transmitter system devoid of rotor mounted power supplies

[DGLR PAPER 71-113] 02 p0232 A72-12735

Two dimensional transonic airfoil section testing at ONERA S3MA wind tunnel, comparing results with helicopter rotor blades test data

[ONERA, TP NO. 1028] 03 p0308 A72-13642

Closed loop fluidic bidirectional jet flap airfoil lift control system, considering application to helicopter rotor blades

05 p0603 A72-16659

Subsonic and transonic compressible potential flow over nonlifting hovering helicopter rotor blades, calculating flow field by three-dimensional nonlinear relaxation scheme

[AIAA PAPER 72-39] 05 p0607 A72-16901

Hingeless rotor helicopter blade steady state response with nonuniform inflow and elastic blade bending

[AIAA PAPER 72-65] 05 p0741 A72-16933

Helicopter rotor blade response to random loads treated by theory of linear dynamic systems with time-varying coefficients

[AIAA PAPER 72-169] 05 p0613 A72-16940

Articulated rotor blade flapping at 0-0.24 advance ratios and constant lift, discussing effects of shaft tilt and collective pitch variations

07 p0910 A72-20205

Pressure sensor measurements of fluctuating aerodynamic forces on rotor blades related to compressor noise generation

[ASA PAPER H 6] 08 p1107 A72-21486

General solution for thin airfoil rectilinear motion in ideal incompressible gas, applying to rotor blade lift calculation

09 p1260 A72-22860

Turbulent boundary layer characteristics of rotating helical blade in annulus contained fluid, calculating boundary layer growth and streamline angles via momentum integral equations

10 p1466 A72-24296

Fan-in-wing model noise due to cross flow generated in- and outflow distortions and unsteady rotor blade forces

[ASME PAPER 72-GT-92] 11 p1571 A72-25666

Integral equation for calculation of unsteady aerodynamic forces on helicopter lifting rotor blades, taking into account air compressibility

[ONERA, TP NO. 1081] 13 p1895 A72-29671

Hughes 500 and OH-6 helicopter tail rotor cambered blades, comparing thrust and stall characteristics with symmetrical blades

14 p2072 A72-30290

Nonlinear analysis of helicopter rotor blade free transverse vibration under air and centrifugal loadings during forward flight, using matrix method

15 p2323 A72-31407

A study of loss of radial equilibrium solution in axial-flow blade row design calculations.

24 p3393 A72-45358

Prediction of velocity profiles for turbulent boundary layers on the blading of radial impellers.

24 p3393 A72-45360

An approximate method for the calculation of the characteristics of axial-flow fans.

24 p3363 A72-45369

Flow analysis in the axial-flow compressor impeller with meridional stream acceleration.

24 p3394 A72-45371

ROTOR BLADES (TURBOMACHINERY)

Sound radiation from axial flow fans running in turbulent flow, evaluating fluctuating lift on rotor blades due to incident gusts

01 p0002 A72-10220

Forged Inconel alloy 718 metal powder preforms for dense aircraft engine compressor rotor blades

02 p0233 A72-11441

Multiple pure tone noise generation from turbofan blade to blade nonuniformities in rotor geometry, using two dimensional inviscid flow model

04 p0565 A72-15568

Centrifugal compressor diagonal type impeller profiling through ruled surfaces delineated by rectilinear generatrices, calculating velocity field of rotating cascade

05 p0603 A72-16626

Boundary conditions in steady and unsteady heat conduction for gas turbine rotors, using blade-disk temperature relation

08 p1222 A72-20944

High speed rotating test rig development for vibration testing of turbine blades, describing design layout

08 p1147 A72-22131

Shrouded propellers and rotor blades free vibrations determination by variational method, showing Coriolis effect on critical flutter speed 11 p1732 A72-25536

Rotor blades setting angle and twist influence on steam turbine wheels vibrational modes and frequency spectra 11 p1732 A72-25537

Noise reduction effects of wake interaction between rotor blade rows in axial flow compressor, cancelling velocity defect at stator position [ASME PAPER 72-GT-15] 11 p1569 A72-25614

Supersonic turbine stator and rotor blading design corrected for boundary layer displacement thickness, discussing limitations due to normal shock wave at flow separation [ASME PAPER 72-GT-63] 11 p1571 A72-25653

Hot corrosion effects on Inconel-700 and Inconel-X gas turbine rotor blades during burning of high sulfur concentration residual oil fuels [ASME PAPER 72-GT-87] 11 p1656 A72-25662

Composite turbofan blades for high temperature applications, discussing weight reduction and design procedure 12 p1816 A72-28102

Profile losses at turbine rotor blade in unsteady gas flow from experimental data analysis, noting effect of turbulence caused by trailing edge wakes 13 p1893 A72-28783

Lift fan blade interaction discrete frequency noise, discussing potential and viscous interactions relation to rotor-stator spacing 15 p2297 A72-32019

Temperature field of a gas turbine rotor blade externally cooled by an air-liquid mixture 19 p2849 A72-38043

Filament winding techniques for rotor blade applications. 19 p2808 A72-38165

Calculation of the plane potential flow past rotating radial blade cascades 19 p2746 A72-38547

An advanced stochastic model for threshold crossing studies of rotor blade vibrations. 20 p2885 A72-39622

Formulation of boundary conditions in the statement of thermal problems for bladed rotors of gas turbines 20 p2987 A72-39926

Analytical method for combining the interaction of inlet distortion and turbulence. 23 p3247 A72-43330

ROTOR DISKS
U TURBINE WHEELS

ROTOR HUBS
U HUBS
U ROTORS

ROTOR LIFT
Critical lift and flow separation on helicopter rotor under dynamic loading as function of flow and blade characteristics 11 p1568 A72-25285

Flow separation effects on critical lift of helicopter rotor, using blade angle of attack criterion 11 p1573 A72-26893

Helicopter maneuverability factors, discussing flight direction change ability, acceleration limitations and rotor thrust requirements [AHS PREPRINT 640] 17 p2490 A72-34500

Helicopter design figure of merit weight ratios definition in terms of rotor thrust coefficient, substituting pure airframe structure weight for conventionally used empty weight [SAWE PAPER 916] 23 p3250 A72-43463

ROTOR SPEED
Altitude-velocity dependence of turboprop engine equivalent horse power, propeller output and specific fuel consumption, discussing performance characteristics relation to ambient air temperature 05 p0708 A72-17100

Gyroscopic effects on elastically supported high speed rotors, examining critical velocity and disturbance behavior via equations of motion 11 p1686 A72-25723

Transient torsional vibration of asymmetric rotor with limited power supply near critical speed calculated by asymptotic method 16 p2463 A72-32874

Hydrodynamic pivoting-pad vane tips for high-speed vane pumps. 18 p2694 A72-36046

ROTORCRAFT
U ROTARY WING AIRCRAFT

ROTORCRAFT AIRCRAFT
Rotorcraft based on VTOL concept for aircraft noise reduction in urban transportation 06 p0758 A72-18248

Crashproof rotorcraft STOL aircraft for rescue operation, discussing orthodox rigid and special rotary wings design, air tunnel experiment and flight tests 06 p0760 A72-18582

ROTORS
NT COMPRESSOR ROTORS
NT FLYWHEELS
NT IMPELLERS

NT LIFTING ROTORS
NT PUMP IMPELLERS
NT RIGID ROTORS
NT ROTARY WINGS
NT TILTING ROTORS
NT TIP DRIVEN ROTORS
NT TURBINE WHEELS

Axial and radial displacements determination in rotor center of gravity for gyroscope with elastic suspension 03 p0360 A72-13560

Dynamic analysis of vertical rotor rotating in elastic sliding bearings, analyzing precession stability and self oscillation zone 04 p0594 A72-15748

Mental rehearsal and physical practice relation to learning rate for rotary pursuit tracking skill acquisition 07 p0925 A72-18801

Mathematical model for multiple bearing supported isotropic undamped rotors with arbitrary stiffness and mass distribution, taking into account horizontal/vertical motion coupling 07 p1096 A72-20529

Dynamical equivalence between vehicles with motor-driven constant speed rotor under bearing friction and freely spinning torque free rotor, deriving equations of motion 08 p1108 A72-21174

Vibrations causes and degrees of freedom relationship in rotor machines at critical velocities, determining rotor imbalance from amplitude characteristics 08 p1243 A72-21232

Monograph on rotor-bearing stability and sliding bearing calculation covering rigid and flexible supports, gyroscopic effects, cavitation, load capacity, etc 15 p2243 A72-31349

Solid and composite rotor induction motors, comparing predicted characteristics based on analytical and numerical analyses 15 p2182 A72-31779

Rotor displacement measurement of electrostatic gyroscope by capacitive sensor using spherical electrode 15 p2236 A72-31899

New hubs for multi-bladed tail rotors. [AHS PREPRINT 602] 17 p2489 A72-34491

Vibration technology: Balancing flexible rotors; Conference, Technische Universitat Berlin, Berlin, West Germany, March 23, 24, 1970, Summaries 18 p2731 A72-36064

Survey regarding present views, directives and standards, and the customary approaches for balancing flexible rotors 18 p2731 A72-36065

Orthogonal functions application to flexible rotors balance, expressing deflections vs angular velocity as sum of eigenvectors 18 p2731 A72-36066

Comparison of the balancing of a flexible rotor following the methods Ferner-Kellenberger and Moore. 18 p2731 A72-36067

Flexible rotors balancing theory based on Fredholm integral equations, considering two- and three-bearing supported shafts with arbitrary mass distribution 18 p2731 A72-36068

Flexible rotor balancing over operational rotational speeds, deriving matrix equation for general conditions based on distributed and concentrated unbalance concept 18 p2732 A72-36071

Balancing of a flexible rotor by means of mode separation. 18 p2732 A72-36072

Calculation of the tightness of threshold joints of gas turbine engine rotor bearings 20 p2979 A72-39589

Non-linear rotor bearing behavior. 21 p3061 A72-41518

ROUGHNESS
NT SEA ROUGHNESS
NT SURFACE ROUGHNESS

ROUND TRIP TRAJECTORIES
Thrust power optimization for spacecraft earth-planet round trip trajectories 01 p0127 A72-10357

ROUNDED LEADING EDGES
U LEADING EDGES

ROVER PROJECT
Nuclear rocket propulsion program, discussing solid refractory core technology, Rover project and NERVA engine development and tests 15 p2273 A72-31811

ROVING VEHICLES
NT LUNAR ROVING VEHICLES

Unmanned remotely controlled planetary rovers for Mars surface exploration, discussing design concepts 15 p2214 A72-32316

ROVINGS
Physical and chemical surface characteristics investigation methods for fiberglass rovings to consider suitability as reinforcement for synthetic resins 16 p2414 A72-33302

Plastic composite container cylindrical wall fabrication by two stage procedure combining radial and cross winding of glass fiber rovings 16 p2398 A72-33305

RUBBER
NT ELASTOMERS
NT SILICONE RUBBER
NT SYNTHETIC RUBBERS
NT THIOPLASTICS

Hollow rubber impact absorber stiffness and deformation characteristics derivation by classical elasticity theory, noting accuracy 06 p0895 A72-17797

German monograph on tire rubber friction on dry and wet rough surfaces, taking into account loading, velocity and temperature effects 09 p1332 A72-22323

Mechanical characteristics of natural and synthetic rubber, noting features of cork filled urethane 10 p1502 A72-24861

Stored energy function for multiaxial stress state in rubberlike materials from tensile data based on Valanis-Landel theory 16 p2472 A72-33838

Friction of rubber on ice. 17 p2560 A72-35225

Linear physical and nonlinear geometric formulation of design problem for prestressed rubber parts based on elasticity theory in terms of assembly requirements 19 p2871 A72-37428

Determination of the natural frequencies and modes of oscillation of a spherical resinous shell 19 p2873 A72-37662

RUBIDIUM
NT RUBIDIUM ISOTOPES

Southern Great Basin upper Cenozoic high Sr87/Sr86 and Sr/Rb ratio basalt initial composition, showing mantle material derivation 05 p0655 A72-16043

Temperature and physical state effects on rubidium optical constants at 0.3-2.4 microns 07 p1050 A72-20522

Optical transmission, reflection and absorption of thin rubidium films for parallel and perpendicularly polarized monochromatic radiation, investigating volume and surface plasma oscillations 07 p1050 A72-20523

Third harmonic radiation generation in phase matched mixture of Rb vapor and Xe, observing nonlinear susceptibility [AD-739764] 08 p1211 A72-21197

Rb87 vapor laser with optical pumping, measuring nitrogen or nitrogen argon mixture buffer gas partial pressure effect on power output 10 p1493 A72-24911

Liquid Rb and Cs density and thermal expansion measurements near fusion point, discussing temperature dependence and gamma ray irradiation method 11 p1746 A72-26237

Nonlinear radiation absorption and resonance molecular fluorescence of saturated diatomic Rb vapors excited by Q switched ruby laser 14 p2109 A72-30353

Oscillator strength and ground state photoionization cross sections computation for Na, K, Rb and Cs atoms, including core polarization correction to dipole moment 16 p2431 A72-33724

RUBIDIUM COMPOUNDS
Superconductivity observation in Na, K and Rb intercalates of molybdenum disulfide comparing transition temperatures 09 p1368 A72-22561

RUBIDIUM ISOTOPES
Rb 87 line shift produced by rare buffer gases and molecular nitrogen measured from applied magnetic field magnitude and hyperfine structure of D lines 10 p1490 A72-24040

Apollo 12 and 14 lunar soils K, Rb and Sr isotopic composition evaluation, noting microbreccia as major nonbasaltic constituent 11 p1723 A72-26497

Buffer gas mixture and pumping light effects on shifts from ground state hyperfine frequency in Rb-85 maser frequency standard 14 p2109 A72-30196

RUBY
Ruby use for submillimeter range optically pumped quantum paramagnetic amplifier 08 p1183 A72-21770

Wear resistance of artificial and natural diamond grindstones in ruby cutting, noting tests for grain geometry and fabrication technique effects 12 p1814 A72-27765

Circularly polarized photon echo decay measurement as function of Cr concentration in ruby, noting relationships to temperature, pulse separation and external magnetic field 15 p2295 A72-32545

Heavily doped ruby optical properties review, discussing N-lines, absorption and fluorescence spectra, interactions with phonon and photon fields and ionic reactions 16 p2441 A72-33522

- Development of phosphorescence during ruby irradiation 23 p3323 A72-43412
- RUBY LASERS**
- Gas bubble damage centers in organic glass produced by quasi-steady ruby laser pulse induced high temperature heating, using high speed photography 01 p0079 A72-10373
- Action kinetics and radiation spectra of multiruby lasers, determining effect of crystal C axes angular orientation relative to ruby pairs geometrical axes 01 p0079 A72-10374
- Cloud energy dissipation coefficient determination by ruby laser device, applying to water content and liquid particle concentration, vapor cloud and aerosol concentration 01 p0094 A72-10562
- Magnetic field effects on ruby laser radiation kinetics and spectral composition, studying crystal heating and light emission 01 p0080 A72-10577
- Multimode Q switched ruby laser temporal coherence, comparing theoretical with experimental results from Michelson two-beam interferometer measurements 01 p0080 A72-10849
- Instabilities in dye switched ruby lasers emission distribution, investigating filament modes 01 p0081 A72-11314
- Hypersonic projectiles wake visualization with holography, using single mode ruby laser and reflected diffuse light techniques 02 p0224 A72-11742
- Low temperature plasma electron density measurements using ruby laser light scattering method 02 p0264 A72-12210
- Pulsed ruby laser with complex mirror resonator including optical delay line, observing mode locking effects in emission dynamics 02 p0238 A72-12290
- Phototropic substance effect on spatial structure of passive Q switched ruby laser emission, considering gallium phthalocyanine solution 02 p0239 A72-12568
- Geos B satellite laser range experiment, discussing ruby oscillator and amplifier as transmitter and optical Schmidt system as receiver 03 p0365 A72-12950
- Ruby ring laser single mode operation with Fabry-Perot etalons for selective feedback, discussing laser emission spectrograms 03 p0366 A72-13194
- Ruby laser radiation nonlinear absorption by azule solutions derived by taking into account two-photon transitions for comparison with measurement 03 p0366 A72-13367
- Spectral and energetic characteristics of ruby laser radiation with two types of three-level radiation centers 03 p0367 A72-13582
- Multiphotonic ionization of atomic cesium jet by Q switched ruby laser beam 03 p0392 A72-14061
- Self focusing effect of Q switched single mode ruby laser emission in CdS crystal, noting 60 kw minimum threshold power 03 p0369 A72-14064
- High power Q switched ruby laser beam one dimensional penetration depth into metal as function of time, emphasizing ionization and plasma heating 04 p0528 A72-14536
- Ultrahigh speed holographic camera for three-dimensional photographs and interferograms, using ruby laser output 04 p0522 A72-15139
- Tunable optical and IR radiation source by rotating lithium niobate crystal in front of Q switched ruby laser 04 p0550 A72-15599
- Giant pulse ruby laser operated at 6 Hz, describing shutter, shutter control unit, cooling system and electrical power supply and control circuits 05 p0667 A72-16035
- Ultrashort light pulse emission during mode locking in ruby lasers in free emission operation, examining first spike radiation 05 p0668 A72-16413
- Self induced transparency effect in ruby laser, investigating light transmission and pulse delay and broadening as function of input energy 05 p0670 A72-17171
- Pulsed ruby laser and photopolymer materials applications to holography, considering research programs for surmounting difficulties 06 p0813 A72-17427
- Airborne ruby lidar application to cirrus and haze layers measurements, deriving optical parameters 06 p0777 A72-18448
- Pulsed ruby laser mode structure effects on quartz damage, noting dependence on propagation and polarization directions with crystal 07 p1001 A72-19196
- Ruby laser emission losses for free lasing modes and threshold and above threshold pumping 07 p1007 A72-20122
- Ruby laser telemetry station operated at 0.7 microns, describing telescope pointing system 07 p0947 A72-20257
- Nanosecond solid dielectric discharger fired by Q switched ruby laser for commutation of coaxial line forming high amplitude voltage pulses 07 p1008 A72-20509
- Optimal location of nonreciprocal disk shaped YIG element traveling wave quantum ruby paramagnetic amplifier for weak magnetic levels 08 p1138 A72-20795
- Signal detection in ruby element quantum paramagnetic amplifier operating at liquid nitrogen temperature 08 p1141 A72-21377
- Ruby laser power output losses at 80 K with spectral line suppression dependence on surface reflection coefficient of plane parallel plate in resonator 08 p1183 A72-22026
- Passive optical shutter implementation for unidirectional emission from traveling wave ruby laser, using diffraction grating 08 p1184 A72-22037
- Two photon absorption of ruby laser emission in mixed zinc cadmium sulfide crystals, plotting laser light damping vs beam power density 09 p1322 A72-22212
- German monograph on luminous intensity amplification by means of solid state lasers covering experiments with GaAs and ruby lasers and traveling wave amplifiers 09 p1322 A72-22331
- Positive pressure cooling of cryogenic baths of liquid nitrogen by helium gas addition for frequency shift of ruby laser 09 p1326 A72-23411
- Ruby laser radiation modulation by mirror ultrasonic vibrations, discussing mechanism 09 p1326 A72-23681
- Pulsed ruby laser with complex mirror resonator with optical delay line, observing mode locking effects in emission dynamics 10 p1488 A72-23764
- Acoustic waves generation in liquids by Q-switched ruby laser, noting transition from plane to spherical waves with dye concentration and focusing configuration variations 10 p1490 A72-23954
- Quantum yield of ruby crystals luminescence for excitation in UV region, noting Cr concentration effect 10 p1490 A72-24043
- Intracavity modulation of ruby laser with frequency near neighboring axial oscillations frequency difference, describing Q switch based on transverse electro-optical effect in KDP crystal 10 p1490 A72-24047
- Inversion spatial nonuniformity effects on spectrum and kinetics of ruby laser, using spherical mirrors 10 p1491 A72-24361
- Heavy ion acceleration from strong electron beam in metallic plasma obtained with ruby laser and positive voltage pulses 10 p1524 A72-25034
- Low temperature plasma electron density measurements using ruby laser light scattering method 11 p1693 A72-25706
- Mode locked ruby laser having triangular ring cavity with four prisms to obtain reliable single-transverse-mode Q switched and normal operation 11 p1647 A72-26150
- Ruby laser coherent light scattering by cylindrical electron beam under longitudinal magnetic field 12 p1820 A72-27586
- Q switched ruby laser radiation spatial coherence, considering modes relationship to permittivity inhomogeneities and changes due to holes burning in population inversion 12 p1821 A72-27591
- Giant pulses generation by ruby laser under self Q switching conditions 12 p1821 A72-27592
- High power pulse generation by ruby laser under free oscillation, using resonator with dielectric mirrors 12 p1821 A72-27597
- Emission characteristics of single mode ring ruby laser under free oscillation conditions, discussing mode selection difficulties 12 p1821 A72-27598
- Ruby laser electro-optical modulator with low modulation voltage, discussing layout, operating principle and laser energy characteristics 12 p1822 A72-27611
- Mode selection in high coherence ruby laser using KDP Q switch 12 p1823 A72-27618
- Spark interferometry of plasma filaments in gases from self focused single mode ruby laser beam 12 p1852 A72-27869
- Magnetic field effect on ruby laser generated plasma in solid target, measuring thermal ion energy increase 12 p1852 A72-27879
- Statistical method of Pearson moments applied to temperature regimes effects on ruby laser output energy distribution 13 p1968 A72-29506
- Spatial coherence measurement of ruby laser light by interference method, calculating diffraction pattern contrast curves 13 p1968 A72-29510
- High power Q switched ruby laser radiation transmission through optically dense plasma, noting bleaching and increased absorptivity 13 p2016 A72-29521
- Optimal energy response conditions for single pulse emission by noninstantaneous switching of ruby and Nd glass lasers 13 p1969 A72-29612
- Temporal, energetic and spectral properties of stimulated emission from Cr doped ruby laser irradiated by Co 60 gamma rays 13 p1969 A72-29613
- Ruby laser emission second harmonic generation effectiveness in organic polycrystals from comparison to lithium niobate 13 p1970 A72-29689
- Semiconducting glass filter time dependent transition, absorption coefficient and luminescent spectral dependences, using monopulsed ruby laser 13 p1971 A72-29909
- Co 60 gamma radiation effect on stimulated ruby laser emission delay time, pulse duration, energy curve and intensity 13 p1972 A72-30005
- Mass spectroscopic determination of vapor composition during GaAs and GaP single crystals exposure to ruby laser radiation 14 p2109 A72-30316
- Nonlinear radiation absorption and resonance molecular fluorescence of saturated diatomic Rb vapors excited by Q switched ruby laser 14 p2109 A72-30353
- Acousto-optical method and equipment for atmospheric gases absorption lines recording with ruby laser for radiation source 14 p2111 A72-30812
- Two beam high speed frame holographic recording of dynamic processes, using passive shutter ruby laser with diaphragmed resonator 15 p2233 A72-31417
- Flashlamp pumped cryptocyanine Q switched high peak power ruby lasers, noting UV radiation responsible for methanolic solution photochemical decomposition 15 p2249 A72-32156
- High speed photography ultrafast shutter based on polymethine cyanide dyes saturability for measuring mode locked ruby laser pulse duration 15 p2241 A72-32553
- Passive shutter power absorption effect on periodically triggered pulsed ruby laser output instability, showing optical inhomogeneity interferograms 16 p2400 A72-33189
- Inversion spatial nonuniformity effects on spectrum and kinetics of ruby laser with spherical mirrors 17 p2563 A72-34960
- Nonpeaked emission from a ruby laser obtained with the aid of bleachable solutions 17 p2563 A72-35306
- Breakdown of some transparent dielectrics under the action of neodymium and ruby lasers in free light emission modes 19 p2810 A72-37542
- Laser-beam-scattering measurement of ion temperature in a theta-pinch plasma and evidence for thermonuclear reactions. 19 p2840 A72-37548
- Interferometric holography of laser-produced gas breakdown. 19 p2798 A72-37623
- Analogy in the evolution of surface and bulk damage features produced by laser radiation in transparent glasses 19 p2812 A72-38541
- Macroscopic photon echo polarization and radiation intensity in Cr ion doped ruby laser stimulated by coherent light pulses 19 p2814 A72-38780
- Investigation of radiation field distribution in a ruby laser with a SFR high speed camera 20 p2931 A72-39318
- Shock waves resulting from interaction of laser radiation with transparent solids. 20 p2933 A72-39522
- An investigation of a possible correlation between the laser output of a ruby rod and the chromous ion concentration. 20 p2934 A72-39643
- High power pulsed ruby laser and sapphire rods optical contacting technique 21 p3063 A72-40622
- Optimal energy response conditions for single pulse emission by noninstantaneous switching of ruby and Nd glass lasers 21 p3063 A72-40665
- Temporal, energy and spectral properties of Cr laser output, considering ruby absorption before/after Co 60 gamma irradiation and radiation density distribution during pumping flashes 21 p3063 A72-40666

Stimulated thermal scattering of picosecond laser pulses. 21 p3063 A72-40779

Light pulse structure and bandwidth bounds in ruby laser with delay line inside variable effective length resonator 21 p3066 A72-40799

Observation of transient behavior of picosecond laser pulses. 21 p3064 A72-41380

Emission synchronization in pulsed lasers 21 p3064 A72-41741

Nonpeaked emission of a ruby laser with frequency tuning and selection 22 p3184 A72-42103

Influence of single-pulse emission from a ruby laser on the plasma of a mercury vapor lamp 22 p3184 A72-42105

Usability of a graphite dish for atom absorption analyses of laser collected samples 22 p3176 A72-42175

Nature of radiation defects formed by ruby laser emission on the surface of solids 22 p3185 A72-42273

Simultaneous recording of laser radiation and signal related to secondary processes, using ruby luminescence for oscillograph triggering 22 p3185 A72-42274

Co 60 gamma radiation effect on stimulated ruby laser emission delay time, pulse duration, energy curve and intensity 22 p3186 A72-42731

German monograph - Amplification measurements and investigation of 'super radiation' characteristics in the case of optically pumped rubies. 22 p3187 A72-43065

Attenuation of ruby laser radiation in the boundary layer of the atmosphere during the temperature-dependent variations of the wavelength 24 p3411 A72-45424

Control of laser pulse duration by nonlinear absorption in semiconductors. 24 p3411 A72-45605

Periodic control of the emission from a ruby laser achieved by a Q switch utilizing the transverse electrooptical effect. 24 p3412 A72-45618

RUDDERS

NT AERIAL RUDDERS

RULES

NT FLIGHT RULES

NT INSTRUMENT FLIGHT RULES

NT WHITHAM RULE

RUMBLE INSTABILITY

U ACOUSTIC INSTABILITY

RUN TIME (COMPUTERS)

Stellar attitude reference and navigation associative processor with high computational speed for radar approach control in ATC 02 p0256 A72-12033

Computational time and computer storage requirements for discrete Kalman filter, comparing simultaneous and sequential types of measurement processing 02 p0198 A72-12806

Different pair potentials for simulating vacancy in Al, discussing program planning for relaxations calculation around vacancy to effect computing time reduction 03 p0378 A72-14253

Backward differentiation formulas application to differential algebraic equations, obtaining efficient algorithm as compared to Gear-Nordsieck method 06 p0779 A72-17479

Linear system digital simulation by matrix exponentiation with generalized hold order algorithm for accuracy improvement at less computer time 06 p0839 A72-17630

Truncated series use in laminar boundary layer calculation, noting computer time saving 06 p0756 A72-18115

Digital simulation for steady state and transient thermal responses of LSI with metal within substrate, considering computer time cost 07 p0954 A72-19176

Interactive simulation language-8 for minicomputer and programming procedures for nonlinear differential equations solution, considering integration step size and computational accuracy and speeds 07 p0951 A72-20334

Conditional mean state estimate approximation for nonlinear systems by parallel computation to reduce computer time 08 p1145 A72-20868

Time shared computer systems output maximization via degenerate exponential distribution function modeling, noting reducibility to Markov processes 11 p1601 A72-25900

Integrals utilization in numerical integration of n body gravitational systems, discussing accuracy and reduced computation time 12 p1874 A72-27903

Time response analysis for digital computer speed evaluation 13 p1925 A72-29270

Simultaneous operation of digital computer units to reduce input times and prolong useful computer operation time 13 p1925 A72-29944

Fast numerical solution for supersonic flow past flat-faced blunt body by integration from stagnation point, noting computing time on CDC 6600 16 p2341 A72-32840

Passive and active electric circuit analysis by structural numbers method with computer time and space advantages, noting application to transistor circuits 16 p2370 A72-32851

Group perturbation method for accuracy analysis of nonlinear stochastic automatic control systems, noting computer time reduction 16 p2371 A72-33091

Fast computational techniques for generalized two dimensional Wiener filtering. 17 p2532 A72-34402

An analog computer technique for estimating sample times for digital simulation. 18 p2663 A72-36305

Computation of optimal controls by a method combining quasi-linearization and quadratic programming. 18 p2673 A72-36824

Memory requirements and computation times for implementing reduced consensus algorithms. 20 p2905 A72-39434

Computerized design for cylindrical cage antenna, using polynomial approximation of current to reduce computer size and time requirements 21 p3028 A72-40511

Efficient method to multiply successively functions of the companion matrix and applying the method to evaluate transient response. 23 p3309 A72-43862

Finite Boolean function computation on sequential machine models, developing exchange inequalities between storage, time, et cetera, for relation of combinational and time complexities 24 p3383 A72-45650

Computer programming for minimization of time required for retranslation with compilers, discussing finite state machine modeling with circulating page loose system 24 p3383 A72-45670

RUNGE-KUTTA METHOD

Finite inflation of toroidal shell with edges bonded to rigid rim, using Runge-Kutta method to solve differential equations based on Mooney strain energy function [ASME PAPER 71-WA/APM-20] 05 p0733 A72-15960

Nonadiabatic real gas nozzle flow with friction and heat transfer to wall, obtaining solution by Runge-Kutta method 05 p0610 A72-17066

Nonlinear vibrational relaxation equations for expanding carbon dioxide-helium-nitrogen laser gas mixture, obtaining mode temperatures and gain coefficients by Runge-Kutta technique 08 p1149 A72-21261

Fifth order modified Runge-Kutta integration algorithm, presenting truncation error estimation method and computation procedure flow chart 10 p1505 A72-24091

High order explicit Runge-Kutta method for linear autonomous systems of differential equations, using interpolation formulas integration 11 p1680 A72-26962

Higher order differential equations solutions for viscoelastic stress-strain functional relationships, recommending Runge-Kutta integration technique 14 p2168 A72-30929

An automated gradient projection algorithm for optimal control problems. 17 p2576 A72-35244

Variable-step truncation error estimates for Runge-Kutta methods of order 4 or less. 22 p3199 A72-42746

High order explicit Runge-Kutta methods construction conditions, discussing error bounds and expansions 24 p3419 A72-45299

RUNOFFS

U DRAINAGE

RUNUP

U ENGINE TESTS

RUNWAY CONDITIONS

Airport cold fog attenuation by propane atomization technique, discussing application at Orly 04 p0508 A72-14686

Crosswind landing under adverse runway conditions, illustrating technique with sketches 07 p0911 A72-18833

Airport fog dispersion methods review, noting seeding and hot air injection techniques 08 p1201 A72-21920

Runway fog dispersal system based on underground installed flight-discarded turbojet engines, discussing system efficiency and economics 09 p1292 A72-22910

Runway unevenness and landing gear characteristics effects on SST vibration during taxiing, taking off and landing 09 p1263 A72-23459

Airport lights system design for optical landing aids, discussing runway illumination conditions 12 p1795 A72-27402

FAA airport fog dispersal program, discussing techniques effectiveness evaluation vs defined goals 13 p1992 A72-28843

Low level vertical wind shear effect on aircraft control, considering runway selection with respect to surface wind conditions 13 p1993 A72-28862

Aeronautical requirements for meteorological reporting and instruments at aerodromes, discussing surface wind, visibility, runway range, weather, temperature and pressure observations 13 p1938 A72-28868

Airport runway fog dispersal in UK, discussing cost projection for chemical seeding system combined with lidar remote sensing 16 p2418 A72-33500

Runway marking requirements for visibility under day and night conditions, considering night reflection value, color stability, durability, noninterference with flight operations, etc 17 p2535 A72-34243

Airport improvements needed for safety. 18 p2675 A72-36784

Airfield flexible pavement design - A state of the art paper. 18 p2675 A72-36787

Airlines and aircraft manufacturers requirements for airport pavement evaluation/data system, discussing relationships between strength, landing gear design, aircraft weight, range, etc 18 p2675 A72-36789

Day-to-day operational airplane-airport relationship, discussing runway grooving impact and friction coefficient measurement [AIAA PAPER 72-813] 19 p2750 A72-38118

Visibility variations at Schiphol-Airport, Amsterdam. 22 p3202 A72-42886

RUNWAY LIGHTS

Automatic instrumental measurement of runway visual range at airport 04 p0508 A72-14679

Airport lights system design for optical landing aids, discussing runway illumination conditions 12 p1795 A72-27402

Airport runway lighting systems development, noting lamp for night flights and control console 13 p1940 A72-30119

RUNWAYS

Airport apron surface pavement strain measurements under field loading conditions, considering static and dynamic loads with finite element method 01 p0047 A72-10192

Atmospheric temperature and pressure altitude effects on runway lengths and aircraft takeoff weights [ASCE PREPRINT 1242] 01 p0047 A72-10193

Lime, cement, fly ash and sand combination airport pavement design and testing, discussing material structural and chemical properties, compressive strength, costs, etc 02 p0200 A72-12023

Spiralport design for maximum utilization of airport runways for landings and takeoffs 05 p0644 A72-16693

Anthropotechnical aspects of aircraft taxiing guidance in airfield runway areas, suggesting computerized operational system 09 p1269 A72-22779

Optimal high capacity runway systems for major airports, discussing multiple systems in anticipation of future mass air traffic requirements 10 p1459 A72-24169

Runway motion stability of aircraft with three wheel landing gear, assuming elastic response to moment induced drift 12 p1753 A72-27235

Future short haul aircraft transportation systems, discussing aircraft forms, noise reduction technology and runway requirements 12 p1754 A72-27660

Atlanta airport redesign and expansion program including runway reconfiguration taxiway relocation and passenger and cargo terminal system improvement to relieve congestion 18 p2675 A72-36781

Independent parallel runway landing system to relieve air traffic congestion, investigating minimum spacing required to minimize collision risk 22 p3203 A72-43130

RUPTURING

Fragment velocity for bursting gas containers in vacuum [ASME PAPER 71-PVP-14] 02 p0295 A72-12473

Rupture strength of disk with surface crack under concentrated loads, applying integral equation to stressed state 07 p1092 A72-19777

Sudden pilot incapacitation and death due to subarachnoid hemorrhage secondary to ruptured intracranial aneurysm 10 p1429 A72-23742

- Increased volume fraction effect on transverse rupture strength and fracture toughness of hot pressed and annealed composites of polycrystalline magnesium oxide
13 p1980 A72-29828
- Deformation modes for deep drawing of extramild steel sheets, noting susceptibility and rupture criteria
16 p2396 A72-32872
- Work hardening and anisotropy coefficients effects on deep drawing limit curves for extramild steel, noting rupture strain and deformation trajectories
16 p2396 A72-32873
- Deformation and failure characteristics of joints in a Ni-Al system under the action of high thermal pulses
20 p2942 A72-39822
- The bursting speed of a symmetrical conical disk with radial holes.
22 p3238 A72-42835

RUTHENIUM

NT RUTHENIUM COMPOUNDS

RUTHENIUM ALLOYS

- Phase diagrams of Ru binary and ternary systems, noting admixtures interactions
14 p2123 A72-30992
- Ru-Nb-Zr alloys phase diagrams from physicochemical analysis, noting components interaction
14 p2123 A72-30993
- Absolute thermoelectric power of chromium-ruthenium alloys.
20 p2942 A72-39988
- Phase diagrams, solubility and alloying of Pt, Pd, Ru, Ir and Rh with noble, alkali earth, rare earth and transition metals
22 p3191 A72-42810

RUTHENIUM COMPOUNDS

- Osarsite, a new osmium-ruthenium sulfarsenide from California.
22 p3172 A72-42450

RUTILE

- Tantalum and tungsten vanadium trirutile oxides crystallographic order ratio from diffraction spectrum intensities and overstructure lines disappearance
05 p0675 A72-16699
- Rutile creep resistant substructure recovery at 1000-1040 C, discussing stress relaxation mechanism due to dislocation walls or subgrain boundaries migration
07 p1023 A72-18800

RVAN MILITARY AIRCRAFT

U MILITARY AIRCRAFT

RYDBERG SERIES

- Formaldehyde photoionization and absorption spectrum measurements in vacuum UV region, using single configuration self consistent field procedure for Rydberg states and model
03 p0321 A72-13856
- HD absorption spectrum measurements in vacuum UV region for Rydberg states and ionization energy determination
16 p2431 A72-33583

S

S BAND

U SUPERHIGH FREQUENCIES

S GLASS

- S-glass fiber bundles and composites under quasi-static loads, investigating strength characteristics and failure mechanism
04 p0592 A72-15474
- Stress rupture data from S glass composite matrix effectiveness tests, noting skewed lifetime distribution in statistical patterns
08 p1192 A72-21683
- S glass/epoxy composites strength retention properties under long duration tensile load, proposing use of stress rupture data for reliable safe structural design
10 p1501 A72-24263
- Strength of S-glass fiber.
21 p3072 A72-40554
- Stress-rupture of simple S-glass/epoxy composites.
23 p3305 A72-34392

S MATRIX THEORY

- Computer program for microwave circuit scattering matrix sensitivity, applying to stripline elliptic low pass filters and thin-film negative resistance transistor amplifier
01 p0034 A72-10688
- High frequency diffraction problems, using matrix formulation in spectral domain
04 p0489 A72-15396
- Electron tunneling probabilities through slowly varying potential energy barrier with potential holes evaluated by T scattering matrix interaction formalism
04 p0563 A72-15471
- Electric network scattering matrix and associated incident and reflected wave variables concepts applications in linear optimal control problem
04 p0507 A72-15528
- Thermodynamic quantities expression in terms of S matrix to formulate questions pertaining to statistical

mechanics-particle physics boundary, applying to cosmology
09 p1355 A72-22750

Closed loop system stability, considering small gain and passivity theorems interrelationship and scattering matrix
11 p1612 A72-26470

Scattering matrix derivation for parallel plate waveguide array terminated in infinite plane, determining neighboring guides TEM modes mutual coupling
13 p1921 A72-29345

Two sided error estimates for electrodynamic impedance, admittance and scattering matrices in diffraction theory
18 p2657 A72-36104

Radiation scattering matrix derivation with allowance for phase correlation, deriving method of radiation transfer equations solution for magnetic field
19 p2834 A72-37819

Wave reflection and transmission characteristics of angled rectangular waveguide, deriving scattering matrix
19 p2764 A72-37938

Atmospheric surface layer light scattering matrices from nighttime air flows, showing climatic variability and similarity between Crimean and Moscow measurements
20 p2948 A72-39014

The Mueller matrix for scattering - Including the effects of interference.
20 p2970 A72-39754

On the comparison of phase and multi-layer techniques for numerical solution of the scattering problems.
22 p3154 A72-42305

S WAVES

- Earth mantle shear velocity model derived from S waves travel time gradient direct measurement, disregarding deep depth lateral homogeneity assumption
04 p0519 A72-15578
- Velocity field time history of interacting shear waves in infinite homogeneous chemically reacting fluid for turbulent combustion studies
05 p0747 A72-16367
- Dynamic stress concentration around elliptical discontinuities in elastic medium, considering rigid and empty cavity scatterers for compression and vertically polarized shear incident waves
10 p1554 A72-24180
- Many electron pseudopotential method for electron-atom scattering, calculating singlet s wave and p wave phase shifts
12 p1848 A72-27429

Velocity behavior of shear waves propagating in uniaxially prestressed isotropic elastic body
12 p1886 A72-27982

Antiplane shear wave diffraction by two coplanar Griffith cracks in infinite isotropic homogeneous elastic medium
16 p2464 A72-32919

Elastic longitudinal or shear wave scattering by movable rigid sphere embedded in elastic solid, showing inverse Rayleigh limit dependence
16 p2423 A72-32988

Hulthen and Schwarzschild potentials in the Klein-Gordon equation.
18 p2711 A72-36515

S-N DIAGRAMS

- Cyclic deformation and energy dissipation during fatigue breakdown in steels under tension-compression and torsion
03 p0372 A72-13590
- Secondary fatigue curves for determining service life of metal specimens under unsteady loads
03 p0445 A72-13592
- Beta structure effect on cyclic fatigue strength in Ti alloy under various heat treatments
03 p0372 A72-13595
- Stepwise thermomechanical treatment effect on improved cyclic fatigue strength of Ni-Cr sheet steel with tension and rolling deformations
03 p0372 A72-13598
- Approximate S-N fatigue testing/digital computer method for quasi-static boundary value problems in plasticity theory, applying to continuum models
03 p0453 A72-14210
- Nickel base alloy under axisymmetric tension compression tests, obtaining breaking load diagrams and fatigue and creep curves
06 p0833 A72-18638
- The use of airborne magnetic tape recorders for fatigue life monitoring.
17 p2553 A72-34812
- Surface cold-working as a means of increasing the short-term fatigue endurance of machine elements
19 p2808 A72-38015
- Influence of the structure of VTZ-1 and VT-18 alloys on the fatigue strength for an asymmetrical loading cycle
19 p2819 A72-38017
- An advanced concept of the Woehler diagram and a new calculating procedure for the application of the

extreme-value method to experimental data in the calculation of fatigue strength
20 p2926 A72-39572

Fatigue strength of welded aluminum-connections - Investigation with the aid of multiparameter life length lines
20 p2930 A72-39941

Low carbon steel S-N diagram for stresses ranging to fatigue limit, noting cyclic creep, macroplastic cyclic stress and fatigue failure
21 p3122 A72-41333

Strain multiplier with S-N fatigue life gages, discussing design and performance
22 p3179 A72-42708

Fracture mechanics and cumulative damage of simulated solid propellant under dynamic loads, obtaining low cycle fatigue curve
23 p3325 A72-43706

Investigation of the thermal fatigue of Khl8N10T steel under complex stress-strain state conditions
23 p3301 A72-43956

The fatigue strength under varying mean stress.
24 p3455 A72-44629

S-18 SATELLITE

U OAO

S-49 SATELLITE

U OGO-A

S-3 AIRCRAFT

S-3A Viking land based antisubmarine warfare maritime and reconnaissance aircraft, describing flight controls, structural design, underslung podded engines and operational equipment
06 p0758 A72-17583

S-3A Viking systems.

- Aerodynamic design and development of the Lockheed S-3A Viking.
[AIAA PAPER 72-746]
19 p2751 A72-38122
- Use of fixed and moving base flight simulators for the aerodynamic design and development of the S-3A airplane.
[AIAA PAPER 72-764]
20 p2888 A72-40052
- S-3A aircraft weight control program organization and methods, considering cost and schedule performance
[SAWE PAPER 906]
23 p3250 A72-43453

S-67 HELICOPTER

- S-67 flight test program.
[AHS PREPRINT 653]
17 p2488 A72-34479
- Flight investigation of design features of the S-67 winged helicopter.
[AHS PREPRINT 601]
17 p2488 A72-34485
- SAAB AIRCRAFT
Development of the Saab-Scania Viggen.
19 p2748 A72-37749

SACCHARIDES

U CARBOHYDRATES

SADDLE POINTS

NT SADDLE POINTS [GAME THEORY]

SADDLE POINTS [GAME THEORY]

Absolute and convective plasma instabilities distinction in one dimensional linear infinite system, discussing saddle points method
11 p1697 A72-26585

SAFETY

NT AIRCRAFT SAFETY

NT FLIGHT SAFETY

NT INDUSTRIAL SAFETY

NT REACTOR SAFETY

Literature review of structural safety, treating load, strength, dynamic structural and structural reliability analyses and design aspects
10 p1560 A72-25174

Polymers flammability tests for research, safety and acceptance purposes, noting ignition limits, decomposition and testing procedures
11 p1746 A72-26044

SAFETY DEVICES

NT EJECTION SEATS

NT ESCAPE CAPSULES

NT HELMETS

NT SEAT BELTS

NT SPACE SUITS

Helmet systems for head protection from concussion and deformation, discussing design and testing
08 p1126 A72-21568

Collision avoidance systems requirements and criteria, evaluating Eros time frequency and Secant interrogation-and-reply systems
09 p1349 A72-22822

Superconducting magnetic suspension systems safety aspects, discussing relief valves for He boil-off, flowmeters, cryostat temperature monitors, power supply diodes and safety interlocks
10 p1462 A72-24774

General aviation crashworthy personnel restraint systems, discussing strap take-up devices, comfort, fit and ease of use
13 p1908 A72-28726

Preventive and remedial space flight safety engineering, discussing escape capsules and onboard and earth-launched rescue systems
17 p2620 A72-34427

Some aspects of survival and rescue of astronauts in polar regions.

- 17 p2507 A72-34435
- An assessment of energy absorbing devices for prospective use in aircraft impact situations.
- 22 p3237 A72-42764
- Detection of hazards associated with aerospace operations.
- 23 p3287 A72-43424
- Nuclear safety in nuclear power and propulsion devices for space.
- 24 p3424 A72-45180

SAFETY FACTORS

- Pressure altimeter system minimum safe performance standards for subsonic aircraft operation, describing test procedures
 - [SAE AS 942] 01 p0064 A72-10386
 - Aircraft interior materials selection relative to fire hazards and smoke emission properties
 - [PI PAPER 18] 03 p0380 A72-13249
 - Pressure vessels with cracks, formulating stress analysis for safety factors
 - 03 p0443 A72-13452
 - Space shuttle safety problems, discussing hydrogen pump bearings and air breathing turbofan blades failures and fuel tank fire hazards
 - 03 p0441 A72-13694
 - Safety factors of aircraft flight instruments, discussing altimeter and artificial horizon reading errors and modifications
 - 03 p0319 A72-13698
 - Oxygen hazards, mishaps and safety programs in NASA operations, considering material, design, cleaning and procedural deficiencies and failures
 - 04 p0564 A72-14436
 - Book on system safety engineering covering systems analysis and engineering, evolution of safety philosophy, product reliability and liability, etc
 - 04 p0477 A72-14573
 - Rotating shaft fatigue under variable stress cycles, determining safety, bending and torque coefficients
 - 04 p0594 A72-15750
 - Strength margin estimation in materials sustaining cumulative static and damage under cyclic thermal loads
 - 05 p0735 A72-15994
 - Leads and booster explosives replacements for tetryl, discussing military specifications and safety criteria of various newly developed compounds and mixtures
 - 08 p1220 A72-20770
 - Safety evaluation for pyrotechnic devices during life cycle including R and D, production, loading, handling, shipment, storage, maintenance and disposal
 - 08 p1221 A72-20773
 - Safety factor distribution function for plastic collapse of structure with random resistance members, discussing variance-expected value ratio
 - 09 p1406 A72-23075
 - Safe exposure times for men working in high temperature environments, showing hyperbolic heat collapse relationship to environmental severity
 - 10 p1432 A72-24990
 - Reliability, operational safety and system concept interrelationship in automatic meteorological stations
 - 10 p1463 A72-25011
 - Safe aircraft fuels crashworthiness evaluation in terms of ignition susceptibility parameter, noting full scale crash environment simulation
 - [ASME PAPER 72-GT-27] 11 p1702 A72-25623
 - Argon and mercury ion engines operation, performance and control, evaluating safety and ease of handling from laboratory test data
 - 13 p2026 A72-28931
 - Hot wire and exploding bridgwire detonators, design characteristics, handling safety and hazard situations
 - 16 p2442 A72-33358
 - Geometry comparisons for weight and safety of multiwatt radioisotope heaters.
 - 17 p2579 A72-35352
 - Concrete airport pavement thickness determination methods comparison, noting design life dependence on safety factors
 - 18 p2675 A72-36786
 - Pressure vessels with cracks, formulating stress analysis for safety factors
 - 24 p3458 A72-44927
 - Safety design of space station against collision hazards with artificial orbiting bodies.
 - 24 p3449 A72-45143
 - Strength margin estimation in materials sustaining cumulative static and cyclic damage under thermo-cyclic loads
 - 24 p3460 A72-45736
- SAFETY HAZARDS**
- U HAZARDS**
- SAFETY MANAGEMENT**
- Pyrotechnic hazard classification for property and personnel protection in event of accidental explosion
 - 08 p1220 A72-20768
 - Safety design review for Skylab program based on experience from prior space projects and ground tests
 - 10 p1550 A72-23990

- General aviation equipment standards in light of air traffic system safety needs, emphasizing Technical Standard Order system
 - [SAE PAPER 720307] 11 p1748 A72-25571
 - Storage and handling of cryogenics.
 - 19 p2784 A72-38827
 - Relative safety afforded operator by various hydrogen pressure gage case designs, recommending specific features and mounting requirements
 - 19 p2755 A72-38833
 - Apollo/Saturn 5 spacecraft liquid propellants safety procedures in event of fire on explosion in operations building at Kennedy Space Center
 - 23 p3343 A72-43552
 - Weather satellites - Their role in the application of environmental services to the marine industries.
 - 24 p3420 A72-44648
 - Toxicity of rocket fuels
 - 24 p3433 A72-44781
- SAGITTARIUS CONSTELLATION**
- High resolution Galactic center interferometric observations at 5 GHz, showing compact components in Sagittarius A
 - 04 p0580 A72-15511
 - Soft X ray survey of galactic plane from Sagittarius to Vela by proportional counter, observing radiation sources
 - 06 p0873 A72-17890
- SAHA EQUATIONS**
- Hydrogen plasma ionization equilibrium and thermodynamic stability existence condition based on Saha equation
 - 07 p1044 A72-19889
 - Saha equation for plasma ionization energy lowering, using three particle distribution function and BBGKY hierarchy
 - 08 p1212 A72-20939
 - Hydrogen plasma ionization equilibrium and thermodynamic stability existence condition based on Saha equation
 - 17 p2590 A72-35137
- SAILPLANES**
- U GLIDERS**
- SAILS**
- NT SAILWINGS
 - NT SOLAR SAILS
- SAILWINGS**
- Sail rotors for hovering platform, calculating rotor performance based on ideal two-dimensional flexible airfoil section characteristics
 - [AIAA PAPER 72-66] 05 p0612 A72-16925
 - Preliminary design of a sailplane wing for dynamic gust loads
 - 24 p3368 A72-44992
- SAINT VENANT FLEXURE PRINCIPLE**
- U SAINT VENANT PRINCIPLE**
- SAINT VENANT PRINCIPLE**
- Saint Venant problem solutions of cylindrical beam in linear theory of micropolar elasticity in terms of three functions
 - 01 p0137 A72-10318
 - Rheological properties of Maxwell fluid-St Venant solid model for solids, noting slip lines direction during plastic flow
 - 02 p0259 A72-12238
 - Saint Venant problem for orthotropic almost cylindrical beams, investigating elongation, bending due to couple and transversal loads and torsion due to torque
 - 04 p0594 A72-15747
 - Cosserat strip bending by singular shear stresses, normal stress dipoles and spin moments, confirming Saint Venant principle
 - 15 p2324 A72-31484
- SALINE SOILS**
- U SOILS**
- SALINITY**
- Satellite earth resources remote sensing in visible, IR and microwave regions for plant disease and salinity evaluation
 - 15 p2229 A72-32049
- SALIVA**
- Parotid fluid 17-hydroxycorticoid steroid level relation to hyperthermia stress at various heat levels during thermal environmental testing
 - 12 p1768 A72-28335
- SALT BATHS**
- Stainless steel electrodes resistive and capacitive properties in contact with saline solutions of various concentrations and over extensive frequency range and current densities
 - 03 p0318 A72-12953
 - Electrochemical crevice corrosion process of Ti in hot concentrated chloride solution, discussing temperature, set potential and surface treatment
 - 03 p0374 A72-13714
 - Autoradiographic study of stress intensity factor influence on hydrogen distribution at crack tips in Ti-Al-V alloy, using tritium doped salt water as corrosive medium
 - 10 p1496 A72-24234
 - Stress corrosion crack initiation and propagation for Ti alloy in sodium chloride solutions, noting anodic dissolution
 - 15 p2253 A72-31295

- Ti alloy initial H content effect on resistance to hot salt stress corrosion embrittlement and cracking, discussing annealing treatment influence
 - 15 p2253 A72-31296
- SALT SPRAY TESTS**
- Fatigue testing of blade materials at high temperatures with periodic spray moistening by liquid corrosive medium
 - 12 p1829 A72-27459
- SALTS**
- Positive electrode materials for high energy density batteries with Li negative electrode, calculating discharge emf for various salts
 - 06 p0760 A72-17575
 - Effect of salt on activity, stability and allosteric properties of catabolic threonine deaminase from extremely halophilic bacteria
 - 09 p1275 A72-22535
 - IR refractivity measurement for atmospheric aerosol substances and sea salts
 - [AD-744397] 11 p1620 A72-25306
 - Studies in prebiotic synthesis. VII - Solid-state synthesis of purine nucleosides.
 - 23 p3262 A72-43567
- SALYUT SPACE STATION**
- Medical investigations during Salut space station flight, discussing weightlessness effects and efficiency evaluation of preventive measures for crewmembers high performance in space flight
 - 15 p2189 A72-31918
 - Construction and optical equipment of astrophysical observatory Orion onboard Salyut space station, discussing mirror telescope, spectrograph and star tracker
 - 15 p2242 A72-32741
 - Alpha Lyra and beta Cen spectrograms by Orion observatory onboard Salyut space station, noting veiled and overexposed photographic films
 - 15 p2316 A72-32742
 - Spectrograph for Orion spaceborne astronomical observatory on Salyut space station calibrated with synchrotron radiation from particle accelerator
 - 15 p2242 A72-32744
- SAMARIUM**
- Gd and Sm isotopic composition measurement in Luna 16 soil with largest low energy neutron fluence
 - 09 p1380 A72-22265
 - Sm and Eu binary alloys, investigating physicochemical interactions and phase diagrams
 - 15 p2289 A72-31187
 - Eu, La and Sm in sunspot spectra.
 - 20 p2973 A72-39884
- SAMARIUM COMPOUNDS**
- Samaria distribution effect on Ni-Cr alloy oxidation rate for various oxygen pressures, discussing behavior of electroplated and bulk specimens
 - 09 p1332 A72-23585
 - Surface tension, density, and volume change on melting of Al₂O₃ systems, Cr₂O₃, and Sm₂O₃.
 - 24 p3417 A72-44925
- SAMARIUM ISOTOPES**
- Neutron capture effect on isotopic composition variations of Sm in Apollo lunar samples, comparing with terrestrial abundance
 - 10 p1537 A72-24156
 - Gd and Sm isotope composition in Apollo 15 soils and drill stem samples, discussing lunar sedimentary processes dating from neutron capture dependence on depth
 - 18 p2729 A72-36974
- SAMOS**
- U.S. reconnaissance satellites development, discussing RAND project, Agena, Discoverer, Samos and Midas
 - 12 p1876 A72-27109
- SAMPLED DATA**
- U DATA SAMPLING**
- SAMPLED DATA SYSTEMS**
- U DATA SAMPLING**
- SAMPLERS**
- Molecular sieve adsorption sampler for stratospheric carbon 14 measurements from balloon collected carbon dioxide samples
 - 06 p0807 A72-17824
- SAMPLING**
- NT AIR SAMPLING
 - NT CORE SAMPLING
 - NT DATA SAMPLING
 - NT PARTICULATE SAMPLING
 - NT RANDOM SAMPLING
 - Conditional distribution density formation for signal-noise mixture based on learning sampling with dependent values
 - 07 p0943 A72-19517
 - Tolerance intervals in multiple type acceptance sampling plans with attribute-based inspection
 - 11 p1749 A72-26790
 - Nonrandomized distribution-free ranking and selection procedures under subset selection formulation, considering application to reliability problems
 - 13 p1962 A72-28366
 - Optimal multistep sampling procedures for production quality control, discussing methods for minimization of error probabilities and total sampling volume
 - 13 p1965 A72-29167

- Procedure for the continuous sampling and measurement of gaseous emissions from aircraft turbine engines.
[SAE ARP 1256] 18 p2721 A72-36532
- SAMPLING DEVICES**
- U SAMPLERS**
- SAN MARCO SATELLITE**
Long range ionospheric guided hf signal propagation from low orbiting San Marco 1 and 2 satellites
04 p0492 A72-15440
Upper atmosphere density measurement techniques used by Sputnik 3 and San Marco 1 and 2 satellites
12 p1802 A72-27683
Solar array for San Marco C satellite to study neutral atmosphere structure, discussing interior mounting design features
12 p1758 A72-28038
- SANDS**
Effect of a distributed sand roughness on the spectrum of wall pressure pulsations in a turbulent flow in a tube
17 p2541 A72-35542
Microwave emission from geological materials - Observations of interference effects.
20 p2917 A72-39477
- SANDWICH CONSTRUCTION**
- U SANDWICH STRUCTURES**
- SANDWICH PLATES**
- U PLATES [STRUCTURAL MEMBERS]**
- U SANDWICH STRUCTURES**
- SANDWICH STRUCTURES**
Structural sandwich panel design, establishing simple stress and deflection formulas under transverse loading based on tests evaluating balsa as laminate core
01 p0138 A72-10723
Ti alloy honeycomb core sandwich panels fabricated by brazing or spot diffusion bonding, investigating elevated temperature effects on mechanical properties
[ASM PAPER W 71-23.3] 01 p0086 A72-10875
Thin walled sandwich cylindrical shells under internal pressure, calculating elastic-plastic zone propagation
01 p0141 A72-11001
Minimum weight web-core sandwich panels under axial compression loads, presenting numerical results for boron-epoxy and graphite-epoxy composites
01 p0142 A72-11131
Edge effect equations for stability, vibration and deflection of asymmetric three layer circular plate and cylindrical shell with filler
02 p0288 A72-11605
Fourier series terms number effect on sandwich plate critical shear stress calculation accuracy
02 p0294 A72-12438
Aeroelastic stability of flat anisotropic sandwich plates in supersonic compressible fluid flow
02 p0297 A72-12614
Circular cylindrical sandwich panel and rectangular sandwich plates dynamic stability under periodic external loads derived from mathematical model
02 p0298 A72-12664
Three layer plates elastoplastic stability, describing breakdown conditions by five differential equations with five unknown variables
02 p0299 A72-12690
Computer program for buckling loads of shallow stiffened eccentrically orthotropic sandwich shells
[DGLR PAPER 71-109] 02 p0299 A72-12703
Complex geometry inhomogeneous sandwich plate, calculating temperature field with R functions
03 p0456 A72-13738
Critical load and stability analysis for three layer orthotropic cylindrical shell with filler under nonuniform external pressure
03 p0448 A72-13906
Stress concentration around circular and elliptical holes in isotropic three layer spherical shells with rigid and lightweight fillers
03 p0449 A72-14104
Three layer plates stability with light fillers, noting filler thickness effect on approximate solutions accuracy
03 p0454 A72-14377
Frequency response and I-V characteristics of metal/chalcogenide glass/metal diode structures
04 p0498 A72-15079
Sandwich beam design, deriving linear programming formulation suitable for computer treatment
04 p0590 A72-15191
Shock response of simply supported sandwich beam with viscoelastic core, using four element model for dynamic shear properties
04 p0591 A72-15274
Minimum weight design of perfectly plastic continuous sandwich beams with two equal spans for movable loads
04 p0593 A72-15647
Three layer bipolar transistor structure with negative resistance region in I-V characteristics
04 p0503 A72-15668
Optimal design of statically determinate sandwich beams for given deflection at specified cross section
05 p0737 A72-16119
- Axially compressed semi-sandwich corrugated ring-stiffened cylindrical shell crippling local buckling and general instability prediction by finite difference energy method
[AIAA PAPER 72-138] 05 p0740 A72-16892
L instability in rocket motors with heterogeneous propellants, investigating sideways sandwich model
[AIAA PAPER 72-33] 05 p0703 A72-16897
Two dimensional network class port behavior equivalence to three layer structures of linear passive isotropic materials based on depth and surface properties analysis
06 p0793 A72-17595
Error analysis of finite element solutions for elastic-plastic sandwich plates
07 p1086 A72-18779
Quench combustion studies with two dimensional propellant sandwiches with ammonium perchlorate oxidizer and various binders, using high pressure combustion vessel for deflagration characteristics determination
07 p1051 A72-19277
Minimum weight design of elastic sandwich beam with segmentwise constant stiffness under displacement and stress constraints, using iterative solution and finite element analysis
[AD-745488] 07 p1092 A72-19825
Limit analysis of ductile fiber reinforced structures, obtaining critical load of composite sandwich ring
07 p1093 A72-19950
Finite element method for elastic plastic sandwich plates analysis, presenting Lagrange multipliers interpretation
07 p1093 A72-19951
Energy dissipation associated with transverse vibrations of sandwich metallic samples with damping coatings
07 p1094 A72-20135
Quasi-static stability of sandwich plates hinged over edge in finite difference formulation
07 p1094 A72-20213
Poisson equation boundary value problems summary representation formulas for three layer annular sector with Dirichlet or Neumann conditions
08 p1205 A72-20963
Stress-strain state of circular three layer laminar plates freely supported at circumference and loaded at edge
09 p1399 A72-22694
Boundary value problems for buckling and initial postbuckling of clamped shallow spherical and conical thin walled sandwich shells under uniformly distributed hydrostatic pressure
[ASME PAPER 71-APM-YY] 10 p1554 A72-24182
Thermal shielding and reduced resistance determination of flat thermoelectric battery in sandwich solar cell assembly
10 p1422 A72-24313
Nonlinear bending and buckling of axisymmetric sandwich shells based on finite element approach
[AIAA PAPER 72-356] 11 p1729 A72-25385
Variational equations of motion for three layered laminated sandwich beam vibrations, assuming small elastic deformations and axial and bending motion
[AIAA PAPER 72-399] 11 p1731 A72-25420
Asymmetric three layer beam design for elastic impact, proposing functional equation integration by computer method
11 p1732 A72-25531
Thermoplastic polypropylene sandwich molds stiffness variation with time, noting three point bending and creep tests
11 p1673 A72-25550
Layered anisotropic fiber composite /Tetra-Core/ for sandwich construction and aircraft applications, discussing design, fabrication and strength characteristics
[SAE PAPER 720343] 11 p1638 A72-25599
Transverse bending theory for sandwich plates, considering core and face equilibrium and compatibility equations
11 p1737 A72-26587
Lossless distributed rectangular microwave structure with dielectrics interposed between two conductive metallic layers, noting existence of transmission zeros and filter properties
11 p1607 A72-26990
Bending problem for circular three layer plate with rigid circular insert, studying deflection under bending moment
12 p1879 A72-27090
Crowded photographic emulsions, predicting granularity of multilayer sandwich as function of layers number
12 p1808 A72-27676
Shallow spherical sandwich shells limiting equilibrium for material with different tension and compression yield stresses
12 p1885 A72-27974
Strain energy calculation for stability analysis of cylindrical and conical sandwich shells, using Euler-Poisson equations
12 p1885 A72-27975
- Fiberglass replacement by organic fiber for L-1011 interior sandwich panels and laminates, considering Nomex fiber in woven fabric
12 p1835 A72-28099
Heated three layer plate with load-carrying layers of different materials, thicknesses and temperatures, calculating stability under uniaxial tension
13 p2055 A72-28736
Resonant frequencies of two thin walled cylindrical panels connected by elastic filler, considering symmetric and asymmetric vibration modes
13 p2058 A72-29146
Compacting kinetics of fiber reinforced sandwich composites during hot pressing controlled by plastic matrix sliding velocity
13 p1967 A72-30103
Fatigue life tests of structural sandwich plates with honeycomb layer, considering temperature effects, material scattering and defects inside honeycomb by nondestructive methods
14 p2164 A72-30280
Nonlinear equilibrium, stability and vibration equations of shallow sandwich shells with isotropic outer layer and rigid compressible filler obtained by variational method
14 p2166 A72-30700
Sandwich beams structural optimization for given deflection by iterative finite element procedure
14 p2168 A72-30927
Honeycomb sandwich beams dynamic analysis by finite element method with three degrees of freedom per discrete element, obtaining flexural, in-plane and shearing modes
14 p2169 A72-31146
Heat flux nondestructive inspection methods for laminate and sandwich structures and electronic components
15 p2232 A72-31322
Optimal plastic design of doubly symmetric closed ring and frame structures of idealized sandwich section under uniform internal pressure
15 p2322 A72-31346
Optimal geometrical and physical properties of sandwich plates with rigid cores under compressive load, discussing critical stress and structural stability
15 p2322 A72-31359
Nonlinear creep failure of imperfect sandwich structures under time variable loading, considering rod and cylindrical shell
15 p2324 A72-31490
Random temperature variations effect on life of Euler column with sandwich cross section under constant axial compressive load, using Norton nonlinear creep law
15 p2324 A72-31494
Local buckling analysis for triangular-corrugated core sandwich panels in compression, noting buckling mode nodal line features
15 p2326 A72-31709
Transverse shear deformations in laminated anisotropic plates from generalized treatment for isotropic and sandwich plates with homogeneous cores
[AD-745613] 16 p2375 A72-32846
Equilibrium equations and boundary conditions for elastic buckling of open cylindrical sandwich shell under compressive forces applied to freely supported edges
16 p2467 A72-33116
Elastic buckling of simply supported sandwich panels with fiber reinforced laminated face plates and honeycomb cores subjected to uniform end loading
16 p2469 A72-33405
Sandwich structures buckling calculation by transfer matrices with allowance for cross section shearing
16 p2471 A72-33680
Elastic sandwich plates analysis with core layer as orthotropic Cosserat surface supporting force and moment stresses
16 p2471 A72-33787
Metal-insulator-metal tunnel junctions, investigating effect of nonparabolic band structure energy-momentum relation on I-V characteristics
16 p2370 A72-34101
Exact analysis of a thick sandwich conical shell by forward integration.
[ASME PAPER 71-APMW-20] 17 p2624 A72-34312
Anisotropic laminated plates theories reliability comparison, noting applications to thin and sandwich plates
17 p2625 A72-34326
Electron currents injected through dielectrics
17 p2529 A72-34753
Bending and vibration of multilayered sandwich plates, presenting static and dynamic analysis method
17 p2635 A72-35976
Buckling of orthotropic, curved, sandwich panels subjected to edge shear loads.
18 p2735 A72-36770
Contribution to the theoretical calculation of sandwich structures with tube core
18 p2736 A72-36939

Symmetrical and antisymmetrical wrinkling of sandwich panels. 18 p2736 A72-37056

Variational principle based three dimensional elasticity theory of micropolar anisotropic sandwich plates, considering transverse shear and strains and rotary inertia 18 p2737 A72-37057

A sandwiched layer of dissimilar material weakened by crack-like imperfections. 18 p2737 A72-37058

Internal buckling of a laminated medium. 18 p2737 A72-37059

Free vibrations of multilayer sandwich plates in the presence of in-plane loads. 19 p2876 A72-38020

Elastic impact on a three-layer plate in the presence of concentrated masses and nonlinear restraints. 19 p2877 A72-38159

Experimental investigation of the stability of compressed heated three-layer plates beyond the proportional limit 20 p2981 A72-39920

Vibration measurements of temperature dependent dynamic moduli of Al/resin/Al sandwich bars with cyanocrylate adhesives 21 p3118 A72-40720

Calculation of sandwich shells of revolution at large elastic-plastic deflections. 21 p3125 A72-41512

Thermal conductivity of honeycomb sandwich panels for space applications. 22 p3244 A72-42650

Optimum design of circular sandwich plates. 22 p3239 A72-42843

On eigenvalue boundary problems of transversely vibrating sandwich beams. 22 p3240 A72-42910

Aeroelastic optimization of a panel in high Mach number supersonic flow. 23 p3343 A72-43327

A crack stopper concept for filamentary composite laminates. 23 p3305 A72-43498

A nonlinear problem of pure bending of a three-layer plate with a corrugated sheet filler 23 p3346 A72-43655

Longitudinal compression of a three-layer plate with initial deflection and a physical nonlinearity of the middle layer /the filler/ 23 p3346 A72-43673

Elastodynamic theory of natural symmetrical vibrations of sandwich plates, assuming filler motion and layer displacements governed by Lamé and Kirchhoff equations 23 p3348 A72-43790

Variational analysis of sandwich beams under static loads, presenting shear deformation and normal stress distributions [ASME PAPER 72-APM-R] 23 p3350 A72-44055

Equilibrium equations of sandwich shell element with weak core and thin membrane facings under large transverse normal and shear strains, showing analogy to Cosserat surface theory 23 p3351 A72-44103

Nonlinear sandwich shell and Cosserat surface theory. 23 p3351 A72-44107

Triangular element for multilayer sandwich plates. 23 p3351 A72-44108

Forced vibration analysis of sandwich beams with viscoelastic core. 23 p3354 A72-44253

Zeta core for sandwich construction with rigidity-to-weight ratio comparable to honeycomb core, discussing elastic properties and cost 23 p3355 A72-44495

A sandwich plate with a part-through and a debonding crack. 24 p3456 A72-44813

The damping properties of elastically supported sandwich plates. 24 p3458 A72-44915

Action of a moving load on a composite shell with elastic filler 24 p3459 A72-45262

SANITATION

Sanitary-hygienic evaluation of the extraction method for water recycling in atmospheric moisture condensates 21 p3006 A72-40435

SAPPHIRE

Surface damage effect on strength of c-axis sapphire filaments, assessing impact on sapphire reinforced metal technology 02 p0249 A72-11992

Basal dislocations determination in sapphire single crystals, using X ray transmission topography 05 p0701 A72-16018

Mechanical strength and microstructural characterization of sapphire ribbons and continuous filaments for composite materials 07 p1023 A72-19929

Nonbasal deformation modes activation in Czochralski sapphire and fine grained alumina polycrystals deformation, noting water weakening 09 p1335 A72-22395

Temperature effects on electrical conductivity and transport mechanisms in sapphire from measurements under protection against surface and gas phase conduction 09 p1335 A72-22400

Chemical interaction effects on single crystal sapphire filament strength in Ni and Ni alloy matrices during heat treatment in inert atmosphere 13 p1974 A72-28661

Sapphire filament mechanical property considerations of importance to Al₂O₃ reinforced metals. 17 p2572 A72-35658

Magnesium aluminate spinel reinforced with sapphire whiskers, investigating whisker content, temperature and deflection rate effects on yield strength 17 p2572 A72-35661

High power pulsed ruby laser and sapphire rods optical contacting technique 21 p3063 A72-40622

SARCOMA

U CANCER

SAS

U SMALL ASTRONOMY SATELLITES

SAS-A

PCM/PM 136 MHz telemetry system of SAS-A satellite, describing operation in record and playback modes 03 p0326 A72-14396

Fully redundant relay and data command system for SAS-A satellite, discussing operation and reliability tests 03 p0442 A72-14397

SAS-A satellite attitude control and determination systems, discussing momentum wheel development, nutation damper and magnetic torquing 03 p0442 A72-14398

SAS-A thermal control design and tests, considering solar cells, attitude control, command system, telemetry and data storage 15 p2320 A72-31805

Nutational stability of a dual-spin satellite under the influence of applied reaction torques. [AIAA PAPER 72-885] 20 p2976 A72-39116

SAS-D

SAS-D borne TV type UV sensitive detector with camera tubes for high resolution astronomical spectroscopy 08 p1169 A72-21954

SATAN [SENSOR]

U TERRAIN ANALYSIS

SATELLITE ANTENNAS

Far field patterns of hourglass reflector phased array for electronic despin of communications antenna on spin stabilized satellite 01 p0029 A72-10666

Nozzle shaped antenna for synchronous satellite, obtaining radiation patterns 01 p0043 A72-11245

World Administrative Radio Conference for Space Telecommunications data on geostationary orbit utilization, covering stationkeeping and satellite antenna pointing accuracies 02 p0177 A72-12387

Plasma resonances due to satellite antenna from ionospheric topside sounder observations 02 p0222 A72-12838

Flexible antennas effect on three dimensional motion stability of gravity gradient satellite, using coupled rigid-elastic analysis 05 p0727 A72-16470

ATS F and G satellites with 30 foot deployable antennas as three axis stabilized platforms in geostationary orbit with high pointing accuracy 07 p1085 A72-19275

French Geole satellite system for geodetic survey, discussing frequency selection, antenna problems, distance measuring equipment and instrument errors 08 p1158 A72-21206

Communication and data relay satellites multibeam antennas characteristics, discussing multiple feed reflectors, bootlace lens configuration and phased arrays [AIAA PAPER 72-530] 12 p1789 A72-27355

Communication satellites design and technology for future launchings, discussing ion engine development, antenna beams and thermal control [AIAA PAPER 72-540] 12 p1780 A72-27363

Earth stations synchronization to switched sequences of multiple access and cyclically interconnected multispot beam antennas satellite controlled by stable onboard clock [AIAA PAPER 72-545] 12 p1781 A72-27368

Flight prototype satellite communications repeater with two transponder channels and dual beam antenna, discussing design parameters and advanced systems application [AIAA PAPER 72-579] 12 p1789 A72-27381

Communication satellites microwave circular array antenna for wideband circularly polarized isotropic radiation [AIAA PAPER 72-529] 12 p1789 A72-27419

Space technology application to ATS F and G program, discussing high power requirements, parabolic antenna design, tracking accuracy and ground station simplification 12 p1870 A72-27523

Pit shielded antenna measurements for communications satellite earth stations in 4 and 6 GHz bands, considering position range and erosion effects 15 p2196 A72-31794

A multi-channel rotary joint for spacecraft applications. 19 p2770 A72-37260

Reflector antennas for satellite communication, discussing hybrid mode, dielectric and lens feeds, spherical and stepped reflectors, and high efficiency paraboloid antennas 21 p3028 A72-40513

An antenna principle with universally polydirectional radiation for large spin-stabilized flight devices 21 p3030 A72-40532

Polar orbiting Aeros aeronomy satellite turnstile antenna system with nearly spherical radiation pattern, discussing design modifications for optimization 21 p3030 A72-40533

Shaped coverage patterns with satellite array antennas. 21 p3019 A72-40884

TV-radio satellite receiver equipment, considering power requirements, antenna, energy supply and placing into 24-hour orbit 23 p3262 A72-43300

SATELLITE ATTITUDE CONTROL

Satellite attitude and libration control by solar radiation pressure 01 p0135 A72-10928

Hybrid computer simulation of spinning satellite dynamic behavior during flexible booms deployment and attitude control maneuvers, deriving equations of motion from Lagrange equations 02 p0286 A72-12658

Two constituent gaseous propellant micropropulsion engines for satellite orbit correction and attitude control, discussing thermodynamic and reaction kinetics problems [DGLR PAPER 71-102] 02 p0271 A72-12711

Solar radiation effects on planar librational motion and attitude of gravity oriented satellites at high altitudes 03 p0434 A72-13613

SAS-A satellite attitude control and determination systems, discussing momentum wheel development, nutation damper and magnetic torquing 03 p0442 A72-14398

AEROS scientific satellite attitude control system, considering control and measuring electronics, axis and spin control coils and spin stabilization 04 p0503 A72-15649

Dynamic test facility for Symphony satellite attitude control, discussing sun and earth sensors and analog computer for motion simulator 05 p0643 A72-16432

Spherical air bearing supported test facility for satellite attitude control system performance testing, discussing motion simulator and automatic balancing system 05 p0643 A72-16435

Kalman linear filtering technique for spinning satellite attitude restitution, evaluating reliability by model for simulation of measurements by sensors [ONERA, TP NO. 953] 05 p0724 A72-16436

Meteorological satellite stabilization and attitude control in synchronous equatorial orbit for two years life, emphasizing nutation damper optimal dynamic characteristics 05 p0725 A72-16437

Relay systems stability in orientation control of flexible satellites 05 p0725 A72-16439

Satellite attitude control in circular orbit by actively varying inertia via angular rate sensing and use of fluid transfer logic 05 p0725 A72-16440

Satellite attitude estimation on elliptic orbits by Kalman filters with periodic coefficients, demonstrating efficiency by earth pointing satellite using different instrumentation noise models 05 p0685 A72-16442

Satellite attitude control with gimbaled reaction wheel digital system, discussing logic and computerized design, implementation, fabrication and performance tests 05 p0726 A72-16458

Long term spin and misalignment in orbit of Azur satellite with passive magnetic attitude control system 05 p0727 A72-16466

Attitude control of satellite with proinruding stabilizing booms from analysis of gravity gradient stabilization systems dynamics, discussing rotation about mass center 05 p0727 A72-16469

AEROS satellite active magnetic attitude control system, describing magnetometer system, sun and IR earth sensors, spin stabilization and axis and spin rate control torque generation 05 p0727 A72-16473

Liapunov direct method based approaches to hybrid dynamical systems stability, applying to attitude stability of flexible earth pointing satellite
[AIAA PAPER 72-18] 05 p0729 A72-16867

Direct earth radiation, albedo and shadow effects on attitude dynamics of gravity orientated satellites
05 p0730 A72-16995

Gas jet control for spinning satellites attitude correction, deriving relations between satellite and control system parameters, response time and fuel consumption
05 p0731 A72-17196

Hydrazine and ammonia resisto-jet systems for satellites orbit and attitude control, discussing component redundancy and mass requirements in terms of system optimization
07 p1054 A72-19603

Computer simulation prediction program for attitude disturbance torques for Tiros series spacecraft rotational motion control
07 p1086 A72-20361

Nonspinning satellite earth-pointing attitude control for elliptic orbits using active regulation of pitch moment of inertia
08 p1204 A72-21605

Star sensor with image disector as pickup tube for Astronomical Netherlands Satellite attitude control system
08 p1171 A72-21974

German monograph on optimal attitude control of satellites with rotors and simultaneous spin reduction, covering motion equations for stable equilibrium and circular orbit
09 p1394 A72-22330

TD-1A satellite functional description for stellar UV spectroscopy and solar and cosmic ray experiments, emphasizing attitude control subsystem
09 p1396 A72-23263

ITOS-1 (Tiros M) satellite design, describing structure, thermal and attitude control, primary and secondary sensor subsystems, power supply and operational goals
09 p1396 A72-23373

Earth pointing rotating satellites attitude control system based on two-degree of freedom gyroscope, determining conditions for rotor spin axis fixation in inertial space
10 p1509 A72-24646

Communication satellite technology trends, discussing channel capacity, attitude stabilization, antenna pointing accuracy, energy conversion and storage, frequency reuse and onboard switching
11 p1725 A72-25254

Communications Technology Satellite attitude control system design, taking into account dynamic interactions with large flexible solar cell array
11 p1593 A72-25913

Orbital eccentricity and angular momentum management scheme stability for satellite large attitude maneuver followed by trim maneuver sequence
11 p1719 A72-25978

Electric thruster for orbit and attitude control of nonspinning geostationary communications satellite
[AIAA PAPER 72-436] 11 p1727 A72-26178

French R and D work on ion propulsion systems for communication satellite stabilization, discussing principal characteristics, mathematical modeling, design and economic problems
[AIAA PAPER 72-437] 11 p1727 A72-26179

Attitude determination during transfer orbit operation of SKYNET and NATO synchronous communications satellites
[AIAA PAPER 72-544] 12 p1876 A72-27367

Synchronous communication satellites body stabilized three axis attitude control superiority over dual spin techniques, emphasizing single large pitch momentum wheel configuration with magnetic torquing
[AIAA PAPER 72-572] 12 p1876 A72-27380

Canada-NASA communications technology satellite /CTS/ for 12 and 14 GHz TV transmission, considering mission profile, spacecraft design, attitude control system and ion thruster
[AIAA PAPER 72-580] 12 p1877 A72-27382

Thermal storage type resistojets design for satellite attitude control, discussing heat loss minimization
13 p2026 A72-28927

Structurally integrated ion thruster (SIT-5) for synchronous satellites attitude control and station-keeping, presenting design and performance data
[AIAA PAPER 72-492] 13 p2027 A72-28950

Design and tests of dual deflectable beam strip ion thruster, noting application to two axes satellite attitude control and stationkeeping
[AIAA PAPER 72-494] 13 p2027 A72-28951

Operational evaluation for sun stabilized attitude control system in Aeros satellite, describing laboratory equipment and component static and dynamic tests
[DGLR PAPER 72-026] 13 p2052 A72-28967

Communication satellites auxiliary propulsion systems surveyed for attitude and stationkeeping systems selection
[AIAA PAPER 72-515] 13 p2052 A72-28978

Intelsat 3 global multichannel wideband multiple access communication system, describing technological

advancements in communication performance, attitude control and testing procedures
[AIAA PAPER 72-534] 13 p1918 A72-28982

Digital autopilot for SKYLAB orbital assembly attitude control during docking, discussing jet selection logic, inter-axis dependence and onboard computer
15 p2269 A72-32183

Stability analysis of gyrostad satellites possible equilibria under gravitational torques, considering inertia, equilibrium and angular momentum parameters
15 p2321 A72-32586

Geomagnetic attitude control of an axisymmetric spinning satellite.
17 p2619 A72-34201

Satellite orientation and stabilization systems aerodynamic compensation for circular orbit perturbations
17 p2621 A72-35034

A horizon sensor with a bolometer and electrooptical modulators
17 p2556 A72-35385

Gravitational stabilization of a satellite in a fixed inertial orientation.
17 p2622 A72-35487

Optimal aerodynamic attitude stabilization of near-earth satellites.
17 p2622 A72-35488

Limit-cycle bounds of a satellite attitude-control system.
17 p2622 A72-35529

Attitude control of satellites with large flexible solar arrays.
[AIAA PAPER 72-733] 18 p2730 A72-36541

TD-1A - Europe's largest and most advanced satellite.
18 p2731 A72-37011

French monograph - Optimal impulse corrections for near-circular orbits - Comparison of various thruster configurations
19 p2856 A72-37491

Attitude stability and performance of a dual-spin satellite with nutation damping.
19 p2862 A72-38022

Attitude control of a spinning Skylab.
[AIAA PAPER 72-889] 20 p2975 A72-39112

Attitude dynamics of a three-axis stabilized satellite with a large flexible solar array.
[AIAA PAPER 72-857] 20 p2976 A72-39137

Periodic libration solutions in attitude control stability study of slowly spinning satellites under gravity gradient torques, using Floquet theory
20 p2968 A72-39195

An automatic mass-trim system for spinning spacecraft.
20 p2977 A72-39603

Polarization follower tracking linear vector transmitted by satellite with high precision, noting spacecraft attitude control and Faraday rotation measurements applications
21 p3021 A72-40907

Effect of bearing flexibility on dual-spin satellite attitude stability.
21 p3115 A72-41303

Liapunov stability analysis of hybrid dynamical systems with multi-elastic domains.
21 p3086 A72-41519

Solar pressure control of a spinning satellite with a stabilized platform.
[AIAA PAPER 72-918] 21 p3115 A72-41563

Performance optimization of satellite semipassive aerodynamic attitude controller for near-earth orbits, considering damping time and pointing error
[AIAA PAPER 72-923] 21 p3082 A72-41567

Attitude control of satellites using the solar radiation pressure.
22 p3231 A72-42871

Alignment of the figure axis of a spin-stabilized spacecraft perpendicular to sun and earth
23 p3343 A72-43621

Aerodynamic solar semipassive hybrid system for continuous three dimensional attitude control of axisymmetric satellite in near-earth orbits, discussing operation, design and optimization
24 p3450 A72-45146

The on-board computer of the Astronomical Netherlands Satellite (ANS).
24 p3382 A72-45163

SATELLITE ATTITUDE DISTURBANCE
U ATTITUDE STABILITY
U SPACECRAFT STABILITY
SATELLITE COMMUNICATIONS
U SPACECRAFT COMMUNICATION
SATELLITE CONFIGURATIONS
Frequency shift and mode shapes for equatorial vibrations of flexible boom on spin stabilized satellite, applying to thermal flutter resonance and nutational stability
15 p2320 A72-31803

HEAO satellite to carry instruments required in high energy astrophysics missions, discussing observational objectives, configuration and experiments
24 p3453 A72-45538

SATELLITE CONTROL
NT SATELLITE ATTITUDE CONTROL

Spurious commands at high altitudes due to hf disturbances in Azur satellites, discussing telecommand system
05 p0626 A72-16137

Ground based satellite control center data processing for Azur satellite, using automatic guidance
05 p0632 A72-16138

Spinning drag-free satellite trapping control phenomenon due to proof mass effect on translation controller design
05 p0725 A72-16445

Unified single rf channel tracking, telemetry and command control systems for guidance of unmanned vehicles, including pilotless aircraft and satellites
05 p0685 A72-16556

Satellites and spacecraft flight control systems, discussing approaches for stationkeeping and orbit determination/correction
05 p0729 A72-16746

ERTS A and B satellite systems for multispectral imaging of earth surface, discussing sensors, operational control and data processing requirements and implementation
07 p1085 A72-19276

Nonlinear multivariable system optimal control with respect to time and fuel consumption, discussing Gauss-Newton and Davidson methods and application to geostationary satellite
07 p0962 A72-19719

Analog simulation of dual-spin satellite dynamics and control, emphasizing Hughes gyrostad spacecraft
07 p1086 A72-20352

Hardware monitor and associated analysis programs to evaluate real time satellite command and control digital computer system performance
10 p1442 A72-23817

Ground satellite control station network, including tracking stations for measuring Doppler effect with IRIS receivers
[DGLR PAPER 72-009] 13 p1938 A72-28960

AEROS research satellite control program, describing system objectives, operational testing, error analysis and command verification
[DGLR PAPER 72-023] 13 p1918 A72-28968

Three stage linear damping of satellite roll and yaw oscillations, using slip motion procedure
15 p2319 A72-31492

Optimal feedback controller design based on cooperative game described by quadratic cost functional under linear differential equation constraints, applying to satellite terminal rendezvous
15 p2267 A72-31789

SAS-A thermal control design and tests, considering solar cells, attitude control, command system, telemetry and data storage
15 p2320 A72-31805

Systems management in major projects exemplified by the German Satellite Control Center
19 p2783 A72-38303

Analysis of effects of fluid energy dissipation on spinning satellite control dynamics.
[AIAA PAPER 72-886] 20 p2976 A72-39115

Analytic partial derivatives for estimating low-thrust parameters.
22 p3231 A72-42865

SATELLITE DESIGN
ESRO polar orbiting meteorological satellite, discussing design features and operational instruments
01 p0126 A72-10186

Satellite electrical power, discussing energy converters, satellite feeder subsystem and voltage requirements
03 p0311 A72-13639

Azur satellite temperature control system for protection against internal heat dissipation and external thermal loads due to earth radiation and albedo
04 p0582 A72-15651

Spinning drag-free satellite trapping control phenomenon due to proof mass effect on translation controller design
05 p0725 A72-16445

Spinning satellite with rigid central body and flexible appendages, deriving equations of motion and Liapunov stability
06 p0892 A72-17652

RAE-1 measurements of If radio phenomena in magnetosphere, solar corona and Galaxy, discussing design, calibration and performance
08 p1137 A72-21984

TD-1A satellite functional description for stellar UV spectroscopy and solar and cosmic ray experiments, emphasizing attitude control subsystem
09 p1396 A72-23263

DIAL aeronomy satellite design and operational features, describing in-flight behavior
10 p1551 A72-24030

Satellite surface coating materials photoemission properties, discussing reflectance, work function, photoyield and photoelectron energy distributions
12 p1844 A72-27280

AMSAT-OSCAR-B series of radio communication satellite for worldwide use with low cost terminals in amateur and education services
[AIAA PAPER 72-521] 12 p1779 A72-27351

Communication satellites design and technology for future launchings, discussing ion engine development, antenna beams and thermal control
[AIAA PAPER 72-540] 12 p1780 A72-27363

Canada-NASA communications technology satellite /CTS/ for 12 and 14 GHz TV transmission, considering mission profile, spacecraft design, attitude control system and ion thruster
[AIAA PAPER 72-580] 12 p1877 A72-27382

ATS F/G spacecraft thermal control design verification by chamber thermal balance tests and performance prediction mathematical model of earth viewing module and orbital environment
12 p1877 A72-27527

Indian national satellite /Insat/ design for continental TV coverage and urban center telecommunication linkage
[AIAA PAPER 72-576] 12 p1785 A72-27866

Solar array for San Marco C satellite to study neutral atmosphere structure, discussing interior mounting design features
12 p1758 A72-28038

Propulsion modes compared for communication satellites design optimization, discussing attitude and longitude control, orbit inclination control, station change and orbit raising
[AIAA PAPER 72-517] 13 p2052 A72-28979

Military geostationary communication satellite Skynet 2 subsystems design development and testing
13 p2052 A72-29856

SAS-A thermal control design and tests, considering solar cells, attitude control, command system, telemetry and data storage
15 p2320 A72-31805

Communication satellite modeling into subsystems to formulate parametric relationships among power, mass and cost, comparing computerized design alternatives
17 p2512 A72-34263

The identification of parameters in nonlinear thermal networks with the aid of a Kalman filter
17 p2533 A72-34827

International UV Explorer synchronous satellite program objectives and technology, describing spacecraft design, instrumentation, ground system, telescope control and data handling
17 p2621 A72-34900

TD-1A - Europe's largest and most advanced satellite.
18 p2731 A72-37011

Commercial satellite communication system development, considering external constraints, orbital geometry, frequency allocations, multiple access transmission techniques, and satellite and earth station designs
21 p3021 A72-40921

NASA developed geostationary weather and environmental satellite for launch in 1973, discussing ground station equipment, antenna system and data collection service
23 p3343 A72-43551

Safety design of space station against collision hazards with artificial orbiting bodies.
24 p3449 A72-45143

Aerodynamic solar semipassive hybrid system for continuous three dimensional attitude control of axisymmetric satellite in near-earth orbits, discussing operation, design and optimization
24 p3450 A72-45146

SATELLITE DRAG
Draconitic-sidereal orbital period difference estimation formula for near-circular orbit satellites with air drag
02 p0279 A72-12048

Al finished and Au plated triple calibration sphere as multispectral optical sensor for testing Cook hypothesis concerning satellite drag dependence on surface material
04 p0500 A72-15305

Upper atmosphere density fluctuations associated with solar activity and local time values, using Cosmos 14 satellite drag data
05 p0659 A72-17037

Microaccelerometer for satellite drag measurement and compensating thrust control
06 p0892 A72-18260

Latitude dependent discrepancy between low latitude satellite drag deduced densities at high latitudes and Jacchia model
07 p0976 A72-19167

Numerical simulation of gas atom scattering from solid surface and satellite drag coefficient calculation
07 p0910 A72-20106

Gas-surface interaction parameters and atmospheric density determination from satellite drag induced orbital decay measurements
07 p0910 A72-20116

Thermosphere and lower exosphere density and temperature variations from satellite decay
11 p1621 A72-25843

Satellite aerodynamics effect on atmospheric density determination, discussing drag coefficient dependence on altitude
13 p1990 A72-28821

Atmospheric oxygen concentration latitudinal and diurnal variations from incoherent scatter and satellite drag data, noting compatibility with Jacchia model
13 p1951 A72-29389

Upper atmosphere density from orbital drag on Cannon Ball II and Musket Ball satellites
15 p2227 A72-31963

Explorer 19 satellite drag evidence for neutral exosphere He concentration asymmetry between Northern and Southern Hemispheres over entire solar activity cycle
15 p2228 A72-31977

Thermospheric variations due to solar activity changes based on satellite drag data
15 p2228 A72-31979

Free molecular flow over rotating sphere satellite, deriving aerodynamic forces on differential surface to determine drag and lift coefficients
16 p2341 A72-32844

Atomic and molecular beams fluid dynamic applications in rarefied gas flows exemplified by satellite drag coefficient measurement
16 p2429 A72-33052

Atmospheric properties effect on satellite aerodynamic characteristics, noting gas composition and upper atmospheric winds
[AIAA PAPER 72-659] 16 p2347 A72-34075

Lift and drag on conical, cylindrical and spherical artificial satellites from spatial impulsive interaction model depending on gas temperature and surface conditions
16 p2347 A72-34167

The variation of air density at 240 and 280 km from April to November 1967.
20 p2916 A72-39235

Atmospheric density from spacecraft drag data by successive optimization of control laws, using quadratic programming
23 p3277 A72-44003

SATELLITE GROUND SUPPORT
Ground station systems of operational control and data processing for satellites and space probes projects Aeros, Symphonie and Helios
03 p0326 A72-14309

Systems management in major projects exemplified by the German Satellite Control Center
19 p2783 A72-38303

Geostationary satellite direct TV broadcasting system extension to 12 GHz band, considering receiving installations, antennas, performance and costs
21 p3018 A72-40876

SATELLITE GUIDANCE
Characteristic thrust concept introduced to classify propulsion system tasks related to geosynchronous communications spacecraft, developing approximate analytical models
[AIAA PAPER 72-514] 13 p2052 A72-28977

SATELLITE INSTRUMENTS
NT LASER ALTIMETERS
Integrated receiver module for satellite transponders, including tunnel diode amplifier, Schottky barrier mixer, Gunn oscillator and low pass filter
01 p0041 A72-10701

Frequency planning for Symphonie German-French telecommunication satellite microwave equipment
01 p0030 A72-10710

Astronomical Netherlands Satellite automatic stabilized detection system for soft celestial X rays measurement, describing various modes of operation
03 p0354 A72-13048

Small astronomy satellite program for X ray experiments and mapping, discussing structure design, systems, testing and launching
03 p0441 A72-14395

Si monolithic multispectral image photosensor array for satellite application, presenting fabrication and spectral response data
04 p0500 A72-15304

Vacuum chamber simulation of solar radiation effects on space satellites and components at 300-400 miles, using short arc xenon lamps
05 p0643 A72-16386

Satellite time-of-day code generator for data recording time identification, using ICs mounted on thick film multilayer printed ceramic substrates
07 p0944 A72-19605

ERTS program, discussing orbit selection and sensor equipment
07 p1085 A72-20305

Photogrammetric measurement with photodiode sensor arrays substitution for film in cameras and yielding real time readout of stellar and satellite coordinates
08 p1169 A72-21700

SAS-D borne TV type UV sensitive detector with camera tubes for high resolution astronomical spectroscopy
08 p1169 A72-21954

Digitized SEC vidicon detector for OSO-H satellite coronagraph, describing optics
08 p1170 A72-21959

TD-1 satellite mounted slow analysis camera with supervidicon image tube to observe cosmic ray tracks in spark chamber
08 p1170 A72-21961

Star sensor with image dissector as pickup tube for Astronomical Netherlands Satellite attitude control system
08 p1171 A72-21974

Image dissector application to D2B astronomical satellite position field plotting in solar and stellar UV photometry
08 p1172 A72-21976

Nimbus 4 satellite-borne selective chopper radiometer design characteristics, obtaining maps of stratospheric warmings in both hemispheres
08 p1173 A72-22168

Radiation resistance of Si photodetectors for star sensors in satellites, using electrical and optical tests
09 p1369 A72-22653

Russian book on satellite-borne electro-optical IR radiometers design for celestial bodies spectral radiance and energy distribution measurement
11 p1634 A72-26376

Surface pressure via satellite-borne measurements of atmospheric transmission near absorption band
12 p1802 A72-27710

Satellite altimetry based on ocean backscattering, analyzing received signal model and altitude errors
13 p1955 A72-28533

Neutral atmospheric density profiles measurements in lower thermosphere by satellite-borne accelerometers, noting longitudinal variations at high latitudes
13 p1948 A72-28833

Experimental communications satellite system of ATS F and G geostationary satellites for specific application, discussing system performance measurement instruments
[AIAA PAPER 72-578] 13 p1918 A72-28986

German aeronomy research satellite Aeros mission objectives, discussing orbit layout, onboard equipment and operation
13 p2050 A72-30079

Satellite sensor cooling systems, considering cryogenic heat pipes, sublimation, radiation cones and surface treatment
15 p2319 A72-31240

Satellite instrument to observe atmospheric composition by energy analysis of incoming gas stream, using velocity mass spectrometer for neutral particles measurement
15 p2236 A72-31966

Satellite Prospero onboard micrometeoroid detector data analysis for near earth flux
15 p2310 A72-31987

Relativistic electron characteristics in interplanetary space from onboard satellite detector measurements beyond magnetospheric influence
[IGPP-UCK-72-11] 15 p2300 A72-31998

Linear ICs application to RF probe for ionospheric electron density measurements from rockets or satellites
15 p2240 A72-32389

International UV Explorer synchronous satellite program objectives and technology, describing spacecraft design, instrumentation, ground system, telescope control and data handling
17 p2621 A72-34900

Reliability of HgTe-CdTe photovoltaic detectors
18 p2670 A72-37139

Use of a loaded silicon elastomer for insulation of channel multipliers of onboard electrons
18 p2670 A72-37140

TOP 1369 traveling wave amplifier tube
18 p2671 A72-37147

Early data from the ultraviolet sky-scan telescope in the TDI satellite.
19 p2857 A72-37524

German Aeros satellite mission and payload, noting mass spectrograph, EUV spectrometer for UV solar radiation and neutral particles temperature measuring instrument
20 p2974 A72-39935

Star scanner attitude determination for the OSO-7 spacecraft.
[AIAA PAPER 72-922] 21 p3082 A72-41566

SATELLITE LAUNCHING
U SPACECRAFT LAUNCHING
SATELLITE LIFETIME
Artificial planetary satellites lifetime estimation from atmospheric drag, discussing critical height/atmospheric density relationship, satellite design and initial orbit height
05 p0722 A72-17042

Spacecraft mean time to failure /MTTF/ and launch success probability /LSP/ effects on annual satellite system costs
09 p1395 A72-22775

Satellite long life assurance, investigating shuttle era spacecraft program cost relationship to mean time to failure
[AIAA PAPER 72-225] 10 p1551 A72-24436

SATELLITE MANEUVERS
U SPACECRAFT MANEUVERS
SATELLITE NAVIGATION SYSTEMS
Closed form solution for Doppler satellite navigation for arbitrary orbits with ellipsoid Earth model and straight path signal transmission
05 p0686 A72-16561

Worldwide satellite navigation system for precise position and velocity of military aircraft, ships and ground vehicles

13 p1996 A72-28758

Aircraft antennas design for radio links to satellites for aeronautical communication and ATC, proposing use of beam steering system

13 p1932 A72-29347

Satellite communications and position finding for ships and aircraft compared with costs and reliability of ionospheric radio communication

15 p2193 A72-31300

Radio navigation satellite systems for ship and aircraft location determination, using time-frequency measurements

15 p2199 A72-32071

Satellite-star optical navigation data from Mariner program, describing objectives and performance of preflight and real time activities leading to successful performance

15 p2271 A72-32196

The role of time/frequency in Navy navigation satellites.

22 p3202 A72-42749

Satellite relay and Omega navigation system for distress signal transmission and reception in global rescue alarm network serving ships, aircraft and spacecraft

24 p3467 A72-45134

Utilization of a satellite system for navigation and control of shipping

24 p3422 A72-45224

Potential of the navy navigation satellite system in predicting ionospheric characteristics.

24 p3447 A72-45555

SATELLITE NETWORKS

Initial Canadian domestic satellite communication system plans and progress

02 p0177 A72-12382

Multiple access techniques in satellite telecommunication systems, discussing clean mesh type network

02 p0182 A72-12699

National TV distribution by Canadian domestic satellite system, discussing design simplicity and payload weight maximization

07 p0944 A72-19654

International and national satellite TV systems, discussing technical and operational characteristics, artificial emission dispersion and costs

07 p0944 A72-19656

Combined educational and TV network satellite distribution system for public broadcasting service, discussing cost reduction techniques

10 p1435 A72-24035

French-U.S. Eole meteorological satellite project to map Southern Hemisphere winds, describing system based on pressurized balloons for data acquisition

11 p1680 A72-25813

Intelsat V satellite system with large telephone channels capacity and full earth station network connectivity, discussing system concepts and technology [AIAA PAPER 72-536]

12 p1780 A72-27359

TDMA system for Intelsat 4 and subsequent satellites, discussing automatic synchronization acquisition, terrestrial network-satellite transmission channel modular interface, etc

12 p1780 A72-27361

Satellite supplement to domestic communication systems, discussing network management, system reliability, broadband capacity, earth station flexibility and market proposals

12 p1781 A72-27374

Ground satellite control station network, including tracking stations for measuring Doppler effect with IRIS receivers

13 p1938 A72-28960

International telephone hierarchical earth network organization for satellite communication extension, considering guidelines and constitution

15 p2193 A72-31179

Economic analysis of satellite network construction program, suggesting Italian national center formation for space exploration

15 p2319 A72-31231

Geostationary Intelsat satellite networks for retransmission of data received by earth resources satellites

15 p2221 A72-31243

Intelsat 4 multichannel communication network earth station equipment components and characteristics experimental system/SPADE/ study to realize demand assignment

18 p2659 A72-36272

Satellite communications and the Pleumeur-Bodou centre.

18 p2659 A72-36273

Near-field Cassegrain antennas of high surface efficiency for satellite communication links

21 p3029 A72-40520

Mission model for European communication satellite system based on estimated future traffic requirements

21 p3017 A72-40853

Techniques for dealing with the effects of bad weather in satellite communications systems.

21 p3017 A72-40856

Spacing limitations of geostationary satellites using multilevel coherent PSK signals.

23 p3265 A72-44183

SATELLITE OBSERVATION

Earth surface thermal radio emission measurements by UHF radiometry onboard Cosmos 243 satellite, showing brightness profiles of water, ice and land areas

01 p0053 A72-10363

Lindauer electron density profile for maximum F layer over sunspot cycle using frequency dependent radio ground echo in satellite ionograms

01 p0054 A72-10421

Statistical analysis of ionospheric electron content observations over European stations with nonstationary satellites, taking into account solar radiation and magnetic activity

01 p0054 A72-10422

Aerosol and atmospheric scattering layers observability by satellite mounted optical detector at 3000-7000 Å, comparing wide angle receiver and limited view field steerable telescope

[AIAA PAPER 71-1110]

01 p0058 A72-10554

Global satellite horizon-scanning monitoring technique permitting scattered solar radiation horizon profile conversion into aerosol vertical distribution [AIAA PAPER 71-1111]

01 p0058 A72-10555

Longitudinal variations of inner radiation belt particle flux density at low altitudes from Proton 2 satellite data

01 p0119 A72-10604

Atmospheric water vapor vertical distribution from satellite IR spectrometer measurements, noting effects, absorption coefficients and temperature profiles errors

01 p0095 A72-10831

Ionospheric total electron content measurement with geostationary ATS 3 satellite during solar eclipse of 7 March 1970, plotting Faraday rotation as function of time

01 p0059 A72-10838

Cosmic ray neutron leakage flux and energy spectrum measurements in 0.01-10 MeV range by OGO 6 satellite-borne neutron detector

01 p0119 A72-10877

Magnetic field and plasma sheet variations observation by IMP 3 satellite in distant magnetotail during magnetospheric substorms

01 p0060 A72-10888

Outer zone energetic electron precipitation, elf whistler and plasmopause location measurements by polar satellite OV-3-3 instruments

01 p0120 A72-10890

Stable red arc 6300 Å emission calculation from satellite electron temperature and density data during geomagnetic storms

01 p0061 A72-10893

Auroral electron flux and energy spectrum observations by synchronous ATS 5 and polar OV-1-17 satellites

01 p0061 A72-10894

Positive Fe ion concentration relationship to equatorial spread F from OGO 6 satellite observation near magnetic equator

01 p0062 A72-10902

Nimbus 3 and 4 satellite technological and meteorological performance, discussing atmospheric temperature humidity and ozone vertical sounding for numerical weather forecasting models

01 p0130 A72-10955

Cloud temperature determination from satellite IR images, presenting error corrections for various U.S.S.R. locations

01 p0095 A72-10956

Earth radiation climatology, noting qualitative agreement between calculated and satellite measured outgoing radiation data with allowance for inaccuracies due to albedo levels overrating

01 p0095 A72-10958

Atmospheric thermal sounding from meteorological satellites, reviewing measurement accuracy, equation kernel, spectral resolution, optimum measuring condition and interpretation techniques

01 p0070 A72-10959

Total ozone estimation by interpolation from Nimbus 4 satellite data on backscattered UV earth radiance attenuation

01 p0096 A72-11285

Soyuz 6 multispectral aerogeophysical measurements of Usturt plateau and Caspian and Aral Seas, discussing remote sensing information yield on earth water/land and atmosphere properties

02 p0208 A72-11785

Atmospheric pollutants time and spatial profiles monitoring by geosynchronous satellite remote sensors

02 p0211 A72-11806

Quantitative cloud information from satellite IR thermal imagery and vertical temperature profile data

02 p0211 A72-11808

Automated operational procedure for sea surface temperature determination from ITOS IR data, discussing error analysis

02 p0211 A72-11810

Orbiting multispectral scanner with independent land and oceanographic spectrometers for ground controlled dual mode operation

02 p0226 A72-11823

Earth surface feature recognition with IR imagery, evaluating Meteor satellite data

02 p0213 A72-11836

Chesapeake Bay aquatic ecosystems observations, using satellite remote sensing multispectral photography and imagery

02 p0215 A72-11885

Vertical concentration profile and diurnal variations of N and NO vs solar activity from satellite horizon airglow experiment

02 p0217 A72-11925

Laser station coordinate and Geos B satellite position compensation with simultaneous optical and laser observations

02 p0219 A72-12045

Laser station coordinate determination by geometrical method and satellite observations

02 p0219 A72-12046

Papers on world geomagnetic survey 1957-1969 covering land, sea, airplane and polar-orbiting geophysical observatory satellite observations, magnetic anomalies and reference field

02 p0219 A72-12080

Geomagnetic survey by Cosmos-49 satellite as international program, discussing data analysis and observation accuracy

02 p0219 A72-12082

Geomagnetic storms and anomaly observation by Satellite 1964 83C telemetry data transmission to ground stations network

02 p0219 A72-12083

Magnetosphere and adjacent regions magnetic surveys by OGO 1 and 3 satellites, discussing magnetopause, bow shock, magnetosheath, geomagnetic tail, ring current and polar substorms

02 p0220 A72-12084

Upper cloud boundary height determination using Cosmos 320 satellite combined reflected solar and intrinsic radiation measurements

02 p0253 A72-12213

Anomalous earth bow shock locations during 1969 from plasma and magnetic observations aboard European satellite Heos-1

02 p0274 A72-12461

Cosmos 65 global ozone contour data similarity with geomagnetic L shells configuration, discussing South Pacific region depletion area

02 p0221 A72-12466

Ageostrophic vertical wind field determination from satellite cloudiness data, including geopotential pressure equations

02 p0253 A72-12537

Satellite measurements of tropospheric and earth surface state parameters for long term numerical weather forecasting, discussing data fluctuations

02 p0255 A72-12789

Celestial gamma rays arrival direction and energy spectra measurement and spectrum analysis using ESRO satellite COS-B data

03 p0408 A72-13029

Solar corona X ray data from SOLRAD satellites, detailing spectral energy distribution, ionization balance, continuum radiation and line emission

03 p0410 A72-13219

Bidirectional reflectance at several wavelengths from moonlit earth observations by airglow photometer on OGO-4 satellite

03 p0433 A72-13428

Polar cap region solar particle fluxes from Esro 1/Aurorae satellite recordings, noting north-south asymmetry

03 p0348 A72-13506

Oso-3 satellite observation of solar flare associated EUV bursts, comparing with microwave radio bursts [AD-739641]

03 p0413 A72-13529

Rf interference measurements on guided hf ionospheric propagation in OV-4-1 dual satellite experiment

03 p0324 A72-14042

Tropical hurricanes and storm outflow layer wind analyses from ATS 3 satellite data, noting cyclonic eddy asymmetric structure

03 p0384 A72-14144

Temperature reduction produced by partial cloud cover effect on radiation received by Nimbus 3 IR radiometer

03 p0385 A72-14226

Time variations of zonal averages of albedo and absorbed solar radiation derived from brightness data of digitized satellite pictures

03 p0385 A72-14228

Central peaked Martian crater distribution from Mariners 6 and 7 photographs, comparing south polar region to equator

03 p0440 A72-14310

Earth triaxiality from satellite data, obtaining non-zero values for harmonic coefficients

03 p0351 A72-14327

- Laser satellite range measurement at Ondrejov astronomical observatory, describing radar system and experiment design 03 p0326 A72-14332
- Cloud streeting in earth atmosphere, discussing satellite observations and theoretical formation mechanisms 04 p0541 A72-14457
- Fe line emission during solar X-ray flares recorded by Bragg crystal spectrometers on OSO-6, resolving fine structure components of hydrogenic Ar 04 p0566 A72-14560
- Daytime cloud cover space-time patterns from satellite sensed brightness values during 1967-1971 04 p0542 A72-14690
- D-2A satellite antisolar mission, examining Lyman alpha emission from geocorona and interstellar hydrogen wind 04 p0582 A72-15688
- D-2B satellite mission, describing attitude, orbit and experiments on zodiacal light, stellar radiation and antisolar data 04 p0583 A72-15689
- Optimization algorithm in measurement conditions selection for satellite thermal sounding of atmosphere in 15 micron carbon dioxide band 05 p0655 A72-16174
- Primary cosmic ray proton energy spectrum in 50 Ge V to 300 Te V range, using Proton 1, 2 and 3 satellite-borne counters 05 p0709 A72-16231
- Electron flux and energy spectra measurements at 200-600 km altitude by Cerenkov counters onboard Proton 1 and 2 05 p0709 A72-16254
- Automatic interplanetary station adapter to obtain reflected signals amplitude-altitude-frequency characteristics during ionospheric probes 05 p0657 A72-16271
- Energetic solar flare particles release from sun, describing satellite observations of solar electromagnetic radiation 05 p0710 A72-16522
- Magnetospheric electron cyclotron and Langmuir plasma frequencies ratio determination from satellite observed electron and ion density data 05 p0659 A72-16765
- Ionospheric ion density distribution at 600 km height and medium and low latitudes from Cosmos 184 satellite data analysis 05 p0659 A72-16766
- Integral and differential electron energy spectra in inner radiation belt from Cosmos 219 satellite observation 05 p0711 A72-16768
- Fast charged particles measurement in inner radiation belt by Cerenkov counter mounted on Cosmos 137 satellite indicating presence of high energy electrons 05 p0711 A72-17035
- Ionospheric geocoronal L alpha emission intensity related to solar activity level from Cosmos 215 satellite data 05 p0659 A72-17038
- Ionospheric electron content from Faraday rotation observed on satellite radio signals at various frequencies 05 p0659 A72-17095
- Satellite surface temperature measurements changes due to atmospheric specific humidity, noting increase in water vapor absorption coefficient with content 06 p0806 A72-17671
- Soviet book on geometrical space geodesy covering satellite observation, Keplerian laws, two body problem and orbit element determination 06 p0879 A72-17817
- Image enhancement techniques for sea-ice mapping from satellite IR data, discussing gray scale contrast augmentation scheme for visual quantitative information 06 p0807 A72-17825
- Brightness profiles of earth daytime horizon from Soyuz spacecraft photographic photometry, deriving atmospheric scattering coefficient relation to optical thickness vertical distribution 06 p0808 A72-18040
- Remote sensing possibilities by aerial photographic methods based on scanning, scatterometer, radiometer and vidicon systems, discussing ground resolution, data automation and satellite observation [DGLR PAPER 71-128] 06 p0818 A72-18234
- Soviet book on terrestrial studies by satellite observation covering meteorology, hydrology, oceanography, geomorphology, geobotanics, geography, pedology, atmospheric physics and TV and photographic analysis 06 p0810 A72-18523
- Combined solution for station coordinates determination by geometric and dynamic satellite geodesy 07 p0974 A72-18887
- Pitch angle distributions of energetic protons for different geomagnetic activity levels as function of invariant latitude and magnetic local time from ESRO IB satellite measurements 07 p1057 A72-19141
- Imp 5 magnetic field measurements at high geomagnetic latitudes in outer magnetosphere near noon meridian, noting depressed field region centered on polar cusp 07 p0975 A72-19146
- Ogo 6 ionospheric measurement of proton whistlers wave-normal vector, investigating propagation modes 07 p1057 A72-19148
- Remote sensing history and techniques, describing ERTS instrumentation for earth science studies 07 p0976 A72-19177
- Satellite system for telemetering environmental and physiological data from winter den of hibernating black bear, discussing instrumentation and equipment performance 07 p0931 A72-19913
- Spherical harmonic representations of geomagnetic field including magnetosphere and tail regions based on ground based and low altitude spacecraft measurements within several earth radii 07 p0977 A72-20026
- European local geodetic datum centering by Doppler measurements of navigation and geodetic satellites [DFVLR-SONDDR-139] 07 p1033 A72-20273
- Galactic cosmic ray particle intensity decrease relationship to low energy proton flux increase based on interplanetary Zond 3 and Venera probes measurements 07 p1063 A72-20626
- Primary cosmic rays energy spectrum at .100-1000 TeV from Proton 4 satellite data 07 p1064 A72-20629
- Primary cosmic ray particles disappearance and proton spectrum slope rise in 1 TeV energy region from Proton satellites data 07 p1064 A72-20630
- Primary cosmic rays alpha particles and protons energy spectra similarity and intensity difference at .05 to 1.6 TeV, using Proton satellites data 07 p1064 A72-20631
- Cosmos satellite measurements of high energy gamma quanta from Crab Nebula region, indicating excess flux association with Taurus constellation point source 07 p1064 A72-20636
- Ionospheric integral electron concentration data from measurements of Elektron 1 and 3 satellites coherent radio wave emission 08 p1155 A72-20800
- Interplanetary medium physical parameters from spacecraft measurements, noting solar wind properties, magnetic fields and MHD discontinuities 08 p1228 A72-20826
- Polar orbiting satellite ESRO-1A 1-13 keV electron measurements compared to bottomside ionosonde measurements for auroral particle precipitation and F region electron density 08 p1226 A72-21099
- Meteorost geostationary satellite international program for earth cloud cover observation and meteorological data relays between ground stations as part of Global Atmospheric Research Program 08 p1241 A72-21204
- Local interstellar hydrogen survey from OAO-2 observations of Lyman alpha absorption at 1216 A for B2 or earlier stars 08 p1235 A72-21392
- Solar energetic particle access characteristics to magnetosphere from PCA riometer and satellite measurements, determining relationship between earth dipole field and interplanetary field 08 p1228 A72-21497
- X ray observatory with gas filled proportional counters, discussing pulse height analyzer, command system, calibration and power distribution 08 p1167 A72-21512
- Periodic intensity and period variations of X ray pulsating source Cen X-3 caused by occulting binary system from Uhuru satellite observation 09 p1382 A72-22289
- Atmospheric temperature profiles real time retrieval from Nimbus 4 satellite IR spectrometer observation, describing method used in dynamical weather forecasting 09 p1345 A72-22440
- Sensor spatial resolution effects on satellite estimation of earth cloud cover, simulating cloud distribution and size 09 p1345 A72-22450
- Diurnal phase anomaly in upper atmospheric density and temperature inferred from satellite drag and incoherent scattering observations 09 p1298 A72-22590
- Earth bow shock laminar profile at low Mach number by crossing satellites on 12 February 1969, determining mean velocity along normal 09 p1387 A72-23004
- Vlf hiss with lower hybrid resonance cut-off recorded by Alouette 1, emphasizing midlatitude events and electromagnetic energy transportation by multion duct in topside ionosphere 09 p1279 A72-23007
- OGO 4 satellite observed band limited ELF hiss characteristics explanation by model based on generation at large wave normal angle in equatorial region 09 p1279 A72-23008
- Differential photoelectron fluxes at 560 km altitude observed by OV1-18 satellite on 22 March 1969, noting latitudinal variation 09 p1378 A72-23013
- Uhuru satellite development history and preliminary X ray observation, analysis of radiation source emission characteristics, locations and identifications 10 p1533 A72-23892
- ESSA satellite observation of meridional circulation, noting roles of subsidence sinks, storm depressions and melting fronts 10 p1506 A72-24059
- Satellite photometric observation of diffuse celestial sources such as Milky Way, zodiacal light and gegenschein 10 p1546 A72-24863
- Ionospheric electron content determination at different latitudes from geostationary satellite signal Faraday rotation 10 p1475 A72-24955
- Equatorial Faraday rotation measurements for night ionospheric electron density peak structures during equinoctial months, using ATS-C geostationary satellite radiation 10 p1476 A72-24958
- Space environment and astronomical studies with sounding rockets, satellites and orbiting solar observations 10 p1548 A72-24974
- Satellite IR spectrometer sounding measurements reduction for atmospheric temperature profiles, obtaining coefficients by statistical regression and minimum information solutions 10 p1508 A72-25081
- Successful operational satellite sounding probabilities with normal global cloud cover by vertical temperature profile radiometer 10 p1508 A72-25082
- Atmospheric humidity vertical profile determination by measuring microwave radiation from satellite 11 p1620 A72-25274
- Gulf Stream surface front structure, temperature and salinity observation from ship, aircraft and satellite 11 p1620 A72-25348
- Autumnal stratospheric temperature variations in northern and southern hemispheres from Nimbus 3 IR spectrometer 11 p1680 A72-25761
- Natural oscillations of magnetosphere and trapped radiation transport by electromagnetic pulses as possible mechanism for disturbances from thermonuclear explosion reaction on particles in natural radiation belt 11 p1712 A72-25935
- Fast charged particle flux measurement in inner radiation belt by Cosmos 137 satellite in January-February 1967 11 p1713 A72-25947
- Dayside magnetosphere stably trapped radiation zone high latitude boundary determination from energetic electron intensity spatial distribution observation by Imp 3 satellite 11 p1713 A72-26106
- Upper atmospheric satellite and rocket soundings reliability and utility, covering ionospheric radio propagation, numerical weather prediction and gravity waves 11 p1623 A72-26390
- Explorer 35 observations of solar wind electron density and temperature, noting anisotropy direction correlation with magnetic field vector alignment 11 p1713 A72-26392
- Earth bow shock nonuniform structure observation correlation with interplanetary field orientation, using Explorer 33 and 35 data 11 p1722 A72-26395
- Midlatitude stable auroral red arcs observation from OV1-10, showing generation at plasmopause due to turbulent dissipation of ring current energy 11 p1624 A72-26401
- Atmospheric neutral density measurement near 400 km during daytime by microphone density gage on OGO 6 11 p1625 A72-26407
- Atmospheric temperature measurement by neutral particle wake method, using satellite-borne mass spectrometer 11 p1634 A72-26408
- Atmospheric density annual and diurnal variations in lower ionosphere, from satellite radar tracking data, considering drag coefficient modeling and orbit determination techniques 11 p1625 A72-26410
- Simultaneous Esro satellites observation of spatial and temporal particle flux variations over polar caps 11 p1714 A72-26418

Semiannual exospheric temperature and density variations from satellite observation and ionosonde measurements

11 p1626 A72-26420

Geomagnetic tail and substorm activity structure from IMP-3 magnetic data, discussing plasma sheet thickness changes and magnetic flux distribution

11 p1627 A72-26533

Atmospheric vertical motions velocities prediction based on satellite cloud data

11 p1683 A72-26887

ATS observed ionospheric columnar electron content variation during March 1970 solar eclipse, discussing neutral winds effects

12 p1801 A72-27155

Research measurement error determination for two frequency Doppler measurement of artificial satellites

12 p1782 A72-27532

NASA Earth Resources Survey program review, discussing satellite and aircraft observation application to agriculture, geology, hydrology, geography, oceanography and environment pollution

12 p1877 A72-27688

Recoverable-observation Cosmos satellites, discussing launch frequency, recovery beacons, binary coded Morse code transmissions and flight duration relation to resolution

12 p1877 A72-27689

Ionospheric irregularities-magnetospheric parameters relationship from satellite scintillation measurement, noting use as indirect electron precipitation indicator

12 p1803 A72-27772

Satellite and ground station observed ionospheric plasma parameters comparison, considering electron density and temperature and ion temperature and composition

12 p1804 A72-27785

Simultaneous determination of chord length and direction by artificial earth satellite geodetic observations in Arctic and Antarctic regions

13 p1945 A72-28493

Computer and meteorological satellite effects on weather support for manned space missions, discussing Gemini 5 and Apollo 11 landing weather predictions and cloud climatology

13 p1989 A72-28804

Four dimensional atmospheric model providing global moisture, temperature, pressure and density profiles as attenuation model inputs for earth resources satellite mission simulation

13 p1989 A72-28805

Clear line-of-sight probabilities for atmosphere from whole sky photos, visual cloud cover, sunshine recorder traces, satellite and in-flight observations

13 p1989 A72-28809

Weather forecasting support of NASA programs involving earth oriented viewing and sensing experiments from aircraft and spacecraft

13 p1990 A72-28816

Regression technique for determining temperature profiles in upper stratosphere from satellite measured radiances, noting accuracy

13 p1990 A72-28822

Satellite radiance data for altitude and amplitude monitoring of stratospheric warming, comparing with rocketsonde and radiosonde observations

13 p1991 A72-28823

Satellite radiance data to determine stratospheric layer thickness, comparing empirical regression equations to mean weighted temperatures

13 p1991 A72-28824

Hybrid forecast model for hydrometeors short range prediction based on meteorological satellites cloud pattern observations and quasi-Lagrangian advection analog

13 p1993 A72-28858

Vertical concentration profile and diurnal variations of N and NO vs solar activity from satellite horizon airglow experiment

13 p1948 A72-29237

Daytime 30 MHz PCA from satellite and riometer measurements, noting linear relationship to square root of integral and differential solar proton fluxes

13 p2030 A72-29339

Inner Van Allen zone proton energy spectrum at 30-300 MeV from ESRO 2 satellite measurements

13 p2031 A72-29383

Whistler mode signals observation in conjugate region of 200 kHz broadcast station by satellite-borne narrow band receiver, considering field-aligned ducted and nonducted propagation

13 p1950 A72-29384

Solar flare X-ray emission occultation observed during 7 March 1970 eclipse by NRL instrument on OSO-5 satellite

13 p2031 A72-29549

Predicting electron density for type 3 solar burst excitation by LF satellite radio observations

13 p2032 A72-29723

Solar relativistic electrons and particle events spectra during 1967-1969 from IMP-4 observations

13 p1033 A72-29746

Satellite measurements of exospheric density variations during June 1968-December 1970 at 1070 and 900 km, discussing solar activity effect

13 p1952 A72-29803

Low energy particles spectrometer channels calibration for satellite auroral observation, discussing photomultiplier detector properties

13 p1960 A72-29843

Data acquisition, reduction, quick-look data and standard and special programs for ESRO 1A and B auroral particle satellite experiment

13 p1925 A72-29868

Solar transition zone and corona EUV lines formation heights measurement from OSO-4 spectroheliograms

13 p2050 A72-29939

Global atmospheric circulation barotropic spectral model application to satellite asymptotic data continuous processing

14 p2127 A72-30258

Solar cyclic intensity variation of excessive radiation with respect to galactic radiation background at low altitudes from satellite data analysis

14 p2146 A72-30475

Uhuru satellite observation of transient X ray source in constellation Lupus, discussing five month period intensity variation

14 p2157 A72-30572

Composition of radiation excess over primary cosmic ray background recorded by Cosmos satellites below midlatitude belt region

14 p2147 A72-30626

Primary cosmic rays antinuclei content upper limit from emulsions investigations with balloons and satellites

14 p2148 A72-30885

United Nations activity in international space program for earth resources and environmental pollution surveillance by satellites

15 p2220 A72-31227

Satellite observation of earth surface, discussing remote sensing techniques application in pollution control and ecology

15 p2319 A72-31232

Monitoring system for ionospheric disturbances prediction from satellite observation, discussing optimum locations for space stations

15 p2220 A72-31233

Atmospheric air pollution study by space techniques via thermal radiation spectral measurements and laser sounding, considering spaceborne photography

15 p2220 A72-31237

Unitary and interdisciplinary information processing of remote satellite observations of earth resources, noting ground station requirement for Italy

15 p2222 A72-31253

Solar wind thermal properties from positive component energy distribution observation by ESRO Heos 1 satellite

15 p2298 A72-31518

Cosmic ray chemical composition from particle sampling by rockets and satellites, comparing galactic rays, solar rays and sun

15 p2299 A72-31648

Energetic electrons generation and relaxation in narrow belt near 2.8 L measured with Cosmos 137 Cerenkov counter

15 p2299 A72-31909

Geomagnetic field aligned electron anisotropies at high latitudes for energies 1 and 6 keV observed by ESRO satellite, noting two regions of maximum occurrence frequency

15 p2226 A72-31928

Nighttime molecular nitrogen and oxygen number density profiles at 130-220 km over Sardinia from ESRO mass spectrometer measurements

15 p2226 A72-31938

Program for orbital determination and prediction of satellite positions from observations at one station

15 p2268 A72-31941

Annual variations of singly charged positive He ion density distribution in solar wind from Vela 3 observations

15 p2299 A72-31944

Extraterrestrial He I 584 A background radiation suggested from rocket and satellite observations, noting interstellar medium temperature determination from isophotes

15 p2309 A72-31945

Satellite charged particle observations and polar cap riometer absorption measurements during solar cosmic ray events, noting electrons and protons contributions

15 p2300 A72-31965

Satellite instrument to observe atmospheric composition by energy analysis of incoming gas stream, using velocity mass spectrometer for neutral particles measurement

15 p2236 A72-31966

Geomagnetically trapped protons pitch angle distribution from ESRO 2 semiconductor telescope measurements

15 p2300 A72-31991

Interplanetary particles intensity relationship with solar activity based on Heos A1 observations during 1969-1971

15 p2300 A72-31992

Report to COSPAR on UK ground based, rocket and satellite-borne space research experiments and 1971-1972 programs

15 p2337 A72-32005

Norwegian report to COSPAR on space scientific activities and application program, including satellite geodesy and earth resources research

15 p2338 A72-32009

Satellite earth resources remote sensing in visible, IR and microwave regions for plant disease and salinity evaluation

15 p2229 A72-32049

Magnetosphere description based on satellite observation data, discussing particle distributions, solar wind, shock wave, magnetic sheath and magnetopause

15 p2315 A72-32400

Vertical temperature profile retrieval from satellite radiance measurements for insertion into numerical atmospheric circulation model, discussing sensitivity test

15 p2267 A72-32728

Ion density and electron acceleration region location from satellite-borne solar flare X-ray measurements

15 p2302 A72-32790

Solar wind He enrichment origin in solar flares connection with type 2 radio emission from analysis of Vela 3 spectra

15 p2302 A72-32791

Interplanetary high energy electron flux association with solar flares from HEOS-A1 data

15 p2302 A72-32792

Ionospheric gravity waves spectral frequency distribution from ATS 3 electron concentration measurements, using numerical filters for statistical frequency analysis

16 p2382 A72-32891

Autocorrelation analysis of Mariner 2 data for solar wind velocity, noting 27 day recurrences

16 p2444 A72-32954

Low energy outer zone electrons high latitude boundary variation with interplanetary magnetic field direction and with geomagnetic activity from Alouette and Explorer data

16 p2382 A72-32957

Spin effects on satellite-borne cylindrical probe electron density measurements, considering satellite wake and geomagnetic field effects

16 p2389 A72-32962

Solar vacuum UV flux measurement by photon ion chambers aboard WRESAT I satellite, obtaining 4600 K brightness temperature

16 p2452 A72-33040

OSO 1 observation of 300 second oscillation in solar transition region and coronal extreme UV emission line intensity

16 p2453 A72-33137

Zodiacal light brightness and polarization measurement from OSO-5 with photometers at 4180 and 6820 A

16 p2385 A72-33467

Diffuse galactic light polarization characteristics from OSO-5 observations, discussing model of starlight scattering by interstellar dust

16 p2446 A72-33468

Atmospheric absorption height determination from orbital elements during solar radiation satellite observation

16 p2386 A72-33603

Soft X-ray spectral studies of plasma dynamics in solar flares from Bragg crystal spectrometer OSO 6 recordings

16 p2449 A72-33918

MHD fluid model for collisionless shock waves in turbulent plasma with enhanced transport coefficients, noting laboratory experiments and satellite and radio observations

16 p2439 A72-33932

Melting snow and ice packs detection by multispectral/visible and near IR/ remote sensing from earth satellites

16 p2387 A72-33999

Upper atmospheric trace constituents global mapping by laser radar probing from satellite, discussing feasibility and comparison with ground based system [AIAA PAPER 72-660]

16 p2365 A72-34074

Satellite measurement of ground-based CW Ar laser source scintillation, deriving log amplitude variance, probability distribution and power spectral density from telemetered data

17 p2513 A72-34289

Computer program algorithm for processing local landmark and cloud motion data recorded by satellite observation

17 p2520 A72-34410

Automated cloud tracking using precisely aligned digital ATS pictures.

17 p2521 A72-34411

Spatial characteristics of magnetic field fluctuation in the magnetosheath.

17 p2545 A72-34474

- Flare-time temperature in soft X-ray sources.
17 p2598 A72-34537
- Experimental evidence of an electron temperature enhancement in the wake of an ionospheric satellite.
17 p2545 A72-34633
- Alouette 2 plasma resonances observation near ionospheric electron cyclotron frequency harmonics, interpreting frequency shift as wave dispersion effects
17 p2546 A72-34692
- Mars and its satellites as viewed by Mariner 9
17 p2607 A72-34752
- ESRO 2 satellite observation of solar X-ray emission from active limb prominence, obtaining temperatures and emission measures as function of time
17 p2608 A72-35085
- Satellite beacons observations from 1964 to 1970.
17 p2547 A72-35125
- Ion concentration inhomogeneities in the ionosphere at an altitude of 600 km
17 p2547 A72-35207
- Low-energy proton observations in July and August, 1970, on the 'Molniya-1' satellite
17 p2600 A72-35208
- Magnetospheric electron cyclotron and Langmuir plasma frequencies ratio determination from satellite observed electron and ion density data
17 p2548 A72-35268
- Ionospheric ion density distribution at 600 km height and medium and low latitudes from Cosmos 184 satellite data analysis
17 p2548 A72-35269
- Integral and differential electron energy spectra in inner radiation belt from Cosmos 219 satellite observation
17 p2600 A72-35271
- Photographic observation of artificial earth satellites without the aid of time recording devices. II
17 p2517 A72-35384
- Explorer 33 and 35 plasma observations of magnetosheath flow.
17 p2548 A72-35587
- High latitude observation of precipitating electron spikes by polar orbiter OGO 4 satellite, noting population dependence on local trapping limit
17 p2601 A72-35591
- Low energy auroral electron precipitation associated ELF noise band observation by polar-orbiting satellite INJUN 5
17 p2517 A72-35593
- Observation of very-low-frequency whistler-mode waves in the region of the radiation-belt slot.
17 p2517 A72-35598
- Turbulence of electrostatic electron cyclotron harmonic waves observed by Ogo 5.
17 p2549 A72-35599
- Atomic oxygen green line emission in nightglow from OGO-F photometer observations, calculating tropical F region electron density spatial distribution
17 p2549 A72-35604
- Solar flares in the extreme ultraviolet. I - The observations.
17 p2602 A72-35710
- Some space instruments for the study of micrometeoroids.
17 p2558 A72-35940
- A comparison of measurements of the charge spectrum of solar cosmic rays from nuclear emulsions and the Explorer 35 solid-state detector.
18 p2721 A72-35988
- Midlatitude red arc observations by satellite and ground station, suggesting thermal conduction theory of formation from ionospheric electron and ion temperatures and densities
18 p2685 A72-35989
- Satellite measurements of the moon's magnetic field - A preliminary report.
18 p2724 A72-36287
- Operational earth observation systems and resources management - A global program.
18 p2725 A72-36539
- [IAIA PAPER 72-735] Orbiting astronomical observatory - Review of scientific results.
18 p2731 A72-36555
- Secular variation of the geomagnetic field in epoch 1965 to 1970 according to observatory and satellite data
18 p2689 A72-36871
- Measurement of integral parameters of the nighttime ionosphere by observations of signals from the 'Intercosmos 2' artificial earth satellite
18 p2689 A72-36877
- Evaluation of 15th-order harmonics in the geopotential.
18 p2729 A72-36986
- The potentialities of space technology in relation to oceanography and surface meteorology.
19 p2790 A72-37924
- Solution of the problem of cosmic triangulation by the generalized method of synchronous and quasi-synchronous straight lines
19 p2861 A72-37971
- Terrestrial and lunar orbital and rotational motion behavior, discussing kinematic theory and ground and space vehicle based observation techniques
19 p2865 A72-38479
- The determination of the vertical structure of the atmosphere from satellite measurements
19 p2792 A72-38700
- Azimuthal propagation of low-energy solar-flare protons as observed from spacecraft very widely separated in solar azimuth.
19 p2852 A72-38726
- Several observations of low-energy solar-proton spectra and possible interpretations.
19 p2852 A72-38727
- Geomagnetic cutoffs for cosmic-ray protons for seven energy intervals between 1.2 and 39 Mev.
19 p2852 A72-38728
- Explorer 35 observation of geomagnetic tail low energy electrons, noting plasma sheet extension to lunar distance and correlation with solar wind
19 p2853 A72-38737
- Airborne optical measurement comparison with satellite observation for auroral emissions and particle precipitation at noon, suggesting electron precipitation role
19 p2868 A72-38738
- Local-time survey of plasma at low altitudes over the auroral zones.
19 p2792 A72-38739
- Studies of outer belt and slot region protons at low altitudes.
19 p2853 A72-38740
- A satellite survey of vector electric fields in the ionosphere at frequencies of 10 to 500 hertz. I - Isotropic, high-latitude electrostatic emissions.
19 p2768 A72-38742
- A satellite survey of vector electric fields in the ionosphere at frequencies of 10 to 500 hertz. II - The electric component of ELF hiss.
19 p2768 A72-38743
- A satellite survey of vector electric fields in the ionosphere at frequencies of 10 to 500 hertz. III - Low-frequency equatorial emissions and their relationship to ionospheric turbulence.
19 p2768 A72-38744
- He abundance relationship to solar wind bulk speed and temperature from Explorers 34 and 43 observations, noting dependence on sunspot number
19 p2853 A72-38749
- A new method for in situ electron temperature determinations from plasma wave phenomena.
19 p2793 A72-38758
- Complex analysis of satellite data for electromagnetic emission measurements in the radio, infrared and optical wavelength ranges
19 p2829 A72-38770
- Aircraft and spacecraft high latitude optical measurements of magnetosphere-related emissions, discussing red arcs, IR auroras, X-ray pulsations, conjugate effects, etc
20 p2918 A72-39539
- Observation of ultraviolet radiation from a rocket exhaust plume at high altitudes.
20 p2984 A72-39641
- Remote sensing of urban 'heat islands' from an environmental satellite.
20 p2919 A72-39717
- An albedo horizon sensor using hybrid circuitry.
21 p3050 A72-40122
- Regression technique for determining temperature profiles in the upper stratosphere from satellite-measured radiances.
21 p3052 A72-40249
- Fundamental geodetic parameters of the earth's figure and the structure of the earth's gravity field derived from satellite data.
21 p3048 A72-40494
- Zodiacal light, airglow and lightning monitoring by wide field broad bandpass OSO-5 experiment, obtaining height profile, cell size and intensity variations of nightglow
21 p3054 A72-40619
- First approximation for spacecraft observations of noctilucent clouds from circular orbits with optimal optical axis orientations
21 p3049 A72-41438
- The composition of the Martian atmosphere - Minor constituents.
21 p3110 A72-41458
- Air motions in the tropical stratosphere deduced from satellite tracking of horizontally floating balloons.
21 p3078 A72-41612
- Martian topography according to ground-based radar measurements and the CO₂ absorption observed from the earth and from the Mariner 6 and 7 spacecraft
21 p3114 A72-41766
- Distribution of total ozone content in the atmosphere according to spacecraft observations
21 p3050 A72-41797
- Some results of measurements of short-wave and long-wave radiation fluxes from the Cosmos-320 satellite
22 p3168 A72-41875
- Corrections to star catalogues from satellite observations.
22 p3220 A72-41997
- Some topside electron density measurements from Ariel III satellite during the geomagnetic storm of 25-27 May 1967.
22 p3169 A72-42017
- Spatial distribution of excess-radiation intensity at low altitudes
22 p3218 A72-42212
- Longitudinal magnetospheric currents contribution to auroral electrojet from satellite observation data, noting magnetosphere electric field excitation of meridional Pedersen and Hall currents
22 p3169 A72-42225
- Magnetically symmetric detection of the mid-latitude electron density trough by Ariel 3 satellite.
22 p3170 A72-42372
- High energy electron spatial distribution in plasma sheet from Ogo 5 magnetometer experiments
22 p3211 A72-42406
- Magnetospheric substorm onset examined via simultaneous balloon X ray and electric field measurements, discussing ATS 5 observations
22 p3170 A72-42409
- Spatial and temporal variations of thermal plasma ion and electron densities as function of L at 3000-5700 km from polar orbiting OV 3-1 satellite observation
22 p3211 A72-42414
- Polar-cap measurements of solar-flare protons with energies down to 12.4 keV.
22 p3218 A72-42425
- Thermospheric atomic oxygen and molecular nitrogen densities from OGO 6 neutral atmospheric composition experiment, comparing with prediction by Jacchia models
22 p3172 A72-42431
- Esro 1 (Aurorae) satellite electron intensity measurements, explaining disparities between different experiments by detectors low-energy thresholds difference
22 p3173 A72-42648
- Satellite measurements of solar X-ray flux and their use for interpretation of sudden ionospheric disturbances.
22 p3219 A72-42884
- Injun 5 satellite measurements of magnetospheric convection electric fields via double probe technique, discussing substantiation with OGO 6 results
22 p3174 A72-42901
- ULF wave observation by satellite, considering geomagnetic activity control of magnetospheric wave occurrence
22 p3174 A72-42902
- Gravitational constant time variations measurement by high flying laser tracked satellite, considering non-conservative forces effects on orbital perturbations
22 p3174 A72-42925
- The equatorial electrojet according to measurements from the Cosmos 321 satellite
23 p3328 A72-43369
- CAT probabilities relationship to temperature radiance gradients determined by IR spectrometers on-board Nimbus satellites
23 p3310 A72-43614
- Backscattering of desorbed gas molecules from spacecraft
23 p3284 A72-43618
- Potsdam correction from the satellite determined geopotential.
23 p3285 A72-43944
- Satellite-observed Southern Hemisphere cloud vortices in relation to conventional observations.
23 p3285 A72-44145
- Investigation of the angular distribution of particles on the basis of Cosmos-219 satellite data
23 p3343 A72-44174
- Model for the uneven illumination of polar caps by solar protons.
23 p3286 A72-44502
- Compressions and rarefactions in the solar wind - Vela 3.
23 p3332 A72-44509
- Pioneer 8 observation of diffuse magnetosphere-magnetopause boundary, noting proton flux intensity and flow angle
23 p3341 A72-44512
- Outer magnetosphere near midnight at quiet and disturbed times.
23 p3341 A72-44513
- Measurements of magnetotail plasma flow made with Vela 4B.
23 p3342 A72-44514
- Source and identification of heavy ions in the equatorial F layer.
23 p3286 A72-44516
- Electron polar cap and the boundary of open geomagnetic field lines.
23 p3286 A72-44522
- Detection of earthward flow of keV protons in the geomagnetic tail at lunar distances.
23 p3333 A72-44532
- Electric field variations during substorms - OGO-6 measurements.
24 p3396 A72-44854
- HEOS-2 in orbit - Its technical performance.
24 p3449 A72-45108

Exact localization of isolated points on earth surface with Geole system satellite observation, noting applications in geodetic survey, geodynamics and geophysics 24 p3398 A72-45228

Russian book - Space research 1970: Investigation of the gravitational fields and shapes of the earth, other planets, and the moon on the basis of spacecraft observations. 24 p3443 A72-45399

NASA X ray satellite UHURU and HEAO-C instruments and observational data on supernova remnants, pulsars, extars quasars, radio galaxies and galactic clusters 24 p3446 A72-45539

SATELLITE ORBIT CALCULATION
U ORBIT CALCULATION
SATELLITE ORBITS
 NT PARKING ORBITS
 NT POLAR ORBITS
 NT STATIONARY ORBITS
 NT TWENTY-FOUR HOUR ORBITS
 Criticism of artificial satellite theory for small eccentricities 01 p0123 A72-10016

Orbital plane rotation and terminal impact ascending node and inclination of satellite during ballistic reentry 01 p0052 A72-10078

Lunar gravitational field for placing spacecraft into static earth satellite orbit with standing position with respect to rotating earth 01 p0127 A72-10351

Satellite low orbit transfer to stationary orbit, emphasizing stage and payload recovery effects on performance 01 p0130 A72-10936

Satellite in eccentric Keplerian orbit transgressing Roche limit about rigid sphere, considering time dependent evolution problem with various centrifugal and tidal forces 01 p0134 A72-11145

Draconitic-sidereal orbital period difference estimation formula for near-circular orbit satellites with air drag 02 p0279 A72-12048

World Administrative Radio Conference for Space Telecommunications data on geostationary orbit utilization, covering stationkeeping and satellite antenna pointing accuracies 02 p0177 A72-12387

Two constituent gaseous propellant micropulsion engines for satellite orbit correction and attitude control, discussing thermodynamic and reaction kinetics problems [DGLR PAPER 71-102] 02 p0271 A72-12711

Satellite orbit determination accuracy from radio interferometer tracking data containing systematic errors, using digital computer techniques on Symphonie transfer orbit [DFVLR-SONDDR-212] 02 p0182 A72-12744

Rotating earth oblateness and equator ellipticity influence on near-equatorial synchronous satellite behavior, using nonlinear mechanics asymptotic method 03 p0436 A72-13835

Long period perturbations arising in orbits of artificial satellites with large surface to mass ratio under solar radiation pressure and earth oblateness effects 04 p0572 A72-14637

Spatial motion of two three-coupled bodies along satellite circular orbit, discussing system equilibrium position stability and phase trajectories 04 p0582 A72-15003

D-2B satellite mission, describing attitude, orbit and experiments on zodiacal light, stellar radiati on and antisolar data 04 p0583 A72-15689

Extremum of satellite orbit perigee or apogee height in Hohmann transfer 05 p0713 A72-16006

Atmospheric density near 150 km altitude from Cosmos 316 orbital decay, noting density increases during geomagnetic storms 05 p0655 A72-16070

Artificial earth satellites orbit plane determination accuracy in terms of local vertical sensor errors and gyroscope drift 05 p0717 A72-16441

Closed form solution for Doppler satellite navigation for arbitrary orbits with ellipsoid Earth model and straight path signal transmission 05 p0686 A72-16561

Satellite motion state vector accuracy estimate algorithm based on angular measurements of stellar positions relative to satellite sent probe 05 p0687 A72-16762

Artificial planetary satellites lifetime estimation from atmospheric drag, discussing critical height/atmospheric density relationship, satellite design and initial orbit height 05 p0722 A72-17042

Spacecraft power system with Maximum Power Point Tracker, discussing German Aeros satellite and orbit simulation program 07 p0914 A72-19090

Regional communications coverage by controlled satellite constellations with low altitude circular orbits, developing analog or digital simulation method for mission planning 07 p0945 A72-19690

Earth gravitational field determination based on long periodic perturbations in orbital motion of satellites, estimating tesseral coefficients errors 07 p0976 A72-19817

ERTS program, discussing orbit selection and sensor equipment 07 p1085 A72-20305

Design and operation of hand control of automatic camera for astrogodesy used for measuring artificial earth satellites orbits 08 p1165 A72-21021

Local and integral ionospheric electron concentrations and horizontal gradients effects on reduced Doppler frequency shift difference along satellite orbit 08 p1132 A72-21144

High order harmonic equations in gravitational potential from Transit 1B orbit inclination, comparing with Ariel 3 08 p1158 A72-21216

Hill variable modification of Brouwer satellite theory algorithm for simplified orbital element and perturbation calculations and orbital eccentricity generalization 08 p1237 A72-21749

Near earth satellite orbit parameters correction, discussing least squares approach 09 p1387 A72-22770

Satellite circular orbit trajectory plane time optimal relocation, examining turn angle angular position and modulus of maximum lateral acceleration 11 p1718 A72-25928

Orbital eccentricity and angular momentum management scheme stability for satellite large attitude maneuver followed by trim maneuver sequence 11 p1719 A72-25978

Satellite orbit tracking data accuracy estimation by partial differentiation, using Doppler and interferometer methods 11 p1593 A72-26097

Near circular orbit elements determination as functions of satellite initial speed and coordinates deviation by mathematical expectation procedure 11 p1724 A72-26912

Earth shadow effects on light artificial satellite orbital motion 13 p2051 A72-28440

German aeronomy research satellite Aeros mission objectives, discussing orbit layout, onboard equipment and operation 13 p2050 A72-30079

Statistical data processing method for accuracy evaluation of satellite orbits parameters obtained from onboard measurements of two stars angular positions 14 p2151 A72-30454

Optimum elliptic orbit characteristics of planetary artificial satellite based on earth-planet-earth flight 14 p2151 A72-30472

Computer calculation of artificial satellite ephemerides from Smithsonian mean orbital elements, comparing observed and computed toponetric equatorial coordinates 14 p2087 A72-30480

Dynamic system motion stability estimation with Liapunov function in quadratic form, applying to circular satellite orbit stability in axisymmetric gravitational field 14 p2161 A72-31079

Stability analysis of satellite motions in Newton planetary field by Liapunov method, considering ellipsoid of revolution under gravitation of sphere 14 p2162 A72-31081

Approximate periodic solution of satellite equation of motion based on Schwarzschild metric integration, noting relativistic effects 14 p2162 A72-31108

Orbiting satellite environment and self contamination, calculating pressure, density and condensation rates and adsorption layers on critical surfaces 15 p2321 A72-31870

Program for orbital determination and prediction of satellite positions from observations at one station 15 p2268 A72-31941

Skyнет 1 synchronous satellite orbit determinations and longitude acceleration due to tesseral harmonics of earth gravity, using tracking station range data 15 p2321 A72-31949

Geopotential harmonics of fifteenth order obtained from decaying satellite orbits analysis 15 p2311 A72-32001

Preflight and real time gravity sensing for Mariner 9 satellite orbit determination during Mars 1971 mission 15 p2270 A72-32186

Algorithm for minimax parameter optimization by linear and quadratic programming with application to earth orbiting satellite orbital transfer 16 p2366 A72-33191

Small amplitude libration stability and damping system for gravitationally stabilized tethered orbiting radio interferometer satellite system 16 p2462 A72-34020

Solar radiation pressure effects on balloon satellite behavior, noting orbital eccentricity variations 16 p2463 A72-34182

Long-term prediction of artificial satellite motion along almost circular orbits allowing for a random number of zonal harmonics 17 p2607 A72-35033

Upper atmosphere zonal winds speed vs local time from data based on Cosmos 316 orbit analysis 17 p2547 A72-35075

Satellite motion state vector accuracy estimate algorithm based on angular measurements of stellar positions relative to satellite launched probe 17 p2578 A72-35265

Earth gravitational field determination based on long periodic perturbations in orbital motion of synchronous satellites, estimating tesseral coefficient errors 17 p2550 A72-35742

Influence of the Galilean Jovian satellites on the motion of an artificial satellite of Callisto 17 p2618 A72-35811

On the effects of gravitational absorption on orbits of artificial earth satellites. 18 p2728 A72-36761

The determination of zonal harmonic coefficients of the terrestrial potential 19 p2790 A72-38173

Ephemeris of a highly eccentric orbit - Explorer 28. 20 p2968 A72-39194

Local and integral ionospheric electron concentrations and horizontal gradients effects on reduced Doppler frequency shift difference along satellite orbit 20 p2903 A72-39249

Determination of the orbits of artificial satellites by the integrated Doppler effect method 20 p2974 A72-40023

Representation of the coordinates of a satellite of a spheroidal planet with the aid of series expansions 21 p3102 A72-40099

Satellite orbit computations using gravity anomalies. 21 p3104 A72-40493

Orbital and frequency sharing between the broadcasting-satellite service and the fixed-satellite service. 21 p3018 A72-40877

Commercial satellite communication system development, considering external constraints, orbital geometry, frequency allocations, multiple access transmission techniques, and satellite and earth station designs 21 p3021 A72-40921

International space telecommunication law and UN resolution concerning geostationary satellite orbit use for radio transmission 21 p3132 A72-41319

First order theory of satellite orbit determination with time difference data for synchronous equatorial spacecraft, applying to VLBI experiments with ATS-3 [AIAA PAPER 72-924] 21 p3112 A72-41568

Orbit prediction for artificial satellites via numerical averaging technique, presenting algorithm for planetary equations solution [AIAA PAPER 72-934] 21 p3112 A72-41572

Equinoctial orbit elements - Application to artificial satellite orbits. 21 p3112 A72-41575

[AIAA PAPER 72-937] 21 p3112 A72-41575

Long-term orbit prediction using two-variable asymptotic expansions and the automated manipulation capabilities of the FORMAC language. 21 p3113 A72-41576

[AIAA PAPER 72-938] 21 p3113 A72-41576

Secular perturbations in the motion of artificial earth satellites 21 p3114 A72-41770

Equations for 15th-order geopotential coefficients from the orbit of Transit 1B. 22 p3169 A72-42009

Least squares method for satellite motion parameters determination in orbital plane, using altimeter distance to planet surface measurements 22 p3223 A72-42202

Transcendental equations solution for satellite Kepler orbit determination from coordinates, velocity and time components, using Lambert-Euler relation 22 p3223 A72-42204

Analytic partial derivatives for estimating low-thrust parameters. 22 p3231 A72-42865

Luni-solar perturbations of the geostationary vehicle at arbitrary latitude. 24 p3448 A72-44990

Earth resources technology satellites [ERTS/ program requirements, considering coverage, spectral characteristics, system performance, photographic interpretation and information extraction 24 p3398 A72-45115

Velocity space maps and transforms of tracking observations, for orbital trajectory state analysis. 24 p3440 A72-45135

The estimation of accuracy of short-term atmosphere density prediction. 24 p3398 A72-45173

Satellite orbital motion numerical integration method, using Picard iteration relative to reference

orbit to calculate short-term anomalistic period intervals
[AIAA PAPER 72-909] 24 p3443 A72-45428
Mariner 9 Mars orbital trajectory analysis from earth based radio data, considering gravity field, n-body perturbation and solar radiation pressure effects [AIAA PAPER 72-928] 24 p3443 A72-45434
A thermospheric model from satellite orbital decay densities and incoherent scatter temperatures. 24 p3400 A72-45595

SATELLITE ORIENTATION

Recurrence relation derived for general normalized satellite inclination function with three parameters in series expansion for geogravitational potential 01 p0123 A72-10012
Spacecraft attitude determination with single-axis sensor and single natural radiation source with relative mutual motion, deriving error equations 01 p0032 A72-11224
Relay systems stability in orientation control of flexible satellites 05 p0725 A72-16439
Pulsed relay control system for stabilizing spacecraft orientation in flight, allowing for changes in characteristics of guidance sensor systems and slave mechanisms 05 p0731 A72-17031
Angular position of sun disoriented artificial earth satellites with angular velocities not exceeding 0.5 deg/sec, using harmonic analysis of magnetometric data 05 p0631 A72-17033
Rotating dumbbell shaped satellites orientation optimization by system of jets, calculating energy losses 05 p0731 A72-17043
Misalignment angle of Azur satellite orientation axis relative to geomagnetic field vector 06 p0892 A72-18145
Proton 2 and 4 and Cosmos 196 orientation by quick response algorithm from onboard three component magnetometer readings 08 p1240 A72-21138
Flexibly stabilized satellite orientation determination by stellar sensors and magnetic damping of rotation 08 p1240 A72-21139
Stationary motions stability of four rotor vertical gyroscopic system on satellite in circular orbit in Newtonian central force field 08 p1205 A72-21804
Observation errors effects on satellite attitude best least squares estimate based on direction measurements, using Monte Carlo method computer simulation 10 p1438 A72-24692
Spin stabilized satellites attitude dynamics during rigid booms extension, deriving equations of motion approximate solution 11 p1726 A72-25915
Tansei satellite spin axis orientation measurement by two flux-gate magnetometers and sun sensor 15 p2272 A72-32334
Gravitational stabilization of a satellite in a fixed inertial orientation. 17 p2622 A72-35487
Proton 2 and 4 and Cosmos 196 orientation by high speed algorithm from onboard three component magnetometer readings 20 p2976 A72-39243
Loosely stabilized satellite orientation determination by stellar sensors and magnetic damping of rotation 20 p2976 A72-39244
An automatic mass-trim system for spinning spacecraft. 20 p2977 A72-39603
First approximation for spacecraft observations of noctilucent clouds from circular orbits with optimal optical axis orientations 21 p3049 A72-41438
Star scanner attitude determination for the OSO-7 spacecraft. [AIAA PAPER 72-922] 21 p3082 A72-41566
Dynamics of spin-stabilized satellites having flexible appendages. 24 p3449 A72-45140

SATELLITE PERTURBATION
Liapunov stability of rigorous particular solutions /corresponding to libration points/ of three body problem, determining motions of satellite influenced by two spherical bodies 03 p0436 A72-13823
Perturbed satellite motion in gravitational field of aspherical rotating planet 06 p0892 A72-18036
Soviet book on celestial mechanics and astrodynamics covering classical and contemporary theory, many body problem, satellite perturbation, optimal and boundary value problems, etc 07 p1078 A72-19952
Secular perturbations of artificial earth satellites Keplerian orbital elements from arbitrary-order zonal harmonics in geopotential series expansion 07 p1078 A72-19982

Rotational perturbation of three bodies in space tied by flexible elastic ropes, relating physical parameters to stable motion regions boundaries 08 p1240 A72-21141
Longitude dependent perturbation inducing portion of geopotential as function of artificial earth satellite orbital elements 08 p1158 A72-21160
Satellite orbital inclination change due to rotating upper atmosphere with day-to-night density variation, deriving resonance conditions 08 p1241 A72-21640
Mathematical model of solar radiation pressure effects on earth satellite orbit 08 p1237 A72-21643
Book on perturbation theory in celestial mechanics, covering absolute perturbation, Hill lunar theory and application to Jupiter satellites 09 p1389 A72-23247
Secular and periodic variations of orbital elements of Mars satellites due to oblateness and solar attraction 10 p1541 A72-24471
Solar radiation pressure effects on orbital evolutions of light artificial earth satellites 10 p1543 A72-24632
Satellite coordinates calculation for arbitrary inclinations and orbit eccentricity below Laplace limit 10 p1543 A72-24633
Perturbed satellite motion in gravitational field of aspherical rotating planet 11 p1727 A72-25972
Time dependent geopotential as function of position weighted atmospheric density from Poisson equation, noting satellite orbit perturbations due to mass shifts in planetary atmospheres 12 p1838 A72-27022
Geostationary artificial satellite orbital parameters calculation, taking into account lunar, solar and light pressure perturbations 14 p2150 A72-30451
Stochastic atmospheric density fluctuations effect on circular-orbiting satellite roll-yaw oscillations stability 15 p2319 A72-31457
Fourier analysis for geopotential resonance effect on satellite orbits, calculating 13th harmonic influence on GEOS 2 and BE-C mean longitude 15 p2309 A72-31939
Longitude dependent perturbation inducing portion of geopotential as function of artificial earth satellite orbital elements 17 p2545 A72-34451
Influence of the diurnal effect in the atmospheric density distribution on the braking of a satellite 17 p2546 A72-35032
Satellite orientation and stabilization systems aerodynamic compensation for circular orbit perturbations 17 p2621 A72-35034
Influence of the Galilean Jovian satellites on the motion of an artificial satellite of Callisto 17 p2618 A72-35811
Undisturbed eccentric anomaly difference as the independent variable in the perturbation differential equations. 19 p2856 A72-37520
Resonant attitude instabilities for a symmetric satellite in a circular orbit. 21 p3115 A72-41046
Attitude perturbations of a spinning Jupiter Orbiter spacecraft. [AIAA PAPER 72-920] 21 p3115 A72-41565
Long term stability of earth and lunar orbiters - Theory and analysis. [AIAA PAPER 72-936] 21 p3112 A72-41574
Secular perturbations in the motion of artificial earth satellites 21 p3114 A72-41770
The equilibrium potential of a magnetospheric satellite in an eclipse situation. 22 p3168 A72-42003
Small oscillations of gravity gradient satellite in circular near-equatorial orbit, discussing operational efficiency of magnetic damping systems 22 p3230 A72-42223
Luni-satellite perturbations of the geostationary vehicle at arbitrary latitude. 24 p3448 A72-44990
Relative equilibrium positions and their stability for a general gyrostat-satellite in a circular orbit. 24 p3449 A72-45142
On the tidal effects in the motion of artificial satellites. 24 p3441 A72-45233
To the problem of satellite's perturbed motion under the influence of solar radiation pressure. 24 p3442 A72-45237
Satellite orbital motion numerical integration method, using Picard iteration relative to reference orbit to calculate short-term anomalistic period intervals [AIAA PAPER 72-909] 24 p3443 A72-45428

Explorer 34 satellite orbit perturbation, noting earth gravitational tesseral harmonic effect on perigee passage time 24 p3399 A72-45557
Omega-Dot law for time optimum approximation of rotating satellites wobble damping with control moment gyroscopes, calculating wobble rates by energy sink method 24 p3453 A72-45777

SATELLITE RENDEZVOUS
U ORBITAL RENDEZVOUS
SATELLITE ROTATION
Integrability of rotating satellite differential equation of motion in axially symmetric gravitational field 01 p0122 A72-10008
Control axes misalignment effects on spinning satellite wobble damping and requirements for active momentum exchange controllers 02 p0286 A72-12267
Hybrid computer simulation of spinning satellite dynamic behavior during flexible booms deployment and attitude control maneuvers, deriving equations of motion from Lagrange equations 02 p0286 A72-12658
Kalman linear filtering technique for spinning satellite attitude restitution, evaluating reliability by model for simulation of measurements by sensors [ONERA, TP NO. 953] 05 p0724 A72-16436
Spinning drag-free satellite trapping control phenomenon due to proof mass effect on translation controller design 05 p0725 A72-16445
Magnetic damper for gravity gradient stabilized satellite rotational and librational motions, deriving formula for calculating damping coefficients 05 p0726 A72-16463
Universal ball-in-tube nutation dampers for spinning satellites, noting cost savings 05 p0729 A72-16756
Rotating dumbbell shaped satellites orientation optimization by system of jets, calculating energy losses 05 p0731 A72-17043
Mathematical model for dissipative dual-spin satellite analysis, making use of high speed rotor symmetry to permit quasi-holonomic transformation 07 p1085 A72-19280
German monograph on optimal attitude control of satellites with rotors and simultaneous spin reduction, covering motion equations for stable equilibrium and circular orbit 09 p1394 A72-22330
Axisymmetric satellite rotation about center of mass in circular orbit under Newtonian gravitational field, considering precessional stability 13 p2052 A72-30002
Spin effects on satellite-borne cylindrical probe electron density measurements, considering satellite wake and geomagnetic field effects 16 p2389 A72-32962
Geomagnetic attitude control of an axisymmetric spinning satellite. 17 p2619 A72-34201
A test of the effect of satellite spin on two-way Doppler range-rate measurements. 19 p2830 A72-37278
Permanent rotations of an equatorial satellite in the geomagnetic field 19 p2869 A72-37437
An automatic mass-trim system for spinning spacecraft. 20 p2977 A72-39603
Resonant attitude instabilities for a symmetric satellite in a circular orbit. 21 p3115 A72-41046
Mass attraction reduction by integral control in spinning drag-free satellites. 21 p3115 A72-41304
Satellite vibration-rotation motions studied via canonical transformations. [AIAA PAPER 72-919] 21 p3115 A72-41564
Attitude perturbations of a spinning Jupiter Orbiter spacecraft. [AIAA PAPER 72-920] 21 p3115 A72-41565
Axisymmetric satellite rotation about center of mass in circular orbit under Newtonian gravitational field, considering precessional stability 22 p3231 A72-42730
To apparent equatorial radius, taking into account distortion due to Jupiter effects on rotation and tides 24 p3436 A72-44701
Omega-Dot law for time optimum approximation of rotating satellites wobble damping with control moment gyroscopes, calculating wobble rates by energy sink method 24 p3453 A72-45777

SATELLITE TELEVISION
Molniya-Orbit communication satellite system, discussing operational quality, maintenance, television transmission facsimile, sound broadcast and multichannel telephony 01 p0023 A72-10046
ERTS satellite return beam vidicon TV system and multispectral scanner images, describing photogrammetric and cartographic evaluations 01 p0065 A72-10449

Educational satellites - Conference, Nice, France, May 1971, covering space communication, TV, performance, data handling, economics, etc

01 p0147 A72-11277

Regional geological surveying by satellite-borne TV, discussing image interpretation methodology

02 p0208 A72-11780

Space TV images use in hydrospherical temperature discontinuity from location, examining cloud cover distributions over Sea of Japan

02 p0214 A72-11872

ATIS-F educational TV experiment in India, discussing domestic communication satellite development and nationwide coverage problems

02 p0278 A72-11960

Communication satellites for European radio and TV broadcasts, discussing use of American, CETSC and Symphonic satellites

04 p0494 A72-15677

TV programs direct broadcasting by satellites, discussing frequency range, amplitude vs frequency modulation, satellite stabilization and economic aspects

04 p0494 A72-15678

Symphonic communication satellite applications in radio and TV broadcasting, discussing Retelsat network, Socrate and Memini projects, educational TV, etc

04 p0494 A72-15680

Meteorological satellites TV, visual and IR cloud imaging and atmospheric sounding techniques for short and long range weather forecasting

06 p0892 A72-18066

Meteorological satellites data gathering equipment including TV cameras, temperature humidity, ozone and radiation measuring devices, discussing data processing and evaluation for weather forecasting

[DGLR PAPER 71-131]

06 p0892 A72-18231

Multispectral TV camera systems for satellite recording of earth surface electromagnetic radiation at separate wavelengths

[DGLR PAPER 71-135]

06 p0817 A72-18232

Soviet book on terrestrial studies by satellite observation covering meteorology, hydrology, oceanography, geomorphology, geobotanics, geography, pedology, atmospheric physics and TV and photographic analysis

06 p0810 A72-18523

National TV distribution by Canadian domestic satellite system, discussing design simplicity and payload weight maximization

07 p0944 A72-19654

Anik communications satellite for Canadian domestic television and radio broadcasting networks

07 p0944 A72-19655

International and national satellite TV systems, discussing technical and operational characteristics, artificial emission dispersion and costs

07 p0944 A72-19656

International TV broadcasting satellite system, discussing technical problems and cost effectiveness in competition with conventional TV systems

08 p1132 A72-21205

UHF band satellite TV broadcasting system with FM, calculating required field strength and transmitter power

10 p1435 A72-24033

Technical standards for educational and community TV by satellite, considering picture quality requirement, modulations, SNR, threshold and fade margin, and channel width

10 p1435 A72-24034

Combined educational and TV network satellite distribution system for public broadcasting service, discussing cost reduction techniques

10 p1435 A72-24035

TV reception from satellite broadcasting systems in hostile environment of remote and inaccessible villages over large land areas

[AIAA PAPER 72-524]

12 p1779 A72-27353

Franco-German Symphonic project of point to point communication and TV distribution by satellite, describing spacecraft and ground station characteristics

[AIAA PAPER 72-549]

12 p1794 A72-27372

Canada-NASA communications technology satellite /CTS/ for 12 and 14 GHz TV transmission, considering mission profile, spacecraft design, attitude control system and ion thruster

[AIAA PAPER 72-580]

12 p1877 A72-27382

Economic and social implications of Indian national satellite for television and telecommunication, noting data links need

[AIAA PAPER 72-583]

12 p1781 A72-27384

Ground and satellite based TV broadcasting compared in terms of economic, political and pedagogical implications to solve educational problems in developing countries

[AIAA PAPER 72-525]

12 p1891 A72-27662

TV network distribution systems cost, comparing video tape shipping, terrestrial interconnection with delay for time zones and indirect and direct satellite transmission

[AIAA PAPER 72-552]

13 p1918 A72-28983

Photointerpretation and computerized radiometric analysis of ERTS multispectral TV and scanner imagery of Israel

15 p2221 A72-31242

A/D and D/A converter for color TV signal digital transmission over communication satellites, discussing system design features

17 p2524 A72-34262

Incore thermionic reactor application to meet European TV broadcasting satellite and submarine and underwater laboratory power requirements

18 p2644 A72-36166

Receiver terminals for satellite television systems.

18 p2662 A72-36849

ERTS-borne return beam vidicon camera using high resolution TV sensors coaligned to view identical scene in different spectral bands

19 p2795 A72-37576

Controlled-carrier transmission of AM/VSB television from space.

21 p3016 A72-40770

Utilization of frequency bands allocated to satellite broadcasting for regional or domestic systems.

21 p3018 A72-40875

Geostationary satellite direct TV broadcasting system extension to 12 GHz band, considering receiving installations, antennas, performance and costs

21 p3018 A72-40876

Orbital and frequency sharing between the broadcasting-satellite service and the fixed-satellite service.

21 p3018 A72-40877

Television transmission performance of an experimental small aperture earth station.

21 p3018 A72-40878

Shaped coverage patterns with satellite array antennas.

21 p3019 A72-40884

An orthographic photomap of the South Pole of Mars from Mariner 7.

21 p3110 A72-41455

TV-radio satellite receiver equipment, considering power requirements, antenna, energy supply and placing into 24-hour orbit

23 p3262 A72-43300

Direct satellite TV broadcasting for complete community or individual home coverage, discussing requirements, technical performance and economic factors in Europe

24 p3380 A72-45553

SATELLITE TEMPERATURE

Azur satellite flight data evaluation of thermal behavior, measuring temperature with thermistors

05 p0746 A72-16139

Thermal control concept evaluation for a ten-year life modular space station.

[ASME PAPER 72-ENAV-30]

20 p2894 A72-39147

SATELLITE TRACKING

German vhf ground telemetry satellite tracking system radio interferometer, discussing specifications and performance

[DGLR PAPER 71-124]

02 p0182 A72-12732

Satellite tracking radio interferometer with 1 deg sec directional accuracy, discussing low noise level and precise time allocation requirements

[DGLR PAPER 71-125]

02 p0182 A72-12738

Satellite tracking by combined optimal estimation and control techniques with Kalman filter, considering radio antenna and optical tracking systems

02 p0285 A72-12812

Earth gravity field representation by simple layer potential from Doppler tracking of satellites

04 p0514 A72-14565

Geophysical and gravimetric measurement time recording techniques, describing satellite tracking photochronograph and electronic printing chronographs

04 p0525 A72-15571

Earth gravity field, movement and temporal form variation determination by satellite tracking, long base interferometry or lunar observation

04 p0520 A72-15723

Propagation delays for clock synchronization from synchronous satellite tracking by range measurements

05 p0628 A72-16563

Satellite angular coordinates determination by laser ranging from single station, using echo recording by Schmidt telescope

07 p0947 A72-20255

Laser ranging techniques application to ground baseline measurements, discussing maximum range of satellites tracking laser system

07 p0947 A72-20264

Elevation angle and range error correction equations for satellite tracking data processing with assumed spherical tropospheric refractivity

09 p1281 A72-23510

Semiautomatic tracking device for satellites comprising laser telemetry equipment

13 p1939 A72-29674

Photographic observation of satellites to sixth magnitude with K-24 aerial camera on Polaroid 3000 and 10,000 ASA film, recording time signals on magnetic tape

14 p2084 A72-30235

Balloon flight tracking by Nimbus D satellite to sound tropical stratosphere air motions, noting northward drift maximum in Northern Hemisphere winter

14 p2128 A72-30350

Low cost optimal earth resources technology satellite station for satellite tracking and image data reception and recording

15 p2213 A72-31246

Sonar techniques application to radar, stressing utilization of preformed channels in rapid and distant detection of satellites and ballistic missiles

15 p2197 A72-31874

Laser ranging instrument for satellite distance measurement, discussing four-axial mounting, guiding telescope, receiving optics and performance

15 p2247 A72-31935

Role satellite observed meteorological balloon data analysis, obtaining mean zonal velocity, meridional velocity and temperature vs latitude from statistical estimates

15 p2266 A72-31980

Report to COSPAR on Polish space program covering artificial satellites tracking, aerospace medicine, meteorology and bioastronautics

15 p2337 A72-32004

Gravitational absorption investigation from lunisolar attraction observed by tracking high flying satellite in eccentric polar orbit

16 p2382 A72-32892

Error analysis of East European triangulation network photographic observations of Echo and Pageos satellites from ground stations

16 p2387 A72-33798

Satellites use for position determination and data acquisition systems application to earth sciences and industry

17 p2603 A72-34398

Use of satellites for the transmission of meteorological data and the tracking of observation stations

17 p2603 A72-34399

Steerable directional VHF antenna design for radio interferometric tracking and ranging of Symphonic satellite

[DFVLR-SONDDR-222]

17 p2536 A72-35432

Role - The tracking and collection of data applicable to meteorology

17 p2622 A72-35718

Role program for tracking and gathering information from drifting buoys at sea

17 p2617 A72-35720

A geopotential model /APL 5.0-1967/ determined from satellite Doppler data at seven inclinations.

18 p2685 A72-36029

Geostationary or orbital satellite tracking radio receiver with steerable antenna for beacon signal detection and locking, discussing system design and performance

18 p2661 A72-36847

A test of the effect of satellite spin on two-way Doppler range-rate measurements.

19 p2830 A72-37278

Solution of the problem of cosmic triangulation by the generalized method of synchronous and quasi-synchronous straight lines

19 p2861 A72-37971

Accuracy of the determination of the positions of stars and artificial satellites from an aircraft

19 p2861 A72-37973

Doppler effect characteristics and applications to artificial satellite tracking, considering computer program in orbit parameter calculations

19 p2765 A72-38172

Russian book - Algorithms for calculation of navigation data on spacecraft position.

21 p3103 A72-40460

Polarization follower tracking linear vector transmitted by satellite with high precision, noting spacecraft attitude control and Faraday rotation measurements applications

21 p3021 A72-40907

Gravitational constant time variations measurement by high flying laser tracked satellite, considering non-conservative forces effects on orbital perturbations

22 p3174 A72-42925

On application of Kalman filtering technique to on-line orbit estimation of a launching vehicle.

22 p3203 A72-43142

Triaxial mount for electrophotometric observations of satellites during their transit into the shadow of the earth

23 p3290 A72-44040

Determination of the mutual position of points on the earth's surface from synchronous laser observations of artificial earth satellites

24 p3397 A72-44860

SATELLITE TRANSMISSION

Forward error correction code performance on hf troposcatter and satellite channels, considering adaptive and nonadaptive convolutional and cyclic coding

01 p0026 A72-10338

Tropospheric effects on vhf satellite signal transmission noted from time lags between observed and calculated satellite rise time

01 p0027 A72-10409

Annual movements of satellite signals scintillation boundary in subauroral ionosphere

Time division multiple access systems for satellite transmission, discussing burst transmission control problem associated with transmitting end synchronization

Orbital elements and onboard transmitter frequency drift of active satellite from Doppler and angle data recorded at single receiving station

Modulation/demodulation techniques for optical one-gigabit/sec intersatellite data transmission link system, comparing per-unit data costs for system selection

Beacon satellite transmission determination of ionosphere total electron content, describing equivalent slab thickness and diurnal, seasonal and solar cycle behavior

L band in satellite system for aerial navigation aid, discussing position accuracy, data transmission and voice communication and modulation methods

Microstrip double down-converter receiver in civil satellite earth stations for reduced interface problems, increased reliability and minimum initial cost

Air surveillance using satellite range-difference measurement from noninterrogated aircraft beacons for ATC

Long range satellite signal Faraday fading rate revealing electron density profile near F layer peak

High latitude scintillation effects on vhf and S band polar orbiting satellite transmissions, examining ionospheric irregularities

Long range ionospheric guided hf signal propagation from low orbiting San Marco 1 and 2 satellites

Time division multiple access (TDMA) satellite communication system optimal design, discussing earth stations, satellites and transmission path characteristics

Ionospheric turbulence induced scintillations of Intelsat geostationary satellite signals at 4 and 6 GHz [AIAA PAPER 72-179]

Recovered carrier phase ambiguity resolution in four-phase PSK digital satellite communications system

FSK transmission experiments on uhf satellite link, noting threshold convolutional decoding contribution to SNR

Digital speech detector with increased voice signal and reduced noise sensitivity for satellite capacity improvement

TDMA satellite communication system with convolutional encoding and Viterbi decoding, evaluating data buffering and control configurations

Earth-space path attenuation statistics and fade duration at 15.3 GHz, using ATS 5 satellite transmission and radiometric sun/sky techniques

F region irregularity contours from correlation analysis of satellite amplitude scintillations, showing axially symmetric field-aligned and north-south elongated planes

Fole satellite relay system for weather balloon location and data collection and transmission to ground stations

Ionospheric inhomogeneity studies from angle of arrival recordings of satellite beacon transmissions, using phase radiometer interferometry

Ionospheric electron content determination at different latitudes from geostationary satellite signal Faraday rotation

Noise threshold improvement of PCM signals for satellite transmission, using quality detector and error detecting codes

Ionospheric total electron content measurement by satellite radio emissions

Digital adaptive echo cancellation mathematical technique for voice circuits derived from satellite transmission [AIAA PAPER 72-539]

Satellite technology for TV broadcasting service to Canadian remote areas, considering new frequency band allocation [AIAA PAPER 72-553]

Recoverable-observation Cosmos satellites, discussing launch frequency, recovery beacons, binary coded Morse code transmissions and flight duration relation to resolution

Ground reflections effect on satellite transmission link fading characteristics, computing transmitter field intensity fluctuations as function of terrain profile elevation angle

Error analysis of ionospheric parameter measurement by satellite transmitted or reflected multiple frequency pulsed radiation signal, using perturbation method

U.S.-Canadian Alouette/ISIS satellites case history, considering hardware, lunar sample analysis and satellite transmitted radio beacon signal reception and analysis

Microwave propagation delay due to atmosphere in satellite-to-earth communication based on spherical smoothly varying model and geometrical optics techniques

Present state of development and extension plans of the German satellite earth station at Raisting.

Intelsat 4 multichannel communication network earth station equipment components and characteristics experimental system (SPADE) study to realize demand assignment

Satellite communications and the Pleumeur-Bodou centre.

The use of satellites to meet future press requirements.

Determination of the orientation of ionospheric irregularities causing scintillation of signals from earth satellites.

Observations of scintillations of two satellite beacons near the boundary of the irregularity region.

Transmission efficiency of gas chromatography algorithmic data compression and coding for spacecraft atmosphere studies

Low noise receiver for satellite broadcasting.

Data link design for planetary video data transmission back to earth based on rate distortion theory generalization of information theory

Suppressed clock pulse duration modulation for noisy voice communication channels with hard limiting satellite repeaters, discussing system design and test data

Ground, satellite, terrestrial glass fiber channel and waveguide radiation systems for laser communications

Spacing limitations of geostationary satellites using multilevel coherent PSK signals.

Minicomputers application for long distance data transmission, noting multipurpose use of VT 1010/B computer in satellite operation program

SATELLITE-BORNE INSTRUMENTS

Cosmic gamma rays at 0.3-3.7 MeV measured by Na/Tl crystal detector 64-channel spectrometer onboard Cosmos 135 and 163

ESRO polar orbiting meteorological satellite, discussing design features and operational instruments

Spaceborne Fourier interference spectrometer for environmental pollutant sensor, discussing IR detection systems, instrument servo, data reduction and handling systems and optical tolerance [AIAA PAPER 71-1108]

Aerosol and atmospheric scattering layers observability by satellite mounted optical detector at 3000-7000 Å, comparing wide angle receiver and limited view field steerable telescope [AIAA PAPER 71-1110]

Nonflammable coolants for Saturn instrument unit environmental control systems, considering component materials compatibility with selected dielectric fluids

Cosmic ray neutron leakage flux and energy spectrum measurements in 0.01-10 MeV range by OGO 6 satellite-borne neutron detector

Venus atmospheric investigation by Venera 4, 5 and 6 probes, discussing satellite components and instrumentation, and atmospheric composition, depth, density, pressure, temperature and model

SATELLITE-BORNE INSTRUMENTS

Aeros satellite mass spectrometer design, discussing operation mode ion detection system, power supply, logarithmic electrometer and modulator

Cosmic X ray sources polarization, spectra and locations measurement, describing Skylark experiments and UK-5 satellite-borne instruments

TD-1, HEOS-B and COS-B satellite-borne experiments, discussing X ray and gamma astronomy

X ray and gamma astronomy, discussing satellite-borne experiments for electromagnetic and nuclear reaction rates and antimatter existence in cosmic radiation

Onboard equipment layout effect on dynamic stability against liquid propellant sloshing in spacecraft

Dipolar rf probe admittance measurements in simulated ionosphere for satellite plasma experiments

Remote sensing history and techniques, describing ERTS instrumentation for earth science studies

Biomedical telemetry instrumentation for radio sensing and transmitting biological information from animals and man, including location by satellite-borne receivers

Plasmasphere structure as outermost ionospheric region from direct measurements by particle traps, ion mass spectrometers and Langmuir probes on satellites

Tracking efficiency of laser telemetry on reflector carrying satellites

Tracking efficiency calculation for laser telemetry with laser reflector on nonstabilized satellite

Operational optimization of ion traps with dc amplifiers mounted on nonoriented earth satellite, proposing control circuit

Primary cosmic ray high energy gamma quanta flux measurements on Cosmos 208 satellite-borne instruments

Atmospheric ozone inference from satellite IR horizon radiance measurements

Neutral upper ionosphere temperature measurement with manometer device onboard Cosmos 320 satellite, noting equatorial fluctuations at 250 km

Ballistic density and wind determination from radiances observed by satellite IR spectrometer (SIRS) onboard Nimbus 3

Solar long term X-ray emitting regions from grazing incidence X ray telescope onboard OSO-4

Satellite-borne low energy electron and proton spectrometer for measuring auroral electron and proton spectra

Cylindrical electrostatic analyzers in rocket and satellite instruments for space low energy charged particles measurements

High resolution observations of UV stellar spectra by ESRO-borne spectrophotometer, emphasizing Mg II lines

Satellite IR telescopes in oceanography for data acquisition on ocean state, circulation, surface temperature, salinity, pollution, etc

Satellite anemometry for ocean waves and weather forecasting, discussing Skylark microwave radiometer-scatterometer potential design

Spaceborne and airborne remote sensing methods and applications for earth resources observation

EUV open channel photomultipliers satellite-borne long term performance degradation, attributing sensitivity loss to grating contamination

Ionospheric neutral density profile measurement by ultrasensitive triaxial electrostatic force rebalance accelerometer onboard Cannon Ball 2

Background spallation source errors in satellite measurements of diffuse cosmic X ray spectrum with crystal scintillators

Polar/midlatitude model of atmospheric density variations from LOGACS low altitude satellite accelerometer experiment

Satellite-borne semiconductor particle detector telescope for C and Mn isotopes identification in

heavy primary cosmic rays, considering scintillation counter and mass resolutions 16 p2389 A72-32883

Centaurus region hard X ray flux temporal variations from OSO-3 X ray telescope observations 16 p2446 A72-33458

Heavy cosmic ray nuclei tracks in etched plastic sheets flown in satellites and balloons, discussing detector response as function of velocity 16 p2447 A72-33730

Investigation of energetic charged particles and VLF emissions on the 'Intercosmos-3' satellite 17 p2600 A72-35209

X ray astronomy observational procedures, discussing source location and models, X ray detectors, satellite-borne equipment, correlation maps and diffuse X ray background studies 17 p2612 A72-35377

Design of a 14/12 GHz transponder for the Communications Technology Satellite. [AIAA PAPER 72-734] 18 p2660 A72-36540

Bistatic radar measurements of the surface of Mars with Mariner 1969. 21 p3110 A72-41453

OA0 3 satellite Copernicus onboard equipment, discussing UV reflecting and X ray telescopes, altitude sensor, star tracker, solar sensor and computer 22 p2321 A72-42985

Neutral upper ionosphere temperature measurement with manometer device onboard Cosmos 320 satellite, noting equatorial fluctuations at 250 km 24 p3402 A72-45086

Polar orbiting operational weather satellites. 24 p3451 A72-45197

Precision X-ray telescopes on HEAO-C. 24 p3403 A72-45202

Space astronomical observatory mission planning, analysis and operation and data utilization in terms of space and ground facility instruments and support subsystems 24 p3382 A72-45530

OA0 IR instruments development to observe IR stars, diffuse galactic objects, galactic center and extragalactic objects 24 p3446 A72-45534

HEAO satellite to carry instruments required in high energy astrophysics missions, discussing observational objectives, configuration and experiments 24 p3453 A72-45538

NASA X ray satellite UHURU and HEAO-C instruments and observational data on supernova remnants, pulsars, extars quasars, radio galaxies and galactic clusters 24 p3446 A72-45539

OSO and Skylab astronomical instruments technology, emphasizing precision pointing, spatial and spectral resolution and photometric efficiency problems 24 p3405 A72-45545

SATELLITE-BORNE PHOTOGRAPHY

Direct readout ground system /DRGS/ for receiving, recording and displaying visible and IR imagery collected by Itos and synchronous meteorological satellite radiometers 01 p0047 A72-10452

Computer programs for global disk and landmarks registration of cloud motions from satellite data for ocean weather monitoring applications 01 p0070 A72-10871

WINDCO interactive man-computer system for automated cloud motion tracking using precisely aligned digital ATS satellite pictures 01 p0070 A72-10872

NASA earth resources satellite R and D program for acquiring data on agriculture, forestry, geography, geology, hydrology, mineralogy and marine resources 01 p0063 A72-10949

Earth resources information systems using satellite and aerial IR terrain photography and ground teams for international cooperation, emphasizing timber inventory 01 p0063 A72-10950

Lake effect cloud examination by TIROS and ESSA photography, noting parallel bands with larger dimensions than cloud streets 01 p0095 A72-11280

IR scanner for Indian land areas and oceans thermal mapping, using satellite-borne multispectral photography 02 p0225 A72-11777

Environments susceptibility to low resolution imaging for land-use mapping, relating landscapes spatial frequency distributions to expected ERTS resolutions 02 p0210 A72-11796

Computer enhancement of multispectral satellite-and air-photographs and imagery for earth resources 02 p0186 A72-11801

Synoptic sea surface temperature mapping off Eastern United States using NASA ITOS satellite IR imagery data 02 p0211 A72-11813

ERTS return beam vidicon imagery simulation, predicting resolvability of ground targets as function of

target size, contrast, spectral distribution and radiance level 02 p0226 A72-11833

Information content in simulated ERTS space photographs as function of various levels of image resolution 02 p0212 A72-11834

Geophysical satellites high resolution imaging systems data redundancy reduction, using Apollo 9 photographs for computerized statistical analysis of picture structure 02 p0226 A72-11837

Digital fast transform methods application to satellite image processing, comparing with nontransform algorithms 02 p0227 A72-11843

Crop, soil and geological mapping from digitized multispectral satellite photography, discussing data processing requirements and surface features distinguishable from satellite altitudes 02 p0214 A72-11876

Hyperaltitude photography evaluation for geological mapping, comparing Gemini 4 and aerial photographs 02 p0216 A72-11891

Satellite photography application to morphological cartography of Baja California 02 p0216 A72-11892

Improved Tiros operational satellite visual and IR scanning radiometer data processing for polar and mercator map projection 02 p0173 A72-12127

Astronomical method of satellite photograph reduction in geodesy using photogrammetric technique 02 p0231 A72-12602

Mesometeorological processes in tropic and subtropic zone based on cloud photographs obtained from aircraft and satellites 02 p0255 A72-12792

Satellite photograph interpretations, discussing wind direction indication, cloud structure, automatic mapping and hydrographic exploration 03 p0351 A72-14306

Photogrammetric coordinate relation of points on lunar surface and stereo panoramas of scanning photographs by Luna 9 and 13 orbiters 05 p0660 A72-15832

Satellite photographs of Himalayan-Indian Ocean tectonic patterns, showing major left and right lateral shear belts as evidence of wrench movements 05 p0655 A72-16040

Facsimile bandwidth compression by picture elements reduction with contrast preservation, discussing analog processing algorithm and application to weather satellite photographs 06 p0772 A72-17406

Satellite-borne multispectral photographic line-scan system with direct optoelectrical signal conversion for photogrammetric and cartographic applications 06 p0815 A72-17757

Meteorological satellites TV, visual and IR cloud imaging and atmospheric sounding techniques for short and long range weather forecasting 06 p0892 A72-18066

Remote sensing methods in geology, discussing air/satellite-borne black and white, color and multispectral photographic, TV, multispectral scanning, IR and radar techniques 06 p0809 A72-18228

Meteorological satellites and Gemini and Apollo earth photographs, showing annual and diurnal oceanographic, hydrologic and geologic dynamic features 06 p0810 A72-18614

Multiple projection assembly for topographic maps preparation by satellite photographs optical projection onto model surfaces, exemplifying by reverse lunar hemisphere 08 p1165 A72-21155

Snow lines determination from ESSA-APT weather satellite pictures, comparing with ground data 09 p1303 A72-23295

Geomorphological and thermographic reconnaissance of Central Sahara, using orbital photographs 09 p1303 A72-23297

Worldwide inventory and monitoring of ice and snow aggregations via satellite photography, discussing climatological aspects 09 p1303 A72-23302

Life detection on earth from satellite 100 meter resolution photographs, discussing potential false positives and implications for Mars probes 10 p1471 A72-23718

Automatic cloud cover mapping from satellite photographs, describing three step procedure of texture edge detection and cleaning, region coloring and map cleaning 10 p1478 A72-23782

Aeolian transport and surface roughness of Mars Hellas basin, using Mariner 1969 photographs 10 p1536 A72-24151

Regional geologic features of Alaska and Western Canada from Nimbus 4 satellite image dissection camera system /IDCS/ photographs 10 p1477 A72-25109

Color enhanced black and white IR satellite images for oceanographic applications 11 p1620 A72-25346

Internal gravity waves effects on energy budgets and vertical angular momentum transport over mountainous terrain in southwestern U.S. from handheld camera pictures on Apollo 9 11 p1682 A72-26472

Cloud top temperature measurement by satellite through comparison of visible and IR cloud images with concurrent airborne radar and lidar measurements 13 p1944 A72-28444

Numerical wind profiles calculation over Mediterranean based on satellite photograph sequences of clouds 15 p2220 A72-31235

Stable air clouds localization from meteorological satellite photographs, noting atmospheric air pollution 15 p2265 A72-31236

Geographical interpretations of ESSA and Nimbus weather satellite pictures for earth resources applications, noting ERTS project 15 p2221 A72-31248

High-orbital satellite global photographs and TV pictures, discussing planetary geographical and topographical data interpretation 15 p2225 A72-31807

Coastal environment remote sensing from satellite and aircraft imaging platforms for geological, oceanographic and ecological investigations 15 p2232 A72-32622

Alpha Lyra and beta Cen spectrograms by Orion observatory onboard Salyut space station, noting veiled and overexposed photographic films 15 p2316 A72-32742

Photographic characteristics of high resolution film for Orion spaceborne astronomical observatory spectrograms, discussing aerospace environment effect on sensitivity and physicochemical properties 15 p2243 A72-32745

Multiple projection assembly for topographic maps preparation by satellite photographs optical projection onto model surfaces, exemplifying by reverse lunar hemisphere 20 p2924 A72-39260

Measurement of the optical transfer function of an onboard objective in the space environment 24 p3403 A72-45225

SATELLITE-BORNE RADAR

Satellite-borne radar altimetry pulse compression, discussing signal return statistics, receiver models and detected wavenumber relation to altitude, attitude and antenna beamwidth errors 02 p0172 A72-11870

Geodetic and oceanographic applications of radar equipped satellites in polar orbits for measuring heights along geoid 06 p0809 A72-18259

Surface pressure and vector wind fields computerized analysis from satellite radar radiometer simulation and conventional data 13 p1995 A72-29619

Skylab radar altimeter for earth surface features remote sensing with high range resolution mode for ocean wave height determination 15 p2236 A72-31995

Methods of radar studies of the moon and planets from spacecraft 21 p3103 A72-40307

SATELLITES

NT AEROS SATELLITE
NT ALOUETTE SATELLITES
NT APPLICATIONS TECHNOLOGY SATELLITES
NT ARTIFICIAL SATELLITES
NT AZUR SATELLITE
NT BEACON SATELLITES
NT COMMUNICATION SATELLITES
NT COS-B SATELLITE
NT COSMOS SATELLITES
NT DEIMOS
NT DIAL SATELLITE
NT DISCOVERER SATELLITES
NT EARTH RESOURCES TECHNOLOGY SATELLITES
NT EARTH SATELLITES
NT ELEKTRON SATELLITES
NT ENVIRONMENTAL RESEARCH SATELLITES
NT EOLE SATELLITES
NT EOSS
NT ESSA SATELLITES
NT EXPLORER SATELLITES
NT GEODETIC SATELLITES
NT GEOPHYSICAL SATELLITES
NT GRAVITY GRADIENT SATELLITES
NT HEOS B SATELLITE
NT HEOS SATELLITES
NT IAPETUS
NT INTERSAT SATELLITES
NT INTERCOSMOS SATELLITES
NT ISIS SATELLITES
NT LUNAR ORBITER
NT LUNAR SATELLITES
NT METEOROLOGICAL SATELLITES

NT MIDAS SATELLITES
 NT MOLNIYA SATELLITES
 NT MOON
 NT NATURAL SATELLITES
 NT NAVIGATION SATELLITES
 NT NAVSTAR SATELLITES
 NT NIMBUS SATELLITES
 NT OAO
 NT OGO
 NT OGO-A
 NT OGO-B
 NT OGO-D
 NT OGO-E
 NT ORBITAL SPACE STATIONS
 NT ORBITAL WORKSHOPS
 NT OSO
 NT OSO-E
 NT OSO-G
 NT OSO-H
 NT PAGEOS SATELLITE
 NT PAS
 NT PASSIVE SATELLITES
 NT PHOBOS
 NT PROTON SATELLITES
 NT RADIO ASTRONOMY EXPLORER SATELLITE
 NT RELAY SATELLITES
 NT SAMOS
 NT SAN MARCO SATELLITE
 NT SAS-A
 NT SAS-D
 NT SCIENTIFIC SATELLITES
 NT SIRIO SATELLITE
 NT SKYNET SATELLITES
 NT SMALL ASTRONOMY SATELLITES
 NT SYMPHONIE SATELLITES
 NT SYNCHRONOUS METEOROLOGICAL SATELLITE
 NT SYNCHRONOUS SATELLITES
 NT SYNCOM SATELLITES
 NT TIROS SATELLITES
 NT TRANSIT SATELLITES
 NT UHURU SATELLITE
 NT VENERA SATELLITES
 Satellite solar power stations, considering energy conversion, microwave generators and beam transfer to earth 02 p0155 A72-11770

SATURABLE REACTORS
 Automatic electromagnetic suspensions using tuned RLC saturable reactor control 10 p1460 A72-24761

SATURATION
 Saturation effect on power gain-bandwidth product of carbon dioxide regenerative ring laser amplifiers operating below threshold 03 p0366 A72-12964
 Diffusion saturation effects on thermal stress concentration in plate with circular hole under edge heating and lateral surface heat transfer 03 p0451 A72-14124
 Binary system molar energy diagram plotting, covering superheated, saturation and liquid phase regions 08 p1255 A72-22170
 Diode junction parameters and inverse saturation current measurements as function of current density and temperature 09 p1289 A72-23418
 Laser resonator transverse and longitudinal mode selection techniques, considering single frequency stabilization, gain saturation theory and applications 12 p1826 A72-27964
 Refractory steels heat resistance improvement by surface saturation with Be and subsequent oxidation in air at 900-1000 C, comparing with aluminized steels 15 p2255 A72-31574
 Rate of molybdenum solution in carbon-saturated liquid iron. 22 p3193 A72-43027

SATURN (PLANET)
 NT SATURN RINGS
 Rotation production in giant planets by gaseous impact, discussing Jupiter and Saturn formation 02 p0282 A72-12331
 Near resonance due to commensurability between Jupiter-Saturn mean motions, discussing effect on planetary system secular disturbing function 06 p0877 A72-17659
 Hydrogen and helium thermal dissociation and ionization at Jupiter and Saturn adiabatic atmospheric models conditions 08 p1211 A72-11277
 UV absorption measurements across Saturn disk at 3300-4800 A, considering rings and distribution in short wave region 08 p1238 A72-21829
 Venus, Mars, Jupiter and Saturn UV spectra from OAO-2 objective grating spectrophotometry, obtaining planetary albedos from G-type stars observations 09 p1382 A72-22288
 Saturn radio emission detection and measurement at 49.5 cm, determining equivalent disk brightness temperature 10 p1531 A72-23710

Photographic measurements of Saturn, observing atmospheric belt latitudes, ring dimensions and southern hemisphere bright spot rotation 10 p1531 A72-23711
 Jupiter, Saturn, Uranus, Neptune and Pluto state of knowledge, noting angular momentum fraction, red spot, albedos, densities, atmospheric compositions, natural satellites, etc 12 p1870 A72-27345
 Jupiter and Saturn gravitational moments from available models, taking into account rotation, density and radius 12 p1871 A72-27744
 Rotation production in giant planets by gaseous impact, discussing Jupiter and Saturn formation 13 p2039 A72-29215
 Titan and Galilean satellites effective temperatures from broadband observations, suggesting low surface emissivity or high opacity for Titan 13 p2041 A72-29417
 Jupiter, Saturn and earth atmospheric circulation seasonal variation data analogies, noting factors governing planetary atmospheric temperature 13 p2048 A72-29813
 Saturn thermal radio emission brightness temperature calculations for subcloud atmosphere ammonia abundance evaluation 14 p2152 A72-30490
 Monochromatic brightness coefficient measurements for Jupiter and Saturn disk centers and Uranus geometric albedo 14 p2152 A72-30491
 Jupiter and Saturn atmosphere composition, structure and radiative properties, presenting two zone stratosphere-troposphere model 14 p2161 A72-31072
 Polarization observations of Saturnian satellite Iapetus leading and trailing hemispheres, showing albedo difference consistent with light curve amplitude 16 p2453 A72-33139
 Titan spectrum absorption features, estimating hydrogen abundances 17 p2606 A72-34540
 Saturn rotation period latitudinal difference, presenting graphic plots derived from various visual observations 17 p2619 A72-35958
 Secular variations of the first order of elements for the four major planets - Comparison with Le Verrier and Gaillot 18 p2727 A72-36734
 Gravitational fields of Jupiter and Saturn 19 p2857 A72-37734
 Determination of major planet coordinates by an expeditionary astrophotograph 19 p2861 A72-37986
 Saturn thermal radio emission brightness temperature calculations for subcloud atmosphere ammonia abundance evaluation 19 p2864 A72-38319
 Monochromatic brightness coefficient measurements for Jupiter and Saturn disk centers and Uranus geometric albedo 19 p2864 A72-38320
 Statistical mechanics of light elements at high pressure. II - Hydrogen and helium alloys. 21 p3106 A72-41044
 Photometric characteristics of Jupiter and Saturn at wavelengths between 0.48 to 0.33 micron 22 p3219 A72-41915
 Mariner spacecraft Jupiter-Saturn 1977 gravity assisted flyby, discussing mission objectives and trajectory options 24 p3444 A72-45438
 [ALAA PAPER 72-943]
 The possibility of a trans-Saturnian belt of particulate matter. 24 p3446 A72-45472

SATURN LAUNCH VEHICLES
 Nonflammable coolants for Saturn instrument unit environmental control systems, considering component materials compatibility with selected dielectric fluids 01 p0091 A72-10769
 Saturn systems holddown acoustic efficiency and normalized acoustic power spectrum. 24 p3433 A72-44681

SATURN RINGS
 Giant planets internal constitution models, discussing Jupiter visual magnitude variability, Saturn ring system, cold matter equations of state and He abundances 03 p0418 A72-13111
 Saturn radio emission and brightness temperature measurements, determining rings optical thickness upper limit 03 p0438 A72-13977
 Saturn ring motion stability factors for atomized material resistance to gravitational field, discussing ring thickness, density and other parameters 08 p1231 A72-21128
 UV absorption measurements across Saturn disk at 3300-4800 A, considering rings and distribution in short wave region 08 p1238 A72-21829

Saturn rings gas-dust atmosphere, thickness and motion, considering planetary radio emission and brightness temperature 14 p2161 A72-31073
 Photometric behaviour of Saturn's rings as a function of the saturnocentric latitudes of the earth and the sun. 18 p2727 A72-36735
 Saturn ring thickness estimates according to observations in 1966 19 p2863 A72-38075

SATURN S-2 STAGE
 Finite element analysis of hydroelastic properties of Saturn 5 full scale S-2 LOX tank, comparing with water tests [ALAA PAPER 72-173] 05 p0740 A72-16833

SATURN 5 LAUNCH VEHICLES
 Acoustic ray tracing of long range infrasonic signals from launch and reentry of Saturn 5 rockets 11 p1690 A72-26512
 Absolute stability analysis of attitude control systems for large boosters. 17 p2622 A72-35489
 A 10,000-gpm liquid hydrogen transfer system for the Saturn/Apollo program. 19 p2784 A72-38829
 Apollo/Saturn 5 spacecraft liquid propellants safety procedures in event of fire on explosion in operations building at Kennedy Space Center 23 p3343 A72-43552
 High level cleanliness maintenance and contamination control for instrument unit ring guidance system in Saturn 5 launch vehicle 24 p3388 A72-45297

SAWTOOTH WAVEFORMS
 Reactive two terminal pair network synthesis for shaping sawtooth current pulses in inductive load for given input function 02 p0193 A72-12222
 Sawtooth voltage generator with switching circuit to achieve small retrace time via blocking generator 11 p1605 A72-26320
 Final stages of transistorized sweep generators 22 p3158 A72-42114

SC-1 AIRCRAFT
 Flying experience with the SC1 research aircraft and the P1127 prototype at the Royal Aircraft Establishment, Bedford, England. 22 p3136 A72-42324

SCALARS
 Hollow waveguide problem considering numerical solution with scalar field approximation, Green function and conformal transformation 02 p0191 A72-11692
 Passive scalar field diffusion in homogeneous turbulence, solving Fourier transformed flow equations by iterative procedure 02 p0204 A72-12174
 Coupled thermoelasticity in infinite body with cavity, introducing Sommerfeld type scalar potential and temperature radiation conditions 02 p0259 A72-12236
 Parametric solution of Brans-Dicke cosmological equations for flat Friedmann type expanding universe for time, density, expansion parameter and scalar field 07 p1074 A72-19525
 Modified Riemann geometry for scalar-tensor theory of gravitation, emphasizing scalar field role relation to vector length change during point-to-point transport 07 p1036 A72-20196
 Turbulent diffusion of scalar contaminant passively advected by homogeneous stationary flow, expanding velocity and scalar fields in stochastic Wiener-Hermite functionals 10 p1469 A72-24606
 Scalar and vector partitions of forecasts probability score in two state situation 11 p1681 A72-26078
 Diffraction coefficients of scalar field for higher order edges and vertices, noting far field behavior of boundary layer expansion 11 p1617 A72-26158
 Conservation laws and symmetry properties of scalar tensor gravitational theories in terms of Einstein, von Freud, Moller and Komar extensions 12 p1847 A72-28153
 Elementary formulas for scalar and matrix valued functions gradient calculation, including continuum mechanics application 15 p2262 A72-31587
 Computer aided study of nondiffusive plane convection mixing of scalar field by isotropic turbulence of single velocity modes 18 p2678 A72-36017
 Representation of solenoidal vector fields in bounded domains by poloidal and toroidal scalar potentials, discussing applications in fluid mechanics, elastic vibrations and electromagnetic theory 23 p3313 A72-43716
 Dispersion relations of scalar hereditary theory of nonlinear viscoelasticity, representing integral operators as orthonormalized function series in Fourier space 24 p3459 A72-45264

SCALE

Experimental comparisons of the international pyrheliometric scale with the absolute radiation scale.

23 p3290 A72-42724

SCALE [CORROSION]

Ni corrosion by hydrogen sulfide, determining nickel sulfide scale chemical composition and crystallographic orientation by electron and X ray diffraction

06 p0828 A72-17606

Boron addition effects on scaling resistance of Ni-Cr steel at high temperatures

07 p1012 A72-19738

Oxide scale formation on zirconium diboride materials, observing microstructural features as function of temperature and reaction time

[AD-737020] 09 p1333 A72-22380

High temperature oxide scale adherence on Fe-Cr-Al alloys with Y or Sc additions as promoting agents

16 p2410 A72-33817

Effects of scale porosity, second-phase oxides, and doping in the high-temperature oxidation of cobalt and dilute cobalt-chromium alloys.

21 p3067 A72-40845

Effect of oxygen on the scale resistance of titanium-titan alloys

23 p3300 A72-43592

SCALE [RATIO]

Image scale selection for topographic map revision in orthophotograph production considering economics and suitability

09 p1311 A72-22968

Al single crystals, investigating scale factor effects on stepwise deformation at 1.4 K

14 p2115 A72-30410

Multiple decision procedures, discrete populations and multinomial and multivariate normal distributions in subset selection formulation

14 p2126 A72-30998

Three dimensional transformation for continental scale geodetic grids photogrammetry by satellite method, noting scale alteration and Euler angles determination

16 p2387 A72-33799

SCALE EFFECT

Deformation kinetics relationship to scale effect in notched samples during elastoplastic loading phase

03 p0443 A72-13455

Scale factor and surface imbedded inserts effect on bending cyclic fatigue strength of nonhardened and roll hardened Al-Ti alloy

03 p0372 A72-13596

Glass ceramics mechanical properties as function of temperature during bending, taking into account scale factor

09 p1337 A72-22742

Equilibrium thermodynamics of critical points, discussing phase transition theory and scaling hypothesis for single component systems

10 p1562 A72-24400

Helicopter rotor blades bending vibrations, examining scale effects, dynamic similarity and natural frequencies via series of Legendre polynomials

[AD-745569] 11 p1734 A72-25733

Aeroelastic model response comparison to amplitudes of sectional and linear wind tunnel models, indicating incorrectness of direct scaling

16 p2342 A72-32904

Chemical reactions in inhomogeneous mixtures - The effect of the scale of turbulent mixing.

17 p2543 A72-35640

Integral scales existence as necessary condition for asymptotical independence of stationary process, showing relationship of conditions for central limit and related theorems

18 p2677 A72-36002

The stress gradient as a cause for the manifestation of the scale effect in brittle fracture of materials

21 p3123 A72-41364

The effects of protuberances and scaling parameters on the aerodynamic characteristics of an air-to-air cruciform missile.

[AIAA PAPER 72-969] 22 p2321 A72-42342

Solid powder metallurgy tungsten alloys, determining scale factor effect on bending strength and fatigue limit

23 p3301 A72-43751

Deformation kinetics relationship to scale effect in notched samples during elastoplastic loading phase

24 p3458 A72-44930

SCALE HEIGHT

Lunar surface details absolute and relative heights, estimating accuracy by comparison of data from different catalogs

06 p0884 A72-18034

Lunar surface features absolute and relative heights, estimating accuracy by comparison of data from different catalogs

11 p1719 A72-25970

Atmospheric model for local mesometeorological deviations from large scale field distributions, taking into account synoptic scale influence

16 p2418 A72-33601

Atmospheric pressure, density and scale height calculated from H Lyman-alpha absorption allowing for the variation in cross-section with wavelength.

19 p2793 A72-38859

Sunrise effects on the latitudinal variations of top-side ionospheric densities and scale heights.

24 p3399 A72-45552

SCALE MODELS

Structural analysis of cable stayed bridge scale model with fractional and full loading, showing system linear behavior with small displacements and real nonlinearities, respectively

[SESA PAPER 1896] 02 p0199 A72-11515

High speed jet noise source physical properties interpretation by theory and scale-model experiments for supersonic transport aircraft noise suppression problem

02 p0154 A72-11973

Ring-plane type slow wave structure hot tested near 3 cm for scale modeling in mm range

07 p0938 A72-18854

Laboratory electromagnetic scale modelling for studying geophysical and propagation boundary value problems

10 p1512 A72-24741

Spacecraft cabin atmosphere thermal scale modeling based on radiative-convective-convective heat transfer, obtaining adequate thermal similitude through mass flux and heat transfer coefficient preservation

[AIAA PAPER 72-288] 11 p1741 A72-25226

Microwave scale model of ILS glide path, considering interference and aircraft taxiing effects

14 p2129 A72-30944

Atmospheric energy spectra from two dimensional synoptic scales applicable to pressure or geopotential surface variables

15 p2266 A72-32721

Scale model tests of high thrust engine blast deflection fence combinations for protection of adjacent roadway traffic

16 p2374 A72-33698

Atmospheric boundary layer and diffusion over three dimensional mountainous terrain by laboratory simulation with meteorological wind tunnel and scale model

[AIAA PAPER 72-648] 16 p2419 A72-34085

On the prediction of acceleration response of air cushion vehicles to random seaways and the distortion effects of the cushion inherent in scale models.

[AIAA PAPER 72-598] 18 p2642 A72-36538

Thermal scale models utilization to predict spacecraft radiator system performance, presenting criteria for modeling fluid system with combined convection, conduction and radiation effects

[ASME PAPER 72-ENAV-29] 20 p2894 A72-39148

Design modeling of external and internal cooling systems for bodies exposed to high temperature gas flow, discussing operation similarity conditions

21 p3129 A72-41052

Shadow shields for minimizing radiant heat transfer into cryogenic propellant tanks on interplanetary missions, predicting performance for comparison with scale model experiment

21 p3130 A72-41181

The stress gradient as a cause for the manifestation of the scale effect in brittle fracture of materials

21 p3123 A72-41364

Characteristics of an ejector-type engine simulator for STOL model testing.

[AIAA PAPER 72-1028] 21 p3042 A72-41607

Model studies of plate and shell stability

22 p3233 A72-42055

SCALERS

Time resolution buffer for multichannel scaler, applying to digital signal averaging

11 p1632 A72-25701

SCALING

Electrical and nuclear propulsion plasma containment problems, discussing simulation experiments and scaling devices feasibility

01 p0117 A72-10938

Scaling of energy spectrum of particles emitted in high energy nucleon-nucleon collisions

10 p1529 A72-24527

Lunar semidiurnal variations of the geomagnetic field determined from the 2.5-min data scalings.

17 p2545 A72-34691

Gaussian elimination with floating point arithmetic, discussing algorithm for least squares scaling of matrices with less error than row and column norms equilibration

21 p3076 A72-41317

SCALING LAWS

Open cycle gas core nuclear rocket engine, determining scaling laws for buoyancy force effect on fuel containment at various flow parameters

01 p0099 A72-11348

Scaling hypothesis testing by angular distributions from cosmic ray experiments

05 p0711 A72-17125

Self induced electron beam collapse prevention by external magnetic field, determining required field strength by scaling law based on simple orbit model

06 p0854 A72-17418

Scaling laws for vibrating beams and plates, stressing shear and rotatory inertia effects

06 p0894 A72-17769

Electron bombardment ion engines scaling laws, considering electron energy, current density, propellant properties and magnetic flux density

07 p1054 A72-19602

Hearing damage scaling methods, discussing audiometric frequencies effect and damage risk criteria

07 p0932 A72-20169

Intermittency and scale similarity in turbulent flow structure, analyzing eddies distribution inhomogeneity

07 p0973 A72-20319

Scaling invariance hypothesis for local structure of turbulence, using quantum field theory methods

13 p1943 A72-29994

Scaling hypothesis and limiting fragmentation mechanism for cosmic ray muon production, noting energy independent charge ratio

15 p2298 A72-31289

Supersonic jet noise mechanisms and scaling laws, studying acoustic fields for rectangular and axisymmetric nozzle configurations

[AIAA PAPER 72-641] 16 p2381 A72-34091

Wind tunnel simulation of full scale vortices.

[AHS PREPRINT 623] 17 p2483 A72-34477

Test of scale invariance in pion production at high energies using cosmic ray primary nucleon and sea level muon intensities.

17 p2599 A72-34875

Gravitation theory in terms of scalar and tensor field, noting Lyra general reference system transformations and scale invariance

18 p2711 A72-36713

Turbulent combustion induced noise, discussing scaling rules for sound power and directional characteristics of radiated sound

20 p2984 A72-39557

Test of hadronic scaling at cosmic ray energies.

21 p3100 A72-40831

SCANDIUM

Scandium substitution for lanthanum in lanthanum hexaboride crystal lattice, investigating effect on thermionic characteristics

12 p1854 A72-27309

Phase diagram of cast and annealed Cr-Sc alloys by differential thermal, X ray, metallographic and microhardness analyses

13 p1981 A72-29953

Deformable magnesium alloys with scandium and yttrium

22 p3192 A72-42820

Simultaneous neutron-activation analyses of scandium, cobalt, iron, and zinc in biological objects with the aid of a total-absorption gamma spectrometer

23 p3259 A72-43347

SCANDIUM COMPOUNDS

Scandium alloys properties based on phase diagrams, noting corrosion resistance

15 p2289 A72-31186

SCANNERS

NT FLYING SPOT SCANNERS

NT HORIZON SCANNERS

NT INFRARED SCANNERS

NT OPTICAL SCANNERS

Two dimensional scanning electron beam pumped laser, describing production of coherent emission

01 p0079 A72-10522

Electronically scanned monopulse cavity backed quadratic spiral antenna array at 1.54-1.66 GHz for maritime satellite communications

01 p0039 A72-10662

Limited scan microwave antenna design, discussing angular coverage, feed motion and focal field distribution

01 p0039 A72-10670

High density digital tape recorder with combined phase encoded digital electronics and helical scan video transport

02 p0229 A72-12152

Interim automatic scanning multichannel data acquisition system for environmental test laboratory, using programmable calculator

02 p0200 A72-12477

Nimbus satellite image dissector camera system for continuous meteorological scanning, noting special suitability for cloud and ice features discrimination from brightness changes

08 p1171 A72-21967

Low energy scanning electron beam gun with retarding field mode for microelectronic device evaluation

10 p1446 A72-23936

Image dissector system fabrication for two dimensional area scanning, applying to photograph digitization

11 p1631 A72-25688

Image intensifier tube scanner replacement of slit and multiplier tube of spectrograph, discussing application to rockets

11 p1631 A72-25689

Computer controlled coude and Cassegrain scanner telescope spectrometers at McDonald Observatory, discussing design, instrument performance and computer program

11 p1632 A72-25698

Scanning photoelectric image conversion /photoanalyzing/ systems for data telemetry from remote optical sensors

11 p1634 A72-26461

Low energetic efficiency of semiconductor microwave scanning converters for radio images of fog obscured objects

13 p1932 A72-29297

Solid state stepping motor drive controller to provide constant angular shaft velocity for scanner applications

13 p1933 A72-29767

Ultrasonic imaging system based on side-looking synthetic aperture radar principles, using B-scan technique

19 p2798 A72-37624

SCANNING

NT CONICAL SCANNING
NT FREQUENCY SCANNING
NT PANORAMIC SCANNING
NT RADAR SCANNING

ERTS satellite image processing for multispectral scanning system, discussing distortion from geometrical properties

01 p0066 A72-10458

Scanned reference beam holography techniques with limited exposure time, noting use of hypersensitized photographic plates

07 p0985 A72-19418

Phase errors and main lobe orientation changes during beam scanning of two reflector Cassegrain antennas

08 p1139 A72-20934

Low cost microwave scanning beam landing systems for interim instrument landing system replacement in civil aviation

15 p2272 A72-32217

Digitally pressure-scanned Fabry-Perot interferometer for studying weak spectral lines

23 p3289 A72-43891

Scanning electron microscope stereophotographic picture synthesis from sequential holographic recording of three dimensional objects

23 p3290 A72-43904

Acoustical holography with a scanned linear array

24 p3401 A72-44705

SCANNING DEVICES

U SCANNERS
SCARS [GEOLOGY]
U EROSION

SCAT

U SUPERSONIC COMMERCIAL AIR TRANSPORT

SCATTER PROPAGATION

NT IONOSPHERIC F-SCATTER PROPAGATION

Polarization diversity radar power law relations from measurements with size and shape distributed scatterers in comparison with linearly polarized system

01 p0030 A72-10832

Bistatic radar scatter communication effective coverage analysis, considering dependence on equipment and target locations and properties

03 p0321 A72-13092

Tropospheric forward electromagnetic scatter propagation path loss prediction by modified Yeh method with empirically derived correction function

03 p0323 A72-14031

Turbulent tropospheric temperature fluctuations effects on optical waves propagation with random scattering, considering amplitude, phase, angle-of-arrival and polarization

04 p0548 A72-14736

Tropospheric scatter path characteristics as communication channel with random fluctuations, deriving signal autocorrelation function from mean power pulse response

08 p1132 A72-21329

Multiplicative noise envelope distribution for ionospheric scatter channel from single and diversity radio reception, noting meteor trails effects on electromagnetic wave propagation

12 p1782 A72-27627

Propagation theory and quantum electrodynamics for light transmission in scattering media

13 p2002 A72-28511

Ionospheric attenuation of 3-100 MHz radio waves, interpreting scatter mode propagation mechanism as total reflection from lower ionizational irregularities

14 p2086 A72-30658

Transmission and phase coefficient logarithmic decrements for wave propagation in random discrete scatterers

19 p2767 A72-38614

Energy characteristics of radio signals scattered by statistically uneven surface, proposing statistical variables substitution

20 p2900 A72-38892

SCATTERED CLOUDS

U CLOUDS [METEOROLOGY]

SCATTERERS

U SCATTERING

SCATTERING

NT ACOUSTIC SCATTERING
NT ATMOSPHERIC SCATTERING

NT BACKSCATTERING

NT COHERENT SCATTERING

NT COMPTON EFFECT

NT ELASTIC SCATTERING

NT ELECTROMAGNETIC SCATTERING

NT ELECTRON SCATTERING

NT FORWARD SCATTERING

NT INCOHERENT SCATTERING

NT INELASTIC SCATTERING

NT ION SCATTERING

NT IONOSPHERIC F-SCATTER PROPAGATION

NT LIGHT SCATTERING

NT MICROWAVE SCATTERING

NT MIE SCATTERING

NT NEUTRON SCATTERING

NT NUCLEAR SCATTERING

NT NUCLEON-NUCLEON SCATTERING

NT PROTON SCATTERING

NT RADAR SCATTERING

NT RAMAN SPECTRA

NT RAYLEIGH SCATTERING

NT RESONANCE SCATTERING

NT THOMSON SCATTERING

NT TROPOSPHERIC SCATTERING

NT WAVE SCATTERING

NT X RAY SCATTERING

Reactive and nonreactive channels full particle scattering amplitudes using coupled integral equations

02 p0262 A72-11910

Monatomic gas atoms scattering by solid surfaces, using classical three dimensional lattice model

07 p0969 A72-20064

Neutral unexcited gas atoms or molecules scattering at solid surfaces, interpreting molecular beam experimental results in terms of classical dynamics

07 p0969 A72-20065

Numerical simulation of gas atom scattering from solid surface and satellite drag coefficient calculation

07 p0910 A72-20106

Fiberglass heat transfer mathematical model, noting scattering effect and thermal conductivity

08 p1191 A72-21452

Direct and inverse problems of scattering theory for hyperbolic system of equations on plane, emphasizing unsteady approach and integral equation class with kernels

13 p2004 A72-29468

Two band model explanation of Hall effect in dirty type-II transition metal superconductors near upper critical field, noting interband impurity scattering role

15 p2295 A72-32542

Perturbation theory for field moments in inhomogeneous media

21 p3016 A72-40780

SCATTERING AMPLITUDE

Duality concept in elementary particle physics, discussing pion-nucleon scattering, amplitude exchange degeneracy, Regge poles and Veneziano models

05 p0692 A72-17077

SCATTERING COEFFICIENTS

Invariant imbedding theory of aerosols multiple scattering induced telephotometric errors, determining scattering coefficients relative to optical thickness by Monte Carlo method

01 p0066 A72-10531

Differential thermal radiation scattering coefficients of submicron W refractory particles in hydrogen and nitrogen at temperatures to 1080 K

01 p0112 A72-11341

Alkali ion scattering by NbTi alloy and SiC and components, comparing scattering coefficients

03 p0401 A72-13424

Atmospheric short wave radiation angular and vertical distribution relation to aerosol scattering parameters, using transport equation

05 p0658 A72-16291

Spherical ice and graphite particles absorption, scattering and radiation pressure coefficients and albedo, noting application to interstellar extinction

06 p0875 A72-17296

Aerosol scattering coefficient in atmosphere, determining statistical characteristics of vertical and spectral structure

06 p0842 A72-18043

Atmospheric directional scattering coefficients from vertical measurements of IR spectral sky brightness near solar almucantar and direct radiation

06 p0842 A72-18048

Deschamps graphical method application to multiport waveguide junction scattering coefficient measurement with averaging and least square fitting for error reduction

06 p0787 A72-18379

Fog and cloud microstructure and density distributions from directional light scattering coefficient /halo indicatrix/

11 p1683 A72-26883

Light beams propagation in clouds and fog, discussing scattering and attenuation coefficients

13 p1988 A72-28517

Antennas scattering coefficients measurement by ground and atmospheric radiation, permitting antenna noise temperature components determination

15 p2206 A72-31652

SCATTERING CROSS SECTIONS

IR carbon dioxide laser radar with heterodyne detection, measuring SNR and atmospheric scattering coefficients for various weather conditions

17 p2516 A72-35192

Fog and cloud microstructure and particle size distributions from directional light scattering coefficient /halo indicatrix/

20 p2948 A72-39570

Stationary expressions for scattering coefficients of rectangular waveguides with dielectric plugs constituting a finite planar array

21 p3027 A72-40371

A practical evaluation of earth-backscatter simulation and an estimate of the HF ground-scatter coefficient

24 p3380 A72-45636

SCATTERING CROSS SECTIONS

Scattering cross section of electromagnetic wave by collisionless plasma perpendicular to applied magnetic field

01 p0105 A72-10025

Environmental pollution sensing by vibrational laser Raman scattering probe measuring species constituency and temperature, discussing fluorescence, scattering cross sections and band shape

01 p0067 A72-10541

Modified Born approximation for electromagnetic backscattering cross section from turbulent plasmas, noting attenuation leading to saturation and cross-polarization

01 p0031 A72-10846

Electrical conductivities dependence on assumed values of elastic collision cross sections of electrons with neutral and charged particles in low temperature plasma

01 p0110 A72-11205

Composite scattering theory mathematical model for radar backscattering cross section relation to ocean surface conditions and wind velocity

02 p0172 A72-11868

Three dimensional angle dependent model for three body problem, considering exact quantum mechanical reactive scattering cross sections

02 p0262 A72-11911

Electromagnetic wave scattering by electron charge density fluctuations in plane waveguide with magnetoactive plasma, showing cross section spectrum function of plasma properties

02 p0183 A72-12766

Atomic data for UV and X ray astronomy, considering atomic wave functions and energy levels, radiative transition probabilities and electron-ion collision cross sections

03 p0420 A72-13125

Time harmonic electromagnetic wave diffraction by thin conducting circular disk at different media plane interface, calculating induced surface current density and scattering cross section

03 p0322 A72-13237

Raman scattering cross section measurement for atmospheric nitrogen tetroxide, using Q switched ruby laser excitation source

03 p0367 A72-13601

Effective cross sections of ion collisions with gaseous target and argon atoms collision with argon target by molecular beam intensity attenuation method

03 p0392 A72-14060

Se and Zn doped n and p type gallium arsenide point defects, considering thermal conductivity, relaxation time and phonon scattering cross section effects

03 p0404 A72-14239

Heuristic theory of positron-helium elastic scattering phase shifts and cross sections

03 p0393 A72-14399

Proton elastic scattering by deuterons in backward hemisphere, examining normal and center of mass scattering angle and differential cross section

04 p0551 A72-14437

Transport coefficients of relativistic gas by method of moments, assuming constant differential cross section of particle interactions in center of mass system

04 p0547 A72-14630

Measuring apparatus for differential cross sections of charge transfer and elastic scattering of atomic projectiles by gas targets

04 p0553 A72-15539

Master equation for vibrational relaxation of diatomic dilute gases, discussing restrictions on experimental initial conditions and scattering cross sections

04 p0553 A72-15634

Atomic and molecular hydrogen mixture viscosity measurement, considering mutual diffusion coefficient, collision cross sections and interaction potentials

04 p0553 A72-15637

Freundlich red shift of wavelengths in solar spectrum, deriving scattering cross sections

05 p0719 A72-16527

Cosmic ray hadrons inelastic collision cross sections and partial K-neutral pion inelasticity factor in ionization calorimeter

06 p0868 A72-17262

Inelasticity factor dependence on particle energy spectra to explain nucleon flux calculations and

Proton satellite data, considering scattering cross sections

06 p0869 A72-17264

Scattering cross section for excited oxygen atoms production by electron impact dissociation of molecular oxygen

07 p1037 A72-18964

Ideally conducting convex body mean differential monostatic scattering cross section, considering wavelength to body dimensions ratio

07 p0938 A72-19018

Mg ion excitation by electron collision in solar chromosphere studies, calculating scattering cross sections

07 p1081 A72-20234

Stokes Q branch fundamental vibrational Raman light scattering cross sections and depolarization ratio measurement for molecular gases

07 p1038 A72-20292

Electron impact cross section and energy deposition in molecular hydrogen, using generalized oscillator strength in Born-Bethe approximation

07 p1038 A72-20567

Atmospheric acoustic attenuation measurement on sailplane, assessing turbulence backscattering cross section

07 p1031 A72-20597

Lyman alpha radiation emission cross sections due to H/2p and H/2s formation in protons and hydrogen atoms collisions with hydrogen molecules

07 p1038 A72-20678

Differential and integral scattering cross sections for helium excitation by electron impact from ground state to 2/super I/S state

07 p1038 A72-20679

Electromagnetic wave diffraction on arbitrary spheres, calculating scattering cross sections and attenuation by four water droplets

08 p1131 A72-20789

Laser radar observations of mesosphere and lower thermosphere optical scattering cross section variations due to tide-caused atmospheric density fluctuations

08 p1156 A72-21100

Temperature dependence of scattering cross sections for cold and hot neutrons colliding with oxygen and deuterium molecules

08 p1211 A72-21872

Radio absorption and scattering cross sections of thin cylinder with arbitrary electron density distribution in ionosphere, observing resonance effects

08 p1239 A72-21890

Quasi-elastic scattering differential cross section for nonpolarized IR radiation in electron plasma of semiconductors in strong elastic fields

09 p1366 A72-22210

Vacuum UV excitation cross sections measurement by electron impact on nitric oxide, tabulating threshold energies and transition probabilities

09 p1357 A72-22857

Post-threshold translational energy dependence of endoergic cross sections for vibrational excitation and reactive scattering of diatomic molecules by atomic or molecular impact

09 p1357 A72-22858

Foreign gas collisional broadening of nitrous oxide absorption lines, obtaining optical collision cross sections

09 p1276 A72-23332

Coulomb interactions within dense Boltzmann plasma in transition from ideal to nonideal state, proposing effective Coulomb pair cross section concept

10 p1517 A72-23834

Low energy elastic scattering cross section measurements for helium-nitrogen system, using two collimated aerodynamically intensified crossed molecular beams

10 p1515 A72-24338

Electron impact excitation of nitric oxide in vacuum UV, measuring absolute cross sections for emission features

[AD-742536]

10 p1515 A72-24341

Frequency and angular correlation function relationship for signal scattering cross section of extensive bodies

10 p1436 A72-24586

Average electric field and power density of electromagnetic wave scattered from rough layer with plane interface, calculating scattering cross sections

10 p1512 A72-24744

Particle-proton total cross section from cosmic ray data on proton-iron inelastic cross sections

11 p1712 A72-25884

Collisional ionization cross sections measurement for gaseous metal atoms in hydrogen-oxygen flames at 2000-2800 K

11 p1591 A72-26659

Mercury vapor physicochemical processes kinematics in shock tube, determining electron gas energy balance equations and atom-atom collision cross sections

11 p1699 A72-26760

Radar backscattering cross section and power of conducting cylindrical spacecraft in compressible electron-ion plasma environment

12 p1779 A72-27173

Electron impact excitation spectrum of molecular oxygen, investigating angular behavior of differential scattering cross sections and energy dissipation

12 p1848 A72-27851

Excitation cross section in dipole approximation of semiclassical impact parameter and Born approximation, using asymptotic expansion of hydrogen-like atoms oscillator strength

13 p2040 A72-29411

Strong circularly polarized electromagnetic wave scattering by plasma electron with radiation reaction, determining cross section as function of amplitude and magnetic field strength

13 p2015 A72-29427

Nonequilibrium plasma wave scattering cross section dependence on energy bands shape and field orientation in semiconductors

13 p2023 A72-29992

Ar and K electron cross section determination for momentum transfer, using dc conductivity measurement of high pressure plasma

14 p2134 A72-30803

Quasi-classical mechanical approximation in molecular scattering, using Monte Carlo methods for Jacobian determinant evaluation

14 p2134 A72-30836

Hydrogen negative ion electron detachment collision process cross section calculation using Coulomb trajectory impact-parameter method

14 p2135 A72-30884

Resonant and semiweak process production cross sections for massive Lee-Wick spin-zero and spin-one bosons at high energies

15 p2280 A72-31290

Cooperative enhanced scattering cross section of far IR laser radiation from nonthermal theta pinch plasmas in weak magnetic field

15 p2288 A72-32417

Electron impact low energy cross sections for transitions between highly excited states, obtaining upper bound via quantum impact parameter theory

15 p2315 A72-32715

High energy resolution spectrometric measurement of relative emission cross section for electron impact excited molecular nitrogen second positive system bands

16 p2428 A72-32922

High and medium energy molecular beam detection for large dispersion angle collision cross sections determination, using photographic plates

16 p2389 A72-33060

Spatial distribution of nitrogen molecular beam scattering from solid nitrogen surface as function of beam energy and incidence angle

16 p2430 A72-33063

Differential collision cross sections for argon pairs with neon, methane and ethane at angular region of two crossed nozzle molecular beams

16 p2431 A72-33070

Elastic wave diffraction by rigid ellipsoid, deriving scattering cross section for incident P wave from integral equation solution

16 p2426 A72-33659

Li, Be and B spallation reactions in galactic cosmic rays from observations of cross sections of energetic protons incident on C and O targets

16 p2447 A72-33734

Cross section measurement for low energy proton reactions with N 14 and O 16 targets observing Be 7 and C 11 in N 14

16 p2447 A72-33735

Bidirectional optical scattering from dielectric materials of various pigmentation and surface roughnesses, obtaining cross section data to determine angular, spectral and polarization behavior

16 p2427 A72-33839

Three dimensional electron density fluctuations scattering spectra in Mach 16 spherical projectile turbulent wakes from fine wire electron collection probe measurements

[AIAA PAPER 72-673]

16 p2432 A72-34066

Calculation procedure involving wave function for vibrational correction to electron scattering cross section of hydrogen molecule in Born approximation

17 p2585 A72-34261

Conducting body radar scattering control by reactive loading, discussing field pattern synthesis for real current with least mean-square approximation

17 p2513 A72-34358

Electron transmission spectroscopy - Core-excited resonances in diatomic molecules.

17 p2586 A72-35771

Radar meteorology in the Soviet Union - 1970.

18 p2707 A72-36719

Absolute differential cross sections of electrons classically scattered on neon atom.

18 p2713 A72-36952

The use of known helium line cross sections for investigation of unknown transition in neon.

18 p2713 A72-36954

An integral test of the inelastic cross sections of Pb and Mo using measured neutron spectra.

19 p2837 A72-37634

Charge states and charge-changing cross sections of fast heavy ions penetrating through gaseous and solid media.

19 p2837 A72-37849

Elastic scattering of 600-MeV protons from H, D, He-3, and He-4.

19 p2837 A72-38025

Yields of gamma rays emitted following capture of negative muons by Si28 and Mg24.

19 p2837 A72-38026

Nonelastic interactions of nucleons and pi mesons with complex nuclei at energies below 3 GeV.

19 p2837 A72-38027

Saturn ring thickness estimates according to observations in 1966

19 p2863 A72-38075

Electromagnetic wave scattering by electron charge density fluctuations in plane waveguide with magnetoactive plasma, showing cross section spectrum function of plasma properties

20 p2903 A72-39072

Interpretation of experimental differential elastic scattering cross section for H/+ + Ne.

20 p2956 A72-39721

Application of the Harris-Nesbet method to a dipole coupling potential.

21 p3083 A72-40103

Cross sections calculations for electron-oxygen scattering using the polarized orbital close coupling theory.

21 p3087 A72-40472

Electron loss in atom-molecule collisions.

21 p3087 A72-40473

Scattering cross section glory undulations relationship to potential energy of interaction of two molecules with minimum containing one or more bound states

21 p3087 A72-40561

Angular distribution of electrons elastically scattered from N2.

21 p3088 A72-40777

Book - Excitation in heavy particle collisions.

21 p3088 A72-41525

Interpolation formulae for the electron impact excitation of ions in the H-, He-, Li-, and Ne-sequences.

22 p3224 A72-42379

Electron deposition in water vapor, with atmospheric applications.

22 p3171 A72-42420

Electron impact excitation cross sections and energy degradation in CO.

22 p3172 A72-42422

Elastic electron-neutral interaction in argon in the vicinity of the Ramsauer minimum

22 p3211 A72-42642

Polarization characteristics and wave vector direction effect on cross section of incident and diffuse light scattered in liquid, determining frequency shift functions

23 p3312 A72-43318

Study of microwave scattering in a plasma-beam discharge

23 p3321 A72-44212

Effective cross section of the inelastic interaction of hadrons with lead-atom nuclei at energies from 3 to 30 TeV

23 p3330 A72-44410

Energy dependence of muon-nucleon inelastic interaction, calculating photonuclear cross section for high energy interactions in iron

23 p3331 A72-44429

Coherent cross section effects on primary particle energy in inelastic proton interaction with carbon nuclei at 20-600 GeV

23 p3332 A72-44439

Electronic excitation of N2 and dissociative excitation of O2 by proton impact.

23 p3317 A72-44520

Scattering of obliquely incident waves by inhomogeneous fibers.

24 p3379 A72-44710

Electron scattering by molecules with and without vibrational excitation. IV - Elastic scattering and excitation of the first vibrational level for N2 and CO at 20 eV.

24 p3427 A72-45304

Electron scattering by molecules with and without vibrational excitation. V - Elastic scattering and non-resonant vibrational excitation of N2 at 30-83 eV.

24 p3427 A72-45305

The effect of the subsurface on the depolarization of rough-surface backscatter.

24 p3380 A72-45635

SCATTERING FUNCTIONS

Bidirectional scattering of electromagnetic waves from rough surfaces in plane of incidence restricted only by tangent plane approximation, comparing with other models

02 p0170 A72-11467

Electromagnetic wave scattering characteristics at arbitrarily configured body with dimensions smaller

than primary field wavelength, determining electric and magnetic moments

02 p0181 A72-12595

Coherence properties of polarized radiation in weak magnetic fields, considering scattering redistribution for normal Zeeman triplet

03 p0427 A72-13292

Scattering function of ellipsoidal gas molecules with translational and rotational degrees of freedom

04 p0552 A72-14629

Thermostated integrating sphere for low temperature measurements of reflection and transmission coefficients of materials with arbitrary scattering functions

06 p0816 A72-17838

Narrow light beam attenuation and scattering characteristics in turbid medium as function of distance from source from transport equation solution

06 p0774 A72-17938

Homogeneous isotropically scattering spherical media atmospheric model for radiative transfer problem, using combined operational method

06 p0842 A72-18083

Atomic variational scattering calculation by method of models, using modified Hamiltonian form to avoid difficulties due to inexact target wave functions

09 p1355 A72-22787

Scattering computations of albedo reflectance for model media as function of incidence angle

09 p1299 A72-22808

Fermi level and scattering phase function nomograms for semiconductors with parabolic and isotropic energy bands, noting charge transfer effects

11 p1700 A72-25781

Computer algorithms for scattering functions of condensed aluminum or magnesium oxides in combustion products for various temperatures and particle sizes

11 p1747 A72-26966

Gas surface interactions models, computing scattering kernels by reduction to boundary value problem

14 p1234 A72-30880

Surface roughness effects on Mars photometric properties, allowing for scattering in terms of Minnaert law

15 p2311 A72-32085

Narrow light beam attenuation and scattering characteristics in turbid medium as function of distance from source from transport equation solution

16 p2426 A72-33779

Solar corona emission line polarization numerical computation based on magnetic dipole transition scattering function for interpretation in terms of magnetic field direction

17 p2608 A72-35084

Book - Angular scattering functions for spheroids

17 p2582 A72-35457

Soft collision plasma scattering function, conductivity and particle energy loss from simplified Fokker-Planck collision model

17 p2592 A72-35621

Albedo and surface illuminance of a planet having a nonhomogeneous purely scattering atmosphere

21 p3050 A72-41796

Measurement of the temperature of flames containing scattering particles on the basis of IR radiation

23 p3356 A72-43678

SCATTERING MATRIX

U S MATRIX THEORY

SCATTEROMETERS

Resonance rail line scattering range using flat parallel conductor transmission line for radar cross section measurement

01 p0032 A72-11251

NASA/MSC earth observation aircraft program radar scatterometers, presenting system evaluation

02 p0172 A72-11849

Microwave radiometer and scatterometer sensing for earth surface and subsurface measurements

06 p0815 A72-17784

Spaceborne scatterometer measurement standard deviation derivation, noting integration time, signal bandwidth and SNR effects on accuracy

12 p1783 A72-27636

SCAVENGING

V-Ti alloys interstitial scavenging action dependence on titanium concentration via internal friction study

17 p2567 A72-34732

Low inlet pressure performance of gerotor lube and scavenge pumps.

18 p2694 A72-36047

SCF

U SELF CONSISTENT FIELDS

SCHEDULES

NT COUNTDOWN

Airline schedule keeping by Sud Lear all-weather landing system, discussing crew training

04 p0544 A72-14688

Airline operational problems from traffic volume increase, discussing flight safety, passenger comfort, schedule adherence and economy aspects

24 p3467 A72-44618

SCHEDULING

NT PREDICTION ANALYSIS TECHNIQUES

DELTA flow chart and network method for R and D projects planning and scheduling

04 p0598 A72-15456

Automated scheduling algorithm for aircraft from terminal area to touchdown, discussing system features and STOL air traffic computerized simulation

05 p0688 A72-16905

Control, prediction and risk optimization in scheduling problems with incomplete random information

06 p0793 A72-17729

Radar tracking pulse scheduling in dense target environment with position estimation error constraints to avoid false return with track correlations

08 p1134 A72-21407

Work administration system for aerospace applications, considering contractual statements, corporate requirements, schedule accomplishment and cost effectiveness

[AIAA PAPER 72-244]

10 p1564 A72-24449

Control, prediction and risk optimization in scheduling problems with incomplete random information

11 p1608 A72-25331

Decision diagrams use in logic analysis for aircraft maintenance schedule testing relative to operational reliability control

13 p1967 A72-30041

Federal legislation impact on airport and airway system planning, considering budget and schedule requirements

18 p2743 A72-36777

Factors to be considered in airline scheduling.

19 p2883 A72-37745

Algorithm for solving the schedule planning problem in mass production

[AD-742589]

21 p3132 A72-41790

S-3A aircraft weight control program organization and methods, considering cost and schedule performance

[SAWE PAPER 906]

23 p3250 A72-43453

Lockheed airline system simulation and aircraft scheduling models.

24 p3466 A72-44579

Cost effective algorithm for optimal route aircraft scheduling for airlines by mixed integer multi-commodity flow technique and Dantzig-Wolfe decomposition

24 p3466 A72-44582

Heuristic procedure solution for least cost commercial airline crew scheduling, emphasizing combinatorial space size reduction

24 p3466 A72-44584

SCHHEELITE

Spectroluminescent and lasing properties of Nd ions in anisotropic scheelite crystal structures

07 p1007 A72-20121

Single crystal scheelite material for Nd doped intermediate gain laser host substance, considering optimum growth conditions, lasing parameter and Nd concentration

15 p2292 A72-32030

SCHEMATICS

U CIRCUIT DIAGRAMS

SCHIFF BASES

U IMINES

SCHLIEREN PHOTOGRAPHY

Clad-to-core bond testing in radioisotope irradiation strips by pulsed laser ultrasonic schlieren system

01 p0080 A72-10811

Schlieren photography for visualizing ultrasonic pulse propagation and reflection in solids and liquids, applying to crack detection in steel tubes

01 p0071 A72-11022

Solid particle influence on underexpanded gas jet shock structures, using schlieren photographs

03 p0342 A72-13840

Laser schlieren measurement of density gradients in laminar hypersonic boundary layer interacting with corner expansion wave in shock tunnel

[AIAA PAPER 72-75]

05 p0606 A72-16879

Supersonic turbulent boundary layer interaction with compression corner, noting static pressure distributions, flow visualization and schlieren photographs

[AIAA PAPER 72-114]

05 p0610 A72-16976

Flow visualization in supersonic axial compressor by short exposure schlieren photography of shock wave patterns in rotating annular cascade of compressor blades

[ONERA, TP NO. 1026]

05 p0708 A72-17192

Schlieren cinematographic and holographic diagnostic of giant pulse ruby laser produced plasma in Xe

[CLEA PAPER 12,2]

07 p1040 A72-19393

Comparative IR schlieren and interferometry techniques for measuring electron density profiles from refractive index effects of rotationally symmetric plasmas

07 p0986 A72-19613

Schlieren optics for visualization and differentiation of density gradients with color and brightness distinctions, applying to supersonic flow through tandem grid

09 p1316 A72-23669

Supersonic axisymmetric turbulent jet density fluctuations measurement by single beam schlieren system, using preheater to reduce jet static/ambient temperature difference

10 p1466 A72-24292

Color schlieren technique for simultaneous photographic recording of flow fields and heat transfer patterns in aerodynamic heating, noting application to shock-boundary layer interactions

11 p1629 A72-25257

Schlieren photographic investigation of shock wave propagation over narrow slit, noting cylindrical expansion wave origin at slit upstream edge

11 p1616 A72-25920

Schlieren observation of generation and convergence of shock waves produced in He and Ar by capacitor bank discharge in parallel rail type device

11 p1695 A72-25921

Schlieren visualization of radiated wave fronts for Al plates illuminated with short acoustical pulses in water, comparing with Lamb theory

11 p1687 A72-26057

Schlieren method for qualitative study of optical inhomogeneities produced by temperature field in cylindrical solid body

14 p2106 A72-31162

Spark discharge light source for shock wave multiple exposure schlieren photography, describing pulse separator and spark trigger circuits

15 p2240 A72-32437

Wall contour effect on shock wave shape, comparing Whitham theory with schlieren photographs from shock tube tests

15 p2219 A72-32595

German monograph on supersonic flow past blunt sharp edged cones, comparing Van Dyke and method of characteristics results with schlieren photos and shadowgraphs

16 p2343 A72-33505

A two-dimensional color schlieren technique.

17 p2554 A72-34933

Quantitative schlieren techniques applied to high current arc investigations.

19 p2797 A72-37588

Three dimensional flow field visualization, data acquisition and reduction via holography, noting applications in schlieren and interferometric techniques

19 p2798 A72-37620

Heat transfer measurements with a Wollaston prism schlieren interferometer.

[ASME PAPER 72-HT-9]

20 p2927 A72-39680

Comparison of information takeoff from a shadow-indication instrument by television and photographic techniques

20 p2928 A72-40049

Method of characteristics for ideal gas flow in annular space of axisymmetric plug nozzle, noting flow visualization by schlieren photography

22 p3166 A72-42263

Measurements of the local velocity of shock and detonation waves by schlieren interferometry of Doppler-shifted laser light.

22 p3178 A72-42455

A laser interferometer for combustion, aerodynamics and heat transfer studies.

24 p3402 A72-44950

Chapman-Jouguet surface characteristics in flow field behind steady gaseous detonation wave, using schlieren photography

24 p3462 A72-45031

SCHMIDT CAMERAS

Geos B satellite laser range experiment, discussing ruby oscillator and amplifier as transmitter and optical Schmidt system as receiver

03 p0365 A72-12950

Aberration correction in collimator of Schmidt spectrograph camera by changing surface geometry and grating positioning

03 p0362 A72-14358

Faint planetary nebulae classification and measurement in northern Milky Way between Cygnus and Perseus from Schmidt camera survey

07 p1070 A72-19084

Apollo 16 far-ultraviolet camera/spectrograph - Earth observations.

21 p3105 A72-40600

Polarization of emission in the IC 4592 and IC 4601 nebulae

23 p3338 A72-44032

SCHMIDT METHOD

Curve and surface fitting with Schmidt potential functions, including polynomial and straight line fit

02 p0252 A72-12601

SCHMIDT NUMBER

Binary gas mixtures calculation for Schmidt, Prandtl and Lewis number dependence on pressure, temperature and chemical composition

07 p1101 A72-20600

Tangential and radial eddy diffusivity effects on nonsymmetric turbulent diffusion in plain impervious tube as function of Schmidt number

14 p2096 A72-31069

SCHOTTKY EFFECT

U WORK FUNCTIONS

SCHROEDINGER EQUATION

Noninteracting Fermi gas in finite square-well potential, obtaining quantum mechanical solution of Schroedinger equation

02 p0262 A72-11671

- Field-dynamic equilibrium of macroparticle motion in central field, comparing with Schrodinger equation 06 p0890 A72-18418
- Wave mechanics theory of turbulence based on Schrodinger equation, discussing resonance and flutter aspects 07 p0971 A72-20095
- Reduction of governing equation for thin non-stretching vortex filament in incompressible inviscid fluid to nonlinear Schrodinger equation describing helical motion propagation 10 p1466 A72-24293
- Variables separability conditions within Riemann space for Schrodinger and Laplace equations 15 p2264 A72-32278
- Stochastic electrodynamics based on zero electromagnetic field motion, deriving Schrodinger equation and electromagnetic model of gravitation 17 p2584 A72-35912
- New demonstration of the adiabatic theorem for conservative systems in wave mechanics 18 p2711 A72-36473
- Formula for the product of semigroups which is determined by the method of bilinear forms, and the application of the formula to the Schrodinger equation 19 p2825 A72-37735
- A general method for integrating the Schrodinger equation with a singular right-hand side in a homogeneous and constant electromagnetic field 19 p2843 A72-38855
- Determination of accurate potential strengths to yield specified eigenvalues of the radial Schrodinger equation. 21 p3086 A72-40109

SCHULER TUNING

- High accuracy north-seeking course-attitude inertial reference system for air navigation, using platform unit and automatic alignment for Schuler tuned operation 07 p0990 A72-20282

SCHUMANN-RUNGE BANDS

- Continuum UV radiation absorption by vibrationally excited molecular oxygen in Schumann-Runge system 02 p0221 A72-12457
- Molecular oxygen photodissociation in Schumann-Runge bands, discussing determination of solar radiation penetration depth into chemosphere 03 p0412 A72-13886
- French monograph - Determination of the absolute value of the absorption in the bands of the Schumann-Runge system of molecular oxygen 19 p2836 A72-37476
- Worldwide thunderstorm activity model selection from Schumann resonance observations, using ELF noise measurements in lowest earth-ionosphere cavity modes 24 p3380 A72-45100

SCHWARTZ INEQUALITY

- Uniqueness theorems for linearized Boltzmann equation with Maxwell boundary conditions, using Gauss theorem and Schwartz inequality 08 p1149 A72-21252

SCHWARTZ METHOD

- Schwartz method application to stripline fields and impedance calculations for different cross sections and internal conductor dimensions 08 p1133 A72-21370

SCHWARZSCHILD ANTENNAS

- Broadband high gain large aperture Schwarzschild antenna systems design, considering compromises and tradeoffs in scan angle, F/D ratio and surface shapes 01 p0039 A72-10672

SCHWARZSCHILD METRIC

- Particle motion in uniform acceleration field via Schwarzschild line element of general relativity, applying to clock paradox 03 p0388 A72-13227
- Precessing elliptical orbits stability in Schwarzschild field 04 p0571 A72-14559
- Maxwell equation spinor formulation for Schwarzschild gravitational field effects on spherical electromagnetic waves propagation 05 p0689 A72-16165
- General theory of relativity for symmetric field, discussing DE Donder incompressible fluid model and Tolman-Schwarzschild metrics 06 p0847 A72-17682
- Baryon number nonmeasurability of Schwarzschild black hole by strong interactions, extending results to Kerr-Newman holes 09 p1387 A72-22875
- Gravitational radiation spectrum and energy computation from point test particle falling radially into Schwarzschild black hole 09 p1393 A72-23646
- Bright black holes from quasars condensation toward Schwarzschild radius, investigating primeval galaxies angular momentum increase and core concentration due to frictional effects 10 p1535 A72-23909

- Wave equation derivation for electromagnetic and gravitational radiations in Schwarzschild field, obtaining third order corrections for scalar waves 10 p1514 A72-25168

- Approximate periodic solution of satellite equation of motion based on Schwarzschild metric integration, noting relativistic effects 14 p2162 A72-31108

- Synchrotron radiation-like angular distribution of gravitational synchrotron radiation produced by ultrarelativistic geodesic particle orbits in Schwarzschild geometry 17 p2583 A72-35820

- Pulses of gravitational radiation of a particle falling radially into a Schwarzschild black hole. 18 p2711 A72-36714

- Quantum fields interaction with classical sources on Schwarzschild background, noting mass, charge and angular momentum as sole measurable quantum numbers of black hole 18 p2726 A72-36716

- Polarization characteristics of Schwarzschild black hole gravitational synchrotron radiation in terms of Stokes parameters 21 p3107 A72-41215

- Fluid sphere of uniform density and vanishing pressure at periphery, expressing internal motion in terms of Schwarzschild mass and radius and central pressure 22 p3205 A72-42451

SCIATIC REGION

- Frog and rabbit sciatic nerve afferent impulse recordings during prolonged sinusoidal vibration of foot 04 p0474 A72-15235

SCIENTIFIC SATELLITES

- NT APPLICATIONS TECHNOLOGY SATELLITES
NT AZUR SATELLITE
NT DIAL SATELLITE
NT ENVIRONMENTAL RESEARCH SATELLITES

- Scientific satellite with simple inertial system, deriving discrete feedback reentry guidance algorithms based on closed-form equations solvable by onboard computer 01 p0098 A72-10944

- AEROS scientific satellite attitude control system, considering control and measuring electronics, axis and spin control coils and spin stabilization 04 p0503 A72-15649

- Space real time data links during processing of French D2 scientific satellite for hydrogen frequency bands investigation 05 p0628 A72-16447

- Computer controlled vacuum optical calibration bench for astronomical satellites, describing pumping system 05 p0644 A72-16755

- UK-5 satellite all sky X ray monitor consisting of pinhole camera, position sensitive proportional counter and data processing electronics 08 p1228 A72-21513

- Image dissector application to D2B astronomical satellite position field plotting in solar and stellar UV photometry 08 p1172 A72-21976

- German aeronomy research satellite Aeros mission objectives, discussing orbit layout, onboard equipment and operation 13 p2050 A72-30079

- Report to COSPAR on UK ground based, rocket and satellite-borne space research experiments and 1971-1972 programs 15 p2337 A72-32005

- Japanese report to COSPAR on space research by sounding rockets, balloons and SHINSEI scientific satellite 15 p2338 A72-32011

- TD-1A - Europe's largest and most advanced satellite. 18 p2731 A72-37011

- The on-board computer of the Astronomical Netherlands Satellite /ANS/. 24 p3382 A72-45163

- Design and operation objectives and constraints for German scientific spacecrafts, discussing orbital performance and reliability and quality control requirements 24 p3451 A72-45205

SCIENTISTS

- Social factors of labor organization and control in scientific teams for industry 02 p0304 A72-11728

- Nonmeteorological scientists and engineers views on meteorology and weather forecasting, discussing uses, problem areas and knowledgeability 03 p0384 A72-13637

SCINTILLATION

- Annual movements of satellite signals scintillation boundary in subauroral ionosphere 01 p0031 A72-10920

- Ionospheric small scale electron density irregularity structure from power spectral analysis of radio source scintillation observations 03 p0345 A72-12985

- High latitude scintillation effects on vhf and S band polar orbiting satellite transmissions, examining ionospheric irregularities 04 p0487 A72-14952

- Radio stars wave amplitude scintillation during passage through ionosphere observed by interferometer, noting association with geomagnetic field fluctuation 04 p0567 A72-14953

- Interplanetary media plasma density fluctuations and power law spectra effects on radio wave scintillation 05 p0695 A72-16068

- Latitudinal, diurnal, seasonal and solar cycle variations in vhf-uhf scintillation producing irregularities in F layer electron density 05 p0630 A72-16617

- Ionospheric scintillation fading observations by NASA satellite tracking and data acquisition networks, noting frequency dependence in auroral regions [AIAA PAPER 72-220] 05 p0631 A72-16858

- Scintillation effects on synchronous satellite communications systems at 250 MHz in equatorial region, discussing diversity techniques and composite diffraction refraction theory [AIAA PAPER 72-178] 05 p0631 A72-16906

- Ionospheric turbulence induced scintillations of Intelsat geostationary satellite signals at 4 and 6 GHz [AIAA PAPER 72-179] 05 p0631 A72-16966

- Geophysical aspects of ionospheric scintillation problems, considering correlation with spread F and sporadic E 06 p0889 A72-18282

- Interplanetary scintillation and angular dimensions of radio sources at 81.5 MHz, using diffraction theory 06 p0889 A72-18327

- Ionospheric scintillations relationship to airglow emission spectrum at 6300 A 07 p0974 A72-18895

- Interplanetary scintillation of two pulsars, discussing scattering and amplitude modulation of incident radiation propagated through interstellar medium 07 p1069 A72-19073

- Angle scintillation in laser radar return from retroreflector, comparing measurement with theoretical derivation in terms of phase fluctuation parameter [CLEA PAPER 2,1] 07 p0942 A72-19377

- Scintillation measurement of transverse component of wind blowing across laser beam, using correlation method [CLEA PAPER 2,3] 07 p0942 A72-19378

- Scattering and scintillations of rf radiation from distant discrete astronomical sources as measure of interplanetary plasma irregularities 07 p1079 A72-20020

- F region irregularity contours from correlation analysis of satellite amplitude scintillations, showing axially symmetric field-aligned and north-south elongated planes 08 p1156 A72-21105

- Aperture filtering effects on amplitude scintillation power spectra of paraboloid radio telescope over millimeter wave propagation path 08 p1136 A72-21982

- Solar wind velocity determination from interplanetary scintillation, deriving equations by smooth perturbations method 09 p1375 A72-22285

- Physical optics approximation study of gravitational waves effect on electromagnetic propagation, noting unobservability of local scintillation effect 09 p1351 A72-22683

- Pulsars CP 0328 and NP 0531 twinkling explained by interstellar electron density fluctuations due to Alfvén wave passage and coupling of cosmic rays to interstellar gas 09 p1377 A72-22753

- Turbulent LF electric field fluctuations relationship with disturbed F region, spread F and scintillations of radio stars and satellites 09 p1300 A72-23025

- Magnetic field line connection between F region irregularities causing scintillation and ionospheric conditions inducing spread E 11 p1625 A72-26405

- Transmitter aperture size and focus effects on scintillations of laser beam propagating through turbulent atmosphere 12 p1791 A72-27678

- Ionospheric irregularities-magnetospheric parameters relationship from satellite scintillation measurement, noting use as indirect electron precipitation indicator 12 p1803 A72-27772

- Regular cyclic fading of HF and VHF radio signals due to ionospheric scintillation, noting consistency with two ray interference formula 13 p1952 A72-29665

- Probability density for interplanetary scintillation at 74 MHz, noting log normal distribution 16 p2450 A72-32953

Radio source power spectra modulation dependence on distance and thickness of solar wind scattering region and on wind velocity component multiplicity
16 p2451 A72-33034

Radio source scintillation observations by arms of one mile radio telescope at Molonglo Observatory
16 p2451 A72-33035

Satellite measurement of ground-based CW Ar laser source scintillation, deriving log amplitude variance, probability distribution and power spectral density from telemetered data
17 p2513 A72-34289

On the size distribution of turbulent elements in the earth's atmosphere.
17 p2549 A72-35717

Study of the solar wind using the power spectrum of interplanetary scintillation of radio sources.
18 p2722 A72-36730

Determination of the orientation of ionospheric irregularities causing scintillation of signals from earth satellites.
19 p2794 A72-38866

Seasonal, diurnal and magnetic dependence of ionospheric scintillation at 64 deg invariant latitude.
20 p2916 A72-39226

Observations of scintillations of two satellite beacons near the boundary of the irregularity region.
20 p2916 A72-39227

Experimental effects of finite transmitter-apertures on scintillations.
20 p2932 A72-39500

Experiments on turbulence characteristics and multiwavelength scintillation phenomena.
21 p3048 A72-40140

Simplified equation for amplitude scintillations in a turbulent atmosphere.
21 p3083 A72-40143

Ground humidity and wind velocity effects on terrestrial scintillation, considering adiabatic temperature stratification factor
21 p3007 A72-40738

Characteristics of the abrupt scintillation boundary.
22 p3170 A72-42363

Error sensitivity of statistical models with pattern rearrangement for analysis of interplanetary scintillation in ecliptic plane
22 p3218 A72-42402

Power-law wavenumber spectrum deduced from ionospheric scintillation observations.
22 p3171 A72-42416

Variation of the output of radioluminescence of organic scintillators with energy loss and the number of charges of ionizing particles
22 p3180 A72-42938

Cross correlated interstellar scintillation patterns of circumpolar pulsar PSR 0329+54 at 408 MHz, interpreting transverse velocities in Galaxy
23 p3334 A72-43253

Relative movements of mid-latitude trough and scintillation boundary.
23 p3282 A72-43267

The scintillation of extended radio sources when the receiver has a finite bandwidth. III - Further methods.
23 p3341 A72-44396

Solar wind velocity determination from radio sources interplanetary scintillation observations, noting magnitude and direction variations with time
23 p3333 A72-44529

Observations of the interplanetary medium and of the structure of radio sources using higher moments of interplanetary scintillations.
24 p3437 A72-44830

Interplanetary scintillation of radio sources observed through solar corona, deriving higher central moments from skewness coefficient of probability density function
24 p3437 A72-44831

SCINTILLATION COUNTERS

Computer controlled scintiscanning for pulmonary blood flow distribution, discussing real time data monitoring, contour plots and three dimensional and wall reflection maps
01 p0020 A72-11038

Scintillation counter to determine neutrons number and distribution in time in pulses generated in hot plasma
02 p0263 A72-11419

Human left ventricular volume determined by peripheral venous scintillation angiocardigraph isotope method, comparing with X ray method
02 p0157 A72-11475

Neutron albedo flux recording instrument with composite scintillation crystal and photomultiplier scanning to monitor near space
02 p0273 A72-11934

Linear energy transfer response of polyvinyltoluene plastic scintillator, presenting data on quality factor and radiation dose equivalent determinations in mixed radiation field
02 p0168 A72-12071

Gamma ray detection system using scintillation counter and active anticoincidence shield
03 p0352 A72-13028

Stilbene scintillator detector for gamma ray spectrometry in energy range 0.5-5 MeV, separating gamma rays from neutrons by pulse shape discrimination technique
03 p0408 A72-13031

Scintillator crystal system with monitoring streak camera for flash X ray burst time measurements
04 p0523 A72-15482

High resolution electrons image intensifier for particle spectrographs, using channel plate, scintillator and fiber optics
04 p0524 A72-15536

Solar neutrons search near solar maximum with plastic scintillator counter, discussing irregular excess in counting rate
05 p0719 A72-16524

Transient effect in electron-photon shower on readings of ionization chamber and scintillation counter
06 p0871 A72-17291

X ray detection on Jupiter with actively collimated balloonborne scintillation counter, noting decametric emission due to electron precipitation
06 p0872 A72-17445

Vacuum chamber sputtering techniques for CsI/Tl and NaI/Tl thin films for soft proton scintillation detector
06 p0816 A72-17834

Scintillation crystal light yield dependence on emission energy in particle flux measurements with semiconductor spectrometer
06 p0816 A72-17835

Image photon counting technique using digital accumulation of individual events registered by high gain image intensifier and TV camera and stored in on-line computer
08 p1170 A72-21960

High energy cosmic ray hadrons energy measurement using glass scintillator ionization spectrometer
09 p1309 A72-22523

Energetic solar X-ray burst of 11 February 1970 observed by balloon-borne NaI scintillation detector launched from Antarctica, comparing to OSO 5 data
09 p1377 A72-22930

Atmospheric turbulence inner scale measuring configuration consisting of light transmitter and two scintillation counter detectors
09 p1314 A72-23343

Penetrating particles effect on low energy scintillation spectrometers sensitivity in various regions of magnetosphere
11 p1632 A72-25934

Neutron albedo flux recording instrument with composite scintillation crystal and photomultiplier scanning to monitor near space
13 p2030 A72-29246

Molniya 1 satellite slow neutron monitor with photomultiplier scanned scintillator, noting limiting effect of geomagnetic perturbations
14 p2105 A72-30628

Scintillation and semiconductor counters - IEEE/AEC/NBS Conference, Washington, D.C., March 1972
15 p2233 A72-31529

Miniature high gain photomultiplier for pulse counting applications in close-packed arrays and mosaics for scintillation imaging and spectrum analyzing
15 p2234 A72-31534

Background spallation source errors in satellite measurements of diffuse cosmic X ray spectrum with crystal scintillators
15 p2300 A72-31986

Scintillation telescopes for muon angular distribution, designing test device for photomultiplier tubes selection
17 p2556 A72-35437

Liquid scintillation counters application in search for relativistic quarks in cosmic rays, setting upper confidence limits on particle intensity
17 p2601 A72-35471

The use of a scintillation counter to measure diagnostic X-ray tube kilovoltage, radiation exposure rates and contamination by low energy gamma emitters.
18 p2655 A72-37197

German monograph - A method for the determination of the differential albedo for photons in the range from 1-17 MeV
19 p2836 A72-37484

Upper limits on vertical fluxes of 1/3 e and 2/3 e charged quarks in cosmic rays from observations with scintillation counter telescope
21 p3101 A72-41450

SCINTILLATION SPECTROMETERS
U SCINTILLATION COUNTERS
U SPECTROMETERS
SCINTILLATORS
U SCINTILLATION COUNTERS
SCINTILLOMETERS
U SCINTILLATION COUNTERS
SCORPIO CONSTELLATION
U SCORPIUS CONSTELLATION

SCORPIUS CONSTELLATION

X ray rocket observations of time variation of SCO X-1 energy spectrum and optical luminosity at 2-20 keV
02 p0281 A72-12307

Scorpius X-1 and Cygnus X-1 pulsed radio emission search by sensitive de-dispersing technique
07 p1073 A72-19422

Spectrum of hot hydrogen plasma continuum radiation, discussing models for Scorpius X-1 source and inhomogeneous clouds
09 p1391 A72-23536

X ray effect from Scorpio XR-1 on lower ionosphere long wave transmissions, considering transit times and field intensity variations
09 p1305 A72-23572

Beta Scorpii occultation by Jupiter, obtaining light curves, atmospheric scale height and stratification
10 p1548 A72-24968

Photoelectric observation of beta Scorpii occultation by Jovian satellite Io, noting Fresnel diffraction effects
10 p1548 A72-24969

Polarization of emission in the IC 4592 and IC 4601 nebulae
23 p3338 A72-44032

SCOUT LAUNCH VEHICLE
Aigol 3 solid propellant rocket motor design for Scout D and E launch vehicles first stage, considering high total impulse, payload/mass capability and propellant grains
01 p0115 A72-10261

Nondestructive radiographic tests for void and unbond detection in Scout solid propellant rocket motors
01 p0114 A72-10812

The Scout launch vehicle system.
24 p3450 A72-45165

SCR [RECTIFIERS]
U SILICON CONTROLLED RECTIFIERS
SCRAMJET ENGINES
U SUPERSONIC COMBUSTION RAMJET ENGINES
SCRAMJETS
U SUPERSONIC COMBUSTION RAMJET ENGINES
SCREEN EFFECT
Distribution moments mathematical method for partially coherent light beam propagation through random phase screens in linear and nonlinear media
02 p0181 A72-12589

Plane wave intensity fluctuations behind random phase screen, discussing phase structural function relation to field statistical properties and fluctuation dispersion
02 p0181 A72-12590

Fresnel diffraction on opaque half plane screens with statistically rough surfaces, using Kirchhoff approximation
02 p0183 A72-12755

Focused laser beam interaction with liquid metal particles, discussing fluid phase light screening effect, droplet evaporation and mass expulsion characteristics
03 p0368 A72-13668

Frequency characteristics of selectively reflecting screens in multichannel parabolic mirror antennas and determination of Fresnel coefficients dependence on polarized plane wave incidence angle
04 p0499 A72-15241

Electromagnetic plane wave diffraction by infinite slit in screen with surface impedance, deriving field and transmission coefficient by asymptotic numerical solution
06 p0771 A72-17352

Spatial boundary layer variations in low speed wind tunnel working section due to settling chamber screens, discussing mesh variations effects on Preston tube measured pressure coefficient distributions
07 p0966 A72-19061

Flat electrically conducting screen with periodic filamentary structure as possible analog converter of electromagnetic field information
09 p1291 A72-23433

Radiant flux from finite cylindrical volume to coaxial screen calculated under quasi-homogeneous medium and arbitrary optical thickness assumptions
10 p1561 A72-23841

Electrically conducting plane screen with periodic filamentary structure as possible analog converter of electromagnetic field information
19 p2782 A72-38516

Fresnel diffraction on opaque half plane screens with statistically rough surfaces, using Kirchhoff approximation
20 p2902 A72-39061

Short distance behaviour of the pair correlation function for classical plasmas.
21 p3091 A72-40570

Bessel series solution to electromagnetic field and pulse function of cylindrical conducting screen located in monochromatic plane wave
22 p3155 A72-42667

Measurement of the modulation transfer functions of focusing screens.
24 p3425 A72-44770

SCREENS

Acoustical field from streamlined body of revolution moving in homogeneous gaseous medium past semiinfinite rigid screen, using Wiener-Hopf method for diffraction radiation

03 p0340 A72-12916

Stereoscopic projection screens for three dimensional image display, discussing classification by diffusing properties, surface types and applications

06 p0814 A72-17440

Velocity distribution downstream of nonuniform single and multiple smoothing screens, presenting theory based on energy losses and flow direction changes

13 p1940 A72-30100

Jet noise reduction by screen placed across jet flow, investigating acoustic properties, velocity and pressure in mixing zone

[ALAA PAPER 72-644]

16 p2381 A72-34088

Wind tunnel investigation of shapes for balloon shelters.

20 p2885 A72-38967

SCREW DISLOCATIONS

Yield stress of solid solution iron and Fe-Ge alloys with bcc structure, obtaining interaction energy between screw atoms and screw dislocation

03 p0402 A72-13974

Isotropic continuum model of elastic interaction of edge and screw dislocation with nearby inclusion

06 p0894 A72-17492

Numerical analysis of passing screw dislocation arrays under stress for computerized work hardening model

07 p1097 A72-20556

Plastic slip in notched half plane undergoing antiplane deformation, using screw dislocation continuous distribution theory

09 p1403 A72-22747

Screw dislocation with free surface interaction in inhomogeneous elastic medium with continuously varying elastic moduli

12 p1881 A72-27253

Interaction energy and force between screw dislocation and spherical inhomogeneity, discussing voids growth in irradiated materials

18 p2718 A72-36510

Cracks and screw dislocation arrays in anisotropic bimaterial plates.

20 p2937 A72-39291

Edge and screw dislocations induced stress fields in isotropic medium, using Kauderer nonlinear elasticity theory

23 p3345 A72-43622

The stress distribution near the tip of an array of screw dislocations piled-up against an inclusion

24 p3460 A72-45694

SCREWS

Screw connections high temperature behavior, discussing creep induced tension relaxation and cyclic loads long term tolerance

03 p0363 A72-13375

Concentric double and single screw seals in laminar Newtonian fluid flow operation, using mathematical methods for optimum thread geometry and maximum sealing coefficients

08 p1178 A72-21930

Sealing pressure and optimal groove form for concentric running screw viscosity seals in laminar flow

08 p1178 A72-21931

Test apparatus and measurement of sealing pressure and temperature in threads of concentric running screw viscosity seals in laminar flow

08 p1178 A72-21932

Investigation of the screw turn magnitude of a contact micrometer attached to the Toepfer meridian circle on the basis of observed right ascensions of stars

19 p2802 A72-37975

Longitudinal-torsional vibrations of a screw beam under axial excitation

22 p3240 A72-42954

SEA ICE

Lake ice surveillance via airborne radar, presenting images of ice forms and land features

02 p0211 A72-11805

SEA LAUNCHING

Helicopter/ship dynamic interface testing for launch and recovery capabilities under sea environment conditions, discussing visual landing aids, wind, visibility and ship motions

[AHS PREPRINT 650]

17 p2491 A72-34505

SEA OF JAPAN

Space TV images use in hydrospherical temperature discontinuity front location, examining cloud cover distributions over Sea of Japan

02 p0214 A72-11872

SEA ROUGHNESS

Sea waves energy spectra from optical Fourier analysis of ocean photographs under particular skylight irradiance

02 p0211 A72-11809

Statistical characteristics of rough sea compared with variable magnetic fields near Crimean coast in Black Sea

02 p0218 A72-11951

Statistical characteristics of rough sea compared with variable magnetic fields near Crimean coast in Black Sea

13 p1949 A72-29263

German monograph - A proposal for a radar device with two simultaneously emitted radar frequencies which has a reduced susceptibility to disturbances produced by sea echoes

19 p2764 A72-37481

SEA STATES

Microwave emission characteristics of oil slicks, showing dependence on oil type, film thickness and sea state

[ALAA PAPER 71-1071]

01 p0057 A72-10533

Synoptic sea surface temperature mapping off Eastern United States using NASA ITOS satellite IR imagery data

02 p0211 A72-11813

Composite scattering theory mathematical model for radar backscattering cross section relation to ocean surface conditions and wind velocity

02 p0172 A72-11868

Ocean wave height measurements with nanosecond radar, using ground truths to relate radar measurements to actual sea conditions

02 p0172 A72-11869

Target detection in sea clutter, showing non-Rayleigh distributed high resolution radar envelope return

02 p0178 A72-12400

Cloud interference-free sea surface temperatures, using techniques to reduce noise effect in Nimbus IR radiometer data

03 p0385 A72-14227

Aerial photographic determination of sea state, using reflection at water surface of natural light diffuse component radiated by sky-sun combination

04 p0525 A72-15563

Sky wave backscattering with narrow beam antenna coupled with signal modulations and Doppler shift as means of sea state observation and environmental monitoring

08 p1134 A72-21493

Sea surface roughness mapping by airborne microwave radiometry with correction for viewing angle and atmospheric effects

09 p1297 A72-22525

Electromagnetic theory of HF radio ground wave backscattering from gently rippled sea surfaces, discussing approximations for separated transmitting and receiving antennas case

10 p1438 A72-24742

SEA WATER

Electromagnetic wave line-of-sight propagation based on geometrical optics for different refractivity profiles above sea, noting earth surface reflection role

01 p0026 A72-10404

Automated operational procedure for sea surface temperature determination from ITOS IR data, discussing error analysis

02 p0211 A72-11810

Microwave measurement and interpretation of oceanic thermal emission in terms of molecular temperature

02 p0214 A72-11866

Sea depth determination in coastal waters based on solar reflection aerial photographs interpretation, presenting formula as function of swell parameters

09 p1303 A72-23307

Sea foam emission and reflection characteristics at microwave frequencies from radiometric measurements, correlating data as functions of frequency and angle

10 p1475 A72-24749

Physical and numerical experiments on layered convection in a density-stratified fluid.

17 p2543 A72-35764

Studies in prebiotic synthesis. VII - Solid-state synthesis of purine nucleosides.

23 p3262 A72-43567

Detection of waste water effluents and of their surface spread in the English channel, the North sea and the Baltic sea, through determination of the surface temperature of the sea by means of infrared air pictures taken by satellites

24 p3398 A72-45223

SEALANTS

U SEALERS

SEALERS

Aircraft power plants sealing materials, emphasizing porous cermet seals heat resistance under thermal cyclic loads

06 p0797 A72-18658

SEALING

Fluid sealing - Conference, Coventry, England, March-April 1971

08 p1177 A72-21926

Fluid sealing theory based on surface tension effects at roughness asperities within seal film

08 p1177 A72-21928

Sealing pressure and optimal groove form for concentric running screw viscosity seals in laminar flow

08 p1178 A72-21931

Test apparatus and measurement of sealing pressure and temperature in threads of concentric running screw viscosity seals in laminar flow

08 p1178 A72-21932

Stress-deformation effects on gasket joint of metal seals at high pressures

08 p1178 A72-21933

A comparison of sealed and vented Ni/Cd battery characteristics.

17 p2498 A72-35567

Hermetic sealing of electronic subsystems with plastics

23 p3294 A72-44142

SEALS [STOPPERS]

NT GASKETS

NT HERMETIC SEALS

NT O RING SEALS

NT PACKINGS [SEALS]

NT PLUGS

Fiber reinforced plastic composite seals for liquid hydrogen and nuclear radiation environments, stressing polyquinoxaline fitness

01 p0075 A72-10773

Hydrostatic pressurized gas seals for rotating shafts under extreme operating conditions, discussing design requirements for small clearances and avoidance of pneumatic instabilities

02 p0236 A72-12425

Continuum gas viscoelastic performance, comparing two seal groove aspect ratio geometries

02 p0237 A72-12850

Power law sealant effects on high aspect ratio viscoelastic performance under laminar isothermal conditions

02 p0237 A72-12851

Algorithm for gas turbine labyrinth seals design, presenting flow chart for seal leakage analysis [ASME PAPER 72-LUB-C]

06 p0821 A72-17803

Friction coefficient, standard wear and surface layer temperature of seal for dry friction pairs in jet engines, investigating crystal lattice parameters

07 p0996 A72-19768

Rarefied gas sealant viscoelastic performance prediction by analytical models, comparing results with experiments on multiple grooved samples

08 p1177 A72-21929

Concentric double and single screw seals in laminar Newtonian fluid flow operation, using mathematical methods for optimum thread geometry and maximum sealing coefficients

08 p1178 A72-21930

Under-lip temperatures and thermal conductivity in rotary shaft seals, using heat transfer analysis

08 p1178 A72-21934

Compressibility effects on straight through labyrinth seal performance in regenerative turbomachine

08 p1178 A72-21935

Bushing seal with pressure dependent clearance for reciprocating piston rod or rotating shaft, presenting laminar and turbulent axial flow theory

08 p1178 A72-21936

Pressure gradient relations for viscous fluid flow in clearance seals at high pressures

08 p1178 A72-21937

Pipe joint flexible metal seal development and testing for Concorde Olympus 593 under thermal and pressure cycling

08 p1178 A72-21938

Metallic four-lip seal performance, discussing force cycle, mechanical spring-back, reusability at room and higher temperatures and thermal shock behavior

08 p1179 A72-21939

Clam seals comparison with elastomers, discussing aircraft use, contamination, inspection, corrosion and erosion, surface finish, service life and cost

08 p1179 A72-21941

Hydrodynamically lubricated mechanical seal design, predicting duty variation effects on performance

08 p1179 A72-21942

Mechanical seal for airborne Stirling cycle cryogenic refrigerator, noting He cross leaks and sealing faces galling and blistering

[ASLE PREPRINT 72AM 16]

13 p1964 A72-28973

Externally pressurized automatic barrier seals for high pressure applications in chemical industry, nuclear power plants and deep - submergence vessels, discussing theory, design and test results

[ASLE PREPRINT 72AM 17]

13 p1964 A72-28974

Materials selection for contact and clearance type seals for various environment conditions

[ASLE PREPRINT 72AM 23]

13 p1964 A72-28975

Mechanical seals for high temperature heat transfer fluids, noting configuration and construction materials

[ASLE PREPRINT 72AM 30]

13 p1964 A72-28976

Ceramic-to-metal seal development for thermionic fuel elements.

18 p2695 A72-36156

SEAMS [JOINTS]

Continuous seam diffusion bonding application to Ti and superalloys lap, butt and T joints production

[SME PAPER AD 71-264]

01 p0076 A72-10970

Thermal stresses in elastic cylinder for variable linear expansion coefficient and temperature, noting welded seam between two constant temperature cylinders

13 p2059 A72-29492

German monograph - Contribution to the ultrasonic seam welding of metals

19 p2807 A72-37655

SEARCH PROFILES

Algorithms for optimal adaptive control of steady motions of single channel discrete extremal systems with independent search, studying quality functional behavior

09 p1291 A72-23437

Algorithm for optimal binary search tree construction with minimum weighted and restricted maximum path lengths

11 p1676 A72-25354

Algorithms for optimal adaptive control of steady motions of single channel discrete extremal systems with independent search, studying quality functional behavior

19 p2782 A72-38520

Space shuttle ascent trajectory optimization by Davidson/Broyden crude search technique for matrix updating

[AIAA PAPER 72-907] 21 p3111 A72-41556

SEARCH RADAR

Search radar performance environmental model using clutter and interference returns

02 p0178 A72-12389

Meteor trail radar operated under digital controller synchronization and programmed for alternate and simultaneous two orthogonal directions search

10 p1438 A72-24715

Operation analysis of automatic range finders in pulse radars regarding target search and lock-on functions

11 p1595 A72-26300

Search radar constant false alarm rate receiver circuit for background noise and clutter compensation, using matched dispersive delay lines flanking hard limiter

16 p2365 A72-33762

Overall detection probability for fluctuating and nonfluctuating target models.

19 p2763 A72-37294

German monograph - A search procedure for electronic radar.

22 p3156 A72-43054

SEARCHING

NT SEARCH PROFILES

Extremum search algorithm in multicomponent mixture optimization problem, using gradient method adaptation

13 p1924 A72-28460

Target and surrounding nontarget stimuli size differences effect on visual search time for displays with large fields

14 p2083 A72-31153

A statistical information theory for extremum search of a function

19 p2827 A72-38576

Simple algorithm for a search of the global extremum of a function of several variables and its application to the functional approximation problem

19 p2828 A72-38582

Optimal search in the presence of Poisson-distributed false targets.

21 p3075 A72-40837

Optimal search with uncertain sweep width.

23 p3308 A72-43805

Mathematical model for digit summation task search time distribution dependence on size of visual display with randomly arranged three digit numbers

24 p3374 A72-44558

SEAS

NT CASPIAN SEA
NT MEDITERRANEAN SEA
NT SEA OF JAPAN

SEASONAL VARIATIONS

U ANNUAL VARIATIONS

SEASONS

NT SUMMER
NT WINTER

SEAT BELTS

Crashworthy upper torso restraint systems for general aviation, incorporating strap takeup devices

08 p1126 A72-21578

Dynamic deceleration anthropomorphic dummy tests of general aviation occupant lap belt/shoulder harness restraint systems

[SAE PAPER 720325] 11 p1583 A72-25588

Impact tests on anthropomorphic dummies for protection effectiveness evaluation of lap belt, Air Force shoulder harness-lap belt and airbag-lap belt restraints

[AD-741530] 12 p1769 A72-27471

Deceleration attenuation effectiveness of airbag restraint systems compared with seat belt-shoulder harness for aircraft occupants crash protection

15 p2191 A72-32605

SEATS

NT BARANY CHAIR
NT EJECTION SEATS

Energy absorbing seat design for light aircraft, describing development and static and dynamic testing

[SAE PAPER 720322] 11 p1583 A72-25585

Flight and centrifuge tested aircrew tilting supinating seats biomedical and technical adequacy as acceleration protective man machine system

19 p2761 A72-38707

SECANTS

U TRIGONOMETRIC FUNCTIONS

SECONDARY AIR

U AIR

SECONDARY COSMIC RAYS

Atmospheric primary and secondary cosmic ray propagation with close reference to two-fire-ball, H-quantum and excited baryon models of multiple meson production

01 p0121 A72-11122

Magnetosphere model for low energy cosmic ray proton propagation mode to synchronous orbit satellite, calculating geomagnetic cutoffs and penetration regions

[AD-741079]

02 p0274 A72-12453

Inelastic nuclear interactions between 200-GeV cosmic ray particles and polyethylene targets, correlating similarity property, angular momentum spectra and secondary particle pairs

06 p0868 A72-17258

Secondary cosmic ray shower charged particles angular distribution asymmetry in C-system and azimuthal plane related to single fireball formation

06 p0868 A72-17263

Measuring equipment for charged particles spatial distribution in cosmic ray showers, considering multiaxial and secondary young showers

08 p1226 A72-21077

Balloon sounding observations of lower stratosphere secondary cosmic radiation bursts due to solar activity

10 p1529 A72-24069

High energy inelastic interactions in cosmic ray showers from Wilson chamber and ionization calorimeter observations, noting secondary particles occurrence dependence on primary energy

23 p3330 A72-44406

S-system motion effect on angular distribution of secondary high energy particle cluster in showers formed by primary and neutral particles, considering nucleon collision line

23 p3331 A72-44436

SECONDARY EMISSION

Electron motion equations for threshold input signal of M type amplifiers with secondary emission cathode in interaction space

02 p0190 A72-11571

Biological efficiency of secondary radiations from 70 GeV protons interaction with target, discussing dose dependences and restoration process relative rates

[CERN-71-16]

02 p0161 A72-12057

Air ionization, secondary electron emission and Compton currents at W-Be interfaces under Co 60 gamma radiation

03 p0403 A72-14083

Velocity dependence of ionization cross section of Ar, Kr and Xe during thermal energy metastable neon atoms impact, obtaining secondary electron ejection efficiency

04 p0553 A72-15640

Secondary particles in pion-nucleon and coherent interactions, measuring momentum from multiple Coulomb scattering

06 p0870 A72-17272

Electron beam welding induced secondary X rays observation with pinhole X ray movie camera to determine beam-metal interactions during penetration

07 p0997 A72-20003

Solar cosmic ray energy spectrum from calculation of secondary emission neutron component generation multiplicities

08 p1225 A72-20723

Auroral emission rates for various transitions from cross section data and secondary electron spectra measurements

08 p1227 A72-21114

Gas rotation temperature measurement by means of high energy electron beam probe with allowance for secondary electrons

[ONERA, TP NO. 1069]

10 p1480 A72-24222

Calibration model for UV stellar photometer using secondary electron conduction/SEC/vidicon

11 p1631 A72-25684

Secondary molecular ion emission of Li as function of atoms number

11 p1701 A72-26506

Graphite band structure investigated by secondary electron emission, observing electron transitions to higher excited states

15 p2260 A72-31856

Secondary electron emission and molecule passage during in-depth interaction of high energy molecular beam with thin gold foil

16 p2430 A72-33067

SECONDARY INJECTION

Solar cosmic ray energy spectrum from calculation of secondary emission neutron component production multiplicities

19 p2852 A72-38351

Investigation by the method of secondary ion-ion emission of the initial phase of the formation process of a silver vacuum condensate on a nickel substrate

21 p3068 A72-40960

Energy and angular distributions of secondary electrons resulting from ionizing collisions of electrons with helium and krypton.

21 p3088 A72-41493

Simultaneous recording of laser radiation and signal related to secondary processes, using ruby luminescence for oscillograph triggering

22 p3185 A72-42274

Controlled secondary electron emission and some possibilities for its application in particle detectors

23 p3316 A72-44159

High energy inelastic interactions in cosmic ray showers from Wilson chamber and ionization calorimeter observations, noting secondary particles occurrence dependence on primary energy

23 p3330 A72-44406

High energy nucleon inelastic collision characteristics dependence on secondary particle energy and meson velocity, using Wilson chamber measurement

23 p3291 A72-44445

Mathematical model for secondary electron production fall-off, calculating ionization cross section from electron distribution

24 p3400 A72-45592

SECONDARY FLOW

Two dimensional transient inviscid flow field from secondary injection in missile control, describing distribution with artificial viscosity finite difference method

01 p0097 A72-10940

Ejector nozzle design criteria, analyzing primary/secondary flow interactions and diameter, spacing and temperature ratio effects

[AIAA PAPER 72-46]

05 p0609 A72-16963

Navier-Stokes equations numerical solution for viscous incompressible fluid in circular cylinder with rotating top disk, computing secondary flow at Reynolds numbers to 400

06 p0802 A72-18526

Correlation for Prandtl number effect on laminar forced convective heat transfer with secondary flow

07 p1100 A72-19629

Secondary gas flow effect on energy transfer distributions from plasma torches, obtaining radial distributions of current and energy flux

07 p1046 A72-20546

Secondary flow types and measurement in axial flow compressor cascades, discussing energy losses

09 p1260 A72-22633

Secondary losses reduction procedure in axial flow turbine stages, using boundary layer fences on blades profile suction side

09 p1374 A72-22634

Centrifugal turbomachine diffuser with high enlargement area compared with logarithmic spiral types, discussing boundary layers, secondary flow, shapes and aerodynamic parameters

10 p1463 A72-23747

Secondary flows effect on turbulent longitudinal velocity distribution in square ducts, using Navier-Stokes and continuity equations

10 p1463 A72-23864

Fully developed laminar flows in ducts with secondary motions, considering annuli with rotating core, pipe with swirl generator and straight rectangular duct

10 p1463 A72-23865

Secondary flow measurements in rotating ducts, obtaining pressure distributions and cross-flow velocities

[ASME PAPER 72-GT-17]

11 p1569 A72-25616

Incompressible viscoelastic isotropic fluid stability in Couette flow, discussing physical parameters effect on critical Reynolds number and cells shape of secondary flow

12 p1797 A72-27169

Secondary flows in ducts of square cross-section.

19 p2789 A72-38795

Resonant growing standing internal gravity waves, considering transient behavior, numerical results, break due to local gravitational instability, maximum amplitude and secondary flow generation

21 p3048 A72-40648

Investigation of the influence of nonuniform conditions at the inlet and of secondary flows on the flow parameters in arbitrarily twisted channels

21 p3045 A72-41067

An experimental study of flows in planar nozzles.

[ASME PAPER 72-FLCS-2]

23 p3249 A72-44066

SECONDARY FRONTS

U FRONTS (METEOROLOGY)

SECONDARY HARMONIC GENERATION

U HARMONIC GENERATIONS

SECONDARY INJECTION

Solid propellant rocket engine thrust vector control by four movable exhaust nozzles, nozzle exit cone secondary injection and flexible bearing nozzle

13 p2026 A72-28928

SECONDARY RADAR

- Ground secondary radar interrogator system using monopulse technique for bearing measurement, accuracy and interference reduction 04 p0493 A72-15523
- Secondary surveillance radar systems design and planning for ATC application 13 p1917 A72-28698
- ATC services configuration with secondary surveillance radar and primary radar data acquisition system, discussing signal processing by automated decoder 21 p3080 A72-40288
- Air traffic density effect on secondary surveillance radar operation in ATC for aircraft identification and position determination, proposing selective address system 21 p3080 A72-40289

SECONDARY WAVES

U S WAVES

SECRETIONS

- NT ENDOCRINE SECRETIONS
- NT HORMONES
- NT INSULIN
- NT SWEAT

SECULAR PERTURBATION

U LONG TERM EFFECTS

SECURITY

- Earth satellite legal aspects under space treaty, discussing orbiting military remote sensing devices, national obligations and security issues 07 p1105 A72-19476

SEDATIVES

- Hypnotic drug use effect on pilot performance and flight safety, using glutethimide, flurazepam and placebo in double blind study 07 p0933 A72-20188

SEDIMENTARY ROCKS

- NT CARBONACEOUS ROCKS
- NT SHALES

Sedimentary rocks remote multispectral analysis by aerial data covering UV to microwave spectral regions 02 p0209 A72-11788

Fluid inclusions in quartz crystals from calcite in Precambrian metasedimentary rocks in South-West Africa 07 p0975 A72-18907

SEDIMENTS

NT GRAVELS

NT SANDS

Sedimentology of Apollo 11 and 12 soils, investigating grain size distribution 03 p0440 A72-14325

Constant cosmic spherule influx rate measured on quaternary deep sea sediments 05 p0722 A72-17153

Geochemistry of amino acid enantiomers - Gas chromatography of their diastereomeric derivatives. 19 p2762 A72-38224

SEEBECK COEFFICIENT

U SEEBECK EFFECT

SEEBECK EFFECT

Thermoelectric generators theory, design and performance characteristics, discussing Seebeck, Peltier and Thomson effects 15 p2182 A72-31375

A thermal oscillator using the thermo-electric /Seebeck/ effect in silicon. 18 p2667 A72-36978

SEEDING (INOCULATION)

U INOCULATION

SEEDS

Chromosome aberrations and germination speedup in Soyuz 5 carried oat seeds, noting stimulating effect by preflight ethylenimine treatment 05 p0623 A72-16777

Cytological, genetic and physiological analyses of space flight factors effects on seeds and plants aboard Zond 5 probe 15 p2186 A72-31828

Chromosome aberrations and germination speedup in Soyuz 5 carried barley seeds, noting stimulating effect by preflight ethylenimine treatment 17 p2505 A72-35280

Analysis of vegetable seedlings grown in contact with Apollo 14 lunar surface films. 17 p2505 A72-35925

Influence of temperature shocks on seed formation after irradiation of pollen from *Tradescantia paludosa*. 19 p2761 A72-38642

Influence of Cosmos 368 space flight conditions on radiation effects in yeasts, hydrogen bacteria and seeds of lettuce and pea. 23 p3254 A72-43390

SEEKERS

U HOMING DEVICES

SEEPAGE

Hydraulic analogy application to heat conduction problems, considering seepage and network pipe flow models for complex heat flux phenomena representation 01 p0145 A72-11174

SEGREGATION

U SEPARATION

SEISMIC ENERGY

Crab Nebula and Vela pulsar constant elastic energy density contours, discussing micro and macroquakes 06 p0886 A72-18095

Mathematical model of seismic isolation block and pneumatic suspension for inertial guidance component tests to describe design factors effects on vibration behavior [AIAA PAPER 72-844] 20 p2950 A72-39085

Pneumatically isolated test platform local gravity vector active control to investigate seismic level disturbance effects on precision inertial components evaluation [AIAA PAPER 72-843] 20 p2923 A72-39086

SEISMIC WAVES

NT LOVE WAVES

NT MICROSEISMS

NT RAYLEIGH WAVES

Elastic dislocation theory of Chandler wobble excitation by earthquakes 09 p1299 A72-22802

Long range air coupled seismic wave recording from Apollo landings, using microphones and seismographs arrays 11 p1690 A72-26514

Seismic wave prediction from high altitude nuclear detonation, using ground reflected spherical shock parameters 11 p1627 A72-26519

Ultrasonic signal propagation with distance along steel sphere surface compared with lunar seismic signal, discussing surface dent and lunar crater effects 13 p2035 A72-28619

Moonquakes and meteorite and manmade impacts as sources of seismic signals detected by Apollo lunar seismic stations 13 p2037 A72-28988

Laboratory studies on seismic and electrical properties of the moon. 18 p2724 A72-36282

Velocity structure and properties of the lunar crust. 18 p2725 A72-36292

Quasi-static loading of the earth by propagating air waves. 22 p3172 A72-42468

SEISMOGRAPHS

NT LUNAR SEISMOGRAPHS

Holographic weak signal enhancement technique in presence of strong noise for seismic and oceanographic applications 07 p0992 A72-20563

Improvements in the wide-band vertical quartz torsion accelerometer. 18 p2689 A72-36030

Three dimensional seismic monitoring system developed from inertial guidance gyroscopes and accelerometers, noting pole shift observation, tilting during earth tides and earthquakes forecasting [AIAA PAPER 72-840] 20 p2923 A72-39088

Linear and rotational quartz fiber accelerometers suitable for geophysical and inertial use. [AIAA PAPER 72-822] 20 p2923 A72-39103

SEISMOLOGY

NT MOONQUAKES

Seismic and underwater effects of sonic booms, comparing theory with experiments 08 p1162 A72-21907

Viking Lander seismic investigations for Martian tectonic activity, internal structure and composition, core size and conditions of formation 10 p1540 A72-24389

ALSEP seismic records from Apollo 12 lunar module and Apollo 13 rocket stage impact, showing ringing phenomenon due to sphere curvature-caused energy dissipation 13 p2035 A72-28618

Moonquakes and meteorite and manmade impacts as sources of seismic signals detected by Apollo lunar seismic stations 13 p2037 A72-28988

Lunar interior structure and crust composition from artificial impact data recorded by Apollo seismometers 15 p2314 A72-32377

Relation between tectonic processes on the earth and moon 19 p2860 A72-37958

Continuous natural background sources of microseismic motions due to atmospheric and ocean loading, wind, flowing water and local disturbances [AIAA PAPER 72-819] 20 p2915 A72-39104

SEISMOMETERS

U SEISMOGRAPHS

SEIZURES

Rat central nervous system oxygen toxicity seizure susceptibility relation to circadian rhythms 04 p0472 A72-14867

Hydrogen peroxide formation relationship to lipid peroxidation and seizures in brain during high pressure oxygen exposure 12 p1766 A72-28300

SELECTION

NT PERSONNEL SELECTION

NT PILOT SELECTION

Exercise capacity in a population of domestic fowl - Effects of selection and training. 17 p2499 A72-34726

SELECTIVITY

Selective attention and short term memory encoding, using tachistoscopic visual display arrangements of capital letters 02 p0166 A72-11549

Compensation of nonlinear selectivity distortions in radio receivers with broadband preamplification stages, noting circuit diagrams for preselector correctors 13 p1927 A72-28412

Selectivity evaluation for regenerative amplifiers of complex design 13 p1929 A72-28898

Optimal selectivity digital recorders for meteor trails radar observations, considering input process quantization rate and spectral width selection 13 p1929 A72-29031

Design and analysis of transistorized, selective HF amplifiers with allowance for sensitivity properties 17 p2532 A72-35978

Preliminary frequency selection during matched signal filtering 21 p3021 A72-40941

SELECTORS

The effect of an interferometer selector on the spectrum of the characteristic frequencies of a dispersion resonator 22 p3176 A72-42245

SELENIDES

NT CADMIUM SELENIDES

NT GALLIUM SELENIDES

NT ZINC SELENIDES

Cold pressed powdered boron nitride, Mo, W, Nb disulfides and diselenides, investigating thermal dissociation in He by X ray analysis 03 p0380 A72-13551

Epitaxy and vacancy structure of TiSe with type B8 ordering 10 p1495 A72-24077

Optical weak absorption measurements in amorphous semiconductors As₂S₃, GeAs and GeSbSe₂, showing dependence on band gap localized states 13 p2022 A72-29629

Study of the mechanism of radiative recombination in vitreous and monocrystalline arsenic selenide. 19 p2844 A72-37684

Fundamental infrared lattice vibration spectrum and the laser-excited Raman spectrum of MoSe₂. 22 p3185 A72-42321

Antifunction and electrical properties of WSe₂-NbSe₂ quasi-binary alloys 23 p3299 A72-43292

Investigation of the fast recombination channel in InSe during excitation by neodymium laser light 23 p3295 A72-43339

SELENIUM

Thermodynamic solids theory generalized for internal strains in perfect non-Bravais crystals, applying to trigonal Se and Te structure 04 p0562 A72-15470

Se and Te additions effects on low carbon steels formability and machinability from metallurgical examination and workability tests 07 p0994 A72-19480

Sealed-off He-Se laser construction and performance, comparing with He-Cd, He-Zn and He-Ne lasers 08 p1182 A72-21437

Effective current carrier electron and hole lifetime in amorphous photodiodelectric semiconducting Se and As-Se films with randomly distributed capture levels 09 p1366 A72-22418

Thin Se film for recording mode structure of 10.6 micron carbon dioxide laser emission, describing optical equipment 11 p1652 A72-26795

SELENIUM COMPOUNDS

NT CADMIUM SELENIDES

NT GALLIUM SELENIDES

NT SELENIDES

NT ZINC SELENIDES

Gas phase photodetachment of electron from selenide ion, determining affinity and spin-orbit coupling constant for SeH negative ion 16 p2360 A72-33580

Effect of selenium on the formation of the electrical potential in the retina 22 p3148 A72-41898

SELENOGRAPHY

Two-layer lunar model from variable viscosity media isostatic processes selenological investigation, suggesting hard top crust and deeper asthenosphere 04 p0569 A72-14505

Lunar volcanology, discussing domes, crater chains, halos, sinuous rills, mare wrinkle ridges, dark smooth level material and ring dike-like structures 04 p0581 A72-15619

Selenographic coordinate system development, using lunar craters as reference point selection criteria 07 p1067 A72-18869

Copernicus rays and ejecta blanket V-features form and distribution, suggesting association with satellite craters of secondary impact origin
07 p1067 A72-18872

Optimal method selection for astronomical measurements on lunar surface, discussing instrumental and technical difficulties with selenographic longitudes and latitudes determination
08 p1231 A72-21130

Determination method for selenographic coordinates of points on lunar surface, discussing astronomical observations from moon
08 p1231 A72-21131

Selenodetic catalog centers mutual positions determination from lunar near side hypsometric charts
11 p1724 A72-26911

Comparative study of lunar objects selenodetic coordinates catalogs based on continuous media deformation theory
13 p2037 A72-28987

Determination of mutual orientation in Euler angles for nine selenodetic catalogs
19 p2863 A72-38076

A catalog of selenographic coordinates of points of the libration zones and the reverse side of the moon
21 p3114 A72-41767

A new unified system for designating objects on the lunar surface
21 p3114 A72-41780

Comments on the figure of the moon from Apollo landmark tracking.
22 p3226 A72-42534

SELENOLOGY
NT LUNAR CORE
Lunar gravitational potential determination from Stokes and selenocentric constant
03 p0440 A72-14326

Lunar gravitational field, relief and internal structure, suggesting two layer model and crust thickness change relation to field characteristics
06 p0881 A72-17926

Papers on moon geology and physics covering lunar volcanic lava flow, water and crater origin
06 p0886 A72-18216

Lunar center of mass position with respect to visible hemisphere physical surface calculated from photogrammetric analysis and Lunar Orbiter 1 data
08 p1232 A72-21158

Lunar interior thermal history discussing mathematical models for radioactive heat source, initial conditions, temperature distribution and time dependent fractionation
12 p1870 A72-27336

Terrestrial volcanic lava conduits origin and development association with lunar maria channels and sinuous rills
13 p2037 A72-28992

Lunar gravitational field, relief and internal structure, suggesting two layer model and crust thickness change relation to field characteristics
18 p2730 A72-37151

Lunar center of mass position with respect to visible hemisphere physical surface calculated from photogrammetric analysis and Lunar Orbiter 1 data
20 p2969 A72-39263

SELF ABSORPTION
Galactic center region neutral hydrogen self absorbing cold cloud, discussing matter, spatial and radial velocity distributions and cloud temperature and density
12 p1867 A72-27208

Radio sources with straight spectra and spectral index of 0.3, noting relationship to self absorption, electron energy distribution and cosmological evolution
16 p2457 A72-33685

Slab band absorbance for molecular gas radiation.
23 p3316 A72-44327

SELF ADAPTIVE CONTROL SYSTEMS
Self adjustment for time optimal nonstationary system control, developing algorithm for flutter
02 p0196 A72-11675

Self adaptive controlled robot velocipedist, discussing speed control and equations of motion
04 p0505 A72-14984

Adaptive control system synthesis by steepest descent method, obtaining algorithms for parameters self adjustment loop construction
06 p0795 A72-18661

Optimal algorithms for analysis, synthesis and correcting filter of self adaptive control systems
13 p1936 A72-29154

Self adaptive two channel iteration servosystems for input reconstruction by successive approximations, determining signal and noise error operators
13 p1936 A72-29155

Linear and nonlinear continuous self adaptive frequency converter filters with minimum error under SNR change
13 p1936 A72-29156

Statistical superoptimal search strategies of self optimizing systems, applying to one dimensional step type and multiextremal problems
13 p1936 A72-29160

Redundant and nonredundant self adaptive systems reliability, discussing statistical random process characteristics
13 p1936 A72-29170

Optimal viability of complex system with ambient medium interaction, using stochastic game theory
13 p1936 A72-29174

Dynamic programming for optimal statistical control of self adaptive systems with fixed learning experiments, noting structural constraints for suboptimality
13 p1965 A72-29178

Hill-climbing controller for plants with any dynamics and rapid drifts.
18 p2673 A72-36819

Self-tuning and self-programming antenna matching devices for the frequency range 1.5-30 MHz and their application
21 p3031 A72-40538

Readjustment algorithm for searchless self adaptive control system with reference standard by direct Liapunov method
22 p3205 A72-42186

Analytical design of adaptive systems with stabilized dynamic characteristics
23 p3276 A72-43783

A learning approach to the parameter-adaptive self-organizing control problem.
23 p3277 A72-44198

SELF ALIGNMENT
Self calibration of surveying cameras for three dimensional object photography without control points, using homologous ray method
06 p0815 A72-17754

Time optimal self alignment of inertial platforms using gyros and accelerometers with Kalman-Bucy filter
07 p0989 A72-20279

High accuracy north-seeking course-attitude inertial reference system for air navigation, using platform unit and automatic alignment for Schuler tuned operation
07 p0990 A72-20282

Readjustment algorithm for searchless self adaptive control system with reference standard by direct Liapunov method
22 p3205 A72-42186

SELF CONSISTENT FIELDS
Formaldehyde photoionization and absorption spectrum measurements in vacuum UV region, using single configuration self consistent field procedure for Rydberg states and model
03 p0321 A72-13856

Hf circularity polarized field strength and plasma density self consistent stationary distribution in weakly inhomogeneous constant magnetic field
04 p0558 A72-15175

Computer models for simulating self consistent collisionless stellar systems evolution under gravitational field
06 p0885 A72-18081

Statistical hypothesis of Van Allen radiation belts, using Vlasov equations for self consistent plasma fields
07 p1055 A72-18805

Self consistent problem solution for planar magnetron diode with low cathode field and charge density not exceeding density of Brillouin zone
08 p1142 A72-21703

Self consistent collisionless theory of turbulent low Mach number ion-acoustic shocks, noting resistive heating
09 p1360 A72-22872

Variational and statistical methods for adiabatic electron plasma with self consistent field interaction in terms of Lagrange, Hamilton and Liouville formalization
12 p1850 A72-27185

Laser quantum theory for single mode emission fluctuations and instability region with high density of excited atoms, noting self consistent field effects
20 p2931 A72-39376

Magnetic neutral sheet model in terms of self consistency between current and tail field in reversal region
20 p2919 A72-39548

The self-consistent test-particle approach to relativistic kinetic theory.
20 p2955 A72-40013

Coupled multiconfigurational self-consistent-field method of atomic dipole polarizabilities. I - Theory and application to carbon.
21 p3087 A72-40776

Self-consistent description of the magnetotail current system.
22 p3172 A72-42429

Self-consistent electromagnetic waves in relativistic Vlasov plasmas.
24 p3430 A72-45569

SELF DEPLOYING SPACE STATIONS
U SELF ERECTING DEVICES
U SPACE STATIONS
SELF DIFFUSION
U DIFFUSION

SELF ERECTING ANTENNAS
U ANTENNAS
U SELF ERECTING DEVICES
SELF ERECTING DEVICES
Flexible rolled-up solar array /FRUSA/ operational performance from spaceborne accelerometers, strain gages and temperature sensors telemetered data, noting damage-free extension-retraction exercises
[AIAA PAPER 72-510] 13 p2051 A72-28952

SELF EXCITATION
Motional feedback systems comparison for ultrasonic transducers operated as resonant emitters, describing circuitry for self excitation
01 p0070 A72-11019

Harmonium reed self excited oscillation mechanism, describing flow visualization, jet instability potential flow and aerodynamic forces
01 p0002 A72-11232

Geomagnetic dynamo theory postulating magnetic field by self excitation due to electric currents within earth core
02 p0220 A72-12086

Time and coordinate dependence of magnetic field for steady symmetric flows of compressible conducting fluid at large Reynolds numbers, investigating self excitation conditions
03 p0398 A72-14001

Ionization waves linear theory for low pressure noble gas strong current column, showing self excitation limit and temperature dependence of energy loss rate
03 p0400 A72-14351

Gunn diode microwave oscillator with moving reflector as self-excited mixer and load variation detector, analyzing performance by I-V characteristics model
04 p0497 A72-17113

Rotary self excitation of helical flows in incompressible liquids, using Navier-Stokes equation
06 p0798 A72-17730

Cylindrically symmetrical low viscosity fluid distortion and homogeneous spiral flow stability under rotational self excitation
06 p0799 A72-17981

Autoparametric excitation in relation to divergence and flutter of autonomous mechanical cantilever systems under nonpotential circulatory forces
06 p0851 A72-18726

Parametric oscillations of nonlinear systems prone to self excitation, using asymptotic method
08 p1206 A72-21243

Rotary self excitation of helical flows in incompressible liquids, using Navier-Stokes equation
11 p1614 A72-25333

Tropical hurricane model describing initial whirlwind and self exciting wind velocity development and dependence on ocean surface temperature
11 p1682 A72-26879

Self excited oscillator using emitter follower circuit and distributed active RC phase shifter network
13 p1927 A72-28404

Rotating machines self excited lateral vibration and instability avoidance and identification
[ASME PAPER 72-DE-21] 14 p2167 A72-30865

Two cavity self exciting SHF microwave oscillator with resistance coupling through low Q-factor resonant diaphragm, noting frequency stability
14 p2090 A72-31121

Nonlinear oscillation systems mathematical model, determining periodic mode parameters, self excitation and damping mechanisms by point mapping method
14 p2133 A72-31126

Nonlinear self excited oscillations with negative hysteresis in automatic control systems
14 p2091 A72-31127

Quasi-conservative optimal nonlinear self excited oscillation systems theory for automatic control, telemechanics and computer applications
14 p2133 A72-31130

Nonlinear approximation of slowly changing standing waves in self excited parametric oscillators with distributed and bulk structures
14 p2090 A72-31131

Self excited increasing thermal wave generation models, using hyperbolic wave heat conduction and thermoelasticity equations
15 p2336 A72-32285

Automatically controlled delay in self-excited pulsating systems based on artificial muscles
19 p2761 A72-38464

Self-excited parametric oscillations at the second harmonic in a parametric system with a triple-post ferromagnetic core
19 p2774 A72-38586

Frequency distortions of signals in frequency-modulated self-excited oscillators
21 p3032 A72-40782

Multiloop LC oscillators with negative resistance and nonlinear capacitances
23 p3271 A72-43838

Excitation of oscillations in transistor oscillators
23 p3271 A72-43840

Self-excitation of oscillations in a system consisting of a delay line, inductance, and tunnel diodes
24 p3384 A72-44895

SELF FOCUSING

Self focusing effect of Q switched single mode ruby laser emission in CdS crystal, noting 60 kw minimum threshold power

03 p0369 A72-14064

Thin electrostatically self focusing electron streams in mercury vapor, analyzing energy distributions of ions and electrons ejected radially from beam

04 p0554 A72-14407

Laser produced spark plasma, calculating threshold conditions for onset of stimulated scattering process and self focusing

04 p0559 A72-15346

Self focusing of electromagnetic waves in isotropic plasma, investigating nonlinear relaxation processes

04 p0489 A72-15391

Self focusing of laser amplifier beam with Gaussian transverse intensity profile, discussing sample length and beam diameter, convergence and divergence [AD-741092]

07 p0941 A72-19240

Differential equation solution for plane self focusing and one dimensional self modulation of waves interacting in nonlinear media

08 p1209 A72-21718

Thermoelastic stresses in solid transparent isotropic homogeneous dielectric under self-focused laser beam

11 p1648 A72-26334

Transparent dielectrics destruction by mode-locked laser ultrashort pulses, discussing filamentary defect presence indication of radiation self focusing

12 p1853 A72-27068

Optical waveguide maximum length determination based on self focusing pulse channel growth rate relationship to striction nonlinearity

12 p1823 A72-27619

Spark interferometry of plasma filaments in gases from self focused single mode ruby laser beam

12 p1852 A72-27869

Spark interferometry of plasma filaments in gases from self focused single mode-locked ruby laser pulses

16 p2439 A72-33978

Oriental Kerr effect direct observation via birefringence relaxation time measurement in self focusing region of mode locked Q switched laser picosecond pulses

17 p2561 A72-34190

Focusing of intense electromagnetic waves in ducts with saturating nonlinearity.

18 p2659 A72-36293

Galactic center emitted gravitational wave discrepancy with astrophysics explained by self focusing and trapping concepts

18 p2729 A72-36985

New proposition of the mechanism of self-focusing of laser beams in semiconductors.

19 p2811 A72-37945

Filaments formation behind nonlinear focus and frequency shift in transient self focusing of light beam in medium with given time dependent permittivity

20 p2953 A72-39502

Anatomy and thermal history of laser self-focusing damage tracks in glass.

21 p3062 A72-40245

Explanation of limiting diameters of the self-focusing of light.

21 p3062 A72-40337

Study of the thermal self-focusing of electromagnetic waves in a plasma

22 p3211 A72-42652

Self focusing effect on wave beam propagation in optical lens waveguides, discussing system nonlinearity

22 p3186 A72-42656

Influence of steric effects and compressibility on nonlinear response to laser pulses and the diameters of self-trapped filaments.

23 p3296 A72-43873

Transparent dielectrics destruction by mode-locked laser ultrashort pulses, discussing filamentary defect presence indication of radiation self focusing

24 p3432 A72-45721

SELF INDUCED VIBRATION

NT PANEL FLUTTER
NT SUBSONIC FLUTTER
NT SUPERSONIC FLUTTER
NT TRANSONIC FLUTTER

One dimensional unsteady flow in turbine engines rotating and static vane cascades, discussing vibrations propagation

02 p0202 A72-11584

Three dimensional velocity field excitation by thin airfoil vibrations in supersonic flow, deriving function in semispace to satisfy boundary constrained wave equation

06 p0756 A72-18111

Periodic vortex formation and shedding in flows past bluff bodies, considering cylinder forced and self excited vibrations and interaction with wake

18 p2679 A72-36389

Electromagnetic self induced vibrations in homogeneous unbounded electron beam moving with time dependent velocity, noting longitudinal and transverse wave generation

19 p2842 A72-38527

SELF LUBRICATING MATERIALS

Plasma jet technique for self lubricating antifriction Ni, Sn or Cu coatings for MoS₂ particle oxidation protection

04 p0527 A72-15664

Filler particles orientation effects on plastic bearing materials friction and wear properties, discussing experimental testing methods

06 p0836 A72-18595

Self lubricating polytetrafluoroethylene and polyimide composites transfer film formation tests, studying film thickness and uniformity

06 p0824 A72-18596

Polyarylates, polyimides and thermosetting polymers role in sliding friction of self lubricating plastics, noting temperature effects

06 p0837 A72-18599

Properties of internally lubricated glass-fortified thermoplastics for gears and bearings.

19 p2822 A72-37896

Book - Solid lubricants and self-lubricating solids.

21 p3073 A72-41529

SELF LUBRICATION

Hydrodynamic journal gas bearing with herringbone grooved portion for self generating air supply pump hydrostatic starting and stopping

[ASME PAPER 71-WA/DE-7]

05 p0664 A72-15944

Modified PV criterion for self lubricated dry bearings, observing bearing length and diameter effect on steady state temperature

06 p0823 A72-18594

Self lubricating materials for maintenance-free clocks antifriction bearings, discussing friction and wear behavior

09 p1319 A72-23562

SELF ORGANIZING SYSTEMS

Mathematics for pattern recognition, discussing perceptions, combinatorics and statistics, feature selection, cybernetic methods and fuzzy sets

01 p0034 A72-10465

Self organizing adaptive aircraft control system with C criterion pitch axis performance and failure compensation

03 p0337 A72-12920

Biological self replicative description and function in chemical reaction networks in search of life origin from non-life-like matrix

04 p0482 A72-14756

Parameter adaptive self organizing control of linear discrete time systems, presenting stochastic approximation algorithms for feedback systems identification

06 p0791 A72-17306

Self organizing control system for optimal performance of navigation instruments, using adaptive algorithm for statistical error filtration

13 p1996 A72-29157

Unknown plant self organizing time optimal controller with variable switching surface and adaptation logic net, noting effectiveness by computer simulation

21 p3037 A72-40639

A learning approach to the parameter-adaptive self-organizing control problem.

23 p3277 A72-44198

Problems of complex object modeling based on heuristic self-organization

24 p3376 A72-45509

SELF OSCILLATION

Random background noise effect on nonlinear self oscillation envelope passage time moments, discussing relationship between amplitude and frequency stabilities

01 p0035 A72-10032

Output power, efficiency and fundamental frequency resistance of Gunn microwave self oscillator in single and multiresonant mode

01 p0037 A72-10638

Harmonium reed self excited oscillation mechanism, describing flow visualization, jet instability potential flow and aerodynamic forces

01 p0002 A72-11232

Self sustained oscillations of mechanical system with infinite number of degrees of freedom, considering application to diffusion in porous medium

02 p0258 A72-11496

Pneumatic hammer /self oscillation/ in gas lubricated externally pressurized annular thrust bearing, presenting stability maps

[ASME PAPER 71-LUB-U]

02 p0234 A72-11527

Mode locked oscillation in ring cavity Nd glass laser, showing satellite pulse and spectral broadening due to self phase modulation

02 p0238 A72-12203

Self oscillations and drift motion of gyroscopic integrator of linear accelerations under hf vibrations, assuming ideal relay gimbal compensation

02 p0231 A72-12567

Frequency fluctuations in nonlinear self oscillating system in presence of periodic nonstationary random noise effects

02 p0195 A72-12586

Describing function method for nonlinear systems under stochastic input, considering statistical optimizations/linearization and self oscillation under noise

03 p0337 A72-13074

Self oscillating system resonant vibrations excitation for fatigue tests, determining frequency and amplitude relationship

03 p0443 A72-13456

Self oscillating dc-to-dc converters performance and design, considering switching frequency, duty cycles, line and load regulation and peak-to-peak ripple

04 p0465 A72-14487

Self oscillating system stability under parametric excitation and harmonic force for large and small natural frequency mismatch

04 p0549 A72-15046

Dynamic analysis of vertical rotor rotating in elastic sliding bearings, analyzing precession stability and self oscillation zone

04 p0594 A72-15748

Spontaneous oscillations generation on transverse surface wave, discussing experimental realization with semiconducting CdS single crystals

05 p0626 A72-16282

Solar self oscillation interference from magnetographic observation, noting power concentration in space and frequency

05 p0718 A72-16502

Controlled motion dynamics of spacecraft performing maneuvers, applying point transformation to third-order nonlinear system moving about center of mass in lateral motion

05 p0730 A72-17029

Higher order nonlinear autonomous oscillation system limit cycle and stability determination by numerical solution based on Andronov point transformation and Liapunov theory

06 p0838 A72-17377

Self-excited lf oscillations in inhomogeneous rf collisional plasma, determining frequency as function of tube length, axial magnetic field and gas neutral pressure

06 p0857 A72-17533

Vertical shaft stability on elastic sliding bearings, considering passage through self oscillation zone

06 p0894 A72-17683

IMPATT diode avalanche region microwave self oscillation mechanism explanation by cavity resonator and feedback theories

06 p0787 A72-18383

Nonlinear self excited oscillations in uniformly distributed oscillators interacting with traveling transverse or surface waves of elastic body

06 p0849 A72-18698

Nonlinear self oscillation solution for systems with two degrees of freedom, comparing with harmonic linearization method for error of small parameter method

06 p0851 A72-18721

Dielectric substrate layer surface wave parasitic resonance effects on microstripline waveguide conductor

07 p0958 A72-18855

Amplifier amplitude characteristic nonlinearity effect on dynamic properties of autooscillatory temperature controller

07 p0981 A72-18926

IMPATT diode microwave oscillator stabilized by two external resonant circuits, investigating self oscillation characteristics

08 p1138 A72-20745

Self excited oscillations and transient responses of spacecraft stabilization relay system with delayed feedback, analyzing time delay effects in actuator circuit

08 p1241 A72-21176

Thomson autooscillatory systems synchronization and small external sinusoidal emf effect with hard and soft bounding of amplitude deviations

08 p1142 A72-21769

Frictional stick-slip autooscillations suppression by resonance effect during forced vibration in normal direction

08 p1181 A72-22181

LF self oscillation processes associated with burning powders, showing origin in thermal relaxation instability in heated condensed phase layer

09 p1411 A72-22883

Russian monograph on self oscillatory noise generation during gas jet ejection covering single, parallel, supersonic, flat and cylindrical jets stability

11 p1617 A72-26066

Ridge dimensions determination and causes of self oscillation in solid surface layers deformation under sliding friction

12 p1817 A72-28182

Laminar channel flow stability loss dependence on Reynolds number and wave number, discussing conditions for separated flow self oscillations

13 p1941 A72-28765

Meteorological rising balloon systems accuracy limitation, noting response to wind field changes, aerodynamic self oscillations and radar tracking errors

13 p1990 A72-28817

Small parameter method for analysis of encounter waves nonlinear self oscillations in ring gas laser, noting periodic energy transfer

14 p2111 A72-31104

Amplitude and frequency characteristics of avalanche diode microwave oscillator loaded with resonant circuits, noting Q value effect on self oscillations 14 p2089 A72-31109

Self oscillations of microwave autodyne oscillator loaded by two resonant cavities, noting radio spectroscopic applications 14 p2089 A72-31110

Nonlinear autooscillation systems forced vibration under random perturbations, calculating dynamic processes by statistical linearization 14 p2132 A72-31114

Ferroresonant circuit with inductor, resistor, nonlinear ferrocapacitor and voltage source, deriving oscillation stability condition 14 p2090 A72-31119

Van der Pol oscillator periodic pulling behavior under weak perturbation near natural frequency, analyzing Fourier frequency spectrum 14 p2132 A72-31122

Van der Pol oscillator acted upon by weak random noise, evaluating oscillations envelope dispersion from probability density function and phase derivation 14 p2132 A72-31123

Nonlinear oscillation systems mathematical model, determining periodic mode parameters, self excitation and damping mechanisms by point mapping method 14 p2133 A72-31126

Flow-plasma system described by hydrodynamic equations, comparing self oscillatory process features with other systems 14 p2141 A72-31129

Nonlinear processes in oscillatory systems with semiconductor diodes, calculating amplitude and phase characteristics in steady state and transient conditions 14 p2090 A72-31133

Van der Pol and nonlinear parametric oscillators fluctuations due to random noises analyzed by averaging method and discrete Markov processes 14 p2133 A72-31134

Frequency stabilized self-oscillating microwave up-converter with transferred electron diodes, noting maximum power output and bandwidth 16 p2369 A72-33764

Rocket body longitudinal autooscillation modes, taking into account pipeline fluid discontinuous cavitation oscillations 17 p2620 A72-34469

Frictional stick-slip autooscillations suppression by resonance effect during forced vibration in normal direction 18 p2695 A72-36238

Frequency dependent loss in self-pulsing ring laser. 18 p2697 A72-36337

Fluid transition through critical value, considering self oscillation onset mode frequency 18 p2681 A72-36663

Growth rate and frequency dispersion characteristics of drift waves in an RF collisional plasma. 18 p2716 A72-36924

On the performance and design of self-oscillating dc-to-dc converters. 19 p2754 A72-37850

Natural oscillations of type-I comet tails 19 p2864 A72-38081

Contractile and muscle-like fibers and autopulsation systems for polymer engine and spring action studies 19 p2760 A72-38200

Possibility of the occurrence of alternating current in a circuit with a semiconductor sample exhibiting a recombinational instability 19 p2846 A72-38449

The locking effect in an autooscillatory system with two degrees of freedom 19 p2783 A72-38580

Self excited LC and RC oscillator networks based on FETs, discussing frequency tuning and FM methods 20 p2906 A72-38899

Self-induced pulsations in the light output from double-heterostructure injection lasers. 20 p2934 A72-39710

Problem of oscillation self-excitation due to the dependence of the normal velocity of a flame on the thermodynamic parameters of a gas 21 p3129 A72-40985

Investigation of the self-oscillations of a continuous medium arising at a stability loss in operation steadiness 22 p3164 A72-41907

Influence of fluctuations on the synchronization of frequency-modulated oscillators 22 p3159 A72-42658

Approximate harmonic linearization method of stability analysis of nonlinear periodic systems, identifying fictitious oscillations due to computation errors 23 p3277 A72-44007

Self oscillating system resonant vibrations excitation for fatigue tests, determining frequency and amplitude relationship 24 p3458 A72-44931

Constrained proportional controller dynamic equation solution on analog computer, determining limit cycle phase shift and nonlinearity effects on self oscillation parameters 24 p3403 A72-45322

SELF PROPAGATION
Sequential sulfidation and oxidation effects on sulfur self propagation in Ni-Cr alloy 05 p0677 A72-17110

SELF REGULATING
U AUTOMATIC CONTROL
SELF REPAIRING DEVICES
STAR self testing and repairing fault tolerant digital computer for outerplanet exploration spacecraft, discussing architecture, reliability analysis, software and peripheral system automatic maintenance 02 p0184 A72-11482

Time shared performance test monitor function, operation and self repair of corporate fed array radars with computer control for long time internal reliability 03 p0321 A72-13165

Fast acting nonmechanical self healing mercury fuse for high current circuit protection 03 p0335 A72-14203

SELF STIMULATION
Negative /painful/ stimulus cessation relation to emotionally positive zone activation in rat brain during self stimulation experiments 20 p2892 A72-39410

SELF SUSTAINED EMISSION
Fabrication and accelerated life tests of self sustained electron emission cathode with Cr film vapor deposition on Cu disk base 21 p2997 A72-40790

SELSYNS (TRADEMARK)
U SERVOMOTORS
SEMICIRCULAR CANALS
Human centrifuge tests for semicircular canal gyroscopic stimulation during sensory deprivation, discussing angular acceleration detection thresholds 04 p0478 A72-14865

Mathematical model for semicircular canal dynamic response to angular acceleration, emphasizing role of perilymph over endolymph in cupula displacement 07 p0917 A72-19491

Semicircular canal function correlation to thresholds, aftereffects and power functions in pilot vestibular tests 12 p1764 A72-28259

The vestibular apparatus. I - The physics and physiology of the otoliths and the semicircular canals 22 p3146 A72-42787

SEMICONDUCTING FILMS
Lf noise measurements of mercury telluride and Cd-Hg-Te semiconducting thin films using vacuum tube preamplifier and step-up transformer 02 p0268 A72-11523

Thermal effects on reversible threshold switching in amorphous semiconductor thin films involving current controlled negative resistance [AD-741462] 02 p0268 A72-12202

Preparation and electrical properties of thin cadmium antimonide and arsenide layers, comparing to single crystal films 02 p0268 A72-12281

Electric and photoelectric properties of CdTe films, describing solar cells preparation 04 p0465 A72-14593

Semiconductor film compound decomposition, chemical composition and metastable modifications presence during condensation in vacuum, discussing defect formation in crystal structure 05 p0701 A72-15752

CdTe condensed films hexagonal modification and twinning boundaries birefringence reflection, using electron microscope and diffraction analysis 07 p1047 A72-18856

Electron wave attenuation technique for current transit determination through semiconducting films with various crystal structures 09 p1284 A72-22209

Sintered cadmium sulfide films microstructure analyzed by X rays, discussing structural changes effects on dark resistance and photosensitivity 09 p1366 A72-22414

Effective current carrier electron and hole lifetime in amorphous photodiode semiconductor Se and As-Se films with randomly distributed capture levels 09 p1366 A72-22418

Recrystallization effects on thin ZnTe film structure, electrical and optical properties 09 p1367 A72-22421

Josephson dc and ac effects in plane junctions with thin semiconducting film barrier of evaporated material between two superconductors 09 p1370 A72-22800

Growth rate of semiconductor epitaxial films obtained by forced cooling from liquid phase 09 p1372 A72-23360

Nonstabilized Ni-P thin films electrical conductivity at 50-280 C, using mass spectrographic, thermal differential, X ray diffraction and electron microdiffraction analyses 10 p1495 A72-24076

SEMICONDUCTING FILMS
Electron tunneling into amorphous InSb and GaSb films, discussing effects of temperature, voltage, coevaporation doping and Cu and Au diffusion 10 p1527 A72-24874

Semiconductor film impedance vs resistivity in free space electric field 11 p1700 A72-25778

Electromagnetic properties of semiconductor diffusion films, using impedance measurements 11 p1700 A72-25779

Space charge limited current theory of thin film organic semiconductor systems, investigating energy spectrum of traps and free carrier capture kinetics 11 p1700 A72-25783

Charge carrier photoproduction and energy structure of trans-bis-indonylene /TBB/ semiconductor thin films 11 p1700 A72-25784

Oxygen chemisorption surface states effects on electrical conductivity of CdS single crystals and evaporated films 11 p1701 A72-25855

Metal surface smoothing during electrochemical dissolution prior to polishing, involving electrolyte diffusion processes or semiconductor oxide film formation 11 p1640 A72-26259

Surface piezoelectric effects of mechanical bending of noncentrosymmetric CdS semiconductor wafers 13 p2020 A72-28524

Semiconductor layers alloying by directional crystallization of compressed melts doped by contact with Ag, Ge, Te, Al and Sb films 13 p2020 A72-28564

Uniaxial elastic deformation pressure effects on electronic conduction in tetrahedrally bonded amorphous semiconducting thin films as function of temperature 13 p2021 A72-28574

Epitaxial film system parameters determination based on variational technique of computing electromagnetic waves reflectance and transmissivity in semiconductor structures 14 p2142 A72-30811

Piezoelectric substrate covered with semiconductor layers, calculating sound amplification characteristics at microwave frequencies 15 p2197 A72-31893

Structure and properties of transition layers formed in the epitaxy process. 18 p2718 A72-36340

Industrial production of high-quality active semiconductor components 18 p2670 A72-37123

Transport coefficient of multi-layer film of semiconductors. 19 p2843 A72-37401

Thickness dependence of the electrical transport properties of germanium films. 19 p2844 A72-37685

Twinning faults in epitaxial films of germanium telluride and GeTe-SnTe alloys. 19 p2844 A72-37688

Investigation of resistance strain gauges based on zinc telluride and cadmium telluride semiconductor films 19 p2845 A72-38206

Photoluminescence and photoconductivity of hole-type cadmium telluride single crystal films. 19 p2845 A72-38403

On the theory of electrical conductivity in semiconducting thin films under a high electric field. 20 p2959 A72-39216

Temperature dependence of electroconductivity and photosensitivity in CdS films 20 p2959 A72-39223

As-Te-Ge amorphous semiconductor film optical memory effect due to crystallization and re vitrification during exposure to pulsed laser beam, noting writing and erasing characteristics 20 p2961 A72-39708

Measurement of substrate impurity profile of MIS field-effect transistors. 21 p3035 A72-41488

The switching behaviour of thin films of chalcogenide glass. 22 p3214 A72-42319

Influence of nonuniformities of the built-in field on the collection efficiency of a semiconductor photocell 22 p3140 A72-43190

Strain gage resistor with BiTeSb compound semiconductor film vacuum deposited on dielectric substrate, noting high sensitivity and operation without amplifiers 23 p3287 A72-43348

Temperature and polarization dependence of arsenic sulfide single crystals and thin films intrinsic absorption edge, determining forbidden bandwidth and transitions types 23 p3324 A72-43688

Effect of substrate temperature on electrical properties of amorphous germanium films. 23 p3324 A72-44069

Reflection amplification in thin layers of n-GaAs. 24 p3385 A72-44971

- Preswitching electrical properties, 'forming,' and switching in amorphous chalcogenide alloy threshold and memory devices. 24 p3385 A72-44982
- SEMICONDUCTOR DEVICES**
- NT AVALANCHE DIODES
 - NT FIELD EFFECT TRANSISTORS
 - NT GALLIUM ARSENIDE LASERS
 - NT GERMANIUM DIODES
 - NT JUNCTION DIODES
 - NT JUNCTION TRANSISTORS
 - NT METAL OXIDE SEMICONDUCTORS
 - NT MIS [SEMICONDUCTORS]
 - NT NEURISTORS
 - NT PARAMETRIC DIODES
 - NT PHOTODIODES
 - NT PHOTOTRANSISTORS
 - NT PHOTOVOLTAIC CELLS
 - NT SEMICONDUCTOR LASERS
 - NT SILICON TRANSISTORS
 - NT THERMISTORS
 - NT THYRISTORS
 - NT TRANSISTOR AMPLIFIERS
 - NT TRANSISTORS
 - NT VARACTOR DIODES
 - NT VARISTORS
- Punch-through transit time negative resistance semiconductor device utilizing injection from Schottky barrier, deriving small signal theory for microwave impedance 01 p0042 A72-10787
- Theorems derived for bulk semiconductor device static negative differential resistance exhibition 01 p0114 A72-10790
- Mm and sub mm wave generation by semiconductor devices, showing power vs frequency plots for IMPATT, Gunn and LSA oscillator diodes 02 p0268 A72-11694
- Book on microelectronics covering integrated circuits, semiconductors, p-n junctions, transistors, Schottky and MOS structures, epitaxy, ion implantation, photomechanical operation, fabrication techniques, etc 02 p0194 A72-12574
- Hybrid circuit production, considering face down assembly of flip chip and beam lead semiconductor devices 02 p0195 A72-12608
- Oscillographically measured semiconductor element I-V characteristics plotting optimization by considering measuring instrument and sampling signal shape and frequency effects on hysteresis 03 p0330 A72-12968
- Au distribution parameters in Si semiconductor devices, using radioactive isotope diagnostic methods 03 p0400 A72-12970
- Electroacoustic magnetic and Hall effects in semiconductors in strong electric field involving phonon production by supersonic electron drift 03 p0401 A72-13088
- Book on field effect electronics covering junction and insulated gate transistors and allied devices, monolithic and film IC and design techniques 03 p0333 A72-13846
- Staged corrector, transformer and low pass filter two terminal pair matching network for resonant circuits using semiconductor elements 03 p0333 A72-13897
- Semiconductor devices potential interference and biological exposure hazards in microwave leakage field, considering shielding and filtering methods for reducing susceptibility 03 p0320 A72-14032
- Voltage contrast mode scanning electron microscopy application to defect and failure analysis of semiconductor memories 03 p0336 A72-14288
- Current transport and I-V characteristics of metal-semiconductor-metal structures with back-to-back contact interfaces 04 p0562 A72-15128
- Submillimeter waves development, discussing materials research, lasers, semiconductor and electron tube sources, system components and applications in space communication, imagery, metrology and sensing 04 p0550 A72-15591
- Anisotropic effects use in passive semiconductor magnetoplasma for submillimeter isolators and circulators based on Faraday rotation 04 p0563 A72-15600
- Low temperature Ga doped Ge bolometer for IR detection, improving sensitivity by load resistance noise elimination 05 p0662 A72-16195
- Photomultiplier operation pulsed control in semiconductor circuit for background cosmic radiation noise error minimization in atmospheric shower station 06 p0811 A72-17294
- Piezoelectric interaction between Lamb waves and charge carriers in piezoelectric plate inserted into semiconductor 06 p0865 A72-17388

- Scintillation crystal light yield dependence on emission energy in particle flux measurements with semiconductor spectrometer 06 p0816 A72-17835
- Closed magnetic fields of helical ring currents on concentric spheres surrounded by semiconductor /Tornado trap/ 06 p0863 A72-18405
- High power efficiency CW Gunn devices design and fabrication, discussing GaAs preparation techniques and device physics 06 p0789 A72-18478
- Papers on thin film and semiconductor IC and contact and connection technology 06 p0790 A72-18570
- Semiconductor device physical behavior, discussing energy levels, impurity conduction, p-n junction capacitance and bipolar and unipolar transistor I-V characteristics 06 p0790 A72-18575
- Semiconductor device IC encapsulation, thermal design, stress analysis, testing and applications 06 p0791 A72-18577
- Exponential conduction increase of semiconductors in strong magnetic fields, determining three dimensional random network resistance with percolation theory 07 p1047 A72-18918
- Two terminal semiconductor strain tensor based on evaporated piezoelectric layer for modulation of forward I-V characteristics of thin film diode 08 p1164 A72-20925
- Schottky barrier semiconductor devices characteristics, fabrication and application to pulse microwave diodes and IC elements 08 p1139 A72-21053
- Five layer resonant transparent semiconductor device structures for microwave amplifiers, reactive elements, low current rectifiers and filters 08 p1139 A72-21059
- High resolution rocket-borne X ray spectrometer with cooled lithium drifted semiconductor detectors for measuring differential X ray energy spectrum of SCO XR-1 08 p1168 A72-21518
- Magnetodiode model of intrinsic semiconductor slab under Lorentz force and double injection inducing ambipolar drift and carrier redistribution 08 p1142 A72-21746
- Quasi-elastic scattering differential cross section for nonpolarized IR radiation in electron plasma of semiconductors in strong elastic fields 09 p1366 A72-22210
- Noncontacting measurements by miniature CW Doppler radar with semiconductor microwave generator 09 p1285 A72-22691
- Static strain measurement errors due to nonstationary thermal conditions in semiconductor resistance gages 09 p1310 A72-22739
- Background noise in active semiconductor devices - Conference, Toulouse, France, September 1971 09 p1286 A72-23101
- Microbarrier mechanisms of 1/f noise for resistive materials and semiconductor devices 09 p1280 A72-23102
- Current carrier flow parameter fluctuations associated with steady state transport noise in semiconductor devices, considering generation-recombination processes, drift, diffusion and dielectric relaxation 09 p1288 A72-23125
- Avalanche carrier multiplication influence on semiconductor device p-n junction quality, discussing current distribution and I-V characteristics during avalanche breakdown 10 p1446 A72-23849
- Microelectronic IC functional logic systems design with S-type semiconductor devices, describing procedures for logic functions, shift register and directional transmission line 10 p1448 A72-24278
- Semiconductor IC transducers for electrical readout of optical radiation, mechanical stress and magnetic field strength 10 p1448 A72-24282
- Selective surfaces and coatings for solar energy conversion systems, discussing semiconductor photoconverters, white-black surfaces, cooling systems and optimal optical properties 10 p1422 A72-24315
- Semiconductor air-air heat pumps with solar cell feed current, determining hot air flow temperature effects and energy conversion efficiency 10 p1423 A72-24319
- Model for large signal losses prediction in charge coupled devices due to fast interface state trapping 10 p1526 A72-24625
- German book on HF semiconductor electronics covering planar and field effect transistors, varactors, n-p, p-i-n, avalanche and Schottky barrier diodes, Gunn devices, etc 10 p1452 A72-24699

- Laser apparatus for resonant frequencies and oscillation amplitudes measurement of semiconductor devices structural elements 11 p1649 A72-26348
- Thermal and shot noise and distortion in charge-coupled semiconductor devices used for imaging applications 12 p1791 A72-27673
- GaAs semiconductor devices role in microwave communications, discussing physical properties and potential applications 12 p1792 A72-27736
- Semiconductor strain gage design and environmental performance for flight control systems 12 p1812 A72-27962
- Semiconductor devices with extended slow wave-carrier interaction region for vacuum traveling wave tube replacement 13 p1927 A72-28401
- Mobility-field characteristics of GaAs below Gunn threshold with magnetoresistance technique, relating to device performance and other material parameters 13 p2021 A72-28573
- Semiconductor devices series production control and analysis by statistical procedures, noting computer controlled data acquisition system for silicon diodes production 13 p1965 A72-29166
- Low energetic efficiency of semiconductor microwave scanning converters for radio images of fog obscured objects 13 p1932 A72-29297
- Electroacoustomagnetic and Hall effects in semiconductors within strong electric field involving phonon production by supersonic electron drift 13 p2022 A72-29437
- Chalcogenide semiconductor monostable threshold and bistable memory switching devices, discussing fabrication and performance 13 p1934 A72-30090
- Physical operation principles of semiconductor sensors using deformation potential for mechanical stress detection and measurement 14 p2104 A72-30445
- Transmission lines with nonlinear capacitance semiconductor diodes, investigating electromagnetic traveling and standing waves instabilities and self amplitude modulation 14 p2086 A72-30795
- Microwave power generation via semiconductor devices, discussing circuit problems due to negative resistance 14 p2088 A72-30833
- Microwave semiconductor diode technology review and development prospects in terms of fabrication processes and materials 14 p2088 A72-30834
- Two dimensional numerical solution of semiconductor steady state transport equations, applying to MOS and bipolar transistors 14 p2142 A72-30847
- Regenerative semiconductor parametric amplifier under dc through p-n junction, analyzing nonlinear phenomena 14 p2090 A72-31124
- Nonlinear processes in oscillatory systems with semiconductor diodes, calculating amplitude and phase characteristics in steady state and transient conditions 14 p2090 A72-31133
- Semiconductor devices quality assurance based on electrical and mechanical performance tests at every stage of product manufacture from initial design 14 p2091 A72-31164
- Scintillation and semiconductor counters - IEEE/AEC/NBS Conference, Washington, D.C., March 1972 15 p2233 A72-31529
- Semiconductor devices application to gamma ray, X ray and nuclear radiations detection and analysis 15 p2235 A72-31644
- Microwave waveguide semiconductor modulator with p-n-n diode as control element, taking into account semiconductor control element conductivity change along waveguide wall 15 p2206 A72-31662
- Gunn diode elements design, operation, performance, efficiency, heat dissipation, lifetime and applications as microwave oscillators 15 p2208 A72-32500
- Three section stepped structure to satisfy requirements for multifunction matching four-pole in signal network with active semiconductor component 15 p2210 A72-32708
- Satellite-borne semiconductor particle detector telescope for C and Mn isotopes identification in heavy primary cosmic rays, considering scintillation counter and mass resolutions 16 p2389 A72-32883
- Charge carrier motion in semiconductor with electron interactions, considering heating in presence of negligible electric field 16 p2441 A72-33278

Laser apparatus for natural resonant frequencies and oscillation amplitudes measurement of semiconductor devices structural elements

16 p2402 A72-33701
Nonlinear characteristics of semiconductor diode multiplier circuits for frequency converters
16 p2370 A72-33951
Thermal resistance of planar semiconductor structures.

17 p2594 A72-34296
Semiconductor low-energy X-ray spectrometry
17 p2552 A72-34335

Controlled self heating effect in semiconducting barium titanate positive temperature coefficient resistor substrate heater for planar Si devices
17 p2527 A72-34680

An investigation of amorphous semiconductor memory devices utilizing thick film fabrication techniques.
17 p2527 A72-34682

Device for ac induction measurements in air, using the Gauss effect in germanium semiconductor diodes
17 p2529 A72-34767

Influence of carrier diffusion on the intrinsic response time of semiconductor avalanches.
18 p2717 A72-36083

Multimedia versus annular construction for high average power in semiconductor devices.
18 p2666 A72-36455

Report on Flip Chip and Beam Lead bonding for electronic circuits.
18 p2666 A72-36528

Improved geometry for a semiconductor surface-wave oscillator.
18 p2667 A72-36685

LSA diode relaxation oscillator loading effect on oscillation damping, calculating optimum loading as function of conductance
18 p2667 A72-36690

Measurement of Hall mobility of current carriers in inhomogeneous semiconductor samples
18 p2720 A72-36964

Detection of defects in semiconductor structures by means of recording the temperature and electric fields.
18 p2693 A72-37106

The detection of unreliable contacts by noise measurements.
18 p2720 A72-37111

Reliability of semiconductor optoelectronic components - Analysis of the long-term behavior
18 p2670 A72-37138

Electronic and optical phenomena in semiconductors.
19 p2844 A72-37445

German monograph - Measurement of 'oscillation impedances' and optimization of frequency noise effects of microwave-semiconductor oscillators tunable over a wide frequency range
19 p2772 A72-37477

Possibility of the occurrence of alternating current in a circuit with a semiconductor sample exhibiting a recombinational instability
19 p2846 A72-38449

The static current-voltage characteristic of four-layer structures in two-collector operation at a low injection level
19 p2846 A72-38573

Metal-insulator-semiconductor-insulator-metal structure light pulse amplification investigating power gain and photocurrent dependences on applied voltage and applicability as radiation detector
20 p2960 A72-39517

Amplification of acoustic surface waves under transverse magnetic field in coupled intrinsic semiconductor-piezoelectric systems.
20 p2960 A72-39703

A new type of switching and memory effect by controlling the polarized field in semiconductor interface.
20 p2961 A72-39709

Stress sensitive device based on anisotropic conductivity of multivalley semiconductor under uniaxial stress
20 p2961 A72-39713

Burn-in technique cost effectiveness in semiconductor and IC reliability enhancement, noting failure rate relationship to operating time
20 p2909 A72-39770

Photoanodic engraving process produced high bit density surface relief holograms on semiconductor crystals for data storage, retrieval and replication applications
21 p3054 A72-40614

Pressure dependence of electrical characteristics of semiconductor sensors using deformation potential for mechanical stress detection and measurement
21 p3056 A72-41109

Quantitative derivation of large signal equivalent circuit of Gunn element in domain mode based on current and space charge characteristics
21 p3034 A72-41401

Miniaturized IC semiconductor device fabrication and failure under electrical load, using scanning electron microscope
21 p3035 A72-41492

Effect of the video signal shaping mechanism in a photosensitive scanistor sensor on the optical data processing accuracy
21 p3058 A72-41735

Analytical calculation of unsteady heat fields in planar devices
22 p3158 A72-42116

Automatic hermetic-sealing systems for semiconductor devices prepared by electron-beam welding
22 p3158 A72-42124

Masking techniques for thin film and semiconductor devices and ICs fabrication, discussing conventional and computerized optical and electron beam systems
22 p3159 A72-42634

Cascade computer controlled system for LSI devices testing, considering interim buffer storage and programmable pattern generator
22 p3160 A72-42823

Measurement of surface leakage currents in a semiconductor photoelectric converter
22 p3140 A72-43188

Electronic superregeneration in semiconductor photosensitive structures with negative resistance
23 p3268 A72-43345

Impedance of a unipolar semiconductor diode under conditions of space-charge limited current with allowance for recombination
23 p3270 A72-43630

Mathematical description and calculation of the steady-state regime of a microwave power stabilizer with a semiconductor attenuator
23 p3270 A72-43766

Frequency-variable semiconductor-oscillator in the microwave region.
23 p3272 A72-43948

Negative resistance, transit time and limited space charge accumulation modes of semiconductor devices operation with electron transitions
23 p3272 A72-44138

Physical limits of semiconductor devices miniaturization for electronic computers, considering thermal energy dissipation, electrical resistance and high current density induced electromigration effects
23 p3273 A72-44332

SEMICONDUCTOR JUNCTIONS

NT JOSEPHSON JUNCTIONS

NT N-N JUNCTIONS

NT N-P-N JUNCTIONS

NT P-I-N JUNCTIONS

NT P-N JUNCTIONS

NT P-N-P JUNCTIONS

NT P-N-P-N JUNCTIONS

NT SILICON JUNCTIONS

Metal-semiconductor-metal Schottky barrier

microwave diode impedance and shot noise calculation
02 p0191 A72-11894

Copper sulfide-cadmium sulfide single crystal photovoltaic heterojunctions, showing optically induced and thermal effects on short circuit current degradation
03 p0389 A72-13603

Metal-insulator-metal tunneling junction, calculating effect of localized impurity states in barrier on tunneling current
03 p0404 A72-14267

N- and p-type semiconductors energy band structure bending near interface
05 p0702 A72-16197

Semiconductor lasers at room temperature, discussing hetero structures and diffused and epitaxial homostructures from basic operation modes and GaAs laser CW operation
06 p0825 A72-17771

Fast algorithm for space charge layer and semiconductor junction capacitance calculation, applying to impurity profile determination
07 p0954 A72-19120

GaAs junction laser, determining second order dispersion in mode locking and self pulsing from output field amplitude correlation measurement
07 p1001 A72-19198

Energy level and V-I characteristics of solid state heterojunction devices, discussing diodes, transistors, thyristors and optoelectronic structures
08 p1139 A72-21054

Physical and operating principles of CW heterojunction injection lasers at room temperature
08 p1181 A72-21056

LF excess flicker noise in metal semiconductor Schottky barrier diodes due to barrier height fluctuation
09 p1287 A72-23114

Local level filling and Fermi distribution in metal semiconductor contact as function of voltage and level location
09 p1372 A72-23355

IMPATT diode junction temperature measurement with accuracy from breakdown voltage by pulse techniques
10 p1449 A72-24304

Photovoltaic effect and energy band model of solar cell cadmium-sulfide-copper-disulfide heterojunctions
12 p1855 A72-28007

Low photon IR photovoltaic response of CdS-metal junction, noting energy conversion efficiency
12 p1855 A72-28009

Solar photosensitive elements prepared p-type GaAs liquid epitaxy on n-type GaAs substrate, measuring dark and light I-V characteristics and spectral response
14 p2142 A72-30225

Experimentally observed admittance properties of the semiconductor-insulator-semiconductor /SIS/ diode.
19 p2772 A72-37568

Behavior of spontaneous emission across threshold in GaAs junction lasers.
19 p2811 A72-37865

Design and frequency characteristics of cylindrical waveguide diode for microwave range, noting semiconductor junction effect on device efficiency
21 p3036 A72-41837

Static and dynamic characteristics of double-injection currents in p'-n-n' diode structures with deep impurities and nonideally injecting junctions
23 p3268 A72-43346

Capacitance voltage characteristics instability of metal-aluminum oxide-silicon dioxide-silicon (MAOS) structures, suggesting polarization effect in layer formed during deposition and annealing
23 p3324 A72-44070

SEMICONDUCTOR LASERS

NT GALLIUM ARSENIDE LASERS

Precision phase indicating pulsed optical range finder, using uncoupled semiconductor laser
01 p0080 A72-10621

Mode guiding improvement in p-n junction of symmetrical AlGaAs-GaAs heterojunction laser diode with narrow active region, obtaining low room temperature threshold current
01 p0080 A72-10788

Laser generator research, discussing metallic vapor, heterojunction semiconductor, liquid, neodymium and organic colorant types
02 p0237 A72-11696

Minimum threshold current density of double heterojunction injection lasers
03 p0367 A72-13412

Lasing onset moments distribution over emitting surface of injection lasers at room temperature
04 p0531 A72-15082

Tunable semiconductor and spin-flip Raman lasers for IR applications [AD-738713]
05 p0667 A72-15788

Semiconductor lasers at room temperature, discussing hetero structures and diffused and epitaxial homostructures from basic operation modes and GaAs laser CW operation
06 p0825 A72-17771

Junction lasers operating principles and device capabilities, considering reliability and mode properties
06 p0827 A72-18462

Optically pumped indium-gallium-arsenides laser coherent emission at room temperature, measuring total power conversion efficiency
07 p0999 A72-18882

Optically pumped semiconductor lasers, discussing two photon absorption, emission from compounds and mixed crystals and smooth frequency variation
07 p1006 A72-20118

Physical and operating principles of CW heterojunction injection lasers at room temperature
08 p1181 A72-21056

Resonator dielectric waveguide structure in electron beam pumped semiconductor laser, noting reduction of diffraction losses and of laser action threshold
08 p1184 A72-22089

Gas, solid state and semiconductor lasers review, discussing applications
09 p1322 A72-22594

Semiconductor lasers with high energy electron pencil beam excitation for high capacity computer storage application
10 p1492 A72-24513

Semiconductor laser continuous emission conditions at room temperature, assuming output power drop with increasing current due to p-n junction heating
10 p1492 A72-24582

Semiconductor laser thermal resistance and time constant evaluation, obtaining operating temperature range and maximum attainable pulse width
11 p1647 A72-25808

Semiconductor laser threshold current dependence on doping degree and temperature based on optical transition model and energy band theory
11 p1647 A72-26327

Semiconductor injection laser with distributed radiative loss, calculating radiation line shape and width and quantum efficiency
11 p1648 A72-26329

Injection semiconductor laser mode selection and output enhancement by introducing external spectrally selective elements into resonator
12 p1821 A72-27589

Optical interaction of inhomogeneously excited semiconductor injection laser diodes, noting power efficiency increase with inhomogeneity

12 p1822 A72-27606

Many element GaAs and CdS semiconductor laser achieving high power output by electron beam pumping

12 p1822 A72-27616

Low threshold current mesa-stripe-geometry double heterostructure injection lasers, eliminating current spreading by etching method

12 p1823 A72-27838

Lightly doped InP and vapor epitaxial GaAs laser, observing long wavelength shift in photoemission spectra peak

14 p2108 A72-30182

CdS crystals lasing in air at atmospheric pressure and room temperature by low voltage electron beam pumping through Ni film

15 p2245 A72-31319

CW tunable semiconductor laser measurement of CO laser amplifier gain line shape for several vibration-rotation lines

15 p2245 A72-31382

Radiation coherence enhancement in pulsed semiconductor injection laser by voltage controlled barium zirconite piezoceramic element

15 p2245 A72-31416

Photon loss coefficients and gain measurement in CdS electron beam pumped lasers, noting absorption mechanism and efficiency

15 p2246 A72-31668

Room temperature GaAlAs single-heterojunction diode lasers structure, fabrication, threshold current density and quantum efficiency dependence on wavelength and temperature

15 p2247 A72-32032

Lightweight man-portable uncooled semiconductor laser illuminator design for field use in night vision applications

15 p2248 A72-32047

Computer designed optical integrating devices for semiconductor laser arrays, considering diode, collection, projection and zoom parameters

15 p2248 A72-32048

Coherent orange emission and bright electroluminescence from indium gallium phosphides vapor grown p-n junction laser diodes

15 p2251 A72-32532

Proton bombarded stripe geometry heterojunction lasers for 300 K CW operation compared with oxide insulated lasers

16 p2403 A72-33757

Resonator dielectric waveguide structure in electron beam pumped semiconductor laser, noting reduction of diffraction losses and of laser action threshold

17 p2562 A72-34660

Certain characteristics of an electron-pumped pulsed laser of small dimensions

17 p2562 A72-34839

Laser computer technology - Today and tomorrow. III

17 p2523 A72-35186

Book - Semiconductor diode lasers

17 p2563 A72-35300

Saturated absorption in optically pumped semiconductor lasers

17 p2563 A72-35303

Tunable output dye and semiconductor lasers application to absorption spectroscopy and air pollution monitoring

17 p2564 A72-35381

Quantum noise in semiconductor lasers.

18 p2697 A72-36345

Radiation coherence in a monopulse single-mode semiconductor injection laser

19 p2811 A72-37736

Reduction in the rate of increase of spontaneous emission from double-heterostructure injection lasers at threshold.

19 p2811 A72-37866

Coherent radiation emission by indium antimonide in a transverse magnetic field

19 p2845 A72-38176

Influence of the refractive index nonlinearity on the dynamics of emission from semiconductor lasers.

20 p2932 A72-39504

Injection laser under self-Q-switching conditions.

20 p2933 A72-39515

High-resolution spectroscopy using magnetic-field-tuned semiconductor lasers.

20 p2933 A72-39561

GaAsSb-AlGaAsSb double heterojunction lasers.

21 p3063 A72-40696

Mode-coupling effects in thin platelet semiconductor lasers.

21 p3064 A72-41381

Lasing properties of yttrium orthoaluminate doped with rare-earth metals

22 p3187 A72-42943

A cathode-ray tube with a semiconductor laser screen

23 p3272 A72-43925

Utilization of a composite resonator for improving the monochromaticity of a semiconductor laser with electron-beam excitation

23 p3297 A72-44468

Time variations in the far-field diffraction patterns of spatial modes from electron-beam-pumped semiconductor lasers.

24 p3409 A72-44712

Commutation switch based on an injection semiconductor laser.

24 p3412 A72-45620

SEMICONDUCTORS [MATERIALS]

NT ACCEPTOR MATERIALS

NT AMORPHOUS SEMICONDUCTORS

NT DONOR MATERIALS

NT METAL OXIDE SEMICONDUCTORS

NT MIS (SEMICONDUCTORS)

NT N-TYPE SEMICONDUCTORS

NT ORGANIC SEMICONDUCTORS

NT P-TYPE SEMICONDUCTORS

NT PHOTOCONDUCTORS

Dember-Hall voltage ratio for low magnetoconcentration in intrinsic semiconductor

01 p0113 A72-10044

Nonlinear skin effects in gas discharge and semiconductor plasmas during electromagnetic wave propagation and dissipation, obtaining wave amplitude and carrier temperature dependence on reflection parameters

01 p0102 A72-10974

Organic semiconductor developments in chemistry and physicochemistry of multiconjugate systems and polymer complexes with charge transfer

01 p0114 A72-11074

Niobium trifluoride synthesis, noting semiconductor and paramagnetic properties

02 p0243 A72-12170

Semiconducting crystal superconductivity in laser field by interaction between electron conduction band and light induced polarization

02 p0269 A72-12883

Multivalley semiconductors electrical pinch effect during electron heating, considering Sasaki effect and sample depletion

02 p0269 A72-12886

Hall effect and conductivity dependence on applied electric field in multivalley semiconductor for power dependent intervalley scattering time

02 p0269 A72-12887

Gunn effect and associated phenomena, covering semiconductor domain formation and movement, space charge waves and thin samples with dielectric coatings

02 p0270 A72-12889

Hall effect mobility dependence on dispersion law in degenerate electron gas on semiconductor surface

02 p0270 A72-12890

Equivalent circuit models in semiconductor transport for thermal, optical, Auger-impact and tunneling recombination-generation-trapping processes

03 p0401 A72-13585

Minority carriers localized surface distribution effect on helicon propagation modes reflectivity in semiconductor

03 p0402 A72-13797

Pulsed Nd laser drilling and welding of metal, metal-semiconductor and semiconductor elements, discussing bond penetration and character, mechanical strength and I-V characteristics

03 p0363 A72-13860

Carrier mobility measurement in inhomogeneous semiconductors based on bulk photovoltaic and photomagnetolectric effects

03 p0402 A72-13862

Carrier transport effects in semiconductors for carrier recombination time approaching relaxation time

03 p0333 A72-13863

Low energy electron beam irradiation of aluminum-silicon nitride-silicon structures for elimination of bias polarization effects on I-V characteristics

03 p0402 A72-13865

Charge state effects on defect production mechanisms, configurations, mobility, annealing kinetics, interaction and dissociation in displacement damage in covalent semiconductors

03 p0403 A72-14077

Se and Zn doped n and p type gallium arsenide point defects, considering thermal conductivity, relaxation time and phonon scattering cross section effects

03 p0404 A72-14239

Periodic lattice one-electron Green function calculation based on pseudopotential matrix element, applying to impurity levels in semiconductors

03 p0404 A72-14268

Semiconductors with diamond and zincblende structures, calculating dielectric function by empirical pseudopotential method

03 p0405 A72-14270

Semiconductor-thermoplastic-dielectric hybrid ICs reliability, discussing interelement adhesive bonding properties and thermally induced strains effects

03 p0337 A72-14294

Deep seated substitutional acceptor impurity levels in semiconductors

04 p0561 A72-15076

Supersaturated semiconductor solid solutions decay kinetic equations and time constants, noting free current carriers effect

04 p0561 A72-15081

Gradient-recombination current instability in high resistance compensated semiconductors

04 p0561 A72-15084

Dynamic negative differential conductivity in bulk semiconductors, analyzing relation to impulse responses

04 p0562 A72-15129

Fe group transition metal impurities in semiconductors, calculating ground state wave functions and photoionization cross section dependence on wavelength

04 p0563 A72-15473

Semiconductor slab electroconductivity measurement based on circularly polarized microwave propagation in circular waveguide

04 p0502 A72-15533

Computer controlled automatic system for measuring electroconductivity and Hall effect in semiconductors, noting data acquisition instrumentation

04 p0496 A72-15534

Sb 124 dopant redistribution in Ge semiconductor during diffusion alloying with In at 750-850 C

05 p0701 A72-15751

Semiconductor-dielectric system for controlling space charge and valley population redistribution by external field

05 p0702 A72-16201

Spontaneous oscillations generation on transverse surface wave, discussing experimental realization with semiconducting CdS single crystals

05 p0626 A72-16282

Transverse acoustoelectric surface wave domain in piezo-semiconducting body, obtaining gain coefficient and generation threshold criterion

05 p0702 A72-16283

Screened impurity scattering determination in heavily doped covalent semiconductors from Hall mobility and thermoelectric power measurements

05 p0702 A72-17073

Two dimensional space charge wave propagation in semiconductors with anisotropic small signal mobility, investigating stability

05 p0632 A72-17097

Parallel and perpendicular magnetic field effects on optically injected electron-hole plasma diffusion in Ge from density measurement by infrared beam absorption technique

05 p0702 A72-17167

Lamb waves interaction with conduction electrons in piezosemiconductor, deriving dispersion equation for CdS wafers

06 p0865 A72-17393

Hydrostatic pressure effects on I-V characteristics of amorphous semiconductor germanium telluride sulfide arsenide

06 p0865 A72-17493

Electron states in glassy amorphous semiconductors, constructing trial wave functions for valence band

06 p0866 A72-18180

Bulk semiconductor material complex microwave conductivity and dielectric constant measurements by cavity perturbation techniques

06 p0786 A72-18371

Metals, insulators, semiconductors and ceramics thermophysical parameters measurement during monotonic heating or cooling at 123-3273 K

06 p0904 A72-18514

Book on electronic processes in noncrystalline materials covering liquid metals, semimetals and semiconductors, Hall effect, phonons and polarons, thermoelectricity, photoconductivity, etc

06 p0866 A72-18516

Electron theories of chemisorption and catalysis on semiconductor surfaces, considering band theory applicability range

07 p1048 A72-19561

Transport phenomena theory for semiconductors in strong electric fields, examining negative differential conductivity and nonmonotonic current behavior

07 p1048 A72-19637

Strong electric field recombinational domains in semiconductors with mobile holes and electrons during band-band illumination or double injection

07 p1048 A72-19638

Semiconductors cyclotron echo signals from dipole interactions of electrons with alternating magnetic fields, discussing frequency doubling and excitation mechanism

07 p1048 A72-19639

Semiconductors theory for multivalley energy spectrum and multivalued equilibrium distribution of carriers during electron phonon interactions

07 p1048 A72-19641

Anomalous Hall effect of polarized electrons spin-orbit interactions in semiconductors, involving emf appearance in electric field and polarized light

07 p1048 A72-19642

Thermodynamic and electrical properties of tantalum nitride powders and thin films for semiconductor IC technology

07 p1049 A72-19935

Semiconductor structure investigation by measuring photoresponses to optical probe motion
07 p1049 A72-19963

Reverse biased p-n diffused junction design with two impurities in nonhomogeneous semiconductors, calculating depleted space charge region thickness
08 p1140 A72-21062

Intraband multiphoton conduction-electron transfer probability in semiconductor under electromagnetic wave action in uniform magnetic field
08 p1216 A72-21066

Transverse and longitudinal current fluctuations in degenerate nonparabolic semiconductors in strong electric field
08 p1216 A72-21074

Multiphonon capture of charge carriers by deep impurity centers in homopolar semiconductors from generalized Lucovsky model
08 p1216 A72-21094

Temperature controller with linear time variation for semiconductors thermally stimulated conductivity and thermoluminescence measurements at 90-300 K operating range
08 p1166 A72-21438

Electron plasma fluctuations in semiconductor with nonparabolic conduction band under external electric and magnetic fields
08 p1218 A72-21877

Numerical solution of theta pinch in electron-hole plasma of Ge semiconductor under surface recombination as contactless method of current carrier injection
08 p1218 A72-22178

Fast neutron radiation damage to glass ceramics and amorphous semiconductors electrical properties
09 p1336 A72-22405

Antimony compounds single crystal whiskers permittivity determination at microwave frequencies from power reflection and transmission coefficients
09 p1366 A72-22417

Forbidden band thermal deformation effect on homogeneous steady state stability of semiconductor
09 p1367 A72-22492

Energy operator diagonalization of interacting valence electrons in semiconductor and metal models
09 p1352 A72-23356

Double beam single detector wavelength modulation spectrometer for background elimination from observed spectra, noting application to semiconductors band structure determination
09 p1315 A72-23402

Dielectric and semiconductor crystals surface defects, considering electric polarization structures
10 p1525 A72-23761

Temperature dependence of emf coefficient Hall constant and conductivity in solid and liquid phases of InSe semiconductor during melting
10 p1526 A72-24267

Monolithic IC semiconductor components layout density evaluation for isolation, active and edge regions utilization efficiency
10 p1449 A72-24287

Transport theory Boltzmann equation and Monte Carlo methods applied to semiconductor negative differential mobility calculation
10 p1526 A72-24398

Semiconductor measurement technology at extremely low currents, discussing dc characteristics and ac amplification
10 p1452 A72-24815

Book on semiconductors covering electrical properties, energy band structure, impurities, epitaxial growth, silicon dioxide, surface properties, p-n junctions and measurement techniques
10 p1528 A72-25123

Transition from metallic to activation conductivity in doped semiconductors, noting activation energy dependence on compensation degree
11 p1700 A72-25720

Gas etching of Ge and Si semiconductors with vapors of chemical elements, emphasizing hydrogen chloride
11 p1700 A72-25776

Semiconductor materials etching and surface coating with protective silicon dioxide film in low temperature oxygen plasma
11 p1700 A72-25777

Fermi level and scattering phase function nomograms for semiconductors with parabolic and isotropic energy bands, noting charge transfer effects
11 p1700 A72-25781

Transverse negative differential conductivity in semiconductors, discussing effect of locations and shapes of energy surfaces in k-space and favorable crystal orientations
11 p1701 A72-25856

Ternary chalcopyrite semiconductors refractivity measurement over range of wavelengths and optical nonlinear coefficient for second harmonic generation from carbon dioxide laser
11 p1701 A72-26148

Small signal theory of emitter current limited injection in negative mobility semiconductors at zero doping limit
12 p1788 A72-27165

Zn, Ge and P based semiconductor alloy specimens chemical composition determination via ac polarograms
12 p1854 A72-27443

Microwave time of flight method for measuring electron drift velocity in GaAs semiconductors
12 p1855 A72-27667

Thermoelectric cooling devices materials figure of merit upper limits above room temperature, using semiconductors parameters experimental values
12 p1755 A72-27722

Resonant interaction and self transparency effect of coherent ultrashort light pulse passing through semiconductor
12 p1824 A72-27868

P-n thin film solar cell based on thermally and electrochemically stable II-IV semiconductors with graded energy gaps
12 p1756 A72-28013

Radiation effects in semiconductors - Conference, State University of New York, Albany, August 1970
12 p1856 A72-28051

Irradiated semiconductors defects theory, considering electronic structure in rigid lattice and lattice distortion near defects
12 p1856 A72-28052

Lattice disorder effects in ion implanted Si and compound semiconductors, using IR and EPR measurements
12 p1859 A72-28074

Lattice damage measurement of Cd ion implanted GaAs semiconductors by optical reflection and scanning electron microscope
12 p1859 A72-28075

Double doping effect on electrical properties of Te and Hg doped and Te and In doped CdSb single crystals
13 p2020 A72-28565

Electron paramagnetic resonance investigation of III-V compound semiconductor crystals, observing large magnetic moments, heteropolar chemical bonding and impurities
13 p2021 A72-28572

I-V characteristics of metal-semiconductor-metal structures based on oxide glasses, noting temperature dependence and current limitation
13 p2021 A72-28688

Temperature and charge carrier density dependence of conduction electron optical effective mass in semiconductor compounds
13 p2021 A72-28788

Mathematical random fluctuation models for noise and energy spectra of pulsed processes during current passage through semiconductors
13 p2021 A72-29064

Semiconducting glass filter time dependent transition, absorption coefficient and luminescent spectral dependences, using monopulsed ruby laser
13 p1971 A72-29909

Spectral analysis for Cu, Cl, Br and I impurity distribution in doped bismuth telluride crystals prepared by Bridgeman method
13 p2023 A72-29979

Energy absorption inelastic surface mechanisms effect on I-V characteristics profile for bounded semiconductors with negative differential conductivity
13 p2023 A72-29991

Nonequilibrium plasma wave scattering cross section dependence on energy bands shape and field orientation in semiconductors
13 p2023 A72-29992

Impurity concentration relationship to electrons and holes density and potential fluctuations in completely compensated crystalline semiconductors with randomly distributed donors and acceptors
13 p2024 A72-29993

Epitaxial GaAs carrier concentration profile, deep traps detection and properties determination, using Schottky barrier on semiconductors
13 p2024 A72-30035

Electron beam-helicons interaction in semiconductor plasma, determining instabilities onset conditions for unbounded system
14 p2141 A72-30172

Strong LF electromagnetic wave propagation in semiconductors with inelastic scattering of current carriers by optical phonons, calculating harmonics reflection coefficients
14 p2142 A72-30361

Charge carrier cooling in nonhomogeneous semiconductors by static electric field, plotting average electron temperature as function of current
14 p2142 A72-30362

Semiconductor gamma ray detectors development, using cadmium dichlorides, dibromides, diiodides and difluorides as doping agents in CdTe crystal growth
14 p2142 A72-30549

Microwave semiconductor diode technology review and development prospects in terms of fabrication processes and materials
14 p2088 A72-30834

Localized electronic states size near mobility edge in semiconductor, considering eigenfunction behavior in random lattice problem
14 p2143 A72-30878

Phase diagrams of rare earth ternary alloys with transition metals and Si, noting semiconductor properties
15 p2289 A72-31189

Chalcogenide semiconductor compounds of b-sub-group transition elements, discussing binary system diagrams, stoichiometric composition and electrical properties
15 p2290 A72-31193

Adiabatic conditions influence on charge carriers dispersion determination of semiconductors based on Nernst-Ettingshausen effect
15 p2291 A72-31390

Electric field and volume charge density distribution in bipolar conductivity semiconductor with recombination instability
15 p2291 A72-31392

Photoelectric emission usefulness for investigation of energy parameters and optical transitions of semiconductor surfaces
15 p2276 A72-31865

Surface treatment effects on light and X ray irradiated surface photoconductivity of InSb semiconductor single crystals at liquid nitrogen temperature
15 p2292 A72-31866

Beta-conductive method improvement for semiconductor electric field intensity measurement by pulsed electron beam
15 p2238 A72-32240

Superconductivity, temperature and tunneling effects in low carrier density semiconductor systems /tin, germanium and indium tellurides, lanthanum triselenide and strontium titanium oxide/
15 p2293 A72-32325

Microwave antenna near field apparent image and phase-amplitude distribution measurement with photocontrolled semiconductor panel
15 p2209 A72-32672

HF electric field effect on ultrasound wave propagation in semiconductor, noting amplification factor dependence on electron heating
15 p2279 A72-32739

Molecular adsorption on semiconducting surfaces, discussing conditions for formation of local surface levels in forbidden gap
15 p2296 A72-32760

Thermally stimulated current measurement application to Ag doped Si semiconductor for energy level and electron capture cross section determination
16 p2441 A72-32859

Piezosemiconductor crystals acoustoelectric surface domain waveguide effect for classical and transverse surface waves
16 p2441 A72-33596

Semiconductor thermal diffusivity and heat capacity measurements, using carbon bolometer and high sensitivity point microthermistor
16 p2442 A72-33855

Resonant interaction and self transparency effect of coherent ultrashort light pulse passing through semiconductor
16 p2403 A72-33977

Semiconductor optoelectronic devices, discussing light emitting indicator diodes, data display systems, photosensitive arrays and optical data transmission links
17 p2594 A72-34332

Semiconductor quadrupole optical links consisting of electroluminescent diode and photoreceptor, discussing operation and design principles
17 p2594 A72-34333

Forbidden band thermal deformation effect on homogeneous steady state stability of semiconductor
17 p2595 A72-34656

Russian book - Characteristics of radiation damage caused by high energy particles in semiconductors
17 p2595 A72-34700

Evaluation of plastic materials for semiconductor encapsulation.
17 p2570 A72-34716

Instrument for Hall and Gauss effects measurement in semiconductors and metals, noting instrument error analysis
17 p2529 A72-34758

Measurement of mobility in high-resistivity semiconductor layers by the van Heek method
17 p2530 A72-35067

Contributions to the study of the macro- and microstructures of semiconductor materials fabricated in our country
17 p2595 A72-35123

Rayleigh wave propagation on a piezoelectric-semiconductor boundary
17 p2596 A72-35541

Luminescence behavior of single-crystal semiconductor compounds under electron bombardment
17 p2596 A72-35721

Equipment for nondestructive measurements of the resistivity of semiconductor epitaxial layers by the three-point probe technique
17 p2557 A72-35755

Instabilities in semiconductors with negative differential mobility.

19 p2844 A72-37465

Stimulated effects in the radiative recombination from electron-hole liquid in semiconductors.

19 p2844 A72-37932

Infrared dispersion of second-order electric susceptibilities in semiconducting compounds.

19 p2844 A72-37944

New proposition of the mechanism of self-focusing of laser beams in semiconductors.

19 p2811 A72-37945

Minority-carrier trapping and the luminescence time response of semiconductors.

19 p2844 A72-37946

Peritectic interaction and phase diagrams of quasi-binary semiconductor CdAs-CdTe and CdP-CdSe systems

19 p2845 A72-38404

Anbipolar diffusion noise in a semiconductor in the presence of a magnetic field.

19 p2846 A72-38599

Calculation of electrostatic potential distribution in semiconductor's contact region during passage of injecting into blocking contact due to illumination.

19 p2846 A72-38626

Hall field occurrence conditions in small semiconductor plates, discussing Hall generator design and layer temperature as function of time

19 p2776 A72-38725

Measurement of the thermal diffusivity of semiconductors by the light pulse technique

21 p3095 A72-40133

Magnetoplasma surface waves in polar semiconductors: Retardation effects.

21 p3096 A72-40344

Vitrification in ternary diamond-like semiconductors

21 p3096 A72-40380

Pinch effect in a germanium electron-hole plasma

21 p3096 A72-40414

Resonance between spin waves and magnetohydrodynamic waves in antiferromagnetic semiconductors and metals

21 p3096 A72-40415

Cooling associated with minority carriers exclusion effect in semiconductors, discussing influence of electroconductivity and forbidden bandwidth

21 p3097 A72-40788

On some aspects of low-temperature and anodic oxidation of metals and semiconductors.

21 p3067 A72-40914

The field strength conditions for measuring the carrier lifetime in semiconductor crystals by the light flash method

21 p3098 A72-41487

Electromechanical, photomechanical and concentration effects of impurities in semiconductors

21 p3098 A72-41677

Scattering by a cylindrical semiconductor rod of anisotropic permittivity perpendicular to the electric field in a rectangular waveguide.

21 p3023 A72-41836

Semiconductor/IC Processing and Production Conference, Anaheim, Calif., February 8-10, 1972 and New York, N.Y., June 13-15, 1972, Proceedings of the Technical Program.

22 p3160 A72-42822

Interpretation of steady-state surface photovoltage measurements in epitaxial semiconductor layers.

22 p3215 A72-43087

Compound tellurides and their alloys for Peltier cooling - A review.

22 p3215 A72-43088

Model of degenerate semiconductor near semiconducting phase transformation, noting superconducting state at low temperatures with corresponding impurity concentrations

23 p3323 A72-43317

Indirect transitions and absorption in the mid-IR region of the spectrum in SbBr crystals

23 p3323 A72-43337

Charge, direction and temperature dependence of semiconductor electrotransmission in dc field, considering metals diffused in Ge, Se, Te, Si, BiTe, GaAs and InAs

23 p3324 A72-43642

Free electrons and holes concentration calculated for quadratic dispersion law in doped semiconductors without degeneration, noting additive atoms effect

23 p3324 A72-43849

The pressure dependence of the E2 reflectivity peak and of the dielectric constant in III-V semiconductors.

23 p3324 A72-44321

Transport phenomena theory for semiconductors in strong electric fields, examining negative differential conductivity and nonmonotonic current behavior

24 p3427 A72-44569

Strong electric field recombinational domains in semiconductors with mobile holes and electrons during band-band illumination or double injection

24 p3431 A72-44570

Semiconductors cyclotron echo signals from dipole interactions with alternating magnetic fields,

discussing frequency doubling and excitation mechanism

24 p3431 A72-44571

Semiconductors theory for multivalley energy spectrum and multivalued equilibrium distribution of carriers during electron phonon interactions

24 p3431 A72-44572

Anomalous Hall effect of polarized electrons spin-orbit interactions in semiconductors, involving emf appearance in electric field and polarized light

24 p3431 A72-44573

Application of a strongly doped semiconductor model to the study of thermodynamic and conductivity properties

24 p3432 A72-45068

Control of laser pulse duration by nonlinear absorption in semiconductors.

24 p3411 A72-45605

SEMIEMPIRICAL EQUATIONS

Energy balance equation of free turbulent boundary layer in incompressible fluid, deriving semiempirical formulas for turbulent viscosity coefficient

16 p3800 A72-34022

Rotary wing head weight estimation for helicopter preliminary design and parametric studies, deriving semiempirical trend formula [SAWE PAPER 914]

23 p3344 A72-43461

SENDERS

U TRANSMITTERS

SENSATIONS

U PERCEPTION

SENSE ORGANS

NT BARORECEPTORS

NT CHEMORECEPTORS

NT CHOROID MEMBRANES

NT COCHLEA

NT CORNEA

NT EAR

NT EARDRUMS

NT EYE [ANATOMY]

NT FOVEA

NT GRABIRECEPTORS

NT LABYRINTH

NT MIDDLE EAR

NT OCULOMOTOR NERVES

NT OTOLITH ORGANS

NT PHOTORECEPTORS

NT PROPRIORECEPTORS

NT PUPILS

NT RETINA

NT SEMICIRCULAR CANALS

NT THERMORECEPTORS

NT VESTIBULES

German book - Hearing, voice, balance /Physiology of the senses III.

22 p3146 A72-42784

SENSES

U SENSORY PERCEPTION

SENSIBILITY

U SENSITIVITY

SENSITIVITY

NT IMPACT RESISTANCE

NT LIGHT ADAPTATION

NT NOTCH SENSITIVITY

NT PAIN SENSITIVITY

NT PHOTOSENSITIVITY

NT PHOTOTROPISM

NT PROPELLANT SENSITIVITY

NT RADIATION TOLERANCE

Pt coated W hot-wire anemometers sensitivities in supersonic turbulent flow at low Reynolds numbers

[ONERA, TP NO. 1024] 01 p0064 A72-10037

Automatic control systems sensitivity, presenting literature survey

01 p0044 A72-10299

Network sensitivity analysis emphasizing first, higher and mixed higher derivatives computation and iterative synthesis techniques

02 p0197 A72-12114

Radio interferometer sensitivity dependence on interrogation frequency for amplitude and time quantization of input signal spectra

05 p0660 A72-15830

Direct and inverse problems of sensitivity theory, discussing solvability conditions, search optimization and applicability in automatic control

05 p0640 A72-16206

Linear single and multiloop control system synthesis for sensitivity reduction by introducing signals proportional to sensitivity functions with analyzer

05 p0640 A72-16207

Parameter adjustment algorithm for simplified sensitivity model in adaptive nonsearching control system of linear plant with polynomial transfer function

05 p0641 A72-16318

Data uncertainties effects on thermal analysis, discussing Monte Carlo method combination with sensitivity analysis

[AIAA PAPER 72-60] 05 p0749 A72-16930

Condenser microphones sensitivity and frequency response characteristics measurement at normal and elevated atmospheric pressures in hyperbaric chamber air and He-air environments

06 p0766 A72-17808

Sensitivity functions for differential equations describing aircraft perturbed motion, noting dependence on time derivatives, system parameters and coordinates

07 p1032 A72-18977

Sensitivity of optical autodyne quantum receiver in presence of output noise, using photomultiplier signal model

07 p1000 A72-19022

Sensitivity predictions of boundary layer pressure fluctuations for round, square and rectangular transducers

07 p0986 A72-19596

Two-fold congruency tests of penetrant inspection system sensitivity using hydrophilic and lipophilic removers /emulsifiers/

07 p0995 A72-19650

Linear time-invariant controllable plant, determining semiclosed loop nominally equivalent control realization for reduced sensitivity to plant parameter perturbations

07 p0961 A72-19705

Linear multivariable discrete time cyclic system sensitivity model yielding sensitivity functions with respect to any system parameters and initial conditions

07 p0961 A72-19706

Eigenvalue sensitivity in optimal feedback control systems with state estimation

07 p0962 A72-19716

Aircraft altitude two-loop feedback control system designed by compensation parameter variation technique, determining correlation between system sensitivity computations and observations

07 p0963 A72-20592

Nonlinear closed loop system reduction of differential trajectory sensitivity to continuous variations or external disturbance

09 p1340 A72-22245

Sensitivity comparison of equivalent open and closed loop optimal control systems, extending performance index formulas to instantaneous and isoperimetric constraints

10 p1456 A72-24456

Parameter adjustment algorithm for simplified sensitivity model in adaptive nonsearching control system of linear plant with polynomial transfer function

10 p1458 A72-25072

Lumped-distributed active network function sensitivity formulas in terms of immitance parameters

11 p1610 A72-25747

Book on sensitivity theory covering continuous and sampled data systems, linear, nonlinear and self exciting dynamic systems, optimal systems, large systems, controllability, etc

11 p1611 A72-26021

Sensitivity limits in moire picture application to holographic interferometry

13 p1958 A72-29514

Quantitative measure for sensitivities of natural frequencies to perturbations leaving modes invariant

15 p2278 A72-32279

Sensitivity design of multiple input controller for dynamic optimization applied to linear systems with quadratic performance index

15 p2212 A72-32795

Radio interferometer sensitivity dependence on interrogation frequency for amplitude and time quantization of input signal spectra

23 p3287 A72-43438

SENSITIZING

Sensitizing by annular surrounds, tracing early light and dark adaptation curves

03 p0317 A72-13936

Scanned reference beam holography techniques with limited exposure time, noting use of hypersensitized photographic plates

07 p0985 A72-19418

Cooperative and sequential sensitization effect on He emissive states population in polycrystalline barium and yttrium fluorides with trivalent Yb

10 p1525 A72-24044

Repression-sensitization and duration of visual attention.

18 p2654 A72-36917

SENSOR-AIRBORNE TERRAIN ANALYSIS

U SENSORS

U TERRAIN ANALYSIS

SENSORIMOTOR PERFORMANCE

NT PSYCHOMOTOR PERFORMANCE

NT PSYCHOSOMATICS

Neural substrates of sensory tactile vision substitution for information mediation in blind subjects, using TV camera

01 p0011 A72-10470

Sensorimotor preconditions of single image impression in human binocular vision

01 p0018 A72-10477

Synaptic mechanisms of vestibulospinal and reticulospinal effect on transmission to lumbar motoneurons in monkeys

02 p0158 A72-11760

Retina, tectum opticum and Rostral brain structures role in analysis and processing of visual sensory stimuli in toad distinguishing between prey and enemies

07 p0915 A72-18775

Hand steadiness during unrestricted linear arm movements and eye-hand coordination tasks, showing tremor occurrence in up-down plane

10 p1432 A72-25113

Multichannel information processing task complexity relation to operator performance for rapidly increasing input conditions

10 p1433 A72-25115

Stimulus complexity effect on amplitude of human cyclofusal response, evaluating relative roles of compensatory eye movements and central responses

10 p1427 A72-25180

Sleep loss effect on reaction and movement times during information processing in step tracking task

11 p1580 A72-26680

Self estimated distractibility in subjects related to attention lapses during perceptual motor performance, indicating psychophysiological changes

12 p1776 A72-28307

Pressure chamber training effects on rats chain motor reflexes hypoxia adaptation, noting sinocarotid receptors importance in compensatory-adaptive reactions

13 p1902 A72-28641

Prevention of weightlessness effects on blood hydrostatic pressure, musculoskeletal system and sensorimotor performance, discussing space flight training and space environment simulation tests

13 p1909 A72-28787

Target acquisition by systems with unlagged acceleration control or rate control with exponential time lag, discussing number of approach and control stick movements

13 p1911 A72-29819

Statistical periodic analysis of cyclic activity in human perceptual-motor performance

13 p1911 A72-29845

Human brain sensorimotor region EEG dependence on proprioceptive influence, instruction for active movement and preparation passive movement of hand

16 p2353 A72-32992

Multilevel motion control

17 p2504 A72-35018

Behavioral properties of somatosensory-motor interhemispheric transfer.

17 p2505 A72-35463

The effect of chlorthalidopexide on visual field, extraocular muscle balance, colour matching ability and hand-eye co-ordination in man.

17 p2505 A72-35915

Rotary pursuit task practice effects on transfer of motor skill from slower to faster speeds

18 p2654 A72-36915

Vertical posture control mechanisms in man

19 p2757 A72-37992

Supplementary cues and delayed-alternation performance of frontal monkeys.

20 p2892 A72-39372

Intracellular study of rubrospinal neurons and of their synaptic activation during the stimulation of the sensorimotor cortical region

21 p2999 A72-40586

Synaptic potentials of sensor and motor neurons of trigeminal nuclei during corticofugal stimulation

21 p2999 A72-40587

Participation of supraspinal structures in the formation and control of a system of arbitrary cyclic motions of man

21 p2999 A72-40594

Effect of electrical excitation of various auditory analyzer levels on a conditioned motor reflex

21 p3001 A72-40805

An assembly for studying the perceptive motor reactions of man under one-dimensional follow-up conditions

21 p3008 A72-40810

The functional organisation of object directed human intended-movement and the forming of a mathematical model.

21 p3011 A72-41422

Motor activity capability of an astronaut in flight

22 p3149 A72-42220

Intermittent movement control theory for prediction of visual correction applied to target aiming during illumination loss

22 p3142 A72-42546

Tactile information transmission for orientation and motor control, discussing somatic sensitivity peripheral mechanism

22 p3146 A72-42778

Sensorimotor mechanism of proprioceptors in muscles and tendons, considering reflexive control of position and motion

22 p3146 A72-42781

Visually directed pointing as a function of target distance, direction, and available cues.

22 p3151 A72-42929

Electrophysiological analysis of limbic-reticular interaction during the orientating reflex

23 p3257 A72-44081

Eye movements evoked by collicular stimulation in the alert monkey.

24 p3371 A72-44906

SENSORS

Fluidic sensors for flow velocity and fluid pressure, temperature and density measurements, emphasizing analog transducers with output signal FM and AM

01 p0006 A72-10151

Experiment sensors impact on on-orbit vehicle configurations and operations in NASA program, synthesizing and cost analyzing common module sets

01 p0135 A72-10945

Fluidic sensors methods for position, angular velocity, fluid level, flow rate and temperature measurement

02 p0155 A72-11998

Zero crossing photoelectric autoreflector pickoffs for readout gyro systems with suspended spherical rotors, classifying systems according to modulation type

05 p0661 A72-16036

Photogrammetric measurement with photodiode sensor arrays substitution for film in cameras and yielding real time readout of stellar and satellite coordinates

08 p1169 A72-21700

Sensors measurement accuracy for rainfall amount and duration determination by automatic remote transmitting meteorological station

10 p1483 A72-25017

Inertial sensing principles interrelationship, stressing electric and magnetic procedures

12 p1809 A72-27788

Steel components contact fatigue kinetics measurement by emf increase of inductive sensor

12 p1887 A72-28245

Sensor measurements correlation to human visibility via sensor equivalent visibility /SEV/ concept, discussing data processing scheme

13 p1992 A72-28846

Roughened and smooth spherical wind sensors lift and drag, calculating aerodynamic coefficient spectra from velocity

13 p1894 A72-29620

Unsteady heat flux sensor types and characteristics, considering flux level, measurement time and frequency response

15 p2233 A72-31374

The effect of atmospheric turbulence on the error of an optoelectronic angle sensor.

17 p2554 A72-34941

Hand tremor measurement methods, discussing pickup system selection for given tasks

21 p3012 A72-41521

SENSORY DEPRIVATION

Human centrifuge tests for semicircular canal gyroscopic stimulation during sensory deprivation, discussing angular acceleration detection thresholds

04 p0478 A72-14865

Auditory flutter fusion frequency changes in humans during prolonged visual deprivation

12 p1769 A72-27418

Human electrophysiological changes during perceptual isolation from EEG, EMG, vertical eye movements and electrodermal measurements

12 p1771 A72-27484

Development of a defensive conditioned reflex to a light stimulus after previous visual deprivation

23 p3257 A72-44078

SENSORY DISCRIMINATION

NT BRIGHTNESS DISCRIMINATION

NT TACTILE DISCRIMINATION

NT VISUAL DISCRIMINATION

Auditory pathway neuron discharge response to complex sound stimuli and frequency discrimination of pattern recognition in cats

01 p0012 A72-10483

High and low pass filtered clicks lateralization tests, suggesting lateral position discrimination dependence on lf content and cochlear partition apical end

04 p0550 A72-15297

Binaural frequency discrimination in masking level difference /MLD/ noise under homophasic and antiphase conditions

13 p2006 A72-29771

Response bias and sensitivity variations in psychophysical test of rats discrimination between standard and attenuated auditory signal intensities

16 p2356 A72-33648

SENSORY FEEDBACK

Sensory psychophysical invariance formation for perceptual functions in human visual system

01 p0011 A72-10468

Statistical evaluation of feedback role in simple movements in terms of Index of Preprogramming

15 p2187 A72-32761

High performance jet aircraft variable feel flight control systems for simulation of aerodynamic reaction forces proportional to dynamic pressure

21 p3039 A72-41069

Parametric adjustment to a shifting target alternating with saccades to a stationary reference point.

21 p3009 A72-41250

Elaboration of steady changes in the firing rate of cortical neuron populations

24 p3370 A72-44587

The reflex and mechanical response of the inspiratory muscles to an increased airflow resistance.

24 p3372 A72-44958

SENSORY PERCEPTION

NT AUDITORY PERCEPTION

NT AUTOKINESIS

NT CONSCIOUSNESS

NT CRITICAL FLICKER FUSION

NT EXTRASENSORY PERCEPTION

NT KINESTHESIA

NT OLFACTORY PERCEPTION

NT PAIN

NT PAIN SENSITIVITY

NT PROPRIOCEPTION

NT SPACE PERCEPTION

NT TACTILE DISCRIMINATION

NT TASTE

NT VERTICAL PERCEPTION

NT VISUAL DISCRIMINATION

NT VISUAL PERCEPTION

Contrast reversal or distance paradox in temperature perception aftereffect

01 p0013 A72-10716

Artificial gravity effects on space station crews performance, discussing unusual mechanical and perceptual phenomena

06 p0766 A72-17715

Sensor systems terminals location in cats colliculus anterior through electrical response measurement to light and sound signals and skin stimulation

07 p0915 A72-18865

Biologist view of behavioristic approach to psychoacoustics, criticizing mechanical concept of living organism as inadequate for understanding human sensory system

11 p1583 A72-25732

Human electrophysiological changes during perceptual isolation from EEG, EMG, vertical eye movements and electrodermal measurements

12 p1771 A72-27484

Microwave induced cutaneous heat and pain perception thresholds, noting usefulness as possible radiation hazard warning

15 p2188 A72-31506

Subjective and objective sensory physiology, discussing transformation processes in sensory receptors and nerves, psychophysical scaling methods, chemoreceptors and peripheral adaptation

22 p3146 A72-42777

Pain perception anatomical and neurophysiological mechanism, discussing human response to mechanical, thermal and chemical pain inducing stimuli

22 p3146 A72-42780

Taste organs neurophysiological structure and functioning, considering stimuli and excitation parameters effects on perception threshold

22 p3146 A72-42783

Relation between a pilot's sensory perception of linear accelerations and the aircraft motion.

24 p3377 A72-45654

SENSORY STIMULATION

Psychological threshold for successiveness, tabulating probabilities for correct guesses of stimuli order

01 p0013 A72-10713

Pyramidal tract neuron reactions to antidromic and afferent stimuli in cats, determining somatosensory cortical neurons responses by intra- and extracellular potential outlets

02 p0159 A72-11768

Physiological effects of localized ventilation, noting human comfort improvement association with reductions in average skin temperature and sweat rate

02 p0159 A72-11955

Human vestibulo-ocular responses to oscillatory rotational stimulation during various sleep and arousal stages, discussing Sugie-Jones reflex system mathematical model

04 p0474 A72-15249

Analgesic electrical stimulation in rat brainstem with other sensory modes unaffected

04 p0475 A72-15361

Single olfactory bulb units under cyclic stimulation, observing activity related to inhalation cycle and odor quality

05 p0617 A72-16162

Visceral afferentation role in vestibular system activity from experiments on rabbit stomach and rectum mechanoreceptor stimulation effects on vestibulo-oculomotor reflexes

05 p0618 A72-16630

Human taste papillae sensitivity to chemical stimuli, showing stable quality and intensity response patterns

05 p0620 A72-17129

Vestibulometric swing to obtain measured doses of receptor stimulation in otolith apparatus and semicircular labyrinth ducts with simultaneous physiological data recording

06 p0769 A72-18200

Sensor systems terminals location in cats colliculus anterior through electrical response measurement to light and sound signals and skin stimulation

07 p0915 A72-18865

EEG study of cortical aftereffects to peripheral stimulation in cats

07 p0915 A72-18866

Hypothalamic single neuron unit discharge pattern response to acoustic, light and somatosensory stimulation in cats

08 p1116 A72-21471

Bulbar respiratory neuron discharge pattern response to nasal and tracheal receptor stimulation in cats, relating changes in neuronal activity and intratracheal pressure

08 p1117 A72-21473

Temporal summation function form change during dark adaptation, noting relationship to change under other stimulus manipulations

09 p1269 A72-22616

Efferent vestibular activity in response to horizontal plane rotary stimulation in frog, showing efferent relations between both ears

10 p1426 A72-25099

Behavioral properties of somatosensory-motor interhemispheric transfer.

17 p2505 A72-35463

Role of afferent and efferent connections in the formation and reproduction of trace processes in man

21 p3001 A72-40807

SENTENCES

NT SYLLABLES

NT WORDS [LANGUAGE]

SEPARATED FLOW

NT BOUNDARY LAYER SEPARATION

Two dimensional wedge shaped body base heat transfer to separated nonreattaching flow region in subsonic wind tunnel

[ASME PAPER 71-HT-D] 02 p0152 A72-12314

Heat transfer and temperature profiles in separated flow generated by transverse rectangular notch in flat plate

02 p0303 A72-12700

Turbulent supersonic separated flow field analysis and pressure measurements for two dimensional and axisymmetric internal and external flow models [DGLR PAPER 71-076]

02 p0152 A72-12710

Symmetrically deformed delta wing in supersonic flow, considering leading edge flow separation induced vortices effects on downwash, pressure distribution and aerodynamic characteristics

04 p0463 A72-15741

Flow separation of turbulent boundary layer ahead of inward-projecting normal step predicted by rotational flow analysis via iterative solution

[ASME PAPER 71-WA/FE-32] 05 p0599 A72-15924

Tangential blowing and wall cooling effects on axisymmetric models flow separation at Mach 6, comparing pressure distribution with Busemann formula

05 p0601 A72-16227

Wake outflow concept application to flow separation phenomena, enabling determination of base pressure for drag calculations

[DFVLR-SONDDR-176] 05 p0603 A72-16702

Unsteady boundary layer on hemisphere embedded on infinite plane during normal liquid impingement, using inner and outer expansions method to study separation time

05 p0653 A72-17003

Increased Reynolds number simulation with roughness set on aircraft model in transonic flow, investigating flow separation by parietal visualization technique

06 p0758 A72-17846

Wall blowing discontinuity effect on two dimensional incompressible turbulent boundary layers, discussing flow relaxation length separation by penetration point trajectory

07 p0966 A72-18841

Attached and separated turbulent viscous regions resulting from shock wave-boundary layer interactions in hypersonic flow

[AIAA PAPER 72-74] 07 p0966 A72-18949

Hot gas heat transfer measurements in separation, reattachment and redevelopment regions downstream of abrupt circular channel expansion

[ASME PAPER 71-HT-DD] 08 p1251 A72-20881

Flow analysis and dimensioning data for parallel walled radial diffusers, stating flow separation criterion

09 p1260 A72-22629

Wind tunnel diffuser design for separated region spread reduction based on egg box principle

10 p1416 A72-23859

Laminar and turbulent boundary layer flow stability with forward separation areas

10 p1418 A72-24535

Supersonic flow around thin cruciform wing with antisymmetrical angle of attack distribution and horizontal plane with leading edge, considering flow separation at edges

10 p1420 A72-25118

Separation flow field measurements for space shuttle cylindrical configurations in hypersonic streams, using pressure heat transfer and visualization techniques

[AIAA PAPER 72-294] 11 p1567 A72-25232

Critical lift and flow separation on helicopter rotor under dynamic loading as function of flow and blade characteristics

11 p1568 A72-25285

Flow separation reduction by transverse jet blowing, illustrating flow patterns by water tunnel visualization on cylinders, perpendicular flat plates, contoured walls, steps, wings, etc [ONERA, TP NO. 1070]

11 p1572 A72-25814

Transverse outflow effects on flow field characteristics of hypersonic finite span separated flows with turbulent boundary layer

11 p1572 A72-26004

Flow separation effects on critical lift of helicopter rotor, using blade angle of attack criterion

11 p1573 A72-26893

Incompressible laminar subcritical flow with separated wake past symmetric two dimensional bluff body, calculating upstream pressure distribution and separation point

12 p1751 A72-27172

Measurement techniques for separated gas flows mean and fluctuating aerodynamic properties, discussing improved optical geometry for laser Doppler anemometer

13 p1956 A72-28632

Laminar channel flow stability loss dependence on Reynolds number and wave number, discussing conditions for separated flow self oscillations

13 p1941 A72-28765

Swirling flow in round pipe with sudden expansion, discussing separation and reversal characteristics

13 p1942 A72-29640

Subsonic flow in separation zones of three dimensional turbulent boundary layer forming in front of cylindrical projections, rectangular parallelepipeds and shields

13 p1895 A72-29881

Pressure distribution and heat transfer in flow separation zone of cone tipped cylindrical body, using shadowgraph photography for flow visualization

14 p2070 A72-31005

Ideal liquid theory application for unsteady separated flow calculation around arbitrary shape bodies, noting numerical solution for plane flow around circular cylinder

14 p2070 A72-31010

Temperature distribution and heat transfer coefficients in turbulent separated flow region downstream of rearward step in subsonic wind tunnel, using Mach-Zehnder interferometer

15 p2333 A72-31204

Deflection and energy dissipation of thin cascade profiles in transonic flow for given pressure distribution, noting boundary layers and separated flow

15 p2178 A72-31501

Reattachment heat transfer for laminar or turbulent separated shear layers, comparing predictions with measurements for cavities, ramps, spiked-nose bodies and forward facing step

16 p2344 A72-34031

Flat plate leading edge blunting and wall cooling effects on supersonic laminar flow ramp-induced separation

[AIAA PAPER 72-716] 16 p2344 A72-34032

Shock wave interactions with nozzle wall turbulent boundary layer, discussing shock strength variation to produce unseparated, incipient and fully separated flow fields

[AIAA PAPER 72-715] 16 p2380 A72-34033

Unsteady flow at the junction of a branched duct.

17 p2539 A72-34971

Self-similar separation flows in a laminar magnetohydrodynamic boundary layer during injection and suction

18 p2716 A72-36886

Calculation of an unsteady separation flow past a slender profile

18 p2642 A72-36900

Numerical tests of resolution of detached flows on thick bodies

18 p2684 A72-37198

Ultimate configuration of the self-similar separated flow of an ideal fluid

19 p2785 A72-37396

Experimental investigation of the flow past a cylinder with a flat nose

19 p2745 A72-37397

Study of flow in a passage in the presence of transverse alternating pressure gradients.

19 p2785 A72-37467

Simple proof of fluid line growth in stationary homogeneous turbulence.

19 p2787 A72-38427

Book - Combustion aerodynamics.

19 p2882 A72-38722

Flow separation at the edges of some types of tail sections used in supersonic aircraft and in rocket technology

20 p2885 A72-39597

An approximate method for solving problems involving separated flows past bodies

21 p2990 A72-41088

Heat transfer in separated regions in supersonic and hypersonic flows.

[ICAS PAPER 72-14] 21 p2991 A72-41139

Experimental investigations of separated flows on wing-body combinations with very slender wings at free-stream Mach numbers from 0.5 to 2.2.

[ICAS PAPER 72-25] 21 p2991 A72-41150

Numerical solution to the Navier-Stokes equations in the problem of a gas flow past a rectangle

22 p3166 A72-42252

Delta wing separation can dominate shuttle dynamics.

[AIAA PAPER 72-976] 22 p3230 A72-42336

Analysis and correlation of data on pressure fluctuations in separated flow.

23 p3247 A72-43331

Length of the separation region behind a bluff body in a bounded flow

23 p3248 A72-43685

Transverse oscillations of a jet in a jet-splitter system.

[ASME PAPER 72-FLCS-1] 23 p3281 A72-44065

The sweepback effect in the subsonic region in the lower atmosphere and in the hypersonic region at high altitudes

24 p3359 A72-44983

Three dimensional shock wave configurations in front of cylindrical body on supersonic wing or of fluid jet injected into main supersonic flow, examining high pressure gradient regions

24 p3361 A72-45113

SEPARATION

Solidification, microsegregation and homogenization of austenitic stainless steels containing delta ferrite

05 p0672 A72-16142

Microsegregation in Ti-Mo, Ti-V and commercial Ti alloys, investigating cooling rate and alloying elements contents effects

11 p1655 A72-25506

Al microsegregation in Ti-Al and commercial Ti alloys, investigating effects of cooling rate from beta phase and of Al content

11 p1655 A72-25507

Heat resistant alloys conjugate phases extraction, separation and chemical analysis, discussing control of minor phases as precipitation products

13 p1978 A72-29443

Gas mixtures separation in Kantowitz-Grey under-expanded molecular jet background as function of rarefaction degree, using electron beam fluorescence technique for concentration measurements

16 p2429 A72-33054

Effective separation technique for small diameter whiskers.

17 p2572 A72-35662

SEPARATORS

NT AIR FILTERS

NT DESICCATORS

NT DIVIDERS

NT DUST COLLECTORS

NT ELECTROSTATIC PRECIPITATORS

NT EVAPORATORS

NT FLUID FILTERS

Battery separator materials requirements derived from in-cell environment and battery mission, evaluating present technology for R and D area concentration

03 p0313 A72-14235

C-54 A/B aircraft engine air particle separator antice system design features, manufacturing techniques and testing

07 p1053 A72-18769

Ion trajectories equations of motion solution for E x B type mass separator, presenting curves for mass species dispersion inside separator channel

10 p1509 A72-23942

Nb superconducting resonant cavities application to linear accelerator and RF particle separator structures in GHz region for wall energy loss reduction

13 p1922 A72-29348

SEPTUM

Visual cortex repetitive stimulation effect on primary response habituation in young normal rabbits and adults with septum pellucidum lesion

14 p2076 A72-30596

SEQUENCING

Hookes law formulation by multindex sequences for stereomechanical multiple system optimization

09 p1354 A72-23611

Huffman sequence synthesis by z transform zero pattern selection to obtain high energy for given peak amplitude, noting signal ambiguity functions

10 p1437 A72-24679

Automata with behavior defined by input stimuli sequence and independent on initial state, considering neuron nets as example

15 p2203 A72-32173

Dipeptidyl aminopeptidase. I - Application in sequencing of peptides.

17 p2511 A72-35167

Methods using Walsh functions for multiplexing and transmitting signals

19 p2765 A72-37942

SEQUENTIAL ANALYSIS

High speed decision sequential decoder design and tests for digital errors, white noise and real channels

01 p0026 A72-10341

Single malfunction diagnosis models in systems failures, describing fixed and sequential testing schedules

02 p0186 A72-11689

Sequential analysis of statistical hypotheses applied to radar detection and coded communications systems

02 p0181 A72-12643

- Pattern recognition by automatic clustering methods without fixed definitions for number and specification of classes, using sequential diagnosis
05 p0632 A72-16075
- Optimal sequential multiple decision procedures for radar receiver using Monte Carlo method
05 p0628 A72-16565
- Switching sequence analysis of gas bearing gyros for low cost inertial sensors in short risetime navigation devices
07 p0989 A72-20281
- Sequential testing of actual and calculated error covariances consistency in recursive nonlinear estimators, noting method application to linear filters
08 p1197 A72-20857
- Targets discovery in predetermined direction by phased array radar, using sequential analysis
09 p1278 A72-22896
- Sequential analysis of statistical hypotheses in radar target detection and in communications systems
09 p1282 A72-23680
- Adaptive filter techniques application to maneuvering reentry vehicle tracking, using Wald sequential test, decision theory and stochastic approximation
10 p1509 A72-23779
- Confidence level determination in terms of reliability index /MTBF/ for MIL-STD-781 truncated sequential probability ratio tests
10 p1444 A72-23989
- Radar sequential detector for digital processing of signal masked by noise, determining false alarm and detection probabilities and mean test duration
10 p1439 A72-24908
- Automatic search for Huffman sequential logic circuit breakdown detection sequence, using VEGA program through matrices and graphs utilization
11 p1612 A72-26549
- Fault detecting sequences observation in sequential circuits with shift registers as memory elements
12 p1794 A72-27496
- Statistical principles of reliability assessment and sequential testing of complex systems, considering confidence level, probability of acceptance and cost factors
13 p1984 A72-28361
- Signal detection sequential procedure duration probability distribution at frequency discriminator output for arbitrarily shaped background noise energy spectrum
13 p1915 A72-28474
- Space-averaged sound pressure measurement by sequentially sampled microphone arrays, considering scanning rate and rms detector time constants effect
13 p1958 A72-29565
- Structural design optimization procedure based on sequence of linearizations with iterative convergence through series of least critical intermediate solutions in hyperspace
15 p2331 A72-32551
- Data transmission systems with decision feedback in presence of burst noise, calculating statistical relations among received sequences as function of duration and spacing
16 p2372 A72-33795
- A sequential algorithm for covariance matrix calculations.
17 p2574 A72-34416
- Asymptotically optimal procedures for certain types of moments of cutoff and terminal decisions in sequential estimation
17 p2576 A72-35419
- Telemetric frame synchronization with the aid of distributed and concentrated frame periods
21 p3024 A72-40329
- Kullback-Leibler information function and the sequential selection of experiments to discriminate among several linear models.
21 p3075 A72-41187
- Estimation and prediction of Gumbel and Frechet distribution parameters, noting statistical decision in tests, sequential analysis and graphical procedures
22 p3199 A72-42968
- Sequential analysis algorithm for data channel detection of received signal represented by Poisson sequence of quantum transitions under large SNR
23 p3266 A72-44206
- The random-sampling procedure in oscilloscope technology
23 p3273 A72-44348
- Optimal cost effective sequencing model for component reliability tests, applying to complex electronic equipment
24 p3467 A72-44654
- An interactive approach for the generation and verification of test sequences in a logic system
24 p3382 A72-44662
- Estimation, confidence intervals, and incentive plans for sequential three way decision procedures.
24 p3406 A72-44667
- Random and algorithmic procedures employing three-valued logic system for sequential circuits fault detection test sequence generation
02 p0185 A72-11486
- Sequential machine realization with trigger or flip-flop elements and Boolean function feedback
10 p1445 A72-24401
- Finite Boolean function computation on sequential machine models, developing exchange inequalities between storage, time, et cetera, for relation of combinational and time complexities
24 p3383 A72-45650
- SEQUENTIAL CONTROL**
- Sequential interpolating estimation algorithm derivation for distributed-parameter noisy dynamic systems described by nonlinear partial differential equations
04 p0538 A72-14669
- M-ary orthogonal signal phase noncoherent detection in sequential decision feedback, comparing performance with optimal coherent reception
06 p0773 A72-17596
- Sequential behavior and inherent tolerance to memory faults in terms of minimum redundancy
07 p0950 A72-19300
- Algorithm for asynchronous multilevel sequential circuits design, stressing NOR networks
07 p0963 A72-20387
- Sequential reliability control and analysis in low run production with plan optimization and tests number reduction
08 p1181 A72-22069
- Sequential control using computer program for signal processing, noting machine tool, die casting, elevator and warehouse applications
09 p1290 A72-22240
- Automaton model with sequential description of control systems operations, discussing structure with states code recorded on shift register
16 p2366 A72-33088
- Finite group homomorphic sequential systems generalization from linear system theory, developing controllability, observability, minimality and realizability concepts
17 p2523 A72-35526
- Spacecraft rendezvous trajectories and targeting maneuvers onboard sequential computation, taking into account maneuver constraints and state vector update information
24 p3450 A72-45172
- SEQUENTIAL DETECTION**
- U SEQUENTIAL ANALYSIS**
- SERIES [MATHEMATICS]**
- NT ASYMPTOTIC SERIES
- NT FOURIER SERIES
- NT PADE APPROXIMATION
- NT POWER SERIES
- NT TAYLOR SERIES
- Recurrence relation derived for general normalized satellite inclination function with three parameters in series expansion for geogravitational potential
01 p0123 A72-10012
- Mixed boundary value problem of Laplace equation solution by dual trigonometric series equations approach, applying to microstrip transmission line capacitance determination
01 p0093 A72-10508
- Linear heat transfer boundary value problem series solution in Cartesian and cylindrical coordinate systems
01 p0145 A72-10575
- Uniform progressing wave expansion solution to wave equation for transition region boundary value problems
03 p0388 A72-12988
- Spreading currents in parabolic rotating coordinates, determining magnetic field components consistent with Laplace equation series expansion
03 p0311 A72-13565
- Quasi-linear tensor operator derived in form of series converging inside circle, proving theorem concerning reciprocity conditions and existence of potential
03 p0445 A72-13579
- Biharmonic problem of displacements in plane theory of elasticity, analyzing stress-strain state by iterative solution in series form
03 p0454 A72-14312
- Trigonometric series solution of Tricomi problem for Chaplygin-type equation in half plane
04 p0461 A72-14628
- Asymptotically diagonal systems for variational expansions applied to elliptic partial differential equations, estimating convergence rate
04 p0540 A72-15374
- Orthogonal expansion of estimators and estimands in Hermite series for Monte Carlo computation
04 p0540 A72-15631
- Infinite series summation in terms of rapidly convergent definite integrals
05 p0682 A72-15808
- Radio signal group trajectory in ionosphere expressed as series expansion in terms of increasing power of beam reflection height
05 p0626 A72-16250
- Low deviation FM wave spectral density estimation as infinite series by low pass Gaussian random process
06 p0772 A72-17407
- Truncated series use in laminar boundary layer calculation, noting computer time saving
06 p0756 A72-18115
- Wiener-Hermite random variable expansion technique with time dependent base for turbulence applied to Burger equation
07 p0967 A72-19502
- Transcendental series solution of Chini-Painleve nonlinear differential equations describing vehicle and meteorite oscillation during planetary atmospheric entry
07 p0964 A72-20594
- Geomagnetic field optimal model with expansion of spherical harmonic series by least squares method
07 p0980 A72-20657
- Optimal filtering for state estimation of nonlinear dynamic models observed with discrete noisy observations by retaining second order terms in series approximation
08 p1145 A72-20863
- Linear time optimal problem with analytical perturbations of initial conditions, determining optimal control switching points from convergent series representation
08 p1145 A72-21466
- Atmospheric boundary layer pressure field expansion into dual series of natural time dependent components to separate fluctuations within monthly period for weather forecasts
08 p1203 A72-22125
- Poised and nonpoised Hermite-Birkhoff interpolation problems application to quadratic formulas and expansions and completely convex functions
11 p1732 A72-25504
- Spreading currents in parabolic rotating coordinates, determining magnetic field components consistency with Laplace equation series expansion
11 p1607 A72-26752
- Iterative formula for constructing Liapunov functions in convergent series form
12 p1836 A72-27073
- Atmospheric optics inverse problem solution, comparing orthogonal functions series expansion and regularization method algorithms
12 p1841 A72-27992
- Book on applied functions of complex variable covering infinite series, Cauchy theorem, singularities, Laurent series, residue theorem, conformal mapping, Fourier and Laplace transforms, etc
13 p1985 A72-28433
- F 2 layer parameter forecasting by computer based on series coefficients dependence on Wolf number
13 p1946 A72-28597
- Analysis of errors generated by Kotelnikov series representation of finite signals during quantization by delta functions, finite duration sampling and constant amplitude sampling
13 p1919 A72-29044
- Series representations of p-analytic functions in Legendre functions of first and second kind, applying to axisymmetric problems solution in elasticity theory
13 p2057 A72-29079
- Waldman-Snyder equation application to sound absorption and dispersion in dilute polyatomic gases, presenting truncation procedure for perturbation function expansion in irreducible Cartesian tensors
14 p2131 A72-30673
- Orthogonal vibration damping matrix numerical evaluation, comparing Caughey series and direct approaches
15 p2326 A72-31711
- On the first-excursion probability in stationary narrow-band random vibration. II.
[ASME PAPER 72-APM-16]
17 p2628 A72-34800
- Expansion solution for subsonic compressible flow.
18 p2679 A72-36124
- Multipole expansion of sound radiation from moving rigid bodies.
18 p2710 A72-36404
- Series solution for electromagnetic wave propagation in radially and axially nonuniform media - Geometrical-optics approximation.
18 p2712 A72-37024
- An improved method for the solution of the heat equation in Chebyshev series.
19 p2879 A72-37370
- Backscatter from gated fluctuating regions - A Bremmer series approach.
21 p3015 A72-40361
- Atmospheric optics inverse problem solution, comparing orthogonal functions series expansion and statistical regularization method algorithms
22 p3202 A72-43006
- Series solution of the three-dimensional elasticity problem of a layer.
23 p3350 A72-44049
- Field expressions for a circular loop antenna in terms of a new set of functions.
24 p3379 A72-44707
- Differential equations of motion of two mutually perturbing bodies, noting series expansion of perturbation

- bation function for close commensurability of mean motions
24 p3437 A72-44761
- F 2 layer parameter forecasting by computer based on series coefficients dependence on Wolf number
24 p3398 A72-45097
- Explicit series solutions for the frequencies of motion around the Lagrangean points in the restricted problem of three bodies.
24 p3440 A72-45136
- SERIES EXPANSION**
U SERIES [MATHEMATICS]
- SEROTONIN**
Insulin injection or carbohydrate consumption effects on serotonin and tryptophan concentrations in rat brains
02 p0165 A72-12845
- Light-dark cycles and physiological stress stimuli effects on circadian rhythm in rat blood serum serotonin levels
08 p1115 A72-21081
- Serotonin precursor 5-oxytryptophan effects on hypothalamic-hypophyseal-adrenal complex under complete deafferentation of medial-basal hypothalamus
13 p1907 A72-30016
- SERT [ROCKET TESTS]**
U SPACE ELECTRIC ROCKET TESTS
- SERT 2 SPACECRAFT**
Electron bombardment SERT II ion thruster operation using Xe, Kr, Ar, Ne, He, nitrogen and carbon dioxide
10 p1528 A72-23964
- Current flow across double layer plasma in SERT 2 type hollow cathode ion thruster, using Langmuir probes
[AIAA PAPER 72-418] 11 p1706 A72-26168
- Space simulation facility for one year SERT 2 mercury ion thruster testing, discussing cryogenic operation and electrical and thermal insulation
[AIAA PAPER 72-430] 11 p1613 A72-26174
- SERUMS**
Serum enzyme activity changes response to constant test exercise, discussing relation to maximum oxygen uptake
04 p0472 A72-14897
- Quantitation of serum proteins on whole blood-electroimmunodiffusion technique applicable to capillary blood.
22 p3150 A72-42495
- SERVICE LIFE**
Charging methods for Ni-Cd batteries used in satellites, noting life increase and weight reduction
01 p0007 A72-11054
- Nonlinear boundary value problem of creep for isotropic bodies with random mechanical properties under random loads, calculating structural component reliability and service life
02 p0289 A72-11619
- Temperature and loading conditions effects on structural element service life, showing partial healing process of microdefects
03 p0443 A72-13454
- Secondary fatigue curves for determining service life of metal specimens under unsteady loads
03 p0445 A72-13592
- Long life magnetic tape recorder for onboard data storage in space flights, discussing two motor tape transport and static memories for improved reliability
[IEEE PAPER 12.4] 03 p0360 A72-13767
- Laminate materials, sockets and connectors for cost-effective high temperature accelerated life testing of IC
03 p0336 A72-14283
- Mean stress and overload effects on mild steel service life, using fatigue damage summation method
04 p0592 A72-15475
- Orbiting space vehicle life extension by momentum management using gravity gradient torques
05 p0727 A72-16467
- Fatigue behavior of notched or cracked aircraft structure parts, examining service life prediction problem
06 p0895 A72-17811
- Self regenerating molten seed electrodes for open cycle MHD power generators longevity, regulating combustion chamber and gas flow seeding
06 p0862 A72-18336
- Steel sheet creep, plastic deformation and service life under temperature and stress cycles
06 p0899 A72-18558
- Thermal resistance estimation for machine parts of heat resistant alloys under real working conditions
06 p0833 A72-18559
- Lubrication with thin molybdenum disulfide solid film under various temperatures and atmospheric pressures, examining friction and lifetime
06 p0823 A72-18587
- Plastic deformation, creep rupture strength, endurance limit and service life of prestressed strain hardenable material
06 p0900 A72-18681

- Lubrication system filtration effects on rolling element bearing life and extended mean time to failure of gas turbine engines
07 p1052 A72-18754
- Aircraft performance parameters in terms of effect on lifting system service and fatigue life and on design
07 p0912 A72-19111
- Stress redistribution in statically indeterminate structures under creep, discussing effects on time to brittle fracture and service life determinations
07 p1088 A72-19259
- Mechanical energy consumption effects of thermal dissipation and cyclic straining methods during sample life tests
07 p1089 A72-19260
- Long life aerospace explosive components, examining material degradation mechanisms and effects of pressure, temperature, moisture, chemical reactions and impurities
08 p1219 A72-20759
- Wilga 3 aircraft structure service life from structural fatigue theory and tests, emphasizing operational load distribution measurement
08 p1110 A72-21634
- Machine metals fatigue life, creep theory and stress and strain kinetics in severe environments, formulating physical equations
08 p1246 A72-21805
- Clam seals comparison with elastomers, discussing aircraft use, contamination, inspection, corrosion and erosion, surface finish, service life and cost
08 p1179 A72-21941
- Reliability theory distribution function construction for failure analysis in physical processes, considering mechanical system service life and living organisms life span
08 p1180 A72-22062
- Twin triodes type parameters stability in microwave region as function of cathode service life and temperature
09 p1284 A72-22243
- Turbine blade root attachment service life determination from fatigue tests with T shaped models
09 p1373 A72-22300
- Electron fractographic investigation of fracture properties via removal of metal oxide film accumulated on crack surface during service life of steel structures
09 p1309 A72-22639
- Thin wall airframe wire insulation relative thermal life and temperature rating evaluation procedure using Arrhenius plot
09 p1339 A72-23270
- High power Ar ion laser with plasma tube using current conducting graphite bore for stable long life operation
10 p1489 A72-23944
- Bayesian analysis application to reliability and life parameter estimation for Weibull failure model, using Monte Carlo simulation
10 p1503 A72-23978
- Time to failure determination in complex service systems, examining Markov processes
11 p1609 A72-25435
- Flutter analysis of propeller whirl flutter, twin boom aircraft, T tail configuration, servo tabs and all-moving tail, discussing structural variations effects on service life
[SAE PAPER 720309] 11 p1575 A72-25573
- Russian book on aircraft engine reliability covering defects, fractures and failure analysis, service life prediction, production deficiencies and operational conditions
11 p1706 A72-26068
- Monolithic micropower command receiver to extend lifetime of implanted biotelemetry system
11 p1586 A72-26564
- Aircraft windscreen design, discussing high impact strength glass, electroconductive film, transparency service life and weight reduction
12 p1753 A72-27006
- Lifetime limitations of ion extraction systems for electron bombardment ion thrusters due to sputter erosion of electrode by ion beam
[AIAA PAPER 72-477] 12 p1860 A72-27421
- Model for supervised repairable system reliability, assuming system life and repair times as exponential probability distributions with deterministic supervisor active and inactive times
12 p1814 A72-27555
- Silicon solar cell fabrication technology developments for long mission life performance reliability over wide temperature and radiation intensity ranges
12 p1757 A72-28029
- Silicon solar cell interconnectors design for 5-10 years mission life, considering launch induced vibration stresses and thermal cycling stresses during mission
12 p1758 A72-28037
- Long life leak-proof hermetic compression seals for alkaline batteries, describing design, fabrication and accelerated thermal cycle test method
[ECS PAPER 72] 13 p1899 A72-28434

- Stress-service life relations for duralumin samples from impact and nonimpact tensile tests with cyclic axial loads, noting notch sensitivity
13 p1978 A72-29147
- Reliability analysis of automatic systems with structural changes accumulated during operation, noting service life determination and damage prevention
13 p1936 A72-29169
- Mathematical models for passenger aircraft market forecast, discussing stock measurement and life expectancies
13 p2067 A72-30125
- Environmental effects on aircraft structure operational reliability, discussing failure removal and protective coating lifetime
14 p2072 A72-30285
- Rocket propellants, propulsive charges and explosives lifetime - Conference, Karlsruhe, Germany, September-October 1971
14 p2143 A72-30751
- Explosives life limitation due to aging phenomena, discussing chemical and physical processes and environmental effects
14 p2143 A72-30752
- Thermochemical methods for plasticized/stabilized cellulose nitrate kinetic constants determination for lifetime estimation, presenting isothermal decomposition curves
14 p2144 A72-30753
- Propellant powders safe life prediction based on short-time tests, discussing aging effects on chemical stability after 7-11 years air conditioned storage
14 p2144 A72-30756
- Double base solid propellants life determination from accelerated aging tests at elevated temperatures, discussing surface properties effect on weight loss and autocatalytic decomposition
14 p2144 A72-30757
- Cast double base propellant rocket motors safe storage and service life assessment, examining environmental storage conditions and accelerated temperature effects
14 p2144 A72-30758
- U.S. Army missile systems rocket motors life cycle reliability programs based on propellant laboratory analyses, motors static tests and field firings statistical evaluation
14 p2146 A72-30759
- Solid rocket propellants storage life analysis and prediction by mathematical modeling of physical-chemical failure generating processes
14 p2145 A72-30762
- Rolling-element bearings life estimation based on ASME engineering design guide, taking into account materials properties and processing, misalignment, speed and lubrication characteristics
[ASME PAPER 72-DE-29] 14 p2108 A72-30870
- Thin film resistor manufacture and evaluation for stability and long-life characteristics
14 p2091 A72-31171
- Limited energy source operational time comparison for continuous and pulse mode operations
15 p2196 A72-31785
- Edge and surface modification of Nb alloys prior to coating with fused silicide for oxidation life extension
15 p2244 A72-32134
- Vibrational diagnostics of operational conditions of machines for wear, design faults and efficiency evaluation
16 p2425 A72-33408
- Compressed initially bent Shanley column analyzed for geometric imperfection coupling and material behavior effects on critical time to creep collapse
16 p2474 A72-34131
- Achieving fail safe design in rotors.
[AHS PREPRINT 673] 17 p2491 A72-34513
- Neutron irradiation effects on thermionic converter materials, performance and service life
18 p2707 A72-36140
- Concrete airport pavement thickness determination methods comparison, noting design life dependence on safety factors
18 p2675 A72-36786
- SRET-1 'solar cells'
19 p2869 A72-37822
- Effect of fuel on gas corrosion in jet engine combustion chambers
19 p2849 A72-38091
- Combined reliability and durability estimation for machines and devices under working conditions with the use of indicators of service life consumption
19 p2808 A72-38219
- Fatigue tests at low cyclic loads of smooth and notched Ti alloy specimens, noting surface hardening effect on service life
20 p2941 A72-39580
- Aircraft engine lifetime and turbine blade reliability
20 p2963 A72-39916
- Analytical fracture mechanics application to stress corrosion cracking test methods for examining crack growth kinetics and time-to-failure
21 p3067 A72-40913

- Erosion effects on gas turbine engine compressor blades due to dust ingestion, discussing means for alleviating performance and service life losses [ICAS PAPER 72-02] 21 p3099 A72-41127
- Life estimation and prediction of fighter aircraft. 22 p3139 A72-42972
- Detection of structural deterioration and associated airline maintenance problems. [SAWE PAPER 918] 23 p3293 A72-43465
- Reliability estimation in life testing in the presence of an outlier observation. 23 p3309 A72-43807
- Elastic stiffness and ductility of refractory materials of long service life, noting creep diagrams and tensile strength 23 p3301 A72-43959
- A concept of service life for estimating the reliability of machines and devices 24 p3405 A72-44623
- Evaluation of guided missile system in-service reliability. 24 p3448 A72-44658
- Estimation, confidence intervals, and incentive plans for sequential three way decision procedures. 24 p3406 A72-44667
- Lifetime estimation, optimal experimental design and stress level severity prediction in parametric and nonparametric accelerated life tests 24 p3406 A72-44671
- Agricultural aircraft flight loads - Typical spectra and some observations on airworthiness. 24 p3366 A72-44734
- Economic and operational aspects of fatigue - Figures of a Swiss ground attack/fighter aircraft. 24 p3367 A72-44742
- Temperature and loading conditions effects on structural element service life, showing partial healing process of microdefects 24 p3458 A72-44929
- Operational support of space shuttle transportation and payload systems with modular checkout and test equipment, noting service life and economy of operations 24 p3388 A72-45111
- SERVICE MODULES**
- Orbiting lunar spacecraft Endeavor radio transmission postocclusion reception, considering surface wave propagation and mountain formation prismatic refraction 02 p0171 A72-11753
- Design of Salyut manned orbital laboratory combined with Soyuz service module 12 p1876 A72-27107
- Aircraft hydraulic control systems modular design for maintainability, emphasizing component removal with minimum hydraulic fluid loss and air entrainment 22 p3140 A72-42294
- SERVICES**
- NT MEDICAL SERVICES**
- NT METEOROLOGICAL SERVICES**
- Computer-controlled queuing system with service interruptions. 23 p3275 A72-43605
- SERVO LOOPS**
- U FEEDBACK CONTROL**
- U SERVOCONTROL**
- SERVOACTUATORS**
- U ACTUATORS**
- U SERVOMOTORS**
- SERVOCONTROL**
- Linear regulator and servomechanism theories modification to account for fluctuation disturbances, obtaining deterministic controller design to maintain set point regulation or servotracking 02 p0198 A72-12803
- Computer servocontrolled granite stage and measuring microscope, discussing mechanical and optical construction, control electronics and applications 04 p0522 A72-15477
- Conventional open and closed loop servo analysis methods applied to Naval aircraft approach power compensator systems, using pilot model concepts [AIAA PAPER 72-124] 05 p0612 A72-16922
- German book on control technology development covering historic periods, symbols and representations, stability, integral transformations, computers, servos, relays and multivariable systems, optimization, etc 08 p1145 A72-21478
- Loaded hydraulic cylinder response to step inputs in on-off servos with three position valves, considering cavitation effect on system natural frequency [ASME PAPER 72-AUT-A] 10 p1423 A72-25052
- Servo systems operational reliability analysis for variable intensity of fluctuating interference, discussing Markov process probability determination and Kolmogoroff equations solution 11 p1609 A72-25441
- Error analysis of measurement-type servo systems with constant product /or quotient/ of dependent and independent variables applying to phase loop AFC operation 11 p1595 A72-26301
- Additional operator method application to nonlinear servosystems self adjusting circuits design, presenting system simulation results 13 p1935 A72-28611
- Self adaptive two channel iteration servosystems for input reconstruction by successive approximations, determining signal and noise error operators 13 p1936 A72-29155
- Hydraulic servosystem performance analysis, determining transfer function for time variant input-output relationship, gain levels and stability assurance 14 p2073 A72-30420
- Dynamic motion analysis of digital servo system with proportional bang-bang control by trajectory mapping on phase plane 15 p2211 A72-31895
- Servo pump nozzle area controls for gas turbines. 18 p2694 A72-36048
- Constant coefficients for linearized flow rate equation of hydraulic throttle servodrive in closed circuit stability solution by Liapunov theorem 22 p3139 A72-41873
- Synthesis problems of optimum quick-response engine control systems 22 p3216 A72-42190
- An inertially balanced servo. 23 p3311 A72-43866
- SERVO MECHANISMS**
- NT SERVOMOTORS**
- Linear regulator and servomechanism theories modification to account for fluctuation disturbances, obtaining deterministic controller design to maintain set point regulation or servotracking 02 p0198 A72-12803
- State space method application to power servomechanism analysis, discussing transition matrices and state equations 03 p0338 A72-13645
- Optimal nonlinear logical filters for noise protection of space vehicle servosystems 05 p0726 A72-16460
- Pulsed relay control system for stabilizing spacecraft orientation in flight, allowing for changes in characteristics of guidance sensor systems and slave mechanisms 05 p0731 A72-17031
- Low pressure gauge with compensation of dry friction forces in servomechanism with respect to mean value 07 p0982 A72-18929
- Accuracy criterion for master mechanism position reproduction by slave mechanism of master-slave manipulator 07 p0914 A72-19261
- Zero velocity lag servomechanism transient response sensitivity from intuitive approach to convolution problem, noting feedback compensation advantages in sensitivity reduction 07 p0964 A72-20593
- Hydraulic actuator servomechanism performance dependence on asymmetrical spool valve lap and closed loop system stability 08 p1113 A72-22153
- Servomechanism with nonlinear static and Coulomb friction under autonomous operation, predicting stability boundaries by analog computer simulation 08 p1113 A72-22154
- Bistable hydraulic servomechanisms limit cycle stable oscillations from bang-bang control and cavitation effects, discussing valve driving gear hysteresis and time lag 08 p1113 A72-22155
- Servo systems precision analysis with coefficients of output signal error caused by response inertia 11 p1609 A72-25431
- Hydraulic feedback servomechanism for dynamic response characteristics control, discussing design parameters and fluid properties influence on system performance 11 p1578 A72-26981
- Solid state ac square law function generator based on fixed elements and operating on electrical servo system principle 13 p1933 A72-29973
- Electromechanical redundant activating mechanism for F-4 aircraft dual tandem hydraulic power servo, noting application to fly by wire control 14 p2072 A72-30422
- Russian book on high precision servo systems synthesis covering combined feedback and open loop controls, accuracy improvement and root-mean-square errors minimization 15 p2210 A72-31273
- Servomechanism and reduction gear ratio selection for arc welding voltage regulator, taking into account welded joints properties 15 p2244 A72-31611
- Orion spaceborne astronomical observatory automatic control system for instrument orientation and star tracking, discussing servomechanism and pulse duration modulation 15 p2242 A72-32743
- State space approach to linear multivariable servomechanism problem, deriving controllability conditions and design procedure 15 p2213 A72-32801
- State feedback control law for linear multiinput multioutput time-invariant dynamic system under disturbance to obtain output with zero steady state error 18 p2672 A72-36054
- Servo action in human voluntary movement. 18 p2654 A72-36999
- Rational selection of structures and parameters for photoelectric meters and follow-up systems 19 p2801 A72-37964
- A method of realizing servo links imposed on a mechanical system. I 19 p2835 A72-38587
- Evaluation of the mean time to tracking failure in a nonlinear pulsed servo with irregular signal input 21 p3038 A72-40708
- Investigation of the stability of a hydraulic servo motor with rigid feedback 22 p3139 A72-41858
- Choice of loop gain for a hydraulic servo system 22 p3140 A72-42921
- SERVOMOTORS**
- Three-axis flight table with dc torque motors, discussing servo loops design and mechanical oscillations frequencies 02 p0257 A72-12541
- Mathematical models for hydraulic position servo, deriving time optimal controllers 08 p1113 A72-22156
- SERVOSTABILITY CONTROL**
- U SERVOCONTROL**
- SET THEORY**
- NT BOREL SETS**
- NT EQUIVALENCE**
- NT THRESHOLD LOGIC**
- Reachable sets calculation for linear dynamical system control, suggesting iterative procedures for numerical approximations 01 p0034 A72-11124
- Computer aided circuit design and analysis, emphasizing algebra of structural numbers as synthesis technique without system structure restriction 02 p0186 A72-11693
- Nonstable oscillating motions positive measure set in dynamic system with noncompact phase space, considering elastically rebounded falling sphere on horizontal plate 08 p1210 A72-22188
- Hilbert space filling curves for solutions of sets of nonlinear equations 09 p1340 A72-22244
- Singular control problems calculation in trajectory optimization using sufficient conditions for control values set form 09 p1291 A72-23432
- Differential games with deviation from encounter, considering strategies for continuous, programmed and discontinuous controlled motion onto given set 10 p1511 A72-24426
- Phenomenological symmetry for spatial, mechanical and relativistic physical laws, providing invariance to subsets of described objects 10 p1512 A72-24781
- Statistical analysis of entire set based on subsets, discussing problem formulation in probabilistic language 10 p1506 A72-25117
- Retrieval model based on probability distribution defined on set of all admissible arrays of elements in loci set 10 p1446 A72-25191
- Nonrandomized distribution-free ranking and selection procedures under subset selection formulation, considering application to reliability problems 13 p1962 A72-28366
- Random retrieval algorithms in finite set of preset movement directions, considering quadratic function minimization 13 p1924 A72-28610
- Multiple decision procedures, discussing location, scale parameters, discrete populations and multinomial and multivariate normal distributions in subset selection formulation 14 p2126 A72-30998
- Limit set configuration of optimal nonlinear feedback control scheme in n-dimensional state space 15 p2213 A72-32797
- Linear normed space subsets approximation by sums based on Fourier-Laplace series 16 p2417 A72-34009
- Stochastic optimal path selection via N discrete points set, discussing probability distributions and computer requirements 18 p2672 A72-36055
- Intermediate space concept extension to Sobolev-Orlicz spaces defined over subset with Lebesgue measure, generalizing trace theorems 18 p2704 A72-36460
- Existence theorems for dynamical systems admissible controls for avoidance of given set of state spaces,

- considering control process governed by ordinary differential equations
[ASME PAPER 72-AUT-C] 19 p2778 A72-37723
Necessary and sufficient conditions for differentiable non-scalar-valued functions to attain extrema.
19 p2826 A72-38244
- Singular control problems calculation in trajectory optimization using sufficient conditions for control values set form
19 p2782 A72-38515
- Variable metric algorithms - Necessary and sufficient conditions for identical behavior of nonquadratic functions.
21 p3074 A72-40227
- Communication network vertex and mixed cutset definitions and computation from interchange graph of given finite connected undirected graph without loops and multiple edges
21 p3015 A72-40634
- Extension of the range of convergence of precise iterative methods
22 p3200 A72-43133
- Uniform estimate of the residual term in a multidimensional limiting theorem for homogeneous Markov chains on the basis of a class of all measurable convex sets. I
23 p3307 A72-43344
- Electric dipole moment of diatomic molecules by configuration interaction. IV.
24 p3426 A72-44870
- Spline functions application to approximation theory problem of determining diameters of subspaces and manifolds in Banach space
24 p3419 A72-45548
- SETTLING**
Displacements in nonhomogeneous elastic layer, investigating uniformly distributed load surface settling behavior dependence on layer depth relationship to loaded area width
03 p0455 A72-14387
- SEWAGE**
Reclaimed surface, ground and sewage water oxidizability measurement, studying oxidation kinetics of potassium bichromate distilled urine condensate admixtures
13 p1910 A72-29313
- Some transport techniques for liquid human wastes and wash water under space flight conditions
21 p3006 A72-40436
- SEX**
Sex differences of chronical effect of environmental stress on blood pressure and information processing in rats, observing neurotic hypertonic blood pressure irregularity
07 p0925 A72-20660
- Echocardiographic investigation of heart rate, sex and normal aging effects on mitral valve leaflet movement in healthy subjects
22 p3148 A72-43021
- SEX GLANDS**
NT GONADS
NT TESTES
- SEXTANTS**
Stellar intensity effect on angular navigation sighting accuracy attainable between star and lunar limb using Apollo T2 sextant
01 p0097 A72-10566
- Gyroscopic device for compensating displacement of sextants or binoculars optical axis due to spontaneous hand movements
07 p0988 A72-19894
- SHADOWGRAPH PHOTOGRAPHY**
NT SCHLIEREN PHOTOGRAPHY
Shock wave impact at flat/spherical end surface of cylindrical body in supersonic nitrogen flow, using pulsed ruby laser for shadow photography
02 p0151 A72-12280
- Holographic investigation of acoustical fields, describing shadowgraph recording apparatus for sound pressure amplitude distribution
03 p0352 A72-12918
- White light shadowgram production during holographically recorded distorted wavefront reconstruction, discussing illuminating slit performance, image producing diaphragm, lenses and collimator
06 p0815 A72-17790
- Pulsating flame spread on liquid alcohol surface over range of liquid temperatures, using shadow streak photography
07 p1099 A72-19375
- Shock wave impact at flat/spherical end surface of cylindrical body in supersonic nitrogen flow, using pulsed ruby laser for shadow photography
11 p1571 A72-25702
- Shadowgraph photography method for supersonic air flow pattern around porous cone in uniform injection, noting pressure distribution dependence
12 p1752 A72-27986
- Pressure distribution and heat transfer in flow separation zone of cone tipped cylindrical body, using shadowgraph photography for flow visualization
14 p2070 A72-31005
- German monograph on supersonic flow past blunt sharp edged cones, comparing Van Dyke and method

of characteristics results with schlieren photos and shadowgraphs
16 p2343 A72-33505

Photoemissive method of recording Mertz shadowgrams and vibrating electrode technique for reading out images in reconstruction of X ray sources original distribution
21 p3051 A72-40219

SHADOWGRAPHS

U SHADOWGRAPH PHOTOGRAPHY

SHADOWS

NT LUNAR SHADOW

NT PENUMBRAS

Magnetic field strengths from umbral spectral lines in sunspots
03 p0428 A72-13301

Fine structure features of sunspot magnetic fields and umbral dots, showing magnetic and thermal or mechanical forces interaction
03 p0430 A72-13334

Short wave asymptotic formulas for shadow zone of plane diffraction, discussing asymptotic solutions for field from point source
04 p0489 A72-15386

Sunspots penumbral and umbral areas ratio in eleven year solar activity cycle, noting larger umbras at second maximum
07 p1082 A72-20295

Ground surface shadow bands observations during 7 March 1970 solar eclipse by photoelectric detection, indicating atmospheric turbulence effect
12 p1800 A72-27142

Forbidden O I lines brightness and shadow bands properties during 7 March 1970 solar eclipse, comparing with rocket measurements
12 p1800 A72-27143

Earth shadow effects on light artificial satellite orbital motion
13 p0521 A72-28440

Photoelectric observations of Fraunhofer ionized metal lines in sunspot spectrum relating to umbral dots
16 p2458 A72-33687

Shadowing function calculation as rough surface point illumination probability by point source radiation, assuming surface elevation as random process
18 p2710 A72-36407

A working model for sunspot umbrae.
18 p2727 A72-36740

Diatomic carbon lines search in sunspot umbras spectrum from solar telescope observations
21 p3108 A72-41285

SHAFTS [MACHINE ELEMENTS]

NT TURBOSHAFTS

Cylindrical shafts with deep circumferential grooves, determining effective stress concentration under axial tension or bending
03 p0451 A72-14125

Cylindrical shaft with circumferential groove, obtaining approximate solution for stress concentration at groove contour under torsion
03 p0452 A72-14130

Elastic shaft bonded to dissimilar elastic disk, considering torsion problem
04 p0583 A72-14449

Natural torsional vibrations of curved shafts, discussing oscillating system with varying flywheels
04 p0584 A72-14470

Torsional vibrations of shaft with multiple flywheels, presenting computer generated graphs for vibration modes
04 p0584 A72-14517

Dynamic analysis of straight shaft with constant noncircular section and internal friction forces, delineating trajectories for shaft center of symmetry
04 p0593 A72-15707

Vertical shaft stability on elastic sliding bearings, considering passage through self oscillation zone
06 p0894 A72-17683

Resolved shear stress formula for shafts under simultaneous tangential bending and torsion acting at dangerous points of cross section
06 p0899 A72-18643

Random vibrations and antitorque moments of rigid shaft with precision bearings, considering effects of geometrical fabrication defects and nonuniform film thickness
06 p0824 A72-18722

Motion and stable equilibrium position of horizontal rotor with nonlinear elastic and internal damping properties, discussing stress-strain-time relations of shaft filaments
09 p1409 A72-23613

Tangential stresses, rigidity characteristics and stress functions of prismatic grooved circular shafts, showing summary representations and integral transformations methods interrelationship
13 p2057 A72-29062

Steels shafts fatigue failure under cyclic loading and fretting corrosion, indicating fatigue strength increase through surface layer wear resistance augmentation
13 p1979 A72-29476

Kinematic equations of motion for elastic shaft with circular plate under external forces and moments, noting transverse and torsional vibrations
16 p2469 A72-33250

Influence of coupling behavior on the quietness of multiply supported shaft systems
18 p2694 A72-36070

Shaft support improvement by combining rolling and hydrodynamic journal bearings, noting wear and friction torque reduction
21 p3060 A72-40928

Deterioration of shaft bearings of electromotor driving aircraft centrifugal fuel pump, determining lateral force acting on impeller
23 p3252 A72-43663

Bearing supports elasticity effect on pendulum vibration of rigid rotating shaft with disk, noting vibrational frequencies relation to resonant frequencies
23 p3293 A72-43668

High accuracy contactless torque-measuring shaft with strain gage as sensor, describing circuit wiring
24 p3403 A72-45296

SHAKERS

Oscillatory shock pulse reproduction with specified spectrum for performing shock testing with electrodynamic or electrohydraulic shaker-amplifier-equalizer system
07 p0965 A72-20199

SHAKING

NT DITHERS

SHALES

Colorado Green River Formation oil shale extracts, determining nitrogenous compounds content with high resolution mass spectrometry
03 p0320 A72-13741

Mass spectrometric studies of solvent extractable acid methyl esters of oil shale from Colorado Green River Formation
03 p0320 A72-13742

Paleomicrobiological analysis of northwest Scotland Stoer Formation black shale pre-Paleozoic spheroidal unicellular fossils as probable form of marine phytoplankton
05 p0655 A72-16042

SHALLOW SHELL EQUATIONS

Initial interaction phase between thin shallow conical shell vibrating axisymmetrically and ideal incompressible fluid, determining hydrodynamic pressure effects
01 p0050 A72-10574

Laminated orthotropic plates and shallow shells structural analysis using finite element program
01 p0140 A72-10984

Static and dynamic buckling behavior of clamped shallow conical shells under axisymmetric loads
02 p0291 A72-11963

Stress concentration in shallow cylindrical shell with circular hole under axial tension, torsion and internal pressure loading
02 p0295 A72-12472

Computer program for buckling loads of shallow stiffened eccentrically orthotropic sandwich shells [DGLR PAPER 71-109]
02 p0299 A72-12703

Anisotropic shell supercritical deformation, deriving formula for lower critical load for shallow orthotropic spherical segment under external pressure
03 p0447 A72-13729

Stress-strain state of shallow shells of positive Gaussian curvature loaded by arbitrary concentrated force
03 p0450 A72-14106

Stress-strain state of shallow shell with crack along principal curvature line, discussing membrane stresses in plates and spherical shells
03 p0453 A72-14140

Shallow spherical shell natural vibration frequencies, deflection and stress function, discussing effects of internal pressure, dimensions and material properties
03 p0453 A72-14209

Soviet book on nonlinear problems of inhomogeneous shallow shell theory covering bending, stability, bearing capacity, plasticity criteria, compressibility, etc
03 p0454 A72-14225

Dynamic analysis of shallow shells with doubly-curved triangular finite element, investigating natural frequencies, mode shapes and convergence
04 p0585 A72-14844

Stochastic aerodynamic heating of shallow shell in supersonic turbulent flow by Monte Carlo method
05 p0599 A72-15845

Stress state of variable thickness long elastic shallow shell in bending and torsion, applying equations to large turbine blades
05 p0735 A72-15986

Triangular/KLI/ and quadrilateral/KQT/ thin shallow shell elements with 20 degrees of freedom, basing bending behavior on discrete Kirchhoff formulation
05 p0739 A72-16549

Singular solutions for nonaxially symmetric shallow shells under concentrated normal or thermal loading
06 p0897 A72-18319

Thin walled elastic isotropic shallow shell with thermal boundary conditions, obtaining thermoelastic solution in series form
06 p0899 A72-18657

Shallow axially symmetrical spherical shell flexural vibrations, obtaining equations iterative solution
06 p0901 A72-18705

Shallow spherical shell equations solution for vibration mode and natural frequencies from analogous vibrating plate solution
07 p1089 A72-19489

Dynamic buckling of elastic shallow structures under periodic loading, determining critical load upper and lower bounds by energy method
07 p1090 A72-19731

Equilibrium equations for thin walled shallow paraboloid shell of revolution, solving boundary value problem for edge fastened loaded circular planform region
07 p1091 A72-19757

Dynamic buckling of shallow circular cylindrical hinged panel under axial compression
08 p1249 A72-22087

Stress-strain state of shallow shells of revolution for large displacements, reducing determination to system of nonlinear differential equations
09 p1400 A72-22714

Circumferential crack in closed shallow cylindrical shell under tension, computing stress singularities strength
09 p1404 A72-22912

Boundary value problems for buckling and initial postbuckling of clamped shallow spherical and conical thin walled sandwich shells under uniformly distributed hydrostatic pressure
[ASME PAPER 71-APM-YY] 10 p1554 A72-24182

Dynamic stability of rapidly heated shallow cylindrical shells, formulating nonlinear equations
12 p1877 A72-27076

Shallow isotropic and orthotropic shells vibration, investigating dynamic rigidity for concentrated mass
12 p1878 A72-27079

Dynamics snap-through instability existence conditions in nonlinear plane deformation of shallow circular cylindrical elastic shell under impulsive loading
12 p1880 A72-27241

Nonlinear stability and vibrations of shallow shells eccentrically stiffened by oblique angled ribs under critical loads
12 p1885 A72-27971

Shallow spherical sandwich shells limiting equilibrium for material with different tension and compression yield stresses
12 p1885 A72-27974

Nonlinear first order differential equation for carrying capacity of anisotropic circular plates, curved elongate disks and shallow shells of revolution
13 p2054 A72-28457

Shallow spherical shells axisymmetric vibrations under time varying loads, discussing transverse shear and rotatory inertia effects in terms of Fourier-Bessel series
13 p2056 A72-28880

Dynamic stability of doubly curved planar rectangular shallow shell, using method of summary representation
13 p2057 A72-29066

Tangential displacements of spherical and circular cylindrical shallow shells calculated from stress function
13 p2059 A72-29490

K-order differential equation solution obtained for system of polynomial functions for shallow spherical shell under uniform pressure, using Bubnov-Galerkin and collocation methods
13 p2062 A72-29947

Differential equations for shallow orthotropic shells with variable thickness obtained by Bubnov-Galerkin variational method, presenting error assessment
14 p2163 A72-30195

Carrying capacity of rigidly hinged shell of revolution with concentric reinforcing rib, applying to shallow spherical shell under uniform external pressure
14 p2166 A72-30687

Shallow rectangular shell vibrations induced by moving band load, deriving frequency equation and load critical speed
14 p2166 A72-30688

Nonlinear equilibrium, stability and vibration equations of shallow sandwich shells with isotropic outer layer and rigid compressible filler obtained by variational method
14 p2166 A72-30700

Stochastic aerodynamic heating of shallow shell in supersonic turbulent flow by Monte Carlo method
15 p2178 A72-31264

Stress function method for calculating stress-strain state in homogeneous shallow spherical shell under arbitrary load
15 p2324 A72-31485

Elastic plates and shallow shells in finite deflection, obtaining iterative solution with good convergence for thermal stresses
15 p2324 A72-31488

Dynamic buckling of shallow circular cylindrical hinged panel under axial compression
17 p2626 A72-34665

Numerical solution for the mean first-passage-time for snap-through of shells.
18 p2737 A72-37061

On the accuracy and application of the point matching method for shallow shells.
18 p2739 A72-37090

Mathematical analogies in a theory of shallow spherical shells and plates allowing for transverse shear
19 p2872 A72-37540

Complex transforms method for Timoshenko theory of elastic shells, deriving transverse shear strain equations for shallow shells
19 p2876 A72-38154

Investigation of the snap-through of rigidly clamped shallow spherical shells under the action of a dynamic stepped load
19 p2877 A72-38163

Behavior of viscoelastic shallow spherical shells subjected to dynamic pressure.
21 p3122 A72-41245

Multilayer shell theories with allowance for transverse shear and transverse normal deformation of layers, noting viscoelastic material and anisotropic shallow shells
21 p3125 A72-41537

Reissner nonlinear equations for stability analysis of shallow shells of revolution, noting critical loads range and error analysis
22 p3232 A72-41856

Solution for shallow shells of revolution with allowance for large deflections by the method of integral relations
22 p3232 A72-41869

A collocation solution of the nonlinear equations for axisymmetric bending of shallow spherical shells.
22 p3232 A72-41938

Nonlinear buckling of cylindrical shells.
22 p3236 A72-42607

Limiting equilibrium of shallow conical shells of variable thickness
23 p3348 A72-43787

Dynamic response of viscoelastic shallow spherical shells.
23 p3349 A72-43972

Response of shallow spherical shells to pulse pressure loads.
24 p3454 A72-44605

Forced and free vibrations of shallow cylindrical shell in rectangular duct filled with ideal fluid
24 p3459 A72-45004

Variable thickness shallow spherical shells of revolution axisymmetric loads carrying capacity, determining limit equilibrium through application of Tresca yield point concept
24 p3460 A72-45725

Stress state of variable thickness long elastic shallow shell in bending and torsion, applying equations to large turbine blades
24 p3460 A72-45728

SHANKS
U JOINTS (JUNCTIONS)
SHANNON INFORMATION THEORY
U INFORMATION THEORY
SHAPED CHARGES
Emergency systems for helicopter crew and passenger survivability improvement, discussing use of ejection seats, extraction systems parachute bail-out and shaped explosive charges
08 p1109 A72-21581

SHAPES
NT CONVEXITY
NT ELLIPTICITY
NT LINE SHAPE
NT ROSETTE SHAPES
Soviet book on structural shape effects of machine parts on durability, covering production, gear transmissions shafts, axles, threaded joints, etc
03 p0364 A72-13966

Extruded superalloy powder structural shapes preparation by filled billet technique for improved chemical and mechanical properties
07 p0994 A72-19483

Shape factors of heat conduction for fin arrangements with isothermal boundaries, using conformal mapping
09 p1412 A72-23688

Meaningful shape coding for aircraft switch knobs.
17 p2510 A72-35944

Thermal design of hybrid modules and assemblies.
22 p3161 A72-43172

Structural design optimization via area ratio method, developing shape factor design charts
[SAWE PAPER 937] 23 p3344 A72-43477

SHARING
U COORDINATION
SHARP LEADING EDGES
Supersonic flow patterns near yawed obstacles around flat plate sharp leading edge with high pressure regions in reversed separated flow zone
06 p0756 A72-18122

Heat transfer rates of impingement cooling in gas turbine airfoils, noting leading edge sharpness effects for slot and circular jet configurations
[ASME PAPER 72-GT-7] 11 p1703 A72-25610

Viscous interaction over concave and convex surfaces at hypersonic speeds.
23 p3249 A72-44308

SHATTERING
U FRAGMENTATION
SHEAR DISTURBANCES
U S WAVES

SHEAR FATIGUE
U SHEAR STRESS
SHEAR FLOW
Equilibrium shear flow of stratified brine in cyclically continuous rectangular tank, discussing stable density region erosion by turbulent layers, Richardson numbers, transition layer and entrainment
01 p0051 A72-11228

Slit element flow in shear flow turbopump rotors, presenting solutions for laminar and turbulent flow between two parallel disks rotating with same angular velocity
02 p0204 A72-12227

Boundary layers nonlinear resonant instability, investigating Tollmien-Schlichting wave triads interactions with energy transfer from primary shear flow to disturbance
03 p0340 A72-13160

Self similar solutions for unsteady shear flows of conducting Newtonian fluids with rheological power law under transverse magnetic field
03 p0397 A72-13997

Flat plate in turbulent shear flow polymer solution, predicting maximum drag reduction with interactive layer concept
03 p0343 A72-14322

Turbulent shear flow mean velocity profiles, calculating eddy diffusivity for momentum and Reynolds stress
03 p0343 A72-14323

Barotropic stability of stratified shear flow to non-geostrophic disturbances by linear analysis
04 p0541 A72-14453

Sound propagation in acoustic ducts with shear flow and wall lining by Ritz-Galerkin technique
04 p0511 A72-14848

Slow motion in shear flow of doublet of two spheres in contact, using Stokes equations solution
04 p0511 A72-14860

Laminar shear flow over impulsively started wedges, describing flow field by Goldstein-Rosenhead method of approximate series expansion
04 p0590 A72-15190

Complex perturbation potential of constant vortex shear flows around airfoil activated by motion in presence of rectilinear wall
05 p0600 A72-16122

German book on turbulent flow theory and applications covering isotropic and homogeneous nonisotropic fields, shear flows, pipe flows, free turbulence, boundary layers, etc
05 p0649 A72-16286

Hot-wire anemometers signals resolution into velocity-temperature fluctuations correlations in compressible flow with shear turbulence wakes
[AIAA PAPER 72-117] 05 p0664 A72-16822

Turbulence effects in stratified shearing flow, determining relationship between measured mass flux and overall Richardson number
06 p0798 A72-17762

Continuum plasma turbulent boundary layer structure in shear flow, showing electron to ion saturation currents ratio decrease from laminar case
[AIAA PAPER 72-107] 07 p1040 A72-18953

Droplets coalescence in clouds, considering microturbulence effects due to laminar shear flow
07 p1030 A72-19102

Polar night jet idealized model with zero tropospheric and constant vertical stratospheric shear, considering instability due to small wave disturbances
07 p1030 A72-19103

Sound generation in shear flow turbulence, discussing dependence on mean flow velocity and temperature
07 p0909 A72-20097

Turbulence measurements in shear flow systems including pipe, tank and multijet reactor configurations
09 p1292 A72-22306

Atmospheric vertical shear at visible cloud level in Jupiter equatorial zone from blue and red wavelength photographs
10 p1531 A72-23712

Turbulent shear stress and kinetic energy characteristics of subsonic air flow in straight conical diffuser, using hot-wire anemometry measurements
10 p1416 A72-23862

Aerodynamic forces calculation for constant vortex shear flows around airfoil fixed between rectilinear walls, noting resultant perpendicularity to Ox axis
10 p1465 A72-24115

Inviscid parallel stratified shear flow stability to two dimensional disturbances, solving Taylor-Goldstein stability equation for eigenvalues by computerized numerical integration
10 p1466 A72-24329

Cavity flow driven by buoyancy and shear, obtaining flow and temperature fields from Navier-Stokes equation numerical solution
10 p1467 A72-24366

Internal Alfvén gravity waves propagation in rotating Boussinesq inviscid adiabatic conducting fluid shear flow within transverse magnetic field, considering electromagnetic and Coriolis forces effects
10 p1511 A72-24470

Transverse shear flow stability analysis based on disturbance energy balance determination, applying to ducted and jet stream boundary layer flows

10 p1469 A72-24531

Turbulent free shear flow intermittency factor determination by electronic circuit, discussing calibration and errors

11 p1617 A72-25997

Viscous effects on turbulent diffusion shear flow past semiinfinite flat plate, using Wiener-Hopf equations

[DFVLR-SONDDR-171] 11 p1617 A72-26370

Rain droplets growth by collision and coalescence during fall through sheared air flow, discussing discrepancies between calculated and experimental collision efficiencies

11 p1619 A72-26642

Heat and momentum transfer properties and storm propagation speed under steeply convective overturning in shear, considering cumulonimbus convection scale of atmospheric motion

12 p1840 A72-27704

Effect of magnetic field superimposed on turbulent shear flow of electrically conducting fluid, discussing turbulent friction in plane flow

13 p2010 A72-28764

CAT forecasting based on fluid mechanics experimental studies of stratified shear flows stability and meteorological analyses of aircraft CAT encounters

13 p1994 A72-28866

Clear air turbulence nonlinear generation mechanism based on finite amplitude periodic waves in stratified shear flow critical layers, considering buoyancy, viscosity and heat conduction effects

14 p2127 A72-30226

Differential turbulent shear flow equation reduction to deduce similarity criteria for velocity pulsations, using Karman transformation

14 p2094 A72-30292

Plane acoustic-gravity wave reflection, refraction and amplification at interface separating two fluids in relative motion, noting shear flow speed effect

16 p2383 A72-32968

Shear-layer flow regimes and wave instabilities and reattachment lengths downstream of an abrupt circular channel expansion.

[ASME PAPER 72-APM-2] 17 p2538 A72-34811

Sound attenuation in acoustically lined circular ducts in the presence of uniform flow and shear flow.

17 p2582 A72-35411

Eddies memory in turbulent shear flow from experiments on plane turbulent wakes undergoing equilibrium transition under impulsive pressure gradient effect

18 p2680 A72-36476

Reynolds stress development in wall region of turbulent shear flow of oil investigated by hot film measurement technique and anemometer signal analysis

18 p2680 A72-36478

Free convection similarity and measurements in flows with and without shear.

18 p2706 A72-36634

The forces on a flat plate in a Couette flow.

18 p2683 A72-36996

Stokes fluids nonlinearity effects on turbulent flow with lateral shear in terms of stress and deformation tensors

19 p2785 A72-37470

Relation between impurity shear dispersion in the atmospheric ground layer and the turbulence characteristics

19 p2829 A72-38772

Momentum transport by gravity waves in a perfectly conducting shear flow.

19 p2788 A72-38792

The mechanics of an organized wave in turbulent shear flow. II - Experimental results.

19 p2789 A72-38793

The mechanics of an organized wave in turbulent shear flow. III - Theoretical models and comparisons with experiments.

19 p2789 A72-38794

The generation of magnetic fields in astrophysical bodies. IX - A solar dynamo based on horizontal shear.

20 p2966 A72-38910

The calculation of low-Reynolds-number phenomena with a two-equation model of turbulence.

[ASME PAPER 72-HT-20] 20 p2914 A72-39688

The stability of a coupled wave-turbulence system in a parallel shear flow.

20 p2948 A72-39797

Large-scale instabilities of turbulent wakes.

21 p3044 A72-40116

Magnetic field effects on turbulent shear flow of electrically conducting fluid, discussing turbulence level, friction stress and heat exchange

21 p3089 A72-40260

Karman vortex street in a uniform shear flow.

21 p2992 A72-41247

Burgers model equation for shear flow turbulence with complex physical processes and nonlinearities in governing equations

21 p3047 A72-41637

Diffusion toward a particle in the case of shear flow of a viscous liquid - Approximation of the diffusion boundary layer

22 p3165 A72-41910

Diffusion flame in homologous turbulent shear flows.

24 p3395 A72-45564

SHEAR LAYERS

Wall shear layers effect on sound attenuation spectra in acoustically lined rectangular ducts, noting dependence on Mach number

04 p0462 A72-14842

Noise generation from turbulent supersonic shear layers, including low supersonic and transonic ranges for jet noise applications

04 p0463 A72-15566

Initial boundary layer effect on turbulent free shear layer velocity profiles, deriving procedure applicable at any streamwise station

05 p0645 A72-15795

Computerized calculations of turbulent shear layers with compressibility, heat transfer, three dimensionality or unsteady flow, using differential equation

[ASME PAPER 71-WA/FE-8] 05 p0646 A72-15934

Fluctuating flow in idealized model of turbulent shear layer composed of many discrete two dimensional vortices, analyzing noise generation

[AIAA PAPER 72-155] 05 p0609 A72-16955

Rotating homogeneous incompressible fluid flow field over step with interior geostrophic regions, horizontal surfaces Ekman layers and vertical shear layers

05 p0653 A72-17008

Compressibility and total enthalpy difference effects on laminar free shear layer from numerical integration of equations of motion

05 p0653 A72-17011

Shear layer finite thickness and magnetic field effects on Kelvin-Helmholtz MHD instability of earth magnetopause boundary

[AD-746435] 07 p0974 A72-18892

Median true height atmospheric profile model synthesis from propagation parameters, using polynomial representations and alpha-Chapman layers

08 p1157 A72-21106

Uniform flow past semiinfinite flat plate for large Reynolds numbers and strong blowing, noting injected fluid region separation from free stream by shear boundary layer

10 p1467 A72-24369

Turbulent shear layer flow in reattachment region downstream of backward facing step and non-monotonic return to ordinary boundary layer state, noting eddy length scale decrease

10 p1468 A72-24467

Drazin method application to thermal stratification effects on unbounded jets and shear layers stability characteristics

11 p1615 A72-25552

Turbulent separating and reattaching supersonic boundary layer flows in two dimensional compression corner, noting Reynolds number effect on separated shear layer length

11 p1618 A72-26634

Stability of free shear layer in wind tunnel two layered temperature differentiated air flow against small periodic disturbances, noting critical Richardson number

11 p1619 A72-26638

Aviation hazards due to stably stratified shear and turbulence zones, discussing meteorological analysis of 747 jumbo jet turbulence incident

13 p1994 A72-28865

Prandtl number effect on stratified free shear layer stability, comparing critical Richardson number to linear inviscid theory result

13 p1942 A72-29111

Supersonic jet exhaust noise radiation from turbulent shear layer instability waves, noting acoustic energy flux dependence on streamwise distance

13 p2028 A72-29581

Reattachment heat transfer for laminar or turbulent separated shear layers, comparing predictions with measurements for cavities, ramps, spiked-noise bodies and forward facing step

[AIAA PAPER 72-717] 16 p2344 A72-34031

Shear-layer flow regimes and wave instabilities and reattachment lengths downstream of an abrupt circular channel expansion.

[ASME PAPER 72-APM-2] 17 p2538 A72-34811

Sound propagation in duct shear layers.

17 p2582 A72-35413

Transmission of sound in ducts with thin shear layers - Convergence to the uniform flow case.

18 p2710 A72-36405

Behavior of spherical balloons in wind shear layers.

18 p2643 A72-36963

Optimization of acoustic linings in presence of wall shear layers.

21 p3083 A72-40334

Transition in compressible free shear layers.

21 p2993 A72-41310

Transverse velocity shear instabilities within a magnetically confined plasma.

21 p3093 A72-41628

Turbulent flow experimental and theoretical investigation, discussing Reynolds stress transport equations, shear layers and turbulence models in context of digital prediction methods

21 p3047 A72-41639

Incompressible free shear layers instability, considering Reynolds number, velocity profile, disturbances and compressibility effects

22 p3167 A72-42579

SHEAR PROPERTIES

NT SHEAR STRENGTH

Dynamic theory of thin elastic beams under large deflection, taking into account shear deformation and axial stress results

[ASME PAPER 71-APM-EE] 04 p0590 A72-15183

Earth mantle shear velocity model derived from S waves travel time gradient direct measurement, disregarding deep depth lateral homogeneity assumption

04 p0519 A72-15578

Random filament misalignment effects on rigidity and tensile strength of unidirectional graphite composites under shear loading

08 p1192 A72-21681

Torsion test determination of interlayer and intralayer-plane shear moduli in annular specimens of glass fiber reinforced plastics

08 p1194 A72-21756

Nondestructive determination of glass reinforced plastics normal elastic and shear moduli and strength characteristics by vibrational, pulsed and acoustic methods

08 p1195 A72-21773

Boron and carbon fiber reinforced plastics anisotropic stress-strain properties, considering fiber misalignments curvature and low shear resistance effects

08 p1196 A72-21857

Bending under concentrated load of laminated cantilever plate with low interlaminar rigidity, taking into account low shear resistance effects

08 p1248 A72-21860

Interlaminar shear testing of composite materials, discussing short beam, scissor and torsional methods

[PI PAPER 7] 09 p1337 A72-22542

Stiffness, stress and deformation analysis of discretely attached corrugated shear webs, using minimum potential energy and calculus of variations methods

[AIAA PAPER 72-351] 11 p1728 A72-25380

Heterogeneous shear deformation effect on dynamic response of laminated plates for various local elastic deformation and interface conditions

[AIAA PAPER 72-398] 11 p1731 A72-25419

Interlaminar shear properties of polymer matrix composites from dual element beam moment test

11 p1671 A72-25465

Elastic body transverse impact against vibrating rectangular plate with allowance for rotatory inertia and shearing forces, using wave equation

11 p1732 A72-25532

Russian monograph on three dimensional deformable bodies stability covering linearized equations for subcritical deformations and strength analysis of low shear rigidity structures

12 p1888 A72-28337

Mixed triangular finite element model for plate bending problems including shear deformation effects, discussing error analysis and convergence

15 p2326 A72-31716

Experimental investigation of the interlaminar shear properties of composite materials.

[SESA PAPER 1985A] 17 p2631 A72-34824

Young and shear moduli of binary Fe base alloys as functions of composition and temperature by ultrasonic pulse echo technique

20 p2937 A72-39287

Shear modulus of liquids at elastohydrodynamic lubrication pressures.

21 p3059 A72-40688

Dependence of linear elasticity solutions on the elastic constants. II - Dependence on the shear modulus in elastostatics.

21 p3119 A72-41106

SHEAR STRAIN

Webbing joints stitching strain, considering nylon and flax yarns stretching properties and various stitching patterns strengths

01 p0005 A72-10315

Tensile plastic flow and fracture behavior of PdSi based alloys in glassy microcrystalline and crystalline states, noting shear deformation bands

09 p1339 A72-23382

Von Mises yield criterion extended to thin walled circular cylinder plastic torsional straining, noting variations of anisotropic parameters and yield stresses with shear strain

[ASME PAPER 71-MET-Y] 11 p1735 A72-25877

Harmonic equation for antiplane shear deformation of elastic composite materials with multiple circular inclusions

12 p1883 A72-27562

Rigid smooth body pressing into elastic plate surface subjected to cylindrical bending, discussing contact problem and transverse shear strain

13 p2062 A72-29950

Shear strains and elastic anisotropy of transversely isotropic cylindrical shell with circular hole under uniform internal pressure, using shallow shell equations 14 p2165 A72-30438

Combined axial compression and shear deformation effect on elastic columns buckling behavior, evaluating third order polynomials eigenvalues by computerized Newton-Raphson technique 14 p2168 A72-30934

Plastic deformation in metals and highly crystalline polymers as function of shear strain, strain rate, frequency and vibrational amplitude 15 p2328 A72-31840

Transverse shear deformations in laminated anisotropic plates from generalized treatment for isotropic and sandwich plates with homogeneous cores [AD-745613] 16 p2375 A72-32846

Test equipment for high strain rates in shear with torsional split-Hopkins pressure bar 16 p2373 A72-33196

On a laminated orthotropic shell theory including transverse shear deformation. [ASME PAPER 72-APM-7] 17 p2629 A72-34807

Shear deformation in heterogeneous anisotropic plates. 17 p2633 A72-35294

Contribution to the theoretical calculation of sandwich structures with tube core 18 p2736 A72-36939

Variational principle based three dimensional elasticity theory of micropolar anisotropic sandwich plates, considering transverse shear and strains and rotatory inertia 18 p2737 A72-37057

Timoshenko finite element beam theory application to flexural vibration problems, considering shear deformation and rotary inertia effects 18 p2740 A72-37206

Complex transforms method for Timoshenko theory of elastic shells, deriving transverse shear strain equations for shallow shells 19 p2876 A72-38154

The octahedral shear strain theory and its relation to biaxial cumulative fatigue damage. 20 p2978 A72-39202

Time dependent deformation of isotropic viscoelastic materials, discussing rectilinear shear, circular cylinder torsion, spiral shear of layer and conical layer torsion 21 p3119 A72-41075

Strength and deformation characteristics of fiberglass under torsional and compressive shear loads, investigating temperature effects on elastic modulus 23 p3306 A72-43730

Shear-strain-rate effects in a high-strength aluminum alloy. 23 p3302 A72-43983

Variational analysis of sandwich beams under static loads, presenting shear deformation and normal stress distributions [ASME PAPER 72-APM-R] 23 p3350 A72-44055

SHEAR STRENGTH

Brazed joints shear strength and ductility tests, discussing deformation, hardness, corrosion, irradiation, structure and microanalysis 01 p0074 A72-10285

Ti alloys for aircraft structures, emphasizing weldability, tensile fatigue and residual strengths, shear-carrying qualities and fuselage shell design 03 p0373 A72-13616

Unidirectional and orthogonally cross-ply carbon fiber reinforced plastics laminates, determining interlaminar shear strength and fatigue life [PI PAPER 8] 09 p1337 A72-22543

Dynamic shear modulus and damping of polystyrene composites filled with glass, salt and foam, including skin effect correction 10 p1500 A72-24260

Random filament misalignment effect on reinforced composite strength, discussing bundle, tensile and shear strengths 11 p1673 A72-25486

Variable shear modulus circular isotropic plate torsion by rigid circular stamp, obtaining stresses and displacements by Fourier analysis 12 p1881 A72-27319

Ice adhesive shear strength to steel bearing surfaces coated with bonded solid lubricants, describing low temperature test apparatus and results [ASLE PREPRINT 72AM 4] 13 p1964 A72-28970

Pure shear testing method and apparatus, verifying validity of method by chromoplastic test specimens 16 p2469 A72-33231

Carbon fiber structure at graphitization temperatures to 3100 C in terms of surface energy and internal stress accounting for low shear strength 17 p2572 A72-35660

Adhesion characteristics of alpha-aluminum oxide-nickel system from shear strength measurements, investigating effects of sintering parameters and Ti and Zr alloying components 20 p2940 A72-39445

Crystal structure and shear strength of solids and imperfections in metals in framework of X ray diffraction and dislocation theory 20 p2942 A72-39998

The use of a torsion machine to measure the shear strength and modulus of unidirectional carbon fibre reinforced plastic composites. 23 p3306 A72-43562

Strength and deformation characteristics of fiberglass under torsional and compressive shear loads, investigating temperature effects on elastic modulus 23 p3306 A72-43730

SHEAR STRESS

NT TORSIONAL STRESS

Slow viscous flow shear stress and velocity field analysis, using photoviscosity and bubble technique [SESA PAPER 1902] 02 p0201 A72-11508

Fourier series terms number effect on sandwich plate critical shear stress calculation accuracy 02 p0294 A72-12438

Laminar two dimensional hypersonic flow over stepwise accelerated flat plate at zero angle of attack, obtaining time dependent velocity and temperature profiles by linearized flow equations 03 p0442 A72-13236

Slip line field for plane strain extrusion of strain hardening material, calculating shear stress 03 p0363 A72-13708

Buoyancy effect on shear stress and heat transfer in horizontal boundary layer, considering Boussinesq approximation 03 p0343 A72-14320

Flexible surface effects on shear stress fluctuations beneath turbulent boundary layer, using fiber optic displacement probe 03 p0343 A72-14324

Ekman boundary layer shear stress due to laminar and turbulent flow over hills 03 p0386 A72-14336

Velocity and shear stress in laminar boundary layer flow on flat plate with narrow suction slot 04 p0461 A72-14461

Shear stress and stability of composite elastic double layer with plane circular crack under torsion 04 p0588 A72-15054

Thermoelasticity theory coupled linear equations for thin orthotropic shells, taking into account rotatory inertia and lateral shear 04 p0588 A72-15060

Turbulence intensities and shear stress measurements in wake of thin flat plate by rotating single hot-wire anemometer 04 p0524 A72-15498

Viscoelastic fluid flow past infinite plane porous wall with time dependent suction, investigating mean velocity profile and wall shear stress 04 p0514 A72-15704

Sensors and circuit design for flow angle and shear stress measurements using heated film and wires [ASME PAPER 71-WA/FE-17] 05 p0661 A72-15930

Local plastic deformation relation to tangential shear stresses, deriving expressions to determine critical levels 05 p0734 A72-15982

Stress-strain characteristics of nylon-polyurethane coated fabric under biaxial tension and shear forces 05 p0736 A72-16108

Torsional vibration induced by periodic circumferential shear force on composite circular cylinder with varying rigidity and density, obtaining solutions for various boundary conditions 05 p0740 A72-16727

Helicopter rotor boundary layer, comparing analytical shear stress and velocity distributions obtained by momentum integral techniques with hot wire probe experimental data [AIAA PAPER 72-38] 05 p0607 A72-16900

Turbulent shear stress, intensity and velocity field in coflowing axisymmetric jets, using eddy viscosity model [AIAA PAPER 72-47] 05 p0652 A72-16926

Fiber pull-out from elastic matrix, calculating shear stress and load distribution dependence on elastic properties and fiber length 06 p0897 A72-18152

Shear and direct stresses on fuselage model cross section due to concentrated radial loads on frame comparing measurement with prediction by matrix force analysis 06 p0898 A72-18322

Resolved shear stress formula for shafts under simultaneous tangential bending and torsion acting at dangerous points of cross section 06 p0899 A72-18643

Interaction surfaces for structural members under combined axial, shear force and bending moment, investigating shear effect on yielding of arches 07 p1090 A72-19730

Basal and prismatic crystal dislocations in Be, measuring critical resolved shear stress dependence on temperature at 300-500 K 08 p1185 A72-20991

Oriented glass fiber reinforced plastics fatigue strength and creep under interlayer shear and compression 08 p1194 A72-21752

Cicala formulas generalization and plasticity theory for deformation strain anisotropy, sliding and elastic strains influence on shear stress 08 p1246 A72-21806

Transverse shear effect during bending of cantilever plates with low shear rigidity 08 p1248 A72-21864

Stress and couple stress fields near antiplane shear crack tip, determining eigenfunctions to satisfy field equations and boundary conditions 09 p1402 A72-22744

Crack propagation in elastic layer under antiplane state of deformation for arbitrarily distributed shearing forces on crack surface 09 p1404 A72-22766

Stress-strain curve determination for shear of twisted conical elastic bar, using torque and angle distribution 09 p1404 A72-22774

Parametric instability of flat rectangular plates under periodic or shear sinusoidal in-plane boundary loads 09 p1408 A72-23463

Equivalent stress and plastic strain rates, based on shear stress hypothesis for theory of anisotropic plasticity of plastic materials under combined stress 10 p1553 A72-23745

Turbulence models application to internal flow prediction, using two-, three- and five-equation models and shear stress hypothesis 10 p1463 A72-23854

Turbulent shear stress calculation from mean velocity data for complex flows with inappropriate boundary layer approximations, using method of characteristics 10 p1463 A72-23866

Rotational, centrifugal and Coriolis force effects on turbulent boundary layer development, discussing changes in structure and shear stress distribution 10 p1464 A72-23870

Asymmetric flow in plane channel characterized by diffusional transport of turbulent shear stress and kinetic energy from rough to smooth wall regions 10 p1467 A72-24368

Stress distribution determination by shear stress difference method in curvilinear orthogonal coordinate systems 10 p1557 A72-24405

Photoelastic investigation of star shaped models for loading direction influence on shear stress distribution at notch tip region in uniform tensile field 10 p1559 A72-24897

Fluctuating turbulent stresses effects on flow over wavy boundary, comparing calculated with measured pressure distributions [AD-742545] 10 p1470 A72-25066

Helical turbulent flow through concentric annulus with rotating inner cylinder, examining axial and tangential velocity distribution and shear stresses 10 p1471 A72-25190

Shear stress and traveling wave response of plate bonded to randomly vibrating viscoelastic half space for soil vibration studies 11 p1688 A72-26062

Noncoincidence of maximum velocity and zero shear stress due to asymmetric turbulent velocity profiles, considering effect on momentum, heat and mass transfer in noncircular channels 11 p1618 A72-26534

Aircraft windscreen reliability, discussing delamination, interface shear stress effects and analogy to metal fatigue 12 p1812 A72-27011

Critical resolved shear stress and solute atom concentrations relationship in solid solution hardening of metal crystals 12 p1853 A72-27101

Stability of transversely isotropic cylindrical shell with elastic filler under axial compression, deriving approximate equations for transverse shear stress effect 13 p2055 A72-28556

Collapse loads of symmetrically tapered cantilever beams under uniformly distributed end shear, considering optimum tapering angle for minimum weight 13 p2059 A72-29596

Magnetoelastic coupling existence between shearing stresses and linear deformation, noting influence on Poynting effect experimental results 13 p1980 A72-29782

Von Karman constant in low Reynolds number turbulent flows, observing shear stress gradients effects on viscous sublayer 13 p1944 A72-30027

Solar rotation effects on solar wind magnetic energy transport by magnetic shear stress near sun 14 p2147 A72-30557

Shear stress distribution and local heat flux at surface of axisymmetric bodies for laminar and turbulent boundary layer flows 14 p2071 A72-31163

Unsteady laminar boundary layer on body of revolution with axial and torsional oscillations, calculating velocity distribution and shear stress variation
15 p2178 A72-31402

Stability analysis of thin walled circular cylindrical shell under shearing force action to one end, calculating buckling modes
15 p2324 A72-31483

Cosserat strip bending by singular shear stresses, normal stress dips and spin moments, confirming Saint Venant principle
15 p2324 A72-31484

Singularities of cylindrical shell under concentrated twisting couple, investigating axial and circumferential deformations and shear stress distribution
15 p2329 A72-32139

Power law fluids impulsively started flow over plate, presenting analytical expressions for velocity distribution, shear stress and boundary layer thickness
16 p2375 A72-32833

Fully developed turbulent air flow through concentric annuli, measuring inner wall shear stress distribution by zero-shear position location and sliding sleeve technique
16 p2375 A72-32875

Dynamic analysis of transient impact response of finite crack opened by in-plane shear tractions
16 p2464 A72-32920

Pressure, shear stress and yaw angle measurements in flow through aircraft intake S-shaped ducts with turbulent boundary layer at entry, noting vortex generation
16 p2377 A72-33403

Transient elastic wave propagation in circular cylinder during sudden torsional shear stress application to end surface, noting surface particle velocity and stress
16 p2426 A72-33660

Shear stress and dimensionless velocity profiles of plane incompressible fluid wall jet propagation along curved surface
16 p2380 A72-33856

Heat generation in oscillating torsional spring modeled by viscoelastic hollow cylinder subjected to sinusoidal shear stresses, calculating stress and temperature distribution and displacement
17 p2635 A72-34232

A fracture mechanics analysis of adhesive failure in a single lap shear joint.
[SESA PAPER 1990A]
17 p2630 A72-34815

Shear buckling of an elastically supported fiber.
17 p2633 A72-35290

Shear stresses distribution in isothermal incompressible turbulent boundary layer with positive pressure gradient by diffusers in open jet wind tunnel
17 p2544 A72-35931

Non-analytic character of the shear-tensor distribution function in incompressible turbulence.
18 p2678 A72-36012

Nonuniformly thick combined cylindrical shell vibrations, studying radial displacement, bending moment and shearing force
18 p2735 A72-36695

An integral analysis of condensing annular-mist flow.
18 p2682 A72-36720

Buckling of orthotropic, curved, sandwich panels subjected to edge shear loads.
18 p2735 A72-36770

Effect of fiber end, fiber orientation and spacing in composite materials.
18 p2738 A72-37086

On the accuracy and application of the point matching method for shallow shells.
18 p2739 A72-37090

On the use of the Preston tube in elliptical ducts.
18 p2676 A72-37094

Yielding of fiber reinforced Tresca material.
19 p2873 A72-37695

Similarity predictions for shear stress and heat flux cospectral behavior in atmospheric turbulent boundary layer
19 p2829 A72-38560

Kramer and Couette flows using the Bhatnagar-Gross-Krook model.
20 p2913 A72-39418

Photoelastic determination of mixed mode stress intensity factors.
20 p2981 A72-39963

A hyperboloidal notch in a transversely isotropic material under pure shear.
21 p3119 A72-41105

Transverse shear effect on thin shells collapse load, considering influence on Shapiro yield surfaces
21 p3121 A72-41213

Measurements of Reynolds shear stress fluctuations in a turbulent boundary layer.
21 p3047 A72-41638

Turbulent flow experimental and theoretical investigation, discussing Reynolds stress transport equations, shear layers and turbulence models in context of digital prediction methods
21 p3047 A72-41639

Dislocation pile-ups in periodic internal stresses.
22 p3214 A72-42316

Wind tunnel measurement for demonstrating similarity of atmospheric turbulent boundary layer mean velocity and shear stress at high Reynolds number
22 p3201 A72-42598

Wind profile development above a locally adjusted sea surface.
22 p3202 A72-42600

On the diffusion of a load from a semi-infinite stringer bonded to a sheet.
22 p3238 A72-42833

Fe-Ni-C martensite reverse transformation to austenite during large and rapid applied shear, evaluating shear zone neighboring partially pierced hole
22 p3193 A72-43031

Limiting equilibrium of shells of revolution and circular plates with allowance for shear stresses
23 p3348 A72-43789

Improved method for determining shear stresses and checking the strength of circular cylinders in transverse bending
23 p3349 A72-43968

Incompressible continuous media three dimensional boundary problems solution by pure shear state analysis, discussing application to plasticity theory
23 p3314 A72-44222

Stress induced birefringence in an isolated and a shortcircuited KH2PO4 crystal.
23 p3324 A72-44322

A sandwich plate with a part-through and a debonding crack.
24 p3456 A72-44813

The structure of turbulent flows adjacent to walls.
24 p3390 A72-45001

The effect of shear on a penny-shaped crack at the interface of an elastic half-space and a rigid foundation.
24 p3459 A72-45250

Local plastic deformation relation to tangential shear stresses, deriving expressions to determine critical levels
24 p3460 A72-45724

SHEAR WAVES

U S WAVES

SHEARING

Sandwich structures buckling calculation by transfer matrices with allowance for cross section shearing
16 p2471 A72-33680

SHEARING STRESS

U SHEAR STRESS

SHEATHS

NT ION SHEATHS

NT PLASMA SHEATHS

SHEET METAL

U METAL SHEETS

SHEETS

Experimental and theoretical study of the fracture of sheet materials in the presence of cracks
23 p3349 A72-43958

SHELL STABILITY

Barrel shaped cylindrical shell stability and free vibrations under torque, evaluating distortion influence by small parameter method
01 p0142 A72-11364

Geometrical method in nonlinear shell theory for supercritical elastic deformation determination, considering stability loss and dynamics problems
02 p0289 A72-11612

Flexible viscoelastic orthotropic plates and shells obeying linear heredity relations, solving stability and bending problems by Laplace transform
02 p0290 A72-11625

Elastic equilibrium in circular conical orthotropic shells of linearly variable thickness, investigating stresses under arbitrary loads
02 p0297 A72-12615

Truncated conical shell buckling under combined torsion and internal pressure load, discussing prebuckling stress conditions
02 p0298 A72-12666

Highly elastic cylindrical layer reinforced with anisotropic shell, deriving stress-strain state and nonlinear elastic stability
02 p0299 A72-12687

Infinitely long orthotropic cylindrical shell partially filled with elastic media under compression load, determining local stability
02 p0299 A72-12688

Creep buckling of cylindrical finite two-layer shell under external hydrostatic pressure, considering rigidly clamped and hinged end conditions
03 p0444 A72-13574

Thick walled rigid plastic cylinders under pressure, obtaining uniqueness and stability of finite deformation
03 p0446 A72-13706

Plastic stability of cylindrical shells under combined internal pressure and axial compression loads
03 p0448 A72-13904

Critical load and stability analysis for three layer orthotropic cylindrical shell with filler under nonuniform external pressure
03 p0448 A72-13906

Axisymmetric load influence on stability of eccentrically reinforced shells of revolution, determining critical loads and linear and nonlinear relations for moment-subcritical states
04 p0587 A72-15014

Soft uniaxial crosswise reinforced shell stability under internal pressure, determining equilibrium state
04 p0587 A72-15015

Linearized equilibrium equations for thin spherical shell with internal pressure, obtaining free vibration modes
04 p0587 A72-15018

Cylindrical shell stability and load capacity at large plastic deformations under internal pressure
04 p0587 A72-15019

Convergence of iterative schemes for calculating stress state of thin shells with allowance for nonlinear terms in differential equilibrium equations
04 p0587 A72-15048

Critical load limit and stability of elastic isotropic and orthotropic cylindrical shells, using net-point method for end conditions
04 p0588 A72-15053

Elastic equilibrium of circular conical orthotropic shells with linearly varying thickness, determining real and complex roots of stress state characteristic equation
04 p0594 A72-15710

Variable thickness shallow spherical shells of revolution axisymmetric loads carrying capacity, determining limit equilibrium through application of Tresca yield point concept
05 p0734 A72-15983

Thin cylindrical shell bending deformation from axisymmetrical temperature distribution generated by narrow heating element
05 p0736 A72-16113

Thin elastic shell postbuckling behavior from asymptotic integration solution for differential equations, permitting dynamic effect modeling
05 p0738 A72-16425

Meridional curvature effect on thin walled cylindrical shell buckling under external constant directional lateral pressure
05 p0739 A72-16546

Equilibrium conditions of closed elastic spherical shell under uniform nearly critical compression loads, determining shell deformation in Hilbert spaces
05 p0739 A72-16587

Supercritical deformation, bulging and instability of spherical edge clamped shell under external pressure, applying variational principle
05 p0742 A72-17210

Asymptotic solution to nonlinear Donnell equations of elastic conical shells, applied to buckling of frustum under axial load
06 p0893 A72-17303

Rib reinforced cylindrical shells deformation under local load, examining stress-strain distribution
06 p0899 A72-18641

Load bearing capacity of shells of revolution, applying viscoplastic strain hardenable material model
06 p0899 A72-18656

Shallow elastic shell under periodic distributed torque loading, investigating static stability enhancement through nonlinear boundary value problem periodic solutions
06 p0900 A72-18697

External pressure effects on stability of closed toroidal shell with circular cross section
07 p1087 A72-18993

Axisymmetric deformation of infinite cylindrical shell under stress-strain state arising from internal pressure in statistically inhomogeneous Winklerian medium
07 p1088 A72-19258

Buckling of arbitrary open cylindrical shells, investigating noncircularity effect
07 p1093 A72-19949

Asymptotic eigenvalue density estimates for edge-hinged thin elastic rectangular shell, determining shell stability linear equation solution conditions
07 p1095 A72-20324

Critical values of compressive loads applied to mid-section of cylindrical shell weakened by circular holes
08 p1244 A72-21241

Stability and postbuckling equilibrium of nearly cylindrical shells of revolution under axial compression
08 p1244 A72-21291

Elastic filler rigidity effect on cylindrical glass fiber reinforced plastic shells stability loss and critical load value under axial compression
08 p1245 A72-21503

Orthotropic hinged cylindrical shell stability under uniform external pressure, deriving linearized three dimensional differential equations
08 p1246 A72-21711

Strength analysis of thin elatoplastic shell with allowance for compressibility, relating loads and moments to deformation of middle surface
08 p1246 A72-21712

Elastic shell geometry and rigidity effects on critical load in pure bending within structurally orthotropic theory, taking into account reinforcing rib eccentricity 08 p1247 A72-21816

Dynamic buckling and plate to shell transition of thick spherical caps under large amplitude axisymmetric flexural vibrations 08 p1249 A72-22135

Nonuniformly heated infinite elastic cylindrical shell stability under axial compression loads 09 p1402 A72-22735

Axisymmetrically heated orthotropic multilayer cylindrical shell with shear sensitive couplings and elastic stiffener, investigating stability and critical force under compression 09 p1402 A72-22735

Temperature and internal pressure effects on circular cylindrical shell stability under tension and compression, deriving critical temperature and loads 09 p1402 A72-22736

Imperfection influence on nonlinear stability of long circular cylindrical shells subject to critical hydrostatic pressure 09 p1403 A72-22763

Torsional behavior of twisted elastic orthotropic cylindrical shells after stability loss, using energy method 09 p1404 A72-22771

Stability loss in thin convex shells of revolution under axisymmetric stress, obtaining integrals for equilibrium equations 10 p1557 A72-24630

Supercritical deformation, bulging and instability of spherical edge clamped shell under external pressure, applying variational principle 11 p1727 A72-25341

Nonlinear equilibrium equations and elastic stability of cylindrical shell weakened by circular hole 12 p1878 A72-27080

Static stability of long cylindrical shells under external pressure, using Euler-Lagrange equations 12 p1880 A72-27228

Two dimensional static solutions for cylindrical shells with nonhomogeneous boundary conditions, discussing numerical results for circular shell 12 p1880 A72-27230

Boundary surfaces during plastic buckling of hollow cylindrical shell under combined loading by external pressure and axial force 12 p1880 A72-27231

Stress-strain state determination for closed cracked cylindrical shell, using Fredholm integral equations 12 p1880 A72-27236

Dynamics snap-through instability existence conditions in nonlinear plane deformation of shallow circular cylindrical elastic shell under impulsive loading 12 p1880 A72-27241

Vibration of free and fluid loaded uniform or rib reinforced cylindrical shells, solving equations of motion for natural frequencies 12 p1882 A72-27341

Linearized elastic equilibrium stability equations for orthotropic cylindrical shell under critical axial compression 12 p1885 A72-27970

Nonlinear stability and vibrations of shallow shells eccentrically stiffened by oblique angled ribs under critical loads 12 p1885 A72-27971

Axial compression stability critical load and buckling of cylindrical shells resting on Winklerian elastic base, using dynamic programming 12 p1885 A72-27972

Nonuniform heating effect on stability of eccentrically stiffened smooth cylindrical shells under combined loading 12 p1885 A72-27973

Strain energy calculation for stability analysis of cylindrical and conical sandwich shells, using Euler-Poisson equations 12 p1885 A72-27975

Iterative solution existence for elastic equilibrium problem of thin plates and shells near boundary layer 12 p1886 A72-27997

Closed thin circular cylindrical shells external pressure pulse and structural parameters effects on stability under dynamic loading 12 p1886 A72-28129

Stability of transversely isotropic cylindrical shell with elastic filler under axial compression, deriving approximate equations for transverse shear stress effect 13 p2055 A72-28556

Cylindrical shell stability with variable thickness and moderate length under distributed ring load and uniform pressure, determining critical load 13 p2058 A72-29459

Inhomogeneous viscoelastic shell stability, determining correlation functions for first approximations of sag, stress functions and critical time alterations 13 p2062 A72-29886

Truncated orthotropic conical shells thermostability at different temperature gradients, using Ritz method 14 p2163 A72-30193

Shallow rectangular shell vibrations induced by moving band load, deriving frequency equation and load critical speed 14 p2166 A72-30688

Nonlinear equilibrium, stability and vibration equations of shallow sandwich shells with isotropic outer layer and rigid compressible filler obtained by variational method 14 p2166 A72-30700

Distributed parameter system approximation by system with finite freedom degrees number, solving stability and vibration of elastic shells for eigenvalue densening case 15 p2327 A72-31739

Thin walled elastic shells stability under finite deformations, deriving equilibrium conditions and constitutive equations 15 p2330 A72-32464

Axially compressed cylindrical shells buckling behavior, deriving formula based on equivalent axisymmetric imperfections concept in terms of shell radius/thickness ratio 15 p2331 A72-32553

Nonlinear stress-strain-curvature problem applied to noncircular cylindrical membrane shell under lateral pressure 16 p2464 A72-32917

Dynamic structural analysis of viscoplastic thin walled shells, noting time dependent profile of deflection 16 p2467 A72-33122

Axisymmetrical stability loss in elastic cylindrical shell under longitudinal and transverse impact waves, discussing buckling and similarity parameter for simulation 16 p2468 A72-33159

Linear stability and critical stress formulas for isotropic cylindrical shells with stepwise variable wall thickness under torsion 16 p2470 A72-33411

Nonlinear critical stability of truncated conical shell uniformly loaded by external hydrostatic pressure, using Bubnov-Galerkin method 16 p2470 A72-33412

On the flutter of thin cylindrical shells conveying fluid. 17 p2634 A72-35415

Free vibration mode shapes mapping of spherical and paraboloidal plastic shells under acoustic excitation via noncontact fiber optics instrumentation 18 p2690 A72-36372

Ritz method for truncated conical shell vibrations investigation, assuming deflection expanded in exponential power series 18 p2735 A72-36694

Numerical solution for the mean first-passage-time for snap-through of shells. 18 p2737 A72-37061

Forced axisymmetric response of fluid filled spherical shells. 18 p2684 A72-37063

A comparison of initial velocities for dynamic instability of a shallow arch. 18 p2738 A72-37080

A proof of the accuracy of a set of simplified buckling equations for circular cylindrical elastic shells. 18 p2739 A72-37091

Further results on the stability of a finitely deformed thin cylindrical shell. 19 p2871 A72-37415

German monograph - A contribution to the clarification of the carrying characteristics of closed isotropic circular cylindrical shells 19 p2871 A72-37478

Mathematical analogies in a theory of shallow spherical shells and plates allowing for transverse shear 19 p2872 A72-37540

Equilibrium conditions of closed elastic spherical shell under uniform nearly critical compression loads, determining shell deformation in Hilbert spaces 19 p2872 A72-37558

Oscillations, statics and transfer matrices of composite shells of revolution contacting elastic bases, using initial parameters method 19 p2876 A72-38156

Buckling of circular cylindrical shells under compression. III - Solutions based on the Donnell type equations considering prebuckling edge rotations. 19 p2878 A72-38299

Selection of optimal parameters of waffle structures from the condition of minimum weight 20 p2980 A72-39905

Stability of a twisted orthotropic cylindrical shell with a jump-wise variable wall rigidity 21 p3118 A72-40815

Calculation of rib-reinforced minimum-weight cylindrical shells under external pressure by the random search method 21 p3119 A72-41099

Rational utilization of the strength capabilities of thermal-expansion compensators 21 p3127 A72-41702

Reissner nonlinear equations for stability analysis of shallow shells of revolution, noting critical loads range and error analysis 22 p3232 A72-41856

Influence of elastic constants on the stability margins and weight characteristics of fiberglass-reinforced shells 22 p3196 A72-41864

A collocation solution of the nonlinear equations for axisymmetric bending of shallow spherical shells. 22 p3232 A72-41938

Determination of the critical temperatures of cylindrical shells of variable thickness 22 p3243 A72-42053

Numerical solution of boundary value problems in the statics of axisymmetric shells by the method of reducing to Cauchy problems 22 p3233 A72-42054

Plastic model shells design, construction and instrumentation for elastic stability studies in NDT, discussing deformation measurements for critical condition prediction 22 p3163 A72-42694

Nondestructive stability evaluation of large shell structures by direct computer controlled testing. 22 p3157 A72-42695

Buckling of circular cylindrical shells under axial compression. 22 p3239 A72-42840

Axisymmetric-multilobe creep buckling transition in thin walled circular cylindrical shells under uniformly distributed axial compressive load 22 p3239 A72-42844

Dangerous structural failure characteristics due to idealized design optimization, discussing shell buckling instabilities 22 p3240 A72-42895

Nonaxisymmetric vibrations of arbitrarily thick circular cylindrical shells 23 p3345 A72-43624

Strength of a cylindrical shell of variable thickness located in a temperature field 23 p3346 A72-43653

Limiting equilibrium of orthogonally coupled cylindrical shells 23 p3346 A72-43656

Ribbed cylindrical shells modeling method for stress-strain state and stability 23 p3347 A72-43745

Longitudinal rib reinforced cylindrical shell under axial compression loads, determining equilibrium stability with approximation of transcendental equations 23 p3347 A72-43748

Limiting equilibrium of shallow conical shells of variable thickness 23 p3348 A72-43787

Limiting equilibrium of shells of revolution and circular plates with allowance for shear stresses 23 p3348 A72-43789

Equilibrium equations of sandwich shell element with weak core and thin membrane facings under large transverse normal and shear strains, showing analogy to Cosserat surface theory 23 p3351 A72-44103

Nonlinear sandwich shell and Cosserat surface theory. 23 p3351 A72-44107

Variable thickness shallow spherical shells of revolution axisymmetric loads carrying capacity, determining limit equilibrium through application of Tresca yield point concept 24 p3460 A72-45725

SHELL THEORY

Differential equations derived for elastic-plastic behavior of rotationally symmetric shells, approximating in finite difference forms and solved by elimination method 01 p0138 A72-10394

Electric field induced splitting of drift shells composed of trapped particles, taking into account non-dipole field components to lowest order 01 p0062 A72-10905

Wave propagation in thin elastic shells by similar formation of shell and nonlinear elasticity theories equations 01 p0142 A72-11197

Nonclassical shell theory development from three dimensional boundary value problems solution in elasticity theory 02 p0288 A72-11606

Geometrical method in nonlinear shell theory for supercritical elastic deformation determination, considering stability loss and dynamics problems 02 p0289 A72-11612

Vibration and buckling analysis of doubly curved composite monocoque plates and shells of positive and negative Gaussian curvature, examining stacking sequence effect 02 p0292 A72-11990

General equations of thick shells for arbitrary material and large deflections, considering thermodynamic and velocity damping properties 02 p0293 A72-12344

Bending stresses in composite shell at conical interface between metal and fiberglass reinforced plastic portions under internal pressure

02 p0298 A72-12683

Soviet book on nonlinear problems of inhomogeneous shallow shell theory covering bending, stability, bearing capacity, plasticity criteria, compressibility, etc

03 p0454 A72-14225

First approximation of linear elastic shell theory using split constitutive equation of stress tensor

03 p0454 A72-14341

Mathematical models of elastic shells and rods, discussing virtual work, operator classifications, deformations and constitutive equations

03 p0454 A72-14344

Iteration method error estimates for thin elastic shell basic stressed state and simple fringe effect relation to boundary stressed state

04 p0586 A72-15012

Thermoelasticity theory coupled linear equations for thin orthotropic shells, taking into account rotatory inertia and lateral shear

04 p0588 A72-15060

Papers on aerospace structure by N. J. Hoff covering aircraft framework, stress analysis, structural stability, shell theories, bending, buckling, monocoque and sandwich structures, etc

04 p0591 A72-15238

Shell bending and Timoshenko-type theory to solve stresses of semiinfinite elastic circular cylindrical shells produced by radial pressure pulses [ASME PAPER 71-WA/APM-16]

05 p0733 A72-15964

Asymptotic two dimensional theory of shell structures, comparing with axiomatic formulation

05 p0738 A72-16349

Slot length effect on buckling load of cylindrical shell with circular holes

05 p0739 A72-16543

Intrusion of pointed dies into cross section circumference sections of semiinfinite cylindrical shell, solving shell theory equations without allowance for friction effects

05 p0739 A72-16586

Small deflection theory for dynamic elastic buckling of stringer-stiffened cylindrical shells under axial impact, discussing optimum stiffener geometry

05 p0742 A72-17248

Shallow axially symmetrical spherical shell flexural vibrations, obtaining equations iterative solution

06 p0901 A72-18705

Pitch angle and radial diffusions relationship in presence of drift shell splitting at arbitrary equatorial pitch angle

07 p1057 A72-19147

Semimomentless theory of closed cylindrical plastic shells subject to random gust loads, obtaining normal circumferential force, shear, transverse bending moment and shell thickness

07 p1092 A72-19851

Axially nonuniform thin cylindrical shells dynamic analysis, obtaining free flexural vibration characteristics by hybrid of finite element and classical shell theories

07 p1097 A72-20531

Elastic-plastic deformation of thin membrane shells

08 p1244 A72-21290

Thermoelasticity theory for transversely isotropic shells, obtaining variational formulation of noncoupled quasi-static problem

08 p1247 A72-21811

Thin shell theory analysis of thin walled cylindrical shell necking phenomenon as tensile deformation nonuniformity

08 p1248 A72-21821

Optimal temperature gradients determination over thickness of shell of revolution under axisymmetric heating, formulating variational problem for conditional extremum of elastic energy functional

09 p1399 A72-22706

Book on tensor analysis and continuum mechanics covering strain, permutation and stress tensors, vector and tensor comparison, application to elasticity and shell theory, etc

09 p1406 A72-23000

Nonstationary temperature field of semitransparent shell with nonuniformly distributed heat sources

09 p1412 A72-23184

Nonlinear vibrations of thin circular cylindrical shells under arbitrary boundary and loading conditions

09 p1407 A72-23456

Book on plastic analysis and plate, shell and disk theories and design covering stress-strain concepts, laws and theorems

10 p1553 A72-23749

Elasticity theory for unsymmetric deformation of nonhomogeneous anisotropic cylindrical shells, using Donnell equations

10 p1555 A72-24252

Natural axisymmetric vibration of thin elastic shell of revolution, deriving eigenvalues convergence to spectrum lower bound by asymptotic method

10 p1557 A72-24429

Plate and thin and thick walled shells treated as three dimensional solids, noting finite element method limitation

10 p1559 A72-24925

Intermediate length open noncircular cylindrical shells analysis based on Vlasov semimembrane theory

10 p1559 A72-24992

Violation effect of moment equilibrium about normal in shell of revolution and helical shell theory, discussing distribution

10 p1560 A72-25171

Finite element generalization of plate displacement functions to shell analysis, using strain energy tensor concept

10 p1560 A72-25187

Computer analysis of shells bifurcation buckling, presenting graphical results

[AIAA PAPER 72-352] 11 p1729 A72-25381

Nonlinear bending and buckling of axisymmetric sandwich shells based on finite element approach

[AIAA PAPER 72-356] 11 p1729 A72-25385

Computer program for bifurcation buckling analysis of shells under collapse load, using strain energy methods and two dimensional finite difference grid

11 p1736 A72-25980

Finite difference method for free vibration of axisymmetric shells, using inertia force terms in shell bending theory equilibrium equations

11 p1737 A72-26429

Dynamic stability of rapidly heated shallow cylindrical shells, formulating nonlinear equations

12 p1877 A72-27076

Shallow isotropic and orthotropic shells vibration, investigating dynamic rigidity for concentrated mass

12 p1878 A72-27079

Nonlinear equilibrium equations and elastic stability of cylindrical shell weakened by circular hole

12 p1878 A72-27080

Finite difference equations for plate and shell calculations with various boundary conditions

12 p1878 A72-27089

Energy method based approximate calculation for natural frequencies of single layer compound shells of revolution

12 p1886 A72-28144

Proximate equations of two dimensional orthotropic shell theory obtained by asymptotic integration method, examining anisotropy effect

13 p2053 A72-28391

Lagrange multiplier method derivation of variational functional for finite element method and applications to plate and shell problems

13 p2055 A72-28623

Vibrations and plane wave propagation in laminated elastic plates and cylinders, noting finite element method for conical shells

[AIAA PAPER 72-406] 13 p2056 A72-28959

Dynamic stability of doubly curved planar rectangular shallow shell, using method of summary representation

13 p2057 A72-29066

Computer algorithm for plates and shells internal forces and moments and stress-strain state determination from strain gage data

13 p2058 A72-29144

Oscillations and acoustic emission by interacting elastic shells in connecting medium, using quadratures with Green function

13 p2004 A72-29208

Mohr formulas construction for composite structures including frames and cylindrical and conical shells

13 p2058 A72-29460

Monge surface shells reduced to bodies of revolution by small parameter method for solution of momentless theory equations

13 p2058 A72-29489

Tangential displacements of spherical and circular cylindrical shallow shells calculated from stress function

13 p2059 A72-29490

System of equations derived for unsteady temperature field of arbitrary multilayer shell, using polynomial expression as temperature approximation for shell thickness

13 p2066 A72-29949

Stress-strain state of complex configured thin walled shell, deriving computer algorithm via tensor analysis and finite difference scheme

14 p2165 A72-30686

Carrying capacity of rigidly hinged shell of revolution with concentric reinforcing rib, applying to shallow spherical shell under uniform external pressure

14 p2166 A72-30687

Shallow rectangular shell vibrations induced by moving band load, deriving frequency equation and load critical speed

14 p2166 A72-30688

Viscoplastic flow of inhomogeneous shells of revolution obeying Tresca condition, noting plastic deformation velocity relation to stresses

15 p2325 A72-31605

Deformation and stress in shells with discontinuous wall thickness variations, noting cylinder with ribs under internal pressure

15 p2326 A72-31705

Elastic shell initial stress effects on dynamic response in all free vibration modes, considering transverse shear and normal strains

15 p2328 A72-32021

Thin walled elastic shells stability under finite deformations, deriving equilibrium conditions and constitutive equations

15 p2330 A72-32464

Longitudinal, transverse and bending waves propagation in elastic shells, using Hadamard method within linear shell theory

16 p2465 A72-3298

Linear theory for spirally sinusoidal stress distributions in elastic helicoidal shells applied to pure bending problem

16 p2465 A72-33003

Constitutive and equilibrium equations for theory of thin shells with slowly varying curvature based on Novoshilov and Koiter assumptions

16 p2465 A72-33004

Nonlinear theory of two dimensional and three dimensional discrete elastic Cosserat media, noting application to reinforced shells and lattice type structures

16 p2425 A72-33592

Deflection of plate on elastic support from equilibrium equations based on shell theory

16 p2472 A72-34015

Exact analysis of a thick sandwich conical shell by forward integration.

[ASME PAPER 71-APMW-20] 17 p2624 A72-34312

Longitudinal impact of cylindrical shells with discontinuous cross-sectional area.

[ASME PAPER 72-APM-24] 17 p2628 A72-34793

On a laminated orthotropic shell theory including transverse shear deformation.

[ASME PAPER 72-APM-7] 17 p2629 A72-34807

Elastic wave propagation in a joined cylindrical-conical-cylindrical shell.

[SESA PAPER 1983] 17 p2630 A72-34819

Thin spherical shells in equilibrium with displacement and stress fields, satisfying virtual work, kinematic and static requirements

17 p2633 A72-35351

Buckling of shells with cutouts - Experiment and analysis.

17 p2634 A72-35404

Finite bending of a compressible anisotropic rectangular block into a hyperbolic shell.

17 p2634 A72-35438

An approximate theoretical study of the dynamic plastic behavior of shells.

18 p2732 A72-36077

Shell of revolution natural vibration spectrum, investigating moment and momentless type systems of differential equations

18 p2735 A72-36665

On the transient response of a closed spherical shell to a local radial impulse.

18 p2739 A72-37089

On the accuracy and application of the point matching method for shallow shells.

18 p2739 A72-37090

Mathematical analogies in a theory of shallow spherical shells and plates allowing for transverse shear

19 p2872 A72-37540

Impression of pointed dies onto cross section circumference sections of semiinfinite cylindrical shell, solving shell theory equations without allowance for friction effects

19 p2872 A72-37557

Thin shell and oriented surface theories.

19 p2873 A72-37694

Loading rig in which axially compressed thin cylindrical shells buckle near theoretical values.

19 p2783 A72-37730

Complex transforms method for Timoshenko theory of elastic shells, deriving transverse shear strain equations for shallow shells

19 p2876 A72-38154

Stress analysis of shell junctions fabricated by the filament-winding method.

19 p2877 A72-38169

Experimental creep buckling of circular cylindrical shell under uniform compression.

20 p2978 A72-38883

Introduction of two resolving functions into the equations for nonshallow shells

20 p2979 A72-39405

Dispersion of flexural waves in circular cylindrical shells.

20 p2982 A72-39975

Stresses in a circular cylindrical shell having two circular cutouts.

20 p2982 A72-40063

Finite element large deflection analysis of elastic-plastic shells of revolution subjected to axisymmetric loading.

20 p2982 A72-40064

The influence of end plate and bulkhead on the shell of variable rectangular profile subjected to simultaneous torsion and bending at middle planes. 20 p2982 A72-40065

Constant strength shells theory generalization from axially symmetric to nonsymmetric case, using Von Mises yield condition 21 p3117 A72-40680

Differential equation reduction via coordinate transformation to algebraic form for problems characterization in elastic shell Cosserat surface theory 21 p3119 A72-41103

Study on an incremental variational principle and its applications to finite element method and incremental thin shell theory. 21 p3121 A72-41240

Numerical solution of a boundary value problem arising in the deflection of beams and shells. 21 p3122 A72-41311

Bent plates and shells equations and rupture modes, characterizing cracks and stress intensity 21 p3122 A72-41338

Constitutive equations and boundary value problems in discrete theory of elasticity, noting linear systems of prismatic rods and lattice type shells 21 p3123 A72-41390

Buckling of inelastic cylindrical shells under axial impact. 21 p3124 A72-41507

Calculation of sandwich shells of revolution at large elastic-plastic deflections. 21 p3125 A72-41512

Multilayer shell theories with allowance for transverse shear and transverse normal deformation of layers, noting viscoelastic material and anisotropic shallow shells 21 p3125 A72-41537

Equilibrium and elastic deformation equations for closed cylindrical shells with arbitrary cross section and variable wall thickness 21 p3126 A72-41551

Method of calculating rotating disk of complex profile 21 p3127 A72-41701

Solution for shallow shells of revolution with allowance for large deflections by the method of integral relations 22 p3232 A72-41869

An inverse problem in the momentless theory of shells of revolution situated in a temperature field 22 p3232 A72-41895

Steady-state creep of shells of revolution in the case of the Tresca criterion 22 p3233 A72-42051

Symmetry transformations for thin elastic shells. 22 p3234 A72-42398

Finite difference and extended Newton methods application to transient and steady state creep deformation in shells of revolution under high temperature and high stress 22 p3235 A72-42482

The dynamic plastic behavior of shells. 22 p3236 A72-42756

Analysis of the transient response of shell structures by numerical methods. 22 p3237 A72-42762

Multilayer shells structural analysis via equilibrium equations transformation into system of equivalent equations 22 p3238 A72-42836

Stresses in a circular cylindrical shell with arbitrary holes. 22 p3238 A72-42837

Buckling of integrally stiffened cylindrical shells - A review of experiment and theory. 22 p3239 A72-42846

Dynamic loading of a fluid-filled spherical shell. 22 p3240 A72-42891

Rigid-body motions and strain-displacement equations of curved shell finite elements. 22 p3240 A72-42892

Finite element method optimization of orthotropic layered shells of revolution under mechanical and thermal loadings, considering stress-strain relationships [SAWE PAPER 939] 23 p3344 A72-43479

Limiting equilibrium of orthogonally coupled cylindrical shells 23 p3346 A72-43656

Stresses around an axial crack in a pressurized cylindrical shell. 23 p3346 A72-43705

Pointwise displacement errors in linear shell theory resulting from errors in the stress-strain relations. 23 p3347 A72-43720

First order constraints in three dimensional continuous elastic fibrous media and thin shells, presenting equilibrium equations 23 p3349 A72-43825

A note on buckling of spherical caps with initial asymmetric imperfections. 23 p3351 A72-44060

Equilibrium equations of sandwich shell element with weak core and thin membrane facings under large transverse normal and shear strains, showing analogy to Cosserat surface theory 23 p3351 A72-44103

Asymmetric imperfections effect on spherical elastic shell buckling strength under uniform external pressure 23 p3351 A72-44104

Nonlinear sandwich shell and Cosserat surface theory. 23 p3351 A72-44107

Line spring analysis model for long part-through surface cracks in walls of plate or shell structures, formulating constitutive laws 23 p3353 A72-44234

Vibration characteristics of cylindrical shells with several axially equispaced constraints. 23 p3355 A72-44371

Laminated thick plate and shell analysis by the assumed stress hybrid model. 24 p3453 A72-44601

Nonlinear theory for static analysis of moderately thick circular cylindrical shells under axisymmetric loads applied to pyrolytic graphite 24 p3454 A72-44603

Parametric influences on the response of structural shells. 24 p3454 A72-44604

Response of shallow spherical shells to pulse pressure loads. 24 p3454 A72-44605

Triangular facet finite element application in thin cylindrical shell analysis by displacement method 24 p3456 A72-44792

Theory of thin elastic shells applied to pipe bends subjected to bending and internal pressure. 24 p3456 A72-44795

A finite element model for shells based on the discrete Kirchhoff hypothesis. 24 p3457 A72-44876

Vibration of simply supported cylindrical shells with longitudinal stiffeners. 24 p3457 A72-44882

A linear asymptotic theory for anisotropic shells. 24 p3460 A72-45473

Mechanical behavior of fiber reinforced cylindrical shells. 24 p3461 A72-45783

SHELLS [STRUCTURAL FORMS]

NT ANISOTROPIC SHELLS

NT CIRCULAR SHELLS

NT CONICAL SHELLS

NT CORRUGATED SHELLS

NT CYLINDRICAL SHELLS

NT DOMES [STRUCTURAL FORMS]

NT ELASTIC SHELLS

NT HEMISPHERICAL SHELLS

NT LIQUID FILLED SHELLS

NT METAL SHELLS

NT ORTHOTROPIC SHELLS

NT PERFORATED SHELLS

NT RADOMES

NT REINFORCED SHELLS

NT SPHERICAL CAPS

NT SPHERICAL SHELLS

NT THIN WALLED SHELLS

NT TOROIDAL SHELLS

Prismatic shells membrane and bending fields induced by concentrated forces, applying Fourier analysis to semiinfinite plates geometry 02 p0296 A72-12527

Shells finite element analysis, discussing inplane and normal displacements interpolation schemes and convergence rates 02 p0296 A72-12532

[AD-739747]

Ring finite elements use in analysis of shells of revolution under axisymmetric loads 05 p0732 A72-15880

[ASME PAPER 71-WA/HT-22]

Spectral properties of differential displacement equations system describing natural vibrations of shell of revolution with m waves along parallel 06 p0897 A72-17990

Neutral rotating mass shell surrounding concentric stationary electrically charged insulation, calculating induced dipole-like magnetic field from coupled linearized general relativity field equations 06 p0853 A72-18423

P-analytical functions application to strength analysis of zero moment shells of revolution with positive Gaussian curvature under concentrated loads 08 p1242 A72-20905

Nonlinear structural analysis of circular plates and shells of revolution with geometric and inelastic material nonlinearities, using direct stiffness method [AIAA PAPER 72-353] 11 p1729 A72-25382

Spectral properties of differential displacement equations system describing natural vibrations of shell of revolution with m waves along parallel 14 p2163 A72-30217

Finite element models with rigid displacement for nonrigid structure analysis, noting curved beam and shells 18 p2739 A72-37173

Gravitational field of arbitrarily thick steadily rotating shell in general relativity, using successive approximation method 20 p2955 A72-40010

Mapping of large dynamic deflections of structures. 24 p3454 A72-44606

SHELTERS

Wind tunnel investigation of shapes for balloon shelters. 20 p2885 A72-38967

SHIELDING

NT ELECTROMAGNETIC SHIELDING

NT ELECTROSTATIC SHIELDING

NT HEAT SHIELDING

NT MAGNETIC SHIELDING

NT RADIATION SHIELDING

NT RADIO FREQUENCY SHIELDING

NT REENTRY SHIELDING

NT SOLAR RADIATION SHIELDING

NT SPACECRAFT SHIELDING

Transparent aircraft polycarbonate glazing systems shielding properties for projectile and bird impacts 12 p1832 A72-27015

SHIFT REGISTERS

Pulse amplitude modulated tester with shift register generated sequence and conventional data /PCM/ bit synchronizer and detector 02 p0192 A72-12148

Large scale integrated circuits for digital differential analyzers, giving operational specifications for shift registers, adders and integrators 10 p1448 A72-24276

Microelectronic IC functional logic systems design with S-type semiconductor devices, describing procedures for logic functions, shift register and directional transmission line 10 p1448 A72-24278

Digital signal analyzer design based on fast Fourier transform algorithm shift register coupled with single flow-through arithmetic unit 10 p1446 A72-25062

Phase shift methods for data transmission vestigial sideband signal generation, providing shaping functions by shift registers, weighting resistors, summing amplifiers and low pass filters 11 p1592 A72-25890

MOS specifications and application to shift registers, considering maximum ratings, clock pulse level and width and pulse rate 11 p1611 A72-26387

Fault detecting sequences construction based on input-output sequences observation in sequential circuits with shift registers as memory elements 12 p1794 A72-27496

Binary PSK signals optimized on minimax and quadratic criteria, noting design of coders and decoders on shift registers with external logic 13 p1914 A72-28415

SHIMS

U COMPENSATORS

SHIP PROPULSION

U MARINE PROPULSION

SHIPS

NT AIRCRAFT CARRIERS

NT SUBMARINES

NT TANKER SHIPS

Discosures geostationary satellites project for Atlantic and Pacific ocean air and ship traffic safety based on radar tracking and multiplex numerical data transmission 09 p1396 A72-23400

Helicopter landing on ships, discussing wind, visibility limitations and flight deck motions vs aircraft stability and handling characteristics 12 p1754 A72-27413

A comparison of voice communication techniques for aeronautical and marine applications. 17 p2512 A72-34267

Potential response of maritime services to craft and persons in distress at sea. 17 p2488 A72-34431

Helicopter/ship dynamic interface testing for launch and recovery capabilities under sea environment conditions, discussing visual landing aids, wind, visibility and ship motions 17 p2491 A72-34505

[AHS PREPRINT 650]

Spatial simulator of tactical navigation 19 p2783 A72-37798

Utilization of a satellite system for navigation and control of shipping 24 p3422 A72-45224

SHIVERING

NT DITHERS

Pulse activity of neurons in the thermal regulation center of the anterior hypothalamus during chill shivering 24 p3371 A72-44594

SHOCK ABSORBERS

Shock isolator model, using passive elements and variable Coulomb friction force to minimize transmitted shock and relative displacement 01 p0047 A72-10218

Impact dampers with spring connection of masses, analyzing periodic motion 02 p0298 A72-12617

Higher order forces effect on shock absorbing systems of masses interconnected by elastic and damping members of aircraft landing gears
09 p1318 A72-22861

Vertical drop rig test equipment for measuring shock attenuation of crash helmets, discussing shock absorption criteria for impact protection
11 p1584 A72-26016

Equipment vibration isolation principles, discussing damping, viscoelastic materials and shock absorbers
18 p2731 A72-35992

SHOCK DIFFUSERS

U DIFFUSERS

U SHOCK WAVE ATTENUATION

SHOCK DISCONTINUITY

Solar wind reverse and forward oblique slow shocks, examining discontinuities from Pioneer 6 plasma and magnetic field data
01 p0120 A72-10882

Rarefied plasma hydrodynamic equations for rotational discontinuities in solar wind, discussing magnetic field modulus jumpwise changes
02 p0272 A72-11915

Unsteady supersonic flow disturbance by slender bodies in strong contact discontinuities in shock tube studies
04 p0462 A72-15507

Discontinuities in electrohydrodynamics, discussing surface charge generation at shock front and shock wave structure determination
05 p0690 A72-16580

Curved shocks discontinuities in nonequilibrium dissociative gas flows, investigating flow gradient variables
05 p0653 A72-17080

Strong normal shock wave structure upstream and downstream of discontinuity due to nonequilibrium radiation and collisional ionization
06 p0902 A72-18106

Hydromagnetic wave theory for solar wind, noting tangential discontinuities, perpendicular and Alfvén shocks and forward and reverse fast and slow shocks
07 p1058 A72-19354

Collisionless plasma electronic shock waves /stationary heat discontinuity/ observation, proving stationary shock wave existence
07 p1043 A72-19874

Shock wave propagation and structure in elastoplastic material with translational work hardening, obtaining closed system of discontinuity equations
07 p1093 A72-19977

Solar wind tangential discontinuities and shock waves determination from flux velocity vector, magnetic field and particle density measurements
08 p1227 A72-21154

Rarefied plasma hydrodynamic equations for rotational discontinuities in solar wind, discussing magnetic field modulus jumpwise changes
13 p2030 A72-29227

Radiation effect on isothermal discontinuity amplitude for stationary shock wave structure with heat transfer and dissipation
15 p2335 A72-32099

Time dependent finite difference /fluid-in-cell/ method for supersonic aerodynamic problems concerning inviscid compressible flow with contact surface and shock discontinuities
16 p2342 A72-32884

Vorticity jump across stationary MHD discontinuity generalization from gas dynamics problem, noting results validity for shock and detonation waves
16 p2435 A72-33011

First and second order shock discontinuity waves propagation in thermoelastic incompressible solids, deriving Piola-Kirchhoff stress tensor via Clausius-Duhem relation
16 p2423 A72-33109

Self similar breakdown problem of two dimensional shock discontinuity in gas dynamics
16 p2377 A72-33154

Triangular and conical wings in hypersonic flow with Mach reflection of shock waves from leading edge with optimal L/D ratio
18 p2642 A72-36893

Propagation of an electromagnetic shock discontinuity in a non-linear isotropic material.
18 p2712 A72-36992

Discontinuities in electrohydrodynamics, discussing surface charge generation at shock front and shock wave structure determination
19 p2834 A72-37551

Solar wind tangential discontinuities and shock waves determination from flux velocity vector, magnetic field and particle density measurements
20 p2964 A72-39259

Influence of viscosity on the characteristics of compressor blades for supersonic flow conditions
20 p2963 A72-39912

Radiation effects on isothermal discontinuity amplitude for stationary shock wave structure with heat transfer and dissipation
21 p3128 A72-40266

Small disturbances propagation effect on self similar flow due to point explosion in medium with density varying according to distance from center
24 p3390 A72-44786

SHOCK FRONTS

Microwave propagation on nonlinear transmission lines by examination of energy dissipation in shock front, considering distributed and lumped-parameter models
01 p0029 A72-10692

Combustion fronts in relativistic hydrodynamics, considering theorem of detonation and deflagration velocity distribution
01 p0145 A72-11179

Analog circuit method for slender profile flow field shock front boundary value problem for simple profile variation, using known mapping plane solutions [DGLR PAPER 71-069]
02 p0153 A72-12743

Atomic oxygen coupled electron excitation and ionization by electron-atom and atom-atom collisions in nonequilibrium relaxation zone behind shock wave
02 p0207 A72-12896

Detection of atmospheric gravity waves produced by focusing of shock front generated by supersonic aircraft, calculating flight trajectories
03 p0345 A72-12984

Excited Hg atom and electron concentration measurement behind shock front in nonstationary plasma by continuous displacement recording of interference bands
03 p0357 A72-13374

Electron density and diffusion measurements in ionized air in front of strong shock wave with resonant microwave probe and electromagnetic induction technique
05 p0648 A72-16211

Energetic charged particles penetration into magnetosphere by auroral simulation experiments with artificial solar wind, observing magnetic field microfluctuations behind collisionless shock front
06 p0805 A72-17469

Cornered axisymmetric blunt body sonic line in steady supersonic flow, showing incomparability with sonic shoulder of sphere
06 p0757 A72-18138

Differential equations describing dynamic behavior of unsteady plane exothermic reaction front in gasless system
06 p0903 A72-18204

Chemical reaction delayed effect on triple shock front confluence point trajectory in detonations, developing qualitative detonation cell model
06 p0904 A72-18530

Initial /premaximal/ phase model of chromospheric flare in terms of explosion theory, determining temperature, shock front and plasma velocities
07 p1077 A72-19809

Nonlinear acoustic propagation in chemically reacting media, discussing quasi-frozen and quasi-equilibrium flow processes behind shock fronts
07 p0969 A72-19974

Solar cosmic rays propagation between shock front and solar flare hot plasma, examining fine structure from Explorer 34 and Venera 6 data
07 p1063 A72-20628

Ignition time delay measurement between leading shock front and hydroxyl emission onset in two phase detonation of decane-oxygen
08 p1255 A72-22041

Self-similar adiabatic expansion of gas behind shock wave front sustained by radiation, describing gas pressure, density and velocity profiles
08 p1152 A72-22049

Aerodynamic field around singular stagnation point of blunt body tip with detached shock, using Legendre functions
09 p1261 A72-22932

Ionospheric disturbances due to shock front from Apollo 15 launching, using split signal observation in ion acoustic and normal mode
09 p1397 A72-23569

Extragalactic clouds supersonic collisions with galactic gases, discussing high velocity neutral hydrogen gas result of recombination following post-shock surplus energy radiation
10 p1538 A72-24248

Phase plane method for one dimensional stationary problem solution in radiative gas dynamics, calculating temperature behind shock wave front
10 p1469 A72-24544

Quasars energy source and structure in terms of kinetic energy conversion to radiation in shock fronts of colliding gas clouds
10 p1544 A72-24671

Axisymmetric shock wave propagation in continuous inhomogeneous medium, taking into account shock geometry orthogonality conditions and flow hydrodynamics behind shock
11 p1616 A72-25864

Self similar blast waves propagation, studying flow field in terms of shock front velocity and ambient atmospheric density variation ahead of front
12 p1889 A72-27832

Sound radiation by shock wave front in cesium vapors, describing experimental shock tube
13 p2017 A72-29608

Shock waves amplification by interaction with burning gas-liquid mixture, noting triangular profile of pressure variations behind wave front
13 p2065 A72-29888

Closed form solutions for one dimensional nonlinear waves in strain rate-sensitive elastoplastic material, describing dispersed wave motion behind propagating shock front
14 p2164 A72-30298

Interferometric investigation of impurities effects on electron density distribution in ionization-relaxation zone behind shock waves in monatomic gas
15 p2215 A72-31213

Electric and magnetic fields fluctuations in region between shock wave front and magnetosphere boundary, noting resulting energy dissipation
15 p2225 A72-31902

Transient flow induced in convergent-divergent nozzles by shock front impingement, investigating nozzle shape and Mach number effects on formation process of reflected shock
15 p2179 A72-32143

Transient flow induced by shock front impingement on Laval nozzles observed by schlieren method, noting time variations of temperature and pressure
15 p2179 A72-32144

Spherical, cylindrical or plane piston motion in nonuniform medium with radiative energy transfer, obtaining approximate analytic solutions and temperature profile behind shock front
15 p2336 A72-32394

Postfrontal ion acoustic shock turbulence as function of Mach number and electron/ion temperature ratio, using particle in cell technique
15 p2281 A72-32424

Shock wave generation by high current pulsed discharges, determining shock front velocity as function of magnetic pressure on current sheath
16 p2434 A72-32909

Analytical method of characteristics to determine front shock and sonic boom due to flat delta wing with supersonic leading edges [DFVLR-SONDDR-205]
16 p2348 A72-33401

Diatom gas flow behind blast wave, discussing vibrational nonequilibrium effects and solution of governing equations via characteristics method
16 p2378 A72-33440

Control volume method for finite amplitude shock front propagation in hyperelastic materials, solving steady state conservation equations
16 p2427 A72-33830

Electron density measurements in bow shock stagnation and conical afterbody regions during blunt body atmospheric reentry, using flush mounted electrostatic probes [AIAA PAPER 72-694]
16 p2345 A72-34047

Initial /premaximal/ phase model of chromospheric flare in terms of explosion theory, determining temperature, shock front and plasma velocities
17 p2602 A72-35734

Numerical and shock tube experiments for variation of bound electron temperature and nonequilibrium chemical and radiative relaxation behind normal shock waves in air, using atom-molecule collision model
18 p2681 A72-36564

Boundary layer closure in the conical shock tube
19 p2788 A72-38431

Experiments concerning the contact surface in a membrane shock tube
20 p2911 A72-39017

Shock front radius of subsonic radiation front driven by plasma fireball during final stages of decaying laser spark
20 p2934 A72-39844

Nonlinear acoustic propagation in chemically reacting media, discussing quasi-frozen and quasi-equilibrium flow processes behind shock fronts
20 p2955 A72-40031

Motion of a strong shock front in a nonuniform atmosphere
21 p3044 A72-40128

Sound radiation generation by shock wave front in Cs vapors, describing experimental shock tube
21 p3091 A72-40662

Resonance absorption of laser emission by methane behind the shock front
21 p3063 A72-40986

Propagation of magnetohydrodynamic shock waves in a medium with diminishing density
21 p3094 A72-41653

Determination of the parameters of a fluid in the neighborhood of the junction of wavefronts by the Legras method
22 p3165 A72-41927

Propagation of radiative shock waves in an inhomogeneous cosmic medium.
22 p3225 A72-42452

Electron diffusion across a shock wavefront in metals
22 p3208 A72-43184

Combustion product gas dynamic motion effects on detonation front propagation, discussing reacting blast wave and finite kinetic rate models and asymptotic results
24 p3391 A72-45027

Method of measuring the fine structure of detonation fronts in solid explosives.
24 p3463 A72-45039

SHOCK HEATING
Whole rock Rb-Sr measurements of hypersthene /including black/ chondrites for shock and reheating effects, noting data conformance to 4.5-4.6 gigayear isochron
04 p0571 A72-14566

Pulse shock tube synthesis of amino acids in primitive environments, discussing thermodynamic relations and conversion efficiency
04 p0482 A72-14761

Carbon dioxide-carbon monoxide vibrational energy transfer rate at 730-2325 K from measurements following heating in shock tube
04 p0553 A72-15641

Plasma velocity, gas pressure, wall heat flux and shock heated region extent measured in electrical discharge shock tube, discussing ionization relaxation process
05 p0693 A72-15849

Shock interference heating in hypersonic flows, measuring pressure and heat transfer in wind tunnels [ALAA PAPER 72-78]
05 p0604 A72-16805

Solar Fe I oscillator strengths determination by hook method on shock heated gases
07 p1037 A72-19349

Shock tube spectroscopy role in laboratory astrophysics, stressing hook method effectiveness for quantitative analysis of shock heated gases in solar abundances determination
08 p1146 A72-21017

Equation of state data of solids from shock vaporization, using spectroscopic technique
09 p1351 A72-22856

Cen X-3 model with X ray emission from atmosphere heated by shock waves generated by surface pulsations of white dwarf
10 p1544 A72-24668

Liquid film transpiration cooling concept application to space shuttle leading edge heating and shock heating [ALAA PAPER 72-389]
11 p1744 A72-25410

Shock heated methane-oxygen-argon mixtures ignition delay time from reaction kinetics calculations
12 p1778 A72-27852

Shock induction melting and vaporization in metals, investigating initial porosity effect
14 p2113 A72-30185

Lunar rock and mineral shock melting and vaporization from hypervelocity meteoroid impacts, calculating entropy, phase changes and thermal equilibrium
14 p2155 A72-30520

Shock heating caused material phase transformation effects on bumper shield performance, studying thin metal sheets response to like-material spheres impact
14 p2168 A72-30921

Plasma velocity, gas pressure, wall heat flux and shock heated region length measured in electrical discharge shock tube without diaphragms, discussing ionization relaxation process
15 p2283 A72-31268

Electron-ion heating in high beta perpendicular collisionless shock waves by plasma cylinder magnetic compression using theta pinch
16 p2439 A72-33936

High temperature oxidation of ammonia.
17 p2511 A72-34904

Comments upon shock-initiated oxidations by nitrous oxide.
17 p2511 A72-34905

Vibrational relaxation of the bending mode of shock-heated CO2 by laser-absorption measurements.
18 p2697 A72-36562

IR emission of nitrogen layer heated by reflected shock wave, noting absorption cross sections under free-free electron transitions in neutral particle fields
19 p2835 A72-38776

Regime factor and stress concentration parameter for sudden heating of solid cylinders and disks, noting thermal stability criterion with allowance for statistical strength
21 p3123 A72-41361

Formation of clusters of galaxies - Photocluster fragmentation and intergalactic gas heating.
22 p3224 A72-42377

Investigation of the heating of the plasma ion component by a collisionless shock wave
23 p3318 A72-43310

Caloric state equation for isentropes and temperature calculation of nonideal Cs plasma produced in high density vapors by shock wave compression
23 p3318 A72-43320

Quartz and feldspar glasses produced by natural and experimental shock.
23 p3285 A72-44136

Shock waves role in coronal heating, solar wind and energy and material transfer to earth and in solar system
24 p3439 A72-45019

3.39 micron resonance line absorption in shocked methane.
24 p3410 A72-45044

Formation of a jet of shock-heated gas outflowing into evacuated space.
24 p3391 A72-45046

Chemical aspects in the shock initiation of fuel droplets.
24 p3433 A72-45051

SHOCK LAYERS
Free stream and shock layer disturbances effect on hypersonic boundary layer transition in wind tunnels from hot wire measurements
02 p0230 A72-12274

Thin shock layer theory of lifting properties of reentry caret and flat delta wings and waveriders at high incidence angles and Mach number
02 p0152 A72-12345

Thermodynamic properties of atomic hydrogen-helium plasma for postulated conditions present in stagnation shock layer of spacecraft entering Jupiter atmosphere
08 p1254 A72-21598

Shock layer emission associated with hypersonic air flow past spherical segment, solving flow equations by iteration technique
10 p1418 A72-24539

Nonequilibrium partially ionized viscous shock layer on blunt body, determining electron temperature and electron-ion density profiles
11 p1744 A72-25560

Numerical analysis of inviscid hypersonic flow characteristics in shock layer between bow shock and cone at angles of attack, taking into account laminar separated flow
14 p2069 A72-30328

Viscous shock layer analysis application to blunt nosed reentry vehicle plasma layer nonequilibrium flow species distribution, considering electron density [ALAA PAPER 72-689]
16 p2346 A72-34053

Three-dimensional wings in hypersonic flow.
19 p2747 A72-38797

Proper equations and similar approximations in the hypersonic merged layer.
20 p2885 A72-39621

Instability of hypersonic viscous shock layer with finite rate chemistry.
20 p2886 A72-39635

Taylor instability in the shock layer on a Jovian atmosphere entry probe.
22 p3136 A72-42873

Radiative transfer in a gray isothermal spherical layer.
24 p3461 A72-44805

Raindrop breakup in the shock layer of a high-speed vehicle.
24 p3395 A72-45780

Influence of a temperature dependent spectral absorption coefficient on radiative flux.
24 p3466 A72-45791

SHOCK LOADS
NT BLAST LOADS
Ribbon parachutes drop tests at Mach 0.57-1.70, measuring opening shock loads and functioning time sequence
01 p0004 A72-10312

Equation of state for porous metals at high temperatures under strong shock compression, considering phase transitions
02 p0258 A72-11469

Composites response to shock loading via Hugoniot synthesis based on theory of mixtures, expressing mass, momentum and energy balance
02 p0291 A72-11986

Shock precompression effect on dynamic fracture strength of steel and Al alloy, investigating crack initiation and growth
04 p0533 A72-14541

Shock response of simply supported sandwich beam with viscoelastic core, using four element model for dynamic rarefactions
04 p0591 A72-15274

Approximate maximum shock stress analysis for curved bar bending vibration due to longitudinal impact by disregarding elements inertia with regard to axial motion
05 p0737 A72-16285

Shock transformed chondrite texture observed in thin plates by UV fluorescence
05 p0722 A72-17151

Explosive shock loading effect on materials mechanical properties, describing test equipment
06 p0797 A72-18659

Shock metamorphism in Luna 16 soil sample, indicating regolith formation by meteorite impact
09 p1380 A72-22259

Shock response of two constituent composites /Elkonites/, predicting Hugoniot states with allowance for thermal energy transfer
10 p1556 A72-24259

Cumulative shock loading fatigue in solids, describing experimental setup and fracture morphologies
10 p1560 A72-25124

Hugoniot equation of state measurements on iron-silicate garnet, showing shock induced transition to high pressure phase
11 p1627 A72-26524

Shock deformation microstructures in Apollo 14 breccia and comparative terrestrial minerals, using transmission electron microscopy
11 p1724 A72-26951

Shock wave reduction, microcracks and dislocation density of hot pressed titanium, zirconium and niobium carbide powders, using X ray crystal analysis
13 p1982 A72-30110

Natural remanent magnetism creation in meteorites via shock passage in collisional fragments
16 p2451 A72-32990

Forced vibration solution and wind tunnel investigation of shallow cylindrical shells under moving pulsating pressure discontinuities, noting compression shock effects
21 p3122 A72-41352

Fracture mechanics and cumulative damage of simulated solid propellant under dynamic loads, obtaining low cycle fatigue curve
23 p3325 A72-43706

Aircraft structures shock and blast loading characteristics from internal detonation, comparing computer program results with available data
24 p3365 A72-44610

SHOCK MEASURING INSTRUMENTS
Fast response pressure gage for short duration shock reflection measurements in shock tubes, using dual capacitive sensing elements with signal differencing for ionized gases
09 p1315 A72-23401

Laser-interferometer instrumentation for shock stress wave measurements in solids, using velocity and displacement techniques
12 p1808 A72-27638

Piezoelectric shock transducers system performance tests, assessing previously recorded shock signatures
16 p2393 A72-33636

SHOCK RESISTANCE
NT IMPACT RESISTANCE
Shock hardened delayed transmission pulse code modulated system for artillery projectile instrumentation with in-barrel and in-flight monitoring capability
02 p0175 A72-12155

Characteristic overpressure concept for sonic bangs effect on structures and dynamic magnification factor engineering formula
06 p0758 A72-17858

Hot pressed baron nitride and composite oxidation tests in atmospheric arc jet, noting fabrication and composition effects on thermal shock and oxidation resistance
09 p1333 A72-23279

Thermal shock resistant composite materials with carbide or oxide matrices based on concept of crack propagation prevention, noting superiority from thermal simulation tests
09 p1334 A72-22384

Yttria stabilized hafnia based graphite and tungsten composites, investigating factors affecting thermal shock resistance
09 p1327 A72-22385

Silicon nitride ceramics resistance to thermal shock and stress in severe environments
09 p1334 A72-22386

Hot pressed silicon nitride with high strength and good oxidation and thermal shock resistance for gas turbine applications [ASME PAPER 72-GT-19]
11 p1673 A72-25618

Rods resistance to thermal shock under coupled thermoelasticity conditions, calculating critical thermal flux during thermodynamic compression waves propagation
13 p2053 A72-28399

Prediction of thermal-shock resistance during heating at very high rates.
22 p3241 A72-43000

SHOCK SENSITIVITY
U SHOCK RESISTANCE
SHOCK SPECTRA
Van der Waal broadening of shock excited emission lines at 5000 K for astrophysical applications
06 p0852 A72-18053

Linear Z plasma pinch in Ar as spectroscopic source, investigating effects on shock-piston separation
06 p0865 A72-18544

Oscillatory shock pulse reproduction with specified spectrum for performing shock testing with electrodynamic or electrohydraulic shaker-amplifier-equalizer system
07 p0965 A72-20199

Analysing vibration and shock data. I - Data acquisition and pre-processing.
24 p3382 A72-45287

SHOCK TESTS

- Computer model of dislocation motion acted on by viscous drag through point obstacle array for tensile stress and shock deformation tests
[AD-737978] 04 p0584 A72-14528
- Dynamic yielding of annealed and cold worked Fe-Ti alloy determined in shock compression tests
05 p0679 A72-17121
- Shock testing machine based on free falling weight striking resilient block, describing design details and electrical circuitry
09 p1292 A72-23472
- Quantified design criteria for vibration and shock test fixtures to insure test repeatability, proposing chart inclusion in military test standards
15 p2215 A72-32619
- Aeroacoustic, vibration and shock environments for the space shuttle orbiter.
24 p3448 A72-44679

SHOCK TUBES

- NT MAGNETIC ANNULAR SHOCK TUBES
- NT SHOCK TUNNELS
- Wall friction effect on current sheet speed of magnetically driven shock tube, establishing steady state existence
01 p0105 A72-10027
- High velocity plasma generation in induction hydrodynamic shock tube and flow into rail type plasma accelerator, investigating possible T layer formation
01 p0110 A72-11203
- Magnetoplasma dynamic supersonic ring duct as electromagnetic shock tube or plasma gun, emphasizing plasma flow-magnetic field interaction
01 p0110 A72-11204
- Shock tube gas temperature measuring equipment using spectrum line reversal method
01 p0072 A72-11217
- Shock tube technique for opacity measurement at high pressures in seeded hydrogen for gas core nuclear rockets
01 p0099 A72-11342
- Carbon dioxide and hydrogen mixtures in shock tube, noting rotational- and translational-vibrational energy transfer role from relaxation time measurement
02 p0203 A72-12028
- Real gas tailored shock tube Mach numbers by analytical method, investigating driver temperature effect
02 p0205 A72-12269
- Computer investigation of three fluid electrical current sheet model, solving magnetic annular shock tube problem
[SRL-TR-71-0021] 02 p0200 A72-12659
- Electron impact broadening of ionized Be and Ba lines in electric shock tube plasma, measuring electron density and temperatures
03 p0393 A72-13020
- Mercury vapor physicochemical processes kinematics in shock tube, determining electron gas energy balance equations
03 p0395 A72-13572
- High temperature CIF reaction kinetics in thermal decomposition shock tube study, using chlorine atom two-body emission
04 p0484 A72-15463
- Arc driven shock tubes performance prediction, presenting correlation equations for velocity calculation
[AD-738275] 04 p0510 A72-15499
- Dutch monograph on heat transfer of gas with vibrational relaxation at shock tube end wall covering mathematical model, induced velocity effect on pressure, etc
05 p0648 A72-16045
- One dimensional continuous electrode shock tube driven MHD accelerator, analyzing unsteady flow behind ionizing shock wave by method of characteristics
[AIAA PAPER 72-102] 05 p0697 A72-16973
- Aerodynamic and thermodynamic phenomena in Hartmann-Sprenger tube with converging walls and excited by subsonic or adapted supersonic jet
06 p0901 A72-17559
- Radiative cooling effect on enthalpy distribution in air behind incident shock waves produced in explosively driven shock tubes
06 p0904 A72-18529
- Compensation of shock wave attenuation due to boundary layer by varying shock tube driver chamber area, using central body of suitable length and profile.
06 p0797 A72-18546
- Shock wave collision induced population inversion in electromagnetic shock tubes, measuring plasma absorption coefficient
07 p1044 A72-20074
- High performance shock tube using electromagnetically compressed and heated driver gas
07 p0965 A72-20559
- Shock tubes - Conference, London, July 1971
[AD-736510] 08 p1148 A72-21013
- Blast and detonation wave phenomena applications in war and peace, discussing hypervelocity launchers, shock tubes and explosive weapons
08 p1146 A72-21014

- Shock tube spectroscopy role in laboratory astrophysics, stressing hook method effectiveness for quantitative analysis of shock heated gases in solar abundances determination
08 p1146 A72-21017
- Laminar and turbulent wall boundary layer and shock attenuation effects on flow uniformity in shock tubes
08 p1149 A72-21018
- Population inversion in plasma via colliding waves generated by symmetric electrodeless electromagnetic shock tube
08 p1147 A72-21304
- Sonic boom simulation devices and techniques, including wind tunnels, ballistic ranges, spark discharges and shock tubes
08 p1147 A72-21906
- Fast response pressure gage for short duration shock reflection measurements in shock tubes, using dual capacitive sensing elements with signal differencing for ionized gases
09 p1315 A72-23401
- Observation and ionization relaxation times of Ar plasma produced in shock tube at Mach 10-13, describing experimental arrangement
10 p1519 A72-24056
- Diaphragmless electrothermal shock tube for collision in preheated Ar, using RF plasma heater
10 p1459 A72-24410
- Diffuser performance and idling characteristics in shock tube at Mach 8, discussing pressure recovery factor laminar and transition flows in boundary layer
10 p1419 A72-24545
- Cylindrical tube geometry and electrode separation effects on normal ionizing shock waves, showing speed proportional to azimuthal drive and axial magnetic fields
10 p1470 A72-24794
- T-tube plasma flow velocity measurement via shock wave attenuation recording technique
11 p1693 A72-25561
- Shock tube rotational relaxation time measurements in cryogenic hydrogen, using laser schlieren optical system
11 p1691 A72-26008
- Mercury vapor physicochemical processes kinematics in shock tube, determining electron gas energy balance equations and atom-atom collision cross sections
11 p1699 A72-26760
- Nonequilibrium Faraday MHD generator performance examined by double diaphragm shock tube within ionization region
13 p2013 A72-29357
- Sound radiation by shock wave front in cesium vapors, describing experimental shock tube
13 p2017 A72-29608
- In-line high vacuum conductance valve with attached diffusion pump for shock tube evacuation
13 p1959 A72-29758
- One dimensional blast wave theory for trajectory analysis of shocks driven by solid explosives in linear shock tubes
14 p2093 A72-30179
- First positive and first negative nitrogen emission excitation kinetic mechanisms, investigating shock tube measurements of nonequilibrium radiation
14 p2134 A72-30837
- Plasma velocity, gas pressure, wall heat flux and shock heated region length measured in electrical discharge shock tube without diaphragms, discussing ionization relaxation process
15 p2283 A72-31268
- Fine wire thermocouple probe use for measurement of total temperature in shock tube lasers
15 p2241 A72-32524
- Wall contour effect on shock wave shape, comparing Whitham theory with schlieren photographs from shock tube tests
15 p2219 A72-32595
- Shock wave propagation velocity increase in combustion shock tubes through intermediate pressure chamber, using streak camera and microwave Doppler technique for velocity measurements
16 p2375 A72-32839
- Shock tube diaphragm rupture effect on density distribution in rarefaction wave as function of time, using mirror laser interferometer measurement
16 p2390 A72-33161
- Low pressure gas heating expediency for stagnation temperature increase in gas flow of shock tube
16 p2480 A72-34168
- HF vibrational relaxation measurements using the combined shock tube-laser-induced fluorescence technique.
17 p2511 A72-34735
- Shock tube investigation of low-density heated fluid element dynamic reaction to reflected shock wave passage, noting similarity to atmospheric thermals
17 p2542 A72-35615
- Accelerated propagation of a shock wave in a shock tube
18 p2682 A72-36670
- Generating high Reynolds-number flows.
19 p2787 A72-38222

- Boundary layer closure in the conical shock tube.
19 p2788 A72-38431
- Experiments concerning the contact surface in a membrane shock tube
20 p2911 A72-39017
- Shock tube boundary layers in ionized argon-helium mixtures.
20 p2914 A72-39639
- Sound radiation generation by shock wave front in Cs vapors, describing experimental shock tube
21 p3091 A72-40662
- Performance and limitations of shock tubes with imploding detonation drivers.
21 p3128 A72-40767
- The simulation of high pressure hydrogen/oxygen rocket engines.
[AIAA PAPER 72-1027] 21 p3042 A72-41606
- A shock tube determination of the electronic transition moment of the CN red band system.
23 p3316 A72-44329
- Instabilities in the reaction zones of detonation waves.
24 p3462 A72-45029
- Measurement of thermal relaxation time of vibration of polyatomic molecules by the impact tube method
24 p3402 A72-45045

SHOCK TUNNELS

- Refinements in high-Reynolds-number shock-tunnel technology.
[AIAA PAPER 72-996] 21 p3040 A72-41582
- A thermal mapping technique for shock tunnels and a practical data reduction procedure.
[AIAA PAPER 72-1031] 24 p3389 A72-45408
- SHOCK WAVE ATTENUATION
- Shock wave damping and droplet atomization function of relaxation zone in noncombustible two phase gas-liquid mixtures
02 p0202 A72-11592
- Acoustic absorption materials weak shock wave reflection and attenuation determination by shadow-graph-schlieren photography and pressure transducers
02 p0259 A72-12177
- Slender projectile supersonic flight in fluid with nonequilibrium transformations, comparing theoretical shock decay angle with Wegener-Klikoff measurements
03 p0307 A72-13158
- Sonic boom generation, propagation and minimization, discussing atmospheric conditions and ground characteristics influence and means for boom signature reduction
04 p0464 A72-14815
- Sonic boom generation, propagation and minimization, discussing atmospheric turbulence and temperature gradients and aircraft configuration effects
[AIAA PAPER 72-194] 05 p0612 A72-16849
- Shock wave deceleration and boundary layer mass loss effects on electron density and ionization levels of air in shock tube
05 p0700 A72-17225
- Compensation of shock wave attenuation due to boundary layer by varying shock tube driver chamber area, using central body of suitable length and profile.
06 p0797 A72-18546
- Stainless steel circular tubes size and fittings effects on pneumatic pulse wave distortion and attenuation in fluidic pulse generation system
08 p1111 A72-20928
- Laminar and turbulent wall boundary layer and shock attenuation effects on flow uniformity in shock tubes
08 p1149 A72-21018
- Earth Love waves and toroidal oscillations attenuation, presenting frequency dependent model of internal friction
09 p1299 A72-22801
- T-tube plasma flow velocity measurement via shock wave attenuation recording technique
11 p1693 A72-25561
- Shock wave propagation and damping in system of constant density gas bubble suspension in liquid flow with uniform velocity
13 p1940 A72-28436
- Reflection of weak shock waves from permeable materials.
17 p2581 A72-35250
- Decay of a diamond shock pattern.
20 p2913 A72-39606
- Flow quality improvements in a blowdown wind tunnel using a multiple shock entrance diffuser.
[AIAA PAPER 72-1002] 21 p3041 A72-41587
- A new concept for correcting the attenuation effects in a shock tube.
24 p3388 A72-44985
- SHOCK WAVE CONTROL
- Shock wave shape and strength alteration by radioisotope emissions from body surface in supersonic airstream
05 p0654 A72-17226
- SHOCK WAVE GENERATORS
- NT MAGNETIC ANNULAR SHOCK TUBES
- NT SHOCK TUBES
- NT SHOCK TUNNELS

Exploding wire restrike mechanisms, discussing shock generation for arc channels

02 p0260 A72-12362

Acceleration phase of solar cosmic rays and relativistic electrons in solar flare of 7 July 1966, discussing MHD shock waves generation

03 p0407 A72-12942

High velocity impact reduced temperature increase due to shock compression in metals, discussing pressure and charge effects

03 p0442 A72-13240

Confined small diameter PETN, RDX and tetryl columns longitudinal detonations, using focused Q switched ruby laser

03 p0367 A72-13604

Pulsed cylindrical converging shock wave generation in decreasing density medium by axial explosion-implosion discharge

05 p0700 A72-17233

Oscillatory shock pulse reproduction with specified spectrum for performing shock testing with electrodynamic or electrohydraulic shaker-amplifier-equalizer system

07 p0965 A72-20199

Schlieren observation of generation and convergence of shock waves produced in He and Ar by capacitor bank discharge in parallel rail type device

11 p1695 A72-25921

Shock wave generation by high current pulsed discharges, determining shock front velocity as function of magnetic pressure on current sheath

16 p2434 A72-32909

SHOCK WAVE INTERACTION

High speed interstellar gas dynamic resonant hydromagnetic wave interaction with cosmic ray shocks

01 p0121 A72-11140

Real gas tailored shock tube Mach numbers by analytical method, investigating driver temperature effect

02 p0205 A72-12269

Shock wave impact at flat/spherical end surface of cylindrical body in supersonic nitrogen flow, using pulsed ruby laser for shadow photography

02 p0151 A72-12280

High velocity boundary layer problems for space shuttle, investigating free interaction with detachment, shock wave, penetration, air bubbles in circulation and adherence conditions

03 p0308 A72-13699

Plane shock wave and blunt body interaction in supersonic gas flow in two-diaphragm shock tube

04 p0461 A72-14639

Collisionless shock wave interaction with particle stream in upper solar corona from decameter radio observation

05 p0708 A72-15764

Hypersonic air inlet of revolution with mixed supersonic compression, analyzing shock-boundary layer interaction process

[ONERA, TP NO. 977] 05 p0599 A72-15857

Monograph on head-on collision of combustion wave with shock wave and rarefaction wave covering gas dynamics, interactions, reflection process, etc

05 p0746 A72-16046

Blunt bodies-shock wave interaction in shock tubes, using interferometer with laser light source and high speed streak camera

05 p0601 A72-16225

Laser schlieren measurement of density gradients in laminar hypersonic boundary layer interacting with corner expansion wave in shock tunnel

[AIAA PAPER 72-75] 05 p0606 A72-16879

Macroscopic boundary conditions of gas-solid interface interaction as function of gas temperature and transport coefficients variation in shock reflection problems

06 p0902 A72-18107

Attached and separated turbulent viscous regions resulting from shock wave-boundary layer interactions in hypersonic flow

[AIAA PAPER 72-74] 07 p0966 A72-18949

Pulsed radiography of X ray absorption by plasma behind incident shock wave in Cs vapors, noting mirror behind shock front and wave reflection

07 p1044 A72-19887

Shock wave collision induced population inversion in electromagnetic shock tubes, measuring plasma absorption coefficient

07 p1044 A72-20074

Shock wave excitation by moving solar wind discontinuity in geomagnetic tail as cause of active phase of magnetospheric substorm

08 p1153 A72-20716

Growth rate estimation of negative energy Bernstein and ion acoustic waves explosive interaction, noting collisionless shock turbulence

08 p1212 A72-21248

Population inversion in plasma via colliding waves generated by symmetric electrodeless electromagnetic shock tube

08 p1147 A72-21304

Two dimensional two step difference scheme for shock wave interaction with cylinder in supersonic flow

08 p1150 A72-21443

Boundary layer transition effect on three dimensional shock interactions due to blunt protuberances and axial compression corner

[AD-743741] 08 p1150 A72-21629

Stagnation conditions of magnetoradiative supersonic flow through shock waves for temperature dependent specific heat parameter

08 p1255 A72-21795

Supercooled cloud water droplets in free fall shattered by shock waves measuring ice crystal formation probability

09 p1345 A72-22446

Book on ideal and real compressible fluid dynamics covering supersonic flow past airfoils and shock wave interaction with laminar boundary layer

09 p1295 A72-23045

Two dimensional shock wave interaction with bends in rectangular duct, showing far wall Mach reflection

10 p1464 A72-23879

Sintered prepolarized perovskite type ferroelectric ceramics adiabatic depolarization and energy conversion under shock wave action

10 p1422 A72-24128

Shock wave passage through curved interface from low to high density medium, showing interaction dependence on density ratio

10 p1469 A72-24541

Vorticity effect on shock wave-boundary layer interactions on blunt edged compression surfaces of hypersonic inlets

10 p1419 A72-24649

Shock wave impact at flat/spherical end surface of cylindrical body in supersonic nitrogen flow, using pulsed ruby laser for shadow photography

11 p1571 A72-25702

Two dimensional Lagrangian hydrodynamic code for stability of shock acceleration perturbed interface between two gases of different density

13 p1942 A72-29114

Shock waves amplification by interaction with burning gas-liquid mixture, noting triangular profile of pressure variations behind wave front

13 p2065 A72-29888

Hypersonic blowdown tunnel investigation of turbulent shock-boundary layer interactions at two dimensional wedge compression corner

13 p1944 A72-30030

Shock wave interaction with supersonic moving plate, calculating plate lift as function of time

14 p2071 A72-31024

Approximate model of weak shock wave interaction with laminar MHD boundary layers for perfectly conducting supersonic streams

15 p2284 A72-31633

Liquid and solid explosives detonation, initiation and shock interaction with inert materials for precision work

16 p2476 A72-33352

Shock wave interactions with nozzle wall turbulent boundary layer, discussing shock strength variation to produce unseparated, incipient and fully separated flow fields

[AIAA PAPER 72-715] 16 p2380 A72-34033

Viscous boundary layer generated weak shock wave effects on gas dynamic laser medium density homogeneity

[AIAA PAPER 72-709] 16 p2380 A72-34037

Atomization of liquid droplets in a convective gas stream

17 p2540 A72-35044

Pulsed radiography of X ray absorption by plasma behind incident shock wave in Cs vapors, noting mirror behind shock front and wave reflection

17 p2590 A72-35135

Pressure distribution on a yawed wedge interacted by an oblique shock

17 p2485 A72-35239

Acceleration of burning by a shock wave interacting with the flame

18 p2740 A72-36240

Fast magnetoacoustic wave interaction with shock wave propagating in ideal electrically conducting gas, showing magnetic field stabilizing effect

18 p2711 A72-36812

Magnetospheric and ionospheric conjugate point phenomena as solar events manifestations via solar wind shock wave interaction with geomagnetic field

19 p2790 A72-37858

Shock wave excitation by moving solar wind discontinuity in geomagnetic tail as cause of active phase of magnetospheric substorm

19 p2791 A72-38344

Strong shock propagation through decreasing density

19 p2789 A72-38796

Correlations of peak heating in shock interference regions at hypersonic speeds

21 p2992 A72-41309

Transition in compressible free shear layers

21 p2993 A72-41310

Pressure fluctuations resulting from the interaction between a shock wave and a turbulent boundary layer

24 p3359 A72-44682

Mach stem generation by colliding spherical pressure waves in spark ignited combustible gas, noting simultaneous deflagration wave characteristics

24 p3462 A72-45028

SHOCK WAVE LUMINESCENCE

Shock layer emission associated with hypersonic air flow past spherical segment, solving flow equations by iteration technique

10 p1418 A72-24539

SHOCK WAVE PROFILES

Rate-type viscoelastic materials, deriving weak shock structure by wave front, ray and singular surface theories and asymptotic expansions

01 p0101 A72-10033

Hypersonic source flow past wedges and cones, calculating flow nonuniformities effects on shock shape, velocity, pressure and density by perturbation analysis

01 p0033 A72-11394

Sonic line neighborhood of uniform axisymmetric supersonic air jet impinging on perpendicular disk plate, measuring shock shapes and surface pressures

01 p0002 A72-11398

Hydrogen shock waves density profiles measurement, noting uncoupled translational and rotational relaxation processes

02 p0263 A72-12360

Solid particle influence on underexpanded gas jet shock structures, using schlieren photographs

03 p0342 A72-13840

Nonsteady molecular beam approximation for strong shock structure problem, considering Boltzmann equation

03 p0399 A72-14053

Transverse shock waves fine structure and saturation of ion-acoustic turbulence in collisionless plasma, using magnetic field probe and MHD equations

03 p0399 A72-14068

Plasma shock wave oscillation profile dependence on ion and electron friction and viscosity

04 p0555 A72-14620

Shock wave structure in monatomic gases, using Fokker-Planck model for particle collisions and Mott-Smith distribution for shock front

04 p0512 A72-15162

Steady normal shock wave analysis in binary inert monatomic gas mixtures using kinetic theory moment method

04 p0513 A72-15340

Discontinuities in electrohydrodynamics, discussing surface charge generation at shock front and shock wave structure determination

05 p0690 A72-16580

Laminar leading edge of collisionless plasma perpendicular shock structure and distribution functions, considering instability calculations

05 p0654 A72-17227

Strong normal shock wave structure upstream and downstream of discontinuity due to nonequilibrium radiation and collisional ionization

06 p0902 A72-18106

Shape and structure of shock wave moving along plane wall in gas, comparing experimental results with De Boer theory

07 p0971 A72-20096

Charge separation effects on plasma shock wave profile in perpendicular propagation to magnetic field, using moment equations derived from Boltzmann equations for electrons and ions

08 p1213 A72-21254

Earth bow shock laminar profile at low Mach number by crossing satellites on 12 February 1969, determining mean velocity along normal

09 p1387 A72-23004

Shock wave profile equation derivation based on minimal entropy rate variational principle for stationary irreversible processes, using local potential for Boltzmann type equation

09 p1295 A72-23473

Shock wave patterns near sonic line in accelerating or decelerating nonhomotropic flows, extending Busemann homotropic flow description

10 p1419 A72-24841

Wedge reflected shock profiles, comparing results for various Mach numbers and incidence angles with predictions based on Whitham theory

11 p1616 A72-25918

Constant density solutions for flow fields behind concave shock waves, noting approximation for transonic free stream Mach numbers

11 p1572 A72-25919

Numerical algorithm for Boltzmann equation solution with application to shock structure in one dimensional flow

13 p1985 A72-28617

Collisional plasma shock waves structure in electromagnetic shock tube with strong transverse bias magnetic field, using two fluid Navier-Stokes equations

13 p2011 A72-29119

- Shock waves amplification by interaction with burning gas-liquid mixture, noting triangular profile of pressure variations behind wave front
13 p2065 A72-29888
- Shock waves internal structure in gas of elastic spheres, solving nonlinear Boltzmann equation
13 p1944 A72-30029
- Wall contour effect on shock wave shape, comparing Whitham theory with schlieren photographs from shock tube tests
15 p2219 A72-32595
- Interstellar H I region strong polarization shock structure, obtaining charge separation field via beam continuum distribution and Mott-Smith approach
16 p2453 A72-33168
- Earth bow shock wave structure model based on development of strong density gradient in magnetic field-free cosmic plasma
16 p2387 A72-33935
- Shock-wave structure using nonlinear model Boltzmann equations.
17 p2542 A72-35614
- Discontinuities in electrohydrodynamics, discussing surface charge generation at shock front and shock wave structure determination
19 p2834 A72-37551
- Propagation and growth of shock waves in inhomogeneous fluids.
19 p2787 A72-38430
- Experimental investigation of pressure profiles in a helical shock wave irregularly reflected in plexiglass cylinders
21 p3045 A72-40988
- Supersonic flow past a suddenly set plate
22 p3136 A72-42906
- One dimensional steady conducting gas flow in nonaccelerating coordinate system under magnetic field, calculating pressure, density and temperature variations with boundary shock wave
23 p3281 A72-44265
- Earth collisionless plasma bow shock oblique structure assessment by pulsation index I_p devised from empirical results
23 p3341 A72-44511
- Three dimensional shock wave configurations in front of cylindrical body on supersonic wing or of fluid jet injected into main supersonic flow, examining high pressure gradient regions
24 p3361 A72-45113
- Shock wave structure in radiation spectrum of photon-electron interaction via induced Compton effect
24 p3431 A72-45709
- SHOCK WAVE PROPAGATION**
Transient shock produced plasma flow interactions with transverse magnetic field
01 p0105 A72-10020
- Explosion induced plane shock wave propagation in gas medium with exponential density distribution, determining gas flow behavior by difference approximation method
02 p0201 A72-11578
- Detonation waves collision in variable gas medium with plane, cylindrical or spherical obstruction, determining gas parameters behind reflected shock wave
02 p0201 A72-11579
- Shock wave propagation from channel in free space for various Mach numbers, using method of characteristics
02 p0202 A72-11590
- Hugoniot analysis of shock disturbance propagation with steady velocity through composite material, deriving conservation equations
02 p0248 A72-11982
- Free electron density, electron temperature and gas ionization during shock wave propagation in Ar-filled shock tube from microwave radiation measurements
02 p0263 A72-12020
- Hydromagnetic cylindrical blast wave propagation in self gravitating polytropic gas, obtaining graphs for velocity, pressure, density and magnetic field distributions
02 p0264 A72-12181
- Straight beams and rectangular frames stress-strain calculation under pulsed loading, taking into account shock waves finite propagation velocity and internal damping
02 p0300 A72-12855
- Liquid breakdown and subsequent propagation by focused high power laser irradiation, presenting short term photography of event sequence
03 p0368 A72-13606
- Linear and nonlinear MHD shock wave propagation and stability, investigating Hugoniot relation
03 p0396 A72-13688
- Anisotropic elasticity effects on plane shock wave propagation for arbitrary loading directions in plate impact experiments
04 p0585 A72-14538
- Sonic boom generation, propagation and minimization, discussing atmospheric conditions and ground characteristics influence and means for boom signature reduction
04 p0464 A72-14815

- Linearized constant temperature hot-wire anemometer calibration for shock tube unsteady flow velocity measurements with low strength wave propagation
04 p0521 A72-14920
- One-dimensional compression/expansion shock waves propagation in elastic nonheat conducting bodies, deriving differential equation for shock amplitude time rate of change
04 p0592 A72-15547
- Varying energy and gamma/quasi-steady models for point source blast waves from high speed solids impact, comparing 1100-0-aluminum shock decay data
05 p0736 A72-16101
- Flow field due to diffraction of shock wave at wedge moving at supersonic speed
05 p0600 A72-16212
- Nonstationary plane shock wave propagation in elastic medium with soil properties, discussing boundary problem solution and numerical analysis
05 p0689 A72-16284
- Sonic boom generation, propagation and minimization, discussing atmospheric turbulence and temperature gradients and aircraft configuration effects [AIAA PAPER 72-194]
05 p0612 A72-16849
- Existence conditions for steady MHD shock waves propagating in collisionless plasma along magnetic field, observing dependence on pressure anisotropy
05 p0698 A72-17016
- Electron temperature gradient instability in collisionless shocks propagating across magnetic field
05 p0700 A72-17228
- Interplanetary magnetic field effect on flare-generated weak shock wave propagation speed and transit time
06 p0875 A72-17461
- Shock tube experimental techniques for studying fast processes coupled to shock wave propagation in reactive gases, describing pressure, density and temperature measurement methods
06 p0800 A72-18120
- Flow parameters behind shock waves propagating in carbon dioxide-nitrogen mixtures at Mach numbers from 5 to 10
07 p0966 A72-18936
- Point explosion in cosmic spheroid with exponential density distribution, observing shock wave propagation along symmetry axis direction
07 p1075 A72-19583
- Ground focus line location of sonic bang propagating in stratified atmosphere with wind for transonically accelerating aircraft
07 p0912 A72-19645
- Shock wave propagation and structure in elastoplastic material with translational work hardening, obtaining closed system of discontinuity equations
07 p1093 A72-19977
- Chemical composition, thermal properties and shock propagation in solar wind plasma
07 p1061 A72-20018
- Solar wind discontinuities and shock waves in interplanetary medium at magnetospheric boundary related to geomagnetic impulses
07 p1061 A72-20024
- Self similar solutions for piston driven shock wave motion, examining Whitham approximation rule validity
07 p0970 A72-20075
- Two dimensional detonation wave structure and propagation calculated numerically, comparing to exact solutions
07 p0971 A72-20086
- Aerodynamic characteristics of hypersonic velocity meteor traveling in earth atmosphere and shock wave propagation generated by explosion in air and on ground
07 p1081 A72-20094
- Shape and structure of shock wave moving along plane wall in gas, comparing experimental results with De Boer theory
07 p0971 A72-20096
- Charge separation effects on plasma shock wave profile in perpendicular propagation to magnetic field, using moment equations derived from Boltzmann equations for electrons and ions [AD-742533]
08 p1213 A72-21254
- Numerical analysis of capture area ratio effect on shock wave propagation from free stream into moving flowing duct
08 p1150 A72-21619
- Maneuvering aircraft sonic boom propagation and signatures prediction in stratified atmosphere by geometric acoustic method
08 p1110 A72-21904
- Instabilities development in flow field generated by shock wave propagation in exothermic gas mixture
08 p1255 A72-22042
- One dimensional shock wave propagation in inhomogeneous elastic materials, showing wave amplitude behavior dependence on critical jump in strain gradient
09 p1405 A72-22990

- Hugoniot equation of state for impact shock wave propagation along fiber direction in Al epoxy matrix composites
09 p1407 A72-23235
- Sonic booms generation and propagation, discussing effects on animate and inanimate objects
09 p1262 A72-23316
- Plane shock wave propagation in polytropic plastic body with elastic unloading properties, deriving closed form solution for time dependent stepwise decreasing load
09 p1353 A72-23554
- Self similar flow patterns due to cylindrical ionizing symmetrical strong shock and detonation wave propagation outwards into gas at rest
09 p1295 A72-23564
- Steady compressible fluid flow and plane shock wave propagation in pipe bends, discussing parameter effects and boundary conditions
10 p1464 A72-23878
- Shock wave propagation in ducts with abrupt area expansion, discussing vortices generation and wave diffraction and reflection effects on ducted flow
10 p1464 A72-23880
- Curvature and thickness corrective terms in Rankine-Hugoniot relation for shock wave propagation of ideal gases binary mixture
10 p1417 A72-24117
- Nonlinear diffraction of weak shock waves near rigid wall with sharp bend, obtaining approximate solution by matched asymptotic expansion method
10 p1468 A72-24432
- Shock wave passage through curved interface from low to high density medium, showing interaction dependence on density ratio
10 p1469 A72-24541
- Plane ionizing shock wave stability in MHD channel within magnetic field
10 p1522 A72-24542
- Cylindrical tube geometry and electrode separation effects on normal ionizing shock waves, showing speed proportional to azimuthal drive and axial magnetic fields
10 p1470 A72-24794
- Blast wave propagation in uniform or gravitationally stratified media, using Brinkley-Kirkwood shock propagation theory
10 p1471 A72-25069
- Shocked flow and pressure loss computation for axial flow compressor cascades, using time dependent finite difference technique [ASME PAPER 72-GT-31]
11 p1569 A72-25627
- Axisymmetric shock wave propagation in continuous inhomogeneous medium, taking into account shock geometry orthogonality conditions and flow hydrodynamics behind shock
11 p1616 A72-25864
- Schlieren photographic investigation of shock wave propagation over narrow slit, noting cylindrical expansion wave origin at slit upstream edge
11 p1616 A72-25920
- Schlieren observation of generation and convergence of shock waves produced in He and Ar by capacitor bank discharge in parallel rail type device
11 p1695 A72-25921
- Relativistic shock propagation and search for electromagnetic pulses from supernovae, plotting kinetic energy factor vs external mass fraction
11 p1721 A72-26126
- Critical shock wave velocity for ionization front propagation with photoionization of hydrogen by radiation, using pinch discharge tube measurements [AIAA PAPER 72-410]
11 p1706 A72-26161
- Characteristic shocks propagation velocity, showing exceptionality of hyperbolic conservative system multiple waves
11 p1689 A72-26479
- Shock wave generation and propagation from Apollo rockets at orbital altitudes
11 p1690 A72-26513
- Seismic wave prediction from high altitude nuclear detonation, using ground reflected spherical shock parameters
11 p1627 A72-26519
- Boundary reflection and transmission of N-shaped acoustic shock wave radiated from circular pipe into free air space
12 p1844 A72-27262
- Molecular dynamic techniques for simulating one dimensional shock wave motion in three dimensional solid, using rare gas solid model
12 p1881 A72-27282
- Self similar blast waves propagation, studying flow field in terms of shock front velocity and ambient atmospheric density variation ahead of front [AD-745816]
12 p1889 A72-27832
- Shock wave propagation and damping in system of constant density gas bubble suspension in liquid flow with uniform velocity
13 p1940 A72-28436
- Weak ion-acoustic quasi-shock wave propagation in collisionless plasma, determining long time behavior of precursor ion stream reflected by electrostatic potential
13 p2012 A72-29125

Approximate calculation of correction to universal law of propagation of one dimensional shock waves in stationary polytropic gas

13 p1943 A72-29882

Strong shock wave formation and propagation in interplanetary space after chromospheric flares calculated by gas dynamic approximation, determining magnetic field configuration

13 p2050 A72-29955

Acoustic shock wave diffraction at moving or static plate immersed in ideal gas

13 p1943 A72-30011

One dimensional blast wave theory for trajectory analysis of shocks driven by solid explosives in linear shock tubes

14 p2093 A72-30179

Hypervelocity impact parameters calculated from shock wave equations of motion, discussing viscosity effect on velocity and stress distributions

14 p2164 A72-30297

Tungusk meteorite explosion energy values for various altitudes from investigation of shock wave propagation in variable density atmosphere

14 p2152 A72-30492

Diatom molecular vibrational excitation and dissociation effects on imploding shock waves, comparing shock tube data to prediction

15 p2192 A72-32148

Shock wave propagation velocity increase in combustion shock tubes through intermediate pressure chamber, using streak camera and microwave Doppler technique for velocity measurements

16 p2375 A72-32839

Shock wave propagation in gas with discrete velocity distribution, comparing solutions based on Euler, exact and Navier-Stokes equations respectively

16 p2375 A72-32861

Shock wave generation by high current pulsed discharges, determining shock front velocity as function of magnetic pressure on current sheath

16 p2434 A72-32909

Solar wind thermal anisotropy effects on least squares estimates of interplanetary shock parameters and associated normals from Rankine-Hugoniot equations

16 p2444 A72-32973

Imploding spherical and cylindrical shocks, considering rear flow field with nonadiabatic isothermal flow and zero temperature gradient

16 p2376 A72-33009

Heat conductivity effect on structure and critical Mach number of shock wave propagation across magnetic field in cold rarefied plasma

16 p2435 A72-33152

Shock wave propagation produced by explosive detonation in contact with inert solid, considering spallation occurrence and prevention

16 p2469 A72-33356

Shock wave propagation in incompressible elastic Mooney-Rivlin material for arbitrary homogeneous strain state

16 p2426 A72-33788

Control volume method for finite amplitude shock front propagation in hyperelastic materials, solving steady state conservation equations

16 p2427 A72-33830

Conservation equations for wave and/or turbulence momentum and energy flux in interplanetary space shock vicinity, developing modifications for electron temperature calculations

16 p2459 A72-33913

Mathematical model for deuterium slab solid and plasma under laser pulses irradiation, noting shock wave propagation and slab acceleration

[AIAA PAPER 72-721]

16 p2439 A72-34027

Q switched laser produced hemispherical shock waves in Ar and He plasmas, determining primary and secondary wave trajectories

[AIAA PAPER 72-720]

16 p2439 A72-34028

Influence of reflected ions on the magnetic structure of a collisionless shock front.

17 p2592 A72-35819

Theoretical and experimental studies of the focus of sonic booms.

18 p2642 A72-36506

Accelerated propagation of a shock wave in a shock tube

18 p2682 A72-36670

Determination of shock wave velocity in the interplanetary medium

18 p2728 A72-36875

High-speed photography of a plasma focus.

18 p2716 A72-36946

Propagation of an electromagnetic shock discontinuity in a non-linear isotropic material.

18 p2712 A72-36992

Interplanetary-gas motion induced by a solar flare

19 p2855 A72-37391

Shock wave propagation in the solar corona as the cause of type II radio bursts

19 p2851 A72-38064

Tungusk meteorite explosion energy values for various altitudes from investigation of shock wave propagation in variable density atmosphere

19 p2864 A72-38321

Propagation and growth of shock waves in inhomogeneous fluids.

19 p2787 A72-38430

Strong shock propagation through decreasing density.

19 p2789 A72-38796

Solution of some boundary value problems in the theory of potential gas flows and weak shock wave propagation

20 p2913 A72-39404

Propagation of weak shock waves through turbulence.

21 p3044 A72-40114

Motion of a strong shock front in a nonuniform atmosphere

21 p3044 A72-40128

Propagation of magnetohydrodynamic shock waves in a medium with diminishing density

21 p3094 A72-41653

Propagation of spherical and cylindrical shock waves in an inhomogeneous atmosphere with allowance for back pressure

21 p3047 A72-41662

Asymptotic behavior of the flow created by a shock wave incident on a wedge-shaped cavity

21 p3047 A72-41668

Diffraction of an elastic wave at a disk

21 p3127 A72-41669

Solution method for some boundary problems of nonlinear hyperbolic-type equations and propagation of weak shock waves

22 p3164 A72-41904

Sudden impulses in the geomagnetotail and the vicinity.

22 p3168 A72-42002

Problem of uniform-jet flow around an airfoil

22 p3133 A72-42271

Propagation of radiative shock waves in an inhomogeneous cosmic medium.

22 p3225 A72-42452

Acoustic shock wave diffraction at moving or stationary flat plate immersed in ideal gas

22 p3206 A72-42732

Theoretical interpretation of emf generation between noncompressed parts of bimetal junction traversed by shock wave, taking into account radiation pressure of phonon gas

22 p3207 A72-43050

Al powder bonding during compaction by explosively driven plates, measuring shock wave amplitudes, pressure drop, layer separation and critical pressures in spall plane

22 p3184 A72-43183

Ion acoustic instability in collisionless shocks.

23 p3320 A72-43522

Perpendicular collisionless shock wave instability.

23 p3320 A72-43523

One-dimensional shock waves in heat conducting materials with memory. I - Thermodynamics.

23 p3314 A72-44341

Association between interplanetary shock waves and delayed solar particle events.

23 p3332 A72-44503

Non-steady shock waves in metals with phase transitions and hardening by explosion.

24 p3414 A72-45025

Combustion product gas dynamic motion effects on detonation front propagation, discussing reacting blast wave and finite kinetic rate models and asymptotic results

24 p3391 A72-45027

Shock wave velocity, combustion front and pressure measurements of unstable detonations in propane-oxygen-nitrogen mixtures, comparing with double discontinuity theory

24 p3462 A72-45030

Smoked foil observation technique for transient behavior produced by perturbing equilibrium configuration detonation waves

24 p3462 A72-45033

Propagation of blast waves in a combustible gas.

24 p3462 A72-45034

Weak shock wave propagation in a relaxing gas.

24 p3391 A72-45042

Model for shock wave propagation through gas-liquid drop medium based on liquid phase atomization by boundary layer stripping

24 p3391 A72-45049

Effects of upstream unsteadiness on hypersonic flow past a wedge.

24 p3364 A72-45565

SHOCK WAVES

NT DETONATION WAVES

NT MACH CONES

NT NORMAL SHOCK WAVES

NT OBLIQUE SHOCK WAVES

NT RIEMANN WAVES

NT SONIC BOOMS

Characteristic scale lengths of stationary ionic collisional shocks in Q device perpendicular to magnetic field, presenting shock thickness variation with Mach number and density

01 p0105 A72-10028

Similarity theory for electrostatic and magnetic collisionless shocks at zero ion temperature, using numerical simulation results

01 p0106 A72-10029

Aligned fields in MHD shock polar equation, obtaining magnetic induction polar variables

01 p0106 A72-10135

Collisionless plasma shock wave measurements in magnetic field, determining plasma temperature and free electron densities

01 p0108 A72-10236

Strong ionizing shock waves production in hydrogen and deuterium gases, measuring plasma electron temperature, axial electric field and density and magnetic field compression

[AD-734469]

01 p0108 A72-10237

Nonlocal behavior of ion sound instability in collisionless nonuniform confined plasma shock wave

01 p0108 A72-10240

X-type pseudoshock at high Mach number compared with lambda-da-type pseudoshock, discussing loss at duct center by leading shock wave

01 p0050 A72-10397

Earth magnetosphere boundary position, bow shock wave, transition region thickness and magnetopause currents magnetic fields during geomagnetic storms

01 p0059 A72-10605

Pioneer 8 plasma wave measurements at distant bow shock crossings, considering solar wind magnetosheath interaction

01 p0062 A72-10903

Kinetics of shock wave pyrolysis of pentafluoroethane dilute mixture in Ar at 1180-1470 K

02 p0170 A72-11520

Difference schemes for continuous computation of supersonic steady gas flows with internal compression shock waves

02 p0150 A72-11737

Jupiter decimeter radio burst possibility as indicator of high velocity fluxes and shock waves in solar wind

02 p0273 A72-11935

Real gas effects in atmosphere to make sonic bang shock wave full dispersion and thickness wide variations

02 p0154 A72-11972

Supersonic and hypersonic flows with attached shock waves over delta wing at angle of attack, deriving unified theory for flow field

02 p0150 A72-12030

High temperature and pressure detonation gas expansion as shock wave from cylindrical volume, calculating flow velocity, pressure and density

02 p0302 A72-12285

Helium shock wave two step collisional ionization model comparison to observed profile data from laser Fabry-Perot interferometer

02 p0266 A72-12368

Anomalous earth bow shock locations during 1969 from satellite and magnetic observations aboard European satellite Heos-1

02 p0274 A72-12461

Solar wind plasma flow through earth bow shock, deriving specific heats ratio based on one-fluid theory and conservation equations

03 p0412 A72-13509

French papers on shock waves in fluids and solids covering gas flows in thermodynamic equilibrium and across conic shocks of revolution

03 p0341 A72-13683

Plane and conical shock waves, presenting graphs and tables for numerical applications

03 p0341 A72-13684

Curved shock waves in steady flow of perfect fluid, confirming Hugoniot relations validity

03 p0341 A72-13685

Shocks structure and kinetic theory of gases, discussing density profiles, velocity and temperature measurement techniques

03 p0341 A72-13686

Shock waves in solids, investigating Hugoniot curve for condensed and porous media and phase transformation effects in polycrystals

03 p0446 A72-13689

Laminar boundary layers on heated plane wall behind shock wave in dissociating oxygen for thermodynamic and frozen flow

03 p0344 A72-14342

Random method solution of Boltzmann equation for pseudoshock /relaxation mixing/, applying to random collisions of molecular beams

04 p0551 A72-14519

Shock wave contributions from micrometeorites, meteors, meteorites and thunder to organic compounds formation in primeval atmosphere

04 p0572 A72-14760

Radiative cooling effects on flow field and heat transfer behind reflected shock wave

[AD-737423]

04 p0597 A72-15338

Boltzmann equation collision integral statistical models, solving shock structure in monatomic gas

04 p0513 A72-15339

Flow distribution behind shock wave with intense laser radiation absorption and laser-triggered thermonuclear reactions

[AD-736299]

04 p0559 A72-15351

Nonstationary behavior of collisionless shock waves in plasma wind tunnel, suggesting interpretation of magnetosphere magnetic field structure near earth bow shock

04 p0559 A72-15468

Suspended compression shock construction near supersonic point in plane nonuniform ideal gas flow by hodograph technique

05 p0600 A72-16213

Contact surface turbulent mixing instability in free piston high enthalpy shock tunnel waves with test air and argon gases

05 p0644 A72-16548

One dimensional continuous electrode shock tube driven MHD accelerator, analyzing unsteady flow behind ionizing shock wave by method of characteristics [AIAA PAPER 72-102]

05 p0697 A72-16973

Electron heating model in perpendicular collisionless plasma shock waves based on electron trapping by turbulent electric field

05 p0697 A72-17014

Longitudinal electrostatic waves in perpendicular collisionless plasma shock, investigating stability

05 p0698 A72-17021

MHD shock waves stability, showing Hall term effect on number of shock boundary conditions

05 p0699 A72-17025

Magnetosonic, Alfvén, shock and infinitesimal waves and corresponding rays in relativistic hydrodynamics and magnetohydrodynamics, using tensor distributions

06 p0847 A72-17253

Ion-acoustic collisionless shock generation by initial plasma density discontinuity in Q machine, correlating experimental results with numerical simulation

06 p0856 A72-17520

Plane supersonic ionizing shock wave in magnetic field under small wave plane perturbation from equilibrium position, calculating stability from linearized equations

06 p0798 A72-17678

Interplanetary shock wave inclination to ecliptic plane dependence on chromospheric flare and earth projection heliolatitude differences

06 p0884 A72-18027

Asymptotic developments in transonic flows, considering three dimensional flows near shock and plane viscous and heat conducting flow

06 p0756 A72-18105

Steady two dimensional magnetodynamic flow past nonconducting wedge with perpendicular magnetic field at different shock attachment angles

06 p0861 A72-18113

Ice particles and frozen droplets formation on nuclei in supercooled cloud by shock waves under laboratory conditions

06 p0843 A72-18452

Radiative cooling effect on enthalpy distribution in air behind incident shock waves produced in explosively driven shock tubes

06 p0904 A72-18529

Transverse ionizing shock waves in gaseous hydrogen at speeds to 4000 km/sec, presenting magnetic shock structure and magnetic field jump measurements [AD-738620]

06 p0863 A72-18531

Earth bow shock magnetic field data correlation withOGO 5 flux gate magnetometer, using Tidman-Northrop theory

07 p0975 A72-19145

MHD shock normals calculation by magnetic coplanarity formula, applying to bow shock crossing of Pioneer 6

07 p1040 A72-19157

Micron sized particle velocity relaxation measurement in shock wave, using laser Doppler methods [CLEA PAPER 11,3]

07 p1005 A72-19389

Book on compressible fluid dynamics covering steady flow, shock waves and self similar motions

07 p0967 A72-19448

Radiative cooling effects in absorbing-emitting gas behind reflected shock waves, using expansion procedure in small density ratio across shock front [AD-738781]

07 p0967 A72-19503

Stationary high beta plasma shock waves generated in plasma wind tunnel by impinging on magnetic field, comparing with earth bow shock

07 p1042 A72-19617

Collisionless plasma electronic shock waves (stationary heat discontinuity/ observation, proving stationary shock wave existence

07 p1043 A72-19874

Nonlinear difference schemes for quasi-linear transfer equation in gas dynamics and shock wave computations

07 p0971 A72-20085

Flow structure between bow shock wave and blunted cone surface, studying interior shock waves by numerical solution via finite difference methods

07 p0910 A72-20108

Side force and shock wave induced by obstacle on rocket engine nozzle wall, investigating pressure distribution

07 p1055 A72-20250

Axial arc column interaction with shock waves and high velocity gas flow effects in forced convection, proposing heat transfer theory

07 p1047 A72-20548

Shock wave properties in RR Lyra type star atmospheres, discussing high temperature region structure behind wave front and emission line profiles

08 p1229 A72-20841

Chemical reactions in shock waves, discussing diatomic molecules dissociation and combustion processes

08 p1148 A72-21016

Strong shock wave diffraction from wedge reduced to Hilbert problem, noting nonregular refraction theory nonexistence

08 p1151 A72-21662

Fluid motion near wave front junction point, expanding unknown functions and independent variables into series of parameters characterizing shock wave and angular distances

08 p1152 A72-21945

Nova outbursts hydrodynamic processes, studying mass loss mechanism based on direct shock wave ejection and pulsational instability

09 p1382 A72-22283

Large amplitude electrostatic ion acoustic shock production by superposing pulsed photoionized plasma slab on dc background

09 p1360 A72-22871

Self consistent collisionless theory of turbulent low Mach number ion-acoustic shocks, noting resistive heating

09 p1360 A72-22872

Single- and multiphase theories of slowly varying nonlinear dispersive waves, noting stability solutions to large scale variations and shocks

09 p1351 A72-22942

Strong shock wave acceleration during passage through decreasing density region observed in experiments with explosions in Ar-H mixture

09 p1295 A72-22961

Electron plasma oscillations distribution upstream from earth bow shock, evaluatingOGO-E plasma wave detector data

09 p1300 A72-23019

Sonic boom effects on structures, discussing ground motion, direct excitation by shock waves and damages

09 p1304 A72-23318

Stable large amplitude high Mach number ion acoustic shocks in collisionless plasma, obtaining electron density as function of time

09 p1364 A72-23445

Loading process behind reflected and refracted shock waves in plastic layered media with linear elastic unloading

09 p1353 A72-23555

High temperature and pressure detonation gas expansion as shock wave from cylindrical volume, calculating flow velocity, pressure and density

10 p1561 A72-23759

Ionization kinetics influence on light absorption zone behind plane stationary shock wave in hydrogen

10 p1467 A72-24358

Pressure jumps lower bounds across supersonic transports induced shock waves in homogeneous atmosphere, using Whitham function in terms of Riemann integral

10 p1420 A72-24846

Astronomical models of solar wind interaction with interstellar medium, determining magnetic field effects on shock wave

11 p1713 A72-25946

Interplanetary shock wave inclination to ecliptic plane dependence on chromospheric flare and earth projection heliolatitude differences

11 p1719 A72-25963

Trajectory determination of supersonically traveling object from shock arrival times observations at ground locations

11 p1617 A72-25994

Steady state plasma interactions with electromagnetic force field in plasma accelerators, showing shock wave formation

[AIAA PAPER 72-413]

11 p1706 A72-26163

Shock-induced flow acceleration in Ar plasma, studying shock front behavior from high-speed photographs

11 p1696 A72-26374

Magnetosheath pressure, magnetic field, temperature, particle density and stream velocity computed for earth bow shock in oblique interplanetary field with solar wind

11 p1723 A72-26526

Skew magnetic structure of ionizing shock waves with ohmic dissipation as dominant diffusion mechanism

11 p1618 A72-26605

Automatic switched Shuman filter for shock waves numerical computation, noting third and fourth order accurate finite difference schemes

11 p1619 A72-26668

Shock wave structure in radiation spectrum of photon-electron interaction via induced Compton effect

12 p1848 A72-27056

Raman effect application to study of gas vibration relaxation downstream of shock wave

12 p1888 A72-27180

Quasi-stationary supersonic plasma flare generation by lamp-pumped rhodamine laser, studying shock wave structure by high speed cinematography

12 p1825 A72-27882

Hydrocarbon-air mixtures reaction in incident shock waves of pressure greater than 25 atmospheres, correlating with shock tube results

13 p2063 A72-28549

Shock wave solutions of nonlinear hyperbolic system of conservation laws, considering case of zero viscosity

13 p1940 A72-28616

Unsteady state propagation of weak nonlinear plasma waves in magnetic field, discussing shock wave formation and compression pulse evolution

13 p2012 A72-29124

Jupiter decameter radio bursts as indicator of high velocity fluxes and shock waves in solar wind

13 p2030 A72-29247

Earth-solar wind bow shock structure fromOGO-5 observations during passage from interplanetary medium into magnetosheath

13 p1950 A72-29379

Two phase flow model of cloud and star formation by galactic shocks in quasi-steady interstellar gas flow in spiral gravitational field

13 p2040 A72-29404

Mathematical model for gas turbine engine inlet noise caused by shock wave impingement, noting dynamic wave system with overpressure and distortion

13 p2028 A72-29576

Low energy proton flux increases associated with geomagnetic storms due to interplanetary shock waves occurring during solar cosmic ray flare event decay

13 p2032 A72-29724

Investigation method for shock wave induced demagnetization in YIG, noting impact study of magnetic properties

13 p1959 A72-29757

Carbon dioxide laser light scattering measurements of turbulence in high beta collisionless plasma shock wave

13 p2018 A72-29853

Shock wave and isentropic compression/expansion in plasma with anomalous thermodynamic properties due to strong particle interactions, discussing phase transitions types

13 p2019 A72-29904

Unsteady spherical shock wave effect on thin infinite elastic plate covering acoustic semispaces, using integral transformation method

13 p1943 A72-29946

Comet-like interaction of Venus atmosphere with solar wind from Venus probe data, noting absence of bow shock wave and ionospheric tail

13 p2050 A72-29956

Visible light flash emission due to strong shock wave of laser spark, investigating strong external magnetic field effect and time variation of luminous intensity

13 p1972 A72-29983

Plasma radiation from collisionless MHD shock waves, discussing waves generation and angular distribution

14 p2138 A72-30555

Limiting ratio between ideal gas densities before and behind vertical shock wave in elastic thermal insulators

15 p2334 A72-31475

Electrical conductivity of shock wave produced Xe plasma measured by probe, noting dependence on Mach number

15 p2284 A72-31583

Numerical analysis of steady one dimensional quasi-shock waves in collisionless plasma within longitudinal uniform magnetic field, noting oscillations behind wave front

15 p2284 A72-31584

Noise measurements during shock free and underexpanded operation modes of supersonic cold model jet at moderate exit Mach number

15 p2179 A72-32017

Mach 26 shock wave in nitrogen investigated by electron beam fluorescence technique, determining population distribution among rotational states

15 p2281 A72-32404

Piston generated magnetosonic shocks, investigating ion and electron pressure effects on formation

15 p2281 A72-32415

Spark discharge light source for shock wave multiple exposure schlieren photography, describing pulse separator and spark trigger circuits

15 p2240 A72-32437

Gas ionization buildup behind hypersonic shock waves, calculating onset point properties from plasma conservation and electron energy equations

16 p2434 A72-32902

Vorticity jump across stationary MHD discontinuity generalization from gas dynamics problem, noting results validity for shock and detonation waves

16 p2435 A72-33011

- Interplanetary scintillation technique application to structure of flare induced shocks and corotating streams within interplanetary medium
16 p2451 A72-33033
- First and second order shock discontinuity waves propagation in thermoelastic incompressible solids, deriving Piola-Kirchhoff stress tensor via Clausius-Duhem relation
16 p2423 A72-33109
- Theory for plasma radiation from collisionless MHD shock waves applied to Type 2 solar radio bursts, comparing to type 4 bursts
16 p2446 A72-33461
- Precursor ionization upstream from shock wave due to shock emitted radiation absorption by easily ionizable impurity species
16 p2379 A72-33512
- MHD fluid model for collisionless shock waves in turbulent plasma with enhanced transport coefficients, noting laboratory experiments and satellite and radio observations
16 p2439 A72-33932
- Autoignition behind reflected shock waves for hydrocarbon-oxygen mixtures, demonstrating two ignition modes via schlieren photographic records
16 p2479 A72-34002
- Onboard radiometric measurement of bow shock generated UV radiation during atmospheric reentry of experimental sphere
[AIAA PAPER 72-692] 16 p2462 A72-34050
- The hodograph transformation in plastic waves with discontinuous loading conditions.
[ASME PAPER 71-APMW-12] 17 p2624 A72-34308
- Flow distribution for inviscid nonconducting uniform supersonic stream past unyawed semiinfinite circular cone with attached shock wave
17 p2483 A72-34325
- Self-adjusting hybrid schemes for shock computations.
17 p2575 A72-34648
- Ionization kinetics influence on light absorption zone behind plane stationary shock wave in hydrogen
17 p2539 A72-34957
- Measurement of the parameters and the structure of a wet vapor flow with interphase heat and mass transfer in the relaxation zone behind the front of a shock wave.
17 p2637 A72-35130
- Shock tube investigation of low-density heated fluid element dynamic reaction to reflected shock wave passage, noting similarity to atmospheric thermals
17 p2542 A72-35615
- Electron cyclotron drift instability linear theory application to controlled fusion and collisionless shocks, proving anomalous resistance to current flow normal to magnetic field
17 p2592 A72-35624
- Strong shock wave acceleration during passage through decreasing density region observed in experiments with gas discharges and Ar-H mixture explosions
17 p2544 A72-35890
- Rotary shocks and waves of relativistic magnetohydrodynamics
17 p2593 A72-35908
- One-dimensional theory of flows with combustion
18 p2740 A72-36246
- Gas dynamics and chemistry of lightning-produced shock waves /thunder/ in postulated primordial reducing atmosphere, noting amino acid production
18 p2650 A72-36443
- Turbulent heating of electrons and ions in a collisionless shock wave.
18 p2715 A72-36599
- Classification of shock waves in a radiating gas
18 p2682 A72-36806
- Calculation of spatial ideal gas flows without a symmetry plane
18 p2642 A72-36901
- Longitudinal waves in a perpendicular collisionless plasma shock. IV - Gradient B.
19 p2838 A72-37329
- Electron-plasma-wave shocks in a bounded plasma.
19 p2840 A72-37719
- Structure of ion acoustic solitons and shock waves in a two-component plasma.
19 p2841 A72-38440
- Method of characteristics for nonlinear equations of perturbed motion of fluid near contact point between shock and diffraction waves
20 p2912 A72-39023
- Shock waves resulting from interaction of laser radiation with transparent solids.
20 p2933 A72-39522
- Ionization behind shock waves in nitrogen-oxygen mixtures.
20 p2958 A72-39601
- Particle charging behind shock waves in suspensions.
20 p2914 A72-39627
- Numerical solution of quasi-conservative hyperbolic systems - The cylindrical shock problem.
21 p3043 A72-40101
- Pioneer 7 observations of the August 29, 1966, interplanetary shock-wave ensemble.
21 p3104 A72-40481
- Experimental study of flows in supersonic compressors
[ICAS PAPER 72-11] 21 p2990 A72-41136
- Closed form solution for the sonic boom in a polytropic atmosphere.
21 p2992 A72-41258
- Formation of a shock wave around a blunt conical body placed in a rarefied hypersonic flow
21 p2993 A72-41340
- Book - A theory of supercritical wing sections, with computer programs and examples.
21 p2993 A72-41534
- Jet noise generation theory /Lighthill-Ffowcs Williams/ verification by model tests, discussing means of reducing or eliminating shock cells
[ICAS PAPER 72-55] 21 p3047 A72-41852
- Rarefaction wave generation by solar wind shock wave interaction with magnetosphere, noting geomagnetic field weakening during magnetic storm
22 p3217 A72-41894
- The heating of the solar plasma due to microwave phenomena correlated with type II meter bursts.
22 p3222 A72-42041
- Magnetohydrodynamic theory for the interaction of an interplanetary double-shock ensemble with the earth's bow shock.
22 p3170 A72-42404
- Comparison of solar-flare energy estimates made by analytical and numerical techniques.
22 p3219 A72-42426
- Measurements of the local velocity of shock and detonation waves by schlieren interferometry of Doppler-shifted laser light.
22 p3178 A72-42455
- German monograph - Ionization of nitrogen-oxygen gas mixtures by shock waves.
22 p3209 A72-43073
- Polish book - Fluid mechanics. Volume 2 - Gasdynamics.
22 p3168 A72-43199
- Modification of the Rankine-Hugoniot relations for shocks in space.
23 p3341 A72-44510
- Weak electrostatic turbulence observation in earth bow shock magnetic field gradient, suggesting cyclotron drift instability role
23 p3342 A72-44523
- Pressure and magnetic field probe measurements in transverse shock waves in ionizing hydromagnetic regimes, investigating bow shock effects on accuracy
24 p3390 A72-44708
- Two-dimensional supersonic flow with flame sheets.
24 p3360 A72-44988
- Transonic flow past a wavy wall with compression shocks
24 p3360 A72-44999
- Propagation of blast waves in a combustible gas.
24 p3462 A72-45034
- Heat addition to supersonic flow by shock induced combustion studied by spherical and conical projectiles shot into explosive gas mixtures
24 p3360 A72-45038
- Some infrared diagnostic techniques in high temperature gasdynamics.
24 p3402 A72-45043
- Pressure and temperature change on the wall surface in strong shock wave diffraction.
24 p3391 A72-45047
- The breakup of liquid droplet columns by shock waves.
24 p3391 A72-45048
- Conical caret wings supersonic characteristics, examining flow transition from weak to strong attached shock waves
24 p3361 A72-45114
- Axisymmetric and two-dimensional flow with attached shock waves.
24 p3361 A72-45161
- The shock-combustion /expansion-combustion/ polar with allowance for variation of the specific heat ratio of a gas passing through a flame front
24 p3465 A72-45446
- Gas dynamics and shock wave physics of supersonic flow in two phase media, noting evaporation, condensation and phase transformations
24 p3364 A72-45525
- Mach reflection from overexpanded nozzle flows.
24 p3365 A72-45794
- SHORAN**
Shoran systems with onboard computers for aircraft position and trajectory parameters, noting coordinate plotting for flight path recovery maneuvers
13 p1996 A72-28785
- SHORT CIRCUITS**
Copper sulfide-cadmium sulfide single crystal photovoltaic heterojunctions, showing optically induced and thermal effects on short circuit current degradation
03 p0389 A72-13603
- Electronic system for electrodischarge machining, considering thyristor spark control and circuitry design for automatic feed down and short circuit clearance
04 p0502 A72-15530
- Si solar cells nonpenetrating proton damage model in satellite radiation environment, showing open and short circuit current dependence on proton energy
07 p0914 A72-20492
- Negative resistance devices, stability under open and short circuits from dc I-V characteristic shape
16 p2368 A72-32857
- Short-circuit current in silicon solar cells - Dependence on cell parameters.
19 p2753 A72-37567
- SHORT HAUL AIRCRAFT**
Future aircraft design trends for transcontinental and short haul operation, considering traffic forecasts, current transport aircraft and potential derivatives and technology
[SAE PAPER 710749] 01 p0002 A72-10248
- Short haul air transport system need for future short takeoff and landing aircraft, considering airports, airways, economics and navigation and landing aids
02 p0154 A72-11719
- Short haul operating systems in air transportation environments, discussing terminal vs cruise configurations, costs and noise abatement
03 p0309 A72-13422
- VFW-614 short range twin jet passenger transport aircraft, analyzing service performance and economic efficiency requirements influence on design characteristics
03 p0310 A72-13643
- Short-short haul STOL network economics for commuter ports in Detroit region, estimating service demand, aircraft number and maintenance costs
03 p0459 A72-13696
- Civil aviation R and D policy study, showing priorities for aircraft noise and congestion abatement and short haul systems
05 p0611 A72-15780
- Airbus A-300 B design and characteristics for passenger transport on short and medium haul routes
05 p0612 A72-16694
- Single satellite angle system and multiple satellite ranging and range difference systems in short haul air navigation, comparing with VORTAC
06 p0844 A72-17335
- STOL transport passenger market demand model selection based on estimation of traffic patterns between two population centers and service frequency and fare considerations
06 p0905 A72-17586
- Mercury short haul transport aircraft, emphasizing lightweight structural design with extensive use of integral machined components for fatigue safety
07 p0913 A72-20310
- V/STOL development for short haul air transportation, discussing requirements for quiet pollution-free operation, ATC systems, navigation and landing aids
08 p1108 A72-21010
- Turbofan engine trends for short haul conventional and STOL aircraft, considering variable pitch fans, reduction gears, thrust reversal and noise and environmental pollution
[ASME PAPER 72-GT-86] 11 p1705 A72-25661
- Future short haul aircraft transportation systems, discussing aircraft forms, noise reduction technology and runway requirements
12 p1754 A72-27660
- V/STOL aircraft potential for short haul civil air traffic, discussing present technology and investment costs in comparison with advanced ground transportation systems
13 p1898 A72-30076
- Quiet RTOL /reduced takeoff and landing/ short haul aircraft cost comparison with Trident 3 aircraft up to design range stage length
15 p2180 A72-31320
- Short haul airlines on-time operation, discussing ATC, weather, cargo and aircraft ground handling, cabin and flight services and aircraft reliability effects
15 p2339 A72-32452
- Ultrashort haul common carrier air transportation system based on VTOL aircraft for suburban-to-city center trips, comparing with land based transport
16 p2480 A72-33113
- Short haul air transportation system economic and political problems, noting community acceptance and passenger service standards
16 p2481 A72-33310
- NASA R and D for STOL short haul transportation systems, discussing propulsive lift, blown flap and augmentor wing concepts, noise reduction, etc
17 p2487 A72-34238
- All weather landing for a STOL system.
[AIAA PAPER 72-788] 19 p2831 A72-38105
- The DHC-7, first generation transport category STOL - Particular design challenges.
[AIAA PAPER 72-809] 19 p2750 A72-38115
- STOL-based short haul transportation feasibility for airport congestion alleviation from airline viewpoint,

discussing system requirements, economic factors and safety
[AIAA PAPER 72-807] 19 p2750 A72-38120
Safety in commuter airline operation.
20 p2988 A72-39748
Landing 'in the backyard' with quiet aircraft
21 p2994 A72-40376
Short haul intercity air transportation systems requirements for successful competition with lower cost ground modes
[ICASP PAPER 72-16] 21 p2995 A72-41141
Prototype interurban IFR STOL transportation system demonstration project, considering area navigation, scanning beam microwave landing systems and STOL port planning
[ICASP PAPER 72-41] 21 p3040 A72-41166
German monograph - Model-analytical investigation of short-haul air traffic with VTOL aircraft in the Federal Republic of Germany.
22 p3245 A72-43068
An assessment of repeated loads on general aviation and transport aircraft.
24 p3366 A72-44736

SHORT RANGE NAVIGATION U SHORAN

SHORT TAKEOFF AIRCRAFT
STOL transport aircraft technology assessment, analyzing airports growth problems
[SAE PAPER 710751] 01 p0003 A72-10250
Augmentor wing jet STOL research aircraft development progress report covering design, engine tests, performance prediction, control simulation and stability augmentation
[SAE PAPER 710757] 01 p0003 A72-10254
Industry assisted state of art assessment of high lift turbofan configurations for USAF STOL tactical transport technology program
[SAE PAPER 710758] 01 p0003 A72-10255
Mach 0.80 quiet intercity STOL transport design comparison for turbofan, prop-fan and turboprop systems
[SAE PAPER 710759] 01 p0003 A72-10256
STOL aircraft for solving noise reduction and land use problems in future transportation systems, discussing airport location and layout for growing air traffic
01 p0005 A72-11153
STOL and VTOL aircraft performance and efficiency, discussing landing and takeoff distances reduction
01 p0006 A72-11258
Handling qualities simulation program for augmentor wing jet STOL research aircraft considering control devices design
02 p0154 A72-11654
STOL aircraft roll moment control possibility for externally-blown jet flap due to engine failure
02 p0154 A72-11700
Short haul air transport system need for future short takeoff and landing aircraft, considering airports, airways, economics and navigation and landing aids
02 p0154 A72-11719
Q/STOL jet aircraft engines design for low noise levels, describing takeoff thrust, bypass ratio and turbine stages
02 p0271 A72-12501
Externally blown flaps for STOL characteristics in medium and heavy jet transport aircraft, demonstrating aerodynamic and flight mechanical feasibility
02 p0155 A72-12502
Aladin 2 noiseless STOL jet aircraft project, describing exhaust nozzle configuration, design and economics
02 p0155 A72-12503
STOL aircraft integrated landing approach flight control system with elevator and thrust control coupling to angle of attack, altitude and other state variables
02 p0155 A72-12705
[DGLR PAPER 71-063] 02 p0155 A72-12705
Short-short haul STOL network economics for commuter ports in Detroit region, estimating service demand, aircraft number and maintenance costs
03 p0459 A72-13696
Prop-fan engine for quiet STOL propulsion, discussing noise characteristics, weight advantage, response and reduced fuel consumption
03 p0406 A72-13697
Canadian STOL design, development, production, airports and civil air transportation applications
05 p0751 A72-15775
Feedback gains for STOL aircraft display pilot interactive flight director design, using computerized approach-touchdown simulation and optimal control theory
[ASME PAPER 71-WA/AUT-9] 05 p0684 A72-15956
Automated scheduling algorithm for aircraft from terminal area to touchdown, discussing system features and STOL air traffic computerized simulation
[AIAA PAPER 72-120] 05 p0688 A72-16905
Jet peak velocity decay in single and multielement nozzles for STOL aircraft externally blown flaps, noting noise reduction due to flow mixing
[AIAA PAPER 72-48] 05 p0608 A72-16927

Low wing loading STOL transport with ride smoothing automatic control system, noting thrust-weight ratio
[AIAA PAPER 72-64] 05 p0613 A72-16942
Aerodynamic characteristics of STOL aircraft with externally blown jet augmented flaps, predicting interference between lifting surfaces and turbofan engines
[AIAA PAPER 72-63] 05 p0609 A72-16953
STOL transport passenger market demand model selection based on estimation of traffic patterns between two population centers and service frequency and fare considerations
06 p0905 A72-17586
Tail first /canard/ and tandem wing configurations for natural STOL, discussing low cost aerial work aircraft
06 p0758 A72-18285
Crashproof rotorcraft STOL aircraft for rescue operation, discussing orthodox rigid and special rotary wings design, air tunnel experiment and flight tests
06 p0760 A72-18582
Externally blown flap noise tests at various nozzle exhaust velocities for STOL aircraft noise reduction
[AIAA PAPER 72-129] 07 p0908 A72-18962
Jet-STOL augmentor wing consisting of moderately thick airfoil with full span leading edge slat and double surface trailing edge flap
08 p1110 A72-21899
Future civil air transport trends, considering passenger and cargo growth, travel frequency per capita income and STOL market
08 p1257 A72-22150
Variable pitch fans for STOL aircraft thrust/shaft engine, noting short field capability and quietness
09 p1374 A72-23447
STOL and V/STOL transport aircraft design requirements consideration based on common propulsion and lift engine types use, noting fan lift solution superiority
10 p1421 A72-24865
STOL aircraft systems development coordination, considering vehicle design, airport facilities and related ground environment, transportation modes interface and airspace management
11 p1574 A72-25255
Variable pitch ultrahigh bypass ratio ducted fan engine design for STOL transport aircraft
[ASME PAPER 72-GT-61] 11 p1704 A72-25652
Turboprop engine trends for short haul conventional and STOL aircraft, considering variable pitch fans, reduction gears, thrust reversal and noise and environmental pollution
[ASME PAPER 72-GT-86] 11 p1705 A72-25661
STOL aircraft role in civil aviation, discussing short range operation, ATC, reduced noise and weather capability
12 p1754 A72-27518
STOL, VTOL and V/STOL air transportation systems development, characteristics and requirements, presenting economic forecast
12 p1754 A72-27661
Acoustic measurements for STOL turboprop transport aircraft propeller configurations under static, taxi and flyover conditions, discussing quiet propeller noise signature
13 p1897 A72-29571
Quiet RTOL /reduced takeoff and landing/ short haul aircraft cost comparison with Trident 3 aircraft up to design range stage length
15 p2180 A72-31320
Buoyancy systems and parawings application in short haul passenger transportation, discussing VTOL and STOL operations
16 p2348 A72-33183
STOL aircraft for civil transport applications, considering optimum design concepts, noise reduction and terminal facility requirements
16 p2348 A72-33331
STOL aircraft minimum noise takeoff trajectories determination, taking into account engine thrust and listeners distance from noise source
[AIAA PAPER 72-665] 16 p2349 A72-34072
NASA R and D for STOL short haul transportation systems, discussing propulsive lift, blown flap and augmentor wing concepts, noise reduction, etc
17 p2487 A72-34238
STOL airports planning objectives, discussing ground and airspace congestion relief, terminal locations, flight safety and community acceptance
17 p2535 A72-34239
The flight mechanics of STOL aircraft.
17 p2488 A72-34241
An experimental investigation of STOL longitudinal flying qualities in the landing approach using the variable stability X-22A aircraft.
[AHS PREPRINT 642] 17 p2490 A72-34502
NASA R and D programs for quiet STOL aircraft and engines development
18 p2721 A72-36503
Development of the Saab-Scania Viggem.
19 p2748 A72-37749
All weather landing for a STOL system.
[AIAA PAPER 72-788] 19 p2831 A72-38105
STOL ride quality criteria - Passenger acceptance.
[AIAA PAPER 72-790] 19 p2749 A72-38107

Noise generated by STOL core-jet thrust reversers.
[AIAA PAPER 72-791] 19 p2849 A72-38108
Forward flight effects on mixer nozzle design and noise considerations for STOL externally blown flap systems.
19 p2746 A72-38109
[AIAA PAPER 72-792] 19 p2746 A72-38109
Investigation of the commonality in development of military and commercial STOL transports.
[AIAA PAPER 72-808] 19 p2750 A72-38114
The DHC-7, first generation transport category STOL - Particular design challenges.
[AIAA PAPER 72-809] 19 p2750 A72-38115
STOL-based short haul transportation feasibility for airport congestion alleviation from airline viewpoint, discussing system requirements, economic factors and safety
[AIAA PAPER 72-807] 19 p2750 A72-38120
Use of the flight simulator in the design of a STOL research aircraft.
[AIAA PAPER 72-762] 19 p2751 A72-38129
Methodology for estimating STOL aircraft high lift systems characteristics.
[AIAA PAPER 72-779] 19 p2752 A72-38138
STOL transport stability and control derivative prediction methods and accuracy requirements.
[AIAA PAPER 72-780] 19 p2752 A72-38139
A method for increasing thrust reverser utilization on STOL aircraft.
[AIAA PAPER 72-782] 19 p2752 A72-38141
4-D guidance system design with application to STOL air traffic control.
19 p2832 A72-38252
Test of direct lift control in the case of the experimental aircraft DFVLR-HFB 320
20 p2888 A72-39934
STOL performance criteria for military transport aircraft.
[AIAA PAPER 72-806] 20 p2889 A72-40055
Design, operation and testing of integrated STOL flight control system, noting approach accuracy and passenger comfort improvement
21 p3080 A72-40292
Landing 'in the backyard' with quiet aircraft
21 p2994 A72-40376
Augmentor wing design for Buffalo STOL aircraft, discussing operational principle and wind tunnel test results
21 p2994 A72-40684
Prototype interurban IFR STOL transportation system demonstration project, considering area navigation, scanning beam microwave landing systems and STOL port planning
[ICASP PAPER 72-41] 21 p3040 A72-41166
Noise control technology for jet-powered STOL vehicles.
[ICASP PAPER 72-50] 21 p2995 A72-41175
Characteristics of an ejector-type engine simulator for STOL model testing.
[AIAA PAPER 72-1028] 21 p3042 A72-41607
An investigation of parameters and factors governing manual control of STOL aircraft in landing approach.
[AIAA PAPER 72-987] 24 p3369 A72-45415

SHORT WAVE RADIATION NT DECIMETER WAVES NT MICROWAVES NT MILLIMETER WAVES NT SUBMILLIMETER WAVES

Receiving equipment in 23 cm band for Krakow 15 m radio telescope
03 p0339 A72-13173
Short wave asymptotic formulas for shadow zone of plane diffraction, discussing asymptotic solutions for field from point source
04 p0489 A72-15386
Atmospheric short wave radiation angular and vertical distribution relation to aerosol scattering parameters, using transport equation
05 p0658 A72-16291
Asymptotic solution to short wave diffraction by convex cylinder, constituting geometrical optic expansion and caustic curves for illuminated and shadow region
05 p0628 A72-16411
Russian papers on mathematical problems of wave propagation and diffraction theory, covering elastic and short waves and point sources
11 p1688 A72-26377
Short wave oscillations point source problem near convex curve, deriving asymptotic expression for Green function
11 p1678 A72-26379
Waveguide point source field, analyzing short wave asymptotic properties of Helmholtz equation Green function in inhomogeneous medium
11 p1689 A72-26382
Book on information theory of atmospheric visibility covering vision threshold conditions, eye as radiation detector and short waves field near ground
11 p1691 A72-26697
Arrival angles of radio wave reflected from ionosphere for remote short wave transmitter direction finding
13 p1917 A72-28601

Physical interpretation of electromagnetic waves atenuation function HF singularity during diffraction over spherical surface, applying to short wave diffraction in tropospheric model
15 p2195 A72-31651

Pulse and monochromatic short wave signals phase/amplitude autocorrelation functions and probability distributions during oblique incidence reflection from ionosphere
15 p2197 A72-31876

Some results of measurements of short-wave and long-wave radiation fluxes from the Cosmos-320 satellite
22 p3168 A72-41875

Arrival angles of radio wave reflected from ionosphere for remote short wave transmitter direction finding
24 p3380 A72-45101

SHORT WAVE RADIO TRANSMISSION
Spanish winter anomalous ionospheric short wave absorption observed by high precision ground based measurements
01 p0055 A72-10434

Ionospheric neutral gas wind and altitude effects on Spanish short wave absorption winter anomaly
01 p0055 A72-10435

Equatorial E region short wave oblique incidence propagation experiment showing transmitted impulse delay increase with frequency decrease
01 p0056 A72-10437

Spread F effects on transequatorial ionospheric short wave oblique incidence path great circle deviations
01 p0056 A72-10438

Auroral backscatter echoes observations in ionospheric short wave propagation, using satellite oblique propagation ionograms and magnetograms
01 p0056 A72-10439

Short wave radio reception and signal path at magnetically conjugate point in Southern Hemisphere, using 40-110 msec delay times
01 p0028 A72-10592

Short wave skip distance calculation as function of path inclination to ionospheric layer for linear and parabolic ionization distributions
01 p0028 A72-10612

Conducting half space electric dipole model of radio propagation through earth at 1-10 MHz
01 p0033 A72-11254

Ricocheting mechanism in short radio wave propagation in ionosphere, using ray trajectories and field intensities equations
04 p0492 A72-15439

Short waves damping or increasing in bounded thick waveguide with real or complex refraction index
04 p0492 A72-15446

Quasi-specular and Lambert reflection of short radio waves from lunar surface dependent on central portion of near side
05 p0631 A72-17039

Round-the-world short wave signals propagation and waveguides effective volume and attenuation characteristics, relating ionospheric effects and non-linear beam defocusing
08 p1130 A72-20704

Reflected short wave signal frequency shift due to reflecting ionospheric layer movement and electron concentration changes, considering oblique incidence on isotropic and anisotropic layers
10 p1436 A72-24576

F region critical frequencies deviation from median due to solar cycle phase, latitude and time, discussing short waves radio communications reliability
11 p1593 A72-26271

Ionospheric and magnetic disturbances effects on short wave radio links, using directional antennas and 1.5-24 MHz frequencies
11 p1594 A72-26279

Equatorial spread F spatial and temporal distribution from short wave side reflection observations along Lindau-Tsumeb transequatorial HF radio transmission path
12 p1803 A72-27778

Statistical model for short wave radio signal fading at oblique signal reflection from ionosphere, determining pulse amplitude and duration distribution laws
13 p1915 A72-28468

Investigation of the characteristics of short wave propagation along the auroral radio path
17 p2519 A72-35877

On an anomaly in long-range short-wave propagation from the equatorial region to central Europe
18 p2657 A72-36232

Properties of plane asymmetric plasma waveguides in applications to the propagation of short radio waves along inhomogeneities in the outer ionosphere
18 p2662 A72-36855

Circumterrestrial short wave signals propagation and waveguides effective volume and attenuation characteristics, relating ionospheric effects and non-linear beam defocusing
19 p2765 A72-38332

Short-wave asymptotic representation of the solution to the problem of diffraction by a circular disk
19 p2769 A72-38849

New combination of logarithmic-periodic dipole antennas for the short wave range
21 p3031 A72-40537

Self-tuning and self-programming antenna matching devices for the frequency range 1.5-30 MHz and their application
21 p3031 A72-40538

Diffraction of a plane wave by a ribbon grating in the case of short wavelengths
23 p3264 A72-43527

Evaluation of the reliability of diversity reception by antennas of different polarizations
23 p3271 A72-43777

SHOT NOISE
Metal-semiconductor-metal Schottky barrier microwave diode impedance and shot noise calculation
02 p0191 A72-11894

Noise in optical output of small area electroluminescent GaAs diffused junction diodes, comparing with theoretical shot noise limit
09 p1286 A72-23087

Excess, shot and channel thermal noises performance-limiting effects on junction FETs in high input impedance applications, considering minimization method
09 p1287 A72-23111

Thermal and shot noise and distortion in charge-coupled semiconductor devices used for imaging applications
12 p1791 A72-27673

Shot noise coefficient calculated from static I-V characteristics for modified thermionic diode with low potential virtual cathode
13 p1915 A72-28467

X ray source Cygnus X-1 pulsation periodicity analysis, showing random shot noise characteristics
14 p2156 A72-30571

Distributed tunnel diode traveling wave amplifier load noise thermal and shot components, noting impedance boundaries
15 p2206 A72-31663

Electrical fluctuations in ideal straight-staggered nondegenerate diodes
21 p3033 A72-40945

Cumulants of multidimensional response of linear and nonlinear systems to Poisson distributed impulses, estimating joint probability distribution and evaluating threshold statistics
23 p3314 A72-44368

SHOT PEENING
Metallic coatings effect on high-strength steels fatigue properties, noting beneficial effect of shot peening
10 p1494 A72-24024

Constraining U-shaped frames for blade edges protection during hydrojet shot blasting of compressor blades for gas turbine engines
11 p1642 A72-26819

Helicopter rotor blade spars shot peening in centrifugal vibrator, optimizing Cr-Mo-Ni steel surfaces work hardening
11 p1642 A72-26820

Shot peen contouring of Boeing 747 wing skins combined with incremental chip forming, noting principles and manufacturing process
12 p1817 A72-28160

Vibrational shot peening as a method of increasing the fatigue strength of critical aircraft elements
20 p2929 A72-39802

SHRINKAGE
Photothermoelastic analysis of shrinkage stresses near discontinuity in fiber composite material, relating matrix cracking to fiber packing
06 p0835 A72-17800

Iron powder specific surface and particle size effect on shrinkage during sintering
13 p1966 A72-29800

Shrinkage concentration behavior of two phase systems /Co-Ni, Co-Fe, Fe-Ni, Fe-Cu/ in sintering correlated with diffusion parameters
19 p2808 A72-38280

SHROUDED BODIES
U SHROUDS
SHROUDED NOZZLES
Boundary conditions in heat conduction for nozzle blades with shrouds exposed to cooling air on one side
08 p1222 A72-20945

SHROUDED PROPELLERS
Shrouded propellers and rotor blades free vibrations determination by variational method, showing Coriolis effect on critical flutter speed
11 p1732 A72-25536

Streamlines and fluid diffusion determination for axisymmetric irrotational and rotational flows in arbitrarily shaped domain onto rectangle
12 p1751 A72-27168

Surface vorticity theory for axisymmetric potential flow past annular aerofoils and bodies of revolution with application to ducted propellers and cowls
19 p2747 A72-38554

SHROUDED TURBINES
Steady heat conduction solution for gas turbine shrouded blade and disk of hyperbolic profile with central hole
08 p1223 A72-20949

Numerical integration of unsteady heat conduction equations for gas turbine rotor with shrouded blades, using grid method
08 p1223 A72-20950

Radial turbine flow analysis, comparing calculated shroud static pressure distribution and outlet velocity profile with measured data
11 p1570 A72-25642

SHROUDS
Pressure distribution around circular cylinder with shrouds of various geometry for suppressing flow induced vibrations at subcritical and transition Reynolds number
09 p1261 A72-23315

Jet turbine engine front fans with and without snubbers, estimating flow field by streamline curvature technique
11 p1568 A72-25607

Small radial inflow turbines for space applications, considering blade-shroud clearance, blade loading and exit diffuser design
11 p1704 A72-25636

Hub and shroud boundary layer growth in centrifugal compressor vaneless diffusers, comparing predicted and measured performance at high pressure ratio per stage
11 p1570 A72-25645

Space simulation shrouds cryogenically cooled with liquid carbon dioxide, discussing automatic temperature control and operating cost savings
15 p2214 A72-32611

SHUNTS
U BYPASSES
U CIRCUITS
SHUTTERS
Passive shutter power absorption effect on periodically triggered pulsed ruby laser output instability, showing optical inhomogeneity interferograms
16 p2400 A72-33189

Single-crystal, electro-optic shutter for Q-switching lasers emitting unpolarized radiation
18 p2698 A72-36698

Emission synchronization in pulsed lasers
21 p3064 A72-41741

SHUTTLE ORBITERS
U SPACE SHUTTLE ORBITERS
SIBERIA
Meteoritic cosmic catastrophe, interpreting flat depression in northern Siberian plateau Khatanga river basin
05 p0713 A72-15977

SIC [COEFFICIENT]
U STRUCTURAL INFLUENCE COEFFICIENTS
SICKNESSES
NT ALTITUDE SICKNESS
NT DECOMPRESSION SICKNESS
SID [IONOSPHERIC DISTURBANCES]
U SUDDEN IONOSPHERIC DISTURBANCES
SIDE-LOOKING RADAR
NT RADAR IMAGERY
Crop discrimination with manual and automatic computerized side-looking radar imagery analysis for microtexture pattern recognition
01 p0065 A72-10451

Agricultural land use analysis by remote sensing, discussing side-looking airborne radar systems and image interpretation for local needs
01 p0056 A72-10456

Agriculture and natural vegetation remote sensing programs, discussing dichotomous keys for side-looking airborne radar imagery analysis
01 p0056 A72-10457

Spatial alignment for low noise difference picture detection in side-looking radar imagery
01 p0129 A72-10874

Remote sensor viewing angle effect on detectability of geological faults in side-looking airborne radar image data by optical spatial frequency analysis
02 p0209 A72-11791

Side-looking airborne radar imagery for sea ice drift size, shape and surface characteristics determination
02 p0215 A72-11882

RADAM /Radar Amazon/ side-looking radar imagery and multiband aerial photography for mineral, vegetation, soil and water resources mapping in Brazil
02 p0216 A72-11890

Side-looking airborne radar /SLAR/ images comparison with small-scale low-sun black and white aerial photographs
05 p0661 A72-16041

AS-11A stereoplotter computerized adaptation to stereo-modeling of SLAR terrain mapping
06 p0818 A72-18330

Receiving antennas polarization parameters selection in side-looking synthetic aperture radars
10 p1453 A72-24905

Pulse excitation of traveling wave antenna array, describing spectral method of solving high resolution side-looking radar limitation

13 p1915 A72-28526

Microwave radiometry for celestial body emitted or reflected radiation observation, discussing radar cartography with emphasis on side-looking and synthetic aperture radars advantages

15 p2232 A72-31251

Computerized analytical system for side-looking radar imagery interpretation by isodensitracer scanned density data multivariate analysis applied to environmental discrimination

15 p2198 A72-32064

Transformation of points from sidelooking radar images into the map system.

17 p2555 A72-35336

Digital technique for automatic change detection in aerial reconnaissance side-looking radar imagery, discussing image correlators

17 p2557 A72-35554

SIDE BANDS

Acquisition time for sideband modulated noiseless phase lock loops

03 p0325 A72-14191

Trapped ion instability in collisionless plasma ion acoustic waves, discussing sideband waves frequency spectrum and growth rate

06 p0859 A72-17545

IMPATT diode microwave oscillators and amplifiers calculating noise sideband correlation factor at randomly large signal frequencies

06 p0788 A72-18464

Hybrid carrier and modulation tracking loops exploiting sideband coherency for phase coherent tracking, telemetry and command system performance improvements

07 p0939 A72-19066

Phase shift methods for data transmission vestigial sideband signal generation, providing shaping functions by shift registers, weighting resistors, summing amplifiers and low pass filters

11 p1592 A72-25890

Signal spectrum sidebands asymmetry of LF waves in plasma with electric current and ion stream, suggesting amplitude and frequency modulation

15 p2284 A72-31650

Time sharing radio communication system analysis with amplitude modulated carrier, noting power reduction, sideband content and multiplexing

15 p2201 A72-32566

Sideband waves excitation by large amplitude ion-acoustic waves in collisionless plasma, noting frequency spectrum and growth rate agreement with trapped particles theory

21 p3094 A72-41629

SIDE BAND REDUCTION

Microwave half blinder for side lobe reduction in large horn reflector antennas in E plane radiation for horizontal polarization

01 p0043 A72-11243

Wideband high power radars alignment and testing, including range side lobes reduction

02 p0178 A72-12392

Radar signal digital processing for replacing analog circuitry, discussing rf signal representation, side lobe reduction, coherent processors and filter design

02 p0178 A72-12396

Antenna side lobe radiation probability assessment for directional gain

03 p0333 A72-13832

Horn lens antennas for millimeter wave radiometric applications, discussing medium gain polystyrene lens design to obtain low peak side lobes

04 p0503 A72-15608

Antenna pattern side lobe control for line sources and uniformly spaced linear arrays, using iterative sampling method

06 p0782 A72-17359

Yagi antenna radiation pattern parameters optimization for maximum directional gain, minimum side lobe and optimal slope curvature

07 p0952 A72-18852

Linear array antenna radiation pattern synthesis for minimum side lobe level outside of given intervals, calculating current distribution

07 p0953 A72-19005

Element position design of pencil beam thin phased arrays with low side lobes

07 p0941 A72-19256

Corrugated surface wave antenna design with low side lobe level radiation pattern, finding relief modulated impedance parameters

07 p0955 A72-19514

Linear antenna synthesis for minimum side lobe level, eliminating superdirectivity effect

07 p0956 A72-19567

Random antenna radiation patterns probability distribution law and Dolph-Chebyshev array design, calculating minimum statistical side lobe level

08 p1138 A72-20930

Range side lobe suppression technique for Barker type phase reversal codes in digital processor for pulse compression

08 p1133 A72-21404

Minimum side lobe radiation level of circular aperture antennas as function of gain and direction finding characteristics

11 p1597 A72-26709

Optimal sum-difference characteristics of nonsuperdirective convex slot spherical antennas for maximum directive gain and minimum spatial side lobe radiation

11 p1598 A72-26713

Parasitic side lobe suppression in radiation patterns of phase switching linear antenna array without gain loss

11 p1598 A72-26717

Launching horn effect on radiation pattern of dielectric cone feeds, proposing wide angle side lobe reduction via absorbent sheath

12 p1791 A72-27669

Phase distribution randomization in switched antenna array, noting radiation pattern side lobe compensation application

15 p2209 A72-32666

A synthesis of array antennas for high directivity and low side lobes.

17 p2525 A72-34354

Quadratic phase feed for phased arrays as method of preventing degradation of side lobe level of patterns due to quantization

17 p2526 A72-34384

Statistical estimate of the attainable side lobe level in phase-switched antenna arrays with a nonlinear initial phase lead

17 p2529 A72-34833

Cylindrical phased arrays - Beam scanning and side lobe control.

17 p2531 A72-35573

Technique for compensating for reflector-antenna-surface errors with long correlation lengths.

18 p2667 A72-36691

Near side lobes in Cassegrain antenna systems.

18 p2668 A72-37039

Phase shifter number reduction effects on phased radar array radiation pattern distortion and side lobe reduction

20 p2907 A72-39268

The optimum design of small nonuniformly spaced arrays.

21 p3027 A72-40362

Correcting effects of corrugated boundaries on coaxial radiators asymmetry and side lobes, investigating waveguide hybrid modes induced transverse fields

21 p3029 A72-40516

Dyadic correlation function method for structured radar signal side lobe suppression during reception, noting Walsh function role

21 p3020 A72-40901

Plexiglas spheres and cubes effect on circular and rectangular waveguide aperture antennas directive radiation patterns and side lobe reduction

21 p3021 A72-40904

Linear antenna synthesis for minimum side lobe level, eliminating superdirectivity effect

22 p3158 A72-42085

Random phasing algorithms to reduce phase quantization side lobes for radiation patterns of commutated phased array antennas

23 p3268 A72-43428

SIDE LOBES

Low side lobe pencil beam thinned phased arrays design involving element position selection

01 p0039 A72-10664

Highly directional circular array antennas radiation characteristics calculation, showing side lobe size dependence on aperture angle

04 p0499 A72-15240

Computer simulated phased arrays with randomly located elements, deriving peak side lobe level for comparison with measurement

07 p0945 A72-17973

Conical scalar horn for paraboloidal reflector illumination, discussing half flare angle calculation for prescribed side lobe realization

10 p1435 A72-24302

Uncertainty functions side maxima for phase manipulated signals with low side lobe levels in autocorrelation functions, noting Doppler frequency shift effect

10 p1440 A72-24916

Characteristics of nonuniform regions responsible for microwave signals auroral scattering, noting observations with two side lobes radio interferometer

13 p1946 A72-28584

Statistical analysis of random mismatched tapped delay line filters effect on binary phase shift keying pulse compression codes peak-to-side lobe and SNR

15 p2196 A72-31792

Theoretical and experimental investigations, conducted with the aid of a plate containing holes, concerning the simulation of a statistically arranged antenna group

21 p3028 A72-40505

Side and back lobe structures of directive antennas.

21 p3020 A72-40903

SIDESLIP

Aircraft steering dynamics model with translational and rotational equations, considering zero sideslip and acceleration and lift bank angle transfer functions

05 p0611 A72-16112

Flight initial spin testing, discussing aircraft autorotation due to stalled angle of attack and sideslip

06 p0759 A72-18492

Airplane sideslip and yaw rate perturbations by continuous random vertical and side gusts, using low pass filtered white noise representation for mathematical modeling

12 p1755 A72-28125

Special control of spiral flight curves with the neutral and maneuver points as ultimate positions of the indifference points

18 p2643 A72-36942

A study of dedicated control surfaces for direct sideforce control.

24 p3368 A72-45344

SIGHT

U VISUAL PERCEPTION

SIGNAL ANALYSIS

Linear stochastic-parameter output channel, examining signal quadrature components statistical characteristics

01 p0024 A72-10199

Spectral characteristics of ionospheric signal by phase lags introduced in multichannel field recorder

02 p0172 A72-11926

Radar detection and resolution, discussing computer analysis of interval modulated signal ambiguity properties and synthesis method

02 p0181 A72-12648

Power spectrum analysis of multilevel digital signals phased modulated by arbitrary pulse shapes, giving examples for rectangular and raised-cosine pulses

02 p0183 A72-12797

Limiting approximation theorems for synthesis of linear circuits and signals in time-frequency domains

03 p0338 A72-13896

Lf spectrum analysis instrumentation, describing stored data signals Fourier series parameters analog computation techniques

04 p0523 A72-15487

CW 100 GHz Si IMPATT diodes with nearly abrupt junctions, discussing output power and dc and small signal analyses

04 p0502 A72-15594

Integral equations derived for single and composite radio signals with maximum energy concentration in given time interval or frequency band

05 p0625 A72-15824

Radio interferometer sensitivity dependence on interrogation frequency for amplitude and time quantization of input signal spectra

05 p0660 A72-15830

Nonlimited phase locked loop analysis for AM signal by Fokker-Planck equation

05 p0637 A72-16554

Linear time-varying system under modulated signal excitation, obtaining quasi-stationary response by separable system approximation with parameter optimization

06 p0771 A72-17379

Ground and atmospheric scattered radiation discrimination by ground modulation based on chopper signal frequency analysis, considering feasibility from airborne tests results

06 p0814 A72-17587

Wide range bias dependence of planar bipolar transistor dc and small signal current gain, comparing analytical findings with Si junction experiment

06 p0783 A72-17608

Statistical model of signal amplitude distribution and thermoelectron noise of photoelectron multiplier

06 p0816 A72-17837

Binary detector with dual gating function between first and second quantization processes, estimating false alarm and rejection probabilities

07 p0937 A72-18851

Stochastic approximation algorithm with nonstationary regression function for signal parameter estimation, considering convergence, mean square error bound and applications

07 p1027 A72-19291

Bayesian estimate of signal parameters in random noise background under mutually exclusive hypotheses about statistical properties

07 p0943 A72-19515

Optimal Bayesian system synthesis for simultaneous discrimination and parameter estimation of several signals in noise background

07 p0943 A72-19516

Conditional distribution density formation for signal-noise mixture based on learning sampling with dependent values

07 p0943 A72-19517

Weak signal detection in additive mixture on non-Gaussian random-correlated noise, deriving algorithms for discrete- and continuous-time and coherent detection problems

07 p0943 A72-19521

SIDERITE METEORITES

U IRON METEORITES

- Abrupt junction Si IMPATT diodes large signal analysis, discussing subharmonic modes and second harmonics effects 07 p0956 A72-19591
- Narrow band signal envelope analysis of astronomically observed quasi-monochromatic emission sources 08 p1135 A72-21731
- Angle tracking radar receiver signal analysis simplification by use of complex variables 10 p1437 A72-24684
- Linear least mean square estimate of additive white noise-corrupted signal considered as purely nondeterministic process of multiplicity one 11 p1591 A72-25352
- Narrow band process signal model for phase and amplitude difference distribution densities of alternating period compensation system output signal 11 p1596 A72-26310
- Holographic method of correlation and spectral analysis of radio signals applied to stable oscillator, randomly inhomogeneous media fields and stereophonic transmission measurements 11 p1636 A72-26726
- Small signal theory of emitter current limited injection in negative mobility semiconductors at zero doping limit 12 p1788 A72-27165
- Continuous signal representations in time and frequency domains by Fourier series 12 p1783 A72-27628
- Spectrum analysis of PCM/AM-FM and PCM/FM-FM telemetry signals, using approximation technique to Fourier transform time signal to frequency domain 13 p1919 A72-29025
- Real time interferential spectrum analysis of deterministic signals in form of partially summed Fourier series 13 p1919 A72-29041
- Dispersion method for real time spectral analysis of signals by Fourier transform for class of integrable functions with finite energy 13 p1919 A72-29042
- Modulated filter theory for AM signal analysis in linear resonant circuits, noting use for superheterodyne amplifier and phase discriminator design 13 p1930 A72-29046
- Spectral characteristics of ionospheric signal by phase lags introduced in multichannel field recorder 13 p1920 A72-29238
- Broadband correlation meter with multiplier using vacuum thermal converters for 1.5 KHz-15 MHz range and variable signal delay 13 p1961 A72-29920
- Single pulses and random samplings signal spectrum analysis on real time scale by ultrasonic dispersion waveguide 13 p1934 A72-30018
- Noiselike FM signals shaping by numerical periodic sequences, analyzing FSK signals 14 p2085 A72-30337
- EHF double-drift IMPATT oscillator small and large signal behavior analysis with computer program, noting second harmonic tuning and single frequency operation possibilities 15 p2204 A72-31314
- Instrumental errors estimation in photomultipliers and photodiodes during measurement of short time phase fluctuations in quasi-harmonic signals 15 p2246 A72-31424
- IMPATT diode junction temperature effects on operation explained by small signal analysis 15 p2206 A72-31545
- Linear stochastic-parameter output channel, examining signal quadrature components statistical characteristics 15 p2195 A72-31623
- Signal with bounded spectrum, obtaining higher derivatives by reduction to stationary random process filtering problem solvable with Kolmogorov-Wiener and Kalman-Bucy techniques 15 p2207 A72-32171
- Limiting approximation theorems for synthesis of linear circuits and signals in time-frequency domains 15 p2212 A72-32707
- Nonstationary fluctuation signal analysis into predetermined frequency band by passing digitized information through resonant LCR filter mathematical analog 16 p2362 A72-32855
- Three-dimensional small-signal analysis of bipolar transistors. 17 p2530 A72-35099
- Optimal signal design for digital center of gravity feedback communications over white noise channels, using energy ratio functions 18 p2659 A72-36316
- Signal recognizing algorithms for class of large number of normal distributions with unknown probabilities, using statistical complex hypothesis verification 19 p2770 A72-38466
- A large-signal theory for current-driven frequency multipliers. 19 p2775 A72-38609
- Analysis of the correlation functions of space-time wideband signals received by linear antennas 19 p2775 A72-38657
- Representation of real narrowband signals through nonuniformly displaced basal functions with positive coefficients 19 p2768 A72-38668
- Correlation and indeterminate functions of signals with discrete frequency-time structure, noting linear frequency modulation of signal element 19 p2768 A72-38669
- Calculation of pulsed signal amplitudes at linear filter output in optical communication systems 19 p2768 A72-38671
- Computer program to simulate electromagnetic signal densities, data rates and power from land based radar transmitters as functions of time and location 20 p2902 A72-38992
- Optical information processing analysis for coherent optics and holography, discussing characteristic spectral bands, sampling and signal averaging 20 p2922 A72-39035
- Mean value of noisy signal quantized by analog/digital converter, noting input noise level relation to estimate accuracy 20 p2904 A72-39785
- Signal voltage density, pulse shape and noise power spectrum analysis of matched filter configurations in IR scanning system model 21 p3033 A72-41078
- Signal voltage density, pulse shape and noise power spectrum analysis of running integrator output in IR scanner model 21 p3056 A72-41086
- Determination of the spectra of modulated pulse trains by the spectral function method 22 p3154 A72-42122
- Integral equations derived for single and composite radio signals with maximum energy concentration band in given time interval or frequency 23 p3263 A72-43432
- Radio interferometer sensitivity dependence on interrogation frequency for amplitude and time quantization of input signal spectra 23 p3287 A72-43438
- Statistical analysis of the turbulence near a wall by conditional sampling 24 p3392 A72-45066
- On the S/N-characteristics in PCM systems for a class of signals with representative amplitude distributions. 24 p3380 A72-45282
- Large-signal analysis of efficiency and nonlinear phase distortion in a phase velocity tapered traveling-wave tube. 24 p3385 A72-45283
- Frequency multiplication with a traveling-wave tube. I - Computation of the current harmonics in a traveling-wave tube by the large-signal theory. 24 p3386 A72-45284
- Frequency multiplication with a traveling-wave tube. II - Numerical analysis of a traveling-wave frequency multiplier by the large-signal theory. 24 p3386 A72-45285
- ## SIGNAL ANALYZERS
- He-Ne traversing laser velocimeter for instantaneous axial fluid velocity measurement, describing signal analyzing system, construction and calibration 02 p0224 A72-11744
- Linear single and multiloop control system synthesis for sensitivity reduction by introducing signals proportional to sensitivity functions with analyzer 05 p0640 A72-16207
- Optimal pulse height analyzer with quadratic transfer function for gamma ray spectrometer on OSO-H 08 p1167 A72-21516
- Digital signal analyzer design based on fast Fourier transform algorithm shift register coupled with single flow-through arithmetic unit 10 p1446 A72-25062
- Associative impulse analyzer for measurement of probability density functions in electronic memories 11 p1602 A72-26446
- Quasi-one dimensional spectral analysis of input signal by delay line circulator, discussing ring frequency characteristic influence on harmonic signal buildup efficiency 13 p1930 A72-29043
- Signal analyzer for LF real time measurement of mechanical impedance by Fourier integral analysis 15 p2215 A72-32628
- A meter giving the number of overshoots of the realization of a steady random process 21 p3058 A72-41732
- Low frequency measurement of mechanical impedance and frequency response. 22 p3164 A72-42700
- ## SIGNAL DETECTION
- ### NT CORRELATION DETECTION
- Time division multiple access systems transmitting and receiving end synchronization control criteria derivation, discussing code pattern selection for reliable detection 01 p0033 A72-11304
- Imperfect timing degradation of direct detection /noncoherent/ optical system using pulse position modulation bits 02 p0174 A72-12141
- Receiver detection characteristics for multiplicative processing of coherent signal pulses with unknown initial phase and slowly fluctuating amplitude 02 p0176 A72-12215
- Optimal filter and polarity coincidence correlator signal detection efficiency for arbitrary noise distribution 02 p0176 A72-12217
- Pulsed Doppler radar loss of detection probability due to echo signal misalignment, discussing distance measurement refinement by interpolation 02 p0179 A72-12571
- Signals detection under unknown direction and arrival time conditions, developing performance evaluation method based on detection probability-false alarm curves 02 p0180 A72-12573
- Autocorrelation signal detection method application to spectrometry by modulation amplitude, investigating SNR 04 p0521 A72-14973
- Optimal detection of Markov radio signals with intrapulse FM using nonlinear filtration theory 04 p0487 A72-15146
- Optimal two stage signal search in frequency vs arrival time indeterminacy plane of communication system 04 p0487 A72-15148
- Neuroelectric signal recognition system with computerized compensation for variations due to small random changes, slow trends and interference potentials 04 p0481 A72-15253
- Cross correlation model for interpreting empirical results on binaural noise masking level differences in sinusoidal signal detection, comparing with equalization-cancellation model 04 p0550 A72-15296
- High purity epitaxial GaAs frequency response, determining heterodyne detection in millimeter and submillimeter regimes 04 p0563 A72-15613
- Recurrent algorithms for optimal signal detection on background of random noise, using Markov processes 05 p0627 A72-16406
- Three frequency IR laser signal heterodyne detection with 40-MHz if narrow-band reception, measuring SNR 05 p0669 A72-16607
- M-ary orthogonal signal phase noncoherent detection in sequential decision feedback, comparing performance with optimal coherent reception 06 p0773 A72-17596
- Stochastic differential equations for a posteriori probability distribution in problems of Markov process parameter estimation, adaptive filtering and signal detection 06 p0794 A72-18301
- Soviet book on laser communication statistical theory covering coherent and noncoherent optical signal detection and discrimination, SNR optimal reception, beam scanning, etc 06 p0777 A72-18518
- Gaussian rf noise effect on optical detection signal fluctuations in optically pumped frequency standards 07 p0938 A72-19013
- Optimal signal detection relative to Neumann-Pearson criterion invariant with respect to amplitude and random noise intensity in radio location 07 p0938 A72-19019
- Digital speech detector with increased voice signal and reduced noise sensitivity for satellite capacity improvement 07 p0939 A72-19067
- Asymptotically optimal rank algorithms for signal resolution at phase and amplitude detectors outputs 07 p0943 A72-19518
- Signal detection in noise, investigating quantiles position optimization in nonparametric test statistics 07 p0943 A72-19519
- Signal detection in stationary, Markov and other noise background, discussing functional method of statistical and probabilistic representation 07 p0943 A72-19520
- Weak signal detection in additive mixture on non-Gaussian random-correlated noise, deriving algorithms for discrete- and continuous-time and coherent detection problems 07 p0943 A72-19521
- Automatic digital detection of fluctuating Rice-distributed signals in presence of Gaussian noise, using M-out-of-N threshold detection criteria 07 p0947 A72-20194
- Combined signal detection and trajectory estimation functions optimization application to Monte Carlo simulation for trajectory moving across two dimensional grid 08 p1144 A72-20858
- Signal detection in ruby element quantum paramagnetic amplifier operating at liquid nitrogen temperature 08 p1141 A72-21377

Periodic and synchronously recurrent transient signal detectability in time-varying noise environment 08 p1134 A72-21406

Microwave signals detection with virtual cathode in klystron repeller by electrons screening at velocity modulated electron beam 08 p1136 A72-21766

Optimal signal discrimination on arbitrary noise background, choosing functional from class of integral polynomials 09 p1277 A72-22475

Gating duration influence in reception channel on singular signal detection in normal noise 09 p1278 A72-22571

Radio receiver-transmitter system for synchronous heterodyne signal detection of 6 GHz band electromagnetic channel pulsed response, discussing operational principles and accuracy 09 p1280 A72-23353

Information theory and ambiguity concept generalization for signal distinction by phase displacement in time and frequency 09 p1281 A72-23470

Asymptotically optimal detection/discrimination algorithms for weak signals on correlated noise background 10 p1436 A72-24508

Optimal detection of rectangular radio signal pulse envelope distortions by multiplex fluctuations over white noise background 10 p1436 A72-24516

Error probability and reception stability in synchronous detection of phase manipulated signals with additive Gaussian noise at multiplied carrier frequency 10 p1436 A72-24587

Binary split phase FSK signal noncoherent detection by multiple predetection filtering, noting probability of error per bit 10 p1437 A72-24686

Noncoherent detection of sinusoidal signal imbedded in clutter and Gaussian noise, obtaining probability density as function of SNR and clutter-to-noise ratio 10 p1437 A72-24691

Synchronous detector technique for statistical properties improvement in phase comparison AM radio altimeter signal 11 p1633 A72-26304

Optimal synthesis and analysis of quasi-deterministic signal detection system with simultaneous parameter measurement on background noise 11 p1596 A72-26312

Weak signals detection at visible wavelengths with background noise, examining photoelectric recording and optimal detection characteristics of receiver 11 p1596 A72-26314

Period modulation of HF oscillation by symmetrical and asymmetrical signals applied to detection in noise 11 p1597 A72-26318

Bibliography on infrasonic sound wave generation, propagation and detection at ground level and ionospheric heights 11 p1690 A72-26520

Radio pulse synchronous detection with wideband preamplifier, evaluating frequency mismatch effects on signal distortion by transient response analysis 12 p1783 A72-27631

Signal detection sequential procedure duration probability distribution at frequency discriminator output for arbitrarily shaped background noise energy spectrum 13 p1915 A72-28474

Analog simulation of Josephson superconducting junctions dc characteristics for two mixed microwave frequencies, discussing signal detection sensitivity improvement 13 p2021 A72-28648

Stochastic differential equations for a posteriori probability distribution in problems of Markov process parameter estimation, adaptive filtering and signal detection 13 p1937 A72-29441

Tunable wide field birefringent element/filter magnetograph to separate polarized magnetic signal from selected spectral line width 13 p2045 A72-29706

Fourth order linear filter function suggested for pulse signal detection from gravitational antennas, noting parameters optimization 14 p2086 A72-30800

Extrasolar civilization search via possibly used electromagnetic signal types, discussing frequency and time domains 15 p2302 A72-31292

Experimental testing of theory of signal detectability derived psychophysical models application to two-pulse visual stimuli temporal discrimination 15 p2184 A72-31379

Adaptive reception of weak repetitive signals on background of intense fluctuating noise, synthesizing adaptive detection system for multipath propagation and small SNR 15 p2195 A72-31658

Probability functional formulas for quasi-determinate signal on unsteady normal noise background for use in false alarm and correct detection 15 p2195 A72-31664

RF receiver predetection SNR measurement from average postdetection signal-plus-noise and noise-only voltages, tabulating computed results 15 p2196 A72-31782

Optimum processing structure/likelihood functional/ determination for signal sequence detection given noisy common background image sets 15 p2196 A72-31783

Transient phase object high sensitivity measurement by He-Ne laser beam transmission through differential interferometer and signal detection with p-i-n photodiode 15 p2235 A72-31784

Asymptotic receiver characteristics, discussing signal detection in spherically invariant noise 15 p2196 A72-31871

Photodiode assembly for fast laser pulses and optical signal detection, utilizing Hewlett-Packard 5082-4220 diode in impedance matched holder 15 p2208 A72-32432

Emitted phonon spectrum effects on detected signal response in superconducting Sn diodes, noting deviation from linearity 15 p2209 A72-32541

Random errors in arrival time measurements of sinusoidal radio signal under noise and pulse interference 15 p2202 A72-32704

Digital phase locked loop realization for near-optimum demodulation of continuous-time FM signal using stochastic estimation theory 16 p2362 A72-33213

Carrier synchronization and polyphase signal detection in digital communication network for high speed data transmission, deriving reconstructed noisy signal error probability 16 p2363 A72-33218

A method of phase detection of the beat signal in FM-CW radar. 17 p2514 A72-34383

Institute of Electrical and Electronics Engineers, Southwestern Annual Conference and Exhibition, 24th, Dallas, Tex., April 19-21, 1972, Record. 17 p2514 A72-34413

Signal detection by receivers with modulus processing 17 p2515 A72-34836

Detection of a two-frequency signal against a noise background of unknown intensity 17 p2516 A72-34849

Detection and recognition of colored signal lights. 17 p2510 A72-35691

Difference frequency signal from two sinusoidal voltages linear detection, estimating amplitude modulation envelope representation accuracy by Fourier series 17 p2518 A72-35781

Theory of optimum M-ary laser detection. 18 p2661 A72-36683

Complex detection - A waveform preserving technique for single-sideband demodulation. 18 p2661 A72-36844

Geostationary or orbital satellite tracking radio receiver with steerable antenna for beacon signal detection and locking, discussing system design and performance 18 p2661 A72-36847

Postdetection integration loss for logarithmic detectors. 19 p2763 A72-37295

Frequency detection with digital resonators without damping 19 p2773 A72-37939

Differentially coherent detection scheme with error-correcting capability by means of decision patterns. 19 p2766 A72-38605

Design of band-limited signal with no intersymbol interference - An extension of sampling function. 19 p2767 A72-38606

Theoretical and experimental investigations of a second-order phase-coordinate receiver 19 p2775 A72-38658

Effect of fringe on masking-level difference when gating from uncorrelated to correlated noise. 21 p2997 A72-40346

Signal transmission and detection in differentially encoded coherent multiple phase shift keyed digital communication systems, discussing carrier suppression-induced resolution ambiguity 21 p3017 A72-40861

Team size and decision rule in the performance of simulated monitoring teams. 21 p3008 A72-41016

The detectability of a brief gap in a pulse of light as a function of its temporal location within the pulse. 21 p3002 A72-41023

Detection of Doppler radio signals on a receiver with an additive noise blip number counter 21 p3022 A72-41116

Separation and detection of signals in the presence of nonadditive noise 21 p3023 A72-41746

Signal classification through quasi-singular detection with applications in mechanical fault diagnosis. 22 p3158 A72-41976

Parametric method of statistical synthesis with incomplete initial information on signal and noise distribution, discussing signal detection in white noise with unknown spectral density 22 p3154 A72-42230

Investigation of the threshold properties of a phase-locked AFC detecting a sinusoidally frequency modulated signal against a noise background 22 p3154 A72-42231

Characteristics of an optimal algorithm for detecting Gaussian signals against a pulse noise background for receivers with a logarithmic amplifier 22 p3154 A72-42238

ASW aircraft magnetic anomaly detection (MAD)/ system range limitation due to residual maneuver noise, discussing real time compensation for geomagnetic gradient interference 22 p3177 A72-42322

Symbol synchronization advances impact on PCM bit synchronizers design, discussing symbol detection and timing extraction circuits 22 p3155 A72-42706

Simultaneous detection and recognition of chromatic flashes. 22 p3152 A72-42933

Performance characterization for L-orthogonal signal transmission and detection, discussing tradeoffs between error probability, SNR and bandwidth by numerical evaluation 23 p3265 A72-44180

Sequential analysis algorithm for data channel detection of received signal represented by Poisson sequence of quantum transitions under large SNR 23 p3266 A72-44206

Effectiveness of certain easily realized rank detection algorithms for noise-masked signals 23 p3266 A72-44216

Analysis of optimal space-time signal discrimination 23 p3266 A72-44217

Signal detection analysis of meridional variations to vertical and horizontal gratings. 23 p3259 A72-44389

Gating duration influence in reception channel on singular signal detection in normal noise 24 p3379 A72-44750

Effects of bandlimiting on the coherent detection of PSK, ASK and FSK signals. 24 p3380 A72-44900

SIGNAL DETECTORS

Microwave oscillator detector Gunn diode as inexpensive alarm device for Doppler radar application 01 p0028 A72-10647

Narrow-band radar/sonar signal optimal detection under known direction and uncertain phase/arrival time conditions, considering statistical signal sampling 02 p0180 A72-12572

Radio signal electron-phonon detector design and experimental realization, considering requirements for minimum transduction and surface wave propagation loss 05 p0626 A72-16281

Noise statistics sensitivity of two sample Mann-Whitney nonparametric detector for radar application. 05 p0629 A72-16576

Filter configuration for detecting pulse excitation smaller than kT, noting SNR and resolving time 05 p0631 A72-17075

Binary detector with dual gating function between first and second quantization processes, estimating false alarm and rejection probabilities 07 p0937 A72-18851

Estimation-correlation principle and optimal detector for incomplete a priori information signal reception on random and white noise background 08 p1131 A72-20790

Data transmission interference protection under extreme noise, using tolerance detectors with redundancy coding 09 p1278 A72-22851

Detectors for deterministic signals in noise with rational spectral density, considering analog filter for continuous input sampling and discrete filter for point sampling 10 p1436 A72-24511

Optimal correlating detector of fluctuating two frequency radar signals in unknown random noise 10 p1436 A72-24515

Sensitivity loss from approximation to radar and sonar signal square law detectors in quadrature systems with postdetection integration 10 p1437 A72-24690

Noise threshold improvement of PCM signals for satellite transmission, using quality detector and error detecting codes 10 p1441 A72-25102

QRS wave detectors for arrhythmia and hemodynamic data analysis, using standardized FM magnetic tape containing various artifacts for evaluation 11 p1582 A72-25499

- Stall warning system for general aviation aircraft, using signal discriminator for rough or gusting air [SAE PAPER 720331] 11 p1630 A72-25592
- Average time between successive false target indications in surveillance binary signal detector with variable storage capacity 11 p1595 A72-26295
- Multifilter detection system with phase autocorrelator, discussing design based on correction detection probability vs mismatch between signal and filter central frequencies 11 p1597 A72-26315
- Switch detector output random process energy spectrum and autocorrelation function, noting distortion reduction by proper parameter choice 11 p1605 A72-26317
- Linear detectors for broadband and high intermediate frequency measurements in radio astronomy 12 p1793 A72-27810
- Digital evoked brain potential detector using multichannel amplitude analyzers 13 p1908 A72-28645
- Stochastic signal reflection by passive element, synthesizing optimal echo-signal detector for space diversity reception 15 p2197 A72-31877
- Computer simulation for performance of carbon dioxide laser heterodyne communication system with photoconductive n-type mercury-cadmium telluride detector/mixer 15 p2198 A72-32062
- Estimation-correlation principle application to harmonic signal receiver with unknown carrier frequency, using searching phase locked AFC circuit as estimation unit 15 p2202 A72-32667
- Measures of effectiveness for special signal detectors of simple structure 17 p2516 A72-35222
- Problem of improving the accuracy of differential meters with commutation of the compared harmonic signals 17 p2519 A72-35788
- Adaptive nonlinear optimization of the signal-to-noise ratio of an array subject to a constraint. 18 p2660 A72-36507
- Classical nonlinear electronic relaxation oscillators as EPR and NMR signal detectors, reconstructing resonance lines from absorption induced oscillator waveform changes 18 p2662 A72-36993
- Effect of magnetic field on the performance of millimeter-wave detectors using bulk InSb. 19 p2772 A72-37570
- SHF signal power influence on detector current, noting sign dependence on virtual cathode potential and signal power 19 p2774 A72-38410
- Capture of a signal with a linearly varying frequency in an astatic phase autotuning system 19 p2766 A72-38420
- Receiver processing for direct-detection optical communication systems. 21 p3017 A72-40859
- Complex detection - A waveform preserving technique for single-sideband demodulation. 21 p3017 A72-40862
- Optical direct detection using avalanche devices. 21 p3018 A72-40867
- Statistical estimation of the signal-to-noise ratio beyond a linear detector 21 p3022 A72-41073
- Analysis of noise immunity of two-channel eddy-current flaw detector. 21 p3057 A72-41723
- Adaptive signal-discrimination system using signals for observation of the channel characteristics. 21 p3023 A72-41838
- Statistical characteristics of an optimal detector of randomly fading pulse signals 22 p3154 A72-42229
- Real time correlator design and operation with signal delay at 40 Hz-20 kHz, using Stieltjes principle 22 p3176 A72-42244
- Nonlinear distortion coefficient measurement in broadband FM signal generator 03 p0333 A72-13898
- Computerized simulation for AM radio receiver waveform performance degradation under pulsed interference 03 p0324 A72-14035
- Angle modulation distortions and measurements in broadband FM microwave links 04 p0485 A72-14466
- Interstellar electron density and magnetic field fluctuations effects on Faraday rotation and signal dispersion measure in radio band 04 p0487 A72-14901
- Rectangular pulse propagation through inhomogeneous medium as plasma diagnostics, investigating electron collisions effect on signal distortion 04 p0556 A72-14946
- Intermodulation noise distortion due to multipath transmission over FM/FDM microwave links, deriving distortion probability distribution for Nakagami-Rice randomly distributed signal reception 04 p0493 A72-15517
- Distortion measuring equipment for determining FM signal transmission errors due to amplitude and group delay frequency response deficiencies and AM/PM conversion 05 p0626 A72-16299
- Periodic quasi-noise spectrum and amplitude modulation of lf pulsed signals from earth in magnetosphere plasma 05 p0696 A72-16605
- Pulsed FM radio pulse signal reflection from inhomogeneous plasma or ionosphere calculating electron collision loss effects on distortion 06 p0854 A72-17487
- AM/PM distortion intermodulation in FM/FDM radio systems during two-path propagation, using Fourier series method for noise power spectra calculation 06 p0775 A72-18239
- Waveform distortion of strong field amplitude modulated plane electromagnetic wave propagating in anisotropic plasma 06 p0862 A72-18338
- Upper bound on rate distortion function for discrete ergodic sources with memory, applying to pictorial data processing 06 p0776 A72-18390
- FM mf equipment for 2700-channel Hertzian beam, considering thermal noise, intermodulation and equivalent distortion of amplifiers, discriminator, limiter, etc 07 p0954 A72-19190
- Picosecond pulse distortion under multimode conditions in optical fiber communication systems 07 p0940 A72-19231
- Cross modulation relationship to intermodulation product based on third order distortions in nonlinear system 07 p0941 A72-19255
- Laser beam diffraction effects on self induced thermal distortion in crosswind, noting dependence on Fresnel number 07 p0942 A72-19379
- Slip effect in diurnal phase and amplitude cycles of vlf signals in lower ionosphere due to wave interference at transmitting point 08 p1130 A72-20710
- Polarization distortion of partially polarized wave emission and reception by two channel horn antennas, noting radio astronomy, radar and optics applications 08 p1138 A72-20788
- Digital image processing for TV camera noise suppression and photometric and geometric distortions calibration and rectification 08 p1172 A72-21977
- Material dispersion contribution to signal envelope delay distortion in weakly guiding dielectric optical fiber waveguides 09 p1314 A72-23340
- Lunar seismograms for LM and S-4B impacts in Apollo 12 experiment, indicating modulation mirage effect on signal distortion 10 p1536 A72-24153
- Optimal detection of rectangular radio signal pulse envelope distortions by multiplex fluctuations over white noise background 10 p1436 A72-24516
- Servo systems precision analysis with coefficients of output signal error caused by response inertia 11 p1609 A72-25431
- Canonical equations for frequency demodulator using feedback, calculating harmonic distortion for sinusoidal modulating signal 11 p1593 A72-25891
- PCM and FDM/FM systems noise and signal distortion analysis by digital simulation with FORTRAN language based on fast Fourier transform 11 p1601 A72-26043
- Message distortions analysis in PCM communications systems due to phase fluctuations of synchronization signal 11 p1598 A72-26728
- First order systems steady state frequency response to general harmonic amplitude modulated input, noting signal attenuation and absence of distortion 12 p1845 A72-27540
- Bandpass filter harmonic signal phase shift distortion effect on transient response in PSK of multichannel transmission 12 p1783 A72-27630
- Radio pulse synchronous detection with wideband preamplifier, evaluating frequency mismatch effects on signal distortion by transient response analysis 12 p1783 A72-27631
- Thermal and shot noise and distortion in charge-coupled semiconductor devices used for imaging applications 12 p1791 A72-27673
- FM distortion in injection phase locked oscillator amplifiers from generalized Alder equation 12 p1793 A72-27965
- Wideband push-pull transistorized power amplifier free of nonlinear distortions due to scattering inductance of load transformer 13 p1926 A72-28378
- Compensation of nonlinear selectivity distortions in radio receivers with broadband preamplification stages, noting circuit diagrams for preselector correctors 13 p1927 A72-28412
- Linearization method to determine changes in principal harmonic resulting from nonlinear device characteristic deformation due to HF components 13 p1937 A72-30019
- Pulse distortion and amplitude smear calculation for electron beam measurements of distance from space vehicles to deployable structure measurements on space vehicles 14 p2103 A72-30198
- Minimum amplitude and phase distortion selective bandpass filters/equalizers for satellite communications, noting realizability in UHF and microwave bands 14 p2089 A72-31048
- Laser amplifier nonlinear properties by simplification of partial differential equations of amplitude and phase behavior, considering signal pulse deformation 14 p2111 A72-31113
- Multimode millimeter waveguides and optical fibers, deriving signal transmission distortion from transfer function and corresponding impulse response statistics 15 p2193 A72-31351
- Signal distortion minimization for random waveguides with frequency-dependent optimum coupling based on transfer function covariance and impulse response time domain statistics 15 p2194 A72-31352
- Fraunhofer holograms wavelength dependent distortion reduction by system parameters optimization, applying to color holotape 15 p2239 A72-32357
- Mean value, repetition and discontinuity errors of spectral-transposition method involving memory storage and compressed signal processing 15 p2212 A72-32703
- Nonlinear distortion coefficient measurement in broadband FM signal generator 15 p2210 A72-32709
- Nonlinear and phase delay distortion of FM modulation in tuned and detuned injection phase-locked oscillator-amplifiers 16 p2369 A72-33760
- Baseband distortion caused by intermodulation in multicarrier FM systems. 17 p2512 A72-34266
- A mode-averaging diversity combiner. 17 p2513 A72-34360
- Quantization and other nonlinear distortions of the hologram transmittance. 17 p2553 A72-34724
- Rate distortion theory model for visual communication fidelity assessment via weighted noise measurement and K rating 18 p2657 A72-36251
- Video data transmission minimum channel capacity requirement calculation from rate distortion function of source with known probability distribution 18 p2657 A72-36253
- Recent developments in digital image processing at the image processing laboratory at the Jet Propulsion Laboratory. 18 p2658 A72-36255
- Reflection of microwave through laboratory plasma. 18 p2716 A72-36947
- Wiener filter design for optimal processing of AM signals distorted during transmission through randomly dispersive medium 19 p2763 A72-37288
- Phase detector data distortion in phase-lock loop receivers. 19 p2763 A72-37297
- Long range holography theory based on reference beam technique for removing distorting effects of atmosphere on imaging, discussing visible light use 19 p2796 A72-37579

SIGNAL DISCRIMINATORS

U SIGNAL DETECTORS

SIGNAL DISTORTION

Balanced negative feedback circuits for reducing nonlinear distortions in distributed gain power amplifiers

02 p0193 A72-12223

Oscillographically measured semiconductor element I-V characteristics plotting optimization by considering measuring instrument and sampling signal shape and frequency effects on hysteresis

03 p0330 A72-12968

Loran C system time tick transmission delay during solar eclipse of 7 March 1970, discussing atmospheric electron density effects

03 p0322 A72-13533

Mean value, repetition and discontinuity errors of spectral transposition method involving memory storage and compressed signal processing

03 p0338 A72-13892

- Slip effect in diurnal phase and amplitude cycles of VLF signals in lower ionosphere due to wave interference at transmitting point 19 p2765 A72-38338
- Transmission of two partially time coincident linearly frequency modulated signals through limiter-filter system, noting distortion and satellite signals generation 19 p2766 A72-38419
- Combinational distortions and cross distortions in parametric microwave systems 19 p2768 A72-38665
- Frequency distortions of signals in frequency-modulated self-excited oscillators 21 p3032 A72-40782
- Convolution noise and distortion in FDM/FM systems. 21 p3020 A72-40893
- Intermodulation distortion of FDM-FM in injection locked oscillator. 21 p3020 A72-40899
- FM signal distortion during passage through two element antenna array to determine usable bandwidth from transmission characteristics viewpoint 21 p3022 A72-41265
- Cross-modulation in tuning circuits with nonlinear capacitances. 21 p3039 A72-41830
- Local-oscillator-circuit optimisation for minimum distortion in double-balanced modulators. 23 p3270 A72-43603
- A high-accuracy radio direction finder with a moving antenna 23 p3270 A72-43769
- Signal frequency distortions in frequency-modulated oscillators with feedback delay 23 p3266 A72-44209
- Large-signal analysis of efficiency and nonlinear phase distortion in a phase velocity tapered traveling-wave tube. 24 p3385 A72-45283
- SIGNAL ENCODING**
- Regulated dc-to-dc converter for voltage step-up or step-down with input-output isolation, using bistable comparator output voltage control through encoder 04 p0465 A72-14488
- Run length encoding for removing redundancy from video signals, determining upper bound on compression ratio based on first order Markov model 06 p0773 A72-17488
- Signal coding for discrete information in multichannel systems using multiple differential phase shift keying 06 p0773 A72-17500
- Source permutation code optimum encoding for long block length, comparing performance with rate distortion function bound and various quantization schemes 06 p0776 A72-18391
- Review of 1971 Picture Coding Symposium at Purdue University, discussing intraframe, interframe and color TV signal coding 09 p1279 A72-22899
- Huffman sequence synthesis by z transform zero pattern selection to obtain high energy for given peak amplitude, noting signal ambiguity functions 10 p1437 A72-24679
- Data transmission bandwidth requirements compression for band-limited functions, investigating feasibility through analog signal routing 11 p1592 A72-25887
- Noise immunity and code sequence rejection probability in real multifrequency communications systems with multipositional frequency shift keying 11 p1598 A72-26729
- Voice digital data rate reduction technique by exploiting zero and one bits imbalance in PCM TDM bit stream output encoding, discussing hardware implementation 12 p1785 A72-27845
- Data compression for spacecraft borne signal measurement, discussing nonlinear quantizing, histogram parameter extraction, and signal encoding [DFVLR-SONDDR-204] 13 p1921 A72-29346
- Modified run-length encoding system for text and drawing documents to obtain higher data reduction ratio 13 p1922 A72-29349
- Analog to digital converter for sinusoidal voltage amplitude pickup and subsequent digital coding with correction for conversion characteristic nonlinearity 13 p1934 A72-30020
- Performance criteria for transform data coding schemes evaluation under computational constraints, presenting numerical examples for Fourier, Walsh, Haar and Karhunen-Loeve transforms 16 p2366 A72-33214
- Grid modulation information encoding technique for image features extraction with simple Fourier filtering to replace heuristic method 16 p2365 A72-33752
- Encoding and decoding of color information using two-dimensional spatial filtering. 17 p2556 A72-35537

- Intraframe coding for picture transmission. 18 p2657 A72-36252
- Picture coding via linear transformation and quantization on subpictures with applications to monochromatic image processing 18 p2658 A72-36254
- Octal Reed-Solomon code to obtain decoding error probability approximation improvement over minimum distance bound 18 p2658 A72-36266
- Signal transmission and detection in differentially encoded coherent multiple phase shift keyed digital communication systems, discussing carrier suppression-induced resolution ambiguity 21 p3017 A72-40861
- Mathematical model for lattice-type error distribution of parallel channels communication system, noting metric for algebraic signal coding method 22 p3154 A72-42234
- Communication systems with binary convolutional signal encoding and threshold decoding, discussing orthogonal checkout sums distribution for correct and erroneous synchronization 22 p3154 A72-42235
- SIGNAL FADEOUT**
- U SIGNAL FADING**
- SIGNAL FADING**
- Wideband FSK receiver for space telemetry, calculating error probability in multipath signal fading due to planetary surface reflections 01 p0025 A72-10329
- Rain, snow and hail precipitation effects on radio link signal attenuation, scattering and fading along various transmission paths at millimeter and centimeter wavelengths 01 p0027 A72-10407
- Centimeter waves fading due to interference from tropospheric multipath propagation 01 p0027 A72-10412
- Radio signal fading analysis by ray tracing for transmission in spherically stratified atmosphere, assuming refractivity linear variation with height 02 p0179 A72-12414
- Fading medium transfer function estimation via homomorphic and Kalman filtering, considering multiplicative noise 03 p0326 A72-14195
- Long range satellite signal Faraday fading rate revealing electron density profile near F layer peak 04 p0486 A72-14883
- Diurnal phase and amplitude variations of long radio waves at great distances, explaining sunrise and sunset fadings 04 p0492 A72-15443
- Probability amplitude analysis of statistical behavior of fading signal envelope 04 p0493 A72-15457
- Ionospheric scintillation fading observations by NASA satellite tracking and data acquisition networks, noting frequency dependence in auroral regions [AIAA PAPER 72-220] 05 p0631 A72-16858
- Block orthogonal M-ary communication over fading dispersive channel with intermittent on-off noiseless feedback, calculating upper and lower bounds on error probability 06 p0776 A72-18389
- Earth-space path attenuation statistics and fade duration at 15.3 GHz, using ATS 5 satellite transmission and radiometric sun/sky techniques 07 p0948 A72-20496
- Wave-like ionospheric disturbance effect on phase polarization fading of vertical sounding signal, using numerical integration by computer 08 p1130 A72-20709
- Fading method measurement of normal and sporadic E region drift, reviewing height gradient data 08 p1161 A72-21539
- Error probability estimates in two channel diversity reception systems with allowance for fading correlation and incomplete signal separation 09 p1278 A72-22572
- Single pulse radio echo fading dependence on sporadic E layer critical and screening frequencies 11 p1595 A72-26282
- First order systems steady state frequency response to general harmonic amplitude modulated input, noting signal attenuation and absence of distortion 12 p1845 A72-27540
- Ground reflections effect on satellite transmission link fading characteristics, computing transmitter field intensity fluctuations as function of terrain profile elevation angle 12 p1785 A72-27800
- Line-of-sight radio link attenuation by atmospheric precipitation and phase interference fading during multipath propagation in 7-15 GHz range 12 p1785 A72-27802
- Statistical model for short wave radio signal fading at oblique signal reflection from ionosphere, determining pulse amplitude and duration distribution laws 13 p1915 A72-28468

- Regular cyclic fading of HF and VHF radio signals due to ionospheric scintillation, noting consistency with two ray interference formula 13 p1952 A72-29665
- SHF signal propagation through troposphere at low elevation angles, comparing fading measurements in winter and summer 15 p2194 A72-315500
- TWT off-transmission band area exponentially fading wave effects on electron beam modulation and amplification 15 p2209 A72-326700
- Adaptive reception in a channel with slow communication fading 17 p2515 A72-34835
- Spatial diversity technique based on predetector equal-gain combining for fast fading reduction of AM radio receiver, using phase shifter 18 p2661 A72-36845
- Correlation between two base-station antennas affected by local scatterers and directions of incoming mobile radio waves. 18 p2661 A72-36846
- Wave-like ionospheric disturbance effect on phase polarization fading of vertical sounding signal, using numerical integration by computer 19 p2765 A72-38337
- Determination of the orientation of ionospheric irregularities causing scintillation of signals from earth satellites. 19 p2794 A72-38866
- Reliability aspects of fading in microwave line of sight using digital transmission. 21 p3019 A72-40887
- Horizontal and vertical electron drifts in the F-region at Thumba. 21 p3049 A72-41324
- Optimal receivers for measuring time lags of pulses signals in the presence of fading 22 p3154 A72-42123
- Statistical characteristics of an optimal detector of randomly fading pulse signals 22 p3154 A72-42229
- Error probability estimates in two channel diversity reception systems of digital data transmission with allowance for fading correlation and incomplete signal separation 24 p3379 A72-44751
- SIGNAL FLOW GRAPHS**
- Irrundant multiple output combinational logic network fault detection and diagnosis theorems derivation from structural models in labeled directed graph form 02 p0184 A72-11478
- Signal flow graph theory based computer diagnosis using blocking gate approach, constructing algorithm for gates optimal locations determination for maximum faults distinguishability 02 p0184 A72-11479
- Reliable combinational logic networks, deriving conditions for fault locatability from directed graph formal model 02 p0185 A72-11491
- Flow graph analysis of optimal operation of frequency multipliers with idler circuits using nonlinear n-p junction capacitance 08 p1140 A72-21061
- Automatic search for Huffman sequential logic circuit breakdown detection sequence, using VEGA program through matrices and graphs utilization 11 p1612 A72-26549
- Reliability analysis of an intermittently used system with N types of failure. 18 p2693 A72-36024
- Communication network vertex and mixed cutset definitions and computation from interchange graph of given finite connected undirected graph without loops and multiple edges 21 p3015 A72-40634
- Digraphs application to electronic linear networks analysis, developing computer program 21 p3024 A72-40992
- Generalized numbers method for analysis and synthesis of linear circuits described by signal flow graph, noting algorithms for computer programming 23 p3269 A72-43443
- SIGNAL GENERATORS**
- NT FREQUENCY SYNTHESIZERS**
- NT FUNCTION GENERATORS**
- Polyphase signal generators, using reversed flux region propagation in saturable ring core controlled by switching transistors operation [IEEE PAPER 17.5] 03 p0322 A72-13773
- Nonlinear distortion coefficient measurement in broadband FM signal generator 03 p0333 A72-13988
- Digital sine wave generator, discussing advantages over conventional RC and LC oscillators due to superior phase constancy 05 p0634 A72-15814
- Dynamic response predictions of fluidically controlled pulsatile hydraulic flow and pressure generator for biomedical systems 07 p0914 A72-18820

Optical sweep generator using single frequency He-Ne lasers with Michelson interferometer for mode selection to provide smooth tuning throughout Doppler width
07 p1000 A72-19010

Solid state sinusoidal signal generator based on current density oscillation effect in high resistivity p-type InSb with transmutation doping
09 p1288 A72-23191

Double balanced frequency converter design for selective microwave generation by combination of CW or swept signal with local oscillator source
10 p1448 A72-24038

Noise measurements of AM and FM microwave generators and amplifiers in nonlinear regime
10 p1452 A72-24643

Russian book on random signal generation covering ultralow and audio frequency spectra, random number and pseudorandom signals simulation and automatic control
12 p1786 A72-28347

Modulation oscillations in ferromagnetic core-based LF signal generators and frequency doublers, deriving differential equations for converter operation and formulas for static characteristics
13 p1930 A72-29049

SSB signal generation without Nyquist filter or auxiliary equipment for PM modems in data transmission
15 p2195 A72-31620

Nonlinear distortion coefficient measurement in broadband FM signal generator
15 p2210 A72-32709

Signal generator designed for calibration and control of interferometric radar station to observe and study radio echoes induced by meteor trails
17 p2519 A72-35959

Video signals generation from binary data and mixing with analog information from cameras or tape recorders for simultaneous display on cathode ray tubes
19 p2769 A72-37936

SIGNAL MEASUREMENT

Directional ionosonde aerials and instrumentation for ionospheric reflection angle of arrival measurements
01 p0053 A72-10091

Generation-recombination model of large signal silicon transistor operating in IC microwatt range
02 p0188 A72-11521

Random errors in arrival time measurements of sinusoidal radio signal under noise and pulse interference
03 p0323 A72-13893

Nonlinear distortion coefficient measurement in broadband FM signal generator
03 p0333 A72-13898

Stochastic signal method for measuring dynamic viscoelastic properties of isometric frog sartorius muscle at rest and contraction, using white noise vibrations
04 p0480 A72-15221

Radio wave absorption during oblique propagation through ionosphere from vertical measurements, using rhombic antenna at 25 MHz
05 p0657 A72-16267

Legibility criterion of records from X-Y recorders, applying to Lissajous figures of stationary signals and phase trajectories
06 p0817 A72-18165

Noise contaminated pulse signal transit time measurement by receiver using digital filters
07 p0939 A72-19051

Shf resonator small resonant frequency shift and Q factor changes measurement based on FM signal envelope shape analysis
07 p1046 A72-20508

Electronic correlator for plasma wave induced coherent signals cross correlation measurement, producing 1 microsecond time delays by automatically switching lumped circuit delay line
07 p0958 A72-20582

Statistical noise characteristics and conditional signal distribution function measurements at output of standard FM demodulator
09 p1277 A72-22570

Microwave transistor noise factor measurement for various geometries and parameter values correlation with predictions
09 p1286 A72-23104

Criterion for signals records legibility obtained by analog recorders, deriving relationship between normalized root-mean-square error and apparent frequency
09 p1316 A72-23663

Frequency measurements of square wave signal with unknown amplitude by two mismatched channels, comparing rms error with effective estimate variance
10 p1436 A72-24509

Ionospheric total electron content measurement by satellite radio emissions
11 p1632 A72-25840

Radial small-signal gain profile measurement in carbon dioxide laser discharge tube explained by axial gas temperature increase with discharge current
11 p1647 A72-26145

Russian papers on radar theory and techniques covering signal measurement, MTI, clutter suppression, false alarm, bearing errors, automatic ranging and tracking, etc
11 p1595 A72-26293

Optimal synthesis and analysis of quasi-deterministic signal detection system with simultaneous parameter measurement on background noise
11 p1596 A72-26312

Digital correlator systems design for nonstationary signals, presenting circuit diagrams for multichannel centering system and memory operation
11 p1602 A72-26445

Associative impulse analyzer for measurement of probability density functions in electronic memories
11 p1602 A72-26446

Linear multiple section binary filters analysis and synthesis, discussing mesh functions spectra for signal measurement in automatic control systems
11 p1612 A72-26452

VLF recorder for measurement of incident direction, polarization, phase and amplitude of 16 and 60 kHz transmitter signals
12 p1796 A72-27791

CO-He laser vibrational population distribution and small signal gain measurements, comparing with prediction based on V-V anharmonic exchange relaxation
12 p1827 A72-28222

Dual threshold temporal fixation of pulse signal from two points on leading edge
13 p1914 A72-28410

Analysis of errors generated by Kotelnikov series representation of finite signals during quantization by delta functions, finite duration sampling and constant amplitude sampling
13 p1919 A72-29044

Optimal quantization parameters for pseudonoise signals at radio receiver output, estimating static error in correlation function measurement
13 p1919 A72-29048

Data compression for spacecraft borne signal measurement, discussing nonlinear quantizing, histogram parameter extraction, and signal encoding [DFVLR-SONDDR-204]
13 p1921 A72-29346

Measuring technique importance for aircraft R and D, emphasizing quartz tensometer, digital control and signal processing
14 p2092 A72-30286

Doppler carrier frequency shift measurement accuracy, finding relationships in errors for coherent and noncoherent pulse trains
15 p2195 A72-31657

Polynomial approximation of measurement signals with variability, comparing Taylor, Abdulaev and Newton formulas
15 p2235 A72-31848

Random errors in arrival time measurements of sinusoidal radio signal under noise and pulse interference
15 p2202 A72-32704

Nonlinear distortion coefficient measurement in broadband FM signal generator
15 p2210 A72-32709

Frequency marker measurement of nuclear quadrupole resonance (NQR) signal in pulsed radio spectrometer compared with zero beat method
16 p2390 A72-33078

Results of simultaneous measurements of the spectrum of auroral radio echoes at two frequencies
17 p2519 A72-35874

Novel and accurate methods for measuring small-signal and large-signal impedances of IMPATT diodes
18 p2664 A72-35997

Construction, analysis, and design of FM digital devices for controlling and measuring rapidly varying quantities
19 p2776 A72-37303

Russian book - Methods of measurement-information conversion and separation from harmonic signals
19 p2764 A72-37449

An improved design and measurement of attenuation characteristics of RF suppressors.
20 p2902 A72-38997

Feedback quantization noise effects on differential PCM systems, showing SNR relation to noise optimized prediction
21 p3017 A72-40860

An irregular signal phase discriminator
21 p3033 A72-40943

Extending the range of attenuation measurements.
21 p3022 A72-40999

Measurement of a radio signal nonenergetic parameter at high additive and modulation noise levels
21 p3022 A72-41117

A threshold device for establishing the time of pulsed signals
21 p3035 A72-41727

A high-frequency transmitted power meter using a laser signal
21 p3064 A72-41730

A method of calculating the lag of the phase photoelectric installation of a time service
21 p3058 A72-41769

Simultaneous recording of laser radiation and signal related to secondary processes, using ruby luminescence for oscillograph triggering
22 p3185 A72-42274

Faraday effect of incoherently scattered radar signals
23 p3263 A72-43365

Wideband pulsed-RF phase measurement.
23 p3270 A72-43575

Multimoded components wavefront arrival angle from measurements of signal induced in linear array, discussing numerical calculation from linear equation solution and polynomial roots
23 p3264 A72-43601

Statistical noise characteristics and conditional signal distribution function measurements at output of standard FM demodulator
24 p3379 A72-44749

SIGNAL MIXING

Digital telemetry data transmitter featuring triangular wave generator and signal mixer for reducing sensitivity to transmission path characteristics variations
02 p0179 A72-12415

Tunable coherent IR signal generation and propagation by mixing carbon dioxide laser and millimeter wave klystron output in GaAs loaded waveguide
04 p0532 A72-15614

Signal injection through laser transmitting window, showing effects on resonant frequency and locking mode [AD-738988]
07 p1009 A72-20680

Superheterodyne radiometers for millimeter and submillimeter waves, using Mach-Zehnder interferometer frequency mixer for parasitic signal suppression
08 p1140 A72-21265

Single band optical mixer heterodyne spectrum analyzer for laser radiation image spectrum suppression
08 p1182 A72-21375

Microwave source four hundredth order harmonic mixing with laser radiation, using Josephson junction and maser
12 p1827 A72-28221

Difference-frequency mixing of pulsed carbon dioxide lasers with non-phase-matched GaAs for submillimeter wave generation
15 p2290 A72-31384

Computer simulation for performance of carbon dioxide laser heterodyne communication system with photoconductive n-type mercury-cadmium telluride detector/mixer
15 p2198 A72-32062

Filtering with perfectly correlated measurement noise.
17 p2533 A72-35240

Fundamental, harmonic and combination frequency components amplitude analysis via dual input describing function for nonlinear element response under two incommensurate frequency sinusoidal signals
18 p2671 A72-36051

Mixing process at the emitter-base junction of a high-frequency transistor.
18 p2667 A72-36948

SIGNAL NOISE

U SIGNAL TO NOISE RATIOS

SIGNAL PROCESSING

Optical radar target range estimation, determining suboptimum post detection signal processing algorithms in photon counting mode
01 p0024 A72-10047

VLF modulation/demodulation system performance prediction by atmospheric noise model, comparing results with measurements
01 p0025 A72-10327

Optimal inertialess transformation of output signals from several devices, noting method application to analog data processing systems
01 p0045 A72-10571

Two dimensional digital pictorial signal processing - Conference, University of Missouri, Columbia, October 1971
01 p0069 A72-10865

Circuit design techniques used for wideband signal processing systems, considering 1000 MB/S microwave communication link
02 p0176 A72-12163

Telemetry standards for transmitting, receiving and signal processing equipment at missile test ranges
02 p0176 A72-12164

Receiver detection characteristics for multiplicative processing of coherent signal pulses with unknown initial phase and slowly fluctuating amplitude
02 p0176 A72-12215

Phase comparison direction finder with successive signals comparison using commutation of two antenna elements for target acquisition and tracking operations
02 p0176 A72-12219

Noisy radar signal processing by spectral analysis method
02 p0177 A72-12225

Radar signal digital processing for replacing analog circuitry, discussing rf signal representation, sidelobe reduction, coherent processors and filter design
02 p0178 A72-12396

Data transmission and distribution systems interface, using semiconductor technology in multiplexing, asynchronous data transfer, A-D and D-A data conversion and sensor signal conditioning
02 p0194 A72-12404

Real time coherent optical processor of pulse Doppler radar signals with Fresnel diffraction masks for PCW target range rate determination
03 p0322 A72-13437

Electropneumatic converter for pneumatic pulse transformation into dc or ac signal, using corona discharge current
03 p0311 A72-13556

Pulse coded processing system EMC performance measurement, considering CW and pulsed interference effects and application to ATC radar beacon system transponders
03 p0324 A72-14033

Radar signal processing by digital computer modeling, presenting apparent target splitting probability and azimuth estimate distribution for shifting window target detectors
03 p0326 A72-14361

Optimal nonlinear discrete filters with finite memory for polynomial signals, discussing synthesis with aid of minimax method
04 p0505 A72-14998

Telemetry systems with discrete compression-expansion function, calculating noise stability improvement as compared to linear and nonlinear signal conversion operations
04 p0487 A72-15000

Hot-wire anemometers signals resolution into velocity-temperature fluctuations correlations in compressible flow with shear turbulence wakes
[AIAA PAPER 72-117] 05 p0664 A72-16822

Surface wave parametric signal processing, obtaining cross correlation of digitally coded input signals
05 p0631 A72-17074

Fourier, Hadamard and Karhunen-Loeve transformations for digital speech processing, comparing bit rate requirements
06 p0772 A72-17405

Amplitude and phase modulated radar pulse train representation by complex number sequences, discussing generation, processing, and Z transform application to combination codes
06 p0773 A72-17495

Adaptive sampling of continuous measurement signals, calculating mean sampling rate
06 p0773 A72-17572

Optimal radio signal processing system on background of correlated interference, calculating detection characteristics
07 p0937 A72-18850

Suboptimum linear quadratic algorithm for optical radar signals postdetection processing and target range estimation
07 p0943 A72-19522

Radio direction finding with discrete antenna scanning and multilevel beacon signal quantization, investigating accuracy
07 p0943 A72-19523

Optimal PSK signals selection and synthesis from random sequences ensuring minimum value of maximum side peak of autocorrelation function
07 p0943 A72-19564

Pontryagin maximum principle application to optimal linear filtration for multivariable systems with signal processing
08 p1133 A72-21374

Multipath angle error reduction using multiple radar target signal processor with angle tracking of wave fronts
08 p1134 A72-21408

ATC radar performance monitoring, considering advances in radar signal processing and digital display techniques
08 p1134 A72-21525

Digital filter synthesis for radar signal processing applications, discussing frequency sampling method extension with advantage of known waveform and reduced computations
08 p1146 A72-21916

Sequential control using computer program for signal processing, noting machine tool, die casting, elevator and warehouse applications
09 p1290 A72-22240

Two dimensional optical signals Fourier transform properties and local frequency filtering methods
09 p1351 A72-22982

Multichannel signal processing system for spatial optical filters synthesized by orthogonal functions
09 p1314 A72-23342

Dynamic programming method application to signal processing components selection for cascaded communication links to satisfy overall gain and noise figure
09 p1281 A72-23415

Stochastic projected gradient algorithm to maximize SNR subject under linear or nonlinear constraints, applying to detector antenna array processing
10 p1456 A72-23808

Wide bandwidth electron beam analog recorder and reproducer, using signal processing electronics and silver halide film
10 p1479 A72-23931

Integrated circuits fabrication and design, describing internal physical processes, input and output signal values, functional operations and topological features
10 p1448 A72-24283

Constant false alarm rate signal processors for several electromagnetic interference types, using distribution-free methods and maximum likelihood estimation in radar target detection
10 p1437 A72-24683

Radar sequential detector for digital processing of signal masked by noise, determining false alarm and detection probabilities and mean test duration
10 p1439 A72-24908

Uncertainty functions side maxima for phase manipulated signals with low sidelobe levels in autocorrelation functions, noting Doppler frequency shift effect
10 p1440 A72-24916

Optimal filter for narrow band stochastic signal processing, using Wiener theory
10 p1441 A72-25103

Pulse amplitude system with finite data recording time, deriving transfer function for signal shaper
11 p1609 A72-25444

Time resolution buffer for multichannel scaler, applying to digital signal averaging
11 p1632 A72-25701

Amplitude-time quantization of radar pulse signals in analog-digital converter, improving noise threshold and ranging accuracy
11 p1595 A72-26294

Statistical error analysis of phase comparison FM radio altimeter during signal processing, investigating range finding strength distribution of echo reflectance
11 p1633 A72-26305

Discrete automatic monitoring and measuring systems with discrete random sequence and continuous process reconstructed output signals, deriving probability criteria for reading frequency determination
11 p1611 A72-26438

Random process quantization interval search algorithm based on signal approximation by n-th degree polynomial
11 p1602 A72-26439

Monotonic signal rejection by connecting line insertion to sensor and central electrical measuring device input galvanic decoupling
11 p1611 A72-26440

Phase metering information converters with digital analog computation, discussing analysis of prototype semiconductor model with ten-digit binary codes
11 p1602 A72-26449

Semiautomatic analog to digital converter for pulse signals time dependent parameters, examining block diagrams and tunnel diode operation
11 p1605 A72-26456

Self balancing ac bridge with double conversion of unbalance-signal and low capacitance sensor for displacement measurement
11 p1634 A72-26459

Signal filtration algorithms and parameter estimation in additive non-Gaussian noise background by conditional Markov process theory
12 p1783 A72-27633

Optoacoustic processing of large time-bandwidth signals, calculating insertion loss vs delay time
12 p1810 A72-27935

Electro-optical processing of phased array signal reception, using electron beam addressing system with potassium diduterium phosphate target crystal
12 p1785 A72-27954

Optimal parameters of electro-optical signal processor for phased array antennas, noting optical subsystem correspondence to optoacoustical spectrum analyzer
13 p1926 A72-28374

Optimal radar recording systems for meteor trail observations providing signal detection, processing and storage triggering and echo discrimination
13 p1929 A72-29030

Automatic real time processing of meteor radar echoes, using digital computers
13 p1924 A72-29033

Circuit of two parallel connected vacuum pentodes with different reactances to provide exact voltage division of ac signals by another
13 p1930 A72-29045

Linear product demodulator for quadrature double sideband signal, evaluating channel noise and phase jitter effect on carrier
13 p1920 A72-29105

Surface wave devices signal processing for space communication, developing fast lock up spread spectrum communication link breadboard
13 p1920 A72-29106

Forward loop signal attenuation and phase shift diagrams for design of feedback amplifier and compensation network for dc flyback converter
13 p1899 A72-29110

Self adaptive two channel iteration servosystems for input reconstruction by successive approximations, determining signal and noise error operators
13 p1936 A72-29155

FAA airborne OMEGA development program covering signal monitoring, airborne data collection and system operational evaluation
13 p1998 A72-29195

Noise resistance techniques for calculating linear signal interpolation errors in adaptive quantizers
13 p1931 A72-29268

Spatial-temporal coherent processing technique application to thermal radio emission random signal reception, deriving ambiguity function
13 p1920 A72-29282

Sampling theorem with small truncation error for band limited signals, discussing applications to pulse transmission filter design
13 p1922 A72-29397

Multidimensional non-Gaussian signals filtration in presence of time correlated noise with discrete values of argument
13 p1937 A72-29638

Noise suppression by time exposure oscilloscope photography to enhance repetitive electric signals obscured by noise of equal amplitude
13 p1959 A72-29754

Signal discretization frequency upper bounds determination to satisfy prescribed level of mean square error in continuous signal restoration
13 p1925 A72-30021

Measuring technique importance for aircraft R and D, emphasizing quartz tensometer, digital control and signal processing
14 p2092 A72-30286

Measuring tape recorder, properties and utilization for signal recording and processing, discussing digital computer techniques and compensation for interference effects
14 p2104 A72-30287

ECG amplifier and cardiostachometer for exercise studies, using digital algorithm for heart rate computation and ECG signal preprocessing for R wave detection
14 p2080 A72-30707

Avionics equipment for signal processing onboard civil aircraft to improve flight safety, discussing uses of OMEGA navigation system and digital computers
15 p2193 A72-31178

Conical scanning system for Pioneer Jupiter spacecraft pointing control, discussing signal processor, spacecraft dynamic behavior, system stability and error budget
15 p2320 A72-31791

Automata with behavior defined by input stimuli sequence and independent on initial state, considering neuron nets as example
15 p2203 A72-32173

Discrete representation of continuous time signals and sequences by digital means, using frequency warping function
16 p2365 A72-33753

Exponential signal reconstruction sampling rate restriction derivation based on pole-zero cancellations in Z transform
16 p2365 A72-33756

Structural information model for data compression algorithm synthesis, using piecewise signal approximation
16 p2395 A72-33954

Book on basic acoustics covering mathematical methods, diffraction phenomena, statistical theory of signal processing, wave acoustics, membrane sound radiation, music, source array theory, etc
16 p2427 A72-33973

Two Dimensional Digital Signal Processing Conference, University of Missouri, Columbia, Mo., October 6-8, 1971, Proceedings.
17 p2520 A72-34401

Relationship between antenna synthesis for a given radiation pattern and the synthesis of spatial signal processing systems
17 p2515 A72-34832

Signal detection by receivers with modulus processing
17 p2515 A72-34836

Fourier transform of two-dimensional signals. II
17 p2516 A72-35185

Design of nonlinear networks with a prescribed small-signal behavior.
17 p2533 A72-35199

Discrete-time demodulation of continuous-time signals.
17 p2516 A72-35332

Spectrum transformation in differential amplitude indicators with commutation of the harmonic signals being compared
17 p2518 A72-35780

Time-optimality of a class of extremal systems with statistical signal processing
17 p2518 A72-35782

Image processing in the context of a visual model.
18 p2658 A72-36256

The use of linear programming to design digital filters from impulse-response specifications.
18 p2663 A72-36304

An adaptive processor for RF antenna arrays.
18 p2659 A72-36329

Surveillance radar for clutter rejection and signal loss reduction at airports, discussing system design features
18 p2662 A72-37046

Wiener filter design for optimal processing of AM signals distorted during transmission through randomly dispersive medium
19 p2763 A72-37288

A differential-integral amplitude-time converter of nanosecond-range pulses
19 p2771 A72-37305

Investigation of the structure of processes in discrete automatic control systems by the application of graph theory
19 p2779 A72-38180

Precise transfer function of a clamper for a commutation switch with a finite closing time
19 p2782 A72-38463

Exponentially weighted noncoherent integration of pulsed signals in the presence of Gaussian noise and random impulse noise.
19 p2767 A72-38623

An algorithm for linearly constrained adaptive array processing.
20 p2904 A72-39777

Effects of finite register length in digital filtering and the fast Fourier transform.
20 p2904 A72-39780

Thermal imaging with pyroelectric IR detector arrays, discussing signal processing by digital technique to eliminate voltage offset variations effects in preamplifiers
20 p2928 A72-39968

ATC services configuration with secondary surveillance radar and primary radar data acquisition system, discussing signal processing by automated decoder
21 p3080 A72-40288

Telemetric frame synchronization with the aid of distributed and concentrated frame periods
21 p3024 A72-40329

Canonic model representations for communication receiver to analyze and simulate input-output behavior as nonlinear signal processing black box
21 p3019 A72-40889

Preliminary frequency selection during matched signal filtering
21 p3021 A72-40941

Digital processing for motion compensation in high resolution airborne synthetic aperture radar imagery in presence of simultaneous longitudinal, lateral and vertical maneuvers
21 p3022 A72-41076

Analysis of a procedure for the transmission of low-frequency signals in time-compressed, analog form
21 p3023 A72-41399

Analysis of the basic metrological characteristics of Vernier time-pulse converters
21 p3035 A72-41729

Effect of the video signal shaping mechanism in a photosensitive scintistor sensor on the optical data processing accuracy
21 p3058 A72-41735

Separation and detection of signals in the presence of nonadditive noise
21 p3023 A72-41746

Optimal invariant conversion of information from a turbine flow meter and a capacitive fuel gauge
21 p3058 A72-41801

Dispersion signal recording for klystron AFC radio spectrometer by low frequency magnetic field modulation
22 p3175 A72-41900

Optimal PSK signals selection and synthesis from random sequences, ensuring minimum value of maximum side peak of autocorrelation function
22 p3153 A72-42082

Communication systems with binary convolutional signal encoding and threshold decoding, discussing orthogonal checkout sums distribution for correct and erroneous synchronization
22 p3154 A72-42235

Parameter estimation of reflected signal in multichannel communication system with discrete readings, considering receiver with optimal signal processing under low noise level
22 p3154 A72-42239

Ultrasonic holography in large phase disturbance.
23 p3290 A72-43950

Electronic devices with Rayleigh ultrasonic acoustic surface wave excitation for storage, recognition and separation of electrical signals usually requiring computerized operation
23 p3314 A72-44148

Optimal equalization of discrete signals passed through a random channel.
23 p3265 A72-44178

Influence of modulating /multiplicative/ noise on signal processing in a phased-array-antenna/receiver system
23 p3265 A72-44205

Optimal signal processing in systems with multiple reception elements /channels/
23 p3266 A72-44219

Signal-to-energy conversion function in the photometry of solar soft X-radiation with broad-band detectors.
23 p3329 A72-44238

SIGNAL RECEPTION
NT SYLLABLES
NT SYMBOLS
NT TELEVISION RECEPTION

Coded multiple FSK in presence of random variable phase, predicting optimum reception performance relationship to phase distribution and SNR
01 p0025 A72-10330

AFC for suppressed-carrier SSB voice signal reception, using phase locking procedure or comparative zero-crossing-rate measurement
01 p0025 A72-10333

Atmospheric wave propagation mode parameters frequency dependence analysis from duct model, calculating received signal time behavior by waveguide transfer function
01 p0027 A72-10408

Diurnal and seasonal changes in occurrence frequency of rapid phase fluctuations in vlf received at Franz Josef Land correlated with geophysical observations
02 p0172 A72-11922

Telemetry receiver signal data quality in terms of RF, if AGC, AFC and AM rejection circuitry requirements
02 p0192 A72-12149

Estimation algorithm for arbitrary parameter of narrow band radio signal with unknown amplitude and phase during reception on additive normal noise background
02 p0176 A72-12218

Signal waveform ensuring maximum reception stability on correlated noise background with peak limiting
02 p0183 A72-12760

Soviet book on statistical theory of digital data transmission through parallel channels covering optimal and suboptimal reception systems under signal fading and interference
03 p0323 A72-13968

Near optimum limiting and blanking levels /error probability/ selection for binary signal matched filter reception in Gaussian and impulse noise, discussing performance simulation
04 p0486 A72-14485

Signal fluctuation effect on directional properties of multipole receiving antenna, calculating radiation pattern
04 p0499 A72-15143

Receiver arrangement for polarization selection based on multiplication of heterodyne-converted and amplified signals taken from dual-input antenna receiving elliptically polarized field
05 p0635 A72-16332

Radio direction finding techniques using amplitude-trigonometric interpolation between signals received at circular antenna array
05 p0628 A72-16555

SNR effect on rms bearing error by amplitude comparison for nonscanning nontracking receiving system with two antenna lobes of arbitrary shape
05 p0629 A72-16577

RF transmission between two parallel whip antennas in warm plasma, noting received signal increase at probe resonant frequency
06 p0860 A72-17747

Digital decision directed suboptimal receiver design for random multipath channel communication with intersymbol interference, predicting performance for steady state probability of correct decision
07 p0941 A72-19272

Multicarrier communications satellite signal power, center frequency and rms deviation computer controlled monitoring system with frequency shift radiometer principle
07 p0948 A72-20491

Optical signal heterodyne reception, discussing atmospheric distortion effects reduction
08 p1131 A72-20749

Optimum pulse duration for ionospheric oblique backscatter sounding, determining receiver signal power input dependence on pulse duration
08 p1131 A72-20820

Orthogonal functions representation of received signals in ideal signal sequences transmission in linear systems with matched filters and frequency band limitation
08 p1132 A72-21326

Potential noise stability of wideband communications systems during discrete signal reception on combined background of quasi-white noise and spectrally lumped interference
09 p1277 A72-22569

Vertical angle estimation for HF sky wave multimode signals arrival, noting validity for arbitrary antenna elements polarization
09 p1281 A72-23513

Nonlinear filtering synthesis of optimal receiver for pseudorandom phase shift keyed signal with arbitrary modulation angle and white noise background
10 p1436 A72-24510

Estimate of effectiveness of utilization of composite signals to combat external interference with available a priori data
10 p1436 A72-24580

Error probability and reception stability in synchronous detection of phase manipulated signals with additive Gaussian noise at multiplied carrier frequency
10 p1436 A72-24587

Maximum likelihood receiver performance for optical detection of multimode laser or scattered radiation, considering photocounting distribution, decision threshold and error probability
10 p1452 A72-24681

Angle tracking radar receiver signal analysis simplification by use of complex variables
10 p1437 A72-24684

Amplitude comparison direction finding systems, calculating error due to clutter from incident signal and noise angular distribution relationship to measured arrival angle
10 p1439 A72-24803

Modulating /multiplicative/ noise effects on output signal characteristics of receiver designed for optimal reception on background of Gaussian noise
10 p1439 A72-24906

Receivers for PPM optical communication and pulsed signal detection in background light, evaluating upper bounds on error probability based on photoelectron Poisson statistics
11 p1591 A72-25311

Position and minimum scattering algorithms for narrow band signal source received by spaced receivers forming antenna arrays with large separations
11 p1598 A72-26715

Received signal spectrum gravity center and effective antenna centers of airborne Doppler velocimeter in horizontal flight
11 p1606 A72-26730

Optimal reception system synthesized for FM signal with phase fluctuation masked by narrow band AM and white noise
13 p1914 A72-28414

Satellite altimetry based on ocean backscattering, analyzing received signal model and altitude errors
13 p1955 A72-28533

Paraboloid and elliptical mirrors in 100 m radio telescope for Helios space probe signals reception, noting device compatibility for data exchange with NASA [DGLR PAPER 72-019]
13 p1939 A72-28964

Diurnal and seasonal changes in occurrence frequency of rapid phase fluctuations in VLF received at Franz Josef Land correlated with geophysical observations
13 p1920 A72-29234

Spatial-temporal coherent processing technique application to thermal radio emission random signal reception, deriving ambiguity function
13 p1920 A72-29282

PSK signal cross-correlated receiver output SNR in presence of random misalignments with respect to carrier frequency and arrival signal time
13 p1921 A72-29283

Optical communications with FDM digital data channels, examining signal optimal reception and noise stability
14 p2084 A72-30331

Digital FM signal receiver with postdetector integration, determining error probability as function of input SNR and noise stability
14 p2084 A72-30332

Delay-lock discriminator to measure spatial delay time of noise-like signal received by two spaced antennas
14 p2088 A72-30336

Cosmos 381 onboard ionospheric station signals received from magnetically conjugate region by ground wideband antennas
14 p2085 A72-30476

Submillimeter plane monochromatic waves propagation in ground layer of turbulent atmosphere, deriving received signals levels fluctuations
15 p2195 A72-31653

Adaptive reception of weak repetitive signals on background of intense fluctuating noise, synthesizing adaptive detection system for multipath propagation and small SNR
15 p2195 A72-31658

Laser communication lines in atmospheric ground layer, comparing SNR for direct-reception and superheterodyne video systems
15 p2247 A72-31887

Time transfer measurement between two locations using nearly simultaneous reception times from optical pulsar signal transmission
15 p2199 A72-32076

FM/FM multiplex receiver with carrier and subcarrier demodulators, deriving average click rate, output noise spectrum and SNR from Rice model
16 p2362 A72-33212

Data transmission systems with decision feedback in presence of burst noise, calculating statistical relations among received sequences as function of duration and spacing
16 p2372 A72-33795

A mode-averaging diversity combiner
17 p2513 A72-34360

Adaptive reception in a channel with slow common fading
17 p2515 A72-34835

Signal waveform ensuring maximum reception stability on correlated noise background with peak limiting
20 p2903 A72-39066

Effectiveness of error-correcting codes during reception on the whole in the presence of additive normal white noise
21 p3014 A72-40310

Performance of antennas in random fields
21 p3026 A72-40355

Optimal frequency-difference communications system with manipulated amplitudes
22 p3154 A72-42237

Parameter estimation of reflected signal in multichannel communication system with discrete readings, considering receiver with optimal signal processing under low noise level
22 p3154 A72-42239

Phase modulated data transmission with partial pilot signals, interpolating reference demodulation signals at receiving end by maximum cross correlation
23 p3264 A72-43771

Linear antenna directivity loss for fluctuating signal reception, noting effects of signal to noise ratio and antenna length
23 p3265 A72-44204

Optimal signal processing in systems with multiple reception elements /channels/
23 p3266 A72-44219

Potential noise stability of wideband communications systems during discrete signal reception on combined background of quasi-white noise and spectrally lumped interference
24 p3379 A72-44748

SIGNAL REFLECTION

Optical aurora relationship to radio counterpart, showing backscattered signal peak amplitude close correlation to magnetic bay peaks
01 p0056 A72-10440

Wind velocity spatial derivative determination by radar observation of signal reflection from atmospheric water particles
03 p0383 A72-13483

Covariance matrix of coordinate fluctuations of instantaneous radar center of reflection from set of scatterers
04 p0487 A72-15144

Automatic interplanetary station adapter to obtain reflected signals amplitude-altitude-frequency characteristics during ionospheric probes
05 p0657 A72-16271

Pulsed FM radio pulse signal reflection from inhomogeneous plasma or ionosphere calculating electron collision loss effects on distortion
06 p0854 A72-17487

Horizontally modulated reflected light signals phase shift and demodulation, assuming single scattering
06 p0848 A72-18047

Semiconductors cyclotron echo signals from dipole interactions of electrons with alternating magnetic fields, discussing frequency doubling and excitation mechanism
07 p1048 A72-19639

Sky wave backscattering with narrow beam antenna coupled with signal modulations and Doppler shift as means of sea state observation and environmental monitoring
08 p1134 A72-21493

Electromagnetic impulse wave impingement on semfinite isotropic plasma slabs with arbitrary incidence angle and polarization, calculating signal reflection in terms of Bessel functions
08 p1137 A72-21990

Meteorological radar signal reflectivity probability and quantization error dependence on incoherent storage device parameters from computer simulation
08 p1201 A72-21995

Cloud and precipitation dynamic processes effects on reflected radar signal statistical characteristics
08 p1137 A72-21996

Cloud and precipitation elementary processes effects on reflected radar signal fluctuation spectrum during hydrometeor formation
08 p1201 A72-21997

Diffusion bonded joints tensile strength determination from ultrasonic pulse echo and attenuation measurements, discussing contamination and SNR effects
10 p1485 A72-23814

Instantaneous frequency statistical characteristics of passive noise spectra and fluctuating signals reflected from nonpoint moving radar targets
10 p1436 A72-24514

Reflected short wave signal frequency shift due to reflecting ionospheric layer movement and electron concentration changes, considering oblique incidence on isotropic and anisotropic layers
10 p1436 A72-24576

Doppler spectral width of radar signal reflected from sea surface as function of illuminated region dimensions, waviness scale and emission factors
10 p1439 A72-24904

Wind velocity spatial derivative determination by radar observation of signal reflection from atmospheric water particles
11 p1682 A72-26253

Diurnal variations of F 2 region critical frequencies and quiet and perturbed ionosphere N/h profiles during solar cycle, estimating signal reflection altitudes
11 p1594 A72-26274

Adcock direction finder errors due to diurnal and sporadic ionospheric variations and tilting layers effects on reflected signal
12 p1804 A72-27780

Ground reflections effect on satellite transmission link fading characteristics, computing transmitter field intensity fluctuations as function of terrain profile elevation angle
12 p1785 A72-27800

Error analysis of ionospheric parameter measurement by satellite transmitted or reflected multiple frequency pulsed radiation signal, using perturbation method
13 p1920 A72-29276

Gravity wave observation in nighttime F region by measuring phase path length changes of stable CW signal reflected obliquely from ionosphere
13 p1953 A72-29814

Ionospheric radio signal reflection fields verified via quantitative statistical reliability criterion
14 p2100 A72-30634

Meter and decimeter wave reflected signals distribution and surface backscattering patterns effective beamwidth investigation by method based on Doppler effect
14 p2086 A72-30792

Pulse and monochromatic short wave signals phase/amplitude autocorrelation functions and probability distributions during oblique incidence reflection from ionosphere
15 p2197 A72-31876

Stochastic signal reflection by passive element, synthesizing optimal echo-signal detector for space diversity reception
15 p2197 A72-31877

Lunik 14 spacecraft radio signal reflection from lunar surface, showing energy spectrum dependence on surface roughness
15 p2202 A72-32655

Correlation of noise-like emission reflected from a statistically uneven surface
17 p2583 A72-35543

Signal reflection height seasonal variations effect on radio waves absorption estimation from vertical ionospheric sounding
18 p2662 A72-36881

Quasi-periodic variation in F 2 layer reflected signal field strength, noting predominance during periods with type 4 bursts, auroras and geomagnetic disturbances
19 p2792 A72-38639

The effects of transmitter source and load impedance on harmonic output spectrum - A new measurement method.
20 p2921 A72-38996

Response of the average pressure acting on the surface of an emitting circular transducer due to different reflecting objects.
21 p3055 A72-40948

Parameter estimation of reflected signal in multichannel communication system with discrete readings, considering receiver with optimal signal processing under low noise level
22 p3154 A72-42239

High power radio transmitter for structural investigation of ionospheric D and E regions by signal reflection and electron concentration profiles
23 p3263 A72-43378

Semiconductors cyclotron echo signals from dipole interactions with alternating magnetic fields, discussing frequency doubling and excitation mechanism
24 p3431 A72-44571

SIGNAL STABILIZATION

Supercritically doped transferred electron microwave amplifiers stabilization mechanisms, considering cathode contact, anode diffusion current and active region temperature gradient roles
01 p0036 A72-10636

Spatially periodic coupled cavity slow wave structures for multibeam microwave tube stabilization without absorber
02 p0190 A72-11575

Thermal zero signal instabilities and error reduction in devices using reluctance sensors
02 p0231 A72-12562

Signal waveform ensuring maximum reception stability on correlated noise background with peak limiting
02 p0183 A72-12760

Single frequency and mode carbon dioxide laser frequency and power stabilization by phase control with electronic servosystem
16 p2402 A72-33621

Amplitude-controlled harmonic oscillator transient response time reduction by sampling techniques in control loop without introducing distortion
16 p2369 A72-33763

Study of unsteady processes in the ionosphere and outer space by using quantum frequency stabilizers
18 p2687 A72-36853

Stabilization of relaxation oscillators with components having an S-shaped current-voltage characteristic
20 p2906 A72-38891

Signal waveform ensuring maximum reception stability on correlated noise background with peak limiting
20 p2903 A72-39066

SIGNAL TO NOISE RATIOS

PM communication systems with Gaussian and clipped noise carriers, calculating SNR
01 p0024 A72-10129

Incoherent optical communications fixed receiver passband, determining SNR for pulse time and code modulation with discrete time
01 p0024 A72-10198

Coded multiple FSK in presence of random variable phase, predicting optimum reception performance relationship to phase distribution and SNR
01 p0025 A72-10330

Bit error rate estimation for narrow band digital communication in presence of atmospheric radio noise bursts
01 p0025 A72-10334

Clutter suppression by amplitude weighted pulse trains in coherent radar, obtaining optimum weights and signal-to-clutter gain as function of Doppler frequency
01 p0030 A72-10789

Spatial alignment for low noise difference picture detection in side-looking radar imagery
01 p0129 A72-10874

Statistical model for communication probability estimate based on signal-to-interference and SNR criteria
01 p0031 A72-10997

Coherent demodulation of continuous phase binary FSK signals in additive white noise, determining error probability
02 p0174 A72-12135

Intermodulation noise in multichannel frequency division multiplex telemetry systems due to nonlinearities in transmitter-receiver links and tape recorder
02 p0175 A72-12145

Approximate signal-clutter ratio formulas for airborne pulse radar system, eliminating computer calculations
02 p0176 A72-12216

Estimation algorithm for arbitrary parameter of narrow band radio signal with unknown amplitude and phase during reception on additive normal noise background
02 p0176 A72-12218

Noisy radar signal processing by spectral analysis method
02 p0177 A72-12225

Circular polarization parasitical signal reduction in variable profile antennas by curved wire grating, noting application to solar magnetic field studies by radio methods
03 p0331 A72-13289

Submillimeter wave stratospheric emission spectra measurement by aircraft- or balloon-borne phase modulated Fourier spectrometry, noting SNR and small errors
03 p0348 A72-13399

Doubly multiplexing dispersive spectrometer, noting high SNR and Littrow mode operation
03 p0359 A72-13446

MnBi magnetic film optical memory system characteristics evaluation, considering laser power requirement, bit packing density and SNR
03 p0332 A72-13754

Correlation functions of signal and noise at output of discrete channel, determining SNR or speech intelligibility
03 p0323 A72-13891

PCM/NRZ signal band limiting effect on bit error probability, presenting SNR degradation as function of bandwidth-bit duration product and bit patterns
03 p0325 A72-14192

Near optimum limiting and blanking levels /error probability/ selection for binary signal matched filter reception in Gaussian and impulse noise, discussing performance simulation
04 p0486 A72-14485

All digital IC FM discriminator design, computing output SNR above threshold 04 p0486 A72-14489

Autocorrelation signal detection method application to spectrometry by modulation amplitude, investigating SNR 04 p0521 A72-14973

Detection characteristics of optimal interperiod processing radar pulse systems for arbitrary correlation of signal and noise fluctuations 04 p0487 A72-15145

Cross correlation model for interpreting empirical results on binaral noise masking level differences in sinusoidal signal detection, comparing with equalization-cancellation model 04 p0550 A72-15296

Antenna arrays performance optimization, emphasizing directivity and signal to noise power ratio 04 p0499 A72-15301

Strain gage system for low amplitude strain measurement, discussing SNR and installation technique 04 p0523 A72-15495

Cu-Be electron multipliers SNR restoration by removing surface contamination on dynodes by chemical etching and cleaning 04 p0524 A72-15500

Gravitational radiation short bursts detector, treating SNR by fluctuations method 05 p0715 A72-16183

Phase locked loop bandwidth, acquisition time and SNR for Doppler tracking deep space communications for Venus and Jupiter probes 05 p0629 A72-16575

SNR effect on rms bearing error by amplitude comparison for nonscanning nontracking receiving system with two antenna lobes of arbitrary shape 05 p0629 A72-16577

Three frequency IR laser signal heterodyne detection with 40-MHz if narrow-band reception, measuring SNR 05 p0669 A72-16607

Filter configuration for detecting pulse excitation smaller than KT , noting SNR and resolving time 05 p0631 A72-17075

FSK transmission experiments on uhf satellite link, noting threshold convolutional decoding contribution to SNR 06 p0773 A72-17599

Bearing estimation performance of monopulse tracking with passive linear arrays, using computer simulation for various integration times and input S/N ratios 06 p0774 A72-17809

SNR expressions for image transmission through turbid medium, showing quality dependence on energy transfer, contrast frequency and sensor phonon illumination level 06 p0774 A72-17936

Low noise IMPATT diode design for arbitrary signal levels, using Read model 06 p0787 A72-18382

Soviet book on laser communication statistical theory covering coherent and noncoherent optical signal detection and discrimination, SNR optimal reception, beam scanning, etc 06 p0777 A72-18518

Passive radio interference filtration analysis, obtaining SNR maximization by ambiguity function partial volume minimization 07 p0937 A72-18848

Nonorthogonality noise at matched radar filter output between stations operating simultaneously in same frequency band in discrete address wideband communication system, defining minimum SNR conditions 07 p0937 A72-18849

Optimal signal detection relative to Neumann-Pearson criterion invariant with respect to amplitude and random noise intensity in radio location 07 p0938 A72-19019

Mathematical expectation of angularly modulated signal in unsteady linear random noise, using Marchenko formula 07 p0939 A72-19020

Variance estimate of second order moment by nonlinear correlator in presence of additive amplitude and phase modulation and normal noise 07 p0939 A72-19021

Phase lock loop receiving system digital simulation for estimating mean time to indicate lock and probability distribution function for wide SNR range 07 p0939 A72-19065

Digital speech detector with increased voice signal and reduced noise sensitivity for satellite capacity improvement 07 p0939 A72-19067

Wideband laser communication for space applications, comparing carbon dioxide and Nd-YAG systems on basis of SNR 07 p0941 A72-19239

Concatenated coded command system for low error probabilities at moderate SNR, emphasizing spaceborne portions implementation 07 p0949 A72-19299

Conditional distribution density formation for signal-noise mixture based on learning sampling with dependent values 07 p0943 A72-19517

Parametric converter mixers with FM and AM signal and pump oscillator, investigating SNR behavior 07 p0956 A72-19658

Linear active two-port networks, considering concept of noise figures F less than 1 in signal and noise transmission 07 p0944 A72-19659

Perceived noise level correction for background noise effects based on frequency band SNR 07 p0932 A72-20170

Holographic weak signal enhancement technique in presence of strong noise for seismic and oceanographic applications 07 p0992 A72-20563

Double beam spectrophotometer with automatic gain controlled preamplifier to achieve insensitivity to signal strength change in noise at low cost 07 p0992 A72-20579

Periodic and synchronously recurrent transient signal detectability in time-varying noise environment 08 p1134 A72-21406

Small signal microwave transistors design with arsenic and phosphorus diffused emitters, comparing performance in terms of power gain-bandwidth product, maximum frequency and noise figure 08 p1142 A72-21743

Optimal signal discrimination on arbitrary noise background, choosing functional from class of integral polynomials 09 p1277 A72-22475

Phase and amplitude error effects on image reconstruction in conventional and weak signal enhancement holography 09 p1312 A72-23242

Stochastic projected gradient algorithm to maximize SNR subject under linear or nonlinear constraints, applying to detector antenna array processing 10 p1456 A72-23808

Technical standards for educational and community TV by satellite, considering picture quality requirement, modulations, SNR, threshold and fade margin, and channel width 10 p1435 A72-24034

Hot thermistor and hot-wire anemometer principles for phonocardiographic transducer design, using theory of hydraulic amplification with high SNR 10 p1430 A72-24374

Optimal antennas statistical synthesis for minimum noise power for given signal gain 10 p1436 A72-24505

Asymptotically optimal detection/discrimination algorithms for weak signals on correlated noise background 10 p1436 A72-24508

Detectors for deterministic signals in noise with rational spectral density, considering analog filter for continuous input sampling and discrete filter for point sampling 10 p1436 A72-24511

Radar detection performance calculation with post-detection integration using single valued loss and ideal curves in terms of SNR 10 p1437 A72-24689

Noncoherent detection of sinusoidal signal imbedded in clutter and Gaussian noise, obtaining probability density as function of SNR and clutter-to-noise ratio 10 p1437 A72-24691

Tuned laser radar detection and ranging of high altitude Ba ion cloud by photon counting, discussing SNR requirement 10 p1440 A72-24963

X and gamma ray astronomy with multiple pinhole cameras and a posteriori image synthesis, obtaining SNR gain 11 p1629 A72-25313

Combined probability density of amplitude and phase difference distribution of signal and noise sum in moving target selection radar systems 11 p1596 A72-26307

Probability distribution density of phase difference between noise and signal-noise sum for radar system efficiency estimation, using Bessel and Whittaker functions 11 p1596 A72-26308

Probability distribution density of amplitude difference of target signal and correlated noise sum for radar efficiency estimation 11 p1596 A72-26309

Period modulation of HF oscillation by symmetrical and asymmetrical signals applied to detection in noise 11 p1597 A72-26318

Noise factor formula of antenna matched multiple loop radio receiver input network with series connected coupled stages 11 p1598 A72-26732

Capacitive memory storage for filtration of repetitive pulse radio signals mixed with additive noise 11 p1598 A72-26734

Exposure conditions and film processing parameters effects on sensitivity, diffraction efficiency and SNR of holograms recorded with continuous and pulsed radiation sources 11 p1637 A72-26796

Holograms with high diffraction efficiency, describing bleaching experiments and SNR measurements in reconstructed image 12 p1810 A72-27887

Probability density functions for output process in frequency discriminator under action of additive mixture of fluctuating radio signal and random noise 13 p1914 A72-28411

Linear and nonlinear continuous self adaptive frequency converter filters with minimum error under SNR change 13 p1936 A72-29156

Preproduction OMEGA aircraft receivers and antennas development and flight testing, noting signal loss problems in high noise or precipitation static environments 13 p1998 A72-29198

Narrow band linear filter output SNR relationship to orthogonal radiating elements system directional gain and radiation patterns 13 p1931 A72-29281

PSK signal cross-correlated receiver output SNR in presence of random misalignments with respect to carrier frequency and arrival signal time 13 p1921 A72-29283

Multidimensional non-Gaussian signals filtration in presence of time correlated noise with discrete values of argument 13 p1937 A72-29638

Digital FM signal receiver with postdetector integration, determining error probability as function of input SNR and noise stability 14 p2084 A72-30332

HF radio signal reception behavior near maximum usable frequency during evening and at midnight, noting SNR 14 p2085 A72-30656

Incoherent optical communications fixed receiver passband, determining SNR for pulse time and code modulation with discrete time 15 p2195 A72-31622

RF receiver predetection SNR measurement from average postdetection signal-plus-noise and noise-only voltages, tabulating computed results 15 p2196 A72-31782

Statistical analysis of random mismatched tapped delay line filters effect on binary phase shift keying pulse compression codes peak-to-sidelobe and SNR 15 p2196 A72-31792

Asymptotic receiver characteristics, discussing signal detection in spherically invariant noise 15 p2196 A72-31871

Laser communication lines in atmospheric ground layer, comparing SNR for direct-reception and super-heterodyne video systems 15 p2247 A72-31887

Modulated laser beam record wideband signals on photographic film, discussing noise sources and compensation methods for SNR improvement 15 p2248 A72-32039

Laser Doppler velocimeter designs for atmospheric applications, discussing illuminating techniques, SNR, performance comparison and system selection 15 p2327 A72-32051

Correlation functions of signal and noise at output of discrete channel, determining SNR or speech intelligibility 15 p2202 A72-32702

Laguerre filters parameters choice for correlator input networks application, noting output SNR improvement 16 p2368 A72-33089

Jet turbulence interaction and velocity effects on noise level of proportional fluid amplifiers 16 p2350 A72-33177

Gaussian beam laser Doppler velocimeter system under high scattering center concentrations and steady flow conditions, deriving noise spectral densities and SNR 16 p2390 A72-33210

Asymptotic formula for approximation of mean cycle-slip time of phase locked loops with low SNR and steady state phase error 16 p2371 A72-33211

FM/FM multiplex receiver with carrier and subcarrier demodulators, deriving average clip rate, output noise spectrum and SNR from Rice model 16 p2362 A72-33212

Noise stability of frequency-time adaptive transmission systems for discrete information, using resolving feedback circuits 16 p2363 A72-33266

SNR expressions for image transmission through turbid medium, showing quality dependence on energy transfer, contrast frequency and sensor phonon illumination level 16 p2426 A72-33777

Additive noise effect on accuracy of integrating digital voltmeters using pulse frequency and pulse time converters

16 p2370 A72-33955

Holograms with high diffraction efficiency, describing bleaching experiments and SNR measurements in reconstructed image

16 p2395 A72-33996

Noise-to-carrier ratio and rms frequency deviation evaluation for X band Gunn and Si and GaAs avalanche diode oscillators

16 p2370 A72-34177

A fast numerical method for determining the optimum SNR of an array subject to a Q factor constraint.

17 p2514 A72-34372

Signal-to-noise performance of cryogenic electrically small receiving antennas.

17 p2525 A72-34375

Sampled imagery transfer function compensation by inverse function, noting truncation effects on processing array SNR performance

17 p2521 A72-34412

Avalanche diode oscillators.

17 p2526 A72-34563

IR carbon dioxide laser radar with heterodyne detection, measuring SNR and atmospheric scattering coefficients for various weather conditions

17 p2516 A72-35192

IR heterodyne radiometer SNR and spectral resolution, noting application to solar physics and air pollution detection

17 p2555 A72-35196

Measures of effectiveness for special signal detectors of simple structure

17 p2516 A72-35222

Error rate of phase-shift keying in the presence of discrete multipath interference.

17 p2516 A72-35334

Output fluctuations of CW-pumped Nd:YAG lasers.

17 p2564 A72-35345

Optimal number of parallel transistor connections in feedback amplifier to improve SNR

18 p2665 A72-36108

Output signal-to-noise ratio of a nonlinear device and bandpass filter.

18 p2666 A72-36334

Adaptive nonlinear optimization of the signal-to-noise ratio of an array subject to a constraint.

18 p2660 A72-36507

Variants of conventional FM demodulation having the aim of improving poor signal-to-noise ratios.

18 p2661 A72-36843

Evaluation of the basis parameters of a frequency-code receiver with a generalized differential circuit.

19 p2771 A72-37304

Nonautonomous phase system of equations with a small parameter, containing invariant tori and rough homoclinic curves

19 p2828 A72-38579

Design of band-limited signal with no intersymbol interference - An extension of sampling function.

19 p2767 A72-38606

Exponentially weighted noncoherent integration of pulsed signals in the presence of Gaussian noise and random impulse noise.

19 p2767 A72-38623

Additive fluctuation noise rejection during the quasi-coherent reception of phase-manipulated signals

20 p2900 A72-38896

The theory and measurement of the signal-to-noise ratio of second generation image intensifiers.

20 p2922 A72-39039

Incoherent radiation imaging system analysis from detector-display characteristics, target response function and noise characteristics

20 p2922 A72-39044

Effects of errors in the direction of incidence on the performance of an adaptive array.

20 p2904 A72-39786

Radio astronomical event visible image generation by electro-optical processing comparing SNR performance and electronic complexity with conventional technique

20 p2904 A72-39787

A unified analysis on laser Doppler velocimeters.

21 p3061 A72-40211

Theoretical model prediction for matched filter selectivity and noise effects on strained object deformation in optical correlation applications, comparing results with experiments

21 p3053 A72-40611

Optical communication channel optimization with binary signals preamplified in optical parametric amplifier, noting amplifier gain and SNR

21 p3016 A72-40783

Signal-to-noise ratio of a photodetector with a virtual cathode

21 p3055 A72-40802

Feedback quantization noise effects on differential PCM systems, showing SNR relation to noise optimized prediction

21 p3017 A72-40860

Reciprocal of normalized mean square error [MSE] and output SNR as performance measures in optimal and suboptimal demodulators

21 p3017 A72-40863

Suppressed clock pulse duration modulation for noisy voice communication channels with hard limiting satellite repeaters, discussing system design and test data

21 p3020 A72-40898

Intermodulation distortion of FDM-FM in injection locked oscillator.

21 p3020 A72-40899

Preliminary frequency selection during matched signal filtering

21 p3021 A72-40941

Extending the range of attenuation measurements.

21 p3022 A72-40999

Statistical estimation of the signal-to-noise ratio beyond a linear detector

21 p3022 A72-41073

Signal voltage density, pulse shape and noise power spectrum analysis of matched filter configurations in IR scanning system model

21 p3033 A72-41078

SNR improvement by negative feedback and deterioration by positive feedback in amplifiers, discussing input circuit thermal noise

21 p3034 A72-41123

Optimum spatial filter for an anisotropic background-noise.

21 p3036 A72-41839

Threshold noise of an FM receiver at small signal-to-noise ratios

22 p3154 A72-42236

ASW aircraft magnetic anomaly detection (MAD)/system range limitation due to residual maneuver noise, discussing real time compensation for geomagnetic gradient interference

22 p3177 A72-42322

Noise-cancelling signal difference method for optical velocity measurements.

22 p3177 A72-42394

FM receiver noise figure measurement - A simplified method.

22 p3155 A72-42704

Application of digital techniques to the measurement of PCM signal power.

22 p3155 A72-42705

Optimal discrimination rule for dual frequency radar targets with inadequate echo signal and background noise level parameters

23 p3263 A72-43429

Influence of a nonlinearity in a coherent accumulator of pulse signals on the gain in the signal-to-noise ratio

23 p3264 A72-43762

Reciprocal mean-square error and signal-to-noise ratio as distinct performance measures in below-threshold communication.

23 p3265 A72-44177

Performance characterization for L-orthogonal signal transmission and detection, discussing tradeoffs between error probability, SNR and bandwidth by numerical evaluation

23 p3265 A72-44180

Linear antenna directivity loss for fluctuating signal reception, noting effects of signal to noise ratio and antenna length

23 p3265 A72-44204

Sequential analysis algorithm for data channel detection of received signal represented by Poisson sequence of quantum transitions under large SNR

23 p3266 A72-44206

Linear filtration of random signals based on the criterion of maximum signal-to-noise ratio

23 p3273 A72-44215

Effectiveness of certain easily realized rank detection algorithms for noise-masked signals

23 p3266 A72-44216

Optimal signal processing in systems with multiple reception elements/channels/

23 p3266 A72-44219

Optimum reception algorithms in communication systems with decision feedback in presence of noise in forward and return channel

24 p3379 A72-44747

Amplitude dependence of frequency in oscillators.

24 p3385 A72-44964

On the S/N-characteristics in PCM systems for a class of signals with representative amplitude distributions.

24 p3380 A72-45282

Noise characteristics of a digital system of light-beam deflection

24 p3410 A72-45323

Evaluation of the performance of an ionospheric sounder with incoherent scatter

24 p3381 A72-45768

SIGNAL TRANSMISSION

NT BIOTELEMETRY

NT DATA TRANSMISSION

NT DOUBLE SIDEBAND TRANSMISSION

NT IONOSPHERIC F-SCATTER PROPAGATION

NT IONOSPHERIC PROPAGATION

NT MESSAGES

NT MICROWAVE ATTENUATION

NT MICROWAVE TRANSMISSION

NT MULTIPATH TRANSMISSION

NT PCM TELEMETRY

NT PULSE FREQUENCY MODULATION

TELEMETRY

NT RADAR TRANSMISSION

NT RADIO TELEMETRY

NT RADIO TRANSMISSION

NT SATELLITE TRANSMISSION

NT SHORT WAVE RADIO TRANSMISSION

NT SINGLE SIDEBAND TRANSMISSION

NT TELEMETRY

NT TELEVISION TRANSMISSION

NT TRANSEQUATORIAL PROPAGATION

Analogue FM multiplex signal intermodulation formula based on time-variable electromagnetic waves tropospheric scatter propagation

01 p0027 A72-10411

Complete suppression of one signal in dual frequency mode of TWT operation, showing electron beam current and accelerating potential dependence on signal amplitude

02 p0189 A72-11565

Low loss wideband characteristics of groove and H guides for efficient signal transmission

02 p0190 A72-11679

Spatial pulse modulation of optical signals for use in picture transmission, cinematography and holography

03 p0358 A72-13440

Soviet book on linear automatic control systems with variable parameters covering pulse transfer function determination algorithms, signal transmission characteristics and systems stability

03 p0339 A72-14245

Transient signal propagation in unbounded time-spatial dispersive hot plasmas, using convolution integral equations

04 p0490 A72-15402

Long range ionospheric guided hf signal propagation from low orbiting San Marco 1 and 2 satellites

04 p0492 A72-15440

Moving object trajectory determination by a posteriori Poisson signal transmission analysis with random parameters

05 p0626 A72-16205

Thermal signal propagation in flowing fluid, plane, line and point sources of varying heat, calculating temperature distribution with conduction and convection heat transfer equation

05 p0746 A72-16299

Distortion measuring equipment for determining FM signal transmission errors due to amplitude and group delay frequency response deficiencies and AM/PM conversion

05 p0626 A72-16299

Closed form solution for Doppler satellite navigation for arbitrary orbits with ellipsoid Earth model and straight path signal transmission

05 p0686 A72-16561

Two dimensional space charge wave propagation in semiconductors with anisotropic small signal mobility, investigating stability

05 p0632 A72-17097

Nonlinear scattering of microwave signals incident on unmagnetized cold plasma column

06 p0859 A72-17547

Ionospheric movements measured by frequency spectra of signals incoherently scattered by ionospheric electrons

06 p0808 A72-18087

Signal design for coherent M-ary communication systems by stochastic gradient algorithm for minimizing error rate

07 p0959 A72-19285

Linear active two-port networks, considering concept of noise figures F less than 1 in signal and noise transmission

07 p0944 A72-19659

Signal statistical model parameter evaluation by selection of operators in form of dimensionless quantile ratios

08 p1130 A72-20724

Scattered signal power approximation during ionospheric oblique backscatter sounding, using geometrical optics method

08 p1130 A72-20733

Orthogonal functions representation of received signals in ideal signal sequences transmission in linear systems with matched filters and frequency band limitation

08 p1132 A72-21326

Fluctuating signal propagation in plane laminar medium acting as spatial frequency filter, determining electron density distribution curvature radius in plasma layers

08 p1135 A72-21732

Multichannel integral commutators with MOSFET as switching elements, calculating transmission errors

10 p1449 A72-24288

Continuous signals discrete values for analysis and synthesis of control systems with variable parameters, obtaining recurrent formulas and error estimate

11 p1609 A72-25445

Conversion losses as function of signal power and circuit impedance in narrow band triode frequency converter under large amplitude operating conditions
11 p1598 A72-26733

Maximum transmission delay in microwave TWT delay lines as function of electron beam size, current, shape and velocity distribution
12 p1782 A72-27436

AM/PM conversion and transfer in nonlinear signal transmission systems, calculating coefficients as function of multicarrier powers for intelligible crosstalk
12 p1782 A72-27554

Signal propagation along homogeneous drifting electron beam focused by strong magnetic field, obtaining phase velocity and space charge density
13 p1914 A72-28373

Coherent brain model for evolution mechanisms of biological resonance in neuron network signal flow
13 p1908 A72-28455

Pulse signal transmission through bandpass error free wideband PCM communications systems
13 p1919 A72-29055

Minimum phase systems application for linear estimation of steady random sequences of signals, obtaining transfer function for optimal frequency filter
13 p1937 A72-29999

Given motion realization in presence of constantly acting perturbations by pulsed correction, applying to signal transmission accuracy implementation
13 p2007 A72-30082

Fluid amplification principles, discussing bistable and proportional amplification, signal transmission and transduction to and from fluid signals
[ASME PAPER 72-DE-20] 14 p2073 A72-30864

Signal transmission through LSI logic circuit chains, discussing time delay measurement by step function testing
15 p2211 A72-31846

Discrete frequency modulated signals with frequency shifted identical envelope pulses, discussing transmission, construction and correlation functions
15 p2197 A72-31878

Whistler mode VLF signal transmission in ground transmitter and magnetically conjugate zones, observing spectrum broadening and AM in magnetosphere
15 p2197 A72-31919

Digital communication system for analog signal transmission by digital modulation techniques, presenting detection schemes
15 p2201 A72-32565

Propagation of pulsed-carrier signals in random media.
17 p2514 A72-34380

Optimal predistortion efficiency for multiplicative disturbances in radio signal transmitting channel, noting Rayleigh distribution of signal fluctuations
17 p2518 A72-35778

Wiener filter design for optimal processing of AM signals distorted during transmission through randomly dispersive medium
19 p2763 A72-37288

Methods using Walsh functions for multiplexing and transmitting signals
19 p2765 A72-37942

Transmission of a fluidic signal at intermediate distances.
19 p2754 A72-38046

Development of coordinate signal transmission and data processing equipment for operation supervision in space travel
19 p2765 A72-38305

Geophysical signal statistical model parameter evaluation by selection of operators in form of dimensionless quantile ratios
19 p2765 A72-38352

Scattered signal power approximation during ionospheric oblique backscatter sounding, using geometrical optics method
19 p2766 A72-38361

Transmission of two partially time coincident linearly frequency modulated signals through limiter-filter system, noting distortion and satellite signals generation
19 p2766 A72-38419

A possible anatomical basis for descending control of impulse transmission through the dorsal horn.
21 p2998 A72-40578

Signal transmission and detection in differentially encoded coherent multiple phase shift keyed digital communication systems, discussing carrier suppression-induced resolution ambiguity
21 p3017 A72-40861

Analysis of a procedure for the transmission of low-frequency signals in time-compressed, analog form
21 p3023 A72-41399

Optimal frequency-difference communications system with manipulated amplitudes
22 p3154 A72-42237

Performance characterization for L-orthogonal signal transmission and detection, discussing tradeoffs between error probability, SNR and bandwidth by numerical evaluation
23 p3265 A72-44180

Semaphore channel signaling reliability, presenting error protection and correction system
24 p3381 A72-45770

SIGNALS
Inflight validation of laboratory scaled-down simulation experiments on optimal hierarchy of colors for markers and signals
[AD-737901] 08 p1147 A72-21582

Rescue signaling devices design and operation, discussing pinpoint markers, rocket boosted panel markers, strobe units, antennas and balloon marker
08 p1112 A72-21584

SIGNATURE ANALYSIS
Backscatter hf radar signature analysis in relation to medium scale traveling ionospheric disturbances, using computer ray tracing technique
01 p0030 A72-10837

Sonic boom pressure signatures during F-104 overflights at Mach 1.3 and 30,000 ft, explaining variations by atmospheric turbulence
01 p0006 A72-11158

Airborne sensors terrain classification, considering sample points clustering approach and signature analysis
02 p0227 A72-11844

Sonic boom signature by bicharacteristic method, correcting zeroth order /free stream/ characteristics to obtain solution to compressible fluid exact equations of motion
[AIAA PAPER 72-195] 05 p0652 A72-16907

SST operational maneuver effects on sonic boom, discussing steady flight and acceleration-to-cruise pressure signatures
[AIAA PAPER 72-196] 05 p0613 A72-16981

Atmospheric effects on remotely sensed earth surface signature recognition, considering scattering, absorption and emission effects
[DGLR PAPER 72-130] 06 p0809 A72-18233

Maneuvering aircraft sonic boom propagation and signatures prediction in stratified atmosphere by geometric acoustic method
08 p1110 A72-21904

Crop classification by airborne multispectral observations, suggesting sample regions selection method for spectral signatures identification based on statistical similarities
11 p1628 A72-26985

Remote sensing system for oil pollution spectral signature properties, analyzing UV, IR, visible light, radar and microwave data
15 p2242 A72-32624

A positive signature for the recognition of gravitational radiation.
23 p3337 A72-43943

SIGNATURES
NT MAGNETIC SIGNATURES
NT RADAR SIGNATURES
NT SPECTRAL SIGNATURES

SIGNIFICANCE
Significance criteria for comparing strength parameter against expectation from random group of vectors in variance matrix applications
09 p1341 A72-23023

SIGNS (SYMBOLS)
U SYMBOLS

SIGNS AND SYMPTOMS
NT ASPHYXIA
NT BRADYCARDIA
NT HEADACHE
NT LEUKOPENIA
NT VERTIGO

Arrhythmias relation to coronary artery disease, discussing conduction defects, sudden death prodromata and prevention and digitalis as antiarrhythmic agent
02 p0157 A72-11476

Propranolol as adrenergic beta receptor inhibiting agent for hyperthyroidism symptom amelioration
08 p1118 A72-21550

Blood serum proteins thermal stability in patients with vegetative vascular and neuroendocrine syndromes, discussing AT effects
09 p1266 A72-22877

Anatomy, pathology, etiology, diagnosis and therapy of posterior tibial nerve compression lesion, discussing tarsal tunnel syndrome
21 p3005 A72-40396

Toxicity of rocket fuels
24 p3433 A72-44781

SIKHOTE-ALIN METEORITE
Sikhote-Alin meteorite shower individual specimens mass distribution with respect to distance from crater center
14 p2153 A72-30496

Sikhote-Alin meteorite shower individual specimens mass distribution with respect to distance from crater center
19 p2864 A72-38325

Instrumental neutron-activation analysis of the troilite of the Sikhote-Alin meteorite
22 p3225 A72-42472

SILANES
NT CHLOROSILANES

Adverse environmental effects on epoxy composites resin-glass interface properties, investigating epoxy-compatible silanes contribution to composite performance
08 p1194 A72-21696

SILENCERS
French jet aircraft noise reduction research facilities, discussing in-flight and overfly noise measurements, various silencer configurations and Concorde engine tests
03 p0406 A72-13680

SILICA
U SILICON DIOXIDE
SILICA GLASS
Fused silica optical transmittance at elevated temperatures during high energy electron bombardment, noting optical absorption at short wavelengths
01 p1013 A72-11357

Silicate glasses fatigue in dynamic and static tests, discussing fracture stress dependence on time of loading
05 p0681 A72-16422

Static fatigue of borosilicate glass, fused silica and polycrystalline alumina, presenting log stress vs log failure time plots
09 p1335 A72-22398

Tensile plastic flow and fracture behavior of PdSi based alloys in glassy microcrystalline and crystalline states, noting shear deformation bands
09 p1339 A72-23382

Refractory glass formulation principles, compositions and properties, discussing vitreous silica production
10 p1501 A72-24727

Cation self diffusion coefficients in potassium oxide-strontium oxide-silicon dioxide glass, using radioactive tracers and sequential etching technique
13 p1912 A72-28625

Simulated Nimbus orbital electron, proton and UV radiation effects on wide bandpass glass and narrow bandpass thin film interference filters and fused silicas
15 p2277 A72-32157

Time-temperature correlated phase transformations in zirconia nucleated magnesium-aluminum-silicon oxide glass ceramics for isothermal heat treatment
16 p2413 A72-33205

Investigation of radiation paramagnetic defects in alkaline-silicate glass subjected to the action of high quasi-hydrostatic pressures - Structure of hole defects
24 p3417 A72-45421

SILICATES
NT ALUMINUM SILICATES
NT ANDESITE
NT ARAGONITE
NT ENSTATITE
NT FAYALITE
NT FELDSPARS
NT FLUOROSILICATES
NT FORSTERITE
NT GARNETS
NT KAOLINITE
NT PYROPHYLLITE
NT PYROXENES
NT SODIUM SILICATES
NT TALC
NT YTTRIUM-ALUMINUM GARNET
NT YTTRIUM-IRON GARNET

Silicate rocks mapping from aerial IR data, discussing method for discriminating emission from background radiation
02 p0208 A72-11787

Chemical composition and morphology of silicate spherules, comparing to lunar rocks, meteorites and tektites
02 p0280 A72-12283

Silicate microspherules distribution anomaly in peats of Tunguska meteorite fall area
02 p0281 A72-12293

IR spectra of rock forming terrestrial and meteoritic silicates important in cosmic silicate dust
02 p0284 A72-12635

Xe and Kr abundance and isotopic composition in silicate inclusions of iron meteorites
03 p0435 A72-13690

Microscopic and electron microprobe analyses of silicate melt inclusions and glasses in lunar soil fragments from Lunik 16 core sample
09 p1379 A72-22255

Xenolithic origin for silicate inclusions in anatase of Landes meteorite from West Virginia
13 p2036 A72-28753

Broad scale remote mapping of spectral composition of silicate rocks from thermal IR scanner data
14 p2099 A72-30321

Chondrule like spherules from supercooled molten oxide and silicate droplets by carbon dioxide laser heating compared with meteoritic chondrules
15 p2303 A72-31306

High energy storage laser material Nd-doped silicate oxyapatite refractivity temperature dependence characteristics measurement
15 p2249 A72-32167

Accretionary processes in the early solar system - An experimental approach.
17 p2618 A72-35836

SILICIDES

NT DISILICIDES

Nb alloy silicide coating thickness data correlation by thermoelectric, metallographic and pointed micrometer techniques, discussing state of art in thickness control, penalties and substrate independence

01 p0075 A72-10750

Field repair of fused slurry silicide coating for oxidation protection of Nb alloys in space shuttle environment

01 p0075 A72-10759

Silicide precipitation in Ti-Zr-Al-Si system, discussing microstructure correlation with mechanical properties

03 p0374 A72-13927

Enthalpy measurements of niobium silicides at 1200-2200 K by mixing method, using isothermal calorimeter

06 p0833 A72-18431

Metal silicide phase formation for Nb, Ta, Mo and W, examining Si diffusion and transport processes

11 p1664 A72-26859

Transition metals silicides additions effect on sintering and oxidation resistance at high temperatures of Ti and Zr diborides

11 p1665 A72-26874

Fusion silicide protective coatings performance for Ta alloys under simulated reentry conditions, noting oxidation rate, ductile brittle bend transition temperature and mechanical properties

[ASM PAPER W 72-13,6] Vanadium emission spectra studies of energy band structure in vanadium silicides, showing p-subzone splitting

13 p1980 A72-29798

Thermomechanical manipulation of precipitate shape in a titanium-base alloy.

22 p3194 A72-43044

Isobar-isothermal potentials, entropy and formation heat of chromium silicides from thermoelectromotive force measurements of high temperature galvanic elements

23 p3298 A72-43286

SILICON

GaAs, Si and alumina performance as substrates in integrated microwave circuits

01 p0046 A72-10700

Single crystal Si defect accumulation and transition to amorphous state under Xe, Ar, Ne, O and P ion irradiation, using EPR

02 p0269 A72-12884

Solar active regions and flares X ray spectroscopic data, observing ionized silicon emission lines

03 p0423 A72-13217

Vacuum deposited films on CsI, AgCl, TiBr and TiCl for IR antireflection coatings on silicon

03 p0380 A72-13431

Li-diffused Si compared to conventionally doped materials under neutron irradiation, considering carrier removal

03 p0403 A72-14078

Annealing defects in n-type silicon, observing anomalous heat treatment temperatures of A and E centers

04 p0560 A72-14529

Isothermal annealing measurements of zero-phonon line luminescence at 0.97 eV in electron irradiated Si, obtaining activation energy

04 p0560 A72-14546

Early solar system nucleosynthesis of Al 26, discussing silicon and carbon burning and spallation

04 p0567 A72-14912

Solar silicon abundance from low excitation forbidden Si I lines

04 p0579 A72-15326

GaAs and Si millimeter wave Schottky barrier mixer diodes fabrication, noting low noise broadband mixer/preamp

06 p0790 A72-18486

Low temperature Si photoconverters transparent in IR solar spectrum tested on Cosmos satellites

07 p0915 A72-20616

Background noise in amplification and oscillation in Si and GaAs avalanche diodes

09 p1287 A72-23119

Radiation induced extrinsic photoconductivity in Li doped Si, examining localized energy levels in forbidden gap

09 p1372 A72-23238

Piezoresistance magnitude and temperature dependence changes of electron irradiated n-type silicon due to oxygen vacancy complex /A center/

09 p1372 A72-23239

Microwave diagnostics of P doped Si semiconductor crystal prism determining relation between complex permittivity and reflection factor by variational method

10 p1450 A72-24404

Si burning in stellar explosions, discussing initial composition and neutron enrichment

10 p1544 A72-24666

Photoionization cross sections for atoms and ions of Al, Si and Ar on basis of Hartree-Fock bound-electron

and close coupling approximation free-electron wave functions

10 p1516 A72-24669

GaAs solar batteries for spacecraft power supplies, comparing effectiveness with Si cells for optimum utilization

11 p1578 A72-25940

Metal silicide phase formation for Nb, Ta, Mo and W, examining Si diffusion and transport processes

11 p1664 A72-26859

French R and D programs on Si and various thin film photovoltaic solar cells, considering efficiency, reliability, and weight and cost reduction problems

12 p1756 A72-28002

German Si and polycrystalline solar cells development survey, discussing interconnection techniques, module design and filter applications for performance improvements

12 p1756 A72-28003

Li dopant radiation damage inhibiting effect on electron irradiated n-type silicon, discussing EPR and photoconductivity experimental results

12 p1856 A72-28023

Lithium diffusion into silicon by evaporation and homogenization technique, discussing dislocations and oxygen effects from aging in Ar at 150 C

12 p1757 A72-28025

Point defects investigation in Si and Ge by diffusion techniques, precipitation from supersaturated solid solutions, quenching from high temperatures and plastic deformation

12 p1856 A72-28053

Irradiation produced defects and electrical properties of n and p-type Si, discussing radiation damage due to neutron and ion implantation

12 p1857 A72-28058

Radiation damage in carbon doped silicon irradiated at low temperatures by 2 MeV electrons, noting isotope shifts

12 p1857 A72-28059

EPR for point defects produced in Si by fast neutron irradiation, emphasizing damage cluster model

12 p1858 A72-28060

Recombination luminescence in irradiated Si, investigating uniaxial stress and temperature variations effects

12 p1858 A72-28061

Recombination luminescence in irradiated Si, investigating thermal annealing and Li impurity effects

12 p1858 A72-28062

Li defect interactions in electron irradiated n-type single crystal Si from electron paramagnetic resonance measurements

12 p1858 A72-28063

Introduction rate and annealing of defects produced in Li-diffused float zone n-type Si by 30 MeV electrons and fission neutrons

12 p1858 A72-28064

Surface damage equations for heavy ion irradiated Si and GaAs single crystals in terms of incident fluence

13 p2020 A72-28430

Forward voltage vs temperature characteristics for Si planar p-n junction diodes, determining zero temperature energy gaps for silicon, germanium and GaAs

13 p1933 A72-29824

Si phase identification in super alpha Ti alloys, using electron transmission microscopy and diffraction analyses

14 p2120 A72-30616

Si solar cell efficiency in synchronous orbit radiation field increase via improvement in diffusion profile, low resistivity material and diode characteristics

15 p2183 A72-32131

Silicon dislocation density relationship to solar cell current loss at low temperature, presenting temperature-diffusion length and I-V characteristics

15 p2183 A72-32132

Electron trapping data in neutron irradiated high purity Si, using space charge limited current measurements

15 p2294 A72-32514

Surface defects evaluation on GaAs and Si wafers by metallographic and electrochemical techniques

15 p2296 A72-32758

Thermally stimulated current measurement application to Ag doped Si semiconductor for energy level and electron capture cross section determination

16 p2441 A72-32859

Be doped p-type Si piezoresistance and hole transport properties dependence on temperature, crystal orientation and doping concentration

16 p2442 A72-33834

Comparison of infrared and activation analysis results in determining the oxygen and carbon content in silicon.

17 p2511 A72-35330

Comments on thermal cycles of silicon power transistors

18 p2667 A72-36794

Measurement of carrier lifetime in the base of silicon diodes - Application to the control of manufacturing techniques.

18 p2669 A72-37108

Study of the spectrally variable silicon Ap star 56 Ari

19 p2862 A72-38055

Interaction of titanium diboride with titanium disilicide and silicon at high temperatures

19 p2819 A72-38284

Subthreshold radiation effect in silicon

20 p2959 A72-38953

Four-terminal Si controlled switches, discussing negative resistance and linear amplification I-V characteristics and applications in oscillators and modulators

20 p2907 A72-39274

Harmonic oscillation characteristics of avalanche Si diode with nonlinear and negative resistance characteristics

20 p2908 A72-39705

Differential negative resistance /DNR/ in n-channel MOSFETS of silicon.

20 p2961 A72-39711

Effects of impurities on gamma-irradiated silicon crystal examined by photovoltaic effect of p-n junction diode.

21 p3097 A72-40693

Pure and compensated Ge and Si far IR spectral properties at liquid He temperatures for bolometer detector application

21 p3013 A72-40822

Thermally-stimulated current from the gold acceptor trapping level in silicon.

21 p3097 A72-40996

Influence of irradiation by 1.2-MeV electrons on the electrophysical properties of p-Si single crystals grown in a hydrogen atmosphere

21 p3098 A72-41686

I-V, spectral and temperature characteristics of autophotocathode emission in p-type silicon cathodes with varying acceptor concentrations

21 p3098 A72-41692

High value thin-film-on-silicon resistors for hybrid applications.

22 p3160 A72-42825

Physical and electrical properties of thin-film barium titanate prepared by RF sputtering on silicon substrates.

22 p3215 A72-42999

Physicochemical problems in silicon and germanium heat treatment, covering solubility and solid solutions stability and saturation variation with temperature

23 p3324 A72-43687

SILICON ALLOYS

Silicide precipitation in Ti-Zr-Al-Si system, discussing microstructure correlation with mechanical properties

03 p0374 A72-13927

Low temperature heat capacity of chromium silicide, observing superconducting transition and magnetic susceptibility

03 p0377 A72-14024

Fe-Cr-Al and Fe-Cr-Si type ferritic steels, investigating additives effects on ductile-brittle transition temperature

05 p0672 A72-16012

Al and Al-Si alloy thermal expansion at low temperatures, noting near-eutectic crystalline composition

07 p1019 A72-20156

Internal oxidation behavior of Cu-Cr-Si ternary alloys microstructure comparison with Cu-Si binary alloys, discussing oxide-matrix interface nucleation

07 p1021 A72-20439

Na additions effects on Si growth velocity and morphology in Al-Si alloys, considering coupled zone adsorption mechanism

13 p1975 A72-28664

Modified Al-Si eutectic solidification behavior and microstructure, investigating LF mechanical vibration effects

14 p2120 A72-30617

Ti-Si system phase diagram and equilibrium states, noting crystal lattices and thermograms

14 p2123 A72-30986

Phase diagrams of rare earth ternary alloys with transition metals and Si, noting semiconductor properties

15 p2289 A72-31189

Stabilization of laves and intermediate phases in Nb-Fe-Si and Nb-Co-Si systems

16 p2409 A72-33805

Radiographic examination of rhenium-aluminum-boron and rhenium-silicon-boron ternary systems

19 p2822 A72-38679

Effects of modification and additional elements on the solidification of Al-Si alloy - Studies on the solidification of Al-Si alloys in a shell mold. II.

21 p3067 A72-40937

Investigation of phase equilibria in alloys of silicon with molybdenum and titanium

22 p3188 A72-42150

Effect of the process of crystallization of the liquid phase under pressure on the properties of Silumil

22 p3192 A72-42959

Physical properties and electronic structure of /V1-x Crx/3Si ternary alloys

22 p3192 A72-43014

Superconducting transition temperature increase in Nb-Al-Si alloys as function of composition under tetragonal lattice crystallization

22 p3192 A72-43020

SILICON CARBIDES

Materials stability testing in high temperature propane-butane combustion product flow, selecting compact silicon carbide for structural use in redox medium

02 p0251 A72-12866

Alkali ion scattering by NbTi alloy and SiC and components, comparing scattering coefficients

03 p0401 A72-13424

Trimethylchlorosilane film boiling for silicon carbide deposit on vertical heated tungsten filaments, investigating mass transport rate

04 p0595 A72-14600

Ti-alloyed SiC based material microstructure investigation by X ray metallography, optical and electron microscopy

08 p1188 A72-22099

Refractivity measurement of pure hexagonal structure 2H SiC over visible range, determining birefringence from curve fitting of data to Cauchy dispersion equation

09 p1309 A72-22603

Recrystallized silicon carbide and reaction bonded silicon nitride as construction materials for gas turbine engine components, describing thermal and mechanical properties

[ASME PAPER 72-GT-20] 11 p1673 A72-25619

Dense silicon nitride and carbide ceramics for gas turbines, discussing critical properties for thermal stress calculation

[ASME PAPER 72-GT-56] 11 p1674 A72-25647

Low temperature solid state phase transformations in 2H silicon carbide single crystals, noting time and temperature dependence

12 p1854 A72-27276

Cubic SiC film growth rate on Si substrate by methyltrichlorosilane decomposition in hydrogen flow, noting dependence on mixture flow rate and temperature

12 p1860 A72-28114

Microfiber extrusion of plasticized mixtures based on titanium and silicon carbides, showing optimum extrusion rate deformation and strengthening

13 p1967 A72-30102

Refractory fiber metal reinforcement and matrix incorporation, considering SiC fiber reinforced Al

14 p2107 A72-30532

Silicon carbide rotating rectifier alternator with solid lubricated bearings for high altitude environments, noting applicability to supersonic aircraft

17 p2498 A72-35565

High strength alumina, boron, silicon carbide and graphite reinforcing fibers for composite materials

17 p2572 A72-35656

Oxidation resistance at high temperatures of refractory materials based on silicon nitride and carbide in various concentrations, showing time and temperature dependence

18 p2703 A72-36096

Aluminum oxide and silicon carbide whiskers fabrication by homogeneous gas reaction process, discussing gas composition, temperature and substrate effects on production yield

20 p2940 A72-39440

SILICON COMPOUNDS

NT ALUMINUM SILICATES

NT ANDESITE

NT ARAGONITE

NT CHLOROSILANES

NT COESITE

NT DISILICIDES

NT ENSTATITE

NT FAYALITE

NT FELDSPARS

NT FLUOROSILICATES

NT FORSTERITE

NT GARNETS

NT KAOLINITE

NT ORGANIC SILICON COMPOUNDS

NT PYROPHYLLITE

NT PYROXENES

NT QUARTZ

NT SILANES

NT SILICATES

NT SILICIDES

NT SILICON CARBIDES

NT SILICON DIOXIDE

NT SILICON NITRIDES

NT SILICON OXIDES

NT SODIUM SILICATES

NT TALC

NT YTTRIUM-ALUMINUM GARNET

NT YTTRIUM-IRON GARNET

Mechanical and thermochemical erosion during ablation of silicophenolic material

04 p0597 A72-15554

Hydrated iron silicon fluoride internal motion pressure dependence examined by wideline and NMR

techniques, noting corrections of second moments for bulk paramagnetic effects

13 p1914 A72-30061

SILICON CONTROLLED RECTIFIERS

Series inverter silicon controlled rectifier 2800 watt dc power supply, noting high efficiency, low weight and stable voltage regulation

01 p0008 A72-11064

Transcendent Si power rectifier with high current and power dissipation capacity, discussing design, fabrication and performance tests

08 p1111 A72-21413

Metal inert gas (MIG) welding of thin sheets, using Si controlled rectifier power source

09 p1320 A72-23627

Condenser charging by dc-dc converter consisting of SCR series inverter, transformer and rectifier-filter circuit, considering power consumption

11 p1577 A72-25278

SCR trigger circuits design generating short control pulses for converters based on SCR elements, presenting circuit diagrams

11 p1603 A72-25280

Characteristics of nonredundant auxiliary and prime propulsion power processors for electron bombardment ion thruster in communication satellites, discussing modular transistorized and SCR systems

[AIAA PAPER 72-518] 13 p2027 A72-28980

A digital computer simulation model for an SCR dc to dc voltage converter.

19 p2754 A72-38267

SILICON DIOXIDE

NT COESITE

NT QUARTZ

Silica based surface insulation material for space shuttle thermal protection system, discussing cyclic tests in simulated environment and fiber purity effects on crystallization

01 p0091 A72-10764

Transparent fused silica wall irradiation induced optical absorption and heat deposition in nuclear light bulb engine

01 p0103 A72-11356

Vacuum UV irradiation of silicon dioxide, discussing positive charging for photon energies above threshold for electron-hole pair creation

03 p0403 A72-14080

Vitreous silica and silicon-silicon dioxide interface defect structure and behavior during ionizing or particle irradiation

03 p0403 A72-14081

P-channel MOS devices radiation hardening by thermal silicon dioxide gate insulator optimization, applying to circuit fabrication

03 p0403 A72-14082

Artificial microfossil permineralization of blue green algae in silica, simulating Precambrian geochemical preservation

04 p0514 A72-14415

Silicon-silicon dioxide system, investigating effect of heating in dry and moist He on capture-center and recombination parameters by thermal and pyrolytic techniques

08 p1216 A72-21068

Slip cast fused silica ablation in high temperature hydrogen-oxygen environment, comparing analytical results with measured data from rocket motor exhaust experiments

08 p1191 A72-21601

Thickening properties of butoxyacrosil products of butyl alcohol vapor and silicon dioxide surface reactions for use as oil lubricant additives

09 p1336 A72-22500

Mullite as part of aluminum oxide-silicon dioxide system, discussing formation, structure, physical chemistry, additives effects and high alumina refractories

10 p1501 A72-24729

Fusion cast zirconia-alumina-silica refractories manufacturing process, phase diagrams, chemical and physical properties and industrial applications

10 p1502 A72-24734

Book on semiconductors covering electrical properties, energy band structure, impurities, epitaxial growth, silicon dioxide, surface properties, p-n junctions and measurement techniques

10 p1528 A72-25123

Semiconductor materials etching and surface coating with protective silicon dioxide film in low temperature oxygen plasma

11 p1700 A72-25777

Sr isotope data indication of Glass Mountain rhyolite lava as part of parent silicic magma

11 p1623 A72-26240

Cation self diffusion coefficients in potassium oxide-strontium oxide-silicon dioxide glass, using radioactive tracers and sequential etching technique

13 p1912 A72-28625

Apollo heat shield silica reinforcement fiber and ablation char reactions in laboratory and actual reentry tests

14 p2172 A72-30922

Antioxidant additives effect on chemical stability and rheological properties of silica gel lubricants with SU type mineral oil dispersion medium

16 p2413 A72-33173

Conductance associated with interface states in MOS tunnel structures.

21 p3032 A72-40701

Diffusion in the system K₂O-SrO-SiO₂. IV - Mobility model, electrostatic effects, and multicomponent diffusion.

21 p3097 A72-40935

Spectroscopic study of the interaction of oxides with metallic surfaces. II - SiO₂-Fe /Cu, Al, Ni, Co, Ti, W systems

22 p3189 A72-42197

Auger spectroscopic observation of Si-Au mixed-phase formation at low temperatures.

22 p3178 A72-42616

MOS devices instability caused by water and hydroxyl molecules on silicon dioxide surface, noting optimal conditions for chemical stabilization

24 p3431 A72-44821

SILICON FILMS

Anodized aluminum metallization for reducing electromigration induced failure modes in silicon wafers

03 p0365 A72-14286

High electric power output Si solar cell development, discussing increased energy conversion efficiency

12 p1757 A72-28026

Improved geometry for a semiconductor surface-wave oscillator.

18 p2667 A72-36685

One MeV electron irradiation of new technology silicon solar cells.

19 p2754 A72-37777

Si solar cell design for high power/weight ratio and extreme environmental operating conditions, describing technological innovations for reliability and efficiency enhancement

19 p2754 A72-37780

Measurement of surface leakage currents in a semiconductor photoelectric converter

22 p3140 A72-43188

SILICON JUNCTIONS

Fluorinated ethylene propylene encapsulated N/P Si solar cells, investigating simulated micrometeoroid exposure effects on I-V performance in shock tube

01 p0006 A72-10381

Au distribution parameters in Si semiconductor devices, using radioactive isotope diagnostic methods

03 p0400 A72-12970

Vitreous silica and silicon-silicon dioxide interface defect structure and behavior during ionizing or particle irradiation

03 p0403 A72-14081

Transient radiation effects on silicon diodes in avalanche breakdown, considering voltage regulating diode response and temperature compensating junction effects

03 p0334 A72-14090

Matched Si junction FET under neutron burst and pulsed gamma radiation, investigating device parameters degradation

03 p0335 A72-14093

MOS Si-gate arrays for static, dynamic and programmable read-only memories, investigating information storage reliability

03 p0336 A72-14282

Alloying elements and grain size effects on thermally induced surface reconstruction of Al film metallization on Si devices from thermal cycling tests

03 p0364 A72-14285

N-p silicon solar cells damage at room temperature by proton and deuteron irradiation, considering particle mass and energy functions and illuminating light wavelength effects

04 p0561 A72-14574

Avalanche breakdown voltage of Gaussian Si planar p-n junctions for design and impurity diffusion evaluation

04 p0561 A72-15126

Space charge recombination in forward biased diffused p-n junction silicon diodes

04 p0562 A72-15127

Si p-n-p and Cr-n-p junction transit time diode oscillators microwave and dc characteristics comparison, noting similarity

04 p0499 A72-15206

Si monolithic multispectral image photosensor array for satellite application, presenting fabrication and spectral response data

04 p0500 A72-15304

CW 100 GHz Si IMPATT diodes with nearly abrupt junctions, discussing output power and dc and small signal analyses

04 p0502 A72-15594

Si planar unijunction transistor fabrication, operation principles, parameter measurements and applications

05 p0635 A72-16196

Refractory metal multilevel interconnection systems, comparing materials fabrication, yield and

circuit performance with diffused Si planar runs and polycrystalline Si films

05 p0636 A72-16362

Silicon Schottky barrier photodiodes development for photographic, photometric and analytical instrumentation, comparing sensitivity, time response and fatigue characteristics with classical photodetectors

06 p0813 A72-17428

Noise spectra of double sided CW silicon TRAPATT oscillator comparable to silicon IMPATT oscillator

06 p0783 A72-17482

Monolithic Si IC design and fabrication including resistors, capacitors, diodes, n-p-n, p-n-p, n-p-n-p and field effect transistors and inductors

06 p0791 A72-18576

Si p-n-p punchthrough X band oscillator, discussing wideband tuning and low noise properties and applications

07 p0955 A72-19252

Abrupt junction Si IMPATT diodes large signal analysis, discussing subharmonic modes and second harmonics effects

07 p0956 A72-19591

Energy spectrum of radiation defects in proton bombarded n-type Si crystals from Hall effect and electroconductivity measurements

07 p1049 A72-19901

Silicon-silicon dioxide system, investigating effect of heating in dry and moist He on capture-center and recombination parameters by thermal and pyrolytic techniques

08 p1216 A72-21068

Si diode array vidicon for ground based and spaceborne planetary and stellar imaging, noting integration time, storage and slow scan capabilities extension through cooling

08 p1171 A72-21970

Burst noise relationship to Si crystal dislocations and defects near emitter-base junction and surface zone in bipolar transistors

09 p1286 A72-23106

Metal probe potentials during mechanical displacement along surface of n-region of forward biased Si diode

09 p1288 A72-23362

Electrical properties of Te/p-Si/N heterodiodes at room and liquid air temperatures

10 p1527 A72-24937

Si Pd-n-p/plus/ transit time diode microwave oscillator, discussing fabrication, FM noise spectrum and bias current fluctuation

11 p1604 A72-25748

Time dependent light emission from mesoplasmas in Si p-n junctions in pulse mode, showing carrier heating effect

11 p1700 A72-25780

Boron doped n-type Si planar diode and n-p-n epitaxial planar Si transistor junctions investigating hydrostatic pressure effects on static characteristics and breakdown voltage

12 p1789 A72-27314

Annealing effects on gamma ray irradiated Li compensated p-type B doped Si semiconductor

12 p1858 A72-28065

Lattice disorder effects in ion implanted Si and compound semiconductors, using IR and EPR measurements

12 p1859 A72-28074

Pulsed Si p-n junction mesoplasma dynamic I-V characteristics explained by mechanism based on hot carrier annihilation

12 p1853 A72-28113

Laser light induced high-low impedance switch in Cd doped n-type Si diodes with p-p-n junctions and negative resistance

13 p1928 A72-28676

Acceptor level study of thermally diffused Be and Be-Li complexes in single crystal Si after quenching and annealing

13 p2022 A72-29628

Defect annealing in neutron irradiated Si by deep trap concentrations, using space charge limited current (SCLC)

13 p2022 A72-29630

Back surface electric field Si cell characteristics and fabrication using alloyed-through contact process

15 p2182 A72-32130

Conductance measurements for metal oxide-amorphous silicon junctions, showing temperature dependent tunneling

16 p2442 A72-33620

Si p-n junction solar cell fill factor for electric power available to load, noting discrepancy between calculated and measured values due to recombination

17 p2494 A72-34264

A thermal oscillator using the thermo-electric /Seebeck/ effect in silicon.

18 p2667 A72-36978

Properties of 1 MeV electron-irradiated defect centers in p-type silicon.

19 p2844 A72-37687

The effect of junction temperature on the output power of a silicon IMPATT diode.

19 p2773 A72-38145

A solid-state transponder source using high-efficiency silicon avalanche oscillators.

19 p2774 A72-38400

A theoretical investigation on the generation current in silicon p-n junctions under reverse bias.

21 p3097 A72-40703

Auger spectroscopic observation of Si-Au mixed-phase formation at low temperatures.

22 p3178 A72-42616

X-band silicon double-drift IMPATT diodes using multiple epitaxy.

23 p3273 A72-44334

Shielded silicon gate complementary MOS integrated circuit.

24 p3385 A72-44972

SILICON NITRIDES

Low energy electron beam irradiation of aluminum-silicon nitride-silicon structures for elimination of bias polarization effects on I-V characteristics

03 p0402 A72-13865

Silicon nitride ceramics resistance to thermal shock and stress in severe environments

09 p1334 A72-22386

Hot pressed silicon nitride with high strength and good oxidation and thermal shock resistance for gas turbine applications

[ASME PAPER 72-GT-19]

11 p1673 A72-25618

Recrystallized silicon carbide and reaction bonded silicon nitride as construction materials for gas turbine engine components, describing thermal and mechanical properties

[ASME PAPER 72-GT-20]

11 p1673 A72-25619

Dense silicon nitride and carbide ceramics for gas turbines, discussing critical properties for thermal stress calculation

[ASME PAPER 72-GT-56]

11 p1674 A72-25647

Normal modulus of elasticity of filamentary silicon nitride crystals with three orientations, calculating elastic liabilities

13 p1984 A72-30117

Oxidation resistance at high temperatures of refractory materials based on silicon nitride and carbide in various concentrations, showing time and temperature dependence

18 p2703 A72-36096

Production and properties of materials of the Si₃N₄-Cr₂O₃ system

23 p3298 A72-43283

SILICON OXIDES

NT COESITE

NT QUARTZ

NT SILICON DIOXIDE

Silicon solar cells antireflection coatings for performance loss minimization, obtaining improvement with titanium dioxide compared to silicon monoxide coatings

12 p1757 A72-28027

SiO transitions radiative lifetimes and absolute oscillator strengths from RKR Franck-Condon factors

13 p2008 A72-30054

Compensation of Fabry-Perot surface defects. II - Silicon oxide compensating layers.

21 p3053 A72-40608

Carrier transport and storage effects in Au ion implanted SiO₂ structures.

21 p3097 A72-40699

Application of a field-emission microscope to the investigation of the work function of tungsten coated with a thin layer of silicon oxide and with tantalum

24 p3432 A72-44891

Field-emission microscopy of tungsten coated with a silicon oxide film

24 p3432 A72-44892

SILICON POLYMERS

NT METHYL POLYSILOXANE

NT SILICONE RESINS

NT SILICONES

NT SILOXANES

Heat resistant reinforced plastics from glass and pyrolytic carbon fibers by silicoorganic polymer treatment

06 p0835 A72-17735

SILICON RADIATION DETECTORS

Nondestructive identification of alloy elements by nondispersive X ray fluorescence spectroscopy using Si/Li/ detectors and radioisotope sources for mobile applications

01 p0069 A72-10805

X ray pulse spectra measurement from Z-pinch plasma focus devices, describing Ross filter system with silicon diode detector capable of nanosecond time resolution

04 p0524 A72-15537

Proton recording equipment onboard automatic interplanetary stations Zond 4 and 5 at 1.5-50 MeV using silicon drift counters

06 p0814 A72-17699

Radiation resistance of Si photodetectors for star sensors in satellites, using electrical and optical tests

09 p1369 A72-22653

Integrating two dimensional silicon diode array vidicon astronomical photometer for telescope use

09 p1313 A72-23330

Efficiency response of covered Si detectors to monoenergetic gamma rays, considering Lucite, Al, Cu and Pb absorbers

13 p1954 A72-28429

Radiation effects measurement on neutron, proton and electron irradiated Li-drifted Si detectors by IR response technique, comparing characteristics with photovoltage effect

15 p2234 A72-31538

Needle type solid state detectors for in vivo measurement of tracer activity.

18 p2655 A72-37194

Some aspects of the use of small needle-shaped semiconductor detectors in the determination of regional distribution and transport of labelled compounds.

18 p2655 A72-37195

Relation between diffusion and defect formation rates in silicon detectors exposed to gamma radiation

20 p2959 A72-38956

SILICON SOLAR CELLS

U SOLAR CELLS

SILICON TRANSISTORS

Generation-recombination model of large signal silicon transistor operating in IC microwatt range

02 p0188 A72-11521

Failure modes of IC containing MOS devices, considering threshold voltage variations, oxide and silicon defects and leakage

02 p0194 A72-12443

P-channel MOS/silicon-on-sapphire transistor logic circuits for aerospace systems, investigating radiation hardness and performance potential

03 p0334 A72-14086

N-channel Si MOS microwave transistor, discussing fabrication, design, power gain, stability, noise figure, equivalent circuit and applications

05 p0636 A72-16361

Wide range bias dependence of planar bipolar transistor dc and small signal current gain, comparing analytical findings with Si junction experiment

06 p0783 A72-17608

Si MOSFET substrate resistivity effect on surface state noise spectra

06 p0783 A72-17609

Normally off Si MESFET for simple dc coupled circuits, computing threshold voltage with two dimensional device model

08 p1141 A72-21426

Acoustic wave detection in strain transducer consisting of silicon insulated gate field effect transistor with piezoelectric film incorporated in insulator region

08 p1168 A72-21556

Temperature dependence and error compensation of Si strain sensors, using coupled dc generators

09 p1316 A72-23649

Quasi-linear approximation of input impedance of epitaxial n-type Si unijunction transistors for predominant drift conditions

13 p1927 A72-28406

Permanent operational characteristics changes of Si and Ge transistors bombarded by gamma and neutron radiation

13 p1928 A72-28700

Emitter-dip model of diffusion anomalies of n-p-n Si HF transistors doped with B and P

21 p3035 A72-41489

SILICONE RESINS

Wear behavior of molybdenum disulfide and antimony trioxide bonded solid film lubricant with air curing silicone resin, noting temperature and pretreatment effects

06 p0823 A72-18593

SILICONE RUBBER

Thermal conductivity of two- and three phase solid mixtures of silicone rubber and Al, Pb, Ni and Bi powders, using line source method

11 p1744 A72-25264

Silicone based elastomers acoustic excitation damping properties at 213-423 K, discussing testing technique and results at 200-1000 Hz

13 p1957 A72-29090

Recent developments in silicone elastomers for microencapsulation.

20 p2944 A72-39492

SILICONES

NT METHYL POLYSILOXANE

NT SILOXANES

Elastomeric silicone ablator heat shields thermal characteristics from NASA Planetary Atmosphere Experiments Test vehicle earth atmosphere entry measurements

[AIAA PAPER 72-326]

13 p2064 A72-28953

SILICONIZING

Thermodynamics of Mo silicidation reactions from gas phase in silicon chloride and hydrogen media, discussing glow discharge maximum yield

07 p0937 A72-20417

SILOS [MISSILE STORAGE]

U MISSILE SILOS

SILOXANES

Testing of plastic lubricants in ball bearings with rocking motion on the TsKB 16-T test stand

23 p3307 A72-43975

SILTS

U SEDIMENTS

SILVER

Water disinfection by Ag coated filters obtained by silver nitrate reduction with ascorbic acid, hydroquinone, formaldehyde and sodium tartrate activated carbon and ion exchange resin surfaces

05 p0622 A72-16637
High strength Al-Zn-Mg-Cu alloys, testing heat treatment and Ag addition effects on tensile strength

05 p0677 A72-17112
Ag addition effects on high strength Al-Zn-Mg-Cu alloys tensile properties and resistance to stress corrosion cracking

05 p0677 A72-17113
ESRO findings on optimal resistance welding of solar cell interconnections for silver coated metals and pure silver

12 p1814 A72-28030
Sulfur dioxide and carbon dioxide interaction with clean silver surface at ultrahigh vacuum, using Auger electron spectroscopy and work function measurement

13 p1912 A72-28684
Out-of-plane density distribution and in-plane velocity distribution measurements for low energy helium scattering inelastically from 550 K silver

15 p2276 A72-31861
Thermally stimulated current measurement application to Ag doped Si semiconductor for energy level and electron capture cross section determination

16 p2441 A72-32859
Investigation by the method of secondary ion-ion emission of the initial phase of the formation process of a silver vacuum condensate on a nickel substrate

21 p3068 A72-40960
Solar silver abundance from spectral scans for Ag 3280.7 and 3382.9 A resonance lines, using spectral synthesis method, model atmosphere and limb darkening observations

22 p3221 A72-42028

SILVER ALLOYS

Alloying and heat treatment ordering effect on hydrogen diffusion coefficients, penetrability and solubility in Pd-Ag alloys

03 p0376 A72-14016
Temperature and stress dependence of steady state creep rate for dispersion strengthened Ag-gallium oxide alloys, noting grain size effect on activation energy

16 p2411 A72-34094

SILVER BROMIDES

Latent image formation in radiographic emulsion of AgBr crystals dispersed in gelatin layer, considering crystal structure and X and gamma rays energy recording

07 p0991 A72-20424
Organic dye desensitization of bleached AgBr phase holograms against printout darkening by Ar ion laser light

12 p1811 A72-27949
Investigation of certain complex compounds of tri-aryl phosphines /phosphites/ in optically sensitized photographic emulsions

21 p3052 A72-40390

SILVER CADMIUM BATTERIES

Electrical power subsystem design in Pioneer F/G spacecraft, using SNAP 19 deployable radioactive thermoelectric generators supplemented by Ag-Cd battery

01 p0008 A72-11065

SILVER COMPOUNDS

NT SILVER BROMIDES

NT SILVER HALIDES

SILVER HALIDES

NT SILVER BROMIDES

Absorption and exposure characteristics of silver halide photochromic glasses for hologram recording

01 p0068 A72-10622
Impurity centers formation and development in AgBr/I photographic emulsion under ultrasonic irradiation

11 p1636 A72-26794
Image forming mechanism in photographic silver halide emulsions due to incident optical signals, considering latent image amplification process efficiency

19 p2800 A72-37857
Laser beam scanning and recording in two dimensional pattern on silver halide, evaluating systems performance based on signal response, granularity and noise characteristics

20 p2930 A72-39040

SIMICOR [IMAGE CORRELATOR]

U IMAGE CORRELATORS

SIMILARITIES

U ANALOGIES

SIMILARITY NUMBERS

Relative motion of active interceptor spacecraft approaching passive craft in central gravitational field, using dimensionless differential equations similarity coefficients method

05 p0728 A72-16592

Differential equations similarity analysis, using Lie infinitesimal contact transformation group as search method for other possible transformation groups

10 p1503 A72-23922
Relative motion of active interceptor spacecraft approaching passive craft in central gravitational field, using dimensionless differential equations similarity coefficients method

19 p2869 A72-37564
Stagnation-point heat transfer - The effect of the first Damkoehler similarity parameter.

[ASME PAPER 72-HT-44] 20 p2985 A72-39666

SIMILARITY THEOREM

Momentum jet and electric discharge from same hole in plane wall bounding viscous incompressible conducting fluid, investigating flow field with similarity solutions

01 p0107 A72-10139
Affine similarity in static problems with mixed boundary conditions for inhomogeneous anisotropic linearly and nonlinearly elastic and viscoelastic and elastoplastic bodies

02 p0288 A72-11607
Critique of self similar solutions for physical property models of laminar boundary layer separation due to adverse pressure gradients, noting viscosity-enthalpy relation

02 p0204 A72-12265
Soviet book on gas turbine engines control systems design based on similarity theory, determining optimal controller formula from engine parameters

02 p0271 A72-12543
Two and three dimensional turbulent boundary layer development in incompressible and compressible flows, obtaining boundary layer equations similarity solutions via mixing length model

[DGLR PAPER 71-066] 02 p0206 A72-12719
Newtonian fluid laminar free convection over curved wall with arbitrary temperature variation, investigating similarity solutions existence by method of free parameters

04 p0596 A72-15193
Book on similarity laws and modeling covering dimensional analysis, transformations, differential equations, gas flows and nonequilibrium processes

04 p0513 A72-15675
Fluid properties for mechanically similar flow fields, discussing dissociating and thermally radiating gas flow

[DFVLR-SONDDR-172] 05 p0648 A72-16064
Similarity and finite difference solutions of parabolic differential equations, exemplifying by heat conduction and boundary layer equations

[ASME PAPER 71-WA/APM-6] 05 p0682 A72-16151
Two dimensional transonic and hypersonic shock structures, discussing flow equations, mathematical properties and similarity rules

06 p0799 A72-17960
Similarity solution for nonlinear viscoplastic semi-infinite rod under constant velocity impact

07 p1088 A72-19115
Self similar solutions for piston driven shock wave motion, examining Whitham approximation rule validity

07 p0970 A72-20075
Similarity theory for turbulently stratified fluid with horizontal and vertical dimensionalities analysis, discussing Karman constant dependence

07 p1031 A72-20698
One dimensional nonviscous dynamic plasticity theory applicability to impacting rod problems tested experimentally using results from three dimensional and viscous similarity considerations

09 p1408 A72-23557
Similarity analysis group theory methods application to dimensional analysis, discussing incompressible fluid mechanics case

10 p1503 A72-23917
Similarity method solution of differential equations of motion for supersonic laminar boundary near symmetry plane of cone at angle of incidence

10 p1418 A72-24326
Biological similarity theory for numerical relationships of morphometric and physiometric organization in mammals, using allometric growth equations and body weight correlations

10 p1432 A72-25098
Boundary value problems in boundary layer theory, discussing Falkner-Skan equation similar solutions existence theorems

11 p1677 A72-25525
Dimensional analysis and similarity theories application to biological organisms relationships between body size and metabolism

11 p1585 A72-26074
Sunspot magnetic field depth variations model, using configuration conditioned by Schlueter-Temesvary similarity law

13 p2048 A72-29740
German book on principles and applications of similarity theory in physical-technical research covering coherent dimensional units and invariance principle, physical dimensions, etc

15 p2218 A72-31900

Pseudo-one dimensional dissociative nonequilibrium nozzle flow, presenting governing equations transformation via similarity parameter for oxygen

16 p2375 A72-32906
Self similar breakdown problem of two dimensional shock discontinuity in gas dynamics

16 p2377 A72-33154
Flows between stationary surfaces of revolution, having similarity solutions.

[ASME PAPER 72-APM-4] 17 p2537 A72-34304
Fluid dynamics problems self similar solutions as descriptions of intermediate asymptotic behavior of solutions for initial, boundary and mixed problems

18 p2709 A72-36388
Free convection similarity and measurements in flows with and without shear.

18 p2706 A72-36634
Recent results on the effect of longitudinal curvature on a laminar layer

18 p2685 A72-37213
Similarity theory of planetary atmosphere circulations applied to solar atmosphere in terms of radius and rotatory Mach number

19 p2863 A72-38066
Similarity theory for turbulence in stratified fluid from horizontal and vertical dimensional analysis approach, discussing Karman constant dependence

20 p2948 A72-39013
Proper equations and similar approximations in the hypersonic merged layer.

20 p2885 A72-39621
Wind tunnel measurement for demonstrating similarity of atmospheric turbulent boundary layer mean velocity and shear stress at high Reynolds number

22 p3201 A72-42598
Extension of the Prandtl-Glauert similarity rule to loss including cascade flow.

24 p3363 A72-45352
Similarity problems of a non-isothermal boundary layer of an incompressible non-linear viscous medium with regard for dissipation.

24 p3395 A72-45634

SIMILITUDE LAW

Power law bodies lift and drag coefficients interrelationship under Newtonian nonaffine similarity laws, presenting rules for equivalent transformations identification

02 p0151 A72-12273
Similitude solutions for turbulent boundary layers in compressible flow with pressure gradient and heat transfer at wall, obtaining velocity and enthalpy profiles

06 p0798 A72-17845
Two and three dimensional turbulent boundary layers integral calculation method, presenting similarity solutions based on extended mixing length model

10 p1469 A72-24653
Spacecraft cabin atmosphere thermal scale modeling based on radiative-convective-convective heat transfer, obtaining adequate thermal similitude through mass flux and heat transfer coefficient preservation

11 p1741 A72-25226
[AIAA PAPER 72-288] Geometric similitude of lunar and terrestrial craters.

17 p2615 A72-35681
Ultimate configuration of the self-similar separated flow of an ideal fluid

19 p2785 A72-37396
Design modeling of external and internal cooling systems for bodies exposed to high temperature gas flow, discussing operation similarity conditions

21 p3129 A72-41052

SIMPLE HARMONIC MOTION

Optimization problems in gravitational attraction, considering homogeneous ellipsoids interaction and free particle simple harmonic motion

06 p0851 A72-18740
Mathematical model of earth liquid core dynamo mechanism for magnetic field maintenance based on simple motions with spherical harmonic form

21 p3048 A72-40400

SIMULATED ALTITUDE

Functional development of the altitude convulsion mechanism in mice and rabbits [Research note].

18 p2650 A72-36445

SIMULATION

NT ACOUSTIC SIMULATION

NT ALTITUDE SIMULATION

NT ANALOG SIMULATION

NT ATMOSPHERIC ENTRY SIMULATION

NT COMPUTERIZED SIMULATION

NT CONTROL SIMULATION

NT DIGITAL SIMULATION

NT ENVIRONMENT SIMULATION

NT EXHAUST FLOW SIMULATION

NT FLIGHT SIMULATION

NT LANDING SIMULATION

NT RHEOELECTRICAL SIMULATION

NT SPACE ENVIRONMENT SIMULATION

NT THERMAL SIMULATION

NT WEIGHTLESSNESS SIMULATION

Magnetic simulation of gravity for wind tunnel investigations of aircraft jettison processes, considering

Froude number and relationships between model and full scale aircraft

10 p1462 A72-24775

Theoretical and experimental investigations, conducted with the aid of a plate containing holes, concerning the simulation of a statistically arranged antenna group

21 p3028 A72-40505

SIMULATOR TRAINING

U TRAINING SIMULATORS

SIMULATORS

NT COCKPIT SIMULATORS
NT CONTROL SIMULATION
NT ENVIRONMENT SIMULATORS
NT FLIGHT SIMULATORS
NT SOLAR SIMULATORS
NT SPACE SIMULATORS
NT TARGET SIMULATORS
NT TRAINING SIMULATORS
NT VIBRATION SIMULATORS

Dynamic characteristics of turbomotor simulator supported on gas lubricated foil bearings of reduced length with starting and stopping unaided by external pressurization

[ASME PAPER 71-LUB-16] 02 p0235 A72-11538

DC 9 aircraft integrated data system simulator to facilitate interacting systems checking, input circuit integrity, performance degradation and calibration

06 p0796 A72-18284

Ergonomic simulators for testing individual mental working capacity, using stress-strain and fatigue relation

09 p1272 A72-23140

Turbojet simulator for supersonic wind tunnel models, simulating inlet mass flow ratio and exhaust nozzle pressure ratio

[ASME PAPER 72-GT-89] 11 p1705 A72-25664

Starry sky energetic simulator design, analyzing comparative brightness of stars

13 p1945 A72-28494

Twin-turboprop transport aircraft, helicopter and all-terrain ground vehicle simulators, discussing control load, visual attachment, cabin motion and sound subsystems

14 p2092 A72-30845

Russian book on thermal simulation of spacecraft and space environment covering heat transfer, cosmic radiation, vacuum chambers, radiant flux simulators, etc

15 p2319 A72-31275

Simulator for physical forces experienced by carrier aircraft during catapult launches and arrested landings, considering external stores safe suspension

15 p2215 A72-32620

Dynamic and static characteristics of jet engine simulators

23 p3327 A72-44286

SIMULTANEOUS EQUATIONS

Optimization algorithm for simultaneous solutions to bivalent 0-1 Knapsack problems with linear target function and linear restrictions, using ALGOL

05 p0632 A72-15817

Necessary and sufficient equilibrium stability conditions for differential equations systems with quasi-homogeneous right sides

06 p0838 A72-17382

Finite difference schemes with splitting operator for mixed type differential equations systems, considering solutions stability and convergence properties

06 p0839 A72-18117

Linear plants time optimal control, deriving auxiliary equations system solution in accordance with Pontryagin maximum principle

07 p0959 A72-19127

Linear difference equations solved by indefinite Z transformations technique using Cramer rule for simultaneous algebraic equations

11 p1678 A72-26664

Schaefer equilibrium and compatibility equations and Reissner constitutive equations for orthotropic cylindrical shells reduction to four simultaneous third-order equations

16 p2466 A72-33023

Approximate solutions of problems involving simultaneous multifunctional nonlinear partial differential equations, noting rectangular plate deflection under lateral pressure

[ASME PAPER 72-APM-47] 17 p2627 A72-34780

On the calculation of variances of solutions to linear simultaneous equation.

21 p3075 A72-41233

On the solution of non-linear simultaneous equations with particular reference to fluid-dynamics.

22 p3199 A72-42325

German monograph - Internal-analytic methods in systems of linear equations with interval coefficients and relations to error analysis.

22 p3200 A72-43061

SIMULTANEOUS IMAGE CORRELATOR

U IMAGE CORRELATORS

SINE

U TRIGONOMETRIC FUNCTIONS

SINE WAVES

Nonuniform sinusoidal electric field anomalous influence on ion motion in gas with allowance for ion-atom collisions

04 p0547 A72-14622

Digital sine wave generator, discussing advantages over conventional RC and LC oscillators due to superior phase constancy

05 p0634 A72-15814

Charged particle acceleration by nonstationary sinusoidal electric fields in earth magnetosphere based on mathematical model

05 p0709 A72-16256

Spectral analysis with sinusoids and Walsh functions, using Rademacher function

05 p0628 A72-16564

Noncoherent detection of sinusoidal signal imbedded in clutter and Gaussian noise, obtaining probability density as function of SNR and clutter-to-noise ratio

10 p1437 A72-24691

Network synthesis for various second and third order sinusoidal oscillators consisting of linear passive or active RC circuits and amplifier

10 p1452 A72-24802

Dynamic calibration of inclined and crossed hot-wire flowmeters for absolute turbulence intensity measurements, using known sinusoidal oscillations in steady flow

11 p1636 A72-26637

Masking functions for intensity discrimination of pulsed sinusoids with and without noise masker

13 p2006 A72-29772

Analog to digital converter for sinusoidal voltage amplitude pickup and subsequent digital coding with correction for conversion characteristic nonlinearity

13 p1934 A72-30020

Fundamental, harmonic and combination frequency components amplitude analysis via dual input describing function for nonlinear element response under two incommensurate frequency sinusoidal signals

18 p2671 A72-36051

An aspect of the problem of pitch dependence on the duration of short sinusoidal signals

20 p2897 A72-39217

Spectra of a frequency-shift-keyed signal amplitude-modulated by a sinusoidal wave.

20 p2904 A72-39771

Spectrally shaped transient forcing functions for frequency response testing.

22 p3206 A72-42463

Stationary solitary, snoidal and sinusoidal ion acoustic waves.

23 p3320 A72-43520

SINGLE CRYSTALS

NT WHISKERS [SINGLE CRYSTALS]

Minority carriers similarity in graphite natural single crystals and pyrolytic samples

01 p0114 A72-11035

Preparation and electrical properties of thin cadmium antimonide and arsenide layers, comparing to single crystal films

02 p0268 A72-12281

Secondary slip in impact loaded Al single crystal disks, interpreting face deformation bands

02 p0247 A72-12819

Single crystal Si defect accumulation and transition to amorphous state under Xe, Ar, Ne, O and P ion irradiation, using EPR

02 p0269 A72-12884

CdS single crystal field emission spectral characteristics at room and cryogenic temperatures, discussing intrinsic and impurity levels

02 p0269 A72-12888

CoO single crystal creep rate at different temperatures, stresses and oxygen pressures, noting slip occurrence

03 p0373 A72-13647

Rolling workability of pure W single crystals grown by electron beam zone melting technique, discussing crack occurrence

03 p0374 A72-13718

Epitaxial layer preparation on GaSb single crystal by liquid phase method, discussing crystal orientation effects

03 p0402 A72-13859

Substructure variations and crystal lattice periods dependence on compression stress in beryllium single crystals during plastic deformation due to base slip

03 p0376 A72-14018

Fine structure of Mo-Re alloys single crystals in solid solution region as function of Re content

03 p0377 A72-14019

Impurity diffusion of Ag, Cd, In, Sn and Sb in magnesium single crystals, observing valence effect on activation energy

03 p0378 A72-14254

Portevin-Le Chatelier effect in Al-Mg single crystals during tensile tests, investigating strain rate influence on stress

03 p0378 A72-14257

Cu single crystal fatigue life explanation by work hardening using statistical theory of slip

03 p0379 A72-14258

Flow stress measurements in disordered and partially ordered Ni-Ta alloy single crystals, correlating with ordered phase volume fraction and domain size

04 p0534 A72-15272

Mono- and polycrystalline Ni high temperature creep kinetics, investigating substructural changes

05 p0671 A72-16000

Basal dislocations determination in sapphire single crystals, using X ray transmission topography

05 p0701 A72-16018

Internal friction changes in aluminum single crystal after uniaxial plastic deformation and irradiation

05 p0673 A72-16148

Photoelectrically excited electrons diffusion and dc effect in ZnO single crystals, calculating drift mobility and lifetime product

05 p0667 A72-16158

Subgrain rotation induced angular anisotropy of plastic deformation of oriented Mo single crystals during rolling

05 p0674 A72-16354

C 14 diffusion coefficients in W and W-Re alloys single crystals at 1500-1800 C, discussing tracer activation energy and frequency factor

05 p0676 A72-16731

Physical theory of plasticity, considering mathematical hypotheses and assumptions, single crystals dislocations and plastic deformation, polycrystals homogeneous strain analysis, slip theories, etc

06 p0896 A72-17962

Flux lines interaction with dislocations in twisted superconducting niobium single crystals, measuring flux gradient and dislocation arrangement

06 p0830 A72-18055

Hopping electroconductivity of n-type GaS single crystals, observing frequency dependence

06 p0866 A72-18181

Mo-Nb alloys single crystals work function, obtaining thermionic emission pattern

06 p0832 A72-18414

Steady creep rates in Ni poly- and single crystals in presence of dislocation stresses

06 p0835 A72-18748

Optical holographic storage in lithium niobate single crystals, noting erasability and rewritability

07 p0981 A72-18890

Reflection mode high energy electron diffraction study of titanium carbide single crystal surfaces in ultrahigh vacuum environment

07 p1019 A72-20408

Plasticity conditions of monocrystals of higher symmetry tetragonal system, using energy density and deformation relations

08 p1242 A72-20938

Al single crystals relationship between stress, strain and dislocation density ring elevated temperature creep by direct observation of etch pits

08 p1185 A72-20990

IR luminescence and photoconductivity in p-type GaSe single crystals alloyed with Sn and Ge impurities

08 p1216 A72-21069

Mo single crystal internal dislocational friction and ultrasound damping dependence on oscillation amplitude, exposure time and annealing temperature

08 p1185 A72-21073

Monocrystals elastic anisotropy effects on polycrystalline sinter matrix minimum porosity, thermal conductivity, mechanical and elastic properties, thermal stress resistance and Hugoniot elastic limit

08 p1186 A72-21441

Metal single crystals use for corrosion tests, noting anisotropy, adsorption, oxidation and pitting

08 p1189 A72-22111

Dielectric dispersion in SrSi filamentary single crystals as function of Curie temperature in If and shf range

09 p1367 A72-22422

Chemisorbed oxygen effect on electrical properties of monocrystalline cadmium sulfide thin plates with high resistivity

10 p1525 A72-24211

Various restrain dislocation distributions effect on mechanical twinning behavior in purified Nb single crystals

10 p1497 A72-24824

Subgrain rotation induced angular anisotropy of plastic deformation of oriented Mo single crystals during rolling

11 p1652 A72-25339

Quasi-continuous charge carrier traps in molecular single crystals associated with polarization energy dissipation

11 p1700 A72-25782

Dielectric and optical constants of p-type GaSb single crystals, interpreting singularities by energy bands diagram

11 p1689 A72-26485

Ga alloying effect on Al single crystals work hardening, noting Portevin-Chatelier effect at higher Ga contents

11 p1662 A72-26739

Synthetic diamond single crystals, investigating impurities and inclusions effects on ferromagnetic properties and heat resistance

12 p1833 A72-27768

IR absorption bands in mechanically and chemically polished GaAs single crystals irradiated with varying neutron and electron doses

12 p1859 A72-28069

Te single crystal electrical resistivity and Hall coefficient effects of electron irradiation, suggesting point defects and dislocations interaction

12 p1859 A72-28073

Double doping effect on electrical properties of Te and Hg doped and Te and In doped CdSb single crystals

13 p2020 A72-28565

Re single crystal LEED diffraction pattern, showing surface carbon structure

13 p2021 A72-28800

Cu-Al-Ni alloys single crystals internal friction temperature dependence during martensitic transformations

13 p1977 A72-28912

Microhardness anisotropy of hardened and aged Be single crystal as function of purity

13 p1978 A72-29023

Al and AlMg single crystals static recovery and stacking fault energy at 77-500 K in plastic deformation, noting cross slip onset at 500 K

13 p1978 A72-29222

Dislocations with Burgers vector during Zr single crystals deformation at different temperatures, examining shear plane foils by electron microscope

13 p1978 A72-29223

Acceptor level study of thermally diffused Be and Be-Li complexes in single crystal Si after quenching and annealing

13 p2022 A72-29628

X ray milliprobe apparatus adaptation for examining single crystals from lunar samples

13 p1960 A72-29839

Plastic deformation in bcc metal single crystals, discussing glide and work hardening, dislocations, core structure and atomic calculations

13 p2061 A72-29874

Sulfur alloyed CdTe single crystals IR absorption spectrum, noting temperature effects

13 p2023 A72-29918

Refractory compounds single crystals preparation, emphasizing hot pressing under high pressures

13 p1982 A72-30113

Mo single crystal weakening after hot rolling and annealing, showing decreased dislocation density and hardness recovery by electron microscopy

14 p2112 A72-30160

Free carrier mobility dependence on excitation light intensity in CdSe single crystals with negative photoconductivity

14 p2141 A72-30169

Quasi-longitudinal and quasi-transverse plane wave propagation in anisotropic elastic-plastic solids, approximating Be single crystal behavior

14 p2163 A72-30176

Al single crystals, investigating scale factor effects on stepwise deformation at 1.4 K

14 p2115 A72-30410

Electric current pulses effect on Zn monocrystals plastic deformation before brittle rupture, noting critical normal stresses increase

14 p2115 A72-30411

Octahedral TiC single crystals oxidation at high temperature in oxygen, carbon dioxide and mixtures, investigating oxygen partial pressure effects on kinetics

14 p2121 A72-30772

Decomposition mechanism of Cn, Ag and Au solid solutions in InAs single crystals, using isotopic radiography

14 p2143 A72-30961

Time to failure under axial tension determined for gallium selenide single crystals at constant temperatures, noting tensile strength dependence

15 p2290 A72-31387

Ultrasonic wave propagation in single crystals, discussing linear elastic wave attenuation, anisotropic interactions, particle displacement polarization and energy flux deviation

15 p2292 A72-31834

Single crystal scheelite material for Nd doped intermediate gain laser host substance, considering optimum growth conditions, lasing parameter and Nd concentration

15 p2292 A72-32030

Current noise spectra in single crystals and polycrystals of transition metal compounds, discussing flicker noise origin

15 p2293 A72-32384

Tensor analysis for planar magnetoresistivity and Hall effect in Ni single crystal thin films, noting anisotropy effects in ferromagnetic crystals

15 p2294 A72-32386

CdTe single crystals photoplastic characteristics, detailing illumination effect on yield stress and resistivity

15 p2294 A72-32501

Trapped charge effect on photovoltaic properties of copper sulfide-cadmium sulfide single crystal heterojunction in terms of tunneling by photocapacitance technique

15 p2294 A72-32520

Multiple plastic and viscoplastic potentials for single crystal and polycrystal with mean densities and mean lengths of dislocations as internal variables

16 p2470 A72-33615

Work functions of some emitting and collecting refractory metal single crystals.

17 p2595 A72-34601

Single crystal disk substrate design with electron bombardment heating for LEED and Auger electron spectroscopy studies in ultrahigh vacuum

17 p2553 A72-34642

Orientation dependence of slip in tantalum single crystals.

17 p2567 A72-34748

Mo-Nb alloys single crystals work function, obtaining thermionic emission pattern

17 p2567 A72-34863

Comparison of infrared and activation analysis results in determining the oxygen and carbon content in silicon.

17 p2511 A72-35330

Preparation and properties of nonheat-treated single crystal Cu₂S-CdS heterojunctions.

17 p2595 A72-35331

Luminescence behavior of single-crystal semiconductor compounds under electron bombardment

17 p2596 A72-35721

Work function dependence on crystal orientation for W with special emphasis to the variation near the $\{110\}$ orientation.

18 p2656 A72-36130

Undamped photocurrent fluctuations in CdSe single crystals

18 p2718 A72-36348

The effects of environment on the elevated temperature fatigue behavior of nickel-base superalloy single crystals.

18 p2700 A72-36587

Single-crystal, electro-optic shutter for Q-switching lasers emitting unpolarized radiation.

18 p2698 A72-36698

Flash desorption spectrum and LEED studies of CO adsorption on W single crystal planes, measuring work function increase as function of coverage

18 p2657 A72-37040

Vapor grown solid state single crystal oxide thin films characteristics and synthesis by thermal vaporization, chemical vapor deposition and sputtering

19 p2843 A72-37443

Hall and resistance measurements on single crystal HgTe-InTe alloy systems for high pressure phases in terms of conduction state, band structure and impurity effects

19 p2844 A72-37464

The plastic deformation behavior of Mo single crystals under compression.

19 p2816 A72-37689

Anisotropy of angular distribution of radiation due to positron annihilation on the surface of Mo single crystals.

19 p2844 A72-37691

Determination, by X-ray photometry, of the frequencies of thermal oscillations which propagate themselves, following the axes of symmetry in a potassium chloride single crystal, at temperatures of 295, 80, and 5 K

19 p2844 A72-37791

Variations as a function of the temperature of the moduli of elasticity of monocrystalline P-type GaSb

19 p2846 A72-38542

Electroconductivity, thermal emf and Hall coefficient for single crystals of Bi-Sb alloys with Cd, In and Sn additions

19 p2847 A72-38683

Investigation of the viscosity and density of solution melts intended for growing yttrium-iron garnet /YIG/ single crystals

19 p2847 A72-38684

Fluorescence of anthracene single crystals whose surface is disturbed by an impurity

19 p2847 A72-38781

Comment on "The deflagration of single crystals of ammonium perchlorate."

19 p2848 A72-38873

The influence of the surface orientation on yield in Mo single crystals.

20 p2935 A72-39007

Optically induced variation of birefringence in ferroelectric materials.

20 p2959 A72-39045

Influence of cerium additions on the luminescence of europium and samarium ions in NaF single crystals

20 p2932 A72-39414

Recrystallized Al monocrystals applications to optics and X ray spectroscopy, describing preparation methods

21 p3065 A72-40085

Electrical conductivity of tungsten trioxide /WO₃/

21 p3096 A72-40198

Parallel pumping of spin waves in yttrium garnet single crystals

21 p3096 A72-40413

LF circularly polarized electromagnetic waves /helicon/ resonance crystal plates, deriving magnetoresistivity and Hall coefficient

21 p3066 A72-40624

Investigation by the mass transfer method of the diffusion of nickel at a $\{110\}$ surface of tungsten single crystals

21 p3068 A72-40955

Quantum limit studies in single crystal and pyrolytic graphite.

21 p3097 A72-41186

Gas adsorption by refractory metal single crystals.

22 p3187 A72-41940

Photovoltaic properties of single-crystal CdS-Cu₂S cells.

22 p3214 A72-42457

Physical metallurgy of single crystals of high-melting and rare metals and alloys

22 p3191 A72-42807

Physicochemical investigation of the thermionic emission properties of metals and alloys

22 p3191 A72-42811

Rotational hysteresis in single crystals of powdered nickel

22 p3192 A72-43011

Pure Co single crystals allotropic transformation effects on deformation behavior, noting flow stress and work hardening rate relationship to history

22 p3193 A72-43034

The kinetics of the reaction between oxygen and sulfur on a Ni/ $\{111\}$ surface.

24 p3378 A72-44951

Cadmium sulfide single crystals suitable for electron-beam-pumped lasers.

24 p3432 A72-45607

SINGLE SIDEBAND DEMODULATION

U SINGLE SIDEBAND TRANSMISSION

SINGLE SIDEBAND MODULATION

U SINGLE SIDEBAND TRANSMISSION

SINGLE SIDEBAND RECEIVERS

U SINGLE SIDEBAND TRANSMISSION

SINGLE SIDEBAND TRANSMISSION

Wideband data transmission on group-band communication channels, using dual single-sideband modulation with basic transmission rate of 48 kbit/sec

01 p0024 A72-10113

AFC for suppressed-carrier SSB voice signal reception, using phase locking procedure or comparative zero-crossing-rate measurement

01 p0025 A72-10333

Gas laser longitudinal mode locking during single sideband modulation with nonuniform broadening in mode intensity distribution

03 p0366 A72-13365

Binary single sideband phase modulation with simultaneous AM by signal and Hilbert transformation

06 p0776 A72-18395

Soviet book on radio receiver design covering military applications, bandwidth requirements, network synthesis and AM, FM, SSB, Doppler, phase metering, PCM and radar equipment

11 p1604 A72-26045

Single sideband AM microwave analog transmission systems using frequency division multiplex techniques

11 p1595 A72-26289

Three centimeter balanced ring modulator with carrier and sideband suppression using amplitude and phase relations

11 p1605 A72-26321

Solid state RC network for single sideband frequency converter using phase difference carrier suppression

11 p1598 A72-26731

SSB signal generation without Nyquist filter or auxiliary equipment for PM modems in data transmission

15 p2195 A72-31620

Complex detection - A waveform preserving technique for single-sideband demodulation.

18 p2661 A72-36844

Controlled-carrier transmission of AM/VSB television from space.

21 p3016 A72-40770

Complex detection - A waveform preserving technique for single-sideband demodulation.

21 p3017 A72-40862

Carrier phase jitter extraction method for VSB and SSB data transmission systems.

21 p3021 A72-40910

SINGLE STAGE ROCKET VEHICLES

NT AGENA ROCKET VEHICLES

NT BLACK KNIGHT ROCKET VEHICLE

NT VIKING ROCKET VEHICLE

SINGLE-PHASE FLOW

Single- and multiphase theories of slowly varying nonlinear dispersive waves, noting stability solutions to large scale variations and shocks

09 p1351 A72-22942

SINGULAR INTEGRAL EQUATIONS

Airfoil theory singular integrodifferential equation reduction to integral equations with quasi-regular and regular kernels, applying to jet flapping wing problem

03 p0381 A72-12987

Circular disk with external radial cracks, obtaining limiting equilibrium stress-strain state through singular integral equation solution

03 p0451 A72-14115

Plane wave diffraction by infinite strip grating, providing closed form solution by boundary value problem reduction to singular integral equation

04 p0490 A72-15411

Diffraction anomaly from infinitely extended strip grating solution by successive approximation technique combination with singular integral equation

04 p0491 A72-15418

Singular integral equation in radiative transfer theory with polynomial scattering indicatrices

04 p0597 A72-15643

Numerical solution of integral equations with singular and weakly singular kernels by weighted residuals method

07 p1025 A72-18781

Singular integral equations numerical solution from Gauss-Chebyshev formulas for mixed boundary value problems

07 p1026 A72-18808

Boundary value problems in micropolar theory of elasticity, obtaining displacement and rotation vectors from singular integral equations

09 p1402 A72-22745

Singular integral representations of displacement and rotation vectors for homogeneous isotropic centrosymmetric body, using Nowacki couple stress theory of thermoelasticity

16 p2465 A72-32984

Existence and uniqueness theorems for Cauchy problem solution for linear singular integrodifferential operator equation

16 p2417 A72-34010

Calculation of coefficients and error estimation for the interpolation quadrature formulas of simplest Cauchy-type integrals and singular open-contour integrals

18 p2705 A72-36808

A general method for integrating the Schrodinger equation with a singular right-hand side in a homogeneous and constant electromagnetic field

19 p2843 A72-38855

The lift coefficient of a supercavitating jet-flapped foil in a free jet.

21 p2992 A72-41236

Conditions for complete continuity of integral operators with stationary features in a space of continuous functions

23 p3307 A72-43224

Application of the method of mechanical quadratures to the approximate solution of nonlinear singular integral equations

24 p3419 A72-45646

SINGULARITY [MATHEMATICS]

Deformation, stress and singularity in cylindrical shells under concentrated circumferential loads, comparing with two dimensional elasticity and plate bending

02 p0291 A72-11662

Fast hyperbolic MHD flow past point source, considering geometry and disturbances singularities of MHD Mach cones

02 p0266 A72-12369

General theory of relativity, examining differences between singularities in stationary and nonstationary fields from gravitational equations solutions

02 p0261 A72-12675

Discrete system high order optimality sufficient conditions and methods for singular and nonsingular controls study

04 p0505 A72-14996

Expanding rotating shearing Bianchi type IX universe, investigating rotation effects on singularity

04 p0549 A72-15290

Multiple-input multiple-output linear time invariant feedback systems stability, investigating continuous-time case

04 p0507 A72-15694

Elastic analysis of circular cylinders with stress singularities from boundary discontinuities, mixed displacement and axial load conditions [ASME PAPER 71-WA/APM-18]

05 p0733 A72-15962

Penalty function method validity for singular solutions to optimal trajectory control problems with state variable inequality constraints

05 p0641 A72-16531

Approximations and bifurcations in flight dynamic system, investigating singular point motion over trajectory during partition process

05 p0611 A72-16582

Existence and bifurcation conditions of singular point consisting of spliced focus spliced out of ordinary trajectories, investigating stability

05 p0690 A72-16593

Lemma for determining relatively prime relationship between two multivariable polynomials, considering singularities of second kind

06 p0783 A72-17485

Optimal final value control systems in phase-variable canonical form, discussing feedback gain singularity structure for single and multiple input systems

06 p0793 A72-17954

N-body gravitational problem numerical integration treatment of close approaches, using transformations for eliminating differential equations of motion singularities

06 p0885 A72-18079

Singular controls calculation based on Poisson brackets, applying to nuclear reactor

06 p0849 A72-18300

Dirichlet and Volterra problem with prescribed singularities for plane with rectilinear boundary slits, applying to fluid mechanics

07 p0971 A72-20092

Matrices of fundamental solutions constructed for loading singularities and Green method in unbounded micropolar elastic continuum

07 p1095 A72-20243

Stress distribution near corner point in interface section of body with two prismatic components, noting state singularity investigation reduction to transcendental equation solution

08 p1249 A72-21944

Potential equations and singularities methods comparison for two dimensional flow field cascades and stress distribution elasticity theories

09 p1260 A72-22627

Functional analysis techniques for existence of holonomic solutions to linear differential equation systems with singular points

09 p1342 A72-23254

Singular control problems calculation in trajectory optimization using sufficient conditions for control values set form

09 p1291 A72-23432

Optimality conditions for dynamic control systems, considering multidimensional singular controls and state space transformations

11 p1608 A72-25324

Viscous liquid impulsive flow past semiinfinite plate, showing leading edge effects and boundary layer singularity existence

11 p1614 A72-25351

Flight mechanics of point with limited power propulsion system and energy storage unit, investigating variational maximum payload problem with singular control optimization

11 p1727 A72-25932

Lossless distributed rectangular microwave structure with dielectrics interposed between two conductive metallic layers, noting existence of transmission zeros and filter properties

11 p1607 A72-26990

Velocity dominated singularities generalized to solutions of Einstein equations with irrotational perfect fluid sources within hydrodynamic cosmological models

12 p1870 A72-27410

Gravitational theory strong discontinuity conditions, using basis variational equation for field and media model construction in general relativity theory

13 p2002 A72-28711

Singular moment stress homogeneous solutions of plane problem with semiinfinite cut in elasticity theory

13 p2056 A72-28773

Singular controls calculation based on Poisson brackets, applying to nuclear reactor

13 p1937 A72-29440

Gradient catastrophe /solution derivative discontinuity/ occurrence time for quasi-linear hyperbolic differential equations describing elastic string oscillations

14 p2130 A72-30194

Eigenvalues examination for self adjoint singular differential operators in Hilbert space by finite difference methods

14 p2126 A72-30619

Singularities of cylindrical shell under concentrated twisting couple, investigating axial and circumferential deformations and shear stress distribution

15 p2329 A72-32139

Singularity method treatment of vortex distribution induced velocity perturbations on flat plate at angle of attack, noting results similarity to lifting surface theory

15 p2180 A72-32466

Three dimensional potential flow with lift about solid body calculated by distribution of sink, source and vortex type singularities satisfying Laplace equation

16 p2342 A72-32896

A method of calculating acoustic resonance phenomena generated by the unsteadiness of singular pressure losses in the pipes

17 p2580 A72-34279

Magnetohydrodynamic flow in the region of a conductivity discontinuity at the wall

17 p2587 A72-34460

The collision singularity in a perturbed n-body problem.

17 p2609 A72-35107

Eigenfunction technique development to incorporate stress singularities at circumference of end planes into problem of solid cylinder compression between rough rigid stamps

17 p2633 A72-35403

Structure of a family of trajectories in the neighborhood of a singular point of a first-order differential equation of degree two

17 p2577 A72-35723

On the behavior of the electromagnetic field with crests

17 p2584 A72-35913

Binomial electronic filter design for nonnegative impulse transient response to obtain fast rise times via inline pole-zero configuration

18 p2672 A72-36053

Determination of the parameters associated with a singular pressure loss permitting the calculation of acoustic resonance phenomena and the role of these parameters

18 p2680 A72-36465

A singular multi-parameter eigenvalue problem in second order ordinary differential equations.

18 p2705 A72-36615

Boundary value problems for second order, ordinary differential equations involving a parameter.

18 p2705 A72-36619

Wave-front singularities for two-dimensional anisotropic elastic waves.

18 p2739 A72-37175

Approximations and bifurcations in flight dynamic system, investigating singular point motion over trajectory during partition process

19 p2748 A72-37553

Existence and bifurcation conditions of singular point consisting of focus fused from ordinary trajectories, investigating dynamic system stability

19 p2834 A72-37565

Singular control problems calculation in trajectory optimization using sufficient conditions for control values set form

19 p2782 A72-38515

Solutions to certain elliptic equations, which are positive in the vicinity of an isolated singular point

20 p2947 A72-39867

Singular moment stresses in homogeneous solutions of plane problem with semiinfinite cut within elasticity theory

21 p3116 A72-40274

Construction of a general cosmological solution of the Einstein equations with a singularity with respect to time

21 p3103 A72-40403

Comparison of the classical and the global solutions of the ideal resonance problem.

21 p3085 A72-41047

General solution of a system of differential equations with an irregular singular point

21 p3075 A72-41095

Singular stress concentration at sharp edge of wedge in contact with half plane in elastostatics

21 p3119 A72-41104

Elastic conservative structural systems stability with many degrees of freedom, discussing critical singular points effect

21 p3120 A72-41206

Combined tension-torsion elastic-plastic waves as propagating singular surfaces.

21 p3121 A72-41244

Line integral expressions along line singularity loop for elastic strain and curvature, observing plastic dislocations, distortions and rotations

21 p3125 A72-41511

Disclinations theory described by plastic and elastic distortions, considering line singularity and dislocation loop

21 p3125 A72-41513

Gravitational theory strong discontinuity conditions, using fundamental variational equation for field and media model construction in general relativity theory

22 p3204 A72-42089

Singular points in conical flow streamline patterns, considering rotational and irrotational flows

22 p3135 A72-42580

Widely convergent method for finding multiple solutions of simultaneous nonlinear equations.

23 p3308 A72-43400

Formal solution of a system of differential equations of fractional rank with an irregular singular point

23 p3308 A72-43579

Infinitely distant points of a differential equation

23 p3309 A72-43846

Application of the method of hydrodynamic singularities to the calculation of the velocity distribution in doubly-periodic infinite blade cascade systems

24 p3390 A72-44874

Determination of pressure losses in turbomachines.

24 p3393 A72-45353

Best finite elements distribution around a singularity.

24 p3420 A72-45786

SINKS
NT HEAT SINKS

SINTERED ALUMINUM POWDER

Al alloy powder metallurgy part production, discussing sintering procedures in nitrogen and dis-
solved ammonia in vacuum 02 p0233 A72-11440

SINTERING

Ti-Al-V alloy powders electrically activated pressure sintering /spark sintering/, considering mechanical properties and economic factors 02 p0240 A72-11428

Plastic flow material transport during sintering, considering dislocation nucleation mechanism 02 p0232 A72-11429

Dislocations forces during sintering of loose and cold-pressed metal powders, using photoelasticity for stress estimation and electron microscopy for defects structure 02 p0232 A72-11430

Thermal treatment for delayed and reduced crystal grain growth during sintering of oxides, metals and alloys 02 p0232 A72-11431

Metal powders sintering activation mechanism, considering heterogeneous metals particles diffusion flow, mutual solubility and crystal lattices distortion 02 p0232 A72-11432

Mechanical constraints effects on loose spherical metal particles sintering rates, considering one, two and three dimensional arrays 02 p0232 A72-11433

Oxygen content and stoichiometry effects on metal carbides grain growth in liquid phase sintering, discussing carbide-metal interface solution reaction as rate controlling mechanism 02 p0240 A72-11434

Ti powder technology, discussing pressed and sintered parts, forging and extrusion preforms and composites 02 p0233 A72-11437

Hydropressed sintered U-700 superalloy powder, noting weakened particle grain boundary conditions from mechanical properties and fracture studies 02 p0240 A72-11444

Holes dispersion hardening in sintered metal powder, discussing dispersed particle effects 02 p0233 A72-11446

Aluminum oxide dispersion hardened ferritic heat resisting Cr steel, describing liquid phase sintering effects on high temperature tensile strength 02 p0241 A72-11448

Corrosion effect on mechanical properties of sintered powder iron and bronze parts, describing test procedure for corrosion resistance determination 02 p0241 A72-11459

Presintering effects on dimensional change of iron powder compacts, using dilatometric, thermogravimetric, differential thermal analyses and resistivity measurements 02 p0233 A72-11461

Sintering and heat treatment effects on mechanical properties of atomized and mixed powders of Ni-Mo steel 02 p0234 A72-11462

Microstructure of prealloyed and premixed specimens of sintered steel 02 p0242 A72-11463

Press and sinter production of Ni maraging steel powder metallurgy parts 02 p0234 A72-11464

Transition metal oxides hot extrusion sintering, discussing temperature and pressure effects on compacting density 02 p0244 A72-12349

Powdered chromium carbide-nickel alloys phosphorus addition effects on sintering temperature, shrinkage, density and hardness 03 p0372 A72-13546

Heat treated single-phase Pr-Co powder compacts, measuring coercivity as function of annealing or sintering temperature [IEEE PAPER 7.3] 03 p0402 A72-13756

Ni-based metal graphite materials, investigating sintering process control variables effects on structure and phase composition responses 05 p0665 A72-16090

Steady and unsteady creep stages in porous body sintering and hot compacting, using three dimensional viscous flow theory 05 p0665 A72-16092

Co and carbide containing alloys, investigating milling and sintering temperature effects on technological and physical properties 06 p0829 A72-17831

Hot pressing of sintered refractory metal oxide powders of Ti, Zr, U, Nb and Cr, showing improved compacting by raising temperature 06 p0822 A72-18427

Phase composition and electrical and mechanical properties of compacted zirconium diboride/tungsten alloys after sintering in argon, carbonaceous medium and vacuum 06 p0832 A72-18428

Thin film formation techniques including evaporation, sputtering, anodization, chemical vapor deposi-

tion, electrodeposition and sintering, discussing surface scattering, tunneling, Schottky emission and conduction mechanisms 06 p0790 A72-18571

Optimum exposure time for sintering in Ar flow of porous rolled product of Ti powders determined from physicomechanical properties changes 07 p0996 A72-19964

WC powder milling and sintering, investigating strain and dislocation density effects on behavior by scanning electron microscope 08 p1176 A72-21440

Sintered cadmium sulfide films microstructure analyzed by X rays, discussing structural changes effects on dark resistance and photosensitivity 09 p1366 A72-22414

High temperature sintering induced dislocations in refractory materials, studying material and diffusion transport processes 10 p1496 A72-24244

Sintering and aging effects on mechanical behavior of low carbon copper steel 10 p1488 A72-24696

Powder metallurgy sintering process variables for dimensional control of bronze parts, discussing strength and porosity level specifications 11 p1640 A72-26243

Superconductive behavior of cold-worked sintered Nb wires, examining effects of aluminum oxide addition on residual resistivity, magnetization behavior and critical current density 11 p1662 A72-26742

Ball milling effects on alumina and tungsten carbide powder sinterability due to particle comminution and microstrains 11 p1642 A72-26827

Dislocation slip motions as densification kinetics mechanism in refractory materials sintering process, discussing electron microscopic observations of partially sintered MgO and W compacts 11 p1643 A72-26834

Ni additive effects on tungsten trioxide reduction with hydrogen and W powder sinterability 11 p1643 A72-26835

Mo powder sintering kinetics and disperse mechanism in isothermal and nonisothermal conditions 11 p1643 A72-26836

Work hardening and recrystallization grain structure of sintered and electron bombardment melted Ta after annealing 11 p1644 A72-26839

Antioxidation coatings of Ta and Ta alloys for high temperature long term operation, emphasizing sintered molybdenum disilicide 11 p1663 A72-26840

Solid state reactions in powder metallurgical production and working of Mo alloy, considering sintering process 11 p1644 A72-26846

Sintered Mo diffusion weld strength dependence on contact surface flatness and smoothness 11 p1644 A72-26847

Oxygen, carbon and boron effect on liquid phase sintering behavior and mechanical properties of Ni base superalloys 11 p1645 A72-26848

Isolation and sintering techniques and thermoelectric properties of lanthanum, yttrium and gadolinium borides 11 p1645 A72-26858

Chemical and physical activation mechanisms of sintering metal powder compacts 11 p1645 A72-26862

Cermets technology applications, discussing powder metallurgy role and sintering mechanism 11 p1665 A72-26871

Transition metals silicides additions effect on sintering and oxidation resistance at high temperatures of Ti and Zr diborides 11 p1665 A72-26874

W-Ni-Mo alloys obtained by powdered metals sintering, investigating mechanical properties, phase distribution and composition 11 p1666 A72-26876

Fracture micromechanism in liquid-phase sintered W-Fe-Ni powder composites, using scanning electron microscopy 11 p1668 A72-26942

Device for comparing powders friability to ascertain quality of compacts fabricated on automatic sintering presses, noting applications in ceramic, chemical and pharmaceutical industry 12 p1795 A72-27468

Iron powder specific surface and particle size effect on shrinkage during sintering 13 p1966 A72-29800

Sintering of binary systems Co-Ni Co-Fe and Fe-Ni with infinite mutual solubility at different temperatures 13 p1966 A72-29954

High porosity nichrome fiber materials sintering at 1000-1350 C, considering size, electric conductivity, shear strength, interfibrillar contact and briquet quality 13 p1967 A72-30105

Porous Ti alloys production with Mo, Cr and Pd, considering optimum sintering temperatures and hydrogenation 13 p1981 A72-30106

Deep diffused layer sintering of metal-ceramic cutting alloys with variable Co content for increased wear resistance and tensile strength 13 p1982 A72-30112

Pressed and sintered preforms of Ti and alloys for forge and extrusion operations, noting processing time reduction and smooth surface 13 p1982 A72-30120

Elastic deformations of porous Cu, Mo and W fiber materials after pressing and sintering due to residual stress relaxation 14 p2106 A72-30151

Sintering and melting preparation effects on mechanical properties of refractory W-Re alloys, considering sigma phase in solid alpha solution 14 p2116 A72-30530

Modified geometrical model for sintering Ni-doped W, including surface tension effect at Ni-vapor interface 14 p2121 A72-30770

Ferrite powder relative density as function of temperature, sintering time and pressure during hot pressing, noting creep activation energy and vacancy motion 14 p2107 A72-30775

Oxide inclusions induced reductions in Nabarro-Herring creep and sintering rates of metals, discussing effect of inclusions diffusional mobility in metal matrix 15 p2257 A72-32112

Notch sensitivity of sintered stainless steel powder as function of density from application of sharp crack fracture mechanics methods to plane strain fracture toughness 16 p2408 A72-33700

Electric spark activated hot pressing application for sintered composite structures, noting process parameters optimization for superalloy powders 16 p2411 A72-34093

Hot forging of sintered stainless steel 19 p2815 A72-37592

Shrinkage concentration behavior of two phase systems /Co-Ni, Co-Fe, Fe-Ni, Fe-Cu/ in sintering correlated with diffusion parameters 19 p2808 A72-38280

Hot pressing of transition metal nitrides and their properties 19 p2808 A72-38281

HfB2 and ZrN alloys 19 p2845 A72-38409

Electrical conductivity of pressed cadmium antimonide 20 p2959 A72-39218

Fabrication and properties of carbon-containing iron fibers and fiber sinter bodies 20 p2939 A72-39439

Mg-Al powder mixtures sintering and coining, describing fabrication procedure, microstructure and mechanical properties 21 p3067 A72-40832

Changes in the phase composition of metal-glass materials depending on the sintering temperature 21 p3073 A72-41370

Phase diagrams, microhardness and composition of sintered binary B compounds with Zr, Hf, Ta, Cr, Mo, W, Re, Fe, Ni, and Si 21 p3070 A72-41371

Solid-state reactions during the production of TZM molybdenum alloy by powder metallurgical methods 22 p3187 A72-41972

The effect of mixed milling on the sintering of WC-Co hardmetals. 22 p3188 A72-41975

German monograph - Contribution to the investigation of the fatigue strength of sintered iron. 22 p3194 A72-43066

Electrical resistivity changes in nichrome films sintering of various thickness with different heat treatment conditions, noting heat stability and thermal shock tests 23 p3292 A72-43280

Influence of the protective medium during sintering on the properties of iron-base cermets 23 p3299 A72-43289

Influence of the cooling rate after sintering on the structure and properties of the ZrGr1.5D2.5 cermet 23 p3303 A72-44014

Influence of the sintering medium on the quality of metalceramic hard alloys containing zirconium and hafnium carbides 23 p3303 A72-44017

SINUSES

NT PARANASAL SINUSES

Bainbridge reflex mechanism, showing sinus ganglion role in tachycardia onset 02 p0165 A72-12514

Regular sinus rhythm bundle branch block effect on ballistocardiogram dynamics 03 p0314 A72-13143

Frontal sinus hematoma incidence in flying personnel and scuba divers, discussing diagnosis and clinical treatment 12 p1765 A72-28275

SINUSOIDS

U SINE WAVES

SIPHONS

Dielectric siphons, using weak polarization force density exerted on insulating dielectric liquids by nonuniform electric field 04 p0520 A72-14416

SIRIO SATELLITE

Controversy surrounding Sirio satellite project related to microwave atmospheric propagation above 10 GHz with possible application in earth-to-space communication systems 17 p2623 A72-35918

SITES

NT LANDING SITES

NT LAUNCHING SITES

NT LUNAR LANDING SITES

SITTING POSITION

Leg cooling effect improving tolerance to positive headward acceleration in sitting position 04 p0479 A72-15210

Human vestibular stability under frontal and sagittal head tilts in rotating chairs, discussing motion sickness onset 05 p0622 A72-16640

Equal comfort contours for whole body vertical, pulsed sinusoidal vibration. 20 p2897 A72-39551

SIZE (DIMENSIONS)

Effects of yielding and size upon fracture of plates and pressure cylinders. 17 p2565 A72-34251

SIZE DETERMINATION

NT PRECIPITATION PARTICLE MEASUREMENT

Optimum cylindrical handle size determination by muscle electromyography, considering gripping task, routine performance and fatigue test 01 p0017 A72-10119

Chlorella algae size distribution curves by combining device for counting electrical conductivity pulses with discriminator for gamma scintillation spectrometry 01 p0017 A72-10400

Flat hole model for defect size definition from ultrasonic inspection as function of echo amplitude and depth 01 p0076 A72-10809

DGS diagrams for defect size determination in ultrasonic NDT 01 p0070 A72-11016

NGC 5128 nucleus radio emission flux density measurement, noting angular size 01 p0132 A72-11090

Object proportions estimation algorithms in single resolution element of airborne multispectral scanner 02 p0227 A72-11839

Photometric meteor mass determination, using models relating radiation intensity, meteor velocity, atmospheric density and instantaneous luminous flux 02 p0282 A72-12334

Size determination for stationary space charge clouds in streaming media from theoretical model of tanks filled with electrostatically chargeable inflammable fluids 02 p0261 A72-12554

Supernovae remnants intrinsic luminosity-diameter correlations from soft X ray emission data, taking into account interstellar medium 03 p0408 A72-13008

Inverse electromagnetic field problem for one dimensional resonator, determining size change from intrinsic mode 05 p0627 A72-16408

Radio sources fine structure survey at 81.5 MHz, finding angular diameters by interplanetary scintillation technique 07 p1081 A72-20231

Galactic clusters size determination from known red shift relation, discussing distribution inhomogeneities, evolution, universe expansion and Hubble constant correction 08 p1234 A72-21282

Rhesus monkey retinal image diameter estimation during exposure to Ar and He-Ne laser irradiation, using microphotometer scans 11 p1582 A72-25314

Photometric meteor mass determination, using models relating radiation intensity, meteor velocity, atmospheric density and instantaneous luminous flux 13 p2039 A72-29218

Target and surrounding nontarget stimuli size differences effect on visual search time for displays with large fields 14 p2083 A72-31153

Interstellar OH maser size determination, discussing scattering by inhomogeneities in electron distribution 16 p2456 A72-33473

Nomogram for heat detector size determination from thermal inertia index and Biot number 16 p2395 A72-33968

Sizing new generation aircraft wire and circuit breakers utilizing computer techniques. 17 p2498 A72-35568

On the size distribution of turbulent elements in the earth's atmosphere. 17 p2549 A72-35717

Analysis of grain- and particle-size distributions in metallic materials. 17 p2569 A72-35922

Photometric radii of Io and Europa. 17 p2619 A72-35946

Grain size distribution in recrystallized alpha-titanium. 19 p2820 A72-38297

Condensed zinc particle size determined by a time discrete sampling apparatus. 20 p2913 A72-39608

SIZE PERCEPTION

U SPACE PERCEPTION

SIZING

Sizing an external-fueled in-core thermionic reactor. 17 p2495 A72-34588

SKELETON

U MUSCULOSKELETAL SYSTEM

SKEWNESS

An equivalent grid framework for skew plates in flexure. 20 p2980 A72-39689

Non-linear flexural vibration of orthotropic skew plates. 23 p3355 A72-44375

SKILLS

U ABILITIES

SKIN (ANATOMY)

NT EPITHELIUM

NT LEATHER

Noceptive chemical action in cat skin vessels, showing fiber types for impulse transmission 02 p0164 A72-12511

Human skin thermal radiation properties, presenting data on reflection, emission, transmission and complex refraction [ASME PAPER 71-WA/HT-37] 05 p0620 A72-15888

Sympathetic responses in human skin nerves with accompanying vasomotor reactions induced by emotional, thermal and respiratory stimuli 10 p1424 A72-24241

Forearm skin and muscle blood flow change measurements during whole body heating, using plethysmography, isotopic labeling and blood sampling techniques 11 p1587 A72-26617

Chamois leather mechanical response, comparing stress relaxation and frequency response characteristics to human skin for applications in anthropometric dummy construction 15 p2191 A72-32606

Lipid peroxidation on the human skin surface following erythrogenic UV irradiation 19 p2757 A72-38087

Measurement of specific mechanical impedance of the skin - Effects of static force, site of stimulation, area of probe, and presence of a surround. 21 p3005 A72-40347

Resistance and capacitance vessels of the skin in permanent and temporary residents at high altitude. 22 p3144 A72-42595

Temperature sensitivity neurophysiological mechanism, discussing cold and heat sensitive receptors localized distribution in human skin and thermoregulatory function 22 p3146 A72-42779

Elaboration of steady changes in the firing rate of cortical neuron populations 24 p3370 A72-44587

SKIN (STRUCTURAL MEMBER)

Coated Nb alloys as radiative thermal protection system skin materials for space shuttle, investigating flaw growth 01 p0085 A72-10757

Thermoelastic effect on flutter and vibration of built up delta wings with solid, stiffened and honeycomb/corrugated sandwich skins [AIAA PAPER 72-174] 05 p0740 A72-16834

Corrosion resistant fabrication methods in jumbo jetliners components to reduce maintenance and repair downtime, discussing clad wing and fuselage skins 10 p1487 A72-24025

Rectangular skin panel vibration modes aerodynamic damping dependence on Mach number, dynamic pressure, mode shape and turbulent boundary layer thickness [AIAA PAPER 72-402] 11 p1568 A72-25423

Shotpeen contouring of Boeing 747 wing skins combined with incremental chip forming, noting principles and manufacturing process 12 p1817 A72-28160

Stress levels and fatigue in aircraft structures subjected to jet noise, noting stress calculation for skin panels and control surfaces 13 p1898 A72-29579

SKIN FRICTION

NT AERODYNAMIC DRAG

NT FRICTION DRAG

NT SUPERSONIC DRAG

NT VISCOUS DRAG

Increasing lift and Reynolds number effects on displacement and skin friction of three dimensional turbulent boundary layer on infinite swept wing 01 p0002 A72-11395

Skin friction measurement in nonisobaric subsonic flow with pressure gradient over airfoil section by surface impact probes 02 p0151 A72-12275

Local skin friction evaluation in compressible flow, using incompressible Clauser charts and sublayer methods for adiabatic and nonadiabatic situations 03 p0341 A72-13614

Steady two dimensional symmetric viscous flow past parabolic cylinder in uniform stream, correlating calculated nose skin friction with boundary layer theory 05 p0610 A72-17012

Navier-Stokes equation solution for laminar incompressible flow past parabolic cylinder, investigating skin friction and pressure drag 06 p0798 A72-17782

Pressure gradient effects on hypersonic turbulent skin friction and boundary layer temperature, velocity and Mach number distributions and shape factors [AIAA PAPER 72-215] 06 p0799 A72-17923

Second order effects in incompressible boundary layer flow with heat transfer, deriving numerical solutions for skin friction 07 p0968 A72-19625

Skin friction response to angle and perturbation in flow past axisymmetric body with unsteady main stream 13 p1941 A72-28887

Hypersonic limit for equilibrium laminar constant pressure boundary layer equations of planetary entry, obtaining skin friction and heat transfer parameters 14 p2071 A72-31052

Heated thin film gages calibration for skin friction measurements in laminar and turbulent flows, discussing wall temperature distribution and turbulence effects 15 p2241 A72-32577

Sharp flat plate laminar, transitional and turbulent skin friction via finite difference integration of compressible boundary layer equations 15 p2180 A72-32596

Simultaneous hypersonic skin friction and heat transfer measurements on sharp-edged flat plate, using thin-skin heat transfer gages and boundary layer pitot rake 15 p2219 A72-32598

Skin friction effects due to Hall currents in conducting unsteady slip flow over porous flat plate under transverse magnetic field 16 p2435 A72-33108

Drag of a flat plate with transition in the absence of pressure gradient. 18 p2641 A72-36775

A method of computing skin friction and adiabatic wall temperature in a laminar boundary-layer without pressure gradient. 21 p3046 A72-41202

Flat compressible turbulent boundary layers of air, predicting foreign gas injection effects on mass and heat transfer Stanton numbers and skin friction 22 p3165 A72-41958

Second order boundary layer solutions on a curved surface. [ASME PAPER 72-FE-21] 23 p3280 A72-44063

Frictionless core flow and friction layers at turbomachine walls and blades for real two dimensional cascade flow modeling 24 p3394 A72-45370

Integrodifferential equations for curved walls effect on laminar boundary layer characteristics, noting wall friction, layer thickness and transverse pressure 24 p3394 A72-45447

Measurements of skin friction on the wall of a hypersonic nozzle. 24 p3365 A72-45792

SKIN FRICTION DRAG

U FRICTION DRAG

SKIN RESISTANCE

Dynamic bioelectric impedance level of tissue area between active electromyograph electrodes related to human skeletal muscle fatigue 13 p1905 A72-29332

GaAs varactor diode design optimization based on calculation of cut-off frequency vs carrier concentration with consideration of skin effect 14 p2088 A72-30588

Skin effect in large hot tokamaks predicted by computer studies based on empirical transport coefficients, discussing suppression by moving limiter 16 p2433 A72-32812

Integral equation for electromagnetic field in diffuse boundary plasma, noting anomalous skin effect 21 p3090 A72-40409

SKIN TEMPERATURE [BIOLOGY]

Skin and hypothalamic temperature effects on human thermoregulatory responses, developing control mechanism for peripheral effects on skin sensors
02 p0160 A72-12041

Heat transfer through fabrics by convection, conduction, radiation and vaporization related to skin temperature and thermal injury
03 p0319 A72-13700

Leg cooling effect improving tolerance to positive headward acceleration in sitting position
04 p0479 A72-15210

Peripheral modifications to exercise induced central drive for sweating, determining rates as functions of internal temperature
04 p0479 A72-15212

Regulation of sweat secretion on skin surfaces overlying active and nonactive muscle tissue during skin or core temperature alterations
04 p0480 A72-15216

Human temperature regulation during upright and supine exercise, showing nonlinear relationships between perspiration and skin and core temperatures
07 p0922 A72-20275

Thermoregulation in deeply hibernating rodents during separate chilling and steady hibernation temperature maintenance of skin and brain
12 p1762 A72-27827

Underwater tests of instrument system for combined skin temperature and direct heat flow measurement in thermally stressful environments
12 p1768 A72-28334

Heat, noise and vibration stress combined effects on skin and rectal temperature, heart rate, weight loss and biochemical urinalysis
17 p2508 A72-34551

Skin temperatures in warm environments and the control of sweat evaporation.
17 p2506 A72-35969

The use of cholesteric liquid crystals in the study of skin temperature and their applications in aviation medicine
21 p3009 A72-41192

Heat strain in hot and humid environments.
22 p3150 A72-42492

SKUA ROCKET VEHICLES

Wind tunnel tests for correction of temperature profile data in stratosphere and lower mesosphere obtained from SKUA rocket sounding
14 p2105 A72-30807

SKULL

NT CRANIUM
NT INTRACRANIAL CAVITY

SKY
NT NIGHT SKY

SKY BRIGHTNESS

Atmospheric aerosols size/altitude distribution via sun aureole sky brightness and airborne particle counterpoint sampling measurements
02 p0213 A72-11860

Thermal IR radiation attenuation by atmospheric particulates, comparing computer simulated brightness temperatures with airborne radiometer and Nimbus 3 observed data
02 p0213 A72-11863

Daytime cloud cover space-time patterns from satellite sensed brightness values during 1967-1971
04 p0542 A72-14690

Brightness profiles of earth daytime horizon from Soyuz spacecraft photographic photometry, deriving atmospheric scattering coefficient relation to optical thickness vertical distribution
06 p0808 A72-18040

Azimuthal IR radiation distribution of atmospheric brightness cross sections at various zenith angles from balloon programmed-control radiometer data
06 p0808 A72-18042

Atmospheric directional scattering coefficients from vertical measurements of IR spectral sky brightness near solar aluminantar and direct radiation
06 p0842 A72-18048

Water and ice clouds spectral brightness coefficients in IR region of spectra from aircraft measurements
06 p0842 A72-18049

Telescopic requirements posed by Venus near sun, discussing sky brightness in image plane, atmospheric dust and Rayleigh scattering
08 p1230 A72-20993

Spectrophotometric measurements of sky radiance distribution to determine atmospheric pollution, ozone content and radiation attenuation by clouds
10 p1476 A72-25085

Starry sky energetic simulator design, analyzing comparative brightness of stars
13 p1945 A72-28494

Daytime sky brightness and scattered light polarization, emphasizing atmospheric radiation field characteristics
13 p1945 A72-28516

Sky spectral brightness, transmittance and indicatrix measurements at near IR wavelengths
15 p2222 A72-31398

X ray observation inadequacy in detection of background radiation surface brightness fluctuations due to irregular distribution within galactic cluster sources
18 p2729 A72-37006

Connection of the brightness indicatrices with the optical thickness of the atmosphere
22 p3200 A72-41874

Skylight intensity, polarization and airglow measurements during the total solar eclipse of 30 May 1965.
22 p3170 A72-42371

Brightness temperature of the terrestrial sky at 2.66 GHz.
22 p3173 A72-42516

SKY RADIATION

NT AIRGLOW
NT DAYGLOW
NT GEOCORONAL EMISSIONS
NT NIGHTGLOW
NT TWILIGHT GLOW

Sky light polarization, cloudiness and view angle effects on oil remote detection over water surface, describing passive radiometric techniques
[AIAA PAPER 71-1075] 01 p0057 A72-10536

Millimeter wave sky noise temperature measurement with 16 and 35 GHz radiometers, including antenna loss and rain and cloud effects
02 p0171 A72-11665

German monograph on sky scanner for short term sky spectral density distribution using glass fiber bundles for spectral components simultaneous measurement
07 p0983 A72-19266

UK-5 satellite all sky X ray monitor consisting of pinhole camera, position sensitive proportional counter and data processing electronics
08 p1228 A72-21513

Sun vicinity skylight polarization influence on polarimetric K corona observations, discussing inaccuracy sources
09 p1392 A72-23544

Coma constellation hard X ray intensity sky map at 20-150 keV from balloon observations
10 p1530 A72-24948

Daytime sky polarimetry of scattered light in atmosphere during solar eclipses
12 p1800 A72-27141

F region parameters relationship to night sky optical emission, considering electron distribution produced by dissociative recombination
12 p1802 A72-27308

Radio attenuation by rain at 37 GHz using sun as source compared with sky emission observations, noting apparent absorber temperature effect
12 p1783 A72-27665

Clear sky atmospheric thermal radiation from all-wave radiation and air temperature measurements, showing diurnal and desert condition induced deviations from empirical formula
12 p1840 A72-27706

Variation of tropospheric slant-path attenuation in the UK at 11.75 and 17 GHz.
22 p3155 A72-42751

A meteor spectrum in the infrared region.
23 p3341 A72-44473

SKY WAVES

NT WHISTLERS

Sky wave propagation over multisectionally homogeneous plane ground, calculating ground loss profile along path by compensation theorem
02 p0181 A72-12604

Geomagnetic field-hf sky wave orthogonality conditions, discussing ray tracing for signals reflected in ionosphere
05 p0630 A72-16619

Sky wave backscattering with narrow beam antenna coupled with signal modulations and Doppler shift as means of sea state observation and environmental monitoring
08 p1134 A72-21493

Vertical angle estimation for HF sky wave multimode signals arrival, noting validity for arbitrary antenna elements polarization
09 p1281 A72-23513

Sky wave propagation curves from MF observations for 7500 km distances
12 p1784 A72-27784

Polynomial surface approximation to OMEGA sky wave corrections for small computer compatible with automatic receiver
13 p1925 A72-29187

Sky wave correction /Swanson/ model and computer program for real time propagation prediction for airborne OMEGA system
13 p1997 A72-29190

OMEGA navigation system in civil maritime application, discussing single frequency, composite, difference and differential configurations and sky wave corrections
13 p1998 A72-29193

Automatic transmission and application of sky wave corrections with differential OMEGA navigation, discussing test equipment, procedures and results
22 p3203 A72-42948

Potential of the navy navigation satellite system in predicting ionospheric characteristics.
24 p3447 A72-45555

SKYLAB PROGRAM

Gimbale control moment gyro for Skylab telescope mount stringent pointing requirements, investigating normal and clamped operation modes and dynamic response of attitude control
01 p0097 A72-10382

Skylink project as prospective joint American-Soviet space mission, combining Skylab and Soyuz spacecraft
05 p0731 A72-17092

Skylab experimental space station, discussing environment comfort, Apollo spacecraft rendezvous for crew rotation and onboard experiments in earth resources, biomedicine, astronomy, etc
06 p0893 A72-18611

NASA space programs, discussing future Apollo, Skylab, orbiting space station, space shuttle and deep space projects
08 p1230 A72-21002

Skylab launch and mission program, describing modular components, crew training, checkout, launch and docking procedures, flight plan and crew working schedules, rescue and reentry procedures, etc
08 p1240 A72-21008

Skylab S-193 altimeter experimental mission objectives and spacecraft instrumentation, considering precision designs, oceanographic surface remote sensing and electromagnetic scattering measurement
09 p1306 A72-22317

NASA space station activities, describing Skylab missions and capabilities in physical and life sciences, earth resources surveying and technology experimentation
09 p1395 A72-22935

Safety design review for Skylab program based on experience from prior space projects and ground tests
10 p1550 A72-23990

Design review as management tool for complex systems quality and reliability assurance, discussing Skylab program
10 p1486 A72-24005

NASA ERTS and Skylab programs review, presenting information on spacecraft design, orbits, attitudes, sensors, image characteristics, data handling and processing, etc
10 p1539 A72-24323

Space maintainability experiment aboard submersible during 30 day drift mission, noting application to Skylab manpower distribution
10 p1431 A72-24442

Skylab earth resources experiment package, examining crew tasks
10 p1472 A72-24444

Space tools and support equipment for earth orbital systems maintenance, replacement and repair, discussing Skylab requirements and teleoperator applications
10 p1488 A72-25049

Skylab communications system, discussing voice, data, TV and command mission requirements and microwave instrumentation
12 p1781 A72-27366

Menu selection for SKYLAB astronauts by computer technique based on mixed integer programming code, using measure of pleasure lists
12 p1769 A72-27442

Cartographic and environmental surveys by Skylab orbiting stations and ERTS satellite using panoramic and mapping cameras and laser altimeter
15 p2232 A72-31247

Skylab radar altimeter for earth surface features remote sensing with high range resolution mode for ocean wave height determination
15 p2236 A72-31995

Digital autopilot for SKYLAB orbital assembly attitude control during docking, discussing jet selection logic, inter-axis dependence and onboard computer
15 p2269 A72-32183

Limit-cycle bounds of a satellite attitude-control system.
17 p2622 A72-35529

Passive stability of a spinning Skylab.
18 p2730 A72-36314

Operational earth observation systems and resources management - A global program.
18 p2725 A72-36539

Orbiting space laboratories for earth resources program, discussing satellites and Skylab missions and international cooperation
18 p2742 A72-36547

Space science advances and NASA Planetary Program, noting solar system evolution, life origin and Skylab and Space Shuttle programs
19 p2855 A72-37274

Attitude control of a spinning Skylab.
20 p2975 A72-39112

Skylab regenerable carbon dioxide removal system.
20 p2896 A72-39173

Mercury-cadmium telluride photoconductive detectors array for S-192 multispectral scanner for Skylab earth scanning experiments
23 p3288 A72-43879

New space processing experiments for the Skylab missions.

24 p3407 A72-45125

Rescue operation capability for Skylab, discussing mission requirements, response time and vehicle configuration

24 p3449 A72-45132

Skylab project participation by students to stimulate interest in science and technology, giving winning experiment proposals

24 p3467 A72-45158

Skylab solar astronomical observation programs and instruments, discussing X ray and H alpha telescopes, coronagraphs, spectroheliographs and UV spectrographs

24 p3453 A72-45528

OSO and Skylab astronomical instruments technology, emphasizing precision pointing, spatial and spectral resolution and photometric efficiency problems

24 p3405 A72-45545

SKYLARK

U SKYLARK ROCKET VEHICLE

SKYLARK ROCKET VEHICLE

Cosmic X ray sources polarization, spectra and locations measurement, describing Skylark experiments and UK-5 satellite-borne instruments

03 p0409 A72-13042

High resolution UV stellar spectroscopy in star stabilized Skylark rocket vehicle, using Cassegrain echelle optics and image intensification

03 p0354 A72-13056

High performance sounding rockets design, discussing Skylark propulsion system improvement and new rocket vehicle design for 200 kg payload capability with existing motor hardware

08 p1241 A72-21172

Skylark 904 sounding rocket cosmic X ray experiment, discussing detector and counter operation and data retrieval technique

10 p1529 A72-24198

SKYNET SATELLITES

Altitude determination during transfer orbit operation of SKYNET and NATO synchronous communications satellites

[AIAA PAPER 72-544] 12 p1876 A72-27367

British defense and civil communications satellite program, discussing Skynet, INTELSAT, ESRO and New Space Technology Program activities

[AIAA PAPER 72-548] 12 p1781 A72-27371

Military geostationary communication satellite Skynet 2 subsystems design development and testing

13 p2052 A72-29856

Skynet 1 synchronous satellite orbit determinations and longitude acceleration due to tesseral harmonics of earth gravity, using tracking station range data

15 p2321 A72-31949

SLABS

Infinite slab, cylindrical or spherical shells with nonuniform heat generation sources and equal surface temperatures, obtaining maximum internal temperature from error bounds

01 p0145 A72-10511

Heat transfer coefficients to both sides of finite one dimensional slab subject to phase-change coating technique boundary conditions, deriving thin wing correction factors

03 p0457 A72-13956

Electromagnetic scattering of square pulse from lossy dielectric slab mounted on perfectly conducting planar ground surface

07 p0945 A72-19660

Elastic wave scattering by moving slab, calculating reflection and transmission coefficients for various incidence angles, frequencies and motion velocities

15 p2219 A72-32476

SLAGS

Russian book on Nb in ferrous metallurgy covering physicochemical properties, steels, slags, ore reduction and smelting for Nb alloys production

11 p1659 A72-26048

Slag powdery material moisture content determination by absolute pyridine adsorption method of moisture extraction

12 p1813 A72-27450

Metal particle decomposition products composition in slags from smelted Cr, Ti, Ni and Zr alloys, using X ray microanalysis

14 p2112 A72-30157

Capillary heat convective diffusion model of liquid layer sandwiched between two planes for calculating slag and metal movement rates

16 p2476 A72-33157

SLANT PERCEPTION

U SPACE PERCEPTION

SLATER ORBITALS

Integrals for atomic wave functions of Slater orbitals, obviating numerical snags by Euler transformation

02 p0262 A72-11980

SLATS

U LEADING EDGE SLATS

SLEDS

NT ROCKET PROPELLED SLEDS

Use of a linear air bearing sled for dynamic calibration of velocity transducers.

22 p3179 A72-42693

SLEEP

NT HYPNOSIS

NT INSOMNIA

EEG and electrooculogram recording of chimpanzee sleep, noting rapid eye movement stages

01 p0009 A72-10074

Monotonous auditory stimulation frequency effects on human orienting reaction habituation and sleep onset

02 p0169 A72-12494

Human vestibulo-ocular responses to oscillatory rotational stimulation during various sleep and arousal stages, discussing Sugie-Jones reflex system mathematical model

04 p0474 A72-15249

Human male gonadotropin secretion relation to sleep stages, using electrophysiologic recordings and radioimmunoassay techniques

05 p0620 A72-17128

Circadian rhythms variations for sleep, EEG, temperature and activity in monkeys, indicating acrophase, amplitude and level regulation

07 p0918 A72-19528

Sleep pattern relation to duty hours of aircrew operating worldwide east-west routes

07 p0932 A72-20178

Isolation stress effect on circadian rhythmic patterns of EEG activity during sleep-wake and sleep cycles in unrestrained chimpanzee

[AD-739469] 07 p0921 A72-20181

Acoustic tests of jet aircraft noise and sonic boom effects on sleep pattern and human performance, using EEG analysis

[ASA PAPER W 11] 08 p1125 A72-21487

Physiology of sleep phases and dreams, discussing data on highly organized and interacting neurohumoral mechanisms exhibiting alternating forms of brain bioelectric activity

08 p1118 A72-21838

Electrophysiological, neurophysiological, metabolic, vegetative, psychological, chemical and pathological aspects of sleep, noting disturbance and wakefulness mechanisms for various clinical disorders

09 p1264 A72-22223

Neurophysiological mechanisms of sleep, studying sleep and wakefulness state evoked potentials relation to cortex and subcortical activity levels

09 p1264 A72-22224

Day/night workers sleep patterns in terms of intrasleep REM-NREM ultradian cycle, noting sleep temporal instability for night workers

10 p1428 A72-23730

EEG measurement of sleep behavior patterns, discussing sleep stages, temporal patterns, circadian rhythm, intrasleep process stability and age factor

11 p1580 A72-26679

Sleep, lack of sleep and circadian rhythm effects on psychometric test performance

11 p1581 A72-26684

Short sleep period and oxygen breathing effects on arousal level of air traffic controller during detection task performance

11 p1588 A72-26686

Sleep-wakefulness cycle variations effect on reaction time and spontaneous tempo during time isolation experiment, showing tendency toward circadian rhythm

11 p1581 A72-26687

Jet aircraft noise effect on sleeping EEG and subsequent waking performance, showing presence of carry-over effects

12 p1770 A72-27474

Deep brain structure biopotential correlations during man sleep development, using electrosuicortograms

13 p1901 A72-28634

Nocturnal primate *Aotus trivirgatus* wakefulness-sleep cycles during dark/light periods expressed in REM/non-REM percentages

13 p1903 A72-29300

Slow neural recovery processes during sleep, characterizing cerebral neurons synchronized and desynchronized sleep phases for mammals

16 p2355 A72-33557

Cerebral blood flow and metabolic changes during wakefulness, sleep, coma and epileptic seizures in terms of homeostatic mechanisms

16 p2356 A72-33558

Biotelemetry and computer analysis techniques for sleep states and wakefulness studies during aerospace flight

16 p2356 A72-33560

Sleep factors and limitations during prolonged space flights, considering weightlessness, hypokinesia, nervous tension, cabin confinement, rhythm, environment and noise effects

16 p2356 A72-33561

REM period functional maintenance of coordinated eye movement facilitation and binocular depth perception accuracy following sleep

17 p2509 A72-35462

EEG investigation of circadian variations in qualitative and quantitative RNA content in human leukocytes, noting changes during sleep

18 p2651 A72-36624

Dynamics of the electrical activity of various regions of the neocortex during the sleep-wakefulness cycle

22 p3147 A72-42955

Human prolactin - 24-hour pattern with increased release during sleep.

23 p3316 A72-43977

SLEEP DEPRIVATION

Time zone shift and p-chlorophenylalanine desynchronizing effects on sleep alteration and circadian rhythms in monkeys

03 p0318 A72-13071

Cerebral neurons population electric stimulation effect on deep sleep duration in Parkinsonism patients

04 p0476 A72-15585

Transmeridian flight psychological effects on aircrews, discussing anxiety, stress, circadian rhythm disruption and sleep loss effects on performance deterioration

06 p0766 A72-17816

Rapid eye movement sleep deprivation and hyperbaric oxygenation influence on gamma-aminobutyric acid levels in mice brains, suggesting protective mechanism against nerve cell oxygen intoxication

07 p0922 A72-20191

Sleep disturbance due to sonic booms, discussing laboratory findings and experimental techniques standardization

09 p1273 A72-23319

Diurnal rhythm and loss of sleep effects on human efficiency - Conference, Strasbourg, July 1970

11 p1580 A72-26676

Sleep deprivation effects relation to work duration, time of day, circadian rhythm, memory function, task performance, environmental factors, drug use and age

11 p1580 A72-26678

Sleep loss effect on reaction and movement times during information processing in step tracking task

11 p1580 A72-26680

Mental performance tests in sleep deprived subjects for indication of recuperative function of slow wave and REM sleep stages

11 p1580 A72-26682

Cumulative partial sleep deprivation effects on human performance in auditory vigilance, routine addition and running digit span tests, observing circadian rhythms

11 p1581 A72-26683

Sleep, lack of sleep and circadian rhythm effects on psychometric test performance

11 p1581 A72-26684

Sleep interruption, sleep deprivation and continuous darkness effects on circadian rhythms in human performance

11 p1581 A72-26685

Sleep loss and work-rest cycle effects on combat efficiency, considering psychomotor reactivity, vigilance and decision making capacity

11 p1588 A72-26688

Work-rest scheduling and sleep loss effect on operator performance in watchkeeping and active multiple visual tasks

11 p1589 A72-26689

Cumulative sleep deficit, preceding sleep or wakefulness period duration and body temperature effects on reaction time in multiple choice visual task

11 p1581 A72-26690

Sleep deprivation effect on circadian rhythms in human performance, psychological fatigue ratings, catecholamine excretion and urine flow

11 p1581 A72-26692

Sleep deprivation effects on diurnal urine potassium excretion, showing individual circadian rhythm variations

13 p1904 A72-29320

Biochemical analysis of cat brain regions for gamma-aminobutyric, aspartic and glutamic acids, glycogen and phosphatidolipid concentrations during paradoxical sleep deprivation

16 p2356 A72-33559

An objective test for evaluating the functional state of the oculomotor system during somnolence states

19 p2756 A72-37876

Sonic boom effects on sleep - A field experiment on military and civilian populations.

23 p3261 A72-44370

SLENDER BODIES

NT SLENDER CONES

Analog circuit method for slender profile flow field shock front boundary value problem for simple profile variation, using known mapping plane solutions [DGLR PAPER 71-069]

02 p0153 A72-12743

Multivortex model of vortex sheet development on slender axisymmetric bodies at angle of attack

03 p0307 A72-12919

Axial flow effect on vortex filaments stability by slender body analysis of force balance between Kutta-Joukowski lift and momentum flux inside filament [AD-740965]

03 p0307 A72-13157

Slender projectile supersonic flight in fluid with nonequilibrium transformations, comparing theoretical shock decay angle with Wegener-Klikoff measurements 03 p0307 A72-13158

Residence time of foreign gas introduced within wake recirculation region behind slender body in axisymmetric supersonic laminar/turbulent flow [AD-733525] 03 p0308 A72-13633

Unsteady supersonic flow disturbance by slender bodies in strong contact discontinuities in shock tube studies 04 p0462 A72-15507

Aerodynamic interference between parallel bodies for estimating aerodynamic characteristics of rocket engine with auxiliary boosters, obtaining flow field by slender body theory 05 p0600 A72-16005

Wake instabilities and vortices spacing, position and strength behind slender cylindrical bodies at large incidence with subcritical cross flow Reynolds numbers 05 p0610 A72-17010

Contact discontinuity motion past slender body of revolution in shock tube, solving unsteady supersonic flow problem by method of integral transformation 07 p0909 A72-20072

Iterative solution to gas dynamics equations for hypersonic flow past slender three dimensional body, applying to Cauchy problem 08 p1107 A72-20971

Slender body theory for flow calculation past low aspect ratio delta wing with straight trailing edge, noting lifting vortices distribution 10 p1420 A72-25131

Stokes flow about slender particle with nonuniform cross section under distributed force, obtaining solution to integral equation for twisted particle by perturbation scheme 12 p1798 A72-27834

Slender profile in nonuniform flow, deriving lift, normal force distribution and moment from vortex and source distribution induced flow field 13 p1894 A72-29005

Velocity perturbation functions in linear theory for bounded stream flow past slender profile 14 p2070 A72-31018

Slender rotating body aeroelastic behavior under inertial, gravitational, thrust, servocontrol, elastic and aerodynamic forces, presenting equilibrium equations in matrix form 15 p2319 A72-31210

Three dimensional boundary layer separation on slender bodies, delta wings and propulsion intake systems, reviewing computing techniques for interfering inviscid flow fields 16 p2341 A72-32826

Sonic boom induced flow field at supersonic/hypersonic speeds, using shock expansion method and hypersonic equivalence principle for sharp and blunt nosed bodies [AIAA PAPER 72-652] 16 p2349 A72-34082

Resonant mode sound field radiated by nonuniform slender circular cross section free-free beams, using dipole array modeling 18 p2710 A72-36410

Weak waves, characteristics, and the problem of flows past slender profiles in electrohydrodynamics 18 p2716 A72-36896

Aerodynamics of a slender cone with asymmetric nose bluntness at Mach 14. 20 p2886 A72-39634

Uniformly exact solution of the problem of the flow past a slender profile 20 p2886 A72-39904

Influence of thermal instability on the convective heat transfer coefficient for flows past slender bodies of arbitrary configuration 20 p2987 A72-39914

Correlation of Magnus force data for slender spinning cylinders. [AIAA PAPER 72-966] 22 p3135 A72-42344

Coning motion, autorotation, and vortex systems of slender flight vehicles 22 p3231 A72-42904

Determination of slender bodies of minimum total drag in hypersonic flow using Newton-Busemann pressure coefficient law. 23 p3249 A72-44267

Roll dynamic behavior of a very slender reentry vehicle. 24 p3452 A72-45348

Occurrence and inhibition of large yawing moments during high-incidence flight of slender missile configurations. [AIAA PAPER 72-968] 24 p3364 A72-45411

Hypersonic leading edge problem - Wedges and cones. 24 p3364 A72-45778

SLENDER CONES

Wind tunnel disturbances effects on hypersonic boundary layer transition on sharp cones, comparing hot-wire anemometer and surface pressure measurements [AIAA PAPER 72-181] 05 p0605 A72-16825

Finite difference integration based on theoretical model analysis of three dimensional turbulent boundary layer on sharp cone at angle of attack in supersonic flow [AIAA PAPER 72-187] 05 p0650 A72-16842

Forebody blowing induced dynamic instability effect on slender cones at hypersonic speeds, presenting theory based on unsteady imbedded Newtonian flow concepts [AIAA PAPER 72-311] 05 p0607 A72-16919

Three degrees of freedom motions of slender cones with slight compounded asymmetries in hypersonic flight wind tunnel stability tests [AIAA PAPER 72-28] 05 p0608 A72-16939

Nonsymmetrical aerodynamic damping moments on 10 deg cone at supersonic speeds and large angles of attack, comparing Newtonian theory prediction with wind tunnel test results [AIAA PAPER 72-29] 05 p0609 A72-16947

Laminar near wake solutions for slender ablating cone under supersonic atmospheric entry conditions including boundary layer reactions [AIAA PAPER 72-116] 07 p0907 A72-18954

Boundary layer transition on slender cone in hypersonic flow as function of nose bluntness, free stream Reynolds number and angle of attack [AIAA PAPER 72-216] 07 p0908 A72-18961

Turbulent wake of slender cone at Mach 12.5, measuring density and temperature fluctuations simultaneously [AIAA PAPER 72-118] 10 p1479 A72-24080

Magnetic balance measurements of aerodynamic forces on spheres and slender cones in hypersonic low density wind tunnels, noting sting effect 10 p1462 A72-24771

Base pressure distribution measurement for free flying sharp cone at hypersonic speeds and high angles of attack [AIAA PAPER 72-316] 11 p1567 A72-25250

Three dimensional laminar boundary layer on slender circular cone at angle of attack in supersonic flow, determining separated flow region via finite difference method 11 p1572 A72-25818

Experimental determination of the aeroacoustic environment about a slender cone. [AIAA PAPER 72-706] 17 p2486 A72-35482

Hypersonic wake aerodynamics at high Reynolds numbers. [AIAA PAPER 72-701] 17 p2486 A72-35484

Prediction of nose shape effects on nonlinear stability characteristics of slender cones. 20 p2886 A72-39628

Turbulent base heating on a slender re-entry vehicle. 21 p2992 A72-41308

Comparison of three oscillatory techniques for cones at incidence. [AIAA PAPER 72-1015] 21 p3042 A72-41595

German monograph - Pressure variation along a plane slender wedge and along a slender cone of revolution at decelerated flight in the supersonic range near sonic velocity. 22 p3136 A72-43074

Asymmetric nose bluntness effects on the aerodynamics of a slender cone at Mach 14. 24 p3363 A72-45342

SLENDER WINGS

Finite element discrete model for large aspect ratio wing transverse vibrations, using inhomogeneous elements with various stiffness-length relations 03 p0442 A72-13189

Nonlinear unsteady potential flow of incompressible fluid past slender wing, using linearized vortex distribution method 05 p0600 A72-16214

Viscous incompressible flow past longitudinally cambered small aspect ratio slender wing near solid interface 05 p0600 A72-16215

HP-115 slender wing research aircraft linear motion and undamped Dutch roll oscillations at high angles of attack [AIAA PAPER 72-62] 05 p0613 A72-16932

Nonuniform propeller streams effects on aerodynamic characteristics of high aspect ratio wing, using airfoil theory [AD-745477] 07 p0908 A72-19092

Static aerodynamic characteristics of bulbous based cone models and slender wings at subsonic speed, using magnetic suspension and balance system 10 p1461 A72-24769

Inviscid incompressible flow past longitudinally curved small aspect ratio slender wing, investigating aerodynamic characteristics 13 p1893 A72-28729

Aerodynamic center and center of pressure of slender small aspect ratio wing near solid or free surface, determining angle of attack effect 13 p1894 A72-29131

Vortex sheet simulation method for slender wing-canard surface nonlinear interaction investigation 16 p2458 A72-33695

Calculation of an unsteady separation flow past a slender profile 18 p2642 A72-36900

Experimental investigations of separated flows on wing-body combinations with very slender wings at free-stream Mach numbers from 0.5 to 2.2. [ICAS PAPER 72-25] 21 p2991 A72-41150

SLEWING

Interference suppression design of switching circuits utilizing slewing rates. 20 p2906 A72-38982

SLIDES

U CHUTES

SLIDING

Friction and wear properties of carbon fiber reinforced polymers sliding against metals in pure and sea water and aqueous solutions 16 p2396 A72-33123

SLIDING CONTACT

Spiral grooves gas bearing theory, taking into account sliding and gas compressibility effects on load carrying capacity 02 p0236 A72-11585

Dynamic analysis of vertical rotor rotating in elastic sliding bearings, analyzing precession stability and self oscillation zone 04 p0594 A72-15748

Sliding bearing structural features and materials effects on running and friction behavior at contact surface 07 p0998 A72-20524

The testing of contact materials for slip rings and brushes for space application. 18 p2698 A72-36117

On the stability of rotor-and-bearing systems and on the calculation of sliding bearings. 18 p2696 A72-36708

Installation for the simultaneous measurement of the functional properties of sliding contacts 20 p2928 A72-39936

Investigation of the nature of photostimulated exoelectronic emission during the friction of precision contacts 22 p3183 A72-43158

SLIDING FRICTION

Cobalt and lanthanum with face and body centered lattices, studying plastic deformation during allotropic transformations under sliding friction and gripping 01 p0074 A72-10579

Ultralow sliding friction during bombardment of polypropylene, molybdenum disulfide and graphite surfaces with charged helium atoms at room temperature in vacuum chamber 02 p0249 A72-12282

Sliding friction and wear behavior of carbon fiber reinforced composites with thermosetting resins, thermoplastic polymers and metal base materials 04 p0537 A72-14747

Nimonic 75 sliding pin and rotating disk frictional force, wear rate and surface temperature 06 p0830 A72-18156

Polyarylates, polyimides and thermosetting polymers role in sliding friction of self lubricating plastics, noting temperature effects 06 p0837 A72-18599

Molybdenum disulfide lubricating effectiveness improvement with finer particles at aggravated sliding conditions, suggesting surface roughness qualifications 06 p0837 A72-18605

Steel/teflon sliding friction in high vacuum at stepwise controlled oscillation frequencies, sliding rates and loads 07 p0964 A72-18863

Solid lubricant additives effects in oils and fats, discussing molybdenum disulfide and zinc pyrophosphate solid film formation on metal surfaces under contact friction conditions 07 p1024 A72-20395

Sliding bearing structural features and materials effects on running and friction behavior at contact surface 07 p0998 A72-20524

Sliding friction and normal force adhesion under ultrahigh vacuum environment, describing test apparatus for real time analysis via contact resistance measurement 08 p1176 A72-21436

Cicala formulas generalization and plasticity theory for deformation strain anisotropy, sliding and elastic strains influence on shear stress 08 p1246 A72-21806

Wear mechanism of lead-bronze dry sliding in air on hardened steel ring 11 p1638 A72-25510

Ultralow sliding friction during bombardment of polypropylene, molybdenum disulfide and graphite surfaces with charged helium atoms at room temperature in vacuum chamber 11 p1639 A72-25707

Reciprocating O ring seal sliding friction behavior prediction by elastohydrodynamic theory, noting dwell time, acceleration rate and previous deceleration effects 12 p1816 A72-28110

Ridge dimensions determination and causes of self oscillation in solid surface layers deformation under sliding friction 12 p1817 A72-28182

Sliding dry friction of hard refractory metals and ceramics, discussing surface changes as function of load, sliding speed, temperature and mechanical properties

12 p1817 A72-28184

Resonant contact vibrations of sliding element in direction normal to friction surface, noting lubrication damping effect

12 p1818 A72-28188

Wear micromechanism in hard and brittle chromium steels under cyclic slide friction loads

12 p1818 A72-28194

Characteristic friction curves /Mohr circle envelopes/ to describe stressed state region with various stresses produced by slide friction in steel due to indentation

12 p1819 A72-28198

High vacuum mass spectroscopic analysis of volatile products released under friction from solid synthetic resin lubricants with molybdenum disulfide as antifriction filler

12 p1835 A72-28199

Temperature effects on synthetic rubber sliding friction characteristics against smooth steel surfaces under compression loads in vacuum and air at 10-140 C

13 p1962 A72-28554

Molybdenum disulfide-tantalum compact solid lubricant wear rate as function of load and sliding velocity, presenting test data statistical interpretation [ASLE PREPRINT 72AM 15]

13 p1964 A72-28972

Jet fuel hydrocarbon group chemical composition effects on antiwear characteristics in sliding friction and rolling simulation experiments

13 p2024 A72-29073

Monograph on rotor-bearing stability and sliding bearing calculation covering rigid and flexible supports, gyroscopic effects, cavitation, load capacity, etc

15 p2243 A72-31349

Negative slip reversal effect formation mechanism during friction, discussing elimination via oleic acid as lubricant additive

17 p2559 A72-34663

Tribological properties of gold for electric contacts.

18 p2693 A72-35980

Friction, wear and noise of slip ring and brush contacts for synchronous satellite use.

18 p2693 A72-35982

Frictional stick-slip autooscillations suppression by resonance effect during forced vibration in normal direction

18 p2695 A72-36238

Application of boundary layer concepts to turbulent lubrication theory of bearings and seals.

18 p2696 A72-37052

Characteristics of a closed-type aerostatic slider bearing

19 p2809 A72-38565

Method of investigating the wear of hard tungsten carbide cobalt alloys in a liquid nitrogen medium.

20 p2941 A72-39715

Technological utilization of Weissenberg viscoelastic effect for sliding bearings centripetal pressure lubrication, noting analogy with human and animal skeletal joints lubrication

22 p3183 A72-42875

German monograph - Control performance as a function of the transmission ratio and the Coulomb friction in the operational element.

22 p3152 A72-43052

Manifestation of the effect of adsorptive reduction in strength under conditions of selective transport during boundary friction

22 p3183 A72-43138

Influence of the degree of strain-hardening and roughness of friction surfaces on wear rate and carrying capacity

22 p3183 A72-43157

Investigation of the nature of photostimulated exoelectronic emission during the friction of precision contacts

22 p3183 A72-43158

Infrared spectroscopy for chemical composition of inorganic and organic products formed on friction surfaces of gas turbine parts immersed in hydrocarbon fuels

23 p3325 A72-43974

SLIP

Critique of theoretical and experimental findings on slip geometry in bcc metals, especially Fe-Si alloy single crystals

01 p0089 A72-11300

Secondary slip in impact loaded Al single crystal disks, interpreting face deformation bands

02 p0247 A72-12819

Cu single crystal fatigue life explanation by work hardening using statistical theory of slip

03 p0379 A72-14258

Velocity /viscous/ slip coefficient and diffusion slip velocity in multicomponent gas mixtures by linearized Boltzmann equation

04 p0513 A72-15334

Negative slip reversal effect formation mechanism during friction, discussing elimination via oleic acid

08 p1181 A72-22092

Plastic slip in notched half plane undergoing antiplane deformation, using screw dislocation continuous distribution theory

09 p1403 A72-22747

Velocity slip effect on squeeze film between porous rectangular plates, calculating pressure, load carrying capacity, film thickness and response time

10 p1488 A72-24820

Numerical solution of two massive rigid bodies impact with variable slipping direction using Routh momentum change theorem

11 p1735 A72-25769

Slip and mechanical twinning in nickel-nickel niobide directionally solidified eutectic alloy, showing variation with temperature of stress-strain curves

11 p1667 A72-26935

Orientation dependence of slip in tantalum single crystals.

17 p2567 A72-34748

On basic principles of the slip theory of plasticity.

21 p3121 A72-41241

SLIP BANDS

U EDGE DISLOCATIONS

SLIP CASTING

Slip cast fused silica ablation in high temperature hydrogen-oxygen environment, comparing analytical results with measured data from rocket motor exhaust experiments

08 p1191 A72-21601

Slip casting process for ceramics, cermets and metal powders, discussing slurry preparation, deflocculating agents, binders and molding process

10 p1502 A72-24733

SLIP FLOW

Gas slip flow and transverse oscillations boundary value problems solution, using Wiener Hopf integral equation

02 p0205 A72-12355

Approximate solution in gas kinetic theory, considering temperature jump, velocity and viscous slip problems

02 p0205 A72-12356

Grain size effect on age hardened Mg-Zn alloy yield and flow stress, using tensile test and electron and optical microscopy at various temperatures

03 p0374 A72-13716

Asymptotic integration method solution of heat transfer equation with constant wall temperature for low speed slip flow regime

[ASME PAPER 71-WA/HT-5] 05 p0599 A72-15866

Centrifugal impeller slip factor prediction from three dimensional flow influences, discussing fluid passage guidance, flow separation, eddy and viscous effects

05 p0610 A72-17247

Thermomagnetic slip produced by certain temperature gradient and magnetic field combinations in rarefied polyatomic gas channel flow

07 p0973 A72-20399

Galerkin method for numerical simulation of incompressible boundary flows in box geometries with periodic and free slip conditions, noting Taylor-Green vortex decay

09 p1294 A72-22941

Temperature-slip problem in rarefied gases, obtaining exact solution by generalized BGK scattering model and Wiener Hopf technique

14 p2095 A72-30882

Binary gas mixture slipping rate determination from joined solution of Hamel kinetic model linearized equations, and Navier-Stokes and Boltzmann equations

14 p2096 A72-31013

Skin friction effects due to Hall currents in conducting unsteady slip flow over porous flat plate under transverse magnetic field

16 p2435 A72-33108

Hypersonic viscous, slip flow over insulated wedges.

20 p2885 A72-39612

One dimensional variable slip and homogeneous model predictions of momentum flux in two phase two component low quality flow

21 p3130 A72-41179

Two dimensional MHD fluctuating flow of incompressible electrically conducting rarefied gas past infinite porous wall for slip-flow regime with variable suction

21 p3095 A72-41784

Effect of gas slipping on drag in a system of parallel cylinders at low Reynolds numbers

22 p3133 A72-42268

Falkner-Skan flows with slip.

23 p3281 A72-44068

SLIPSTREAMS

NT PROPELLER SLIPSTREAMS

Plane laminar semibounded incompressible fluid jet propagation into slipstream along moving plate, solving boundary layer equations

10 p1471 A72-25136

Slipping stream instability of a self-gravitating hydromagnetic gas cloud.

17 p2613 A72-35501

Circular-elliptical transformation of jet propagating in homogeneous slipstream within unperturbed uniform transverse magnetic field, using linearized three dimensional boundary layer equations

18 p2716 A72-36815

Structure of turbulent underexpanded jets expelled into a submerged space and into a slipstream

18 p2642 A72-36884

Analytical prediction of vortex-ring boundaries for helicopters in steep descents.

20 p2886 A72-38949

Mixing of slipstreams in a channel of constant cross section in the presence of a recirculation zone

21 p3129 A72-40982

Experimental and design investigation of a supersonic wall jet in a supersonic slipstream

22 p3133 A72-42254

Laminar to turbulent transition in axisymmetrical submerged jets and slipstream flows of air and He, discussing Reynolds number effect

22 p3166 A72-42270

SLITS

Photomaterial nonlinear effects on contour distortion in holographic recording of Fourier image slit for graphic memory use

04 p0522 A72-15150

Axisymmetric thermoelastic state of isotropic infinitely long circular cylinder with external annular cut, determining cut plane normal thermal stresses

08 p1245 A72-21668

High resolution Hadamard transform IR spectrometer with single slit and multiplex scan operation modes determined by signal strength, noise characteristics and scanning time

09 p1313 A72-23327

Schlieren photographic investigation of shock wave propagation over narrow slit, noting cylindrical expansion wave origin at slit upstream edge

11 p1616 A72-25920

Spectrometer entrance slit diffraction effects on observed fast beam spectral line width

15 p2280 A72-31383

The precise simulation of image transfer systems with the aid of an optical convolution obtained with a rotating slit of prescribed form

23 p3261 A72-44361

SLOPES

NT GLIDE PATHS

Slope angle determination with respect to photograph surface from visible horizon line configuration

15 p2238 A72-3212

Mars - The effects of topography on baroclinic stability.

22 p3225 A72-42504

SLOSHING

U LIQUID SLOSHING

SLOT ANTENNAS

Radiation patterns of symmetrical dipoles or small apertures on perfectly conducting sphere, using dyadic Green function analysis

01 p0030 A72-10844

Automatically retrodirective performance from circular arrays and circularly continuous aperture antennas, applying method to cylindrical antennas

01 p0043 A72-11248

Parallel longitudinal resonant slots in rectangular waveguide broad wall, determining mutual impedance from magnetic field reaction

02 p0173 A72-12109

Dielectric loaded cavity or waveguide slot antennas for telemetry applications, describing design and fabrication

02 p0192 A72-12157

Rectangular slot antennas radiation through inhomogeneous plasma layer with dielectric window, obtaining input admittances by fields modal expansion

04 p0554 A72-14412

Arbitrarily located inclined resonant slot in waveguide antenna, obtaining condition for circularly polarized radiation from scattering parameters analysis

04 p0499 A72-15205

Feld modification for integrodifferential equation solution for voltage on exponentially narrow waveguide slit, discussing further changes in method

04 p0501 A72-15409

Radiation field from slot antennas on semiinfinite conducting cone surface, evaluating patterns for various cone angles, slot positions and azimuthal variations

06 p0781 A72-17342

Slot excited conical antenna, calculating first order diffraction coefficients by integral expressions for radiation field

06 p0781 A72-17343

Half wavelength antenna radiation admittance into warm lossy two layer plasma half space, using effects of slot width and electron collision frequency

06 p0781 A72-17348

Ground plane curvature effect on aperture admittance of waveguide fed axial slot on teflon coated metal cylinder for underdense plasma

06 p0771 A72-17354

Dual integral equations solutions to electromagnetic wave diffraction at plane conducting slotted screen
06 p0773 A72-17689

Single slotted waveguide linear arrays, discussing microwave antenna design and feeding and cross polarization suppression
06 p0784 A72-17740

Microwave attenuation due to ohmic losses in periodic linear arrays of metallic cylinders, ribbons and slots in metallic ground plane
06 p0786 A72-18372

Ground plane absorption coefficient effects on admittance of slot antenna radiating into warm lossy plasma
07 p0957 A72-19797

Statistical analysis of magnetic energy-density antenna performance in mobile communication, comparing two-crossed-slot design to three element unit
07 p0957 A72-19801

Synthesis of slot antenna on metallic wedge for amplitude radiation pattern, determining RMS approximation and fixed phase diagram
10 p1436 A72-24506

Optimum synthesis of antenna array of slot radiators with passive elements, using nonlinear programming
11 p1597 A72-26708

Optimal sum-difference characteristics of nonsuperdirective convex slot spherical antennas for maximum directive gain and minimum spatial sidelobe radiation
11 p1598 A72-26713

Optimal directional gain and slope difference characteristics of cylindrical nonsuperdirective slot antennas, relating sidelobe-main lobe radiation
13 p1927 A72-28408

Rectangular slots linear array and feed network performance in reentry plasma environment, obtaining self and mutual impedances, gain and radiation pattern
13 p1916 A72-28537

Electromagnetic cylindrical wave diffraction by linear emitter in parabolic cylinder with slots
13 p1917 A72-28709

Combination antenna unit with vertical monopole and two perpendicular slots in horizontal plane to yield steerable cardioid-shaped pattern for vertically polarized waves
15 p2206 A72-31776

Narrow strongly radiating slot voltage distribution, investigating cavity coupling with integral equation
15 p2209 A72-32659

Analysis of antennas on finite circular cylinders with conical or disk end caps.
17 p2525 A72-34361

The monopole slot - A small broad-band unidirectional antenna.
17 p2525 A72-34367

Frequency-scanned X-band waveguide array.
17 p2525 A72-34374

The transient radiated field of a coaxial aperture antenna.
18 p2660 A72-36331

Analysis and element pattern design of periodic arrays of circular apertures on conducting cylinders.
21 p3026 A72-40351

Wave equation for infinitely long slotted screen in elliptic cylindrical coordinates, noting radiation pattern for phased antenna array of metallized hyperbolic striplines
21 p3028 A72-40507

Ground-based Doppler navigation waveguide slot antenna design for optimal directional multilobe reception from aircraft
21 p3028 A72-40509

Plexiglas spheres and cubes effect on circular and rectangular waveguide aperture antennas directive radiation patterns and sidelobe reduction
21 p3021 A72-40904

SLOTS

NT WING SLOTS

Linearly polarized wave excitation with specified phase shift and predetermined amplitude ratio by waveguide slots, giving slot configuration design formulas
04 p0487 A72-15243

Stability control of rotating circular plates with edge slots and membrane stresses by finite element method [ASME PAPER 71-WA/AUT-2] 05 p0733 A72-15951

Reciprocal effects of rectangular guide-slot radiators with circular polarization, analyzing field ellipticity factor change for cross-cut slot under neighboring array slots influence
05 p0635 A72-16336

Polarization and energy characteristics of two mutually orthogonal slots cut in rectangular guide, allowing for reciprocal effects of slot arms
05 p0635 A72-16337

Slot length effect on buckling load of cylindrical shell with circular holes
05 p0739 A72-16543

Longitudinal and transverse nonresonant slots on waveguide, calculating susceptance, conductance, reflectance and transmittance as function of wavenumber
07 p0952 A72-18843

Laminar-turbulent incompressible boundary layer transition prevention by suction slots on bodies of revolution, determining optimal suction power/slot distance conditions by variational methods
07 p0968 A72-19737

Monograph on slotted circular waveguide analysis covering boundary value problem solution by Wiener-Hopf and Galerkin procedures and application to far field determination
09 p1279 A72-22925

Double slot laminar film cooling, considering tangential gas injection velocities into laminar boundary layer and heat transfer to wall [AIAA PAPER 72-290] 11 p1741 A72-25228

Parabolic boundary layer finite difference model for predicting film cooling and heat transfer near flush injection slots in gas turbine combustors
11 p1614 A72-25229

Comparison of experimental and numerical results concerning a hollow photoelastic bar with a slot subjected to torsion
21 p3122 A72-41337

An experimental study of film cooling through a rearward-facing slot.
23 p3356 A72-43971

Reduction of end losses in cascades of cambered blades
23 p3248 A72-44025

SLOTTED ANTENNAS

U SLOT ANTENNAS

SLOTTED WIND TUNNELS

A new method for the evaluation of slotted wind tunnel interference parameters applicable to subsonic oscillatory tests.
21 p3043 A72-41642

SLOW NEUTRONS

U THERMAL NEUTRONS

SLURRIES

Niobium alloy for reentry vehicle heat shields, describing slurry coating process reliability
01 p0077 A72-10982

SLUSH

Slush, boiling methane and methane mixture characteristics, noting advantages as potential rocket, aircraft and motor vehicle fuels
04 p0564 A72-15542

SMALL ASTRONOMY SATELLITES

Small astronomy satellite program for X ray experiments and mapping, discussing structure design, systems, testing and launching
03 p0441 A72-14395

High energy X ray and gamma ray astronomy for galactic and extragalactic observations, noting SAS satellite and HEAO program
05 p0712 A72-15773

SMALL PERTURBATION FLOW

Subsonic linearized theory for symmetrical cranked wings at zero incidence, presenting corrected formulas for streamwise and spanwise perturbation velocity components due to wing thickness
01 p0001 A72-11154

Hydrodynamic stability small perturbation theory, considering potential flow in contact with flexible membrane
07 p0969 A72-20067

Free convection effect on plane crystallization front instability under conditions of phase transition, using method of small perturbations
08 p1151 A72-21661

Relaxation hypothesis of cavitation erosion based on small perturbations, eliminating theory-experiment contradictions
13 p1941 A72-28776

Three dimensional ideal incompressible fluid flows under small velocity perturbation, using linearized Euler equations with respect to steady flow
16 p2375 A72-32932

Nonlinear instability of two dimensional unbounded incompressible viscous fluid flows under periodic small perturbation
16 p2376 A72-32933

Three dimensional small perturbation effects on laminar and turbulent low and high speed boundary layer flows [AIAA PAPER 72-713] 16 p2344 A72-34034

Instability of a moving plane-parallel layer
18 p2682 A72-36883

Mechanism for relaxation of cavitation erosion based on small perturbations, eliminating theory-experiment contradictions
21 p3044 A72-40271

The development of inlet flow distortions in multi-stage axial compressors of high hub-tip ratio. [ICAS PAPER 72-20] 21 p3099 A72-41145

Plane potential flow stability with respect to small perturbation flow of bounded and free hollow vortices, using conformal mapping method
22 p3165 A72-42093

Theory of a boundary layer with abruptly varying boundary conditions
22 p3166 A72-42259

SMELL

U OLFACTORY PERCEPTION

SMELTING

Russian book on Nb in ferrous metallurgy covering physicochemical properties, steels, slags, ore reduction and smelting for Nb alloys production
11 p1659 A72-26048

Metal particle decomposition products composition in slags from smelted Cr, Ti, Ni and Zr alloys, using X ray microanalysis
14 p2112 A72-30157

Lower oxide mechanism in reduction-oxidation reactions during Ti steels electrosmelting with slag and gas phases
14 p2112 A72-30158

SMOKE

Smoke plume opacity or particulate content measurement by laser backscatter, using Q switched ruby and Nd lidars [AIAA PAPER 71-1087] 01 p0058 A72-10544

Flammability smoke hazards and combustion product toxicity tests of plastics [PI PAPER 2] 03 p0379 A72-13243

Army aircraft gas turbine engines pollution potential evaluation program, considering smoke emission, noise and invisible pollutants
07 p1053 A72-18772

Physical properties, combustion characteristics and applications of pyrotechnic castable composition for smoke generation
08 p1222 A72-20785

Smoke development of plastics under various fire parameters.
17 p2570 A72-34718

SMOKE ABATEMENT

Aircraft interior materials selection relative to fire hazards and smoke emission properties [PI PAPER 18] 03 p0380 A72-13249

National Aviation System technology, discussing wide body jets, smokeless turbofans, all-weather operational capability, collision avoidance and noise reduction
04 p0597 A72-14824

Combustion research for reducing jet aircraft pollutant emissions, discussing fuel atomization improvement, smoke reduction and combustor design techniques
11 p1705 A72-26037

Exhaust composition and smoke emission reduction from aircraft with gas turbine power plants
12 p1860 A72-27270

SMOKE TRAILS

Aircraft engine exhaust geometry effects on smoke plume visibility, describing carbon particles light absorption characteristics by Beer-Lambert law [ASME PAPER 71-WA/GT-10] 05 p0704 A72-15903

Apollo 6 photogrammetric, photometric and neutron activation analysis of smoke plume, determining eddy diffusivity
06 p0819 A72-18439

Aircraft gas turbine engines smoke emission sampling by stained filter technique, comparing Navy specifications AS 1833 with SAE method ARP 1179
07 p1053 A72-18770

Smoke trail motions in winds with constant shear, considering potential, vorticity and stratified flows [AD-742738] 10 p1475 A72-24748

Smoke generator for fluid flow visualization, presenting photographs of turbulent rotating air flow in cylindrical enclosure [AD-746416] 11 p1613 A72-26540

Smoke-trail method for obtaining wind profiles.
22 p3202 A72-43144

SMOOTHING

NT DATA SMOOTHING

Optimal smoothing for continuous-time systems with multiple time delays.
17 p2534 A72-35536

SMS

U SYNCHRONOUS METEOROLOGICAL SATELLITE

SNAKES

Effect of activity and temperature on metabolism and water loss in snakes.
22 p3144 A72-42669

SNAKING

U LATERAL OSCILLATION

SNAP

NT SPACE POWER UNIT REACTORS

SNAP 19

Electrical power subsystem design in Pioneer F/G spacecraft, using SNAP 19 deployable radioactive thermoelectric generators supplemented by Ag-Cd battery
01 p0008 A72-11065

SNATCHING

U SPACECRAFT RECOVERY

SNOW

Soyuz manned spacecraft meteorological observations, dealing cloud cover in various climatic zones, atmospheric turbidity and snow cover in mountain areas
02 p0253 A72-11731

Natural and artificial snowpacks microwave brightness temperature variations with snow depth,

free water content and underlying material characteristics

02 p0212 A72-11832

Aerial Radiological Measurement System for environmental radiation detection and tracking, emphasizing snow mass prediction by terrain radiation attenuation measurement

02 p0215 A72-11884

Computerized synoptic weather map forecasting of heavy snowfall in Colorado

04 p0542 A72-14685

Radar instrument for measuring snow density, water content, layer depth and inhomogeneity based on snow cover electrical properties effects on echo characteristics

06 p0805 A72-17591

Worldwide inventory and monitoring of ice and snow aggregations via satellite photography, discussing climatological aspects

09 p1303 A72-23302

Snow accumulation determination from snow intensity based on visibility estimates, noting application to forecasting

11 p1682 A72-26085

Radar range reduction by snowfall, considering path attenuation and clutter power backscattered from near target precipitation

13 p1917 A72-28699

Fog, cloud, rain and snow detection by acoustic echo sounding, noting effects of energy scattered from atmospheric boundary layer velocity and temperature fluctuations

15 p2267 A72-32725

A presumptive formula for snowfall attenuation of radio waves.

21 p3023 A72-41829

SNOW COVER

Snow lines determination from ESSA-APT weather satellite pictures, comparing with ground data

09 p1303 A72-23295

Joint ocean-atmosphere model response to solar zenith angle seasonal variation, noting snow cover and ocean surface effects on lower troposphere warming

11 p1620 A72-25766

Aircraft or helicopter-borne IR radiometer for surface temperature of snow covers and glaciers and air-snow energy balance measurements

15 p2232 A72-31244

Spectroscopic sounding of clouds and snow and ice covers from below /earth surface/ and above /space or planet/

16 p2417 A72-33288

Melting snow and ice packs detection by multispectral /visible and near IR/ remote sensing from earth satellites

16 p2387 A72-33999

SNOW PACKS

U SNOW

SNOWFALL EFFECT

U PLASMA DYNAMICS

SOAPS

Properties of lithium greases as a function of the saturation level of commercial 12-oxytetraric acid

19 p2823 A72-38093

SOCIAL FACTORS

Social factors of labor organization and control in scientific teams for industry

02 p0304 A72-11728

Urban geographic social-spatial pattern determination with aerial photographic interpretation

02 p0229 A72-12019

Water based offshore and floating island airports planning and construction, discussing economic, technical and social aspects

05 p0644 A72-16695

Human biology, including evolution, organism structure, organizations of people, degeneracy, interactions with environment and philosophical concepts

06 p0765 A72-18315

Educational and social applications of communication and meteorological satellite data dissemination, discussing learning and teaching model development

06 p0777 A72-18624

Economic and social implications of Indian national satellite for television and telecommunication, noting data links need

12 p1781 A72-27384

Future spacecraft habitable compartment layout from psychophysiological viewpoint, considering human visual and motor field parameters and crew members social needs

13 p1910 A72-29321

Aerospace technology economic and social effects, relating U.S. space expenditures and gross national product

14 p2174 A72-30682

Airport economic and social impact on environs in terms of community development

16 p2373 A72-33309

Commercial transport aircraft engine technology contribution to world air transportation, considering social and ecological compatibility with community

16 p2348 A72-33314

Social and emotional crises with respect to isolation, confinement and group dynamics of astronaut crews during long duration space flight

16 p2354 A72-33545

What's new in airport planning.

18 p2675 A72-36780

Economic and social aspects of commercial aviation at supersonic speeds.

[ICAS PAPER 72-51] 21 p2996 A72-41851

Space structures and materials technology utilization and transfer to world economic and social problems, considering thermal control, NDT, systems analysis and design

24 p3407 A72-45154

SOCIAL ISOLATION

Abdominal injected barbarnyl somnifacient and toxic effect on mice subjected to hypokinesia and isolation

05 p0622 A72-16650

Confinement, physical deconditioning and hypercapnia effects on human musculoskeletal protein by chromatographic method for quantifying urinary peptides and free amino acids

06 p0767 A72-17869

Isolation stress effect on excretory products in unrestrained chimpanzee, suggesting Ca to P excretion ratio as physiological stress indicator

[AD-739467] 07 p0921 A72-20179

Isolation stress effect on micturition circadian rhythm and diuresis occurrence in unrestrained chimpanzee under entrained and free running conditions

[AD-739468] 07 p0921 A72-20180

Isolation stress effect on circadian rhythmic patterns of EEG activity during sleep-wake and sleep cycles in unrestrained chimpanzee

[AD-739469] 07 p0921 A72-20181

Heart rate change regularities during inverted work-rest cycle of isolated man, noting relation to circadian rhythm

13 p1904 A72-29317

Hermetic chamber medico-engineering experiment for long term isolation effects on human intestinal microflora, showing reduction and disappearance of certain microbe populations

13 p1904 A72-29323

Human respiratory rate diurnal rhythm adjustments during inverted work-rest cycles in isolation chamber with controlled comfortable atmospheres

14 p2075 A72-30390

Social and emotional crises with respect to isolation, confinement and group dynamics of astronaut crews during long duration space flight

16 p2354 A72-33545

Circadian rhythms in physiological and psychological functions related to jet travel, studying body temperature variations and psychomotor performance during isolation and varying light-dark cycle conditions

20 p2897 A72-39723

Exogenous modifications of circadian rhythms of adrenal hormones in man.

22 p3147 A72-42978

SOCIAL PSYCHIATRY

General aircraft accident investigation approach, using subsequent psychosocial reconstruction of pilot lifestyle to explain accident-producing behavior

14 p2082 A72-31095

Sonic boom effects on sleep - A field experiment on military and civilian populations.

23 p3261 A72-44370

SOCIOLOGY

NT SOCIAL FACTORS

Space technological advance effects on human extraterrestrial, scientific, economic and sociological progresses

19 p2867 A72-38545

SODALITE

High contrast and sensitivity thermal erase cathodochromic sodalite for storage and display applications, measuring contrast ratio versus electron beam flux

15 p2240 A72-32362

SODIUM

NT LIQUID SODIUM

NT SODIUM VAPOR

Nighttime sodium layer observation by tuned laser beam resonance scattering technique, measuring seasonal variation in Na abundance and height distribution

01 p0063 A72-10915

Low energy phase shifts for elastic scattering of electrons by Li and Na

03 p0391 A72-13745

Interstellar sodium lines intensities and widths as discriminants for two component models of galactic H I cloud regions

04 p0578 A72-15310

Upper atmosphere Na abundance compared to radio meteor rate after diurnal effects elimination

06 p0876 A72-17645

Na deactivation effect on carbon dioxide-nitrogen gas dynamic laser gain

07 p1008 A72-20564

Aortic constriction and release effects on kidney glomerulotubular balance in saline- and water-loaded dogs, studying sodium reabsorption changes

08 p1115 A72-21084

Atmospheric Na, Li and K layers height, width, abundance and thickness from twilight glow measurements, using birefringent filter type photometers

08 p1159 A72-21224

Cross sections of Li nonresonant capture of Na ion charge, interpreting quasi-oscillatory structure

10 p1517 A72-25047

Model potential method for calculating positively charged diatomic sodium molecular ions potential energy curves and resonance charge transfer cross sections

12 p1848 A72-28350

Ca and Na ionization equilibrium ratio in dust filled interstellar clouds, considering cosmic ray and charge transfer influence

13 p2040 A72-29405

Na-He atomic collisions induced D lines broadening, fine structure transitions cross sections and multiple polarization resonance levels relaxation

15 p2283 A72-32651

Upper atmospheric Na abundance from daytime spectroscopic absorption measurement compared with twilight glow observation

16 p2384 A72-32970

Oscillator strength and ground state photoionization cross sections computation for Na, K, Rb and Cs atoms, including core polarization correction to dipole moment

16 p2431 A72-33724

The determination of diffusion coefficient for Na in dc arc plasma by measurements of intensity distribution of emitted light.

18 p2716 A72-36959

Interrelationship of hemodynamic alterations of valvular heart disease and renal function - Influences on renal sodium reabsorption.

19 p2756 A72-37872

Decarburization kinetics of low alloy ferritic steels in sodium.

22 p3194 A72-43042

Study of the Stark effect in the resonance lines of sodium by an atomic jet method

22 p3209 A72-43048

Capillary circulation as a regulator of sodium reabsorption and excretion.

23 p3257 A72-43995

Metabolism of angiotensin II in sodium depletion and hypertension in humans.

23 p3257 A72-43998

Relationship of sodium deprivation to +Gz acceleration tolerance.

24 p3377 A72-45653

SODIUM ALLOYS

Na additions effects on Si growth velocity and morphology in Al-Si alloys, considering coupled zone adsorption mechanism

13 p1975 A72-28664

SODIUM CHLORIDES

Plasma renin activity during supine physical exercise as function of salt loading

04 p0480 A72-15214

Solute rejection in hyperfiltration of sodium chloride and urea with porous glass ion exchange membrane as function of pressure, temperature and concentration

07 p0937 A72-20601

Paint coatings aging effect on D16T type alloy corrosion fatigue in NaCl solution, noting protective efficiency decrease

13 p1984 A72-29486

Extractability of antioxidative additions from fuels by means of water and NaCl solutions

17 p2596 A72-35179

Studies of the electron transport chain of extremely halophilic bacteria. VII - Solubilization properties of menadiene reductase.

19 p2755 A72-37649

Evidence of crystal structure in some sputtered MoS₂ films.

19 p2823 A72-37897

SODIUM COMPOUNDS

NT NEMBUTAL [TRADEMARK]

NT SODIUM CHLORIDES

NT SODIUM FLUORIDES

NT SODIUM IODIDES

NT SODIUM SILICATES

NT TALC

Mossbauer spectra measurement of metallic iron, sodium nitroprusside, sodium ferrocyanide and ferrocyanide absorbers at 78-293 K, fitting temperature dependencies and resonant velocity to models

01 p0114 A72-10324

Superconductivity observation in Na, K and Rb intercalates of molybdenum disulfide comparing transition temperatures

09 p1368 A72-22561

SODIUM COOLING

Nb heat pipe design with Na coolant for high temperature operation, discussing slopes effect on transmitted power

21 p3129 A72-41051

SODIUM D-LINE

U D LINES
SODIUM FLUORIDES

Influence of cerium additions on the luminescence of europium and samarium ions in NaF single crystals
20 p2932 A72-39414

SODIUM IODIDES

Vacuum chamber sputtering techniques for CsI/Tl and NaI/Tl thin films for soft proton scintillation detector
06 p0816 A72-17834

SODIUM SILICATES

NT TALC
Isotope effect measurements application to determination of sodium diffusion mechanism and rate in sodium silicate glass
22 p3196 A72-42794

SODIUM VAPOR

Sodium heat pipes sonic limit, describing vapor dissociation-recombination and homogeneous vapor condensation phenomena
[ASME PAPER 71-WA-HT-11] 05 p0743 A72-15871

SODIUM 22

Lunar rheolite cosmogenic Al 26 and Na 22 distribution in Lunik 16 sample interpreted by lunar surface soil impact induced mixing
08 p1240 A72-22190

Vertical macroturbulence diffusion coefficient and Na 22 and Be 7 flux from stratosphere to troposphere estimated using ground level measurements and two layer model
09 p1376 A72-22416

SOFT LANDING

Digital computer investigation of radio signals transmitted by Vener 7 during Venus soft landing, describing spectral analysis and telemetric data detection methods
05 p0630 A72-16770

Venera 7 satellite data during descent through Venus atmosphere and activity after soft landing on 25 December 1970, noting temperature and pressure measurements
11 p1718 A72-25937

Digital computer investigation of radio signals transmitted by Venera 7 during Venus soft landing, describing spectral analysis and telemetric data detection methods
17 p2516 A72-35273

Stochastically optimal terminal control system synthesis for loss function dependence on finite phase coordinates of dynamic system, considering soft landing of flight vehicle
23 p3275 A72-43781

SOFT LANDING SPACECRAFT

NT APOLLO SPACECRAFT
NT LUNAR MODULE
NT MERCURY SPACECRAFT
NT SURVEYOR LUNAR PROBES
NT VOSKHOD MANNED SPACECRAFT
NT VOSTOK SPACECRAFT

SOFT RECOVERY

U SOFT LANDING

SOFTENING

Metal fatigue mechanisms in subcreep temperature range, discussing response to cyclic loading including hardening, softening and inhomogeneous plastic strain development
02 p0295 A72-12496

Metal surface layers structural changes under external loading, noting hardening, softening and phase transformations of active layer material
12 p1818 A72-28190

Alloying effects on high temperature softening due to crystal lattice, stacking fault energy and decreased mobility interactions
15 p2254 A72-31564

Transition metals additives effect on binary Mo alloys softening, noting influence of temperature and electron concentration change
15 p2258 A72-32135

Impurity controlled deformation mechanism for softening control of interstitial bcc alloys, discussing low temperature and composition effects
18 p2699 A72-36341

SOFTWARE [COMPUTERS]

U COMPUTER PROGRAMS
U COMPUTER SYSTEMS PROGRAMS

SOIL MAPPING

IR scanner for Indian land areas and oceans thermal mapping, using satellite-borne multispectral photography
02 p0225 A72-11777

Crop, soil and geological mapping from digitized multispectral satellite photography, discussing data processing requirements and surface features distinguishable from satellite altitudes
02 p0214 A72-11876

Digital computer mapping of terrain by clustering techniques, using color IR film emulsion layers as three band spectrometer
02 p0215 A72-11879

Automatic soil type mapping, using multispectral remote sensing and computerized pattern recognition
02 p0215 A72-11881

RADAM /Radar Amazon/ side-looking radar imagery and multiband aerial photography for mineral, vegetation, soil and water resources mapping in Brazil
02 p0216 A72-11890

Aerial photography for rural soil mapping, considering geographic, ecologic and agricultural production interpretation
09 p1301 A72-23279

Color interpretation of pedological factors from aerial photographs in relation to agricultural seasons and use of panchromatic and false color emulsions
09 p1304 A72-23313

Multispectral photography in soil moisture determination and soil series differentiation.
18 p2686 A72-36320

SOIL MECHANICS

Lunar surface bearing strength vs penetration curves from Surveyor 3 soil sample, comparing with in-situ remote measurements
07 p1067 A72-18873

Surface orientation reconstruction of Apollo 14 lunar rocks from microstereoscopic studies of microcraters, soil covers and glass coatings, determining micrometeoroid erosion
11 p1719 A72-25975

Shear stress and traveling wave response of plate bonded to randomly vibrating viscoelastic half space for soil vibration studies
11 p1688 A72-26062

Lunar ash flows - Isothermal approximation.
18 p2723 A72-36026

A photoelastic material with variable modulus of elasticity.
19 p2822 A72-37731

Soil mechanical properties at the Apollo 14 site.
24 p3447 A72-45556

SOIL SCIENCE

Apollo 11 and 12 lunar soil samples, calculating mixing models by least squares and end member groups by Q mode factor analysis
01 p0124 A72-10057

Visible and near IR reflectance spectra of soil mineralized trees, using multispectral photographic filters
02 p0209 A72-11789

Ponderosa pine foliage visible and near IR spectra, investigating soil copper contents effect on foliage spectral reflectance
02 p0209 A72-11790

Remote sensing for land use soil limitations recognition and mapping, using color encoded density slicing analysis
02 p0209 A72-11793

Topmost soil layer moisture content measurement by reflected visible light polarization enhancement
02 p0209 A72-11794

Soil surface moisture content and temperature profile determination by remote microwave sensing
02 p0214 A72-11871

Earth surface remote sensing with thermal IR radiation, investigating uncovered soils with heat balance equations under various weather conditions and times of day
02 p0172 A72-12017

Lunar mare soil deformation and cracking from Surveyor and Apollo photographs
04 p0574 A72-14918

Spectral reflectance of various soils and vegetation, measuring solar energy reflection as function of sun elevation in UV, visible and near IR regions
06 p0810 A72-18446

Lunar soil electric properties, density, microhardness, abrasive properties and frictional and shear resistance determinations by Tor 1 operating in high vacuum
07 p1075 A72-19562

Low power X ray diffractometer with multiwire proportional counter detector array for remote mineralogical analysis of lunar, planetary or asteroid soils detector array
08 p1167 A72-21507

Opaque mineralogy of Luna 16 soil sample, emphasizing compositional variations of Fe-Ti-Cr-Al-Mg spinels
09 p1380 A72-22261

Cosmos 243 microwave radiation analysis over cultivated terrain, showing radio brightness temperature dependence on soil temperature and humidity effect on emissivity
09 p1297 A72-22495

Soil science and climatology use for archeological site detection on aerial photographs
09 p1303 A72-23296

Vacuum and inert gas TOR-1 device for studying physical properties of lunar soil and terrestrial analogs
10 p1478 A72-27354

Luna 16 lunar soil sample tests, comparing friction coefficients and microhardness with terrestrial analogs
10 p1532 A72-23755

Lunar soil dielectric constant and loss-tangent and electrical resistivity measurement by Q meter method, noting resemblance to dense terrestrial rock powders
10 p1532 A72-23756

Viking Lander carbon 14 assimilation experiment for life detection in Martian soils
10 p1540 A72-24385

Viking Lander physical properties experiments for Martian soil, studying bearing strength, cohesion, adhesion, grain size, porosity, thermal properties and internal friction
10 p1540 A72-24390

Automatic hydrometeorological stations standardized sensors, describing data converters for atmospheric pressure, precipitation, humidity and wind and water and soil temperature measurements
10 p1483 A72-25014

Lunar topsoil density variations from Lunik and Surveyor radio wave, alpha and gamma scattering data, discussing Lunik 13 and Surveyor 7 landing sites
11 p1724 A72-26909

Viking orbiter/lander spacecraft instrumentation for Mars soil biological life experiments, discussing pyrolytic and labeled release, light scattering and gas exchange techniques
13 p1956 A72-29024

Urease-active colloidal organo-complex extraction from Dublin clay loam soil, describing filtration procedure
13 p1913 A72-29399

Lunar topsoil-solid bodies interaction in terms of hardness and friction, discussing simulation equipment
14 p2161 A72-31074

SOILS

NT GRAVELS
NT LUNAR DUST
NT LUNAR SOIL
NT SANDS

Remote sensing of environment - Conference, University of Michigan, May 1971
02 p0207 A72-11776

Nonstationary plane shock wave propagation in inelastic medium with soil properties, discussing boundary problem solution and numerical analysis
05 p0689 A72-16284

SOLAR ACTIVITY

NT FACULAE
NT SOLAR FLARES
NT SOLAR PROMINENCES
NT SOLAR STORMS
NT SPICULES
NT SUNSPOTS

Lunar tidal variations of ionospheric electron density at fixed heights for different solar hours over Huan-cayo and Puerto Rico
01 p0053 A72-10089

Neutral H concentration in upper atmosphere during solar minimum, using ion thermal energies from rocket and satellite mass spectrometric, radio and proton whistler measurements
01 p0053 A72-10361

Correlation coefficients for galactic cosmic rays relation to solar activity indices in interplanetary space
02 p0273 A72-11937

Broadband geomagnetic micropulsations relations to magnetospheric, interplanetary and solar phenomena
[AD-739038] 02 p0222 A72-12869

Coronal events in 5303 A wavelength, discussing loops and arches and slow and fast events from photographic recordings
03 p0422 A72-13209

Nonoptical and optical observation derived coronal condensations models for active regions and flare associated events
03 p0423 A72-13211

Areas index relationship to different phenomena in chromosphere, corona and interplanetary space, investigating coronal radio diameter during solar cycle and cosmic rays
03 p0423 A72-13214

Quiet sun radio emission observation, considering statistical minimum value and time varying structure
03 p0424 A72-13220

Sunspot and active region magnetic fields and thermodynamic structure from umbral and penumbral models, discussing magnetic fine structure
03 p0427 A72-13296

Magnetic field measurements at different depths of solar atmosphere active regions by Crimean Astrophysical Observatory double magnetograph, showing close correlation
03 p0428 A72-13302

Solar magnetic field configuration evolution in active region of photosphere, using solar magnetograph
03 p0428 A72-13305

Statistical model of small scale discrete structure of magnetoplasma in solar active regions
03 p0430 A72-13335

Coronal magnetic fields above slowly changing active regions
03 p0431 A72-13342

Magnetic field structure in active solar corona, discussing optical and radio observations
03 p0431 A72-13345

Solar active region properties at millimeter wavelengths, suggesting chromospheric magnetic field measurement possibility from polarization

03 p0432 A72-13348

Solar cycle models physical mechanisms, discussing surface activities and nonaxisymmetric steady state solutions

03 p0433 A72-13357

Time variation of mean values for magnetic field elements strength and size in solar polar regions, noting solar activity maximum effect

03 p0436 A72-13830

Large scale magnetic field distribution and solar activity, discussing granular pattern, differential rotation, magnetic flux near surface and background field pattern

03 p0437 A72-13870

Solar disk active centers X ray emission, using rocket mounted pinhole cameras

04 p0567 A72-15164

Atmospheric composition and temperature effects on F 1 region ion concentration structure from 140 to 220 km for low solar activity conditions

05 p0657 A72-16261

Solar chromospheric fine structure at active region, magnetic polarity boundaries from high resolution H-alpha filtergrams

05 p0718 A72-16508

Solar activity asymmetry on two hemispheres in 1959-1969, considering spots, faculae, prominences and corona

05 p0718 A72-16511

Electron content measurement for low latitude station obtained at sunspot maximum by Syncom 3, observing seasonal variation and winter anomaly effect

06 p0874 A72-18089

Magnetospheric structure models during quiet solar periods

06 p0809 A72-18277

Solar photosphere active regions and large scale flow patterns from Greenwich sunspot statistics

07 p1068 A72-18886

Large scale magnetic fields and activity patterns in solar atmosphere, considering supergranules and active longitude and latitude development

07 p1078 A72-20007

Solar active regions properties observation, noting correlation with magnetic field, flares, sunspots, magnetic knots, pores, umbral flashes, etc

07 p1079 A72-20009

Active region sources of solar proton streams, discussing 27-day recurrence, acceleration and confinement in interplanetary space

07 p1060 A72-20010

Long term variations in height of solar activity maxima and sunspot numbers during 11 year cycle

07 p1079 A72-20016

Comet characteristics as indicators of cosmic space conditions, including relation to solar activity

07 p1081 A72-20272

Electroconductivity distribution and vertical gradients in photospheric layers of solar active region, using approximate model

07 p1082 A72-20293

Sunspots penumbral and umbral areas ratio in eleven year solar activity cycle, noting larger umbras at second maximum

07 p1082 A72-20295

Solar active regions temperature measurements from 2 cm radioheliograms, using high resolution radio telescope

07 p1082 A72-20296

Solar cosmic ray heavy nuclei acceleration independence from solar activity phenomena, based on Elektron 4 satellite observation

07 p1064 A72-20632

F region ionization anomalous evening enhancement, discussing seasonal variations, solar activity and geomagnetic coordinates maximum in Yakutsk

08 p1153 A72-20707

Sunspot group number and average lifetimes in solar activity cycle

09 p1390 A72-23397

Transportable radio telescope for atmospheric attenuation and solar activity observations

09 p1316 A72-23509

Geometric parameters variations of ionospheric N/h profiles and characteristics during magnetic storm, discussing prognosis procedures from solar activity, latitude and season

11 p1594 A72-26273

Correlation coefficients for galactic cosmic rays relationship to solar activity indices in interplanetary space

13 p2030 A72-29249

Low energy relativistic cosmic ray electrons temporal intensity variations from IMP satellite measurements, considering correlation with solar activity

13 p2030 A72-29376

Solar disk 10 cm radio emission during 7 March 1970 solar eclipse, discussing occultation of McMath plage active region

13 p2044 A72-29550

Spectral radio observations of 7 March 1970 solar eclipse, noting McMath plages intense activity source flux characteristics and weaker source bremsstrahlung emission

13 p2044 A72-29551

Mg filterheliogram comparison with Ca spectroheliogram, noting correlation coefficient between location and intensity of bright features on sun

13 p2045 A72-29708

Photographic records of sunspot umbrae showing bright penumbral filament penetration

13 p2045 A72-29713

Short lived chromospheric absorbing features in H alpha wings, noting development into active center

13 p2046 A72-29717

Sunspot cycle 21 behavior prediction, explaining solar activity forecasting based on 80 year cycle

13 p2046 A72-29727

Latitude dependent time variations of solar differential rotation and global activity distribution asymmetry, assuming large scale convection due to angular momentum transport

13 p2046 A72-29730

Photoelectron precipitation induced dissociation of atmospheric nitrogen molecules during moderate solar activity

14 p2102 A72-30659

Earth electrical conductivity radial distribution effect on solar quiet day geomagnetic field variations

14 p2103 A72-30666

Quiet and active models for solar structure and processes in terms of elementary physical concepts

15 p2302 A72-31276

Solar activity correlation with filaments disintegration during transit across solar disk, analyzing statistical data

15 p2318 A72-32782

Magnetic field rapid dissipation induced by stochastic topology of lines of force, discussing implications for hydromagnetic turbulence, solar activity and cosmic ray diffusion

16 p2378 A72-33454

Numerical method for force-free magnetic field structures in solar active regions, discussing rotation effects

16 p2455 A72-33462

Space observations of the solar corona

17 p2611 A72-35326

Polarization of solar active regions at 9.5 mm wavelength

17 p2617 A72-35707

Occurrence frequency of F 2 layer sporadic ionization in auroral zone, noting solar activity effect

17 p2551 A72-35867

Solar activity centers characteristics cyclic variations in decreasing and increasing parts of sunspot activity cycles, discussing latitude-longitude distribution

19 p2851 A72-37906

Initial phase in the development of activity centers in the photosphere

19 p2860 A72-37951

Sunrise and sunset period of helio-geophysical processes in terms of optical, X ray, corpuscular and radio characteristics of solar activity

19 p2868 A72-38637

Velocity oscillations in the solar atmosphere

21 p3107 A72-41278

Balloon-borne telescope search for solar neutrons and gamma rays during enhanced solar activity periods

21 p3101 A72-41298

Study of the chromosphere in the D3He line during the eclipse of September 22, 1968

21 p3114 A72-41764

Short period geomagnetic variations, discussing origin by different solar activity mechanisms

22 p3173 A72-42544

Second positive system of nitrogen bands in the day airglow from Cosmos-224 data

23 p3282 A72-43356

Dayglow nitrogen ion 3914 A emission profiles for average solar activity at 110-240 km heights from Cosmos 224 observations

23 p3282 A72-43357

Families of geomagnetic storms, direction of the interplanetary magnetic field, and solar activity

23 p3283 A72-43371

Variation of the cosmic-ray gradient during a solar activity cycle

23 p3328 A72-43374

Solar activity research review, discussing sunspots, magnetic fields, solar atmosphere, rotation, radio bursts, flares, X ray emission, etc

23 p3338 A72-43976

Photographic processing method for solar activity macrostructural distributions determination, suppressing minor and sporadic formations by defocusing technique

23 p3340 A72-44239

SOLAR ACTIVITY EFFECTS

L-chondrite Assam, determining He, Ne and Ar concentrations and isotopic compositions and galactic and solar flare irradiation track densities

01 p0124 A72-10060

Cosmic ray density distribution inside cosmic ray modulating spherical cone in solar wind, noting modulation depth quasi-periodic variation

01 p0119 A72-10606

Cosmic ray energetic spectrum variation from observed latitudinal effects during 1954-1962 solar activity cycle

01 p0119 A72-10607

F 2 layer critical frequency variations relation to solar radio flux intensity, using mathematical approximations

01 p0059 A72-10613

Long term galactic cosmic ray intensity modulation correlation to 5303 A coronal intensity during rising part of solar activity cycle

01 p0120 A72-10909

Middle geographic latitude sporadic E-layer initial height variations during 1957-1968 solar cycle

01 p0064 A72-11103

Cosmic ray exposure thindown tracks in human tissue from solar minimum to maximum at SST flight level

02 p0163 A72-12079

Cosmic ray intensity long term modulation and 27 day recurrence relationship to solar activity

03 p0407 A72-12945

Sunspot cycle 1958/70 effects on D region ionospheric absorption and stratospheric temperature measured by radiosonde

03 p0345 A72-12978

Altitude, photon wavelength and solar activity effects on photoionization yield of ionospheric monatomic and diatomic oxygen and nitrogen via Monte Carlo simulation

03 p0345 A72-12983

Ionospheric effects of X ray flare on 8 July 1968, estimating ionizing radiation spectral characteristics from SID observation

03 p0407 A72-12986

Solar magnetic field variations in McMath Regions, using longitudinal magnetograms time sequences

03 p0430 A72-13327

Auroral behavior observation at midlatitude station, exhibiting correlation with solar activity as regards solar cycle recurrence and phase

04 p0515 A72-14882

Ionospheric electron content over New Delhi, observing seasonal and solar cycle variations of diurnal changes

04 p0515 A72-14930

Height profiles for volume emission rate and intensity of second positive band of nitrogen molecule excited by photoelectron impact, noting solar activity effects

04 p0518 A72-14962

Solar effects contradictory relationships with earth atmosphere, discussing geomagnetic disturbance, annual variations, stratospheric transport and high energy particles

05 p0656 A72-16233

Ionospheric neutral composition variations as function of height, local time and solar activity

05 p0656 A72-16235

Latitudinal distribution of electron temperature in F 2 layer during summer daytime period of low solar activity from electron density profile geometrical parameters

05 p0656 A72-16248

Arctic polar region geomagnetic perturbations during IQSY, noting diurnal variations

05 p0658 A72-16278

Active solar regions effects on galactic cosmic ray intensity

05 p0710 A72-16526

Upper atmosphere density fluctuations associated with solar activity and local time values, using Cosmos 14 satellite drag data

05 p0659 A72-17037

Ionospheric geocoronal L alpha emission intensity related to solar activity level from Cosmos 215 satellite data

05 p0659 A72-17038

Background phonon X ray and gamma quanta intensities dependence on solar activity from Geiger counter recordings in deep space

05 p0711 A72-17046

Statistical criteria of geomagnetic activity, considering solar corpuscular radiation effect

06 p0803 A72-17369

Semidiurnal lunar variation, solar and sidereal effects on cosmic radiation intensity, using zenith pointed particle telescopes

06 p0873 A72-17490

Ionospheric disturbance in American zone during IGY-IGC, showing latitudinal, annual and diurnal solar variations effects and regional geomagnetic anomaly

06 p0806 A72-17641

Electron density distribution inhomogeneities from vhf Faraday rotation measurements, noting diurnal, seasonal, sunspot cycle and geomagnetic activity effects

06 p0806 A72-17642

- Sunspot cycles effect on F region drifts and irregularities from observations at Ibadan during 1966/67, noting seasonal and diurnal variations
06 p0806 A72-17643
- Geomagnetic field intensity fluctuations due to events in atmosphere, ionosphere, magnetosphere and in interplanetary space connected with solar activity
06 p0809 A72-18276
- Solar modulated galactic cosmic rays radial gradient idealized model for comparable deceleration and convection effects
07 p1057 A72-19138
- Interplanetary magnetic sector structure at 1962-1969 solar maxima, noting Pioneer 9 magnetometer experiment observations
[AD-740308] 07 p1071 A72-19161
- Cosmic ray nuclei intensity and energy spectrum measurement in nuclear emulsions stack, noting no charge dependence in solar modulation process
07 p1059 A72-19582
- Exact cosmological solutions in Brans-Dicke scalar tensor theory, noting consequences for solar relativistic effects
07 p1075 A72-19584
- Cosmic ray heavy nuclear component during solar activity minimum, using Cerenkov counters onboard Elektron satellites
07 p1060 A72-19872
- Ionospheric effects of solar flares, relating sudden ionospheric disturbances with solar X-rays, radio bursts, H alpha emissions and cosmic rays
07 p1062 A72-20037
- Solar modulation of cosmic ray intensity in stratosphere, examining relationship to sunspots group number and heliographic latitudes over 11 year period
07 p1065 A72-20641
- Solar active regions effects on galactic cosmic ray distribution and interplanetary magnetic field structure
07 p1065 A72-20646
- Diurnal, sporadic and yearly variations in cosmic ray flux based on neutron component data, noting relation to solar activity cycles
07 p1066 A72-20647
- Solar unipolar magnetic regions relation to geomagnetic disturbances variability, discussing 11 year cycle
08 p1155 A72-20808
- Solar modulation process for galactic cosmic ray particle time variation, discussing interplanetary magnetic fields and plasma, energy losses from solar wind deceleration, etc
08 p1227 A72-21188
- Model calculation for electron production rates due to photoionization and particle precipitation below 100 km at midlatitude during solar minimum and maximum years
09 p1375 A72-22357
- D and E region electron density profile, investigating geographical, diurnal, seasonal and sunspot cycle variations
09 p1376 A72-22370
- Geomagnetic activity annual variations from daily international magnetic character figures analysis by time series numerical filter method, discussing sunspot cycle effect
09 p1298 A72-22584
- Polar orbiting satellite observations of energetic solar proton entrance into polar cap during March 1970 solar event
09 p1376 A72-22588
- Trapped He, Ne and Ar isotopic variations presence in meteorites due to rare gas ions implantation by solar wind and flares
09 p1385 A72-22599
- Potential gradient and air-earth current increases during period of increasing solar activity, discussing H alpha flare effects
09 p1378 A72-23264
- Geomagnetic field short term variations as function of solar activity from solar radiation data harmonic analysis, relating large amplitude fluctuation to seasonal variations
09 p1304 A72-23503
- Balloon sounding observations of lower stratosphere secondary cosmic radiation bursts due to solar activity
10 p1529 A72-24069
- Atmospheric electricity problems, considering air pollution effects on ion concentration and air conductivity and solar activity effects on ionosphere-earth potential difference
10 p1473 A72-24528
- Atmospheric wind velocity time variations at 80-100 km altitudes from ionospheric drift data, finding planetary oscillation periodicities relationship to solar activity cycle
11 p1620 A72-25273
- E and F region apparent and true drifts over magnetic equator correlated to solar activity, comparing electron density sensitivity to geomagnetic range
11 p1623 A72-26104
- Whistler dispersion and occurrence rate characteristics at low latitudes during solar cycle, noting annual variations and magnetospheric electron density
11 p1623 A72-26105
- Ionospheric disturbances and prediction dependence on solar and geophysical activities, discussing SID, pca, auroral absorption and F 2 region
11 p1623 A72-26267
- Anomalous F region ionization in darkened high latitudes during solar activity growth and abatement
11 p1623 A72-26270
- F region critical frequencies deviation from median due to solar cycle phase, latitude and time, discussing short waves radio communications reliability
11 p1593 A72-26271
- F 2 region critical radio frequencies forecasts from solar cycles, ionospheric disturbances data, latitude and annual and diurnal variations
11 p1594 A72-26272
- Noontime N/h profiles forecasts and annual variation in F region, relating solar activity levels to vertical distribution of electron concentration
11 p1594 A72-26277
- Sporadic E layer cyclic variations during solar activity cycle, noting time dependence of occurrence probability and critical frequency
11 p1623 A72-26281
- Solar activity maximum annual variations effect on ionospheric parameters
12 p1868 A72-27306
- Seasonal atmospheric composition changes relation to midlatitude F 2 layer seasonal anomaly during high solar activity
12 p1803 A72-27776
- Ionospheric absorption measurements during sunspot cycle at fixed frequencies, noting monthly and seasonal variations
12 p1804 A72-27782
- Russian papers on solar activity effects on earth atmosphere and biosphere covering climate, vegetation, animals and man
12 p1763 A72-28206
- Solar activity relation to geophysical phenomena, discussing atmospheric circulation and climatic variation cyclicity and sunspot corpuscular fluxes
12 p1842 A72-28207
- Quasi-steady and sporadic corpuscular fluxes as basic solar activity effect on troposphere, showing magnetosphere interaction time relation to meridional atmospheric circulation changes
12 p1842 A72-28208
- Solar activity effects in magnetosphere and ionosphere relation to geomagnetic activity and biospheric development, noting 11 year geomagnetic perturbation cycles
12 p1805 A72-28209
- Solar activity effects on biospheric processes for biological and physicochemical systems in unsteady state, considering maximum effects on man at certain electromagnetic wave frequencies
12 p1773 A72-28211
- Solar activity effects on bismuth chloride hydrolysis tests from statistical results following solar flares
12 p1773 A72-28212
- Solar activity effects on biosphere processes, discussing radiation-induced molecular activation mechanisms in water and biological plasma calcium ion concentration changes
12 p1763 A72-28213
- Variations of F 1 layer thickness and maximum ionization height for high and low solar activity periods obtained from vertical ionospheric sounding
13 p1946 A72-28595
- Solar activity effects on atmospheric electricity during favorable weather conditions, discussing troposphere potential gradient and earth air current
13 p2029 A72-28622
- OMEGA phase shifts in auroral region due to solar phenomena, discussing methods eliminating PCA induced errors
13 p1997 A72-29185
- Daytime 30 MHz PCA from satellite and riometer measurements, noting linear relationship to square root of integral and differential solar proton fluxes
13 p2030 A72-29339
- Solar flare flux effects on D region effective ion recombination coefficient decrease, discussing electron and negative ion densities
13 p1913 A72-29654
- Solar flare induced vortex ring formation, describing photographic observations by Okayama Astrophysical Observatory solar telescope on 30 October 1970
13 p2048 A72-29741
- Satellite measurements of exospheric density variations during June 1968-December 1970 at 1070 and 900 km, discussing solar activity effect
13 p1952 A72-29803
- Radio waves field strength measurement and recording for D region behavior during partial solar eclipse of 25 February 1971
13 p1961 A72-30050
- Nightglow ground based spectrophotometric observations of hydroxyl emission intensity and rotational temperature variations related with solar and geophysical activity
14 p2098 A72-30144
- Long term atmospheric pressure fluctuations in relationship to solar activity over Northern Hemisphere, confirming 22 year cycle
14 p2101 A72-30648
- Weber experiment gravitational signals correlation to solar and geomagnetic activity and cosmic ray intensity
14 p2160 A72-30886
- Solar event-related ionospheric horizontal electric fields derived from balloon measurement of mid-European and equatorial ionosphere potentials
15 p2223 A72-31556
- Solar activity long term effects on Jupiter cloud structure rotational periods, using Chree superposition analysis
15 p2308 A72-31930
- Thermospheric variations due to solar activity changes based on satellite drag data
15 p2228 A72-31979
- Interplanetary particles intensity relationship with solar activity based on Heos A1 observations during 1969-1971
15 p2300 A72-31992
- Sudden decreases of atmospheres due to solar flares effects on lower ionosphere, discussing noise propagation
15 p2230 A72-32256
- Solar activity effects on integrated ion production rates at sunrise using atmospheric model
15 p2301 A72-32266
- Interplanetary scintillation technique application to structure of flare induced shocks and corotating streams within interplanetary medium
16 p2451 A72-33033
- Ionospheric electron content semiannual and seasonal variations as function of solar and geomagnetic activity from low and mid-northern latitude observations
16 p2385 A72-33378
- Day to day variation of Schumann resonance frequency and occurrence of Pc 1 in view of solar activity
17 p2548 A72-35464
- Cosmic ray electron spectrum and its modulation near solar maximum
17 p2601 A72-35583
- Book on ionosphere and magnetosphere covering solar radiation effects, ionospheric layers, currents and storms, charged particle movement and various wave propagations
17 p2550 A72-35850
- Comprehensive investigation of individual geomagnetic storms
18 p2686 A72-36226
- Geomagnetic activity and the solar situation in the neighbourhood of proton effects
18 p2686 A72-36227
- Sudden commencements of geomagnetic storms at the turn of two solar cycles
18 p2686 A72-36228
- Whistler activity in central Europe during the period of increasing solar activity from 1964 to 1968
18 p2657 A72-36230
- Sunspot control of ionospheric absorption
18 p2686 A72-36231
- Physical observations of comets. XVII
18 p2726 A72-36722
- Ionospheric magnetic disturbances during March 1970 related to solar flare corpuscular and proton fluxes, generating ring current and PCA absorption
18 p2688 A72-36857
- The north-south anisotropy and the cosmic-ray radial gradient in the vicinity of the earth
18 p2722 A72-37164
- Model ionosphere for D region at summer noon during sunspot maximum
18 p2689 A72-37207
- Features of zonal circulation in the stratosphere and lower mesosphere of the equatorial region during the period of increasing solar activity /1967-1968/
19 p2790 A72-37999
- F region ionization anomalous evening enhancement, discussing seasonal variations, solar activity effects and maximum value dependence on geomagnetic latitude and longitude
19 p2790 A72-38335
- Solar activity effects on sun-earth space physical processes, considering galactic cosmic rays, comets, ionospheric disturbances, and noctilucent clouds
19 p2867 A72-38629
- Rotation period variation in long term behavior of interplanetary magnetic sector structure during nearly four solar cycles
19 p2868 A72-38731
- He abundance relationship to solar wind bulk speed and temperature from Explorers 34 and 43 observations, noting dependence on sunspot number
19 p2853 A72-38749
- Sodium emission from the atmosphere during a solar eclipse
19 p2793 A72-38857
- Characteristics of interplanetary electron inhomogeneities according to observations in the period from 1967 to 1969
21 p3114 A72-41765

Sudden impulses in the geomagnetotail and the vicinity.

22 p3168 A72-42002

Magnetic field change rate related to chromospheric activity in McMath Regions 8863, 10385 and 11415, discussing flare associated effects and total flux

22 p3217 A72-42039

Magnetic field structure in flare-associated solar-wind disturbances.

22 p3219 A72-42428

Ozone measurements in the mesosphere during the solar proton event of 2 November 1969.

22 p3173 A72-42509

Free oscillations of the sun and their possible stimulation by solar flares.

22 p3219 A72-42570

The sunspot cycle and solar and lunar daily variations in H.

22 p3228 A72-42882

August solar activity and its geophysical effects.

22 p3174 A72-42982

Variations of the planetary values of the F2 layer thickness and the parameters of the neutral atmosphere

23 p3284 A72-43375

Energy and mass content of high-speed solar-wind streams.

23 p3332 A72-44508

Detection of interplanetary electrons from 18 keV to 1.8 MeV during solar quiet times.

23 p3333 A72-44546

The cosmic-ray spectral modulation above 2 GV. IV - The influence on the attenuation coefficient of the nucleonic component.

24 p3434 A72-44783

Variations of F1 layer thickness and maximum ionization height for high and low solar activity periods obtained from vertical ionospheric sounding

24 p3398 A72-45095

SOLAR ARRAYS

High voltage solar array technology, studying power conditioning control system design and array-space plasma interactions

13 p1899 A72-28942

Solar radiation simulators and the measurements of solar battery and cell characteristics [Survey/

17 p2498 A72-35514

Solar array cost reduction.

19 p2754 A72-37642

SOLAR ATMOSPHERE

NT SOLAR GRANULATION

Asymptotic methods application to differential equations in nonlinear solar convection theory at high Rayleigh number, noting discrepancy from numerical integration

02 p0276 A72-11644

Steady state convection in solar atmosphere outer layers, plotting physical parameters as functions of geometrical depth

02 p0276 A72-11645

Temperature fluctuations and fine structures in solar atmosphere from Ca II IR lines

03 p0414 A72-12926

Solar streamline flow patterns analysis test on terrestrial wind data

03 p0414 A72-12928

Solar chromosphere fine structure at limb, measuring spicules and bright mottles lifetime

03 p0415 A72-12930

Coronal magnetic fields effects on energy and mass flux from lower solar atmosphere levels into corona, discussing plasma instabilities, solar flares, radio bursts, etc

03 p0422 A72-13206

Active and quiet solar atmosphere models from OSO satellite data, presenting emission lines and continua from abundant elements

03 p0423 A72-13215

Solar outer corona steamer density and temperature data from type 3 solar radio burst observation by space radio astronomy

03 p0424 A72-13223

Solar magnetic field measurements using electromagnetic radiation, atmospheric structure /MHD effects/ and energy equipartition

03 p0427 A72-13277

Absorption line formation in magnetic field for magnetograph interpretation of solar atmosphere

03 p0427 A72-13291

Magnetic field measurements at different depths of solar atmosphere active regions by Crimean Astrophysical Observatory double magnetograph, showing close correlation

03 p0428 A72-13302

Magnetograph scans of solar disk center supergranulation, showing downdrafts relation to magnetic field strength and chromosphere and photosphere brightness

03 p0429 A72-13307

Magnetic and velocity fields and brightness in solar atmosphere, using double magnetograph

03 p0429 A72-13309

Supergranule velocity and magnetic fields concentrations in solar atmosphere

03 p0429 A72-13311

Spectroheliogram movies of magnetic, velocity and intensity field in solar atmosphere, showing time resolution of line spectra

03 p0429 A72-13314

Solar hydrodynamic dynamo theories concerning convective zone large scale velocity fields and magnetic activity cycle

03 p0433 A72-13360

Short periodical pulsations in solar atmosphere related to magnetosound propagation in area of temperature minimum with directed perpendicular magnetic field

03 p0436 A72-13813

Gamma ray and neutron emissions from sun, considering acceleration of charged particles in solar atmosphere

04 p0566 A72-14724

Dispersion equation derived for acoustic-gravity type natural modes in solar atmosphere

05 p0712 A72-15769

Goldberg-Unno method accuracy for solar photospheric microturbulent velocities, discussing correction for damping effect and LTE deviation

05 p0718 A72-16503

Fine H alpha fibrils in middle chromosphere, discussing optical thickness and absorption features

05 p0718 A72-16506

Temperature and density fluctuations in photosphere from Fe and Mg line intensities, noting variations due to granulation in solar atmosphere model

06 p0876 A72-17579

Solar chromosphere radiative transfer and thermal conduction coupling, applying singular perturbation method to Frisch analysis

07 p1070 A72-19087

Solar magnetic field regularities analogy with terrestrial cyclones instead of convection cells in vertical heat transport

07 p1074 A72-19558

Fine structure elements of chromosphere, discussing spicules, fibrils and thermal effects

07 p1077 A72-19808

Radiation temperature of carbon monoxide molecules in solar atmosphere from vibratory-rotatory spectral measurements

07 p1077 A72-19811

Large scale magnetic fields and activity patterns in solar atmosphere, considering supergranules and active longitude and latitude development

07 p1078 A72-20007

Non-LTE effects on mechanical heating in gray atmosphere applied to nonradiative energy input estimates for solar chromosphere from negative hydrogen ion emission

08 p1235 A72-21391

Solar five minute oscillations in isothermal atmosphere by base pressure fluctuations

09 p1382 A72-22287

Solar atmosphere low energy positron production by solar particle fluxes demodulated according to cosmic ray transport equations

09 p1378 A72-23022

Solar chromosphere double limb effect attributed to instrument, discussing application to height measurement

11 p1717 A72-25905

Solar wind ion temperature association with influx of neutral hydrogen from heliosphere boundary

11 p1714 A72-26527

Ionization and associated energy loss effects on particles acceleration in solar atmosphere, emphasizing Fermi mechanisms

12 p1863 A72-27303

Model solar atmosphere from mm and cm wavelength high resolution observations of chromosphere by lunar limb antenna tracking during 7 March 1970 eclipse

13 p2042 A72-29532

Spectrographic observation of flash spectrum during 7 March 1970 solar eclipse, showing significant coronal line emission origin in chromosphere interspersal regions

13 p2042 A72-29534

Lower solar chromosphere two dimensional models, noting effects of macroscopic velocity fields

13 p2045 A72-29709

Short lived chromospheric absorbing features in H alpha wings, noting development into active center

13 p2046 A72-29717

Energetic electron and proton trapping in lower solar atmosphere magnetic field, discussing particle injection, bremsstrahlung and gyro synchrotron radiation

13 p2046 A72-29719

Semiempirical line blanketing in solar model atmospheres, including limb darkening predictions

13 p2047 A72-29735

Directional dependence of sound wave emission by convective turbulence in solar atmosphere, considering cut-off frequency effects on transmitted acoustic spectrum

13 p2048 A72-29926

Solar photosphere velocity field photoelectric measurements, emphasizing long periods and low spatial wave numbers in deep layers

13 p2048 A72-29927

Solar photospheric fluctuations, applying fast Fourier transform to power coherence and phase spectra calculations

13 p2049 A72-29928

Undisturbed and active solar photospheric turbulent velocity determination by comparing half widths of observed weak Fraunhofer line profiles with model calculation

13 p2049 A72-29929

Equatorial quiet solar atmosphere model for chromosphere-corona transition region based on cm radio observation and hydrodynamical conservation equations

13 p2049 A72-29933

Radio bursts and X ray emissions associated with 15-16 November 1970 solar chromosphere flares, noting brightness maximum differences

14 p2146 A72-30483

Geomagnetic storms caused by quasi-stationary directed corpuscular streams resulting from solar chromosphere flares

14 p2147 A72-30487

Diffusion effects on stellar surface chemical composition, emphasizing solar atmosphere conditions

15 p2305 A72-31342

Sunspot area east-west asymmetry dependence on location in chromospheric facula or plage, considering solar atmosphere optical and geometric depth changes

15 p2318 A72-32787

Temperature profile derivation for uppermost convection region of two solar convection zone models from finite amplitude convection theory

16 p2451 A72-33037

Rotation effect on total heat transport and cell size in solar convection zone

16 p2451 A72-33038

Solar chromosphere bright mottles and spicules lifetime relationship from H alpha photograph isophotometry of limb

16 p2456 A72-33509

Fraunhofer lines emergent intensity fluctuation caused by temperature and pressure perturbation in solar atmosphere

17 p2608 A72-35080

Solar chromosphere-corona transition region structure and energy balance calculation by static planar model compared with XUV resonance line observations

17 p2608 A72-35083

Space observations of the solar corona.

17 p2611 A72-35326

Plasma turbulence in solar atmosphere upper layers related to chromospheric flares and radio bursts

17 p2612 A72-35349

Metallic abundances in the solar chromosphere.

17 p2613 A72-35498

On the choice of boundary conditions for integration of transfer equations.

17 p2577 A72-35695

On the temperature of the helium emission regions in the solar atmosphere.

17 p2616 A72-35699

Fine structure elements of chromosphere, discussing spicules, fibrils and thermal effects

17 p2617 A72-35733

Radiation temperature of carbon monoxide molecules in solar atmosphere from vibratory-rotatory spectral measurements

17 p2618 A72-35736

Terrestrial and solar atmospheres general circulations from laboratory experiments on rotating cylinders filled with differentially heated fluids, noting solar equatorial acceleration

17 p2551 A72-35941

Radial velocities and brightness distribution in active and quiet solar atmosphere from magnetograph measurements, discussing motion directions in photosphere and chromosphere

19 p2858 A72-37818

Similarity theory of planetary atmosphere circulations applied to solar atmosphere in terms of radius and rotatory Mach number

19 p2863 A72-38066

Geomagnetic storms caused by quasi-stationary directional corpuscular streams resulting from solar chromosphere flares

19 p2851 A72-38316

Homologous complex radio bursts of type IV-II in the solar atmosphere

19 p2852 A72-38498

On the acceleration time of particles in the solar atmosphere.

19 p2852 A72-38634

On the filamentary nature of solar magnetic fields.

20 p2971 A72-39762

Investigation of physical conditions in the solar photosphere by a curve of growth technique

21 p3102 A72-40097

- Gravitational perturbations as source for solar oblateness fluctuations, considering density in upper convective zone 21 p3106 A72-41039
- Linear and nonlinear aspects of ion-sound current instability for solar atmosphere conditions of full ionization, noting implications for flare mechanism 21 p3100 A72-41040
- Probability interpretation of radiative transfer to calculate magnetic field-originating spectral line formation dependence on solar atmosphere mean optical depth 21 p3107 A72-41276
- Atmospheric model for numerical simulation of five minute oscillation field properties of solar granular convection-excited gravity waves 21 p3107 A72-41277
- Velocity oscillations in the solar atmosphere. 21 p3107 A72-41278
- Intensity ratios of He I and H lines in a prominence and the chromosphere. 21 p3109 A72-41329
- Molecular abundances and gas-to-electron pressure ratios as function of temperatures and pressures in solar composition gaseous mixture of late type stellar atmospheres 21 p3'10 A72-41446
- Observation procedures in high resolution spectrophotometry of solar chromospheric spectral fine structures 22 p3221 A72-42031
- The decay characteristics of models of solar hard X-ray bursts. 22 p3217 A72-42040
- The density dependent ionization balance of carbon, oxygen and neon in the solar atmosphere. 23 p3334 A72-43252
- Photometric elements of corporeal unstable AH Vir eclipsing binary at 4400 and 5600 Å, comparing stellar gas stream and solar chromosphere densities 23 p3338 A72-44028
- The quiet sun brightness distributions at millimeter wavelengths and chromospheric inhomogeneities. 24 p3438 A72-44840
- Solar atmosphere fine structure observation limitations in terms of solar telescope angular resolution 24 p3404 A72-45529
- SOLAR AZIMUTH**
U AZIMUTH
U SOLAR POSITION
- SOLAR CELLS**
Fluorinated ethylene propylene encapsulated N/P Si solar cells, investigating simulated micrometeoroid exposure effects on I-V performance in shock tube 01 p0006 A72-10381
- Integrated electronics digital-analog solar cell array control unit, discussing circuit design and radiation hardening 01 p0042 A72-11059
- Electrical power subsystem for Initial Defense Communications Satellite Program/Augmentation, noting solar cells for power conversion and Ni-Cd batteries for energy storage 01 p0008 A72-11066
- ESRO satellite power supply solar paddles deployment mechanism, describing simulated zero gravity tests [DGLR PAPER 71-112] 02 p0286 A72-12713
- Li-containing solar cell damage and recovery characteristics measurement under 1-MeV electron irradiation, deriving diffusion-length damage coefficient 03 p0312 A72-14092
- Two dimensional solar cell model with partial differential equation relating arbitrary point potential to cell parameters for I-V characteristics prediction 04 p0465 A72-14480
- N-p silicon solar cells damage at room temperature by proton and deuteron irradiation, considering particle mass and energy functions and illuminating light wavelength effects 04 p0561 A72-14574
- Electric and photoelectric properties of CdTe films, describing solar cells preparation 04 p0465 A72-14593
- AEROS aeronomy satellite solar cell array power supply system simulation tests under space conditions 04 p0466 A72-15650
- Spacecraft initial solar orientation techniques estimation and classification 05 p0685 A72-16444
- Fatigue failure tests of soldered joint in solar cell interconnector designs under extended temperature cycling 05 p0615 A72-16552
- Cylindrical solar array absorbance as function of solar flux vector inclination, using Gier-Dunkle integrating sphere [AIAA PAPER 72-57] 05 p0616 A72-16909
- Lunar mineral resources from analyses of moon samples, discussing solar cell and vacuum process manufacturing 05 p0722 A72-17099
- Solar cells with improved photoelectric efficiency, describing use of noncorroding Ti-Pd-Ag contacts, titanium oxide antireflection layer and welded cell joints 06 p0760 A72-17751
- Si solar cells nonpenetrating proton damage model in satellite radiation environment, showing open and short circuit current dependence on proton energy 07 p0914 A72-20492
- Neutron irradiation produced lattice disorder in Li doped float zone melted n-p type Si solar cells 08 p1216 A72-21182
- Solar cells in satellite power supplies, discussing design, environment effects, reconditioning, microwave performance and testing 10 p1422 A72-24150
- Cosmic radiation effects and damage on solar cells, discussing shielding, stability improvement, space environments, minority carrier lifetime and photosensitivity spectral distribution 10 p1422 A72-24312
- Thermal shielding and reduced resistance determination of flat thermoelectric battery in sandwich solar cell assembly 10 p1422 A72-24313
- Cooling system based on vaporization of solar cell preheated solution drawn through chamber with atomizing injector 10 p1422 A72-24314
- Thermoelectric cooling battery performance of solar cell system, determining low temperature current requirements under various thermal loads 10 p1423 A72-24317
- Semiconductor air-air heat pumps with solar cell feed current, determining hot air flow temperature effects and energy conversion efficiency 10 p1423 A72-24319
- Communications Technology Satellite attitude control system design, taking into account dynamic interactions with large flexible solar cell array 11 p1593 A72-25913
- GaAs solar batteries for spacecraft power supplies, comparing effectiveness with Si cells for optimum utilization 11 p1578 A72-25940
- Electrostatic rocket exhaust materials deposits effects on solar cells optical, thermal and electrical performance characteristics, using optical thin film theory [AIAA PAPER 72-447] 11 p1578 A72-26184
- Electric propulsion spacecraft design for ion thruster systems testing with circular solar cells array as gyroscopic stable platform [AIAA PAPER 72-466] 11 p1578 A72-26200
- Performance and environmental tests of large lightweight solar array unit, measuring structural members displacements with electro-optical instruments [AIAA PAPER 72-569] 12 p1755 A72-27377
- Solar cells - Conference, Toulouse, France, July 1970 12 p1755 A72-28001
- French R and D programs on Si and various thin film photovoltaic solar cells, considering efficiency, reliability, and weight and cost reduction problems 12 p1756 A72-28002
- German Si and polycrystalline solar cells development survey, discussing interconnection techniques, module design and filter applications for performance improvements 12 p1756 A72-28003
- British thin Si solar cells for large flexible lightweight arrays, considering radiation resistance, specific mass, area, contact material and antireflection coatings 12 p1756 A72-28004
- Photovoltaic effects in solar cell p-n homojunctions and heterojunctions at low and high excitation levels 12 p1855 A72-28006
- Photovoltaic effect and energy band model of solar cell cadmium-sulfide-copper-disulfide heterojunctions 12 p1855 A72-28007
- Thin film Cu-CdS solar cell electrochemical plating potential and solution composition effects on copper sulfide surface layer formation and cell efficiency 12 p1855 A72-28008
- Postdip heat treatment effects on thin film copper sulfide-cadmium sulfide junction solar cells spectral response, diode parameters and resistance 12 p1855 A72-28010
- Recombination diffusion length of minority carriers in thin layer cuprous sulfide solar cells 12 p1856 A72-28011
- P-n thin film solar cell based on thermally and electrochemically stable II-IV semiconductors with graded energy gaps 12 p1756 A72-28013
- Improved efficiency of cadmium sulfide-copper sulfide thin film solar cells, noting optimization of layer formation, gridding and encapsulation 12 p1756 A72-28016
- CdTe thin film solar cell room temperature prolonged operation instability, thermal degradation and performance improvement by gas adsorption removal 12 p1756 A72-28017
- Photoelectric properties of cadmium telluride thin film solar cells, discussing energy gap temperature dependence, work function and current variations anomalies 12 p1756 A72-28018
- Heat treatment and electron irradiation tests for spatial reliability of CdS and CdTe thin film solar cells, noting photovoltaic properties 12 p1757 A72-28019
- Cadmium sulfide solar cells stress analysis in relation to degradation caused by fabrication technology, discussing barrier layer formation process 12 p1757 A72-28020
- Radiovoltaic generator energy conversion by thin film solar cells, noting performance dependence on semiconductor band gap and radioisotope characteristics 12 p1757 A72-28021
- Electron irradiation effects on Li doped silicon solar cells, noting changes in donor concentration and defects formation 12 p1757 A72-28022
- Electron bombardment effects on transport properties and carrier lifetime degradation of Li doped Si solar cells 12 p1856 A72-28024
- High electric power output Si solar cell development, discussing increased energy conversion efficiency 12 p1757 A72-28026
- Silicon solar cells antireflection coatings for performance loss minimization, obtaining improvement with titanium dioxide compared to silicon monoxide coatings 12 p1757 A72-28027
- Titanium dioxide thin film antireflection coating to minimize reflection losses in Si solar cells, discussing fabrication and optical and electrical characteristics 12 p1757 A72-28028
- Silicon solar cell fabrication technology developments for long mission life performance reliability over wide temperature and radiation intensity ranges 12 p1757 A72-28029
- ESRO findings on optimal resistance welding of solar cell interconnections for silver coated metals and pure silver 12 p1814 A72-28030
- Integral diode cell for solar arrays compared with bypass configuration, discussing design, advantages and electrical performance test data 12 p1757 A72-28031
- Silicon solar cells IR reflectance improvement by reflecting back electrode, obtaining 10 percent efficiency increase 12 p1758 A72-28032
- Solar cells array design and assembly techniques, discussing tests for Esro satellites aerospace environments 12 p1758 A72-28033
- Structural design, performance and costs of rigid or semirigid solar panels for geostationary satellites power supplies 12 p1758 A72-28034
- Solar cell array tests for high intensity application up to 0.3 AU from sun under simulated space environment 12 p1758 A72-28035
- Flexible solar cell array module design technique, discussing electric welding procedure and equipment parameters effects on breaking strength and reliability 12 p1758 A72-28036
- Silicon solar cell interconnectors design for 5-10 years mission life, considering launch induced vibration stresses and thermal cycling stresses during mission 12 p1758 A72-28037
- Solar array for San Marco C satellite to study neutral atmosphere structure, discussing interior mounting design features 12 p1758 A72-28038
- Soft solder cracking and breaking alleviation in welding technique for solar cells, noting resistance to thermal cycles 12 p1814 A72-28039
- Silicon solar cell calibrations for space applications, discussing equivalent diagram, I-V characteristics and stratospheric balloon measurement 12 p1758 A72-28040
- Solar cells calibration by high altitude aircraft, using extrapolation method to zero air density 12 p1758 A72-28041
- Solar cell calibration in uncollimated sunlight, obtaining standards for solar simulator intensity 12 p1759 A72-28042
- Secondary standard solar cells calibration method based on solar spectral response comparison with primary standard, discussing error correction method 12 p1759 A72-28043
- Solar cells testing and array performance evaluation for communication satellites at Comsat laboratories, noting electron irradiation and proton damage studies 12 p1759 A72-28044
- Proton and electron radiation effects on silicon solar cells electric and photovoltaic properties, determining

- damage coefficients via minority carriers diffusion length measurement 12 p1759 A72-28045
- Monoenergetic electrons and low energy protons radiation damage effect on Si solar cell electrical and optical properties 12 p1759 A72-28046
- ESRO satellites solar array performance under orbital environmental conditions, discussing radiation damage and earth albedo effects 12 p1759 A72-28047
- Solar array degradation effect on electric propulsion spacecraft performance, presenting power allocation strategy during mission [AIAA PAPER 72-444] 13 p2037 A72-28943
- Flexible rolled-up solar array /FRUSA/ operational performance from spaceborne accelerometers, strain gages and temperature sensors telemetered data, noting damage-free extension-retraction exercises [AIAA PAPER 72-510] 13 p2051 A72-28952
- Solar cells insulating dielectrics breakdown tests in dilute Ar plasma at positive bias voltages to 20 kV 14 p2140 A72-30926
- Permanent manned lunar stations electrical power systems, discussing nuclear energy, solar cells and electrochemical power cells 15 p2214 A72-31814
- Back surface electric field Si cell characteristics and fabrication using alloyed-through contact process 15 p2182 A72-32130
- Si solar cell efficiency in synchronous orbit radiation field increase via improvement in diffusion profile, low resistivity material and diode characteristics 15 p2183 A72-32131
- Silicon dislocation density relationship to solar cell current loss at low temperature, presenting temperature-diffusion length and I-V characteristics 15 p2183 A72-32132
- Cost analysis for solar cell space power systems, considering array area and module standardization 15 p2338 A72-32133
- Silicon solar energy conversion for electrical power generation on spacecraft. 17 p2494 A72-34186
- Si p-n junction solar cell fill factor for electric power available to load, noting discrepancy between calculated and measured values due to recombination 17 p2494 A72-34264
- Effects of junction depth on the radiation damage of silicon solar cells. 17 p2594 A72-34388
- Solar radiation simulators and the measurements of solar battery and cell characteristics [Survey] 17 p2498 A72-35514
- Attitude control of satellites with large flexible solar arrays. [AIAA PAPER 72-733] 18 p2730 A72-36541
- Short-circuit current in silicon solar cells - Dependence on cell parameters. 19 p2753 A72-37567
- One MeV electron irradiation of new technology silicon solar cells. 19 p2754 A72-37777
- Si solar cell design for high power/weight ratio and extreme environmental operating conditions, describing technological innovations for reliability and efficiency enhancement 19 p2754 A72-37780
- SRET-1 'solar cells' 19 p2869 A72-37822
- Minimisation of the solar array generated electrical interference on the GEOS satellite. 20 p2889 A72-38990
- Attitude stability of a dual-spin satellite with a large flexible solar array. [AIAA PAPER 72-887] 20 p2975 A72-39114
- Attitude dynamics of a three-axis stabilized satellite with a large flexible solar array. [AIAA PAPER 72-857] 20 p2976 A72-39137
- Infrared testing of solar cell arrays. 20 p2890 A72-39339
- Measurement of surface leakage currents in a semiconductor photoelectric converter 22 p3140 A72-43188
- Determination of the optimum concentration level of solar radiation in solar batteries with different types of cooling 22 p3140 A72-43189
- SOLAR CHROMOSPHERE**
- U CHROMOSPHERE**
- U SOLAR ATMOSPHERE**
- SOLAR COLLECTORS**
- NT SOLAR REFLECTORS**
- Methods for the quality control of the reflecting surfaces of solar energy condensers [Survey] 22 p3140 A72-43187
- Mechanical tests of laminated plastics in solar installations 22 p3197 A72-43192
- SOLAR CONSTANT**
- Solar radiative constant and stratospheric volcanic dust effects on circulation and climate anomalies 06 p0840 A72-17623

Evaluating the light from the sun.

19 p2790 A72-37933

SOLAR CONVERTERS**U SOLAR GENERATORS****SOLAR CORONA**

Quiet solar corona thermal emission flux at 169 MHz, showing constant brightness and electron temperatures during cycle 01 p0123 A72-10045

MHD wave modes nonlinear coupling by quantum field approach with Hamiltonian formulation, applying to solar coronal heating 01 p0129 A72-10797

Line splitting in emission near plasma frequency in drift pair solar radio bursts, considering causes by model involving electrons bunching through solar corona 02 p0276 A72-11646

Solar coronal MHD disturbance off eastern limb correlation with complex radio event observed simultaneously with white light coronameter and Culgoora radioheliograph 02 p0276 A72-11647

Periodic solar flare modulation by pulsating structure, attributing radiation to synchrotron radiation emitted by electrons in magnetic flux tube embedded in solar corona 02 p0274 A72-12412

Gyroresonance plasma wave absorption in corona, investigating solar radio bursts fine structure 03 p0415 A72-12935

Solar U-type radio bursts in outer corona at 0.7 MHz related to magnetic bottle 03 p0406 A72-12937

Solar corona transition probabilities in intermediate coupling between Fe XVII configurations, including full configuration mixing 03 p0416 A72-13006

Solar UV and X radiation, considering chromospheric temperature and density profiles and coronal electron densities 03 p0409 A72-13123

Physics of solar corona - NATO Conference, Athens, September 1970 03 p0421 A72-13201

Solar corona research, discussing radio and radar astronomy and UV spectrum observations 03 p0422 A72-13202

Solar corona atomic states radiative and collisional transitions, inferring radiative recombination cross section from bound-free absorption coefficient 03 p0422 A72-13203

Solar corona MHD and plasma physical structure, considering macroscopic and microscopic properties 03 p0422 A72-13204

Extreme UV observations of solar chromosphere-corona transition region, evaluating various theoretical and empirical models 03 p0422 A72-13205

Coronal magnetic fields effects on energy and mass flux from lower solar atmosphere levels into corona, discussing plasma instabilities, solar flares, radio bursts, etc 03 p0422 A72-13206

Solar coronal magnetic field large scale structure relation to photospheric and interplanetary sector patterns [AD-734628] 03 p0422 A72-13207

Solar coronal monochromatic optical emission, inferring electron density and ionization or temperature distributions and variations with time 03 p0422 A72-13208

Coronal events in 5303 A wavelength, discussing loops and arches and slow and fast events from photographic recordings 03 p0422 A72-13209

Solar corona shape, structure and brightness changes during 11 year cycle from monochromatic and total eclipse white light observations 03 p0423 A72-13210

Nonoptical and optical observation derived coronal condensations models for active regions and flare associated events 03 p0423 A72-13211

Areas index relationship to different phenomena in chromosphere, corona and interplanetary space, investigating coronal radio diameter during solar cycle and cosmic rays 03 p0423 A72-13214

Solar far UV spectrum observations for chromospheric coronal structure determination, reviewing ionization balance, relative abundances and limb/disk ratios 03 p0423 A72-13216

Solar corona X ray data from SOLRAD satellites, detailing spectral energy distribution, ionization balance, continuum radiation and line emission 03 p0410 A72-13219

Solar chromosphere-corona transition region models based on UV resonance emission lines intensity, deriving temperature gradient from radio data 03 p0424 A72-13222

Solar outer corona steamer density and temperature data from type 3 solar radio burst observation by space radio astronomy 03 p0424 A72-13223

Flare- and prominence-associated solar radio outburst, describing preflash phase and type 2 and moving type 4 bursts relation to coronal instability 03 p0410 A72-13321

Solar turbulent magnetic field in lower corona associated with expanding limb microwave burst of 30 March 1969 03 p0410 A72-13325

Small scale magnetic field theories, concerning solar prominence structure, chromospheric and coronal heating and particle production in flares 03 p0430 A72-13333

Helmet streamer interaction of coronal material with magnetic fields, considering inertial, pressure, gravitational and magnetic forces 03 p0431 A72-13339

Large scale solar magnetic field properties, discussing rotation, patterns and effects on corona 03 p0431 A72-13341

Coronal magnetic fields above slowly changing active regions 03 p0431 A72-13342

Magnetic fields orientation in solar corona from polarization measurements in green line 03 p0431 A72-13343

Magnetic field structure in active solar corona, discussing optical and radio observations 03 p0431 A72-13345

Large-scale solar coronal magnetic field from optical and radio observations for corpuscular propagation in corona and interplanetary medium 03 p0432 A72-13346

Solar moving type 4 bursts and coronal magnetic fields evidence from 80 MHz radioheliograph data 03 p0411 A72-13347

Radio-astronomical evidence for magnetohydrodynamical pulsations in corona, considering solar radio burst model of pulsating structure due to synchrotron radiation 03 p0432 A72-13349

OSO-G satellite spectroheliograms of chromospheric, transition zone and coronal lines, indicating magnetic field spread with height 03 p0432 A72-13351

Coronal rotation determination by spectroscopic method for mean rotation rate vs heliographic latitude, confirming high latitude phenomena dependence of low latitude magnetic fields 03 p0432 A72-13352

Solar magnetic field sector boundaries, discussing photospheric field direction, activity regions, flares, coronal enhancements, faculae and geomagnetic response [AD-734627] 03 p0433 A72-13359

Solar corona observations during total eclipse of 22 September 1968, presenting photographs, polarization measurements, photometric data, structure and isophotes 03 p0434 A72-13492

Solar limb flare observations on 4 November 1968, presenting photographs and intensive green coronal luminescence 03 p0434 A72-13493

Solar K corona intensity and electron density determination from photographs without eclipse 04 p0574 A72-14924

Collisionless shock wave interaction with particle stream in upper solar corona from decimeter radio observation 05 p0708 A72-15764

Solar coronal total dielectronic recombination coefficient simple relationships for isoelectronic sequences of H, He, Ne, K-Ni and Li-F, Na-A and Cu-Kr 05 p0718 A72-16510

Solar activity asymmetry on two hemispheres in 1959-1969, considering spots, faculae, prominences and corona 05 p0718 A72-16511

Electron density profiles as function of position in enhanced coronal region from Ni XV and Fe XIII emission lines observation 05 p0719 A72-16517

Moving type 4 radio burst observation with radioheliograph, suggesting isolated self contained synchrotron emitting plasmoid and relation to coronal magnetic field 05 p0710 A72-16521

Solar wind velocity correlation with 5303 A coronal intensity 05 p0710 A72-16523

Solar wind structure from long lived inhomogeneities in corona, allowing for velocity, density and temperature perturbations 06 p0872 A72-17444

Solar type 3 bursts from high resolution radio spectrographs, deriving coronal temperatures from decay times 06 p0876 A72-17576

- Structure, absolute photometry and polarization of corona from solar eclipse observation on 22 September 1968 06 p0883 A72-18026
- He and heavy ions properties and behavior in solar wind from expanding solar corona theoretical models 06 p0874 A72-18065
- Neutral current sheath formation from plane dipole magnetic field extension by plasma flow, discussing solar corona streamers and geomagnetic tail 07 p1039 A72-18914
- Ionization mechanisms of quiescent prominence of He II 4686 line luminescence under coronal UV radiation at high temperatures 07 p1077 A72-19812
- Solar corona structure and dynamics in context of energy transfer processes of dissipation, radiation, heat conduction and hydrodynamic expansion 07 p1078 A72-20006
- Solar magnetic fields configuration in corona in relation to energetic proton escape into interplanetary space 07 p1060 A72-20015
- Transfer characteristics of solar radio radiation in scattering corona 07 p1062 A72-20230
- Solar corona abundance and intensity measurements during 30 May 1965 eclipse 07 p1081 A72-20233
- Coronal condensation of 10 September 1970, observing iron and calcium emission lines 07 p1082 A72-20297
- Isophote equidensity role in astronomical photometric investigation of solar corona, galactic nebulas, comets and extragalactic stellar systems 07 p1082 A72-20301
- Solar corona structure during 22 September 1968 total eclipse noting N-S asymmetry and correspondence of large details to formations in photosphere and chromosphere 08 p1228 A72-20825
- Radio observation of flare sources and emission areas above coronal condensations during 22 September 1968 solar eclipse 08 p1228 A72-20828
- Solar coronal plasma radiative capacity and temperature structure from cooling function in thermal balance equation 08 p1231 A72-21124
- RAE-1 measurements of 1f radio phenomena in magnetosphere, solar corona and Galaxy, discussing design, calibration and performance 08 p1137 A72-21984
- Sun vicinity skylight polarization influence on polarimetric K corona observations, discussing inaccuracy sources 09 p1392 A72-23544
- Coronal nonthermal radio emissions occurrence in absence of visible flares due to chromospheric perturbation 10 p1529 A72-24525
- Ions classification by ionization potential to explain existence of empirically defined classes for visible solar corona lines 10 p1542 A72-24614
- Solar chromosphere-corona transition region theoretical and empirical models, studying acoustic flux generated above convective zone 11 p1717 A72-25906
- Structure, absolute photometry and polarization of corona from solar eclipse observation on 22 September 1968 11 p1719 A72-25962
- Hydrodynamic approximation for solar wind nonuniformity in ecliptic plane, noting linear disturbances caused by nonuniform velocity of plasma flow from corona 13 p2029 A72-28577
- Outer corona and interplanetary space magnetic fields calculated from photosphere magnetic fields measured during 7 March 1970 solar eclipse 13 p2041 A72-29528
- OSO-6 Mg X spectroheliogram data for corona electron density map construction during 7 March 1970 solar eclipse period 13 p2031 A72-29529
- Slit spectrogram and direct photograph observation of inner corona fine structure during 7 March 1970 solar eclipse, describing line and continuum intensities 13 p2042 A72-29533
- Spectrographic observation of flash spectrum during 7 March 1970 solar eclipse, showing significant coronal line emission origin in chromosphere interspersal regions 13 p2042 A72-29534
- Inner corona spectral data of 7 March 1970 solar eclipse, noting line half widths and emission line origin area relationship 13 p2042 A72-29535
- Spectrophotometry of inner corona and quiescent prominence during 7 March 1970 solar eclipse, discussing Balmer line analysis 13 p2042 A72-29536
- Solar corona IR Fe XIII lines during 12 November 1966 solar eclipse, discussing proton collisions as line-producing excitation mechanism 13 p2042 A72-29537
- Fourier transform spectrometer observation of IR coronal emission lines during 7 March 1970 solar eclipse from high altitude aircraft 13 p2042 A72-29538
- Aerobee rocket far UV flash spectrum observations of chromosphere and corona during 7 March 1970 solar eclipse 13 p2042 A72-29539
- Wavelength, intensity and spatial distribution identification of far UV solar coronal forbidden lines observed during 7 March 1970 solar eclipse 13 p2043 A72-29540
- Rocket-borne photographic measurement of Lyman alpha corona brightness during 7 March 1970 eclipse, comparing limb white light variations 13 p2043 A72-29541
- White light and XUV coronas on 7 March 1970 from rocket photographs, comparing with X ray, Lyman alpha, Fe XIV and IR eclipse photographs 13 p2031 A72-29542
- Rocket-borne coronagraph photometry of solar corona during 7 March 1970 eclipse for streamer analysis 13 p2043 A72-29543
- Polarization-color effect in K corona during 7 March 1970 eclipse observation, using Wollaston prism and filter combination 13 p2043 A72-29544
- Jet aircraft photographic observation of solar corona polarization during March 1970 solar eclipse 13 p2043 A72-29545
- Satellite photometric observatory for solar corona intensity and polarization measurements during 7 March 1970 total eclipse 13 p2043 A72-29546
- Photographic polarimeter measurement of linear polarization of coronal emission lines during 7 March 1970 solar eclipse 13 p2043 A72-29547
- Solar corona spectral line width and wavelength measurements during 7 March 1970 total eclipse, using Fabry-Perot photographic interferometer 13 p2043 A72-29548
- Relative brightnesses along solar radius from density photometry of corona at eclipses 13 p2046 A72-29715
- Solar corona intensification analysis based on ionized Fe monochromatic emission spectra, investigating spectral lines behavior as function of temperature and electron density 13 p2047 A72-29736
- Equatorial quiet solar atmosphere model for chromosphere-corona transition region based on cm radio observation and hydrodynamical conservation equations 13 p2049 A72-29933
- Solar coronal magnetic field structure and energy content from synoptic data analysis, noting differential rotation effects 13 p2050 A72-29938
- Solar transition zone and corona EUV lines formation heights measurement from OSO-4 spectroheliograms 13 p2050 A72-29939
- Solar X-ray spectral lines at 1-60 A from coronal ion relative abundances obtained from Jordan ionization equilibrium calculations 13 p2034 A72-29940
- Coronal condensation X ray sources from heliograms, discussing relation to active region evolution 14 p2146 A72-30204
- Solar proton flare on 2 November 1969, investigating active region magnetic field development and spatial structure, near limb and coronal phenomena 14 p2160 A72-30909
- Lunar orbital photography of astronomical and geophysical phenomena during Apollo 15 flight, noting solar corona and Milky Way 15 p2236 A72-31974
- Coronal scattering effects on type 3 solar bursts, using radio sources scintillation model and Monte Carlo ray tracing technique 15 p2316 A72-32752
- Eleven year period solar photospheric magnetic field evolution, comparing latitudinal variation with sunspots, faculae and prominences distribution and green-line corona intensity 15 p2317 A72-32778
- Solar corona Ca ion abundance from emission line measurements and electron density determination 15 p2318 A72-32785
- Inner solar corona electron density distribution as function of heliographic latitude, longitude and radial distance from K-coronameter polarization-brightness data 15 p2318 A72-32786
- Coronal randomly distributed anisotropic density inhomogeneities induced refraction and scattering effects on solar radio sources at 80 MHz 16 p2452 A72-33042
- Near earth interplanetary electron source detection related to coronal site type 3 bursts, using 80 MHz radioheliograph observations 16 p2445 A72-33044
- German monograph on solar wind-coronal magnetic field interactions, presenting numerical calculation of time dependent coronal states 16 p2445 A72-33425
- Photographic technique to obtain isophotic contours of solar corona polarized light during total eclipse 16 p2393 A72-33624
- Particle excitation processes in solar corona, ionosphere and astrophysics, discussing electron affinities, ion-molecule reactions, forbidden atomic transitions and Fe II problem 16 p2432 A72-34150
- The possibility of single-valued determination of electron concentration from results of phase measurements 17 p2585 A72-35031
- Solar chromosphere-corona transition region structure and energy balance calculation by static planar model compared with XUV resonance line observations 17 p2608 A72-35083
- Solar corona emission line polarization numerical computation based on magnetic dipole transition scattering function for interpretation in terms of magnetic field direction 17 p2608 A72-35084
- Charged particle stream neutralization and stabilization in solar corona, noting plasma wave and relation to type 3 radio bursts 17 p2608 A72-35093
- Transport of cosmic rays in the solar corona 17 p2599 A72-35094
- Space observations of the solar corona 17 p2611 A72-35326
- A model for drift pair and hook burst emission from the solar corona 17 p2617 A72-35712
- Ionization mechanisms for quiescent prominence He II 4686 line emission under coronal UV radiation and high temperature conditions 17 p2618 A72-35737
- Solar flares and radio bursts significance for chromosphere and corona studies, considering radiation frequency-source location relations 17 p2603 A72-35957
- Pulsating modulations and peculiar absorptions of type IV emissions from the solar corona 18 p2721 A72-36651
- Density of the solar corona from occultations of NP 0532 19 p2855 A72-37242
- Shock wave propagation in the solar corona as the cause of type II radio bursts 19 p2851 A72-38064
- Neutral current sheath formation from plane dipole magnetic field extension by plasma flow, discussing solar corona streamers and geomagnetic tail 20 p2957 A72-39380
- Computer program for solar corona emission line polarization computation to interpret measurements in terms of coronal magnetic field direction 20 p2971 A72-39757
- Temperature and emission measure deduced by coronal visible lines 20 p2974 A72-39896
- Multiple-frequency operation of the Culgoora radioheliograph 21 p3053 A72-40397
- Solar coronal F component separation from K component by utilizing elongation dependence differences in scattering populations, computing F for wide range of parameters 21 p3106 A72-41041
- OSO-4 observations of coronal EUV hole, considering association with regions of diverging magnetic fields 21 p3106 A72-41042
- Various ground configuration level intervals from gaseous nebulas and solar coronal forbidden transitions observations and laboratory investigations of resonance lines 21 p3108 A72-41286
- Hydrodynamical study of the large northeast coronal streamer observed during the eclipse of March 7, 1970 21 p3100 A72-41287
- Coronagraphic observations of an enhanced coronal region. II - Temperature and density structure through the enhanced region 21 p3108 A72-41288
- Faraday rotation of linearly polarized radio waves from the Crab Nebula by the solar corona 21 p3109 A72-41327
- The derivation of temperature gradient and electron density maps from EUV spectroheliograms 22 p3222 A72-42036
- Alpha force-free magnetic field representation for solution of boundary value problem for chromosphere and lower corona magnetic fields 22 p3222 A72-42037

A possibly direct measurement of coronal magnetic field strengths.

22 p3222 A72-42042

Interpolation formulae for the electron impact excitation of ions in the H-, He-, Li-, and Ne-sequences.

22 p3224 A72-42379

Mathematical models from UV, IR and radio observations of chromosphere and transition region to corona, noting temperature effects of shock wave dissipation

22 p3229 A72-42903

Coronal condensation X ray sources from heliograms, discussing relation to active region evolution

23 p3328 A72-43234

Coronal lines photometry systematic error dependence on aureola spectral intensity, line half width, gradation curve slope, and neutral filter transmission coefficient

23 p3340 A72-44240

Shock waves role in coronal heating, solar wind and energy and material transfer to earth and in solar system

24 p3439 A72-45019

Hydrodynamic approximation for solar wind nonuniformity in ecliptic plane, noting linear disturbances caused by nonuniform velocity of plasma flow from corona

24 p3435 A72-45077

Physical conditions in the solar corona from spectral observations of the eclipse of March 7, 1970

24 p3448 A72-45684

SOLAR CORPUSCULAR RADIATION NT SOLAR PROTONS

Polar cap region solar particle fluxes from Esro 1/Aurora satellite recordings, noting north-south asymmetry

03 p0348 A72-13506

Nuclear charge composition and energy spectra measurement for hydrogen, helium and medium nuclei in 12 April 1969 solar particle event

04 p0567 A72-15325

Heavy nuclei enrichment in solar accelerated particles, discussing differential energy spectra, photospheric and coronal abundances, satellite observation and agreement with galactic cosmic rays

04 p0568 A72-15366

Azur satellite for investigating polar regions, inner radiation belt and solar particle emission

05 p0715 A72-16135

Solar neutrons search near solar maximum with plastic scintillator counter, discussing irregular excess in counting rate

05 p0719 A72-16524

Statistical criteria of geomagnetic activity, considering solar corpuscular radiation effect

06 p0803 A72-17369

Proton measurements with Azur satellite during solar particle events of March 1970, considering diffusion and convection transport theories

07 p1056 A72-18901

Solar discrete particle events classification and emission and acceleration mechanisms in relation to flare development

07 p1060 A72-20011

Diffusion models of energetic solar particles in interplanetary medium, considering impulsive emission from solar flares

07 p1061 A72-20023

Comet brightness variations correlation with geomagnetic field and solar corpuscular flux variations in interplanetary space

08 p1231 A72-21132

Solar energetic particle access characteristics to magnetosphere from PCA riometer and satellite measurements, determining relationship between earth dipole field and interplanetary field

08 p1228 A72-21497

Radiation damage by heavy solar particles in soil grains from Lunik 16 and landing Apollo sites

09 p1381 A72-22269

Solar particles latitudes dayside profiles as function of geomagnetic activity, suggesting closed field lines limit location

09 p1378 A72-23002

Solar atmosphere low energy positron production by solar particle fluxes demodulated according to cosmic ray transport equations

09 p1378 A72-23022

D region ionization by solar corpuscular streams, considering formation of charged particle concentration profiles

11 p1622 A72-25948

Quasi-steady and sporadic corpuscular fluxes as basic solar activity effect on troposphere, showing magnetosphere interaction time relation to meridional atmospheric circulation changes

12 p1842 A72-28208

Solar relativistic electrons and particle events spectra during 1967-1969 from IMP-4 observations

13 p1033 A72-29746

Geomagnetic storms caused by quasi-stationary directed corpuscular streams resulting from solar chromosphere flares

14 p2147 A72-30487

Evidence for solar particle production above approximately 75 GeV.

17 p2600 A72-35365

The absorption length for solar particles in the earth's atmosphere - Solar proton event November 18, 1968.

17 p2602 A72-35760

Sudden commencements of geomagnetic storms at the turn of two solar cycles.

18 p2686 A72-36228

Possibility of estimating an energetic particle stream in the ionospheric D region at sunrise and under daytime conditions

18 p2688 A72-36858

Experimental nuclear physics and theoretical solar structure and evolution explanations of disagreement between calculated and observed solar neutrino flux

18 p2722 A72-37007

Geomagnetic storms caused by quasi-stationary directional corpuscular streams resulting from solar chromosphere flares

19 p2851 A72-38316

Coordinate system for use with high-latitude energetic-particle phenomena.

19 p2853 A72-38729

Reconnection of the geomagnetic tail deduced from solar-particle observations.

19 p2792 A72-38730

Aluminum 26 and manganese 53 produced by solar-flare particles in lunar rock and cosmic dust.

20 p2970 A72-39472

Balloon-borne telescope search for solar neutrons and gamma rays during enhanced solar activity periods

21 p3101 A72-41298

Sea level tropospheric pressure distribution persistence correlation to solar corpuscular radiation measured by planetary scale geomagnetic disturbance

22 p3219 A72-42517

Magnetic storm classification from geomagnetic field H and Z components behavior, associating with solar corpuscular flux

22 p3174 A72-42952

Solar neutrino flux dependence on gravitational effects, discussing Brans-Dicke gravitation theory and general relativity equations

22 p3229 A72-42957

Solar neutrino and dilaton theory of non-Newtonian gravity.

23 p3329 A72-44315

Association between interplanetary shock waves and delayed solar particle events.

23 p3332 A72-44503

SOLAR COSMIC RAYS

Solar cosmic ray cutoff rigidity increase during polar cap absorption related to geomagnetic perturbation onset

02 p0273 A72-11938

Acceleration phase of solar cosmic rays and relativistic electrons in solar flare of 7 July 1966, discussing MHD shock waves generation

03 p0407 A72-12942

Astronomical model for solar cosmic ray bursts propagation including anisotropic particle diffusion along interplanetary magnetic field

03 p0407 A72-12944

Areas index relationship to different phenomena in chromosphere, corona and interplanetary space, investigating coronal radio diameter during solar cycle and cosmic rays

03 p0423 A72-13214

Cosmic ray decreases correlation to solar flare occurrence by epoch analysis of monitor data, proposing mechanism for explanation

03 p0412 A72-13528

Cosmic ray energy changes in interplanetary space by model for solar X-ray bursts

03 p0413 A72-13534

Polar cap absorption event, investigating solar high energy protons precipitation effects

05 p0709 A72-16239

Energetic solar flare particles release from sun, describing satellite observations of solar electromagnetic radiation

05 p0710 A72-16522

Solar cosmic rays propagation between shock front and solar flare hot plasma, examining fine structure from Explorer 34 and Venera 6 data

07 p1063 A72-20628

Solar cosmic ray heavy nuclei acceleration independence from solar activity phenomena, based on Elektron 4 satellite observation

07 p1064 A72-20632

Solar cosmic ray flare recording in stratosphere in Murmansk and Antarctic regions during February-April 1969

07 p1066 A72-20649

Solar cosmic ray flare of 11-18 April 1969, investigating effect on polar cap absorption in lower ionosphere

07 p1066 A72-20650

Solar cosmic ray energy spectrum from calculation of secondary emission neutron component generation multiplicities

08 p1225 A72-20723

Solar cosmic ray spectra at time of ejection from flare region and arrival near earth

08 p1226 A72-20812

Solar cosmic ray diffusion in interplanetary medium, describing solar flare proton and heavy nuclei propagation in terms of time of arrival measurements

08 p1227 A72-21157

Solar atmosphere low energy positron production by solar particle fluxes demodulated according to cosmic ray transport equations

09 p1378 A72-23022

Enhanced abundances of low energy heavy elements in solar cosmic rays due to preferential acceleration within flare region

10 p1530 A72-24673

High energy solar and galactic cosmic ray chemical composition, considering electron component abundances and beryllium-boron ratio

12 p1863 A72-27426

Solar cosmic ray cut-off rigidity increase during PCA related to geomagnetic perturbation onset

13 p2030 A72-29250

Low energy proton flux increases associated with geomagnetic storms due to interplanetary shock waves occurring during solar cosmic ray flare event decay

13 p2032 A72-29724

Solar cosmic rays spectrum and geomagnetic cut-off rigidity determination from ion production rates in lower ionosphere

14 p2147 A72-30627

Cosmic ray chemical composition from particle sampling by rockets and satellites, comparing galactic rays, solar rays and sun

15 p2299 A72-31648

Satellite charged particle observations and polar cap riometer absorption measurements during solar cosmic ray events, noting electrons and protons contributions

15 p2300 A72-31965

Transport of cosmic rays in the solar corona.

17 p2599 A72-35094

Spatial distribution and temporal nature of the entry of solar cosmic rays into the polar cap

17 p2603 A72-35870

A comparison of measurements of the charge spectrum of solar cosmic rays from nuclear emulsions and the Explorer 35 solid-state detector.

18 p2721 A72-35988

Solar cosmic ray anisotropy 27-day variations during IGY from global network stations neutron component data

18 p2722 A72-36876

Solar cosmic ray energy spectrum from calculation of secondary emission neutron component production multiplicities

19 p2852 A72-38351

Radiobiological problems caused by supersonic transport /With a survey of the first results established by tests performed on board the Concorde prototype/.

19 p2762 A72-38713

Solar cosmic ray diffusion in interplanetary medium, describing solar flare proton and heavy nuclei propagation in terms of time of arrival measurements

20 p2964 A72-32962

Solar flare associated relativistic electron acceleration relationship to cosmic ray and type 4 radio burst production

22 p3217 A72-42010

Particle flux measurements from rockets during a solar cosmic-ray flare in April, 1969

22 p3218 A72-42226

Production of light elements in the solar system.

23 p3335 A72-43487

Some characteristics of microwave type IV radio bursts and the acceleration of solar cosmic rays.

23 p3328 A72-43616

SOLAR CYCLES

NT SUNSPOT CYCLE

Oscillatory hydromagnetic dynamo model of variable sign large scale solar magnetic field, using Benard convective cell with Coriolis velocity disturbance

01 p0128 A72-10585

Balloon measurements for differential energy spectra of cosmic ray protons and He over half solar cycle 1965-1969, using Geiger tube hodoscope

[AD-745870]

01 p0119 A72-10876

Middle geographic latitude sporadic E-layer initial height variations during 1957-1968 solar cycle

01 p0064 A72-11103

Criticism of cyclonic reversal mechanism and dynamo theory for solar 22-year cycle, proposing penetrating magnetic and general field theory

02 p0276 A72-11641

Beacon satellite transmission determination of ionosphere total electron content, describing equivalent slab thickness and diurnal, seasonal and solar cycle behavior

02 p0221 A72-12460

Solar corona shape, structure and brightness changes during 11 year cycle from monochromatic and total eclipse white light observations

03 p0423 A72-13210

Solar cycle models physical mechanisms, discussing surface activities and nonaxisymmetric steady state solutions

03 p0433 A72-13357

- Solar magnetic field and solar cycle dynamo theory based on mean field MHD 03 p0433 A72-13361
- Viscous torsional vibrations inadequacy for interpreting solar activity cycles relative to magnetic field 03 p0436 A72-13811
- Solar magnetic field generation by gyrotropic turbulence, noting inadequacy of Steenbeck explanation for quantitative estimates of solar cycle parameters 03 p0436 A72-13825
- Auroral behavior observation at midlatitude station, exhibiting correlation with solar activity as regards solar cycle recurrence and phase [AD-739061] 04 p0515 A72-14882
- Ionospheric electron content over New Delhi, observing seasonal and solar cycle variations of diurnal changes 04 p0515 A72-14930
- Latitudinal, diurnal, seasonal and solar cycle variations in vhf-uhf scintillation producing irregularities in F layer electron density 05 p0630 A72-16617
- Long time variations of proton energy spectra in inner radiation belt during solar cycle 05 p0710 A72-16767
- Statistical analysis of sunspot activity, forecasting solar cycle events 05 p0723 A72-17176
- Diurnal variation of lower ionosphere, analyzing nature and behavior of absorption long range variations over solar activity cycle 05 p0660 A72-17182
- Short and long term spectral modulation of primary cosmic rays above 2 GV during solar cycle 19 descending phase, presenting neutron monitors calibration procedure 06 p0874 A72-18160
- Long term variations in height of solar activity maxima and sunspot numbers during 11 year cycle 07 p1079 A72-20016
- Solar modulation of cosmic ray intensity in stratosphere, examining relationship to sunspots group number and heliographic latitudes over 11 year period 07 p1065 A72-20641
- Diurnal, sporadic and yearly variations in cosmic ray flux based on neutron component data, noting relation to solar activity cycles 07 p1066 A72-20647
- Solar unipolar magnetic regions relation to geomagnetic disturbances variability, discussing 11 year cycle 08 p1155 A72-20808
- Ionospheric drift patterns diurnal, seasonal and solar cycle variations from synoptic measurements over east Siberia by closely spaced receivers, using Briggs similar fades method 08 p1160 A72-21530
- Solar five minute oscillations in isothermal atmosphere by base pressure fluctuations 09 p1382 A72-22287
- Diurnal, seasonal and solar cycle variations in cosmic noise absorption during 1957-1966, showing various ionospheric layers contribution 09 p1385 A72-22586
- Ionospheric potential and thunderstorm activity annual variations during 1959-70 solar cycle from radiosonde measurements in free atmosphere 09 p1301 A72-23265
- Sunspot group number and average lifetimes in solar activity cycle 09 p1390 A72-23397
- Atmospheric wind velocity time variations at 80-100 km altitudes from ionospheric drift data, finding planetary oscillation periodicities relationship to solar activity cycle 11 p1620 A72-25273
- Whistler dispersion and occurrence rate characteristics at low latitudes during solar cycle, noting annual variations and magnetospheric electron density 11 p1623 A72-26105
- F region critical frequencies deviation from median due to solar cycle phase, latitude and time, discussing short waves radio communications reliability 11 p1593 A72-26271
- F 2 region critical radio frequencies forecasts from solar cycles, ionospheric disturbances data, latitude and annual and diurnal variations 11 p1594 A72-26272
- Diurnal variations of F 2 region critical frequencies and quiet and perturbed ionosphere N/h_p profiles during solar cycle, estimating signal reflection altitudes 11 p1594 A72-26274
- Sporadic E layer cyclic variations during solar activity cycle, noting time dependence of occurrence probability and critical frequency 11 p1623 A72-26281
- Magnetic disturbances recurrence relationship to even- and odd-numbered sunspot cycles, noting existence of 22-year solar cycle 12 p1803 A72-27773
- F region mean electron density profile seasonal and solar cycle dependence, using Chapman function for nighttime F layer description 12 p1803 A72-27775
- Sunspots, Doppler shifts, geophysical changes and statistical evaluation of diffuse objects motion in sun, discussing solar magnetic fields and 22 year cycle 13 p2044 A72-29701
- Eighty year cycle representation deduced from yearly means of sunspot relative numbers without use of averaging or smoothing method 13 p2046 A72-29728
- Solar cycle dynamo theory and Babcock and Leighton model inadequacies, considering alternative theory based on deep magnetic field 13 p2046 A72-29729
- Solar maps from quiet sun center limb microwave radio telescope observations during cycle maximum 13 p2048 A72-29742
- Solar cyclic intensity variation of excessive radiation with respect to galactic radiation background at low altitudes from satellite data analysis 14 p2146 A72-30475
- Harmonic analysis of solar wind geometry and geomagnetic activity levels during even and odd cycles based on cosmic ray intensity variations for 1900-1969 period 14 p2147 A72-30651
- Explorer 19 satellite drag evidence for neutral exosphere He concentration asymmetry between Northern and Southern Hemispheres over entire solar activity cycle 15 p2228 A72-31977
- Blanketing sporadic E layer latitude seasonal variations near geographic equator, noting spread F occurrence and solar cycle effects 15 p2231 A72-32265
- Eleven year period solar photospheric magnetic field evolution, comparing latitudinal variation with sunspots, faculae and prominences distribution and green-line corona intensity 15 p2317 A72-32778
- Long term variations of proton flux and energy spectra in inner radiation belt during solar cycle 17 p2600 A72-35270
- On the temporal distribution of type IV burst-active centres over the solar cycle [Research note]. 17 p2602 A72-35715
- Cosmic ray anisotropy and conditions in the interplanetary medium during a solar cycle 17 p2603 A72-35871
- Sudden commencements of geomagnetic storms at the turn of two solar cycles. 18 p2686 A72-36228
- Nature of the 80-90 year cycle of solar activity 19 p2860 A72-37952
- Rotation period variation in long term behavior of interplanetary magnetic sector structure during nearly four solar cycles 19 p2868 A72-38731
- Observations of the radial gradient of galactic cosmic radiation over a solar cycle. 20 p2964 A72-39337
- One dimensional migratory dynamo model for alpha effect turbulence controlled by increasing magnetic field, considering oscillatory antisymmetric solutions relation to solar cycle 20 p2972 A72-39877
- Change in the eleven-year modulation at the time of the June 8, 1969, Forbush decrease. 22 p3172 A72-42424
- Variation of the cosmic-ray gradient during a solar activity cycle 23 p3328 A72-43374
- Annual and solar-magnetic-cycle variations in the interplanetary magnetic field, 1926-1971. 23 p3286 A72-44504
- Energy and mass content of high-speed solar-wind streams. 23 p3332 A72-44508
- SOLAR DISK**
U SUN
SOLAR ECLIPSES
Ionospheric total electron content measurement with geostationary ATS 3 satellite during solar eclipse of 7 March 1970, plotting Faraday rotation as function of time 01 p0059 A72-10838
- L alpha limb flux during total solar eclipse of 12 November 1966 from rocket measurements, comparing with chromosphere model 03 p0415 A72-12931 [AD-739763]
- Radio observations of filaments in absorption against solar disk during 11 September 1969 and 7 March 1970 eclipses 03 p0415 A72-12939
- Solar corona shape, structure and brightness changes during 11 year cycle from monochromatic and total eclipse white light observations 03 p0423 A72-13210
- Solar corona observations during total eclipse of 22 September 1968, presenting photographs, polarization measurements, photometric data, structure and isophotes 03 p0434 A72-13492
- Loran C system time tick transmission delay during solar eclipse of 7 March 1970, discussing atmospheric electron density effects 03 p0322 A72-13533
- F 2 layer critical frequency deviations and negative disturbance zones during solar eclipse of 22 September 1968 05 p0657 A72-16264
- Partial solar eclipse observation at 9 mm wavelength on 25 February 1971, noting limb brightening 05 p0718 A72-16509
- Vlf propagation and D region aeronomy model for vlf phase behavior predictions and observations during two solar eclipses 05 p0630 A72-16618
- Sporadic E ionization during 1955 partial solar eclipse, considering gravity waves effect due to fast moving shadow region cooling spot 06 p0805 A72-17466
- Structure, absolute photometry and polarization of corona from solar eclipse observation on 22 September 1968 06 p0883 A72-18026
- Solar corona abundance and intensity measurements during 30 May 1965 eclipse 07 p1081 A72-20233
- Solar corona structure during 22 September 1968 total eclipse noting N-S asymmetry and correspondence of large details to formations in photosphere and chromosphere 08 p1228 A72-20825
- Radio observation of flare sources and emission areas above coronal condensations during 22 September 1968 solar eclipse 08 p1228 A72-20828
- Differential photoelectron flux in lower ionosphere during 7 March 1970 solar eclipse observed by Nike-Apache rockets 09 p1378 A72-23012
- Ionospheric electron concentrations and temperatures determined by time dependent continuity equations model during 11 September 1969 solar eclipse 09 p1390 A72-23518
- Photographic observation of times of first and second contact and maximum phase for 15 February 1971 partial solar eclipse, discussing instruments and materials 11 p1717 A72-25903
- Structure, absolute photometry and polarization of corona from solar eclipse observation on 22 September 1968 11 p1719 A72-25962
- Atmospheric electricity measurements at Waldorf observatory during 7 March 1970 solar eclipse 12 p1799 A72-27139
- Atmospheric electricity, turbulence and pseudosunrise effect during solar eclipse, analyzing space charge density and power spectra decay 12 p1800 A72-27140
- Daytime sky polarimetry of scattered light in atmosphere during solar eclipses 12 p1800 A72-27141
- Ground surface shadow bands observations during 7 March 1970 solar eclipse by photoelectric detection, indicating atmospheric turbulence effect 12 p1800 A72-27142
- Forbidden O I lines brightness and shadow bands properties during 7 March 1970 solar eclipse, comparing with rocket measurements 12 p1800 A72-27143
- Upper atmosphere neutral particle pressure, temperature and density profiles during 7 March 1970 solar eclipse from pitot tube soundings 12 p1800 A72-27144
- Solar UV radiation and Lyman alpha flux observation during 7 March 1970 solar eclipse with Nike-Apache rocket photometer soundings 12 p1862 A72-27145
- Solar X-rays absorption profiles and residual fluxes in D and E layers during 7 March 1970 eclipse from rocket measurements 12 p1863 A72-27146
- Solar Lyman alpha radiation flux over disk during solar eclipse from rocket measurements 12 p1863 A72-27147
- Electron density and ionization changes in lower ionosphere during 7 March 1970 solar eclipse from 2.66 MHz absorption and Langmuir probe rocket measurements 12 p1800 A72-27148
- Electron recombination loss coefficients and concentration profiles for D region during solar eclipses from rocket measurements 12 p1800 A72-27149
- Nitric oxide and oxygen molecular ion composition of lower ionosphere during solar eclipses from rocket measurements 12 p1801 A72-27150
- Ionospheric electron and ion densities during 12 November 1966 solar eclipse from rocket probe measurements 12 p1863 A72-27151
- Thermospheric ion, electron and neutral particle concentration, composition and temperature changes during 7 March 1970 solar eclipse from rocket measurements 12 p1778 A72-27152
- Conjugate point photoelectron flux measurements in ionosphere during 7 March 1970 solar eclipse, using

retarding potential analyzer onboard Nike-Tomahawk rocket

12 p1801 A72-27153

Ionosonde observations and Faraday rotation measurements of E and F region total electron content during two solar eclipses

12 p1801 A72-27154

ATS observed ionospheric columnar electron content variation during March 1970 solar eclipse, discussing neutral winds effects

12 p1801 A72-27155

Traveling ionospheric disturbances observations during March 1970 solar eclipse from ATS 3 total electron content measurements

12 p1801 A72-27156

Ionospheric HF Doppler dispersion during 7 March 1970 solar eclipse, noting traveling ionospheric disturbance

12 p1801 A72-27157

Traveling ionospheric disturbances radio sounding during 7 March 1970 solar eclipse time, noting wave front orientation

12 p1801 A72-27158

Solar eclipse 1970 - Conference, Seattle, June 1971

13 p2041 A72-29526

Solar eclipse timings by photoelectric, photographic and visual observation for comparison of Newcombe sun tables and improved lunar ephemeris reference systems

13 p2041 A72-29527

Outer corona and interplanetary space magnetic fields calculated from photosphere magnetic fields measured during 7 March 1970 solar eclipse

13 p2041 A72-29528

OSO-6 Mg X spectroheliogram data for corona electron density map construction during 7 March 1970 solar eclipse period

13 p2031 A72-29529

Spectral line variations in transition region from photosphere to chromosphere during March 1970 solar eclipse

13 p2041 A72-29530

Solar radial brightness distribution, using mm observations during 7 March 1970 solar eclipse for improved angular resolution

13 p2042 A72-29531

Model solar atmosphere from mm and cm wavelength high resolution observations of chromosphere by lunar limb antenna tracking during 7 March 1970 eclipse

13 p2042 A72-29532

Slit spectrogram and direct photograph observation of inner corona fine structure during 7 March 1970 solar eclipse, describing line and continuum intensities

13 p2042 A72-29533

Spectrographic observation of flash spectrum during 7 March 1970 solar eclipse, showing significant coronal line emission origin in chromosphere interspersed regions

13 p2042 A72-29534

Inner corona spectral data of 7 March 1970 solar eclipse, noting line half widths and emission line origin area relationship

13 p2042 A72-29535

Spectrophotometry of inner corona and quiescent prominence during 7 March 1970 solar eclipse, discussing Balmer line analysis

13 p2042 A72-29536

Solar corona IR Fe XIII lines during 12 November 1966 solar eclipse, discussing proton collisions as line-producing excitation mechanism

13 p2042 A72-29537

Fourier transform spectrometer observation of IR coronal emission lines during 7 March 1970 solar eclipse from high altitude aircraft

13 p2042 A72-29538

Aerobee rocket far UV flash spectrum observations of chromosphere and corona during 7 March 1970 solar eclipse

13 p2042 A72-29539

Wavelength, intensity and spatial distribution identification of far UV solar coronal forbidden lines observed during 7 March 1970 solar eclipse

13 p2043 A72-29540

Rocket-borne photographic measurement of Lyman alpha corona brightness during 7 March 1970 eclipse, comparing limb white light variations

13 p2043 A72-29541

White light and XUV coronas on 7 March 1970 from rocket photographs, comparing with X ray, Lyman alpha, Fe XIV and IR eclipse photographs

13 p2031 A72-29542

Rocket-borne coronagraph photometry of solar corona during 7 March 1970 eclipse for streamer analysis

13 p2043 A72-29543

Polarization-color effect in K corona during 7 March 1970 eclipse observation, using Wollaston prism and filter combination

13 p2043 A72-29544

Jet aircraft photographic observation of solar corona polarization during March 1970 solar eclipse

13 p2043 A72-29545

Satellite photometric observatory for solar corona intensity and polarization measurements during 7 March 1970 total eclipse

13 p2043 A72-29546

Photographic polarimeter measurement of linear polarization of coronal emission lines during 7 March 1970 solar eclipse

13 p2043 A72-29547

Solar corona spectral line width and wavelength measurements during 7 March 1970 total eclipse, using Fabry-Perot photographic interferometer

13 p2043 A72-29548

Solar flare X-ray emission occultation observed during 7 March 1970 eclipse by NRL instrument on OSO-5 satellite

13 p2031 A72-29549

Solar disk 10 cm radio emission during 7 March 1970 solar eclipse, discussing occultation of McMath plage active region

13 p2044 A72-29550

Spectral radio observations of 7 March 1970 solar eclipse, noting McMath plages intense activity source flux characteristics and weaker source bremsstrahlung emission

13 p2044 A72-29551

E region ionosonde observations to reconstruct ionizing X ray and far UV radiation source distribution over solar disk during March 1970 total solar eclipse

13 p2044 A72-29552

Relative brightnesses along solar radius from density photometry of corona at eclipses

13 p2046 A72-29715

Radio waves field strength measurement and recording for D region behavior during partial solar eclipse of 25 February 1971

13 p1961 A72-30050

Air pressure and temperature changes during 7 March 1970 solar eclipse, showing primary wave structure with Fourier analysis

14 p2128 A72-30351

Photographic technique to obtain isophotic contours of solar corona polarized light during total eclipse

16 p2393 A72-33624

Digital computer program for automatic processing of rocketsonde and radar digitized data, presenting graphical output from meteorological rocket soundings during 7 March 1970 solar eclipse

16 p2419 A72-33944

Thermospheric molecular oxygen from solar extreme-ultraviolet occultation measurements

17 p2614 A72-35602

The chromosphere in continuum emission observed at the total solar eclipse on 7 March 1970

17 p2616 A72-35698

Sodium emission from the atmosphere during a solar eclipse

19 p2793 A72-38857

Hydrodynamical study of the large northeast coronal streamer observed during the eclipse of March 7, 1970

21 p3100 A72-41287

The chromospheric continuum observed at the total solar eclipse of 12 November 1966 and a model of the low chromosphere

21 p3109 A72-41328

Study of the chromosphere in the D3He line during the eclipse of September 22, 1968

21 p3114 A72-41764

Skylight intensity, polarization and airglow measurements during the total solar eclipse of 30 May 1965

22 p3170 A72-42371

Physical conditions in the solar corona from spectral observations of the eclipse of March 7, 1970

24 p3448 A72-45684

SOLAR ELECTRIC PROPULSION

Cruise guidance, trajectory and navigation analysis for solar electric Mercury orbiter, considering engine performance, thrust and terminal errors

[AIAA PAPER 72-427]

11 p1684 A72-26172

Trajectory shaping advantages for outer planet orbiter solar electric propulsion, considering radiation belt constraints, dual launch and target orbit geometries

[AIAA PAPER 72-423]

13 p2036 A72-28938

Guidance and navigation techniques for a solar electric Mercury orbiter

[AIAA PAPER 72-917]

21 p3082 A72-41562

SOLAR ENERGY

Solar energy exchange by thermal radiation, investigating monochromatic emission factors at 0.3-15 micron

04 p0596 A72-14702

Neutrino emission process effects on solar C-N-O cycle energy generation and C 12/C 13 abundance ratio

04 p0567 A72-14911

Spectral reflectance of various soils and vegetation, measuring solar energy reflection as function of sun elevation in UV, visible and near IR regions

06 p0810 A72-18446

Solar energy conversion as pollution-free power source, discussing silicon solar cells, power transmission techniques, satellite solar power stations and system control and guidance

06 p0893 A72-18625

Solar energy sources and dissipation and emission mechanisms, considering radiant flux of convection zone and photosphere and solar variabilities

07 p1078 A72-20005

OSO-H solar X ray instrument for solar flares energy release investigation via thermal and nonthermal electrons X ray emission

08 p1167 A72-21514

Selective surfaces and coatings for solar energy conversion systems, discussing semiconductor photoconverters, white-black surfaces, cooling systems and optimal optical properties

10 p1422 A72-24315

Cost efficiency and relative economic merits prediction for solar energy conversion systems

10 p1423 A72-24316

Sunspot energy deficit relation to model depth deriving facular model with two dimensional radiative transfer analysis

13 p2045 A72-29712

A universal power characteristic of a high-temperature solar heat source

17 p2498 A72-35516

Large-scale concentration and conversion of solar energy

18 p2643 A72-36075

The impact of aerospace technology on energy conversion in the 70's

[ASME PAPER 72-AERO-11]

22 p3140 A72-43147

Shock waves role in coronal heating, solar wind and energy and material transfer to earth and in solar system

24 p3439 A72-45019

SOLAR ENERGY ABSORBERS

Solar absorptance and thermal emittance of thermal control coatings contaminated by thruster exhaust in vacuum environment

[AIAA PAPER 72-263]

12 p1846 A72-27865

Methods for the quality control of the reflecting surfaces of solar energy condensers /Survey/

22 p3140 A72-43187

Calculation of the solar radiation incident on an inclined ribbed surface

22 p3140 A72-43194

SOLAR FACULAE

U FACULAE

SOLAR FLARES

Steady motion effect on sunspot magnetic field stability related to force-free configurations and solar flare origin

01 p0118 A72-1008

Type 3 and 3/5 solar radio bursts coupling with microwave bursts, considering connection with H-alpha flares and X ray emission

01 p0118 A72-10414

Solar X rays angular distribution during solar flares, considering anisotropy connection with short wave fadeouts correlation with H alpha flares and X ray bursts center-to-limb variation

01 p0118 A72-10420

Solar flares forecasting based on group total sunspot area, largest spot area and spots number observations

01 p0118 A72-10570

Flare region curved absorption lines interpreted as photospheric and chromospheric mass motions

01 p0129 A72-10800

Solar flares far UV radiation time structure correlation with hard X rays

02 p0272 A72-11773

Periodic solar flare modulation by pulsating structure, attributing radiation to synchrotron radiation emitted by electrons in magnetic flux tube embedded in solar corona

02 p0274 A72-12412

Acceleration phase of solar cosmic rays and relativistic electrons in solar flare of 7 July 1966, discussing MHD shock waves generation

03 p0407 A72-12942

Solar flare EUV flashes from sudden ionospheric frequency deviation observations

03 p0407 A72-12946

Ionospheric effects of X ray flare on 8 July 1968, estimating ionizing radiation spectral characteristics from SID observation

03 p0407 A72-12986

Solar observation survey, considering sounding rockets, OSO, balloons, orbiting observatories, spectral resolution, spectral features and solar flare

03 p0409 A72-13050

Short wavelength continuous solar X-radiation polarization and angular distribution measurements, revealing physical processes in solar flares

03 p0409 A72-13126

Nonoptical and optical observation derived coronal condensations models for active regions and flare associated events

03 p0423 A72-13211

Flare associated waves suggested by optically observed phenomena, using time lapse photography of solar chromosphere

03 p0423 A72-13212

Solar flare surges with hot spectrum and violent activity, analyzing trajectories

03 p0423 A72-13213

Solar active regions and flares X ray spectroscopic data, observing ionized silicon emission lines
03 p0423 A72-13217

Solar flare 1.9 A line feature identification from X ray observation by OSO-4 proportional counter spectrometer
03 p0424 A72-13218

Radiation exposure during high altitude flights, considering normal radiation levels due to galactic radiation and short term increases due to solar flares
03 p0315 A72-13234

H alpha solar flare association with photospheric magnetic field patterns, discussing flare insertion and relation to magnetic structure evolution
03 p0410 A72-13320

Flare- and prominence-associated solar radio outburst, describing preflash phase and type 2 and moving type 4 bursts relation to coronal instability
03 p0410 A72-13321

MHD processes responsible for solar flares in polarity boundaries of magnetic fields, determining magnetic energy change and flux
03 p0410 A72-13322

High energy electrons behavior and sunspot magnetic fields in solar flares, using hard X ray and microwave radio burst balloon observations
03 p0410 A72-13323

Solar proton flare connection with strong electric currents, discussing net magnetic flux changes and electric conductivity and field strength
03 p0410 A72-13326

Solar flare associated magnetic field behavior and radio emission polarization in October 1968 active center, describing polarity flux variations
03 p0411 A72-13328

Equatorial-western shifts of flare positions related to field maximum in sunspot groups
03 p0411 A72-13329

Photospheric vortex motions effect on flare productive magnetic patterns in solar active regions
03 p0411 A72-13330

Magnetic-channel solar flare volume characteristics based on proton flare H alpha pictures, using Petschek model
03 p0411 A72-13331

Dash phenomenon in eruptive loop prominences representing solar flare process at all levels of atmosphere, discussing pinch effect instability
03 p0411 A72-13332

Filamentary magnetic structure production on plasma current sheath of coaxial deuterium operated accelerator for laboratory observations of solar flare processes
03 p0411 A72-13338

Solar magnetic field sector boundaries, discussing photospheric field direction, activity regions, flares, coronal enhancements, faculae and geomagnetic response
03 p0433 A72-13359

Solar limb flare observations on 4 November 1968, presenting photographs and intensive green coronal luminescence
03 p0434 A72-13493

Cosmic ray decreases correlation to solar flare occurrence by epoch analysis of monitor data, proposing mechanism for explanation
03 p0412 A72-13528

Oso-3 satellite observation of solar flare associated EUV bursts, comparing with microwave radio bursts
03 p0413 A72-13529

Hf plasma turbulence in solar flares due to nonlinear conversion of ion-acoustic plasmons to Langmuir plasmons
03 p0413 A72-13812

Solar flare, galactic and magnetically trapped /Van Allen/ nuclear particle radiation environments calculation for three outer planet Grand Tour missions
03 p0413 A72-14095

Solar chromospheric flare spectrophotometric data on 8 July 1966, presenting line spectra, ground state and populations in excited energy levels
03 p0413 A72-14242

Sudden cosmic noise absorption from D region N-H profile during solar X ray flares on 13 April 1966
04 p0566 A72-14512

Fe line emission during solar X-ray flares recorded by Bragg crystal spectrometers on OSO-6, resolving fine structure components of hydrogenic Ar
04 p0566 A72-14560

Nonthermal electron spectra hardness limit during flash phase of solar flares from OGO-5 observation
04 p0566 A72-14561

Magnetic and gravitational energy release by resistive MHD instabilities responsible for solar flares
04 p0571 A72-14578

Solar flares, presenting line width changes curves, chromospheric observation by spectrohelioscope and solar flux measurements
04 p0567 A72-14923

Solar radiation effects on earth atmosphere with MR-12 and M-100 meteorological rockets launched at onset of chromospheric flare, noting atmospheric parameters measurements
04 p0580 A72-15453

Type 4 solar radio bursts peak flux spectra center to limb variation association with proton flares
05 p0709 A72-16073

Time behavior of temperature and emission measure in X ray flares observed from Vela 5 spacecraft
05 p0709 A72-16518

Anisotropic angular distribution of solar flare associated hard X-rays
05 p0709 A72-16519

Extreme UV observations of flare surge at solar limb
05 p0710 A72-16520

Energetic solar flare particles release from sun, describing satellite observations of solar electromagnetic radiation
05 p0710 A72-16522

Solar flare X-ray emission Compton backscattering from Fe lines examination
05 p0710 A72-16720

Sunspot magnetic field strength rapid variation, discussing spot group development and flare activity
05 p0722 A72-17155

Filament activations caused by disturbances originating in solar flares
05 p0711 A72-17201

Interplanetary magnetic field effect on flare-generated weak shock wave propagation speed and transit time
06 p0875 A72-17461

Solar flare effectiveness relation to magnetic field orientation from magnetic storms development analysis
06 p0873 A72-17984

Interplanetary shock wave inclination to ecliptic plane dependence on chromospheric flare and earth projection heliolatitude differences
06 p0884 A72-18027

Sudden ionospheric disturbance occurrence probability with solar X-ray flares, noting relaxation time
06 p0874 A72-18086

Ionospheric effects of solar flares, considering flare spectrum below 10 A, flare X-rays relationship to sudden ionospheric disturbances and electron density profiles
06 p0874 A72-18087

Ionospheric electron density profiles and time variation of electron production rate for X-ray flare of 30 January 1968, observing decrease in effective recombination coefficient
06 p0874 A72-18088

Rocket astronomy development, reviewing V-2, Aerobee rocket and balloon-rocket flights for solar X rays and flares and galactic and extragalactic experiments
07 p1076 A72-19675

Initial /premaximal/ phase model of chromospheric flare in terms of explosion theory, determining temperature, shock front and plasma velocities
07 p1077 A72-19809

Type 4 solar burst spectral characteristics relationship to flare class and magnetic field configuration in spot group
07 p1077 A72-19814

Solar active regions properties observation, noting correlation with magnetic field, flares, sunspots, magnetic knots, pores, umbral flashes, etc
07 p1079 A72-20009

Solar discrete particle events classification and emission and acceleration mechanisms in relation to flare development
07 p1060 A72-20011

Thermal plasma origin of solar X-ray emission and far UV flash observation during 28 August 1966 proton flare
07 p1060 A72-20013

Particle acceleration and plasma ejection in solar flares, using model of nonstationary cumulative flow near magnetic neutral line
07 p1060 A72-20014

Solar proton flares forecasting methods in connection with active region developments for spacecraft radiation shielding
07 p1061 A72-20017

Diffusion models of energetic solar particles in interplanetary medium, considering impulsive emission from solar flares
07 p1061 A72-20023

Ionospheric effects of solar flares, relating sudden ionospheric disturbances with solar X-rays, radio bursts, H alpha emissions and cosmic rays
07 p1062 A72-20037

Solar surges /plasma ejections/ relation to spot groups and flares, correlating various observational data
07 p1063 A72-20294

Solar cosmic rays propagation between shock front and solar flare hot plasma, examining fine structure from Explorer 34 and Venera 6 data
07 p1063 A72-20628

Solar cosmic ray flare recording in stratosphere in Murmansk and Antarctic regions during February-April 1969
07 p1066 A72-20649

Solar cosmic ray flare of 11-18 April 1969, investigating effect on polar cap absorption in lower ionosphere
07 p1066 A72-20650

Nucleon and electromagnetic component generation, energy spectrum and diffusion during solar flares
07 p1066 A72-20651

Solar cosmic ray spectra at time of ejection from flare region and arrival near earth
08 p1226 A72-20812

Radio observation of flare sources and emission areas above coronal condensations during 22 September 1968 solar eclipse
08 p1228 A72-20828

High resolution multiple particle spectrometer for measuring energetic protons, electrons and alpha particles during solar particle events
08 p1167 A72-21509

OSO-H solar X ray instrument for solar flares energy release investigation via thermal and nonthermal electrons X ray emission
08 p1167 A72-21514

Apollo 15 lunar subsatellite particle experiment subsystem design for studying magnetosphere dynamics, plasmas-moon interaction and solar flare physics
08 p1168 A72-21519

Effective electron loss rates in lower D region from ionization changes during solar X ray flares, noting water cluster ions destruction
09 p1376 A72-22369

Potential gradient and air-earth current increases during period of increasing solar activity, discussing H alpha flare effects
09 p1378 A72-23264

Solar wind kinetic energy from flare associated solar wind disturbances relation to types 2 and 4 radio bursts, using satellite observations
09 p1378 A72-23399

Enhanced abundances of low energy heavy elements in solar cosmic rays due to preferential acceleration within flare region
10 p1530 A72-24673

Interplanetary shock wave inclination to ecliptic plane dependence on chromospheric flare and earth projection heliolatitude differences
11 p1719 A72-25963

SID coincident with solar photon burst, showing vertical variations of electron concentration
11 p1713 A72-26269

E layer effective recombination coefficient determination from solar flare enhanced electron density and solar X-ray flux measurements and ionospheric relaxation time constant evaluation
11 p1627 A72-26766

Upper atmosphere electric fields derived from ionosphere-earth electric potential measurements following solar flare activity
12 p1804 A72-27805

Solar activity effects on bismuth chloride hydrolysis tests from statistical results following solar flares
12 p1773 A72-28212

Charged particles propagation in magnetic field and scattering medium with constant and variable transport paths, applying to proton propagation for solar flares
13 p2029 A72-28576

Solar flare X-ray emission occultation observed during 7 March 1970 eclipse by NRL instrument on OSO-5 satellite
13 p2031 A72-29549

Solar flare flux effects on D region effective ion recombination coefficient decrease, discussing electron and negative ion densities
13 p1913 A72-29654

Flare related impulsive EUV solar emission lines enhancement in chromosphere-corona transition region
13 p2032 A72-29720

Time evolution of chromosphere layer heated by energetic particle stream during solar flare, noting cooling by Lyman continuum radiation transfer
13 p2032 A72-29721

Electron temperature and emission measures during solar X-ray flares, studying effects of gradual and rapid radiation flux increases
13 p2032 A72-29722

Solar flare induced vortex ring formation, describing photographic observations by Okayama Astrophysical Observatory solar telescope on 30 October 1970
13 p2048 A72-29741

High energy electron heating of solar flare plasma with X-ray emission due to thermal and nonthermal bremsstrahlung
13 p1033 A72-29745

Energy storage in chromospheric magnetic flux ropes in solar flares, discussing kink perturbation instability suppression
13 p2049 A72-29936

Strong shock wave formation and propagation in interplanetary space after chromospheric flares calculated by gas dynamic approximation, determining magnetic field configuration
13 p2050 A72-29955

Cosmic ray anomalous absorption height dependence on zenith distance in midlatitude ionosphere during solar flare emission from polarization study

14 p2146 A72-30461

Cycle 20 solar flare and sunspot distribution along heliographic longitude, using isoline analysis method

14 p2152 A72-30482

Radio bursts and X ray emissions associated with 15-16 November 1970 solar chromosphere flares, noting brightness maximum differences

14 p2146 A72-30483

Geomagnetic storms caused by quasi-stationary directed corpuscular streams resulting from solar chromosphere flares

14 p2147 A72-30487

Solar proton flare prediction, examining diurnal rotation of axis connecting two stable spots and change in horizontal gradient of spots magnetic field

14 p2147 A72-30649

Solar proton flare on 2 November 1969, investigating active region magnetic field development and spatial structure, near limb and coronal phenomena

14 p2160 A72-30909

Solar proton flare induced X ray bursts maximum flux, total radiated energy, electron temperature and emission from satellite measurements

14 p2160 A72-30910

Solar X-ray flux daily changes before and after proton flare, using zero-epoch superposition method

14 p2148 A72-30911

Rocket-borne spectrometric measurement of small solar flare O VII and Ne IX resonance lines and 5 keV X-ray continuum emission, analyzing data via nonisothermal model

15 p2300 A72-31990

Sudden decreases of atmospheric due to solar flares effects on lower ionosphere, discussing noise propagation

15 p2230 A72-32256

Solar flare and neutral sheet simulation by investigating behavior of plasma current through magnetic neutral point created by capacitor discharges

15 p2301 A72-32342

Solar flares induced magnetic field configurations, considering open and closed current sheets instabilities as flare sources

15 p2301 A72-32788

Solar white light flares relationship to EUV emission based on sudden frequency deviations observations, noting coincidence with H alpha flare areas

15 p2302 A72-32789

Ion density and electron acceleration region location from satellite-borne solar flare X-ray measurements

15 p2302 A72-32790

Solar wind He enrichment origin in solar flares connection with type 2 radio emission from analysis of Vela 3 spectra

15 p2302 A72-32791

Interplanetary high energy electron flux association with solar flares from HEOS-A1 data

15 p2302 A72-32792

Two dimensional unsteady solutions to MHD equations, describing matter compression near zero line of magnetic field for solar flares and z pinch studies

16 p2435 A72-33151

Solar flare producing regions statistical correlation to SC/SL events accounting for geomagnetic storms and Forbush decreases in terms of interplanetary streams

16 p2445 A72-33376

Radiation hazards in space with respect to galactic radiation shielding, solar flare prediction and conventional terrestrial safety standards

16 p2358 A72-33556

Soft X-ray spectral studies of plasma dynamics in solar flares from Bragg crystal spectrometer OSO 6 recordings

16 p2449 A72-33918

Fine structure similarities between solar flares and current sheath in laboratory hot plasma coaxial accelerator, noting X ray and high energy particles production mechanism

16 p2438 A72-33919

Stellar X ray emission flux calculation for UV Ceti flares, using similarities between solar and stellar flares

16 p2450 A72-34161

Flare-time temperature in soft X-ray sources.

17 p2598 A72-34537

Solar flares and prominences rotational motions from spectrographic observations of atomic Al absorption line periodic asymmetry

17 p2608 A72-35086

Note on the characteristics of sunspot groups which produce solar proton flares.

17 p2608 A72-35087

A physical mechanism for the production of solar flares.

17 p2608 A72-35088

Soft X-ray and microwave observations of hot regions in solar flares.

17 p2608 A72-35089

A search for high energy gamma-rays from solar active regions.

17 p2599 A72-35092

Helium and H alpha emission relationship observation in 11 February 1970 solar flare from photometric reduction of filtergrams

17 p2599 A72-35117

Solar flare initial, explosive and decay phases related to plasma motion, soft X-rays and radio emission

17 p2600 A72-35348

Plasma turbulence in solar atmosphere upper layers related to chromospheric flares and radio bursts

17 p2612 A72-35349

On polarimetry in solar active regions. V - The magnetic field immediately before and after a flare.

17 p2617 A72-35706

Spectral analysis of highly inhomogeneous chromospheric flares.

17 p2617 A72-35709

Solar flares in the extreme ultraviolet. I - The observations.

17 p2602 A72-35710

Solar flares in the extreme ultraviolet. II - Comparisons with other observations.

17 p2602 A72-35711

Initial/premaximal/phase model of chromospheric flare in terms of explosion theory, determining temperature, shock front and plasma velocities

17 p2602 A72-35734

Type 3 solar burst spectral characteristics relationship to flare class and magnetic field configuration in spot group

17 p2618 A72-35739

Solar flares and radio bursts significance for chromosphere and corona studies, considering radiation frequency-source location relations

17 p2603 A72-35957

Theoretical studies of the flux and energy spectrum of gamma radiation from the sun.

18 p2721 A72-35993

Geomagnetic storms correlation with chromospheric flare series and with central meridian passages of recurrent positive plagues

18 p2723 A72-36087

Ionospheric magnetic disturbances during March 1970 related to solar flare corpuscular and proton fluxes, generating ring current and PCA absorption

18 p2688 A72-36857

Time-dependent ionization equilibrium and line radiation under flarelike conditions.

19 p2849 A72-37241

Interplanetary-gas motion induced by a solar flare

19 p2855 A72-37391

Solar flare composition and energy spectra of heavy nuclei from 1971 rocket observations comparing to cosmic ray abundances

19 p2850 A72-37509

Energy exchange processes in solar flares, noting initial derivation of energy from changing magnetic fields within solar atmosphere

19 p2850 A72-37782

Solar radio burst time profiles comparison with H alpha line emission curves for corresponding flares, noting neutral hydrogen emission relation to electrons acceleration

19 p2850 A72-37802

Continuous emission localization in solar flare nuclei

19 p2850 A72-37814

Tabulation of physical conditions in proton and non-proton solar flares from observations and H alpha line width measurements

19 p2851 A72-37815

Solar chromospheric flare details motion differences from spectrum analysis and H alpha line frame photography, noting radial velocities difference

19 p2851 A72-37816

Relation between chromosphere flare motion and ejections and the magnetic field

19 p2851 A72-37817

Periodic heating mechanism in solar flares.

19 p2851 A72-37888

Plasma heating by fast electrons, and nonthermal X rays during solar flares

19 p2851 A72-38063

Geomagnetic storms caused by quasi-stationary directional corpuscular streams resulting from solar chromosphere flares

19 p2851 A72-38316

Structure of solar active zones in the mm wave range

19 p2866 A72-38496

Ionospheric D region, a sensitive detector of hard X-rays of solar subflares.

19 p2852 A72-38628

Azimuthal propagation of low-energy solar-flare protons as observed from spacecraft very widely separated in solar azimuth.

19 p2852 A72-38726

Rocket observation of Ar XII-XVI, Ca XIV-XVIII, and Fe XIV, XV, XXIV in the extreme-ultraviolet spectrum of a solar flare.

20 p2963 A72-38913

Aluminum 26 and manganese 53 produced by solar-flare particles in lunar rock and cosmic dust.

20 p2970 A72-39472

Linear and nonlinear aspects of ion-sound current instability for solar atmosphere conditions of full ionization, noting implications for flare mechanism

21 p3100 A72-41040

X-ray and HF microwave bursts correspondence shown in observations of 24 October 1969 impulsive solar flare and of XUV and radio emissions

21 p3108 A72-41290

Thick target processes during hard X ray emission, noting electron bombardment during solar flare impulsive phase and white light flare optical continuum production

21 p3100 A72-41292

New measurements of the polarization of X-ray solar flares.

21 p3101 A72-41293

Solar soft X-rays and solar activity. II - Observational assessment of the role of the type III acceleration mechanism in establishment of the soft X-ray source volume.

21 p3101 A72-41294

Change of solar flare proton to alpha ratios during an energetic storm particle event.

21 p3101 A72-41297

Solar flare associated relativistic electron acceleration relationship to cosmic ray and type 4 radio burst production

22 p3217 A72-42010

Some aspects of flare properties versus magnetic boundary morphology.

22 p3217 A72-42038

Magnetic field change rate related to chromospheric activity in McMath Regions 8863, 10385 and 11415, discussing flare associated effects and total flux

22 p3217 A72-42039

Particle flux measurements from rockets during a solar cosmic-ray flare in April, 1969

22 p3218 A72-42226

Polar-cap measurements of solar-flare protons with energies down to 12.4 keV.

22 p3218 A72-42425

Comparison of solar-flare energy estimates made by analytical and numerical techniques.

22 p3219 A72-42426

Magnetic field structure in flare-associated solar-wind disturbances.

22 p3219 A72-42428

Free oscillations of the sun and their possible stimulation by solar flares.

22 p3219 A72-42570

Solar wind noble gases and solar flare emitted Fe group nuclei energetic tracks in chondrite Weston, considering galactic cosmic ray generated tracks

22 p3228 A72-42863

August solar activity and its geophysical effects.

22 p3174 A72-42982

The great solar flares of August, 1972.

22 p3219 A72-42984

A comparison of field-strengths of 164 kHz radio waves transmitted from Tashkent and received at Ahmedabad with flare-time solar X-ray emissions measured in satellites.

23 p3262 A72-43275

Association between interplanetary shock waves and delayed solar particle events.

23 p3332 A72-44503

Charged particles propagation in magnetic field and scattering medium with constant and variable transport mean free path, applying to proton propagation for solar flares

24 p3435 A72-45076

On some plasma rotation phenomena on the sun.

24 p3445 A72-45469

SOLAR FLUX

Quiet solar corona thermal emission flux at 169 MHz, showing constant brightness and electron temperatures during cycle

01 p0123 A72-10045

Neutrino flux from solar models differing in opacity, equations of state and nuclear cross section factors

01 p0122 A72-11146

Microwave solar radio bursts occurrence and intensity distribution at 19 GHz during July 1967-December 1969

03 p0407 A72-12941

Solar UV flux measurements by balloon-borne grating monochromator, using FM-FM analog and PCM telemetry systems for computerized data analysis

03 p0409 A72-13051

Solar flares, presenting line width changes curves, chromospheric observation by spectrohelioscope and solar flux measurements

04 p0567 A72-14923

Type 4 solar radio bursts peak flux spectra center to limb variation association with proton flares

05 p0709 A72-16073

Cylindrical solar array absorptance as function of solar flux vector inclination, using Gier-Dunkle integrating sphere

05 p0616 A72-16909

Solar wind flux velocity diurnal variations relation to magnetic activity index based on Mariner 2 and 4, Pioneer 6 and Vela satellites data

08 p1226 A72-20821

D region extraionization and solar X-ray flux from vlf data, emphasizing solar spectral shape and use of continuity equation for ionization time history 08 p1227 A72-21116

Solar wind tangential discontinuities and shock waves determination from flux velocity vector, magnetic field and particle density measurements 08 p1227 A72-21154

Solar atmosphere low energy positron production by solar particle fluxes demodulated according to cosmic ray transport equations 09 p1378 A72-23022

Solar wind termination distance as function of flux, velocity and interstellar hydrogen density, velocity and magnetic field strength 10 p1528 A72-23716

Solar radio astronomy instrumental requirements for 20 meter wavelength interferometry, metric and decametric flux and polarization measurements 12 p1872 A72-27815

Quasi-steady and sporadic corpuscular fluxes as basic solar activity effect on troposphere, showing magnetosphere interaction time relation to meridional atmospheric circulation changes 12 p1842 A72-28208

Experimental nuclear physics and theoretical solar structure and evolution explanations of disagreement between calculated and observed solar neutrino flux 18 p2722 A72-37007

Solar wind tangential discontinuities and shock waves determination from flux velocity vector, magnetic field and particle density measurements 20 p2964 A72-39259

Magnetic storm classification from geomagnetic field H and Z components behavior, associating with solar corpuscular flux 22 p3174 A72-42952

Solar oblateness and neutrino flux measurement experiments, discussing agreement with solar interior and evolution models 24 p3446 A72-45527

SOLAR FLUX DENSITY
NT SOLAR CONSTANT

Dicke-type microwave radiometer for daily measurements of 2800 MHz solar flux, discussing antenna system and dynamic range 04 p0522 A72-15163

Monograph on solar IR limb profiles covering intensity observations, apparatus, instrumental distortions and data reduction and analysis 08 p1236 A72-21489

Solar X ray burst analysis from individual quantum/energy and time recordings by Lunokhod 1 spectrometer 13 p2032 A72-29700

Solar UV Lyman alpha radiation intensity measurements, using Vertikal-1 rocket-borne photometer and photoelectron analyzer 14 p2128 A72-30465

Solar vacuum UV flux measurement by photon ion chambers aboard WRESAT I satellite, obtaining 4600 K brightness temperature 16 p2452 A72-33040

Quantitative evolution model for time variable flux densities and polarization characteristics of isolated moving type 4 events 16 p2444 A72-33041

Influence of solar flux and the equatorial electrojet on the diurnal development of the latitude distribution of total electron content in the 'equatorial anomaly'. 19 p2794 A72-38868

SOLAR FURNACES

High temperature and vacuum solar furnace processing of refractory metals in space or on moon 19 p2857 A72-37675

Investigation of the possibility of using radiant solar energy for welding and soldering of materials 24 p3407 A72-45126

SOLAR GENERATORS
NT SOLAR CELLS

Satellite solar power stations, considering energy conversion, microwave generators and beam transfer to earth 02 p0155 A72-11770

High efficiency solar electricity converters utilizing wave-like properties of radiation interacting with absorber-converter elements, discussing cost and fabrication advantages [ASME PAPER 71-WA/SOL-1] 05 p0614 A72-15891

Pollution free electrical power generation from solar energy, discussing microwave transmission to earth, power shortages, thermal pollution and solar cell manufacture cost [ASME PAPER 71-WA/SOL-2] 05 p0614 A72-15892

Solar energy conversion as pollution-free power source, discussing silicon solar cells, power transmission techniques, satellite solar power stations and system control and guidance 06 p0893 A72-18625

American and European solar generator technology development review, discussing roll-up arrays, flexible panels, and stowage and deployment system components 12 p1756 A72-28005

Solar photosensitive elements prepared p-type GaAs liquid epitaxy on n-type GaAs substrate, measuring dark and light I-V characteristics and spectral response 14 p2142 A72-30225

Thermodynamic analysis and parameter optimization of a solar thermoelectric power plant with heat removal by radiation 17 p2497 A72-35509

A universal power characteristic of a high-temperature solar heat source 17 p2498 A72-35516

Parallel operation of the solar generator and battery on the Symphonie satellite 18 p2648 A72-36681

SOLAR GRANULATION

Sunspot formation due to magnetic flux concentration in active region and formation of invisible pores with suppressed granular motion 14 p2148 A72-30205

Atmospheric model for numerical simulation of five minute oscillation field properties of solar granular convection-excited gravity waves 21 p3107 A72-41277

Sunspot temperature increase stimulation of supergranule motion leading to spot decay and magnetic field diurnal fluctuation development 21 p3114 A72-41762

Sunspot formation due to magnetic flux concentration in active region and formation of invisible pores with suppressed granular motion 23 p3333 A72-43235

Sunspots and solar granulation recording and imaging with 64-element array of PbS IR detector for obtaining high SNR and resolution 23 p3288 A72-43883

SOLAR GRAVITATION

Earth motion nutations, considering external forces effects from sun and moon 04 p0575 A72-15030

Solar gravitational field precision measurements for gravitation theory validity verification 05 p0713 A72-16050

Solar gravitational red shift measurement from solar and laboratory potassium absorption line comparison, using atomic beam resonance scattering technique 10 p1541 A72-24415

Error sources in numerical integration of spacecraft equations of motion in solar and planetary gravitational fields, suggesting methods for improving accuracy 14 p2151 A72-30453

Gravitational absorption investigation from lunisolar attraction observed by tracking high flying satellite in eccentric polar orbit 16 p2382 A72-32892

Photospheric faculae brightness influence on solar gravitational oblateness determination, considering criticism of Dicke-Goldenberg argument on Mercury excess perihelion motion 19 p2855 A72-37239

Lunar and solar gravitational effects on earth atmosphere, describing latitudinal distribution of cyclone centers by momentum distribution of horizontal tide-generating forces 23 p3310 A72-43249

Luni-solar perturbations of the geostationary vehicle at arbitrary latitude. 24 p3448 A72-44990

SOLAR HEAT FLOW
U HEAT FLUX
U SOLAR FLUX

SOLAR HEATING

Small scale magnetic field theories, concerning solar prominence structure, chromospheric and coronal heating and particle production in flares 05 p0430 A72-13333

Solar pole-equator difference in effective temperature and mechanical heating, using atmospheric model 13 p2044 A72-29702

Thermospheric density annual and semiannual variations due to solar heat input into ozone layer and Joule heating, discussing decomposition into Fourier terms 15 p2229 A72-32255

Thermodynamic analysis and parameter optimization of a solar thermoelectric power plant with heat removal by radiation 17 p2497 A72-35509

Periodic heating mechanism in solar flares. 19 p2851 A72-37888

Investigation of the possibility of using radiant solar energy for welding and soldering of materials 24 p3407 A72-45126

SOLAR INSTRUMENTS
NT SPECTROHELIOGRAPHS

Optics and electronics of digitized birefringent filter solar magnetograph to isolate magnetic sensitive lines 03 p0337 A72-13287

Narrow band electrically controlled interferential polarization filter with fine tuning capability for solar physical research, discussing design and operation 03 p0357 A72-13369

Solar prominence telescope design using two prism reflectors for ray path deflection 07 p0982 A72-19125

Image dissector application to D2B astronomical satellite position field plotting in solar and stellar UV photometry 08 p1172 A72-21976

Precision radiometric techniques in meteorology and geostrophysics, discussing references, pyroheliometric scale, transfer calibrations and solar radiation measurements 10 p1485 A72-25097

Solar radio astronomy instrumental requirements for 20 meter wavelength interferometry, metric and decametric flux and polarization measurements 12 p1872 A72-27815

Solar instruments and methods for photosphere magnetic field measurement, noting spectroheliographic mapping in violet spectral region 15 p2306 A72-31647

Solar tracking via automatic 5-GHz radiometer with paraboloid antenna, using continuous polar axis rotation in one direction 18 p2691 A72-36433

A line-profile Stokesmeter - Preliminary results on non-sunspot fields. 20 p2971 A72-39761

A non imaging approach to solar oblateness measurements. 22 p3222 A72-42046

Modulation transfer function for solar telescopes and atmospheric turbulence. 22 p3175 A72-42047

Image motion in the Culgoora solar magnetograph - The role of vibration. 23 p3278 A72-43617

Sunspots and solar granulation recording and imaging with 64-element array of PbS IR detector for obtaining high SNR and resolution 23 p3288 A72-43883

Skylab solar astronomical observation programs and instruments, discussing X ray and H alpha telescopes, coronagraphs, spectroheliographs and UV spectrographs 24 p3453 A72-45528

Solar atmosphere fine structure observation limitations in terms of solar telescope angular resolution 24 p3404 A72-45529

OSO and Skylab astronomical instruments technology, emphasizing precision pointing, spatial and spectral resolution and photometric efficiency problems 24 p3405 A72-45545

SOLAR LIMB

Solar chromosphere fine structure at limb, measuring spicules and bright mottles lifetime 03 p0415 A72-12930

L alpha limb flux during total solar eclipse of 12 November 1966 from rocket measurements, comparing with chromosphere model [AD-739763] 03 p0415 A72-12931

Solar limb flare observations on 4 November 1968, presenting photographs and intensive green coronal luminescence 03 p0434 A72-13493

Solar photospheric facula blue light limb photographs, determining spatial variation in contrast levels 03 p0434 A72-13494

Type 4 solar radio bursts peak flux spectra center to limb variation association with proton flares 05 p0709 A72-16073

Extreme UV observations of flare surge at solar limb 05 p0710 A72-16520

Monograph on solar IR limb profiles covering intensity observations, apparatus, instrumental distortions and data reduction and analysis 08 p1236 A72-21489

Turbulent earth atmosphere optical inhomogeneities determination from solar limb image characteristics in motion pictures of solar disk edge 09 p1305 A72-22233

Solar chromosphere double limb effect attributed to instrument, discussing application to height measurement 11 p1717 A72-25905

Brightenings and surgelike spikes associated with low amplitude soft solar X-ray background flux in H alpha above limb, assessing energy budget 13 p2032 A72-29718

Semiempirical line blanketing in solar model atmospheres, including limb darkening predictions 13 p2047 A72-29735

Solar maps from quiet sun center limb microwave radio telescope observations during cycle maximum 13 p2048 A72-29742

Spicular field morphology near solar limb from photographs taken with H alpha filter 15 p2305 A72-31512

Arch prominence outside west limb on 24 April 1971, noting H alpha monochromatic image, internal motion of matter and radio emission 17 p2614 A72-35503

- A first order analysis of variations of the limb darkening and the shapes for solar Fraunhofer lines.
17 p2616 A72-35694
- Theoretical explanation of the solar limb effect.
17 p2618 A72-35895
- New measurements of the polarization of photospheric light near the solar limb
18 p2727 A72-36739
- Faculae and the solar oblateness.
19 p2855 A72-37240
- Observation error in time determination of solar limb contact with optical instrument hair, noting effect on accuracy of time and longitude measurement
24 p3438 A72-44859
- Human observation error effect on astronomical refraction calculation from time determination of solar limbs passing across optical instrument reticle
24 p3438 A72-44863
- SOLAR LONGITUDE**
- Cycle 20 solar flare and sunspot distribution along heliographic longitude, using isoline analysis method
14 p2152 A72-30482
- SOLAR MAGNETIC FIELD**
- Steady motion effect on sunspot magnetic field stability related to force-free configurations and solar flare origin
01 p0118 A72-10083
- Narrow-band type 4 bursts behavior comparison with synchrotron radiation in media with refractive index less/equal unity, determining magnetic field and electron energy
01 p0118 A72-10415
- Oscillatory hydromagnetic dynamo model of variable sign large scale solar magnetic field, using Benard convective cell with Coriolis velocity disturbance
01 p0128 A72-10585
- Solar sector magnetism cross correlation, showing difference from classical Babcock model in boundary direction, rigid rotation and identical solar hemisphere polarities
01 p0134 A72-11267
- Criticism of cyclonic reversal mechanism and dynamo theory for solar 22-year cycle, proposing penetrating magnetic and general field theory
02 p0276 A72-11641
- Type 4 solar radio burst multiple magnetic loop structure and polarization observation by 80 MHz heliography
02 p0272 A72-11648
- Rotating solar magnetic dipole with 26 7/8 day period from polar geomagnetic and spacecraft interplanetary field observations
02 p0277 A72-11899
- Brightness correlation and mapping of weak photospheric magnetic fields and faculae using CN 3883-A spectroheliograms
03 p0414 A72-12927
- Topological features of force free magnetic field near bipolar sunspots, considering chromospheric fibrils and filaments in H alpha lines
03 p0415 A72-12932
- Solar U-type radio bursts in outer corona at 0.7 MHz related to magnetic bottle
03 p0406 A72-12937
- Coronal magnetic fields effects on energy and mass flux from lower solar atmosphere levels into corona, discussing plasma instabilities, solar flares, radio bursts, etc
03 p0422 A72-13206
- Solar coronal magnetic field large scale structure relation to photospheric and interplanetary sector patterns
[AD-734628] 03 p0422 A72-13207
- Solar magnetic fields - Conference, College de France, Paris, August-September 1970
03 p0427 A72-13276
- Solar magnetic field measurements using electromagnetic radiation, atmospheric structure [MHD effects] and energy equipartition
03 p0427 A72-13277
- Solar magnetic fields time fluctuation determination using longitudinal, intensity and line of sight velocity measurements
03 p0356 A72-13278
- Digital videomagnetograph providing real time display of line of sight component of solar magnetic fields
03 p0356 A72-13281
- Kitt Peak 40 channel magnetograph using fiber optic probe for spectral and spatial resolution in weak photospheric field detection
03 p0356 A72-13282
- Magnetic atomic beam absorption filter for high resolution solar field observations
03 p0357 A72-13290
- Absorption line formation in magnetic field for magnetograph interpretation of solar atmosphere
03 p0427 A72-13291
- Collisional relaxation rate effects of atomic level polarization on spectral line formation in solar magnetic regions
03 p0427 A72-13294
- Sunspot and active region magnetic fields and thermodynamic structure from umbral and penumbral models, discussing magnetic fine structure
03 p0427 A72-13296

- Magnetic field and turbulence in sunspots, studying local variations of saturation and Doppler broadening
03 p0428 A72-13297
- Magnetographic observations of magnetic fields in quiescent solar prominences, using Zeeman effect on H, He, and metal lines
03 p0428 A72-13298
- Fine structure of magnetic field distribution in umbra and penumbra of sunspots
03 p0428 A72-13299
- Spatial distribution of total magnetic vector and of electric currents in unipolar sunspot
03 p0428 A72-13300
- Magnetic field strengths from umbral spectral lines in sunspots
03 p0428 A72-13301
- Magnetic field measurements at different depths of solar atmosphere active regions by Crimean Astrophysical Observatory double magnetograph, showing close correlation
03 p0428 A72-13302
- Sunspot magnetic field evolution in time and space from four-camera spectral scanning method, obtaining magnetic flux and radial velocity field
03 p0428 A72-13303
- Solar magnetic field structure determination in active regions from H alpha morphology obtained with chromospheric magnetograph, discussing emerging flux region role
03 p0428 A72-13304
- Solar magnetic field configuration evolution in active region of photosphere, using solar magnetograph
03 p0428 A72-13305
- Magnetic field fine structure in undisturbed photosphere for high latitude solar regions, constructing model to explain magnetograph response
03 p0428 A72-13306
- Magnetograph scans of solar disk center supergranulation, showing downflows relation to magnetic field strength and chromosphere and photosphere brightness
03 p0429 A72-13307
- High resolution magnetographic and spectrographic observations of plage fields and photospheric effects in weakly active regions
03 p0429 A72-13308
- Magnetic and velocity fields and brightness in solar atmosphere, using double magnetograph
03 p0429 A72-13309
- Solar magnetic field measurement with 10,830 A He I line photoelectric spectroheliograms, observing filamentary fine structure in active regions
03 p0429 A72-13310
- Supergranule velocity and magnetic fields concentrations in solar atmosphere
03 p0429 A72-13311
- Plage magnetic fields associated with downward velocities from magnetograph filtergrams of opposite circular polarizations in CA I absorption line
03 p0429 A72-13312
- Solar magnetic field fine structure from filter magnetograms, tabulating magnetic elements frequency distributions
03 p0429 A72-13315
- Solar magnetic field observations with birefringent filter for 5324 A Fe I line, showing H alpha fine structure
03 p0430 A72-13316
- Zeeman spectroheliograms of photospheric magnetic fields in Ca I 6102.7 A line
03 p0430 A72-13317
- Solar magnetic fields time fluctuation determination using longitudinal, intensity and line of sight velocity measurements
03 p0430 A72-13318
- Five-minute plasma oscillations in solar photospheric and low chromospheric magnetic fields, discussing evidence, properties and production mechanism [AD-743346] 03 p0430 A72-13319
- H alpha solar flare association with photospheric magnetic field patterns, discussing flare insertion and relation to magnetic structure evolution
03 p0410 A72-13320
- MHD processes responsible for solar flares in polarity boundaries of magnetic fields, determining magnetic energy change and flux
03 p0410 A72-13322
- High energy electrons behavior and sunspot magnetic fields in solar flares, using hard X ray and microwave radio burst balloon observations
03 p0410 A72-13323
- Corona X ray emitting structures comparison to photospheric magnetic field distribution
03 p0410 A72-13324
- Solar turbulent magnetic field in lower corona associated with expanding limb microwave burst of 30 March 1969
03 p0410 A72-13325
- Solar proton flare connection with strong electric currents, discussing net magnetic flux changes and electric conductivity and field strength
03 p0410 A72-13326
- Solar magnetic field variations in McMath Regions, using longitudinal magnetograms time sequences
03 p0430 A72-13327

- Solar flare associated magnetic field behavior and radio emission polarization in October 1968 active center, describing polarity flux variations
03 p0411 A72-13328
- Equatorial-western shifts of flare positions related to field maximum in sunspot groups
03 p0411 A72-13329
- Photospheric vortex motions effect on flare productive magnetic patterns in solar active regions
03 p0411 A72-13330
- Magnetic-channel solar flare volume characteristics based on proton flare H alpha pictures, using Petschek model
03 p0411 A72-13331
- Small scale magnetic field theories, concerning solar prominence structure, chromospheric and coronal heating and particle production in flares
03 p0430 A72-13333
- Fine structure features of sunspot magnetic fields and umbral dots, showing magnetic and thermal or mechanical forces interaction
03 p0430 A72-13334
- Steady state turbulent solar magnetic fields dynamic evolution, considering weak random magnetic excitation in electrically conducting fluid under varying kinematic conditions
03 p0430 A72-13336
- Solar magnetic field distribution in sunspots surface layers, considering photospheric three dimensional magnetohydrostatic model
03 p0431 A72-13337
- Helmet streamer interaction of coronal material with magnetic fields, considering inertial, pressure, gravitational and magnetic forces
03 p0431 A72-13339
- Solar magnetic field origin in fine structure elements of photosphere and sunspots
03 p0431 A72-13340
- Large scale solar magnetic field properties, discussing rotation, patterns and effects on corona
03 p0431 A72-13341
- Coronal magnetic fields above slowly changing active regions
03 p0431 A72-13342
- Magnetic fields orientation in solar corona from polarization measurements in green line
03 p0431 A72-13343
- Time evolution of large scale solar magnetic field observing zonal harmonics
03 p0431 A72-13344
- Magnetic field structure in active solar corona discussing optical and radio observations
03 p0431 A72-13344
- Large-scale solar coronal magnetic field from optical and radio observations for corpuscular propagation in corona and interplanetary medium
03 p0432 A72-13346
- Solar moving type 4 bursts and coronal magnetic fields evidence from 80 MHz radioheliograph data
03 p0411 A72-13347
- Solar active region properties at millimeter wavelengths, suggesting chromospheric magnetic field measurement possibility from polarization
03 p0432 A72-13348
- Solar magnetic field vector distribution in quiescent prominence plasma with components both along and perpendicular to long axis
03 p0432 A72-13350
- OSO-G satellite spectroheliograms of chromospheric, transition zone and coronal lines, indicating magnetic field spread with height
03 p0432 A72-13351
- Coronal rotation determination by spectroscopic method for mean rotation rate vs heliographic latitude, confirming high latitude phenomena dependence of low latitude magnetic fields
03 p0432 A72-13352
- Solar polar and general magnetic field fine structure and statistical nature, discussing time fluctuations and interplanetary field
03 p0432 A72-13353
- Solar magnetic field large scale patterns and apparent regularities, noting active longitude 27-day rotation periods and polarity differences
03 p0432 A72-13354
- Solar longitudinal magnetic field measurements in polar prominence, noting configuration similarity to arc
03 p0432 A72-13355
- Solar polar magnetic fields, discussing inversion line location, observations, data analysis, general field and computer reduction
03 p0432 A72-13356
- Large-scale solar magnetic field dynamics, considering joint transport action by regular velocity field, diffusion, sinking and sources of origin and destruction
03 p0433 A72-13358
- Solar magnetic field sector boundaries, discussing photospheric field direction, activity regions, flares, coronal enhancements, faculae and geomagnetic response [AD-734627] 03 p0433 A72-13359

Solar hydrodynamic dynamo theories concerning convective zone large scale velocity fields and magnetic activity cycle

03 p0433 A72-13360

Solar magnetic field and solar cycle dynamo theory based on mean field MHD

03 p0433 A72-13361

Large scale solar magnetic field dynamo model in terms of force-free constituents series, deducing periodic solution by eigenvalue method

03 p0433 A72-13362

Viscous torsional vibrations inadequacy for interpreting solar activity cycles relative to magnetic field

03 p0436 A72-13811

Short periodical pulsations in solar atmosphere related to magnetosound propagation in area of temperature minimum with directed perpendicular magnetic field

03 p0436 A72-13813

Solar magnetic field generation by gyrotropic turbulence, noting inadequacy of Steenbeck explanation for quantitative estimates of solar cycle parameters

03 p0436 A72-13825

Time variation of mean values for magnetic field elements strength and size in solar polar regions, noting solar activity maximum effect

03 p0436 A72-13830

Solar magnetic fields small scale structure with emphasis on photospheric measurements, discussing sunspots fields

03 p0437 A72-13869

Large scale magnetic field distribution and solar activity, discussing granular pattern, differential rotation, magnetic flux near surface and background field pattern

03 p0437 A72-13870

Rotating dipole sector structure of interplanetary and solar photospheric magnetic fields from spacecraft observations

03 p0437 A72-13871

Solar prominences, considering heavy gas suspension in magnetic arches with grooved tops

05 p0708 A72-15976

Large scale alternating solar magnetic field generation by outer shell convective flow, constructing oscillatory hydromagnetic dynamo model

05 p0715 A72-16232

H alpha fine structure, investigating chromospheric magnetic field distribution

05 p0718 A72-16507

Solar chromospheric fine structure at active region, magnetic polarity boundaries from high resolution H-alpha filtergrams

05 p0718 A72-16508

Moving type 4 radio burst observation with radioheliograph, suggesting isolated self contained synchrotron emitting plasmoid and relation to coronal magnetic field

05 p0710 A72-16521

Sunspot magnetic field strength rapid variation, discussing spot group development and flare activity

05 p0722 A72-17155

Solar flare effectiveness relation to magnetic field orientation from magnetic storms development analysis

06 p0873 A72-17984

Solar magnetic field filamentary structure based on analysis of photospheric photographs and presunrise spectrograms obtained during Soviet stratospheric observatory flight

06 p0886 A72-18100

Magnetic vector directions determination in sunspots by fringe technique with corrections for instrumental polarization in line spectrum

06 p0889 A72-18326

Magnetic field decay in solar microwave burst region evaluated from circular polarization degree time profile

06 p0891 A72-18505

Solar magnetic field regularities analogy with terrestrial cyclones instead of convection cells in vertical heat transport

07 p1074 A72-19558

Type 4 solar burst spectral characteristics relationship to flare class and magnetic field configuration in spot group

07 p1077 A72-19814

Large scale magnetic fields and activity patterns in solar atmosphere, considering supergranules and active longitude and latitude development

07 p1078 A72-20007

Local structure of solar magnetic fields in sunspots as complexes of microspots

07 p1079 A72-20008

Solar active regions properties observation, noting correlation with magnetic field, flares, sunspots, magnetic knots, pores, umbral flashes, etc

07 p1079 A72-20009

Particle acceleration and plasma ejection in solar flares, using model of nonstationary cumulative flow near magnetic neutral line

07 p1060 A72-20014

Solar magnetic fields configuration in corona in relation to energetic proton escape into interplanetary space

07 p1060 A72-20015

Solar unipolar magnetic regions relation to geomagnetic disturbances variability, discussing 11 year cycle

08 p1155 A72-20808

Transverse magnetic field measurement over sunspot in chromosphere, noting fan-shaped field line divergence

08 p1232 A72-21135

Solar magnetic fields forced latitudinal drift rate due to differential rotation, taking into account turbulent friction and pressure forces

09 p1382 A72-22286

Solar general magnetic field nature, origin, fine structure and temporal variations, evaluating sunspots and active plage areas as field sources

09 p1387 A72-22752

Solar rotation as function of heliographic altitude from measurements of Fe and H lines, sunspots and magnetic field in photosphere

10 p1541 A72-24569

Active chromosphere coupling to magnetic field determined by subphotospheric motions, discussing active regions rotation period

11 p1720 A72-26117

Magnetic field gradient in sunspot umbrae from magnetically split line profiles

12 p1867 A72-27206

Solar magnetic field variation during solar rotation from sunspot observations, noting similarity to magnetic stars and behavior as quadrupole magnetic rotator

12 p1871 A72-27746

Outer corona and interplanetary space magnetic fields calculated from photosphere magnetic fields measured during 7 March 1970 solar eclipse

13 p2041 A72-29528

Sunspots, Doppler shifts, geophysical changes and statistical evaluation of diffuse objects motion in sun, discussing solar magnetic fields and 22 year cycle

13 p2044 A72-29701

Photospheric network, magnetic fields, Ca emission and continuum faculae from multichannel magnetograph observations

13 p2045 A72-29705

Solar video magnetographic observations of magnetic and H alpha plage correspondence on 21 March 1971

13 p2045 A72-29707

Energetic electron and proton trapping in lower solar atmosphere magnetic field, discussing particle injection, bremsstrahlung and gyro synchrotron radiation

13 p2046 A72-29719

Solar cycle dynamo theory and Babcock and Leighton model inadequacies, considering alternative theory based on deep magnetic field

13 p2046 A72-29729

Solar magnetic field fine structure from chromospheric morphology, using high resolution H alpha filtergram and magnetogram

13 p2046 A72-29731

Sunspot magnetic field depth variations model, using configuration conditioned by Schlueter-Temessvary similarity law

13 p2048 A72-29740

Solar magnetic fields filamentary structure from Mount Wilson magnetograph recordings in Fe I 5250 A and Fe I 5233 A spectral lines

13 p2049 A72-29934

Solar magnetogram recorded mean photospheric magnetic field cross correlation with interplanetary magnetic field

13 p2049 A72-29935

Energy storage in chromospheric magnetic flux ropes in solar flares, discussing kink perturbation instability suppression

13 p2049 A72-29936

Alfven wave transmission in sunspot umbral magnetic flux tube, noting standing progressive waves and energy dissipation in facular regions

13 p2049 A72-29937

Solar coronal magnetic field structure and energy content from synoptic data analysis, noting differential rotation effects

13 p2050 A72-29938

Sunspot formation due to magnetic flux concentration in active region and formation of invisible pores with suppressed granular motion

14 p2148 A72-30205

Solar rotation effects on solar wind magnetic energy transport by magnetic shear stress near sun

14 p2147 A72-30557

Solar proton flare on 2 November 1969, investigating active region magnetic field development and spatial structure, near limb and coronal phenomena

14 p2160 A72-30909

Solar instruments and methods for photospheric magnetic field measurement, noting spectroheliographic mapping in violet spectral region

15 p2306 A72-31647

Alpha effect solar dynamo model magnetic field and velocity expansion in spherical harmonics, solving mean field induction equation

15 p2316 A72-32755

Eleven year period solar photospheric magnetic field evolution, comparing latitudinal variation with sunspots, faculae and prominences distribution and green-line corona intensity

15 p2317 A72-32778

Solar flares induced magnetic field configurations, considering open and closed current sheets instabilities as flare sources

15 p2301 A72-32788

German monograph on solar wind-coronal magnetic field interactions, presenting numerical calculation of time dependent coronal states

16 p2445 A72-33425

Numerical method for force-free magnetic field structures in solar active regions, discussing rotation effects

16 p2455 A72-33462

Solar wind structure from observations and mathematical models, discussing effects of relativistic protons, heat transfer from electrons to protons and magnetic fields

16 p2449 A72-33909

Solar rotational properties in photosphere, solar wind and magnetic fields, including long lived sunspots and magnetic dipole observations

16 p2459 A72-33917

Solar corona emission line polarization numerical computation based on magnetic dipole transition scattering function for interpretation in terms of magnetic field direction

17 p2608 A72-35084

Note on the characteristics of sunspot groups which produce solar proton flares.

17 p2608 A72-35087

Chromospheric structure, magnetic field configuration, radiative transfer and energy balance relationship to solar prominences formation from corona

17 p2616 A72-35693

Photographic magnetograms comparison with H alpha filtergrams, investigating chromospheric features relationship to photospheric magnetic fields

17 p2616 A72-35702

H alpha loops incompatibility with stable filaments/prominences/ noting magnetic loops existence between regions of opposite polarity

17 p2617 A72-35704

On polarimetry in solar active regions. V - The magnetic field immediately before and after a flare.

17 p2617 A72-35706

Type 3 solar burst spectral characteristics relationship to flare class and magnetic field configuration in spot group

17 p2618 A72-35739

Relation between chromosphere flare motion and ejections and the magnetic field

19 p2851 A72-37817

Correlation of polarization in type III solar radio bursts at frequencies of 23.5 and 30 MHz

19 p2851 A72-38065

The generation of magnetic fields in astrophysical bodies. IX - A solar dynamo based on horizontal shear.

20 p2966 A72-38910

Solar magnetic fields derived from hydrogen alpha filtergrams.

20 p2969 A72-39338

The redistribution function of polarized light in the presence of collisions and of small magnetic fields - Discussion of the polarization of the solar line Ca I 4227 A.

20 p2971 A72-39756

Computer program for solar corona emission line polarization computation to interpret measurements in terms of coronal magnetic field direction

20 p2971 A72-39757

A line-profile Stokesmeter - Preliminary results on non-sunspot fields.

20 p2971 A72-39761

On the filamentary nature of solar magnetic fields.

20 p2971 A72-39762

New observations of solar magnetic and brightness fields.

20 p2971 A72-39763

On the filamentary nature of active-region magnetic fields.

20 p2971 A72-39764

Energy spectrum of small scale solar magnetic fields.

20 p2971 A72-39765

One dimensional migratory dynamo model for alpha effect turbulence controlled by increasing magnetic field, considering oscillatory antisymmetric solutions relation to solar cycle

20 p2972 A72-39877

OSO-4 observations of coronal EUV hole, considering association with regions of diverging magnetic fields

21 p3106 A72-41042

Probability interpretation of radiative transfer to calculate magnetic field-originating spectral line for-

- dependence on solar atmosphere mean optical
21 p3107 A72-41276
- Spectroheliogram absorption features cor-
related magnetic field regions and H alpha struc-
21 p3108 A72-41279
- Method to calculate electric currents in quiescent
21 p3108 A72-41282
- Coexisting weak and strong opposite-polarity mag-
netic field regions as cause of sunspot umbra Zeeman
component splitting
21 p3108 A72-41283
- Sunspot temperature increase stimulation of super-
granule motion leading to spot decay and magnetic
field diurnal fluctuation development
21 p3114 A72-41762
- Solar polar regions magnetic fields polarity and
strength during 1960-1971
22 p3221 A72-42026
- Observations of the horizontal velocity field sur-
rounding sunspots.
22 p3221 A72-42033
- Alpha force-free magnetic field representation for
solution of boundary value problem for chromosphere
and lower corona magnetic fields
22 p3222 A72-42037
- Some aspects of flare properties versus magnetic
boundary morphology.
22 p3217 A72-42038
- Magnetic field change rate related to chromospheric
activity in McMath Regions 8863, 10385 and 11415,
discussing flare associated effects and total flux
22 p3217 A72-42039
- A possibly direct measurement of coronal magnetic
field strengths.
22 p3222 A72-42042
- Magnetic field structure in flare-associated solar-
wind disturbances.
22 p3219 A72-42428
- The sunspot cycle and solar and lunar daily varia-
tions in H.
22 p3228 A72-42882
- The great solar flares of August, 1972.
22 p3219 A72-42984
- Sunspot formation due to magnetic flux concentra-
tion in active region and formation of invisible pores
with suppressed granular motion
23 p3333 A72-43235
- Solar activity research review, discussing sunspots,
magnetic fields, solar atmosphere, rotation, radio
waves, flares, X ray emission, etc
23 p3338 A72-43976
- Annual and solar-magnetic-cycle variations in the
interplanetary magnetic field, 1926-1971.
23 p3286 A72-44504
- Substorm related changes in the geomagnetic tail -
the growth phase.
24 p3397 A72-44856
- SOLAR NEBULA**
U SOLAR CORONA
SOLAR NOISE
U SOLAR RADIO EMISSION
SOLAR OBSERVATORIES
NT OSO
NT OSO-E
NT OSO-H
- Solar observation survey, considering sounding
rockets, OSO, balloons, orbiting observatories, spec-
tral resolution, spectral features and solar flare
03 p0409 A72-13050
- Preliminary analysis of the solar image quality in the
'Amici' dome of the Arcetri Astrophysical Observa-
tory
18 p2728 A72-36767
- SOLAR ORBITS**
NT APHELIONS
NT PERIHELIONS
- Solution of N planets equations of motion around
sun with recurrent power series in time
01 p0123 A72-10014
- Computerized series solution of relativistic motion
of planet Mercury for Schwarzschild and isotropic
coordinates
02 p0260 A72-12306
- Venus transit, across solar face, detailing black drop
effect on computation of exact ingress moment
01 p0581 A72-15620
- Mercury trajectory across solar disk plotted by
telescope lens cameras, for determining position an-
gles, disk contact times and relative angular velocity
06 p0882 A72-17934
- Short period comets orbital evolution and major
planets gravitational effects, discussing cometary cloud
formation, diffusion, motion and discovery
07 p1078 A72-19981
- Evolutionary processes /tidal dissipation, close ap-
proach and collision/ responsibility for commensura-
bility relations between orbital periods and orbital-spin
periods in solar system
07 p1083 A72-20465
- Outer planet mass determination limitations from
mutual motion perturbations
08 p1236 A72-21636

- Short period comets origin and orbital evolution,
discussing Jupiter perturbations and statistical study
10 p1536 A72-24143
- Heliocentric orbit from modified Laplace and
Leuschner method with optimal time interval between
five successive observations
14 p2149 A72-30233
- Sub-Mercurial planet Vulcan observation data, cal-
culating orbital elements, angular size and velocity
radial distance and object diameter
14 p2149 A72-30234
- Trajectory analysis for swingly technique using
Jovian gravitational field for leaving ecliptic plane
along heliocentric orbit and for solar flyby at specified
distance
14 p2150 A72-30452
- Earth capture of dust particles moving in ecliptic
plane heliocentric orbits, using three gravitational
bodies analysis
14 p2153 A72-30494
- Contact time determinations during 9 May 1970
Mercury passage across solar disk
14 p2153 A72-30498
- Asteroids and comets orbit perturbation equations
for small eccentricity values
14 p2161 A72-31080
- Mercury trajectory across solar disk plotted by
telescope lens cameras to determine position angles,
disk contact times and relative angular velocity
18 p2730 A72-37158
- Earth capture of dust particles moving in ecliptic
plane heliocentric orbits, using three gravitational
bodies analysis
19 p2864 A72-38323
- Contact time determinations during 9 May 1970
Mercury passage across solar disk
19 p2864 A72-38327
- Perturbation guidance for minimum time flight paths
of spacecraft.
21 p3082 A72-41560
- [AIAA PAPER 72-915] Spectral investigations of the comet Bennett 1970 II
(1969 i)
23 p3337 A72-43646
- A determination of the motion of the ecliptic.
23 p3337 A72-43833
- Critical inclinations and eccentricities concepts for
N planet problem, applying results to general three
body problem
24 p3442 A72-45239
- The possibility of a trans-Saturnian belt of particu-
late matter.
24 p3446 A72-45472

SOLAR PHYSICS

- Interplanetary medium spherical solid component
model from radio meteor orbit catalog, discussing den-
sity of interplanetary dust, meteor matter and cosmic
fallout on sun
02 p0282 A72-12332
- Physics of solar corona - NATO Conference,
Athens, September 1970
03 p0421 A72-13201
- Flare associated waves suggested by optically ob-
served phenomena, using time lapse photography of
solar chromosphere
03 p0423 A72-13212
- Steady state turbulent solar magnetic fields dynamic
evolution, considering weak random magnetic excita-
tion in electrically conducting fluid under varying
kinematic conditions
03 p0430 A72-13336
- Large-scale solar magnetic field dynamics, con-
sidering joint transport action by regular velocity field,
diffusion, sinking and sources of origin and destruc-
tion
03 p0433 A72-13358
- Large scale solar magnetic field dynamo model in
terms of force-free constituents series, deducing
periodic solution by eigenvalue method
03 p0433 A72-13362
- Cosmic ray decreases correlation to solar flare oc-
currence by epoch analysis of monitor data, proposing
mechanism for explanation
03 p0412 A72-13528
- Solar model for capture rate in C1 37 neutrino ex-
periment, comparing different stellar evolution pro-
grams
04 p0566 A72-14562
- Energy dependence of solar proton-proton reaction,
generating p-p wave function from Schroedinger equa-
tion
05 p0718 A72-16501
- Solar self oscillation interference from magneto-
graphic observation, noting power concentration in
space and frequency
05 p0718 A72-16502
- Thin solar convection zone relation to sunspot cy-
cle, noting magneto-kinematical model
06 p0886 A72-18099
- Solar-terrestrial physics - Conference, Leningrad,
May 1970
07 p0977 A72-20004
- Solar model inconsistencies, considering He and Fe
abundances and solar age approximation
07 p1083 A72-20464

- Solar current flow penetration to 1 AU in interplane-
tary medium, discussing inhibition of field line recon-
nection across neutral sheet
11 p1714 A72-26528
- Interplanetary medium spherical solid component
model from radio meteor orbit catalog, discussing den-
sity of interplanetary dust, meteor matter and cosmic
fallout on sun
13 p2039 A72-29216
- Solar plasmas intensity ratios of He-like ion line
emission, showing dependence on atomic number and
electron temperature
13 p2018 A72-29737
- Quiet and active models for solar structure and
processes in terms of elementary physical concepts
15 p2302 A72-31271
- Report to COSPAR on East German space program
covering ionosphere, geomagnetic phenomena and
solar physics
15 p2338 A72-32013
- Meson exchange effects on solar pion-production
process, using low energy Adler theorem with cross
section correction factor
16 p2456 A72-33476
- Easterly and westerly polar electrojets intensity
diurnal variations with respect to universal time and
geo- and heliophysical phenomena
19 p2791 A72-38368
- Solar activity effects on sun-earth space physical
processes, considering galactic cosmic rays, comets,
ionospheric disturbances, and noctilucent clouds
19 p2867 A72-38629
- Sunrise and sunset period of helio-geophysical
processes in terms of optical, X ray, corpuscular and
radio characteristics of solar activity
19 p2868 A72-38637
- Investigation of physical conditions in the solar
photosphere by a curve of growth technique
21 p3102 A72-40097
- Gravitational perturbations as source for solar
oblateness fluctuations, considering density in upper
convective zone
21 p3106 A72-41039
- Solar coronal F component separation from K com-
ponent by utilizing elongation dependence differences
in scattering populations, computing F for wide ranges
of parameters
21 p3106 A72-41041
- Solar oblateness and neutrino flux measurement ex-
periments, discussing agreement with solar interior
and evolution models
24 p3446 A72-45552
- Skylab solar astronomical observation programs
and instruments, discussing X ray and H alpha
telescopes, coronagraphs, spectroheliographs and UV
spectrographs
24 p3453 A72-45528
- Physical conditions in the solar corona from spectral
observations of the eclipse of March 7, 1970
24 p3448 A72-45684
- SOLAR PLASMA (RADIATION)**
U SOLAR WIND
SOLAR POSITION
- Time between noontime and evening maxima in F2
layer critical frequency compared with evening max-
imum period, showing dependence on noontime solar
zenith angle
01 p0059 A72-10615
- Lunisolar precession and equinox motion from
Cepheids proper motion, using recently determined
distance values
04 p0576 A72-15038
- Ionospheric electron concentration and temperature
as function of solar zenith angle from rocket sounding
08 p1154 A72-20734
- Geocoronal hydrogen Lyman alpha glow intensity,
and zenith angle dependence from observations by
rocket-borne extreme UV photometers
09 p1298 A72-22593
- Lunar surface roughness effect on temperature dis-
tribution, noting solar elevation and observation angles
dependence
11 p1715 A72-25244
- Joint ocean-atmosphere model response to solar
zenith angle seasonal variation, noting snow cover and
ocean surface effects on lower troposphere warming
11 p1620 A72-25766
- D region electron density profiles calculated as
function of solar zenith angles, noting LF radio wave
propagation
13 p1945 A72-28582
- Sea surface albedo for short wave solar radiation in
terms of sun altitude and atmospheric transmittance,
noting wind and surface roughness effects
18 p2687 A72-36642
- Right ascensions of the sun, Mercury, and Venus
observed with the transit instrument at Nikolaev dur-
ing 1966-1967
19 p2861 A72-37982
- Declinations of the sun, Mercury, and Venus in the
FK4 system as deduced from observations with the
vertical circle of the Nikolaev Observatory during
1966-1967
19 p2861 A72-37983

- Ionospheric electron concentration and temperature as function of solar zenith angle from rocket sounding 19 p2791 A72-38362
- Solar altitude nomogram for estimating terrestrial ground objects heights from shadow length on aerial photographs 22 p3181 A72-43196
- An approximate method of determining the azimuth from observations of the passage of the solar disk across the horizontal thread of the instrument's telescope 24 p3437 A72-44755
- D region electron density profiles calculated as function of solar zenith angles, noting LF radio wave propagation 24 p3397 A72-45082
- ### SOLAR POWER GENERATION
- #### U SOLAR GENERATORS
- #### SOLAR POWER SOURCES
- #### U SOLAR GENERATORS
- ### SOLAR PROBES
- Helios solar probe mission, describing project management, data reception system, trajectory monitoring and international cooperation [DGLR PAPER 71-052] 02 p0284 A72-12720
- German-American interplanetary solar probes Helios A and B mission characteristics and ground operations system, discussing planning phase [DGLR PAPER 71-122] 02 p0285 A72-12741
- Spin stabilized axisymmetric probe altitude deviation due to solar pressure in elliptic orbits 06 p0892 A72-17655
- Search coil magnetometer for measurement of weak alternating magnetic fields encountered by Helios solar probe in space 11 p1632 A72-25804
- Helios solar probe-borne zodiacal light photometer for diffuse light measurements in interplanetary space 11 p1632 A72-25805
- Ferrite core memory for storage of Helios probe perisolar space data before transmission to telemetry system 11 p1601 A72-25806
- Helios solar probe project command station design, discussing equipment details and command transmission operation sequence [DGLR PAPER 72-018] 13 p1939 A72-28963
- Investigation of the optical and pyrometric behavior of surface coatings for the Helios probe 19 p2880 A72-37493
- Structural problems of the helios solar probe. 24 p3449 A72-45122
- Helios solar probe development, discussing scientific experiments, structural, thermal and engineering models and systems tests 24 p3451 A72-45214
- ### SOLAR PROMINENCES
- Solar prominence oscillatory motion on 26 March 1964 association with plasmoids generated by pinch tube plasma 02 p0278 A72-12044
- Topological features of force free magnetic field near bipolar sunspots, considering chromospheric fibrils and filaments in H alpha lines 03 p0415 A72-12932
- Radio observations of filaments in absorption against solar disk during 11 September 1969 and 7 March 1970 eclipses 03 p0415 A72-12939
- Solar prominence telescope design parameters and structural dimensions calculation using lens equation 03 p0356 A72-13197
- Solar flare surges with hot spectrum and violent activity, analyzing trajectories 03 p0423 A72-13213
- Magnetographic observations of magnetic fields in quiescent solar prominences, using Zeeman effect on H, He, and metal lines 03 p0428 A72-13298
- Flare- and prominence-associated solar radio outburst, describing preflare phase and type 2 and moving type 4 bursts relation to coronal instability 03 p0410 A72-13321
- Dash phenomenon in eruptive loop prominences representing solar flare process at all levels of atmosphere, discussing pinch effect instability 03 p0411 A72-13332
- Small scale magnetic field theories, concerning solar prominence structure, chromospheric and coronal heating and particle production in flares 03 p0430 A72-13333
- Solar magnetic field vector distribution in quiescent prominence plasma with components both along and perpendicular to long axis 03 p0432 A72-13350
- Solar longitudinal magnetic field measurements in polar prominence, noting configuration similarity to arc 03 p0432 A72-13355
- Solar prominences, considering heavy gas suspension in magnetic arches with grooved tops 05 p0708 A72-15976
- Solar activity asymmetry on two hemispheres in 1959-1969, considering spots, faculae, prominences and corona 05 p0718 A72-16511
- High dispersion spectroscopic study of H alpha and K lines profile and velocity structure in quiescent prominences 05 p0719 A72-16516
- Filament activations caused by disturbances originating in solar flares 05 p0711 A72-17201
- Solar prominence telescope design using two prism reflectors for ray path deflection 07 p0982 A72-19125
- Ionization mechanisms of quiescent prominence of He II 4686 line luminescence under coronal UV radiation at high temperatures 07 p1077 A72-19812
- Solar eruptive prominence observations and photographs on 3 May 1971 at 0903-1029 UT with maximum height of 540,000 km 07 p1082 A72-20298
- Telescope construction for solar prominences observation, discussing reflection prisms effect on light rays path and image displacement 08 p1165 A72-21088
- He ionization and excitation in optically thick solar prominences, considering recombination excitation for observed triplet-level populations at 5000-10,000 K electron temperature 08 p1231 A72-21123
- AS type solar prominence kinematics of 10 September 1956, noting hyperbolic spiral knot motion from recorded data analysis 09 p1390 A72-23398
- Spectrophotometry of inner corona and quiescent prominence during 7 March 1970 solar eclipse, discussing Balmer line analysis 13 p2042 A72-29536
- Eleven year period solar photospheric magnetic field evolution, comparing latitudinal variation with sunspots, faculae and prominences distribution and green-line corona intensity 15 p2317 A72-32778
- Macroscopic velocity fields in solar prominence based on solar spectra and monochromatic photographs, proposing helical model 15 p2318 A72-32779
- Quiescent solar prominences internal motions from fine structure wavelength shift observations in Ca II K line spectra 15 p2318 A72-32780
- Spectroscopic analysis of condensations density and intensity variations in solar eruptive prominences, discussing hypothetical magnetic field effects 15 p2318 A72-32781
- ESRO 2 satellite observation of solar X-ray emission from active limb prominence, obtaining temperatures and emission measures as function of time 17 p2608 A72-35085
- Solar flares and prominences rotational motions from spectrographic observations of atomic Al absorption line periodic asymmetry 17 p2608 A72-35086
- Possible long-period oscillations in solar radio emission at microwaves. 17 p2608 A72-35091
- Arch prominence outside west limb on 24 April 1971, noting H alpha monochromatic image, internal motion of matter and radio emission 17 p2614 A72-35503
- Chromospheric structure, magnetic field configuration, radiative transfer and energy balance relationship to solar prominences formation from corona 17 p2616 A72-35693
- H alpha loops incompatibility with stable filaments/prominences/ noting magnetic loops existence between regions of opposite polarity 17 p2617 A72-35704
- Ionization mechanisms for quiescent prominence He II 4686 line emission under coronal UV radiation and high temperature conditions 17 p2618 A72-35737
- He II line emission in cold regions of solar prominences and chromosphere, noting hydrogen, metal and He I emissions 21 p3108 A72-41281
- A method to calculate electric currents in quiescent prominences. 21 p3108 A72-41282
- Hydrodynamical study of the large northeast coronal streamer observed during the eclipse of March 7, 1970 21 p3100 A72-41287
- Intensity ratios of He I and H lines in a prominence and the chromosphere. 21 p3109 A72-41329
- Simultaneous measurements of H alpha and H beta Balmer lines and He D3 line in faint prominences, showing emission intensity ratios dependence on layer total optical thickness 22 p3221 A72-42034
- Millimeter absorption features corresponding with H alpha dark filaments on disk and emissive regions in
- solar prominences, discussing electron temperature and densities 22 p3221 A72-42034
- The great solar flares of August, 1972. 22 p3219 A72-42984
- On some plasma rotation phenomena on the sun 24 p3445 A72-45082
- ### SOLAR PROPULSION
- #### NT SOLAR ELECTRIC PROPULSION
- Power processing requirements for solar electric propulsion in deep space mission, noting use of electron bombardment ion thruster with hollow cathode 01 p0007 A72-11055
- Multimission capability of solar electric propulsion /SEP/ spacecraft, analyzing payload variation, propellant requirements, thrusting time limitations and throttling range [AIAA PAPER 72-51] 10 p1582
- Solar electric low thrust unmanned missions, considering spacecraft subsystems and swingby trajectories [AIAA PAPER 72-425] 11 p1721
- Solar electric propulsion upper stage for space exploration missions, discussing spacecraft performance, configurations and program plans [AIAA PAPER 72-464] 11 p1709 A72-26224
- Solar electric propulsion application to cometary rendezvous and docking CARD mission sample return [AIAA PAPER 72-470] 11 p1722 A72-26220
- Solar electric propulsion subsystem performance tested on breadboard model, noting electrical power conversion, command, thrust vector control and propellant supply [AIAA PAPER 72-507] 11 p1711 A72-26224
- Multimission and engine performance requirements for solar electric spacecraft propulsion stage configurations, considering launch vehicle compatibility integration payload and environmental extreme effects [AIAA PAPER 72-465] 11 p1712 A72-26325
- Solar electric propulsion for satellite transport into geostationary orbit, discussing launchers, energy supply, electrostatic ion thruster and mass/power ratio [AIAA PAPER 72-505] 12 p1860 A72-26325
- Encounter trajectory design for solar electric propulsion rendezvous with low mass celestial bodies noting target characteristics [AIAA PAPER 72-424] 13 p2036 A72-28959
- Encounter sequences determination techniques for multitarget flyby and rendezvous missions to asteroids and comets by spacecraft using solar electric propulsion [AIAA PAPER 72-429] 13 p2037 A72-28959
- Structural evaluations and dynamic testing of electric propulsion components, surveying power conditioning plan model frequencies by holographic interferometry technique [AIAA PAPER 72-442] 13 p1899 A72-28959
- Solar array degradation effect on electric propulsion spacecraft performance, presenting power allocation strategy during mission [AIAA PAPER 72-444] 13 p2037 A72-28959
- Solar electric multimission spacecraft /SEMME/ concept, investigating Mariner, Viking and TOP technologies applicability to postulated mission/science objectives [AIAA PAPER 72-469] 13 p2026 A72-28959
- ### SOLAR PROTONS
- Higher moment Vlasov equations of collisionless fully ionized plasma for studying solar wind proton thermal anisotropy, heat flux and distribution function 01 p0119 A72-10888
- Solar proton flux and energy spectra from 1968-1969 ESRO 2 satellite measurements, detailing 11 November 1968 event 02 p0273 A72-12077
- Apollo 11 and 12 rock samples depth profiles for Al, Na, Mn, S, V, Ca, P, Co, Fe, Cu and Sc isotopic contents, estimating solar proton flux 02 p0282 A72-12077
- Solar proton entry observations over polar regions in relation to magnetosphere, magnetotail and magnetopause models 02 p0275 A72-12077
- Low energy solar proton propagation and interplanetary magnetic field measurements, comparison with population in solar wind 03 p0407 A72-13333
- Solar proton flare connection with strong electric currents, discussing net magnetic flux changes at electric conductivity and field strength 03 p0410 A72-13333
- Magnetic-channel solar flare volume characteristics based on proton flare H alpha pictures, using Petschek model 03 p0411 A72-13333
- Solar wind protons adiabatic spatial cooling relation to temperature anisotropy 05 p0709 A72-15976
- Polar cap absorption event, investigating solar energy protons precipitation effects 05 p0709 A72-15976

Solar wind proton penetration through earth magnetosphere, taking into account drift, force lines curvature and nonstationary plasma boundary

05 p0709 A72-16255

Solar wind model of electrons, protons and alpha particles velocity and temperature differences dependence on distance from sun

06 p0873 A72-18025

Proton measurements with Azur satellite during solar particle events of March 1970, considering diffusion and convection transport theories

07 p1056 A72-18901

Monte Carlo calculations of lunar photon albedo from galactic and solar proton bombardment for lunar soil composition information

07 p1070 A72-19139

Radionuclides formation rate as function of depth in moon for bombardments by galactic cosmic ray particles and by solar protons

07 p1057 A72-19140

Solar electrons and protons measurements in interplanetary space and in magnetotail, noting access to north polar cap

[AD-744404] 07 p1058 A72-19156

Active region sources of solar proton streams, discussing 27-day recurrence, acceleration and confinement in interplanetary space

07 p1060 A72-20010

Thermal plasma origin of solar X-ray emission and far UV flash observation during 28 August 1966 proton flare

07 p1060 A72-20013

Solar magnetic fields configuration in corona in relation to energetic proton escape into interplanetary space

07 p1060 A72-20015

Solar proton flares forecasting methods in connection with active region developments for spacecraft radiation shielding

07 p1061 A72-20017

Solar protons propagation from instantaneous injection source and inhomogeneities interaction description by mean free path and scattering angle specification

07 p1063 A72-20627

Cometary carbon dioxide molecules annihilation by recharging and dissociative charge exchange with solar protons

08 p1229 A72-20830

Polar orbiting satellite observations of energetic solar proton entrance into polar cap during March 1970 solar event

09 p1376 A72-22588

Solar wind model of electrons, protons and alpha particles velocity and temperature differences dependence on distance from sun

11 p1713 A72-25961

SID coincident with solar photon burst, showing vertical variations of electron concentration

11 p1713 A72-26269

Solar proton event classification system with index of three digits representing proton flux, absorption and sea level neutron monitor response measurements

11 p1714 A72-26425

VLF phase changes due to particle precipitation into geomagnetic anomaly during solar proton events explained by exponential ionospheric models with effective reflecting height

11 p1599 A72-26765

Charged particles propagation in magnetic field and scattering medium with constant and variable transport paths, applying to proton propagation for solar flares

13 p2029 A72-28576

Apollo 11 and 12 rock samples depth profiles for cosmogenic Al, Na, Mn, S, V, Ca, P, Co, Fe, Cu and Sc isotopic contents, estimating solar proton flux

13 p2039 A72-29211

Daytime 30 MHz PCA from satellite and riometer measurements, noting linear relationship to square root of integral and differential solar proton fluxes

13 p2030 A72-29339

Model of solar wind expansion beyond heliosphere, taking into account effect of relative motion between cool interstellar atomic hydrogen and solar wind protons

13 p1033 A72-29801

Solar proton flare prediction, examining diurnal rotation of axis connecting two stable spots and change in horizontal gradient of spots magnetic field

14 p2147 A72-30649

Solar proton flare on 2 November 1969, investigating active region magnetic field development and spatial structure, near limb and coronal phenomena

14 p2160 A72-30909

Solar proton flare induced X ray bursts maximum flux, total radiated energy, electron temperature and emission from satellite measurements

14 p2160 A72-30910

Solar X-ray flux daily changes before and after proton flare, using zero-epoch superposition method

14 p2148 A72-30911

Solar proton flux density angular and latitude distribution in polar regions magnetosphere from satellite observation

15 p2299 A72-31921

Solar proton events end prediction from flux decay rates observation, noting particle energy effect on accuracy

15 p2301 A72-31999

HF radiation in type 3 burst sources, discussing amplification by proton and electron streams

15 p2316 A72-32753

Magnetospheric particles and interplanetary magnetic field measurements for solar proton event of March 1970, noting polar cap structures

16 p2444 A72-32956

Solar radio bursts time sequence and positions observation during 24 January 1971 proton event, noting relation to relativistic particles acceleration into interplanetary field

16 p2445 A72-33045

Solar wind structure from observations and mathematical models, discussing effects of relativistic protons, heat transfer from electrons to protons and magnetic fields

16 p2449 A72-33909

Note on the characteristics of sunspot groups which produce solar proton flares.

17 p2608 A72-35087

Transport of cosmic rays in the solar corona.

17 p2599 A72-35094

A two-fluid solar wind model with anisotropic proton temperature.

17 p2599 A72-35097

A new model for estimating space proton dose to body organs.

17 p2508 A72-35354

Entry of high-energy solar protons into the distant geomagnetic tail.

17 p2601 A72-35588

Geomagnetic activity and the solar situation in the neighbourhood of proton effects.

18 p2686 A72-36227

Heos 1 data on interplanetary magnetic field, solar wind and proton characteristics, noting barium cloud experiment

19 p2850 A72-37492

Tabulation of physical conditions in proton and non-proton solar flares from observations and H alpha line width measurements

19 p2851 A72-37815

Azimuthal propagation of low-energy solar-flare protons as observed from spacecraft very widely separated in solar azimuth.

19 p2852 A72-38726

Several observations of low-energy solar-proton spectra and possible interpretations.

19 p2852 A72-38727

Collisionless solar wind protons - A comparison of kinetic and hydrodynamic descriptions.

19 p2853 A72-38732

Persistent particle anisotropies and magnetospheric models.

20 p2916 A72-39233

Solar cosmic ray diffusion in interplanetary medium, describing solar flare proton and heavy nuclei propagation in terms of time of arrival measurements

20 p2964 A72-39262

Change of solar flare proton to alpha ratios during an energetic storm particle event.

21 p3101 A72-41297

Polar-cap measurements of solar-flare protons with energies down to 12.4 keV.

22 p3218 A72-42425

Ozone measurements in the mesosphere during the solar proton event of 2 November 1969.

22 p3173 A72-42509

Model for the uneven illumination of polar caps by solar protons.

23 p3286 A72-44502

Compressions and rarefactions in the solar wind - Vela 3.

23 p3332 A72-44509

Charged particles propagation in magnetic field and scattering medium with constant and variable transport mean free path, applying to proton propagation for solar flares

24 p3435 A72-45076

SOLAR RADIATION

NT SOLAR CORPUSCULAR RADIATION

NT SOLAR COSMIC RAYS

NT SOLAR PROTONS

NT SOLAR RADIO BURSTS

NT SOLAR RADIO EMISSION

NT SOLAR WIND

NT SOLAR X-RAYS

NT SUNLIGHT

Book on solar and galactic cosmic rays covering collisions with matter, propagation through geomagnetic field and atmosphere and origin

01 p0118 A72-10170

Satellite attitude and libration control by solar radiation pressure

01 p0135 A72-10928

Upper cloud boundary height determination using Cosmos 320 satellite combined reflected solar and intrinsic radiation measurements

02 p0253 A72-12213

Polarization and atmospheric inhomogeneity effects on solar radiative transfer in turbid atmospheres, using diffused reflection and transmission matrices

02 p0222 A72-12836

Solar coronal monochromatic optical emission, inferring electron density and ionization or temperature distributions and variations with time

03 p0422 A72-13208

Real time complete Stokes vector scanning photoelectric polarimeter with 16 cm aperture for measuring visible radiation of solar disk, corona, moon and planets

03 p0356 A72-13275

Solar UV radiation role in mesosphere, investigating absorption cross sections of ozone and molecular oxygen

03 p0411 A72-13385

Molecular oxygen photodissociation in Schumann-Runge bands, discussing determination of solar radiation penetration depth into chemosphere

03 p0412 A72-13388

Relaxation and heating rate due to solar radiation absorption by 2.7 and 4.3 micron vibration-rotation bands of carbon dioxide

03 p0347 A72-13387

Solar radiation effects on planar librational motion and attitude of gravity oriented satellites at high altitudes

03 p0434 A72-13613

Time variations of zonal averages of albedo and absorbed solar radiation derived from brightness data of digitized satellite pictures

03 p0385 A72-14222

Long period perturbations arising in orbits of artificial satellites with large surface to mass ratio under solar radiation pressure and earth oblateness effects

04 p0572 A72-14637

Solar radiation characteristics, calculating concentration and spectral energy distribution

04 p0572 A72-14707

Temperature variations in 30-100 km region of atmosphere, investigating solar radiation effects

04 p0516 A72-14933

Solar radiation effects on earth atmosphere with MR-12 and M-100 meteorological rockets launched at onset of chromospheric flare, noting atmospheric parameters measurements

04 p0580 A72-15471

Equilibrium temperature distribution on radiatively adiabatic smooth and rough planes uniformly irradiated by collimated solar flux

[AIAA PAPER 72-59] 05 p0749 A72-16874

APZ-2 daytime actinometric radiosonde measuring long wave radiation balance in presence of short wave solar radiation

06 p0814 A72-17624

International comparison of standard solar radiation measurement pyranometers

06 p0816 A72-17921

Solar radiation angular field structure from upper atmospheric boundary scattering, taking into account underlying surface albedo fluctuations

06 p0807 A72-17942

Atmospheric directional scattering coefficients from vertical measurements of IR spectral sky brightness near solar almucantar and direct radiation

06 p0842 A72-18044

Total atmospheric water vapor content from solar radiation absorption observation at millimeter wavelengths

06 p0817 A72-18099

Solar radiation pressure effects on gravity oriented satellites librational dynamics, using digital computer aided numerical analysis and analog simulation

07 p1067 A72-18789

Environmental forces effects on gravity oriented satellites attitude dynamics, considering earth atmosphere aerodynamic and solar radiation forces effects

07 p1085 A72-19064

Wave front division interferometry for small scale solar features study at visible wavelengths

07 p1076 A72-19599

Intercosmos 4 solar radiation equipment, including Lyman, optical and X ray photometers, spectroheliographs, polarimeters and optical orientation system

07 p0986 A72-19641

Atmospheric aerosols optical thickness evaluation from solar radiation integral intensity

07 p1031 A72-19851

Solar energy sources and dissipation and emission mechanisms, considering radiant flux of convection zone and photosphere and solar variabilities

07 p1078 A72-20001

Solar corona structure and dynamics in context of energy transfer processes of dissipation, radiation heat conduction and hydrodynamic expansion

07 p1078 A72-20004

Algorithm for solving boundary value problem of integrodifferential equations describing temperature

- field inside hollow thin walled rod within solar radiation field in vacuum 07 p1028 A72-20207
- Transfer characteristics of solar radio radiation in scattering corona 07 p1062 A72-20230
- Interstellar gas role in cosmic ray yearly variations determined from solar short wave radiation induced gas ionization 07 p1065 A72-20640
- Nucleon and electromagnetic component generation, energy spectrum and diffusion during solar flares 07 p1066 A72-20651
- Excess radiation and primary cosmic ray intensity variations at 200-350 km during 1965-1969 solar cycle from Cosmos satellite data 08 p1227 A72-21156
- Mathematical model of solar radiation pressure effects on earth satellite orbit 08 p1237 A72-21643
- Radiative transfer equation for solar irradiance penetration of turbid atmosphere and plant canopy, using four point quadrature method 09 p1297 A72-22442
- High energy UV solar radiation transfer by photospheric aerosols to biosphere, considering radiation injury to human lung 09 p1298 A72-22662
- Geomagnetic field short term variations as function of solar activity from solar radiation data harmonic analysis, relating large amplitude fluctuation to seasonal variations 09 p1304 A72-23503
- Heat transfer through glass plate in solar radiation flux, discussing temperature distribution and thermal flux meter design 10 p1562 A72-24318
- Solar radiation pressure effects on orbital evolutions of light artificial earth satellites 10 p1543 A72-24632
- Stellar spectra differential analysis from solar curve of growth for Fe I with revised gf-scale, noting van der Waals broadening and microturbulence 10 p1547 A72-24868
- Book on earth environment covering atmospheric structure, terrestrial magnetic field, solar radiation, micrometeorites, ionosphere and van Allen belts 10 p1478 A72-25173
- Model atmosphere with n homogeneous layers and ground surface for solar radiation flux calculation [AD-744410] 11 p1620 A72-25307
- Solar UV radiation and Lyman alpha flux observation during 7 March 1970 solar eclipse with Nike-Apache rocket photometer soundings 12 p1862 A72-27145
- Solar Lyman alpha radiation flux over disk during solar eclipse from rocket measurements 12 p1863 A72-27147
- Upper atmospheric measurement of incident solar UV radiation penetration to lower levels, discussing measuring instruments 13 p2030 A72-28826
- Diurnal and annual temperature variations at 30-60 km from statistical analysis of rocketsonde data, obtaining solar radiation errors magnitude 13 p1947 A72-28829
- Solar radial brightness distribution, using mm observations during 7 March 1970 solar eclipse for improved angular resolution 13 p2042 A72-29531
- Fourier transformations for convolution integral calculation in image distortion correction by ground visual observations of solar intensity distribution, noting successive approximations method 13 p2046 A72-29726
- Carbon origin in comets associated with propyne photodissociation by solar 1216 A Lyman alpha radiation 13 p2050 A72-29995
- Solar UV Lyman alpha radiation intensity measurements, using Vertikal-1 rocket-borne photometer and photoelectron analyzer 14 p2128 A72-30465
- Solar cyclic intensity variation of excessive radiation with respect to galactic radiation background at low altitudes from satellite data analysis 14 p2146 A72-30475
- High resolution atmospheric millimeter wave spectrum of attenuated solar radiation from sea level observations, using Fourier type IR techniques 15 p2224 A72-31671
- Pageos balloon satellite orbital perturbations due to erratic solar radiation pressure induced accelerations, comparing modified Smith perturbation model calculations with photometric observations 15 p2228 A72-31975
- Report to COSPAR on Netherlands space research covering solar and stellar radiation, cosmic gamma and X rays, photometry and satellite geodesy 15 p2338 A72-32010
- Report to COSPAR on West German space program covering meteorology, aeronomy, ionospheric physics, magnetosphere, solar wind and radiation, solar system and life sciences 15 p2338 A72-32014
- Unmodulated solar radiation effect on electro-optical photoreceptors voltage sensitivity, noting photomultipliers and silicon photodiodes 15 p2237 A72-32121
- Circumsolar radiation measurement discrepancy explanation based on comparison with results obtained by international pyrheliometer scale 15 p2238 A72-32169
- Molecular oxygen concentrations from solar Lyman alpha radiation absorption profile in mesosphere, using rocket-borne nitric oxide filled ion chamber 15 p2230 A72-32264
- Solar and geocoronal hydrogen Lyman alpha radiation detector, discussing ion chamber with magnesium difluoride window and nitric oxide gas 15 p2239 A72-32336
- Solar radiation absorption measurements in 2150 A region as function of altitude to obtain oxygen and ozone densities 16 p2384 A72-32975
- Solar radiation anisotropic nonconservative scattering in semiinfinite atmosphere, calculating plane and spherical albedo by exponential kernel approximation 16 p2446 A72-33463
- Atmospheric absorption height determination from orbital elements during solar radiation satellite observation 16 p2386 A72-33603
- Solar radiation angular field structure from upper atmospheric boundary scattering, taking into account underlying surface albedo fluctuations 16 p2386 A72-33783
- Solar radiation absorption and scattering by particles in atmosphere, emphasizing absorption/backscatter ratio explanation 16 p2388 A72-34023
- Solar radiation pressure effects on balloon satellite behavior, noting orbital eccentricity variations 16 p2463 A72-34182
- Monte Carlo treatment of Lyman-alpha radiation in a plane-parallel atmosphere 17 p2598 A72-34538
- Backscatter of solar resonance radiation. I. 17 p2598 A72-34626
- A search for high energy gamma-rays from solar active regions. 17 p2599 A72-35092
- Solar radiation simulators and the measurements of solar battery and cell characteristics /Survey/ 17 p2498 A72-35514
- Calculation of solar radiation incident on a cylindrical surface 17 p2498 A72-35515
- On the size distribution of turbulent elements in the earth's atmosphere. 17 p2549 A72-35717
- Book - The earth's atmosphere 17 p2550 A72-35797
- Theoretical studies of the flux and energy spectrum of gamma radiation from the sun. 18 p2721 A72-35993
- Predictions of solar induced response of thin-walled open-section booms for design. 18 p2733 A72-36364
- Atmospheric ozone and the history of life. 18 p2686 A72-36626
- Sea surface albedo for short wave solar radiation in terms of sun altitude and atmospheric transmittance, noting wind and surface roughness effects 18 p2687 A72-36642
- Studies on radiation balance at a tropical station. 18 p2722 A72-36759
- Correlation study of geodetic refraction effect on astronomical refraction anomalies for solar light source observation at large zenith distances 19 p2855 A72-37348
- French monograph - Determination of the absolute value of the absorption in the bands of the Schumann-Runge system of molecular oxygen 19 p2836 A72-37476
- Excess radiation and primary cosmic ray intensity variations at 200-350 km during 1965-1969 solar cycle from Cosmos satellite data 20 p2964 A72-39261
- New observations of solar magnetic and brightness fields. 20 p2971 A72-39763
- Mathematical model for moving radiometer system for reflected solar radiation measurement, discussing instrument time constant effect on surface emittance variations reproduction 20 p2927 A72-39795
- Solar radiant energy reflection and absorption by cloud layers 21 p3049 A72-41795
- Some results of measurements of short-wave and long-wave radiation fluxes from the Cosmos-320 satellite 22 p3168 A72-41875
- The effect of cloud scattering on the absorption of solar radiation by atmospheric dust. 22 p3201 A72-42512
- Directional far IR emission from lunar surface, determining brightness temperature as function of observer and sun elevation angles and surface parameters 22 p3226 A72-42537
- Integration sphere facility with water cooled long arc xenon sources for pyranometer calibration, discussing operation theory and system design 22 p3163 A72-42692
- Attitude control of satellites using the solar radiation pressure. 22 p3231 A72-42871
- Calculation of the solar radiation incident on an inclined ribbed surface 22 p3140 A72-43194
- Cloud structure and cover determination from actinometric short wave solar radiation and IR cloud radiation measurements 23 p3311 A72-43627
- Calculation of middle ultraviolet radiation detector response to solar radiation as a function of altitude. 23 p3289 A72-43897
- Solar activity research review, discussing sunspots, magnetic fields, solar atmosphere, rotation, radio bursts, flares, X ray emission, etc 23 p3338 A72-43976
- Experimental comparisons of the international pyrheliometric scale with the absolute radiation scale. 23 p3290 A72-44274
- Solar control over the evolution of F2-layer after sunrise. 24 p3395 A72-44822
- Aerodynamic solar semipassive hybrid system for continuous three dimensional attitude control of axisymmetric satellite in near-earth orbits, discussing operation, design and optimization 24 p3450 A72-45146
- To the problem of satellite's perturbed motion under the influence of solar radiation pressure. 24 p3442 A72-45237
- SOLAR RADIATION OBSERVATION**
- U SOLAR RADIATION**
- SOLAR RADIATION SHIELDING**
- Solar proton flares forecasting methods in connection with active region developments for spacecraft radiation shielding 07 p1061 A72-20017
- SOLAR RADIO BURSTS**
- Multichannel hf spectrograph for decimeter wave solar burst spectrum fine structure analysis, noting operation at any desired frequency and channel separation 01 p0065 A72-10416
- Line splitting in emission near plasma frequency in drift pair solar radio bursts, considering causes by model involving electrons bunching through solar corona 02 p0276 A72-11646
- Jet-like structure formation by close juxtaposition of 80 MHz sources observed in late phase of complex solar burst, presenting model for explanation 02 p0272 A72-11649
- Gyroresonance plasma wave absorption in corona, investigating solar radio bursts fine structure 03 p0415 A72-12935
- Rain type periodic solar radio bursts interpreted on basis of stream instability pulsating regime, considering plasma waves excitation 03 p0406 A72-12936
- Solar U-type radio bursts in outer corona at 0.7 MHz related to magnetic bottle 03 p0406 A72-12937
- Polarization distribution and inversion of solar impulsive microwave bursts at 17 GHz 03 p0407 A72-12940
- Microwave solar radio bursts occurrence and intensity distribution at 19 GHz during July 1967-December 1969 03 p0407 A72-12941
- Radio Astronomy Explorer Satellite data on solar bursts, interstellar medium ionized component distribution, cosmic rays and galactic halo magnetic fields 03 p0330 A72-13067
- Solar decimeter and hectometer wavelength radio burst generation, examining dynamic spectra and source position as function of frequency and time 03 p0424 A72-13221
- Flare- and prominence-associated solar radio outburst, describing preflare phase and type 2 and moving type 4 bursts relation to coronal instability 03 p0410 A72-13321
- High energy electrons behavior and sunspot magnetic fields in solar flares, using hard X ray and microwave radio burst balloon observations 03 p0410 A72-13323
- Solar turbulent magnetic field in lower corona associated with expanding limb microwave burst of 30 March 1969 03 p0410 A72-13325
- Radio-astronomical evidence for magnetohydrodynamical pulsations in corona, considering solar radio burst model of pulsating structure due to synchrotron radiation 03 p0432 A72-13349

Oso-3 satellite observation of solar flare associated EUV bursts, comparing with microwave radio bursts [AD-739641] 03 p0413 A72-13529

Solar radio recombination lines observation at hydrogen and helium frequencies 04 p0568 A72-15328

Statistical investigations of solar burst time dependent fine structure, giving data for multichannel spectrograph and recording system design 05 p0708 A72-15767

Solar microwave bursts impulsive and gradual rise and fall type comparison, noting frequency response and distribution 05 p0713 A72-16022

Solar radio spike bursts, discussing categorization by high time resolution dynamic spectra and drift 06 p0876 A72-17578

Magnetic field decay in solar microwave burst region evaluated from circular polarization degree time profile 06 p0891 A72-18505

Automatic zero suppression system for recording solar bursts time functions and data reduction without information loss 07 p0982 A72-19052

Solar radio bursts classification, discussing normal and magnetic bremsstrahlung and plasma waves conversion 07 p1079 A72-20012

Statistical analysis of solar microwave bursts, examining radiation source development and emission mechanism 12 p1872 A72-27814

Narrow antenna radiation beam used for size and location determination of solar microwave radio burst observed with radio telescope 13 p2048 A72-29743

Radio bursts and X ray emissions associated with 15-16 November 1970 solar chromosphere flares, noting brightness maximum differences 14 p2146 A72-30483

Solar radio bursts time sequence and positions observation during 24 January 1971 proton event, noting relation to relativistic particles acceleration into interplanetary field 16 p2445 A72-33045

Microwave spectrograph with broadband superheterodyne total-power radiometer for time-shared recording solar burst dynamic spectra 17 p2552 A72-34191

Correlation of solar radio bursts and sudden increases of the total electron content (STEC) of the ionosphere. 17 p2598 A72-34698

Solar thermal radio burst temperature and emission measure determination from flux spectrum, noting consistency with radio observation 17 p2608 A72-35090

Plasma turbulence in solar atmosphere upper layers related to chromospheric flares and radio bursts 17 p2612 A72-35349

Frequency separation in structure of solar continuum radio bursts. 17 p2602 A72-35713

Solar flares and radio bursts significance for chromosphere and corona studies, considering radiation frequency-source location relations 17 p2603 A72-35957

Observation of linear polarization of solar microwave bursts. 18 p2722 A72-36997

Solar radio burst time profiles comparison with H alpha line emission curves for corresponding flares, noting neutral hydrogen emission relation to electrons acceleration 19 p2850 A72-37802

Heat conduction as mechanism for solar microwave bursts attenuation, noting effect of gyromagnetic absorption layers 19 p2852 A72-38497

X-ray and HF microwave bursts correspondence shown in observations of 24 October 1969 impulsive solar flare and of XUV and radio emissions 21 p3108 A72-41290

Measurement of the electron temperature of small 3-cm radio bursts /Research note/. 21 p3100 A72-41291

Quasi-periodic solar radio pulsations at decimetric wavelengths. 22 p3222 A72-42045

SOLAR RADIO EMISSION

NT SOLAR RADIO BURSTS

Redundancy reduction method for multichannel spectrometer solar radio data processing, using least squares technique 01 p0128 A72-10418

F 2 layer critical frequency variations relation to solar radio flux intensity, using mathematical approximations 01 p0059 A72-10613

Quiet sun radio emission observation, considering statistical minimum value and time varying structure 03 p0424 A72-13220

Solar flare associated magnetic field behavior and radio emission polarization in October 1968 active center, describing polarity flux variations 03 p0411 A72-13328

Meteorological elements, upper ionospheric data and solar radio emission intensities during winter stratospheric temperature rises 03 p0383 A72-13477

Total flux and polarization of solar S-component at mm wavelengths, obtaining radio source optical depth by evaluation of QL propagation based on magnetoionic theory 07 p1069 A72-19080

Solar radio emission, considering sources of slowly varying waves, brightness temperature distribution, frequency spectra and fluctuations 08 p1228 A72-20827

Radio observation of flare sources and emission areas above coronal condensations during 22 September 1968 solar eclipse 08 p1228 A72-20828

Coronal nonthermal radio emissions occurrence in absence of visible flares due to chromospheric perturbation 10 p1529 A72-24525

Meteorological elements, upper ionospheric data and solar radio emission intensities during winter stratospheric temperature rises 11 p1682 A72-26247

Atmospheric carbon monoxide and nitrous oxide telluric line contours and line centers optical thickness, measuring solar radio emission transmissivity 11 p1628 A72-26881

Radio attenuation by rain at 37 GHz using sun as source compared with sky emission observations, noting apparent absorber temperature effect 12 p1783 A72-27665

Solar radio astronomy instrumental requirements for 20 meter wavelength interferometry, metric and decametric flux and polarization measurements 12 p1872 A72-27815

Solar disk 10 cm radio emission during 7 March 1970 solar eclipse, discussing occultation of McMath place active region 13 p2044 A72-29550

Spectral radio observations of 7 March 1970 solar eclipse, noting McMath places intense activity source flux characteristics and weaker source bremsstrahlung emission 13 p2044 A72-29551

Solar radio emission map at 1.2 mm wavelength obtained with He cooled Ge bolometer connected radio telescope 13 p2046 A72-29716

Coronal randomly distributed anisotropic density inhomogeneities induced refraction and scattering effects on solar radio sources at 80 MHz 16 p2452 A72-33042

Soft X-ray and microwave observations of hot regions on solar flares. 17 p2608 A72-35089

Possible long-period oscillations in solar radio emission at microwaves. 17 p2608 A72-35091

Correlation studies of solar X-ray and radio bursts. 17 p2600 A72-35318

Solar flare initial, explosive and decay phases related to plasma motion, soft X-rays and radio emission 17 p2600 A72-35348

Slowly varying component spectrum of the solar radio emission at millimetre wavelengths. 17 p2617 A72-35708

Results of observation of spectra and polarization of meter solar radio emission with high time resolution - May-June, 1969. 17 p2602 A72-35714

Pulsating modulations and peculiar absorptions of type IV emissions from the solar corona. 18 p2721 A72-36651

Polarization observations of solar radio emission at the 3.15-cm wavelength 19 p2858 A72-37801

Structure of solar active zones in the mm wave range 19 p2866 A72-38496

Atmospheric carbon monoxide and nitrous oxide telluric line contours and optical thickness in line centers, measuring solar radio emission transmissivity 20 p2919 A72-39568

Characteristics of interplanetary electron inhomogeneities according to observations in the period from 1967 to 1969 21 p3114 A72-41765

The quiet sun brightness distributions at millimeter wavelengths and chromospheric inhomogeneities. 24 p3438 A72-44840

SOLAR RADIO WAVES

U SOLAR RADIO EMISSION

SOLAR REFLECTORS

Solar rudder for spacecraft steering in form of right circular cone with ideally reflecting surface 11 p1727 A72-25943

Determination of the quality of the reflective properties of mirrors used in photoelectric converter assemblies 17 p2498 A72-35510

SOLAR ROTATION

Solar sector magnetism cross correlation, showing difference from classical Babcock model in boundary direction, rigid rotation and identical solar hemisphere polarities 01 p0134 A72-11267

Rotating solar magnetic dipole with 26 7/8 day period from polar geomagnetic and spacecraft interplanetary field observations 02 p0277 A72-11899

Large scale solar magnetic field properties, discussing rotation, patterns and effects on corona 03 p0431 A72-13341

Coronal rotation determination by spectroscopic method for mean rotation rate vs heliographic latitude, confirming high latitude phenomena dependence of low latitude magnetic fields 03 p0432 A72-13352

Solar magnetic field large scale patterns and apparent regularities, noting active longitude 27-day rotation periods and polarity differences 03 p0432 A72-13354

Rotating dipole sector structure of interplanetary and solar photospheric magnetic fields from spacecraft observations [AD-740309] 03 p0437 A72-13871

Angular momentum and Li diffusive transport induced by mild thermally driven turbulence associated with Goldreich-Schubert-Fricke instability, discussing solar rotation slowdown [AD-735988] 05 p0720 A72-16718

Solar wind speed variations, examining velocity structure recurrence at various rotations, time interval of steady state flow and temporal evolution effects 06 p0872 A72-17442

Mercury trajectory across solar disk plotted by telephoto lens cameras, for determining position angles, disk contact times and relative angular velocity 06 p0882 A72-17934

Solar magnetic fields forced latitudinal drift rate due to differential rotation, taking into account turbulent friction and pressure forces 09 p1382 A72-22286

Solar rotation as function of heliographic altitude from measurements of Fe and H lines, sunspots and magnetic field in photosphere 10 p1541 A72-24569

Relativistic explanation for excess motion of Mercury perihelion in terms of solar oblateness and interior rotation mechanism [AD-745666] 11 p1715 A72-25350

Active chromosphere coupling to magnetic field determined by subphotospheric motions, discussing active regions rotation period 11 p1720 A72-26117

Solar magnetic field variation during solar rotation from sunspot observations, noting similarity to magnetic stars and behavior as quadrupole magnetic rotator 12 p1871 A72-27746

Mean linear velocity of rotation on solar equator to improve Hart rotatory velocity fluctuation values, giving expressions for statistical reestimation of mean square errors 13 p2035 A72-28441

Latitude dependent time variations of solar differential rotation and global activity distribution asymmetry, assuming large scale convection due to angular momentum transport 13 p2046 A72-29730

Solar coronal magnetic field structure and energy content from synoptic data analysis, noting differential rotation effects 13 p2050 A72-29938

Complex eigenvalues of frequency for Laplace tidal equation with negative equivalent depth, noting unstable modes role in solar differential rotation 14 p2100 A72-30344

Solar rotation effects on solar wind magnetic energy transport by magnetic shear stress near sun 14 p2147 A72-30557

Rotation effect on total heat transport and cell size in solar convection zone 16 p2451 A72-33038

Solar rotational properties in photosphere, solar wind and magnetic fields, including long lived sunspots and magnetic dipole observations 16 p2459 A72-33917

On the dependence of the linear velocity of solar rotation on latitude and optical depth. 17 p2607 A72-35076

The evolution of the solar inner rotation by the Eddington-Sweet type circulation under the influence of the solar wind torque. 17 p2613 A72-35497

Similarity theory of planetary atmosphere circulations applied to solar atmosphere in terms of radius and rotatory Mach number 19 p2863 A72-38066

Solar activity research review, discussing sunspots, magnetic fields, solar atmosphere, rotation, radio bursts, flares, X ray emission, etc

23 p3338 A72-43976

SOLAR SAILS

Analysis of the possibility of planetary escape by means of the solar sail

22 p3230 A72-43072

SOLAR SENSORS

Soviet book on electro-optical devices for space vehicles orientation and navigation covering vertical plotters and sun, planet and star trackers

02 p0256 A72-12125

Thermal heliotrope adaptation to terrestrial applications, discussing solar radiation energy input dominance assurance and wind effect minimization [ASME PAPER 71-WA/SOL-10]

05 p0614 A72-15893

Dynamic test facility for Symphony satellite attitude control, discussing sun and earth sensors and analog computer for motion simulator

05 p0643 A72-16432

AEROS satellite active magnetic attitude control system, describing magnetometer system, sun and IR earth sensors, spin stabilization and axis and spin rate control torque generation

05 p0727 A72-16473

Operational evaluation for sun stabilized attitude control system in Aeros satellite, describing laboratory equipment and component static and dynamic tests [DGLR PAPER 72-026]

13 p2052 A72-28967

Tansei satellite spin axis orientation measurement by two flux-gate magnetometers and sun sensor

15 p2272 A72-32334

A multislut shadow sensor of direction to a luminous object

21 p3052 A72-40308

Nimbus limb radiometer, Apollo fine sun sensor, and Skylab multispectral scanner.

23 p3288 A72-43882

SOLAR SIMULATORS

Vacuum chamber simulation of solar radiation effects on space satellites and components at 300-400 miles, using short arc xenon lamps

05 p0643 A72-16386

Solar cell calibration in uncollimated sunlight, obtaining standards for solar simulator intensity

12 p1759 A72-28042

Solar radiation simulators and the measurements of solar battery and cell characteristics

17 p2498 A72-35514

SOLAR SPECTRA

Line radiation from theta pinch with oscillatory ion and electron density applied to solar spectral studies

01 p0106 A72-10098

Flare region curved absorption lines interpreted as photospheric and chromospheric mass motions

01 p0129 A72-10800

Line splitting in emission near plasma frequency in drift pair solar radio bursts, considering causes by model involving electrons bunching through solar corona

02 p0276 A72-11646

H alpha spectra and combined filtergram observations of chromospheric fine structure, using Becker model

03 p0414 A72-12929

L alpha limb flux during total solar eclipse of 12 November 1966 from rocket measurements, comparing with chromosphere model

03 p0415 A72-12931

Prominent Zeeman multiplets in photosphere, penumbra, umbra and sunspot spectra, presenting ratios for temperature sensitivity measurements

03 p0415 A72-12933

Spectral and polarization characteristics of type 4 bursts with respect to energetic particle emission and solar-terrestrial phenomena

03 p0407 A72-12938

Solar observation survey, considering sounding rockets, OSO, balloons, orbiting observatories, spectral resolution, spectral features and solar flare

03 p0409 A72-13050

High spectral resolution balloon-borne spectrograph for near UV solar Mg II resonance lines

03 p0354 A72-13053

Real time ground control optimization of data acquisition of solar spectra scans from OSO 6

03 p0417 A72-13060

Solar spectral radiation intensity calibration methods in 10-4000 A range, including black body source, tungsten lamp, carbon arc, detectors, synchrotron radiation, etc

03 p0355 A72-13064

Solar UV line spectrum identification and intensity analysis, emphasizing electron spectra in soft X ray region and forbidden transitions

03 p0420 A72-13124

Solar flare surges with hot spectrum and violent activity, analyzing trajectories

03 p0423 A72-13213

Solar far UV spectrum observations for chromospheric coronal structure determination, reviewing

ionization balance, relative abundances and limb/disk ratios

03 p0423 A72-13216

Solar flare 1.9 A line feature identification from X ray observation by OSO-4 proportional counter spectrometer

03 p0424 A72-13218

Sunspot magnetic field evolution in time and space from four-camera spectral scanning method, obtaining magnetic flux and radial velocity field

03 p0428 A72-13303

Solar magnetic field measurement with 10,830 A He I line photoelectric spectroheliograms, observing filamentary fine structure in active regions

03 p0429 A72-13310

Solar spectra photographic recording technique, using spectra-spectroheliography method with data reduction

03 p0429 A72-13313

Solar limb flare observations on 4 November 1968, presenting photographs and intensive green coronal luminescence

03 p0434 A72-13493

Solar chromospheric flare spectrophotometric data on 8 July 1966, presenting line spectra, ground state and populations in excited energy levels

03 p0413 A72-14242

Solar silicon abundance from low excitation forbidden Si I lines

04 p0579 A72-15326

Missing solar UV opacity from band adsorption coefficient comparison between photospheric diatomic molecules and metals and hydrogen

04 p0579 A72-15327

Solar radio recombination lines observation at hydrogen and helium frequencies

04 p0568 A72-15328

Type 4 solar radio bursts peak flux spectra center to limb variation association with proton flares

05 p0709 A72-16073

Horizontally averaged nonthermal velocities determination in lower solar chromosphere, observing Doppler widths of weak rare earth emission lines in H and K wings

05 p0718 A72-16504

Intensity variations of CN photospheric and K line chromospheric network with time

05 p0718 A72-16505

Water molecules absorption lines in sunspots umbral near IR spectrum, noting improved spectrometric apparatus

05 p0719 A72-16515

High dispersion spectroscopic study of H alpha and K lines profile and velocity structure in quiescent prominences

05 p0719 A72-16516

Freundlich red shift of wavelengths in solar spectrum, deriving scattering cross section

05 p0719 A72-16527

Emission line of neutral carbon in solar spectrum at 1993.6 A from balloon-borne spectrography

06 p0876 A72-17566

Solar radio spike bursts, discussing categorization by high time resolution dynamic spectra and drift

06 p0876 A72-17578

Solar Fraunhofer line profiles determination by digital data recording double-pass spectrophotometer, presenting observed atomic Ni and Fe lines intensity distributions

06 p0884 A72-18028

Ionospheric effects of solar flares, considering flare spectrum below 10 A, flare X-rays relationship to sudden ionospheric disturbances and electron density profiles

06 p0874 A72-18087

Solar MgH isotopic abundance ratios and photospheric lines, correcting previous overestimation for sunspot spectra analyses

07 p1071 A72-19179

Solar Fe I oscillator strengths determination by hook method on shock heated gases

07 p1037 A72-19349

Turbulent micro and macromotion velocities in solar photosphere from CN molecule vibrational band line contours

07 p1077 A72-19810

Type 4 solar burst spectral characteristics relationship to flare class and magnetic field configuration in spot group

07 p1077 A72-19814

Low temperature Si photoconverters transparent in IR solar spectrum tested on Cosmos satellites

07 p0915 A72-20616

D region extraionization and solar X-ray flux from vlf data, emphasizing solar spectral shape and use of continuity equation for ionization time history

08 p1227 A72-21116

Monograph on solar IR limb profiles covering intensity observations, apparatus, instrumental distortions and data reduction and analysis

08 p1236 A72-21489

Relative intensity of solar XUV emission lines of Li isoelectronic sequence ions, taking into account transitional collision strengths

09 p1391 A72-23532

Jupiter spectral observations, discussing presence of deuterated methane in atmosphere and comparison with solar spectra for telluric features identification

10 p1539 A72-24347

Solar gravitational red shift measurement from solar and laboratory potassium absorption line comparison, using atomic beam resonance scattering technique

10 p1541 A72-24415

Solar rotation as function of heliographic altitude from measurements of Fe and H lines, sunspots and magnetic field in photosphere

10 p1541 A72-24569

Ions classification by ionization potential to explain existence of empirically defined classes for visible solar corona lines

10 p1542 A72-24614

Stratospheric methane measurements over North America from solar absorption spectra observed from aircraft

11 p1622 A72-25911

Solar Fraunhofer line profiles determination by digital data recording double-pass spectrophotometer, presenting observed atomic Ni and Fe lines intensity distributions

11 p1719 A72-25964

He-like lines in solar X-ray spectrum observed by Bragg crystal spectrometer, noting absolute wavelengths determination with shaft encoder for angle readout

11 p1714 A72-26572

Solar curve of iron growth, noting damping dependence on excitation potentials

12 p1867 A72-27204

Secondary standard solar cells calibration method based on solar spectral response comparison with primary standard, discussing error correction method

12 p1759 A72-28043

Diatomic carbon negative ion search in HD 201626 and solar spectra, noting rotational lines coincidence with absorption features

13 p2038 A72-29010

Solar spectrum measurements at 2100-3200 A by Aerobee rocket mounted Ebert-Fastie spectrometer with LIF diffusion plates

13 p2040 A72-29408

OSO-6 Mg X spectroheliogram data for corona electron density map construction during 7 March 1970 solar eclipse period

13 p2031 A72-29529

Spectral line variations in transition region from photosphere to chromosphere during March 1970 solar eclipse

13 p2041 A72-29530

Slit spectrogram and direct photograph observation of inner corona fine structure during 7 March 1970 solar eclipse, describing line and continuum intensities

13 p2042 A72-29533

Inner corona spectral data of 7 March 1970 solar eclipse, noting line half widths and emission line origin area relationship

13 p2042 A72-29535

Spectrophotometry of inner corona and quiescent prominence during 7 March 1970 solar eclipse, discussing Balmer line analysis

13 p2042 A72-29536

Solar corona IR Fe XIII lines during 12 November 1966 solar eclipse, discussing proton collisions as line-producing excitation mechanism

13 p2042 A72-29537

Fourier transform spectrometer observation of IR coronal emission lines during 7 March 1970 solar eclipse from high altitude aircraft

13 p2042 A72-29538

Wavelength, intensity and spatial distribution identification of far UV solar coronal forbidden lines observed during 7 March 1970 solar eclipse

13 p2043 A72-29540

Photographic polarimeter measurement of linear polarization of coronal emission lines during 7 March 1970 solar eclipse

13 p2043 A72-29547

Solar corona spectral line width and wavelength measurements during 7 March 1970 total eclipse, using Fabry-Perot photographic interferometer

13 p2043 A72-29548

UV solar spectrum recorded by rocket-borne spectrograph with diffraction grating echelle in Czerny-Turner arrangement

13 p2044 A72-29703

Solar video magnetographic observations of magnetic and H alpha plage correspondence on 21 March 1971

13 p2045 A72-29707

Bright point intensity distribution on CN spectroheliogram of sunspot penumbra on 4 July 1970

13 p2045 A72-29710

Umbral model effect on Li abundance determination from sunspot spectra

13 p2045 A72-29711

Flare related impulsive EUV solar emission lines enhancement in chromosphere-corona transition region

13 p2032 A72-29720

Comparative spectroheliograms of He 10830 A and H alpha lines in chromosphere

13 p2047 A72-29733

Observed continuous solar spectrum intensity comparison with photospheric models, noting bend-off due to veiled line haze

13 p2047 A72-29734

Solar corona intensification analysis based on ionized Fe monochromatic emission spectra, investigating spectral lines behavior as function of temperature and electron density

13 p2047 A72-29736

Crossover and magneto-optical effects of line splitting in sunspot spectra, considering instrumental circular polarization

13 p2047 A72-29738

Spectroheliograph study of fine structure of Evershed effect, determining radial velocity in penumbra along dark filaments and interfilamentary space

13 p2047 A72-29739

Solar relativistic electrons and particle events spectra during 1967-1969 from IMP-4 observations

13 p1033 A72-29746

Solar H alpha profile formation from non-LTE radiative transfer solutions through model atmosphere by integro-differential equation technique

13 p2049 A72-29931

Solar chromosphere model based on Lyman spectra observations, calculating temperature, gas and electron pressure and particle densities as function of height

13 p2049 A72-29932

Solar transition zone and corona EUV lines formation heights measurement from OSO-4 spectroheliograms

13 p2050 A72-29939

Solar X-ray spectral lines at 1-60 Å from coronal ion relative abundances obtained from Jordan ionization equilibrium calculations

13 p2034 A72-29940

Solar cosmic rays spectrum and geomagnetic cut-off rigidity determination from ion production rates in lower ionosphere

14 p2147 A72-30627

Solar spectrum Mg I multiplet lines hyperfine structures, examining emission lines with Fabry-Perot and Fourier transform spectrometers

14 p2158 A72-30730

Rocket-borne spectrometric measurement of small solar flare O VII and Ne IX resonance lines and 5 keV X-ray continuum emission, analyzing data via nonisothermal model

15 p2300 A72-31990

Sunspot umbral TiO gamma system photoelectric spectra examination for less abundant stable Ti isotopes

15 p2314 A72-32372

Tabulation of diatomic molecular lines observed in sunspot spectra with rotation branch, quantum number and vibration band

15 p2316 A72-32750

Solar photosphere and low chromosphere spectral lines non-LTE empirical analysis, relating coefficients of departure from LTE to elemental state temperatures

15 p2317 A72-32771

Solar Mg abundance and hyperfine structure from oscillator strengths measurement by comparing absorption lines at furnace temperatures

15 p2317 A72-32774

Large sunspot umbra high resolution spectrogram obtained by beam splitter with monochromatic polarization optics, noting blends near Zeeman lines

15 p2317 A72-32775

Solar photospheric resonance oscillation power spectrum observation, noting statistical significance

15 p2317 A72-32777

Macroscopic velocity fields in solar prominence based on solar spectra and monochromatic photographs, proposing helical model

15 p2318 A72-32779

Quiescent solar prominences internal motions from fine structure wavelength shift observations in Ca II K line spectra

15 p2318 A72-32780

Solar O VI, Ne VIII and Mg X spectral lines intensity ratios from XUV rocket measurements, comparing data with Jordan-Allen-Dupree ionization equilibrium calculations

Solar Fe XIII IR lines intensity ratio at 10747 and 10798 Å, deriving electron density as function of dilution factor with allowance for proton impact effect

15 p2318 A72-32784

OSO 1 observation of 300 second oscillation in solar transition region and coronal extreme UV emission line intensity

16 p2453 A72-33137

Photoelectric observations of Fraunhofer ionized metal lines in sunspot spectrum relating to umbral dots

16 p2458 A72-33687

Soft X-ray spectral studies of plasma dynamics in solar flares from Bragg crystal spectrometer OSO 6 recordings

16 p2449 A72-33918

Microwave spectrograph with broadband superheterodyne total-power radiometer for time-shared recording solar burst dynamic spectra

17 p2552 A72-34191

On the dependence of the linear velocity of solar rotation on latitude and optical depth.

17 p2607 A72-35076

The solar abundance of gold.

17 p2607 A72-35077

Measurements of the limb darkening in the forbidden Mg I line at 4571.1 Å.

17 p2608 A72-35078

Spectral analyses of solar photospheric fluctuations. II.

17 p2608 A72-35081

Photoelectric observation of H alpha, sodium deuteride and He solar umbral line profiles, using pressure scanning spectrometer

17 p2608 A72-35082

Solar corona emission line polarization numerical computation based on magnetic dipole transition scattering function for interpretation in terms of magnetic field direction

17 p2608 A72-35084

Solar flares and prominences rotational motions from spectrographic observations of atomic Al absorption line periodic asymmetry

17 p2608 A72-35086

The identification of the 1-0 and 2-1 bands of HCl in the infrared sunspot spectrum.

17 p2611 A72-35299

The solar spectrum - Wavelengths and identifications from 60 to 385 angstroms.

17 p2600 A72-35319

A first order analysis of variations of the limb darkening and the shapes for solar Fraunhofer lines.

17 p2616 A72-35694

Some new Dy II identifications in the solar spectrum.

17 p2616 A72-35696

Space and time variations of the solar Na D line profiles.

17 p2616 A72-35697

EUV observations of solar quiet region with OSO 6 spectroheliometer, noting chromospheric network structure

17 p2616 A72-35703

Doppler shift of solar photospheric spectral lines related to downward motions over plages

17 p2617 A72-35705

Turbulent micro and macromotion velocities in solar photosphere from CN molecule vibrational band line contours

17 p2617 A72-35735

Type 3 solar burst spectral characteristics relationship to flare class and magnetic field configuration in spot group

17 p2618 A72-35739

Theoretical studies of the flux and energy spectrum of gamma radiation from the sun.

18 p2721 A72-35993

A working model for sunspot umbrae.

18 p2727 A72-36740

Continuous emission localization in solar flare nuclei

19 p2850 A72-37814

Spectral line contours in the solar chromosphere, hydrogen line. IV - Contours in the chromosphere on the disk

19 p2859 A72-37905

Evaluating the light from the sun.

19 p2790 A72-37933

Spectral line profiles of the solar chromosphere. III - Relationship between the line profiles and their intensity gradients

19 p2860 A72-37950

Effect of photographic factors on the line intensities in the Fraunhofer spectrum of the sun

19 p2860 A72-37960

Rocket observation of Ar XII-XVI, Ca XIV-XVIII, and Fe XIV, XV, XXIV in the extreme-ultraviolet spectrum of a solar flare.

20 p2963 A72-38913

Radiative lifetimes for some resonance transitions of Fe I and Fe II in the region between 2300 Å and 3050 Å, and the application to iron abundance determinations in the sun and in the QSO PHL 938.

20 p2966 A72-38915

The redistribution function of polarized light in the presence of collisions and of small magnetic fields - Discussion of the polarization of the solar line Ca I 4227 Å.

20 p2971 A72-39756

A line-profile Stokesmeter - Preliminary results on non-sunspot fields.

20 p2971 A72-39761

New observations of solar magnetic and brightness fields.

20 p2971 A72-39763

The type IIIb burst - A precursor of decametre type III radio-burst.

20 p2965 A72-39882

Eu, La and Sm in sunspot spectra.

20 p2973 A72-39884

Calculation of solar CO vibration-rotation line profiles and equivalent widths.

20 p2973 A72-39889

Temperature and emission measure deduced by coronal visible lines.

20 p2974 A72-39896

Investigation of physical conditions in the solar photosphere by a curve of growth technique

21 p3102 A72-40092

OSO-4 observations of coronal EUV hole, considering association with regions of diverging magnetic fields

21 p3106 A72-41042

Thermal oscillations in the high solar photosphere.

21 p3107 A72-41275

Probability interpretation of radiative transfer to calculate magnetic field-originating spectral line formation dependence on solar atmosphere mean optical depth

21 p3107 A72-41276

Velocity oscillations in the solar atmosphere.

21 p3107 A72-41277

Characteristics of the Ca II K-line profiles in the quiet sun.

21 p3108 A72-41280

Coexisting weak and strong opposite-polarity magnetic field regions as cause of sunspot umbra Zeeman spectra pi-component splitting

21 p3108 A72-41283

Photoelectrically observed diatomic carbon absorption lines in sunspot spectra for two energy bands

21 p3108 A72-41284

Diatomic carbon lines search in sunspot umbrae spectrum from solar telescope observations

21 p3108 A72-41285

Coronagraphic observations of an enhanced coronal region. II - Temperature and density structure through the enhanced region.

21 p3108 A72-41288

The chromospheric continuum observed at the total solar eclipse of 12 November 1966 and a model of the low chromosphere.

21 p3109 A72-41328

Intensity ratios of He I and H lines in a prominences and the chromosphere.

21 p3109 A72-41329

Study of the chromosphere in the D3He line during the eclipse of September 22, 1968

21 p3114 A72-41764

Behavior of carbon monoxide in the upper photosphere

21 p3114 A72-41773

The solar abundance of calcium and collisional broadening of Ca I- and Ca II-Fraunhofer lines by hydrogen.

22 p3221 A72-42037

Solar photospheric fluctuations measured from time sequence of Sacramento Peak Observatory spectrograms, using power, coherence and phase spectra computed by fast Fourier transform

22 p3221 A72-42038

Micro- and macroturbulent motions and the velocity spectrum of the solar photosphere.

22 p3221 A72-42039

Observation procedures in high resolution spectrophotometry of solar chromospheric spectral fine structures

22 p3221 A72-42039

High resolution spectroscopy of the disk chromosphere. II - Time sequence observations of Ca II H and K emissions.

22 p3221 A72-42032

Millimeter absorption features corresponding with H alpha dark filaments on disk and emissive regions in solar prominences, discussing electron temperatures and densities

22 p3221 A72-42033

The decay characteristics of models of solar hard X-ray bursts.

22 p3217 A72-42040

Peculiar absorption and emission microstructures in the type IV solar radio outburst of March 2, 1970.

22 p3217 A72-42044

Absolute measurement of the solar brightness in the spectral region between 100 and 500 microns.

22 p3225 A72-42389

Low abundance of solar photosphere iron from Fe excitation and ionization computations, showing LTH departure effects on spectral lines

22 p3228 A72-42569

The great solar flares of August, 1972.

22 p3219 A72-42984

Stellar and Uranus photometric measurements for solar (B-V) and (U-B) color indices determination using K and H delta lines and G band filters

23 p3337 A72-43613

Coronal lines photometry systematic error dependence on aureola spectral intensity, line half width, gradation curve slope, and neutral filter transmission coefficient

23 p3340 A72-44240

Physical conditions in the solar corona from spectral observations of the eclipse of March 7, 1970

24 p3448 A72-45684

SOLAR SPECTROMETERS
Multichannel hf spectrograph for decimeter wave solar burst spectrum fine structure analysis, noting operation at any desired frequency and channel separation

01 p0065 A72-10410

Redundancy reduction method for multichannel spectrometer solar radio data processing, using least squares technique
01 p0128 A72-10418

Rocket-borne spectrometers calibration for observing absolute intensity and center-to-limb variations of sun in vacuum UV region
03 p0355 A72-13066

Statistical investigations of solar burst time dependent fine structure, giving data for multichannel spectrograph and recording system design
05 p0708 A72-15767

Sunspot umbra spectrophotometric scans with spatial cancellation techniques, finding 4200 K umbral temperature with 0.60 photosphere contrast
07 p1069 A72-19081

Programmed electro-optical systems of multichannel solar spectrometer for ground observations of X ray and EUV emission regions
11 p1630 A72-25680

Solar X ray burst analysis from individual quanta/energy and time recordings by Lunokhod 1 spectrometer
13 p2032 A72-29700

UV solar spectrum recorded by rocket-borne spectrograph with diffraction grating echelle in Czerny-Turner arrangement
13 p2044 A72-29703

Photoelectric observation of H alpha, sodium deuteride and He solar umbral line profiles, using pressure scanning spectrometer
17 p2608 A72-35082

A multislot shadow sensor of direction to a luminous object
21 p3052 A72-40308

SOLAR STORMS
Auroral X ray radiation measurements in midnight sector during solar storm of 8 March 1970
08 p1155 A72-20806

Change of solar flare proton to alpha ratios during an energetic storm particle event.
21 p3101 A72-41297

SOLAR STREAMS
U SOLAR CORPUSCULAR RADIATION

SOLAR SYSTEM
Planetary mass distribution in solar system from gravitational contraction of nebula formed by accretion of ring shaped particle cloud
02 p0282 A72-12311

Inner solar system particle propagation model solved for radial gradient of galactic protons, comparing to Mariner 4 measurements
03 p0412 A72-13527

Early solar system nucleosynthesis of Al 26, discussing silicon and carbon burning and spallation
04 p0567 A72-14912

Solar system data processing system (SSDPS)/ computer solution for major planetary masses from optical, radar and radio tracking data
04 p0575 A72-15034

Near resonance due to commensurability between Jupiter-Saturn mean motions, discussing effect on planetary system secular disturbing function
06 p0877 A72-17659

Evolutionary processes /tidal dissipation, close approach and collision/ responsibility for commensurability relations between orbital periods and orbital-spin periods in solar system
07 p1083 A72-20465

Elemental nucleosynthesis, considering cosmological, stellar, galactic and solar system evolution and atomic nuclei energetic levels
07 p1083 A72-20466

Solar wind propagation limitations by galactic magnetic field and cosmic rays and solar system motion relative to interstellar gas
08 p1225 A72-20701

Soviet papers on astronomical studies covering coordinate systems motion and stellar and celestial body position determination in solar system
09 p1388 A72-23051

Jacobi integrals in restricted three body problem of small bodies with massive sun and Jupiter in solar system
09 p1389 A72-23394

Apollo, Luna and Zond lunar exploration contribution to solar system formation knowledge, discussing post-Apollo lunar and planetary exploration programs
11 p1715 A72-25252

Gas rich meteorites and lunar materials solar rare gases component observed and predicted relative abundance agreement indicating absence of fractionation in solar nebula formation
11 p1721 A72-26118

Outer solar system - AAS Conference, Seattle, June 1971
12 p1870 A72-27344

Optical and electronic imaging systems optimization for solar system exploration, discussing effects on public support for national funding
12 p1807 A72-27346

Space technology developments during 1970s and 1980s, discussing solar system exploration, space

shuttle systems, cost effectiveness, international cooperation, nuclear propulsion systems, etc
13 p2051 A72-28453

Protoplanet cloud model of solar system as flat gas-dust disk, discussing density profile, gravitational stability and mass loss
14 p2148 A72-30206

Model for textural features and mineralogical composition of Ca and Al-rich inclusions in C3 chondrites during condensation in primitive solar nebula
14 p2157 A72-30585

Earth-moon system mass from ratio of solar mass to sum of terrestrial and lunar masses, discussing solar attraction effects and radar distance measurements
15 p2306 A72-31598

Chemical equilibrium models of low temperature condensation from solar nebula relating to planetary composition
15 p2311 A72-32083

Low energy cosmic ray deuteron and He 3 source spectra observation implications for adiabatic deceleration in solar cavity, discussing interstellar propagation
16 p2448 A72-33743

Astronomical model for primitive solar nebula showing planetary evolution in hot initial state under centrifugal forces
17 p2614 A72-35677

Lunar composition as a clue to the early history of the solar system.
17 p2614 A72-35678

Accretionary processes in the early solar system - An experimental approach.
17 p2618 A72-35836

A possible mechanism for the capture of micrometeoritic particles by the earth and other planets of the solar system.
17 p2619 A72-35939

Evidence for objects of lunar mass in the early solar system.
18 p2724 A72-36284

Planetary volcanic activity and matter disintegration as source of development in solar system, using density and rotational energy data
18 p2725 A72-36521

The north-south anisotropy and the cosmic-ray radial gradient in the vicinity of the earth.
18 p2722 A72-37164

Space science advances and NASA Planetary Program, noting solar system evolution, life origin and Skylab and Space Shuttle programs
19 p2855 A72-37274

Russian book - Physics of the earth and planets: Figures and internal structure
19 p2856 A72-37474

Russian book - Water in the universe
19 p2789 A72-37743

Solar wind propagation limitations by galactic magnetic field and cosmic ray pressure and solar system motion relative to interstellar gas
19 p2851 A72-38329

Chronology of first phases of formation of solar system solid objects, meteorites and primitive lunar rocks, describing models
19 p2867 A72-38548

Metal/silicate fractionation in the solar system.
20 p2967 A72-39177

Ordinary chondrite chemical and mineralogical properties establishment during solar system formation, noting fractionation events
20 p2969 A72-39334

Recent developments in the history of the nucleosynthesis of the solar system.
20 p2971 A72-39837

Jet streams development in rotating gaseous disk at discrete orbital distances in solar system
20 p2972 A72-39859

Generalization of the sphere of interaction for the restricted four-body problem
20 p2975 A72-40073

Terminal orbit of comet 1937 V /Finisler/
22 p3220 A72-41917

Book on moons and planets covering celestial mechanics, solar system origin, stellar formation, comets, asteroids, meteorites, planetary interiors, surfaces, atmospheres, etc
22 p3228 A72-42750

Protoplanet cloud model of solar system as flat gas-dust disk, discussing density profile, gravitational stability and mass loss
23 p3333 A72-43236

Solar system thin disk form planet formation in equatorial plane from nebula dust component, discussing gravitational effects and mass increase rate
23 p3335 A72-43261

Production of light elements in the solar system.
23 p3335 A72-43487

Inconsistency of gravitational constant variability in inverse proportion to time from viewpoint of stellar and solar system age, life development and physical three dimensional space
23 p3338 A72-44037

Saturn-Jupiter rebound - A method of high-speed spacecraft ejection from the solar system.
23 p3340 A72-44323

Flyby missions to comets, asteroids and meteors for obtaining solar system geological information, considering space dynamics feasibility
23 p3340 A72-44351

Lunar composition in terms of evolutionary mode based on inhomogeneous planetary accretion and high temperature condensation
24 p3439 A72-44977

From plasma to planet; Proceedings of the Twenty-First Nobel Symposium, Saltsjobaden, Sweden, September 6-10, 1971.
24 p3444 A72-45451

Origin of the planetary systems astronomical evidence in other stars.
24 p3444 A72-45453

A gasdynamical view on the motion, heating and accretion of solid bodies in the solar system.
24 p3444 A72-45456

Chemical effects in plasma condensation.
24 p3429 A72-45457

Conditions in the early solar system, as inferred from meteorites.
24 p3445 A72-45458

On certain aerodynamic processes for asteroids and comets.
24 p3445 A72-45463

Investigation of solar system evolution by automatic vehicles on the moon.
24 p3445 A72-45466

Potential contributions of the United States space program to exploration of the solar system.
24 p3445 A72-45467

SOLAR TEMPERATURE
Temperature fluctuations and fine structures in solar atmosphere from Ca II IR lines
03 p0414 A72-12926

Short periodic pulsations in solar atmosphere related to magnetosound propagation in area of temperature minimum with directed perpendicular magnetic field
03 p0436 A72-13813

Temperature variation with latitude in upper solar photosphere from photoelectric meridional and equatorial limb-darkening scans
05 p0719 A72-16710

Solar type 3 bursts from high resolution radio spectrographs, deriving coronal temperatures from decay times
06 p0876 A72-17576

Sunspot umbra spectrophotometric scans with spatial cancellation techniques, finding 4200 K umbral temperature with 0.60 photosphere contrast
07 p1069 A72-19081

Initial /premaximal/ phase model of chromospheric flare in terms of explosion theory, determining temperature, shock front and plasma velocities
07 p1077 A72-19809

Radiation temperature of carbon monoxide molecules in solar atmosphere from vibratory-rotatory spectral measurements
07 p1077 A72-19811

Solar active regions temperature measurements from 2 cm radioheliograms, using high resolution radio telescope
07 p1082 A72-20296

Solar pole-equator difference in effective temperature and mechanical heating, using atmospheric model
13 p2044 A72-29702

Photoelectric measurement of solar photosphere pole-equator temperature differences, analyzing statistical and systematic errors
15 p2317 A72-32770

Initial /premaximal/ phase model of chromospheric flare in terms of explosion theory, determining temperature, shock front and plasma velocities
17 p2602 A72-35734

Radiation temperature of carbon monoxide molecules in solar atmosphere from vibratory-rotatory spectral measurements
17 p2618 A72-35736

Coronagraphic observations of an enhanced coronal region. II - Temperature and density structure through the enhanced region.
21 p3108 A72-41288

Sunspot temperature increase stimulation of supergranule motion leading to spot decay and magnetic field diurnal fluctuation development
21 p3114 A72-41762

Free oscillations of the sun and their possible stimulation by solar flares.
22 p3219 A72-42570

SOLAR VELOCITY
Turbulent micro and macromotion velocities in solar photosphere from CN molecule vibrational band line contours
07 p1077 A72-19810

Statistical investigations of motions and distances of planetary nebulae
19 p2860 A72-37969

SOLAR WIND
Lunar crater population and distribution time development under meteoroid and solar wind bombardment, developing model for absolute formation ages
01 p0124 A72-10056

Collisionless motion of solar wind ions in helical magnetic field, giving transfer function of charged particles

01 p0118 A72-10360

Tago-Sato-Kosaka and Bennett comets plasma tails interaction with interplanetary magnetic field, demonstrating cometary events correlatability with solar wind data

01 p0128 A72-10419

Interplanetary magnetic field angular gradient and sectorial effects on solar wind, discussing wind velocity

01 p0118 A72-10583

Cosmic ray density distribution inside cosmic ray modulating spherical cone in solar wind, noting modulation depth quasi-periodic variation

01 p0119 A72-10606

Quiet solar wind kinetic model, comparing with exospheric, semikinetic and hydrodynamic models

01 p0119 A72-10878

Solar wind two component model with protons collisionless beyond ten solar radii, discussing effects of variable electron temperature

01 p0119 A72-10879

Higher moment Vlasov equations of collisionless fully ionized plasma for studying solar wind proton thermal anisotropy, heat flux and distribution function

01 p0119 A72-10880

Quiet time solar wind temperature profile calculation from energy equation using observed velocity profile data at earth orbit

[AD-742176] 01 p0120 A72-10881

Solar wind reverse and forward oblique slow shocks, examining discontinuities from Pioneer 6 plasma and magnetic field data

01 p0120 A72-10882

Microscale MHD wave and stationary structure fluctuations in interplanetary medium solar wind, considering theoretical constraints

01 p0129 A72-10883

Pioneer 8 plasma wave measurements at distant bow shock crossings, considering solar wind-magnetosheath interaction

01 p0062 A72-10903

Magnetospheric diagnostics from ground stations data, considering dimensions, cusp, ring current, tail flux, electric fields, radiation zone, solar wind and interplanetary field

01 p0132 A72-11072

Solar wind electron density variations, discussing radio source interplanetary scintillation and angular distribution measurements at various distances from sun

02 p0277 A72-11902

Solar wind plasma spherically symmetrical outflow allowing for equations of motion of velocity components, discussing interplanetary field and single fluid MHD

02 p0278 A72-11914

Rarefied plasma hydrodynamic equations for rotational discontinuities in solar wind, discussing magnetic field modulus jumpwise changes

02 p0272 A72-11915

Galactic cosmic ray-solar wind nonlinear interaction effects on solar wind geometry near and far from sun

02 p0272 A72-11917

Jupiter decimeter radio burst possibility as indicator of high velocity fluxes and shock waves in solar wind

02 p0273 A72-11935

Magnetosphere deformation by solar wind, comparing accuracy of free molecular flow and double dipole models

02 p0218 A72-11948

Long period geomagnetic pulsation generation at boundary of magnetosphere and incoming solar wind, considering possibility from idealized model

02 p0218 A72-11950

Idealized model for small scale internal structure of magnetopause separating distorted geomagnetic field in magnetosphere from solar plasma flow in magnetosheath

02 p0218 A72-11977

Solar wind induced atmospheric mass loss from magnetic field-free planets, using mass, momentum and energy conservation laws

02 p0275 A72-12465

Lunar surface magnetic field variations, considering solar wind effect

02 p0285 A72-12871

Damped geomagnetic pulsations associated with geomagnetic storms interpreted as interaction between hydromagnetic oscillations and solar wind induced magnetospheric motions, discussing modified mathematical model

02 p0222 A72-12872

Low energy solar proton propagation and interplanetary magnetic field measurements, comparing with population in solar wind

03 p0407 A72-12943

Lunar induced and permanent magnetism, discussing solar wind dynamic pressure effects and Apollo data

03 p0418 A72-13109

Solar wind 10-9900 eV electron flux, evaluating energy transport in plasma rest frame

03 p0412 A72-13507

Solar wind plasma flow through earth bow shock, deriving specific heats ratio based on one-fluid theory and conservation equations

03 p0412 A72-13509

Jupiter decametric radio emission relation to solar wind, geomagnetic activity and shock waves causing Forbush decreases

03 p0436 A72-13820

Solar wind effects on storms and structure of magnetosphere and radiation belt maintenance

03 p0350 A72-14304

Nonuniform solar wind velocity effect on interplanetary medium and on cosmic radiation, observing diurnal variations

04 p0567 A72-14928

Solar wind protons adiabatic spatial cooling related to temperature anisotropy

05 p0709 A72-16067

Solar wind proton penetration through earth magnetosphere, taking into account drift, force lines curvature and nonstationary plasma boundary

05 p0709 A72-16255

Comet Bennett tail and coma surface brightness distribution, estimating solar wind velocity

05 p0717 A72-16426

Solar wind velocity correlation with 5303 A coronal intensity

05 p0710 A72-16523

Cosmic plasma phenomena in astrophysics, discussing distribution, ionospheric disturbances, magnetospheric waves, solar wind, etc

05 p0723 A72-17217

Worldwide magnetic storm due to solar wind interaction with geomagnetic field, discussing field deformation

06 p0803 A72-17368

Collisionless solar wind in spiral interplanetary magnetic field, using two fluid model with hydrodynamically treated electrons

06 p0872 A72-17441

Solar wind speed variations, examining velocity structure recurrence at various rotations, time interval of steady state flow and temporal evolution effects

06 p0872 A72-17442

Solar wind stream-stream interactions, studying time profiles, velocity variations, corotating spiral, increased pressure due to radial compression and zonal flow directions

06 p0872 A72-17443

Solar wind structure from long lived inhomogeneities in corona, allowing for velocity, density and temperature perturbations

06 p0872 A72-17444

Circularly polarized hydromagnetic wave propagation upstream in solar wind, noting Doppler shifted whistler and slow electron cyclotron modes

06 p0872 A72-17449

Energetic charged particles penetration into magnetosphere by auroral simulation experiments with artificial solar wind, observing magnetic field microfluctuations behind collisionless shock front

06 p0805 A72-17469

Inviscid solar wind equations supersonic solutions existence domain from critical point boundary conditions

06 p0881 A72-17894

Solar wind model of electrons, protons and alpha particles velocity and temperature differences dependence on distance from sun

06 p0873 A72-18025

He and heavy ions properties and behavior in solar wind from expanding solar corona theoretical models

06 p0874 A72-18065

Low latitude surface horizontal magnetic field intensity depression due to quiet time ring current in magnetosphere as function of solar wind velocity

07 p1055 A72-18884

Magnetized solar wind velocities and fields obtained by three dimensional model using perturbation technique with spherically symmetric boundary conditions

07 p1057 A72-19142

Discrete wave packets observed in solar wind, discussing mechanism similar to echo phenomenon in plasma physics

07 p1057 A72-19143

Solar wind perturbations downstream of moon outside of diamagnetic cavity, considering lunar surface magnetized areas as possible sources

07 p1057 A72-19144

Hydromagnetic wave theory for solar wind, noting tangential discontinuities, perpendicular and Alfvén shocks and forward and reverse fast and slow shocks

07 p1058 A72-19354

Initial/premaximal/phase model of chromospheric flare in terms of explosion theory, determining temperature, shock front and plasma velocities

07 p1077 A72-19809

Particle acceleration and plasma ejection in solar flares, using model of nonstationary cumulative flow near magnetic neutral line

07 p1060 A72-20014

Chemical composition, thermal properties and shock propagation in solar wind plasma

07 p1061 A72-20018

Solar wind radial velocity variations effects on interplanetary magnetic field spiral structure

07 p1079 A72-20019

Galactic cosmic ray modulation by interplanetary medium, including solar wind boundary problem

07 p1061 A72-20021

Solar wind discontinuities and shock waves in interplanetary medium at magnetospheric boundary related to geomagnetic impulses

07 p1061 A72-20024

Solar wind and geomagnetic tail interaction with moon, discussing lunar Mach cone evidence for anisotropic wave propagation in magnetized collisionless warm plasma

07 p1061 A72-20025

Auroral forms dynamics dependence on solar wind and DP intensity in magnetosphere

07 p0977 A72-20030

Geomagnetic tail role in magnetospheric substorms, discussing solar wind energy storage, magnetic merging process and plasma sheet origin

07 p0977 A72-20032

Carbon chemistry of Apollo 14 size-fractionated fines, noting solar wind activity effect

07 p1082 A72-20290

Simulation study of lunar carbon chemistry, noting hydrocarbon production by solar wind interaction with fines

07 p1082 A72-20291

Distributions and average values for proton speed, azimuthal and polar flow directions and proton temperature and density in solar wind from Pioneer data

07 p1063 A72-20380

Hall effect influence on magnetospheric boundary magnetic field generation by solar wind perturbation, using beam-magnetic field interface model

07 p0980 A72-20407

Solar wind magnetic fields characteristics relative to 11 year cosmic ray modulation in interplanetary space

07 p1065 A72-20642

Nonstationary and asymmetric cosmic ray modulation theory, discussing moving boundary problem and solar wind model with spherical singularity

07 p1065 A72-20643

Diffusion and stochastic variations of galactic cosmic rays in solar wind

07 p1066 A72-20648

Solar wind propagation limitations by galactic magnetic field and cosmic rays and solar system motion relative to interstellar gas

08 p1225 A72-20701

Space-time relationship derivation to estimate traveling time of discontinuities running against magnetosphere in unperturbed solar wind

08 p1153 A72-20714

Geomagnetic effect of solar wind rotational discontinuity observed by Explorer 34, noting high latitude nonstationary ionospheric current attenuation and magnetic disturbances

08 p1225 A72-20715

Shock wave excitation by moving solar wind discontinuity in geomagnetic tail as cause of active phase of magnetospheric substorm

08 p1153 A72-20716

Geomagnetic field fluctuations during storms, considering Alfvén waves generation and propagation in solar wind and magnetosphere

08 p1153 A72-20717

Solar wind plasma parameter spatial perturbation problem solution by method of characteristics

08 p1225 A72-20721

Outer radiation belt parameters dependence on interplanetary magnetic field sectorial structure and solar wind velocity

08 p1226 A72-20811

Solar wind flux velocity diurnal variations relation to magnetic activity index based on Mariner 2 and 4, Pioneer 6 and Vela satellites data

08 p1226 A72-20821

Artificial magnetosphere interaction with 8 keV electrons in hydrogen plasma beam simulating solar wind, noting penetration caused by boundary instability

08 p1156 A72-20823

Interplanetary medium physical parameters from spacecraft measurements, noting solar wind properties, magnetic fields and MHD discontinuities

08 p1228 A72-20826

Lunar dust grain fossil coatings of ultrathin metamictized amorphous layers resulting from solar wind ion implantation

08 p1230 A72-20982

Solar wind tangential discontinuities and shock waves determination from flux velocity vector, magnetic field and particle density measurements

08 p1227 A72-21154

Solar wind velocity determination from interplanetary scintillation, deriving equations by smooth perturbations method

09 p1375 A72-22285

- Mariner 4 trajectory relation to proposed location of bow wave caused by solar wind interaction with Mars ionosphere, noting planet orbit aberration effects
09 p1385 A72-22581
- Comet gas production and interaction with solar wind, discussing visible plasma tail within flow pattern
09 p1387 A72-22755
- Solar wind properties and discontinuity characteristics, describing particle densities, wind speed, magnetic field level and near earth electron and ion temperatures
09 p1377 A72-22756
- Interplanetary magnetic field perturbations by solar wind and moon, noting lunar wake anomalies positive correlation with plasma beta value
09 p1387 A72-23003
- Low energy ions and negative particle fluxes simultaneous enhancements due to Apollo 14 lunar module impact, suggesting solar wind and gas cloud interaction as acceleration mechanism
09 p1388 A72-23018
- Solar wind kinetic energy from flare associated solar wind disturbances relation to types 2 and 4 radio bursts, using satellite observations
09 p1378 A72-23399
- Lunar surface darkening caused by solar wind effect, noting Fe valence state changes evaluation from photoelectronic spectroscopy of foil samples exposed to ion bombardment
09 p1394 A72-23665
- Solar wind termination distance as function of flux, velocity and interstellar hydrogen density, velocity and magnetic field strength
10 p1528 A72-23716
- Satellite, space probe and observatory data impact on space physics, considering solar wind, interplanetary magnetic field, Van Allen belt and Chapman-Ferraro theory
10 p1538 A72-24268
- Geomagnetic field and magnetosphere variations due to solar wind interactions, using rocket, satellite and indirect measurements
11 p1621 A72-25841
- Astronomical models of solar wind interaction with interstellar medium, determining magnetic field effects on shock wave
11 p1713 A72-25946
- Solar wind model of electrons, protons and alpha particles velocity and temperature differences dependence on distance from sun
11 p1713 A72-25961
- Low latitude geomagnetic field diurnal variations caused by solar wind associated component, noting evening side depression
11 p1713 A72-26109
- Explorer 35 observations of solar wind electron density and temperature, noting anisotropy direction correlation with magnetic field vector alignment
11 p1713 A72-26392
- Heavy ions from interplanetary dust, estimating contribution to solar wind flux
11 p1713 A72-26393
- Magnetosheath pressure, magnetic field, temperature, particle density and stream velocity computed for earth bow shock in oblique interplanetary field with solar wind
11 p1723 A72-26526
- Solar wind ion temperature association with influx of neutral hydrogen from heliosphere boundary
11 p1714 A72-26527
- Interplanetary plasma microinstabilities within framework of underlying electron-proton solar exosphere, discussing solar wind high beta effects
11 p1714 A72-26529
- Supergranular motions source of Alfvén waves dominating solar wind microstructure at earth orbit
11 p1724 A72-26530
- Geomagnetic tail model with plasma cylinder immersed into solar wind, obtaining dispersion equation for oscillations
11 p1627 A72-26532
- Method of characteristics for three dimensional supersonic flow of guiding center plasma, noting application to solar wind-moon interaction
11 p1573 A72-26601
- Spacecraft propulsion based on electric energy extraction from solar wind or energy transfer from ground via plasma arcs
11 p1712 A72-26779
- Cosmic and solar wind abundance analysis for D and He-3 in protosolar gas, noting chemical equilibrium reaction role in D enrichment
12 p1868 A72-27216
- Remanent lunar magnetic field compression by solar wind from magnetic measurements at Apollo landing sites
12 p1871 A72-27691
- Russian book on geomagnetic field cosmic rays covering charged particle motion theory, extraionosphere currents, magnetosphere tail and solar wind effects, etc
12 p1864 A72-28345
- Hydrodynamic approximation for solar wind nonuniformity in ecliptic plane, noting linear disturbances caused by nonuniform velocity of plasma flow from corona
13 p2029 A72-28577
- Solar wind distortion of stellar anisotropy of galactic cosmic rays, associating annual particle density variation with earth revolution about sun
13 p2029 A72-28590
- Solar wind plasma spherically symmetrical outflow allowing for equations of motion of velocity components, discussing interplanetary field and single fluid MHD
13 p2039 A72-29226
- Rarefied plasma hydrodynamic equations for rotational discontinuities in solar wind, discussing magnetic field modulus jumpwise changes
13 p2030 A72-29227
- Galactic cosmic ray-solar wind nonlinear interaction effects on solar wind geometry near and far from sun
13 p2030 A72-29229
- Jupiter decameter radio bursts as indicator of high velocity fluxes and shock waves in solar wind
13 p2030 A72-29247
- Magnetosphere deformation by solar wind, comparing accuracy of free molecular flow and double dipole models
13 p1949 A72-29260
- Long period geomagnetic pulsation generation at boundary of magnetosphere and incoming solar wind, considering possibility from idealized model
13 p1949 A72-29262
- Interplanetary electrons quiet-time intensity increases, considering trans-earth-orbital modulating region due to solar wind transport of photospheric field lines
13 p2030 A72-29377
- Large amplitude interplanetary solar wind discontinuities observed by OGO-5 plasma spectrometer and magnetometers, considering magnetic drift waves mechanism for plasma turbulence generation
13 p2031 A72-29378
- Earth-solar wind bow shock structure from OGO-5 observations during passage from interplanetary medium into magnetosheath
13 p1950 A72-29379
- Magnetosheath electron precipitation effect on dayside auroral-oval plasma density and conductivity, relating precipitation heat flux to solar wind energy density
13 p1950 A72-29381
- Burgers binary and Shkarofsky multiple collision theory numerical application to electrical conductivity in partially ionized solar magnetoplasma
13 p2018 A72-29714
- Nonradial oscillations and energy transport in nonmagnetic stationary rotating stellar wind in local theory limit
13 p2033 A72-29725
- Model of solar wind expansion beyond heliosphere, taking into account effect of relative motion between cool interstellar atomic hydrogen and solar wind protons
13 p1033 A72-29801
- Two dimensional mathematical model of magnetosphere with neutral sheet for oblique incidence of solar wind, noting magnetic field minimum energy
13 p1954 A72-29850
- Comet-like interaction of Venus atmosphere with solar wind from Venus probe data, noting absence of bow shock wave and ionospheric tail
13 p2050 A72-29956
- Mathematical model for magnetized solar wind with one fluid MHD and polytrope state equations, calculating magnetic field variables at earth
13 p2034 A72-29958
- Gas dynamics of steady rotating azimuthally dependent solar wind under magnetic field influence, calculating azimuthal distribution of radial velocity near earth orbit
13 p2034 A72-29960
- Electron temperature radial dependence in two fluid models of solar wind, noting unrealistic assumption of heat conduction dominated electron gas energy equation
13 p2034 A72-29961
- Anomalies detected in Mars 3 solar wind recordings interpreted as possibly caused by geomagnetic tail crossed by interplanetary probe
13 p2034 A72-30010
- Cylindrical model of interplanetary magnetic field-moon interaction, taking into account solar wind flow boundary condition asymmetries
14 p2154 A72-30514
- Solar rotation effects on solar wind magnetic energy transport by magnetic shear stress near sun
14 p2147 A72-30557
- Minimum magnetic field energy of two dimensional magnetosphere with neutral sheet for arbitrary dipole inclination to solar wind as function of potential difference on boundary points
14 p2101 A72-30643
- Harmonic analysis of solar wind geometry and geomagnetic activity levels during even and odd cycles based on cosmic ray intensity variations for 1900-1969 period
14 p2147 A72-30651
- Unipolar steady electromagnetic bow shock interaction of Mercury with solar wind, calculating planetary surface temperature
15 p2303 A72-31305
- Solar wind thermal properties from positive component energy distribution observation by ESRO Heos 1 satellite
15 p2298 A72-31518
- Low energy electron flux in magnetosphere, discussing relation to geophysical phenomena, solar wind, interplanetary magnetic field and charged particle longitudinal drift trajectories
15 p2225 A72-31903
- Annual variations of singly charged positive He ion density distribution in solar wind from Vela 3 observations
15 p2299 A72-31944
- Unshocked solar wind detection by ATS 5 satellite during 8 March 1970 geomagnetic storm
15 p2299 A72-31960
- Pioneer spacecraft intermittent solar wind streams data temporal variations analysis to account for anomalous type 3 bursts
15 p2299 A72-31964
- Solar wind model dividing interplanetary space in one fluid and two fluid collisionless regions, discussing proton thermal anisotropy
15 p2300 A72-31996
- Solar wind and planetary atmosphere interaction observation by simulation of ionization mechanism in comet, using gun produced plasma stream and gas cloud
15 p2301 A72-32341
- Magnetosphere description based on satellite observation data, discussing particle distributions, solar wind, shock wave, magnetic sheath and magnetopause
15 p2315 A72-32400
- Solar wind He enrichment origin in solar flares connection with type 2 radio emission from analysis of Vela 3 spectra
15 p2302 A72-32791
- Autocorrelation analysis of Mariner 2 data for solar wind velocity, noting 27 day recurrences
16 p2444 A72-32954
- Solar wind thermal anisotropy effects on least squares estimates of interplanetary shock parameters and associated normals from Rankine-Hugoniot equations
16 p2444 A72-32973
- Interplanetary scintillation technique application to structure of flare induced shocks and corotating streams within interplanetary medium
16 p2451 A72-33033
- Radio source power spectra modulation dependence on distance and thickness of solar wind scattering region and on wind velocity component multiplicity
16 p2451 A72-33034
- German monograph on solar wind-coronal magnetic field interactions, presenting numerical calculation of time dependent coronal states
16 p2445 A72-33425
- Solar wind velocity near Jupiter correlated to Io geocentric phase during radio bursts, noting plasma-sphere models
16 p2459 A72-33904
- Solar wind heat flux measurements comparison with collision dominated heat transfer theory in ionized medium, noting deviations from Maxwellian velocity distribution
16 p2449 A72-33908
- Solar wind structure from observations and mathematical models, discussing effects of relativistic protons, heat transfer from electrons to protons and magnetic fields
16 p2449 A72-33909
- Solar wind expansion analysis with allowance for interaction with neutral interstellar matter, discussing kinetic energy loss due to EUV ionization of interstellar gas
16 p2449 A72-33910
- H-He ions solar wind expansion absence for case of equal gas temperature, noting mass flux relationship to He ion temperature
16 p2449 A72-33911
- Alfvén wave propagation in interplanetary medium for solar wind microscale fluctuations, using stationary spherically symmetrical model
16 p2449 A72-33912
- Comets Tago-Sato-Kosaka and Bennett UV observational data interpretation for origin, constitution and interaction with solar wind, emphasizing total gas production
16 p2459 A72-33914
- Venus comet-like interaction with solar wind explained via He outer atmosphere with preferential heating by wind
16 p2459 A72-33915
- Solar rotational properties in photosphere, solar wind and magnetic fields, including long lived sunspots and magnetic dipole observations
16 p2459 A72-33917
- Alfvén wave firehose instability relaxation calculation to include nonlinear terms for explanation of solar wind temperature anisotropies by collisionless mechanism
16 p2449 A72-33933

- The solar wind H and He/ \pm content.
17 p2598 A72-34627
- Critical point regularity conditions and asymptotic solutions to the time stationary, linearized, inhomogeneous solar wind flow problem.
17 p2599 A72-35095
- On neutral sheets in the solar wind.
17 p2599 A72-35096
- A two-fluid solar wind model with anisotropic proton temperature.
17 p2599 A72-35097
- Observations of the region of interaction between the solar-wind plasma and Mars
17 p2600 A72-35219
- The evolution of the solar inner rotation by the Eddington-Sweet type circulation under the influence of the solar wind torque.
17 p2613 A72-35497
- Heat conduction in a turbulent magnetic field, with application to solar-wind electrons.
17 p2601 A72-35584
- An analysis of Pioneer 9 low-frequency wave observations near interplanetary discontinuities.
17 p2614 A72-35585
- Explorer 33 and 35 plasma observations of magnetosheath flow.
17 p2548 A72-35587
- Velocity and flux dependence of the solar-wind helium abundance.
17 p2602 A72-35607
- Detection of solar-wind electron plasma frequency fluctuations in an oblique nonlinear magnetohydrodynamic wave.
17 p2602 A72-35610
- Hydrogen and helium velocities in the solar wind.
17 p2602 A72-35716
- Magnetic dipole field interaction with plasma flow ions, noting qualitative model of solar wind flow past magnetosphere
17 p2593 A72-35905
- Satellite measurements of the moon's magnetic field - A preliminary report.
18 p2724 A72-36287
- Study of the solar wind using the power spectrum of interplanetary scintillation of radio sources.
18 p2722 A72-36730
- Determination of shock wave velocity in the interplanetary medium
18 p2728 A72-36875
- Lunar electrical conductivity.
18 p2729 A72-37000
- Heos 1 data on interplanetary magnetic field, solar wind and proton characteristics, noting barium cloud experiment
19 p2850 A72-37492
- Observations of the solar wind with the European satellite Heos-1
19 p2850 A72-37785
- Magnetospheric and ionospheric conjugate point phenomena as solar events manifestations via solar wind shock wave interaction with geomagnetic field
19 p2790 A72-37858
- Natural oscillations of type-I comet tails
19 p2864 A72-38081
- Solar wind propagation limitations by galactic magnetic field and cosmic ray pressure and solar system motion relative to interstellar gas
19 p2851 A72-38329
- Space-time relationship derivation to estimate traveling time of discontinuities running against magnetosphere in unperturbed solar wind
19 p2791 A72-38342
- Geomagnetic effect of solar wind rotational discontinuity observed by Explorer 34, noting magnetic storm initial phase relation to high latitude nonstationary ionospheric current attenuation
19 p2852 A72-38343
- Shock wave excitation by moving solar wind discontinuity in geomagnetic tail as cause of active phase of magnetospheric substorm
19 p2791 A72-38344
- Geomagnetic field fluctuations during storms, considering Alfvén waves generation and propagation in solar wind and magnetosphere
19 p2791 A72-38345
- Solar wind plasma parameter spatial perturbation problem solution by method of characteristics
19 p2852 A72-38349
- Numerical calculation of the lunar wake in a magnetohydrodynamic model.
19 p2864 A72-38435
- Reconnection of the geomagnetic tail deduced from solar-particle observations.
19 p2792 A72-38730
- Collisionless solar wind protons - A comparison of kinetic and hydrodynamic descriptions.
19 p2853 A72-38732
- One fluid solar wind model prediction from corona base density and temperature for parameters at earth
19 p2853 A72-38733
- Explorer 35 observation of geomagnetic tail low energy electrons, noting plasma sheet extension to lunar distance and correlation with solar wind
19 p2853 A72-38737
- He abundance relationship to solar wind bulk speed and temperature from Explorers 34 and 43 observations, noting dependence on sunspot number
19 p2853 A72-38749
- Radial penetration of a hot plasma associated with a large-scale electric field in the magnetosphere, and some related problems.
20 p2916 A72-39228
- Relationship of interplanetary magnetic field structure with development of substorm and storm main phase.
20 p2968 A72-39232
- Solar wind tangential discontinuities and shock waves determination from flux velocity vector, magnetic field and particle density measurements
20 p2964 A72-39259
- Magnetospheric shapes, flows and substorms in terms of magnetotail flux, solar wind pressure, dipole moment and plasma sheet interaction
20 p2919 A72-39546
- Midday auroras and polar cap auroras.
20 p2920 A72-39978
- Pioneer 7 observations of the August 29, 1966, interplanetary shock-wave ensemble.
21 p3104 A72-40481
- Solar wind models of energy transport mechanisms and nonthermal heating requirements, comparing predictions with spacecraft observation
21 p3100 A72-40484
- Characteristics of interplanetary electron inhomogeneities according to observations in the period from 1967 to 1969
21 p3114 A72-41765
- Rarefaction wave generation by solar wind shock wave interaction with magnetosphere, noting geomagnetic field weakening during magnetic storm
22 p3217 A72-41894
- Solar-wind and interplanetary electron measurements on the Apollo 15 subsatellite.
22 p3218 A72-42403
- Simultaneous solar-wind plasma and magnetic-field measurements in the expected region of the extended geomagnetic tail.
22 p3170 A72-42405
- Comparison of solar-flare energy estimates made by analytical and numerical techniques.
22 p3219 A72-42426
- Upper limit of the torque of the solar wind on the earth.
22 p3219 A72-42427
- Magnetic field structure in flare-associated solar-wind disturbances.
22 p3219 A72-42428
- Solar wind noble gases and solar flare emitted Fe group nuclei energetic tracks in chondrite Weston, considering galactic cosmic ray generated tracks
22 p3228 A72-42863
- Solar-wind parameter variation, magnetic activity, and electrons in the magnetospheric tail and outer radiation belt
23 p3283 A72-43367
- Variation of the cosmic-ray gradient during a solar activity cycle
23 p3328 A72-43374
- Electromagnetic instabilities produced by neutral-particle ionization in interplanetary space.
23 p3332 A72-44506
- Interaction of the solar wind with the neutral component of the interstellar gas.
23 p3332 A72-44507
- Energy and mass content of high-speed solar-wind streams.
23 p3332 A72-44508
- Compressions and rarefactions in the solar wind - Vela 3.
23 p3332 A72-44509
- Solar wind velocity determination from radio sources interplanetary scintillation observations, noting magnitude and direction variations with time
23 p3333 A72-44529
- Substorm related changes in the geomagnetic tail - The growth phase.
24 p3397 A72-44856
- Shock waves role in coronal heating, solar wind and energy and material transfer to earth and in solar system
24 p3439 A72-45019
- Hydrodynamic approximation for solar wind nonuniformity in ecliptic plane, noting linear disturbances caused by nonuniform velocity of plasma flow from corona
24 p3435 A72-45077
- Solar wind distortion of stellar anisotropy of galactic cosmic rays, associating annual particle density variation with earth revolution about sun
24 p3435 A72-45090
- Impacting polar plasma thermalization during comet close approach to sun, considering solar wind-comet interaction role
24 p3445 A72-45470
- Solar X rays angular distribution during solar flares, considering anisotropy connection with short wave fadeouts correlation with H alpha flares and X ray bursts center-to-limb variation
01 p0118 A72-10420
- Solar flares far UV radiation time structure correlation with hard X rays
02 p0272 A72-11773
- EUV and soft X ray images of sun from sounding rocket experiments
03 p0415 A72-12934
- Ionospheric effects of X ray flare on 8 July 1968, estimating ionizing radiation spectral characteristics from SID observation
03 p0407 A72-12986
- High energy solar and celestial X ray experiment with OSO 5, measuring spectrum as function of time, intensity and spatial distribution
03 p0353 A72-13044
- High spatial resolution solar X-ray and far UV instruments, employing glancing incidence optics
03 p0353 A72-13045
- Holographically produced zone plates for solar X ray imaging, using Ar laser produced interference figure
03 p0354 A72-13046
- Apodized Fresnel zone plate construction for solar X-ray image formation
03 p0354 A72-13047
- Solar UV and X radiation, considering chromospheric temperature and density profiles and coronal electron densities
03 p0409 A72-13123
- Solar UV line spectrum identification and intensity analysis, emphasizing electron spectra in soft X ray region and forbidden transitions
03 p0420 A72-13124
- Short wavelength continuous solar X-radiation polarization and angular distribution measurements, revealing physical processes in solar flares
03 p0409 A72-13126
- Solar active regions and flares X ray spectroscopic data, observing ionized silicon emission lines
03 p0423 A72-13217
- Solar flare 1.9 A line feature identification from X ray observation by OSO-4 proportional counter spectrometer
03 p0424 A72-13218
- Solar corona X ray data from SOLRAD satellites, detailing spectral energy distribution, ionization balance, continuum radiation and line emission
03 p0410 A72-13219
- Corona X ray emitting structures comparison to photospheric magnetic field distribution
03 p0410 A72-13324
- Cosmic ray energy changes in interplanetary space by model for solar X-ray bursts
03 p0413 A72-13534
- Solar X-ray control of E and sporadic E layers during November 1966-July 1968, discussing blanketing frequency
03 p0413 A72-13535
- Sudden cosmic noise absorption from D region N-h profile during solar X ray flares on 13 April 1966
04 p0566 A72-14512
- Fe line emission during solar X-ray flares recorded by Bragg crystal spectrometers on OSO-6, resolving fine structure components of hydrogenic Ar
04 p0566 A72-14560
- Gamma ray and neutron emissions from sun, considering acceleration of charged particles in solar atmosphere
04 p0566 A72-14724
- Solar disk active centers X ray emission, using rocket mounted pinhole cameras
04 p0567 A72-15164
- Time behavior of temperature and emission measure in X ray flares observed from Vela 5 spacecraft
05 p0709 A72-16518
- Anisotropic angular distribution of solar flare associated hard X-rays
05 p0709 A72-16519
- Solar flare X-ray emission Compton backscattering from Fe lines examination
05 p0710 A72-16720
- Sudden ionospheric disturbance occurrence probability with solar X-ray flares, noting relaxation time
06 p0874 A72-18086
- Ionospheric effects of solar flares, considering flare spectrum below 10 A, flare X-rays relationship to sudden ionospheric disturbances and electron density profiles
06 p0874 A72-18087
- Ionospheric electron density profiles and time variation of electron production rate for X-ray flare of 30 January 1968, observing decrease in effective recombination coefficient
06 p0874 A72-18088
- Rocket astronomy development, reviewing V-2, Aerobee rocket and balloon-rocket flights for solar X rays and flares and galactic and extragalactic experiments
07 p1076 A72-19675

Thermal plasma origin of solar X-ray emission and far UV flash observation during 28 August 1966 proton flare

07 p1060 A72-20013

D region extraionization and solar X-ray flux from vlf data, emphasizing solar spectral shape and use of continuity equation for ionization time history

08 p1227 A72-21116

OSO-H solar X ray instrument for solar flares energy release investigation via thermal and nonthermal electrons X ray emission

08 p1167 A72-21514

Effective electron loss rates in lower D region from ionization changes during solar X ray flares, noting water cluster ions destruction

09 p1376 A72-22369

Energetic solar X-ray burst of 11 February 1970 observed by balloon-borne NaI scintillation detector launched from Antarctica, comparing to OSO 5 data

09 p1377 A72-22930

He-like lines in solar X-ray spectrum observed by Bragg crystal spectrometer, noting absolute wavelengths determination with shaft encoder for angle readout

11 p1714 A72-26572

E layer effective recombination coefficient determination from solar flare enhanced electron density and solar X-ray flux measurements and ionospheric relaxation time constant evaluation

11 p1627 A72-26766

Solar X-rays absorption profiles and residual fluxes in D and E layers during 7 March 1970 eclipse from rocket measurements

12 p1863 A72-27146

Exponential functions model for D region vertical distribution of electron density profiles, taking into account solar X- and cosmic rays

13 p1945 A72-28581

Solar flare X-ray emission occultation observed during 7 March 1970 eclipse by NRL instrument on OSO-5 satellite

13 p2031 A72-29549

E region ionosonde observations to reconstruct ionizing X ray and far UV radiation source distribution over solar disk during March 1970 total solar eclipse

13 p2044 A72-29552

Solar X ray burst analysis from individual quantum/energy and time recordings by Lunokhod 1 spectrometer

13 p2032 A72-29700

Brightenings and surgelike spikes associated with low amplitude soft solar X-ray background flux in H alpha above limb, assessing energy budget

13 p2032 A72-29718

Electron temperature and emission measures during solar X-ray flares, studying effects of gradual and rapid radiation flux increases

13 p2032 A72-29722

Solar long term X-ray emitting regions from grazing incidence X ray telescope onboard OSO-4

13 p1033 A72-29744

High energy electron heating of solar flare plasma with X-ray emission due to thermal and nonthermal bremsstrahlung

13 p1033 A72-29745

Multiplicative factors for energy scale corrections of OSO-3 ion chamber for solar X-ray monitoring

13 p1033 A72-29748

Solar X-ray spectral lines at 1-60 A from coronal ion relative abundances obtained from Jordan ionization equilibrium calculations

13 p2034 A72-29940

Solar X-ray data normalization, using conversion factors independent of incident photons spectrum

13 p2034 A72-29941

Coronal condensation X ray sources from heliograms, discussing relation to active region evolution

14 p2146 A72-30204

Radio bursts and X ray emissions associated with 15-16 November 1970 solar chromosphere flares, noting brightness maximum differences

14 p2146 A72-30483

Solar proton flare induced X ray bursts maximum flux, total radiated energy, electron temperature and emission from satellite measurements

14 p2160 A72-30910

Solar X-ray flux daily changes before and after proton flare, using zero-epoch superposition method

14 p2148 A72-30911

K-2 astrophysical rocket observatory for far UV and X ray solar radiation recording, discussing trajectory, orientation and stabilization, electric and spectrophotographic instrumentation

14 p2163 A72-30970

Rocket-borne spectrometric measurement of small solar flare O VII and Ne IX resonance lines and 5 keV X-ray continuum emission, analyzing data via nonisothermal model

15 p2300 A72-31990

Ion density and electron acceleration region location from satellite-borne solar flare X-ray measurements

15 p2302 A72-32790

Soft X-ray spectral studies of plasma dynamics in solar flares from Bragg crystal spectrometer OSO 6 recordings

16 p2449 A72-33918

Flare-time temperature in soft X-ray sources

17 p2598 A72-34537

ESRO 2 satellite observation of solar X-ray emission from active limb prominence, obtaining temperatures and emission measures as function of time

17 p2608 A72-35085

Soft X-ray and microwave observations of hot regions in solar flares

17 p2608 A72-35089

Correlation studies of solar X-ray and radio bursts

17 p2600 A72-35318

Solar flare initial, explosive and decay phases related to plasma motion, soft X-rays and radio emission

17 p2600 A72-35348

Day to day variation of Schumann resonance frequency and occurrence of Pc 1 in view of solar activity

17 p2548 A72-35464

Nonthermal solar X-ray bursts origin in non-Maxwellian electron fluxes interactions with surrounding plasma, reviewing energy spectra

18 p2721 A72-36093

Time-dependent ionization equilibrium and line radiation under flarelike conditions

19 p2849 A72-37241

Periodic heating mechanism in solar flares

19 p2851 A72-37888

Plasma heating by fast electrons, and nonthermal X rays during solar flares

19 p2851 A72-38063

Ionospheric D region, a sensitive detector of hard X-rays of solar subflares

19 p2852 A72-38628

Photometric analysis of X-ray photographs of sun obtained with rocket-borne zone plate camera in XUV region

21 p3108 A72-41289

X-ray and HF microwave bursts correspondence shown in observations of 24 October 1969 impulsive solar flare and of XUV and radio emissions

21 p3108 A72-41290

Thick target processes during hard X ray emission, noting electron bombardment during solar flare impulsive phase and white light flare optical continuum production

21 p3100 A72-41292

New measurements of the polarization of X-ray solar flares

21 p3101 A72-41293

Solar soft X-rays and solar activity. II - Observational assessment of the role of the type III acceleration mechanism in establishment of the soft X-ray source volume

21 p3101 A72-41294

The decay characteristics of models of solar hard X-ray bursts

22 p3217 A72-42040

The solar X-ray spectrum deduced from a proportional counter experiment and the resultant production of ionization in the mesosphere

22 p3170 A72-42368

Satellite measurements of solar X-ray flux and their use for interpretation of sudden ionospheric disturbances

22 p3219 A72-42884

Coronal condensation X ray sources from heliograms, discussing relation to active region evolution

23 p3328 A72-43234

A comparison of field-strengths of 164 kHz radio waves transmitted from Tashkent and received at Ahmedabad with flare-time solar X-ray emissions measured in satellites

23 p3262 A72-43275

The effective recombination coefficient in the ionospheric D region

23 p3283 A72-43364

Signal-to-energy conversion function in the photometry of solar soft X-radiation with broad-band detectors

23 p3329 A72-44238

Exponential functions model for D region vertical distribution of electron density profiles, taking into account solar X- and cosmic rays

24 p3397 A72-45081

SOLDERED JOINTS

Fatigue failure tests of soldered joint in solar cell interconnector designs under extended temperature cycling

05 p0615 A72-16552

Electrical resistance and thermal joint conductance measurements at perfect contact interfaces from electroplating, soldering and explosive bonding

05 p0666 A72-16859

Printed circuit boards and RC elements soldered connections reliability under high temperature and excessive current conditions, discussing test procedure and evaluation criteria

07 p0994 A72-19247

SOLDERING

High alumina ceramics metallization and hard soldering to metals for manufacturing vacuum jacket of transmitting thermionic tubes

10 p1488 A72-24642

B-Al metal matrix composites joining together and to Al and Ti, considering soldering, brazing, bonding and mechanical fastening

11 p1638 A72-25388

Microwelding and microsoldering equipment control systems, discussing ac phase cut-off, dual pulse, dc and intermediate frequency units

11 p1639 A72-25810

Investigation of the possibility of using radiant solar energy for welding and soldering of materials

24 p3407 A72-45126

SOLENOID VALVES

Proportional-integral control of reactants supply for hydrazine-oxygen fuel cells with pulse controlled solenoids

06 p0867 A72-18290

SOLENOIDS

Cu clad N8-Ti wire wound superconducting solenoids with large fields at 1.6-5.2 K

10 p1446 A72-23762

High reliability long life grid pulsed L band traveling wave tube with integral solenoid focusing for high power radar use

14 p2089 A72-31046

Representation of solenoidal vector fields in bounded domains by poloidal and toroidal scalar potentials, discussing applications in fluid mechanics, elastic vibrations and electromagnetic theory

23 p3313 A72-43716

SOLID LUBRICANTS

Plasma jet technique for self lubricating antifriction Ni, Sn or Cu coatings for MoS2 particle oxidation protection

04 p0527 A72-15664

Solid lubricant antifriction properties test methods and measuring apparatus design for wide temperature range

05 p0665 A72-16096

Molybdenum disulfide and layer lattice materials lubricating mechanism and effectiveness from sulfur atoms strong polarization, using scanning electron microscope

06 p0822 A72-18157

Heat resistance of magnesium, barium and calcium fluorides as solid lubricants in air, hydrogen and water vapor at 100-1100 C

06 p0836 A72-18433

Solid lubrication - Conference, Denver, August 1971

06 p0823 A72-18583

Friction and wear characteristics at high temperature of plain bearing embedded with pellets of graphite, sodium fluoride and tungsten disulfide lubricating mixture

06 p0823 A72-18584

Thin solid film lubricants for use with roller bearings at ambient and elevated temperatures, discussing surface treatment

06 p0823 A72-18585

Molybdenum disulfide lubricating film and wear-in study by scanning electron microscopy and testing machine

06 p0836 A72-18586

Lubrication with thin molybdenum disulfide solid film under various temperatures and atmospheric pressures, examining friction and lifetime

06 p0823 A72-18587

Molybdenum disulfides with varying purity level evaluated as solid lubricants and as lubricant additives in standard lubricating testing devices

06 p0836 A72-18588

Solid lubricant coatings adherence to porous materials, discussing porosity acquired by sulfuration treatment in melted salts bath on soft steel surface

06 p0823 A72-18590

Resin bonded solid lubricant film thickness optimization from statistical analysis of bench and machine element test data

06 p0823 A72-18591

Methyl phenyl polysiloxane bonded solid film lubricants, discussing air curing at ambient temperatures and performance tests

06 p0836 A72-18592

Wear behavior of molybdenum disulfide and antimony trioxide bonded solid film lubricant with air curing silicone resin, noting temperature and pretreatment effects

06 p0823 A72-18593

Graphite fluoride as solid lubricant, investigating friction coefficient and wear resistance

06 p0837 A72-18598

Oxidation resistant solid lubricants for high temperature air and gaseous environments applications, considering oxide and fluoride coatings with silicate additives for wear life improvement

06 p0837 A72-18600

Lubricating mixtures of mineral oil with inorganic phosphates, hydroxides and sulfides, discussing lubrication mechanism and physical properties

06 p0837 A72-18603

Molybdenum disulfide lubricating effectiveness improvement with finer particles at aggravated sliding conditions, suggesting surface roughness qualifications

06 p0837 A72-18605

Adherent solid lubricant films electrochemical deposition, noting method application to metal forming techniques

06 p0824 A72-18606

Sputtered molybdenum disulfide lubrication on polished metal surfaces with low friction coefficient, strong adherence, high density and small particle size

06 p0824 A72-18607

Graphite and molybdenum disulfide powders lubricating properties relation to surface crystalline orientation

06 p0824 A72-18608

Solid lubricant additives effects in oils and fats, discussing molybdenum disulfide and zinc pyrophosphate solid film formation on metal surfaces under contact friction conditions

07 p1024 A72-20395

Soviet monograph on solid inorganic compounds as high temperature lubricants covering powder lubricants mechanism under different friction conditions, gas media, temperature effects, etc

08 p1191 A72-20913

Soviet book on temperature resistance of lubrication boundary layers and solid lubrication coatings during friction of metals and alloys

08 p1179 A72-22023

Al alloy and brass deformation compression tests inadequacy for friction determination and boundary agents, EP additives and hydrodynamic and solid lubricants evaluation

08 p1181 A72-22195

High vacuum mass spectroscopic analysis of volatile products released under friction from solid synthetic resin lubricants with molybdenum disulfide as antifriction filler

12 p1835 A72-28199

Chemical reactions between solids during boundary friction, presenting literature review on mechanochemical or tribo-chemical reactions between solid lubricants and metal surfaces

[ASLE PREPRINT 72AM 1] 13 p1964 A72-28969

Ice adhesive shear strength to steel bearing surfaces coated with bonded solid lubricants, describing low temperature test apparatus and results

[ASLE PREPRINT 72AM 4] 13 p1964 A72-28970

Molybdenum disulfide-tantalum compact solid lubricant wear rate as function of load and sliding velocity, presenting test data statistical interpretation

[ASLE PREPRINT 72AM 15] 13 p1964 A72-28972

Metallic, ceramic, polymeric, composite and solid film lubricant friction and wear properties and testing

[ASME PAPER 72-DE-28] 14 p2108 A72-30869

Lubrication with solids

19 p2807 A72-37771

Investigation of the lubricant properties of molybdenum disulfide, graphite, and phthalocyanine

19 p2823 A72-38094

Book - Solid lubricants and self-lubricating solids

21 p3073 A72-41529

Influence of the protective medium during sintering on the properties of iron-base cermets

23 p3299 A72-43289

SOLID NITROGEN

Spatial distribution of nitrogen molecular beam scattering from solid nitrogen surface as function of beam energy and incidence angle

16 p2430 A72-33063

SOLID PHASES

Germanium nitride thermolysis, discussing allotropic alpha and beta phases stability and activation energies

01 p0023 A72-10191

Transmission electron microscopic investigation of heterogeneous nucleation of Al-Ag alloys metastable gamma prime phase, noting association with four dislocation types

01 p0083 A72-10209

VT22 high strength Ti alloy beta phase decomposition kinetics studies under heat treatment, noting omega and alpha phases role for low plasticity

02 p0244 A72-12247

Heat treatment, quenching and aging caused metastable and stable alpha and beta structures effects on nitrogen diffusion rate in Ti alloy during nitriding

02 p0244 A72-12248

Ti-Cr alloys omega phase formation by measurements of hardness, Young modulus and internal friction

02 p0246 A72-12672

Superalloy compositions prealloyed powders strengthening by secondary gamma phase precipitation, noting high temperature strength without ductility loss after thermomechanical treatment and aging

02 p0247 A72-12856

Solid phase friction welding, discussing metallurgy and engineering applications

03 p0362 A72-12990

X ray diffraction analysis of dilute Nb-C alloys epsilon phase, discussing Bravais lattice and unit cell dimensions

03 p0375 A72-13932

Sigma phase formation in chromous ferrite, investigating vacuum diffusion, hot and cold working, welding and additives effects

03 p0375 A72-13940

Phase composition and structure of Be alloys containing Ru, Os, Rh or Ir, noting isomorphous beryllides existence

03 p0375 A72-13942

Ductile plastics solid phase forming, discussing forging, extrusion deep drawing and rubber cushion forming techniques

04 p0538 A72-15451

Transition metals distribution of IV-VI and VIII a groups in metastable refractory nickel alloys gamma and gamma-prime phases

07 p1012 A72-19678

Nb-Mo alloys behavior in aggressive boron containing medium at high temperatures, relating boride phases growth rate to component percentages

07 p1012 A72-19680

Aluminized layer phase and chemical composition on heat resistant iron and nickel alloys

07 p1013 A72-19748

Hf-Co-Al system phase equilibria determination by partial microstructural and X ray analysis

07 p1017 A72-19991

Transition metal borides chemical bonding mechanism from Nb and Cr boride phases thermal emf and expansion, resistivity, Hall coefficient and carrier mobility

07 p1017 A72-19992

Ni-Cr-Ti alloy hardening during intermetallic phases precipitation, discussing atom segregations, Guinier-Preston zones and fcc and hcp lattices

07 p1019 A72-20152

Heat treatment, water quenching and aging effects on Ti-V alloys hardening and structural properties, discussing omega phase formation

07 p1023 A72-20667

Soviet papers on phase transformations covering supersaturated solid solutions decomposition, Nb-Al-Ge system phase diagram, martensite decomposition, etc

08 p1186 A72-21776

Explosive loading effect on Cr-Ni stainless steel structure with electron microscope study of gamma, alpha and epsilon phases

08 p1187 A72-21780

Cold shortness of W and related refractory metals, noting oxide phases and impurities effects on mechanical properties temperature dependence

09 p1326 A72-22226

Electrical conductivity relationship to phase composition in thin CdTe films deposited on mica bases and annealed in Cd vapor

09 p1367 A72-22420

Fe-Cr-Mn alloys structural changes during high temperature oxidation, noting subscale layer thickening and alpha phase detection after heat treatment

11 p1655 A72-25498

VT22 high strength Ti alloy beta phase decomposition kinetics under heat treatment, noting omega and alpha phases formation effect on ductility

11 p1660 A72-26133

Heat treatment produced metastable and stable alpha and beta structures effects on nitrogen diffusion rate in Ti alloy during nitriding

11 p1660 A72-26134

Lunar and terrestrial pyroxenes phase structure electron microscopic investigation, using ion-thinned samples

11 p1725 A72-26952

Ti alloy metastable phases classification, including alpha-prime, secondary alpha, omega, beta and alpha phases

12 p1828 A72-27290

Electrochemical conditions for separation of gamma prime phase from heat resistant Ni alloys by electrolysis

12 p1828 A72-27446

Angular annihilation photon distribution curves from positron-electron annihilation method for metallic phase interaction with crystal lattice in synthetic diamonds

12 p1833 A72-27764

Papers on high pressure-high temperature research techniques covering laboratory procedures for control, calibration and measurement of solid-vapor and liquid-vapor equilibria

12 p1778 A72-28103

Liquid quenched Sb-transition metal binary alloy constitution, finding metastable phases in quenched Cr-Sb and Mn-Sb alloys

13 p1975 A72-28672

Two phase structure solidification of monovariant eutectic Co-Cr-C alloys near pseudobinary cut

13 p1976 A72-28674

Thermal effects on phase structure of welded joints of Al alloy with Cu addition

13 p1978 A72-29022

Ti-Ni alloy strengthening by titanium nickelide intermetallic epsilon phase formation control via heat treatment

13 p1981 A72-29829

Diffusion kinetics and thermodynamic characteristics of solid phase interactions in systems cobalt-transition metal carbides

13 p1981 A72-30104

Zirconium oxycarbide formation, solubility and one phase properties by X ray diffraction, chemical and metallographic analyses

13 p1982 A72-30107

Ni, Si and Mn alloying effect on structural transformations, phase composition and mechanical properties of cast Cr-Ni steels

14 p2114 A72-30273

Zr-Cu-Mo system phase diagram from microscopy X ray analysis and mechanical tests, noting beta solid solution transformation into alpha, omega and beta phase mixtures

14 p2122 A72-30978

Electronic energy band structures for alpha and gamma phase Ce, using exchange potential and plane wave method

15 p2293 A72-32227

Solid phase reaction kinetics in zirconium beryllide alloys with Ta and Nb at 900-1400 C, noting Be diffusion effect

16 p2408 A72-33535

Geometric/chemical model of lattice dimensions of Laves phases of binary alloy bcc and fcc structures

16 p2409 A72-33801

Si stabilization of laves and intermediate phases in Nb-Fe-Si and Nb-Co-Si systems

16 p2409 A72-33805

Amorphous structure analysis of sput quenched Cu-Zr noncrystalline phase, using electron microscopy

16 p2410 A72-33814

As-quenched and aged form of omega phase in Ti-Nb alloys investigated by electron microscopy and X ray diffraction

16 p2410 A72-33818

Electron diffraction patterns of previously deformed Ti-Nb alloy containing unequal populations of omega phase variants, noting anisotropy

17 p2566 A72-34673

Solid-gas phase equilibria and thermodynamic properties of cadmium selenide

17 p2511 A72-35329

Formation of deformation martensite in Fe-Ni-C alloys which do not undergo transformation on cooling

21 p3066 A72-40270

Peritectic solid phase transformations in cast homogenized Al-Cu-Li-Mn-Cd alloy, noting Li strengthening effect

23 p3303 A72-44099

SOLID PROPELLANT IGNITION

Boron containing solid propellant combustion efficiency and fuel-air ratio determination from particle laden plume nonequilibrium effects in ducted subsonic flow

[AIAA PAPER 72-36] 05 p0750 A72-16972

Critical conditions for self ignition of solid fuel particles suspended in gas

06 p0903 A72-18203

Solid propellant reaction kinetics at gaseous fuel and catalyst-containing ammonium perchlorate interface, studying ignition and deflagration

07 p1051 A72-19367

Heterogeneous composite solid propellants ignition behavior under exposure to hot oxidizing gas, using gas phase model with species and energy radial diffusion

07 p1051 A72-19726

Solid propellant gas generators, discussing propellant processing, grain, ignition, insulation and restrictions

09 p1263 A72-23600

Boron ignition and combustion in air-augmented rocket afterburners

17 p2636 A72-34902

Combustion of solid-propellant layer in contact with a solid-oxidizer layer

18 p2720 A72-36239

Ignition moment of solid propellant particles monodispersive aggregate uniformly distributed in gaseous oxidizer

19 p2879 A72-37359

Ignition of a mixture of ammonium perchlorate and starch by incandescent wires

19 p2847 A72-37367

Measurements of radiation flux at the moment of ignition of a solid propellant

[ONERA, TP NO. 1067] 19 p2800 A72-37759

SOLID PROPELLANT ROCKET ENGINES

NT ALGOL ENGINE

Solid rocket on-off and acceleration control, discussing motor concepts, thrust modulation and potential technology applications

[SAE PAPER 710767] 01 p0116 A72-10262

Nondestructive radiographic tests for void and un-bond detection in Scout solid propellant rocket motors

01 p0114 A72-10812

French missile and rocket weapon systems based on solid propellants, describing various ground-to-ground, short and medium range, antitank and other missile types 03 p0441 A72-13644

Low cost large solid rocket boosters technology, discussing propellant, case material, insulation, nozzle ablatives and thrust vector control 04 p0565 A72-14435

Dynamic characteristics of buoyant low altitude clouds formed by solid rocket motor launches, determining initial temperature by motion pictures combined with conservation equations [ASME PAPER 71-WA/FE-33] 05 p0724 A72-15923

Optimal design criteria for multigrain solid propellant rockets, considering powder weight, burning time and combustion chamber length 05 p0704 A72-16351

Plane two dimensional flow in channel of rocket engine with solid propellant combustion, obtaining burning rates 06 p0867 A72-18207

Nonequilibrium chemistry effects on electrical properties of solid propellant rocket motors turbulent afterburning exhaust plumes, describing free electron sources 07 p0935 A72-19359

Solid propellant rocket engine thrust vector control by four movable exhaust nozzles, nozzle exit cone secondary injection and flexible bearing nozzle 13 p0206 A72-28928

Waxwing solid propellant rocket motor design for third stage propulsion of Black Arrow satellite launcher 13 p0206 A72-28932

Solid propellant pulsed plasma microthruster performance tests, describing engine design and operation [AIAA PAPER 72-460] 13 p0206 A72-28945

Launch center for solid-liquid propellant rocket probes, Diamant and Europa 2, describing payload preparation hall [DGLR PAPER 72-0137] 13 p1939 A72-28962

Metallized solid propellants burning rate augmentation by internal ballistics effect of spinning rocket motor, deriving relationship between burning rate, pressure level and acceleration 13 p0205 A72-29302

Two stage solid propellant sounding rocket, discussing engine design, operation and tests 13 p0205 A72-29859

Composite and double base solid propellant rocket motors storage, considering ingredients and materials compatibility and ignition temperatures effects on spontaneous inflammation potential 14 p2144 A72-30761

Russian book on solid propellant rocket engines covering combustion chamber and nozzle layouts, working cycle and thrust control 16 p2443 A72-33350

Pressurized crack behavior in two-dimensional rocket motor geometries. 17 p2596 A72-34203

German book - Solid-propellant rocket engines I: Introduction and fundamentals 17 p2597 A72-35453

Linear theory of a solid propellant rocket motor with modulated exhaust 24 p3433 A72-45116

SOLID PROPELLANTS

NT CASE BONDED PROPELLANTS

NT COMPOSITE PROPELLANTS

NT DOUBLE BASE ROCKET PROPELLANTS

NT METAL PROPELLANTS

NT SOLID ROCKET PROPELLANTS

Aluminized solid propellant transient burning rate augmentation as function of acceleration vector magnitude and orientation, applying centrifugal accelerations of zero to 140 g 01 p0114 A72-10378

Pure solid and composite propellants combustion theory based on laminarized solutions to energy and flow conservation equations 02 p0270 A72-11766

Chemical efficiency improvement of aluminum combustion with nitric acid in organic solid fuel 03 p0405 A72-13540

Burner design for solid propellants burning properties dynamic testing, using broadband tuned Helmholtz resonator for instability onset delay 04 p0509 A72-15497

Solid propellant flame spectral and temporal details during unstable and stable combustion, using middle infrared spectrometer [AIAA PAPER 72-32] 05 p0703 A72-16896

Wall thermal radiation influence on solid propellants burning rate in electrically heated tube furnace, noting correlation with laminar flame theory [AIAA PAPER 72-35] 05 p0703 A72-16938

Solid propellant reaction kinetics at gaseous fuel and catalyst-containing ammonium perchlorate interface, studying ignition and deflagration 07 p1051 A72-19367

Quench combustion studies with two dimensional propellant sandwiches with ammonium perchlorate oxidizer and various binders, using high pressure combustion vessel for deflagration characteristics determination 07 p1051 A72-19727

Barium styphnate replacement for discontinued SR-4990 smokeless powder as propellant base charge in MK 24 actuator 08 p1222 A72-20784

Automated mechanical system for solid propellant sheet stretch tests in two directions as function of time 08 p1147 A72-21331

Small perturbation stability of discontinuous solution of equations of motion for solid fuel combustion processes 08 p1253 A72-21463

Solid propellant gas generators, discussing propellant processing, grain, ignition, insulation and restrictions 09 p1263 A72-23600

Parallel rail solid fuel pulsed electric microthruster performance, noting mathematical model for mass ablation and plasma acceleration mechanism [AIAA PAPER 72-458] 11 p1708 A72-26194

Solid propellants oscillatory burning with gas phase time lag, solving nonsteady governing differential equations by numerical integration 13 p0205 A72-29301

Metallized solid propellants burning rate augmentation by internal ballistics effect of spinning rocket motor, deriving relationship between burning rate, pressure level and acceleration 13 p0205 A72-29302

Solid propellants burning rate dynamic response to rapid pressure changes, discussing equations applicability to combustion extinction prediction as function of pressure decay rate 13 p0205 A72-29304

Effective stabilizer content measurement in smokeless powder propellants, discussing nitrogen dioxide generation by cellulose nitrate and glycerin trinitrate decomposition 14 p2144 A72-30755

Double base solid propellants life determination from accelerated aging tests at elevated temperatures, discussing surface properties effect on weight loss and autocatalytic decomposition 14 p2144 A72-30757

Carboxy-terminated polybutadiene/ammonium perchlorate base solid propellants aging properties under long time storage conditions at 243-353 K, considering mechanical, dimensional and combustion properties 14 p2145 A72-30763

Insulation and bonding materials effects on double base solid propellants stability, using vacuum reactivity testing technique 14 p2145 A72-30766

The effects of various cure cycles upon the viability of *Bacillus subtilis* var. *niger* spores within solid propellant. 18 p2652 A72-36437

Qualitative determination of organometallic substances in solid propellants by thin layer chromatography 23 p3262 A72-43598

Fracture mechanics and cumulative damage of simulated solid propellant under dynamic loads, obtaining low cycle fatigue curve 23 p3325 A72-43706

The transient processes in hybrid solid propellant combustion chamber throttled by supersonic nozzle. 24 p3434 A72-45198

SOLID ROCKET PROPELLANTS

NT DOUBLE BASE ROCKET PROPELLANTS

NT METAL PROPELLANTS

Fracture analysis of two dimensional thermal loaded solid propellant rocket grain models under cooldown [SESA PAPER 1927A] 02 p0270 A72-11513

Na and K trace amounts detection in Al based solid rocket propellants by neutron activation analysis, using gamma ray spectroscopy for nondestructive analysis 02 p0270 A72-11959

Combustion of composite solid propellants with ammonium perchlorate base and pyrolyzable binder, investigating perchlorate grain size, binder concentration and catalyst effects 06 p0867 A72-17574

Solid charge design for hybrid rocket engine with constant liquid propellant component consumption, deriving differential equation for perforated grain burning rate 07 p1053 A72-18994

Particle mass spatial distribution effect on particulate damping of combustion acoustic vibrations in solid rocket combustors 08 p1224 A72-21617

German monograph on flight performance optimization of solid propellant rockets covering thrust values, burning time, rocket design and orbits within earth atmosphere 10 p1550 A72-23770

Solid teflon pulsed plasma thruster quasi-steady and short pulse discharge operations, discussing propulsion system performance and erosion behavior [AIAA PAPER 72-459] 11 p1709 A72-26195

Combustion surface acoustic admittance model of blended solid propellant with allowance for foam zone inertia and solid/gas interface reactions 12 p1889 A72-27980

Solid rocket propellant combustion instability research, discussing data acquisition and reduction, motor instrumentation, motors and burning rate measurements 13 p0204 A72-28929

Solid rocket propellants storage life analysis and prediction by mathematical modeling of physical-chemical failure generating processes 14 p2145 A72-30762

Case bonded solid rocket propellants mechanical strength characteristics determination by photoelastic stress measurements or viscoelastic calculation 14 p2145 A72-30765

High efficiency hybrid rocket motor based on polyester fuel and RFNA oxidizer, determining correlation between burning rate, oxidizer and total flow rates 15 p2297 A72-31207

German book - Solid-propellant rocket engines I: Introduction and fundamentals 17 p2597 A72-35453

Investigation of the resonant combustion of a rocket charge with longitudinal slots 18 p2720 A72-36241

Solid rocket propellant erosion burning in turbulent gas flow, discussing burning velocity dependence on Pobedonostsev criterion 19 p2878 A72-37351

Nonlinear equations solutions for interior ballistics parameters of solid rocket propellants combustion during rocket engine nozzle opening 19 p2878 A72-37352

Erosion combustion effect on unsteady solid rocket propellant burning stability during engine nozzle opening, noting combustion velocity and surface temperature 19 p2879 A72-37353

Development of a solid fuel on a polyurethane basis for a hybrid rocket propulsion system with 98% nitric acid as oxidizer 20 p2962 A72-39416

Burn-up rate of a solid-propellant slab in contact with a solid-oxidizer layer 22 p3245 A72-43180

A nonacoustic wave instability of processes in a solid-fuel engine 22 p3217 A72-43182

SOLID ROTATION

U ROTATING BODIES

SOLID SOLUTIONS

Carbon atoms thermodynamic properties in bcc and fcc Fe-Si-C solid solutions from equilibrium measurements with hydrogen-methane gas mixtures as function of temperature and carburizing gas composition 01 p0083 A72-10207

Coarse grained dispersion strengthened Al alloys, investigating solute solutions effects on steady state creep behavior 01 p0087 A72-11025

Matrix hardening in dispersion strengthened powder products, discussing dispersion, grain boundary and solid solution hardening 02 p0241 A72-11457

Atomic structural mechanism of solid solution decomposition by nucleation and equilibrium phase particles in Fe-Co-Ti alloy, using X ray analysis and transmission microscopy 02 p0242 A72-12008

Niobium anomalous oxidation below 600 C, noting suboxide formation between solid solutions and heat resistance reduction 02 p0243 A72-12214

Titanium and aluminum variations effects on eta and gamma prime solvus temperatures and on mechanical properties of iron-nickel superalloy 02 p0245 A72-12508

Fan shaped precipitate formation during supersaturated Al-Zr solid solution decomposition, discussing interpretation as grain boundary migration 02 p0247 A72-12820

Niobium-oxygen-nitrogen system solid solution, noting gas composition effects on hardness and electrical resistivity 03 p0369 A72-12958

Nb-Mo-N solid solution nitrogen solubility equilibrium at various temperatures and pressures 03 p0370 A72-12962

Ta and Nb addition effects on W solid solution strengthening, determining W-Nb-Ta alloys phase diagram and melting point 03 p0375 A72-13943

Y-Mn-Al ternary alloy solid solution phase diagram isothermal section construction from X ray structural data 03 p0376 A72-13945

Fibrous structure of precipitates produced at bottom of trace due to friction in work hardened Al-Cu alloy solid solution

03 p0376 A72-13970

Yield stress of solid solution iron and Fe-Ge alloys with bcc structure, obtaining interaction energy between solute atoms and screw dislocation

03 p0402 A72-13974

Fine structure of Mo-Re alloys single crystals in solid solution region as function of Re content

03 p0377 A72-14019

Temperature dependence of X ray interference lines for Al-V alloy obtained at high cooling rate, noting metastable solid solution thermal stability

03 p0377 A72-14022

Ni-C solid solution, determining room temperature neutron irradiation effects on C distribution during decomposition

03 p0378 A72-14251

Statistical mechanical calculation of thermodynamic properties of interstitial solid solutions involving second nearest neighbor solute atom mutual interactions based on Kirkwood expansions

03 p0459 A72-14252

Supersaturated semiconductor solid solutions decay kinetic equations and time constants, noting free current carriers effect

04 p0561 A72-15081

Ni-Mo-N system alpha-solid solution thermodynamic analysis, deriving reaction enthalpies/entropies, free energy and interaction coefficients

05 p0676 A72-16795

Alloying elements effects upon iron mechanical properties, investigating lattice parameters, temperature dependence of yielding and plastic flow, solid solution strengthening and softening, etc

05 p0676 A72-17101

Electron transmission microscope study of quenched Mo-N alloys supersaturated solid solution low temperature aging behavior, investigating recovery processes

06 p0830 A72-18056

Short range order and X ray diffused scattering in Ti-WC solid solution, using least squares method

06 p0834 A72-18741

Solid solution yield strengthening and weakening of V-Ti alloys, investigating strain rate sensitivity temperature dependence as indication of two deformation mechanisms

07 p1021 A72-20434

Bcc solid solutions formation in Cr-W binary alloys, investigating interface reaction and two phase grain boundary diffusion by X ray diffraction and microscopy

08 p1185 A72-21246

Precipitation effect on microstructure, coercive force, resistivity and cell formation changes in heterogeneous decomposition of supersaturated solid solutions and aging alloys

08 p1218 A72-21777

Nonstoichiometric solid solutions based on ZrC and NbC, investigating microhardness variation due to differing valences of atoms in metal sublattices

08 p1188 A72-22100

Cast Nb alloys plasticity enhancement by heat treatment, discussing solid solution decay kinetics and carbides composition of Nb-Mo-Zr-C system

09 p1327 A72-22229

Opaque mineralogy of Luna 16 soil sample, emphasizing compositional variations of Fe-Ti-Cr-Al-Mg spinels

09 p1380 A72-22261

Transition metal superconductors transition temperatures survey, considering d-band solid solution alloys and intermetallics and ferromagnetic element compounds

09 p1367 A72-22552

X ray K absorption edges in binary solid solutions of Co, Fe and Ni with localized hole increases

09 p1371 A72-22846

Al alloys solid binary solution soft X ray emission spectra interpretation by rigid band and virtual bound state models

09 p1371 A72-22847

Environment and grain size effect on steady state creep and creep rupture properties of Ni-W solid solution

09 p1331 A72-23381

Mo-Zr solid solutions internal bonding, discussing diffusion controlled process and hardness dependence on Zr

10 p1494 A72-23833

Differential sputtering yield of Ni-Cu alloy solid solution bombarded by Ar ions

10 p1495 A72-24057

Lattice source interference method for detection of X ray diffraction in Al-Zn solid solutions, taking into account precipitation effects

10 p1499 A72-24981

Polarization characteristics of ferroelectric barium strontium titanates in solid solution at 4-100 K

10 p1527 A72-24984

Temperature dependence of Ni and Ni alloys and solid solutions microhardness, noting strengthening effect of Ti, Cr, Al and B additions

11 p1654 A72-25491

Solid solutions of stabilized Zr in cubic form prepared from zirconium and yttrium oxide mixture by ammonia precipitation and heat treatment

11 p1660 A72-26486

Fe-Mo solid solutions transient creep behavior as function of applied stress, noting temperature effect

11 p1662 A72-26656

Carbon solubility in Nb at 1500-2150 C, determining saturation concentrations from electrical resistivity vs reaction time curves

11 p1662 A72-26740

Thermodynamic description of metal rich side of Nb-Mo-N solid solution, determining equilibrium nitrogen solubility as function of pressure and temperature

11 p1664 A72-26842

Critical resolved shear stress and solute atom concentrations relationship in solid solution hardening of metal crystals

12 p1853 A72-27101

Electron microprobe analysis of solute segregation near grain boundaries in Al-Zn-Mg alloy after quenching and aging heat treatment

13 p1973 A72-28652

High temperature steady state tensile creep behavior of Ni-W solid solutions, showing creep rate relation to stress and stacking fault energy

13 p1975 A72-28668

Al-Zn alloy supersaturated solid solution decomposition during aging, studying single crystal lattice characteristics via X ray diffusive scattering techniques

13 p1976 A72-28902

Tin lead telluride rock salt structure solid solutions phase stability at 356-500 C, using room temperature lattice parameter measurements

13 p1913 A72-29750

Zirconium oxycarbide formation, solubility and one phase properties by X ray diffraction, chemical and metallographic analyses

13 p1982 A72-30107

Mechanical strength of interstitial solid tantalum-oxygen solutions obtained by electron beam fusion, thermal cycling and saturation as function of temperature and oxygen contents

14 p2112 A72-30163

Tungsten and carbon combined solubility in solid niobium at 2000, 1700 and 1100 C

14 p2113 A72-30165

Room temperature negative photoconductivity of p-type ZnTe-CdTe solid solutions mixed crystals within model with electron and hole capture levels

14 p2141 A72-30173

Hydrogen gas solubility measurement in solid Mo at atmospheric pressure and 905-1521 C, noting quasi-regular linearity of Arrhenius plot

14 p2113 A72-30246

U-Zr-Nb and U-Nb-Mo alloys gamma solid solution phase isothermal transformation kinetics at 500-600 C from dilatometric, microstructural and X ray analyses, noting decomposition

14 p2114 A72-30403

Mutual solid solubilities of rare earth metals with Zr extended by splat quenching, noting metastable low temperature allotropic forms of solid solutions

14 p2119 A72-30609

Alpha solid solution of nitrogen in Nb-Mo alloys, obtaining excess partial quantities and activity and interaction coefficients at high temperatures

14 p2121 A72-30773

Decomposition mechanism of Cn, Ag and Au solid solutions in InAs single crystals, using isotopic radiography

14 p2143 A72-30961

Nb-Ti-Zr-Hf system phase diagram from X ray analysis, observing beta solid solution below solid curve

14 p2122 A72-30977

Phase composition of Nb-O-Hf and Nb-O-Zr ternary alloys, noting O solubility decrease

14 p2122 A72-30980

Mo-W-C system high temperature phase equilibria from X ray and microstructural analysis, noting decrease of C solid solubility with temperature

14 p2123 A72-30984

Binary systems phase diagrams qualitative and quantitative analysis based on free atoms electron state energy ratios, formulating solid solubility criterion

14 p2123 A72-30994

Russian papers on light and nonferrous alloys structure and properties covering phase diagrams, alloying effects, reduction, crystallization and recrystallization, solid solutions decomposition, etc

14 p2123 A72-31027

Phase equilibrium of Mg base solid solutions of Mg-Li-Sn system at 200-500 C, analyzing microstructure, microhardness and electrical resistivity

14 p2124 A72-31029

Mn, Zr and Cr alloying effects on grain size and solid solution decomposition of cast Al-Zn-Mg alloy bars

14 p2125 A72-31039

Surface energy effect on alloy structure formation, analyzing crystal growth and formation from supersaturated solutions

15 p2253 A72-31221

Russian papers on alloying and properties of heat resistant alloys covering creep, solid solution and dispersion hardening, chemical interactions and protective coatings

15 p2254 A72-31557

Chemical interaction within crystals for generation of stacking fault vacancies and phenomena associated with solid solution microheterogeneity dislocations discussing heat resistance

15 p2254 A72-31558

Structural decomposition and hardening of supersaturated Al-Cu, Al-Cu-Ag, Al-Zn, Cu-Sn and Cu-Ni-Co solid solutions

15 p2255 A72-31565

Concentration dependence of interdiffusion coefficient in binary metallic systems with continuous and bounded solid solutions

15 p2243 A72-31572

Solution kinetics of secondary phases in cast dendritic and nondendritic Mg-Zn and Mg-Zn-Zr alloys, using cylindrical and spherical diffusion models

15 p2257 A72-32119

Ti-Mo binary solid solution, investigating superconducting transition temperature, lattice instability and electron-to-atom ratio by calorimetric measurements

15 p2295 A72-32544

Heat capacity data analysis for solid solutions of superconducting Nb-Ti system, investigating electronic structure

15 p2296 A72-32692

Co-Cr-C system carbon activity and solubility at 950-1200 C, deriving equation for temperature dependence and solid solution-carbide precipitation zone boundaries

16 p2407 A72-33441

Al-Mg solid solution creep at 570-800 K, discussing creep rate controlling mechanism due to Mg atoms interactions with dislocations

16 p2407 A72-33442

Strain rate and temperature effects on supersaturated Al-Cu-Mg solid solution mechanical properties considering ultimate tensile strength and hardening

16 p2407 A72-33443

Grain-size dependence of Snoek peaks in niobium

17 p2566 A72-34678

High temperature solid-solubility limit and phase studies in the system tantalum-oxygen

17 p2567 A72-34733

High-temperature resistant cobalt alloys

17 p2567 A72-35171

Thermodynamics and phase relations in refractory metal solid solutions containing carbon, nitrogen, and oxygen

18 p2699 A72-36576

Phase structure and solution kinetics of cast and wrought Al alloys after plastic deformation by rolling

18 p2700 A72-36583

Diffusion in the nickel-rich, Ni-Al solid solution at 1260 C

18 p2701 A72-36593

Thermodynamic description of the metal-rich part of the system niobium-molybdenum-nitrogen

18 p2701 A72-36597

Solid-state phase transformations

19 p2815 A72-37442

Characteristics of temperature dependences for the thermal conductivity coefficients of niobium-zirconium solid solutions

19 p2817 A72-37739

Electrical and thermoelectrical effects in GaAs-InAs solid solutions

19 p2844 A72-37752

Phase diagrams of AlSb-GaSb and InAs-GaAs systems, noting mixing energy for liquid and solid phases

19 p2845 A72-38207

Interaction of titanium diboride with titanium disilicide and silicon at high temperatures

19 p2819 A72-38284

Formation of fluorine-containing solid solutions based on barium titanate

19 p2845 A72-38407

X-ray analysis of iron-chrome solid solutions

19 p2821 A72-38572

Activity-composition relations in the fayalites-forsterite solid solution between 900 and 1300 C at low pressures

20 p2915 A72-39178

Decomposition, solubility and coherent phase stability of modulated structure Co-Ni-Ti system at high nucleation temperatures

20 p2939 A72-39312

Investigation of solid solution decay in cobalt-titanium, iron-cobalt-titanium-aluminum and iron-nickel-titanium-aluminum alloys

20 p2939 A72-39314

Interdiffusion in nickel-molybdenum and palladium-molybdenum systems 20 p2939 A72-39315

The effect of Si, Zr, Al and Mo on the structure and strength of Ti martensite. 20 p2941 A72-39792

Effect of alloying on the decay of an aluminum-magnesium solid solution 20 p2942 A72-39823

Mutual interdiffusions of thorium, lanthanides, and bismuth in Th-Ln-Bi solutions - Evidence for the formation of ThLnBi₃ compounds. 20 p2942 A72-39986

Precipitation thermodynamics of unstable and metastable solid solutions, discussing interfaces, vacancies, spinodal decomposition, nucleation, reversion and macroscopic diffusion 20 p2943 A72-40000

Beta to omega phase transformation and structure in Zr and Ti alloys bcc solid solutions by dark field electron microscopy, diffraction and ultrasonic technique. 21 p3065 A72-40092

Conditions and mechanism of formation of suboxide phases in the niobium-oxygen system 21 p3066 A72-40381

The nature of solid solutions of the titanium-vanadium-oxygen and titanium-vanadium-aluminum-oxygen systems 21 p3068 A72-40962

Mechanism of high temperature creep of aluminum-magnesium solid solution alloys. 21 p3069 A72-41299

Physical properties and electronic structure of V_{1-x}Cr_x/SSi ternary alloys 22 p3192 A72-43014

Compound tellurides and their alloys for Peltier cooling - A review. 22 p3215 A72-43088

Contact interaction between high-melting compounds and liquid metals. I - Interaction between subgroup IVA metals and metals of the iron family 23 p3299 A72-43287

X ray, microstructural and differential thermal analysis for binary Zr alloys, noting formation of ternary phases and solid solutions 23 p3300 A72-43588

Physicochemical problems in silicon and germanium heat treatment, covering solubility and solid solutions stability and saturation variation with temperature 23 p3324 A72-43687

Investigation of the influence of the gas medium on the phase composition and certain properties of refractory materials containing zirconium 23 p3306 A72-43690

Contribution to the study of some HfO₂-MO systems 23 p3302 A72-43999

Solid solution, subsolidus reduction and compositional characteristics of spinels in some Apollo 15 basalts. 23 p3262 A72-44135

Relationship between the electrical resistivity and solute concentration in the solid solution of tantalum-hydrogen system. 24 p3412 A72-44718

Influence of boron on the structure and properties of electron-beam melted molybdenum 24 p3414 A72-45380

Co-V solid solution decomposition by equilibrium phase precipitation at aging temperatures, using electron microscopic and X ray analysis 24 p3414 A72-45382

Physicomechanical properties of titanium-tungsten solid alloys with deficiency of carbon in the carbide solid solution lattice 24 p3415 A72-45385

SOLID STATE

Normal, highly conducting and ion-exchanging solid electrolytes structure and conductivity, with particular attention to rechargeable silver halide batteries 16 p2352 A72-33899

Optical constants of cesium in the wavelength range from 0.3 to 2.5 microns and their dependence on temperature and state of matter 24 p3426 A72-44800

SOLID STATE DEVICES

NT AVALANCHE DIODES

NT CRYOTRONS

NT FIELD EFFECT TRANSISTORS

NT GALLIUM ARSENIDE LASERS

NT GERMANIUM DIODES

NT JUNCTION DIODES

NT JUNCTION TRANSISTORS

NT METAL OXIDE SEMICONDUCTORS

NT MIS [SEMICONDUCTORS]

NT NEURISTORS

NT PARAMETRIC DIODES

NT PHOTODIODES

NT PHOTOTRANSISTORS

NT PHOTOVOLTAIC CELLS

NT RUBY LASERS

NT SEMICONDUCTOR DEVICES

NT SEMICONDUCTOR LASERS

NT SILICON TRANSISTORS

NT SOLID STATE LASERS

NT THERMISTORS

NT THYRISTORS

NT TRANSISTOR AMPLIFIERS

NT TRANSISTORS

NT VARACTOR DIODES

NT VARISTORS

NT YAG LASERS

Phased array antennas design and performance characteristics, examining feeding and electronic scanning problems with special attention to all-solid-state designs 01 p0038 A72-10659

Low noise phase locked power microwave sources for solid state radio links with 960 voice channels, discussing design 01 p0006 A72-10712

Shf electromagnetic radiation interaction with solid body plasma, explaining wave propagation in solid state plasma waveguides 02 p0170 A72-11561

Book on microwave electronics covering electron beam microwave devices and solid state microwave oscillators and amplifiers 03 p0331 A72-13233

Narrow band medium power X, Ku and C band solid state amplifiers, demonstrating TWT replacement with GaAs and avalanche diodes 03 p0334 A72-14072

Solid state tunnel diode amplifier-rectifier expander for microwave pulse regenerators 03 p0335 A72-14184

Hf solid state and quantum electronic devices - Conference, Cornell University, August 1971 06 p0787 A72-18453

Transferred electron effect in GaAs, presenting three level solid state microwave oscillator advantages 06 p0866 A72-18454

System potential of microwave solid state generation and amplification, comparing IMPATT, TRAPATT, Gunn, LSA, transistor and transistor-multiplier devices 06 p0787 A72-18456

Pulsed and CW solid state microwave oscillator EM noise as function of power level and locking parameters 06 p0788 A72-18465

Solid state Ku-band local Gunn oscillator for airborne radar applications, discussing design and batch process fabrication 06 p0789 A72-18480

Solid state microwave power amplifier with unidirectional transmission line loaded by negative resistance diode series, calculating large signal characteristics 08 p1142 A72-21558

Solid state microwave devices, discussing varactor, varistor, tunnel, Gunn, IMPATT and TRAPATT diodes and power transistors characteristics and applications 09 p1285 A72-22567

Inexpensive solid state microwave sources development and applications considering spectrum allocations, health hazards and reliability problems 09 p1285 A72-22595

HF thermal noise in single and double injection space charge limited solid state diodes 09 p1288 A72-23124

Solid state sinusoidal signal generator based on current density oscillation effect in high resistivity p-type InSb with transmutation doping 09 p1288 A72-23191

Magnetic integrated circuits design and fabrication problems involving branched and logic circuits and solid state structures controlled domains 10 p1448 A72-24279

Power-combining methods for synchronous detuned solid state microwave oscillators with stable large signal locking characteristics, noting feasibility 10 p1449 A72-24306

Solid state RC network for single sideband frequency converter using phase difference carrier suppression 11 p1598 A72-26731

VOR and Doppler VOR ground station equipment based on reliable solid state radio transmitters and signal generating devices for aircraft navigation 12 p1779 A72-27104

Solid state array camera based on diffused junction phototransistors, discussing sensor technology and fabrication 12 p1810 A72-27931

Solid state InP sources for microwave transferred electron oscillators and amplifiers with improved conversion efficiencies, comparing with GaAs 13 p2020 A72-28432

OMEGA receiver with digital solid state circuits for remote unmanned platform positioning, discussing ship to shore tests and design features 13 p1925 A72-29184

Solid state ac square law function generator based on fixed elements and operating on electrical servo system principle 13 p1933 A72-29973

Solid state dc power controller design functional requirements, considering system overcurrent protection, power control by low voltage signals, power output to load status, etc 15 p2182 A72-31219

Carrier wave propagation at semiconductor surface with electron drift, discussing solid state traveling wave amplifier design 15 p2290 A72-31288

Solid state modular ground based distance measuring equipment /DME/ receiver for en route aircraft navigation and landing 16 p2420 A72-33521

High-frequency ultrasonic devices. 17 p2526 A72-34564

Image pickup and display devices. 17 p2552 A72-34568

Characterization of a bilateral DC converter as a DC transformer. 17 p2497 A72-34705

Modular I-band solid-state microwave amplifier. 17 p2528 A72-34711

Solid state phased arrays for ECM applications. 17 p2531 A72-35569

Airborne waveguide element reliable advanced solid state radar /RASSR/ phased array radiation patterns and design 17 p2531 A72-35571

Thermal noise in double injection diodes operating in the insulator regime. 18 p2667 A72-36979

An all solid-state MIC transmit-receive module. 19 p2771 A72-37268

Radio astronomical observations in the 0.9 to 1.5 mm band using a 22-m radio telescope with an n-InSb receiver 19 p2858 A72-37803

Fast response solid state phase lock refractometer for airborne measurement of atmospheric refractive index 19 p2802 A72-38225

Book - Solid state electronic devices. 20 p2907 A72-39024

Measurements of electron detection efficiencies in solid state detectors. 20 p2925 A72-39401

Conference on Solid State Devices, 3rd, Tokyo, Japan, September 1, 2, 1971, Proceedings. 20 p2960 A72-39701

Reliable advanced solid state radar /RASSR/ array design featuring transmit-receive elements arranged in triangular grid and built-in test equipment 20 p2904 A72-39732

Disk and toroidal solid state computer storage cell arrays without boundary cells, comparing read- and write-time characteristics with conventional organizations 20 p2910 A72-39966

Raman scattering techniques applied to problems in solid state physics. 21 p3096 A72-40602

A solid-state 'flux-drive' control circuit for latching-ferrite-phaser applications. 23 p3275 A72-43574

Solid state microwave devices, discussing varactor, varistor, tunnel, Gunn, IMPATT, and TRAPATT diodes and power transistors characteristics and applications 24 p3384 A72-44746

SOLID STATE LASERS

NT RUBY LASERS

Axial mode locking and equidistant frequency generation in solid state lasers due to active medium saturation, using self consistent equations with broadened amplification line 01 p0079 A72-10347

Solid state laser emission angular divergence, considering active medium optical inhomogeneity and cavity parameters effects 01 p0081 A72-10976

Active and passive parameters correlations of solid state laser ruby crystals and Nd glass, using mechanical, thermal, chemical, optical, spectroscopic and electrical measurements 01 p0081 A72-11183

Solid state Q switched laser emission frequency drift from Fabry-Perot rings interferograms 02 p0237 A72-12108

High resolution atmospheric transmission measurement of wavelength dependence of absorption losses in carbon dioxide of solid state Er laser radiation 02 p0238 A72-12201

Mode locked oscillation in ring cavity Nd glass laser, showing satellite pulse and spectral broadening due to self phase modulation 02 p0238 A72-12203

Picosecond pulse production and measurement from mode locked Nd glass laser 02 p0238 A72-12492

Neodymium laser plasma dispersion and diffusion in magnetic field, using electrostatic injection of LiH particles 03 p0393 A72-13081

Ruby and Nd lasers fundamental emission effects on excitation of stimulated Raman scattering in liquid and crystalline media by second harmonics 03 p0366 A72-13364

Single mode solid state laser periodic Q switching effects on spike pulse shape and synchronization by harmonic analysis with convergent series

03 p0366 A72-13371

Internal Q switching in CdS laser activated by exciton recombination, observing lag in emission onset after input pulses delivery

04 p0528 A72-14575

Pulsed Nd laser beam polarization components energy measurement by double reflecting plate calorimeter, checking accuracy against NBS liquid cell calorimeter

04 p0531 A72-15479

Spectral heterogeneous lasing media with asymmetric luminescence bands, considering neodymium phosphate and germanate glass

06 p0824 A72-17392

Pinched vortex tube high current arc discharges for continuous pumping of ion crystal YAG-Nd lasers

06 p0825 A72-17839

Single pulse Nd laser with KDP cascade multipliers and tunable frequency converter using organic dye solution

06 p0825 A72-17841

Temporal characteristics of emission line broadening in lasers with dispersive resonators for Nd ion activated phosphate glasses and disordered crystals

06 p0826 A72-18011

Laser beam welding by solid state pulsed lasers, discussing heat conduction relation to power density utilization

06 p0822 A72-18254

Continuously pumped repetitively Q switched Nd-yttrium-aluminum trioxide laser, discussing mode selection technique based on gain excess over hold-off loss

07 p1000 A72-19045

High power UV light pulse generation using Nd-YAG laser with frequency doubling

07 p1002 A72-19202

Ho doped YLF and YAG laser threshold and slope characteristics at room temperature, considering Q-switched operation lifetime

07 p1004 A72-19233

Lamp pumped IR solid state laser obtaining 20 W output and 4 percent efficiency from transition of Ho ion in sensitized YAG

07 p1004 A72-19234

Continuous TEM power from single longitudinal mode Nd-YAG laser pumped with tungsten-iodine lamp

07 p1004 A72-19235

Thermal distortion insensitive TEM mode beam of hf YAG laser for high precision drilling machine

07 p1004 A72-19236

Wideband laser communication for space applications, comparing carbon dioxide and Nd-YAG systems on basis of SNR

07 p0941 A72-19239

Neodymium-glass laser emission spectral and temporal correlations during Q switching by rotating prisms and passive shutter

07 p1006 A72-19633

Laser applications in industrial machining and welding, describing theory and operation of optically pumped ruby, glass-Nd, YAG-Nd, Ar and carbon dioxide lasers

07 p1007 A72-20224

High speed rotating mirror camera adapted to solid state laser radiation, noting continuous recording and simultaneous imaging

07 p0990 A72-20401

Laser triggered spark gaps characteristics initiated by switched out picosecond pulse from mode locked Nd-glass laser, investigating breakdown formation time delay

07 p1008 A72-20547

Continuous laser action in Nd-yttrium aluminum oxide rod, determining terminal state loss coefficient in stimulated emission

08 p1217 A72-21322

Nd-glass laser time characteristics and radiation ordering from cavity lengthening

08 p1183 A72-21771

Nd smooth pulsed laser action with narrow spectral line and emission amplification from Nd doped phosphate and silicate glass rods

08 p1183 A72-22027

German monograph on luminous intensity amplification by means of solid state lasers covering experiments with GaAs and ruby lasers and traveling wave amplifiers

09 p1322 A72-22331

Gas, solid state and semiconductor lasers review, discussing applications

09 p1322 A72-22594

Stimulated emission and spectroscopic properties of activated ferroelectric crystal laser, noting Stark effect

09 p1323 A72-22981

CW Kr arc lamps for high power Nd-YAG laser pumping, testing operating life and electrical and spectral characteristics as function of design

09 p1324 A72-23080

Single picosecond light pulses from mode locked Nd-glass laser, discussing temporal structure, spectral energy distribution and pulse shape measurements

09 p1324 A72-23082

FM mode locked Nd-YAG pulsed laser controlled bistable phase position operation, using modulator cut as Brewster angle prism

09 p1325 A72-23089

Electro-optical Q switching of solid state laser sources without linear energy polarization in optical resonator

09 p1326 A72-23422

High power Nd-glass laser systems, discussing oscillator and amplifier operating parameters optimization

10 p1489 A72-23945

Near field characteristics of solid state laser frequency converters emission, determining medium transluence during single pulse excitation of organic phosphors

10 p1490 A72-24052

Solid state laser with slow relaxation bleachable filter, calculating modes self synchronization probability statistics relationship to relaxation time

10 p1492 A72-24512

IR radiation generation by Raman scattering and difference frequency mixing with Q switched Nd-YAG laser, noting peak power and photon conversion efficiency

11 p1647 A72-26149

Vortex discharge in Ar as optical pumping source for ionic crystal CW lasers, comparing efficiency with YAG-Nd crystal pumping

11 p1648 A72-26331

Pumping conditions relationship to tube filling in Nd-YAG pulsed laser

11 p1649 A72-26344

Multilayer dielectric reflective coatings performance in solid state laser pumping systems

11 p1649 A72-26345

Populations modulation and spatial harmonics influence on gas and solid state laser radiation characteristics, discussing uniform and nonuniform line broadening

11 p1650 A72-26353

Polyhedral radiation energy guides for laser sources and amplifiers, presenting solid state resonator design computation methods

11 p1650 A72-26354

Multichannel monopulse Nd glass laser design characteristics, describing input generator, preamplifier and amplifier channel beam distribution

11 p1651 A72-26363

Angular spectra and frequency characteristics of quasi-continuous monomode and two mode Nd-YAG lasers with spherical resonator

12 p1819 A72-27054

High power Nd glass laser with stepwise pulse amplification for intensive heating of solid target plasmas

12 p1849 A72-27061

High power light pulse generation with steep leading edges in Nd-glass laser, noting duration change based on transparency increase under light transmission

12 p1820 A72-27583

Second, third and fourth optical harmonics generation of Nd-doped YAG laser radiation under Q switching fast repetition pulse conditions

12 p1821 A72-27594

Solid state laser resonator inhomogeneous dielectric and mirror elements matching effects on Q factor and output power

12 p1822 A72-27609

Temperature gradient and thermoelastic stresses in Nd-YAG laser active elements under continuous pumping conditions, noting refractivity radial distribution

12 p1822 A72-27614

Nd-glass amplifier gain saturation by 1.06 micron light pulses determined by two laser states lifetimes and degeneracies and thermalization rates

12 p1792 A72-27752

Nd laser second harmonic generation by organic crystalline powders, noting suitability of benzophenone, xanthone, benzimidazole and resorcin

12 p1823 A72-27854

Active elements for high power Nd-glass laser facility to generate short and ultrashort pulses

12 p1825 A72-27881

Nd-fiberglass laser intensity fluctuations due to fibers absorption centers, deriving population inversion threshold, pumping power and center formation rate from kinetic equations

12 p1825 A72-27884

Frequency tuning and intracavity high efficiency extraction of second harmonic radiation from prism type Nd laser

12 p1825 A72-27885

Second harmonic conversion of CW YAG-Nd laser radiation on lithium metaniobate crystals, discussing conversion coefficient optimization

12 p1825 A72-27886

Crystal growth, physical and spectroscopic properties and laser performance of Nd and Ho doped crystals with apatite structure

12 p1825 A72-27927

Q switched YAG-Nd laser implementation into target designators and range finders, stressing temperature insensitive design with electronic compensation and thermal equalization

12 p1825 A72-27928

Nd-YAG laser bibliography covering oscillation, dynamics, engineering, materials and harmonic generation

12 p1826 A72-27957

Gas and solid state lasers amplitude and phase fluctuations calculated from Langevin equations, noting spectral line width and collision waves

12 p1826 A72-28050

Picosecond pulse efficient second harmonic generation by crystals inside high power dye mode locked Nd-glass laser folded cavity

12 p1826 A72-28220

Nd laser irradiation of LiH particles in magnetic trap, investigating resultant plasma expansion and diffusion

13 p2015 A72-29431

Periodic motions of weakly interacting modes in solid state lasers, using active matter pellet-resonator model

13 p1969 A72-29517

Angular spectrum of second harmonic generation during two frequency interactions in KDP laser

13 p1969 A72-29524

Energy conversion efficiency of xanthene dye laser pumped by mode-locked Nd-glass laser second harmonic, discussing effect of excited molecules transition to triplet state

13 p1970 A72-29686

High power monopulse Nd laser, obtaining single longitudinal frequency stabilized mode with anisotropic spar or quartz plates

13 p1971 A72-29922

Giant pulse radiation in Q factor modulated Nd glass laser frequency stabilization by molecular Cs vapor

15 p2245 A72-31411

Pulsed solid state lasers with large area Si photodiode for output measurement in feedback control system to compensate flash lamp aging

15 p2247 A72-32027

Nd glass laser drilling and welding applications and tests on materials to evaluate feasibility and operational advantages, identifying optimal pulse energies and durations

15 p2244 A72-32028

High power CW Nd-YAG laser efficiency improvement by optical pump wavelength, power coupling and balance factors, noting krypton arc lamp contribution

15 p2247 A72-32029

Single crystal scheelite material for Nd doped intermediate gain laser host substance, considering optimum growth conditions, lasing parameter and Nd concentration

15 p2292 A72-32030

Avalanche photodiodes for Nd and injection lasers radiation detection, reducing noise equivalent power

15 p2247 A72-32035

Tunable monochromatic IR laser based on magneto-Raman scattering from conduction electrons in n-type InSb, discussing physical processes and experimental techniques

15 p2250 A72-32393

Spiking response of luminescent diode pumped CW Nd-YAG laser to sinusoidal modulation, showing agreement with relaxation oscillation resonance prediction

15 p2250 A72-32526

Q switched laser operation with electro-optic switch mechanism, measuring initial photon number per mode of Nd-glass and Nd-YAG lasers

16 p2399 A72-33014

Q switched and free emission mode locking of neodymium glass and ruby lasers via liquid bleachable dye filter

16 p2400 A72-33296

Populations modulation and spatial harmonics influence on gas and solid state laser radiation characteristics, discussing uniform and nonuniform line broadening

16 p2402 A72-33706

Polyhedral radiation energy guides for laser sources and amplifiers, presenting solid state resonator design computation methods

16 p2402 A72-33707

Multichannel monopulse Nd glass laser design characteristics, describing input generator, preamplifier and amplifier channel beam distribution

16 p2403 A72-33715

Active elements for high power Nd-glass laser facility to generate short and ultrashort pulses

16 p2404 A72-33990

Nd-fiberglass laser intensity fluctuations due to fibers absorption centers, deriving population inversion threshold, pumping power and center formation rate

16 p2404 A72-33993

Frequency tuning and intracavity high efficiency extraction of second harmonic radiation from prism type Nd laser

16 p2404 A72-33994

Second harmonic conversion of CW YAG-Nd laser radiation on lithium metaniobate crystals, discussing conversion coefficient optimization
16 p2404 A72-33995

Laser systems.
17 p2562 A72-34567

Output fluctuations of CW-pumped Nd:YAG lasers.
17 p2564 A72-35345

Multicomponent structure of Nd-glass laser radiation, observing active medium gain band portions in interrelationships in free running and stimulated emission operation modes
17 p2564 A72-35507

Off-axis hologram recording on thin bismuth film with picosecond pulse train from mode-locked Nd-glass laser
17 p2558 A72-35817

Effects of thermal lensing in glass lasers.
19 p2810 A72-37512

Experimental evidence of an X-ray laser /Coherent radiation/copper/II/ gel target/neodymium-glass pump/.
19 p2811 A72-37774

Active Q switching technique for producing high laser power in a single longitudinal mode.
19 p2811 A72-37845

Relation between the plasma ion current and the surface defects produced by ruby and neodymium laser emission
19 p2812 A72-38210

Properties of stimulated neodymium laser emission under the action of Co 60 gamma emission
19 p2812 A72-38214

Nonlinear optics with picosecond laser pulses.
19 p2812 A72-38379

Harmonic mode locking of the Nd:YAG laser.
19 p2813 A72-38688

Multipulsing behavior of electrooptically Q-switched lasers.
19 p2813 A72-38692

Single-mode laser with a continuously variable pulse duration.
20 p2933 A72-39511

Influence of gas pressure in arc lamps on the pumping efficiency of CW garnet lasers.
20 p2933 A72-39513

Diffraction of a laser beam by domains in yttrium iron garnet.
20 p2933 A72-39521

Frequency-tunable stimulated IR parametric fluorescence produced by barium sodium niobate crystal pumped with picosecond pulses from frequency-doubled mode locked Nd-glass laser
20 p2933 A72-39560

Flash lamp optimal operating parameters determination by impedance matching to driving circuit and spectral matching to material of optically pumped solid state pulsed lasers
21 p3061 A72-40204

Solid state laser sources, light modulators and silicon avalanche photodiode detectors for fiber optical communication, discussing performance and limitations from system design viewpoint
21 p3018 A72-40866

A stable neodymium-glass laser harmonic generator
21 p3064 A72-41739

Study of the operation of a neodymium glass laser under nonsteady thermal conditions, with thermal insulation of the active element by air
22 p3185 A72-42172

Gas absorption lines detection based on multiple light passage through absorbing medium during generation process, noting radiation spectra of neodymium glass laser
23 p3295 A72-43305

Investigation of the fast recombination channel in InSe during excitation by neodymium laser light
23 p3295 A72-43339

Optical signal envelopes recording and reproduction with parametric superregenerative frequency converters, noting optical pumping by continuous wave YAG laser emission
23 p3292 A72-44471

Neodymium-glass laser emission spectral and temporal correlations during Q switching by rotating prisms and passive shutter
24 p3408 A72-44565

Nanosecond and picosecond laser-produced CD2 plasmas.
24 p3427 A72-44709

The effect of a harmonic-oscillator velocity distribution on an ideal solid-state laser.
24 p3409 A72-44953

Investigation of the uniformity of neodymium-glass laser emission
24 p3410 A72-45419

Increase in the ratio of the energy of ultrashort laser pulses to the energy of the background radiation.
24 p3411 A72-45613

Threshold characteristics of receivers with optical quantum amplifiers.
24 p3412 A72-45617

High power Nd glass laser with stepwise pulse amplification for intensive heating of solid target plasmas
24 p3431 A72-45714

SOLID STATE PHYSICS

Solids static electrification models based on solid state physics, considering contact, deformation and cleavage charging processes
02 p0269 A72-12552

Solid state colloidal plasma physics, discussing statistical ionization mechanics, electron emission and recombination, rocket exhausts, MHD generation, metal vapors electrostatic precipitation, etc
02 p0267 A72-12842

Electron beam interaction with bounded solid state plasma, deriving slow wave dispersion relations
04 p0561 A72-15080

Thermal expansion in simple solids and structural composites due to anharmonic vibrations, using atomic density model
15 p2322 A72-31257

Oscillatory current characteristics of Stark ladder electron with weak LO phonon coupling in solids
15 p2293 A72-32218

Book - Topics in solid state and quantum electronics
17 p2594 A72-34560

Solid state physics - An overview.
17 p2594 A72-34561

Physics of strengthening mechanisms in crystalline solids.
19 p2843 A72-37444

Charge states and charge-changing cross sections of fast heavy ions penetrating through gaseous and solid media.
19 p2837 A72-37849

Quantum crystals in the single-particle picture.
19 p2844 A72-37943

Russian book - Radiation effect method in the investigation of the structure and properties of solids.
20 p2958 A72-38951

Diffusion effects in solids caused by radiation exposure, calculating diffusion coefficients of additions and defects
20 p2958 A72-38952

Solid state physics experiment for conduction electrons effective mass determination in ultrapure n-type InSb by means of magnetophonon effect
21 p3096 A72-40203

SOLID SURFACES

NT CRYSTAL SURFACES

Solid thermal motion influence on atom colliding with solid surface linear semifinite atomic chain, presenting accommodation coefficient calculation method
06 p0853 A72-18140

Thermal emittance measuring methods for solids at temperatures above 1500 K, discussing emittance dependence on surface characteristics
06 p0818 A72-18253

High intensity laser beams for solid surface material removal by vaporization and explosion, noting surface and subsurface temperature relations
07 p1002 A72-19210

Numerical simulation of gas atom scattering from solid surface and satellite drag coefficient calculation
07 p0910 A72-20106

German monograph on lattice and solid metal surface transport processes, discussing atom migration, activation energies, impurity atom diffusion, Kossel-Stranski model, etc
08 p1212 A72-22173

Optical measurement of point velocity on surface of moving solid, applying to Mylar foil accelerated by plasma gun
09 p1310 A72-22773

Compressible turbulent boundary layer with arbitrary pressure gradients on solid or permeable surfaces, using extended mixing length theory
11 p1616 A72-25917

Conductive heat propagation with finite rate for semibound solid body under periodic surface temperature fluctuations dependent on relaxation time
12 p1890 A72-28174

Hertz formulas for undulate solid surface height distribution
12 p1819 A72-28196

Conjugate unsteady problem of convective heat transfer for uniform flow over solid body with matching boundary conditions at interface
13 p2064 A72-28889

Solid surface inspection by X ray diffraction, electron microscopy and chemical techniques
14 p2131 A72-30693

Laminar boundary layer separation point in steady two dimensional constant density flow past solid surface, deriving pressure-vorticity gradient relationship
15 p2218 A72-32467

Velocity distributions of molecular beams evaporating into vacuum from polycrystalline hexachlorobenzene and sulfur surfaces
16 p2429 A72-33058

Spatial distribution of nitrogen molecular beam scattering from solid nitrogen surface as function of beam energy and incidence angle
16 p2430 A72-33063

Numerically computed momentum and energy accommodation coefficients and angular distributions of gas molecules reflected from solid crystalline surfaces applied to satellite drag calculation
16 p2430 A72-33065

Aerodynamic coefficients determination from momentum and energy exchange between low velocity molecular jet and solid surfaces, describing time of flight measurement technique
16 p2390 A72-33069

Solid-body-surface and thin-layer analyses by the static method of secondary-ion mass spectroscopy
18 p2719 A72-36830

Solid surface geometry, atomic composition and electronic structure observations, discussing Auger spectroscopy, field ion microscopy and electron diffraction and scattering techniques
19 p2803 A72-38389

Electron spectroscopic investigation of solid surfaces chemical composition and atomic binding states and structure, discussing methods of inducing electron emission
20 p2927 A72-39695

Water film formation and breakdown during motion over solid surfaces, predicting flow rate difference due to contact angle hysteresis
21 p3085 A72-41178

A re-evaluation of material effects on microbial release from solids.
23 p3253 A72-43383

SOLID SUSPENSIONS

Cascade wind tunnel and water table determination for trajectories and velocities of suspended particles in fluid flow through axial compressor stage
07 p0907 A72-18756

SOLID-SOLID INTERFACES

Finite element method extension using computer program for solving problems of elastic bodies in contact with stiffness method advantages
01 p0141 A72-11047

Two dimensional contact problems solutions for nonclassical elastic regions for layer and strip
02 p0288 A72-11603

Vitreous silica and silicon-silicon dioxide interface defect structure and behavior during ionizing or particle irradiation
03 p0403 A72-14081

Air ionization, secondary electron emission and Compton currents at W-Be interfaces under Co 60 gamma radiation
03 p0403 A72-14083

Slow motion in shear flow of doublet of two spheres in contact, using Stokes equations solution
04 p0511 A72-14860

N- and p-type semiconductors energy band structure bending near interface
05 p0702 A72-16197

Metal polymer interface synthesis based on linearly cyclic oligoelementary high molecule compounds, analyzing heat and thermal oxidation resistances
05 p0680 A72-16202

Point contact realization between helical transmission wheels teeth
05 p0667 A72-17058

Differential thermal and X ray analyses of ignition and preignition solid-solid reactions in Zr-Mo trioxide delay system over 440-475 C
08 p1219 A72-20756

Integral contact temperatures and heat balance calculation for heat transfer between contacting bodies with rotational motions
08 p1252 A72-21444

Water effect at epoxy resin-steel interface on adhesive bond strength as function of vitrification temperature
08 p1196 A72-21863

Tensionless contact area between beam and elastic half space determined by approximate technique
09 p1398 A72-22623

Tractions at interface between fiber and matrix in fiber reinforced composites, considering axially symmetric deformations and stress fields
09 p1339 A72-23173

Stress wave reflection and transmission at interfaces between homogeneous isotropic linear elastic materials
09 p1353 A72-23501

Metallic foils effects on thermal joint resistance of interface between lathe turned and optically flat surfaces, noting optimal thickness
11 p1685 A72-25223

[AIAA PAPER 72-283]

Wear mechanism of lead-bronze dry sliding in air on hardened steel ring
11 p1638 A72-25510

Alloying addition effects on structural stability and particle-matrix cohesion in metal-alumina composites
11 p1665 A72-26864

Uniqueness and existence theorems for nonideal thermal contact between three dimensional solid parts in heat conduction theory, noting case of two dimensional body
12 p1889 A72-27996

Surface roughness effects on seizure and friction of contacting metal plates under atmospheric pressure and vacuum
12 p1819 A72-28197

Tribochemical effects during friction of non-lubricated amorphous and crystalline polymer surfaces under mild and hard contacting conditions
12 p1835 A72-28200

- Conjunction mechanism of two real contacting bodies with rough surfaces under normal load
12 p1819 A72-28202
- Chemical reactions between solids during boundary friction, presenting literature review on mechano-chemical or tribo-chemical reactions between solid lubricants and metal surfaces
[ASLE PREPRINT 72AM 1] 13 p1964 A72-28969
- Rigid smooth body pressing into elastic plate surface subjected to cylindrical bending, discussing contact problem and transverse shear strain
13 p2062 A72-29950
- Tangential force distribution at fiber surface in composite material under tensile stress without displacement at fiber axis
15 p2260 A72-31743
- Elastic dilatational field association with twist dislocation loop interaction with free surface of two phase system interface
15 p2331 A72-32504
- Mathematical model and simulation for contact problems involving elastic half spaces and viscoelastic and friction effects
18 p2734 A72-36371
- Thickness-punch size ratio effects on stress state response of elastic plates and beams in flat contact under symmetric loads due to rigid punches
18 p2734 A72-36378
- Transport coefficient of multi-layer film of semiconductors.
19 p2843 A72-37401
- Contact interactions of smooth rigid punch impressing into thin laminar anisotropic reinforced plastic plate
19 p2872 A72-37541
- Adhesive wear theoretical model based on asperity interactions number, area and volume, considering implications for friction and surface temperature analysis
19 p2809 A72-38377
- Stress concentration around circular crack on interface between two bonded dissimilar isotropic elastic half spaces
20 p2982 A72-40020
- Polymer adsorption as a cause of changes in contact interaction intensity between two solid surfaces
21 p3059 A72-40083
- Phenomena and interpretation of the transients caused by temperature change on capacitance of metal-oxide-metal systems.
21 p3097 A72-40690
- Conductance associated with interface states in MOS tunnel structures.
21 p3032 A72-40701
- Observation on phenomena associated with a slowly varying surface barrier at niobium oxide and aluminum interface.
21 p3097 A72-40702
- Photovoltaic properties of single-crystal CdS-Cu2S cells.
22 p3214 A72-42457
- Capacitance voltage characteristics instability of metal-aluminum oxide-silicon dioxide-silicon (MAOS) structures, suggesting polarization effect in layer formed during deposition and annealing
23 p3324 A72-44070
- ### SOLIDIFICATION
- Directional solidification of off-eutectic Al-Be alloy, obtaining ultimate strength, elastic modulus and concentration perturbation caused by freezing rate changes
[AD-738212] 02 p0242 A72-11985
- Steel cleanliness conditions for formation and decantation of inclusions due to deoxidation during production up to solidification
03 p0371 A72-13198
- Solidification, microsegregation and homogenization of austenitic stainless steels containing delta ferrite
05 p0672 A72-16142
- Rapidly and unidirectionally solidified Al alloys microstructure, discussing crystal dislocation origins and patterns
07 p1019 A72-20240
- Nucleation mechanism for weld solidification in electron beam and tungsten-inert gas welding processes
09 p1332 A72-23641
- Coupling of interstitial liquid and porous elastic medium deformation, calculating solidification by numerical integration of partial differential equations system of Lamé type
10 p1465 A72-24116
- Acoustic measurement of solid-liquid interface motion and solidification during freezing of Hg and paraffins
10 p1563 A72-25044
- Solidification mode of weld metal in Inconel 718, using optical and electron transmission microscopy, etch-pit technique and electron-microprobe analysis
11 p1653 A72-25344
- Vibration viscometer measurement of viscosity of alkali metals Rb, Cs, Na and K near solidification temperature, studying oxygen effects on metal surface
11 p1746 A72-26236
- Ultrasonic oscillations effects on alloy castings grain size and heat resistance, suggesting waveguide direction for oriented solidification
11 p1642 A72-26822
- Weld solidification synthesis with crystalline organic materials, investigating substructure size, growth rate and thermal gradients
13 p1966 A72-29424
- Modified Al-Si eutectic solidification behavior and microstructure, investigating LF mechanical vibration effects
14 p2120 A72-30617
- Al-Zn-Mg alloys hot cracking during solidification, discussing chemical composition, Al purity, temperature, aging, dissolved gases and grain refining additives effects
15 p2256 A72-31774
- Temperature and pressure requirements for producing superfluid liquid molecular hydrogen, noting use of solid deuterium or Ne walls to prevent hydrogen solidification
16 p2422 A72-32911
- Isotropic fiber coarsening in unidirectionally solidified eutectic alloys, showing effect on alloy microstructure
16 p2409 A72-33802
- Pure metal unidirectional solidification as function of liquid superheat, metal/mold heat transfer coefficient and mold material
16 p2399 A72-33804
- Chill zone structures in Al-Cu alloys as function of heat sink, surface microprofile and liquid metal fluid flow
16 p2409 A72-33810
- Separation of iron and annealing-out of lattice defects in rapidly-solidified aluminum-iron alloys. I - Microstructure and properties of quenched samples. II - Tempering behavior
17 p2567 A72-35174
- Filler wire composition effects on solidification cracking resistance in weldable Al-Zn-Mg alloy
18 p2699 A72-36426
- Calculation of residual stresses in wound materials produced by a layer-on-layer solidification process
19 p2872 A72-37532
- Study of the solidification of cryogenic fluids by means of evacuation
19 p2881 A72-38039
- Rates of solidification of Apollo 11 basalt and Hawaiian tholeiite.
20 p2967 A72-39181
- Metals and alloys solidification concepts, applying to casting techniques development
20 p2936 A72-39211
- Unidirectionally oriented pseudobinary eutectic solidification in ternary systems, investigating crystallographic and mechanical characteristics of ZrCuSi fibers embedded in Cu matrix
20 p2940 A72-39441
- Effects of modification and additional elements on the solidification of Al-Si alloy - Studies on the solidification of Al-Si alloys in a shell mold. II.
21 p3067 A72-40937
- Metastable phases in very rapidly solidified aluminum-germanium alloys
21 p3070 A72-41644
- ### SOLIDIFIED GASES
- #### NT SOLID NITROGEN
- Southern Martian polar cap seasonal change, describing variation at vernal equinox and dry ice hypothesis
04 p0581 A72-15621
- ### SOLIDS
- #### NT SOLIDIFIED GASES
- Perturbed vibrational motion in isotropic elastic solid, using nonlinear Truesdell equations
01 p0101 A72-10039
- Griffith crack stress intensity factor and crack face displacement in elastic solid, detailing symmetrical, antisymmetrical and point body force distributions
01 p0136 A72-10185
- Stokes and Love integral representations for elastodynamic displacement fields in elastic solid deduced by potential theory method
01 p0138 A72-10513
- Kink movement and cutting forest dislocation models of creep in thermally activated crystalline solids
01 p0140 A72-10857
- Calorimetric and radiometric methods for thermal radiation properties of solids, considering reflectance, absorbance, transmittance and spectral emittance
02 p0223 A72-11499
- Solid body surface strain field optical determination, using diffraction gratings
[SESA PAPER 1751] 02 p0199 A72-11512
- Rheological properties of Maxwell fluid-St Venant solid model for solids, noting slip lines direction during plastic flow
02 p0259 A72-12238
- Optimal stabilization of permanent rotation of solid body with arbitrary mass distribution by controlled gyroscope
02 p0230 A72-12337

Anelastic solid energy dissipation linear memory models based on viscoelasticity theory, applied to earth and metals experimental data and dynamic loading problems
02 p0294 A72-12447

Solids static electrification models based on solid state physics, considering contact, deformation and cleavage charging processes
02 p0269 A72-12552

Surface subsidence in semiinfinite resilient elastic solid mass supporting annular load distributed over circular ring
02 p0297 A72-12616

Resistive force on moving dislocations at low temperature in solids and crystal defect studies by ultrasonic methods, determining temperature dependence of mechanical properties
03 p0362 A72-13224

Shock waves in solids, investigating Hugoniot curve for condensed and porous media and phase transformation effects in polycrystals
03 p0446 A72-13689

Solid materials inelastic constitutive relations, developing internal variable thermodynamic formalism for microstructural rearrangements
03 p0446 A72-13710

Linear viscoelastic solid defined by constitutive equations replacing bounded domain in time interval on real axis, deriving theorem regarding solution of second problem of limits
03 p0447 A72-13787

Specific quantitative trace analysis technique for solids using spark source mass spectrometry
03 p0361 A72-13849

High temperature thermal conductivity measurements of solids at 800-1500 C using heat pipe technique
04 p0547 A72-14544

Plane periodic oscillations of solid body on elliptic orbit, characterizing stability of motion equations periodic solutions
04 p0582 A72-14632

Seminfinite elastic solid response to arbitrary axially directed line load, transforming simultaneous partial differential equations by Hankel transforms
[ASME PAPER 71-APMW-1] 04 p0589 A72-15180

Thermodynamic solids theory generalized for internal strains in perfect non-Bravais crystals, applying to trigonal Se and Te structure
04 p0562 A72-15470

Geometric displacements and space-time derivatives determining velocity and strain fields in solids under deformation
05 p0738 A72-16529

Plastic deformation of solid body in terms of slip dislocations displacement rate
06 p0894 A72-17687

Solid bodies crack development theory, emphasizing crack tip fine and hyperfine structures concepts and time dependent effects
06 p0898 A72-18554

Free solid body kinetic moment vector effects on long period motion in resonant state during transition from rotational to somersaulting mode
06 p0849 A72-18699

Finite element and finite difference formulations for solid continua by variational principles, including potential energy, complementary energy and Reissner principles
07 p1087 A72-18792

Surface relief effect on radiative properties of solid body with random surface roughness distribution
07 p1098 A72-18934

Test facility for thermal diffusivity measurements in solids by method of plane temperature waves using periodic optical heating at 1500 K
07 p0982 A72-18942

High intensity pulsed laser beam heating of solid transparent materials
07 p1002 A72-19212

Unsteady thermal conductivity and heat transfer in solid bodies heated by radiation, using cascade linearization method
07 p1100 A72-19884

Motion equations order reduction for solid body with fixed point
08 p1207 A72-21340

Transformation of integrodifferential equation of motion of heavy solid body about fixed point
08 p1207 A72-21341

Solid body motion about fixed point, determining moving and fixed angular velocity hodographs
08 p1208 A72-21351

Helical line deformation in solid body motion about fixed point
08 p1209 A72-21366

Optimal stabilization of permanent rotation of solid body with arbitrary mass distribution by controlled gyroscope
08 p1168 A72-21552

Asymptotic analysis of activation energy limit for radiant ignition of reactive solid with in-depth absorption
[AD-741533] 08 p1255 A72-22044

- High strength solids compositional, heat treatment and chemical environmental effects on fracture strength, considering alumina as example
09 p1334 A72-22387
- Thermal diffusion in solids subject to deformation, using classical elasticity theory body force analogy for variational and reciprocal theorems
09 p1403 A72-22757
- Equation of state data of solids from shock vaporization, using spectroscopic technique
09 p1351 A72-22856
- Perturbed motion of rotating solid body with viscous fluid filled cavity, linearizing motion and Navier-Stokes equations
09 p1295 A72-23487
- Stress intensity factor for circular crack embedded in finite thickness solid under uniform tension, noting semielliptical surface flaw in brittle material [ASME PAPER 71-APMW-6]
10 p1554 A72-24183
- Heat conduction and thermoelasticity in solids, discussing thermomechanical coupling, structural analysis and thermal stresses and deformations [SMRT PAPER L 1/1]
10 p1556 A72-24394
- Solid body elastic deformation potential energy and structure calculation on computer by finite element method and calculus of variations
10 p1559 A72-24924
- Cumulative shock loading fatigue in solids, describing experimental setup and fracture morphologies
10 p1560 A72-25124
- Laser stimulated Raman scattering and IR absorption on crystal defects leading to atomic migration in solids
11 p1647 A72-26144
- Axisymmetric stress field in infinite homogeneous isotropic elastic solid with crack surrounding cylindrical cavity, solving elastic equilibrium equations
11 p1738 A72-26720
- Physical properties of atoms, molecules and solid material in ultrastrong magnetic field, using quantum drift approximation
12 p1847 A72-27055
- Molecular dynamic techniques for simulating one dimensional shock wave motion in three dimensional solid, using rare gas solid model
12 p1881 A72-27282
- Impulse and kinetic momentum equations for dynamics of variable mass solid using mechanical model
12 p1846 A72-27543
- Dead load static stability of elastic solids in terms of zero moment condition of Beatty theory
12 p1883 A72-27557
- Stress intensity factor of Griffith crack in elastic solid opened by thin symmetric wedge, using triple integral equations
12 p1883 A72-27558
- Laser-interferometer instrumentation for shock stress wave measurements in solids, using velocity and displacement techniques
12 p1808 A72-27638
- Acceleration waves propagation in elastic-plastic strain hardening rate independent solids, obtaining solution for discontinuity change in strength in homogeneously prestressed medium
12 p1846 A72-27729
- Cryogenic microwave equipment for solids study provided by adiabatic demagnetization cooling system, noting relaxation time measurement in magnetic fields
12 p1796 A72-27856
- Russian papers on solid bodies friction mechanism and properties covering adhesion, lubricants effects, wear in presence of aircraft fuels and temperature effects
12 p1817 A72-28180
- Solids deformation resistance increased by active lubricants effects on coupled friction surfaces, noting damage localization to thin surface layers
12 p1817 A72-28181
- Temperature effects on crystalline solids adhesion, noting friction rise above seizure point
12 p1818 A72-28187
- Solid deformable body mean stress determination by statistical summation of stress squares on faces of parallelepiped rotated within Euler angle limits
12 p1887 A72-28233
- Stability in mechanics of continuous solids - Conference, University of Waterloo, Ontario, Canada, October 1970-September 1971
13 p2054 A72-28476
- Thermomechanical interactions between elastic waves and nonstationary temperature fields in solid continua, considering coupled and uncoupled theories
13 p2064 A72-29093
- Three dimensional steady temperature field calculation for solid bodies under concentrated heat source, using flow kinetic heat conduction method
13 p2065 A72-29151
- Three grid LEED-Auger display system for electron emission from solids at low primary beam energies
13 p1932 A72-29751
- Axisymmetric hypersonic motion around thin solid of revolution, taking into account boundary layer interaction with inviscid external flow
13 p1895 A72-29847
- Numerical solution of algebraic equation encountered in aerodynamics of hypersonic boundary layer interacting with external flow on thin solids of revolution
13 p1895 A72-29848
- Microinhomogeneous solid bodies elastic fields and effective moduli calculation method within framework of random field theory, using singular approximation
13 p2062 A72-29884
- Variational problem solution for solid strained body with nonlinear stress-strain relation, applying finite element method
14 p2130 A72-30189
- Solid bodies microanalysis by mass spectrum microscopy based on secondary ion-ion emission, discussing ion source and focusing systems
14 p2104 A72-30449
- Elastoplastic equilibrium theorems for solid subjected to variable external effects, considering perfectly plastic and arbitrary hardening materials
14 p2165 A72-30574
- Russian papers on relaxation mechanisms in solids covering microscopic theory, mechanical, electrical, chemical, thermal and magnetic processes, equipment and techniques
14 p2121 A72-30951
- Mobile point defects interaction with moving dislocation in inelastic solid bodies, considering energy dissipation due to impurity relaxation
14 p2169 A72-30954
- Energy losses due to hysteresis friction during oscillations of dislocations in elastic field of point defect in solids, discussing temperature and amplitude effects
14 p2121 A72-30955
- Relaxation methods of magnetic and acoustic spectrography for studies of gravitational and inertial dipoles and quadrupoles in molecules and nuclei of solid bodies
14 p2143 A72-30963
- Dislocation motions as internal friction mechanism in solids due to medium frequency acoustic waves, considering motional energy transfer to thermal phonons and lattice vibrations
15 p2292 A72-31833
- Displacement and stress field for elastic solid containing cruciform crack with unequal length arms
15 p2330 A72-32292
- Nearly incompressible elastic solid compressibility effects theory, applying to annular wedge straightening, stretching and shearing and cylindrical tube telescopic shear problems
15 p2330 A72-32477
- Strain release method for investigating thermally activated microflow mechanisms in solids, discussing technique for activation energy and relaxation strength measurements
16 p2372 A72-32822
- Three dimensional potential flow with lift about solid body calculated by distribution of sink, source and vortex type singularities satisfying Laplace equation
16 p2342 A72-32896
- Limit displacement or solids parameters optimization for perfectly locking bodies, presenting mathematical models based on extremum energy theorems
16 p2423 A72-33104
- First and second order shock discontinuity waves propagation in thermoelastic incompressible solids, deriving Piola-Kirchhoff stress tensor via Clausius-Duhem relation
16 p2423 A72-33109
- Exponential representation of isotropy groups of simple solids, noting conditions for conjugation of unimodular to orthogonal group subgroups
16 p2423 A72-33111
- Magnetic field effect on ruby laser generated plasma in solid target, measuring thermal ion energy increase
16 p2439 A72-33988
- Note on dynamic fracture toughness measurement
17 p2566 A72-34257
- Unsteady thermal conductivity and heat transfer in solid bodies heated by radiation, using cascade linearization method
17 p2637 A72-35132
- Stress analysis of axisymmetric solids with asymmetric properties
17 p2632 A72-35227
- Temperature distribution in solids under laser irradiation
17 p2564 A72-35355
- Simultaneous determination of the thermokinetic characteristics of solids by a variable regime method
17 p2638 A72-35749
- Distortion of the semi-infinite solid due to transient surface heating
17 p2635 A72-35974
- Wave-front singularities for two-dimensional anisotropic elastic waves
18 p2739 A72-37175
- Book - Annual review of materials science. Volume 1
19 p2843 A72-37441
- Optical holography and holographic interferometry applications in solid mechanics, considering surface physics, bomb breakup, transverse wave propagation, nondestructive testing and vibration analysis
19 p2797 A72-37603
- A photoelectric method for measuring the temperature pulsations of solids
19 p2799 A72-37664
- Plane bending problems in the theory of elasticity for nonhomogeneous solids
19 p2877 A72-38162
- Semiempirical method for determining electron wave-function parameters in solids
20 p2959 A72-38955
- Criteria for delayed fracture in solids and their experimental verification
20 p2981 A72-39954
- The vertical stress distribution due to parabolical strip load and uniform load over an ellipse in the interior of a semi-infinite solid
21 p3121 A72-41243
- Radiant conduction heat transfer in semitransparent solid materials
22 p3243 A72-41955
- Coherent/incoherent elastic/inelastic neutron scattering in amorphous solids, presenting neutron intensity and correlation functions
22 p3206 A72-42799
- Plane waves in a new theory of thermoelasticity
22 p3239 A72-42856
- Inverse problems of the dynamics of a ponderous solid with one fixed point
23 p3312 A72-43219
- Computer simulation of fracture spreading in a visco-elastic solid
23 p3267 A72-43702
- Statistical strength and plasticity criterion for materials in a complex stress-strain state
23 p3349 A72-43953
- Reissner-Sagoci problem for semiinfinite elastic solid stress and displacement determination, discussing generalization to nonhomogeneous media with circular part under axisymmetric twisting
23 p3314 A72-44266
- Physical properties of atoms, molecules and solid material in ultrastrong magnetic field, using quantum drift approximation
24 p3427 A72-45708
- SOLIDS FLOW**
Solid cylinder stress-strain state under thermal and mechanical loads, obtaining analytical solutions via flow theory based on Von Mises yield condition
09 p1401 A72-22723
- Kinetic freezing effects of supersonic gas flow with solid particles into vacuum, analyzing continuous to collisionless transition flow for Maxwell molecules
14 p2094 A72-30295
- Two phase flow types defined as flow problems of two-phase matter mixtures /solid, liquid, gas or plasma/ and interface interaction
20 p2915 A72-39971
- SOLIDUS**
Nb-Ti-B ternary system melts hardened in vacuum, determining solidus temperature and surface from phase diagram
03 p0370 A72-13186
- Nonequilibrium subsolidus reduction of lunar spinels at low oxygen fugacities based on Cr-Al ulvöspinel and olivine decomposition
03 p0439 A72-14298
- Yttrium alloys isoperiodic lines, solidus isotherms, equal hardness lines and resistivity presented diagrammatically
15 p2289 A72-31185
- SOLITHANES**
The fracture energy and some mechanical properties of a polyurethane elastomer
19 p2823 A72-38450
- SOLSTICES**
F 2 layer midlatitude local centers of anomalous nighttime ionization during winter and summer solstices
11 p1623 A72-26283
- SOLUBILITY**
Metal powders sintering activation mechanism, considering heterogeneous metals particles diffusion flow, mutual solubility and crystal lattices distortion
02 p0232 A72-11432
- Hydrogen diffusivity and solubility in alpha-Ti alloys, considering absorption effect on stress corrosion cracking
02 p0244 A72-12481
- Nb-Mo-N solid solution nitrogen solubility equilibrium at various temperatures and pressures
03 p0370 A72-12962
- Phosphate solubilization and activation on primitive earth, using apatite solubility as function of pH
04 p0483 A72-14769
- Carburization of various irons in methane-hydrogen atmosphere at 750 C, comparing activity coefficients and solubility limits
04 p0533 A72-14978

- Nitrogen interaction with liquid binary Ni alloys, investigating solubility as function of temperature and pressure and titanium nitrides existence conditions
07 p1011 A72-19547
- Cast Nb-C alloys carbon solubilities of 1.4 and 0.25 percent at 2100 and 1200 C, showing molten microstructure and measuring procedures
07 p1023 A72-20669
- Temperature dependence of Ge solubility in CdSb single crystals from microstructural observations and measurements of microhardness and electrical properties
09 p1372 A72-23480
- Isotope effect calculation hydrogen and deuterium solubility in fcc metals, analyzing elastic vibrational spectrum of crystal with impurity atom in internode
10 p1498 A72-24873
- Carbon solubility in Nb at 1500-2150 C, determining saturation concentrations from electrical resistivity vs reaction time curves
11 p1662 A72-26740
- Nitrogen solubility, degassing kinetics and diffusion coefficients for Mo-N, W-N and Re-N systems for 1300-3050 C
11 p1663 A72-26841
- Thermodynamic description of metal rich side of Nb-Mo-N solid solution, determining equilibrium nitrogen solubility as function of pressure and temperature
11 p1664 A72-26842
- High temperature solubility and diffusion coefficient of nitrogen in rhenium
12 p1827 A72-27138
- Binary ordering alloys with fcc lattice, studying volume effects on solubility of impurity atoms in interstices
13 p2023 A72-29907
- Hydrogen gas solubility measurement in solid Mo at atmospheric pressure and 905-1521 C, noting quasi-regular linearity of Arrhenius plot
14 p2113 A72-30246
- Solute quenching technique to determine hydrogen solubility in Ta to liquid He temperature, comparing with equilibrium measurements
15 p2259 A72-32640
- Co-Cr-C system carbon activity and solubility at 950-1200 C, deriving equation for temperature dependence and solid solution-carbide precipitation zone boundaries
16 p2407 A72-33441
- Hydrogen solubility in Zr-Nb-Hf systems as function of composition, temperature and hydrogen equilibrium pressure
16 p2410 A72-33816
- Studies of the electron transport chain of extremely halophilic bacteria. VII - Solubilization properties of menadiene reductase.
19 p2755 A72-37649
- Rate of molybdenum solution in carbon-saturated liquid iron.
22 p3193 A72-43027
- Physicochemical problems in silicon and germanium heat treatment, covering solubility and solid solutions stability and saturation variation with temperature
23 p3324 A72-43687
- Immiscible materials processing experiments in near weightlessness environments during Apollo 14 mission and on NASA short duration low gravity test facilities
24 p3407 A72-45155
- The mutual solubilities of titanium and boron in pure aluminum.
24 p3415 A72-45482

SOLUTES

- Maximum volatile solute vaporization escape prior to droplet solidification during metal vapor chemical release process
08 p1128 A72-21618
- Solute dispersion distribution over tube cross section with flowing solvent, comparing with Gaussian distribution
10 p1466 A72-24330

SOLUTIONS

- NT AQUEOUS SOLUTIONS
NT DETONABLE GAS MIXTURES
NT GAS MIXTURES
NT NUCLEAR EMULSIONS
NT PHOTOGRAPHIC EMULSIONS
NT SOLID SOLUTIONS
Calculation of the surface properties of elastic polymer molecules in athermal solutions by the Guggenheim method
21 p3095 A72-40078
- Concentration dependence of surface tension in solutions of surface-inactive polymers
21 p3072 A72-40079

SOLVENT EXTRACTION

- Determination of copper, iron, cobalt, nickel, and manganese in biological samples of vegetable origin
23 p3260 A72-43924

SOLVENTS

- Solute dispersion distribution over tube cross section with flowing solvent, comparing with Gaussian distribution
10 p1466 A72-24330

SOMMERFELD APPROXIMATION

- Altitude dependence of vlf field of vertical electric dipole in spherical waveguide of radially inhomogeneous ionosphere and earth, using Sommerfeld integral representations
08 p1130 A72-20736
- Wire antenna half-space problem analysis by Sommerfeld integral approach and plane wave reflection coefficient approximation
14 p2085 A72-30338
- Altitude dependence of VLF field of vertical electric dipole in spherical waveguide of radially inhomogeneous ionosphere and earth, using Sommerfeld integral representations
19 p2766 A72-38364

SOMMERFELD WAVES

- Coupled thermoelasticity in infinite body with cavity, introducing Sommerfeld type scalar potential and temperature radiation conditions
02 p0259 A72-12236
- Microwave resonators excited in coupled and E sub zero modes, determining equivalent circuit and Sommerfeld resonator Q factor and guide wavelength
11 p1605 A72-26369

SONAR

- Double ended scan converters for multisensor data display in radar, sonar and TV applications
02 p0193 A72-12394
- Narrow-band radar/sonar signal optimal detection under known direction and uncertain phase/arrival time conditions, considering statistical signal sampling
02 p0180 A72-12572
- Regulating amplifier with optoelectronic coupler for sonar sea bed layer measurements
09 p1284 A72-22239
- Operator independence test for human performance reliability modelling based on symptom detection and fault location of sonar system failure
10 p1429 A72-24002
- Sensitivity loss from approximation to radar and sonar signal square law detectors in quadrature systems with postdetection integration
10 p1437 A72-24690
- Sonar techniques application to radar, stressing utilization of preformed channels in rapid and distant detection of satellites and ballistic missiles
15 p2197 A72-31874

SONDES

- NT IONOSONDES
NT RADIOSONDES
NT RAWINSONDES
Free atmosphere vertical temperature structure at mesoscale, using continuous recording sonde
[AD-739147] 04 p0519 A72-15158

SONIC BOOMS

- Finite element method for determining transient response of box-type structure to traveling sonic pressure wave
01 p0136 A72-10219
- Sonic boom pressure signatures during F-104 overflights at Mach 1.3 and 30,000 ft, explaining variations by atmospheric turbulence
01 p0006 A72-11158
- Real gas effects in atmosphere to make sonic bang shock wave full dispersion and thickness wide variations
02 p0154 A72-11972
- Transonic air transport design, discussing wind tunnel tests, supercritical flow technology, sonic beam avoidance, cruising speed, operating costs and transport family development
03 p0310 A72-13487
- Sonic boom generation, propagation and minimization, discussing atmospheric conditions and ground characteristics influence and means for boom signature reduction
04 p0464 A72-14815
- N-wave dynamic magnification factors for sonic bangs response on complicated structures
04 p0464 A72-14849
- Sonic boom generation, propagation and minimization, discussing atmospheric turbulence and temperature gradients and aircraft configuration effects
[AIAA PAPER 72-194] 05 p0612 A72-16849
- Sonic boom signature by bicharacteristic method, correcting zeroth order/free stream characteristics to obtain solution to compressible fluid exact equations of motion
[AIAA PAPER 72-195] 05 p0652 A72-16907
- SST operational maneuver effects on sonic boom, discussing steady flight and acceleration-to-cruise pressure signatures
[AIAA PAPER 72-196] 05 p0613 A72-16981
- Characteristic overpressure concept for sonic bangs effect on structures and dynamic magnification factor engineering formula
06 p0758 A72-17858
- Simulated sonic boom effect on tracking performance and autonomic response, noting heart rates, skin conductance and startle reflex
06 p0767 A72-17868
- Ground focus line location of sonic bang propagation in stratified atmosphere with wind for transonically accelerating aircraft
07 p0912 A72-19645

Turbojet and turbofan engines noise signatures and sonic boom effects, discussing frequency spectra, atmospheric attenuation and noise suppression systems
07 p0912 A72-20163

Booms generated on ground by supersonic aircraft flying at high altitude through stratified atmosphere
08 p1149 A72-21019

Acoustic tests of jet aircraft noise and sonic boom effects on sleep pattern and human performance, using EEG analysis
[ASA PAPER W11] 08 p1125 A72-21487

Sonic booms - Conference, Houston, November 1970
08 p1110 A72-21901

Sonic booms generation theory and prediction methods for supersonic aircraft during nonaccelerated flight in quiet atmosphere
08 p1110 A72-21902

Sonic boom minimization, obtaining positive phase signature pressures as function of altitude, Mach number, weight and length
08 p1110 A72-21903

Maneuvering aircraft sonic boom propagation and signatures prediction in stratified atmosphere by geometric acoustic method
08 p1110 A72-21904

Atmospheric stratification irregularities effects on sonic boom propagation, obtaining probability density functions
08 p1111 A72-21905

Sonic boom simulation devices and techniques, including wind tunnels, ballistic ranges, spark discharges and shock tubes
08 p1147 A72-21906

Seismic and underwater effects of sonic booms, comparing theory with experiments
08 p1162 A72-21907

Building structures response to transient pressures caused by sonic booms, discussing three dimensional loading effects, air cavity coupling and nonlinearities influence
08 p1249 A72-21908

Animal response to sonic booms, considering mink reactions in detail
08 p1119 A72-21909

Human response to sonic booms, discussing super-sonic commercial flights acceptability
08 p1127 A72-21910

Concorde sonic boom measurement, discussing structural vibrational response
08 p1111 A72-21911

Sonic boom exposure effect on humans based on visual performance and tracking tests
08 p1127 A72-21912

Sonic booms generation and propagation, discussing effects on animate and inanimate objects
09 p1262 A72-23316

Sonic boom research facilities and techniques emphasizing applicability to other environmental problems
09 p1262 A72-23317

Sonic boom effects on structures, discussing ground motion, direct excitation by shock waves and damages
09 p1304 A72-23318

Sleep disturbance due to sonic booms, discussing laboratory findings and experimental techniques standardization
09 p1273 A72-23319

Human reactions to sonic boom acoustic stimuli, noting startle reflex responses
09 p1267 A72-23320

Human annoyance reactions to sonic booms, discussing field and laboratory findings
09 p1273 A72-23321

Sonic booms effects on domestic and wild animals, discussing field and laboratory findings
09 p1267 A72-23322

Field and laboratory sonic boom simulators, noting required characteristics
09 p1292 A72-23323

Summary of 1971 Stockholm workshop on sonic boom effects, discussing humans, animals and structure exposure and interdisciplinary aspects
09 p1273 A72-23324

Mechano-acoustical network model for room-hallway-window system response to sonic booms or other transient loads, determining damping ratios
11 p1686 A72-25729

Hypersonic vehicle far field behavior for sonic boom strength, position and positive phase duration
11 p1617 A72-26002

Window response to sonic booms, establishing upper bounds by mechano-acoustical network modeling of one and two degree of freedom dynamic systems
13 p2057 A72-29091

Supersonic jet noise and sonic boom sources, propagation and reduction, considering airport community disturbances, aircraft cabin noise and fatigue problems
13 p1898 A72-29578

Sonic boom magnitude and location in stratified atmosphere calculated from gas dynamical equations for lifting body of revolution
13 p1898 A72-29585

Maximum overpressures of supersonic aircraft maneuvering-produced sonic booms occurring at geometrical acoustic ray focus points [acoustic cusps]
13 p1898 A72-29586

Acoustically scaled simulation of sonic boom N-wave energy penetration into ocean for flat air-water interface
13 p1951 A72-29587

Far field sonic boom approach effects, describing Whitham theory extension for ultimate N wave deviations for body configurations with continuous or discontinuous tangent
16 p2347 A72-33010

Analytical method of characteristics to determine front shock and sonic boom due to flat delta wing with supersonic leading edges
[DFVLR-SONDDR-205] 16 p2348 A72-33401

Sonic boom induced pressure wave propagation and attenuation in water, comparing ballistic range measurements with theoretical predictions
[AIAA PAPER 72-654] 16 p2349 A72-34080

Sonic boom alleviation by flow field alteration near supersonic aircraft, considering finite rise times, reduced overpressures and shock pressure rises
[AIAA PAPER 72-653] 16 p2349 A72-34081

Sonic boom induced flow field at supersonic/hypersonic speeds, using shock expansion method and hypersonic equivalence principle for sharp and blunt nosed bodies
[AIAA PAPER 72-652] 16 p2349 A72-34082

An estimate of sonic boom damage to large windows.
17 p2623 A72-34234

Sonic boom duration effects on thin circular elastic plate transient axisymmetric vibration via Hankel and Laplace transforms
18 p2734 A72-36409

Sonic jet noise pressure source model for radiated sound power and jet pressure frequency spectra ratio derivation with application to noise suppression
18 p2680 A72-36414

Theoretical and experimental studies of the focus of sonic booms.
18 p2642 A72-36506

Supersonic aircraft wing form influence on sonic boom, discussing supersonic wind tunnel tests for noise reduction
20 p2888 A72-39931

Canadian sonic boom simulation facilities.
[ICAS PAPER 72-26] 21 p3040 A72-41151

Closed form solution for the sonic boom in a polytropic atmosphere.
21 p2992 A72-41258

Supersonic aircraft focused sonic boom suppression by slowing down during turning flight, obtaining conditions for focus cut-off at ground by atmospheric refraction
23 p3251 A72-44125

Sonic boom effects on sleep - A field experiment on military and civilian populations.
23 p3261 A72-44370

Sonic boom startle - A field study in Meppen, West Germany.
24 p3374 A72-44916

SONIC FLOW
U TRANSONIC FLOW
SONIC SPEED
U ACOUSTIC VELOCITY
SONIC WAVEGUIDES
U ACOUSTIC DELAY LINES
SONOGRAMS
Intercoms 3 satellite vlf radiation and natural signals recording with circular antenna, whistler recorders, sonograms and spectroanalizers
08 p1157 A72-21146

Magnetosphere thermal plasma densities determination from hydromagnetic whistler digital sonograms and modified normalized dispersion curves
15 p2283 A72-31430

Intercoms 3 satellite VLF radiation and natural signals recording with circular antenna, whistler recorders, sonograms and spectroanalizers
20 p2903 A72-39251

SOOT
Soot oxidation rate from diffusion flame measurements extrapolated for gas turbine combustion chambers
05 p0747 A72-16368

Mean emissivity of a luminous flame - Spray combustion of liquid fuel.
18 p2740 A72-36148

SORBENTS
NT ADSORBENTS
SORPTION
NT ADSORPTION
NT CHEMISORPTION
Anion sorption mechanisms and product composition in anodic aluminum oxide filled with phosphate, chromate and sulfate solutions, discussing chemisorptive compound formation and oxide dehydration
05 p0624 A72-17053

Sorption properties of anodic aluminum oxides prepared in orthophosphoric and chromic acid solu-

tions, determining dependence on pH by isotopic labeling method
05 p0624 A72-17055

Heat stretching-induced changes effect on strength, sorption and structural properties of polyformaldehyde fibers, noting structural orientation enhancement and porosity growth
08 p1194 A72-21757

Equipment and techniques for He sorption by condensed gas layers at 0.1 picotorr
09 p1364 A72-23227

Thermogravimetric design, using electromagnetic microbalances and turbomolecular pump for automatic sorption isotherm measurements in surface area and pore size analyses
11 p1636 A72-26788

High temperature low pressure reaction kinetics of nitrogen sorption by titanium foil, using ultrahigh vacuum microbalance
12 p1777 A72-27045

SORTING
U CLASSIFYING
SOUND
U ACOUSTICS
SOUND ABSORPTION
U SOUND TRANSMISSION
SOUND AMPLIFICATION
Coupling between chemical kinetics and sound propagation, discussing conditions for amplification and attenuation of acoustic wave
13 p1912 A72-28547

Piezoelectric substrate covered with semiconductor layers, calculating sound amplification characteristics at microwave frequencies
15 p2197 A72-31893

Plane acoustic-gravity wave reflection, refraction and amplification at interface separating two fluids in relative motion, noting shear flow speed effect
16 p2383 A72-32968

SOUND BARRIER
U ACOUSTIC VELOCITY
SOUND DETECTORS
U SOUND TRANSDUCERS
SOUND FIELDS
Wideband acoustic pressure field sensing by moving receivers and sensors, calculating motion effects on response including directional pattern and gain
02 p0259 A72-12176

Sound reflection by dense doubly periodic grating parallel to rigid baffle, describing asymptotic characteristics by double lattice virtual mass including mirror image
03 p0387 A72-12914

Acoustical field from streamlined body of revolution moving in homogeneous gaseous medium past seminfinitesimal rigid screen, using Wiener-Hopf method for diffraction radiation
03 p0340 A72-12916

Acoustic field hf asymptotic characteristics after sound transmission through elastic shell, using integro-differential equations system
03 p0388 A72-12917

Holographic investigation of acoustical fields, describing shadowgraph recording apparatus for sound pressure amplitude distribution
03 p0352 A72-12918

Optical acoustic field recordings application to turbulent characteristics measurement for transparent media
05 p0660 A72-15848

Acoustic /ultrasonic/ holography techniques for acoustic field recording and image reconstruction in coherent light, including applications
07 p0981 A72-18920

Sound field measurement in circular and rectangular air duct with sound-absorbing walls /mufflers/, deriving empirical formula for attenuation frequency characteristics
09 p1354 A72-23683

Vibration of infinite thin plate coupled with acoustic field in surrounding fluid, using Fourier transformation
10 p1511 A72-24223

Two dimensional low Mach number sound field from line vortex passage around rigid half plane edge, calculating space-time variation by perturbation methods
10 p1468 A72-24370

Radiation resistance for natural modes of rectangular panel from far field acoustic radiation energy distribution
11 p1687 A72-26059

Acoustic /ultrasonic/ holography techniques for acoustic field recording and image reconstruction in coherent light, including applications
13 p1957 A72-29206

Unstable discharge regime of nonisothermal axisymmetric subsonic turbulent jet in acoustic field with local perturbations
13 p1943 A72-29883

Lighthill method for ohmic dissipation pulsation effect on sound field generated by turbulent flow of conducting fluid
14 p2141 A72-31001

Optical acoustic field recordings application to turbulent characteristics measurement for transparent media of fluid flows
15 p2232 A72-31267

Blowdown wind tunnel internal and external noise fields prediction by empirical method, considering valves, burners, turbulent boundary layers and exhaust jets as sources
[AIAA PAPER 72-668] 16 p2374 A72-34070

Supersonic jet noise mechanisms and scaling laws, studying acoustic fields for rectangular and axisymmetric nozzle configurations
[AIAA PAPER 72-641] 16 p2381 A72-34091

Space-modulated lateral emission of an ultrasonic beam in a solid
17 p2583 A72-35546

Multipole expansion of sound radiation from moving rigid bodies.
18 p2710 A72-36404

Separation and analysis of the acoustic field scattered by a rigid sphere.
18 p2710 A72-36408

Resonant mode sound field radiated by nonuniform slender circular cross section free-free beams, using dipole array modeling
18 p2710 A72-36410

Spheroids with surface vibration at specified normal velocity distributions, calculating acoustic radiation by Green function approach
18 p2710 A72-36412

The acoustics of axial flow machines.
18 p2685 A72-37204

Numerical study of the characteristic magnitudes of turbulence on the far sound field radiated by a subsonic jet
[ONERA, TP NO. 1058] 19 p2786 A72-37761

Uniform moving source radiated sound field from equivalent stationary source distribution via transformation based on retarded-time position and Doppler frequency shift
22 p3205 A72-42461

Holographic techniques in high intensity acoustic fields analysis, applying to chemistry, medicine and engineering
23 p3287 A72-43549

SOUND GENERATORS
Acoustic pulse generation and transmission loss characteristics measurement by single pulse method with simple shape to facilitate Fourier analysis
03 p0388 A72-12955

Sound generation in shear flow turbulence, discussing dependence on mean flow velocity and temperature
07 p0909 A72-20097

Circular jets sound generation analysis, using Lighthill equation and Michalke spectral method
[DFVLR-SONDDR-179] 07 p0910 A72-20100

Sonic booms generation theory and prediction methods for supersonic aircraft during nonaccelerated flight in quiet atmosphere
08 p1110 A72-21902

Field and laboratory sonic boom simulators, noting required characteristics
09 p1292 A72-23323

Acoustic waves generation in liquids by Q-switched ruby laser, noting transition from plane to spherical waves with dye concentration and focusing configuration variations
10 p1490 A72-23954

Turbulence generated sound due to interaction with sound absorbent liners, investigating dynamic process via rigid boundary model with homogeneous array of circular orifices or pistons
10 p1511 A72-24424

Matched acoustic generator for sweep frequency testing of power gain of fluoric amplifiers
[ASME PAPER 71-WA/FLCS-2] 10 p1423 A72-25051

Flexural vibrating free edge plate transducer with stepped thickness for high directional ultrasonic radiation generation in fluids
11 p1687 A72-26060

Sound generation by fluid flow interaction with sharp-edged vibrator, predicting sound radiation pressure by quasi-steady analysis based on reed velocity
13 p2005 A72-29562

Sound generation by finite rectangular plate vibrations, deriving radiated power as function of aspect ratio and vibration pattern
13 p2005 A72-29564

Moving sound sources spectral analysis techniques, discussing computer controlled one-third octave band and narrowband analysis
13 p2005 A72-29566

Fan noise estimation from equation involving delivery volume and pressure to correct ratings to generated sound power levels
16 p2377 A72-33323

Blowdown wind tunnel internal and external noise fields prediction by empirical method, considering valves, burners, turbulent boundary layers and exhaust jets as sources
[AIAA PAPER 72-668] 16 p2374 A72-34070

The acoustics of axial flow machines.
18 p2685 A72-37204

Linear acoustic model to predict axial flow turbomachinery aerodynamic sound generation including flow effects on radiation 19 p2788 A72-38568

Use of acoustic emission for the detection of weld and stress corrosion cracking. 20 p2925 A72-39283

Observation and analysis of simulated ultrasonic acoustic emission waves in plates and complex structures. 20 p2925 A72-39284

Theoretical model for acoustic emission relationship to fiber cracking during rising load tensile test on fiber reinforced composites 20 p2925 A72-39285

Acousto-optic modulation with coupled Gunn oscillator-piezoelectric structure. 20 p2960 A72-39702

Canadian sonic boom simulation facilities. 21 p3040 A72-41151 [ICAS PAPER 72-26]

Jet noise generation theory /Lighthill-Ffowkes Williams/ verification by model tests, discussing means of reducing or eliminating shock cells 21 p3047 A72-41852 [ICAS PAPER 72-55]

Uniform moving source radiated sound field from equivalent stationary source distribution via transformation based on retarded-time position and Doppler frequency shift 22 p3205 A72-42461

SOUND INTENSITY

Jet noise simple-source theory experimental verification, determining relation of measured sound power and jet pressure levels of turbojet engine 06 p0867 A72-17856

Mark VII ear performance calculation procedure for perceived loudness or noisiness levels relation to sound pressure, using experimental frequency weighting contours 08 p1127 A72-21895

Monaural perstimulatory loudness adaptation measurement by delayed and single simultaneous balance methods, discussing intensity, frequency and duration effects 08 p1127 A72-21896

Auditory adaptation tests confirmation of Small loudness model prediction of lower adaptation for test tone greater than adapting tone intensity 08 p1127 A72-21897

High intensity sound effects on electronic equipment and components in aircraft noise environment, noting whisker diode and printed circuit board damage 15 p2209 A72-32621

Auditory induction of fainter by louder sounds as perceptual phenomenon cancelling masking effects 16 p2354 A72-33170

Response bias and sensitivity variations in psychophysical test of rats discrimination between standard and attenuated auditory signal intensities 16 p2356 A72-33648

Sound reduction by barriers on the ground. 17 p2580 A72-34235

Determination of the functional state of the auditory analyzer through the action of short-term acoustic stimuli of increasing intensity 20 p2893 A72-38939

Turbulent combustion induced noise, discussing scaling rules for sound power and directional characteristics of radiated sound 20 p2984 A72-39557

Acoustic pressure and sound intensity levels and noise annoyance international standards for civil aircraft noise reduction 20 p2888 A72-39803

Reaction time to the second of two shortly spaced auditory signals both varying in intensity. 22 p3142 A72-42549

SOUND LOCALIZATION

Directional hearing perception threshold in normal and auditory-defective patients, studying frontal and median planes for rising and falling noise frequencies 02 p0158 A72-11740

Human cerebral hemodynamic changes during arousal and orienting reactions to auditory stimuli 16 p2353 A72-32993

SOUND MEASUREMENT

U ACOUSTIC MEASUREMENTS

SOUND PERCEPTION

U AUDITORY PERCEPTION

SOUND PRESSURE

Wideband acoustic pressure field sensing by moving receivers and sensors, calculating motion effects on response including directional pattern and gain 02 p0259 A72-12176

Hypersonic boundary layer transition in presence of wind tunnel noise, indicating rms sound pressure relationship to transition Reynolds number 02 p0151 A72-12278

Holographic investigation of acoustical fields, describing shadowgraph recording apparatus for sound pressure amplitude distribution 03 p0352 A72-12918

White noise mean square sound pressure in turbulent flow in cylindrical duct, using cross correlation technique [ASME PAPER 71-WA/FE-5] 05 p0647 A72-15936

Axial sound sources number, strengths and phases in jets, using experimental measurements of audio pressure in near field 05 p0652 A72-16910 [AIAA PAPER 72-159]

Sound pressure levels and acoustic fatigue tests for 11,200 and 9,300 pound thrust J-52 engines comparison in A-6A aircraft 07 p0910 A72-18757

Sound pressure in liquid layer bounded by oscillating plate under bending as function of boundary acoustic impedance 07 p1034 A72-18923

JT8D engine exhaust noise field, considering internal noise sources contribution from exhaust duct sound pressure measurements 07 p1054 A72-19331

Mean sound pressure level measurement with mobile microphone carriers, noting difference from mean energy density measurement 08 p1165 A72-21297

Mark VII ear performance calculation procedure for perceived loudness or noisiness levels relation to sound pressure, using experimental frequency weighting contours 08 p1127 A72-21895

Subsonic jet noise directivity prediction from acoustic pressure measurements 11 p1706 A72-26041

Sound generation by fluid flow interaction with sharp-edged vibrator, predicting sound radiation pressure by quasi-steady analysis based on reed velocity 13 p2005 A72-29562

Space-averaged sound pressure measurement by sequentially sampled microphone arrays, considering scanning rate and rms detector time constants effect 13 p1958 A72-29565

Compressor directivity determination at discrete frequencies by tone power separation from noise background, using Fourier analysis of sound pressure autocorrelation 13 p2028 A72-29572

Acoustic mode propagation and interaction in hard walled cylindrical ducts, determining pressure and power spectral densities from pressure cross spectrum measurements 15 p2277 A72-32018

Turbulence induced sound pressure level measurement for noise generated by grill in air flow, using streamlined probe microphone 16 p2344 A72-34001

Data correlation of jet noise total sound power and peak sideline overall sound pressure level for subsonic and supersonic convergent exhaust nozzles 16 p2381 A72-34089 [AIAA PAPER 72-643]

Design requirements for a quiet helicopter. 17 p2488 A72-34484 [AHS PREPRINT 604]

Sound propagation in duct shear layers. 17 p2582 A72-35413

Experimental determination of the aeroacoustic environment about a slender cone. 17 p2486 A72-35482 [AIAA PAPER 72-706]

The estimation of nonstationary spectra from moving acoustic source distributions. 17 p2583 A72-35486 [AIAA PAPER 72-667]

Sonic jet noise pressure source model for radiated sound power and jet pressure frequency spectra ratio derivation with application to noise suppression 18 p2680 A72-36414

A new approach to the measurement of very low acoustic noise levels. 20 p2953 A72-39554

Acoustic pressure and sound intensity levels and noise annoyance international standards for civil aircraft noise reduction 20 p2888 A72-39803

Response of the average pressure acting on the surface of an emitting circular transducer due to different reflecting objects. 21 p3055 A72-40948

Evaluation of transonic and supersonic wind-tunnel background noise and effects of surface pressure fluctuation measurements. 21 p3041 A72-41588 [AIAA PAPER 72-1004]

SOUND PROPAGATION

NT VOICE

Sound propagation and absorption mechanism in liquid-base foams explored by bubble pulsation and coupling mathematical model and distributed parameter mechanical analog 01 p0115 A72-10161

Sound wave propagation velocity in partially dissociated and ionized gas, discussing attenuation coefficient, chemical process relaxation time and high temperature oxygen and nitrogen calculations 01 p0051 A72-11212

Sound propagation in acoustic ducts with shear flow and wall lining by Ritz-Galerkin technique 04 p0511 A72-14848

Sound propagation within and radiated from annular duct flow, measuring acoustic distributions for single and multimode excitations 05 p0691 A72-16924 [AIAA PAPER 72-197]

Carbon fibers elastic modulus inference from electrical conductivity inverse correlation with sound propagation rates 08 p1191 A72-21498

Acoustic approximation of pressure step discontinuity sound propagation in attenuating and dispersive ionosphere 08 p1162 A72-22139

Combined translational and internal relaxation theory of sound propagation in polyatomic gases, using 17 moment approximation 11 p1687 A72-26054

Wave equation for sound velocity propagation in suspensions based on mass and momentum balances 11 p1687 A72-26056

Atmospheric infrasound measurement techniques and instrumentation for long distance propagation, considering wind and temperature effects 11 p1635 A72-26509

Coupling between chemical kinetics and sound propagation, discussing conditions for amplification and attenuation of acoustic wave 13 p1912 A72-28547

Electron contribution to phonon damping in anharmonic metal for collision-free regime, evaluating relaxation times 15 p2277 A72-31890

Atmospheric sound absorption prediction based four-gases composition and energy transfer mechanisms, comparing results with experiments at different humidities 15 p2277 A72-32020

Relativistic hydrodynamics and gravitational instability. 17 p2581 A72-35356

Sound propagation in duct shear layers. 17 p2582 A72-35413

Acoustic refraction and attenuation in cylindrical and annular ducts. 17 p2582 A72-35414

Space-modulated lateral emission of an ultrasonic beam in a solid 17 p2583 A72-35546

Theory of sound propagation in mixtures of monatomic gases. 17 p2583 A72-35613

Theoretical and experimental studies of the focus of sonic booms. 18 p2642 A72-36506

Vibration of an infinite thin plate coupled with a fluid 18 p2736 A72-37002

Sound propagation in ionized gases and electro acoustic effect. 21 p3085 A72-40993

A model of low-frequency sound propagation in a lined duct. 21 p3085 A72-41112

Thermal properties of polymers below 4 K. 22 p3197 A72-42800

The propagation of sound in a circular duct of continuously varying cross-sectional area. 22 p3207 A72-42911

Radiation properties of the semi-infinite vortex sheet. 24 p3359 A72-44918

SOUND TRANSDUCERS

NT ELECTROACOUSTIC TRANSDUCERS

NT MICROPHONES

Log-periodic interdigital transducer design to obtain wide bandwidth for acoustic surface waves 06 p0784 A72-18241

Acoustic wave detection in strain transducer consisting of silicon insulated gate field effect transistor with piezoelectric film incorporated in insulator region 08 p1168 A72-21556

Interdigital acoustic surface wave transducer impedance characteristics calculation from equivalent circuit, demonstrating effectiveness on delay lines [AD-743552] 09 p1316 A72-23421

Hot thermistor and hot-wire anemometer principles for phonocardiographic transducer design, using theory of hydraulic amplification with high SNR 10 p1430 A72-24374

Atmospheric turbulent coherent noise in pipe arrays design for infrasonic wave detection 11 p1689 A72-26511

SOUND TRANSMISSION

Resonant and nonresonant sound transmission through cylinder walls, using statistical analysis 02 p0260 A72-12374

Acoustic field hf asymptotic characteristics after sound transmission through elastic shell, using integro-differential equations system 03 p0388 A72-12917

Wall shear layers effect on sound attenuation spectra in acoustically lined rectangular ducts, noting dependence on Mach number 04 p0462 A72-14842

Cat and rabbit middle ear muscles contraction by electric stimulation of motor nerves, noting sound transmission reduction 08 p1115 A72-21136

Turbulence generated sound due to interaction with sound absorbent liners, investigating dynamic process via rigid boundary model with homogeneous array of circular orifices or pistons

10 p1511 A72-24424

Sound transmission loss through double leaf walls, noting correction for LF calculations

11 p1687 A72-26038

Boundary reflection and transmission of N-shaped acoustic shock wave radiated from circular pipe into free air space

12 p1844 A72-27262

Statistical energy analysis of sound-structural interaction, considering sound transmission through complex walls and piping systems and fluid filled container vibrations

13 p2005 A72-29556

Sound transmission loss and diffraction measurements by combined correlation and Fourier techniques

13 p2006 A72-29768

Waldman-Snyder equation application to sound absorption and dispersion in dilute polyatomic gases, presenting truncation procedure for perturbation function expansion in irreducible Cartesian tensors

14 p2131 A72-30673

Transmission of sound in ducts with thin shear layers - Convergence to the uniform flow case.

18 p2710 A72-36405

The utility of the Galerkin method for the acoustic transmission in an attenuating duct.

21 p3083 A72-40332

Bending waves propagation through flat plate forming rigid sound bridge between two parallel plates, calculating energy transfer at LF oscillations

22 p3234 A72-42128

Sound absorption in atmosphere at 20°C, predicting relaxation times and strengths in 100 Hz to 1 MHz as functions of relative humidity

23 p3285 A72-44112

Acoustic transmission and reflection by a shear discontinuity separating hot and cold regions.

23 p3315 A72-44373

SOUND VELOCITY

U ACUSTIC VELOCITY

SOUND WAVES

NT AERODYNAMIC NOISE

NT AIRCRAFT NOISE

NT ELECTROACOUSTIC WAVES

NT ENGINE NOISE

NT JET AIRCRAFT NOISE

NT LAMB WAVES

NT NOISE [SOUND]

NT ROCKET ENGINE NOISE

NT SONIC BOOMS

NT THERMAL NOISE

LF large scale oblique Alfvén wave propagation in turbulent ion acoustic plasma, investigating dispersion relation, Landau damping and interactions

01 p0107 A72-10137

Acoustic power radiated by jet aircraft fuselage structure exposed to turbulent boundary layer pressure field, evaluating noise reduction treatments

01 p0002 A72-10216

Sound radiation from axial flow fans running in turbulent flow, evaluating fluctuating lift on rotor blades due to incident gusts

01 p0002 A72-10220

Small harmonic oscillations of isothermal atmosphere due to acoustic-gravity wave downward reflection caused by kinematic viscosity increase with altitude

01 p0102 A72-10229

MHD waves nonlinear interaction in magnetosphere, calculating transverse Alfvén and magnetosonic and longitudinal acoustic wave decay instabilities

01 p0109 A72-10618

Zinc oxide longitudinal acoustic microwave transducer, measuring untuned insertion loss and electroacoustic coupling constant

01 p0042 A72-10705

Unstable sound waves in uranium plasma, taking into account fission power density, radiation diffusion and ionization variations

01 p0112 A72-11336

Moving load effect on circular cylindrical shell in acoustic medium, discussing free axisymmetric vibration mode, shape and frequencies

02 p0290 A72-11627

Papers on noise and vibration control covering acoustics in free space, outdoors, small enclosures and rooms, measurement, analysis and design problems

02 p0258 A72-12100

Unstiffened cylinders natural frequency equations, determining modal density distribution and acoustic radiation efficiency

02 p0293 A72-12373

Noise reduction by acoustic interference, using sound generators operating in antiphase mode to noise input

02 p0262 A72-12897

Dynamic calibration by sound wave of hot wire operated by constant resistance method, using open

resonance tube in homogeneous incompressible air flow

03 p0356 A72-13235

Apodized interdigital transducers acoustic surface wave front distortion, describing perturbation and compensation method

03 p0360 A72-13602

Hf electric field influence on electron drift instability and slow ion-acoustic waves for inhomogeneous magnetized plasma stabilization

04 p0555 A72-14617

Ionospheric hydromagnetic and acoustic gravity wave interactions, examining stratified nonisothermal atmospheric model

04 p0516 A72-14934

Nonstationary hydroacoustic wave diffraction at curvilinear rigid surface, deriving transfer function and radiation pressure

04 p0589 A72-15062

Closed form solution of wave equation for sound wave scattering by rotating cylinders and spheres

04 p0550 A72-15567

Dispersion equation derived for acoustic-gravity type natural modes in solar atmosphere

05 p0712 A72-15769

Acoustic radiation pressure of small radius spherical obstacle in high level harmonic plane field for application to microphone calibration [ONERA, TP NO. 1008]

05 p0661 A72-16023

Pressure source model of sound radiated by sonic jet, deriving frequency spectra ratio and jet pressure

05 p0600 A72-16105

Ion-acoustic instability in ionosphere in presence of fast particles inhomogeneity, estimating ions and electrons drift velocities

05 p0656 A72-16245

Sound effect on diffusion flames, presenting vortex model

05 p0747 A72-16701

Dispersion properties of drift waves in low-beta weakly collisional plasma in presence of ion acoustic or Langmuir waves parallel to magnetic lines

05 p0698 A72-17019

Acoustic waves generation in afterglow of weakly ionized low pressure He plasma, using electrostatic probe

05 p0699 A72-17083

Ion-acoustic waves and ionization waves instabilities in gas discharge plasmas

05 p0699 A72-17222

Perturbed density and ion velocity distribution functions of grid-excited ion acoustic waves in collisionless plasma in single ended Q device

06 p0855 A72-17511

Pseudowaves and ion acoustic waves simulation, calculating time evolution of ion distribution for oscillating negative plasma potentials applied at grid

06 p0855 A72-17512

Parametric excitation of ion-acoustic waves in Q machine plasma, controlling electron temperature by amplitude modulated rf heating

06 p0855 A72-17513

Plasma microinstabilities due to ion acoustic waves propagation with double-humped ion velocity distribution function in Q machine

06 p0855 A72-17516

Energy absorption measurements of ion heating by ion-acoustic waves in ion streaming plasma

06 p0856 A72-17518

Ion acoustic wave excitation in plasma by modulated energetic electron beam, compared with grid excitation

06 p0856 A72-17519

Cylindrical plasma ion-acoustic resonance measurements from various excitation methods for noise component identification

06 p0856 A72-17523

Ion acoustic waves instability from electron-ion temperature difference in homogeneous collisional ionized plasma, using fluid equations perturbation analysis

06 p0856 A72-17524

Wake behind body moving in plasma parallel to magnetic field, observing coupling with parallel ion acoustic waves and with perpendicular Bernstein modes

06 p0875 A72-17525

Trapped ion instability in collisionless plasma ion acoustic waves, discussing sideband waves frequency spectrum and growth rate

06 p0859 A72-17545

Ion sound waves decay instability induced by large amplitude Bernstein mode in plasma

06 p0859 A72-17546

Ion heating caused by ion acoustic waves in ion streaming argon plasma

06 p0860 A72-17746

Ion acoustic and cyclotron harmonic plasma waves parametric excitation by hf electric field, measuring thresholds and growth rates agreeable with theory

06 p0861 A72-17827

Acoustic waves refraction, reflection and transmission from moving medium layer with space-dependent

velocity, considering Poiseuille flow three sublayer approximation

06 p0848 A72-17852

Weighted acoustic surface wave dispersive microwave filter apodized interdigital array design modification for phase error correction to reduce distortion

06 p0787 A72-18380

Spacecraft incipient failure detection, stressing acoustic energy release techniques

07 p0964 A72-18829

Oscillations and acoustic emission by interacting elastic shells in connecting medium, using quadratures with Green function

07 p1034 A72-18922

Ion-acoustic solitary waves formation and interaction in collisionless warm plasma, using Vlasov equation for ions and Boltzmann distribution for electrons

07 p1041 A72-19507

Laser probes for acoustic surface wave amplitude and phase measurements

07 p1008 A72-20385

Ion-sound plasma turbulence theory, considering collisionless shock waves data and anomalous resistivity calculations

07 p1045 A72-20480

Nonlinear ion acoustic instability in plasma for sub-harmonic and harmonic forcing oscillations similar to Van der Pol effect

07 p1046 A72-20541

Acoustic and gravity waves nonlinear propagation and structural deformation in isothermal and incompressible atmospheres with traveling wave induction

07 p0981 A72-20696

Moving plasma heating by fast large amplitude hf magnetoacoustic wave, noting Doppler effect resonance splitting

08 p1212 A72-21070

Growth rate estimation of negative energy Bernstein and ion acoustic waves explosive interaction, noting collisionless shock turbulence

08 p1212 A72-21248

Sound wave propagation in plasma, attributing acoustic cavity resonance curve sharpening to collisional energy transfer from electrons to neutrals

08 p1213 A72-21256

Slow and fast longitudinal ion acoustic waves in plasma cylinder under axial magnetic field

08 p1215 A72-21873

Electron Larmor radius effect on hf hose and mirror instabilities of fast magnetoacoustic and ion acoustic waves in nonisothermal plasma

08 p1215 A72-21874

Ray trace of sound refraction by point source on jet flow axis, numerically calculating directivity pattern

08 p1152 A72-21893

Sound refraction by sinusoidal point source in subsonic jet flow, obtaining solution by finite difference method for comparison with ray tracing results

08 p1152 A72-21894

Quartz crystals ultrasonic vibrations produced by laser beam, noting light modulation depth dependence on effective cross section and amplitude

09 p1322 A72-22415

Self consistent collisionless theory of turbulent low Mach number ion-acoustic shocks, noting resistive heating

09 p1360 A72-22872

Propagating crack properties characterization during fatigue cycling, using ultrasonic flaw detection and acoustic emission

09 p1310 A72-22922

Stable large amplitude high Mach number ion acoustic shocks in collisionless plasma, obtaining electron density as function of time

09 p1364 A72-23445

Ar/He plasma acoustic wave properties, expressing phase velocity and damping as function of ion-electron temperature ratio and relative species densities

10 p1520 A72-24300

Sound waves radiative damping in isothermal atmosphere, discussing relaxation influence on model response to body force and chromosphere dissipation effect on oscillation

10 p1543 A72-24622

Phase velocity and Landau damping of ion acoustic waves propagating through plasma boundary layer at conducting sphere or cylinder based on two fluid model

10 p1523 A72-24746

Surface acoustic wave technology in communication systems, discussing analog and digital matched filters and navigation, ATC and collision avoidance applications

10 p1483 A72-24940

Burning gunpowder surface reactions relative to temperature, chemical enthalpy and acoustic waves of pressure, velocity and density

11 p1744 A72-25337

Grid produced LF electrostatic perturbations propagation and damping in near isothermal plasma, discussing ion ballistic contributions to ion acoustic waves

11 p1692 A72-25520

Fracture surface energy and acoustic emission of boron fiberepoxy resin composite, using linear elastic fracture mechanics and compliance variation methods 11 p1674 A72-25858

Schlieren visualization of radiated wave fronts for Al plates illuminated with short acoustical pulses in water, comparing with Lamb theory 11 p1687 A72-26057

Radiation resistance of baffled beam modes from far field acoustic power intensity 11 p1687 A72-26058

Sound radiation impedance of vibrating prolate spheroids as function of nearfield variation 11 p1688 A72-26064

Negative auroral arc infrasonic wave observations during substorm poleward expansions at Inuvik, Canada 11 p1627 A72-26516

Bibliography on infrasonic sound wave generation, propagation and detection at ground level and ionospheric heights 11 p1690 A72-26520

Plasma sheath from plane negatively biased electrode immersed in low pressure discharge investigated by ion acoustic waves and hot probe 12 p1850 A72-27279

Acoustic pressure wave effect on motion of elastic conical shell fastened in rigid screen, using Timoshenko theory 13 p2055 A72-28772

Plane sound wave scattering by acoustically soft sphere at constant subsonic velocity 13 p2003 A72-28797

Infinite plane plates sound radiation due to bending waves interactions with density and stiffness fluctuations in material 13 p2004 A72-29094

Weak ion-acoustic quasi-shock wave propagation in collisionless plasma, determining long time behavior of precursor ion stream reflected by electrostatic potential 13 p2012 A72-29125

Parametric decay instability of Langmuir and acoustic plasma waves induced by incident electromagnetic wave near plasma frequency, noting application to ionospheric instabilities 13 p2012 A72-29126

Oscillations and acoustic emission by interacting elastic shells in connecting medium, using quadratures with Green function 13 p2004 A72-29208

Acoustic dipole radiation by wall pressure fluctuations in turbulent boundary layer flow over rigid and plane surface at low Mach number 13 p1894 A72-29583

Alternating magnetic field effect on collisionless nonhomogeneous magnetoplasma ion acoustic oscillations stability, examining parametric excitation of Langmuir oscillations 13 p2016 A72-29604

Sound radiation by shock wave front in cesium vapors, describing experimental shock tube 13 p2017 A72-29608

Radio aurora ion-acoustic wave propagation direction divergence due to magnetic field distortion by large ionospheric horizontal sheet current [AD-746367] 13 p1923 A72-29662

Dispersion characteristics of ion-acoustic waves in positive gas discharge plasma column 13 p2019 A72-29912

Directional dependence of sound wave emission by convective turbulence in solar atmosphere, considering cut-off frequency effects on transmitted acoustic spectrum 13 p2048 A72-29926

Stationary nonlinear ion acoustic oscillations in dense weakly ionized current carrying plasma, considering wave propagation velocity and instability process 13 p2019 A72-29988

Ion-acoustic oscillations effect on turbulent plasma electric conductivity within weak external electric field 13 p2019 A72-29990

Acoustic shock wave diffraction at moving or static plate immersed in ideal gas 13 p1943 A72-30011

Ion sound turbulence in dense plasma within magnetic field, representing global equilibrium spectrum 14 p2137 A72-30356

Acoustic wave diffraction at fixed plate boundary, determining velocity field by inverting Volterra-type integral equations 14 p2070 A72-31016

Dislocation motions as internal friction mechanism in solids due to medium frequency acoustic waves, considering motional energy transfer to thermal phonons and lattice vibrations 15 p2292 A72-31833

High amplitude ultrasonic stress waves effect on metals elastic and plastic deformation characteristics, verifying model for sound waves-lattice structure interactions 15 p2328 A72-31842

Acoustic mode propagation and interaction in hard walled cylindrical ducts, determining pressure and power spectral densities from pressure cross spectrum measurements 15 p2277 A72-32018

Ion acoustic and guided electron plasma waves excitation by grid antenna produced LF signals in cylindrical plasma column 15 p2289 A72-32650

Acoustic emission from carbon fiber-epoxy composite during continuous tensile stress cycling 16 p2413 A72-32868

Plane acoustic-gravity wave reflection, refraction and amplification at interface separating two fluids in relative motion, noting shear flow speed effect 16 p2383 A72-32968

Nondestructive vibration analysis of mechanical structures, using digital computer technique for sound wave spectrum analysis 16 p2397 A72-33220

Acoustic tunnel effect in elastic waveguide, noting penetration coefficient and quantum mechanics potential barrier 16 p2364 A72-33588

Plasmapause and geomagnetic micropulsations correlation from universal magnetospheric instability model, noting drift waves conversion to sound or Alfvén waves 16 p2387 A72-33906

Book on basic acoustics covering mathematical methods, diffraction phenomena, statistical theory of signal processing, wave acoustics, membrane sound radiation, music, source array theory, etc 16 p2427 A72-33973

Acoustic radiation from multiple spheres 17 p2579 A72-34226

Ion heating via turbulent ion acoustic waves 17 p2588 A72-34873

A modified Navier-Stokes equation, and its consequences on sound dispersion 17 p2540 A72-35146

Damping coefficient measurement for sound waves inside cylindrical tube closed at one end and excited at other end by loudspeaker 17 p2582 A72-35426

The steepening of the wavefront due to nonlinearities /An electric model test regarding the origin of shock waves/ 17 p2582 A72-35428

Sonic discontinuities in a radiative gas 17 p2582 A72-35435

Acoustic power spectrum of a subsonic jet 17 p2541 A72-35544

A stability mechanism for the ion-acoustic waves 17 p2592 A72-35625

Beam-generated collisionless ion-acoustic shocks 17 p2592 A72-35626

Nonlinear saturation of 'type I' irregularities in the equatorial electrojet 18 p2685 A72-35990

High-speed image scanning devices using acoustic surface waves and photodiode array 18 p2658 A72-36267

Multipole expansion of sound radiation from moving rigid bodies 18 p2710 A72-36404

The radiation of sound from vibrating composite membranes 18 p2711 A72-36757

Independent moving vibrational /acoustic/ source-induced wave losses during friction of two elastic bodies 18 p2696 A72-36966

Vibration of an infinite thin plate coupled with a fluid 18 p2736 A72-37002

Nature of sound dispersion in a plasma 18 p2717 A72-37178

Short-wave asymptotic representation of the solution to the problem of diffraction by a circular disk 19 p2769 A72-38849

Acoustic and gravity waves nonlinear propagation and structural deformation in isothermal and incompressible atmospheres with traveling wave induction 20 p2915 A72-39011

Acoustic emission; Proceedings of the Symposium, Bal Harbour, Fla., December 7, 8, 1971. 20 p2924 A72-39276

Acoustic emission testing and microcracking processes 20 p2924 A72-39277

Acoustic emission experiments design based on piezoelectric transducer, discussing signal detection and data acquisition methods 20 p2924 A72-39278

Factors affecting acoustic emission response from materials 20 p2924 A72-39279

Dislocation motion as a source of acoustic emission 20 p2924 A72-39280

Correlation analysis techniques to characterize acoustic emission pulses from Mg alloys, obtaining time varying spectra 20 p2924 A72-39281

Crack growth behavior correlation to acoustic emission signal amplitude distribution in high strength steel heat treated to different fracture toughness values 20 p2924 A72-39282

Turbulent combustion induced noise, discussing scaling rules for sound power and directional characteristics of radiated sound 20 p2984 A72-39557

Amplification of acoustic surface waves under transverse magnetic field in coupled intrinsic semiconductor-piezoelectric systems 20 p2960 A72-39703

Acoustic emissions and energy transfer during crack propagation 20 p2981 A72-39925

Experimental investigation of the influence of acoustic oscillations on the evaporation intensity of liquid droplets 20 p2987 A72-40037

Microwave scattering from a radially propagating ion acoustic wave in a positive column 21 p3089 A72-40203

Plane acoustic pressure wave effect on motion of thin elastic truncated conical shell fastened in rigid screen, using Timoshenko theory 21 p3116 A72-40263

Nonexistence of ion acoustic waves and Landau damping driven electrostatically in an ideal Q machine 21 p3090 A72-40348

Alternating magnetic field effect on ionoacoustic oscillations stability of collisionless nonhomogeneous magnetoplasma, examining parametric excitation of Langmuir oscillations 21 p3091 A72-40658

Sound radiation generation by shock wave front in Cs vapors, describing experimental shock tube 21 p3091 A72-40662

Coulomb-collision corrected ion-acoustic linear profiles 21 p3092 A72-40819

Excitation of volume ion-acoustic oscillations in an inhomogeneous dense plasma by the field of an electromagnetic wave 21 p3092 A72-40836

Linear and nonlinear aspects of ion-sound current instability for solar atmosphere conditions of full ionization, noting implications for flare mechanism 21 p3100 A72-41040

Wall temperature, thermal conductivity and acoustic vibration frequency as function of critical heat flux density for unstable water film boiling conditions 21 p3130 A72-41065

Sideband waves excitation by large amplitude ion acoustic waves in collisionless plasma, noting frequency spectrum and growth rate agreement with trapped particles theory 21 p3094 A72-41626

Quasi-static loading of the earth by propagating acoustic waves 22 p3172 A72-42466

Acoustic shock wave diffraction at moving or stationary flat plate immersed in ideal gas 22 p3206 A72-42732

Reflection and transformation of sound waves in a superfluid liquid at a solid boundary 22 p3207 A72-42956

Electromagnetic waves interaction with transverse waves of thin piezoelectric plate in waveguide, noting transformation into acoustic waves 23 p3312 A72-43407

Stationary solitary, snoidal and sinusoidal ion acoustic waves 23 p3320 A72-43520

Electronic devices with Rayleigh ultrasonic acoustic surface wave excitation for storage, recognition and separation of electrical signals usually requiring computerized operation 23 p3314 A72-44148

Acoustical holography with a scanned linear array 24 p3401 A72-44702

Diffraction of an acoustic wave by a stationary plate 24 p3360 A72-44987

A bibliographical survey of acoustic emission 24 p3408 A72-45293

High-frequency instabilities in a plasma with a nonlinear ion-acoustic wave 24 p3429 A72-45489

Effects of pseudosonic and electroacoustic waves on the radiation of a plasma-coated spherical antenna 24 p3386 A72-45642

SOUND-SOUND INTERACTIONS

Lift fan blade interaction discrete frequency noise; discussing potential and viscous interactions relation to rotor-stator spacing 15 p2297 A72-32019

SOUNDERS

U SOUNDING

SOUNDING

NT BALLOON SOUNDING

NT IONOSPHERIC SOUNDING

NT ROCKET SOUNDING

- Mesosphere meteorological sounding by acoustic grenade and pitot probe techniques, investigating seasonal and latitudinal variations
03 p0383 A72-13384
- Spectroscopic sounding of clouds and snow and ice covers from below /earth surface/ and above /space or planet/
16 p2417 A72-33288
- ### OUNDING ROCKETS
- NT SKUA ROCKET VEHICLES
NT SKYLARK ROCKET VEHICLE
- Sounding rockets spin rate sensor, describing apparatus operation and size and weight reduction
01 p0071 A72-11173
- EUV and soft X ray images of sun from sounding rocket experiments
03 p0415 A72-12934
- Motion equations of constrained split fairing for avoiding contamination of sounding rocket payload environment by uncontained explosive actuation device
05 p0724 A72-16102
- Three-axis attitude control and stabilization system for sounding rocket payload, discussing performance from simulation and ground test results
05 p0728 A72-16478
- Sounding rocket programs and balloon implemented upper atmosphere research in Australia
07 p1070 A72-19088
- Sounding rocket radio tracking systems with real time trajectory plotting, developing computer program for exoatmospheric trajectory determination
07 p0939 A72-19089
- Photometer using rotating wedge interference filter as wavelength scanning element near 6300 Å for high altitude sounding rocket application
07 p0985 A72-19403
- Parachute design for very high altitude sounding rockets, discussing stability and descent velocity requirements and test methods
07 p1085 A72-19604
- Attitude reference platforms in ASTRID and DACHS control systems for high altitude research rockets
07 p0990 A72-20283
- High performance sounding rockets design, discussing Skylark propulsion system improvement and new rocket vehicle design for 200 kg payload capability with existing motor hardware
08 p1241 A72-21172
- Sounding rocket payloads environmental testing, discussing test techniques for shock, vibration, temperature, humidity, pressure, contamination, corrosion effects during handling, storage, launch, flight and recovery
08 p1241 A72-21173
- ESRO sounding rockets program survey, discussing launchings in terms of number, vehicle types and sites, member participation, payload integration policy and success rate
10 p1551 A72-24197
- Space environment and astronomical studies with sounding rockets, satellites and orbiting solar observations
10 p1548 A72-24974
- Low cost meteorological sounding rocket evolution, including Arcas, Lokidart and Viper Dart systems for various altitude ranges
10 p1552 A72-25090
- Sounding rocket heat pipe experiment in zero gravity, testing spiral and pedestal arteries and plain groove designs
11 p1739 A72-25204
- [AIAA PAPER 72-259]
Stability criteria for limiting oscillatory motion of coasting sounding rocket exiting atmosphere
13 p2051 A72-28886
- Two stage solid propellant sounding rocket, discussing engine design, operation and tests
13 p2052 A72-29859
- Upper atmosphere research rockets missions, payloads and measurements, describing various international aeronomy research projects
13 p2052 A72-30081
- Equipment for ground and sea recovery of sounding rocket payloads, discussing airbrakes, buoy and parachute assemblies
15 p2319 A72-31690
- Parachute systems and flotation gear used to recover sounding rocket payloads and components after water landings
15 p2320 A72-31691
- Report to COSPAR on Australian space program covering earth atmosphere, cosmic and synchrotron radiation, X ray astronomy, weather satellites, deep space and sounding rockets
15 p2338 A72-32007
- Japanese report to COSPAR on space research by sounding rockets, balloons and SHINSEI scientific satellite
15 p2338 A72-32011
- Report to COSPAR on Argentina space program covering sounding rockets and balloons and Experimental Inter-American Meteorological Network meteorological rocket launchings
15 p2338 A72-32015
- ESRO report to COSPAR on satellites in orbit and under development and on 1971 sounding rocket program
15 p2338 A72-32016
- Sounding rocket experiment on nonlinear interaction between two electron plasma waves and ion acoustic wave in ionosphere to investigate artificial realization feasibility
15 p2331 A72-32333
- Mobile launching facility for high altitude sounding rockets, describing telemetered data recording, radar and optical tracking, range safety and payload recovery equipment
16 p2374 A72-33499
- [DGLR PAPER 72-012]
Reusable two-stage meteorological rocket vehicle, discussing design, performance, second stage recovery technique and cost
17 p2619 A72-34185
- Simulation in plasma wind tunnels of the environmental conditions for sounding rocket experiments
20 p2912 A72-39928
- Ground and flight tests of the Ramzes rocket sonde
21 p3115 A72-41499
- The dynamics of the ascending flight of sounding rockets
22 p3231 A72-42582
- [ONERA, TP NO. 1056]
Sounding rockets for astronomical research, discussing rocket types, payloads, launch sites, advantages over satellites, economic factors and future prospects
22 p3231 A72-42983
- ### SOUTHEAST ASIA
- Plate convergence, transcurent faults, and internal deformation adjacent to Southeast Asia and the Western Pacific.
20 p2917 A72-39479
- ### SOUTHERN HEMISPHERE
- NT ANTARCTIC REGIONS
- French-U.S. Eole meteorological satellite project to map Southern Hemisphere winds, describing system based on pressurized balloons for data acquisition
11 p1680 A72-25813
- Global horizontal sounding technique balloon flights, determining Southern Hemisphere temperate latitude circulation climatology
13 p1988 A72-28443
- Explorer 19 satellite drag evidence for neutral exosphere He concentration asymmetry between Northern and Southern Hemispheres over entire solar activity cycle
15 p2228 A72-31977
- Stratospheric winds and winter warmings in the Southern Hemisphere.
20 p2948 A72-39862
- Satellite-observed Southern Hemisphere cloud vortices in relation to conventional observations.
23 p3285 A72-44145
- ### SOYUZ SPACECRAFT
- Soyuz 9 flight crew physiological data, discussing mental and physical performance and adaptation and readaptation to space-earth environments
01 p0020 A72-10933
- Soyuz manned spacecraft meteorological observations, dealing cloud cover in various climatic zones, atmospheric turbidity and snow cover in mountain areas
02 p0253 A72-11731
- Natural formation interpretation from spectrophotometric measurements of underlying earth surface from manned spacecraft Soyuz 7 and Soyuz 9
02 p0228 A72-11887
- Radiation doses received by cosmonauts in manned Soyuz 3-9 from mission retrieved thermoluminescent glass dosimeters
02 p0168 A72-12075
- [CERN-71-16]
Soviet manned space flight history and characteristics, discussing Vostok, Voskhod and Soyuz vehicles
03 p0440 A72-13475
- Manual orbital control used on Soyuz spacecraft in orbital flight, investigating equations of motion and pilot work load
05 p0725 A72-16438
- Soyuz 5 satellite vehicle space flight factors effect on chlorella cells, investigating survival rates and mutability
05 p0623 A72-16776
- Skylink project as prospective joint American-Soviet space mission, combining Skylab and Soyuz spacecraft
05 p0731 A72-17092
- Design of Salyut manned orbital laboratory combined with Soyuz service module
12 p1876 A72-27107
- Soyuz 9 spectrophotometry of earth surface features, comparing manned spacecraft-obtained and conventional spectrographs
14 p2100 A72-30464
- Design features of Soyuz life support and launch escape systems and Vostok rocket booster stage
23 p3343 A72-44335
- ### SPACE BIOLOGY
- U EXOBIOLOGY
- ### SPACE CAPSULES
- NT ESCAPE CAPSULES
NT MERCURY SPACECRAFT
- ### SPACE CHARGE
- Monograph on electron beam welding covering space charge effect, equipment, metallurgical and mechanical aspects, production engineering, economics and applications
01 p0073 A72-10167
- High efficiency transferred electron microwave oscillators operated in short LSA mode, noting pulse-operated diode power appearance time delay behavior
01 p0036 A72-10634
- Size determination for stationary space charge clouds in streaming media from theoretical model of tanks filled with electrostatically chargeable inflammable fluids
02 p0261 A72-12554
- Gunn effect and associated phenomena, covering semiconductor domain formation and movement, space charge waves and thin samples with dielectric coatings
02 p0270 A72-12889
- Moving plasma beam capture by transverse magnetic field due to polarization space charges electrostatic separation
03 p0396 A72-13657
- Dc flow through p-n junction by modified Melehy force field method, discussing space charge variation in depletion layer
03 p0338 A72-13866
- Space charge recombination in forward biased diffused p-n junction silicon diodes
04 p0562 A72-15127
- Space charge layer /ion sheath/ effects on impedance of lf transmitting electric dipole in ionospheric plasma
04 p0490 A72-15399
- Semiconductor-dielectric system for controlling space charge and valley population redistribution by external field
05 p0702 A72-16201
- High pressure gas lasers excitation, determining energy introduction and space charge stability
05 p0668 A72-16415
- Two dimensional space charge wave propagation in semiconductors with anisotropic small signal mobility, investigating stability
05 p0632 A72-17097
- Separatrix structure and stability of helical Tornado trap magnetic field from electron space charge measurements
06 p0863 A72-18407
- LSA oscillators performance and control optimization, discussing multiaxis radial microwave cavity effectiveness in oscillation starting and coupling to coaxial transmission line
06 p0789 A72-18481
- High power GaAs LSA transmitter oscillator refinements, noting pulsers development to change load and thermal environment frequency stability
06 p0789 A72-18482
- Fast algorithm for space charge layer and semiconductor junction capacitance calculation, applying to impurity profile determination
07 p0954 A72-19120
- Physical parameters of transistor, discussing carrier transfer, space charge and potential drop as function of current and voltage changes
08 p1139 A72-21058
- Reverse biased p-n diffused junction design with two impurities in nonhomogeneous semiconductors, calculating depleted space charge region thickness
08 p1140 A72-21062
- Plasma potential determination near probe by space charge layer reactance observation
09 p1361 A72-22962
- HF thermal noise in single and double injection space charge limited solid state diodes
09 p1288 A72-23124
- Width of space charge layer of reverse-biased p-n junction in p-n-p-n structure effect on current density, mobile charge carriers and constituent transistors gain coefficients
10 p1526 A72-24584
- Space charge limited current theory of thin film organic semiconductor systems, investigating energy spectrum of traps and free carrier capture kinetics
11 p1700 A72-25783
- Signal propagation along homogeneous drifting electron beam focused by strong magnetic field, obtaining phase velocity and space charge density
13 p1914 A72-28373
- Field mill measurement of atmospheric electric space charge density, discussing effects of snow melting and artificial charge sources
13 p1952 A72-29666
- P channel MOS transistors hardening against ionizing radiation based on positive space charge density and electrode injection efficiency
13 p2023 A72-29837
- Nonlinear plasma oscillations effect on electron bunching in microwave devices, noting space charge waves of finite amplitude
14 p2089 A72-31106
- GaAs Gunn diode LSA operation mode in multiloop circuit to extend high frequency limit
15 p2207 A72-31888

Space charge electron flow between parallel conducting walls, developing relativistic method for potential and field distribution time variation

15 p2279 A72-32510

Electron trapping data in neutron irradiated high purity Si, using space charge limited current measurements

15 p2294 A72-32514

Plasma accumulation in electrostatic potential well produced by electron space charges, determining diocotron instability as function of electron plasma and gyrofrequency ratio

16 p2434 A72-32819

Pulsed discharge development mechanism relationship to carbon dioxide laser lasing process, considering positive space charge ion role

16 p2401 A72-33369

Separatrix shape, presence and position and electron lifetime and space charge in helical Tornado trap magnetic field

17 p2588 A72-34857

Propagation and instability characteristics of small signal electro-fluid-mechanical space charge and polarization waves in nonhomogeneous fluids

17 p2542 A72-35612

Plasma potential determination near probe by space charge layer reactance observation

17 p2593 A72-35892

LSA diode relaxation oscillator loading effect on oscillation damping, calculating optimum loading as function of conductance

18 p2667 A72-36690

Electromagnetic and space charge disturbance transmission and reflection at plasma boundary and oblique incidence, discussing isotropic Vlasov plasma

19 p2839 A72-37336

Dynamics of stratified liquids in the presence of space charge.

19 p2788 A72-38432

Interpretation of the preswitching behaviour of chalcogenide-glass switches in terms of a space-charge-injection mechanism.

21 p3034 A72-41466

Influence of a surface space charge on certain photoelectric properties of p-type gallium arsenide

21 p3098 A72-41684

Impedance of a unipolar semiconductor diode under conditions of space-charge limited current with allowance for recombination

23 p3270 A72-43630

Negative resistance, transit time and limited space charge accumulation modes of semiconductor devices operation with electron transitions

23 p3272 A72-44138

The negative space-charge density distribution and the potential distribution in a Penning discharge cell

23 p3324 A72-44211

The ionization of caesium vapour by the method of space charge amplification.

23 p3316 A72-44344

SPACE COMMUNICATION

NT LUNAR COMMUNICATION

NT REENTRY COMMUNICATION

NT SPACECRAFT COMMUNICATION

Convolutional coding, Viterbi decoding and binary phase shift keyed modulation for reliable communication on power limited satellite and space channels

01 p0026 A72-10342

Educational satellites - Conference, Nice, France, May 1971, covering space communication, TV, performance, data handling, economics, etc

01 p0147 A72-11277

Extraterrestrial life and civilization possibility in other planetary systems in universe, suggesting communication by hydrogen line frequency low harmonics

02 p0276 A72-11642

Multichannel space station communications using PCM-PSK-PM interplex modulation for reducing cross modulation loss

02 p0174 A72-12131

High data rate convolutional coding for space station telemetry links, considering sequential and cascaded Viterbi decoding

02 p0174 A72-12132

International frequency allocation table revision by World Administrative Radio Conference for Space Telecommunications

02 p0177 A72-12385

Frequency sharing criteria for terrestrial and space services, showing improved radio spectrum utilization and permissible interference

02 p0178 A72-12388

Book on global communication law covering maritime transport, civil aviation, radio, space communication postal services, international cooperation, etc

02 p0305 A72-12575

Book on radio wave propagation covering ground, tropospheric and ionospheric waves, atmospheric and cosmic noise, reflection, attenuation, signal distortion, space communication, etc

04 p0487 A72-15269

Millimeter wave and laser space-to-space communication links comparison, considering chf system based

on size, weight, power consumption and communication parameters calculations

04 p0493 A72-15609

Geodetic determination of geoid shape by computerized laser-effect space telemetry ground stations

04 p0495 A72-15724

Space real time data links during processing of French D2 scientific satellite for hydrogen frequency bands investigation

05 p0628 A72-16447

Noise parameters of space communication systems ground receiving antennas, considering noise effects on gain and radiation patterns

06 p0783 A72-17499

Wideband laser communication for space applications, comparing carbon dioxide and Nd-YAG systems on basis of SNR

07 p0941 A72-19239

Concatenated coded command system for low error probabilities at moderate SNR, emphasizing spaceborne portions implementation

07 p0949 A72-19299

International space communication systems legal and operational aspects, discussing Intelsat and Intersputnik systems

07 p1104 A72-19470

Space communication application for information, education and cultural exchange, noting need for international cooperation

07 p1104 A72-19473

International cooperation in space law problems, considering space communication systems, geostationary orbits use, frequency band allocation, world weather watch and earth resources survey programs

07 p1105 A72-19475

Laser communication systems for terrestrial and space data transmission, discussing line-of-sight requirements and atmospheric effects

07 p0947 A72-20225

Layer-like atmosphere discontinuities effects on earth-space communications, noting electromagnetic waves alteration and reflection by grazing incidence

09 p1279 A72-22898

Auto and cross correlation functions of combined binary pseudorandom sequences in digital space communication systems

10 p1439 A72-24907

Trojan deep space communications systems, maintaining powerful relay satellites in equilibrium at Lagrangian points of earth, Mars and Venus orbits

10 p1548 A72-24975

NASA program for acquisition, analysis and dissemination of space propagation and interference data for space systems designers, operators and regulatory agencies

[AIAA PAPER 72-577]

13 p1918 A72-28985

Limitations of technological state-of-the-art with satellite and space communications above 10 GHz.

19 p2765 A72-37940

Book - Eleventh report by the International Telecommunication Union on telecommunication and the peaceful uses of outer space.

20 p2988 A72-39025

Low noise microwave parametric amplifier design for space communication receivers, using inverted diode balanced mixers

21 p3025 A72-40304

The 20 and 30 GHz communications system for the ATS-F millimeter wave experiment.

21 p3019 A72-40882

Linguistic message decoding algorithms for communication with extraterrestrial intelligences, considering unified procedure and key problems solutions

24 p3382 A72-45226

SPACE DEBRIS

Daily mean amount of cosmic matter falling on earth

09 p1389 A72-23195

SPACE DENSITY

Cosmological density fluctuations in hadron stage, examining relativistic free particle and high temperature hadron gas models

03 p0426 A72-13273

Vlasov equation phase space boundary integration for evolution of one dimensional self gravitating collisionless stellar systems with constant density

05 p0714 A72-16056

Collective relaxation of two phase space density collisionless one dimensional self gravitating stellar systems, following boundary curve motion

05 p0714 A72-16057

Four phase space density collisionless one dimensional stellar system evolution in time by following motion of boundary curves

06 p0876 A72-17577

Space densities and time scales of Seyfert galaxies, radio galaxies and quasi-stellar objects

10 p1534 A72-23905

Rapid perturbation growth conditions for expanding universe, discussing background density decrease with time

10 p1543 A72-24661

One and two boundary curves systems for Vlasov equation of one dimensional collisionless self gravitating

stellar systems evolution with constant phase space density

12 p1874 A72-27911

Boundary curves for collective relaxation in one dimensional collisionless two phase space density self gravitating stellar system evolution, noting velocity dispersions dependence

12 p1875 A72-27911

Intercloud atomic H gas density distribution from 21 cm line width variations with galactic longitude

19 p2867 A72-38511

Fluid sphere of uniform density and vanishing pressure at periphery, expressing internal motion in terms of Schwarzschild mass and radius and central pressure

22 p3205 A72-42453

On irrotational Bianchi-type universes in the Brans-Dicke cosmology.

23 p3314 A72-44311

SPACE DETECTION AND TRACKING SYSTEM

Hybrid carrier and modulation tracking loops exploiting sideband coherency for phase coherent tracking, telemetry and command system performance improvements

07 p0939 A72-19066

SPACE DIVERSITY

U RECEPTION DIVERSITY

SPACE ELECTRIC ROCKET TESTS

Aerospace reliability methods, discussing distribution functions, sampling, accelerated life testing and case histories of space electric rocket and microthruster power conditioner tests

04 p0526 A72-14444

Space simulation facility for one year SERT 2 mercury ion thruster testing, discussing cryogenic operation and electrical and thermal insulation

[AIAA PAPER 72-430]

11 p1613 A72-26177

SPACE ENVIRONMENT

U AEROSPACE ENVIRONMENTS

SPACE ENVIRONMENT SIMULATION

NT WEIGHTLESSNESS SIMULATION

Silica based surface insulation material for space shuttle thermal protection system, discussing cyclic tests in simulated environment and fiber purity effects on crystallization

01 p0091 A72-10766

Microbial survivability in deep space environmental simulation experiments, describing aerospace ecology and panspermia avoidance

01 p0019 A72-10833

Multiprogrammed digital computer controlled acquisition and processing of quasi-static analog transmitter data during spacecraft environmental simulation tests

02 p0200 A72-12477

Space environment simulator with ultrahigh vacuum chamber and UV and corpuscular radiation for material samples physical properties in-situ measurement

02 p0201 A72-12704

Polymer fractionation in simulated Jovian atmosphere according to molecular weight, suggesting substance responsible for red color

04 p0572 A72-14777

AEROS aeronomy satellite solar cell array power supply system simulation tests under space conditions

04 p0466 A72-15654

Laboratory ionization chamber measurement of ion chemistry and production rates from partial simulation of disturbed nighttime ionosphere at 300 K

09 p1275 A72-22366

Thermal nodal analysis of spacecraft hull-canister model from space simulation test, using least squares estimation and regression analysis

09 p1412 A72-23498

Micrometeoroid simulation by accelerated microparticles bombardment of metal targets, discussing energy partition as function of impact velocity

09 p1409 A72-23666

ATS specular thermal control louver system performance in simulated solar vacuum environment as function of sun and blade angle, noting white paint effect

[AIAA PAPER 72-268]

11 p1740 A72-25209

Laboratory irradiation tests with van de Graaff generator for simulation of spacecraft component radiation damage due to high energy space protons and electrons

12 p1863 A72-27551

Solar cell array tests for high intensity application up to 0.3 AU from sun under simulated space environment

12 p1758 A72-28031

Prevention of weightlessness effects on blood hydrostatic pressure, musculoskeletal system and sensorimotor performance, discussing space flight training and space environment simulation tests

13 p1909 A72-28781

Amitetrayite /biological protectant/ effect on natural immunity state of dogs exposed to chronic gamma irradiation simulating space flight environment

14 p2074 A72-30388

Russian book on thermal simulation of spacecraft and space environment covering heat transfer, cosmic

radiation, vacuum chambers, radiant flux simulators, etc

15 p2319 A72-31275

Spacecraft thermal control materials research, discussing surface selection, coatings, space simulation and environmental effects

15 p2260 A72-31806

Solar wind and planetary atmosphere interaction observation by simulation of ionization mechanism in comet, using gun produced plasma stream and gas cloud

15 p2301 A72-32341

Space simulation shrouds cryogenically cooled with liquid carbon dioxide, discussing automatic temperature control and operating cost savings

15 p2214 A72-32611

Experimental motion sickness studies in slow rotation room simulating rotating spacecraft conditions, noting relation between subject susceptibility and number of head motions

16 p2354 A72-33542

German book on vacuum technology covering theory, measurement techniques and applications in nuclear physics research facilities, electronic tubes, space environment simulation, mass transfer, etc

18 p2709 A72-36250

Space environment simulation and testing techniques, considering vacuum systems, low temperature, solar radiation and motion simulation

18 p2676 A72-36833

Survival of common terrestrial microorganisms under simulated Jovian conditions.

19 p2755 A72-37721

Thermal control techniques used in space simulation laboratory testing.

22 p3164 A72-42997

SPACE ENVIRONMENTAL LUBRICATION

U SPACECRAFT LUBRICATION

SPACE ERECTABLE STRUCTURES

NT BEACON SATELLITES

ESRO satellite power supply solar paddles deployment mechanism, describing simulated zero gravity tests

[DGLR PAPER 71-112] 02 p0286 A72-12713

Integral and modular space stations objectives, construction and utilization for astronomy, scientific experiments and technology

03 p0441 A72-14308

Spin stabilized satellites attitude dynamics during rigid booms extension, deriving equations of motion approximate solution

11 p1726 A72-25915

Flexible rolled-up solar array /FRUSA/ operational performance from spaceborne accelerometers, strain gages and temperature sensors telemetered data, noting damage-free extension-retraction exercises

[AIAA PAPER 72-510] 13 p2051 A72-28952

Spacecraft boom deployment dynamics environmental simulation and testing for preflight system reliability evaluation

15 p2321 A72-32627

SPACE EXPLORATION

NT VIKING MARS PROGRAM

Book on earth, moon and planet space photography, discussing synoptic meteorological data, mapping, surface detail inspection and planetary exploration

03 p0438 A72-14099

Extraterrestrial life on Mars and Venus and Jupiter atmospheres, discussing abiogenesis failures on life-supportable planets

04 p0471 A72-14805

Exobiology research objectives, discussing planetary exploration data on origin, nature and distribution of life, spacecraft contamination, manned and unmanned missions and specific mission targets

05 p0714 A72-16133

Anthropomorphic robots design and performance for space exploration

05 p0644 A72-16448

Automatic craft for planet surface exploration, classifying propulsion gear

05 p0644 A72-16449

Soviet book on space exploration in U.S.S.R. covering Elektron, Proton and Cosmos research satellites, communication and meteorological satellites, lunar and manned spacecraft, etc

06 p0879 A72-17815

Future deep space missions, discussing exploration of interplanetary conditions outside ecliptic plane and solar system Grand Tour with outer planets flyby

07 p1068 A72-19059

Limitations on principle of freedom of exploration and use in space treaty, discussing meaning and implications of benefit and interests terms

07 p1103 A72-19458

Legal status of outer space, defining human activities in space

07 p1104 A72-19465

UN agencies role in communication satellites technology exploitation, discussing international cooperation in outer space peaceful use and exploration and development of space law

07 p1074 A72-19468

Image tube, film and mechanical scan camera imaging systems comparison for spacecraft-borne planetary photography based on maximum data return at acceptable cost

08 p1170 A72-21964

Soviet book on radiation hazards and protection in space covering detection, radiobiology and effects on human organism

11 p1713 A72-26050

Solar electric propulsion upper stage for multiple space exploration missions, discussing spacecraft performance, configurations and program plans

[AIAA PAPER 72-464] 11 p1709 A72-26199

Optical and electronic imaging systems optimization for solar system exploration, discussing effects on public support for national funding

12 p1807 A72-27346

International cooperation in space operations and exploration - AAS Conference, Washington, D.C., March 1971

14 p2175 A72-31135

NASA space plans for 1970s including lunar, planetary and universe explorations, cost reduction, human living and working capability, technology applications and international cooperation

14 p2162 A72-31136

U.S.-U.S.S.R. space cooperation, considering Eisenhower and Kennedy initiatives, NASA-Soviet Academy negotiations and current situation

14 p2176 A72-31145

Economic analysis of satellite network construction program, suggesting Italian national center formation for space exploration

15 p2319 A72-31231

Mars and Venus automatic station data transmission systems for surface and atmosphere studies, discussing relay and direct transmission modes

15 p2203 A72-31823

Report to COSPAR on 1971 Soviet space programs, discussing moon, planets, cosmic radiation, interplanetary medium, magnetosphere, upper atmosphere, meteorological, orbital station and biomedical studies

15 p2337 A72-32002

Report to COSPAR on U.S. space program covering stellar astronomy, lunar and planetary research upper atmospheric physics, earth and life sciences, etc

15 p2337 A72-32006

High accuracy approach guidance system for outer planet exploration.

[AIAA PAPER 72-867] 20 p2951 A72-39132

ESOC Darmstadt - ESRO's European center of operations for space exploration

20 p2988 A72-39415

Russian book - Equipment for space studies.

21 p3014 A72-40301

Spacecraft and missions for Jupiter exploration, discussing launch vehicle requirements, solar electric propulsion for midcourse correction, Pioneer flyby and orbiter missions, TOPS mission, etc

21 p3103 A72-40457

Data link design for planetary video data transmission back to earth based on rate distortion theory generalization of information theory

21 p3019 A72-40891

'Mars-2,' 'Mars-3' observatories exploring the 'red' planet.

21 p3109 A72-41318

Mariner spacecraft 1973 for flyby Venus and encounter Mercury, discussing launch and arrival conditions and aiming zones selection to maximize science return

[AIAA PAPER 72-942] 21 p3113 A72-41578

Flyby missions to comets, asteroids and meteors for obtaining solar system geological information, considering space dynamics feasibility

23 p3340 A72-44351

Two early missions to comets in 1977-1980 as precursors to more ambitious missions in 1984-1986, discussing exploration objectives and spacecraft configurations

23 p3340 A72-44352

Viking Mars exploration project, discussing orbiter and lander design and operational features and scientific experiments relevant to existence of life

24 p3440 A72-45123

NASA space science, exploration and applications plans and policies in view of space shuttle capabilities, emphasizing cost reduction

24 p3440 A72-45162

Comparative merits of manned and unmanned /automated/ space exploration, considering lunar observations, earth orbiting space stations and interplanetary missions

24 p3441 A72-45220

Potential contributions of the United States space program to exploration of the solar system.

24 p3445 A72-45467

The results of Soviet research into Mars.

24 p3447 A72-45559

SPACE FLIGHT

NT APOLLO FLIGHTS

NT HYPERBOLIC REENTRY

NT HYPERSONIC REENTRY

NT INTERPLANETARY FLIGHT

NT INTERSTELLAR TRAVEL

NT MANNED REENTRY

NT MANNED SPACE FLIGHT

NT MERCURY FLIGHTS

NT RETURN TO EARTH SPACE FLIGHT

NT SPACECRAFT REENTRY

NT VIKING MARS PROGRAM

Space flight biological effects on lysogenic bacteria and human cells in culture

01 p0011 A72-10365

Effective dose change after repeated radiation exposures as function of time intervals between fractions, evaluating space flight radiation hazards

[CERN-71-16] 02 p0161 A72-12059

Azur satellite flight data evaluation of thermal behavior, measuring temperature with thermistors

05 p0746 A72-16139

Dynamic system optimal design with various degrees of maneuver parameters information, considering space flight mechanics problem of payload maximization for limited propulsive power

06 p0849 A72-18306

Space flight experience application to human factors engineering problems in air and maritime navigation, considering use of small digital computers, display and sensing devices

09 p1348 A72-22785

Bioastronautic results of Apollo space flight biomedical operations, discussing weightlessness, sleep impairment, motion sickness, preventive medicine, etc

15 p2189 A72-31827

Medical investigations during Salut space station flight, discussing weightlessness effects and efficiency evaluation of preventive measures for crewmembers high performance in space flight

15 p2189 A72-31918

Book on man machine system experiments covering ATC, air defense, logistics organizations, space flight, battlefield operation, police dispatching, communications, etc

16 p2359 A72-33796

SPACE FLIGHT FEEDING

Apollo 14 food system, describing new items, improvements in production methods, packaging and preparation with emphasis on rehydratable foods

02 p0166 A72-11706

Biochemical and physiological effects of Apollo flight diet, noting no significant variations in serum electrolytes, endocrine values, body fluids and hematologic parameters

02 p0167 A72-11707

Menu selection for SKYLAB astronauts by computer technique based on mixed integer programming code, using measure of pleasure lists

12 p1769 A72-27442

Synthetic carbohydrates toxicity effects on rat liver lysosomes application to astronaut potential food sources

14 p2074 A72-30381

Dihydroxyacetone /DHA/ as nutrient in growing rats diet, showing unsuitability of regenerated DHA-containing formose mixtures for space crew diets

16 p2354 A72-33371

Biochemical and physiological evaluation of nourishment of subjects feeding on dehydrated products in test chamber with regenerative life support system, discussing metabolic data and hormone function

24 p3375 A72-45128

Spacecraft food synthesis, using carbon dioxide and water from chemically regenerated human metabolic and waste products

24 p3376 A72-45277

SPACE FLIGHT STRESS

Soviet book on astronaut activity psychological features covering space flight living conditions, space and time perception psychophysiological mechanism changes and weightlessness effects

03 p0317 A72-14246

Optimum duration of human circadian cycle with respect to energy cost during work hours, relating normal cycle change to prolonged space mission stresses

05 p0619 A72-16639

Space flight effects on chlorella cell survival and mutability in Zond automatic stations

05 p0623 A72-16775

Chromosome aberrations and germination speedup in Soyuz 5 carried oat seeds, noting stimulating effect by preflight ethylenimine treatment

05 p0623 A72-16777

Medicobiological investigations of prolonged weightlessness effects on astronaut physiological system based on Soyuz flight program

10 p1425 A72-24409

Space flight ecology and physiology, discussing atmospheric temperatures and radiation, biological effects of acceleration, deceleration and weightlessness and physiological stresses

11 p1584 A72-26018

Russian book on pathophysiological principles of air and space pharmacology covering stress and fatigue reduction and pilots and astronauts performance improvement

12 p1772 A72-27926

- Red cell mass plasma volume decrease in Apollo mission crews, indicating erythropoiesis inhibition 12 p1765 A72-28266
- Integrated medical and behavioral laboratory for detection and measurement of space flight stresses, specific etiologies and human tolerances and adaptivity 12 p1796 A72-28279
- Russian book on functional morphology under extremal space flight conditions covering overloads, hypoxia and hyperoxia effects on organism and cellular structure and metabolism 14 p2077 A72-30996
- Technology R and D program to qualify man for long term weightlessness, assessing space flight stress effects on physiology and psychology 16 p2358 A72-33544
- Social and emotional crises with respect to isolation, confinement and group dynamics of astronaut crews during long duration space flight 16 p2354 A72-33545
- Long term space flight weightlessness and hypodynamic effects on orthostatic and vestibular tolerances, infection susceptibility and drug reactivity 16 p2355 A72-33550
- Sleep factors and limitations during prolonged space flights, considering weightlessness, hypokinesia, nervous tension, cabin confinement, rhythm, environment and noise effects 16 p2356 A72-33561
- Space flight effects on chlorella cell survival and mutability in Zond automatic stations 17 p2504 A72-35278
- Soyuz 5 satellite vehicle space flight factors effect on chlorella cells, investigating survival rates and mutability 17 p2505 A72-35279
- Chromosome aberrations and germination speedup in Soyuz 5 carried barley seeds, noting stimulating effect by preflight ethylenimine treatment 17 p2505 A72-35280
- Problem of artificial gravitation in terms of experimental physiology 21 p3006 A72-40441
- Psychological principles of active rest during long space flights 21 p3006 A72-40446
- Psychic adaptation of man to a long-duration stay in space 22 p3149 A72-41988
- The prediction of the condition of man during a space flight 22 p3149 A72-42067
- The effect of space flight conditions and prolonged hypokinesia on the kidney function in man 22 p3149 A72-42068
- Motor activity capability of an astronaut in flight 22 p3149 A72-42220
- Effects of the space flight environment on man's immune system. I - Serum proteins and immunoglobulins. 22 p3150 A72-42493
- Effects of weightlessness on astronauts - A summary. 23 p3253 A72-43385
- Effects of an 18-day flight on the human body. 23 p3253 A72-43386
- Studies on weightlessness in a primate in the Biosatellite 3 experiment. 23 p3253 A72-43388
- Human organism and space flight stress endurance limits and manned space mission rescue capabilities requirements, considering cabin decompression, anoxia, radiation, onboard illness, etc 24 p3376 A72-45218
- ### SPACE FLIGHT TRAINING
- Prevention of weightlessness effects on blood hydrostatic pressure, musculoskeletal system and sensorimotor performance, discussing space flight training and space environment simulation tests 13 p1909 A72-28787
- ### SPACE GLIDERS
- ### U LIFTING REENTRY VEHICLES
- ### SPACE LABORATORIES
- NT MANNED ORBITAL LABORATORIES
- NT MANNED ORBITAL RESEARCH LABORATORIES
- Nonlinear and digital synthesis of computerized optimal control systems for long-life orbital stations and laboratories 05 p0724 A72-16434
- Orbiting space laboratories for earth resources program, discussing satellites and Skylab missions and international cooperation [AIAA PAPER 72-741] 18 p2742 A72-36547
- ### SPACE LAW
- Space law existence, contents and legal sources, discussing international decisions on outer space and celestial bodies use 01 p0147 A72-11108
- Committee organization and international law concepts on outer-space peaceful uses, detailing Ukrainian delegation position 05 p0752 A72-16203
- United Nations international space law development, discussing concepts of state jurisdiction, territorial sovereignty, damage liability, etc 06 p0905 A72-17814
- Space law - IAF Conference, Konstanz, West Germany, October 1970 07 p1102 A72-19452
- United Nations activities in space law, discussing creation of Committee on Peaceful Uses of Outer Space 07 p1102 A72-19453
- United Nations role as center of international cooperation in space law norms elaboration 07 p1102 A72-19454
- Structure and organization of UN bodies concerned with space activities, discussing legal contribution 07 p1102 A72-19455
- International space agency necessity, discussing registry of space objects, claims settlement, cooperation and space rescue 07 p1103 A72-19456
- Space treaties, discussing factors of UN contribution success 07 p1103 A72-19457
- Limitations on principle of freedom of exploration and use in space treaty, discussing meaning and implications of benefit and interests terms 07 p1103 A72-19458
- Liability for space activities, considering international organizations status before international tribunals 07 p1103 A72-19459
- Liability for damage caused by space objects, noting UN resolution 07 p1103 A72-19460
- Legal aspects of international manned orbiting laboratories, discussing space objects registry and liability for damage 07 p1103 A72-19461
- Manned orbital laboratories within framework of space treaty 07 p1103 A72-19462
- UN registry of space vehicles, reviewing historical development of registration procedures in U.S. and U.S.S.R. 07 p1103 A72-19463
- United Nations proposals concerning legal principles for use of natural resources of celestial bodies and ocean floor 07 p1103 A72-19464
- Legal status of outer space, defining human activities in space 07 p1104 A72-19465
- Space and atmosphere contamination by industrial wastes, aircraft and spacecraft exhaust and radioactive waste disposal, considering legal safeguards 07 p1104 A72-19466
- UN agencies role in communication satellites technology exploitation, discussing international cooperation in outer space peaceful use and exploration and development of space law 07 p1074 A72-19468
- European space organization with scientific and technological research objectives, noting jurisdictional status 07 p1105 A72-19474
- International cooperation in space law problems, considering space communication systems, geostationary orbits use, frequency band allocation, world weather watch and earth resources survey programs 07 p1105 A72-19475
- Conventions on international responsibility for damage caused by space objects, studying UN juridical subcommittee resolution 08 p1255 A72-21076
- Book - Law and politics in outer space: A bibliography. 21 p3132 A72-41535
- Government, military safety, police permission and insurance regulations for European rocket activities 24 p3467 A72-45124
- ### SPACE MAINTENANCE
- Human role in space shuttle on-orbit maintenance vs space station modules earth return, considering feasibility and cost effectiveness 10 p1487 A72-24440
- Space maintainability experiment aboard subsatellite during 30 day drift mission, noting application to Skylab manpower distribution [AIAA PAPER 72-232] 10 p1431 A72-24442
- Design considerations and reliability analysis for long duration manned space missions, noting redundancy and inflight maintenance requirement [AIAA PAPER 72-239] 10 p1487 A72-24446
- Space tools and support equipment for earth orbital systems maintenance, replacement and repair, discussing Skylab requirements and teleoperator applications [AIAA PAPER 72-230] 10 p1488 A72-25049
- In orbit servicing of spacecraft. [AIAA PAPER 72-731] 18 p2730 A72-36543
- Man serviced spacecraft systems reliability and maintainability optimization methodology, developing parametric data based on failure modes analysis, components MTBF, duty cycles, redundancy and costs [SAWE PAPER 943] 23 p3343 A72-43483
- ### SPACE MANUFACTURING
- Extraterrestrial environment utilization, describing space power plants, manufacturing operations in earth orbit and planetary mineral resources 12 p1871 A72-27625
- High temperature and vacuum solar furnace processing of refractory metals in space or on moon 19 p2857 A72-37675
- Environmental characteristics and advantages of manufacturing in space, considering gravity, vacuum, temperature, pressure and radiation effects on materials and products processing 21 p3060 A72-40968
- New space processing experiments for the Skylab missions. 24 p3407 A72-45125
- Investigation of the possibility of using radiant solar energy for welding and soldering of materials 24 p3407 A72-45126
- Immiscible materials processing experiments in near weightlessness environments during Apollo 14 mission and on NASA short duration low gravity test facilities 24 p3407 A72-45155
- Laser spin melting experiments for glass production in space from high melting metal and rare earth oxide ceramics 24 p3417 A72-45156
- Economic materials processing in orbiting spacecraft under zero gravity conditions, emphasizing single crystal electronic materials and high purity biologicals 24 p3407 A72-45157
- ### SPACE MECHANICS
- NT ASTRODYNAMICS
- NT CELESTIAL MECHANICS
- NT KEPLER LAWS
- NT ORBITAL MECHANICS
- ### SPACE MISSIONS
- Nuclear gas core and fusion rocket engines performance potential for various space missions, comparing capabilities in terms of payload ratio 01 p0099 A72-11328
- Nuclear radiation interference and damage effects in galactic and solar cosmic ray measurements during charged particle experiments by deep space missions. 03 p0438 A72-1408-
- Future deep space missions, discussing exploration of interplanetary conditions outside ecliptic plane and solar system Grand Tour with outer planets flyby 07 p1068 A72-19054
- Manned space flight escape, rescue and survival systems based on onboard, prepositioned aid and earth launched concepts, considering earth orbit, lunar and interplanetary missions 09 p1395 A72-23151
- International standardization of manned spacecraft components for rescue efforts and joint multinational space missions 09 p1395 A72-23154
- Lunar landing mission escape and rescue concepts, considering emergencies during earth orbit, translunar, lunar orbit, surface and rendezvous, transearth and earth reentry phases 09 p1396 A72-23157
- Trajectory optimization for low thrust mission and system analysis, exemplifying by Jupiter flyby and comet rendezvous missions 11 p1721 A72-26171
- Multimission and engine performance requirements for solar electric spacecraft propulsion stage configurations, considering launch vehicle compatibility integration payload and environmental extreme effects [AIAA PAPER 72-465] 11 p1712 A72-26325
- Space Shuttle supported manned earth orbital laboratories for operational communication and navigation systems, discussing mission program, design and equipment [AIAA PAPER 72-533] 12 p1876 A72-27357
- Solar electric multimission spacecraft /SEMMS/ concept, investigating Mariner, Viking and TOPS technologies applicability to postulated mission/science objectives [AIAA PAPER 72-469] 13 p2026 A72-28946
- Second generation European multi-mission launcher system for scientific and application satellites, using high energy propulsion modular design 15 p2320 A72-31804
- Deep space navigation requirements for interplanetary missions /1978-1990/ 15 p2269 A72-32178
- International space cooperation, emphasizing arrangements and prospects between U.S. and U.S.S.R. [AIAA PAPER 72-740] 18 p2743 A72-36549
- German Aros satellite mission and payload, noting mass spectrograph, EUV spectrometer for UV solar radiation and neutral particles temperature measuring instrument 20 p2974 A72-39935
- An integrated medical system for long-duration space missions. 21 p3009 A72-41305

Two early missions to comets in 1977-1980 as precursors to more ambitious missions in 1984-1986, discussing exploration objectives and spacecraft configurations

23 p3340 A72-44352

SPACE NAVIGATION

NT INTERPLANETARY NAVIGATION

Apollo spacecraft guidance and control systems, reviewing navigation objectives, concepts and performances during cislunar, rendezvous and landing maneuver phases

01 p0097 A72-10943

Soviet book on electro-optical devices for space vehicles orientation and navigation covering vertical plotters and sun, planet and star trackers

02 p0256 A72-12125

Nighttime airglow layer effect application to autonomous navigation and orientation of piloted space vehicles

02 p0256 A72-12289

Soviet book on space navigation covering dimensional spaces, navigation functions, relativistic phenomena, position finding, motion parameters, statistical methods, etc

02 p0256 A72-12297

Kalman filter divergence due to errors, applying to orbital navigation

02 p0198 A72-12805

Book on orbit determination, space navigation and celestial mechanics covering two body problem integration, units and constants, perturbation theory, orbit correction, etc

05 p0712 A72-15862

Optimal linear filtering for unmodeled time correlated driving disturbances of forcing function, applying to space navigation

05 p0685 A72-16461

Spacecraft, aircraft and ship navigation by satellites, noting Navy Navigation Satellite System

05 p0687 A72-16747

Iterative process convergence in least squares and maximum likelihood methods of processing measurements in spacecraft trajectory control, space navigation and geodesy systems

05 p0633 A72-16761

Spacecraft planetary approach navigation with TV camera onboard Mariner 9 giving images of Mars natural satellites against star background, discussing optical data processing programs

07 p1032 A72-18946

Outer planets Grand Tour trajectory correction requirements, examining combined radio/onboard navigation system and delta V estimates

07 p1068 A72-18947

Nonoptimality of Lawden spiral for minimum fuel transfer orbits in space navigation

07 p1033 A72-20246

Nighttime airglow layer effect application to autonomous navigation and orientation of piloted space vehicles

10 p1508 A72-23758

Space navigation - Conference, Orlando, Florida, March 1972

15 p2269 A72-32176

Low thrust spacecraft navigation requirements for minimum propellant guidance, using neighboring external law

15 p2270 A72-32194

Recursive filtering techniques in space navigation, describing initialization procedure to account for state vector errors correlation

17 p2532 A72-34214

Iterative process convergence in least squares and maximum likelihood methods of processing measurements in spacecraft trajectory control, space navigation and geodesy systems

17 p2523 A72-35264

Spectral factorization in periodically time-varying systems and application to navigation problems

17 p2578 A72-35492

Enlarging the region of convergence of Kalman filters that encounter nonlinear elongation of measured range

20 p2907 A72-39121

An adaptive technique for a redundant-sensor navigation system

20 p2952 A72-39134

Russian book - Algorithms for calculation of navigation data on spacecraft position

21 p3103 A72-40460

Analytical assessment of the accuracy of autonomous space navigation from measurements of the flight altitude and zenithal distance of one reference star

22 p3202 A72-42222

An attitude reference system with discrete-correction capability

22 p3203 A72-42864

Viewing Phobos and Deimos for navigating Mariner 9

24 p3423 A72-45433

[AIAA PAPER 72-927]

SPACE ORIENTATION

Psychophysical perceived orientation experiments on Poggendorff illusion (transversal interrupted by parallel lines)

01 p0013 A72-10717

Dust grain orientation parameter from Fokker-Planck equation, considering magnetic relaxation time, nearly spherical grains and oblate spheroids

02 p0283 A72-12627

Earth bow shock nonuniform structure observation correlation with interplanetary field orientation, using Explorer 33 and 35 data

11 p1722 A72-26395

Hypergravity effects on bats spatial orientation, noting resistance to head-pelvis and pelvis-head accelerations

13 p1907 A72-30015

Optical sensors for spacecraft attitude determination, discussing operation principles based on solar radiation, albedo, IR contrast and stellar radiation detection

16 p2389 A72-32849

Control simulation models of three dimensional joint angle motions, including circle, ellipse and straight line trajectories and orientations in space

22 p3162 A72-42187

SPACE PERCEPTION

NT AUTOKINESIS

Object size erroneous perception by apparent distance alteration

01 p0012 A72-10478

Neuronal mechanisms of binocular vision and space perception from tests on cats and men, discussing neurophysiological models of stereopsis

01 p0012 A72-10479

Stereopsis spring coupled magnetic dipole model of binocular stereoscopic depth perception in man

01 p0012 A72-10480

Poggendorff illusion depth processing theory, noting noncollinear line resolution effects on projective relationships within figure

01 p0013 A72-10714

Contrast reversal or distance paradox in temperature perception aftereffect

01 p0013 A72-10716

Position constancy and motion perception tests of head movement feedback calibration of perceived direction of optical motions

01 p0013 A72-10719

Perspective effects on direction of rotation judgments, using figures with rectangular and trapezoidal contours

02 p0167 A72-11898

Stereoscopic depth movement perception sensitivity compared to monocular movement

02 p0169 A72-12209

Classical optical measurement and holographic methods of flow field visualization, discussing operating principles, measurement sensitivity, three dimensional and depth-focusing properties

02 p0230 A72-12300

Binocular depth perception based on two retinal images spatial frequency content

02 p0164 A72-12486

Soviet book on astronaut activity psychological features covering space flight living conditions, space and time perception psychophysiological mechanism changes and weightlessness effects

03 p0317 A72-14246

Successive visual motion illusion during perception of rotating kymograph drum by human eye

04 p0476 A72-15588

Pilot perception tests on estimating flight path inclination, ground image and touchdown time under poor visibility

05 p0684 A72-16180

Geometric central projection properties of optical illusions, including Muller-Lyer, Zollner and Hering configurations

05 p0689 A72-16194

Oculomotor accommodation and convergence as distance perception cues, showing size perception change relation to glasses adaptation

06 p0765 A72-17411

Perceived common rotary motion of ambiguous stimuli as criterion of perceptual grouping

06 p0765 A72-17413

Oculomotor cue-based distance perception, discussing glasses adaptation-caused accommodation and convergence changes in stereoscopic depth perception

06 p0765 A72-17414

Recognition algorithms of moving objects for patterns alone and in symbolic and motion context, indicating possible recognition mechanism degradation

06 p0780 A72-18257

Visual space geometry and perception experiments, demonstrating size-distance relations for various visual cues

07 p0926 A72-19031

Counteradaptation and cue discrepancy as perceptual adaptation basis, considering changes in registered and apparent distance of luminous object moving in dark

08 p1115 A72-20988

Adjustment to subjective horizontal, vertical and 45 deg tilt in dark as function of age in 3-20 year old subjects

08 p1124 A72-20989

Stereoscopic acuity for photometrically matched background wavelengths at scotopic and photopic levels, plotting variable depth error as function of retinal illuminance

10 p1425 A72-24269

Natural visual capture result of vision and touch conflict in bilateral comparisons of object length

10 p1430 A72-24270

Character recognition experiments to determine attention control and temporal-spatial capacity limitation during visual information processing

12 p1768 A72-27074

Slant range visibility measurements by lidar for aircraft landing operations under low clouds and fog at coastal region

13 p1992 A72-28847

Individual differences in motion-in-depth detection from Lissajous pattern test for judgment of object approach, receding and movement rate

14 p2081 A72-30965

Airplane attitude display motion relationship to external world as factor in pilot error due to visual frame of reference shift

14 p2083 A72-31151

Disparity-associated depth sensation masking, suggesting visual signal processing inhibitory mechanisms for crossed and uncrossed stimuli

15 p2184 A72-31366

Visual stimulus orientation effect on movement perception, relating physiological and psychological factors

15 p2184 A72-31368

Head-up display for aircraft three dimensional sky path observation during navigation and landing, discussing computer units, CRT and image generating subsystems

15 p2268 A72-32042

Size scaling rate from retinal image size comparison judgment time during observation of briefly presented concentric rectangles of varying size and orientation

15 p2187 A72-32762

Voluntary eye movement and convergence effects on relation between binocularly perceived and physical distance ratios

16 p2358 A72-33647

Visual depth perception response functions for sine and square wave modulated binocular parallax

17 p2498 A72-34293

Effect of target-background luminance contrast on binocular depth discrimination at photopic levels of illumination

17 p2508 A72-34879

REM period functional maintenance of coordinated eye movement facilitation and binocular depth perception accuracy following sleep

17 p2509 A72-35462

Peripheral contrast thresholds for moving images

17 p2509 A72-35688

The relative importance of contrast and motion in visual detection

17 p2509 A72-35689

Congruent and spurious motion in the learning and performance of a compensatory tracking task

17 p2510 A72-35692

The tracking of targets located outside of Panum's area

17 p2505 A72-35916

Effect of selective adaptation on detection of simple and compound parafoveal stimuli

18 p2651 A72-36607

Optokinetic thresholds in the normal monkey

18 p2651 A72-36610

Vergence eye movements to pairs of disparity stimuli with shape selection cues

18 p2651 A72-36612

Division and orientation in the vertical-horizontal illusion

18 p2651 A72-36913

The neurophysiology of binocular vision

19 p2755 A72-37250

Discontinuity of seen motion reduces the visual motion aftereffect

19 p2760 A72-37600

Psychophysical procedures to investigate selective visual adaptation to light of different wavelengths from test gratings with various orientations and spatial frequencies

19 p2756 A72-37829

Target distance and adaptation in distance perception in the constancy of visual direction

21 p3008 A72-41022

Apparent movement and change in perceived location of a stimulus produced by a change in accommodative vergence

21 p3002 A72-41024

Interactions between spatial and kinetic dimensions in movement aftereffect

21 p3003 A72-41254

Book - Aspects of motion perception

21 p3012 A72-41531

- Visually directed pointing as a function of target distance, direction, and available cues.
22 p3151 A72-42929
- Moving spot detection threshold measurement for varying exposures, noting product of stimulus duration and velocity for comparison with Bloch law
22 p3151 A72-42930
- Visual angle and apparent size of objects in peripheral vision.
22 p3152 A72-42932
- Role of eye movements in the perception of apparent motion.
23 p3259 A72-43804
- Motion thresholds for fovea and peripheral retina with/without correction for peripheral refractive error
23 p3260 A72-43978
- Conjugate and disjunctive optokinetic eye movements in the rabbit, evoked by rotatory and transitory motion.
23 p3257 A72-44243
- On a long-term temporal aspect of stereoscopic depth sensation.
23 p3258 A72-44381
- Line length detectors in the human visual system - Evidence from selective adaptation.
23 p3258 A72-44384
- Signal detection analysis of meridional variations to vertical and horizontal gratings.
23 p3259 A72-44389
- Visual stimuli distance estimation with head stationary or moving, discussing performance after monocular motion parallax training
24 p3374 A72-44557
- Optical directionality of retinal receptors and corresponding points. I - Nasal-temporal asymmetry of retinal spatial values and orientation of receptors: Are the corresponding points cones. II - Variation of form of the experimental horoptera, and possibility of reorganization of the retinal correspondence according to the orientation of the eyes
24 p3371 A72-44907
- SPACE PHOTOGRAPHY**
U SPACEBORNE PHOTOGRAPHY
SPACE POWER REACTORS
NT SPACE POWER UNIT REACTORS
A small, 1400 K, reactor for Brayton space power systems.
19 p2833 A72-37635
- SPACE POWER UNIT REACTORS**
Angular quadrature effects on two dimensional space power reactor radiation shield calculation for manned space station application
04 p0546 A72-14426
- NASA-Lewis experiences with multigroup cross sections and shielding calculations.
19 p2833 A72-37633
- On-board nuclear power plants in space
24 p3423 A72-45119
- United States Space Nuclear Electric Power Program.
24 p3424 A72-45179
- SPACE PROBES**
NT JUPITER PROBES
NT LUNAR PROBES
NT LUNIK LUNAR PROBES
NT MARINER SPACE PROBES
NT MARINER SPACECRAFT
NT MARS PROBES
NT PIONEER SPACE PROBES
NT RANGER LUNAR PROBES
NT SOLAR PROBES
NT SURVEYOR LUNAR PROBES
NT VENERA SATELLITES
NT VENUS PROBES
NT VIKING MARS PROGRAM
Ground station systems of operational control and data processing for satellites and space probes projects Aeros, Symphonie and Helios
03 p0326 A72-14309
- Automatic control of ESRO drag-free deep space probe for measuring Robertson matrix beta and gamma constants
[ONERA, TP NO. 952] 05 p0727 A72-16468
- Deep space probe MULTIPAC data system computer repairable during flight via command and telemetry links by reprogramming failed unit
05 p0633 A72-16573
- Thermodynamic parameters correlation of planetary atmosphere with planetary probe parachute descent rate applied to Venera 5 and 6 data
05 p0721 A72-16769
- Paraboloid and elliptical mirrors in 100 m radio telescope for Helios space probe signals reception, noting device compatibility for data exchange with NASA
[DGLR PAPER 72-019] 13 p1939 A72-28964
- Pontyragin maximum principle for optimal terminal velocity control of automatic space probe descent in Mars atmosphere
14 p2162 A72-30456
- Minimum weight phase change thermal control device for planetary descent probes, discussing test over various heat loads
[AIAA PAPER 72-287] 14 p2171 A72-30826

- Planetary atmosphere thermodynamic parameters correlation between spacecraft parachute descent rate and measured data, noting Venera spacecraft example
17 p2610 A72-35272
- Radiation gasdynamics of planetary entry - Concepts and recent advances.
24 p3361 A72-45188
- SPACE PROGRAMS**
NT APOLLO PROGRAM
NT EUROPEAN SPACE PROGRAMS
NT FRENCH SPACE PROGRAMS
NT LUNAR PROGRAMS
NT U.S.S.R. SPACE PROGRAM
Space shuttle system purposes, noting space program cost reduction
04 p0582 A72-15265
- Space operations cost effectiveness improvement by earth-to-orbit shuttle, discussing space utilization growth and economics
[SD-71-780] 05 p0724 A72-16048
- Space technology development importance for future of mankind, discussing terrestrial environment conservation, extraterrestrial raw materials recovery and power generation, etc
05 p0753 A72-16309
- Space for mankind benefit - Conference, Huntsville, November 1971
06 p0891 A72-18609
- Educational programs for increasing public interest in space program benefits, describing summer teacher workshop on Apollo lunar and Skylab space station missions
06 p0906 A72-18623
- Structure and organization of UN bodies concerned with space activities, discussing legal contribution
07 p1102 A72-19455
- Book on dividends from space covering contributions to home and industry, health and medicine, systems approach to human problems, earth monitoring, communications, etc
07 p1105 A72-20202
- Escape systems evolution for manned space flight, considering X-15, Mercury, Gemini and Apollo programs and future space stations and planetary missions
09 p1395 A72-23153
- Satellite long life assurance, investigating shuttle era spacecraft program cost relationship to mean time to failure
[AIAA PAPER 72-225] 10 p1551 A72-24436
- Cost effective innovations in space programs management, discussing communication, problem solving and reward and punishment
[AIAA PAPER 72-246] 10 p1564 A72-24451
- Product assurance cost aspects on high reliability space programs, discussing design, packaging, failure trends, acceptance testing and Apollo program
[AIAA PAPER 72-247] 10 p1551 A72-24452
- Aerospace management systems effectiveness in design, development, test and engineering areas, discussing cost, scheduling and technical performance factors
[AIAA PAPER 72-243] 10 p1565 A72-25050
- Space projects technological developments and benefits, discussing communications, transportation, computers, education, holography, power and life support systems, manufacturing in space and earth resources
11 p1748 A72-25253
- Short and long range contributions of NASA space program to life quality improvement, discussing land and crop surveys, communications and environment modification
11 p1748 A72-26098
- NASA space program impact on U.S. technology, discussing performance levels, precision, reliability and industry stimulation
11 p1748 A72-26099
- International cooperation in space operations and exploration - AAS Conference, Washington, D.C., March 1971
14 p2175 A72-31135
- NASA space plans for 1970s including lunar, planetary and universe explorations, cost reduction, human living and working capability, technology applications and international cooperation
14 p2162 A72-31136
- Space applications benefits through international cooperation, emphasizing environmental problems
14 p2175 A72-31143
- Space activity in fields of ecology and earth resources - Conference, Rome, Italy, March 1972
15 p2220 A72-31226
- United Nations activity in international space program for earth resources and environmental pollution surveillance by satellites
15 p2220 A72-31227
- Report to COSPAR on Australian space program covering earth atmosphere, cosmic and synchrotron radiation, X ray astronomy, weather satellites, deep space and sounding rockets
15 p2338 A72-32007

- Japanese report to COSPAR on space research by sounding rockets, balloons and SHINSEI scientific satellite
15 p2338 A72-32011
- Report to COSPAR on Indian space program covering organizations, ground station facilities, atmosphere and astronomy studies and international collaborations
15 p2338 A72-32012
- Report to COSPAR on Argentina space program covering sounding rockets and balloons and Experimental Inter-American Meteorological Network meteorological rocket launchings
15 p2338 A72-32015
- International UV Explorer synchronous satellite program objectives and technology, describing spacecraft design, instrumentation, ground system, telescope control and data handling
17 p2621 A72-34900
- The El Arenosillo launch base, a rocket test center in Huelva province
17 p2536 A72-34944
- Canadian industrial participation in domestic, U.S. and overseas space projects, emphasizing technology advancement as national objective
[AIAA PAPER 72-738] 18 p2742 A72-36544
- International space cooperation, emphasizing arrangements and prospects between U.S. and U.S.S.R.
[AIAA PAPER 72-740] 18 p2743 A72-36549
- Reliability of HgTe-CdTe photovoltaic detectors
18 p2670 A72-37139
- Development of planetary quarantine in the United States.
23 p3259 A72-43382
- RAM - A concept for reducing space payload costs.
[SAWE PAPER 942] 23 p3343 A72-43482
- Aircraft/spacecraft design approach and performance data, considering space shuttle program
24 p3467 A72-45159
- Cost prediction of space projects.
24 p3468 A72-45211
- Helios solar probe development, discussing scientific experiments, structural, thermal and engineering models and systems tests
24 p3451 A72-45214
- Mission objectives, hardware development and international cooperation aspects in U.S. future space flight programs, discussing space shuttle, space tug, Apollo 17 and Skylab
24 p3441 A72-45219
- SPACE RADIATION**
U EXTRATERRESTRIAL RADIATION
SPACE RADIATORS
U SPACECRAFT RADIATORS
SPACE RENDEZVOUS
NT EARTH ORBITAL RENDEZVOUS
NT ORBITAL RENDEZVOUS
Comet rendezvous and outer planet exploration mission operations by unmanned nuclear electric propulsion (NEP) system with inciner thermionic reactors for electric power generation
[AIAA PAPER 72-428] 11 p1722 A72-26177
- Solar electric propulsion application to comet and asteroid rendezvous and docking CARD missions without sample return
[AIAA PAPER 72-470] 11 p1722 A72-26201
- Encounter sequences determination techniques for multitarget flyby and rendezvous missions to asteroids and comets by spacecraft using solar electric propulsion
[AIAA PAPER 72-429] 13 p2037 A72-28947
- Functional equations for optimal spacecraft or rocket interception by similar vehicle within limits of dense atmosphere
17 p2621 A72-35121
- Iterative method for the calculation of two-impulse spacecraft rendezvous maneuvers
17 p2622 A72-35216
- Spacecraft rendezvous trajectories and targeting maneuvers onboard sequential computation, taking into account maneuver constraints and state vector update information
24 p3450 A72-45172
- SPACE RENDEZVOUS MANEUVERS**
U SPACE RENDEZVOUS
U SPACECRAFT MANEUVERS
SPACE SCIENCES
U AEROSPACE SCIENCES
SPACE SHUTTLE ORBITERS
Real time estimation of trajectory for lifting reentry vehicle of shuttle orbiter type, discussing iterated nonlinear filter and adaptive filter
[AIAA PAPER 72-874] 20 p2966 A72-39126
- Significant factors in environmental and thermal control/life support system design for space shuttle orbiter
[ASME PAPER 72-ENAV-21] 20 p2895 A72-39156
- Comparative evaluation of environmental control and life support systems for the space shuttle orbiter.
[ASME PAPER 72-ENAV-19] 20 p2895 A72-39158
- Computer simulation of the space shuttle orbiter environmental thermal control system.
[ASME PAPER 72-ENAV-12] 20 p2896 A72-39165

- Influence of discontinuity stresses on main propellant tankage of a space shuttle orbiter.
[ICAS PAPER 72-10] 21 p3120 A72-41135
- Delta wing separation can dominate shuttle dynamics.
[AIAA PAPER 72-976] 22 p3230 A72-42336
- Space shuttle mission and orbiter element description, discussing European participation
23 p3343 A72-44366
- ### SPACE SHUTTLES
- Aerospike rocket engine system for orbit-to-orbit space shuttle, discussing light-weight regeneratively cooled thrust chamber performance tests
[SAE PAPER 71070] 01 p0116 A72-10264
- Space shuttle materials - Conference, Huntsville, Alabama, October 1971, Volume 3
01 p0090 A72-10726
- Composite materials application for space shuttle structures, relating structural weight to payloads
01 p0090 A72-10727
- Boron-epoxy tubular struts for one third scale space shuttle booster thrust truss structure, discussing design, analysis, fabrication, weight, test and quality control
01 p0138 A72-10735
- Hat section stiffened compression panel of graphite/epoxy composite for space shuttle, discussing quality control procedures
01 p0139 A72-10736
- Fiberglass overwrapped Al alloy for space shuttle cryogenic hydrogen and oxygen tanks, noting weight reduction and impeding effect on cyclic loading induced crack growth rate
01 p0139 A72-10738
- Composite space shuttle booster and orbiter engine support structures design and analysis, stressing weight savings
01 p0139 A72-10740
- Titanium alloys and superalloys selection for elevated temperature use on space shuttle
01 p0084 A72-10743
- Multiple reentry effects on space shuttle thermal protective superalloys mechanical properties, presenting cyclic simulation results for different temperatures, pressures and stresses
01 p0084 A72-10754
- Test program to evaluate metallic materials candidates for space shuttle booster thermal protection system
01 p0085 A72-10755
- Coated Nb alloys as radiative thermal protection system skin materials for space shuttle, investigating flaw growth
01 p0085 A72-10757
- Field repair of Nb alloy panels with protective coatings designed as part of space shuttle thermal protection system
01 p0091 A72-10758
- Field repair of fused slurry silicide coating for oxidation protection of Nb alloys in space shuttle environment
01 p0075 A72-10759
- High temperature insulation for radiative thermal protection system of space shuttle orbiter, evaluating survival chances under acoustic, vibration and thermal loads
01 p0091 A72-10760
- Space shuttle reusable surface insulation thermal protection system, discussing thermal stress distribution, failure modes and mechanical properties
01 p0091 A72-10761
- Reusable external thermal insulation multilayer for space shuttle vehicle, presenting conductivity, expansion coefficient, specific heat, stability, tensile strength and strain capability
01 p0091 A72-10762
- Silica based surface insulation material for space shuttle thermal protection system, discussing cyclic tests in simulated environment and fiber purity effects on crystallization
01 p0091 A72-10764
- Space shuttle low density ablative thermal protection systems, emphasizing low cost refurbishment techniques
01 p0091 A72-10766
- Electrochemical carbon dioxide concentrator materials compatibility to space shuttle life support environment, comparing with LiOH method
01 p0018 A72-10768
- Impact sensitivity of space shuttle materials in liquid and gaseous oxygen at high pressures
01 p0102 A72-10772
- High pressure gaseous hydrogen effect on space shuttle main engine components alloys under static loads, using surface flawed flat plate PTC samples
01 p0085 A72-10774
- Corrosion and stress corrosion cracking prevention on space shuttle by materials selection
01 p0085 A72-10775
- Refractory material development for space shuttle hydrogen tank reusable internal gas layer insulation
01 p0139 A72-10777
- Space shuttle cryogenic tanks self evacuating multilayer insulation, evaluating thermal and dynamic performance
01 p0139 A72-10778
- Temperature and compressive loading cycles effects on high performance multilayer insulation materials and composites, discussing application to space shuttle orbiter
01 p0092 A72-10779
- Characterization of graphite/polyimide composites for space shuttle applications
01 p0092 A72-10784
- Space shuttle oriented polyimide reinforced Ti matrix composites properties, noting weight saving
01 p0139 A72-10785
- Space shuttle thermal protection system, discussing oxidation resistant coatings, refractory metals, heat shield technology, ballistic reentry programs, weight and cost
01 p0135 A72-10935
- Plasma arc testing of space shuttle Nb and Co alloys thermal protection materials, using IR radiometric and photographic techniques
01 p0048 A72-10977
- Arc jet simulation tests of thorium dispersed Ni and Co alloys for space shuttle Metallic Thermal Protection System, determining material degradation
01 p0086 A72-10978
- Nondestructive tests of Nb alloy radiative thermal protection heat shield design for space shuttle requirements
01 p0048 A72-10980
- Power conditioning requirements and tradeoff considerations for space shuttle, warning against central power conversion use on orbiter and booster vehicles
01 p0007 A72-11052
- Aircraft and spacecraft integrated avionics systems design with emphasis on telemetry, discussing space shuttle subsystems integration
02 p0179 A72-12403
- Space shuttle orbiter flight instrumentation, data handling and communication requirements, discussing data gathering methods, crew displays, computer processing, recording and digital data bus telemetry
02 p0179 A72-12406
- Space shuttle optimal boost trajectories, showing payload increase by flying pitch profiles optimization
[AAS PAPER 71-325] 02 p0286 A72-12423
- Post Apollo program, considering space shuttle design, operation, transportation and payload cost reduction, rocket developments and plans for Mars expedition
03 p0440 A72-13612
- Space shuttle safety problems, discussing hydrogen pump bearings and air breathing turbofan blades failures and fuel tank fire hazards
03 p0441 A72-13694
- Space shuttle cryogenics technology, flight and ground operations, checkout, maintenance and safety
03 p0441 A72-13695
- High velocity boundary layer problems for space shuttle, investigating free interaction with detachment, shock wave, penetration, air bubbles in circulation and adherence conditions
03 p0308 A72-13699
- Space shuttle system purposes, noting space program cost reduction
04 p0582 A72-15265
- Space operations cost effectiveness improvement by earth-to-orbit shuttle, discussing space utilization growth and economics
[SD-71-780] 05 p0724 A72-16048
- Three dimensional supersonic flow about space shuttle, comparing method-of-characteristics and shock-capturing computations
[AIAA PAPER 72-191] 05 p0729 A72-16845
- Space shuttle flow field fluid dynamic hyperbolic equations numerical solution by noncentered finite difference schemes, noting advantages in programming logic simplicity and multidimensional generalizations
[AIAA PAPER 72-193] 05 p0729 A72-16848
- Wind tunnel study of space shuttle longitudinal dynamic stability at supersonic speeds, discussing damping-in-pitch
[AIAA PAPER 72-135] 05 p0730 A72-16890
- Reusable shuttle for cost reduction, including reusability rate, expanded orbit capabilities and flight frequency
06 p0906 A72-18171
- Shuttle ascent guidance and control, discussing self targeting, trajectory optimization problems and flight phases
06 p0892 A72-18178
- Space shuttle program evaluation, discussing national economic benefits relative to aerospace industry employment, domestic production, balance of trade, etc
06 p0893 A72-18612
- NASA materials science and manufacturing in space program involving space shuttle reusable equipment and weightlessness applications experiments
06 p0797 A72-18621
- Space shuttle payloads and space manufacturing candidate materials and methods, discussing float-zone refined semiconductors, electronic crystals, viral insecticides, vaccines and biological cells
06 p0824 A72-18622
- Supersonic transition flight mode of reusable two stage space shuttle booster for orbiter launching, comparing with subsonic and high lift to drag designs
[AIAA PAPER 72-133] 07 p0104 A72-18963
- Space shuttle vehicle configurations with reusable booster and orbiter modules, discussing cargo capacity, maneuvering capability, mission duration, engine characteristics and acceleration constraints
07 p1085 A72-19058
- Stochastic simulation model for space shuttle fleet operations, using closed loop queuing system approach
07 p0965 A72-20330
- Digital simulation for predicting performance of data communication networks with computerized switching centers, detailing space shuttle interior communication system
07 p0952 A72-20364
- Onboard orbital navigation system analysis on space shuttle radio range and range rate measurement data relative to ground beacon, using Kalman filter
08 p1203 A72-20856
- Space shuttle, tug and orbital station transportation system benefits and applications, noting European economic implications
08 p1229 A72-20977
- NASA research and applications module (RAM) for interim space station development and possible missions with space shuttle
08 p1240 A72-20978
- NASA space programs, discussing future Apollo, Skylab, orbiting space station, space shuttle and deep space projects
08 p1230 A72-21002
- Space shuttle phase B design studies regarding configurational alternatives, propulsion systems, displays and controls, simulations and flight test programs
08 p1240 A72-21009
- Satellite long life assurance, investigating shuttle era spacecraft program cost relationship to mean time to failure
[AIAA PAPER 72-225] 10 p1551 A72-24436
- Space shuttle flight crew/computer interface display and control functional requirements optimization by real time digital simulation
[AIAA PAPER 72-226] 10 p1460 A72-24437
- Unpowered shuttle orbiter piloted control during approach and landing, discussing energy management technique based on fixed base six degree of freedom simulation
[AIAA PAPER 72-227] 10 p1551 A72-24438
- Human role in space shuttle on-orbit maintenance vs space station modules earth return, considering feasibility and cost effectiveness
[AIAA PAPER 72-229] 10 p1487 A72-24440
- Econometric approach to space shuttle design for optimum operational redundancy levels, using payload-cost effectiveness criterion
[AIAA PAPER 72-242] 10 p1551 A72-24448
- Metallic materials for delta wing space shuttle configuration with metallic thermal protection system
10 p1498 A72-24876
- Space shuttle orbiter thermal protection system metallic interaction with chemical environment during reentry, emphasizing degradation in dissociated oxygen
[AIAA PAPER 72-262] 11 p1590 A72-25206
- Heat pipe applications for waste heat rejection, cooling and temperature control in space shuttle, discussing design and performance
[AIAA PAPER 72-272] 11 p1725 A72-25212
- Separation flow field measurements for space shuttle cylindrical configurations in hypersonic streams, using pressure heat transfer and visualization techniques
[AIAA PAPER 72-294] 11 p1567 A72-25232
- Thermal boundary layer interaction with distortions in shape or material of adjacent surface for space shuttle design
[AIAA PAPER 72-312] 11 p1614 A72-25246
- Rarefied flow fields and heating rates for space shuttle orbiter reentry at high angles of attack, using Monte Carlo simulation technique
[AIAA PAPER 72-314] 11 p1567 A72-25248
- Laminar and turbulent convective heating distributions on delta wing space shuttle boosters with interference effects
[AIAA PAPER 72-315] 11 p1567 A72-25249
- Liquid propellants coupling effects on parallel stage space shuttle configuration structural dynamics, using forty degree of freedom analytical model
[AIAA PAPER 72-347] 11 p1725 A72-25376
- Orthotropic point-supported rectangular panel vibration and flutter analysis for natural frequencies and flutter boundaries, applying to space shuttle design
[AIAA PAPER 72-350] 11 p1728 A72-25379

Space shuttle orbiter vehicle structural design configurations development and evaluation with respect to overall system weight and program cost
[AIAA PAPER 72-373] 11 p1726 A72-25397

Space shuttle thermal protection refurbishment labor costs and techniques, noting motion studies results for maintenance tasks in terms of manpower and performance time
[AIAA PAPER 72-374] 11 p1726 A72-25398

Unsteady airfoil stall and stall flutter analysis, discussing application to space shuttle configuration
[AIAA PAPER 72-380] 11 p1730 A72-25404

Space shuttle heat shield metallic refractory, superalloy and composite materials joining, discussing vacuum furnace brazing of Al/B matrix structures
[AIAA PAPER 72-387] 11 p1638 A72-25408

Reusable external insulation materials for space shuttle thermal protection, evaluating local heat transfer at interface areas in plasma arc test facility
[AIAA PAPER 72-388] 11 p1744 A72-25409

Liquid film transpiration cooling concept application to space shuttle leading edge heating and shock heating
[AIAA PAPER 72-389] 11 p1744 A72-25410

Hot versus shielded aerodynamic surfaces trade study for space shuttle booster wings and fins design, considering materials, structural weight and cost estimates
[AIAA PAPER 72-390] 11 p1726 A72-25411

Space shuttle booster and orbiter thermal protection systems, examining heat sink, metallic radiative, reusable surface insulation and surface cooled designs
[AIAA PAPER 72-391] 11 p1726 A72-25412

Boron-epoxy reinforced Ti tubular truss for application to space shuttle booster thrust structure, evaluating performance
[AIAA PAPER 72-393] 11 p1730 A72-25414

Boron-epoxy reinforced composite metal shear web design for space shuttle orbiter main engine thrust beam structure
[AIAA PAPER 72-395] 11 p1726 A72-25416

Manufacturing process for dispersion strengthened nickel-chromium-thorium dioxide alloys for space shuttle thermal protection system panels, discussing joining optimization and mechanical properties
11 p1659 A72-26035

Space shuttle orbiter reentry heat shield materials, considering hot structures and hot radiative metallic, ceramic insulative and ablative heat shields
11 p1660 A72-26245

Space Shuttle supported manned earth orbital laboratories for operational communication and navigation systems, discussing mission program, design and equipment
[AIAA PAPER 72-533] 12 p1876 A72-27357

Space shuttle cost savings from viewpoints of reusable system, launch rate, vehicle life and overall program
12 p1877 A72-27514

Space technology developments during 1970s and 1980s, discussing solar system exploration, space shuttle systems, cost effectiveness, international cooperation, nuclear propulsion systems, etc.
13 p2051 A72-28453

Atmospheric model effects on space shuttle ascent and reentry trajectories and aerodynamic heating
13 p1990 A72-28813

Atmospheric model for random density variations effects on space shuttle reentry parameters, using Monte Carlo trajectories for delta wing orbiter
13 p1990 A72-28814

LB 21 and space shuttle orbiter aerodynamic testing, discussing computer program supplanting reentry vehicle free flight aerodynamic testing
13 p1894 A72-28934

Space shuttle applications as spacecraft launcher, unmanned instrumentation platform and manned laboratory, discussing advantages to space research
13 p2051 A72-28935

Structural design characteristics of low density fiber ceramic materials coated with refractory ceramics for space shuttle reusable surface insulation thermal protection systems
[AIAA PAPER 72-372] 13 p2056 A72-28957

Teleoperator manipulator for payload handling in space shuttle, noting design features and simulations of master-slave remote control system
[AIAA PAPER 72-238] 13 p1909 A72-29075

European programs on space stations, tugs, shuttles, propulsion and avionics and consideration for participation in NASA programs for 1970s and 1980s
14 p2175 A72-31137

U.S. industry views on NASA plans for 1970s, emphasizing interplanetary nuclear propulsion, space transportation, shuttle costs and economics
14 p2175 A72-31139

Space shuttle umbilical systems for mating, connection and checkout of carrier assemblies and couplings for cryogenic, electrical, pneumatic and hydraulic services
15 p2213 A72-31695

Space Shuttle Orbiter onboard ultrasonic system for structural integrity tests and assessment, noting limitations factors due to configuration and vehicle launch noise effects
15 p2256 A72-31698

Failure detection techniques for Space Shuttle redundant multiple gimbaled inertial measurement units, using simulated boost and entry trajectories
15 p2270 A72-32189

Space shuttle payload design for weight and cost reduction, discussing refurbishable modular design concept
15 p2321 A72-32317

Longitudinal dynamic stability of hypersonic shuttle vehicle designed for operation to planetary atmosphere rim
16 p2462 A72-34019

Inviscid surface streamlines and laminar, transitional and turbulent heating of blunt nose shuttle configurations in hypersonic flow
[AIAA PAPER 72-703] 16 p2345 A72-34041

Finite difference method computation of multishocked three dimensional wing-body supersonic flow fields with real gas effects, applying to delta winged space shuttle
[AIAA PAPER 72-702] 16 p2345 A72-34042

The earth orbit shuttle as a space rescue vehicle.
17 p2620 A72-34437

Space shuttle program, discussing configurational concepts, payload carrying capacity variants and cost reduction design changes
17 p2621 A72-34869

Carbon-carbon composites for space shuttle reentry thermal protection.
17 p2572 A72-35667

Design of model-reference adaptive control systems using Liapunov functions.
18 p2672 A72-36326

The manufacture of mullite reusable surface insulation materials for space shuttle.
[SME PAPER EM 72-714] 18 p2695 A72-36527

In orbit servicing of spacecraft.
[AIAA PAPER 72-731] 18 p2730 A72-36543

Space shuttle configuration, discussing payload accommodation requirements, accessories, mission operations and reusable tug
[AIAA PAPER 72-737] 18 p2731 A72-36546

Space science advances and NASA Planetary Program, noting solar system evolution, life origin and Skylab and Space Shuttle programs
19 p2855 A72-37274

Development of a GH2/GO2 pulsejet engine with 6.7 kN thrust for the attitude control system of the space shuttle
19 p2848 A72-37495

Long term storage and propellant transfer capabilities of propellant depot system design to act in earth orbit as resupply station for cargo/personnel shuttles
19 p2870 A72-38831

An explicit automatic terminal energy management guidance technique for space shuttle.
[AIAA PAPER 72-833] 20 p2950 A72-39094

Space shuttle terminal navigation with conventional navigation aids.
[AIAA PAPER 72-832] 20 p2950 A72-39095

Thermally controlled entry guidance for shuttle.
[AIAA PAPER 72-831] 20 p2951 A72-39096

Constrained payload-optimum extremal ascent trajectories for space shuttle vehicles.
[AIAA PAPER 72-829] 20 p2966 A72-39097

Modular heat rejection system to accommodate widely varying thermal loads in space shuttles and future spacecraft, emphasizing commonality design philosophy for cost reduction
[ASME PAPER 72-ENAV-34] 20 p2976 A72-39144

Structural thermal protection systems for Space Shuttle, noting reusable surface insulation with active cooling
[ASME PAPER 72-ENAV-32] 20 p2976 A72-39145

Thermal control design for research applications module (RAM) shuttle compatible payload carriers, using Freon 21-water system
[ASME PAPER 72-ENAV-31] 20 p2894 A72-39146

Development of a laboratory prototype spraying flash evaporator.
[ASME PAPER 72-ENAV-28] 20 p2894 A72-39149

Multi-cycle plasma arc evaluation of oxidation inhibited carbon-carbon material for shuttle leading edges.
[ASME PAPER 72-ENAV-26] 20 p2894 A72-39151

Optimal shuttle research applications module (RAM) environmental control and life support system for sortie missions
[ASME PAPER 72-ENAV-20] 20 p2895 A72-39157

Space shuttle environmental temperature control-life support system program changes, discussing air cooled electronic equipment, cryogenic stores, crew size and mission duration
[ASME PAPER 72-ENAV-18] 20 p2895 A72-39159

Modular environmental control/life support system design for low cost shuttle launched space station, evaluating humidity, carbon dioxide, water and waste management
[ASME PAPER 72-ENAV-17] 20 p2895 A72-39160

Space shuttle waste collection system development, discussing human-interface requirements, zero gravity effects and operational considerations
[ASME PAPER 72-ENAV-13] 20 p2896 A72-39164

Development of a desiccant CO2 adsorbent tailored for shuttle application.
[ASME PAPER 72-ENAV-11] 20 p2896 A72-39166

Panel-flutter analysis of a thermal protection-shield concept for the space shuttle.
20 p2980 A72-39623

European participation in space shuttle and space tug programs, discussing funding and technical aspects
21 p3103 A72-40456

Space shuttle technological evolution prospects, discussing cooperative development phases toward space transportation system with globally dispersed launch and landing bases
21 p3132 A72-40966

Laminar and turbulent boundary-layer studies at hypersonic speeds.
[ICASE PAPER 72-09] 21 p2990 A72-41134

The optimum configuration and the optimum reentry trajectory of space shuttle vehicles.
[ICASE PAPER 72-27] 21 p2991 A72-41152

Shuttle flight opportunities between stations orbiting the earth and moon.
21 p3108 A72-41302

Space shuttle ascent trajectory optimization by Davidson/Broyden crude search technique for matrix updating
[AIAA PAPER 72-907] 21 p3111 A72-41556

Structural dynamics and aeroelasticity analysis of space shuttle, covering vibration modes, thermal protection system dynamics, ground winds, flutter, buffet and noise
22 p3237 A72-42761

RAM - A concept for reducing space payload costs.
[SAWE PAPER 942] 23 p3343 A72-43482

Space shuttle mission and orbiter element description, discussing European participation
23 p3343 A72-43666

Space Shuttle landing navigation using precision distance measuring equipment.
24 p3421 A72-44637

Aeroacoustic, vibration and shock environments for the space shuttle orbiter.
24 p3448 A72-44679

Diffusion bonded columbium panels for the shuttle heat shield.
24 p3406 A72-44886

Boron-aluminum structural component for Shuttle.
24 p3458 A72-44899

Operational support of space shuttle transportation and payload systems with modular checkout and test equipment, noting service life and economy of operations
24 p3388 A72-45111

Extending the utility of the Space Shuttle as a space rescue vehicle.
24 p3449 A72-45130

Utilization of advanced composite materials for spacecraft and space shuttle applications.
24 p3417 A72-45153

Aircraft/spacecraft design approach and performance data, considering space shuttle program
24 p3467 A72-45159

NASA space science, exploration and applications plans and policies in view of space shuttle capabilities, emphasizing cost reduction
24 p3440 A72-45162

Space shuttle design evolution for program cost minimization, discussing refurbishment, payload impact, management cost and mission specifications and objectives
24 p3450 A72-45171

Transportation of radioactive waste-materials into the sun.
24 p3450 A72-45184

Optimal guidance for the space shuttle transition.
24 p3422 A72-45186

Study of shuttle-based systems for high-energy planetary missions.
24 p3441 A72-45189

NASA's management concept for the Space Shuttles Program.
24 p3468 A72-45194

The Agena orbit transfer stage as an interim space tug.
24 p3451 A72-45195

The effect of space shuttle payload design techniques on total space program cost.
24 p3451 A72-45210

Energy management during the space shuttle transition.
24 p3452 A72-45347

Space shuttle optimal entry trajectories for thermal protection system weight minimization, considering constant and variable angles of attack
[AIAA PAPER 72-977] 24 p3452 A72-45414

SPACE SIMULATORS
Space environment simulator with ultrahigh vacuum chamber and UV and corpuscular radiation for material samples physical properties in-situ measurement
02 p0201 A72-12701

Star sky simulation in testing and training stands, using spherical mirror, collimator and imbedded spheres
09 p1310 A72-22949

Closed loop life support systems, discussing manned ninety day test in space station simulator, Soviet experiments and water and oxygen regeneration
10 p1432 A72-24973

Space simulation facility for one year SERT 2 mercury ion thruster testing, discussing cryogenic operation and electrical and thermal insulation
[AIAA PAPER 72-430] 11 p1613 A72-26174

Dynamical motion simulation facility for Symphonie satellite, using sensors, attitude control electronics and analog computer in closed loop system [DEVLR-SONDDR-201] 12 p1795 A72-27659

Dual spin spacecraft simulation on three axis air bearing ball in atmosphere testing propellant tank dissipation and spacecraft stability in autotrack mode
[AIAA PAPER 72-860] 20 p2911 A72-39108

Theory of an experiment in an orbiting space laboratory to determine the gravitational constant.
20 p2968 A72-39200

SPACE STATIONS

NT HALO ORBIT SPACE STATION

NT ORBITAL SPACE STATIONS

NT ORBITAL WORKSHOPS

NT SALYUT SPACE STATION

Manned space station design for astronomy, space physics and biology, earth surveys, aerospace medicine, materials science and advanced technologies applications
01 p0135 A72-10937

Multichannel space station communications using PCM-PSK-PM interplex modulation for reducing cross modulation loss
02 p0174 A72-12131

High data rate convolutional coding for space station telemetry links, considering sequential and cascaded Viterbi decoding
02 p0174 A72-12132

Integral and modular space stations objectives, construction and utilization for astronomy, scientific experiments and technology
03 p0441 A72-14308

Angular quadrature effects on two dimensional space power reactor radiation shield calculation for manned space station application
04 p0546 A72-14426

Spin dynamics model of space station with counterweight connected by multiple cables, using linearized motion equations
[AIAA PAPER 72-172] 05 p0730 A72-16882

Triaxial space station orbit around oblate earth, presenting equations of motion, Hamiltonian and integration methods
06 p0878 A72-17663

Artificial gravity effects on space station crews performance, discussing unusual mechanical and perceptual phenomena
06 p0766 A72-17715

Educational programs for increasing public interest in space program benefits, describing summer teacher workshop on Apollo lunar and Skylab space station missions
06 p0906 A72-18623

NASA space station activities, describing Skylab missions and capabilities in physical and life sciences, earth resources surveying and technology experimentation
09 p1395 A72-22935

Malfunction detection for space station environmental/thermal control and life support system, using onboard computer
[AIAA PAPER 72-241] 10 p1423 A72-24447

Closed loop life support systems, discussing manned ninety day test in space station simulator, Soviet experiments and water and oxygen regeneration
10 p1432 A72-24973

High temperature biowaste resistojets with electrically conducting ceramic heaters, discussing lifetime and space station power systems adaptability
[AIAA PAPER 72-454] 11 p1708 A72-26190

High reliability long life heat pipe thermal control system for space station application
[AIAA PAPER 72-261] 14 p2171 A72-30835

European programs on space stations, tugs, shuttles, propulsion and avionics and consideration for participation in NASA programs for 1970s and 1980s
14 p2175 A72-31137

Monitoring system for ionospheric disturbances prediction from satellite observation, discussing optimum locations for space stations
15 p2220 A72-31233

Aerial IR line scanner systems for forest fire detection, considering escalation from aircraft to space platform
15 p2221 A72-31250

Elastic damping of spin stabilized space stations nutational oscillations induced by time-variant moments of inertia
15 p2319 A72-31458

Habitability factors in a rotating space station.
18 p2652 A72-36436

Stability and CMG wobble damping of flexible, spinning space stations.
[AIAA PAPER 72-888] 20 p2975 A72-39113

Space station prototype environmental/thermal control and life system - A current overview.
[ASME PAPER 72-ENAV-35] 20 p2894 A72-39143

Thermal control concept evaluation for a ten-year life modular space station.
[ASME PAPER 72-ENAV-30] 20 p2894 A72-39147

Design criteria for the modular space station environmental control and life support system selection.
[ASME PAPER 72-ENAV-25] 20 p2894 A72-39152

Space station atmospheric revitalization system design, covering temperature, humidity, carbon dioxide, contaminant and oxygen generation and composition control and vehicle configuration
[ASME PAPER 72-ENAV-24] 20 p2894 A72-39153

Environmental control and life support subsystem conceptual design studies for shuttle launched 6-12 man crew modular space station
[ASME PAPER 72-ENAV-22] 20 p2895 A72-39155

Modular environmental control/life support system design for low cost shuttle launched space station, evaluating humidity, carbon dioxide, water and waste management
[ASME PAPER 72-ENAV-17] 20 p2895 A72-39160

Water and waste management subsystem design for a space station prototype.
[ASME PAPER 72-ENAV-8] 20 p2896 A72-39169

Safety design of space station against collision hazards with artificial orbiting bodies.
24 p3449 A72-45143

SPACE SUITS

Calculation procedures for some parameters of space suit gas medium supply systems
21 p3006 A72-40449

SPACE SURVEILLANCE [GROUND BASED]

Visible displays of millimeter and submillimeter wave images for all-weather ground surveillance, discussing image conversion
[AD-736578] 04 p0494 A72-15612

SPACE SURVEILLANCE [SPACEBORNE]

Air surveillance using satellite range-difference measurement from noninterrogated aircraft beacons for ATC
04 p0545 A72-14826

Terrestrial surface observation from space platform, considering atmospheric effects, surface spectral properties and information resolution and transmission
08 p1170 A72-21965

Computer processed image enhancement applications to spacecraft returned photoreconnaissance, discussing data transmission and resolution vs recognition and color quality
17 p2520 A72-34408

SPACE SYSTEMS ENGINEERING
U AEROSPACE ENGINEERING

SPACE TOOLS

Space tools and support equipment for earth orbital systems maintenance, replacement and repair, discussing Skylab requirements and teleoperator applications
[AIAA PAPER 72-230] 10 p1488 A72-25049

Recommendations for selection and use of torque wrenches for aerospace propulsion systems applications.
[SAE AIR 1268] 18 p2648 A72-36531

SPACE TRANSPORTATION

Post Apollo program, considering space shuttle design, operation, transportation and payload cost reduction, rocket developments and plans for Mars expedition
03 p0440 A72-13612

Atmospheric rendezvous concept to increase space transportation system efficiency and flexibility, discussing structural weight savings
[AIAA PAPER 72-134] 05 p0730 A72-16889

Space shuttle, tug and orbital station transportation system benefits and applications, noting European economic implications
08 p1229 A72-20977

U.S. industry views on NASA plans for 1970s, emphasizing interplanetary nuclear propulsion, space transportation, shuttle costs and economics
14 p2175 A72-31139

Expendable space transportation - A 1972 assessment.
[AIAA PAPER 72-732] 18 p2730 A72-36542

Space shuttle technological evolution prospects, discussing cooperative development phases toward space transportation system with globally dispersed launch and landing bases
21 p3132 A72-40966

Transportation of radioactive waste-materials into the sun.
24 p3450 A72-45184

Implications of new transport vehicles and cost analysis of supplying and maintaining a manned lunar laboratory.
24 p3441 A72-45209

Flight mechanics aspects in space transportation system for international rescue, analyzing potential crises situations requiring emergency action
24 p3451 A72-45217

SPACE TUGS

European reusable space tug, discussing computer controlled attitude stabilization and maneuvering system design for orbital rendezvous and docking
05 p0725 A72-16446

Reusable space tug mission profile for interplanetary spacecraft recovery, using branched trajectory, steepest descent optimization and propellant minimization
[AIAA PAPER 72-13] 05 p0730 A72-16949

Space shuttle, tug and orbital station transportation system benefits and applications, noting European economic implications
08 p1229 A72-20977

European Special Space Tug electronic subsystem requirements, considering strapdown inertial measuring unit, remote sensors, computer and fail-safe backup system
09 p1396 A72-23258

European Special Space Tug structural and configurational layouts and problems
09 p1396 A72-23259

Nuclear rocket for space tug, comparing performance and operational costs with chemical propulsion
13 p2000 A72-28926

Space tug for recoverable reusable system with winged manned boost-glide vehicle, discussing feasibility in economics and engineering
13 p2051 A72-28930

Space tug design constraints, configurational alternatives, subsystem arrangements, docking system, propellant tank pressurization system, main engine and power supply, etc
13 p2051 A72-28933

European programs on space stations, tugs, shuttles, propulsion and avionics and consideration for participation in NASA programs for 1970s and 1980s
14 p2175 A72-31137

Space shuttle configuration, discussing payload accommodation requirements, accessories, mission operations and reusable tug
[AIAA PAPER 72-737] 18 p2731 A72-36546

European participation in space shuttle and space tug programs, discussing funding and technical aspects
21 p3103 A72-40456

Aerospace tug using atmospheric braking during return from geostationary orbit, discussing radiative thermal protection, mass, design and advantages
23 p3340 A72-44275

Extending the utility of the Space Shuttle as a space rescue vehicle.
24 p3449 A72-45130

The Agena orbit transfer stage as an interim space tug.
24 p3451 A72-45195

The space tug orbital operations.
24 p3451 A72-45196

The space tug optimum cost evaluation.
24 p3468 A72-45212

SPACE VEHICLE CHECKOUT PROGRAM

Space shuttle cryogenics technology, flight and ground operations, checkout, maintenance and safety
03 p0441 A72-13695

Structure-borne acoustic nondestructive testing for readiness assessment, fault isolation and automatic checkout of space vehicle mechanical devices
15 p2214 A72-31699

Operational support of space shuttle transportation and payload systems with modular checkout and test equipment, noting service life and economy of operations
24 p3388 A72-45111

SPACE VEHICLE CONTROL
U SPACECRAFT CONTROL

SPACE VEHICLES
U SPACECRAFT

SPACE-TIME CONTINUUM
U RELATIVITY

SPACE-TIME FUNCTIONS

Nonlinear hydromagnetic waves in finite beta collisionless plasma, calculating space-time evolution with nonlinear integrodifferential equation
01 p0107 A72-10143

Electromagnetic waves diffusion by space-time fluctuations in plasma electron density
[ONERA, TP NO. 1043] 01 p0110 A72-11180

Gravitational biology theory problems, discussing possibility of applying relativistic phenomena to living organisms in inertial or noninertial systems
02 p0160 A72-12016

Spatial-temporal correlation functions of field due to electromagnetic waves backscattering from random inhomogeneities in extended layer
02 p0180 A72-12580

Anisotropic universe model based on Einstein equations for metric with cosmological term
03 p0388 A72-13193

Gravitational field of bounded and isolated material in empty four-dimensional locally Minkowskian space-time, emphasizing radiation zone and gravitational waves
04 p0570 A72-14556

Human body kinematics numerical analysis, obtaining spacetime resolution by photogrammetric restitution and electronic data processing of photographic recordings 04 p0478 A72-14710

Metric tensor components of isotropic inhomogeneous cosmological model obtained from Einstein equations 07 p1072 A72-19340

Wightman field theory generalization for application to gravitational field quantization, describing curved space-time by strongly geodesically complete manifolds 07 p1036 A72-20198

Space-time relationship derivation to estimate traveling time of discontinuities running against magnetosphere in unperturbed solar wind 08 p1153 A72-20714

Probabilistic derivation of quantum mechanics wave equations for Brownian motion and spatial-temporal diffusion 10 p1505 A72-24071

Equations of motion with gravitational radiation reaction terms for gravitating system as source of asymptotically flat space 10 p1511 A72-24416

Godel metric type MHD universes, using Maxwell and conservation equations 10 p1524 A72-24857

Radiative displacement of molecular beam sidebands by spatiotemporal modulation of irradiating RF field 10 p1492 A72-24858

Time-space nonholonomic characteristics of curvature tensor for three dimensional physical space in gravitational and inertial fields 12 p1843 A72-27049

Space-time model locally identical with Minkowski space in geometrical and causality features, implying non-Doppler red shift and cosmology 12 p1868 A72-27218

Space-time correlation of field amplitude and phase in plane waveguide with statistically irregular boundary, using Born approximation and perturbation theory method 13 p1928 A72-28471

Dipole antenna radiation patterns in sinusoidal space-time periodic media 13 p1915 A72-28531

Conformally flat linear axial symmetry chronometrically invariant cosmological models, discussing various types of spaces realized during model evolution 13 p2036 A72-28759

Spatial-temporal coherent processing technique application to thermal radio emission random signal reception, deriving ambiguity function 13 p1920 A72-29282

Luminosity variation of star in circular orbit around extreme Kerr black hole due to Doppler effects and gravitational field light focusing 13 p2041 A72-29416

Electromagnetic waves backscattering in magnetoactive plasma containing random inhomogeneities of electron density, calculating field spatial-time and cross correlation functions 14 p2086 A72-30789

Anisotropic and isotropic descriptions of physical process speeds in special relativity theory space-time metric 15 p2279 A72-32768

Curved space cosmological bounds on time variation of gravitational constant in terms of Brans-Dicke theory for Friedmann expanding cosmologies 16 p2450 A72-32864

Lorentz-covariant procedure for equations of structure and motion of particles represented by singularities in Einstein relativistic field theory 16 p2422 A72-32880

Information propagation time direction of cosmological models in terms of conventional electrodynamic theory, contrasting with Wheeler-Feynman theory 16 p2424 A72-33286

Electromagnetic wave propagation and wave-vector diagram in space-time periodic media 17 p2514 A72-34381

Relativistic kinetic theory combined with surface layer theory in curved space-time to study counter-rotating disks with fine central red shift 17 p2582 A72-35389

Correlation of noise-like emission reflected from a statistically uneven surface 17 p2583 A72-35543

Structural analysis of gravitational field in asymptotic limit at spatial infinity, introducing three dimensional spacelike surface carrying initial data for space-time 17 p2583 A72-35824

Conformally flat linear axisymmetric chronometrically invariant cosmological models, discussing various types of spaces realized during model evolution 18 p2724 A72-36237

Isotropic, space-like, Maxwellian particles of real mass and of time-like velocity 18 p2710 A72-36472

Universe expansion induced electromagnetic wave backscattering absence in Robertson-Walker space-time as consequence of motion equations conformal invariance 18 p2711 A72-36711

Equations of motion in the linear approximation. 19 p2835 A72-38174

Space-time relationship derivation to estimate traveling time of discontinuities running against magnetosphere in unperturbed solar wind 19 p2791 A72-38342

Electromagnetic wave dispersion in ionized cosmic medium for spatially flat Brans-Dicke cosmology 20 p2969 A72-39265

Introduction of time and space into a point system endowed with a signal 20 p2946 A72-39574

The geometry of free fall and light propagation. 20 p2954 A72-40005

Minkowski space-times for impulsive gravitational waves, considering idealized plane fronted wave form and limiting case of Robinson-Trautman null spherically fronted wave 20 p2955 A72-40007

Plane-symmetric similarity solutions for self-gravitating fluids. 20 p2955 A72-40009

Construction of a general cosmological solution of the Einstein equations with a singularity with respect to time 21 p3103 A72-40403

Spatially homogeneous general relativistic Bianchi cosmological models with diagonal metrics, noting field equations simplicity 21 p3104 A72-40569

Electron processes in nonrelativistic electron streams against stationary ion background as wave packet envelope deformation in space and time 21 p3094 A72-41652

On the cosmological equations in a universe with small scale condensations. 22 p3220 A72-41998

First derivative discontinuities of space-time metric tensor in Einstein equations solution for nonisotropic and isotropic hypersurfaces, proving coordinate system existence for continuity 23 p3312 A72-43302

Generalization of the Taub-Kazner cosmological metric in the scalar-tensor gravitation theory. 23 p3313 A72-43500

Analysis of optimal space-time signal discrimination 23 p3266 A72-44217

Mathematical consequences of physical laws invariance hypothesis under space-time-dependent changes in unit length, discussing conformally covariant and cosmological theories interrelationship 24 p3447 A72-45626

Time-space nonholonomic characteristics of curvature tensor for three dimensional physical space in gravitational and inertial fields 24 p3425 A72-45702

SPACE-TIME METRIC U SPACE-TIME FUNCTIONS SPACEBORNE ASTRONOMY

Space astronomy experiments with TV scanning, discussing data from Telescope catalog of UV observations and photometric and astrometric accuracy 08 p1170 A72-21957

Spaceborne Uvicon/Telescope astronomical observatory for stellar UV TV pictures, discussing system design requirements 08 p1170 A72-21958

Electronography in space astronomy, discussing use of Lallemand electronic camera as photon receptor onboard balloons or rockets 08 p1170 A72-21963

Image dissector application to D2B astronomical satellite position field plotting in solar and stellar UV photometry 08 p1172 A72-21976

Space environment and astronomical studies with sounding rockets, satellites and orbiting solar observations 10 p1548 A72-24974

Spacecraft-based observations of gamma and X radiation resulting from planetary surface and atmosphere processes to obtain source medium chemical composition 10 p1530 A72-25060

Large space telescope /LST/ project, discussing instrumentation, observation program and operational characteristics 11 p1630 A72-25681

Astronomical observations from astrophysical observatory onboard orbital space station controlled by astronaut, discussing telescope orientation outside of spacecraft 15 p2242 A72-32740

Construction and optical equipment of astrophysical observatory Orion onboard Salyut space station, discussing mirror telescope, spectrograph and star tracker 15 p2242 A72-32741

Orion spaceborne astronomical observatory automatic control system for instrument orientation and

star tracking, discussing servomechanism and pulse duration modulation 15 p2242 A72-32743

Spectrograph for Orion spaceborne astronomical observatory on Salyut space station calibrated with synchrotron radiation from particle accelerator 15 p2242 A72-32744

Photographic characteristics of high resolution film for Orion spaceborne astronomical observatory spectrograms, discussing aerospace environment effect on sensitivity and physicochemical properties 15 p2243 A72-32745

Extra-atmospheric astronomical studies and instruments, discussing spaceborne, X ray and heavy orbiting telescopes and ground-space radio interferometer designs 16 p2462 A72-33516

Space observations of the solar corona. 17 p2611 A72-35326

Sounding rockets for astronomical research, discussing rocket types, payloads, launch sites, advantages over satellites, economic factors and future prospects 22 p3231 A72-42983

OA0 3 satellite Copernicus onboard equipment, discussing UV reflecting and X ray telescopes, attitude sensor, star tracker, solar sensor and computer 22 p3231 A72-42985

The on-board computer of the Astronomical Netherlands Satellite /ANS/. 24 p3382 A72-45163

Astronomy from a space platform; Proceedings of the Symposium, Philadelphia, Pa., December 27, 28, 1971. 24 p3446 A72-45526

Skylab solar astronomical observation programs and instruments, discussing X ray and H alpha telescopes, coronagraphs, spectroheliographs and UV spectrographs 24 p3453 A72-45528

Space astronomical observatory mission planning, analysis and operation and data utilization in terms of space and ground facility instruments and support subsystems 24 p3382 A72-45530

UV and IR observations of galactic and intergalactic matter from space stations, noting spatial resolution increase 24 p3446 A72-45532

Future orbital observatory modules for stellar and galactic astronomy. 24 p3453 A72-45533

Unmanned OA0 spacecraft series and experiment packages, discussing space astronomy scientific achievements, mission plans and space shuttle role 24 p3453 A72-45535

Radiation pressure supported stars, degenerate dwarfs, neutron stars and black holes high energy observations from space platforms 24 p3446 A72-45536

HEAO satellite to carry instruments required in high energy astrophysics missions, discussing observational objectives, configuration and experiments 24 p3453 A72-45538

NASA X ray satellite UHURU and HEAO-C instruments and observational data on supernova remnants, pulsars, extars quasars, radio galaxies and galactic clusters 24 p3446 A72-45539

Charged and neutral cosmic rays radioactive isotope and momentum distribution measuring techniques in high energy particle astronomy observatories /HEAO/ 24 p3404 A72-45540

Spaceborne astronomy by synthetic aperture optics for high resolution without cost and weight disadvantages of large telescopes, considering Michelson stellar interferometer 24 p3404 A72-45541

Electronic imaging devices for astronomy from a space platform. 24 p3404 A72-45542

Future giant-aperture orbital space telescope design based on active optics and electro-optical techniques, discussing laser interferometry and precise servomechanisms roles 24 p3405 A72-45544

OSO and Skylab astronomical instruments technology, emphasizing precision pointing, spatial and spectral resolution and photometric efficiency problems 24 p3405 A72-45545

Manned and unmanned space-based astronomical observatory systems pros and cons, discussing experiment management complexity and cost reduction 24 p3447 A72-45546

SPACEBORNE PHOTOGRAPHY NT SATELLITE-BORNE PHOTOGRAPHY

Interpretation model for aircraft and spacecraft remote sensing of tropical agricultural systems 02 p0210 A72-11798

High altitude aircraft and Apollo 9 multispectral photography and simulated ERTS-A imagery evaluation, comparing with ground observations in Arizona 02 p0210 A72-11799

Meteorological precipitation and earth surface under cloud characteristics from airborne microwave radiation measurements using millimeter and centimeter waves

02 p0216 A72-11889

Space and high altitude aerial photography agricultural ground data collection and processing for Arizona survey evaluation

02 p0220 A72-12200

Integral image tube optical systems for far UV narrow band and broad bandpass photography from spacecraft outside atmosphere

03 p0355 A72-13063

Book on earth, moon and planet space photography, discussing synoptic meteorological data, mapping, surface detail inspection and planetary exploration

03 p0438 A72-14099

Mars surface topographic characteristics relationship to earth features, using Mariner 6 and 7 photographs

04 p0569 A72-14501

Atmospheric contrast degradation and turbulence effects on photography from space with computerized optimization of ground resolution

06 p0813 A72-17431

Image resolutions for ERTS return beam vidicon TV, Skylab multispectral cameras and Gemini/Apollo photographs

06 p0818 A72-18328

Apollo 6 photogrammetric, photometric and neutron activation analysis of smoke plume, determining eddy diffusivity

06 p0819 A72-18439

Soviet book on terrestrial studies by satellite observation covering meteorology, hydrology, oceanography, geomorphology, geobotany, geography, pedology, atmospheric physics and TV and photographic analysis

06 p0810 A72-18523

International legal aspects of earth resources survey from space

07 p1104 A72-19467

Image tube, film and mechanical scan camera imaging systems comparison for spacecraft-borne planetary photography based on maximum data return at acceptable cost

08 p1170 A72-21964

Si diode array vidicon for ground based and spaceborne planetary and stellar imaging, noting integration time, storage and slow scan capabilities extension through cooling

08 p1171 A72-21970

Mass and energy exchange in tropical convective cloud systems from ATS cloud photographs

09 p1344 A72-22430

Mars surface lineament systems from Mariner photographs, noting global and radial type associated with Hellas and South Pole basins

12 p1868 A72-27259

Apollo mapping camera system synchronized laser altimetry utilization in astro-photogrammetric triangulation

12 p1872 A72-27816

Image deformation sources correction in space photography, discussing stationary and moving cameras and panoramic and complex sensing systems

12 p1809 A72-27817

Atmospheric air pollution study by space techniques via thermal radiation spectral measurements and laser sounding, considering spaceborne photography

15 p2220 A72-31237

Lunar orbital photography of astronomical and geophysical phenomena during Apollo 15 flight, noting solar corona and Milky Way

15 p2236 A72-31974

Apollo 9, Skylab and Earth Resources Technology Satellite-borne multiband cameras performance requirements and tolerances comparison, considering geometric and spectroradiometric properties

16 p2395 A72-34103

Multispectral angular reflectivity effect on optimum filter combinations for spaceborne multiband photography sensing mission in visible and near IR regions

16 p2395 A72-34104

Determination of the parameters of a satellite camera

17 p2556 A72-35360

Recent developments in digital image processing at the image processing laboratory at the Jet Propulsion Laboratory.

18 p2658 A72-36255

Photomorphologic units for regional analysis from hyperaltitude and spacecraft remote sensing data

18 p2690 A72-36321

The new Mariner 9 map of Mars.

18 p2729 A72-36988

A detailed analysis of Mariner nine TV navigation data.

20 p2977 A72-40061

Photogrammetric method for determining the deflection of light beams by spacecraft windows during flight

21 p3052 A72-40305

Mars photographic mapping and UV/IR spectrometric investigation by Mariner 9, discussing Martian surface features and atmospheric composition

21 p3105 A72-40967

First approximation for spacecraft observations of noctilucent clouds from circular orbits with optimal optical axis orientations

21 p3049 A72-41438

An orthographic photomap of the South Pole of Mars from Mariner 7.

21 p3110 A72-41455

The location of the Mountains of Michel and evidence for their nature in Mariner 7 pictures.

21 p3110 A72-41456

Jupiter - Its Red Spot and disturbances in 1970-1971.

24 p3435 A72-44690

Mariner 9 spacecraft systems and photographs of Martian surface details

24 p3441 A72-45170

High resolution imagery with the large space telescope.

24 p3404 A72-45537

SPACEBORNE TELESCOPES

TV tube type image sensors to replace photographic film for space telescope, discussing design and performance

08 p1169 A72-21956

Limiting magnitudes of stars in visual telescopic observations /Ground and extraatmospheric locations of instrument and observer/

19 p2859 A72-37907

Fine guidance pointing stability of a 120-inch /3 meter/ large space telescope /LST/.

[AIAA PAPER 72-853]

20 p2949 A72-39076

Precision X-ray telescopes on HEAO-C.

24 p3403 A72-45202

Orbiting telescopes improved angular resolution and access to UV spectra as advantages in determining stellar composition, mass, luminosity and distance

24 p3446 A72-45531

Future orbital observatory modules for stellar and galactic astronomy.

24 p3453 A72-45533

High resolution imagery with the large space telescope.

24 p3404 A72-45537

Future giant-aperture orbital space telescope design based on active optics and electro-optical techniques, discussing laser interferometry and precise servomechanisms roles

24 p3405 A72-45544

SPACECRAFT

Aircraft and spacecraft conceptual definitions in national and international law

11 p1749 A72-26561

SPACECRAFT ANTENNAS

Microwave breakdown prediction models for antenna system in ionized reentry environment

04 p0486 A72-14531

Spacecraft antenna radiation pattern numerical analysis using combined electric and magnetic integral equations

04 p0500 A72-15407

Radiation pattern of spacecraft dipole antenna mounted on conducting finite length cone calculated by superposition of radiated and diffracted waves

09 p1282 A72-23524

Electra method of plasma diagnosis around reentry vehicle head, describing onboard antennas impedance measurements and use of triple Langmuir probe mounted on telescopic mast

10 p1552 A72-24659

Autotracking antenna effect on dual spin spacecraft nutational stability, using averaging, eigenvalues and digital simulation techniques

[AIAA PAPER 72-571]

12 p1876 A72-27379

Test facility for aircraft and spacecraft antennas radiation patterns and optimal installation determination

12 p1795 A72-27412

Digital simulations of effects of two-antenna interference on space vehicle guidance.

19 p2830 A72-37292

Selection of an optimal design for a spacecraft antenna system

21 p3025 A72-40311

Circular-polarization antennas with controlled radiation patterns

21 p3026 A72-40314

Microwave filters in antenna circuit feeder systems of space vehicles

21 p3026 A72-40318

Spacecraft antenna feeder channel parameter control in flight

21 p3026 A72-40319

Controlling the directive gain of weakly directional antennas during space-vehicle flight

21 p3026 A72-40324

Certain problems in designing highly directional spacecraft antennas

21 p3026 A72-40325

Radiation patterns of wideband horn antenna loaded by dielectric belt, noting satellite and terrestrial radio relay applications

21 p3036 A72-41832

SPACECRAFT CABIN ATMOSPHERES

Miniaturized magnetic mass spectrometer for trace contaminants continuous monitoring and control, discussing applications to closed atmospheric systems in spacecraft and undersea environments

[AIAA PAPER 71-1122]

01 p0608 A72-10558

Rat brain acetylated and unacetylated coenzyme A aberration in marginally hyperoxic space capsule environments

06 p0763 A72-17875

Spacecraft cabin atmosphere thermal scale modeling based on radiative-convective-convective heat transfer, obtaining adequate thermal similitude through mass flux and heat transfer coefficient preservation

[AIAA PAPER 72-288]

11 p1741 A72-25226

Space station atmospheric revitalization system design, covering temperature, humidity, carbon dioxide, contaminant and oxygen generation and composition control and vehicle configuration

[ASME PAPER 72-ENAV-24]

20 p2894 A72-39153

Spacecraft atmosphere trace contaminant sensor system using mass spectrometric analysis of contaminants concentrated on sorbents in monitor inlet system

[ASME PAPER 72-ENAV-15]

20 p2896 A72-39162

Development of a desiccant CO₂ adsorbent tailored for shuttle application.

[ASME PAPER 72-ENAV-11]

20 p2896 A72-39166

Six-month test program of two water electrolysis systems for spacecraft cabin oxygen generation.

[ASME PAPER 72-ENAV-5]

20 p2896 A72-39172

Expired air as a source of spacecraft environment carbon monoxide contamination

24 p3375 A72-45120

SPACECRAFT CABINS

Future spacecraft habitable compartment layout from psychophysiological viewpoint, considering human visual and motor field parameters and crew members social needs

13 p1910 A72-29321

SPACECRAFT COMMUNICATION

NT REENTRY COMMUNICATION

Diurnal and seasonal variations of scintillations in short wave radio signals of earth satellites and spacecraft

01 p0053 A72-10359

Spacecraft-ground communications system, discussing electromagnetic wave propagation and frequency bands

01 p0027 A72-10445

Grid controlled 100 W microwave transmitter power triode for space applications, noting high reliability and stability through use of metal dispenser cathode

01 p0009 A72-11223

Orbiting lunar spacecraft Endeavor radio transmission postocclusion reception, considering surface wave propagation and mountain formation prismatic refraction

02 p0171 A72-11753

Initial Canadian domestic satellite communication system plans and progress

02 p0177 A72-12382

Space shuttle orbiter flight instrumentation, data handling and communication requirements, discussing data gathering methods, crew displays, computer processing, recording and digital data bus telemetry

02 p0179 A72-12406

Multiple access techniques in satellite telecommunication systems, discussing clean mesh type network

02 p0182 A72-12699

High speed digital communication over space to earth satellite links by quadriphase modulation, discussing modulator, receiver and system technology for maximizing data transfer

04 p0485 A72-14477

Phase locked loop bandwidth, acquisition time and SNR for Doppler tracking deep space communications for Venus and Jupiter probes

05 p0629 A72-16575

Scintillation effects on synchronous satellite communications systems at 250 MHz in equatorial region, discussing diversity techniques and composite diffraction refraction theory

[AIAA PAPER 72-178]

05 p0631 A72-16906

Recovered carrier phase ambiguity resolution in four-phase PSK digital satellite communications system

06 p0772 A72-17409

Error coding techniques application to communication satellite links, discussing computer simulation results

07 p0948 A72-20495

Parameters affecting communication and rescue time constraints for emergency astronaut return from low earth orbits

09 p1395 A72-23155

Terminal guidance systems and techniques application to manned space flight rescue operations, discussing emergency location and rescue spacecraft communication and guidance

09 p1396 A72-23158

Frequency bands for space-earth links in broadcasting satellite service, stressing application to educational television

10 p1435 A72-24032

Microwave equipment and technology application for instrument landing, terminal ATC, millimeter wave CAT detection and satellite communications

10 p1509 A72-24036

Space communications period forecasting algorithm for limited power ground based transmitters and spacecraft in earth orbit

11 p1598 A72-26735

Simultaneous measurements of ionospheric electrons number vertical distribution by incoherent ground radio wave scattering and coherent signals from Intercoms 2 and Cosmos 321 satellites

11 p1628 A72-26918

Intelsat 4 satellite communication transponder design for broadband multicarrier operation, using frequency and pulse modulation techniques

[AIAA PAPER 72-535]

12 p1780 A72-27358

SkyLab communications system, discussing voice, data, TV and command mission requirements and microwave instrumentation

[AIAA PAPER 72-543]

12 p1781 A72-27366

Franco-German Symphonie project of point to point communication and TV distribution by satellite, describing spacecraft and ground station characteristics

[AIAA PAPER 72-549]

12 p1794 A72-27372

Flight prototype satellite communications repeater with two transponder channels and dual beam antenna, discussing design parameters and advanced systems application

[AIAA PAPER 72-579]

12 p1789 A72-27381

Experimental earth station for wave propagation studies in satellite communications using frequency range above 10 GHz

12 p1785 A72-27801

Ground terminals spatial diversity for earth satellite mm wave communication systems to avoid attenuations by rainfall

13 p1989 A72-28810

Data compression for spacecraft borne signal measurement, discussing nonlinear quantizing, histogram parameter extraction, and signal encoding

[DFVLR-SONDDR-204]

13 p1921 A72-29346

Spacecraft-borne computer and electronic systems interface for radio reception, transmission and TV imagery applications

21 p3014 A72-40309

Optical communication with distant spacecraft, discussing electro-optical transducers, light sources and receivers

21 p3014 A72-40321

Telemetric frame compression coefficient and shaping algorithm for spacecraft data processing systems for arbitrary number of active channels

21 p3014 A72-40326

Statistical analysis of information from remote space vehicles

21 p3015 A72-40327

A priori estimation of the quality of a data-compression system from the statistical characteristics of the sensors employed

21 p3024 A72-40328

Reflector antennas for satellite communication, discussing hybrid mode, dieguide and lens feeds, spherical and stepped reflectors, and high efficiency paraboloid antennas

21 p3028 A72-40513

Planning of a broadcast-satellite service

21 p3016 A72-40771

Computer simulation of a digital satellite communications link

21 p3024 A72-40854

Error correcting codes applied to satellite channels

21 p3018 A72-40874

Phase noise types in digital satellite communication links, discussing continuous binary phase shift keyed modulation systems with coherent detection

21 p3020 A72-40896

Economic considerations for low-traffic satellite earth stations

21 p3022 A72-41320

Relation between satellite radio signal scintillations and magnetic activity

23 p3264 A72-43850

SPACECRAFT COMPONENTS

NT SERVICE MODULES

NT SPACECRAFT CABINS

NT SPACECRAFT MODULES

Microbiological examination of space hardware, discussing viable organisms neutralization buried inside solid materials, sampling procedures and culture media

01 p0019 A72-10820

Space flight hardware sterilization, considering dry heat and chemical destruction

01 p0019 A72-10822

Nonsterile space flight hardware effects on planetary quarantine, evaluating contamination sources, design and mission parameters, cleanliness conditions and biohazard

01 p0020 A72-10824

Long life aerospace explosive components, examining material degradation mechanisms and effects of

pressure, temperature, moisture, chemical reactions and impurities

08 p1219 A72-20759

International standardization of manned spacecraft components for rescue efforts and joint multinational space missions

09 p1395 A72-23154

Vehicle components oxidation in thermal control coatings, investigating resistance to oxidation by UV photoproduct ZnO electronic holes

[AIAA PAPER 72-264]

11 p1699 A72-25207

Reliability, quality and testing assurance in ATS F and G system, discussing computerized handling of spacecraft parts information

12 p1814 A72-27524

Laboratory irradiation tests with van de Graaff generator for simulation of spacecraft components radiation damage due to high energy space protons and electrons

12 p1863 A72-27552

Heat losses due to spacecraft installation discontinuities on aluminized Mylar multilayer insulation, predicting blanket performance

[AIAA PAPER 72-285]

14 p2171 A72-30829

French aerospace industry difficulties in procuring parts, suggesting purchasing centralization or setting up of parts stocks

17 p2639 A72-35951

Problems encountered in aerospace material components procurement, considering purchase centralization and inventories creation policies

18 p2743 A72-37125

Modular heat rejection system to accommodate widely varying thermal loads in space shuttles and future spacecraft, emphasizing commonality design philosophy for cost reduction

[ASME PAPER 72-ENAV-34]

20 p2976 A72-39144

Boron-aluminum structural component for Shuttle

24 p3458 A72-44890

SPACECRAFT CONFIGURATIONS

NT APOLLO TELESCOPE MOUNT

NT SATELLITE CONFIGURATIONS

Experiment sensors impact on on-orbit vehicle configurations and operations in NASA program, synthesizing and cost analyzing common module sets

01 p0135 A72-10945

Integral and modular space stations objectives, construction and utilization for astronomy, scientific experiments and technology

03 p0441 A72-14308

Space shuttle vehicle configurations with reusable booster and orbiter modules, discussing cargo capacity, maneuvering capability, mission duration, engine characteristics and acceleration constraints

07 p1085 A72-19058

Space shuttle phase B design studies regarding configurational alternatives, propulsion systems, displays and controls, simulations and flight test programs

08 p1240 A72-21009

European Special Space Tug structural and configurational layouts and problems

09 p1396 A72-23259

Liquid propellants coupling effects on parallel stage space shuttle configuration structural dynamics, using forty degree of freedom analytical model

[AIAA PAPER 72-347]

11 p1725 A72-25376

Unsteady airfoil stall and stall flutter analysis, discussing application to space shuttle configuration

[AIAA PAPER 72-380]

11 p1730 A72-25404

Solar electric propulsion upper stage for multiple space exploration missions, discussing spacecraft performance, configurations and program plans

[AIAA PAPER 72-464]

11 p1709 A72-26199

Space shuttle program, discussing configurational concepts, payload carrying capacity variants and cost reduction design changes

17 p2621 A72-34869

Parameters influencing dynamic stability characteristics of Viking-type entry configurations at Mach 1.76

17 p2622 A72-35494

Space shuttle configuration, discussing payload accommodation requirements, accessories, mission operations and reusable tug

[AIAA PAPER 72-737]

18 p2731 A72-36546

Russian book - Space ergonomics

21 p3004 A72-40300

Viking configuration pitch damping derivatives as influenced by support interference and test technique at transonic and supersonic speeds

[AIAA PAPER 72-1012]

21 p3041 A72-41593

Configuration analysis as applied to aerospace vehicle design synthesis

[SAWE PAPER 911]

23 p3342 A72-43458

Two early missions to comets in 1977-1980 as precursors to more ambitious missions in 1984-1986, discussing exploration objectives and spacecraft configurations

23 p3340 A72-44352

Rescue operation capability for Skylab, discussing mission requirements, response time and vehicle configuration

24 p3449 A72-45132

SPACECRAFT CONSTRUCTION MATERIALS

Space shuttle materials - Conference, Huntsville, Alabama, October 1971, Volume 3

01 p0090 A72-10726

Composite materials application for space shuttle structures, relating structural weight to payloads

01 p0090 A72-10727

Continuous casting of metallic tubular structural elements reinforced with boron filaments, stressing application to space shuttle structures

01 p0074 A72-10731

High temperature testing of metal matrix composites mechanical properties, noting aerospace structural applications

01 p0084 A72-10732

Hat section stiffened compression panel of graphite/epoxy composite for space shuttle, discussing quality control procedures

01 p0139 A72-10736

Composite space shuttle booster and orbiter engine support structures design and analysis, stressing weight savings

01 p0139 A72-10740

Space shuttle mechanical fastener design, discussing drives, threads, manufacturing and refractory alloys

01 p0075 A72-10751

TD nickel as construction material for rocket thrust chambers, discussing spin-forming, welding, machining, electric discharge machining and electroforming operations

01 p0075 A72-10753

Test program to evaluate metallic materials candidates for space shuttle booster thermal protection system

01 p0085 A72-10755

Adhesive materials based on room temperature vulcanizing silicone elastomers for space shuttle vehicle reusable surface insulation bonding

01 p0075 A72-10763

Silica based surface insulation material for space shuttle thermal protection system, discussing cyclic tests in simulated environment and fiber purity effects on crystallization

01 p0091 A72-10764

Zirconium diboride-silicon carbon-graphite composition for lifting entry vehicle hot leading edges, investigating mechanical behavior by tension and flexural tests

01 p0091 A72-10767

Refractory material development for space shuttle hydrogen tank reusable internal gas layer insulation

01 p0139 A72-10777

Oxidation screening at 2200 F of Ni, Fe and Co wrought alloys for space shuttle thermal protection system, noting microstructural changes

01 p0085 A72-10781

Characterization of graphite/polyimide composites for space shuttle applications

01 p0092 A72-10784

Combustion chamber and nozzle materials for fluorine and/or metal combustibles high energy propellant rocket engines, considering cooled and uncooled nozzles and spoiler plates

01 p0117 A72-10941

High modulus high strength graphite composites for aerospace structures, noting materials, machining properties and applications

[SME PAPER EM 71-191]

01 p0092 A72-10965

Macroscopic metal crystal plastic deformation applications to aircraft and spacecraft materials production, considering internal friction and energy conversion into strain energy and heat

01 p0071 A72-11020

Strain gage tests on three dimensional composites for reentry vehicle structural design evaluation

02 p0287 A72-11506

Optical mirrors contamination by condensation of outgassed spacecraft materials in vacuum under UV irradiation, describing test apparatus and results with various materials

[AIAA PAPER 72-267]

11 p1637 A72-25208

Thermal emittance, reflectance, absorptance and transmittance of aerospace materials

[AIAA PAPER 72-307]

11 p1742 A72-25241

Dimensional stability and micromechanical properties of materials for use in OAO, investigating residual stresses, creep properties and stress relaxation

[AIAA PAPER 72-325]

11 p1653 A72-25362

Reusable external insulation materials for space shuttle thermal protection, evaluating local heat transfer at interface areas in plasma arc test facility

[AIAA PAPER 72-388]

11 p1744 A72-25409

Beryllium sheet and foil application to lightweight space structures, discussing mechanical properties

[AIAA PAPER 72-404]

11 p1726 A72-25425

Satellite surface coating materials photoemission properties, discussing reflectance, work function, photoyield and photoelectron energy distributions

12 p1844 A72-27280

Environmental effects on spacecraft materials, structures and design, discussing sterilization, gravity, vacuum, micrometeoroids, radiation, etc

15 p2320 A72-31802

The manufacture of mullite reusable surface insulation materials for space shuttle.
[SME PAPER EM 72-714] 18 p2695 A72-36527

Interferometric holography for bond inspection in aerospace composite materials and honeycomb structures
19 p2806 A72-37607

Multi-cycle plasma arc evaluation of oxidation-inhibited carbon-carbon material for shuttle leading edges.
[ASME PAPER 72-ENAV-26] 20 p2894 A72-39151

Thermal conductivity of honeycomb sandwich panels for space applications.
22 p3244 A72-42650

Nonlinear elastic torsion analysis for aerospace materials.
23 p3354 A72-44251

Construction of a high-performance resistojel for satellite propulsion.
23 p3328 A72-44324

Utilization of advanced composite materials for spacecraft and space shuttle applications.
24 p3417 A72-45153

SPACECRAFT CONTAMINATION

Planetary quarantine microbiological and engineering problems, discussing cost, international policies, contamination and sterilization
01 p0019 A72-10818

Apollo 12 retrieved Surveyor 3 TV camera mirror surface and camera-shroud organic contamination attributed to spacecraft outgassing and engine exhaust products
03 p0415 A72-12948

Motion equations of constrained split fairing for avoiding contamination of sounding rocket payload environment by uncontained explosive activation device
05 p0724 A72-16102

Exobiology research objectives, discussing planetary exploration data on origin, nature and distribution of life, spacecraft contamination, manned and unmanned missions and specific mission targets
05 p0714 A72-16133

Rocket plume contamination effect on transmitting and reflecting materials optical properties, noting predominant absorption and scattering effects
[AIAA PAPER 72-56] 05 p0750 A72-16967

Forecasting technique for accumulated particulate contamination on spacecraft assemblies, discussing cleanliness optimization and test procedures
07 p0915 A72-18763

Surface contamination effect on alpha particle resolution of surface barrier detector/preamplifier combination for use in space environment
08 p1168 A72-21517

Temperature effects on microorganism survival in deep space vacuum, using molecular sink test
09 p1265 A72-22641

Spacecraft critical surfaces protection from molecular and particulate contamination sources including gloves, tissues, and covering or packaging materials
12 p1768 A72-27042

Orbiting satellite environment and self contamination, calculating pressure, density and condensation rates and adsorption layers on critical surfaces
15 p2321 A72-31870

Surface contamination effect on electron temperature measurement using rocket-borne Langmuir probe in lower ionosphere
15 p2236 A72-31926

Survival of common terrestrial microorganisms under simulated Jovian conditions.
19 p2755 A72-37721

Spacecraft atmosphere trace contaminant sensor system using mass spectrometric analysis of contaminants concentrated on sorbents in monitor inlet system
[ASME PAPER 72-ENAV-15] 20 p2896 A72-39162

Development of planetary quarantine in the United States.
23 p3259 A72-43382

A re-evaluation of material effects on microbial release from solids.
23 p3253 A72-43383

Effects of aeolian erosion on microbial release from solids.
23 p3253 A72-43384

Spacecraft functional properties degradation due to surface contamination with outgassing vapors, discussing contaminant materials transport and sorption characteristics
23 p3254 A72-43619

Microflora accumulation prevention methods during spacecraft flight, noting bacterial filters for air purification and wiping with disinfectants for surface contamination reduction
24 p3376 A72-45213

SPACECRAFT CONTROL

NT SATELLITE ATTITUDE CONTROL

NT SATELLITE CONTROL

Optimal control algorithm for spacecraft descent in atmosphere at speed near escape velocity, using game theory
01 p0135 A72-10298

Group matrix representation theory application to elastic spacecraft stabilization
01 p0135 A72-10497

Apollo spacecraft guidance and control systems, reviewing navigation objectives, concepts and performance during cislunar, rendezvous and landing maneuver phases
01 p0097 A72-10943

Control axes misalignment effects on spinning satellite wobble damping and requirements for active momentum exchange controllers
02 p0286 A72-12267

Nighttime airglow layer effect application to autonomous navigation and orientation of piloted space vehicles
02 p0256 A72-12289

Roll control algorithm for parabolic velocity spacecraft reentry, using successive stepwise extrapolation of approach trajectory parameters
05 p0685 A72-16431

Nonlinear and digital synthesis of computerized optimal control systems for long-life orbital stations and laboratories
05 p0724 A72-16434

Manual orbital control used on Soyuz spacecraft in orbital flight, investigating equations of motion and pilot work load
05 p0725 A72-16438

Spacecraft initial solar orientation techniques estimation and classification
05 p0685 A72-16444

Language for description of onboard control system location and attitude control operations during spacecraft maneuvering
05 p0726 A72-16456

Three dimensional global spacecraft attitude control system analytical design technique based on system stability considerations
05 p0726 A72-16457

Spacecraft precision off-on attitude control by pure jet torquing, using electronics based on control system idealized model
05 p0726 A72-16459

Optimal nonlinear logical filters for noise protection of space vehicle servosystems
05 p0726 A72-16460

Automatic control of ESRO drag-free deep space probe for measuring Robertson matrix beta and gamma constants
[ONERA, TP NO. 952] 05 p0727 A72-16468

Spacecraft attitude control system reliability and performance improvement through nonorthogonal coordinates application, using matrix technique
05 p0728 A72-16477

Gas jet attitude control systems for spacecraft, discussing accuracy and time of active operation
05 p0728 A72-16479

Satellites and spacecraft flight control systems, discussing approaches for stationkeeping and orbit determination/correction
05 p0729 A72-16746

Control system design computerized optimization technique based on high speed repetitive simulations and gradient minimization, considering application to reusable and expendable boost vehicles
[AIAA PAPER 72-98] 05 p0729 A72-16812

Large space vehicles automatic docking guidance and control system design, using single plane and six degrees of freedom analysis
[AIAA PAPER 72-99] 05 p0729 A72-16874

Spacecraft banking control during reentry, deriving dynamic equations of angular motion
05 p0730 A72-17026

Dynamic stability of controlled spacecraft with liquid propellant rocket engines, considering acceleration and braking sections of trajectory
05 p0730 A72-17027

Controlled motion dynamics of spacecraft performing maneuvers, applying point transformation to third-order nonlinear system moving about center of mass in lateral motion
05 p0730 A72-17029

Pulsed relay control system for stabilizing spacecraft orientation in flight, allowing for changes in characteristics of guidance sensor systems and slave mechanisms
05 p0731 A72-17031

Shuttle ascent guidance and control, discussing self targeting, trajectory optimization problems and flight phases
06 p0892 A72-18178

Space shuttle phase B design studies regarding configurational alternatives, propulsion systems, displays and controls, simulations and flight test programs
08 p1240 A72-21009

Nighttime airglow layer effect application to autonomous navigation and orientation of piloted space vehicles
10 p1508 A72-23758

Solar rudder for spacecraft steering in form of right circular cone with ideally reflecting surface
11 p1727 A72-25943

Parabolic velocity atmospheric reentry navigation algorithm for spacecraft control, demonstrating guidance accuracy to landing point
11 p1684 A72-26899

Spacecraft motion control algorithm for reentry at escape velocity based on object motion model
11 p1684 A72-26900

Spacecraft optimal control after transfer from hyperbolic trajectory to planetary satellite orbit by atmospheric drag, minimizing engine thrust
14 p2129 A72-30470

European synchronous meteorological satellite system Meteosat, discussing mission, control and data acquisition
15 p2265 A72-31345

Conical scanning system for Pioneer Jupiter spacecraft pointing control, discussing signal processor, spacecraft dynamic behavior, system stability and error budget
15 p2320 A72-31791

Flexible space vehicle multiple closed loop attitude control system design, discussing stability, structure interaction and performance by analog simulation
15 p2321 A72-32587

Russian book - Mathematical methods of modeling in space studies
17 p2607 A72-35026

A method of realization of the functions of a program timer on a computer used in a spacecraft on-board equipment control system
17 p2522 A72-35028

Controlled systems with discontinuous couplings and means of optimization of their control
17 p2621 A72-35035

Synthesis of a nonlinear law for spacecraft motion control in the earth's atmosphere
17 p2621 A72-35201

Synthesis of a nonlinear law for the control of spacecraft motion in the atmosphere of the earth
17 p2621 A72-35202

Parabolic switching boundaries method for optimal fuel consumption control of manned orbital space vehicles
18 p2672 A72-36325

Design of model-reference adaptive control systems using Liapunov functions.
18 p2672 A72-36326

Astroelasticity in design and analysis of flexible space vehicles, presenting dynamics and control considerations
18 p2738 A72-37082

Invariant poles feedback control of flexible, highly variable spacecraft.
19 p2869 A72-38240

Development of coordinate signal transmission and data processing equipment for operation supervision in space travel
19 p2765 A72-38305

Constrained payload-optimum extremal ascent trajectories for space shuttle vehicles.
[AIAA PAPER 72-829] 20 p2966 A72-39097

The development of a 150,000 watt-inch variable conductance heat pipe for space vehicle thermal control.
[ASME PAPER 72-ENAV-14] 20 p2896 A72-39163

Proportional control of space vehicles with the aid of auxiliary jet engines
20 p2977 A72-39593

A control algorithm for the orbital reentry of a space vehicle
22 p3223 A72-42206

Motor activity capability of an astronaut in flight
22 p3149 A72-42220

An attitude reference system with discrete-correction capability.
22 p3203 A72-42864

A simple algorithmic method for the simulation of a spacecraft with flexible appendages.
23 p3343 A72-44552

SPACECRAFT DESIGN

NT SATELLITE DESIGN

Manned space station design for astronomy, space physics and biology, earth surveys, aerospace medicine, materials science and advanced technologies applications
01 p0135 A72-10937

Space vehicles development and fabrication cost estimation, deriving statistical-analytical formulas with allowance for technical complexity and learning factor
01 p0147 A72-11219

Aerodynamic design of atmospheric reentry vehicles forebody, considering maximum drag for hypersonic bodies
02 p0149 A72-11726

Post Apollo program, considering space shuttle design, operation, transportation and payload cost reduction, rocket developments and plans for Mars expedition
03 p0440 A72-13612

Small astronomy satellite program for X ray experiments and mapping, discussing structure design, systems, testing and launching
03 p0441 A72-14395

Lifting reentry vehicle Bumerang design and development, discussing experimental verification of theoretical design concepts by aircraft launched unmanned flying model

05 p0724 A72-16312

Time optimal and fuel optimal control of spin stabilized space vehicle for body-fixed and gimbaled jets, using maximum principle

05 p0728 A72-16476

Extrapolation procedure for determining small-scale wind shear definition from Rawinsonde vertical wind profiles statistical data for aerospace vehicle design

07 p1085 A72-19687

Space shuttle phase B design studies regarding configurational alternatives, propulsion systems, displays and controls, simulations and flight test programs

08 p1240 A72-21009

Delta wing configuration design with anhedral heat shield for high lift reentry in 6-20 Mach number range [AIAA PAPER 72-132]

09 p1259 A72-22501

Soviet interplanetary spacecraft Mars 2 and 3, describing design, mission objectives, onboard systems and instrumentation

09 p1395 A72-22974

Emergency reentry manned spacecraft remedial concepts, mission constraints and system designs in terms of cost effectiveness

09 p1396 A72-23159

ITOS-1/Tiros M/ satellite design, describing structure, thermal and attitude control, primary and secondary sensor subsystems, power supply and operational goals

09 p1396 A72-23373

Safety design review for Skylab program based on experience from prior space projects and ground tests

10 p1550 A72-23990

Statistical-analytical cost models for spacecraft development and fabrication, taking into account various technical and management factors

10 p1564 A72-24026

Econometric approach to space shuttle design for optimum operational redundancy levels, using payload-cost effectiveness criterion

10 p1551 A72-24448

Product assurance cost aspects on high reliability space programs, discussing design, packaging, failure trends, acceptance testing and Apollo project

10 p1551 A72-24452

Multimission capability of solar electric propulsion (SEP) spacecraft, analyzing payload variations, propellant requirements, thrusting time limitations and throttling range

10 p1552 A72-25125

Thermal boundary layer interaction with distortions in shape or material of adjacent surface for space shuttle design

11 p1614 A72-25246

Computerized structural design of aerospace vehicle, stressing automated routines for finite element models generation

11 p1727 A72-25367

Spacecraft structural dynamics, design and testing, using Fourier transform and analog vibration simulation

11 p1728 A72-25378

Electric propulsion spacecraft design for ion thruster systems testing with circular solar cells array as gyroscopic stable platform

11 p1578 A72-26200

Design of Salyut manned orbital laboratory combined with Soyuz service module

12 p1876 A72-27107

Space Shuttle supported manned earth orbital laboratories for operational communication and navigation systems, discussing mission program, design and equipment

12 p1876 A72-27357

Space technology application to ATS F and G program, discussing high power requirements, parabolic antenna design, tracking accuracy and ground station simplification

12 p1870 A72-27523

Space tug design constraints, configurational alternatives, subsystem arrangements, docking system, propellant tank pressurization system, main engine and power supply, etc

13 p2051 A72-28933

Mars 3 probe design and mission details, covering trajectory correction lander separation, engine start-up, aerodynamic braking and dust storm data

14 p2151 A72-30477

Environmental effects on spacecraft materials, structures and design, discussing sterilization, gravity, vacuum, micrometeoroids, radiation, etc

15 p2320 A72-31802

Second generation European multi-mission launcher system for scientific and application satellites, using high energy propulsion modular design

15 p2320 A72-31804

Space shuttle payload design for weight and cost reduction, discussing refurbishable modular design concept

15 p2321 A72-32317

Flexible space vehicle multiple closed loop attitude control system design, discussing stability, structure interaction and performance by analog simulation

15 p2321 A72-32587

Bumerang lifting body design for reentry vehicles, discussing optimal configurations and experimental flight testing

16 p2462 A72-33050

Space shuttle program, discussing configurational concepts, payload carrying capacity variants and cost reduction design changes

17 p2621 A72-34869

Astroelasticity in design and analysis of flexible space vehicles, presenting dynamics and control considerations

18 p2738 A72-37082

Compact expressions for maximum and minimum eclipse durations of spacecraft circular orbit, presenting numerical data as aid to spacecraft design

19 p2862 A72-38021

Recent development on thermal design of spacecraft

21 p3115 A72-41125

Viking configuration pitch damping derivatives as influenced by support interference and test technique at transonic and supersonic speeds

21 p3041 A72-41593

Configuration analysis as applied to aerospace vehicle design synthesis

23 p3342 A72-43458

Structural problems of the helios solar probe

24 p3449 A72-45122

Viking Mars exploration project, discussing orbiter and lander design and operational features and scientific experiments relevant to existence of life

24 p3440 A72-45123

OSO pointing accuracy improvement through dual spin stabilization, discussing OSO design evolution

1962-72

24 p3449 A72-45145

Aircraft/spacecraft design approach and performance data, considering space shuttle program

24 p3467 A72-45159

Space shuttle design evolution for program cost minimization, discussing refurbishment, payload impact, management cost and mission specifications and objectives

24 p3450 A72-45171

The Agena orbit transfer stage as an interim space tug

24 p3451 A72-45195

Design and operation objectives and constraints for German scientific spacecrafts, discussing orbital performance and reliability and quality control requirements

24 p3451 A72-45205

The effect of space shuttle payload design techniques on total space program cost

24 p3451 A72-45210

The space tug optimum cost evaluation

24 p3468 A72-45212

Helios solar probe development, discussing scientific experiments, structural, thermal and engineering models and systems tests

24 p3451 A72-45214

SPACECRAFT DOCKING

Large space vehicles automatic docking guidance and control system design, using single plane and six degrees of freedom analysis

05 p0729 A72-16874

Spaceborne laser radar for target acquisition and tracking in spacecraft rendezvous and docking applications

07 p0943 A72-19387

Apollo 14 mission report covering crew training, launch, docking, lunar landing and surface activities

08 p1230 A72-21006

Skylab launch and mission program, describing modular components, crew training, checkout, launch and docking procedures, flight plan and crew working schedules, rescue and reentry procedures, etc

08 p1240 A72-21008

Solar electric propulsion application to comet and asteroid rendezvous and docking CARD missions with sample return

11 p1722 A72-26201

Space tug design constraints, configurational alternatives, subsystem arrangements, docking system, propellant tank pressurization system, main engine and power supply, etc

13 p2051 A72-28933

The space tug orbital operations

24 p3451 A72-45196

SPACECRAFT ELECTRONIC EQUIPMENT

NT AIRBORNE/SPACEBORNE COMPUTERS

Spacecraft electronic equipment requirements, discussing effects of planned missions

02 p0196 A72-12739

Spacecraft electronic equipment design criteria for maintainability and installation, discussing mockup zero g demonstration tests of new packaging concepts

10 p1487 A72-24445

Electric power supply systems for satellites, discussing packaging standardization of electronic circuits modules

13 p1900 A72-30096

Survey of current component reliability problems and methods for prevention

18 p2668 A72-37102

Spaceflight-qualified tunable C-band parametric amplifier system

19 p2770 A72-37253

S-band high power microstrip switches with p-i-n diodes for spacecraft radio systems

19 p2770 A72-37257

Thermal control system incorporation into lunar roving vehicle (LRV) for electronic component protection during translunar transportation and lunar surface operation

[ASME PAPER 72-ENAV-27] 20 p2894 A72-39150

Navigation satellite system based on triangular distance measurement between two satellites and aircraft, noting simplification of air- and satellite-borne equipment requirements

21 p3080 A72-40285

Spacecraft-borne computer and electronic systems interface for radio reception, transmission and TV imagery applications

21 p3014 A72-40309

Biological instrumentation for the Viking 1975 mission to Mars

23 p3259 A72-43396

SPACECRAFT ENVIRONMENTS

MORL and Orbital Biomedical Laboratory projects, reviewing crew accommodation, spacecraft and booster requirements and biomedical measurements

05 p0724 A72-16177

Chromosome aberrations and germination speedup in Soyuz 5 carried oat seeds, noting stimulating effect by preflight ethylenimine treatment

05 p0623 A72-16777

Skylab experimental space station, discussing environmental comfort, Apollo spacecraft rendezvous for crew rotation and onboard experiments in earth resources, biomedicine, astronomy, etc

06 p0893 A72-18611

Weightlessness effects on human organism, discussing physiological changes, artificial gravity by spacecraft rotation and exercise to counter adverse reactions

11 p1589 A72-26891

Radar backscattering cross section and power of conducting cylindrical spacecraft in compressible electron-ion plasma environment

12 p1779 A72-27173

ESRO satellites solar array performance under orbital environmental conditions, discussing radiation damage and earth albedo effects

12 p1759 A72-28047

Meteorological-astronomical diurnal and seasonal environmental rhythm simulation for psychological stresses alleviation in long term space missions

13 p1910 A72-29322

Russian book on thermal simulation of spacecraft and space environment covering heat transfer, cosmic radiation, vacuum chambers, radiant flux simulators, etc

15 p2319 A72-31275

Orbiting satellite environment and self contamination, calculating pressure, density and condensation rates and adsorption layers on critical surfaces

15 p2321 A72-31870

Radiation hazards in space with respect to galactic radiation shielding, solar flare prediction and conventional terrestrial safety standards

16 p2358 A72-33556

Sleep factors and limitations during prolonged space flights, considering weightlessness, hypokinesia, nervous tension, cabin confinement, rhythm, environment and noise effects

16 p2356 A72-33561

Astronauts red cell mass changes associated with space flight due to space and earth environment differences

16 p2356 A72-33564

Soyuz 5 satellite vehicle space flight factors effect on chlrella cells, investigating survival rates and mutability

17 p2505 A72-35279

Habitability factors in a rotating space station

18 p2652 A72-36436

Space station prototype environmental/thermal control and life system - A current overview

[ASME PAPER 72-ENAV-35] 20 p2894 A72-39143

Modular environmental control/life support system design for low cost shuttle launched space station, evaluating humidity, carbon dioxide, water and waste management

[ASME PAPER 72-ENAV-17] 20 p2895 A72-39160

Development of a spacecraft wet oxidation waste processing system

[ASME PAPER 72-ENAV-3] 20 p2896 A72-39174

Dry incineration of wastes for aerospace waste management systems

[ASME PAPER 72-ENAV-2] 20 p2896 A72-39175

Toxicological evaluation of some synthetic materials designed for airtight space equipment
21 p2998 A72-40434

Some transport techniques for liquid human wastes and wash water under space flight conditions
21 p3006 A72-40436

Influence of Cosmos 368 space flight conditions on radiation effects in yeasts, hydrogen bacteria and seeds of lettuce and pea.
23 p3254 A72-43390

The problem of decontaminating and preserving drinking water in spacecraft water supply systems
24 p3375 A72-45121

SPACECRAFT GUIDANCE

NT SATELLITE GUIDANCE

Optimal control for thrusting rocket guidance with controllable steering angle rate during insertion into circular orbit, using flat earth approximation
01 p0097 A72-10383

Minimum propellant impulsive optimal spacecraft guidance and trajectory problem, developing deterministic theory in discrete linear quadratic form with second order perturbation analysis
01 p0130 A72-10929

Apollo spacecraft guidance and control systems, reviewing navigation objectives, concepts and performances during cislunar, rendezvous and landing maneuver phases
01 p0097 A72-10943

Soviet book on electro-optical devices for space vehicles orientation and navigation covering vertical plotters and sun, planet and star trackers
02 p0256 A72-12125

Space vehicles guidance with UV optical systems, describing photometric celestial images with various receptors and different wavelength bandwidth selection
03 p0354 A72-13054

Spacecraft soft orbital rendezvous guidance involving orbital transfer maneuver for velocity vector directional coincidence to reduce terminal relative velocity
05 p0729 A72-16757

Large space vehicles automatic docking guidance and control system design, using single plane and six degrees of freedom analysis
05 p0729 A72-16874

Shuttle ascent guidance and control, discussing self targeting, trajectory optimization problems and flight phases
06 p0892 A72-18178

Explicit analytic guidance technique for hyperbolic approach phases of lunar and interplanetary spacecraft trajectories from first order solution for perturbed planet centered trajectory
07 p1032 A72-18944

German monograph on optimal guidance of spin stabilized space bodies for combined attitude and angular velocity control and time optimal rotation damping
08 p1241 A72-21847

German monograph on inertial platform stabilization by optical sensors for space vehicle guidance covering aircraft position determination
09 p1394 A72-22334

Terminal guidance systems and techniques application to manned space flight rescue operations, discussing emergency location and rescue spacecraft communication and guidance
09 p1396 A72-23158

Spacecraft interplanetary guidance trajectory correction, deriving algorithm for optimal accuracy and minimum fuel expenditure
11 p1718 A72-25931

Cruise guidance, trajectory and navigation analysis for solar electric Mercury orbiter, considering engine performance, thrust and terminal errors
11 p1684 A72-26172

Aerospace guidance multiprocessor with memory units attached to time-multiplexed data bus, predicting performance in terms of queueing theory, Markov process and simulation
12 p1786 A72-27433

Outer planets masses and ephemerides, noting guidance system and fuel quantity for orbit corrections on interplanetary flight
15 p2312 A72-32181

Low thrust spacecraft navigation requirements for minimum propellant guidance, using neighboring extremal law
15 p2270 A72-32194

Steering algorithm for fail-safe guidance of continuously thrusting interplanetary spacecraft to maintain ballistic intercept target objective
15 p2271 A72-32195

Optimal deterministic guidance for bounded-thrust spacecrafts.
17 p2609 A72-35101

Analytical guidance in the neighborhood of optimal multi-impulse trajectories.
17 p2609 A72-35102

Spacecraft soft orbital rendezvous guidance involving orbital transfer maneuver for velocity vector directional coincidence to reduce terminal relative velocity
17 p2622 A72-35260

Digital simulations of effects of two-antenna interference on space vehicle guidance.
19 p2830 A72-37292

Spacecraft orientation according to reference celestial bodies direction determination, noting successive orientation permissible time intervals
19 p2831 A72-38149

An explicit automatic terminal energy management guidance technique for space shuttle.
20 p2950 A72-39094

High accuracy approach guidance system for outer planet exploration.
20 p2951 A72-39132

A detailed analysis of Mariner nine TV navigation data.
20 p2977 A72-40061

Perturbation guidance for minimum time flight paths of spacecraft.
21 p3082 A72-41560

Computer simulation of retargeting procedure with closed form iterative solution and parameter optimization for nonlinear low thrust spacecraft guidance scheme
21 p3082 A72-41561

Guidance and navigation techniques for a solar electric Mercury orbiter.
21 p3082 A72-41562

Evaluation of optical data for Mars approach navigation.
24 p3422 A72-44646

On required guidance for transfer from hyperbolic trajectory to the planetary satellite orbit by aerodynamic drag in atmosphere.
24 p3450 A72-45176

Optimal guidance for the space shuttle transition.
24 p3422 A72-45186

High level cleanliness maintenance and contamination control for instrument unit ring guidance system in Saturn 5 launch vehicle
24 p3388 A72-45297

SPACECRAFT INSTRUMENTS

NT LASER ALTIMETERS

NT SATELLITE INSTRUMENTS

NT SPACECRAFT POSITION INDICATORS

Space shuttle orbiter flight instrumentation, data handling and communication requirements, discussing data gathering methods, crew displays, computer processing, recording and digital data bus telemetry
02 p0179 A72-12406

NASA spacecraft instrumentation for high energy phenomena measurements, discussing collimated proportional counters, wire grid digitized spark chambers and modulation and slit collimators
03 p0353 A72-13038

Coarsely stabilized spacecraft-borne Michelson interferometer, obtaining high resolution by computerized spectrum reconstruction with fast Fourier transform
03 p0354 A72-13055

Spacecraft-borne UV spectroheliograph with spherical mirror, considering moving part weight reduction
03 p0355 A72-13057

Long life magnetic tape recorder for onboard data storage in space flights, discussing two motor tape transport and static memories for improved reliability
03 p0360 A72-13767

Impedance determination for symmetrical spherical probes and spacecraft housing with flat screen separation, using partial capacitance formula
05 p0662 A72-16268

Proton recording equipment onboard automatic interplanetary stations Zond 4 and 5 at 1.5-50 MeV using silicon drift counters
06 p0814 A72-17699

OSO-H solar X ray instrument for solar flares energy release investigation via thermal and nonthermal electrons X ray emission
08 p1167 A72-21514

Gamma ray spectrometer with antiCompton shield for OSO-7 spacecraft
08 p1167 A72-21515

Surface contamination effect on alpha particle resolution of surface barrier detector/preamplifier combination for use in space environment
08 p1168 A72-21517

ESRO program in imaging detector development for UV and soft X ray space missions, presenting image storage target details
08 p1171 A72-21971

High resolution vidicons, image orthicons, esicons and ebicons design for space missions
08 p1171 A72-21972

Bimetallic actuator for spacecraft thermal control with design emphasis on external power source elimination, high reliability, frictionless operation, simplicity and low weight
09 p1305 A72-22249

SkyLab S-193 altimeter experimental mission objectives and spacecraft instrumentation, considering precision designs, oceanographic surface remote sensing and electromagnetic scattering measurement
09 p1306 A72-22317

European Special Space Tug electronic subsystem requirements, considering strapdown inertial measur-

ing unit, remote sensors, computer and fail-safe backup system
09 p1396 A72-23258

Energetic particle flux measurement on spacecraft based on statistics of overflowing register counting Poisson process
09 p1312 A72-23261

Spacecraft orientation angle measurement by inertial sensors, analyzing equipment kinematic efficiency and limitations
11 p1684 A72-26913

Spaceborne scatterometer measurement standard deviation derivation, noting integration time, signal bandwidth and SNR effects on accuracy
12 p1783 A72-27636

Apollo 15 orbital science payload instruments for exploring lunar origin and evolution to relate to earth history
15 p2310 A72-31984

Spacecraft onboard compact low-power coherent optical data processing system, using GaAs laser and paraboloid mirror segments
15 p2248 A72-32052

Space and upper atmosphere environmental effects on spacecraft and instrument surfaces, considering high energy particle radiation, interstellar and lunar dust effects, etc
18 p2712 A72-36832

Russian book - Equipment for space studies.
21 p3014 A72-40301

Photogrammetric method for determining the deflection of light beams by spacecraft windows during flight
21 p3052 A72-40305

Space applications of Fabry-Perot modulator as alternative to mechanical devices, presenting optical and electrical performance data for different temperatures
21 p3055 A72-40824

A bivariate normal theory maximum-likelihood technique when certain variances are known.
21 p3075 A72-40826

Analysis of cryogenic suspensions for use in spacecraft
22 p3230 A72-42208

Evaluation of optical data for Mars approach navigation.
24 p3422 A72-44646

Extraterrestrial electromagnetic radiation and particle flux characteristics of low and medium energy, considering onboard spacecraft measuring instruments and data processing systems
24 p3404 A72-45398

SPACECRAFT LANDING

NT LUNAR LANDING

NT MARS LANDING

NT PLANETARY LANDING

Unpowered shuttle orbiter piloted control during approach and landing, discussing energy management technique based on fixed base six degree of freedom simulation
10 p1551 A72-24438

Spacecraft reentry into random medium atmosphere, determining optimal control procedure for prescribed arrival region and time with simulation equation
11 p1686 A72-25930

Landing control algorithm using onboard digital computer for spacecraft hyperbolic velocity reentry, discussing simulation test results
11 p1684 A72-26898

Spacecraft rescue/recovery capabilities, discussing in-flight escape, ground egress and descent systems, performance and technical and human factors
24 p3450 A72-45147

SPACECRAFT LAUNCHING

Guiana Space Center launch complexes for Diamant B and Europa satellite launchers and rocket probes, discussing trajectory, telemetry and safety measures
03 p0339 A72-12912

Apollo 14 mission report covering crew training, launch, docking, lunar landing and surface activities
08 p1230 A72-21006

Spacecraft mean time to failure (MTTF) and launch success probability /LSP/ effects on annual satellite system costs
09 p1395 A72-22775

Ionospheric disturbances due to shock front from Apollo 15 launching, using split signal observation in ion acoustic and normal mode
09 p1397 A72-23569

Titan 3 family systems analysis for delivering multiple communication satellites to geostationary orbits
12 p1870 A72-27378

Spacecraft propulsion into orbit by ground based high-power lasers via thrust generation by material evaporation, emphasizing advantages in launching small payloads
13 p2025 A72-28454

Waxwing solid propellant rocket motor design for third stage propulsion of Black Arrow satellite launcher
13 p2026 A72-28932

Space shuttle applications as spacecraft launcher, unmanned instrumentation platform and manned laboratory, discussing advantages to space research

13 p2051 A72-28935

Booster launch vehicle guidance scheme for critical aborts from staging through burnout, minimizing aerodynamic phases for different landing sites

15 p2269 A72-32182

Resource allocation for minimum cost launch vehicle assignment to space missions, using network and dynamic programming algorithm

16 p2482 A72-33498

Controlled systems with discontinuous couplings and means of optimization of their control

17 p2621 A72-35035

Real-time launch vehicle steering program selection. [AIAA PAPER 72-830]

20 p2977 A72-40058

Minimum energy trajectory and propellant consumption considerations for launch windows to Mars and Venus planets with Grand Tour mission possibilities

23 p3336 A72-43553

Optimization of altitude and inclination change schedules during low thrust ascent to geosynchronous orbit.

24 p3440 A72-45150

SPACECRAFT LUBRICATION

Self lubricating polytetrafluoroethylene and polyimide composites transfer film formation tests, studying film thickness and uniformity

06 p0824 A72-18596

SPACECRAFT MANEUVERS

Transfer from high elliptical to circular orbit, using successive spacecraft braking maneuvers in planetary atmosphere with incomplete information

01 p0130 A72-10927

Optimal dynamic system design for maneuvers with complete statistical information applied to limited power space flight

05 p0641 A72-16313

European reusable space tug, discussing computer controlled attitude stabilization and maneuvering system design for orbital rendezvous and docking

05 p0725 A72-16446

Language for description of onboard control system location and attitude control operations during spacecraft maneuvering

05 p0726 A72-16456

Spacecraft soft orbital rendezvous guidance involving orbital transfer maneuver for velocity vector directional coincidence to reduce terminal relative velocity

05 p0729 A72-16757

Controlled motion dynamics of spacecraft performing maneuvers, applying point transformation to third-order nonlinear system moving about center of mass in lateral motion

05 p0730 A72-17029

Adaptive filter techniques application to maneuvering reentry vehicle tracking, using Wald sequential test, decision theory and stochastic approximation

10 p1509 A72-23779

Optimal dynamic system design for maneuvers with complete statistical information applied to limited power space flight

11 p1610 A72-25796

Elliptical orbiting spacecraft minimum fuel consumption rendezvous maneuver, formulating variational extremum problem with constraints

14 p2150 A72-30329

Iterative method for the calculation of two-impulse spacecraft rendezvous maneuvers

17 p2622 A72-35216

Spacecraft soft orbital rendezvous guidance involving orbital transfer maneuver for velocity vector directional coincidence to reduce terminal relative velocity

17 p2622 A72-35260

Nonlinear on-line rapid estimation scheme with application to trajectory maneuvering vehicles.

19 p2781 A72-38258

Experimental and simulation study results on the development of a planetary landing site selection system.

[AIAA PAPER 72-868]

20 p2951 A72-39131

High accuracy approach guidance system for outer planet exploration.

[AIAA PAPER 72-867]

20 p2951 A72-39132

Optimal three dimensional maneuvering of a rocket powered hypervelocity vehicle.

24 p3450 A72-45151

Thrust-weight ratio optimization for spacecraft orbit inclination change maneuver, deriving motion kinematics via point mass gravitational model

24 p3440 A72-45167

Spacecraft rendezvous trajectories and targeting maneuvers onboard sequential computation, taking into account maneuver constraints and state vector update information

24 p3450 A72-45172

A teleoperator system for space application.

24 p3407 A72-45174

Maneuver design and implementation for the Mariner 9 mission.

[AIAA PAPER 72-913]

24 p3443 A72-45429

Maneuver strategies for multi-planet missions.

[AIAA PAPER 72-914] 24 p3443 A72-45431

SPACECRAFT MODELS

Imperfect thermal modeling of spacecraft based on error states representation in multidimensional Euclidean space, evaluating approximate total error effect

03 p0441 A72-13635

Lifting reentry vehicle Bumerang design and development, discussing experimental verification of theoretical design concepts by aircraft launched unmanned flying model

05 p0724 A72-16312

Si solar cells nonpenetrating proton damage model in satellite radiation environment, showing open and short circuit current dependence on proton energy

07 p0914 A72-20492

Thermal nodal analysis of spacecraft hull-canister model from space simulation test, using least squares estimation and regression analysis

09 p1412 A72-23497

Finite element equations for hybrid coordinate dynamic analysis of interconnected rigid bodies with elastic flexible appendages for use in spacecraft simulation

12 p1876 A72-27257

SPACECRAFT MODULES

NT LUNAR MODULE

Experiment sensors impact on on-orbit vehicle configurations and operations in NASA program, synthesizing and cost analyzing common module sets

01 p0135 A72-10945

Space shuttle vehicle configurations with reusable booster and orbiter modules, discussing cargo capacity, maneuvering capability, mission duration, engine characteristics and acceleration constraints

07 p1085 A72-19058

NASA research and applications module /RAM/ for interim space station development and possible missions with space shuttle

08 p1240 A72-20978

Skylab launch and mission program, describing modular components, crew training, checkout, launch and docking procedures, flight plan and crew working schedules, rescue and reentry procedures, etc

08 p1240 A72-21008

Human role in space shuttle on-orbit maintenance vs space station modules earth return, considering feasibility and cost effectiveness

10 p1487 A72-24440

Thermal control design for research applications module /RAM/ shuttle compatible payload carriers, using Freon 21-water system

[ASME PAPER 72-ENAV-31]

20 p2894 A72-39146

Design criteria for the modular space station environmental control and life support system selection.

[ASME PAPER 72-ENAV-25]

20 p2894 A72-39152

Environmental control and life support subsystem conceptual design studies for shuttle launched 6-12

man crew modular space station

[ASME PAPER 72-ENAV-22]

20 p2895 A72-39155

Optimal shuttle research applications module /RAM/ environmental control and life support system for sortie missions

[ASME PAPER 72-ENAV-20]

20 p2895 A72-39157

Future orbital observatory modules for stellar and galactic astronomy.

24 p3453 A72-45533

SPACECRAFT MOTION

German book on gyroscope theory and applications, covering artificial satellites motion in gravitational field

03 p0360 A72-13675

Relative motion of active interceptor spacecraft approaching passive craft in central gravitational field, using dimensionless differential equations similarity coefficients method

05 p0728 A72-16592

Earth satellite plane periodic oscillations damping with respect to center of mass in orbital plane during motion on elliptical Kepler orbit

05 p0730 A72-17030

Center of mass motion of spacecraft in central gravitational field, analyzing programming of size and position of elements in mass geometry leading to arbitrarily large displacements

05 p0731 A72-17032

Aberration introduced by high satellite velocities, investigating application to laser telemetry

07 p0947 A72-20258

Moment of forces on spacecraft with low angular velocities in variable magnetic field, using electrodynamics equations

08 p1240 A72-21140

Earth-moon system gravitational effect on Venera automatic interplanetary stations motion away from earth

08 p1239 A72-22086

Spacecraft motion stabilization about mass center and optimal angular velocity control using minimax technique

11 p1684 A72-26903

Dynamical motion simulation facility for Symphonie satellite, using sensors, attitude control electronics and analog computer in closed loop system [DFVLR-SONDDR-201]

12 p1795 A72-27659

Oscillations of spacecraft with on-off attitude control under constant perturbation moment, calculating energy expenditures for desired orientation maintenance

14 p2162 A72-30459

Earth-moon system gravitational effect on Venera automatic interplanetary stations motion away from earth

17 p2606 A72-34655

Spacecraft oscillatory motion as function of attitude control impulse and slave mechanism efficiency

17 p2622 A72-35205

Relative motion of active interceptor spacecraft approaching passive craft in central gravitational field, using dimensionless differential equations similarity coefficients method

19 p2869 A72-37564

Moment of forces on spacecraft with low angular velocities in variable magnetic field, using electrodynamics equations

20 p2976 A72-39245

Influence of the terrestrial magnetic field on the motion of a satellite around its center of gravity

21 p3106 A72-41048

Kepler second law based moment of gyration concept application to spacecraft and missiles mechanics and kinematics, proposing Skylab weightless environment experiment for validation [SAWE PAPER 931]

23 p3342 A72-43471

SPACECRAFT ORBITS

NT INTERPLANETARY TRANSFER ORBITS

NT PARKING ORBITS

NT POLAR ORBITS

NT SATELLITE ORBITS

NT STATIONARY ORBITS

NT TRANSFER ORBITS

NT TROJAN ORBITS

NT TWENTY-FOUR HOUR ORBITS

Orbiting space vehicle life extension by momentum management using gravity gradient torques

05 p0727 A72-16467

Satellites and spacecraft flight control systems, discussing approaches for stationkeeping and orbit determination/correction

05 p0729 A72-16746

Rocket orbit in mass point gravitational field, studying KS variables separability, elliptic functions and equivalent problems

06 p0877 A72-17656

Shock wave generation and propagation from Apollo rockets at orbital altitudes

11 p1690 A72-26511

Error sources in numerical integration of spacecraft equations of motion in solar and planetary gravitational fields, suggesting methods for improving accuracy

14 p2151 A72-30457

Data processing method for optimal prediction of spacecraft orbital elements, using dynamic and quadratic programming

14 p2151 A72-30455

Spacecraft optimal control after transfer from hyperbolic trajectory to planetary satellite orbit by atmospheric drag, minimizing engine thrust

14 p2129 A72-30476

First approximation for spacecraft observations of nocturnal clouds from circular orbits with optimal optical axis orientations

21 p3049 A72-41438

Spacecraft local vertical estimation and error limits in meridional and equatorial planes based on terrestrial IR radiation measuring instruments

22 p3223 A72-42205

A control algorithm for the orbital reentry of a space vehicle

22 p3223 A72-42206

Dynamic characteristics, stability and steady state accuracy for orbital gyroscope with digital control, noting bit density requirements of onboard computer

22 p3202 A72-42207

SPACECRAFT PERFORMANCE

Satellite low orbit transfer to stationary orbit, emphasizing stage and payload recovery effects on performance

01 p0130 A72-10936

Spacecraft attitude control system reliability and performance improvement through nonorthogonal coordinates application, using matrix technique

05 p0728 A72-16477

Solar electric propulsion upper stage for multiple space exploration missions, discussing spacecraft performance, configurations and program plans [AIAA PAPER 72-464]

11 p1709 A72-26199

Solar array degradation effect on electric propulsion spacecraft performance, presenting power allocation strategy during mission

[AIAA PAPER 72-444]

13 p2037 A72-28943

Intelsat 3 global multichannel wideband multiple access communication system, describing technological advancements in communication performance, attitude control and testing procedures

[AIAA PAPER 72-534]

13 p1918 A72-28982

Experimental communications satellite system of ATS F and G geostationary satellites for specific ap-

- plication, discussing system performance measurement instruments
[AIAA PAPER 72-578] 13 p1918 A72-28986
- Description and in-orbit performance of the Orbiting Solar Observatory control system.
[AIAA PAPER 72-852] 20 p2975 A72-39077
- HEOS-2 in orbit - Its technical performance.
24 p3449 A72-45108
- Design and operation objectives and constraints for German scientific spacecrafts, discussing orbital performance and reliability and quality control requirements
24 p3451 A72-45205
- SPACECRAFT POSITION INDICATORS**
- Flight laser altimeter for Apollo vehicle height measurements above lunar surface, using telescope relay and quartz crystal oscillator
05 p0660 A72-15786
- Atomic clocks application to spacecraft position determination, discussing ground stations synchronization and accuracy improvement by lasers [ONERA, TP NO. 1020] 05 p0660 A72-15858
- Three axis angular deviations measurement by flexure monitor system for spacecraft, using pulsed light sources, autocollimator and porro reflectors
[AIAA PAPER 72-855] 20 p2951 A72-39106
- Choice of parameters to be measured in determination of a spacecraft trajectory
22 p3223 A72-42201
- Spacecraft local vertical estimation and error limits in meridional and equatorial planes based on terrestrial IR radiation measuring instruments
22 p3223 A72-42205
- SPACECRAFT POWER SUPPLIES**
- Aerospace radioisotope power systems, discussing heat source technology, shielding, safety and thermoelectric integration
[SAE AIR 1213] 01 p0098 A72-10387
- Charging methods for Ni-Cd batteries used in satellites, noting life increase and weight reduction
01 p0007 A72-11054
- Design and performance of Intelsat III dual TWT power supply, noting space, weight and cost savings
01 p0007 A72-11056
- Dc-dc converter input filter requirements and design for spacecraft power processing equipment
01 p0007 A72-11058
- Multiphase, 2 kw, high voltage, regulated, conditioned power supply for space application, discussing efficiency, weight, design and performance
01 p0008 A72-11063
- Electrical power subsystem design in Pioneer F/G spacecraft, using SNAP 19 deployable radioactive thermoelectric generators supplemented by Ag-Cd battery
01 p0008 A72-11065
- Electrical power subsystem for Initial Defense Communications Satellite Program/Augmentation, noting solar cells for power conversion and Ni-Cd batteries for energy storage
01 p0008 A72-11066
- ESRO satellite power supply solar paddles deployment mechanism, describing simulated zero gravity tests
[DGLR PAPER 71-112] 02 p0286 A72-12713
- Satellite electrical power, discussing energy converters, satellite feeder subsystem and voltage requirements
03 p0311 A72-13639
- Nuclear Brayton space power systems, discussing efficiency, isotope decay and reactor design
04 p0546 A72-14423
- AEROS aeronomy satellite solar cell array power supply system simulation tests under space conditions
04 p0466 A72-15650
- Heat pipe radiator with 50 kW heat rejection capability for potassium working fluid of Rankine cycle space power system, discussing design, fabrication and testing
[ASME PAPER 71-WA/HT-16] 05 p0744 A72-15875
- Power supply and converters for satellite and spacecraft, discussing fuel cells, radioisotopes, nuclear reactors, etc
05 p0615 A72-16745
- Ion engine performance optimization by power sharing with secondary batteries on synchronous equatorial satellites
[AIAA PAPER 72-206] 05 p0706 A72-16852
- Spacecraft power system with Maximum Power Point Tracker, discussing German Aeros satellite and orbit simulation program
07 p0914 A72-19090
- Kilowatt rotary dc-dc power transformer in modular sections for spacecraft applications, discussing electrical and mechanical designs and characteristics
08 p1112 A72-21414
- Uranium mononitride as nuclear reactor fuel for space vehicle power supply applications, discussing fabrication techniques and irradiation behavior
09 p1349 A72-22406
- ITOS-1/Tiros M/ satellite design, describing structure, thermal and attitude control, primary and secondary sensor subsystems, power supply and operational goals
09 p1396 A72-23373
- Solar cells in satellite power supplies, discussing design, environment effects, reconditioning, microwave performance and testing
10 p1422 A72-24150
- Lunar roving vehicle reliability program and design features of mobility, electrical power and navigation subsystems
[AIAA PAPER 72-233] 10 p1460 A72-24443
- GaAs solar batteries for spacecraft power supplies, comparing effectiveness with Si cells for optimum utilization
11 p1578 A72-25940
- Structural design, performance and costs of rigid or semirigid solar panels for geostationary satellites power supplies
12 p1758 A72-28034
- Silicon solar cell calibrations for space applications, discussing equivalent diagram, I-V characteristics and stratospheric balloon measurement
12 p1758 A72-28040
- Space tug design constraints, configurational alternatives, subsystem arrangements, docking system, propellant tank pressurization system, main engine and power supply, etc
13 p2051 A72-28933
- Electric power supply systems for satellites, discussing packaging standardization of electronic circuits modules
13 p1900 A72-30096
- Cost analysis for solar cell space power systems, considering array area and module standardization
15 p2338 A72-32133
- Silicon solar energy conversion for electrical power generation on spacecraft.
17 p2494 A72-34186
- Thermionic reactor system for auxiliary power and electric propulsion.
17 p2494 A72-34579
- Auxiliary power and electric propulsion applications of thermionic reactor power systems in manned and unmanned space missions
18 p2644 A72-36168
- Controlled dc to dc converter for a space-qualified thermionic-reactor.
18 p2644 A72-36170
- Voltage-conversion for incore-thermionic-reactors.
18 p2645 A72-36182
- A comparison of thermionic reactor designs employing a common thermionic fuel element.
18 p2645 A72-36183
- An out-of-core thermionic-converter system for nuclear space power.
18 p2645 A72-36187
- Parallel operation of the solar generator and battery on the Symphonie satellite
18 p2648 A72-36681
- Power regulation in the Symphonie satellite
18 p2648 A72-36682
- Solar array cost reduction.
19 p2754 A72-37642
- Hydrogen oxygen fuel cell development for spacecraft power supply systems, emphasizing service life and reliability under elevated temperature and high current density
19 p2754 A72-37643
- Minimisation of the solar array generated electrical interference on the GEOS satellite.
20 p2889 A72-38990
- Thermal conductivity measurements of nickel-cadmium aerospace cells. II - Component conductivities.
21 p2997 A72-40841
- Nuclear rocket reactor and radioisotope power technology for propulsion and electricity requirements in spacecraft and space stations
24 p3423 A72-45166
- SPACECRAFT PRELAUNCH TESTS**
- U SPACE VEHICLE CHECKOUT PROGRAM**
- SPACECRAFT PROPULSION**
- NT ELECTROMAGNETIC PROPULSION
- NT ELECTROSTATIC PROPULSION
- NT ION PROPULSION
- NT PHOTONIC PROPULSION
- NT PLASMA PROPULSION
- NT SOLAR PROPULSION
- High temperature gaseous U fission plasma core reactor engine concepts for space propulsion
01 p0099 A72-11327
- Space vehicle with solid-liquid propulsion system, determining optimal initial mixing ratio for cylindrical configuration
[DGLR PAPER 71-101] 02 p0271 A72-12706
- Maximum propellant utilization in electron bombardment ion thruster for space applications
04 p0564 A72-14432
- Controlled thermonuclear fusion for space propulsion, discussing magnetic-confinement and laser-plasma fusion engines
04 p0556 A72-14889
- Gas core nuclear rocket reactor program for 60 day Mars, shuttle and Skylab applications
05 p0688 A72-15778
- Automatic craft for planet surface exploration, classifying propulsion gear
05 p0644 A72-16449
- Current and future rocket and spacecraft propulsion systems based on chemical propellants, nuclear thermoelectric, electrostatic and electromagnetic power generators
05 p0705 A72-16743
- Space shuttle phase B design studies regarding configurational alternatives, propulsion systems, displays and controls, simulations and flight test programs
08 p1240 A72-21009
- Quasi-steady MPD propulsion systems for astronautical applications, describing electric energy storage bank, mass supply system, accelerator and operation principle
09 p1374 A72-22934
- High energy rocket propellants for space probe propulsion systems, evaluating various propellant combinations in terms of specific impulse, toxicity, corrosiveness, cost and availability
11 p1702 A72-25299
- Biowaste resistojet propulsion system development program, discussing design, propellant management and control subsystems
[AIAA PAPER 72-448] 11 p1707 A72-26185
- System tradeoffs for high performance pulsed MPD thruster in space mission application
[AIAA PAPER 72-457] 11 p1708 A72-26193
- RF ion thruster for spacecraft propulsion, discussing tests and digital computer calculations to optimize design parameter
[AIAA PAPER 72-474] 11 p1709 A72-26205
- ESRO electric propulsion systems R and D, discussing various concepts in terms of weight, cost, thrust level, efficiency, simplicity, exhaust velocity and development potential
[AIAA PAPER 72-478] 11 p1710 A72-26207
- Electric propulsion systems assessment for military spacecraft, discussing ion, colloid, pulsed and quasi-steady plasma thrusters
[AIAA PAPER 72-493] 11 p1711 A72-26217
- Spacecraft nuclear electric propulsion system multimission performance evaluation, discussing launch mode and vehicle capability factors in system size selection
[AIAA PAPER 72-503] 11 p1685 A72-26226
- Multimission and engine performance requirements for solar electric spacecraft propulsion stage configurations, considering launch vehicle compatibility integration payload and environmental extreme effects
[AIAA PAPER 72-465] 11 p1712 A72-26325
- Spacecraft propulsion based on electric energy extraction from solar wind or energy transfer from ground via plasma arcs
11 p1712 A72-26779
- Ion thruster module design for primary electric propulsion systems, discussing optical configurations, discharge chamber, control and performance tests
[AIAA PAPER 72-508] 12 p1860 A72-27423
- Liquid fuel rocket engines design for space applications, describing combustion chambers, thrust and vector control systems and propellant mixtures physicochemical properties
12 p1861 A72-27861
- Spacecraft propulsion into orbit by ground based high-power lasers via thrust generation by material evaporation, emphasizing advantages in launching small payloads
13 p2025 A72-28454
- Nuclear rocket for space tug, comparing performance and operational costs with chemical propulsion
13 p2000 A72-28926
- Encounter sequences determination techniques for multitarget flyby and rendezvous missions to asteroids and comets by spacecraft using solar electric propulsion
[AIAA PAPER 72-429] 13 p2037 A72-28940
- Solar electric multimission spacecraft (SEMMS)/concept, investigating Mariner, Viking and TOPS technologies applicability to postulated mission/science objectives
[AIAA PAPER 72-469] 13 p2026 A72-28946
- Communication satellites auxiliary propulsion systems surveyed for attitude and stationkeeping systems selection
[AIAA PAPER 72-515] 13 p2052 A72-28978
- Propulsion modes compared for communication satellites design optimization, discussing attitude and longitude control, orbit inclination control, station change and orbit raising
[AIAA PAPER 72-517] 13 p2052 A72-28979
- Second generation European multi-mission launcher system for scientific and application satellites, using high energy propulsion modular design
15 p2320 A72-31804
- Nonchemical space propulsion systems for lunar and planetary flights, discussing fission, fusion and electric rockets
15 p2297 A72-31810
- Nuclear rocket propulsion program, discussing solid refractory core technology, Rover project and NERVA engine development and tests
15 p2273 A72-31811

Small power nuclear propulsion engines for Europa launching systems, discussing heat exchange reactor using hydrogen propellant

15 p2273 A72-31812

Laser pulse produced high temperature plasma engine propulsion system, noting thrust/power ratio and requirements for orbital applications

[AIAA PAPER 72-719] 16 p2443 A72-34029

Prediction of tank pressure history in a blowdown propellant feed system.

17 p2537 A72-34211

Mixed-mode propulsion - Optimum burn profile for two-mode systems.

17 p2596 A72-34212

Thermonuclear fusion spacecraft propulsion systems operation principles, interplanetary orbit-to-orbit mission capabilities and environmental safeguard problems

17 p2598 A72-35953

Thermionic reactor electric propulsion system requirements.

18 p2720 A72-36167

Auxiliary power and electric propulsion applications of thermionic reactor power systems in manned and unmanned space missions

18 p2644 A72-36168

Development of a digital control system for a spacecraft propulsion test facility.

19 p2783 A72-37641

Hydrazine thrusters for space application.

21 p3098 A72-40123

Development of a digital control system for a spacecraft propulsion test facility.

22 p3163 A72-42685

Saturn-Jupiter rebound - A method of high-speed spacecraft ejection from the solar system.

23 p3340 A72-44323

Construction of a high-performance resistor for satellite propulsion.

23 p3328 A72-44324

Nuclear rocket reactor and radioisotope power technology for propulsion and electricity requirements in spacecraft and space stations

24 p3423 A72-45166

Development and testing of a radioisotope-fueled thruster for spacecraft propulsion.

24 p3434 A72-45178

SPACECRAFT RADIATORS

Heat pipe radiator with 50 kW heat rejection capability for potassium working fluid of Rankine cycle space power system, discussing design, fabrication and testing

[ASME PAPER 71-WA/HT-16] 05 p0744 A72-15875

Precision temperature control system for spacecraft equipment thermal loads rejection by space radiator, using acetone variable conductance heat pipes

[AIAA PAPER 72-270] 11 p1740 A72-25211

Thermal scale models utilization to predict spacecraft radiator system performance, presenting criteria for modeling fluid system with combined convection, conduction and radiation effects

[ASME PAPER 72-ENAV-29] 20 p2894 A72-39148

SPACECRAFT RECOVERY

Satellite low orbit transfer to stationary orbit, emphasizing stage and payload recovery effects on performance

01 p0130 A72-10936

Reusable space tug mission profile for interplanetary spacecraft recovery, using branched trajectory, steepest descent optimization and propellant minimization

[AIAA PAPER 72-13] 05 p0730 A72-16949

Reusable two-stage meteorological rocket vehicle, discussing design, performance, second stage recovery technique and cost

17 p2619 A72-34185

International Space Rescue Symposium, 4th, Brussels, Belgium, September 21, 1971, Proceedings.

17 p2620 A72-34426

Spacecraft rescue and recovery capabilities assessment based on anticipated U.S. space programs, discussing mission design, recovery response, weather prediction and communications

17 p2620 A72-34429

International Space Rescue Symposium, 1st, New York, N.Y., October 14, 1968, Proceedings.

20 p2977 A72-39550

Spacecraft rescue/recovery capabilities, discussing in-flight escape, ground egress and descent systems, performance and technical and human factors

24 p3450 A72-45147

Despinning and detumbling satellites in rescue operations.

24 p3450 A72-45160

SPACECRAFT REENTRY

Scientific satellite with simple inertial system, deriving discrete feedback reentry guidance algorithms based on closed-form equations solvable by onboard computer

01 p0098 A72-10944

Spacecraft reentry trajectory parameter selection and optimal control algorithm under random atmospheric density variation

05 p0685 A72-16429

Spacecraft reentry communications, discussing plasma sheaths, blackout alleviation and flight experiments

05 p0628 A72-16562

Emergency reentry manned spacecraft remedial concepts, mission constraints and system designs in terms of cost effectiveness

09 p1396 A72-23159

Space shuttle orbiter thermal protection system metal interaction with chemical environment during reentry, emphasizing degradation in dissociated oxygen

[AIAA PAPER 72-262] 11 p1590 A72-25206

Rarefied flow fields and heating rates for space shuttle orbiter reentry at high angles of attack, using Monte Carlo simulation technique

[AIAA PAPER 72-314] 11 p1567 A72-25248

Ablation phase duration during spacecraft decelerated hypersonic reentry flight, using theoretical model based on quasi-steady assumptions

11 p1745 A72-25815

Spacecraft reentry into random medium atmosphere, determining optimal control procedure for prescribed arrival region and time with simulation equation

11 p1686 A72-25930

Two step spacecraft reentry guidance involving skip trajectory at parabolic speeds, proposing algorithm for running coordinate and speed vector components values

11 p1684 A72-26896

Spacecraft roll stabilization during parabolic earth atmosphere reentry, developing single parameter multistep algorithm

11 p1684 A72-26897

Landing control algorithm using onboard digital computer for spacecraft hypersonic velocity reentry, discussing simulation test results

11 p1684 A72-26898

Parabolic velocity atmospheric reentry navigation algorithm for spacecraft control, demonstrating guidance accuracy to landing point

11 p1684 A72-26899

Spacecraft motion control algorithm for reentry at escape velocity based on object motion model

11 p1684 A72-26900

Synthesis of a nonlinear law for spacecraft motion control in the earth's atmosphere

17 p2621 A72-35201

Synthesis of a nonlinear law for the control of spacecraft motion in the atmosphere of the earth

17 p2621 A72-35202

Analytical evaluation of the spacecraft descent range for hyperbolic reentry trajectories

17 p2610 A72-35203

The development of the Apollo entry thermal protection system.

21 p3115 A72-41124

A control algorithm for the orbital reentry of a space vehicle

22 p3223 A72-42206

Explorer satellites and Pioneer space probes development program, discussing launching rockets, reentry tests, payloads, radio communication, Van Allen belts discovery, etc

23 p3358 A72-44353

Optimization of spacecraft reentry into a planetary atmosphere

24 p3453 A72-45597

SPACECRAFT RELIABILITY

Space shuttle cryogenics technology, flight and ground operations, checkout, maintenance and safety

03 p0441 A72-13695

Oxygen hazards, mishaps and safety programs in NASA operations, considering material, design, cleaning and procedural deficiencies and failures

04 p0564 A72-14436

Statistical distribution of maximum response for reliability-based optimum spacecraft structural design for random excitations from booster shutdown

05 p0724 A72-16103

Spacecraft attitude control system reliability and performance improvement through nonorthogonal coordinates application, using matrix technique

05 p0728 A72-16477

Spacecraft incipient failure detection, stressing acoustic energy release techniques

07 p0964 A72-18829

Spacecraft mean time to failure /MTTF/ and launch success probability /LSP/ effects on annual satellite system costs

09 p1395 A72-22775

Failure modes, effects and criticality analysis method for evaluating spacecraft reliability characteristics

10 p1485 A72-23974

Safety design review for Skylab program based on experience from prior space projects and ground tests

10 p1550 A72-23990

Communication satellite systems reliability assessment using figure of merit method

10 p1435 A72-23991

High reliability long life heat pipe thermal control system for space station application

14 p2171 A72-30835

Development of electronic part failure rates for long-duration space missions.

17 p2527 A72-34684

Man serviced spacecraft systems reliability and maintainability optimization methodology, developing parametric data based on failure modes analysis, components MTBF, duty cycles, redundancy and costs

[SAWE PAPER 943] 23 p3343 A72-43483

Design and operation objectives and constraints for German scientific spacecrafts, discussing orbital performance and reliability and quality control requirements

24 p3451 A72-45205

SPACECRAFT RENDEZVOUS

U SPACE RENDEZVOUS

SPACECRAFT SENSORS

U SPACECRAFT INSTRUMENTS

SPACECRAFT SHIELDING

Space shuttle thermal protection system, discussing oxidation resistant coatings, refractory metals, heat shield technology, ballistic reentry programs, weight and cost

01 p0135 A72-10935

Active shielding against radiation in space using charged particle deflection by electric and magnetic fields

[CERN-71-16] 02 p0258 A72-12076

Zirconium dioxide white pigment coatings for spacecraft thermal control, discussing impurities effects on optical absorption properties

07 p1023 A72-19692

Solar proton flares forecasting methods in connection with active region developments for spacecraft radiation shielding

07 p1061 A72-20017

Hot versus shielded aerodynamic surfaces trade study for space shuttle booster wings and fins design, considering materials, structural weight and cost estimates

[AIAA PAPER 72-390] 11 p1726 A72-25411

Spacecraft thermal control coating damage by energetic Hg ion bombardment, using absorbance measurements

[AIAA PAPER 72-445] 11 p1746 A72-26183

Apollo heat shield silica reinforcement fiber and ablation char reactions in laboratory and actual reentry tests

14 p2172 A72-30922

Spacecraft thermal control materials research, discussing surface selection, coatings, space simulation and environmental effects

15 p2260 A72-31806

Panel-flutter analysis of a thermal protection-shield concept for the space shuttle.

20 p2980 A72-39622

Shadow shields for minimizing radiant heat transfer into cryogenic propellant tanks on interplanetary missions, predicting performance for comparison with scale model experiment

21 p3130 A72-41181

SPACECRAFT STABILITY

Group matrix representation theory application to elastic spacecraft stabilization

01 p0135 A72-10497

Symphonie satellite stability during perigee, apogee and orbital transfer, considering propellant motion in tank and spinning top containing liquid

02 p0287 A72-12717

Astronomical Netherlands Satellite automatic stabilized detection system for soft celestial X rays measurement, describing various modes of operation

03 p0354 A72-13048

Autonomous star mapping attitude reference technique for providing three-axes attitude information on inertially stabilized or slowly spinning spacecraft

03 p0387 A72-13952

TV programs direct broadcasting by satellites, discussing frequency range, amplitude vs frequency modulation, satellite stabilization and economic aspects

04 p0494 A72-15678

Meteorological satellite stabilization and attitude control in synchronous equatorial orbit for two years life, emphasizing nutation damper optimal dynamic characteristics

05 p0725 A72-16437

Three dimensional global spacecraft attitude control system analytical design technique based on system stability considerations

05 p0726 A72-16457

Magnetic damper for gravity gradient stabilized satellite rotational and librational motions, deriving formula for calculating damping coefficients

05 p0726 A72-16463

Steady state angular motion stability of passive magnetically stabilized satellites, using Liapunov method

05 p0726 A72-16464

Spin-axis attitude stability in torque-free environment of dual spin spacecraft with energy losses in both bodies

05 p0730 A72-16964

Onboard equipment layout effect on dynamic stability against liquid propellant sloshing in spacecraft

05 p0730 A72-17028

Tracking efficiency calculation for laser telemetry with laser reflector on nonstabilized satellite 07 p0947 A72-20260

Laser tracking of magnetically and gravity gradient stabilized satellites, noting latitude effect on efficiency 07 p0947 A72-20263

Flexibly stabilized satellite orientation determination by stellar sensors and magnetic damping of rotation 08 p1240 A72-21139

Librational transverse oscillations boundary value problems of heavy thread on orbiting satellite, determining equilibrium and eigenfunctions 08 p1240 A72-21142

Self excited oscillations and transient responses of spacecraft stabilization relay system with delayed feedback, analyzing time delay effects in actuator circuit 08 p1241 A72-21170

Liquid filled spinning projectiles and satellites flight stability based on Stewartson gyroscope analysis method 08 p1168 A72-21600

Stationary motions, stability of satellite with rotary gyroscope and gimbals in circular orbit and central Newtonian force field 08 p1241 A72-21801

Image dissector, silicon photodiode and vidicon behavior comparison for medium resolution star mappers design for three axis stabilized vehicles 08 p1172 A72-21975

Liapunov direct method in synthesis of frequency-pulse system for automatic stabilization of spacecraft position 09 p1397 A72-23427

Compensator improvement for relative stability and frequency response of large space vehicle, using nonlinear programming 10 p1442 A72-23791

Thrust profile shaping for spin stabilized vehicles, analyzing effect on wobble motion and pointing error 10 p1552 A72-24647

Coupled librational motion of gravity oriented satellite in circular orbit under aerodynamic forces, discussing limiting stability and periodic solutions 11 p1726 A72-25914

French R and D work on ion propulsion systems for communication satellite stabilization, discussing principal characteristics, mathematical modeling, design and economic problems [AIAA PAPER 72-437] 11 p1727 A72-26179

Spacecraft roll stabilization during parabolic earth atmosphere reentry, developing single parameter multilevel algorithm 11 p1684 A72-26897

Spacecraft motion stabilization about mass center and optimal angular velocity control using minimax technique 11 p1684 A72-26903

Autotracking antenna effect on dual spin spacecraft nutational stability, using averaging, eigenvalues and digital simulation techniques [AIAA PAPER 72-571] 12 p1876 A72-27379

Gravitational stabilization systems parameters determination for minimum amplitude of satellite eccentric vibrations 14 p2162 A72-30457

Optimal efficiency of satellite passive nutation damper, noting system moment of inertia and flywheel axis relationship and viscous friction coefficient 14 p2162 A72-30458

Stability analysis of satellite motions in Newton planetary field by Liapunov method, considering ellipsoid of revolution under gravitation of sphere 14 p2162 A72-31081

Optimum design parameters for a spin-stabilized spacecraft nutation damper. 17 p2619 A72-34208

Satellite orientation and stabilization systems aerodynamic compensation for circular orbit perturbations 17 p2621 A72-35034

Gravitational stabilization of a satellite in a fixed inertial orientation. 17 p2622 A72-35487

Passive stability of a spinning Skylab. 18 p2730 A72-36314

Attitude control of satellites with large flexible solar arrays. [AIAA PAPER 72-733] 18 p2730 A72-36541

Attitude stability and performance of a dual-spin satellite with nutation damping. 19 p2862 A72-38022

Dual spin spacecraft simulation on three axis air bearing ball in atmosphere testing propellant tank dissipation and spacecraft stability in autotrack mode [AIAA PAPER 72-860] 20 p2911 A72-39108

Stability of dual spin spacecraft containing tracking payloads. [AIAA PAPER 72-890] 20 p2975 A72-39111

Stability and CMG wobble damping of flexible, spinning space stations. [AIAA PAPER 72-888] 20 p2975 A72-39113

Nutational stability of a dual-spin satellite under the influence of applied reaction torques. [AIAA PAPER 72-885] 20 p2976 A72-39116

Loosely stabilized satellite orientation determination by stellar sensors and magnetic damping of rotation 20 p2976 A72-39244

Librational transverse oscillations boundary value problems of heavy thread on orbiting satellite, determining equilibrium and eigenfunctions 20 p2977 A72-39247

Solar pressure control of a spinning satellite with a stabilized platform. [AIAA PAPER 72-918] 21 p3115 A72-41563

Small oscillations of gravity gradient satellite in circular near-equatorial orbit, discussing operational efficiency of magnetic damping systems 22 p3230 A72-42223

OSO pointing accuracy improvement through dual spin stabilization, discussing OSO design evolution 1962-72 24 p3449 A72-45145

SPACECRAFT STERILIZATION

Papers on planetary quarantine covering microbial survival in deep space, contamination by nonsterile flight hardware and sterilization 01 p0019 A72-10817

Planetary quarantine microbiological and engineering problems, discussing cost, international policies, contamination and sterilization 01 p0019 A72-10818

Microbiological examination of space hardware, discussing viable organisms neutralization buried inside solid materials, sampling procedures and culture media 01 p0019 A72-10820

Space flight hardware sterilization, considering dry heat and chemical destruction 01 p0019 A72-10822

Dry heat resistance of bacillus spores on spacecraft metal surfaces for different pressures, atmospheres and materials 04 p0475 A72-15261

The effects of various cure cycles upon the viability of *Bacillus subtilis* var. *niger* spores within solid propellant. 18 p2652 A72-36437

A stochastic bioburden model for spacecraft sterilization. 18 p2652 A72-36442

Application of planetary quarantine methodology and spacecraft sterilization technology to improved health care delivery. 24 p3375 A72-45148

SPACECRAFT STRUCTURES

Space shuttle safety problems, discussing hydrogen pump bearings and air breathing turbofan blades failures and fuel tank fire hazards 03 p0441 A72-13694

Adhesive bonded components in aircraft and aerospace structures, discussing manufacturing, metal surface preparation, inspection and environmental exposure [SAE PAPER 720118] 06 p0835 A72-17325

Mars 3 spacecraft structure and experiments, noting central hypergolic fuel tanks, S-band directional antenna and solar panels 06 p0892 A72-17400

European Special Space Tug structural and configurational layouts and problems 09 p1396 A72-23259

ITOS-1/Tiros M/ satellite design, describing structure, thermal and attitude control, primary and secondary sensor subsystems, power supply and operational goals 09 p1396 A72-23373

Thermal nodal analysis of spacecraft hull-canister model from space simulation test, using least squares estimation and regression analysis 09 p1412 A72-23497

Viking conical aeroshell structural prototype design, analysis and testing, comparing buckling failure data with theoretical predictions 11 p1725 A72-25395

Space shuttle orbiter vehicle structural design configurations development and evaluation with respect to overall system weight and program cost [AIAA PAPER 72-373] 11 p1726 A72-25397

Arc cast vacuum melted Mo base alloy properties, production and applications to heat pipes, aerospace structures and pressure vessels 11 p1644 A72-26844

Composite materials mechanical and thermal properties for ATS reflector supporting truss, noting graphite fiber reinforced epoxy plastic design, fabrication and tests 12 p1886 A72-28158

Energetic Hg ion bombardment erosive and chemical effects on spacecraft surfaces downstream of electrostatic rockets [AIAA PAPER 72-446] 13 p1983 A72-28944

Space Shuttle Orbiter onboard ultrasonic system for structural integrity tests and assessment, noting limita-

tion factors due to configuration and vehicle launch noise effects 15 p2256 A72-31698

Environmental effects on spacecraft materials, structures and design, discussing sterilization, gravity, vacuum, micrometeoroids, radiation, etc. 15 p2320 A72-31802

Flow area computerized prediction for multicompart ment series-parallel spacecraft venting satisfying pressure differential requirements [AIAA PAPER 72-707] 16 p2462 A72-34038

Predictions of solar induced response of thin-walled open-section booms for design. 18 p2733 A72-36364

Combined spot weld-adhesive bonding to join sheet metal parts with applications to propellant tanks and spacecraft and aircraft structures [SME PAPER AD 72-710] 18 p2695 A72-36526

Impact tests for aid in data interpretation of measured meteor particles impact on spacecraft structures, noting transducer response dependence on impact angle 22 p3234 A72-42218

Structural problems of the helios solar probe. 24 p3449 A72-45122

SPACECRAFT TELEVISION

NT SATELLITE TELEVISION

Adaptive variable length coding for efficient compression of spacecraft TV data of Grand Tour missions 06 p0771 A72-17401

Mariner 9 television reconnaissance of Mars surface and satellites, observing south polar cap and dark spots with crater features 06 p0889 A72-18341

Channel coding/decoding schemes compatibility with TV data compressor for planetary missions in real time transmission 07 p0941 A72-19274

Space astronomy experiments with TV scanning, discussing data from Telescope catalog of UV observations and photometric and astrometric accuracy 08 p1170 A72-21957

Spaceborne Uvicorn/Telescope astronomical observatory for stellar UV TV pictures, discussing system design requirements 08 p1170 A72-21958

Mars observation by Mariner 9, discussing TV pictures of surface, UV and IR spectroscopy of atmosphere, S band experiment and Phobos and Deimos studies 10 p1538 A72-24309

Mariner 9 TV experiment image data display, processing and production for real time analysis, noting computer algorithms 15 p2236 A72-31982

Spacecraft-borne computer and electronic systems interface for radio reception, transmission and TV imagery applications 21 p3014 A72-40309

SPACECRAFT TRACKING

NT SATELLITE TRACKING

Nonlinear theory of cascaded two-way coherent spacecraft tracking system model, obtaining steady state probability density functions of phase and Doppler error 02 p0174 A72-12137

Error correcting data decoder assembly for mission independent sequential decoding at all stations in deep space tracking network, discussing design and performance 07 p0949 A72-19298

Spaceborne laser radar for target acquisition and tracking in spacecraft rendezvous and docking applications [CLEA PAPER 9,5] 07 p0943 A72-19387

Closed loop covariances prediction in reentry vehicle tracking and data compression, presenting simulation results 08 p1144 A72-20846

Compression of data from measurements in real time nonlinear estimation to reduce data processing requirements without performance deterioration, applying to reentry vehicle tracking 10 p1442 A72-23802

Satellite orbit tracking data accuracy estimation by partial differentiation, using Doppler and interferometer methods 11 p1593 A72-26097

Cosmological geodetic survey network construction via spacecraft tracking and laser beams, calculating power required for balloon satellite photography 13 p1922 A72-29631

Space tracking stations in Spain. I - The Madrid space station and its activities 17 p2536 A72-34945

Spectral factorization in periodically time-varying systems and application to navigation problems. 17 p2578 A72-35492

Global network of ground based facilities /infrastructure/ including spacecraft launching, tracking, communication and readout sites for international space operations [AIAA PAPER 72-739] 18 p2742 A72-36545

Low noise microwave receiving systems on a 64 m antenna. 19 p2763 A72-37255

Location estimation for spacecraft landed on Mars surface via statistical techniques application to earth based radio tracking data, taking into account ephemeris biases [AIAA PAPER 72-903] 21 p3082 A72-41554

SPACECRAFT TRAJECTORIES

NT EARTH-MARS TRAJECTORIES

NT EARTH-MOON TRAJECTORIES

NT EARTH-VENUS TRAJECTORIES

NT INTERPLANETARY TRAJECTORIES

NT LUNAR TRAJECTORIES

NT MOON-EARTH TRAJECTORIES

Spacecraft flight trajectory parameters from unknown second moment matrix of navigation measurement errors 01 p0127 A72-10352

Accuracy of spacecraft trajectory determination by complex expressions in multidimensional geometric representation 01 p0127 A72-10353

Optimal measurement programs for instrument controlled spacecraft trajectory sections, using maximum likelihood method 01 p0127 A72-10354

Soviet book on space navigation covering dimensional spaces, navigation functions, relativistic phenomena, position finding, motion parameters, statistical methods, etc 02 p0256 A72-12297

Spacecraft trajectories optimization by gradient method combination with Euler equations in calculus of variations 04 p0571 A72-14631

Interplanetary spacecraft trajectory error analysis by closed form approximation to state transition matrix, enabling rapid estimation with computer program 05 p0718 A72-16443

Dynamic system observation accuracy in spacecraft trajectory measurement, deriving processing algorithm based on state-estimate error correlation matrix analysis with maximum likelihood procedure 05 p0721 A72-16760

Iterative process convergence in least squares and maximum likelihood methods of processing measurements in spacecraft trajectory control, space navigation and geodesy systems 05 p0633 A72-16761

Polynomial class random process realization based on statistical methods of processing spacecraft orbital measurement data, considering random and systematic errors 05 p0683 A72-16763

Methodical errors in spacecraft local vertical determination due to variability of physical effects, considering planet oblateness, atmospheric refraction, incident radiation fluctuations, etc 05 p0721 A72-16764

Dynamic stability of controlled spacecraft with liquid propellant rocket engines, considering acceleration and braking sections of trajectory 05 p0730 A72-17027

Explicit analytic guidance technique for hyperbolic approach phases of lunar and interplanetary spacecraft trajectories from first order solution for perturbed planet centered trajectory [AIAA PAPER 72-15] 07 p1032 A72-18944

Recursive and nonrecursive real time spline methods for nonlinear estimation of independent trajectory parameters for vehicle entering earth atmosphere 08 p1197 A72-20862

Disturbing parameters effect on spacecraft trajectory X coordinate values estimation, including planetary masses and coordinates, astronomical unit and light speed 08 p1232 A72-21151

Liapunov direct method in synthesis of frequency-pulse system for automatic stabilization of spacecraft position 09 p1397 A72-23427

Pioneer 10 probe survival hazards during passage through asteroids belt and intense Jupiter radiation fields 10 p1551 A72-24272

Interplanetary single impulse flight trajectories optimization and computation, determining geometrical and kinematic characteristics 11 p1718 A72-25927

Spacecraft trajectories for reentry at hyperbolic velocity, examining aerodynamic control loads and characteristics in atmospheric skip 11 p1718 A72-25929

Atmospheric model effects on space shuttle ascent and reentry trajectories and aerodynamic heating 13 p1990 A72-28813

Trajectory shaping advantages for outer planet orbiter solar electric propulsion, considering radiation belt constraints, dual launch and target orbit geometries [AIAA PAPER 72-423] 13 p2036 A72-28938

Space center tractography and telemetry systems, including radar stations, interferometric equipment, optical methods and interlinked computers [DGLR PAPER 72-014] 13 p1938 A72-28961

Vibration stability and interference transfer function of onboard transponder with phase lock AFC used in Doppler system for measuring spacecraft trajectory parameters 13 p1958 A72-29456

Multiple probe targeting from spacecraft for 1977 Venus mission, considering trajectory, spin, release, attack angle, location and navigation and control accuracy effects 15 p2312 A72-32193

Spacecraft free fall trajectory calculation, using numerical optimization procedure based on Hamilton principle for two point boundary value problems 16 p2460 A72-34021

Synthesis of a nonlinear law for spacecraft motion control in the earth's atmosphere 17 p2621 A72-35201

Dynamic system observation accuracy in spacecraft trajectory measurement, deriving processing algorithm based on state-estimate error correlation matrix analysis with maximum likelihood procedure 17 p2610 A72-35263

Iterative process convergence in least squares and maximum likelihood methods of processing measurements in spacecraft trajectory control, space navigation and geodesy systems 17 p2523 A72-35264

Polynomial class random process realization based on statistical methods of processing spacecraft orbital measurement data, considering random and systematic errors 17 p2576 A72-35266

Methodical errors in spacecraft local vertical determination due to variability of physical effects, considering planet oblateness, atmospheric refraction, incident radiation fluctuations, etc 17 p2610 A72-35267

Disturbing parameters effect on spacecraft trajectory X coordinate values estimation, including planetary masses and coordinates, astronomical unit and light speed 20 p2969 A72-39256

About the interaction between a satellite and its environmental ionospheric plasma. 21 p3090 A72-40454

N-burn analytic solution for propellant-optimal transfer trajectories in vacuum, taking into account gravitational effects [AIAA PAPER 72-929] 21 p3112 A72-41569

Choice of parameters to be measured in determination of a spacecraft trajectory 22 p3223 A72-42201

Nonlinear problems of analyzing the observability of the trajectories of spacecraft motion on the basis of measured data 22 p3223 A72-42203

Saturn-Jupiter rebound - A method of high-speed spacecraft ejection from the solar system. 23 p3340 A72-44323

Rendezvous at specified destinations through optimum transfer paths 24 p3442 A72-45281

Mission strategy for combined comet-asteroid flybys. [AIAA PAPER 72-939] 24 p3444 A72-45436

Minimum-time entry of space vehicles into a planetary atmosphere 24 p3452 A72-45442

SPACECREWS

Spacecraft and aircraft crew survival after emergency landing in adverse environments, discussing water and food requirements, survival supplies and medical and first aid equipment 05 p0621 A72-16629

Soviet space crews selection and training based on professional and scientific background, emphasizing psychological qualities for working compatibility in space environment 09 p1274 A72-23672

Rest and activity patterns effect on space crews well-being and operational effectiveness during prolonged extraterrestrial missions, noting work load effect on long-haul transport aircrews 10 p1427 A72-23727

Ground and flight crews coordinated effort in Apollo mission operations, noting experts on ground and spacecraft spot judgments capability [AIAA PAPER 72-236] 11 p1586 A72-26557

Red cell mass plasma volume decrease in Apollo mission crews, indicating erythropoiesis inhibition 12 p1765 A72-28266

Future spacecraft habitable compartment layout from psychophysiological viewpoint, considering human visual and motor field parameters and crew members social needs 13 p1910 A72-29321

Social and emotional crises with respect to isolation, confinement and group dynamics of astronaut crews during long duration space flight 16 p2354 A72-33545

Spacecrews rescue requirements, considering escape capsules earth-based and orbit-based rescue systems and flight hazards 17 p2620 A72-34438

International Space Rescue Symposium, 1st, New York, N.Y., October 14, 1968, Proceedings. 20 p2977 A72-39550

An integrated medical system for long-duration space missions. 21 p3009 A72-41305

SPACING

NT AIRCRAFT APPROACH SPACING

Reynolds number and cylindrical spacing effect on Karman vortex street formation from smoke visualizations of single and tandem cylinder wakes 09 p1261 A72-22931

SPADATS [TRACKING SYSTEM]

U SPACE DETECTION AND TRACKING SYSTEM

SPAIN

Spanish winter anomalous ionospheric short wave absorption observed by high precision ground based measurements 01 p0055 A72-10434

SPALLATION

Pu-244 fission Xe isotopic composition parameters in achondrite meteorites, using lunar spallation systematics 01 p0124 A72-10058

Apollo 12 lunar igneous rocks 12004, 12040, 12051 and 12053, obtaining Kr 78/Kr 83 and Xe 131/Xe 126 spallation component ratios correlation line 01 p0124 A72-10065

Early solar system nucleosynthesis of Al 26, discussing silicon and carbon burning and spallation 04 p0567 A72-14912

Proton bombarded CsI crystal spallation-caused radioactive decay products contribution to background rate in satellite X ray telescope detector 06 p0853 A72-18084

Largest Apollo 15 lunar rock mass spectrometry analyses of noble gases with gas retention age estimation and spallation Kr data 06 p0888 A72-18267

Mathematical model for superheavy cosmic ray production by spallation on interstellar hydrogen, assuming single source for particle injection with given charge spectrum 07 p1062 A72-20197

Lunar glass particle micrometeorite crater morphology, showing radial fracture and spallation zone relationships 13 p2036 A72-28755

Spallation origin of anomalous He 3/He 4 ratio in 3 Centauri A, considering thermonuclear processes model 14 p2158 A72-30731

Light elements production from primary cosmic rays spallation in interstellar gas, noting diffusion coefficient of relativistic particles in galaxy 15 p2301 A72-32754

Shock wave propagation produced by explosive detonation in contact with inert solid, considering spallation occurrence and prevention 16 p2469 A72-33356

Li, Be and B spallation reactions in galactic cosmic rays from observations of cross sections of energetic protons incident on C and O targets 16 p2447 A72-33734

Li, Be and B nuclei production via nuclear spallation reactions generated by Galactic cosmic ray bombardment of interstellar gas 16 p2448 A72-33737

Nonelastic interactions of nucleons and pi mesons with complex nuclei at energies below 3 GeV. 19 p2837 A72-38027

Recent developments in the history of the nucleosynthesis of the solar system. 20 p2971 A72-39837

SPALLING

Shock precompression effect on dynamic fracture strength of steel and Al alloy, investigating crack initiation and growth 04 p0533 A72-14541

Prediction of thermal-shock resistance during heating at very high rates. 22 p3241 A72-43000

SPARE PARTS

Electronic data processing in airline materiel supplies operations, discussing procedural efficiency improvement through reduction of stochastic effects inherent in aircraft maintenance operations 14 p2174 A72-30823

SPARK CHAMBERS

Optical multiplate spark chamber in balloon-borne gamma ray telescope, describing triggering signal from plastic scintillator directional Cerenkov counter and photographic recording system 03 p0353 A72-13035

NASA spacecraft instrumentation for high energy phenomena measurements, discussing collimated proportional counters, wire grid digitized spark chambers and modulation and slit collimators 03 p0353 A72-13038

Spark calorimeter calibration by particle accelerator induced high energy pions, noting neutral and charged particles track detectors high geometric resolution
06 p0811 A72-17292

Wide gap spark chamber feeding technique for compensation of charged particle track drift due to avalanches
07 p0988 A72-19956

Multiple-wire spark counter characteristics for alpha particle detection, discussing electrodes surface finish and gas filling
08 p1164 A72-20941

TD-1 satellite mounted slow analysis camera with supervidicon image tube to observe cosmic ray tracks in spark chamber
08 p1170 A72-21961

Spatial spark jitter measurements of highly charged nuclei for optical spark chambers.
21 p3055 A72-41003

A transmitting television tube for collecting information from streamer spark chambers
23 p3290 A72-44160

A study of the mechanisms of formation of penetrating particle groups by the spark calorimeter method
23 p3291 A72-44430

Electric field orientation, magnetic field strength and high voltage pulse delay effects on spark chamber track displacement from true particle trajectory
23 p3291 A72-44441

SPARK DISCHARGES
U ELECTRIC SPARKS
SPARK GAPS

Laser triggered spark gaps characteristics initiated by switched out picosecond pulse from mode locked Nd-glass laser, investigating breakdown formation time delay
07 p1008 A72-20547

Ignition energy measurement by nanosecond electric sparks produced by transmission line method, recording voltage pulses onto spark gap
10 p1563 A72-25138

Electrode gap current and temperature distributions during electrochemical precision processing of metals, studying gas and electrolyte flow
11 p1613 A72-26258

Spark interferometry of plasma filaments in gases from self focused single mode ruby laser beam
12 p1852 A72-27869

Vacuum gap discharge conditions as function of electron beam parameters and metal vapor pressure
13 p2017 A72-29611

Spark interferometry of plasma filaments in gases from self focused single mode-locked ruby laser pulses
16 p2439 A72-33978

SPARK IGNITION

Secondary explosive spark detonators design and performance, determining ambient pressure variations effects on firing characteristics
08 p1219 A72-20758

Ignition energy measurement by nanosecond electric sparks produced by transmission line method, recording voltage pulses onto spark gap
10 p1563 A72-25138

SPARK MACHINING

Multilead electrical spark discharge machining for mass production technology, noting carburetor slot cutting and data processing equipment applications
01 p0078 A72-11097

Electronic system for electrodischarge machining, considering thyristor spark control and circuitry design for automatic feed down and short circuit clearance
04 p0502 A72-15530

Minimum charging resistance in relaxation generators for spark machining as function of supply voltage, using thyristor and voltage source circuit model
07 p0956 A72-19594

Thermomechanical model for calculating craters formed by short pulses in electro discharge machining
08 p1173 A72-21028

Electrical erosion efficiency of metal working under increased pressure in discharge gap in air and water
08 p1174 A72-21029

Automatic control of electroerosion machining by process computer, using pulse-voltage-metal removal relation
08 p1174 A72-21030

Technological characterization of electric discharge machines by metal removal rate, volumetric electrode wastage and machined surface roughness
08 p1174 A72-21031

Electroerosion machining with optimal control of electrical parameters, number of passes and electrode wear, using nonlinear programming and critical path method
08 p1174 A72-21032

Optimization for maximum productivity of electric spark machining with vibrating electrode, noting erosion product removal difficulties
08 p1174 A72-21033

Dielectric sulfur activated liquids for high productivity electroerosion machining of steels and metallic carbides, comparing with petroleum
08 p1174 A72-21034

Pulse energy and heat distribution in dielectric and metal during electroerosive machining
08 p1174 A72-21035

Surface structure changes in metal worked by electroerosion, discussing temperature and electrical tension effects
08 p1174 A72-21036

Oscillographic transient analysis of electric spark machining processes with electrode natural or forced vibrations
08 p1174 A72-21037

Transistorized static pulse generators for spark erosion machining, discussing operating principle, design, applications, automatic control system and maintenance procedures
08 p1146 A72-21038

Optimization criteria for electroerosion machining, determining objective functions
08 p1175 A72-21039

Complex erosion machining control and optimization, investigating current and tension effects
08 p1175 A72-21042

Electrochemical machining with forward speed control via hydraulic means
08 p1175 A72-21043

Realisation of a high-efficiency electrodischarge-machining power supply.
19 p2807 A72-37846

SPARK SHADOWGRAPH PHOTOGRAPHY
U SHADOWGRAPH PHOTOGRAPHY
SPARKS

NT ELECTRIC SPARKS

Laser spark plasma initial development phase showing high electron temperature and concentration, continuous spectrum emission, line broadening and shock wave formation
02 p0237 A72-11405

Shock front radius of subsonic radiation front driven by plasma fireball during final stages of decaying laser spark
20 p2934 A72-39844

SPASMS

Hyperventilation relationship with spasmophilia, noting psychoemotional cause and neuromuscular excitability
07 p0922 A72-20384

Description of an easy and simplified test for electromyographic diagnosis of latent spasmophilia in flight personnel
19 p2760 A72-37878

SPATIAL DEPENDENCIES

Nonlinear dynamic response of deformable solids under time and space dependent thermal and mechanical loads determined by finite element method
08 p1248 A72-21822

Hydrometeorological parameters spatial-temporal variations analysis and forecasting based on association functions and conditional probability distribution functions
08 p1202 A72-22116

Surveyor spacecraft lunar thermal data, comparing spatial resolution with earth based measurements
12 p1869 A72-27329

Spatial and time dependence of electron velocity in short channel microwave FET, using Monte Carlo method
12 p1790 A72-27434

Polarization and spatial and frequency characteristics of ground signal resulting from finite source Pc 1 micropulsation disturbance
13 p1922 A72-29391

Spatial and temporal summation characteristics and relationship in human peripheral retina investigated for stimuli viewed at eccentricity against luminous background
13 p1907 A72-29970

Impulse excited spatial systems of rigid bodies linked by pivot joints with arbitrary kinematics, applying Maxwell-Betti theorem
15 p2323 A72-31461

Transversely excited pulsed carbon dioxide laser with and without hydrogen addition, observing gain spatial and temporal dependence
15 p2251 A72-32529

Space and time variations of the solar Na D line profiles.
17 p2616 A72-35697

Models of neurons reacting to input signal alternation in space and time
19 p2759 A72-37424

Quiet day daily geomagnetic field variability associated with equatorial ionospheric upheavals, noting longitudinal extent
19 p2794 A72-38869

Atmospheric transmittance measurements time and spatial representativeness optimization by allowing for fog element caused discontinuities
20 p2947 A72-38971

Positive geomagnetic bays in evening high-latitudes and their possible connection with partial ring current.
21 p3049 A72-41387

SPATIAL DISTRIBUTION

Time scales and correlations in a turbulent boundary layer.
21 p3047 A72-41626

Investigation of laser light spatial correlation by the photon coincidence method
21 p3064 A72-41691

Conditions for space invariance in optical data processors used with coherent or incoherent light.
23 p3288 A72-43887

Semigray approximation to nongray radiative transfer, taking into account mean absorption coefficient variation with spatial position and photon propagation direction
23 p3314 A72-44328

SPATIAL DISTRIBUTION
NT STAR DISTRIBUTION

Interstellar medium physical properties and distribution, discussing ionization heating by starlight, cosmic X rays and subcosmic rays
01 p0128 A72-10413

Plasma potentials spatial distribution measurement, describing switching circuit and probe design
01 p0109 A72-10580

Sporadic E layer occurrence frequency distribution during 1958-1960, investigating characteristics over equatorial, temperate and auroral zones
01 p0059 A72-10596

Spatial alignment for low noise difference picture detection in side-looking radar imagery
01 p0129 A72-10874

Precipitated electron energy latitude and time variations from auroral-height measurement during IQSY, using meridian scanning photometers
01 p0120 A72-10896

Critique on luminosity volume test for quasars, considering space distribution and luminous function
01 p0133 A72-11126

Fabry-Perot interferometer for studying spatial distribution of plasma electron concentration, discussing resolution using solid state gas laser light source
02 p0223 A72-11403

Spatial distribution of plasma density from phase shift measurement in millimeter waves based on microwave multichannel probes
02 p0263 A72-11412

Multifrequency interferometer for inhomogeneous plasma density soundings, determining time dependence, spatial distribution and plasma layer size
02 p0263 A72-11413

Atmospheric pollutants time and spatial profiles monitoring by geosynchronous satellite remote sensors
02 p0211 A72-11806

Urban geographic social-spatial pattern determination with aerial photographic interpretation
02 p0229 A72-12019

Bright galaxies and quasars associations based on spatial distribution and red shift considerations, discussing probability analysis
02 p0279 A72-12188

Incompressible two dimensional plane jet spatial stability analysis, presenting disturbance vorticity, Reynolds stress and energetics distribution in cross stream direction
02 p0152 A72-12352

Phototrophic substance effect on spatial structure of passive Q switched ruby laser emission, considering gallium phthalocyanine solution
02 p0239 A72-12568

Dust grain existence at large distances from galactic plane by computing interstellar radiation field pressure effects on grains
02 p0283 A72-12629

Dust particle dynamical behavior during cloud collisions, discussing grain distribution in resultant cloud
02 p0284 A72-12638

Galactic superclusters and matter distribution in universe, considering systematic catalog errors and uncertainty of statistical tests
03 p0421 A72-13172

Magellanic Clouds star clusters spatial distribution, color-magnitude diagrams, structures, dynamics and origins
03 p0425 A72-13254

Magellanic Clouds neutral hydrogen distribution, concentrations and velocity structure, noting H II correlation with supergiant stars
03 p0425 A72-13256

Spatial distribution of total magnetic vector and of electric currents in unipolar sunspot
03 p0428 A72-13300

Magnetic field fine structure in undisturbed photosphere for high latitude solar regions, constructing model to explain magnetograph response
03 p0428 A72-13306

Solar photospheric facula blue light limb photographs, determining spatial variation in contrast levels
03 p0434 A72-13494

Comet hypotheses, examining orbit axes and perihelions spatial distribution as possible interstellar origin
03 p0438 A72-13978

Spatial distribution of gaseous nitrogen molecules scattered from metal surface, estimating beam capture coefficient
03 p0392 A72-14056

Central peaked Martian crater distribution from Mariners 6 and 7 photographs, comparing south polar region to equator

03 p0440 A72-14310

Spatial transformation in geodesy, considering point in space as position function for orthogonal and curvilinear coordinates

03 p0351 A72-14329

Closed-loop nonlinear sampled-data systems with sampler and finite Hankel transformable distributed elements, deriving frequency domain stability criteria

04 p0504 A72-14662

Iterative procedure for computing optimal controls in distributed parameter systems described by linear parabolic differential equations, applying to metal slab temperature profile problem

04 p0504 A72-14664

Dual variational principles application to distributed parameter system suboptimal control strategy evaluation, considering control variable and feedback gain as piecewise function of time

04 p0505 A72-14665

Distributed parameter control system optimal control problems, formulating existence with minimum norm technique

04 p0505 A72-14667

Distributed systems modeled by partial differential equations, identifying unknown parameters by Galerkin method using steepest descent method and nonlinear filter

04 p0505 A72-14674

Spatial dispersion effects in crystal optics, obtaining dispersion law for normal waves in crystals via electromagnetic field tensor equations

04 p0548 A72-14739

Spatial structure coherence in sublayer of turbulent boundary layer, using spanwise flow hot-wire anemometer measurements

04 p0462 A72-15116

N galaxies and quasars properties comparison, suggesting continuous distribution and luminosity function

04 p0578 A72-15285

Quasar red shifts and spatial density with statistical approach, confirming cosmological distances and uniform distribution in accompanying space

04 p0580 A72-15452

Three dimensional temperature distribution at thermally insulated crack in plate

04 p0593 A72-15658

Low velocity neutral hydrogen spur coincidence with radio continuum Loop IV, discussing average excess surface density and total mass

05 p0711 A72-15765

Distributed parameter state regulator system, investigating order of spatial discretization error in finite difference approximation to optimal response, control and performance cost

05 p0639 A72-15805

Asteroids origin, discussing Phaethon model, masses, distribution, fragmentation and disintegration

05 p0713 A72-15980

Refraction theory applied to isotropic absorbing media, noting spatial distribution of incoherent components according to polarization states

05 p0689 A72-16173

Galactic high energy electron differential spectrum, estimating spatial distribution and random magnetic field intensity

05 p0709 A72-16237

F 2 region electron density spatial and temporal distribution, investigating plasma vertical drift effects

05 p0657 A72-16263

Neutral hydrogen distribution in spiral and irregular galaxies, discussing H II regions

05 p0716 A72-16371

Stable molecules spatial concentration profiles in high intensity combustion chamber, using quartz sampling probe and gas chromatograph

05 p0751 A72-17088

Optimal averaging of control in distributed random parameter system described by hyperbolic partial differential equations, considering boundary values on characteristics as control functions

05 p0683 A72-17133

Extensive air showers radio emission polarization, spatial distribution and electric field strength, noting geomagnetic mechanism effect

06 p0870 A72-17278

Electrons spatial and temporal response in collisionless plasma to externally applied voltage pulse

06 p0856 A72-17522

Double and multiple galaxies relative number and space distribution with respect to single galaxies number from sky survey map analysis

06 p0882 A72-18005

High radial velocity neutral hydrogen outside galactic plane, noting inability to correlate with radio spurs, absorption and emission regions

07 p1069 A72-19082

Atmospheric eddy flux spatial variations in constant flux layer, noting heat and momentum flux variability of less than 10 percent

07 p1030 A72-19107

Numerical solution of equations for asteroidal mass distribution under collisional fragmentation

07 p1071 A72-19180

M supergiants in Carina arm, discussing photometric studies at 4-18 microns, interstellar extinction uncertainties and spatial distribution

07 p1072 A72-19344

Magnetospherically trapped particles sources, losses and transport processes, presenting time averaged proton, electron and alpha particle distributions in trapping and pseudo-trapping regions

07 p1062 A72-20028

Plasma sheet distribution in magnetosphere from low energy particle observations in equatorial region of magnetotail

07 p0977 A72-20031

Upper atmosphere minor component distribution rearrangement, investigating transition time to diffusion equilibrium

08 p1155 A72-20803

Measuring equipment for charged particles spatial distribution in cosmic ray showers, considering multiaxial and secondary young showers

08 p1226 A72-21077

Spatial-temporal temperature distribution on CW laser irradiated materials, noting application to water film

08 p1252 A72-21289

Frost rule for meteoroid spatial sorting as basis for Allende meteorite shower strewn field examination of fragment mass and position

08 p1237 A72-21651

Spatial structure of sinusoidally modulated light beam propagating in medium with forward extended scattering characteristics

08 p1136 A72-21742

Quasi-stellar radio sources spectroscopic and photometric observations, determining spatial distribution and bivariate radio and optical luminosity function

09 p1382 A72-22279

Differential photoelectron fluxes at 560 km altitude observed by OVI-18 satellite on 22 March 1969, noting latitudinal variation

09 p1378 A72-23013

Quasar redshift distribution and optical and radio luminosity functions analysis

10 p1534 A72-23904

Inversion spatial nonuniformity effects on spectrum and kinetics of ruby laser, using spherical mirrors

10 p1491 A72-24361

Time optimal control of distributed systems with random properties, considering n integral relations and flying wing vehicle torsional vibration problems

10 p1421 A72-24427

Spiral galaxy density wave maintenance mechanism from rotating disk star-gas system model description of stellar birth and disintegration effects

10 p1547 A72-24869

Spatial distribution of electron beam excited plasma wave spectrum, determining wavenumber, amplitude and frequency by incoherent microwave scattering

11 p1693 A72-25564

Dayside magnetosphere stably trapped radiation zone high latitude boundary determination from energetic electron intensity spatial distribution observation by Imp 3 satellite

11 p1713 A72-26106

Planetary nebula classification based on forbidden line ratios and morphology, discussing galactic plane distribution, radial velocities and evolution

12 p1867 A72-27209

Russian book on spectral, spatial and time characteristics of lasers covering luminescence and resonator theories, electromagnetic field structure and radiation dispersion

12 p1820 A72-27500

ATS F/G radio beacon experiments for study of exosphere and ionosphere integrated electron content, spatial structure and time dependent behavior

12 p1782 A72-27526

Spatial characteristics of equal energy visual stimuli in metacontrast design for targets and masks of constant separation and varying width, deriving weighting functions

12 p1762 A72-27680

High level Canberra flight for three dimensional picture of wind and temperature fields, showing CAT, gravity waves and smooth flight characteristics

12 p1841 A72-27709

Equatorial spread F spatial and temporal distribution from short wave side reflection observations along Lindau-Tsumeb transequatorial HF radio transmission path

12 p1803 A72-27778

Plasma ionization traveling disturbances velocity and spatial structure in strong electromagnetic waves field

13 p1915 A72-28469

Estimated peak regional concentration of SST exhaust in stratosphere from expected flight operation levels

13 p1991 A72-28837

Time varying magnetospheric electric field spatial distribution effect on plasmasphere temporal evolution, considering fine structure due to periodic gusts in convection electric field

13 p1953 A72-29804

Solar photosphere velocity field photoelectric measurements, emphasizing long periods and low spatial wave numbers in deep layers

13 p2048 A72-29927

Electron energy distribution, ions mass spectral composition and spatial charge concentration of currentless photoresonant Ce plasma obtained by associative ionization

14 p1236 A72-30175

Refraction theory applied to isotropic absorbing media, noting spatial distribution of incoherent components according to polarization states

14 p2130 A72-30242

Dc arc plasma, investigating applied magnetic field, trace elements and gap spacing effects on spectral line intensity spatial distribution

14 p2139 A72-30783

Solar proton flare on 2 November 1969, investigating active region magnetic field development and spatial structure, near limb and coronal phenomena

14 p2160 A72-30909

Voluntary saccade length dependence on visual field nontarget stimuli number, locus and distance from target

14 p2077 A72-30966

Gravity waves parametric generation on liquid surface, presenting threshold values for space distribution of amplitudes and phases

14 p2097 A72-31111

Particular and general exact solutions of Einstein equations for matter filled space under assumption of spherically symmetric distribution of perfect fluid

15 p2305 A72-31343

Surface electrode distance, area and pressure effects on electromyogram recording of large skeletal muscle electrical activity during defined muscular tensions

15 p2190 A72-32490

Spatial distribution of nitrogen molecular beam scattering from solid nitrogen surface as function of beam energy and incidence angle

16 p2430 A72-33063

Face centered solid crystal cell spatial distribution effect on body surface-reflected molecular beam intensity distribution

16 p2430 A72-33066

Spatial flow velocity fields of incompressible continuous media with family of instantaneously inextensible planes, applying plastic flow theory

16 p2423 A72-33107

Variational principle by imposing time-independent spatial variation on hypothetical system governed by differential equation

16 p2416 A72-33664

Mode locked lasers, investigating effect of grating-induced phase and spatial modulations by multiple transverse modes on pulse compression across beam cross section

16 p2403 A72-33840

Spatial characteristics of magnetic field fluctuation in the magnetosheath

17 p2545 A72-34474

Inversion spatial nonuniformity effects on spectrum and kinetics of ruby laser with spherical mirrors

17 p2563 A72-34960

Spectral analysis of highly inhomogeneous chromospheric flares

17 p2617 A72-35709

Spatial distribution and temporal nature of the entry of solar cosmic rays into the polar cap

17 p2603 A72-35870

Spatial distribution of galactic globular clusters stars from Palomar sky survey

18 p2724 A72-36092

X ray observation inadequacy in detection of background radiation surface brightness fluctuations due to irregular distribution within galactic cluster sources

18 p2729 A72-37006

The structure of the Coma cluster of galaxies

19 p2854 A72-37229

Ignition moment of solid propellant particles monodisperse aggregate uniformly distributed in gaseous oxidizer

19 p2879 A72-37359

Bright nebulae near concentrations of high-velocity gas

19 p2856 A72-37504

All sky photography of auroral arcs alignment, noting oval distribution pattern

19 p2793 A72-38750

OH airglow IR observation from high altitude sites with bandpass filter, noting average spatial and diurnal fluctuations

19 p2794 A72-38861

Noise and stimuli current time and spatial distribution effect on visual performance of eye with image intensifier

21 p3054 A72-40742

Three-dimensional pattern of instability development during the interaction between a modulated electron beam and a plasma
21 p3092 A72-40800

Effects of thermo-optical distortion on the radiation loss magnitude and spatial-angular radiation characteristics for a lamp-pumped rhodamine-6G laser
22 p3185 A72-42173

High energy electron spatial distribution in plasma sheet from Ogo 5 magnetometer experiments
22 p3211 A72-42406

Plasma sheet characteristics of geomagnetic tail at 60 earth radii, inferring spatial distribution of magnetic field magnitude and plasma energy density
22 p3211 A72-42407

Spatial and temporal variations of thermal plasma ion and electron densities as function of L at 3000-5700 km from polar orbiting OV 3-1 satellite observation
22 p3211 A72-42414

Light scattering studies in amorphous media.
22 p3206 A72-42798

Light scattering in a sphere in the presence of an arbitrary source distribution
22 p3207 A72-42965

The effect of meteoric ion processes on radio studies of meteoroids.
23 p3336 A72-43558

Optimally sensitive control for distributed parameter systems.
23 p3275 A72-43612

Spatial and temporal temperature distribution in plasma from a low-voltage aperiodic spark discharge in an atmosphere of argon
23 p3320 A72-43677

Equivalence conditions for classes of linear and non-linear distributed parameter systems.
23 p3277 A72-44369

Fluctuations of the spatial distribution of the number of particles in showers generated by muons in heavy material
23 p3331 A72-44431

Behavior of the spatial distribution function of shower particles near the axis of a cascade shower
23 p3331 A72-44432

Lensless multiplication of images and their spatial frequency spectra with the aid of Fresnel holograms
23 p3292 A72-44470

Identification of four novae and a super-nova in Palomar Sky Atlas.
23 p3341 A72-44474

SPATIAL FILTERING

Wave front sampling points in spatial filtering of nonequidistant discrete holograms of flat objects
02 p0232 A72-12751

Spatial pulse modulation of optical signals for use in picture transmission, cinematography and holography
03 p0358 A72-13440

Nonlinear spatial filter synthesis by one-to-one signal-to-reference beam ratio and optimum exposure condition
05 p0663 A72-16676

Sunspot umbra spectrophotometric scans with spatial cancellation techniques, finding 4200 K umbral temperature with 0.60 photosphere contrast
07 p1069 A72-19081

Fluctuating signal propagation in plane laminar medium acting as spatial frequency filter, determining electron density distribution curvature radius in plasma layers
08 p1135 A72-21732

Linear analysis and synthesis of three dimensional interference system stationary in space and time domains
09 p1278 A72-22573

Spatial filtering techniques and numerical classification methods for pattern recognition in automated photointerpretation
09 p1312 A72-23305

Multichannel signal processing system for spatial optical filters synthesized by orthogonal functions
09 p1314 A72-23342

Holographic image structure spatial filtering resulting from nonlinear distortions in hologram recording
10 p1479 A72-24048

Radiographic image enhancement based on mathematical concepts of image convolution, Fourier transformation and spatial frequency filtering, discussing hardware and computer needs
10 p1481 A72-24322

Rotating mirror image position sensor for high angular resolution optical tracking, discussing performance improvement by computer generated variable density spatial filter
11 p1591 A72-25312

Phi-spatial filter method for straight or curved line geometric feature extraction of characters, using coherent optical system
12 p1820 A72-27494

Amplitude and phase local distribution analysis by filtering of spatial frequencies, examining holographic system by Hilbert and Fourier transformation
12 p1812 A72-27952

Frequency-specific color aftereffects as result of alternate exposure of subject to inspection gratings of different spatial frequencies
13 p1901 A72-28615

Relationship between antenna synthesis for a given radiation pattern and the synthesis of spatial signal processing systems
17 p2515 A72-34832

Encoding and decoding of color information using two-dimensional spatial filtering.
17 p2556 A72-35537

Computational algorithms compared for spatial frequency image filtering, considering tradeoffs between direct convolution and fast Fourier transform under equal point-spread functions assumption
18 p2658 A72-36263

Use of amplitude filter to improve the partially space coherent diffraction of a defocused circular aperture.
19 p2833 A72-37402

Wave front sampling points in spatial filtering of nonequidistant discrete holograms of flat objects
20 p2923 A72-39057

Optimum spatial filter for an anisotropic background-noise.
21 p3036 A72-41839

Visual information space-time dependent filtering by retinal and geniculate body neural nets
22 p3142 A72-42299

Comparison of theoretical and experimental results concerning spatial filtering in coherent optics
23 p3288 A72-43724

Linear analysis and synthesis of three dimensional interference system stationary in space and time domains
24 p3379 A72-44752

SPATIAL ISOTROPY

U ISOTROPY

U SPATIAL DISTRIBUTION

SPATIAL ORIENTATION

U ATTITUDE (INCLINATION)

SPECIES DIFFUSION

Stress induced oxygen diffusion in alpha Zr, attributing temperature dependent internal friction peak to oxygen-titanium interactions
02 p0247 A72-12818

Au distribution parameters in Si semiconductor devices, using radioactive isotope diagnostic methods
03 p0400 A72-12970

Pure metals creep or self diffusion activation energy from hot-hardness data, noting temperature and elastic modulus effects
03 p0375 A72-13931

Impurity diffusion of Ag, Cd, In, Sn and Sb in magnesium single crystals, observing valence effect on activation energy
03 p0378 A72-14254

Annealing effects in plated-wire memory elements, investigating Cu and Permalloy interdiffusion at low temperatures by X ray diffraction and electron beam microprobe
04 p0503 A72-15715

Reactive diffusion in binary systems, explaining diffusive saturation process from phenomenological viewpoint
05 p0701 A72-15753

Pure Al self diffusion at 130-200 C, determining activation energy from prismatic loop annealing rates
05 p0677 A72-17109

Diffusive mobility of C in Mo single crystals and Mo-Re alloy, using autoradiography and electron microscopy
06 p0829 A72-17733

Heterogeneous composite solid propellants ignition behavior under exposure to hot oxidizing gas, using gas phase model with species and energy radial diffusion
07 p1051 A72-19726

Diffusion kinetics in Nb-Al system for varying time and temperatures
07 p1015 A72-19930

Neutral species chemical reactions in D and E regions, taking into account effects of photodissociation and transport by horizontal and vertical flow and molecular diffusion
07 p0936 A72-20039

Bcc solid solutions formation in Cr-W binary alloys, investigating interface reaction and two phase grain boundary diffusion by X ray diffraction and microscopy
08 p1185 A72-21246

Defects high temperature diffusion effect on Mossbauer spectral lines width and positions in crystals with quantum transfer between multiplet sublevels in fine structure
09 p1372 A72-23038

Mo-Zr solid solutions internal bonding, discussing diffusion controlled process and hardness dependence on Zr
10 p1494 A72-23833

Interdiffusion of tight contact welded ring Ti-W pairs at high temperature, using X ray analysis and electron beam techniques
10 p1497 A72-24785

Diffusive mobility of C in Mo single crystals and Mo-Re alloy, using autoradiography and electron microscopy
11 p1652 A72-25340

Metal silicide phase formation for Nb, Ta, Mo and W, examining Si diffusion and transport processes
11 p1664 A72-26859

Electron microscope observed dislocation splitting in bent thin tantalum carbide sheet, analyzing results in terms of strain rate law and carbon diffusion model
11 p1669 A72-26948

Lithium diffusion into silicon by evaporation and homogenization technique, discussing dislocations and oxygen effects from aging in Ar at 150 C
12 p1757 A72-28025

Mo addition effect on Al and Ti diffusion from inter-metallic compounds into Ni matrix, noting increased high temperature stress rupture life
13 p1975 A72-28670

Gaseous species diffusion in carrier gas under various geometries and flow conditions, using finite element method
14 p2095 A72-30928

Ionized and neutral specie concentration in rarefied hypersonic wake flow behind cone, using electrostatic and electron density probes
15 p2177 A72-31209

Solution kinetics of secondary phases in cast dendritic and nondendritic Mg-Zn and Mg-Zn-Zr alloys, using cylindrical and spherical diffusion models
15 p2257 A72-32119

Boltzmann-Matano analysis of substitutional interstitial diffusion profiles of Zn in GaAs by radio tracer techniques
16 p2441 A72-33209

Chemical diffusion in the titanium-aluminum system
17 p2510 A72-34275

Binary diffusion of a jet embedded in a boundary layer.
17 p2541 A72-35238

Studies of the influence of CVD tungsten depositing conditions on the formulation of pores resulting from interdiffusion in the emitters of thermionic converters.
18 p2698 A72-36145

Diffusion in the nickel-rich, Ni-Al solid solution at 1260 C.
18 p2701 A72-36593

Diffusion effects in solids caused by radiation exposure, calculating diffusion coefficients of additions and defects
20 p2958 A72-38952

Relation between diffusion and defect formation rates in silicon detectors exposed to gamma radiation
20 p2959 A72-38956

Self-diffusion of cobalt in coarse grained polycrystalline Ni-Co alloys at low temperature.
20 p2935 A72-39016

Developments in the field of metallic diffusion protective layers employed against high-temperature corrosion
20 p2944 A72-39450

Surface reactions in similar boundary layers.
20 p2915 A72-40014

Russian book - Heat and mass transfer: A reference book.
21 p3128 A72-40350

Iron transport in chondrites - Evidence from the Warrenite meteorite.
21 p3104 A72-40491

Investigation by the mass transfer method of the diffusion of nickel at a /110/ surface of tungsten single crystals
21 p3068 A72-40955

Application of Tolubinskii's integral method to the solution of boundary value problems of nonstationary convective diffusion
21 p3129 A72-41056

Diffusion of cobalt in Ni-Co alloys at temperatures up to 1000 C
21 p3070 A72-41645

Isotope effect measurements application to determination of sodium diffusion mechanism and rate in sodium silicate glass
22 p3196 A72-42794

German monograph - Determination of the diffusion coefficient of hydrogen in the binary iron-nickel system at 25 and 58 C.
22 p3194 A72-43057

Kinetic equations solution approximation for two species isothermal reactions in homogeneous turbulent mixing
24 p3392 A72-45059

SPECIFIC HEAT

NT HEAT OF SOLUTION

Tungsten heat capacity, electrical resistivity and thermal radiation measurement over 2000-3600 K range by pulse heating technique
01 p0082 A72-10174

Positive and negative deviations of linear electrical resistance of d-transition metals at high temperatures as function of Debye temperature and Fermi level
02 p0242 A72-12006

Solar wind plasma flow through earth bow shock, deriving specific heats ratio based on one-fluid theory and conservation equations

03 p0412 A72-13509

Quasi-static measurement and electron phonon interpretation of specific heat of metals at low temperature

03 p0456 A72-13843

Method of characteristics calculations of inviscid free jet flow with low specific heat ratios for perfect gas at 1.10 Mach number

03 p0309 A72-13926

Low temperature heat capacity of chromium silicide, observing superconducting transition and magnetic susceptibility

03 p0377 A72-14024

Electron correlation effects on low temperature thermodynamics of amorphous semiconductors, predicting Curie law magnetic susceptibility and equilibrium electronic specific heat dependence on temperature

04 p0562 A72-15153

Tantalum carbide specific heat and other thermodynamic properties over 0-3000 K range

05 p0672 A72-16097

Thermal conductivity, electrical resistivity, emissivity and specific heat of polycrystalline vanadium under electron bombardment heating at 1200 to 1800 K

06 p0828 A72-17613

Niobium carbide thermodynamic properties tabulated for 0-3000 K, deriving equation for heat capacity from low temperature experiments

06 p0832 A72-18430

Electroconductivity, thermal conductivity and diffusivity, specific heat and emissivities of Ti at 1000-1700 K

07 p1010 A72-18935

Test facility for studying temperature dependence of thermal diffusivity and true heat capacity of metals between minus 150 and plus 400 C

07 p0982 A72-18941

Thermal diffusivity and heat capacity measurement by temperature vs time curve shape by laser pulse absorption, using thermocouple

07 p1101 A72-19890

Critique of paper on heat capacity and thermal conductivity of Apollo 11 lunar rocks at liquid helium temperatures, noting constraints imposed by Mossbauer data

07 p1084 A72-20521

Unsteady heat conductivity equation for finite dimensions parallelepiped, noting temperature dependence of specific heat and thermal conductivity

08 p1252 A72-21321

Stagnation conditions of magnetoradiative supersonic flow through shock waves for temperature dependent specific heat parameter

08 p1255 A72-21795

Thermal diffusivity and conductivity and specific heat of hard electrode graphite intermediate medium in hydraulic hot extrusion of metals

08 p1181 A72-22072

Thermal conductivity, diffusivity and specific heat of lunar soil and basalt analogs, using Luna 16 samples

10 p1532 A72-23753

Levitron calorimetry for solid and liquid Mo enthalpy measurement, calculating specific heat and heat of fusion

10 p1496 A72-24243

Fiber reinforced plastics thermophysical properties, thermal conductivity and heat capacity, determining effects of reinforcement fiber type, resin amount and type

[AIAA PAPER 72-366] 11 p1669 A72-25391

Hot wire cell measurement of specific heat in low pressure gases, determining thermal conductivity and accommodation coefficient

11 p1634 A72-26367

Specific heat temperature coefficient measurement of W at 2000 to 3600 K for defect and phase transition studies

11 p1661 A72-26625

Isochoric heat capacity peaks of water and argon near boundary in two phase region at critical state

11 p1747 A72-26964

Energy capacity margin of heat absorbing liquid /water/ in cooling system, considering specific heat and maximum critical heat flux

11 p1747 A72-26969

Apollo 11 and 12 lunar samples thermal properties, presenting diffusivity, conductivity and specific heat

12 p1869 A72-27334

Experimental data gathering, processing and presentation for materials enthalpy, heat capacity, thermal conductivity, compressibility and volume over wide pressure and temperature ranges

14 p2130 A72-30599

Orthogonal projection method for nonstationary heat conduction boundary value problem with thermal conductivity and specific heat as prescribed functions of position

14 p2126 A72-31049

Temperature measurement error due to solid body and temperature sensor specific heat differences for unsteady heat transfer

14 p2106 A72-31160

Benzene isochoric specific heat curves along saturation line in biphasic and single phase states, noting variations near critical point

15 p2334 A72-31393

Debye-Waller factors measurement for Mo and Cr surfaces near normal incidence based on LEED

15 p2292 A72-31857

Heat capacity data analysis for solid solutions of superconducting Nb-Ti system, investigating electronic structure

15 p2296 A72-32692

Semiconductor thermal diffusivity and heat capacity measurements, using carbon bolometer and high sensitivity point microthermistor

16 p2442 A72-33855

Thermal conductivity and heat capacity measurement by temperature vs time curve shape by laser pulse absorption, using thermocouple

17 p2637 A72-35138

Enthalpy and heat capacity of boron carbide at temperatures ranging from 273 to 2600 K

18 p2704 A72-37191

Determination of the temperature dependence of the thermophysical characteristics of solid materials by the method of successive approximations

19 p2881 A72-38044

Elastic constants of niobium-molybdenum alloys in the temperature range -190 to +100 C

19 p2821 A72-38591

Liquid dielectrics specific heat determination by adiabatic calorimeter with monotonic heating

21 p3059 A72-41819

Enthalpy and specific heat of tantalum carbide over the temperature range from 273 to 3600 K

22 p3187 A72-41890

Thermal properties of polymers below 4 K

22 p3197 A72-42800

Apparatus for measurement of specific heats between 0.3 and 3 K in the oscillating thermal region

22 p3180 A72-42936

Specific-heat and magnetic measurements in superconducting Ta-Nb alloys

23 p3323 A72-43273

Thermal and electrical conductivities, thermal expansion and specific heat of commercial graphite obtained by precipitation of methane pyrolysis products on hot surface

23 p3306 A72-43689

Application of a strongly doped semiconductor model to the study of thermodynamic and conductivity properties

24 p3432 A72-45068

The shock-combustion /expansion-combustion/ polar with allowance for variation of the specific heat ratio of a gas passing through a flame front

24 p3465 A72-45446

Phonon dispersion relations and Debye characteristic temperature for Ti, Hf and Y hcp lattices

24 p3415 A72-45629

SPECIFIC IMPULSE

Algol 3 solid propellant rocket motor design for Scout D and E launch vehicles first stage, considering high total impulse, payload/mass capability and propellant grains

[SAE PAPER 710765] 01 p0115 A72-10261

Fluorine-ammonia as high energy liquid bipropellant for rocket engines, presenting ground test results regarding velocity and specific impulse characteristics as functions of mixture ratio

01 p0114 A72-11220

Nozzle and cavity wall cooling limitations on uranium plasma nuclear rocket specific impulse, discussing wall heat flux and transpirational cooling by propellant flow

03 p0387 A72-14383

Rocket propellants R and D toward higher specific impulses, discussing liquid, solid, hybrid and tribrid systems

05 p0702 A72-16744

Specific impulse, mass and propellant efficiency characteristics of miniature motors using cryogenic fuels for auxiliary rocket thrusters

07 p0914 A72-18983

High energy rocket propellants for space propulsion systems, evaluating various propellant combinations in terms of specific impulse, toxicity, corrosiveness, cost and availability

11 p1702 A72-25299

ATS F ion thruster system for north-south station-keeping, discussing specific impulse, thrust vectoring, propellant system and power conditioning circuitry

[AIAA PAPER 72-439] 11 p1707 A72-26180

Duration test and performance of annular colloid thruster, noting specific impulse increase and electrostatic vectoring

[AIAA PAPER 72-483] 11 p1710 A72-26209

Generalized relations for determining specific impulse losses in nonequilibrium two-phase nozzle flows

20 p2914 A72-39909

SPECIFICATIONS

NT AIRCRAFT SPECIFICATIONS

NT EQUIPMENT SPECIFICATIONS

Proposed gas turbine procurement standards for gaseous and liquid fuel specifications emphasizing fuel contaminants

[ASME PAPER 71-WA/GT-3] 05 p0703 A72-15896

SPECIMENS

Vacuum mold preparation and flexural testing of miniature carbon fiber reinforced composite specimens

11 p1671 A72-25468

A study of the vestigial records of cosmic rays in lunar rocks using a thick section technique

23 p3341 A72-44459

SPECTRA

NT ABSORPTION SPECTRA

NT ATOMIC SPECTRA

NT BALMER SERIES

NT D LINES

NT ELECTROMAGNETIC SPECTRA

NT ELECTRONIC SPECTRA

NT EMISSION SPECTRA

NT ENERGY SPECTRA

NT FRAUNHOFER LINES

NT H ALPHA LINE

NT H BETA LINE

NT H GAMMA LINE

NT H LINES

NT HERZBERG BANDS

NT INFRARED SPECTRA

NT K LINES

NT LINE SPECTRA

NT LYMAN SPECTRA

NT MASS SPECTRA

NT MICROWAVE SPECTRA

NT MOLECULAR SPECTRA

NT NEUTRON SPECTRA

NT NOISE SPECTRA

NT OXYGEN SPECTRA

NT PASCHEN SERIES

NT PHOTOLUMINESCENT BANDS

NT PLASMA SPECTRA

NT POWER SPECTRA

NT RADIATION SPECTRA

NT RADIO SPECTRA

NT RAMAN SPECTRA

NT RYDBERG SERIES

NT SCHUMANN-RUNGE BANDS

NT SHOCK SPECTRA

NT SOLAR SPECTRA

NT SPECTRAL BANDS

NT STELLAR SPECTRA

NT TELLURIC LINES

NT UV SPECTRA

NT ULTRAVIOLET SPECTRA

NT VEGARD-KAPLAN BANDS

NT VIBRATIONAL SPECTRA

SPECTRAL ABSORPTION

U ABSORPTION SPECTRA

SPECTRAL ANALYSIS

U SPECTRUM ANALYSIS

SPECTRAL BANDS

NT ABSORPTION SPECTRA

NT FRAUNHOFER LINES

NT HERZBERG BANDS

NT PHOTOLUMINESCENT BANDS

NT SCHUMANN-RUNGE BANDS

NT TELLURIC LINES

NT VEGARD-KAPLAN BANDS

Green and blue-green algae reflectance and transmittance characteristics, selecting spectral bands for multispectrum scanning of algal suspensions in water bodies

02 p0213 A72-11857

Nonisothermal gas layer IR radiation in multiatomic molecular vibrational-rotational band range, determining lowest level energy for wide line spectrum

04 p0547 A72-14657

Fluorescence polarization and intensities of nitric oxide vibrational bands from Cd line and continuum excitation for spectrometer calibration

04 p0552 A72-14893

Height profiles for volume emission rate and intensity of second positive band of nitrogen molecule excited by photoelectron impact, noting solar activity effects

04 p0518 A72-14962

Intensity-height profiles for molecular oxygen first and second negative bands in F region, using equilibrium velocity distribution of photoelectrons

04 p0518 A72-14963

White dwarf Grw plus 70 deg 8247 circular polarization spectral structure with molecular absorption bands coincident with Minkowski bands

04 p0580 A72-15368

Artificial barium oxide clouds band spectrum analysis, calculating rotational and vibrational temperatures in total wavelength region

05 p0655 A72-16069

Martian atmospheric pressure determination from carbon dioxide bands spectroscopic measurements

06 p0884 A72-18032

Radio sources sky survey with radio telescope, discussing 5C1 and 5C2 spectral distributions

07 p1069 A72-19074

German monograph on sky scanner for short term sky spectral density distribution using glass fiber bundles for spectral components simultaneous measurement

07 p0983 A72-19266

Martian height gradients from 1.6 micron carbon dioxide band intensity, using telescopes with prismatic quartz spectrometer

08 p1231 A72-21125

Einstein A coefficients, band oscillator strengths and absolute band strengths calculation for comet tail band system of CO cations

09 p1355 A72-22789

CO Cameron system band intensity from measurements of equivalent widths of resolved rotational lines, using Doppler growth curve for line strength conversion

10 p1514 A72-24095

Radiative displacement of molecular beam sidebands by spatiotemporal modulation of irradiating RF field

10 p1492 A72-24858

Martian atmospheric pressure determination from carbon dioxide bands spectroscopic measurements

11 p1719 A72-25968

Cameron bands phosphorescent yield of carbon monoxide from carbon dioxide photodissociation in helium buffer

11 p1590 A72-26013

Carbon dioxide laser vibrational-rotational band small signal gain factor dependence on time elapsing after breakdown of equilibrium distribution

13 p2008 A72-29503

Absolute cross sections for Werner band system excitation of molecular hydrogen by electron impact, discussing relative spectral response calibration

13 p2009 A72-30065

Ferric ion traces evidenced in lunar and meteoritic titanates by charge transfer bands observations during heating, interpreting origin as caused by cosmic radiation

14 p2154 A72-30515

Methane spectral band tetrahedral fine structure analysis, using vibration-rotation Hamiltonian

14 p2084 A72-30523

CO overtone band and vibrational transitions in CW carbon disulfide-oxygen chemical laser, discussing pressure effects

15 p2250 A72-32525

Band model and scaling approximation validity for computation of transmission profile in V4 band of methane in Jovian atmosphere

16 p2461 A72-34099

Application of dispersion techniques to molecular band intensity measurements. I - Principles of 'fringe shift' and 'fringe slope' band analysis procedures

17 p2586 A72-35832

Fringe shift and slope analysis of interferometric spectrogram formed by NO-gamma system spectral band

17 p2586 A72-35833

New observations on the Kuiper bands of Uranus.

21 p3106 A72-41043

Temperature range estimation method for planetary atmospheric component generating spectral lines, applying to Venus observations at 7820 A carbon dioxide band

21 p3106 A72-41045

Quantitative spectroscopy of the aurora. I - The spectrum of bright aurora between 7000 and 9000 A at 7.5 A resolution.

21 p3049 A72-41724

Second positive system of nitrogen bands in the day airglow from Cosmos-224 data

23 p3282 A72-43356

A shock tube determination of the electronic transition moment of the CN red band system.

23 p3316 A72-44329

Interpretation of X-ray emission bands of AIII-BV compounds

24 p3432 A72-44914

SPECTRAL CORRELATION

Spectral correlation and transition probabilities of mutually dependent orthogonal binary random signals

11 p1595 A72-26299

SPECTRAL EMISSION

Materials spectral emission properties measurement, comparing with absolute black body model

04 p0596 A72-14652

Quasar radio structure, investigating morphology, statistical characteristics, angular size of spectra and red shift correlations from interferometer measurements

05 p0716 A72-16377

Temperature inhomogeneity effect on plasma column microwave resonant behavior in presence of axial magnetic field, ascribing spectral shifts to electron density and temperature profiles changes

06 p0854 A72-17417

Terrestrial surface observation from space platform, considering atmospheric effects, surface spectral properties and information resolution and transmission

08 p1170 A72-21965

Apollo lunar fine samples total emittance as function of temperature, using spectral emittance measurement technique

09 p1388 A72-23028

Regional observation of atmospheric spectral transmittance by Bouguer and high/low star methods

13 p2044 A72-29650

Electric field excited stable auroral red arc time dependent behavior, noting inconsistency with satellite and ground observation of 6300 A emission for electron energy

13 p1953 A72-29812

Emission line polarization prediction for planetary nebula C IV ion emitted spectrum via theory for energy level population

16 p2458 A72-33689

Spectral emittance of Apollo-12 lunar fines.

20 p2970 A72-39486

Spectral reflectance and emittance of Apollo 11 and 12 lunar material.

20 p2970 A72-39609

Peculiar absorption and emission microstructures in the type IV solar radio outburst of March 2, 1970.

22 p3217 A72-42044

Photochemistry of the airglow continuum.

22 p3153 A72-42889

Spectral investigations of the comet Bennett 1970 II (1969 i)

23 p3337 A72-43646

SPECTRAL ENERGY DISTRIBUTION

RF interference in angle-modulated system with predetection linear bandpass filter, calculating output power spectral density in baseband

01 p0045 A72-10332

Cosmic ray energetic spectrum variation from observed latitudinal effects during 1954-1962 solar activity cycle

01 p0119 A72-10607

Irregular, spiral and elliptical galaxies radio continuum measurements at 1420 MHz, presenting positions flux densities and brightness distributions

01 p0131 A72-11005

Galactic clusters red shifts and absolute spectral energy distributions, inferring evolutionary effects by comparison with giant elliptical galaxies light energy distribution

02 p0279 A72-12185

Space observation of stars and interstellar medium, considering stellar energy distributions and line spectra, interstellar absorption lines, galactic nebulae and X ray sources

03 p0420 A72-13122

Solar corona X ray data from SOLRAD satellites, detailing spectral energy distribution, ionization balance, continuum radiation and line emission

03 p0410 A72-13219

Solar radiation characteristics, calculating concentration and spectral energy distribution

04 p0572 A72-14701

Spectral energy distributions of peculiar galaxies and quasars by photoelectric spectrometry, observing emission lines strength

05 p0716 A72-16373

Mf/hf/vhf scattering from sea, deriving received power and spectral energy density dependence on grazing angle, frequency, range and surface impedance

06 p0770 A72-17338

Quasars red shift distribution apparent maximum for Z near 2.0, investigating possible sources of observational selection

06 p0882 A72-18000

Solar Fraunhofer line profiles determination by digital data recording double-pass spectrophotometer, presenting observed atomic Ni and Fe lines intensity distributions

06 p0884 A72-18028

Early type stars photoelectric spectra obtained with Mariner 9 UV spectrometer, obtaining resonant line features and spectral energy distribution

06 p0890 A72-18347

Spectral distributions of laser emission as dynamic variables of electromagnetic field modes and active medium excitations, using perturbation theory

07 p1007 A72-20120

High temperature black body model based on induction heating of graphite crucible, noting application to stellar energy spectral distribution determination

07 p0991 A72-20404

Optimum lasing conditions and spectral characteristics of organic dye lasers at 3,100-11,000 A

07 p1009 A72-20613

Spectral density curves for intensity fluctuations of stimulated emission from low and ultralow frequency gas lasers as function of thermal oscillation, mode interference and heat effects

08 p1182 A72-21379

Fabry-Perot spectrometer/premonochromator assembly integral transmissivity as function of spectral tuning noting selectivity by amplitude modulation

08 p1172 A72-22035

Spectral distribution characteristics of geomagnetic field mean intensity variations, relating longitudinal

SPECTRAL ENERGY DISTRIBUTION

specific resistance and integral conductivity of top rock layer

09 p1296 A72-22236

Single picosecond light pulses from mode locked Nd-glass laser, discussing temporal structure, spectral energy distribution and pulse shape measurements

09 p1324 A72-23082

LF noise spectral density measurements in avalanche diodes as function of frequency, considering mean square voltage drift

09 p1287 A72-23118

Simulated superposed coherent and chaotic thermal radiation of arbitrary spectral shape, using laser beam modulation and photocount statistics

09 p1352 A72-23240

Spectral indices of extragalactic radio sources at 1.4 GHz independent on flux density

10 p1545 A72-24807

Spectral distribution of signal power in AM, FM and PM PCM systems with time division multiplexing

10 p1439 A72-24909

Solar Fraunhofer line profiles determination by digital data recording double-pass spectrophotometer, presenting observed atomic Ni and Fe lines intensity distributions

11 p1719 A72-25964

Semiconductor injection laser with distributed radiative loss, calculating radiation line shape and width and quantum efficiency

11 p1648 A72-26329

Russian book on satellite-borne electro-optical IR radiometers design for celestial bodies spectral radiance and energy distribution measurement

11 p1634 A72-26376

Turbulent plasma electric field energy density spectrum from statistical mechanics investigation based on canonical formalism for electron plasma

12 p1851 A72-27387

Negative photoconductivity effect in high resistance n-type indium phosphide single crystals, noting photocurrent spectral distribution and I-V characteristics

13 p2022 A72-29647

Signal level fluctuations line spectra energy characteristics comparison for oblique and oblique-backscatter sounding, noting changes in harmonics intensity and period

14 p2085 A72-30638

Stellar UV radiation spectral energy distribution investigation of stellar composition and atmosphere and interstellar gas, discussing observation restriction by earth atmosphere absorption

15 p2302 A72-31284

List of galaxies with UV continuum, noting emission lines, Seyferts, quasars and spectral energy distribution

15 p2304 A72-31326

Venus long wave radiation spectral composition, angular distribution and carbon dioxide transmission from thermal, structure and vertical radiation absorption profile

15 p2305 A72-31394

Spectral intensity distribution of vibrational electron interaction with strong coupling during polymerization of monomer cyanine dye and dimer molecules

15 p2280 A72-31410

B type main sequence star absolute energy flux envelope from ground based and OAO 2 observations, comparing with model atmosphere prediction

15 p2311 A72-31997

IR radiant energy emission from conical jet exhaust of turbojet aircraft

15 p2298 A72-32399

Emitted phonon spectrum effects on detected signal response in superconducting Sn diodes, noting deviation from linearity

15 p2209 A72-32541

Torch temperature measurements in vacuum by spectral radiative energy distribution method

16 p2476 A72-33258

Determination of the parameters of minority carriers in semiconductor photocells from a spectral sensitivity curve

17 p2498 A72-35512

Evaluating the light from the sun.

19 p2790 A72-37933

IR chemiluminescence technique /method of arrested relaxation/ to measure spectral energy distribution among Cl and HI and DI reaction products

19 p2763 A72-38802

Rate constant determination for reaction product molecule in vibrational and rotational quantum states, obtaining spectral energy distribution

19 p2763 A72-38803

Energy distribution among reaction products. VI - F + H2, D2.

19 p2763 A72-38804

An analysis of the spectral scanning technique for determining the temperature distribution in a semi-transparent medium.

20 p2986 A72-39677

Velocity oscillations in the solar atmosphere.

21 p3107 A72-41278

A spectral study of the nebula NGC 7635 and the star BD +60.2522 deg

21 p3113 A72-41755

Type II supernova spectral intensity minima due to blueshifted absorption lines of hydrogen and Fe II based on observed and synthetic spectra wavelength comparison

23 p3334 A72-43257

Galactic submillimeter background radiation energy density limit, taking into account recalibrated gamma ray flux measurements agreement with cosmic ray-interstellar matter interactions

23 p3329 A72-43942

Spectrometric zonal standards - Selection of stars and methodology of their study

23 p3338 A72-44031

Orion nebula continuum spectrum energy distribution from spectrophotometric measurements, comparing color temperature with previously obtained data

24 p3438 A72-44839

Angular spectra and frequency characteristics of quasi-continuous monomode and two mode Nd-YAG lasers with spherical resonator

24 p3412 A72-45707

SPECTRAL LINE WIDTH

Self broadened rotational half widths for Lorentzian line shape and slit function in CO fundamental, using line center transmission measurements

01 p0104 A72-10095

Spectral distribution of total continuous emission coefficient for LTE hydrogen plasma over 8000-16,000 K and 400-15,000 Å ranges, observing Stark broadening

01 p0108 A72-10175

Orion A and M17 radio recombination line width increases, discussing Stark broadening functional dependence on principal quantum number

01 p0131 A72-11010

Line profile shape analysis of X ray diffraction broadening from deformed W, showing close approximation to Voigt distribution

01 p0088 A72-11046

Laser spark plasma initial development phase showing high electron temperature and concentration, continuous spectrum emission, line broadening and shock wave formation

02 p0237 A72-11405

Spectral broadening in laser Doppler velocimeter, showing identity of wave vectors spread for incident and detected fields and scattering center finite volumetric stay

02 p0229 A72-12094

Electron impact broadening of ionized Be and Ba lines in electric shock tube plasma, measuring electron density and temperatures

03 p0393 A72-13020

Single electron approximation of Stark broadening of hydrogen spectral lines without constraints of collision and quasi-static theories

03 p0391 A72-13079

Magnetic field and turbulence in sunspots, studying local variations of saturation and Doppler broadening

03 p0428 A72-13297

Fluctuation theory for single mode laser detuning effect on photon intensity and spectral line width

03 p0368 A72-13671

Electron impact Stark broadening of ionized chlorine lines in pulsed arc plasma using laser interferometric and spectroscopic measurements

03 p0396 A72-13748

Optical excitation of divergent alkali atomic beam by radiation absorption, deriving absorption coefficient for line broadening and/or Doppler effect

03 p0393 A72-14062

Eclipsing variable system AW Peg spectrophotometric data, examining spectral line geometries and intensities and atmospheric conditions

03 p0439 A72-14244

Curve of line width correlation application to alpha Orionis OH lines, determining atmospheric turbulence and thermal velocities

04 p0571 A72-14558

Pressure broadened water vapor line shape resonance dispersion at 22 GHz, deriving expression for instrument induced deviation from Lorentzian behavior

04 p0552 A72-14891

Blanketing effect of strong line spectra collisionally broadened wings, evaluating stellar atmospheric model computation

04 p0573 A72-14907

Solar flares, presenting line width changes curves, chromospheric observation by spectrohelioscope and solar flux measurements

04 p0567 A72-14923

Stark contours of hydrogen spectral lines in turbulent plasma with high noise level due to hf Langmuir oscillations

04 p0557 A72-14986

Interstellar sodium lines intensities and widths as discriminants for two component models of galactic H I cloud regions

04 p0578 A72-15310

Plasma satellite linewidth broadening due to density inhomogeneity, considering evidence based on light scattering from Ar plasma jet

04 p0559 A72-15355

Two mode lasers with photon intensity coupling near threshold treated by fluctuation theory detailing intensity, correlations and line widths

05 p0667 A72-16017

Horizontally averaged nonthermal velocities determination in lower solar chromosphere, observing Doppler widths of weak rare earth emission lines in H and K wings

05 p0718 A72-16504

He-Ne laser amplitude fluctuations with hot and cold cathode discharge tube operation, determining emission spectral line width

05 p0669 A72-16613

Be stars emission line profile broadening due to surrounding gaseous ring in circular motion according to Kepler law

06 p0880 A72-17892

Temporal characteristics of emission line broadening in lasers with dispersive resonators for Nd ion activated phosphate glasses and disordered crystals

06 p0826 A72-18011

Flare spectra of AD Leo during strong burst, comparing Balmer discontinuity and line widths with UV Cet stars

06 p0883 A72-18020

Red shift and spectral line broadening model based on emitting and absorbing atom effects

06 p0883 A72-18023

Van der Waal broadening of shock excited emission lines at 5000 K for astrophysical applications

06 p0852 A72-18053

Gas laser emission fluctuations of total radiation energy, polarized field components and line widths in longitudinal magnetic field

07 p0999 A72-18911

Doppler broadening elimination in red Balmer line of atomic hydrogen at 6563 Å by high resolution saturation spectroscopy

07 p1037 A72-19132

Coupled mode locking equations solved for homogeneously broadened lasers modulated near axial mode separation frequency

07 p1001 A72-19192

Spontaneous emission from driven Doppler broadened gas of two level atoms radiating into free space, predicting power spectrum

07 p0940 A72-19194

High gain xenon laser spectral narrowing dependence on line-broadening mechanism including saturation and distributed loss effects

07 p1001 A72-19201

Energy transfer rates and spectral line inhomogeneity of narrow band oscillation phosphate glass and inorganic liquid lasers with Nd

07 p1004 A72-19227

Carbon dioxide IR absorption lines broadening at 298 and 207 K by evacuated high-resolution Czerny-Turner spectrograph, comparing with values based on fixed collision cross section

07 p1038 A72-19834

Single mode laser line width calculation by reduction to non-Hermitian eigenvalue problem using Fokker-Planck equation

07 p1008 A72-20440

Plasma If waves nonlinear spectral broadening in magnetic field based on degeneracy splitting

07 p1045 A72-20443

Laser induced line narrowing effects in coupled Doppler broadened transitions within standing wave field

07 p1039 A72-20682

Internal asynchronous modulation of multifrequency He-Ne laser with Doppler broadened transition line

08 p1181 A72-20793

Coalescence /collapse/ of overlapping spectral lines due to nonadiabatic broadening for Stark structure of hydrogen and helium lines in discharge plasma

08 p1211 A72-21717

Nd smooth pulsed laser action with narrow spectral line and emission amplification from Nd doped phosphate and silicate glass rods

08 p1183 A72-22027

Hydrogen line broadening in plasma theory with limitations of Stark component intensity distribution by quasi-static and impact approximations

09 p1358 A72-22493

Carbon monoxide in carbon dioxide atmosphere, determining IR absorption lines broadening at reduced temperatures

09 p1351 A72-22612

Pressure broadened atomic line shapes calculation for Cs resonance line pressurized by Ar, using Lennard-Jones potentials

09 p1354 A72-22663

Mossbauer lines diffusion broadening and weakening in crystals impurity atoms nuclear spectra

09 p1371 A72-23030

Defects high temperature diffusion effect on Mossbauer spectral lines width and positions in crystals

with quantum transfer between multiplet sublevels in fine structure

09 p1372 A72-23038

Laser pulse description by Fourier analysis, showing broadened spectral line widths relationship to cavity modes

09 p1324 A72-23078

Foreign gas collisional broadening of nitrous oxide absorption lines, obtaining optical collision cross sections

09 p1276 A72-23332

Xenon plasma produced in cascaded arcs, investigating spectral line widths, temperature and electron density profiles, transition probabilities and I-V characteristics

09 p1364 A72-23392

Methane absorption line profile, intensity and width studied with magnetically tuned He-Ne laser

10 p1490 A72-24041

Smooth variation of He-Ne laser spectral line width in single to multifrequency mode transition, passing laser beam through coated quartz plate

10 p1490 A72-24051

CO Cameron system band intensity from measurements of equivalent widths of resolved rotational lines, using Doppler growth curve for line strength conversion

10 p1514 A72-24095

Radio recombination lines broadening in hydrogen by electron collisions, using Baranger impact theory

10 p1435 A72-24142

Laser source spectroscopic determination of pure and nitrogen perturbed carbon dioxide transition lines half-widths

10 p1491 A72-24227

Transition probabilities and line shapes and widths of unimolecular problem computed using numerical methods for scattering processes

10 p1514 A72-24337

Optical hyperfine structure of Ne 21 excited states and quadrupole moment obtained by laser induced line narrowing techniques

10 p1515 A72-24601

Stellar absorption spectral line fineness indication for cold interstellar molecular clouds between observer and star

10 p1546 A72-24848

Stellar spectra differential analysis from solar curve of growth for Fe I with revised gf-scale, noting van der Waals broadening and microturbulence

10 p1547 A72-24868

Doppler spectral width of radar signal reflected from sea surface as function of illuminated region dimensions, waviness scale and emission factors

10 p1439 A72-24904

Paschen beta emission line equivalent width variation in IR spectra of omicron Ceti

11 p1716 A72-25679

Flare spectra of AD Leonis during strong burst, comparing Balmer discontinuity and line widths with UV Cet stars

11 p1718 A72-25956

Red shift and spectral line broadening model based on emitting and absorbing atom effects

11 p1718 A72-25959

Carbon dioxide laser cross relaxation effects on hole burning process in Doppler broadened gain or absorption line

11 p1647 A72-26146

Semiconductor injection laser with distributed radiative loss, calculating radiation line shape and width and quantum efficiency

11 p1648 A72-26329

He-Ne laser with absorption cell, investigating high contrast power resonances due to Lamb dip at nonuniformly broadened absorption line center

11 p1649 A72-26340

Two axial modes competition in He-Ne laser with uniform line broadening, noting application for high stability frequency standards

11 p1649 A72-26349

Populations modulation and spatial harmonics influence on gas and solid state laser radiation characteristics, discussing uniform and nonuniform line broadening

11 p1650 A72-26353

HD 4180 shell H lines width variations comparison with Be stars, noting thirty year period emission decrease followed by outer shell absorption

12 p1867 A72-27213

Gas and solid state lasers amplitude and phase fluctuations calculated from Langevin equations, noting spectral line width and collision waves

12 p1826 A72-28050

Single electron approximation of Stark broadening of hydrogen spectral lines without constraints of collision and quasi-static theories

13 p2007 A72-29429

Adiabatic characteristics of impact to quasi-static transition during electron induced Stark hydrogen line broadening in plasmas

13 p2016 A72-29516

- Inner corona spectral data of 7 March 1970 solar eclipse, noting line half widths and emission line origin area relationship 13 p2042 A72-29535
- Solar corona spectral line width and wavelength measurements during 7 March 1970 total eclipse, using Fabry-Perot photographic interferometer 13 p2043 A72-29548
- Interaction between generating lines in coupled channels with arbitrary line broadening, studying radiation generation regimes in cascade circuit 13 p1970 A72-29680
- Tunable wide field birefringent element /filter magnetograph/ to separate polarized magnetic signal from selected spectral line width 13 p2045 A72-29706
- Nitrous oxide band intensities, half widths and pressure broadening coefficients 13 p2008 A72-30059
- Phononless lines shift and broadening and electron phonon interaction in lanthanum trifluoride-Nd crystal, obtaining temperature dependence of non-radiative transition probability 14 p2142 A72-30359
- Methane collision broadened rotational fundamental line, calculating line width dependence on temperature 14 p2135 A72-30893
- HCl and HF in carbon dioxide atmosphere, determining line intensities, halfwidths and shapes at room temperature 14 p2135 A72-30894
- Fundamental and overlapping bands integrated intensities and nitrogen broadened half widths of rotational lines in nitrous oxide obtained from absorption measurements 14 p2135 A72-30895
- Ionized plasma line widths and intensities due to Landau and collisional damping, observing effects by light scattering techniques 14 p2140 A72-30901
- Noncoherent isotropic scattering in plane parallel finite layer, considering Doppler line broadening 15 p2273 A72-31331
- Spectrometer entrance slit diffraction effects on observed fast beam spectral line width 15 p2280 A72-31383
- Singly ionized Ca and Mg electron impact broadened resonance lines from rapid scanning Fabry-Perot spectrometer measurements in shock tube generated high temperature plasma 15 p2282 A72-32643
- Na-He atomic collisions induced D lines broadening, fine structure transitions cross sections and multipole polarization resonance levels relaxation 15 p2283 A72-32651
- Minimum values estimation of amplitude fluctuations dispersion and spectral line width for conventional and quartz crystal controlled oscillators 15 p2210 A72-32735
- Sodium D lines broadening and shift parameters under atomic H and He collisions effect, calculating low lying states interatomic potentials 15 p2317 A72-32772
- Spectral line width measurement accuracy based on digital autocorrelation of photon counting fluctuations, noting light field and photoelectric process limiting effects 16 p2357 A72-32949
- High gain laser amplifier spectral linewidth dependence on external signal or spontaneous emission source, noting saturation role and relevance to interstellar medium radiation 16 p2453 A72-33166
- Two axial modes competition in He-Ne laser with uniform line broadening, noting application for high stability frequency standards 16 p2402 A72-33702
- Populations modulation and spatial harmonics influence on gas and solid state laser radiation characteristics, discussing uniform and nonuniform line broadening 16 p2402 A72-33706
- Hydrogen line broadening in plasma theory with limitations of Stark component intensity distribution by quasi-static and impact approximations 17 p2588 A72-34657
- Papers on kinetic equations covering axiomatics, quantum and relativistics, plasma kinetic theory role in spectral line width, etc 17 p2590 A72-35151
- A first order analysis of variations of the limb darkening and the shapes for solar Fraunhofer lines. 17 p2616 A72-35694
- Space and time variations of the solar Na D line profiles. 17 p2616 A72-35697
- Improved Stark-profile calculations for the He II lines at 256, 304, 1085, 1216, 1640, 3203, and 4686 Å. 17 p2585 A72-35768
- Forbidden line intensities in cesium plasmas. 19 p2840 A72-37776
- Tabulation of physical conditions in proton and non-proton solar flares from observations and H alpha line width measurements 19 p2851 A72-37815
- Spectral line contours in the solar chromosphere, hydrogen line. IV - Contours in the chromosphere on the disk 19 p2859 A72-37905
- Early star absolute magnitude from equivalent H gamma and delta line widths and Balmer hydrogen series line 19 p2859 A72-37908
- Measurement of the equivalent widths of oxygen A-band absorption lines at different pressures 19 p2837 A72-37959
- Absorption line profile and equivalent line width derivation for planetary atmosphere with low and high optical thicknesses, assuming arbitrary scattering coefficients 19 p2863 A72-38071
- Measurements of the laser linewidth due to quantum phase and quantum amplitude noise above and below threshold. I. 19 p2811 A72-38084
- H and K emission intensity and line width dependence on stars age and luminosity, discussing dwarf stars and giants 19 p2866 A72-38503
- Investigation of the 0.63-micron line shift in an He-Ne/20/ laser with an absorbing cell 19 p2814 A72-38787
- Balloon-borne UV spectrophotometer observation of Mg II resonance doublet at 2795 and 2802 Å in stellar spectra, comparing to Ca II line widths 20 p2965 A72-38907
- Hot star with broad H lines with weak variable central emission, noting Ca II and He I 20 p2966 A72-38920
- Gas laser emission fluctuations of total radiation energy, polarized field components and line widths in longitudinal magnetic field 20 p2931 A72-39377
- Observation of quantum-phase and quantum-amplitude noise for a laser below and above threshold. 20 p2934 A72-39813
- Calculation of solar CO vibration-rotation line profiles and equivalent widths. 20 p2973 A72-39889
- Anomalous line broadening in the low temperature X-ray diffraction pattern of niobium. 20 p2942 A72-39989
- A unified analysis on laser Doppler velocimeters. 21 p3061 A72-40211
- Influence of polarization of laser fields on nonlinear interference effects 21 p3062 A72-40405
- Shapes and widths of ammonia lines collision-broadened by hydrogen. 21 p3013 A72-40817
- Speed-dependent collisional width and shift parameters in spectral profiles. 21 p3088 A72-40820
- Electron impact effects on Ba I, Ba II and Sr I selected spectral line Doppler widths calculated for laser-generated plasmas for chemical release simulation 21 p3092 A72-40821
- Spectrophotometry of the Wolf-Rayet type stars HD 195765, HD 192163, and HD 192103 21 p3109 A72-41437
- Kinetic theory of the lasing bandwidth in a spectrally inhomogeneous medium 21 p3064 A72-41695
- Behavior of carbon monoxide in the upper photosphere 21 p3114 A72-41777
- The solar abundance of calcium and collision broadening of Ca I- and Ca II-Fraunhofer lines by hydrogen. 22 p3221 A72-42027
- Broadening and shift of magnesium lines by van der Waals interaction with argon atoms and by microfields. 22 p3208 A72-42388
- Lyman alpha resonance line asymmetry calculation in dense hydrogen plasma, noting disagreement between theory and experiment 22 p3212 A72-42917
- Study of the Stark effect in the resonance lines of sodium by an atomic jet method 22 p3209 A72-43048
- Investigation of several nebulae in Cassiopeia with a Fabry-Perot interferometer. 23 p3333 A72-43233
- Spectral line identification computer program determining wavelength and equivalent line width for photometric measurements 23 p3267 A72-44029
- A new method of measuring temperature, inversion ratio, and pressure-broadened linewidth in a CW molecular laser. 23 p3297 A72-44188
- Light spectral width and constant frequency shift during spontaneous diffusion in ideal gas for fixed photon wave 23 p3315 A72-44479
- Laser-source spectroscopy. II - Experimental study of line broadening for the 00 1-1/10 0, 02 0/ transition of CO2 disturbed by N2: Application of the theory of Anderson, Tsao, and Curnutte to the calculation of pure and N2-disturbed CO2 linewidths 23 p3298 A72-44535
- A study of cold-worked titanium-aluminum alloys by X-ray diffraction. 24 p3413 A72-44720
- Rhodamine laser emission spectral band control by plane parallel plates and polarizing prisms, noting band widening by resonator loss modulation with Fabry-Perot interferometer 24 p3410 A72-45418
- Gain and line width in stimulated Brillouin scattering in gases. 24 p3412 A72-45616
- Critical-point anomalies in the electron-paramagnetic-resonance linewidth and in the zero-field relaxation time of antiferromagnets. 24 p3432 A72-45674
- Stellar spectra analysis from measured truncated equivalent spectral line widths, calculating curves of growth for given truncations, source functions and absorption coefficients 24 p3447 A72-45680
- SPECTRAL LINES**
U LINE SPECTRA
- SPECTRAL NOISE**
U WHITE NOISE
- SPECTRAL RECONNAISSANCE**
IR detector specifications, construction and applications to industry science and military 23 p3291 A72-44393
- Earth resources technology satellites /ERTS/ program requirements, considering coverage, spectral characteristics, system performance, photographic interpretation and information extraction 24 p3398 A72-45115
- SPECTRAL REFLECTANCE**
Grasslands mapping for ecosystem analysis, determining spectroradiance/reflectance characteristics by aerial and satellite-borne multispectral scanner imagery, aerial and ground photography and spectrometry 02 p0208 A72-11783
- Visible and near IR reflectance spectra of soil mineralized trees, using multispectral photographic filters 02 p0209 A72-11789
- Ponderosa pine foliage visible and near IR spectra, investigating soil copper contents effect on foliage spectral reflectance 02 p0209 A72-11790
- Natural formations optical spectral reflectance optimal coding with speedy digital computer processing advantage for remote sensing of earth surface 02 p0187 A72-11811
- Spectral texture effects on remotely sensed high altitude automatic IR image interpretation, using Bayesian probability techniques 02 p0228 A72-11873
- Bidirectional reflectance at several wavelengths from moonlit earth observations by airglow photometer on OGO-4 satellite 03 p0433 A72-13428
- Vacuum deposited films on CsI, AgCl, TiBr and TiCl for IR antireflection coatings on silicon [AD-734261] 03 p0380 A72-13431
- Spectral reflectance of various soils and vegetation, measuring solar energy reflection as function of sun elevation in UV, visible and near IR regions 06 p0810 A72-18446
- Spectral reflectance properties of lunar surface areas, discussing materials identification and maria depth determination 09 p1393 A72-23664
- Blackness degree calculation for semitransparent film on nontransparent substrate with layer temperature gradients, allowing for polarization emission and multiple reflections 14 p2130 A72-30296
- Vacuum UV reflectance dependence of Re and W vapor-deposited films on substrate temperature during deposition, film thickness and aging in air 15 p2274 A72-31377
- Multispectral angular reflectivity effect on optimum filter combinations for spaceborne multiband photography sensing mission in visible and near IR regions 16 p2395 A72-34104
- Spectral reflectance and emittance of Apollo 11 and 12 lunar material. 20 p2970 A72-39609
- Temperature effects on water refractive index from normal incidence IR spectral reflectance measurements 21 p3012 A72-40150
- SPECTRAL RESOLUTION**
Pohlman cell for ultrasonic hologram production, describing construction, resolution and real time reconstruction 02 p0225 A72-11751
- Far UV astronomical studies with moderate spectral and spatial resolution instruments, discussing Lyman alpha line background 03 p0417 A72-13049

High spectral resolution UV space astronomy spectrographs with echelle gratings

03 p0354 A72-13052

High spectral resolution balloon-borne spectrograph for near UV solar Mg II resonance lines

03 p0354 A72-13053

Kitt Peak 40 channel magnetograph using fiber optic probe for spectral and spatial resolution in weak photospheric field detection

03 p0356 A72-13282

Astronomical spectroscopy using ultravioletable resolution single Fabry-Perot interferometer in tandem with echelle Hilger monochromator

12 p1811 A72-27942

Spectral transmittance enhancement in Fabry-Perot narrow band light filter by wavelength shifted dielectric mirror technique

15 p2233 A72-31414

Computerized analysis of overlapping Raman and IR spectral lines, describing routine for resolving complex spectrum into component lines via operator intervention

16 p2366 A72-33027

IR heterodyne radiometer SNR and spectral resolution, noting application to solar physics and air pollution detection

17 p2555 A72-35196

Evaluation of the possibilities of IR diffraction spectrometers

19 p2801 A72-37965

High resolution Michelson interferometer for spectral investigations of lasers.

21 p3062 A72-40610

Fast Fourier transform algorithm for astronomical line spectra resolution enhancement, estimating central line intensity, line width parameter and line shape

24 p3438 A72-44841

SPECTRAL SIGNATURES

Crop classification by airborne multispectral observations, suggesting sample regions selection method for spectral signatures identification based on statistical similarities

11 p1628 A72-26985

Remote sensing system for oil pollution spectral signature properties, analyzing UV, IR, visible light, radar and microwave data

15 p2242 A72-32624

Gases and vapors spectral signatures application in correlation spectroscopy and interferometry for aerospace monitoring of earth resources and pollution

16 p2393 A72-33630

SPECTRAL THEORY

Spectral theory of Taylor vortices. I - Structure of unstable modes.

19 p2788 A72-38550

SPECTROGRAMS

Classification-dispersion spectrograms of early decline of Nova Serpentis 1970, discussing diffuse enhanced absorption system behavior

07 p1071 A72-19338

Zeeman patterns and energy level Lande g factors from spectrograms of As ion electrodeless discharge tubes in presence of 24,025 G magnetic field

07 p0987 A72-19832

Soyuz 9 spectrophotometry of earth surface features, comparing manned spacecraft-obtained and conventional spectrograms

14 p2100 A72-30464

Alpha Lyra and beta Cen spectrograms by Orion observatory onboard Salyut space station, noting veiled and overexposed photographic films

15 p2316 A72-32742

Photographic characteristics of high resolution film for Orion spaceborne astronomical observational spectrograms, discussing aerospace environment effect on sensitivity and physicochemical properties

15 p2243 A72-32745

Temporal properties of Ca II K line profile in solar disk nonmagnetic regions, noting time sequences of spectrograms and spectroheliograms

15 p2317 A72-32773

Characteristics of the Ca II K-line profiles in the quiet sun.

21 p3108 A72-41280

SPECTROGRAPHS

U SPECTROMETERS

SPECTROHELIOGRAPHS

Spacecraft-borne UV spectroheliograph with spherical mirror, considering moving part weight reduction

03 p0355 A72-13057

High resolution magnetographic and spectrographic observations of plage fields and photospheric effects in weakly active regions

03 p0429 A72-13308

Solar magnetic field measurement with 10,830 Å He I line photoelectric spectroheliograms, observing filamentary fine structure in active regions

03 p0429 A72-13310

Solar spectra photographic recording technique, using spectra-spectroheliography method with data reduction

03 p0429 A72-13313

Spectroheliogram movies of magnetic, velocity and intensity field in solar atmosphere, showing time resolution of line spectra

03 p0429 A72-13314

Zeeman spectroheliograms of photospheric magnetic fields in Ca I 6102.7 Å line

03 p0430 A72-13317

OSO-G satellite spectroheliograms of chromospheric, transition zone and coronal lines, indicating magnetic field spread with height

03 p0432 A72-13351

Intercomos 4 solar radiation equipment, including Lyman, optical and X ray photometers, spectroheliographs, polarimeters and optical orientation system

07 p0986 A72-19643

Extreme UV solar images televised in flight with rocket-borne SEC vidicon system, noting pictures reconstruction enhancement

12 p1810 A72-27930

OSO-6 Mg X spectroheliogram data for corona electron density map construction during 7 March 1970 solar eclipse period

13 p2031 A72-29529

Slit spectrogram and direct photograph observation of inner corona fine structure during 7 March 1970 solar eclipse, describing line and continuum intensities

13 p2042 A72-29533

Aerobee rocket far UV flash spectrum observations of chromosphere and corona during 7 March 1970 solar eclipse

13 p2042 A72-29539

Mg filterheliogram comparison with Ca spectroheliogram, noting correlation coefficient between location and intensity of bright features on sun

13 p2045 A72-29708

Comparative spectroheliograms of He 10830 Å and H alpha lines in chromosphere

13 p2047 A72-29733

Spectroheliograph study of fine structure of Evershed effect, determining radial velocity in penumbra along dark filaments and interfilamentary space

13 p2047 A72-29739

Solar transition zone and corona EUV lines formation heights measurement from OSO-4 spectroheliograms

13 p2050 A72-29939

Coronal condensation X ray sources from heliograms, discussing relation to active region evolution

14 p2146 A72-30204

Cycle 20 solar flare and sunspot distribution along heliographic longitude, using isoline analysis method

14 p2152 A72-30482

Solar instruments and methods for photosphere magnetic field measurement, noting spectroheliographic mapping in violet spectral region

15 p2306 A72-31647

Temporal properties of Ca II K line profile in solar disk nonmagnetic regions, noting time sequences of spectrograms and spectroheliograms

15 p2317 A72-32773

Microwave spectrograph with broadband superheterodyne total-power radiometer for time-shared recording solar burst dynamic spectra

17 p2552 A72-34191

On the dependence of the linear velocity of solar rotation on latitude and optical depth.

17 p2607 A72-35076

A compact grating spectroheliograph for the MgII resonance lines.

17 p2554 A72-35079

EUV observations of solar quiet region with OSO 6 spectroheliometer, noting chromospheric network structure

17 p2616 A72-35703

A new project of 8-cm radioheliograph.

18 p2691 A72-36434

Initial phase in the development of activity centers in the photosphere

19 p2860 A72-37951

Solar magnetic fields derived from hydrogen alpha filtergrams.

20 p2969 A72-39338

Multiple-frequency operation of the Culgoora radioheliograph.

21 p3053 A72-40397

He-D3 spectroheliogram absorption features correlation with magnetic field regions and H alpha structures

21 p3108 A72-41279

Characteristics of the Ca II K-line profiles in the quiet sun.

21 p3108 A72-41280

Measurement of the electron temperature of small 3-cm radio bursts /Research note/.

21 p3100 A72-41291

Coronal condensation X ray sources from heliograms, discussing relation to active region evolution

23 p3328 A72-43234

SPECTROHELIOSCOPES

U SPECTROHELIOGRAPHS

SPECTROMETERS

NT EBERT SPECTROMETERS

NT FABRY-PEROT SPECTROMETERS

NT INFRARED SPECTROMETERS

NT MASS SPECTROMETERS

NT NEUTRON SPECTROMETERS

NT SOLAR SPECTROMETERS

NT SPECTROHELIOGRAPHS

NT TIME OF FLIGHT SPECTROMETERS

NT ULTRAVIOLET SPECTROMETERS

Apollo 12 liquid oxygen cloud spectrum observations, describing spectrograph with off axis zone plate for transmission grating and sieve plate collimator

01 p0071 A72-11172

Microwave spectrometer remote sensing of atmospheric temperature and water vapor, discussing cloud, topography and sea state effects and multiple regression statistical method

02 p0228 A72-11859

Stilbene scintillator detector for gamma ray spectrometry in energy range 0.5-5 MeV, separating gamma rays from neutrons by pulse shape discrimination technique

03 p0408 A72-13031

X ray astronomy techniques survey, covering image forming telescopes, detectors, nondispersive spectrometers and polarimeters

03 p0353 A72-13037

Bragg crystal spectrometer for Sco X-1 spectrum scanning, using Aerobee 170 rocket

[AD-736552] 03 p0353 A72-13039

Pressure scanning Fabry-Perot magnetometer using KDP crystal and Glan-Thompson prism with echelle interferometer spectrograph for polarized Zeeman components

03 p0356 A72-13283

Jones matrix representation of optical instruments applied to Fourier interferometers /spectrometers and spectropolarimeters/

03 p0358 A72-13434

Doubly multiplexing dispersive spectrometer, noting high SNR and Littrow mode operation

03 p0359 A72-13446

Apparatus for emission spectroscopic studies on high density molecular jets excited by slow electron bombardment

03 p0392 A72-14054

Aberration correction in collimator of Schmidt spectrograph camera by changing surface geometry and grating positioning

03 p0362 A72-14358

Airborne gamma ray spectrometer investigation circle, considering altitude, air density, source density and gamma ray attenuation coefficient effects

04 p0520 A72-14564

Fluorescence polarization and intensities of nitric oxide vibrational bands from Cd line and continuum excitation for spectrometer calibration

04 p0552 A72-14891

Autocorrelation signal detection method application to spectrometry by modulation amplitude, investigating SNR

04 p0521 A72-14972

Apollo 14 charged particle lunar environment experiment, describing ALSEP particle spectrometer

04 p0508 A72-15097

Ion transit time in ion cyclotron resonance spectrometer, using combination of pulsed ion formation and time dependent trapping conditions

04 p0523 A72-15484

High resolution electrons image intensifier for particle spectrographs, using channel plate, scintillator and fiber optics

04 p0524 A72-15536

Microwave spectrometer crystal current leveler for broadband video detector and rotary wave attenuator control

04 p0524 A72-15541

Fiber optics system for H beta line shape measurement in transient high temperature plasma, using narrow slits at spectrograph exit plane

[AIAA PAPER 72-106] 05 p0663 A72-16816

Spectrometers for phase audible frequencies, discussing linearization theory and application to spectrum analyzer calculation

07 p0983 A72-19186

Sound velocity and attenuation variations with magnetic field from ultrasonic continuous wave spectrometry

07 p0984 A72-19321

Multichannel modular spectrometer with electrostatic analyzers for low energy electron and proton flux measurement

07 p0988 A72-19954

Spectrometers with electrostatic analyzers alternating with shielding and suppressing gratings for low energy electron flux measurement

07 p0988 A72-19955

High resolution multiple particle spectrometer for measuring energetic protons, electrons and alpha particles during solar particle events

08 p1167 A72-21509

Gamma ray spectrometer with antiCompton shield for OSO-7 spacecraft

08 p1167 A72-21515

Optimal pulse height analyzer with quadratic transfer function for gamma ray spectrometer on OSO-H

08 p1167 A72-21516

- IR spectral emittance measurement with airborne spectrometer for geological mapping over Pisgah Crater /California/ 08 p1162 A72-22017
- Spectroscope model design using ruby laser highly monochromatic light pulses, electro-optical scanning and high speed photography to study atmospheric gases absorption spectra 09 p1322 A72-22205
- Cumulus cloud microstructure measurement by single particle optical spectrometer, inferring transition from water to ice phase regions from droplet size and number distributions 09 p1307 A72-22444
- High energy cosmic ray hadrons energy measurement using glass scintillator ionization spectrometer 09 p1309 A72-22523
- Spectrometric oil analysis program /SOAP/ method for turbid and helicopter transmissions damage monitoring and flight safety 09 p1319 A72-22933
- Field compensated Michelson spectrometer systems, discussing tolerances, usefulness, resolution luminosity products, stigmatism and astigmatism 09 p1313 A72-23328
- Double beam single detector wavelength modulation spectrometer for background elimination from observed spectra, noting application to semiconductors band structure determination 09 p1315 A72-23402
- High resolution NMR spectrometer conversion from continuous wave to Fourier transform operation, permitting computer systems and pulse amplifiers use 09 p1316 A72-23408
- Continuous scan diffraction spectrometer for thermal sounding experiment on Meteor satellite, presenting vertical temperature and humidity profiles 09 p1347 A72-23588
- Optical properties of nuclei of normal, Seyfert and N-type galaxies and quasars from spectrographic and photometric observations 10 p1534 A72-23902
- Martian atmosphere water vapor detection and mapping during Viking missions, discussing experimental approach and spectrometer choice 10 p1539 A72-24378
- Interferometric photoelectric scans of interstellar Ca K lines in stellar spectra, noting interstellar Na lines presence 10 p1544 A72-24663
- Image intensifier tube scanner replacement of slit and multiplier tube of spectrograph, discussing application to rockets 11 p1631 A72-25689
- Automated echelle spectrograph data handling using computer control 11 p1716 A72-25693
- Penetrating particles effect on low energy scintillation spectrometers sensitivity in various regions of magnetosphere 11 p1632 A72-25934
- He-like lines in solar X-ray spectrum observed by Bragg crystal spectrometer, noting absolute wavelengths determination with shaft encoder for angle readout 11 p1714 A72-26572
- Antimatter search in primary cosmic rays by balloon-borne superconducting magnetic spectrometer capable of direct matter-antimatter separation 12 p1863 A72-27296
- Satellite-borne low energy electron and proton spectrometer for measuring auroral electron and proton spectra 13 p1960 A72-29841
- Low energy particles spectrometer channels calibration for satellite auroral observation, discussing photomultiplier detector properties 13 p1960 A72-29843
- Relative cross sections for gas phase photodetachment of electrons from amide and arsenide ions using ion cyclotron resonance spectrometer 13 p1914 A72-30064
- Photon correlation spectrometer for laboratory wind tunnel measurement of laser Doppler signals backscattered from dust particles 14 p2111 A72-30854
- Spectrometer entrance slit diffraction effects on observed fast beam spectral line width 15 p2280 A72-31383
- Soft X ray appearance potential spectrometer construction and operation for metal film diffusion detection in microcircuit technology 15 p2241 A72-32442
- Construction and optical equipment of astrophysical observatory Orion onboard Salyut space station, discussing mirror telescope, spectrograph and star tracker 15 p2242 A72-32741
- Spectrograph for Orion spaceborne astronomical observatory on Salyut space station calibrated with synchrotron radiation from particle accelerator 15 p2242 A72-32744
- Construction, tuning and characteristics of high resolution spectrometers with scanning interferometers for He-Ne laser radiation analysis 16 p2400 A72-33080
- Comet Tago-Sato-Kosaka /1969g/ L alpha emission image recorded by f/2 objective-grating spectrograph aboard Aerobee rocket, discussing ice sublimation in nucleus 16 p2455 A72-33466
- Computer simulation of airborne gamma ray spectrometer with prescribed photopeak windows from flight over surfaces with arbitrary-dimension radiation sources 16 p2392 A72-33617
- Spectral measurements of atomic level populations in a plasma 17 p2591 A72-35307
- Photon count circuit conjugation with photomultiplier for spectrometric measurement of lines emitted by atomic barium jet excited by slow electron beam 19 p2799 A72-37671
- Low-temperature part of a spectrometer for gigahertz-ultrasonics and ultrasonic paramagnetic resonance. 21 p3051 A72-40215
- Investigation of the structural content and the determination of the optimal image of focus series in light and electron microscopy with the aid of Fraunhofer diffraction /structure spectroscopy/ 21 p3055 A72-40747
- A simple, low power, multiple pulse NMR spectrometer. 21 p3056 A72-41005
- Astrospectrography with a mirror telescope. II - One-prism spectrograph with 60 deg flint prism 22 p3178 A72-42545
- Spectrometer for absolute stellar spectroscopy 23 p3290 A72-44039
- SPECTROMETRY**
U SPECTROMETERS
SPECTROPHOTOGRAPHY
Spectrophotographic recording of UV auroral emissions during rocket probe flight, noting excitation by electron impact on molecular nitrogen 08 p1159 A72-21225
- K-2 astrophysical rocket observatory for far UV and X ray solar radiation recording, discussing trajectory, orientation and stabilization, electric and spectrographic instrumentation 14 p2163 A72-30970
- Apollo 16 far-ultraviolet camera/spectrograph - Earth observations. 21 p3105 A72-40600
- Spectrographic, photometric and chemical identification of Giacobinid /Draconid/ meteoroids, noting compositional similarity to carbonaceous and olivine-bronzite chondrites 23 p3336 A72-43600
- SPECTROPHOTOMETERS**
NT INFRARED SPECTROPHOTOMETERS
NT ULTRAVIOLET SPECTROPHOTOMETERS
Spectrophotometer and tristimulus mask calorimeter using double grating mirror dispersion system 03 p0358 A72-13427
- Laboratory spectrophotometer calibration for specular light over 0.5-2.5 micron range by means of stacked glass plates, noting accuracy 04 p0524 A72-15535
- Solar Fraunhofer line profiles determination by digital data recording double-pass spectrophotometer, presenting observed atomic Ni and Fe lines intensity distributions 06 p0884 A72-18028
- Time range extension methods for rapid readout dual wavelength spectrophotometers 07 p0983 A72-19319
- Optical bidirectional modulator for two beam spectrophotometer, using tuning fork as oscillatory system 07 p0988 A72-19962
- Double beam spectrophotometer with automatic gain controlled preamplifier to achieve insensitivity to signal strength change in noise at low cost 07 p0992 A72-20579
- Total ozone measurements by selective transmission filter ozonometer comparable to Dobson spectrophotometer 09 p1307 A72-22453
- Solar Fraunhofer line profiles determination by digital data recording double-pass spectrophotometer, presenting observed atomic Ni and Fe lines intensity distributions 11 p1719 A72-25964
- Spherical mirror camera for southern galaxy planar photometry, discussing photographic calibration methods 15 p2306 A72-31597
- Balloon-nacelle for small scale photography and multispectral photometric ground measurements, describing automatic adjustment device for photographic lens diaphragm 16 p2349 A72-33633
- Spectrophotometers and photometers calibration and standardization, emphasizing necessity for periodic control of instrument parameters 16 p2394 A72-33872
- Modified Dobson ozone spectrophotometer with revised electronic design circuitry, considering high voltage power supply, photomultiplier tube circuit, amplifier and electromechanical phase sensitive rectifier 20 p2921 A72-38968
- A multislot shadow sensor of direction to a luminous object 21 p3052 A72-40308
- Pulsed photoexcitation /flash photolysis/ spectrophotometers in terms of light sources, recording sensitivity enhancement, data processing, laser use and performance requirements 21 p3058 A72-41726
- Spectrophotometer linearity testing using the double-aperture method. 23 p3289 A72-43894
- SPECTROPHOTOMETRY**
NT STELLAR SPECTROPHOTOMETRY
Natural formation interpretation from spectrophotometric measurements of underlying earth surface from manned spacecraft Soyuz 7 and Soyuz 9 02 p0228 A72-11887
- Mars carbon dioxide distribution map determination of surface topography from spectrophotometric observations of equatorial region 04 p0569 A72-14499
- Photoelectric spectrophotometric measurements of Jupiter atmosphere optical properties and structure, showing methane absorption band intensity latitudinal variations 06 p0881 A72-17928
- Camera tube used in Faust program of spatial and astronomical UV photometry and spectrophotometry 08 p1169 A72-21953
- Auroral spectrophotometric measurements in /S-1/ region and of O I line /5577/, discussing digital recording and computer averaging techniques 10 p1474 A72-24745
- Spectrophotometric measurements of sky radiance distribution to determine atmospheric pollution, ozone content and radiation attenuation by clouds 10 p1476 A72-25085
- Heatable chamber burners design to increase sensitivity of flame spectrophotometry, separating solvent from aerosols 13 p1958 A72-29525
- Spectrophotometry of inner corona and quiescent prominence during 7 March 1970 solar eclipse, discussing Balmer line analysis 13 p2042 A72-29536
- Soyuz 9 spectrophotometry of earth surface features, comparing manned spacecraft-obtained and conventional spectrographs 14 p2100 A72-30464
- Mars topography variations from earth based surface height radar ranging and Mariner spectrophotometric observation of Mars atmosphere 15 p2313 A72-32346
- Mars surface mapping from spectrophotometric studies of surface materials photometric function, composition and distribution, suggesting color due to limonite-stained soil particles 16 p2457 A72-33616
- Slope-gradient diagram of galaxies and quasars 17 p2607 A72-34919
- Photoelectric spectrophotometric measurements of Jupiter atmosphere optical properties and structure, showing methane absorption band intensity latitudinal variations 18 p2730 A72-37153
- Emission lines and optical continuum of Seyfert radio galaxy 3C 120 from spectrophotometric scans 20 p2965 A72-38905
- Tilting-filter measurements in dayglow rocket photometry. 23 p3289 A72-43893
- A differential spectrophotometric extraction method of determining yttrium-subgroup rare-earth elements /REE/ in complex objects 23 p3324 A72-44164
- Spectrophotometry of the comet Tago-Sato-Kosaka 1969 IX 23 p3339 A72-44168
- Coronal lines photometry systematic error dependence on aureola spectral intensity, line half width, gradation curve slope, and neutral filter transmission coefficient 23 p3340 A72-44240
- SPECTRORADIOMETERS**
Stabilized hydrogen plasma arc spectral radiation as light source for vacuum UV radiometry, comparing output with W strip and carbon sources 01 p0073 A72-11400
- Extended wavelength field spectroradiometry for multispectral scanner data interpretation in airborne observations 02 p0228 A72-11853
- Automated scanning spectroradiometer for color vision test stimuli and luminescence measurements, applying computer analysis of spectral data 12 p1811 A72-27944
- Apollo 9, Skylab and Earth Resources Technology Satellite-borne multiband cameras performance

requirements and tolerances comparison, considering geometric and spectroradiometric properties

16 p2395 A72-34103

The techniques of present-day radioastronomy,

24 p3439 A72-44946

SPECTROSCOPES

U SPECTROMETERS

SPECTROSCOPIC ANALYSIS

Hydrogen iodide flash photolysis in presence of nitrous oxide, carbon dioxide and water investigated by kinetic spectroscopy, observing imidogen as intermediate reaction product

01 p0023 A72-11114

Far IR Fourier spectrometer with built-in real time digital computer for routine physical and chemical spectroscopy

04 p0520 A72-14523

Self absorption and temperature gradient effects on fluorine-hydrogen flame spectroscopic temperature determination, comparing calculated and theoretical Lorentz intensity profile

04 p0596 A72-14890

German monograph on spectroscopic investigation of Cs plasma electron density and temperature and excited atom density in various operational states of thermionic converter

04 p0560 A72-15699

Spectrographic measurement of electron temperature and ion density profiles in cesium plasma thermionic converter

06 p0862 A72-18309

Artificial intelligence applications for chemical inference, discussing modified heuristic DENDRAL computer program for cyclic structure and linear molecule identification

07 p0936 A72-19498

Two channel high resolution spectrometric measurements of plasma velocity from intrinsic radiation in optical range by Doppler effect

07 p1044 A72-19885

Shock tube spectroscopy role in laboratory astrophysics, stressing hook method effectiveness for quantitative analysis of shock heated gases in solar abundances determination

08 p1146 A72-21017

X ray emission spectroscopy of electronic structure of transition metals and alloys, obtaining electron energy spectrum

09 p1370 A72-22841

Electron spectroscopy for chemical analysis /ESCA/ application to band structure measurements in transition metals, discussing photoexcitation, energy loss and escape depth

09 p1371 A72-22843

Standard deviation in ghost lines size due to random sampling position errors of monochromatic spectral line in Fourier transform spectroscopy

09 p1314 A72-23344

Spectroscopic techniques for high temperature materials research program, studying light emission from plasmas generated by intense electron beam

10 p1518 A72-23937

Turbojet engine oil circuit contamination rate determination by spectrometric analysis, obtaining mathematical theory for data interpretation

[SAE PAPER 720303]

11 p1703 A72-25567

Spectral analysis for Cu, Cl, Br and I impurity distribution in doped bismuth telluride crystals prepared by Bridgman method

13 p2023 A72-29979

Atomic spectroscopy role in modern physics, discussing 1913 genesis, golden age in 1930s and revival in 1960s

14 p2133 A72-30577

Spectroscopic binary orbital elements calculated by FORTRAN IV computer programs, considering period, radial velocity Fourier coefficients and element improvement by least squares method

14 p2159 A72-30736

Pulsed Ar plasma temperature and charged particle concentration obtained as functions of elapsed discharge time by spectroscopic observation

14 p2139 A72-30780

Pavel stony meteorite microspectral analysis to obtain metallic elements weight percentages in chondrules, matrix and core, using laser source for local vaporization and excitation

14 p2159 A72-30785

Hemoglobin determination in whole blood with Specol-Zeiss spectrophotometry, comparing accuracy to cyanmethemoglobin measurements

14 p2080 A72-30787

Atmospheric air pollution study by space techniques via thermal radiation spectral measurements and laser sounding, considering spaceborne photography

15 p2220 A72-31237

Low energy electron spectroscopy measurement of thin oxide layer growth on Al surface, noting oxidation uniformity dependence on residual gas water content

15 p2276 A72-31859

Chondrite Pavel microspectral analysis with laser beam vaporization of sample from microzone

16 p2450 A72-32850

Spectroscopic sounding of clouds and snow and ice covers from below /earth surface/ and above /space or planet/

16 p2417 A72-33288

Electron spectroscopy for chemical analysis /ESCA/ technique for nondestructive elemental analysis of lunar and terrestrial minerals

16 p2454 A72-33447

Two channel high resolution spectrometric measurements of plasma velocity from intrinsic radiation in optical range by Doppler effect

17 p2590 A72-35133

Solid surface geometry, atomic composition and electronic structure observations, discussing Auger spectroscopy, field ion microscopy and electron diffraction and scattering techniques

19 p2803 A72-38389

Heat-pipe plasma oven for microwave and spectroscopic measurements.

20 p2912 A72-39433

Electron spectroscopic investigation of solid surfaces chemical composition and atomic binding states and structure, discussing methods of inducing electron emission

20 p2927 A72-39695

Comparative studies of various spectral lamp designs for atom-absorption analyses and use of double-discharge multielement lamps to account for non-selective interference

22 p3176 A72-42170

Sensitivity enhancement of atom absorption measurements by the method of pulse vaporization from the microprobe into the flame

22 p3176 A72-42174

Usability of a graphite dish for atom absorption analyses of laser collected samples

22 p3176 A72-42175

Spectroscopic study of the parameters of a turbulent plasma

22 p3213 A72-43107

Standard Ti bars samples for spectral determination of H concentration and distribution in Ti alloys, using mathematical statistical method

23 p3287 A72-43676

The presence of P700 in chloroplast fragments prepared by short time incubation with Triton X-100.

23 p3258 A72-44325

SPECTROSCOPIC TELESCOPES

NT STRATOSCOPE TELESCOPES

Red interference filter design for high performance prominence telescope for H alpha line observation

01 p0064 A72-10203

Telescopic phase retardation effect on Zeeman triplet Fe of polar sunspot umbrae in Stokes parameter measurements

03 p0357 A72-13288

Computer controlled coude and Cassegrain scanner telescope spectrometers at McDonald Observatory, discussing design, instrument performance and computer program

11 p1632 A72-25698

Orbiting telescopes improved angular resolution and access to UV spectra as advantages in determining stellar composition, mass, luminosity and distance

24 p3446 A72-45531

SPECTROSCOPY

NT ABSORPTION SPECTROSCOPY

NT ASTRONOMICAL SPECTROSCOPY

NT AUROREAL SPECTROSCOPY

NT GAS SPECTROSCOPY

NT INFRARED SPECTROSCOPY

NT MAGNETIC SPECTROSCOPY

NT MASS SPECTROSCOPY

NT MOLECULAR SPECTROSCOPY

NT NUCLEAR RADIATION SPECTROSCOPY

NT OPTICAL EMISSION SPECTROSCOPY

NT RADIO SPECTROSCOPY

NT RAMAN SPECTROSCOPY

NT SPECTROPHOTOGRAPHY

NT SPECTROPHOTOMETRY

NT SPECTROSCOPIC ANALYSIS

NT STELLAR SPECTROPHOTOMETRY

NT ULTRAVIOLET SPECTROSCOPY

NT VACUUM SPECTROSCOPY

NT X RAY SPECTROSCOPY

Electron scattering off atoms, diatomic and polyatomic molecules in impact spectroscopy, applying simple group theory

02 p0262 A72-11913

Miniature vacuum furnace for Mossbauer spectroscopic samples heating to 1000 C, discussing temperature control, use of inert atmospheres, etc

04 p0523 A72-15481

Statistical analysis of spectrographic plasma temperature measurements, obtaining numerical solution to Abel integral equation

12 p1852 A72-27685

Spectroscopy by synthesis of two or more fixed or moving diffraction gratings, obtaining transfer functions for total information increase

12 p1811 A72-27943

High speed frame photography application in spectroscopic studies of plasma jet in cylindrical pulsed accelerator with dielectric

15 p2283 A72-31418

Electron transmission spectroscopy - Core-excited resonances in diatomic molecules.

17 p2586 A72-35771

SPECTRUM ANALYSIS

Radiation spectral properties in mode locking region of He-Ne 20 laser at 0.63 microns, generating three axial modes

01 p0078 A72-10154

Electrostatic potential fluctuations spectrum in turbulent hot ion plasma confined between magnetic mirrors, investigating mode coupling, energy cascading and electron concentration

01 p0108 A72-10242

Multichannel hf spectrograph for decimeter wave solar burst spectrum fine structure analysis, noting operation at any desired frequency and channel separation

01 p0065 A72-10416

Error fluctuation component spectral density determination in closed automatic nonlinear system for controlling random vibration spectrum

01 p0045 A72-10505

Gas filter correlation spectral analysis technique for measuring pollutant concentrations in presence of interfering gases, describing application to hydrochloric and hydrofluoric acids monitoring

[AIAA PAPER 71-1049]

01 p0066 A72-10525

Magnetic field effects on ruby laser radiation kinetics and spectral composition, studying crystal heating and light emission

01 p0080 A72-10577

Spectral analyses of Mira-type variable stars near light maximum, discussing empirical curve of growth, Doppler velocity, damping constant and electron pressures

01 p0129 A72-10792

Flare region curved absorption lines interpreted as photospheric and chromospheric mass motions

01 p0129 A72-10800

Cygnus X-6 soft X ray source location, presenting polycarbonate pulse-height spectrum and counter response to different model source energy spectra

01 p0121 A72-11096

Apollo 12 liquid oxygen cloud spectrum observations, describing spectrograph with off axis zone plate for transmission grating and sieve plate collimator

01 p0071 A72-11172

Statistical long term speech spectrum analysis and perceptual evaluation, using digital bandpass filter technique

02 p0171 A72-11660

Compact extragalactic radio source spectrum analysis, discussing successive uncorrelated outburst models

02 p0277 A72-11774

Sedimentary rocks remote multispectral analysis by aerial data covering UV to microwave spectral regions

02 p0209 A72-11783

Spectrum analysis of synchronous recordings of Pi irregular pulsations and auroral brightness at Sogra fo ionospheric electric fields

02 p0216 A72-11924

Spectral characteristics of ionospheric signal wave phase lags introduced in multichannel field recorder

02 p0172 A72-11926

Mountaintop high resolution spectral observations of diffuse isotropic submillimeter atmospheric and sky emission

02 p0274 A72-12194

Grating spectra of Jupiter North Equatorial Belt, noting absorption feature at 4.73 microns

02 p0280 A72-12200

Noisy radar signal processing by spectral analysis method

02 p0177 A72-12222

Ionospheric small scale electron density irregularity structure from power spectral analysis of radio source scintillation observations

03 p0345 A72-12985

Celestial gamma rays arrival direction and energy spectra measurement and spectrum analysis using ESO satellite COS-B data

03 p0408 A72-13029

High energy solar and celestial X ray experiment with OSO 5, measuring spectrum as function of time intensity and spatial distribution

03 p0353 A72-13044

Scanning Fabry-Perot interferometer for He-Ne laser spectral composition, discussing transmission coefficient, resolution, resonator dissipative losses, active medium saturation and light field spatial nonuniformity

03 p0356 A72-13190

Magellanic Clouds supergiant stars intrinsic colors: observing in five spectral bands to separate from Galactic foreground stars

03 p0425 A72-13260

Sunspot magnetic field evolution in time and space from four-camera spectral scanning method, obtaining magnetic flux and radial velocity field

03 p0428 A72-13301

Spectroscopic characteristics of continuous wave neutral argon laser using helium and chlorine wave power enhancement

03 p0367 A72-13432

- Mean value, repetition and discontinuity errors of spectral transposition method involving memory storage and compressed signal processing
03 p0338 A72-13892
- Photopic spectral curves of relative luminous efficiency for congenital deficiencies of color vision, using optical bench, interference filters and Bachstein flicker photometer
03 p0316 A72-13935
- Meteor spectrum analysis, presenting tables for Soviet observations
03 p0438 A72-13979
- Planetary nebula IC 418 reddening constant from Paschen line intensities of IR spectrum
04 p0570 A72-14554
- Curve of line width correlation application to alpha Orionis OH lines, determining atmospheric turbulence and thermal velocities
04 p0571 A72-14558
- Materials spectral emission properties measurement, comparing with absolute black body model
04 p0596 A72-14652
- Spectral line data on terminal flare and wake of double-station meteor 38421
04 p0574 A72-14922
- Interstellar propagation of 2-8 Z galactic cosmic ray nuclei at 10-1000 MeV/nucleon, analyzing differential kinetic energy spectra
04 p0567 A72-15323
- White dwarf Grw plus 70 deg 8247 circular polarization spectral structure with molecular absorption bands coincident with Minkowski bands
04 p0580 A72-15368
- Gas cloud motions in Seyfert galaxy NGC 7469 center from image tube spectra, discussing size, mass and radial velocities
04 p0580 A72-15370
- NGC 5128 X ray spectrum from sounding rocket and balloon observations, presenting inverse Compton models
04 p0568 A72-15372
- High frequency diffraction problems, using matrix formulation in spectral domain
04 p0489 A72-15396
- Electromagnetic wave propagation in plane and spherical waveguide channels with conducting lower wall, investigating transverse wave spectrum dependence on curvature and boundary conditions
04 p0492 A72-15441
- Lf spectrum analysis instrumentation, describing stored data signals Fourier series parameters analog computation techniques
04 p0523 A72-15487
- On-line digital spectrum analysis based on fast Fourier transform algorithm, exemplifying by plasma density fluctuations correlation
04 p0496 A72-15488
- Airglow considered as faint light emission during atomic and molecular dissociations in atmosphere, yielding clues to physical and chemical processes from spectrum
04 p0520 A72-15642
- Digital data reduction techniques for stellar spectrograms, discussing digital noise smoothing for SNR improvement
05 p0632 A72-15762
- Artificial barium oxide clouds band spectrum analysis, calculating rotational and vibrational temperatures in total wavelength region
05 p0655 A72-16069
- Radio absorption spectra sounding for planetary atmospheric impurities calculating water vapor content in Venus cloud level
05 p0715 A72-16169
- Optical spectra of compact objects, reviewing emission line spectra of quasars
05 p0716 A72-16372
- Spectral analysis with sinusoids and Walsh functions, using Rademacher function
05 p0628 A72-16564
- Computational model of post mixer spectra of periodic FM altimeters with area target returns, using radar scattering coefficient
05 p0637 A72-16568
- Digital computer investigation of radio signals transmitted by Vener 7 during Venus soft landing, describing spectral analysis and telemetric data detection methods
05 p0630 A72-16770
- Solid propellant flame spectral and temporal details during unstable and stable combustion, using middle infrared spectrometer
05 p0703 A72-16896
- Low deviation FM wave spectral density estimation as infinite series by low pass Gaussian random process
06 p0772 A72-17407
- Acquisition and processing of plasma fluctuation data using fast Fourier transform analog-digital spectral analysis technique
06 p0859 A72-17548
- Variance spectral techniques in detecting wave modes of synoptic scale tropospheric wind in midlatitudes and tropics
06 p0841 A72-17634
- Radio galaxy spectra determination from measurements over various frequencies, noting correlation with physical parameters
06 p0879 A72-17859
- Argon ion spectra overlap with satellites to carbon and boron Lyman alpha lines, employing theta pinch
06 p0852 A72-17897
- Extragalactic radio sources, discussing galactic radiation, quasars, nonthermal emissions, energy dissipation and spectrum analysis
06 p0886 A72-18172
- Hybrid computer method of nonstationary spectrum analysis of aircraft noise, applying to flyover and jet aircraft noise abatement under operational conditions
07 p0911 A72-18778
- Spectral analysis of light reflected from Nd laser produced deuterium plasma, observing Doppler shift
07 p1039 A72-18888
- Spectral composition of emitted radiation, emissivity and absorptivity of Venus atmosphere at high temperatures
07 p1068 A72-18933
- Radially conducting cone wave spectrum calculation for noncoplanar excitation, noting circularly polarized TEM and elliptically polarized TM wave amplitudes
07 p0938 A72-19003
- Midlatitude geomagnetic micropulsations polarization and spectral characteristics, explaining behavior in terms of MHD wave propagation theories
07 p0975 A72-19152
- Spectral intensity measurements of noctiluculent clouds with scanning spectrophotometer
07 p0975 A72-19155
- F and G dwarf stars synthetic spectra and colors computation from chemical abundance, Doppler broadening velocity and damping constant
07 p1071 A72-19181
- Spectrometers for phase audible frequencies, discussing linearization theory and application to spectrum analyzer calculation
07 p0983 A72-19186
- Superconducting magnetic spectrometer for cosmic ray nuclei spectrum analysis, describing design, calibration and operation
07 p0983 A72-19315
- Solar Fe I oscillator strengths determination by hook method on shock heated gases
07 p1037 A72-19349
- X ray spectrum analysis of Sco XR-1 sources, showing plasma sheath with high electron temperature
07 p1076 A72-19804
- Circular jets sound generation analysis, using Lighthill equation and Michalke spectral method [DFVLR-SONDDR-179]
07 p0910 A72-20100
- Ultrapur metals microimpurities determination from crystal lattice and atomic properties, comparing spectral analysis activation, mass spectrometric, thermophysical, recrystallization and kinetic methods
07 p1049 A72-20149
- Computer simulation of empirical confidence limits for variance spectra, applying to Gaussian random noise data stochastic model
07 p0951 A72-20360
- Carbon determination in Cr-Ni steels and Ni alloys by layerwise spectral analysis, using electrode gap with He
07 p0993 A72-20609
- Venus clouds composition from spectral and polarization data, considering hydrochloric acid particles model
08 p1230 A72-20980
- Spectral density estimates for discrete time models of steady nonGaussian random processes, noting dispersion in asymptotic expression
08 p1198 A72-20996
- Spectral characteristics of continuous radio emission of extragalactic binary objects, discussing model of binary radio source formation from dipole nucleus
08 p1231 A72-21118
- Semiregular variable CH Cygni observations from 1967 to 1969 with continuous spectrum variations comparison to monochromatic brightness changes
08 p1233 A72-21278
- Spectral response and vision thresholds of human eye for light detection and color sensation
08 p1125 A72-21332
- Single band optical mixer heterodyne spectrum analyzer for laser radiation image spectrum suppression
08 p1182 A72-21375
- Radio meteor observations of upper atmosphere long period wind variations, determining oscillation spectra peaks by harmonic analysis
08 p1161 A72-21537
- Spectrum shape of Doppler radar return from two dimensional random rough surface model using helmholtz integral approach and Kirchhoff approximation
09 p1277 A72-22314
- Al alloys solid binary solution soft X ray emission spectra interpretation by rigid band and virtual bound state models
09 p1371 A72-22847
- Gravitational radiation spectrum and energy computation from point test particle falling radially into Schwarzschild black hole
09 p1393 A72-23646
- Spectral reflectance properties of lunar surface areas, discussing materials identification and maria depth determination
09 p1393 A72-23664
- Methane absorption line profile, intensity and width studied with magnetically tuned He-Ne laser
10 p1490 A72-24041
- Spectral position of spontaneous self regulatory systems, comparing to classical wave spectra
10 p1511 A72-24221
- Spectrographic analysis of K-type supergiant epsilon Pegasi for effective temperature, surface gravity and heavy and light element abundances
10 p1543 A72-24621
- Data window for digital spectrum estimation of random data by fast Fourier transform techniques, noting bandwidth increase by various data smoothing sequences
10 p1439 A72-24804
- Stellar spectra differential analysis from solar curve of growth for Fe I with revised gf-scale, noting van der Waals broadening and microturbulence
10 p1547 A72-24868
- Spectral measurements of temperature in low temperature plasma, describing line reversal method
10 p1485 A72-25110
- Spectral density of frequency deviation process for performance predictions from oscillator testing and frequency noise calibration, discussing sample averages convergence to statistical values
11 p1593 A72-25892
- Electromagnetic interference measurement by wide dispersion type spectrum analyzer electronically tuned over octave frequency range [SAE AIR 1255]
11 p1632 A72-26027
- Auroral spectrum analysis in 1200-4000 A band, obtaining photon emission rates
11 p1624 A72-26402
- Cometary spectra analysis, noting resonance fluorescence mechanism of emissions
11 p1722 A72-26433
- Holographic method of correlation and spectral analysis of radio signals applied to stable oscillator, randomly inhomogeneous media fields and stereophonic transmission measurements
11 p1636 A72-26726
- Magnetic field gradient in sunspot umbrae from magnetically split line profiles
12 p1867 A72-27206
- Russian book on spectral, spatial and time characteristics of lasers covering luminescence and resonator theories, electromagnetic field structure and radiation dispersion
12 p1820 A72-27500
- Distant thunderstorm center location with VLF atmospherics, determining delay time difference of Fourier spectrum groups of 6 and 8 kHz
12 p1841 A72-27793
- Automated scanning spectroradiometer for color vision test stimuli and luminescence measurements, applying computer analysis of spectral data
12 p1811 A72-27944
- X ray and Mossbauer spectral analyses of thermomagnetically treated nickel ferrite samples containing Co, investigating ordering mechanism
13 p2020 A72-28490
- X ray spectral analysis of Ti-Mo system alloys, investigating K and L lines and electronic structure
13 p1972 A72-28491
- Spectrum analysis of PCM/AM-FM and PCM/FM-FM telemetry signals, using approximation technique to Fourier transform time signal to frequency domain
13 p1919 A72-29025
- Real time interferential spectrum analysis of deterministic signals in form of partially summed Fourier series
13 p1919 A72-29041
- Dispersion method for real time spectral analysis of signals by Fourier transform for class of integrable functions with finite energy
13 p1919 A72-29042
- Quasi-one dimensional spectral analysis of input signal by delay line circulator, discussing ring frequency characteristic influence on harmonic signal buildup efficiency
13 p1930 A72-29043
- Spectrum analysis of synchronous recordings of Pi 1 irregular pulsations and auroral brightness at Sogra for ionospheric electric fields
13 p1948 A72-29235
- Spectral characteristics of ionospheric signal by phase lags introduced in multichannel field recorder
13 p1920 A72-29238
- Moving sound sources spectral analysis techniques, discussing computer controlled one-third octave band and narrowband analysis
13 p2005 A72-29566
- Solar corona intensification analysis based on ionized Fe monochromatic emission spectra, in-

investigating spectral lines behavior as function of temperature and electron density

13 p2047 A72-29736

Natural instabilities development in laminar boundary layer of incompressible flow, considering AM spectrum and abscissa-ordinate development compared to Orr-Sommerfeld equation solution

13 p1943 A72-29784

Ti, B, Zr and Be trace additions effect on Al alloy grain refining from spectrochemical analysis

13 p1913 A72-29838

Solar photospheric fluctuations, applying fast Fourier transform to power coherence and phase spectra calculations

13 p2049 A72-29928

Single pulses and random samplings signal spectrum analysis on real time scale by ultrasonic dispersion waveguide

13 p1934 A72-30018

Collisional relaxation and rotational intensity distributions in aeronomic spectra, including radiative losses effects from weak interaction model

13 p2008 A72-30057

Radio absorption spectra sounding for planetary atmospheric impurities calculating water vapor content in Venus cloud level

14 p2149 A72-30238

K beta emission spectrum of metallic Cr, discussing structural X ray analysis revealed cubic structure

14 p2116 A72-30414

Spectral changes of light reflected back from plasma during heating by mode locked Nd laser, noting equidistant lines presence

14 p2138 A72-30447

Apollo 12 lunar fines spectral and thermal radiation properties as function of bulk density, presenting emittance as function of temperature and solar reflectance

14 p2154 A72-30513

Spectral line identifications and classifications of Li like spectra of elements K through Mn in extreme UV region, detailing extrapolation procedures

14 p2133 A72-30563

Spectral line profile of optical transition spontaneous radiation during resonance with strong field on adjacent transition

14 p2110 A72-30781

Spectrochemical trace analyses in electric arc plasma, examining external magnetic field effects on spectral line intensity variation

14 p2139 A72-30784

Elliptical and barred spiral Markarian galaxies, discussing starlike and diffuse spectra dependence on morphology

15 p2304 A72-31327

Spectral brightness coefficient and photodensity measurements for remote vegetation productivity sensing in visible band

15 p2222 A72-31396

Control theory of second order linear hyperbolic partial differential equations, discussing relation to harmonic and spectral analysis

15 p2263 A72-31757

Boundary value problems for discrete spectrum of nonlinear ordinary differential operators on unbounded intervals

15 p2263 A72-31760

Jovian synchrotron emission measurements by radioheliograph at 80 MHz, passing square low detector outputs through RC integrators

15 p2307 A72-31799

Whistler mode VLF signal transmission in ground transmitter and magnetically conjugate zones, observing spectrum broadening and AM in magnetosphere

15 p2197 A72-31919

Signal with bounded spectrum, obtaining higher derivatives by reduction to stationary random process filtering problem solvable with Kolmogorov-Wiener and Kalman-Bucy techniques

15 p2207 A72-32171

Mean value, repetition and discontinuity errors of spectral-transposition method involving memory storage and compressed signal processing

15 p2212 A72-32703

Spectral index-luminosity relation for radio galaxies and quasi-stellar sources with power law spectra

15 p2315 A72-32714

Computerized analysis of overlapping Raman and IR spectral lines, describing routine for resolving complex spectrum into component lines via operator intervention

16 p2366 A72-33027

Nondestructive vibration analysis of mechanical structures, using digital computer technique for sound wave spectrum analysis

16 p2397 A72-33220

Stellar velocity dispersion in elliptical galaxy NGC 7332 from coude spectrum obtained by SEC vidicon TV camera and telescope

16 p2454 A72-33453

Planetary nebula M2-9 spectrum analysis, discussing IR excess, internal motions and Fe II emission lines

16 p2455 A72-33459

Quasars and emission line objects red shift distribution using power spectrum analysis method

16 p2457 A72-33625

Gaussian electromagnetic radiation beam propagation in turbulent medium, calculating broadening dependence on outer scale by modified Karman spectrum characterization

17 p2580 A72-34291

Study by Mossbauer spectrometry of the iron distribution in mineralogical fractions separated from lunar rocks brought back by Apollo 12

17 p2607 A72-34917

High speed spectrum analyzer/hissa and its application to the study of geomagnetic pulsations. I - S-type hissa.

17 p2554 A72-35061

Spectral analyses of solar photospheric fluctuations. II.

17 p2608 A72-35081

Low-energy proton observations in July and August, 1970, on the 'Molniya-1' satellite

17 p2600 A72-35208

Digital computer investigation of radio signals transmitted by Venera 7 during Venus soft landing, describing spectral analysis and telemetric data detection methods

17 p2516 A72-35273

On the temperature of the helium emission regions in the solar atmosphere.

17 p2616 A72-35699

Spectral analysis of highly inhomogeneous chromospheric flares.

17 p2617 A72-35709

Results of observation of spectra and polarization of meter solar radio emission with high time resolution - May-June, 1969.

17 p2602 A72-35714

X ray spectrum analysis of Sco X-1 type sources, showing plasma sheath with high electron temperature

17 p2617 A72-35727

Application of dispersion techniques to molecular band intensity measurements. I - Principles of 'fringe shift' and 'fringe slope' band analysis procedures.

17 p2586 A72-35832

Radio galaxies monochromatic luminosity-spectral index relationship from 3CR spectra studied at 10 MHz to 10,700 MHz

18 p2726 A72-36621

Pm existence evidence for HR 465 from analysis of Pm II spectral line data

18 p2727 A72-36738

Some aspects of cosmic ray differential spectrum measurements

18 p2722 A72-36852

Flash desorption spectrum and LEED studies of CO adsorption on W single crystal planes, measuring work function increase as function of coverage

18 p2657 A72-37040

Comparison of theoretical and experimental limits of detection in atomic absorption spectrometry using air-acetylene and nitrous oxide-acetylene flames.

19 p2762 A72-37725

Theoretical study of the Zeeman spectrum and of the magnetic resonance in the evanescent wave of Fresnel - Case of the magnetic transverse mode

19 p2834 A72-37790

Solar chromospheric flare details motion differences from spectrum analysis and H alpha line frame photography, noting radial velocities difference

19 p2851 A72-37816

Table for reduction of stellar radial velocities to the center of the sun

19 p2859 A72-37909

Solution of the problem of a fast Fourier transform in a homogeneous associative parallel processor

19 p2779 A72-37993

Study of the spectrally variable silicon Ap star 56 Ari

19 p2862 A72-38055

Galactic radio emission spectrum analysis via horn antennas with wavelength proportional apertures, calculating full beam antenna temperatures for selected radio frequencies

19 p2852 A72-38484

Spectral characteristics of surface-layer turbulence.

19 p2829 A72-38559

Geomagnetic activity index Ap variation spectral data analysis, noting correlation to sunspot number variation

19 p2793 A72-38747

Correlation analysis techniques to characterize acoustic emission pulses from Mg alloys, obtaining time varying spectra

20 p2924 A72-39281

Statistical analysis for best fit of compact X ray object spectra to black body, bremsstrahlung and power law models

20 p2969 A72-39387

Expanding ring in Galactic center from analysis of microwave spectroscopic data, measuring expansion and rotation velocities

20 p2972 A72-39860

H II region fine structure from 11 and 3.7 cm observations, deducing physical parameters from continuum

21 p3105 A72-41031

Electron paramagnetic resonance spectrum of vanadyl acetylacetonate dissolved in liquid crystal or isotropic solvent

21 p3013 A72-41177

Hydrogen sulfide detection in Galactic sources via observation of single line corresponding to rotational transition, comparing abundance to formaldehyde, CS, HCN and CO

21 p3107 A72-41271

Jupiter atmospheric C12/C13 ratio for methane from equivalent width measurements in R[2] multiplet

21 p3107 A72-41271

Application of holographic Fourier spectroscopy to the analysis of the microwave radiation spectrum

21 p3058 A72-41733

Statistical tests for spectral correlation analysis of continuum VHF radio emission fluctuations from noise storms

21 p3102 A72-41778

Airglow observations with a Hadamard photometer.

22 p3169 A72-42022

Solar photospheric fluctuations measured from time sequence of Sacramento Peak Observatory spectrograms, using power, coherence and phase spectra computed by fast Fourier transform

22 p3221 A72-42029

Type 3 solar burst distinction from auroral type high pass noise via spectrum analysis

22 p3222 A72-42043

Spectral analysis of microwave pulses by a ferrite transducer

22 p3158 A72-42119

Determination of the spectra of modulated pulse trains by the spectral function method

22 p3154 A72-42122

Electronic analyzer of structural vibration frequency characteristics and mutual spectra, considering bandpass filter and automatic frequency spectrum recorder

22 p3176 A72-42134

Determination of optical transfer functions by Fourier transformation in spatially incoherent light

22 p3205 A72-42296

Spectrophotometry 0/3 to 1.1 micron/ of visited and proposed Apollo lunar landing sites.

22 p3225 A72-42506

Observations of the airglow continuum.

22 p3174 A72-42818

Some results of an analysis of Pc4-type steady geomagnetic pulsations at a network of stations

23 p3283 A72-43371

The analysis of the small Magellanic Cloud supergiant HD 7583.

23 p3336 A72-43558

Digitally pressure-scanned Fabry-Perot interferometer for studying weak spectral lines.

23 p3289 A72-43806

Spectral line identification computer program determining wavelength and equivalent line width from photometric measurements

23 p3267 A72-44027

Spectral characteristics of the scattering field of uniformly traveling and rotating impedance cylinder

23 p3265 A72-44201

The lunar conductivity profile and the nonuniqueness of electromagnetic data inversion.

24 p3436 A72-44606

Stellar spectra analysis from measured truncated equivalent spectral line widths, calculating curves of growth for given truncations, source functions and absorption coefficients

24 p3447 A72-45688

SPECULAR REFLECTION

Aqueous solutions specular reflectance measurement, using organic dye laser spectrophotometer at 360-650 nm and reflectometer equipped spectrophotometer at 0.2-20 micron wavelengths

02 p0226 A72-11831

Laboratory spectrophotometer calibration for specular light over 0.5-2.5 micron range by means of stacked glass plates, noting accuracy

04 p0524 A72-15531

Quasi-specular and Lambert reflection of short radio waves from lunar surface dependent on central portion of near side

05 p0631 A72-17031

Thin films thickness and refraction index calculation from curves of specularly reflected X ray intensity vs grazing angle, obtaining surface roughness variance

07 p1050 A72-20403

Pseudo-hemispherical properties applied to radiative transfer in absorbing-emitting medium involving specular directional surfaces

09 p1351 A72-22674

ATS specular thermal control louver system performance in simulated solar vacuum environment as function of sun and blade angle, noting white paint effect

[AIAA PAPER 72-268]

11 p1740 A72-25202

Roughness effects on radiant heat transfer between interacting surfaces based on Beckman reflectance model
[AIAA PAPER 72-305] 11 p1742 A72-25239

Spherical specularly reflecting nonresonant cavities for use as absorption cells in far IR spectroscopy, predicting performance
11 p1629 A72-25301

Specular components of thermal reflectance as function of directional incident intensity variations
11 p1746 A72-25993

Laser induced transparent dielectrics surface fracture mechanism determination based on electron microscopic photograph analysis and disturbed specular reflection under predischARGE conditions study
11 p1648 A72-26333

Kinetic model for electromagnetic field fluctuations in bounded isotropic plasma half space with specular reflection of electrons at boundary
14 p2135 A72-30170

Kinematic intensity recovery from LEED data of specular and nonspecular beams from Ni(111) surface, noting multiple scattering interference elimination
15 p2276 A72-31855

Effect of fluidization on the polarization of reflected light from lunar dust layers.
18 p2729 A72-36987

Effect of polarization on the apparent emittance of rectangular groove cavities.
20 p2954 A72-39629

Design of a specular aspheric surface to uniformly radiate a flat surface using a nonuniform collimated radiation source.
[ASME PAPER 72-HT-J] 20 p2984 A72-39653

Methods for the quality control of the reflecting surfaces of solar energy condensers (Survey)
22 p3140 A72-43187

Formation of defects in reflecting coatings under the action of high temperatures
22 p3197 A72-43193

PEECH
NT SYLLABLES
NT WORDS (LANGUAGE)

Air flow and acoustic characteristics of speech sounds produced with turbulence noise at glottal constriction, using flow equations
[AD-744389] 01 p0101 A72-10162

Breathing control during speech, noting carbon dioxide response, hyperventilation and apnea
04 p0480 A72-15218

Right ear prevalence in hearing process determined by dichotic speech audition
04 p0476 A72-15584

Fourier, Hadamard and Karhunen-Loeve transformations for digital speech processing, comparing bit rate requirements
06 p0772 A72-17405

German book - Hearing, voice, balance /Physiology of the senses III/.
22 p3146 A72-42784

Human vocal apparatus anatomical and neural structure, considering linguistic sounds composition
22 p3147 A72-42789

Features of a speech signal during cumulative action of Coriolis accelerations
23 p3257 A72-44154

PEECH DISCRIMINATION
U SPEECH RECOGNITION
PEECH RECOGNITION

Voice quality improvement in He atmospheres by on-line segment dilation
01 p0101 A72-10158

Human touch deficiency in artificial pattern recognizers regarding handwriting, speech and pattern recognition involving nonevents
01 p0017 A72-10464

Earplugs effect on passenger speech reception and intelligibility in rotary wing aircraft, noting protection against noise annoyance, fatigue and deafening
01 p0022 A72-11294

Statistical long term speech spectrum analysis and perceptual evaluation, using digital bandpass filter technique
02 p0171 A72-11666

Correlation functions of signal and noise at output of discrete channel, determining SNR or speech intelligibility
03 p0323 A72-13891

Formant-coded voiced speech parameters smoothing and quantizing effects subjective evaluation, obtaining average quantization threshold levels
04 p0487 A72-15298

Digital speech detector with increased voice signal and reduced noise sensitivity for satellite capacity improvement
07 p0939 A72-19067

Noise rating methods for speech communication effectiveness evaluation, presenting charts and tables for intelligibility limits with various communication techniques and equipment
07 p0932 A72-20167

Design criteria for transportation system noise regulation, considering ambient noise, hearing damage, speech interference and subjective reactions
07 p0932 A72-20173

Human cortical auditory evoked response to speech and sound effects, relating EEG interhemispheric wave amplitude asymmetry to stimulus meaningfulness
08 p1115 A72-20984

Air traffic control messages syllabic and word prominence patterns, discussing impact on continuous speech recognition by machine
09 p1274 A72-23581

PCM speech transmission systems, comparing pseudorandomly dithered quantization with fixed level method by intelligibility and subjective appreciation tests and statistical analysis
14 p2087 A72-30942

Correlation functions of signal and noise at output of discrete channel, determining SNR or speech intelligibility
15 p2202 A72-32702

Language and speech capacity of the right hemisphere.
19 p2757 A72-38150

Speech intelligibility during exercise at normal and increased atmospheric pressures.
22 p3150 A72-42496

SPEED
U VELOCITY
SPEED CONTROL

Self adaptive controlled robot velocipedist, discussing speed control and equations of motion
04 p0505 A72-14984

Aircraft turbo-alternator speed control for constant frequency power supply, presenting theoretical relationships for electrohydraulic or mecano-hydraulic control loops
04 p0466 A72-15462

Electrochemical machining with forward speed control via hydraulic means
08 p1175 A72-21043

Dynamic structural analysis of system formed by engine, variable ratio differential and working machine, calculating differential ratio for constant shaft rotation speed
15 p2182 A72-31609

Monitor and regulator for automatic speed control and flow velocity measurement in wind tunnel
16 p2392 A72-33609

A new instrument for the measurement of low dynamic torque.
18 p2692 A72-36820

Optoelectronic speed control for replacing mechanical gear drives for precisely variable shaft speed ratios
21 p2997 A72-40259

Optimal control of the speed of a two-shaft helicopter turbine
23 p3326 A72-44278

SPEED INDICATORS
NT ANEMOMETERS
NT HOT-FILM ANEMOMETERS
NT HOT-WIRE ANEMOMETERS
NT TACHOMETERS

Doppler system with navigation radar device, computer unit and data transmitter for continuous recording of aircraft position and speed
02 p0258 A72-12749

Display device for engine rotational speed nonuniformity parameters indication on oscilloscope without supplementary computation
05 p0662 A72-16125

Received signal spectrum gravity center and effective antenna centers of airborne Doppler velocimeter in horizontal flight
11 p1606 A72-26730

SPEED REGULATION
U SPEED CONTROL
SPEED REGULATORS

Investigation of the dynamic characteristics of the speed governor of a hydropneumatic feed drive
23 p3253 A72-44022

SPEEDMETERS
U SPEED INDICATORS
SPHALERITE
U ZINCBLENDE
SPHERES

NT CELESTIAL SPHERE
NT FALLING SPHERES
NT POINCARÉ SPHERES
NT ROTATING SPHERES

Gravity and magnetic anomalies interpretation in terms of buried spherical bodies, calculating bodies size and depth of burial
01 p0064 A72-11101

Mechanical constraints effects on loose spherical metal particles sintering rates, considering one, two and three dimensional arrays
02 p0232 A72-11433

Contact problem of rigid sphere intrusion into viscoelastic half space, obtaining solution by Green function construction and integral-operator equation formulation
02 p0289 A72-11615

Magnetosonic perturbations caused by ideally conducting sphere expansion in cold plasma, determining electric field and magnetic induction time dependences
02 p0217 A72-11939

Half range differential approximation for spherically symmetric radiative transfer in concentric spheres with and without internal heat sources
02 p3032 A72-12259

Concentric spherical heat exchanger, showing heat transfer coefficient decrease with coolant flow rate increase
02 p3033 A72-12320

Motion stability of sphere and homogeneous semi-infinite rotating cylinder in circular orbits and monoenergetic streams, integrating by trajectories
02 p0285 A72-12832

Radiative cooling system for nearly spherical or polyhedral bodies using radially attached diverging conical elements
02 p3034 A72-12863

Static isotropic elastic body first and second boundary value problems solutions for inside and outside m dimensional sphere
02 p3030 A72-12876

Hard sphere liquid Bernal model with cell method extension, determining liquid argon behavior near melting
03 p0388 A72-13151

Viscous fluid flow at small Reynolds numbers past porous permeable sphere, obtaining drag formula
04 p0511 A72-14858

Slow motion in shear flow of doublet of two spheres in contact, using Stokes equations solution
04 p0511 A72-14860

Hydrodynamic field around sphere moving along Poiseuille flow axis determined by least squares method, formulating flow resistance
04 p0511 A72-14968

Small sphere hydrodynamic drag in ionized gas at local thermodynamic equilibrium, taking into account nonlinear transport properties variations with temperature
[ASME PAPER 71-APM-CC] 04 p0558 A72-15176

Al finished and Au plated triple calibration sphere as multispectral optical sensor for testing Cook hypothesis concerning satellite drag dependence on surface material
04 p0500 A72-15305

Hf electromagnetic wave scattering and diffraction by smooth dielectric cylinder and sphere based on Lorentz excitation theory
04 p0490 A72-15397

Flat plate, sphere and circular cylinder drag and lift coefficients in free molecular flow
04 p0463 A72-15645

Multimoment solutions to convective heat transfer from sphere, discussing maximum drag coefficient and validity at all Knudsen numbers
[ASME PAPER 71-WA/HT-1] 05 p0743 A72-15863

High frequency electric field backscattering by plane electromagnetic wave incident on perfectly conducting sphere with radially inhomogeneous dielectric coating
05 p0630 A72-16621

Thermostated integrating sphere for low temperature measurements of reflection and transmission coefficients of materials with arbitrary scattering functions
06 p0816 A72-17838

Dynamic behavior of stiffened hollow viscoelastic cylinder and elastic shell-contained sphere, taking into account compressibility and internal pressure
07 p0900 A72-19751

Sphere unsteady motion in viscoelastic liquids, noting falling-ball technique use for elastic parameters determination
07 p0973 A72-20549

Elasticity and potential theory axisymmetric problems solution for sphere and spherical cavity, constructing x-analytic functions for boundary surfaces
08 p1242 A72-20908

German monograph on steady flow past sphere and cylinder near wall, discussing drag, lift and flow visualization
08 p1108 A72-21950

Light scattering by spherical particles, noting cost effectiveness of logarithmic derivatives calculation method
09 p1350 A72-22412

Local and macroscopic thermal transport in turbulent air stream, discussing measurement from calorimeter instrumented sphere
10 p1417 A72-24148

Autonomous combustion of Al sphere in controlled atmospheres oxygen-argon, nitrogen and air, identifying products
10 p1562 A72-24238

Radial vibrations of isotropic homogeneous sphere and cylinder bonded to thin nonhomogeneous casting outside
10 p1557 A72-24406

Shock layer emission associated with hypersonic air flow past spherical segment, solving flow equations by iteration technique
10 p1418 A72-24539

Magnetic balance measurements of aerodynamic forces on spheres and slender cones in hypersonic low density wind tunnels, noting sting effect

10 p1462 A72-24771

Spheres drag coefficient measurements in laminar flow as function of Reynolds number, using wind tunnel model magnetic suspension system

10 p1419 A72-24772

Hydrodynamic field generated by sphere motion along viscous fluid filled cylinder axis beyond Stokes regime

10 p1470 A72-24852

Time dependent viscous flow past impulsively started sphere using numerical solutions for governing equations based on Legendre series expansion of stream and vorticity functions

11 p1615 A72-25551

Slow drop of heavy rigid spheres through vertical tube filled with viscous liquid, noting minimization of errors due to temperature and trajectory path

11 p1617 A72-26501

Unsteady flow evolution at sphere and elliptical cylinder obtained by flow visualization techniques, showing streamline sequence dependence on angle of attack

12 p1797 A72-27469

Ultrasonic signal propagation with distance along steel sphere surface compared with lunar seismic signal, discussing surface dent and lunar crater effects

13 p2035 A72-28619

Plane sound wave scattering by acoustically soft sphere at constant subsonic velocity

13 p2003 A72-28797

Nonuniform concentration mechanism for observed drag reduction in flows with high molecular weight polymer additives, considering boundary layer with varying viscosity on sphere

13 p1942 A72-29113

Nonlinear heat conduction in rarefied gases between concentric cylinders and spheres, using series expansion in terms of temperature difference for closed-form solution

13 p2064 A72-29118

Magnetosonic perturbations caused by ideally conducting sphere expansion in cold plasma, determining electric field and magnetic induction time dependences

13 p1949 A72-29251

Nonequilibrium dissociating inviscid nitrogen flow pattern over spheres and circular cylinders, obtaining temperature, pressure and density fields

13 p1895 A72-30032

Wind tunnel investigation of wake pressure and vortex shedding characteristics of flow past spheres as function of Reynolds number

13 p1896 A72-30099

Convective heat transfer of sphere in rarefied gas subsonic flow, comparing calculation with measurement

14 p2071 A72-31023

Stress-strain state of spherical body in centrally symmetric temperature field, noting elastoplastic interface and continuity conditions

15 p2327 A72-31742

Elastic wave diffraction on multiconnected cylindrical or spherical regions in nonsymmetric elasticity theory, determining constants of series solution

15 p2330 A72-32290

Thermal force exerted on spherical particle between two flat plates in stagnant monatomic rarefied gas, using moment solution to Boltzmann equation

15 p2336 A72-32403

Spherical particle accelerated motion in stationary viscous fluid, using numerical integration technique for velocity and displacement computations

16 p2375 A72-32907

Radial vibrations and plane wave propagation in elastic deforming sphere with superimposed time dependent displacement field

16 p2467 A72-33117

Onboard radiometric measurement of bow shock generated UV radiation during atmospheric reentry of experimental sphere

[AIAA PAPER 72-692]

16 p2462 A72-34050

Spatial diffusion dynamics, spin, and the Pauli equation

17 p2573 A72-34193

Acoustic radiation from multiple spheres.

17 p2579 A72-34226

Motion of a sphere in an electrically conducting rotating fluid.

18 p2714 A72-36123

Separation and analysis of the acoustic field scattered by a rigid sphere.

18 p2710 A72-36408

Heat transfer from a slowly rotating sphere.

18 p2741 A72-36934

Negative index polytropic sphere gravitational collapse structure, noting application to interstellar gas clouds thermal equilibrium

19 p2857 A72-37794

Thermal stress induced flow around constant temperature solid sphere in rarefied gas with uniform temperature gradient, using asymptotic theory

19 p2788 A72-38433

Critical levitation loci for spheres on cryogenic fluids.

19 p2836 A72-38844

Unsteady heat transfer and temperature for Stokesian flow about a sphere.

[ASME PAPER 72-HT-C]

20 p2983 A72-39482

Sting-free measurements of sphere drag in laminar flow.

21 p2989 A72-40110

A flow induced by thermal stress in rarefied gas.

21 p2989 A72-40193

Plexiglas spheres and cubes effect on circular and rectangular waveguide aperture antennas directive radiation patterns and sidelobe reduction

21 p3021 A72-40904

Force-time investigations for the elastic impact between a rigid sphere and a thin layer.

21 p3121 A72-41212

Transverse mass flow past a sphere at small Reynolds numbers

21 p3047 A72-41664

Influence of blowing on the resistance of a sphere in laminar viscous fluid flow

21 p3047 A72-41665

Determination of the velocity field of the wake of a hypersonic sphere with the aid of ion probe arrays

21 p3057 A72-41725

Fluid sphere of uniform density and vanishing pressure at periphery, expressing internal motion in terms of Schwarzschild mass and radius and central pressure

22 p3205 A72-42451

New method for determining the distribution of delta-g anomalies for a sphere, horizontal cylinder, and vertical material half-line

22 p3173 A72-42574

Light scattering in a sphere in the presence of an arbitrary source distribution

22 p3207 A72-42965

German monograph - Cooling of geometrically simple bodies /flat plate, cylinder, sphere/ by convection and radiation.

22 p3244 A72-43062

Viscous torque on sphere immersed in Newtonian and non-Newtonian fluids in rotating cylinder, comparing experimental results with Collins theory

23 p3280 A72-43714

Stress distribution in a homogeneous elastic sphere containing a penny shaped crack of prescribed shape.

23 p3354 A72-44268

SPHERICAL ANTENNAS

Spherical reflector antenna phase aberration correction by planar array feeds, discussing synthesis procedure for mean square error minimization

06 p0781 A72-17344

Optimal sum-difference characteristics of nonsuperdirective convex slot spherical antennas for maximum directive gain and minimum spatial sidelobe radiation

11 p1598 A72-26713

A wideband antenna array

17 p2531 A72-35766

Cross-polarized radiation from convex spherical antennas with a phase-opposed field distribution

19 p2774 A72-38414

Spherical reflector as possible antenna for millimeter wave astronomy, discussing feed design for spherical aberration corrections

21 p3029 A72-40519

Luneburg lens spherical antenna microwave radiation pattern, computing Maxwell equations via Tai method

21 p3030 A72-40529

Effects of pseudosonic and electroacoustic waves on the radiation of a plasma-coated spherical antenna.

24 p3386 A72-45645

SPHERICAL CAPS

Dynamic buckling and plate to shell transition of thick spherical caps under large amplitude axisymmetric flexural vibrations

08 p1249 A72-22135

Axisymmetric stability of spherical cap rigidly clamped at contour of shells of revolution, using variational difference method for uniformly distributed external pressure

13 p2053 A72-28393

Spherical cap dynamic buckling under impulsive loading, comparing prediction by energy criterion with experiment using spray deposited explosive

15 p2323 A72-31405

A note on buckling of spherical caps with initial asymmetric imperfections.

23 p3351 A72-44060

SPHERICAL HARMONICS

Spherical harmonics method utilization in radiative transfer calculations, describing characteristic equations roots determination technique

03 p0389 A72-13795

Earth gravitational potential, including surface density, crystal thickness, potential coefficients, contour maps and spherical harmonic expansion

06 p0877 A72-17657

Spherical harmonic representations of geomagnetic field including magnetosphere and tail regions based on ground based and low altitude spacecraft measurements within several earth radii

07 p0977 A72-20026

Geomagnetic field optimal model with expansion of spherical harmonic series by least squares method

07 p0980 A72-20657

Nonuniform non-Lambertian diffusely scattering surface optical transfer characteristics and initial radiance distribution inside sphere, discussing spherical harmonic moment measurement

09 p1309 A72-22610

Geomagnetic data testing by including monopoles term in spherical harmonic reduction

13 p1951 A72-29394

Spherical analyses of the principal geomagnetic field for the years 1550 through 1800

18 p2689 A72-36874

Mathematical model of earth liquid core dynamo mechanism for magnetic field maintenance based on simple motions with spherical harmonic form

21 p3048 A72-40400

Earth main magnetic field description by cartography and analytic methods based on dipole or spherical harmonic series representations

23 p3283 A72-43366

SPHERICAL SHELLS

NT SPHERICAL CAPS

Infinite slab, cylindrical or spherical shells with nonuniform heat generation sources and equal surface temperatures, obtaining maximum internal temperature from error bounds

01 p0145 A72-10511

Variable volume spherical cavity motion in ideal liquid near plane surface

02 p2020 A72-11586

Tube and hollow sphere revolving in thermal flux under surface pressure load, obtaining stress-strain state and random temperature dependences of creep

02 p2289 A72-11618

Fluid filled fiber reinforced spherical shells extensional vibrations, evaluating equivalent elastic orthotropic compliance constants, natural frequencies and mode shapes

03 p0443 A72-13403

Elastoplastic stress distribution in thin spherical metallic shells with cylindrical branch pipe under internal pressure

03 p0448 A72-13905

Stress concentration around circular and elliptical holes in isotropic three layer spherical shells with rigid and lightweight fillers

03 p0449 A72-14104

Shallow spherical shell natural vibration frequencies, deflection and stress function, discussing effects of internal pressure, dimensions and material properties

03 p0453 A72-14200

Linearized equilibrium equations for thin spherically shell with internal pressure, obtaining free vibration modes

04 p0587 A72-15018

Nonlinear elastoplastic deformations of flexible shells of revolution, calculating stress concentration at circular hole in spherical shell

04 p0588 A72-15049

Constitutive equations derivation for electrical conduction due to small deformation superposition, applying to deformed spherical shell current density determination

04 p0549 A72-15254

Variable thickness shallow spherical shells of revolution axisymmetric loads carrying capacity, determining limit equilibrium through application of Tresca yield point concept

05 p0734 A72-15983

Equilibrium conditions of closed elastic spherical shell under uniform nearly critical compression loads, determining shell deformation in Hilbert spaces

05 p0739 A72-16587

Telemetry system on board beryllium sphere reentry vehicle for hypersonic gas dynamics and wake chemistry experiments, using flush mounted antennas with isotropic radiation pattern

[AIAA PAPER 72-176]

05 p0631 A72-16836

Supercritical deformation, bulging and instability of spherical edge clamped shell under external pressure, applying variational principle

05 p0742 A72-17210

Shallow axially symmetrical spherical shell flexural vibrations, obtaining equations iterative solution

06 p0901 A72-18705

Optimal rigid-plastic limit load analysis of spherical shells under nonsymmetrical loadings, using SUMT and Rosenbrock method

07 p1087 A72-18791

Shallow spherical shell equations solution for vibration mode and natural frequencies from analogous vibrating plate solution

07 p1089 A72-19489

Stress-strain state of thin walled spherical shell in contact with internal rigid sphere, determining contact area size

07 p1091 A72-19756

Wave propagation in hollow elastic/viscoplastic sphere under impact load, assuming Mises condition, isotropic hardening and incompressibility

07 p1096 A72-20429

Trapped modes structure of rotating fluid in thin spherical shell, noting constitution of free oscillation periods

07 p0973 A72-20455

Dynamic characteristics and nonlinear oscillations of liquid in spherical shell of revolution, modifying Lukovskii approximation method

08 p1148 A72-20962

Green matrix computation algorithm extensible to spherical and toroidal closed shells of revolution for stress-strain state determination

08 p1246 A72-21672

Temperature fields produced in viscoelastic cylindrical, conical and spherical shells by cyclic loads, calculating displacements from zero moment stress theory formulas

09 p1399 A72-22701

Continuum model for cylindrical and spherical elastic laminated composites deformation, using balance and constitutive equations

09 p1405 A72-22992

Boundary value problems for buckling and initial postbuckling of clamped shallow spherical and conical thin walled sandwich shells under uniformly distributed hydrostatic pressure

[ASME PAPER 71-APM-YY]

10 p1554 A72-24182

Gas role in radiative transfer and free convection between concentric spheres, noting gray gas assumption validity

[AIAA PAPER 72-280]

11 p1740 A72-25220

Supercritical deformation, bulging and instability of spherical edge clamped shell under external pressure, applying variational principle

11 p1727 A72-25341

Pressure loaded shallow spherical shells with reinforced circular holes, noting stress concentration increase due to reinforcement bead eccentricity

11 p1734 A72-25736

Mixed variational formulation and finite element method for axisymmetric cylindrical, conical, spherical and ellipsoidal shells

12 p1879 A72-27195

Hollow elastic momentless spherical shell translatory displacements in compressible fluid under nonstationary spherical wave

12 p1880 A72-27234

Shallow spherical sandwich shells limiting equilibrium for material with different tension and compression yield stresses

12 p1885 A72-27974

Thermal stresses near pole of spherical reservoir during cooling, using thermoelastic equations of shell of revolution

12 p1887 A72-28242

Shallow spherical shells axisymmetric vibrations under time varying loads, discussing transverse shear and rotatory inertia effects in terms of Fourier-Bessel series

13 p2056 A72-28880

Tangential displacements of spherical and circular cylindrical shallow shells calculated from stress function

13 p2059 A72-29490

K-order differential equation solution obtained for system of polynomial functions for shallow spherical shell under uniform pressure, using Bubnov-Galerkin and collocation methods

13 p2062 A72-29947

Radiative energy transfer through gray gas layer between black concentric spheres at different temperatures

13 p2066 A72-30055

Carrying capacity of rigidly hinged shell of revolution with concentric reinforcing rib, applying to shallow spherical shell under uniform external pressure

14 p2166 A72-30687

Creep deformation transition theory in spherical shells, using generalized strain measure for asymptotic solution

14 p2169 A72-30999

Stress function method for calculating stress-strain state in homogeneous shallow spherical shell under arbitrary load

15 p2324 A72-31485

Elastic deformation of thin walled spherical and cylindrical shells and associated rings under external loads for small displacements

15 p2325 A72-31604

Stress and displacement solution to Lamé problem for multilayer spherical vessels and cylindrical tubes in nonlinear elasticity theory

15 p2333 A72-32679

Surface stress solution for elastic half space weakened by spherical cut under internal pressure

15 p2333 A72-32681

Vibrational frequency density analysis of thin spherical and cylindrical shells of revolution, using asymptotic integration method

16 p2464 A72-32935

Natural vibration frequency spectra of circular cylindrical and spherical shells of revolution, using Bessel function

16 p2465 A72-32936

Perturbation scheme for branching analysis of postbuckling behavior in elastic spherical shells

16 p2465 A72-33001

Temperature and stress fields generated by pulsating internal pressure in viscoelastic hollow sphere with temperature dependent material properties, using iterative numerical procedure

16 p2473 A72-34122

Numerical procedure for spherical and cylindrical shells creep behavior, taking into account stress redistribution due to interaction between elastic and creep strains

16 p2473 A72-34125

Asymptotic singular perturbation solution to thick spherical shell with circular hole under axisymmetric external pressure

16 p2474 A72-34157

Contact pressure between an elastic spherical shell and a rigid plate.

[ASME PAPER 72-APM-31]

17 p2628 A72-34788

The shielding effect of metallic spherical envelopes with respect to very short EM waves and pulses

17 p2530 A72-35223

Thin spherical shells in equilibrium with displacement and stress fields, satisfying virtual work, kinematic and static requirements

17 p2633 A72-35351

Numerical solution of problems of large deformations for spherical elastic shells

17 p2634 A72-35421

Fracture of cylindrical and spherical shells containing a crack.

17 p2634 A72-35645

Free vibration mode shapes mapping of spherical and paraboloidal plastic shells under acoustic excitation via noncontact fiber optics instrumentation

18 p2690 A72-36372

Free vibrations of a spherically isotropic hollow sphere.

18 p2736 A72-37004

Forced axisymmetric response of fluid filled spherical shells.

18 p2684 A72-37063

On the transient response of a closed spherical shell to a local radial impulse.

18 p2739 A72-37089

On the accuracy and application of the point matching method for shallow shells.

18 p2739 A72-37090

Mathematical analogies in a theory of shallow spherical shells and plates allowing for transverse shear

19 p2872 A72-37540

Equilibrium conditions of closed elastic spherical shell under uniform nearly critical compression loads, determining shell deformation in Hilbert spaces

19 p2872 A72-37558

Determination of the natural frequencies and modes of oscillation of a spherical resinous shell

19 p2873 A72-37662

Investigation of the snap-through of rigidly clamped shallow spherical shells under the action of a dynamic stepped load

19 p2877 A72-38163

Behavior of viscoelastic shallow spherical shells subjected to dynamic pressure.

21 p3122 A72-41245

A collocation solution of the nonlinear equations for axisymmetric bending of shallow spherical shells.

22 p3232 A72-41938

Model studies of plate and shell stability

22 p3233 A72-42055

Rotatory vibration of a thick spherical shell of isotropic non-homogeneous elastic material.

22 p3240 A72-42880

Dynamic loading of a fluid-filled spherical shell.

22 p3240 A72-42891

Dynamic response of viscoelastic shallow spherical shells.

23 p3349 A72-43972

Asymmetric imperfections effect on spherical elastic shell buckling strength under uniform external pressure

23 p3351 A72-44104

Response of shallow spherical shells to pulse pressure loads.

24 p3454 A72-44605

Collapse of massless nonrotating gas particle nonuniform spheroidal shell contracting around gravitating massive point nucleus, interpreting galactic evolution

24 p3438 A72-44844

The transient electromagnetic response of a spherical shell of arbitrary thickness.

24 p3381 A72-45638

Variable thickness shallow spherical shells of revolution axisymmetric loads carrying capacity, determining limit equilibrium through application of Tresca yield point concept

24 p3460 A72-45725

SPHERICAL TANKS

Optimal composite structures of multilayer spherical vessels in terms of elastic deformation under critical loads in thermal field

16 p2467 A72-33158

SPHERICAL WAVES

Atmospheric turbulence induced laser beam spread estimation from spherical wave modulation transfer function

03 p0367 A72-13442

Maxwell equation spinor formulation for Schwarzschild gravitational field effects on spherical electromagnetic waves propagation

05 p0689 A72-16165

Asymmetrical profile calculation of spherical multiple wave interference patterns at finite distance with nonparallel mirror Fabry-Perot interferometer

05 p0662 A72-16193

Multifrequency plane, spherical and beam waves propagation, calculating temporal frequency spectra in turbulent atmosphere

06 p0771 A72-17339

Source distribution estimate in radar mapping, comparing prolate spherical wave functions inverse versus truncated Fourier transform methods

07 p0946 A72-17992

Spherical wave functions in analysis of infinite systems of algebraic equations describing elastic wave diffraction in sequence of spherical cavities

08 p1246 A72-21706

German monograph on pulsed laser induced spherical unsteady blast waves in stationary and flowing gases

09 p1325 A72-23161

Laser heating of plasma based on heat conduction mechanism of spherical thermal wave, taking into account nuclear fusion heat generation

09 p1365 A72-23551

Acoustic waves generation in liquids by Q-switched ruby laser, noting transition from plane to spherical waves with dye concentration and focusing configuration variations

10 p1490 A72-23954

Closed form solution for spherical and cylindrical wave propagation in laser conductively heated plasma, considering account of nuclear fusion energy recovery

10 p1522 A72-24721

Turbulence theory 2/3 law applicability to optical spherical wave propagation through turbulent atmosphere, comparing to von Karman model

11 p1686 A72-25772

Hollow elastic momentless spherical shell translatory displacements in compressible fluid under nonstationary spherical wave

12 p1880 A72-27234

Numerical accuracy of electromagnetic field spherical wave expansions, considering horn antenna radiation pattern

12 p1791 A72-27670

Unsteady spherical shock wave effect on thin infinite elastic plate covering acoustic semispaces, using integral transformation method

13 p1943 A72-29946

Imploding spherical and cylindrical shocks, considering rear flow field with nonadiabatic isothermal and zero temperature gradient

16 p2376 A72-33009

Q switched laser produced hemispherical shock waves in Ar and He plasmas, determining primary and secondary wave trajectories

16 p2439 A72-34028

Propagation of spherical waves in a weak static gravitational field

17 p2581 A72-35170

Strong intensity fluctuations of a spherical wave propagating in a randomly refractive medium

18 p2661 A72-36659

Near sidelobes in Cassegrain antenna systems.

18 p2668 A72-37039

Minkowski space-times for impulsive gravitational waves, considering idealized plane fronted wave form and limiting case of Robinson-Trautman null spherically fronted wave

20 p2955 A72-40007

Scattering of a spherical wave at a spherical discontinuity with an arbitrary radial distribution of the refractive index

21 p3016 A72-40793

Averaged equations of simultaneous hydrodynamic expansion and thermal heating of two-temperature plasma, taking the recovery of thermonuclear fusion into account. I - The plane problem. II - The spherical problem.

21 p3093 A72-41476

Propagation of spherical and cylindrical shock waves in an inhomogeneous atmosphere with allowance for back pressure

21 p3047 A72-41662

Alternative description of laser plasma heating for spherical thermal wave, the fusion energy being taken into account.

22 p3211 A72-42629

SPHEROIDS

NT OBLATE SPHEROIDS

NT PROLATE SPHEROIDS

Extraterrestrial magnetic spheroid concentrations observed in October 1967 and 1969 proposing relationship to rainfall frequency

08 p1226 A72-21109

- Sound radiation impedance of vibrating prolate spheroids as function of nearfield variation
11 p1688 A72-26064
- Book - Angular scattering functions for spheroids
17 p2582 A72-35457
- Spheroids with surface vibration at specified normal velocity distributions, calculating acoustic radiation by Green function approach
18 p2710 A72-36412
- Boundary value problem approximate solution for Stokes flow of unbounded viscous Newtonian fluid past single body, applying algorithm to spheroidal shapes
19 p2784 A72-37369

SPHERULES

- Chemical composition and morphology of silicate spherules, comparing to lunar rocks, meteorites and tektites
02 p0280 A72-12283
- Silicate microspherules distribution anomaly in peats of Tunguska meteorite fall area
02 p0281 A72-12293
- Constant cosmic spherule influx rate measured on quaternary deep sea sediments
05 p0722 A72-17153
- Microscopic, chemical and morphological studies of ultralarge meteoric spherules in Yakut ASSR, noting composition
08 p1229 A72-20838
- Lunar crater region ray systems origin and brightness variation mechanism from surface vitreous spherules examination
11 p1715 A72-25300
- Chondrule like spherules from supercooled molten oxide and silicate droplets by carbon dioxide laser heating compared with meteoritic chondrules
15 p2303 A72-31306

SPICULES

- Toroidal magnetic ring development and interaction with poloidal magnetic field, considering relationships to sunspots bright rings and spicules dynamics
05 p0719 A72-16512
- Fine structure elements of chromosphere, discussing spicules, fibrils and thermal effects
07 p1077 A72-19808
- Spicular field morphology near solar limb from photographs taken with H alpha filter
15 p2305 A72-31512
- Solar chromosphere bright mottles and spicules lifetime relationship from H alpha photograph isophotometry of limb
16 p2456 A72-33509
- Fine structure elements of chromosphere, discussing spicules, fibrils and thermal effects
17 p2617 A72-35733

SPIKE ANTENNAS

U MONOPOLE ANTENNAS

SPIKE POTENTIALS

- Multichannel IC spike height discriminator for separating electrical activity of neural units recorded with microelectrode
04 p0481 A72-15223
- Ultrashort light pulse emission during mode locking in ruby lasers in free emission operation, examining first spike radiation
05 p0668 A72-16413
- Retinal ganglion cell spikes timing in mammalian retina, using electroretinography and computer analysis
06 p0762 A72-17721
- Neuronal spike activity changes in rabbit visual and sensorimotor neocortex and hippocampus during EEG activation
13 p1902 A72-28643
- Cat hypothalamus regions neurons background activity characterized by single nonrhythmic spikes with large interspike intervals, noting frequency of discharge bursts
24 p3370 A72-44588

SPIKES

- Plasma interpretation of solar type 3 and spike bursts associations from high time resolution radiospectrographic observations
09 p1392 A72-23540

SPIKING

- Instantaneous and averaged spiking emission spectra of injection laser under spontaneous pulsation as function of oscillation mode and photon distribution
16 p2404 A72-33984

SPIN

- NT ELECTRON CAPTURE
- NT ELECTRON SPIN
- NT ISOTOPIC SPIN
- NT NUCLEAR SPIN
- NT PARTICLE SPIN
- NT SPIN-ORBIT INTERACTIONS
- Sounding rockets spin rate sensor, describing apparatus operation and size and weight reduction
01 p0071 A72-11173
- SPIN DECOUPLING
- NT SPIN
- Measurement of longitudinal relaxation times for spin-decoupled protons.
24 p3427 A72-45400

SPIN DYNAMICS

NT SPIN

- Galactic rotation origin, discussing tidal, vortex and spinning core theories
01 p0127 A72-10290
- Linear spin-down of stratified rotating Boussinesq fluid in circular cylinder as function of Prandtl number, noting solar interior problem
01 p0051 A72-11231
- Aircraft spin characteristics due to superstall, comparing three stall types with respect to recovery, yaw damping and rate of rotation
02 p0155 A72-12718
- [DGLR PAPER 71-057]
- Ball bearings rolling and spinning friction coefficients determination as function of stress at contact point, race and ball diameter
03 p0363 A72-13561
- Spin dynamics model of space station with counterweight connected by multiple cables, using linearized motion equations
05 p0730 A72-16882
- [AIAA PAPER 72-172]
- Thermally expanding surface effects on aerodynamic roll torques on smoothly ablating spinning cones, comparing analytic study and hypersonic wind tunnel test results
05 p0608 A72-16923
- [AIAA PAPER 72-30]
- Spinning satellite with rigid central body and flexible appendages, deriving equations of motion and Liapunov stability
06 p0892 A72-17652
- Mathematical model for dissipative dual-spin satellite analysis, making use of high speed rotor symmetry to permit quasi-holonomic transformation
07 p1085 A72-19280
- Analog simulation of dual-spin satellite dynamics and control, emphasizing Hughes gyrostat spacecraft
07 p1086 A72-20352
- Dynamical equivalence between vehicles with motor-driven constant speed rotor under bearing friction and freely spinning torque free rotor, deriving equations of motion
08 p1108 A72-21174
- Liquid filled spinning projectiles and satellites flight stability based on Stewartson gyroscopic analysis method
08 p1168 A72-21600
- Spin excitation effects in superconductors, noting impurity concentration effects on transition temperature and thermodynamic properties
09 p1368 A72-22558
- Earth pointing rotating satellites attitude control system based on two-degree of freedom gyroscopes, determining conditions for rotor spin axis fixation in inertial space
10 p1509 A72-24646
- Linear impulsive spin down from rigid body rotational equilibrium of radiation penetrated opaque compressible fluid in circular cylinder
11 p1680 A72-25555
- Metallized solid propellants burning rate augmentation by internal ballistics effect of spinning rocket motor, deriving relationship between burning rate, pressure level and acceleration
13 p2025 A72-29302
- Dynamic spin disorder effect on electrical and thermal conductivity, noting low resonant frequency in metal atom magnon spectrum
15 p2290 A72-31388
- Terrestrial and lunar orbital and rotational motion behavior, discussing kinematic theory and ground and space vehicle based observation techniques
19 p2865 A72-38479
- High angular velocity device design problems, considering gyroscopes, ultracentrifuges, yarn-spinning textile machinery and dental drill
19 p2809 A72-38544
- Characteristics of models of detonation spinning in various combustible media
20 p2987 A72-40045
- Analytic prediction of aircraft spin characteristics and analysis of spin recovery.
22 p3136 A72-42329
- [AIAA PAPER 72-985]
- Development of design criteria for predicting departure characteristics and spin susceptibility of fighter-type aircraft.
22 p3136 A72-42330
- [AIAA PAPER 72-984]
- Generalized subharmonic response of a missile with slight configurational asymmetries.
22 p3134 A72-42339
- [AIAA PAPER 72-972]
- Dynamics of spin-stabilized satellites having flexible appendages.
24 p3449 A72-45140
- Spin response of symmetric ablating vehicle at zero angle of attack, noting spin-up by ablation-induced grooving and spin-down by crosshatching effects
24 p3362 A72-45339
- SPIN EXCHANGE
- Direct fitting of spin wave energies to interatomic exchange parameters in the ferromagnetic rare earth metals.
21 p3097 A72-40625
- SPIN REDUCTION
- German monograph on optimal attitude control of satellites with rotors and simultaneous spin reduction,

covering motion equations for stable equilibrium and circular orbit
09 p1394 A72-22330

Stability of linear systems with constraint damping and integrals of the motion.
19 p2856 A72-37519

Despinning and detumbling satellites in rescue operations.
24 p3450 A72-45160

SPIN RESONANCE

- Hyperfine magnetic field reduction produced in Fe-Cr alloy single crystal by Cr atoms observed by Mossbauer method, proposing spin disturbance mechanism
15 p2293 A72-32230
- Dynamics of the optical-pumping cycle of F centers in alkali halides - Theory and application to detection of electron-spin and electron-nuclear-double-spin resonance in the relaxed-excited state.
18 p2719 A72-36709
- Resonance between spin waves and magnetohydrodynamic waves in antiferromagnetic semiconductors and metals
21 p3096 A72-40415
- Gamma ray scattering asymmetries of Fe 57 nucleus, discussing hyperfine structure and conjugate spin transition
22 p3209 A72-42924

SPIN STABILIZATION

- Far field patterns of hourglass reflector phased array for electronic despin of communications antenna on spin stabilized satellite
01 p0029 A72-10666
- AEROS scientific satellite attitude control system, considering control and measuring electronics, axis and spin control coils and spin stabilization
04 p0503 A72-15649
- AEROS satellite active magnetic attitude control system, describing magnetometer system, sun and IR earth sensors, spin stabilization and axis and spin rate control torque generation
05 p0727 A72-16473
- Time optimal and fuel optimal control of spin stabilized space vehicle for body-fixed and gimbaled jets, using maximum principle
05 p0728 A72-16476
- Universal ball-in-tube nutation dampers for spinning satellites, noting cost savings
05 p0729 A72-16756
- Gas jet control for spinning satellites attitude correction, deriving relations between satellite and control system parameters, response time and fuel consumption
05 p0731 A72-17194
- Spin stabilized axisymmetric probe attitude deviation due to solar pressure in elliptic orbits
06 p0892 A72-17655
- German monograph on optimal guidance of spin stabilized space bodies for combined attitude and angular velocity control and time optimal nutation damping
08 p1241 A72-21847
- Thrust profile shaping for spin stabilized vehicles analyzing effect on wobble motion and pointing error
10 p1552 A72-24647
- Spin stabilized satellites attitude dynamics during rigid booms extension, deriving equations of motion approximate solution
11 p1726 A72-25915
- Synchronous communication satellites body stabilized three axis attitude control superiority over dual spin techniques, emphasizing single large pitch momentum wheel configuration with magnetic torquing
12 p1876 A72-27386
- [AIAA PAPER 72-572]
- Elastic damping of spin stabilized space stations nutational oscillations induced by time-variant moments of inertia
15 p2319 A72-31458
- Frequency shift and mode shapes for equatorial vibrations of flexible boom on spin stabilized satellite, applying to thermal flutter resonance and nutational stability
15 p2320 A72-31803
- Optimum design parameters for a spin-stabilized spacecraft nutation damper.
17 p2619 A72-34208
- Passive stability of a spinning Skylab.
18 p2730 A72-36314
- Attitude stability and performance of a dual-spin satellite with nutation damping.
19 p2862 A72-38022
- Stability and CMG wobble damping of flexible, spinning space stations.
20 p2975 A72-39113
- [AIAA PAPER 72-888]
- Attitude stability of a dual-spin satellite with a large flexible solar array.
20 p2975 A72-39114
- [AIAA PAPER 72-887]
- Analysis of effects of fluid energy dissipation on spinning satellite control dynamics.
20 p2976 A72-39115
- [AIAA PAPER 72-886]
- An antenna principle with universally polydirectional radiation for large spin-stabilized flight devices
21 p3030 A72-40532
- Effect of bearing flexibility on dual-spin satellite attitude stability.
21 p3115 A72-41303

Mass attraction reduction by integral control in spinning drag-free satellites. 21 p3115 A72-41304

Solar pressure control of a spinning satellite with a stabilized platform. [AIAA PAPER 72-918] 21 p3115 A72-41563

Flight mechanics of spin stabilized rotating disks for special ordnance delivery, considering aerodynamic parameters relation to dynamic stability and orientation. [AIAA PAPER 72-982] 22 p3134 A72-42332

Effects of rifling and N-vanes on the Magnus characteristics of bodies of revolution. [AIAA PAPER 72-970] 22 p3135 A72-42341

Spin stabilized ballistic air-to-ground or ground-to-ground rocket, discussing dynamic stability-impact error relationship [SAWE PAPER 928] 23 p3342 A72-43468

Alignment of the figure axis of a spin-stabilized spacecraft perpendicular to sun and earth. 23 p3343 A72-43621

Dynamics of spin-stabilized satellites having flexible appendages. 24 p3449 A72-45140

OSO pointing accuracy improvement through dual spin stabilization, discussing OSO design evolution 1962-72. 24 p3449 A72-45145

Spin stabilization dispersive effect on marginally stable bodies due to precession rate, comparing analytical results with aeroballistic range measurements. 24 p3362 A72-45340

SPIN TESTS

NT SPIN

Boeing 347 helicopter program, discussing simulation, wind tunnel, whirl tower, bench testing, flight test development and demonstration. 05 p0614 A72-16993

F-14 Tomcat test program for hydraulic systems, spinning, low speed performance, stalling, afterburning turbofan engines, in-flight refueling and automatic telemetry equipment. 06 p0758 A72-17582

Flight initial spin testing, discussing aircraft autorotation due to stalled angle of attack and sideslip. 06 p0759 A72-18492

Status of U.S. Navy stall/post-stall/spin flight testing. [AIAA PAPER 72-787] 19 p2749 A72-38104

SPIN-LATTICE RELAXATION

Microwave diode switch operating at 35 GHz for spin lattice relaxation time measurement, discussing insertion loss, and rise and decay times characteristics. 16 p2369 A72-33623

Dynamics of the optical-pumping cycle of F centers in alkali halides - Theory and application to detection of electron-spin and electron-nuclear-double-spin resonance in the relaxed-excited state. 18 p2719 A72-36709

SPIN-ORBIT INTERACTIONS

NT ELECTRON CAPTURE

Long term spin and misalignment in orbit of Azur satellite with passive magnetic attitude control system. 05 p0727 A72-16466

Anomalous Hall effect of polarized electrons spin-orbit interactions in semiconductors, involving emf appearance in electric field and polarized light. 07 p1048 A72-19642

Gas phase photodetachment of electron from selenide ion, determining affinity and spin-orbit coupling constant for SeH negative ion. 16 p2360 A72-33580

Low field magnetization measurements at 4.2 K on bulk and thin film niobium nitride, discussing Pauli spin paramagnetism and spin-orbit scattering. 16 p2442 A72-33843

Observability of hyperfine structure and Lamb, nuclear-volume shifts in ^{151}Sm transitions of heli-unlike ions. 19 p2837 A72-37544

Gravitational spin interaction. 19 p2835 A72-38425

Anomalous Hall effect of polarized electrons spin-orbit interactions in semiconductors, involving emf appearance in electric field and polarized light. 24 p3431 A72-44573

SPINAL CORD

NT SPINE

Spinal reflexes through electric stimulation of gastrocnemius and soleus human leg muscles, attributing increased tendon reflex amplitudes to gamma motoneurons hyperactivation. 04 p0467 A72-14704

Seat cushion evaluation for behavior during helicopter crash or aircraft ejection and spinal injury probability. 08 p1126 A72-21577

Albino rats spinal cord capillaries ultrastructure upon hypothermy, noting endothelial cells sinking to lower levels from microscopic observation. 12 p1760 A72-27304

High threshold afferents role in dorsal surface potential formation in cat spinal cord. 13 p1905 A72-29327

Supraspinal effects on different work regimes of supplementary respiratory muscles, using interference electromyograms cross correlation analysis. 13 p1905 A72-29328

Human spinal segment functional state before voluntary movement during water immersion, using H-reflex for spinal cord motoneuron excitability evaluation. 14 p2073 A72-30255

Nucleic acid contents in cholinergic and adrenergic spinal cord neurons and in their glial satellite-cells during hypoxic hypoxia and a post-hypoxia period. 19 p2756 A72-37742

Russian book - Mechanisms of descending control of spinal cord activities. 21 p2998 A72-40577

A possible anatomical basis for descending control of impulse transmission through the dorsal horn. 21 p2998 A72-40578

Neuronal fiber and synaptic axonal contact structure of cat spinal gray matter in corticospinal, rubrospinal and reticulospinal terminal zones by Golgi method. 21 p2998 A72-40579

Morphological changes in spinal cord neurons of animals due to the decreased intensity of supraspinal stimulation. 21 p2998 A72-40580

The ultrastructure of the lateral basilar region of the spinal cord. 21 p2998 A72-40581

Neuronal organization of descending systems of the spinal cord. 21 p2998 A72-40582

Propriospinal ducts of the lateral funiculus and their possible role in transmission of pyramidal stimuli. 21 p2998 A72-40583

Synaptic suprasegmental control mechanisms of spinal cord motor neurons. 21 p2998 A72-40584

Study of the conductivity of the motor neuron membrane during supraspinal stimulation. 21 p2998 A72-40585

Intracellular study of rubrospinal neurons and of their synaptic activation during the stimulation of the sensorimotor cortical region. 21 p2998 A72-40586

Influence of a preceding afferent stimulation on the pyramidal activation of spinal motor neurons. 21 p2998 A72-40588

Systems analysis approach to the study of spinal mechanisms. 21 p2998 A72-40590

Role of pyramidal and extrapyramidal components of cortically-induced efferent stimuli in the mechanism of cortical motor activity coordination. 21 p2998 A72-40591

Possible role of supraspinal formations in the fixation of trace alterations at the segmental apparatus level of the spinal cord. 21 p2998 A72-40592

Cerebrum sections and related efferent processes as activator of automatic neuron mechanism control of motor activity, discussing segmentary spinal cord changes. 21 p2998 A72-40593

Role of efferent influences of temporo-rhinencephalic cerebral structures in pre-adjustment alterations of spinal motor neuron excitability. 21 p2998 A72-40596

Vasomotor reflexes and the principle of descending control. 21 p2998 A72-40597

Hypothalamic control of the electrical activity of the spinal cord. 21 p3000 A72-40598

Supraspinal effects in the activity of preganglionic sympathetic neurons delivering axons to the cervical sympathetic nerve. 21 p3000 A72-40599

Cortico-visceral studies of spinal cord reticular formation stimulation and destruction effects on electroencephalogram, cardiac activity and interoceptive glycemic reflexes. 21 p3000 A72-40757

Effects of physical exercise on spinal reflectivity in man. 21 p3003 A72-41524

Electromyographic investigation of diaphragm cross contraction following spinal cord section in cats, noting diaphragm motoneurons excitation by breathing center pulses. 22 p3142 A72-42281

Spinal cord heating and cooling effects on body temperature, respiratory and heart rates and arterial blood pressure, investigating feeding and drinking behaviors. 22 p3150 A72-42672

Classification of neurons in the lumbosacral section of the spinal cord according to their discharge during evoked locomotion. 23 p3257 A72-44092

Influence of the sympathetic nervous system on the presynaptic inhibition of the dorsal surface potential of the spinal cord. 24 p3370 A72-44589

SPINDLES

Experimental research on the wave resistance of a thin spindle with an annular shield in a supersonic axial flow. 24 p3364 A72-45393

SPINE

Human spine elastic deformation due to bending stresses, presenting statistical data on caudocephalad acceleration effects in vertebral column injuries. 01 p0016 A72-10111

Synaptic mechanisms of vestibulospinal and reticulospinal effect on transmission to lumbar motoneurons in monkeys. 02 p0158 A72-11760

Aircraft ejection simulation by human thoraco-lumbar spine flexion dynamic model, using strength of materials theory and shear effects for curved elastic beam. [ASME PAPER 71-WA/BHF-7] 05 p0620 A72-15947

Aircraft accident in the Faroe Islands in 1970 - Observations from a medical point of view, with special reference to spinal fractures. 17 p2508 A72-34556

The scoliosis of congenital heart disease. 24 p3370 A72-44560

SPINEL

Apollo flight lunar spinels compositional variations, formulating modified Johnstone prism projections. 01 p0134 A72-11162

Nonequilibrium subsolidus reduction of lunar spinels at low oxygen fugacities based on Cr-Al ulvospinel and olivine decomposition. 03 p0439 A72-14298

Chromian pleonaste and aluminous picotite in Apollo 14 fine grained microbreccias comparing with spinel composition in lunar basalts. 06 p0878 A72-17672

Opaque mineralogy of Luna 16 soil sample, emphasizing compositional variations of Fe-Ti-Cr-Al-Mg spinels. 09 p1380 A72-22261

Oxide spinels crystallographic structure determination, stability relationships, covalent bondings and physical properties. 10 p1501 A72-24730

Electron microprobe analysis of chromian spinels from Apollo 14 rocks indicating crystallization from high aluminum low iron magma. 12 p1865 A72-27113

Absorption spectrum of Cr cations in magnesium aluminate spinel crystals excited by strong optical pumping. 12 p1854 A72-27596

Magnesium aluminate spinel reinforced with sapphire whiskers, investigating whisker content, temperature and deflection rate effects on yield strength. 17 p2572 A72-35661

Room temperature operation of microwave acoustic delay lines with magnesium aluminate spinel, discussing acoustic mode conversion and shear wave piezoelectric transducers. 19 p2800 A72-37875

Elasticity of some mantle crystal structures. I - Pleonaste and hercynite spinel. 20 p2917 A72-39478

Occurrence of chromian, hercynitic spinel /'pleonaste' in Apollo-14 samples and its petrologic implications. 22 p3153 A72-42862

Solid solution, subsolidus reduction and compositional characteristics of spinels in some Apollo 15 basalts. 23 p3262 A72-44135

SPINOR GROUPS

Maxwell equation spinor formulation for Schwarzschild gravitational field effects on spherical electromagnetic waves propagation. 05 p0689 A72-16165

Integrability and identity relations for Newman-Penrose formalism equations in spinor description, assuming Einstein equations validity for vacuum. 10 p1510 A72-24105

Spinor differential equation of generalized unperturbed Kepler motion, using motor method and Lie algebra. 24 p3442 A72-45238

SPIRAL ANTENNAS

NT LOG SPIRAL ANTENNAS

Electronically scanned monopulse cavity backed quadratic spiral antenna array at 1.54-1.66 GHz for maritime satellite communications. 01 p0039 A72-10662

Frequency-independent multimode equiangular/conical spiral antenna with thick wires, calculating current distribution and radiation pattern by numerical program. 07 p0939 A72-19187

Radiation from a directive continuous spiral antenna array. 17 p2526 A72-34376

Experimental investigation regarding Archimedean spiral antennas for the L-band, and radiator groups constructed from them whose radiation directions are controlled by a conduction matrix. 21 p3028 A72-40510

SPIRAL GALAXIES

NT MILKY WAY GALAXY

Irregular, spiral and elliptical galaxies radio continuum measurements at 1420 MHz, presenting positions flux densities and brightness distributions

01 p0131 A72-11005

Spiral galaxies radio continuum emission origin, discussing supernovae and relativistic electrons effects

01 p0131 A72-11006

Milky Way Galaxy spiral structure determination, presenting arms anatomy, gas and star kinetics and radio astronomy data

03 p0417 A72-13104

Galactic spiral arm structure theory, discussing density wave pattern and material objects concepts

03 p0418 A72-13105

Neutral hydrogen distribution in spiral and irregular galaxies, discussing H II regions

05 p0716 A72-16371

Maffei 2 galaxy radio maps and H line studies, discussing distances, intrinsic luminosity, flux density and apparent size

06 p0886 A72-18097

Spiral galaxies hypothesis for higher mass-luminosity ratio of outer parts from undetected cold neutral hydrogen, using model of NGC 300

07 p1068 A72-19071

Stellar dynamical and density wave theories for spiral pattern persistence in Galaxy with differential rotation

07 p1074 A72-19430

Variational principle in equilibrium and stability theory of rotating bodies under magnetic and thermal fields, explaining spiral branch number in galaxies

07 p1077 A72-19806

NGC 3031 spiral galaxy photometry and large scale structure determination by UBV_R integral equidensity curves method

08 p1234 A72-21280

Wolf-Rayet stars identification in spiral galaxy M33/NGC 598/ from narrow band interference filter photographs, tabulating apparent magnitudes and emission indexes

09 p1382 A72-22281

Spiral density waves in galactic model with differentially rotating interstellar gas and stars, deriving dispersion equation by frequency to wave numbers relation

09 p1384 A72-22517

Galactic spiral density waves instability effects, noting local centroid radial motion and apex deviation

09 p1384 A72-22519

Intergalactic matter infall in galaxies, discussing quasar absorption spectra, hydrogen clouds, accretion rate and relations to spiral structure

09 p1386 A72-22660

Interstellar gas streaming velocity due to galactic spiral density waves, deriving mathematical expressions for Oort constant and differential galactic rotation nodes from Lin theory

09 p1391 A72-23538

Radio continuum survey of spiral galaxies M51 and NGC 5195 for study of galactic magnetic field and cosmic rays origin and distribution

10 p1543 A72-24623

Large Magellanic Cloud spiral structure and motion through interstellar gas, determining old and young stars spatial distribution near major spiral arm

10 p1544 A72-24662

Spiral galaxy density wave maintenance mechanism from rotating disk star-gas system model description of stellar birth and disintegration effects

10 p1547 A72-24869

Perseus two armed spiral shock model based on O associations, young open clusters, H II regions, interstellar absorption lines and 21 cm hydrogen maps

11 p1720 A72-26110

Small perturbations in collisionless stellar dynamics, discussing linear modes for flat axisymmetric galaxy and effects introduced by nonlinear theory of spiral structure

12 p1874 A72-27904

Instabilities initiation in spiral arm formation and stellar cluster evolution, noting analogy to hose-pipe instability in plasma physics

12 p1874 A72-27905

Numerical experimentation in collisionless systems for Jeans instability, static self consistent models and spiral patterns

12 p1874 A72-27908

Spiral density wave structure persistence conditions determined from computer simulations of galaxies evolution, noting gravitational azimuthal and radial forces effects

12 p1874 A72-27910

Milky Way spiral structure and star distribution, discussing photometric methods

12 p1875 A72-27967

Two phase flow model of cloud and star formation by galactic shocks in quasi-steady interstellar gas flow in spiral gravitational field

13 p2040 A72-29404

Spiral galaxies radio sources spectral components, noting relativistic electrons radiation and luminosity-surface brightness diagram

14 p2148 A72-30203

Galactic astronomy - Conference, State University of New York, Stony Brook, June-July 1968, covering Galactic structure, spiral shape theories, star migration, etc

14 p2152 A72-30486

H II regions radial velocities in Carina arms from Fabry-Perot interferometric H alpha measurements, determining early stars distances from spectroscopic and photoelectric observations

14 p2159 A72-30740

Elliptical and barred spiral Markarian galaxies, discussing starlike and diffuse spectra dependence on morphology

15 p2304 A72-31327

Spiral galaxy density wave damping by induced large-scale shock in interstellar medium

15 p2315 A72-32718

Spiral structure generation by outward angular momentum transfer, considering gravitational stress tensor, star-spiral wave momentum transfer and galactic secular evolution

16 p2457 A72-33683

Variational principle in equilibrium and stability theory of rotating bodies under magnetic and thermal fields, explaining spiral branch number in galaxies

17 p2617 A72-35730

Galactic spiral structure temporal decay based on density waves hypothesis

17 p2619 A72-35955

Spiral galaxies self gravitating cold disk model, considering equilibrium state, instability, oscillation modes, bending motions, pressure effects and angular momentum distribution

18 p2725 A72-36386

Multicolor photometry of the NGC 5194/5195 double system

19 p2858 A72-37812

Direction of trailing in spiral galaxies

19 p2863 A72-38067

The origin and form of the galactic magnetic field. II.

21 p3104 A72-40479

Gross properties of five Scd galaxies as determined from 21-centimeter observations.

21 p3105 A72-41027

Spiral and halo structure of our galaxy on the basis of optical distance determinations.

22 p3222 A72-42136

A photoelectric study of Messier 81.

22 p3229 A72-42975

Spiral galaxies radio sources spectral components, noting relativistic electrons radiation and luminosity-surface brightness diagram

23 p3333 A72-43232

SPIRALS
Narrow groove theory for spiral groove viscous pump gas bearings generalized to include rarefied gas and turbulence effects

02 p0234 A72-11531

SPIROMETERS
Respiration function testing device using spirometers and gas analyzers

09 p1272 A72-23256

A method for spirometric display of functional residual capacity and other lung volumes.

21 p3005 A72-40427

Radiorespirometry in the case of work and sports activities

22 p3149 A72-42071

SPLASH POINTS

U RECOVERY ZONES

U WATER LANDING

SPLREEN

Dipeptidyl aminopeptidase I preparation from beef spleen and rat liver, discussing contamination with catheptic carboxypeptidase C and Ser-Met dipeptidase

07 p0935 A72-18906

SPLINE FUNCTIONS

Engineering curves and surfaces representation by spline functions, discussing computerized approximation methods for algebraic, transcendental and transfer functions

07 p1024 A72-18777

Interpolation of function of two variables by surface splines method, solving linear equations system by digital computer

07 p1026 A72-19095

Real time recursive algorithms for estimating coefficients of fixed knot spline approximation to trajectory

08 p1197 A72-20849

Recursive and nonrecursive real time spline methods for nonlinear estimation of independent trajectory parameters for vehicle entering earth atmosphere

08 p1197 A72-20862

Increased accuracy cubic spline approximation to two-point boundary value problems for differential equation, noting truncation error

10 p1502 A72-23722

Computer programmed algorithm for conducting smooth piecewise polynomial third order approximation in spline function determination

13 p1986 A72-29065

Polynomial spline function for approximate solution of Cauchy problem for nonlinear differential equations of order n

14 p1216 A72-30716

Holographic strain analysis using spline functions.

19 p2797 A72-37611

Book - Functional analysis and approximation theory in numerical analysis.

20 p2946 A72-39729

Calculation of potential flow about aerofoils using approximation by splines.

22 p3135 A72-42844

Spline transformation of independent variable for free transverse vibration of elastic bars with piecewise constant rigidity, calculating resonant frequencies

23 p3348 A72-43793

Spline functions application to approximation theory problem of determining diameters of subspaces and manifolds in Banach space

24 p3419 A72-45548

SPLINES
Additional deformation work for splines forming in splined circular profiles pressing, deriving characteristic displacement velocity distribution equations

13 p1963 A72-28744

SPLIT FLAPS
Three dimensional wind tunnel investigation of vortex augmented unswept wing with leading edge cusp flap and split upper and lower trailing edge flaps

11 p1568 A72-25584

SPLITS (GEOLOGY)
U GEOLOGICAL FAULTS

SPLITTING
Electric field induced splitting of drift shells composed of trapped particles, taking into account non-dipole field components to lowest order

01 p0062 A72-10905

SPOILERS
Aircraft flight characteristics for landing approach by spoiler-elevator deflection coupling, considering pitch, flight path angle and speed

16 p2343 A72-33423

Jaguar powered flight controls, discussing wing spoilers, slab tailplane, rudder, autostabilization system and integrated packaging of actuators

16 p2353 A72-34144

SPONTANEOUS COMBUSTION
Gaseous diethyl peroxide spontaneous ignition during decomposition in cylindrical vessel, investigating diluents and temperature effects on self heating

02 p3010 A72-12027

Thermal theory of criticality for spontaneous explosion of exothermic reactant mass in bodies of arbitrary shape

03 p0457 A72-13972

Self ignition in hydrogen oxidation kinetics, considering convection, molecular diffusion, mixing and pressure

05 p0625 A72-17212

Turbulent hot gas stream self ignition in oxidizers flow for hydrogen-air and gasoline-air mixtures

14 p2170 A72-30294

Composite and double base solid propellant rocket motors storage, considering ingredients and materials compatibility and ignition temperatures effects on spontaneous inflammation potential

14 p2144 A72-30761

Self-ignited impulsive optical discharge in a laser erosion plasma

23 p3295 A72-43308

SPONTANEOUS EMISSION
Current dependent intensity of spontaneous emission of GaAs injection laser operated at 300 K

02 p0238 A72-12204

Pulsed Ar ion laser quantitative level population mechanism in gas discharges, discussing radiation trapping effects on 4s doublet based on spontaneous emission line data

04 p0529 A72-14602

Neon lower laser level spontaneous emission doublet resonance phenomena, discussing depopulation rates and resonance line profile changes

04 p0531 A72-15138

Spontaneous emission from driven Doppler broadened gas of two level atoms radiating into free space, predicting power spectrum

07 p0940 A72-19194

Temperature dependence of internal quantum efficiency of spontaneous emission as function of beam voltage in electron beam excited p-type GaAs

10 p1526 A72-24559

Instantaneous and averaged emission spectra of injection laser under spontaneous pulsation as function of operation mode and photon distribution

12 p1824 A72-27879

Spectral line profile of optical transition spontaneous radiation during resonance with strong field on adjacent transition

14 p2110 A72-30781

High gain laser amplifier spectral linewidth dependence on external signal or spontaneous emission source, noting saturation role and relevance to interstellar medium radiation

16 p2453 A72-33166

Active medium spontaneous radiation level effect on traveling wave amplifier gain factor, supporting theoretical results by experiments with superluminescent Ne-He active medium

16 p2400 A72-33277

Instantaneous and averaged spiking emission spectra of injection laser under spontaneous pulsation as function of oscillation mode and photon distribution

16 p2404 A72-33984

Behavior of spontaneous emission across threshold in GaAs junction lasers.

19 p2811 A72-37865

Reduction in the rate of increase of spontaneous emission from double-heterostructure injection lasers at threshold.

19 p2811 A72-37866

Spontaneous emission of plasma waves in the presence of a finite amplitude wave.

21 p3093 A72-41494

Effect of increasing beam voltage on the internal quantum efficiency of spontaneous emission in electron-beam-excited p-type GaAs.

22 p3185 A72-42308

Group theory for spontaneous coherent radiation of multilevel sources, noting angular distribution of photon echo effects

23 p3295 A72-43306

Experimental studies of injection lasers - Spontaneous spectrum at room temperature.

24 p3409 A72-44713

PONTANEOUS IGNITION TEMPERATURE

U IGNITION TEMPERATURE

U SPONTANEOUS COMBUSTION

SPORADIC E LAYER

Skyark rocket observations of sporadic E layer magnetic fields, winds and ionization indicating ion divergence region

01 p0052 A72-10086

Sporadic E layer reflection behavior measurements from two closely located stations, deriving drift direction and critical frequencies daily variation

01 p0055 A72-10431

Daily, annual and long term ionosscatter and sporadic E variations above Europe, using hf propagation measurements

01 p0055 A72-10432

Sporadic E layer occurrence frequency distribution during 1958-1960, investigating characteristics over equatorial, temperate and auroral zones

01 p0059 A72-10596

Middle geographic latitude sporadic E-layer initial height variations during 1957-1968 solar cycle

01 p0064 A72-11103

Sporadic E layer motion and spreading under constant horizontal wind action, estimating lifetime

02 p0218 A72-11942

Sporadic E layer shielding frequency correlation to limiting reflection frequency calculated by diurnal data from nine ground stations

02 p0221 A72-12522

Shielding and semitransparent sporadic E layer fine structure characteristics from summer observations data analysis

02 p0222 A72-12523

Reflection and transmission coefficients for radio waves incident upon thin highly ionized layers, comparing with sporadic E reflections

03 p0344 A72-12976

Sporadic E disappearance due to temporary reversal of equatorial electrojet current, observing horizontal geomagnetic field component

03 p0345 A72-12999

Solar X-ray control of E and sporadic E layers during November 1966-July 1968, discussing blanketing frequency

03 p0413 A72-13535

F 2 layer anomalies association with equatorial electrojet, investigating midday critical frequencies of sporadic E layer

04 p0515 A72-14932

Daytime ionogram corrections for underlying ionization in absence of X-trace of sporadic E layer

05 p0657 A72-16265

Geomagnetic pulsations correlation with h type ionospheric sporadic echoes, considering effects on electromagnetic disturbances transmission

05 p0659 A72-16725

Vhf waves transhorizontal propagation and day types correlation with sporadic E ionospheric layers in temperate zone, discussing wind shear theories

05 p0659 A72-16782

Rocket-borne vector magnetometer measurements of midlatitude ionospheric currents near sporadic E, noting nearly uniform vertical distribution

06 p0804 A72-17459

Sporadic E ionization during 1955 partial solar eclipse, considering gravity waves effect due to fast moving shadow region cooling spot

06 p0805 A72-17466

Geophysical aspects of ionospheric scintillation problems, considering correlation with spread F and sporadic E

06 p0889 A72-18282

Metallic ion convergent flow role in sporadic E layer formation in auroral and equatorial ionosphere

06 p0810 A72-18730

PE sub s harmonic components diurnal and seasonal variations and latitudinal dependence, investigating relationship to drift velocity in E region

06 p0811 A72-18749

Unified coordinate system for earth planetary distribution of F2 and sporadic E layer transmission parameters, suggesting geomagnetic longitude and modified magnetic inclination

08 p1153 A72-20726

Polar latitude sporadic E layer diurnal variations with appearance dependence on cutoff frequency

08 p1130 A72-20727

Radar verification of sporadic E layer formation from meteoritic atoms and ions production by meteoritic ablation

08 p1154 A72-20728

Errors in ionospheric sounding of sporadic E layers with auroral presence, discussing continuous reflections duration distribution

08 p1155 A72-20817

Seasonal variation in ionospheric horizontal drift velocities under normal E and sporadic E conditions for middle latitudes

08 p1157 A72-21115

Fading method measurement of normal and sporadic E region drift, reviewing height gradient data

08 p1161 A72-21539

Wind shear theory of midlatitude sporadic E formation, using wind profiles from artificial luminous cloud observations

08 p1161 A72-21540

Sporadic E layer critical frequency relationship to ionospheric wind direction for midlatitudes in summer period

10 p1472 A72-24079

Equatorial sporadic E sudden disappearance associated with magnetic field depressions, noting irregularities and electron velocities role

10 p1475 A72-24956

Temperate latitude sporadic E cause and structure - Conference, Utah State University, Logan, September 1971

10 p1477 A72-25151

Sporadic E layer variations monitoring in 50 MHz band, examining diurnal, seasonal, magnetic and meteoroid showers relationships of oblique incidence paths

10 p1441 A72-25152

Sporadic E layer structure model from radiosonde observation, noting peak plasma frequency variation and total reflection by blobs

10 p1441 A72-25153

Simultaneous rocket observation of wind shear and electron density profile in lower ionosphere, noting sporadic E layer formation

10 p1477 A72-25154

Wind shear theory expectations tested by wind profiles and sporadic E layer observations, stressing time variations significance

10 p1477 A72-25155

Midlatitude sporadic E layer observed by rocket and radio sounding, deriving plasma frequency from peak electron density

10 p1477 A72-25156

Wind shear and midlatitude sporadic E layer theories, discussing metal ions production and loss

10 p1477 A72-25158

Metal ion sheaths in midlatitude sporadic E layer caused by vertical redistribution of neutral ionization, discussing wind shear discontinuities

10 p1477 A72-25159

Temporal variations of sporadic E layer blanketing frequency, virtual height and occurrence rate, calculating electron density profiles and tidal wind influence

10 p1441 A72-25162

Sporadic E layer altitude and density variations caused by lunar influences, using model for electrostatic field and wind shear effects

10 p1478 A72-25163

Small scale sporadic E layer explained by means of cross field instability, proposing numerical solution based on realistic three dimensional perturbation

10 p1478 A72-25164

Electron density maxima position relationship to wind profiles in sporadic E layer with electric fields and vertical ion motion

10 p1530 A72-25165

Sporadic E layer cyclic variations during solar activity cycle, noting time dependence of occurrence probability and critical frequency

11 p1623 A72-26281

Single pulse radio echo fading dependence on sporadic E layer critical and screening frequencies

11 p1595 A72-26282

Sporadic E layer structure and dynamics diurnal and seasonal variations from ionosondes frequency and drift measurements

12 p1804 A72-27781

Sporadic E layer frequency variations from space-diversity sounding data from three ionospheric stations

13 p1946 A72-28599

Sporadic E layer motion and spreading under constant horizontal wind action, estimating lifetime

13 p1949 A72-29254

Diurnal and seasonal variations of ionospheric absorption in D and E regions, discussing blanketing sporadic E presence effect

13 p1922 A72-29392

Midlatitude sporadic E layer formation under wind shear action from artificial cloud data on lower thermosphere wind speed and direction

13 p1951 A72-29589

Auroral sporadic E layer diurnal distribution correlation to charged particle integral flux diurnal variations observed by satellite in winter, noting Kp index effect

14 p2102 A72-30655

Atmospheric gravity waves effects in ionosphere, discussing F region traveling ionospheric disturbances, sporadic E layer and D region radar scattering

15 p2222 A72-31285

Midlatitude nighttime sporadic E layer relationship to geomagnetic field, considering wind shear theory

15 p2224 A72-31798

Blanketing sporadic E layer latitude seasonal variations near geographic equator, noting spread F occurrence and solar cycle effects

15 p2231 A72-32265

Tropical sporadic E reflections and vertical plasma instabilities as function of equatorial electrojet and electron drift ratio based on ionogram observations

16 p2382 A72-32867

Height of the region of principal auroral radio-wave absorption in the presence of a sporadic E layer

17 p2519 A72-33869

Dependence of sporadic ionization in the high-latitude ionospheric E-region on magnetic activity

18 p2688 A72-36860

Unified coordinate system for global distribution of F 2 and sporadic E layer transmission parameters, suggesting geomagnetic longitude and modified magnetic inclination

19 p2791 A72-38354

Polar latitude sporadic E layer diurnal variations with appearance dependence on cut-off frequency

19 p2766 A72-38355

Radar verification of sporadic E layer formation from meteoritic atoms and ions produced by meteoroid ablation

19 p2791 A72-38356

The interpretation of ionospheric radio drift measurements. V - Demonstration of the point effect in time-averaged correlations and drift calculations.

19 p2794 A72-38862

Very-high-frequency wave propagation by the temperate-latitude sporadic-E layer.

22 p3154 A72-42367

Metal ions effect on sporadic E layer formation, noting magnesium ions profile redistribution by vertical gradient in neutral particles wind

23 p3284 A72-43376

Sporadic E layer frequency variations from space-diversity sounding data from three ionospheric stations

24 p3398 A72-45099

SPORADIC METEORIODS

Sporadic meteor orbital parameters measurement by continuous radar, determining out-of-atmosphere rate

02 p0283 A72-12524

Ejected lunar particles in meteoric sporadic background, noting brightness relation to yearly particle concentration

19 p2864 A72-38324

SPORES

Spore survival in dry heat sterilization as function of water activity, indicating entropy-molecular stability relationship

04 p0475 A72-15259

Dry heat resistance of bacillus spores on spacecraft metal surfaces for different pressures, atmospheres and materials

04 p0475 A72-15261

Aliphatic hydrocarbons in phytopathogenic fungi spores, discussing similarity to higher plant alkanes, functional roles and species distribution and occurrence

13 p1906 A72-29834

Aqueous formaldehyde effects on Bacillus subtilis spores, showing sporostasis due to germination inhibition and sporocide due to temperature dependent inactivation

16 p2357 A72-33772

Probability for spore sterilization by aerodynamic heating, considering straight line and decaying circular orbital Mars entry trajectories

16 p2461 A72-34165

The effects of various cure cycles upon the viability of *Bacillus subtilis* var. *niger* spores within solid propellant.

18 p2652 A72-36437

A re-evaluation of material effects on microbial release from solids.

23 p3253 A72-43383

SPOT WELDS

Electron beam welding with filler metal, describing spot and butt welding applications

06 p0819 A72-17498

Spot and seam welding of Cr ferritic stainless steel thin sheets, discussing electric current loading in relation to sheet thickness and contact pressure

07 p0995 A72-19575

Metal inert gas (MIG) spot welding process effects on weld dimensions, shape and strength

09 p1320 A72-23630

Al alloy-graphite composites brazing and welding feasibility, tabulating spot welding parameters

11 p1641 A72-26491

Ultrasound reflection from molten core during spot welding of steel alloys as function of geometrical dimensions and configuration and transition zone dimensions

13 p1965 A72-29152

High speed photographic analysis of spot welding galvanized steel, observing three stage process

13 p1958 A72-29421

A preliminary investigation of joining methods for aluminum-graphite composites.

17 p2561 A72-35665

Combined spot weld-adhesive bonding to join sheet metal parts with applications to spacecraft and aircraft structures [SME PAPER AD 72-710]

18 p2695 A72-36526

SPRAY CHARACTERISTICS

Polydisperse spray device with controllable drop size distribution for two phase detonation research

04 p0509 A72-15486

In-line holography of reacting liquid sprays.

19 p2798 A72-37619

SPRAY NOZZLES

Method of calculating pneumatic spray nozzles

23 p3325 A72-44015

SPRAYED COATINGS

Plasma sprayed tungsten and zirconium dioxide coatings porosity on chromium bronze, Ti and Al alloys and steel

03 p0363 A72-13550

Sprayed single component ceramic coating thermal stability enhancement techniques, noting limitations

05 p0680 A72-16093

Composite plasma sprayed coatings of Cu, Ni and boron nitride, noting antifriction and wear characteristics

06 p0822 A72-18429

Plasma spraying process effects on carbon steel coatings structure and bonding, considering optimal parameters, properties control and phase transformations

07 p0996 A72-19966

Plasma coating formation mechanisms and parameters, studying metal surface and deposited particles temperatures, spraying time effects, etc

10 p1487 A72-24488

Ultrasonic device with magnetostriction vibrator for suspension coating oxide cathodes, noting superiority to spray coating by compressed air

16 p2374 A72-33969

Variables influencing the characteristics of plasma-sprayed coatings.

17 p2561 A72-35920

SPRAYED PROTECTIVE COATINGS

U PROTECTIVE COATINGS

U SPRAYED COATINGS

SPRAYERS

Polydisperse spray device with controllable drop size distribution for two phase detonation research

04 p0509 A72-15486

SPRAYING

NT ARC SPRAYING

NT FLAME SPRAYING

NT METAL SPRAYING

NT PLASMA SPRAYING

SPRAYING APPARATUS

U SPRAYERS

SPRAYS

U SPRAYERS

SPREAD F

Spread F effects on transequatorial ionospheric short wave oblique incidence path great circle deviations

01 p0056 A72-10438

Positive Fe ion concentration relationship to equatorial spread F fromOGO 6 satellite observation near magnetic equator

01 p0062 A72-10902

Ionospheric spread-F mechanism as electromagnetic wave scattering on electron density inhomogeneities, calculating characteristic dependence of height interval on operational frequency

02 p0216 A72-11920

Supermode F range spreading and evening type transequatorial propagation, considering single scattering in east-west plane

03 p0321 A72-12994

Geophysical aspects of ionospheric scintillation problems, considering correlation with spread F and sporadic E

06 p0889 A72-18282

Turbulent LF electric field fluctuations relationship with disturbed F region, spread F and scintillations of radio stars and satellites

09 p1300 A72-23025

Equatorial spread F spatial and temporal distribution from short wave side reflection observations along Lindau-Tsumeb transequatorial HF radio transmission path

12 p1803 A72-27778

Ionospheric spread-F mechanism as electromagnetic wave scattering on electron density inhomogeneities, calculating characteristic dependence of height interval on operational frequency

13 p1948 A72-29232

Range and frequency spread F diurnal and seasonal variations at magnetic equatorial station Thumba, noting geomagnetic activity effect

14 p2097 A72-30130

Spread F association with ionospheric tilts due to total electron content drift, using incoherent scatter radar

15 p2230 A72-32261

Blanketing sporadic E layer latitude seasonal variations near geographic equator, noting spread F occurrence and solar cycle effects

15 p2231 A72-32265

Ground recorded Pc 1 micropulsations occurrence frequency relationship to ionospheric spread F based on long term ionosonde recordings

18 p2685 A72-35987

F 2 layer spread reflections and critical frequencies increase on ionogram recordings during Northern Hemisphere nighttime magnetic storm of 2 December 1967, noting cosmic radio emission decrease

19 p2791 A72-38366

Radar observations of equatorial spread F in a region of electrostatic turbulence.

23 p3286 A72-44528

Equatorial spread F - Recent observations and a new interpretation.

23 p3286 A72-44530

SPREAD REFLECTION

U DIFFUSE RADIATION

SPRINGS [ELASTIC]

Energy-phase time transformations of damped Liapunov system applied to nonlinear spring pendulum and betatron transient oscillations

01 p1013 A72-11387

Springs fracture and vibration in injection pumps by analog model

02 p0236 A72-12437

Impact dampers with spring connection of masses, analyzing periodic motion

02 p0298 A72-12617

Mean-square approximate estimator for standard deviation of natural frequency of two degrees of freedom spring systems, comparing with Monte Carlo simulation

[ASME PAPER 71-WA/APM-7] 05 p0734 A72-15971

Infinitely long Euler-Bernoulli damped periodic aluminum beam with elastic springs, determining distance for steady state sinusoidal response to spatial decay

05 p0736 A72-16111

Damping of lateral oscillatory processes by end terminal displacement compensation, noting spring energy

05 p0691 A72-17132

Impact interaction between free two body system with elastic spring coupling and fixed plane, considering mass ratio and velocity restitution coefficient

08 p1209 A72-21803

Thin walled Bourdon tube manometric spring deformation analysis by Ritz method in second approximation

09 p1397 A72-22349

Mechanical system with inertial vibration sensor and nonlinear spring, obtaining global asymptotic stability of zero solution of differential equations describing natural vibration

09 p1399 A72-22697

Single degree of freedom systems with nonlinear spring characteristics of skew symmetric form, discussing 1/2 subharmonic oscillation analysis by harmonic balance method

09 p1342 A72-23455

Nonlinear elastic suspension system with two springs in parallel, measuring nondimensional load versus deflection curve and frequency response

11 p1736 A72-26007

Coupled nonlinear equations of motion of large deflections of impacted helical springs, comparing with streak photographs

11 p1688 A72-26061

Static deflection effect on nonlinear spring mass system step function response, considering approximate calculation of oscillation period

11 p1688 A72-26372

Natural vibration modes of coupled spring-mass nonlinear system with two degrees of freedom from stability analysis

12 p1844 A72-27245

Heat generation in oscillating torsional spring modeled by viscoelastic hollow cylinder subjected to sinusoidal shear stresses, calculating stress and temperature distribution and displacement

17 p2635 A72-34232

Contractile and muscle-like fibers and autopolusation systems for polymer engine and spring action studies

19 p2760 A72-38200

Electric relay spring design for miniaturization, deriving relation between length and thickness to minimize fiber stress under constant contacting force

19 p2775 A72-3861

Mechanical properties of heat and corrosion resistant nonmagnetic Ni-Cr-Nb spring alloys with W addition tested in aggressive and nitric acid base media

23 p3300 A72-43595

SPUR [REACTORS]

U SPACE POWER UNIT REACTORS

SPUTNIK 1 SATELLITE

Soviet space program review from Sputnik 1 launch, discussing launch sites and vehicles, lunar, planetary and manned missions, civil and military programs and future goals

05 p0722 A72-17091

SPUTNIK 3 SATELLITE

Upper atmosphere density measurement techniques used by Sputnik 3 and San Marco 1 and 2 satellites

12 p1802 A72-27683

SPUTTERING

Sputtered molybdenum disulfide film lubrication, discussing adherence to metal surfaces, particle size, friction experiments and tensile tests

02 p0236 A72-12848

Sputtering sources fabrication by plasma spraying for nitride films deposition with Ta-Hf mixtures

04 p0527 A72-15494

Ni-Cr thick films triode sputtering technique with temperature control by low-energy electron bombardment heating, presenting phase diagram

05 p0675 A72-16393

Thin film formation techniques including evaporation, sputtering, anodization, chemical vapor deposition, electrodeposition and sintering, discussing surface scattering, tunneling, Schottky emission and conduction mechanisms

06 p0790 A72-1857

Sputtered molybdenum disulfide lubrication on polished metal surfaces with low friction coefficients, strong adherence, high density and small particle size

06 p0824 A72-18607

Lunar dust grain fossil coatings of ultrathin metamorphized amorphous layers resulting from solar wind ion implantation

08 p1230 A72-20982

A-15 superconducting films preparation cosputtering method, noting alloying effects and crystal structure stability determinations applications

09 p1368 A72-22554

Noncrystalline Ge film preparation by rf sputtering onto substrate with explosive crystallization triggered by localized transient energy pulse at room temperature

09 p1369 A72-22623

Differential sputtering yield of Ni-Cu alloy solid solution bombarded by Ar ions

10 p1495 A72-24057

Dc and RF sputter deposition in ionized inert gas of thin film coatings solid state microelectronics, solid lubricants and corrosion resistance applications

[ASME PAPER 72-DE-37] 14 p2108 A72-30871

X ray photoelectron spectroscopic measurements of Fe and Cu valence states produced by ion sputtering reduction, applying to multiplet splitting and isoelectronic shifts

16 p2389 A72-33026

Diffusion limitation avoidance at high current densities by fuel cell preparation via Pt thin film sputtering on porous vycor substrates

16 p2352 A72-33893

Thin films deposited by evaporation and sputtering - A comparative study

18 p2696 A72-36834

Effect of structural parameters and temperature on the effective thermal conductivity of plasma-sputtered aluminum oxide

18 p2696 A72-37188

Evidence of crystal structure in some sputtered MoS₂ films.

19 p2823 A72-37897

Physical and electrical properties of thin-film barium titanate prepared by RF sputtering on silicon substrates.

22 p3215 A72-42999

SQUALL LINES

U SQUALLS

SQUALLS

Morning glory, showing squall formation by atmospheric hydrologic jump favored by slack pressure gradients, cloudless skies and low latitudes

11 p1681 A72-26080

SQUARE WAVES

Square wave source gated detector bridge for precise resistance measurement, discussing design and performance, and application in Pt resistance thermometry

06 p0785 A72-18244

Frequency measurements of square wave signal with unknown amplitude by two mismatched channels, comparing rms error with effective estimate variance

10 p1436 A72-24509

Solid state ac square law function generator based on fixed elements and operating on electrical servo system principle

13 p1933 A72-29973

A simple reference generator for lock-in amplifiers.

21 p3025 A72-40206

Shaping circuit for complex RF pulse consisting of simultaneous equallength square pulses with different frequencies, discussing carrier frequencies selection

21 p3022 A72-41118

Parabolic approximation of spatially bounded square and Lorentz two dimensional light pulse propagation in homogeneous isotropic linear medium without dispersion

23 p3313 A72-43682

QUARES [MATHEMATICS]

Laplace equation under Robbin boundary conditions over unit square, discussing numerical solution by difference approximation and iterative procedure

05 p0682 A72-16100

QUEEZING

U COMPRESSING

QUIRRELS

NT GROUND SQUIRRELS

R [REACTORS]

U SATURABLE REACTORS

T VENANT FLEXURE PROBLEM

U SAINT VENANT PRINCIPLE

TABILITY

NT ACOUSTIC INSTABILITY

NT AERODYNAMIC STABILITY

NT AIRCRAFT STABILITY

NT ATTITUDE STABILITY

NT BOUNDARY LAYER STABILITY

NT COMBUSTION STABILITY

NT CONTROL STABILITY

NT DIMENSIONAL STABILITY

NT DIRECTIONAL STABILITY

NT DYNAMIC STABILITY

NT FLAME STABILITY

NT FLOW STABILITY

NT FREQUENCY STABILITY

NT GYROSCOPIC STABILITY

NT HOVERING STABILITY

NT LATERAL STABILITY

NT LONGITUDINAL STABILITY

NT MAGNETOHYDRODYNAMIC STABILITY

NT MAGNETOSPHERIC INSTABILITY

NT MOTION STABILITY

NT ROTARY STABILITY

NT SHELL STABILITY

NT SPACECRAFT STABILITY

NT STATIC STABILITY

NT STORAGE STABILITY

NT STRUCTURAL STABILITY

NT SURFACE STABILITY

NT SYSTEMS STABILITY

NT THERMAL STABILITY

Uniformly and asymptotically stable solutions to linear Volterra integrodifferential equation system, discussing Liapunov stability

02 p0252 A72-11997

Centered difference approximation for atmospheric model advection equation by two step Lax-Wendroff method, discussing computational instability due to lattice separation

11 p1680 A72-25768

Baroclinic instability formulation as initial value problem compared to normal mode studies, considering cyclone development in atmosphere

13 p1945 A72-28446

Stability in mechanics of continuous solids - Conference, University of Waterloo, Ontario, Canada, October 1970-September 1971

13 p2054 A72-28476

Liapunov direct stability method extension to partial differential equations, using functional analysis and wave equation example

13 p1985 A72-28483

Necessary and sufficient conditions for the absolute asymptotic stability of linear systems of differential equations with constant delay

22 p3198 A72-42143

TABILITY AUGMENTATION

U FEEDBACK CONTROL

U STABILIZATION

TABILITY DERIVATIVES

NT PITCHING MOMENTS

NT ROLLING MOMENTS

NT YAWING MOMENTS

Hypersonic vehicles lateral dynamics during great circle flight, using linearized equations of motion and Newtonian theory for stability derivatives estimation

08 p1110 A72-21603

Aerodynamic force and moment measurements on model in magnetic wind tunnel balance system, using field equations

10 p1461 A72-24765

STABILITY TESTS

NT FLIGHT STABILITY TESTS

NT WIND TUNNEL STABILITY TESTS

Contact surface turbulent mixing instability in free piston high enthalpy shock tunnel waves with test air and argon gases

05 p0644 A72-16548

Aerospace explosive components accelerated storage life and stability tests, basing method on Arrhenius reaction rate equation modification

08 p1220 A72-20762

Liquid nitrate ester sensitivity and dissolved water desensitization, using thermal initiation and drop weight impact tests

09 p1373 A72-23145

Plastic model shells design, construction and instrumentation for elastic stability studies in NDT, discussing deformation measurements for critical condition prediction

22 p3163 A72-42694

Nonlinear nonautonomous dynamic systems practical stability conditions for specified settling time, verifying constant matrix Hurwitz property

23 p3309 A72-43858

STABILIZATION

NT SIGNAL STABILIZATION

NT SPIN STABILIZATION

Austenite stabilization in maraging steel by cumulative heat cycling, using dilatometric and X ray analysis techniques

07 p0998 A72-20483

Control system for stabilization of liquid propellant rockets Pogo oscillations, discussing structure, fuel tank and feed system, combustion chamber, control gain and accelerometer installations

10 p1551 A72-24027

Ionic and hydrophobic interactions effects on Micrococcus lysodeikticus membrane stabilization process

14 p2075 A72-30595

Discharge stabilization in closed cycle carbon dioxide electric discharge convection lasers by aerodynamic, RF power and tandem techniques

[AIAA PAPER 72-723]

16 p2404 A72-34026

Stabilizing techniques for holographic recording.

17 p2556 A72-35416

Problems and solutions related to the design of a control augmentation system for a longitudinally unstable supersonic transport.

[AIAA PAPER 72-871]

20 p2887 A72-39128

STABILIZED PLATFORMS

Differential equations of motion for stable member of three-axis gyro stabilized platform

03 p0387 A72-14190

Equations of motion for stable member of three axis gyro stabilized platform for inertial navigation, including friction, inertia and torque motor effects

05 p0662 A72-16557

Inertial navigation system accelerometer error autocompensation, using reversal by accelerator forced rotation in stabilized platform plane

05 p0664 A72-17148

Three component airborne magnetometer design, discussing direction reference system and stabilized platform

06 p0812 A72-17372

ATS F and G satellites with 30 foot deployable antennas as three axis stabilized platforms in geostationary orbit with high pointing accuracy

07 p1085 A72-19275

Nonlinear controls for single axis gyro platforms, using time optimal Luenberger observers

07 p0989 A72-20278

Optimal alignment and calibration of gyrostabilized platforms, using Kalman filter and minimal weighted squared errors

07 p0989 A72-20280

Attitude reference platforms in ASTRID and DACHS control systems for high altitude research rockets

07 p0990 A72-20283

German monograph on inertial platform stabilization by optical sensors for space vehicle guidance covering aircraft position determination

09 p1394 A72-22334

Tethered autostabilized rotor platform for military surveillance, target location and communication, discussing flight vehicle, tethering cable, ground station and guidance-control system

13 p1898 A72-30078

Stable microprecision test platforms construction and microseismic effects on motion sensing instrument calibration including gyroscopes and inertial navigation and guidance systems

[AIAA PAPER 72-893]

20 p2911 A72-39110

Black Arrow satellite launch vehicle attitude control as part of inertial guidance system, describing four-gimbal gyroscopically stabilized platform and associated electronics

21 p3115 A72-40121

STACKING FAULT ENERGY

Vertical flight direction determination by gyrostabilizers with integral compensation, noting variable platform orientation and vibration damping correction

21 p3059 A72-41812

Method of equivalent turns in the kinematics of inertial systems

23 p3311 A72-43583

Kalman filter design considerations for space-stable inertial navigation systems.

24 p3421 A72-44640

STABILIZERS [AGENTS]

Effective stabilizer content measurement in smokeless powder propellants, discussing nitrogen dioxide generation by cellulose nitrate and glycerin trinitrate decomposition

14 p2144 A72-30755

STABILIZERS [FLUID DYNAMICS]

NT HORIZONTAL TAIL SURFACES

Parachute designs and applications to escape systems, paratrooping, supply dropping, aircraft braking, weapons systems stabilization, flight testing aids and sport

01 p0003 A72-10302

Development of an inflatable fabric structure for the early stabilization of the B-1 crew escape capsule.

[AIAA PAPER 72-801]

20 p2888 A72-40053

Flight test investigation of the aerodynamic behavior of various-sized stabilizers on a small helicopter.

24 p3362 A72-45328

STABLE OSCILLATIONS

Integrated PFM feedback control system, investigating stable periodic oscillation based on nonlinear discrete equivalence

04 p0506 A72-15114

Third order nonlinear van der Pol oscillating systems, discussing digital computer verification for existence of stable limit cycles in state space trajectory plots

05 p0639 A72-15806

Higher order nonlinear autonomous oscillation system limit cycle and stability determination by numerical solution based on Andronov point transformation and Liapunov theory

06 p0838 A72-17377

Microwave parametric amplification and conversion in circuits with Josephson junctions, describing stable oscillation measurements

06 p0866 A72-18477

Bistable hydraulic servomechanisms limit cycle stable oscillations from bang-bang control and cavitation effects, discussing valve driving gear hysteresis and time lag

08 p1113 A72-22155

Oscillation development time in phantastron oscillator, using linearization of nonlinear term

10 p1450 A72-24517

Steady state combination oscillations stability, examining geometrical properties of amplitude surfaces

14 p2133 A72-31128

Stochastic atmospheric density fluctuations effect on circular-orbiting satellite roll-yaw oscillations stability

15 p2319 A72-31457

Lasing kinetics in coupled lasers pair, noting generation of steady state oscillations without relaxation

15 p2252 A72-32696

Frequency/temperature characteristics of Gunn devices.

18 p2667 A72-36684

Nonsymmetric oscillations in certain symmetric nonautonomous systems

19 p2777 A72-37436

STACKING FAULT ENERGY

Hexagonal close packed Ti-Al alloys, determining stacking fault probability with X ray powder diffraction line profiles and Fourier analysis

01 p0087 A72-11029

Rolled metals and alloys with various lattice types and packing defect energies, showing elastic properties isotropy and Young modulus anisotropy

03 p0371 A72-13188

Dislocation substructure in fatigued Al and Ni polycrystals surface layer and interior due to high and low stress cycling, discussing stacking fault energy influence

04 p0534 A72-15577

Dislocation splitting and stacking fault energy variation during plastic deformation of TaC at 2200 C, using bending tests and microscope observations

[ONERA, TP NO. 1005]

05 p0670 A72-15861

Thermodynamic estimation of transition metal stacking fault energy, discussing relation to lattice stability and structural changes

05 p0679 A72-17149

FET devices stacking faults induced leakage currents, pinpointing critical processing steps by diagnostic X ray charts

06 p0782 A72-17364

Martensitic transformations induced by plastic deformation in Fe-Ni-Cr-C system, noting stacking fault energy dependence on temperature

07 p1015 A72-19928

Three and four layer vacancy defects annealing in quenched Al for stacking fault removal

07 p1020 A72-20412

Impurities effects on stress corrosion and work hardening induced dislocation structures in stainless steels, considering stacking fault energy relationship

10 p1496 A72-24231

High temperature steady state tensile creep behavior of Ni-W solid solutions, showing creep rate relation to stress and stacking fault energy

13 p1975 A72-28668

Al and AlMg single crystals static recovery and stacking fault energy at 77-500 K in plastic deformation, noting cross slip onset at 500 K

13 p1978 A72-29222

Chemical interaction within crystals for generation of stacking fault vacancies and phenomena associated with solid solution microheterogeneity dislocations, discussing heat resistance

15 p2254 A72-31558

Alloying effects on high temperature softening due to crystal lattice, stacking fault energy and decreased mobility interactions

15 p2254 A72-31564

High-temperature resistant cobalt alloys

17 p2567 A72-35173

Measurement of the stacking-fault energy of gold using the weak-beam technique of electron microscopy

22 p3177 A72-42320

A study of cold-worked titanium-aluminum alloys by X-ray diffraction

24 p3413 A72-44720

The creep of dispersion-strengthened Ni-Co alloys

24 p3413 A72-44923

Measurement of stacking fault energy in CrMnNiN austenitic steel by the method of extended nodes

24 p3415 A72-45397

STACKING FAULTS

U CRYSTAL DEFECTS

STACKS

Mica polymorph distribution among space groups from unit layer and stacking sequence characteristics

12 p1802 A72-27512

Mass spectrometer sampling system for measuring effluent concentrations downwind of stacks at various positions in turbulent flow within atmospheric simulation facility

[AIAA PAPER 72-649]

17 p2536 A72-35478

STAGE SEPARATION

Altitude chamber simulation of reentry bodies separation from ballistic missiles, examining body shape, nozzle dimensions, gas pressure and distance effects

[ONERA, TP NO. 1029]

05 p0645 A72-17198

Detonating cut-off pyrotechnic chain of explosive devices for stage separation involving primers, relays and fuses

08 p1221 A72-20777

Plume impingement force during tandem stage separation at high altitudes

22 p3231 A72-42872

Dynamic behavior of M-4S rocket devices for strap-on booster separation and nose cone and flare deployment

22 p3232 A72-43143

Extending the utility of the Space Shuttle as a space rescue vehicle

24 p3449 A72-45130

STAGGERING

M-type amplifier operation with two electron beams and staggered dual section cathode

02 p0190 A72-11570

Equivalent-damping and generalized-stagger distributions in single-circuit stagger-stage IF amplifiers at critical staggering

20 p2906 A72-38894

Allowance for transistor parameter dispersion in transistor IF amplifier designs with staggered-cascade pairs

20 p2906 A72-38895

STAGING (ROCKETS)

U STAGE SEPARATION

STAGNATION

U STAGNATION POINT

STAGNATION FLOW

Flowing plasma ionization density measurement by stagnation probe, comparing measured with calculated plasma sheath convection current values

[AD-738692]

01 p0110 A72-11189

Premixed combustible system in laminar axisymmetric stagnation flow, considering steady state and transient response of state variables, blow off extinction, ignition and heat flux

[AD-73387]

03 p0458 A72-14222

Combustion reactions of water catalyzed gas-phase oxidation of carbon monoxide in premixed stagnation flow at atmospheric pressure

[AD-743563]

03 p0459 A72-14223

Low Reynolds number nonequilibrium stagnation heat transfer with helium, argon and hydrogen injection into air boundary and thin viscous shock layers

[ASME PAPER 71-WA/HT-19]

05 p0744 A72-15878

Surface pressure fluctuations near axisymmetric stagnation point in flow over simple impinged body, showing fluid strain suppression of turbulence

06 p0757 A72-18133

Stagnation conditions of magnetoradiative supersonic flow through shock waves for temperature-dependent specific heat parameter

08 p1255 A72-21795

Mathematical model for flow field inside raindrop under aerodynamic transient stresses before impingement at stagnation point of blunt body in supersonic flight

13 p1942 A72-29224

Thermodynamic properties of axisymmetric and planar stagnation flows of air with gas injection, taking into account mass transfer effects on heat transfer rate

16 p2477 A72-33428

Electron density measurements in bow shock stagnation and conical afterbody regions during blunt body atmospheric reentry, using flush mounted electrostatic probes

[AIAA PAPER 72-694]

16 p2345 A72-34047

Radiative and convective heat transfer for stagnation point flow of emitting carbon dioxide and nitrogen gas mixture, assuming thermodynamic equilibrium in shock layer

17 p2636 A72-34470

The boundary layer of higher order at the stagnation line of a yawed cylinder in the case of strong suction or injection

23 p3249 A72-44297

Effect of a flow with a stagnation point on the rate of variation of the total entropy of a fluid mixture

24 p3465 A72-45074

On the unsteady magnetohydrodynamic flow over yawed infinite cylinder

24 p3395 A72-45599

STAGNATION POINT

Two dimensional unsteady incompressible boundary layer near forward stagnation point of infinite plane wall with uniform suction or injection, obtaining iterative solution

01 p0050 A72-11106

Radiative heat transfer between gas flow and axisymmetric ablating body near stagnation point, considering ablation products effects under boundary layer chemical equilibrium conditions

02 p0300 A72-11577

Electron temperature profile across nonequilibrium stagnation point boundary layer in partially ionized gas, investigating charged particles interaction with body in ionosphere

02 p0262 A72-12268

Gas flow fluctuations near stagnation point on hot wall, taking into account laminar boundary layer compressibility effects

[ASME PAPER 71-APM-RR]

04 p0462 A72-15178

Nonequilibrium stagnation heat transfer mathematical models for injecting He, Ar or H into ionizing air laminar viscous layers at low Reynolds numbers

[ASME PAPER 71-WA/HT-18]

05 p0744 A72-15877

Hypersonic axially symmetric laminar boundary layer electrically conducting fluid flow in blunt body stagnation region in presence of radial magnetic field

05 p0600 A72-16063

Inviscid variable density core flow in thin compressible boundary layer near stagnation point of smooth blunt body

05 p0601 A72-16216

Nonstationary oncoming flow temperature effect on heat transfer in thermal boundary layer at forward stagnation point

05 p0746 A72-16217

Hypersonic melting ablation waves simulation near stagnation region by frozen oil models

[AIAA PAPER 72-92]

05 p0750 A72-16977

Convergent power series solution in powers of time for unsteady viscous flow near stagnation after impulsive motion of bluff body from vorticity distribution viewpoint

06 p0757 A72-18135

Monatomic ionized radiating gas nonequilibrium flow in blunt body stagnation region behind shock wave during hypersonic atmospheric reentry

07 p0909 A72-20083

Free convection velocity fields measurements and stagnation point location around horizontal torus in air, using fine particle trajectories

[ASME PAPER 71-HT-X]

08 p1163 A72-20877

Boundary condition for plane or axisymmetric stagnation point flow of micropolar fluid over flat plate, giving numerical solutions for turbulent characteristics

09 p1293 A72-22621

Aerodynamic field around singular stagnation point of blunt body tip with detached shock, using Legendre functions

09 p1261 A72-22932

Viscous boundary layer equations for MHD flow near rear stagnation point at small Reynolds number

09 p1296 A72-23674

Two dimensional unsteady stagnation point flow against plane wall with impulsive motion

10 p1470 A72-25040

Flow fields and inviscid core of two dimensional diffuser with fluid extraction on diverging walls, describing streamline patterns, stagnation region and stall conditions

[ASME PAPER 72-GT-2]

11 p1568 A72-25605

Three dimensional free convection boundary layer equations solution at two dimensional isothermal stagnation point with various Prandtl numbers

11 p1747 A72-26662

Cylindrical pitot tube displacement effects on stagnation point and static pressure angle in impeller nonuniform peripheral flow

14 p2094 A72-30720

Aerothermochemical analysis of thermosetting hydrocarbon plastic ablation rate under heat transfer at reentry vehicle hypersonic stagnation point, describing pyrolysis by chemical kinetic equation

15 p2335 A72-32149

Counterflow diffusion flame gas dynamic structure analysis in porous cylinder forward stagnation region, using surface and boundary layer approximations

15 p2336 A72-32310

Fast numerical solution for supersonic flow past flat-faced blunt body by integration from stagnation point, noting computing time on CDC 6600

16 p2341 A72-32840

Grid-generated turbulence distortion approaching two dimensional bluff body stagnation region

16 p2344 A72-33569

Blunt nose cone flow field characteristics microwave measurement at stagnation point during atmospheric reentry, using plasma diagnostic sensors with antennas and electrostatic probes

[AIAA PAPER 72-693]

16 p2345 A72-34049

Foreign gas injection into three-dimensional stagnation point flows

17 p2483 A72-34205

Liquid fuel droplet transient combustion in supercritical hot stagnant oxidizing environment, solving conservation equations

17 p2636 A72-34903

Influence of a trailing vortex on friction pulsations in the near-wall region of the leading stagnation point of a cylinder in transverse flow

19 p2786 A72-38041

Motion of particles injected from the surface into stagnation-point flow

20 p2913 A72-39611

Instability of hypersonic viscous shock layer with finite rate chemistry

20 p2886 A72-39631

Stagnation-point heat transfer - The effect of the first Damkohler similarity parameter

[ASME PAPER 72-HT-44]

20 p2985 A72-39668

Ablative nose shape change effects on re-entry vehicle aerodynamic performance

[AIAA PAPER 72-974]

22 p3230 A72-42337

Behavior of the lines of flow in the proximity of the stagnation points of blunt bodies

22 p3136 A72-42907

Second order boundary layer solutions on a curved surface

[ASME PAPER 72-FE-21]

23 p3280 A72-44063

A new concept for correcting the attenuation effects in a shock tube

24 p3388 A72-44985

STAGNATION PRESSURE

Cooled miniature pneumometric probes for high temperature gases dynamic or stagnation pressure and velocity measurement

01 p0072 A72-11213

Compressible gas subsonic or transonic flow in front of obstacle, determining stagnation pressure with thermal relaxation time by numerical and wind tunnel methods

02 p0151 A72-12097

Average stagnation pressure measurement in low velocity ducted gas flow with nonuniform velocity profiles, discussing mathematical technique and computer program

[ASME PAPER 71-WA/PUR-1]

05 p0645 A72-15910

Supersonic molecular jet improvement via expansion chamber residual gas pressure reduction and nozzle stagnation pressure increase

16 p2429 A72-33053

A new stagnation pressure probe having a high pressure recovery in supersonic flow

22 p3179 A72-42687

STAGNATION REGION

U STAGNATION POINT

STAGNATION TEMPERATURE

Nozzle boundary layer effects on reisojets performance, presenting conical design model in heated stagnation conditions

03 p0405 A72-12973

Local stagnation temperature measurement in supersonic flow, using hot-wire anemometer

03 p0309 A72-13789

Low pressure gas heating expediency for stagnation temperature increase in gas flow of shock tube

16 p2480 A72-34168

Fine wire thermocouple probes for stagnation temperature measurements in hypersonic mixing layers

[AIAA PAPER 72-1023]

21 p3057 A72-41601

STAINING
The distribution of the long wave photoreceptors in the compound eye of the honey bee as revealed by selective osmic staining. 17 p2500 A72-34877

STAINLESS STEELS
NT AUSTENITIC STAINLESS STEELS
NT FERRITIC STAINLESS STEELS
NT MARTENSITIC STAINLESS STEELS
High chromium ferritic stainless steels weldability and mechanical properties, showing C, N, Ti and residuals effects on recrystallization, toughness, tensile behavior and corrosion resistance
01 p0083 A72-10283
Nondestructive determination of temperature dependence of elastic moduli of Al alloy and Ni and stainless steels by resonant frequency method
01 p0084 A72-10518
Cryogenically formed prestressed stainless steel glass fiber reinforced vessels, demonstrating structural performance for space shuttle life support oxygen/nitrogen high pressure gas tanks
01 p0139 A72-10770
Porous stainless steels as filter medium, describing manufacturing techniques, properties and applications
02 p0233 A72-11449
Deformable stainless steels empirical diagram for structural state estimation from chemical composition, considering various austenite, martensite and ferrite combinations
02 p0243 A72-12241
Organophosphorus antiwear additives in neopentyl polyol ester lubricants on 440C stainless steel surfaces, using four ball wear test machine
[AD-740055] 02 p0250 A72-12849
Stainless steel electrodes resistive and capacitive properties in contact with saline solutions of various concentrations and over extensive frequency range and current densities
03 p0318 A72-12953
Corrosion resistance of stainless steels in acid solutions, describing electrochemical cell for recording potential/current density and polarization curves
04 p0533 A72-15236
Impact fatigue testing apparatus, presenting results for stainless steel
04 p0524 A72-15549
Wear, bending and corrosion resistance of stainless steels with Cr thermal vacuum diffused coating
04 p0535 A72-15661
Heat transfer for water at pressures near atmospheric in wicks formed of stainless steel screen layers, obtaining steady and maximum evaporation rates
[ASME PAPER 71-WA/HT-12] 05 p0744 A72-15872
Ar, Kr, methane and nitrogen physisorption isotherms on stainless steel in low pressure cryogenic baths calculating mean adsorption energies
05 p0624 A72-16395
Ferritic stainless steel roping /buckling/ morphology and texture explanation by anisotropic plastic flow
05 p0677 A72-17105
Stainless steels with improved formability developed through assessment of stress-strain curve slope and plastic strain ratio
07 p1011 A72-19477
Oxygen effect on structure and mechanical, technological and corrosive properties of stainless steel melted in open and vacuum furnaces
07 p1013 A72-19739
Carbide precipitation effect on strength of auroless hardenable hypoeutectoid and hypereutectoid stainless steels
07 p1016 A72-19943
Metallographic properties of vacuum brazed, heat treated and gas quenched Al alloys, low alloy steels and corrosion resistant steel alloys
07 p1017 A72-20001
Vacancy supersaturation effect on enhanced precipitation by high flux electron irradiation in stainless steel
07 p1033 A72-20410
Stainless steel saturation with Al and Cr, investigating structure, microhardness, linear expansion and contact surface seizure reduction
07 p1020 A72-20419
Explosive loading effect on Cr-Ni stainless steel structure with electron microscope study of gamma, alpha and epsilon phases
08 p1187 A72-21780
Oxygen jet-carbon dioxide laser beam cutting in mild and stainless steels, noting speed and material thickness limitations
09 p1321 A72-23639
Impurities effects on stress corrosion and work hardening induced dislocation structures in stainless steels, considering stacking fault energy relationship
10 p1496 A72-24231
Low temperature resistant stainless steels mechanical properties, microstructure and weldability, discussing compositions and heat treatments
10 p1498 A72-24838

Eddy current extensometer for monitoring long term creep in diameter of pressurized tubular stainless steel specimens
11 p1613 A72-25821
Metallographic examination of stainless steel specimens exposed to long term creep rupture tests, noting carbides precipitation and stress induced grain boundary migration
11 p1658 A72-25832
Deformable wrought stainless steels phase diagram for structural state estimation from chemical composition, considering various austenite, martensite and ferrite combinations
11 p1659 A72-26127
Filler wires development for inert gas welding of stainless maraging steel
11 p1660 A72-26488
Ferritic stainless weld metal ductility, investigating yield and fracture stresses after heat treatment
11 p1661 A72-26494
Stainless steels sensitivity to pitting corrosion under sulfides action, measuring rupture potential
11 p1661 A72-26648
Cyclic stress ratio effects on stainless steel fatigue crack propagation at 1000 F, using linear elastic fracture mechanics
12 p1829 A72-27663
High strength low alloy steel and stainless steel recrystallization after hot working at plastic deformation temperature
13 p1973 A72-28654
Precipitated carbide role in Cr-Ni stainless steels high temperature properties and creep rupture strength
13 p1979 A72-29447
Chromium stainless steel fatigue life reduction due to embrittlement in gaseous hydrogen atmosphere at room temperature, noting alleviating effect of atmosphere contaminants
13 p1979 A72-29484
Ni-Cr-Mo stainless maraging steel, investigating yield strength, toughness, corrosion resistance and weldability
14 p2113 A72-30270
Aluminum-stainless steel and Ni-Mo composites prepared by dynamic hot pressing, determining bond strength between fibers and reinforced metal matrix
14 p2107 A72-30431
Heat treatment hardening effect on stress corrosion resistance of ultrapure maraging and stainless steels, emphasizing hydrogen embrittlement
14 p2117 A72-30540
Accelerated intergranular corrosion and grain boundary precipitation mechanisms in stainless steel Fe-Ni-Cr alloy, using Huey, acid and Strauss tests
14 p2118 A72-30548
Low carbon and nitrogen concentrations in chromium ferritic stainless steel obtained with gas rinsing at reduced pressure, noting weldability and corrosion resistance
14 p2119 A72-30606
Stainless steel surface alloy composition characterization as function of vacuum annealing temperature, using proton-induced X rays
15 p2258 A72-32527
Mo and stainless Ni-Cr steel surfaces chemical composition determination by Auger electron spectroscopy during heating in high vacuum
16 p2406 A72-33251
Notch sensitivity of sintered stainless steel powder as function of density from application of sharp crack fracture mechanics methods to plane strain fracture toughness
16 p2408 A72-33700
Deformation substructures in stainless steels under low cycle high strain fatigue tests evaluation for application as fuel cladding for fast breeder reactors
16 p2411 A72-33825
Hot forging of sintered stainless steel.
19 p2815 A72-37592
Temperature effects on the strainrange partitioning approach for creep-fatigue analysis.
19 p2815 A72-37638
Hydrogen and nitrogen desorption phenomena associated with a stainless steel 304 low energy electron diffraction (LEED) and molecular beam assembly.
19 p2762 A72-38023
Fracture behavior of stainless steel fibers in Sn-Pb alloy matrix.
19 p2820 A72-38373
Stress dependent cyclic creep rupture tests of Ti and Co-base alloys and stainless steel at 1300 F
20 p2938 A72-39305
Stainless steels high temperature creep rupture strength relationship to carbide precipitation morphology
21 p3069 A72-41013
Fatigue properties of 18-8 stainless steel at cryogenic temperatures.
21 p3071 A72-41845
Magnetostriction of stainless steels as a function of heat treatment
23 p3300 A72-43596

Some preliminary observations on the extension of cracks under static loadings at elevated temperatures.
23 p3301 A72-43712
Materials creep behavior and elevated temperature design.
24 p3453 A72-44553
Fatigue-crack growth in 20% cold-worked Type 316 stainless steel at elevated temperatures.
24 p3435 A72-44555

STALL
U BOUNDARY LAYER SEPARATION
STALLING
Two dimensional airfoil unsteady stall in incompressible flow, comparing calculated loading during transient and sinusoidal pitching motions with measured values
[AIAA PAPER 72-37] 05 p0607 A72-16899

STAMPING
Axisymmetric contact problem for circular flat stamp on laminated half space, using matrix calculus and Hankel transforms
03 p0448 A72-13903
Variational solution to axisymmetric problem of rigid stamp quasi-static impression into elastoplastic half space
13 p2053 A72-28387
Wiener Hopf integral equation for problem of smooth stamp impression into elastic wedge face, solving by gamma and hypergeometric functions
13 p2059 A72-29500
Dynamic contact problems of stamps bands oscillation on elastic layer surface or cylinder, analyzing vibrationally induced elastic waves
14 p2163 A72-30223
Eigenfunction technique development to incorporate stress singularities at circumference of end planes into problem of solid cylinder compression between rough rigid stamps
17 p2633 A72-35403

STANDARD ATMOSPHERES
U REFERENCE ATMOSPHERES
STANDARD DEVIATION
Mean-square approximate estimator for standard deviation of natural frequency of two degrees of freedom spring systems, comparing with Monte Carlo simulation
[ASME PAPER 71-WA/APM-7] 05 p0734 A72-15971
System natural frequency standard deviation estimator, using Monte Carlo method
[ASME PAPER 71-WA/APM-8] 05 p0734 A72-15972
Vertical two-point longitudinal velocity differences or wind shear in atmospheric boundary layer, obtaining standard deviation from turbulence measurements
06 p0841 A72-17666
Standard deviation in ghost lines size due to random sampling position errors of monochromatic spectral line in Fourier transform spectroscopy
09 p1314 A72-23344
Spaceborne scatterometer measurement standard deviation derivation, noting integration time, signal bandwidth and SNR effects on accuracy
12 p1783 A72-27636
Aircraft pilot reaction capability for switch activation in response to voice countdown, tone initiation and termination, noting standard deviation
15 p2188 A72-31787

STANDARDIZATION
Aircraft high pressure oxygen cylinder system filler valve optimum standards, discussing automatic fill rate and pressure sensitive closing control, design, construction and performance
[SAE AS 1225] 01 p0006 A72-10385
International standardization of manned spacecraft components for rescue efforts and joint multination space missions
09 p1395 A72-23154
Sleep disturbance due to sonic booms, discussing laboratory findings and experimental techniques standardization
09 p1273 A72-23319
Vacuum gage calibration standardization by piston manometer method of pressure determination from direct force-area measurement
12 p1805 A72-27037
Aeronautical navigation/guidance standardization in conjunction with OMEGA, covering sensor and computer equipment life cycles
13 p1999 A72-29199
Electric power supply systems for satellites, discussing packaging standardization of electronic circuits modules
13 p1900 A72-30096
Standardization of microwave irradiation experiments on animals, discussing power density level evaluations and local vs whole-body irradiation effects
14 p2080 A72-30746
Standardization of positive directions for parameters in materials strength theory, noting systems of coordinates, moments, forces, angles and stresses
15 p2325 A72-31502
Spectrophotometers and photometers calibration and standardization, emphasizing necessity for periodic control of instrument parameters
16 p2394 A72-33872

- Airborne equipment electric power supply standards to provide characteristics limits for compatibility with ground support systems
[SAE AS 1212] 18 p2648 A72-36535
- Standardization and reliability assurance on the national and European levels
18 p2743 A72-37128
- Standardization and quality assurance of electronic devices on the national and European levels
18 p2743 A72-37129
- Standardized programming routine operations independent of problem and language for controlling computer program design, discussing advantages and applications
23 p3267 A72-43991
- STANDARDS**
- NT FREQUENCY STANDARDS**
- NT REFERENCE ATMOSPHERES**
- Aerospace wire and cables testing methods standards for evaluating mechanical, electrical and chemical properties, coating thicknesses, continuity flaws, flammability, geometrical characteristics, etc
[SAE AS 1198] 01 p0006 A72-10384
- Pressure altimeter system minimum safe performance standards for subsonic aircraft operation, describing test procedures
[SAE AS 942] 01 p0064 A72-10386
- Telemetry standards for transmitting, receiving and signal processing equipment at missile test ranges
02 p0176 A72-12164
- Bayard-Albert ionization vacuum meter use as primary standard, investigating ion orbiting and collecting processes
03 p0361 A72-13880
- Ac and dc electric power transient test equipment satisfying MIL-STD-704A requirements
03 p0312 A72-14038
- Proposed gas turbine procurement standards for shipment and installation preparation
[ASME PAPER 71-WA/GT-4] 05 p0703 A72-15897
- Europa 2 launch vehicle standardized PCM/FM and FM/PM telemetry system compared with Europa 1
05 p0630 A72-16751
- International comparison of standard solar radiation measurement pyranometers
06 p0816 A72-17925
- Thin wall airflow wire insulation relative thermal life and temperature rating evaluation procedure using Arrhenius plot
09 p1339 A72-23270
- Confidence level determination in terms of reliability index (MTBF) for MIL-STD-781 truncated sequential probability ratio tests
10 p1444 A72-23989
- Technical standards for educational and community TV by satellite, considering picture quality requirement, modulations, SNR, threshold and fade margin, and channel width
10 p1435 A72-24034
- Airborne VHF omni-range (VOR) systems minimum operational standards for navigation and communication in air traffic control
10 p1509 A72-24725
- General aviation equipment standards in light of air traffic system safety needs, emphasizing Technical Standard Order system
[SAE PAPER 720307] 11 p1748 A72-25571
- Pathophysiology of exposure to UV, IR, coherent, microwave and RF radiations, discussing potential hazards, damage, human tolerance threshold, protection guides and safety standards
12 p1772 A72-27963
- Solar cell calibration in uncollimated sunlight, obtaining standards for solar simulator intensity
12 p1759 A72-28042
- Secondary standard solar cells calibration method based on solar spectral response comparison with primary standard, discussing error correction method
12 p1759 A72-28043
- FAA policy in issuing civil airport operating certificates and establishing minimum safety standards
16 p2373 A72-33330
- Thermoemission ion gage stability and design aspects, discussing application as secondary standard for vacuum measurements
16 p2394 A72-33871
- Method for calibration and verification of automatic liquidborne particle counter/light method/
[SAE ARP 1192] 18 p2692 A72-36533
- Attitude instruments, pitch and roll. I - Minimum performance standard for equipment.
[SAE AS 1162] 18 p2692 A72-36534
- Continuous flow general aviation oxygen masks.
[SAE AS 1224] 18 p2653 A72-36536
- Standard iron wavelengths for determining the radial velocities of stars
19 p2859 A72-37910
- Acoustic pressure and sound intensity levels and noise annoyance international standards for civil aircraft noise reduction
20 p2888 A72-39803
- Criteria for valid plane strain fracture toughness testing dealing with straightness of fatigue crack front of metal specimens
20 p2981 A72-39958

- Standard Ti bars samples for spectral determination of H concentration and distribution in Ti alloys, using mathematical statistical method
23 p3287 A72-43676
- Spectrometric zonal standards - Selection of stars and methodology of their study
23 p3338 A72-44031
- STANDING WAVE RATIOS**
- Broadband dipole antenna design based on method of moments, noting VSWR and current distribution
01 p0043 A72-11241
- Mutual microwave coupling effects on element VSWR in linear dipole log periodic antenna array
01 p0043 A72-11242
- Frequency response of passive dipole antennas fed by transistor circuit, investigating power gain, bandwidth and voltage SWR
04 p0503 A72-15670
- Reflection and transmission characteristics of circularly polarized horn antenna, discussing bandwidth properties, phase differences, polarization characteristics and voltage SWR
05 p0635 A72-16334
- STANDING WAVES**
- Ultrasonic bonding tip design for densely wired electronic circuit boards, analyzing standing wave phenomena and resonant frequency
[SAE PAPER 710789] 01 p0074 A72-10279
- Elastic systems nonlinear oscillations with moving inertial loads, noting standing waves superposition
06 p0901 A72-18706
- Laser induced line narrowing effects in coupled Doppler broadened transitions within standing wave field
07 p1039 A72-20682
- Laser holographic imagery of plane and three dimensional objects for supersonic field representation of standing wave in isotropic liquid
08 p1165 A72-21078
- Stationary waves properties dependence on weak skin effect in distributed tunnel diode type of nonlinear active transmission lines
10 p1453 A72-24902
- Standing wave and colliding wave lasing and synchronization region in ring laser using active gas isotope mixture
13 p1968 A72-29511
- Alfvén wave transmission in sunspot umbral magnetic flux tube, noting standing progressive waves and energy dissipation in facular regions
13 p2049 A72-29937
- Kinetic instability bursts during heating of electron plasma in cylindrical resonator with standing electromagnetic waves
14 p2136 A72-30308
- Transmission lines with nonlinear capacitance semiconductor diodes, investigating electromagnetic traveling and standing waves instabilities and self amplitude modulation
14 p2086 A72-30795
- Nonlinear approximation of slowly changing standing waves in self excited parametric oscillators with distributed and bulk structures
14 p2090 A72-31131
- Some comments on the generation of electromagnetic traveling and standing waves for inductive acceleration of plasmas
[DFVLR-SONDDR-209] 17 p2589 A72-34895
- High power microwave nanosecond pulse generator with waveguide standing wave resonator, noting power gain and pulse shape
19 p2776 A72-38672
- Resonant growing standing internal gravity waves, considering transient behavior, numerical results, break due to local gravitational instability, maximum amplitude and secondary flow generation
21 p3048 A72-40648
- Kinetic instability bursts during heating of electron plasma in cylindrical resonator with standing electromagnetic waves
23 p3317 A72-43210
- STANDS**
- U SUPPORTS**
- STANNIDES**
- NT NIOBIUM STANNIDES**
- STANTON NUMBER**
- Reynolds analogy based correlation method for Stanton number prediction for turbulent heat and mass transfer in smooth tubes
06 p0903 A72-18186
- Flat compressible turbulent boundary layers of air, predicting foreign gas injection effects on mass and heat transfer Stanton numbers and skin friction
22 p3165 A72-41958
- STAR CLUSTERS**
- NT VIRGO STAR CLUSTER**
- Radiative, segregation and evaporation processes of ice particles surrounding early type stars of Orion association, justifying ice particle model for dust grains
01 p0129 A72-10794
- Trapezium type star systems photographic observations, presenting rectangular coordinates and relative positions
02 p0286 A72-12878

- Globular cluster NGC 6838 membership from relative proper motions
03 p0415 A72-13001
- He abundances in universe, discussing stellar structure and evolution, He production, variable stars and globular clusters H-R diagrams shape
03 p0418 A72-13112
- Magellanic Clouds star clusters spatial distribution, color-magnitude diagrams, structures, dynamics and origins
03 p0425 A72-13254
- Small Magellanic Cloud NGC 371 region photometric studies for cepheids period-luminosity relations, noting domination by young supergiant stars
03 p0425 A72-13258
- Stellar field structure in NGC 2129 cluster direction, discussing interstellar radiation absorption and star distribution
03 p0433 A72-13491
- Relative stellar orbit determination in clusters NGC 5460, 5617, 6067, 6405 and 6494, presenting gravitational potential, orbital elements and anomalistic period
03 p0434 A72-13495
- Stellar systems existence with positive total energy, using numerical integration of equations of motion for members of Orion Trapezium
03 p0435 A72-13808
- Globular clusters with inhomogeneous composition, deriving partial densities of masses
03 p0436 A72-13826
- Gravitational waves proposed origin, considering black holes, star collapse, white dwarf and neutron star formation and galaxy center neutron star clustering
04 p0576 A72-15074
- Globular clusters NGC 1851 and 2808, reducing plate material with iris photometer
05 p0711 A72-15761
- UBV magnitude measurement for stars in open clusters NGC 6613 and 6716, determining spectral classes, absorption and distances
05 p0712 A72-15768
- Photoelectric photometry of Ca K-line for A stars of population I clusters
05 p0712 A72-15797
- Young cluster NGC 2264 stellar radiation flux measurements, suggesting surrounding circumstellar shells producing observable IR excesses
05 p0720 A72-16716
- Four phase space density collisionless one dimensional stellar system evolution in time by following motion of boundary curves
06 p0876 A72-17577
- Galactic star clusters dynamic evolution, using King type equilibrium and stellar mass distribution models
06 p0879 A72-17860
- Star cluster stability in form of Einstein model of rotating spherically symmetrical mass system, using Newton approximation
06 p0883 A72-18018
- Stellar velocity distribution functions in nonrotating clusters, considering encounter multiplicity effects and dissipation increase from masses dispersion
06 p0883 A72-18024
- Southern globular clusters (NGC 6362 and NGC 6752) photometric standards, stellar photographic and color-magnitude diagrams
07 p1069 A72-19076
- Stellar evolution, pulsation and atmosphere theories for globular cluster stars comparison with observation in bulk properties estimation
07 p1071 A72-19332
- Galactic cluster M67 blue stragglers in pseudohorizontal branch, determining stellar mass relative to turnoff point stars and zero-age main sequence
07 p1071 A72-19335
- Radio emission of galactic clusters at 1.4 and 2.7 GHz, computing mean electron density and hydrogen gas mass
07 p1075 A72-19577
- Population I stars and open cluster age determination methods based on stellar evolution theory, discussing inherent uncertainties effects
07 p1083 A72-20467
- Population II stars age determination by main sequence turnover luminosity and other methods, noting cosmological and galactic evolution implications
07 p1083 A72-20468
- IR emission sources in NGC 2264, IC 2087 and M1-82 H II regions
08 p1236 A72-21397
- Stability solutions of collective oscillations of spherical star cluster rotating in near circular orbits in self consistent field
08 p1239 A72-22180
- Model stability of globular star cluster with nonzero rotational moment, discussing gravitational effects
09 p1383 A72-22494
- Rotating stellar system with stars and interstellar gas within magnetic field, discussing gravitational and magnetic effects on gas pressure
09 p1384 A72-22511

Markov processes in stellar dynamics, discussing relaxation and evaporation times and star velocity distribution for galactic cluster models

09 p1390 A72-23504

Membership probabilities for open cluster IC 4665 based on relative proper motions

09 p1391 A72-23531

Galaxy and globular cluster ages in relation to Hubble constant, deceleration parameter and Friedmann expansion time

10 p1535 A72-23911

Schwarzschild solution to Vlasov equation for velocity distribution function of self gravitating stellar system

10 p1535 A72-24112

Photoelectric UBV photometry for galactic cluster NGC 7039 region stars, discussing MK spectral classifications and peculiar A stars

10 p1545 A72-24827

Peculiar A stars in open cluster Tr 2 region from objective prism plate searches, showing membership by photometrical characteristics and proper motions

10 p1545 A72-24828

Total mass content of early type star clusters associated with reflection nebulosities

10 p1548 A72-24966

Large grazing incidence X ray telescope mirrors for IEO-C mission observations, noting single stars resolution in clusters and galaxies study

11 p1630 A72-25682

Star cluster stability in form of Einstein model of rotating spherically symmetrical mass system, using Newton approximation

11 p1718 A72-25954

Stellar velocity distribution functions in nonrotating clusters, considering encounter multiplicity effects and dissipation increase from masses dispersion

11 p1719 A72-25960

Perseus two armed spiral shock model based on O associations, young open clusters, H II regions, interstellar absorption lines and 21 cm hydrogen maps

11 p1720 A72-26110

IR and optical observations of cluster surrounding Ierbig Be type star BD plus 40.4124, noting extreme outflow of group

11 p1721 A72-26122

Probability and collisional relaxation in stellar systems, discussing gravitational polarization, collective interactions and spatial inhomogeneity

12 p1872 A72-27891

Dynamical evolution of spherical star cluster under effect of internal encounters, using Monte Carlo models

12 p1873 A72-27896

Galactic cluster lifetimes from observed age distribution comparison to evaporation times by numerical experiments with star cluster models

12 p1873 A72-27897

Galactic tidal field and multiple encounters role in stellar escape from star clusters, noting escape rates and kinetic energy involved

12 p1873 A72-27898

Binary evolution in star cluster models from numerical methods of direct integration, noting domination by heavy binary and double star formation and disruption

12 p1873 A72-27899

Runaway stars trajectories stability tested from clusters study, noting preservation of energy, velocity and position and reproducibility

12 p1873 A72-27900

Instabilities initiation in spiral arm formation and stellar cluster evolution, noting analogy to hose-pipe instability in plasma physics

12 p1874 A72-27905

Monte Carlo scheme for dynamical evolution of physical star clusters, considering stellar dense core, gaseous relaxation and escape

12 p1875 A72-27919

Star escape and accumulation in halo from stellar random gravitational encounters in spherical system dense central core

13 p2040 A72-29402

Field stars near NGC 2168 /M 35/ cluster, segregating main sequence stars by proper motion dispersions with allowance for interstellar extinction

14 p2159 A72-30742

Pleiades slow flareup in photosphere, comparing with Orion flare stars

15 p2304 A72-31329

Massive stars velocity distribution function in clusters, determining escape rate and energy dissipation

15 p2305 A72-31339

Studies of extremely young clusters. VI - Spectroscopic observations of the ultraviolet-excess stars in the Orion Nebula cluster and NGC 2264.

17 p2605 A72-34530

Pre-main-sequence stars. II - Stellar polarization in GC 2264 and the nature of circumstellar shells.

17 p2605 A72-34531

Model stability of globular star cluster with nonzero angular momentum, discussing gravitational effects

17 p2606 A72-34658

The reddening, distance modulus, chemical composition and age of the galactic cluster NGC 752.

17 p2607 A72-34675

Clustering properties of the luminosity function in galactic globular clusters.

18 p2723 A72-36091

Stability solutions of collective oscillations of spherical star cluster rotating in near circular orbits in self consistent field

18 p2724 A72-36236

Photometric study of the open cluster NGC 2232.

18 p2728 A72-36742

The colour-magnitude diagram of the globular cluster NGC 6981.

19 p2855 A72-37342

The colour-magnitude diagram of the globular cluster NGC 7099.

19 p2855 A72-37343

Catalog of individual motions of stars in the open star cluster NGC 6866 and vicinity

19 p2860 A72-37918

Absolute magnitudes and color indexes of red giant concentration centers on a color-luminosity diagram

19 p2863 A72-38069

Radial density distribution and luminosity functions for stars in alpha Persei cluster

19 p2863 A72-38070

The kinematics of open star clusters

19 p2865 A72-38488

Models concerning the kinematics of star clusters

19 p2866 A72-38489

Star cluster age relation to mass ratios of stars and interstellar hydrogen and dust

19 p2867 A72-38511

Galactic structure at galactic longitudes from 230 to 355 deg on the basis of photoelectric UBV H beta photometry of 55 southern open star clusters

19 p2867 A72-38513

Structure of spherically symmetrical clusters in the relaxation phase

20 p2974 A72-40022

Model of a stationary star cluster of high binding energy

21 p3103 A72-40401

Pulsating variables in the Pleiades cluster.

21 p3105 A72-41032

Computer-aided numerical experiment of cluster mass increase by accretion in protostar evolution

21 p3113 A72-41754

Bright red giants of the globular clusters M 3, M 5, and M 13

21 p3113 A72-41756

Nebulae of the Southern Milky Way - An atlas.

21 p3114 A72-41847

On circumstellar gas emission among pre-main-sequence stars in Ie Orionis and NGC 2264.

22 p3227 A72-42555

Homogeneous stellar system with purely gravitational interactions, predicting oscillatory relaxation time

22 p3207 A72-42853

Investigation of type-A star condensations in the Perseus and Cassiopeia constellations

22 p3229 A72-42951

Spectral classification of stars with respect to unbroadened low-dispersion spectra. IV - Catalog of spectra of faint stars about the NGC 2129 cluster

24 p3447 A72-45679

STAR DISTRIBUTION

Stellar pair scale technique for determining multiplying factor of ocular micrometer drum in universal astronomical instrument

01 p0064 A72-10197

Soviet book on cool carbon stars covering spectral features, atmospheric composition and temperatures

02 p0281 A72-12296

Globular cluster NGC 6838 membership from relative proper motions

03 p0415 A72-13001

Pulsar observation data, presenting period histogram, intensity, shape and polarization variations, position distribution, physical nature and spectra

03 p0417 A72-13102

Astronomical catalog of 42 novae, presenting tables of exact positions

03 p0433 A72-13489

Stellar field structure in NGC 2129 cluster direction, discussing interstellar radiation absorption and star distribution

03 p0433 A72-13491

Autonomous star mapping attitude reference technique for providing three-axes attitude information on inertially stabilized or slowly spinning spacecraft

03 p0387 A72-13952

Differential equations systems formulation and numerical integration in gravitational problem of stellar n-bodies, discussing close approaches

05 p0713 A72-16052

Equilibrium temperatures of interstellar grains around early stars, discussing dependency on grain size and stellar distance

06 p0875 A72-17297

Photoelectric lunar occultation measurements of multiple star systems, determining separate colors from simultaneous multichannel observations

06 p0880 A72-17862

Stellar velocity distribution functions in nonrotating clusters, considering encounter multiplicity effects and dissipation increase from masses dispersion

06 p0883 A72-18024

Ultrashort period cepheids presence in blue stragglers of old disk population

07 p1071 A72-19334

M supergiants in Carina arm, discussing photometric studies at 4-18 microns, interstellar extinction uncertainties and spatial distribution

07 p1072 A72-19344

Pulsar and supernova remnant relative space position based on runaway pulsar hypothesis, discussing pulsar period-luminosity relation from evolutionary standpoint

08 p1233 A72-21180

NGC 3031 spiral galaxy photometry and large scale structure determination by UBVR integral equidensity curves method

08 p1234 A72-21280

Image dissector, silicon photodiode and vidicon behavior comparison for medium resolution star mappers design for three axis stabilized vehicles

08 p1172 A72-21975

Geodetic azimuth determination by multiple observations of bright stars near meridian

09 p1297 A72-22485

Star sky simulation in testing and training stands, using spherical mirror, collimator and imbedded spheres

09 p1310 A72-22949

Mathematical model of block adjustment and star coordinate accuracy in photographic astrometry

09 p1392 A72-23541

Data reduction for photographic catalog of AGK2-AGK3 stars in terms of random and systematic errors in plate constants

09 p1392 A72-23543

Galactic nuclei origins, evolution, observational evidence and activity relation to cosmological problems, examining Milky Way, spiral and radio galaxies and quasars

10 p1532 A72-23884

Pulsar electrodynamic properties, radiation mechanism, galactic distribution and pulse shape, period distribution and propagation characteristics, reviewing Crab Nebula pulsar features

10 p1533 A72-23888

Galactic nuclei evolution and stellar content models from nearby stars spectral synthesis

10 p1533 A72-23895

Relative orientation of major axes of double radio sources, comparing with Brown ordering of galaxies on megaparsec scale

10 p1541 A72-24472

OB star distribution in Puppis from UBV and H beta photometry, noting correlation with hydrogen concentration

10 p1542 A72-24615

Large Magellanic Cloud spiral structure and motion through interstellar gas, determining old and young stars spatial distribution near major spiral arm

10 p1544 A72-24662

Light curve of TW Delphini from visual observations, noting relationship to RV Tauri-type stars

10 p1546 A72-24830

Stellar velocity distribution functions in nonrotating clusters, considering encounter multiplicity effects and dissipation increase from masses dispersion

11 p1719 A72-25960

Milky Way spiral structure and star distribution, discussing photometric methods

12 p1875 A72-27967

Stellar population in Galactic nuclear bulge, considering interstellar reddening and variable stars

13 p2038 A72-29011

Quasi-stationary spherical system structure model for stars of different masses with isotropic velocity distribution

14 p2149 A72-30212

Galactic supernova remnants radio frequency absorption line observations, deriving distances, radio luminosity function and distribution

14 p2158 A72-30726

Galactic tidal interactions, computing mass loss for hyperbolic collisions and giant system formation from density distribution models

14 p2161 A72-31043

Average interstellar electron and early star density in Galactic disk, examining hot stars ionizing photons and H II regions photoionization

14 p2161 A72-31044

Spiral galaxy density wave damping by induced large-scale shock in interstellar medium

15 p2315 A72-32718

Optical identification of two radio source samples from astronomical B2 catalog, providing finding charts and reference star positions for investigated fields

15 p2316 A72-32749

Local population II stars density upper limit in terms of mass-luminosity ratio based on U, B and V photometric observations

17 p2604 A72-34442

Spatial distribution of galactic globular clusters stars from Palomar sky survey

18 p2724 A72-36092

Investigation of the Talcott levels of zenith telescopes and determination of their division value

19 p2802 A72-37980

Radial density distribution and luminosity functions for stars in alpha Persei cluster

19 p2863 A72-38070

Pulsars as stellar population, considering physical models, pulse emission radiation mechanism and use in galaxy studies

19 p2865 A72-38476

Stellar rings and stellar cavities as random phenomena

19 p2866 A72-38492

Initial results of a PM study in the Hydra ring

19 p2866 A72-38493

Structure and motions in the Carina spiral feature.

20 p2973 A72-39880

Model of a stationary star cluster of high binding energy

21 p3103 A72-40401

The kinematics of semi-regular red variables in the solar neighbourhood.

21 p3111 A72-41473

Bright red giants of the globular clusters M 3, M 5, and M 13

21 p3113 A72-41756

A more accurate determination of the structural features of the instability strip of classical Cepheids from Gascoigne's photoelectric data in the Small Magellanic Cloud

21 p3113 A72-41757

Corrections to star catalogues from satellite observations.

22 p3220 A72-41997

Spiral and halo structure of our galaxy on the basis of optical distance determinations.

22 p3222 A72-42136

Investigation of type-A star condensations in the Perseus and Cassiopeia constellations

22 p3229 A72-42951

Quasi-stationary spherical system structure model for stars of different masses with isotropic velocity distribution

23 p3334 A72-43242

Identification of four novae and a super-nova in Palomar Sky Atlas.

23 p3341 A72-44474

STAR FIELDS

U STAR DISTRIBUTION

STAR TRACKERS

Soviet book on electro-optical devices for space vehicles orientation and navigation covering vertical plotters and sun, planet and star trackers

02 p0256 A72-12125

Gimbale telescope/UV spectrophotometer combination with star tracking facilities for use on ESRO TD-1 A satellite

03 p0355 A72-13061

Thermal heliotrope adaptation to terrestrial applications, discussing solar radiation energy input dominance assurance and wind effect minimization [ASME PAPER 71-WA/SOL-10]

05 p0614 A72-15893

Flexibly stabilized satellite orientation determination by stellar sensors and magnetic damping of rotation

08 p1240 A72-21139

Star sensor with image dissector as pickup tube for Astronomical Netherlands Satellite attitude control system

08 p1171 A72-21974

Radiation resistance of Si photodetectors for star sensors in satellites, using electrical and optical tests

09 p1369 A72-22653

Optical radiation from Hg bombardment ion thrusters downstream regions due to excited atoms radiative decay, examining exhaust interference with star tracker

[AIAA PAPER 72-441]

11 p1707 A72-26182

Construction and optical equipment of astrophysical observatory Orion onboard Salyut space station, discussing mirror telescope, spectrograph and star tracker

15 p2242 A72-32741

Orion spaceborne astronomical observatory automatic control system for instrument orientation and star tracking, discussing servomechanism and pulse duration modulation

15 p2242 A72-32743

Loosely stabilized satellite orientation determination by stellar sensors and magnetic damping of rotation

20 p2976 A72-39244

Star scanner attitude determination for the OSO-7 spacecraft.

21 p3082 A72-41566

STAR TRACKING

U STAR TRACKERS

STARCHES

Ignition of a mixture of ammonium perchlorate and starch by incandescent wires

19 p2847 A72-37367

STARK EFFECT

Spectral distribution of total continuous emission coefficient for LTE hydrogen plasma over 8000-16,000 K and 400-15,000 Å ranges, observing Stark broadening

01 p0108 A72-10175

Molecular Stark effect modulation of IR carbon dioxide laser radiation, using density matrix technique

01 p0079 A72-10515

Orion A and M17 radio recombination line width increases, discussing Stark broadening functional dependence on principal quantum number

01 p0131 A72-11010

Single electron approximation of Stark broadening of hydrogen spectral lines without constraints of collision and quasi-static theories

03 p0391 A72-13079

Electron impact Stark broadening of ionized chlorine lines in pulsed arc plasma using laser interferometric and spectroscopic measurements

03 p0396 A72-13748

Carbon dioxide laser modulation by molecular Stark effect in deuterated ammonia, observing pressure broadening coefficient

04 p0528 A72-14585

Stark contours of hydrogen spectral lines in turbulent plasma with high noise level due to hf Langmuir oscillations

04 p0557 A72-14986

Carbon dioxide laser Q switching by molecular gases intracavity Stark modulation with sine or square wave electric field, using methyl chloride and difluoroethane

05 p0669 A72-16609

Carbon dioxide laser IR radiation modulation by application of Stark effect in various molecular absorbers, showing absence of saturation

07 p1000 A72-19035

Doppler broadening elimination in red Balmer line of atomic hydrogen at 6563 Å by high resolution saturation spectroscopy

07 p1037 A72-19132

Gases for carbon dioxide laser lines modulation by molecular Stark effect, presenting data for fluoroethane, monomethylamine, methyl mercaptan, vapors methanol and trichloroethylene

07 p1001 A72-19193

Coalescence /collapse/ of overlapping spectral lines due to nonadiabatic broadening for Stark structure of hydrogen and helium lines in discharge plasma

08 p1211 A72-21717

Hydrogen line broadening in plasma theory with limitations of Stark component intensity distribution by quasi-static and impact approximations

09 p1358 A72-22493

Stimulated emission and spectroscopic properties of activated ferroelectric crystal laser, noting Stark effect

09 p1323 A72-22981

Hydrogen atom emission spectrum calculation in uniform rotating electric field, applying to charged particles collisions and Stark broadening of plasma H lines

10 p1514 A72-24039

Saturated absorption spectroscopy of ammonia, considering Stark effect on IR transition

10 p1491 A72-24122

Relativistic Zeeman-Stark effect on molecular jet due to molecular translational motion in continuous magnetic field

10 p1514 A72-24135

Charged particles effect on plasma negative ions, examining Stark effect in energy level

11 p1693 A72-25714

Single electron approximation of Stark broadening of hydrogen spectral lines without constraints of collision and quasi-static theories

13 p2007 A72-29429

Adiabatic characteristics of impact to quasi-static transition during electron induced Stark hydrogen line broadening in plasmas

13 p2016 A72-29516

Electronic density measurement in ionized Cs vapor by observation of fundamental series lines mixture, comparing to Stark widening theory based profiles

14 p1314 A72-30852

Oscillatory current characteristics of Stark ladder electron with weak LO phonon coupling in solids

15 p2293 A72-32218

High power carbon dioxide laser produced dense He plasma, comparing experimental and theoretical Stark profile of forbidden and allowed transitions

15 p2285 A72-32223

Early B stars with normal helium abundances and small rotational velocities, deducing gravity from H lines and ESW Stark broadening

15 p2316 A72-32751

Energy difference measurement between 2S and 2P levels of multiply charged O 16 positive ion, using Stark quenching technique

16 p2432 A72-33768

Hydrogen line broadening in plasma theory with limitations of Stark component intensity distribution by quasi-static and impact approximations

17 p2588 A72-34657

Improved Stark-profile calculations for the He II lines at 256, 304, 1085, 1216, 1640, 3203, and 4686 Å.

17 p2585 A72-35768

Measurement of nonthermal oscillations at the plasma frequency and its harmonics in a magnetized arc plasma, using the high-frequency Stark effect.

22 p3212 A72-42916

Study of the Stark effect in the resonance lines of sodium by an atomic jet method

22 p3209 A72-43048

STARS

NT A STARS

NT B STARS

NT BINARY STARS

NT BLACK HOLES [ASTRONOMY]

NT CEPHEID VARIABLES

NT COMPANION STARS

NT DWARF STARS

NT EARLY STARS

NT ECLIPSING BINARY STARS

NT EXTARS

NT GIANT STARS

NT HOT STARS

NT INFRARED STARS

NT MAGNETIC STARS

NT MAIN SEQUENCE STARS

NT NEUTRON STARS

NT NOVAE

NT O STARS

NT PROTOSTARS

NT PULSARS

NT RADIO STARS

NT REFERENCE STARS

NT STELLAR GRAVITATION

NT SUBDWARF STARS

NT SUN

NT SUPERGIANT STARS

NT SUPERNOVAE

NT T TAURI STARS

NT VARIABLE STARS

NT WHITE DWARF STARS

Electromechanical system for wire drive along stellar right ascension of meridian circle of Odessa Astronomical Observatory

09 p1311 A72-2306

Computer processing of star meridian observations: concerning reduction to visible area, declinations right ascensions and conversion

09 p1283 A72-23063

Star declinations from simultaneous observations at upper and lower culminations

09 p1388 A72-23064

Eight color intermediate band photometric three-dimensional star classification system, taking into account spectral classes, absolute magnitudes, Fe/H ratios and interstellar reddening

09 p1392 A72-23546

Corrections to the right ascensions of FK4 according to observations of fundamental star series with the meridian circle of the Cerro Calan Observatory /Chile/

19 p2859 A72-37911

Effective temperatures of massive stars as a function of chemical composition and mass.

22 p3227 A72-42560

Russian book - Problems of the physics of nebulas and unsteady stars.

23 p3338 A72-44026

Compilation of azimuth tables for the North star /for the tropical zone/

24 p3438 A72-44866

Application of the restricted hyperbolic three-body problem to a star-sun-comet system.

24 p3442 A72-45234

STARS [MATHEMATICS]

Multidimensional time dependent flow field analysis by split finite difference operator technique, using star mesh of quadrilateral cells

[AIAA PAPER 72-154]

05 p0609 A72-16950

STARTERS

NT ENGINE STARTERS

STARTING

Jacketed tubular chemical reactor optimal startup control, presenting distributed maximum principle for diffusional parameter system

02 p0301 A72-12093

STATE EQUATIONS

U EQUATIONS OF STATE

STATE ESTIMATION

U ORBITAL POSITION ESTIMATION

STATE VECTORS

Optimal limited state variable feedback controllers design for static and dynamic linear systems [AD-738770]

02 p0198 A72-12809

Nonlinear plant and observation models with white Gaussian noise and continuous data, obtaining state vector a posteriori probability density for optimal prediction

04 p0506 A72-15112

Modal theory of state observers for control of multivariable time-invariant linear systems with plant matrices possessing distinct eigenvalues
04 p0507 A72-15529

Computational algorithm for optimal control problem with variable terminal point constrained on state space surface, using iteration technique for satisfying transversality condition
[ASME PAPER 71-WA/AUT-6] 05 p0640 A72-15957

Penalty function method validity for singular solutions to optimal trajectory control problems with state variable inequality constraints
05 p0641 A72-16531

Error covariance matrix evaluation at end of orbit extrapolation in terms of state vectors at measurement, discussing computation and interpretation
05 p0720 A72-16753

Dynamic system observation accuracy in spacecraft trajectory measurement, deriving processing algorithm based on state-estimate error correlation matrix analysis with maximum likelihood procedure
05 p0721 A72-16760

Satellite motion state vector accuracy estimate algorithm based on angular measurements of stellar positions relative to satellite sent probe
05 p0687 A72-16762

Generalized matrix inverse application to dynamic system state vector estimation, determining covariance matrix for comparison with optimal Kalman type procedure
05 p0641 A72-17089

Conjugate gradient iterative method for optimal control problems with state variable constraint, noting optimal trajectory cases
06 p0793 A72-17953

Optimal control of distributed parameter systems with incomplete state information by dynamic programming and Liapunov methods
07 p1034 A72-18981

Feasible solutions to automatic control problems satisfying multiple state and control variable inequality constraints, discussing algorithmic numerical implementation
07 p0959 A72-19281

Minimax terminal state estimator existence and structure for linear discrete system, applying to stochastic pursuit evasion games of LQG variety
07 p1027 A72-19283

Multiinput and multioutput linear and nonlinear dynamic system maximum likelihood identification based on state vector formulation and optimal filter use
07 p0959 A72-19286

Algorithm for low order linear state variable models construction from measured data
07 p0950 A72-19701

Algebraic algorithm for reducing to state form multivariable control systems defined by linear constant differential operators
07 p0950 A72-19702

Linear multivariable control system state observation by sampling with arbitrary but fixed distribution of sampling instants, emphasizing dual control by step functions
07 p0961 A72-19707

Time optimal closed loop control system synthesis by phase space technique verifying results by state variable approach
07 p0964 A72-20595

Compensated Kalman filter as suboptimal state estimator to eliminate steady state bias errors in use with mismatched asymptotic time-invariant case
08 p1144 A72-20845

Omega radio navigation system lanning problem, discussing ambiguity resolution by multiple state vector Kalman filter
08 p1144 A72-20860

Optimal filtering for state estimation of nonlinear dynamic models observed with discrete noisy observations by retaining second order terms in series approximation
08 p1145 A72-20863

Orbit determination using Kalman-Bucy filter to estimate state and unmodeled acceleration approximated as first order stationary Gauss-Markov process
08 p1145 A72-20867

Conditional mean state estimate approximation for nonlinear systems by parallel computation to reduce computer time
08 p1145 A72-20868

Algorithm for asymptotic behavior approximation of semi-Markov processes with splitting set of states by Markov chain
08 p1198 A72-20997

State estimation for nonlinear discrete-time system based on quantized data, presenting maximum likelihood estimate solution and Monte Carlo simulation results
09 p1290 A72-23095

Optimal probing signals design for state vector parameter estimation, considering Fisher information matrix function as optimality criterion
10 p1454 A72-23786

Optimal nonlinear estimation problem with nonlinear plant and observation models obtaining state vector a posteriori probabilities for prediction and smoothing via partition theorem
[AD-736521] 10 p1455 A72-23803

Optimality conditions for dynamic control systems, considering multidimensional singular controls and state space transformations
11 p1608 A72-25324

Optimal state space synthesis of discrete linear computer controlled systems with quadratic cost function, using Liapunov, Pontryagin, and Bellman techniques
15 p2212 A72-32765

State space approach to linear multivariable servomechanism problem, deriving controllability conditions and design procedure
15 p2213 A72-32801

System models for R and D processes in terms of state variables and control vectors, deriving algorithm for optimization
16 p2482 A72-33864

Recursive filtering techniques in space navigation, describing initialization procedure to account for state vector errors correlation
17 p2532 A72-34214

State space technique application to discrete linear control systems synthesis, discussing time-optimal and quadratic-cost problems, and pole assignment method
17 p2532 A72-34246

State dependent state variable feedback method to control multiple input multiple output nonlinear and/or time varying systems
17 p2532 A72-34420

Dynamic system observation accuracy in spacecraft trajectory measurement, deriving processing algorithm based on state-estimate error correlation matrix analysis with maximum likelihood procedure
17 p2610 A72-35263

Satellite motion state vector accuracy estimate algorithm based on angular measurements of stellar positions relative to satellite launched probe
17 p2578 A72-35265

Optimal regulator inverse problem analysis for multiinput systems with integral type performance indices, using state variable canonical form
17 p2534 A72-35527

Nonlinear dynamic feedback control systems modeling by parameter estimation scheme with polynomial representation for state variables
18 p2672 A72-36057

Criteria for nonlinear systems controllability in terms of state variable analytic function and derivatives, implying strong accessibility for manifolds including Euclidean spaces
18 p2673 A72-36616

Design of digital filters using state-space realization.
18 p2674 A72-36943

Direct and inverse transformations between phase variable and canonical forms.
19 p2826 A72-38230

Linear control system design with parameter uncertainties, using stochastic control approach based on minimization of state vector-dependent quadratic performance index expected value
19 p2780 A72-38239

Nonlinear on-line rapid estimation scheme with application to trajectory maneuvering vehicles.
19 p2781 A72-38258

Decoupling and synthesis of certain nonlinear systems.
19 p2827 A72-38275

Decoupling of linear discrete time systems by state variable feedback.
19 p2827 A72-38563

State vector moments of nonlinear mechanical systems under stochastic excitation, using Fokker-Planck equation for transition probability and differential equations derivation
21 p3084 A72-40679

Nonlinear problems of analyzing the observability of the trajectories of spacecraft motion on the basis of measured data
22 p3223 A72-42203

Analog and digital automatic control systems for aerospace and process applications, discussing transfer function and state variable methods
22 p3162 A72-42714

Infinite-time reachability of state-space regions by using feedback control.
23 p3274 A72-43538

The application of Monte Carlo methods to the nonlinear filtering problem.
23 p3274 A72-43541

On discrete linear time-invariant systems with singular transition matrix.
23 p3275 A72-43545

Optimally sensitive control for distributed parameter systems.
23 p3275 A72-43612

Nonlinear differential equations control systems, determining conditions for observability of initial state and vector of constant parameters extended from time-varying linear systems
23 p3310 A72-44548

Velocity space maps and transforms of tracking observations, for orbital trajectory state analysis.
24 p3440 A72-45135

STATIC AERODYNAMIC CHARACTERISTICS
All-moving tail plane parameters influence on glider static and dynamic characteristics, discussing lateral and longitudinal stability, maneuverability and pilot induced oscillations
08 p1110 A72-21632

Static aerodynamic characteristics of bulbous based cone models and slender wings at subsonic speed, using magnetic suspension and balance system
10 p1461 A72-24769

Determination of the statistical characteristics of a turbine stage and a group of turbine stages
23 p3328 A72-44295

STATIC DEFORMATION
Initial crack effect on slender column compression load carrying capacity, deflection and stress intensity factor
01 p0140 A72-10989

Exoelectronic emission method for examining deformation induced structural changes and interactions with ambient medium of metals and alloys surfaces
07 p0989 A72-20157

Static deflections determination of thin rectangular plates with point clamped restraints, using Ritz method with Lagrange multipliers
10 p1555 A72-24193

Strain work per unit time for static and dynamic pressing processes, taking into account inertial forces
13 p1966 A72-29466

Static deformation of laminar orthotropic shells of revolution with variable rigidity, using integral correlation method
13 p2061 A72-29795

Particulate composite model deformation and failure behavior under plane uniaxial compressive stress, using finite element method
15 p2258 A72-32556

Transverse isotropy effects on beams static behavior, considering Green functions, deflection under distributed loads and beam-column deflection
20 p2980 A72-39613

STATIC DISCHARGERS
Electrically charged low mobility droplet production by water vapor condensation on to gaseous ions from aircraft static discharger
02 p0231 A72-12556

STATIC ELECTRICITY
Static electrification - Conference, London, May 1971
02 p0260 A72-12551

Solids static electrification models based on solid state physics, considering contact, deformation and cleavage charging processes
02 p0269 A72-12552

Transistor damage by electrostatic discharges, noting charge stored by humans and protection techniques
08 p1140 A72-21064

Charge carrier cooling in nonhomogeneous semiconductors by static electric field, plotting average electron temperature as function of current
14 p2142 A72-30362

Radiation from a particle in static electric and magnetic fields.
20 p2956 A72-39459

Static electricity in fueling of superjets.
21 p3040 A72-41375

STATIC FRICTION
Servomechanism with nonlinear static and Coulomb friction under autonomous operation, predicting stability boundaries by analog computer simulation
08 p1113 A72-22154

Friction and molecular structure - The behaviour of some thermoplastics.
20 p2945 A72-39974

STATIC INVERTERS
Time optimal bang-bang response control of two pole single phase static inverter, giving output current transient response data
01 p0008 A72-11062

Series inverter silicon controlled rectifier 2800 watt dc power supply, noting high efficiency, low weight and stable voltage regulation
01 p0008 A72-11064

STATIC LOADS
Static loads effect on natural vibrations of thin truncated conical shells by shallow shell theory, determining resonant frequency spectrum due to prestressing
01 p0142 A72-11362

Test equipment for glass and polymer fibers strength and lifetime in vacuum and inert bases under static loads
01 p0093 A72-11382

Static and dynamic load measurements for stress-strain behavior and load-time characteristics of aerodynamic decelerator canopy fabrics, using metal foil strain gages
02 p0287 A72-11507

Static and dynamic buckling behavior of clamped shallow conical shells under axisymmetric loads
02 p0291 A72-11963

Rupture induced perturbation loads in pressurized orthotropic circular cylindrical shells

02 p0299 A72-12704

Static load transfer to discontinuous elastic filament in fiber reinforced composite, determining fiber force longitudinal distribution by approximation to Fredholm integral equation

03 p0455 A72-14384

Rectangular plates nonlinear vibrations under combined static and vibrational loads, using Bubnov-Galerkin method on Karman type nonlinear differential equations

04 p0588 A72-15061

Uniform circular plates axisymmetric elastic deformation under various static loadings and boundary conditions, solving flexural equilibrium equations

04 p0590 A72-15184

S-glass fiber bundles and composites under quasi-static loads, investigating strength characteristics and failure mechanism

04 p0592 A72-15474

Automatic testing machine for mechanical properties of metals under static loading

06 p0796 A72-18365

Gas turbine blades thermal fatigue test and analysis, investigating static tensile loading effects on heat resistance under thermal cycling

06 p0899 A72-18556

Recrystallized and unrecrystallized deformed semirigid wrought Al alloy under cyclic and static loads, investigating macrofracture kinetics

07 p1014 A72-19840

Fiberglass reinforced plastics fatigue failure prediction based on test demonstrated correlation between static and cyclic strainability

08 p1195 A72-21856

Vibration string static strain gage for high temperature operation, proposing relations for measurement error calculation

09 p1310 A72-22741

Thick steel plate diffusion welding in air with dead-weight loading and autogenous surface cleaning

11 p1637 A72-25343

Static loading and monochromatic excitation influence on transverse vibrations of eccentrically prestressed metallic beam

11 p1732 A72-25535

Two coordinate oscillograph recording device with automatic reversing for stress-strain tests under static and cyclic loads

11 p1637 A72-26814

Linear programming simplex method for static load limit of circular arch

11 p1739 A72-26921

Optimal design of elastic structures, emphasizing stability and response under applied static and dynamic loads

13 p2054 A72-28487

Testing machine for creep resistance of foam plastics under simultaneous static and vibration loads

14 p2092 A72-30591

Atmospheric humidity, temperature, vibrational and static loads effects on composite and double base rocket propellants strength and safety characteristics

14 p2145 A72-30764

Variational principle based Pian hybrid finite element procedure for static cylindrical shell analysis extended to plate and shell vibration

14 p2169 A72-31149

Buckling behavior of simply supported elastic folded plate structures without and with transverse stiffeners under symmetrical and asymmetrical uniform vertical loads

15 p2332 A72-32562

Singular perturbation methods for deflections, frequencies and eigenmodes of statically loaded or freely vibrating circular or annular membrane

16 p2467 A72-33106

Optimal design of static laterally loaded fiber reinforced plates, determining optimum load-path directions at all plate points

16 p2475 A72-34174

Static and tension fatigue and free edge delamination damage induced by uniaxial tensile loads in flat graphite/epoxy laminate coupons

17 p2571 A72-35291

Possibility of determining the fracture toughness of materials on the basis of the form of static bend test fracture samples.

20 p2941 A72-39714

Effect of inertial loading on the compression of powdered materials by a vibration process

21 p3061 A72-41369

Comparison of the resistance to fracture of the K1c of the AK4-IT1, V95T1, and D16T aluminum alloys and VT8 and VT9 titanium alloys under static and cyclic loading

21 p3071 A72-41705

Numerical solution of boundary value problems in the statics of axisymmetric shells by the method of reducing to Cauchy problems

22 p3233 A72-42054

Analysis of static deflections by holographically recorded vibration modes.

22 p3177 A72-42397

A new creep rupture testing machine with loading by tubular springs and electronic temperature control

22 p3164 A72-42860

Aluminum matrix composites fracture mechanism dependence on static loading conditions and reinforcing filament type, investigating failure modes in tension and compression tests

23 p3299 A72-43497

Some preliminary observations on the extension of cracks under static loadings at elevated temperatures.

23 p3301 A72-43712

Fatigue test equipment for 293-233 K and 50-100 ton static or 25-50 ton cyclic loads, using Freon 22 as coolant

23 p3278 A72-43759

Variational analysis of sandwich beams under static loads, presenting shear deformation and normal stress distributions

[ASME PAPER 72-APM-R] 23 p3350 A72-44055

Automatic recording of cyclic creep and strain curves for metals under low cycle static tension

24 p3458 A72-44943

Strength margin estimation in materials sustaining cumulative static and cyclic damage under thermocyclic loads

24 p3460 A72-45736

Automatic testing machine for mechanical properties of metals under static loading

24 p3389 A72-45751

The influence of static stresses on the dissipation of energy due to forced oscillations.

24 p3461 A72-45767

Mechanical behavior of fiber reinforced cylindrical shells.

24 p3461 A72-45783

STATIC PRESSURE

NT HYDROSTATIC PRESSURE

Flight test procedures for subsonic transport aircraft pitot static pressure system, recommending trailing cone calibration method

[SAE ARP 921] 01 p0064 A72-10389

Altitude hypoxia human pulmonary compliance relation between static transpulmonary pressure and inspired volume

02 p0159 A72-11958

Supersonic turbulent boundary layer interaction with compression corner, noting static pressure distributions, flow visualization and schlieren photographs

[AIAA PAPER 72-114] 05 p0610 A72-16976

Cavitation erosion of Al in liquid oxygen as function of static pressure and ultrasound frequency

07 p1034 A72-18921

Static pressure tube calibration for surface pressure measurements in flow over flat plate and airfoil

09 p1261 A72-22937

Radial turbine flow analysis, comparing calculated shroud static pressure distribution and outlet velocity profile with measured data

[ASME PAPER 72-GT-50] 11 p1570 A72-25642

Cavitation erosion of Al in liquid oxygen as function of static pressure and ultrasound frequency

13 p1942 A72-29207

Cylindrical pitot tube displacement effects on stagnation point and static pressure angle in impeller nonuniform peripheral flow

14 p2094 A72-30720

Turbulent boundary layer separation zone subsonic flow before two dimensional rectangular step, examining flow pattern and static pressure distribution

14 p2096 A72-31020

Microscale static pressure fluctuation measurements in lower atmospheric boundary layer turbulent flow using Eulerian measurements

15 p2265 A72-31618

Pressure, shear stress and yaw angle measurements in flow through aircraft intake S-shaped ducts with turbulent boundary layer at entry, noting vortex generation

16 p2377 A72-33403

Relationship between static pressure error/position error and measurable flight parameters for different aircraft weights and configurations

16 p2393 A72-33637

Turbulent boundary layer static pressure and heat exchange dependence on gas injection through porous surface

20 p2912 A72-39363

Instrumentation for measuring static pressure fluctuations within the atmospheric boundary layer.

20 p2927 A72-39799

Errors in static pressure measurements due to protruding pressure taps.

21 p3050 A72-40117

Application of piezoelectric transducers for the measurement of static pressures

21 p3035 A72-41811

STATIC STABILITY

NT DIMENSIONAL STABILITY

NT SHELL STABILITY

NT STRUCTURAL STABILITY

Optimal shape calculation for partially elastic and elastoplastic column under conservative load based on static stability criterion

03 p0447 A72-13851

Atmospheric static stability effect on turbulence layer thickness under nonuniform temperature, using correction factor dependent on Richardson number

03 p0386 A72-14334

Spatial motion of two thread-coupled bodies along satellite circular orbit, discussing system equilibrium position stability and phase trajectories

04 p0582 A72-15003

Optimal fixed point hovering rotor design for improved static performance by pulse theory

05 p0601 A72-16350

Shallow elastic shell under periodic distributed torque loading, investigating static stability enhancement through nonlinear boundary value problem periodic solutions

06 p0900 A72-18697

Conical and spherical nose shapes effects on drag and static stability at Mach 10

07 p0908 A72-19695

Static and dynamic analysis of legged planetary instrument landers, taking into account structural flexibility, elastic-plastic gear load characteristics and soil properties

[AIAA PAPER 72-371] 11 p1725 A72-25396

Static stability of long cylindrical shells under external pressure, using Euler-Lagrange equations

12 p1880 A72-27228

Two dimensional static solutions for cylindrical shells with nonhomogeneous boundary conditions, discussing numerical results for circular shell

12 p1880 A72-27230

Dead load static stability of elastic solids in terms of zero moment condition of Beatty theory

12 p1883 A72-27557

Radiative-dynamic model for static stability of rotating atmospheres, deriving mean equilibrium value of Richardson number in troposphere

14 p1217 A72-30341

Wheel balancing by static and dynamic trial method, using Churchill Mark 3 apparatus

15 p2213 A72-31635

Euler method limitations in static stability analysis, noting criterion for follow-type problem of buckling

16 p2466 A72-33016

Stability loss condition for long rectangular cross section band from nonlinear elastic material with internal constraints, discussing critical loads and deformations

16 p2467 A72-33120

Elastic stability theory of compressible and incompressible composite media

19 p2871 A72-37530

Methods of studying three-dimensional problems of stability in the presence of highly elastic strains

21 p3126 A72-41538

Model studies of plate and shell stability

22 p3233 A72-42055

Control requirements for control configured vehicles.

24 p3368 A72-45349

STATIC TESTS

Linear and nonlinear material static and dynamic structural analysis using NASTRAN digital computer program with finite element approach

01 p0140 A72-10983

Static properties of circular hydrostatic thrust gas bearings with curved surfaces, comparing theory with measurements

[ASME PAPER 71-LUB-22] 02 p0236 A72-11542

Silicate glasses fatigue in dynamic and static tests, discussing fracture stress dependence on time of loading

05 p0681 A72-16422

Monostable three output fluid amplifier models with curved walls in turbulent jet flow, comparing wall design in dynamic and static tests

09 p1263 A72-22931

Statistical failure characteristics and probability evaluation of the static strength of structural components made of composite polymer materials

20 p2943 A72-38942

Surface flaws measurement devices and quasi-static fracture tests, discussing cyclic crack growth, elastic compliance derivative method and stress intensity equations

23 p3353 A72-44229

Dynamic and static characteristics of jet engine simulators

23 p3327 A72-44286

Fan jet Falcon design and certification tests.

24 p3366 A72-44731

Stepwise fatigue testing of high temperature alloy, noting strain hardening phenomena in prestressed samples

24 p3416 A72-45755

STATIC THRUST

Thrust stand for evaluation of thrust vectoring nozzle performance.

[AIAA PAPER 72-1029] 24 p3389 A72-45406

STATICS

NT ELECTROSTATICS

NT HYDROSTATICS

NT MAGNETOHYDROSTATICS

Axiomatic development of mechanics from geometrically formulated kinematics to statics of rigid bodies and systems, using virtual rate of work and reaction principles
13 p2000 A72-28477

Presupposition, aim and methods for teaching transducer technology to users and designers, reviewing transducer static and dynamic performance characteristics and classifications
16 p2393 A72-33632

Conventional aircraft flight mechanics, reviewing vector analytical treatment of rigid body statics
17 p2493 A72-35794

Boundary value problems of lattice plates statics for transversally loaded homogeneous strip, noting elastically supported continuous plates
21 p3123 A72-41394

STATIONARY FRONTS
U FRONTS (METEOROLOGY)
STATIONARY ORBITS
Satellite low orbit transfer to stationary orbit, emphasizing stage and payload recovery effects on performance
01 p0130 A72-10936

Magnetosphere model for low energy cosmic ray proton propagation mode to synchronous orbit satellite, calculating geomagnetic cutoffs and penetration regions
[AD-741079] 02 p0274 A72-12453

Frequency allocation effectiveness and mutual interference calculation for adjacent geostationary communication satellites
07 p0943 A72-19563

Electric thruster for orbit and attitude control of nonspinning geostationary communications satellite
[AIAA PAPER 72-436] 11 p1727 A72-26178

Ion thruster development for Communications Technology Satellite, discussing synchronous orbit stationkeeping requirements, thrust vector control and mounting positions
[AIAA PAPER 72-491] 11 p1711 A72-26216

Frequency allocation effectiveness and mutual interference calculation for adjacent geostationary communication satellites
22 p3153 A72-42081

Celestial mechanics principles application to geostationary satellites in equatorial plane and in earth-moon system libration points, considering Jupiter and Saturn stationary satellites
22 p3222 A72-42141

Optimization of altitude and inclination change schedules during low thrust ascent to geosynchronous orbit.
24 p3440 A72-45150

The Symphonie transponder in the integration phase
24 p3380 A72-45273

STATIONKEEPING
World Administrative Radio Conference for Space Telecommunications data on geostationary orbit utilization, covering stationkeeping and satellite antenna pointing accuracies
02 p0177 A72-12387

Satellites and spacecraft flight control systems, discussing approaches for stationkeeping and orbit determination/correction
05 p0729 A72-16746

ATS F ion thruster system for north-south stationkeeping, discussing specific impulse, thrust vectoring, propellant system and power conditioning circuitry
[AIAA PAPER 72-439] 11 p1707 A72-26180

Ion thruster development for Communications Technology Satellite, discussing synchronous orbit stationkeeping requirements, thrust vector control and mounting positions
[AIAA PAPER 72-491] 11 p1711 A72-26216

Structurally integrated ion thruster /SIT-5/ for synchronous satellites attitude control and stationkeeping, presenting design and performance data
[AIAA PAPER 72-492] 13 p2027 A72-28950

Design and tests of dual deflectable beam strip ion thruster, noting application to two axes satellite attitude control and stationkeeping
[AIAA PAPER 72-494] 13 p2027 A72-28951

Communication satellites auxiliary propulsion systems surveyed for attitude and stationkeeping systems selection
[AIAA PAPER 72-515] 13 p2052 A72-28978

STATIONS
NT EOSS
NT GLOBAL TRACKING NETWORK
NT GROUND STATIONS
NT HALO ORBIT SPACE STATION
NT ORBITAL SPACE STATIONS
NT ORBITAL WORKSHOPS
NT SALYUT SPACE STATION
NT SPACE DETECTION AND TRACKING SYSTEM
NT SPACE STATIONS
NT TRACKING STATIONS
NT WEATHER STATIONS

STATISTICAL ANALYSIS
NT AMPLITUDE DISTRIBUTION ANALYSIS
NT BIVARIATE ANALYSIS
NT CORRELATION COEFFICIENTS
NT FACTOR ANALYSIS

NT KOLMOGOROFF-SMIRNOFF TEST
NT MANN-WHITNEY-WILCOXON U TEST
NT MAXWELL-BOLTZMANN DENSITY FUNCTION
NT MULTIVARIATE STATISTICAL ANALYSIS
NT NONPARAMETRIC STATISTICS
NT NORMAL DENSITY FUNCTIONS
NT PEARSON DISTRIBUTIONS
NT POISSON DENSITY FUNCTIONS
NT PROBABILITY DENSITY FUNCTIONS
NT PROBABILITY DISTRIBUTION FUNCTIONS
NT RANK TESTS
NT RAYLEIGH DISTRIBUTION
NT REGRESSION ANALYSIS
NT SEQUENTIAL ANALYSIS
NT STANDARD DEVIATION
NT STATISTICAL CORRELATION
NT STATISTICAL DECISION THEORY
NT STATISTICAL TESTS
NT VARIANCE [STATISTICS]
NT WEIBULL DENSITY FUNCTIONS

EEG parameters estimation and statistical uncertainty calculation by computer program
01 p0016 A72-10073

Error probability distributions in navigational statistics involving single or identical and diverse instruments or operators
01 p0096 A72-10176

Statistical analysis of track keeping Strumble VOR data for lateral navigation separation standards and collision risk in continental environment
01 p0097 A72-10179

Linear stochastic-parameter output channel, examining signal quadrature components statistical characteristics
01 p0024 A72-10199

Large structural systems dynamic mathematical models, predicting eigenvalue and eigenvector with statistical analysis
[SAE PAPER 710785] 01 p0137 A72-10276

Statistical methods application to parachute materials evaluation, using factorial experiments for multiple variables simultaneous effects analysis
01 p0005 A72-10317

Statistical analysis of ionospheric electron content observations over European stations with nonstationary satellites, taking into account solar radiation and magnetic activity
01 p0054 A72-10422

Statistical analysis of atmospheric average arrival time distribution, using simultaneous data from Berlin and equatorial latitude positioned research ship Meteor
01 p0056 A72-10443

Statistical model for communication probability estimate based on signal-to-interference and SNR criteria
01 p0031 A72-10997

Learning-identification of unknown nonlinear discrete systems, using local estimation results for global function learning
01 p0046 A72-11199

Space vehicles development and fabrication cost estimation, deriving statistical-analytical formulas with allowance for technical complexity and learning factor
01 p0147 A72-11219

Combined bending/torque fatigue test machines design, operation, calibration and results, developing probabilistic S-N diagram from cycles-to-failure data statistical analysis
02 p0199 A72-11514

Stress-strain characteristics of stochastically reinforced materials of high rigidity orthotropic elastic layers alternating with isotropic elastic or viscoelastic layers
02 p0248 A72-11623

Statistical long term speech spectrum analysis and perceptual evaluation, using digital bandpass filter technique
02 p0171 A72-11666

Computerized statistical identification of aerial photograph ground patterns, comparing elliptical boundary condition with minimum distance to mean classification models
02 p0187 A72-11842

Neutron cosmic ray spectrograph method of separating recorded data by energies, using statistical analysis of data combinations with different dead times
02 p0229 A72-11936

Steerable receiving antennas L/S band solar calibration error statistical analysis, obtaining 0.5 db uncertainty by monitoring antenna gain-to-noise temperature ratio
02 p0192 A72-12159

Quasar evolution models statistics suggesting relationship to radio galaxies, discussing continuity equation for density and luminosity changes
02 p0279 A72-12187

Resonant and nonresonant sound transmission through cylinder walls, using statistical analysis
02 p0260 A72-12374

Radar target cross section parameters statistical analysis, discussing real target categories and relative measuring methods
02 p0181 A72-12641

Statistical synthesis of antenna arrays using phase amplitude distribution equivalent to reference array radiation pattern
02 p0196 A72-12758

Thermal advection statistical relation to vertical motion, discussing conventional synoptic meteorological empirical facts utilization in numerical models for long term weather forecasting
02 p0254 A72-12779

Describing function method for nonlinear systems under stochastic input, considering statistical optimizations/linearization and self oscillation under noise
03 p0337 A72-13074

RR Lyrae stars absolute magnitude determination by statistical parallaxes method
03 p0421 A72-13139

Book on random data analysis and measurement procedures covering physical systems dynamic response properties, random processes, statistical sampling, data acquisition and processing, etc
03 p0327 A72-13175

Quiet sun radio emission observation, considering statistical minimum value and time varying structure
03 p0424 A72-13220

Statistical model of small scale discrete structure of magnetoplasma in solar active regions
03 p0430 A72-13335

Relativistic plasma with particles interacting through electromagnetic field, constructing statistical description by reduced distribution functions and correlation patterns
03 p0395 A72-13626

Statistical investigation of 1500 galaxies in MCG catalog with weak surface brightness, noting sculpture type spheroidal galaxies in Virgo cluster
03 p0435 A72-13807

Statistical processing of phase dependence of Martian integral brightness at 0.3-1.1 microns, noting abrupt reflectivity decrease
03 p0436 A72-13816

Soviet book on statistical theory of digital data transmission through parallel channels covering optimal and suboptimal reception systems under signal fading and interference
03 p0323 A72-13968

Ultrasonic defectoscope sensitivity, discussing statistical character of random signal level distribution and test conditions
03 p0364 A72-13988

Electromagnetic noise and effects on communication systems, considering statistical parameters definition and measurements
03 p0324 A72-14036

Composite incidental man-made radio noise data correlation to envelope statistic transformation hypothesis based on vlf airborne measurements of metropolitan area noise
03 p0324 A72-14041

Code performance evaluation over real digital channels, characterizing channel error process by multipag statistics
03 p0325 A72-14183

Statistical methods of stress and reliability analyses of elastic systems under random external loads
03 p0453 A72-14206

Homogeneous first order solutions to Lamé equations in statistical elasticity theory, yielding harmonic surface displacement for elastic body
03 p0454 A72-14371

Statistical properties of random-phase modulated laser beams, calculating coherence functions of optical fields
04 p0528 A72-14580

Cyclic phenomena periodicity by expected mean square deviation statistical analysis of observational data samples, using null hypothesis and unequally spaced sample intervals
04 p0574 A72-14908

Statistical analysis of low latitude F 2 layer disturbances associated with sudden commencement type geomagnetic storms, investigating critical frequencies
04 p0516 A72-14937

Lunar surface small crater statistical analysis and age prediction based on density and diameter correlation from Soviet Lunar Rover panoramic pictures
04 p0576 A72-15065

Lunar stone distribution statistical analysis according to size on Soviet Lunar Rover panoramic pictures, estimating rock ages
04 p0576 A72-15067

Error distribution computation for combined Rayleigh-Gaussian statistics data, applying to antenna radiation beam-pointing example
04 p0500 A72-15303

Boltzmann equation collision integral statistical models, solving shock structure in monatomic gas
04 p0513 A72-15339

Light transmission in medium with random inhomogeneities in Markov random process approximation, obtaining short wave field statistical characteristics

04 p0488 A72-15380

Average ray direction and mean square deviation formula for electromagnetic wave propagation in random inhomogeneous medium suited for calculation by ray tracing program

04 p0488 A72-15382

Probability amplitude analysis of statistical behavior of fading signal envelope

04 p0493 A72-15457

Statistical calculation of wear rate in friction pair with linear contact, analyzing errors

04 p0528 A72-15711

Statistical investigations of solar burst time dependent fine structure, giving data for multichannel spectrograph and recording system design

05 p0708 A72-15767

Stressed state of radial bearings hollow rollers under loads concentrated along generatrix, evaluating test results by statistical analysis

05 p0665 A72-15984

Statistical characteristics of range-guard intrusions and airspace collision conflicts in terminal area

05 p0611 A72-16110

Statistical description of Brownian particle motion in turbulent flow, using theory of canonical correlations

05 p0648 A72-16171

Quasar radio structure, investigating morphology, statistical characteristics, angular size of spectra and red shift correlations from interferometer measurements

05 p0716 A72-16377

Two dimensional turbulence stationary states from statistical equilibria for Navier-Stokes equation

05 p0649 A72-16686

Characteristic functional for random delayed events and cluster processes, using Blanc-Lapierre statistical model

05 p0693 A72-17079

Statistical solution of analytical design of optimal control system maintaining coarseness/universality/with minimum quality loss

05 p0691 A72-17135

Statistical analysis of sunspot activity, forecasting solar cycle events

05 p0723 A72-17176

Time to failure statistics for communications satellites redundant systems with spares and negative exponential reliability function, discussing perfect and imperfect switching

05 p0731 A72-17250

Statistical criteria of geomagnetic activity, considering solar corpuscular radiation effect

06 p0803 A72-17369

Statistical equations for turbulent fluctuations of energy, concentration and rotation in compressible flows

06 p0797 A72-17557

Aerosol scattering coefficient in atmosphere, determining statistical characteristics of vertical and spectral structure

06 p0842 A72-18043

Soviet book on laser communication statistical theory covering coherent and noncoherent optical signal detection and discrimination, SNR optimal reception, beam scanning, etc

06 p0777 A72-18518

Resin bonded solid lubricant film thickness optimization from statistical analysis of bench and machine element test data

06 p0823 A72-18591

Statistical characteristics of antenna gain threshold as function of link trajectory during radiation pattern shift with respect to fixed orientation

07 p0953 A72-19006

Mathematical expectation of angularly modulated signal in unsteady linear random noise, using Marchenko formula

07 p0939 A72-19020

Atmospheric attenuation due to rain based on links experiment and statistical study of equivalent precipitation for given path length and time percentage

07 p0939 A72-19188

Statistical analysis of eccentricity changes in nearly parabolic comets, showing data samples relation to Bernoulli random variable with two different unknown parameters

07 p1072 A72-19339

Statistical evaluation for forged jet engine parts tensile tests cost reduction, using regression analysis

07 p0995 A72-19484

Conditional distribution density formation for signal-noise mixture based on learning sampling with dependent values

07 p0943 A72-19517

Signal detection in stationary, Markov and other noise background, discussing functional method of statistical and probabilistic representation

07 p0943 A72-19520

Extrapolation procedure for determining small-scale wind shear definition from Rawinsonde vertical wind profiles statistical data for aerospace vehicle design

07 p1085 A72-19687

Axially compressed cylindrical shells with axisymmetric imperfections, analyzing random buckling behavior and failure probability by statistical methods

07 p1089 A72-19689

Statistical analysis of linear systems with additive environmental inputs and behavioral uncertainties, obtaining transfer function matrix, cross covariance matrix and power spectrum

07 p0960 A72-19703

Statistical analysis of magnetic energy-density antenna performance in mobile communication, comparing two-crossed-slot design to three element unit

07 p0957 A72-19801

Book on statistical antenna theory covering radiation patterns and other parameters for large multielement, mirror, and synthetic aperture antennas

07 p0957 A72-19862

Statistical-hydrodynamic description of nonequilibrium gas dynamics of single component and binary mixtures and systems with chemical reactions

07 p0968 A72-19886

Statistical analysis of system component error propagation by digital simulation using Continuous System Modeling program, considering strapped down inertial guidance computer

07 p1033 A72-20347

Laser Doppler velocimeter signals statistical properties, examining bandwidth, counting time and input SNR effects on zero crossing counter output fluctuations rms value

07 p0990 A72-20370

Distributions and average values for proton speed, azimuthal and polar flow directions and proton temperature and density in solar wind from Pioneer data

07 p1063 A72-20380

Strength and strain theory statistical analysis for perfectly brittle and plastic materials, assuming ultimate or elastic limit strain as governing factor

07 p1097 A72-20536

Signal statistical model parameter evaluation by selection of operators in form of dimensionless quantile ratios

08 p1130 A72-20724

Statistical treatment of galaxy clusters shape, using flattening measurement data

08 p1229 A72-20842

Taxonomy for incomplete data problems, developing unified analysis methods based on maximum likelihood estimate

08 p1199 A72-21199

Stationary statistical model for microwave oscillator flicker frequency noise, leading to power spectral density and time domain frequency instability

[ONERA, TP NO. 1085] 08 p1141 A72-21431

Survival rates in USAF accidents during 1965-69, noting visual sighting as primary rescue factor

08 p1109 A72-21564

Statistical analysis of cockpit simulator data on altimetry display for commercial aircraft

08 p1168 A72-21573

Stress rupture data from S glass composite matrix effectiveness tests, noting skewed lifetime distribution in statistical patterns

08 p1192 A72-21683

Planetary and lunar surface relief reconstruction from photographic imagery, discussing statistical morphological characteristics determination from relief

08 p1238 A72-21833

German monograph on computerized statistical analysis of Al alloy fatigue test data, considering welded samples and thin plates

08 p1188 A72-21848

Mean monthly statistical characteristics of wind regime from meteor trail drifts observations

08 p1162 A72-21885

Cloud and precipitation dynamic processes effects on reflected radar signal statistical characteristics

08 p1137 A72-21996

Radio system operational reliability analysis by mathematical methods with use of digital computer, discussing statistical modeling algorithm

08 p1143 A72-22065

Adaptive statistical system with feedback loop for weather analysis and forecasting, examining learning process features

08 p1202 A72-22113

Statistical characteristics of wind elements from vertical-temporal structure of wind field

08 p1202 A72-22118

Statistical analysis of temperature characteristics based on natural orthogonal components expansion for weather forecasting application

08 p1203 A72-22120

Atmospheric surface layer meteorological elements representative values determination as optimal filtration problem, examining data correlation with errors in initial statistical characteristics

08 p1203 A72-22121

Discriminatory analysis application in hydrometeorological forecasts, discussing use of bunch map analysis

08 p1203 A72-22122

Sigma algebra and statistics system for optimal stopping of stochastic processes for continuous time case

09 p1340 A72-22424

Equilibrium statistics of randomly forced two dimensional viscous flow three mode representation constructed by numerical integration of nonlinear equations system

09 p1293 A72-22459

Averaging process in thermodynamic systems energy transformation description

09 p1410 A72-22635

Radar data statistical evaluation, emphasizing near Doppler shift for aircraft radial velocity calculation

09 p1278 A72-22897

Star catalogs comparison and stellar positional differences and motion studies using random field theory

09 p1388 A72-23052

Energetic particle flux measurement on spacecraft based on statistics of overflowing register counting Poisson process

09 p1312 A72-23261

Black and white aerial photographs quantitative evaluation for differentiation and identification of land use patterns by microdensitometry, using statistical methods

09 p1313 A72-23306

One degree of freedom mechanical system with jump-like variable mass, determining displacement and velocity statistical characteristics under random excitation and mass addition

09 p1353 A72-23608

Statistical analysis of piezoelectric transducer voltage-displacement characteristic, determining linearity deviations magnitude

09 p1317 A72-23676

Monte Carlo and convolution methods for statistical analysis of ladder filters, describing programs for determining attenuation probabilistic distribution as function of components dispersions

09 p1289 A72-23679

Probability model of statistical independence relationships among two events and environmental event, examining all combinations of definition statements for reliability analysis

10 p1504 A72-24015

Statistical-analytical cost models for spacecraft development and fabrication, taking into account various technical and management factors

10 p1564 A72-24026

Statistical solution of steady natural turbulent convection at large Grashof numbers

10 p1465 A72-24103

Short period comets origin and orbital evolution, discussing Jupiter perturbations and statistical study

10 p1536 A72-24143

Statistical analysis of MOS integrated circuits from initial data of electrophysical and geometric distribution laws and covariance matrix

10 p1449 A72-24289

Statistical equilibrium analysis of fluorescent Fe I emission in long period variables

10 p1542 A72-24610

Mathematical statistics application to complex systems modeling, considering group method of data handling, simulation and regression methods

10 p1457 A72-24634

Electronic circuits statistical optimization with Monte Carlo procedure, discussing methods and algorithms for accelerating evolutionary modeling

10 p1452 A72-24638

Stellar statistics method for determining interstellar extinction to reddening ratio in dark cloud area

10 p1546 A72-24836

Statistical evaluation of welded airframe component fatigue damage increment during cyclic loading with constant force amplitude

10 p1559 A72-24922

Statistical analysis of entire test based on subsets, discussing problem formulation in probabilistic language

10 p1506 A72-25117

Russian papers on cybernetic systems accuracy and reliability covering error correction schemes, statistical analysis and computer design

11 p1599 A72-25426

Cybernetic system effectiveness analysis with operations research and statistical theory based on stochastic treatment

11 p1608 A72-25428

Russian papers on discrete control systems covering inertialess Markov objects, pulse amplitude and frequency modulation and statistical analysis

11 p1609 A72-25442

Recurrent algorithms for inertialess Markov objects identification based on statistical solutions theory

11 p1609 A72-25443

Approximate statistical analysis of PFM and combined modulation systems, proposing linearization method

11 p1609 A72-25447

Statistical diagnosis of aeronautical systems reliability and maintenance, using Benzecri factorial analysis for data reduction
11 p1639 A72-25817

Laminated reinforced plastics structural design criteria obtained by statistical and deterministic approach
11 p1737 A72-26235

Statistical analysis of errors in altitude readings of phase comparison AM radio altimeters
11 p1633 A72-26303

Synchronous detector technique for statistical properties improvement in phase comparison AM radio altimeter signal
11 p1633 A72-26304

Statistical error analysis of phase comparison FM radio altimeter during signal processing, investigating range finding strength distribution of echo reflectance
11 p1633 A72-26305

Digital analog converter output voltage variation coefficient derivation, obtaining operational error statistical characteristics estimates and elements parameter
11 p1602 A72-26447

Statistical analysis of strain criteria and stochastic relations for Al alloy fatigue life and minimum creep rate at 175-250 C
11 p1663 A72-26800

Statistical approach to atmospheric optics inverse problems solution, considering application to vertical temperature and humidity profiles determination
11 p1683 A72-26888

Variational and statistical methods for adiabatic electron plasma with self consistent field interaction in terms of Lagrange, Hamilton and Liouville formalization
12 p1850 A72-27185

Technological parameters effects on resistance values dispersion of thick film resistors, reviewing stability test performance
12 p1788 A72-27274

Test conduct inaccuracies effect estimation for statistical spread of experimental creep rate and long term strength values
12 p1813 A72-27456

Volume averages of stress and strain changes induced by Poisson ratio variation in boundary value problems of three dimensional classical elastostatics
12 p1884 A72-27566

Statistical analysis of spectrographic plasma temperature measurements, obtaining numerical solution to Abel integral equation
12 p1852 A72-27685

Intergalactic extinction relationship to large galactic clusters from statistical analysis of fourth and fifth Zwicky catalogs
12 p1872 A72-27759

Statistical analysis of solar microwave bursts, examining radiation source development and emission mechanism
12 p1872 A72-27814

Solar activity effects on bismuth chloride hydrolysis tests from statistical results following solar flares
12 p1773 A72-28212

Solid deformable body mean stress determination by statistical summation of stress squares on faces of parallelepiped rotated within Euler angle limits
12 p1887 A72-28233

Parametric approaches to statistical burn-in or debugging problems in aircraft reliability analysis
13 p1985 A72-28363

Mean linear velocity of rotation on solar equator to improve Hart rotatory velocity fluctuation values, giving expressions for statistical reestimation of mean square errors
13 p2035 A72-28441

Statistical model for short wave radio signal fading at oblique signal reflection from ionosphere, determining pulse amplitude and duration distribution laws
13 p1915 A72-28468

Statistical theory of nonuniform turbulent incompressible fluid flow, presenting approximate formulas of nonisotropic two point correlation tensors
13 p1941 A72-28629

Cloud statistics stratification by climatological regime, month and time of day, extending simulation to drop size distributions and liquid water content
13 p1989 A72-28808

Precipitation exceedance rates charts for various risks, using statistical models
13 p1989 A72-28811

Diurnal and annual temperature variations at 30-60 km from statistical analysis of rocketsonde data, obtaining solar radiation errors magnitude
13 p1947 A72-28829

Automatic statistical analyzer for radio meteor echo multiplicity recording in three coordinate /multivariable/ space, including instrument error allowance
13 p1929 A72-29032

Random vibration statistics of lifting rotors with feedback controls, solving response variance matrix by random inputs shaping filters
13 p2057 A72-29096

Analog and digital computers for automatic statistical analysis of unsteady random process recorded data, calculating correlation functions and expectancy
13 p1925 A72-29165

Semiconductor devices series production process control and analysis by statistical procedures, noting computer controlled data acquisition system for silicon diodes production
13 p1965 A72-29166

Redundant and nonredundant self adaptive systems reliability, discussing statistical random process characteristics
13 p1936 A72-29170

Statistical homogeneity criteria for automatic equipment operation reliability, using Poisson flow model with random fluctuations
13 p1965 A72-29173

Statistical activity analysis procedure for random nerve network model, determining representative point trajectory in phase space via similarity matrix
13 p1909 A72-29176

Statistical analysis for single airport ATC digital simulation using Poisson distribution law, calculating optimal number of channels
13 p1996 A72-29179

Neutron cosmic ray spectrograph method of separating recorded data by energies, using statistical analysis of data combinations with different dead times
13 p1957 A72-29248

Statistical energy analysis of sound-structural interaction, considering sound transmission through complex walls and piping systems and fluid filled container vibrations
13 p2005 A72-29556

Random vibration of two multimodal mechanical systems with point coupling, obtaining power flow spectral density by statistical energy analysis
13 p2005 A72-29563

Statistical description of Brownian particle velocity in turbulent flow, using theory of canonical correlations
14 p2093 A72-30240

Averaged atmospheric IR counter radiation values in cumulus clouds, using statistical characteristics
14 p2099 A72-30249

Welded machine component service history effects on residual fatigue life from statistical evaluation of factor experiment
14 p2107 A72-30278

Non-Maxwellian inhomogeneous collisionless plasma equilibrium and stability, proposing statistical thermodynamic model
14 p2137 A72-30394

PCM speech transmission systems, comparing pseudorandomly dithered quantization with fixed level method by intelligibility and subjective appreciation tests and statistical analysis
14 p2087 A72-30942

Aircraft accident statistical projections from human error review, analyzing situational circumstance limitations
14 p2081 A72-31086

Van der Pol and nonlinear parametric oscillators fluctuations due to random noises analyzed by averaging method and discrete Markov processes
14 p2133 A72-31134

Multimode millimeter waveguides and optical fibers, deriving signal transmission distortion from transfer function and corresponding impulse response statistics
15 p2193 A72-31351

Signal distortion minimization for random waveguides with frequency-dependent optimum coupling based on transfer function covariance and impulse response time domain statistics
15 p2194 A72-31352

Linear stochastic-parameter output channel, examining signal quadrature components statistical characteristics
15 p2195 A72-31623

Eole satellite observed meteorological balloon data analysis, obtaining mean zonal velocity, meridional velocity and temperature vs latitude from statistical estimates
15 p2266 A72-31980

Statistical analysis of photocounts of arbitrary spectral profile Gaussian light, discussing two incoherent beams superposition
15 p2277 A72-32231

Statistical evaluation of feedback role in simple movements in terms of Index of Preprogramming
15 p2187 A72-32761

Photoelectric measurement of solar photosphere pole-equator temperature differences, analyzing statistical and systematic errors
15 p2317 A72-32770

[AD-745809] Autocorrelation analysis of Mariner 2 data for solar wind velocity, noting 27 day recurrences
16 p2444 A72-32954

Critique on experiment to measure gravitational constant differences between two elements, discussing errors in statistical analysis
16 p2426 A72-33769

Statistical analysis of position-fixing general theory for systems with Gaussian errors.
17 p2578 A72-34294

Application of statistical linearization techniques to nonlinear multidegree-of-freedom systems.
[ASME PAPER 71-WA/APM-5] 17 p2624 A72-34315

Book - Elements of applied stochastic processes
17 p2575 A72-34624

Statistical estimate of the attainable sidelobe level in phase-switched antenna arrays with a nonlinear initial phase lead
17 p2529 A72-34833

Price adjusted single sampling with linear indifference.
17 p2560 A72-34943

Statistical-hydrodynamic description of nonequilibrium gas dynamics of single component and binary mixtures and systems with chemical reactions
17 p2540 A72-35134

Measures of effectiveness for special signal detectors of simple structure
17 p2516 A72-35222

Image autocorrelation function models and power spectra, obtaining probability distribution, variance and correlation coefficients of image orthogonal transformations
17 p2518 A72-35672

Focused irradiance fluctuations beyond a layer of turbulent atmosphere.
17 p2518 A72-35754

Identification of periodicities in the structure of natural stochastic processes
17 p2534 A72-35783

Statistical models and turbulence: Proceedings of the Symposium, University of California, La Jolla, Calif., July 15-21, 1971.
18 p2676 A72-36001

Self-consistent statistical models for the gravity anomaly, vertical deflections, and undulation of the geoid.
18 p2723 A72-36028

Application of statistical methods to the study of the rigidity of a dielectric
18 p2720 A72-37116

The diurnal effect of the cosmic rays during the period 15 October 1965-30 June 1966. I - Method of analysis and statistical distribution.
18 p2722 A72-37159

Radar cross section fluctuation statistics description by generalized chi-square distribution, discussing target detection probabilities maximum likelihood estimates
19 p2763 A72-37293

A method for generalized statistical studies of discrete information transmission systems
19 p2764 A72-37301

Conditions for the effectiveness of adaptation algorithms based on an empirical Bayesian approach to statistics
19 p2825 A72-37440

Weight estimation methods.
19 p2871 A72-37451

Statistical characteristics of surface pressure pulsations in turbulent boundary layer of incompressible fluid, discussing effects near smooth flat wall
19 p2785 A72-37472

Study of the flow of air traffic and capacity of a control system
19 p2831 A72-37797

Novae and background stars relative proper motions, deriving and tabulating absolute proper motions via statistical transformation
19 p2860 A72-37970

Geophysical signal statistical model parameter evaluation by selection of operators in form of dimensionless quantile ratios
19 p2765 A72-38352

A statistical information theory for extremum search of a function
19 p2827 A72-38576

Statistical synthesis of antenna arrays using phase amplitude distribution equivalent to reference array radiation pattern
20 p2907 A72-39064

Dynamic electromagnetic scattering pattern of flying object, constructing quasi-ergodicity condition to compute standard statistical descriptions for recognition
20 p2903 A72-39071

Dynamic nonlinear system direct statistical analysis by Covariance Analysis Describing Function Technique with linearization, giving illustrative examples
20 p2905 A72-39124

Statistical analysis for best fit of compact X ray object spectra to black body, bremsstrahlung and power law models
20 p2969 A72-39387

Book - Bayesian statistics: A review.
20 p2946 A72-39728

A statistical method for the determination of the rate of changes of period for eclipsing binaries.
20 p2974 A72-39892

Application of statistical methods to studies of the surface properties of polymers 21 p3072 A72-40080

Quantization error of the coefficients in digital filters with N shift sequences 21 p3025 A72-40223

Data acquisition, storage and processing, discussing data reduction by statistical coding, interpolation, prediction and parameter identification 21 p3014 A72-40322

Statistical analysis of information from remote space vehicles 21 p3015 A72-40327

A priori estimation of the quality of a data-compression system from the statistical characteristics of the sensors employed 21 p3024 A72-40328

Performance of antennas in random fields. 21 p3026 A72-40355

Receiver processing for direct-detection optical communication systems. 21 p3017 A72-40859

Quantitative aspects of reliability in process-control systems. 21 p3038 A72-40922

Statistical estimation of the signal-to-noise ratio beyond a linear detector 21 p3022 A72-41073

Independent cascaded multicomponent random variable system gain statistics relationship to individual component based on moment derivation, obtaining curves from variance equation 21 p3022 A72-41087

Statistical analysis of influence coefficients and unbalance forces measurement errors in balancing of rotors 21 p2996 A72-41229

Diffusion from a continuous source in relation to the Eulerian properties of turbulence. 21 p3046 A72-41248

Location estimation for spacecraft landed on Mars surface via statistical techniques application to earth based radio tracking data, taking into account ephemeris biases [AIAA PAPER 72-903] 21 p3082 A72-41554

Orbit prediction for artificial satellites via numerical averaging technique, presenting algorithm for planetary equations solution [AIAA PAPER 72-934] 21 p3112 A72-41572

Weibull distribution government of dispersion of destructive temperature gradients characteristic of fireproof ceramic materials heat resistance 21 p3074 A72-41713

Analysis of noise immunity of two-channel eddy-current flaw detector. 21 p3057 A72-41723

Application of sample quantiles to the compression of teletext transmission and statistical processing of medical information 22 p3150 A72-42221

Statistical characteristics of an optimal detector of randomly fading pulse signals 22 p3154 A72-42229

Parametric method of statistical synthesis with incomplete initial information on signal and noise distribution, discussing signal detection in white noise with unknown spectral density 22 p3154 A72-42230

Statistical synthesis of navigation aids systems with unsteady random interferences, obtaining optimization criterion by least squares method 22 p3202 A72-42232

Very-high-frequency wave propagation by the temperate-latitude sporadic-E layer. 22 p3154 A72-42367

Atmospheric effects on the surface cosmic ray meson intensity recorded in London. 22 p3218 A72-42369

Error sensitivity of statistical models with pattern rearrangement for analysis of interplanetary scintillation in ecliptic plane 22 p3218 A72-42402

Statistical characteristics of storm-associated Pc 5 micropulsations observed at the synchronous equatorial orbit. 22 p3171 A72-42413

Some effects of cognitive similarity on proactive and retroactive interference in short-term memory. 22 p3142 A72-42548

Noncoherent scattering probabilistic formulation in terms of mean intensity averaged over absorption profile and mean scatterings number required for photon escape 22 p3206 A72-42559

An approximation to midcourse correction direction errors. 22 p3203 A72-42870

Statistical method of failure analysis for redundancy forms selection, noting aircraft safety and reliability 22 p3139 A72-42973

Atmospheric optics inverse problem solution, comparing orthogonal functions series expansion and statistical regularization method algorithms 22 p3202 A72-43006

Einstein equations reduction to friction systems in homogeneous cosmological models, investigating Bianchi models isotropization and statistical analysis. 23 p3335 A72-43301

Statistical analysis of Forbush decreases and the preceding increases in cosmic-ray intensity 23 p3328 A72-43354

Stress-rupture of simple S-glass/epoxy composites. 23 p3305 A72-43492

Statistical strength and plasticity criterion for materials in a complex stress-strain state 23 p3349 A72-43953

Analysis of optimal space-time signal discrimination 23 p3266 A72-44217

Statistical analysis of the sound level distribution of aircraft noise as a function of time 23 p3252 A72-44337

Statistical forecasting models for USAF CONUS outbound cargo airlift requirements by averaging and exponential smoothing models 24 p3466 A72-44578

Statistical techniques for severely censored random samples with known and unknown probability distribution functions 24 p3418 A72-44665

Interplanetary objects in review - Statistics of their masses and dynamics. 24 p3435 A72-44688

An assessment of repeated loads on general aviation and transport aircraft. 24 p3366 A72-44736

Statistical analysis of the turbulence near a wall by conditional sampling 24 p3392 A72-45066

Hodgkins disease post-surgery recurrence hazard rate in flying personnel, developing statistical base for decision regarding return to military flying duty 24 p3377 A72-45661

Statistical analysis of comet observations, calculating relationships between comet head angular diameter and heliocentric and geocentric distances and apparent brightness 24 p3448 A72-45687

Stressed state of radial bearings hollow rollers under loads concentrated along generatrix, evaluating test results by statistical analysis 24 p3408 A72-45726

STATISTICAL COMMUNICATION THEORY U COMMUNICATION THEORY STATISTICAL CORRELATION

Student naval aviator selection by multiple correlation technique using noncognitive college and flight background questionnaire to reduce attrition rate 02 p0166 A72-11704

Statistical characteristics of rough sea compared with variable magnetic fields near Crimean coast in Black Sea 02 p0218 A72-11951

Statistical linearization approach to determine approximate instantaneous correlation matrices of nonlinear structure response to nonwhite excitation 02 p0298 A72-12663

Book on random functions and turbulence covering probability theory, random processes and fields, statistical correlation and spectral methods, numerical weather forecasting, etc 05 p0649 A72-16397

F region irregularity contours from correlation analysis of satellite amplitude scintillations, showing axially symmetric field-aligned and north-south elongated planes 08 p1156 A72-21105

Averaged Bogoliubov-derived chains of kinetic theory gas dynamics equations with strong statistical correlation for macroprocess description 08 p1149 A72-21175

Clutter correlated lognormal random variables generation from statistically independent Gaussian random variables for radar simulations 08 p1134 A72-21423

Zaidenberg correlation method for nonlinear systems dynamic properties under random excitation, determining statistically equivalent linearized terms for equations of motion 09 p1353 A72-23607

Statistical estimation method for brittle metals fracture strength, taking into account stress nonuniformities due to dislocation defects 11 p1738 A72-26803

Radio source and radio quiet quasars identifications for statistical correlation with bright galaxies positions 12 p1871 A72-27742

Statistical characteristics of rough sea compared with variable magnetic fields near Crimean coast in Black Sea 13 p1949 A72-29263

Digital computer estimates of random processes spectral density by statistical correlation method, calculating errors in numerical integration techniques 13 p1937 A72-29495

Statistical data processing method for accuracy evaluation of satellite orbits parameters obtained from onboard measurements of two stars angular positions 14 p2151 A72-30454

Joint photon-count probability distribution measurement of electric field amplitude correlation function for random-Gaussian light fields produced by laser beam scattering 15 p2280 A72-31378

Optical pulse wave field longitudinal and transverse statistical correlations during propagation in turbulent atmosphere 15 p2198 A72-32061

Solar activity correlation with filaments disintegration during transit across solar disk, analyzing statistical data 15 p2318 A72-32782

Electronic circuit reliability prediction model with statistical dependence for detailed failure modes 16 p2371 A72-33349

Statistical correlation techniques applied to jet aircraft autoland system dynamic ground tests with simulated engine and aerodynamic characteristics 16 p2420 A72-33641

Data transmission systems with decision feedback in presence of burst noise, calculating statistical relations among received sequences as function of duration and spacing 16 p2372 A72-33799

Statistical correlation of X-band microwave scattering by overdense intermittently turbulent ionized Ar jet with flux fluctuations from electrostatic probe observations [AIAA PAPER 72-674] 16 p2440 A72-34063

Calculation of correlation matrices for linear systems subjected to nonwhite excitation. [ASME PAPER 71-APMW-10] 17 p2625 A72-34316

An application of the generalized Langevin equations to the study of correlations in simple, classical fluids. 17 p2581 A72-35154

Correlation functions and reconstruction error for quantized Gaussian signals transmitted over discrete memoryless channels. 17 p2516 A72-35333

Role of recursive estimation in statistical image enhancement. 18 p2658 A72-36260

Certain results of the statistical processing of a large series of large-scale television images of stars 19 p2860 A72-37957

General transport theory of noise in pn junction-like devices. II - Carrier correlations and fluctuations from high injection. 22 p3160 A72-43081

STATISTICAL DECISION THEORY

Optimal sequential multiple decision procedures for radar receiver using Monte Carlo method 05 p0628 A72-16561

Statistical inferences on two parameter Weibull reliability function from classical, Bayesian and structural probability viewpoint 15 p2264 A72-31800

Comparison of the quality of empirical and optimal adaptation algorithms in multiple-alternative choice problems 19 p2828 A72-38583

Bayesian decision analysis of the hazard rate for a two-parameter Weibull process. 22 p3198 A72-41981

Determining optimum burn-in and replacement times using Bayesian decision theory. 22 p3182 A72-41982

A stochastic automata theoretical approach to dynamic programming. 22 p3199 A72-42633

Bayesian statistical decision theory and reliability-based design. 22 p3240 A72-42967

Estimation and prediction of Gumbel and Frechet distribution parameters, noting statistical decision in tests, sequential analysis and graphical procedures 22 p3199 A72-42968

Estimation, confidence intervals, and incentive plans for sequential three way decision procedures. 24 p3406 A72-44667

STATISTICAL DISTRIBUTIONS

NT PEARSON DISTRIBUTIONS

NT PROBABILITY DISTRIBUTION FUNCTIONS

NT RAYLEIGH DISTRIBUTION

Electrostatic waves in longitudinally magnetized plasmas with random electron charge distribution and applied magnetic field, finding phase characteristics 01 p0106 A72-10128

Log normal random fluctuations of ionospheric electron concentration in F region from vertical sounding and incoherent scatter data 01 p0059 A72-10609

Amorphous semiconductors dielectric properties based on randomly distributed local electron states in disordered solids, crystalline impurities and polymer aggregates 02 p0269 A72-12450

Critique of quasar model of independent random pulse emitting sources conglomeration, noting brightness fluctuations incompatibility 03 p0435 A72-13802

- Statistical distribution of maximum response for reliability-based optimum spacecraft structural design for random excitations from booster shutdown
05 p0724 A72-16103
- Rice exceedance statistics application to atmospheric turbulence, indicating strong nonGaussian second order distributions
[AIAA PAPER 72-136] 05 p0684 A72-16969
- Logic circuit binary signal autocorrelation determination as function of 0 and 1 signals duration distribution considering AND and OR gates
05 p0632 A72-17094
- Diversity reception during radio wave scattering on statistically uneven surface, using geometrical optics method
07 p0944 A72-19566
- Fokker-Planck equations for charged particle dynamics rederived for random fields, finding pitch angle scattering
08 p1227 A72-21385
- Narrow-band pulsed laser radar photocount distribution statistics in thermal background radiation, noting detection performance dependence on signal and noise absolute level and SNR
08 p1134 A72-21420
- Statistical crack length distribution of flaw sizes in steel parts during manufacturing
09 p1328 A72-22920
- Random elastic modulus variability of building materials test pieces under compression and tensile loads
10 p1557 A72-24403
- Statistical bounding approach to fracture analysis of fiber reinforced composite materials tensile strength
10 p1502 A72-24883
- Local limit theorems for sequence of nonidentically distributed independent integral-valued lattice random variables
11 p1676 A72-25356
- Intermolecular collisions distribution on centerline of freely expanding axisymmetrical jet, using ellipsoidal statistical model and simplified transport equations
11 p1615 A72-25557
- Expected value of two dimensional Gaussian random array gain, assuming two dimensional isotropic noise field of single frequency
11 p1604 A72-26040
- Narrow band process signal model for phase and amplitude difference distribution densities of alternating period compensation system output signal
11 p1596 A72-26310
- Ejection injuries from U.S. Navy aircraft, discussing statistical distribution of vertebral, shoulder, arm/hand, knee, leg, head and face injuries
12 p1774 A72-28273
- Nonrandomized distribution-free ranking and selection procedures under subset selection formulation, considering application to reliability problems
13 p1962 A72-28366
- Hot worked Al alloy machine elements mechanical properties scattering, discussing quality control procedures
14 p2114 A72-30275
- Phase distribution randomization in switched antenna array, noting radiation pattern sidelobe compensation application
15 p2209 A72-32666
- Independent random test values effective sample numbers for mean and variance distributions in meteorological and geophysical statistical tests
16 p2385 A72-33382
- Observations of the variability of dissipation rates of turbulent velocity and temperature fields
18 p2678 A72-36022
- Fourth moment of a wave propagating in a random medium
18 p2712 A72-37025
- Error of the statistical method for determining the dependence of the combustion characteristics of particles upon particle size
19 p2879 A72-37363
- Stellar rings and stellar cavities as random phenomena
19 p2866 A72-38492
- Model random medium with two kinds of dielectric layers stacked in arbitrary proportions, calculating electromagnetic wave propagation characteristics by transmission line analogy
19 p2767 A72-38613
- Energy characteristics of radio signals scattered by statistically uneven surface, proposing statistical variables substitution
20 p2900 A72-38892
- Statistically dilute antenna groups with enhanced minimum distance between elements
21 p3028 A72-40504
- Theoretical and experimental investigations, conducted with the aid of a plate containing holes, concerning the simulation of a statistically arranged antenna group
21 p3028 A72-40505
- Prior distributions fitted to observed reliability data.
22 p3182 A72-41980
- Diversity reception during radio wave scattering on statistically uneven surface, using geometrical optics method
22 p3153 A72-42084
- Multiple scattering of bending waves by random inhomogeneities.
22 p3235 A72-42460
- Estimation and prediction of Gumbel and Frechet distribution parameters, noting statistical decision in tests, sequential analysis and graphical procedures
22 p3199 A72-42968
- Investigation of the applicability of different laws of extremal-value statistics to the approximation of empirical distributions of maximum wind velocities
23 p3310 A72-43535
- Statistics of the radiation from astronomical masers.
23 p3337 A72-43872
- Mathematical model for digit summation task search time distribution dependence on size of visual display with randomly arranged three digit numbers
24 p3374 A72-44558
- Propagation of the mutual coherence of optical waves in a random medium.
24 p3424 A72-44711
- Approximate formulae for mixed modulated coherent and partially polarized chaotic light.
24 p3425 A72-44769
- Linear corrector for laser beam intensity distribution transformation into random distribution with rectangular envelope, noting uniform energy distribution result of spatial fluctuations averaging
24 p3411 A72-45608
- STATISTICAL MECHANICS**
- Closure problem in statistical theory of isotropic turbulent velocity field
03 p0342 A72-13900
- Statistical mechanical calculation of thermodynamic properties of interstitial solid solutions involving second nearest neighbor solute atom mutual interactions based on Kirkwood expansions
03 p0459 A72-14252
- Nonlinear oscillations stochastic instability in dynamic systems, discussing nonequilibrium statistical mechanics
03 p0390 A72-14316
- Turbulent particle diffusion statistical mechanical model, using random walk
03 p0344 A72-14331
- Hydrodynamic equations for non-Lagrangian statistical mechanical particle systems with three degrees of freedom under frictional and velocity dependent forces
04 p0512 A72-15202
- Closure approximation in hierarchy stochastic differential operator equations in statistical mechanics
04 p0540 A72-15257
- Lynden-Bell statistical mechanics predictions compared with most and least violently relaxed one dimensional self gravitating systems, using computer experiments
05 p0714 A72-16055
- Statistical group theory of two component associated gas mixtures, noting erroneous virial coefficient
05 p0692 A72-16356
- Statistical mechanics of N-body self gravitating system one dimensional model, using canonical and microcanonical ensembles
06 p0885 A72-18075
- Statistical hypothesis of Van Allen radiation belts, using Vlasov equations for self consistent plasma fields
07 p1055 A72-18805
- Thermodynamic quantities expression in terms of S matrix to formulate questions pertaining to statistical mechanics-particle physics boundary, applying to cosmology
09 p1355 A72-22750
- Perturbation procedure for weakly coupled oscillators in connection with statistical mechanics ergodic problem and nonlinear interaction models
12 p1844 A72-27248
- Turbulent plasma electric field energy density spectrum from statistical mechanics investigation based on canonical formalism for electron plasma
12 p1851 A72-27387
- Relativistic statistical mechanics invariant formula for coherence degree of plane blackbody radiation beam in arbitrary Lorentz frame, noting transformation law of temperature
12 p1846 A72-27741
- Chandrasekhar statistical stellar dynamics assumption generality compared to Chandrasekhar diffusion process, discussing discontinuous model, relaxation time, escape probability and numerical results
12 p1872 A72-27893
- Statistical mechanics of one dimensional model for many body self gravitating system with canonical and microcanonical ensembles, noting isothermal solution of Vlasov equation
12 p1846 A72-27907
- Covariant statistical mechanics equations system for distribution function of relativistic particles in steady external gravitational field, noting Vlasov equation as limiting case
13 p2035 A72-28465
- Statistical physics multiple wave scattering-phenomenological radiation transfer equation relations, using Green function
13 p2002 A72-28512
- Weak homogeneous turbulence analysis by Bogoliubov statistical mechanics theory, deriving kinetic equations for nonlinear wave interaction
15 p2278 A72-32383
- Atmospheric turbulence statistical theory, discussing random flow field characterization by property expressed in ergodic theorem
17 p2537 A72-34273
- Statistical mechanics of magneto-active plasma.
17 p2590 A72-35144
- The two-particle correlation function in nonequilibrium statistical mechanics.
17 p2581 A72-35164
- Two dimensional turbulence model for charge fluctuations statistical mechanics of nonlinear guiding center plasma
18 p2714 A72-36014
- Statistical model of chemical reactions in nonisothermal low pressure plasma.
18 p2715 A72-36567
- Nonlinear oscillations stochastic instability in dynamic systems, discussing nonequilibrium statistical mechanics
19 p2836 A72-38814
- The relativistic Boltzmann equation.
20 p2955 A72-40012
- Finite difference calculus development of method to express thermodynamic limit of statistical-mechanical average as power series in number density, noting advantages and applicability
21 p3087 A72-40562
- Statistical mechanics of light elements at high pressure. II - Hydrogen and helium alloys.
21 p3106 A72-41044
- Stellar-statistical formulation of the problem of setting up an astronomical radial velocity system.
21 p3109 A72-41439
- Predvoditelev critical revision of hydrodynamic and heat transfer theory based on Navier-Stokes and Boltzmann equations, developing statistical system of molecular interactions
22 p3165 A72-41951
- Statistical mechanics of polymerized materials.
22 p3197 A72-42796
- Power law behavior of autocorrelation and memory functions of statistical mechanics as t approaches infinity
23 p3309 A72-43870
- Information theory and statistical mechanics applications to thermodynamics, discussing entropy and superiority of Georgian to Kelvin temperature scale
24 p3465 A72-45372
- Some reflections on the nature of entropy, irreversibility and the second law of thermodynamics.
24 p3465 A72-45628
- STATISTICAL MOMENTS**
- U DISTRIBUTION MOMENTS**
- STATISTICAL PROBABILITY**
- U PROBABILITY THEORY**
- STATISTICAL TESTS**
- NT KOLMOGOROFF-SMIRNOFF TEST
NT MANN-WHITNEY-WILCOXON U TEST
NT RANK TESTS
- Statistical test plans with improved flexibility, application ease and efficiency for maintainability demonstration
10 p1504 A72-23998
- Loose medium deformations and displacements fluctuations verification by statistical tests, noting inception information from autocorrelation and boundary conditions cross correlation functions
10 p1512 A72-24719
- Indirect statistical quality control procedure for piece goods in batch based on image recognition technique for data classification
13 p1965 A72-29175
- Geomagnetic data testing by including monopole term in spherical harmonic reduction
13 p1951 A72-29394
- Ionospheric radio signal reflection fields verified via quantitative statistical reliability criterion
14 p2100 A72-30634
- Independent random test values effective sample numbers for mean and variance distributions in meteorological and geophysical statistical tests
16 p2385 A72-33382
- Bandpass-filtered geophysical and meteorological time series data statistical evaluation by comparison with filtered test series with same variance and autocorrelation function
16 p2363 A72-33383
- Information criterion for optimal planning of reliability acceptance tests maximizing average effect
21 p3038 A72-40714
- A note on a comparison of confidence interval techniques in truncated life tests.
21 p3075 A72-40828

Statistical tests for spectral correlation analysis of continuum VHF radio emission fluctuations from noise storms
21 p3102 A72-41778

Estimation, confidence intervals, and incentive plans for sequential three way decision procedures.
24 p3406 A72-44667

STATISTICAL WEATHER FORECASTING

Weather forecasting, discussing statistical entropy, numerical and statistical methods and computer technology utilization
02 p0254 A72-12777

Statistical methods in meteorology - Conference, Leningrad, September 1969
08 p1202 A72-22112

Adaptive statistical system with feedback loop for weather analysis and forecasting, examining learning process features
08 p1202 A72-22113

Hydrodynamic models and computational schemes optimization in statistical weather forecasting
08 p1202 A72-22114

Probabilistic-statistical method for recognition and short term forecasting of convective clouds, spring floods, hail, thunderstorms and showers
08 p1202 A72-22115

Hydrometeorological parameters spatial-temporal variations analysis and forecasting based on association functions and conditional probability distribution functions
08 p1202 A72-22116

Averaging period parameters determination for weather climatic norms forecasting with minimum mean square error
08 p1202 A72-22117

Statistical characteristics of wind elements from vertical-temporal structure of wind field
08 p1202 A72-22118

Statistical analysis of temperature characteristics based on natural orthogonal components expansion for weather forecasting application
08 p1203 A72-22120

Discriminatory analysis application in hydrometeorological forecasts, discussing use of bunch map analysis
08 p1203 A72-22122

Probability weather forecasts reliability, considering utility and spherical and logarithmic validities
08 p1203 A72-22124

Atmospheric boundary layer pressure field expansion into dual series of natural time dependent components to separate fluctuations within monthly period for weather forecasts
08 p1203 A72-22125

Prognosis algorithm to infer vector predictor by analogy as basis for statistical weather forecasting
08 p1203 A72-22126

Linear statistical forecasting with noncorrelated predictors by multiple regression equations, showing degradation dependence on sampled cross covariances
13 p1995 A72-29591

Geomagnetic pulsations long term statistical forecast, obtaining averaged yearly pearls activity
15 p2222 A72-31426

Monthly mean air temperature anomalies annual forecasts based on Fourier analysis of 1900-1970 statistical data
16 p2418 A72-33381

Method of constructing a forecast chart of H sub 500 anomalies on the basis of several analogs
19 p2828 A72-38000

Local and regional weather forecasting based on multilinear regression technique
21 p3078 A72-40765

Adjustment of the wind field to geopotential data in a primitive equations model.
22 p3200 A72-42502

Climatology of the occurrences of thundery weather over Gauhati Airport.
22 p3202 A72-42887

STATISTICS

Methods for measurement of the state of health
21 p3005 A72-40395

STATOR BLADES

Stator blade design to shield turbofan from pressure disturbances arising in downstream subsonic duct [AIAA PAPER 72-84]
05 p0707 A72-16883

Noise reduction effects of wake interaction between rotor blade rows in axial flow compressor, cancelling velocity defect at stator position [ASME PAPER 72-GT-15]
11 p1569 A72-25614

Supersonic turbine stator and rotor blading design corrected for boundary layer displacement thickness, discussing limitations due to normal shock wave at flow separation [ASME PAPER 72-GT-63]
11 p1571 A72-25653

Lift fan blade interaction discrete frequency noise, discussing potential and viscous interactions relation to rotor-stator spacing
15 p2297 A72-32019

A study of film-cooling effectiveness of some gas-turbine stator surfaces.
17 p2597 A72-34468

Influence of the angle of attack on the performance of high-deflection stator blades
17 p2484 A72-34889

Flow and energy loss distribution in annular stator nozzle cascades with cylindrical blade profiles of different twist, measuring flow exit angle along blade span
23 p3248 A72-43664

STATORS

Noise generated by free flow turbulence incident on rotor or stator in axial flow fans and compressors, noting sound spectrum dependence
13 p0208 A72-29575

Hysteretic motor in steady synchronous operation with nonsinusoidal supply voltage, computing stator winding current based on superposition with two linear equivalent circuits
13 p1900 A72-29975

STEADY FLOW

NT COUETTE FLOW
NT HARTMANN FLOW

Alternating directional implicit numerical solution for three dimensional steady low density hypersonic flow over finite width flat plate [AD-736572]
01 p0049 A72-10230

Nonlinearity effects on two dimensional steady supersonic dissipative flow governed by Navier-Stokes equations, obtaining expressions for flows past thin airfoil and wedge
02 p0203 A72-11976

Steady sonic flow around three dimensional obstacles by pseudo-axisymmetrical flow approach, revealing singular perturbation of lift downstream at infinity
02 p0150 A72-12096

Least squares and point matching techniques compared for solution of two dimensional steady state heat conduction problems with irregularly shaped boundaries [ASME PAPER 71-HT-P]
02 p0302 A72-12318

Conducting fluid steady MHD pipe flow under transverse magnetic field, obtaining mass flow rate
03 p0394 A72-13241

Curved shock waves in steady flow of perfect fluid, confirming Hugoniot relations validity
03 p0341 A72-13685

Time and coordinate dependence of magnetic field for steady symmetric flows of compressible conducting fluid at large Reynolds numbers, investigating self excitation conditions
03 p0398 A72-14001

Steady laminar viscous conducting fluid flow in infinite rectangular channel in crossed electric and magnetic fields, deriving flow rate and potential distribution
03 p0398 A72-14008

Steady flow of viscous incompressible conducting fluid in rectangular channel with sectional walls under longitudinal external magnetic field, deriving velocity distribution
03 p0398 A72-14009

Navier-Stokes equation analysis of three dimensional steady radial expansion of viscous heat-conducting compressible fluid from spherical sonic source into vacuum
03 p0343 A72-14247

Rotational symmetry solutions to differential equations of stationary barotropic or axisymmetric incompressible flow
03 p0344 A72-14345

Steady two dimensional cavity flow past infinite number of airfoils using linearized theory
04 p0461 A72-14460

Plane steady flow of two viscous fluids in contact, presenting normal and tangential pressure
04 p0510 A72-14513

Linear stability of nearly parallel steady plane viscous flows, using method of multiple scales [ONERA, TP NO. 1044]
04 p0511 A72-14969

Boundary value problem for steady parallel axisymmetric irrotational flow of inviscid incompressible fluid past cylinder having common axis with tube
04 p0512 A72-15056

Sound attenuation in lined rectangular ducts with uniform steady flow, considering aircraft engine noise reduction
04 p0565 A72-15267

Navier-Stokes equations solution by finite difference methods for steady incompressible laminar vapor flow in symmetrical and unsymmetrical heat pipes, calculating pressure losses [ASME PAPER 71-WA/HT-15]
05 p0744 A72-15874

Continuous media stationary motion stability using initial boundary value problem of partial differential equations in perturbations [ASME PAPER 71-WA/APM-17]
05 p0647 A72-15963

Steady inviscid diabatic complex lamellar gas flow geometric properties, correlating stream and vortex lines via Beltrami surfaces in Euclidean space
05 p0747 A72-16667

Internal axisymmetrical steady inviscid rotational flow velocity profiles simulation by means of shaped wire gauze screens [AIAA PAPER 72-165]
05 p0650 A72-16830

Characteristic schemes comparison for three dimensional steady isentropic supersonic flow [AIAA PAPER 72-190]
05 p0605 A72-16844

Steady two dimensional symmetric viscous flow past parabolic cylinder in uniform stream, correlating calculated nose skin friction with boundary layer theory
05 p0610 A72-17011

Stationary plasma flow interaction with axisymmetric spatially periodic magnetic field in presence of Hall effect, determining electric currents structure
05 p0701 A72-17244

Steady two dimensional magnetodynamic flow past nonconducting wedge with perpendicular magnetic field at different shock attachment angles
06 p0861 A72-18131

Flow field quantities for nearly free axisymmetric steady molecular gas flow through circular orifice from high pressure region into vacuum
06 p0800 A72-18111

Steady subsonic potential gas flow in multiply connected regions, determining velocity field via boundary value problem solution for quasi-linear elliptic equations set
06 p0801 A72-18122

Cornered axisymmetric blunt body sonic line in steady supersonic flow, showing incomparability with sonic shoulder of sphere
06 p0757 A72-18133

Plane stationary flow of ideal incompressible fluid past large camber profiles of arbitrary shape and thickness, using computerized Fourier expansion
07 p0908 A72-18977

Difference method for numerical integration of Navier-Stokes equations for two dimensional incompressible steady flow along flat thin plate
07 p0908 A72-19177

Book on compressible fluid dynamics covering steady flow, shock waves and self similar motions
07 p0967 A72-19444

Monograph on three dimensional turbulent boundary layers in unsteady incompressible flow covering flow equations, eddy viscosity and mixing length models, etc
07 p0968 A72-19951

Iterative solution of differential equations for steady plane flow with heat and mass transfer at high Reynolds numbers
07 p0971 A72-20094

Perfect fluid two dimensional steady flow equations solution for viscous flow with specified boundary conditions, considering vortex flow
07 p0971 A72-20094

Steady viscous incompressible fluid flow in circular disk with prescribed velocity components at low Reynolds numbers, considering computer tested numerical method
07 p0972 A72-20104

Parabolic differential equation system for boundary layer behavior of steady plane gas flow
08 p1107 A72-20914

Stream functions for steady two dimensional flow field of viscous liquid near circular whirl
08 p1148 A72-20931

Steady axisymmetrical twisted gas flow parameters in channels with geometries similar to turbojet engine units
08 p1149 A72-21311

Inviscid conducting gas steady one-dimensional MHD flow, using three-dimensional phase diagram for differential equations analysis
08 p1214 A72-21644

Steady flow of dual temperature plasma into vacuum from widening nozzle, taking into account electron thermal conductivity and heat exchange between components
08 p1214 A72-21651

German monograph on steady flow past sphere and cylinder near wall, discussing drag, lift and flow visualization
08 p1108 A72-21954

Rotationally symmetrical cylindrical shell loaded by uniform pressure distribution along length, calculating quasi-steady viscoplastic flow under Huber-Mises condition
09 p1399 A72-22694

Book on steady laminar supersonic and hypersonic wakes covering near and far region solutions, boundary layer separation, etc
09 p1261 A72-23025

Geometrical characterization of steady nondissipative compressible fluid flow described by first order partial differential equations system
09 p1295 A72-23366

Steady turbulent flow and heat transfer downstream of circular pipe sudden enlargement, computing streamline and temperature profiles and wall fluxes
09 p1412 A72-23687

Numerical prediction of inert and reacting steady internal two dimensional recirculating flows by finite difference method, including turbulence and combustion models
10 p1561 A72-23866

Steady inviscid irrotational transonic flow in two dimensional symmetric and axially symmetric nozzle throats

Steady compressible fluid flow and plane shock wave propagation in pipe bends, discussing parameter effects and boundary conditions

Statistical solution of steady natural turbulent convection at large Grashof numbers

Steady two dimensional flow of monatomic rarefied gas past semiinfinite beam

Viscous fluid steady nonaxisymmetric flow past rotating sphere, obtaining antitorque moment expressions and resisting force projections

Turbulent diffusion of scalar contaminant passively advected by homogeneous stationary flow, expanding velocity and scalar fields in stochastic Wiener-Hermite functionals

Steady rarefied gas flow around sphere with radial reflection of particles along normals, calculating gas dynamics variables of conservation equation

Interaction solutions of steady crossed field MHD channel flows for perfect, singly ionizing monatomic and thermodynamically unspecified gases

Equations of motion of steady viscous fluid flow in three dimensional boundary layer on walls of axial flow compressors and turbines, obtaining velocity field

Dynamic and thermal laminar compressible boundary layers on flat plate, noting interaction of two quasi-steady flows

[ONERA, TP NO. 1068]

Limiting form of equations for perfect gas steady two dimensional flow under gravity effects

[ONERA, TP NO. 1087]

Asymptotic behavior of velocity profiles in laminar boundary layers of steady incompressible fluid two dimensional flow past rigid wall

Steady three dimensional viscous vortex within circular cylinder with tangential fluid influx from jets on outer surface and efflux through sink on bottom

[AD-741352]

Steady laminar boundary layer generated by vortex over fixed coaxial disk, solving governing equations by numerical integration

Turbulent mixing length velocity, temperature pulsations and viscous sublayer thickness in steady incompressible fluid flow past infinite plate

Random phase approximation for nonlinear theory of MHD nonequilibrium plasma steady turbulent regime, noting ionization level rise by energy dissipation

Calculation method for steady convective heat transfer in single-flow motion of several media, deriving equation system for characteristic directions and compatibility conditions

Steady nonrotating axisymmetric viscous incompressible flows with zero and negative ring circulation flux, studying solutions in three dimensional phase space

Steady flow of compressible heat conducting fluid, discussing effect of small transfer coefficient on isentropic sonic singularity in Laval nozzle

Magnetic and electric field effects on steady state laminar MHD Couette flow of non-Newtonian fluids governed by Prandtl rheological law or Ostwald-de Waele power law

Third order extension of perturbation method to solve Oseen equations for two dimensional steady viscous flow past cylindrical body at low Reynolds number

Plane nonlinear wave propagation in transonic region of two dimensional and axisymmetric steady flows, considering disturbance at arbitrary point

Two dimensional two phase steady supersonic wedge flow patterns analysis based on equations for flow between wedge surface and shock wave

Stationary heat conduction between stagnant binary gas mixture and two constant temperature plane parallel walls for arbitrary Knudsen numbers

Perfect gas steady flow under gravity action, analyzing limiting equations

[ONERA, TP NO. 1087]

Heat transfer and longitudinal temperature distribution at Hartmann-Sprenger tube inlet calculated approximately on basis of boundary layer data in steady compressible flow

Velocity distributions for slow steady rotational motion of non-Newtonian inelastic viscous fluid contained between two concentric spheres, using successive approximations

Isentropic perfect gas steady compressible flow finite element analysis through nonlinear equations linearization based on perturbation theory

Characteristic parameters of stationary supersonic plasma flow in magnetic de Laval nozzle calculated for collisional and collisionless cases, measuring ion saturation currents

Stationary plasma flow interaction with dipole magnetic field to study geophysical phenomena in upper atmosphere

Steady laminar MHD flow of viscous incompressible electrically conducting fluid between long concentric rotating porous cylinders under radial magnetic field

Backward diffusion statistical properties in time for homogeneous unsharped stationary turbulent flow, using Eulerian velocity

Laminar boundary layer separation point in steady two dimensional constant density flow past solid surface, deriving pressure-vorticity gradient relationship

Stability analysis of ideal incompressible liquid steady flow for given distribution, discussing velocity distribution effect on longitudinal cylindrical flow instability

German monograph on plane steady isentropic flow past obtuse apex angle wedge at zero angle of attack and free stream sonic velocity

Hydrodynamic equations for low speed steady external rarefied gas flows past circular cylinder, noting drag and heat transfer coefficients

Nonlocal fluid dynamics continuum theory with equilibrium and constitutive equations derived by generalizing Stokes Laws, noting steady channel and shear flow

Nonequilibrium steady quasi-one dimensional expanding nozzle flow of chemically reacting gas mixture, using time dependent finite difference technique

[AIAA PAPER 72-684]

Supplement to the asymptotic theory of steady turbulent flows with bubbles

Hydrodynamic characteristics of a cambered hydrofoil with a jet flap.

[ASME PAPER 71-APMW-17]

Prediction of the flow and heat transfer in a rectangular wall cavity with turbulent flow.

[ASME PAPER 72-APM-Q]

Continuity, motion and Maxwell equations for steady MHD flow under constant magnetic flux

Theorem for instability of rectilinear vortices in two dimensional steady flow of ideal liquid with or without submerged obstacle

Axisymmetric rotating flow past a circular disk.

Laminar gas flow in narrow channels of constant and variable cross sections in the presence of heat transfer

Inviscid perfect gas supersonic steady irrotational flow past wedge, investigating analytical solution validity in downstream region behind shock

Nusselt number dependence on Rayleigh number for steady convection in porous medium, explaining heat transport abrupt change by breakdown of Darcy law

Boundary layer and inviscid main stream interaction in asymmetric supersonic steady gas flow incident on circular cone at high Reynolds numbers

Steady flow of conducting fluid in MHD ball bearing clearance between two eccentric spheres, deriving load, friction moment and optimum operation mode

On the steady flow between a rotating and a stationary disk with a uniform suction at the stationary disk.

Convergence and accuracy of three finite difference schemes for a two-dimensional conduction and convection problem.

French monograph - An asymptotic theory of the Boltzmann equation and its application to the study of near continuum flows

On a method of computing the plane steady flow around a profile situated between straight parallel lines.

Generating high Reynolds-number flows.

Numerical analysis of three dimensional steady laminar free convection boundary layer due to heated ellipsoid, solving flow equations

Simple proof of fluid line growth in stationary homogeneous turbulence.

A Monte Carlo model of turbulent mixing for the prediction of NO production in steady-flow combustors.

[WSCI PAPER 72-8]

Surface reactions in similar boundary layers.

An asymptotic solution for steady flow above an infinite rotating disc with suction.

Interaction between the droplets of a polydispersed condensate in a nozzle flow

Steady flow past body fixed in uniform flow of dusty gas, obtaining velocity distribution

Hot wire data corrections in low and in high turbulence intensity flows.

Steady capillary-gravitational waves of finite amplitude generated by pressure periodically distributed along the flow surface of a fluid of finite depth.

Steady two dimensional motion during horizontal motion of body at high Richardson number in stratified fluid, considering blocking mechanism

Interaction of a steady plasma flow with a dipole magnetic field in the presence of a radial electric field.

Steady radiating gas flow past a semi-infinite flat plate at a constant temperature for an optically thick case.

Two-dimensional stationary problem with a free boundary for the Navier-Stokes equations

New results concerning the numerical calculation of the sonic flow around a given airfoil section

Stationary spherical vortices in a perfect fluid.

The internal boundary value problem for the Boltzmann equation in the steady state and weakly nonlinear

Noncoaxial rotations of a disk and a fluid at infinity

One dimensional steady conducting gas flow in nonaccelerating coordinate system under magnetic field, calculating pressure, density and temperature variations with boundary shock wave

Steady two-dimensional viscous flow in a jet.

Plane stationary flow of ideal incompressible fluid past large camber profiles of arbitrary shape and thickness, using computerized Fourier expansion

Mach reflection from overexpanded nozzle flows.

STEADY STATE

Wall friction effect on current sheet speed of magnetically driven shock tube, establishing steady state existence

Steady state turbulent solar magnetic fields dynamic evolution, considering weak random magnetic excitation in electrically conducting fluid under varying kinematic conditions

Surface cycle models physical mechanisms, discussing solar activities and nonaxisymmetric steady state solutions

Nonentraining axially symmetric steady state sloping model of severe storm, discussing validity and limitations

Collisional radiative recombination applicability to time dependent electron density decay in helium afterglow before reaching quasi-steady state

Large signal IMPATT diode microwave oscillator lumped model, considering steady state oscillation

Steady state operational characteristics of two component heat pipes, applying mass and energy conservation

vation laws and thermodynamic phase equilibrium relations
[ASME PAPER 71-WA/HT-30] 05 p0745 A72-15883

Thermodynamics near steady state, considering stability criterion
05 p0746 A72-16159

Steady state geostrophic wind vector variation hodographs in planetary baroclinic boundary layer, considering thermal influence linear superposition on internal friction effects
06 p0841 A72-17667

Heat transfer steady state and transient response problems nodal formulation and numerical solution on digital computer
07 p1101 A72-19918

Control system stability with nonlinear feedback in steady equilibrium state
07 p0963 A72-20321

Transients determined for Cs vapor discharge phases, observing current fluctuations between steady states in negative resistance zone above 0.2 torr
07 p1046 A72-20517

Compensated Kalman filter as suboptimal state estimator to eliminate steady state bias errors in use with mismatched asymptotic time-invariant case
08 p1144 A72-20845

Book on physical cosmology development covering universe expansion, steady state, isotropy, Hubble constant, cosmic time scale, mass density, etc
08 p1236 A72-21480

Transverse electromagnetic field and electron velocity vectors during rectangular pulse incidence on ionization front moving at light speed, describing steady state encounter region
08 p1136 A72-21741

Steady state and temperature relaxation of rarefied gas between two plane parallel plates
08 p1211 A72-21871

German monograph on Ranvier node steady state I-V characteristics transition range and control by altered external solutions and morphological effects on nerve fiber
09 p1264 A72-22336

Forbidden band thermal deformation effect on homogeneous steady state stability of semiconductor
09 p1367 A72-22492

Transient characteristics and steady state off-design operation of mixed and unmixed type turbfan engines, noting peculiarities in control characteristics
09 p1374 A72-22626

Micropolar thermoelasticity steady state axisymmetric problem solution from equilibrium equations, considering uniform surface temperature and surface heat doublet cases
09 p1403 A72-22749

Steady state charged cylindrical electron-ion beam with high current in kinetics model framework, discussing densities proportionality and relativistic factor
09 p1360 A72-22951

Current carrier flow parameter fluctuations associated with steady state transport noise in semiconductor devices, considering generation-recombination processes, drift, diffusion and dielectric relaxation
09 p1288 A72-23125

Algorithms for optimal adaptive control of steady motions of single channel discrete extremal systems with independent search, studying quality functional behavior
09 p1291 A72-23437

General structure steady state response under harmonic forcing in internal resonance relation, noting inertial nonlinear effects on autoparametric interactions and energy flow
09 p1408 A72-23462

Steady state model for Venus atmosphere water vapor loss, noting hydrogen and oxygen escape due to dynamic outflow of constituents from upper region
09 p1393 A72-23657

Steady state operation of automatic control system to stabilize random vibration spectra, noting maximum control accuracy at optimum loop gain
10 p1457 A72-24635

Closed and open loop transfer function coefficients relationship for steady state linear system with proportional elements in feedback and parallel paths
10 p1457 A72-24724

Boundary layer model for laminar transient forced convection film boiling on isothermal flat plate, noting one dimensional conduction, intermediate and steady state regions
[AIAA PAPER 72-289] 11 p1741 A72-25227

Steady state plasma interactions with electromagnetic force field in plasma accelerators, showing shock wave formation
[AIAA PAPER 72-413] 11 p1706 A72-26163

First order systems steady state frequency response to general harmonic amplitude modulated input, noting signal attenuation and absence of distortion
12 p1845 A72-27540

Linearized steady motion of gas with mass sources and sinks, determining resonance onset conditions
13 p1893 A72-28731

Instrument to determine steady and unsteady stress state of elastic fluids in viscometric flow, noting rheological measurements in solved polymers
14 p2094 A72-30421

Two dimensional numerical solution of semiconductor steady state transport equations, applying to MOS and bipolar transistors
14 p2142 A72-30847

Nonlinear resonant circuits analysis, noting steady state operation of ferroresonant circuit with staircase response curve and synchronization conditions
14 p2132 A72-31103

Nonlinear processes in oscillatory systems with semiconductor diodes, calculating amplitude and phase characteristics in steady state and transient conditions
14 p2090 A72-31133

Nodal equations derivation for lumped circuit representation of Gunn diode with steadily propagating domain under steady state and transient conditions
15 p2205 A72-31317

Steady state electron mean energy variation between parallel plates in Ar and He calculated by Monte Carlo simulation for comparison
15 p2285 A72-32222

Magnetized plasma discharge steady state problem of finite cylinder positive column in magnetic field, detailing radial and axial solutions
15 p2288 A72-32508

Theory of the dynamic vibration neutralizer with motion-limiting stops.
[ASME PAPER 71-APMW-14] 17 p2625 A72-34317

Regression analysis for steady state N2 inequality in O2 consumption calculations.
17 p2507 A72-34542

Forbidden band thermal deformation effect on homogeneous steady state stability of semiconductor.
17 p2595 A72-34656

Calculation of steady modes of operation of RC circuits with jumpwise varying parameters
17 p2533 A72-34761

Contributions to the study of the steady-state regime of fluidic amplifiers with jet deflection
17 p2497 A72-35122

Spectral factorization in periodically time-varying systems and application to navigation problems.
17 p2578 A72-35492

Numerical simulation studies of two-dimensional turbulence. I - Models of statistically steady turbulence.
17 p2543 A72-35765

Steady state charged cylindrical electron-ion beam with high current in kinetic model framework, discussing densities proportionality and relativistic factor
17 p2593 A72-35880

Integral scales existence as necessary condition for asymptotical independence of stationary process, showing relationship of conditions for central limit and related theorems
18 p2677 A72-36002

State feedback control law for linear multiinput multioutput time-invariant dynamic system under disturbance to obtain output with zero steady state error
18 p2672 A72-36054

Functional relationships between the conventional steady-state error characteristics and the weighting matrices in the quadratic performance index.
18 p2672 A72-36058

Heat transfer from a slowly rotating sphere.
18 p2741 A72-36934

Algorithms for optimal adaptive control of steady motions of single channel discrete extremal systems with independent search, studying quality functional behavior
19 p2782 A72-38520

Simple conduction model for theoretical steady-state heat pipe performance.
20 p2984 A72-39607

Transient and steady state vorticity generated by horizontal temperature gradients.
20 p2987 A72-40016

Propagation of electromagnetic disturbances and the stability of stationary states in media with a nonlinear Ohm's law
21 p3086 A72-41651

Synthesis of linear stationary systems with the aid of proportional elements
22 p3162 A72-42738

Steady state equations of motion, equilibrium shape and stability derivatives of elastic airplanes evaluated with finite element methods.
22 p3138 A72-42845

Interpretation of steady-state surface photovoltage measurements in epitaxial semiconductor layers.
22 p3215 A72-43087

Steady thermoelastic state in an infinite plate with a moving parabolic cut
23 p3345 A72-43586

Mathematical description and calculation of the steady-state regime of a microwave power stabilizer with a semiconductor attenuator
23 p3270 A72-43766

An algorithm to obtain the steady state response of nonlinear periodic systems.
23 p3267 A72-43852

Necessary conditions for steady state in radiation - Matter interaction and the role of entropy.
24 p3461 A72-44806

STEADY STATE CREEP

Coarse grained dispersion strengthened Al alloys, investigating solute solutions effects on steady state creep behavior
01 p0087 A72-11025

Constant stress and compression creep testing in vacuum conditions, describing simple spring loaded apparatus characteristics and performance
01 p0071 A72-11171

Steady creep rates in Ni poly- and single crystals in presence of dislocation stresses
06 p0835 A72-18748

Steady state high temperature niobium creep in torsion under rarefied oxygen infiltration conditions, discussing surface interactions kinetics
07 p1012 A72-19679

Steady creep rate logarithm and creep limit obedience to normal distribution law
07 p1014 A72-19846

Steady state creep model for high activation energy role in interstitial formation and migration in particle strengthened alloys
08 p1185 A72-20992

Discontinuous rigid or creeping fiber reinforced composite materials, predicting steady state creep behavior
09 p1338 A72-23167

Environment and grain size effect on steady state creep and creep rupture properties of Ni-W solid solution
09 p1331 A72-23381

Functional analytical formulation of steady creep processes, using error estimations in solution of equations with monotonic potential operators in Banach spaces
09 p1409 A72-23567

Steady creep and delayed fracture dependence on metal structure and composition, considering strain hardening at small strain rate and elevated temperature
15 p2254 A72-31559

High temperature steady creep of Nb and niobium-aluminum oxide alloys at 850-1400 C
15 p2254 A72-31561

Steady state creep measurements of lead-phosphor bronze discontinuous fiber composites under nonuniform deformation, comparing to fiber and matrix alone
15 p2261 A72-32299

Steady state creep theory for discontinuous fiber composites, considering rigid and creeping fibers and sliding interface
15 p2261 A72-32300

Recovery-work hardening model of steady state creep for Al, assuming equal internal and applied stress
15 p2259 A72-32642

Temperature and stress dependence of steady state creep rate for dispersion strengthened Ag-gallium oxide alloys, noting grain size effect on activation energy
16 p2411 A72-34094

Steady state creep of composite material with discontinuous fibers, determining random function mean and variance for fiber stress distribution
16 p2412 A72-34115

Relations between the experimental parameters describing the steady-state and transient creep
18 p2732 A72-36343

Steady-state creep of shells of revolution in the case of the Tresca criterion
22 p3233 A72-42051

Finite difference and extended Newton methods application to transient and steady state creep deformation in shells of revolution under high temperature and high stress
22 p3235 A72-42482

Materials creep behavior and elevated temperature design.
24 p3453 A72-44553

The creep of dispersion-strengthened Ni-Co alloys.
24 p3413 A72-44923

STEADY STATE FLOW

U EQUILIBRIUM FLOW

STEAM

Zr alloys hydride distribution after oxidation in steam at 550 C, discussing hydrogen uptake
04 p0534 A72-15362

Zr and Zr-Cr alloys corrosion behavior in steam, noting parabolic rate law breakaway point to linear rate
05 p0676 A72-16797

STEAM FLOW

Catapult steam ingestion test of turbofan engines in A-7 aircraft, correlating compressor stall occurrences with temperature increase rate in distorted region
07 p1052 A72-18760

Critical discharge regimes of two phase steam/water mixture flow from nozzles, using counterpressure effect

11 p1619 A72-26674

Steam-condensate mixture boundary layer flow along curved body surface with arbitrary pressure gradient at low Mach number and constant physical properties

16 p2378 A72-33437

STEAM GENERATORS

U BOILERS

STEAM TURBINES

Nonstationary temperature field determination in steam turbine casing-connector nozzle by difference method based on heat balances, comparing results with electric analog studies

02 p0303 A72-12534

Vibration of reciprocating engine crankshafts and steam turbine, alternator and gas turbine rotor shafts supported on hydrodynamic sleeve bearings

08 p1225 A72-22133

Rotor blades setting angle and twist influence on steam turbine wheels vibrational modes and frequency spectra

11 p1732 A72-25537

TEATITE

U TALC

STEEL STRUCTURES

Upset steel cylinders under axial compression loads, determining localized surface stress and strain critical values at fracture

01 p0141 A72-11032

Strain anisotropy effect on thin walled tubular steel samples with combined bending and torsion, constructing matrix and stress vectors

03 p0445 A72-13578

Electron fractographic investigation of fracture properties via removal of metal oxide film accumulated on crack surface during service life of steel structures

09 p1309 A72-22639

Welded steel airframe residual fatigue life tests by nonstationary random loading, applying to jet trainer aircraft landing gear

14 p2107 A72-30277

Ni-Cr-Ti steel aircraft structural element fatigue life calculation based on failure mechanism involving crack propagation

14 p2164 A72-30429

Ultrahigh tensile strength steel pressure chamber fracture behavior in high stress concentration fields

15 p2330 A72-32345

Resistance to brittle fracture of high-strength steels in various structural states

19 p2819 A72-38014

Effect of residual elements on radiation strengthening in iron alloys, pressure vessel steels, and welds.

20 p2937 A72-39289

Experimental investigation of the carrying capacity in bending of steel box-section beams

22 p3232 A72-41870

STEELS

NT AUSTENITIC STAINLESS STEELS

NT BAINITIC STEEL

NT CARBON STEELS

NT CHROMIUM STEELS

NT FERRITIC STAINLESS STEELS

NT HIGH STRENGTH STEELS

NT MARAGING STEELS

NT MARTENSITIC STAINLESS STEELS

NT NICKEL STEELS

NT STAINLESS STEELS

Acoustic emission characteristics from nuclear reactor irradiated steels during tensile and wedge opening load tests

01 p0068 A72-10803

Steel and Ti-Al-V alloy surface integrity during various machining methods, considering microstructures, residual stress profiles and fatigue characteristics

[SME PAPER IQ 71-237] 01 p0076 A72-10972

Hot formed Cr-Ni-Mo and Ni-Mo prealloyed steel powders fatigue and toughness properties, determining hardness effects by varying draw temperature from 400 to 1000 F

02 p0240 A72-11435

Microstructure of prealloyed and premixed specimens of sintered steel

02 p0242 A72-11463

Hardened steel inhibited crack propagation mechanism, observing striation in microstructure on fracture surface

02 p0243 A72-12212

Heat treated carbonized, cyanided, nitrided and boronized steel fatigue strength dependence on static strength, residual stress, brittleness and stress concentration from test data

02 p0244 A72-12242

Alloy steels temper brittleness analysis, using internal friction characteristics as functions of time and temperature

02 p0247 A72-12816

Steel cleanliness conditions for formation and decantation of inclusions due to deoxidation during production up to solidification

03 p0371 A72-13198

Steel castings made in electric furnace with Al additive, observing magnesium and lime aluminates inclusions

03 p0371 A72-13199

Ductility relationship to plasticity characteristics in cylindrical steel samples with short notch under tension

03 p0443 A72-13458

Steels modulus of elasticity dependence on prestressing level produced by transverse and longitudinal tension

03 p0371 A72-13462

Steels gas-powder facing with boron carbide, testing microhardness and wear resistance

03 p0363 A72-13547

Steel coatings produced by plasma jets on experimental machine parts, determining friction wear resistance by successive tests

03 p0363 A72-13548

Testing temperature effect on intergranular fracture propagation in steel sensitive to tempering brittleness

03 p0372 A72-13599

Steels fatigue life tests as function of stress level, confirming Wohler curves mathematical model

03 p0373 A72-13673

Mo and C additives effects on austenite susceptibility to deformation martensite formation and steel resistance to hydroerosion

03 p0375 A72-13941

Melting effect on recrystallization of overheated tempered steel, discussing rectification under conditions favoring formation of silicon-oxygen compounds

03 p0376 A72-14017

Ferritic steel nil-ductility transition temperature data analysis correlating irradiation results with activation fluences and temperature

04 p0547 A72-14430

Shock precompression effect on dynamic fracture strength of steel and Al alloy, investigating crack initiation and growth

04 p0533 A72-14541

Effective plastic strain for Tresca and von Mises materials, investigating hot rolled mild steel specimens

04 p0590 A72-15187

Mean stress and overload effects on mild steel service life, using fatigue damage summation method

04 p0592 A72-15475

Hydrogen generation mechanism during cadmium plating of steel, describing porosity testing technique

04 p0527 A72-15561

Lamellar tearing and testing of steel sheets in direction of short side by Brodeau test

04 p0527 A72-15561

Strain hardened layers effect on wear resistance of 50Kh steel

04 p0534 A72-15653

Fe-Cr-Al and Fe-Cr-Si type ferritic steels, investigating additives effects on ductile-brittle transition temperature

05 p0672 A72-16012

Al and steel plate penetration, perforation and fragmentation under hard steel sphere impact at and above ballistic velocities, investigating velocity and strain histories

05 p0672 A72-16115

Dissolved oxygen effect on structure and toughness of nonalloyed extruded steels, observing austenite recrystallization kinetics retardation after hot plastic deformation

05 p0672 A72-16143

Unstable propagation and brittle fracture arrest in steels from double cantilever beam test under compression

05 p0677 A72-17107

Mechanical, technological and physical properties of steel with and without molybdenum

05 p0679 A72-17204

Ductile fracture development in steel due to microcracks and pores formation

05 p0679 A72-17205

Fine oxide particle inclusions in mild steel weld metal deposited by carbon dioxide shielded metal arc process, using electron microscopy and diffraction pattern photography

06 p0820 A72-17706

Cyclic loading effects on resistance to brittle fracture of low carbon structural steels, using crack with criterion

06 p0831 A72-18353

Plasticity onset and brittle fracture of annealed steel as function of preceding strains

06 p0831 A72-18354

Maximum temperature-holding time effects on plastic deformation and fracture of steel under thermal cyclic loads

06 p0831 A72-18359

Refractory and structural steels and Al alloys, obtaining low cyclic plastic deformation and breaking stress curves

06 p0898 A72-18549

Steel sheet creep, plastic deformation and service life under temperature and stress cycles

06 p0899 A72-18558

Stress distribution during plastic deformation of steel turbine disk from hardness measurements

06 p0900 A72-18670

Ti influence on ductility of normalized low alloy steel, considering crack initiation and propagation

06 p0834 A72-18687

Thermostable and heat resistant steels and alloys vibration loading frequency effects on fatigues at high temperatures

06 p0834 A72-18688

Special steels - Conference, Nantes, France, May 1971

07 p1010 A72-18969

Steel cutting suitability test, determining optimum cutting conditions for pure iron used in magnetic applications

07 p0994 A72-18973

Austenitizing conditions effects on hardness and microstructure of tempered steel, emphasizing martensite structure and grain size changes produced by controlled heat treatment

07 p0995 A72-19486

Ti, Fe, Co, Ni, Pt and steels phase transformation and thermal defect effects on high temperature thermal conductivity

07 p1012 A72-19548

Radioactive molybdenum disulfide lubrication films distribution on nitrated steel and on magnesium pig iron

07 p0996 A72-19775

Strength differential effect on microstructures of steels, using tensile and compressive stress-strain curves

07 p1015 A72-19927

Ductility and fracture of heat resistant steels at high temperatures and unsteady loading, estimating loading cycle effect on plastic strain buildup to failure

07 p1017 A72-20127

Stress-strain behavior of steel under elastic compression at 4.2 K, observing discontinuous twinning

07 p1020 A72-20413

Heat treatment effect on elastic properties of steel clad material for devices in sulfuric acid, discussing structural changes and optimal conditions

07 p1020 A72-20415

Nondestructive ultrasonic determination of defects in structural steel blanks

07 p0991 A72-20423

Special steels - Conference, Nantes, France, May 1971

07 p1021 A72-20482

Physicomechanical properties of steel with oxide, sulfide, silicon, phosphorus and mixed metal-non-metal inclusions

07 p1022 A72-20618

Gamma radiation source energy and activity determination for radiometric flaw detection in steel

08 p1177 A72-21775

Water effect at epoxy resin-steel interface on adhesive bond strength as function of vitrification temperature

08 p1196 A72-21863

Structural changes of nitrated steel diffusion zone, showing alpha solid solution and hard nitride phases mixture

08 p1188 A72-21880

Statistical crack length distribution of flaw sizes in steel parts during manufacturing

09 p1328 A72-22920

Plastic deformation effect on structure and properties of steel sheet under biaxial tension at liquid nitrogen temperature

09 p1330 A72-23187

Wear resistance of steel and Ti alloys in free abrasive gas jet, noting surface microhardness increase effect

09 p1319 A72-23188

Sintering and aging effects on mechanical behavior of low carbon copper steel

10 p1488 A72-24696

Environmental sensitivity effect on crack propagation rates in steels and Al and Ti alloys, discussing corrosion fatigue

10 p1499 A72-24899

Chemical compositions, properties and heat treatment of Ti, Al alloys and steels used in aircraft industry

11 p1652 A72-25286

Thick steel plate diffusion welding in air with dead-weight loading and autogenous surface cleaning

11 p1637 A72-25343

Phase transformations and recrystallization study of Ti-steel bimetal with emission microscope, observing high temperature formation of titanium and vanadium carbides

11 p1654 A72-25493

Hardened steel inhibited crack propagation mechanism, observing striation in microstructure on fracture surface

11 p1656 A72-25710

Crystal grain size effect on fracture initiation in mild steel under triaxial stress, using notch tests at low temperatures

11 p1657 A72-25756

Locati and Prot methods for metal fatigue limits evaluated by axial and rotating bending tests on steel specimens 11 p1657 A72-25824

Upper yield stress effect on elastoplastic behavior of mild steel in bending and torsion, noting relationship to strain rate 11 p1659 A72-25894

Russian book on Nb in ferrous metallurgy covering physicochemical properties, steels, slags, ore reduction and smelting for Al alloys production 11 p1659 A72-26048

Heat treated carbonized, cyanided, nitrided and boronized steels fatigue limit dependence on static strength, residual stress, brittleness and stress concentration 11 p1659 A72-26128

Mechanical, technological and physical properties of steel with and without molybdenum 11 p1660 A72-26139

Ductile fracture development in steel due to microcracks and pores formation 11 p1660 A72-26140

Electrolyte temperature, pH and mixing rate effects on anodic dissolution of steels and brass in electrochemical precision processing, using thermokinetic data processing 11 p1640 A72-26257

Continuous drive friction welding of mild steel, noting burn-off rate relationship to tensile strength 11 p1641 A72-26492

Low carbon ultrafine grain steel tensile behavior, noting critical grain size for stable/unstable plastic flow transition 11 p1661 A72-26651

Diamond burnishing effect on surface quality and fatigue strength of steel, noting work hardening increase and compressive residual stresses buildup in surface layer 11 p1642 A72-26811

Helicopter rotor blade spars shot peening in centrifugal vibrator, optimizing Cr-Mo-Ni steel surfaces work hardening 11 p1642 A72-26820

Powder metallurgy versus melting and casting of high temperature alloys, tool steels and specialty alloys 11 p1646 A72-26869

Plane titanium and niobium carbide precipitation in microalloyed steels during heat treatment above 1300 C, noting eutectic sulfide effect 12 p1827 A72-27102

Ball bearings lubricated with oils and fire-resistant fluids, testing fatigue life relationship to steel quality, fluid film thickness and viscosity 12 p1816 A72-28108

Characteristic friction curves /Mohr circle envelopes/ to describe stressed state region with various stresses produced by slide friction in steel due to indentation 12 p1819 A72-28198

Isotropy postulate corollary verification for strain vectors measurement of annealed steel tubular specimens under combined tension and internal pressure 12 p1887 A72-28232

Low carbon steel prior plastic deformation effects on mechanical hysteresis loop shape 12 p1887 A72-28234

Crack and notch induced stress concentrations effect on steel mechanical properties at 20-293 K, using static and dynamic test methods 12 p1831 A72-28240

Steel components contact fatigue kinetics measurement by emf increase of inductive sensor 12 p1887 A72-28245

Surface finishing effects on steel sensitivity to stress concentration under variable loads, emphasizing diamond smoothing and roller technique 12 p1831 A72-28246

Ultrafine grained microstructures and mechanical properties of alloy steels developed by cold working followed by annealing 13 p1974 A72-28662

Hardened coarse-grained steels recrystallization during fast heating, investigating martensite phase macro- and microstructural changes by X ray analysis 13 p1977 A72-28908

Room temperature uniaxial tension tests for elastic deformation of steel samples, showing quadratic stress-strain function 13 p1977 A72-29008

Velocity field at strain center during steel channel rolling, deriving relations for center contour calculation 13 p1964 A72-29149

Ultrasound reflection from molten core during spot welding of steel alloys as function of geometrical dimensions and configuration and transition zone dimensions 13 p1965 A72-29152

High speed photographic analysis of spot welding galvanized steel, observing three stage process 13 p1958 A72-29421

Steels shafts fatigue failure under cyclic loading and fretting corrosion, indicating fatigue strength increase through surface layer wear resistance augmentation 13 p1979 A72-29476

Borated steels strength under static bending, cyclic flexure and torsion and impact loads, correlating fatigue strength, residual stresses and core properties 13 p1979 A72-29477

Steels structural and microhardness changes by pulsed laser beam induced local heat treatment, noting needleshaped grain refinement 13 p1979 A72-29482

Aviation fuels and additives effect on steel endurance limit at room temperature 13 p1980 A72-29487

Niobium and molybdenum carbide film deposition on steel substrates by open arc welding with partial carbon burnout 14 p2107 A72-30156

Lower oxide mechanism in reduction-oxidation reactions during Ti steels electrosmelting with slag and gas phases 14 p2112 A72-30158

Temperature effects on critical crack opening as fracture toughness criterion for medium strength steel, taking into account local plasticity and propagation resistance 14 p2118 A72-30590

Hot rolled steel bar strain history effect on isotropic and anisotropic plastic behavior, considering additional tension and torsion data 15 p2325 A72-31527

One dimensional wave pulse propagation, attenuation and dispersion in uniaxially reinforced steel-epoxy resin composites 15 p2325 A72-31528

Refractory steels heat resistance improvement by surface saturation with Be and subsequent oxidation in air at 900-1000 C, comparing with aluminized steels 15 p2255 A72-31574

Mechanical properties of high temperature steels and alloys for gas turbine rotors, disks and blades 15 p2256 A72-31703

Mechanical properties and residual stresses in and adjacent to interface of explosively welded Al-Zn-Mg alloy with steel, noting microcracks effect on weld strength 15 p2257 A72-32111

Mossbauer spectroscopy theory and application to steel technology, discussing spectral characteristics of various iron phases and corrosion and stress effects 16 p2405 A72-32824

Deformation modes for deep drawing of extramild steel sheets, noting susceptibility and rupture criteria 16 p2396 A72-32872

Work hardening and anisotropy coefficients effects on deep drawing limit curves for extramild steel, noting rupture strain and deformation trajectories 16 p2396 A72-32873

Charpy impact tests of neutron irradiated nuclear reactor component steels to determine ductile/brittle transition temperature, describing setup and gas heating and cooling procedures 16 p2373 A72-33222

High temperature strength and ductility study of hot working behavior of steels, using hot impact tension tests 16 p2406 A72-33316

C diffusion mobility and coefficients in W-Mo steels gamma and alpha phases, discussing ionization effect on activation energy increase 16 p2408 A72-33538

Precipitation hardening effects on yield strength, toughness and ductile to brittle transition temperature of low alloy steels containing Nb 16 p2409 A72-33809

Error analysis of dynamic yield point measurements based on residual deformation from impact tests of Al alloy and steel specimens 16 p2472 A72-34016

Steels creep behavior relationship to stress-strain curve shape, defining creep resistance as function of strain hardening coefficient 16 p2412 A72-34146

Differences in the creep characteristics at room temperature of steels with and without distinct yield point 17 p2566 A72-34397

Effects of thickness on fatigue crack initiation and growth in notched mild steel specimens. 17 p2627 A72-34747

Strain history effect on isotropic and anisotropic plastic behavior. [SESA PAPER 1940] 17 p2631 A72-34820

Russian book - Plastic deformation of high-alloy steels and alloys 17 p2568 A72-35454

Influence of cerium, lanthanum, neodymium, and boron on the critical points and the linear expansion coefficient of Kh17N2 steel 17 p2569 A72-35523

Phenomenology and engineering significance of creep recovery in heat resistant steels, stressing ductility and microstructural effects 19 p2816 A72-37707

Investigation of the effect of some surface-active media on the variations in strength characteristics of steel U8 in a high strength state 19 p2817 A72-37738

Investigation of the influence of surface treatment purity and procedure on the strength of the Kh18N10T and Kh16N6 steels and the AMG6 alloy at normal and low temperatures 19 p2819 A72-38016

Possibility of using the eddy-current method to measure the local magnetization of an object. 19 p2805 A72-38761

The use of an electrical induction method for determining the physical condition of a ground steel surface. 19 p2805 A72-38762

Relation between the reliability and allowable stress amplitude in fatigue design. 20 p2977 A72-38879

Testing of hydrogen pressure or stress concentration induced crack propagation theory for steels based on decohesion mechanism 20 p2935 A72-39003

Effect of thickness and orientation on fatigue crack growth rate in 4340 steel. 20 p2937 A72-39294

Cyclic stress-strain induced buckling and fatigue failure in cold-rolled steel and tabulating and diagramming mechanical properties 21 p3065 A72-40233

Influence of the cycling frequency on the fatigue and corrosion fatigue of steel samples with bushings 22 p3242 A72-43155

Investigation of the wear resistance carbonized chromium coatings on various brands of steel 22 p3195 A72-43159

Determination of the mechanical properties of steels by short-time rupture in hydrogen at high temperatures and pressures 22 p3195 A72-43160

Heat resistant steels long time strength determination by graph-analytical time-temperature extrapolation 23 p3301 A72-43739

Strain-rupture criteria for simple and complex loads 23 p3349 A72-43954

Cold shortness of 14Kh2NZMA steel 23 p3303 A72-44023

Ultrasonic attenuation and velocity in hot specimens by the momentary contact method with pressure coupling, and some results on steel to 1200 C. 23 p3294 A72-44116

Cumulative damage stochastic models and distributions of strength of steels and graphite. 24 p3412 A72-44673

Ductility relationship to plasticity characteristics in cylindrical steel samples with short notch under tension 24 p3458 A72-44933

Steels modulus of elasticity dependence on prestressing level produced by transverse and longitudinal tension 24 p3413 A72-44937

Cyclic loading effects on resistance to brittle fracture of low carbon structural steels, using crack width criterion 24 p3416 A72-45740

Plasticity onset and brittle fracture of annealed steel as function of preceding strains 24 p3416 A72-45741

Maximum temperature-holding time effects on plastic deformation and fracture of steel under thermal cyclic loads 24 p3416 A72-45746

Ductility and fracture of heat resistant steels at high temperatures and unsteady loading, estimating loading cycle effect on plastic strain buildup to failure 24 p3416 A72-45753

STEEP GRADIENT AIRCRAFT

U V/STOL AIRCRAFT

STEEPEST ASCENT METHOD

U STEEPEST DESCENT METHOD

STEEPEST DESCENT METHOD

Distributed systems modeled by partial differential equations, identifying unknown parameters by Galerkin method using steepest descent method and non-linear filter 04 p0505 A72-14674

Steepest ascent method for function optimization in arbitrary direction by selecting distance metric and scale dependency 04 p0540 A72-15683

Reusable space tug mission profile for interplanetary spacecraft recovery, using branched trajectory, steepest descent optimization and propellant minimization [AIAA PAPER 72-13] 05 p0730 A72-16949

Adaptive control system synthesis by steepest descent method, obtaining algorithms for parameters self adjustment loop construction 06 p0795 A72-18661

Steepest descent variable step-size algorithm with dynamic programming for mean square error adaptive equalizer, noting convergence 10 p1455 A72-23794

- Point source wave field diffraction on nontransparent circular cone, using steepest descent method and integral transformations 11 p1597 A72-26385
- Minimum drag bodies of revolution in supersonic flow obtained by combining steepest descent method with integral flow model 14 p2069 A72-30231
- Steepest descent path of integral describing transient plane wave propagation in anisotropic cold plasma, relating to evanescent wave arrival 15 p2285 A72-32109
- A modified gradient technique for solving boundary and initial value problems. 20 p2946 A72-39618
- Optimal design of a class of nonlinear networks. 23 p3276 A72-43865
- STEEPNESS**
- U SLOPES**
- STEERABLE ANTENNAS**
- Pulse IMPATT diode Ka band microwave rf head mechanically steered antenna array for airborne monopulse tracker applications 01 p0039 A72-10661
- Large reflector and phased array antennas, discussing synthesis and analysis, active impedance and blind spots, matching, beam steering and implementation 02 p0191 A72-11686
- Large steerable radio reflectors profile measurement with laser system, describing instrument design, accuracy and modifications 02 p0238 A72-12113
- Steerable receiving antennas L/S band solar calibration error statistical analysis, obtaining 0.5 db uncertainty by monitoring antenna gain-to-noise temperature ratio 02 p0192 A72-12159
- Steerable vhf/uhf receiving antennas stellar calibration error analysis, obtaining worst-case uncertainty of 0.4 db by monitoring antenna gain-to-noise temperature ratio 02 p0175 A72-12161
- Metrology and radio performance of steerable antenna paraboloidal reflector, considering profile measurements by optical range finder and laser methods 04 p0493 A72-15518
- Electronic scanning steerable phased array radar beam pointing capability improvement for moving target detection probability 06 p0772 A72-17423
- Electronically scanned steerable antenna array design with interelement coupling, considering maximum gain and radiation pattern control 06 p0773 A72-17497
- Quasi-time optimal nonlinear controller for steerable antennas or telescopes in target acquisition or slew mode, predicting performance by digital simulation 07 p0959 A72-19288
- Iterative algorithm for digital adaptive null steering of RF antenna arrays, demonstrating feasibility by computer simulation 09 p1289 A72-23416
- Single engine aircraft-borne weather radar with electronically scanned steerable phased array antenna [SAE PAPER 720315] 11 p1591 A72-25579
- Aircraft antennas design for radio links to satellites for aeronautical communication and ATC, proposing use of beam steering system 13 p1932 A72-29347
- Combination antenna unit with vertical monopole and two perpendicular slots in horizontal plane to yield steerable cardioid-shaped pattern for vertically polarized waves 15 p2206 A72-31776
- Airborne ground mapping and meteorological radar with steerable phased array antenna without mechanical scanners 15 p2200 A72-32216
- Five-horn feed system design for improving large steerable antenna monopulse performance, discussing weight and cost reductions by focal length selection 17 p2526 A72-34467
- Steerable directional VHF antenna design for radio interferometric tracking and ranging of Symphonie satellite [DFVLR-SONDDR-222] 17 p2536 A72-35432
- A short-wave rotating antenna for 500-kW transmitter output 18 p2666 A72-36676
- Geostationary or orbital satellite tracking radio receiver with steerable antenna for beacon signal detection and locking, discussing system design and performance 18 p2661 A72-36847
- Digital tracking with phased arrays. 19 p2765 A72-38261
- Selection of an optimal design for a spacecraft antenna system 21 p3025 A72-40311
- Circular-polarization antennas with controlled radiation patterns 21 p3026 A72-40314
- Controlling the directive gain of weakly directional antennas during space-vehicle flight 21 p3026 A72-40324
- A high-accuracy radio direction finder with a moving antenna 23 p3270 A72-43769
- STEERING**
- Optimal control for thrusting rocket guidance with controllable steering angle rate during insertion into circular orbit, using flat earth approximation 01 p0097 A72-10383
- Electromechanical nose wheel steering system for general aviation aircraft ground maneuverability improvement, describing design 01 p0006 A72-10963
- Aircraft steering dynamics model with translational and rotational equations, considering zero sideslip and acceleration and lift bank angle transfer functions 05 p0611 A72-16112
- Apollo lunar roving vehicle design requirements based on environmental conditions, emphasizing wheel drive control and steering systems optimization and navigational instrumentation 05 p0643 A72-16428
- An explicit automatic terminal energy management guidance technique for space shuttle. [AIAA PAPER 72-833] 20 p2950 A72-39094
- Real-time launch vehicle steering program selection. [AIAA PAPER 72-830] 20 p2977 A72-40058
- An assembly for studying the perceptive motor reactions of man under one-dimensional follow-up conditions 21 p3008 A72-40810
- STEERING ROCKETS**
- U CONTROL ROCKETS**
- STEFAN-BOLTZMANN LAW**
- Multiphase Stefan problems for bounded and unbounded temperature fields with variable phase volume 06 p0904 A72-18401
- Spatial layer cooling during surface emission according to Stefan-Boltzmann law, assuming heat source inside body 08 p1253 A72-21445
- Multiphase Stefan problems for bounded and unbounded temperature fields with variable phase volume 17 p2636 A72-34852
- Solution of the Stefan problem by the collocation method 21 p3130 A72-41089
- STELLAR ATMOSPHERES**
- NT CHROMOSPHERE**
- NT SOLAR ATMOSPHERE**
- Empirical model with near IR spectra from expanding circumstellar envelope, normal pulsating atmosphere, shock front and relaxation layers and expanding radiative cooling layer 01 p0128 A72-10791
- Pulsar nature and radiation mechanism, examining rotating neutron stars structure and atmospheric dynamics 01 p0131 A72-10973
- Early O and Of spectroscopic and photometric data, evaluating atmospheric properties, surface gravities and temperature scales 01 p0131 A72-11009
- G and K giants atmospheric parameters determination by photoelectric indices, considering effective temperature, chemical composition and surface gravity 01 p0132 A72-11013
- Pulsar magnetosphere axisymmetric and vacuum oblique rotator models, emphasizing electromagnetic field properties 01 p0134 A72-11159
- Soviet book on cool carbon stars covering spectral features, atmospheric composition and temperatures 02 p0281 A72-12296
- Oblique rotator model for time dependent light polarization of red long period variables, considering dust particle alignment in outer atmospheric layers near magnetic poles 02 p0283 A72-12630
- Polycyclic hydrocarbon molecules formation in cool stars atmospheres and gases ejected by supernovae and Seyfert galaxies, discussing Platt particles origin 02 p0284 A72-12634
- Cyanide and carbon molecules and isotopes electronic systems opacity probability distribution functions for stellar equilibrium model atmospheres calculations 03 p0416 A72-13012
- He abundance in population I and II stellar atmospheres 03 p0418 A72-13113
- Differential line shifts in spectrum of supergiant beta Ori attributed to radial spreading of stellar atmosphere 03 p0436 A72-13810
- Eclipsing variable system AW Peg spectrophotometric data, examining spectral line geometries and intensities and atmospheric conditions 03 p0439 A72-14244
- Curve of line width correlation application to alpha Orionis OH lines, determining atmospheric turbulence and thermal velocities 04 p0571 A72-14558
- Blanketing effect of strong line spectra collisionally broadened wings, evaluating stellar atmospheric model computation 04 p0573 A72-14907
- F and early G dwarf stars atmospheric models and line data, deriving temperatures, abundances and gravities 04 p0577 A72-15282
- Photometric standard star 29 Piscium abundance analysis with flux constant hydrogen line blanketed model atmospheres 04 p0578 A72-15317
- Explosive p-process nucleosynthesis limiting conditions in supernova envelopes, using proton capture and neutron photodisintegration rates 04 p0579 A72-15318
- Giant M stars atmospheres absorption coefficient calculation from vibrational and pure rotational bands of H₂O, CO and OH 05 p0715 A72-16167
- Fe I and Ti I excitation temperatures and ionization potentials of late G and K giant stellar atmospheres, comparing with model predictions 07 p1069 A72-19077
- Model atmosphere and spectral analysis for two early B-type supergiant stars, deducing stellar mass and evolutionary phase 07 p1070 A72-19085
- Stellar evolution, pulsation and atmosphere theories for globular cluster stars comparison with observation in bulk properties estimation 07 p1071 A72-19332
- Zeta Orionis spectra at 922-1453 A from rocket spectroscopy, matching lines with stellar atmosphere models 07 p1072 A72-19346
- Energy transport within stellar structure, discussing radiative transfer and opacity relationship to mean free path of radiation 07 p1078 A72-19924
- Shock wave properties in RR Lyrae type star atmospheres, discussing high temperature region structure behind wave front and emission line profiles 08 p1229 A72-20841
- Zeta Puppis visual line spectrum discrepancy from non-LTE stellar atmospheres models, necessitating hydrostatic equilibrium deviations consideration for temperature derivation 08 p1232 A72-21178
- Stellar atmosphere UV spectral line broadening by electron collision, radiative and classical damping 08 p1237 A72-21750
- Cosmic sources of organic compounds from chemical evolution viewpoint, discussing comets, interstellar space, prestellar nebulae and cool stellar atmospheres 08 p1120 A72-22014
- Astrophysical abundances analysis, discussing assumptions of local thermodynamic equilibrium and microturbulence in stellar atmospheres 09 p1386 A72-22659
- Book on stellar atmospheric physics covering gray and nongray atmospheres, radiation emission and absorption, transfer equation, Eddington approximation, spectral lines formation, etc 10 p1532 A72-23725
- T Tauri type variable stars spectral features relation to evolutionary sequences, noting stellar atmosphere nonthermal equilibrium plasma region effects 10 p1549 A72-25056
- Stellar atmospheric structure physical parameters from model atmosphere calculations, applying method to G and K stars 11 p1717 A72-25904
- Abundance in cold stellar atmospheres, noting effect on atmospheric thermal stratification and energy transfer from molecular spectra 11 p1722 A72-26432
- Variable white dwarf radial pulsation periods explained by nonradial oscillations and gravity modes, considering atmospheric mixing with degenerate core 12 p1868 A72-27260
- Nonlinear differential energy equation of static state stellar atmospheres with radiation and heat conduction terms 13 p2036 A72-28890
- Avrett-Krook temperature correction procedure modified to improve, near surface convergence for blanketed model stellar atmospheres 13 p2040 A72-29406
- Goldberg and Unno method application to microturbulent velocity determination in stellar atmosphere with convection 13 p2047 A72-29732
- Magnetic neutron stars /pulsars/ atmosphere, questioning vacuum approximation method applicability 14 p2160 A72-30887
- Stellar UV radiation spectral energy distribution investigation of stellar composition and atmosphere and

interstellar gas, discussing observation restriction by earth atmosphere absorption

15 p2302 A72-31284

Lower zero age main sequence star models uncertainties, comparing nonmixing and mixing length theory for various composition atmospheres

15 p2314 A72-32367

Radiative stellar envelopes circulation velocity calculation for various cylindrical rotation laws using perturbation method

15 p2314 A72-32371

Stellar and planetary atmosphere dynamics, deriving balance equations for variance analysis of angular momentum

16 p2453 A72-33247

Equations of state and equilibrium for electron gas in strong magnetic field, discussing effects in pulsar crusts and atmospheres

16 p2460 A72-33929

Stellar evolution and rotation data acquisition from photometric analysis of B-F main sequence stars, considering different models for rotating atmospheres

16 p2462 A72-34184

Meridian circulation with rapid differential rotation in radiative stellar envelopes.

17 p2605 A72-34532

Transfer of polarized radiation in a stellar atmosphere.

17 p2605 A72-34533

The limb darkening problem in eclipsing binaries.

17 p2612 A72-35382

Limb darkening for B-type main sequence stars in the infrared.

17 p2612 A72-35383

A model atmosphere analysis of the Ap star HR 465.

18 p2727 A72-36736

The metal-to-hydrogen ratio in F1-F5 stars, as determined by a model-atmosphere analysis of photoelectric observations of a group of weak metal lines.

18 p2727 A72-36737

The measurement of polarized 10-micron radiation from cool stars with circumstellar shells.

19 p2854 A72-37232

Studies of hydrodynamic events in stellar evolution. II - Dynamic instabilities in stellar envelopes.

19 p2854 A72-37234

On circumstellar molecules in the Pleiades.

19 p2856 A72-37508

Astronomical observations supporting stellar atmosphere microturbulence concept, noting Cepheid variables high dispersion spectra, supergiants irregular changes and microturbulence hydrodynamic effect

19 p2857 A72-37525

Energy variation curves for direct flare radiation and reflection from eruptive star atmosphere, discussing color variations

19 p2858 A72-37808

Extent of information that can be obtained from the luminosity loss curves of eclipsing systems with extended atmospheres

19 p2860 A72-37953

Two quantum induced photon-plasmon transition probability for hydrogen atom in processes of nebulas and stellar chromospheres

19 p2837 A72-38058

Thermalization lengths and mean numbers of scatterings for line photons.

20 p2956 A72-39759

On the chemical composition of epsilon Pegasi.

20 p2974 A72-39901

Russian book - Large-scale motions in the convective zones of stars and large planets.

21 p3104 A72-40462

Relaxation oscillations in the envelopes of luminous red giants.

21 p3105 A72-41034

Transfer of resonance-line radiation in differentially expanding atmospheres. II - Analytic solution for the case of coherence in the frame of the fluid.

21 p3106 A72-41038

Oxygen abundances of three population II horizontal-branch stars.

21 p3109 A72-41330

Radiative transfer equations solution for stellar spherical atmosphere by Grant-Hunt method, approximating intensity derivative over angular variable with Legendre polynomials

21 p3109 A72-41433

Chou-Tien nonplane-parallel solution to transfer equation for radiation scattering by free electrons in stellar spherical atmosphere by regional averaging procedure

21 p3109 A72-41434

Mechanical equilibrium equation of nongray stellar matter, approximating electron pressure vs temperature in early stellar atmospheres

21 p3109 A72-41435

Mean coefficient of opacity in stellar atmosphere model calculations

21 p3110 A72-41443

Curve of growth analysis of F star beta Cas and 10 UMa atmospheres for Ca, Sc, Ti, Cr, Mn and Ni-to-Fe abundance ratios

21 p3110 A72-41444

Model atmosphere analysis of the A 31a-O supergiant HD 33579 in the Large Magellanic Cloud.

22 p3225 A72-42386

Cool supergiant stars atmospheric model for chemical composition change effects due to nuclear burning cycle

22 p3227 A72-42556

Theory of radiative heat transfer in polytropic atmospheres

22 p3229 A72-42962

Giant stars iron abundance from narrow band spectrophotometric analysis and model atmospheres, isolating super metal rich stars below H-R diagram subgiant branch

23 p3334 A72-43256

Spectral variabilities of magnetic peculiar A stars associated with atmospheric chemical composition anomalies, using inclined rotator model

23 p3335 A72-43297

The influence of ultraviolet line blanketing on the neutral helium triplet lines in B-type stars.

24 p3438 A72-44834

STELLAR DOPPLER SHIFT

U DOPPLER EFFECT

U EXTRATERRESTRIAL RADIATION

STELLAR EVOLUTION

Book on nuclear reactions in stellar surfaces and relations with stellar evolution covering high energy L elements formation, Li-Be observations and thermonuclear and spallation theories

01 p0122 A72-10002

Isothermally contracting turbulent gas sphere for stellar formation from extension of Chandrasekhar work on Jeans criterion for static turbulent medium

01 p0129 A72-10799

Cepheid variables mass discrepancy from evolution and pulsation theories, emphasizing opacity changes, luminosity values and effective temperature

01 p0133 A72-11128

Spectroscopic He abundance in population II stars from viewpoint of big-bang cosmology, taking into account neutrino emission according to photon-neutrino coupling theory

02 p0281 A72-12303

Dust particle formation in circumstellar space accompanying star formation, discussing necessary and sufficient condition for grain escape by fragmentation

02 p0284 A72-12637

Stellar secular stability during complex roots onset in model evolution, discussing radiative heat transport coefficient effects

03 p0416 A72-13004

He abundances in universe, discussing stellar structure and evolution, He production, variable stars and globular clusters H-R diagrams shape

03 p0418 A72-13112

Dense cloud and protostar molecules from molecular line emission, considering mass effects in stellar evolution

03 p0419 A72-13120

Absolute magnitudes and mass-radius relationship of RR Lyrae stars for stellar evolution calculations

03 p0421 A72-13140

Magellanic Clouds cepheid variables compared to Milky Way cepheids, discussing evolution tracks

03 p0425 A72-13261

Massive star evolution, discussing stellar structure theory uncertainties, young clusters, helium burning and evolutionary tracks

03 p0425 A72-13262

Binary systems formation probability during triple encounters, observing dependence on system/potential energy ratio

03 p0435 A72-13809

Stellar evolution in close binary systems, discussing post main sequence stage, hydrodynamical processes and dwarf binaries

03 p0437 A72-13868

Nuclear reactions in anomalous element abundances production for peculiar A stars, considering surface diffusion and surface and internal nuclear processes

03 p0437 A72-13872

Soviet book on long period variable stars covering spectral data photometric characteristics, spatial and kinematic properties, absorption effect and evolution

03 p0439 A72-14224

One zone model formulation and mathematical behavior for evolution of galaxies, discussing stellar birth rate and end states

04 p0570 A72-14551

Solar model for capture rate in C1 37 neutrino experiment, comparing different stellar evolution programs

04 p0566 A72-14562

Gravitational waves proposed origin, considering black holes, star collapse, white dwarf and neutron star formation and galaxy center neutron star clustering

04 p0576 A72-15074

Metal-rich 1.19 solar mass main sequence star evolution to convection onset in core during He flash

04 p0577 A72-15283

Cyg X-1 type X ray sources evolution, discussing white dwarf and supernovae stages, parent mass and angular momentum

04 p0568 A72-15508

Cosmological evolution theories, discussing big bang theory, galactic evolution, quasars, pulsars, gravitational collapse, stellar evolution, supernovae, black holes, etc

05 p0716 A72-16311

White dwarf magnetic fields decay time scale for dipolar and toroidal configurations

06 p0876 A72-17581

Elemental synthesis and energy sources in stellar evolution, hydrogen, helium and advanced burning stages, p-p cycle, e process and nuclear equilibrium

06 p0876 A72-17585

Model computations for population I stars of 0.6, 0.8 and 1.2 solar masses, considering evolutionary sequences correspondence to planetary nebulae evolution

06 p0882 A72-17999

Stellar evolution, pulsation and atmosphere theories: for globular cluster stars comparison with observations in bulk properties estimation

07 p0171 A72-19332

Galactic cluster M67 blue straggler stars in pseudohorizontal branch, determining stellar mass relative to turnoff point stars and zero-age main sequence

07 p0171 A72-19335

Stellar extinction and genesis with Galaxy, discussing Li role in nucleosynthesis and degenerate star structure theory

07 p0173 A72-19427

Hydrogen-helium stars evolution, noting high surface temperature

07 p0175 A72-19581

Neutron star evolution theories, emphasizing neutrino emission processes and stellar collapse

07 p0180 A72-20056

Elemental nucleosynthesis, considering cosmological, stellar, galactic and solar system evolution and atomic nuclei energetic levels

07 p0183 A72-20466

Population I stars and open cluster age determination methods based on stellar evolution theory, discussing inherent uncertainties effects

07 p0183 A72-20467

Population II stars age determination by main sequence turnoff luminosity and other methods, noting cosmological and galactic evolution implications

07 p0183 A72-20467

Astrophysical helium production by massive pulsationally unstable pure hydrogen stars evolving inhomogeneously with mass loss

07 p0184 A72-20691

Soviet monograph on universal gravitation covering prerelativistic theories, inverse square law, relativistic effects, celestial mechanics, stellar structures and evolution, etc

08 p1231 A72-21025

Pulsar and supernova remnant relative space position based on runaway pulsar hypothesis, discussing pulsar period-luminosity relation from evolutionary standpoint

08 p1233 A72-21186

Unstable binary RW Aur spectrophotometric study with stellar evolution and outer atmosphere implications, relating Balmer continuum to UV excess

08 p1233 A72-21277

Initially stationary axisymmetric disk of stars evolution calculated by gravitational potential solver for various values of velocity dispersion

09 p1383 A72-22460

Main sequence star evolution relation to pulsar formation, discussing stellar core density at carbon ignition with respect to critical density limit

09 p1394 A72-23698

Neutron star properties, formation theories, crust composition and internal structure, examining interior neutron behavior, fermion systems superfluidity, magnetic field effects and stellar dynamics

10 p1533 A72-23890

Cepheid instability strip stellar models pulsation properties compared with delta Scuti stars and AI Velorum variables observation data for stellar evolution studies

10 p1542 A72-24611

Hyades member star BD plus 16.516 deg described as late evolution product of binary system with mass exchange and loss through planetary nebula phase

10 p1543 A72-24618

Cepheid variables evolutionary and blue edge calculations reconciled with observation

10 p1544 A72-24665

Stellar evolution from precarbon-burning contraction to presupernova stage with and without neutrino production by electron neutrino interaction

10 p1545 A72-24825

Main sequence, red giant and white dwarf stars convective envelopes evolution, discussing mixing length theory inadequacy

10 p1545 A72-24826

Spiral galaxy density wave maintenance mechanism from rotating disk star-gas system model description of stellar birth and disintegration effects
10 p1547 A72-24869

Hydrogen gas cloud gravitational contraction and fragmentation in expanding universe, noting cooling and massive stars formation
10 p1547 A72-24870

Total mass content of early type star clusters associated with reflection nebulosities
10 p1548 A72-24966

T Tauri type variable stars spectral features relation to evolutionary sequences, noting stellar atmosphere nonthermal equilibrium plasma region effects
10 p1549 A72-25056

Gas and dust cloud evolution with allowance for dimensional finiteness and stellar evolution into red supergiant after hydrogen depletion
11 p1715 A72-25297

One and two boundary curves systems for Vlasov equation of one dimensional collisionless self gravitating stellar systems evolution with constant phase space density
12 p1874 A72-27912

Boundary curves for collective relaxation in one dimensional collisionless two phase space density self gravitating stellar system evolution, noting velocity dispersions dependence
12 p1875 A72-27913

Stellar gravitational collapse to neutron stars and black holes, discussing gravitational wave emission from Galactic center
12 p1875 A72-27958

Two phase flow model of cloud and star formation by galactic shocks in quasi-steady interstellar gas flow in spiral gravitational field
13 p2040 A72-29404

Thermonuclear detonation and reimplosion of dense stellar cores, studying beta-processes effect on post-detonation evolution
13 p2044 A72-29625

Evolution of extreme population I massive stars from main sequence to He exhaustion phase, discussing various development phases in H-R diagram
14 p2158 A72-30727

Near-solar mass star secular stability during gravitational contraction and main sequence phases, considering static and quasi-static models
14 p2158 A72-30734

Nova Delphini evolution from metallic absorption lines observations before December 1967 maximum, obtaining dispersion variation with wavelength
14 p2159 A72-30741

Adiabatic stellar shells stability in cases of rigid and compressible nucleus
15 p2304 A72-31334

Shell formation during star collapse due to rotational instability, discussing relativistic effects
15 p2305 A72-31337

Book on astronomy covering optical and radio telescopes properties and atmospheres of inner and outer planets, stellar lifetimes and evolution, galaxies, cosmology, etc
15 p2306 A72-31516

Algorithmic calculation for composition changes due to nuclear reactions and convective mixing during stellar evolution
15 p2314 A72-32374

Planetary nebulae nuclei evolution, describing shell ejection mechanism with dependence on progenitor star luminosity
16 p2451 A72-33032

Magnitude redshift relation in flat Brans-Dicke cosmology, discussing gravitational constant effects on stellar evolution and galactic luminosity
16 p2455 A72-33471

Helium stars linear and nonlinear pulsation and evolutionary computations, establishing instability strip with two solar mass models
16 p2458 A72-33720

Stellar magnetic oblique rotator internal moment field construction by perturbation technique estimating energy dissipation and turbulent viscosity
16 p2458 A72-33721

Numerical calculation for axisymmetric gas cloud rotation effects on collapse, noting implications for star formation and fragmentation
16 p2458 A72-33722

Model for low energy galactic cosmic ray effects on young and F star Li abundance and H I region heating
16 p2448 A72-33740

Stellar evolution and rotation data acquisition from photometric analysis of B-F main sequence stars, considering different models for rotating atmospheres
16 p2462 A72-34184

Studies of extremely young clusters. VI - Spectroscopic observations of the ultraviolet-excess stars in the Orion Nebula cluster and NGC 2264.
17 p2605 A72-34530

Collapse calculations for 0.25-10 solar mass spherical protostars, discussing stellar core evolution and temperature distribution in infalling cloud
17 p2606 A72-34674

The reddening, distance modulus, chemical composition and age of the galactic cluster NGC 752.
17 p2607 A72-34675

Studies of hydrodynamic events in stellar evolution. I - Method of computation.
17 p2611 A72-35316

Fundamental data for massive stars compared with theoretical models.
17 p2611 A72-35317

Nonspherical perturbations of relativistic gravitational collapse. I - Scalar and gravitational perturbations. II - Integer-spin, zero-rest-mass fields.
17 p2612 A72-35390

Russian book - Theory of gravitation and the evolution of stars
17 p2613 A72-35452

Formation of neutron star spots and its connection with pulsars. I.
17 p2613 A72-35502

Supergiants internal structure, evolution and spectral characteristics, discussing instability phenomena and luminosity calibration
18 p2723 A72-35995

Astrophysical theories of supernovae outbursts as stellar evolutionary nonstationary phase in terms of thermal instability of degenerated matter or stellar explosion
18 p2725 A72-36399

Evolution of close binary systems with intermediate initial mass ratios.
18 p2728 A72-36741

Experimental nuclear physics and theoretical solar structure and evolution explanations of disagreement between calculated and observed solar neutrino flux
18 p2722 A72-37007

Studies of hydrodynamic events in stellar evolution. II - Dynamic instabilities in stellar envelopes.
19 p2854 A72-37234

Variation of evolved blue/red ratio for supergiants as function of stellar mass, discussing status of astrophysical test for neutrino emission
19 p2854 A72-37235

Hydrostatic oxygen burning in stars. II.
19 p2854 A72-37236

Central galactic plane, interstellar medium and spiral arm conditions for star formation in Milky Way
19 p2855 A72-37249

The colour-magnitude diagram of the globular cluster NGC 6981.
19 p2855 A72-37342

Single body and stellar cluster models of quasars and galactic nuclei stability, noting neutron and collapsing star lifetimes
19 p2862 A72-38052

Unsteady hydrodynamic accretion on a neutron star
19 p2862 A72-38053

Secular stability. I - A Population I star near the main sequence.
19 p2864 A72-38099

Pulsars as stellar population, considering physical models, pulse emission radiation mechanism and use in galaxy studies
19 p2865 A72-38476

Protostars formation through interstellar atomic hydrogen clouds gravitational collapse, deriving critical mass, surface temperatures and luminosities
19 p2865 A72-38478

Star cluster age relation to mass ratios of stars and interstellar hydrogen and dust
19 p2867 A72-38511

The influence of local conditions in the interstellar medium upon star formation.
19 p2868 A72-38699

Hydrodynamic model of white dwarf envelope thermonuclear runaway evolution producing nova outburst, computed for various CNO nuclei initial abundances
20 p2966 A72-38908

Gas density as function of galactic radius according to Jeans unstable criterion for star formation from known galaxy rotation curve and gas sound speed
20 p2966 A72-38917

An estimate of stellar wind mass loss during the red giant phase of evolution.
20 p2967 A72-39187

Stellar energy-loss rates in a convergent theory of weak and electromagnetic interactions.
20 p2972 A72-39868

On the influence of the opacity values on static stellar models. I - Horizontal branch stars.
20 p2973 A72-39879

Finite radial oscillations of uniformly rotating gravitating magnetized fluid cylinder model of star formation dynamics
21 p3109 A72-41331

Curve of growth analysis of F star beta Cas and 10 UMa atmospheres for Ca, Sc, Ti, Cr, Mn and Ni-to-Fe abundance ratios
21 p3110 A72-41444

Self similar procedure derived for gas fall to solid surface in constant gravitational field, applying to initial phase of neutron star matter accretion
21 p3113 A72-41753

Computer-aided numerical experiment of cluster mass increase by accretion in protostar evolution
21 p3113 A72-41754

Dark dust nebulae and bright H II clouds, considering light molecules, stellar birth region, radio and IR astronomy
22 p3220 A72-41995

On circumstellar gas emission among pre-main-sequence stars in Ic Orionis and NGC 2264.
22 p3227 A72-42555

Nucleosynthesis theory for advanced thermonuclear evolution models of massive stars from helium burning through final hydrodynamic stages
22 p3227 A72-42561

Approximation of energy generation and nucleosynthesis during hydrostatic carbon burning in massive stars, noting neutrino-dominated evolution effects
22 p3228 A72-42562

Studies of heavy-element synthesis in the galaxy. I - Separation of r- and s-process abundances.
22 p3228 A72-42563

Unsteady phenomena in the world of stars and galaxies
22 p3230 A72-43153

Numerical models for He stars structural evolution, considering main sequence models of 1-8 solar masses and different carbon enrichments
23 p3334 A72-43258

Mixing between stellar envelope and core in advanced phases of evolution. IV - Effect of super-adiabaticity in convective envelope.
23 p3335 A72-43486

Extended horizontal branch loci.
23 p3337 A72-43830

Galactic evolution - Program and initial results.
23 p3337 A72-43832

Inconsistency of gravitational constant variability in inverse proportion to time from viewpoint of stellar and solar system age, life development and physical three dimensional space
23 p3338 A72-44037

Gravitational emission in the scalar-tensor theory of gravitation
23 p3315 A72-44476

Resonance effects on second order anharmonic pulsational amplitudes for polytropic main sequence evolutionary models, classifying Cepheid-type pulsators
24 p3437 A72-44832

Stellar implosion, gas cloud collapse into white dwarf or neutron star and atomic hydrogen cloud collapse, considering effects of cosmic bodies at high velocities
24 p3439 A72-45017

Solar oblateness and neutrino flux measurement experiments, discussing agreement with solar interior and evolution models
24 p3446 A72-45527

STELLAR FIELDS
U STAR DISTRIBUTION
STELLAR GRAVITATION
Stability theory for a star with a toroidal magnetic field
19 p2863 A72-38062

Double water-bag model stability for plane one dimensional stellar system, computing eigenfrequencies and eigenfunctions
22 p3224 A72-42384

STELLAR INERTIAL NAVIGATION
U CELESTIAL NAVIGATION
U INERTIAL NAVIGATION
STELLAR LUMINOSITY
Stellar intensity effect on angular navigation sighting accuracy attainable between star and lunar limb using Apollo T2 sextant
01 p0097 A72-10566

RR Lyrae variables intermediate band photometry, tabulating magnitudes and color of 125 stars
01 p0133 A72-11129

X ray rocket observations of time variation of SCO X-1 energy spectrum and optical luminosity at 2-20 keV
02 p0281 A72-12307

Supernovae remnants intrinsic luminosity-diameter correlations from soft X ray emission data, taking into account interstellar medium
03 p0408 A72-13008

Pulsar observation data, presenting period histogram, intensity, shape and polarization variations, position distribution, physical nature and spectra
03 p0417 A72-13102

Helium abundance in stellar interiors, considering mass-luminosity relations of Hyades
03 p0419 A72-13114

RR Lyrae stars absolute magnitude determination by statistical parallaxes method
03 p0421 A72-13139

Absolute magnitudes and mass-radius relationship of RR Lyrae stars for stellar evolution calculations
03 p0421 A72-13140

Cepheid variables compared for Milky Way and Small and Large Magellanic Clouds, discussing amplitudes, period-luminosity relations and light curves
03 p0425 A72-13255

Magellanic Clouds bright star intermediate band photometry, discussing interstellar extinction and luminous supergiants

03 p0425 A72-13257

Small Magellanic Cloud NGC 371 region photometric studies for cepheids period-luminosity relations, noting domination by young supergiant stars

03 p0425 A72-13258

Eclipsing variable star EQ Taurus photoelectric brightness variation observations in B and V light

03 p0433 A72-13488

Halos around black holes, showing luminosities caused by synchrotron radiation of magnetized plasma

03 p0435 A72-13803

Telescopic meteors light curves, showing maximum point brightness distribution in visible trajectory with respect to stellar magnitudes

03 p0438 A72-13985

Starlight intensity modulation at discrete radio frequencies due to enhanced ionospheric electron density fluctuations

03 p0438 A72-14096

UBV magnitude measurement for stars in open clusters NGC 6613 and 6716, determining spectral classes, absorption and distances

05 p0712 A72-15768

Stellar populations in galaxies as function of luminosity, investigating spectroscopic and photometric properties

05 p0716 A72-16370

GX3 plus 1 identification by sounding rocket during lunar occultations, discussing magnitude

07 p1070 A72-19123

Disk population F-type star photometric luminosities, motions and metal abundance indices, discussing ultrashort period cepheids

07 p1071 A72-19333

Galactic cluster M67 blue straggler stars in pseudohorizontal branch, determining stellar mass relative to turnoff point stars and zero-age main sequence

07 p1071 A72-19335

Pulsars optical counterpart observation, noting Crab Nebula pulsar visual magnitude

07 p1080 A72-20050

Population II stars age determination by main sequence turnoff luminosity and other methods, noting cosmological and galactic evolution implications

07 p1083 A72-20468

N Her 1963 distance, absolute magnitude, stellar mass and explosion-ejected shell mass, using maximum and relative intensity calculation methods

08 p1229 A72-20840

Type R Corona Borealis variable stars luminosity variations attributed to formation of carbon layer from He nuclear transformation process at stellar core-envelope boundary

08 p1231 A72-21086

Pulsar and supernova remnant relative space position based on runaway pulsar hypothesis, discussing pulsar period-luminosity relation from evolutionary standpoint

08 p1233 A72-21180

Semiregular variable CH Cygni observations from 1967 to 1969 with continuous spectrum variations comparison to monochromatic brightness changes

08 p1233 A72-21278

RR Lyrae variables period-luminosity relations explained by linearized pulsation calculations for quenching of first harmonic

08 p1235 A72-21388

Crab pulsar optical pulse stability comparison to radio frequency output, noting negative results in search for polar precession

08 p1235 A72-21396

Wolf-Rayet stars identification in spiral galaxy M33/NGC 598/ from narrow band interference filter photographs, tabulating apparent magnitudes and emission indexes

09 p1382 A72-22281

Spectral types and magnitudes of O and WC stars of binary gamma Velorum system

09 p1382 A72-22282

Stellar magnitude equation for 400 mm photographic telescope, correcting star coordinates measurements

09 p1311 A72-23060

Visual binary star investigations, considering parallaxes, masses, absolute magnitudes and orbit computation

09 p1390 A72-23502

Precessional corrections, solar motion and galactic rotation determination from proper motions by maximum likelihood method, taking into account stars visual magnitude

09 p1391 A72-23535

Stellar brightness variations of T Cep during January 1969-November 1971, considering visual estimates and period length observations

10 p1542 A72-24571

Extragalactic supernovae X ray luminosity upper limits from OSO 3 data, estimating total energies

10 p1544 A72-24667

Visual observations of eclipsing period elements of nova-like variable V Sagittae for estimate of total magnitude of uneclipsed binary

10 p1545 A72-24829

Close binary stars system model for totally eclipsing AW UMa light curves and line profiles, noting very low mass ratio

10 p1550 A72-25195

Stellar physical parameters computed from multicolor photometric data on extraatmospheric magnitudes by maximum likelihood method

11 p1715 A72-25296

Measurement of light pressure-force on Echo 1 satellite based on satellite surface reflection and stellar magnitude as function of phase angle

11 p1718 A72-25939

Close binary stars photometric measurement with electronic camera, noting magnitude difference determination from recorded images

12 p1866 A72-27203

Ap stars with variable periods from magnetic and photometric data analysis

12 p1868 A72-27221

Starry sky energetic simulator design, analyzing comparative brightness of stars

13 p1945 A72-28494

Luminosity variation of star in circular orbit around extreme Kerr black hole due to Doppler effects and gravitational field light focusing

13 p2041 A72-29416

Nonoriented astronomical satellite attitude determination from onboard measurements of geomagnetic field and stellar luminosity

14 p2151 A72-30460

White dwarf background radiation and optical emission variations due to thermal bremsstrahlung from stellar corona

14 p2147 A72-30554

Color photoelectric light pulsations curve of RU Cam variable star during October 1969-August 1970, noting constant mean luminosity and color

14 p2158 A72-30729

Pulsars distance computation, considering period-luminosity relationship and uncertainties inherent in dispersion measure /DM/ method

14 p2159 A72-30738

Fuor luminosity phenomena due to thermal corpuscular radiation emitting energy sources

15 p2304 A72-31330

Photometric characteristics of two types of eruptive binary stars differing in hot spot brightness

15 p2305 A72-31340

Planetary nebulae nuclei evolution, describing shell ejection mechanism with dependence on progenitor star luminosity

16 p2451 A72-33032

Local population II stars density upper limit in terms of mass-luminosity ratio based on U, B and V photometric observations

17 p2604 A72-34442

Occultations of stars by Jupiter

17 p2607 A72-34751

A recalibration of the absolute magnitudes of supergiants.

17 p2609 A72-35115

The limb darkening problem in eclipsing binaries.

17 p2612 A72-35382

Supergiants internal structure, evolution and spectral characteristics, discussing instability phenomena and luminosity calibration

18 p2723 A72-35995

Photometric study of the open cluster NGC 2232.

18 p2728 A72-36742

Consequences of the Stromgren's theorem for radiative envelope stars.

18 p2728 A72-36760

The type II supernova 1969 I in NGC 1058.

18 p2728 A72-36763

Underluminosity and magnetic fields in beta Lyrae.

18 p2729 A72-36982

Luminosities and motions of the F-type stars. II - Metal-deficient stars.

19 p2855 A72-37238

Kinematics of faint M stars near the north galactic pole, and the mass density in the solar neighbourhood.

19 p2855 A72-37341

The association of X-ray sources with bright stars.

19 p2856 A72-37507

Limiting magnitudes of stars in visual telescopic observations /Ground and extraatmospheric locations of instrument and observer/

19 p2859 A72-37907

Early star absolute magnitude from equivalent H gamma and delta line widths and Balmer hydrogen series line

19 p2859 A72-37908

Extent of information that can be obtained from the luminosity loss curves of eclipsing systems with extended atmospheres

19 p2860 A72-37953

Colorimetric and spectrophotometric gradient systems comparison for bright stars used in automatic telescope pointing control, discussing interstellar absorption

19 p2860 A72-37955

Minimum perceivable stellar magnitudes in visual observations by naked eye and telescope, discussing image contrast and angular scale

19 p2860 A72-37961

Declinations of bright and weak stars determined separately from observations in the upper and lower culminations by the Struve-Ertel vertical circle during 1955-1961

19 p2861 A72-37981

Absolute magnitudes and color indexes of red giant concentration centers on a color-luminosity diagram

19 p2863 A72-38069

Radial density distribution and luminosity functions for stars in alpha Persei cluster

19 p2863 A72-38070

The kinematics of open star clusters

19 p2865 A72-38488

Photoelectric photometry of close visual binaries

19 p2866 A72-38499

H and K emission intensity and line width dependence on stars age and luminosity, discussing dwarf stars and giants

19 p2866 A72-38503

Interferometer detection of radio sources near pulsing extar Hercules X-1 during low X ray luminosity period

20 p2963 A72-38918

On the influence of the opacity values on static stellar models. I - Horizontal branch stars.

20 p2973 A72-39879

Structure and motions in the Carina spiral feature.

20 p2973 A72-39880

A study of the interstellar extinction in the Carina-Centaurus region.

20 p2973 A72-39881

Photoelectric light curve of Nova Vulpeculae 1968 N. 1.

20 p2973 A72-39883

Secondary fluctuations in the light curve of epsilon Aur.

20 p2974 A72-39898

Photoelectric observations of the 1971-eclipse of 32 Cyg.

20 p2974 A72-39900

Cosmological model radiation pressure and density calculation by red shift-stellar magnitude ratios from galactic observations

21 p3109 A72-41441

Bright red giants of the globular clusters M 3, M 5, and M 13

21 p3113 A72-41756

Interactions between stars and local dust formations

21 p3113 A72-41758

Stratification of the emission in the envelope of a Wolf-Rayet type eclipsing binary V444 Cyg

21 p3113 A72-41759

Eclipsed binary brightness curve determination by least squares method, using weighted gravity center point observations

21 p3113 A72-41760

Red variables in globular clusters, in the galactic centre and in the solar neighbourhood.

22 p3222 A72-42135

Brightness and polarization structure of four supernova remnants 3C58, IC443, W28, and W44 at 2.8 centimeter wavelength.

22 p3224 A72-42382

The peculiar O6f star HD 148937 and the symmetrically surrounding nebulae.

22 p3227 A72-42557

Physical characteristics of type I supernova envelopes during the initial expansion phase. II - Development of type I supernova spectra after maximum light.

23 p3333 A72-43228

A spectroscopic and photometric study of the pulsating R Coronae Borealis type variable, RY Sagittarii.

23 p3334 A72-43255

Identification of four novae and a super-nova in Palomar Sky Atlas.

23 p3341 A72-44474

Luminosity variation in the one-zone Cepheid model.

24 p3438 A72-44837

Investigation of the variable stars WR-96, GR-29, and WR-96 /2/

24 p3448 A72-45682

Photographic observations of variable stars in the proximity of NGC 6830

24 p3448 A72-45683

STELLAR MAGNETIC FIELDS

NT SOLAR MAGNETIC FIELD

Quasar model proposal as giant pulsar rejected discussing mass, radius, magnetic field strength, luminosity and gamma radiation

01 p0134 A72-11144

Pulsar magnetosphere axisymmetric and vacuum oblique rotator models, emphasizing electromagnetic field properties

01 p0134 A72-11159

Magnetic field role in Ap stars abundance peculiarities model, discussing rotational circulation, convection, accretion and mass loss effects on surface

03 p0416 A72-13010

Pulsars formation rate and connection with supernovae and cosmic rays, discussing stellar magnetic field strength

03 p0421 A72-13134

Electromagnetic pulsar models features and predictions, using rotating neutron stars with strong dipolar magnetic fields 03 p0437 A72-13873

Neutron star and white dwarf strong magnetic field generation mechanism involving thermodynamic equilibrium states of electron gas 05 p0723 A72-17162

White dwarf magnetic fields decay time scale for dipolar and toroidal configurations 06 p0876 A72-17581

X ray pulsations mechanism in Cyg X-1 related to high magnetic fields produced by flare-like events 06 p0873 A72-17636

Pulsar model based on neutron star rotation with skew magnetic field, considering radiated particle acceleration responsible for high energy activity in supernova remnants 07 p1080 A72-20057

Pulsar braking index and period-pulse width distribution calculations within proposed model leading to neutron star surface magnetic field strength estimates 08 p1235 A72-21389

Magnetic star theory, postulating stellar magnetic flux as slowly decaying relic of flux in prestar gas, considering dissipation processes and rotation 09 p1387 A72-22754

Long time behavior of neutron star magnetic fields, noting pulsar evidence for large internal fields in main sequence stars 09 p1389 A72-23393

Magnetic field generation problem in rotating relativistic star for barotropic medium 09 p1391 A72-23537

Neutron star properties, formation theories, crust composition and internal structure, examining interior neutron behavior, fermion systems superfluidity, magnetic field effects and stellar dynamics 10 p1533 A72-23890

Pulsar radiation mechanism study from magnetosphere structure model, taking into account neutron star evaporated gas accumulation in gravitation-centrifugal force balance region 10 p1544 A72-24672

Turbulent plasma dynamo mechanisms of magnetic field origin in astrophysics, noting Steenbeck and Parker theories 14 p2162 A72-31150

Flare mechanism of pulsar radiation near magnetic poles of rotating neutron stars 15 p2298 A72-31627

Pulsar rotating electromagnetic field vectors classification for magnetosphere models 16 p2450 A72-32866

Stellar magnetic oblique rotator internal motion field construction by perturbation technique estimating energy dissipation and turbulent viscosity 16 p2458 A72-33721

The stability of a self-gravitating, nonrotating gas layer with stellar, magnetic, and cosmic-ray components. I. 17 p2611 A72-35313

Underluminosity and magnetic fields in beta Lyræ. 18 p2729 A72-36982

Stability theory for a star with a toroidal magnetic field 19 p2863 A72-38062

Neutron star matter properties and model calculations, investigating magnetic field decay 19 p2865 A72-38482

Line formation in the presence of magnetic fields; Proceedings of the Conference, Boulder, Colo., August 30-September 2, 1971. 20 p2970 A72-39752

Stellar emission and absorption line spectra formation in presence of magnetic field interpreted by radiative transfer equation solution, considering dwarf stars observation 20 p2956 A72-39753

Line spectra and continuum polarization in magnetic white dwarfs. 20 p2971 A72-39760

Magnetic-field variations in 78 Virginis, beta Coronæ Borealis, and 73 Draconis. 21 p3106 A72-41036

Hamiltonian analysis of charged particle motion in the pulsar rotating magnetic field. 21 p3111 A72-41472

Neutron star model for magnetic field and superfluidity effects on cooling during pulsar stage 22 p3228 A72-42565

STELLAR MASS

NT STELLAR GRAVITATION

Cepheid variables mass discrepancy from evolution and pulsation theories, emphasizing opacity changes, luminosity values and effective temperature 01 p0133 A72-11128

Helium abundance in stellar interiors, considering mass-luminosity relations of Hyades 03 p0419 A72-13114

Dense cloud and protostar molecules from molecular line emission, considering mass effects in stellar evolution 03 p0419 A72-13120

Absolute magnitudes and mass-radius relationship of RR Lyræ stars for stellar evolution calculations 03 p0421 A72-13140

Linear nonadiabatic pulsation constants for fundamental mode and first two harmonics of stellar models including Cepheids, observing mass scattering 04 p0579 A72-15319

Model computations for population I stars of 0.6, 0.8 and 1.2 solar masses, considering evolutionary sequences correspondence to planetary nebulae evolution 06 p0882 A72-17999

Close binary system average gravity and effective temperature at Roche limit for 90 deg phase and both conjunctions, taking into account mass ratios and orbital inclination 06 p0882 A72-18002

Stellar velocity distribution functions in nonrotating clusters, considering encounter multiplicity effects and dissipation increase from masses dispersion 06 p0883 A72-18024

Microscopic calculations for nuclear forces, compressibility of neutron matter and maximum mass of neutron stars based on solid state model at high densities 06 p0891 A72-18507

Isolated pulsar or neutron star upper mass limit based on consideration of rotational energy by ejection of low energy cosmic rays or photons 06 p0891 A72-18508

Stellar evolution, pulsation and atmosphere theories for globular cluster stars comparison with observation in bulk properties estimation 07 p1071 A72-19332

Galactic cluster M67 blue straggler stars in pseudohorizontal branch, determining stellar mass relative to turnoff point stars and zero-age main sequence 07 p1071 A72-19335

N Her 1963 distance, absolute magnitude, stellar mass and explosion-ejected shell mass, using maximum and relative intensity calculation methods 08 p1229 A72-20840

Gravitational system dynamics, discussing massive-light star mixtures with collisions and systems with equal mass objects 08 p1231 A72-21121

Synchro-Compton theory for variable compact components in extragalactic radio sources, suggesting stellar mass object collapse as energy source 08 p1233 A72-21181

Visual binary star investigations, considering parallaxes, masses, absolute magnitudes and orbit computation 09 p1390 A72-23502

Main sequence star evolution relation to pulsar formation, discussing stellar core density at carbon ignition with respect to critical density limit 09 p1394 A72-23698

Hyades member star BD plus 16.516 deg described as late evolution product of binary system with mass exchange and loss through planetary nebula phase 10 p1543 A72-24618

Total mass content of early type star clusters associated with reflection nebulosities 10 p1548 A72-24966

Stellar velocity distribution functions in nonrotating clusters, considering encounter multiplicity effects and dissipation increase from masses dispersion 11 p1719 A72-25960

Quasi-stationary spherical system structure model for stars of different masses with isotropic velocity distribution 14 p2149 A72-30212

X ray emitting component Centaurus X-3 mass limit in close eclipsing binary system with regard to Roche lobe principle 14 p2156 A72-30569

Near-solar mass star secular stability during gravitational contraction and main sequence phases, considering static and quasi-static models 14 p2158 A72-30734

Mass exchange and thermal time scales for shell source burning binary components with deep outer convective layers, interpreting numerical results from analytical model 14 p2159 A72-30739

Massive stars velocity distribution function in clusters, determining escape rate and energy dissipation 15 p2305 A72-31339

Opacity corrections of main sequence stellar models of 2.25 solar masses in terms of Cox, Carson and Watson formulas 16 p2452 A72-33130

Local population II stars density upper limit in terms of mass-luminosity ratio based on U, B and V photometric observations 17 p2604 A72-34442

Vibrational stability of supermassive stars stabilized dynamically by a uniform or differential rotation 17 p2613 A72-35461

State equation for superdense stars treated as perfect degenerate tachyon gas, noting dynamic stability for arbitrarily large central densities 18 p2726 A72-36715

Evolution of close binary systems with intermediate initial mass ratios. 18 p2728 A72-36741

Variation of evolved blue/red ratio for supergiants as function of stellar mass, discussing status of astrophysical test for neutrino emission 19 p2854 A72-37235

Determination of the spectrophotometric temperature, mean radius and mass of the star beta Cep 19 p2860 A72-37954

Star cluster age relation to mass ratios of stars and interstellar hydrogen and dust 19 p2867 A72-38511

The influence of local conditions in the interstellar medium upon star formation. 19 p2868 A72-38699

Kinetic equations for ultradense matter neutronization, noting stellar configuration of given mass with variable volume 21 p3086 A72-40096

Two phase stellar structure with polytropic equations of state for shell and core, calculating configuration mass, radius and energy 21 p3102 A72-40098

Computer-aided numerical experiment of cluster mass increase by accretion in protostar evolution 21 p3113 A72-41754

Effective temperatures of massive stars as a function of chemical composition and mass. 22 p3227 A72-42560

Nucleosynthesis theory for advanced thermonuclear evolution models of massive stars from helium burning through final hydrodynamic stages 22 p3227 A72-42561

Approximation of energy generation and nucleosynthesis during hydrostatic carbon burning in massive stars, noting neutrino-dominated evolution effects 22 p3228 A72-42562

Quasi-stationary spherical system structure model for stars of different masses with isotropic velocity distribution 23 p3334 A72-43242

Numerical models for He stars structural evolution, considering main sequence models of 1-8 solar masses and different carbon enrichments 23 p3334 A72-43258

STELLAR MASS EJECTION

Galactic wind formation in elliptical galaxies by stellar ejected gas heating by supernovae, discussing thermally unsteady cores 02 p0279 A72-12189

Wolf-Rayet type stars emission line variations from outer convective zone opening and matter ejection 03 p0439 A72-14243

Ejection behavior of relativistic particle magnetized clouds in radio galaxies central parts, noting interaction with interstellar medium 06 p0891 A72-18503

Astrophysical helium production by massive pulsationally unstable pure hydrogen stars evolving inhomogeneously with mass loss 07 p1084 A72-20691

Nova outbursts hydrodynamic processes, studying mass loss mechanism based on direct shock wave ejection and pulsational instability 09 p1382 A72-22283

Galactic nucleus evolutionary processes, considering mass ejection from newly formed massive stars, gas concentration toward center, kinetic energy exchange and stellar collisions 10 p1535 A72-23907

Monodirectional jet mass ejection from black holes, developing hypothetical model based on squeezed toothpaste analogy 10 p1535 A72-23910

Low mass neutron star source of pulsed X radiation in binary Centaurus X-3 ejected during low energy supernova explosion 14 p2156 A72-30570

Model for hot stars mass outflow due to gas acceleration by radiation absorption in UV resonance lines 15 p2305 A72-31341

Nitrogen existence in galactic cosmic ray sources, considering formation from CNO cycle hydrogen and He burning and ejection from normal stars 16 p2448 A72-33739

The association of X-ray sources with bright stars. 19 p2856 A72-37507

A preliminary model for the shell ionisation of the nova RS Ophiuchi. 19 p2866 A72-38504

An estimate of stellar wind mass loss during the red giant phase of evolution. 20 p2967 A72-39187

A statistical method for the determination of the rate of changes of period for eclipsing binaries. 20 p2974 A72-39892

Physical properties of interstellar matter surrounding binary stars from astronomical spectroscopy, discussing eruptions and photometric changes 20 p2975 A72-40069

Relaxation oscillations in the envelopes of luminous red giants. 21 p3105 A72-41034

The dynamical effects of stellar mass loss on diffuse nebulae. 22 p3224 A72-42380

STELLAR MOTIONS

Source motion effects on Doppler period variations of high velocity pulsars, considering first and second time derivatives 02 p0281 A72-12309

Globular cluster NGC 6838 membership from relative proper motions 03 p0415 A72-13001

Milky Way Galaxy spiral structure determination, presenting arms anatomy, gas and star kinetics and radio astronomy data 03 p0417 A72-13104

Relative stellar orbit determination in clusters NGC 5460, 5617, 6067, 6405 and 6494, presenting gravitational potential, orbital elements and anomalous period 03 p0434 A72-13495

Stellar orbits in galactic symmetry plane, using gravitational potential theories 03 p0434 A72-13496

Precession from proper motions of stars with respect to galaxies, discussing correction for systematic errors 04 p0575 A72-15027

Stellar radial velocities observation with photoelectric spectrometer, discussing catalog errors 04 p0577 A72-15280

Galactic cluster lifetimes compared with star cluster model evaporation times, discussing general galactic and interstellar clouds tidal fields effects 05 p0713 A72-16051

Collisionless stellar dynamics, considering Lin wave interactions for orbital theory 05 p0713 A72-16053

Plasma physics collective phenomena enhancing effect on relaxation processes, emphasizing relevance to stellar dynamics [AD-739801] 05 p0714 A72-16059

Vlasov equation stability properties of collisionless plasma and stellar gas, removing energy variation difficulties with multiple water bag model 05 p0694 A72-16060

Four phase space density collisionless one dimensional stellar system evolution in time by following motion of boundary curves 06 p0876 A72-17577

Stellar motion in asymmetric galaxies with three degrees of freedom, using four dimensional surface of section mapping and stochastic measurement 07 p1034 A72-19072

Disk population F-type star photometric luminosities, motions and metal abundance indices, discussing ultrashort period cepheids 07 p1071 A72-19333

Orbital elements from radial velocity measurements for single line K giant binary star 4 Ursae Minoris 07 p1071 A72-19337

K3-M2 dwarf space motions in solar neighborhood analyzed for sun motion 07 p1073 A72-19347

Stellar dynamical and density wave theories for spiral pattern persistence in Galaxy with differential rotation 07 p1074 A72-19430

Soviet book on compact binary stellar systems with globular components covering disk darkening, eclipsing, absolute dimensions and masses, etc 08 p1229 A72-20910

Generalized many body problem of interacting finite material points motion in isolated stellar systems 08 p1237 A72-21642

Soviet papers on astronomical studies covering coordinate systems motion and stellar and celestial body position determination in solar system 09 p1388 A72-23051

Star catalogs comparison and stellar positional differences and motion studies using random field theory 09 p1388 A72-23052

Star declinations from simultaneous observations at upper and lower culminations 09 p1388 A72-23064

Markov processes in stellar dynamics, discussing relaxation and evaporation times and star velocity distribution for galactic cluster models 09 p1390 A72-23504

Membership probabilities for open cluster IC 4665 based on relative proper motions 09 p1391 A72-23531

Precessional corrections, solar motion and galactic rotation determination from proper motions by maximum likelihood method, taking into account stars visual magnitude 09 p1391 A72-23535

Cassiopeia region galactic structure study via objective prism, cataloging stars radial velocities and distances 09 p1391 A72-23539

Large Magellanic Cloud star membership, comparing Sanduleak catalog based on objective-prism spectroscopy with Fehrenbach-Duflo catalog based on radial velocities 09 p1392 A72-23547

Large Magellanic Cloud spiral structure and motion through interstellar gas, determining old and young stars spatial distribution near major spiral arm 10 p1544 A72-24662

Peculiar A stars in open cluster Tr 2 region from objective prism plate searches, showing membership by photometrical characteristics and proper motions 10 p1545 A72-24828

Secondary component of eclipsing binary beta Lyrae as massive main sequence star in rapid nonuniform motion, refuting black hole suggestion 11 p1717 A72-25869

Triple stellar system evolution and disintegration, discussing energy partitioning and initial velocity effects on stability 12 p1865 A72-27095

Vertex deviation of stellar samples in terms of reflection and galactic potential perturbation 12 p1867 A72-27212

Probability and collisional relaxation in stellar systems, discussing gravitational polarization, collective interactions and spatial inhomogeneity 12 p1872 A72-27891

Polarization and dynamical friction drags on star in uniform infinite media and flat rotation sheet 12 p1872 A72-27892

Chandrasekhar statistical stellar dynamics assumption generality compared to Chandrasekhar diffusion process, discussing discontinuous model, relaxation time, escape probability and numerical results 12 p1872 A72-27893

Galactic disk systems relaxation time due to particle encounters, discussing validity of Boltzmann-Vlasov equation 12 p1872 A72-27894

Galactic tidal field and multiple encounters role in stellar escape from star clusters, noting escape rates and kinetic energy involved 12 p1873 A72-27898

Binary evolution in star cluster models from numerical methods of direct integration, noting domination by heavy binary and double star formation and disruption 12 p1873 A72-27899

Runaway stars trajectories stability tested from clusters study, noting preservation of energy, velocity and position and reproducibility 12 p1873 A72-27900

Massless test star velocity vector deflection in stellar field from numerical integration on relaxation times 12 p1873 A72-27901

Small perturbations in collisionless stellar dynamics, discussing linear modes for flat axisymmetric galaxy and effects introduced by nonlinear theory of spiral structure 12 p1874 A72-27904

Instabilities initiation in spiral arm formation and stellar cluster evolution, noting analogy to hose-pipe instability in plasma physics 12 p1874 A72-27905

Nonsymmetrical stellar motion in galaxies, finding number of isolating integrals in systems with three degrees of freedom from four dimensional mapping 12 p1874 A72-27911

Relaxation processes enhancement by collective particle collisions effects in plasma, stressing application to stellar dynamics 12 p1853 A72-27915

Stability properties for collisionless plasma and encounterless self gravitational stellar gas described by Vlasov equations 12 p1875 A72-27916

Monte Carlo scheme for dynamical evolution of spherical star clusters, considering stellar dense core, spurious relaxation and escape 12 p1875 A72-27919

Computer models for collisionless stellar systems equations of motion, obtaining force from smoothed gravitational field 12 p1875 A72-27920

Luminosity variation of star in circular orbit around extreme Kerr black hole due to Doppler effects and gravitational field light focusing 13 p2041 A72-29416

Quasi-stationary spherical system structure model for stars of different masses with isotropic velocity distribution 14 p2149 A72-30212

Galactic astronomy - Conference, State University of New York, Stony Brook, June-July 1968, covering Galactic structure, spiral shape theories, star migration, etc 14 p2152 A72-30486

Spectroscopic binary orbital elements calculated by FORTRAN IV computer programs, considering period, radial velocity Fourier coefficients and element improvement by least squares method 14 p2159 A72-30736

Field stars near NGC 2168 /M 35/ cluster, segregating main sequence stars by proper motion dispersions with allowance for interstellar extinction 14 p2159 A72-30742

Dynamic behavior of three masses moving under mutual gravitational attraction examined by numerical experiments for binary star formation via third star hyperbolic escape 14 p2160 A72-30877

Circumzenithal instrument for latitude and longitude determination and star transits observation through almucantar 15 p2238 A72-32122

Water bag model in cylindrical rotating two dimensional rod stellar system, showing kinetic energy minimum correspondence to collisionless Boltzmann equation 15 p2315 A72-32717

Stellar velocity dispersion in elliptical galaxy NGC 7332 from coude spectrum obtained by SEC vidicon TV camera and telescope 16 p2454 A72-33453

Singularity of noncircular cross section zero velocity torus circumscribing area with three dimensional orbit of stationary stellar system star 16 p2460 A72-34014

Random gravitational encounters and the evolution of spherical systems. IV - Isolated systems of identical stars. 17 p2605 A72-34528

The equilibria and oscillations of a family of uniformly rotating stellar disks. 17 p2605 A72-34529

The rotation of close binaries 18 p2725 A72-36474

Contribution of Danjon's astrolabe to the study of proper motions 18 p2726 A72-36727

Evolution of close binary systems with intermediate initial mass ratios. 18 p2728 A72-36741

Luminosities and motions of the F-type stars. II - Metal-deficient stars. 19 p2855 A72-37238

Kinematics of faint M stars near the north galactic pole, and the mass density in the solar neighbourhood. 19 p2855 A72-37341

On the optical search for Centaurus X-3. 19 p2856 A72-37506

Least squares method for Y Cyg spectroscopic elements improvement based on radial velocity measurements, noting nonexistence of gamma velocity variability 19 p2858 A72-37809

Double system HD 175514. III - Analysis of 1968 observations 19 p2858 A72-37816

Table for reduction of stellar radial velocities to the center of the sun 19 p2859 A72-37909

Comparison of IDS Catalog double stars having determined individual motions of their components 19 p2859 A72-37917

Catalog of individual motions of stars in the open star cluster NGC 6866 and vicinity 19 p2860 A72-37918

Statistical investigations of motions and distances of planetary nebulae 19 p2860 A72-37969

Novae and background stars relative proper motions, deriving and tabulating absolute proper motions via statistical transformation 19 p2860 A72-37970

Orientation of astrophotographs in observations and measurements 19 p2802 A72-37972

Determination of the aberration constant and the coefficients of short-period nutation terms from observations by the Pulkovo polar tube during the period from 1953 to 1964 19 p2861 A72-37976

Effects of nuclear reactions on the stability of degenerate stars. 19 p2864 A72-38100

The kinematics of open star clusters 19 p2865 A72-38488

Models concerning the kinematics of star clusters 19 p2866 A72-38489

Initial results of a PM study in the Hydra ring 19 p2866 A72-38493

Structure and motions in the Carina spiral feature. 20 p2973 A72-39880

Stellar evaporation in globular clusters passing through galactic plane, considering gravitational perturbation increase of total energy within system 21 p3107 A72-41269

Stellar-statistical formulation of the problem of setting up an astronomical radial velocity system. 21 p3109 A72-41439

The kinematics of semi-regular red variables in the solar neighbourhood. 21 p3111 A72-41473

Bright red giants of the globular clusters M 3, M 5, and M 13 21 p3113 A72-41756

- Homogeneous stellar system with purely gravitational interactions, predicting oscillatory relaxation time 22 p3207 A72-42853
- Investigation of type-A star condensations in the Perseus and Cassiopeia constellations 22 p3229 A72-42951
- Quasi-stationary spherical system structure model for stars of different masses with isotropic velocity distribution 23 p3334 A72-43242
- Iterative solution for adiabatic radial pulsation in massive main sequence star, noting transition to non-linearity via Eddington stability integral extension 24 p3438 A72-44833
- Proper motions of 122 eclipsing variables 24 p3448 A72-45688
- ### STELLAR OCCULTATION
- Jupiter atmospheric hydrogen-helium mixing ratio from binary star beta Sco occultation by planet in May 1971 03 p0416 A72-13009
- Lunar limb structure from occultation traces from point source stars, constructing model with levels and slopes 03 p0420 A72-13129
- Occultation curves for optical and radio lunar occultation analysis of radio sources, considering detection and measurement of binary systems 03 p0420 A72-13130
- Seeing effects on light curve of stellar occultation by moon, calculating limitation on angular resolution 03 p0420 A72-13131
- Filters and color effects on lunar occultation of stars and appropriate deconvolution procedures 03 p0420 A72-13132
- Jupiter equatorial radius and oblateness at atmospheric level from timings of 13-14 May 1971 occultations of beta Scorpii 04 p0571 A72-14615
- Jovian atmosphere effect on photometric observations of beta Sco C occultation by Jupiter on 13 May 1971 06 p0886 A72-18153
- GX3 plus 1 identification by sounding rocket during lunar occultations, discussing magnitude 07 p1070 A72-19123
- Telescope observations of occultations of stars by outer planets, natural satellites and asteroids 09 p1387 A72-22977
- Beta Scorpii occultation by Jupiter, obtaining light curves, atmospheric scale height and stratification 10 p1548 A72-24968
- Photoelectric observation of beta Scorpii occultation by Jovian satellite Io, noting Fresnel diffraction effects 10 p1548 A72-24969
- Occultation of beta Scorpii by Jupiter and Io to determine Jovian equatorial radius and oblateness 10 p1548 A72-24970
- Lunar occultations of IRC plus 10216 for IR radiation distribution, deducing model of late type carbon star surrounded by thermally reemitting dust shell 11 p1721 A72-26123
- Flash symmetry observed during fading and brightening of beta Scorpii A in occultation by Jupiter 12 p1868 A72-27297
- Jupiter occultations of multiple star beta Scorpii and Io close approach to beta sub 2 Sco 12 p1871 A72-27757
- Occultations of stars by Jupiter 17 p2607 A72-34751
- Density of the solar corona from occultations of NP 0532. 19 p2855 A72-37242
- Occultation of beta Scorpii by Jupiter on May 13, 1971. 19 p2859 A72-37890
- Faraday rotation of linearly polarized radio waves from the Crab Nebula by the solar corona. 21 p3109 A72-41327
- The occultation of beta Sco by Jupiter. 24 p3436 A72-44699
- The determination of the diameter of Io from its occultation of beta Scorpii C on May 14, 1971. 24 p3436 A72-44700
- Observation of the occultation of beta Sco C by Io. 24 p3436 A72-44702
- Upper limits for an atmosphere on Io. 24 p3436 A72-44703
- ### STELLAR RADIATION
- #### NT STELLAR WINDS
- Centaurus A NGC 5128 nucleus IR radiation measurement, suggesting small nonstellar core superposed on extended reddened stellar component 01 p0132 A72-11091
- Galactic IR astronomy, discussing findings on emission from H II regions of Orion Nebula and late and early type stars 02 p0276 A72-11643
- Stearable vhf/uhf receiving antennas stellar calibration error analysis, obtaining worst-case uncertainty of 0.4 db by monitoring antenna gain-to-noise temperature ratio 02 p0175 A72-12161
- Interferometric photoelectric scans of interstellar Ca I 4226 line for stars with interstellar Ca II K-lines, discussing deduced electron densities 02 p0280 A72-12197
- B and Be type stars intrinsic polarization, considering UVB spectra and effects on observed polarization 02 p0283 A72-12628
- Reflection nebulae genetic relationship to illuminating stars from catalogs based on Palomar Observatory Sky Survey 02 p0284 A72-12639
- Diffuse reflection of point source /flare/ light emission for cold dwarf star semiinfinite plane parallel atmosphere, calculating polarization 02 p0285 A72-12831
- Electromagnetic emission from pulsar with magnetic force tube on surface of magnetosphere treated as rotating magnetic multipole 02 p0285 A72-12833
- Galactic disk component of diffuse X radiation from unresolved red dwarf flare stars 03 p0408 A72-12993
- Stellar X ray emission polarization measurement using Thomson scattering polarimeter [AD-736550] 03 p0353 A72-13041
- Monochromatic radio emission from decilight years distant stars, discussing search experiment by low noise multichannel receivers 03 p0436 A72-13827
- Pulsar model, discussing polar radiation diagram formation with source motion around neutron star 04 p0573 A72-14903
- Circular polarization change with wavelength in white dwarf Grw plus 70 deg 8247 04 p0580 A72-15367
- Astrophysics of interstellar medium, discussing direct and indirect observations including 21 cm H lines and starlight extinction and polarization 04 p0581 A72-15622
- D-2B satellite mission, describing attitude, orbit and experiments on zodiacal light, stellar radiation and anisolar data 04 p0583 A72-15689
- Young cluster NGC 2264 stellar radiation flux measurements, suggesting surrounding circumstellar shells producing observable IR excesses 05 p0720 A72-16716
- Interstellar extinction curves for stellar far UV radiation, discussing required multicomponent interstellar dust model 05 p0720 A72-16717
- Isolated pulsar or neutron star upper mass limit based on consideration of rotational energy by ejection of low energy cosmic rays or photons 06 p0891 A72-18508
- X ray power density spectrum observation of pulsars, detecting Crab Nebulae pulsar radiation 07 p1080 A72-20051
- Annual variations of calibration factors of star pyranometers for copper-constantan and nichrome-constantan thermocouples 07 p0991 A72-20450
- Cyclotron magnetoacoustic wave generation by planets and binary stars in circular orbits, deriving interstellar gas density variations 08 p1231 A72-21122
- Wolf-Rayet stars identification in spiral galaxy M33 (NGC 598) from narrow band interference filter photographs, tabulating apparent magnitudes and emission indexes 09 p1382 A72-22281
- Hydrogen cloud structure of interstellar medium, assuming UV star Stromgren sphere radiation effects 09 p1390 A72-23526
- Cygnus Loop supernova remnant X ray emission structure from sounding rocket spectral data, showing thermal emission mechanism 09 p1378 A72-23699
- High density models for ambient gas of eta Carinae star from X ray observations 10 p1530 A72-24947
- Stellar OH radical emission amplification by maser effect raising low energy molecules to high energy by pumping 14 p2110 A72-30578
- Stellar radiation and gravitational effects on neutral atoms and dust grains at large distances for various spectral type stars in schematic evolutionary galaxy 14 p2158 A72-30735
- Stellar UV radiation spectral energy distribution investigation of stellar composition and atmosphere and interstellar gas, discussing observation restriction by earth atmosphere absorption 15 p2302 A72-31284
- Fuor luminosity phenomena due to thermal corpuscular radiation emitting energy sources 15 p2304 A72-31330
- B type main sequence star absolute energy flux envelope from ground based and OAO 2 observations, comparing with model atmosphere prediction 15 p2311 A72-31997
- Report to COSPAR on Netherlands space research covering solar and stellar radiation, cosmic gamma and X rays, photometry and satellite geodesy 15 p2338 A72-32010
- Eclipsing binary WZ Sge observation for light curves with 3-sec time resolution, noting amplitude variation similarity to other cataclysmic variables 15 p2314 A72-32368
- Pulsar pulse broadening due to multiple scattering by interstellar medium, finding exponential decay time constant relation to rms broadening of angular size 16 p2457 A72-33686
- Thermal X ray sources associated with rotating collapsed stars, discussing Scorpio X1 plasma shell heating mechanism 16 p2460 A72-33924
- Pulsars radiation mechanism relationship to magnetospheric conditions, considering optical, X ray and gamma radiation 16 p2460 A72-33928
- Stellar X ray emission flux calculation for UV Ceti flares, using similarities between solar and stellar flares 16 p2450 A72-34161
- Soft X-rays from Cygnus X-2 and from Cygnus X-1 in eclipse/. 17 p2600 A72-35297
- Consequences of the Stromgren's theorem for radiative envelope stars. 18 p2728 A72-36760
- Radiative opacity and calculation of stellar models 18 p2728 A72-36766
- The measurement of polarized 10-micron radiation from cool stars with circumstellar shells. 19 p2854 A72-37232
- Energy variation curves for direct flare radiation and reflection from eruptive star atmosphere, discussing color variations 19 p2858 A72-37808
- Unsteady hydrodynamic accretion on a neutron star 19 p2862 A72-38053
- Nuclear energy sources in overdense celestial bodies 19 p2862 A72-38061
- Design and testing of a nine-channel photometer 19 p2804 A72-38500
- A preliminary model for the shell ionization of the nova RS Ophiuchi. 19 p2866 A72-38504
- Non-thermal bremsstrahlung of fast electrons and flare of stars. 20 p2974 A72-39894
- Stratification of the emission in the envelope of a Wolf-Rayet type eclipsing binary V444 Cyg 21 p3113 A72-41759
- Double star components light aberration dependence on relative velocity of source and observer, considering two reference systems 22 p3225 A72-42458
- Calculation of stellar and diffuse radiation for a plane-parallel semiinfinite model of the Galaxy 23 p3338 A72-44027
- Book - Dimensional analysis and group theory in astrophysics. 23 p3341 A72-44500
- ### STELLAR REFRACTION
- #### U ATMOSPHERIC REFRACTION
- #### U STELLAR RADIATION
- ### STELLAR ROTATION
- #### NT SOLAR ROTATION
- Pulsar nature and radiation mechanism, examining rotating neutron stars structure and atmospheric dynamics 01 p0131 A72-10973
- Variational solutions of nonlinear free boundary integrodifferential Euler equations for rotating star models 02 p0252 A72-12540
- Rotating star global axisymmetric dynamic stability, deriving local criteria by variational principle 03 p0417 A72-13021
- Pulsar theory, discussing rotating neutron star principle, kinetic energy, structure, atmosphere, radiation mechanics and supernovae remnants 03 p0417 A72-13103
- Rotating relativistic stellar models, covering coordinate systems injection energy, convection, red shift, external gravitational waves and black holes 03 p0426 A72-13269
- Electromagnetic pulsar models features and predictions, using rotating neutron stars with strong dipolar magnetic fields 03 p0437 A72-13873
- Relaxation time estimation for electron velocity relative to dilute vortex core array in rotating neutron superfluid, applying to pulsar slowdown rate 04 p0571 A72-14590
- Slowly rotating F, G and early K field stars data, computing Li abundance and isotope ratio 04 p0578 A72-15316
- Cyg X-1 type X ray sources evolution, discussing white dwarf and supernovae stages, parent mass and angular momentum 04 p0568 A72-15508
- Tesseral equilibrium shapes of rotating neutron stars emitting gravitational radiation pulses 05 p0719 A72-16602

Stationary stars rigid and differential rotation angular velocity limits, showing analogous conditions in general relativity

06 p0882 A72-18001

Pulsar dynamics and electrodynamic for power derivation from rotational energy, discussing toroidal magnetic field induced nonhydrostatic stress in neutron star

07 p1068 A72-19001

Pulsar rotation and dispersion from polarization and pulse arrival time observations, calculating magnetic field components in path to pulsars

07 p1072 A72-19343

Variational principle in equilibrium and stability theory of rotating bodies under magnetic and thermal fields, explaining spiral branch number in galaxies

07 p1077 A72-19806

Pulsars suggested as rotating neutron stars based on collapsed star magnetic field strength, mass-radius relation and radio flux emission

07 p1080 A72-20055

Pulsar model based on neutron star rotation with skew magnetic field, considering radiated particle acceleration responsible for high energy activity in supernova remnants

07 p1080 A72-20057

Magnetosphere theory of pulsar electrodynamic, discussing uniform inductor with iron sphere having uniform magnetization parallel to rotation axis

07 p1080 A72-20058

White dwarfs rotation parameters relation to angular velocity within general relativity compared to analogous calculations in Newtonian theory

08 p1234 A72-21284

Stability solutions of collective oscillations of spherical star cluster rotating in near circular orbits in self consistent field

08 p1239 A72-22180

Black body X ray sources creation due to neutron stars rotational energy dissipation by strain hysteresis in crust

09 p1382 A72-22284

Spiral density waves in galactic model with differentially rotating interstellar gas and stars, deriving dispersion equation by frequency to wave numbers relation

09 p1384 A72-22517

Landau instability effect on density waves propagation in self gravitating disk of differentially rotating and nonrotating stars populations, noting radial flow of matter

09 p1384 A72-22518

Quasar rotation and pulsation periods within pulsar models, postulating supermassive stars /one million-one billion solar masses/ as energy sources

09 p1385 A72-22536

Rapid rotation effect on weak and intermediate strength early type stellar radiation spectral absorption lines

09 p1390 A72-23527

Gravity darkening effects on rapidly rotating B stars He I and Mg II spectral lines

09 p1391 A72-23530

Magnetic field generation problem in rotating relativistic star for barotropic medium

09 p1391 A72-23537

Binary stars convective zones reaction to periodic gravitational fluctuations due to stellar revolutions asynchronism, using incompressible fluid plane layer model

10 p1543 A72-24631

Mu Cephei light polarization explanation, deriving spatial orientation of rotational axis and rotation period

10 p1546 A72-24832

Relativistic counterpart of Poincare condition for angular velocity of rigidly rotating star, discussing equilibrium disturbance effects

10 p1549 A72-25058

Pulsar speed increase mechanism as metastable flow state transition in neutron star superfluid core

11 p1724 A72-26705

Structural and integral parameters for rotating stellar configurations within Newton gravitation theory, giving equations for gravitational potential, outer surface geometry and multipole moments

13 p2035 A72-28677

Rotating neutron stars stability and radial pulsations by energy method, allowing for relativistic effects

15 p2304 A72-31335

Rotating white dwarfs and neutron stars quasi-radial pulsations frequencies, discussing central densities critical values

15 p2304 A72-31336

Shell formation during star collapse due to rotational instability, discussing relativistic effects

15 p2305 A72-31337

Flare mechanism of pulsar radiation near magnetic poles of rotating neutron stars

15 p2298 A72-31627

Radiative stellar envelopes circulation velocity calculation for various cylindrical rotation laws using perturbation method

15 p2314 A72-32371

Stellar magnetic oblique rotator internal motion field construction by perturbation technique estimating energy dissipation and turbulent viscosity

16 p2458 A72-33721

Stellar MHD, discussing strongly magnetic stars identification and slow rotation origin based on oblique rotator model

16 p2460 A72-33923

Thermal X ray sources associated with rotating collapsed stars, discussing Scorpio X1 plasma shell heating mechanism

16 p2460 A72-33924

Stellar evolution and rotation data acquisition from photometric analysis of B-F main sequence stars, considering different models for rotating atmospheres

16 p2462 A72-34184

Meridian circulation with rapid differential rotation in radiative stellar envelopes.

17 p2605 A72-34532

Field variations of perfect fluid in axisymmetric stationary universe within general relativity theory concept, noting energy extremal properties for rotating stars

17 p2607 A72-34921

Vibrational stability of supermassive stars stabilized dynamically by a uniform or differential rotation

17 p2613 A72-35461

Variational principle in equilibrium and stability theory of rotating bodies under magnetic and thermal fields, explaining spiral branch number in galaxies

17 p2617 A72-35730

Fluid dynamics of convective stellar envelopes.

17 p2618 A72-35933

Stability solutions of collective oscillations of spherical star cluster rotating in near circular orbits in self consistent field

18 p2724 A72-36236

The rotation of close binaries

18 p2725 A72-36474

Rotational velocities of Ap stars.

19 p2855 A72-37237

Linear pulsations and stability of differentially rotating stellar models. I - Newtonian analysis. II - General relativistic analysis.

19 p2855 A72-37247

Density wave detection by local hydrogen gas and young stars radial velocities comparison with Lin theory of galactic spiral structure

19 p2866 A72-38494

Coude spectra, abundance ratios and radial and rotational velocities of He rich stars, using microphotometer equivalent width tracings

19 p2866 A72-38502

Slowly rotating relativistic stars. VI - Stability of the quasi-radial modes.

20 p2966 A72-38909

Tidal perturbation of the non-radial oscillations of a star.

20 p2974 A72-39895

Russian book - Large-scale motions in the convective zones of stars and large planets.

21 p3104 A72-40462

VLF electromagnetic radiation frequency observation for pulsar pulsation or rotation period

21 p3111 A72-41485

Differential rotation of polytropic stellar models by structural equilibrium equations, disproving Porfiriev theory

21 p3114 A72-41775

Spectral variabilities of magnetic peculiar A stars associated with atmospheric chemical composition anomalies, using inclined rotator model

23 p3335 A72-43297

Slowly rotating axisymmetric star gravitational collapse derivation from general relativistic hydrodynamic and gravitational field equations formulated under Bondi-Sachs coordinate condition

23 p3335 A72-43488

Transfer equations for stellar systems

23 p3338 A72-44035

Accretion disc models for compact X-ray sources.

24 p3435 A72-44828

STELLAR SPECTRA

NT SOLAR SPECTRA

Empirical model with near IR spectra from expanding circumstellar envelope, normal pulsating atmosphere, shock front and relaxation layers and expanding radiative cooling layer

01 p0128 A72-10791

Spectral analyses of Mira-type variable stars near light maximum, discussing empirical curve of growth, Doppler velocity, damping constant and electron pressures

01 p0129 A72-10792

CH Cygni spectrum analysis in activity phase, discussing blue continuum, emission and UV absorption lines, radial velocity and stratification effects

01 p0131 A72-11008

Calibrations consistency of UBVY beta and GNMKFM photometries of binary stars with G or K giants and A or F main sequence components

01 p0132 A72-11014

IR radiation variability from circumstellar grains around carbon-rich supergiant R Coronae Borealis, noting spectrum similarity to black bodies

01 p0121 A72-11093

IR point source Becklin star spectrum consistent with highly reddened early-type supergiant with weak absorption masked by low resolution

01 p0133 A72-11094

He emission line star G61-29, discussing spectral features and proper motion limits on maximum distance

01 p0133 A72-11095

Pulse widths formed by relativistic beaming pulsars effect on emission spectra

01 p0133 A72-11130

Eta Carinae model with IR spectrum details described by compact H II region photoionized by hot massive star radiation

02 p0277 A72-11688

Soviet book on cool carbon stars covering spectral features, atmospheric composition and temperatures

02 p0281 A72-12296

Periodicities from power spectrum analysis of light curve of RR Tauri variable

02 p0281 A72-12302

X ray rocket observations of time variation of SCORPUS X-1 energy spectrum and optical luminosity at 2-20 keV

02 p0281 A72-12307

Line spectrum of Of star zeta Puppis at 3150-8600 A, comparing absorption spectrum to 9 Sgr

03 p0416 A72-13014

High resolution UV stellar spectroscopy in star stabilized Skylark rocket vehicle, using Cassegrain echelle optics and image intensification

03 p0354 A72-13056

Pulsar observation data, presenting period histogram, intensity, shape and polarization variations, position distribution, physical nature and spectra

03 p0417 A72-13102

Space observation of stars and interstellar medium, considering stellar energy distributions and line spectra, interstellar absorption lines, galactic nebulae and X ray sources

03 p0420 A72-13122

Magellanic Clouds supergiant stars intrinsic colors, observing in five spectral bands to separate from Galactic foreground stars

03 p0425 A72-13260

Eclipsing variable star EQ Taurus photoelectric brightness variation observations in B and V light

03 p0433 A72-13488

Red, blue and color anomalous rare carbon stars properties determination from comparative analysis of R-N and C classifications

03 p0433 A72-13490

Differential line shifts in spectrum of supergiant beta Ori attributed to radial spreading of stellar atmosphere

03 p0436 A72-13810

Linear polarization of pulsar PSR 22 18 plus 47 radio emission pulses, attributing periodic fine structure of spectrum to rotation of polarization plane in interstellar medium

03 p0436 A72-13824

Soviet book on long period variable stars covering spectral data photometric characteristics, spatial and kinematic properties, absorption effect and evolution

03 p0439 A72-14224

Wolf-Rayet type stars emission line variations from outer convective zone opening and matter ejection

03 p0439 A72-14243

Abundance ratios in quasar PKS 0237-23 from absorption spectrum measurements and explosive nucleosynthesis calculations

04 p0570 A72-14526

Curve of line width correlation application to alpha Orionis OH lines, determining atmospheric turbulence and thermal velocities

04 p0571 A72-14558

Astrogenic and planetogenic environments characteristics examination for stellar spectral classes effect on intelligent life evolutionary pace and existence probability

04 p0573 A72-14887

F and early G dwarf stars atmospheric models and line data, deriving temperatures, abundances and gravities

04 p0577 A72-15282

Early type supergiant far UV spectrum observations, showing broad absorption feature near 1720 A

04 p0578 A72-15315

Slowly rotating F, G and early K field stars data, computing Li abundance and isotope ratio

04 p0578 A72-15316

Photometric standard star 29 Piscium abundance analysis with flux constant hydrogen line blanketed model atmospheres

04 p0578 A72-15317

Pulsar CP 0328 wideband rf spectrum long term periodicity, considering origin during propagation through interstellar medium

04 p0580 A72-15369

- X ray and gamma astronomy, discussing old and blue stars, supernova remnants, radio galaxies, quasars and pulsars 04 p0582 A72-15687
- Digital data reduction techniques for stellar spectrograms, discussing digital noise smoothing for SNR improvement 05 p0632 A72-15762
- UBV magnitude measurement for stars in open clusters NGC 6613 and 6716, determining spectral classes, absorption and distances 05 p0712 A72-15768
- Interstellar dust distribution, nature and physicochemical and dynamic evolution, discussing star and galaxy observation, light diffusion, star reddening and IR sources 06 p0882 A72-17995
- Flare spectra of AD Leo during strong burst, comparing Balmer discontinuity and line widths with UV Cet stars 06 p0883 A72-18020
- Temperature scale for classifying spectra of peculiar and metallic line stars 06 p0883 A72-18021
- Early type stars photoelectric spectra obtained with Mariner 9 UV spectrometer, obtaining resonant line features and spectral energy distribution 06 p0890 A72-18347
- Radio sources sky survey with radio telescope, discussing 5C1 and 5C2 spectral distributions 07 p1069 A72-19074
- MHz IR/OH sources, discussing M type Mira variables or M supergiants photospheric temperature and dust shell structure 07 p1069 A72-19075
- Southern globular clusters (NGC 6362 and NGC 6752) photometric standards, stellar photographic and color-magnitude diagrams 07 p1069 A72-19076
- F and G dwarf stars synthetic spectra and colors computation from chemical abundance, Doppler broadening velocity and damping constant 07 p1071 A72-19181
- Classification-dispersion spectrograms of early decline of Nova Serpentis 1970, discussing diffuse enhanced absorption system behavior 07 p1071 A72-19338
- Astronomical IR spectroscopy of Alpha Ori, discussing OH line formation, LTE, rms turbulence velocity and abundance 07 p1072 A72-19345
- Zeta Orionis spectra at 922-1453 A from rocket spectroscopy, matching lines with stellar atmosphere models 07 p1072 A72-19346
- High temperature black body model based on induction heating of graphite crucible, noting application to stellar energy spectral distribution determination 07 p0991 A72-20404
- Zeta Puppis visual line spectrum discrepancy from non-LTE stellar atmospheres models, necessitating hydrostatic equilibrium deviations consideration for temperature derivation 08 p1232 A72-21178
- Semiregular variable CH Cygni observations from 1967 to 1969 with continuous spectrum variations comparison to monochromatic brightness changes 08 p1233 A72-21278
- Local interstellar hydrogen survey from OAO-2 observations of Lyman alpha absorption at 1216 A for B2 or earlier stars 08 p1235 A72-21392
- Stellar atmosphere UV spectral line broadening by electron collision, radiative and classical damping 08 p1237 A72-21750
- Non-LTE atmospheric model calculations for H, He I and II spectra of O stars, discussing He abundances 08 p1239 A72-21949
- Spectral types and magnitudes of O and WC stars of binary gamma Velorum system 09 p1382 A72-22282
- Long period Cepheids in galactic spherical component, confirming two groups according to spectral characteristics 09 p1384 A72-22514
- Rapid rotation effect on weak and intermediate strength early type stellar radiation spectral absorption lines 09 p1390 A72-23527
- Gravity darkening effects on rapidly rotating B stars He I and Mg II spectral lines 09 p1391 A72-23530
- Cygnus Loop supernova remnant X ray emission structure from sounding rocket spectral data, showing thermal emission mechanism 09 p1378 A72-23699
- Galactic nuclei evolution and stellar content models from nearby stars spectral synthesis 10 p1533 A72-23895
- UBVr colors of supergiants as function of radiation pressure, sphericity, microturbulence and effective temperatures 10 p1542 A72-24609
- Statistical equilibrium analysis of fluorescent Fe I emission in long period variables 10 p1542 A72-24610
- Ca II K line profiles in front of distant OB stars, using pressure scanned Fabry-Perot interferometer and coude spectrograph 10 p1542 A72-24616
- Interferometric photoelectric scans of interstellar Ca K lines in stellar spectra, noting interstellar Na lines presence 10 p1544 A72-24663
- Photoelectric UVB photometry for galactic cluster NGC 7039 region stars, discussing MK spectral classifications and peculiar A stars 10 p1545 A72-24827
- Stellar absorption spectral line fineness indication for cold interstellar molecular clouds between observer and star 10 p1546 A72-24848
- Stellar spectra differential analysis from solar curve of growth for Fe I with revised gf-scale, noting van der Waals broadening and microturbulence 10 p1547 A72-24868
- Simultaneous observations of radio flares from beta Persei on 25-25 January 1972 at 2.8, 3.7 and 11.1 cm, noting spectral characteristics difference from quasi-steady component 10 p1547 A72-24945
- Photoelectric scans of M supergiant alpha Ori and carbon stars from 3400 to 11,000 A, obtaining dominant spectral features 10 p1548 A72-24967
- R Coronae Borealis type variable stars spectral, IR and polarimetric studies, outlining common features and hypotheses for phenomenon explanation 10 p1549 A72-25055
- T Tauri type variable stars spectral features relation to evolutionary sequences, noting stellar atmosphere nonthermal equilibrium plasma region effects 10 p1549 A72-25056
- WR hot stars CIII, NIV and OV emission spectra structure associated with excitation of 2pn and pd ion configurations 10 p1549 A72-25169
- Short period RR Lyrae variables, presenting light curves in UVB system 10 p1550 A72-25198
- Paschen beta emission line equivalent width variation in IR spectra of omicron Ceti 11 p1716 A72-25679
- Lick observatory image-dissector scanner for faint astronomical spectra, describing design and performance of system based on individual photon pulse counting and memory storage 11 p1631 A72-25691
- Flare spectra of AD Leonis during strong burst, comparing Balmer discontinuity and line widths with UV Cet stars 11 p1718 A72-25956
- Temperature scale for classifying spectra of peculiar and metallic line stars 11 p1718 A72-25957
- Abundance in cold stellar atmospheres, noting effect on atmospheric thermal stratification and energy transfer from molecular spectra 11 p1722 A72-26432
- HD 4180 shell H lines width variations comparison with Be stars, noting thirty year period emission decrease followed by outer shell absorption 12 p1867 A72-27213
- Diatomic carbon negative ion search in HD 201626 and solar spectra, noting rotational lines coincidence with absorption features 13 p2038 A72-29010
- High resolution observations of UV stellar spectra by ESRO-borne spectrophotometer, emphasizing Mg II lines 14 p2150 A72-30370
- Quasar color indices and redshift correlation, using catalog data on U, B and V colors 14 p2150 A72-30371
- Model for hot stars mass outflow due to gas acceleration by radiation absorption in UV resonance lines 15 p2305 A72-31341
- UV stellar spectra observation with orbiting stellar spectrophotometer aboard ESRO TDIA satellite, noting Mg II lines 15 p2308 A72-31927
- Cosmic background radiation temperature from interstellar CN band R branch absorption line in star zeta Ophiuchi spectrum 15 p2313 A72-32309
- Alpha Lyra and beta Cen spectrograms by Orion observatory onboard Salyut space station, noting veiled and overexposed photographic films 15 p2316 A72-32742
- Early B stars with normal helium abundances and small rotational velocities, deducing gravity from H lines and ESW stark broadening 15 p2316 A72-32751
- K2 III star Arcturus UV chromospheric emission line spectrum observation with rocket-borne spectrometer, identifying hydrogen L alpha and O I 16 p2453 A72-33136
- Emission line star WRA 795 as optical counterpart of Cen X-3 occulting binary system 16 p2456 A72-33474
- Pulsars 0950 plus 08 and 1133 plus 16 flux density spectra measurements at 1.4-5.0 GHz, noting equivalent continuum break 16 p2456 A72-33477
- Spectral characteristics of hot stars with emission lines, discussing Ba, Of, P Cygni, Wolf-Rayet and B type supergiant stars 16 p2462 A72-34183
- Carbon 12/13 isotope ratio measurement for interstellar ionized CH molecules toward stars with strong interstellar lines 17 p2604 A72-34524
- A recalibration of the absolute magnitudes of supergiants. 17 p2609 A72-35115
- Discoveries on southern objective-prism plates. III - Three new hydrogen-deficient stars and a bright B-type subdwarf. 17 p2609 A72-35116
- Minimum-light spectra of nine M-type variable stars. 17 p2610 A72-35118
- Narrow-band photoelectric photometry of the peculiar Wolf-Rayet eclipsing binary CV Serpentis. 17 p2617 A72-35732
- The helium abundance in thirty-three main sequence B stars. 18 p2726 A72-36726
- Changes in the spectrum of the star Be HD 217050 18 p2727 A72-36733
- Pm existence evidence for HR 465 from analysis of Pm II spectral line data 18 p2727 A72-36738
- Rotational velocities of Ap stars. 19 p2855 A72-37237
- Luminosities and motions of the F-type stars. II - Metal-deficient stars. 19 p2855 A72-37238
- The colour-magnitude diagram of the globular cluster NGC 7099. 19 p2855 A72-37343
- The primary spectrum of the eclipsing binary LR Centauri. 19 p2856 A72-37505
- Early data from the ultraviolet sky-scan telescope in the TDI satellite. 19 p2857 A72-37524
- Astronomical observations supporting stellar atmosphere microturbulence concept, noting Cepheid variables high dispersion spectra, supergiants irregular changes and microturbulence hydrodynamic effect 19 p2857 A72-37525
- Spectrophotometric investigation of Ap stars. I - Two-dimensional quantitative spectral classification 19 p2858 A72-37813
- Spectrographic and photometric observations of supergiants and foreground stars, in the direction of the Large Magellanic Cloud. 19 p2858 A72-37855
- Early star absolute magnitude from equivalent H gamma and delta line widths and Balmer hydrogen series line 19 p2859 A72-37908
- Standard iron wavelengths for determining the radial velocities of stars 19 p2859 A72-37910
- Study of the spectrally variable silicon Ap star 56 Ari 19 p2862 A72-38055
- Secular stability. I - A Population I star near the main sequence. 19 p2864 A72-38099
- Coude spectra, abundance ratios and radial and rotational velocities of He rich stars, using microphotometer equivalent width tracings 19 p2866 A72-38502
- Balloon-borne UV spectrophotometer observation of Mg II resonance doublet at 2795 and 2802 A in stellar spectra, comparing to Ca II line widths 20 p2965 A72-38907
- Hot star with broad H lines with weak variable central emission, noting Ca II and He I 20 p2966 A72-38920
- Photometric and power spectrum observation of peculiar blue variable star, showing low amplitude high frequency luminosity oscillations, hydrogen deficiency and degeneracy 20 p2966 A72-38921
- Line formation in the presence of magnetic fields; Proceedings of the Conference, Boulder, Colo., August 30-September 2, 1971. 20 p2970 A72-39752
- Stellar emission and absorption line spectra formation in presence of magnetic field interpreted by radiative transfer equation solution, considering dwarf stars observation 20 p2956 A72-39753
- Stellar multilevel spectral line formation solution by preconditioning procedure based on core frequency transfer determination by local saturation approximation 20 p2954 A72-39758

Line spectra and continuum polarization in magnetic white dwarfs.

20 p2971 A72-39760

On the chemical composition of epsilon Pegasi.

20 p2974 A72-39901

Pulsating variables in the Pleiades cluster.

21 p3105 A72-41032

Interstellar lines in the ultraviolet spectrum of zeta Ophiuchi.

21 p3105 A72-41035

Magnetic-field variations in 78 Virginis, beta Coronae Borealis, and 73 Draconis.

21 p3106 A72-41036

Oxygen abundances of three population II horizontal-branch stars.

21 p3109 A72-41330

The spectrum of N Del 67 and some remarks on chemical composition of the novae envelopes.

21 p3109 A72-41436

Curve of growth analysis of F star beta Cas and 10 UMa atmospheres for Ca, Sc, Ti, Cr, Mn and Ni-to-Fe abundance ratios

21 p3110 A72-41444

Spectrum of P Cygni in 1968-1969.

21 p3110 A72-41445

Frequency correlation measurement of pulsar spectral fine structure due to radio emission scattering by interstellar plasma

21 p3101 A72-41752

A spectral study of the nebula NGC 7635 and the star BD +60.2522 deg

21 p3113 A72-41755

Stratification of the emission in the envelope of a Wolf-Rayet type eclipsing binary V444 Cyg

21 p3113 A72-41759

Effect of a random magnetic field on the absorption line characteristics of stars

21 p3113 A72-41761

Red variables in globular clusters, in the galactic centre and in the solar neighbourhood.

22 p3222 A72-42135

Transuranium elements in HD 25354.

22 p3224 A72-42381

The peculiar O6f star HD 148937 and the symmetrically surrounding nebulae.

22 p3227 A72-42557

Internal dust effects on nebulae structure and spectrum, solving radiation transfer equation for spherical models with nonisotropic scattering

22 p3227 A72-42558

Spectrophotometric study of the cometary nebula NGC 2261

22 p3229 A72-42961

Physical characteristics of type I supernova envelopes during the initial expansion phase. II - Development of type I supernova spectra after maximum light.

23 p3333 A72-43228

Type II supernova spectral intensity minima due to blueshifted absorption lines of hydrogen and Fe II based on observed and synthetic spectra wavelength comparison

23 p3334 A72-43257

Spectral variabilities of magnetic peculiar A stars associated with atmospheric chemical composition anomalies, using inclined rotator model

23 p3335 A72-43297

The analysis of the small Magellanic Cloud supergiant HD 7583.

23 p3336 A72-43555

Ultraviolet absorption lines in the spectrum of Vega.

23 p3337 A72-43826

Infrared photometry of Northern Wolf-Rayet stars.

23 p3337 A72-43827

Spectrometric zonal standards - Selection of stars and methodology of their study

23 p3338 A72-44031

The influence of ultraviolet line blanketing on the neutral helium triplet lines in B-type stars.

24 p3438 A72-44834

A further high-resolution search for Fe XXV line emission from Scorpius X-1.

24 p3438 A72-44838

Orbiting telescopes improved angular resolution and access to UV spectra as advantages in determining stellar composition, mass, luminosity and distance

24 p3446 A72-45531

Spectral classification of stars with respect to non-broadened low-dispersion spectra. III - Classification method and criteria

24 p3447 A72-45678

Spectral classification of stars with respect to non-broadened low-dispersion spectra. IV - Catalog of spectra of faint stars about the NGC 2129 cluster

24 p3447 A72-45679

Stellar spectra analysis from measured truncated equivalent spectral line widths, calculating curves of growth for given truncations, source functions and absorption coefficients

24 p3447 A72-45680

Titanium oxide molecular spectrum band intensities measurement for vibrational temperature of M supergiant stars, noting atomic absorption effect on measurement accuracy

24 p3448 A72-45681

STELLAR SPECTROPHOTOMETRY

UBV photometric studies of eclipsing variable R Canis Majoris confirming primary component as F1V star, discussing ordinary semidetached system possibility

01 p0129 A72-10793

Early O and Of spectroscopic and photometric data, evaluating atmospheric properties, surface gravities and temperature scales

01 p0131 A72-11009

RR Lyrae variables intermediate band photometry, tabulating magnitudes and color of 125 stars

01 p0133 A72-11129

Six color photometry of F-G supergiants in Large Magellanic Cloud, noting color similarity with galactic stars

03 p0416 A72-13019

Magellanic Clouds bright star intermediate band photometry, discussing interstellar extinction and luminous supergiants

03 p0425 A72-13257

Interstellar absorption in Perseus OB 2 association direction from UVBY-beta photometry of early type stars in four fields

03 p0438 A72-13875

Solar chromospheric flare spectrophotometric data on 8 July 1966, presenting line spectra, ground state and populations in excited energy levels

03 p0413 A72-14242

Eclipsing variable system AW Peg spectrophotometric data, examining spectral line geometries and intensities and atmospheric conditions

03 p0439 A72-14244

Stellar radial velocities observation with photoelectric spectrometer, discussing catalog errors

04 p0577 A72-15280

Photoelectric measurements of Ca K line of southern/equatorial A stars, discussing abundance variation

05 p0712 A72-15796

Photoelectric photometry of Ca K-line for A stars of population I clusters

05 p0712 A72-15797

Photoelectric observations in different colors of eclipsing variable TX Cancri, presenting tables

05 p0723 A72-17199

UV spectrophotometry of late-type giant star /Arc-turus/ from Aerobee rocket, identifying Mg II doublet resonance line for stellar chromosphere

06 p0881 A72-17893

Observed light curve amplitude phase relations in Ap magnetic star UVB system, using oblique rotator model

06 p0882 A72-18008

Computer program for photometric orbital elements determination of eclipsing binary stars

06 p0883 A72-18022

Disk population F-type star photometric luminosities, motions and metal abundance indices, discussing ultrashort period cepheids

07 p1071 A72-19333

UBV photometry for stars near quasars and N and Seyfert galaxies, noting suitability as secondary photoelectric standards or photographic sequences for monitoring programs

07 p1071 A72-19336

M supergiants in Carina arm, discussing photometric studies at 4-18 microns, interstellar extinction uncertainties and spatial distribution

07 p1072 A72-19344

Fabry lens application in stellar photometry, describing technique of image construction on photomultiplier tube cathode

07 p0985 A72-19419

Unstable binary RW Aur spectrophotometric study with stellar evolution and outer atmosphere implications, relating Balmer continuum to UV excess

08 p1233 A72-21277

Spaceborne Uvicorn/Telescope astronomical observatory for stellar UV TV pictures, discussing system design requirements

08 p1170 A72-21958

Metal lines and dwarf stars study by photoelectric photometry based on narrow passbands

10 p1538 A72-24230

OB star distribution in Puppis from UVB and H beta photometry, noting correlation with hydrogen concentration

10 p1542 A72-24615

Spectrophotographic analysis of K-type supergiant epsilon Pegasi for effective temperature, surface gravity and heavy and light element abundances

10 p1543 A72-24621

Blue white dwarf HL Tau-76 rapid variations, suggesting underlying driving mechanism from high speed three color photometric observations

10 p1549 A72-25193

Stellar photometric classification by comparing color indices to indices of standard stars with UPX-YZVS system, outlining computer method

11 p1715 A72-25294

Computed and observed color indices of intermediate band UPX-YZVS and wideband UVB photometric systems, evaluating response curve validity for parameter determination

11 p1715 A72-25295

V 1057 Cyg photometry and polarimetry, considering model with two circumstellar shells stellar flux absorption and reradiation

11 p1716 A72-25678

Calibration model for UV stellar photometer using secondary electron conduction /SEC/ vidicon

11 p1631 A72-25684

Computer program for photometric orbital elements determination of eclipsing binary stars

11 p1718 A72-25958

Russian book on eclipsing binary stars covering limb darkening law, photometric eclipsing phases, computer applications and models

11 p1720 A72-26046

Spectrophotometry of nebulosity associated Ae and Be stars, discussing age, circumstellar dust shells geometry and red stellar objects

11 p1720 A72-26114

Omega Velorum revelation as beta Canis Majoris type variable stars from photoelectric and spectrographic observations

12 p1867 A72-27207

UBV photometric properties and probability of discovery in blue light of detached close binaries models

12 p1867 A72-27214

Regional observation of atmospheric spectral transmittance by Bouguer and high/low star methods

13 p2044 A72-29650

High resolution observations of UV stellar spectra by ESO-borne spectrophotometer, emphasizing Mg II lines

14 p2150 A72-30370

Stellar photometric observations in Magellanic Clouds, presenting photoelectric sequences in UVB system, interstellar reddening and extinction data

14 p2159 A72-30737

UV stellar spectra observation with orbiting stellar spectrophotometer aboard ESO TD1A satellite, noting Mg II lines

15 p2308 A72-31927

Photoelectric photometry of binary VV Pup with 3-sec time resolution, suggesting qualitative model from eclipses identification

15 p2314 A72-32369

Sequential three color photometry of dwarf cepheid DY Pegasi, noting smooth color variation with phase

15 p2314 A72-32370

Stellar evolution and rotation data acquisition from photometric analysis of B-F main sequence stars, considering different models for rotating atmospheres

16 p2462 A72-34184

Optical observations of the supernova in NGC 5253.

18 p2726 A72-36648

Photometric study of the open cluster NGC 2232.

18 p2728 A72-36742

Near-infrared photometry of Mira variables.

18 p2729 A72-37018

The colour-magnitude diagram of the globular cluster NGC 6981.

19 p2855 A72-37342

The colour-magnitude diagram of the globular cluster NGC 7099.

19 p2855 A72-37343

Rocket-borne Cassegrain optic stellar electrophotometer for early star observations in 1300-2000 A region

19 p2796 A72-37585

Double system HD 175514. III - Analysis of 1968 observations

19 p2858 A72-37810

Spectrophotometric study of eclipsing-variable system components. I

19 p2858 A72-37811

Spectrophotometric investigation of Ap stars. I - Two-dimensional quantitative spectral classification

19 p2858 A72-37813

Determination of the spectrophotometric temperature, mean radius and mass of the star beta Cep

19 p2860 A72-37954

Colorimetric and spectrophotometric gradient systems comparison for bright stars used in automatic telescope pointing control, discussing interstellar absorption

19 p2860 A72-37955

Coude spectra, abundance ratios and radial and rotational velocities of He rich stars, using microphotometer equivalent width tracings

19 p2866 A72-38502

Photometric and power spectrum observation of peculiar blue variable star, showing low amplitude high frequency luminosity oscillations, hydrogen deficiency and degeneracy

20 p2966 A72-38921

A study of the interstellar extinction in the Carina-Centaurus region.

20 p2973 A72-39881

Physical properties of interstellar matter surrounding binary stars from astronomical spectroscopy, discussing eruptions and photometric changes

20 p2975 A72-40069

Variation of the spectrophotometric temperature from the center of the disk to the limb of stars of the spectral classes B and A

21 p3102 A72-40094

- Pressure-scanned echelle grating plus Fabry-Perot stellar spectrophotometer. 21 p3053 A72-40609
- Spectrophotometry of the Wolf-Rayet type stars HD 195765, HD 192163, and HD 192103 21 p3109 A72-41437
- Photometry of RR Lyrae variables in the globular cluster NGC 6981. 21 p3111 A72-41475
- A more accurate determination of the structural features of the instability strip of classical Cepheids from Gascoigne's photoelectric data in the Small Magellanic Cloud 21 p3113 A72-41757
- Observation procedures in high resolution spectrophotometry of solar chromospheric spectral fine structures 22 p3221 A72-42031
- Spectrophotometric study of the cometary nebula NGC 2261 22 p3229 A72-42961
- A spectroscopic and photometric study of the pulsating R Coronae Borealis type variable, RY Sagittarii. 23 p3334 A72-43255
- Giant stars iron abundance from narrow band spectrophotometric analysis and model atmospheres, isolating super metal rich stars below H-R diagram subgiant branch 23 p3334 A72-43256
- Stellar and Uranus photometric measurements for solar J/B-V/ and [U-B]/ color indices determination, using K and H delta lines and G band filters 23 p3337 A72-43615
- Infrared photometry of Northern Wolf-Rayet stars. 23 p3337 A72-43827
- Photometric elements of coparcular unstable AH Vir eclipsing binary at 4400 and 5600 Å, comparing stellar gas stream and solar chromosphere densities 23 p3338 A72-44028
- Spectral line identification computer program determining wavelength and equivalent line width for photometric measurements 23 p3267 A72-44029
- Characteristic curve formulas of cosmic objects and stellar focal images for photometric measurement processing on computer 23 p3267 A72-44030
- Spectrometric zonal standards - Selection of stars and methodology of their study 23 p3338 A72-44031
- Spectrometer for absolute stellar spectrometry 23 p3290 A72-44039
- Individual reddening laws of O-type stars. I - Computation method, first results 24 p3437 A72-44829
- ### STELLAR STRUCTURE
- Pulsar nature and radiation mechanism, examining rotating neutron stars structure and atmospheric dynamics 01 p0131 A72-10973
- Helium abundance in stellar interiors, considering mass-luminosity relations of Hyades 03 p0419 A72-13114
- Neutron star surface structure and cooling calculations for pulsar cosmic ray production through surface material acceleration 03 p0421 A72-13136
- Massive star evolution, discussing stellar structure theory uncertainties, young clusters, helium burning and evolutionary tracks 03 p0425 A72-13262
- Loop structure of Monoceros supernova remnant, predicting thermal soft X ray point source as cooling neutron star 07 p1073 A72-19421
- Energy transport within stellar structure, discussing radiative transfer and opacity relationship to mean free path of radiation 07 p1078 A72-19924
- Stellar structure calculation by real gas equation of state, considering He abundances and solar lines of ionizable metal atoms 07 p1078 A72-19925
- Neutron star properties, formation theories, crust composition and internal structure, examining interior neutron behavior, fermion systems superfluidity, magnetic field effects and stellar dynamics 10 p1533 A72-23890
- Structure of lower main sequence stars, considering ionization equilibrium in outer convection zone 10 p1546 A72-24835
- Stellar physical parameters computed from multicolor photometric data on extraatmospheric magnitudes by maximum likelihood method 11 p1715 A72-25296
- Cold static superdense model for white dwarf and neutron stars, using relativity theory and variational principles for stellar structure in hydrostatic equilibrium 11 p1715 A72-25528
- Pulsar speed increase mechanism as metastable flow state transition in neutron star superfluid core 11 p1724 A72-26705
- Thermonuclear detonation and reimplosion of dense stellar cores, studying beta-processes effect on post-detonation evolution 13 p2044 A72-29625
- Adiabatic stellar shells stability in cases of rigid and compressible nucleus 15 p2304 A72-31334
- Diffusion effects on stellar surface chemical composition, emphasizing solar atmosphere conditions 15 p2305 A72-31342
- Fluid dynamics of convective stellar envelopes. 17 p2618 A72-35933
- Supergiants internal structure, evolution and spectral characteristics, discussing instability phenomena and luminosity calibration 18 p2723 A72-35995
- Examples of multiple solutions for equilibrium stars with helium cores. 20 p2973 A72-39878
- On the influence of the opacity values on static stellar models. I - Horizontal branch stars. 20 p2973 A72-39879
- Local Vogt-Russell theorem confirmation by linear approximation for stellar structure nonlinear differential equations, discussing equilibrium model local uniqueness and stellar stability 20 p2973 A72-39888
- Two phase stellar structure with polytropic equations of state for shell and core, calculating configuration mass, radius and energy 21 p3102 A72-40098
- Numerical models for He stars structural evolution, considering main sequence models of 1-8 solar masses and different carbon enrichments 23 p3334 A72-43258
- Mixing between stellar envelope and core in advanced phases of evolution. IV - Effect of superadiabaticity in convective envelope. 23 p3335 A72-43486
- Extended horizontal branch loci. 23 p3337 A72-43830
- Book - Dimensional analysis and group theory in astrophysics. 23 p3341 A72-44500
- Luminosity variation in the one-zone Cepheid model. 24 p3438 A72-44837
- Solar oblateness and neutrino flux measurement experiments, discussing agreement with solar interior and evolution models 24 p3446 A72-45527
- ### STELLAR WINDS
- Galactic wind formation in elliptical galaxies by stellar ejected gas heating by supernovae, discussing thermally unsteady cores 02 p0279 A72-12189
- Stellar winds and breezes classification using energy flux and particles kinetic and thermal energies for criteria, noting coronal temperature effects 15 p2313 A72-32298
- An estimate of stellar wind mass loss during the red giant phase of evolution. 20 p2967 A72-39187
- Inviscid non-monatomic interstellar gas radial flow, considering gravitational and heat conducting effects in stellar winds 20 p2967 A72-39193
- Transfer of resonance-line radiation in differentially expanding atmospheres. II - Analytic solution for the case of coherence in the frame of the fluid. 21 p3106 A72-41038
- The dynamical effects of stellar mass loss on diffuse nebulae. 22 p3224 A72-42380
- ### STELLARATORS
- Plasma density profiles by microwave interferometry technique in Sirius stellerator diverter for two magnetic field configurations and injection methods 04 p0555 A72-14619
- Plasma filament equilibrium in Sirius stellerator during heating by fast magnetosonic wave 09 p1363 A72-23214
- Double helix magnetic field in longitudinal and axial current fields of stellarators, noting rotatory transformation and shear of field lines 09 p1363 A72-23217
- Star stellarator model for hot electron plasma production by steady electron beam injection in closed magnetic traps 09 p1363 A72-23219
- Density and electric field oscillations of plasma in stellarator, considering magnetic field strength effect, stabilization by ionic collisions and energy pumping mechanism 13 p2019 A72-29985
- Plasma capture by stellarator diverter magnetic field, noting stream length controllability by field pulse duration 14 p2135 A72-30168
- Purification of hydrogen plasmas by the magnetic field of an injector-diverter device 19 p2843 A72-38539
- Low beta model of collision dominated plasma flow effect on toroidal confinement, simulating Stellarator, Levitron and Tokamak 20 p2957 A72-39356
- ### STEP FAULTS
- ### U GEOLOGICAL FAULTS
- ### STEP FUNCTIONS
- Soviet book on theory of differential equations with deviating argument covering step methods, existence and uniqueness theorems, solutions stability, approximations, etc 02 p0252 A72-12124
- Avalanche pulse generator with pretrigger output for reflection coefficient and step function response measurements 02 p0195 A72-12605
- Flow separation of turbulent boundary layer ahead of inward-projecting normal step predicted by rotational flow analysis via iterative solution [ASME PAPER 71-WA/FE-32] 05 p0599 A72-15924
- Semiinfinite circular fluid transmission line transient response to step function [ASME PAPER 71-WA/FE-10] 05 p0646 A72-15932
- Metastable Fe-Cr-Ni austenitic stainless steels, demonstrating step phenomenon at elastic limit 05 p0672 A72-16011
- Linear multivariable control system state observation by sampling with arbitrary but fixed distribution of sampling instants, emphasizing dual control by step functions 07 p0961 A72-19707
- Variational solutions to linear integral equations and extremal functions in physical gas dynamics problems, using stepwise constant trial functions 08 p1150 A72-21620
- Convergence of random number sums of independent infinitesimal multidimensional stochastic step processes to generalized Poisson processes 09 p1340 A72-22423
- Static deflection effect on nonlinear spring mass system step function response, considering approximate calculation of oscillation period 11 p1688 A72-26372
- Ideal low pass filter with fastest monotonic step response to permit no signal transmission outside prescribed frequency band 11 p1605 A72-26469
- Quantization background noise during hologram approximation by step function, discussing effect on diffraction field forming reconstructed image 13 p1959 A72-29684
- Approximate periodic solutions of second order nonlinear differential equations via step function 15 p2262 A72-31553
- Signal transmission through LSI logic circuit chains, discussing time delay measurement by step function testing 15 p2211 A72-31846
- An approximate analysis of non-linear non-conservative systems subjected to step function excitation. 17 p2582 A72-35412
- Snap-off diodes for avalanche generators step pulse output rise time steepening, describing circuit diagram and time-volt-ampere characteristics 21 p3035 A72-41650
- Dynamic buckling of axially stiffened imperfect cylinders under axial impulse. 24 p3453 A72-44602
- ### STEPS
- Turbulent shear layer flow in reattachment region downstream of backward facing step and non-monotonic return to ordinary boundary layer state, noting eddy length scale decrease 10 p1468 A72-24467
- ### STEREOCHEMISTRY
- Diastereomeric S-prolyl dipeptide derivatives adaptation of gas chromatographic quantitative estimation of R- and S-leucine enantiomers 11 p1590 A72-26366
- The steric analysis of aliphatic amines with two asymmetric centres by gas-liquid chromatography of diastereoisomeric amides. 17 p2510 A72-34337
- ### STEREOGRAPHY
- ### U STEREOPHOTOGRAPHY
- ### STEREOPHOTOGRAPHY
- Air pollution circulation patterns remote sensing, describing multispectral stereo image pairs digital cross correlation [AIAA PAPER 71-1106] 01 p0067 A72-10551
- Camera slit lamp apparatus design for anterior eye diagnosis in two dimensional and stereoscopic photography and ophthalmic application 04 p0478 A72-14725
- Photogrammetric coordinate relation of points on lunar surface and stereo panoramas of scanning photographs by Luna 9 and 13 orbiters 05 p0660 A72-15832
- Pinhole, fly-eye and holographic stereogram methods, examining resolution relationships, horizontal and vertical parallax and aberrations 05 p0663 A72-16673
- Block triangulation of arbitrary terrain without point transfer, using stereo comparator 06 p0806 A72-17755

Planicart stereoplotter for map compilation and revision in photogrammetry

06 p0815 A72-17756

AS-11A stereoplotter computerized adaptation to stereo-modeling of SLAR terrain mapping

06 p0818 A72-18330

Random bias holographic technique for imaging three dimensional objects, using laser, one mirror, one diffuser and photographic plate
[AD-743777]

07 p0982 A72-19036

Semiautomatic stereophotographic processing of cosmic ray shower particle interaction data from Wilson chamber

07 p0988 A72-19865

Drobyshv stereograph corrector operation for aerial photographs processing with transformed beam of stereoprojector

09 p1308 A72-22483

Aerial stereopair photograph orientation for geodetic coordinate adjustment in terms of collinearity, coplanarity and scaling

09 p1308 A72-22486

Measurement accuracy and reliability of photogrammetric methods in stereoscopic height determinations of wooded areas

09 p1312 A72-23284

Topographical stereo map plotting apparatus with auxiliary device for orthophoto production, describing design for combined photointerpretation-cartographic applications

09 p1313 A72-23309

Visual and automatic stereometric image analysis, citing minimum measurable contrast thresholds for various devices

10 p1478 A72-23826

Viking Lander imaging experiments with stereoscopic camera system to study Martian surface and atmospheric morphology, composition and evolution

10 p1540 A72-24382

Zeiss /Jena/ stereoplanigraph design and operation to obtain purely optical projection for object reconstruction, discussing human operator replacement by objective electro-optical system

16 p2394 A72-33870

Epipolar scanning to convert image correlation from two dimensional to one dimensional task for application to photogrammetric automation

18 p2691 A72-36492

Nonholographic coherent optical correlation for automatic stereoperception.

18 p2691 A72-36493

Stereoplotting instrument concept based on image data selection independence from object space model reconstruction

18 p2691 A72-36498

A new computer-assisted stereocomparator.

18 p2664 A72-36499

The measurement of three-dimensional body movements by the use of photogrammetry.

20 p2898 A72-39806

Russian book - Stereophotogrammetric processing methods for photographs made from a mobile basis.

22 p3175 A72-42025

High resolution lunar surface stereophotographs from pairing overlapping Lunar Orbiter photographs

22 p3230 A72-43195

Scanning electron microscope stereophotographic picture synthesis from sequential holographic recording of three dimensional objects

23 p3290 A72-43904

STEREOSCOPIC PHOTOGRAPHY

U STEREOPHOTOGRAPHY

STEREOSCOPIC VISION

Neuronal mechanisms of binocular vision and space perception from tests on cats and men, discussing neurophysiological models of stereopsis

01 p0012 A72-10479

Stereopsis spring coupled magnetic dipole model of binocular stereoscopic depth perception in man

01 p0012 A72-10480

Stereoscopic depth movement perception sensitivity compared to monocular movement

02 p0169 A72-12209

Oculomotor cue-based distance perception, discussing glasses adaptation-caused accommodation and convergence changes in stereoscopic depth perception

06 p0765 A72-17414

Stereoscopic projection screens for three dimensional image display, discussing classification by diffusing properties, surface types and applications

06 p0814 A72-17440

Stereoscopic acuity for photometrically matched background wavelengths at scotopic and photopic levels, plotting variable depth error as function of retinal illuminance

10 p1425 A72-24269

Visual latencies measurement as function of stimulus luminance and adaptation state by stereoscopic null method, characterizing relationship by inverse power function

13 p1911 A72-29968

Russian book - Eye movements as the basis of spatial vision and as a model of behavior

17 p2509 A72-35459

On the apparent orbit of the Pulfrich pendulum.

18 p2653 A72-36608

Viewing stereoscopically through binocular optical systems.

21 p3054 A72-40728

On a long-term temporal aspect of stereoscopic depth sensation.

23 p3258 A72-44381

STEREOSCOPY

NT STEREOPHOTOGRAPHY

STERILIZATION

NT CHEMICAL STERILIZATION

NT SPACECRAFT STERILIZATION

Planetary quarantine microbial contamination control, considering clean room concept and microbiological barrier techniques

01 p0019 A72-10821

Spore survival in dry heat sterilization as function of water activity, indicating entropy-molecular stability relationship

04 p0475 A72-15259

Probability for spore sterilization by aerodynamic heating, considering straight line and decaying circular orbital Mars entry trajectories

16 p2461 A72-34165

STERILIZATION EFFECTS

NT CHEMICAL EFFECTS

NT CORROSION

NT DECONTAMINATION

NT DEGRADATION

NT THERMAL DEGRADATION

STERNS

U AFTERBODIES

STERNUM

Chin-sternum-heart syndrome from partial parachute failure, with close reference to atrial endocardial and myocardial lacerations

02 p0167 A72-11711

STEROIDS

NT ALDOSTERONE

NT CHOLESTEROL

NT CORTICOSTEROIDS

NT CORTISONE

NT PENICILLIN

Tobacco tissue cultures with Apollo 12 lunar material, determining endogenous sterols and fatty acids concentrations by gas chromatography and mass spectrometry

07 p0920 A72-19850

STIFF STRUCTURES

U RIGID STRUCTURES

STIFFENING

Anisotropic plate with hole stiffened at edge by thin isotropic ring, calculating thermal stress distribution

03 p0450 A72-14113

Pressurized vessel bottoms weakened by central hole with edge stiffened by elastic ring, determining stress-strain state and stress concentration

03 p0451 A72-14120

Elastic stiffener bonded to elastic half plane with different mechanical properties, reducing governing integral equation to infinite system of linear algebraic equations

[ASME PAPER 71-APM-TT] 04 p0589 A72-15182

Doubly symmetric oval ring with stiffeners pair parallel to major or minor axis, investigating stress behavior under radial load

[ASME PAPER 71-WA/DE-14] 05 p0732 A72-15941

Graphite reinforced epoxy stiffeners for variable geometry fuel tank to meet light weight requirement, discussing billet fabrication, assembly and installation

08 p1176 A72-21688

An experimental buckling study of skin-corrugated ring-stiffened curved panels.

[SESA PAPER 1993A] 17 p2630 A72-34818

STIFFNESS

Algorithms for mass and stiffness matrices synthesis from experimental vibration modes applied to cantilever beam

[SAE PAPER 710787] 01 p0137 A72-10278

Unidirectional fiber array reinforced composites with improved longitudinal tensile strength and stiffness compared with structural metals

[SME PAPER EM 71-283] 01 p0092 A72-10966

Torsional stiffness /shear modulus/ of glass fiber reinforced plastic tubes as function of filament winding angle

01 p0141 A72-10999

Finite element method extension using computer program for solving problems of elastic bodies in contact with stiffness method advantages

01 p0141 A72-11047

Thin walled prismatic structural members under uneven axial moment distribution, formulating force deflection equations for torsional-flexural behavior

01 p0141 A72-11049

Stiffness matrix method application to finite deformation theory, noting convergence through use of iterative interpolation in numerical calculations

02 p0298 A72-12667

Bending stress analysis of rectangular plate with variable stiffness applied to marine propeller blade

02 p0298 A72-12673

Complex structures mass and stiffness matrices reduction by automatic condensation, calculating lowest eigenfrequencies and eigenmodes of substitute systems

[DGLR PAPER 71-108] 02 p0299 A72-12721

Ti alloys for airframe shell construction based on room temperature strength, stiffness and densities comparison with Al alloys, stainless steel and Be data

03 p0373 A72-13615

Fiber flexural stiffness determination from bending moment and deflection relation, using bend test

03 p0365 A72-14300

Multipurpose optimal design of elastic structures with piecewise uniform cross section for load states and prescribed stiffness by energy methods

[AD-743418] 03 p0455 A72-14386

Plastic deformation and elastic stiffness of refractory metals, discussing impurities, alloying, temperature, work hardening, strain rate and texture effects

06 p0822 A72-18519

Book on matrix structural analysis covering matrix algebra concepts, direct stiffness matrix methods, lifting surface, nonlinear truss and structural partitioning analysis, etc

07 p1092 A72-19908

Transfer matrix and dynamic stiffness techniques application to critical speed analysis in rotating machinery

08 p1224 A72-22128

Predictor-corrector method for stiff linear differential equations, considering truncation error estimation and system stability

11 p1675 A72-25272

Distributed elastic system discrete model mass, stiffness and damping matrices derivation from dynamic test response data

[AIAA PAPER 72-346] 11 p1728 A72-25375

Stiffness, stress and deformation analysis of discretely attached corrugated shear webs, using minimum potential energy and calculus of variations methods

[AIAA PAPER 72-351] 11 p1728 A72-25380

Thermoplastic polypropylene sandwich molds stiffness variation with time, noting three point bending and creep tests

11 p1673 A72-25550

Composite materials fabrication, emphasizing high strength/stiffness to weight ratio as critical performance requirements

12 p1815 A72-28082

Brittle continuous and crazed anodic oxide coating-effect on Al filament stiffness, comparing with Dow analysis

13 p1974 A72-28666

Infinite plane plates sound radiation due to bending waves interactions with density and stiffness fluctuations in material

13 p2004 A72-29094

Crystalline polymers behavior as multiphase composite solid, calculating supermolecular structures effects on stiffness properties

14 p2163 A72-30181

Stability of compressed elastic rod with continuously varying stiffness, deriving solution via influence function

14 p2166 A72-30691

Finite element displacement field with internal equilibrium application to nine degrees of freedom triangular bending element stiffness matrix calculation

14 p2168 A72-30930

Compressive strength and stiffness improvement for crystalline thermoplastic polymers via solid glass sphere reinforcement

16 p2414 A72-33370

Bending of skew plates of variable rigidity.

17 p2626 A72-34329

Monograph - The finite-element method in plate bending analysis

17 p2634 A72-35547

Contribution to the theoretical calculation of sandwich structures with tube core

18 p2736 A72-36939

Buckling of elastic bars with varying stiffness and nonideal boundary conditions.

21 p3118 A72-40932

Cylindrical shells of optimal torsional stiffness

22 p3233 A72-42112

Simple thickness modes for laminated composite materials.

22 p3235 A72-42465

Iteration process convergence improvement based on stiffness change expression as linear combination of two matrices in structural reanalysis

22 p3235 A72-42602

Elastic stiffness and ductility of refractory materials of long service life, noting creep diagrams and tensile strength

23 p3301 A72-43959

A method of computing numerically integrated stiffness matrices.

24 p3457 A72-44878

Wave propagation in a thin hollow cone by a finite element method.

24 p3458 A72-44886

STIGMATISM
Field compensated Michelson spectrometer systems, discussing tolerances, usefulness, resolution luminosity products, stigmatism and astigmatism 09 p1313 A72-23328

STILBENE
Stilbene scintillator detector for gamma ray spectrometry in energy range 0.5-5 MeV, separating gamma rays from neutrons by pulse shape discrimination technique 03 p0408 A72-13031

STIMULANT
NT CENTRAL NERVOUS SYSTEM STIMULANTS
NT NORADRENALINE
NT NOREPINEPHRINE
Work capacity evaluation from fatigue, biological rhythm, tissue respiration and oxygen consumption studies, discussing pharmacological stimulation effects 14 p2078 A72-30376

STIMULATED EMISSION
Laser produced spark plasma, calculating threshold conditions for onset of stimulated scattering process and self focusing 04 p0559 A72-15346
Stimulated Raman emission in glass fiber optical waveguides with low threshold broadband gain, permitting construction of wideband amplifiers and oscillators 07 p0953 A72-18876
Stimulated emission cross section, loss coefficient and terminal level lifetime of high power Nd-phosphorus oxychloride liquid lasers 07 p1004 A72-19226
He-Ne laser discharge gap oscillation modes observation, noting applied magnetic field, gas parameters and cathode type effects on stimulated emission 07 p1008 A72-20510
Continuous laser action in Nd-yttrium aluminum oxide rod, determining terminal state loss coefficient in stimulated emission 08 p1217 A72-21322
Spectral density curves for intensity fluctuations of stimulated emission from low and ultralow frequency gas lasers as function of thermal oscillation, mode interference and beat effects 08 p1182 A72-21379
Stimulated emission and spectroscopic properties of activated ferroelectric crystal laser, noting Stark effect 09 p1323 A72-22981
Flashlamp and laser pumped cresyl violet laser emission characteristics between 620 and 710 nm, noting self mode locking in 3 component solution 09 p1324 A72-23048
Four-photon parametric frequency selection within broad stimulated emission lines during coherent light interaction, considering dye solution laser pumping 11 p1648 A72-26335
Spectroscopic and stimulated emissive properties of neodymium ions in potassium yttrium tungstate crystals at 77 and 300 K 11 p1701 A72-26362
Stimulated laser emission in vacuum UV by liquid Xe excitation with electron beam, determining threshold current density, radiation divergence and line half width 12 p1820 A72-27582
Laser emission intensity enhancement based on stimulated Brillouin scattering effect by raising pumping level, energy density and pulse duration 12 p1821 A72-27587
Stimulated luminescence in activated Nd glass by pulsed laser radiation at 1060 nm wavelength 13 p1969 A72-29519
Temporal, energetic and spectral properties of stimulated emission from Cr doped ruby laser irradiated by Co 60 gamma rays 13 p1969 A72-29613
Resonance scattering and direct photoelectron excitation contribution to molecular nitrogen first positive bands emission in day airglow from rocket measurements 13 p1953 A72-29808
Angular distribution of first Stokes component for stimulated combinational scattering investigated under various excitation conditions 13 p1972 A72-29982
Stimulated Compton scattering of laser radiation by electron plasma, determining electrons diffusion coefficient and velocity distribution function 13 p1972 A72-29987
Co 60 gamma radiation effect on stimulated ruby laser emission delay time, pulse duration, energy curve and intensity 13 p1972 A72-30005
Molecular nitrogen pulsed laser wavelength measurements, observing IR bands, stimulated emission lines and population inversion mechanisms 15 p2249 A72-32151
Stimulated emission in molecular iodine vapor phase laser optically pumped by Q switched Nd-YAG laser second harmonics 15 p2251 A72-32538

Visible and UV stimulated emission in plasma of direct pinch discharge on Ar II and III ions, discussing application possibility to plasma diagnostics 16 p2400 A72-33297
Pumping current pulse duration effect on lasing threshold of injection lasers with diffusion junctions and heterojunctions in GaAs-AlAs system 16 p2404 A72-33986
Nd-glass laser interaction with singly stimulated two-photon emission and anti-Stokes Raman scattering from metastable state He, calculating cross sections 17 p2565 A72-35831
Dependence of emission on work function variation in metals under tension 18 p2699 A72-36350
Optical polarization effects in a gas laser 18 p2697 A72-36487
Sideband growth in nonlinear Landau wave-particle interaction 19 p2838 A72-37327
Properties of stimulated neodymium laser emission under the action of Co 60 gamma emission 19 p2812 A72-38214
Influence of the refractive index nonlinearity on the dynamics of emission from semiconductor lasers 20 p2932 A72-39504
Frequency-tunable stimulated IR parametric fluorescence produced by barium sodium niobate crystal pumped with picosecond pulses from frequency-doubled mode locked Nd-glass laser 20 p2933 A72-39560
Stimulated thermal scattering of picosecond laser pulses 21 p3063 A72-40779
High-intensity X-ray spectra and stimulated emission from laser plasmas 22 p3210 A72-41990
Co 60 gamma radiation effect on stimulated ruby laser emission delay time, pulse duration, energy curve and intensity 22 p3186 A72-42731
Stimulated emission with pumping by a pulsed electron beam formed in a direct discharge 23 p3295 A72-43319
Stimulated emission in vacuum far ultraviolet during rapid heating of the plasma electrons by ultrashort light pulses 23 p3322 A72-44466
Mass spectra stimulated by O+ and Ar+ interacting with a surface 24 p3378 A72-45312

STIMULATED EMISSION DEVICES
NT ARGON LASERS
NT CARBON DIOXIDE LASERS
NT CARBON MONOXIDE LASERS
NT CHEMICAL LASERS
NT GALLIUM ARSENIDE LASERS
NT GAS LASERS
NT GAS MASERS
NT HCN LASERS
NT HELIUM-NEON LASERS
NT INFRARED LASERS
NT INJECTION LASERS
NT LASERS
NT LIQUID LASERS
NT MASERS
NT ORGANIC LASERS
NT PULSED LASERS
NT Q SWITCHED LASERS
NT RAMAN LASERS
NT RING LASERS
NT RUBY LASERS
NT SEMICONDUCTOR LASERS
NT SOLID STATE LASERS
NT TRAVELING WAVE MASERS
Elements of a theory of CW gasdynamic quantum generators. 23 p3297 A72-44225

STIMULATION
NT AUDITORY STIMULI
NT SENSORY STIMULATION
Biological systems activity in controlling extremal problems of nervous and muscular systems, noting external stimulation minimization 19 p2761 A72-38577
Patterns of spontaneous and reflexly-induced activity in phrenic and intercostal motoneurons. 21 p3003 A72-41462

STIMULI
Maximum aerobic power response and oxygen consumption to training stimulus intensity, duration and frequency, using bicycle ergometer exercise 07 p0916 A72-18965
Pain perception anatomical and neurophysiological mechanism, discussing human response to mechanical, thermal and chemical pain inducing stimuli 22 p3146 A72-42780

STIRLING CYCLE
Mechanical seal for airborne Stirling cycle cryogenic refrigerator, noting He cross leaks and sealing faces galling and blistering [ASLE PREPRINT 72AM 16] 13 p1964 A72-28973

STOCHASTIC PROCESSES
NT MARKOV CHAINS
NT MARKOV PROCESSES

STOCHASTIC PROCESSES
NT RANDOM PROCESSES
NT RANDOM WALK
Linear stochastic-parameter output channel, examining signal quadrature components statistical characteristics 01 p0024 A72-10199
Stochastic differential equations vector solution by two-time method, applying to random harmonic oscillators and wave propagation in random media [AD-733125] 01 p0093 A72-10510
Estimation and control relations separation for discrete time stochastic systems, considering assumptions on linearity, criteria, information pattern, constraints and noise distributions 01 p0047 A72-11306
Stochastic linear-quadratic-Gaussian problem role in optimal closed loop control system design, emphasizing philosophy, modeling and problem formulation [AD-738763] 02 p0198 A72-12801
Linear and quadratic programming procedures in optimal control problems of stochastic and deterministic system design 02 p0198 A72-12807
Discrete-time linear quadratic stochastic control system with perfect measurements of state, obtaining optimal solution by dynamic programming 02 p0198 A72-12808
Bibliography on linear-quadratic-Gaussian problems covering quadratic criteria, state estimation, stochastic control, computations and applications 02 p0198 A72-12813
Describing function method for nonlinear systems under stochastic input, considering statistical optimizations/linearization and self oscillation under noise 03 p0337 A72-13074
Weak solutions of degenerate partial differential equation of dynamic programming, investigating relation to value function of stochastic optimal control problem 03 p0382 A72-13701
Plate under projectile impact, calculating motion response due to random initial velocity distribution over surface by stochastic model 03 p0447 A72-13852
Finite memory uncertain stochastic controller, developing optimal and suboptimal algorithms 03 p0329 A72-14181
Closure schemes and retention of third moments in stochastic dynamic equations for numerical weather prediction, discussing imperfect forcing effects and kinetic energy relations 03 p0385 A72-14230
Nonlinear stochastic systems stability conditions description by Volterra integral equation, applying to distributed parameter feedback control system with nonlinear amplifier of random gain 04 p0504 A72-14663
Stochastic signal method for measuring dynamic viscoelastic properties of isometric frog sartorius muscle at rest and contraction, using white noise vibrations 04 p0480 A72-15221
Closure approximation in hierarchy stochastic differential operator equations in statistical mechanics 04 p0540 A72-15257
Adaptive control algorithm with disturbance prediction for solution of deterministic and stochastic optimization problems of linear equation of state and quadratic performance criteria 05 p0639 A72-15759
Stochastic aerodynamic heating of shallow shell in supersonic turbulent flow by Monte Carlo method 05 p0599 A72-15845
Complex systems stochastic survivability estimates dependence on delay depth and initial conditions of interaction 05 p0640 A72-16204
Missile trajectory stochastic optimal control systems with fuel constraint by mean path deviation optimization 05 p0725 A72-16452
Optimal closed loop control of stochastic nonlinear systems by expanded cost function applied to reduced terminal error atmospheric entry problem 05 p0685 A72-16462
MHD Couette flow stochastic processes optimal control synthesis by dynamic programming 05 p0653 A72-17131
Optimal control synthesis for linear stochastic systems with random piecewise-continuous coefficients as function of time 05 p0683 A72-17139
Optimal control of systems described by stochastic differential equations with delayed argument, using Kozhevnikov mean principle 05 p0683 A72-17140
Optimal control algorithm for nonlinear stochastic systems ensuring probability-wise stability and minimum error, using Liapunov theory and dynamic programming 05 p0691 A72-17141

Minimal energy stochastic controller design for electrically driven vehicles, using dynamic programming

06 p0795 A72-17304

Adaptive control for linear discrete time stochastic systems with unknown gain parameters, considering open loop feedback optimal control using quadratic performance index

[AD-739126] 06 p0791 A72-17305

Parameter adaptive self organizing control of linear discrete time systems, presenting stochastic approximation algorithms for feedback systems identification

06 p0791 A72-17306

Optimally sensitive closed loop control synthesis for systems containing uncertain time varying parameters, applying to stochastic systems

06 p0792 A72-17309

Nonlinear stochastic systems analysis by extended Volterra-functional method for first and higher order linear plants with constant or time varying parameters

06 p0838 A72-17376

Stochastic dynamic equations for atmospheric prediction and numerical weather forecasting, using barotropic model

06 p0841 A72-17633

Discrete stochastic differential games with quadratic payoff function, deriving deterministic, randomized and game optimal control strategies

06 p0793 A72-17956

GERT simulation program as stochastic network analysis technique for modeling policies and processes in performance tests and checkout

06 p0780 A72-17977

GERTS II simulation program for graphically modeling and analyzing complex stochastic systems, discussing applications to assembly line, project management, conveyor and inventory systems

06 p0780 A72-17978

Suboptimal stochastic control strategies class based on game theory and optimin principle, investigating completeness in closed discrete-time systems

06 p0794 A72-18167

Stochastic differential equations for a posteriori probability distribution in problems of Markov process parameter estimation, adaptive filtering and signal detection

06 p0794 A72-18301

Stochastic optimal control for operations of plants with pure lag and two point estimate of performance index investigating systems stability

06 p0795 A72-18662

Stellar motion in asymmetric galaxies with three degrees of freedom, using four dimensional surface of section mapping and stochastic measurement

07 p1034 A72-19072

Minimax terminal state estimator existence and structure for linear discrete system, applying to stochastic pursuit evasion games of LQ/G variety

07 p1027 A72-19283

Signal design for coherent M-ary communication systems by stochastic gradient algorithm for minimizing error rate

07 p0959 A72-19285

Stochastic approximation algorithm with nonstationary regression function for signal parameter estimation, considering convergence, mean square error bound and applications

07 p1027 A72-19291

Dynamic programming for optimal stochastic control problem with Gaussian shot noise involving parabolic or elliptic differential equation in unbounded domain, discussing iterative solution and quasi-linearization

07 p1027 A72-19292

Failure analysis probability for structures excited by randomly varying dynamic loads, comparing Gaussian and filtered Poisson processes

07 p1093 A72-19948

Stochastic simulation model for space shuttle fleet operations, using closed loop queueing system approach

07 p0965 A72-20330

Computer simulation of empirical confidence limits for variance spectra, applying to Gaussian random noise data stochastic model

07 p0951 A72-20360

Diffusion and stochastic variations of galactic cosmic rays in solar wind

07 p1066 A72-20648

Nonlinear filter dynamics for stochastic optimal control for quadratic cost functional, evaluating performance

08 p1145 A72-20866

Algorithm for asymptotic power series for Poisson process residence time function generation in band with delaying screen

08 p1198 A72-20998

Stochastic rule for optimum moment of preventive maintenance of redundant technological systems, predicting system reliability

08 p1180 A72-22056

Convergence of random number sums of independent infinitesimal multidimensional stochastic step processes to generalized Poisson processes

09 p1340 A72-22423

Sigma algebra and statistics system for optimal stopping of stochastic processes for continuous time case

09 p1340 A72-22424

Stochastic approximation for identification of element with second order lag, noting convergence with optimum parameter

09 p1291 A72-23371

Positive to quasi-stochastic matrix reduction by similar variation method, determining largest characteristic number and eigenvector

09 p1343 A72-23490

Monotonicity theorems for functionals and transformations in stochastic models of queueing, reliability and optimality problems

09 p1343 A72-23565

Interplanetary spacecraft midcourse guidance stochastic control, deriving algorithm for computing optimum velocity correction and execution time with allowance for correction-dependent errors

10 p1508 A72-23778

Adaptive filter techniques application to maneuvering reentry vehicle tracking, using Wald sequential test, decision theory and stochastic approximation

10 p1509 A72-23779

Differential geometric methods to extend linear system theory to nonlinear classes, considering differential equations, controllability, optimal control, stochastic processes and bilinear system problems

10 p1503 A72-23788

Quadratic cost, nonlinear optimal adaptive stochastic control of linear plant and measurement models excited by white Gaussian noise and with unknown parameters

10 p1455 A72-23792

Stochastic model for eye movements during fixation on stationary target

10 p1429 A72-23795

Linear least squares estimation of Stratonovich-Kalman-Bucy formulas by innovations method

10 p1503 A72-23801

Stochastic projected gradient algorithm to maximize SNR subject under linear or nonlinear constraints, applying to detector antenna array processing

10 p1456 A72-23808

Stochastic nonlinear system one-step optimal dual control instead of separation control policy for performance improvement

10 p1456 A72-23810

Optimal closed loop control of discrete stochastic nonlinear systems, considering guidance and navigation for space and terrestrial vehicles

10 p1456 A72-23811

Stochastic models of human performance effectiveness functions reliability and correctability from error data generated by tracking and vigilance tasks

10 p1429 A72-24001

Optimal closed loop control of discrete stochastic nonlinear systems, obtaining solution by cost function in power series around deterministic trajectory

10 p1457 A72-24499

Equivalence conditions for optimal control problems for stochastic and deterministic plants in cases of nonrandomized strategies

10 p1457 A72-24637

Stochastic optimization of airborne laser seeker system design parameters to maximize target acquisition probability through regression analysis of data from computerized model

10 p1437 A72-24682

Statistical linearization of stochastic differential equations for optimal terms in mean square distance

10 p1506 A72-24993

Stochastic control theory application to flight problem, discussing aircraft identification and adaptive control over wide environmental range

10 p1458 A72-25146

Cybernetic system effectiveness analysis with operations research and statistical theory based on stochastic treatment

11 p1608 A72-25428

Complex square stochastic matrix spectral inverse, examining nonzero eigenvalues on unit circle

11 p1677 A72-26152

McShane belated stochastic integral existence theorem with quasi-martingale process for sample continuity assumption

11 p1678 A72-26156

Random Fredholm and Volterra integral equations applied to stochastic systems, investigating absolute stability concept

11 p1679 A72-26780

Statistical analysis of strain criteria and stochastic relations for Al alloy fatigue life and minimum creep rate at 175-250 C

11 p1663 A72-26800

Stochastic dynamic prediction of meteorological fields in deterministic and indeterminate atmosphere

12 p1838 A72-27020

Inverted pendulum subjected to small amplitude sinusoidal periodic and stochastic base motion, determining stability boundaries by averaging method

12 p1844 A72-27247

Stochastic time varying patterns classification by Kalman filter, discussing optimum dichotomizer with supervised learning

12 p1790 A72-27498

Nonlinear stochastic partial differential equations solution by graph technique, calculating correlation function and phase change spectrum in phase locked circuit

12 p1837 A72-27575

Optimal allocation of tasks and resources, using asymptotic properties of stochastic approximation method

12 p1837 A72-27823

Reliability and stochastic stability theory relationships for multidimensional and continuous systems

13 p1985 A72-28486

Popov frequency criterion analog for stochastic nonlinear continuous systems with random parameters and disturbances, investigating stability

13 p1935 A72-28608

Sinusoidal signal and stationary quasi-white Gaussian noise mixture effects on stochastic phase locked AFC system operation, noting phase error probability density function

13 p1921 A72-29285

Stochastic differential equations for a posteriori probability distribution in problems of Markov process parameter estimation, adaptive filtering and signal detection

13 p1937 A72-29441

Stochastic aerodynamic heating of shallow shell in supersonic turbulent flow by Monte Carlo method

15 p2178 A72-31264

Stochastic atmospheric density fluctuations effect on circular-orbiting satellite roll-yaw oscillations stability

15 p2319 A72-31457

Hierarchical system of helicopter service terminals, calculating passenger lots for single and multiloop arrangements under given stochastic input conditions

15 p2337 A72-31498

Linear stochastic-parameter output channel, examining signal quadrature components statistical characteristics

15 p2195 A72-31623

Stochastic signal reflection by passive element, synthesizing optimal echo-signal detector for space diversity reception

15 p2197 A72-31877

Generator for data transmission lines stochastic noise bursts simulation with statistically independent burst durations and intervals

15 p2201 A72-32475

Automated problem solving in continuous stochastic processes, using nonergodic representation of Gaussian process with continuous spectral density

15 p2204 A72-32588

Group perturbation method for accuracy analysis of nonlinear stochastic automatic control systems, noting computer time reduction

16 p2371 A72-33091

Nonlinear vibration damper system subject to forced vibrations considered as stochastic processes in form of white noise and stationary and ergodic processes

16 p2467 A72-33144

Digital phase locked loop realization for near-optimum demodulation of continuous-time FM signal using stochastic estimation theory

16 p2362 A72-33213

Application of statistical linearization techniques to nonlinear multidegree-of-freedom systems. [ASME PAPER 71-WA/APM-5]

17 p2624 A72-34315

Book - Elements of applied stochastic processes

17 p2575 A72-34624

Application of a limit theorem to solutions of a stochastic differential equation.

17 p2575 A72-34866

Regional Conference on Control Theory, University of Maryland, Baltimore, Md., August 23-27, 1971, Proceedings.

17 p2533 A72-34948

Discrete-time demodulation of continuous-time signals.

17 p2516 A72-35332

Numerical solution of an optimal control problem with a probability criterion.

17 p2534 A72-35531

Identification of periodicities in the structure of natural stochastic processes

17 p2534 A72-35783

Stochastic electrodynamics based on zero electromagnetic field motion, deriving Schroedinger equation and electromagnetic model of gravitation

17 p2584 A72-35912

Approximations yielding closed equations for isotropic turbulence compared to laboratory and computer experiments, emphasizing Langevin type model equation for velocity

18 p2677 A72-36008

Nonlinear functional homogeneous chaos expansions for stationary stochastic processes in turbulence theory

18 p2678 A72-36011

Dynamo instability and feedback in a stochastically driven system. 18 p2678 A72-36013

Stochastic optimal path selection via N discrete points set, discussing probability distributions and computer requirements 18 p2672 A72-36055

Hybrid processing of empirical functions in mechanics 18 p2710 A72-36423

A stochastic bioburden model for spacecraft sterilization. 18 p2652 A72-36442

Reliability of simulations of asymptotically steady and strictly ergodic stochastic processes 18 p2704 A72-36467

Adaptive nonlinear optimization of the signal-to-noise ratio of an array subject to a constraint. 18 p2660 A72-36507

Optimal control laws for stochastic problems involving intentional errors, caution and probing 18 p2674 A72-36825

Optimal minimal-order observers for discrete-time systems - A unified theory. 18 p2674 A72-37099

Linear stochastic system optimal measurement strategy and matched Kalman type filter computation via transformation into deterministic control problem 18 p2674 A72-37100

Optimal terminal rendezvous as a stochastic differential game problem. 19 p2869 A72-37284

Sufficient conditions for two stage stochastic optimal control difference approximation by finite dimensional extremum problem sequences 19 p2777 A72-37318

Infinite systems of stochastic differential equations arising in optimal nonlinear filtering theory 19 p2824 A72-37323

Certain properties of continuous stochastic approximation procedures 19 p2824 A72-37325

Stochastic analogs of finite-converging learning algorithms for recognition systems 19 p2769 A72-37421

Dynamic programming technique for simultaneous measurement and dynamic control optimization for stochastic systems 19 p2779 A72-38233

Pontryagin Minimum Principle application to stochastic optimal control problems formulated around linear systems with Gaussian noise and general cost criteria 19 p2779 A72-38234

A circle criterion for nonlinear stochastic feedback systems. 19 p2779 A72-38235

Optimal decentralized control of two coupled linear stochastic systems, introducing fake plant white noise for weak coupling effects compensation 19 p2779 A72-38236

Linear control system design with parameter uncertainties, using stochastic control approach based on minimization of state vector-dependent quadratic performance index expected value 19 p2780 A72-38239

Suboptimal stochastic control of a class of linear distributed parameter regulators. 19 p2780 A72-38243

On-line identification of multivariable stochastic feedback systems. 19 p2781 A72-38270

Nonlinear oscillations stochastic instability in dynamic systems, discussing nonequilibrium statistical mechanics 19 p2836 A72-38814

Fourier transformation relating autocorrelation to spectral density of power bounded and energy bounded functions, discussing unsteady stochastic processes 20 p2953 A72-39552

Book - Fundamentals of pattern recognition. 20 p2905 A72-39575

An advanced stochastic model for threshold crossing studies of rotor blade vibrations. 20 p2885 A72-39622

Optimization of controlled plants sequence with stochastic process described by partial differential equations, noting hydropneumatic system of liquid fuel jet engine 20 p2947 A72-39903

State vector moments of nonlinear mechanical systems under stochastic excitation, using Fokker-Planck equation for transition probability and differential equations derivation 21 p3084 A72-40679

Optimal risk equation and solution existence and uniqueness of dual control problems with unknown parameter and additive disturbances 21 p3038 A72-40706

Receiver processing for direct-detection optical communication systems. 21 p3017 A72-40859

Transit time heating in stochastic electromagnetic fields. 21 p3092 A72-41222

Characterization and algorithm for optimal solution of stochastic linear programming to minimize cost 21 p3075 A72-41234

Necessary conditions for continuous parameter stochastic optimization problems. 22 p3198 A72-41932

Stochastic and deterministic relationships between random variables, noting correlation coefficient as measure of regression lines representation accuracy 22 p3178 A72-42449

A stochastic automata theoretical approach to dynamic programming. 22 p3199 A72-42633

Applicability bounds for the equation describing the mean field in a discrete scattering medium with allowance for the correlation of the scatterers 22 p3155 A72-42660

Control and estimation separation in stochastic optimization, discussing Wonham observer matrix reversibility and replacement in closed and closed-open loop systems 22 p3163 A72-42740

Response of linear and nonlinear continuous structures subject to random excitation and the problem of high-level excursions. 22 p3241 A72-42970

German monograph - Stability conditions for a linear homogeneous ordinary differential equation of second order with stochastic parameter excitation. 22 p3199 A72-43055

Particle distribution function evolution effect on turbulent plasma heating by wave interaction, considering stochastic heating of ions 23 p3318 A72-43314

Infinite-time reachability of state-space regions by using feedback control. 23 p3274 A72-43538

Control of jump parameter systems with discontinuous state trajectories. 23 p3275 A72-43547

Empirical support for a stochastic model of evolution. 23 p3254 A72-43565

Output-feedback control law for randomly distributed multivariable system. 23 p3275 A72-43608

Stochastic models for block triangulation by bundle approach, comparing theoretical accuracies obtained from different block adjustment methods 23 p3284 A72-43631

Stochastically optimal terminal control system synthesis for loss function dependence on finite phase coordinates of dynamic system, considering soft landing of flight vehicle 23 p3275 A72-43781

Optimal control of stochastic systems with continuous and discontinuous random disturbances, obtaining problem solution conditions for linear system via dynamic programming 23 p3276 A72-43782

Asilomar Conference on Circuits and Systems, 5th, Pacific Grove, Calif., November 8-10, 1971, Record. 23 p3276 A72-43851

Reduced order observers design for optimal control of linear discrete time stochastic systems, considering velocity-aided tracking filter 23 p3276 A72-43856

Ultrasonic holography in large phase disturbance. 23 p3290 A72-43950

Stochastic coder electronic circuit for random numbers conversion into electrical voltages and vice versa, noting compactness and low cost 23 p3273 A72-44460

Logical groupings of preventive maintenance and replacement policies for stochastically failing items to reduce cost under continuous surveillance 24 p3406 A72-44653

Cumulative damage stochastic models and distributions of strength of steels and graphite. 24 p3412 A72-44673

STOICHIOMETRY

Oxygen content and stoichiometry effects on metal carbides grain growth in liquid phase sintering, discussing carbide-metal interface solution reaction as rate controlling mechanism 02 p0240 A72-11434

Stoichiometry effect on high temperature creep in oxides, relating impurities, point defects concentration and diffusion 09 p1335 A72-22397

Flame structure studies of stabilizing region of near stoichiometric laminar burner methane-air flame 09 p1411 A72-23147

Ignition and incandivity of laser irradiated single micron size Mg particles suspended in stoichiometric methane air mixture 10 p1564 A72-25140

Ni-Mn alloy phase transformation characteristics from neutron diffraction and small angle scattering studies, showing ordered nearly stoichiometric metastable phase for entire temperature range 13 p1976 A72-28903

Chalcogenide semiconductor compounds of b-sub-group transition elements, discussing binary system diagrams, stoichiometric composition and electrical properties 15 p2290 A72-31193

STOKES FLOW

Slow motion in shear flow of doublet of two spheres in contact, using Stokes equations solution 04 p0511 A72-14860

Corrugated cylinder steady rotation in incompressible viscous fluid based on linear or Stokes approximation 09 p1293 A72-22411

Quasi-steady creeping flow in small arrays of spherical, oblate and prolate ellipsoid and circular cylinder lung models, obtaining Stokes equations solutions 10 p1431 A72-24469

Hydrodynamic field generated by sphere motion along viscous fluid filled cylinder axis beyond Stokes regime 10 p1470 A72-24852

Stokes flow about slender particle with nonuniform cross section under distributed force, obtaining solution to integral equation for twisted particle by perturbation scheme 12 p1798 A72-27834

Three dimensional viscous flow near corner, constructing Stokes slow-flow solution 13 p1944 A72-30031

Boundary value problem approximate solution for Stokes flow of unbounded viscous Newtonian fluid past single body, applying algorithm to spheroidal shapes 19 p2784 A72-37369

Stokes fluids nonlinearity effects on turbulent flow with lateral shear in terms of stress and deformation tensors 19 p2785 A72-37470

Unsteady heat transfer and temperature for Stokesian flow about a sphere. [ASME PAPER 72-HT-C] 20 p2983 A72-39482

Note on the symmetries of certain material tensors for a particle in Stokes flow. 21 p3044 A72-40113

STOKES LAW

Real time complete Stokes vector scanning photoelectric polarimeter with 16 cm aperture for measuring visible radiation of solar disk, corona, moon and planets 03 p0356 A72-13279

Calibration of polarimetric measurements in terms of magnetic fields, using Stokes parameters without line formation dependence 03 p0427 A72-13280

Telescopic phase retardation effect on Zeeman triplet Fe of polar sunspot umbrae in Stokes parameter measurements 03 p0357 A72-13288

Lunar gravitational potential determination from Stokes and selenocentric constant 03 p0440 A72-14326

Elliptical polarization and depolarization coefficients for monochromatic radio waves reflected from F 2 ionosphere using Stokes parameters 05 p0656 A72-16241

Nonlocal fluid dynamics continuum theory with equilibrium and constitutive equations derived by generalizing Stokes Laws, noting steady channel and shear flow 16 p2379 A72-33832

The treatment of the Stokes parameters and measurement of magnetic field. 20 p2970 A72-39755

STOKES THEOREM [VECTOR CALCULUS]

Null electromagnetic field propagation in general relativity, applying to Stokes parameters definitions for monochromatic light 02 p0259 A72-12178

Radiation propagation in optically thin anisotropic noncrystalline media, obtaining explicit formulas for Stokes parameters of transmitted and scattered radiation 12 p1865 A72-27052

Photoelastic analysis with Stokes vector and new methods for the determination of characteristic parameters in three dimensional photoelasticity. 23 p3354 A72-44255

Radiation propagation in optically thin anisotropic noncrystalline media, obtaining explicit formulas for Stokes parameters of transmitted and scattered radiation 24 p3425 A72-45705

STOL AIRCRAFT

U SHORT TAKEOFF AIRCRAFT

STONES [ROCKS]

U ROCKS

STONY METEORITES

NT ACHONDRITES

NT AUSTRALITES

NT BEDIASITES

NT BRUDERHEIM METEORITE

NT CARBONACEOUS METEORITES

NT CHONDRITES

NT ORGUEIL METEORITE

NT TEKITTES

- NT TUNGUSK METEORITE**
Terrestrial stony meteorites age determination from C 14 content
09 p1386 A72-22661
- Pavel stony meteorite microspectral analysis to obtain metallic elements weight percentages in chondrites, matrix and core, using laser source for local vaporization and excitation
14 p2159 A72-30785
- Transition element distribution in stony meteorites and in terrestrial and lunar rocks.
17 p2619 A72-35936
- The isotopic composition and elemental abundance of gallium in meteorites and in terrestrial samples.
18 p2723 A72-36061
- Elemental abundances in stone meteorites.
19 p2858 A72-37863
- Non-destructive activation analysis of some elements in stony meteorites by proton- and bremsstrahlen-irradiation.
20 p2899 A72-39833
- Falls of meteorites in Germany: Temporal distribution of the falls and deductions with regard to their origin - Hypotheses concerning the origin of the meteorites as well as further falls and findings in Germany
22 p3227 A72-42542

STOPPING

- Sigma algebra and statistics system for optimal stopping of stochastic processes for continuous time case
09 p1340 A72-22424

STOPPING POWER

- The influence of molecular binding on the stopping power of alpha particles in hydrocarbons.
18 p2655 A72-37193

STORABLE PROPELLANTS

- NT AIRCRAFT FUELS**
- STORAGE BATTERIES**
NT NICKEL CADMIUM BATTERIES
NT SILVER CADMIUM BATTERIES
Battery separator materials requirements derived from in-cell environment and battery mission, evaluating present technology for R and D area concentration
03 p0313 A72-14235
- Rechargeable high energy density battery with Al and Cl electrodes and molten aluminum chloride-alkali chloride eutectic electrolyte
16 p2352 A72-33896

STORAGE STABILITY

- Nitrate ester propellants self ignition hazard and ballistic stability, describing heat generation test at various temperatures for long term storage
14 p2144 A72-30754
- Propellant powders safe life prediction based on short-time tests, discussing aging effects on chemical stability after 7-11 years air conditioned storage
14 p2144 A72-30756
- Cast double base propellant rocket motors safe storage and service life assessment, examining environmental storage conditions and accelerated temperature effects
14 p2144 A72-30758
- Gamma radiation effects on composite propellants stability, investigating polyurethane, polybutadiene, silicone and polyisoprene binders mechanical properties
14 p2144 A72-30760
- Composite and double base solid propellant rocket motors storage, considering ingredients and materials compatibility and ignition temperatures effects on spontaneous inflammation potential
14 p2144 A72-30761
- Solid rocket propellants storage life analysis and prediction by mathematical modeling of physical-chemical failure generating processes
14 p2145 A72-30762
- Insulation and bonding materials effects on double base solid propellants stability, using vacuum reactivity testing technique
14 p2145 A72-30766

STORAGE TANKS

- ELDO launch vehicle cryogenic tanks fabrication, discussing Al alloy selection and mechanical properties at low temperatures, manufacturing processes and thermal insulation
09 p1318 A72-22690
- Determination of the optimal parameters of high-pressure cryogenic fluid storage systems.
20 p2962 A72-39358
- The long fluid storage bag - A contact problem for a closed membrane.
20 p2980 A72-39691

STORMS

- NT CYCLONES**
NT HURRICANES
NT IONOSPHERIC STORMS
NT MAGNETIC STORMS
NT NOISE STORMS
NT POLAR SUBSTORMS
NT RAINSTORMS
NT SOLAR STORMS
NT STORMS [METEOROLOGY]
NT SUDDEN IONOSPHERIC DISTURBANCES
NT THUNDERSTORMS
NT TORNADOES

NT TROPICAL STORMS

- STORMS [METEOROLOGY]**
NT HURRICANES
NT POLAR SUBSTORMS
NT RAINSTORMS
NT THUNDERSTORMS
NT TORNADOES
NT TROPICAL STORMS
Soviet book on calms and storms in upper atmosphere covering energy variations, auroras, geomagnetic storms, weather forecasting, etc
03 p0350 A72-13967
- Nonentraining axially symmetric steady state sloping model of severe storm, discussing validity and limitations
03 p0384 A72-14147
- Storm effects on SST operations, discussing wave initiation at storm top and tropospheric propagation
04 p0542 A72-14683
- Storm forecasts by meteorological satellites, describing TV monitoring of cyclones and hurricanes
05 p0683 A72-15978
- Broadbeam S band radar application to quantitative analysis of severe storms, calculating liquid water content
06 p0843 A72-18442
- Supercell, multicell and sheared severe hailstorms structure and motion observation by radar echoes, noting propagation characteristics
09 p1345 A72-22447
- ESSA satellite observation of meridional circulation, noting roles of subsidence sinks, storm depressions and melting fronts
10 p1506 A72-24059
- Radar echo maximum intensity display by digital comparator with shift register video signals storage in National Severe Storms Laboratory
11 p1591 A72-25762
- Martian storm of 1971, describing development, decline, structure and photographic data
12 p1870 A72-27425
- Heat and momentum transfer properties and storm propagation speed under steady convective overturning in shear, considering cumulonimbus convection scale of atmospheric motion
12 p1840 A72-27704
- Gravity waves on leeward side of Continental Divide in Colorado, noting generation by winds and storms
14 p2128 A72-30343
- Cloud liquid water content measurement via digital radar system, presenting two dimensional display of storm system characteristics
21 p3077 A72-40250
- Further study of the severe storm with a rotating updraft configuration.
21 p3077 A72-40466

STRAIGHT WINGS**U RECTANGULAR WINGS****STRAIN AGING****U PRECIPITATION HARDENING****STRAIN DISTRIBUTION****U STRESS CONCENTRATION****STRAIN ENERGY METHODS**

- Ductile tensile cracking macroscopic simulation with perforated pure Al specimens, determining fracture energy as function of hole size and pattern
01 p0086 A72-10987
- Finite inflation of toroidal shell with edges bonded to rigid rim, using Runge-Kutta method to solve differential equations based on Mooney strain energy function
[ASME PAPER 71-WA/APM-20]
- Cyclic loading failure criteria based on plastic deformation energy concepts, considering material load carrying capacity
05 p0733 A72-15960
- Penny shaped interface crack between elastic layer and half space, calculating stress intensity factors and strain energy release rate for aluminum-epoxy combination
06 p0899 A72-18650

- Computation procedure for crystal lattice electrostatic strain energy derivatives
09 p1398 A72-22530
- Finite element generalization of plate displacement functions to shell analysis, using strain energy tensor concept
09 p1372 A72-23228
- Large deflection of variable thickness square plate under uniform load, using strain energy method
10 p1560 A72-25187
- Book on thermal stress analysis covering equivalent thermal loads, bars, beams and rings extensional and bending deformation, shells, strain energy methods, etc
11 p1737 A72-26588
- Strain energy calculation for stability analysis of cylindrical and conical sandwich shells, using Euler-Poisson equations
11 p1739 A72-26925

- Small amplitude plane wave speed variation with pressure for Na and K at absolute zero temperature, using crystal strain energy formulation
12 p1885 A72-27975
- 13 p2006 A72-29675

- Cylindrical shell rectangular finite element from generalized independent strain functions and corresponding displacement functions
14 p2169 A72-31174

- Book on structural analysis covering statically indeterminate structures, force and displacement methods, flexibility and stiffness matrices, strain energy, virtual work, energy theorems, etc
15 p2325 A72-31517

- Strain energy methods for stability of finitely deformed elastic membranes under conservative loading
16 p2465 A72-33002

- Strain energy method for finite deformation of solid and tubular cylinders of incompressible isotropic elastic material, noting torsional and tensile tests on natural rubber
16 p2468 A72-33198

- Strain energy release rate for radial cracks emanating from a pin loaded hole.
17 p2623 A72-34254

- On strain energy and constitutive relations for alkali metals.
18 p2703 A72-37087

- On a method of analysis of the strain energy changes taking place during the rotatory bending fatigue test of carbon steels and an effect of the pearlite patches to these changes.
20 p2935 A72-38881

- The stress intensity factors of a radial crack in a finite rotating elastic disc.
21 p3124 A72-41397

- On the effect of the form of the strain energy function on the solution of a boundary-value problem in finite elasticity.
22 p3236 A72-42606

- Crack propagation speed measurements with wedge loaded double cantilever beam of PMMA, calculating stress intensity, strain energy release rate and kinetic energy
23 p3346 A72-43709

- Nonlinear elastic torsion analysis for aerospace materials.
23 p3354 A72-44251

- Mixed-displacement finite-element analysis with particular application using plane-stress triangles.
24 p3455 A72-44789

STRAIN FATIGUE**U FATIGUE [MATERIALS]****STRAIN GAGES**

- Strain gage and manganin pressure gage instrumentation for magnetic driven flyer plate facility [MDAC-WD-1700]
02 p0223 A72-11502
- Strain gage tests on three dimensional composites for reentry vehicle structural design evaluation
02 p0287 A72-11506
- Moment sensors for strain gaged beam systems analysis, noting application to bending moments determination
02 p0287 A72-11510
- Contactless optical strain measurement based on speckle pattern change of diffusely reflected laser light
02 p0225 A72-11755
- Strain gage measurements of stress intensity factor for crack propagation in fatigue cracked thin metal sheets
03 p0444 A72-13542
- Strain gage system for low amplitude strain measurement, discussing SNR and installation technique
04 p0523 A72-15495
- High precision strain gage dynamometers design and testing at ONERA Modane test center, discussing accuracy limitation due to hysteresis and creep effects [ONERA, TP NO. 995]
05 p0642 A72-15859
- Principle stress errors in biaxial stress fields expressed in terms of transverse sensitivity, stress and Poisson ratios of material during strain gage calibration
06 p0895 A72-17798
- Residual stress measurements in metals by annular photoelastic gages, obtaining relationship to fringe orders
06 p0818 A72-18317
- Elastic constants measurement using vibrating wire strain gages on diametrically loaded circular disk and ring specimens
06 p0818 A72-18325
- Bridge circuit to minimize parasitic electrical disturbances in resistance strain gage measurements of dynamic stresses in impact tests
06 p0819 A72-18672
- X ray and resistance strain gage techniques for bar and metal plate simultaneous residual stress determination
07 p0993 A72-20606
- High temperature strain measurement accuracy improvement by gage spot welding
08 p1163 A72-20920
- Nuclear radiation effects on ceramic cemented strain gages and polyimide encapsulated epoxy bonded gages
08 p1164 A72-20922

- Two terminal semiconductor strain tensor based on evaporated piezoelectric layer for modulation of forward I-V characteristics of thin film diode
08 p1164 A72-20925
- Acoustic wave detection in strain transducer consisting of silicon insulated gate field effect transistor with piezoelectric film incorporated in insulator region
08 p1168 A72-21556
- Static strain measurement errors due to nonstationary thermal conditions in semiconductor resistance gages
09 p1310 A72-22739
- Vibration string static strain gage for high temperature operation, proposing relations for measurement error calculation
09 p1310 A72-22741
- Temperature dependence and error compensation of Si strain sensors, using coupled dc generators
09 p1316 A72-23649
- Ultrahigh strain rate measurement via diffraction gratings directly impressed into test material surface, recording outputs by high speed cameras or photoelectric techniques
10 p1487 A72-24573
- Embedded strain gage technique for subsurface tensile testing of boron-epoxy composites
11 p1671 A72-25467
- Perforated plates plastic deformation, stresses and strains near holes, using strain gage data in biaxial tensile tests
11 p1733 A72-25540
- Flow measurement instrumentation for turbomachine rotors, noting telemetry type data transmission system with strain gage pressure transducers for turbocompressor
[ASME PAPER 72-GT-55] 11 p1630 A72-25646
- Crack initiation detecting and recording instrument with optical strain gages for double shear fatigue tests of aircraft fasteners
11 p1632 A72-25823
- Bonded strain gage type load cell design, construction and application, explaining methods to achieve high accuracy
12 p1806 A72-27315
- Local heating effect of electrical resistance gages measuring strain across thickness of plane photoelastic Araldite models
12 p1807 A72-27316
- Semiconductor strain gage design and environmental performance for flight control systems
12 p1812 A72-27962
- Computer program to reduce automated multiaxial testing strain gage and applied loads data from tubular or flat specimens including fiber composites
12 p1787 A72-27999
- Computer algorithm for plates and shells internal forces and moments and stress-strain state determination from strain gage data
13 p2058 A72-29144
- Methane absorption stabilized 30 meter laser strain meter with Fabry-Perot geometry for earth tide, nuclear explosion and free earth oscillation observation
14 p2109 A72-30323
- Composite materials stress analysis techniques, discussing strain gages, photoelastic coatings more and holographic applications
[ASME PAPER 72-DE-6] 14 p2167 A72-30861
- Forces and strain rates measurement in elastic elements of dynamic systems under impact, discussing test equipment and strain gage transducers
16 p2395 A72-33964
- Fatigue life gages use in combination with strain multipliers in field applications with random ergodic cyclic strains
17 p2554 A72-34822
- Photoelasticity, holography, moire and strain gage methods in European experimental mechanics research
18 p2733 A72-36357
- Some uncommon electric transducers for the measurement of mechanical quantities.
18 p2690 A72-36369
- High-stability capacitance strain gauge for use at extreme temperatures.
18 p2693 A72-37210
- Strain distribution in and around strain gages.
19 p2870 A72-37225
- Gage-length errors in the resolution of dispersive stress waves.
19 p2800 A72-37729
- Investigation of resistance strain gauges based on zinc telluride and cadmium telluride semiconductor films
19 p2845 A72-38206
- Electro-optical noncontracting torque sensor, using slit diffraction pattern technique
21 p3051 A72-40231
- A ten-inch extensometer measuring small low-frequency strains.
21 p3052 A72-40234
- Electric model of bridging losses and optimal insulation layer thickness for small size resistance strain gages
21 p3056 A72-41367
- An advanced strain level counter for monitoring aircraft fatigue.
22 p3179 A72-42688
- Strain multiplier with S-N fatigue life gages, discussing design and performance
22 p3179 A72-42708
- Strain gage resistor with BiTeSb compound semiconductor film vacuum deposited on dielectric substrate, noting high sensitivity and operation without amplifiers
23 p3287 A72-43348
- Measurement of small strain amplitudes in internal friction experiments by means of a laser interferometer.
24 p3402 A72-44947
- High accuracy contactless torque-measuring shaft with strain gage as sensor, describing circuit wiring
24 p3403 A72-45296
- STRAIN HARDENING**
- Metals mechanical behavior, considering plastic deformability, strain hardening, cohesion and engineering performance prediction
01 p0086 A72-10985
- Circularly symmetrical disks with circular hole and loaded by pressure at edges, calculating linear and power-law strain hardening
02 p0297 A72-12535
- Gamma prime precipitate hardened Ni base alloys, attributing strengthening mechanism to coherency strains and precipitates antiphase boundary energy
02 p0247 A72-12817
- Microinhomogeneous elastoplastic cyclically strain hardenable material under symmetric loading, calculating stress-strain relationship
03 p0443 A72-13453
- Slip line field for plane strain extrusion of strain hardening material, calculating shear stress
03 p0363 A72-13708
- Doubly connected strain-hardened thin plate, calculating stress concentration and stress-strain state by variational principle of least additional potential energy
03 p0451 A72-14122
- Yield point elongated and strain hardened rectangular plates, calculating plastic coefficients in geometrically nonlinear bending problem
04 p0588 A72-15057
- Strain hardening for steel strength increase to 300 kg/sq mm by sequentially combined mechanical and thermal processing, involving plastic deformation, quenching and aging
04 p0527 A72-15454
- Strain hardened layers effect on wear resistance of 50Kh steel
04 p0534 A72-15653
- Ni-NiNb intermetallic unidirectional eutectic alloy crystal structure and high temperature behavior, considering mechanical twinning relationship to strain hardening and ductility
05 p0677 A72-17108
- Stress concentrations at circular holes and inclusions in elastoplastic strain hardening plate under tension and shear
06 p0897 A72-18316
- Deformation stresses and strains in quasi-static low cycle fracture of stabilizing, softening and strain hardening materials
06 p0831 A72-18352
- Hardening mechanisms of interaction between superlattice dislocations and point defects in Ni-Al intermetallic compound mechanical properties strain rate and temperature dependence
06 p0832 A72-18420
- Failure analysis of plastic materials susceptible to cyclic strain hardening under thermal load, considering residual stress concentration
06 p0898 A72-18547
- Load bearing capacity of shells of revolution, applying viscoplastic strain hardenable material model
06 p0899 A72-18656
- Aging creep theory application to anisotropic strain hardenable metals
06 p0900 A72-18680
- Plastic deformation, creep rupture strength, endurance limit and service life of prestressed strain hardenable material
06 p0900 A72-18681
- Aging effect on brittleness and hardening of Fe-Ni-Mn alloy at various temperatures
07 p1016 A72-19939
- Perturbation solution to nonlinear nonuniform torsion of thin walled open elastic beams with strain hardening dependent on torque-rotation behavior
07 p1096 A72-20431
- Strain rate effects on strain hardening of duralumin, copper and lead, noting yield stress sensitivity to deformation induced temperature changes
07 p0998 A72-20527
- Strain hardening law for rigid incompressible material with plastic properties independent of mean normal stress
08 p1248 A72-21820
- Soviet monograph on thermoplastic hardening of high strength martensitic steels and Ti alloys by ordering dislocation structure
09 p1327 A72-22520
- Explosive strain hardening of hard metal-ceramic alloy, presenting photographs of carbide and cobalt phases structural changes after impact loading
09 p1337 A72-22892
- Fracture strength relation to austenite stability in steels with plastic deformation caused by strain induced austenite-martensite transformation
10 p1499 A72-24894
- Creep and low cycle fatigue dynamic behavior, noting stress concentration time dependence, strain hardening and local plastic deformations in dead annealed Al thin walled tubes
11 p1658 A72-25829
- Creep characteristics of weakly strain-hardenable alloy under variable tensile load and temperature conditions
11 p1663 A72-26808
- Reversible stress effects in theory of plastic flow in strain hardened metals at high temperatures
12 p1879 A72-27159
- Acceleration waves propagation in elastic-plastic strain hardening rate independent solids, obtaining solution for discontinuity change in strength in homogeneously prestressed medium
12 p1846 A72-27729
- Large deflection calculation of circular and annular strain hardenable rigid plastic plates under axisymmetric load, using Kirchhoff-Love hypothesis and Tresca flow condition
14 p2165 A72-30440
- Combined heat treatment and machining effects on Mg-Nd alloys structure and mechanical properties, noting strain hardening mechanism
14 p2125 A72-31042
- Material constants for strain hardened polycrystalline metals calculated from mathematical model for plastic deformation
15 p2322 A72-31361
- Viscoelastic model for constitutive nonlinear creep law with combined strain and time hardening assumptions, evaluating material parameters for Al alloys
15 p2254 A72-31554
- Steady creep and delayed fracture dependence on metal structure and composition, considering strain hardening at small strain rate and elevated temperature
15 p2254 A72-31559
- Stress-strain relations for inelastic deformation of anisotropic strain hardenable shells of revolution under arbitrary plasticity conditions
15 p2332 A72-32678
- Constitutive equations for metallic creep analysis based on simultaneous strain hardening and crack propagation processes, calculating creep rupture time
16 p2408 A72-33589
- Composition effect on strain-transformation and precipitation hardening of beta Ti alloys at 800-1100 F
16 p2410 A72-33813
- Approximate method for reactions redistribution and displacements in statically indeterminate structures, using strain hardening hypothesis and creep power law
16 p2473 A72-34119
- Steels creep behavior relationship to stress-strain curve shape, defining creep resistance as function of strain hardening coefficient
16 p2412 A72-34146
- Strengthening mechanism in metals during creep under variable stress for dislocation network structure studies
16 p2475 A72-34164
- Geometric instabilities in isotropic plastic solids under increasing uniaxial compression.
[ASME PAPER 72-APM-28] 17 p2624 A72-34310
- Mathematical models for metallic plastic strain hardening under cyclic loads, introducing internal state parameters
17 p2632 A72-35111
- Application of an analog computer to the calculation of partially plasticized rotating circular disks prepared from strain-hardenable materials
18 p2735 A72-36421
- The structure and properties of thermomechanically treated beta-III titanium.
18 p2700 A72-36586
- The application of a dislocation model to the strain and temperature dependence of the strain hardening exponent n in the Ludwik-Hollomon relation between stress and strain in mild steels.
18 p2701 A72-36589
- Plane stress rupture criterion for age hardening materials during plastic deformation, calculating resistance to shear and torsion of solid and hollow round bars
19 p2818 A72-38009
- Study of the structural stability and mechanical properties of molybdenum subjected to the prolonged action of temperature and stress
19 p2818 A72-38013
- Plastic flow and strain hardening theories for short time tensile creep in high temperature metal formation, applying to Al alloys
21 p3125 A72-41510

Ti based beta alloy strain hardening and failure characteristics, emphasizing initial deformation phase and microdefect onset and development

21 p3071 A72-41716

Strain hardening of maraging steels in liquid nitrogen

22 p3187 A72-41867

Cyclic hardening of Al-Zn single crystals at constant plastic strain amplitude, observing similarity between fatigue hardening and work hardening

22 p3189 A72-42439

Influence of the degree of strain-hardening and roughness of friction surfaces on wear rate and carrying capacity

22 p3183 A72-43157

Strain hardening effect of Ni, Mn and Mo in Cr steel after high temperature annealing

23 p3301 A72-43742

Microinhomogeneous elastoplastic cyclically strain hardenable material under symmetric loading, calculating stress-strain relationship

24 p3458 A72-44928

Deformation stresses and strains in quasi-static low cycle fracture of stabilizing, softening and strain hardening materials

24 p3460 A72-45739

STRAIN RATE

Ground test determination of design data for low supersonic high density air deployable deceleration systems, considering high strain rate effects on parachute materials

01 p0005 A72-10313

Eutectic Ni-Cr alloy temperature effects on deformation rate on plasticity, noting superplasticity point

02 p0244 A72-12243

Yield stress effects at high strain rate on finite crack unsteady motion

03 p0446 A72-13705

Portevin-Le Chatelier effect in Al-Mg single crystals during tensile tests, investigating strain rate influence on stress

03 p0378 A72-14257

Infinite elastic-plastic beam impact by semiinfinite elastic rod, computing strain-time profiles

04 p0583 A72-14447

Substitutional dynamic strain aging effects on Fe-Nb alloys mechanical properties, attributing ductility reduction to work hardening and strain rate effects

04 p0534 A72-15576

Near tip strain criterion validity for ductile crack growth on specimen surface

05 p0673 A72-16307

Test conditions, specimen batch and method effects on accuracy of rapid fatigue limit tests with increasing stress amplitude

05 p0741 A72-17085

Dynamic strain aging significance in titanium, observing reduction of temperature and strain rate effects on stress-strain curves shapes

06 p0830 A72-18054

Low temperature slip discontinuity and strength of pure Al crystals as function of strain rate

06 p0831 A72-18355

Anomalous temperature-strain rate dependence of Ni-Al intermetallic compound mechanical properties from plastic deformation mechanism

06 p0832 A72-18417

Solid solution yield strengthening and weakening of V-Ti alloys, investigating strain rate sensitivity temperature dependence as indication of two deformation mechanisms

07 p1021 A72-20434

Strain rate effects on strain hardening of duralumin, copper and lead, noting yield stress sensitivity to deformation induced temperature changes

07 p0998 A72-20527

Temperature dependence of strain rate sensitivity in low temperature deformation processes, considering inherent lattice conditions and impurity atoms effects

07 p1022 A72-20573

Fiberglass reinforced plastics creep characteristics under high strain rate loading-unloading conditions

08 p1195 A72-21855

Viscoplasticity techniques application to deforming portion strain and strain rate fields of axisymmetric Al alloy extrusion with various flow patterns

08 p1250 A72-22194

High temperature alloy deformation superplasticity and formability relation with microstructure, fine structure and load requirements for hot working with high strain rate

08 p1250 A72-22200

Fracture toughness tests on Al-Cu alloy plate, noting insensitivity to strain rate

09 p1328 A72-22913

Time and cycles to failure diagrams for strain rate and hold periods effects on high temperature metal creep fatigue in design analysis

09 p1407 A72-23199

Fatigue indicators with analytic or visual notched and cracked coupons techniques and strain multipliers for welded structures

09 p1316 A72-23620

Equivalent stress and plastic strain rates, based on shear stress hypothesis for theory of anisotropic plasticity of plastic materials under combined stress

10 p1553 A72-23745

Transient strain in axially impacted hollow non-homogeneous cone with axially varying modulus of elasticity and density

10 p1555 A72-24195

Ultrahigh strain rate measurement via diffraction gratings directly impressed into test material surface, recording outputs by high speed cameras or photoelectric techniques

10 p1487 A72-24573

Torsion testing machine for hot metal workability tests at constant strain rate

11 p1639 A72-25820

Temperature and strain rate effects on superplasticity of Ni-Cr eutectic alloy

11 p1659 A72-26129

Residual stresses and stress relaxation determination in electrochemical galvanic coating with automatic strain curve plotter

11 p1613 A72-26264

Alpha Zr tensile properties tests noting strain aging effects on strain rate, work hardening and ductility anomalies

11 p1661 A72-26595

Electron microscope observed dislocation splitting in bent thin tantalum carbide sheet, analyzing results in terms of strain rate law and carbon diffusion model

11 p1669 A72-26948

Mathematical model for dynamic yield point dependence in strain rate based on similarity and dimensionality theories and Weierstrass theorem

13 p2054 A72-28458

Strain rate controlling mechanisms of superplastic deformation at various stresses and temperatures, considering vacancy and dislocation creep and grain boundary sliding

13 p1974 A72-28657

Temperature and strain rate dependence of austenitic stainless steel fracture by low cycle fatigue at high temperatures, studying striations with scanning electron microscopes

13 p1979 A72-29449

Strain work per unit time for static and dynamic pressing processes, taking into account inertial forces

13 p1966 A72-29466

Closed form solutions for one dimensional nonlinear waves in strain rate-sensitive elastoplastic material, describing dispersed wave motion behind propagating shock front

14 p2164 A72-30298

Low and medium strain rates and temperature effects on bcc structure polycrystalline Nd and Mo, determining mechanical properties of yield and flow

14 p2114 A72-30367

Plastic deformation in metals and highly crystalline polymers as function of shear strain, strain rate, frequency and vibrational amplitude

15 p2328 A72-31840

Mechanical vibrations effect on flow stress and strain rate from tensile and creep tests as function of amplitude

15 p2257 A72-31841

Mobile dislocation density and strain rate sensitivity of bcc Fe-Ni alloys from deformation onset to high temperature plateau

15 p2258 A72-32639

Elastic-viscoplastic solution for deformation of impulsively loaded strain rate sensitive steel rings

16 p2464 A72-32916

Strain rate history effects on stress incremental wave front propagation in elastic bars, considering Taylor-Karman-Rakhmatulin theory

16 p2466 A72-33103

Test equipment for high strain rates in shear with torsional split Hopkins pressure bar

16 p2373 A72-33196

Stress-strain diagrams for constant strain rates in shear of Ti from torsion test machine, deriving constitutive equation for dynamic overstress

16 p2405 A72-33197

Stress-strain curve correction for triaxial stress state and strain rate at arbitrary temperatures, describing instrument for continuous test specimen profile measurement

16 p2469 A72-33232

Al-Mg solid solution creep at 570-800 K, discussing creep rate controlling mechanism due to Mg atoms interactions with dislocations

16 p2407 A72-33442

Strain rate and temperature effects on supersaturated Al-Cu-Mg solid solution mechanical properties, considering ultimate tensile strength and hardening

16 p2407 A72-33443

Forces and strain rates measurement in elastic elements of dynamic systems under impact, discussing test equipment and strain gage transducers

16 p2395 A72-33964

Heteroplastic materials creep characteristics from constant strain rate isothermal traction tests, deriving deformation functions for material behavior beyond elastic range

16 p2412 A72-34120

On uniqueness in ideally elastoplastic problems in case of nonassociated flow rules.

[ASME PAPER 72-APM-33] 17 p2628 A72-34786

An analysis of the split Hopkinson bar technique for strain-rate-dependent material behavior.

[ASME PAPER 72-APM-26] 17 p2628 A72-34792

The dynamic stress-strain behavior in torsion of 1100-O aluminum subjected to a sharp increase in strain rate.

[ASME PAPER 72-APM-6] 17 p2629 A72-34808

Strain rate, stress concentration and temperature effects on hydrogen environment embrittlement of metals

19 p2816 A72-37640

High strain rate and thermal instability torsional impact machines for metal dynamic testing, using shear pin mode control

21 p3039 A72-40229

Simple structures behavior under constant loads, considering low stress levels and creep rupture mechanism with internal damage affecting strain rate.

21 p3117 A72-40673

Effect of the structure of carbon steels on their dynamic properties during dynamic loading

21 p3067 A72-40923

Temperature and strain rate dependences of low cycle fatigue life at high temperatures of austenitic stainless steel, examining crack behavior and stress-strain relations

21 p3069 A72-41010

Dependence of changes in the electronic dissipation-braking force during superconducting transition on the stresses, temperature, and strain rate

23 p3312 A72-43315

Limiting equilibrium of shallow conical shells of variable thickness

23 p3348 A72-43787

Shear-strain-rate effects in a high-strength aluminum alloy.

23 p3302 A72-43983

Characterization of four polymeric materials at strain rates from 0.0001 to 1000 per sec.

24 p3417 A72-44612

Photoelastic verification of a mechanical model for the flow of a granular material.

24 p3460 A72-45697

Low temperature slip discontinuity and strength of pure Al crystals as function of strain rate

24 p3416 A72-45742

STRAIN SOFTENING

U PLASTIC DEFORMATION

STRANDS

Al and Zr single thin strands burning rates at various total oxygen pressures, comparing photographic observation to computations

16 p2479 A72-34001

STRAPDOWN INERTIAL GUIDANCE

Delta and Thor/Agenda satellite launch vehicles, discussing costs, performance and mission planning based on booster design flexibility, incorporating computer programmed strapdown inertial guidance

01 p0136 A72-10952

Quantization errors effect on recursive filter design for strapdown inertial navigation systems, developing suboptimal linear minimum variance

08 p1144 A72-20848

Strapdown inertial guidance and navigation systems: state of art, discussing recent developments in computers, sensors and systems technology

08 p1204 A72-21088

A simplified analysis of the computational requirements for strapdown attitude reference.

[AIAA PAPER 72-827] 20 p2951 A72-39099

Maximum likelihood failure detection for redundant inertial instruments.

[AIAA PAPER 72-864] 20 p2923 A72-39133

STRAPS

A crack stopper concept for filamentary composite laminates.

23 p3305 A72-43498

STRATA

NT SUBSTRATES

STRATEGY

Optimal air defense strategy with budgetary constraints, considering artillery, airborne interceptor and mobile surface to air missile effectiveness against penetrating enemy

03 p0459 A72-14197

Discrete stochastic differential games with quadratic payoff function, deriving deterministic, randomized and game optimal control strategies

06 p0793 A72-17956

Suboptimal stochastic control strategies class based on game theory and optimin principle, investigating completeness in closed discrete-time systems

06 p0794 A72-18167

Game theory application to time optimal control strategy for independent operations set

06 p0794 A72-18168

Optimal strategies for decision chain with controllable connections and finite number of states and decisions, deriving existence theorem

07 p1028 A72-19904

Operator, task level and workload effects on operative strategy, showing controllers methods modification in ATC center 09 p1270 A72-23130

Landing sequence strategy variations for individual ATC operators, indicating dependence on flight progress data variation, existing maneuvering conditions and controller personality traits 09 p1271 A72-23131

Differential games with deviation from encounter, considering strategies for continuous, programmed and discontinuous controlled motion onto given set 10 p1511 A72-24426

Optimality and strategy efficiency in Gaussian elimination on sparse matrix, using graphical method 11 p1678 A72-26496

Multistage pursuit-evasion game on circle, constructing player optimal strategies via measure theory 12 p1836 A72-27511

Differential games extremal strategies with player control action subject to integral constraints 13 p2002 A72-28712

Position differential games of extremal stable evasion strategies for swerving motions with absorption in time 13 p2004 A72-29470

Tracker recovery strategy during temporary target obscuration in pursuit tracking task, analyzing control stick movements 13 p1911 A72-29820

Orbit determination strategy, detailing optimization criterion correlation with measurement errors 15 p2307 A72-31817

On behavior strategy solutions in two-person zero-sum finite extended games with imperfect information. I - A method for determination of minimally complex behavior strategy solutions. 17 p2574 A72-34343

Phase locked loop model based on AGC circuitry, devising optimum control strategies 17 p2532 A72-34419

Second order differential guidance game, formulating strategy for optimal feedback control 18 p2673 A72-36660

Optimal strategies conditions for game problems in conflict controlled system, discussing minimax technique and Bellman equation solution 20 p2947 A72-40028

Differential games extremal strategies with player control action subject to integral constraints 22 p3198 A72-42090

Maneuver strategies for multi-planet missions. [AIAA PAPER 72-914] 24 p3443 A72-45431

STRATHS

U VALLEYS

STRATIFICATION

NT ATMOSPHERIC STRATIFICATION

Blast wave propagation in uniform or gravitationally stratified media, using Brinkley-Kirkwood shock propagation theory 10 p1471 A72-25069

STRATIFIED FLOW

Equilibrium shear flow of stratified brine in cyclically continuous rectangular tank, discussing stable density region erosion by turbulent layers, Richardson numbers, transition layer and entrainment 01 p0051 A72-11228

Linear spin-down of stratified rotating Boussinesq fluid in circular cylinder as function of Prandtl number, noting solar interior problem 01 p0051 A72-11231

Barotropic stability of stratified shear flow to non-geostrophic disturbances by linear analysis 04 p0541 A72-14453

Stratified fluid motion between two parallel infinite disks rotating with different angular velocities 04 p0511 A72-14857

Disk pump driven fluid layer device for density stratified water channel flow measurements, using hydrogen bubble technique 04 p0509 A72-15118

Exact linear dielectric operator for stratified plasma streams with velocity gradients for diagnostics with electromagnetic waves 06 p0861 A72-17748

Turbulence effects in stratified shearing flow, determining relationship between measured mass flux and overall Richardson number 06 p0798 A72-17762

Thermal and momentum diffusivity measurements in turbulent stratified flow, obtaining velocity and temperature profiles [AIAA PAPER 72-80] 07 p0966 A72-18950

Atmospheric kinetic and temperature energy spectral balances in thermally stratified turbulent flow without shear 07 p0980 A72-20454

Similarity theory for turbulently stratified fluid with horizontal and vertical dimensionalities analysis, discussing Karman constant dependence 07 p1031 A72-20698

Turbulence generated by moving obstacle in tank of stably stratified fluid, measuring velocity and concen-

tration fluctuations with hot-film and electrode conductivity probes 09 p1293 A72-22308

Equations of motion for discrete structure fluid, discussing equilibrium pressure and fluid-wall interaction effects 09 p1296 A72-23691

Linear initial value problem of partially mixed cylindrical wave in uniformly stratified fluid, obtaining exact solutions for density and velocity distributions 10 p1466 A72-24299

Inviscid parallel stratified shear flow stability to two dimensional disturbances, solving Taylor-Goldstein stability equation for eigenvalues by computerized numerical integration 10 p1466 A72-24329

Blood flow stratification effect on alveolar gas exchange in liquid filled lungs in dogs from Xe 133 concentration measurements 10 p1425 A72-24481

Smoke trail motions in winds with constant shear, considering potential, vorticity and stratified flows [AD-742738] 10 p1475 A72-24748

Columnar disturbance strengths upstream of obstacle in uniformly stratified or rotating flows relative to validity of Long hypothesis 10 p1470 A72-25063

Drazin method application to thermal stratification effects on unbounded jets and shear layers stability characteristics 11 p1615 A72-25552

Stability of free shear layer in wind tunnel two layered temperature differentiated air flow against small periodic disturbances, noting critical Richardson number 11 p1619 A72-26638

Modified gas dynamic functions of total momentum of plane boundary layer for arbitrarily oriented control surfaces and for stratified flows with potential layer 11 p1574 A72-26973

Atmospheric models for critical flux Richardson number prediction for turbulence maintenance in stratified flows 12 p1840 A72-27702

CAT forecasting based on fluid mechanics experimental studies of stratified shear flows stability and meteorological analyses of aircraft CAT encounters 13 p1994 A72-28866

Prandtl number effect on stratified free shear layer stability, comparing critical Richardson number to linear inviscid theory result 13 p1942 A72-29111

Clear air turbulence nonlinear generation mechanism based on finite amplitude periodic waves in stratified shear flow critical layers, considering buoyancy, viscosity and heat conduction effects 14 p2127 A72-30226

Atmospheric motions prediction with numerical model based on discrete stratified fluid free oscillations 15 p2266 A72-32720

Initial value problem for compressible viscous heat-conducting fluid flows with basic rotation and density stratification in gravitational field 16 p2377 A72-33337

Perturbation methods for density stratified viscous flow past flat plate, using boundary layer and low Reynolds number approximations [AIAA PAPER 72-646] 16 p2381 A72-34086

Finite amplitude disturbances in the flow 8019 of inviscid rotating and stratified fluids over obstacles. 18 p2679 A72-36383

Calculation of airflow over an arbitrary ridge including diabatic heating and cooling. 18 p2706 A72-36629

A theoretical solution of the Lockhart and Martinelli flow model for calculating two-phase flow pressure drop and hold-up. 19 p2787 A72-38392

The enhancement of heat transfer by waves in stratified gas-liquid flow. 19 p2787 A72-38398

Dynamics of stratified liquids in the presence of space charge. 19 p2788 A72-38432

Propagation of Alfvén-gravitational waves in a stratified perfectly conducting flow with transverse magnetic field. 19 p2843 A72-38791

Similarity theory for turbulence in stratified fluid from horizontal and vertical dimensional analysis approach, discussing Karman constant dependence 20 p2948 A72-39013

Rotating fluids density stratification effect on characteristic features of homogeneous Taylor column, noting flow patterns 21 p2989 A72-40652

Steady two dimensional motion during horizontal motion of body at high Richardson number in stratified fluid, considering blocking mechanism 21 p2990 A72-40653

Turbulent boundary layer calculation behind surface cusp, taking into account external flow turbulence and thermal stratification 24 p3390 A72-45008

Tidal waves of a two-layer liquid in a cylindrical basin of revolution rotating about its axis 24 p3392 A72-45073

STRATIGRAPHY

Regional stratigraphy and fabric distribution of volcanic ash flow sheets in northwestern Mogollon Plateau by flow direction technique 15 p2223 A72-31578

Instrumental neutron activation analysis of igneous rock abundances in petrogenic and stratigraphic problems, applying to Colombia River basalts and Apollo 11 rock samples 20 p2899 A72-39829

STRATOCUMULUS CLOUDS

Cumulus and stratocumulus ice crystal and nuclei concentrations, drop size distributions, glaciation differences and enhancement mechanisms 07 p1030 A72-19101

STRATOPAUSE

Methane concentration of air sample from stratopause measured by gas chromatography, discussing sample integrity, analysis method and results 12 p1802 A72-27505

STRATOSCOPE TELESCOPES

High resolution imagery with the large space telescope. 24 p3404 A72-45537

STRATOSCOPE 1 TELESCOPE

U STRATOSCOPE TELESCOPES

STRATOSCOPE 2 TELESCOPE

U STRATOSCOPE TELESCOPES

STRATOSPHERE

Stratospheric aerosol boiling point measurement with photoelectric particle counter, observing sulfate radical as major constituent 01 p0059 A72-10833

Stratospheric CAT relationships to baroclinic zones and Richardson number examined from aircraft observed cross sections data 01 p0096 A72-11282

Mt. Agung volcanic eruption dust effects on monthly-mean lower stratospheric temperatures for tropical stations 01 p0096 A72-11284

Tropospheric processes effects on Northern Hemisphere stratospheric meridional transformations in geopotential field and air circulation 02 p0253 A72-11732

Photochemical models of aeronomic formation and dissociation of hydrogen and ozone in mesosphere and stratosphere 03 p0346 A72-13377

Dynamic modeling of stratospheric and mesospheric circulation and thermal structure 03 p0346 A72-13382

Associative attachment and gas-to-particle conversion mechanisms in positive and negative ion formation up to 50 km 03 p0347 A72-13390

Submillimeter wave stratospheric emission spectra measurement by aircraft- or balloon-borne phase modulated Fourier spectrometry, noting SNR and small errors 03 p0348 A72-13399

Meteorological elements, upper ionospheric data and solar radio emission intensities during winter stratospheric temperature rises 03 p0383 A72-13477

Stratospheric water vapor concentration annual variability from regression analysis of monthly measurements initiated as IQSY program 03 p0385 A72-14148

Air exchange between stratosphere and troposphere from cosmic ray produced radionuclides and fallout comparison with weather development 03 p0351 A72-14359

Stratospheric circulation and air temperature horizontal and vertical distribution, discussing CAT at supersonic transport heights 04 p0541 A72-14676

Water vapor injection into stratosphere by thunderstorms from IR radiometric inference measurements on NASA jet laboratory 04 p0544 A72-15358

French monograph on atmospheric ozone utilization as tracer for troposphere-stratosphere exchanges covering investigations at various locations 05 p0654 A72-15799

Solar effects contradictory relationships with earth atmosphere, discussing geomagnetic disturbance, annual variations, stratospheric transport and high energy particles 05 p0656 A72-16233

Stratospheric rocket sounding on global scale for studies of atmospheric circulation in equatorial zone, polar regions and hemispheres 06 p0840 A72-17620

Quasi-biennial modulation of kinetic energy transfer in stratosphere, comparing with hemispheric energy, eddy transports and tropical zonal wind and temperature 06 p0841 A72-17632

Specific moisture contents in stratosphere over European Soviet Union from balloon measurements 06 p0806 A72-17734

Balloon measurements of lower stratosphere ion conductivity, noting deviation from predicted values based on Thompson ion-ion recombination theory

06 p0808 A72-18094

Ozone content and vertical distribution variations as causes of winter stratospheric warmings in Northern Hemisphere

07 p0973 A72-18861

Atmospheric ozone photochemistry, discussing pure oxygen and moist atmospheres, NO mechanism, tracer applications, stratospheric dynamics and Umkehr observations

07 p0979 A72-20228

Solar modulation of cosmic ray intensity in stratosphere, examining relationship to sunspots group number and heliographic latitudes over 11 year period

07 p1063 A72-20641

Solar cosmic ray flare recording in stratosphere in Murmansk and Antarctic regions during February-April 1969

07 p1066 A72-20649

Mesospheric temperature and wind profiles during stratospheric warming from rocket grenade experiments

08 p1160 A72-21533

Ground based Raman laser backscatter measurement of stratospheric water vapor content, noting 1 ppm accuracy

08 p1161 A72-21825

Nimbus 4 satellite-borne selective chopper radiometer design characteristics, obtaining maps of stratospheric warmings in both hemispheres

08 p1173 A72-22168

Meteorological synoptic analysis of stratospheric planetary wave interaction with lower ionosphere in terms of wind, temperature and ionospheric electron density profiles

09 p1297 A72-22375

Vertical macroturbulence diffusion coefficient and Na 2 and Be 7 flux from stratosphere to troposphere estimated using ground level measurements and two layer model

09 p1376 A72-22416

Horizontal temperature variations relation to stratospheric CAT based on U-2 flight data

09 p1344 A72-22438

Three parameter prognosis model for geopotential vertical profile in troposphere and stratosphere, describing vortex and heat influx in quasi-geostrophic and adiabatic approximations

09 p1297 A72-22549

Stratospheric ozone photochemistry through nitrogen oxides and hydrogen compounds reactions, noting controlling effect of water vapor

09 p1298 A72-22674

Horizontal ozone distribution in middle stratospheric macrosynoptic situations, considering anticyclonic side and jet stream delta region

09 p1301 A72-23194

Balloon sounding observations of lower stratosphere secondary cosmic radiation bursts due to solar activity

10 p1529 A72-24069

Vertical air density gradient in stratosphere as function of altitude

10 p1472 A72-24489

Calibration technique for meteorological superpressure balloon hygrometers designed for horizontal sounding of troposphere and stratosphere

10 p1484 A72-25087

Autumnal stratospheric temperature variations in northern and southern hemispheres from Nimbus 3 IR spectrometer

11 p1680 A72-25761

Stratospheric methane measurements over North America from solar absorption spectra observed from aircraft

11 p1622 A72-25911

Vertical distribution of nitric acid vapor concentration in lower stratosphere from balloon sounding

11 p1622 A72-26086

Meteorological elements, upper ionospheric data and solar radio emission intensities during winter stratomesospheric temperature rises

11 p1682 A72-26247

Stratosphere geopotential height and temperature data observed at Northern Hemisphere radiosonde stations comparison with objectively analyzed data

11 p1682 A72-26474

Numerical model of global scale propagating waves in equatorial stratosphere generated by tropospheric heat sources for Kelvin and Rossby-gravity modes

12 p1839 A72-27029

Coincidence effects of ionospheric extraterrestrial radiation focusing on ionospheric changes and stratospheric warmings

12 p1804 A72-27804

Upper troposphere-lower stratosphere geostrophic wind deviation from rawinsonde and pressure-height data in El Paso-White Sands area, using finite difference method

13 p1988 A72-28447

Transient planetary Rossby waves dynamics in winter stratosphere forced from below, using quasi-geostrophic midlatitude beta plane approximations

13 p1988 A72-28550

Satellite radiance data for altitude and amplitude monitoring of stratospheric warming, comparing with rocketsonde and radiosonde observations

13 p1991 A72-28823

Satellite radiance data to determine stratospheric layer thickness, comparing empirical regression equations to mean weighted temperatures

13 p1991 A72-28824

Mesosphere and stratosphere density and temperature variability with seasons and altitude

13 p1947 A72-28830

Rocket sounding of ozone diurnal variations in upper stratosphere and lower mesosphere

13 p1947 A72-28831

Upper atmosphere water vapor sources and sinks, discussing Hadley cell circulation, convective storm, stratospheric-tropospheric interchange, methane oxidation and volcanic activity

13 p1948 A72-28835

Residence time of water vapor and aerosols in troposphere and lower stratosphere, noting application to air pollution buildup by aircraft

13 p1991 A72-28836

Estimated peak regional concentration of SST exhaust in stratosphere from expected flight operation levels

13 p1991 A72-28837

Stratospheric subsonic and supersonic aircraft emission estimation for water vapor and nitrogen oxides

13 p1991 A72-28838

Stratospheric aerosols physical properties and chemical composition, discussing various measuring techniques and results

13 p1991 A72-28839

Lower stratospheric turbulence and horizontal temperature gradients from RB-57F aircraft meteorological measurements

13 p1993 A72-28864

Synoptic meteorological parameters vs CAT encountered in stratosphere by XB-70 airplane, presenting frequency distributions and probability tables

13 p1994 A72-28867

Stratospheric meteorological characteristics effects on Concorde supersonic flight performance, fuel consumption, dynamic behavior and passenger comfort

13 p1994 A72-28876

SST water vapor and nitrogen oxides exhausts effect on stratospheric composition, developing nonequilibrium photochemical model

13 p1994 A72-28878

Semiannual equatorial wind oscillations in upper stratosphere and lower mesosphere dependence on temperature variations in high and middle latitudes

14 p2099 A72-30259

Balloon flight tracking by Nimbus D satellite to sound tropical stratosphere air motions, noting northward drift maximum in Northern Hemisphere winter

14 p2128 A72-30350

Monthly mean pattern variations for equatorial stratospheric easterly and westerly winds, noting continuity of low latitude regimes

14 p2129 A72-30806

Wind tunnel tests for correction of temperature profile data in stratosphere and lower mesosphere obtained from SKUA rocket sounding

14 p2105 A72-30807

Submillimeter isotropic background limits of stratosphere emission spectrum, using aircraft-borne Michelson interferometer and Rollin far IR detector

15 p2265 A72-31626

Temperature and density data deviation from stratosphere and mesosphere mean season model values at high latitudes

15 p2225 A72-31907

Stratospheric particles analysis by X ray detector on scanning electron microscope, comparing results with data on volcanic particles and cosmic dust

15 p2227 A72-31958

Electrical conductivity in mesosphere and upper stratosphere from rocket sounding by blunt probe technique, suggesting electron density profiles dependence on dissociative recombination variations

15 p2228 A72-31972

Bibliography on SST upper atmosphere environment, listing references to stratospheric structure, composition and physical dynamics, chemical reactions with pollutants, transport properties, etc

16 p2386 A72-33797

Climatic changes due to stratospheric perturbation by propulsion effluents of high altitude aircraft flights [AIAA PAPER 72-658]

16 p2388 A72-34076

SST contrasts stratospheric dispersion by aircraft wake, atmospheric turbulence and exhaust gases temperature induced buoyancy

16 p2388 A72-34084

X-ray bremsstrahlung in the stratosphere and the auroral activity of January 21 and February 3, 1969

18 p2722 A72-36863

Wind patterns at meteor altitudes 75-105 kilometers/above College, Alaska, associated with mid-winter stratospheric warmings.

18 p2689 A72-36962

Numerical prediction of the diffusion of exhaust products of supersonic aircraft in the stratosphere

19 p2748 A72-37824

Features of zonal circulation in the stratosphere and lower mesosphere of the equatorial region during the period of increasing solar activity /1967-1968/

19 p2790 A72-37999

Stratospheric winds and winter warmings in the Southern Hemisphere.

20 p2948 A72-39862

Stratosphere circulation variation in autumns preceding cold winters

20 p2949 A72-39947

Stratospheric winds over Leba rocket sounding station in spring and autumn, 1970.

21 p3049 A72-41500

Stratospheric general circulation patterns from geographical, vertical and annual distribution for Northern Hemisphere temperatures, geopotential heights and winds

21 p3078 A72-41611

Air motions in the tropical stratosphere deduced from satellite tracking of horizontally floating balloons.

21 p3078 A72-41612

Fine structure of temperature stratification in the troposphere and stratosphere

21 p3079 A72-41799

An updated theory for the quasi-biennial cycle of the tropical stratosphere.

22 p3201 A72-42503

Equatorial stratospheric waves induced by diabatic heat sources.

22 p3201 A72-42508

Stratospheric concentration of radioactive carbon from 1961-62 nuclear tests by balloon measurements over European U.S.S.R. territory during 1967-69

23 p3286 A72-44492

On the instability of a three-layer atmosphere with an isentropic stratosphere.

24 p3399 A72-45484

STRATOSPHERE RADIATION

Balloon-borne radiometer-sonde measurement of stratospheric downward emission in absorption spectral region of water vapor rotational band

07 p0982 A72-19105

Stratospheric cosmic ray short period variations at 30 km by spectral density method

07 p1066 A72-20653

High resolution observation of stratospheric submillimeter thermal emission spectrum by helium-cooled InSb electron bolometer on board Comet 2E aircraft

10 p1476 A72-25023

Regression technique for determining temperature profiles in upper stratosphere from satellite measured radiances, noting accuracy

13 p1990 A72-28822

Stratospheric model for bremsstrahlung X ray relation emission to auroral electron flux, considering photon energy release in scintillation counters

17 p2551 A72-35872

Regression technique for determining temperature profiles in the upper stratosphere from satellite-measured radiances.

21 p3052 A72-40249

Seasonal, nonseasonal and synoptic global variations in stratosphere temperature from satellite-measured radiances, discussing latitudinal warming-cooling relationships

21 p3048 A72-40253

STREAM FUNCTIONS [FLUIDS]

Uniqueness of turbomachinery flow calculations using streamline curvature and matrix through-flow methods

03 p0308 A72-13648

Plasma layer growth and equilibrium magnetic fields for astron configurations, solving stream function by finite difference methods

07 p1042 A72-19512

Nonuniform plane parallel plasma streams instability with/without magnetic field, comparing with conducting fluid

07 p1042 A72-19618

Navier-Stokes equation numerical solution methods, expressing boundary conditions by separate equations for vorticity and stream function

07 p0970 A72-20077

Stream functions for steady two dimensional flow field of viscous liquid near circular whirl

08 p1148 A72-20937

Resonant frequencies of viscous liquid in rectangular tank calculated from stream functions, assuming two dimensional oscillations and laminar flow

09 p1295 A72-23074

Turbulent boundary layer characteristics of rotating helical blade in annulus contained fluid, calculating boundary layer growth and streamline angles via momentum integral equations

10 p1466 A72-24296

Mass flow and current distribution in magnetic MPD accelerator thruster plumes calculated from meridional flow stream function equation

11 p1696 A72-26224

Subsonic and supersonic flow around nonaxisymmetric fuselages, deriving streamlines differential equations based on camber line distribution of source, dipole and quadrupole singularities

11 p1573 A72-26578

Streamlines and fluid diffusion determination for axisymmetric irrotational and rotational flows in ducted propellers, noting conformal mapping of arbitrarily shaped domain onto rectangle 12 p1751 A72-27168

Stream surfaces of three dimensional sub and supersonic irrotational gas flows in variable cross section channels and nozzles 13 p1895 A72-30004

Direct integral method to calculate subsonic and supersonic regions in planar and axisymmetric hyper-sonic flow, using stream function for velocity and density [DFVLR-SONDDR-202] 16 p2343 A72-33421

Flow pattern of two impinging circular jets. 17 p2540 A72-35233

Determination of the stream function of a perturbation associated with a plane jet 18 p2680 A72-36470

Slow motion in a two-dimensional semi-infinite channel with moving walls. 18 p2683 A72-37044

Flow of a non-Newtonian fluid in a tube with sinusoidal deformation. 21 p3044 A72-40192

Stewartson transformation correlating three dimensional compressible boundary layer growth on impulsive moving body, assuming small cross flow 21 p3047 A72-41782

Stream surfaces of three dimensional sub and supersonic irrotational gas flows in variable cross section channels and nozzles 22 p3135 A72-42727

Behavior of the lines of flow in the proximity of the stagnation points of blunt bodies 22 p3136 A72-42905

STREAMLINE FLOW
U LAMINAR FLOW
STREAMLINED BODIES
NT FAIRINGS
Acoustical field from streamlined body of revolution moving in homogeneous gaseous medium past seminfinit rigid screen, using Wiener-Hopf method for diffraction radiation 03 p0340 A72-12916

Critical streamline length in axisymmetric and plane ideal gas flows past conical bodies as function of Mach number and form parameter 06 p0755 A72-17677

STREAMLINING
Multiplicity theorem for aligned steady MHD flows of inviscid perfectly conducting gas, assuming constant density along streamline 19 p2840 A72-37405

Streamline and fieldline geometry with applications to MHD flow kinematic properties, discussing field and momentum relations decomposition in terms of sound velocity 23 p3322 A72-44270

STREAMS
NT GAS STREAMS
Axial and tangential velocity distributions within trailing line vortex to large distance downstreams of generating wing extended from available data [AD-743599] 01 p0001 A72-11135

STRENGTH
Strength and plasticity characteristics of hardened multilayer structural steels, investigating layer thickness effect 07 p1013 A72-19746

STRENGTH OF MATERIALS
U MECHANICAL PROPERTIES
STRESS (BIOLOGY)
Sex differences of chronic effect of environmental stress on blood pressure and information processing in rats, observing neurotic hypertonic blood pressure irregularity 07 p0925 A72-20660

Lipid composition of growing and starving cells of *Arthrobacter crystallopoietes*. 17 p2505 A72-35835

STRESS (PHYSIOLOGY)
NT ACCELERATION STRESSES (PHYSIOLOGY)
NT CENTRIFUGING STRESS
Shock-induced fighting effect on pituitary adrenocorticotrophic hormone ACTH and adrenocortical steroids plasma concentration in rats, relating psychological stress to physiological function 05 p0617 A72-16080

Adrenocortical steroids during acute exposure to environmental stresses, noting effects of injected cortisol removal, uptake and release 06 p0763 A72-17874

Hemodynamic response to running exercise stress for aeronautics personnel selection, determining systolic ejection variation measurement and cardiac frequency increase 07 p0927 A72-19242

Isolation stress effect on excretory products in unrestrained chimpanzee, suggesting Ca to P excretion ratio as physiological stress indicator [AD-739467] 07 p0921 A72-20179

Isolation stress effect on micturition circadian rhythm and diuresis occurrence in unrestrained chimpanzee under entrained and free running conditions [AD-739468] 07 p0921 A72-20180

Isolation stress effect on circadian rhythmic patterns of EEG activity during sleep-wake and sleep cycles in unrestrained chimpanzee [AD-739469] 07 p0921 A72-20181

Human performance and exhaustion predictive model from responses to exercise and environmental stresses, considering circulation, thermal regulation, work load and oxygen pressure effects 07 p0934 A72-20358

Light-dark cycles and physiological stress stimuli effects on circadian rhythm in rat blood serum serotonin levels 08 p1115 A72-21081

Behavioral inaction under stress conditions similar to survivable aircraft accident, tabulating hesitation statistics 08 p1109 A72-21570

Human blood serum 11-oxy corticosteroid content after maximum stress exercise, noting heart rate and blood pressure changes 09 p1266 A72-22878

Time series analysis of physiological and work study data in ATC tasks, using heart rate as strain indicator 09 p1271 A72-23137

Elastic lung shaped model for distribution analysis of weight induced stresses, strains and surface pressures in lung 10 p1425 A72-24479

Food deprivation stress effects on urinary excretion values in unrestrained chimpanzees 10 p1426 A72-24822

Electromyogram and myogram responses in phasic stretch reflex under prestrain conditions as index of fusimotor activity level in normal humans 11 p1588 A72-26632

Physiological index changes in parachutists of various ages, considering plasma recalcification, blood prothrombin, heparin time, fibrinolytic activity, pressure and heart beat 11 p1590 A72-26988

Human cardiovascular function change as indication of hypoxic circulatory stress, using noninvasive cardiographic measurements of cardiac electromechanical time intervals 12 p1769 A72-27470

Hemodynamic response to physical exercise stress in dogs with angiotensin-induced acute arterial hypertension 12 p1764 A72-28216

Physiological and subjective responses of physically fit young men to combined exercise-carbon dioxide stress tests 12 p1767 A72-28311

Underwater tests of instrument system for combined skin temperature and direct heat flow measurement in thermally stressful environments 12 p1768 A72-28334

Parotid fluid 17-hydroxycorticosteroid level relation to hyperthermia stress at various heat levels during thermal environmental testing 12 p1768 A72-28335

Human visual accommodation biorhythm and reactions under hard physical work and visual stress 13 p1909 A72-28749

Russian book on functional morphology under extremal space flight conditions covering overloads, hypoxia and hyperoxia effects on organism and cellular structure and metabolism 14 p2077 A72-30996

Noise and vibration stress combined effects on human mental performance as function of time of day, taking into account circadian rhythm factor 14 p2081 A72-31083

Heat chamber treadmill work-induced thermal stress effects on reaction time to foveally and peripherally presented visual stimuli 14 p2078 A72-31154

Monograph on hot environments stress covering heat exchange at skin surface, clothing effect, body temperature regulation and sweating control 15 p2185 A72-31515

Heat, noise and vibration stress combined effects on skin and rectal temperature, heart rate, weight loss and biochemical urinalysis [AD-746083] 17 p2508 A72-34551

Comparison of physical, biophysical and physiological methods of evaluating the thermal stress associated with wearing protective clothing. 20 p2898 A72-39808

Human tryptophan and tyrosine metabolism - Effects of acute exposure to cold stress. 21 p2997 A72-40417

Prediction of vegetative reactions in the case of stress and extreme effects upon the organism 22 p3149 A72-42069

Effects of externally imposed mechanical resistance on breathing dense gas at exercise - Mechanics of breathing. 22 p3150 A72-42489

Heat acclimatization by exercise-induced elevation of body temperature. 22 p3151 A72-42741

Nervous mechanisms of the acoustic stress reaction 22 p3148 A72-43169

Nervous-emotional stress as a problem of modern work physiology 22 p3148 A72-43170

Calcium metabolism under stress and in repose. 23 p3254 A72-43389

STRESS [PSYCHOLOGY]
Vibration space analysis for human voice characteristics change during unintended speech under experimental psychological stresses and actual emergency situations 01 p0017 A72-10213

Phenamine and aminazine effects on subthreshold sound perception and adrenoreactive excitability of unstable subjects under emotional stress 04 p0476 A72-15586

Shock-induced fighting effect on pituitary adrenocorticotrophic hormone ACTH and adrenocortical steroids plasma concentration in rats, relating psychological stress to physiological function 05 p0617 A72-16080

Time shortage as stress factor affecting mental activity of operator in man-flying vehicle system, discussing control signal handling efficiency 05 p0622 A72-16638

Aeromedical diagnostics for aircraft pilot hearing sense tests, considering cockpit environment and stress-produced impairments in central nervous system 05 p0623 A72-16781

Emotional aspects of pilot performance under high stress in emergency situations, discussing psychophysiological training methods 05 p0623 A72-17098

Human immediate memory adaptation to speed stress, discussing response time and performance accuracy relationship to stimuli complexity and input speed 06 p0766 A72-17716

Evoked cortical potentials changes from emotional visual word stimuli stress under amylid anticholinesterase drug influence 08 p1116 A72-21194

ATC operator stress factor evaluation from information theory analysis of radio telecommunication information content 09 p1271 A72-23134

Ergonomic simulators for testing individual mental working capacity, using stress-strain and fatigue relation 09 p1272 A72-23140

Camera shake under stress of tracking moving targets viewed briefly in poor light, considering blur in horizontal and vertical dimension 10 p1483 A72-24986

Increase in skeletal muscle performance during emotional stress in man. 17 p2500 A72-34942

Psychic adaptation of man to a long-duration stay in space 22 p3149 A72-41988

The function of external respiration in mental activity 22 p3150 A72-42284

Nervous mechanisms of the acoustic stress reaction 22 p3148 A72-43169

Nervous-emotional stress as a problem of modern work physiology 22 p3148 A72-43170

STRESS ANALYSIS
NT PHOTOGRAPHIC MEASUREMENT
NT SCHWARTZ METHOD
NT X RAY STRESS ANALYSIS
Structural sandwich panel design, establishing simple stress and deflection formulas under transverse loading based on tests evaluating balsa as laminate core 01 p0138 A72-10723

Stress effects on TiNi compound martensitic transformation, investigating deformation as function of composition and heat treatment 01 p0087 A72-11023

Constant stress and compression creep testing in vacuum conditions, describing simple spring loaded apparatus characteristics and performance 01 p0071 A72-11171

Fiber reinforced composite rotating disks stress-strain state calculation, discussing steady state closed solutions and approximate methods 01 p0142 A72-11175

Analytical and graphical calculations of stress concentration coefficients and stress gradients in machine parts with recesses and finite depth cuts 01 p0144 A72-11377

Analytic yield surface in work hardening including stress in transition range after load change /Bauschinger effect/ 01 p0144 A72-11388

Dislocations forces during sintering of loose and cold-pressed metal powders, using photoelasticity for

stress estimation and electron microscopy for defects structure

02 p0232 A72-11430

Structural analysis of cable stayed bridge scale model with fractional and full loading, showing system linear behavior with small displacements and real nonlinearities, respectively

[SESA PAPER 1896] 02 p0199 A72-11515

Stress and failure analysis of glass-epoxy composite plate with circular hole under uniaxial tension by finite element method

[SESA PAPER 1942] 02 p0248 A72-11517

Isothermal uniaxial stress analysis of material consistent with linear law of heredity theory, determining viscoelastic relaxation function

02 p0290 A72-11621

Deformation, stress and singularity in cylindrical shells under concentrated circumferential loads, comparing with two dimensional elasticity and plate bending

02 p0291 A72-11662

Stress analysis for transverse deformation of fiber reinforced composites

02 p0249 A72-11991

Composite rotating sphere with concentric inhomogeneity of elastic constants and outer boundary free from tractions, calculating stress by digital computer

02 p0259 A72-12180

Elastic quadrant shaped disk loaded on horizontal and vertical edges, determining stress values at arbitrary points

02 p0259 A72-12235

Finite element technique for stress analysis of rotating bodies under axially symmetric stresses

02 p0293 A72-12343

Nonlinear deflections and radial surface stresses in thin elastic circular glass plates with coaxial rings

02 p0249 A72-12418

Inhomogeneous microstructure elastoplastic medium, examining strain and work in plastic deformation

02 p0293 A72-12427

Contact stress between half plane and elastic cover plate, reducing problem to Prandtl type integrodifferential equation with Hilbert kernel

02 p0294 A72-12433

Stress analysis of pressurized ribbed cylindrical shell with intersecting reinforced circular hole under internal pressure

[ASME PAPER 71-PVP-8] 02 p0294 A72-12470

Plastic collapse limit analysis for combined edge and pressure loading on circular cylindrical shells for Tresca yield condition

[ASME PAPER 71-PVP-22] 02 p0295 A72-12474

Improved finite difference solutions for stress in thin cylindrical shells, using Donnell assumptions

[ASME PAPER 71-PVP-24] 02 p0295 A72-12475

Elastic equilibrium in circular conical orthotropic shells of linearly variable thickness, investigating stresses under arbitrary loads

02 p0297 A72-12615

Finite element formulation for nonlinear large deflection elastic analysis of displacements and stresses in thin plate structures

02 p0298 A72-12657

Bending stress analysis of rectangular plate with variable stiffness applied to marine propeller blade

02 p0298 A72-12673

Bending stresses in composite shell at conical interface between metal and fiberglass reinforced plastic portions under internal pressure

02 p0298 A72-12683

Pressure vessels with cracks, formulating stress analysis for safety factors

03 p0443 A72-13452

Nonstationary thermoelastic stress determination in hollow cylinder walls under convective heat transfer

03 p0443 A72-13459

Mechanical response of Al and Cu under complex strain histories conditions, using endochronic theory of viscoplasticity without yield surface

03 p0444 A72-13504

Stresses due to initial elastic deformations in orthotropic thin plate strip, expressing Dirac function by Fourier series and integral

03 p0444 A72-13505

Strain anisotropy effect on thin walled tubular steel samples with combined bending and torsion, constructing matrix and stress vectors

03 p0445 A72-13578

Displacement equations for rotating cylinder of revolution with stress on boundary corresponding to centrifugal force

03 p0445 A72-13625

Yield stress effects at high strain rate on finite crack unsteady motion

03 p0446 A72-13705

Disk shaped frame corner stress under external load, using complex variables and conformal mapping

03 p0448 A72-13886

Axisymmetric Reissner-Sagoci problem in linear micropolar elasticity for stress and displacement under load applied by rigid circular disk

03 p0448 A72-13890

Elastic-plastic stress-strain analysis of beams with uniform cross section under combined loadings by finite element method

03 p0449 A72-13975

Creep rupture test program for Al alloys, circumventing parametric methods limitations by extrapolation procedure with graphical extension of isostress curves

03 p0378 A72-14174

Statistical methods of stress and reliability analyses of elastic systems under random external loads

03 p0453 A72-14206

Biharmonic stress and displacement potentials for two dimensional boundary problems in elasticity theory, using Galerkin method

03 p0453 A72-14207

Mathematical plasticity theory of stress-strain relations under complex loading, including broken line trajectories

03 p0453 A72-14211

Rheological relations of moment-stress plasticity for steady and cyclic loads, using small elastoplastic strains

03 p0453 A72-14212

Iteration method error estimates for thin elastic shell basic stressed state and simple fringe effect relation to boundary stressed state

04 p0586 A72-15012

Thermoviscoelastic stress analysis for hollow circular cylinder with reinforcing interlayer under pressure, axial tension and nonstationary temperature field

04 p0587 A72-15016

Convergence of iterative schemes for calculating stress state of thin shells with allowance for nonlinear terms in differential equilibrium equations

04 p0587 A72-15048

Elastic strip stresses and displacements, using eigenfunctions with coefficients determined by variational principles

[ASME PAPER 71-APMW-24] 04 p0589 A72-15181

Papers on aerospace structure by N. J. Hoff covering aircraft framework, stress analysis, structural stability, shell theories, bending, buckling, monocoque and sandwich structures, etc

04 p0591 A72-15238

Uniaxial stress effect on monocrytalline niobium stannide superconducting transition temperature, considering crystal structure

04 p0562 A72-15293

Mean stress and overload effects on mild steel service life, using fatigue damage summation method

04 p0592 A72-15475

Stress and strain approximate analysis for thin elastic shells by rational derivation of two dimensional differential and constitutive equations

[AD-745612] 04 p0592 A72-15506

Safe stressing of high strength and locally nonbrittle solid bodies, testing hard polymers at room temperature

04 p0593 A72-15656

Non-Newtonian real fluids flow characteristics, determining stress-deformation relationship by tensor analysis, with application to lubrication theory

04 p0528 A72-15742

Boundary collocation method for estimating stress intensity factors for through-thickness interior crack in finite rectangular plate

[ASME PAPER 71-MET-L] 05 p0732 A72-15794

Compounded rotating disks stress-strain analysis from equilibrium and compatibility equations and boundary condition, comparing results with photoelastic and finite difference approximation

05 p0732 A72-15804

Ni alloy stress rupture data correlation and extrapolation from computerized evaluations of time-temperature parameters relative abilities

[ASME PAPER 71-WA/MET-4] 05 p0670 A72-15905

Elastic analysis of circular cylinders with stress singularities from boundary discontinuities, mixed displacement and axial load conditions

[ASME PAPER 71-WA/APM-18]

05 p0733 A72-15962

Shell bending and Timoshenko-type theory to solve stresses of semiinfinite elastic circular cylindrical shells produced by radial pressure pulses

[ASME PAPER 71-WA/APM-16]

05 p0733 A72-15964

Elastic stress field in hollow circular cylindrical anisotropic body under surface tractions expressed as Fourier series

[ASME PAPER 71-WA/APM-13]

05 p0734 A72-15967

Transient stress analysis for sudden twisting of penny-shaped crack in infinite elastic body under torsion, using integral transform

[ASME PAPER 71-WA/APM-10]

05 p0734 A72-15969

Turbine casing components stresses in presence of creep, demonstrating calculation method validity for thick-walled structures by elastoplastic analogy

05 p0734 A72-15985

X ray topography of natural diamond, showing impurity platelet distribution, slip depth, temperature and stress conditions after plastic deformation

05 p0702 A72-16020

Approximate maximum shock stress analysis for curved bar bending vibration due to longitudinal impact by disregarding elements inertia with regard to axial motion

05 p0737 A72-16285

Disk stretching under tensile stresses, determining stress at arbitrary point in half band form connected with quadrant

05 p0737 A72-16294

Asymmetric micropolar elasticity plane problem, solving equilibrium equations with Fourier transformation for displacements, rotation and stresses

05 p0737 A72-16296

Optical interference technique for experimental stress analysis of cracked structures, obtaining crack shape relationship to stress intensity factor

05 p0666 A72-16321

Plastic stress and strain intensity factors for cracked plates in tensile fields

05 p0737 A72-16323

Stress analysis of radial flow impeller disk due to centrifugal force in steady state of high speed rotation by matrix finite element method

05 p0741 A72-16996

Strength analysis of hyperboloidal electric wire joint designs, expressing stress as function of contact loads

05 p0616 A72-17059

Semiempirical stress analysis of cantilevered thin walled cylinder, obtaining local stresses via strain gages

[SAE PAPER 720285] 06 p0893 A72-17324

Stress and displacement solutions to elastic deformation of homogeneous and composite anisotropic near cylindrical bodies, using Almansi algorithm

06 p0894 A72-17688

Axisymmetric stress analysis in various weld configurations of stub end high pressure pipe connections, using finite element method

06 p0820 A72-17709

Photothermoelastic analysis of shrinkage stresses near discontinuity in fiber composite material, relating matrix cracking to fiber packing

06 p0835 A72-17800

Interferometric holography application to photoelastic stress analysis of opaque anisotropic composite plates under static and dynamic transverse and in-plane loads

06 p0898 A72-18349

Diffused failure model as basis for plotting delayed fracture curves in space of principal stresses

06 p0898 A72-18532

Brittle strength characteristics of construction materials with cracks calculated by graphical analysis procedure, considering state of limiting equilibrium

06 p0899 A72-18560

Transverse strains in solid body due to volumetric stresses counteraction to external load stresses

06 p0899 A72-18566

Semiconductor device IC encapsulation, thermal design, stress analysis, testing and applications

06 p0791 A72-18577

Resolved shear stress formula for shafts under simultaneous tangential bending and torsion acting at dangerous points of cross section

06 p0899 A72-18643

Two- and three dimensional photoelastic experiments evaluation to obtain principal stresses differences

07 p1088 A72-19171

Flexure analysis of isotropic Reissner flat plate, bonded by adhesive layer, deriving stress distribution equations in general tensor form

[AIAA PAPER 71-148] 07 p1089 A72-19688

Plane harmonic waves propagation in stressed polycrystalline bodies with slight orthotropy in unstressed state, substantiating theory for initial stress determination by ultrasonic technique

07 p1090 A72-19753

Experimental determination of torsional stresses in rod from moire patterns, describing facility and procedure

07 p1091 A72-19762

Stress analysis of infinite plate with parallel cracks under symmetrical edge loads

07 p1092 A72-19781

Approximate stress calculation in friction pulley shells of multipulley hoisting machines, using method of initial parameters

07 p1094 A72-20134

Method of images solution for stress systems in rectangular plate under general self equilibrant edge tractions

07 p1095 A72-20244

NASTRAN/NASA structural analysis program for computer stress analysis based on finite element method, noting vibration, acoustics, transient motion and random response applications

08 p1138 A72-21325

Book on plasticity theory covering stress and strain as basic concepts of continuum mechanics, differential equations of motion, plastic flow, yield criteria, elastic-plastic equilibrium, plane strain, etc

08 p1244 A72-21477

- Plastics optimal reinforcement in given stressed state by determining shortest path from stress point to strength region 08 p1244 A72-21502
- Uniaxially stressed elastic /soft/ shells with fold formation during compressive strain, formulating equilibrium and boundary conditions for uniaxial region 08 p1247 A72-21812
- Perforated flexible polymer plates stressed state problem with boundary conditions and viscoelastic and creep properties effects 08 p1248 A72-21861
- Stress-deformation effects on gasket joint of metal seals at high pressures 08 p1178 A72-21933
- Secondary normal stresses in fixed flange zone of thin walled nonlinearly elastic pipe under bending moment and torsion 08 p1249 A72-22096
- German monograph on bending theory extension for stress analysis of disks and cylindrical shells 09 p1397 A72-22333
- Somigliani dislocations effect in infinite elastic cylinder, determining stresses in form of eigenfunctions expansions 09 p1398 A72-22491
- Stress analysis of isotropic linearly elastic square plate of constant thickness loaded by concentrated forces at edges 09 p1399 A72-22698
- Thermal stress-strain state analysis of nonlinear elastic medium by small parameter method 09 p1400 A72-22717
- Two dimensional thermoelasticity problem with nonstationary temperature field and external boundary forces, using algorithm to evaluate stress-strain state of welded plates 09 p1401 A72-22725
- Infinite elastic solid deformation in antiplane strain mode, discussing corresponding strain model with continuous distribution of slipping edge dislocations 09 p1405 A72-22919
- Microelastic stress mechanics of thinly laminated orthotropic multilayered plates, taking into account skin effect 09 p1405 A72-22994
- Papers on design for high temperature environments covering structural fatigue, creep interaction and ratchetting deformation and inelastic stress analysis 09 p1406 A72-23196
- Mathematical model and inelastic stress analysis for metal creep-fatigue interaction and progressive deformation in breeder reactors operation 09 p1407 A72-23200
- Influence coefficients for circumferential stress resultants in thin conical shell elements without edges interaction 10 p1555 A72-24192
- Metal creep under multiaxial stress states, proposing technique for numerical stress analysis data collection [SMRT PAPER L 1/3] 10 p1556 A72-24395
- Green function for stress components in circumferentially loaded circular disk, noting conformal mapping for arbitrary shape 10 p1557 A72-24717
- Green function for stress components in straight edge loaded half plane disk, noting conformal mapping for arbitrary shape 10 p1558 A72-24718
- Carbon steel fatigue crack propagation rate dependence on strength and stress history, discussing conditions for crack nonpropagation 10 p1499 A72-24889
- Flugge equations for circular cylindrical shells buckling under compression, considering Donnell theory limits, stress determination and boundary conditions 10 p1560 A72-25025
- Thermal stresses and displacements in elastic medium containing parallel circular cracks, using perturbation technique 10 p1560 A72-25045
- Photothermoelastic analysis of temperature and rupture stress in cryogenic tanker structures, using steel and plastic ship models [AIAA PAPER 72-344] 11 p1728 A72-25373
- Stiffness, stress and deformation analysis of discretely attached corrugated shear webs, using minimum potential energy and calculus of variations methods [AIAA PAPER 72-351] 11 p1728 A72-25380
- Finite element structural analysis for local buckling stresses in flat plates, panels and thin walled columns, deriving elastic and geometric stiffness matrices [AIAA PAPER 72-354] 11 p1729 A72-25383
- Stress analysis of short beam bending of graphite fiber reinforced epoxy composites 11 p1671 A72-25464
- Anisotropic graphite composite laminates cutouts stress analysis by finite element method, predicting structural reinforcement behavior 11 p1672 A72-25475
- Fiberglass-graphite reinforcement of unidirectional epoxy laminates, examining longitudinal composite fracture stress and strain and tensile and compressive stiffness 11 p1672 A72-25485
- Perforated plates plastic deformation, stresses and strains near holes, using strain gage data in biaxial tensile tests 11 p1733 A72-25540
- Torsional stress analysis of rectangular beam composed of two elastic materials, using complex variable and conformal mapping 11 p1733 A72-25544
- Computerized analysis of prismatic rectangular plate assemblies natural frequencies and initial buckling stresses 11 p1734 A72-25731
- Bending stress in oxygen presaturated Nb during oxidation, cooling, dissolution and annealing, using thin film model 11 p1658 A72-25853
- Upper yield stress effect on elastoplastic behavior of mild steel in bending and torsion, noting relationship to strain rate 11 p1659 A72-25894
- Book on turbulence covering Reynolds stresses, kinetic theory of gases, vorticity dynamics and mixing length models 11 p1616 A72-25925
- Thermoelastic stress and displacement in thin finite rod due to distributed time dependent heat sources 11 p1736 A72-25991
- Infinite elastic thick plate with loads symmetrical to axis of revolution and middle plane, analyzing stress functions, Fourier-Bessel expansion and photoelastic experiment 11 p1626 A72-26427
- Plastic materials adaptability to solid and hollow turbine blades, deriving thermally and mechanically induced stresses 11 p1738 A72-26799
- Plastic percentage reduction of area and elongation for circular cylindrical sample in tensile deformation, proposing stress analysis method for metallic sleeves under low cycle loads 11 p1738 A72-26810
- Conventional and explosive compacting effect on density distribution in green briquettes, investigating normal and shear stresses 11 p1643 A72-26830
- Book on thermal stress analysis covering equivalent thermal loads, bars, beams and rings extensional and bending deformation, shells, strain energy methods, etc 11 p1739 A72-26925
- Finite difference method for bending stresses calculation in rotating disks subjected to irregularly distributed temperature, deriving digital computer program algorithm 11 p1712 A72-26976
- Glass sample mechanical strength testing, considering abrasion process, concentric ring stress calculation and laser light scattering techniques 12 p1832 A72-27007
- Bending of unbounded plate coupled to elastic isotropic half space with vertical and horizontal springs, calculating contact stresses by double Fourier transforms 12 p1878 A72-27082
- Stress-strain state approximation for isotropic strip with circular hole, noting method adaptability to computer computations 12 p1880 A72-27232
- Stress-strain state determination for closed cracked cylindrical shell, using Fredholm integral equations 12 p1880 A72-27236
- X ray determination of thermal microstresses in metal specimens surfaces 12 p1807 A72-27447
- Plastic deformation resistance nonuniformity in Al alloys, determining stresses 12 p1829 A72-27457
- Materials selection for models used in thermal stress studies by restrained shrinkage method with emphasis on polyurethanes 12 p1813 A72-27460
- Algebraic equations for displacement and stress vectors at faces and interfaces of elastic multilayered cylinders and infinite wedges, using matrix method 12 p1884 A72-27565
- Volume averages of stress and strain changes induced by Poisson ratio variation in boundary value problems of three dimensional classical elastostatics 12 p1884 A72-27566
- Fiber composites plastic flow and fracture, using plane strain model for analysis 12 p1884 A72-27730
- Cadmium sulfide solar cells stress analysis in relation to degradation caused by fabrication technology, discussing barrier layer formation process 12 p1757 A72-28020
- Transparent materials study by interferometric methods, emphasizing holographic bench advantages for stress analysis and aerodynamic flows observation [ONERA, TP NO. 1037] 12 p1812 A72-28048
- Solid deformable body mean stress determination by statistical summation of stress squares on faces of parallelepiped rotated within Euler angle limits 12 p1887 A72-28233
- Stress calculation in inflexible overlapping cemented joint of orthotropic layers, taking into account joining geometry and elastic properties anisotropy 13 p1962 A72-28396
- Internal pressure induced stresses, displacements and time-variable plasticity radii for thick walled fiber reinforced cylinder with hereditary elastic binder interlayers 13 p2055 A72-28557
- Plane stressed state of elastic rectangular plate solved by method of summary representations 13 p2057 A72-29067
- Series solution for coaxial spherical cavity effect on torsional stress of finite length elastic circular cylinder 13 p2059 A72-29491
- Stress levels and fatigue in aircraft structures subjected to jet noise, noting stress calculation for skin panels and control surfaces 13 p1898 A72-29579
- Small transport aircraft horizontal tail surfaces flow characteristics determination for stress calculation during flight in turbulent atmosphere 14 p2071 A72-30284
- Shear strains and elastic anisotropy of transversely isotropic cylindrical shell with circular hole under uniform internal pressure, using shallow shell equations 14 p2165 A72-30438
- Stress analysis of thick walled hollow viscoelastic circular cylinder enclosed in elastic shell and subjected to nonlinear creep conditions, noting temperature effects 14 p2165 A72-30439
- Average stress and strain across thickness of liquid filled cylindrical elastic thin walled shell with rigid bottom under axial impact loads 14 p2166 A72-30698
- Composite materials stress analysis techniques, discussing strain gages, photoelastic coatings moire and holographic applications [ASME PAPER 72-DE-6] 14 p2167 A72-30861
- Higher order differential equations solutions for viscoelastic stress-strain functional relationships, recommending Runge-Kutta integration technique 14 p2168 A72-30929
- Creep deformation transition theory in spherical shells, using generalized strain measure for asymptotic solution 14 p2169 A72-30999
- Stress analysis and deflection equation for uniformly loaded and heated two layer clamped rectangular plate 15 p2322 A72-31362
- Stress analysis of two coaxially conjugated elastic isotropic cylinders under compression loads in terms of Fourier-Bessel series 15 p2323 A72-31447
- Nonlinear Cosserat continuum theory of elasticity, discussing kinematics and stressed state as functions of angular velocity, acceleration, volume forces and moments 15 p2274 A72-31476
- Approximate values for elastic body stresses and displacements based on finite element method and virtual displacements and minimum potential energy principles equivalence 15 p2323 A72-31477
- Stress analysis of boron fiber-reinforced and isotropic Al panels under identical loading conditions 15 p2323 A72-31479
- Numerical calculation of stresses and displacements in variable radius bodies of revolution under axially symmetric torsional load, using Fredholm type integral equation 15 p2324 A72-31480
- Strain analysis of thin metallic films on low modulus structural substrate by light intensity measurement 15 p2325 A72-31526
- Viscoplastic flow of inhomogeneous shells of revolution obeying Tresca condition, noting plastic deformation velocity relation to stresses 15 p2325 A72-31605
- Deformation and stress in shells with discontinuous wall thickness variations, noting cylinder with ribs under internal pressure 15 p2326 A72-31705
- Rough surface elastic bodies stress calculation, using asymptotic method of boundary conditions 15 p2327 A72-31736
- Structural components design from fiber composites, noting computer programs for structural and stress analysis 15 p2328 A72-32128
- Constant stress effect on propagation velocity of elastic waves in three dimensional body, considering earth crust and earthquake prediction applications 15 p2329 A72-32284
- Thermal stresses in plane elasticity for doubly connected regions, considering temperature distribution, stress state problem formulation and nonconcentric annulus 15 p2329 A72-32287

Higher moments of Reynolds stress fluctuations and velocity components in turbulent boundary layer, obtaining probability density distributions

15 p2218 A72-32401

Large amplitude deflections and induced stresses in uniformly pressure loaded circular plate on elastic foundation, using von Karman coupled nonlinear partial differential equations

15 p2331 A72-32558

Structural averaging of stresses in finite element method hybrid stress model, using additional equilibrium equations

15 p2332 A72-32597

Stress and displacement solution to Lamé problem for multilayer spherical vessels and cylindrical tubes in nonlinear elasticity theory

15 p2333 A72-32679

Thermoelastic stress analysis for hollow cylinder heated along helix, calculating stress function for given surface temperature distribution

15 p2333 A72-32687

Speckle pattern method of laser holography for structural vibration and surface strain study, noting real time operation

16 p2388 A72-32821

Plane stress solution for thin walled cantilever beam with end load extended for beam width effects in composite orthotropic beam bending

16 p2463 A72-32841

Holography application to photoelastic stress analysis, showing information content correspondence to angles of incidence for different model regions

16 p2389 A72-32905

Thermoelastic stress bounds in fiber reinforced composite beams of arbitrary cross section, examining conditions for applicability of elementary beam theory

16 p2464 A72-32915

Membrane and bending stress analysis for thin circular cylindrical shells with elliptic hole

16 p2464 A72-32918

Linearly elastic, transversely isotropic multilayer system, presenting stress and stability problem for two dimensional strain states

16 p2466 A72-33022

Stresses induced by torsional vibration in twisted composite cylindrical shell of cylindrically anisotropic materials for high and low frequencies

16 p2466 A72-33102

Two dimensional fibrous medium model for strain and stress analysis of structural plate formed by three dimensional grid of rods

16 p2467 A72-33115

Stress analysis for brittle body with thermoinsulated crack under mechanical load and temperature field, noting limiting equilibrium equation

16 p2469 A72-33272

Stress analysis for circular disk with diametral crack under symmetric and antisymmetric loads, solving integral equations via factorization

16 p2469 A72-33273

Cosserat couple stresses theory application to time varying concentrated forces induced displacements in infinite elastic space

16 p2469 A72-33385

Analytical solution of stress distribution and load endurance of perforated square plate supported at corners, comparing with photoelastic observations

16 p2470 A72-33410

Stress analysis in circular disk loaded along circumference, noting results identity for stress presentation by Fourier series, Poisson integral and Green function

16 p2470 A72-33593

Elastic sandwich plates analysis with core layer as orthotropic Cosserat surface supporting force and moment stresses

16 p2471 A72-33787

Book on mathematical methods for viscoelasticity problems covering shear stress, viscometric flow, stress analysis, Fourier and Laplace transforms, momentum, equilibrium and constitutive equations, etc

16 p2427 A72-33975

Components creep-rupture life prediction for multiaxial stress from uniaxial test data, discussing crack initiation and propagation phases stress states

16 p2412 A72-34114

Plane-strain compression of rigid plastic material between flat platens, approximating frictional boundary conditions by entrapped viscous fluid lubricant

16 p2428 A72-34171

Permanent traction and torsion strains effect on ratio between pure compression and pure traction yield points of Al alloy

16 p2412 A72-34179

Exact analysis of a thick sandwich conical shell by forward integration

[ASME PAPER 71-APMW-20] 17 p2624 A72-34312

Design and testing a high fuel volume fraction, externally finned, thermionic emitter

17 p2495 A72-34586

Somigliani dislocations effect in infinite elastic cylinder, determining stresses in form of eigenfunctions expansions

17 p2626 A72-34654

Stress and parametric change analysis for failure mode identification and reliability screen tests of LSI

circuits, noting MOS inverter operation and RAM mechanization

17 p2528 A72-34706

Physical determination of fields of displacements and their derivatives in continuous media

[ASME PAPER 72-APM-15] 17 p2629 A72-34801

Stress analysis of axisymmetric solids with asymmetric properties

17 p2632 A72-35227

Elastic behavior of multilayered bidirectional composites

17 p2632 A72-35234

Constitutive equations to characterize rubberlike nonlinear viscoelastic materials under finite deformation stress, obtaining numerical solutions via finite difference technique

17 p2633 A72-35401

Russian book on aircraft design covering flight conditions, structure and control characteristics, production and stress analysis

17 p2492 A72-35448

Russian book - Determination of stresses in the plastic region from the hardness distribution

18 p2732 A72-36300

An approach to the analysis of the nonlinear deformation and fatigue response of components subjected to complex service load histories

18 p2733 A72-36355

Techniques in photoelastic analysis of pressure vessels

18 p2690 A72-36363

A method of analysis for compressible viscoelastic solids

18 p2736 A72-36936

Wave propagation in half plane consisting of two joined elastic quarter planes under in-plane disturbances normal to free surface, obtaining stresses at interface

18 p2738 A72-37069

Effect of fiber end, fiber orientation and spacing in composite materials

18 p2738 A72-37086

The stress boundary value problem for plane strain deformations of an ideal fibre-reinforced material

19 p2870 A72-37371

German monograph - A contribution to the clarification of the carrying characteristics of closed isotropic circular cylindrical shells

19 p2871 A72-37478

German monograph - Finite elements according to a theory of the second order on the basis of an extended variational principle with an application to the stability and stress computation of simple symmetrical I-beams under consideration of the deformation of the cross-section

19 p2871 A72-37479

Anisotropic circular cylinder stress analysis under uniaxial load, calculating elastic deformation

19 p2872 A72-37536

Holographic strain analysis using spline functions

19 p2797 A72-37611

German monograph - Computation of the stress condition in homogeneous anisotropic discs with the aid of an integral equation method

19 p2873 A72-37660

Essential factors in reliability prediction and stress analysis of structural component with wide load and temperature variations

19 p2874 A72-37710

A photoelastic material with variable modulus of elasticity

19 p2822 A72-37731

Elasto-visco-plastic constitutive equations for quasi-static structures calculations

[ONERA, TP NO. 1089] 19 p2875 A72-37763

Stress calculations for lifetime prediction in turbine blades

[ONERA, TP NO. 1097] 19 p2875 A72-37770

Regularities in the deformation and failure of commercial iron in a complex stress state under low-temperature conditions

19 p2818 A72-38005

Applicability of the small parameter method to the estimation of stresses in nonhomogeneous elastic media

19 p2876 A72-38153

Stress analysis of shell junctions fabricated by the filament-winding method

19 p2877 A72-38169

Post-critical deformations of a cylindrical shell subject to the action of external pressure and a temperature field

19 p2878 A72-38472

Electric relay spring design for miniaturization, deriving relation between length and thickness to minimize fiber stress under constant contacting force

19 p2775 A72-38617

Computerized finite element three dimensional stress analysis, taking into account mechanical and thermal stresses

19 p2878 A72-38649

Polarization optical method for analyzing local stress concentrations in structural members

19 p2805 A72-38768

An analytical approach to the non propagating crack problem using the finite element method

20 p2977 A72-38882

On the fatigue crack propagation in polymeric materials

20 p2943 A72-38886

Brittle lacquer of air-drying type, investigating coating ingredients and plasticizers effect on strain sensitivity for various temperature and humidity levels

20 p2920 A72-38890

The temperature dependence of the friction stress for basal dislocations in beryllium in the range 300-500 K

20 p2935 A72-39191

Stress induced martensitic transformation relation ship to shape memory effect compared with superelasticity, transformation plasticity and reversible linear change

21 p3065 A72-40091

Electrical modeling of the plane problem of elasticity theory in terms of stresses

21 p3116 A72-40164

Three-dimensional photoelastic and finite-element analysis of a propellant grain

21 p3052 A72-40237

Central band-type wide angle camera shutter design, noting stress examination in machine parts by optical method

21 p3052 A72-40306

Dependence of linear elasticity solutions on the elastic constants. II - Dependence on the shear modulus in elastostatics

21 p3119 A72-41106

Non-Hertzian contact stresses in a smoothly cradled heavy cylinder

21 p3119 A72-41108

The vertical stress distribution due to parabolic strip load and uniform load over an ellipse in the interior of a semi-infinite solid

21 p3121 A72-41243

Six dimensional vector space of stresses in elastic piecewise linear material divided into separate regions having different linear stress-strain relation

21 p3122 A72-41345

Determination of the limits of applicability of a continuous model when calculating a discrete polar lattice disk

21 p3122 A72-41346

Determination of stresses along the symmetry axis in the isometric problem on the basis of an elastooptical image of isochromes

21 p3122 A72-41347

Stress differentiation procedure for screen technique studies in dynamic photoelasticity, giving expressions for elastic modulus and Poisson coefficient

21 p3123 A72-41363

Optimal compression of constant-thickness media in a plane stress state

21 p3123 A72-41391

Russian book - Design principles in aircraft construction

22 p3136 A72-42074

Stress analysis in two dimensional bending process using the photo-rheological stress analysis

22 p3183 A72-42483

The oriented elastic continuum as a model for the magnetoelastic body

22 p3206 A72-42525

Large deflections of flat arbitrary membranes

22 p3235 A72-42604

Stresses in a circular cylindrical shell with arbitrary holes

22 p3238 A72-42837

Effects of non-homogeneity on the stresses in a rotating cylinder

22 p3240 A72-42877

German monograph - Heat stresses in circular plates subject to finite deflections

22 p3241 A72-43058

Stress-strain state induced by local physicochemical transformations in a layer

22 p3242 A72-43164

Fracture mechanics of composites

23 p3345 A72-43509

Construction of the solution of a two-dimensional mixed boundary value problem for an arbitrary doubly connected region

23 p3345 A72-43629

A finite element stress analysis of a crack in a bi-material plate

23 p3346 A72-43707

Crack propagation speed measurements with wedge loaded double cantilever beam of PMMA, calculating stress intensity, strain energy release rate and kinetic energy

23 p3346 A72-43709

Stress state of arbitrary contour body of revolution under torsion using finite difference method

23 p3347 A72-43744

Thermoviscoelastic problem for semiinfinite plate, determining temperature field and stresses permitting heat propagation

23 p3347 A72-43749

- Inelastic transverse strain coefficient and Poisson ratio dependences on plastic and brittle properties
23 p3348 A72-43752
- Statistical strength and plasticity criterion for materials in a complex stress-strain state
23 p3349 A72-43953
- Investigation of the strength of construction materials for various principal-stress relations
23 p3349 A72-43955
- Improved method for determining shear stresses and checking the strength of circular cylinders in transverse bending
23 p3349 A72-43968
- Stability and vibration of transversely isotropic beams under initial stress.
23 p3350 A72-44057
- The accuracy of Donnell's theory for very high harmonic loading on closed cylinders.
23 p3350 A72-44059
- Line spring analysis model for long part-through surface cracks in walls of plate or shell structures, formulating constitutive laws
23 p3353 A72-44234
- Mixed-displacement finite-element analysis with particular application using plane-stress triangles.
24 p3455 A72-44789
- A sandwich plate with a part-through and a debonding crack.
24 p3456 A72-44813
- Torsion analysis of prismatic bars of different cross sections based on dipolar stress theory, applying to anisotropic media
24 p3457 A72-44872
- Elasto-plastic stress analysis - A generalization for various constitutive relations including strain softening.
24 p3457 A72-44880
- Pressure vessels with cracks, formulating stress analysis for safety factors
24 p3458 A72-44927
- Nonstationary thermoelastic stress determination in hollow cylinder walls under convective heat transfer
24 p3458 A72-44934
- Pure antiplane stress and equilibrium of isotropic elastic beams, considering suspended cylinders
24 p3459 A72-44989
- Double hierarchy in repeated cascade theory of turbulence.
24 p3390 A72-44997
- Turbine casing components stresses in presence of creep, demonstrating calculation method validity for thick-walled structures by elastoplastic analogy
24 p3460 A72-45727
- Method for applying a fatigue crack to impact test specimens made from tough materials.
24 p3417 A72-45765

STRESS CALCULATIONS
U STRESS ANALYSIS
STRESS CONCENTRATION

- Griffith crack stress intensity factor and crack face displacement in elastic solid, detailing symmetrical, antisymmetrical and point body force distributions
01 p0136 A72-10185
- Hydrogen partial molar volume in metal-hydrogen two component systems under externally applied uniform hydrostatic stress field, using thermodynamic analysis
01 p0083 A72-10205
- Flow in turbulent trailing vortex, considering circulation profiles and Reynolds stress distribution
[AD-740436] 01 p0049 A72-10232
- Finite element analysis of creep due to stress and strain in double edge notched plates and round bars
01 p0138 A72-10519
- Aluminum stiffening structural sections selectively reinforced with boron/epoxy composite materials, discussing mechanical properties, cost effectiveness and stress distribution
01 p0139 A72-10737
- Initial crack effect on slender column compression load carrying capacity, deflection and stress intensity factor
01 p0140 A72-10989
- Plane strain analysis of two bonded semiinfinite elastic media with different thermomechanical properties and cracks, calculating stress factors and maximum stress angles
01 p0140 A72-10990
- Stress intensity factors for circular crack near surface of semiinfinite solid, considering pure beam bending and approximate thickness effect for plate deep surface flaw
01 p0140 A72-10991
- Trapezoidal isoparametric and triangular singularity elements for crack tip elastic stress intensity factor for mesh having small number of degrees of freedom
01 p0140 A72-10992
- Two-layered plane strain elastic cylinder with cracked inner bore under internal pressure loading, obtaining stress intensity factors by finite element method
01 p0141 A72-10994

- Maraging and Ni steels stress corrosion cracking rates dependence on stress intensity factor, discussing measurements in salt and distilled water
01 p0086 A72-10995
- Clearance, friction and load effects on turbine blade root fastening stress distribution, comparing finite element method with photoelastic experimental results
01 p0141 A72-11048
- Experimental development of homogeneous field of plane stresses gripped in biaxial traction, considering convex models under constraint
01 p0142 A72-11176
- Turbomachine blade frequency disalignment effects on resonant vibrations and stress distribution, using wheel model and computer solution
01 p0143 A72-11367
- Analytical and graphical calculations of stress concentration coefficients and stress gradients in machine parts with recesses and finite depth cuts
01 p0144 A72-11377
- Solid body surface strain field optical determination, using diffraction gratings
[SESA PAPER 1751] 02 p0199 A72-11512
- Stress tensor asymmetry effects on stress concentration at curvilinear holes in elastic plates under tension
02 p0289 A72-11611
- Stress concentration factors for fiber and matrix in axially loaded unidirectional composite with discontinuous fiber, using linearly elastic finite element analysis
02 p0292 A72-11987
- Elastoplastic problem of stress concentration in orthotropic plate with circular hole under balanced biaxial tension of infinity
02 p0293 A72-12428
- Digital computer programmed numerical calculation based on admittance method for torsional forced vibration spectra of masses and stress distribution in transmission system
02 p0271 A72-12435
- Stress concentration in shallow cylindrical shell with circular hole under axial tension, torsion and internal pressure loading
02 p0295 A72-12472
- [ASME PAPER 71-PVP-9] High strength steels stress corrosion crack propagation velocity relationship to crack tip stress intensity
02 p0295 A72-12482
- Stress and velocity distributions in homogeneous viscoelastic rigid body, deriving uniqueness theorems and minimum principles for limits problem
02 p0297 A72-12596
- Truncated conical shell buckling under combined torsion and internal pressure load, discussing prebuckling stress conditions
02 p0298 A72-12666
- Stress distribution for anisotropic elastic plate containing two or more arbitrary elliptical holes
02 p0298 A72-12674
- Stress distribution analysis of femoral neck, using three dimensional photoelastic model
03 p0318 A72-12952
- Crack notched three point loaded bend specimens plain strain fracture toughness determination, showing relation between elastic work and stress intensity factor
03 p0442 A72-12960
- Stress concentration coefficients calculation at sharp cracks and notches for rods in tension, compression and combined bending and torsion
03 p0443 A72-13457
- Double forces distribution over elastic body surface from Lamé equation describing static defects, discussing Kupradse potential and sources corresponding to plane dislocations and cracks
03 p0444 A72-13501
- Stresses due to initial elastic deformations in orthotropic thin plate strip, expressing Dirac function by Fourier series and integral
03 p0444 A72-13505
- Thermal stress concentration at circular heat-insulated hole in plate with elastoplastic strains, assuming temperature independent mechanical properties
03 p0445 A72-13575
- Crack propagation rates during bending fatigue tests on flat hardened steel as function of stress intensity and plasticity area
03 p0445 A72-13593
- Steels fatigue life tests as function of stress level, confirming Wohler curves mathematical model
03 p0373 A72-13673
- Fracture mechanics of interfacial cracks between two bonded dissimilar anisotropic elastic half spaces, presenting two dimensional analysis of stress fields
03 p0446 A72-13707
- Glass fabric reinforced composite materials stress distribution under longitudinal loading, using finite element method with two dimensional model
03 p0381 A72-13720
- Stress concentration around reinforced curvilinear hole in elastic infinite plate, discussing ring reinforcement rigidity effects
03 p0447 A72-13730

- Stressed state of reinforced physically nonlinear rods under torsion, using theory of functions of complex variables
03 p0447 A72-13731
- Temperature field analysis in locally heated cylindrical shell for stressed state production with lowest elastic energy
03 p0456 A72-13733
- Elastoplastic stress distribution in thin spherical metallic shells with cylindrical branch pipe under internal pressure
03 p0448 A72-13905
- Stress distribution at contour of connected region in plane elasticity solved for half plane and circle
03 p0449 A72-13909
- Soviet papers on stress concentration near holes in plate and shell structures
03 p0449 A72-14101
- Asymptotic methods for complex mixed problems of elasticity related to stress concentration in plates with cracks or inclusions
03 p0449 A72-14102
- Stress concentration around circular and elliptical holes in isotropic three layer spherical shells with rigid and lightweight fillers
03 p0449 A72-14104
- Approximate solution for stress concentration near oval shaped hole in nonlinearly elastic plate, using small parameter and boundary perturbation methods
03 p0449 A72-14105
- Stress concentration near free hole in circular thick compressed plate, using plane elasticity theory
03 p0450 A72-14107
- Stress concentration at eccentric holes and effect on strength of full size rotating turbine disks
03 p0450 A72-14108
- Edge temperature effects on contact stress concentration in anisotropic plate with elliptic hole under mixed boundary conditions of thermoelasticity
03 p0450 A72-14109
- Stress concentration and stability of plates and shells weakened by holes
03 p0450 A72-14110
- Stress concentration at hole in plates after stability loss, using branching and small parameter method
03 p0450 A72-14111
- Elastic plate with two collinear thermally insulated cracks, calculating steady temperature field and stresses for uniform heat flux at infinity
03 p0450 A72-14112
- Anisotropic plate with hole stiffened at edge by thin isotropic ring, calculating thermal stress distribution
03 p0450 A72-14113
- Stress concentration of isotropic rotating multiply connected circular and elliptical plates weakened by two circular holes
03 p0450 A72-14114
- Pressurized vessel bottoms weakened by central hole with edge stiffened by elastic ring, determining stress-strain state and stress concentration
03 p0451 A72-14120
- Stress concentration at circular holes in polyurethane plates under plane compression wave, obtaining interference fringes
03 p0451 A72-14121
- Doubly connected strain-hardened thin plate, calculating stress concentration and stress-strain state by variational principle of least additional potential energy
03 p0451 A72-14122
- Transversely isotropic plates with elastic circular insert, calculating stress concentration at holes under bending
03 p0451 A72-14123
- Diffusion saturation effects on thermal stress concentration in plate with circular hole under edge heating and lateral surface heat transfer
03 p0451 A72-14124
- Cylindrical shafts with deep circumferential grooves, determining effective stress concentration under axial tension or bending
03 p0451 A72-14125
- Time effects on stress concentration around circular and elliptical holes in infinite plate with nonlinear creep
03 p0451 A72-14126
- Stress concentration around circular hole in infinite semibrittle plate under omnidirectional tension at infinity or pressure at hole contour
03 p0452 A72-14127
- Cylindrical shaft with circumferential groove, obtaining approximate solution for stress concentration at groove contour under torsion
03 p0452 A72-14130
- Variable-modulus isotropic material finite elastic deformation, deriving two dimensional stress concentration by dual series expansion
03 p0452 A72-14132
- Stress concentration at circular, elliptical, square, rectangular and triangular holes in isotropic plates stiffened by discontinuous elements under uniaxial tension
03 p0452 A72-14133

Thermal stress concentration at heat insulated holes in orthotropic plate, assuming external-load free contour

03 p0452 A72-14134

Stress concentration at hypotrochoid hole in cylindrical shell under internal pressure and axial tensile stresses

03 p0453 A72-14138

Dynamic stress concentration at circular hole generated by plane bending wave propagation in thin plate, analyzing dependence on vibration frequency

03 p0453 A72-14139

Stress-strain state of shallow shell with crack along principal curvature line, discussing membrane stresses in plates and spherical shells

03 p0453 A72-14140

Cyclic deformation and fatigue testing equipment and techniques for biaxial stress, stress concentration and pure bending

03 p0339 A72-14168

Stress concentration problems in two and three dimensional elastoplasticity, using Ilyushin small deformation theory

03 p0453 A72-14213

Stress channelling in transversely isotropic elastic composites, comparing classical theory with ideal fiber reinforced composite plane deformation theory

03 p0455 A72-14385

Generalized epicycloid properties application to fracture mechanics, considering stress fields of constrained plastic zones around cracks in thin elastic plate

03 p0455 A72-14388

Stress intensity and plane dilatational wave diffraction in elastic material with finite crack

04 p0583 A72-14459

Unitary stress state and deformations in rotating axisymmetric disk, using function applicable to axisymmetric pipes

04 p0584 A72-14471

Variable thickness plate under cylindrical bending, considering stress concentration around circular hole

04 p0586 A72-14991

Forced vibrations of elastic plate with infinite series of identical circular holes, discussing elastic wave diffraction and stresses at/near holes

04 p0587 A72-15017

Nonlinear elastoplastic deformations of flexible shells of revolution, calculating stress concentration at circular hole in spherical shell

04 p0588 A72-15049

Stress distribution at hole in multilayer anisotropic shells of composite glass-plastic or cermet material

04 p0588 A72-15052

Nonlinear hereditary elasticity theory boundary value problem solution using complex potentials in successive approximation algorithm for stress concentration and nonlinear creep analysis

04 p0588 A72-15059

Stress concentration around elliptic hole in infinitely long circular cylindrical shell under torsional loads

04 p0589 A72-15122

Perturbation solution for stress concentration around elliptic hole in cylindrical shell under torsional loading

04 p0589 A72-15123

Magnitude and distribution of stresses produced by external energy sources in thick plate

04 p0593 A72-15657

Elastic equilibrium of circular conical orthotropic shells with linearly varying thickness, determining real and complex roots of stress state characteristic equation

04 p0594 A72-15710

Magnetic stress anisotropy field in plated cylindrical Permalloy films, determining relationships to circumferential composition variation, geometry and easy-axis dispersion

04 p0564 A72-15717

Fatigue strength optimization of bonded double strap metal joints, attributing stress concentration to plastic relaxation

[ASME PAPER 71-MET-Q] 05 p0731 A72-15791

Mechanical behavior of uniaxially loaded multilayered oriented fiber cylindrical composites, observing tensile transverse stresses

[ASME PAPER 71-MET-Q] 05 p0732 A72-15792

Boundary collocation method for estimating stress intensity factors for through-thickness interior crack in finite rectangular plate

[ASME PAPER 71-MET-L] 05 p0732 A72-15794

Doubly symmetric oval ring with stiffeners pair parallel to major or minor axis, investigating stress behavior under radial load

[ASME PAPER 71-WA/DE-14] 05 p0732 A72-15941

Distortional energy theory for predicting failure of orthotropic materials exposed to three dimensional stress state

[ASME PAPER 71-WA/DE-13] 05 p0732 A72-15942

Stressed state of radial bearings hollow rollers under loads concentrated along generatrix, evaluating test results by statistical analysis

05 p0665 A72-15984

Stress state of variable thickness long elastic shallow shell in bending and torsion, applying equations to large turbine blades

05 p0735 A72-15986

Gas turbine wheel design analysis, presenting procedures for estimating revolution rates, blade numbers and component configurations effects on wheel weight for prescribed stresses

05 p0735 A72-15995

Load or compression eccentricity effect on buckling and postbuckling behavior of flat plates, presenting stress distribution curves

05 p0737 A72-16116

Dimpling behavior of metal plate with mode I edge crack, relating flaw depth, applied stress level and crack tip plastic zone

05 p0673 A72-16305

Mass concept for moving crack, relating stress concentrations of elastic field with crack inertia

05 p0673 A72-16306

Stress intensity factors for pair of coplanar Griffith cracks subject to asymmetrical surface tractions

05 p0737 A72-16320

High temperature low cycle fatigue of Cr-Mo-V steel, observing crack growth rate correlation with crack tip stress

05 p0673 A72-16321

Optical interference technique for experimental stress analysis of cracked structures, obtaining crack shape relationship to stress intensity factor

05 p0666 A72-16322

Plastic stress and strain intensity factors for cracked plates in tensile fields

05 p0737 A72-16323

Geometric displacements and space-time derivatives determining velocity and strain fields in solids under deformation

05 p0738 A72-16529

Power parameter determination in rotary swaging of thin conical shells, discussing radial contact stresses

05 p0666 A72-16628

Nb-O and Nb-N alloys, investigating oxygen and nitrogen solute-hardening effects on room temperature flow stress

05 p0675 A72-16729

Unidirectional carbon fiber composites effects and use of stress envelopes in aircraft structure design

05 p0681 A72-16997

Plastic flow stress around dislocations on Ni-Al intermetallic cube and octahedral cross slip systems

05 p0678 A72-17118

Complex potentials for nonlinear elasticity, creep and small elastoplastic deformations, applying to stress concentration at curvilinear hole in infinite plane

05 p0742 A72-17183

Dynamic overstressing and annealing effects on fatigue life of convoluted metal bellows, using dynamic model and strain gage measurements

05 p0742 A72-17245

Stress fields around moving weld arc on Al sheet from isotherm map, calculating compressive and tensile stresses from heat induced material expansion

06 p0820 A72-17705

Critical review on data accuracy of maximum principal elastic stresses and deflections of thin initially-flat square isotropic plates under uniform normal pressure

06 p0894 A72-17796

Principle stress errors in biaxial stress fields expressed in terms of transverse sensitivity, stress and Poisson ratios of material during strain gage calibration

06 p0895 A72-17798

Fatigue crack formation speed relationship to stress intensity factor, investigating crack propagation by fracture mechanics methods

06 p0895 A72-17810

Fiber pull-out from elastic matrix, calculating shear stress and load distribution dependence on elastic properties and fiber length

06 p0897 A72-18152

Stress concentrations at circular holes and inclusions in elastoplastic strain hardening plate under tension and shear

06 p0897 A72-18316

Singular solutions for nonaxially symmetric shallow shells under concentrated normal or thermal loading

06 p0897 A72-18319

Shear and direct stresses on fuselage model cross section due to concentrated radial loads on frame comparing measurement with prediction by matrix force analysis

06 p0898 A72-18322

FORTAN programs for calculating principal stresses, strains and directions from rosette readings

06 p0781 A72-18324

Low frequency biaxial load effect on stress concentration factors for circular and elliptical holes in Plexiglas plates

06 p0898 A72-18350

Fatigue life and creep tests of refractory materials under programmed thermal cycling for different stress levels

06 p0831 A72-18351

Single fiber reinforced plate initial stress distribution due to linear expansion coefficients difference between matrix and fiber, using optical polarization

06 p0836 A72-18557

Temperature stress distribution in infinite plate with time varying heat transfer coefficient

06 p0899 A72-18565

Metal strip with circular hole under tension, calculating plastic strain and stress concentration coefficients

06 p0899 A72-18567

Stress and temperature fields in cooled gas turbine blades with allowance for elasticity, plasticity and creep

06 p0899 A72-18628

Cyclic bending stress distribution in fir tree turbine blade root for arbitrary loading phase

06 p0899 A72-18629

Rib reinforced cylindrical shells deformation under local load, examining stress-strain distribution

06 p0899 A72-18641

Heat resistant metals long time creep prediction at low stresses or temperatures

06 p0834 A72-18668

Stress distribution during plastic deformation of steel turbine disk from hardness measurements

06 p0900 A72-18670

Stress and deflection distribution for circular and elliptical toroidal shells under internal pressure from first order differential equations solutions

07 p1088 A72-19118

Finite element method application to fracture mechanics problems of stress concentration and intensity factors and elastoplastic response to cyclic loading

07 p1088 A72-19130

Moving heat source model of temperature profile and thermal stress propagation for laser drilled holes in alumina ceramic material

07 p0994 A72-19211

Stress redistribution in statically indeterminate structures under creep, discussing effects on time to brittle fracture and service life determinations

07 p1088 A72-19259

Moment stresses and deflections of rigidly clamped hinged and simply supported square elastic plates beyond elastic limit, deriving equilibrium and strain compatibility equations

07 p1091 A72-19759

Rupture strength of disk with surface crack under concentrated loads, applying integral equation to stressed state

07 p1092 A72-19777

Elastoplastic stressed state of thin cylindrical shells with circular hole, using small strain theory

07 p1092 A72-19896

High temperature tensile tests of Mo with helical and circular V grooves, discussing stress concentration sensitivity relations for grooved and smooth samples

07 p1018 A72-20141

Impurities and crystal lattice role in metal brittleness, discussing stress concentration and relaxation, crack initiation and plastic deformation

07 p1018 A72-20145

Stressed state of isotropic nonlinear plate with doubly periodic system of curvilinear holes

07 p1094 A72-20208

Stressed state approximate determination for isotropic slab with randomly positioned circular holes

07 p1094 A72-20210

Stressed state of infinite isotropic plate weakened by curvilinear hole with elastic plug, using asymptotic integration method

07 p1094 A72-20212

Stressed state of isotropic plate with curvilinear holes under tension, using computer techniques

07 p1094 A72-20215

Three dimensional stressed state of isotropic plate with elliptical holes under tension, solving boundary value problems

07 p1095 A72-20216

Maximum stress concentration in two dimensional elasticity theory for half plane and circle as function of contour distribution, using Cauchy-Buniakovskii inequality in Banach space

07 p1095 A72-20325

Strength and strain theory statistical analysis for perfectly brittle and plastic materials, assuming ultimate or elastic limit strain as governing factor

07 p1097 A72-20536

Numerical analysis of passing screw dislocation arrays under stress for computerized work hardening model

07 p1097 A72-20556

Metals cold working mechanics about stress state and yield points, proposing theoretical model for mechanism and applications in extrusion molding, drawing and hollow forging

07 p0999 A72-20599

P-analytical functions application to strength analysis of zero moment shells of revolution with positive Gaussian curvature under concentrated loads

08 p1242 A72-20905

- Longitudinal plane harmonic elastic wave scattering and stress concentration at rough circular hole boundary in thin isotropic plate
08 p1243 A72-21230
- Membrane and bending moment stresses distribution at elliptical hole in circular cylindrical shell, solving boundary value problems
08 p1243 A72-21234
- Stress concentration and elastohedriary values at curvilinear hole in fiberglass reinforced plastic plate under bending moment
08 p1243 A72-21237
- Stress concentration near elliptic and square orifices in plates with nonlinear viscoelastic hereditary creep properties
08 p1244 A72-21242
- Prestressed glass reinforced composites mechanical behavior, taking into account manufacture induced residual stress concentrations
08 p1192 A72-21674
- Plane stability of isotropic plate with straight line series of holes reinforced by complex elements or multicomponent rings, determining stress concentrations
08 p1246 A72-21710
- Glass fiber reinforced polymer composite model for tensile stress: distribution in matrix and fibers and at bond interface
08 p1194 A72-21753
- Dynamic radial vibrations and stresses in thick circular annulus of nonisotropic elastic material, using Hankel transform
08 p1246 A72-21793
- Successive approximations method for stress concentration problem at hole in cylindrical shell
08 p1247 A72-21818
- Radial and axial residual stress components in glass fiber reinforced polyethylene, comparing with adhesion strength obtained by shear method
08 p1196 A72-21862
- Notch length effect on stress concentration in polymethyl methacrylate sample from tensile, impact and bending tests
08 p1196 A72-21867
- Quenched aluminum oxide rod residual stress profile from strain and heat transfer rates measurements and temperature distribution calculation
08 p1196 A72-21918
- Stress distribution near corner point in interface section of body with two prismatic components, noting state singularity investigation reduction to transcendental equation solution
08 p1249 A72-21944
- Plastic deformation friction fracturing, stress concentration, free surface changes and load displacement analysis with upper bound, slip line and finite element methods
08 p1250 A72-22197
- Interaction between two noncoplanar parallel staggered elastic cracks with narrow spacing, calculating stress intensity required for crack propagation
09 p1397 A72-22250
- Fractography of high boron ceramics under ballistic impact, suggesting macroscopic and microscopic textures relationship to stress states and microstructure
09 p1334 A72-22391
- Penny shaped interface crack between elastic layer and half space, calculating stress intensity factors and strain energy release rate for aluminum-epoxy combination
09 p1398 A72-22530
- Stress intensity factor of crack near inclusion in infinite elastic plane, using numerical methods
09 p1398 A72-22531
- Photoelastic measurement of stress concentration in three dimensional fiber reinforced brittle plastic matrix under uniaxial tension
[PI PAPER 1] 09 p1398 A72-22538
- Numerical solution of integral equations for dislocation densities and stress singularities associated with cracks and pile ups in bimetallic media
09 p1398 A72-22622
- Potential equations and singularities methods comparison for two dimensional flow field cascades and stress distribution elasticity theories
09 p1260 A72-22627
- Temperature and thermal stress distribution in cylinder of finite length for mixed heating conditions
09 p1400 A72-22707
- Thermal stress distribution in orthotropic cylindrical shell weakened by circular hole, obtaining general solution by small parameter method
09 p1400 A72-22715
- Thermal stressed state determination for open thin walled cylindrical shells, using method of integral relations
09 p1400 A72-22716
- Elastoplastic stressed state of multilayer cylinder during loading, unloading and cyclic loading processes
09 p1401 A72-22721
- Micropolar elasticity plane problem singular solution based on stress equations and elastic potentials methods, discussing thermal stress concentration
09 p1402 A72-22743
- Stress and couple stress fields near antiplane shear crack tip, determining eigenfunctions to satisfy field equations and boundary conditions
09 p1402 A72-22744
- Crack propagation in elastic layer under antiplane state of deformation for arbitrarily distributed shear forces on crack surface
09 p1404 A72-22766
- Impact detonation mechanism in ammonium perchlorate mixtures with inflammable additions, determining critical detonation triggering stresses
09 p1373 A72-22890
- Central crack in plane orthotropic rectangular sheet under tension, showing stress intensity factors dependence on geometric and elastic constants
09 p1404 A72-22915
- Circumferential crack in cylindrical shell under torsion, presenting membrane and bending components of stress intensity factor ratio
09 p1404 A72-22918
- Rotationally symmetric stress and strain distribution in anisotropic elastic shells of revolution
[AD-745622] 09 p1405 A72-22944
- One dimensional shock wave propagation in inhomogeneous elastic materials, showing wave amplitude behavior dependence on critical jump in strain gradient
09 p1405 A72-22990
- Plane elastostatic problem of stress concentration near flat interface inclusion in bonded dissimilar materials
09 p1405 A72-22997
- Two dimensional creeping flow in fiber reinforced composite under uniform tension, discussing matrix shear stress and fiber direct stress distributions
09 p1338 A72-23168
- Carbon fiber reinforced plastic toughness from strain concentration and plastic flow observation near crack tip by moire technique
09 p1339 A72-23170
- Stress concentration in elastic composite reinforced by two dimensional continuous parallel fiber array with one broken fiber
09 p1339 A72-23172
- Tractions at interface between fiber and matrix in fiber reinforced composites, considering axially symmetric deformations and stress fields
09 p1339 A72-23173
- Stressed state of circular elastic plate with press-fitted equiaxial disk
09 p1406 A72-23181
- Optical simulation of plastic strain distribution with models prepared from organic glass, investigating birefringence effect
09 p1406 A72-23182
- Stress distribution determination for long isotropic elastic cylinder with strip crack on diametral plane by complex variable technique and Fredholm equation solution
09 p1409 A72-23574
- Rotational, centrifugal and Coriolis force effects on turbulent boundary layer development, discussing changes in structure and shear stress distribution
10 p1464 A72-23870
- Light beams diffraction patterns of thin plexiglass plate for load induced thickness variations, noting crack opening and edge sliding modes stress intensity factors
[ASME PAPER 71-APM-QQ] 10 p1553 A72-24178
- Plane harmonic compression waves scattering by circular holes in thin elastic plate, calculating dynamic stresses concentration
10 p1554 A72-24179
- Dynamic stress concentration around elliptical discontinuities in elastic medium, considering rigid and empty cavity scatterers for compression and vertically polarized shear incident waves
[ASME PAPER 72-APM-D] 10 p1554 A72-24180
- Stress intensity factor for circular crack embedded in finite thickness solid under uniform tension, noting semielliptical surface flaw in brittle material
[ASME PAPER 71-APMW-6] 10 p1554 A72-24183
- Stress distribution in general relativity on oriented compact Riemann manifold
10 p1511 A72-24206
- Autoradiographic study of stress intensity factor influence on hydrogen distribution at crack tips in Ti-Al-V alloy, using tritium doped salt water as corrosive medium
[ONERA, TP NO. 1052] 10 p1496 A72-24234
- Stress distribution determination by shear stress difference method in curvilinear orthogonal coordinate systems
10 p1557 A72-24405
- Partial differential equation for thin walled circular cylindrical shells, deriving solutions for displacement and stresses in terms of surface coordinates low degree polynomials
10 p1557 A72-24560
- Optimum thickness variation in annular strip/curved beam/ under bending moment at constant stress based on Mises-Hencky yield criterion
10 p1558 A72-24847
- Crack arrest in transversely loaded elastic plates from fracture mechanics combined with stress intensity factor for tensile and compression loads
10 p1499 A72-24890
- Variational methods for approximate solutions to Fredholm integral equations describing stress intensity factors and plastic regions of Dugdale cracks
[AD-744365] 10 p1558 A72-24892
- Mathematical model for supersonic crack propagation in cubic lattice, deriving velocity-applied stress relation
10 p1558 A72-24895
- Crack shape and plastic energy dissipation rate relation to plate thickness and applied stress for penny-shaped crack in elastic plate
10 p1559 A72-24896
- Photoelastic investigation of star shaped models for loading direction influence on shear stress distribution at notch tip region in uniform tensile field
10 p1559 A72-24897
- Approximate stress intensity factor for corner flaw emanating from quarter infinite solid edge, based on Smith solution for semicircular flaw
10 p1559 A72-24898
- Rough surfaces thermal contact resistance in vacuum for normal height distribution, discussing bolted joint nonuniform stress distribution effect
[AIAA PAPER 72-281] 11 p1741 A72-25221
- Elastic constants and bond stress distribution for discontinuous fiber-reinforced three dimensional composite subjected to uniaxial tension
[AIAA PAPER 72-397] 11 p1731 A72-25418
- Elastic finite element analysis for stress distribution in gripped thin walled tubular anisotropic three dimensional composite specimens
11 p1731 A72-25457
- Stress concentrations around circular openings and failure criteria for orthotropic and anisotropic composite laminated plates subjected to uniaxial, biaxial and shear loading
11 p1732 A72-25474
- Fatigue crack initiation and growth in filament reinforced Al alloys, noting interface crack tip stress distribution effects
11 p1654 A72-25480
- Elastic glass and Thorne fiber/epoxy matrix composite material creep tests, determining creep rate dependence on specimen geometry and stress state
11 p1672 A72-25481
- Moment stress-strain state of two layer circular cylindrical shells under creep conditions
11 p1733 A72-25542
- Bending of rectangular cross section cantilever beam with cylinder reinforced circular opening, calculating interface stress distribution as function of thickness and elasticity moduli ratio
11 p1733 A72-25545
- Pressure loaded shallow spherical shells with reinforced circular holes, noting stress concentration increase due to reinforcement bead eccentricity
11 p1734 A72-25736
- Specimen preparation effects on fracture strength measurements, noting critical stress intensity factor for single edge notch and compact tension high strength steel samples
11 p1657 A72-25825
- Creep and low cycle fatigue dynamic behavior, noting stress concentration time dependence, strain hardening and local plastic deformations in dead annealed Al thin walled tubes
11 p1658 A72-25829
- Constrained zones and stress intensity factors in cracked thin elastic plates under combined tensile and shear loads
11 p1735 A72-25893
- Low temperature tensile strength and plasticity of Ti alloys with zirconium, investigating sensitivity to stress concentrations
11 p1660 A72-26138
- Axisymmetric stress field in infinite homogeneous isotropic elastic solid with crack surrounding cylindrical cavity, solving elastic equilibrium equations
11 p1738 A72-26720
- Mellin transforms for finite elastic disk radial crack stress intensity factor and energy formulae in terms of Fredholm equation solution, considering constant loading case
11 p1738 A72-26724
- Statistical estimation method for brittle metals fracture strength, taking into account stress nonuniformities due to dislocation defects
11 p1738 A72-26803
- Ti alloys fatigue strength, stress concentration sensitivity and grain sizes effects at normal and high temperature under cyclic loads
11 p1663 A72-26821
- Hyperboloidal profile circular disk stress distribution induced by thermal pulse nonuniform temperature field
11 p1739 A72-26979
- Thermal stress distribution in orthotropic plates with variable heat transfer coefficient, using Fourier and Laplace transforms
12 p1878 A72-27084

Equilibrium equations of infinite strip with circular hole, using plane multiply connected domain method for stress field

12 p1878 A72-27087

Fatigue failure criteria under combined stress conditions, considering complex form, thin and thick walled cylinders as test specimens

12 p1828 A72-27317

Stress concentration in infinite elastic isotropic disk with circular hole under internal tensile loading

12 p1882 A72-27320

Green function for stress distribution in plane shaped disk with edge loaded circular hole, noting conformal mapping for arbitrary shape

12 p1883 A72-27391

Stress intensity factor of Griffith crack in elastic solid opened by thin symmetric wedge, using triple integral equations

12 p1883 A72-27558

Micromechanics of deformed continua, discussing atomic structure effects on stress concentrations in composite materials, framed structures and grids

12 p1884 A72-27640

Flow rate limits increase and near homogeneous stress concentration in active hot extrusion of Al alloys

12 p1814 A72-27644

Stress distribution in circular cylindrical shell weakened by two identical holes on common generatrix

12 p1886 A72-27984

Circular cylindrical shell under distributed edge load along circular hole contour, calculating stress concentration by trigonometric series solution for shallow shell equation

12 p1886 A72-28130

Characteristic friction curves /Mohr circle envelopes/ to describe stressed state region with various stresses produced by slide friction in steel due to indentation

12 p1819 A72-28198

Elastoplastic deformation effects on load bearing capacity of samples with stress concentrators under alternating cyclic loading, obtaining nomograms by digital computer

12 p1887 A72-28228

Cylindrical samples with deep circular hyperbolic notch, investigating cyclic inelastic strain induced stress redistribution effects on load bearing capacity

12 p1830 A72-28229

Engineering formula relating crack tip stress intensity coefficient to mechanical properties and structural element size

12 p1887 A72-28236

Crack and notch induced stress concentrations effect on steel mechanical properties at 20-293 K, using static and dynamic test methods

12 p1831 A72-28240

Thermal stresses near pole of spherical reservoir during cooling, using thermoelastic equations of shell of revolution

12 p1887 A72-28242

Surface finishing effects on steel sensitivity to stress concentration under variable loads, emphasizing diamond smoothing and roller technique

12 p1831 A72-28246

Stress-strain concentrations near circular holes in fiberglass reinforced plastic plates under various types of load as function of hole diameter/plate width ratio, anisotropy and load

13 p1983 A72-28560

Microcuts as equivalent mechanical stress concentrators for breakdown energy estimation in flat polymethyl methacrylate glass specimens under impact bending loads

13 p1983 A72-28563

Finite circular cylindrical shell under uniform pressure on outer rim, comparing stresses and displacements

13 p2055 A72-28624

High temperature constant load creep tests on pure powder metallurgy W and tungsten-thoria alloy, discussing stress dependence

13 p1975 A72-28665

Singular moment stress homogeneous solutions of plane problem with seminfinitesimal cut in elasticity theory

13 p2056 A72-28773

Thermal stress distribution determination in isotropic plate with rigid circular insert, using small parameter technique

13 p2056 A72-28913

Tangential stresses, rigidity characteristics and stress functions of prismatic grooved circular shafts, showing summary representations and integral transformations methods interrelationship

13 p2057 A72-29062

Plane stressed state of elastic rectangular plate solved by method of summary representations

13 p2057 A72-29067

Plane plastic deformation during single pass rolling of corrugated metal sheet, determining stress-strain fields for first and second phases

13 p1964 A72-29148

Velocity field at strain center during steel channel rolling, deriving relations for center contour calculation

13 p1964 A72-29149

Notch stress concentration in disk with elastic core under tension, using finite element method

13 p2060 A72-29600

Iron content and stress level effect on flaking corrosion of Al alloy sheets, describing experimental technique

13 p1980 A72-29826

Three dimensional axisymmetric problem for stressed state of elastic homogeneous cylindrical orthotropic bodies of revolution, using method based on small parameters

13 p2062 A72-29948

Modified finite element method application to plane elastic area elementary triangles strained and stressed state description by polynomial algebraic expressions and harmonic functions

14 p2163 A72-30188

Stress distribution variations and wave propagation in viscoelastic rod of finite length under impact

14 p2163 A72-30191

Aircraft landing gear stress spectrum and design data during ground loading on airport runways, using linearized theory for model investigation

14 p2071 A72-30283

Hypervelocity impact parameters calculated from shock wave equations of motion, discussing viscosity effect on velocity and stress distributions

14 p2164 A72-30297

Boundary value problems in dynamics of Cosserat infinite elastic medium with finite crack, noting couple stresses effect on dynamic stress concentration

14 p2164 A72-30299

Instrument to determine steady and unsteady stress state of elastic fluids in viscometric flow, noting rheological measurements in solved polymers

14 p2094 A72-30421

Temperature effects on critical crack opening as fracture toughness criterion for medium strength steel, taking into account local plasticity and propagation resistance

14 p2118 A72-30590

Mill annealed Ti alloy fatigue at 600 F and room temperature, noting critical local stress for slip bands formation and cracking

14 p2120 A72-30611

Anisotropic plate with doubly periodic system of elastic ring stiffened elliptic holes, calculating stresses at holes due to tensile forces applied at infinity

14 p2165 A72-30685

Axisymmetric ductile rotating shaft failure modes, considering fatigue, buckling and impact stress factors [ASME PAPER 72-DE-40]

14 p2167 A72-30873

Optical anisotropy effects in birefringent materials by reflected shadow method and extension of theory for constrained zones around cracked plates under plane stress

14 p2167 A72-30903

Stress concentration in symmetrical U-notched plates, comparing data with Baratta, Neal, Neuber and Heywood formulas

14 p2167 A72-30904

Finite element method with compliance equations determining energy release rates and stress intensity factors for complex crack configurations and loadings

14 p2168 A72-30908

Shear stress distribution and local heat flux at surface of axisymmetric bodies for laminar and turbulent boundary layer flows

14 p2071 A72-31163

Elastic crack tip stress fields, considering weight function

15 p2322 A72-31347

Elastic body stress concentration problem formulation as singular integral operator eigenvalue problem for half space

15 p2323 A72-31478

Metal hardening level evaluation on basis of volume dislocation structure from stress field of dislocation loops

15 p2254 A72-31562

Elastoplastic stress concentration near elliptic hole in plate loaded in smallest axis direction

15 p2325 A72-31606

Numerical solution of singular integral equations system for stress concentration in elastic plane with curvilinear crack

15 p2327 A72-31735

Zero moment stress effect on modal density spectrum of fluctuating thin cylindrical shells and cylindrical panels

15 p2327 A72-31737

Tangential force distribution at fiber surface in composite material under tensile stress without displacement at fiber axis

15 p2260 A72-31743

Mechanical vibrations effect on flow stress and strain rate from tensile and creep tests as function of amplitude

15 p2257 A72-31841

Elastic shell initial stress effects on dynamic response in all free vibration modes, considering: transverse shear and normal strains

15 p2328 A72-32021

Stress concentrations in cylindrical shells with cutouts under uniformly distributed axial tensile load, presenting exact solution of differential equation

15 p2328 A72-32138

Singularities of cylindrical shell under concentrated: twisting couple, investigating axial and circumferential deformations and shear stress distribution

15 p2329 A72-32139

Deep drawing of circular mild steel and aluminum sheets with polyurethane or rubber rings, examining strain distribution, shape and surface roughness

15 p2244 A72-32145

Debonded laminar composite torsional stress intensification analysis near circular shaped imperfection based on Hankel transform and dual integral equations solution

15 p2261 A72-32247

Displacement and stress field for elastic solid containing cruciform crack with unequal length arms

15 p2330 A72-32292

Nonlinear thermoelasticity theory in terms of continuum mechanics terminology, assessing strain gradients and couple stresses effects on stress distribution

15 p2330 A72-32293

Ultrahigh tensile strength steel pressure chamber fracture behavior in high stress concentration fields

15 p2330 A72-32345

Surface stress solution for elastic half space weakened by spherical cut under internal pressure

15 p2333 A72-32681

Rigidity effect of reinforcing rings on stressed state of physically nonlinear perforated elastic plates

15 p2333 A72-32683

Differential equations for stress-strain state of circular cylindrical shell with circular holes resting on elastic base under external pressure

15 p2333 A72-32686

Fully developed turbulent air flow through concentric annuli, measuring inner wall shear stress distribution by zero-shear position location and sliding sleeves technique

16 p2375 A72-32875

Analog simulation method for highly redundant structure optimization based on reproducing structural mechanical behavior in stabilized stress states

16 p2463 A72-32894

Nonlinear stress-strain-curvature problem application to noncircular cylindrical membrane shell under lateral pressure

16 p2464 A72-32917

Linear theory for spirally sinusoidal stress distributions in elastic helicoidal shells applied to pure bending problem

16 p2465 A72-33000

Stress and heat flux constitutive equations dependence on observer reference frame, considering field equation for temperature of gas at rest

16 p2478 A72-33526

Dynamic stress field solution to plane strain crack propagation in elastic body under general loading at constant and nonlinear extension rate

16 p2470 A72-33612

German papers on crack propagation in metal sheets, resonant vibration of cylindrical shells and stress concentration in plastic plates

16 p2470 A72-33676

Stress concentration in elastic layer with circular slot analyzed by reducing mixed boundary value problem to initial condition problem via invariant imbedding

16 p2471 A72-33827

Stored energy function for multiaxial stress state in rubberlike materials from tensile data based on Valanis-Landel theory

16 p2472 A72-33838

Creep tests on Cr martensite stainless steel, showing inapplicability of Garofalo equation for stress dependence of secondary creep rate during variable stress experiment

16 p2412 A72-34112

Steady state creep of composite material with discontinuous fibers, determining random function mean and variance for fiber stress distribution

16 p2412 A72-34115

Energy theorems for creep constitutive relationships, discussing total deformation of body composed of elastic-creeping material with allowance for stress redistribution effects

16 p2473 A72-34118

Temperature and stress fields generated by pulsating internal pressure in viscoelastic hollow sphere with temperature dependent material properties, using iterative numerical procedure

16 p2473 A72-34122

Numerical procedure for spherical and cylindrical shells creep behavior, taking into account stress redistribution due to interaction between elastic and creep strains

16 p2473 A72-34125

Heat generation in oscillating torsional spring modeled by viscoelastic hollow cylinder subjected to sinusoidal shear stresses, calculating stress and temperature distribution and displacement 17 p2635 A72-34232

Buekner formulation combined with finite element method for arbitrary shaped cracked bodies stress intensity factors in framework of linear fracture mechanics 17 p2623 A72-34253

Crack opening displacement and the rate of fatigue crack growth. 17 p2565 A72-34255

On the extension of an infinite elastic plate containing an axisymmetric hole. [ASME PAPER 72-APM-G] 17 p2624 A72-34313

A comparison of flow and deformation theories in a radially stressed annular plate. [ASME PAPER 72-APM-44] 17 p2627 A72-34781

Conservation laws related to energy release rates associated with cavity or crack rotation and expansion, discussing plastic stress distribution around cracks [ASME PAPER 72-APM-22] 17 p2580 A72-34795

Effect of end attachment on the strength of fiber reinforced composite cylinders. [SESA PAPER 1994A] 17 p2630 A72-34817

The evaluation of the stress intensity factors for cracks subjected to tension, torsion, and flexure by an efficient numerical technique. [ASME PAPER 72-MAT-B] 17 p2631 A72-34966

A comparison of numerical methods for determining stress intensity factors. 17 p2631 A72-34973

Thin spherical shells in equilibrium with displacement and stress fields, satisfying virtual work, kinematic and static requirements 17 p2633 A72-35351

Eigenfunction technique development to incorporate stress singularities at circumference of end planes into problem of solid cylinder compression between rough rigid stamps 17 p2633 A72-35403

Shear stresses distribution in isothermal incompressible turbulent boundary layer with positive pressure gradient by diffusers in open jet wind tunnel 17 p2544 A72-35931

Creep of different molybdenum alloys at high temperature and under strong stresses 18 p2698 A72-36144

Strain measure determined plastic stress concentrations around discontinuities in flat plates compared with incremental theory 18 p2733 A72-36359

Mechanical structure and component stress measurement by reinforced concrete, microconcrete, elastic and plastic models 18 p2733 A72-36370

Photoelastic investigation of a Hertzian contact with shallow grooves in the contact area. 18 p2734 A72-36374

Photoelastic study of stress concentration in rectangular panels with inserts. 18 p2734 A72-36376

Thickness-punch size ratio effects on stress state response of elastic plates and beams in flat contact under symmetric loads due to rigid punches 18 p2734 A72-36378

Stress state and velocity fluctuations in a perturbed boundary layer 18 p2680 A72-36464

Similarity solutions to nonlinear equations of motion of n dislocations group in slip plane under stress 18 p2719 A72-36745

Thermo-elastic interactions in an infinite elastic solid due to a concentrated transient heat source. 18 p2735 A72-36754

Analysis of a partially cracked panel. 18 p2735 A72-36771

Bending of rectangular plates of linearly varying thickness 18 p2736 A72-36991

Infinite plate with a supported reinforced circular hole. 18 p2738 A72-37071

Experimental determination of viscoelastic characteristics 18 p2740 A72-37211

Stress distribution and displacements in adhesive bonded lap-jointed aerospace structures, presenting approximate solution 18 p2740 A72-37214

Point-loaded discs and blocks applicable to tensile testing of brittle materials. 19 p2870 A72-37223

Asymmetric collinear internal cracks interaction evaluation by measuring diameter variation and shape distortion of caustic surface impinged upon by retarded laser radiation 19 p2870 A72-37224

Strain distribution in and around strain gauges. 19 p2870 A72-37225

A note on the low frequency diffraction of elastic waves by a Griffith crack. 19 p2870 A72-37414

Some results of an experimental study of stress distribution at monofilament tips 19 p2822 A72-37529

Estimation of the accuracy of the method of measuring the bending of strips in order to determine residual stresses. 19 p2806 A72-37574

Strain rate, stress concentration and temperature effects on hydrogen environment embrittlement of metals 19 p2816 A72-37640

Creep rupture under stress concentration. 19 p2874 A72-37702

Stress criterion for creep rupture in tubes under combined axial load and internal pressure, deriving stress concentration from high temperature tests 19 p2874 A72-37715

Stress redistribution caused by creep in a thick walled circular cylinder under axial and thermal loading. 19 p2874 A72-37716

Crack toughness - Physical and technological significance 19 p2875 A72-37854

Elastic impact on a three-layer plate in the presence of concentrated masses and nonlinear restraints 19 p2877 A72-38159

Solution manifolds for dynamic elasticity equations corresponding to the action of a concentrated load 19 p2878 A72-38213

Effect of stress amplitude and number of vibration cycles on the damping decrement in metals 19 p2878 A72-38217

Polarization optical method for analyzing local stress concentrations in structural members. 19 p2805 A72-38768

Relation between the reliability and allowable stress amplitude in fatigue design. 20 p2977 A72-38879

Features of deformation and stress distribution in a laminated plastic 20 p2944 A72-38948

Testing of hydrogen pressure or stress concentration induced crack propagation theory for steels based on decohesion mechanism 20 p2935 A72-39003

Factors affecting acoustic emission response from materials. 20 p2924 A72-39279

Use of acoustic emission for the detection of weld and stress corrosion cracking. 20 p2925 A72-39283

The unit stress state in a cylindrical tank with a flat bottom and a partly cantilevered shell 20 p2979 A72-39594

Characteristics of the thermal and stressed states of cooled shell-type blades 20 p2963 A72-39911

Stress intensity factors for transversely loaded elastic plates and their application to predictions of crack arrest. 20 p2981 A72-39956

Elastic analysis for a radial crack in a circular ring. 20 p2981 A72-39959

Study of fatigue crack initiation from flaws using fracture mechanics theory. 20 p2981 A72-39961

Crack arrest and crack initiation in a titanium alloy. 20 p2942 A72-39962

Photoelastic determination of mixed mode stress intensity factors. 20 p2981 A72-39963

Stress concentration around circular crack on interface between two bonded dissimilar isotropic elastic half spaces 20 p2982 A72-40020

A method for directly determining surface strain fields using diffraction gratings. 21 p3052 A72-40236

Applicability of the Euler approach to investigate the strain stability of anisotropic nonlinearly elastic bodies under finite subcritical strains. 21 p3116 A72-40273

Singular moment stresses in homogeneous solutions of plane problem with semiinfinite cut within elasticity theory 21 p3116 A72-40274

Russian book - Plates strengthened by composite rings and elastic cover pieces. 21 p3116 A72-40385

Stresses in a perforated, continuously loaded cantilever beam. 21 p3117 A72-40453

Axisymmetric impact of compactible rods subjected to finite deformations. 21 p3117 A72-40455

Crack tip vicinity stress generated by plane transient tension-stress wave diffraction, examining ductility effects on fracture modes 21 p3117 A72-40672

Simple structures behavior under constant loads, considering low stress levels and creep rupture mechanism with internal damage affecting strain rate 21 p3117 A72-40673

Complex stress-intensity factors at bifurcated cracks. 21 p3117 A72-40675

The effect of couple-stresses on stress concentration of a ring inclusion. 21 p3117 A72-40681

Dynamic stress concentration of notched strips. 21 p3117 A72-40715

Stresses around one hole or two holes subjected to internal pressures in semi-infinite or infinite medium. 21 p3118 A72-40717

A study of stress around non-central holes in a rotating tapered disc. 21 p3118 A72-40775

Singular stress concentration at sharp edge of wedge in contact with half plane in elastostatics 21 p3119 A72-41104

A hyperboloidal notch in a transversely isotropic material under pure shear. 21 p3119 A72-41105

Influence of discontinuity stresses on main propellant tankage of a space shuttle orbiter. [ICAS PAPER 72-10] 21 p3120 A72-41135

Fatigue strength of overloaded stiffeners in cracked panels, evaluating stress intensity factor and overload coefficients for fatigue crack propagation via finite element method [ICAS PAPER 72-40] 21 p3120 A72-41165

A measurement of the surface strain distribution by optical differentiation method. 21 p3056 A72-41239

The vertical stress distribution due to parabolic strip load and uniform load over an ellipse in the interior of a semi-infinite solid. 21 p3121 A72-41243

A consistent approach for treating distributed loading in the matrix force method. 21 p3122 A72-41261

Bent plates and shells equations and rupture modes, characterizing cracks and stress intensity 21 p3122 A72-41338

Regime factor and stress concentration parameter for sudden heating of solid cylinders and disks, noting thermal stability criterion with allowance for statistical strength 21 p3123 A72-41361

The stress gradient as a cause for the manifestation of the scale effect in brittle fracture of materials. 21 p3123 A72-41364

Stress distribution at crack tips in elastic plate loaded by two concentrated opposite forces perpendicular to crack 21 p3123 A72-41389

Stresses in bonded materials with a crack perpendicular to the interface. 21 p3124 A72-41396

The stress intensity factors of a radial crack in a finite rotating elastic disc. 21 p3124 A72-41397

Stress distribution in a cylindrical shell with reinforced holes 21 p3126 A72-41542

Stress concentration around curvilinear holes in plates according to Reissner's theory 21 p3126 A72-41543

Equilibrium equations for given stress concentration in circular and annular plates under tensile loads with different yield points in tension and compression 21 p3126 A72-41545

Influence of stress raisers in the form of circular holes on the endurance in symmetric bending of AMg6BM aluminum-alloy sheet 21 p3071 A72-41704

Calculation of the stress concentration at the joint between a cylindrical casing and a branch pipe for internal pressure 21 p3127 A72-41710

Crack tip stress field alteration via elastic pulses for changing crack trajectory or fracturing process termination, using polarization optical method 21 p3061 A72-41824

Approximate calculation of the temperature stresses in the thermal impact zone 22 p3232 A72-41871

Estimation of the effect of stress concentration in nonstationary loading regimes 22 p3232 A72-41922

On the application of the mixed finite element methods to the stress concentration problems of cylindrical shells with a circular cutout or a crack. 22 p3232 A72-41942

Stress-strain state of an isotropic half-plane with an elliptic hole, deformed by concentrated loads 22 p3233 A72-42057

Stress-strain state at holes in plates in the case of asymmetric buckling modes 22 p3233 A72-42059

Stress concentration at an elliptic hole in an elastoplastic body 22 p3233 A72-42060

Photoelastic study of stress concentration in perforated composite pipes under external pressure 22 p3233 A72-42064

Surface distortion and strain fields visualization by grating produced diffraction patterns, discussing different detection techniques

22 p3234 A72-42391

Magnetic tension induced stress balance in plasma sheet, considering pressure gradient along geomagnetic tail axis, plasma flow kinetic energy and pressure anisotropy

22 p3211 A72-42408

Stress amplitude and hysteresis loop width changes in alpha Ti during cyclic work softening-work hardening with constant strain amplitude

22 p3189 A72-42438

Stress analysis in two dimensional bending process using the photo-rheological stress analysis.

22 p3183 A72-42483

Numerical solution of bending stresses in elastic cantilever plates under surface and edge loads, noting boundary layer, load concentration and sweep back effects

22 p3236 A72-42609

Versatile stretching of a disc shaped as a plane with elliptic aperture.

22 p3236 A72-42627

The stretching of a disc shaped as a semi-infinite plate with half-elliptic edge sector.

22 p3236 A72-42628

Stress concentration around holes in plates and shells.

22 p3238 A72-42834

Brittle fracture under dynamic loading conditions.

22 p3239 A72-42848

A simple formula for the maximum stress in a twisted angle or channel.

22 p3240 A72-42894

Reinforcement of structural materials by long strong fibres.

22 p3241 A72-43026

Book - Effect of notches on low-cycle fatigue: A literature survey.

22 p3242 A72-43145

Plane problem of elasticity theory for known normal and tangential stress tensor components at boundary of simply connected region, calculating stress concentration

23 p3344 A72-43353

Stress concentration around a circular hole in an elastoplastic medium under the action of a temperature field and omnidirectional tension

23 p3344 A72-43418

Combined mode crack extension in adhesive joints.

23 p3305 A72-43493

Boundary value problems for concentrated forces acting inside semiinfinite anisotropic plate under plane stress, investigating failure modes of unidirectional composites

23 p3344 A72-43495

Glass fracture mechanics, discussing microcrack stress concentration, Griffith theory, statistical failure theories, static fatigue and strength measurements

23 p3305 A72-43502

Edge and screw dislocations induced stress fields in isotropic medium, using Kauderer nonlinear elasticity theory

23 p3345 A72-43622

Experimental analysis of the stress distribution in the vicinity of a nonwelded rigid circular inclusion in the interior of a plate stressed in monoxal tension

23 p3346 A72-43691

Plane elastostatic analysis of V grooved rectangular plates notch angle and specimen geometry effects on stress intensity factors and fracture toughness measurements

23 p3346 A72-43703

Stresses around an axial crack in a pressurized cylindrical shell.

23 p3346 A72-43705

A finite element stress analysis of a crack in a bi-material plate.

23 p3346 A72-43707

A note on the twisting deformation of a non-homogeneous shaft containing a circular crack.

23 p3346 A72-43708

Load distribution in a single-edge-notch tensile specimen.

23 p3306 A72-43710

Path independent integrals to predict onset of crack instability in an elastic plastic material.

23 p3346 A72-43711

Al alloy sheet panel tests for cracks emanating from stress concentration areas at holes or cutout edge

23 p3347 A72-43713

Fiber reinforced metallic matrix composite under creep, discussing rigidity, stress distribution, rupture strength and failure time

23 p3306 A72-43727

Refractory materials heat resistance criteria, taking into account hollow cylinder thermal stress distribution

23 p3306 A72-43738

Stress state of arbitrary contour body of revolution under torsion using finite difference method

23 p3347 A72-43744

Disk fillets stressed state, determining concentration coefficient and bearing capacity effect

23 p3347 A72-43747

Thermal and mechanical stresses concentration near peripheral notches on ring-shaped graphite, noting notch sensitivity relationship to tip curvature and graphite grain size

23 p3306 A72-43755

Stress function for thermal shock in plate with cylindrical heat source, noting thermal stress concentration in optical materials under electromagnetic radiation

23 p3348 A72-43792

Numerical determination of the stress concentration around a hole in a circular cylindrical shell

23 p3348 A72-43799

Approximate stress-strain state determination in plate weakened by arbitrarily oriented rectilinear cracks and circular holes in elasticity theory

23 p3349 A72-43801

Photoelastic analysis of cardiovascular-magnitude stress pattern produced by flow through gelatin-agar walled channels for analysis of mechanical stresses on blood vessel walls

23 p3260 A72-43936

Stress distribution at defects in the form of rigid sharply-angled inclusions

23 p3349 A72-43952

Photothermoelastic study of stress concentrations in a plate with internal heating.

23 p3349 A72-43986

Determination of the stressed state in a welded joint in plastic deformation

23 p3293 A72-44019

The torsion of a circular cylinder containing a symmetric array of edge cracks.

23 p3350 A72-44048

Variational analysis of sandwich beams under static loads, presenting shear deformation and normal stress distributions

[ASME PAPER 72-APM-R] 23 p3350 A72-44055

On the solution of plane, orthotropic elasticity problems by an integral method.

[ASME PAPER 72-APM-BB] 23 p3350 A72-44056

Transfer matrix approach for determining stresses and displacements in elastostatics of laminated composites

[ASCE PREPRINT 1674] 23 p3351 A72-44105

Stress-strain characterization of part-through crack in plate under tension in terms of stress intensity factor

23 p3352 A72-44227

Stress intensity factors for embedded elliptical crack in semiinfinite solid and for semielliptical surface crack in plate under tension and/or bending

23 p3353 A72-44231

The elastic analysis of the part-circular surface flaw problem by the alternating method.

23 p3353 A72-44232

Numerical evaluation of elastic stress intensity factors by the boundary-integral equation method.

23 p3353 A72-44233

Three-dimensional finite element analysis for fracture mechanics.

23 p3353 A72-44235

Stress distribution in a homogeneous elastic sphere containing a penny shaped crack of prescribed shape.

23 p3354 A72-44268

Thermoelastic contact problem of an elastic layer resting on an elastic foundation.

23 p3354 A72-44269

Stress distributions in a semi-infinite plate with a row of circular holes.

23 p3355 A72-44398

Stress concentration of a cylindrical shell with one or two circular holes.

23 p3355 A72-44399

Mean stress effects on fatigue crack propagation rate from tests at various temperatures, assuming initial, tensile and shear modes and final propagation stages

24 p3454 A72-44627

Polymer fatigue failure mechanism examination on constant deflection type testing machine, investigating applied stress and temperature effects on crack propagation rate

24 p3455 A72-44631

Optimum design of joints - The stress severity factor concept.

24 p3455 A72-44728

Orthotropic photoelasticity methods application to concentrated force on half plane edge and to stress distribution on elliptical hole boundary in tensile strip

24 p3455 A72-44790

Plane-stress fracture toughness testing using a crack-line-loaded specimen.

24 p3456 A72-44810

Crack growth resistance in plane-stress fracture testing.

24 p3456 A72-44811

A sandwich plate with a part-through and a debonding crack.

24 p3456 A72-44813

Linear fracture mechanics in orthotropic materials.

24 p3457 A72-44818

Stress concentration coefficients calculation at sharp cracks and notches for engine parts in tension, compression and combined bending and torsion

24 p3458 A72-44932

Analogy between body force and inelastic strain gradient in all crystal systems.

24 p3459 A72-45247

The effect of shear on a penny-shaped crack at the interface of an elastic half-space and a rigid foundation.

24 p3459 A72-45250

The stress distribution near the tip of an array of screw dislocations piled-up against an inclusion.

24 p3460 A72-45694

Stressed state of radial bearings hollow rollers under loads concentrated along generatrix, evaluating test results by statistical analysis

24 p3408 A72-45726

Stress state of variable thickness long elastic shallow shell in bending and torsion, applying equations to large turbine blades

24 p3460 A72-45728

Gas turbine wheel design analysis, presenting procedures for estimating revolution rates, blade numbers and component configurations effects on wheel weight for prescribed stresses

24 p3460 A72-45737

Fatigue life and creep tests of refractory materials under programmed thermal cycling for different stress levels

24 p3416 A72-45738

High temperature tensile tests of Mo with helical and circular V grooves, discussing stress concentration sensitivity relations for grooved and smooth samples

24 p3417 A72-45766

The influence of static stresses on the dissipation of energy due to forced oscillations.

24 p3461 A72-45767

STRESS CORROSION

Monograph on stress corrosion failure, covering threshold stresses, fracture mechanics, electrochemical processes, hydrogen embrittlement, corrosives, various steels and alloys, environmental effects, etc

01 p0082 A72-10166

Corrosion and stress corrosion cracking prevention on space shuttle by materials selection

01 p0085 A72-10775

Electrochemical potential microstructure and stress intensity factor effect on aqueous stress corrosion crack propagation rate in high strength Ti alloy

01 p0085 A72-10776

Maraging and Ni steels stress corrosion cracking rates dependence on stress intensity factor, discussing measurements in salt and distilled water

01 p0086 A72-10995

Stress corrosion cracking of Cr-Ni austenitic stainless steel with Mo and Cu additions in boiling sulfuric medium

01 p0089 A72-11181

Stress corrosion crack initiation and propagation characteristics computerized simulation validity

02 p0295 A72-12480

Hydrogen diffusivity and solubility in alpha-Ti alloys, considering absorption effect on stress corrosion cracking

02 p0244 A72-12481

High strength steels stress corrosion crack propagation velocity relationship to crack tip stress intensity

02 p0295 A72-12482

Corrosion fatigue cyclic crack growth rate above and below environmental threshold stress in steels as function of frequency and potentials, indicating hydrogen embrittlement

03 p0377 A72-14172

Maraging steel laminates stress corrosion cracking behavior, showing composite base plate and weld structure influence on crack propagation reduction

04 p0534 A72-15569

Ti-Al-Mo-V alloy sustained load stress corrosion crack growth in salt and distilled water environments

04 p0534 A72-15570

Grain boundary region constituents corrosion behavior and solution chemistry within stress corrosion cracks in Al alloys observed from pH changes

04 p0535 A72-15733

Stress corrosion crack tip electrochemical reactions simulation on Ti and alloy surfaces, using modified rotating disk apparatus with pH measurement

04 p0536 A72-15739

Crackline loaded edge crack stress corrosion specimen, investigating crack initiation and propagation

05 p0673 A72-16324

Stress corrosion crack growth in air melted and vacuum arc remelted nickel maraging steel, using stress wave analysis technique

05 p0674 A72-16327

Critique of microstructure effect on strength, toughness and stress corrosion cracking susceptibility of metastable beta titanium alloy, discussing recrystallization conditions

05 p0679 A72-17122

High Cr ferritic steels intergranular and stress corrosion properties and resistance to sea water, organic and inorganic acids and acid mixtures

07 p0995 A72-19572

Prestressing effect on stress corrosion resistance of fatigue precracked high strength steels

07 p1016 A72-19941

Lower confidence bound for reliability and specifications for nonnormally distributed stress corrosion test data, using Weibull statistical distribution

08 p1189 A72-22102

Alloy composition, specimen stressing and surface conditions effects on stress corrosion cracking

08 p1189 A72-22106

Soviet book on corrosion cracking of carbon steels covering chemical composition, structure, mechanical properties, anode and cathode processes role and adsorption losses

08 p1190 A72-22163

Stress corrosion of uranium carbide ceramics in atmospheric environments containing water

09 p1335 A72-22399

Ion and laser microprobes for concentration measurements of hot salt stress corrosion produced hydrogen on Ti alloy on microscopic scale

09 p1276 A72-23477

German monograph on transition elements Cr, Mn and Zr influence on Al-Zn-Mg alloys stress corrosion covering electron microscope studies and loop-bending tests

10 p1493 A72-23769

Impurities effects on stress corrosion and work hardening induced dislocation structures in stainless steels, considering stacking fault energy relationship

10 p1496 A72-24231

Electrochemical and stress corrosion tests of Ti-Ni alloys in acidic chloride solutions at ambient and elevated temperatures [NACE PAPER 30]

10 p1497 A72-24321

Tensile ligament instability model for stress corrosion crack propagation velocity in austenitized steel tempered at 750 F

10 p1499 A72-24888

Hexagonal metals stress corrosion cracking fractographs interpretation, noting striations as prominent feature of transgranular fractures

11 p1652 A72-25288

Stress corrosion crack paths in Al-Zn-Mg alloys, showing normal coincidence with grain boundaries

11 p1652 A72-25289

Aerospace vehicle high tensile strength fasteners stress corrosion cracking and hydrogen embrittlement [AIAA PAPER 72-385]

11 p1653 A72-25407

Al alloys hand forgings fracture strength and stress corrosion characteristics from precracked specimens bending tests in air and sea water

11 p1658 A72-25833

Metal stress corrosion crack propagation rate theory based on film rupture mechanism

11 p1735 A72-25852

Stress corrosion cracking mechanism of low carbon steels to explain transcrystalline brittle mechanical cracks development along grain boundaries

11 p1666 A72-26923

Fractographic study of stress corrosion fractures of low carbon steels with electron microscope

11 p1666 A72-26924

Microstructural effects on high strength Mg, Al and Ti alloys stress corrosion crack growth in aqueous environments, discussing correlations relative to composition and preferred orientation

11 p1668 A72-26946

Al-Zn-Mg alloy tear resistance relationship to stress corrosion cracking from tear, tensile and corrosion tests

12 p1830 A72-27750

Ti alloys hot salt stress corrosion cracking mechanism, discussing cold deformation and heat treatment effects, tensile tests, hydrogen analysis and microscope investigation

14 p2117 A72-30535

Chemical and mechanical properties relationship to stress corrosion in high strength Al-Cu and Al-Zn-Mg alloys, emphasizing grain boundaries cleavage energy

14 p2117 A72-30536

Heat treatment and grain size effects on stress corrosion resistance and life duration of maraging steels, investigating crack initiation and propagation

14 p2117 A72-30539

Heat treatment hardening effect on stress corrosion resistance of ultrahigh maraging and stainless steels, emphasizing hydrogen embrittlement

14 p2117 A72-30540

Anodic salt-chromate stress corrosion resistance test of Al-Zn-Mg alloys, noting time reduction and correlation with natural environment exposures

14 p2117 A72-30541

Microstructural changes relationship to corrosion susceptibility in ternary Al alloy obtained from stress corrosion cracking tests and electron metallography, noting precipitate-free region

14 p2118 A72-30542

Stress corrosion crack initiation and propagation for Ti alloy in sodium chloride solutions, noting anodic dissolution

15 p2253 A72-31295

Ti alloy initial H content effect on resistance to hot salt stress corrosion embrittlement and cracking, discussing annealing treatment influence

15 p2253 A72-31296

Ti-Al-V foil stress corrosion methanol cracking resistance improved by treatment with pentanedione, suggesting metal ions removal from protective film

15 p2253 A72-31297

Ti alloys hot salt stress corrosion during turbine engine operation, noting effects of alloy processing conditions, surface properties and cyclic exposures

15 p2297 A72-32136

Catalytic dissociation, hydrogen embrittlement, and stress corrosion cracking.

17 p2566 A72-34256

Critical species in the transgranular stress corrosion cracking of titanium alloys in aqueous solutions.

17 p2567 A72-34733

Austenitic steel stress corrosion prevention at high temperatures and pressures, investigating inhibitor adsorption properties from capacitance measurements and polarization curves

17 p2568 A72-35474

Interface morphology development during stress corrosion cracking. I - Via surface diffusion.

18 p2700 A72-36583

Active corrosion in aqueous solutions, discussing reactions, adsorption, intergranular attack, pitting, crevice corrosion and stress corrosion cracking

19 p2815 A72-37446

Cathodic protection and hydrogen in stress corrosion cracking.

19 p2817 A72-37765

Stress corrosion cracking of 18% Cr ferritic stainless steels.

19 p2820 A72-38300

Effect of additions of Cu and Zr on stress corrosion cracking of Al-Mg alloys.

19 p2820 A72-38370

A study of the mechanical behaviors of austenitic stainless steels in the process of stress corrosion testing.

19 p2820 A72-38372

The role of metal dissolution in the process of stress corrosion cracking of austenitic stainless steel.

19 p2821 A72-38374

Interpreting electron fractographs of stress corrosion in aluminum alloys.

19 p2821 A72-38387

Effects of small amounts of additional elements on stress corrosion cracking of Al-Zn-Mg alloys. VI.

19 p2821 A72-38555

Use of acoustic emission for the detection of weld and stress corrosion cracking.

20 p2925 A72-39283

Electrochemical protection potential of metals and alloys in pitting, intergranular corrosion and stress corrosion cracking in presence of chlorides

21 p3065 A72-40087

Designing to avoid stress-corrosion and/or fatigue failures.

[AICHE PAPER 15C]

21 p3116 A72-40125

Stress-corrosion cracking of high strength steels and titanium alloys.

21 p3067 A72-40849

Analytical fracture mechanics application to stress corrosion cracking test methods for examining crack growth kinetics and time-to-failure

21 p3067 A72-40913

Brittle striation formation role in corrosion fatigue crack propagation mechanism in Al-Zn-Mg alloy from test in NaCl solution under reversed anodic-cathodic current

22 p3193 A72-43033

Differentiating stress corrosion cracking from hydrogen cracking of ferritic 18-8 stainless steels.

22 p3195 A72-43127

The effect of some electrolytes on the stress corrosion cracking of AISI 4340 steel.

22 p3195 A72-43128

Influence of the cycling frequency on the fatigue and corrosion fatigue of steel samples with bushings

22 p3242 A72-43155

STRESS CYCLES

Metal crystals dislocations movements and interactions with dislocation dipole under applied cyclic stresses for various configurations and starting conditions, using numerical methods

01 p0113 A72-10208

Tensile and fatigue tests on steel, brass and aluminum with starter cracks, showing relation of strength and ductility to crack propagation and stress cycles

01 p0083 A72-10392

Combined bending/torque fatigue test machines design, operation, calibration and results, developing probabilistic S-N diagram from cycles-to-failure data statistical analysis

02 p0199 A72-11514

Automatic recording of cyclic creep and strain curves for metals under low cycle static tension

03 p0444 A72-13468

Fatigue failure under cyclic stress, analyzing surface and temperature effects

03 p0372 A72-13588

Optimal cyclic fatigue strength of low C steel from critical deformation rate during thermomechanical treatment

03 p0372 A72-13597

Fatigue cracks nucleation in steel bearings subjected to cyclic contact stresses

03 p0377 A72-14020

Structural inhomogeneities effect on fatigue phenomenon in rolling motion, discussing stress cycles preceding active surface degradation

04 p0526 A72-14473

Cyclic strain accumulation induced creep behavior prediction via plasticity model, considering non-homogeneous stress states

[ASME PAPER 71-APM-NN]

04 p0589 A72-15179

Vibrations effect on corrosion rate by experimental method, comparing reaction kinetics on two specimens with and without alternating stresses

04 p0591 A72-15237

Dislocation substructure in fatigued Al and Ni polycrystals surface layer and interior due to high and low stress cycling, discussing stacking fault energy influence

04 p0534 A72-15577

Rotating shaft fatigue under variable stress cycles, determining safety, bending and torque coefficients

04 p0594 A72-15750

Elastoplastic creep analysis for cylindrical pressure vessel structural response during cyclic thermal shock, internal pressure and extended high temperature loading [ASME PAPER 71-WA/PVP-12]

05 p0732 A72-15911

Crack growth dependence on applied high stress level cycle number, showing fatigue life inversely proportional to stress exponential function

05 p0673 A72-16304

High temperature low cycle fatigue of Cr-Mo-V steel, observing crack growth rate correlation with crack tip stress

05 p0673 A72-16321

Plastic zone formation and fatigue crack propagation rate during high cyclic bending of metals

05 p0674 A72-16326

Microvolume decohesion hypothesis for crystal lattice defects explaining metal fatigue under variable stresses

06 p0829 A72-17743

Hardened and tempered Ni-Cr-Mo steel, testing rest periods caused fatigue life increase in terms of cycles to failure

06 p0895 A72-17802

Fatigue damage factor and failure probabilities in structural design for multilevel repetitive cyclic stresses

06 p0896 A72-17965

Deformation stresses and strains in quasi-static low cycle fracture of stabilizing, softening and strain hardening materials

06 p0831 A72-18352

Steel sheet creep, plastic deformation and service life under temperature and stress cycles

06 p0899 A72-18558

High temperature fatigue test assembly for symmetric tension compression cycles at 10 kHz with specimen heating in resistance furnace

06 p0797 A72-18568

Small elastoplastic cyclic strain effects on internal friction and energy dissipation in metals during vibrations

06 p0834 A72-18679

Stress variation effect on strength values obtained by low cycle fatigue tests involving bending with rotation

07 p1014 A72-19847

Ni based superrefractory alloy high temperature fatigue tests, studying creep as function of stress load and frequency and temperature

07 p1022 A72-20487

Epoxy and polyester resin fatigue fracture tests for cyclic stress and moisture effects

08 p1192 A72-21680

Mechanical surface strengthening effect on small cycle fatigue life of Ti alloy weakened by stress raiser

08 p1186 A72-21725

German monograph on fracture formation and behavior in Ni maraging steel under repeated stress alternations, considering Al and Ti effects on steel strength

08 p1190 A72-22172

Structural model application to construction material alternate stress description at elevated temperatures

09 p1401 A72-22727

Creep ratchetting deformation and rupture damage from thermal transient stress cycle and constant membrane force under high temperature metal creep conditions

09 p1406 A72-23197

Polycrystalline Mo fatigue behavior under cyclic stresses, discussing grain size effect on fatigue life and relationship between cycle dependent yield and French damage line

11 p1658 A72-25830

Cylindrical samples with deep circular hyperbolic notch, investigating cyclic inelastic strain induced stress redistribution effects on load bearing capacity

12 p1830 A72-28229

Microcrack initiation and propagation in ductile metals at low cycle and ultrasonic frequencies, investigating fatigue fracture mechanism by scanning electron microscope

15 p2256 A72-31838

Acoustic emission from carbon fiber-epoxy composite during continuous tensile stress cycling

16 p2413 A72-32868

Cyclic compressive fatigue cracking tests of prenotched fiber reinforced epoxy materials at low stress

16 p2414 A72-33319

Deformation substructures in stainless steels under low cycle high strain fatigue tests evaluation for application as fuel cladding for fast breeder reactors

16 p2411 A72-33825

Understressing and coxing cycles effect on deeply notched carbon steel fatigue behavior, emphasizing crack initiation and breakdown

16 p2472 A72-33947

Rheological model for creep under intermittent square wave stress pulses, taking into account time dependent dislocation density

16 p2412 A72-34113

Strengthening mechanism in metals during creep under variable stress for dislocation network structure studies

16 p2475 A72-34164

Fatigue crack initiation and propagation in welded structures, considering low and high cyclic stresses, microstructure and environment effects

17 p2635 A72-35919

Creep damage role in governing elevated temperature strain cycling fatigue lives of heat resistant stainless steel and cobalt alloy

19 p2817 A72-37712

A certain generalization of the hysteresis loop contour equations to the case of an asymmetric cycle

19 p2876 A72-38003

Stress dependent cyclic creep rupture tests of Ti and Co-base alloys and stainless steel at 1300 F

20 p2938 A72-39305

Dynamic strength of tangentially wound toothed blade roots

20 p2979 A72-39586

Cyclic stress-strain induced buckling and fatigue failure in cold-rolled steel and tabulating and diagramming mechanical properties

21 p3065 A72-40233

A study on the correlation between thermal fatigue and low-cycle fatigue at elevated temperatures.

21 p3119 A72-41008

Low carbon steel S-N diagram for stresses ranging to fatigue limit, noting cyclic creep, macroplastic cyclic stress and fatigue failure

21 p3122 A72-41353

Thermoplastics fatigue life dependence on stress with allowance for heating laws, noting heat accumulation effect on thermal failure

22 p3196 A72-42164

Dislocation pile-ups in periodic internal stresses.

22 p3214 A72-42316

Effect of cyclic stress wave form on corrosion fatigue crack propagation in Al-Zn-Mg alloys.

22 p3194 A72-43043

Low cycle fatigue under biaxial strain controlled conditions.

23 p3354 A72-44259

A comparison of the axial and reversed-torsional strain cycling low-cycle fatigue strength of several structural materials.

23 p3304 A72-44397

The stress-strain relation in the low-cycle fatigue of metallic materials under rotating-beam bending.

24 p3454 A72-44626

The cyclic plastic strain and cumulative fatigue damage - Fatigue damage caused by the stress below the fatigue limit.

24 p3454 A72-44628

The fatigue strength under varying mean stress.

24 p3455 A72-44629

Automatic recording of cyclic creep and strain curves for metals under low cycle static tension

24 p3458 A72-44943

Deformation stresses and strains in quasi-static low cycle fracture of stabilizing, softening and strain hardening materials

24 p3460 A72-45739

Cyclic loading effects on resistance to brittle fracture of low carbon structural steels, using crack width criterion

24 p3416 A72-45740

STRESS FUNCTIONS

Elastic incompressible isotropic transparent media, deriving photoelastic effect relationship to stress function

01 p0089 A72-10123

Hydrogen chemical permeation through iron and steel as function of compressive and tensile stress

01 p0083 A72-10206

Finite plasticity incremental and total strain theories for nonproportionate loading of circular steel and Al alloy torsion-tension members assuming von Mises yield

[SESA PAPER 1901]

02 p0288 A72-11519

Isothermal uniaxial stress analysis of material consistent with linear law of heredity theory, determining viscoelastic relaxation function

02 p0290 A72-11621

Fatigue breakdown and energy dissipation dependence on stress during bending of cylindrical steel and iron specimens

03 p0372 A72-13589

Shallow spherical shell natural vibration frequencies, deflection and stress function, discussing effects of internal pressure, dimensions and material properties

03 p0453 A72-14209

McNamee-Gibson displacement potential functions generalization to problems for compressible pore fluid in theory of consolidation or thermoelasticity

03 p0455 A72-14389

Effective plastic strain for Tresca and von Mises materials, investigating hot rolled mild steel specimens

04 p0590 A72-15187

Continuous linear elastic systems characteristic vibrations differential operator eigenvalues lower bounds calculation, obtaining Green integral operator first invariant upper bound via stress function

04 p0540 A72-15706

Thermal stresses in thin symmetrically heated disk with time and temperature dependent mechanical properties, deriving integrodifferential equation defining stress function

05 p0740 A72-16624

Dual stress, strain and displacement formulations of linear finite element elasticity, showing Finzi stress function applicability

07 p1087 A72-18780

Stress functions for anisotropic elastic body with uniformly propagating circumferential crack, considering axially orthotropic cylinder

10 p1553 A72-23744

Von Mises yield criterion extended to thin walled circular cylinder plastic torsional straining, noting variations of anisotropic parameters and yield stresses with shear strain

[ASME PAPER 71-MET-Y]

11 p1735 A72-25877

Hybrid cylindrical shell finite element, determining natural frequencies from equilibrium equations, stress functions stress-strain relationships and boundary force transfer matrices

12 p1882 A72-27339

Stress boundary value problems for infinite wedges in linear elasticity theory solved by Mellin transforms

12 p1883 A72-27561

Thick rectangular plate stress functions under linear tensile forces application to longitudinal edges and resultant forces application to transverse edges

13 p2055 A72-28735

Tangential stresses, rigidity characteristics and stress functions of prismatic grooved circular shafts, showing summary representations and integral transformations methods interrelationship

13 p2057 A72-29062

Tangential displacements of spherical and circular cylindrical shallow shells calculated from stress function

13 p2059 A72-29490

Stress function method for calculating stress-strain state in homogeneous shallow spherical shell under arbitrary load

15 p2324 A72-31485

Schaefer stress representation for elastokinetics of linearly elastic isotropic homogeneous body under small deformations and torsions

15 p2324 A72-31486

Thermoelastic stress analysis for hollow cylinder heated along helix, calculating stress function for given surface temperature distribution

15 p2333 A72-32687

On the two-dimensional deformation of a semi-infinite porous elastic medium.

16 p2736 A72-36929

Thermal stability of skewed plates

19 p2871 A72-37430

Plate bending analysis with hybrid triangular and rectangular finite elements, deriving stiffness matrix via optimized stress functions

20 p2979 A72-39556

Stress functions in three-dimensional elastodynamics.

21 p3117 A72-40677

Constant strength shells theory generalization from axially symmetric to nonsymmetric case, using Von Mises yield condition

21 p3117 A72-40680

Non-linear elastic constitutive equations.

21 p3125 A72-41514

Weight minimization for elastic circular plates of variable thickness under uniformly distributed load with given stress function conditions

22 p3232 A72-41896

Glassy materials rheological behavior description in terms of stress function, discussing molecular processes transformation range thermodynamics

22 p3196 A72-42791

Stress-strain state induced by local physicochemical transformations in a layer

22 p3242 A72-43164

Stress function for thermal shock in plate with cylindrical heat source, noting thermal stress concentration in optical materials under electromagnetic radiation

23 p3348 A72-43792

Elastic and plastic deformations in torsional moment loaded rod, noting successive approximation for stress functions

23 p3348 A72-43794

Two-dimensional problem of elasticity theory for an anisotropic inhomogeneous wedge

24 p3459 A72-45263

Castigliano variational theorem for algebraic equation solution of thermal stresses determination in elastic parallelepiped, using Maxwell stress functions as cosine binomial series

24 p3459 A72-45267

STRESS MEASUREMENT

NT X RAY STRESS MEASUREMENT

Airport apron surface pavement strain measurements under field loading conditions, considering static and dynamic loads with finite element method

01 p0047 A72-10192

Tensometric damage detection in rolling contact bearings from bending stress spectrum, using Si strain and wire strain gages

01 p0078 A72-11379

Strain gage measurements of stress intensity factor for crack propagation in fatigue cracked thin metal sheets

03 p0444 A72-13542

Griffith crack propagation in polymethyl methacrylate, examining stress changes by photoelastic method

03 p0380 A72-13719

Flow stress measurements in disordered and partially ordered Ni-Ta alloy single crystals, correlating with ordered phase volume fraction and domain size

04 p0534 A72-15272

Strain gage system for low amplitude strain measurement, discussing SNR and installation technique

04 p0523 A72-15495

Turbulence intensities and shear stress measurements in wake of thin flat plate by rotating single hot-wire anemometer

04 p0524 A72-15498

Stress measurement at surface of polycrystalline bodies by nondestructive X ray diffractometry method

04 p0525 A72-15553

Test conditions, specimen batch and method effects on accuracy of rapid fatigue limit tests with increasing stress amplitude

05 p0741 A72-17085

Principle stress errors in biaxial stress fields expressed in terms of transverse sensitivity, stress and Poisson ratios of material during strain gage calibration

06 p0895 A72-17798

Residual stress measurements in metals by annular photoelastic gages, obtaining relationship to fringe orders

06 p0818 A72-18317

Elastic-plastic strain measurement on flat steel surfaces by moire gratings, using electroluminescent source and crossing jig

06 p0818 A72-18323

Single fiber reinforced plate initial stress distribution due to linear expansion coefficients difference between matrix and fiber, using optical polarization

06 p0836 A72-18557

Bridge circuit to minimize parasitic electrical disturbances in resistance strain gage measurements of dynamic stresses in impact tests

06 p0819 A72-18672

Stress relaxation measurement assembly for polymer film and fiber samples under tensile stresses at 213-573 K

07 p0986 A72-19779

Automatic photoelectric device for measuring internal stresses and deformations of photographic films

07 p0988 A72-19861

Internal strain measurement in solid elastomeric materials by radioactive implant method using pinhole camera or multichannel collimator

07 p0992 A72-20583

Strain measurements by holographic interferometry, considering data input to computer by digitization of video signals

08 p1163 A72-20917

High temperature strain measurement accuracy improvement by gage spot welding

08 p1163 A72-20920

Thermal stress measurement and thermoelastic behavior of carbon-carbon-materials for reentry nose

STRESS DISTRIBUTION

U STRESS CONCENTRATION

cones, describing gage mounting, temperature compensation and data recording
08 p1164 A72-20921

Basal and prismatic crystal dislocations in Be, measuring critical resolved shear stress dependence on temperature at 300-500 K
08 p1185 A72-20991

Automated mechanical system for solid propellant sheet stretch tests in two directions as function of time
08 p1147 A72-21331

Plastic flow properties and stress measurement for metal working conditions with flat ring compression specimens and interfacial friction consideration
08 p1250 A72-22196

X ray method characteristics in thermal interphase microstresses determination, considering spherical silicon inclusion surrounded by concentric Al matrix envelope
09 p1309 A72-22638

Photothermoelasticity method for determining thermal stresses
09 p1402 A72-22737

Static strain measurement errors due to nonstationary thermal conditions in semiconductor resistance gages
09 p1310 A72-22739

Semiconductor IC transducers for electrical readout of optical radiation, mechanical stress and magnetic field strength
10 p1448 A72-24282

Stress distribution determination by shear stress difference method in curvilinear orthogonal coordinate systems
10 p1557 A72-24405

Elastic r-value variation in Ti sheet from direct measurement of width and thickness strains
11 p1659 A72-25895

Isotropy postulate corollary verification for strain vectors measurement of annealed steel tubular specimens under combined tension and internal pressure
12 p1887 A72-28232

Physical operation principles of semiconductor sensors using deformation potential for mechanical stress detection and measurement
14 p2104 A72-30445

Case bonded solid rocket propellants mechanical strength characteristics determination by photoelastic stress measurements or viscoelastic calculation
14 p2145 A72-30765

Holographic interferometry for strain measurements in bodies, obtaining frozen interference fringes for stressed plane mechanical component via double exposure
14 p2105 A72-30840

Embedded piezoelectric quartz crystal transducer with Hopkinson pressure bar to measure internal dynamic stress
15 p2240 A72-32433

Stresses in a welded diaphragm due to boundary contraction and normal uniform pressure.
[SESA PAPER 1811]
17 p2631 A72-34821

Two-phase crystal structure microdeformation measurement by combined holographic interferometry and X ray diffraction
18 p2690 A72-36358

Mechanical structure and component stress measurement by reinforced concrete, microconcrete, elastic and plastic models
18 p2733 A72-36370

Program-controlled machine for the investigation of mechanical properties of materials under a complex stress.
19 p2795 A72-37575

Holographic strain measurement on a tensile specimen.
19 p2798 A72-37615

Ceramic coatings measure the complex stresses in gas-turbine blades.
19 p2875 A72-37732

The effect of wire length and separation on X-array hot-wire anemometer measurements.
19 p2801 A72-37903

Stress sensitive device based on anisotropic conductivity of multivalley semiconductor under uniaxial stress
20 p2961 A72-39713

Pressure dependence of electrical characteristics of semiconductor sensors using deformation potential for mechanical stress detection and measurement
21 p3056 A72-41109

A measurement of the surface strain distribution by optical differentiation method.
21 p3056 A72-41239

Measurements of Reynolds shear stress fluctuations in a turbulent boundary layer.
21 p3047 A72-41638

Chemical etchants and etching procedure for decorating areas of residual tensile elastic surface stresses in ultrahigh strength steels without aging
22 p3183 A72-43045

Experimental investigation of displacements and stresses in a rod during impact loading
23 p3348 A72-43795

Full-field surface-strain and displacement analysis of three-dimensional objects by speckle interferometry.
23 p3349 A72-43984

Unsteady flow field near wall and Reynolds stress measurement in turbulent boundary layer, using conditional sampling technique with digital computer
23 p3282 A72-44304

The structure of turbulent flows adjacent to walls.
24 p3390 A72-45001

STRESS PROPAGATION

Longitudinal stress pulse amplification during propagation along tapered elastic bars in direction of decreasing cross section
[SESA PAPER 1894]
02 p0287 A72-11504

Initially sharp cylindrical pressure pulse propagation and stress wave attenuation in linear elastic fiber reinforced composites
[AIAA PAPER 72-394]
11 p1730 A72-25415

Longitudinal propagation of elastic disturbance in conical rod, discussing Young modulus, material density and periodic and impulsive stress
11 p1737 A72-26589

Geometrically nonlinear structure elastic stress propagation, deformation and dynamic response under impact, using finite element matrix displacement method and computer programs
12 p1879 A72-27189

Fourier transform approximate inversion solution for transient pulse propagation from spherical cavity with surface under impulsive pressure in viscoelastic medium
12 p1844 A72-27196

Stress wave propagation and fracture in composites, discussing micromechanical and homogeneous-continuum theories
13 p2060 A72-29692

Transient stress pulses propagation in obliquely laminated composites, comparing analytically predicted waveforms with experimental results
13 p2060 A72-29693

Interacting continua theory for stress wave propagation in composites with microstructural stress and displacement fields, discussing elastic and viscoelastic materials behavior
13 p2060 A72-29695

Longitudinal impact of cylindrical shells with discontinuous cross-sectional area.
[ASME PAPER 72-APM-24]
17 p2628 A72-34793

Reflection of pulses at the interface between an elastic rod and an elastic half-space.
23 p3314 A72-44119

STRESS RATIO

Cyclic stress ratio effects on stainless steel fatigue crack propagation at 1000 F, using linear elastic fracture mechanics
12 p1829 A72-27663

STRESS RELAXATION

Rheological properties and architecture of arterial walls, using stress relaxation and stress-strain hysteresis tests on dog aorta, iliac and femoral strips
01 p0010 A72-10184

Stress relaxation resistance at elevated temperatures after reloading as function of internal and effective stress
01 p0138 A72-10520

Isothermal uniaxial stress analysis of material consistent with linear law of heredity theory, determining viscoelastic relaxation function
02 p0290 A72-11621

Quenching effects on thoria-dispersed Ni sheet plastic stress relaxation and room temperature mechanical properties
02 p0247 A72-12822

Screw connections high temperature behavior, discussing creep induced tension relaxation and cyclic loads long term tolerance
03 p0363 A72-13375

Thermodynamic and dissipative restrictions on isothermal stress relaxation functions in linear viscoelasticity
04 p0583 A72-14462

Distensibility and stress relaxation characteristics of capacitance and resistance vessels of isolated rabbit ear as function of basal tone
04 p0473 A72-15124

Cylindrical shell under internal pressure, detailing axial thermal stresses relaxation
06 p0900 A72-18669

Rutile creep resistant substructure recovery at 1000-1040 C, discussing stress relaxation mechanism due to dislocation walls or subgrain boundaries migration
07 p1023 A72-18800

Increased microplastic deformation resistance, relaxation stability and aging of beryllium by cyclic heat treatment
07 p1013 A72-19740

Stress relaxation measurement assembly for polymer film and fiber samples under tensile stresses at 213-573 K
07 p0986 A72-19779

Refractory alloys softening under stress relaxation conditions at high temperatures, noting plastic strain hardening effect absence
07 p1018 A72-20138

Polyurethane O ring seals for high pressure applications, discussing stress relaxation /creep/ behavior, resilience and tear and abrasion resistance
08 p1173 A72-21023

Nonlinear viscoelastic body model for stress relaxation of amorphous linear polymers below vitrification temperature for various deformations, temperatures and deformation speeds
08 p1194 A72-21751

Stress and thermal relaxation effects in viscoelastic behavior of turbulent flows of liquids and gases
10 p1464 A72-23867

Dimensional stability and micromechanical properties of materials for use in OAO, investigating residual stresses, creep properties and stress relaxation
[AIAA PAPER 72-325]
11 p1653 A72-25362

Residual stresses and stress relaxation determination in electrochemical galvanic coating with automatic strain curve plotter
11 p1613 A72-26264

Dynamic relaxation critical damping estimation in terms of mass dependent load vector concept involving vibration and Rayleigh principle
12 p1844 A72-27197

Quenched beryllium bronze alloy plastic deformation effects on anomalous and ordinary stress relaxation processes
12 p1828 A72-27292

Stress relaxation in anelastic materials, calculating spectra, complex modulus of elasticity and internal friction
12 p1883 A72-27541

Gamma irradiation effects on epoxy-diane resin creep and stress relaxation properties indicated by loaded specimens birefringence patterns
13 p1984 A72-29481

Strain release method for investigating thermally activated microflow mechanisms in solids, discussing technique for activation energy and relaxation strength measurements
16 p2372 A72-32822

Bauschinger effect analysis based on yield theory, noting effects of stress relaxation and isotropic hardening
16 p2471 A72-33786

Graph-analytic technique to plot Cr steel stress relaxation curve from primary and isochronous creep diagrams
16 p2472 A72-33848

Second order deformation theory for axially held strut during thermal cycling at creep relaxation temperature, using galerkin method with assumed sine wave
16 p2473 A72-34124

Load cycle frequency and time characteristic effects on plastics fatigue behavior, considering relaxation, retardation and internal damping induced heating effects
16 p2416 A72-34145

Grain-boundary relaxations in an Fe-Ni-Cr alloy.
18 p2700 A72-36588

Temperature-time superposition applied to the relaxation properties of a glass fiber reinforced plastic and its binder
19 p2822 A72-37543

Combined stress creep of non-linear viscoelastic material.
19 p2822 A72-37714

Modified Gilman equation relating dislocation velocity to applied effective stress shown in agreement with stress relaxation experiments on Ti
22 p3189 A72-42436

A comparison of single-integral non-linear viscoelasticity theories.
24 p3460 A72-45695

Refractory alloys softening under stress relaxation conditions at high temperatures, noting plastic strain hardening effect absence
24 p3416 A72-45763

STRESS RELIEVING

Ti-Al-V room temperature creep, considering tensile and torsional loading, plastic deformation, stress relief and design limitations
03 p0377 A72-14171

Transverse strains in solid body due to volumetric stresses counteraction to external load stresses
06 p0899 A72-18566

Aircraft light alloy integral construction for stress concentration and fatigue failure avoidance, describing continuous casting process, stress relieving and ultrasonic flaw testing procedures
07 p0995 A72-19725

Heat treated Al alloy forgings stress relief by cold deformation between quench and age, examining effect on tensile properties and residual stresses
[ASM PAPER W 72-53,1]
12 p1817 A72-28165

Stress relieving heat treatment for service failure prevention of stressed austenitic stainless steel components of high temperatures, noting cracking regulation by oxidation mechanism
14 p2117 A72-30538

Flow-stress recovery of nickel-aluminum alloys.
23 p3299 A72-43563

Recovery of high temperature deformed Ni-Al alloys.
23 p3300 A72-43564

STRESS RUPTURE STRENGTH

U CREEP RUPTURE STRENGTH

STRESS TENSORS

- Stress tensor asymmetry effects on stress concentration at curvilinear holes in elastic plates under tension 02 p0289 A72-11611
- Elastoplastic deformation in medium with initial dislocations and temperature field, expressing kinetic stress and distortion tensors by Hamiltonian derivatives 02 p0290 A72-11630
- Polarization and stress tensor characteristics as function of interaction between mechanical, thermal and electromagnetic processes in elastic isotropic dielectrics 03 p0390 A72-14103
- Infinite elastic isotropic multiply connected plate, determining stress-strain state by asymmetric stress tensors and moment stresses 03 p0451 A72-14119
- First approximation of linear elastic shell theory using split constitutive equation of stress tensor 03 p0454 A72-14341
- Continuous bodies incremental deformation and stability under initial stress, discussing relationships for elasticity constants and material stress tensors [ASME PAPER 71-WA/APM-9] 05 p0734 A72-15970
- Subgroup structure of symmetry group G of stress tensor for stored energy function in hyperelasticity 06 p0893 A72-17302
- Isotropic and anisotropic materials strength criteria and boundary surfaces in invariant stress tensor spaces 06 p0898 A72-18553
- Flexure analysis of isotropic Reissner flat plates bonded by adhesive layer, deriving stress distribution equations in general tensor form [AIAA PAPER 71-148] 07 p1089 A72-19688
- Thirteen moment closed system of approximate integral equations for rarefied gases density, velocity, temperature, stress tensor and thermal flux vector 09 p1259 A72-22425
- Boltzmann equation solution in terms of irreducible spherical tensors and Talmi coefficients, calculating stress tensor for fully ionized plasma in strong magnetic field 09 p1341 A72-22681
- Anisotropic plate theory for perfectly plastic flow, expressing yield condition in terms of mixed stress-anisotropy tensors 09 p1403 A72-22765
- Book on tensor analysis and continuum mechanics covering strain, permutation and stress tensors, vector and tensor comparison, application to elasticity and shell theory, etc 09 p1406 A72-23000
- Turbulent flow time averaged description by Navier-Stokes equations, determining Reynolds number dependent stress tensor coefficients 11 p1615 A72-25722
- Elastic inhomogeneous continuum stability dependence on internal stress tensors field and boundary conditions, noting application to composite materials 12 p1843 A72-27171
- Turbulence model based on transport equations for Reynolds stress tensor and energy dissipation rate, deriving simplified version for boundary layer flows 12 p1798 A72-27830
- Almansi strain tensor comparison with Lamé elastostatics equations, noting distinction between strained and unstrained state 15 p2330 A72-32291
- Depolarized light scattering spectra splitting in nonassociated liquids, noting viscoelastic theory with allowance for antisymmetric part of microscopic stress tensor 16 p2428 A72-32950
- Nonlinear thermoelasticity theory extension via entropy production inequality theorem, deriving expressions for stress tensor and heat conduction vector 16 p2465 A72-32980
- First and second order shock discontinuity waves propagation in thermoelastic incompressible solids, deriving Piola-Kirchhoff stress tensor via Clausius-Duhem relation 16 p2423 A72-33109
- Non-analytic character of the shear-tensor distribution function in incompressible turbulence. 18 p2678 A72-36012
- Propagation mechanism of tensor wave in solid elastic body due to impact. 18 p2734 A72-36377
- Microinhomogeneous elastic media with moduli tensor as coordinate random function, investigating stress and strain tensors 18 p2735 A72-36668
- Stokes fluids nonlinear effects on turbulent flow with lateral shear in terms of stress and deformation tensors 19 p2785 A72-37470
- Extension of the Curie principle and constitutive relations for fluids with antisymmetric stress. 22 p3166 A72-42311

Plane problem of elasticity theory for known normal and tangential stress tensor components at boundary of simply connected region, calculating stress concentration 23 p3344 A72-43353

A new variational principle for finite elastic displacements. 23 p3350 A72-44047

Photoelastic verification of a mechanical model for the flow of a granular material. 24 p3460 A72-45697

STRESS WAVES

- Electromagnetic plane stress wave generation by capacitor bank for transient loading of photoelastic models along straight and curved boundaries [SESA PAPER 1907A] 02 p0199 A72-11503
- Beams and plates resting on elastic base with loads moving along line or strip, calculating wave processes based on half space dynamic model 02 p0290 A72-11629
- Stress waves propagation in woven-fabric composites, obtaining dynamic moduli and vibration damping coefficients by resonance technique [AD-736006] 02 p0291 A72-11984
- Finite amplitude stress wave propagation behind shock in unidirectionally reinforced fiber matrix composites under impact loads 04 p0585 A72-14534
- Discrete variable approach for stress wave propagation in axisymmetric layered elastic-plastic solids 04 p0593 A72-15626
- Error bounds on elastic-plastic strain wave measurements, considering one dimensional wave propagation in seminfinitesimal bar [ASME PAPER 71-MET-W] 05 p0731 A72-15789
- Combined stress wave propagation in thin wall prestressed tube under longitudinal and torsional impact loading 06 p0898 A72-18321
- Composite elastic beams equations under initial stress, investigating flexural wave propagation and structural stability 07 p1090 A72-19733
- Brittle fracture dynamics, deriving motion equations and stability conditions of surface cracks under stress waves from energy balance and angular momentum conservation law 09 p1404 A72-22916
- Stress wave reflection and transmission at interfaces between homogeneous isotropic linear elastic materials 09 p1353 A72-23501
- Photoelastic studies of plane stress fields in plate induced by moving loads at subsonic, transonic and supersonic speeds 10 p1553 A72-23746
- Stress wave surfaces in graphite fiber-epoxy matrix anisotropic plates under transverse impact forces, using Mindlin approximation theory 10 p1555 A72-24255
- Two dimensionally reinforced quartz-phenolic composite material dynamic fracture behavior under stress wave loading in uniaxial strain, noting spallation threshold time dependence 11 p1669 A72-25291
- Initially sharp cylindrical pressure pulse propagation and stress wave attenuation in linear elastic fiber reinforced composites [AIAA PAPER 72-394] 11 p1730 A72-25415
- Laser-interferometer instrumentation for shock stress wave measurements in solids, using velocity and displacement techniques 12 p1808 A72-27638
- Stress wave propagation and fracture in composites, discussing micromechanical and homogeneous-continuum theories 13 p2060 A72-29692
- Interacting continua theory for stress wave propagation in composites with microstructural stress and displacement fields, discussing elastic and viscoelastic materials behavior 13 p2060 A72-29695
- One dimensional wave equation for stress wave propagating at variable velocity for case of monotone decreasing rate 15 p2327 A72-31738
- High amplitude ultrasonic stress waves effect on metals elastic and plastic deformation characteristics, verifying model for sound waves-lattice structure interactions 15 p2328 A72-31842
- Strain rate history effects on stress incremental wave front propagation in elastic bars, considering Taylor-Karman-Rakhmatulin theory 16 p2466 A72-33103
- Metal fracture by electron pulse generated stress waves, noting intergranular fracture mechanism 16 p2472 A72-33845
- A lattice model for stress wave propagation in composite materials. [ASME PAPER 72-APM-52] 17 p2627 A72-34778
- An analysis of the split Hopkinson bar technique for strain-rate-dependent material behavior. [ASME PAPER 72-APM-26] 17 p2628 A72-34792

Stress pulse attenuation in cloth-laminate quartz phenolic. 17 p2571 A72-35284

Stress wave propagation observation in rigid high modulus epoxy polymer by slow motion photography, noting photoelastic properties and viscosity effect 18 p2734 A72-36380

Gage-length errors in the resolution of dispersive stress waves. 19 p2800 A72-37729

Strongly coupled stress waves in heterogeneous plates. 20 p2980 A72-39616

Crack tip vicinity stress generated by plane transient tension-stress wave diffraction, examining ductility effects on fracture modes 21 p3117 A72-40672

Use of stress wave emission for nondestructive testing of materials and articles. 21 p3061 A72-41720

STRESS-STRAIN DIAGRAMS

- Solid rectangular beams under bending tests, obtaining tension-compression stress-strain curves 01 p0141 A72-11002
- Static and dynamic load measurements for stress-strain behavior and load-time characteristics of aerodynamic decelerator canopy fabrics, using metal foil strain gages 02 p0287 A72-11507
- Tube and hollow sphere revolving in thermal flux under surface pressure load, obtaining stress-strain state and random temperature dependences of creep 02 p0289 A72-11618
- Creep theory by rheonomic body interpretation as controlled system with unknown vectors at input and output, obtaining stress-strain curves for experimental verification 02 p0289 A72-11620
- Stress-strain characteristics of stochastically reinforced materials of high rigidity orthotropic elastic layers alternating with isotropic elastic or viscoelastic layers 02 p0248 A72-11623
- Nonlinear viscoelasticity theory, considering simplified stress-strain functional relationships with respect to time based on isotropy postulate 02 p0290 A72-11624
- Ultrasonic measurement of orthotropic laminated composites elastic moduli, describing stress-strain response [AD-736007] 02 p0249 A72-11994
- Deformable stainless steels empirical diagram for structural state estimation from chemical composition, considering various austenite, martensite and ferrite combinations 02 p0243 A72-12241
- Yield relationship to coupling of plastic waves, obtaining stress-strain diagrams 02 p0297 A72-12613
- Highly elastic cylindrical layer reinforced with anisotropic shell, deriving stress-strain state and nonlinear elastic stability 02 p0299 A72-12687
- Straight beams and rectangular frames stress-strain calculation under pulsed loading, taking into account shock waves finite propagation velocity and internal damping 02 p0300 A72-12855
- Cumulative damage in metal fatigue, suggesting unified theory applicable to stress or strain controlled conditions 03 p0442 A72-12922
- Microinhomogeneous elastoplastic cyclically strain hardenable material under symmetric loading, calculating stress-strain relationship 03 p0443 A72-13453
- One dimensional heat insulated structure under dynamic loads, showing thermoviscoelastic effects on spontaneous heating and stress-strain state 03 p0444 A72-13460
- Stress-strain state determination for plane orthotropic bodies by optical polarization method, discussing numerical methods for stress and strain tensor components 03 p0445 A72-13580
- Elastic-plastic stress-strain analysis of beams with uniform cross section under combined loadings by finite element method 03 p0449 A72-13975
- Stress-strain state of shallow shells of positive Gaussian curvature loaded by arbitrary concentrated force 03 p0450 A72-14106
- Circular disk with external radial cracks, obtaining limiting equilibrium stress-strain state through singular integral equation solution 03 p0451 A72-14115
- Elastic plates with moduli of elasticity variable in tension and compression, deriving plane stress-strain relations 03 p0451 A72-14118
- Infinite elastic isotropic multiply connected plate, determining stress-strain state by asymmetric stress tensors and moment stresses 03 p0451 A72-14119

Pressurized vessel bottoms weakened by central hole with edge stiffened by elastic ring, determining stress-strain state and stress concentration 03 p0451 A72-14120

Doubly connected strain-hardened thin plate, calculating stress concentration and stress-strain state by variational principle of least additional potential energy 03 p0451 A72-14122

Stress-strain state of transverse isotropic plate with hole under bending and torsional moments 03 p0452 A72-14136

Stress-strain state of shallow shell with crack along principal curvature line, discussing membrane stresses in plates and spherical shells 03 p0453 A72-14140

Anisotropic media elastoplastic behavior, developing plastic deformation theory from stress-strain relationships for linearly elastic media 03 p0454 A72-14216

Biharmonic problem of displacements in plane theory of elasticity, analyzing stress-strain state by iterative solution in series form 03 p0454 A72-14312

Stress-strain increment relations for materials with different compression and tension resistance under orthogonal loading 04 p0586 A72-15007

Stress-strain tensor component relations for isotropic elastic bodies with different tension and compression resistance 04 p0586 A72-15008

Stress-strain state of thin ellipsoidal shell with central stiffened hole, using small elastoplastic deformation theory 04 p0588 A72-15050

Optimal temperature field s and stress-strain state in orthotropic conical and cylindrical shells subject to local heating 04 p0588 A72-15051

Circular conical orthotropic shells of linearly variable thickness loaded by distributed and concentrated forces and moments, analyzing stress-strain state by numerical methods 04 p0594 A72-15749

Griffith fracture theory application to thermal crack propagation, computing stress-strain field and critical temperature [ASME PAPER 71-MET-N] 05 p0731 A72-15790

Compounded rotating disks stress-strain analysis from equilibrium and compatibility equations and boundary condition, comparing results with photoelastic and finite difference approximation 05 p0732 A72-15804

Metal powder materials at high loading rates, obtaining stress state diagram from Cauchy problem solution with inertia components in equilibrium equations 05 p0672 A72-16088

Stress-strain characteristics of nylon-polyurethane coated fabric under biaxial tension and shear forces 05 p0736 A72-16108

Age hardened Al-Cu single crystal anisotropy from stress-strain curves, using plane strain compression tests [AD-743602] 05 p0677 A72-17106

Large deformations of incompressible isotropic materials with parabolic stress-strain relations, deriving constitutive equation from strain energy function 06 p0848 A72-17919

Dynamic strain aging significance in titanium, observing reduction of temperature and strain rate effects on stress-strain curves shapes 06 p0830 A72-18054

Fiber reinforced materials mechanical properties, showing strength dependence on stress-strain behavior of fibers and binders and fiber volumetric proportions 06 p0835 A72-18252

FORTAN programs for calculating principal stresses, strains and directions from rosette readings 06 p0781 A72-18324

Temperature induced bending of thin freely supported rectangular plate, obtaining stress-strain state 06 p0899 A72-18564

Stress-strain diagrams of heat resistant alloys at high temperatures, describing test facility 06 p0834 A72-18684

Axisymmetric deformation of infinite cylindrical shell under stress-strain state arising from internal pressure in statistically inhomogeneous Winklerian medium 07 p1088 A72-19258

Stainless steels with improved formability developed through assessment of stress-strain curve slope and plastic strain rate 07 p1011 A72-19477

Stress-strain state determination in elastic range by net point method and matrix filtering 07 p1091 A72-19754

Stress-strain state of homogeneous isotropic medium bounded by noncanonical surfaces of revolution, using perturbation method 07 p1091 A72-19755

Stress-strain state of thin walled spherical shell in contact with internal rigid sphere, determining contact area size 07 p1091 A72-19756

Acoustic loads effect on carrying capacity and vibration stability of longitudinally stiffened cylindrical metal panels, investigating fatigue strength and stress-strain state 07 p1091 A72-19760

Material anisotropy effect on stress-strain state and limiting load in plane plastic deformation 07 p1091 A72-19764

Stress-strain state in elastic plane with small radial cracks and circular hole under hydrostatic tension 07 p1091 A72-19765

Stress-strain state relationship to crack development morphology in elastic strain region of austenitic steel sample under cyclic bending 07 p1013 A72-19769

Strength differential effect on microstructures of steels, using tensile and compressive stress-strain curves 07 p1015 A72-19927

Elasticity theory axisymmetric problem for hollow cone, analyzing stress-strain state and boundary value problem by asymptotic methods 07 p1093 A72-19980

Stress-strain state in tension of orthogonally stiffened fiberglass-reinforced plastic with cracks in transversely stiffened layers 07 p1094 A72-20128

Test facility for graphites fracture under thermal stresses, considering stress-strain relations calculation method for annular samples 07 p1024 A72-20137

Stress-strain state of unclamped thin elastic zero curvature shell under three component surface load and tangential boundary forces 07 p1095 A72-20313

Computerized dynamic simulation with graphic display of crystal plastic dislocation movement among random obstacles, emphasizing stress-strain, strain rate and thermal activation mechanisms 07 p1095 A72-20338

Stress-strain behavior of steel under elastic compression at 4.2 K, observing discontinuous twinning 07 p1020 A72-20413

Plastic stress-strain anisotropy of metals under forming for mild steel, austenitic stainless steel and Mg, showing nonconformability with Hill criterion 07 p1020 A72-20432

Axisymmetric elasticity theory problems for stress-strain state of space with spherical incision, obtaining solutions with p-analytic functions 08 p1242 A72-20960

Al single crystals relationship between stress, strain and dislocation density ring elevated temperature creep by direct observation of etch pits 08 p1185 A72-20990

Metallic matrix stress-strain properties from phenomenological model based on idealized behavior of system components, noting dependence on fiber volume content 08 p1185 A72-21183

Rheological model of reticular polymers and glass fiber reinforced plastics based on stress-strain relationship during damped creep elastic deformation 08 p1191 A72-21499

Green matrix computation algorithm extensible to spherical and toroidal closed shells of revolution for stress-strain state determination 08 p1246 A72-21672

Cicala formulas generalization and plasticity theory for deformation strain anisotropy, sliding and elastic strains influence on shear stress 08 p1246 A72-21806

Elasticity theory method for nonlinear stress-strain relationships in thin anisotropic shells, discussing fiberglass reinforced cylindrical shell 08 p1247 A72-21810

Boron and carbon fiber reinforced plastics anisotropic stress-strain properties, considering fiber misalignments curvature and low shear resistance effects 08 p1196 A72-21857

Copper, zinc and aluminum mechanical properties comparison by cyclic and steady state compressive load tests, noting stress-strain curve relationship to strain rate 08 p1188 A72-21921

Ceramic materials stress-strain behavior dependence on microstructural factors, discussing point defects, pore size and grain boundaries 09 p1334 A72-22392

Axisymmetric grid plate bending and torsion under normal forces and moment vectors loads, determining stress-strain state from finite difference equations 09 p1398 A72-22692

Grid plates of complex structure, determining stress-strain state by asymptotic solution of boundary value problem for sixth order differential equations 09 p1398 A72-22693

Stress-strain state of circular three layer laminar plates freely supported at circumference and loaded at edge 09 p1399 A72-22694

Stress-strain state produced by asymmetric physical and thermal loads in thin orthotropic viscoelastic shells of revolution 09 p1399 A72-22702

Heat conduction, stress-strain state and thermoelasticity of massive bodies of revolution under nonuniform heating 09 p1400 A72-22709

Stress-strain state of shallow shells of revolution for large displacements, reducing determination to system of nonlinear differential equations 09 p1400 A72-22714

Thermal stress-strain state analysis of nonlinear elastic medium by small parameter method 09 p1400 A72-22717

Stress-strain state of circular conical shell of linearly variable thickness within small elastoplastic deformation theory, assuming specific convective heat transfer at surface 09 p1401 A72-22722

Solid cylinder stress-strain state under thermal and mechanical loads, obtaining analytical solutions via flow theory based on Von Mises yield condition 09 p1401 A72-22723

Computer algorithm for thermoplastic stress-strain state of thin shells of revolution based on plastic flow theory, taking into account loading history 09 p1401 A72-22724

Stresses, strains and moments interrelationship in axisymmetrically loaded circular cylindrical shell under unsteady creep conditions 09 p1401 A72-22729

Stress-strain curve determination for shear of twisted conical elastic bar, using torque and angle distribution 09 p1404 A72-22774

Energy balance criterion application to crack growth under cyclic fatigue loading, considering stress-strain behavior of plastic deformation energy 09 p1404 A72-22911

Single and multiple fractures in brittle matrix fibrous composites, discussing fracture energetics, stress-strain curves and hysteresis effects 09 p1338 A72-23164

Stress-strain characteristics of metal ductile filaments with elastic brittle coatings, noting strengthening effect on anodic oxide coated aluminum 09 p1330 A72-23379

Book on plastic analysis and plate, shell and disk theories and design covering stress-strain concepts, laws and theorems 10 p1553 A72-23749

Axially homogeneous stress and strain in anisotropic thin walled cylindrical shells, considering pure bending, stretching and twisting [ASME PAPER 71-APMW-4] 10 p1554 A72-24181

Charpy impact strength data for unidirectional graphite, boron and glass-resin composites tested in fiber direction, noting tensile stress-strain characteristics importance 11 p1672 A72-25471

Off axis and transverse tensile properties of boron reinforced Al alloys, correlating metallurgical structures with stress-strain curves and fractographic studies 11 p1654 A72-25479

Rigidly connected rectangular plates stress-strain calculation with finite difference method 11 p1733 A72-25538

Fatigue life cumulative damage prediction procedure for engineering metals subjected to complicated stress-strain histories, noting errors in average mean stress method 11 p1658 A72-25831

Constitutive equations for bimodulus elastic materials, postulating rheological model based on anisotropy stress-strain laws 11 p1736 A72-25984

Two coordinate oscillograph recording device with automatic reversing for stress-strain tests under static and cyclic loads 11 p1637 A72-26814

Three dimensional nonlinearly elastic anisotropic body with arbitrary elastic potential examined for large initial deformations, considering stress-strain state 12 p1877 A72-27077

Stress-strain state and temperature distribution in transversely isotropic layer under mixed heat transfer conditions 12 p1878 A72-27085

Reversible stress effects in theory of plastic flow in strain hardened metals at high temperatures 12 p1879 A72-27159

Variable shear modulus circular isotropic plate torsion by rigid circular stamp, obtaining stresses and displacements by Fourier analysis 12 p1881 A72-27319

Energy method for boundary conditions of beam vibrations under linear viscoelastic stress-strain law,

deriving uniqueness, boundedness and stability theorems

12 p1885 A72-27848

Uniqueness theorem for solution to boundary value problem in anisotropic viscoelasticity, considering stress-strain relation in nonlinear Volterra equation form

12 p1886 A72-27983

Unloading wave propagation in semiinfinite elastoplastic cylindrical rod for concave stress-strain diagram with no initial linear segment

13 p2053 A72-28388

Stress-strain state in pure bending for infinite elastic strip with circular central hole, using integral Fourier transforms

13 p2053 A72-28390

Deformation limits in thin and thick walled metal blanks axisymmetric drawing process, determining stress-strain state based on prescribed velocity field

13 p1963 A72-28743

Room temperature uniaxial tension tests for elastic deformation of steel samples, showing quadratic stress-strain function

13 p1977 A72-29008

Computer algorithm for plates and shells internal forces and moments and stress-strain state determination from strain gage data

13 p2058 A72-29144

Stress-strain state of elastic rectangular plate under arbitrary edge forces on displacements

13 p2058 A72-29458

Rheological stress-strain relations in nonlinear viscoelasticity theory, calculating relaxation parameters for isotropic viscoelastic circular cylinder

13 p2059 A72-29493

Variational problem solution for solid strained body with nonlinear stress-strain relation, applying finite element method

14 p2130 A72-30189

Aircraft engine components fatigue life assessment under small cycle temperature conditions, including temperature field and stress-strain determination in critical spot

14 p2145 A72-30279

Disks with inclined face, investigating effects of joint between hub and disk face on stress-strain state

14 p2164 A72-30430

Tubular materials plane stress-strain test facility for combined axial load and internal pressure effects, describing principal components

14 p2092 A72-30442

Stress-strain state of complex configured thin walled shell, deriving computer algorithm via tensor analysis and finite difference scheme

14 p2165 A72-30686

Point heat source induced thermal stresses in elliptic plate with circular holes, determining stress-strain field by two dimensional elasticity theory

14 p2166 A72-30689

Constitutive equations for incremental stress-strain relations in elastoplastic media, noting plane stress and strain in isotropic materials

14 p2131 A72-30715

Higher order differential equations solutions for viscoelastic stress-strain functional relationships, recommending Runge-Kutta integration technique

14 p2168 A72-30929

Crystal lattice and dislocation anharmonicities interdependence and stress-strain correlation in presence of interaction between ultrasonic waves of different frequencies

14 p2169 A72-30959

Stress function method for calculating stress-strain state in homogeneous shallow spherical shell under arbitrary load

15 p2324 A72-31485

Stress-strain state of spherical body in centrally symmetric temperature field, noting elastoplastic interface and continuity conditions

15 p2327 A72-31742

Temperature effects on stress-strain diagram, tensile strength and creep properties of fiber-epoxy resin composites

15 p2260 A72-32137

Displacement and stress field for elastic solid containing cruciform crack with unequal length arms

15 p2330 A72-32292

Plasticity, elastic relaxation and stress-strain relation characterization for Schofield-Scott Blair media, using nonequilibrium thermodynamics method

15 p2331 A72-32482

Stress-strain relations for inelastic deformation of anisotropic strain hardenable shells of revolution under arbitrary plasticity conditions

15 p2332 A72-32678

Plastic deformation and limiting strain curves of Ti alloys in plane stressed state, comparing with yield and rupture conditions

15 p2259 A72-32684

Metal specimens yield point in adiabatic tension determined by thermoelectric method from temperature-stress and stress-strain diagrams

15 p2259 A72-32690

Stress-strain diagrams for constant strain rates in shear of Ti from torsion test machine, deriving constitutive equation for dynamic overstress

16 p2405 A72-33197

Stress-strain curve correction for triaxial stress state and strain rate at arbitrary temperatures, describing instrument for continuous test specimen profile measurement

16 p2469 A72-33232

Stress-strain diagrams for orthotropic glass fiber reinforced plastic plates with circular hole under uniaxial tensile load

16 p2471 A72-33681

Prestrained and annealed elastic materials stress-strain relationship calculation in plastic range, compared with tensile and compression load tests results

16 p2472 A72-33948

Steels creep behavior relationship to stress-strain curve shape, defining creep resistance as function of strain hardening coefficient

16 p2412 A72-34146

Model with lamellae and tie molecules disordered alignments to explain relation between stress-strain behavior and bond fracture in highly oriented polymer fibers

17 p2569 A72-34258

Approximate method for composite materials effective elastic moduli determination from uniform stress-strain field or as second derivative of average strain energy

17 p2625 A72-34322

An analysis of the split Hopkinson bar technique for strain-rate-dependent material behavior.

[ASME PAPER 72-APM-26] 17 p2628 A72-34792

The dynamic stress-strain behavior in torsion of 1100-O aluminum subjected to a sharp increase in strain rate.

[ASME PAPER 72-APM-6] 17 p2629 A72-34808

Strain history effect on isotropic and anisotropic plastic behavior.

[SESA PAPER 1940] 17 p2631 A72-34820

Strain measure determined plastic stress concentrations around discontinuities in flat plates compared with incremental theory

18 p2733 A72-36359

An optical method for the determination of constrained zones at crack-tips.

18 p2733 A72-36368

Direct and indirect creep modelling technique in photoelasticity.

18 p2734 A72-36379

The application of a dislocation model to the strain and temperature dependence of the strain hardening exponent n in the Ludwik-Hollomon relation between stress and strain in mild steels.

18 p2701 A72-36589

A non-linear integral-type theory of inelasticity for transversely isotropic materials.

18 p2738 A72-37075

The matrix fatigue behaviour of fibre composites subjected to repeated tensile loads - Application to B/AI 6061 composites.

20 p2936 A72-39208

The low strain tensile behavior of U-7.5 wt pct Nb-2.5 wt pct Zr.

20 p2938 A72-39303

Elasticity theory axisymmetric problem for hollow cones analyzing stress-strain state and boundary value problem by asymptotic methods

20 p2982 A72-40036

On the stress-strain curve of polyethylene filled with randomly oriented glass fibers.

21 p3073 A72-40721

Stress-strain state of thin circular perforated Cu plate under uniform tensile load, showing applicability of small elastoplastic finite deformation theory

21 p3122 A72-41351

Epoxy-thiocol binder viscoelastic deformation under short and long term loads, noting stress-strain linearity limit

21 p3073 A72-41360

Strain curves of VT-6C and VT-14 titanium alloys in the temperature range between 20 and 400 C

21 p3070 A72-41362

Yielding and fracture of D16T alloy at low temperatures under conditions of complex stress-strain state

21 p3071 A72-41706

Allowance for the hysteresis behavior of a continuous medium in a complex state of stress under conditions of simple cyclic loading

21 p3127 A72-41711

Elastic isotropic plates stability for nonlinear stress-strain relations, noting effect of deformation tensor invariant on critical load magnitude

22 p2324 A72-42275

Stress-strain diagrams and fracture characteristics of fiber-reinforced aluminum alloys

22 p3189 A72-42300

A general program for computer plotting of Mohr's circle.

22 p3156 A72-42608

Some recent experimental investigations in stress-wave propagation and fracture.

22 p2327 A72-42768

Reinforcement of structural materials by long strong fibres.

22 p3241 A72-43026

Book - Effect of notches on low-cycle fatigue: A literature survey.

22 p3242 A72-43145

Analysis of the mechanisms of yield-stress variation during compacting of metal-ceramic materials by rolling

23 p3298 A72-43278

Finite element method optimization of orthotropic layered shells of revolution under mechanical and thermal loadings, considering stress-strain relationships

[SAWE PAPER 939] 23 p3344 A72-43479

Pointwise displacement errors in linear shell theory resulting from errors in the stress-strain relations.

23 p3347 A72-43720

Fibers-matrix force interaction effects in metal composites, analyzing stress-strain state of reinforced plate

23 p3306 A72-43728

Diffusive metal coatings stress-strain state effect on composite Mo material strength, ductility and creep characteristics

23 p3306 A72-43732

Ribbed cylindrical shells modeling method for stress-strain state and stability

23 p3347 A72-43745

Shear-strain-rate effects in a high-strength aluminum alloy.

23 p3302 A72-43983

Determination of the stressed state in a welded joint in plastic deformation

23 p3293 A72-44019

A note on buckling of spherical caps with initial asymmetric imperfections.

23 p3351 A72-44060

Triangular element for multilayer sandwich plates.

23 p3351 A72-44108

Equivalent linear solution for transient free vibration of beams with strain dependent, frequency independent stress-strain hysteresis loop with sharp corners

23 p3352 A72-44120

Stress-strain characterization of part-through crack in plate under tension in terms of stress intensity factor

23 p3352 A72-44227

Nonlinear elastic torsion analysis for aerospace materials.

23 p3354 A72-44251

Reissner-Sagoci problem for semiinfinite elastic solid stress and displacement determination, discussing generalization to nonhomogeneous media with circular part under axisymmetric twisting

23 p3314 A72-44266

The stress-strain relation in the low-cycle fatigue of metallic materials under rotating-beam bending.

24 p3454 A72-44626

The fatigue strength under varying mean stress.

24 p3455 A72-44629

Stress-strain diagrams from high and low temperature tests of Y alloy rods, noting temperature effects on plastic deformation

24 p3413 A72-44724

Development and present-day state of the fatigue-damage theories.

24 p3457 A72-44873

Microinhomogeneous elastoplastic cyclically strain hardenable material under symmetric loading, calculating stress-strain relationship

24 p3458 A72-44928

One dimensional heat insulated structure under dynamic loads, showing thermoviscoelastic effects on spontaneous heating and stress-strain state

24 p3458 A72-44935

Some extremal properties and energy theorems for inelastic materials and their relationship to the deformation theory of plasticity.

24 p3460 A72-45692

On dual energy theorems for a class of elastoplastic problems due to G. Maier.

24 p3460 A72-45693

A power-law model for the multiple-integral theory of non-linear viscoelasticity.

24 p3460 A72-45696

Photoelastic verification of a mechanical model for the flow of a granular material.

24 p3460 A72-45697

Stress-strain state in tension of orthogonally stiffened fiberglass-reinforced plastic with cracks in transversely stiffened layers

24 p3460 A72-45754

Graphites fracture under thermal stresses, considering stress-strain relations calculation method for annular samples

24 p3418 A72-45762

STRESS-STRAIN DISTRIBUTION
U STRESS CONCENTRATION
STRESS-STRAIN RELATIONSHIPS
U STRESS-STRAIN DIAGRAMS

STRESS-STRAIN-TIME RELATIONS

Small dilatation and short time approximate constitutive equations for compressible nonlinear viscoelastic materials, using multiple integrals and kernel functions

01 p0137 A72-10319

Creep behavior during and immediately after loading of Nimonic 90 and H 46 Cr steel under various stresses, temperatures and rates

06 p0829 A72-17801

Viscoplasticity theory thermodynamic foundations, considering stress/strain states time and deformation path dependence

06 p0896 A72-17963

Machine metals fatigue life, creep theory and stress and strain kinetics in severe environments, formulating physical equations

08 p1246 A72-21805

Workability tests from material deformation stress determination and fracture strain rate relation for forging, extrusion and rolling limits predictions

08 p1190 A72-22198

Motion and stable equilibrium position of horizontal rotor with nonlinear elastic and internal damping properties, discussing stress-strain-time relations of shaft filaments

09 p1409 A72-23613

Dislocation velocity-stress relationship in plastically deformed Al at room temperature, noting entropy term in Gibbs free energy equation

11 p1661 A72-26652

Plastic strains and crack growth in Al alloy under static and repeated static loading

13 p1977 A72-28915

Hot rolled steel bar strain history effect on isotropic and anisotropic plastic behavior, considering additional tension and torsion data

15 p2325 A72-31527

Relations between the experimental parameters describing the steady-state and transient creep.

18 p2732 A72-36343

A model of a nonlinear viscoelastic medium allowing for the effects of cumulative damage

19 p2871 A72-37528

Mathematical relationships for primary, secondary and tertiary creep and their use in extrapolation of tensile creep data.

19 p2874 A72-37708

The modulus of elasticity of plastic materials at stress times between .001 and 10,000,000 seconds

22 p3197 A72-42859

Investigation of the thermal fatigue of Kh18N10T steel under complex stress-strain state conditions

23 p3301 A72-43956

STRESSED-SKIN STRUCTURES

Iteration method error estimates for thin elastic shell basic stressed state and simple fringe effect relation to boundary stressed state

04 p0586 A72-15012

STRESSES

AXIAL STRESS

COMBINED STRESS

CRITICAL LOADING

RESIDUAL STRESS

SHEAR STRESS

TENSILE STRESS

THERMAL STRESSES

TORSIONAL STRESS

TRIAXIAL STRESSES

VIBRATIONAL STRESS

STRETCHING

Finite stretching of isotropic incompressible annular plate with inner edge rigid inclusion, noting edge zone thickness variation due to transverse normal strain

02 p0296 A72-12528

Neo-Hookean material circular plate under finite axisymmetric stretching, showing approximately constant deformed thickness

04 p0590 A72-15196

Disk stretching under tensile stresses, determining stress at arbitrary point in half band form connected with quadrant

05 p0737 A72-16294

Automated mechanical system for solid propellant heat stress tests in two directions as function of time

08 p1147 A72-21331

Heat stretching-induced changes effect on strength,orption and structural properties of polyformaldehyde fibers, noting structural orientation enhancement and porosity growth

08 p1194 A72-21757

Repeated stretching effect on triaxetic fibers thermal destruction in vacuum after hot air or steam heat-setting

08 p1194 A72-21759

Axially homogeneous stress and strain in anisotropic thin walled cylindrical shells, considering pure bending, stretching and twisting

ASME PAPER 71-APMW-4) 10 p1554 A72-24181

Versatile stretching of a disc shaped as a plane with elliptic aperture.

22 p2326 A72-42627

The stretching of a disc shaped as a semi-infinite plate with half-elliptic edge sector.

22 p2326 A72-42628

Exponential type equation for carbon steel stretched sample necking profile curve

23 p3348 A72-43753

STRIATION

Moving striations in tapered gaseous discharge tube, noting frequency dependence on tube radius

11 p1698 A72-26644

Brittle striation formation role in corrosion fatigue crack propagation mechanism in Al-Zn-Mg alloy from test in NaCl solution under reversed anodic-cathodic current

22 p3193 A72-43033

STRINGERS

Variable cross section elastic stringer end loaded longitudinal force transmission to stiffened elastic plate

03 p0444 A72-13465

Small deflection theory for dynamic elastic buckling of stringer-stiffened cylindrical shells under axial impact, discussing optimum stiffener geometry

05 p0742 A72-17248

DC 10 aircraft wing stringers fabrication and processing, discussing stress relieving and stretch form contouring techniques, aging and tempering processes and flaw detection

[ASM PAPER W 72-31,3] 12 p1817 A72-28161

On the diffusion of a load from a semi-infinite stringer bonded to a sheet.

22 p3238 A72-42833

Variable cross section elastic stringer end loaded longitudinal force transmission to stiffened elastic plate

24 p3458 A72-44940

Welding airframe structures in titanium using tensile loading to overcome distortion.

24 p3407 A72-45000

STRINGS

Parametric and adaptive non-parametric system identification procedures in boundary value problem of string on elastic foundation, considering various approximation methods

07 p1096 A72-20349

Nonlinear traveling string transverse oscillations frequency, using Panavko direct linearization method

11 p1688 A72-26324

Inhomogeneous strings oscillations determination in nonstationary inverse boundary value problems with integral equations

11 p1689 A72-26381

Random deflection function for taut string on elastic foundation subject to random loads, using invariant imbedding method and Fokker-Planck equations

15 p2273 A72-31311

Asymptotic solutions of inhomogeneous initial boundary value problems for weakly nonlinear partial differential equations.

17 p2574 A72-34342

Determination of the unloading boundary in transverse impact of an elastic-plastic string.

[ASME PAPER 72-APM-12] 17 p2629 A72-34804

STRIP

Equilibrium equations of infinite strip with circular hole, using plane multiply connected domain method for stress field

12 p1878 A72-27087

Estimation of the accuracy of the method of measuring the bending of strips in order to determine residual stresses.

19 p2806 A72-37574

STRIP TRANSMISSION LINES

Mixed boundary value problem of Laplace equation solution by dual trigonometric series equations approach, applying to microstrip transmission line capacitance determination

01 p0093 A72-10508

Self admittance and radiation conductance characteristics of stripline feed slots in waveguide walls

01 p0029 A72-10683

Hybrid microwave integrated circuits, discussing distributed circuits with strip transmission lines and lumped element circuits with inductors and capacitors

01 p0045 A72-10698

Microstrip double down-converter receiver in civil satellite earth stations for reduced interface problems, increased reliability and minimum initial cost

03 p0334 A72-14074

Mathematical model for reciprocal and nonreciprocal magneto-optical effects in magnetized ferrite-filled microstrip transmission lines

04 p0502 A72-15434

Microwave antennas, feed systems, strip transmission lines and test instrumentation, examining radiation patterns, design and polarization characteristics

05 p0635 A72-16330

TEM modes characteristics in shielded stripline with four internal strips, tabulating characteristic impedances at different line parameters

05 p0636 A72-16339

Bandwidth properties and design of shielded asymmetrical striplines filled by dielectric

05 p0636 A72-16340

Coaxial and stripline wideband microwave hybrid ring junctions equivalent to Magic Tees with improved electrical properties

05 p0636 A72-16344

Microwires and microstrips fabrication from high strength deformation resistant aluminum alloys

05 p0680 A72-17207

Microwave thin film microstrip IC tunnel diode amplifiers for broadband high performance receivers, discussing design, construction and performance

06 p0786 A72-18374

GaAs IMPATT diode with plated heat sink for microstrip circuit applications, exemplifying X band oscillator experiment

06 p0787 A72-18385

Dielectric substrate layer surface wave parasitic resonance effects on microstripline waveguide conductor

07 p0958 A72-18855

Digital loaded-line phase shifters for phased array antennas, discussing lossy microstrips effects and P-I-N diode switching shortcomings in design requirements

07 p0954 A72-19048

Schwartz method application to stripline fields and impedance calculations for different cross sections and internal conductor dimensions

08 p1133 A72-21370

Coupled line microstrip circuit for high power and efficiency L and S band TRAPATT diode oscillators

10 p1450 A72-24307

VHF and UHF radio transmitters with strip transmission lines, discussing transistor power amplifier design

10 p1441 A72-25116

Microwires and microstrips fabrication from high strength deformation resistant Al alloys

11 p1660 A72-26142

Microstrip propagation and loss filling factor design formulas for magnetic substrates

11 p1599 A72-26991

Stacked TRAPATT diodes oscillator with microstripline circuit to obtain 1 kw peak power at 1 GHz

12 p1788 A72-27163

Microstrip transmission lines analysis by integral equations approach, assuming TEM mode

12 p1782 A72-27492

Distributed base resistance effect on stripline geometry transistor input characteristic, using equivalent circuit with pseudo-junction having high saturation current

13 p1930 A72-29059

Waveguide model for calculating microstrip discontinuities and T-junctions wave impedances, using orthogonal series procedure

15 p2201 A72-32470

Nonideal component parts effect on behavior of digital microstrip closed circuit X band phase shifter, presenting detailed network analysis

15 p2201 A72-32471

High efficiency and power S-band pulsed oscillator using avalanche diode and microstrip circuit

16 p2369 A72-33759

Microwave integrated circuits.

17 p2527 A72-34570

Determination of the dielectric constants of microwave-striplines

17 p2530 A72-35429

S-band high power microstrip switches with p-i-n diodes for spacecraft radio systems

19 p2770 A72-37257

Microwave filters in antenna circuit feeder systems of space vehicles

21 p3026 A72-40318

Wave equation for infinitely long slotted screen in elliptic cylindric coordinates, noting radiation pattern for phased antenna array of metallized hyperbolic striplines

21 p3028 A72-40507

Computation of single-conductor and symmetric and asymmetric two-conductor stripline characteristics by the relaxation method.

21 p3036 A72-41831

Synthesis method for phase and loss optimized single-stage reflection type phase shifters, determining transformation coefficient

23 p3268 A72-43439

Microstrip matching networks synthesis for microwave integrated circuits, calculating passband of configurations with lumped and distributed elements

23 p3269 A72-43445

STROBOSCOPES

Stroboscopic measurement of elastic untwisting angles of axial compressor rotor vanes under centrifugal and aerodynamic forces

01 p0143 A72-11371

Visual persistence and perceptual moment hypotheses for time-dependent visual illusion from viewing moving stroboscopically illuminated object

05 p0621 A72-16150

Double frequency stroboscopic method for absolute calibration of vibration transducers, analyzing errors

06 p0815 A72-17766

The non-stroboscopic visualisation of vibration patterns by the real time-time averaged hologram interferometry.

20 p2921 A72-39028

STRONTIUM

NT STRONTIUM ISOTOPES

Sunlight resonance scattering by spherically symmetric optically thick artificial Sr clouds, comparing photometric data with computed theoretical isophotes, line profiles and irradiances
09 p1297 A72-22579

Eu and Sr distribution between coexisting feldspars in acidic rocks, using mass spectroscopic isotope dilution method
10 p1472 A72-24166

Electron impact effects on Ba I, Ba II and Sr I selected spectral line Doppler widths calculated for laser-generated plasmas for chemical release simulation
21 p3092 A72-40821

STRONTIUM COMPOUNDS

NT STRONTIUM TITANATES
NT STRONTIUM ZIRCONATES
Cation self diffusion coefficients in potassium oxide-strontium oxide-silicon dioxide glass, using radioactive tracers and sequential etching technique
13 p1912 A72-28625

High refractory gadolinium oxide-strontium oxide system phase diagram and transition temperature by X ray and differential thermal analyses
13 p1984 A72-30109

Phase diagram, isomorphism and temperature dependence of hexagonal, monoclinic and triclinic modifications of Sr-Ba polycrystalline aluminosilicates
21 p3072 A72-40382

Diffusion in the system K₂O-SrO-SiO₂. IV - Mobility model, electrostatic effects, and multicomponent diffusion.
21 p3097 A72-40935

Electron paramagnetic resonance hyperfine spectral observation of double quantum transitions of Ti positive ions in strontium chloride single cubic crystal host
24 p3378 A72-45311

STRONTIUM ISOTOPES

Southern Great Basin upper Cenozoic high Sr⁸⁷/Sr⁸⁶ and Sr/Rb ratio basalt initial composition, showing mantle material derivation
05 p0655 A72-16043

Pb and Sr isotopic composition measurements on eclogites from South Africa
05 p0658 A72-16551

Sr isotope data indication of Glass Mountain rhyolite lava as part of parent silicic magma
11 p1623 A72-26240

Apollo 12 and 14 lunar soils K, Rb and Sr isotopic composition evaluation, noting microbreccia as major nonbasaltic constituent
11 p1723 A72-26497

STRONTIUM TITANATES

Polarization characteristics of ferroelectric barium strontium titanates in solid solution at 4-100 K
10 p1527 A72-24984

STRONTIUM ZIRCONATES

High temperature creep behavior of sintered polycrystalline strontium zirconate as function of temperature, stress, grain size and strain level, using pure bending test method
10 p1497 A72-24275

STRUCTURAL ANALYSIS

NT BERNSTEIN ENERGY PRINCIPLE
NT DYNAMIC STRUCTURAL ANALYSIS
NT ENERGY METHODS
NT EQUILIBRIUM METHODS
NT FLUTTER ANALYSIS
NT MATRIX METHODS
NT STRAIN ENERGY METHODS
Laminated orthotropic plates and shallow shells structural analysis using finite element program
01 p0140 A72-10984

Moment sensors for strain gaged beam systems analysis, noting application to bending moments determination
02 p0287 A72-11510

Structural analysis of cable stayed bridge scale model with fractional and full loading, showing system linear behavior with small displacements and real nonlinearities, respectively
[SESA PAPER 1896] 02 p0199 A72-11515

Soviet papers on strength and plasticity covering elasticity, creep, polymer mechanics, plates and shells, dynamic and high temperature stability, thermoelasticity, soil and free flowing media
02 p0288 A72-11601

Minimum weight beams and frames calculation for random loads taking into account material carrying capacity
02 p0291 A72-11727

Rheomobility and structural creep, correlating mobile, rigid, elastic, viscous and plastic models
02 p0297 A72-12612

Finite element formulation for nonlinear large deflection elastic analysis of displacements and stresses in thin plate structures
02 p0298 A72-12657

Complex structures mass and stiffness matrices reduction by automatic condensation, calculating lowest eigenfrequencies and eigenmodes of substitute systems
[DGLR PAPER 71-108] 02 p0299 A72-12721

Nonlinear thermoviscoelasticity problem exact solution expressed as product of two functions, formulating conditions
03 p0445 A72-13576

Breakdown of three dimensional brittle medium weakened by concentric systems of interconnected circular cracks, using Fredholm integral equations
03 p0447 A72-13732

Book on automated structural analysis covering computer oriented problem solving methods for trusses, plane and space frame es, curved beams, etc
04 p0591 A72-15270

Nonhomogeneous elastic structure with quasi-periodic coefficients, deriving mechanical model by continuum spectral theory
04 p0594 A72-15745

Ring finite elements use in analysis of shells of revolution under axisymmetric loads
[ASME PAPER 71-WA/HT-22] 05 p0732 A72-15880

Asymptotic two dimensional theory of shell structures, comparing with axiomatic formulation
05 p0738 A72-16349

Fatigue limit amplitude diagram schemes and formulas
05 p0740 A72-16625

Static perturbation technique functional form for postbuckling equilibrium path analysis by asymptotic approximation, noting relationship to Koiter method
05 p0742 A72-17244

Free flexural wave propagation in doubly periodic structures, obtaining natural frequencies
06 p0894 A72-17764

Large elastic deformation problems analysis by incremental finite element technique, using variational principles
07 p1087 A72-18782

Stress redistribution in statically indeterminate structures under creep, discussing effects on time to brittle fracture and service life determinations
07 p1088 A72-19259

Iterative and direct modification procedures for structural analysis matrix displacement method, discussing computer program implementation
07 p1089 A72-19329

Book on matrix structural analysis covering matrix algebra concepts, direct stiffness matrix methods, lifting surface, nonlinear truss and structural partitioning analysis, etc
07 p1092 A72-19908

Bounds for impulsively loaded plastic structures, considering fixed end beam with uniform velocity distribution
07 p1093 A72-19947

Limit analysis of ductile fiber reinforced structures, obtaining critical load of composite sandwich ring
07 p1093 A72-19950

Elastic equilibrium of infinite wedge with apical asymmetric notch, reducing to Hilbert problem fo; holomorphic vectors
07 p1093 A72-19976

Mechanical properties and structural strength evaluation methods for metallic materials at low temperatures, describing hydraulic and pneumatic testing facilities
07 p1017 A72-20130

Monte Carlo digital simulation of probabilistic buckling behavior of indeterminate structure under initial stresses due to random geometric lack-of-fit
07 p1095 A72-20348

Axisymmetric elasticity theory problems for stress-strain state of space with spherical incision, obtaining solutions with p-analytic functions
08 p1242 A72-20960

NASTRAN/NASA structural analysis/ program for computer stress analysis based on finite element method, noting vibration, acoustics, transient motion and random response applications
08 p1138 A72-21325

Heavy falling body elastic impact against circular plate center analyzed by Timoshenko type wave equation
08 p1247 A72-21814

Consistent finite element method to analyze random response of complex structures based on standard modal approach
08 p1248 A72-21823

Building structures response to transient pressures caused by sonic booms, discussing three dimensional loading effects, air cavity coupling and nonlinearities influence
08 p1249 A72-21908

Nonlinear beam and plate analysis, obtaining smooth elastic-plastic transition through modified Richard moment-rotation equation application
08 p1249 A72-21923

Nonlinear programming analysis of free vibration of simply supported beam
08 p1249 A72-22136

Structural model application to construction material alternate stress description at elevated temperatures
09 p1401 A72-22727

Mathematical modeling for structural analysis and design from viewpoint of methodology, physical principles, simulation, optimization, constraints and control theory
[SMRT PAPER M 2/3] 10 p1556 A72-24399

Heat conduction and thermoelasticity in solids, discussing thermomechanical coupling, structural stresses and thermal stresses and deformations
[SMRT PAPER L 1/1] 10 p1556 A72-24394

Solid body elastic deformation potential energy and structure calculation on computer by finite element method and calculus of variations
10 p1559 A72-24924

Nonlinear structural analysis of circular plates and shells of revolution with geometric and inelastic material nonlinearities, using direct stiffness method
[AIAA PAPER 72-353] 11 p1729 A72-25383

Finite element structural analysis for local buckling stresses in flat plates, panels and thin walled columns, deriving elastic and geometric stiffness matrices
[AIAA PAPER 72-354] 11 p1729 A72-25383

Viking conical aeroshell structural prototype design, analysis and testing, comparing buckling failure data with theoretical predictions
[AIAA PAPER 72-370] 11 p1725 A72-25395

Two dimensional elastoplastic finite element analysis of structural members under cyclic thermal-mechanical loadings
[ASME PAPER 72-GT-1] 11 p1734 A72-25604

Computerized analysis of prismatic rectangular plate assemblies natural frequencies and initial buckling stresses
11 p1734 A72-25731

Control theory application to nonlinear elastic analysis of trusses, partitioning structure into statically determinate stages
11 p1736 A72-25989

Multilevel structural analysis for multilayered fiber-epoxy and metal matrix composites, using FORTRAN IV
11 p1601 A72-26033

Probability minimization and detection of errors in computerized analysis of civil engineering frameworks, noting graphical output advantages
12 p1786 A72-27190

Stress-strain state approximation for isotropic strip with circular hole, noting method adaptability to computer computations
12 p1880 A72-27232

Long term high temperature test machine to record structural changes of materials
12 p1795 A72-27464

Polymer testing machine for simultaneous structural and mechanical properties measurement of specimens subjected to uniaxial tensile loads for broad temperature range
12 p1795 A72-27464

Stokes-Helmholtz decomposition role in displacement potentials derivation in elasticity
12 p1884 A72-27564

Interactive computer graphics technique for structural analysis, aiding engineering decisions by CRT graphical and numerical information display
12 p1787 A72-27864

Engineering formula relating crack tip stress intensity coefficient to mechanical properties and structural element size
12 p1887 A72-28236

Russian monograph on three dimensional deformable bodies stability covering linearized equations for subcritical deformations and strength analysis of low shear rigidity structures
12 p1888 A72-28337

Structural approach to elastic stability in buckling problems, simplifying deformation concepts and loading condition definition
13 p2054 A72-28474

Structural evaluations and dynamic testing of solar electric propulsion components, surveying power conditioning panel modal frequencies by holographic interferometry technique
[AIAA PAPER 72-442] 13 p1899 A72-28941

Axisymmetric geometry and load finite element structural analysis of isotropic elastic materials for parametric and optimization studies
13 p2062 A72-29875

Finite element method for nonlinear analysis of nuclear reactor structures, noting elasticity, viscoelasticity and elastoplasticity problems
[SMRT PAPER M 2/2] 14 p2166 A72-30724

Sandwich beams structural optimization for given deflection by iterative finite element procedure
14 p2168 A72-30927

Nonlinear creep failure of imperfect sandwich structures under time variable loading, considering rod and cylindrical shell
15 p2324 A72-31490

Book on structural analysis covering statically indeterminate structures, force and displacement methods, flexibility and stiffness matrices, strain energy, virtual work, energy theorems, etc
15 p2325 A72-31517

Structural mechanics computer programs compendium covering subject oriented information according to structure type, load environment and analytical models
15 p2328 A72-31771

- FORTRAN IV program for small structure analysis with maximum 10 deg of indeterminacy
15 p2328 A72-31772
- Structural components design from fiber composites, noting computer programs for structural and stress analysis
15 p2328 A72-32128
- Structural averaging of stresses in finite element method hybrid stress model, using additional equilibrium equations
15 p2332 A72-32597
- Analog simulation method for highly redundant structure optimization based on reproducing structure mechanical behavior in stabilized stress states
16 p2463 A72-32899
- Optimal plane elastic trusses under alternative loads, designing for smallest total volume of bars with upper stress bound
16 p2466 A72-33017
- Cost-saving techniques in helicopter structural test methods, suggesting system simulation, component replacement time calculation and computer techniques
16 p2373 A72-33221
- Nonlinear theory of two dimensional and three dimensional discrete elastic Cosserat media, noting application to reinforced shells and lattice type structures
16 p2425 A72-33592
- Sandwich structures buckling calculation by transfer matrices with allowance for cross section shearing
16 p2471 A72-33680
- Unified description of structures behavior subject to elastic, creep and plastic deformations
16 p2473 A72-34117
- Approximate method for reactions redistribution and displacements in statically indeterminate structures, using strain hardening hypothesis and creep power law
16 p2473 A72-34119
- Three dimensional elastoviscoplastic theory for complex structures static-dynamic creep deformation under time varying stress and temperature fields, generalizing Odqvist-Hoff law
16 p2473 A72-34121
- Bending of skew plates of variable rigidity.
17 p2626 A72-34329
- Finite element analysis of elastoplastic structures with temperature dependent mechanical properties
17 p2631 A72-34947
- Flexure of micropolar elastic beams.
17 p2631 A72-35056
- Elastoplastic structural analysis from design viewpoint, discussing load limits and stability estimates based on large deformation assumption
17 p2632 A72-35113
- Monograph - The finite-element method in plate bending analysis
17 p2634 A72-35547
- Steady state response of nonlinear beam under periodic loading, using finite element techniques for nonlinear differential equation
18 p2732 A72-36078
- Coordinate transformation for perturbation analysis of elastic structural system imperfections influence on elastic buckling
18 p2732 A72-36079
- Analytical foundations of experimental mechanics - Trends in analytical mechanics.
18 p2732 A72-36354
- Clamped flat skew plates stability under inplane stresses in terms of oblique components, calculating elastic buckling coefficients via energy method
18 p2736 A72-36931
- Integral equation method for solution of boundary value problems of structural mechanics. I - Ordinary differential equations. II - Elliptic partial differential equations.
18 p2739 A72-37169
- Finite element models with rigid displacement for nonrigid structure analysis, noting curved beam and shells
18 p2739 A72-37173
- Stress distribution and displacements in adhesive bonded lap-jointed aerospace structures, presenting approximate solution
18 p2740 A72-37214
- Structures and materials performance under creep and plastic deformation, discussing energy theorems implications
19 p2874 A72-37705
- Essential factors in reliability prediction and stress analysis of structural component with wide load and temperature variations
19 p2874 A72-37710
- Elasto-visco-plastic constitutive equations for quasi-static structures calculations.
[ONERA, TP NO. 1089]
19 p2875 A72-37763
- Experimental investigation of flexural vibration damping in supported square plates with coatings
19 p2876 A72-38004
- Mixed boundary value problem in the theory of elasticity for a half-space with circular lines of separation between boundary conditions
19 p2876 A72-38152
- Applicability of the small parameter method to the estimation of stresses in nonhomogeneous elastic media
19 p2876 A72-38153
- Zero-moment reinforced axisymmetric shells
19 p2876 A72-38155
- Plane bending problems in the theory of elasticity for nonhomogeneous solids
19 p2877 A72-38162
- Polarization optical method for analyzing local stress concentrations in structural members.
19 p2805 A72-38768
- Plate bending analysis with hybrid triangular and rectangular finite elements, deriving stiffness matrix via optimized stress functions
20 p2979 A72-39556
- Iterative solution of nonlinear structural problems, using convergence criteria based on displacement quantities
20 p2946 A72-39625
- An equivalent grid framework for skew plates in flexure.
20 p2980 A72-39689
- Elastic analysis for a radial crack in a circular ring.
20 p2981 A72-39959
- Simulation of physically nonlinear multispin beams
21 p3116 A72-40180
- Simple structures behavior under constant loads, considering low stress levels and creep rupture mechanism with internal damage affecting strain rate
21 p3117 A72-40673
- Geometrical non-linear analysis of structures by finite elements.
21 p3120 A72-41204
- Boundary value problems of lattice plates statics for transversally loaded homogeneous strip, noting elastically supported continuous plates
21 p3123 A72-41394
- Theoretical and experimental investigation of the relationship between plastic and creep deformation of structures.
21 p3124 A72-41509
- Method of calculating rotating disk of complex profile
21 p3127 A72-41701
- Estimation of the effect of stress concentration in nonstationary loading regimes
22 p3232 A72-41922
- Limit analysis and plastic design of structural elements of complex shape.
22 p3235 A72-42577
- Iteration process convergence improvement based on stiffness change expression as linear combination of two matrices in structural reanalysis
22 p3235 A72-42602
- Book - Contributions to the theory of aircraft structures.
22 p3238 A72-42826
- Multilayer shells structural analysis via equilibrium equations transformation into system of equivalent equations
22 p3238 A72-42836
- Buckling of integrally stiffened cylindrical shells - A review of experiment and theory.
22 p3239 A72-42846
- Structural stability of anisotropic plates and structures, developing method based on data for corresponding isotropic problem
22 p3239 A72-42847
- Book - Thermal structural analysis programs: A survey and evaluation.
22 p3241 A72-43046
- Longitudinal compression of a three-layer plate with initial deflection and a physical nonlinearity of the middle layer / the filler/
23 p3346 A72-43673
- Lower and upper bounds for the lowest characteristic value of the elastically supported membrane
23 p3347 A72-43717
- Vibration characteristics of cylindrical shells with several axially equispaced constraints.
23 p3355 A72-44371
- Triangular facet finite element application in thin cylindrical shell analysis by displacement method
24 p3456 A72-44792
- Mechanical properties and structural strength evaluation methods for metallic materials at low temperatures, describing hydraulic and pneumatic testing facilities
24 p3416 A72-45756
- High speed radial thrust multipoint ball bearing design, discussing contact resistance, ball motion, ring deflection and centrifugal force effect on performance and service life
01 p0078 A72-11378
- Two stage resonant slow wave structure synthesis for microwave device applications, deriving conditions for required dispersion and coupling impedance characteristics
02 p0190 A72-11574
- Optimal design of elastic beams under alternative loads and constraints on generalized compliance and bending stiffness
02 p0291 A72-11962
- Aircraft design interactive computer graphics technique, using human decision input response to computer output information
02 p0300 A72-12733
- Complex determinate and indeterminate structures weight minimization subject to design constraints relative to size, allowable stress, natural frequencies, etc
03 p0446 A72-13703
- Optimal shape calculation for partially elastic and elastoplastic column under conservative load based on static stability criterion
03 p0447 A72-13851
- Multipurpose optimal design of elastic structures with piecewise uniform cross section for load states and prescribed stiffness by energy methods
03 p0455 A72-14386
- Elastoplastic circular plates optimum shakedown design under cyclic loading
04 p0585 A72-14613
- Carbon fiber reinforced composites properties and design limitations relative to elastic anisotropy in pump and fan applications
04 p0536 A72-14744
- Carbon fiber resin composite characteristics for airframe component design, comparing with metal materials
04 p0537 A72-14746
- Glass fiber reinforced plastic composites design, strain limitation and creep fatigue properties for large structures
04 p0537 A72-14749
- Random search method application to optimal design of closed circular cylindrical shells under axial compressive loading
04 p0587 A72-15020
- Optimal design of solid and three layer rods with prescribed natural frequencies for longitudinal and transverse vibrations, using minimum mass criterion
04 p0587 A72-15047
- ALSEP structural/thermal/ design, outlining package hardware configuration, passive thermal protection and materials selection procedures
04 p0508 A72-15093
- Sandwich beam design, deriving linear programming formulation suitable for computer treatment
04 p0590 A72-15191
- Statically indeterminate and determinate elastic beams optimal design for maximum-minimum deflection under distributed load
04 p0590 A72-15192
- Minimum weight design of perfectly plastic continuous sandwich beams with two equal spans for movable loads
04 p0593 A72-15647
- Composite multilayer fibrous shell structural design optimization, using nonlinear mathematical programming methods
05 p0733 A72-15943
- [ASME PAPER 71-WA/DE-12]
05 p0733 A72-15943
- Statistical distribution of maximum response for reliability-based optimum spacecraft structural design for random excitations from booster shutdown
05 p0724 A72-16103
- Automatic plastic minimum weight design of structural frames comparing with linear programming techniques
05 p0737 A72-16117
- Optimal design of statically determinate sandwich beams for given deflection at specified cross section
05 p0737 A72-16119
- OAO space telescope of 120 inches aperture, discussing structural design, geometric configuration and stabilization and pointing control system
05 p0663 A72-16800
- [AIAA PAPER 72-201]
05 p0663 A72-16800
- S-3A Viking land based antisubmarine warfare maritime and reconnaissance aircraft, describing flight controls, structural design, underslung podded engines and operational equipment
06 p0758 A72-17583
- Fatigue damage factor and failure probabilities in structural design for multilevel repetitive cyclic stresses
06 p0896 A72-17965
- Quasi-linearized solution to nonlinear Volterra equations in design of structures under creep deformations
06 p0897 A72-18318
- Structural design primal and dual linear programming problem decomposition into sum and difference problems with form of original equation
07 p1026 A72-18810

Minimum weight design of elastic sandwich beam with segmentwise constant stiffness under displacement and stress constraints, using iterative solution and finite element analysis [AD-745488] 07 p1092 A72-19825

Thin walled box beam optimal design, noting cross section areas and dimensions with permissible walls and flanges safety and stability 08 p1243 A72-21240

Automated minimum weight design of ring and stringer stiffened conical shells, using membrane theory for prebuckling analysis 08 p1245 A72-21599

Optimal design of anisotropic composite material annular plates by numerical method 08 p1246 A72-21673

German monograph on optimal design of gyroscope using spherical static gas bearing 08 p1173 A72-22174

Titanium-boron-epoxy composite materials selection and fracture mechanics criteria for B-1 bomber structural design 09 p1317 A72-22477

Optimization of load-carrying elastic lattice structures designed on prescribed surface 09 p1402 A72-22746

Papers on design for high temperature environments covering structural fatigue, creep interaction and ratchetting deformation and inelastic stress analysis 09 p1406 A72-23196

Time and cycles to failure diagrams for strain rate and hold periods effects on high temperature metal creep fatigue in design analysis 09 p1407 A72-23199

Design information for machinery to incorporate welding positions and joints, fatigue mechanisms, loads, combined stresses and plate and cast materials properties 09 p1409 A72-23621

Book on plastic analysis and plate, shell and disk theories and design covering stress-strain concepts, laws and theorems 10 p1553 A72-23749

Mathematical modeling for structural analysis and design from viewpoint of methodology, physical principles, simulation, optimization, constraints and control theory [SMRT PAPER M 2/3] 10 p1556 A72-24393

Structural design systematology of statics and dynamics numerical approximate procedures based on variational principles and differential equations [SMRT PAPER M 7/4] 10 p1505 A72-24397

Literature review of structural safety, treating load, strength, dynamic structural and structural reliability analyses and design aspects 10 p1560 A72-25174

Sounding rocket heat pipe experiment in zero gravity, testing spiral and pedestal arteries and plain groove designs [AIAA PAPER 72-259] 11 p1739 A72-25204

Short time stress rupture test data correlation for design, using computerized time-temperature parametric methods [AIAA PAPER 72-327] 11 p1653 A72-25363

Transport aircraft fuselage computerized design, determining optimal structural distribution for strength and displacement constraints [AIAA PAPER 72-330] 11 p1727 A72-25366

Computerized structural design of aerospace vehicle, stressing automated routines for finite element models generation [AIAA PAPER 72-332] 11 p1727 A72-25367

Viking conical aeroshell structural prototype design, analysis and testing, comparing buckling failure data with theoretical predictions [AIAA PAPER 72-370] 11 p1725 A72-25395

Space shuttle orbiter vehicle structural design configurations development and evaluation with respect to overall system weight and program cost [AIAA PAPER 72-373] 11 p1726 A72-25397

Boron-epoxy composite design for aircraft structures, discussing materials variations, strength prediction inadequacies and full scale tests 11 p1670 A72-25454

Asymmetric three layer beam design for elastic impact, proposing functional equation integration by computer method 11 p1732 A72-25531

Flight vehicle structures optimum design for random vibration environment, presenting formulation as nonlinear programming problem 11 p1736 A72-26003

Laminated reinforced plastics structural design criteria obtained by statistical and deterministic approach 11 p1737 A72-26235

Acrylics and polycarbonates properties in aircraft transparencies design, emphasizing cost and optical, mechanical, thermal and chemical properties 12 p1832 A72-27009

Prager-Shield theory for optimal plastic design extended to multicomponent cost functions and load conditions, applying to fiber reinforced plate 12 p1881 A72-27243

Fatigue failure information in structural design, considering low cycle, cumulative damage and time dependent conditions 12 p1884 A72-27641

Structural design, performance and costs of rigid or semirigid solar panels for geostationary satellites power supplies 12 p1758 A72-28034

Optimal design of elastic structures, emphasizing stability and response under applied static and dynamic loads 13 p2054 A72-28487

Dimensional chains calculation in differential method of manufacturing complex precision elements of casings 13 p1962 A72-28740

Hailstone impact simulator for aircraft damage prediction in testing prospective structural designs 13 p1938 A72-28855

A-4 Skyhawk horizontal stabilizer experimental graphite-epoxy composite construction, describing design, manufacturing and testing techniques [AIAA PAPER 72-358] 13 p2056 A72-28954

Optimal design of thin walled minimum weight aircraft shell structures, using linear programming 13 p2058 A72-29143

Fiber glass reinforced plastic structure design based on anisotropy, calculating optimum angle between reinforcement and horizontal axis 13 p2058 A72-29463

Aircraft structures design and development with composite materials, considering materials characteristics relations to structural components dynamic response 13 p2060 A72-29691

Minimum weight elastic structure designs under dynamic loads with constraints on stress displacements and natural oscillation frequencies 13 p2062 A72-30009

Aircraft landing gears structural systems design, taking into account different design criteria imposed by various national impact load norms 13 p1898 A72-30025

Structural design and electrical drive mechanism of helicopter hoist for rescue operations 13 p1912 A72-30097

Minimum weight hinged and unhinged cantilever truss design as variational problem, using dynamic programming method 14 p2166 A72-30690

Navy program for composites technology development in aircraft structures, discussing design, reliability and cost [ASME PAPER 72-DE-3] 14 p2073 A72-30860

High modulus composites structural design applications, considering fatigue performance vs cost [ASME PAPER 72-DE-24] 14 p2167 A72-30866

Control design for dynamic/vibratory loading of high speed rotating machinery, discussing rotor, bearing span and support stiffness and coupling centering [ASME PAPER 72-DE-39] 14 p2167 A72-30872

Optimal plastic design of doubly symmetric closed ring and frame structures of idealized sandwich section under uniform internal pressure 15 p2322 A72-31346

Composite materials for engineering component and structure design, considering mechanical properties and cost-effective performance 15 p2260 A72-31443

Coupled flexural longitudinal vibrations of circular arc girder with symmetrical cross section, discussing optimal design 15 p2324 A72-31487

Arctic environment surface effect vehicle design, considering structures, drag, lift, propulsive power and range 15 p2181 A72-32125

Structural components design from fiber composites, noting computer programs for structural and stress analysis 15 p2328 A72-32128

Structural design optimization procedure based on sequence of linearizations with iterative convergence through series of least critical intermediate solutions in hyperspace 15 p2331 A72-32551

Buckling strain effects on critical stresses in design of longitudinally corrugated shells for axial compression 15 p2333 A72-32680

Structural design optimization by geometric programming, illustrating computerized technique on two bar truss and ship bulkhead problem 16 p2366 A72-32913

Optimal plane elastic trusses under alternative loads, designing for smallest total volume of bars with upper stress bound 16 p2466 A72-33017

Thin walled elastic structures optimization by overall and local buckling coincidence, discussing compression column design 16 p2468 A72-33200

Exact differential equation derived for optimal design of straight nonprismatic column subject to creep buckling 16 p2474 A72-34132

Time and temperature independent permissible deformation limits as basis for dimensioning of cyclically and multiaxially stressed plastics structural components 16 p2416 A72-34147

Elastic-plastic systems under dynamic loadings, discussing compounded shakedown load solution by zero work and direct search methods [ASME PAPER 71-APMW-27] 17 p2624 A72-34309

A computer system for structural design 17 p2522 A72-34743

Elastoplastic structural analysis from design viewpoint, discussing load limits and stability estimates based on large deformation assumption 17 p2632 A72-35113

Multilevel hierarchical structural design optimization, proposing component by component ascent method of dynamic programming 17 p2533 A72-35171

Composite materials technology utilization in structural design, considering stiffness, strength, weight, fatigue properties, adhesive joining and structural reliability 17 p2633 A72-35283

Invariant imbedding and optimum beam design with displacement constraints. 17 p2634 A72-35406

A finite element approach to optimal design of plastic structures in plane stress. 18 p2739 A72-37165

Natural frequencies and dynamic response constraints in optimal structural design, considering mathematical programming aspects 18 p2739 A72-37167

Active controls - Changing the rules of structural design. 19 p2748 A72-37681

Book - Advances in creep design 19 p2874 A72-37701

A rational approach to creep design. 19 p2874 A72-37706

Mathematical relationships for primary, secondary and tertiary creep and their use in extrapolation of tensile creep data. 19 p2874 A72-37707

A flutter optimization program for aircraft structural design. [AIAA PAPER 72-795] 19 p2876 A72-38116

Designing aircraft structure for resistance and tolerance to battle damage. [AIAA PAPER 72-773] 19 p2752 A72-38138

Structural development of the L-1011 Tri-Star. [AIAA PAPER 72-776] 19 p2876 A72-38139

Polymoment homogeneous solution characteristics in the theory of elasticity for design calculations 20 p2979 A72-39587

The carrying capacity of frames under the influence of concentrated forces 20 p2981 A72-39919

Determination of the limits of applicability of a continuous model when calculating a discrete polar lattice disk 21 p3122 A72-41344

Influence of deviations in the shape of the base surface on the precision of turbine blade machining operations 22 p3182 A72-41863

Russian book - Design principles in aircraft construction. 22 p3136 A72-42074

Minimum weight elastic structure designs under dynamic loads with nonlinear constraints on stress displacements and natural oscillation frequencies 22 p3236 A72-42737

Wing flutter prevention in SST structural design, using finite element model and lifting surface aerodynamic theory 22 p3237 A72-42760

Aircraft structural design loads definition by mission analysis criteria, taking into account gust loads via power spectral density method 22 p3138 A72-42828

The influence of production imperfections on design of optimum structures. 22 p3239 A72-42841

Optimum design of circular sandwich plates. 22 p3239 A72-42843

Dangerous structural failure characteristics due to idealized design optimization, discussing shell buckling instabilities 22 p3240 A72-42895

Bayesian statistical decision theory and reliability-based design. 22 p3240 A72-42967

Structural design optimization via area ratio method, developing shape factor design charts [SAWE PAPER 937] 23 p3344 A72-43477

Minimum weight structural design, generalizing method for deriving sufficient optimality conditions

with examples for specified maximum deflection and critical nonconservative loading parameters

23 p3347 A72-43719

Equipment assembly design optimization by operational versions determination and criteria evaluation for optimal conditions, noting rotary wing design

23 p3294 A72-44024

Optimal design of indeterminate truss using geometric programming.

23 p3354 A72-44256

Dynamic programming and the optimum design of rotating disks.

23 p3356 A72-44550

Optimum design of joints - The stress severity factor concept.

24 p3455 A72-44728

Design and certification for executive type aircraft.

24 p3366 A72-44730

Fatigue design and test program for the American SST.

24 p3367 A72-44741

Plastic design of regular orthotropic grids with two adjacent edges fixed, free, or hinged.

24 p3456 A72-44794

Utilization of advanced composite materials for spacecraft and space shuttle applications.

24 p3417 A72-45153

STRUCTURAL DESIGN CRITERIA

Linear physical and nonlinear geometric formulation of design problem for prestressed rubber parts based on elasticity theory in terms of assembly requirements

19 p2871 A72-37428

STRUCTURAL DYNAMICS

U DYNAMIC STRUCTURAL ANALYSIS

STRUCTURAL ENGINEERING

Structural mechanics in reactor technology - Conference, Berlin, Germany, September 1971

10 p1556 A72-24392

Elastoplastic computation of thin cylindrical shells under cyclic loading

23 p3348 A72-43786

STRUCTURAL FAILURE

Monograph on stress corrosion failure, covering threshold stresses, fracture mechanics, electrochemical processes, hydrogen embrittlement, corrosidents, various steels and alloys, environmental effects, etc

01 p0082 A72-10166

Nylon parachute materials failure mechanics, considering friction, light, chemical and thermal effects

01 p0005 A72-10316

Factorial design model of materials fatigue failure under narrow band random vibrations

01 p0140 A72-10942

Tensometric damage detection in rolling contact bearings from bending stress spectrum, using Si strain and wire strain gages

01 p0078 A72-11379

Local buckling and collapse of thin walled lipped channel beams under critical end moments

01 p0144 A72-11396

Boeing 707 rapid decompression at 25,000 feet, noting rivet hole fatigue damage

02 p0167 A72-11715

Plastic collapse limit analysis for combined edge and pressure loading on circular cylindrical shells for Tresca yield condition

[ASME PAPER 71-PVP-22]

02 p0295 A72-12474

Quenched and tempered high strength and maraging steels delayed failure properties from notched-tensile sustained-load tests in distilled water

02 p0246 A72-12560

Mechanical breakdown prediction of loaded fiberglass reinforced plastic by seismoacoustic technique, investigating load effects on seismoacoustic emission

02 p0250 A72-12679

Mechanical breakdown characteristics of polymethyl methacrylate and polystyrene samples exposed to picosecond pulses emitted by Q switched laser

02 p0250 A72-12680

Fatigue breakdown and energy dissipation dependence on stress during bending of cylindrical steel and iron specimens

03 p0372 A72-13589

S-glass fiber bundles and composites under quasi-static loads, investigating strength characteristics and failure mechanism

04 p0592 A72-15474

Fatigue damage factor and failure probabilities in structural design for multilevel repetitive cyclic stresses

06 p0896 A72-17965

Deformation kinetics and failure of refractory Nb and Mo base alloys in plastic state under low cyclic fatigue

06 p0833 A72-18631

Cyclic loading failure criteria based on plastic deformation energy concepts, considering material load carrying capacity

06 p0899 A72-18650

Fractographic analysis of failure kinetics and crack formation in Al alloys, showing microfatigue intrusions and extrusions for various initial stress levels

06 p0834 A72-18653

Compression strength theory for monodirectional reinforced homogeneous anisotropic and piecewise homogeneous composite materials, using microvolume stability loss failure mechanism

06 p0838 A72-18655

Safety factor distribution function for plastic collapse of structure with random resistance members, discussing variance-expected value ratio

09 p1406 A72-23075

Sonic boom effects on structures, discussing ground motion, direct excitation by shock waves and damages

09 p1304 A72-23318

Summary of 1971 Stockholm workshop on sonic boom effects, discussing humans, animals and structure exposure and interdisciplinary aspects

09 p1273 A72-23324

Satellite long life assurance, investigating shuttle era spacecraft program cost relationship to mean time to failure

[AIAA PAPER 72-225]

10 p1551 A72-24436

Fatigue failure modes of composite materials, considering fiber breakage, delamination, matrix cracking, interface debonding and void growth

11 p1670 A72-25461

General aviation aircraft structural safety studied with 1547 accident histories, noting IFR and turbulent weather conditions predominance

[SAE PAPER 720308]

11 p1575 A72-25572

Computer program for bifurcation buckling analysis of shells under collapse load, using strain energy methods and two dimensional finite difference grid

11 p1736 A72-25980

Fatigue failure criteria under combined stress conditions, considering complex form, thin and thick walled cylinders as test specimens

12 p1828 A72-27317

Fatigue failure tests of low carbon Mn steel, analyzing structural damage under cyclic loads in relation to temperature curve

12 p1829 A72-27458

Collapse loads of symmetrically tapered cantilever beams under uniformly distributed end shear, considering optimum tapering angle for minimum weight

13 p2059 A72-29596

Dynamically similar wind tunnel models for transonic aeroelastic studies of aircraft failures or structural damage and flutter margins

[ONERA, TP NO. 1082]

13 p1939 A72-29672

Ni-Cr-Ti steel aircraft structural element fatigue life calculation based on failure mechanism involving crack propagation

14 p2164 A72-30429

Thermal shock produced edge effect, analyzing brittle material heat resistance and failure, using thermoelastic heated cylinder

14 p2165 A72-30437

Cast Al alloys tendency to brittle failure in percussive bending tests estimated from force strain oscillograms

14 p2124 A72-31035

Debonded laminar composite torsional stress intensification analysis near circular shaped imperfection based on Hankel transform and dual integral equations solution

15 p2261 A72-32247

Aerodynamic noise and structural fatigue failure research and test facility, concerning supersonic jet and V/STOL aircraft

16 p2342 A72-32900

Structural failure probability distribution for threshold stress crossings in random vibration, using Poisson approximation

16 p2468 A72-33227

Compressed initially bent Shanley column analyzed for geometric imperfection coupling and material behavior effects on critical time to creep collapse

16 p2474 A72-34131

Achieving fail safe design in rotors.

[AHS PREPRINT 673]

17 p2491 A72-34513

Russian book on metal fatigue and inelasticity covering structural inhomogeneities, static and dynamic loading, failure mechanisms, deformation, temperature effects and test methods

17 p2566 A72-34649

A fracture mechanics analysis of adhesive failure in a single lap shear joint.

[SESA PAPER 1990A]

17 p2630 A72-34815

Analysis of a partially cracked panel.

18 p2735 A72-36771

Numerical solution for the mean first-passage-time for snap-through of shells.

18 p2737 A72-37061

Investigation of the snap-through of rigidly clamped shallow spherical shells under the action of a dynamic stepped load

19 p2877 A72-38163

Statistical failure characteristics and probability evaluation of the static strength of structural components made of composite polymer materials

20 p2943 A72-38942

STRUCTURAL MEMBERS

The broad range detection of incipient failure using the acoustic emission phenomena.

20 p2925 A72-39286

Longitudinal tensile failure of unidirectional fibrous composites.

20 p2944 A72-39789

Fatigue damage of aluminum alloy at high temperature.

21 p3066 A72-40716

Transverse shear effect on thin shells collapse load, considering influence on Shaprio yield surfaces

21 p3121 A72-41213

Perfectly plastic media under the action of multiparameter loads

21 p3123 A72-41393

Facility for studying the failure of structural elements in a supersonic high-temperature flow containing a controlled number of abrasive particles

21 p3043 A72-41717

Limit analysis and plastic design of structural elements of complex shape.

22 p3235 A72-42577

Transport aircraft wing compression panel failure in bending test due to stringer interruptions, analyzing structural deficiency via column and beam bending theories

22 p3183 A72-42827

Aircraft structural safety criteria based on acceptable failure probability, determining critical load levels

22 p3138 A72-42829

Fatigue strength and fail-safe aspects of lug joint in aircraft structures, considering tension-compression load, fretting corrosion, prestress and residual stress

22 p3239 A72-42851

Dangerous structural failure characteristics due to idealized design optimization, discussing shell buckling instabilities

22 p3240 A72-42895

Best linear invariant estimation of Weibull parameters - Samples censored by time and truncated distributions.

22 p3199 A72-42969

Detection of structural deterioration and associated airline maintenance problems.

[SAWE PAPER 918]

23 p3293 A72-43465

Failure and crack formation in gas turbine engine compressor disks under variable stresses from fatigue tests, considering safety factors

23 p3347 A72-43736

The surface flaw in aircraft structures and related fracture mechanics analysis problems.

23 p3352 A72-44228

Polymer fatigue failure mechanism examination on constant deflection type testing machine, investigating applied stress and temperature effects on crack propagation rate

24 p3455 A72-44631

STRUCTURAL FATIGUE

U FATIGUE [MATERIALS]

STRUCTURAL FOUNDATIONS

U FOUNDATIONS

STRUCTURAL INFLUENCE COEFFICIENTS

Determination of influence coefficients for composite structures by holographic interferometry.

19 p2873 A72-37614

Inelastic transverse strain coefficient and Poisson ratio dependences on plastic and brittle properties

23 p3348 A72-43752

STRUCTURAL MATERIALS

U CONSTRUCTION MATERIALS

STRUCTURAL MEMBERS

NT ANISOTROPIC PLATES

NT ANNULAR PLATES

NT BEAMS [SUPPORTS]

NT BOX BEAMS

NT CANTILEVER BEAMS

NT CANTILEVER PLATES

NT CIRCULAR PLATES

NT COLUMNS [SUPPORTS]

NT CORRUGATED PLATES

NT CURVED BEAMS

NT ELASTIC PLATES

NT FLAT PLATES

NT GIRDLERS

NT I BEAMS

NT MEMBRANE STRUCTURES

NT ORTHOTROPIC PLATES

NT PERFORATED PLATES

NT PLATES [STRUCTURAL MEMBERS]

NT POROUS PLATES

NT RECTANGULAR BEAMS

NT REINFORCED PLATES

NT SKIN [STRUCTURAL MEMBER]

NT STRINGERS

NT STRUTS

NT TAPERED COLUMNS

NT TRUSSES

NT WING PANELS

Aluminum stiffening structural sections selectively reinforced with boron/epoxy composite materials, discussing mechanical properties, cost effectiveness and stress distribution

01 p0139 A72-10737

Temperature and loading conditions effects on structural element service life, showing partial healing process of microdefects

03 p0443 A72-13454

Soviet book on structural shape effects of machine parts on durability, covering production, gear transmissions shafts, axles, threaded joints, etc

03 p0364 A72-13966

Hybrid representation for structural component by vibration modes with free or fixed connection points and boundary conditions selection to optimize accuracy

05 p0736 A72-16084

Interaction surfaces for structural members under combined axial, shear force and bending moment, investigating shear effect on yielding of arches

07 p1090 A72-19730

Boron and carbon fiber reinforced plastics applications in aircraft and engine structural components, discussing dynamic and impact damping properties compared to conventional materials

13 p1982 A72-28555

Aircraft structures design and development with composite materials, considering materials characteristics relations to structural components dynamic response

13 p2060 A72-29691

Temperature distribution of structural element with heat shield and metallic layer, determining ablation process for thermal flux at surface

14 p2170 A72-30593

Time and temperature independent permissible deformation limits as basis for dimensioning of cyclically and multiaxially stressed plastics structural components

16 p2416 A72-34147

Linear physical and nonlinear geometric formulation of design problem for prestressed rubber parts based on elasticity theory in terms of assembly requirements

19 p2871 A72-37428

Polarization optical method for analyzing local stress concentrations in structural members.

19 p2805 A72-38768

Temperature and loading conditions effects on structural element service life, showing partial healing process of microdefects

24 p3458 A72-44929

STRUCTURAL RELIABILITY

Nonlinear boundary value problem of creep for isotropic bodies with random mechanical properties under random loads, calculating structural component reliability and service life

02 p0289 A72-11619

Statistical methods of stress and reliability analyses of elastic systems under random external loads

03 p0453 A72-14206

Composite materials durability and strength estimations, using reliability theory for failure rate characteristic

05 p0680 A72-15991

Thin walled box beam optimal design, noting cross section areas and dimensions with permissible walls and flanges safety and stability

08 p1243 A72-21240

Wilga 3 aircraft structure service life from structural fatigue theory and tests, emphasizing operational load distribution measurement

08 p1110 A72-21634

Literature review of structural safety, treating load, strength, dynamic structural and structural reliability analyses and design aspects

10 p1560 A72-25174

Flexible solar cell array module design technique, discussing electric welding procedure and equipment parameters effects on breaking strength and reliability

12 p1758 A72-28036

Reliability analysis of automatic systems with structural changes accumulated during operation, noting service life determination and damage prevention

13 p1936 A72-29169

Minimum weight reliable beams and frames calculation for random loads, using one degree of freedom system to obtain closed form solution

14 p2164 A72-30237

Computer algorithms and programs contribution to aircraft structure operational reliability and fatigue life calculation

14 p2164 A72-30288

Space Shuttle Orbiter onboard ultrasonic system for structural integrity tests and assessment, noting limitation factors due to configuration and vehicle launch noise effects

15 p2256 A72-31698

Composite materials technology utilization in structural design, considering stiffness, strength, weight, fatigue properties, adhesive joining and structural reliability

17 p2633 A72-35283

Aircraft engine lifetime and turbine blade reliability

20 p2963 A72-39916

Experimental investigation of the elastic characteristics of composite bearings in turbine machinery

for the purpose of increasing their efficiency and reliability during nonlinear vibrations of the rotor

22 p3181 A72-41860

ICAO structural airworthiness requirements relation to air transportation safety, considering maneuver and gust loads in terms of limit load concept

22 p3138 A72-42830

International Conference on Structural Safety and Reliability, Washington, D.C., April 9-11, 1969, Proceedings.

22 p3240 A72-42966

Bayesian statistical decision theory and reliability-based design.

22 p3240 A72-42967

Response of linear and nonlinear continuous structures subject to random excitation and the problem of high-level excursions.

22 p3241 A72-42970

Reliability analysis in the estimation of transport-type aircraft fatigue performance.

22 p3241 A72-42971

Testing procedures for the design and life estimation of fatigue-sensitive structures.

22 p3241 A72-42974

Optimal fleet reliability under fatigue and chance overload in service.

24 p3365 A72-44656

Life prediction of expulsion bladders through fatigue test and fold strain analysis.

24 p3455 A72-44672

Reliability analysis based on time to the first failure.

24 p3455 A72-44727

Structural fatigue cost penalties in airline operations, considering inspection, maintenance and carrying capacity reduction

24 p3367 A72-44743

Composite materials durability and strength estimations, using reliability theory for failure rate characteristic

24 p3418 A72-45733

STRUCTURAL RIGIDITY

U STRUCTURAL STABILITY

STRUCTURAL STABILITY

NT SHELL STABILITY

Michelson interferometers with large interference fields for plasma diagnostics emphasizing structural rigidity, monochromatic light pulse power, instruments vibrations resistance, etc

02 p0223 A72-11402

Alumina dispersions structural stability in Fe and Ni based alloys metal matrices

02 p0241 A72-11445

Three dimensional problems in stability, elasticity and plasticity theory for isotropic, anisotropic and inhomogeneous bodies, noting applications to machine construction, civil engineering, geophysics, etc

02 p0288 A72-11602

Edge effect equations for stability, vibration and deflection of asymmetric three layer circular plate and cylindrical shell with filler

02 p0288 A72-11605

Flexible viscoelastic orthotropic plates and shells obeying linear heredity relations, solving stability and bending problems by Laplace transform

02 p0290 A72-11625

Elastic stability of body under conservative loads, deriving energy criterion with thermodynamic laws

02 p0292 A72-12003

Aeroelastic stability of flat anisotropic sandwich plates in supersonic compressible fluid flow

02 p0297 A72-12614

Square orthotropic and isotropic plates stability with square hole under uniformly distributed load

02 p0299 A72-12685

Three layer plates elastoplastic stability, describing breakdown conditions by five differential equations with five unknown variables

02 p0299 A72-12690

Elasticity tensor formulas for wave propagation, vibration and stability of deformed isotropic solids

03 p0448 A72-13887

Stress concentration and stability of plates and shells weakened by holes

03 p0450 A72-14110

Stress concentration at hole in plates after stability loss, using branching and small parameter method

03 p0450 A72-14111

Potential energy principle in equilibrium stability problems for flexible extendable thread, using Liapunov method

03 p0390 A72-14208

Elastoplastic stability of structural rods in unloadable systems, considering load carrying capacity increase by critical state onset delay

03 p0454 A72-14214

Three layer plates stability with light fillers, noting filler thickness effect on approximate solutions accuracy

03 p0454 A72-14377

Cracked rectangular plates vibration and stability, computing eigenvalues, natural frequencies and moment distribution

04 p0583 A72-14448

Point contact Josephson junctions arrangement for millimeter and submillimeter region, showing mechanical stability

04 p0561 A72-14919

Shear stress and stability of composite elastic double layer with plane circular crack under torsion

04 p0588 A72-15054

Time delay effect on stability of viscoelastic cantilever column under retarded follower load

04 p0590 A72-15186

Papers on aerospace structure by N. J. Hoff covering aircraft framework, stress analysis, structural stability, shell theories, bending, buckling, monocoque and sandwich structures, etc

04 p0591 A72-15238

Open resonators stability analysis, describing integral equations eigenfunctions and eigenvalues short wave asymptotic expansions

04 p0502 A72-15435

Vibration and stability of rectangular plates with mixed edge conditions, reducing dual series equations to homogeneous Fredholm integral equations [ASME PAPER 71-WA/APM-21]

05 p0733 A72-15959

Continuous bodies incremental deformation and stability under initial stress, discussing relationships for elasticity constants and material stress tensors [ASME PAPER 71-WA/APM-9]

05 p0734 A72-15970

Elastically supported cantilever stability with continuous lateral restraint under uniform distributed axial load, developing boundary conditions

05 p0737 A72-16118

Structural stabilization of austenitic steels with manganese, maintaining toughness and sensitivity to martensitic transformation by hammer hardening

05 p0673 A72-16145

Structural stabilization of austenitic steels with manganese, noting chemical purity and cleanliness conditions

05 p0673 A72-16146

Transverse vibrations stability of launching rocket body, allowing for propellant sloshing and body elastic deformation

05 p0731 A72-17187

Vertical shaft stability on elastic sliding bearings, considering passage through self oscillation zone

06 p0894 A72-17683

Dispersion strengthened Co alloys structural stability, tensile and creep rupture strengths and hot corrosion properties

06 p0829 A72-17829

Uniformly curved fluid conveying tube free vibration and stability, showing flow velocity, fluid pressure and Coriolis force effects on natural frequency

06 p0821 A72-17853

Mathematical modeling of discrete nonconservative dynamic elastic systems for finite sensitivity, using Liapunov stability

06 p0840 A72-18320

Convergence conditions for Galerkin method, applying to boundary value problems of structural stability and critical buckling loads

07 p1025 A72-18798

Elastic stability of laminated circular plate with rectangular anisotropy under in-plane compression forces along edge

07 p1090 A72-19693

Composite elastic beams equations under initial stress, investigating flexural wave propagation and structural stability

07 p1090 A72-19733

Critical stability and supercritical equilibrium behavior of compressed viscoelastic rod

07 p1091 A72-19761

Stability loss of circular annular plate under compression, determining critical loads with inner edge free and outer edge hinged or clamped

07 p1092 A72-19900

Quasi-static stability of sandwich plates hinged over edge in finite difference formulation

07 p1094 A72-20213

Elastic rods and rings stability under compression beyond elasticity limit, determining equilibrium branching characteristics near bifurcation point

07 p1095 A72-20314

Gravitational field simulation by centrifugal force for structural stability and self weight buckling studies

07 p1096 A72-20428

Local stability of thin walled isotropic elastic cylinder, deriving characteristic equations for critical load calculation

08 p1242 A72-20969

Rational parameters and reinforcement of stiffened laminar plates with instability tendencies under compression loads

08 p1243 A72-21236

Thin walled box beam optimal design, noting cross section areas and dimensions with permissible walls and flanges safety and stability

08 p1243 A72-21240

Critical compressive stresses leading to instability of layer fastened to elastic half space

08 p1244 A72-21368

Elastic stability of nonlinearly elastic anisotropic body analyzed via variational principles in three dimensional theory 08 p1246 A72-21707

Plane stability of isotropic plate with straight line series of holes reinforced by complex elements or multicomponent rings, determining stress concentrations 08 p1246 A72-21710

Elastic rectangular plate instability in pure bending along two perpendicular directions solved by Karman nonlinear equation reduction to partial differential equations integration 08 p1247 A72-21817

Quadrilateral four node nonconforming plate bending finite elements for structural vibration and stability analysis 08 p1250 A72-22142

Necking instability in rectangular elastoplastic plate under biaxial tension, obtaining condition for equilibrium bifurcation by variational method 09 p1398 A72-22532

A-15 superconducting films preparation computer-aided method, noting alloying effects and crystal structure stability determinations applications 09 p1368 A72-22559

Mathematical thermodynamic theory for plastic deformation induced internal structure changes in rheological material, describing homogeneous response by temperature and deformation gradients 09 p1403 A72-22761

Hamiltonian used as Liapunov function in stability evaluation of one dimensional continuous system loaded with polygenic forces 09 p1406 A72-23077

Parametric instability of flat rectangular plates under periodic or shear sinusoidal in-plane boundary loads 09 p1408 A72-23463

Parametric dynamic stability equations and boundary conditions for thin walled open cross section beam under axial load, taking into account longitudinal deformation effect [ASME PAPER 71-APM-LL] 10 p1554 A72-24184

Upper bounds on lumped and continuous dynamic systems motion under loads and perturbations, discussing structure stability conditions [ASME PAPER 71-APMW-3] 10 p1554 A72-24188

Simply supported skew plates stability under combined loading, noting wing and tail design applications for high speed aircraft and missiles 10 p1555 A72-24196

Gradient iterative techniques application to finite element vibration and stability analysis of skew plates 10 p1558 A72-24878

Critical compressive buckling and stability of straight beams under axial and transverse loads calculated by three unknowns methods 10 p1560 A72-25121

Hypersonic nonlinear aerodynamic loading effect on panel flutter, examining stability for various initial conditions [AIAA PAPER 72-345] 11 p1728 A72-25374

Viking conical aeroshell structural prototype design, analysis and testing, comparing buckling failure data with theoretical predictions [AIAA PAPER 72-370] 11 p1725 A72-25395

Prestressed circular ring snap-through under continuously distributed or discrete torsional loads, determining critical torque by asymptotic solution 11 p1734 A72-25721

Alloying addition effects on structural stability and particle-matrix cohesion in metal-alumina composites 11 p1665 A72-26864

Linear programming simplex method for static load limit of circular arch 11 p1739 A72-26921

Elastic inhomogeneous continuum stability dependence on internal stress tensors field and boundary conditions, noting application to composite materials 12 p1843 A72-27171

Plane unstable deformation and stability loss of incompressible laminated composites under highly elastic strains 12 p1880 A72-27229

Linearized thermal viscoelasticity theory for stability, large strain and wave propagation problems, taking into account heat generating effects 12 p1880 A72-27233

Symmetric discrete elastic conservative structural systems stability boundary estimation through reduction to linear equation recursive solution, using perturbation method 12 p1880 A72-27242

Structural effects of meridian imperfections in symmetrically loaded elastic thin shell of revolution 12 p1881 A72-27255

Ultimate safe load estimates for stability of isotropic elastic materials 12 p1883 A72-27563

Structural system dynamic instability regions determination by finite element and conjugate gradient methods 12 p1884 A72-27847

Russian monograph on three dimensional deformable bodies stability covering linearized equations for subcritical deformations and strength analysis of low shear rigidity structures 12 p1888 A72-28337

Axisymmetric stability of spherical cap rigidly clamped at contour of shells of revolution, using variational difference method for uniformly distributed external pressure 13 p2053 A72-28393

Rods resistance to thermal shock under coupled thermoelasticity conditions, calculating critical thermal flux during thermodynamic compression waves propagation 13 p2053 A72-28399

Equilibrium state stability in elastic conservative system, relating system postbuckling behavior to critical branching point 13 p2054 A72-28478

Structural approach to elastic stability in buckling problems, simplifying deformation concepts and loading condition definition 13 p2054 A72-28479

Creep stability of bars and thin plates and shells for given loading force, considering instability criteria 13 p2054 A72-28481

Optimal design of elastic structures, emphasizing stability and response under applied static and dynamic loads 13 p2054 A72-28487

Heated three layer plate with load-carrying layers of different materials, thicknesses and temperatures, calculating stability under uniaxial tension 13 p2055 A72-28736

Critical force instability analysis for rectangular plates with mixed boundary conditions, using deflection forms in Fourier series 14 p2165 A72-30575

Stability of compressed elastic rod with continuously varying stiffness, deriving solution via influence function 14 p2166 A72-30691

Finite element method application to dynamic stability of thin plates and shells, noting nuclear reactor structural analysis [SMRT PAPER M 2/1] 14 p2166 A72-30723

Structural systems stability and natural frequency analysis eigenvalue problems solution by Sturm sequence method, using finite element technique 14 p2168 A72-30931

Optimal geometrical and physical properties of sandwich plates with rigid cores under compressive load, discussing critical stress and structural stability 15 p2322 A72-31359

Stability analysis of thin walled circular cylindrical shell under shearing force action to one end, calculating buckling modes 15 p2324 A72-31483

Unsymmetrical coupled columns stability under nonconservative lateral and end loading, using finite element method 15 p2331 A72-32557

Analog simulation method for highly redundant structure optimization based on reproducing structure mechanical behavior in stabilized stress states 16 p2463 A72-32899

Strain energy methods for stability of finitely deformed elastic membranes under conservative loading 16 p2465 A72-33002

Linearly elastic, transversely isotropic multilayer system, presenting stress and stability problem for two dimensional strain states 16 p2466 A72-33022

Stable bifurcation mode prior to instability in thick walled cylindrical viscoplastic pressure vessel under internal hydrostatic pressure 16 p2474 A72-34129

Stability analysis of a pinned-end beam undergoing non-linear free vibration. 17 p2623 A72-34236

Stability of a beam on an elastic foundation subjected to a follower force. 17 p2626 A72-34331

The elastic stability of two-parameter nonconservative systems. [ASME PAPER 72-APM-43] 17 p2627 A72-34782

Elastoplastic structural analysis from design viewpoint, discussing load limits and stability estimates based on large deformation assumption 17 p2632 A72-35113

Local potential concept based variational method for eigenvalue problems of disturbance damping or amplification in stability analysis 17 p2583 A72-35641

Stability of a dome rigidly clamped over its edge under uniform external pressure 17 p2635 A72-35806

Clamped flat skew plates stability under inplane stresses in terms of oblique components, calculating elastic buckling coefficients via energy method 18 p2736 A72-36931

Some properties pertaining to the stability of circulatory systems. 18 p2737 A72-37060

Elastic stability of folded plate structures of triangular cross-section. 18 p2738 A72-37073

German monograph - Finite elements according to a theory of the second order on the basis of an extended variational principle with an application to the stability and stress computation of simple symmetrical I-beams under consideration of the deformation of the cross-section 19 p2871 A72-37479

Study of the structural stability and mechanical properties of molybdenum subjected to the prolonged action of temperature and stress 19 p2818 A72-38013

Characteristics of the thermal and stressed states of cooled shell-type blades 20 p2963 A72-39911

Experimental investigation of the stability of compressed heated three-layer plates beyond the proportional limit 20 p2981 A72-39920

Applicability of the Euler approach to investigate the strain stability of anisotropic nonlinearly elastic bodies under finite subcritical strains. 21 p3116 A72-40273

On the growth kinetics of Laves phase precipitates in Fe-Ti alloys at elevated temperatures. 21 p3069 A72-41011

Elastic isotropic material mechanical and thermal constitutive equations restrictions investigation to ensure local stability under perturbations of deformation gradient and temperature field 21 p3120 A72-41203

The post-flutter oscillations of discrete symmetric structural systems with circulatory loading. 21 p3120 A72-41207

Simply supported column dynamic stability under axial periodic load, discussing external viscous damping effect 21 p3121 A72-41242

Calculating the stability of centrally compressed thin-walled bars with various profiles 21 p3126 A72-41549

Model studies of plate and shell stability 22 p3233 A72-42055

Investigation of the stability and vibrations of beams of variable rigidity by the method of bilateral estimates 22 p3234 A72-42147

Stability of elastoplastic rod under external conservative and nonconservative forces, discussing nonconservative component effect and critical load magnitude 22 p3234 A72-42149

Elastic isotropic plates stability for nonlinear stress-strain relations, noting effect of deformation tensor invariant on critical load magnitude 22 p3234 A72-42275

Structons /close-neighbor arrangements/ stability and characteristics in anhydrous borate crystals and glasses containing bridging and nonbridging or tribonded oxygens 22 p3197 A72-42795

Structural stability of anisotropic plates and structures, developing method based on data for corresponding isotropic problem 22 p3239 A72-42847

Material properties, metallurgy, production technology and operational factors effects on machinery structural strength 23 p3347 A72-43733

Gas turbine blades of cast ZhS6K heat resistant alloy, investigating structural strength from fatigue test data 23 p3347 A72-43734

Stability and vibration of transversely isotropic beams under initial stress. 23 p3350 A72-44057

Stability of orthotropic stiffened composite plates. 23 p3352 A72-44109

Liapunov method extension to dynamically loaded elastically end-restrained columns stability and frames forced vibration boundedness problems [ASCE PREPRINT 1639] 23 p3352 A72-44110

Stability of an elastoplastic rod of varying resistance to tension and compression with allowance for the initial stresses 23 p3352 A72-44162

The use of bar buckling eigenfunctions in the stability analysis of clamped skew plates. 23 p3355 A72-44456

STRUCTURAL STRAIN

Al and steel plate penetration, perforation and fragmentation under hard steel sphere impact at and above ballistic velocities, investigating velocity and strain histories 05 p0672 A72-16115

Thermoelastic characteristics and crystal phase distribution effect on microstructural stresses and thermal expansion of polycrystalline refractory materials 07 p1018 A72-20133

WC powder milling and sintering, investigating strain and dislocation density effects on behavior by scanning electron microscope 08 p1176 A72-21440

Static and dynamic analysis of legged planetary instrument landers, taking into account structural flexibility, elastic-plastic gear load characteristics and soil properties

[AIAA PAPER 72-371] 11 p1725 A72-25396
Strain work per unit time for static and dynamic pressing processes, taking into account inertial forces

13 p1966 A72-29466

Two dimensional fibrous medium model for strain and stress analysis of structural plate formed by three dimensional grid of rods

16 p2467 A72-33115

Creep in structures - Conference, Goteborg, Sweden, August 1970

16 p2411 A72-34110

Strain-rupture criteria for simple and complex loads

23 p3349 A72-43954

Life prediction of expulsion bladders through fatigue test and fold strain analysis.

24 p3455 A72-44672

Undercarriage loadings of three aircraft - Porter PC-6, Venom DH-112 and Mirage IIIS.

24 p3367 A72-44738

Thermoelastic characteristics and crystal phase distribution effect on microstructural stresses and thermal expansion of polycrystalline refractory materials

24 p3416 A72-45759

STRUCTURAL VIBRATION

NT BENDING VIBRATION

NT BREATHING VIBRATION

NT FLUTTER

NT LINEAR VIBRATION

NT MISSILE VIBRATION

NT PANEL FLUTTER

NT SELF INDUCED VIBRATION

NT SUBSONIC FLUTTER

NT SUPERSONIC FLUTTER

NT TORSIONAL VIBRATION

NT TRANSONIC FLUTTER

Perturbed vibrational motion in isotropic elastic solid, using nonlinear Truesdell equations

01 p0101 A72-10039

Finite element method for determining transient response of box-type structure to traveling sonic pressure wave

01 p0136 A72-10219

Curved beam finite elements comparison for structural vibration problems, obtaining ring natural frequencies

01 p0136 A72-10222

Direct-iterative eigensolution technique for simultaneous determination of structural system lowest frequencies and modal patterns, using reduced generalized coordinates and Stodola-Vianello method [SAE PAPER 710784]

01 p0137 A72-10275

Initial interaction phase between thin shallow conical shell vibrating axisymmetrically and ideal incompressible fluid, determining hydrodynamic pressure effects

01 p0050 A72-10574

Transient response of Al cylindrical shells to longitudinal impact, indicating wave front propagation at plate velocity

[SESA PAPER 1885] 02 p0287 A72-11505

Edge effect equations for stability, vibration and deflection of asymmetric three layer circular plate and cylindrical shell with filler

02 p0288 A72-11605

Thick orthotropic off-axis laminated plates vibration equations solution, presenting natural frequencies spectra and modal functions

02 p0249 A72-11988

Vibration and buckling analysis of doubly curved composite monocoque plates and shells of positive and negative Gaussian curvature, examining stacking sequence effect

02 p0292 A72-11990

Unpredicted structural vibration in Comet and Electra aircraft, Graf Zeppelin dirigible, missile antennas, etc

02 p0292 A72-12002

Papers on noise and vibration control covering acoustics in free space, outdoors, small enclosures and rooms, measurement, analysis and design problems

02 p0258 A72-12100

Springs fracture and vibration in injection pumps by analog model

02 p0236 A72-12437

Two finite conducting cylinders radial vibrations in E polarized electromagnetic wave, detailing pressure distribution and resonance effects

02 p0262 A72-12877

Finite element discrete model for large aspect ratio wing transverse vibrations, using inhomogeneous elements with various stiffness-length relations

03 p0442 A72-13189

Fluid filled fiber reinforced spherical shells extensional vibrations, evaluating equivalent elastic orthotropic compliance constants, natural frequencies and mode shapes

03 p0443 A72-13403

French book on thin elastic structures vibration, describing antivibrational devices and rotating machines balancing

03 p0445 A72-13682

Two dimensional boundary value problem in elasticity for rectangular prism vibrations, considering dynamic stress and frequency characteristics

03 p0449 A72-13908

Linear nongyroscopic conservative system stability from modified Lagrange equations of motion, using pseudo degree of freedom concepts and vibration method

03 p0362 A72-14394

Cracked rectangular plates vibration and stability, computing eigenvalues, natural frequencies and moment distribution

04 p0583 A72-14448

Free vibration and buckling of orthotropic skew plates with different edge conditions, using Ritz variational method

04 p0584 A72-14508

Natural vibration frequencies calculation of straight bars with stepwise variable cross sections by iterative technique based on method of three unknowns

04 p0584 A72-14522

Three dimensional analysis for free vibrations of simply supported viscoelastic rectangular plates

04 p0585 A72-14841

Rectangular plates nonlinear vibrations under combined static and vibrational loads, using Bubnov-Galerkin method on Karman type nonlinear differential equations

04 p0588 A72-15061

Fundamental frequency calculation method for bars and plates with arbitrary fixity of rotations, discussing buckling and vibration with realistic boundary conditions

04 p0591 A72-15275

Step-by-step perturbation method for calculating vibration modes of aerospace structure

[ONERA, TP NO. 968] 04 p0592 A72-15552

Natural frequencies and vibration mode shapes of simply supported symmetric trapezoidal plates

04 p0592 A72-15564

Integral equation for lowest natural frequency of vibrating beams, using eigenfunction theory

04 p0593 A72-15565

Vibration and stability of rectangular plates with mixed edge conditions, reducing dual series equations to homogeneous Fredholm integral equations [ASME PAPER 71-WA/JP-21]

05 p0733 A72-15959

Alloying, thermal and mechanical treatment effects on Mg alloys damping properties under elastic vibrations, showing test results consistency with materials microdeformation theory

05 p0671 A72-15987

Aerospace vehicle noise induced structural vibration, presenting propellers, turbojet engine exhausts and sonic boom waves

05 p0739 A72-16597

Thermoelastic effect on flutter and vibration of built up delta wings with solid, stiffened and honeycomb/corrugated sandwich skins

[AIAA PAPER 72-174] 05 p0740 A72-16834

Flexible elastic plate nonlinear vibration response and noise transmission from turbulent boundary layer by Monte Carlo technique, discussing subsonic and supersonic flow regions

[AIAA PAPER 72-199] 05 p0651 A72-16850

Coriolis force effect on axially symmetric body oscillating slowly along axis in rotating viscous fluid

05 p0610 A72-17081

Longitudinal vibrations stability of launching rocket body, allowing for propellant sloshing, body dynamic deformation and motor dynamics

05 p0731 A72-17186

Transverse vibrations stability of launching rocket body, allowing for propellant sloshing and body elastic deformation

05 p0731 A72-17187

Environment acoustic resonant frequencies effect on flat steel plate vibration under direct and air flow vortex shedding excitations

06 p0894 A72-17768

Scaling laws for vibrating beams and plates, stressing shear and rotatory inertia effects

06 p0894 A72-17769

Algorithm for selective computation of large structural modifications effect on eigenmodes of linear structure

06 p0895 A72-17848

Aerospace structures harmonic vibration tests, discussing structures natural frequency spectrum, mode isolation, eigenmodes and inertial characteristics

06 p0896 A72-17948

Dynamic matrix analysis of vibrating three dimensional frame structures, comparing discrete and continuous mass systems

06 p0897 A72-17971

Spectral properties of differential displacement equations system describing natural vibrations of shell of revolution with m waves along parallel

06 p0897 A72-17990

Test facility for vibrations damping study of structural elements in water flow based on frequency and amplitude measurement at various flow conditions

06 p0796 A72-18364

Energy dissipation of vibrating structures in complex stress state, using generalized stresses and strains as coordinates

06 p0900 A72-18677

Shallow axially symmetrical spherical shell flexural vibrations, obtaining equations iterative solution

06 p0901 A72-18705

Nonlinear solid body system rotating and oscillating parts effect on spatial vibration stability, deriving excitation-natural frequencies relationship

06 p0850 A72-18711

Mixed boundary value problem of partial differential equations describing nonlinear viscoelastic vibration of clamped rods, examining asymptotic solution stability

06 p0901 A72-18716

Random vibrations in rectangular plate clamped on opposite sides by load, determining natural oscillation frequencies by Ritz technique

06 p0901 A72-18719

Numerical approximation of Pochhammer-Chree longitudinal vibration modes in elastic cylinders by quadratic spline functions

07 p1087 A72-18797

Oscillations and acoustic emission by interacting elastic shells in connecting medium, using quadratures with Green function

07 p1034 A72-18922

Natural frequencies and vibration modes of simply supported tapered skew rhombic plates, considering thickness and skew angle effects

07 p1088 A72-19116

Aircraft design for acceptable vibration level, discussing flight vibration and runway response

07 p0928 A72-19269

Periodically supported beams acoustically induced vibration response based on equivalent structural wavelength definition

[ASA PAPER E 14] 07 p1089 A72-19330

Vibration characteristics of simply supported unsymmetric trapezoidal plates

07 p1089 A72-19644

Equivaluminal vibration modes of multipolar elastic plate with traction free faces

07 p1089 A72-19644

Hovercraft noise and vibration source and reduction for improved crew and passenger comfort

07 p0912 A72-19644

Acoustic loads effect on carrying capacity and vibration stability of longitudinally stiffened cylindrical metal panels, investigating fatigue strength and stress-strain state

07 p1091 A72-19766

Random vibrational stress and displacement spectra for linear complex mechanical dissipative systems with strong resistance and finite degrees of freedom

07 p1091 A72-19763

Free vibration determination method for thin rectangular plate with arbitrary boundary conditions and thickness variations

07 p1092 A72-19857

Energy dissipation associated with transverse vibrations of sandwich metallic samples with damping coatings

07 p1094 A72-20135

Magnetoelastic vibrations of thin conducting plate in magnetic field, solving electrodynamic equations

07 p1095 A72-20315

Symmetrically loaded uniform thin circular ring natural vibration frequencies in radial and axial flexural modes, comparing experimental data with values predicted by group theory

07 p1096 A72-20499

Pinned-free beam response to transient support excitation, using pinned-pinned beam modal parameters

07 p1096 A72-20526

External pressure effects on cantilever rotating shaft vibration, determining critical whirling speed as function of pressure and area distribution by energy method

07 p1096 A72-20528

Vibrations causes and degrees of freedom relationship in rotor machines at critical velocities, determining rotor imbalance from amplitude characteristics

08 p1243 A72-21232

Nonlinear large amplitude vibration of beams for various support conditions, using finite element matrix displacement method

08 p1245 A72-21262

Dynamic radial vibrations and stresses in thick circular annulus of nonisotropic elastic material, using Hankel transform

08 p1246 A72-21793

Orthotropic circular cylindrical elastic shell vibration mode shape analysis by Vlasov equations, using asymptotic method

08 p1247 A72-21813

Variable wall thickness influence on axisymmetric vibrations frequencies and reduced masses of cylindrical elastic shell filled with ideal incompressible fluid

08 p1247 A72-21813

Concorde sonic boom measurement, discussing structural vibrational response 08 p1111 A72-21911

Vibrations in rotating systems - Conference, London, February 1972 08 p1224 A72-22127

Vibrational characteristics dependence on structural flexibility in gimbal bearings and supporting structure of two axis free gyroscopes and single axis rate gyroscopes 08 p1173 A72-22129

Vibration modes of bladed turbine wheel, formulating mathematical model 08 p1224 A72-22132

Vibration of reciprocating engine crankshafts and steam turbine, alternator and gas turbine rotor shafts supported on hydrodynamic sleeve bearings 08 p1225 A72-22133

Frequency dependent condensation method for vibration problems in structural dynamics, presenting results for spring-mass system with six degrees of freedom 08 p1250 A72-22143

Fundamental vibrations of long circular cylinder made of micropolar elastic solid, discussing dispersion equations 09 p1398 A72-22620

Two independent damping systems impact vibration analysis from solution of equations of motion by Laplace transformation 09 p1399 A72-22695

Damping coefficient increase in welded bodies under uniform stress and compression, torsion and bending vibration 09 p1406 A72-23076

Nonlinear dynamic motion response analysis of flight vehicles typified by continuously changing vibration damping and frequency 09 p1262 A72-23452

Nonlinear vibrations of thin circular cylindrical shells under arbitrary boundary and loading conditions 09 p1407 A72-23456

Runway unevenness and landing gear characteristics effects on SST vibration during taxiing, taking off and landing 09 p1263 A72-23459

General structure steady state response under harmonic forcing in internal resonance relation, noting inertial nonlinearity effects on autoparametric interactions and energy flow 09 p1408 A72-23462

Transfer matrix method application to rocket vehicles structural dynamics, incorporating axial and aerodynamic lift forces in vibrational analysis 09 p1397 A72-23499

Vibration frequencies of slender beams and circular plates with boundary stiffness and damping [ASA PAPER E 5] 09 p1408 A72-23525

Numerical computation of bilateral bounds for arbitrary vectorial and tensorial field quantities of elastic bodies eigen vibration states, applying to thin rectangular plate 09 p1409 A72-23566

Nonlinear random radial vibration of elastic cylindrical shell under load, using stochastic linearization and correlation analysis 09 p1409 A72-23606

Long wave trains of gravitational waves from vibrating black hole, stressing hole dynamical entity 09 p1394 A72-23697

Maximum dynamic to static deflection ratio for thermally induced vibrations of elastic beams and plates, considering damping and axial load effects [ASME PAPER 71-APM-UU] 10 p1554 A72-24185

Vibration of infinite thin plate coupled with acoustic field in surrounding fluid, using Fourier transformation 10 p1511 A72-24223

Radial vibrations of isotropic homogeneous sphere and cylinder bonded to thin nonhomogeneous casting outside 10 p1557 A72-24406

Nonuniform vortex flow of compressible gas past cascade of plates, noting monochromatic pressure waves at harmonics of plate vibration frequency 10 p1418 A72-24538

Longitudinal vibrations of composite rod under concentrated impact forces at junctions between prismatic sections 10 p1557 A72-24627

Book on continuous elements dynamics covering membrane, torsional, string and elastic beam vibration, four pole techniques, periodic forced motion and surface waves 10 p1557 A72-24674

Dynamic contact problems of die or bandage on elastic layer surface or cylinder, analyzing vibrationally induced elastic waves 10 p1558 A72-24779

Gradient iterative techniques application to finite element vibration and stability analysis of skew plates 10 p1558 A72-24878

Hydrodynamic forces in sinusoidal vibrations of disk in water channel with toroidal vorticity wake pattern, applying results to flapping wing mechanics 10 p1471 A72-25129

Cylindrical shell vibrations in incompressible inviscid fluid near free interface, calculating natural frequencies with Fourier transforms 10 p1471 A72-25130

Free in-plane vibrations of hinged and fixed uniform circular arches, discussing natural frequencies and flexural and extensional vibration modes 10 p1560 A72-25186

Variational equations of motion for three layered laminated sandwich beam vibrations, assuming small elastic deformations and axial and bending motion [AIAA PAPER 72-399] 11 p1731 A72-25420

Vibration characteristics of unidirectional filamentary boron-epoxy composite panels, obtaining nodal patterns, natural frequencies and damping coefficients 11 p1732 A72-25477

Elastic body transverse impact against vibrating rectangular plate with allowance for rotatory inertia and shearing forces, using wave equation 11 p1732 A72-25532

Longitudinal and transverse vibrations and transient response of elastically coupled nonlinear mechanical system 11 p1732 A72-25534

Static loading and monoharmonic excitation influence on transverse vibrations of eccentrically prestressed metallic beam 11 p1732 A72-25535

Aerodynamic damping of turbomachine blade vibrations under varied conditions of stagger angle, pressure ratio and relative velocity, using pure bending mode excitation 11 p1568 A72-25611

Linear maximization of turbine disk natural vibration frequencies combination, solving optimal control problem via Pontryagin maximum principle 11 p1734 A72-25727

Flexural vibration of rectangular orthotropic plates with clamped, simply supported and/or free edges, presenting solution method for coupled characteristic equation pairs 11 p1735 A72-25737

Vibration of simply supported rectangular plate with unidirectional linear thickness variation, using perturbation technique for eigenvalue problem derived by Galerkin method 11 p1735 A72-25739

Matrix displacement method for nonuniform beam vibration problems, using internal nodes concept 11 p1735 A72-25740

Flight vehicle structures optimum design for random vibration environment, presenting formulation as nonlinear programming problem 11 p1736 A72-26003

Proper vibration frequencies of thin imbedded plate obtained by layer potentials method 11 p1737 A72-26477

Rayleigh problem in presence of magnetic field, discussing transpiration effects on MHD flow near oscillating flat plate 11 p1696 A72-26542

Turbine blade alloys vibrational fatigue and creep properties under high and low frequency axisymmetric loads at room and elevated temperatures 11 p1662 A72-26798

Shallow isotropic and orthotropic shells vibration, investigating dynamic rigidity for concentrated mass 12 p1878 A72-27079

Finite element method application to variable thickness circular and annular plates free transverse vibration 12 p1879 A72-27191

Approximate theory for high frequency elastic plate vibrations in terms of thickness mode expansion 12 p1881 A72-27251

Ring stiffened truncated cone shells vibration mode tests, describing air and electrodynamic shakers and mobile noncontacting displacement sensitive sensor system 12 p1882 A72-27340

Vibration of free and fluid loaded uniform or rib reinforced cylindrical shells, solving equations of motion for natural frequencies 12 p1882 A72-27341

Energy method for boundary conditions of beam vibrations under linear viscoelastic stress-strain law, deriving uniqueness, boundedness and stability theorems 12 p1885 A72-27848

Finite difference approximation and Fourier analysis to determine mechanical system eigenfrequency, studying string and membrane vibration 13 p2000 A72-28417

Finite element method for calculating vibrations of thin rectangular plate with four degrees of freedom 13 p2000 A72-28466

Compressor blade vibration indicator measurement by positioning one inductive sensor by rotor blades and another by toothed gear on rotor shaft 13 p1956 A72-28784

Shallow spherical shells axisymmetric vibrations under time varying loads, discussing transverse shear and rotatory inertia effects in terms of Fourier-Bessel series 13 p2056 A72-28880

Thermoelastic vibrations of simply supported rectangular plate produced by temperatures prescribed on faces, obtaining solution in trigonometric series form 13 p2056 A72-28888

Vibrations and plane wave propagation in laminated elastic plates and cylinders, noting finite element method for conical shells [AIAA PAPER 72-406] 13 p2056 A72-28959

Finite element method for in-plane free vibrations of shear wall type structures, noting rectangular plate elements with six degrees of freedom per node 13 p2057 A72-29092

Random vibration statistics of lifting rotors with feedback controls, solving response variance matrix by random inputs shaping filters 13 p2057 A72-29096

Oscillations and acoustic emission by interacting elastic shells in connecting medium, using quadratures with Green function 13 p2004 A72-29208

Frequency converter dynamics, considering transverse vibrations of mechanical system composed of string with centrally lumped mass 13 p1932 A72-29457

Statistical energy analysis of sound-structural interaction, considering sound transmission through complex walls and piping systems and fluid filled container vibrations 13 p2005 A72-29556

Noise and vibration control in industrial and aerospace environments, discussing materials and techniques for structural vibration damping 13 p2059 A72-29557

Sound generation by finite rectangular plate vibrations, deriving radiated power as function of aspect ratio and vibration pattern 13 p2005 A72-29564

Spectral properties of differential displacement equations system describing natural vibrations of shell of revolution with m waves along parallel 14 p1263 A72-30217

Dynamic contact problems of stamps bands oscillation on elastic layer surface or cylinder, analyzing vibrationally induced elastic waves 14 p1263 A72-30223

Gravitational stabilization systems parameters determination for minimum amplitude of satellite eccentric vibrations 14 p1262 A72-30457

Oscillations of spacecraft with on-off attitude control under constant perturbation moment, calculating energy expenditures for desired orientation maintenance 14 p1262 A72-30459

Shallow rectangular shell vibrations induced by moving band load, deriving frequency equation and load critical speed 14 p1266 A72-30688

Nonlinear equilibrium, stability and vibration equations of shallow sandwich shells with isotropic outer layer and rigid compressible filler obtained by variational method 14 p1266 A72-30700

Aileron vibration pressure measurement in plane-parallel transonic flow, evaluating damping characteristics with allowance for shock motion caused nonlinear effects 14 p2071 A72-31026

Variational principle based Pian hybrid finite element procedure for static cylindrical shell analysis extended to plate and shell vibration 14 p1269 A72-31149

Equations of motion and free vibration for trusswork structures under nonperiodic dynamic loads, calculating longitudinal and transverse end forces 15 p2322 A72-31360

Distributed parameter system approximation by system with finite freedom degrees number, solving stability and vibration of elastic shells for eigenvalue densening case 15 p2327 A72-31739

Thermal shock induced thermoelastic vibrations of rectangular plate calculated by Ritz averaging method 15 p2333 A72-32689

Speckle pattern method of laser holography for structural vibration and surface strain study, noting real time operation 16 p2388 A72-32821

First mode ultraharmonics in nonlinear beam vibration with various boundary conditions and structural properties 16 p2463 A72-32845

Vibrational frequency density analysis of thin spherical and cylindrical shells of revolution, using asymptotic integration method 16 p2464 A72-32935

Natural frequency of free beam-like vibration of coupled fluid/structural system of cylindrical rod submerged in ideal fluid enclosed by cylindrical shell 16 p2465 A72-32985

Nondestructive vibration analysis of mechanical structures, using digital computer technique for sound wave spectrum analysis 16 p2397 A72-33220

Vibrational diagnostics of operational conditions of machines for wear, design faults and efficiency evaluation 16 p2425 A72-33408

Natural frequencies and vibration modes of free glider, using symmetrical matrix to replace three dimensional structure by approximate model 16 p2348 A72-33409

Vibration analysis of cylindrical panels 17 p2623 A72-34230

Stability analysis of a pinned-end beam undergoing non-linear free vibration. 17 p2623 A72-34236

Theory of the dynamic vibration neutralizer with motion-limiting stops. [ASME PAPER 71-APMW-14] 17 p2625 A72-34317

Vibration perturbation of slender rotating beam with end masses, using method of matched asymptotic expansions [ASME PAPER 72-APM-B] 17 p2625 A72-34318

Natural bending frequency comparable to rotational frequency in rotating cantilever beam. 17 p2625 A72-34324

Transverse vibration frequencies and mode shapes of clamped or supported orthotropic plates by energy method, using Rayleigh-Ritz technique 17 p2626 A72-34327

Stability of a beam on an elastic foundation subjected to a follower force. 17 p2626 A72-34331

Helicopters vibration reduction through fuselage nodalization, discussing analysis method and dynamic scale model and full scale flight test results [AHS PREPRINT 611] 17 p2489 A72-34487

An energy technique for use in the vibration testing of complex structures. 17 p2626 A72-34720

Nonlinear vibrations of a hinged beam including nonlinear inertia effects. [ASME PAPER 72-APM-51] 17 p2627 A72-34779

Structural system response to white noise excitation, deriving integral equation for first passage time-density function via Markov process model [ASME PAPER 72-APM-11] 17 p2629 A72-34805

Contactless parameter measurements of a vibrating bar. 17 p2554 A72-35148

Nonlinear panel response from a turbulent boundary layer. 17 p2632 A72-35228

Buckling and vibration analysis for stiffened orthotropic shells of revolution. 17 p2632 A72-35242

Equation for nonlinear vibrations of shells. 17 p2633 A72-35246

A method for selection of significant terms in the assumed solution in a Rayleigh-Ritz analysis. 17 p2634 A72-35408

A comparison of approximate methods for solving non-conservative problems of elastic stability. 17 p2634 A72-35410

Structural mode vibration control system design for B-1 aircraft to improve ride during atmospheric turbulence and terrain following 17 p2493 A72-35563

Elastic vibrations in roller bearings. I - The rotating mass is balanced with respect to its own rotation axis 17 p2561 A72-35894

Bending and vibration of multilayered sandwich plates, presenting static and dynamic analysis method 17 p2635 A72-35976

Equipment vibration isolation principles, discussing damping, viscoelastic materials and shock absorbers 18 p2731 A72-35992

Vibration technology: Balancing flexible rotors; Conference, Technische Universitaet Berlin, Berlin, West Germany, March 23, 24, 1970, Summaries 18 p2731 A72-36064

Flat beam linear vibration analysis from mode measurement and moire technique, applying to prototype turbine compressor blade 18 p2734 A72-36375

Sonic boom duration effects on thin circular elastic plate transient axisymmetric vibration via Hankel and Laplace transforms 18 p2734 A72-36409

Spheroids with surface vibration at specified normal velocity distributions, calculating acoustic radiation by Green function approach 18 p2710 A72-36412

Ritz method for truncated conical shell vibrations investigation, assuming deflection expanded in exponential power series 18 p2735 A72-36694

Nonuniformly thick combined cylindrical shell vibrations, studying radial displacement, bending moment and shearing force 18 p2735 A72-36695

On axisymmetric vibration in a transversely isotropic finite cylindrical shell acted upon by a magnetic field. 18 p2711 A72-36755

The radiation of sound from vibrating composite membranes. 18 p2711 A72-36757

Higher vibration modes by matrix iteration. 18 p2736 A72-36772

Hydromagnetic boundary layer flow around an oscillating axisymmetric body. 18 p2683 A72-36932

Plate vibrations and layer potentials 18 p2736 A72-37001

Vibration of an infinite thin plate coupled with a fluid 18 p2736 A72-37002

Bounds on the extremal eigenvalues of the finite element stiffness and mass matrices and their spectral condition number. 18 p2705 A72-37202

Vibration of a stiffened ring considered as a cyclic structure. 18 p2739 A72-37205

Timoshenko finite element beam theory application to flexural vibration problems, considering shear deformation and rotary inertia effects 18 p2740 A72-37206

Experimental determination of viscoelastic characteristics 18 p2740 A72-37211

Determination of the parameters of motion of a container and its load with allowance for their interaction during internal vibrational finishing operations 19 p2824 A72-37426

Calculation of the nonlinear viscoelastic oscillations of a vibronic protective layer 19 p2872 A72-37537

Method of stationary phase for analysis of fringe functions in hologram interferometry. 19 p2796 A72-37582

Applications of holography to vibrations of segmented shells. 19 p2873 A72-37617

Use of a projected-ruling moire method for vibration and deflection measurements of three-dimensional structures. 19 p2799 A72-37629

A stand for quality control of the vibrational characteristics of 'ultraquiet' radial ball bearings 19 p2807 A72-37663

Vibrations of elastically connected ring systems. 19 p2873 A72-37692

Three-dimensional vibrations of orthotropic cylinders. 19 p2873 A72-37693

A certain generalization of the hysteresis loop contour equations to the case of an asymmetric cycle 19 p2876 A72-38003

Free vibrations of multilayer sandwich plates in the presence of in-plane loads. 19 p2876 A72-38020

A flutter optimization program for aircraft structural design. [AIAA PAPER 72-795] 19 p2876 A72-38111

Oscillations, statics and transfer matrices of composite shells of revolution contacting elastic bases, using initial parameters method 19 p2876 A72-38156

Theory for transverse vibrations of beams during elastoplastic deformations 19 p2877 A72-38179

Dynamic characteristics of composite laminates. 20 p2979 A72-39558

An advanced stochastic model for threshold crossing studies of rotor blade vibrations. 20 p2885 A72-39622

Determination of the natural frequencies of cylindrical shells of variable thickness 20 p2980 A72-39906

Vibrations of a concentrated mass on a ring coupled to a thin shell 20 p2981 A72-39908

Simulation of torsional vibrations of rods without concentrated masses 21 p3116 A72-40167

Some problems in the mathematical simulation of blade vibrations in turbomachines 21 p3116 A72-40169

A ten-inch extensometer measuring small low-frequency strains. 21 p3052 A72-40234

Stability and non-stationary vibration of columns under periodic loads. 21 p3116 A72-40336

Russian book - Mechanics of deformable one-dimensional bodies of variable length. 21 p3116 A72-40387

Application of methods in perturbation theory to the calculation of the natural vibrations of rod systems 21 p3119 A72-41097

Randomly coupled flexural and longitudinal vibrations of plates. 21 p3120 A72-41111

A new method of calculating the natural vibrations of a free aeroplane. [ICAS PAPER 72-05] 21 p3120 A72-41130

The post-flutter oscillations of discrete symmetric structural systems with circulatory loading. 21 p3120 A72-41207

Vibration of trapezoidal cantilever plates with partial root chord support. 21 p3121 A72-41225

Free vibrations of a system with a generalized piecewise-continuous characteristic 21 p3122 A72-41349

Non-stationary random vibration of non-linear structures. 21 p3125 A72-41517

Application of a method using slowly changing parameters for the approximate calculation of transverse vibrations of rods 21 p3126 A72-41550

Hydrodynamic forces acting on rigid disk and circular membrane vibrating in ideal incompressible fluid, noting dependence on phase shift between vibration modes 21 p3126 A72-41552

Satellite vibration-rotation motions studied via canonical transformations. [AIAA PAPER 72-919] 21 p3115 A72-41564

Inhomogeneous beam torsional vibration modes and frequencies calculation by initial parameters method, replacing beam by series connected oscillators 22 p3232 A72-41865

Cylindrical shells vibration under external forces with allowance for internal and external friction, obtaining harmonic influence functions in series form 22 p3233 A72-42056

Machine vibration diagnostics and damping, emphasizing filter lattice foundation structures, probability analysis and Bayes formula application 22 p3182 A72-42127

A method and equipment for the investigation of spatial vibrations in rotating reductor unit components 22 p3182 A72-42129

New methods of measuring the parameters of multidimensional vibrations of linear mechanical systems. 22 p3176 A72-42130

Viscoelastic and active vibration isolators for foundation isolation of polyharmonic vibrational effects of operating machines 22 p3182 A72-42131

Machine elements vibration parameters from dynamic model of planetary gears, noting energy spectrum, correlation and amplitude distribution functions 22 p3182 A72-42132

Electronic analyzer of structural vibration frequency characteristics and mutual spectra, considering bandpass filter and automatic frequency spectra recorder 22 p3176 A72-42134

Investigation of the stability and vibrations of beams of variable rigidity by the method of bilateral estimates 22 p3234 A72-42147

Pontryagin maximum principle for fundamental frequency variation limits of longitudinal vibrations of variable cross section rod 22 p3234 A72-42148

Chladni's patterns for random vibration of a plate. 22 p3236 A72-42758

Extensional vibration of a certain type of composite circular plate with a central hole. 22 p3240 A72-42879

Rotatory vibration of a thick spherical shell of isotropic non-homogeneous elastic material. 22 p3240 A72-42880

Torsional vibration of an orthotropic cylindrical shell. 22 p3240 A72-42881

Vibrations of circular plates of variable thickness under an inplane force. 22 p3240 A72-42908

Vibration measurements of an airplane fuselage structure. I - Turbulent boundary layer excitation. II - Jet noise excitation. 22 p3139 A72-42912

Procedures for simple resonance testing of sailplanes 22 p3139 A72-42920

Method of measuring modal characteristics of a structure subjected to a random excitation 22 p3242 A72-43095

Bearing supports elasticity effect on pendulum vibration of rigid rotating shaft with disk, noting vibrational frequencies relation to resonant frequencies 23 p3293 A72-43668

Spline transformation of independent variable for free transverse vibration of elastic bars with piecewise constant rigidity, calculating resonant frequencies 23 p3348 A72-43793

High-frequency fatigue testing facility, U-20P, with programmed control of the sample's vibration amplitude 23 p3278 A72-43970

- Free vibrations of an arbitrary structure in terms of component modes.
[ASME PAPER 72-APM-T] 23 p3350 A72-44054
Stability and vibration of transversely isotropic beams under initial stress. 23 p3350 A72-44057
- Thermomechanical coupling effects in the longitudinal oscillations of a viscoelastic cylinder. 23 p3352 A72-44122
- The vortex street in the wake of a vibrating cylinder. 23 p3281 A72-44302
- Non-linear flexural vibration of orthotropic skew plates. 23 p3355 A72-44375
- Effects of transport velocity of wake vortex on aerofoil oscillations. 23 p3249 A72-44494
- Vibration frequencies and modes determination for clamped rectangular plates of orthotropic material, using weighted residual technique and polynomial approximation 24 p3455 A72-44683
- Multi-node elements model of isoparametric thin shell vibration for turbine blade application 24 p3457 A72-44881
- Vibration of simply supported cylindrical shells with longitudinal stiffeners. 24 p3457 A72-44882
- On the use of a coordinate transformation for analysis of axisymmetric vibration of polar orthotropic annular plates. 24 p3457 A72-44883
- Buckling and lateral vibration of rectangular plates subject to inplane loads - A Ritz approach. 24 p3458 A72-44887
- Hydraulic duct transfer function determination for prediction of liquid-fuel engine space launcher LF vibrations, investigating incompressible flow rate modulation by deformable walls 24 p3392 A72-45117
- The calculation of elastic tanks partially filled with liquids for prediction of the Pogo effect 24 p3392 A72-45152
- Unsteady longitudinal viscoelastic vibrations of a rod of variable thickness at small values of time 24 p3459 A72-45265
- Aerodynamic characteristics of turbine blade cascades in unsteady incompressible and compressible fluid flow, considering axial flow turbine blades vibration 24 p3364 A72-45524
- Alloying, thermal and mechanical treatment effects on Mg alloys damping properties under elastic vibrations, showing test results consistency with materials microdeformation theory 24 p3415 A72-45729
- Energy dissipation associated with transverse vibrations of sandwich metallic samples with damping coatings 24 p3461 A72-45760
- ### STRUCTURAL WEIGHT
- Atmospheric temperature and pressure altitude effects on runway lengths and aircraft takeoff weights [ASCE PREPRINT 1242] 01 p0047 A72-10193
- Composite materials application for space shuttle structures, relating structural weight to payloads 01 p0090 A72-10727
- Composite space shuttle booster and orbiter engine support structures design and analysis, stressing weight savings 01 p0139 A72-10740
- Space shuttle oriented polyimide reinforced Ti matrix composites properties, noting weight saving 01 p0139 A72-10785
- Minimum weight web-core sandwich panels under axial compression loads, presenting numerical results for boron-epoxy and graphite-epoxy composites 01 p0142 A72-11131
- Minimum weight beams and frames calculation for random loads taking into account material carrying capacity 02 p0291 A72-11727
- Complex determinate and indeterminate structures weight minimization subject to design constraints relative to size, allowable stress, natural frequencies, etc 03 p0446 A72-13703
- Upper and lower bounds for expected value and variance of minimum material weight necessary for random resistance structure able to support assigned loads 04 p0593 A72-15648
- Gas turbine wheel design analysis, presenting procedures for estimating revolution rates, blade numbers and component configurations effects on wheel weight for prescribed stresses 05 p0735 A72-15995
- Automatic plastic minimum weight design of structural frames comparing with linear programming techniques 05 p0737 A72-16117
- Atmospheric rendezvous concept to increase space transportation system efficiency and flexibility, discussing structural weight savings [AIAA PAPER 72-134] 05 p0730 A72-16889
- Column axial load carrying capacity optimization vs structural weight, using finite element displacement method for buckling load, mode shape and strain energy density [AIAA PAPER 72-141] 05 p0740 A72-16894
- Carbon fiber laminates for helicopter components weight reduction 05 p0681 A72-16999
- Rotary wing aircraft first flight and envelope expansion at design gross weight 06 p0759 A72-18493
- Minimum weight design of elastic sandwich beam with segmentwise constant stiffness under displacement and stress constraints, using iterative solution and finite element analysis [AD-745488] 07 p1092 A72-19825
- Wing structural weight estimation for civil aircraft preliminary deriving generalized formula based on wing root bending moment for specified flight condition 09 p1262 A72-22909
- Space shuttle orbiter vehicle structural design configurations development and evaluation with respect to overall system weight and program cost [AIAA PAPER 72-373] 11 p1276 A72-25397
- Selective reinforcement with high strength boron filament to achieve cost effectiveness and weight savings for composite structures [AIAA PAPER 72-396] 11 p1731 A72-25417
- Supercritical thick wing for structural weight reduction and increased cruise speeds flight tested on Navy T2-C aircraft [SAE PAPER 720320] 11 p1576 A72-25583
- Computer calculation of minimum weight ribbed plates under axial compression by random search method and linear programming 12 p1878 A72-27083
- Structural weight optimization with piecewise concave cost functionals defined on set in Euclidean space for anisotropic cylindrical shells 12 p1881 A72-27254
- Optimal weight and load capacity of ellipsoidal cylindrical shell of revolution of constant thickness with central circular hole under uniform internal pressure 12 p1885 A72-27977
- British thin Si solar cells for large flexible lightweight arrays, considering radiation resistance, specific mass, area, contact material and antireflection coatings 12 p1756 A72-28004
- Composite materials fabrication, emphasizing high strength/stiffness to weight ratio as critical performance requirements 12 p1815 A72-28082
- Carbon-carbon composite material for high performance aircraft braking systems, noting weight savings and thermal characteristics improvements 12 p1835 A72-28093
- General Dynamics model 401 air superiority single engine fighter design stressing light weight structure and maneuverability at high speeds and angles of attack 13 p1896 A72-28575
- Optimal design of thin walled minimum weight aircraft shell structures, using linear programming 13 p2058 A72-29143
- Minimum weight elastic structure designs under dynamic loads with constraints on stress displacements and natural oscillation frequencies 13 p2062 A72-30009
- Minimum weight reliable beams and frames calculation for random loads, using one degree of freedom system to obtain closed form solution 14 p2164 A72-30237
- Computerized optimal design by nonlinear programming for minimum weight elastic plates crossed with rigid ribs for vibrational loading to meet natural frequencies condition 14 p2165 A72-30576
- Minimum weight hinged and unhinged cantilever truss design as variational problem, using dynamic programming method 14 p2166 A72-30690
- Minimum weight phase change thermal control device for planetary descent probes, discussing test over various heat loads [AIAA PAPER 72-287] 14 p2171 A72-30826
- Weight minimization for simple structures with single natural frequency constraint, solving nonlinear two point boundary value problem by variational and numerical methods 16 p2463 A72-32834
- Relationship between static pressure error /position error/ and measurable flight parameters for different aircraft weights and configurations 16 p2393 A72-33637
- Electrostatic ion thruster and hydrazine monopropellant systems for communication satellites, noting weight savings 17 p2596 A72-34265
- Weight estimation methods. 19 p2871 A72-37451
- Flow and circulation diagrams formed by events involved in optimum aircraft design configuration and structural weight selection, outlining calculation methods 19 p2748 A72-37452
- Fast method for aircraft rebalance. 19 p2748 A72-37453
- Synthesis of optimal cylindrical reinforced-plastic shells under external pressure and axial compression 19 p2872 A72-37534
- Graphite-epoxy composites application to commercial transports for weight and cost reduction 19 p2873 A72-37680
- Active controls - Changing the rules of structural design. 19 p2748 A72-37681
- Aerodynamic design and development of the Lockheed S-3A Viking. [AIAA PAPER 72-746] 19 p2751 A72-38122
- B-52 test vehicle flight demonstration program for control configured vehicles /CCV/ technology concepts validation, noting gross weight reduction [AIAA PAPER 72-747] 19 p2751 A72-38123
- Weight saving, vibration proofing and heat dissipating techniques in avionics packaging, considering B-1 bomber electronic multiplexing system example 20 p2909 A72-39768
- Selection of optimal parameters of waffle structures from the condition of minimum weight 20 p2980 A72-39905
- Calculation of rib-reinforced minimum-weight cylindrical shells under external pressure by the random search method 21 p3119 A72-41099
- Aircraft structures weight reduction through fiber-matrix composite materials, discussing anisotropic elastic and failure behavior of composite light shell structures [ICAS PAPER 72-38] 21 p3120 A72-41163
- Minimum weight design of circular plates with limited thickness. 21 p3125 A72-41515
- Influence of elastic constants on the stability margins and weight characteristics of fiberglass-reinforced shells 22 p3196 A72-41864
- Weight minimization for elastic circular plates of variable thickness under uniformly distributed load with given stress function conditions 22 p3232 A72-41896
- Cylindrical shells of optimal torsional stiffness 22 p3233 A72-42112
- Minimum weight elastic structure designs under dynamic loads with nonlinear constraints on stress displacements and natural oscillation frequencies 22 p3236 A72-42737
- The influence of production imperfections on design of optimum structures. 22 p3239 A72-42841
- Aeroelastic optimization of a panel in high Mach number supersonic flow. 23 p3343 A72-43327
- High strength bimetallic rivets produced by inertia welding Al-Ti alloy shank with pure Ti tail, noting weight and cost reduction for aerospace vehicle production [SAWE PAPER 902] 23 p2393 A72-43452
- Engine selection for specific aircraft design and mission, considering bypass and pressure ratios and turbine temperature effects on performance and weight [SAWE PAPER 910] 23 p2350 A72-43457
- Helicopter design figure of merit weight ratios definition in terms of rotor thrust coefficient, substituting pure airframe structure weight for conventionally used empty weight [SAWE PAPER 916] 23 p2350 A72-43463
- Airline operational weighing and balancing of 747 aircraft, discussing accuracy and calibration procedures for electronic load cells, mobile platform scales and onboard aircraft weighing systems [SAWE PAPER 917] 23 p2351 A72-43464
- Empty weight and cruise performance of very large subsonic jet transports. [SAWE PAPER 919] 23 p2351 A72-43466
- Moment sampling method as selfvalidating aircraft weight and balance accounting procedure [SAWE PAPER 920] 23 p2351 A72-43467
- Aerospace vehicle passive thermal protection systems heat shield and bulk insulation estimation by weight prediction in conceptual phases of design [SAWE PAPER 934] 23 p3356 A72-43474
- Aircraft hydraulic secondary power system weight estimation, presenting components loads and weights breakdown in tables and charts [SAWE PAPER 935] 23 p2352 A72-43475
- Aircraft design structural weight estimation based on post-design analysis of production aircraft, discussing weight factors application to new designs [SAWE PAPER 936] 23 p2351 A72-43476
- Minimum weight structural design, generalizing method for deriving sufficient optimality conditions with examples for specified maximum deflection and critical nonconservative loading parameters 23 p3347 A72-43719

Dynamic programming and the optimum design of rotating disks.

23 p3356 A72-44550

Boron-aluminum structural component for Shuttle.

24 p3458 A72-44890

Gas turbine wheel design analysis, presenting procedures for estimating revolution rates, blade numbers and component configurations effects on wheel weight for prescribed stresses

24 p3460 A72-45737

STRUTS

Boron-epoxy tubular struts for one third scale space shuttle booster thrust truss structure, discussing design, analysis, fabrication, weight, test and quality control

01 p0138 A72-10735

Spanwise velocity distribution effect on drag measurement of short struts in two dimensional turbulent airstreams

10 p1417 A72-23881

Second order deformation theory for axially held strut during thermal cycling at creep relaxation temperature, using galerkin method with assumed sine wave

16 p2473 A72-34124

STUDENTS

SkyLab project participation by students to stimulate interest in science and technology, giving winning experiment proposals

24 p3467 A72-45158

STUDS [STRUCTURAL MEMBERS]

Pneumatic machine for microfriction stud welding of dissimilar metals

09 p1320 A72-23631

STURM-LIOUVILLE OPERATOR

U STURM-LIOUVILLE THEORY

Sufficient criteria for MHD stability derived from lowest eigenvalue bounds of Sturm-Liouville problem.

04 p0557 A72-15168

Recursive algorithm for numerical solution of Sturm-Liouville problem with periodic boundary conditions

11 p1679 A72-26958

Eigenvalue equation, orthogonality theorem and wear eigenfunction expansion for boundary value coupling of second order Sturm-Liouville systems

15 p2262 A72-31588

Book - Riccati differential equations

17 p2577 A72-35798

Asymptotic behavior of the eigenvalues and eigenfunctions of the Sturm-Liouville operator with a complex-valued polynomial potential.

22 p3198 A72-41854

Direct methods of qualitative spectral analysis for the singular Sturm-Liouville equation with an unrestricted operator potential

23 p3308 A72-43578

STYRENE

NT POLYSTYRENE

Glass styrene acrylonitrile bead filled composites tensile behavior, discussing relationship between yield stress, filler content, strain rate and temperature

11 p1673 A72-25487

SUBCARRIER WAVES

U CARRIER WAVES

SUBCIRCUITS

U CIRCUITS

SUBCONTRACTS

Reliable component procurement for Symphonie satellite, discussing parts list, specifications and subcontract monitoring and inspection

18 p2670 A72-37124

SUBCOOLING

U SUPERCOOLING

SUBCRITICAL FLOW

Wake instabilities and vortices spacing, position and strength behind slender cylindrical bodies at large incidence with subcritical cross flow Reynolds numbers

05 p0610 A72-17010

High intensity free stream turbulence effects on flow past circular cylinder at subcritical Reynolds numbers, measuring unsteady lift and drag

11 p1573 A72-26640

Pneumatic amplifiers with controlled pressure during subcritical and supercritical flow, considering jet-resonant choke, conical and membrane systems

11 p1578 A72-26783

Incompressible laminar subcritical flow with separated wake past symmetric two dimensional bluff body, calculating upstream pressure distribution and separation point

12 p1751 A72-27172

Spanwise correlation measurement of vortex shedding behind circular cylinder in subcritical Reynolds number region

16 p2379 A72-33658

SUBDWARF STARS

Growth analysis curve of halo subdwarf Groombridge 1830 relative to sun, noting metal abundance

15 p2314 A72-32373

Discoveries on southern objective-prism plates. III - Three new hydrogen-deficient stars and a bright B-type subdwarf.

17 p2609 A72-35116

Extended horizontal branch loci.

23 p3337 A72-43830

SUBGRAVITY

U REDUCED GRAVITY

SUBGROUPS

Uniform Markov processes properties in Hilbert space, examining operator subgroups

12 p1836 A72-27071

Heisenberg antiferromagnet with noncollinear sublattices and linear dislocation, considering coupled spin wave states and density

13 p2023 A72-29910

SUBHARMONIC GENERATORS

Subharmonic oscillations excited by horizontal vibrations of mathematical pendulum suspension

07 p1036 A72-20323

Subharmonically injected phase locked microwave IMPATT oscillator

09 p1285 A72-22894

Calculation of transient processes in a capacitance parametron by the phase approximation method

23 p3312 A72-43351

SUBLATTICES

U LATTICES [MATHEMATICS]

U SUBGROUPS

SUBLAYERS

U SUBSTRATES

SUBLIMATION

Constituents, processing, fabrication and structure effects on artificial graphitic materials ablation performance in sublimation regime from high temperature tests

[ALAA PAPER 72-298] 11 p1742 A72-25235

Cylindrical diode characteristics with sublimed electrode surfaces.

17 p2527 A72-34607

Carbon and graphite sublimation in inert gas flow at 2800-3000 K, determining rate dependence on temperature under kinetic and diffusive conditions

18 p2704 A72-37186

SUBMARINES

Optimal stochastic /Kalman/ filters application to integrated air and submarine navigation systems, discussing measurement errors modeling as bias and colored noise

02 p0256 A72-12050

Incore thermionic reactor application to meet European TV broadcasting satellite and submarine and underwater laboratory power requirements

18 p2644 A72-36166

Polaris submarine-weapon system autonomous organization and management technique based on team combining Navy and civilian contractors in close working relationship

23 p3358 A72-44358

SUBMERGED BODIES

NT DIVING [UNDERWATER]

Fluid immersed body velocity fluctuations due to irregular molecular impacts

01 p0001 A72-10234

Variable volume spherical cavity motion in ideal liquid near plane surface

02 p0202 A72-11586

Trajectory and flow properties of submerged heated effluents discharging into moving waterway

[ALAA PAPER 72-79] 05 p0659 A72-16912

Thermally induced convection flow characteristics in separated or wake formation regions over heated cylindrical surface submerged in water

07 p1100 A72-19630

Forced heat convection from sphere immersed in inviscid fluid stream at small Peclet number, using matched asymptotic expansions

11 p1747 A72-26669

An integro-differential equation approach to acoustic scattering from fluid-immersed elastic bodies.

21 p3083 A72-40102

Periodic wave of oscillating and stationary two dimensional bodies immersed in uniform incompressible stream, investigating semiinfinite vortex trails relationship to oscillating airfoils

21 p2989 A72-40651

SUBMERGING

Prolonged water immersion effects on renal function and plasma volume in trained and untrained subjects, noting deleterious effect on orthostatic tolerance and work capacity

10 p1428 A72-23738

Space maintainability experiment aboard submersible during 30 day drift mission, noting application to SkyLab manpower distribution

[ALAA PAPER 72-232] 10 p1431 A72-24442

Multihour immersion effects on blood plasma protein and electrolyte concentration in trained and untrained subjects

12 p1770 A72-27480

Human spinal segment functional state before voluntary movement during water immersion, using H-reflex for spinal cord motoneuron excitability evaluation

14 p2073 A72-30255

Hemodynamic changes in man during immersion with the head above water.

17 p2507 A72-34543

Regional lung function in man during immersion with the head above water.

19 p2758 A72-38701

Pulmonary air-trapping induced by water immersion.

19 p2759 A72-38711

Comparison of the vectors of the ventricular depolarization and repolarization of man during immersion in a standing position

24 p3372 A72-44924

SUBMILLIMETER WAVES

Millimeter and submillimeter microwave spectrometric studies of high temperature plasmas and noise emission, discussing instrumentation and absolute measurements

02 p0223 A72-11405

Mm and sub mm wave generation by semiconductor devices, showing power vs frequency plots for IMPATT, Gunn and LSA oscillator diodes

02 p0268 A72-11694

Mountaintop high resolution spectral observations of diffuse isotropic submillimeter atmospheric and sky emission

02 p0274 A72-12194

Submillimeter wave stratospheric emission spectra measurement by aircraft- or balloon-borne phase modulated Fourier spectrometry, noting SNR and small errors

03 p0348 A72-13399

Point contact Josephson junctions arrangement for millimeter and submillimeter region, showing mechanical stability

04 p0561 A72-14919

Submillimeter waves - Conference, New York, March-April 1970

04 p0532 A72-15590

Submillimeter waves development, discussing materials research, lasers, semiconductor and electron tube sources, system components and applications in space communication, imagery, metrology and sensing

04 p0550 A72-15591

Millimeter and submillimeter wave applications, considering environment remote sensing, radar communication, tracking and imagery, wideband communication, plasma diagnostics and spectroscopy

04 p0550 A72-15592

Submillimeter wave sulfur dioxide molecular laser, investigating lasing lines, plasma decay and relaxation line interactions and signal temporal behavior

04 p0532 A72-15595

Submillimeter wavelength HCN laser stabilization describing AFC and phase locking

04 p0532 A72-15596

Millimeter and submillimeter wave molecular beam masers amplification principles and Doppler and collisional broadening elimination capability

04 p0532 A72-15597

Electron tube with Fabry-Perot cavity resonator with grooved and smooth mirrors for millimeter and submillimeter wave generation

04 p0503 A72-15598

Anisotropic effects use in passive semiconductor magnetoplasma for submillimeter isolators and circulators development, describing transmission devices based on Faraday rotation

04 p0563 A72-15600

Pyroelectric detector noise equivalent power limitation factors, discussing heterodyne systems and pulsed submillimeter lasers detection

04 p0551 A72-15602

Near sea level atmospheric effects on submillimeter radiation absorption in terms of dielectric coefficient theory

04 p0551 A72-15606

Atmospheric molecular and aerosol absorption effects on submillimeter radio wave propagation using laser, BWT and liquid He receiver-transmitter devices

04 p0551 A72-15607

Visible displays of millimeter and submillimeter wave images for all-weather ground surveillance, discussing image conversion

04 p0494 A72-15612

Electromagnetic radiation modulators in millimeter and submillimeter wave range using gas-discharge plasma magneto-optical effects in alternating magnetic field

05 p0625 A72-15826

Conical cavity resonator design for submillimeter wave electron beam devices, investigating mode and resonant frequency dependence on cavity size

05 p0632 A72-16364

Nb-Nb point-contact Josephson junctions response to submillimeter radiation from HCN and DCN lasers

07 p0992 A72-20551

Millimeter and submillimeter band frequency conversion in nonlinear bulk n-InSb semiconductor at liquid helium temperature

08 p1140 A72-21060

Superheterodyne radiometers for millimeter and submillimeter waves, using Mach-Zehnder interferometer frequency mixer for parasitic signal suppression

08 p1140 A72-21265

Ruby use for submillimeter range optically pumped quantum paramagnetic amplifier
08 p1183 A72-21770

Atmospheric water vapor submillimeter absorption lines in high resolution radiation transmission measurements with Froome type plasma metal junction device
10 p1472 A72-24175

High resolution observation of stratospheric submillimeter thermal emission spectrum by helium-cooled InSb electron bolometer on board Comet 2E aircraft
10 p1476 A72-25023

Submillimeter plane waves formation by quasi-optical line and diverging lens with phase front adjustment
11 p1598 A72-26719

Millimeter and submillimeter radiation produced by diffraction phenomena during charged particle passage near periodic structures, discussing physical properties and oscillator development
14 p2088 A72-30598

Difference-frequency mixing of pulsed carbon dioxide lasers with non-phase-matched GaAs for submillimeter wave generation
15 p2290 A72-31384

Submillimeter isotropic background limits of stratosphere emission spectrum, using aircraft-borne Michelson interferometer and Rollin far IR detector
15 p2265 A72-31626

Submillimeter plane monochromatic waves propagation in ground layer of turbulent atmosphere, deriving received signals levels fluctuations
15 p2195 A72-31653

Oxygen molecule parameters from frequency data in microwave, submillimeter and IR spectroscopy
15 p2283 A72-32654

Composite quasi-optical-broad waveguide transmission lines for millimeter and submillimeter waves with spectrum phase correction
18 p2664 A72-36106

A two-element telescope of high collecting efficiency for sub-millimetre astronomy.
21 p3055 A72-40825

Conceptual possibilities of studies of moisture content in the atmosphere from thermal radio emission in the submillimeter wavelength range
21 p3078 A72-41798

Electromagnetic radiation modulators in millimeter and submillimeter wave range using gas-discharge plasma magneto-optical effects in alternating magnetic field
23 p3319 A72-43434

Galactic submillimeter background radiation energy density limit, taking into account recalibrated gamma ray flux measurements agreement with cosmic ray-interstellar matter interactions
23 p3329 A72-43942

SUBMINIATURIZATION
Subminiature TV camera using hybrid packaging techniques and digital circuitry for full EIA composite video output format and 450 TV/RH resolution capability
09 p1316 A72-23599

SUBREFLECTORS
Rayleigh distance for reflection from curved surfaces in Cassegrain subreflector geometrical optics design
04 p0499 A72-15207

Conical reflector microwave antenna design including subreflector with horn feed, presenting ray and physical optics analysis for radiation patterns
07 p0957 A72-19786

SUBROUTINES
FORTRAN subroutines for plate bending and plane stress elements stiffness and geometric matrices generation, taking into account anisotropic properties and linear thickness variations
18 p2739 A72-37166

Standardized programming routine operations independent of problem and language for controlling computer program design, discussing advantages and applications
23 p3267 A72-43991

SUBSETS (MATHEMATICS)
U SET THEORY
SUBSONIC AIRCRAFT
Flight test procedures for subsonic transport aircraft pitot static pressure system, recommending trailing cone calibration method
[SAE ARP 921] 01 p0064 A72-10389

Unsolved aerodynamic problems in sub- and transonic civil and military aircraft design, considering flow problems during transonic flight, takeoff and landing
[DGLR PAPER 71-105] 02 p0153 A72-12745

U.S.S.R. high-subsonic freight transport jet aircraft IL-76 for arctic areas, Siberia and Far East, noting independence of large airports availability
03 p0310 A72-13471

Steady and oscillatory subsonic aerodynamic loads prediction based on Doublet-Lattice method and method of images, determining chord and spanwise loading on lifting surfaces
[AIAA PAPER 72-26] 05 p0607 A72-16917

NASA aerodynamic technology program, emphasizing airframe and engine development for next generation subsonic CTOL jet transport requirements
[SAE PAPER 720319] 11 p1575 A72-25582

NASA quiet engine program, discussing noise reduction technology for subsonic civil transport aircraft propulsion system
[ASME PAPER 72-GT-96] 11 p1705 A72-25667

Subsonic jet noise directivity prediction from acoustic pressure measurements
11 p1706 A72-26041

Stratospheric subsonic and supersonic aircraft emission estimation for water vapor and nitrogen oxides
13 p1991 A72-28838

Vortex-lattice method for subsonic aircraft aerodynamic coefficients calculation, verifying results with airbus lifting surface wind tunnel test data
15 p2178 A72-31401

Advanced subsonic transport technology.
19 p2748 A72-37677

Numerical study of the characteristic magnitudes of turbulence on the far sound field radiated by a subsonic jet
[ONERA, TP NO. 1058] 19 p2786 A72-37761

An exploratory study of flying qualities of very large subsonic transport aircraft in landing approach
[ICAS PAPER 72-07] 21 p2995 A72-41132

NASA Quiet Engine program R and D on conventional takeoff and landing subsonic cruise aircraft engine noise
[ICAS PAPER 72-48] 21 p3100 A72-41173

Empty weight and cruise performance of very large subsonic jet transports.
[SAWE PAPER 919] 23 p3251 A72-43466

A systems analysis of subsonic versus supersonic jet travel.
24 p3466 A72-44580

SUBSONIC FLOW
Subsonic linearized theory for symmetrical cranked wings at zero incidence, presenting corrected formulas for streamwise and spanwise perturbation velocity components due to wing thickness
01 p0001 A72-11154

Electron thermal boundary layer effects on Langmuir probe measurements in subsonic cold plasma flow
01 p0071 A72-11191

Book on pressure probe methods for wind speed and direction covering incompressible and subsonic compressible flow pressures, temperature, etc
01 p0072 A72-11273

Straight line computer solution of Chaplygin equation, with application to high subsonic gas flow incident on airfoil with local supersonic zone
02 p0149 A72-11581

Near pressure field within subsonic circular turbulent cold jet potential cone, noting peak in power spectra
02 p0150 A72-11974

Compressible gas subsonic or transonic flow in front of obstacle, determining stagnation pressure with thermal relaxation time by numerical and wind tunnel methods
02 p0151 A72-12097

Skin friction measurement in nonisobaric subsonic flow with pressure gradient over airfoil section by surface impact probes
02 p0151 A72-12275

Low subsonic region unsteady interference effects on harmonically oscillating wing-tailplane model with variable sweep wing
[DGLR PAPER 71-081] 02 p0152 A72-12709

Base pressure determination for subsonic isothermal central and peripheral jets of incompressible fluid discharging into subsonic slipstream
03 p0342 A72-13912

Mass blocking of subsonic isentropic swirling flow through convergent axisymmetric nozzle, considering radial velocity component effect on vorticity
03 p0342 A72-13957

Flow calculations for subsonic and transonic portions of ring nozzles and plane curvilinear channels
05 p0601 A72-16226

Thin wing harmonic oscillation in subsonic flow, developing analytical form of kernel function in generalized Possio integral equation
05 p0603 A72-16707

Computerized analytical model of two dimensional multicomponent airfoil in viscous subsonic flow
[AIAA PAPER 72-2] 05 p0606 A72-16861

Mean velocity and turbulent fluctuation distributions for sub- and supersonic jets in convergent nozzles, obtaining sound power spectra
[AIAA PAPER 72-157] 05 p0651 A72-16872

Stator blade design to shield turbofan from pressure disturbances arising in downstream subsonic duct
[AIAA PAPER 72-84] 05 p0707 A72-16883

Subsonic and transonic compressible potential flow over nonlifting hovering helicopter rotor blades, calculating flow field by three-dimensional nonlinear relaxation scheme
[AIAA PAPER 72-39] 05 p0607 A72-16901

Subsonic oscillating surface theory for wings with partial span controls, noting computer program rapidity
[AIAA PAPER 72-61] 05 p0608 A72-16931

Steady subsonic potential gas flow in multiply connected regions, determining velocity field via boundary value problem solution for quasi-linear elliptic equations set
06 p0801 A72-18123

Cascading turbomachine blades vibration measurement in subsonic and sonic high temperature gas flows, describing test facility
06 p0797 A72-18689

Subsonic three dimensional potential flow computational method lifting aerodynamic configurations analysis and design
[AIAA PAPER 72-188] 07 p0907 A72-18958

Two dimensional subsonic flow behind symmetrical blade cascade, taking into account initial flow turbulence
07 p0909 A72-20078

Interference induced unsteady aerodynamic forces on tandem airfoils in subsonic flow, using two dimensional model
07 p0910 A72-20101

Durando model overprediction of deflected jet vortex strength in subsonic cross flow
08 p1151 A72-21631

Sound refraction by sinusoidal point source in subsonic jet flow, obtaining solution by finite difference method for comparison with ray tracing results
08 p1152 A72-21894

Supersonic and subsonic jet flows coexistence in constant section duct, analyzing pressure on walls and in fluid and schlieren visualization
[ONERA, TP NO. 976] 09 p1294 A72-22813

Mixed subsonic-supersonic flows solution for choked isentropic flow in convergent-divergent nozzle, comparing results with series solution
10 p1561 A72-23721

German monograph on gas dynamic properties of turbulent subsonic compressible flow of ideal gas at insulator walls in MHD generator
10 p1517 A72-23771

Pressure recovery calculation for subsonic adiabatic air flow through diffusers with tail pipes, assuming turbulent inlet boundary layer
10 p1415 A72-23855

Numerical prediction of subsonic and supersonic flow through convergent-divergent nozzle
10 p1416 A72-23874

Iron rotational hysteresis effect in cold magnetic balance wind tunnel system for spinning aircraft configurations and subsonic flow regimes
10 p1462 A72-24776

Subsonic unsteady aerodynamic pressures on blades of compressor wheel rotating freely in air stream
[ONERA, TP NO. 1077] 10 p1420 A72-24854

Hodograph method involving conformal mapping for turbomachine blade subsonic flow profile calculation
[ASME PAPER 72-GT-41] 11 p1570 A72-25635

Subsonic and supersonic flow around nonaxisymmetric fuselages, deriving streamlines differential equations based on camber line distribution of source, dipole and quadrupole singularities
[DFVLR-SONDDR-189] 11 p1573 A72-26578

Nonstationary interaction flow field between subsonic and composite jet on flat plate with vortex formation and reverse currents, using finite difference technique
12 p1799 A72-28168

Vorticity and energy transfer equations for subsonic jet impingement on flat plate, noting turbulent jet effect on friction factor
12 p1799 A72-28171

Wind tunnel investigation of pressure perturbations on plane surface due to gas jet injected from surface into subsonic air drift flow
13 p1894 A72-29637

Subsonic flow in separation zones of three dimensional turbulent boundary layer forming in front of cylindrical projections, rectangular parallelepipeds and shields
13 p1895 A72-29881

Unstable discharge regime of nonisothermal axisymmetric subsonic turbulent jet in acoustic field with local perturbations
13 p1943 A72-29883

Stream surfaces of three dimensional sub and supersonic irrotational gas flows in variable cross section channels and nozzles
13 p1895 A72-30004

Turbulent boundary layer separation zone subsonic flow before two dimensional rectangular step, examining flow pattern and static pressure distribution
14 p2096 A72-31020

Convective heat transfer of sphere in rarefied gas subsonic flow, comparing calculation with measurement
14 p2071 A72-31023

Air and carbon dioxide intensive injection effects on turbulent boundary layer of subsonic channel air flow
14 p2097 A72-31159

Axisymmetric convergent cone profile synthesis to transform parallel flow at inlet to uniform sonic flow at outlet, examining solution convergence

15 p2177 A72-31206

Local subsonic flow region in transonic free flow past airfoil profile, transforming flow differential equations into linear Beltrami equations system via Chaplygin transformation

15 p2178 A72-31473

Subsonic and supersonic steady two dimensional compressible turbulent boundary layer flow past wavy wall, presenting wall pressure and temperature distributions

16 p2341 A72-32828

Inverse Laval problem of three dimensional subsonic and supersonic flows in nozzles and ducts of variable cross section in terms of asymptotic series

16 p2342 A72-32930

Direct integral method to calculate subsonic and supersonic regions in planar and axisymmetric hyper-sonic flow, using stream function for velocity and density

[DFVLR-SONDDR-202] 16 p2343 A72-33421

Subsonic, transonic, and supersonic nozzle flow by the inverse technique.

17 p2483 A72-34206

A new theoretical model for representing jet penetration into a subsonic stream

17 p2538 A72-34888

Acoustic power spectrum of a subsonic jet

17 p2541 A72-35544

Expansion solution for subsonic compressible flow.

18 p2679 A72-36124

Near flow field and aerodynamic loading in subsonic and supersonic flow over body-wing configuration, surveying numerical, kernel function and image methods

18 p2641 A72-36390

Measurement of pressure fluctuations within subsonic turbulent jets.

18 p2681 A72-36575

Jet aircraft noise sources in subsonic and supersonic exhaust mixing process, suppressing noise via turbofan exhaust speed reduction

19 p2849 A72-38380

Downwash distribution at surface of rectangular planform wings with prescribed subsonic aerodynamic loading for various aspect ratios

19 p2747 A72-38809

Evaluation of the downwash integral for rectangular planforms by the BAC subsonic lifting-surface method.

19 p2747 A72-38810

Space correlations of the fluctuating pressure in subsonic turbulent jets.

20 p2913 A72-39555

The effect of entrance configuration on local heat-transfer coefficients in subsonic diffusers.

[ASME PAPER 72-HT-34] 20 p2986 A72-39670

Experimental study of heat transfer in a subsonic jet impinging normally on a plane baffle.

21 p3128 A72-40949

Two-dimensional subsonic linearized theory of the unsteady flow through a blade-row with small steady pitch and camber angle.

[ICAS PAPER 72-12] 21 p2990 A72-41137

The characteristics of a cylindrical probe at high subsonic speeds. I - The case of zero inclination angle.

22 p3135 A72-42484

Stream surfaces of three dimensional sub and supersonic irrotational gas flows in variable cross section channels and nozzles

22 p3135 A72-42727

Calculation of a profile or of a cascade of profiles for a velocity distribution given as a function of potential

22 p3136 A72-43096

Analysis and correlation of data on pressure fluctuations in separated flow.

23 p3247 A72-43331

Modified Newton-Kantorovich variational method for calculating flows in subsonic and transonic portions of circular nozzles, noting savings in computer time

23 p3248 A72-43659

Pressure at the trailing edge and losses in turbine bladings with air injection into the blade wake

23 p3248 A72-43661

Problems of interference between oscillating surfaces in subsonic flow

23 p3248 A72-43809

Extension of the Prandtl-Glauert similarity rule to loss including cascade flow.

24 p3363 A72-45352

Some experiences with the solution of potential flow in the plane cascade on the computer.

24 p3393 A72-45365

Iterative methods for the aerodynamic calculation of thin wings in a subsonic flow

24 p3363 A72-45378

Pressure, temperature, current density, and potential difference fluctuations in subsonic flow of combustion products plasma, noting steadiness, ergodicity and distribution functions

24 p3429 A72-45502

SUBSONIC FLUTTER

Dynamic aspects of Fokker F-28 aircraft design.

22 p3138 A72-42831

SUBSONIC SPEED

High subsonic velocity aerodynamics boundary problem, transforming compressible flow to incompressible

03 p0307 A72-13238

Propulsion twin spool power plant design and dimensioning with selective high pressure cut-off for supersonic aircraft with part of flight in subsonic range [DFVLR-SONDDR-169]

03 p0406 A72-13608

Cross flow effect on lifting fan noise at subsonic blade tip speeds, analyzing radiation pattern change due to inlet flow distortion

[AIAA PAPER 72-128] 05 p0608 A72-16921

Compressible boundary layer stability at subsonic speeds, using orthogonalization calculation method

09 p1293 A72-22409

Photoelastic studies of plane stress fields in plate induced by moving loads at subsonic, transonic and supersonic speeds

10 p1553 A72-23746

Subsonic powered nacelle wind tunnel model for investigation of geometric variables effect on pressure drag

[ASME PAPER 72-GT-14] 11 p1568 A72-25613

Propulsion system design for military VTOL aircraft, emphasizing subsonic cruise to maximum thrust ratio and exhaust downwash characteristics

[ASME PAPER 72-GT-73] 11 p1704 A72-25655

Fluid jets formation in collisions between metal plates for large angles at subsonic velocities

13 p1963 A72-28771

Data correlation of jet noise total sound power and peak sideline overall sound pressure level for subsonic and supersonic convergent exhaust nozzles

[AIAA PAPER 72-643] 16 p2381 A72-34089

Variable sweep wings aerodynamic characteristics in subsonic, transonic and supersonic flight, considering lift, drag, stability and control

18 p2643 A72-36976

Shock front radius of subsonic radiation front driven by plasma fireball during final stages of decaying laser spark

20 p2934 A72-39844

Fluid jets formation region in subsonic collisions between metal plates at large angles

21 p3059 A72-40262

SUBSONIC WIND TUNNELS

Two dimensional wedge shaped body base heat transfer to separated nonreattaching flow region in subsonic wind tunnel

[ASME PAPER 71-HT-D] 02 p0152 A72-12314

Subsonic wind tunnel investigation of aircraft wake far field structure, measuring trailing vortex decay by yawhead pressure probe

[AIAA PAPER 72-40] 05 p0607 A72-16902

Homogeneous compressible turbulence field with large amplitude and density fluctuations generated in subsonic wind tunnel by rapid mixing of hot and cold air streams

[AIAA PAPER 72-119] 05 p0652 A72-16980

Temperature distribution and heat transfer coefficients in turbulent separated flow region downstream of rearward step in subsonic wind tunnel, using Mach-Zehnder interferometer

15 p2333 A72-31204

Subsonic wind tunnel for pulsed flows with speed modulation as periodic function of time

16 p2372 A72-32898

A new method for the evaluation of slotted wind tunnel interference parameters applicable to subsonic oscillatory tests.

21 p3043 A72-41642

SUBSTITUTES

Substitutional-interstitial interactions in bcc alloys.

18 p2699 A72-36396

SUBSTITUTION

U SUBSTITUTES

SUBSTRATES

GaAs, Si and alumina performance as substrates in integrated microwave circuits

01 p0046 A72-10700

Si MOSFET substrate resistivity effect on surface state noise spectra

06 p0783 A72-17609

Thin film materials and fabrication methods, discussing substrate requirements, surface properties, chemical stability, thermal conductivity and preparation of various resistors and capacitors

06 p0790 A72-18572

Cartridge system for substrate heating to 500 C in vacuum chamber during metals or semiconductor vapor deposition, describing carbon block-high intensity quartz lamp assembly

07 p0984 A72-19325

Reactivity evaporated titanium nitride resistors for thin film microcircuits, discussing nitrogen gas pressure and substrate temperature effects on electrical properties during evaporation

09 p1286 A72-22902

Microstrip propagation and loss filling factor design formulas for magnetic substrates

11 p1599 A72-26991

Chemical vapor deposition of boron on carbon monofilament substrate to eliminate fracture and boron damage and achieve good strength

12 p1834 A72-28085

Single crystal disk substrate design with electron bombardment heating for LEED and Auger electron spectroscopy studies in ultrahigh vacuum

17 p2553 A72-34642

Thermal analysis of high performance devices mounted on dielectric substrates.

17 p2527 A72-34677

Controlled self heating effect in semiconducting barium titanate positive temperature coefficient resistor substrate heater for planar Si devices

17 p2527 A72-34680

Substrate utilization and glycolysis in the heart.

17 p2501 A72-34977

Production of prototype hybrid micro-electronic modules using thin film substrates.

20 p2908 A72-39493

The relationship between the thick film conductor and substrate and its influence on conductor properties.

20 p2908 A72-39494

A comparison of manufacturing techniques for hybrid microwave circuits.

20 p2908 A72-39496

The computation of dynamic equilibrium temperature distributions on substrates having a temperature-dependent thermal conductivity.

20 p2908 A72-39499

SUBTRACTION

Real time analog video magnetogram, describing differential photometer for electronic subtraction technique

03 p0357 A72-13286

SUBTRACTORS

U ADDING CIRCUITS

SUBTROPICAL REGIONS

U TEMPERATE REGIONS

U TROPICAL REGIONS

SUBZERO TEMPERATURE

Peripheral thermoregulation in arctic canines, showing subzero bath-immersed foot temperature maintenance above tissue freezing point

08 p1120 A72-22019

SUCCINIMIDES

Zinc dithiophosphate and bisphenol effects on surface activation of additive compositions with succinimide base in lubricant applications

07 p1023 A72-19903

SUCROSE

Influence of hyperosmolality on left ventricular stiffness.

17 p2499 A72-34727

SUCTION

Two dimensional unsteady incompressible boundary layer near forward stagnation point of infinite plane wall with uniform suction or injection, obtaining iterative solution

01 p0050 A72-11106

Velocity profiles of turbulent boundary layers with injection or suction through porous walls as function of momentum thickness by Truckenbrodt method

02 p2022 A72-11663

Incompressible boundary layer theory development: to include second order curvature effects, determining suction velocity to maintain constant displacement thickness on sphere

02 p0204 A72-12104

Two dimensional viscoelastic fluid flow past infinite plate with time dependent suction and constant and periodic free stream velocity

03 p0341 A72-13630

Boundary layer suction intensity and slot location effects on performance of curvilinear annular diffuser for various Mach and Reynolds numbers

03 p0308 A72-13736

Velocity and shear stress in laminar boundary layer flow on flat plate with narrow suction slot

04 p0461 A72-14461

Free convection flow along infinite vertical flat plate under periodically varying suction and with fluctuating plate temperature, analyzing mean velocity and temperature profiles

05 p0747 A72-16668

Laminar-turbulent incompressible boundary layer transition prevention by suction slots on bodies of revolution, determining optimal suction power/slot distance conditions by variational methods

07 p0968 A72-19737

Laminar boundary layer instability to longitudinal vortices onset due to homogeneous suction from slightly concave permeable wall, determining Goertler parameter and wavenumber critical values

10 p1470 A72-25064

Uniform suction effect at stationary plate on longitudinal and transverse velocities of plane Couette flow between parallel plates

13 p1941 A72-28884

Navier-Stokes equation for rotating liquid axial flow past porous plate, noting velocity distribution for suction and thinning effect for blowing

13 p1942 A72-29127

Steady asymptotic suction profiles in free convection laminar boundary layer flows on heated vertical circular cylinder 14 p2096 A72-31070

Navier-Stokes equation for unsteady asymptotic suction flow over flat plate, plotting velocity distribution profiles 15 p2178 A72-31406

Blowing and suction effects on free convection boundary layer on semiinfinite vertical flat plate, taking into account temperature difference between plate and fluid 16 p2477 A72-33429

Blowing and suction effects on heat transfer and friction coefficients of transpired turbulent boundary layer, presenting theoretical models and experimental results 16 p2378 A72-33431

Lateral pressure gradient and suction effects on laminar incompressible boundary layer separation on curved surfaces predicted by generalized tow-layer flow model [AIAA PAPER 72-698] 16 p2380 A72-34045

Viscous dissipation effects on unsteady free convective flow past an infinite, vertical porous plate with constant suction. 17 p2637 A72-35047

Flow over infinite wedge with mass transfer by boundary suction or injection, solving nonlinear boundary layer equations by parametric differentiation method 17 p2485 A72-35230

Self-similar separation flows in a laminar magnetohydrodynamic boundary layer during injection and suction 18 p2716 A72-36886

On the steady flow between a rotating and a stationary disk with a uniform suction at the stationary disk. 18 p2683 A72-36994

Heat transfer at reattachment of a compressible flow over a backward facing step with a suction slot. 20 p2885 A72-39626

An asymptotic solution for steady flow above an infinite rotating disc with suction. 20 p2886 A72-40015

Experimental friction factors for turbulent flow with suction in a porous tube. 21 p3047 A72-41618

Magnetic field and suction effects on unsteady MHD free convection flow of conductive fluid around nonconductive porous flat plate 21 p3095 A72-41787

Rectangular wind tunnel study of suction effect on velocity profiles and characteristics of turbulent boundary layer 24 p3390 A72-45005

Velocity profiles of plane turbulent flow of incompressible fluid on porous surface in presence of suction 24 p3390 A72-45007

Vortex control on an inclined body of revolution. 24 p3362 A72-45335

SUD AVIATION AIRCRAFT
NT CONCORDE AIRCRAFT
SUDDEN ENHANCEMENT OF ATMOSPHERICS
Sudden enhancement and decrease of elf atmospherics, investigating diurnal variations for frequencies 03 p0321 A72-13090

Observation of very-low-frequency whistler-mode waves in the region of the radiation-belt slot. 17 p2517 A72-35598

SUDDEN IONOSPHERIC DISTURBANCES
Magnetospheric substorm model for auroral activity sudden increase and ionospheric current development explanation by shock wave excitation in magnetospheric tail neutral layer 02 p0217 A72-11927

Solar flare EUV flashes from sudden ionospheric frequency deviation observations 03 p0407 A72-12946

Ionospheric effects of X ray flare on 8 July 1968, estimating ionizing radiation spectral characteristics from SID observation 03 p0407 A72-12986

Statistical analysis of low latitude F 2 layer disturbances associated with sudden commencement type geomagnetic storms, investigating critical frequencies 04 p0516 A72-14937

Sudden ionospheric disturbance occurrence probability with solar X-ray flares, noting relaxation time 06 p0874 A72-18086

Ionospheric effects of solar flares, considering flare spectrum below 10 A, flare X-rays relationship to sudden ionospheric disturbances and electron density profiles 06 p0874 A72-18087

Ionospheric effects of solar flares, relating sudden ionospheric disturbances with solar X-rays, radio bursts, H alpha emissions and cosmic rays 07 p1062 A72-20037

Sudden ionospheric perturbation effect on D region vertical distribution profiles, finding sixfold electron concentration increase at 75-80 km 08 p1154 A72-20729

Ionospheric disturbances and prediction dependence on solar and geophysical activities, discussing SID, pca, auroral absorption and F 2 region 11 p1623 A72-26267

SID coincident with solar photon burst, showing vertical variations of electron concentration 11 p1713 A72-26269

Magnetospheric substorm model for auroral activity sudden increase and ionospheric current development explanation by shock wave excitation in magnetospheric tail neutral layer 13 p1948 A72-29239

Experimental evidences for a transient ion layer formation in connection with sudden ionospheric disturbances in the height range 20-50 km. 17 p2545 A72-34630

Correlation of solar radio bursts and sudden increases of the total electron content /SITEC/ of the ionosphere. 17 p2598 A72-34698

Sudden ionospheric disturbance effect on D region vertical distribution profiles, finding sixfold electron concentration increase at 75-80 km 19 p2791 A72-38357

Ionospheric D region, a sensitive detector of hard X-rays of solar subflares. 19 p2852 A72-38628

Satellite measurements of solar X-ray flux and their use for interpretation of sudden ionospheric disturbances. 22 p3219 A72-42884

The effective recombination coefficient in the ionospheric D region 23 p3283 A72-43364

Quadruple conjugate pair observations of the sudden commencement absorption event on June 17, 1965. 23 p3286 A72-44526

Preconditions for the triggering of polar magnetic substorms by storm sudden commencements. 23 p3286 A72-44531

SUGARS
NT GLUCOSE
NT SUCROSE
Cyanogen induced phosphorylation of sugars in aqueous solution, discussing system prebiotic plausibility 04 p0483 A72-14771

SUITS
NT PRESSURE SUITS
NT SPACE SUITS
Water cooled suits efficiency and effectiveness for heat removal, noting importance of head area 14 p2081 A72-31085

SULFATES
NT AMMONIUM SULFATES
Formation mechanism of sodium sulfate from gas turbine fuel combustion, discussing thermodynamic equilibria and reaction kinetics 15 p2297 A72-31294

The role of Sm and Mn as activators in calcium sulphate and lithium tetraborate. 18 p2718 A72-36347

SULFATION
Sequential sulfidation and oxidation effects on sulfur self propagation in Ni-Cr alloy 05 p0677 A72-17110

Thermodynamics of ceramic oxide corrosion by sulphur and oxygen bearing atmospheres, considering formation products and furnace refractory materials choice 09 p1333 A72-22377

Chemical composition, powder particle size, porosity and heat treatment effects on sulfurized iron graphite cermets durability 13 p1984 A72-30118

Lunar pentlandite and sulfidization reactions in microbreccia 14315,9. 18 p2729 A72-36973

Interaction between vanadium in gas turbine fuels and sulfidation attack. 19 p2817 A72-37766

SULFIDES
NT CADMIUM SULFIDES
NT CARBON DISULFIDE
NT COPPER SULFIDES
NT DISULFIDES
NT HYDROGEN SULFIDE
NT LEAD SULFIDES
NT MOLYBDENUM DISULFIDES
NT POLYSULFIDES
NT TROILITE
NT WURTZITE
NT ZINC SULFIDES
NT ZINCBLLENDE
Intercalation complexes of Lewis bases and layered tantalum and niobium disulfide superconductors, noting critical temperatures 01 p0113 A72-10018

Titaniums sulfide initiation of pitting corrosion of Ti stabilized corrosion resistant Cr-Ni-Ti steels 03 p0379 A72-14367

Ni corrosion by hydrogen sulfide, determining nickel sulfide scale chemical composition and crystallographic orientation by electron and X ray diffraction 06 p0828 A72-17606

Hopping electroconductivity of n-type GaS single crystals, observing frequency dependence 06 p0866 A72-18181

Lubricating mixtures of mineral oil with inorganic phosphates, hydroxides and sulfides, discussing lubrication mechanism and physical properties 06 p0837 A72-18603

IR emission of oxygen reaction with carbon oxysulfide, investigating molecular vibrational transitions 10 p1510 A72-24133

Stainless steels sensitivity to pitting corrosion under sulfides action, measuring rupture potential 11 p1661 A72-26648

Thermal stability of sulphides of some metals in iron-base cermets 23 p3298 A72-43285

Temperature and polarization dependence of arsenic sulfide single crystals and thin films intrinsic absorption edge, determining forbidden bandwidth and transitions types 23 p3324 A72-43688

SULFUR
NT SULFUR ISOTOPES
Fe-S segregation role in early chemical and physical history, giving model of early lunar differentiation 03 p0439 A72-14274

Sequential sulfidation and oxidation effects on sulfur self propagation in Ni-Cr alloy 05 p0677 A72-17110

JP-5 fuel sulfur content effect on aircraft engine turbine blades hot corrosion under marine environmental conditions 07 p1010 A72-18752

Dielectric sulfur activated liquids for high productivity electroerosion machining of steels and metallic carbides, comparing with petroleum 08 p1174 A72-21034

Ti-Ce-S alloys phase equilibria with isothermal cross section, discussing eutectic alloys anomalous structure and cerium monosulfide preparation method 08 p1187 A72-21784

Graphite morphology in metallic materials from scanning electron micrographs, discussing sulfur contents effect in tempered cast iron 10 p1500 A72-23825

Sulfur alloyed CdTe single crystals IR absorption spectrum, noting temperature effects 13 p2023 A72-29918

The kinetics of the reaction between oxygen and sulfur on a Ni/111/ surface. 24 p3378 A72-44951

SULFUR CHLORIDES
Fluorescence and absorption spectra from oxygen sulfur dichloride photodissociation in vacuum UV, discussing So formation 11 p1590 A72-26012

SULFUR COMPOUNDS
NT AMMONIUM SULFATES
NT CADMIUM SULFIDES
NT CARBON DISULFIDE
NT COPPER SULFIDES
NT DISULFIDES
NT HYDROGEN SULFIDE
NT LEAD SULFIDES
NT MOLYBDENUM DISULFIDES
NT POLYSULFIDES
NT SULFATES
NT SULFIDES
NT SULFUR CHLORIDES
NT SULFUR FLUORIDES
NT SULFUR OXIDES
NT SULFURIC ACID
NT TROILITE
NT WURTZITE
NT ZINC SULFIDES
NT ZINCBLLENDE
Lubricating action of sulfur-containing additives and chlorine compounds in lubricants and cermet materials, noting effects of iron compounds formation in contact region 07 p0996 A72-19967

Dielectric dispersion in SrS1 filamentary single crystals as function of Curie temperature in lf and shf range 09 p1367 A72-22422

Flame photometric detection of small concentrations of sulfur compounds in ambient air, describing spectrum scanning detector, rotating interference filter and correlation detector 10 p1480 A72-24101

Ni plating by chemical reduction method in boron hydride solution, deducing stabilizing effect of sulfur compounds and Pb salts from catalyst poisoning theory 11 p1641 A72-26265

Antioxidative and antiwear action of S-containing and S-free phosphoric acid ester additives in lubricating oils

12 p1835 A72-28201

Osarsite, a new osmium-ruthenium sulfarsenide from California.

22 p3172 A72-42450

SULFUR FLUORIDES

Airborne gas chromatograph for real time diffusion analyses, describing flight test results with sulfur hexafluoride plumes

09 p1307 A72-22451

Cardiorespiratory response to breathing dense sulfur fluoride-oxygen mixture under physical exercise conditions

12 p1767 A72-28314

Hypersonic sound attenuation and velocity dispersion in sulfur fluoride near critical point determined by light scattering measurement

16 p2422 A72-32946

SULFUR ISOTOPES

Apollo 12 lunar rocks and fines sulfur concentrations and isotope ratios measurement

10 p1538 A72-24168

SULFUR OXIDES

Remote sensing of regional vertical air column pollutants, discussing sulfur dioxide and nitrogen dioxide measurements by correlation spectrometer [AIAA PAPER 71-1060]

01 p0057 A72-10529

Submillimeter wave sulfur dioxide molecular laser, investigating lasing lines, plasma decay and relaxation, line interactions and signal temporal behavior

04 p0532 A72-15595

Population inversion production in sulfur dioxide molecular laser

06 p0827 A72-18459

Sulfur dioxide and carbon dioxide interaction with clean silver surface at ultrahigh vacuum, using Auger electron spectroscopy and work function measurement

13 p1912 A72-28684

Carbon dioxide power laser effects on IR spectra of HCl-ethylene and sulfur dioxide-ethylene mixtures, focusing with Ge lens

13 p1971 A72-29870

Oscillator strength for sulfur monoxide transition band systems calculated from radiative lifetime with Franck-Condon factors

20 p2966 A72-38916

SULFURIC ACID

Heat treatment effect on elastic properties of steel clad material for devices in sulfuric acid, discussing structural changes and optimal conditions

07 p1020 A72-20415

SUMMARIES

NT ABSTRACTS

SUMMER

Shielding and semitransparent sporadic E layer fine structure characteristics from summer observations data analysis

02 p0222 A72-12523

Tropical east-west atmospheric circulation geometrical, thermal and intensity characteristics during northern summer

03 p0384 A72-14143

Latitudinal distribution of electron temperature in F 2 layer during summer daytime period of low solar activity from electron density profile geometrical parameters

05 p0656 A72-16248

Tropical upper tropospheric motion field during Northern Hemisphere summer, computing energy exchange between zonal flow and eddies

06 p0842 A72-18437

Quarter thickness variation and particle temperature dependence on height and frequency in summer daytime F region

08 p1155 A72-20815

Sporadic E layer critical frequency relationship to ionospheric wind direction for midlatitudes in summer period

10 p1472 A72-24079

Slant path radar attenuation events due to rain during summers at 10 GHz, obtaining statistics on frequency of occurrence, extent in azimuth and duration

15 p2200 A72-32103

Summer upper mesosphere and lower thermosphere positive ion composition at high latitudes from Nike Cajon rocket soundings

16 p2383 A72-32966

A diagnostic study of the vorticity balance at 200 mb in the tropics during the Northern summer.

22 p3201 A72-42507

Noctilucent clouds in daytime - Circumpolar particulate layers near the summer mesopause.

22 p3173 A72-42515

SUMS

Summability and absolute convergence of Fourier series in large, proving theorems on boundedness of trigonometric polynomials integral norms sequence

03 p0382 A72-13947

Infinite series summation in terms of rapidly convergent definite integrals

05 p0682 A72-15808

Best approximation estimates for function of many variables by sums of two functions of smaller number of variables

08 p1199 A72-21299

Convergence of random number sums of independent infinitesimal multidimensional stochastic step processes to generalized Poisson processes

09 p1340 A72-22423

An algorithm in arithmetic with a floating point to increase the accuracy of a sum

17 p2575 A72-34906

Necessary and sufficient conditions for space linear operator factorization, noting summation operators theory

18 p2704 A72-36462

SUN

Radio observations of filaments in absorption against solar disk during 11 September 1969 and 7 March 1970 eclipses

03 p0415 A72-12939

K3-M2 dwarf space motions in solar neighborhood analyzed for sun motion

07 p1073 A72-19347

Precessional corrections, solar motion and galactic rotation determination from proper motions by maximum likelihood method, taking into account stars visual magnitude

09 p1391 A72-23535

Contact time determinations during 9 May 1970 Mercury passage across solar disk

14 p2153 A72-30498

Quiet and active models for solar structure and processes in terms of elementary physical concepts

15 p2302 A72-31276

Temporal properties of Ca II K line profile in solar disk nonmagnetic regions, noting time sequences of spectrograms and spectroheliograms

15 p2317 A72-32773

Faculae and the solar oblateness.

19 p2855 A72-37240

Contact time determinations during 9 May 1970 Mercury passage across solar disk

19 p2864 A72-38327

Solar silver abundance from spectral scans for Ag 3280.7 and 3382.9 A resonance lines, using spectral synthesis method, model atmosphere and limb darkening observations

22 p3221 A72-42028

A non imaging approach to solar oblateness measurements.

22 p3222 A72-42046

Observation error in time determination of solar limb contact with optical instrument hair, noting effect on accuracy of time and longitude measurement

24 p3438 A72-44859

Application of the restricted hyperbolic three-body problem to a star-sun-comet system.

24 p3442 A72-45234

SUN SENSORS

U SOLAR SENSORS

SUNLIGHT

Multiple scattering polarization of sunlight reflected by terrestrial water clouds as function of particle shape and size, using doubling method

03 p0384 A72-14145

Jupiter and Venus cloudy atmosphere reflected sunlight circular polarization measurement, noting sense variations with phase angle and location on disk

03 p0439 A72-14150

Sunlight resonance scattering by spherically symmetric optically thick artificial Sr clouds, comparing photometric data with computed theoretical isophotes, line profiles and irradiances

09 p1297 A72-22579

Sun vicinity skylight polarization influence on polarimetric K corona observations, discussing inaccuracy sources

09 p1392 A72-23544

Solar cell calibration in uncollimated sunlight, obtaining standards for solar simulator intensity

12 p1759 A72-28042

Lunar albedo and temperature distribution from simultaneous photoelectric and far IR brightness temperature measurements of sunlit lunar surface

22 p3226 A72-42536

SUNRISE

D region ion and electron density rocket measurement during sunrise, discussing negative ion electron affinity and ion production functions

03 p0347 A72-13397

Nighttime and sunrise period ionospheric electron density profiles with respect to time after sunset and solar zenith angle

08 p1226 A72-21102

Nocturnal F region electrodynamic drift at conjugate point sunrise time, discussing dynamo electrostatic field normal component change as cause of ionosphere vertical movement

09 p1297 A72-22576

Atmospheric electricity, turbulence and pseudosunrise effect during solar eclipse, analyzing space charge density and power spectra decay

12 p1800 A72-27140

Solar activity effects on integrated ion production rates at sunrise using atmospheric model

15 p2301 A72-32266

An investigation of the ionospheric D region at sunrise. I - Time variations of ozone, metastable molecular oxygen, and atomic oxygen. II - Estimation of some photodetachment rates. III - Time variations of negative-ion and electron densities.

18 p2656 A72-36295

Possibility of estimating an energetic particle stream in the ionospheric D region at sunrise and under daytime conditions

18 p2688 A72-36858

On the source of sunrise effects in the low ionosphere.

19 p2792 A72-38627

Sunrise and sunset period of helio-geophysical processes in terms of optical, X ray, corpuscular and radio characteristics of solar activity

19 p2868 A72-38637

Solar control over the evolution of F2-layer after sunrise.

24 p3395 A72-44822

Sunrise effects on the latitudinal variations of topside ionospheric densities and scale heights.

24 p3399 A72-45552

SUNSET

Sunrise and sunset period of helio-geophysical processes in terms of optical, X ray, corpuscular and radio characteristics of solar activity

19 p2868 A72-38637

SUNSPOT CYCLE

Lindauer electron density profile for maximum F layer over sunspot cycle using frequency dependent radio ground echo in satellite ionograms

01 p0054 A72-10421

F 1 layer appearance and critical frequencies average daily variations at Tsumeb, Southwest Africa, as function of sunspot cycle phase

01 p0055 A72-10428

Sunspot cycle 1958/70 effects on D region ionospheric absorption and stratospheric temperature measured by radiosonde

03 p0345 A72-12978

Sunspot cycles effect on F region drifts and irregularities from observations at Ibadan during 1966/67, noting seasonal and diurnal variations

06 p0806 A72-17643

Thin solar convection zone relation to sunspot cycle, noting magneto-kinematical model

06 p0886 A72-18099

Sunspots penumbral and umbral areas ratio in eleven year solar activity cycle, noting larger umbras at second maximum

07 p1082 A72-20295

Geomagnetic activity annual variations from daily international magnetic character figures analysis by time series numerical filter method, discussing sunspot cycle effect

09 p1298 A72-22584

Magnetic disturbances recurrence relationship to even- and odd-numbered sunspot cycles, noting existence of 22-year solar cycle

12 p1803 A72-27773

Ionospheric absorption measurements during sunspot cycle at fixed frequencies, noting monthly and seasonal variations

12 p1804 A72-27782

Sunspot cycle 21 behavior prediction, explaining solar activity forecasting based on 80 year cycle

13 p2046 A72-29727

Cycle 20 solar flare and sunspot distribution along heliographic longitude, using isoline analysis method

14 p2152 A72-30482

Ionospheric radio waves absorption and stratosphere temperature variations with respect to season and sunspot cycles, examining 1963-5 winter anomaly

15 p2195 A72-31555

Solar activity centers characteristics cyclic variations in decreasing and increasing parts of sunspot activity cycles, discussing latitude-longitude distribution

19 p2851 A72-37906

The sunspot cycle and solar and lunar daily variations in H.

22 p3228 A72-42882

SUNSPOTS

Steady motion effect on sunspot magnetic field stability related to force-free configurations and solar flare origin

01 p0118 A72-10083

Feautrier numerical solutions to transfer equation of polarized continuum radiation from sunspot in chromosphere

01 p0101 A72-10096

Midlatitude D layer observations during sunspot minimum, emphasizing atmospheric ionization and ozonospheric parameters

01 p0055 A72-10433

Solar flares forecasting based on group total sunspot area, largest spot area and spots number observations

01 p0118 A72-10570

Topological features of force free magnetic field near bipolar sunspots, considering chromospheric fibrils and filaments in H alpha lines

03 p0415 A72-12932

Telescopic phase retardation effect on Zeeman triplet Fe of polar sunspot umbrae in Stokes parameter measurements

03 p0357 A72-13288

Magnetic splitting of lines dependence on Paschen-Back effect for Li resonance doublet in sunspots
03 p0427 A72-13293

Sunspot and active region magnetic fields and thermodynamic structure from umbral and penumbral models, discussing magnetic fine structure
03 p0427 A72-13296

Magnetic field and turbulence in sunspots, studying local variations of saturation and Doppler broadening
03 p0428 A72-13297

Fine structure of magnetic field distribution in umbra and penumbra of sunspots
03 p0428 A72-13299

Spatial distribution of total magnetic vector and of electric currents in unipolar sunspot
03 p0428 A72-13300

Magnetic field strengths from umbral spectral lines in sunspots
03 p0428 A72-13301

Sunspot magnetic field evolution in time and space from four-camera spectral scanning method, obtaining magnetic flux and radial velocity field
03 p0428 A72-13303

High energy electrons behavior and sunspot magnetic fields in solar flares, using hard X ray and microwave radio burst balloon observations
03 p0410 A72-13323

Equatorial-western shifts of flare positions related to field maximum in sunspot groups
03 p0411 A72-13329

Fine structure features of sunspot magnetic fields and umbral dots, showing magnetic and thermal or mechanical forces interaction
03 p0430 A72-13334

Solar magnetic field distribution in sunspots surface layers, considering photospheric three dimensional magnetohydrostatic model
03 p0431 A72-13337

Solar magnetic field origin in fine structure elements of photosphere and sunspots
03 p0431 A72-13340

Solar magnetic fields small scale structure with emphasis on photospheric measurements, discussing sunspots fields
03 p0437 A72-13869

Radio astronomical observation of two local sources associated with unipolar sunspot group 275 and bipolar group 282, investigating emission directivity and brightness temperature
04 p0572 A72-14636

Ionospheric radio absorption, observing diurnal and seasonal variations and sunspot numbers and solar flares effects
04 p0518 A72-14966

Solar activity asymmetry on two hemispheres in 1959-1969, considering spots, faculae, prominences and corona
05 p0718 A72-16511

Toroidal magnetic ring development and interaction with poloidal magnetic field, considering relationships to sunspots bright rings and spicules dynamics
05 p0719 A72-16512

Magneto-optical effects on circular polarization in sunspots within Fe I 6302.5 Å line
05 p0719 A72-16514

Water molecules absorption lines in sunspots umbral near IR spectrum, noting improved spectrometric apparatus
05 p0719 A72-16515

Sunspot magnetic field strength rapid variation, discussing spot group development and flare activity
05 p0722 A72-17155

Statistical analysis of sunspot activity, forecasting solar cycle events
05 p0723 A72-17176

Electron content measurement for low latitude station obtained at sunspot maximum by Syncom 3, observing seasonal variation and winter anomaly effect
06 p0874 A72-18089

Magnetic vector directions determination in sunspots by fringe technique with corrections for instrumental polarization in line spectrum
06 p0889 A72-18326

Solar photosphere active regions and large scale flow patterns from Greenwich sunspot statistics
07 p1068 A72-18886

Sunspot umbra spectrophotometric scans with spatial cancellation techniques, finding 4200 K umbral temperature with 0.60 photosphere contrast
07 p1069 A72-19081

Solar MgH isotopic abundance ratios and photospheric lines, correcting previous overestimation for sunspot spectra analyses
07 p1071 A72-19179

Type 4 solar burst spectral characteristics relationship to flare class and magnetic field configuration in spot group
07 p1077 A72-19814

Local structure of solar magnetic fields in sunspots as complexes of microspots
07 p1079 A72-20008

Solar active regions properties observation, noting correlation with magnetic field, flares, sunspots, magnetic knots, pores, umbral flashes, etc
07 p1079 A72-20009

Long term variations in height of solar activity maxima and sunspot numbers during 11 year cycle
07 p1079 A72-20016

Solar surges /plasma ejections/ relation to spot groups and flares, correlating various observational data
07 p1063 A72-20294

Solar modulation of cosmic ray intensity in stratosphere, examining relationship to sunspots group number and heliographic latitudes over 11 year period
07 p1065 A72-20641

Transverse magnetic field measurement over sunspot in chromosphere, noting fan-shaped field line divergence
08 p1232 A72-21135

Solar general magnetic field nature, origin, fine structure and temporal variations, evaluating sunspots and active plage areas as field sources
09 p1387 A72-22752

Sunspot group number and average lifetimes in solar activity cycle
09 p1390 A72-23397

Solar rotation as function of heliographic altitude from measurements of Fe and H lines, sunspots and magnetic field in photosphere
10 p1541 A72-24569

Sunspots contact region charged particles acceleration by plasma flow induced electric field, noting Fermi type mechanism
11 p1695 A72-26107

Magnetically unaffected Fe I line profiles in sunspots from high resolution photographic spectra observation
12 p1867 A72-27205

Magnetic field gradient in sunspot umbrae from magnetically split line profiles
12 p1867 A72-27206

Solar magnetic field variation during solar rotation from sunspot observations, noting similarity to magnetic stars and behavior as quadrupole magnetic rotation
12 p1871 A72-27746

Solar activity relation to geophysical phenomena, discussing atmospheric circulation and climatic variation cyclicity and sunspot corpuscular fluxes
12 p1842 A72-28207

New and old sunspot groups proper motions in large scale flow of solar photosphere investigated as function of age, noting angular momentum transport direction
13 p2036 A72-28834

Sunspots, Doppler shifts, geophysical changes and statistical evaluation of diffuse objects motion in sun, discussing solar magnetic fields and 22 year cycle
13 p2044 A72-29701

Bright point intensity distribution on CN spectroheliogram of sunspot penumbra on 4 July 1970
13 p2045 A72-29710

Umbral model effect on Li abundance determination from sunspot spectra
13 p2045 A72-29711

Sunspot energy deficit relation to model depth, deriving facular model with two dimensional radiative transfer analysis
13 p2045 A72-29712

Photographic records of sunspot umbrae showing bright penumbral filament penetration
13 p2045 A72-29713

Eighty year cycle representation deduced from yearly means of sunspot relative numbers without use of averaging or smoothing method
13 p2046 A72-29728

Crossover and magneto-optical effects of line splitting in sunspot spectra, considering instrumental circular polarization
13 p2047 A72-29738

Sunspot magnetic field depth variations model, using configuration conditioned by Schlueter-Temesvary similarity law
13 p2048 A72-29740

Alfven wave transmission in sunspot umbral magnetic flux tube, noting standing progressive waves and energy dissipation in facular regions
13 p2049 A72-29937

Sunspot formation due to magnetic flux concentration in active region and formation of invisible pores with suppressed granular motion
14 p2148 A72-30205

Cycle 20 solar flare and sunspot distribution along heliographic longitude, using isoline analysis method
14 p2152 A72-30482

Solar proton flare prediction, examining diurnal rotation of axis connecting two stable spots and change in horizontal gradient of spots magnetic field
14 p2147 A72-30649

Sunspot umbral TiO gamma system photoelectric spectra examination for less abundant stable Ti isotopes
15 p2314 A72-32372

Tabulation of diatomic molecular lines observed in sunspot spectra with rotation branch, quantum number and vibration band
15 p2316 A72-32750

Large sunspot umbra high resolution spectrogram obtained by beam splitter with monochromatic polarization optics, noting blends near Zeeman lines
15 p2317 A72-32775

Eleven year period solar photospheric magnetic field evolution, comparing latitudinal variation with sunspots, faculae and prominences distribution and green-line corona intensity
15 p2317 A72-32778

Sunspot area east-west asymmetry dependence on location in chromospheric facula or plage, considering solar atmosphere optical and geometric depth changes
15 p2318 A72-32787

Photoelectric observations of Fraunhofer ionized metal lines in sunspot spectrum relating to umbral dots
16 p2458 A72-33687

Note on the characteristics of sunspot groups which produce solar proton flares.
17 p2608 A72-35087

The identification of the 1-0 and 2-1 bands of HCl in the infrared sunspot spectrum.
17 p2611 A72-35299

On the temporal distribution of type IV burst-active centres over the solar cycle /Research note/.
17 p2602 A72-35715

Type 3 solar burst spectral characteristics relationship to flare class and magnetic field configuration in spot group
17 p2618 A72-35739

Sunspot control of ionospheric absorption.
18 p2686 A72-36231

A working model for sunspot umbrae.
18 p2727 A72-36740

Nature of the 80-90 year cycle of solar activity
19 p2860 A72-37952

Correlation of polarization in type III solar radio bursts at frequencies of 23.5 and 30 MHz
19 p2851 A72-38065

Geomagnetic activity index Ap variation spectral data analysis, noting correlation to sunspot number variation
19 p2793 A72-38747

He abundance relationship to solar wind bulk speed and temperature from Explorers 34 and 43 observations, noting dependence on sunspot number
19 p2853 A72-38749

Eu, La and Sm in sunspot spectra.
20 p2973 A72-39884

Coexisting weak and strong opposite-polarity magnetic field regions as cause of sunspot umbra Zeeman spectra pi-component splitting
21 p3108 A72-41283

Photoelectrically observed diatomic carbon absorption lines in sunspot spectra for two energy bands
21 p3108 A72-41284

Diatomic carbon lines search in sunspot umbras spectrum from solar telescope observations
21 p3108 A72-41285

Sunspot temperature increase stimulation of supergranule motion leading to spot decay and magnetic field diurnal fluctuation development
21 p3114 A72-41762

Observations of the horizontal velocity field surrounding sunspots.
22 p3221 A72-42033

The great solar flares of August, 1972.
22 p3219 A72-42984

Sunspot formation due to magnetic flux concentration in active region and formation of invisible pores with suppressed granular motion
23 p3333 A72-43235

Sunspots and solar granulation recording and imaging with 64-element array of PbS IR detector for obtaining high SNR and resolution
23 p3288 A72-43883

SUPERALLOYS
U HEAT RESISTANT ALLOYS
SUPERCAVITATING FLOW
Integrodifferential equation for rigid tunnel walls effect on supercavitating flow past thin jet flapped airfoil, noting lift coefficient derivatives
10 p1469 A72-24562

The lift coefficient of a supercavitating jet-flapped foil in a free jet.
21 p2992 A72-41236

SUPERCAVITATION
U SUPERCAVITATING FLOW
SUPERCONDUCTING MAGNETS
Cu clad Nb-Ti wire wound superconducting solenoids with large fields at 1.6-5.2 K
10 p1446 A72-23762

Superconducting magnetic suspension and balance facility of superersonic wind tunnel for dynamic stability studies
10 p1460 A72-24757

Electrical loss measurements in superconducting magnets at 60 Hz for Nb-Sn ribbon and Nb-Ti cable and multifilament coils
10 p1460 A72-24760

Data acquisition and reduction for model aerodynamics in superconducting magnetic suspension and balance of superersonic wind tunnel facility
10 p1461 A72-24766

Superconducting magnetic suspension systems safety aspects, discussing relief valves for He boil-off, flowmeters, cryostat temperature monitors, power supply diodes and safety interlocks 10 p1462 A72-24774

Antimatter search in primary cosmic rays by balloon-borne superconducting magnetic spectrometer capable of direct matter-antimatter separation 12 p1863 A72-27296

Simplified theory for optimizing the design of a heat shield in an isochorically operated toroidal dewar. 19 p2805 A72-38843

SUPERCONDUCTIVITY

High conductivity superfluid region in cryogenic liquid helium 4 bath with temperature gradient in equilibrium with saturating vapor 01 p0101 A72-10040

Semiconducting crystal superconductivity in laser field by interaction between electron conduction band and light induced polarization 02 p0269 A72-12883

NbN thin film stabilization by metal overlays with reduction in ac losses, discussing superconducting reversibility to normal transition 04 p0560 A72-14542

Superconductivity - Conference, Stanford, California, August 1969 04 p0562 A72-15291

Nb-Ti alloy critical current density increase dependence on temperature, discussing evidence supporting rigidly pinned vortex lattice model 04 p0562 A72-15292

Uniaxial stress effect on monocrystalline niobium stannide superconducting transition temperature, considering crystal structure 04 p0562 A72-15293

NbN film superconducting properties measured as function of thickness, discussing transition temperature, critical current and magnetic field 04 p0562 A72-15294

Critical supercurrents in heat treated and cold worked Nb-Ti wires, proposing pinning model based on enhancement of Ginzburg-Landau parameter in cell walls 08 p1186 A72-21594

Phase diagrams, superconducting properties and annealing critical temperature of Nb-Al-Ge alloys, establishing four phase peritectic equilibria 08 p1218 A72-21778

Josephson effect /superconducting weak link/ devices for low frequency magnetic field sensing, noting applications in magnetocardiography and absolute noise thermometry 08 p1218 A72-21919

Superconductivity in d- and f-band transition metals - Conference, University of Rochester, New York, October 1971 09 p1367 A72-22551

Maximum superconducting transition temperature estimation, discussing optimum resonant frequency for attractive interaction, umklapp electron scattering and lattice instabilities 09 p1367 A72-22553

Ta, Nb and La superconductivity, investigating surface contamination effects on electron tunneling characteristics 09 p1367 A72-22554

Electron phonon coupling in tight-binding approximation for phonon frequency renormalization and transition metal superconductivity coupling constant computation 09 p1368 A72-22555

BCS theory for transition metals and alloys superconductivity, discussing electron phonon coupling, transition temperatures and Cooper pair fluctuations 09 p1368 A72-22556

La superconductivity pressure dependence based on valency considerations, noting actinides metals and alloys localized magnetism explanation by simple model 09 p1368 A72-22557

Transition metal superconducting thin films and rf cavity surface protective coverings, investigating properties by low energy electron diffraction and Auger spectroscopy 09 p1368 A72-22560

Superconductivity observation in Na, K and Rb intercalates of molybdenum disulfide comparing transition temperatures 09 p1368 A72-22561

Phonon dispersion curves from inelastic neutron scattering for actinide and transition metals carbides, noting superconducting properties 09 p1369 A72-22564

NbN family high transition temperature values application to phonon spectrum prediction based on superconductivity microscopic theory 09 p1369 A72-22565

Electron phonon coupling and IR optical constants relationship to superconductivity in transition metals 09 p1369 A72-22566

Magnetic phenomena effects on superconductivity in simple and transition metals and dilute rare earth alloys 11 p1701 A72-26025

Superconductive behavior of cold-worked sintered Nb wires, examining effects of aluminum oxide addition on residual resistivity, magnetization behavior and critical current density 11 p1662 A72-26742

Transition temperature and other superconducting properties of annealed Nb-Al-Ge thin films 12 p1853 A72-27038

Broadband superconducting quantum microwave magnetometer design, operation and performance 12 p1812 A72-28219

Analog simulation of Josephson superconducting junctions dc characteristics for two mixed microwave frequencies, discussing signal detection sensitivity improvement 13 p2021 A72-28648

Parametric regeneration in Josephson superconducting point contacts for combination frequency signal amplification and conversion in microwave application 13 p1932 A72-29298

Critical superconductivity currents measurement in niobium based U shaped and coiled wires within steady magnetic field 13 p2007 A72-30013

Metallurgical and superconducting properties of beta-tungsten structure niobium aluminide with high critical temperature 14 p2119 A72-30607

Hydrogen impregnated Ta superconducting to normal transition and M-H curves, discussing effect on impure surface layer superconducting properties 15 p2293 A72-32242

Superconductivity, temperature and tunneling effects in low carrier density semiconductor systems /tin, germanium and indium tellurides, lanthanum triselenide and strontium titanium oxide/ 15 p2293 A72-32325

In-Ti alloys electron phonon interaction and superconductivity electron tunneling examined by sum rule and mass defect theory 15 p2295 A72-32543

Ti-Mo binary solid solution, investigating superconducting transition temperature, lattice instability and electron-to-atom ratio by calorimetric measurements 15 p2295 A72-32544

Superconductivity. 17 p2594 A72-34565

Dependence of critical supercurrent on normal layer thickness in S-N-S structures. 19 p2846 A72-38631

Stabilization of a superconducting modification of beryllium by an aluminum admixture 20 p2960 A72-39407

Phenomenological models of the electron-phonon interaction and the superconductivity criterion of metals 21 p3098 A72-41688

Critical superconductivity currents measurement in niobium based U shaped and coiled wires within steady magnetic field 22 p3190 A72-42735

Characteristics of superconducting niobium-tin alloys obtained by the vacuum evaporation method 22 p3192 A72-43013

Superconducting transition temperature increase in Nb-Al-Si alloys as function of composition under tetragonal lattice crystallization 22 p3192 A72-43020

Effect of an alternating current on the steady characteristics of Josephson point contacts 22 p3208 A72-43109

Magnetic flux penetration into superconducting thin films. 23 p3323 A72-43271

Dependence of changes in the electronic dislocation-braking force during superconducting transition on the stresses, temperature, and strain rate 23 p3312 A72-43315

Model of degenerate semiconductor near semiconducting phase transformation, noting superconducting state at low temperatures with corresponding impurity concentrations 23 p3323 A72-43317

Laplace equation for homogeneous magnetic field perturbation by superconducting elliptical cylinder and by two parallel circular cylinders 23 p3313 A72-43779

Properties of a superconducting point contact contained in a resonator 23 p3324 A72-44221

SUPERCONDUCTORS

Intercalation complexes of Lewis bases and layered tantalum and niobium disulfide superconductors, noting critical temperatures 01 p0113 A72-10018

Electron microscopy and diffraction analysis of lattice imperfections of layered superconducting transition metal dichalcogenide intercalation complexes 01 p0113 A72-10019

High transition temperature alloys, layered intermetallic and organic superconductors development and properties 01 p0113 A72-10163

Dc and ac Josephson effects in bulk granular superconductor, presenting junction I-V characteristics 02 p0268 A72-11477

Dynamic equations for nonequilibrium stationary state superconductors with electron-phonon and electron-electron inelastic collisions 03 p0401 A72-13089

Propagation modes attenuation and phase shift of electromagnetic plane wave in superconducting coaxial cylindrical waveguide 03 p0321 A72-13170

Strong coupling superconductors transition temperature derivation from Coulomb pseudopotential and Einstein-type phonon spectrum 03 p0402 A72-13672

Longitudinal ultrasonic sound attenuation in superconducting Mo-Re alloys as function of temperature, magnetic field and frequency, using evaporated thin film CdS transducers 04 p0562 A72-15299

Flux lines interaction with dislocations in twisted superconducting niobium single crystals, measuring flux gradient and dislocation arrangement 06 p0830 A72-18055

State density singularities elimination in inhomogeneous superconductors by electron interactions nonuniformities, resulting in tunnel junction current-voltage characteristic fluctuation 07 p1047 A72-18915

Superconducting magnetic spectrometer for cosmic ray nuclei spectrum analysis, describing design, calibration and operation 07 p0983 A72-19315

Abrikosov and Mendelsohn models of nonideal superconductors of second kind in transverse magnetic field, discussing Landau-Ginzburg parameters and critical current density 07 p1049 A72-20153

Critical temperature dependence of Nb-Al-Ge superconducting alloys on composition and heat treatment, discussing phase boundaries and electron state densities 07 p1049 A72-20154

Precipitation hardening of quenched superconducting Nb-Al alloys, examining polycrystalline and single crystal samples and intermetallic phases 07 p1050 A72-20155

Precipitates dispersion and fluxoid pinning /critical current density/ in superconducting Nb-Hf alloy during aging, using transmission electron microscopy 07 p1020 A72-20417

Lattice expansion of metal chalcogenide superconducting organometallic structures with aromatic or aliphatic Lewis bases sandwiched into van der Waals gap 08 p1216 A72-21244

Quasi-particle decay rates by electron-electron scattering in superconductors, noting effect on states tunneling density 08 p1217 A72-21599

Superconducting quantum flux sensors for measuring magnetic fields and susceptibility, voltage and resistance 09 p1308 A72-22466

Transition metal superconductors transition temperatures survey, considering d-band solid solution alloys and intermetallics and ferromagnetic element compounds 09 p1367 A72-22559

Spin excitation effects in superconductors, noting impurity concentration effects on transition temperature and thermodynamic properties 09 p1368 A72-22558

A-15 superconducting films preparation computer-aided method, noting alloying effects and crystal structure stability determinations applications 09 p1368 A72-22559

Pressure effects on transition temperature and electronic structure of narrow band superconductors 09 p1368 A72-22562

Transition temperature pressure dependence determination for d- and f-band superconductor metals, alloys and compounds 09 p1368 A72-22563

Nb-Al-Ge alloy superconductor deposits structure, transition temperature and critical current densities after preparation by triode sputtering and heat treatment 09 p1369 A72-22795

Pinning force of vortex lines and microstructural inhomogeneities in superconductors, using magnetization and critical current measurements 09 p1369 A72-22796

Magnetic induction distribution in second species superconductor cylindrical samples after limited flux jumps, proposing instability propagation model 09 p1369 A72-22797

Inhomogeneous superconductors and proximity effects, calculating conditions for vortex lattice pinning energy as increasing function of magnetic field and temperature 09 p1370 A72-22798

- Josephson dc and ac effects in plane junctions with thin semiconducting film barrier of evaporated material between two superconductors 09 p1370 A72-22800
- Short and long term frequency stability improvement in X band klystron oscillator stabilized by high Q superconducting cavity 10 p1449 A72-24303
- Superconducting levitron machine for trapped hot plasma stability and confinement studies in vacuum, discussing construction and coil performance 10 p1460 A72-24759
- Superconducting coil design for magnetic suspension of supersonic wind tunnel balance 10 p1460 A72-24759
- Abrikosov vortex lattice in superconductors, calculating resonance linewidth and vacancy formation energy 11 p1699 A72-25718
- Strip and line source antennas quality factor, examining relationship to superconductivity ratio 13 p1916 A72-28535
- Friction force electron component for superconducting dynamic dislocation at various temperatures and propagation rates 13 p2021 A72-28901
- Nb superconducting resonant cavities application to linear accelerator and RF particle separator structures in GHz region for wall energy loss reduction 13 p1922 A72-29348
- Dynamic equations for superconductors with electron-phonon and electron-electron inelastic collisions, investigating nonequilibrium stationary states 13 p2022 A72-29438
- Two fluid model application to microbridges between superconductors, investigating superconducting particles number time variation possibility 13 p2023 A72-29789
- Joule heating power density in NbZr superconductor hollow cylinder, estimating temperature changes and instability locations 13 p2023 A72-29855
- German monograph on superconductors transition temperature calculation by iteration method using phonon spectrum approximation 14 p2143 A72-30947
- Superconducting to normal transition field as function of temperature for Ta with thin surface layer variable density impurities 15 p2293 A72-32241
- One electron and Josephson tunneling in superconductors in terms of energy level concepts 15 p2293 A72-32236
- Multifilamentary superconducting Nb-Sn composite wires in ductile metal matrix, determining transition temperature and critical current density 15 p2294 A72-32534
- Thin film superconductors conductivity evaluation above transition temperature through renormalization of impurity-scattering vertex by pair fluctuation effect inclusion 15 p2295 A72-32540
- Emitted phonon spectrum effects on detected signal response in superconducting Sn diodes, noting deviation from linearity 15 p2209 A72-32541
- Two band model explanation of Hall effect in dirty type-II transition metal superconductors near upper critical field, noting interband impurity scattering role 15 p2295 A72-32542
- Heat capacity data analysis for solid solutions of superconducting Nb-Ti system, investigating electronic structure 15 p2296 A72-32692
- Flux quantization in superconductors demonstrated by magnetometer probe measurement of magnetic field trapped in thin In film holes 16 p2441 A72-33225
- Hard superconductors cylindrical samples irreversible magnetization and size effect calculation, comparing results with experiment on Nb-Ti alloy specimens 16 p2441 A72-33523
- Experiments on the phase contrast transfer functions of a superconducting lens 17 p2594 A72-34284
- Superconducting-cavity-stabilised oscillator of high stability. 17 p2530 A72-35386
- Measurements of ultrasonic velocities using a digital averaging technique. 18 p2691 A72-36401
- Anisotropy and strong-coupling effects on the critical-magnetic-field curve of elemental superconductors. 18 p2719 A72-36710
- Voltages induced in superconductors in the absence of transport currents. 18 p2719 A72-36744
- The effect of dislocation tangles on superconducting properties. 18 p2719 A72-36746
- Superconducting energy gaps and transition temperatures of disordered cadmium and zinc films. 19 p2844 A72-37690
- State density singularities elimination in inhomogeneous superconductors by electron interactions nonuniformities, resulting in tunnel junction I-V characteristic fluctuation 20 p2960 A72-39385
- Flux vortices and transport currents in type II superconductors. 20 p2961 A72-39809
- Interactions between dislocations or flux lines moving through hardened crystal, discussing distribution functions method applications to diffuse and localized obstacles 20 p2962 A72-39994
- Electrodynamical analysis of superconducting vortices interaction with cylindrical cavities [pinning], calculating critical currents in type II superconductors in external magnetic field 21 p3096 A72-40416
- Force free fields in type II superconductors. 21 p3096 A72-40573
- Extension of Eliashberg's theory to type-II superconductors. 21 p3097 A72-40574
- Tunneling generation, relaxation, and tunneling detection of hole-electron imbalance in superconductors. 21 p3097 A72-40774
- Phase precipitation structure of superconducting Nb-Ti alloys after cold working and low temperature annealing 21 p3067 A72-40951
- Fabrication studies of Nb3Al superconductors. 21 p3097 A72-41182
- Two band superconductor state density vs energy, noting energy spectrum extremal points 21 p3098 A72-41697
- Ultrasonic evidence against multiple energy gaps in superconducting niobium. 22 p3190 A72-42476
- Superconducting alloys of niobium and vanadium 22 p3191 A72-42808
- Plotting of composition vs property curves for superconducting systems with a digital computer by the method of simplex arrays 22 p3191 A72-42813
- Niobium superconductive tunnel diode integrated circuit arrays. 22 p3161 A72-43090
- Specific-heat and magnetic measurements in superconducting Ta-Nb alloys. 23 p3323 A72-43273
- Thermal conductivity in the two-band model of superconducting transition metals containing nonmagnetic impurities. 23 p3323 A72-43274
- Equilibrium equations for vortex lines with allowance for interaction with boundary of ideal superconductor, calculating extremum values of magnetic field 23 p3312 A72-43316
- Influence of hydraulic extrusion on the composition and properties of the Nb3Sn compound 23 p3323 A72-43597
- Thermal conductivity of superconducting layer in intermediate stage with Andreev electron excitation trajectories in magnetic field, using Green function and impurity distribution technique 23 p3325 A72-44486
- Thermal conductivity in dirty transition-metal superconductors near the upper critical field. 24 p3432 A72-45675
- SUPERCOOLING**
- BiTe crystal critical growth rate calculation based on theory for diffusional supercooling of melt with excess Te 08 p1217 A72-21338
- Supercooled water drops freezing by contact nucleation with AgI and silicate particles, determining effective temperature in updraft wind tunnel experiments 09 p1345 A72-22445
- Supercooled cloud water droplets in free fall shattered by shock waves measuring ice crystal formation probability 09 p1345 A72-22446
- Crystallization discontinuity and layer thickness in welded joints as function of overcooling and isotherm shape 13 p1963 A72-28922
- Subcooling and acceleration effects on nucleate boiling heat flux, comparing heat transfer prediction models with experimental measurements 16 p2477 A72-33433
- Mathematical formulation of ice crystal formation and propagation mechanism in seeded supercooled convective clouds 23 p3311 A72-43722
- SUPERCRITICAL FLOW**
- Supercritical stationary states of dissipative hydromagnetic rotating Couette flow between electrically insulating cylinders within axial magnetic field. 04 p0554 A72-14405
- Pneumatic amplifiers with controlled pressure during subcritical and supercritical flow, considering jet-resonant choke, conical and membrane systems 11 p1578 A72-26783
- Supercritical aerodynamics technology, noting lifting surface cross sectional profile and structural weight reduction 19 p2746 A72-37678
- SUPERCRITICAL PRESSURES**
- Anisotropic shell supercritical deformation, deriving formula for lower critical load for shallow orthotropic spherical segment under external pressure 03 p0447 A72-13729
- Heat transfer in rectangular annular channel during external heating under supercritical pressure, discussing thermal flux, mass flow rates and enthalpy 03 p0457 A72-14152
- Supercritical pressure turbulent forced fluid heat transfer mechanism hypothesis, explaining anomalous transfer improvements and deteriorations 04 p0511 A72-14641
- Supercritical deformation, bulging and instability of spherical edge clamped shell under external pressure, applying variational principle 05 p0742 A72-17210
- Cs and Hg vapors compressibility factor in supercritical range as function of density, considering charged particles and atoms polarization interactions in ionized metal vapors 07 p1040 A72-18943
- Supercritical deformation, bulging and instability of spherical edge clamped shell under external pressure, applying variational principle 11 p1727 A72-25341
- Supercritical pressure convergent nozzle performance prediction by time dependent method of characteristics solution to mixed flow problem, adapting Moretti-Abbott technique [AIAA PAPER 72-680] 16 p2346 A72-34061
- Combustion of liquid propellants under supercritical conditions 17 p2637 A72-34946
- Experimental study of conditions for heat transfer deterioration in a turbulent carbon dioxide flow under supercritical pressure 18 p2742 A72-37185
- A thermal stratification model of a cryogenic tank at supercritical pressures. 19 p2883 A72-38845
- Determination of the optimal parameters of high-pressure cryogenic fluid storage systems. 20 p2962 A72-39358
- A theoretical model for the combustion of droplets in super-critical conditions and gas pockets. 24 p3463 A72-45050
- SUPERCRITICAL WINGS**
- Supercritical thick wing for structural weight reduction and increased cruise speeds flight tested on Navy T2-C aircraft 11 p1576 A72-25583
- [SAE PAPER 720320] Book - A theory of supercritical wing sections, with computer programs and examples. 21 p2993 A72-41534
- SUPERFLUID FLOW**
- U SUPERFLUIDITY**
- SUPERFLUIDITY**
- High conductivity superfluid region in cryogenic liquid helium 4 bath with temperature gradient in equilibrium with saturating vapor 01 p0101 A72-10040
- Relaxation time estimation for electron velocity relative to dilute vortex core array in rotating neutron superfluid, applying to pulsar slowdown rate 04 p0571 A72-14590
- Neutron star properties, formation theories, crust composition and internal structure, examining interior neutron behavior, fermion systems superfluidity, magnetic field effects and stellar dynamics 10 p1533 A72-23890
- Pulsar speed increase mechanism as metastable flow state transition in neutron star superfluid core 11 p1724 A72-26705
- Temperature oscillations associated with surface gravity waves at two fluid model compressible vapor-incompressible superfluid interface 12 p1845 A72-27386
- Temperature and pressure requirements for producing superfluid liquid molecular hydrogen, noting use of solid deuterium or Ne walls to prevent hydrogen solidification 16 p2422 A72-32911
- Two fluid model for qualitative interpretation of turbulent intermittency, noting governing equations analogy to Landau equations for superfluidity 19 p2787 A72-38428
- Heat transfer with the helium II superfluid film. 19 p2883 A72-38839
- Breakdown of superfluidity for cylinders in saturated liquid helium II. 19 p2836 A72-38840
- Thermohydrodynamic conditions at the peak flux of horizontal heaters in superfluid liquid helium II at zero net mass flow. 20 p2984 A72-39647
- Neutron star model for magnetic field and superfluidity effects on cooling during pulsar stage 22 p3228 A72-42565
- Reflection and transformation of sound waves in a superfluid liquid at a solid boundary 22 p3207 A72-42956

SUPERGIANT STARS

Six color photometry of F-G supergiants in Large Magellanic Cloud, noting color similarity with galactic stars

03 p0416 A72-13019

Magellanic Clouds hot supergiants color-magnitude arrays from spectroscopic and photometric measurements

03 p0424 A72-13253

Magellanic Clouds neutral hydrogen distribution, concentrations and velocity structure, noting H II correlation with supergiant stars

03 p0425 A72-13256

Magellanic Clouds bright star intermediate band photometry, discussing interstellar extinction and luminous supergiants

03 p0425 A72-13257

Small Magellanic Cloud NGC 371 region photometric studies for cepheids period-luminosity relations, noting domination by young supergiant stars

03 p0425 A72-13258

Magellanic Clouds supergiant stars intrinsic colors, observing in five spectral bands to separate from Galactic foreground stars

03 p0425 A72-13260

Early type supergiant far UV spectrum observations, showing broad absorption feature near 1720 Å

04 p0578 A72-15315

MHz IR/OH sources, discussing M type Mira variables or M supergiants photospheric temperature and dust shell structure

07 p1069 A72-19075

Model atmosphere and spectral analysis for two early B-type supergiant stars, deducing stellar mass and evolutionary phase

07 p1070 A72-19085

M supergiants in Carina arm, discussing photometric studies at 4-18 microns, interstellar extinction uncertainties and spatial distribution

07 p1072 A72-19344

Astronomical IR spectroscopy of Alpha Ori, discussing OH line formation, LTE, rms turbulence velocity and abundance

07 p1072 A72-19345

Quasar rotation and pulsation periods within pulsar models, postulating supermassive stars /one million-one billion solar masses/ as energy sources

09 p1385 A72-22536

UBVr colors of supergiants as function of radiation pressure, sphericity, microturbulence and effective temperatures

10 p1542 A72-24609

Spectrographic analysis of K-type supergiant epsilon Pegasi for effective temperature, surface gravity and heavy and light element abundances

10 p1543 A72-24621

Photoelectric scans of M supergiant alpha Ori and carbon stars from 3400 to 11,000 Å, obtaining dominant spectral features

10 p1548 A72-24967

Fowler quasars and exploding galaxies model tested by hydrodynamic equations numerical solution for premain sequence contraction and relativistic collapse of nonrotating supermassive star

12 p1866 A72-27202

Stellar photometric observations in Magellanic Clouds, presenting photoelectric sequences in UVB system, interstellar reddening and extinction data

14 p2159 A72-30737

Massive red supergiants radial pulsations from adiabatic theory application to convective envelope models based on mixing length theory and H-He ionization zones

14 p2159 A72-30743

Binary nature of the B supergiant in the error box of the Vela X-ray source.

17 p2604 A72-34521

A recalibration of the absolute magnitudes of supergiants.

17 p2609 A72-35115

Vibrational stability of supermassive stars stabilized dynamically by a uniform or differential rotation

17 p2613 A72-35461

Supergiants internal structure, evolution and spectral characteristics, discussing instability phenomena and luminosity calibration

18 p2723 A72-35995

Variation of evolved blue/red ratio for supergiants as function of stellar mass, discussing status of astrophysical test for neutrino emission

19 p2854 A72-37235

Astronomical observations supporting stellar atmosphere microturbulence concept, noting Cepheid variables high dispersion spectra, supergiants irregular changes and microturbulence hydrodynamic effect

19 p2857 A72-37525

Spectrographic and photometric observations of supergiants and foreground stars, in the direction of the Large Magellanic Cloud.

19 p2858 A72-37855

Structure and motions in the Carina spiral feature.

20 p2973 A72-39880

On the chemical composition of epsilon Pegasi.

20 p2974 A72-39901

Cool supergiant stars atmospheric model for chemical composition change effects due to nuclear burning cycle

22 p3227 A72-42556

Mixing between stellar envelope and core in advanced phases of evolution. IV - Effect of superadiabaticity in convective envelope.

23 p3335 A72-43486

The analysis of the small Magellanic Cloud supergiant HD 7583.

23 p3336 A72-43555

Titanium oxide molecular spectrum band intensities measurement for vibrational temperature of M supergiant stars, noting atomic absorption effect on measurement accuracy

24 p3448 A72-45681

SUPERHARMONICS

Electromagnetic potentials excited by dipole oscillator moving in homogeneous uniformly drifting medium, analyzing frequency spectrum and finite dimensions effect on higher harmonics

08 p1135 A72-21736

Geopotential harmonics of fifteenth order obtained from decaying satellite orbits analysis

15 p2311 A72-32001

ADP or KDP crystal induced second harmonic emission from Ar laser resonator, noting crystal temperature effects on primary/secondary radiation phase synchronism

16 p2400 A72-33281

Langmuir probe dc and second harmonic characteristics measuring system, describing switching circuitry

16 p2392 A72-33608

The superharmonic functions in the axiomatics of M. Brelot associated with a degenerate elliptical operator

24 p3418 A72-44825

SUPERHEATING

Superheating in Zr-oxygen combustion system during autoignition period

08 p1128 A72-21219

Binary system molar energy diagram plotting, covering superheated, saturation and liquid phase regions

08 p1255 A72-22170

Convective heat exchange of metastable liquid during suspension of boiling

19 p2881 A72-38037

Observation of superheat instability in a fully ionized current-carrying plasma.

20 p2958 A72-39854

SUPERHETERODYNE RECEIVERS

Three frequency IR laser signal heterodyne detection with 40-MHz if narrow-band reception, measuring SNR

05 p0669 A72-16607

High sensitivity wideband heterodyne receiver system for spaceborne and ground-based IR laser communications

07 p0940 A72-19238

High resolution stabilized superheterodyne microwave interferometer, noting noise figure and dynamic range

07 p0993 A72-20590

Superheterodyne radiometers for millimeter and submillimeter waves, using Mach-Zehnder interferometer frequency mixer for parasitic signal suppression

08 p1140 A72-21265

Reciprocity theorem for antenna directivity pattern measurement of optical superheterodyne receiver for carbon dioxide laser radiation

08 p1140 A72-21376

Laser communication lines in atmospheric ground layer, comparing SNR for direct-reception and superheterodyne video systems

15 p2247 A72-31887

Use of selective RC amplifiers in the radio-frequency amplifier stages of superheterodyne radio receivers

23 p3271 A72-43775

SUPERHIGH FREQUENCIES

Centimeter waves fading due to interference from tropospheric multipath propagation

01 p0027 A72-10412

Shf electromagnetic radiation interaction with solid body plasma, explaining wave propagation in solid state plasma waveguides

02 p0170 A72-11561

X band gallium arsenide field effect transistor, noting applications for radar receivers, microwave communication links and electronic countermeasures

02 p0193 A72-12184

Parametric excitation of hf and lf plasma oscillations by modulated shf field dependent on field strength at carrier frequency

03 p0394 A72-13086

High latitude scintillation effects on vhf and S band polar orbiting satellite transmissions, examining ionospheric irregularities

04 p0487 A72-14952

Broadbeam S band radar application to quantitative analysis of severe storms, calculating liquid water content

06 p0843 A72-18442

GaAs IMPATT diodes technology and performance at C, X and K band frequencies

06 p0788 A72-18466

Harmonic power extraction from series-stacked high efficiency avalanche diodes at superhigh frequencies on simple microstrip circuits

06 p0788 A72-18468

Low noise GaAs Schottky barrier FET for X and Ku bands applications

07 p0955 A72-19257

Hf and shf power transistor gain, efficiency and electrical characteristics for wideband linear amplifiers

08 p1139 A72-21051

Operational and equivalent circuit characteristics of low noise hf and shf transistors in wideband amplifiers

08 p1139 A72-21052

Viking Mars Orbiter and Lander radio and radars science experiments, noting surface tracking, dual frequency S and X band data and communications system

10 p1539 A72-24380

Tunnel diode amplifier for 8 GHz band, considering gain, bandwidth, noise factor and stability characteristics

12 p1790 A72-27533

Parametric excitation of HF and LF plasma oscillations by AM SHF field, noting dependence on field strength at carrier frequency

13 p2015 A72-29436

High reliability long life grid pulsed L band traveling wave tube with integral solenoid focusing for high power radar use

14 p2089 A72-31046

Dielectric waveguide X band telemetry system for remote power and multiplexing applications in noisy electromagnetic pulse environment

14 p2087 A72-31047

Prototype local oscillator for X band communication satellite, discussing electrical and mechanical characteristics and temperature and noise measurements

15 p2204 A72-31182

SHF signal propagation through troposphere at low elevation angles, comparing fading measurements in winter and summer

15 p2194 A72-31550

Pit shielded antenna measurements for communications satellite earth stations in 4 and 6 GHz bands, considering position range and erosion effects

15 p2196 A72-31794

Venus brightness temperature and phase dependence at 2.7 cm wavelength during 1968-1970

15 p2311 A72-32085

Nonideal component parts effect on behavior of digital microstrip closed circuit X band phase shifter presenting detailed network analysis

15 p2201 A72-32471

Electron beam modulation by SHF noise signal in a plasma-beam system

15 p2289 A72-32698

An X-band paramp with 0.85 dB noise figure /uncooled/ and 500 MHz bandwidth.

19 p2770 A72-37258

Spectral densities of radio emission fluxes from discrete radio sources at the 3.5-cm /8550 MHz/ wavelength

19 p2850 A72-37804

Limitations of technological state-of-the-art with satellite and space communications above 10 GHz.

19 p2765 A72-37940

SHF signal power influence on detector current, noting signal dependence on virtual cathode potential and signal power

19 p2774 A72-38410

Utilization of frequency bands allocated to satellite broadcasting for regional or domestic systems.

21 p3018 A72-40875

High resolution observations of 3C390.3 at 2.7 and 5 GHz.

21 p3111 A72-41471

Quasi-linear theory for the low-frequency instability of a plasma placed in a weak SHF electric field

23 p3321 A72-44172

X-band silicon double-drift IMPATT diodes using multiple epitaxy.

23 p3273 A72-44334

SUPERIMPOSITION [MATHEMATICS]

U SUPERPOSITION [MATHEMATICS]

SUPERMAGNETS

U HIGH FIELD MAGNETS

SUPERNOVAE

Supernova Vela X and local remnants as origin of below 1000 GeV cosmic electrons, deducing existence at 10 to 15 GeV from muon poor showers

01 p0119 A72-10853

Second decrease in Vela Pulsar period, noting time span between discontinuities and supernova remnant Vela X

02 p0277 A72-11904

High velocity interstellar Ca II near Vela pulsar 0833-45, discussing absorption line association with Vela X, Y, Z supernova remnant complex

02 p0279 A72-12191

Polycyclic hydrocarbon molecules formation in cool stars atmospheres and gases ejected by supernovae and Seyfert galaxies, discussing Platt particles origin 02 p0284 A72-12634

Supernovae remnants intrinsic luminosity-diameter correlations from soft X ray emission data, taking into account interstellar medium 03 p0408 A72-13008

Pulsar theory, discussing rotating neutron star principle, kinetic energy, structure, atmosphere, radiation mechanics and supernovae remnants 03 p0417 A72-13103

Pulsars formation rate and connection with supernovae and cosmic rays, discussing stellar magnetic field strength 03 p0421 A72-13134

Papers on Magellanic Clouds covering properties, observational and theoretical approaches, supernovae remnants, color-magnitude diagrams, globular clusters, etc 03 p0424 A72-13251

Explosive p-process nucleosynthesis limiting conditions in supernova envelopes, using proton capture and neutron photodisintegration rates 04 p0579 A72-15318

X ray and gamma astronomy, discussing old and blue stars, supernova remnants, radio galaxies, quasars and pulsars 04 p0582 A72-15687

Distance estimation for supernova remnants and H I regions from H I absorption measurements 05 p0712 A72-15770

Radio emitting giant loops in the Galaxy, considering supernova radiation induced nebulae model to explain spectral and polarization properties 06 p0876 A72-17649

Galactic evolution model, tracing stellar and supernova nucleosynthesis influence on interstellar gas composition 06 p0886 A72-18082

Cosmological red shift and galactic evolution effects on line features in X ray background due to young pulsars in supernova remnants 06 p0891 A72-18509

Interstellar matter cooling and recombination after supernova ionization, comparing X ray and cosmic ray heating mechanisms 07 p1070 A72-19083

Loop structure of Monoceros supernova remnant, predicting thermal soft X ray point source as cooling neutron star 07 p1073 A72-19421

Radio emission of Lupus region believed to contain supernova of 1006 A.D., noting strong polarization 07 p1076 A72-19607

Pulsar model based on neutron star rotation with skew magnetic field, considering radiated particle acceleration responsible for high energy activity in supernova remnants 07 p1080 A72-20057

Pulsar and supernova remnant relative space position based on runaway pulsar hypothesis, discussing pulsar period-luminosity relation from evolutionary standpoint 08 p1233 A72-21180

Hard X radiation source in Vela X supernova remnant direction detected during balloon flight on 25 November 1970 09 p1383 A72-22290

Cygnus Loop supernova remnant X ray emission structure from sounding rocket spectral data, showing thermal emission mechanism 09 p1378 A72-23699

Galactic and universal theories of cosmic ray source mechanisms, energy requirements, particle composition, propagation through interstellar matter and acceleration in supernovae remnants 10 p1533 A72-23889

Si burning in stellar explosions, discussing initial composition and neutron enrichment 10 p1544 A72-24666

Extragalactic supernovae X ray luminosity upper limits from OSO 3 data, estimating total energies 10 p1544 A72-24667

Stellar evolution from precarbon-burning contraction to presupernova stage with and without neutrino production by electron neutrino interaction 10 p1545 A72-24825

High sensitivity search for X rays from supernova remnants in Aquila 11 p1713 A72-26121

Relativistic shock propagation and search for electromagnetic pulses from supernovae, plotting kinetic energy factor vs external mass fraction 11 p1721 A72-26126

Soft X ray emission from supernova remnants, considering maximum linear diameter dependence on remnant distance from galactic plane 12 p1863 A72-27222

Expanding elliptical H I ring with major and minor axes of 1300 and 560 pc from type III supernova in solar neighborhood 13 p2048 A72-29831

Pulsar PSR 1154-62 association with nearby galactic radio source having supernova remnant shell structure and spectrum characteristics 14 p2150 A72-30369

Low mass neutron star source of pulsed X radiation in binary Centaurus X-3 ejected during low energy supernova explosion 14 p2156 A72-30570

Low energy X ray astronomical observation, considering hot plasma existence in old supernova remnants 14 p2157 A72-30676

Galactic supernova remnants radio frequency absorption line observations, deriving distances, radio luminosity function and distribution 14 p2158 A72-30726

Supernovae produced fluorescence pulses search in upper atmosphere by automatic coincident light receivers 15 p2313 A72-32233

Uhuru observed galactic X ray sources related to binary systems or supernova remnants, noting galaxy clusters 16 p2454 A72-33362

Supernova explosion mechanism and quantitative game for galactic chemical evolution, discussing relationship to cosmic rays 16 p2459 A72-33744

Neutron star acceleration of He, Fe and supernova debris into cosmic ray flux throughout Galaxy, discussing magnetic and superfluidity effects 16 p2448 A72-33745

Radio observations of two supernova remnants, HB21 and IC443, at 4170 MHz. 17 p2613 A72-35500

Gamma radiation production through interaction between high energy particles emitted by pulsar originating in supernova core and gas in supernova envelope 18 p2721 A72-36088

Astrophysical theories of supernovae outbursts as stellar evolutionary nonstationary phase in terms of thermal instability of degenerated matter or stellar explosion 18 p2725 A72-36399

Optical observations of the supernova in NGC 5253. 18 p2726 A72-36648

Observations of six supernovae. 18 p2728 A72-36762

The type II supernova 1969I in NGC 1058. 18 p2728 A72-36763

Extragalactic origin of the transient X-ray sources. 19 p2856 A72-37502

Unsteady hydrodynamic accretion on a neutron star 19 p2862 A72-38053

Study of a faint nebula identified as the HB-21 radio source 19 p2862 A72-38054

Observational evidence against supernovae being the source of the universal X-ray background. 20 p2965 A72-38906

Energy spectrum and composition of pulsar-accelerated cosmic rays. 20 p2964 A72-39343

Emission and absorption line spectra of type I supernovae after luminosity maximum interpreted by heating and ionization mechanisms in shell and intensity computation 20 p2973 A72-39886

Convection and diffusion transport equation of galactic cosmic ray electrons with energy loss and absorption allowance for supernova compressed halo models 22 p3217 A72-42210

Brightness and polarization structure of four supernova remnants 3C58, IC443, W28, and W44 at 2.8 centimeter wavelength. 22 p3224 A72-42382

Gum nebula origin as ionized hydrogen cloud from prehistorical supernova explosion, discussing different ionization mechanisms 22 p3227 A72-42543

Polarized radio emission from five supernova remnants. 22 p3229 A72-42994

Polarization measurements of the supernova in M101. 23 p3333 A72-43227

Physical characteristics of type I supernova envelopes during the initial expansion phase. II - Development of type I supernova spectra after maximum light. 23 p3333 A72-43228

Type II supernova spectral intensity minima due to blueshifted absorption lines of hydrogen and Fe II based on observed and synthetic spectra wavelength comparison 23 p3334 A72-43257

A study of galactic supernova remnants. II - Supernova rate, galactic radio emission and pulsars. 23 p3337 A72-43829

Identification of four novae and a super-nova in Palomar Sky Atlas. 23 p3341 A72-44474

Low energy X-ray survey from the Crab Nebula to Cygnus. 24 p3435 A72-44842

SUPERPOSITION [MATHEMATICS]

Continuity of probability distribution functions obtained by superposition 04 p0540 A72-15260

Superposable and self-superposable MGD flows from nonlinear differential equations, considering entropy, flow velocity and magnetic field strength 05 p0694 A72-16030

Variated states superimposed on finite elements in discrete elasticity, noting small oscillations superposition on arbitrary motion of elastic system 12 p1845 A72-27393

Hysteretic motor in steady synchronous operation with nonsinusoidal supply voltage, computing stator winding current based on superposition with two linear equivalent circuits 13 p1900 A72-29975

Superposition principle in test particle method for reducing plasma cloud kinetic theory to determination of conditional probability function involving Vlasov equation 17 p2591 A72-35163

Superposition method for potential distribution in plane tetrode field with unipotential and bipotential grids, noting electro-optical effect in cylindrical lenses 19 p2776 A72-38667

Absolute accuracy of the pulse-echo overlap method and the pulse-superposition method for ultrasonic velocity. 23 p3313 A72-44114

Study of a viscous flow in rotating centrifugal impellers. 24 p3363 A72-45368

SUPERSATURATION

Supersaturated semiconductor solid solutions decay kinetic equations and time constants, noting free current carriers effect 04 p0561 A72-15081

Vacancy supersaturation effect on enhanced precipitation by high flux electron irradiation in stainless steel 07 p1033 A72-20410

Precipitation effect on microstructure, coercive force, resistivity and cell formation changes in heterogeneous decomposition of supersaturated solid solutions and aging alloys 08 p1218 A72-21777

Al-Zn alloy supersaturated solid solution decomposition during aging, studying single crystal lattice characteristics via X ray diffusive scattering techniques 13 p1976 A72-28902

Surface energy effect on alloy structure formation, analyzing crystal growth and formation from supersaturated solutions 15 p2253 A72-31221

Different forms of elimination of quenching lacunae in supersaturation in the case of aging of two alloys, Al-Cu and Al-Mg-Si 22 p3190 A72-42444

SUPERSONIC AIRCRAFT

NT CONCORDE AIRCRAFT

NT JAGUAR AIRCRAFT

NT SUPERSONIC COMMERCIAL AIR TRANSPORT

NT SUPERSONIC TRANSPORTS

B-1 strategic supersonic bomber design, emphasizing variable sweep wing, landing gear, control and instrumentation 02 p0154 A72-12226

Unsolved aerodynamic problems in sub- and transonic civil and military aircraft design, considering flow problems during transonic flight, takeoff and landing [DGLR PAPER 71-105] 02 p0153 A72-12745

Detection of atmospheric gravity waves produced by focusing of shock front generated by supersonic aircraft, calculating flight trajectories 03 p0345 A72-12984

Supersonic Tu 144 aircraft design, discussing engine and aerodynamic characteristics, stabilization and control, propulsion, wing structure, landing gear and operation 03 p0310 A72-13473

Propulsion twin spool power plant design and dimensioning with selective high pressure cut-off for supersonic aircraft with part of flight in subsonic range [DFVLR-SONDDR-169] 03 p0406 A72-13608

Ramjet engine propulsion systems for large aircraft above Mach number 2.5 04 p0565 A72-14450

Convergent-divergent nozzles thrust model measurement on supersonic aircraft afterbody [ONERA, TP NO. 978] 05 p0642 A72-15856

Booms generated on ground by supersonic aircraft flying at high altitude through stratified atmosphere 08 p1149 A72-21019

SR-71 aircraft ejection seat, obtaining ejection survival rate from case histories 08 p1112 A72-21562

Sonic booms generation theory and prediction methods for supersonic aircraft during nonaccelerated flight in quiet atmosphere

Automated optimization for preliminary design of supersonic aircraft wings, noting flutter, stresses and resonant frequency as dynamic constraints [AIAA PAPER 72-333]

Case report of rapid decompression in supersonic trainer aircraft pressurized cabin, discussing physical and blast effects, pressurization safety, decompression sickness and hypoxia

Air bleeding location to cool turbojet engine turbine of supersonic aircraft, presenting graphs

Stratospheric subsonic and supersonic aircraft emission estimation for water vapor and nitrogen oxides

Supersonic jet noise and sonic boom sources, propagation and reduction, considering airport community disturbances, aircraft cabin noise and fatigue problems

Maximum overpressures of supersonic aircraft maneuvering-produced sonic booms occurring at geometrical acoustic ray focus points/caustic cusps/

Sonic boom alleviation by flow field alteration near supersonic aircraft, considering finite rise times, reduced overpressures and shock pressure rises [AIAA PAPER 72-653]

Silicon carbide rotating rectifier alternator with solid lubricated bearings for high altitude environments, noting applicability to supersonic aircraft

Numerical prediction of the diffusion of exhaust products of supersonic aircraft in the stratosphere

Optimum turns to a specified track for a supersonic aircraft.

Flow separation at the edges of some types of tail sections used in supersonic aircraft and in rocket technology

Fuels, lubricating oils and hydraulic fluids for supersonic aircraft, discussing chemical properties, propellant combustion efficiency and production

Supersonic aircraft wing form influence on sonic boom, discussing supersonic wind tunnel tests for noise reduction

Analysis of a lateral-directional airframe/propulsion system interaction of a Mach 3 cruise aircraft. [AIAA PAPER 72-961]

Supersonic aircraft focused sonic boom suppression by slowing down during turning flight, obtaining conditions for focus cut-off at ground by atmospheric refraction

Electrical discharge-produced explosions aboard supertankers during cleaning operation and electrostatic charging of supersonic aircraft during passage through heavy rain, noting water drop disintegration

SUPERSONIC AIRFOILS

Analytical method of characteristics to determine front shock and sonic boom due to flat delta wing with supersonic leading edges [DFVLR-SONDDR-205]

SUPERSONIC BOUNDARY LAYERS

High velocity boundary layer problems for space shuttle, investigating free interaction with detachment, shock wave, penetration, air bubbles in circulation and adherence conditions

Noise generation from turbulent supersonic shear layers, including low supersonic and transonic ranges for jet noise applications

Jet interaction induced supersonic turbulent boundary layer separation, obtaining flat plate pressure measurements and jet plume shadowgraphs

Velocity profile shapes computation in supersonic compressible turbulent boundary layers with adverse pressure gradients, discussing data and theory discrepancy, curvature, and three dimensional effects

Supersonic turbulent boundary layer interaction with compression corner, noting static pressure distributions, flow visualization and schlieren photographs [AIAA PAPER 72-114]

Laminar near wake solutions for slender ablating cone under supersonic atmospheric entry conditions including boundary layer reactions [AIAA PAPER 72-116]

Similarity method solution of differential equations of motion for supersonic laminar boundary near symmetry plane of cone at angle of incidence

Wind tunnel investigation of adiabatic compressible turbulent boundary layer in adverse and favorable pressure gradients at supersonic speed

Adverse pressure gradients effect on two dimensional supersonic turbulent boundary layer, measuring axial distribution of pressure, temperature, mass flow, turbulence intensity and wall shear [AIAA PAPER 72-311]

Supersonic axisymmetric turbulent boundary layer characteristics over circular cone, predicting blowing effect on separation

Impact probe displacement effects in supersonic turbulent boundary layer in terms of Mach number profiles

Turbulent separating and reattaching supersonic boundary layer flows in two dimensional compression corner, noting Reynolds number effect on separated shear layer length

Recovery factors on porous surface within gas screen region in supersonic turbulent boundary layer for various air injection rates

Subsonic and supersonic steady two dimensional compressible turbulent boundary layer flow past wavy wall, presenting wall pressure and temperature distributions

Supersonic interaction effects on boundary layer flow structure in intersecting wedge corner at high Reynolds numbers from surface pressure measurements and oil flow visualization

Numerical solution to stabilization temperatures of supersonic boundary layer under intense surface cooling without constraints on disturbance wave number and Reynolds number

Binary diffusion of a jet embedded in a boundary layer.

Cooled supersonic turbulent boundary layer separated by a forward facing step.

Numerical and asymptotic methods for solving the problem of complete boundary-layer stabilization

Spin induced boundary layer distortion on rotating cone at supersonic speeds via spark shadowgraphs, correlating Magnus and normal force measurements with boundary layer configurations [AIAA PAPER 72-967]

Velocity distribution in the turbulent boundary layer of a supersonic gas flow

Three dimensional shock wave configurations in front of cylindrical body on supersonic wing or of fluid jet injected into main supersonic flow, examining high pressure gradient regions

Turbulent supersonic boundary layer flow in the neighborhood of a 90 deg corner.

SUPERSONIC COMBUSTION

Supersonic diffusion flame in duct configuration to study mixing with combustion of two parallel methane and air flows

Thermal nozzle combustion effects on supersonic flow of chemically reacting gas in thermodynamic equilibrium

Hydrogen fueled supersonic burning combustor testing, determining wall static pressure, hydrogen radial distribution, Pitot pressure and Mach number at combustor exit

Supersonic combustion of liquid fuels, hydrogen and propane, discussing initiation and stabilization in supersonic flow

Thermal nozzle combustion effects on supersonic flow of chemically reacting gas in thermodynamic equilibrium

Supersonic combustion research facility design for studying air-fuel mixing processes, shock wave induced temperature and pressure increments and flame holding devices

Two component reaction kinetics model for numerical analysis of combustion during two- and three dimensional supersonic steady flow of hydrogen-air fuel mixtures

Burning of carbon particles in a supersonic chemically active gas flow

Effect of the temperature on the burn-out of hydrogen diffusion flames in a supersonic flow in a closed channel

Supersonic and hypersonic combustion processes three dimensional characteristics, comparing wind tunnel test data with boundary layer equations numerical integration results [ICAS PAPER 72-21]

Two-dimensional supersonic flow with flame sheets.

Heat addition to supersonic flow by shock induced combustion studied by spherical and conical projectiles shot into explosive gas mixtures

Two-phase detonations with bimodal drop distributions.

Supersonic combustion photochemical initiation feasibility, measuring quantum yields and induction times in hydrogen, oxygen and chlorine mixtures

SUPERSONIC COMBUSTION RAMJET ENGINES

The S4MA hypersonic wind tunnel - Its use for tests of ramjet engines with supersonic combustion of hydrogen

Experiments on methods for improved fuel ignition in scramjet combustion systems. [ICAS PAPER 72-15]

Theoretical and experimental study of a dual-mode ramjet/flight range from Mach 3.5 to 7 [ICAS PAPER 72-24]

Swirling base injection for supersonic combustion ramjets.

SUPERSONIC COMBUSTION RAMJET MISSILE

U RAMJET MISSILES

U SUPERSONIC COMBUSTION RAMJET ENGINES

A systems analysis of subsonic versus supersonic jet travel.

SUPERSONIC COMPRESSORS

Performance similarity of supersonic axial compressors with gas mixtures of different thermodynamic properties, verifying validity of critical Mach number of rotation [ONERA, TP NO. 966]

Hypersonic air inlet of revolution with mixed supersonic compression, analyzing shock-boundary layer interaction process [ONERA, TP NO. 977]

Supersonic axial flow shock-in-rotor type compressor performance tests, discussing factors responsible for low efficiency

Flow visualization in supersonic axial compressor by short exposure schlieren photography of shock wave patterns in rotating annular cascade of compressor blades [ONERA, TP NO. 1026]

Radial velocity distribution at supersonic compressor inlet from duct-cowl and wall pressure measurements [ONERA, TP NO. 975]

Flow data reduction validity for supersonic axial compressors, presenting experimental results for rotating supersonic cascade [ASME PAPER 72-GT-100]

Experimental study of flows in supersonic compressors [ICAS PAPER 72-11]

Jet pumps for compressible fluids at supersonic velocities.

SUPERSONIC DIFFUSERS

Russian book on theory of ramjet and rocket ramjet engines covering supersonic diffuser operational principles and design, nozzle, combustion chamber and ejector

Axisymmetric jet stretcher diffuser performance for ramjet engine inlet configurations, testing at angles of attack and supersonic flow velocities [AIAA PAPER 72-1024]

SUPERSONIC DRAG

Supersonic wind tunnel investigation of drag characteristics of clustered booster configuration in longitudinal flow at Mach 1.5 to 4.0 [DGLR PAPER 71-120]

Minimum drag bodies of revolution in supersonic flow obtained by combining steepest descent method with integral flow model

Experimental results regarding drag in supersonic flow without lift in the case of flight bodies with three in front pointed bodies [DFVLR-SONDDR-215]

SUPERSONIC FLIGHT

Slender projectile supersonic flight in fluid with nonequilibrium transformations, comparing theoretical shock decay angle with Wegener-Klikoff measurements

Book on heat and mass transfer, covering research results over 1953-1969 on supersonic aircraft and mis-

slies cooling problems, rarefied gas dynamics boundary layer flow, etc 05 p0747 A72-16399

Supersonic transition flight mode of reusable two stage space shuttle booster for orbiter launching, comparing with subsonic and high lift to drag designs [AIAA PAPER 72-133] 07 p1084 A72-18963

Liquid fuel elastic rocket motion stability in supersonic flight, using vibration and thrust vector control equations for dynamic properties description 08 p1241 A72-21633

Pitching moments effect on phugoid and height mode stability of aircraft in supersonic flight 09 p1263 A72-23622

Stratospheric meteorological characteristics effects on Concorde supersonic flight performance, fuel consumption, dynamic behavior and passenger comfort 13 p1994 A72-28876

Mathematical model for flow field inside raindrop under aerodynamic transient stresses before impingement at stagnation point of blunt body in supersonic flight 13 p1942 A72-29224

Variable sweep wings aerodynamic characteristics in subsonic, transonic and supersonic flight, considering lift, drag, stability and control 18 p2643 A72-36976

Computer program for automated design of long haul transport aircraft, discussing cost effectiveness of composite materials for aircraft structure [AIAA PAPER 72-794] 19 p2750 A72-38121

German monograph - Pressure variation along a plane slender wedge and along a slender cone of revolution at decelerated flight in the supersonic range near sonic velocity. 22 p3136 A72-43074

Supersonic aircraft energy turns. 23 p3252 A72-44196

Raindrop breakup in the shock layer of a high-speed vehicle. 24 p3395 A72-45780

SUPERSONIC FLOW

Pt coated W hot-wire anemothermometers sensitivities in supersonic turbulent flow at low Reynolds numbers [ONERA, TP NO. 1024] 01 p0064 A72-10037

Discrete ionospheric model of supersonic two dimensional low density plasma flow past large bodies, using quasi-neutrality condition 01 p0001 A72-10588

Difference schemes for continuous computation of supersonic steady gas flows with internal compression shock waves 02 p0150 A72-11737

Supersonic oxygen molecules nozzle beam reactive scattering on barium atoms, detailing exothermic reaction energy in barium oxide formation 02 p0170 A72-11912

Nonlinearity effects on two dimensional steady supersonic dissipative flow governed by Navier-Stokes equations, obtaining expressions for flows past thin airfoil and wedge 02 p0203 A72-11976

Supersonic and hypersonic flows with attached shock waves over delta wing at angle of attack, deriving unified theory for flow field 02 p0150 A72-12030

Circular cone in supersonic flow, obtaining self similar solution for effect of angle of attack on laminar boundary layer by finite difference method 02 p0150 A72-12095

Shock wave impact at flat/spherical end surface of cylindrical body in supersonic nitrogen flow, using pulsed ruby laser for shadow photography 02 p0151 A72-12280

Low density monatomic gas supersonic spherical source flow, presenting departure from translational equilibrium 02 p0205 A72-12359

Aeroelastic stability of flat anisotropic sandwich plates in supersonic compressible fluid flow 02 p0297 A72-12614

Turbulent supersonic separated flow field analysis and pressure measurements for two dimensional and axisymmetric internal and external flow models [DGLR PAPER 71-076] 02 p0152 A72-12710

Closed boundary layer separation regions in super- and hypersonic flow, deriving mathematical model for neutral stability curves calculation 02 p0153 A72-12715

Residence time of foreign gas introduced within wake recirculation region behind slender body in axisymmetric supersonic laminar/turbulent flow [AD-733525] 03 p0308 A72-13633

Local stagnation temperature measurement in supersonic flow, using hot-wire anemothermometer 03 p0309 A72-13789

Interaction forces of gas jet injected into supersonic stream, examining data from thrust vector control gas injection tests 03 p0342 A72-13958

Plane shock wave and blunt body interaction in supersonic gas flow in two-diaphragm shock tube 04 p0461 A72-14639

Unsteady supersonic flow disturbance by slender bodies in strong contact discontinuities in shock tube studies 04 p0462 A72-15507

Symmetrically deformed delta wing in supersonic flow, considering leading edge flow separation induced vortices effects on downwash, pressure distribution and aerodynamic characteristics 04 p0463 A72-15741

Stochastic aerodynamic heating of shallow shell in supersonic turbulent flow by Monte Carlo method 05 p0599 A72-15845

Suspended compression shock construction near supersonic point in plane nonuniform ideal gas flow by hodograph technique 05 p0600 A72-16213

Surface pressure approximation formula for inclined circular cone in supersonic flow 05 p0603 A72-16547

Finite difference integration based on theoretical model analysis of three dimensional turbulent boundary layer on sharp cone at angle of attack in supersonic flow [AIAA PAPER 72-187] 05 p0650 A72-16842

Three dimensional supersonic flow about space shuttle, comparing method-of-characteristics and shock-capturing computations [AIAA PAPER 72-191] 05 p0729 A72-16845

Characteristic schemes comparison for three dimensional steady isentropic supersonic flow [AIAA PAPER 72-190] 05 p0605 A72-16846

Numerical analysis of three dimensional inviscid supersonic flow field about complex vehicle geometry, using finite difference technique and Rankine-Hugoniot relations [AIAA PAPER 72-192] 05 p0606 A72-16847

Supersonic interaction in streamwise corner of intersecting wedges, including pitot traverse, surface pressure and oil flow visualization measurements [AIAA PAPER 72-6] 05 p0606 A72-16862

Nonlinear effects of inviscid supersonic flow field surrounding bodies in coning motion, using shock capturing finite difference technique [AIAA PAPER 72-27] 05 p0607 A72-16918

Optimal airfoil profile for minimum drag in supersonic linearized gas flow with allowance for random fabrication errors and surface melting and sublimation at high temperatures 05 p0610 A72-17136

Shock wave shape and strength alteration by radioisotope emissions from body surface in supersonic airstream 05 p0654 A72-17226

Plane supersonic ionizing shock wave in magnetic field under small wave plane perturbation from equilibrium position, calculating stability from linearized equations 06 p0798 A72-17678

Inviscid solar wind equations supersonic solutions existence domain from critical point boundary conditions 06 p0881 A72-17894

Water vapor condensation in centered rarefaction wave arising in supersonic flow around apex of obtuse angle 06 p0799 A72-17911

Three dimensional velocity field excitation by thin airfoil vibrations in supersonic flow, deriving function in semispase to satisfy boundary constrained wave equation 06 p0756 A72-18111

Numerical solution of supersonic flow past blunt bodies with large mass injection, deriving finite difference equations 06 p0756 A72-18114

Ideal gas flow past blunt body in supersonic stream, discussing sonic lines, characteristics and Mach number 06 p0756 A72-18119

Supersonic flow patterns near yawed obstacles around flat plate sharp leading edge with high pressure regions in reversed separated flow zone 06 p0756 A72-18122

Lax finite difference scheme application to transonic two dimensional Laval nozzle and supersonic blunt body flow with detached shock wave, considering inviscid thermally nonconducting 06 p0756 A72-18126

V-shaped wings supersonic characteristics at 0-15 deg angles of attack, investigating flow structure between wings by pitot tube rake 06 p0757 A72-18129

Cornered axisymmetric blunt body sonic line in steady supersonic flow, showing incomparability with sonic shoulder of sphere 06 p0757 A72-18138

Supersonic near wake flow around blunt and sharp cones with trailing edge turbulent boundary layer 06 p0757 A72-18141

Forced nonlinear oscillations of finite plate in plane supersonic gas flow, considering elastic forces and resonant characteristics deformation 06 p0901 A72-18708

Supersonic hydrogen plasma flow in collapsing postsunset upper ionosphere, noting nonvanishing temperature gradient effect on critical point location 07 p0974 A72-18899

Transitional and turbulent heat transfer measurements on yawed blunt cone nosetip in supersonic air flow at various angles of attack [AIAA PAPER 72-212] 07 p0964 A72-18960

Plate surface temperature during aerodynamic heating in supersonic gas flow, using linearized Pohlhausen method 07 p0909 A72-18991

Contact discontinuity motion past slender body of revolution in shock tube, solving unsteady supersonic flow problem by method of integral transformation 07 p0909 A72-20072

Laser holographic imagery of plane and three dimensional objects for supersonic field representation of standing wave in isotropic liquid 08 p1165 A72-21078

High power visible output gas dynamic lasers, discussing supersonic flow generation 08 p1182 A72-21337

Body drag measurement in low density supersonic gas stream in various Knudsen number ranges 08 p1166 A72-21409

Two dimensional two step difference scheme for shock wave interaction with cylinder in supersonic flow 08 p1150 A72-21443

Evaporation and combustion of liquids injected into high temperature supersonic flow, considering interrelation with pressure variations 08 p1253 A72-21454

Supersonic plasma flow in narrow rectangular channel and free incompressible inviscid conducting liquid jet motion within pulsating transverse magnetic field 08 p1214 A72-21652

Stagnation conditions of magnetoradiative supersonic flow through shock waves for temperature dependent specific heat parameter 08 p1255 A72-21795

Supersonic flow through stationary and rotating cascades, using method of characteristics 09 p1260 A72-22630

Book on ideal and real compressible fluid dynamics covering supersonic flow past airfoils and shock wave interaction with laminar boundary layer 09 p1295 A72-23045

Taylor series truncation method for steady supersonic inviscid gas flow past nonaxisymmetric conical bodies 09 p1295 A72-23498

Schlieren optics for visualization and differentiation of density gradients with color and brightness distinctions, applying to supersonic flow through tandem grid 09 p1316 A72-23669

Mixed subsonic-supersonic flows solution for choked isentropic flow in convergent-divergent nozzle, comparing results with series solution 10 p1561 A72-23721

Flat face cylinders in rarefied supersonic gas flow, investigating perturbed region evolution based on pitot tube method 10 p1415 A72-23751

Mach number distribution along critical streamline in compressed layer in front of cylinder in supersonic flow 10 p1415 A72-23752

Numerical prediction of subsonic and supersonic flow through convergent-divergent nozzle 10 p1416 A72-23874

Pseudoviscous method application to computation of supersonic flow of inviscid ideal gas through two dimensional or annular axisymmetric ducts 10 p1417 A72-23876

Numerical solution for super-Alfvénic supersonic aligned MGD flow over cone with attached shock wave, obtaining surface pressure coefficients, current and vorticity distributions 10 p1418 A72-24463

Pitot tube pressure measurements in supersonic gas flow, calculating free molecular conditions limits 10 p1419 A72-24548

Supersonic flow around thin cruciform wing with antisymmetrical angle of attack distribution and horizontal plane with leading edge, considering flow separation at edges 10 p1420 A72-25118

Linearized method of characteristics application to supersonic flow past oscillating flat plate cascades with supersonic leading edge locus [AIAA PAPER 72-377] 11 p1730 A72-25401

Unsteady aerodynamic loadings of flexible aircraft with nonplanar wings and wing-tail surfaces in supersonic flow 11 p1574 A72-25402

Two dimensional cascades supersonic exit flow field, using Oswatitsch method of characteristics and conservation laws [ASME PAPER 72-GT-49] 11 p1570 A72-25641

Shock wave impact at flat/spherical end surface of cylindrical body in supersonic nitrogen flow, using pulsed ruby laser for shadow photography 11 p1571 A72-25702

Three dimensional laminar boundary layer on slender circular cone at angle of attack in supersonic flow, determining separated flow region via finite difference method

11 p1572 A72-25818

Electrically excited carbon dioxide-nitrogen laser using high repetition rate discharge pulses from pin electrode array transverse to supersonic flow

11 p1647 A72-26147

Subsonic and supersonic flow around nonaxisymmetric fuselages, deriving streamlines differential equations based on camber line distribution of source, dipole and quadrupole singularities

[DFVLR-SONDDR-189]

11 p1573 A72-26578

Method of characteristics for three dimensional supersonic flow of guiding center plasma, noting application to solar wind-moon interaction

11 p1573 A72-26601

Holographic interferometer and fringe analyzer with laser sources, discussing design and application to supersonic flow imaging in wind tunnel

12 p1809 A72-27760

Shadowgraph photography method for supersonic air flow pattern around porous cone in uniform injection, noting pressure distribution dependence

12 p1752 A72-27986

Surface temperature distribution for porous plate in supersonic flow with gas injection into turbulent boundary layer

13 p1893 A72-28917

Vibrational relaxation mechanism in supersonic flows of chemically reacting carbon dioxide-nitrogen mixture, using numerical integration

13 p1913 A72-29502

Wind tunnel investigation of supersonic air flow behavior on rotatable right dihedral formed by two plane plates with sharp edges

13 p1894 A72-29636

Friction drag and heat transfer on long blunt-nosed cylinder in supersonic flow, determining location of transition zone as function of Mach number

13 p1895 A72-29642

Stream surfaces of three dimensional sub and supersonic irrotational gas flows in variable cross section channels and nozzles

13 p1895 A72-30004

Minimum drag bodies of revolution in supersonic flow obtained by combining steepest descent method with integral flow model

14 p2069 A72-30231

Kinetic freezing effects of supersonic gas flow with solid particles into vacuum, analyzing continuous to collisionless transition flow for Maxwell molecules

14 p2094 A72-30295

Initial dihedral wing-body interaction for supersonic leading edges, determining expansion of velocity potential on root chord

14 p2069 A72-30365

Laminar to turbulent boundary layer transition in supersonic flow over flat plate investigated in supersonic wind tunnels, noting unit Reynolds number effect

14 p2069 A72-31004

Two dimensional two phase steady supersonic wedge flow patterns analysis based on equations for flow between wedge surface and shock wave

14 p2070 A72-31011

Ideal gas axisymmetric flow created in supersonic flow interaction with blunt body with strong blowing at surface, obtaining boundary layer approximate solution

14 p2070 A72-31012

Supersonic ideal gas flow in corner formed by intersecting plates, using direct computation method for nonequilibrium flows with detached shock waves

14 p2071 A72-31021

Shock wave interaction with supersonic moving plate, calculating plate lift as function of time

14 p2071 A72-31024

Heat transfer distribution in supersonic arc plasma constrictor of variable cross sectional area ducts, including pressure and compression shock front effects

14 p2141 A72-31071

Stochastic aerodynamic heating of shallow shell in supersonic turbulent flow by Monte Carlo method

15 p2178 A72-31264

Ideal gas supersonic axial flow past circular cylinder, solving Navier-Stokes equations by Van Dyke matched asymptotic expansions method

15 p2178 A72-31463

Isoenergetic and irrotational planar supersonic cascade ideal gas flow computation by analytic method of characteristics

15 p2178 A72-31466

Approximate model of weak shock wave interaction with laminar MHD boundary layers for perfectly conducting supersonic streams

15 p2284 A72-31633

Characteristic parameters of stationary supersonic plasma flow in magnetic de Laval nozzle calculated for collisional and collisionless cases, measuring ion saturation currents

15 p2285 A72-32268

Numerical results of carbon dioxide-nitrogen-water gas dynamic laser comparison with arc-driven supersonic laser in gas dynamic mode

15 p2250 A72-32517

Supersonic interaction effects on boundary layer flow structure in intersecting wedge corner at high Reynolds numbers from surface pressure measurements and oil flow visualization

16 p2341 A72-32830

Probst-Gold viscoelastic model of supersonic flow induced surface cross-hatching assessment against Dowell studies on plates and shells flutter

16 p2463 A72-32838

Fast numerical solution for supersonic flow past flat-faced blunt body by integration from stagnation point, noting computing time on CDC 6600

16 p2341 A72-32840

Linearized supersonic flow past harmonically vibrating cylindrical body, solving boundary value problem by cylindrical integral transformation

16 p2342 A72-32878

Inverse Laval problem of three dimensional subsonic and supersonic flows in nozzles and ducts of variable cross section in terms of asymptotic series

16 p2342 A72-32930

Crococo-Lee theory extension to flow behavior prediction for two dimensional supersonic turbulent near wake behind bluff body during recompression

16 p2343 A72-33402

Direct integral method to calculate subsonic and supersonic regions in planar and axisymmetric hyperbolic flow, using stream function for velocity and density

16 p2343 A72-33421

German monograph on supersonic flow past blunt sharp edged cones, comparing Van Dyke and method of characteristics results with schlieren photos and shadowgraphs

16 p2343 A72-33505

Coordinate perturbation and multiple scale techniques application to supersonic flow field around two dimensional wing and oscillations in closed tube

16 p2379 A72-33576

Faraday ring currents induction by radial magnetic field in low pressure plasma supersonic ring channel flow driven by inductive hydrodynamic shock tube

16 p2437 A72-33749

Supersonic vortex boundary layer flow velocity profiles behind flat plate indentation for Mach numbers 1.7-3.0 and Reynolds numbers to 40,000,000

16 p2380 A72-33857

Flat plate leading edge blunting and wall cooling effects on supersonic laminar flow ramp-induced separation

16 p2344 A72-34032

Supersonic flow aerodynamic window for high power laser beam extraction through nonabsorbing gas medium while supporting pressure difference between cavity and ambient atmosphere

16 p2404 A72-34036

Finite difference method computation of multishocked three dimensional wing-body supersonic flow fields with real gas effects, applying to delta winged space shuttle

16 p2345 A72-34042

Magnetogasdynamic heat transfer to hemispherical body in supersonic low density plasma, noting magnetic field effects on heat flux

16 p2346 A72-34056

Flow distribution for inviscid nonconducting uniform supersonic stream past unyawed semiinfinite circular cone with attached shock wave

17 p2483 A72-34325

Solution of the two-dimensional, unsteady, compressible Navier-Stokes equations using a second-order accurate numerical scheme

17 p2538 A72-34646

Development of transition in the wake of a cylinder perpendicular to a supersonic flow

17 p2484 A72-34769

Numerical calculation of the supersonic flow of a viscous fluid about a parabolic obstacle

17 p2484 A72-34887

Plate surface temperature during aerodynamic heating in supersonic gas flow, using linearized Pohlhausen method

17 p2485 A72-35139

Unified area rule for hypersonic and supersonic wing-bodies

17 p2485 A72-35251

Velocity distribution and Mach number in a supersonic molecular beam of plane symmetry

17 p2486 A72-35423

Turbulence model equations for calculation of supersonic and hypersonic flows, representing Reynolds stresses and turbulent heat flux vector in terms of eddy viscosity

17 p2543 A72-35639

Inviscid perfect gas supersonic steady irrotational flow past wedge, investigating analytical solution validity in downstream region behind shock

17 p2544 A72-35900

Particle motion behind oblique shock wave in two phase supersonic wedge flow, deriving expressions for particle trajectories and velocity equalization time

17 p2487 A72-35926

Spectroscopic determination of the rotational temperature in a rarefied supersonic flow in glowing-discharge excited nitrogen

17 p2544 A72-35928

Inert and reactive gas injection in near wake behind blunt bodies in supersonic flow, considering influence on base pressure and temperature

17 p2487 A72-35930

Fluid jets and droplets deformation in transverse supersonic two phase gas flow

17 p2544 A72-35932

Near flow field and aerodynamic loading in subsonic and supersonic flow over body-wing configuration, surveying numerical, kernel function and image methods

18 p2641 A72-36390

Boundary layer and inviscid main stream interaction in asymmetric supersonic steady gas flow incident on circular cone at high Reynolds numbers

18 p2641 A72-36662

A contribution to the gas dynamics of oblique shocks with change of total enthalpy

18 p2682 A72-36725

A through-type counting method for two-dimensional and spatial supersonic flows. II

18 p2642 A72-36810

Weak waves, characteristics, and the problem of flows past slender profiles in electrohydrodynamics

18 p2716 A72-36896

Calculation of spatial ideal gas flows without a symmetry plane

18 p2642 A72-36901

Experimental investigation of the flow past a cylinder with a flat nose

19 p2745 A72-37397

Generating high Reynolds-number flows

19 p2787 A72-38222

Jet aircraft noise sources in subsonic and supersonic exhaust mixing process, suppressing noise via turbofan exhaust speed reduction

19 p2849 A72-38380

A method of straight-through calculation for two-dimensional and three-dimensional supersonic flows. I

19 p2747 A72-38852

Flow separation at the edges of some types of tail sections used in supersonic aircraft and in rocket technology

20 p2885 A72-39597

Decay of a diamond shock pattern

20 p2913 A72-39606

Influence of viscosity on the characteristics of compressor blades for supersonic flow conditions

20 p2963 A72-39917

Unsteady aerodynamic and aeroelastic effects in turbomachine blade cascades supersonic flow, discussing trends in fan and compressor technology

21 p3118 A72-40969

Heat transfer in separated regions in supersonic and hypersonic flows

21 p2991 A72-41139

Computation of three-dimensional non-equilibrium supersonic flows

21 p2992 A72-41162

The possibility of producing plasma regions at thermonuclear fusion conditions in a supersonic flow by means of high power electron beam

21 p3092 A72-41224

On the conditions for the appearance of the Mach effect in the reflection of an oblique shock wave in supersonic flow

21 p3046 A72-41339

Base mounted cylinders effect on near wake of axisymmetric blunt base in supersonic flow

21 p2993 A72-41594

Three-dimensional supersonic flows at large distances from a body of finite volume

21 p2994 A72-41661

Experimental determination of the vibrational temperature of a supersonic gas flow

22 p3242 A72-41879

A new stagnation pressure probe having a high pressure recovery in supersonic flow

22 p3179 A72-42687

Stream surfaces of three dimensional sub and supersonic irrotational gas flows in variable cross section channels and nozzles

22 p3135 A72-42727

Supersonic flow past a suddenly set plate

22 p3136 A72-42906

Aeroelastic optimization of a panel in high Mach number supersonic flow

23 p3343 A72-43327

Three dimensional supersonic flow past bodies with a smooth generatrix

23 p3248 A72-43651

Velocity distribution in the turbulent boundary layer of a supersonic gas flow

23 p3249 A72-44084

Heat addition to supersonic flow by shock induced combustion studied by spherical and conical projectiles shot into explosive gas mixtures

24 p3360 A72-45038

Conical caret wings supersonic characteristics, examining flow transition from weak to strong attached shock waves

24 p3361 A72-45114

Effect of a line energy source at the boundary of a supersonic flow.

24 p3361 A72-45187

Experimental research on the wave resistance of a thin spindle with an annular shield in a supersonic axial flow

24 p3364 A72-45393

Gas dynamics and shock wave physics of supersonic flow in two phase media, noting evaporation, condensation and phase transformations

24 p3364 A72-45525

SUPERSONIC FLOW INLETS

U SUPERSONIC INLETS

SUPERSONIC FLUTTER

Orthotropy orientation effect on supersonic flutter of infinite-length thin heterogeneous circular cylindrical structures in axisymmetric gas flow

04 p0584 A72-14520

Minimum weight panel designs subject to supersonic flutter constraint, approximating governing differential equations by difference equations

05 p0741 A72-16908

Automated optimization for preliminary design of supersonic aircraft wings, noting flutter, stresses and resonant frequency as dynamic constraints

[AIAA PAPER 72-333] 11 p1727 A72-25368

Supersonic flutter of plane, rectangular, anisotropic, heterogeneous structures

24 p3459 A72-45440

SUPERSONIC HEAT TRANSFER

Plate surface temperature during aerodynamic heating in supersonic gas flow, using linearized Pohlhausen method

07 p0909 A72-19891

Flow field model of convective heat transfer along reattachment surface in planar supersonic turbulent flow

[ASME PAPER 71-HT-W] 08 p1251 A72-20876

Surface patterns from ablating, melting and flowing materials in supersonic flow of wind tunnel, rocket motor and flight test environments, comparing with theory

[AIAA PAPER 72-313] 11 p1743 A72-25247

Plate surface temperature during aerodynamic heating in supersonic gas flow, using linearized Pohlhausen method

17 p2485 A72-35139

Heat transfer at reattachment of a compressible flow over a backward facing step with a suction slot.

20 p2885 A72-39626

SUPERSONIC INLETS

Mach 2.65 axisymmetric mixed-compression inlet system diffuser and boundary layer bleed system performance estimates confirmed by tests

[AIAA PAPER 72-45] 05 p0609 A72-16959

Combined viscous-inviscid analytical procedure for predicting boundary layer effects on supersonic inlet flow field

[AIAA PAPER 72-44] 05 p0609 A72-16975

Radial velocity distribution at supersonic compressor inlet from duct-cowl and wall pressure measurements

[ONERA, TP NO. 975] 09 p1260 A72-22812

Application of quadratic optimization to supersonic inlet control.

23 p3251 A72-44195

Experiment of supersonic air intake buzz.

23 p3249 A72-44496

Supersonic aircraft engine inlet performance in terms of pressure recovery, discussing oblique shock wave formation ahead of entrance to improve efficiency

24 p3360 A72-44991

SUPERSONIC JET FLOW

Sonic line neighborhood of uniform axisymmetric supersonic air jet impinging on perpendicular flat plate, measuring shock shapes and surface pressures

01 p0002 A72-11398

High speed jet noise source physical properties interpretation by theory and scale-model experiments for supersonic transport aircraft noise suppression problem

02 p0154 A72-11973

Induction heated low density supersonic free plasma jet diagnosis, determining velocities and heavy particle temperatures

02 p0265 A72-12361

Method of characteristics calculations of inviscid free jet flow with low specific heat ratios for perfect gas at 1.10 Mach number

03 p0309 A72-13926

Mean velocity and turbulent fluctuation distributions for sub- and supersonic jets in convergent nozzles, obtaining sound power spectra

[AIAA PAPER 72-157] 05 p0651 A72-16872

Gas density distributions in argon and carbon dioxide supersonic jets with low angular divergence in vacuum, using Laval supersonic nozzle

07 p0973 A72-20512

Boundary configuration of supersonic underexpanded jet discharging into stationary medium

09 p1259 A72-22410

Supersonic and subsonic jet flows coexistence in constant section duct, analyzing pressure on walls and in fluid and schlieren visualization

[ONERA, TP NO. 976] 09 p1294 A72-22813

Pressure, temperature and nozzle size effects on molecular cluster formation in expanding supersonic jets of rare gases, nitrogen and carbon dioxide

09 p1294 A72-22853

Charged to neutral particle transformation capacity of wide aperture recharge target formed by supersonic gas jets in magnetic trap with annular nozzle

09 p1363 A72-23224

Cryogenic techniques for high vacuum differential pumping with low conductivity cooled channels and supersonic jet target

09 p1364 A72-23225

Supersonic Ar, He and molecular nitrogen jets, determining electron temperature and concentration and atomic state population in shock waves region by spectroscopic measurement

10 p1517 A72-23837

Supersonic axisymmetric turbulent jet density fluctuations measurement by single beam schlieren system, using preheater to reduce jet static/ambient temperature difference

10 p1466 A72-24292

Aerodynamic noise generation mechanism of ideally expanded supersonic jet based on large scale flow instabilities, deriving mathematical model

10 p1418 A72-24331

Fast iodine ions charge exchange in dense carbon dioxide supersonic jet, determining electron capture cross sections by least squares method

10 p1516 A72-25036

Russian monograph on self oscillatory noise generation during gas jet ejection covering single, parallel, supersonic, flat and cylindrical jets stability

11 p1617 A72-26066

Optimization of high temperature supersonic gas jets for metal powders production by melts atomization, discussing excess air ratio effect on gas parameters

13 p2025 A72-29133

Holographic interferometry of Mach wave field generation by supersonic turbulent jet, noting visible conical wave front from core edge

13 p1898 A72-29580

Supersonic jet exhaust noise radiation from turbulent shear layer instability waves, noting acoustic energy flux dependence on streamwise distance

13 p2028 A72-29581

Reichardt mixing model for turbulent boundary layer calculation in wall flow, noting supersonic and nonisothermal jet flow

14 p2095 A72-31002

Noise measurements during shock free and underexpanded operation modes of supersonic cold model jet at moderate exit Mach number

15 p2179 A72-32017

Supersonic molecular jet improvement via expansion chamber residual gas pressure reduction and nozzle stagnation pressure increase

16 p2429 A72-33053

Perturbations effects on plane symmetry supersonic molecular beam intensity as function of nozzle-skimmer geometry and nozzle pressures

16 p2430 A72-33062

Acoustic attenuation and thrust loss incurred by shrouded multi-tube supersonic jet noise suppressor

[AIAA PAPER 72-642] 16 p2381 A72-34090

Supersonic jet noise mechanisms and scaling laws, studying acoustic fields for rectangular and axisymmetric nozzle configurations

[AIAA PAPER 72-641] 16 p2381 A72-34091

Combustion driven resonance tubes.

17 p2597 A72-34974

Effect on supersonic jet noise of nozzle plenum pressure fluctuations.

17 p2597 A72-35243

Method of characteristics application to supersonic jet and nozzle gas flow with allowance for equilibrium and nonequilibrium condensation

17 p2544 A72-35929

Acoustic efficiency of supersonic annular jets

21 p3045 A72-41098

Discrete component of the noise spectrum of a supersonic annular jet

21 p3045 A72-41100

Wall porosity and angle of attack effects on jet stretcher flow field for supersonic engine inlet testing, using three dimensional method of characteristics

[AIAA PAPER 72-1025] 21 p3042 A72-41603

Experimental and design investigation of a supersonic wall jet in a supersonic slipstream

22 p3133 A72-42254

Numerical integration of three dimensional flow equations for supersonic jets of ideal gas exhausted from elliptical and rectangular nozzles

22 p3133 A72-42264

Problem of uniform-jet flow around an airfoil

22 p3133 A72-42271

Diffusion of a filament of gas injected into a supersonic free jet.

23 p3280 A72-43947

Formation of a jet of shock-heated gas outflowing into evacuated space.

24 p3391 A72-45046

SUPERSONIC NOZZLES

Carbon dioxide-nitrogen-water or He mixtures expansion through supersonic nozzles, showing population inversion of vibrational energy levels

04 p0513 A72-15337

Laser action in carbon monoxide vibrational-rotational bands produced by electrical excitation of carbon monoxide-nitrogen-oxygen-helium mixtures following expansion in supersonic nozzle

07 p1001 A72-19047

Pressure, temperature and nozzle size effects on molecular cluster formation in expanding supersonic jets of rare gases, nitrogen and carbon dioxide

09 p1294 A72-22853

Boundary layer turbulence development by gas flow interaction with arc plasma in supersonic nozzle, causing light emission fluctuations

[AIAA PAPER 72-415] 11 p1617 A72-26165

Electrothermal thruster supersonic convergent-divergent nozzle performance with lithium vapor propellant, predicting exhaust velocity by isentropic flow equations

[AIAA PAPER 72-453] 11 p1708 A72-26189

Laser emission from pulsed transverse electric discharge in supersonic nozzle downstream region gas dynamic cooled mixture

15 p2245 A72-31385

Three dimensional supersonic nozzle exhaust flow field numerical analysis based on reference plane characteristics, deriving difference equations for three coordinate systems

[AIAA PAPER 72-704] 16 p2344 A72-34040

Data correlation of jet noise total sound power and peak sideline overall sound pressure level for subsonic and supersonic convergent exhaust nozzles

[AIAA PAPER 72-643] 16 p2381 A72-34089

Influence of contraction section shape and inlet flow direction on supersonic nozzle flow and performance.

17 p2483 A72-34204

Subsonic, transonic, and supersonic nozzle flow by the inverse technique.

17 p2483 A72-34206

Calculations of the turbulent boundary layer in supersonic nozzles.

17 p2485 A72-35237

Method of characteristics application to supersonic jet and nozzle gas flow with allowance for equilibrium and nonequilibrium condensation

17 p2544 A72-35929

Nozzle beam-mass spectrometer system for studying one-atmosphere flames.

[WSCI PAPER 72-9] 20 p2921 A72-38975

Viscous non-adiabatic laminar flow through a supersonic nozzle - Experimental results and numerical calculations.

[ASME PAPER 72-HT-49] 20 p2985 A72-39662

Study of a reactive nozzle flow associated with solid gas-phase interaction.

24 p3433 A72-45063

The transient processes in hybrid solid propellant combustion chamber throttled by supersonic nozzle.

24 p3434 A72-45198

SUPERSONIC PRESSURE DISTRIBUTION

U PRESSURE DISTRIBUTION

U SUPERSONIC FLOW

SUPERSONIC SPEEDS

Supersonic ribbon parachute testing by transonic wind tunnel, rocket sled and water channel simulator

01 p0004 A72-10305

Ground test determination of design data for low supersonic high density air deployable deceleration systems, considering high strain rate effects on parachute materials

01 p0005 A72-10313

Frictional electrification from supersonic particle impact, determining particle charge and concentration, body intercepting area and velocity variations with speed

02 p0261 A72-12555

Flow field due to diffraction of shock wave at wedge moving at supersonic speed

05 p0600 A72-16212

Nonsymmetrical aerodynamic damping moments on 10 deg cone at supersonic speeds and large angles of attack, comparing Newtonian theory prediction with wind tunnel test results

[AIAA PAPER 72-29] 05 p0609 A72-16947

Plane oblique shock wave diffraction on wedge moving in homogeneous gas flow at supersonic speed, reducing boundary value problem to Hilbert problem

07 p0910 A72-20317

Photoelastic studies of plane stress fields in plate induced by moving loads at subsonic, transonic and supersonic speeds

10 p1553 A72-23746

Mathematical model for supersonic crack propagation in cubic lattice, deriving velocity-applied stress relation

10 p1558 A72-24895

Trajectory determination of supersonically traveling object from shock arrival times observations at ground locations

11 p1617 A72-25994

Supersonic auroral motions relationship to infrasonic waves generation, showing acoustic pulse within electrojet arcs due to collisions with neutral gas of positive ions

11 p1624 A72-26403

Supersonic aerodynamic influence coefficients matrices calculation for wings of arbitrary planform, constructing computer program

12 p1752 A72-28142

Composition dependence of ultrasonic velocity in binary Mg base alloys measured by pulse method

14 p2143 A72-31030

Sonic boom induced flow field at supersonic/hypersonic speeds, using shock expansion method and hypersonic equivalence principle for sharp and blunt nosed bodies

[AIAA PAPER 72-652] 16 p2349 A72-34082

Quasi-homogeneous approximation for wing with curved subsonic leading edges at supersonic speeds.

[ICAS PAPER 72-54] 21 p2992 A72-41176

The diffraction of light by progressive supersonic waves: Oblique incidence of light. I - Approximate solution of the Raman-Nath equations.

22 p3207 A72-42852

Ultrasonic attenuation and velocity in hot specimens by the momentary contact method with pressure coupling, and some results on steel to 1200 C.

23 p3294 A72-44116

SUPERSONIC STRIKE AIRCRAFT

U ATTACK AIRCRAFT

U SUPERSONIC AIRCRAFT

SUPERSONIC TEST APPARATUS

Facility for studying the failure of structural elements in a supersonic high-temperature flow containing a controlled number of abrasive particles

21 p3043 A72-41717

High response two-transducer pressure measurement for evaluating nonuniform and unsteady inlet air flow distortion effects on supersonic jet engine stability and performance

22 p3216 A72-42683

SUPERSONIC TRANSPORTS

NT CONCORDE AIRCRAFT

NT SUPERSONIC COMMERCIAL AIR TRANSPORT

Thin-down intensities for heavy primaries at SST flight levels, using plastic stacks measurements

[CERN-71-16] 02 p0274 A72-12077

In-flight warning meter for solar and cosmic radiation dose equivalent measurements for radiological protection in SST aircraft

[CERN-71-16] 02 p0274 A72-12078

Cosmic ray exposure thindown tracks in human tissue from solar minimum to maximum at SST flight level

[CERN-71-16] 02 p0163 A72-12079

Stratospheric circulation and air temperature horizontal and vertical distribution, discussing CAT at supersonic transport heights

04 p0541 A72-14676

Minimum flight time routes model at SST altitudes, taking into account temperature, meteorological and wind factors

04 p0542 A72-14678

Storm effects on SST operations, discussing wave initiation at storm top and tropospheric propagation

04 p0542 A72-14683

CAT inducing atmospheric conditions effects on SST flight, discussing turbulence in convective clouds and kinetic energy spectra of atmospheric motions

04 p0543 A72-14693

Wave drag reduction by antisymmetric wing and body arrangement, discussing application to transport aircraft at supersonic speeds

05 p0602 A72-16534

SST operational maneuver effects on sonic boom, discussing steady flight and acceleration-to-crest pressure signatures

[AIAA PAPER 72-196] 05 p0613 A72-16981

Probability estimates of aircraft encounters with hail, discussing variations with locality, hailstone size and height and supersonic transport experience

09 p1346 A72-23423

Runway unevenness and landing gear characteristics effects on SST vibration during taxiing, taking off and landing

09 p1263 A72-23459

Pressure jumps lower bounds across supersonic transports induced shock waves in homogeneous atmosphere, using Whitham function in terms of Riemann integral

10 p1420 A72-24846

Flight airworthiness requirements development for supersonic transports, V/STOL and transport and general aviation aircraft, exploring critical control and stability parameters

[SAE PAPER 720306] 11 p1575 A72-25570

Medical and physiological hazards for SST passengers and crews, discussing cumulative cosmic radiation and high altitude decompression risks

11 p1583 A72-25816

Estimated peak regional concentration of SST exhaust in stratosphere from expected flight operation levels

13 p1991 A72-28837

Thunderstorm encounter probability at SST altitudes for selected cross country routes, using radar observation data

13 p1992 A72-28853

SST water vapor and nitrogen oxides exhausts effect on stratospheric composition, developing nonequilibrium photochemical model

13 p1994 A72-28878

Optimum low noise engine selection for transport and combat aircraft relative to range or payload performance, considering CTOL, VTOL, SST and fighter aircraft

15 p2297 A72-32127

Bibliography on SST upper atmospheric environment, listing references to stratospheric structure, composition and physical dynamics, chemical reactions with pollutants, transport properties, etc

16 p2386 A72-33797

SST contrails stratospheric dispersion by aircraft wake, atmospheric turbulence and exhaust gases temperature induced buoyancy

[AIAA PAPER 72-650] 16 p2388 A72-34084

Stratospheric pollution by SST exhaust gases, discussing water vapor and nitrogen oxides effects on ozone concentration

17 p2597 A72-35327

Meteorological effects on SST performance, considering temperature, wind, turbulence, hydrometeors, ozone and radiation effects

17 p2577 A72-35790

Radiobiological problems caused by supersonic transport /With a survey of the first results established by tests performed on board the Concorde prototype/.

19 p2762 A72-38713

Problems and solutions related to the design of a control augmentation system for a longitudinally unstable supersonic transport.

[AIAA PAPER 72-871] 20 p2887 A72-39128

Economic and social aspects of commercial aviation at supersonic speeds.

[ICAS PAPER 72-51] 21 p2996 A72-41851

Wing flutter prevention in SST structural design, using finite element model and lifting surface aerodynamic theory

22 p3237 A72-42760

SUPERSONIC TURBINES

High tip speed low loading transonic fan rotor design for weak oblique shocks with improved efficiency and stall margin

[AIAA PAPER 72-83] 07 p0907 A72-18951

Economical performance of single rim supersonic turbine stage with repeated low level admission of working body

07 p0908 A72-18986

Supersonic turbine cascade flow properties and pressure distributions on blades, comparing calculated results with experimental data

[ASME PAPER 72-GT-47] 11 p1570 A72-25639

Supersonic turbine stator and rotor blading design corrected for boundary layer displacement thickness, discussing limitations due to normal shock wave at flow separation

[ASME PAPER 72-GT-63] 11 p1571 A72-25653

Optimal arrangement of conical nozzles in a segment of a partial supersonic turbine stage

20 p2963 A72-39913

SUPERSONIC WAKES

Finite difference model application to supersonic planar viscous near wake, determining parameter range by physical and numerical restraints

[AIAA PAPER 72-115] 05 p0609 A72-16971

Book on steady laminar supersonic and hypersonic wakes covering near and far region solutions, boundary layer separation, etc

09 p1261 A72-23029

Development of transition in the wake of a cylinder perpendicular to a supersonic flow

17 p2484 A72-34769

SUPERSONIC WIND TUNNELS

Supersonic wind tunnel study of flow induced pressure oscillations in shallow rectangular cavity, investigating resonant frequencies and pressure mode shapes

01 p0049 A72-10221

Wind tunnel study of space shuttle longitudinal dynamic stability at supersonic speeds, discussing damping-in-pitch

[AIAA PAPER 72-135] 05 p0730 A72-16890

Flat plate boundary layer transition equations for supersonic wind tunnels, taking into account free stream turbulence

08 p1150 A72-21616

Laminar/turbulent boundary layer transition on parabolic wing profile in supersonic wind tunnel, noting critical Reynolds number increase with leading edge thickness

09 p1259 A72-22407

Superconducting magnetic suspension and balance facility of supersonic wind tunnel for dynamic stability studies

10 p1460 A72-24757

Superconducting coil design for magnetic suspension of supersonic wind tunnel balance

10 p1460 A72-24759

Data acquisition and reduction for model aerodynamics in superconducting magnetic suspension and balance of supersonic wind tunnel facility

10 p1461 A72-24766

Holographic interferometer and fringe analyzer with laser sources, discussing design and application to supersonic flow imaging in wind tunnel

12 p1809 A72-27760

Laminar to turbulent boundary layer transition in supersonic flow over flat plate investigated in supersonic wind tunnels, noting unit Reynolds number effect

14 p2069 A72-31004

Supersonic aircraft wing form influence on sonic boom, discussing supersonic wind tunnel tests from noise reduction

20 p2888 A72-39931

Flow quality improvements in a blowdown wind tunnel using a multiple shock entrance diffuser.

[AIAA PAPER 72-1002] 21 p3041 A72-41587

Evaluation of transonic and supersonic wind-tunnel background noise and effects of surface pressure fluctuation measurements.

[AIAA PAPER 72-1004] 21 p3041 A72-41588

SUPERSONICS

Time dependent finite difference /fluid-in-cell/ method for supersonic aerodynamic problems concerning inviscid compressible flow with contact surface and shock discontinuities

16 p2342 A72-32884

SUPINE POSITION

Plasma renin activity during supine physical exercise as function of salt loading

04 p0480 A72-15214

Supine human body mechanical impedance under combined stress of vibration and sustained acceleration

12 p1765 A72-28200

Cardiac stroke volume measurements during supine bicycle exercise and recovery period, using indicator dilution technique

14 p2079 A72-30700

Flight and centrifuge tested aircrew tilting supine seats biomedical and technical adequacy as acceleration protective man machine system

19 p2761 A72-38703

Health condition changes in test subjects during strict bed rest in hypokinetic recumbent and antiorthostatic position subject to lower body negative pressure

23 p2259 A72-43913

Rheographic investigation of cerebral, pulmonary and peripheral circulation during bed rest in antiorthostatic position

23 p2255 A72-43914

Metabolic changes in healthy humans caused by prolonged bed rest in horizontal position, noting prevention by physical exercises and electric muscle stimulation

23 p2260 A72-43923

Induction of hemodynamic deterioration by the hypogravic state - An evaluation of mechanisms and prevention.

24 p3373 A72-45191

SUPPORT SYSTEMS

NT GROUND OPERATIONAL SUPPORT SYSTEM

NT GROUND SUPPORT SYSTEMS

Product support functional organization, discussing support systems analysis and engineering, training design, technical proposals and publications, customer training, field service, etc

04 p0597 A72-15220

SUPPORTS

NT PYLONS

Iterative solution for non-Levy rectangular plates with corner supports, assuming small deflection theory

06 p0896 A72-17966

Influence of coupling behavior on the quietness of multiply supported shaft systems

18 p2694 A72-36070

Theoretical analysis of a cryogenic gas bearing with a flexible damped support.

19 p2810 A72-38837

SUPPRESSORS

NT ECHO SUPPRESSORS

Zener diode transient suppressors with electronic thermal switch for ground vehicle and aircraft applications

[AD-741529] 05 p0637 A72-16553

Large scale high aspect ratio multielement suppressor nozzle arrays testing for augmentor wings and internally blown flaps

[AIAA PAPER 72-131] 05 p0612 A72-16886

- Effect of electrical generator parameters on transient suppressors. 19 p2753 A72-37291
- An improved design and measurement of attenuation characteristics of RF suppressors. 20 p2902 A72-38997
- SURFACE CHEMISTRY**
- U SURFACE REACTIONS**
- SURFACE COOLING**
- Neutron star surface structure and cooling calculations for pulsar cosmic ray production through surface material acceleration 03 p0421 A72-13136
- Hg vapor condensation on cooled vertical steel cylinder at 70-185 C, considering heat flux relation to saturated vapor/cooling surface temperature difference 06 p0903 A72-18190
- Steady heat conduction of cooled gas turbine hollow nozzle blades with gas temperature variation along cascade 08 p1223 A72-20948
- Spatial layer cooling during surface emission according to Stefan-Boltzmann law, assuming heat source inside body 08 p1253 A72-21445
- Space shuttle booster and orbiter thermal protection systems, examining heat sink, metallic radiative, reusable surface insulation and surface cooled designs [AIAA PAPER 72-391] 11 p1726 A72-25412
- Thermal stresses near pole of spherical reservoir during cooling, using thermoelastic equations of shell of revolution 12 p1887 A72-28242
- Numerical solution to stabilization temperatures of supersonic boundary layer under intense surface cooling without constraints on disturbance wave number and Reynolds number 16 p2343 A72-33155
- Chill zone structures in Al-Cu alloys as function of heat sink, surface microprofile and liquid metal fluid flow 16 p2409 A72-33810
- Structural thermal protection systems for Space Shuttle, noting reusable surface insulation with active cooling [ASME PAPER 72-ENAV-32] 20 p2976 A72-39145
- Nonisothermal surface cooling for arbitrary temperature distribution and Prandtl number approaching zero, solving thermal boundary layer equations by series expansion 21 p3129 A72-41061
- German monograph - Cooling of geometrically simple bodies /flat plate, cylinder, sphere/ by convection and radiation. 22 p3244 A72-43062
- SURFACE CRACKS**
- Stress corrosion crack tip electrochemical reactions simulation on Ti and alloy surfaces, using modified rotating disk apparatus with pH measurement 04 p0536 A72-15739
- Dimpling behavior of metal plate with mode I edge crack, relating flaw depth, applied stress level and crack tip plastic zone 05 p0673 A72-16305
- Temperature effects on anodic polarization of Ti open surface and corrosion crevices, discussing critical potential relation to pitting 06 p0829 A72-17946
- Rupture strength of disk with surface crack under concentrated loads, applying integral equation to stressed state 07 p1092 A72-19777
- Analytical model for surface fatigue crack configuration during propagation into thick plate under cyclic loading [AD-741575] 07 p1095 A72-20242
- Brittle fracture dynamics, deriving motion equations and stability conditions of surface cracks under stress waves from energy balance and angular momentum conservation law 09 p1404 A72-22916
- Stress intensity factor for circular crack embedded in finite thickness solid under uniform tension, noting semielliptical surface flaw in brittle material [ASME PAPER 71-APMW-6] 10 p1554 A72-24183
- Brittle continuous and crazed anodic oxide coatings effect on Al filament stiffness, comparing with Dow analysis 13 p1974 A72-28663
- Cu surface contamination effect on hot crack susceptibility and weldability of Co based superalloys 13 p1965 A72-29419
- Crack propagation in biaxially stressed and heat treated cylindrical pressure vessel observed by strain gage displacement measurement, noting effects of initial surface cracks 14 p2169 A72-31176
- Surface stress solution for elastic half space weakened by spherical cut under internal pressure 15 p2333 A72-32681
- Surface crack detection in ferrous and nonferrous metals, glass, ceramics and plastics by water-washable dye penetrants process 16 p2397 A72-33239
- Crack depth measurement with surface waves. 19 p2809 A72-38569
- The influence of grain and twin boundaries in fatigue cracking. 21 p3069 A72-41350
- The magnetic field of eddy currents above a surface crack in metal with excitation of them by an applied inductor. 21 p3057 A72-41722
- The surface crack: Physical problems and computational solutions; Proceedings of the Winter Annual Meeting, New York, N.Y., November 26-30, 1972. 23 p3352 A72-44226
- The surface flaw in aircraft structures and related fracture mechanics analysis problems. 23 p3352 A72-44228
- Surface flaws measurement devices and quasi-static fracture tests, discussing cyclic crack growth, elastic compliance derivative method and stress intensity equations 23 p3353 A72-44229
- Experimental characterization of yield induced by surface flaws. 23 p3353 A72-44230
- Stress intensity factors for embedded elliptical crack in semiinfinite solid and for semielliptical surface crack in plate under tension and/or bending 23 p3353 A72-44231
- The elastic analysis of the part-circular surface flaw problem by the alternating method. 23 p3353 A72-44232
- Line spring analysis model for long part-through surface cracks in walls of plate or shell structures, formulating constitutive laws 23 p3353 A72-44234
- Three-dimensional finite element analysis for fracture mechanics. 23 p3353 A72-44235
- Stress distribution in a homogeneous elastic sphere containing a penny shaped crack of prescribed shape. 23 p3354 A72-44268
- SURFACE DEFECTS**
- Extruded anodized AlMgSi alloy matrix precipitate surface defects, noting wood grain effect, segregated bands, microstructural stains and heterogeneous zones 01 p0077 A72-11042
- Breakdown surfaces of thin Ti alloy specimens under tension as function of composition and heat treatment temperature 01 p0088 A72-11079
- Surface damage effect on strength of c-axis sapphire filaments, assessing impact on sapphire reinforced metal technology 02 p0249 A72-11992
- Dye penetrant surface defect indications on 2014-T6 Al gas metal arc weldments heat affected zone, considering minimization by arc stabilization and caustic etch time reduction 02 p0236 A72-12775
- Double forces distribution over elastic body surface from Lamé equation describing static defects, discussing Kupradse potential and sources corresponding to plane dislocations and cracks 03 p0444 A72-13501
- Defective IC device glass surface passivation effects on scanning electron microscope analysis 03 p0365 A72-14287
- Residual stresses and geometrical imperfections effects on compressive strength of thin welded box columns 07 p1088 A72-19114
- Residual stresses effect on technical cohesive strength of welded cylindrical shell with surface defects, presenting plane strain fracture toughness determination method 07 p0997 A72-20131
- Dielectric and semiconductor crystals surface defects, considering electric polarization structures 10 p1525 A72-23761
- Surface defects absence after intergranular creep from Al bicrystals grain boundaries observation by transmission electron microscopy 10 p1495 A72-24084
- Solids deformation resistance increased by active lubricants effects on coupled friction surfaces, noting damage localization to thin surface layers 12 p1817 A72-28181
- Surface contamination effect on electron temperature measurement using rocket-borne Langmuir probe in lower ionosphere 15 p2236 A72-31926
- Optical nondestructive surface flaw detection for steel plates using oblique angle illumination combined with high pass spatial filter 15 p2238 A72-32153
- Surface defects evaluation on GaAs and Si wafers by metallographic and electrochemical techniques 15 p2296 A72-32758
- Line and surface defect treatments of elastic media dislocation field, noting nonuniqueness with respect to Burgers and jump conditions 16 p2467 A72-33141
- Precipitation caused surface defects on Al-Mg-Si alloy extrusions, considering segregation streaks, cooling induced microstructural stains and cold working-annealing produced heterogeneous zones 18 p2699 A72-36225
- Photoelastic investigation of a Hertzian contact with shallow grooves in the contact area. 18 p2734 A72-36374
- Ways of reducing porosity in argon-arc welding of thin titanium sheets. 18 p2695 A72-36428
- Relation between the plasma ion current and the surface defects produced by ruby and neodymium laser emission 19 p2812 A72-38210
- Some considerations on the residual stresses in orthogonal cut surface of aluminium. 20 p2978 A72-38884
- Compensation of Fabry-Perot surface defects. II - Silicon oxide compensating layers. 21 p3053 A72-40608
- Residual stresses effect on technical cohesive strength of welded cylindrical shell with surface defects, presenting plane strain fracture toughness determination method 24 p3408 A72-45757
- SURFACE DIFFUSION**
- Mixed cubic carbide diffusion layer formation on carbon steel surface, using chemical transport reaction analysis 06 p0828 A72-17570
- Structural changes of nitrided steel diffusion zone, showing alpha solid solution and hard nitride phases mixture 08 p1188 A72-21880
- Diffusion measurements during annealing of Pd-V, Pd-Ti and metal-ceramic systems by microprobe 11 p1664 A72-26853
- Deep diffused layer sintering of metal-ceramic cutting alloys with variable Co content for increased wear resistance and tensile strength 13 p1982 A72-30112
- Reactional diffusion in metal surface layers due to chemically active external media involving solid reaction products formation 15 p2255 A72-31570
- Diffusion layer formation on metallic surfaces, discussing saturation, crystallization, phase structure, chemical reactions, thermal and contact conditions 15 p2255 A72-31571
- Soft X ray appearance potential spectrometer construction and operation for metal film diffusion detection in microcircuit technology 15 p2241 A72-32442
- Incore thermionic reactor cylindrical Mo emitter covered with two CVD W layers, discussing first layer adhesion and diffusion characteristics and work function stability 18 p2707 A72-36135
- Interface morphology development during stress corrosion cracking. I - Via surface diffusion. 18 p2700 A72-36583
- Chromizing of steel sheet by diffusion 20 p2929 A72-39581
- Structure and properties of nickel-phosphorus coatings as a function of the temperature and annealing time 20 p2929 A72-39583
- A comparison of the effect of inward and outward diffusion aluminate coatings on the fatigue behavior of nickel-base superalloys. 21 p3067 A72-40916
- Digital parallel correlator with LSI single-chip bipolar transistor construction, discussing triple diffusion process for n-p-n and p-n-p junctions 23 p2374 A72-44453
- Transition of the oxide film on a molybdenum surface from the two-dimensional to the three-dimensional phase 24 p3432 A72-45503
- SURFACE DISTORTION**
- Solid body surface strain field optical determination, using diffraction gratings [SESA PAPER 1751] 02 p0199 A72-11512
- Previous loading effect on contact area and prints number and size distribution and thermal conductance for two nominally flat surfaces in contact [ASME PAPER 71-LUB-M] 02 p0234 A72-11528
- Impending metal fatigue failure holographic detection by optical correlation of coherent light reflection from deformed surface structure as function of time 02 p0294 A72-12442
- Homogeneous first order solutions to Lamé equations in statistical elasticity theory, yielding harmonic surface displacement for elastic body 03 p0454 A72-14371
- Ultrahigh strain rate measurement via diffraction gratings directly impressed into test material surface, recording outputs by high speed cameras or photoelectric techniques 10 p1487 A72-24573
- Thermal boundary layer interaction with distortions in shape or material of adjacent surface for space shuttle design [AIAA PAPER 72-312] 11 p1614 A72-25246

Boundary surfaces during plastic buckling of hollow cylindrical shell under combined loading by external pressure and axial force

12 p1880 A72-27231

Boussinesq solution for elastic surface deflection due to continuous pressure with polynomial distribution over triangular area

12 p1884 A72-27568

Diffraction efficiency of phase holograms formed by surface deformation of light sensitive dichromated gelatin films

12 p1808 A72-27600

Optical measurement of wave front lens or mirror surface contours by laser unequal path interferometer combined with computer data reduction

20 p2922 A72-39034

Conformal mapping procedure for numerical generation of airfoils with local curvature singularities, presenting test problem results for zero trailing edge angle

21 p2992 A72-41259

An immersion interferometer for monitoring the quality of second-order aspherical surfaces

21 p3058 A72-41808

Influence of deviations in the shape of the base surface on the precision of turbine blade machining operations

22 p3182 A72-41863

Investigation of optical inhomogeneities in large fields by holographic methods

22 p3176 A72-42106

Surface distortion and strain fields visualization by grating produced diffraction patterns, discussing different detection techniques

22 p3234 A72-42391

Stress state of arbitrary contour body of revolution under torsion using finite difference method

23 p3347 A72-43744

SURFACE ENERGY

Terrestrial radiation emission mapping from imagery produced by scanning radiometer, discussing remote sensors used to study surface energy phenomena

02 p0210 A72-11804

Surface energy states of CdS basal plane based on photovoltage inversion effect model

03 p0400 A72-12991

Double cantilevered specimen crack growth, computing fracture surface energies from dynamical cleavage analysis

05 p0735 A72-16019

Surface and interfacial energies measurement by multiphase equilibrium method for refractory metal monocarbides with liquid cobalt

07 p1010 A72-19136

Surface active medium effect on free surface energy and strength of pyrographite in ethyl alcohol solution, using crack kinetics experiment

08 p1197 A72-22182

Surface tension determination at immiscible liquids or liquid-gas phase interfaces by capillary rise measurement of droplet

09 p1294 A72-22678

Fracture surface energy and acoustic emission of boron fiber-epoxy resin composite, using linear elastic fracture mechanics and compliance variation methods

11 p1674 A72-25858

Surface energy effect on alloy structure formation, analyzing crystal growth and formation from supersaturated solutions

15 p2253 A72-31221

Orientation and elongation effects on grain boundary correction term in foil surface energy measurement by zero creep, using virtual work method

15 p2258 A72-32637

Fracture-surface energy model for Cu-W fiber metal matrix composites, using plastic flow analysis

16 p2470 A72-33613

Surface energy and cleavage plane observation of brittle fracture for W single crystal in tension as function of orientation and temperature

18 p2702 A72-36750

The fracture energy and some mechanical properties of a polyurethane elastomer.

19 p2823 A72-38450

Manifestation of the effect of adsorptive reduction in strength under conditions of selective transport during boundary friction

22 p3183 A72-43138

SURFACE EROSION

U EROSION

SURFACE FINISHING

Extruded AlMgSi alloy manufacturing conditions effect on strength, surface finish and anodized appearance, discussing evenly distributed fine hardening precipitates, metal purity, etc

01 p0077 A72-11043

Hydraulic sand blasting and annealing effects on Ti alloy sheet bending fatigue strength

06 p0831 A72-18357

Thin solid film lubricants for use with roller bearings at ambient and elevated temperatures, discussing surface treatment

06 p0823 A72-18585

Milling, band grinding, final manual polishing and tumbler polishing effects on fatigue life and surface finish of steel compressor blades

06 p0824 A72-18651

Maximum allowable time between Ti metal surface preparation and agent application in adhesive bonding

07 p1024 A72-20254

Metal structure effect on anodic dissolution and surface microgeometry formation during electrochemical machining

08 p1175 A72-21040

Electrolyte flow rate, electric current intensity and tool electrode shape influence on surface finish quality in precision electrochemical machining

08 p1175 A72-21044

Machine parts surface hardening and smoothing by vibrating hard alloy sphere impact at ultrasonic frequency

08 p1176 A72-21050

Graphite fibers surface treatment and interfacial adhesive bonding, considering resin composites shear strength enhancement by sulfuric acid and sodium chlorate oxidation

08 p1194 A72-21697

Clam seals comparison with elastomers, discussing aircraft use, contamination, inspection, corrosion and erosion, surface finish, service life and cost

08 p1179 A72-21941

Thick steel plate diffusion welding in air with dead-weight loading and autogenous surface cleaning

11 p1637 A72-25343

Hardcoat anodizing of Al surfaces, discussing preparation, racking, equipment and post treatments [SAE PAPER 720341]

11 p1638 A72-25598

Hydroplasma metal removal for surface cleaning of heat resistant alloys, using electric contact plasma arc machine

11 p1641 A72-26673

Diamond burnishing effect on surface quality and fatigue strength of steel, noting work hardening increase and compressive residual stresses buildup in surface layer

11 p1642 A72-26811

Ge field effect dependence on surface roughness and finishing, noting relief elements dimensions ratio and orientation to current flow direction

12 p1855 A72-27859

Surface finishing effects on steel sensitivity to stress concentration under variable loads, emphasizing diamond smoothing and roller technique

12 p1831 A72-28246

Squeeze casting for precision shaping mechanical properties, surface finish and cost reduction in metal working

[ASME PAPER 72-DE-7]

14 p2108 A72-30862

Surface treatment effects on light and X ray irradiated surface photoconductivity of InSb semiconductor single crystals at liquid nitrogen temperature

15 p2292 A72-31866

Surface cold-working as a means of increasing the short-term fatigue endurance of machine elements

19 p2808 A72-38015

Investigation of the influence of surface treatment purity and procedure on the strength of the Kh18N10T and Kh16N6 steels and the AMG6 alloy at normal and low temperatures

19 p2819 A72-38016

Effects of environment on formation of finished surface in drilling aluminum and aluminum alloys.

21 p3060 A72-40936

Flat optical surfaces production methods for Fabry-Perot interferometers, describing Otte polishing process and quality test methods

22 p3177 A72-42446

Wide-band abrasive grinding of complex surfaces with flexible contact wire elements

23 p3293 A72-43672

Crystalline solids surfaces with catalysis, electronics and corrosive reactions, discussing slow electron diffraction, ionic field microscopy and Auger spectroscopy techniques for surface cleanliness measurement

23 p3324 A72-44461

SURFACE GEOMETRY

Geometrical method in nonlinear shell theory for supercritical elastic deformation determination, considering stability loss and dynamics problems

02 p0289 A72-11612

Rayleigh distance for reflection from curved surfaces in Cassegrain subreflector geometrical optics design

04 p0499 A72-15207

Heat transfer, drag and lift coefficients for free molecular flow over concave surfaces, describing Monte Carlo simulation technique

[ASME PAPER 71-WA/HT-17]

05 p0744 A72-15876

Hypersonic boundary layer displacement interaction and surface curvature effects, employing implicit finite difference methods

[AIAA PAPER 72-76]

05 p0603 A72-16803

Program system for computation of surface from set of data points, using piecewise polynomial functions

06 p0815 A72-17753

Surface relief effect on radiative properties of solid body with random surface roughness distribution

07 p1098 A72-18934

Radiative heat transfer characteristics of optimum geometry radiating stainless steel fin

07 p1098 A72-18997

Metal structure effect on anodic dissolution and surface microgeometry formation during electrochemical machining

08 p1175 A72-21040

German monograph on optimum principle for numerical representation of surfaces, discussing association with elasticity theory extremal requirements

09 p1340 A72-22319

Optimization of load-carrying elastic lattice structures designed on prescribed surface

09 p1402 A72-22746

Spacelike hypersurface conformally invariant three geometry role in unconstrained dynamical degrees of freedom of gravitational field

11 p1691 A72-26706

Computer algorithms and programs for complex surface geometrical parameters calculation and discrete curve coordinates determination by interpolation

13 p1924 A72-29141

Green function solution for electric field intensity in space due to electric dipole at another point under boundary conditions on surface of revolution

13 p1921 A72-29341

Computer algorithm to calculate surfaces formed by equidistant conic sections, using successive approximation method

13 p1966 A72-29461

Infinitesimally small slip bendings of sign-variable curved surface of revolution with parabolic boundary parallels

13 p2061 A72-29794

Large astronomical telescopes construction discussing aspherical surfaces control, grinding, polishing and optical testing procedures

15 p2234 A72-31612

Flows between stationary surfaces of revolution having similarity solutions.

[ASME PAPER 72-APM-4]

17 p2537 A72-34304

The analysis of deployable umbrella paraboloid reflectors.

17 p2524 A72-34355

Solid surface geometry, atomic composition and electronic structure observations, discussing Auger spectroscopy, field ion microscopy and electron diffraction and scattering techniques

19 p2803 A72-38338

Condensation on a downward-facing horizontal rough surface.

[ASME PAPER 72-HT-33]

20 p2983 A72-39483

Double exposure holographic interferometry for distinguishing surface deformations by changing illuminating beam inclination in successive exposures

22 p3175 A72-41992

Viscous interaction over concave and convex surfaces at hypersonic speeds.

23 p3249 A72-44308

Investigation of the dependence of the smoothness of rectilinear motion in precision-equipment mechanisms on the form of the microrelief of contacting surfaces

24 p3403 A72-45322

SURFACE INTERACTIONS

U SURFACE REACTIONS

SURFACE IONIZATION

Mass spectrometric investigation of high power laser beam plasma on solid target, determining multicharged ion yield, energy, angular distribution and recombination effect

01 p0079 A72-10344

Electrostatic surface and bulk ionization ion thrusters current densities for propulsive and working fluid utilization efficiency

05 p0705 A72-16777

Cs diode discharge current oscillations in Knudsen plasma containing electron and positive ion fluxes from thermionic emission and surface Cs ionization

09 p1361 A72-22966

Hydrogen atom ground state ionization probability derivation as function of electric field strength and distance to metal surface

15 p2279 A72-32694

Electrostatic surface ionization and electron bombardment ion thrusters current densities for propulsive and working fluid utilization efficiency

17 p2597 A72-35272

Cs diode discharge current oscillations in collisionless Knudsen plasma containing electron and positive ion fluxes from thermionic emission and surface Cs ionization

17 p2593 A72-35888

Nickel single crystal target ionization by high voltage electron beam bombardment, using flight time mass spectroscopic analysis

19 p2835 A72-38666

SURFACE LAYERS

Gas saturated surface layer deformation in rolled Ti alloys as function of specimen thickness reduction

01 p0077 A72-11086

Lateral surface heat transfer effect on thermophysical characteristics in thin layer coatings, discussing temperature gradients in corundum and zirconium oxide on copper
02 p0304 A72-12864

Solar magnetic field distribution in sunspots surface layers, considering photospheric three dimensional magnetohydrostatic model
03 p0431 A72-13337

Surface layers and aging influence on Bauschinger effect in profiled low carbon steel under low tension-compression load cycles
03 p0445 A72-13591

Finite difference schemes for surface and planetary boundary layer solutions using grid spacings proportional to mixing length and eddy viscosity
03 p0386 A72-14337

Displacements in nonhomogeneous elastic layer, investigating uniformly distributed load surface settling behavior dependence on layer depth relationship to loaded area width
03 p0455 A72-14387

Cross section geometry and deformation effects on rods vibration damping, determining surface layer energy absorbing properties for longitudinal and torsional oscillations
05 p0735 A72-15988

Mixed cubic carbide diffusion layer formation on carbon steel surface, using chemical transport reaction analysis
06 p0828 A72-17570

Flexural, longitudinal and torsional vibration damping of various size rods, taking into account surface layer energy loss
06 p0900 A72-18675

Diurnal temperature variations in lunar surface layer from Apollo 12 samples, comparing with Apollo 11 samples and IR measurements
07 p1068 A72-18874

Gas saturation of Ti alloy in air and vacuum at 750-1050 C for 1-6 hr, discussing surface layer microstructure change after heat treatment
07 p1013 A72-19742

High temperature nitriding of martensitically aging steels in ammonia-nitrogen mixtures, obtaining hard nonbrittle diffusion surface layers
07 p1020 A72-20418

Laminar thermal boundary layer analysis, comparing heat transfer characteristics of continuous surface and semiinfinite plate
08 p1254 A72-21613

Ti crystallographic and topographical features determination by hydrogen-ion microscopy, noting temperature effects on surface films and low index facets production
09 p1327 A72-22805

Transitional microstructure of machined surface layer due to built-up edge disintegration
11 p1638 A72-25508

General relativity equations solution for interaction of gravitational radiation and conducting fluids in magnetic field, noting energy absorption in specified depth surface layer
11 p1720 A72-26116

Metal surface layer and microetching process along grain boundaries during electrochemical precision processing, verifying steel microcrack depths with mathematical model
11 p1640 A72-26260

Axial, circumferential and radial residual stresses calculation in polymetallic coatings and cylindrical elements during surface layer removal by electrochemical processing
11 p1737 A72-26263

Pulsating heat source model for physical processes in metal surface layer under fatigue limit stress level, calculating critical volume to limit energy buildup
11 p1738 A72-26801

Lunar topsoil density variations from Lunik and Surveyor radio wave, alpha and gamma scattering data, discussing Lunik 13 and Surveyor 7 landing sites
11 p1724 A72-26909

Temperature dependence of destruction threshold of lithium niobate surface under laser irradiation, noting ferroelectric properties effects
12 p1853 A72-27069

Electron microscope study of hard alloy surface layer formation characteristics during diamond grinding with electrolysis
12 p1814 A72-27766

Solids deformation resistance increased by active lubricants effects on coupled friction surfaces, noting damage localization to thin surface layers
12 p1817 A72-28181

Ridge dimensions determination and causes of self oscillation in solid surface layers deformation under sliding friction
12 p1817 A72-28182

Physicochemical processes in metal surface layers subjected to contact friction with aircraft fuels presence, noting secondary compounds and thermal oxidation acceleration
12 p1817 A72-28183

Oxide thin films effects on surface layers deformation and wear resistance of coated metals under friction, noting electrical resistance changes in annealing
12 p1818 A72-28189

Metal surface layers structural changes under external friction, noting hardening, softening and phase transformations of active layer material
12 p1818 A72-28190

Cumulative damage and structural changes in friction contact areas of steel plates under cyclic pulsed loads, noting microhardness distribution and surface layers microstructure
12 p1818 A72-28191

General relativity equation of motion for spherically symmetric surface layer of ideal gas under central gravitational field
13 p2035 A72-28646

Blackness degree calculation for semitransparent film on nontransparent substrate with layer temperature gradients, allowing for polarization emission and multiple reflections
14 p2130 A72-30296

Ferroelectric nature of superficial layer on barium titanate crystals from scanning electron microscope and optical observations
15 p2291 A72-31681

Superconducting to normal transition field as function of temperature for Ta with thin surface layer variable density impurities
15 p2293 A72-32241

Hydrogen impregnated Ta superconducting to normal transition and M-H curves, discussing effect on impure surface layer superconducting properties
15 p2293 A72-32242

Photoconductivity in depleted surface layer of quasi-monopolar semiconductors with arbitrary diffusion to Debye lengths ratio, noting n-type low resistance gallium arsenide
15 p2296 A72-32694

Lunar surface diurnal temperature variations calculation based on Apollo 12 lunar fines thermophysical properties and surface layer core-tube sample density
16 p2454 A72-33432

Danckwert liquid film surface layer renewal concept as refinement of Reynolds theory of correlation between convective heat transfer and momentum transfer
17 p2637 A72-35050

Relativistic kinetic theory combined with surface layer theory in curved space-time to study counter-rotating disks with fine central red shift
17 p2582 A72-35389

Temperature anomaly in the superficial layers of rubbing surfaces
17 p2638 A72-35422

Some measurements of the fine structure of large Reynolds number turbulence.
18 p2678 A72-36020

Effect of fluidization on the polarization of reflected light from lunar dust layers.
18 p2729 A72-36987

Spectral characteristics of surface-layer turbulence.
19 p2829 A72-38559

Relation between impurity shear dispersion in the atmospheric ground layer and the turbulence characteristics
19 p2829 A72-38772

Brightness matrix of a flat powdered layer with opaque particles in the single-scattering approximation
19 p2836 A72-38783

Stability of a liquid film in a lateral gas flow and the size of droplets during the breaking of the film
20 p2987 A72-39925

Changes in the wear resistance of polymer surface layers in aggressive and biologically active media
21 p3072 A72-40081

Observation on phenomena associated with a slowly varying surface barrier at niobium oxide and aluminum interface.
21 p3097 A72-40702

Surface effects during high-speed impact of metals
22 p3188 A72-42163

An improved pressure-sphere anemometer.
22 p3178 A72-42596

Interpretation of steady-state surface photovoltage measurements in epitaxial semiconductor layers.
22 p3215 A72-43087

Surface layer grain boundary corrosion damage of Ti alloys during vacuum annealing, reducing rupture strength, vibration resistance and bending fatigue limit
23 p3293 A72-43589

Determination of the optical thickness of polymer fracture surface layers from interference phenomena.
23 p3307 A72-44317

Thermal conductivity of superconducting layer in intermediate stage with Andreev electron excitation trajectories in magnetic field, using Green function and impurity distribution technique
23 p3325 A72-44486

The difference in the plastic deformation of the surface and bulk layers of polycrystalline iron under fatigue loading
23 p3304 A72-44490

Transition of the oxide film on a molybdenum surface from the two-dimensional to the three-dimensional phase
24 p3432 A72-45503

Temperature dependence of destruction threshold of lithium niobate surface under laser irradiation, noting ferroelectric properties effects
24 p3432 A72-45722

Cross section geometry and deformation effects on rods vibration damping, determining surface layer energy absorbing properties for longitudinal and torsional oscillations
24 p3460 A72-45730

Al and Ti alloy fatigue after temperature reduction to 253, 77 and 4 K as function of surface purity after machining
24 p3416 A72-45743

Hydraulic sand blasting and annealing effects on Ti alloy sheet bending fatigue strength
24 p3416 A72-45744

SURFACE NAVIGATION
Lunar Roving Vehicle navigation subsystem power converter design, discussing circuits, performance and voltage regulators and preregulators
01 p0009 A72-11069

Maritime and aerial navigation radio aids, discussing recent technological advances
02 p0258 A72-12750

Tethered flying rotor platform for reconnaissance, fire control and radio transmission assignments in naval missions, discussing system characteristics
04 p0465 A72-15652

Space flight experience application to human factors engineering problems in air and maritime navigation, considering use of small digital computers, display and sensing devices
09 p1348 A72-22785

Lunar roving vehicle reliability program and design features of mobility, electrical power and navigation subsystems
[AIAA PAPER 72-233]
10 p1460 A72-24443

Adaptive multibeam experiment for aeronautical and maritime services /AMEAMS/, discussing NASA ATS-G satellite application to small mobile terminal communications system
12 p1842 A72-27383

Detection range, color, brightness and flash subjective response tests to evaluate light signals for nighttime sea navigation and visual collision avoidance
12 p1777 A72-28326

OMEGA short term range precision for broad ocean area navigation, using four range least squares position solution
13 p1997 A72-29181

OMEGA navigation system in civil maritime application, discussing single frequency, composite, difference and differential configurations and sky wave corrections
13 p1998 A72-29193

OMEGA navigation system operation aboard NOAA ship Discoverer in conjunction with satellite system, noting Trans-Atlantic tracklines
13 p1998 A72-29194

Satellite communications and position finding for ships and aircraft compared with costs and reliability of ionospheric radio communication
15 p2193 A72-31300

Landmark navigation with angle measurements for roving vehicle guidance on lunar and planetary surfaces
15 p2268 A72-31790

Landmark navigation rule, a new navigation device.
19 p2830 A72-37296

OMEGA air and maritime navigation system development, test phase and application potential, discussing operational modes, propagation parameters, solar activity effects and signal loss
19 p2831 A72-37796

Spatial simulator of tactical navigation
19 p2783 A72-37798

Remote control and navigation tests for application to long-range lunar surface exploration.
22 p3203 A72-43131

Utilization of a satellite system for navigation and control of shipping
24 p3422 A72-45224

SURFACE PROPERTIES
NT ADHESION
NT COEFFICIENT OF FRICTION
NT INTERFACIAL TENSION
NT SPECTRAL REFLECTANCE
NT SURFACE CRACKS
NT SURFACE DEFECTS
NT SURFACE ENERGY
NT SURFACE ROUGHNESS
NT SURFACE STABILITY
NT SURFACE TEMPERATURE
NT WALL TEMPERATURE
Unsteady flow about two dimensional airfoils, determining surface pressure fluctuations induced by turbulent boundary layers
01 p0001 A72-10217

Estimation method for surface pressure distribution on cascade airfoil in retarded flow, applying to axial

flow turbomachines design with suction performance and efficiency

01 p0001 A72-10396

Inconel 718 surface integrity from various manufacturing processes, tabulating data on surface finish effects on fatigue, microhardness and metallurgical properties

[SME PAPER IQ 71-239] 01 p0076 A72-10967

Steel and Ti-Al-V alloy surface integrity during various machining methods, considering microstructures, residual stress profiles and fatigue characteristics

[SME PAPER IQ 71-237] 01 p0076 A72-10972

Numerical-integral equation approach to plane wave scattering from nonplanar conducting surface with sinusoidal height profile for magnetic field parallel to surface ridges

[AD-735574] 01 p0032 A72-11237

Digital simulation of general atmospheric circulation via spatial finite difference dense grid, considering surface properties and pressure distribution maps

02 p0252 A72-11652

Airborne remote sensing of earth surface physical properties, using panchromatic and IR black and white, true color and IR false color photography

02 p0208 A72-11782

Surface moisture effect on dielectric properties of ultrafine barium titanate particulates of varying particle size

[ACS PAPER 7-E-69F] 02 p0269 A72-12416

Surface subsidence in semiinfinite resilient elastic solid mass supporting annular load distributed over circular ring

02 p0297 A72-12616

Graphite and molybdenum disulfide surface and lubricating properties, examining basal plane proportion relationship with edge sites

02 p0236 A72-12847

Titanium disilicide oxidation mechanism at various temperatures, discussing surface quality effect, growth rate and protective mechanism

03 p0369 A72-12925

Laminar flame front surface area determination, presenting graphical constructions from generatrix of arbitrary segment number

03 p0455 A72-13099

Minority carriers localized surface distribution effect on helicon propagation modes reflectivity in semiconductor

03 p0402 A72-13797

Alloying elements and grain size effects on thermally induced surface reconstruction of Al film metalization on Si devices from thermal cycling tests

03 p0364 A72-14285

Flexible surface effects on shear stress fluctuations beneath turbulent boundary layer, using fiber optic displacement probe

03 p0343 A72-14324

Light phase curve model for nonatmospheric bodies covered with porous or dust-like surface layer

04 p0574 A72-14910

Ti surface oxide films ionic and electronic conductivity properties and correlation with crevice corrosion susceptibility in contact with polytetrafluoroethylene gaskets

04 p0535 A72-15732

Metal oxide powder surface measurement using modified Kozeny-Karman formula, considering porous space, gas kinetic slip and air permeability effects

05 p0665 A72-16087

Near tip strain criterion validity for ductile crack growth on specimen surface

05 p0673 A72-16307

Surface pressure approximation formula for inclined circular cone in supersonic flow

05 p0603 A72-16547

Contact surface turbulent mixing instability in free piston high enthalpy shock tunnel waves with test air and argon gases

05 p0644 A72-16548

Two dimensional network class port behavior equivalence to three layer structures of linear passive isotropic materials based on depth and surface properties analysis

06 p0793 A72-17595

Earth gravitational potential, including surface density, crystal thickness, potential coefficients, contour maps and spherical harmonic expansion

06 p0877 A72-17657

Surface catalytic properties effect on multicomponent gas hypersonic boundary layer with simultaneous vibrational-dissociative relaxation, considering plate and blunt body laminar boundary layer

06 p0757 A72-18130

Thin film materials and fabrication methods, discussing substrate requirements, surface properties, chemical stability, thermal conductivity and preparation of various resistors and capacitors

06 p0790 A72-18572

Basal plane and edge surface areas measurement in graphite/molybdenum disulfide powders

06 p0837 A72-18601

Graphite and molybdenum disulfide powders lubricating properties relation to surface crystalline orientation

06 p0824 A72-18608

Convective conductance meter for continuous measurement of outdoor exposed surface convection coefficient, using electrically heated plaques with known surface radiation properties

07 p0981 A72-18821

Lunar surface bearing strength vs penetration curves from Surveyor 3 soil sample, comparing with in-situ remote measurements

07 p1067 A72-18873

MOS inversion layer mobility theory and surface charge scattering mechanism

07 p0954 A72-19121

Steady two dimensional laminar compressible boundary layer of reacting gas mixture with surface vaporization and fuel injection, using integral method

07 p0967 A72-19129

Surface and thermal effects on hydrogen oxidation, calculating explosion limits and slow reaction rates

07 p0935 A72-19370

Surface processes effect on hydrogen penetration and diffusion into thick Mo membranes

07 p1014 A72-19772

Boundary value problems in supporting surfaces vibrations theory, constructing Green function from part of differential operator

07 p1093 A72-19984

Exoelectronic emission method for examining deformation induced structural changes and interactions with ambient medium of metals and alloys surfaces

07 p0989 A72-20157

Optical high precision surfaces correction method for laser based reflectors on vacuum vapor differential deposition

07 p1007 A72-20262

Stainless steel saturation with Al and Cr, investigating structure, microhardness, linear expansion and contact surface seizure reduction

07 p1020 A72-20419

Electronic characteristics of real CdS surfaces in room atmosphere and ultrahigh vacuum

07 p1050 A72-20458

Surface structure changes in metal worked by electroerosion, discussing temperature and electrical tension effects

08 p1174 A72-21036

Electron microscopy application to dynamic wear studies of Ni on Ni surface and subsurface topography and microstructure in nitrogen atmosphere

08 p1179 A72-21943

Alkali antimonide photocathodes photoelectric yield /quantum efficiency/ relation to reversible variation of surface potential, noting critical current density temperature dependence

08 p1171 A72-21968

Alloy composition, specimen stressing and surface conditions effects on stress corrosion cracking

08 p1189 A72-22106

Surface current density of perfectly conducting polygonal cylinders for axially polarized incident electromagnetic field

09 p1350 A72-22247

Liquid flow cavitation impact on rotating disk surfaces, showing pitting characteristics dependence on physicochemical properties of specimens

09 p1327 A72-22297

German monograph on model concept for erosion mechanism involved in crystalline material surface bombardment covering particle elastic deformation during impact

09 p1397 A72-22324

Permeable porous plate surface properties effect on boundary layer stability

09 p1293 A72-22408

Phase errors in range finding measurements with radio waves reflection from underlying surface

09 p1277 A72-22481

Transition metal superconducting thin films and rf cavity surface protective coverings, investigating properties by low energy electron diffraction and Auger spectroscopy

09 p1368 A72-22560

Laser induced surface damage probability as function of power density, suggesting electron avalanche breakdown as cause

09 p1324 A72-23083

Metal probe potentials during mechanical displacement along surface of n-region of forward biased Si diode

09 p1288 A72-23362

Laser reflection studies of surface morphology of growing or evaporating crystals

09 p1326 A72-23409

Thermal radiative cooling system characteristics determination, taking into account surface material thermal conductivity and blackness degree dependence on temperature

10 p1561 A72-23840

Electric contact phenomena in ultraclean and specifically contaminated metallic systems, noting resistance relationship to load curves and surface conditions

10 p1448 A72-24172

Selective surfaces and coatings for solar energy conversion systems, discussing semiconductor

photoconverters, white-black surfaces, cooling systems and optimal optical properties

10 p1422 A72-24315

Liquid phase epitaxy GaAs growth in rotary reactors from Ga solution, noting thickness, doping uniformity, reproducibility and surface morphology

10 p1526 A72-24556

Metal adhesive forces to clean Fe surface measured with LEED and Auger emission spectroscopy, noting binding energy correlation to oxygen

10 p1497 A72-24821

Stationary waves properties dependence on weak skin effect in distributed tunnel diode type of nonlinear active transmission lines

10 p1453 A72-24902

Multidimensional formulation of surfaces configuration factor in radiative semidiathermanous absorbing media by change of variable method

[AIAA PAPER 72-275] 11 p1685 A72-25215

Metallic foils effects on thermal joint resistance of interface between lathe turned and optically flat surfaces, noting optimal thickness

[AIAA PAPER 72-283] 11 p1685 A72-25223

Configuration factors for radiative heat transfer analysis with partially occluded surfaces, defining areas by computer technique

[AIAA PAPER 72-304] 11 p1742 A72-25238

Radiative heat transfer spectral, temperature and directional dependence on interacting opaque surfaces system properties, noting models with accounted non-gray character

[AIAA PAPER 72-306] 11 p1742 A72-25240

Surface textures in rolled Al sheets, investigating friction and reduction

11 p1638 A72-25509

Measurement of light pressure-force on Echo 1 satellite based on satellite surface reflection and stellar magnitude as function of phase angle

11 p1718 A72-25939

Surface orientation reconstruction of Apollo 14 lunar rocks from microstereoscopic studies of microcraters, soil covers and glass coatings, determining micrometeoroid erosion

11 p1719 A72-25975

Nose blunting, exposure time and initial temperature effects on axisymmetric bodies ablation surface cross hatching patterns, presenting test results on cones with various vertex angles

11 p1572 A72-26006

Russian book on radar studies of moon covering lunar motion, dimensions, mass, density and surface layer thermal and optical properties

11 p1720 A72-26047

Electrochemical metal precision processing discussing steels carbon content, surface purity, electrolyte anion composition and anode potential

11 p1640 A72-26256

Electrochemical precision metal processing accuracy, analyzing electrode gap size and surface nonuniformities effects on prescribed configuration

11 p1640 A72-26262

Laser induced transparent dielectrics surface fracture mechanism determination based on electron microscopic photograph analysis and disturbed specular reflection under predischARGE conditions study

11 p1648 A72-26333

Spacecraft critical surfaces protection from molecular and particulate contamination sources including gloves, tissues, and covering or packaging materials

12 p1768 A72-27042

Transparent dielectric surface photoelectric emission current under laser pulse illumination, noting correlation to surface treatment and damage threshold

12 p1822 A72-27613

Surface pressure via satellite-borne measurements of atmospheric transmission near absorption band

12 p1802 A72-27710

Sliding dry friction of hard refractory metals and ceramics, discussing surface changes as function of load, sliding speed, temperature and mechanical properties

12 p1817 A72-28184

Clean metallic surfaces adhesion coefficients in vacuum at 77-293 K as function of load, loading time and contact cycles

12 p1818 A72-28193

Surface charge density in thermoplastic recording, showing potential-relief modulation dependence on frequency, scanning rate and electron beam properties

13 p1954 A72-28402

Rigidity of developable surfaces with cylindrical connections and without plane domains, subjected to infinitesimally small bendings

13 p2061 A72-29793

Energy absorption inelastic surface mechanisms effect on I-V characteristics profile for bounded semiconductors with negative differential conductivity

13 p2023 A72-29991

Gas surface interactions models, computing scattering kernels by reduction to boundary value problem

14 p2134 A72-30880

Hydrodynamic and molecular velocity characteristics of rarefied gas motion between infinite plane

parallel emitting and absorbing surfaces, using Boltzmann equation

14 p2096 A72-31025

Lunar topsoil-solid bodies interaction in terms of hardness and friction, discussing simulation equipment

14 p2161 A72-31074

Russian papers on physical chemistry of surface effects in melts covering binary and multicomponent alloys, silicates, oxides and salts at high temperatures

15 p2253 A72-31220

Spacecraft thermal control materials research, discussing surface selection, coatings, space simulation and environmental effects

15 p2260 A72-31806

Absolute intensity LEED spectra for clean Ni surfaces, discussing measurement uncertainties

15 p2276 A72-31854

Photoelectric emission usefulness for investigation of energy parameters and optical transitions of semiconductor surfaces

15 p2276 A72-31865

Edge and surface modification of Nb alloys prior to coating with fused silicide for oxidation life extension

15 p2244 A72-32134

IR internal reflection spectroscopy application to dynamic chemical changes study on ammonium perchlorate surface during thermal decomposition, observing crystal lattice transformation

15 p2296 A72-32313

Stainless steel surface alloy composition characterization as function of vacuum annealing temperature, using proton-induced X rays

15 p2258 A72-32527

Molecular adsorption on semiconducting surfaces, discussing conditions for formation of local surface levels in forbidden gap

15 p2296 A72-32760

Small disturbance behavior in laminar boundary layer on elastic surface experiencing deformation under perturbing pressure, noting surface resilience effect

16 p2377 A72-33164

Physical and chemical surface characteristics investigation methods for fiberglass rovings to consider suitability as reinforcement for synthetic resins

16 p2414 A72-33302

Field-ion microscopy as experimental metallurgical technique for metal surface atomic structure studies, discussing image formation, ionization and field evaporation

16 p2392 A72-33444

Impurities and additives effects on electrode properties in Cs vapor thermionic converter, noting coadsorption model for Cs-W-O surface

17 p2496 A72-34598

Study of the surface reactivity of carbon fibers by gas chromatography

17 p2570 A72-34891

Principle of control of aspherical surfaces by holography and moires

17 p2554 A72-34912

Current and capacitance transient responses of MOS capacitor. I - General theory and applications to initially depleted surface without surface states.

18 p2718 A72-36346

High vacuum technology applications in surface physics research, discussing atomic collisions and adsorption processes

18 p2712 A72-36827

On the intrinsic representation of flows with Lamb surfaces.

18 p2684 A72-37085

A critical examination of the validity of simplified models for radiant heat transfer analysis.

19 p2882 A72-38399

Effect of surface heterogeneity on the adsorptive behavior of of orbiting pressure gages.

19 p2869 A72-38752

The use of an electrical induction method for determining the physical condition of a ground steel surface.

19 p2805 A72-38762

The influence of the surface orientation on yield in Mo single crystals.

20 p2935 A72-39007

Surface tilt and vibration measurements by laser speckle pattern photography, comparing with moire fringes in strain analysis

20 p2930 A72-39032

Thermal emissivity and directivity for V groove and rectangular cavities, optimizing geometry and surface properties for maximum focusing of emitted energy [ASME PAPER 72-HT-L]

20 p2984 A72-39651

Mathematical models for radiative heat transfer prediction in real enclosures, noting directional characteristics of heat exchanging surfaces

20 p2984 A72-39652

Calculation of the surface properties of elastic polymer molecules in athermal solutions by the Guggenheim method

21 p3095 A72-40078

A method for directly determining surface strain fields using diffraction gratings.

21 p3052 A72-40236

A measurement of the surface strain distribution by optical differentiation method.

21 p3056 A72-41239

Spherical focusing transducers with Gaussian surface velocity distribution.

21 p3057 A72-41477

Directional far IR emission from sunlit lunar surface, determining brightness temperature as function of observer and sun elevation angles and surface parameters

22 p3226 A72-42537

Study of the flow kinetics of metal melt spread over hard surfaces

23 p3293 A72-43284

The topology of the regularized integral surfaces of the 3-body problem.

23 p3309 A72-43982

Full-range solution for the measurement of thin-film surface densities with proton-excited X rays.

24 p3431 A72-44715

SURFACE REACTIONS

Ni-Cr-Al alloys high temperature oxidation, detailing surface reactions and continuous oxide layer formation

[ECS PAPER 114] 01 p0082 A72-10172

Vapor bubble growth on heated surface with random temperature distribution and liquid microfilm for water and boiling potassium

02 p0303 A72-12862

Structural inhomogeneities effect on fatigue phenomenon in rolling motion, discussing stress cycles preceding active surface degradation

04 p0526 A72-14473

Low energy He ion bombardment effects on Ni alloy single crystal surface, observing defect structure with stacking faults, tangled dislocations and carbide precipitation

04 p0533 A72-15159

X ray spectral analysis of microchemical changes in surface films of titanium alloys during diffusive interaction with silicon carbide abrasive

04 p0534 A72-15654

Knudsen boundary layer role in physicochemical hydrodynamics of heterogeneous reactions and flows with surface reactions, using Boltzmann equation

05 p0746 A72-16209

Burning gunpowder surface reactions relative to temperature, chemical enthalpy and acoustic waves of pressure, velocity and density

05 p0751 A72-17211

Zinc dithiophosphate and bisphenol effects on surface activation of additive compositions with succinimide base in lubricant applications

07 p1023 A72-19903

Neutral monatomic rarefied gas-surface interaction at energy levels 0.1-10 eV, using Boltzmann equation

07 p0969 A72-20061

Temperature fields and mass and heat transfer at surface of solid spherical particle in laminar viscous fluid flow

07 p0973 A72-20318

Thickening properties of butoxyacrosol products of butyl alcohol vapor and silicon dioxide surface reactions for use as oil lubricant additives

09 p1336 A72-22500

Vibrating membrane generated acoustic pressure wave propagation in rarefied gas, applying to solid surface-gas interaction models

09 p1294 A72-22762

Small scale flow and surface effects in multiphase media hydromechanics, obtaining entropy production in mixture for interphase transformations characterization

10 p1468 A72-24430

Surface ignition behavior of M2 double base propellant, analyzing reaction kinetics

10 p1528 A72-25142

Surface patterns from ablating, melting and flowing materials in supersonic flow of wind tunnel, rocket motor and flight test environments, comparing with theory

11 p1743 A72-25247

Burning gunpowder surface reactions relative to temperature, chemical enthalpy and acoustic waves of pressure, velocity and density

11 p1744 A72-25337

Chemical surface treatment effects on mechanically gripped fiberglass rods tensile strength

11 p1674 A72-25827

Surface reaction mechanisms analysis in adhesion, friction, wear and lubrication, using electron diffraction, Auger spectroscopy and ellipsometry techniques

12 p1813 A72-27036

Solid surface inspection by X ray diffraction, electron microscopy and chemical techniques

14 p2131 A72-30693

Hexagonal and cubic boron nitride surface wetting by liquid metals as function of contact interaction and chemical affinity

15 p2253 A72-31224

Surface phonon appearance criteria associated with crystal surface gas adsorption, discussing entropy variation and colliding particle-crystal energy exchange

15 p2280 A72-31858

Clean Ge crystal surface oxidation process investigation by LEED and conductivity measurements

15 p2292 A72-31868

Study of the surface reactivity of carbon fibers by gas chromatography

17 p2570 A72-34891

Contribution to the study of flows with surface chemical reactions in the boundary layer

17 p2541 A72-35455

Tribological properties of gold for electric contacts.

18 p2693 A72-35980

Contact contamination - Formation of carbonaceous deposits on electrical contacts.

18 p2665 A72-36119

Energetic and topological effects in surface chemical reactions, considering intermolecular dispersion and dipole forces and chemisorption

18 p2657 A72-36828

Space and upper atmosphere environmental effects on spacecraft and instrument surfaces, considering high energy particle radiation, interstellar and lunar dust effects, etc

18 p2712 A72-36832

Anisotropy of angular distribution of radiation due to positron annihilation on the surface of Mo single crystals.

19 p2844 A72-37691

Recombination of hydrogen atoms on the surfaces of solid bodies

19 p2838 A72-38199

High and ultrahigh vacuum equipment and components selection, discussing gas-surface interactions, contamination and cleaning problems

19 p2835 A72-38391

Condensation on a downward-facing horizontal rippled surface.

[ASME PAPER 72-HT-33] 20 p2983 A72-39485

The relationship between the thick film conductor and substrate and its influence on conductor properties.

20 p2908 A72-39494

Saturated liquid film boiling on vertical surface, calculating local heat transfer rates as function of height and superheat from turbulent vapor flow model [ASME PAPER 72-HT-38]

20 p2986 A72-39668

Surface reactions in similar boundary layers.

20 p2915 A72-40014

Russian book - Macromolecules at the boundary between phases.

21 p3071 A72-40077

Polymer adsorption as a cause of changes in contact interaction intensity between two solid surfaces

21 p3059 A72-40083

Laser-induced damage in transparent dielectrics - The relationship between surface damage and surface plasmas.

21 p3062 A72-40241

Spectroscopic study of the interaction of oxides with metallic surfaces. II - SiO₂-Fe /Cu, Al, Ni, Co, Ti, W/ systems

22 p3189 A72-42197

Photoemission from surface states on tungsten.

22 p3190 A72-42478

Crystalline solids surfaces with catalysis, electronics and corrosive reactions, discussing slow electron diffraction, ionic field microscopy and Auger spectroscopy techniques for surface cleanliness measurement

23 p3324 A72-44461

MOS devices instability caused by water and hydroxyl molecules on silicon dioxide surface, noting optimal conditions for chemical stabilization

24 p3431 A72-44821

Oxidation of W/110/. I - LEED study of the oxide formation at 1000 K.

24 p3378 A72-44952

Mass spectra stimulated by O⁺ and Ar⁺ interacting with a surface.

24 p3378 A72-45312

Pulsating conditions in the evaporation of optical materials under the influence of CO₂ laser radiation.

24 p3411 A72-45610

SURFACE ROUGHNESS

Fresnel diffraction on opaque half plane screens with statistically rough surfaces, using Kirchhoff approximation

02 p0183 A72-12755

Impulsive spatial interaction model between monoenergetic molecular beam and rough isotropic rigid metal surface in free molecule flow

03 p0392 A72-14058

Free molecular flow heat transfer to rough surface, discussing surface/molecule interaction model for digital simulation

[ASME PAPER 71-WA/HT-8] 05 p0743 A72-15868

Turbulent flow in smooth and rough pipes at Reynolds numbers 30,000-480,000, presenting velocity mean and fluctuating components rms and cross correlation values

[ASME PAPER 71-WA/FE-7] 05 p0647 A72-15935

Critique on condition for planar antennas physical reliability, concerning smoothness of aperture edges

06 p0782 A72-17362

Diversity reception during radio wave scattering on statistically uneven surface, using geometrical optics method

07 p0944 A72-19566

Technological characterization of electric discharge machines by metal removal rate, volumetric electrode wastage and machined surface roughness

08 p1174 A72-21031

Sea surface roughness mapping by airborne microwave radiometry with correction for viewing angle and atmospheric effects

09 p1297 A72-22525

Aeolian transport and surface roughness of Mars Hellas basin, using Mariner 1969 photographs

10 p1536 A72-24151

Fresnel diffraction on opaque absorbing screen half planes with small rough surfaces, deriving field attenuation factor and structure/correlation functions

10 p1435 A72-24502

Rough surfaces thermal contact resistance in vacuum for normal height distribution, discussing bolted joint nonuniform stress distribution effect

11 p1741 A72-25221

Reflecting surface roughness measurement by holographic interferometry, applying to lapped steel specimens

11 p1629 A72-25309

Sintered Mo diffusion weld strength dependence on contact surface flatness and smoothness

11 p1644 A72-26847

Lunar surface roughness mapping by combined IR and radar measurements

12 p1869 A72-27328

Lunar surface roughness thermal characteristics, comparing IR data with three realistic models

12 p1870 A72-27335

Hertz formulas for undulate solid surface height distribution

12 p1819 A72-28196

Conjunction mechanism of two real contacting bodies with rough surfaces under normal load

12 p1819 A72-28202

Full wave analysis of radio wave propagation over rough surfaces characterized by variable impedance and height parameters

13 p1916 A72-28539

Leading angle effects on cutting force components, temperature and surface roughness in drawing of Ti alloys

13 p1963 A72-28746

Turbulent diffusion limiting flux variation with angular rotation velocity of rough rotating disk

15 p2217 A72-31676

Rough surface elastic bodies stress calculation, using asymptotic method of boundary conditions

15 p2327 A72-31736

Deep drawing of circular mild steel and aluminum sheets with polyurethane or rubber rings, examining strain distribution, shape and surface roughness

15 p2244 A72-32145

Heat transfer and friction coefficients for turbulent flow in rough tubes as function of Reynolds and Prandtl number, using von Karman method

16 p2478 A72-33513

The response of a turbulent boundary layer to a step change in surface roughness. II - Rough-to-smooth.

17 p2540 A72-35191

Effect of a distributed sand roughness on the spectrum of wall pressure pulsations in a turbulent flow in a tube

17 p2541 A72-35542

Correlation of noise-like emission reflected from a statistically uneven surface

17 p2583 A72-35543

Comments on the figure of the moon based on preliminary results from laser altimetry

18 p2774 A72-36280

Adhesive wear theoretical model based on asperity interactions number, area and volume, considering implications for friction and surface temperature analysis

19 p2809 A72-38377

Energy characteristics of radio signals scattered by statistically uneven surface, proposing statistical variables substitution

20 p2900 A72-38892

Fresnel diffraction on opaque half plane screens with statistically rough surfaces, using Kirchhoff approximation

20 p2902 A72-39061

Turbulence theory generalization for flow near wall with various surface roughness modes, presenting velocity profiles

20 p2912 A72-39359

Measurements of Reynolds shear stress fluctuations in a turbulent boundary layer.

21 p3047 A72-41638

Diversity reception during radio wave scattering on statistically uneven surface, using geometrical optics method

22 p3153 A72-42084

Influence of the degree of strain-hardening and roughness of friction surfaces on wear rate and carrying capacity

22 p3183 A72-43157

Phase correlation between two sources formed on a diffusing surface - Application to the human retina

23 p3261 A72-44379

Turbulent boundary layer calculation behind surface cusp, taking into account external flow turbulence and thermal stratification

24 p3390 A72-45008

SURFACE ROUGHNESS EFFECTS

Earth surface roughness effects on vertical Hertz dipole electromagnetic field reflection

01 p0027 A72-10447

Momentum exchange coefficient for surface layer neutrally stable flow after surface roughness change, noting error possibility in flow estimates for heterogeneous terrain

01 p0094 A72-10827

Electromagnetic wave scattering from rough surfaces by Kirchhoff approach and small perturbation method, discussing validity near grazing angle

01 p0032 A72-11249

Bidirectional scattering of electromagnetic waves from rough surfaces in plane of incidence restricted only by tangent plane approximation, comparing with other models

02 p0170 A72-11467

Cross flow through in-line tube bank, investigating surface roughness effects on behavior by pressure drop, static pressure and skin friction distributions measurements

02 p0203 A72-12102

Fine scale surface oxide film roughness effects on metal substrate-oxide film system hemispherical emittance

02 p0303 A72-12319

Acoustic attenuation calculation for turbulent flow in rigid tubes, determining critical flow velocity dependence on wall roughness and sound wave frequency

03 p0340 A72-12954

Digital computer simulation of rarefied gas molecular beam-rough metal surface interaction

03 p0392 A72-14057

Conductive heat transfer from rib roughened surfaces in gas cooled reactor fuel elements

04 p0595 A72-14596

Full wave solution for vertically polarized radio wave propagation over rough variable impedance surface by Fourier transform

04 p0492 A72-15437

X ray spectral analysis of microchemical changes in surface films of titanium alloys during diffusive interaction with silicon carbide abrasive

04 p0534 A72-15654

Brightness temperatures and directionality of IR emission from rough lunar surface of crater field

05 p0714 A72-16104

Equilibrium temperature distribution on radiatively adiabatic smooth and rough planes uniformly irradiated by collimated solar flux

05 p0749 A72-16876

Electromagnetic wave scattering from curved rough surfaces and transmission through turbulent medium, obtaining solution by spatial Fourier transform of three transfer functions product

06 p0771 A72-17340

Surface roughness effect on TEM mode propagation, discussing perturbation and Bessel series methods

06 p0774 A72-17738

Increased Reynolds number simulation with roughness set on aircraft model in transonic flow, investigating flow separation by parietal visualization technique

06 p0758 A72-17846

Rough surfaces with orthogonal parallel V grooves, studying shadowing, interreflection and masking effects on bidirectional reflectance from He-Ne laser illumination

06 p0848 A72-17924

Lunar surface temperature-independent and dependent plane homogeneous models for thermal properties study, discussing surface roughness and localized thermal anomalies

06 p0887 A72-18227

Molybdenum disulfide lubricating effectiveness improvement with finer particles at aggravated sliding conditions, suggesting surface roughness qualifications

06 p0837 A72-18605

Surface relief effect on radiative properties of solid body with random surface roughness distribution

07 p1098 A72-18934

Geostrophic drag coefficient for heterogeneous terrain as function of effective roughness length, considering surface friction effects in large scale atmospheric models

07 p1030 A72-19108

Air flow turbulent behavior and dynamic characteristics dependence on underlying surface roughness variations

07 p1031 A72-20695

Brightness distribution and phase dependence measured for spheres with different colors and roughness for Mars surface optical parameters model validity

08 p1238 A72-21830

Fluid sealing theory based on surface tension effects at roughness asperities within seal film

08 p1177 A72-21928

Spectrum shape of Doppler radar return from two dimensional random rough surface model using helmholtz integral approach and Kirchhoff approximation

09 p1277 A72-22314

German monograph on tire rubber friction on dry and wet rough surfaces, taking into account loading, velocity and temperature effects

09 p1332 A72-22323

Runway unevenness and landing gear characteristics effects on SST vibration during taxiing, taking off and landing

09 p1263 A72-23459

Forced convection heat transfer for turbulent flow over flat surface with attached protrusion for varying Reynolds number and boundary layer thickness

10 p1561 A72-23882

Asymmetric flow in plane channel characterized by diffusional transport of turbulent shear stress and kinetic energy from rough to smooth wall regions

10 p1467 A72-24368

Rough surface effects on EM reflection for electromagnetic probing in geophysics, using Rayleigh and Kirchhoff methods

10 p1512 A72-24738

Radio propagation over slightly roughened curved earth surface, using perturbation method and Taylor series in model calculation

10 p1439 A72-24743

Average electric field and power density of electromagnetic wave scattered from rough layer with plane interface, calculating scattering cross sections

10 p1512 A72-24744

Bolted joint thermal conductance, considering interfacial pressure distribution and surface roughness effects

11 p1741 A72-25222

Anomalous refraction maxima in bidirectional plane polarized radiant flux transmittance of roughened dielectric surfaces

11 p1742 A72-25236

Radiative transfer theory for passage wall surface roughness effects on light transmission and reflection

11 p1742 A72-25237

Roughness effects on radiant heat transfer between interacting surfaces based on Beckman reflectance model

11 p1742 A72-25238

Bidirectional reflectance from randomly rough engineering surfaces, using photographic technique

11 p1742 A72-25242

Lunar surface roughness effect on temperature distribution, noting solar elevation and observation angle dependence

11 p1715 A72-25244

Four stage gas turbine, measuring blade surface roughness and profile changes effects on flow characteristics and efficiency

11 p1704 A72-25630

Turbocompressor deceleration cascades blades surface roughness effects on boundary layer, noting pressure and velocity distributions

11 p1570 A72-25640

Surface roughness effects on air flow in turbulent atmospheric boundary layer, using finite difference method

12 p1838 A72-27026

Ge field effect dependence on surface roughness and finishing, noting relief elements dimensions ratio and orientation to current flow direction

12 p1855 A72-27859

Deep groove ball bearing endurance tests to determine running conditions and lubricant film thickness/surface roughness ratio effects on fatigue life

12 p1816 A72-28112

Molecular-mechanical theory of external friction, taking into account surface roughness, time and temperature dependent mechanical properties and chemical processes

12 p1818 A72-28195

Surface roughness effects on seizure and friction of contacting metal plates under atmospheric pressure and vacuum

12 p1819 A72-28197

Surface finishing effects on steel sensitivity to stress concentration under variable loads, emphasizing diamond smoothing and roller technique

12 p1831 A72-28246

High angular resolution optical system to measure light reflection from rough surfaces

13 p2002 A72-28513

Ultrasonic signal propagation with distance along steel sphere surface compared with lunar seismic signal, discussing surface dent and lunar crater effects

13 p2035 A72-28619

Internal rarefied gas flow, taking into account molecular backscattering due to wall surface roughness

13 p1942 A72-29117

Surface roughness effects on Mars photometric properties for scattering in terms of Minnaert law
15 p2311 A72-32085

Lunik 14 spacecraft radio signal reflection from lunar surface, showing energy spectrum dependence on surface roughness
15 p2202 A72-32655

German monograph on surface roughness effects on pressure loss and heat transfer in high temperature turbulent flow, deriving universal laws
16 p2478 A72-33506

Mechanism by which a two-dimensional roughness element induces boundary-layer transition.
17 p2542 A72-35611

Shadowing function calculation as rough surface point illumination probability by point source radiation, assuming surface elevation as random process
18 p2710 A72-36407

Behavior of boundary layers on rough compressor blades
18 p2641 A72-36420

Sea surface albedo for short wave solar radiation in terms of sun altitude and atmospheric transmittance, noting wind and surface roughness effects
18 p2687 A72-36642

Rotational theory of laminar boundary layer separation of incompressible fluid from smooth surface under pressure gradients
18 p2682 A72-36887

Investigation of the influence of surface treatment purity and procedure on the strength of the Kh18N10T and Kh16N6 steels and the AMG6 alloy at normal and low temperatures
19 p2819 A72-38016

Influence of roughness on the thermal radiation emitted by opaque surfaces - Model test
19 p2881 A72-38393

Atmospheric flow turbulent behavior and dynamic characteristics dependence on underlying surface roughness variations
20 p2948 A72-39010

Turbulent boundary layer calculation, investigating surface roughness, pressure gradient and surface temperature effects
20 p2912 A72-39365

Intensity of turbulence within canopies with simple and complex roughness elements.
20 p2948 A72-39798

IR reflectance [or emittance] remote spectroscopy of mineral particulate surfaces, discussing particle size, surface roughness, porosity and mixing ratios effects
22 p3178 A72-42526

Wind profile development above a locally adjusted sea surface.
22 p3202 A72-42600

Initial electron velocity and emitter surface roughness effects on oscillatory velocities dispersion in helical electron beams used in cyclotron resonance masers
22 p3208 A72-42664

Sunlight scattering by double reflection on rough and absorbing surfaces, deriving fractional circular polarization from models for comparison with observation
23 p3334 A72-43254

Study of the dependence of the spectral and integral radiation properties of bodies on the surface roughness.
23 p3357 A72-44538

Investigation of the dependence of the smoothness of rectilinear motion in precision-equipment mechanisms on the form of the microrelief of contacting surfaces
24 p3403 A72-45325

The effect of the subsurface on the depolarization of rough-surface backscatter.
24 p3380 A72-45635

Determination of the reflecting power of a hilly terrain, knowing the reflective power of a flat terrain of the same nature
24 p3381 A72-45769

SURFACE STABILITY
Physical processes of fluids atomization in electric field, discussing droplet surface instability and boundary values of surface tension coefficient
05 p0667 A72-17185

Numerical solution of disintegration and surface stability of gas bubbles under nonspherical free oscillation
08 p1149 A72-21295

Certain class of solutions of the three-dimensional problem for a rigid perfectly plastic material with a family of momentarily inextensible planes
21 p3123 A72-41392

SURFACE TEMPERATURE
NT WALL TEMPERATURE
Infinite slab, cylindrical or spherical shells with nonuniform heat generation sources and equal surface temperatures, obtaining maximum internal temperature from error bounds
01 p0145 A72-10511

Electron work function and electrode physicochemical properties and surface temperature on boundary layer formation and thickness at electrodes in MHD channel
01 p0009 A72-11206

Remote sensing of surface radiation temperature topographic variations by precision radiation thermometer equipped aircraft, calibrating for atmospheric attenuation
02 p0210 A72-11803

Automated operational procedure for sea surface temperature determination from ITOS IR data, discussing error analysis
02 p0211 A72-11810

Synoptic sea surface temperature mapping off Eastern United States using NASA ITOS satellite IR imagery data
02 p0211 A72-11813

Surface temperature measurement by microwave radiometry, noting sensitivity reduction due to moisture effects for resolution cell size targets
02 p0214 A72-11867

Soil surface moisture content and temperature profile determination by remote microwave sensing
02 p0214 A72-11871

Graphite surface temperature and ablation rate for various stagnation pressures, radiative heat fluxes, stagnation enthalpies, heat transfer coefficients and test gas compositions
02 p0249 A72-12021

Boron-containing polymer heterogeneous combustion determination using hybrid regression rate with thermal degradation and surface temperature data
02 p0270 A72-12260

Locally nonsimilar solutions for thermal boundary layer, presenting surface heat transfer and temperature distribution
02 p0302 A72-12313

Thermal simulator of flows with chemical wall reaction, plotting surface temperature variations with distance
03 p0456 A72-13793

Thermal stresses from inner surface temperature of micropolar hollow cylinder in static thermoelasticity problem with vanishing body loads
03 p0448 A72-13889

Unsteady thermal conductivity inverse problems, obtaining heated body surface temperature and heat flux from temperature measurement in interior
03 p0458 A72-14164

Cloud interference-free sea surface temperatures, using techniques to reduce noise effect in Nimbus IR radiometer data
03 p0385 A72-14227

Dry spot formation in nonboiling ethanol thin film on horizontal surface heated from below
04 p0595 A72-14597

Heat conduction model of surface thermal history of moon as function of dust, anorthosite, basalt and dunite layers
04 p0571 A72-14598

Steady heat conduction plane problem solution for infinitely long cylinder with constant surface thermal flux density and temperature
04 p0595 A72-14644

Equilibrium temperature formula derived for surface subjected to aerodynamic heating by gas from heat balance between convective and radiative heat flow
04 p0595 A72-14651

Thermal laminar boundary layer equations solution for power-law velocity distribution in external flow and arbitrary surface temperature distribution
05 p0742 A72-15844

Environmental effects on superalloy high temperature corrosion in gas turbines, noting blade surface temperature as critical factor
05 p0704 A72-15945

Nighttime ground surface temperature prediction by net flux radiometer
05 p0684 A72-16792

Satellite surface temperature measurements changes due to atmospheric specific humidity, noting increase in water vapor absorption coefficient with content
06 p0806 A72-17671

Nimonic 75 sliding pin and rotating disk frictional force, wear rate and surface temperature
06 p0830 A72-18156

Hg vapor condensation on cooled vertical steel cylinder at 70-185 C, considering heat flux relation to saturated vapor/cooling surface temperature difference
06 p0903 A72-18190

Nonlinearly radiating semiinfinite heat conducting solid surface temperature, expressing heating rate as nonnegative integrable function of time
07 p1098 A72-18814

High intensity laser beams for solid surface material removal by vaporization and explosion, noting surface and subsurface temperature relations
07 p1002 A72-19210

SURFACE TEMPERATURE
Friction coefficient, standard wear and surface layer temperature of seal for dry friction pairs in jet engines, investigating crystal lattice parameters
07 p0996 A72-19768

Plate surface temperature during aerodynamic heating in supersonic gas flow, using linearized Pohlhausen method
07 p0909 A72-19891

Integral contact temperatures and heat balance calculation for heat transfer between contacting bodies with rotational motions
08 p1252 A72-21444

Free convection and hydrodynamics of inclined liquid layers in laminar flow and in stepwise change of heat exchange surfaces temperature
08 p1151 A72-21663

Micropolar thermoelasticity steady state axisymmetric problem solution from equilibrium equations, considering uniform surface temperature and surface heat doublet cases
09 p1403 A72-22749

Radiant heat flux measurement during pulsed processes from surface in high temperature emitting gas, using thin film sensor with small time constant
10 p1561 A72-23843

Viking Mars Orbiter IR thermal mapper (IRTM)/to study surface kinetic temperature, thermal balance, anomalous cooling regions, ground frosts and water vapor
10 p1539 A72-24379

Plasma coating formation mechanisms and parameters, studying metal surface and deposited particles temperatures, spraying time effects, etc
10 p1487 A72-24488

Tropical hurricane model describing initial whirlwind and self exciting wind velocity development and dependence on ocean surface temperature
11 p1682 A72-26879

Overlap emissivity of atmospheric carbon dioxide and water vapor for computer simulated earth surface temperature calculations
11 p1628 A72-26986

Papers on thermal characteristics of moon covering earth based and in situ surface temperature measurements, radar mapping, heat flow experiments, etc
12 p1869 A72-27326

Apollo 11 EASEP nickel resistance thermometer lunar surface data, presenting unshadowed equivalent brightness temperature and thermal parameters and emission directional dependence
12 p1869 A72-27330

Ice formation on helicopter rotor blades, discussing atmospheric moisture and temperature conditions, blade surface temperature, centrifugal and aerodynamic forces and preventive measures
12 p1754 A72-27414

Life on Mars, investigating ground based and probe observations of atmospheric composition and pressure, surface temperature and features and UV radiation
12 p1761 A72-27624

Conductive heat propagation with finite rate for semibound solid body under periodic surface temperature fluctuations dependent on relaxation time
12 p1890 A72-28174

Surface temperature distribution for porous plate in supersonic flow with gas injection into turbulent boundary layer
13 p1893 A72-28917

Aircraft or helicopter-borne IR radiometer for surface temperature of snow covers and glaciers and air-snow energy balance measurements
15 p2232 A72-31244

Thermal laminar boundary layer equations solution for power-law velocity distribution in external flow and arbitrary surface temperature distribution
15 p2334 A72-31263

Unipolar steady electromagnetic bow shock interaction of Mercury with solar wind, calculating planetary surface temperature
15 p2303 A72-31305

German monograph on heat transfer and stability limits for boiling and nonboiling falling films covering surface and bubble boiling conditions
15 p2334 A72-31503

Sea surface temperature determination on Nimbus 2 satellite, using three channels in medium resolution IR radiometer
15 p2224 A72-31674

High speed photographic pyrometer for surface temperature measurements on aerodynamic models during free flight in aeroballistic range
15 p2237 A72-32050

Thermal history and early magmatism for lunar models, considering high near-surface temperatures and radionuclides upward transport during melting
15 p2311 A72-32082

Graphite ablation rate inhibition and surface temperature depression by chlorine gas in supersonic high temperature air environment
16 p2475 A72-32842

Plate surface temperature during aerodynamic heating in supersonic gas flow, using linearized Pohlhausen method
17 p2485 A72-35139

- Temperature anomaly in the superficial layers of rubbing surfaces 17 p2638 A72-35422
- Distortion of the semi-infinite solid due to transient surface heating. 17 p2635 A72-35974
- Calculation of thermal fluxes and temperatures on the surfaces of a plate in the presence of heat exchange between fluids incident on the surfaces 18 p2742 A72-37183
- S-band radiometer design for high absolute precision measurement. 19 p2794 A72-37252
- Erosion combustion effect on unsteady solid rocket propellant burning stability during engine nozzle opening, noting combustion velocity and surface temperature 19 p2879 A72-37353
- Steady combustion thermal stability of condensed explosives for burning rate limitation by condensed phase chemical reactions, noting surface temperature effects 19 p2879 A72-37356
- Influence of the earth's outgoing radiation on the temperature of a rotating disk in space 19 p2856 A72-37496
- Thermoprobe - An instrument for determining the temperature of opaque, translucent, and transparent surfaces in the incandescent temperature range. 19 p2795 A72-37513
- Thermally controlled entry guidance for shuttle. [AIAA PAPER 72-831] 20 p2951 A72-39096
- Turbulent boundary layer calculation, investigating surface roughness, pressure gradient and surface temperature effects 20 p2912 A72-39365
- The effect of thermal conductivity and base-temperature depression on fin effectiveness. 20 p2983 A72-39489
- An analysis of the spectral scanning technique for determining the temperature distribution in a semi-transparent medium. [ASME PAPER 72-HT-6] 20 p2986 A72-39677
- Film cooling effect on surface heat transfer in laminarizing mainstream turbulent boundary layer for injection through flush angled two dimensional slots [ASME PAPER 72-HT-11] 20 p2986 A72-39682
- Remote sensing of urban 'heat islands' from an environmental satellite. 20 p2919 A72-39717
- Allowance for the ocean surface temperature in monthly weather forecasts for the Northern Atlantic Ocean 20 p2949 A72-39946
- Numerical and asymptotic methods for solving the problem of complete boundary-layer stabilization 21 p3047 A72-41659
- German monograph - Cooling of geometrically simple bodies (flat plate, cylinder, sphere) by convection and radiation. 22 p3244 A72-43062

SURFACE TENSION

U INTERFACIAL TENSION

SURFACE TO AIR MISSILES

- Miss distance simulation for SAM guided by proportional navigation, using ASIM programming language for digital computer 03 p0386 A72-13611
- Missile systems of U.S., U.S.S.R. and other nations, discussing ground-to-ground, ground-to-air, air-to-ground and air-to-air missiles 05 p0728 A72-16740
- SAM-D control test vehicle trajectory planning and flight test analysis. 24 p3451 A72-45338

SURFACE TO SURFACE MISSILES

- NT ANTITANK MISSILES
- NT INTERCONTINENTAL BALLISTIC MISSILES
- NT INTERMEDIATE RANGE BALLISTIC MISSILES
- NT MINUTEMAN ICBM
- NT POLARIS MISSILES
- NT POSEIDON MISSILES
- Missile systems of U.S., U.S.S.R. and other nations, discussing ground-to-ground, ground-to-air, air-to-ground and air-to-air missiles 05 p0728 A72-16740
- Harpoon air-sea/sea-sea all-weather missile system, describing two phase guidance system based on inertial platform initial phase and radar terminal guidance 07 p1085 A72-20312

SURFACE TREATMENT

U SURFACE FINISHING

SURFACE VEHICLES

- NT AIRCRAFT CARRIERS
- NT AUTOMOBILES
- NT LIFEBOATS
- NT LUNAR ROVING VEHICLES
- NT LUNAR SURFACE VEHICLES
- NT MANNED LUNAR SURFACE VEHICLES
- NT ROCKET PROPELLED SLEDS
- NT ROVING VEHICLES
- NT SLEDS
- NT TANKER SHIPS
- NT WALKING MACHINES

- Zener diode transient suppressors with electronic thermal switch for ground vehicle and aircraft applications [AD-741529] 05 p0637 A72-16553
- Analog dynamic model of tracked air cushion vehicle for high speed ground transportation systems 13 p1896 A72-28704
- Twin-turboprop transport aircraft, helicopter and all-terrain ground vehicle simulators, discussing control load, visual attachment, cabin motion and sound subsystems 14 p2092 A72-30845
- Landmark navigation with angle measurements for roving vehicle guidance on lunar and planetary surfaces 15 p2268 A72-31790
- Arctic environment surface effect vehicle design, considering structures, drag, lift, propulsive power and range 15 p2181 A72-32125

SURFACE WAVES

- NT BAROCLINIC WAVES
- NT CAPILLARY WAVES
- NT GRAVITY WAVES
- NT SOMMERFELD WAVES
- MHD boundary waves properties, noting application to traveling wave nonreciprocal devices and planar structures based on microwave integrated circuits 01 p0029 A72-10703
- Equivalent circuit model for electroacoustic surface microwave transducer, discussing radiation properties determination from excitation fields distribution 01 p0041 A72-10704
- Characteristic equation of surface wave propagation on two dimensional corrugated structures for phased array applications 01 p0030 A72-10845
- Nonreciprocal guiding devices for electromagnetic surface waves, noting large bandwidth and non-rectilinear polarization of alternating magnetic field 01 p0044 A72-11323
- Orbiting lunar spacecraft Endeavor radio transmission postoculation reception, considering surface wave propagation and mountain formation prismatic refraction 02 p0171 A72-11753
- Quasi-static surface waves at Maxwellian plasma boundary with diffuse electron scattering, considering plasma electromagnetic oscillations 02 p0266 A72-12577
- Apodized interdigital transducers acoustic surface wave front distortion, describing perturbation and compensation method 03 p0360 A72-13602
- Tangential stress pulse effects on transversally isotropic half space surface wave motion under torsion 03 p0452 A72-14128
- Nonlinear surface wave propagation on pinched cylindrical plasma, developing asymptotic approach from L undquist equations 04 p0559 A72-15348
- Two dimensional axisymmetric surface waves motion in inviscid incompressible homogeneous electrically conducting fluid under uniform magnetic and electric fields, considering surface tension effects 04 p0560 A72-15744
- Spontaneous oscillations generation on transverse surface wave, discussing experimental realization with semiconducting CdS single crystals 05 p0626 A72-16282
- Transverse acoustoelectric surface wave domain in piezo-semiconducting body, obtaining gain coefficient and generation threshold criterion 05 p0702 A72-16283
- Surface wave parametric signal processing, obtaining cross correlation of digitally coded input signals 05 p0631 A72-17074
- Cracks interactions with transversal and surface elastic waves, relating crack propagation threshold conditions to critical pulse duration 06 p0893 A72-17419
- Light intensity distribution from ultrasonic surface waves reflection to probe surface acoustic propagation characteristics 06 p0848 A72-17851
- Log-periodic interdigital transducer design to obtain wide bandwidth for acoustic surface waves 06 p0784 A72-18241
- Weighted acoustic surface wave dispersive microwave filter apodized interdigital array design modification for phase error correction to reduce distortion 06 p0787 A72-18380
- Nonlinear self excited oscillations in uniformly distributed oscillators interacting with traveling transverse or surface waves of elastic body 06 p0849 A72-18698
- Corrugated surface wave antenna design with low sidelobe level radiation pattern, finding relief modulated impedance parameters 07 p0955 A72-19514

- Love surface wave excitation in thin film layer by line source as function of propagation direction, frequency and film thickness 07 p1089 A72-19683
- Laser probes for acoustic surface wave amplitude and phase measurements 07 p1008 A72-20385
- Phased directional surface wave splitters and microwave and integrated optics elements based on single mode, dielectric and rectangular waveguides 08 p1131 A72-20935
- Linear inverse problem of coefficient matrix eigenvectors, implying surface waves and free oscillations for earth structure 08 p1159 A72-21495
- Electromagnetic wave propagation along open rectangular dielectric waveguide, deriving dispersion equations for surface waves propagation constants 08 p1136 A72-21739
- Rayleigh type transverse surface wave existence in continuous elastic body with nonlocal interaction 09 p1403 A72-22748
- Dielectric permeability tensor operator for surface wave-electron beam interaction in relativistic nonuniform plasma stream with cylindrical geometry 09 p1359 A72-22769
- Interdigital acoustic surface wave transducer immittance characteristics calculation from equivalent circuit, demonstrating effectiveness on delay lines [AD-743552] 09 p1316 A72-23421
- Telecommunications ultrasonic resonators, electromechanical and piezoelectric filters and microacoustic surface elastic wave devices 09 p1281 A72-23468
- Plane stratified earth crust parameters determination from dispersion curve of Rayleigh surface waves fundamental tone 09 p1304 A72-23488
- Book on continuous elements dynamics covering membrane, torsional, string and elastic beam vibration, four pole techniques, periodic forced motion and surface waves 10 p1557 A72-24674
- Book on continuous transitions in open waveguides covering plane directive surface, single wire transmission line and layered waveguide surface wave propagation modes 10 p1436 A72-24675
- Surface acoustic wave technology in communication systems, discussing analog and digital matched filters and navigation, ATC and collision avoidance applications 10 p1483 A72-24946
- Microwave two reflector rectangular backfire antenna with dielectric surface wave structure as waveguide prolongation, obtaining far field radiation pattern 11 p1604 A72-25749
- Surface waves propagation in inhomogeneous elastic body, deriving wave equations asymptotic solutions 11 p1689 A72-26384
- Antisymmetry principle for solving equation of elastic surface wave caused by waveguide 12 p1845 A72-27392
- Surface wave propagation mechanism on dielectric bodies noting compatibility with physical properties involved with optical cables for commercial transmission systems 12 p1782 A72-27556
- Surface wave devices signal processing for space communication, developing fast lock up spread spectrum communication link broadband 13 p1920 A72-29106
- Surface waves generation and absorption by interdigital transducer with uniform finger spacing, discussing parallel equivalent circuit derived in weak coupling approximation 13 p1960 A72-29769
- Dynamic behavior of long-period oscillations of surface wave type in system of inhomogeneous ion beams moving in dense plasma along magnetic field 14 p1236 A72-30307
- Acoustic surface wave chirp filters application in pulse compression radar system, considering various piezoelectric substrate materials characteristics 14 p2089 A72-31045
- Dispersion equations and resonant absorption of plane and cylindrical surface waves in transition layer between plasmas, noting Langmuir oscillations 15 p2286 A72-32385
- Microwave acoustic surface waves attenuation at solid and monatomic gas boundary, detailing frequency, molecular weight, pressure and temperature effects 15 p2278 A72-32505
- Nondispersive guidance structure for acoustic surface waves due to velocity reduction of thin conducting strip on piezoelectric substrate 15 p2278 A72-32506
- Power spectrum of light scattered from surface waves thermally excited on carbon dioxide liquid-vapor interface near critical point 16 p2423 A72-32948

Piezosemiconductor crystals acoustoelectric surface domain waveguide effect for classical and transverse surface waves
16 p2441 A72-33596

Reliable nondestructive microstructure testing via surface ultrasonic waves
16 p2399 A72-33822

Love wave tapping in isotropic microacoustic surface waveguide by partial transduction into bulk wave at discontinuity
16 p2428 A72-34178

Acoustic edge scattering of elastic surface waves.
17 p2579 A72-34227

High-frequency ultrasonic devices.
17 p2526 A72-34564

The surface plasmon resonance effect in holography.
17 p2553 A72-34723

High-speed image scanning devices using acoustic surface waves and photodiode array.
18 p2658 A72-36267

Vlasov and Maxwell equations solution for surface waves dispersion in semiinfinite hot plasma
18 p2716 A72-36925

Excitation of nanosecond waves on positive columns.
19 p2838 A72-37328

Kinetic theory of surface waves in a cylindrical plasma waveguide
19 p2842 A72-38531

Propagation of surface waves along a plane boundary between two magnetoactive plasmas
19 p2842 A72-38532

Crack depth measurement with surface waves.
19 p2809 A72-38569

Analysis of piezoelectric thin-film transducers for elastic surface waves.
19 p2804 A72-38607

Earth density, surface wave velocity and other properties calculation from model consistent with physical and petrological mantle theories
20 p2917 A72-39475

Amplification of acoustic surface waves under transverse magnetic field in coupled intrinsic semiconductor-piezoelectric systems.
20 p2960 A72-39703

Magnetoplasma surface waves in polar semiconductors: Retardation effects.
21 p3096 A72-40344

Dielectric slab surrounding medium gain effects on bound modes amplification via estimation of evanescent surface wave interactions in optical waveguide by perturbation theory
21 p3062 A72-40605

A directional antenna represented by a system of two planes positioned on the generatrix of a relief impedance cylinder
21 p3033 A72-40942

Correction of diffraction errors in acoustic-surface-wave pulse-compression filters.
21 p3034 A72-41464

Quasi-static loading of the earth by propagating air waves.
22 p3172 A72-42468

Use of rotated electrodes for amplitude weighting in interdigital surface-wave transducers.
22 p3178 A72-42619

Propagation of Rayleigh waves on visco-elastic cylindrical surfaces placed in a magnetic field.
22 p3207 A72-42876

On the propagation of Love type waves in an infinite cylinder with rigidity and density varying linearly with the radial distance.
22 p3207 A72-42878

Plasma-electromagnetic interaction with surface wave propagation along boundary, obtaining boundary conditions for longitudinal and transverse wave amplitudes with allowance for particles interaction
22 p3213 A72-43117

Dynamic behavior of long-period oscillations of surface wave type in system of inhomogeneous ion beams moving in dense plasma along magnetic field
23 p3317 A72-43209

Surface wave parametric excitation by weak HF electric field in semibounded plasma, calculating near threshold instability by dispersion equation
23 p3318 A72-43322

Electronic devices with Rayleigh ultrasonic acoustic surface wave excitation for storage, recognition and separation of electrical signals usually requiring computerized operation
23 p3314 A72-44148

SURFACES

Steady and oscillatory subsonic aerodynamic loads prediction based on Doublet-Lattice method and method of images, determining chord and spanwise loading on lifting surfaces
[AIAA PAPER 72-26]
05 p0607 A72-16917

Monge surface shells reduced to bodies of revolution by small parameter method for solution of momentless theory equations
13 p2058 A72-29489

SURGERY

Resumption of flight after retinal surgery
19 p2760 A72-37879

SURGES

Zener diode transient suppressors with electronic thermal switch for ground vehicle and aircraft applications
[AD-741529]
05 p0637 A72-16553

Acoustic stimuli transients rise time and repetition rate effects on loudness, applying various steady state noise calculation methods to transients Fourier transforms
13 p2004 A72-29097

SURVEILLANCE

NT SPACE SURVEILLANCE [GROUND BASED]
NT SPACE SURVEILLANCE [SPACEBORNE]
Air transportation system design for safety and efficiency, discussing navigation facilities and surveillance systems employment for blunder prevention
01 p0098 A72-11117

Synchronous satellite surveillance system for transoceanic ATC, using suboptimal /modified Kalman/ filter for aircraft position and velocity computation
08 p1204 A72-21091

Optimal tracking filter for processing sensor data of imprecisely determined origin in surveillance system by minimizing effects of correlation uncertainties
10 p1455 A72-23787

Trends in civil ATC discussing plans to increase terminal capacity, surveillance system and use of multiple synchronous satellites for ocean travel efficiency improvement
12 p1842 A72-27103

Correlation technique for position location in surveillance and navigation by phase extraction from range tones using synchronous satellites
[AIAA PAPER 72-564]
12 p1842 A72-27375

ATC operational systems, discussing global surveillance and voice and data communication between aircraft and earth station
14 p2129 A72-31141

SURVEILLANCE RADAR

Avionics contribution to airspace decision making problems, considering navigation, surveillance radar, collision avoidance and ATC techniques
01 p0097 A72-10180

Airfield surface radar detection equipment to control aircraft and ground vehicles under reduced visibility and darkness
02 p0173 A72-12105

Tactical ATC display system for airport surveillance, precision approach and landing and operator/aircraft/machine operations by using terminal Area Surveillance Radar
02 p0230 A72-12421

Target trajectory detector optimization, using data and Markovian chain apparatus
03 p0323 A72-13831

Air surveillance using satellite range-difference measurement from noninterrogated aircraft beacons for ATC
04 p0545 A72-14826

Airborne traffic display system using beacon and radar surveillance network and ground computer processing
06 p0844 A72-17329

Aircraft proximity control for ATC system using national secondary surveillance radar /SSR/ for CAS-PWT functions
06 p0844 A72-17330

Suboptimal decision algorithm to correlate sensor data with stored tracks in real time track-while-scan surveillance system
10 p1441 A72-23780

Electronics and data processing technology effects on radar state of art, discussing automated air traffic control surveillance systems
10 p1435 A72-24490

Average time between successive false target indications in surveillance binary signal detector with variable storage capacity
11 p1595 A72-26295

Target angular position measurement by surveillance radar on background of correlated interference
11 p1595 A72-26296

Azimuth-bearing error dispersion in surveillance radar measurements, using Markov chains
11 p1595 A72-26297

Continuous wave Doppler radar with microwave oscillator for ATC measurements and surveillance
12 p1789 A72-27403

Secondary surveillance radar systems design and planning for ATC application
13 p1917 A72-28698

Surveillance radar for clutter rejection and signal loss reduction at airports, discussing system design features
18 p2662 A72-37046

Bearing azimuth measurement accuracy improvement by ATC beacon system/secondary surveillance radar using monopulse technique
18 p2662 A72-37047

ATC IC transponder used with secondary surveillance radar, discussing design features
18 p2662 A72-37048

SURVIVAL

ATC services configuration with secondary surveillance radar and primary radar data acquisition system, discussing signal processing by automated decoder
21 p3080 A72-40288

Air traffic density effect on secondary surveillance radar operation in ATC for aircraft identification and position determination, proposing selective advisory system
21 p3080 A72-40289

Discrete address beacon system /DABS/ development for surveillance and ground-air communications in support of ATC automation
22 p3204 A72-43151

SURVEYING

U SURVEYS

SURVEYOR LUNAR PROBES

Martian surface nature from Surveyor and Apollo missions data on lunar particle size distribution
01 p0132 A72-11037

Lunar surface soil mechanical properties from computer simulation of Surveyor spacecraft observation data for each landing site, estimating cohesion
02 p0275 A72-11595

Lunar mare soil deformation and cracking from Surveyor and Apollo photographs
04 p0574 A72-14918

Surveyor spacecraft lunar thermal data, comparing spatial resolution with earth based measurements
12 p1869 A72-27329

SURVEYOR 3 LUNAR PROBE

Apollo 12 retrieved Surveyor 3 TV camera mirror surface and camera-shroud organic contamination attributed to spacecraft outgassing and engine exhaust products
03 p0415 A72-12948

Lunar surface bearing strength vs penetration curves from Surveyor 3 soil sample, comparing with in-situ remote measurements
07 p1067 A72-18873

SURVEYS

NT GEODETIC SURVEYS

Urban area aerial photography survey for large scale photomaps, discussing building feature examination and universal stereophotogrammetric instruments utilization
03 p0362 A72-14311

Terminal area ATC specialists and trainees job attitude and motivation from questionnaire on challenge, tasks, salary, work schedule, etc.
06 p0766 A72-17865

Frankfurt Airport air traffic controller opinion survey of attitudes toward work and working environment
09 p1271 A72-23138

SURVIVAL

Microbial survivability in deep space environmental simulation experiments, describing aerospace ecology and panspermia avoidance
01 p0019 A72-10823

Hazard rate of recurrence in patients with malignant melanoma, investigating survival
02 p0167 A72-11713

Complex systems stochastic survivability estimates dependence on delay depth and initial conditions of interaction
05 p0640 A72-16204

Spacecraft and aircraft crew survival after emergency landing in adverse environments, discussing water and food requirements, survival supplies and medical and first aid equipment
05 p0621 A72-16629

High performance aircraft takeoff and landing accidents, investigating survival rates
08 p1109 A72-21563

Survival rates in USAF accidents during 1965-69, noting visual sighting as primary rescue factor
08 p1109 A72-21564

Pilot survival probabilities under various conditions of high performance aircraft takeoff and landing accidents, suggesting emergency action guidelines for pilot training
10 p1428 A72-23732

Passenger behavioral inaction in survivable aircraft accidents, suggesting maladaptive behavior counteraction by leadership and/or training
13 p1908 A72-28727

Effect of Acetazolamide /Diamox/ at different dose levels on survival time of rats under acute hypoxia and on Na⁺/K⁺/ATP-ase activity of rat tissue microsomes.
17 p2499 A72-34546

Stress and adaptation responses to repeated acute acceleration.
17 p2500 A72-34729

Analysis of survival and cause of death statistics for mice under single and duration-of-life gamma irradiation.
23 p3254 A72-43394

A study of USAF survival accidents 1 Jan. 1965-31 Dec. 1969.
23 p3259 A72-43425

Evidence for a metabolic limitation of survival in hypothermic hamsters.
23 p3258 A72-44364

SURVIVAL EQUIPMENT

Spacecraft and aircraft crew survival after emergency landing in adverse environments, discussing water and food requirements, survival supplies and medical and first aid equipment

05 p0621 A72-16629

Survival and flight equipment - Conference, Las Vegas, September 1971

08 p1109 A72-21560

Single Integrated Signal Device to aid in locating downed airmen awaiting rescue in dense jungle terrain by Search and Rescue aircraft

08 p1112 A72-21580

Emergency systems for helicopter crew and passenger survivability improvement, discussing use of ejection seats, extraction systems parachute bail-out and shaped explosive charges

08 p1109 A72-21581

Emergency Life Saving Instant Exit system in aircraft fuselage for use after crash landing, discussing design and ground testing

08 p1109 A72-21583

Manned space flight escape, rescue and survival systems based on onboard, prepositioned aid and earth launched concepts, considering earth orbit, lunar and interplanetary missions

09 p1395 A72-23152

Thermally protective life rafts and clothing evaluation for cold sea survival potential assessment and tolerance limit determination

14 p2081 A72-31088

Survival equipment for life raft in conjunction with Mercury, Gemini, Apollo, Skylab and space shuttle NASA programs

17 p2620 A72-34433

Medical and technical aspects of rescue and survival of astronauts in high mountain and mountainous remote areas.

17 p2507 A72-34434

Some aspects of survival and rescue of astronauts in polar regions.

17 p2507 A72-34435

SUSCEPTIBILITY [MAGNETISM]

U MAGNETIC PERMEABILITY

SUSPENDING [HANGING]

NT MAGNETIC SUSPENSION

Axial and radial displacements determination in rotor center of gravity for gyroscope with elastic suspension

03 p0360 A72-13560

Angular rigidity of support shaft elastic suspension of dynamically adjustable gyroscope

09 p1307 A72-22348

Nonlinear elastic suspension system with two spring pairs in parallel, measuring nondimensional load versus deflection curve and frequency response

11 p1736 A72-26007

Elastic deformation and rigidity of rectangular, circular and elliptic gimbals for gyroscope suspension

13 p1957 A72-29272

Equations of motion for contactless suspension gyroscope in force field

15 p2235 A72-31726

Stability and control dynamics of helicopter hovering with heavy sling load, analyzing maneuvers for minimal excitation of pendulous motion

[AHS PREPRINT 630] 17 p2489 A72-34488

Behavioral features of a composite hydrostatic suspension of a gyrocompass under conditions of vibration

21 p3058 A72-41807

SUSPENDING [MIXING]

Ignition and incandescence of laser irradiated single micron size Mg particles suspended in stoichiometric methane air mixture

10 p1564 A72-25140

Turbulent friction values diminished by reading errors in pitot tube flow measurement of solid particles suspensions and polymer solutions caused by viscoelastic associations

14 p2106 A72-31007

Particle charging behind shock waves in suspensions.

20 p2914 A72-39627

Determination of the characteristics of the averaged motion of the carrier medium in turbulent gas flow with suspended particles

21 p3044 A72-40126

Performance and flow properties change through a rocket turbine by presence of solid particles.

24 p3361 A72-45206

SUSPENSION SYSTEMS [VEHICLES]

Deterministic optimization of aircraft undercarriage suspension characteristics for taxiing induced vibration minimization, discussing damping and stiffness functions and hybrid computer solution

09 p1407 A72-23458

Combined hydrostatic suspension Hg cushion effects on gyrocompass response precision during irregular roll of platform

13 p1961 A72-30022

Design of vibration absorbers minimizing human discomfort.

21 p3009 A72-41231

SUSPENSIONS

Balance laws of micromorphic theory for polycrystalline mixtures, granular composites and fluid suspensions involving motions with wavelength comparable to intrinsic discontinuities in materials

01 p0102 A72-10320

Thermal conductivity, electrical conductivity, viscosity and diffusivity of ionized gas-solid suspension in electric field, using transport equations and particle interaction potentials

01 p0111 A72-11332

Time characteristics preceding self-ignition of solid particle system suspended in gas, discussing quasi-steady state duration

06 p0903 A72-18202

Critical conditions for self ignition of solid fuel particles suspended in gas

06 p0903 A72-18203

Wave equation for sound velocity propagation in suspensions based on mass and momentum balances

11 p1687 A72-26056

Conjugate-flow theory for heterogeneous compressible fluids, with application to non-uniform suspensions of gas bubbles in liquids.

21 p3044 A72-40120

SWAGING

NDT holographic interference pattern technique to determine Advanced Test Reactor fuel element swage joint tightness

01 p0078 A72-11110

Tungsten wire deformation structure from swaging or rolling and drawing processes, noting cylindrical texture superimposed on fiber texture

03 p0375 A72-13933

Power parameter determination in rotary swaging of thin conical shells, discussing radial contact stresses

05 p0666 A72-16628

Brazed-welded lightweight high pressure aerospace tube-fittings.

17 p2560 A72-34939

SWEAT

Peripheral modifications to exercise induced central drive for sweating, determining rates as functions of internal temperature

04 p0479 A72-15212

Regulation of sweat secretion on skin surfaces overlying active and nonactive muscle tissue during skin or core temperature alterations

04 p0480 A72-15216

Body thermal stress, local heating and arterial occlusion effects on sweat electrolyte content

07 p0929 A72-19437

Myoepithelial mechanism of high frequencies pulsatile discharge of human sweat glands

07 p0930 A72-19444

Galvanic skin response techniques for palmar and dorsal sweat detection during motion sickness by vestibular stimulation, comparing arousal and thermal sweat response

07 p0933 A72-20185

Calorimetric measurements of human body temperature and of hot saline solution drinking effects on sweating rate

09 p1267 A72-23440

Calorimetric study of sweating man response to drinking hot saline solution as function of temperature, volume and salinity of ingested liquid

09 p1267 A72-23441

Thermodynamic analysis of heat of evaporation of sweat, considering ambient temperature and humidity effects, body heat storage and presence of solutes

11 p1586 A72-26610

Thermoregulation changes during simulated weightlessness of prolonged bed rest, noting lower sweating threshold and decreased vasodilation/autonomic dysfunction/

12 p1767 A72-28301

Environmental temperature effect on motion sickness sweating, discussing nausea and discomforting symptomatology prediction

12 p1775 A72-28302

Human diaphoretic system physiology, discussing skin surface sweat excretion intensity relation to optimal balancing process in thermoregulation

14 p2076 A72-30672

Skin temperatures in warm environments and the control of sweat evaporation.

17 p2506 A72-35969

Sweat depression during controlled hyperthermia in man - Effects on the sweat rate and sweat electrolytes

20 p2892 A72-39591

SWEAT COOLING

Heat and mass transfer equations for unsteady transpiration cooling, taking into account temperature gradient between coolant and surface

03 p0457 A72-14154

Nozzle and cavity wall cooling limitations on uranium plasma nuclear rocket specific impulse, discussing wall heat flux and transpirational cooling by propellant flow

03 p0387 A72-14383

Surface heat transfer and pressure measurements for downstream effects of transpiration cooled nose tip, using nitrogen as injectant fluid

[AIAA PAPER 72-185] 05 p0605 A72-16840

One dimensional two phase flow transpiration cooling through porous metals

[AIAA PAPER 72-24] 05 p0749 A72-16915

Two phase heat transfer in porous metal transpiration cooling system, comparing measured with calculated temperature distribution

[AIAA PAPER 72-25] 05 p0749 A72-16916

Transpiration cooling of laminar tangential Newtonian flow in annuli, obtaining temperature distribution

07 p1100 A72-19631

Liquid film transpiration cooling concept application to space shuttle leading edge heating and shock heating

[AIAA PAPER 72-389] 11 p1744 A72-25410

Gas side, coolant side and interstitial heat transfer in gas turbines transpiration air cooling

12 p1860 A72-27350

Boundary layer approach to local potential solution of diffusion equations, applying to transpiration cooled half space and heat conduction in melting solid

13 p2064 A72-28885

SWEATING

U PERSPIRATION

SWEDEN

Report to COSPAR on Swedish space research, discussing activities of astronomical, ionosphere and geophysical observatories and space technology, physics and cosmic ray groups

15 p2338 A72-32008

SWEEP ANGLE

NT LEADING EDGE SWEEP

SWEEP CIRCUITS

Final stages of transistorized sweep generators

22 p3158 A72-42114

SWEEP EFFECT

Laminar three dimensional boundary layer nonequilibrium effects at hypersonic wing swept leading edge with intensively cooled surface, considering sweep induced crossflow effect

[VPI-E-71-23] 02 p0152 A72-12422

SWEEP FREQUENCY

Optical sweep generator using single frequency He-Ne lasers with Michelson interferometer for mode selection to provide smooth tuning throughout Doppler width

07 p1000 A72-19010

Matched acoustic generator for sweep frequency testing of power gain of fluoric amplifiers

[ASME PAPER 71-WA/FLCS-2] 10 p1423 A72-25051

Biological system transfer-function extraction using swept-frequency and correlation techniques.

22 p3151 A72-42773

SWEEPBACK

NT LEADING EDGE SWEEP

SWELLING

Effect of neutron spectra on the swelling of ceramic insulators and implications for thermionic reactor design.

18 p2703 A72-36146

SWEPT WINGS

NT ARROW WINGS

NT DELTA WINGS

NT SWEPTBACK WINGS

Subsonic linearized theory for symmetrical cranked wings at zero incidence, presenting corrected formulas for streamwise and spanwise perturbation velocity components due to wing thickness

01 p0001 A72-11154

Increasing lift and Reynolds number effects on displacement and skin friction of three dimensional turbulent boundary layer on infinite swept wing

01 p0002 A72-11395

Laminar three dimensional boundary layer nonequilibrium effects at hypersonic wing swept leading edge with intensively cooled surface, considering sweep induced crossflow effect

[VPI-E-71-23] 02 p0152 A72-12422

A-300B European Airbus cantilever wing design and manufacture, discussing skin forming, skin-stringer and torsion-box assembly, automatic riveting and root-end profile machining procedures

03 p0365 A72-14301

Incompressible boundary layer velocity profile on swept wings, comparing critical Reynolds number to straight wing value

13 p1894 A72-29639

Elliptic-hyperbolic relaxation algorithm for solution to three dimensional nonlinear transonic small disturbance potential equation for flow about swept wings

[AIAA PAPER 72-677] 16 p2346 A72-34063

Aerodynamic test facility data on swept wings, peaky airfoils, aircraft flutter and transonic flow, discussing shock tubes and wind tunnels development

20 p2912 A72-39846

SWEPTBACK WINGS

NT ARROW WINGS

NT DELTA WINGS

Flutter analysis and unsteady pressure fields induced by pitching motions of wall mounted sweptback wing, verifying experimentally lifting surface theory in high subsonic range

22 p3241 A72-43094

- The sweepback effect in the subsonic region in the lower altitudes and in the hypersonic region at high altitudes 24 p3359 A72-44983
- SWIMMING**
Cardiorespiratory functions in child swimmers and nonathletes during growth, relating training to oxygen transport system dimensions 08 p1123 A72-20894
- SWINE**
Pigs role as ideal experimental animal in human biomedical research, discussing investigations to emphasize similarities 18 p2649 A72-36440
- SWINGBY TECHNIQUE**
Planetary swingby optimum transfer between hyperbolic asymptotes with less than maximum natural turn angle 10 p1552 A72-24487
Trajectory analysis for swingby technique using Jovian gravitational field for leaving ecliptic plane along heliocentric orbit and for solar flyby at specified distance 14 p2150 A72-30452
Mission design and navigation for a 1977-1978 Venus Swingby/Mercury Orbiter. [AIAA PAPER 72-941] 21 p3113 A72-41577
Saturn-Jupiter rebound - A method of high-speed spacecraft ejection from the solar system. 23 p3340 A72-44323
- SWIRLING**
Numerical solution for swirling ideal gas flow in Laval nozzle, determining swirling effects on nozzle performance 02 p0149 A72-11583
Multicellular viscous vortex core embedded in unsteady outer potential swirling flow, obtaining numerical solution 02 p0253 A72-11971
Mass blocking of subsonic isentropic swirling flow through convergent axisymmetric nozzle, considering radial velocity component effect on vorticity 03 p0342 A72-13957
Laminar boundary layer velocity profiles in convergent nozzle incompressible swirling flow, considering boundary layer growth effects on free stream axial and tangential velocities 10 p1471 A72-25068
Reynolds analogy for twisted liquid flow in tube with swirl vanes 11 p1619 A72-26968
Swirling flow effects on annular conical diffuser performance in axial flow turbomachines, showing stagnation region and inner body diameter dependence 14 p2069 A72-30580
Fuel injection, mixing and combustion processes investigation in model cylindrical swirl chamber, describing flow visualization method for turbulence observation 15 p2297 A72-32297
Solution existence for singular boundary value problem involving swirling flow, corresponding to problem of axisymmetric flow above rotating disk 16 p2377 A72-33186
Numerical finite difference prediction of inert turbulent boundary layer swirling jet flow, using nonisotropic energy-length model [AIAA PAPER 72-699] 16 p2380 A72-34044
Swirling flows vortex breakdown in nozzles, diffusers and combustion chambers, considering analogy to boundary layer separation 18 p2641 A72-36385
Calculation of axisymmetric swirling and non-swirling turbulent jets 18 p2682 A72-36890
Characteristics of the propagation of swirling jets of variable density 22 p3166 A72-42255
Reacting and nonreacting swirl recirculation bubble gasdynamic structure in fuel combustion systems, noting anisotropic turbulence from hot-wire anemometer measurements 24 p3461 A72-45024
The damping of precessing vortex cores by combustion in swirl generators. 24 p3464 A72-45060
Decay of swirl in a straight pipe flow /with hub at the entrance/. 24 p3394 A72-45367
Swirling base injection for supersonic combustion ramjets. 24 p3434 A72-45785
- SWIRLING WAKES**
U TURBULENT WAKES
- SWITCHES**
NT CAPACITANCE SWITCHES
NT CRYOTRONS
NT ELECTRIC RELAYS
NT ELECTRIC SWITCHES
NT FLUID SWITCHING ELEMENTS
NT PRESSURE SWITCHES
NT SWITCHING CIRCUITS
NT THERMOSTATS
NT TRIGATRONS
- Frequency response of spectral noise amplitude in chalcogenide glass switches 09 p1366 A72-22215
- SWITCHING**
NT BEAM SWITCHING
NT MAGNETIC SWITCHING
NT MICROWAVE SWITCHING
Response of discrete linear systems to forcing functions with inequality constraints. 20 p2910 A72-39604
A new type of switching and memory effect by controlling the polarized field in semiconductor interface. 20 p2961 A72-39709
Isochronic corner generated difficulties avoidance in linear multivariable system minimum time controller, noting association with switchings 21 p0307 A72-40638
An iterative technique for determining the minimal number of variables for a totally symmetric function with repeated variables. 23 p3308 A72-43421
- SWITCHING CIRCUITS**
NT FLUID SWITCHING ELEMENTS
Plasma potentials spatial distribution measurement, describing switching circuit and probe design 01 p0109 A72-10580
Low driving power resistive gate MOSFET microwave switch with performance approaching P-I-N diode 01 p0038 A72-10658
Ionization chamber for direct measurement of radiation dose equivalent, describing high voltage switching circuit [CERN-71-16] 02 p0168 A72-12072
Thermal effects on reversible threshold switching in amorphous semiconductor thin films involving current controlled negative resistance 02 p0268 A72-12202
Millimeter wave pulse signal transmission path length modulator with P-I-N diode switch, discussing system design and experimental results 02 p0196 A72-12798
Polyphase signal generators, using reversed flux region propagation in saturable ring core controlled by switching transistors operation [IEEE PAPER 17-5] 03 p0322 A72-13773
Bistable fluidic amplifiers switching dynamics, developing analytic performance prediction method from flow visualization studies [ASME PAPER 71-WA/FLCS-8] 05 p0615 A72-15916
Book on transistors in pulse circuits covering switching diodes and circuits, multivibrators, blocking oscillators, etc 05 p0640 A72-16288
Switching contacts performance principles, noting inductive energy role in electrical breakdown voltage determination 06 p0791 A72-18579
Digital loaded-line phase shifters for phased array antennas, discussing lossy microstrips effects and P-I-N diode switching shortcomings in design requirements 07 p0954 A72-19048
Digital simulation for predicting performance of data communication networks with computerized switching centers, detailing space shuttle interior communication system 07 p0952 A72-20364
Ac and dc power regulation by switched capacitor, analyzing voltage spectrum for resistive load 07 p0958 A72-20389
Switching characteristics of MOS channel transistors, solving nonlinear differential equations describing current and potential distribution 08 p1140 A72-21267
Six channel integrated MOS switch, discussing MOS transistor operation and circuits structure 09 p1288 A72-23363
German monograph on electric arc behavior in narrow channel with plasma cooling by channel wall and continuously decreasing current for switching applications 10 p1517 A72-23773
Switching behavior and attenuation of space division multiplex crosspoint circuit with end marking, discussing realization in thick film technology 11 p1604 A72-25908
Switch detector output random process energy spectrum and autocorrelation function, noting distortion reduction by proper parameter choice 11 p1605 A72-26317
Sawtooth voltage generator with switching circuit to achieve small retrace time via blocking generator 11 p1605 A72-26320
Aluminum-silicon Schottky diode clamped transistor-transistor logic circuits parameters optimization for high switching speed and IC applications 11 p1606 A72-26568
Parasitic sidelobe suppression in radiation patterns of phase switching linear antenna array without gain loss 11 p1598 A72-26717
- Fall time calculation and junction capacitance effect in diodes with nonuniform base doping switched off by voltage and current generators 11 p1607 A72-26963
Electroluminescent matrix display system with amorphous semiconductor threshold switches for isolation and memory, discussing performance and address waveforms 12 p1788 A72-27239
Reversible threshold switching in amorphous semiconductor alloys by carrier transport and recombinative electron injection 12 p1854 A72-27431
Second order systems time optimal control with delay, determining maximum number of switching points for control function 12 p1794 A72-28141
P-n-p-n junction thyristor turnoff process under reverse anode voltage at high injection level, examining current voltage curve and switching time constant 13 p1932 A72-29293
Metal-dielectric-semiconductor junction transistor HF response analysis by digital computer, deriving switching time as function of impurity concentration and electrode voltage 13 p1932 A72-29294
Chalcogenide semiconductor monostable threshold and bistable memory switching devices, discussing fabrication and performance 13 p1934 A72-30090
Reliability modeling principles, concepts and implementation techniques for switching system design 14 p2091 A72-31167
Fluidic digital logic devices vs electromechanical-electronic equivalents, describing Coanda effect application to bistable jet amplifiers /flip-flops/ as switching or memory devices 15 p2182 A72-31218
High voltage dc arc interrupter for use in high power pulse generators and switching application in high voltage dc power transmission system 15 p2201 A72-32569
Phase distribution randomization in switched antenna array, noting radiation pattern sidelobe compensation application 15 p2209 A72-32666
Langmuir probe dc and second harmonic characteristics measuring system, describing switching circuitry 16 p2392 A72-33608
An investigation of amorphous semiconductor memory devices utilizing thick film fabrication techniques. 17 p2527 A72-34682
Switch properties of thermionic diodes with cesium vapor. 18 p2645 A72-36178
S-band high power microstrip switches with p-i-n diodes for spacecraft radio systems 19 p2770 A72-37257
Contactless relay circuits employing a branched-core magnetic modulator with second-harmonic output 19 p2771 A72-37302
Switching curves and lobesweeping in origin seeking time optimal control for Duffing oscillator, using Pontryagin maximum principle 19 p2777 A72-37373
Symbol generators for the representation of switching circuits by data display devices according to the television principle 19 p2769 A72-37935
Amplitude and harmonic oscillation characteristics of quaternary RC parametron using tunnel diodes 19 p2773 A72-38211
Precise transfer function of a clamper for a commutation switch with a finite closing time 19 p2782 A72-38463
Interference suppression design of switching circuits utilizing slewing rates. 20 p2906 A72-38982
Realization of static /combination/ logic switches with the aid of TRIMELOG pneumatic elements. II 20 p2890 A72-39423
Analysis of the characteristics of an MOS transistor as a switching element 21 p3025 A72-40163
Switches for high-frequency channels 21 p3026 A72-40317
Interpretation of the preswitching behaviour of chalcogenide-glass switches in terms of a space-charge-injection mechanism. 21 p3034 A72-41466
Parameters and properties of special avalanche transistors 21 p3035 A72-41809
The relative merits of thyristors and power transistors for fast power-switching applications. 22 p3159 A72-42306
The switching behaviour of thin films of chalcogenide glass. 22 p3214 A72-42319
A CW Gunn diode bistable switching element. 22 p3159 A72-42610

Ferrite component for waveguide commutator used as microwave switching element and modulator, noting application in navigation instruments and avionics

23 p3270 A72-43768

Preswitching electrical properties, 'forming,' and switching in amorphous chalcogenide alloy threshold and memory devices.

24 p3385 A72-44982

Commutation switch based on an injection semiconductor laser.

24 p3412 A72-45620

A near-time-optimal control circuit with a large number of relay elements

24 p3387 A72-45699

SWITCHING ELEMENTS

U SWITCHING CIRCUITS

SWITCHING FUNCTIONS

U BOOLEAN FUNCTIONS

U SWITCHING

SWITCHING THEORY

Switching operations in TDMA system, noting availability of signaling channels with broadcast mode

01 p0033 A72-11305

Sign behavior of switching function defined for plane fuel-optimal flight on elliptical coast trajectories

05 p0728 A72-16705

Quasi-time optimal control synthesis of two-control variable system by equivalent switching signum function method

07 p0961 A72-19712

Linear time optimal problem with analytical perturbations of initial conditions, determining optimal control switching points from convergent series representation

08 p1145 A72-21466

Laser light induced high-low impedance switch in Cd doped n-type Si diodes with p-p-n junctions and negative resistance

13 p1928 A72-28676

Parabolic switching boundaries method for optimal fuel consumption control of manned orbital space vehicles

18 p2672 A72-36325

SYLLABLES

NT MESSAGES

Cortical responses to visually displayed word and nonsense syllable stimuli, using EEG and computer techniques

04 p0474 A72-15248

SYMBIOSIS

Hereditary endosymbiotic model of microbial evolution of Precambrian prokaryotic and eukaryotic cells

04 p0471 A72-14800

Phylogenetic origin of cytoplasmids from Cyanophyceae alga involved in endosymbiosis with colorless Cryptophyte

13 p1907 A72-29996

SYMBOLIC PROGRAMMING

NT COMPUTER PROGRAMMING

SYMBOLS

NT MESSAGES

Symbol generation with black-and-white or color display devices and time shared computer for man-machine communication

01 p0034 A72-10484

Exploratory test of extrasensory perception to identify random order of symbols in space during Apollo 14 flight with four subjects on earth

04 p0565 A72-14888

Pattern recognition in mental process automation, noting character transformations, written symbols content analysis and syntactic description

12 p1786 A72-27576

Electronic head-up displays for aircraft instrument indication in symbolic form at pilot eye level

15 p2188 A72-31513

Symbol generators for the representation of switching circuits by data display devices according to the television principle

19 p2769 A72-37935

SYMMETRICAL BODIES

NT AXISYMMETRIC BODIES

NT BODIES OF REVOLUTION

NT CELESTIAL SPHERE

NT CONICAL BODIES

NT CYLINDRICAL BODIES

NT ELLIPSOIDS

NT FAIRINGS

NT PARABOLIC BODIES

NT POINCARÉ SPHERES

NT ROTATING CYLINDERS

NT ROTATING SPHERES

NT SLENDER CONES

NT SPHERES

NT STREAMLINED BODIES

NT TORUSES

Motion of two symmetrical rigid bodies connected by frictionless spherical hinge positioned at dynamic symmetry axes intersection

08 p1206 A72-21168

Dynamic and kinematic equations of attitude and translational motions of symmetric rigid body under body fixed force

09 p1351 A72-22991

Stress concentration in symmetrical U-notched plates, comparing data with Baratta, Neal, Neuber and Heywood formulas

14 p2167 A72-30904

An approximate method for solving problems involving separated flows past bodies

21 p2990 A72-41088

SYMMETRY

Phenomenological symmetry for spatial, mechanical and relativistic physical laws, providing invariance to subsets of described objects

10 p5152 A72-24781

Radiative properties of charged particles moving in attractive Coulomb fields related to repulsive fields by symmetry relationships

12 p1848 A72-28155

Linear differential equations solution symmetry properties, using Lie algebraic methods and finite dimensional linear systems theory

15 p2264 A72-31761

The solution of sharp-cone boundary-layer equations in the plane of symmetry.

21 p2989 A72-40650

Symmetry transformations for thin elastic shells.

22 p3234 A72-42398

Compensating fields of homomorphic imaging problems in space symmetry, discussing quasi-tensors, covariant derivatives and Poincaré group

23 p3312 A72-43336

SYMPATHETIC NERVOUS SYSTEM

Stellate ganglion stimulation and hypoxia effects on hemodynamics and coronary circulation in dogs, discussing myocardial oxygen consumption, sympathetic nerve vasoconstrictor effect and vasodilatory response

05 p0617 A72-16153

Myorelaxant 3,5-dimethyl-4-bromopyrazol injection effect on rabbit and dog heart during direct extracardiac nerve stimulation

05 p0618 A72-16358

Cardiac acceleration by voluntary muscle contractions of minimal duration in men due to vagal tone inhibition

07 p0929 A72-19442

Vagal control of ventilation and respiratory muscles during elevated pressures in cats

07 p0917 A72-19446

Stimulation transmission tracts, synaptic mechanisms and tonic activity of cat sympathetic ganglia

07 p0924 A72-20617

Propranolol as adrenergic beta receptor inhibiting agent for hyperthyroidism symptom amelioration

08 p1118 A72-21550

Sympathetic responses in human skin nerves with accompanying vasomotor reactions induced by emotional, thermal and respiratory stimuli

10 p1424 A72-24241

Physiological and psychological effects of noise noting vulnerability of circulatory apparatus, neurovegetative system and stomach

14 p2079 A72-30696

Effect of beta-adrenergic blockade on plasma volume in human subjects.

19 p2757 A72-38029

Vasomotor reflexes and the principle of descending control

21 p2999 A72-40597

Supraspinal effects in the activity of preganglionic sympathetic neurons delivering axons to the cervical sympathetic nerve

21 p3000 A72-40599

Polysynaptic sympatho-reticular and somatic afferent visceral links between internal organs and cerebrum in interoceptive reflex fields

21 p3000 A72-40755

Unresponsiveness of pial precapillary vessels to catecholamines and sympathetic nerve stimulation.

22 p3140 A72-41934

Influence of the sympathetic nervous system on the presynaptic inhibition of the dorsal surface potential of the spinal cord

24 p3370 A72-44589

SYMPATHOMIMETICS

U ADRENERGICS

SYMPHONIE SATELLITES

Telemetry equipment of network tracking stations for CNES Symphonie satellites at 136-138 and 148 MHz

[DGLR PAPER 72-015]

13 p1939 A72-28966

Parallel operation of the solar generator and battery on the Symphonie satellite

18 p2648 A72-36681

Power regulation in the Symphonie satellite

18 p2648 A72-36682

Reliable component procurement for Symphonie satellite, discussing parts list, specifications and subcontract monitoring and inspection

18 p2670 A72-37124

Integrated systems design procedures as exemplified by Europa 1, 2 and 3 rockets and Symphonie communication satellite development

19 p2869 A72-38302

The Franco-German telecommunications satellite Symphonie

24 p3451 A72-45230

The Symphonie transponder in the integration phase

24 p3380 A72-45273

SYMPTOMOLOGY

Asymmetrical hypertrophic cardiomyopathy symptoms simulating mitral stenosis, suggesting electrocardiography, chest X ray and hemodynamic studies as diagnostic procedures

06 p0761 A72-17380

Environmental temperature effect on motion sickness sweating, discussing nausea and discomforting symptomatology prediction

12 p1775 A72-28302

SYMPTOMS

U SIGNS AND SYMPTOMS

SYNAPSES

Postsynaptic electric potential responses to click on auditory cortex neurons in cats

02 p0158 A72-11757

Synaptic mechanisms of vestibulospinal and reticulospinal effect on transmission to lumbar motoneurons in monkeys

02 p0158 A72-11760

Blink reflexes in man during sleep and wakefulness, discussing electromyographically recorded orbicularis oculi mono- and polysynaptic responses to electrical stimuli

04 p0474 A72-15250

Synaptic contacts in vertebrate retinas, reviewing bipolar terminals, ganglion cells and amacrine responses from electron microscopy

06 p0762 A72-17719

Marine gastropod mollusk synaptic transmission mechanism, discussing various chemical transmitters, two phase potential, receivers, electrical interaction and electrophysiological conditioning

06 p0764 A72-17996

Field and intracellular potentials in cat trochlear nucleus following vestibular nerve and nuclei stimulation for synaptic organization study of vestibulo-ocular reflex

07 p0923 A72-20501

Stimulation transmission tracts, synaptic mechanisms and tonic activity of cat sympathetic ganglia

07 p0924 A72-20617

Motoneuron pool fraction determination in human monosynaptic response of healthy and neuropathological subjects, comparing diagnostic methods

07 p0924 A72-20619

Visual cortex neuronal background activity in unanesthetized rabbits under stimulation and depression of lateral geniculate body and mesencephalic reticular formation, considering synaptic organization

12 p1761 A72-27646

Synaptic patterns in the superficial layers of the superior colliculus of the monkey, Macaca mulatta.

19 p2758 A72-38647

Neuronal fiber and synaptic axonal contact structure of cat spinal gray matter in corticospinal, rubrospinal and reticulospinal terminal zones by Golgi method

21 p2998 A72-40579

The ultrastructure of the lateral basilar region of the spinal cord.

21 p2998 A72-40581

Neuronal organization of descending systems of the spinal cord

21 p2998 A72-40582

Synaptic suprasegmental control mechanisms of spinal cord motor neurons

21 p2999 A72-40584

Study of the conductivity of the motor neuron membrane during supraspinal stimulation

21 p2999 A72-40585

Intracellular study of rubrospinal neurons and of their synaptic activation during the stimulation of the sensorimotor cortical region

21 p2999 A72-40586

Synaptic potentials of sensor and motor neurons of trigeminal nuclei during corticofugal stimulation

21 p2999 A72-40587

Pyramidal control of the activity of interneurons related to various types of peripheral afferents

21 p2999 A72-40589

Possible role of supraspinal formations in the fixation of trace alterations at the segmental apparatus level of the spinal cord

21 p2999 A72-40592

Polysynaptic sympatho-reticular and somatic afferent visceral links between internal organs and cerebrum in interoceptive reflex fields

21 p3000 A72-40755

Synaptic events during specific and nonspecific inhibition of visual cortex neurons

23 p3257 A72-44088

SYNCHRONISM

NT BIT SYNCHRONIZATION

NT FREQUENCY SYNCHRONIZATION

Optimal two stage signal search in frequency vs arrival time indeterminacy plane of communication system

04 p0487 A72-15148

Atomic clocks application to spacecraft position determination, discussing ground stations synchronization and accuracy improvement by lasers

05 p0660 A72-15858

Eros and ATA /Air Transport Association/ time-frequency collision avoidance systems, discussing synchronization methods, back-up mode operation, threat computation and displays

09 p1349 A72-22823

Haag synchronization theory generalization through precision improvement and extension to almost periodical systems

10 p1510 A72-24123

Optimum decision rule for sync word location in binary data frame, noting sum maximization of correlation and energy correction terms

11 p1592 A72-25888

Earth stations synchronization to switched sequences of multiple access and cyclically interconnected multipot beam antennas satellite controlled by stable onboard clock

[AIAA PAPER 72-545]

12 p1781 A72-27368

Relaxation oscillator synchronized by quartz crystal between emitter and base of unijunction transistor, obtaining sinusoidal output by series-connected RC load

13 p1926 A72-28377

Parametric resonance suppression in annular laser by steady noise perturbation, discussing beat signal spectrum

13 p1968 A72-29505

Synchronization theory for digital data transmission with random changes in channel characteristics

14 p2085 A72-30333

Nonlinear resonant circuits analysis, noting steady state operation of ferroresonant circuit with staircase response curve and synchronization conditions

14 p2132 A72-31103

Tunnel diode harmonic relaxation frequency divider, obtaining large division factors and wide synchronization bands with sinusoidal output signal

15 p2206 A72-31666

Extractop model for time signal decoding for worldwide synchronization using Transit satellite system

15 p2199 A72-32078

ATS-3 C band dual transponders for geographically distant clocks time synchronization, using Cs clocks for accuracy verification

15 p2200 A72-32080

Automata with specific properties of diagnostic, arranging and synchronizing word sets

16 p2366 A72-33086

Train synchronism of second harmonic excitation/pumping/ by periodic sequence of ultrashort light pulses

16 p2402 A72-33493

Synchronizing electronic equipment for digital computers input graphic data recording fidelity improvement ensuring proper timing of set and reset pulses

16 p2367 A72-34018

Synchronization and noise performance of mutually coupled oscillators.

18 p2668 A72-37036

Time synchronized ranging system (TSRS) providing high-speed real-time two-way data link between community members

19 p2764 A72-37904

Synchronization in the work of motor neurons during arbitrary motor activity of various types

21 p2999 A72-40595

Analysis of a single-loop parametric amplifier by the phase plane method

24 p3384 A72-44893

SYNCHRONIZED OSCILLATORS

Synchronized multiple microwave oscillators power and noise characteristics at microwave and millimeter frequencies, discussing magic T configuration

01 p0037 A72-10648

Solid state oscillator phase and frequency synchronization by injection of stable sinusoidal uhf signal modulated by 0-180 deg phase jump

02 p0194 A72-12569

Phase stabilization of synchronized tracking oscillator with resonant frequency regulated by output voltage

03 p0333 A72-13895

Mechanical system of elastically coupled bodies carrying identical vibrators, examining self synchronization behavior

06 p0850 A72-18713

Phase locking loop synchronized quartz oscillator for integral frequency multiplication in wideband carrier frequency systems

07 p0954 A72-19174

Thomson autooscillator systems synchronization and small external sinusoidal emf effect with hard and soft bounding of amplitude deviations

08 p1142 A72-21769

Phase stabilization of synchronized tracking oscillator with resonant frequency regulated by output voltage

15 p2209 A72-32706

Determination of the locking range from the reactive power balance of the oscillator.

17 p2530 A72-35430

The locking effect in an autooscillator system with two degrees of freedom

19 p2783 A72-38580

Influence of fluctuations on the synchronization of frequency-modulated oscillators

22 p3159 A72-42658

Reciprocal synchronization of generators connected by a long line section

23 p3272 A72-44210

SYNCHRONIZERS

Branch synchronizer for convolutional decoders, noting design adaptability to nonsystematic codes of different constraint lengths

02 p0188 A72-12410

Synchros as electromechanical function generators and receivers for analog computers, examining errors in standard resolvers operation

03 p0328 A72-13841

Synchronization system for remote control and performance checking of motion picture projectors with running film, discussing recording equipment and stroboscopic pulsed illuminator operations

04 p0521 A72-14711

Myocardium biopulse-controlled cardio-synchronizer as key component of biocontrol systems for cardiological studies

11 p1585 A72-26455

SYNCHRONOUS COMMUNICATION SATELLITES

U SYNCOM SATELLITES

SYNCHRONOUS DETECTORS

U CORRELATORS

SYNCHRONOUS METEOROLOGICAL SATELLITE

Direct readout ground system (DRGS) for receiving, recording and displaying visible and IR imagery collected by ItoS and synchronous meteorological satellite radiometers

01 p0047 A72-10452

Hydrologic data collection via ATS 1 satellite for river and flood forecast of National Weather Service, planning geostationary operational environmental satellites /GOES/

09 p1296 A72-22315

European synchronous meteorological satellite system Meteosat, discussing mission, control and data acquisition

15 p2265 A72-31345

SYNCHRONOUS MOTORS

Vibration measurements of gyromotors with aerodynamic spherical and ball bearings

09 p1263 A72-22347

Hysteretic motor in steady synchronous operation with nonsinusoidal supply voltage, computing stator winding current based on superposition with two linear equivalent circuits

13 p1900 A72-29975

Transistorized oscillators for variable-frequency generators designed to feed synchronous motor drives of equatorial telescopes

14 p2073 A72-30683

Digital computer studies of control loop parameters and configurations effects on performance of synchronous turbogenerator with two field windings

15 p2183 A72-32793

SYNCHRONOUS SATELLITES

NT AEROS SATELLITE

NT SIRIO SATELLITE

NT SYNCHRONOUS METEOROLOGICAL SATELLITE

NT SYNCOM SATELLITES

Nozzle shaped antenna for synchronous satellite, obtaining radiation patterns

01 p0043 A72-11245

Atmospheric pollutants time and spatial profiles monitoring by geosynchronous satellite remote sensors

02 p0211 A72-11806

World Administrative Radio Conference for Space Telecommunications data on geostationary orbit utilization, covering stationkeeping and satellite antenna pointing accuracies

02 p0177 A72-12387

Magnetosphere model for low energy cosmic ray proton propagation mode to synchronous orbit satellite, calculating geomagnetic cutoffs and penetration regions

[AD-741079]

02 p0274 A72-12453

Europa 3 candidate propulsion modules system analysis, considering payload, mission flexibility, orbital injection precision, synchronous satellite design influence, satellite-booster interfaces and costs

02 p0287 A72-12731

Rotating earth oblateness and equator ellipticity influence on near-equatorial synchronous satellite behavior, using nonlinear mechanics asymptotic method

03 p0436 A72-13835

Ionospheric electron content changes during 25-26 May 1967 magnetic storm event from geostationary satellite monitoring

04 p0516 A72-14940

Meteorological satellite stabilization and attitude control in synchronous equatorial orbit for two years life, emphasizing nutation damper optimal dynamic characteristics

05 p0725 A72-16437

Propagation delays for clock synchronization from synchronous satellite tracking by range measurements

05 p0628 A72-16563

SYNCHRONOUS SATELLITES

Ion engine performance optimization by power sharing with secondary batteries on synchronous equatorial satellites

[AIAA PAPER 72-206]

05 p0706 A72-16852

Spacecraft charging at synchronous orbit, constructing mathematical model of ATS 5

07 p1058 A72-19150

ATS F and G satellites with 30 foot deployable antennas as three axis stabilized platforms in geostationary orbit with high pointing accuracy

07 p1085 A72-19275

Nonlinear multivariable system optimal control with respect to time and fuel consumption, discussing Gauss-Newton and Davidson methods and application to geostationary satellite

07 p0962 A72-19719

Geostationary communication satellites and terrestrial radio relays frequency sharing, controlling interference by flux density and transmitter power limitation

07 p0948 A72-20490

Synchronous satellite surveillance system for transoceanic ATC, using suboptimal /modified Kalman/ filter for aircraft position and velocity computation

08 p1204 A72-21091

Aerosat program for ATC and communications via four geostationary satellites over Atlantic and Pacific Oceans, discussing technical and financial international provisions

08 p1256 A72-21203

Meteosat geostationary satellite international program for earth cloud cover observation and meteorological data relays between ground stations as part of Global Atmospheric Research Program

08 p1241 A72-21204

Dioscures geostationary satellites project for Atlantic and Pacific ocean air and ship traffic safety based on radar tracking and multiplex numerical data transmission

09 p1396 A72-23400

Ionospheric electron content determination at different latitudes from geostationary satellite signal Faraday rotation

10 p1475 A72-24955

Electric thruster for orbit and attitude control of nonspinning geostationary communications satellite

[AIAA PAPER 72-436]

11 p1727 A72-26178

Point motion in random error region applied to synchronous satellite trajectory control by single impulse correction

11 p1684 A72-26902

Geostationary satellites spacing dependence on quantifying factors, describing space environment experiments for satellite attitude stability and ground station antenna patterns and polarization effects

[AIAA PAPER 72-542]

12 p1780 A72-27365

Attitude determination during transfer orbit operation of SKYNET and NATO synchronous communications satellites

[AIAA PAPER 72-544]

12 p1876 A72-27367

Correlation technique for position location in surveillance and navigation by phase extraction from range tones using synchronous satellites

[AIAA PAPER 72-564]

12 p1842 A72-27375

Aircraft and water vehicles mobile communications via stationary satellite, discussing optimum multiple access and repeater configuration

[AIAA PAPER 72-565]

12 p1781 A72-27376

Titan 3 family systems analysis for delivering multiple communication satellites to geostationary orbits

[AIAA PAPER 72-570]

12 p1870 A72-27378

Synchronous communication satellites body stabilized three axis attitude control superiority over dual spin techniques, emphasizing single large pitch momentum wheel configuration with magnetic torquing

[AIAA PAPER 72-572]

12 p1876 A72-27380

Solar electric propulsion for satellite transport into geostationary orbit, discussing launchers, energy supply, electrostatic ion thruster and mass/power ratio

[AIAA PAPER 72-505]

12 p1860 A72-27422

Structural design, performance and costs of rigid or semirigid solar panels for geostationary satellites power supplies

12 p1758 A72-28034

Structurally integrated ion thruster /ISIT-5/ for synchronous satellites attitude control and station-keeping, presenting design and performance data

[AIAA PAPER 72-492]

13 p2027 A72-28950

Characteristic thrust concept introduced to classify propulsion system tasks related to geosynchronous communications spacecraft, developing approximate analytical models

[AIAA PAPER 72-514]

13 p2052 A72-28977

Experimental communications satellite system of ATS F and G geostationary satellites for specific application, discussing system performance measurement instruments

[AIAA PAPER 72-578]

13 p1918 A72-28986

Proton and electron fluxes limits in synchronous orbit, investigating local time dependence

13 p2031 A72-29393

Military geostationary communication satellite Skynet 2 subsystems design development and testing

13 p2052 A72-29856

- Seasonal changes in magnetospheric directional fluxes at synchronous altitudes due to solar wind induced field line knee effect and drift shell asymmetry 14 p2097 A72-30131
- Geostationary artificial satellite orbital parameters calculation, taking into account lunar, solar and light pressure perturbations 14 p2150 A72-30451
- Barbados oceanographic meteorological experiment /BOMEX/ sea air interaction program in equatorial Atlantic, using real time synchronous satellite information 15 p2225 A72-31808
- Skyнет 1 synchronous satellite orbit determinations and longitude acceleration due to tesseral harmonics of earth gravity, using tracking station range data 15 p2321 A72-31949
- Anisotropic electron pitch angle distributions at synchronous altitude due to wave-particle scattering and ionospheric acceleration along field lines 15 p2299 A72-31961
- Report on photo-sheath calculations for the satellite GEOS. 17 p2553 A72-34629
- Europa III preparatory phase. 17 p2621 A72-34899
- International UV Explorer synchronous satellite program objectives and technology, describing spacecraft design, instrumentation, ground system, telescope control and data handling 17 p2621 A72-34900
- A horizon sensor with a bolometer and electrooptical modulators 17 p2556 A72-35385
- The collection of data by geostationary meteorological satellites 17 p2622 A72-35719
- Earth gravitational field determination based on long periodic perturbations in orbital motion of synchronous satellites, estimating tesseral coefficients errors 17 p2550 A72-35742
- Friction, wear and noise of slip ring and brush contacts for synchronous satellite use. 18 p2693 A72-35982
- The use of satellites to meet future press requirements. 18 p2743 A72-37012
- A nomogram for look angles to geostationary satellites. 19 p2869 A72-37298
- Factors affecting frequency and orbit utilization by high power transmission satellite systems. 19 p2857 A72-37644
- Geostationary satellite system for air navigation via voice and data communication, discussing ground facilities and avionics 21 p3080 A72-40284
- Geostationary satellite direct TV broadcasting system extension to 12 GHz band, considering receiving installations, antennas, performance and costs 21 p3018 A72-40876
- International space telecommunication law and UN resolution concerning geostationary satellite orbit use for radio transmission 21 p3132 A72-41319
- First order theory of satellite orbit determination with time difference data for synchronous equatorial spacecraft, applying to VLBI experiments with ATS-3 [AIAA PAPER 72-924] 21 p3112 A72-41568
- Celestial mechanics principles application to geostationary satellites in equatorial plane and in earth-moon system libration points, considering Jupiter and Saturn stationary satellites 22 p3222 A72-42141
- NASA developed geostationary weather and environmental satellite for launch in 1973, discussing ground station equipment, antenna system and data collection service 23 p3343 A72-43551
- Spacing limitations of geostationary satellites using multilevel coherent PSK signals. 23 p3265 A72-44183
- Luni-solar perturbations of the geostationary vehicle at arbitrary latitude. 24 p3448 A72-44990
- Optimization of altitude and inclination change schedules during low thrust ascent to geosynchronous orbit. 24 p3440 A72-45150
- On the utilization of thermonuclear propulsion for an upper stage of the Europa III launcher 24 p3424 A72-45227
- SYNCHROSCOPES**
- High speed spectrum analyzer /hissa/ and its application to the study of geomagnetic pulsations. I - S-type hissa. 17 p2554 A72-35061
- SYNCHROTRON NOISE**
- U ELECTROMAGNETIC NOISE
- U SYNCHROTRON RADIATION
- SYNCHROTRON RADIATION**
- Narrow-band type 4 bursts behavior comparison with synchrotron radiation in media with refractive

index less/equal unity, determining magnetic field and electron energy 01 p0118 A72-10415

Synchrotron radiation from incoming auroral electrons based on Schwinger equation, accounting for hf backscatter sounder noise 01 p0060 A72-10839

Photometric calibration of long wavelength vacuum UV standards by synchrotron and plasma black body radiation 01 p0073 A72-11399

Fast cyclotron and synchrotron transverse waves noise measurement in electron flux, using resonator with homogeneous electric field 02 p0190 A72-11573

Periodic solar flare modulation by pulsating structure, attributing radiation to synchrotron radiation emitted by electrons in magnetic flux tube embedded in solar corona 02 p0274 A72-12412

Synchrotron and thermal H II region radio emission in Magellanic Clouds 03 p0425 A72-13259

Radio-astronomical evidence for magnetohydrodynamical pulsations in corona, considering solar radio burst model of pulsating structure due to synchrotron radiation 03 p0432 A72-13349

Charged particle motion in pulsar electromagnetic fields, discussing coherent synchrotron radiation and charge bunching 03 p0438 A72-13874

Absorption effects on circular polarization in synchrotron radiation, discussing frequency and magnetic field dependence 04 p0570 A72-14550

Coherent synchrotron radiation from model with charge distribution moving on ring, applying to pulsars 04 p0566 A72-14555

Spontaneous and induced Compton scattering of high frequency waves by relativistic electrons in synchrotron sources 04 p0487 A72-14902

Moving type 4 radio burst observation with radioheliograph, suggesting isolated self contained synchrotron emitting plasmoid and relation to coronal magnetic field 05 p0710 A72-16521

Synchrotron emission source identification from spectral index dependence on frequency 07 p1059 A72-19807

Steady state problem of energy spectrum of variable magnetic field accelerated electrons, considering synchrotron X ray emission of Crab pulsar and nebula 08 p1231 A72-21119

Synchro-Compton theory for variable compact components in extragalactic radio sources, suggesting stellar mass object collapse as energy source 08 p1233 A72-21181

Quasars and Seyfert galaxies radiation, discussing dust clouds, synchrotron and unstable plasma models 08 p1234 A72-21383

Cosmic electrons energy spectrum between 1 and 25 GeV from balloon observations, noting Compton/synchrotron loss effects [AD-745871] 09 p1377 A72-23001

Nonthermal emission and ejection of matter from galactic nuclei, discussing radio, optical and IR synchrotron sources and background radiation 10 p1535 A72-23906

Cygnus X-1 model with hard X rays from inverse Compton scattering of B star UV photons and IR synchrotron radiation from other component 10 p1530 A72-24944

Gravitational wave observation interpretations, discussing Weber theory of galactic nucleus isotropic radiation and synchrotron radiation sources in terms of black hole existence 11 p1717 A72-25883

Relativistic analysis for synchrotron gravitational radiation emitted by particle in circular orbit around Schwarzschild black hole, noting astrophysical implications 13 p2007 A72-30123

Gyrosynchrotron radiation fields from mildly relativistic electrons in magnetoactive plasma, studying radiative transfer problem 14 p2138 A72-30556

Ionized gas effect on interstellar space synchrotron emission, noting magnetic field orientation-dependent low frequency cut-off 14 p2156 A72-30559

Crab Nebula X ray emission synchrotron model confirmation by sounding rocket polarimeter polarization detection data 14 p2156 A72-30565

Jovian synchrotron emission measurements by radioheliograph at 80 MHz, passing square low detector outputs through RC integrators 15 p2307 A72-31799

Spectrograph for Orion spaceborne astronomical observatory on Salyut space station calibrated with synchrotron radiation from particle accelerator 15 p2242 A72-32744

Quantum mechanics framework for electron movement perpendicular to intense magnetic field, predicting energy broadening with time for initially monoenergetic electron beam 16 p2422 A72-32888

Synchrotron emission source identification from spectral index dependence on frequency 17 p2602 A72-35733

Synchrotron radiation-like angular distribution or gravitational synchrotron radiation produced by ultrarelativistic geodesic particle orbits in Schwarzschild geometry 17 p2583 A72-35820

Polarization characteristics of Schwarzschild black hole gravitational synchrotron radiation in terms of Stokes parameters 21 p3107 A72-41211

Conditions for magnetoactive plasma longitudinal waves with phase velocity near light velocity existence, investigating increments during synchrotron instability due to relativistic particles 23 p3262 A72-43311

SYNCHROTRONS

NT BEVATRON

SYNCLINAL VALLEYS

U VALLEYS

SYNCOM SATELLITES

Scintillation effects on synchronous satellite communications systems at 250 MHz in equatorial region, discussing diversity techniques and composite diffraction refraction theory [AIAA PAPER 72-178] 05 p0631 A72-16900

SYNCOPE

NT BLACKOUT [PHYSIOLOGY]

NT BLACKOUT PREVENTION

Student pilot syncope during altitude chamber training, discussing physiological mechanism from cardiovascular studies and psychiatric evaluation 06 p0767 A72-17877

Case report of pilot near-syncope episode with bradycardia due to hyperactive right carotid sinus reflex 12 p1771 A72-27488

Tilt table tests for orthostatic tolerance, measuring heart rate, blood pressure and responses of fainter and nonfainters 21 p3008 A72-41000

SYNDROMES

U SIGNS AND SYMPTOMS

SYNOPTIC MEASUREMENT

Papers on world geomagnetic survey 1957-1960 covering land, sea, airplane and polar-orbiting geophysical observatory satellite observations, magnetic anomalies and reference field 02 p0219 A72-12008

Magnetic survey worldwide earth coverage by land, sea and airplane measurements data 02 p0220 A72-12008

Ionospheric drift patterns diurnal, seasonal and solar cycle variations from synoptic measurements over east Siberia by closely spaced receivers, using Briggs similar fades method 08 p1160 A72-21510

Synoptic measurement of midlatitude D region electron density diurnal and seasonal variations under quiet conditions, using differential absorption partial reflection experiment 09 p1376 A72-22370

Reference radiosondes for quality control of global high altitude temperature, pressure and humidity measurements, discussing dual soundings and synoptic comparison 10 p1484 A72-25076

Ground based synoptic measurement of mesospheric electron densities, noting variations relationship to solar radiation changes 11 p1626 A72-26428

Barbados Oceanographic and Meteorological Experiment to compare synoptic scale-measured vertical vapor fluxes over tropical ocean 16 p2417 A72-33160

Upper atmospheric trace constituents global mapping by laser radar probing from satellites, discussing feasibility and comparison with ground based system [AIAA PAPER 72-660] 16 p2365 A72-34071

SYNOPTIC METEOROLOGY

Kinematic vertical motions computation from radiosonde wind observations, correlating with synoptic features 01 p0095 A72-10858

Synoptic sea surface temperature mapping off Eastern United States using NASA ITOS satellite II imagery data 02 p0211 A72-11811

Thermal advection statistical relation to vertical motion, discussing conventional synoptic meteorological empirical facts utilization in numerical models for long term weather forecasting 02 p0254 A72-12777

Book on earth, moon and planet space photography, discussing synoptic meteorological data, mapping surface detail inspection and planetary exploration 03 p0438 A72-14090

Computerized synoptic weather map forecasting of heavy snowfall in Colorado
04 p0542 A72-14685

Variance spectral techniques in detecting wave modes of synoptic scale tropospheric wind in midlatitudes and tropics
06 p0841 A72-17634

Stationary-nonstationary temporal sampling for synoptic meteorological networks, illustrating oceanic wind speed measurements
06 p0842 A72-18436

Synoptic and dynamic aspects of tornado-producing thunderstorms development from ATS 3 and aerological data, observing mesoscale convective disturbances
06 p0842 A72-18438

Weather forecasting techniques improvement by synoptic meteorology analysis
07 p1031 A72-20449

Synoptic velocity fluctuations from empirical structural functions of wind fields, proposing spectral kinetic energy distribution model for atmospheric turbulence
07 p1031 A72-20694

Meteorological synoptic analysis of stratospheric planetary wave interaction with lower ionosphere in terms of wind, temperature and ionospheric electron density profiles
09 p1297 A72-22375

Horizontal ozone distribution in middle stratospheric macrosynoptic situations, considering anticyclonic side and jet stream delta region
09 p1301 A72-23194

Upper atmospheric dynamics and electrodynamic processes for evaluation of meteor trail radar observations in synoptic meteorology
10 p1473 A72-24702

Monthly weather forecasting synoptic method development prospects, noting macroprocesses phasing and global experiment program realization impact
11 p1683 A72-26885

Thunderstorm-associated aircraft mishaps relation to surrounding synoptic scale meteorological conditions, discussing storm interior condition contribution to flight stability upset
13 p1992 A72-28851

Synoptic meteorological parameters vs CAT encountered in stratosphere by XB-70 airplane, presenting frequency distributions and probability tables
13 p1994 A72-28867

Persistent intense CAT in upper level frontal zone, discussing synoptic features, vertical wind shears, radar echoes and turbulence intensity
13 p1995 A72-29622

Book on dynamic meteorology covering synoptic disturbance model, numerical weather prediction and baroclinic waves origin
15 p2266 A72-31875

Atmospheric energy spectra from two dimensional synoptic scales applicable to pressure or geopotential surface variables
15 p2266 A72-32721

Atmospheric model for local mesometeorological deviations from large scale field distributions, taking into account synoptic scale influence
16 p2418 A72-33601

Method of constructing a forecast chart of H sub 500 anomalies on the basis of several analogs
19 p2828 A72-38000

Complex analysis of satellite data for electromagnetic emission measurements in the radio, infrared and optical wavelength ranges
19 p2829 A72-38770

Synoptic velocity fluctuations from empirical structural functions of wind fields, proposing spectral kinetic energy distribution model for atmospheric turbulence
20 p2948 A72-39009

Seasonal, nonseasonal and synoptic global variations in stratosphere temperature from satellite-measured radiances, discussing latitudinal warming-cooling relationships
21 p3048 A72-40253

Quasi-two dimensional turbulence model of energy spectra and potential enstrophy transfer in synoptic large scale quasi-horizontal atmospheric motions
21 p3049 A72-41793

Earth surface and background wind effects on mesoscale and large scale meteorological processes in free stably stratified atmosphere
21 p3078 A72-41794

Russian book - Aviation meteorology
22 p3200 A72-42024

Description of global-scale circulation cells in the tropics with a 40-50 day period.
22 p3201 A72-42506

Satellite-observed Southern Hemisphere cloud vortices in relation to conventional observations.
23 p3285 A72-44145

SYNTAX

NT SYLLABLES
NT WORDS [LANGUAGE]
SYNTHETIC ARRAYS

Supersynthesis antenna array design by analytical approach involving isolation and separate optimization

of parameters effects on spatial frequency component sampling
06 p0771 A72-17341

Receiving antennas polarization parameters selection in side-looking synthetic aperture radars
10 p1453 A72-24905

Ultrasonic imaging system based on side-looking synthetic aperture radar principles, using B-scan technique
19 p2798 A72-37624

Linear HF radar antenna array aperture synthesis for ionospherically propagated signal reception in air-plane for achievement of ideal directivity without ionospheric compensation
21 p3022 A72-41080

SYNTHETIC FIBERS
NT GLASS FIBERS
NT NYLON [TRADEMARK]
Microfibrillar superlattice with vacancy defect and point dislocation in microcrack formation and propagation in nylon 6 fibers
05 p0681 A72-16308

Stress relaxation measurement assembly for polymer film and fiber samples under tensile stresses at 213-573 K
07 p0986 A72-19779

Inorganic single crystal titanate whisker fibers with high modulus strength for plastic reinforcement, noting mechanical, thermal and physical properties
08 p1193 A72-21685

Test procedures and apparatus for short and long term creep of polymer monofilaments under radial compression
08 p1194 A72-21758

Morphology and physicomechanical properties of carbonized polyacrylonitrile fibers by scanning electron microscopy, discussing macro and microdefects effects on strength characteristics
08 p1195 A72-21762

Carbonized and ion beam thinned polyacrylonitrile copolymer fibers examination by low angle electron scattering electromicroscopy technique
09 p1339 A72-23190

Model with lamellae and tie molecules disordered alignments to explain relation between stress-strain behavior and bond fracture in highly oriented polymer fibers
17 p2569 A72-34258

SYNTHETIC RESINS
NT ACRYLIC RESINS
NT EPOXY RESINS
NT FURAN RESINS
NT NYLON [TRADEMARK]
NT PHENOLIC RESINS
NT POLYAMIDE RESINS
NT POLYESTER RESINS
NT POLYMETHYL METHACRYLATE
NT THERMOPLASTIC RESINS
NT THERMOSETTING RESINS
NT VINYL COPOLYMERS
High vacuum mass spectroscopic analysis of volatile products released under friction from solid synthetic resin lubricants with molybdenum disulfide as antifriction filler
12 p1835 A72-28199

SYNTHETIC RUBBERS
NT ELASTOMERS
NT THIOPLASTICS
Liquid polysulfide rubber, discussing fabrication method and physical properties
07 p1024 A72-20603

Mechanical characteristics of natural and synthetic rubber, noting features of cork filled urethane
10 p1502 A72-24861

Temperature effects on synthetic rubber sliding friction characteristics against smooth steel surfaces under compression loads in vacuum and air at 10-140 C
13 p1962 A72-28554

SYSTEM EFFECTIVENESS
Multivariable control systems, discussing effects of interaction vs noninteraction /decoupling/ on system performance and energy requirements
07 p0962 A72-19715

Computerized and analytic techniques for estimating multiplexed systems output probability distribution, considering system effectiveness, reliability and survivability
10 p1486 A72-23977

Communication satellite systems reliability assessment using figure of merit method
10 p1435 A72-23991

Aerospace management systems effectiveness in design, development, test and engineering areas, discussing cost, scheduling and technical performance factors
10 p1565 A72-25050

[AIAA PAPER 72-243]
Cybernetic system effectiveness analysis with operations research and statistical theory based on stochastic treatment
11 p1608 A72-25428

Data acquisition and transfer efficiency and reliability in computerized automatic control systems for communications, listing probability and expectation criteria
11 p1600 A72-25436

Radar systems of effectiveness for moving target selection with alternating period compensation devices, allowing for signals and noise statistical properties
11 p1596 A72-26306

Probability distribution density of phase difference between noise and signal-noise sum for radar system efficiency estimation, using Bessel and Whittaker functions
11 p1596 A72-26308

Effectiveness and reliability criteria for information and monitoring systems performance evaluation, suggesting use of revenue ratio
11 p1611 A72-26437

Optimization of diagnostic tests for monitoring industrial system efficiency, obtaining compromise between costs and utilization
11 p1611 A72-26441

Laser beam scanning and recording in two dimensional pattern on silver halide, evaluating systems performance based on signal response, granularity and noise characteristics
20 p2930 A72-39040

Digital computer hierarchical structure based on tree model using request/service resources as nodes, examining parallelor multiple-stream organizations effectiveness
20 p2906 A72-39735

Unknown plant self organizing time optimal controller with variable switching surface and adaptation logic net, noting effectiveness by computer simulation
21 p3037 A72-40639

Book on complete technological system reliability assessment covering performance requirement and achievement, transfer characteristics, sampling, estimation, confidence, synthesis problem, etc
23 p3294 A72-44499

Estimate of the operational efficiency of a human operator in the follow-up mode of a closed-loop control system
24 p3376 A72-45516

SYSTEM FAILURES
Single malfunction diagnosis models in systems failures, describing fixed and sequential testing schedules
02 p0186 A72-11689

Redundancy configuration effect on electronic system reliability, discussing MTBF and cost analysis
02 p0194 A72-12445

Self organizing adaptive aircraft control system with C criterion pitch axis performance and failure compensation
03 p0337 A72-12920

Regenerative system reliability, examining oscillation mode selector
03 p0333 A72-13833

Oxygen hazards, mishaps and safety programs in NASA operations, considering material, design, cleaning and procedural deficiencies and failures
04 p0564 A72-14436

Economically optimal operation of protection circuit for plant subject to stationary random process, determining failure rate of plant
04 p0496 A72-14995

Sequential behavior and inherent tolerance to memory faults in terms of minimum redundancy
07 p0950 A72-19300

Soviet papers on digital computers application to reliability problems solution for recoverable, failing, controlled, redundant and electronic systems
08 p1179 A72-22051

Reliability analysis of redundant and nonredundant systems with different component failures, using probability theory
08 p1180 A72-22053

Functional readiness of periodically inspected recoverable systems with different failure causes
08 p1180 A72-22055

Computerized and analytic techniques for estimating multiplexed systems output probability distribution, considering system effectiveness, reliability and survivability
10 p1486 A72-23977

Reliability program for SAAB 37 Viggen airborne computer, discussing prototype and components operating tests and failure rates
10 p1443 A72-23984

Computer reliability in terms of design criteria to minimize faults incidence, discussing failures detection and correction, fault diagnosis and system maintenance
10 p1444 A72-23985

Reliability statistics of third generation computer systems failure causes, emphasizing cumulative effects of hardware and software
10 p1444 A72-23986

Reliability and time to failure prediction for degradation-prone systems via Markov processes theory
10 p1504 A72-23988

Communication satellite systems reliability assessment using figure of merit method
10 p1435 A72-23991

Operator independence test for human performance reliability modelling based on symptom detection and fault location of sonar system failure
10 p1429 A72-24002

System reliability improvement technique for identification and prevention of failures, using Experience Storage Program for design problem documentation collecting, storage and retrieval
10 p1486 A72-24021

Mathematical model for digital systems reliability, determining probability of success and of various failure modes
13 p1923 A72-28356

Reliability prediction of system with components having independent and constant rate failures
13 p1961 A72-28357

Failure rate function nonparametric estimators comparison on basis of asymptotic and Monte Carlo mean square errors
13 p1985 A72-28364

Mathematical models for complex system debugging in initial life period, noting maximum likelihood estimates for failure rate functions
13 p1962 A72-28365

Magnetic compass use in instrument flight conditions, suggesting emergency procedures during aircraft system failures
15 p2238 A72-32212

Aircraft industry product support role in time delays minimization for aircraft operators, discussing malfunction report, minimum equipment decision and fault diagnosis
15 p2339 A72-32456

Avionics effects on airline operations timekeeping, considering gains due to all-weather capability and engine monitoring vs possible losses due to equipment failures
15 p2208 A72-32461

Man serviced spacecraft systems reliability and maintainability optimization methodology, developing parametric data based on failure modes analysis, components MTBF, duty cycles, redundancy and costs [SAWE PAPER 943]
23 p3343 A72-43483

Allocating optimum time for systems malfunction search.
24 p3406 A72-44661

SYSTEM LIFE
U RELIABILITY
SYSTEMIZATION
U SYSTEMS ENGINEERING
SYSTEMS ANALYSIS

Nonautonomous systems periodic solutions through Liapunov functions construction, considering application to nth-order dynamic systems forced oscillations
02 p0251 A72-11498

NASA/MSC earth observation aircraft program radar scatterometers, presenting system evaluation
02 p0172 A72-11849

Europa 3 candidate propulsion modules system analysis, considering payload, mission flexibility, orbital injection precision, synchronous satellite design influence, satellite-booster interfaces and costs
02 p0287 A72-12731

Symplectic structure of continuous system, constructing relativistic free vibrating cord without linearization
03 p0389 A72-13792

Mathematical modeling methodology for communication receiver life cycle EMC decisions, considering analysis and prediction problems with emphasis on nonlinear circuits and systems
03 p0324 A72-14034

Automated system pathfinder application to systems design and analysis for engineering information exchange
03 p0326 A72-14198

Systems analysis for equipment performance and data management in aerospace programs
03 p0460 A72-14199

Fully redundant relay and data command system for SAS-A satellite, discussing operation and reliability tests
03 p0442 A72-14397

Complex systems stochastic survivability estimates dependence on delay depth and initial conditions of interaction
05 p0640 A72-16204

Synergic control of computer-manipulators, evaluating system
05 p0621 A72-16450

Conventional open and closed loop servo analysis methods applied to Naval aircraft approach power compensator systems, using pilot model concepts [AIAA PAPER 72-124]
05 p0612 A72-16922

Time domain infinite matrices analysis methods for linear stationary and nonstationary multivariable systems, presenting recursion formulae
06 p0792 A72-17310

Third order nonlinear systems phase plane analysis, noting applicability to unity feedback closed-loop systems with linear memory
06 p0792 A72-17313

Nonlinear stochastic systems analysis by extended Volterra-functional method for first and higher order linear plants with constant or time varying parameters
06 p0838 A72-17376

Optimal synthesis of multiparametric machine systems by LP search /determinate analog of random search/, applying to oscillatory models
06 p0821 A72-17726

Book on discrete event computer simulation for complex systems synthesis and analysis covering random numbers use, languages, and interactive man machine applications
06 p0779 A72-17812

Collection of papers on control systems theory and applications covering optimal control, final value control systems, discrete stochastic differential games, linear estimation, etc
06 p0793 A72-17952

GERTS II simulation program for graphically modeling and analyzing complex stochastic systems, discussing applications to assembly line, project management, conveyor and inventory systems
06 p0780 A72-17978

Nonlinear mechanical oscillation systems analysis by analog computer, exemplifying pendulum rotating about vertical axis
06 p0851 A72-18725

Collisional avoidance system operation evaluation, noting protected airspace volume requirement
07 p1032 A72-18835

System properties of information patterns in complex hierarchical automatic control systems
07 p0949 A72-18927

Time-variable multivariable systems reduction to completely controllable and observable systems by subdivision and transformation procedures, using subsystems order matrices
07 p1026 A72-19271

Suboptimal Kalman filter design for system state estimation in presence of plant dynamics uncertainties and measurements noise, optimizing tradeoff between sensitivity and estimation error
07 p0959 A72-19302

Two-variable second order system for multivariable systems predictive control, deriving algorithm for near time optimal control
07 p0961 A72-19709

Multivariable control systems, discussing effects of interaction vs noninteraction /decoupling/ on system performance and energy requirements
07 p0962 A72-19715

Airfield surface system fast-time computer simulation model for airport planning systems analysis
07 p0965 A72-20341

Averaging method for systems with shocks, assessing exact and approximate solutions discrepancy over finite time intervals
08 p1206 A72-20967

Reliability of complex systems performing function with time dependent quantity
08 p1180 A72-22061

Reliability theory distribution function construction for failure analysis in physical processes, considering mechanical system service life and living organisms life span
08 p1180 A72-22062

Automatic systems efficiency determination, using characteristic equation roots sensitivity with respect to system parameters changes
08 p1146 A72-22063

Minimal dynamic systems invariant Borel probabilistic measure with metric space and topological entropy equality
08 p1210 A72-22187

Adaptive algorithms for dynamic systems observation based on extremal data processing systems construction
09 p1283 A72-22219

Ground based ATC information processing systems analysis, considering controllers work load
09 p1348 A72-22778

ATC systems analysis by computerized real time environmental simulation, taking into account new aircraft types, navigation and supervision aids
09 p1348 A72-22782

Generalized polynomial operators for nonlinear systems analysis, presenting local invertibility theorem
09 p1341 A72-23092

Human operator role in ATC systems analysis, evaluating tasks with respect to job demands and personal fulfillment
09 p1270 A72-23127

Air traffic control systems efficiency evaluation, discussing measures for criteria conflict solution
09 p1270 A72-23128

ATC system analysis by fast time arithmetic simulation techniques, describing ground model development
09 p1272 A72-23141

One degree of freedom mechanical system with jump-like variable mass, determining displacement and velocity statistical characteristics under random excitation and mass addition
09 p1353 A72-23608

Analog to digital conversion system analysis and design with linear converter and nonlinear logarithmic amplifier, noting small signal resolution
09 p1284 A72-23678

Hammerstein form nonlinear systems class invertibility and reproducibility criteria derivation, noting decoupling possibility by dynamic precompensation and nonlinear state feedback
10 p1502 A72-23781

Systems analysis and mathematical modeling role in planning transportation networks from control theory viewpoint
10 p1442 A72-23796

Maximum likelihood method of combining system and component data for reliability estimates
10 p1444 A72-24016

Analytical design of pulse width modulated systems with time constant and delay for electronic control using Z transform
10 p1457 A72-24458

System diagnosis based on ordered statistical samples, discussing Kolmogoroff-Smirnov detector use for on-line computers in testing noisy systems
10 p1482 A72-24597

Methods of moments, rational transform approximation, Taylor series expansion and modulating functions used for process identification model, determining system transfer functions
11 p1607 A72-25283

Sampling theorem application to time varying systems, considering Hankel transform as example
11 p1675 A72-25293

Probabilistic analysis of technological systems precision, estimating distribution functions of random output parameters
11 p1609 A72-25430

Reliability analysis of repairable redundant systems with random replenishment of reserves, using discrete time Markov process theory
11 p1600 A72-25440

Continuous signals discrete values for analysis and synthesis of control systems with variable parameters, obtaining recurrent formulas and error estimate
11 p1609 A72-25445

Approximate statistical analysis of PFM and combined modulation systems, proposing linearization method
11 p1609 A72-25447

ATC system, discussing flight data and radar processing functions and terminal automation program
11 p1683 A72-25875

Weighting patterns application to linear finite dimensional systems analysis and synthesis, presenting discrete time realizability condition
11 p1677 A72-26154

Trajectory optimization for low thrust mission and system analysis, exemplifying by Jupiter flyby and comet rendezvous missions [AIAA PAPER 72-426]
11 p1721 A72-26171

Correlations analysis method for homogeneous and inhomogeneous systems under external field based on BBGKY hierarchy and decomposition of reduced distribution functions
11 p1689 A72-26480

Finite difference equations of motion for conservative and nonconservative dynamic systems with finite degrees of freedom, obtaining numerical solution by Hamilton principle
12 p1844 A72-27193

Titan 3 family systems analysis for delivering multiple communication satellites to geostationary orbits [AIAA PAPER 72-570]
12 p1870 A72-27378

First order systems steady state frequency response to general harmonic amplitude modulated input, noting signal attenuation and absence of distortion
12 p1845 A72-27540

Model for supervised repairable system reliability, assuming system life and repair times as exponential probability distributions with deterministic supervisor active and inactive times
12 p1814 A72-27555

Second order systems time optimal control with delay, determining maximum number of switching points for control function
12 p1794 A72-28141

Complete aircraft systems reliability and maintainability, discussing extraordinary variances causes, faulty data inferences and operational testing for equipment specifications validation
13 p1896 A72-28358

Statistical principles of reliability assessment and sequential testing of complex systems, considering confidence level, probability of acceptance and cost factors
13 p1984 A72-28361

Reliability lower confidence limit estimation for serial systems with failure in any subsystems resulting in overall failure
13 p1962 A72-28362

Reliability analysis of automatic systems with structural changes accumulated during operation, noting service life determination and damage prevention
13 p1936 A72-29169

Hydraulic servosystem performance analysis, determining transfer function for time variant input-output relationship, gain levels and stability assurance 14 p2073 A72-30420

Mechanical and electrical technologies unification, discussing systems and balances 15 p2211 A72-31873

Time sharing radio communication system analysis with amplitude modulated carrier, noting power reduction, sideband content and multiplexing 15 p2201 A72-32566

Discontinuity problems in optimal control of systems describable by ordinary differential equations, deriving Weierstrass optimality conditions 16 p2371 A72-32939

Optimization of noise impeding observation of dynamic system subjected to random perturbations, discussing optimal control based on least square estimate 16 p2371 A72-33090

Iterative computational procedure for system parameter identification and optimization, using multilevel technique 16 p2371 A72-33192

Correlation technique for transient response of a hysteretically-damped dynamic system to stationary random excitation. 17 p2579 A72-34231

Nuclear electric propulsion systems performance evaluation for various escape missions 17 p2606 A72-34577

Discrete and continuous systems spurious solutions avoidance through Hamilton principle reciprocal form derivation of geometric compatibility conditions [ASME PAPER 72-APM-54] 17 p2627 A72-34777

Nonlinear system consisting of gas filled tube with pressure sensitive heat source, noting oscillation evolution due to equilibrium perturbation [ASME PAPER 72-APM-21] 17 p2580 A72-34796

Russian book on numerical methods in optimal control systems theory covering functional extremum, dynamic programming, control synthesis and statistical linearization of nonlinear systems 17 p2533 A72-35458

Digital simulation for sampled electro-optical imaging system performance prediction and optimization 17 p2557 A72-35552

New description of a first harmonic approximation for nonlinear distributed parameter systems 17 p2534 A72-35722

The effects of damping on a non-linear system with two degrees of freedom. 18 p2709 A72-36080

Mathematical modeling assumptions and procedures in experimental mechanics, considering transfer function, impedance and human factor roles 18 p2709 A72-36353

Optimally sensitive adaptive control techniques for systems with unknown time-varying parameters, suggesting applicability to ATC 19 p2776 A72-37289

Generalized dynamic systems and process prediction 19 p2833 A72-37378

Mathematical model of class of complex control systems composed of structures obtained from aggregates of ordered sets and random operators 19 p2777 A72-37380

Analysis of discrete automatic control systems with variable parameters by the method of orthogonal expansions. I, II 19 p2778 A72-37438

The output control of linear time-invariant multivariable systems with unmeasurable arbitrary disturbances. 19 p2779 A72-38231

Effects of incomplete adaptation and disturbance in adaptive control. 19 p2781 A72-38263

Parameter identification of a class of multiple input/multiple output linear discrete-time systems. 19 p2826 A72-38269

Feedback loop equations and discrete measuring point methods for synthesis of optimal control systems with location dependent controlled variables 19 p2782 A72-38311

Two state system analytic modelling as nonlinear heat transfer problem 19 p2882 A72-38445

Study of the stability of a polar coordinate compensator 19 p2783 A72-38581

A method of realizing servo links imposed on a mechanical system. I 19 p2835 A72-38587

Book - An introduction to engineering systems. 20 p2945 A72-38925

Incoherent radiation imaging system analysis from detector-display characteristics, target response function and noise characteristics 20 p2922 A72-39044

Synthesis and analysis of a fly-by-wire flight control system for an F-4 aircraft. [AIAA PAPER 72-880] 20 p2887 A72-39119

Dynamic nonlinear system direct statistical analysis by Covariance Analysis Describing Function Technique with linearization, giving illustrative examples [AIAA PAPER 72-875] 20 p2905 A72-39124

System analysis and synthesis for B-52 Control Configured Vehicle program, discussing flutter mode and maneuver load control and augmented stability configurations [AIAA PAPER 72-869] 20 p2887 A72-39130

Nonlinear system described by three generalized coordinates, noting dynamic response stability equivalence to two degrees of freedom system 20 p2953 A72-39553

Use of the multidimensional Laplace transform for the analysis of nonlinear systems with variable parameters 21 p3036 A72-40185

Topological analysis of the sensitivity of a digital system 21 p3036 A72-40222

An application of the concepts and methods of linear systems analysis to the scattering of resonance radiation by an atomic vapour. 21 p3084 A72-40470

Systems analysis approach to the study of spinal mechanisms. 21 p2999 A72-40590

Failure diagnostics in mathematical models of automatic control systems 21 p3038 A72-40712

Mission model for European communication satellite system based on estimated future traffic requirements 21 p3017 A72-40853

Impulse noise in FM receivers in the presence of adjacent channel interference and thermal noise. 21 p3020 A72-40894

Carrier phase jitter extraction method for VSB and SSB data transmission systems. 21 p3021 A72-40910

Quantitative aspects of reliability in process-control systems. 21 p3038 A72-40922

System analysis for an airline operational environment through a computerized network simulation model. 21 p3025 A72-41077

Independent cascaded multicomponent random variable system gain statistics relationship to individual component based on moment derivation, obtaining curves from variance equation 21 p3022 A72-41087

Analysis of impact vibrations by delta-function method - Case of one degree-of-freedom system. I - Perfectly elastic collision. 21 p3121 A72-41238

Extended Kalman filter application to delayed systems for state and time delay estimation, discussing two nonlinear estimators [AIAA PAPER 72-902] 21 p3039 A72-41553

Global asymptotic stability of two classes of control system with pulse-width and pulse-frequency modulation 22 p3162 A72-42184

Polynomial operators for nonlinear systems analysis. 23 p3308 A72-43599

Design of controllers for open-loop unstable multivariable system using inverse Nyquist array. 23 p3275 A72-43609

Asilomar Conference on Circuits and Systems, 5th, Pacific Grove, Calif., November 8-10, 1971, Record. 23 p3276 A72-43851

Berner simulation method /BERSIM/ based on lumping recurring combinations of operations into component subsystems representing specified transformations of input into output variables 23 p3267 A72-44143

A systems analysis of subsonic versus supersonic jet travel. 24 p3466 A72-44580

The heavy lift helicopter - An operations research/technology/performance blend. 24 p3466 A72-44581

A survey and comparison of methods for determining confidence bounds on system reliability from subsystem data. 24 p3406 A72-44652

Robert Bruce's spider problem extended - Reliability of adaptive experimental systems. 24 p3406 A72-44666

Linear analysis and synthesis of three dimensional interference system stationary in space and time domains 24 p3379 A72-44752

Mathematical model for life support system optimization in terms of reduced mass minimization as quality criteria for energy conversion and metabolic processes 24 p3375 A72-45133

Evaluation of the danger of damage to mechanical systems exposed to random vibrations 24 p3459 A72-45449

SYSTEMS COMPATIBILITY

Test facilities for aeropropulsion systems, emphasizing utilization, cost and technical advantages, aircraft inlet-engine systems compatibility and test types [AIAA PAPER 72-1034] 24 p3388 A72-45401

SYSTEMS DESIGN

U SYSTEMS ENGINEERING

SYSTEMS ENGINEERING

Cassegrain type astronomical reflecting telescope design, describing auxiliary equipment 01 p0047 A72-10202

Airline Propulsion Team approach to DC-10 aircraft power plant design for maximum operational effectiveness [SAE PAPER 710778] 01 p0116 A72-10270

Error correction techniques of convolutional coding with Viterbi maximum likelihood decoding for communications systems design, using computer simulation 01 p0026 A72-10344

Multidimensional variable structure systems synthesis for automatic optimization of inertialess technological plants in presence of constraints 01 p0045 A72-10498

Gradient method for optimization control system construction with cross couplings between channels 01 p0045 A72-10501

FM/CW laser radar technique for smoke plume opacity remote measurement, discussing eye safety [AIAA PAPER 71-1081] 01 p0080 A72-10539

Systems approach to space technology application, covering Global Atmospheric Research Program and Earth Resources Technology Satellites 01 p0146 A72-10952

Design and performance of Intelsat III dual TWT power supply, noting space, weight and cost savings. 01 p0007 A72-11056

Electrical power subsystem design in Pioneer F/G spacecraft, using SNAP 19 deployable radioactive thermoelectric generators supplemented by Ag-Cd battery 01 p0008 A72-11065

Electrical power subsystem for Initial Defense Communications Satellite Program/Augmentation, noting solar cells for power conversion and Ni-Cd batteries for energy storage 01 p0008 A72-11066

Air transportation system design for safety and efficiency, discussing navigation facilities and surveillance systems employment for blunder prevention 01 p0098 A72-11117

Inertial navigation role in automatic ATC systems, discussing path control accuracies, environmental conditions, noise and air pollution, etc 01 p0098 A72-11118

Time division multiple access systems for communication satellites, discussing performance and application in Intelsat network 01 p0033 A72-11301

Plasma diagnostics facilities design, circuit diagrams and operation based on Q switched ruby laser and optical recording system 02 p0237 A72-11407

Homodyne frequency converter design using microwave oscillator with bitonal frequency modulation 02 p0223 A72-11415

Anglo-Australian astronomical optical telescope construction, summarizing project organization, components and system design 02 p0199 A72-11640

ATC system decision making problem and future technological and administrative improvements 02 p0255 A72-11718

Hybrid system to process multispectral photographic data from aircraft and spacecraft sensors, assessing data quality, cost effectiveness and delay reduction 02 p0228 A72-11883

Optimum power allocation in design of phase-coherent receiver having bandpass limiter, extending technique from single channel to two channel system 02 p0174 A72-12136

Digital telemetry/communication laser link system design for operation at 1 gigabit/sec 02 p0174 A72-12143

Frame synchronization performance tests for PCM telemetry system, considering code selection, frame length and data recovery 02 p0175 A72-12147

Microwave aircraft landing system development, discussing contract definition, feasibility, prototype development, management planning and program costs 02 p0304 A72-12377

Discrete address ATC radar beacon system operation and design 02 p0256 A72-12378

MTI radar system design philosophy for target detection in land clutter environment 02 p0178 A72-12390

Aircraft and spacecraft integrated avionics systems design with emphasis on telemetry, discussing space shuttle subsystems integration

02 p0179 A72-12403

Multiplex FM recording system parameters effect on system design, considering SNR, deviation ratio, wow and flutter, tape speed errors, crosstalk and FM filters

02 p0230 A72-12409

Visual display systems for man-machine communications, discussing applications, data processing, hardware designs and human engineering

02 p0230 A72-12419

Computer-aided interactive graphic displays for ATC, discussing subsystems, data processing flow and operational capabilities

02 p0257 A72-12420

Soviet book on gas turbine engines control systems design based on similarity theory, determining optimal controller formula from engine parameters

02 p0271 A72-12543

German-American interplanetary solar probes Helios A and B mission characteristics and ground operations system, discussing planning phase [DGLR PAPER 71-122]

02 p0285 A72-12741

Stochastic linear-quadratic-Gaussian problem role in optimal closed loop control system design, emphasizing philosophy, modeling and problem formulation [AD-738763]

02 p0198 A72-12801

Linear and quadratic programming procedures in optimal control problems of stochastic and deterministic system design

02 p0198 A72-12807

Linear multivariable interacting feedback control system optimal design by heuristic approach to determine input-output pairing and controller settings for satisfactory disturbance attenuation

03 p0337 A72-12905

Pulse shaped small parameter variation effects on performance index of minimum fuel control systems with initial and final manifolds

03 p0337 A72-12906

Concorde aircraft electrical power systems design, noting dc and emergency supplies and installation

03 p0311 A72-12910

Book on human factors engineering covering systems design requirements and interface equipment for man machine interaction implementation

03 p0318 A72-13023

Systems, man and cybernetics - IEEE Conference, Anaheim, California, October 1971

03 p0318 A72-13161

Linear time optimal control system with retardations in controls, discussing controllability, existence and uniqueness, synthesis techniques and dynamic programming [AD-737927]

03 p0338 A72-13406

Services and systems integration into total aircraft design, considering utilization and type effects

03 p0309 A72-13413

Magnetic bubble repertory dialer memory design, noting bit storage capacity and random access [IEEE PAPER 28,1]

03 p0328 A72-13782

Analog computer simulation for filtering, phasing, multiplication and addition in AM communication system

03 p0329 A72-14182

Automated system pathfinder application to systems design and analysis for engineering information exchange

03 p0326 A72-14198

High speed digital communication over space to earth satellite links by quadriphase modulation, discussing modulator, receiver and system technology for maximizing data transfer

04 p0485 A72-14477

ATS F and G ground station mobile terminal, discussing system flexibility, utility and reliability features and parabolic antenna design

04 p0485 A72-14478

Chain and branched type electrical and mechanical systems, establishing algorithms with linear flow graphs

04 p0504 A72-14516

Self oscillating dc-dc converter analysis and optimal design, modeling by single loop nonlinear feedback system

04 p0465 A72-14571

Book on system safety engineering covering systems analysis and engineering, evolution of safety philosophy, product reliability and liability, etc

04 p0477 A72-14573

Distributed systems modeled by partial differential equations, identifying unknown parameters by Galerkin method using steepest descent method and nonlinear filter

04 p0505 A72-14674

Collision avoidance systems and pilot warning instruments, minimizing cost by pilot detection, evaluation and avoidance execution

04 p0545 A72-14823

Discrete system high order optimality sufficient conditions and methods for singular and nonsingular controls study

04 p0505 A72-14996

Control system synthesis from transient process estimates with Liapunov functions, proposing optimality criteria based on Gaussian minimum constraint principle extension

04 p0505 A72-14997

ALSEP design and development, discussing reliability, power sources and astronaut interface constraints

04 p0577 A72-15092

Minimal order precompensator with state feedback for decoupling linear time-invariant multivariable control system, discussing design parameters determination from linear equations

04 p0506 A72-15109

Optimal control systems with terminal state constraints, presenting algorithm based on constraint-space conjugate gradient method for function minimization

04 p0506 A72-15111

Product support functional organization, discussing support systems analysis and engineering, trainer design, technical proposals and publications, customer training, field service, etc

04 p0597 A72-15224

Refractory metal thermocouple research program, describing design and performance of ultrahigh vacuum high temperature furnace system

04 p0524 A72-15550

Integrated data processing system organizational model methodology for individual firms, emphasizing interdependence on program groups

05 p0632 A72-15815

Thermal heliotrope adaptation to terrestrial applications, discussing solar radiation energy input dominance assurance and wind effect minimization [ASME PAPER 71-WA/SOL-10]

05 p0614 A72-15893

Structure, controllability and synthesis of n-dimensional invariant systems under perturbation vector, using governing equations

05 p0641 A72-16352

Anthropomorphic robots design and performance for space exploration

05 p0644 A72-16448

Three dimensional global spacecraft attitude control system analytical design technique based on system stability considerations

05 p0726 A72-16457

Heat transfer rate prediction in cooling system design for gas turbines [ALAA PAPER 72-10]

05 p0707 A72-16865

NASA closed cycle MHD facility for power generation, discussing system components, design and operation [ALAA PAPER 72-103]

05 p0616 A72-16936

Aircraft collision avoidance system design and evaluation, developing closed form method for system alarm rate estimation

05 p0688 A72-16945

Adaptive model following control systems design by hyperstability approach for flight control and simulation [ALAA PAPER 72-95]

05 p0613 A72-16956

HF and/or HF-carbon dioxide transfer laser potential power output and design criteria, considering deuterium and fluorine combustion, reaction product expansion and mixing rate [ALAA PAPER 72-147]

05 p0670 A72-16970

Linear time-varying control system synthesis for specific input and maximum admissible error, considering various weighting functions and constraints

06 p0792 A72-17311

Optimal linear multivariable control systems design with prescribed eigenvalues, presenting method for corresponding weighting matrix elements

06 p0792 A72-17315

Raman laser radar (LIDAR) for remote probing, discussing design, construction, testing, atmospheric scattering, and intensity and polarization measurements

06 p0824 A72-17588

Design, development and operation of liquid hydrogen plant, using production for rocket thrust chamber tests and tank pressurization studies

06 p0867 A72-17593

Book on discrete event computer simulation for complex systems synthesis and analysis covering random numbers use, languages, and interactive man machine applications

06 p0779 A72-17812

Earth resources technology satellite program, discussing mission requirements, payload, orbital characteristics, earth stations, data processing, system design and international features [DGLR PAPER 71-139]

06 p0892 A72-18230

Computerized Eros II airborne collision avoidance time frequency system design, considering radar transmission, synchronization and ground stations

06 p0845 A72-18247

Optimal design of dynamic system with universality for series of maneuvers with various degrees of informativeness, considering flight mechanics of limited power engine system

06 p0848 A72-18299

Optimal control systems synthesis with allowance for given reliability, finding extremal value of quality function with constraint on probability of fail-safe operation

06 p0794 A72-18305

Dynamic system optimal design with various degrees of maneuver parameters information, considering space flight mechanics problem of payload maximization for limited propulsive power

06 p0849 A72-18306

Narrow beam radiometer design and performance for atmospheric radiation studies including water vapor continuum absorption and high layer clouds emissivity

06 p0819 A72-18447

C-54 A/B aircraft engine air particle separator anti-ice system design features, manufacturing techniques and testing

07 p1053 A72-18769

Multichannel communication system in adaptive system based on random parameter extremum criterion, deriving average usage time of extremal channel

07 p0938 A72-19008

Systems science - Conference, University of Hawaii, January 1972

07 p0949 A72-19270

First passage time boundary value problem for first order phase locked loop systems, determining probability density function of time to cycle-slip

07 p0959 A72-19273

Algorithmic procedure in compensator design for hyperstable discrete model reference adaptive systems [MRAS/]

07 p1027 A72-19294

Aerospace subsystem alternate designs and cost effectiveness evaluation and optimization, considering algorithm of three functions with minimal coupling

07 p1105 A72-19552

Multivariable plant optimization, considering oil field operations, n-paired transceiver power loads, Laplace and Poisson equations described systems and interindustrial balance

07 p0962 A72-1972

Linear multivariable feedback control system design techniques

07 p0963 A72-1972

Integrated systems approach to computer simulation with functional modules to achieve control processor independent expansion and optimization

07 p0951 A72-20331

Computer simulation requirements for air around transportation system, emphasizing mathematical models capable of system performance relation to design parameters

07 p0952 A72-20362

High resolution digital integrator design based on second order differences

07 p0963 A72-20388

Interactive graphics technique for design of single input linear feedback systems described by state equations or cascaded transfer functions

07 p0963 A72-20391

Single-channel-per-voice-carrier transmission system application to data communication and small earth station operation, discussing modular design and performance

07 p0948 A72-20494

Time optimal closed loop control system synthesis by phase space technique verifying results by state variable approach

07 p0964 A72-20595

Explosive/pyrotechnics performance monitoring for acceptance, lot qualification, comparison testing and system design guidelines

08 p1219 A72-20760

Biased estimator as alternative to linear unbiased estimator for dynamic system model states and parameters optimization and regulation, noting squared errors sum

08 p1144 A72-20852

Test pilot role in attack aircraft avionics systems integration consisting of head-up display, projected map, digital computer, inertial platform, radar and Doppler systems, etc

08 p1165 A72-21012

White Sands Missile Range and Range-Rate system design and verification to meet midcourse tracking requirements under severe target dynamics

08 p1133 A72-21402

Apollo 15 lunar subsatellite particle experiment subsystem design for studying magnetosphere dynamics, plasmas-moon interaction and solar flare physics

08 p1168 A72-21519

Radio communication system optimization from viewpoints of global synthesis, including economics and partial synthesis based on noise stability, precision and reliability

08 p1136 A72-21845

- System reliability improvement by redundancy, noting independence of distribution law type
08 p1180 A72-22057
- Adaptive statistical system with feedback loop for weather analysis and forecasting, examining learning process features
08 p1202 A72-22113
- Soviet papers on industrial plants automatic control systems organization, design and teleautomatic arrangement, covering information handling requirements and man machine interfaces
08 p1256 A72-22144
- Automated administrative control systems design, discussing man machine interactions in industrial and economic enterprises management
08 p1256 A72-22145
- Data transmission system design in computerized administrative control system for industrial enterprise management
08 p1257 A72-22148
- Three phase bidirectional pulsating flow hydraulic control system, discussing design, performance and applications
08 p1114 A72-22162
- Redundant polystable element designs with autonomous redundant state breakdown controls for reliability improvement in automatic control systems
09 p1290 A72-22547
- Systems approach to technological forecasting for short range research, considering consumer, market and organizational resources
09 p1413 A72-22950
- Nonlinear systems controllers design based on Liapunov functions and time domain ratio criterion, presenting digital computer algorithm
09 p1290 A72-23090
- Linear time invariant multirate sampled data control systems characteristic equation simplification
09 p1290 A72-23099
- Numerical algorithm for optimal coefficient equations in analytical design of complex control plants
09 p1291 A72-23426
- Optimal control synthesis for linear passive stationary plants with symmetrical coefficient matrices of minimized functional
09 p1291 A72-23431
- Man machine automatic control system structural synthesis, treating system operation as nonlinear programming problem
09 p1291 A72-23438
- Nonlinear systems optimal design mathematical modeling, discussing synthesis, manufacturing, production, exploitation and evaluation
09 p1343 A72-23610
- Analog to digital conversion system analysis and design with linear converter and nonlinear logarithmic amplifier, noting small signal resolution
09 p1284 A72-23678
- Quadratic performance index generation for optimal design of completely controllable, scalar linear system with state feedback
10 p1454 A72-23783
- Optimal probing signals design for state vector parameter estimation, considering Fisher information matrix function as optimality criterion
10 p1454 A72-23786
- Nonlinear programming and parameter optimization algorithms for constrained feedback control system design
10 p1441 A72-23790
- System methodology application to filter design for inertial reference unit calibration in digital test station for FB-111 aircraft navigation system
10 p1456 A72-23820
- Task oriented maintainability engineering relationship to systems engineering and logistics support requirements
10 p1564 A72-23852
- Lunar roving vehicle reliability program and design features of mobility, electrical power and navigation subsystems
10 p1460 A72-24443
[AIAA PAPER 72-233]
- Weak signal turnaround transponder design for pseudonoise coded ranging systems, discussing bandwidth optimization and performance comparison between various receiver configurations
10 p1452 A72-24688
- Cumulative index of papers on radar systems published in IRE/IEEE journals since World War II
10 p1438 A72-24694
- Avionics systems electrical interface connection design information document creation and dissemination, using EMPRENT computer program
10 p1453 A72-24864
- RCA SECANT aircraft collision avoidance system avionics design using nonsynchronous techniques
10 p1509 A72-24866
- Time division multiplexing system for asynchronous high data rate telemetry, discussing design features
10 p1440 A72-25061
- STOL aircraft systems development coordination, considering vehicle design, airport facilities and related ground environment, transportation modes interface and airspace management
11 p1574 A72-25255
- Structure, controllability and synthesis of n-dimensional invariant systems under perturbation vector, using governing equations
11 p1608 A72-25328
- Time to failure determination in complex service systems, examining Markov processes
11 p1609 A72-25435
- Optimal parameters selection for natural vibrations maximum damping rate, applying method to two mass electromechanical system
11 p1686 A72-25533
- Design and development program for air conditioning system of twin engine unpressurized Piper Navajo, noting flight test results
[SAE PAPER 720328] 11 p1577 A72-25590
- Hale observatories computer system design for telescope control and data handling, using solid state techniques
11 p1601 A72-25696
- Optimal dynamic system design for maneuvers with complete statistical information applied to limited power space flight
11 p1610 A72-25796
- Communications Technology Satellite attitude control system design, taking into account dynamic interactions with large flexible solar cell array
11 p1593 A72-25913
- Electromagnetic compatibility system design checklist, noting usefulness to project personnel
[SAE AIR 1221] 11 p1604 A72-26026
- Weighting patterns application to linear finite dimensional systems analysis and synthesis, presenting discrete time realizability condition
11 p1677 A72-26154
- Biowaste resistojet propulsion system development program, discussing design, propellant management and control subsystems
[AIAA PAPER 72-448] 11 p1707 A72-26185
- Integrated display system design with navigation update, weapon delivery, reconnaissance, bomb damage assessment, threat and terrain avoidance capabilities for multicrew military aircraft
11 p1684 A72-26292
- FAA automated ATC system, discussing subsystems related to operational and nonoperational computer program components, data entry and display, communication, personnel and environments
11 p1684 A72-27000
- Communication systems design with error control, applying algebraic codes to biphasic and multiphase modulation systems
12 p1782 A72-27488
- Reliability, quality and testing assurance in ATS F and G system, discussing computerized handling of spacecraft parts information
12 p1814 A72-27524
- Tactical satellite communication system and ground terminal design options for efficiency improvement, considering power sharing, priority system frequency allocation and system control concepts
12 p1785 A72-27844
- American and European solar generator technology development review, discussing roll-up arrays, flexible panels, and stowage and deployment system components
12 p1756 A72-28005
- Automatic control system synthesis by computer-aided version of grapho-analytical method
13 p1934 A72-28459
- Variable structure automatic control relay system design with reduced insensitivity zone and given transient process requirements
13 p1935 A72-28612
- Aircraft electrical power systems design dependence on latitude, minimum weight requirement, reliability degree, environmental conditions and acceleration
13 p1899 A72-28693
- Secondary surveillance radar systems design and planning for ATC application
13 p1917 A72-28698
- Model determining system responses to nominal profiles of atmospheric parameters from orbital to 25 km altitudes
13 p1989 A72-28807
- Hailstone size estimation to design exposed equipment for irreversible impact damage prevention
13 p1993 A72-28854
- High voltage solar array technology, studying power conditioning control system design and array-space plasma interactions
[AIAA PAPER 72-443] 13 p1899 A72-28942
- Experimental communications satellite system of ATS F and G geostationary satellites for specific application, discussing system performance measurement instruments
13 p1918 A72-28986
- Early design phase reliability analysis of large adaptive systems in terms of domination and graph theories
13 p1965 A72-29171
- Signal system design with digital displays for deviation control in complex multiparameter technological processes, using algorithm to estimate efficiency
13 p1936 A72-29177
- Visual display units as manifold input output devices in data processing systems, discussing structure, characteristics and applications
13 p1925 A72-29343
- Optimal design of dynamic system with universality for series of maneuvers with various degrees of informativeness, considering flight mechanics of limited power engine system
13 p2052 A72-29439
- Linear automatic control systems diagnostics and synthesis
13 p1937 A72-29998
- Process computer technology, discussing data recognition, on-line open loop operation and system characteristics
13 p1926 A72-30051
- Optimal control systems synthesis with allowance for given reliability, finding extremal value of quality function with constraint on probability of fail-safe operation
13 p1937 A72-30073
- Aerospace critical systems and future technologies, presenting illustrative diagram for functions combination and interrelations
14 p2175 A72-31140
- Reliability modeling principles, concepts and implementation techniques for switching system design
14 p2091 A72-31167
- Adaptive reception of weak repetitive signals on background of intense fluctuating noise, synthesizing adaptive detection system for multipath propagation and small SNR
15 p2195 A72-31658
- Stage removal and addition effect on multistage axial compressor for application in engine design
15 p2179 A72-31706
- Human waste management system evaluation in zero gravity flight tests, presenting design concept for collection by air flow technique
15 p2189 A72-31825
- Electro-optical systems design - Conference, New York, September 1971
15 p2247 A72-32026
- Time-frequency dissemination system design, discussing radio propagation, time signals, noise effects, synchronous satellite transponders and TV use, accuracy, geographical coverage and costs
15 p2198 A72-32065
- Fraunhofer holograms wavelength dependent distortion reduction by system parameters optimization, applying to color holotape
15 p2239 A72-32357
- Total system approach to time scheduled aircraft operations - Conference, London, May 1972
15 p2339 A72-32451
- Accessory reliability relation to on-time performance, discussing production route in terms of specification, design, development and manufacture
15 p2339 A72-32463
- Sensitivity design of multiple input controller for dynamic optimization applied to linear systems with quadratic performance index
15 p2212 A72-32795
- Numerical methods for Liapunov linear matrix equations solution in control systems analysis and design
15 p2265 A72-32798
- Discrete system feedback design based on complex number plane mapping, determining gain
15 p2213 A72-32800
- State space approach to linear multivariable servomechanism problem, deriving controllability conditions and design procedure
15 p2213 A72-32801
- Automatic systems design for monitoring dynamic control systems, noting feedback control system performance prediction based on subsystems characteristics
16 p2371 A72-33085
- Observability conditions for nonlinear and unsteady linear systems, noting control systems design
16 p2371 A72-33092
- Integrated airborne-ground based instrumentation system for variable stability X-22A aircraft flying qualities research, discussing telemetry, mobile van, landing aids and airplane design
16 p2348 A72-33628
- Airborne flight test data acquisition system modular design to provide digital readings from monitoring transducers analog signal
16 p2364 A72-33645
- Thermoemission ion gage stability and design aspects, discussing application as secondary standard for vacuum measurements
16 p2394 A72-33871
- A/D and D/A converter for color TV signal digital transmission over communication satellites, discussing system design features
17 p2524 A72-34262
- Communication satellite modeling into subsystems to formulate parametric relationships among power, mass and cost, comparing computerized design alternatives
17 p2512 A72-34263

Intelsat satellite SPADE demand-assignment multiple access system design for increased communication flexibility and efficiency

17 p2512 A72-34269

Comparison of circuit call capacity of demand-assignment and preassignment operation.

17 p2512 A72-34270

Thermionic reactor system for auxiliary power and electric propulsion.

17 p2494 A72-34579

Thermionic reactor power conditioner design for nuclear electric propulsion.

17 p2495 A72-34582

Optimized 100 We multicell thermionic power supply design with high reliability, noting isomote converter performance characteristics

17 p2495 A72-34583

Design features, fabrication technology and in-pile testing of thermionic reactor fuel elements

17 p2495 A72-34584

Design of an external-fueled thermionic diode for in-pile testing.

17 p2495 A72-34585

Process computer system design, discussing structural units, data flow coordination with storage, input/output channels and periphery coupling problems

17 p2523 A72-35443

Structural mode vibration control system design for B-1 aircraft to improve ride during atmospheric turbulence and terrain following

17 p2493 A72-35563

Design and analysis of transistorized, selective HF amplifiers with allowance for sensitivity properties

17 p2532 A72-35978

Intelsat 4 multichannel communication network earth station equipment components and characteristics experimental system/SPADE/ study to realize demand assignment

18 p2659 A72-36272

Practical problems and solutions in modeling physical systems with time-domain input-output measurements or specifications.

18 p2663 A72-36327

Systems approach to integrated planning of airfield pavements design, construction, operation and maintenance, emphasizing need for mathematical models, constitutive parameters and limiting criteria

18 p2675 A72-36788

Surveillance radar for clutter rejection and signal loss reduction at airports, discussing system design features

18 p2662 A72-37046

Model reference adaptive control systems design based on optimal control, parametric optimization, stability and statistical estimation theory

19 p2778 A72-37722

Realisation of a high-efficiency electrodischarge-machining power supply.

19 p2807 A72-37846

A computerized system for the preliminary design of commercial airplanes.

19 p2749 A72-38110

Area navigation and its affect on aircraft operation and systems design.

[AIAA PAPER 72-754] 19 p2831 A72-38125

Designing aircraft structure for resistance and tolerance to battle damage.

[AIAA PAPER 72-773] 19 p2752 A72-38133

Structural-matrix methods for discrete automatic control system designs

19 p2779 A72-38185

Design techniques for model-reference adaptive control systems.

19 p2781 A72-38266

Linear dynamic systems parameter identification via optimal input design, noting eigenfunction dependence on positive self adjoint operator

19 p2781 A72-38271

Decoupling and synthesis of certain nonlinear systems.

19 p2827 A72-38275

Integrated systems design procedures as exemplified by Europa 1, 2 and 3 rockets and Symphonie communication satellite development

19 p2869 A72-38302

Systems management in major projects exemplified by the German Satellite Control Center

19 p2783 A72-38303

Design and testing of a nine-channel photometer

19 p2804 A72-38500

A development study for a 65-m radio telescope for the mm wave range

19 p2804 A72-38510

Optimal control synthesis for linear passive stationary plants with symmetrical coefficient matrices of minimized functional

19 p2782 A72-38514

Man machine automatic control system structural synthesis, treating system operation as nonlinear programming problem

19 p2782 A72-38521

Optical communications in Japan.

19 p2766 A72-38602

A 10,000-gpm liquid hydrogen transfer system for the Saturn/Apollo program.

19 p2784 A72-38829

Long term storage and propellant transfer capabilities of propellant depot system design to act in earth orbit as resupply station for cargo/personnel shuttles

19 p2870 A72-38831

Book - An introduction to engineering systems.

20 p2945 A72-38925

Partially coherent light for image formation of objects with amplitude, phase and complex variations, discussing system concepts, coherence control, apodization and techniques

20 p2931 A72-39048

Application of optimization techniques to the problem of determining optical constants of thin films.

20 p2959 A72-39052

Error analyses of Euler angle transformations arising in design of precision pointing systems, guidance sensors and instruments with gimballs

[AIAA PAPER 72-851] 20 p2949 A72-39078

Design analysis and performance characteristics of a circular test base.

[AIAA PAPER 72-845] 20 p2911 A72-39084

Problems and solutions related to the design of a control augmentation system for a longitudinally unstable supersonic transport.

[AIAA PAPER 72-871] 20 p2887 A72-39128

System analysis and synthesis for B-52 Control Configured Vehicle program, discussing flutter mode and maneuver load control and augmented stability configurations

[AIAA PAPER 72-869] 20 p2887 A72-39130

Development of a laboratory prototype spraying flash evaporator.

[ASME PAPER 72-ENAV-28] 20 p2894 A72-39149

Design criteria for the modular space station environmental control and life support system selection.

[ASME PAPER 72-ENAV-25] 20 p2894 A72-39152

Significant factors in environmental and thermal control/life support system design for space shuttle orbiter

[ASME PAPER 72-ENAV-21] 20 p2895 A72-39156

Space shuttle waste collection system development, discussing human-interface requirements, zero gravity effects and operational considerations

[ASME PAPER 72-ENAV-13] 20 p2896 A72-39164

Water and waste management subsystem design for a space station prototype.

[ASME PAPER 72-ENAV-8] 20 p2896 A72-39169

NERVA flight engine control system design.

21 p3083 A72-40764

Public policy, regulatory controls, market strategies and systems economics considerations for future U.S. domestic communication satellite system

21 p3132 A72-40865

Solid state laser sources, light modulators and silicon avalanche photodiode detectors for fiber optical communication, discussing performance and limitations from system design viewpoint

21 p3018 A72-40866

Television transmission performance of an experimental small aperture earth station.

21 p3018 A72-40878

Suppressed clock pulse duration modulation for noisy voice communication channels with hard limiting satellite repeaters, discussing system design and test data

21 p3020 A72-40898

A procedure for the design of asynchronous time division multiplexers.

21 p3021 A72-40909

Improving R & D management through prototyping

21 p3132 A72-40970

Defense systems development based on balance between theoretical studies and hardware prototyping for uncertainty reduction in performance and cost

21 p3132 A72-40971

Optimum design of MHD generator combustion chamber, noting effects of heating temperature, oxygen enrichment degree and flow velocities

21 p2997 A72-41065

Future trends in air traffic control and landing.

[ICAS PAPER 72-04] 21 p3082 A72-41129

Comparison of design procedures of vibration absorbers for systems with random excitations.

21 p3121 A72-41230

Design of vibration absorbers minimizing human discomfort.

21 p3009 A72-41231

Probabilistic approach to design of control systems.

21 p3038 A72-41232

Anthropotechnics/human engineering/ approach to man machine system optimization, discussing task allocation and adaptations of machine dynamics, displays and controls to human operator

21 p3009 A72-41403

Display device layout based on human operator manual control information requirements consideration, discussing functional categories, motion compatibility, indicators relation and integration

21 p3009 A72-41404

Human engineering requirements in aircraft system development.

21 p3011 A72-41423

Design and development of the United Aircraft Research Laboratories acoustic research tunnel.

[AIAA PAPER 72-1005] 21 p3041 A72-41589

Synthesis of statistically optimal multiloop control systems containing essentially nonlinear elements

22 p3162 A72-42183

Statistical synthesis of navigation aids systems with unsteady random interferences, obtaining optimization criterion by least squares method

22 p3202 A72-42233

Aircraft hydraulic control systems modular design for maintainability, emphasizing component removal with minimum hydraulic fluid loss and air entrainment

22 p3140 A72-42294

Digital computer technique and real time monitoring software application to instrumentation data acquisition system, discussing design guidelines and gas turbine engine test example

22 p3156 A72-42683

Integration sphere facility with water cooled long arc xenon sources for pyranometer calibration/ discussing operation theory and system design

22 p3163 A72-42692

A near real time data acquisition/reduction facility for the Boeing wind tunnels.

22 p3164 A72-42699

Book - Computer simulation of dynamic systems.

22 p3157 A72-43083

Technical and economic processes representation on radioelectronic equipment synthesis optimization using elementary random magnitudes involving output parameters deterioration rates and fabrication tolerances

23 p3269 A72-43442

Computerized weight data storage, recording and information system to aid in aerospace vehicle design [SAWE PAPER 933] 23 p3266 A72-43473

Space subsystems cost optimization technique for minimization of total spacecraft plus boost cost, studying orbital logistics spacecraft

[SAWE PAPER 941] 23 p3342 A72-43488

Integration of safety engineering into a cost optimized development program.

[SAWE PAPER 945] 23 p3358 A72-43489

Electrohydraulic stand for vibration strength testing, discussing system design, specifications, frequency-amplitude characteristics and applications

23 p3278 A72-43760

Stochastically optimal terminal control system synthesis for loss function dependence on finite phase coordinates of dynamic system, considering soft landing of flight vehicle

23 p3275 A72-43781

Design optimization of an integrated-circuit direct access memory unit

23 p3267 A72-43840

Equipment assembly design optimization by operational versions determination and criteria evaluation for optimal conditions, noting rotary wing design

23 p3294 A72-44024

Aerospace tug using atmospheric braking during return from geostationary orbit, discussing radiative thermal protection, mass, design and advantages

23 p3340 A72-44277

Basic considerations concerning the design of control systems

23 p3326 A72-44279

Systems approach to airport passenger terminal planning.

24 p3387 A72-44583

SECANT midair collision avoidance system based on nonsynchronous microsec pulse transmission and receiving via randomly selected frequency, describing modular components and operating principles

24 p3422 A72-44646

Invariant transformation of the control laws in ergodic systems

24 p3376 A72-45510

Selection of an optimizing functional in control system synthesis

24 p3387 A72-45512

Analytical designing of regulators for second-order nonlinear systems

24 p3387 A72-45519

Theoretical-experimental method for parametric synthesis of director-type control systems

24 p3377 A72-45522

SYSTEMS MANAGEMENT

Pilots in aircraft systems management involving machine and air traffic environment

03 p3039 A72-13419

Cost reduction by integration of assurance technologies from complex systems development risk management model

[AIAA PAPER 72-245] 10 p1487 A72-24450

Satellite supplement to domestic communication systems, discussing network management, system reliability, broadband capacity, earth station flexibility, and market proposals

[AIAA PAPER 72-554] 12 p1781 A72-27374

Reliability role in commercial and military telecommunications satellite system planning, discussing economic factors, earth station redundancies and maintenance, spare levels and control systems

13 p2051 A72-28352

Expendable space transportation - A 1972 assessment.
[AIAA PAPER 72-732] 18 p2730 A72-36542
Implementation status of the Omega Navigation System.
22 p3203 A72-42945

SYSTEMS STABILITY

Triangular points stability in restricted three body problem by computer program

01 p0122 A72-10004
Stability of and motion about L4 in restricted three body problem with 3 to 1 commensurability between long and short periods of motion

01 p0122 A72-10010
French monograph on extremum values of function with two variables and nonlinear feedback control systems stability, using associate recurrence solutions properties

01 p0044 A72-10164
Frequency conditions of absolute stability for closed automatic control system with nonlinear unsteady units

01 p0045 A72-10499
Plasma column equilibrium position feedback control stability based on combination principle, analyzing system stability

01 p0109 A72-10502
Closed linear systems optimal stabilization determining transfer function from Wiener Hopf equation

01 p0045 A72-10572
Bulk InP three level transferred electron microwave oscillators, observing current-controlled instabilities and operation modes

01 p0036 A72-10632
Sixth order nonlinear differential equation isolated equilibrium point stability determination, constructing Liapunov function

01 p0094 A72-11125
Nonlinear mechanics and stability - Conference, Rome, February 1970

02 p0251 A72-11492
Linear systems partial stability via Liapunov second method, examining relation between uniformly and exponentially asymptotic partial stability

02 p0251 A72-11493
Stability relative to part of variables of n-dimensional vector equation, considering applications to solid bodies with fluid filled cavities and gyrostatt satellite optimal stabilization

02 p0251 A72-11494
Stability theorems reformulation with one-parameter families of Liapunov functions, discussing applications to Matrosov and Rouche asymptotic stability theorems

02 p0251 A72-11495
Stability theory invariance principle extension to generalized dynamical systems, considering problems in thermoelasticity, viscoelasticity and distributed nonlinear networks

02 p0251 A72-11497
Nonlinear systems absolute stability calculation, considering time lag, backlash type nonlinearity and process controller

02 p0196 A72-11674
Varactor diode microwave parametric amplifiers for radio astronomy interferometer, discussing system design features for gain and phase stabilities

02 p0192 A72-12043
Stability properties of functional differential system solutions, discussing Liapunov functions construction

02 p0252 A72-12173
Electroluminescent image converter with positive optical feedback, investigating steady state bistable operation mode stability

02 p0193 A72-12341
Linear regulator and servomechanism theories modification to account for fluctuation disturbances, obtaining deterministic controller design to maintain set point regulation or servotracking

02 p0198 A72-12803
Linear multivariable interacting feedback control system optimal design by heuristic approach to determine input-output pairing and controller settings for satisfactory disturbance attenuation

03 p0337 A72-12905
Stability and perturbation of oscillator system with frequency fixed by all pass ring transmission function with delayed amplitude regulation

03 p0331 A72-13410
Frequency criteria for stability of nonlinear multivariable RLC networks with bounded solutions approaching equilibrium

03 p0338 A72-13411
Gas-liquid bipropellant rocket motor system instability boundaries under various operating and design conditions, interpreting experimental results via time lag model

03 p0406 A72-13632
Stability criterion for system representing amplitude modulation amplifiers development, noting applicability to excitation functions

03 p0338 A72-13791
Liapunov stability of rigorous particular solutions /corresponding to libration points/ of three body

problem, determining motions of satellite influenced by two spherical bodies

03 p0436 A72-13823
Finite time motion stability of systems with small parameter, using method of averaging and matching principle

03 p0390 A72-13910
Solution stability of linear differential equations systems with harmonic coefficients, using Jordan canonical forms and perturbation method

03 p0382 A72-13918
Soviet book on linear automatic control systems with variable parameters covering pulse transfer function determination algorithms, signal transmission characteristics and systems stability

03 p0339 A72-14245
Nonlinear oscillations stochastic instability in dynamic systems, discussing nonequilibrium statistical mechanics

03 p0390 A72-14316
Linear nongyroscopic conservative system stability from modified Lagrange equations of motion, using pseudo degree of freedom concepts and vibration method

03 p0362 A72-14394
Nonconservative stability problems, obtaining eigenvalues with adjoint variational methods [AD-742170]

04 p0583 A72-14446
Stability conditions for direct control systems in critical case, assuming pair of imaginary conjugated and zero characteristic numbers

04 p0538 A72-14623
Plane periodic oscillations of solid body on elliptic orbit, characterizing stability of motion equations periodic solutions

04 p0582 A72-14632
Closed-loop nonlinear sampled-data systems with sampler and finite Hankel transformable distributed elements, deriving frequency domain stability criteria

04 p0504 A72-14662
Nonlinear stochastic systems stability conditions description by Volterra integral equation, applying to distributed parameter feedback control system with nonlinear amplifier of random gain

04 p0504 A72-14663
Liapunov functionals synthesis for continuous system stability study, discussing linear combinations of moments of governing partial differential operators

04 p0538 A72-14671
Unsteady radial flow between fixed and oscillating walls, obtaining flow equations and air bearings stability conditions

04 p0511 A72-14970
Telemetry systems with discrete compression-expansion function, calculating noise stability improvement as compared to linear and nonlinear signal conversion operations

04 p0487 A72-15000
Self oscillating system stability under parametric excitation and harmonic force for large and small natural frequency mismatch

04 p0549 A72-15046
Time-varying systems with observer for feedback control, investigating stability

04 p0506 A72-15108
Numerical instability of gravitational n-body problem considering differences between computed systems and exact solutions to differential equations

04 p0581 A72-15629
Multiple-input multiple-output linear time invariant feedback systems stability, investigating continuous-time case

04 p0507 A72-15694
Stability-instability criterion of time varying linear systems, using canonical form of differential equations [ASME PAPER 71-WA/AUT-20]

05 p0682 A72-15953
Dynamic systems stability under periodic impulsive parametric excitation, deriving simple closed-form analytic stability criteria for special cases from general theory [ASME PAPER 71-WA/APM-19]

05 p0733 A72-15961
Continuous media stationary motion stability using initial boundary value problem of partial differential equations in perturbations [ASME PAPER 71-WA/APM-17]

05 p0647 A72-15963
Encounterless one-dimensional constant density self gravitating system stability for symmetric disturbances, using analytic treatment and computer experiments

05 p0713 A72-16054
Stability characteristics of finite difference schemes based on lumped-parameter model and numerical integrator for wave propagation in continuous media

05 p0735 A72-16081
Structure, controllability and synthesis of n-dimensional invariant systems under perturbation vector, using governing equations

05 p0641 A72-16352
Stability-instability zones of solutions of Whittaker equation in vibration theory

05 p0690 A72-16353

Relay systems stability in orientation control of flexible satellites

05 p0725 A72-16439
Three dimensional global spacecraft attitude control system analytical design technique based on system stability considerations

05 p0726 A72-16457
Existence and bifurcation conditions of singular point consisting of spliced focus spliced out of ordinary trajectories, investigating stability

05 p0690 A72-16593
Liapunov direct method based approaches to hybrid dynamical systems stability, applying to attitude stability of flexible earth pointing satellite [AIAA PAPER 72-18]

05 p0729 A72-16867
Linear time-varying control systems with one feedback nonlinearity, determining combined time-frequency condition for stability

05 p0642 A72-17090
Tunnel diode amplifier stability under parameter variation due to fabrication tolerances, aging, heating, etc

05 p0638 A72-17189
On-off control system stability with feedback proportional to square of velocity, determining system frequency response

06 p0793 A72-17316
Higher order nonlinear autonomous oscillation system limit cycle and stability determination by numerical solution based on Andronov point transformation and Liapunov theory

06 p0838 A72-17377
Necessary and sufficient equilibrium stability conditions for differential equations systems with quasi-homogeneous right sides

06 p0838 A72-17382
Triangular points linear stability in elliptic restricted three body problem, determining exponents by convergent iteration method

06 p0878 A72-17664
Star cluster stability in form of Einstein model of rotating spherically symmetrical mass system, using Newton approximation

06 p0883 A72-18018
Transit instrument system year-to-year stability in astronomical time determination, considering seasonal wave causes and star coordinate errors

06 p0885 A72-18037
Frequency criterion of weak instability in nonlinear control systems

06 p0794 A72-18304
Stochastic optimal control for operations of plants with pure lag and two point estimate of performance index investigating systems stability

06 p0795 A72-18662
Forced vibrations and stability of one degree of freedom system with damping proportional to velocity, determining amplitude and phase resonance curves

06 p0901 A72-18710
Stability analysis of steady control systems acted upon by random signal in single valued one dimensional nonlinearity form, using statistical linearization

07 p0959 A72-18989
Book on asymptotic behavior and stability in ordinary differential equations covering linear and nonlinear systems, Liapunov and analytical-topological methods

07 p1026 A72-19184
Light amplifier steady state pulse local instability against amplitude perturbations in absence of relaxation or inhomogeneous broadening

07 p1002 A72-19204
Hyperstable algorithm for multiinput and output systems identification through equation error method, representing scheme as equivalent time varying nonlinear feedback system

07 p1027 A72-19290
Singular perturbation of absolute stability of Lure-Postnikov nonlinear systems described by differential equations with small parameters at higher derivatives

07 p1027 A72-19293
Closed system equilibrium correlation functions relationships based on total momentum conservation, discussing application to solids or liquids electrical conductivity via nuclei dynamics

07 p1035 A72-19669
Absolute stability region of linear portion of single loop automatic control system with one nonlinear element determined by frequency criteria

07 p0963 A72-19898
Reduction principle validity in perturbed motion stability theory for near-critical systems with gyro horizon application

07 p1035 A72-19972
Asymptotic method applications to differential equations solution construction and stability analysis and to stochastic systems

07 p1028 A72-20206
Stability requirement of gyro systems in generalized Thomson-Tait theory

07 p0989 A72-20277
Minimum dimensionality determination for control process stabilizing linear mechanical system equilibrium position, obtaining necessary and sufficient conditions

07 p1036 A72-20320

Control system stability with nonlinear feedback in steady equilibrium state 07 p0963 A72-20321

Stability and local error of difference formulas derived from characteristic polynomial for first order ordinary differential equation solution 07 p1028 A72-20472

F region electron-ion gas dynamic model with stability dependence on periodic solutions convergence of continuity equations 08 p1153 A72-20725

Convergence and stability criteria of monotonic difference schemes for linear parabolic differential equations with interface boundary conditions 08 p1199 A72-21286

Nonlinear differential equations system stability conditions for arbitrary initial perturbations of zero solution, using Liapunov functions 08 p1199 A72-21461

Small perturbation stability of discontinuous solution of equations of motion for solid fuel combustion processes 08 p1253 A72-21463

Linear system oscillations and stability under random disturbances, using Laplace transform and Sh-tokalo method 08 p1146 A72-21730

Electroluminescent image converter with positive optical feedback, investigating steady state bistable operation mode stability 08 p1143 A72-21947

Hydraulic actuator servomechanism performance dependence on asymmetrical spool valve lap and closed loop system stability 08 p1113 A72-22153

Stability solutions of collective oscillations of spherical star cluster rotating in near circular orbits in self consistent field 08 p1239 A72-22180

Asymptotic motion stability for part of periodic and continuous systems variables, deriving solution uniqueness sufficient conditions 09 p1350 A72-22206

Potential noise stability of wideband communications systems during discrete signal reception on combined background of quasi-white noise and spectrally lumped interference 09 p1277 A72-22569

Mechanical system with inertial vibration sensor and nonlinear spring, obtaining global asymptotic stability of zero solution of differential equations describing natural vibration 09 p1399 A72-22697

Pod-mounted jet engine follower force instability, analyzing two degrees of freedom system dynamics 09 p1374 A72-22938

Stability analysis of composite systems, applying scalar and vector Liapunov function approach to specific examples 09 p1290 A72-23091

Linear multivariable system stabilization by output feedback technique based on gradient approach 09 p1290 A72-23097

Hyperstability conditions generalization for model reference adaptive systems, using positive definite kernels properties 09 p1290 A72-23098

Difference equation inequalities in sampled data system stability analysis, discussing solution asymptotic behavior 09 p1342 A72-23252

Stability degree analysis of linear feedback control systems with dead time, presenting proportional and integral compensation diagrams produced with digital computer program 09 p1291 A72-23370

Liapunov theory solutions stability for oscillations along galactic axis of symmetry 09 p1390 A72-23396

Motion stability of linear discrete deterministic and random systems over finite time interval 09 p1291 A72-23428

Liapunov functional stability analysis in structural dynamics problems including wave equations with nonlinear damping 09 p1407 A72-23457

Differential equations solutions stability for physical discrete systems with delayed argument, impact excitation, variable mass or structure, disturbances or weak couplings 09 p1343 A72-23601

Dynamic systems stability problems, differential equations linearization and random processes 09 p1343 A72-23603

Hartman-Olech theorem to prove asymptotic stability of mechanical system with nonlinear elastic characteristic, analyzing differential equations of motion 09 p1343 A72-23612

Computer aided design of linear time-invariant multivariable feedback control systems, given specifications in frequency domain in stability margin form 10 p1455 A72-23789

Stability criteria for continuous dynamic system under parametric excitation derived by Liapunov

direct method, using time dependent functionals and Rayleigh operators quotients 10 p1510 A72-24187

Upper bounds on lumped and continuous dynamic systems motion under loads and perturbations, discussing structure stability conditions 10 p1554 A72-24188

Perturbation method for stability boundaries of Hill equation with three independent parameters 10 p1505 A72-24190

Predictor-corrector method for stiff linear differential equations, considering truncation error estimation and system stability 11 p1675 A72-25272

Discrete time systems with periodic feedback gain, deriving stability conditions and Nyquist plot from linear operator spectral theory 11 p1608 A72-25318

Input-output stability of linear time invariant multivariable closed loop control systems 11 p1608 A72-25327

Structure, controllability and synthesis of n-dimensional invariant systems under perturbation vector, using governing equations 11 p1608 A72-25328

Stability-instability zones of solutions of Whittaker equation in vibration theory 11 p1685 A72-25334

Absolute stability conditions of zero solution for PAM automatic control systems equations in terms of transfer function 11 p1609 A72-25446

Extremal feedback control system operation with integral PFM in extremum drift mode, determining equations of motion and steady state regime 11 p1610 A72-25449

Asymptotic stability of astatic pulse frequency modulated feedback control systems with discrete correction, obtaining sufficient conditions in closed form with Liapunov method 11 p1610 A72-25450

Pump and unloading valve hydraulic system model with waves processes allowance in connecting pipe, discussing liquid mass and leakage effects on stability 11 p1578 A72-25770

Stiffly stable implicit linear multistep algorithm for deriving stability properties from extended complex plane transformation 11 p1677 A72-25860

Numerical stability in linear algebraic equations, considering mapping from input data to desired output information 11 p1677 A72-25861

Equilibrium stability of hyperelastic bodies under finite strain, deriving differential equations and boundary conditions of critical equilibrium states 11 p1686 A72-25916

Star cluster stability in form of Einstein model of rotating spherically symmetrical mass system, using Newton approximation 11 p1718 A72-25954

Transit instrument system year-to-year stability in astronomical time determination, considering seasonal wave causes and star coordinate errors 11 p1719 A72-25973

Linearization and Liapunov stability analysis of nongyroscopic holonomic conservative dynamic differential equations system 11 p1677 A72-25979

Self balanced microwave static calorimeter with substantial delay time, discussing system instability conditions 11 p1634 A72-26450

Closed loop system stability, considering small gain and passivity theorems interrelationship and scattering matrix 11 p1612 A72-26470

Design analysis of emitter- and collector-base gain stabilized junction transistor amplifier at elevated temperatures using passive elements 11 p1606 A72-26569

Random Fredholm and Volterra integral equations applied to stochastic systems, investigating absolute stability concept 11 p1679 A72-26780

Triple stellar system evolution and disintegration, discussing energy partitioning and initial velocity effects on stability 12 p1865 A72-27095

Natural vibration modes of coupled spring-mass nonlinear system with two degrees of freedom from stability analysis 12 p1844 A72-27245

Holographic recording systems stabilization with intermittent exposure control for interference patterns fidelity 12 p1806 A72-27263

Approximation for mechanical system equilibrium perturbation anharmonic analysis based on Fourier series with real multiplication factors of fundamental pulsation 12 p1845 A72-27542

Antoniou bridge type gyrator circuit stability, showing sensitivity to resistors ratio variations 12 p1792 A72-27698

Steady bifurcating time periodic solutions stability for flows in bounded domain with complex conjugate simple eigenvalues at critical Reynolds number 12 p1837 A72-27712

Asymptotic stability of mechanical system with two mathematical pendulums and rod subjected to axial follower, correcting aerodynamic and dissipative forces 12 p1847 A72-27979

Binary logic circuits with interconnected repeaters and inverters, discussing signal level selection to ensure maximum noise stability 12 p1786 A72-28120

Limiting stability cases of vehicle with linear attitude control and pointed at star by two power gyroscopes in conical suspensions 13 p2051 A72-28383

Analytical solution to difference stability equations evaluating adequacy of difference scheme for circular cylindrical shell and rectangular hinged plate under compression 13 p2053 A72-28389

Time constant limited stability of numerical integration procedures for systems of kinetic equations, examining causes and effects of stiffness 13 p1985 A72-28419

Single frequency generation stability of one dimensional model of traveling wave laser using inhomogeneously broadened active material 13 p1967 A72-28470

Equilibrium state stability in elastic conservative system, relating system postbuckling behavior to critical branching point 13 p2054 A72-28478

Stability and oscillation in linear and nonlinear systems, examining existence of T-periodic solutions/harmonic forced vibrations/ 13 p2000 A72-28484

Reliability and stochastic stability theory relationships for multidimensional and continuous systems 13 p1985 A72-28486

Popov frequency criterion analog for stochastic nonlinear continuous systems with random parameters and disturbances, investigating stability 13 p1935 A72-28608

Suboptimal controls of linear multidimensional plants with variable parameters, considering asymptotic stability 13 p1935 A72-28609

Control parameters required for stabilization of motion in systems with nonholonomic couplings by dynamic programming method of summary representations 13 p2003 A72-29068

Associated system instability related to difficulties encountered in maximum principle application to optimization problems solution 13 p2003 A72-29069

Homogeneous difference schemes stability for ordinary differential equation of arbitrary order with discontinuous coefficients, analyzing positive definite operators class 13 p1986 A72-29076

Coefficient stability of homogeneous difference schemes using irregular networks for fourth order differential equation with discontinuous coefficients 13 p1986 A72-29087

Liapunov functions and integral inequalities for study of finite time stability of motion, noting small parameter system subjected to continuous disturbances 13 p2004 A72-29496

Kalman filter stability analysis by mathematical modeling, using floating point computer algorithm 13 p1934 A72-30006

Frequency criterion of weak instability in nonlinear control systems 13 p1937 A72-30072

Hydraulic servosystem performance analysis, determining transfer function for time variant input-output relationship, gain levels and stability assurance 14 p2073 A72-30420

Second order moments of system with parametric excitation by filtered white noise calculated with Fokker-Planck equation, giving condition for mean-square-stability 14 p2131 A72-30711

Ferroresonant circuit with inductor, resistor, nonlinear ferrocapacitor and voltage source, deriving oscillation stability condition 14 p2090 A72-31119

Periodic two-parameter solution families of dynamic systems having first integral, showing stability and bifurcation existence criteria relationships to dimensionality and Hamiltonian systems 15 p2261 A72-31309

Spectral stability characteristics of difference schemes for hyperbolic differential equations in gas dynamics involving triangular and tetragonal bases 15 p2178 A72-31444

Instability regions of vibratory system with two degrees of freedom under random parametric effect, calculating bounds by numerical and analytical methods 15 p2275 A72-31608

- Numerical integration of equations of motion in finite element methods, investigating explicit methods stability 15 p2326 A72-31717
- Linear autonomous differential equations finite time stability theory, extending to systems driven by white noise 15 p2264 A72-31764
- Conical scanning system for Pioneer Jupiter spacecraft pointing control, discussing signal processor, spacecraft dynamic behavior, system stability and error budget 15 p2320 A72-31791
- Multidimensional asynchronous FM pulse systems stability, considering continuous linear part transmission matrix poles located on imaginary axis 15 p2212 A72-32172
- Saturating nonlinear feedback systems stability under bounded input excitation, discussing error signals magnitude and duration 15 p2212 A72-32246
- Quasi-optical transmission line stability improvement, investigating pulsating light beam concept 15 p2202 A72-32663
- Limit cycle stability of third and higher order feedback systems predicted from negative slope of describing function 15 p2213 A72-32796
- Liapunov functions for nonlinear autonomous difference equations stability analysis, defining difference gradient, principal sum and definite sum 15 p2265 A72-32802
- Negative resistance devices, stability under open and short circuits from dc I-V characteristic shape 16 p2368 A72-32857
- Mechanical system nonlinear perturbation effect on equations of motion solutions, deriving boundedness and stability conditions via inequality theorems 16 p2423 A72-33101
- Nonparametric probability density function modeling algorithms comparison for convergence rate and limit cycle stability relative to implementation ease 16 p2367 A72-33867
- Thermoemission ion gage stability and design aspects, discussing application as secondary standard for vacuum measurements 16 p2394 A72-33871
- The numerical solution of hyperbolic systems using bicharacteristics. 17 p2574 A72-34449
- Nonlinear system consisting of gas filled tube with pressure sensitive heat source, noting oscillation evolution due to equilibrium perturbation [ASME PAPER 72-APM-21] 17 p2580 A72-34796
- Comparison principle and finite time stability of control systems. 17 p2581 A72-35052
- Transmission line with feedback, deriving Nyquist stability from Michailov criterion with application to liquid fuel rocket model 17 p2621 A72-35100
- Hamiltonian system evolutionary stability via area preserving mapping, using Bartlett eigenvector method 17 p2547 A72-35108
- Continuous elastic systems flutter and divergence instability under nonconservative loading, determining slopes of loading-frequency curves 17 p2633 A72-35255
- On the stability of axisymmetric systems to axisymmetric perturbations in general relativity. I - The equations governing nonstationary, stationary, and perturbed systems. 17 p2611 A72-35315
- Absolute stability analysis of attitude control systems for large boosters. 17 p2622 A72-35489
- Stability and transient behavior of composite nonlinear systems. 17 p2534 A72-35530
- Equivalent predictions of the circle criterion and an optimum quadratic form for a second-order system 17 p2577 A72-35534
- Stability of linear time-invariant distributed parameter single-loop feedback systems. 17 p2534 A72-35535
- Lyapunov functionals for a class of delay-differential systems. 18 p2709 A72-36052
- Feedback controller synthesis from nonlinear system modeling by linear equations, proving theorem relating stability properties 18 p2672 A72-36060
- Stability solutions of collective oscillations of spherical star cluster rotating in near circular orbits in self consistent field 18 p2724 A72-36236
- Russian book - Introduction to the theory of stability of motion 18 p2711 A72-36523
- Linear homogeneous system of differential equations as model for perturbation problems including functions with retarded and/or advanced arguments 18 p2705 A72-36614
- A-stable, accurate averaging of multistep methods for stiff differential equations. 18 p2705 A72-37019
- Trajectories behavior and finite time stability of differential equations system, using Liapunov techniques 19 p2833 A72-37375
- Complex systems dynamics and stability problems, deriving equations of motion and boundary conditions from principle of least action 19 p2784 A72-37388
- Extension of the frequency-type unconditional stability criterion of controlled systems with one nonlinear nonstationary element 19 p2777 A72-37431
- Stability of nonlinear automatic systems with double pulse modulation, discussing systems with linear and nonlinear pulse elements 19 p2777 A72-37435
- Stability of linear systems with constraint damping and integrals of the motion. 19 p2856 A72-37519
- Existence and bifurcation conditions of singular point consisting of focus fused from ordinary trajectories, investigating dynamic system stability 19 p2834 A72-37565
- Model reference adaptive control systems design based on optimal control, parametric optimization, stability and statistical estimation theory 19 p2778 A72-37722
- A circle criterion for nonlinear stochastic feedback systems. 19 p2779 A72-38235
- Variable stability simulation techniques for nonlinear, rate dependent systems. 19 p2780 A72-38241
- Distributed parameter linear and nonlinear systems analysis, deriving theorem for solution stability of linear partial differential equations 19 p2826 A72-38247
- Hyperstability concepts and their application to discrete control systems. 19 p2780 A72-38248
- A stability theory for perturbed difference equations. 19 p2826 A72-38249
- Control theory stability criteria applied to discrete time feedback systems, investigating numerical integration methods for initial value problems solution 19 p2826 A72-38250
- Recent results concerning a graphical test for checking the stability of a linear time-invariant system. 19 p2826 A72-38251
- Liapunov theory application to stability analysis of large scale dynamic systems, developing methods for vector Liapunov functions construction 19 p2781 A72-38262
- Measurement transducers in industrial process control, discussing requirements for dynamic properties, stability, linearity and computer applications 19 p2803 A72-38315
- F region electron-ion gas dynamic model with stability dependence on continuity equations periodic solutions convergence 19 p2791 A72-38353
- Study of the stability of a polar coordinate compensator 19 p2783 A72-38581
- Binary logic circuits with interconnected repeaters and inverters, discussing signal level selection to ensure maximum noise stability 19 p2767 A72-38621
- Tunnel diode amplifier stability under parameter variation due to fabrication tolerances, aging, heating, etc 19 p2775 A72-38625
- Nonlinear system described by three generalized coordinates, noting dynamic response stability equivalence to two degrees of freedom system 20 p2953 A72-39553
- A theorem of the Liapunov theorem type for the stability of a multidimensional system 20 p2954 A72-39866
- HCN laser mechanical, pressure, temperature and voltage environmental factors effects on output power stability 20 p2934 A72-39967
- Reduction principle validity in perturbed motion stability theory for near-critical systems with gyro horizon application 20 p2955 A72-40029
- Instability conditions for holonomic system with stationary constraints, applying to pendulum and to rectilinear motion of material point 20 p2955 A72-40033
- Numerical solution of quasi-conservative hyperbolic systems - The cylindrical shock problem. 21 p3043 A72-40101
- Stable current-to-frequency converter with continuous integration of analog input signal providing digital output suitable for input to scaler 21 p2996 A72-40207
- Using the quasi-homogeneity of differential equations in modeling physical systems 21 p3083 A72-40377
- Bounded-input bounded-output stability of nonlinear discrete systems by a method of comparison 21 p3037 A72-40645
- Geometric criterion for the design of a non-oscillatory dynamical system. 21 p3037 A72-40647
- Linear equilibrium stability relationship to wave propagation through elastic medium, considering Hadamard theorem proofs 21 p3085 A72-41102
- Avalanche transistor circuit with controlled S shaped I-V characteristics, discussing equivalent circuits and operating points stability 21 p3034 A72-41119
- Elastic conservative structural systems stability with many degrees of freedom, discussing critical singular points effect 21 p3120 A72-41206
- Instability of the equilibrium position of a multidimensional system consisting of 'neutrally' unstable subsystems 21 p3126 A72-41546
- Inductive frequency converter with a characteristic having enhanced linearity 21 p3058 A72-41802
- Stabilities and settling times of nonlinear and time-varying feedback systems. 22 p3161 A72-41937
- Multidimensional asynchronous FM sampled data systems stability, considering continuous linear part transfer matrix poles located on imaginary axis 22 p3162 A72-42080
- Construction of Liapunov functions for time-dependent systems containing inertialess nonlinearities 22 p3205 A72-42176
- Global asymptotic stability of two classes of control system with pulse-width and pulse-frequency modulation 22 p3162 A72-42184
- Double water-bag model stability for plane one dimensional stellar system, computing eigenfrequencies and eigenfunctions 22 p3224 A72-42384
- On the stability of axisymmetric systems to axisymmetric perturbations in general relativity. II - A criterion for the onset of instability in uniformly rotating configurations and the frequency of the fundamental mode in case of slow rotation. 22 p3206 A72-42566
- On the perturbation method in the stability analysis of continuous systems. 22 p3206 A72-42842
- Reduction principle application to solution stability of system of differential equations in critical cases, noting instability of free gyroscope in gimbal suspension 23 p3287 A72-43416
- Decision surface estimate of nonlinear system stability domain by Lie series method. 23 p3274 A72-43540
- Singular small parameter perturbation effect on absolute stability of high order derivatives in Lure-Postnikov nonlinear systems 23 p3274 A72-43544
- Stability bounds for nonlinear systems designed via frequency domain stability criteria. [ASME PAPER 72-AUT-L] 23 p3275 A72-43636
- Asymptotic behavior of solutions of systems of conservative differential equations 23 p3308 A72-43693
- A method for partitioning the phase space into regions with constant-sign increments of phase coordinates 23 p3275 A72-43780
- Sufficient condition formulation for Lure type nonlinear continuous control system exponential absolute stability 23 p3309 A72-43854
- Regions of absolute ultimate boundedness for discrete-time systems. 23 p3309 A72-43857
- Nonlinear nonautonomous dynamic systems practical stability conditions for specified settling time, verifying constant matrix Hurwitz property 23 p3309 A72-43858
- Linear inequalities and P matrices, with applications to stability of nonlinear systems. 23 p3309 A72-43859
- Recent results in convolution feedback systems. 23 p3276 A72-43861
- Synthesis of hyperstable discrete model reference adaptive systems. 23 p3276 A72-43867
- Laser radiation geometric divergence and variation of transmitted intensity with mirror transmissivity at centerline for unstable cavity viewed as oscillator-amplifier 23 p3296 A72-43902
- Approximate harmonic linearization method of stability analysis of nonlinear periodic systems, identifying fictitious oscillations due to computation errors 23 p3277 A72-44007
- Gravitational instability of perturbed and unperturbed matter distribution in form of density and

velocity fluctuations associated with continuity relationship between wavelength and rotation direction
23 p3338 A72-44036

Stabilization of the motion of certain nonlinear systems by a linear approximation
23 p3313 A72-44045

A difference method for plane problems in magnetoelectrodynamics.
[ASME PAPER 72-APM-A] 23 p3321 A72-44051

On the sufficiency of the energy criterion for the stability of certain nonconservative systems of the follower-load type.
[ASME PAPER 72-APM-E] 23 p3350 A72-44052

Stability criteria for phase-locked oscillators.
23 p3272 A72-44192

Determination and quality estimation of stability in discrete linear systems
24 p3386 A72-44722

Potential noise stability of wideband communications systems during discrete signal reception on combined background of quasi-white noise and spectrally lumped interference
24 p3379 A72-44748

On exponential-asymptotic stability properties of Boltzmann's equation and a class of its modifications.
24 p3426 A72-44911

A general theory of convergence for numerical methods.
24 p3419 A72-45300

Analytical designing of regulators for second-order nonlinear systems
24 p3387 A72-45519

Allowable regions for stability multiplier characteristics.
24 p3420 A72-45787

SYSTOLE

Extrastolic potentiation of ventricular contraction effect on dog mitral valve function, using roentgen videodensitometry
01 p0015 A72-11036

Canine and human ventricular myocardium microelectrophysiologic studies of postextrastolic T wave change relation to cellular repolarization and contractile potentiation magnitude
02 p0157 A72-11474

Beta-adrenergic and vagal blockage altered autonomous control effects on left ventricular function in conscious dogs, noting heart rate, stroke volume and end-diastolic and end-systolic diameters
02 p0163 A72-12090

Single linear measure of systolic pressure gradient for calculation of aortic valve area in stenosis severity assessment
12 p1762 A72-27734

Determination of systolic time intervals using the apex cardiogram and its first derivative.
19 p2759 A72-38817

Factors limiting the increase in stroke volume obtainable by positive inotropism - Investigations regarding the sufficient heart in the case of continued postextrastolic potentiation
22 p3145 A72-42748

SYSTOLIC PRESSURE

If subaudible chest wall vibration recordings, discussing external, epicardial surface and intraventricular pressure precordial displacement tracings
01 p0017 A72-10120

Automated constant cuff-pressure system to measure average systolic and diastolic blood pressure in man.
17 p2507 A72-34298

T

T TAIL SURFACES

Dynamic aspects of Fokker F-28 aircraft design.
22 p3138 A72-42831

T TAURI STARS

T Tauri type variable stars spectral features relation to evolutionary sequences, noting stellar atmosphere nonthermal equilibrium plasma region effects
10 p1549 A72-25056

T-2 AIRCRAFT

Mitsubishi T-2 two-place supersonic trainer, describing prototype airframe and propulsion system design and operational features
07 p0913 A72-20306

Supercritical thick wing for structural weight reduction and increased cruise speeds flight tested on Navy T2-C aircraft.
[SAE PAPER 720320] 11 p1576 A72-25583

T-33 AIRCRAFT

Flight test of direct side force control by rudder deflection and asymmetrical drag on T-33 airplane, noting use in dive bombing
12 p1754 A72-27520

Flight experiments to determine horizontal visual restriction effects on T-33 aircraft front cockpit during approaches and landings
15 p2180 A72-31697

T-53 ENGINE

Portable self contained ultrasonic field inspection equipment for nondestructive crack detection in T53 gas turbine compressor disks
01 p0076 A72-10814

Metallographic and fractographic analyses of cracking in T53-L13 gas turbine engine compressor disks
01 p0085 A72-10816

T-63 ENGINE

T63/250 engine program current status, covering turboshaft helicopter engine and fixed wing aircraft powerplant models and applications
[SAE PAPER 720350] 11 p1703 A72-25601

TABLES [DATA]

NT MATHEMATICAL TABLES

Chemical analysis of iron meteorites, tabulating Ni, Co, P and C content
01 p0126 A72-10108

RR Lyrae variables intermediate band photometry, tabulating magnitudes and color of 125 stars
01 p0133 A72-11129

International frequency allocation table revision by World Administrative Radio Conference for Space Telecommunications
02 p0177 A72-12385

Minor planet Eros photographic observations by long-focus refracting telescopes and Ross cameras at various Yale observatories, tabulating ephemerides [AD-737017] 02 p0286 A72-12894

Plane and conical shock waves, presenting graphs and tables for numerical applications
03 p0341 A72-13684

Meteor spectrum analysis, presenting tables for Soviet observations
03 p0438 A72-13979

Earth nutation tables, comparing precession-nutations and tidal potential
04 p0575 A72-15031

Planetary mass determination tables, presenting mass inverse value in constants system with international ephemerides
04 p0575 A72-15032

Photoelectric observations in different colors of eclipsing variable TX Cancri, presenting tables
05 p0723 A72-17199

Niobium carbide thermodynamic properties tabulated for 0-3000 K, deriving equation for heat capacity from low temperature experiments
06 p0832 A72-18430

Observational parameters of 61 pulsars, tabulating names, right ascension and declination, galactic longitude and latitude and period and dispersion measures
08 p1233 A72-21179

Tabulation of calculated rotational line intensities relative to integrated vibration-rotation band intensity for various electron transitions of nitrous oxide
09 p1276 A72-22665

Tago-Sato-Kosako comet positions determination from plates obtained with photographic telescope, tabulating averaged spherical coordinates
09 p1389 A72-23068

Radio emission variations of eclipsing binary stars beta Persei and beta Lyrae tabulated
10 p1547 A72-24946

Atmospheric metal ion chemistry, tabulating thermal energy binary and three body reaction rate data
10 p1434 A72-25160

Experimental data on twin vortices formed behind impulsively started or uniformly accelerated circular cylinders
11 p1572 A72-26375

Lunar transient phenomena during 1540-1970, tabulating observation reports
15 p2312 A72-32093

Tabulation of diatomic molecular lines observed in sunspot spectra with rotation branch, quantum number and vibration band
15 p2316 A72-32750

Jupiter Red Spot position determinations by East German observers tabulated
16 p2456 A72-33496

Liquid metals thermodynamic properties tabulation, including high melting transition metals, based on levitation data and periodic table correlations
16 p2479 A72-34000

Book - Angular scattering functions for spheroids
17 p2582 A72-35457

Some new Dy II identifications in the solar spectrum.
17 p2616 A72-35696

Period changes in eclipsing variables. II - The system VW Cephei.
18 p2723 A72-36084

Tabulation of physical conditions in proton and non-proton solar flares from observations and H alpha line width measurements
19 p2851 A72-37815

Positions of the major planets and the moon observed at the 0.33 M photographic equatorial
19 p2858 A72-37856

Table for reduction of stellar radial velocities to the center of the sun
19 p2859 A72-37909

Novae and background stars relative proper motions, deriving and tabulating absolute proper motion via statistical transformation
19 p2860 A72-37977

A tabulation of pulsar observations.
20 p2969 A72-39399

Mathematical determination of decibel-loudness index, tables for various frequencies.
20 p2956 A72-40077

Spectrum of P Cygni in 1968-1969.
21 p3110 A72-41444

Mesospheric noctilucent clouds tables listing weather stations geographical coordinates, observation time periods, elevation above northern horizon and azimuth
22 p3173 A72-42575

Magnetism of meteorites - A review of Russian studies.
23 p3339 A72-44122

Minerals discovered in meteorites, tabulating formula and occurrence and plagioclase composition
23 p3262 A72-44133

Observations of minor planets at the Crimean Astrophysical Observatory AN SSSR. XVIII
24 p3437 A72-44766

TACAN

Tactical ATC display system for airport surveillance, precision approach and landing and operator/aircraft/machine operations by using terminal Area Surveillance Radar
02 p0230 A72-12422

VOR, Direct Measuring Equipment and TACAN polar coordinate radio navigation systems history, improvements and future development
02 p0257 A72-12644

Operational requirements for VORTAC system improvements, including precision VOR, navigation, broadcast, DME capacity and CAS signal synchronization
06 p0845 A72-17330

Integrated inertial-VOR-DME or inertial-TACAN navigation system, presenting slant range and bearing adjustment procedure via least squares method
16 p2421 A72-34130

TACHISTOSCOPES

Selective attention and short term memory encoding, using tachistoscopic visual display arrangements of capital letters
02 p0166 A72-11544

Perception of tachistoscopic binary patterns, examining reproduction accuracy with respect to pattern length and fixation and end-segregation reference points
18 p2653 A72-36914

TACHOMETERS

Sounding rockets spin rate sensor, describing apparatus operation and size and weight reduction
01 p0071 A72-11112

High resolution angular velocity measurement by high speed digital transducer feeding photosensor pick-up pulses into pulse shaping circuit
14 p2103 A72-30199

TACHYCARDIA

Paroxysmal supraventricular tachycardia initiated by sinus beats in patient, observing A-V nodal conduction delay by ECG and electrophysiological methods
02 p0156 A72-11422

Bainbridge reflex mechanism, showing sinus ganglion role in tachycardia onset
02 p0165 A72-12514

Tachycardia role in coronary vascular bed hemodynamic response to severe exercise in dogs
10 p1426 A72-24488

Aortic regurgitation variation with respiratory sinus arrhythmia and respiratory cycle in dogs during tachycardia and bradycardia
22 p3151 A72-42674

TACHYONS

Tachyon generation of gravitational radiation analogous to Cerenkov emission of electromagnetic radiation
05 p0711 A72-17160

State equation for superdense stars treated as perfect degenerate tachyon gas, noting dynamical stability for arbitrarily large central densities
18 p2726 A72-36715

TACTICAL AIR NAVIGATION

U TACAN

TACTICS

Game theoretical modeling of fighter aircraft turning tactics competition in pursuit combat, using minimax technique
[AIAA PAPER 72-950] 22 p3138 A72-42359

TACTILE DISCRIMINATION

Neural substrates of sensory tactile vision substitution for information mediation in blind subjects, using TV camera
01 p0011 A72-10470

Intervening discrete elements effects on filled duration illusion in auditory, tactual and visual presentation
01 p0014 A72-10720

Natural visual capture result of vision and touch conflict in bilateral comparisons of object length
10 p1430 A72-24270

- Visual and haptic perception in angle reproduction matching task, noting performance differences relation to nature of form discrimination and task
10 p1433 A72-25126
- Visual-tactile senses conflict experimental examination, discussing vision as dominant modality
17 p2507 A72-34249
- Meaningful shape coding for aircraft switch knobs.
17 p2510 A72-35944
- Russian book - Neurophysiological background of tactile perception.
21 p2998 A72-40464
- German book - Somatic sensitivity, smell and taste.
22 p3145 A72-42776
- Tactile information transmission for orientation and motor control, discussing somatic sensitivity peripheral mechanism
22 p3146 A72-42778
- TAGGING**
U MARKING
TAIL PLANES
U HORIZONTAL TAIL SURFACES
TAIL SURFACES
NT HORIZONTAL TAIL SURFACES
NT T TAIL SURFACES
NT TRAPEZOIDAL TAIL SURFACES
Unsteady aerodynamic loadings of flexible aircraft with nonplanar wings and wing-tail surfaces in supersonic flow
[AIAA PAPER 72-378] 11 p1574 A72-25402
Small transport aircraft horizontal tail surfaces flow characteristics determination for stress calculation during flight in turbulent atmosphere
14 p2071 A72-30284
- Problems of interference between oscillating surfaces in subsonic flow
23 p3248 A72-43809
- TAKEOFF**
NT VERTICAL TAKEOFF
Aircraft copilot assistance to pilot in flight phases, emphasizing takeoff and landing and man machine system reliability
14 p2072 A72-30815
U.S.S.R. civil aviation regulations on takeoff and landing minimum conditions for cloud ceilings and visibility range for various aircraft characteristics and equipment
14 p2129 A72-30820
Meteorological and takeoff and landing information transmission by proposed automated meteorological and information service, discussing air-ground data link
21 p3080 A72-40287
- TAKEOFF RUNS**
Atmospheric temperature and pressure altitude effects on runway lengths and aircraft takeoff weights
[ASCE PREPRINT 1242] 01 p0047 A72-10193
TU-154 lift and drag augmenting devices for takeoff and landing characteristics improvement
03 p0310 A72-13472
High performance aircraft takeoff and landing accidents, investigating survival rates
08 p1109 A72-21563
Buccaneer Mk 2 and F-4K Phantom takeoff and landing performance improvement due to boundary layer control by leading and trailing edge blowing
09 p1262 A72-22973
Pilot survival probabilities under various conditions of high performance aircraft takeoff and landing accidents, suggesting emergency action guidelines for pilot training
10 p1428 A72-23732
Turbulent jets effectiveness in protection of aircraft surfaces from rain, describing wind tunnel simulation of takeoff and landing
10 p1463 A72-25137
Propulsion system flexibility in V/STOL aircraft with one lift-cruise engine, discussing takeoff thrust requirements and cruise fuel consumption efficiency
[ASME PAPER 72-GT-105] 11 p1576 A72-25670
Application of electronic data processing airport analysis in airlines operations and for manufacturers.
19 p2747 A72-37277
- TAKEOFF SYSTEMS**
U AIRCRAFT LAUNCHING DEVICES
ALC
The effect of firing temperature on properties of natural steatite and pyrophyllite.
17 p2569 A72-34666
- TALKING**
NT SYLLABLES
NT WORDS [LANGUAGE]
TANDEM WING AIRCRAFT
Tail first/canard/ and tandem wing configurations for natural STOL, discussing low cost aerial work aircraft
06 p0758 A72-18285
Interference induced unsteady aerodynamic forces on tandem airfoils in subsonic flow, using two dimensional model
07 p0910 A72-20101
- TANGENTS**
Trajectory optimization problems solution with terminal state constraints using combined parallel tangents/penalty function approach
02 p0280 A72-12264
- Tangent methods for nonlinear equations iterative solution using alternate tangent and derivative values
07 p1026 A72-19039
- TANK GEOMETRY**
Nonlinear oscillations of liquids in complex geometrically shaped moving vessels, using approximation methods for boundary value problem solution in Cartesian coordinate system
06 p0802 A72-18712
Free small steady oscillations of liquid in solid tanks, considering HF modes
16 p2375 A72-32931
- TANKER SHIPS**
Photothermoelastic analysis of temperature and rupture stress in cryogenic tanker structures, using steel and plastic ship models
[ALAA PAPER 72-344] 11 p1728 A72-25373
- TANKERS**
Electrical discharge-produced explosions aboard supertankers during cleaning operation and electrostatic charging of supersonic aircraft during passage through heavy rain, noting water drop disintegration
24 p3368 A72-44979
- TANKS [CONTAINERS]**
NT CYLINDRICAL TANKS
NT FUEL TANKS
NT PROPELLANT TANKS
NT SPHERICAL TANKS
NT STORAGE TANKS
NT WING TANKS
Free oscillations of liquid masses contained in tanks, analyzing variational and Ritz methods
04 p0513 A72-15557
Coupled oscillations of inviscid homogeneous liquid with free surface under vacuum or gas filled space in elastic cylindrical container
15 p2217 A72-31472
Plastic composite container cylindrical wall fabrication by two stage procedure combining radial and cross winding of glass fiber rovings
16 p2398 A72-33305
Transient turbulent free convection in a closed container with heating at the sides only.
17 p2638 A72-35642
Transient laminar free convection in closed spherical containers.
[ASME PAPER 72-HT-37] 20 p2986 A72-39669
- TANTALUM**
Hydrogen diffusion, electron transfer and density distribution in Ta as function of temperature and field strength
02 p0242 A72-12009
V, Nb and Ta deoxidizing capability in liquid Fe from oxide phase formation identification by electronographic and X ray analyses
07 p1011 A72-19545
Ta, Nb and La superconductivity, investigating surface contamination effects on electron tunneling characteristics
09 p1367 A72-22554
Ta and W X ray spectra fine structure measurement, providing electron states density in unoccupied regions of energy bands of solids
09 p1370 A72-22842
Polymorphism in Ta vacuum condensates, observing beta-alpha phase transformation in films
09 p1329 A72-23041
Work hardening and recrystallization grain structure of sintered and electron bombardment melted Ta after annealing
11 p1644 A72-26839
Phase composition, structure and strength properties of aluminizing coatings on Ni-Al alloys, noting plasticity increase due to Ta addition
13 p1980 A72-29485
Ta thermal conductivity and electric resistance at various temperatures
13 p1981 A72-29897
Mechanical strength of interstitial solid tantalum-oxygen solutions obtained by electron beam fusion, thermal cycling and saturation as function of temperature and oxygen contents
14 p2112 A72-30163
Superconducting to normal transition field as function of temperature for Ta with thin surface layer variable density impurities
15 p2293 A72-32241
Hydrogen impregnated Ta superconducting to normal transition and M-H curves, discussing effect on impure surface layer superconducting properties
15 p2293 A72-32242
Solute quenching technique to determine hydrogen solubility in Ta to liquid He temperature, comparing with equilibrium measurements
15 p2259 A72-32640
High temperature solid-solubility limit and phase studies in the system tantalum-oxygen.
17 p2567 A72-34731
Orientation dependence of slip in tantalum single crystals.
17 p2567 A72-34748
Iridium and tantalum foils for spaceflight neutron dosimetry.
17 p2558 A72-35901
- Relation between hydrogen embrittlement and the formation of hydride in the group V transition metals.
18 p2700 A72-36578
The influence of interstitial nitrogen on the asymmetry of the yield stress of tantalum.
20 p2935 A72-39006
Experimental setup for the investigation of the spectral radiative capability of metals
22 p3175 A72-41893
Oxidation protection of tantalum and tantalum alloys at up to 1500 C
22 p3188 A72-41973
Relationship between the electrical resistivity and solute concentration in the solid solution of tantalum-hydrogen system.
24 p3412 A72-44718
Application of a field-emission microscope to the investigation of the work function of tungsten coated with a thin layer of silicon oxide and with tantalum
24 p3432 A72-44891
- TANTALUM ALLOYS**
Ta-Ra-B ternary alloy, investigating phase equilibria and isothermal cross sections with X ray analysis
03 p0374 A72-13739
Ta-Co system phase diagram from differential thermal, X ray, and microstructural analyses, determining composition, temperature, structural type and lattice constant
03 p0374 A72-13740
Ta-W-Hf alloy ultrahigh vacuum high temperature creep tests, showing deoxidation effect on creep behavior and early test stage oxygen-associated dynamic strain aging
05 p0674 A72-16392
Mo- and Ta-base refractory alloys creep tests, determining interactions between creep strength, fatigue life and strain aging by fatigue vibration application
05 p0677 A72-17111
Oxidation and hot corrosion tests of coated Ta and Ta based alloys between 800 and 1500 C in still air and in oxidizing gas stream
06 p0828 A72-17614
Electron beam welding of W-base alloy to Ta-base alloy, avoiding Re induced embrittlement by pure Mo transition piece
06 p0821 A72-17710
Phase diagram of Ta-B system by thermal, X ray and microstructural analyses
06 p0833 A72-18434
Magnetic properties, electrical resistivity and hardness of vacuum melted Ni-Fe-Ta alloys
11 p1655 A72-25512
Antioxidation coatings of Ta and Ta alloys for high temperature long term operation, emphasizing sintered molybdenum disilicide
11 p1663 A72-26840
Grain boundary network of allotropic phase change for ductility enhancement in Fe-Ta alloys
11 p1668 A72-26941
Fusion silicide protective coatings performance for Ta alloys under simulated reentry conditions, noting oxidation rate, ductile brittle bend transition temperature and mechanical properties
[ASM PAPER W 72-13.6] 12 p1835 A72-28162
W and Nb effect on Ta base alloys high temperature oxidation behavior
14 p2118 A72-30547
Ta-W-Hf alloy mechanical properties impairment from oxygen contamination, noting hafnium dioxide precipitate in reaction zone
14 p2121 A72-30769
Disilicide coated Ta-W alloy system oxidation behavior at 927-1482 C, using thermogravimetric, X ray diffraction and electron microprobe analyses
14 p2121 A72-30771
Ta alloys fusion weld ductility, discussing welding parameters, alloy components, interstitial impurities and weldment microstructure effects
15 p2244 A72-31775
Phase diagrams for W-Ta-Ti alloys at 1600 C from metallographic and X ray analysis
16 p2407 A72-33533
Solid phase reaction kinetics in zirconium beryllide alloys with Ta and Nb at 900-1400 C, noting Be diffusion effect
16 p2408 A72-33535
Precipitation reactions during tempering of Ti-Ta alloys, studying hcp and orthorhombic martensitic phases from electron microscope observations
16 p2408 A72-33619
The effect of oxygen on tantalum-sodium compatibility.
20 p2938 A72-39297
Oxidation protection of tantalum and tantalum alloys at up to 1500 C
22 p3188 A72-41973
Oxidation rate anisotropy investigation on coupon specimen of Ta-Mo alloy at 950 C
22 p3190 A72-42770
Alloying and impurity effects on mechanical and recrystallization properties of Ta obtained by arc, electron beam and zone melting
22 p3191 A72-42809

Specific-heat and magnetic measurements in superconducting Ta-Nb alloys.

23 p3323 A72-43273

TANTALUM CARBIDES

Dislocation splitting and stacking fault energy variation during plastic deformation of TaC at 2200 C, using bending tests and microscope observations [ONERA, TP NO, 1005]

05 p0670 A72-15861

Tantalum carbide specific heat and other thermodynamic properties over 0-3000 K range

05 p0672 A72-16097

Electron microscope observed dislocation splitting in bent thin tantalum carbide sheet, analyzing results in terms of strain rate law and carbon diffusion model

11 p1669 A72-26948

Structure of the energy bands of titanium, hafnium, and tantalum monocarbides

20 p2939 A72-39311

Structural and reaction kinetic characteristics of W, Ti and Ta/C-Co systems, considering solubility, surface energy, diffusion, segregation and grain growth

21 p3071 A72-41849

Enthalpy and specific heat of tantalum carbide over the temperature range from 273 to 3600 K

22 p3187 A72-41890

TANTALUM COMPOUNDS

NT TANTALUM CARBIDES

NT TANTALUM NITRIDES

NT TANTALUM OXIDES

Intercalation complexes of Lewis bases and layered tantalum and niobium disulfide superconductors, noting critical temperatures

01 p0113 A72-10018

Tungsten, molybdenum and tantalum disulfides oxidation rate determination by fluidized bed technique, calculating kinetic and diffusive processes activation energy

03 p0370 A72-13184

Sputtering sources fabrication by plasma spraying for nitride films deposition with Ta-Hf mixtures

04 p0527 A72-15494

Electro-optic KTN/potassium tantalate niobate/crystals for modulators, deflectors, phase shifters and polarization rotator devices

20 p2922 A72-39047

Investigation of tantalum-compound films at the surface of acicular tungsten microcrystals

21 p3068 A72-40964

TANTALUM NITRIDES

Thermodynamic and electrical properties of tantalum nitride powders and thin films for semiconductor IC technology

07 p1049 A72-19935

TANTALUM OXIDES

Tantalum and tungsten vanadium trinitride oxides crystallographic order ratio from diffraction spectrum intensities and overstructure lines disappearance

05 p0675 A72-16699

Stoichiometric composition, crystal structure and chemical bond variations in Ta-O system

15 p2290 A72-31197

TAPE MERGING

U DATA PROCESSING

U MAGNETIC TAPES

TAPE RECORDERS

Notch noise loading tests on predetection tape recording of FM carriers, showing noise power ratio dependence on record level and bias levels and output equalization

02 p0175 A72-12146

Multichannel high-speed high-density digital recorder, describing tape transport and signal system

02 p0187 A72-12151

High density digital tape recorder with combined phase encoded digital electronics and helical scan video transport

02 p0229 A72-12152

Long life magnetic tape recorder for onboard data storage in space flights, discussing two motor tape transport and static memories for improved reliability [IEEE PAPER 12.4]

03 p0360 A72-13767

Impulse noise reproduction for temporary threshold shift and impulse noise measurements, considering rise time, frequency response and limitations of tape recorders

04 p0521 A72-14847

Arterial pressure data recording technique using magnetic tape recorder and automatic conversion to digital form

12 p1772 A72-27649

Measuring tape recorder, properties and utilization for signal recording and processing, discussing digital computer techniques and compensation for interference effects

14 p2104 A72-30287

The use of airborne magnetic tape recorders for fatigue life monitoring.

17 p2553 A72-34812

High speed, high density digital recording.

22 p3175 A72-41933

Broadband magnetic tape predetection recording of data modulated carrier MHz radio telemetry signals, applying to Aris, Mercury and Gemini programs

24 p3385 A72-45269

TAPER

U TAPERING

TAPERED COLUMNS

Improved bounds for buckling loads of tapered elastic columns.

17 p2626 A72-34330

TAPERED WINGS

U SWEPT WINGS

TAPERING

Longitudinal stress pulse amplification during propagation along tapered elastic bars in direction of decreasing cross section

[SESA PAPER 1894]

02 p0287 A72-11504

Tapered I-beams elastic twisting and flexural-torsional buckling, considering critical loads as function of taper ratio

08 p1249 A72-21924

Tapered elastic rod transient behavior under end impact due to mass striking, computing fixed end stress, struck end velocity and impact time duration

15 p2323 A72-31404

Cantilever beam tapered linearly in horizontal and vertical planes, obtaining computer solution for free transverse vibration fundamental frequency and harmonics

15 p2328 A72-32022

Engineering approach to the design of tapered dielectric-rod and horn antennas.

17 p2530 A72-35362

Computerized numerical integration for nonlinear bending of tapered slender cantilever beams under concentrated tip loads

17 p2635 A72-35975

TAPES

Numerically controlled composite tape laying machine, discussing production run simulation, raw material quality effect and control corrective devices

12 p1815 A72-28078

TARE [DATA REDUCTION]

U DATA REDUCTION

TARGET ACQUISITION

Phase comparison direction finder with successive signals comparison using commutation of two antenna elements for target acquisition and tracking operations

02 p0176 A72-12219

MTI radar system design philosophy for target detection in land clutter environment

02 p0178 A72-12390

Clear air atmospheric target detection, comparing bistatic and monostatic radar techniques [AIAA PAPER 72-175]

05 p0630 A72-16835

Response surface methodology/RSM/ techniques application to operator target acquisition performance prediction, describing multivariable functional relationship by multiple regression polynomial equation

06 p0773 A72-17714

Pulsed coherent radar with pulse position random modulation, discussing subclutter visibility, target attenuation and blind speeds cancellation and radial speed measurement without range ambiguities

06 p0775 A72-18184

Quasi-time optimal nonlinear controller for steerable antennas or telescopes in target acquisition or slew mode, predicting performance by digital simulation

07 p0959 A72-19288

Spaceborne laser radar for target acquisition and tracking in spacecraft rendezvous and docking applications

[CLEA PAPER 9.5]

07 p0943 A72-19387

Programmed minimax target acquisition in rendezvous game between conflictively controlled motion and given set of vectors

07 p1028 A72-19969

Spurious target generation due to hard limiting in pulse compression radars with three phase coded signals superposed at input, comparing with digital simulation

08 p1134 A72-21416

Reduced data storage requirement of synthetic aperture radar for target classification by fast Fourier transform

08 p1134 A72-21422

Minimum time duration rocket interception, calculating trajectory parameters and target orbits in Earth gravitational field

09 p1393 A72-23573

Sequential analysis of statistical hypotheses in radar target detection and in communications systems

09 p1282 A72-23680

Stochastic model for eye movements during fixation on stationary target

10 p1429 A72-23795

Instantaneous frequency statistical characteristics of passive noise spectra and fluctuating signals reflected from nonpoint moving radar targets

10 p1436 A72-24514

Stochastic optimization of airborne laser seeker system design parameters to maximize target acquisition probability through regression analysis of data from computerized model

10 p1437 A72-24682

Agile beam electronically scanned multitarget phased array tracking radar, dwell allocation strategy and trajectory extrapolation algorithm effects on target handling capacity

10 p1437 A72-24685

Target angular position measurement by surveillance radar on background of correlated interference

11 p1595 A72-26294

Radar systems of effectiveness for moving target selection with alternating period compensation devices, allowing for signals and noise statistical properties

11 p1596 A72-26304

Combined probability density of amplitude and phase difference distribution of signal and noise sum in moving target selection radar systems

11 p1596 A72-26307

Passive detection radar system for bombers, calculating target distance during horizontal flight

11 p1597 A72-26314

Detection probability for moving small targets embedded in random white noise on TV display, comparing machine processed pattern recognition techniques and human performances

12 p1843 A72-27933

Circadian rhythms of visual accommodation responses and physiological correlations during target tracking, recording monocular focus state by IR optometer

12 p1767 A72-28304

Target acquisition by systems with unlagged acceleration control or rate control with exponential time lag, discussing number of approach and control stick movements

13 p1911 A72-29811

Visual acuity measurement by dynamic and statistics as function of target velocity and exposure time

13 p1911 A72-30044

Cassiopeia attitude control apparatus flight tests on Tacite rocket, describing aiming accuracy, target acquisition and gas consumption

15 p2321 A72-31824

Hypoxia and peripheral visual stimulus position effects on response time during monitoring of centrally located stimulus light

16 p2357 A72-34094

Search density function optimality for random moving target in n dimensional space with location probability density function satisfying given partial differential equation

17 p2574 A72-34344

Radar cross section fluctuation statistics description by generalized chi-square distribution, discussing target detection probabilities maximum likelihood estimates

19 p2763 A72-37734

Overall detection probability for fluctuating and nonfluctuating target models.

19 p2763 A72-37734

Discrete optimal terminal control, with application to missile guidance.

19 p2780 A72-38274

Visual optical system evaluation from viewpoint of human operator target detection under field conditions in terms of resolution, transfer functions, aberrations and eye movements

20 p2893 A72-39044

Real time homing guidance geometry and interceptor/sensor tradeoff studies based on reachable sets and target states analysis

20 p2951 A72-39104

Tactical aircraft weapon system development describing navigation, target acquisition, release point guidance and delivery modes

20 p2951 A72-39104

Programmed minimax target acquisition in rendezvous game between conflict controlled motion and given set of vectors

20 p2947 A72-40024

Intermittent movement control theory for prediction of visual correction applied to target aiming during illumination loss

22 p3142 A72-42544

Visually directed pointing as a function of target distance, direction, and available cues.

22 p3151 A72-42924

TARGET DRONE AIRCRAFT

BQM-34A and E/F target drone aircraft versatile automatic flight control system flight test program and results for basic and advanced flight modes

05 p0687 A72-16664

Unmanned systems flight testing by test bed vehicle conversion to man operated mode, discussing T-33 jet trainer conversion to drone operation

05 p0623 A72-16664

TARGET PENETRATION

U TERMINAL BALLISTICS

TARGET RECOGNITION

Atmospheric scattering and absorption effects on target/background discrimination in environmental remote sensing at 0.4-3.0 microns spectral region

02 p0213 A72-11854

Target detection in sea clutter, showing non-Rayleigh distributed high resolution radar envelope return

02 p0178 A72-12404

Target trajectory detector optimization, using data and Markovian chain apparatus

03 p0323 A72-13834

Radar signal processing by digital computer modeling, presenting apparent target splitting probability and azimuth estimate distribution for shifting window target detectors
03 p0326 A72-14361

Optimal discrimination rule for dual frequency radar targets with inadequate echo signal and background noise level parameters
05 p0625 A72-15821

Targets discovery in predetermined direction by phased array radar, using sequential analysis
09 p1278 A72-22896

Adaptive optical antenna array detection of unknown spatial location radar targets, noting tradeoff between array size and signal energy with respect to performance
10 p1434 A72-23809

Constant false alarm rate signal processors for several electromagnetic interference types, using distribution-free methods and maximum likelihood estimation in radar target detection
10 p1437 A72-24683

Target position information for radar energy potential calculation and detection quality, describing transmitter power reduction for normal range distribution density
11 p1596 A72-26313

Q switched YAG-Nd laser implementation into target designators and range finders, stressing temperature insensitive design with electronic compensation and thermal equalization
12 p1825 A72-27928

White background noise intensity effects on human visual target detection performance considering display difficulty levels, target location, detection time and error
14 p2083 A72-31156

Effect of target-background luminance contrast on binocular depth discrimination at photopic levels of illumination
17 p2508 A72-34879

The relative importance of contrast and motion in visual detection
17 p2509 A72-35689

Determining the detectability range of camouflaged targets
17 p2510 A72-35690

The tracking of targets located outside of Panum's area
17 p2505 A72-35916

Time-compressed displays for target detection
17 p2510 A72-35945

Incoherent radiation imaging system analysis from detector-display characteristics, target response function and noise characteristics
20 p2922 A72-39044

An application of atmospheric light scattering for contrast analysis in electro-optical detection systems
20 p2923 A72-39056

Automatic air targets recognition via digital radar data processing, discussing methods for noise signals suppression
21 p3081 A72-40547

Optimal search in the presence of Poisson-distributed false targets
21 p3075 A72-40837

Optimal discrimination rule for dual frequency radar targets with inadequate echo signal and background noise level parameters
23 p3263 A72-43429

Optimal search with uncertain sweep width
23 p3308 A72-43805

TARGET SIMULATORS

ERTS return beam vidicon imagery simulation, predicting resolvability of ground targets as function of target size, contrast, spectral distribution and radiance level
02 p0226 A72-11833

Target motion simulator with photographic recording of image velocity and motion compensation in cameras, discussing errors
03 p0356 A72-13226

RF simulator design for missile systems performance tests, discussing requirements, target array and anechoic chamber
20 p2911 A72-39125 [ALAA PAPER 72-861]

ARGENT THICKNESS

Triatomic hydrogen positive ions dissociation at 410, 510 and 550 keV in molecular hydrogen gas, measuring atoms yield as function of target thickness
01 p0104 A72-11148

Thick target processes during hard X ray emission, noting electron bombardment during solar flare impulsive phase and white light flare optical continuum production
21 p3100 A72-41292

TARGETS

NT PARTICLE ACCELERATOR TARGETS

NT RADAR TARGETS

Charged to neutral particle transformation capacity of wide aperture recharge target formed by supersonic gas jets in magnetic trap with annular nozzle
09 p1363 A72-23224

Multiple probe targeting from spacecraft for 1977 Venus mission, considering trajectory, spin, release, attack angle, location and navigation and control accuracy effects
15 p2312 A72-32193

The effect of target absorption on the attenuation characteristics of bremsstrahlung generated at constant medium potentials
21 p3087 A72-40474

TASK COMPLEXITY

Problem solving research, discussing trouble shooting, logic, light pattern, search, fire control, code transformation, perceptual maze and computer administered tasks
01 p0020 A72-11192

Skill acquisition in performance of three phase code transformation task
01 p0021 A72-11193

Time sharing three phase code transformation multitask effects on sustained performance
01 p0021 A72-11194

Twelve hour light-dark-dark cycle phase shift effects on monkey feeding behavior and serial task performance
02 p0157 A72-17103

Book on sustained attention (vigilance), discussing effects of signal frequency, magnitude and distribution, task complexity, noise, age, intelligence, etc
07 p0930 A72-19910

Operator mental processes during ATC task performance, discussing work load effect, mental representation and operator algorithm definition
09 p1270 A72-23129

Operator, task level and workload effects on operative strategy, showing controllers methods modification in ATC center
09 p1270 A72-23130

Time analyses of ATC approach controller tasks, developing flow diagram for task component sequencing and quantifying
09 p1271 A72-23133

ATC task analysis by subjective rating of work load, discussing information processing measures, scoring method and observer rating procedure
09 p1271 A72-23135

Acceptable load standards in ATC tasks, defining moments of conscious brain control as mental load measure
09 p1271 A72-23139

Human performance prediction dependence on task and equipment variables effects, using experimental data for performance classification system
10 p1429 A72-24003

Choice reaction task times for responses to signals by middle, little and index fingers
10 p1432 A72-24985

Multichannel information processing task complexity relation to operator performance for rapidly increasing input conditions
10 p1433 A72-25115

Vigilance performance prediction for difficulty-matched auditory and loosely and closely coupled visual intensity discrimination tasks
10 p1433 A72-25127

Work-rest scheduling and sleep loss effect on operator performance in watchkeeping and active multiple visual tasks
11 p1589 A72-26689

Workload modification effects on pilot neurological changes during Boeing 707 letdown, approach and landing
12 p1775 A72-28290

Divided attention effect localization, using choice tracking task reaction times in sequential stage model for human information processing
13 p1911 A72-29852

Time perception distortion level in simulated and real flight due to task complexity-related pilot emotional stress
14 p2078 A72-30392

High temperature and altitude combined effects on performance of tracking, monitoring and mental arithmetic complex task
14 p2083 A72-31155

Aircraft electronic display for pilot precise control in complex tasks, discussing clarity, stability and readability of CRT images
15 p2181 A72-32632

Rotary pursuit task practice effects on transfer of motor skill from slower to faster speeds
18 p2654 A72-36915

Finite Boolean function computation on sequential machine models, developing exchange inequalities between storage, time, et cetera, for relation of combinational and time complexities
24 p3383 A72-45650

TASK SEQUENCERS

U CONTROL EQUIPMENT

U SEQUENTIAL CONTROL

TASKS

NT AUDITORY TASKS

NT VISUAL TASKS

Optimal allocation of tasks and resources, using asymptotic properties of stochastic approximation method
12 p1837 A72-27823

TASTE

Human taste papillae sensitivity to chemical stimuli, showing stable quality and intensity response patterns
05 p0620 A72-17129

Taste organs neurophysiological structure and functioning, considering stimuli and excitation parameters effects on perception threshold
22 p3146 A72-42783

TAURUS CONSTELLATION

Periodicities from power spectrum analysis of light curve of RR Tauri variable
02 p0281 A72-12302

Cas A, Tau A, Cyg A and Orion Nebula absolute flux density measurements at centimeter wavelengths
04 p0578 A72-15313

Cosmos satellite measurements of high energy gamma quanta from Crab Nebula region, indicating excess flux association with Taurus constellation point source
07 p1064 A72-20636

Cassiopeia A secular flux density decrease relative to Cygnus A and Taurus A at 1.4 and 3 GHz, discussing application to antennas and radio telescopes calibration
09 p1390 A72-23529

TAXIING

Anthropotechnical aspects of aircraft taxiing guidance in airfield runway areas, suggesting computerized operational system
09 p1269 A72-22779

Deterministic optimization of aircraft undercarriage suspension characteristics for taxiing induced vibration minimization, discussing damping and stiffness functions and hybrid computer solution
09 p1407 A72-23458

ICAO standardized taxiing guidance and airports surface traffic control procedures
10 p1459 A72-24171

TAXONOMY

DNA primary structure variability relation to origin and evolution, discussing taxon scale in existing animal, plant and microorganism systems
04 p0470 A72-14792

Taxonomy for incomplete data problems, developing unified analysis methods based on maximum likelihood estimate
08 p1199 A72-21199

TAYLOR INSTABILITY

Dynamic stabilization of Rayleigh-Taylor instability at interface between two heavy fluids by viscosity and interfacial tension
01 p0108 A72-10231

Distributed impedance controller synthesis for stabilization of plane fluid flows, investigating Rayleigh-Taylor instability
01 p0050 A72-10504

Finite Larmor radius effect on Rayleigh-Taylor plasma instability in vertical magnetic field, characterizing solution by variational principle
04 p0557 A72-15022

Fluid dynamics stability of double radial sources in intergalactic medium, discussing evolution, ram pressure mechanism and Rayleigh-Taylor and Kelvin-Helmholtz effects
10 p1550 A72-25196

Larmor frequency influence on Rayleigh-Taylor instability of viscous Hall plasma with magnetic field
11 p1698 A72-26604

Rayleigh-Taylor instability in a composite medium
21 p3104 A72-40478

Rotating fluids density stratification effect on characteristic features of homogeneous Taylor column, noting flow patterns
21 p2989 A72-40652

Taylor instability in the shock layer on a Jovian atmosphere entry probe
22 p3136 A72-42873

TAYLOR SERIES

Taylor type antenna radiation distribution for aperture edge behavior realization in E or H planes
07 p0945 A72-19785

Taylor series truncation method for steady supersonic inviscid gas flow past nonaxisymmetric conical bodies
09 p1295 A72-23498

Radio propagation over slightly roughened curved earth surface, using perturbation method and Taylor series in model calculation
10 p1439 A72-24743

Methods of moments, rational transform approximation, Taylor series expansion and modulating functions used for process identification model, determining system transfer functions
11 p1607 A72-25283

Polynomial approximation of measurement signals with variability, comparing Taylor, Abdulaev and Newton formulas
15 p2235 A72-31848

A method for selection of significant terms in the assumed solution in a Rayleigh-Ritz analysis
17 p2634 A72-35408

Computer-aided vector Taylor series approximation of fundamental matrix of ordinary first order differential equations with variable coefficients

21 p0376 A72-41785

Equilibrium equation for unsteady creep of thin truncated conical shell under internal pressure, solving in successive time steps with Taylor series expansion

22 p3233 A72-42062

TAYLOR THEOREM

U TAYLOR SERIES

TD-1 SATELLITE

TD-1, HEOS-B and COS-B satellite-borne experiments, discussing X ray and gamma astronomy

04 p0582 A72-15690

TD-1 satellite mounted slow analysis camera with supervidicon image tube to observe cosmic ray tracks in spark chamber

08 p1170 A72-21961

TD-1A satellite functional description for stellar UV spectroscopy and solar and cosmic ray experiments, emphasizing attitude control subsystem

09 p1396 A72-23263

TD-1A - Europe's largest and most advanced satellite.

18 p2731 A72-37011

Early data from the ultraviolet sky-scan telescope in the TD1 satellite.

19 p2857 A72-37524

TEA LASERS

U CARBON DIOXIDE LASERS

TEACHING

U EDUCATION

TEACHING MACHINES

Instructor station design for automated flight training systems, considering human factors and informational requirements

07 p0928 A72-19277

TEAMS

Social factors of labor organization and control in scientific teams for industry

02 p0304 A72-11728

Team size and decision rule in the performance of simulated monitoring teams.

21 p3008 A72-41016

TEARING

Lamellar tearing and testing of steel sheets in direction of short side by Brodeau test

04 p0527 A72-15561

Semibrittle tears and fractures by progressive cracking in metallic structures, discussing metal fatigue and environmental stress

06 p0897 A72-18297

Tacky adhesive tearing between two flexible strips, solving Newtonian viscous fluid slow flow problem by iterative numerical scheme

12 p1798 A72-27831

TECHNIQUES

U METHODOLOGY

TECHNOLOGICAL FORECASTING

Commercial transport market and technology forecasting, considering all-cargo, STOL, SST and CTOL aircraft

[SAE PAPER 710750] 01 p0002 A72-10249
Space technology development importance for future of mankind, discussing terrestrial environment conservation, extraterrestrial raw materials recovery and power generation, etc

05 p0753 A72-16309

Technological forecasting method evaluation for R and D planning, fitting trend curves to sets of technological data

07 p1105 A72-20268

Technology transfer model in terms of donor-recipient activities for information implementation, forecasting and long range planning in developing countries and regional economics

07 p1106 A72-20271

Technology forecasting and risk assessment in V/STOL transport area, examining mission issues and selection criteria

09 p1261 A72-22473

Systems approach to technological forecasting for short range research, considering consumer, market and organizational resources

09 p1413 A72-22950

Reliability growth curves for product assessment as technical management forecasting technique

10 p1564 A72-24004

Space projects technological developments and benefits, discussing communications, transportation, computers, education, holography, power and life support systems, manufacturing in space and earth resources

11 p1748 A72-25253

Dynamic modeling application to technological forecasting, discussing mathematical simulation for R and D management planning in project selection and budget allocation

11 p1748 A72-26284

Technological forecasting and long range planning in transportation, considering roles of expert opinion, trend extrapolation, normative models and social impact

11 p1748 A72-26285

Space technology developments during 1970s and 1980s, discussing solar system exploration, space shuttle systems, cost effectiveness, international cooperation, nuclear propulsion systems, etc

13 p2051 A72-28453

Technological forecasting in venture analysis and planning for long-term growth objectives, engineering project selection and resource allocation

[ASME PAPER 72-DE-26] 14 p2174 A72-30868

Air transport development between the UK and Europe - The next twenty years.

18 p2743 A72-37092

Economic impact of applying advanced technologies to transport airplanes.

[AIAA PAPER 72-758] 19 p2751 A72-38128

Space technological advance effects on human extraterrestrial, scientific, economic and social progresses

19 p2867 A72-38545

Public policy, regulatory controls, market strategies and systems economics considerations for future U.S. domestic communication satellite system

21 p3132 A72-40865

Space shuttle technological evolution prospects, discussing cooperative development phases toward space transportation system with globally dispersed launch and landing bases

21 p3132 A72-40966

German monograph - Model-analytical investigation of short-haul air traffic with VTOL aircraft in the Federal Republic of Germany.

22 p3245 A72-43068

Forecasting as a means for scientific and technological policy control.

23 p3358 A72-44350

Economic materials processing in orbiting spacecraft under zero gravity conditions, emphasizing single crystal electronic materials and high purity biologicals

24 p3407 A72-45157

Forecasting costs and completion dates for defense research and development contracts.

24 p3468 A72-45479

TECHNOLOGIES

NT BIOTECHNOLOGY

NT MARINE TECHNOLOGY

NT MILITARY TECHNOLOGY

NT REACTOR TECHNOLOGY

Aerospace critical systems and future technologies, presenting illustrative diagram for functions combination and interrelations

14 p2175 A72-31140

Book - Treatise on materials science and technology, Volume I

18 p2718 A72-36392

TECHNOLOGY ASSESSMENT

STOL transport aircraft technology assessment, analyzing airports growth problems

[SAE PAPER 710751] 01 p0003 A72-10250
Industry assisted state of art assessment of high lift turbofan configurations for USAF STOL tactical transport technology program

[SAE PAPER 710758] 01 p0003 A72-10255
Aerospace radioisotope power systems, discussing heat source technology, shielding, safety and thermoelectric integration

[SAE AIR 1213] 01 p0098 A72-10387
Radio astronomy technology developments, discussing antennas, receivers and data processing

01 p0047 A72-10417
Battery separator materials requirements derived from in-cell environment and battery mission, evaluating present technology for R and D area concentration

03 p0313 A72-14235
National Aviation System technology, discussing wide body jets, smokeless turbofans, all-weather operational capability, collision avoidance and noise reduction

04 p0597 A72-14824

Aircraft air breathing propulsion technology, discussing two-place aircraft, turbofan power plants, helicopter engines and V/STOL, CTOL, subsonic transports and supersonic aircraft

04 p0565 A72-14825

Submillimeter waves development, discussing materials research, lasers, semiconductor and electron tube sources, system components and applications in space communication, imagery, metrology and sensing

04 p0550 A72-15591

Civil aircraft technological constraints and requirements, discussing noise, congestion and performance characteristics of rotorcraft, STOL, VTOL, hypersonic and supersonic transports

05 p0611 A72-15774

Aircraft and reusable spacecraft propulsion systems current status and future development, discussing noise and exhaust emission problems, V/STOL bypass and fan engines, ramjets, etc

05 p0705 A72-16735

Flight navigation technology current state and development trends, discussing transition from Doppler to inertial systems, use of computers and satellites, collision avoidance, etc

05 p0687 A72-16737

Rockets and spacecraft technology developments in U.S., U.S.S.R. and other nations, discussing satellite boosters, ballistic missiles, manned and unmanned spacecraft, lunar and interplanetary probes, etc

05 p0728 A72-16742

Gas dynamic laser technology advances, discussing water content, temperature and Na effects and nozzle design

[AIAA PAPER 72-143] 05 p0669 A72-16895

Materials selection problems due to wide variety of new products, discussing technologically and economically optimal decisions on product design, development and future substitutions

06 p0906 A72-18255

Technological advances and program risks assessment by operations research and systems analysis techniques, applying to cost overruns and schedule slippages in weapon systems

07 p1106 A72-20270

Holographic technique development review, discussing current and future applications and unsolved problems

09 p1315 A72-23375

Electron, ion and laser beam technology - IEEE Conference, Boulder, Colorado, May 1971

10 p1517 A72-23926

Reliability growth curves for product assessment as technical management forecasting technique

10 p1564 A72-24004

Communication satellite technology trends, discussing channel capacity, attitude stabilization, antenna pointing accuracy, energy conversion and storage, frequency reuse and onboard switching

11 p1725 A72-25254

Remotely manned systems technology for military, industrial, scientific and civil applications for hostile or difficult environments

11 p1612 A72-25256

Furnace technology review, stressing need for higher sintering temperatures, better automatic atmosphere controls and faster preforms transfer to forging operation

11 p1640 A72-26242

Ball, globe, gate, butterfly, Y-type and safety-and-relief valves assessed for cryogenic applications

11 p1642 A72-26777

Cermets technology applications, discussing powder metallurgy role and sintering mechanism

11 p1665 A72-26871

Electronic structure of technological processes in powder metallurgy of high temperature materials

11 p1646 A72-26873

Composite powders preparation by metals deposition from aqueous solution onto core materials by gaseous hydrogen at high temperature and pressure, noting coating application

11 p1646 A72-26873

Communication satellites design and technology for future launches, discussing ion engine development, antenna beams and thermal control

[AIAA PAPER 72-540] 12 p1780 A72-27363

Solid state array camera based on diffused junction phototransistors, discussing sensor technology and fabrication

12 p1810 A72-27931

Silicon solar cell fabrication technology developments for long mission life performance reliability over wide temperature and radiation intensity ranges

12 p1757 A72-28029

Cost effectiveness model for evaluating general aviation weather dissemination techniques, stressing design variables and time periods

13 p1994 A72-28871

Civil aviation approach and landing guidance systems evolution, discussing ILS development, state of art and future requirements

13 p1996 A72-29014

V/STOL aircraft potential for short haul civil air traffic, discussing present technology and investment costs in comparison with advanced ground transportation systems

13 p1898 A72-30076

Hovercraft state of development and utilization potential, comparing performance to other transportation modes

14 p2073 A72-30818

Microwave semiconductor diode technology review and development prospects in terms of fabrication processes and materials

14 p2088 A72-30834

French quality assurance of electronic components, discussing organizational links with international bodies

14 p2174 A72-30848

Adhesive and abrasive wear technology assessment, considering design equations use for prediction

[ASME PAPER 72-DE-2] 14 p2108 A72-30859

Fluid amplification principles, discussing bistable and proportional amplification, signal transmission and transduction to and from fluid signals

[ASME PAPER 72-DE-20] 14 p2073 A72-30864

Space applications benefits through international cooperation, emphasizing environmental problems

14 p2175 A72-31143

- Aeronautical communication satellite technical and economic survey, considering wave propagation, noise, aircraft antennas and VHF and UHF links 15 p2193 A72-31180
- Rare earth metals and alloys technology assessment and utilization covering quantum mechanics concepts application to Fermi surface 15 p2289 A72-31184
- Nd glass laser drilling and welding applications and tests on materials to evaluate feasibility and operational advantages, identifying optimal pulse energies and durations 15 p2244 A72-32028
- Magneto-optics materials for use in data storage, discussing quality evaluation based on figure of merit reflecting heat sensitivity and readout requirements 15 p2203 A72-32352
- Recyclable holographic recording media performance parameters comparison to develop tradeoffs for storage and imaging applications 15 p2239 A72-32360
- European unity as prerequisite for technological and scientific progress with respect to U.S. and Soviet superiority 16 p2480 A72-32893
- Metal-air batteries with alternately polarizable oxygen electrodes, discussing current state of technology 16 p2350 A72-33670
- Design features, fabrication technology and in-pile testing of thermionic reactor fuel elements 17 p2495 A72-34584
- Development of the insulating multilayer collector system for ITR /Status report/. 17 p2559 A72-34594
- Microwave technology - A five year prospective. 17 p2528 A72-34709
- Monoplastic solid encapsulant for n-p-n and p-n-p silicon planar passivated signal transistors 17 p2528 A72-34715
- International UV Explorer synchronous satellite program objectives and technology, describing spacecraft design, instrumentation, ground system, telescope control and data handling 17 p2621 A72-34900
- Helicopters technical and marketing projections for 1980s, emphasizing reliability, maintainability and maneuverability in design philosophy 17 p2491 A72-34926
- Digital methods of frequency measurement - A comparison. 17 p2530 A72-35363
- Aerospace computer software validation and verification methods application to complex systems, discussing code execution and analysis tools, program diagnostics, cost and schedules 17 p2524 A72-35582
- Composites technology, costs and performance review covering metal matrix composites, ceramic reinforced plastics and whisker composites 17 p2571 A72-35652
- Vibration technology: Balancing flexible rotors; Conference, Technische Universitaet Berlin, Berlin, West Germany, March 23, 24, 1970, Summaries 18 p2731 A72-36064
- Thermionic fuel element development status summary. 18 p2708 A72-36151
- Multicell thermionic fuel element fabrication technology. 18 p2708 A72-36152
- German book on vacuum technology covering theory, measurement techniques and applications in nuclear physics research facilities, electronic tubes, space environment simulation, mass transfer, etc 18 p2709 A72-36250
- Expendable space transportation - A 1972 assessment. [AIAA PAPER 72-732] 18 p2730 A72-36542
- Limitations in microelectronics. II - Bipolar technology. 18 p2667 A72-36980
- Polish aircraft industry production and fabrication techniques, discussing metal working, digital controlled machining and cost reduction 18 p2696 A72-37010
- Development of a complementary MOS technology of high reliability 18 p2671 A72-37142
- Advanced subsonic transport technology. 19 p2748 A72-37677
- Propulsion technology advance factors, stressing noise and exhaust emissions reduction, economic considerations and aircraft performance 19 p2848 A72-37679
- Fluidics - A potential technology for aircraft engine control. 19 p2849 A72-38047
- Fluidics control technology applications to thrust reversal, turbine engine speed, pressure valves, nozzle and fuel flow, discussing life and reliability 19 p2849 A72-38050
- B-52 test vehicle flight demonstration program for control configured vehicles /CCV/ technology concepts validation, noting gross weight reduction [AIAA PAPER 72-747] 19 p2751 A72-38123
- Satellite communications in Japan. 19 p2766 A72-38603
- Cryobiology phenomena and applications, considering mode of action of various substances for freezing injury protection 19 p2762 A72-38828
- Laser beam scanning and recording in two dimensional pattern on silver halide, evaluating systems performance based on signal response, granularity and noise characteristics 20 p2930 A72-39040
- A review of the science, technology, and applications of dispersion strengthened Ni-Cr- and Co-Cr-base alloys. 20 p2936 A72-39209
- Technology and performance of n-channel MOS-LSIs using depletion-type load elements. 20 p2961 A72-39712
- Rocks and meteorites analysis techniques evaluation, using Apollo 11 fines results to evaluate activation analysis for geochemistry and cosmochemistry applications 20 p2899 A72-39827
- Boron fiber reinforced composites technology assessment and utilization, stressing cost reduction [ICAS PAPER 72-30] 21 p2995 A72-41155
- Electron beam diameter measurement technique and welding technology review, describing experimental apparatus 22 p3183 A72-42448
- Technological aspects concerning the structural elements in the development of resistance furnaces under vacuum 22 p3163 A72-42636
- An assessment of energy absorbing devices for prospective use in aircraft impact situations. 22 p3237 A72-42764
- Niobium superconductive tunnel diode integrated circuit arrays. 22 p3161 A72-43090
- Teleoperator technology development, discussing remote operators, mobile manipulators and autonomous robots for man capability extension and industrial application [ASME PAPER 72-AERO-18] 22 p3245 A72-43150
- Forecasting as a means for scientific and technological policy control. 23 p3358 A72-44350
- Rocketry and space age inauguration, considering technical, engineering, management and political problem areas 23 p3358 A72-44354
- Book on complete technological system reliability assessment covering performance requirement and achievement, transfer characteristics, sampling, estimation, confidence, synthesis problem, etc 23 p3294 A72-44499
- Point-to-point national data communication geostationary satellite system associated with computers, discussing organization, earth station equipment and technical and economical feasibility 24 p3380 A72-44975
- Spacecraft rescue/recovery capabilities, discussing in-flight escape, ground egress and descent systems, performance and technical and human factors 24 p3450 A72-45147
- United States Space Nuclear Electric Power Program. 24 p3424 A72-45179
- Streamflow forecasting project to assess feasibility of air and spaceborne remote sensed data acquisition application to watershed hydrological behavior prediction 24 p3398 A72-45215
- OSO and Skylab astronomical instruments technology, emphasizing precision pointing, spatial and spectral resolution and photometric efficiency problems 24 p3405 A72-45545
- TECHNOLOGY TRANSFER**
- Book on NASA technology transfer program covering regional university-based dissemination center evaluation and comparison with other transfer mechanisms 07 p1102 A72-19182
- Technology transfer model in terms of donor-recipient activities for information implementation, forecasting and long range planning in developing countries and regional economics 07 p1106 A72-20271
- NASA space program impact on U.S. technology, discussing performance levels, precision, reliability and industry stimulation 11 p1748 A72-26099
- Aerospace technology transfer to and utilization by industry for product development and improvement, discussing NASA structural analysis computer program /NASTRAN/ [ASME PAPER 72-DE-60] 14 p2175 A72-30875
- Mechanical and electrical technologies unification, discussing systems and balances 15 p2211 A72-31873
- NASA technology transfer from information dissemination and service to product development, noting firemen breathing system 17 p2639 A72-35506
- The impact of aerospace technology on energy conversion in the 70's. [ASME PAPER 72-AERO-11] 22 p3140 A72-43147
- Space structures and materials technology utilization and transfer to world economic and social problems, considering thermal control, NDT, systems analysis and design 24 p3407 A72-45154
- TECHNOLOGY UTILIZATION**
- Channel clearing through clouds by laser beam, considering cross section expansion dynamics, channel growth rate, cloud motion and blurring 01 p0078 A72-10155
- Hybrid microwave integrated circuits, discussing distributed circuits with strip transmission lines and lumped element circuits with inductors and capacitors 01 p0045 A72-10698
- Cb alloy processing technology from ores to manufactured finished fabricated, joined and coated hardware, discussing reduction methods, annealing, forming, joining, etc 01 p0075 A72-10745
- Systems approach to space technology application, covering Global Atmospheric Research Program and Earth Resources Technology Satellites 01 p0146 A72-10952
- Satellite photography application to morphological cartography of Baja California 02 p0216 A72-11892
- ERTS-A orbital earth resources data utilization, describing user community size and character and central repository data center 02 p0305 A72-12381
- Weather forecasting, discussing statistical entropy, numerical and statistical methods and computer technology utilization 02 p0254 A72-12777
- Pulsed Nd laser drilling and welding of metal, metal-semiconductor and semiconductor elements, discussing bond penetration and character, mechanical strength and I-V characteristics 03 p0363 A72-13860
- Low cost large solid rocket boosters technology, discussing propellant, case material, insulation, nozzle ablatives and thrust vector control 04 p0565 A72-14435
- ATC technology impact on flight operations and public value of aviation, discussing microwave landing system economic aspects 04 p0544 A72-14810
- Millimeter and submillimeter wave applications, considering environment remote sensing, radar communication, tracking and imagery, wideband communication, plasma diagnostics and spectroscopy 04 p0550 A72-15592
- Symphonic communication satellite technology application to subsequent satellites, discussing three axes stabilization, use of microwave frequencies, components and subsystems reliability 04 p0494 A72-15681
- Thermal heliotrope adaptation to terrestrial applications, discussing solar radiation energy input dominance assurance and wind effect minimization [ASME PAPER 71-WA/SOL-10] 05 p0614 A72-15893
- Space operations cost effectiveness improvement by earth-to-orbit shuttle, discussing space utilization growth and economics [SD-71-780] 05 p0724 A72-16048
- Book on computer applications to engineering analysis covering mathematical models, numerical techniques, program usage, programming and design 05 p0632 A72-16106
- Space technology development importance for future of mankind, discussing terrestrial environment conservation, extraterrestrial raw materials recovery and power generation, etc 05 p0753 A72-16309
- Water based offshore and floating island airports planning and construction, discussing economic, technical and social aspects 05 p0644 A72-16695
- Holography utilization effectiveness in three dimensional image displays, information storage, image multiplication and recording, interferometry, coding, lens corrosion, pattern recognition, etc 06 p0816 A72-17951
- GERTS II simulation program for graphically modeling and analyzing complex stochastic systems, discussing applications to assembly line, project management, conveyor and inventory systems 06 p0780 A72-17978
- Laser radiation pressure applications to isotope and particle separation, optical levitation, high velocity acceleration and atomic beam analysis 06 p0826 A72-18176

Computer technological development effects on professional engineers education and work, considering impacts of computerized design, simulation, etc
06 p0780 A72-18235

Computer aided design in electronics, discussing interactive computing with time sharing teletype keyboards or CRT graphics and applications in IC, network analysis and optimization
06 p0780 A72-18236

Automated navigation aids interface with human operator, discussing Apollo flight experience and technology utilization in air and marine navigation
06 p0846 A72-18288

Book on lasers and applications covering theories of light, polarization, coherence, resonators, mirrors, modes, electro-optical effect, communication, holography, etc
06 p0827 A72-18524

Semiconductor device IC encapsulation, thermal design, stress analysis, testing and applications
06 p0791 A72-18577

Aerospace waste and water management technologies for community and household applications
06 p0769 A72-18617

Power generation for electrical, thermal and transportation needs, considering technology use for air, noise, thermal, water and nuclear pollution reduction
06 p0761 A72-18627

Semifinished product production technology influence on heat resistant alloys mechanical properties, considering forging, rolling, casting, melting, diffusion welding and powder metallurgy
06 p0834 A72-18647

Weather modification as example of government managed and funded technological innovation, discussing various evolutionary R and D and operational phases
07 p1102 A72-18974

Nd-YAG laser system generating gold conductor patterns on ceramic substrates, using numerical control system for Si production
07 p1002 A72-19213

UN agencies role in communication satellites technology exploitation, discussing international cooperation in outer space peaceful use and exploration and development of space law
07 p1074 A72-19468

Space communication application for information, education and cultural exchange, noting need for international cooperation
07 p1104 A72-19473

Laser technology applications, considering economic factors in terms of market oriented products
07 p1105 A72-19554

Papers on high temperature physics and chemistry covering peaceful nuclear explosions, radiative transfer, hydrodynamics, stellar opacity and solar He abundance
07 p1078 A72-19922

Book on dividends from space covering contributions to home and industry, health and medicine, systems approach to human problems, earth monitoring, communications, etc
07 p1105 A72-20202

Laser applications in industrial machining and welding, describing theory and operation of optically pumped ruby, glass-Nd, YAG-Nd, Ar and carbon dioxide lasers
07 p1007 A72-20224

Collaboration of World Health Organization and various international astronomical organizations for space technology applications to man-environment relationships and medical and communication sciences
07 p0933 A72-20300

French space applications program for telecommunications, meteorology, natural resources survey and air/sea traffic control
08 p1256 A72-21201

Industrial applications of lasers, considering programmable machining, distance measurement, computer memories, communication, night clubs, machine shops, aircraft manufacture and tunnel boring machine alignment
08 p1182 A72-21207

Space applications of camera tubes - Conference, Paris, November 1971
08 p1169 A72-21951

Gas, solid state and semiconductor lasers review, discussing applications
09 p1322 A72-22594

Inexpensive solid state microwave sources development and applications considering spectrum allocations, health hazards and reliability problems
09 p1285 A72-22595

Space flight experience application to human factors engineering problems in air and maritime navigation, considering use of small digital computers, display and sensing devices
09 p1348 A72-22785

Multiple charge Al and C ions X-UV spectra use for studying laser produced plasmas build up and expansion regions
09 p1359 A72-22830

NASA space station activities, describing Skylab missions and capabilities in physical and life sciences, earth resources surveying and technology experimentation
09 p1395 A72-22935

Holographic interferometry application to weak inhomogeneities visualization in gas flows, using photographic emulsion nonlinear properties
09 p1311 A72-22965

Automatic computer-controlled system with laser technology for quality inspection of mass produced automobile master brake cylinders
09 p1319 A72-22979

Electromagnetic velocity and flow measurements techniques application to cardiovascular patients, discussing utilization problems
09 p1272 A72-23275

Materials processing with carbon dioxide lasers, noting cutting, welding and hole drilling applications
10 p1485 A72-23969

Microwave equipment and technology application for instrument landing, terminal ATC, millimeter wave CAT detection and satellite communications
10 p1509 A72-24036

Monolithic, thin film and LSI technology development trends in microelectronics, noting heteroepitaxy, ion implantation and laser beam techniques
10 p1454 A72-25175

Space projects technological developments and benefits, discussing communications, transportation, computers, education, holography, power and life support systems, manufacturing in space and earth resources
11 p1748 A72-25253

Remotely manned systems technology for military, industrial, scientific and civil applications for hostile or difficult environments
11 p1612 A72-25256

Transport aircraft aerodynamic design technology application to general aviation propeller driven twin engine aircraft, discussing wing loading and aspect ratio optimization
11 p1576 A72-25595

Commercial applications of quiet light aircraft technology, discussing cost and noise reduction
11 p1576 A72-25596

Short and long range contributions of NASA space program to life quality improvement, discussing land and crop surveys, communications and environment modification
11 p1748 A72-26098

Boron/epoxy and graphite/epoxy composites application to aircraft structural design, discussing flight test and developmental programs
11 p1577 A72-26234

Complementary metal oxide semiconductor applications, noting device power dissipation, high noise immunity, good switching speeds and cost reduction
11 p1701 A72-26386

High performance low power complementary MOS memories based on silicon-on-sapphire technology, noting quiescent power dissipation
11 p1606 A72-26565

High temperature materials powder metallurgy for space applications, discussing melting points
11 p1665 A72-26866

Cermets technology applications, discussing powder metallurgy role and sintering mechanism
11 p1665 A72-26871

Composite powders preparation by metals deposition from aqueous solution onto core materials by gaseous hydrogen at high temperature and pressure, noting coating application
11 p1646 A72-26875

Weather satellite data use to obtain forecasts for aircraft and ships in Southern Hemisphere and for Antarctic research stations
11 p1683 A72-26890

Commercially available laser systems applications to welding, drilling, scribing and other machining operations
11 p1652 A72-26984

TV reception from satellite broadcasting systems in hostile environment of remote and inaccessible villages over large land areas
12 p1779 A72-27353

Space techniques application to meteorological prediction, noting Meteosat and Eole satellites capabilities
12 p1840 A72-27506

Space technology application to ATS F and G program, discussing high power requirements, parabolic antenna design, tracking accuracy and ground station simplification
12 p1870 A72-27523

Surface pressure via satellite-borne measurements of atmospheric transmission near absorption band
12 p1802 A72-27710

NASA reliability and quality assurance methodology to improve hospital biomedical equipment, using space electric rocket test example
12 p1814 A72-27960

Surface integrity machining practices application to jet engines production, noting cost reduction and process selection and quality control improvement
12 p1862 A72-28163

Worldwide satellite navigation system for precise position and velocity of military aircraft, ships and ground vehicles
13 p1996 A72-28750

Slant Visual Range/Approach Light Contact Height Measurement System utilizing state of art technology for airport applications
13 p1938 A72-28844

High cruise altitude operational advantages for commercial transport aircraft utilizing technological innovations in structures, propulsion, controls, avionics and aerodynamics
13 p1996 A72-28877

Solar electric multimission spacecraft /SEMMS/ concept, investigating Mariner, Viking and TOPS technologies applicability to postulated mission/science objectives
13 p2026 A72-28944

Long range transport aircraft structures and composite materials technology for airframe and engine systems
13 p1897 A72-28955

Gas dynamic lasers and combustion driven devices design, operation, performance and industrial applications
13 p1965 A72-29424

Aerospace technology economic and social effects relating U.S. space expenditures and gross national product
14 p2174 A72-30683

Hovercraft state of development and utilization potential, comparing performance to other transportation modes
14 p2073 A72-30814

High power carbon dioxide laser construction specifications and operation for applications to laboratory and industrial processing of glass, ceramics and metals
14 p2111 A72-30855

Navy program for composites technology development in aircraft structures, discussing design, reliability and cost
14 p2073 A72-30864

Aerospace technology transfer to and utilization by industry for product development and improvement, discussing NASA structural analysis computer program /NASTRAN/
14 p2175 A72-30874

Rare earth metals and alloys technology assessment and utilization covering quantum mechanics concepts application to Fermi surface
15 p2289 A72-31174

Russian book on man and computer covering interaction systems technological capabilities, mathematical aspects and applications
15 p2188 A72-31277

NASA ATS F/G satellites for educational TV broadcasting in foreign countries, discussing technologies and case histories
15 p2196 A72-31824

Sonar techniques application to radar, stressing utilization of preformed channels in rapid and distant detection of satellites and ballistic missiles
15 p2197 A72-31877

Lightweight man-portable uncooled semiconductor laser illuminator design for field use in night vision applications
15 p2248 A72-32047

Time/frequency technology application to reliable aircraft collision avoidance system, discussing precision time-ordered techniques, frequency control and synchronization and flying clocks
15 p2268 A72-32072

Flexible wing applications to passenger and cargo transport, discussing gliding and soaring sport, emergency use, powered flight, rocket payload recovery etc
16 p2347 A72-33182

S-64 Skycrane helicopter current and anticipated applications in commerce and industry, considering logging operations in ecologically sensitive or rugged areas, bridge construction, etc
16 p2348 A72-33182

Microwave transmission phenomenon and application to NDT, discussing various methods and examples
16 p2391 A72-33233

Univac 1616 computer design featuring uses of 16-bit word technology, medium and large scale integration, and transistor-transistor logic
16 p2366 A72-33247

F-100 and F-401 turbofan engine design and development for F-15 and F-14, discussing impingement cooling, Ti alloys, powder metallurgy and metal composites, etc
17 p2597 A72-34390

Re applications technology, discussing production methods, mechanical and physical properties, plasma spraying, annealing and alloying techniques
17 p2567 A72-34825

Composite materials technology utilization in structural design, considering stiffness, strength, weight, fatigue properties, adhesive joining and structural reliability
17 p2633 A72-35283

Electrothermal cutting processes using a CO2 laser. [IEEE PAPER TOD-71-118]
17 p2560 A72-35644

Canadian industrial participation in domestic, U.S. and overseas space projects, emphasizing technology advancement as national objective [AIAA PAPER 72-738]
18 p2742 A72-36544

High vacuum technology applications in surface physics research, discussing atomic collisions and adsorption processes
18 p2712 A72-36827

Economic impact of applying advanced technologies to transport airplanes. [AIAA PAPER 72-758]
19 p2751 A72-38128

Cryobiology phenomena and applications, considering mode of action of various substances for freezing injury protection
19 p2762 A72-38828

Book - Solid state electronic devices.
20 p2907 A72-39024

Potential applications of NASA-developed technology to problems of the environment. [ASME PAPER 72-ENAV-23]
20 p2895 A72-39154

A review of the science, technology, and applications of dispersion strengthened Ni-Cr- and Co-Cr-base alloys.
20 p2936 A72-39209

Electric power generation by thermionic converters, discussing physical principles of operation and technology utilization in communications, meteorology, geophysics, oceanography and space exploration
20 p2890 A72-39940

Advanced technology applications to present and future transport aircraft. [AIAA PAPER 72-759]
20 p2888 A72-40051

Microminiaturization, microprogramming, multiprocessing, and processing and memory module design technology of aerospace computers in different size ranges
21 p3025 A72-41113

Boron fiber reinforced composites technology assessment and utilization, stressing cost reduction [ICAS PAPER 72-30]
21 p2995 A72-41155

Technological utilization of Weissenberg viscoelastic effect for sliding bearings centripetal pressure lubrication, noting analogy with human and animal skeletal joints lubrication
22 p3183 A72-42875

Some contributions to energetics by the Lewis Research Center and a review of their potential non-aerospace applications. [ASME PAPER 72-AERO-12]
22 p3245 A72-43148

Solutions to transportation problems using time/frequency technology.
24 p3422 A72-44649

Application of planetary quarantine methodology and spacecraft sterilization technology to improved health care delivery.
24 p3375 A72-45148

Space structures and materials technology utilization and transfer to world economic and social problems, considering thermal control, NDT, systems analysis and design
24 p3407 A72-45154

Commercial space applications economics, discussing meteorological, navigational traffic control and communications satellites, nuclear waste disposal, space manufacturing, solar power generation, etc
24 p3441 A72-45216

Control configured fighter and bomber aircraft based on flight control technology, discussing development programs
24 p3369 A72-45386

Direct satellite TV broadcasting for complete community or individual home coverage, discussing requirements, technical performance and economic factors in Europe
24 p3380 A72-45553

T E C T O N I C M O V E M E N T
U T E C T O N I C S

Northern Alps geology, hydrology, lithology and tectonic survey, using aircraft-borne thermal IR scanner remote sensor
02 p0209 A72-11795

Lunar passive seismic experiment deducing internal structure constitution and tectonic processes
03 p0418 A72-13108

Satellite photographs of Himalayan-Indian Ocean tectonic patterns, showing major left and right lateral shear belts as evidence of wrench movements
05 p0655 A72-16040

Viking Lander seismic investigations for Martian tectonic activity, internal structure and composition, core size and conditions of formation
10 p1540 A72-24389

Mariner and Mars space probe data on Mars surface and atmosphere, suggesting possibility of tectonic activity
16 p2461 A72-34181

Tectonic dewatering and strain in the Michigamme Slate, Michigan.
18 p2686 A72-36223

Relation between tectonic processes on the earth and moon
19 p2860 A72-37958

T E E T H
Influence of ionizing radiation on the tooth organ
22 p3141 A72-41987

T E F L O N [T R A D E M A R K]
Photoemission from polyethylene, Kapton, Teflon and polyvinyl chloride under photon irradiation
03 p0403 A72-14084

Steel/teflon sliding friction in high vacuum at stepwise controlled oscillation frequencies, sliding rates and loads
07 p0964 A72-18863

Teflon diffusion membrane for in vivo blood and intramycardial tissue gas tension measurement by mass spectroscopy without chemically bonded heparin surface
08 p1124 A72-20901

Solid teflon pulsed plasma thruster quasi-steady and short pulse discharge operations, discussing propulsion system performance and erosion behavior [AIAA PAPER 72-459]
11 p1709 A72-26195

Teflon-bonded hydrophobic gas diffusion electrode performance prediction by mathematical treatment of flooded catalyst agglomerate model
16 p2352 A72-33892

A parametric study of the transient ablation of Teflon. [ASME PAPER 72-HT-32]
20 p2986 A72-39671

Thermal anomalies in stressed Teflon.
24 p3417 A72-44766

T E K T I T E S
NT AUSTRALITES
NT BEDIASITES

Chemical composition and morphology of silicate spherules, comparing to lunar rocks, meteorites and tektites
02 p0280 A72-12283

Cosmic ray exposure age of australites and far-east tektites, using C14 content as indication of terrestrial age
06 p0878 A72-17761

Atmospheric abundance ratios of gas inclusions in Muong Nong and Libyan Desert glass tektites by mass spectrometric analysis, indicating terrestrial origin
12 p1866 A72-27117

Geological verification in search for origin of vagabond tektites, commenting on Caribbean label bediasite find
15 p2303 A72-31307

Czech book - Moldavites and tektites.
21 p3111 A72-41536

Shock damaged zircon, corundum, rutile, monazite and quartz crystalline inclusions in Muong Nong-type indochinite /tektite/, noting production from detrital sedimentary materials as possible terrestrial origin
23 p3335 A72-43398

T E L E C H I R I S
U R E M O T E H A N D L I N G
T E L E C O M M U N I C A T I O N

NT AIRCRAFT COMMUNICATION
NT BIOTELEMETRY
NT BROADCASTING
NT CLOSED CIRCUIT TELEVISION
NT COLOR TELEVISION
NT COMMUNICATION
NT DATA LINKS
NT DEFENSE COMMUNICATIONS SATEL-LITE SYSTEM
NT EDUCATIONAL TELEVISION
NT FACSIMILE COMMUNICATION
NT GROUND-AIR-GROUND COMMUNICA-TIONS
NT LUNAR COMMUNICATION
NT MULTICHANNEL COMMUNICATION
NT OPTICAL COMMUNICATION
NT PULSE COMMUNICATION
NT PULSE FREQUENCY MODULATION TELEMETRY
NT RADIO COMMUNICATION
NT RADIO RELAY SYSTEMS
NT RADIO TELEGRAPHY
NT RADIO TELEMETRY
NT RADIOTELEPHONES
NT REENTRY COMMUNICATION
NT SATELLITE TELEVISION
NT SPACE COMMUNICATION
NT SPACECRAFT ANTENNAS
NT SPACECRAFT COMMUNICATION
NT SPACECRAFT TELEVISION
NT TELEMETRY
NT TELEPHONY
NT TELEPHOTOMETRY
NT TRANSOCEANIC COMMUNICATION
NT VIDEO COMMUNICATION
NT VOICE COMMUNICATION
NT VOICE DATA PROCESSING
NT WIDEBAND COMMUNICATION

Book on global communication law covering maritime transport, civil aviation, radio, space com-munication postal services, international cooperation, etc
02 p0305 A72-12575

Sequential analysis of statistical hypotheses applied to radar detection and coded communications systems
02 p0181 A72-12643

Electromagnetic noise and effects on communication systems, considering statistical parameters definition and measurements
03 p0324 A72-14036

Analog computer simulation for filtering, phasing, multiplication and addition in AM communication system
03 p0329 A72-14182

Noise, delay and interruption caused communication degradation effects on feedback control system performance, considering air navigation and computer aided command and control on battlefield
06 p0794 A72-18242

Unified design charts for communication systems filter networks with inverse Chebyshev and elliptic function responses
06 p0787 A72-18400

Phase coherent frequency synthesizer as modulation source for multiple feature communication system, noting noise resistance, navigation capability, Doppler correction and transmitter to receiver ranging
06 p0777 A72-18619

French space applications program for telecommunications, meteorology, natural resources survey and air/sea traffic control
08 p1256 A72-21201

Telecommunications ultrasonic resonators, electromechanical and piezoelectric filters and microacoustic surface elastic wave devices
09 p1281 A72-23468

Sequential analysis of statistical hypotheses in radar target detection and in communications systems
09 p1282 A72-23680

Global NASA communications network /NASCOM/ reliability, discussing design and performance goals
10 p1435 A72-23992

Data acquisition and transfer efficiency and reliability in computerized automatic control systems for communications, listing probability and expectation criteria
11 p1600 A72-25436

Communication systems design with error control, applying algebraic codes to biphasic and multiphase modulation systems
12 p1782 A72-27488

Indian national satellite /Insat/ design for continental TV coverage and urban center telecommunication linkage [AIAA PAPER 72-576]
12 p1785 A72-27866

Error probabilities estimates for communication systems using orthogonal multiposition signals in information transmission, noting techniques applicability to diversity reception systems with self selection
13 p1918 A72-28893

Ground station with control, communication and information processing centers, discussing automation, data transfer, system control and emergencies [DGLR PAPER 72-007]
13 p1939 A72-28965

Apollo centralized ground support and communication system, describing network support team, mission control center, instrumentation support team and manned space flight network
13 p1940 A72-29860

Satellites for long distance telecommunications, noting ATS, Intelsat, military systems and Canadian domestic system Anik
14 p2085 A72-30363

Parametric amplifiers for satellite microwave communication systems, discussing frequency stability, noise temperature and gain relationships
16 p2369 A72-33520

Short- and long-range terrestrial telecommunication using energetic collimated beams of muons
17 p2519 A72-35837

Communication network vertex and mixed cutset definitions and computation from interchange graph of given finite connected undirected graph without loops and multiple edges
21 p3015 A72-40634

Annual International Conference on Communications, 8th, Philadelphia, Pa., June 19-21, 1972, Conference Record.
21 p3016 A72-40851

Adaptive signal-discrimination system using signals for observation of the channel characteristics.
21 p3023 A72-41838

Communication systems with binary convolutional signal encoding and threshold decoding, discussing orthogonal checkout sums distribution for correct and erroneous synchronization
22 p3154 A72-42235

Optimal frequency-difference communications system with manipulated amplitudes
22 p3154 A72-42237

Field reporting system for reliability analysis on telecommunication equipment.
24 p3384 A72-44657

- The Franco-German telecommunications satellite
Symphonie 24 p3451 A72-45230
- TELEMETERS**
U TELEMETRY
TELEMETRY
NT BIOTELEMETRY
NT PCM TELEMETRY
NT PULSE FREQUENCY MODULATION TELEMETRY
NT RADIO TELEMETRY
Report on U.S. telecommunications telemetry information theory in period 1966-1969, discussing ionospheric and tropospheric data transmission 02 p0171 A72-11687
Telemetry - Conference, Washington, D.C., September 1971 02 p0173 A72-12126
High data rate convolutional coding for space station telemetry links, considering sequential and cascaded Viterbi decoding 02 p0174 A72-12132
Digital telemetry/communication laser link system design for operation at 1 gigabit/sec 02 p0174 A72-12143
Computerized bias optimization of telemetry timing accuracy applied to Minuteman system 02 p0174 A72-12144
ERTS multispectral scanner data telemetry decom-mutator/processor capable of decommutating five spectral bands of digital video data 02 p0175 A72-12162
Telemetry standards for transmitting, receiving and signal processing equipment at missile test ranges 02 p0176 A72-12164
Telemetry applications in aerospace industry - ISA Conference, Las Vegas, May 1971 02 p0179 A72-12402
Aircraft and spacecraft integrated avionics systems design with emphasis on telemetry, discussing space shuttle subsystems integration 02 p0179 A72-12403
Computer controlled telemetry data acquisition station, noting cost effectiveness 02 p0179 A72-12407
German vhf ground telemetry satellite tracking system radio interferometer, discussing specifications and performance [DGLR PAPER 71-124] 02 p0182 A72-12732
German ground operation system for satellites and space probes, discussing telemetric data processing, handling and flow [DGLR PAPER 71-123] 02 p0201 A72-12742
Scientific balloon data management system, discussing airborne and ground station equipment for telemetry, command and flight control 03 p0327 A72-13725
Dynamic damping coefficient extraction from reentry vehicle flight test telemetered lateral rate data 03 p0441 A72-13951
Automated telemetry system providing real time analytical capability and reduction of flight test time for F-14 04 p0486 A72-14592
Cloud base altitude measurement by optical telemetry using TNN 1000 apparatus, noting reduced maintenance 04 p0521 A72-14691
Automated meteorological telemetry and interrogation response system with terminal extensions for Paris airport 04 p0508 A72-14695
Geodetic determination of geoid shape by computerized laser-effect space telemetry ground stations 04 p0495 A72-15724
Europe-Africa geodetic link in spatial triangulation of passive Pageos satellite, discussing laser telemetry operation 04 p0520 A72-15725
International Satellite Geodesy Experiment based on laser telemetry technique, discussing ground stations network and tracking cameras 04 p0520 A72-15726
High accuracy laser reflector telemetric measurement for earth-moon distance variation in time by correlation method 04 p0495 A72-15727
Azur satellite ground station network with polar stations for telemetry reception 05 p0643 A72-16140
Telemetry system on board beryllium sphere reentry vehicle for hypersonic gas dynamics and wake chemistry experiments, using flush mounted antennas with isotropic radiation pattern [AIAA PAPER 72-176] 05 p0631 A72-16836
Geodetic satellite systems applications, describing trajectory beacons, telecontrol and telemetry stations and computing and operations center of French Geole system 06 p0809 A72-18258
Laser telemetry performance, considering means of noise reduction 07 p0947 A72-20256

- Aberration introduced by high satellite velocities, investigating application to laser telemetry 07 p0947 A72-20258
Tracking efficiency of laser telemetry on reflector carrying satellites 07 p0947 A72-20259
Tracking efficiency calculation for laser telemetry with laser reflector on nonstabilized satellite 07 p0947 A72-20260
Book on telemetry and remote control covering information theory, analog/digital techniques, signal transmission, data processing and coding, etc 10 p1436 A72-24550
Standardized automatic telemetering hydrometeorological station, discussing structure, operation, working principles and sensors 10 p1462 A72-25009
Air, wet bulb and soil temperature indications from automatic telemetering meteorological stations, comparing with Hg thermometer readings 10 p1483 A72-25012
Automatic telemetering meteorological stations and visual observation data processor control 10 p1507 A72-25020
Time division multiplexing system for asynchronous high data rate telemetry, discussing design features 10 p1440 A72-25061
Scanning photoelectric image conversion [photoanalyzing] systems for data telemetry from remote optical sensors 11 p1634 A72-26461
Space center trajectory and telemetry systems, including radar stations, interferometric equipment, optical methods and interlinked computers [DGLR PAPER 72-014] 13 p1938 A72-28961
Spectrum analysis of PCM/AM-FM and PCM/FM-FM telemetry signals, using approximation technique to Fourier transform time signal to frequency domain 13 p1919 A72-29025
Linear negative feedback dc current magnetic transducers for telemetry input signals, discussing operation principles and design 16 p2370 A72-33862
Potential value of turn-rate telemetry in tracking of aircraft equipped with discrete address beacon system /DABS/ for ATC, discussing tracking algorithms design 19 p2830 A72-37282
Real time telemetry processing systems, describing display features and limitations [AIAA PAPER 72-783] 19 p2752 A72-38142
- TELEMETRY AUTO REDUCTION SYSTEM**
U DATA REDUCTION
U TELEMETRY
TELEOPERATORS
Space tools and support equipment for earth orbital systems maintenance, replacement and repair, discussing Skylab requirements and teleoperator applications [AIAA PAPER 72-230] 10 p1488 A72-25049
Teleoperator manipulator for payload handling in space shuttle, noting design features and simulations of master-slave remote control system [AIAA PAPER 72-238] 13 p1909 A72-29075
NASA teleoperator-robot development program, discussing technology and design studies related to space shuttle and stations, satellites and planetary vehicles 15 p2190 A72-32315
Human or computer control role in teleoperator remote control mechanisms, discussing control modes, sensing and transmission time delay problems 21 p3011 A72-41416
Computerized supervisory control for interpretation of subgoal statements from human operator to permit teleoperator interaction with environment without long time delay 21 p3011 A72-41417
Remote control and navigation tests for application to long-range lunar surface exploration. 22 p3203 A72-43131
Teleoperator technology development, discussing remote operators, mobile manipulators and autonomous robots for man capability extension and industrial application [ASME PAPER 72-AERO-18] 22 p3245 A72-43150
A teleoperator system for space application. 24 p3407 A72-45174
- TELEPHONES**
NT RADIOTELEPHONES
Message circuit noise evaluation in commercial telephone system, discussing noise measurements and weighting curves 15 p2202 A72-32575
- TELEPHONY**
Molniya-Orbit communication satellite system, discussing operational quality, maintenance, television transmission facsimile, sound broadcast and multichannel telephony 01 p0023 A72-10046
S band transistor power amplifier design and performance, noting application for 960 telephone channel radio relay system 01 p0038 A72-10657

- Adjacent channel interference effects in multicarrier telephony FM communications system 07 p0948 A72-20493
Intelsat V satellite system with large telephone channels capacity and full earth station network connectivity, discussing system concepts and technology [AIAA PAPER 72-536] 12 p1780 A72-27359
International telephone hierarchical earth network organization for satellite communication extension, considering guidelines and constitution 15 p2193 A72-31179
Bandpass filters set synthesis in crab eye configuration, noting design principles and telephone techniques 17 p2524 A72-34295
Potential response of maritime services to craft and persons in distress at sea. 17 p2488 A72-34431
Adaptive equalization of data transmission rate in telephonic systems, considering criteria and iterative algorithms 18 p2661 A72-36790
Orbital and frequency sharing between the broadcasting-satellite service and the fixed-satellite service. 21 p3018 A72-40877
Signal quality monitoring of computer data transmission. [ASME PAPER 72-AERO-1] 22 p3156 A72-43146
- TELEPHOTOMETERS**
U TELEPHOTOMETRY
TELEPHOTOMETRY
Invariant imbedding theory of aerosols multiple scattering induced telephotometric errors, determining scattering coefficients relative to optical thickness by Monte Carlo method [AIAA PAPER 71-1062] 01 p0066 A72-10531
- TELESCOPES**
NT APOLLO TELESCOPE MOUNT
NT ASTRONOMICAL TELESCOPES
NT CELESCOPES
NT HELIOMETERS
NT PARTICLE TELESCOPES
NT PYROHELIOMETERS
NT RADIO TELESCOPES
NT REFLECTING TELESCOPES
NT REFRACTING TELESCOPES
NT SCHMIDT CAMERAS
NT SPACEBORNE TELESCOPES
NT SPECTROSCOPIC TELESCOPES
NT STRATOSCOPE TELESCOPES
NT X RAY TELESCOPES
Solar prominence telescope design using two prism reflectors for ray path deflection 07 p0982 A72-19125
Telescope performance reciprocity in laser transmitter or optical heterodyne receiver functioning, considering atmospheric turbulence effects 11 p1636 A72-26750
One-to-one telescope with pressurized Ar gas for nanosecond and picosecond laser output pulse sensitive detection via gas breakdown and energy absorption 21 p3062 A72-40618
- TELEVISION CAMERAS**
Airborne high resolution multispectral TV camera system, describing special objective configuration for improved ground resolution 02 p0227 A72-11850
Apollo 12 retrieved Surveyor 3 TV camera mirror surface and camera-shroud organic contamination attributed to spacecraft outgassing and engine exhaust products 03 p0415 A72-12948
Multispectral TV camera systems for satellite recording of earth surface electromagnetic radiation at separate wavelengths [DGLR PAPER 71-135] 06 p0817 A72-18232
Image resolutions for ERTS return beam vidicon TV, Skylab multispectral cameras and Gemini/Apollo photographs 06 p0818 A72-18328
Spacecraft planetary approach navigation with TV camera onboard Mariner 9 giving images of Mars natural satellites against star background, discussing optical data processing programs [AIAA PAPER 72-53] 07 p1032 A72-18946
Performance tests of return beam vidicon multispectral television camera system for ERTS program 07 p0986 A72-19657
SAS-D borne TV type UV sensitive detector with camera tubes for high resolution astronomical spectroscopy 08 p1169 A72-21954
UV/visible image converter for use with TV camera tubes for astronomical photometry and spectroscopy from satellites and sounding rockets 08 p1169 A72-21955
Nimbus satellite image dissector camera system for continuous meteorological scanning, noting special suitability for cloud and ice features discrimination from brightness changes 08 p1171 A72-21967

Digital image processing for TV camera noise suppression and photometric and geometric distortions calibration and rectification 08 p1172 A72-21977

Subminiature TV camera using hybrid packaging techniques and digital circuitry for full EIA composite video output format and 450 TV/RH resolution capability 09 p1316 A72-23599

Design and operation of digital image recorder based on single stage intensifier and silicon target-inertial television camera tube coupled to large memory 11 p1631 A72-25685

Image-to-signal conversion by TV tube in automatic contactless measuring systems, producing mosaics of object by optical, X ray and ultrasonic techniques 11 p1634 A72-26460

Apollo 15 and 16 TV, still and movie cameras, discussing astronomical activities of astronauts 12 p1807 A72-27546

Low level light TV camera with Si intensifier target tube for fire control system to improve AH-IG Cobra helicopter night reconnaissance and attack capabilities 17 p2557 A72-35555

ERTS-borne return beam vidicon camera using high resolution TV sensors coaligned to view identical scene in different spectral bands 19 p2795 A72-37576

Electro-optical TV technique with laser source illumination to provide engineering metrology and NDT procedure resembling real time holographic interferometry 20 p2930 A72-39038

A detailed analysis of Mariner nine TV navigation data. [AIAA PAPER 72-866] 20 p2977 A72-40061

High resolution multispectral camera system for ERTS A & B. 24 p3402 A72-45182

TELEVISION EQUIPMENT

NT IMAGE DISSECTOR TUBES

NT TELEVISION CAMERAS

NT TELEVISION RECEIVERS

TV time lapse interferometry and contouring for photoelastic nondestructive testing, comparing with photographic techniques 03 p0358 A72-13436

TV tube type image sensors to replace photographic film for space telescope, discussing design and performance 08 p1169 A72-21956

Celestial pole region photographs obtained with TV equipment, emphasizing observations of faint meteoroids and gas trails 13 p2044 A72-29648

TV speckle pattern recording for coherent laser light measurement of mechanical vibrations in micrometer range 13 p1961 A72-30026

Venus observation experiment with the aid of a television system 19 p2858 A72-37820

A transmitting television tube for collecting information from streamer spark chambers 23 p3290 A72-44160

TELEVISION RECEIVERS

Digital computers data output alphanumeric display by commercially available TV sets, describing system design 03 p0355 A72-13075

Alphanumeric data representation by TV receivers, describing coding device and gate system for video signal generation 05 p0634 A72-15813

Color TV tube design without difference current generator, describing scanning unit saddle coils fabrication technique 18 p2667 A72-36678

Receiver terminals for satellite television systems. 18 p2662 A72-36849

TELEVISION RECEPTION

TV reception from satellite broadcasting systems in hostile environment of remote and inaccessible villages over large land areas [AIAA PAPER 72-524] 12 p1779 A72-27353

Detection probability for moving small targets embedded in random white noise on TV display, comparing machine processed pattern recognition techniques and human performances 12 p1843 A72-27933

Geostationary satellite direct TV broadcasting system extension to 12 GHz band, considering receiving installations, antennas, performance and costs 21 p3018 A72-40876

TELEVISION SYSTEMS

NT CLOSED CIRCUIT TELEVISION

NT COLOR TELEVISION

NT EDUCATIONAL TELEVISION

NT SATELLITE TELEVISION

NT SPACECRAFT TELEVISION

Visual film, TV and optical data systems unified classification for performance criteria based on equa-

tion similar to ideal imaging system description by Rose 03 p0329 A72-14188

Single scan TV-radiography system for providing A-D converter analog signal for digital data acquisition, obtaining transfer functions 04 p0522 A72-15226

Low light television camera tubes application to navigation safety in congested areas, reconnaissance and other watchkeeping system 07 p1032 A72-19070

National TV distribution by Canadian domestic satellite system, discussing design simplicity and payload weight maximization 07 p0944 A72-19654

International and national satellite TV systems, discussing technical and operational characteristics, artificial emission dispersion and costs 07 p0944 A72-19656

International TV broadcasting satellite system, discussing technical problems and cost effectiveness in competition with conventional TV systems 08 p1132 A72-21205

Astronaut training obtained visually in lunar module simulator via film, spacecraft models and landing site relief models as sources for complex TV system 08 p1147 A72-21335

Frequency bands for space-earth links in broadcasting satellite service, stressing application to educational television 10 p1435 A72-24032

TV microscopic system for on-line measurement of cat omentum microvessels diameter relative to heart action 11 p1587 A72-26621

Indian national satellite /Insat/ design for continental TV coverage and urban center telecommunication linkage [AIAA PAPER 72-576] 12 p1785 A72-27866

Extreme UV solar images televised in flight with rocket-borne SEC vidicon system, noting pictures reconstruction enhancement 12 p1810 A72-27930

Intensified electron bombarded Si camera tube performance in low light level TV systems, predicting sensor resolution vs irradiance characteristics 12 p1810 A72-27934

TV network distribution systems cost, comparing video tape shipping, terrestrial interconnection with delay for time zones and indirect and direct satellite transmission [AIAA PAPER 72-552] 13 p1918 A72-28983

Regional microwave ground distribution facility for TV service organized for satellite relay transmitted video signals accommodation [AIAA PAPER 72-557] 13 p1918 A72-28984

Alphanumeric characters for small TV type raster displays, describing legibility experiment for character height optimization 13 p1911 A72-29821

Time data dissemination techniques, discussing astronomical and atomic time scales, frequency standards, broadcasting and TV, navigation and satellite systems 14 p2085 A72-30364

Holographic prerecorded TV system, discussing coherent light noise elimination and redundancy effects on image quality 15 p2239 A72-32356

Factors affecting frequency and orbit utilization by high power transmission satellite systems. 19 p2857 A72-37644

Experimental observations of the instability of stellar images from a bichromatic two-channel television system 19 p2860 A72-37956

Certain results of the statistical processing of a large series of large-scale television images of stars 19 p2860 A72-37957

Comparison of information takeoff from a shadow-indication instrument by television and photographic techniques 20 p2928 A72-40049

TELEVISION TRANSMISSION

Molniya-Orbit communication satellite system, discussing operational quality, maintenance, television transmission facsimile, sound broadcast and multichannel telephony 01 p0023 A72-10046

Educational satellites - Conference, Nice, France, May 1971, covering space communication, TV, performance, data handling, economics, etc 01 p0147 A72-11277

ATS-F educational TV experiment in India, discussing domestic communication satellite development and nationwide coverage problems 02 p0278 A72-11960

Communications and TV broadcasting antenna feeder cost-efficient designs, relating climatology, oscillation theory and structural aerodynamic stability 07 p0955 A72-19513

Review of 1971 Picture Coding Symposium at Purdue University, discussing intraframe, interframe and color TV signal coding 09 p1279 A72-22899

UHF band satellite TV broadcasting system with FM, calculating required field strength and transmitter power 10 p1435 A72-24033

TV reception from satellite broadcasting systems in hostile environment of remote and inaccessible villages over large land areas [AIAA PAPER 72-524] 12 p1779 A72-27353

Satellite technology for TV broadcasting service to Canadian remote areas, considering new frequency band allocation [AIAA PAPER 72-553] 12 p1781 A72-27373

Ground and satellite based TV broadcasting compared in terms of economic, political and pedagogical implications to solve educational problems in developing countries [AIAA PAPER 72-525] 12 p1891 A72-27662

Regional microwave ground distribution facility for TV service organized for satellite relay transmitted video signals accommodation [AIAA PAPER 72-557] 13 p1918 A72-28984

NASA ATS F/G satellites for educational TV broadcasting in foreign countries, discussing technologies and case histories 15 p2196 A72-31829

Range coding application to TV and visiohphone images, stressing plug memory 17 p2518 A72-35675

A polydirectional antenna in polygon reflector design with cosecant-type elevation directional diagram for providing television in the 12-GHz frequency range 21 p3029 A72-40524

Broad-band television transmitting antenna with polydirectional characteristics for the UHF-region 21 p3031 A72-40542

Horizontally polarized polydirectional or beam antenna, which is slightly out of round and consists of beam units, for television and FM radio 21 p3031 A72-40544

Television transmission performance of an experimental small aperture earth station. 21 p3018 A72-40878

Shaped coverage patterns with satellite array antennas. 21 p3019 A72-40884

Analysis of a procedure for the transmission of low-frequency signals in time-compressed, analog form 21 p3023 A72-41399

Remote transmission of telescope coordinate readings by industrial television 21 p3056 A72-41448

Direct satellite TV broadcasting for complete community or individual home coverage, discussing requirements, technical performance and economic factors in Europe 24 p3380 A72-45553

TELLEGEN THEORY

U GYRATORS

U NETWORK ANALYSIS

U NETWORK SYNTHESIS

TELLURIC CURRENT MICROPULSATIONS

U MICROPULSATIONS

U TELLURIC CURRENTS

TELLURIC CURRENTS

Photogeological remote sensing of high voltage dc power transmission system induced ground current paths, discussing X-15 near IR photographic recordings 02 p0212 A72-11826

Solar activity effects on atmospheric electricity during favorable weather conditions, discussing troposphere potential gradient and earth air current 13 p2029 A72-28622

DR ring current belt formation due to electron and proton gradient drift in inhomogeneous geomagnetic field, calculating charged particles trajectories 14 p2101 A72-30646

Earth electrical conductivity radial distribution effect on solar quiet day geomagnetic field variations 14 p2103 A72-30666

Kinematic dynamo theory of electric currents flow in earth liquid core, discussing model, field electrodynamics and hydromagnetic dynamo 16 p2385 A72-33340

A contribution to the numerical treatment of the electromagnetism field /H-polarization/ in horizontally non-homogeneous models of the earth. 21 p3048 A72-40498

TELLURIC FIELDS

U ELECTRIC FIELDS

U TELLURIC CURRENTS

TELLURIC LINES

Oxygen telluric lines contours shape analysis, allowing for atmospheric nonisothermicity and inhomogeneity 06 p0852 A72-18050

Atmospheric carbon monoxide and nitrous oxide telluric line contours and line centers optical thickness, measuring solar radio emission transmissivity 11 p1628 A72-26881

Atmospheric carbon monoxide and nitrous oxide telluric line contours and optical thickness in line centers, measuring solar radio emission transmissivity 20 p2919 A72-39568

TELLURIDES

NT BISMUTH TELLURIDES
NT CADMIUM TELLURIDES
NT INDIUM TELLURIDES
NT LEAD TELLURIDES
NT MERCURY TELLURIDES
NT TIN TELLURIDES
NT ZINC TELLURIDES
Compound tellurides and their alloys for Peltier cooling - A review.

22 p3215 A72-43088

TELLURIUM

Thermodynamic solids theory generalized for internal strains in perfect non-Bravais crystals, applying to trigonal Se and Te structure

04 p0562 A72-15470

Se and Te additions effects on low carbon steels formability and machinability from metallurgical examination and workability tests

07 p0994 A72-19480

Electrical properties of Te/p-Si/N heterodiodes at room and liquid air temperatures

10 p1527 A72-24937

Te single crystal electrical resistivity and Hall coefficient effects of electron irradiation, suggesting point defects and dislocations interaction

12 p1859 A72-28073

Target anion effect on radioactive Sb and Te distribution formed by high energy proton irradiation of cesium salts containing oxygen

15 p2282 A72-32485

CW laser transitions in singly ionized Te vapor spectrum at 4843-9378 Å, indicating charge transfer as dominant excitation mechanism

16 p2401 A72-33394

TELLURIUM ALLOYS

Sn additions influence on Te structural characteristics relation to microhardness and current carrier mobility variations

09 p1322 A72-22204

TELLURIUM COMPOUNDS

NT BISMUTH TELLURIDES
NT CADMIUM TELLURIDES
NT INDIUM TELLURIDES
NT LEAD TELLURIDES
NT MERCURY TELLURIDES
NT TELLURIDES
NT TIN TELLURIDES
NT ZINC TELLURIDES

TEMPER [METALLURGY]

Alloy steels temper brittleness analysis, using internal friction characteristics as functions of time and temperature

02 p0247 A72-12816

Internal friction peak in fresh tempered martensite from Fe-Ni-C alloy cooled to 77 K, suggesting hypothetical carbon atoms interactions with mobile dislocations

10 p1496 A72-24232

Vacancy annealing effect on beta phase transformation during tempering of Ti alloy with Mo, showing strain hardening and contraction increase

14 p2124 A72-31032

TEMPERATE REGIONS

Midlatitude vhf phase detection of magnetic field aligned ionospheric irregularities

01 p0031 A72-10916

Anomalous changes in ionospheric radio absorption during winter at midlatitudes, investigating diurnal and seasonal variations and stratospheric warming

04 p0518 A72-14967

Vhf waves transhorizontal propagation and day types correlation with sporadic E ionospheric layers in temperate zone, discussing wind shear theories

05 p0659 A72-16782

Temperate latitude sporadic E cause and structure - Conference, Utah State University, Logan, September 1971

10 p1477 A72-25151

Global horizontal sounding technique balloon flights, determining Southern Hemisphere temperate latitude circulation climatology

13 p1988 A72-28443

Test flights into weather at midlatitudes and tropical systems with airborne OMEGA navigation system, discussing E field and H field antennas

13 p1999 A72-29203

Very-high-frequency wave propagation by the temperate-latitude sporadic-E layer.

22 p3154 A72-42367

TEMPERATURE

NT AMBIENT TEMPERATURE
NT ATMOSPHERIC TEMPERATURE
NT AURORAL TEMPERATURE
NT BODY TEMPERATURE
NT BRIGHTNESS TEMPERATURE
NT COMBUSTION TEMPERATURE
NT CRITICAL TEMPERATURE
NT CURIE TEMPERATURE
NT FLAME TEMPERATURE
NT GAS TEMPERATURE
NT HIGH TEMPERATURE
NT IGNITION TEMPERATURE
NT ION TEMPERATURE
NT IONOSPHERIC TEMPERATURE
NT LOW TEMPERATURE

NT LUNAR TEMPERATURE
NT NOISE TEMPERATURE
NT OPERATING TEMPERATURE
NT PLANETARY TEMPERATURE
NT PLASMA TEMPERATURE
NT ROOM TEMPERATURE
NT SATELLITE TEMPERATURE
NT SKIN TEMPERATURE [BIOLOGY]
NT SOLAR TEMPERATURE
NT STAGNATION TEMPERATURE
NT SUBZERO TEMPERATURE
NT SURFACE TEMPERATURE
NT TRANSITION TEMPERATURE
NT WALL TEMPERATURE
NT WATER TEMPERATURE

TEMPERATURE COMPENSATION

Temperature compensated high dielectric constant material, discussing low loss at microwave frequencies, reproducibility and mechanical properties

01 p0044 A72-11308

Transient radiation effects on silicon diodes in avalanche breakdown, considering voltage regulating diode response and temperature compensating junction effects

03 p0334 A72-14090

Aerodynamic compensation for ambient medium temperature effect on fluidic standard components and timing devices

04 p0466 A72-14993

Constant temperature hot-wire anemometer compensation for thermal lag of wire or film resistance thermometer

09 p1306 A72-22307

Fast response thermal compensation system for gas laser resonator length and frequency stabilization, discussing fabrication and design calculation

12 p1822 A72-27607

Light emitting diodes, photodiodes and photon coupled pair temperature compensation schemes, including uses of n-p-n transistors, operational amplifier and thermistor-resistor network

15 p2247 A72-32034

Rational utilization of the strength capabilities of thermal-expansion compensators

21 p3127 A72-41702

Simultaneous measurements of temperature and velocity in heated flows.

23 p3292 A72-44541

TEMPERATURE CONTROL

Cavity resonator thermal stabilization, using gas pressure controlled membrane

02 p0196 A72-12698

Thermal control methods for high density packaging, discussing cooling techniques for hybrid circuit consisting of semiconductor chips and/or thin film components

03 p0337 A72-14293

Closed-loop temperature distribution optimal control by heater-sensor spatial configuration design for highest steady state temperature stiffness under heat flux disturbance

04 p0504 A72-14661

Iterative procedure for computing optimal controls in distributed parameter systems described by linear parabolic differential equations, applying to metal slab temperature profile problem

04 p0504 A72-14664

Nonsteady high-rate heat transfer control in boundary layer by conjugate problem treatment and reduction to Volterra equation, considering limiting-regime and stability

04 p0596 A72-14666

Laser ranging retroreflector deployed by Apollo missions, discussing array design, structural support and thermal control

04 p0509 A72-15099

Nerve structures localized cooling device using vacuum insulated closed circuit controlled cryogenic probe with cooling range of plus/minus 20 C

04 p0481 A72-15252

Azur satellite temperature control system for protection against internal heat dissipation and external thermal loads due to earth radiation and albedo

04 p0582 A72-15651

Ni-Cr thick films triode sputtering technique with temperature control by low-energy electron bombardment heating, presenting phase diagram

05 p0675 A72-16393

Amplifier amplitude characteristic nonlinearity effect on dynamic properties of autooscillatory temperature controller

07 p0981 A72-18926

Zirconium dioxide white pigment coatings for spacecraft thermal control, discussing impurities effects on optical absorption properties

07 p1023 A72-19692

Ti honeycomb brazing, discussing filler metals, furnace temperature and atmosphere control and use of protected graphite as furnace material

07 p0998 A72-20288

Temperature controller with linear time variation for semiconductors thermally stimulated conductivity and thermoluminescence measurements at 90-300 K operating range

08 p1166 A72-21438

Bimetallic actuator for spacecraft thermal control with design emphasis on external power source elimination, high reliability, frictionless operation, simplicity and low weight

09 p1305 A72-22249

Electromagnetic field forces on finite conducting bodies, discussing heating rates and temperatures with ambient air convection and machine design recommendations

09 p1359 A72-22679

ITOS-1/Tiros M/ satellite design, describing structure, thermal and attitude control, primary and secondary sensor subsystems, power supply and operational goals

09 p1396 A72-23373

High purity fine particle pigment materials preparation for spacecraft thermal control coatings discussing hydrothermal, cryochemical and vapor phase processes

10 p1500 A72-24145

Vaporizer temperature effect on ion propulsion system thrust vector, presenting temperature control loop circuit diagram

10 p1528 A72-24652

Thermal diode heat pipe for advanced thermal control flight experiment, discussing engineering model analysis, design, fabrication and test

[AIAA PAPER 72-260]

11 p1739 A72-25205

ATS specular thermal control louver system performance in simulated solar vacuum environment as function of sun and blade angle, noting white paint effect

[AIAA PAPER 72-268]

11 p1740 A72-25209

Experimental cold plates provided with heat pipes for thermal control of electronic equipment

[AIAA PAPER 72-269]

11 p1740 A72-25210

Precision temperature control system for spacecraft equipment thermal loads rejection by space radiator, using acetone variable conductance heat pipes

[AIAA PAPER 72-270]

11 p1740 A72-25211

Heat pipe applications for waste heat rejection, cooling and temperature control in space shuttle, discussing design and performance

[AIAA PAPER 72-272]

11 p1725 A72-25212

Aircraft cockpit electrical heating system, converting three phase ac energy from alternator with economy and safety

[SAE PAPER 720329]

11 p1577 A72-2559

Human body thermoregulatory processes under varying environmental conditions and metabolic rates, discussing role of blood circulation, sweating, nervous stimuli, hormones, etc

11 p1584 A72-2607

Compact photomultiplier housing with controlled cooling, discussing temperature control and measurement

12 p1806 A72-2726

Communication satellites design and technology for future launchings, discussing ion engine development, antenna beams and thermal control

[AIAA PAPER 72-540]

12 p1780 A72-27363

Polymer testing machine for simultaneous structural and mechanical properties measurement of specimens subjected to uniaxial tensile loads for broad temperature range

12 p1795 A72-27465

ATS F/G spacecraft thermal control design verification by chamber thermal balance tests and performance prediction mathematical model of earth viewing module and orbital environment

12 p1877 A72-27527

Turbine inlet gas temperature limiting systems design and operation in turboprop engines, describing blocking mechanism, delaying element and altitude compensation

12 p1861 A72-27863

Electronic heating test arrangement for high temperature testing of metals and electrically conducting ceramics in vacuum, describing temperature control systems

12 p1796 A72-28249

Vacuum induction melting process for high temperature steels and superalloys fabrication, emphasizing control over temperature, pressure, beneficial trace elements and harmful impurities

13 p1964 A72-29100

Time constant of aircraft gas turbine engines gas temperature regulating system, using two thermocouples with different rise times

13 p2028 A72-29138

Temperature control and measurement in electric wire annealing for standard Pt-Pt-10 Rh thermocouples

13 p1960 A72-29766

Single automatic potentiometer based maximum-minimum temperature control unit, noting elimination of dual temperature regulators

14 p2104 A72-30444

Minimum weight phase change thermal control device for planetary descent probes, discussing test over various heat loads

[AIAA PAPER 72-287]

14 p2171 A72-30826

High reliability long life heat pipe thermal control system for space station application

[AIAA PAPER 72-261]

14 p2171 A72-30835

Space simulation shrouds cryogenically cooled with liquid carbon dioxide, discussing automatic temperature control and operating cost savings

15 p2214 A72-32611

Constant voltage and constant emitter-temperature control schemes dynamics in thermionic reactor, showing closed loop responses to load changes, converter failures and reactivity perturbations

17 p2494 A72-34581

Controlled self heating effect in semiconducting barium titanate positive temperature coefficient resistor substrate heater for planar Si devices

17 p2527 A72-34680

Electronic temperature-flattening of thermionic reactors.

18 p2644 A72-36172

A high-accuracy temperature stabilizing and control device also operating in the cryogenic range

19 p2804 A72-38645

Space station prototype environmental/thermal control and life system - A current overview.

[ASME PAPER 72-ENAV-35] 20 p2894 A72-39143

Thermal control design for research applications module (RAM) shuttle compatible payload carriers, using Freon 21-water system

[ASME PAPER 72-ENAV-31] 20 p2894 A72-39146

Thermal control concept evaluation for a ten-year life modular space station.

[ASME PAPER 72-ENAV-30] 20 p2894 A72-39147

Development of a laboratory prototype spraying flash evaporator.

[ASME PAPER 72-ENAV-28] 20 p2894 A72-39149

Thermal control system incorporation into lunar roving vehicle (LRV) for electronic component protection during translunar transportation and lunar surface operation

[ASME PAPER 72-ENAV-27] 20 p2894 A72-39150

Significant factors in environmental and thermal control/life support system design for space shuttle orbiter

[ASME PAPER 72-ENAV-21] 20 p2895 A72-39156

Space shuttle environmental temperature control-life support system program changes, discussing air cooled electronic equipment, cryogenic stores, crew size and mission duration

[ASME PAPER 72-ENAV-18] 20 p2895 A72-39159

The development of a 150,000 watt-inch variable conductance heat pipe for space vehicle thermal control.

[ASME PAPER 72-ENAV-14] 20 p2896 A72-39163

Computer simulation of the space shuttle orbiter environmental thermal control system.

[ASME PAPER 72-ENAV-12] 20 p2896 A72-39165

Integration of an automated onboard data management system with a manned spacecraft environmental thermal control and life support system.

[ASME PAPER 72-ENAV-6] 20 p2896 A72-39171

A temperature adjustment process in a Boussinesq fluid via a buoyancy-induced meridional circulation.

21 p3044 A72-40112

Electronic simulator for calculating effective temperatures in the establishment of climatological procedures

21 p3077 A72-40166

A novel specimen stage permitting high-resolution electron microscopy at low temperatures.

21 p3051 A72-40218

A new creep rupture testing machine with loading by tubular springs and electronic temperature control

22 p3164 A72-42860

Thermal control techniques used in space simulation laboratory testing.

22 p3164 A72-42997

R and D on environmental and thermal control/life support system application to lunar base mission, discussing reliability and food regeneration

24 p3375 A72-45164

TEMPERATURE DIFFERENCES

U TEMPERATURE GRADIENTS

TEMPERATURE DISTRIBUTION

Infinite slab, cylindrical or spherical shells with nonuniform heat generation sources and equal surface temperatures, obtaining maximum internal temperature from error bounds

01 p0145 A72-10511

Thermal stresses, temperature distribution and displacement fields in elastic solid with spherical cavity and external crack

01 p0144 A72-11385

Forced air cooling of cylindrical body with distributed thermal input, calculating temperature distribution and optimum mechanical dimensions for temperature rise minimization

02 p0189 A72-11560

Turbulent boundary layer flow past surface with arbitrary temperature distribution, presenting approximate heat transfer solution with allowance for pressure gradient and Reynolds number

02 p0201 A72-11582

Elastoplastic deformation in medium with initial dislocations and temperature field, expressing kinetic stress and distortion tensors by Hamiltonian derivatives

02 p0290 A72-11630

Temperature fields and stresses in thin elastic non-ferromagnetic electrically conducting cylindrical shells heated by induction determined from heat source distribution and thin shell theory relations

02 p0290 A72-11631

Thermal conductivity and boundary conditions for unsteady thermal fields in thin anisotropic plates with heat emission

02 p0291 A72-11635

Wall conduction effect on heat transfer to laminar boundary layer, obtaining temperature distributions at plate surface by energy transport equation

02 p0202 A72-11670

Space TV images use in hydrothermal temperature discontinuity front location, examining cloud cover distributions over Sea of Japan

02 p0214 A72-11872

Locally nonsimilar solutions for thermal boundary layer, presenting surface heat transfer and temperature distribution

[ASME PAPER 71-HT-L] 02 p0302 A72-12313

Radiative heat transfer within nonisothermal air plasma, presenting centerline temperature data for various boundary pressures and temperatures

[ASME PAPER 71-HT-G] 02 p0302 A72-12316

Nonstationary temperature field determination in stream turbine casing-connector nozzle by difference method based on heat balances, comparing results with electric analog studies

02 p0303 A72-12534

Lee waves characteristics relationship to air flow and temperature layers in troposphere based on satellite pictures

02 p0255 A72-12791

Velocity and temperature distributions for unsteady plane Poiseuille flow of viscous incompressible fluid between two parallel plates

03 p0340 A72-13000

Solar coronal monochromatic optical emission, inferring electron density and ionization or temperature distributions and variations with time

03 p0422 A72-13208

Ground based atmospheric vertical temperature profiles measurement by Raman backscatter from molecular nitrogen

03 p0348 A72-13430

Two dimensional elasto-viscous incompressible fluid flow past porous wall with variable suction, analyzing temperature field of laminar thermal boundary layers

03 p0341 A72-13500

Current lines and temperature fields in square cavity with one movable wall and viscous flow and heat transfer, solving equations numerically

03 p0456 A72-13629

Temperature field analysis in locally heated cylindrical shell for stressed state production with lowest elastic energy

03 p0456 A72-13733

Complex geometry inhomogeneous sandwich plate, calculating temperature field with R functions

03 p0456 A72-13738

Temperature stresses near thermally insulated square holes in unbounded plane, determining temperature distribution

03 p0449 A72-13914

Curvilinear material anisotropy effects on temperature distributions of thin walled cylindrical shells of revolution

03 p0449 A72-13919

Small signal gain and radiant power of carbon dioxide gas dynamic laser, presenting temperature distribution and population inversion

03 p0368 A72-13920

Cross flow blown two dimensional stationary plasma arc deflection and temperature distribution as function of collisional drift velocity and electric field

03 p0397 A72-13921

Elastic plate with two collinear thermally insulated cracks, calculating steady temperature field and stresses for uniform heat flux at infinity

03 p0450 A72-14112

Small parameter method solutions to linear viscoelasticity problems with nonhomogeneous temperature field applied to reinforced tube under internal pressure

03 p0454 A72-14217

Heat transfer to liquid fuel burning from sandfilled pan burner, measuring burning rate, wick temperature distribution and flame radiation heat flux distribution as function of time

03 p0458 A72-14221

Thermal boundary layer of incompressible fluid unsteady laminar flow, obtaining temperature field from energy equation for various wall temperature conditions

03 p0343 A72-14314

Transformation of differential equations describing interaction between electric arc and gas flow by taking temperature as independent variable, considering Laval nozzle example

03 p0344 A72-14392

TEMPERATURE DISTRIBUTION

Freezing of hot fluid flowing onto flat cold wall, solving nonlinear integrodifferential equation for temperature distribution by iteration method

04 p0595 A72-14650

Closed-loop temperature distribution optimal control by heater-sensor spatial configuration design for highest steady state temperature stiffness under heat flux disturbance

04 p0504 A72-14661

Optimal temperature fields and stress-strain state in orthotropic conical and cylindrical shells subject to local heating

04 p0588 A72-15051

Nearly free molecular slit flow of gas from reservoir at finite pressure and temperature ratios

04 p0512 A72-15120

Newtonian fluid laminar free convection over curved wall with arbitrary temperature variation, investigating similarity solutions existence by method of free parameters

04 p0596 A72-15193

Underexpanded nitrogen jet from sonic orifice, investigating axial rotational temperature distribution

04 p0597 A72-15335

Lunar thermal history and radioactivity upper limits determination consistent with proposed temperature distribution and Apollo chondrite data, implying low uranium content

04 p0581 A72-15579

Optimal temperature fields in locally heated orthotropic cylindrical shells, determining rigidities effect

04 p0593 A72-15655

Three dimensional temperature distribution at thermally insulated crack in plate

04 p0593 A72-15658

Thermal laminar boundary layer equations solution for power-law velocity distribution in external flow and arbitrary surface temperature distribution

05 p0742 A72-15844

Piecewise linear approximation of inverse nonstationary conductive heat transfer through unbounded plate with arbitrary temperature distribution and asymmetric boundary conditions

05 p0742 A72-15847

Nitrogen heat pipe axial temperature distribution and vapor pressure measurement, noting effective thermal conductivity variation with power load and inclination angle

[ASME PAPER 71-WA/HT-28] 05 p0744 A72-15881

Steady state heat transfer problem solutions in living tissue modeled as cylindrical shells, discussing blood flow and temperature distributions in extremities

[ASME PAPER 71-WA/HT-34] 05 p0745 A72-15885

Turbulent flow and heat transfer characteristics of non-Newtonian fluids on flat plate, measuring velocity and temperature distributions

05 p0648 A72-16003

Electric field strength, radiated power and radial temperature distribution measurements in high pressure Ar cascade arc

05 p0695 A72-16156

Two dimensional stationary temperature fields determination in ribs, cylinders and pipes with temperature independent heat conductivity

05 p0746 A72-16188

Thermal signal propagation in flowing fluid, plane, line and point sources of varying heat, calculating temperature distribution with conduction and convection heat transfer equation

05 p0746 A72-16295

Time behavior of temperature and emission measure in X ray flares observed from Vela 5 spacecraft

05 p0709 A72-16518

Temperature variation with latitude in upper solar photosphere from photoelectric meridional and equatorial limb-darkening scans

[AD-744409] 05 p0719 A72-16710

Gegenbauer/ultraspherical/ polynomials and Meijer G-functions for solution of heat production and diffusion in cylinder with internal sources leading to axisymmetric temperature distribution

05 p0747 A72-16791

Radiative transfer in gray medium with prescribed spatial temperature distribution in rectangular enclosures with nonisothermal walls, deriving exact solutions by radiation transport theory

[AIAA PAPER 72-21] 05 p0748 A72-16869

Turbulent jets interaction with cross flow, presenting longitudinal and transverse velocity, temperature and turbulence distributions

[AIAA PAPER 72-149] 05 p0651 A72-16870

Equilibrium temperature distribution on radiatively adiabatic smooth and rough planes uniformly irradiated by collimated solar flux

[AIAA PAPER 72-59] 05 p0749 A72-16876

Incompressible fluid unsteady kinetic energy equation periodic solution for harmonic oscillation viscous dissipation influence on temperature field, considering Couette steady flow solution

05 p0750 A72-17007

Partially insulated homogeneous cylinder temperature distribution from heat conductivity boundary value problem equations

05 p0751 A72-17142

Thermoelasticity equations for thermal shock effect on freely supported circular plate, describing deformation and temperature field interactions

05 p0741 A72-17147

Solar wind structure from long lived inhomogeneities in corona, allowing for velocity, density and temperature perturbations

06 p0872 A72-17444

Temperature and density fluctuations in photosphere from Fe and Mg line intensities, noting variations due to granulation in solar atmosphere model

06 p0876 A72-17579

Velocity and temperature pulsations as function of stratification parameter in atmospheric boundary layer

06 p0842 A72-18044

Multiphase Stefan problems for bounded and unbounded temperature fields with variable phase volume

06 p0904 A72-18401

Multilayer heat reflective coating optical thickness effect on temperature distributions, taking into account interlayer contact resistance and thermal radiation volume absorption

06 p0904 A72-18511

Complex bodies time dependent temperature distribution from temperature measurements at arbitrary points, using Duhamel integral

06 p0904 A72-18512

Kinetic theory of wall temperature jump and near-wall temperature distribution in polyatomic gases, solving simultaneous singular linear integral equations by numerical methods

06 p0904 A72-18528

Temperature stress distribution in infinite plate with time varying heat transfer coefficient

06 p0899 A72-18565

Stress and temperature fields in cooled gas turbine blades with allowance for elasticity, plasticity and creep

06 p0899 A72-18628

Power series method with Cauchy formula for non-linear partial differential equations solution in unsteady periodic temperature oscillations

06 p0905 A72-18727

Laplace equation internal Dirichlet and Neumann boundary value problems solution procedure for thermal potential of steady temperature field

07 p1098 A72-18988

Temperature distribution in composite media with internal heat generation, solving diffusion equation via Vodicka type orthogonality relationship

07 p1100 A72-19626

Temperature distribution in infinite slab during and after heat generation by plane source of finite duration

07 p1100 A72-19627

Transpiration cooling of laminar tangential Newtonian flow in annuli, obtaining temperature distribution

07 p1100 A72-19631

Hydrogen halide rotational relaxation to thermal distribution without intermediate quantum number peak, discussing IR chemiluminescence data correction method

07 p0936 A72-19673

Temperature pulsation spectra of turbulent mercury flow in horizontal pipe at various Reynolds numbers, showing dependence on magnetic field

07 p1100 A72-19882

Axisymmetric single phase Stefan problem with boundary condition of second kind, obtaining temperature distribution along solidifying zone

07 p1101 A72-19892

Algorithm for solving boundary value problem of integrodifferential equations describing temperature field inside hollow thin walled rod within solar radiation field in vacuum

07 p1028 A72-20207

Temperature fields and mass and heat transfer at surface of solid spherical particle in laminar viscous fluid flow

07 p0973 A72-20318

Thermomolecular pressure gradients and temperatures in flow between parallel plates for statistical gas models at arbitrary Knudsen numbers

07 p1101 A72-20513

Solar radio emission, considering sources of slowly varying waves, brightness temperature distribution, frequency spectra and fluctuations

08 p1228 A72-20827

Unsteady temperature field and conductive heat accumulating properties of bodies with dihedral and polyhedral angles

08 p1251 A72-20954

Three dimensional nonstationary heat conduction of hollow circular cylinder in medium with different temperature

08 p1251 A72-20972

Spatial-temporal temperature distribution on CW laser irradiated materials, noting application to water film

08 p1252 A72-21289

Temperature and concentration fields of liquid solution droplets during unsteady vaporization process in high temperature gas media

08 p1252 A72-21308

Uniform and crowded temperature distribution in large geometry power transistor, solving time dependent heat diffusion equation

08 p1141 A72-21419

Temperature distribution and zone melting in carbon thin films heated by electron beam, using Sn crystal indicators

08 p1253 A72-21446

Nonuniform temperature distribution effect on heat conduction coefficient of hot-wire cell, using computerized net point method

08 p1166 A72-21449

Mesospheric temperature and wind profiles during stratospheric warming from rocket grenade experiments

08 p1160 A72-21533

Spherically symmetric Stefan problem with boundary condition of second kind, obtaining temperature distribution

08 p1255 A72-21671

Under-lip temperatures and thermal conductivity in rotary shaft seals, using heat transfer analysis

08 p1178 A72-21934

Statistical analysis of temperature characteristics based on natural orthogonal components expansion for weather forecasting application

08 p1203 A72-22120

Weather analysis for mountainous terrain from potential temperature surface maps and vertical cross sections

09 p1344 A72-22431

Temperature fields produced in viscoelastic cylindrical, conical and spherical shells by cyclic loads, calculating displacements from zero moment stress theory formulas

09 p1399 A72-22701

Temperature and thermal stress distribution in cylinder of finite length for mixed heating conditions

09 p1400 A72-22707

Two dimensional thermoelasticity problem with nonstationary temperature field and external boundary forces, using algorithm to evaluate stress-strain state of welded plates

09 p1401 A72-22725

Thermal buckling of parallelogram shaped plate under stationary temperature field and uniformly distributed forces, deriving critical load

09 p1402 A72-22733

German book on unsteady heat conduction and temperature field equalization covering mathematical treatment with Laplace transformations

09 p1412 A72-23175

Nonstationary temperature field of semitransparent shell with nonuniformly distributed heat sources

09 p1412 A72-23184

Radial temperature distribution in Ar plasma jet, assuming local thermodynamic equilibrium

09 p1364 A72-23387

Kinematic and thermal turbulent fluctuations isolation by means of hot-wire anemometric probe

10 p1479 A72-24055

Asymmetry and intermittency factors of temperature and velocity fluctuations in viscous substrate of hot plate turbulent boundary layer

10 p1464 A72-24064

Radial temperature distribution determination in nitrogen plasma jet from continuous spectral background intensity measurement

10 p1519 A72-24131

Heat transfer through glass plate in solar radiation flux, discussing temperature distribution and thermal flux meter design

10 p1562 A72-24318

Cavity flow driven by buoyancy and shear, obtaining flow and temperature fields from Navier-Stokes equation numerical solution

10 p1467 A72-24366

Thin circular plate quasi-static thermal stresses induced by transient temperature distribution on upper face, obtaining series form solution in terms of Bessel functions

10 p1558 A72-24720

Two dimensional transverse subsonic hot-air jet interaction with freestream flow at various jet/freestream velocity ratios, measuring jet velocity and temperature distributions

[AIAA PAPER 72-292]

11 p1567 A72-25230

Lunar surface roughness effect on temperature distribution, noting solar elevation and observation angle dependence

[AIAA PAPER 72-310]

11 p1715 A72-25244

Temperature distributions in constant viscosity incompressible Couette flow with additional pressure gradients

11 p1743 A72-25262

Drazin method application to thermal stratification effects on unbounded jets and shear layers stability characteristics

11 p1615 A72-25552

Global sea surface temperature distribution determination with ITOS 1 radiation measurements and composite histogram, discussing RMS errors

11 p1620 A72-25767

Numerical calculation of temperature distribution and tempering depth for inductive hardening process with automatic material feed, taking into account temperature dependent material properties

11 p1639 A72-25899

Electrode gap current and temperature distributions during electrochemical precision processing of metals studying gas and electrolyte flow

11 p1613 A72-26255

Laser light intensity relationship to temperature distribution in completely ionized plasma, defining optimal heating conditions

11 p1696 A72-26344

Thermal stresses in cylindrical shell under moving hot spot with cooling effect of surrounding media

11 p1737 A72-26423

Thermal stresses in homogeneous isotropic and composite curved beams for temperature distribution in polynomial form with coefficients representing functions of two remaining coordinates

11 p1737 A72-26664

Pressure and temperature fields expansion in natural orthogonal components, considering application to long range forecasts construction

11 p1683 A72-26888

Finite difference method for bending stresses calculation in rotating disks subjected to irregularly distributed temperature, deriving digital computer program algorithm

11 p1712 A72-26970

Hyperboloidal profile circular disk stress distribution induced by thermal pulse nonuniform temperature field

11 p1739 A72-26979

Stress-strain state and temperature distribution in transversely isotropic layer under mixed heat transfer conditions

12 p1878 A72-27083

Two heat conducting phases free boundary problem with temperature distribution within phases, proving existence and uniqueness theorems

12 p1836 A72-27124

Lunar interior thermal history discussing mathematical models for radioactive heat source, initial conditions, temperature distribution and time dependence fractionation

12 p1870 A72-27314

Temperature distribution and dissipation effects in compressible isothermal atmosphere Lamb waves vertical structure

12 p1839 A72-27514

Thermal flux on contact area and temperature distribution on specimen surface during diamond grinding

12 p1814 A72-27717

Temperature distribution and heat dissipation calculations for CW and pulsed laser optical elements

12 p1824 A72-27877

Gas turbine engine combustion chamber, investigating swirl vane air flow rate effects on circumferential nonuniformity of gas temperature field at outlet

12 p1861 A72-28132

Radial and circular thermal stresses in free and end-constrained orthotropic cylinders with axisymmetric temperature distributions, determining relations between temperature and thermoelastic coefficients

13 p2055 A72-28561

Axisymmetric temperature problem with arbitrary load duration for disk-shaped crack fracture mechanics, using Fredholm equation with symmetrical kernel for temperature field determination

13 p2055 A72-28720

Temperature distribution in rotating cylinder with moving surface source, allowing for heat transfer to ambient medium

13 p2064 A72-28916

Surface temperature distribution for porous plate in supersonic flow with gas injection into turbulent boundary layer

13 p1893 A72-28917

Thermomechanical interactions between elastic waves and nonstationary temperature fields in solid continua, considering coupled and uncoupled theories

13 p2064 A72-29093

Three dimensional steady temperature field calculation for solid bodies under concentrated heat source, using flow kinetic heat conduction method

13 p2065 A72-29151

Ethanol liquid fuel counterflow diffusion flame stabilization and thermal structure determination by interferometry

13 p1913 A72-29306

Two point correlation description of MHD plasma properties subject to electrothermal instability, calculating electron number density and temperature fluctuations

13 p2015 A72-29373

Avrett-Krook temperature correction procedure modified to improve, near surface convergence for blanketed model stellar atmospheres

13 p2040 A72-29406

Plastic properties of locally heated refractory metals in hot pressing calculated from temperature distribution
13 p1966 A72-29465

Cs vapors thermal conductivity at various temperatures and pressures, using low emissivity Ni cylinders
13 p2065 A72-29896

Isothermal vertical plate turbulent thermal boundary layer during free convection, noting temperature pulsations dispersion
13 p2066 A72-29899

System of equations derived for unsteady temperature field of arbitrary multilayer shell, using polynomial expression as temperature approximation for shell thickness
13 p2066 A72-29949

Mars upper cover temperature, representing diurnal variations at different areographic latitudes as harmonic series
14 p2148 A72-30207

Interferometric investigation of temperature fields and heat transfer in air layers between vertical, inclined and horizontal parallel walls
14 p2170 A72-30251

Aircraft engine components fatigue life assessment under small cycle temperature conditions, including temperature field and stress-strain determination in critical spot
14 p2145 A72-30279

Composite two-material circular sector two dimensional stationary temperature field determined for certain thermal conduction coefficient ratios
14 p2170 A72-30573

Temperature distribution of structural element with heat shield and metallic layer, determining ablation process for thermal flux at surface
14 p2170 A72-30593

Relaxation method for thermal computation programs to solve nonlinear heat exchange equations for steady state temperature distribution, discussing numerical instability due to linearization
14 p2170 A72-30684

Electric arc plasma, predicting elements addition and electron density alteration effects on radial temperature distribution
14 p2139 A72-30778

Electric arc plasma, investigating reaction energy effects on radial temperature distribution
14 p2139 A72-30779

Schlieren method for qualitative study of optical inhomogeneities produced by temperature field in cylindrical solid body
14 p2106 A72-31162

Temperature distribution and heat transfer coefficients in turbulent separated flow region downstream of rearward step in subsonic wind tunnel, using Mach-Zehnder interferometer
15 p2333 A72-31204

Thermal laminar boundary layer equations solution for power-law velocity distribution in external flow and arbitrary surface temperature distribution
15 p2334 A72-31263

Piecewise linear approximation of inverse nonstationary conductive heat transfer through unbounded plate with arbitrary temperature distribution and asymmetric boundary conditions
15 p2334 A72-31266

Heat conductivity equation solution for laminar gas flow in tubes, calculating temperature field and heat removal for molecular lasers with gas pumping
15 p2245 A72-31421

Thermal stress and temperature distribution in rigidly bounded elastic half-space, taking into account coupling effects
15 p2325 A72-31637

Heat transfer and longitudinal temperature distribution at Hartmann-Sprenger tube inlet calculated approximately on basis of boundary layer data in steady compressible flow
15 p2217 A72-31685

Stress-strain state of spherical body in centrally symmetric temperature field, noting elastoplastic interface and continuity conditions
15 p2327 A72-31742

Closed form solution for transient temperatures between two thermocouple readings, using Laplace transformation
15 p2336 A72-32583

Velocity and temperature distribution for viscous incompressible fluid unsteady flow between two parallel plates with pressure gradient linearly varying with time
15 p2199 A72-32599

Thermoelastic stress analysis for hollow cylinder heated along helix, calculating stress function for given surface temperature distribution
15 p2333 A72-32687

Subsonic and supersonic steady two dimensional compressible turbulent boundary layer flow past wavy wall, presenting wall pressure and temperature distributions
16 p2341 A72-32828

Temperature profile derivation for uppermost convection region of two solar convection zone models from finite amplitude convection theory
16 p2451 A72-33037

Unsteady heat conduction in hollow cylinder suddenly heated by temperature field moving along outer and inner side surfaces
16 p2475 A72-33114

Stress analysis for brittle body with thermoinsulated crack under mechanical load and temperature field, noting limiting equilibrium equation
16 p2469 A72-33272

Steady state temperature field and heat flux at wall for metallic coolant flow in thin walled axisymmetric pipe with nonhomogeneous Neumann boundary condition
16 p2477 A72-33434

Wall and ambient temperature distribution effects on free convection heat transfer from nonisothermal vertical flat plate in temperature stratified medium for Prandtl number range
16 p2477 A72-33434

German monograph on pressure loss and heat transfer in heat exchangers, taking into account hydrodynamic and thermal inflow velocity and temperature distribution
16 p2478 A72-33504

Magnetothermoelastic temperature distribution effects due to linear heat source in infinite circular cylinder acted upon by magnetic field
16 p2425 A72-33595

Temperature field in flat plate with selective radiation absorption coefficient, using asymptotic representations for internal heat flux radiation component
16 p2479 A72-33858

Temperature distribution and heat dissipation calculations for CW and pulsed laser optical elements
16 p2403 A72-33982

Steady state magnetically balanced cross flow arc, calculating flow and temperature fields and boundary shape under assumption of two independent variables [AIAA PAPER 72-687]
16 p2439 A72-34055

Temperature and stress fields generated by pulsating internal pressure in viscoelastic hollow sphere with temperature dependent material properties, using iterative numerical procedure
16 p2473 A72-34122

Prediction of the flow and heat transfer in a rectangular wall cavity with turbulent flow.
[ASME PAPER 72-APM-Q]
17 p2636 A72-34305

A first initial boundary value problem for a semilinear heat equation.
17 p2573 A72-34339

Reactor core length, externally configured thermionic converter.
17 p2495 A72-34589

Collapse calculations for 0.25-10 solar mass spherical protostars, discussing stellar core evolution and temperature distribution in infalling cloud
17 p2606 A72-34674

Computer thermal analysis of hybrid microcircuits.
17 p2521 A72-34679

The identification of parameters in nonlinear thermal networks with the aid of a Kalman filter
17 p2533 A72-34827

Multiphase Stefan problems for bounded and unbounded temperature fields with variable phase volume
17 p2636 A72-34852

Onset of convection near a suddenly heated horizontal wire.
17 p2637 A72-35048

Temperature distribution in solids under laser irradiation.
17 p2564 A72-35355

Unsteady temperature distribution for laminar flow in a porous straight channel.
17 p2541 A72-35434

Turbulent boundary layer with discontinuity in wall temperature and concentration
17 p2638 A72-35746

Distortion of the semi-infinite solid due to transient surface heating.
17 p2635 A72-35974

Observations of the variability of dissipation rates of turbulent velocity and temperature fields.
18 p2678 A72-36022

Geochemically and geophysically consistent model of lunar accretion process to explain initial temperature distribution
18 p2725 A72-36291

Solution of heat transfer problems with the aid of Laplace transforms. I - Development of analytical solutions for two specific boundary value problems
18 p2740 A72-36422

Multimesa versus annular construction for high average power in semiconductor devices.
18 p2666 A72-36455

Convective cells formation in fluid unsteady flow between two horizontal rigid boundaries with time periodic temperature distribution
18 p2681 A72-36483

TEMPERATURE DISTRIBUTION

Thermo-elastic interactions in an infinite elastic solid due to a concentrated transient heat source.
18 p2735 A72-36754

Unsteady-state temperature distribution in a connecting fin of constant area.
18 p2741 A72-36935

Viscoelastic analysis of graphite under neutron irradiation and temperature distribution.
18 p2704 A72-37088

Solution of the general heat transfer problem by the integral Tolubinskii method for a longitudinal flow past cylindrical bodies
18 p2742 A72-37182

Calculation of the temperature field of a heated zone of complex form consisting of a chassis and built-in components
18 p2742 A72-37187

Thermal displacements and stresses in cylindrical shells due to instantaneous line heat sources.
19 p2870 A72-37272

Experimental investigation of nonstationary heat exchange for flow around a flat plate
19 p2880 A72-37665

Temperature probes for flows at high enthalpy [ONERA, TP NO. 1074]
19 p2800 A72-37767

Ulcera meteorite - Determination of differential atmospheric heating using its natural thermoluminescence.
19 p2858 A72-37859

Solution of boundary value problems in heat conduction by the method of the successive averaging of a desired function
19 p2881 A72-38042

Temperature field of a gas turbine rotor blade externally cooled by an air-liquid mixture
19 p2849 A72-38043

Post-critical deformations of a cylindrical shell subject to the action of external pressure and a temperature field
19 p2878 A72-38472

Temperature distribution in hot wires in high-enthalpy low-density flows [DFVLR-SONDDR-216]
19 p2804 A72-38685

Discussion of the thermal state of an open air premixed methane-oxygen flame.
19 p2883 A72-38871

Rotationally symmetric temperature distribution in region between two coaxial circular cones for isothermal and adiabatic conditions, solving heat conduction equation
20 p2983 A72-39329

Temperature distribution control in n-dimensional space via quasi-inversion method with Fourier transformation for Cauchy problem solution of heat conductivity equation
20 p2983 A72-39466

Unsteady heat transfer and temperature for Stokesian flow about a sphere.
[ASME PAPER 72-HT-C]
20 p2983 A72-39482

Straight fins with periodic base temperature variation, calculating design parameters effects on heat transfer rates, temperature distributions and efficiencies
[ASME PAPER 72-HT-E]
20 p2983 A72-39484

The effect of thermal conductivity and base-temperature depression on fin effectiveness.
20 p2983 A72-39489

Microelectronic component system temperature distribution measurement by IR microscope and electrical technique to determine beam-lead IC thermal performance
20 p2908 A72-39498

The computation of dynamic equilibrium temperature distributions on substrates having a temperature-dependent thermal conductivity.
20 p2908 A72-39499

Temperature distribution in a helically heated tube
20 p2984 A72-39648

An analytical solution of wall-temperature distribution for transpiration and local mass injection over a flat plate.
[ASME PAPER 72-HT-57]
20 p2985 A72-39659

Thermal remote sensing of temperature distribution in semitransparent solids - A numerical experiment.
[ASME PAPER 72-HT-5]
20 p2986 A72-39676

An analysis of the spectral scanning technique for determining the temperature distribution in a semi-transparent medium.
[ASME PAPER 72-HT-6]
20 p2986 A72-39677

Remote sensing of urban 'heat islands' from an environmental satellite.
20 p2919 A72-39717

Calculation of a plane stationary temperature field in the presence of a heat source
20 p2987 A72-39915

Digital simulation of the SEI-1 static electrointegrator for solving heat-type equations
21 p3127 A72-40160

Nonisothermal surface cooling for arbitrary temperature distribution and Prandtl number approaching zero, solving thermal boundary layer equations by series expansion
21 p3129 A72-41061

Application of the elementary-balance method to the calculation of the nonstationary temperature fields and aerodynamic characteristics of several versions of a surface-type heat exchanger

21 p3130 A72-41064

Elastic isotropic material mechanical and thermal constitutive equations restrictions investigation to ensure local stability under perturbations of deformation gradient and temperature field

21 p3120 A72-41203

Stresses and strains in the plastic range in an annular disk due to steady-state radial temperature variation.

21 p3121 A72-41210

Steady radiating gas flow past a semi-infinite flat plate at a constant temperature for an optically thick case.

21 p3131 A72-41497

Buildup of thermal equilibrium in a fluid near the critical point

22 p3242 A72-41882

An inverse problem in the momentless theory of shells of revolution situated in a temperature field

22 p3232 A72-41895

Temperature distribution and heat flux in infinite length rectangular and finite length cylindrical fins, examining validity of one dimensional approximation

22 p3243 A72-41961

Axisymmetric temperature problem with arbitrary load duration for disk-shaped crack fracture mechanics, using Fredholm equation with symmetrical kernel for temperature field determination

22 p3233 A72-42097

Analytical calculation of unsteady heat fields in planar devices

22 p3158 A72-42116

Lunar albedo and temperature distribution from simultaneous photoelectric and far IR brightness temperature measurements of sunlit lunar surface

22 p3226 A72-42536

Effective temperatures of massive stars as a function of chemical composition and mass.

22 p3227 A72-42560

Mars upper cover temperature, representing diurnal variations at different areographic latitudes as harmonic series

23 p3333 A72-43237

A current instability in the neutral layer of the tail of the earth's magnetosphere

23 p3283 A72-43368

Stress concentration around a circular hole in an elastoplastic medium under the action of a temperature field and omnidirectional tension

23 p3344 A72-43418

Three dimensional temperature distribution of internally cooled hollow airfoil section turbine blades, deriving heat transfer equations for digital computation

23 p3325 A72-43667

Spatial and temporal temperature distribution in plasma from a low-voltage aperiodic spark discharge in an atmosphere of argon

23 p3320 A72-43677

Temperature distribution in a perforated stiffener

23 p3356 A72-43684

Probability distribution of velocities and temperatures near a wall

23 p3279 A72-43696

On the approximation of the thermal conductivity of rigid heat conductors as a Cauchy problem.

23 p3356 A72-43721

Thermoviscoelastic problem for semiinfinite plate, determining temperature field and stresses permitting heat propagation

23 p3347 A72-43749

Test equipment for heat resistance determination of brittle refractory material, noting data processing procedure and formulas for temperature distribution and thermal stress

23 p3278 A72-43962

On free vibrations at temperature-dependent material properties and transient temperature fields. [ASME PAPER 72-APM-J]

23 p3350 A72-44053

Determination of the stationary temperature field in a plate with a crack in the presence of heat release from the lateral surfaces

23 p3357 A72-44086

Thermomechanical coupling effects in the longitudinal oscillations of a viscoelastic cylinder.

23 p3352 A72-44122

An experimental study of heat transfer downstream of a rearward-facing step with small coolant injection.

23 p3357 A72-44271

Temperature calculation in a multilayered wall acted on by a thermal pulse.

23 p3357 A72-44537

Latitudinal variation of temperature in the lower thermosphere /80 to 100 km/

24 p3395 A72-44635

Dual analysis for heat conduction problems by finite elements.

24 p3461 A72-44877

Laminar high speed mixing of nonequilibrium dissociating gases.

24 p3392 A72-45056

Developing turbulent flow and heat transfer in concentric annuli.

[CSME PAPER 71-39] 24 p3465 A72-45253

Plane thermoelastic one-dimensional waves in an inhomogeneous medium with allowance for connectedness

24 p3459 A72-45266

Partial differential heat conduction equation for temperature distribution in rectangular plate, comparing with finite difference solution

24 p3465 A72-45268

Calculation of the temperature field in a ventilated cassette-type radio electronic device

24 p3386 A72-45324

Approximate temperature distribution for a diffuse, highly reflecting material.

24 p3465 A72-45790

TEMPERATURE EFFECTS

Sphene U-Pb age resistance to thermal metamorphism, discussing zircon U-Pb and biotite and hornblende K-Ar ages within thermal aureole

01 p0052 A72-10069

Tungsten heat capacity, electrical resistivity and thermal radiation measurement over 2000-3600 K range by pulse heating technique

01 p0082 A72-10174

Spectral distribution of total continuous emission coefficient for LTE hydrogen plasma over 8000-16,000 K and 400-15,000 A ranges, observing Stark broadening

01 p0108 A72-10175

Nb alloys bend ductility at various temperatures, showing silicide coatings and electron beam and gas tungsten arc welding effects on mechanical properties

01 p0083 A72-10284

Hydrostatic pressure and temperature effects on growth of psychrophilic marine bacterium, emphasizing inhibited amino acid transport and respiration

01 p0011 A72-10322

Mossbauer spectra measurement of metallic iron, sodium nitroprusside, sodium ferrocyanide and ferrocyanide absorbers at 78-293 K, fitting temperature dependences and resonant velocity to models

01 p0114 A72-10324

Heat transfer in turbulent flow of equilibrium dissociating nitrogen tetroxide within round tube, considering pressure, temperature and mass flow rate effects

01 p0145 A72-10490

Nondestructive determination of temperature dependence of elastic moduli of Al alloy and Ni and stainless steels by resonant frequency method

01 p0084 A72-10518

Stress relaxation resistance at elevated temperatures after reloading as function of internal and effective stress

01 p0138 A72-10520

CW X-band Gunn oscillator in coaxial cavities, investigating frequency variation with ambient temperature

01 p0037 A72-10641

Contrast reversal or distance paradox in temperature perception aftereffect

01 p0013 A72-10716

Thermal and environmental exposure effects on high temperature mechanical properties of graphite/polyimide composites

01 p0090 A72-10730

Temperature and compressive loading cycles effects on high performance multilayer insulation materials and composites, discussing application to space shuttle orbiter

01 p0092 A72-10779

Ionized argon recombination rate constant determination as function of temperature, using dual frequency laser interferometry measurement of corner expansion flow

01 p0050 A72-10851

Ti alloy honeycomb core sandwich panels fabricated by brazing or spot diffusion bonding, investigating elevated temperature effects on mechanical properties

[ASM PAPER W 71-23.3] 01 p0086 A72-10875

Hydrogen diffusion kinetics in Nb under various temperatures during gas-metal absorption experiments, observing room temperature hardness profile

01 p0087 A72-11026

Breakdown surfaces of thin Ti alloy specimens under tension as function of composition and heat treatment temperature

01 p0088 A72-11079

Recrystallization and rolling temperature effects on W strength and plasticity

01 p0088 A72-11083

Optimal conditions for energy conversion in MHD generator, observing ion seeding effect on plasma temperature

01 p0009 A72-11207

Turbine blades adaptability limits to temperature variations, considering rectangular cross section plastic rod under programmed thermal and tensile load cycles

01 p0143 A72-11372

Optical distortion induced by heated windows in high power laser systems, deriving figures of merit for window materials

02 p0237 A72-11470

Annealed pure Al polycrystals fatigue behavior data under elevated temperatures, using transmission electron microscopy

02 p0242 A72-11525

Tube and hollow sphere revolving in thermal flux under surface pressure load, obtaining stress-strain state and random temperature dependences of creep

02 p0289 A72-11618

Low impulsive loading effect on strength creep resistance of polycrystalline Al at elevated temperatures

02 p0243 A72-12011

Gaseous diethyl peroxide spontaneous ignition during decomposition in cylindrical vessel, investigating diluents and temperature effects on self heating

02 p0301 A72-12027

Thermal conductivity measurement of dissociating nitrogen dioxide over 548-792 K and 1-30 atm

02 p0170 A72-12091

Thermal effects on reversible threshold switching in amorphous semiconductor thin films involving current controlled negative resistance

[AD-741462] 02 p0268 A72-12202

Niobium anomalous oxidation below 600 C, noting suboxide formation between solid solutions and heat resistance reduction

02 p0243 A72-12214

Eutectic Ni-Cr alloy temperature effects on deformation rate on plasticity, noting superplasticity point

02 p0244 A72-12243

Real gas tailored shock tube Mach numbers by analytical method, investigating driver temperature effect

02 p0205 A72-12269

Dielectric properties of high purity polycrystalline barium titanate, observing temperature effects as function of heat treatment

[AD-737022] 02 p0269 A72-12417

Temperature effects on strength and deformability of randomly reinforced fiberglass polyamides

02 p0250 A72-12678

Cathode and anode temperatures effect on effective heat of condensation of electrons at anode for particular current density and different cesium vapor pressures

02 p0156 A72-12858

CdS single crystal field emission spectral characteristics at room and cryogenic temperatures, discussing intrinsic and impurity levels

02 p0269 A72-12888

Titanium disilicide oxidation mechanism at various temperatures, discussing surface quality effect, growth rate and protective mechanism

03 p0369 A72-12925

Heat treatable high strength steels fracture toughness dependence on temperature, examining surfaces with electron scanning microscope

03 p0369 A72-12959

High velocity impact reduced temperature increase due to shock compression in metals, discussing pressure and charge effects

03 p0442 A72-13240

Nonperiodically moving object holographic interferometry by time-averaging method, considering single exposure technique advantage over multiple exposure in thermal deformation observation

03 p0357 A72-13373

Temperature and loading conditions effects on structural element service life, showing partial healing process of microdefects

03 p0443 A72-13454

Testing temperature effect on intergranular fracture propagation in steel sensitive to tempering brittleness

03 p0372 A72-13599

Copper sulfide-cadmium sulfide single crystal photovoltaic heterojunctions, showing optically induced and thermal effects on short circuit current degradation

03 p0389 A72-13603

CoO single crystal creep rate at different temperatures, stresses and oxygen pressures, noting slip occurrence

03 p0373 A72-13647

Thermocouple efficiency with respect to Thomson effect and electric resistivity temperature dependence

03 p0360 A72-13651

Heat treated single-phase Pr-Co powder compacts, measuring coercivity as function of annealing or sintering temperature

[IEEE PAPER 7.3] 03 p0402 A72-13756

Computerized design algorithm for ferrite core memory system, considering cross-temperature effect under worst driving conditions

[IEEE PAPER 11.8] 03 p0327 A72-13766

Thermal stresses from inner surface temperature of micropolar hollow cylinder in static thermoelasticity problem with vanishing body loads

03 p0448 A72-13889

Zr and V linear thermal expansion coefficients explanation by alpha Zr hexagonal crystal lattice anisotropy

03 p0376 A72-13946

- Temperature dependence of X ray interference lines for Al-V alloy obtained at high cooling rate, noting metastable solid solution thermal stability 03 p0377 A72-14022
- Edge temperature effects on contact stress concentration in anisotropic plate with elliptic hole under mixed boundary conditions of thermoelasticity 03 p0450 A72-14109
- Metals thermophysical characteristics temperature dependence determination by analog computer, using one dimensional temperature fields in thin infinite plates and cylindrical or spherical surfaces 03 p0458 A72-14165
- Temperature reduction produced by partial cloud cover effect on radiation received by Nimbus 3 IR radiometer 03 p0385 A72-14226
- Polymer adhesives chemistry and properties in 450 F air, discussing weight loss and strength values 03 p0381 A72-14233
- Ionization waves linear theory for low pressure noble gas strong current column, showing self excitation limit and temperature dependence of energy loss rate 03 p0400 A72-14351
- Low temperatures and deformation rates effect on martensitic phase formation in Cr-Ni austenitic stainless steel under compression and tension 03 p0379 A72-14378
- Ferritic steel nil-ductility transition temperature data analysis correlating irradiation results with activation fluences and temperature 04 p0547 A72-14430
- Electrochemical machining electrode processes thermodynamic and kinetic characteristics, discussing temperature, electrolyte viscosity and flow rate and current density effects on metal removal rate 04 p0526 A72-14475
- Carbon monoxide oxidation by hydroxyl radicals at high and low temperatures from transition state theory, confirming flame and shock tube results [WSCI PAPER 71-36] 04 p0482 A72-14584
- Turbulent tropospheric temperature fluctuations effects on optical waves propagation with random scattering, considering amplitude, phase, angle-of-arrival and polarization 04 p0548 A72-14736
- Inorganic phosphates-nucleoside hypohydrous thermal reaction mechanism, discussing thermal polymerization of orthophosphates for phosphorylation and condensing agents in primordial synthesis 04 p0483 A72-14770
- Heat input, interpass temperature and panel width effects on butt welds strength in Al alloy plate 04 p0526 A72-14838
- Ionospheric plasma drift instability, showing electric and magnetic fields, electron density and temperature effects 04 p0517 A72-14956
- Carburization of various irons in methane-hydrogen atmosphere at 750 C, comparing activity coefficients and solubility limits 04 p0533 A72-14978
- Unsteady approach to nonisothermal flow theory for Couette flow, making general assumptions concerning rheological law and temperature dependence of fluidity 04 p0512 A72-14985
- Temperature dependence of quantizing thin films electroconductivity in case of scattering at neutral impurities 04 p0561 A72-15078
- High resolution electron microscope observation of voids in amorphous Ge films, noting density dependence on substrate temperature 04 p0562 A72-15152
- Small sphere hydrodynamic drag in ionized gas at local thermodynamic equilibrium, taking into account nonlinear transport properties variations with temperature [ASME PAPER 71-APM-CC] 04 p0558 A72-15176
- Nb-Ti alloy critical current density increase dependence on temperature, discussing evidence supporting rigidly pinned vortex lattice model 04 p0562 A72-15292
- Longitudinal ultrasonic sound attenuation in superconducting Mo-Re alloys as function of temperature, magnetic field and frequency, using evaporated thin film CdS transducers 04 p0562 A72-15295
- Radiative cooling effects on flow field and heat transfer behind reflected shock wave [AD-737423] 04 p0597 A72-15338
- Zr alloys hydride distribution after oxidation in steam at 550 C, discussing hydrogen uptake 04 p0534 A72-15362
- Arrhenius model and graphical methods for temperature accelerated life tests in electrical insulation systems 04 p0500 A72-15364
- Weak magnetic moments measurement under pressure and over wide temperature range by Faraday method, discussing magnetometer and cryogenic equipment modifications [AD-740076] 04 p0522 A72-15478
- German monograph on refractory materials elasticity modulus determination at elevated temperatures, describing device based on characteristic vibrations frequency relation to temperature 04 p0510 A72-15698
- Supermendur magnetization and ac core loss temperature dependence under slow temperature cycling in vacuum, noting anomalous Barkhausen effect 04 p0564 A72-15718
- Sb 124 dopant redistribution in Ge semiconductor during diffusion alloying with In at 750-850 C 05 p0701 A72-15751
- Thermal load effect on convective heat transfer in turbulent flow in circular duct 05 p0742 A72-15843
- Water heat pipes transient thermal impedance, monitoring evaporator, vapor space and condenser temperature [ASME PAPER 71-WA/HT-9] 05 p0743 A72-15869
- Mean and fluctuating temperature dependence of gas discharging from orifice to atmosphere on pressure vessel wall heat transfer [ASME PAPER 71-WA/HT-32] 05 p0745 A72-15884
- Temperature, flow, end conditions and branching on small signal sinusoidal amplitude frequency response of pneumatic lines, investigating transfer functions [ASME PAPER 71-WA/AUT-5 [FLCS]] 05 p0615 A72-15958
- Temperature and compression rate effects on metal powder packing density, obtaining activation energy from Boltzmann equation 05 p0665 A72-16089
- Thin cylindrical shell bending deformation from axisymmetrical temperature distribution generated by narrow heating element 05 p0736 A72-16113
- Nonstationary oncoming flow temperature effect on heat transfer in thermal boundary layer at forward stagnation point 05 p0746 A72-16217
- Fluid motion model with gas bubbles, noting energy dependence on temperature and density 05 p0649 A72-16224
- Atmospheric temperature effect on solar diurnal variation of muon component, considering asymptotic characteristics of cosmic ray anisotropy 05 p0709 A72-16257
- Temperature, pressure and crystallization time effects on artificial diamond crystal growth of various morphological shapes 05 p0681 A72-16355
- Quasar primordial He content prediction from primordial temperature fluctuations necessary for galaxy formation 05 p0717 A72-16384
- Metastable He atoms concentration in plasma from absorption characteristics at temperatures 4-300 K and pressures 1-70 mm Hg 05 p0696 A72-16612
- Surface oxide film effects on hydrogen liberation rate from Al and alloys in high vacuum at 20-450 C 05 p0675 A72-16627
- Nb alloy oxidation behavior dependence on temperature in 550-1316 C range 05 p0676 A72-16732
- Thermoelastic effect on flutter and vibration of built up delta wings with solid, stiffened and honeycomb/corrugated sandwich skins [AIAA PAPER 72-174] 05 p0740 A72-16834
- Turbine blade row coolant flow velocity, injection location and temperature effects on kinetic energy output [AIAA PAPER 72-12] 05 p0707 A72-16866
- Gas dynamic laser technology advances, discussing water content, temperature and Na effects and nozzle design [AIAA PAPER 72-143] 05 p0669 A72-16895
- Analytical models for predicting mass transfer cooling effects on blade row efficiency of turbine airfoils [AIAA PAPER 72-11] 05 p0707 A72-16943
- Hydraulic fluids behavior under extreme temperature, pressure and filtration conditions, considering viscosity, wear and corrosion resistance 05 p0681 A72-17084
- Prolonged heatings effect on heat resistant magnesium alloys microstructure and mechanical properties 05 p0680 A72-17208
- Electrical resistance, Hall coefficient and magnetic susceptibility of transition metal nitrides at low and room temperatures 06 p0827 A72-17386
- Homologous temperature method to compare mechanical properties of metals tested at different temperatures 06 p0827 A72-17399
- Temperature inhomogeneity effect on plasma column microwave resonant behavior in presence of axial magnetic field, ascribing spectral shifts to electron density and temperature profiles changes 06 p0854 A72-17417
- Co and carbide containing alloys, investigating milling and sintering temperature effects on technological and physical properties 06 p0829 A72-17831
- Automatic frequency adjustment of pair of He-Ne lasers with different oscillation frequency fluctuations under various heating conditions 06 p0825 A72-17840
- Temperature effects on anodic polarization of Ti open surface and corrosion crevices, discussing critical potential relation to pitting 06 p0829 A72-17946
- Dynamic strain aging significance in titanium, observing reduction of temperature and strain rate effects on stress-strain curves shapes 06 p0830 A72-18054
- Flow in gas lubricated conical bearings, considering analytical and numerical solutions for axisymmetric flow model with temperature dependent viscosity and dissipation coefficients 06 p0801 A72-18124
- Bacteriophage synergistic inactivation by heat and ionizing radiation from kinetic model describing dose rate and temperature dependences 06 p0768 A72-18185
- High energy chemical propellant combustion under adiabatic and nonadiabatic conditions, calculating product equilibrium state as functions of temperature and pressure with computer program 06 p0903 A72-18212
- Internal friction spectrum peaks in Fe-Ni alloy at 20-1100 C upon heating and cooling, explaining by grain boundary relaxation and martensitic transformations 06 p0830 A72-18293
- Internal friction in annealed and deformed tungsten at room temperature to 950 C, examining carbon contents, dislocations and temperature effects on carbon Snoek peak 06 p0830 A72-18295
- High temperature and ZrO2 ceramic electrolyte effects on ionic partial conductivity and fuel cells longevity 06 p0760 A72-18337
- Al and Ti alloy fatigue after temperature reduction to 253, 77 and 4 K as function of surface purity after machining 06 p0831 A72-18356
- Compressive strength of Cu-W fiber metal matrix composite as function of temperature, comparing to cermets 06 p0832 A72-18363
- Anomalous temperature-strain rate dependence of Ni-Al intermetallic compound mechanical properties from plastic deformation mechanism 06 p0832 A72-18417
- Plastic deformation and elastic stiffness of refractory metals, discussing impurities, alloying, temperature, work hardening, strain rate and texture effects 06 p0822 A72-18519
- Thermally activated crystal microcrack initiation by fusion of leading and following dislocations 06 p0898 A72-18551
- Approximate trigonometric solution to thermoelastic boundary value problem of plate with doubly periodic system of holes under unsteady temperature and thermal stress fields 06 p0899 A72-18563
- Temperature induced bending of thin freely supported rectangular plate, obtaining stress-strain state 06 p0899 A72-18564
- Graphite and molybdenum disulfide, investigating temperature effect, thermal stability and oxidation effect on weight by TGA and DTA 06 p0837 A72-18602
- Temperature dependent directional differences of modulus of elasticity of Mo sheet, using resonance technique 06 p0833 A72-18632
- Temperature and deformation velocity effects on elasticity and tensile strength of Mo and Nb alloys 06 p0833 A72-18636
- Sheet metal fatigue test method for transverse 100-1000 Hz bending at normal and high temperatures, applying to 1.5 mm Ti alloy sheet 06 p0900 A72-18671
- Polymers mechanical losses temperature-frequency dependence, using nonlinear viscoelastic theory 06 p0838 A72-18678
- Rectangular capacitor overheating calculation with allowance for heat transfer from all surfaces, discussing chassis heat removing action computation during natural cooling 07 p0953 A72-18930
- Test facility for studying temperature dependence of thermal diffusivity and true heat capacity of metals between minus 150 and plus 400 C 07 p0982 A72-18941
- Welding thermal energy effect on residual ferrite of austenitic chrome-nickel steel deposits 07 p1010 A72-18971
- Third harmonic generation in Ge induced by conduction nonlinearity during bulk heating of charge carriers by microwave fields 07 p1047 A72-19023
- Low frequency modulation noise generation due to conductance fluctuations in Gunn oscillators, measuring noise spectra temperature dependence 07 p0954 A72-19050

Nonstationary thermal interaction between thermally inert circular disk in bounded cylinder with controlled temperature, describing control process by third order differential equation

07 p1098 A72-19263

Analog simulation of normal thermal explosions and cool flames, observing oscillations limits, time dependence of parameters and effect of changes in activation energy or initial temperature

07 p1098 A72-19366

Surface and thermal effects on hydrogen oxidation, calculating explosion limits and slow reaction rates

07 p0935 A72-19370

Pulsating flame spread on liquid alcohol surface over range of liquid temperatures, using shadow streak photography

07 p1099 A72-19375

Temperature dependence of carbon monoxide reaction rate with hydroxyl, noting activation energy

07 p0935 A72-19376

Thermal blooming of laser beams in liquids and gases, investigating short and long time behavior under thermal conduction and viscosity effects

07 p1005 A72-19408

Nitrogen interaction with liquid binary Ni alloys, investigating solubility as function of temperature and pressure and titanium nitrides existence conditions

07 p1011 A72-19547

Ti, Fe, Co, Ni, Pt and steels phase transformation and thermal defect effects on high temperature thermal conductivity

07 p1012 A72-19548

Steady state high temperature niobium creep in torsion under rarefied oxygen infiltration conditions, discussing surface interactions kinetics

07 p1012 A72-19679

Pure and doped ammonium perchlorate deflagration rate sensitivity due to sample temperature and environmental pressure changes

07 p1051 A72-19729

Tungsten alloy filaments as reinforcing agent of heat resistant composite chromium alloy, investigating long term high temperature effects

07 p1013 A72-19745

Hydrodynamic flow parameters in laminar incompressible water boundary layer on heated plate, noting plate surface heating effect on velocity profile

07 p0968 A72-19766

Tempering temperature effect on hydrogen penetration level and brittleness of hardened carbon steel

07 p1014 A72-19773

Cu, Al and Pb bcc metals, investigating dislocation structure and creep characteristics change mechanism at transition from low to high temperature

07 p1014 A72-19822

Deformation rate and temperature effects on optimum strength and ductility of die forged and extruded Mo-Ti alloys

07 p1014 A72-19845

Book on materials low temperature mechanical properties covering metals, polymers, ceramics and composites, temperature effects on deformation processes, fracture mechanics, test methods, etc

07 p1015 A72-19909

Martensitic transformations induced by plastic deformation in Fe-Ni-Cr-C system, noting stacking fault energy dependence on temperature

07 p1015 A72-19928

Diffusion kinetics in Nb-Al system for varying time and temperatures

07 p1015 A72-19930

Transition metal borides chemical bonding mechanism from Nb and Cr boride phases thermal emf and expansion, resistivity, Hall coefficient and carrier mobility

07 p1017 A72-19992

Refractory alloys softening under stress relaxation conditions at high temperatures, noting plastic strain hardening effect absence

07 p1018 A72-20138

Test temperature effect on phase composition, mechanical properties and resistance to cavitation of unstable austenitic steels, describing test facility

07 p1018 A72-20140

Kinetics of heat inactivation of phosphoglycerate kinase in soluble fraction from hydrogenomonas facilis

07 p0922 A72-20237

Al wrought alloys dynamic elasticity modulus and Poisson ratio dependence on temperature, using ultrasonic measurement method

07 p1019 A72-20239

High turbine entry temperature effects on gas turbine engine specific power and fuel consumption, noting thrust/weight ratio increase in turbojet and turbofan engines

07 p1055 A72-20311

Temperature effects on hot-wire anemometer calibrations, plotting Nusselt number variation with Reynolds number

07 p0990 A72-20369

Solid solution yield strengthening and weakening of V-Ti alloys, investigating strain rate sensitivity tem-

perature dependence as indication of two deformation mechanisms

07 p1021 A72-20434

Temperature and alloy composition effects on coarsening rate of metal carbide particles in dissimilar metallic matrix

07 p1021 A72-20436

Ni based superrefractory alloy high temperature fatigue tests, studying creep as function of stress load and frequency and temperature

07 p1022 A72-20487

Inhomogeneous high-collision finite pressure plasma stability, finding thermal instability development under uniform temperature and arbitrary pressure

07 p1046 A72-20514

Temperature and physical state effects on rubidium optical constants at 0.3-2.4 microns

07 p1050 A72-20522

Strain rate effects on strain hardening of duralumin, copper and lead, noting yield stress sensitivity to deformation induced temperature changes

07 p0998 A72-20527

Temperature dependence of strain rate sensitivity in low temperature deformation processes, considering inherent lattice conditions and impurity atoms effects

07 p1022 A72-20573

Temperature dependence of electrical resistance and thermal conductivity in duralumin quenched at 77 K

07 p1022 A72-20663

Electrical resistance and thermal conductivity dependence on temperatures in duralumin quenched at 77 K

07 p1022 A72-20666

Temperature effects elimination from underground muon intensity measurements

08 p1226 A72-20813

Gas mixture properties at high temperatures, pressures and densities, applying to thermal ionization of adiabatically compressed air

08 p1210 A72-20942

Basal and prismatic crystal dislocations in Be, measuring critical resolved shear stress dependence on temperature at 300-500 K

08 p1185 A72-20991

Plasma beam cutting of Al sheets, discussing heat effect on surface oxides and microstructure and plasmagenic gas influence

08 p1176 A72-21047

Silicon-silicon dioxide system, investigating effect of heating in dry and moist He on capture-center and recombination parameters by thermal and pyrolytic techniques

08 p1216 A72-21068

Polycarbonate yield dependence on temperature in uniaxial compression and tensile tests described by modification of Eyring theory of non-Newtonian viscosity

08 p1191 A72-21184

Unsteady heat conductivity equation for finite dimensions parallelepiped, noting temperature dependence of specific heat and thermal conductivity

08 p1252 A72-21321

Conductive heat flux propagation rate in gases as function of absolute temperature

08 p1253 A72-21447

Heat transfer in shield-vacuum thermal insulation layers at various temperatures and pressures, noting conductivity anisotropy

08 p1253 A72-21451

Glass fiber reinforced plastics irreversible cumulative damage under axial cyclic tension compression loads with heat production

08 p1191 A72-21500

Wind shear, turbulence, precipitation, temperature, visibility and ceiling effects on airport capacity, suggesting weather data integration into ATC system for pilots information

08 p1147 A72-21521

X ray diffuse scattering from Al crystal at 100-500 V, considering phonon modes effects on anharmonicity and atomic deformation

08 p1186 A72-21591

Turbulized combustion product plasma electrical conductivity, noting temperature dependent variation

08 p1214 A72-21649

Gas temperature variation effects on powder burning stability in rocket combustion chamber from unsteady powder burning theory

08 p1255 A72-21659

Nonlinear viscoelastic body model for stress relaxation of amorphous linear polymers below vitrification temperature for various deformations, temperatures and deformation speeds

08 p1194 A72-21751

Impurities and temperature effects on microdeformation of Mo single crystals under dynamic loads

08 p1188 A72-21789

Temperature dependence of scattering cross sections for cold and hot neutrons colliding with oxygen and deuterium molecules

08 p1211 A72-21872

Metallic four-lip seal performance, discussing force cycle, mechanical spring-back, reusability at room and higher temperatures and thermal shock behavior

08 p1179 A72-21939

Reduced air pressure effect on He-Ne laser output power via self heating

08 p1184 A72-22033

Thermal self disturbance effect on second harmonic generation in crystals and CW and pulsed lasers

08 p1184 A72-22034

Temperature dependence of intrinsic light absorption band edge characteristics in p-type InSb

09 p1366 A72-22213

Cold shortness of W and related refractory metals, noting oxide phases and impurities effects on mechanical properties temperature dependence

09 p1326 A72-22226

Twin triodes type parameters stability in microwave region as function of cathode service life and temperature

09 p1284 A72-22243

German monograph on tire rubber friction on dry and wet rough surfaces, taking into account loading velocity and temperature effects

09 p1332 A72-22323

Oxygen, nitric oxide and water cluster positive ion composition from mass spectrometer experiments in lower ionosphere, noting ion production and low temperature effects

09 p1375 A72-22363

High temperature radiographic techniques for measurements of molten ceramics density, melting point, phase transitions, surface tension and viscosity up to 3000 C

09 p1333 A72-22378

Oxide scale formation on zirconium diboride materials, observing microstructural features as function of temperature and reaction time [AD-737020]

09 p1333 A72-22380

Temperature effects on electrical conductivity and transport mechanisms in sapphire from measurements under protection against surface and gas phase conduction

09 p1335 A72-22400

Thermomechanical treatment effects on microstructure and mechanical properties of Al alloy

09 p1327 A72-22470

Carbon monoxide in carbon dioxide atmosphere determining IR absorption lines broadening at reduced temperatures

09 p1351 A72-22612

Temperature effects on microorganism survival in deep space vacuum, using molecular sink test

09 p1265 A72-22646

Cryostat for high resolution tensile measurements of thermally activated processes during plastic deformation

09 p1398 A72-22657

Temperature induced stresses and displacements in fiberglass reinforced plastic cylindrical shell

09 p1399 A72-22704

Creep properties in turbine disks of heat resistant alloy under plastic deformation due to nonstationary thermal conditions

09 p1401 A72-22730

Nonuniformly heated infinite elastic cylindrical shell stability under axial compression loads

09 p1402 A72-22734

Temperature and internal pressure effects on cylindrical shell stability under tension and compression, deriving critical temperature and loads

09 p1402 A72-22736

Static strain measurement errors due to nonstationary thermal conditions in semiconductor resistance gages

09 p1310 A72-22739

Glass ceramics mechanical properties as function of temperature during bending, taking into account scale factor

09 p1337 A72-22742

Modal behavior and temperature tuning of pulsed room temperature GaAs laser, using hyperfine energy level separation

09 p1323 A72-22768

Polyatomic ions interaction with neutral molecules in gases, calculating ion mobility as function of temperature from core model representation

09 p1355 A72-22784

Inhomogeneous superconductors and proximity effects, calculating conditions for vortex lattice pinning energy as increasing function of magnetic field and temperature

09 p1370 A72-22794

Ti crystallographic and topographical features: determination by hydrogen-ion microscopy, noting temperature effects on surface films and low index facets production

09 p1327 A72-22801

Molecular hydrogen dissociation by He, observing molecule initial quantum states effect on temperature dependent reaction cross section

09 p1357 A72-22851

- Q factor over temperature range of microwave resonator coupled with drifting indium antimonide plasma 09 p1285 A72-22895
- Apollo lunar fine samples total emittance as function of temperature, using spectral emittance measurement technique 09 p1388 A72-23028
- Transistor LF flicker background noise generation mechanism in terms of bulk effect due to temperature fluctuation or phonon electron interactions 09 p1286 A72-23107
- P-channel MOS transistor LF background noise components analysis for different dependencies on gate bias and temperature 09 p1286 A72-23109
- Liquid nitrate ester sensitivity and dissolved water desensitization, using thermal initiation and drop weight impact tests 09 p1373 A72-23145
- Piezoresistance magnitude and temperature dependence changes of electron irradiated n-type silicon due to oxygen vacancy complex /A center/ 09 p1372 A72-23239
- Temperature effects on low pressure calibration in vacuum gage metrology 09 p1312 A72-23249
- Laser beam induced thermal blooming in absorbing gases from combined fluid dynamics and eikonal geometric optics theory, considering wind effects 09 p1352 A72-23333
- Parabolic oxidation kinetics of Ni-Ti alloy compound at elevated temperatures 09 p1330 A72-23358
- Beta-III Ti alloy mechanical properties dependence on heat treatment and elevated temperature exposure, illustrating associated microstructures 09 p1331 A72-23384
- Diode junction parameters and inverse saturation current measurements as function of current density and temperature 09 p1289 A72-23418
- Electrical conductivity and thermal emf as function of temperature in CdSb, discussing energy spectrum and crystallization 09 p1372 A72-23479
- Temperature dependence of Ge solubility in CdSb single crystals from microstructural observations and measurements of microhardness and electrical properties 09 p1372 A72-23480
- Vapor pressure and composition in As-I system, investigating entropy and enthalpy changes and temperature dependence of equilibrium constant 09 p1373 A72-23481
- Niobium carbide resistors properties, investigating temperature dependence of electrical resistance and thermal stability 09 p1331 A72-23483
- Temperature dependence and error compensation of Si strain sensors, using coupled dc generators 09 p1316 A72-23649
- Temperature effects on blood electrobioluminescence, relating luminescence peaks to protein and lipid molecular structure changes 09 p1268 A72-23694
- Hot-stage optical microscopes for microhardness measurements at elevated temperatures, describing techniques to determine heat resistant alloys mechanical and physical properties temperature dependence 10 p1478 A72-23827
- Optical and electron microscopic study of Inconel 625 precipitation and recrystallization behavior over temperature range under plastic deformation 10 p1494 A72-23829
- Thermal radiative cooling system characteristics determination, taking into account surface material thermal conductivity and blackness degree dependence on temperature 10 p1561 A72-23840
- Stress and thermal relaxation effects in viscoelastic behavior of turbulent flows of liquids and gases 10 p1464 A72-23867
- Nonstabilized Ni-P thin films electrical conductivity at 50-280 C, using mass spectrographic, thermal differential, X ray diffraction and electron microdiffraction analyses 10 p1495 A72-24076
- Temperature effects on kinetics of methane decomposition on carbon fiber at high temperatures, showing characteristics relationship to carbon gasification reactions 10 p1433 A72-24086
- Thermal shock and temperature cycling environmental testing, discussing military specifications, components thermal lag characteristics, environmental test chambers and various cooling methods 10 p1459 A72-24144
- Maximum dynamic to static deflection ratio for thermally induced vibrations of elastic beams and plates, considering damping and axial load effects [ASME PAPER 71-APM-UU] 10 p1554 A72-24185
- Quenched specimen anisotropic surface heating effect in liquid vaporization characteristics determination 10 p1561 A72-24207
- Tempering effects on weakly doped n-InSb electrical properties at 77 K, discussing diffusion and activation energies in reversible/irreversible defect change processes 10 p1526 A72-24242
- Temperature dependence of emf coefficient Hall constant and conductivity in solid and liquid phases of InSe semiconductor during melting 10 p1526 A72-24267
- High temperature creep behavior of sintered polycrystalline strontium zirconate as function of temperature, stress, grain size and strain level, using pure bending test method 10 p1497 A72-24275
- Semiconductor air-air heat pumps with solar cell feed current, determining hot air flow temperature effects and energy conversion efficiency 10 p1423 A72-24319
- Positive plasma column theory for longitudinal cylindrical discharge problem in ambipolar conditions, stressing surface and bulk temperature effects 10 p1521 A72-24357
- CW X band Gunn microwave oscillators, measuring frequency variation relationship to ambient temperature 10 p1450 A72-24555
- Alloy p-n-p junction transistor diffusion capacity variation with emitter current as function of temperature at 80-320 K 10 p1451 A72-24558
- Temperature dependence of internal quantum efficiency of spontaneous emission as function of beam voltage in electron beam excited p-type GaAs 10 p1526 A72-24559
- Temperature dependence of gas flow coefficients at low pressures, determining isothermal permeability and heats of transport of He, Ne and Ar capillary flow 10 p1469 A72-24600
- Vaporizer temperature effect on ion propulsion system thrust vector, presenting temperature control loop circuit diagram 10 p1528 A72-24652
- Glass content and temperature effects on fabric reinforced plastic laminates static behavior, analyzing tensile and bending strength and elastic moduli 10 p1501 A72-24660
- Thermolabile triose phosphate isomerase in psychrophilic Clostridium at moderate temperatures 10 p1426 A72-24750
- Interdiffusion of tight contact welded ring Ti-W pairs at high temperature, using X ray analysis and electron beam techniques 10 p1497 A72-24785
- Electron tunneling into amorphous InSb and GaSb films, discussing effects of temperature, voltage, coevaporation doping and Cu and Au diffusion 10 p1527 A72-24874
- Vacuum arc stationary cathode mechanism theoretical analysis, determining cathodic temperature and current density 10 p1524 A72-24930
- Electrical properties of Te/p-Si/In heterodiodes at room and liquid air temperatures 10 p1527 A72-24937
- Radiative heat transfer spectral, temperature and directional dependence on interacting opaque surfaces system properties, noting models with accounted non-gray character [AIAA PAPER 72-306] 11 p1742 A72-25240
- Pendulum impact resistance of tungsten fiber-metal matrix composites, noting heat treatment and test temperature effects 11 p1653 A72-25473
- Temperature dependence of Ni and Ni alloys and solid solutions microhardness, noting strengthening effect of Ti, Cr, Al and B additions 11 p1654 A72-25491
- Test assembly design for microstructural studies of metal and alloy fatigue in vacuum during heating, describing electrical resistance measurement and stroboscopic illumination 11 p1612 A72-25492
- Drazin method application to thermal stratification effects on unbounded jets and shear layers stability characteristics 11 p1615 A72-25552
- Aircraft gas turbine engines exhaust emission characteristics identification, considering ambient temperature and humidity effects [ASME PAPER 72-GT-75] 11 p1705 A72-25657
- Hot corrosion effects on Inconel-700 and Inconel-X gas turbine rotor blades during burning of high sulfur concentration residual oil fuels [ASME PAPER 72-GT-87] 11 p1656 A72-25662
- High efficiency CW performance of InP transferred electron microwave oscillator with anomalous I-V characteristics temperature dependence 11 p1604 A72-25750
- Grain size and carbon content effects on recrystallized Mo wire ductility at room and low temperatures 11 p1657 A72-25758
- Be elastic constants at 25-300 C, using ultrasonic pulse technique 11 p1657 A72-25774
- Nose blunting, exposure time and initial temperature effects on axisymmetric bodies ablation surface cross hatching patterns, presenting test results on cones with various vertex angles 11 p1572 A72-26006
- Temperature and strain rate effects on superplasticity of Ni-Cr eutectic alloy 11 p1659 A72-26129
- Prolonged heating effect on heat resistant Mg alloys microstructure and mechanical properties 11 p1660 A72-26143
- Electrolyte temperature, pH and mixing rate effects on anodic dissolution of steels and brass in electrochemical precision processing, using thermokinetic data processing 11 p1640 A72-26257
- Semiconductor laser threshold current dependence on doping degree and temperature based on optical transition model and energy band theory 11 p1647 A72-26327
- Frequency modulation of CW GaAs laser emission by injection current, noting temperature effects 11 p1648 A72-26337
- Interstellar free radicals and molecules spectra, noting catalyzers, temperature and abundances role 11 p1722 A72-26434
- Design analysis of emitter- and collector-base gain stabilized junction transistor amplifier at elevated temperatures using passive elements 11 p1606 A72-26569
- Fe-Mo solid solutions transient creep behavior as function of applied stress, noting temperature effect 11 p1662 A72-26656
- Nb-Ti alloy elasticity modulus temperature dependence, considering foreign atoms interactions with dislocations 11 p1662 A72-26737
- Nonlinear thermal effects of atmospheric absorption for high power carbon dioxide laser beams 11 p1651 A72-26747
- Thermionic converter model analysis for performance stability and inhomogeneities in Cs diode, considering emission current dependence on temperature 11 p1578 A72-26759
- Turbine blade alloys vibrational fatigue and creep properties under high and low frequency axisymmetric loads at room and elevated temperatures 11 p1662 A72-26798
- Low temperature mechanical properties of Ti-base alloys, examining notched samples impact strength as function of temperature and notch depth 11 p1663 A72-26806
- Creep characteristics of weakly strain-hardenable alloy under variable tensile load and temperature conditions 11 p1663 A72-26808
- Test device for reinforced plastics mechanical properties under heating and pressure with allowance for gas permeability 11 p1613 A72-26813
- Ti alloys fatigue strength, stress concentration sensitivity and grain sizes effects at normal and high temperature under cyclic loads 11 p1663 A72-26821
- Thermodynamic description of metal rich side of Nb-Mo-N solid solution, determining equilibrium nitrogen solubility as function of pressure and temperature 11 p1664 A72-26842
- NASA program to develop heat resistant materials for aerospace applications, discussing refractory carbides, nitrides and borides temperature dependent behavior and properties 11 p1664 A72-26857
- Temperature, oxygen pressure and exposure time effects on oxidation characteristics of molybdenum-zirconium oxide cermets 11 p1665 A72-26865
- Dislocation structure and strength of Ti at low and intermediate temperatures, investigating strain, grain size and interstitial solute hardening 11 p1666 A72-26927
- Lunar surface neutral gas pressure measurement by Apollo 14 cold cathode ionization gage, determining day and night temperature effects on vacuum quality 12 p1805 A72-27041
- Temperature dependence of destruction threshold of lithium niobate surface under laser irradiation, noting ferroelectric properties effects 12 p1853 A72-27069
- High temperature dislocation rearrangement in lightly cold deformed Nb as function of time and temperature, using etch pit technique for evaluation 12 p1827 A72-27136
- Linearized thermal viscoelasticity theory for stability, large strain and wave propagation problems, taking into account heat generating effects 12 p1880 A72-27233
- Low temperature solid state phase transformations in 2H silicon carbide single crystals, noting time and temperature dependence 12 p1854 A72-27276

Mathematical model for thermal lensing of IR laser window, discussing aberrations effect on diffraction-limited far field focus time

12 p1819 A72-27284

Living organisms defense and preservation via refrigeration and vacuum combined use in lyophilization technique

12 p1769 A72-27293

Local heating effect of electrical resistance gages measuring strain across thickness of plane photoelastic Araldite models

12 p1807 A72-27316

Temperature oscillations associated with surface gravity waves at two fluid model compressible vapor-incompressible superfluid interface

12 p1845 A72-27386

Astronomical reflector telescope design, describing thermal effects on Al mirror and image intensification

12 p1807 A72-27428

Niobium diffusion into copper as function of time and temperature, obtaining rates by electrical resistance measurements

12 p1828 A72-27448

Fatigue failure tests of low carbon Mn steel, analyzing structural damage under cyclic loads in relation to temperature curve

12 p1829 A72-27458

Temperature distribution and dissipation effects on compressible isothermal atmosphere Lamb waves vertical structure

12 p1839 A72-27504

Radio attenuation by rain at 37 GHz using sun as source compared with sky emission observations, noting apparent absorber temperature effect

12 p1783 A72-27665

Austenizing temperature relationship to quenching rate in ultrahigh strength steels with high fracture toughness, recommending two step quench technique

12 p1829 A72-27695

Circuitry and operational characteristics of variable output voltage regulator with low temperature coefficient, noting suitability for monolithic integration

12 p1792 A72-27740

Thermoregulation in deeply hibernating rodents during separate chilling and steady hibernation temperature maintenance of skin and brain

12 p1762 A72-27827

Photoelectric properties of cadmium telluride thin film solar cells, discussing energy gap temperature dependence, work function and current variations anomalies

12 p1756 A72-28018

Recombination parameters in low resistivity gamma irradiated n-type Ge, obtaining energy levels and temperature dependence of electron and hole capture probabilities

12 p1857 A72-28056

Recombination luminescence in irradiated Si, investigating uniaxial stress and temperature variations effects

12 p1858 A72-28061

Cubic SiC film growth rate on Si substrate by methyltrichlorosilane decomposition in hydrogen flow, noting dependence on mixture flow rate and temperature

12 p1860 A72-28114

Friction characteristics of high melting point metal chalcogenides as function of load and temperature, noting friction coefficient variations

12 p1817 A72-28185

Temperature effects on crystalline solids adhesion, noting friction rise above seizure point

12 p1818 A72-28187

Clean metallic surfaces adhesion coefficients in vacuum at 77-293 K as function of load, loading time and contact cycles

12 p1818 A72-28193

Molecular-mechanical theory of external friction, taking into account surface roughness, time and temperature dependent mechanical properties and chemical processes

12 p1818 A72-28195

Heat resistant blade alloy test temperature effects on fatigue life, tensile strength, hardness and chemical composition

12 p1831 A72-28230

Tensile strength, plastic properties and notch sensitivity from low temperature tests of binary Ti alloys, noting effects of Sn content and temperature

12 p1831 A72-28239

Environmental temperature effect on motion sickness sweating, discussing nausea and discomforting symptomatology prediction

12 p1775 A72-28302

Ear site body temperature measurement relation to radiant heating of scalp and upper face

12 p1768 A72-28333

Spatially resolved gain measurements in carbon dioxide laser amplifier, considering gas mixture, flow rate, temperature, pressure and current effects

13 p1967 A72-28448

Heating rate effects on residual stresses in thick walled cylinders produced by winding heated binder impregnated fiberglass tape on cold spool

13 p1982 A72-28553

Temperature effects on synthetic rubber sliding friction characteristics against smooth steel surfaces under compression loads in vacuum and air at 10-140 C

13 p1962 A72-28554

Radial and circular thermal stresses in free and end-constrained orthotropic cylinders with axisymmetric temperature distributions, determining relation between temperature and thermoelastic coefficients

13 p2055 A72-28561

Uniaxial elastic deformation pressure effects on electronic conduction in tetrahedrally bonded amorphous semiconducting thin films as function of temperature

13 p2021 A72-28574

Laplace transformation for mechanical response of piezoelectric composite transducer under action of thermal field and electric potential, noting time dependent modulus of elasticity

13 p1955 A72-28621

Strain rate controlling mechanisms of superplastic deformation at various stresses and temperatures, considering vacancy and dislocation creep and grain boundary sliding

13 p1974 A72-28657

Tempered or recrystallized chromium steels tensile behavior at 0 to 700 C, showing strength dependence on martensite transformation induced dislocation structure

13 p1975 A72-28667

Polycrystalline alpha Ti work hardening at low temperatures and different purities, discussing plastic strain effects

13 p1975 A72-28671

Holographic system stability tested by diffraction efficiency-exposure curves obtained in real time from probing holograms sequence, emphasizing temperature effects

13 p1956 A72-28685

I-V characteristics of metal-semiconductor-metal structures based on oxide glasses, noting temperature dependence and current limitation

13 p2021 A72-28688

Diamond powder lattice parameter changes during fast electron irradiation at various temperatures, discussing crystal defect stability and neutron irradiation comparison

13 p1983 A72-28760

Temperature and charge carrier density dependence of conduction electron optical effective mass in semiconductor compounds

13 p2021 A72-28788

Thermoelastic vibrations of simply supported rectangular plate produced by temperatures prescribed on faces, obtaining solution in trigonometric series form

13 p2056 A72-28888

Co-Cu alloy phase formation and separation morphology changes with temperature and anomalous diffusive X ray scattering in solid solutions

13 p1976 A72-28905

Hardened coarse-grained steels recrystallization during fast heating, investigating martensite phase macro- and microstructural changes by X ray analysis

13 p1977 A72-28908

Cu-Al-Ni alloys single crystals internal friction temperature dependence during martensitic transformations

13 p1977 A72-28912

Hg flow and hollow cathode temperature effects on ion thruster neutralizer stability and lifetime capability, using bell jar tests

13 p2026 A72-28937

Thermal effects on phase structure of welded joints of Al alloy with Cu addition

13 p1978 A72-29022

Temperature dependent small signal operation of junction transistors at low supply voltage

13 p1930 A72-29058

Silicone based elastomers acoustic excitation damping properties at 213-423 K, discussing testing technique and results at 200-1000 Hz

13 p1957 A72-29090

Atomic hydrogen viscosity and thermal conductivity coefficients for 1-100,000 K, using quantum theory for low temperatures and classical mechanics for high temperatures

13 p2065 A72-29299

Fusion welding of Ti-W and Ti-graphite composites, determining weldability and effect of weld thermal energy on fiber matrix reactions

13 p1966 A72-29423

Temperature and strain rate dependence of austenitic stainless steel fracture by low cycle fatigue at high temperatures, studying striations with scanning electron microscopes

13 p1979 A72-29449

Statistical method of Pearson moments applied to temperature regimes effects on ruby laser output energy distribution

13 p1968 A72-29506

Temperature dependent electron density of state and dc resistivity of disordered binary alloys, using single band thermal disorder model

13 p2022 A72-29626

Thermal vacuum tests of rhenium disulfide decomposition as function of temperature at 800-1200 C, using thermogravimetric method

13 p2023 A72-29649

Ammonium perchlorate burning rate temperature dependence as function of pressure and oxidizer particles size, noting low pressure deflagration limit [ONERA, TP NO. 1079]

13 p2025 A72-29669

Variational form to determine equations and boundary conditions for elastic isotropic homogeneous nonferromagnetic body subjected to external load, temperature and electromagnetic field actions

13 p2061 A72-29797

Forward voltage vs temperature characteristics for Si planar p-n junction diodes, determining zero temperature energy gaps for silicon, germanium and GaAs

13 p1933 A72-29824

Joule heating power density in NbZr superconductor hollow cylinder, estimating temperature changes and instability locations

13 p2023 A72-29855

High melting point transition metals carbides, nitrides, borides, silicides and oxides thermal conductivity as function of characteristic temperature

13 p1981 A72-29905

Electrical characterization of GaAs by Hall and magnetoresistance measurements, analyzing temperature dependence of carrier concentration

13 p2024 A72-30034

Temperature and extracellular Ca level effects on mammalian ventricular myocardium force-frequency relationships, determining contractile tension, velocity and phase duration

13 p1907 A72-30045

Al inhibitive of Ti oxidation at 800-1000 C due to interatomic bonds, lower oxygen solubility and diffusion rates

14 p2113 A72-30166

Fatigue life tests of structural sandwich plates with honeycomb layer, considering temperature effects, material scattering and defects inside honeycomb by nondestructive methods

14 p2164 A72-30286

Phononless lines shift and broadening and electron phonon interaction in lanthanum trifluoride-Nd crystal, obtaining temperature dependence of non-radiative transition probability

14 p2142 A72-30359

Low and medium strain rates and temperature effects on bcc structure polycrystalline Nd and Mo determining mechanical properties of yield and flow

14 p2114 A72-30367

Microstructure effects on thermomechanically processed dispersion strengthened Ni alloys yield strength at various temperatures

14 p2114 A72-30368

Tungsten-rhenium alloys and tungsten self diffusion coefficient temperature dependence investigation, noting Re addition effects

14 p2114 A72-30402

Heterogeneous order-disorder transformation in Ni-Mo alloy at 78 K after annealing, using ion field emission microscopy

14 p2116 A72-30416

Stress analysis of thick walled hollow viscoelastic circular cylinder enclosed in elastic shell and subjected to nonlinear creep conditions, noting temperature effects

14 p2165 A72-30439

Lunar breccia and crystalline rocks thermomagnetic magnetization characteristics, presenting alternating field and thermal demagnetization curves

14 p2154 A72-30507

Apollo 12 fines thermal conductivity in vacuum at 200-400 K, using least squares technique for curve fit

14 p2154 A72-30509

Magnetization and temperature interrelationship in high constant magnetic field for Apollo 11, 12 and 14 rocks, obtaining magnetic hysteresis curves

14 p2155 A72-30517

Apollo 11 and 12 lunar surface rocks electrical conductivity at 300-1200 K in vacuum, Ar, He and H₂ hydrogen atmospheres, noting large hysteresis above 500 C

14 p2155 A72-30518

Welded Al alloys at temperatures above 100 C, discussing traditional and powder metallurgy and mechanical properties dependence on time, temperature and creep

14 p2116 A72-30528

Creep rate dependence on high temperature oxidation in austenitic steel, noting preformed oxide layer and environment cycling effects

14 p2117 A72-30537

Heat treatment and grain size effects on stress corrosion resistance and life duration of maraging steels, investigating crack initiation and propagation

14 p2117 A72-30539

Co-Cr alloy oxidation as function of temperature and oxygen partial pressure, discussing solid state diffusion

14 p2118 A72-30544

W and Nb effect on Ta base alloys high temperature oxidation behavior

14 p2118 A72-30547

Temperature effects on critical crack opening as fracture toughness criterion for medium strength steel, taking into account local plasticity and propagation resistance
14 p2118 A72-30590

Cast double base propellant rocket motors safe storage and service life assessment, examining environmental storage conditions and accelerated temperature effects
14 p2144 A72-30758

Atmospheric humidity, temperature, vibrational and static loads effects on composite and double base rocket propellants strength and safety characteristics
14 p2145 A72-30764

Octahedral TiC single crystals oxidation at high temperature in oxygen, carbon dioxide and mixtures, investigating oxygen partial pressure effects on kinetics
14 p2121 A72-30772

Alpha solid solution of nitrogen in Nb-Mo alloys, obtaining excess partial quantities and activity and interaction coefficients at high temperatures
14 p2121 A72-30773

Ferrite powder relative density as function of temperature, sintering time and pressure during hot pressing, noting creep activation energy and vacancy motion
14 p2107 A72-30775

Zirconium diboride oxidation processes at temperatures above 520 C, noting zirconium oxide formation
14 p2121 A72-30850

Hg vapor absorptivity dependence on wave number, atomic density and temperature in 2537 A resonance line region, discussing measurement by magnetic scanning or monochromator
14 p2131 A72-30853

Temperature effects on nonelastic behavior of turbine rotor disk for steady and cyclic loading, noting creep solutions, transient stress and plastic strain
14 p2167 A72-30906

Temperature aftereffect in heating and cooling of metals with cubic and noncubic lattices in relation to relaxation and hereditary deformation
14 p2143 A72-30952

Relaxation and internal friction characteristics of beta-rhombohedral B at 80-1000 K, using LF vacuum oscillator with inverted torsion pendulum
14 p2122 A72-30958

Phase diagram of quaternary W-Mo-Nb-Ta alloy system, noting dependence of hardness on composition and temperature
14 p2122 A72-30982

Al-Mu-Li alloys phases mechanical and thermal properties under tensile and fatigue tests at room and elevated temperatures
14 p2124 A72-31037

Heat treated light alloy bar deformation, temperature and time factor effects macrostructure and mechanical properties
14 p2124 A72-31038

Li addition effects on Mg mechanical properties temperature dependence and notch sensitivity of binary Mg-Li alloys
14 p2125 A72-31041

Heat chamber treadmill work-induced thermal stress effects on reaction time to foveally and peripherally presented visual stimuli
14 p2078 A72-31154

High temperature and altitude combined effects on performance of tracking, monitoring and mental arithmetic complex task
14 p2083 A72-31155

Thermal expansion of carbon-carbon composites as function of temperature and fiber orientation by dilatometric measurements
15 p2260 A72-31256

Thermal expansion measurements of simulated volcanic and nonvolcanic lunar rocks as function of temperature
15 p2222 A72-31258

Thermal load effect on convective heat transfer in turbulent flow of viscous incompressible liquid in circular tube
15 p2334 A72-31262

Temperature dependent Mg and Fe hyperfine doublets in lunar olivine, indicating slow cooling crystallization
15 p2303 A72-31302

Temperature dependent optical constants of Ti and W crystal surfaces cleaned by ion bombardment in ultrahigh vacuum
15 p2274 A72-31376

Random temperature variations effect on life of Euler column with sandwich cross section under constant axial compressive load, using Norton nonlinear creep law
15 p2324 A72-31494

Calibrated thermal emission spectra under extreme temperature, surface reststrahlen and cloud conditions from Nimbus 4 IR spectroscopy
15 p2223 A72-31510

IMPATT diode junction temperature effects on operation explained by small signal analysis
15 p2206 A72-31545

Thermal stress and temperature distribution in rigidly bounded elastic half-space, taking into account coupling effects
15 p2325 A72-31637

Al-Zn-Mg alloys hot cracking during solidification, discussing chemical composition, Al purity, temperature, aging, dissolved gases and grain refining additives effects
15 p2256 A72-31774

Room temperature GaAlAs single-heterojunction diode lasers structure, fabrication, threshold current density and quantum efficiency dependence on wavelength and temperature
15 p2247 A72-32032

Transition metals additives effect on binary Mo alloys softening, noting influence of temperature and electron concentration change
15 p2258 A72-32135

Temperature effects on stress-strain diagram, tensile strength and creep properties of fiber-epoxy resin composites
15 p2260 A72-32137

High energy storage laser material Nd-doped silicate oxyapatite refractivity temperature dependence characteristics measurement
15 p2249 A72-32167

Excess white noise source in photomultiplier as function of temperature from voltage, intensity and ion pulse measurements, noting effect on photon counting statistics
15 p2207 A72-32238

Superconducting to normal transition field as function of temperature for Ta with thin surface layer variable density impurities
15 p2293 A72-32241

Stellar winds and breezes classification using energy flux and particles kinetic and thermal energies for criteria, noting coronal temperature effects
15 p2313 A72-32298

Superconductivity, temperature and tunneling effects in low carrier density semiconductor systems /tin, germanium and indium tellurides, lanthanum triselenide and strontium titanium oxide/
15 p2293 A72-32325

Thermal force exerted on spherical particle between two flat plates in stagnant monatomic rarefied gas, using moment solution to Boltzmann equation
15 p2336 A72-32403

Stainless steel surface alloy composition characterization as function of vacuum annealing temperature, using proton-induced X rays
15 p2258 A72-32527

Thin film superconductors conductivity evaluation above transition temperature through renormalization of impurity-scattering vertex by pair fluctuation effect inclusion
15 p2295 A72-32540

Temperature and pressure requirements for producing superfluid liquid molecular hydrogen, noting use of solid deuterium or Ne walls to prevent hydrogen solidification
16 p2422 A72-32911

Angular distribution and intensity of light scattered by carbon dioxide near critical point, noting temperature dependence of isothermal compressibility and long range correlation length
16 p2422 A72-32945

Solar radiation induced molecular oxygen photodissociation rate as function of column density and temperature in mesosphere and lower thermosphere
16 p2383 A72-32967

Sudden heating-induced deflection of rectangular plate fitted into equal sized excavation in elastic foundation with relatively very low thermal conductivity
16 p2475 A72-33148

Nb-Mo alloys elastic constants anomalous temperature dependence, proposing phase changes role and relationship to neutron diffraction and specific heat
16 p2405 A72-33167

Temperature effect on bonding strength between ceramic whiskers or fibers and metal matrices attributed to thermal expansion coefficients disparity
16 p2413 A72-33206

Temperature effect on fatigue crack growth in high strength annealed Ti-Al-V alloy in water, oxygen/hydrogen and vacuum environments
16 p2406 A72-33320

Design criteria for fiber reinforced thermoplastic resins performance optimization, discussing temperature, humidity and chemicals effects
16 p2415 A72-33417

Al-Mg solid solution creep at 570-800 K, discussing creep rate controlling mechanism due to Mg atoms interactions with dislocations
16 p2407 A72-33442

Strain rate and temperature effects on supersaturated Al-Cu-Mg solid solution mechanical properties, considering ultimate tensile strength and hardening
16 p2407 A72-33443

Carbon monoxide oxidation reactions temperature dependence, correlating high to low temperature results via transition state theory
16 p2360 A72-33511

Forming techniques and heat treatment effects on recrystallization characteristics of heat resistant Cr alloy, noting high temperature influence on crystal structure
16 p2407 A72-33531

C concentration and temperature dependence of graphite wetting by liquid Ni and Co and melts of Ni-C and Co-C alloys, noting nonequilibrium effect
16 p2415 A72-33537

Nonlinear viscoelastic behavior of isotropic unoriented crystalline polyethylene terephthalate at 70-100 C, using creep, recovery and load tests
16 p2416 A72-33614

Conductance measurements for metal oxide-amorphous silicon junctions, showing temperature dependent tunneling
16 p2442 A72-33620

Temperature dependent elastoplastic wing assemblies and continua analysis via matrix displacement method
16 p2471 A72-33791

Discontinuous precipitation and site nucleation in quenched and aged Al based Zn alloys as function of temperature
16 p2410 A72-33812

Hydrogen solubility in Zr-Nb-H systems as function of composition, temperature and hydrogen equilibrium pressure
16 p2410 A72-33816

Graphic procedure for strength test data conversion from test temperature to design temperature based on equivalent damageability concept
16 p2411 A72-33847

Temperature and stress dependence of steady state creep rate for dispersion strengthened Ag-gallium oxide alloys, noting grain size effect on activation energy
16 p2411 A72-34094

Thermal resistance of planar semiconductor structures.
17 p2594 A72-34296

Visible and invisible nonionizing radiation produced human injuries, considering visual and retinal effects and induced thermal stresses
17 p2499 A72-34300

Signal-to-noise performance of cryogenic electrically small receiving antennas.
17 p2525 A72-34375

Plane problem of thermal creep at high temperatures
17 p2636 A72-34473

Parametric optimization of a cylindrical converter with a molybdenum emitter and niobium collector.
17 p2497 A72-34610

Decay rate coefficients at 250-370 K for three-body recombination kinetics of O and CO, considering CO, carbon dioxide and nitrogen as third body
17 p2511 A72-34736

Finite element analysis of elastoplastic structures with temperature dependent mechanical properties
17 p2631 A72-34947

Soft X-ray and microwave observations of hot regions in solar flares.
17 p2608 A72-35089

Characteristics of Gunn elements CGY 11 to 14 and their application as microwave oscillators. II
17 p2530 A72-35150

Friction of rubber on ice.
17 p2560 A72-35225

Characteristics of cosmic ray diurnal variation from Deep River neutron and meson data and temperature effects.
17 p2601 A72-35400

Investigation of the dependence of the electrical characteristics of a 'Fotovol'-type high-voltage matrix photoconverter on the radiation intensity and temperature
17 p2498 A72-35511

Temperature dependence of electrical and thermal conductivity for transition metals at 20 to 1200 C, noting periodic variations associated with atomic structures periodicity
17 p2568 A72-35519

Radiant interchange among suspended particles and its effect on thermal relaxation in gas-particle mixtures. (DFVLR-SONDDR-210)
17 p2638 A72-35643

Magnesium aluminate spinel reinforced with sapphire whiskers, investigating whisker content, temperature and deflection rate effects on yield strength
17 p2572 A72-35661

Dislocation mechanisms in creep.
17 p2635 A72-35921

Incident thermal flux parameters and wall temperature effects on flow characteristics in preseparation zone of laminar boundary layer and separation point location
17 p2487 A72-35927

Oxidizability of boron-carbon compounds at high temperatures, determining chemical composition effect on oxidation resistance
18 p2703 A72-36095

Plasma immersion probe measurements of electron work function.
18 p2690 A72-36127

Thermionic characteristics of carburized tungsten-rhenium alloys.

18 p2656 A72-36131

The stability of structure of physical mechanical properties of molybdenum and tungsten after irradiation and thermal influence

18 p2698 A72-36153

Noise in bipolar junction transistors at low temperatures.

18 p2666 A72-36323

FET noise at high temperatures.

18 p2666 A72-36324

Experimental determination of ultrasonic wave velocities in plastics, elastomers, and syntactic foam as a function of temperature.

18 p2703 A72-36415

Gas shielded arc welding of Ni, discussing current density, energy, arc length and preheating temperature effects on welds porosity

18 p2695 A72-36427

Thermal effects in JFET and MOSFET devices at cryogenic temperatures.

18 p2666 A72-36453

Temperature dependence of low-frequency excess noise in junction-gate FET's.

18 p2666 A72-36454

Expanding universe models showing particle pairs annihilation at critical temperatures

18 p2725 A72-36525

Thermoregulation during positive and negative work at different environmental temperatures.

18 p2650 A72-36559

The application of a dislocation model to the strain and temperature dependence of the strain hardening exponent n in the Ludwik-Hollomon relation between stress and strain in mild steels.

18 p2701 A72-36589

Temperature dependence of the electron thermal conductivity in rare gas plasmas.

18 p2716 A72-36958

Thermal modulation and FM noise of Gunn oscillators.

18 p2668 A72-37038

On the numerical solution of a class of nonlinear problems in dynamic coupled thermoelasticity.

18 p2738 A72-37078

Effect of structural parameters and temperature on the effective thermal conductivity of plasma-sputtered aluminum oxide

18 p2696 A72-37188

A graphite calorimeter

18 p2693 A72-37192

Steady combustion thermal stability of condensed explosives for burning rate limitation by condensed phase chemical reactions, noting surface temperature effects

19 p2879 A72-37356

Thermal expansion at elevated temperatures. III - A hemispherical laminar composite of pyrolytic graphite, silicon carbide and its constituents between 300 and 800 K.

19 p2822 A72-37463

Effects of thermal lensing in glass lasers.

19 p2810 A72-37512

Temperature effects on the strainrange partitioning approach for creep-fatigue analysis.

19 p2815 A72-37638

Strain rate, stress concentration and temperature effects on hydrogen environment embrittlement of metals

19 p2816 A72-37640

Characteristics of temperature dependence for the thermal conductivity coefficients of niobium-zirconium solid solutions

19 p2817 A72-37739

Specific fuel consumption and specific thrust optimization methods in turbofan cycles, noting optimum fan pressure ratio increase with turbine inlet temperature

19 p2848 A72-37746

Determination, by X-ray photometry, of the frequencies of thermal oscillations which propagate themselves, following the axes of symmetry in a potassium chloride single crystal, at temperatures of 295, 80, and 5 K

19 p2844 A72-37791

Oxygen diffusion coefficient variation with temperature observed during dissolution in alpha-zirconium, noting oxygen content effect on oxygen atom elementary jump length

19 p2817 A72-37795

Effect of temperature on the base resistance and the noise factor of a bipolar junction transistor.

19 p2773 A72-37848

Method for determining thermal strains in astronomical mirrors

19 p2801 A72-37968

Heat resistant alloys stress-rupture strength tests for operating temperatures based on equivalent high temperatures damageability

19 p2818 A72-38008

Determination of the temperature dependence of the thermophysical characteristics of solid materials by the method of successive approximations

19 p2881 A72-38044

Volume and enthalpy changes at critical point of condensed state, noting Ar enthalpy dependence on temperature

19 p2881 A72-38045

The effect of junction temperature on the output power of a silicon IMPATT diode.

19 p2773 A72-38145

Atomic oxygen-ozone gas phase reaction rate constant direct measurement in steady state flow system at 269-409 K under excess ozone conditions

19 p2762 A72-38221

Thermal and athermal components of the flow stress in zone-refined titanium.

19 p2820 A72-38298

Effect of chemical reaction reversibility on the temperature and pressure dependence of burning rates

19 p2882 A72-38455

Thermal effects in the seam area during impact welding

19 p2809 A72-38461

Variations as a function of the temperature of the moduli of elasticity of monocrystalline P-type GaSb

19 p2846 A72-38542

The temperature dependence of the critical current of a double Josephson junction.

19 p2846 A72-38556

Elastic constants of niobium-molybdenum alloys in the temperature range -190 to +100 C.

19 p2821 A72-38591

Influence of temperature shocks on seed formation after irradiation of pollen from *Tradescantia paludosa*.

19 p2761 A72-38642

Vacuum thermal decompositions of the nitrate salts of hydrazine.

19 p2848 A72-38876

Brittle lacquer of air-drying type, investigating coating ingredients and plasticizers effect on strain sensitivity for various temperature and humidity levels

20 p2920 A72-38890

Influence of cooling of the sensor region of the cerebral cortex on the neurons of the mesencephalic reticular formation

20 p2890 A72-38926

Numerical climatic-change experiments - The effect of man's production of thermal energy.

20 p2947 A72-38962

The temperature dependence of the friction stress for basal dislocations in beryllium in the range 300-500 K.

20 p2935 A72-39191

Electrical conductivity of pressed cadmium antimonide

20 p2959 A72-39218

Temperature dependence of electroconductivity and photosensitivity in CdS films

20 p2959 A72-39223

The effect of elastic anisotropy on dislocations in Ni₃Fe.

20 p2937 A72-39293

The effect of oxygen on tantalum-sodium compatibility.

20 p2938 A72-39297

Elevated temperature ductility minimum in Hastelloy alloy X.

20 p2938 A72-39304

Interdiffusion in nickel-molybdenum and palladium-molybdenum systems

20 p2939 A72-39315

Turbulent boundary layer calculation, investigating surface roughness, pressure gradient and surface temperature effects

20 p2912 A72-39365

The plastic behavior of pure and dispersion-hardened nickel in the temperature range from 20 to 600 C

20 p2940 A72-39455

Heat transfer coefficient measurement and thermal network analysis computer program for improving performance and reliability of microelectronic package/board and chip/substrate systems

20 p2908 A72-39497

Time characteristics of heterojunction injection lasers.

20 p2933 A72-39516

The universal high temperature emissometer.

[ASME PAPER 72-HT-1]

Some results of testing M.O.S. transistors at elevated temperatures.

20 p2909 A72-39774

Low-temperature reduction of molybdenum and tungsten oxides

20 p2941 A72-39820

Fast-neutron-compensated n-germanium as a model of amorphous semiconductors.

20 p2961 A72-39853

The use of pre-cracked Charpy specimens to determine dynamic fracture toughness.

20 p2981 A72-39964

HCN laser mechanical, pressure, temperature and voltage environmental factors effects on output power stability

20 p2934 A72-39967

Phase diagram study of Cr-Ga alloys, investigating intermetallic compounds presence and polymorphic transformation and temperature effects

20 p2942 A72-39987

Absolute thermoelectric power of chromium-ruthenium alloys.

20 p2942 A72-39988

The mechanisms of diffusion in metals and alloys.

20 p2962 A72-39999

Induction period, particle size distribution and medium temperature effects on thermal ignition of metal particles under exothermal oxidation reaction on surface

20 p2987 A72-40040

Temperature effects on water refractive index from normal incidence IR spectral reflectance measurements

21 p3012 A72-40150

Electrical conductivity of tungsten trioxide/WO₃.

21 p3096 A72-40198

Deformation-induced martensitic transformation in isothermal and athermal Fe-Ni-C alloys.

21 p3066 A72-40272

Characteristics of the low temperature effect of an electric field on the sensitivity of photographic emulsions

21 p3053 A72-40391

Processing of carbon/carbon composites - An overview.

21 p3072 A72-40552

An experimental investigation of yield surfaces at elevated temperatures.

21 p3117 A72-40678

Shear modulus of liquids at elastohydrodynamic lubrication pressures.

21 p3059 A72-40688

Phenomena and interpretation of the transients caused by temperature change on capacitance of metal-oxide-metal systems.

21 p3097 A72-40690

Correlation of irradiation data using activation fluences and irradiation temperature.

21 p3083 A72-40763

Temperature effects on modulation sensitivity and vibrational spectra in Gunn diode oscillators, suggesting frequency stability improvement method

21 p3032 A72-40792

Temperature dependence of thermionic emission current density of Pt additive powdered zirconium carbide deposit on diode cathode working surface

21 p2997 A72-40801

Space applications of Fabry-Perot modulator as alternative to mechanical devices, presenting optical and electrical performance data for different temperatures

21 p3055 A72-40824

Fracture toughness of the heat-affected zone in 14CrMoV69 steel and 18Ni maraging steel.

21 p3067 A72-40850

Kinetics of carbothermal reduction of quartz under vacuum.

21 p3073 A72-40934

Strain aging of pure aluminum annealed from pre-melting temperature

21 p3060 A72-40954

Reagent concentration and temperature fluctuation effects on turbulent burning rate, noting temperature pulsations influence on energy balance

21 p3128 A72-40976

Effect of the temperature on the burn-out of hydrogen diffusion flames in a supersonic flow in a closed channel

21 p3129 A72-40983

Determination of the concentration range of flame propagation at elevated temperatures

21 p3129 A72-40984

Thermally-stimulated current from the gold acceptor trapping level in silicon.

21 p3097 A72-40996

Temperature and strain rate dependences of low cycle fatigue life at high temperatures of austenitic stainless steel, examining crack behavior and stress-strain relations

21 p3069 A72-41010

Optimum design of MHD generator combustion chamber, noting effects of heating temperature, oxygen enrichment degree and flow velocities

21 p2997 A72-41065

Theoretical and experimental features and methods of creep.

21 p3069 A72-41170

Hematological modifications due to acute exposure to heat

21 p3002 A72-41191

He II line emission in cold regions of solar prominences and chromosphere, noting hydrogen, metal and He I emissions

21 p3108 A72-41281

Bending vibration test of glass-textolites, noting temperature effect on vibration damping properties

21 p3073 A72-41357

Strain curves of VT-6C and VT-14 titanium alloys in the temperature range between 20 and 400 C

21 p3070 A72-41362

Changes in the phase composition of metal-glass materials depending on the sintering temperature

21 p3073 A72-41370

Nonpolar thermodynamics of thermoelastic differential materials in terms of deformation gradient, temperature and Clausius-Duhem constraints
21 p3131 A72-41478

Wave propagation in thermal rate dependent thermoelastic materials.
21 p3131 A72-41479

Reynolds number and drive power variation with Mach number, pressure and temperature in cryogenic wind tunnel
[AIAA PAPER 72-995] 21 p3040 A72-41581

Diffusion of cobalt in Ni-Co alloys at temperatures up to 1000 C
21 p3070 A72-41645

I-V, spectral and temperature characteristics of auto-photoelectron emission in p-type silicon cathodes with varying acceptor concentrations
21 p3098 A72-41692

Influence of the test temperature on the fracture energy of graphite
21 p3074 A72-41714

Thermal expansion coefficients of some fiberglass-reinforced plastics and their components under conditions of low and high temperatures
21 p3074 A72-41715

Influence of high temperature on the onset of motion sickness
21 p3004 A72-41749

Sunspot temperature increase stimulation of supergranule motion leading to spot decay and magnetic field diurnal fluctuation development
21 p3114 A72-41762

Behavior of carbon monoxide in the upper photosphere
21 p3114 A72-41777

Fatigue properties of 18-8 stainless steel at cryogenic temperatures.
21 p3071 A72-41845

Temperature dependence of the thermal electromotive force and of the Nernst-Ettingshausen effect in nickel-cobalt alloys
22 p3187 A72-41855

Kinetic theory of a modified Knudsen's absolute manometer.
22 p3175 A72-41941

Variational formulation and computer solution for thermal boundary layer flow over flat plate in entrance region, assuming temperature dependent thermal conductivity and viscosity
22 p3156 A72-41959

Effects of thermooptical distortion on the radiation loss magnitude and spatial-angular radiation characteristics for a lamp-pumped rhodamine-6G laser
22 p3185 A72-42173

Matthiessen rule on binary alloy electrical resistivity temperature derivative, discussing data deviations in substitutional alloys after quenching, radiation damage and plastic deformation
22 p3189 A72-42298

Heat transfer effects on reentry vehicle surfaces boundary layer stability and aerodynamic characteristics, noting stall angle reduction and drag increase from wind tunnel tests
[AIAA PAPER 72-960] 22 p3137 A72-42357

Atmospheric effects on the surface cosmic ray meson intensity recorded in London.
22 p3218 A72-42369

Current noise and conductance-temperature characteristics of thin discontinuous Pt films on glass substrate interpreted by quantum mechanical electron tunneling model
22 p3214 A72-42453

Deposition of finishes and dyes in materials dried using microwave heating.
22 p3183 A72-42480

The effect of a thermal and ultrahigh vacuum environment on the strength of precompressed granular materials.
22 p3173 A72-42528

Versatile stretching of a disc shaped as a plane with elliptic aperture.
22 p3236 A72-42627

On the formation of plastic adiabatic bands in a thin tube subjected to a dynamic torsion
22 p3236 A72-42638

Effect of activity and temperature on metabolism and water loss in snakes.
22 p3144 A72-42669

Spinal cord heating and cooling effects on body temperature, respiratory and heart rates and arterial blood pressure, investigating feeding and drinking behaviors
22 p3150 A72-42672

Electron spin resonance of divalent Mn ion doped in thallous azide single crystals, investigating temperature effects on spin Hamiltonian parameters
22 p3152 A72-42716

Ablation rate growth phenomenon in fusible material with diminished thermal flux, discussing quartz glass characteristics
22 p3244 A72-42728

Influence of temperature on the mechanical properties of metallic compounds
22 p3191 A72-42804

Plane waves in a new theory of thermoelasticity.
22 p3239 A72-42856

The modulus of elasticity of plastic materials at stress times between .001 and 10,000,000 seconds
22 p3197 A72-42859

Two-dimensional model for thermal compression.
22 p3136 A72-42868

Mathematical models from UV, IR and radio observations of chromosphere and transition region to corona, noting temperature effects of shock wave dissipation
22 p3229 A72-42903

X-ray structural examination of phase transformations in the VT14 titanium alloy during heating
22 p3192 A72-43015

Grain size and temperature effects on Cr and Al diffusion coefficients and mobility in Ni-20Cr and thoriated dispersed NiCr alloys from measurement at 1038-1200 C
22 p3193 A72-43028

High-temperature thermodynamic properties of the chromium carbides determined using the torsion-effusion technique.
22 p3193 A72-43029

A study of the rates of carbon-carbon dioxide reaction in the temperature range 839 to 1050 C.
22 p3153 A72-43037

Constitution of the Ni-Cr-Fe system from 0 to 40 pct Fe including some effects of Ti, Al, Si, and Nb.
22 p3194 A72-43038

Decarburization kinetics of low alloy ferritic steels in sodium.
22 p3194 A72-43042

Thermal conductivity in the two-band model of superconducting transition metals containing nonmagnetic impurities.
22 p3323 A72-43274

Dependence of changes in the electronic dislocation-braking force during superconducting transition on the stresses, temperature, and strain rate
22 p3312 A72-43315

High strength boron and borsic fiber reinforced aluminum composites.
22 p3299 A72-43491

Temperature-time effects on fracture failure mode and strength of polymeric glasses in terms of Ludwik brittle-ductile transition hypothesis and Griffith theory
22 p3305 A72-43503

Microscopic aspects of fracture in ceramics.
22 p3305 A72-43504

Perpendicular collisionless shock wave instability.
22 p3320 A72-43523

Recovery of high temperature deformed Ni-Al alloys.
22 p3300 A72-43564

Strength of a cylindrical shell of variable thickness located in a temperature field
22 p3346 A72-43653

Physicochemical problems in silicon and germanium heat treatment, covering solubility and solid solutions stability and saturation variation with temperature
22 p3324 A72-43687

Temperature and polarization dependence of arsenic sulfide single crystals and thin films intrinsic absorption edge, determining forbidden bandwidth and transitions types
22 p3324 A72-43688

Influence of wall temperature on heat transfer in a compressible three-dimensional turbulent boundary layer
22 p3248 A72-43694

Plasma-beam interaction in limited geometry: Temperature effects
22 p3321 A72-43700

Gas turbine blade models of heat resistant ZrSiO₄ alloy under operational temperature variations, observing fatigue strength
22 p3347 A72-43735

Postoperative states of turbine disk alloys at 280-500 and 550-630 C, noting lower durability values
22 p3347 A72-43737

Heat resistant steels long time strength determination by graph-analytical time-temperature extrapolation
22 p3301 A72-43739

Effect of overheating on the creep resistance of metastable alloys
22 p3301 A72-43927

Creep and fracture of OT-4 titanium alloy in the temperature range from 400 to 550 C
22 p3302 A72-43960

Technical cohesive strength of welded joints at various temperatures and loading rates
22 p3293 A72-43961

Some strength characteristics of graphite/zirconium carbide composites
22 p3307 A72-44013

On free vibrations at temperature-dependent material properties and transient temperature fields.
[ASME PAPER 72-APM-J] 22 p3350 A72-44053

Effect of substrate temperature on electrical properties of amorphous germanium films.
22 p3324 A72-44069

Heat conduction with allowance for the temperature dependence of the coefficient of thermal conductivity.
II - Correctness of the variational formalism
22 p3357 A72-44085

Ultrasonic attenuation and velocity in hot specimens by the momentary contact method with pressure coupling, and some results on steel to 1200 C.
23 p3294 A72-44116

Aircraft gas turbine engine controllers and fuel pump testing under extreme fuel temperatures, noting cavitation characteristics
23 p3327 A72-44287

Heat treatment effects in multipass weldments of a high-strength steel.
23 p3304 A72-44310

Study of the dependence of the spectral and integral radiation properties of bodies on the surface roughness.
23 p3357 A72-44538

Polymer fatigue failure mechanism examination on constant deflection type testing machine, investigating applied stress and temperature effects on crack propagation rate
24 p3455 A72-44631

Stress-strain diagrams from high and low temperature tests of Y alloy rods, noting temperature effects on plastic deformation
24 p3413 A72-44724

The influence of the atmosphere on the wavelength of the He-Ne laser and the solution of corrections of the laser interferometer.
24 p3409 A72-44771

Optical constants of cesium in the wavelength range from 0.3 to 2.5 microns and their dependence on temperature and state of matter
24 p3426 A72-44800

An experimental investigation of radiative properties of aluminum oxide particles.
24 p3461 A72-44809

Phase transformations in chromium-titanium compounds.
24 p3413 A72-44922

The creep of dispersion-strengthened Ni-Co alloys.
24 p3413 A72-44923

Temperature and loading conditions effects on structural element service life, showing partial healing process of microdefects
24 p3458 A72-44929

Frequency stability of Gunn oscillators with variation of ambient temperature.
24 p3385 A72-44980

Turbulent boundary layer calculation behind surface cusp, taking into account external flow turbulence and thermal stratification
24 p3390 A72-45008

3.39 micron resonance line absorption in shocked methane.
24 p3410 A72-45044

Temperature-sensitive neurons in the brain stem - Their responses to brain temperature at different ambient temperatures.
24 p3373 A72-45232

Hall generator operation characteristics under load, power, temperature and nuclear radiation conditions
24 p3385 A72-45270

The mutual solubilities of titanium and boron in pure aluminum.
24 p3415 A72-45482

Similarity problems of a non-isothermal boundary layer of an incompressible non-linear viscous medium with regard for dissipation.
24 p3395 A72-45634

Temperature dependence of destruction threshold of lithium niobate surface under laser irradiation, noting ferroelectric properties effects
24 p3432 A72-45722

Al and Ti alloy fatigue after temperature reduction to 253, 77 and 4 K as function of surface purity after machining
24 p3416 A72-45743

Compressive strength of Cu-W fiber metal matrix composite as function of temperature, comparing to ceramics
24 p3416 A72-45750

Refractory alloys softening under stress relaxation conditions at high temperatures, noting plastic strain hardening effect absence
24 p3416 A72-45763

Influence of a temperature dependent spectral absorption coefficient on radiative flux.
24 p3466 A72-45791

TEMPERATURE FIELDS
U TEMPERATURE DISTRIBUTION
TEMPERATURE GRADIENTS
NT THERMOCLINES
Temperature gradient induced in Lost City /Oklahoma/ olivine-bronzite chondrite by atmospheric friction from thermoluminescent emission measurements
01 p0126 A72-10109

Lateral surface heat transfer effect on thermophysical characteristics in thin layer coatings, discussing temperature gradients in corundum and zirconium oxide on copper
02 p0304 A72-12864

Solar chromosphere-corona transition region models based on UV resonance emission lines intensity, deriving temperature gradient from radio data
03 p0424 A72-13222

Magnetoplasma with skin current characterized by current and electron temperature nonuniformity, analyzing instabilities for perturbations above ion gyrofrequency

03 p0396 A72-13713

Temperature gradients measurements in transit-instrument pavilion and errors in time determination for two year period

03 p0361 A72-13822

Thermodynamic theory of rheological materials with internal changes accounting for higher gradients of deformation and temperature

03 p0448 A72-13888

Heat and mass transfer equations for unsteady transpiration cooling, taking into account temperature gradient between coolant and surface

03 p0457 A72-14154

Laser beam deflection as temperature sensor in optically inhomogeneous medium discussing gas density and temperature gradient relations

04 p0531 A72-15136

Temperature fluctuation structure in turbulent wake behind heated circular cylinder, investigating thermal convection, production and diffusion

[AD-740540]

04 p0596 A72-15330

Heat pipe temperature gradient initial conditions for ideal gas model, introducing two phase Mach number for choking phenomena analysis

[AIAA PAPER 72-22]

05 p0749 A72-16913

Local or radiative-convective heat transfer coefficient determinatin at porous surface in presence of two dimensional temperature field, using temperature gradient method

05 p0751 A72-17070

Transverse hydromagnetic plane waves existence in uniformly heated electrically conducting fluid under temperature gradient and magnetic field

07 p1045 A72-20442

Temperature gradients and dynamics of transient heating and cooling processes in metallic thermistors connected in series to power supplies

08 p1252 A72-21307

Anisotropy effect on glass fiber reinforced plastics cyclic deformability and heating kinetics under cyclic tension compression loads

08 p1191 A72-21501

Horizontal temperature variations relation to stratospheric CAT based on U-2 flight data

09 p1344 A72-22438

Optimal temperature gradients determination over thickness of shell of revolution under axisymmetric heating, formulating variational problem for conditional extremum of elastic energy functional

09 p1399 A72-22706

Alfven waves development and high pressure plasma hydrodynamic and kinetic instabilities dependence on magnetic field to temperature gradients ratio

09 p1360 A72-22954

Convective motions in rotating laterally heated annulus with contacting rigid lid, determining radial temperature difference for transition to vortex regime

10 p1506 A72-24420

High temperature gradients in pulsed heated Mo specimen under vacuum, using photomicrographic technique

11 p1629 A72-25267

Stability of free shear layer in wind tunnel two layered temperature differentiated air flow against small periodic disturbances, noting critical Richardson number

11 p1619 A72-26638

ALSEP heat flow experiment design and calibration, presenting independent vertical temperature gradient and thermal conductivity measurements in regolith

12 p1869 A72-27331

Temperature gradient and thermoelastic stresses in Nd-YAG laser active elements under continuous pumping conditions, noting refractivity radial distribution

12 p1822 A72-27614

Streak photography for three dimensional structure of thermal convection in rotating fluid under horizontal temperature gradient, noting time variations of baroclinic waves

12 p1809 A72-27701

Near-ground daytime temperature and humidity fine structure relation to heat flux, net radiation and temperature and wind gradients

12 p1841 A72-27711

Lower stratospheric turbulence and horizontal temperature gradients from RB-57F aircraft meteorological measurements

13 p1993 A72-28864

Nonlinear heat conduction in rarefied gases between concentric cylinders and spheres, using series expansion in terms of temperature difference for closed-form solution

13 p2064 A72-29118

Electrode boundary layer electrical breakdown mechanism with allowance for steep temperature gradients at surface, considering Joule heating or electrostatic field effect as causes

13 p2013 A72-29361

Horizontal and vertical scales of atmospheric boundary layer turbulence for various temperature stratifications, noting space and time correlations for longitudinal wind velocity component

13 p1995 A72-29592

Convective clouds effect on air temperature gradient and turbulent heat fluxes in near-surface layers

13 p1995 A72-29593

Truncated orthotropic conical shells thermostability at different temperature gradients, using Ritz method

14 p2163 A72-30193

Laminar Ekman boundary layer instability for incompressible fluid over rigid boundary with fixed vertical temperature gradient, investigating internal gravity waves generation

14 p2100 A72-30347

Metal creep activation energy determination during plastic deformation process, using temperature differential method

14 p2115 A72-30412

Nighttime lunar surface thermal properties from differential IR flux scans with earth based Cassegrain telescope, noting difference in brightness temperature gradients between highlands and maria

14 p2153 A72-30503

Large deflection vibrations of free circular plate of lenticular section with constant temperature gradient through thickness, noting thermal stresses effect

15 p2325 A72-31552

Photoelectric measurement of solar photosphere pole-equator temperature differences, analyzing statistical and systematic errors

[AD-745809]

15 p2317 A72-32770

Imploding spherical and cylindrical shocks, considering rear flow field with nonadiabatic isothermal flow and zero temperature gradient

16 p2376 A72-33009

Thermodynamic theory of materials with memory depending on temperature gradient summed history

16 p2425 A72-33587

Alfven waves development and high pressure plasma hydrodynamic and kinetic instabilities dependence on magnetic field to temperature gradients ratio

17 p2593 A72-35883

Pure and thoriated W compatibility with uranium carbide alloys at 1800 C, noting thermal gradient and thorium noneffects

18 p2699 A72-36163

Thermoluminescence lunar samples - Measurement of temperature gradients in core material

18 p2724 A72-36278

Electrical properties and fabrication details of integral diode matrices with controllable avalanche breakdown produced from zone melted silicon under temperature gradient

19 p2774 A72-38416

Thermal stress induced flow around constant temperature solid sphere in rarefied gas with uniform temperature gradient, using asymptotic theory

19 p2788 A72-38433

Reduction of temperature difference in shielding pipes for light-beam transmission

20 p2903 A72-39267

Transient and steady state vorticity generated by horizontal temperature gradients

20 p2987 A72-40016

Variation of the spectrophotometric temperature from the center of the disk to the limb of stars of the spectral classes B and A

21 p3102 A72-40094

Weibull distribution government of dispersion of destructive temperature gradients characteristic of fireproof ceramic materials heat resistance

21 p3074 A72-41713

The derivation of temperature gradient and electron density maps from EUV spectroheliograms

22 p3222 A72-42036

Extension of the Curie principle and constitutive relations for fluids with antisymmetric stress

22 p3166 A72-42311

Comparative cut-bar thermal conductivity apparatus

22 p3180 A72-42710

Physical characteristics of type I supernova envelopes during the initial expansion phase. II - Development of type I supernova spectra after maximum light

23 p3333 A72-43228

Ion acoustic instability in collisionless shocks

23 p3320 A72-43522

CAT probabilities relationship to temperature radiance gradients determined by IR spectrometers on-board Nimbus satellites

23 p3310 A72-43614

Photothermoelastic study of stress concentrations in a plate with internal heating

23 p3349 A72-43986

Acoustic transmission and reflection by a shear discontinuity separating hot and cold regions

23 p3315 A72-44373

TEMPERATURE INDICATORS

U INDICATING INSTRUMENTS

U TEMPERATURE MEASURING INSTRUMENTS

TEMPERATURE INSTRUMENTS

U TEMPERATURE MEASURING INSTRUMENTS

TEMPERATURE INVERSIONS

NT CENTRIFUGING STRESS

NT INTERFACIAL TENSION

NT STRUCTURAL STRAIN

NT VOLUMETRIC STRAIN

Clear air turbulence radiometric detection by IR vertical scan technique, associating atmospheric lapse rate anomalies with CAT related temperature inversions

02 p0225 A72-11820

Clear air turbulence association with rapid temperature change over Bahrain, suggesting convectionally induced internal wave dissipation in inversion layer as turbulence mechanism

09 p1346 A72-23424

Some features of the behavior of an intense light beam in a nonideal gas

24 p3411 A72-45609

TEMPERATURE MEASUREMENT

Cloud temperature determination from satellite IR images, presenting error corrections for various U.S.S.R. locations

01 p0095 A72-10956

Subsurface discontinuity detection by microwave radiometry, noting microwave temperature correlation with moisture patterns

02 p0209 A72-11792

Automated operational procedure for sea surface temperature determination from ITOS IR data, discussing error analysis

02 p0211 A72-11810

Stratospheric and lower mesospheric temperature measurement by ground based passive microwave sensing, calculating oxygen absorption band lines brightness temperature emission spectra

02 p0213 A72-11861

Microwave measurement and interpretation of oceanic thermal emission in terms of molecular temperature

02 p0214 A72-11868

Surface temperature measurement by microwave radiometry, noting sensitivity reduction due to moisture effects for resolution cell size targets

02 p0214 A72-11867

Fluidic sensors methods for position, angular velocity, fluid level, flow rate and temperature measurement

02 p0155 A72-11948

Electrical thermometer mounted on breathing mask for electropneumograms, measuring temperature change in respiration air flow

02 p0169 A72-12514

Prominent Zeeman multiplets in photospheric penumbra, umbra and sunspot spectra, presenting ratios for temperature sensitivity measurements

03 p0415 A72-12933

Ground based atmospheric vertical temperature profiles measurement by Raman backscatter from molecular nitrogen

03 p0348 A72-13438

Rocket fuel combustion products composition and combustion chamber temperature determination

03 p0405 A72-13474

Local stagnation temperature measurement in supersonic flow, using hot-wire anemothermometer

03 p0309 A72-13789

Temperature gradients measurements in transit-instrument pavilion and errors in time determination for two year period

03 p0361 A72-13822

Motion picture technique for studying vapor bubbles formation, determining temperature fluctuations on heated surface below active region

03 p0457 A72-14151

Unsteady thermal conductivity inverse problems obtaining heated body surface temperature and heat flux from temperature measurement in interior

03 p0458 A72-14164

Temperature reduction produced by partial cloud cover effect on radiation received by Nimbus 3 IR radiometer

03 p0385 A72-14226

Direct display plasma density and temperature meter, using floating double probe method

04 p0520 A72-14531

Self absorption and temperature gradient effects on fluorine-hydrogen flame spectroscopic temperature determination, comparing calculated and theoretical Lorentz intensity profile

04 p0596 A72-14898

ALSEP lunar heat flow experiment, describing instrument for temperature and thermal conductivity measurements in lunar subsurface

04 p0577 A72-15094

Mathematical analysis of Vuilleumier refrigerator calculating internal pressures, temperatures and gas flow rates via computer program

[ASME PAPER 71-WA/HT-33]

Radiation thermometry trends, considering photodetectors, optical pyrometers and filters

[ASME PAPER 71-WA/TEMP-3]

05 p0661 A72-15901

- Dynamic characteristics of buoyant low altitude clouds formed by solid rocket motor launches, determining initial temperature by motion pictures combined with conservation equations
[ASME PAPER 71-WA/FE-33] 05 p0724 A72-15923
- X ray topography of natural diamond, showing impurity platelet distribution, slip depth, temperature and stress conditions after plastic deformation
05 p0702 A72-16020
- Optimization algorithm in measurement conditions selection for satellite thermal sounding of atmosphere in 15 micron carbon dioxide band
05 p0655 A72-16174
- Pressure modulated carbon dioxide radiometer for remote temperature sounding in upper atmosphere
05 p0663 A72-16692
- Gas turbine blade temperature measurement by radiation pyrometer, discussing thermal radiation sensing and fiber optics transmission, signal processing and real time temperature characteristic display
[SAE PAPER 720159] 06 p0812 A72-17321
- Aluminum oxide cloud formation for thermosphere temperature determinations, describing methane/oxygen payloads, spectrographs, photometers and atmospheric models
06 p0806 A72-17646
- Satellite surface temperature measurements changes due to atmospheric specific humidity, noting increase in water vapor absorption coefficient with content
06 p0806 A72-17671
- Shock tube experimental techniques for studying fast processes coupled to shock wave propagation in reactive gases, describing pressure, density and temperature measurement methods
06 p0800 A72-18120
- Reciprocal temperature changes in dogs during constant thermomodulation for coronary sinus blood flow measurement
06 p0769 A72-18197
- Cathode temperature measurement in erosion and heat transport reduction by cesium seeding of Ar plasma arc
06 p0862 A72-18334
- Complex bodies time dependent temperature distribution from temperature measurements at arbitrary points, using Duhamel integral
06 p0904 A72-18512
- Test facility for thermal diffusivity measurements in solids by method of plane temperature waves using periodic optical heating at 1500 K
07 p0982 A72-18942
- Nimbus 4 satellite selective chopper IR radiometer atmospheric temperature measurements from earth surface to 50 km altitude, describing instrument design, operation and performance
07 p1029 A72-19097
- Atmospheric vapor pressure and temperature direct measurement, using copper-constantan thermocouples for wet-bulb temperature rapid fluctuations and thermistor for mean wet-bulb temperature
07 p0982 A72-19106
- Thermal diffusivity and heat capacity measurement by temperature vs time curve shape by laser pulse absorption, using thermocouple
07 p1101 A72-19890
- Photoelectric temperature measurements in contact zone during grinding of aluminum oxide ceramic materials by synthetic diamond disks
07 p0997 A72-20252
- Atmospheric turbulence, wind velocity, temperature and density measurements at 90-250 km, using explosive contaminants release from Skylark rockets
07 p0979 A72-20265
- Solar active regions temperature measurements from 2 cm radioheliograms, using high resolution radio telescope
07 p1082 A72-20296
- Nonideal black body temperature measurement with IR radiometer, discussing error dependence on object temperature and emissivity and background temperature
07 p0993 A72-20692
- Upper atmosphere temperature measurement by homodyne detection of excited atoms and molecules radiation, using photodiode beat frequencies produced by spectral line emission
08 p1154 A72-20739
- Various work-rest cycles and environmental temperature effects on body temperature, determining external auditory canal and core temperature relationship
08 p1123 A72-20886
- Temperature measurements of axial gas turbine rotor for start-up heating and cooling tests
08 p1223 A72-20953
- Heat exchange effects in thermal diffusivity measurements in dielectrics by plane temperature wave method, applying to rock and mineral studies
08 p1251 A72-21095
- Atmospheric temperature vertical profiles by laser Raman backscatter measurements
09 p1307 A72-22439
- Contactless induction multipoint current sensor design and operation principles for turbomachine rotating component temperature measurement
09 p1310 A72-22740
- Ionic and atomic temperature measurement in low pressure Ar plasma by X ray absorption spectroscopy
09 p1360 A72-22832
- Thermal behavior of explosively welded metals, describing test facility for temperature measurements of joints
09 p1319 A72-22891
- Thermal conductivity measurement for gases and gas mixtures with water vapor, describing methods and results
09 p1413 A72-23689
- Turbulent wake of slender cone at Mach 12.5, measuring density and temperature fluctuations simultaneously
[AIAA PAPER 72-118] 10 p1479 A72-24080
- Gas rotation temperature measurement by means of high energy electron beam probe with allowance for secondary electrons
[ONERA, TP NO. 1069] 10 p1480 A72-24222
- IMPATT diode junction temperature measurement with accuracy from breakdown voltage by pulse techniques
10 p1449 A72-24304
- Plasma coating formation mechanisms and parameters, studying metal surface and deposited particles temperatures, spraying time effects, etc
10 p1487 A72-24488
- Vanadium enthalpy and heat of fusion measurement with massive copper calorimeter
10 p1497 A72-24784
- Low resistance thermometry with transformer coupled potentiometer circuit to obtain size reduction and ability for direct exposure to fluid
10 p1482 A72-24806
- Temperature indetermination and large scale weather patterns in winter from 70 year temperature records
10 p1507 A72-25003
- Air, wet bulb and soil temperature indications from automatic telemetering meteorological stations, comparing with Hg thermometer readings
10 p1483 A72-25012
- Automatic hydrometeorological stations standardized sensors, describing data converters for atmospheric pressure, precipitation, humidity and wind and water and soil temperature measurements
10 p1483 A72-25014
- LiCl dew point hygrometer operation investigated by double ventilation psychrometers, noting measurement error dependence on relative humidity and temperature
10 p1483 A72-25015
- Atmospheric temperature measurement up to 2 km height, reviewing sounding equipment and techniques
10 p1508 A72-25091
- Spectral measurements of temperature in low temperature plasma, describing line reversal method
10 p1485 A72-25110
- Optical method based on spectral line center intensity recording to measure plasma temperature in MHD generators channels and combustion chambers
10 p1525 A72-25111
- Venera 7 satellite data during descent through Venus atmosphere and activity after soft landing on 25 December 1970, noting temperature and pressure measurements
11 p1718 A72-25937
- Molecular energy levels population inversions calculated from vibrational temperatures in carbon dioxide laser discharge plasma
11 p1649 A72-26339
- Atmospheric temperature measurement by neutral particle wake method, using satellite-borne mass spectrometer
11 p1634 A72-26408
- Digital precision measurement of thermocouple thermal emf at 200-1000 C, examining block diagram
11 p1634 A72-26457
- Spectropyrometric device for pulsed light or plasma source temperature measurement, noting operation in 2000-40000 C range
11 p1635 A72-26465
- Electron temperature determination from rate of ionization due to collisions between electrons and neutral particles in plasma
11 p1697 A72-26586
- Specific heat temperature coefficient measurement of W at 2000 to 3600 K for defect and phase transition studies
11 p1661 A72-26625
- Thermosphere temperature measurement by free velocity probe, admitting atmospheric sample via free molecular flow inlet
12 p1806 A72-27044
- Compact photomultiplier housing with controlled cooling, discussing temperature control and measurement
12 p1806 A72-27265
- Papers on thermal characteristics of moon covering earth based and in situ surface temperature measurements, radar mapping, heat flow experiments, etc
12 p1869 A72-27326
- Surveyor spacecraft lunar thermal data, comparing spatial resolution with earth based measurements
12 p1869 A72-27329
- Apollo 11 EASEP nickel resistance thermometer lunar surface data, presenting unshadowed equivalent brightness temperature and thermal parameters and emission directional dependence
12 p1869 A72-27330
- Measurement circuit for temperature dependence of thermal emf and electrical conductivity in thermoelectric materials
12 p1807 A72-27452
- Statistical analysis of spectrographic plasma temperature measurements, obtaining numerical solution to Abel integral equation
12 p1852 A72-27685
- Radial temperature and water vapor concentration profiles of radiating combustion source from optical method, using IR band model
12 p1811 A72-27945
- Ear site body temperature measurement relation to radiant heating of scalp and upper face
12 p1768 A72-28333
- Underwater tests of instrument system for combined skin temperature and direct heat flow measurement in thermally stressful environments
12 p1768 A72-28334
- Cloud top temperature measurement by satellite through comparison of visible and IR cloud images with concurrent airborne radar and lidar measurements
13 p1944 A72-28444
- Neutral upper ionosphere temperature measurement with manometer device onboard Cosmos 320 satellite, noting equatorial fluctuations at 250 km
13 p1955 A72-28586
- Titan and Galilean satellites effective temperatures from broadband observations, suggesting low surface emissivity or high opacity for Titan
13 p2041 A72-29417
- Continuous volume-temperature dilatometer measurement of small liquid samples in biological application
13 p1959 A72-29752
- Temperature control and measurement in electric wire annealing for standard Pt/Pt-10 Rh thermocouples
13 p1960 A72-29766
- Pyrometric obturation devices effect on sample temperature level during high temperature tests with radiant heating
13 p1960 A72-29903
- Correcting electronic transducer for rapidly changing temperature measurement, discussing design peculiarities for superior metrological characteristics
13 p1961 A72-30024
- Hydroxyl emission bands intensity, and vibrational and rotational temperatures sporadic and harmonic components in seasonal and diurnal variations
14 p2098 A72-30142
- Vanadium enthalpy and heat of fusion measurement using massive copper calorimeter with isothermal jacket
14 p2113 A72-30222
- Temperature difference between steadily flowing fluid and solid sphere due to viscous dissipation determined for simultaneous conduction and radiation
[DFVLR-SONDDR-220] 14 p2105 A72-30710
- Ionospheric rotational temperature and density measurement, using fluorescence produced by rocket-borne electron beam gun
14 p2106 A72-30974
- Temperature measurement error due to solid body and temperature sensor specific heat differences for unsteady heat transfer
14 p2106 A72-31160
- Gas temperature from Raman rotational line intensities generated by lidar techniques applied to inelastic Raman scattering
15 p2232 A72-31373
- Sea surface temperature determination on Nimbus 2 satellite, using three channels in medium resolution IR radiometer
15 p2224 A72-31674
- Mesosphere and lower thermosphere temperature measurement by rocket-borne manometer, relating temperature variations to corpuscular flux intensity and sun generated geomagnetic excitations
15 p2225 A72-31910
- High temperature lattice and radiative thermal conductivity measurements utilizing carbon dioxide laser and IR detector for diffusivity and mean extinction coefficient phase data
15 p2250 A72-32507
- Fine wire thermocouple probe use for measurement of total temperature in shock tube lasers
15 p2241 A72-32524
- Metal specimens yield point in adiabatic tension determined by thermoelectric method from temperature-stress and stress-strain diagrams
15 p2259 A72-32690

Photoelectric measurement of solar photosphere pole-equator temperature differences, analyzing statistical and systematic errors [AD-745809] 15 p2317 A72-32770

Torch temperature measurements in vacuum by spectral radiative energy distribution method 16 p2476 A72-33258

Uranus, Neptune and Pluto disk temperature observations via National Radio Astronomy Observatory interferometer 16 p2455 A72-33464

Microwave /60 GHz/ radiometer for air temperature measurement outside aircraft during icing conditions 16 p2393 A72-33631

Semiconductor thermal diffusivity and heat capacity measurements, using carbon bolometer and high sensitivity point microthermistor 16 p2442 A72-33855

Critical analysis of Senfleben modified hot-wire method for gas heat conductivity measurement 16 p2479 A72-33861

Small temperature variation measurement by temperature sensor switching, using multipoint electronic automatic recording bridge with polarized relay 16 p2395 A72-33967

Thermal relationship between tympanic membrane and hypothalamus in conscious cat and monkey. 17 p2499 A72-34344

Thermal conductivity and heat capacity measurement by temperature vs time curve shape by laser pulse absorption, using thermocouple 17 p2637 A72-35138

Measurement of the error of temperature sensors in flowing gases. 17 p2555 A72-35247

Temperature anomaly in the superficial layers of rubbing surfaces 17 p2638 A72-35422

Russian book on pyrometry principles covering high temperature measurement, error analysis, heat transfer and brightness temperature 17 p2556 A72-35447

Spectroscopic determination of the rotational temperature in a rarefied supersonic flow in glowing-discharge excited nitrogen. 17 p2544 A72-35928

Plasma immersion probe measurements of electron work function. 18 p2690 A72-36127

Thermoluminescence lunar samples - Measurement of temperature gradients in core material. 18 p2724 A72-36278

The Apollo 15 lunar heat-flow measurement. 18 p2724 A72-36285

Temperature sounding experiments for the Jovian planets. 18 p2726 A72-36641

Detection of defects in semiconductor structures by means of recording the temperature and electric fields. 18 p2693 A72-37106

Clinical IR thermography with Thermovision camera for body temperature discontinuity detection, discussing image resolution 18 p2655 A72-37196

A photoelectric method for measuring the temperature pulsations of solids 19 p2799 A72-37664

Experimental investigation of nonstationary heat exchange for flow around a flat plate 19 p2880 A72-37665

Determination of the spectrophotometric temperature, mean radius and mass of the star beta Cep 19 p2860 A72-37954

Upper atmosphere temperature measurement by homodyne detection of excited atoms and molecules radiation, using photodiode beat frequencies produced by spectral line emission 19 p2791 A72-38367

Spectral characteristics of surface-layer turbulence. 19 p2829 A72-38559

Effect of plasma resistance on electron temperature measurement by means of an electrostatic probe. 19 p2804 A72-38593

A new method for in situ electron temperature determinations from plasma wave phenomena. 19 p2793 A72-38758

Experiments concerning the contact surface in a membrane shock tube 20 p2911 A72-39017

Microelectronic component system temperature distribution measurement by IR microscope and electrical technique to determine beam-lead IC thermal performance 20 p2908 A72-39498

Thermal remote sensing of temperature distribution in semitransparent solids - A numerical experiment. [ASME PAPER 72-HT-5] 20 p2986 A72-39676

Arc furnace for thermal analysis of ultrarefractory materials 21 p3039 A72-40208

'Mars-2', 'Mars-3' observatories exploring the 'red' planet. 21 p3109 A72-41318

Ground and flight tests of the Ramzes rocket sonde. 21 p3115 A72-41499

Fine wire thermocouple probes for stagnation temperature measurements in hypersonic mixing layers [AIAA PAPER 72-1023] 21 p3057 A72-41601

Pulsed GaAs injection laser heating application to thermal conductivity coefficient measurement in thin films, discussing lasing spectra kinetics 21 p3064 A72-41740

Experimental determination of the vibrational temperature of a supersonic gas flow 22 p3242 A72-41879

CAT probabilities relationship to temperature radiance gradients determined by IR spectrometers on-board Nimbus satellites 23 p3310 A72-43614

Measurement of the temperature of flames containing scattering particles on the basis of IR radiation 23 p3356 A72-43678

Ground-based sensing of temperature profiles from angular and multi-spectral microwave emission measurements. 23 p3285 A72-44147

A new method of measuring temperature, inversion ratio, and pressure-broadened linewidth in a CW molecular laser. 23 p3297 A72-44188

Experimental study of heat transfer during cooling of a high-temperature gas flow in a pipe. 23 p3357 A72-44539

Simultaneous measurements of temperature and velocity in heated flows. 23 p3292 A72-44541

Temperature change direct measurement and annealing experiment via differential power analysis to determine stored energy release in metal plastic flow during compression 24 p3405 A72-44613

A thermal mapping technique for shock tunnels and a practical data reduction procedure. [AIAA PAPER 72-1031] 24 p3389 A72-45408

TEMPERATURE MEASURING INSTRUMENTS

NT OPTICAL PYROMETERS

NT PNEUMATIC PROBES

NT PYROMETERS

NT RADIATION PYROMETERS

NT RESISTANCE THERMOMETERS

NT TEMPERATURE PROBES

NT THERMOMETERS

Optical/electrical apparatus for measuring high brightness temperatures in 6,000-100,000 K range 01 p0068 A72-10620

Shock tube gas temperature measuring equipment using spectrum line reversal method 01 p0072 A72-11217

Digital magnetic temperature transducer using permeability discontinuity at Curie temperature for high stability and reproducibility without calibration [IEEE PAPER 8,5] 03 p0332 A72-13758

Measurement techniques for electrically heated temperature probes in flames, considering wire sensor diameter and radiative transfer 03 p0456 A72-13925

Thermography capabilities and limitations for design analysis and quality control in nondestructive testing of material test vehicle carbon-carbon composite cones 03 p0364 A72-14026

IR ray thermography, discussing application to tires testing and rubber manufacture 07 p0991 A72-20422

Microwave temperature sensor for radiation environment use, discussing cavity resonator design and operation, thermal cycling tests and comparative radiometer technique 07 p0993 A72-20677

Differential thermal analysis for electrical insulation thermal degradation and thermogram shape, combining equations for required life line 09 p1339 A72-23271

Ti-Si system phase diagram and equilibrium states, noting crystal lattices and thermograms 14 p2123 A72-30986

Temperature measuring instrument with thermocouple for differential thermal analysis equipment used in phase diagram construction 14 p2106 A72-30995

Thermoprobe - An instrument for determining the temperature of opaque, translucent, and transparent surfaces in the incandescent temperature range. 19 p2795 A72-37513

Temperature probes for flows at high enthalpy [ONERA, TP NO. 1074] 19 p2800 A72-37767

Thermistor temperature observation and correction for errors due to refraction anomalies in latitude measurements 19 p2801 A72-37913

Apparatus for measurement of specific heats between 0.3 and 3 K in the oscillating thermal region 22 p3180 A72-42936

Air temperature measurement errors due to instrument inertia under various meteorological conditions and atmospheric stratification 23 p3310 A72-43536

Neutral upper ionosphere temperature measurement with manometer device onboard Cosmos 320 satellite, noting equatorial fluctuations at 250 km 24 p3402 A72-45086

TEMPERATURE PHOTOMETERS

U PHOTOMETERS

U TEMPERATURE MEASURING INSTRUMENTS

TEMPERATURE PROBES

NT PNEUMATIC PROBES

Alternative heating local heat clearance probes for human muscle blood flow measurement 09 p1273 A72-23442

Thermosphere temperature measurement by high velocity probe, admitting atmospheric sample via free molecular flow inlet 12 p1806 A72-27044

Fine wire thermocouple probes for stagnation temperature measurements in hypersonic mixing layers [AIAA PAPER 72-1023] 21 p3057 A72-41601

TEMPERATURE PROFILES

Temperature, concentration and heat conductivity profiles of chemically reacting gas mixtures with thermal gradient, using classical transfer equations 01 p0023 A72-10489

Quiet time solar wind temperature profile calculation from energy equation using observed velocity profile data at earth orbit 01 p0120 A72-10881

Ground based passive remote sensing of low altitude vertical temperature profiles by microwave radiometry 02 p0211 A72-11807

Quantitative cloud information from satellite IR thermal imagery and vertical temperature profile data 02 p0211 A72-11808

Temperature profiles calculation for laminar boundary layer outside vibratory equilibrium 02 p0203 A72-11969

Flame propagation and overdrive heating in laser beam created plasma, calculating density and temperature profiles by one dimensional continuum hydrodynamic theory 02 p0238 A72-12363

Heat transfer and temperature profiles in separated flow generated by transverse rectangular notch in flat plate 02 p0303 A72-12700

Laminar two dimensional hypersonic flow over stepwise accelerated flat plate at zero angle of attack obtaining time dependent velocity and temperature profiles by linearized flow equations 03 p0442 A72-13236

Iterative procedure for computing optimal control in distributed parameter systems described by linear parabolic differential equations, applying to metal slabs temperature profile problem 04 p0504 A72-14664

Bright O, C and carbon dioxide emissions in Martian airglow from temperature profile models based on Mariner UV spectrometry 06 p0803 A72-17448

Radiative heat transfer damping rates of turbulent temperature pulsations in upper planetary atmospheres, assuming Kirchhoff radiation law validity 06 p0882 A72-17938

Radar observed apparent land breeze front off Wallops Island, giving temperature and wind profiles 06 p0843 A72-18441

Thermal and momentum diffusivity measurements in turbulent stratified flow, obtaining velocity and temperature profiles [AIAA PAPER 72-80] 07 p0966 A72-18956

Mars atmosphere temperature profiles inferred from outgoing radiation spectral characteristics, constructing atmospheric model 08 p1232 A72-21147

Biot variational principle for phase change problem with constant heat flux boundary condition and without melt removal, noting linear temperature profile choice 08 p1254 A72-21611

Atmospheric temperature profiles real time retrieval from Nimbus 4 satellite IR spectrometric observations describing method used in dynamical weather forecasting 09 p1345 A72-22440

Dinitroxydiethyl nitramine burning, describing experimental facilities used to determine temperature profile of combustion front 09 p1411 A72-22884

Xenon plasma produced in cascaded arcs, investigating spectral line widths, temperature and electron density profiles, transition probabilities and I-V characteristics 09 p1364 A72-23393

Continuous scan diffraction spectrometer for thermal sounding experiment on Meteor satellite, presenting vertical temperature and humidity profiles 09 p1347 A72-23588

Jupiter atmosphere thermospheric temperature profile from heat conduction equation, noting radiative and convective transfer 09 p1393 A72-23656

- Steady turbulent flow and heat transfer downstream of circular pipe sudden enlargement, computing streamline and temperature profiles and wall fluxes
09 p1412 A72-23687
- Satellite IR spectrometer sounding measurements reduction for atmospheric temperature profiles, obtaining coefficients by statistical regression and minimum information solutions
10 p1508 A72-25081
- Successful operational satellite sounding probabilities with normal global cloud cover by vertical temperature profile radiometer
10 p1508 A72-25082
- Lower atmosphere vertical temperature profiles determination from clear air ground based measurements of microwave thermal emission by oxygen
11 p1591 A72-25764
- Ground based radiometric measurements of vertical temperature profiles in planetary boundary layer, describing data reduction technique
11 p1681 A72-26083
- Statistical approach to atmospheric optics inverse problems solution, considering application to vertical temperature and humidity profiles determination
11 p1683 A72-26888
- Ionospheric and neutral atmospheric temperature profile, composition and electron density and energy measurements by MR-12 rocket
11 p1628 A72-26905
- Vertical electron concentration and temperature profiles at 80-170 km measured by rocket launched on 10 July 1969 at Volgograd
11 p1628 A72-26917
- High level Canberra flight for three dimensional picture of wind and temperature fields, showing CAT, gravity waves and smooth flight characteristics
12 p1841 A72-27709
- Turbulent mixing length velocity, temperature pulsations and viscous sublayer thickness in steady incompressible fluid flow past infinite plate
12 p1799 A72-28179
- Regression technique for determining temperature profiles in upper stratosphere from satellite measured radiances, noting accuracy
13 p1990 A72-28822
- One dimensional unsteady flow of dense magnetized plasma, investigating time evolution of temperature profile in wall layer and thermal conductivity
13 p2018 A72-29876
- Lunar interior temperature profile estimation from electrical conductivity distribution based on forsteritic olivine composition
14 p2153 A72-30505
- Lunar interior electrical conductivity from surface magnetic field measurements by Apollo magnetometers, calculating temperature profile for olivine moon model
14 p2154 A72-30508
- Wind tunnel tests for correction of temperature profile data in stratosphere and lower mesosphere obtained from SKUA rocket sounding
14 p2105 A72-30807
- Boundary layer temperature profile for ablating asbestos-plastic composite samples measured under combined convection and radiant heat fluxes
14 p2172 A72-31003
- Velocity and temperature profiles of plane Poiseuille flow with finite amplitude convection and longitudinal vortices, investigating uniform axial temperature gradient effect
14 p2173 A72-31063
- Heat and mass transfer in steady viscous flow through curved circular tubes, investigating velocity and temperature profiles
14 p2173 A72-31064
- Temperature and electric field profiles in two TRAPATT diode structures in nonoscillatory state under dc bias, comparing geometrical limitations on diamond heat sinks
15 p2205 A72-31316
- Spherical, cylindrical or plane piston motion in nonuniform medium with radiative energy transfer, obtaining approximate analytic solutions and temperature profile behind shock front
15 p2336 A72-32394
- Vertical temperature profile retrieval from satellite radiance measurements for insertion into numerical atmospheric circulation model, discussing sensitivity test
15 p2267 A72-32728
- Radiative heat transfer damping rates of turbulent temperature pulsations in upper planetary atmospheres, assuming Kirchhoff radiation law validity
16 p2459 A72-33776
- Optically thick plasma temperature profile determination by extended brightness emissivity method
16 p2440 A72-34100
- Heat transfer by free convection from a longitudinally vibrating vertical plate.
17 p2637 A72-35045
- Water vapor, CO₂ and particulate effects on the atmospheric temperature profile.
17 p2549 A72-35636
- Some results of a numerical experiment in the reconstruction of a temperature profile by a 'regularized' iteration method
19 p2829 A72-38769
- Lunar temperature profiles from electrical conductivity profile of olivine single crystal as lunar interior material representative sample
20 p2967 A72-39179
- Mars atmosphere temperature profiles inference from outgoing radiation spectral characteristics, constructing atmospheric model
20 p2968 A72-39252
- Turbulent gas jets formed in cryogenic substance discharge into gas at supercritical pressure and gas into gas of different molecular weight and temperature
20 p2912 A72-39366
- Motion due to a moving internal heat source.
21 p3044 A72-40115
- Regression technique for determining temperature profiles in the upper stratosphere from satellite-measured radiances.
21 p3052 A72-40249
- Mathematical models for temperature profiles and heat transfer rates in two-stream and multistream cross flow heat exchanger
21 p3128 A72-40931
- Venus atmosphere constituent abundances and temperature and pressure profiles from Venera probe data
21 p3110 A72-41451
- Ground-based sensing of temperature profiles from angular and multi-spectral microwave emission measurements.
23 p3285 A72-44147
- Thermal equilibrium calculations of the lower Venus atmosphere.
24 p3439 A72-44955
- ## TEMPERATURE SCALES
- Temperature scale for classifying spectra of peculiar and metallic line stars
06 p0883 A72-18021
- Temperature scale for classifying spectra of peculiar and metallic line stars
11 p1718 A72-25957
- Information theory and statistical mechanics applications to thermodynamics, discussing entropy and superiority of Georgian to Kelvin temperature scale
24 p3465 A72-45372
- ## TEMPERATURE SENSORS
- ### NT THERMISTORS
- High temperature properties of composite contact stack composed of alternating thermal flux sensors and heaters, determining heat conductivity and energy dissipation
03 p0458 A72-14160
- Thermal flux sensors high temperature calibration, using vacuum chamber technique
03 p0362 A72-14163
- Closed-loop temperature distribution optimal control by heater-sensor spatial configuration design for highest steady state temperature stiffness under heat flux disturbance
04 p0504 A72-14661
- Laser beam deflection as temperature sensor in optically inhomogeneous medium discussing gas density and temperature gradient relations
04 p0531 A72-15136
- Jimsonde high resolution temperature sensor for FPS-16 Radar/Jimisphere wind system, analyzing rms errors
04 p0522 A72-15157
- Fluidic sensors for temperature measurement at gas turbine inlet, noting long life and fast dynamic response
06 p0811 A72-17320
- Turbine inlet temperature sensor for gas turbine engines, using noble metal thermoelements with high signal level
06 p0812 A72-17322
- Fluid oscillator temperature sensor, noting fast dynamic response and application in high temperature environments
08 p1164 A72-20926
- Calibration technique for conductive thermal flux sensors operating at low temperatures
08 p1166 A72-21315
- Contactless induction multipoint current sensor design and operation principles for turbomachine rotating component temperature measurement
09 p1310 A72-22740
- Airborne thermal sensors time constants, giving temperature perturbation wavelength estimates
13 p1958 A72-29623
- Temperature measurement error due to solid body and temperature sensor specific heat differences for unsteady heat transfer
14 p2106 A72-31160
- Small temperature variation measurement by temperature sensor switching, using multipoint electronic automatic recording bridge with polarized relay
16 p2395 A72-33967
- Nomogram for heat detector size determination from thermal inertia index and Biot number
16 p2395 A72-33968
- Measurement of the error of temperature sensors in flowing gases.
17 p2555 A72-35247
- Clinical IR thermography with Thermovision camera for body temperature discontinuity detection, discussing image resolution
18 p2655 A72-37196
- Turbine engine sensors for high temperature applications.
19 p2802 A72-38048
- Optimization of the structural parameters of galvanic laminar heat-flux sensors
21 p3056 A72-41058
- The use of cholesteric liquid crystals in the study of skin temperature and their applications in aviation medicine
21 p3009 A72-41192
- Nitrogen temperature determination in arc tunnel air flows.
21 p3042 A72-41600
- Fluidic heat sensors for measuring fuel temperature in jet engines
23 p3326 A72-44280
- ## TEMPERATURE TRANSDUCERS
- ### U TEMPERATURE MEASURING INSTRUMENTS
- ### U TEMPERATURE SENSORS
- #### TEMPERING
- Testing temperature effect on intergranular fracture propagation in steel sensitive to tempering brittleness
03 p0372 A72-13599
- Tempered Fe-Cr-C-Co steels microstructural and mechanical properties, investigating martensite and bainite
03 p0375 A72-13929
- Melting effect on recrystallization of overheated tempered steel, discussing recrystallization under conditions favoring formation of silicon-oxygen compounds
03 p0376 A72-14017
- Quenched and tempered Ni-Cr-Nb-Co alloy, describing cellular precipitation mechanism
04 p0533 A72-14977
- Hardened and tempered Ni-Cr-Mo steel, testing rest periods caused fatigue life increase in terms of cycles to failure
06 p0895 A72-17802
- Tempering temperature effect on hydrogen penetration level and brittleness of hardened carbon steel
07 p1014 A72-19773
- Long-time isothermal temper embrittlement in Ni-Cr-Mo-V steels, noting tensile ductility decrease and intergranular fracture
07 p1015 A72-19932
- Internal friction measurements of tempered martensitic Cr steel quenched from 1100 C, connecting friction peaks with precipitation phenomena
07 p1021 A72-20486
- Martensite first stage decomposition mechanism and kinetics during tempering of quenched Re steels with varying carbon concentration
08 p1187 A72-21779
- Tempering effects on weakly doped n-InSb electrical properties at 77 K, discussing diffusion and activation energies in reversible/irreversible defect change processes
10 p1526 A72-24242
- Tempered or recrystallized chromium steels tensile behavior at 0 to 700 C, showing strength dependence on martensite transformation induced dislocation structure
13 p1975 A72-28667
- Precipitation reactions during tempering of Ti-Ta alloys, studying hcp and orthorhombic martensitic phases from electron microscope observations
16 p2408 A72-33619
- Study of point defects produced in aluminum by tempering and irradiation with electrons
18 p2702 A72-36705
- Fe-Ni-C alloys internal damping, martensitic structure and mechanical properties after quenching and tempering, discussing Mo and Cr additions
19 p2806 A72-37418
- Tempered hardness and tensile strength of ausforming Mn-Cr-B spring steels at low temperatures in austenite stable phase by electron microscopy
21 p3066 A72-40718
- ## TEMPLATES
- Thin film deposition of carbon on polypropylene, noting morphological templates role in enhancement of polymer nucleation during recrystallization
23 p3305 A72-43269
- ## TENSILE CREEP
- Creep behavior during and immediately after loading of Nimonic 90 and H 46 Cr steel under various stresses, temperatures and rates
06 p0829 A72-17801
- Fiber thermoplastics matrix breakdown and mechanical properties enhancement, examining lateral and longitudinal strain during uniaxial tensile creep and recovery
09 p1337 A72-22541
- Metal creep fatigue analysis and life prediction by inelastic strain ranges partitioning into reversed tensile and compressive plasticity and creep components
09 p1406 A72-23198

High temperature steady state tensile creep behavior of Ni-W solid solutions, showing creep rate relation to stress and stacking fault energy

13 p1975 A72-28668

Hydrostatic pressure effect on tensile creep and creep rupture of polycrystalline metals at high temperatures

13 p2058 A72-29450

Creep rupture characteristics of alloy in uniaxial tension, considering transient, steady state and accelerated phases

13 p1981 A72-29890

Maxwell rheological creep model verification by tensile tests on Mg alloy at 150 C under step loadings, treating thermodynamics of ideal creep

16 p2412 A72-34111

Mathematical relationships for primary, secondary and tertiary creep and their use in extrapolation of tensile creep data.

19 p2874 A72-37708

Plastic flow and strain hardening theories for short time tensile creep in high temperature metal formation, applying to Al alloys

21 p3125 A72-41510

Quadrisectional facility for studying creep and fatigue strength under deep freezing conditions

21 p3057 A72-41719

TENSILE DEFORMATION

Low temperatures and deformation rates effect on martensitic phase formation in Cr-Ni austenitic stainless steel under compression and tension

03 p0379 A72-14378

Thin shell theory analysis of thin walled cylindrical shell necking phenomenon as tensile deformation nonuniformity

08 p1248 A72-21821

Tensile plastic flow and fracture behavior of PdSi based alloys in glassy microcrystalline and crystalline states, noting shear deformation bands

09 p1339 A72-23382

Plastic percentage reduction of area and elongation for circular cylindrical sample in tensile deformation, proposing stress analysis method for metallic sleeves under low cycle loads

11 p1738 A72-26810

Thin walled tubular carbon steel specimen deformation pattern under biaxial tension and internal pressure at normal and low temperatures

12 p1830 A72-28227

Metal specimens yield point in adiabatic tension determined by thermoelectric method from temperature-stress and stress-strain diagrams

15 p2259 A72-32690

Tensile deformation of Co single crystal in high temperature fcc phase, noting dislocations effect on work hardening

16 p2410 A72-33819

Optimization of thermo-mechanical deformation parameters for Ti-6Al-4V.

19 p2821 A72-38385

Deformation and fracture of dispersion-strengthened nickel charged with hydrogen.

20 p2935 A72-39004

Large elastic deformations of an incompressible material heteroresistant to tensile and compressive strains

20 p2978 A72-39021

Deformation-induced martensitic transformation in isothermal and athermal Fe-Ni-C alloys.

21 p3066 A72-40272

Stress concentration at an elliptic hole in an elastoplastic body

22 p3233 A72-42060

Width/thickness ratio effect on steel, brass and molybdenum sheet specimens plasticity and deformation under tension at room temperature

23 p3301 A72-43758

TENSILE PROPERTIES

Precipitation hardened Al-Cu alloy microstructure relation to fatigue and tensile properties, emphasizing particle size and distribution, moving dislocations and grain boundary effects

01 p0088 A72-11044

Al-AiCu intermetallic unidirectionally solidified eutectic composite structure and heat treatment effects on room temperature tensile properties

05 p0676 A72-17104

Static and fatigue strength in tension of welded joints composed of low carbon and austenitic steel

07 p0996 A72-19767

Tensile ligament instability model for stress corrosion crack propagation velocity in austenitized steel tempered at 750 F

10 p1499 A72-24888

Off axis and transverse tensile properties of boron reinforced Al alloys, correlating metallurgical structures with stress-strain curves and fractographic studies

11 p1654 A72-25479

Glass styrene acrylonitrile bead filled composites tensile behavior, discussing relationship between yield stress, filler content, strain rate and temperature

11 p1673 A72-25487

Tensile properties of continuously cast aluminum-carbon fiber composites, discussing fiber outgassing and metal coating for wetting promotion

11 p1659 A72-25859

Alpha Zr tensile properties tests noting strain aging effects on strain rate, work hardening and ductility anomalies

11 p1661 A72-26595

Low carbon ultrafine grain steel tensile behavior, noting critical grain size for stable/unstable plastic flow transition

11 p1661 A72-26651

Heat treated Al alloy forgings stress relief by cold deformation between quench and age, examining effect on tensile properties and residual stresses

[ASM PAPER W 72-53,1]

12 p1817 A72-28165

Tempered or recrystallized chromium steels tensile behavior at 0 to 700 C, showing strength dependence on martensite transformation induced dislocation structure

13 p1975 A72-28667

Tensile properties from high temperature and room temperature tests of Ti alloys containing Ga correlated with creep resistance at 1000 F, noting activation energy

14 p2120 A72-30614

Adhesion effects on tensile and thermal expansion properties of aluminum oxide particles filled epoxy-urethane polymer at ambient and liquid nitrogen temperatures

16 p2415 A72-33415

Stored energy function for multiaxial stress state in rubberlike materials from tensile data based on Valanis-Landel theory

16 p2472 A72-33838

A comparison between the tensile and compressive creep behaviour of an 11 per cent chromium steel.

19 p2814 A72-37222

The transverse tensile properties of boron fiber reinforced aluminum matrix composites.

20 p2938 A72-39302

The low strain tensile behavior of U-7.5 wt pct Nb-2.5 wt pct Zr.

20 p2938 A72-39303

Transverse tensile properties of an unbonded model composite.

20 p2941 A72-39790

Book - Metal matrix composites.

21 p3070 A72-41528

Investigation of the strength and deformability of thin composite materials of magnetic recorder type. I - Strength and deformability at elevated temperatures

21 p3073 A72-41707

TENSILE STRENGTH

Unidirectional fiber array reinforced composites with improved longitudinal tensile strength and stiffness compared with structural metals

[SME PAPER EM 71-283]

01 p0092 A72-10966

Hot pressed Ti alloy powders, evaluating strength and toughness at cryogenic temperatures

02 p0240 A72-11439

Thorium oxide dispersion strengthened Ni powder metallurgy alloys, noting thermomechanical processing effects on tensile strength

02 p0241 A72-11447

Aluminum oxide dispersion hardened ferritic heat resisting Cr steel, describing liquid phase sintering effects on high temperature tensile strength

02 p0241 A72-11448

Winding fiber reinforced plastics, investigating fiber curvature effects on elastic constants and tensile strength optimization

02 p0248 A72-11626

Ti-Nd and Ti-Nd-Al alloys heat treatment effects on tensile and bending strengths

02 p0244 A72-12245

Hereditarily elastic body model with various tensile and compressive strengths, using elasticity theory with differing moduli

02 p0294 A72-12429

Ti alloys for aircraft structures, emphasizing weldability, tensile fatigue and residual strengths, shear-carrying qualities and fuselage shell design

03 p0373 A72-13616

Ti-Al-V room temperature creep, considering tensile and torsional loading, plastic deformation, stress relief and design limitations

03 p0377 A72-14171

Heat treatable Al alloys tensile and compressive moduli of elasticities data from USAF programs, comparing to long-accepted typical values

03 p0378 A72-14175

Stress-strain increment relations for materials with different compression and tension resistance under orthogonal loading

04 p0586 A72-15007

Stress-strain tensor component relations for isotropic elastic bodies with different tension and compression resistance

04 p0586 A72-15008

Elasticity theory relations for material with tension- and compression-varying modulus of elasticity, representing elastic strain energy as quadratic form potential

04 p0586 A72-15009

S-glass fiber bundles and composites under quasi-static loads, investigating strength characteristics and failure mechanism

04 p0592 A72-15474

Composite materials durability and strength estimations, using reliability theory for failure rate characteristic

05 p0680 A72-15991

High temperature brazing of heat resistant alloys, determining tensile strengths

05 p0666 A72-16189

High strength Al-Zn-Mg-Cu alloys, testing heat treatment and Ag addition effects on tensile strength

05 p0677 A72-17112

Ag addition effects on high strength Al-Zn-Mg-Cu alloys tensile properties and resistance to stress corrosion cracking

05 p0677 A72-17113

Low temperature tensile strength and plasticity of Ti alloys containing zirconium

05 p0679 A72-17203

Dispersion strengthened Co alloys structural stability, tensile and creep rupture strengths and hot corrosion properties

06 p0829 A72-17829

Tensile strength of tungsten reinforced nickel, determining temperature effect on fibers deformation after vacuum rolling simultaneously with plastic matrix

06 p0832 A72-18362

Deformability and strength of soft fiber reinforced plastics under biaxial tension, determining low temperature critical tensile stresses and elongation ratios

06 p0836 A72-18562

Temperature and deformation velocity effects on elasticity and tensile strength of Mo and Nb alloys

06 p0833 A72-18636

High pressure hydrogen effects on austenitic stainless steel embrittlement, determining yield, tensile and fracture strength

07 p1011 A72-19479

Alumoborosilicate glass fibers vacuum tensile strength tests, noting fiber strength increase with vacuum and exposure time

07 p1023 A72-19778

Al-Mg alloy with Ti, Zr, Mo and B additions under tensile and impact loads, investigating mechanical properties, strength and crack formation

07 p1014 A72-19834

Tensile strength enhancement of dislocated martensites in Fe alloys by precipitate dispersion in austenite prior to transformation

07 p1016 A72-19934

Interfacial dislocations and failure in tension of directionally solidified Al-Cu-Mg eutectic

07 p1016 A72-19937

Tensile strength estimation for two dimensional composite with brittle matrix and randomly orientated discontinuous elastic fibrous reinforcement

08 p1244 A72-21324

Random filament misalignment effects on rigidity and tensile strength of unidirectional graphite composites under shear loading

08 p1192 A72-21681

Gamma radiation effect on cracking and tensile strength of polycapromide/capron film

08 p1196 A72-21876

Diffusion bonded joints tensile strength determination from ultrasonic pulse echo and attenuation measurements, discussing contamination and SNR effects

10 p1485 A72-23814

Tensile strength of notched carbon and glass fiber reinforced epoxy resin composites as function of crack size

10 p1500 A72-24253

Glass content and temperature effects on fabric reinforced plastic laminates static behavior, analyzing tensile and bending strength and elastic moduli

10 p1501 A72-24660

Statistical bounding approach to fracture analysis of fiber reinforced composite materials tensile strength

10 p1502 A72-24883

Aerospace vehicle high tensile strength fasteners stress corrosion cracking and hydrogen embrittlement [AIAA PAPER 72-385]

11 p1653 A72-25407

Boron fibers tensile and transverse strengths, relating severe anisotropy to residual stress pattern from preexistent flaws

11 p1672 A72-25484

Fiberglass-graphite reinforcement of unidirectional epoxy laminates, examining longitudinal composite fracture stress and strain and tensile and compressive stiffness

11 p1672 A72-25485

Random filament misalignment effect on reinforced composite strength, discussing bundle, tensile and shear strengths

11 p1673 A72-25486

Chemical surface treatment effects on mechanically gripped fiberglass rods tensile strength

11 p1674 A72-25827

Ti-Nb and Ti-Nb-Al alloys heat treatment effects on tensile and bending strengths

11 p1659 A72-26131

Low temperature tensile strength and plasticity of Ti alloys with zirconium, investigating sensitivity to stress concentrations 11 p1660 A72-26138

Continuous drive friction welding of mild steel, noting burn-off rate relationship to tensile strength 11 p1641 A72-26492

Cold working effect on precipitation-recrystallization interaction in Cu-Ni-Zn alloy, discussing superposed strengthening mechanism during annealing 11 p1641 A72-26738

Cold working effect on Cu-Ni-Si-Mg and Cu-Ni-Si-Cr alloys age hardening behavior, presenting hardness and tensile strength vs aging time at 350 and 400 C 11 p1662 A72-26743

Glass textolites and high strength oriented plastics fracture mechanism in tension and bending, noting equalizing effect through proper cohesion characteristics between layers 11 p1674 A72-26804

Heat treatment effects on martensitic bainitic steel hardness, tensile strength and impact endurance, examining carbide and alpha phases 11 p1666 A72-26922

Al-Zn-Mg alloy tear resistance relationship to stress corrosion cracking from tear, tensile and corrosion tests 12 p1830 A72-27750

Al alloy plate material microstructural variations and specimen orientation effects on tensile and fracture toughness properties 12 p1830 A72-28080

Graphite fiber with high tensile strength and modulus and good elongation at low cost for aerospace applications 12 p1834 A72-28084

Particulate fillers bulk effects on epoxy resin compositions flexural, compressive and tensile strengths and moduli 12 p1834 A72-28089

Heat resistant blade alloy test temperature effects on fatigue life, tensile strength, hardness and chemical composition 12 p1831 A72-28230

Boron and carbon reinforced fiberglass plastics tensile strength characteristics, presenting static fatigue curves vs Poisson coefficient and elastic modulus for various fiber contents 13 p1982 A72-28552

Tensile strength of fiber glass reinforced plastic elements joined by cover plates and nonlinearly elastic adhesives 13 p1962 A72-28737

Tensile, creep and creep rupture strength hot hardness tests for metallic and nonmetallic materials 13 p1958 A72-29442

Time to failure under axial tension determined for gallium selenide single crystals at constant temperatures, noting tensile strength dependence 15 p2290 A72-31387

Tensile strength and martensitic transformation effect on stainless steel plastic deformation at cryogenic temperatures 15 p2253 A72-31521

Temperature effects on stress-strain diagram, tensile strength and creep properties of fiber-epoxy resin composites 15 p2260 A72-32137

Ultrahigh tensile strength steel pressure chamber fracture behavior in high stress concentration fields 15 p2330 A72-32345

Foam content effect on fiberglass reinforced thermoplastic foam tensile and impact strength, thermal distortion and mold shrinkage properties 16 p2415 A72-33418

High strength-high modulus boron vapor deposited on a carbon monofilament substrate. 17 p2572 A72-35657

Ultrasonic tests for incipient fatigue, hardness and elastic constants-tensile strength relationship in metals 18 p2690 A72-36125

Metallurgical aspects in the development of AlMgSi alloys with a low sensitivity to quenching 18 p2699 A72-36224

Strength and plasticity of molybdenum during short-term tests 19 p2819 A72-38218

Tensile and compressive flow strength and work hardening behavior in maraging steels, attributing strength differential to nonlinear elastic interactions between interstitials and dislocations 20 p2939 A72-39306

Longitudinal tensile failure of unidirectional fibrous composites. 20 p2944 A72-39789

Strength of S-glass fiber. 21 p3072 A72-40554

Tempered hardness and tensile strength of ausforming Mn-Cr-B spring steels at low temperatures in austenite stable phase by electron microscopy 21 p3066 A72-40718

Effect of the structure of carbon steels on their dynamic properties during dynamic loading 21 p3067 A72-40923

Strength of welded joints of high-strength stainless steels at cryogenic temperatures 21 p3061 A72-41365

Probabilistic model for tensile strength of brittle fibers, discussing clamping effects at various gauge lengths and Weibull flaw structure 23 p3305 A72-43490

Heat treatment effect on tensile and bending fatigue strength of Al alloy thin sheet 23 p3301 A72-43743

Solid powder metallurgy tungsten alloys, determining scale factor effect on bending strength and fatigue limit 23 p3301 A72-43751

Lutetium strength and plastic deformation characteristics under tension, presenting temperature and strain rate effects 23 p3301 A72-43754

Investigation of the strength of construction materials for various principal-stress relations 23 p3349 A72-43955

Elastic stiffness and ductility of refractory materials of long service life, noting creep diagrams and tensile strength 23 p3301 A72-43959

Stability of an elastoplastic rod of varying resistance to tension and compression with allowance for the initial stresses 23 p3352 A72-44162

Fracture of WC-Co from a continuum viewpoint. 24 p3413 A72-44815

The mechanism of void formation, void growth, and tensile fracture in an alloy consisting of two ductile phases. 24 p3415 A72-45481

Composite materials durability and strength estimations, using reliability theory for failure rate characteristic 24 p3418 A72-45733

Tensile strength of tungsten reinforced nickel, determining temperature effect on fibers deformation after vacuum rolling simultaneously with plastic matrix 24 p3416 A72-45749

TENSILE STRESS

Yield-fracture criterion for angle ply laminate cylinders wound with filament in biaxial tension 01 p0090 A72-10521

Torsional prestrain effects on 1100-F Al alloy thin walled tubes yield locus, calculating distortion degree by statistical characteristics 01 p0086 A72-11000

Solid rectangular beams under bending tests, obtaining tension-compression stress-strain curves 01 p0141 A72-11002

Turbine blades adaptability limits to temperature variations, considering rectangular cross section plastic rod under programmed thermal and tensile load cycles 01 p0143 A72-11372

Finite plasticity incremental and total strain theories for nonproportionate loading of circular steel and Al alloy torsion-tension members assuming von Mises yield [SESA PAPER 1901] 02 p0288 A72-11519

Dynamic response of infinitely wide perfectly flexible foil bearings to small sinusoidal tensile variations [ASME PAPER 71-LUB-20] 02 p0235 A72-11540

Elastoplastic problem of stress concentration in orthotropic plate with circular hole under balanced biaxial tension of infinity 02 p0293 A72-12428

Stress concentration coefficients calculation at sharp cracks and notches for rods in tension, compression and combined bending and torsion 03 p0443 A72-13457

Ductility relationship to plasticity characteristics in cylindrical steel samples with short notch under tension 03 p0443 A72-13458

Steels modulus of elasticity dependence on prestressing level produced by transverse and longitudinal tension 03 p0371 A72-13462

Cylindrical shafts with deep circumferential grooves, determining effective stress concentration under axial tension or bending 03 p0451 A72-14125

Stress concentration around circular hole in infinite semibrittle plate under omnidirectional tension at infinity or pressure at hole contour 03 p0452 A72-14127

Optimum variable thickness reinforcement around circular hole in flat elastic sheet under radial tension 04 p0583 A72-14463

Computer model of dislocation motion acted on by viscous drag through point obstacle array for tensile stress and shock deformation tests 04 p0584 A72-14528 [AD-737978]

Creep surface in Al alloy under combined tension and torsion, obtaining strain rate vectors from probes 04 p0590 A72-15195

Mechanical behavior of uniaxially loaded multilayered oriented fiber cylindrical composites, observing tensile transverse stresses [ASME PAPER 71-MET-O] 05 p0732 A72-15792

Stress-strain characteristics of nylon-polyurethane coated fabric under biaxial tension and shear forces 05 p0736 A72-16108

Disk stretching under tensile stresses, determining stress at arbitrary point in half band form connected with quadrant 05 p0737 A72-16294

Plastic stress and strain intensity factors for cracked plates in tensile fields 05 p0737 A72-16323

Combined tension-torsion creep testing of polymers, discussing equivalent stress and strain concept, testing apparatus and preliminary results for polythene 06 p0835 A72-17795

Nonheat treated extruded Mo alloy under tension and vacuum conditions at various temperatures, investigating cylindrical samples size effects on mechanical properties 06 p0833 A72-18635

Bending tests of beam with different creep characteristics in tension and compression 06 p0899 A72-18639

Static hydrogen fatigue of high strength steels, deriving relationship between time to cracking and tensile stresses magnitude for cadmium-plated steel 07 p1014 A72-19774

Stress relaxation measurement assembly for polymer film and fiber samples under tensile stresses at 213-573 K 07 p0986 A72-19779

Stressed state of isotropic plate with curvilinear holes under tension, using computer techniques 07 p1094 A72-20215

Three dimensional stressed state of isotropic plate with elliptical holes under tension, solving boundary value problems 07 p1095 A72-20216

Tensile load elastostatic transfer from rectangular cross section web to two infinite parallel sheets, deriving Cauchy type integral equation for adhesive bond force density 07 p1095 A72-20241

Circular elastoplastic beam under combined torsion and tension via Mindlin elastic model for materials with microstructure, taking into account work hardening 07 p1097 A72-20534

Glass fiber reinforced polymer composite model for tensile stress distribution in matrix and fibers and at bond interface 08 p1194 A72-21753

Biaxial tension and combined tension-torsion induced initial yield surfaces and plastic deformation onset, using localized strain theory 08 p1195 A72-21852

Necking instability in rectangular elastoplastic plate under biaxial tension, obtaining condition for equilibrium bifurcation by variational method 09 p1398 A72-22532

Photoelastic measurement of stress concentration in three dimensional fiber reinforced brittle plastic matrix under uniaxial tension [PI PAPER 1] 09 p1398 A72-22538

Circumferential crack in closed shallow cylindrical shell under tension, computing stress singularities strength 09 p1404 A72-22912

Cracks interaction with other cracks or boundaries under tension, determining critical loads for rapid fracture initiation by optical measurement 09 p1404 A72-22914

Central crack in plane orthotropic rectangular sheet under tension, showing stress intensity factors dependence on geometric and elastic constants 09 p1404 A72-22915

Crack propagation in two dimensional geometry with isotropic homogeneous and linearly elastic properties under in-plane tension loading 09 p1405 A72-22921

Loading path effect on yield surfaces of pure Al at elevated temperatures under tension 09 p1328 A72-22993

Microstructural transformations in preaged Ti alloys with unstable beta phase under external tensile stresses 09 p1328 A72-23032

Ti, Zr, Mo, B and Mn additives effect on rupture characteristics of cast Al-Mg alloy under uniaxial tensile stress 09 p1328 A72-23033

Two dimensional creeping flow in fiber reinforced composite under uniform tension, discussing matrix shear stress and fiber direct stress distributions 09 p1338 A72-23168

Tensile microstrain and cyclic loading behavior of carbon fiber reinforced plastic composites at elevated temperature 09 p1338 A72-23169

Elastoplastic deformation of Zn single crystals under uniaxial tensile loads, noting critical stresses relationship to current pulses

10 p1553 A72-23766

Stress intensity factor for circular crack embedded in finite thickness solid under uniform tension, noting semielliptical surface flaw in brittle material

[ASME PAPER 71-APMW-6] 10 p1554 A72-24183

Photoelastic investigation of star shaped models for loading direction influence on shear stress distribution at notch tip region in uniform tensile field

10 p1559 A72-24897

Elastic constants and bond stress distribution for discontinuous fiber-reinforced three dimensional composite subjected to uniaxial tension

[ALAA PAPER 72-397] 11 p1731 A72-25418

Charpy impact strength data for unidirectional graphite, boron and glass-resin composites tested in fiber direction, noting tensile stress-strain characteristics importance

11 p1672 A72-25471

Test assembly for Brinell microhardness measurements of metal and alloy surfaces under tension during vacuum heating and in protective gas media

11 p1612 A72-25490

Ni and Ni alloys microstructure under tensile stress, determining Cr and Ti effects on plastic deformation at high temperature

11 p1654 A72-25494

Tensile stress effect on formation of suboxide needles, microcracks and oxide wedges during low temperature Nb oxidation

11 p1658 A72-25854

Creep characteristics of weakly strain-hardenable alloy under variable tensile load and temperature conditions

11 p1663 A72-26808

Stress concentration in infinite elastic isotropic disk with circular hole under internal tensile loading

12 p1882 A72-27320

Stressed state induced in compound thick walled cylinder for testing residual tensile stresses effect on machine parts wear resistance

12 p1814 A72-27461

Isotropy postulate corollary verification for strain vectors measurement of annealed steel tubular specimens under combined tension and internal pressure

12 p1887 A72-28232

Frequency equation for torsional wave phase velocity in solid circular rod under initial tension, plotted for various propagation modes

13 p2002 A72-28620

Thick rectangular plate stress functions under linear tensile forces application to longitudinal edges and resultant forces application to transverse edges

13 p2055 A72-28735

Heated three layer plate with load-carrying layers of different materials, thicknesses and temperatures, calculating stability under uniaxial tension

13 p2055 A72-28736

Notch stress concentration in disk with elastic core under tension, using finite element method

13 p2060 A72-29600

Transverse strain coefficient for steel box-section beam under tension, presenting test values for deformations before and beyond elastic limit

14 p2166 A72-30692

Creep velocity and rupture strength calculated for tensile stress, noting high temperature tests of austenitic steel

14 p2121 A72-30697

Tangential force distribution at fiber surface in composite material under tensile stress without displacement at fiber axis

15 p2260 A72-31743

Acoustic emission from carbon fiber-epoxy composite during continuous tensile stress cycling

16 p2413 A72-32868

Al-Cu-Mg alloys room temperature age hardening, determining effects of tension load up to plastic deformation from measurements of mechanical properties and electrical resistance

[DFVLR-SONDDR-188] 16 p2408 A72-33674

Stress-strain diagrams for orthotropic glass fiber reinforced plastic plates with circular hole under uniaxial tensile load

16 p2471 A72-33681

Low recession graphite nosetip design for ballistic reentry, considering blunt and sharp configurations in terms of thermally induced tensile strain survival

[ALAA PAPER 72-705] 16 p2472 A72-34039

Plastic deformation at a stably growing crack tip

17 p2569 A72-34252

The evaluation of the stress intensity factors for cracks subjected to tension, torsion, and flexure by an efficient numerical technique

[ASME PAPER 72-MAT-B] 17 p2631 A72-34966

Failure mechanism for carbon fibers in epoxy novolac matrices under tensile loads

17 p2633 A72-35286

Static and tension fatigue and free edge delamination damage induced by uniaxial tensile loads in flat graphite/epoxy laminate coupons

17 p2571 A72-35291

Fracture of cylindrical and spherical shells containing a crack.

17 p2634 A72-35645

Dependence of emission on work function variation in metals under tension

18 p2699 A72-36350

Flexible cable in uniform flow field, calculating coupling between longitudinal and transverse modes to obtain centripetal acceleration effects on tension

18 p2734 A72-36418

Influence of twinned growth crystals on the texture of nickel work hardened in tension

18 p2702 A72-36703

Secondary recrystallization of nickel 270 work-hardened by tension

18 p2702 A72-36704

On the measurement of mechanical tension in plastic encapsulated devices by means of piezo-resistance.

18 p2669 A72-37112

Holographic strain measurement on a tensile specimen.

19 p2798 A72-37615

The comparison of torsion and tension creep data for a 0.18 per cent carbon steel.

19 p2816 A72-37709

Creep delay in low-carbon steel at room temperature

19 p2818 A72-38011

Load capacity of tension-bent and compression-bent circular plates

19 p2877 A72-38161

On the cumulative fatigue damage of glass fiber reinforced plastics subjected to repeated tensile impact load.

20 p2943 A72-38888

The matrix fatigue behaviour of fibre composites subjected to repeated tensile loads - Application to B/AI 6061 composites.

20 p2936 A72-39208

Tensile and compressive stress coarsening effects on coherent gamma prime precipitate yield strength of Ni-base superalloy single crystals

20 p2938 A72-39299

Electrostatic, reticular vorticity, turbulence effects and equivalences with tensional and spectral elastic fields.

20 p2953 A72-39419

The unit stress state in a cylindrical tank with a flat bottom and a partly cantilevered shell

20 p2979 A72-39594

Crack tip vicinity stress generated by plane transient tension-stress wave diffraction, examining ductility effects on fracture modes

21 p3117 A72-40672

The effect of couple-stresses on stress concentration of a ring inclusion.

21 p3117 A72-40681

Bursting of wire reinforced composite tubes under biaxial tension stresses.

21 p3121 A72-41209

Circular cracks in tension and torsion.

21 p3123 A72-41395

Equilibrium equations for given stress concentration in circular and annular plates under tensile loads with different yield points in tension and compression

21 p3126 A72-41545

The accumulation of damage in a glass-reinforced plastic under tensile and fatigue loading.

22 p3196 A72-42456

Chemical etchants and etching procedure for decorating areas of residual tensile elastic surface stresses in ultrahigh strength steels without aging

22 p3183 A72-43045

Stress concentration around a circular hole in an elastoplastic medium under the action of a temperature field and omnidirectional tension

23 p3344 A72-43418

Experimental analysis of the stress distribution in the vicinity of a nonwelded rigid circular inclusion in the interior of a plate stressed in monoaxial tension

23 p3346 A72-43691

Al alloy rupturing analysis in complex stress state, noting sublimation and self diffusion values of activation energy in torsional to tensile state transition

23 p3301 A72-43957

Stress-strain characterization of part-through crack in plate under tension in terms of stress intensity factor

23 p3352 A72-44227

Experimental characterization of yield induced by surface flaws.

23 p3353 A72-44230

Stress intensity factors for embedded elliptical crack in semiinfinite solid and for semielliptical surface crack in plate under tension and/or bending

23 p3353 A72-44231

Stress distributions in a semi-infinite plate with a row of circular holes.

23 p3355 A72-44398

Stress concentration of a cylindrical shell with one or two circular holes.

23 p3355 A72-44399

Fatigue crack closure at positive stresses.

24 p3457 A72-44819

Stress concentration coefficients calculation at sharp cracks and notches for engine parts in tension, compression and combined bending and torsion

24 p3458 A72-44932

Ductility relationship to plasticity characteristics in cylindrical steel samples with short notch under tension

24 p3458 A72-44933

Steels modulus of elasticity dependence on prestressing level produced by transverse and longitudinal tension

24 p3413 A72-44937

Welding airframe structures in titanium using tensile loading to overcome distortion.

24 p3407 A72-45000

TENSILE TESTERS

U TENSILE TESTS

TENSILE TESTS

Bare and coated Nb alloy in high temperature vacuum conditions, discussing tensile and bend tests and mechanical properties

01 p0084 A72-10747

Constant high tensile stress and rapid aerodynamic heating effect on maraging steels and Ti and Al alloys, evaluating test and simulation procedures for design data development

01 p0084 A72-10749

High speed tensile impact test for polymers at large loading rate, describing equipment design and test technique

01 p0048 A72-10782

Acoustic emission characteristics from nuclear reactor irradiated steels during tensile and wedge opening load tests

01 p0068 A72-10803

Acoustic emission evaluation of damage of filament wound composite materials under tensile loading applied to spherical test shapes

01 p0069 A72-10804

Crack angle effect on high strength metals fracture toughness, using Al alloys and tool steel ASTM-type single edge notch tension specimens

01 p0086 A72-10988

Breakdown surfaces of thin Ti alloy specimens under tension as function of composition and heat treatment temperature

01 p0088 A72-11079

Postshear buckling, diagonal tension behavior of rectangular laminated boron-epoxy plates clamped on each side, observing stacking sequence effect

02 p0249 A72-11995

VT3-1 Ti alloy with Al, Mo, Cr and Fe additives, investigating ductile type fracture after heat treatment by electron microscopy and tensile tests

02 p0244 A72-12249

Quenched and tempered high strength and maraging steels delayed failure properties from notched-tensile sustained-load tests in distilled water

02 p0246 A72-12560

Portevin-Le Chatelier effect in Al-Mg single crystals during tensile tests, investigating strain rate influence on stress

03 p0378 A72-14257

Validity hypothesis for total creep rate potential in strain-hardenable materials, discussing carbon steel torsion and tensile tests

04 p0586 A72-15006

Tensile ductile-brittle transition temperature and slip mechanism of thoriated Cr, comparing with unalloyed Cr

05 p0678 A72-17117

Statistical evaluation for forged jet engine parts tensile tests cost reduction, using regression analysis

07 p0995 A72-19484

Jerky flow /serrated yielding/ in Co-Ni-Cr-C fcc alloys during tensile testing, noting no correlation to dislocation-precipitate interactions

07 p1016 A72-19940

Stress-strain state in tension of orthogonally stiffened fiberglass-reinforced plastic with cracks in transversely stiffened layers

07 p1094 A72-20128

High temperature tensile tests of Mo with helical and circular V grooves, discussing stress concentration sensitivity relations for grooved and smooth samples

07 p1018 A72-20141

Polycarbonate yield dependence on temperature in uniaxial compression and tensile tests described by modification of Eyring theory of non-Newtonian viscosity

08 p1191 A72-21184

Dispersion strengthening of electrolytically deposited nickel-aluminum oxide alloys, comparing tensile tests to theoretical values

08 p1186 A72-21442

Notch length effect on stress concentration in polymethyl methacrylate sample from tensile, impact and bending tests

08 p1196 A72-21867

Epoxy resin tensile specimen fabrication and testing, discussing factors controlling data scatter

09 p1337 A72-22650

- Cryostat for high resolution tensile measurements of thermally activated processes during plastic deformation 09 p1398 A72-22657
- Tensile and fatigue tests of dissimilar metal joints made by friction pressure welding 09 p1321 A72-23640
- S glass/epoxy composites strength retention properties under long duration tensile load, proposing use of stress rupture data for reliable safe structural design 10 p1501 A72-24263
- Random elastic modulus variability of building materials test pieces under compression and tensile loads 10 p1557 A72-24403
- Al alloy notch-bend and compact-tension specimens thickness and crack length effects on plane-strain fracture toughness test results 10 p1498 A72-24886
- Tensile, plane strain fracture toughness and fatigue tests of high strength Al alloy cylinders, discussing unstable crack growth conditions 10 p1498 A72-24887
- Embedded strain gage technique for subsurface tensile testing of boron-epoxy composites 11 p1671 A72-25467
- Perforated plates plastic deformation, stresses and strains near holes, using strain gage data in biaxial tensile tests 11 p1733 A72-25540
- Specimen preparation effects on fracture strength measurements, noting critical stress intensity factor for single edge notch and compact tension high strength steel samples 11 p1657 A72-25825
- Ductile type fracture after heat treatment of VT3-1 Ti alloy with Al, Mo, Cr and Fe additives investigated by electron microscopy and tensile tests 11 p1660 A72-26135
- Automated microdynamometer for thin plastic specimens microtension tests with continuous microscopic observation and automatic diagram plotting 11 p1633 A72-26288
- Filament reinforced boron-aluminum composites multiple fracture behavior dependence on cross section geometry from tensile test 11 p1668 A72-26944
- Polymer testing machine for simultaneous structural and mechanical properties measurement of specimens subjected to uniaxial tensile loads for broad temperature range 12 p1795 A72-27465
- Tensile plastic deformation effect on structural evolution of Ti-Ni alloy under anisothermal heat treatment 12 p1830 A72-27738
- Room temperature uniaxial tension tests for elastic deformation of steel samples, showing quadratic stress-strain function 13 p1977 A72-29008
- Tensile properties from high temperature and room temperature tests of Ti alloys containing Ga correlated with creep resistance at 1000 F, noting activation energy 14 p2120 A72-30614
- Transverse strain coefficient for steel box-section beam under tension, presenting test values for deformations before and beyond elastic limit 14 p2166 A72-30692
- Mechanical vibrations effect on flow stress and strain rate from tensile and creep tests as function of amplitude 15 p2257 A72-31841
- Strain energy method for finite deformation of solid and tubular cylinders of incompressible isotropic elastic material, noting torsional and tensile tests on natural rubber 16 p2468 A72-33198
- Equipment for low cycle fatigue bending, torsion and tension-compression tests, considering design and performance 16 p2394 A72-33846
- Prestrained and annealed elastic materials stress-strain relationship calculation in plastic range, compared with tensile and compression load tests results 16 p2472 A72-33948
- Heteroplastic materials creep characteristics from constant strain rate isothermal traction tests, deriving deformation functions for material behavior beyond elastic range 16 p2412 A72-34120
- Point-loaded discs and blocks applicable to tensile testing of brittle materials. 19 p2870 A72-37223
- Asymmetric collinear internal cracks interaction evaluation by measuring diameter variation and shape distortion of caustic surface impinged upon by retarded laser radiation 19 p2870 A72-37224
- Fatigue limits of cylindrical test pieces in rotative bending and in tension-compression, investigating strain gradient effect 19 p2875 A72-37788
- Strength and plasticity of molybdenum during short-term tests 19 p2819 A72-38218
- Fiberglass reinforced plastics tensile test specimens aspect ratio effect on tensile properties, considering deformation of orthotropic rectangular plate with uniform forced displacement 20 p2943 A72-38889
- Theoretical model for acoustic emission relationship to fiber cracking during rising load tensile test on fiber reinforced composites 20 p2925 A72-39285
- Photoelastic determination of mixed mode stress intensity factors. 20 p2981 A72-39963
- Investigation of the strength and deformability of thin composite materials of magnetic recorder type. I- Strength and deformability at elevated temperatures 21 p3073 A72-41707
- Fatigue properties of 18-8 stainless steel at cryogenic temperatures. 21 p3071 A72-41845
- Studies on sizes and shapes of tensile test specimens for thin sheet materials of aluminum alloys. 22 p3195 A72-43125
- Application of cylindrical samples to the determination of the resistance to crack propagation of materials 22 p3242 A72-43163
- High strength boron and borsic fiber reinforced aluminum composites. 23 p3299 A72-43491
- Aluminum matrix composites fracture mechanism dependence on static loading conditions and reinforcing filament type, investigating failure modes in tension and compression tests 23 p3299 A72-43497
- Heat treatment effectiveness criteria for thermomechanically strengthened steels, using creep rupture, fatigue, bending and tensile tests 23 p3300 A72-43643
- Load distribution in a single-edge-notch tensile specimen. 23 p3306 A72-43710
- Strain-rupture criteria for simple and complex loads 23 p3349 A72-43954
- Determination of the stressed state in a welded joint in plastic deformation 23 p3293 A72-44019
- Bending evaluation of test section in tensile tests with axial loads and resistance strain gages, noting friction moment role 24 p3456 A72-44791
- Estimation of creep and fatigue behaviour under cyclic loading. 24 p3456 A72-44793
- Computation of post-yield behaviour in notch-bend and tension testpieces. 24 p3456 A72-44796
- Equation of state relating time variations of stress and strain in elastoplastic material under tension 24 p3459 A72-45069
- Contribution to the study of the creep behavior of 18 per cent-nickel maraging steel 24 p3415 A72-45600
- High temperature tensile tests of Mo with helical and circular V grooves, discussing stress concentration sensitivity relations for grooved and smooth samples 24 p3417 A72-45766
- TENSIOLOGIES**
- High pressure oxygen control for synthesis and vapor phase equilibria, discussing tensiometric measurements and cold seal pressure vessel techniques 12 p1778 A72-28105
- TENSION**
- Lutetium strength and plastic deformation characteristics under tension, presenting temperature and strain rate effects 23 p3301 A72-43754
- TENSION TESTERS**
- U TENSILE TESTS**
- TENSIOLOGIES**
- Tensometric damage detection in rolling contact bearings from bending stress spectrum, using Si strain and wire strain gages 01 p0078 A72-11379
- Fast and slow human muscle fibers temporal response characteristics, using tensiometric recording 03 p0317 A72-13989
- Measuring technique importance for aircraft R and D, emphasizing quartz transducer, digital control and signal processing 14 p2092 A72-30286
- TENSOR ANALYSIS**
- Viscoelastic fluids continuum mechanical theory, discussing constitutive equation and tensor analysis [AD-736009] 02 p0203 A72-12004
- Hydrogen molecular ion g tensor calculation, determining approximate ground state wave functions 03 p0391 A72-13152
- Elasticity tensor formulas for wave propagation, vibration and stability of deformed isotropic solids 03 p0448 A72-13887
- Spatial dispersion effects in crystal optics, obtaining dispersion law for normal waves in crystals via electromagnetic field tensor equations 04 p0548 A72-14739
- Tensor-tensor theory of gravitation, introducing first effect of Mach principle 04 p0573 A72-14905
- Non-Newtonian real fluids flow characteristics, determining stress-deformation relationship by tensor analysis, with application to lubrication theory 04 p0528 A72-15742
- Tensor calculus theorem application to elastic isotropic materials finite deformation, considering acceleration waves propagation and moduli of elasticity 05 p0735 A72-16029
- Cosmological models dynamics and structural evolution feedback from density inhomogeneities energy momentum tensor, using hf approximation 05 p0715 A72-16166
- Homogeneous turbulence with rotatory anisotropy, determining alternating tensor with moment equations 06 p0800 A72-17988
- Classical elasticity displacement problem solution by integral equation method based on Betti tensor counterpart of Green procedure in potential theory 07 p1026 A72-18813
- Exact cosmological solutions in Brans-Dicke scalar tensor theory, noting consequences for solar relativistic effects 07 p1075 A72-19584
- Tensor analysis of electromagnetic energy localization in space, generating gravitational field and space curvature via equation to Einstein tensor 07 p1035 A72-19685
- Gravitational field potential energy-momentum pseudotensor component determination in general relativity theory 08 p1207 A72-21301
- Impulse-energy tensor for heat flow-crossed continuum subjected to electromagnetic field, using energy balance and quantity of movement equations 09 p1351 A72-22673
- Book on tensor analysis and continuum mechanics covering strain, permutation and stress tensors, vector and tensor comparison, application to elasticity and shell theory, etc 09 p1406 A72-23000
- Asymmetrical mechanics theory of nematic liquid crystals, noting relation for local moment of inertia and tensor analysis of kinematic characteristics 13 p2022 A72-29497
- Homogeneous turbulence with rotatory anisotropy, determining alternating tensor with moment equations 14 p2093 A72-30214
- Waldman-Snyder equation application to sound absorption and dispersion in dilute polyatomic gases, presenting truncation procedure for perturbation function expansion in irreducible Cartesian tensors 14 p2131 A72-30673
- Coherence narrowing during multiple scattering of resonance radiation in atomic vapor, treating polarization transfer in terms of classical tensors 15 p2281 A72-32221
- Almansi strain tensor comparison with Lamé elastostatics equations, noting distinction between strained and unstrained state 15 p2330 A72-32291
- Tensor analysis for planar magnetoresistivity and Hall effect in Ni single crystal thin films, noting anisotropy effects in ferromagnetic crystals 15 p2294 A72-32386
- Gosiewski vorticity tensor formula generalization from moving unit vector associated with material point to vector field relative to moving continuum 16 p2423 A72-33112
- Gravitational field potential energy-momentum pseudotensor component determination in general relativity theory 17 p2580 A72-34659
- On motions with a history of constant deformation 18 p2680 A72-36463
- Gravitation theory in terms of scalar and tensor field, noting Lyra general reference system transformations and scale invariance 18 p2711 A72-36713
- Book on classical relativity theory covering relativistic kinematics and mechanics, tensor calculus, electrodynamics, gravitational fields and effects, elastic continua mechanics, thermomechanics and cosmology 18 p2712 A72-36850
- On Maxwell's equations in three-dimensional anisotropic periodic media - Tensor formulation of the problem and the N-beam approximation 20 p2962 A72-40019
- Note on the symmetries of certain material tensors for a particle in Stokes flow. 21 p3044 A72-40113
- Reflection and refraction of radio waves from the ionosphere in presence of time-varying irregularities. 22 p3154 A72-42302
- First derivative discontinuities of space-time metric tensor in Einstein equations solution for nonisotropic

- and isotropic hypersurfaces, proving coordinate system existence for continuity 23 p3312 A72-43302
- Longitudinal dielectric tensor for an electron gas in a uniform magnetic field. 23 p3321 A72-43808
- Multicomponent plasmas with static magnetic field, deriving dielectric tensor and dispersion relation for wave propagation by linearization technique 24 p3428 A72-44967
- Perturbation methods in atmospheric flight mechanics. 24 p3368 A72-45350
- On the gauge groups of linear conservative gravitational theories. 24 p3447 A72-45630
- TENSOR FIELDS**
U TENSORS
- TENSORS**
NT STRESS TENSORS
- Gravitational potential tensor and equations of motion of relativistic mechanics for isolated system of masses 01 p0127 A72-10345
- Energy-momentum tensor for radiation and radiative viscosity in optically thick matter having Thomson scattering with photon absorption and emission processes 01 p0129 A72-10798
- Tensor description of laser beam second harmonic generation in dc magnetic field, using group theory derivation of nonzero element relations for all crystallographical classes 03 p0365 A72-12963
- Quasi-linear tensor operator derived in form of series converging inside circle, proving theorem concerning reciprocity conditions and existence of potential 03 p0445 A72-13579
- Spatio-temporal tensorial structure of fluid magnetodynamic equations in terms of electromagnetism and continuum mechanics 06 p0861 A72-18103
- Metric tensor components of isotropic inhomogeneous cosmological model obtained from Einstein equations 07 p1072 A72-19340
- Modified Riemann geometry for scalar-tensor theory of gravitation, emphasizing scalar field role relation to vector length change during point-to-point transport 07 p1036 A72-20196
- Dielectric tensor for electromagnetic waves in weakly inhomogeneous anisotropic media, taking into account permittivity and conductivity fluctuations 09 p1280 A72-23230
- Metric tensors as alternate to coordinate transformation equations for computer program inputs in automatic problem formulation 10 p1443 A72-23923
- Preresonance Raman scattering tensor in Born-Oppenheimer approximation of molecular wave functions 10 p1491 A72-24110
- Asymmetric Einstein equations with impulse-energy tensor in canonical form derived from variational principle, defining space-time continuum as pseudo-Riemann manifold 10 p1510 A72-24120
- Electromagnetic field interaction with nonconducting polarizable and magnetizable continuum from theory based on total impulse energy tensor, deriving force density from relativistic balance approximation 10 p1510 A72-24124
- Gruneisen tensor relationship to elastic and thermal properties of anisotropic quartz fiber-phenolic composite 10 p1500 A72-24251
- Time-space nonholonomic characteristics of curvature tensor for three dimensional physical space in gravitational and inertial fields 12 p1843 A72-27049
- Conservation laws and symmetry properties of scalar tensor gravitational theories in terms of Einstein, von Freud, Moller and Komar extensions 12 p1847 A72-28153
- Uniqueness principle application to construction of gravitational field generated by complex of elastic bodies for mass tensor 16 p2424 A72-33366
- Finite range gravitation theory extension to generally covariant massive two-tensor field gravitation theory containing eight dynamically independent degrees of freedom 20 p2953 A72-39342
- Motion concept formulation by linear algebra of n dimensional spaces, emphasizing tensor character of velocity and acceleration 21 p3084 A72-40816
- Time-space nonholonomic characteristics of curvature tensor for three dimensional physical space in gravitational and inertial fields 24 p3425 A72-45702

TERBIUM

Cr-Tb alloys monotectic, eutectic and eutectoidal phase transformations study with differential thermal, metallographic, X ray structural and durometric analysis 08 p1187 A72-21781

TEREPHTHALATE

NT POLYETHYLENE TEREPHTHALATE

TERMINAL BALLISTICS

- Al and steel plate penetration, perforation and fragmentation under hard steel sphere impact at and above ballistic velocities, investigating velocity and strain histories 05 p0672 A72-16115
- Alumina microstructure, grain size and impurities effects on ballistic performance, discussing results in terms of microplasticity 09 p1334 A72-22390
- Fractography of high boron ceramics under ballistic impact, suggesting macroscopic and microscopic textures relationship to stress states and microstructure 09 p1334 A72-22391
- The forces for projectile penetration of aluminum. 19 p2871 A72-37461
- Simple analyses for the non-symmetric dynamic expansion of cylindrical cavities. 22 p3240 A72-42893

TERMINAL FACILITIES

- Airport efficiency improvement measures, considering boarding gates, parking space, baggage handling, fire protection, monitoring and central control 02 p0200 A72-17177
- Airport terminal flow and interface transportation systems, discussing access, passenger traffic and cargo handling and government controls 03 p0339 A72-13414
- ATS F and G ground station mobile terminal, discussing system flexibility, utility and reliability features and parabolic antenna design 04 p0485 A72-14478
- Lens type beam waveguide for optical trunk communication, discussing transmission medium, terrain layout, bandwidth, terminal equipment, misalignment and multibeam application 04 p0497 A72-14483
- Remote meteorological elements sensing in terminal area, discussing radar, ceilings, thunderstorm warning, slant range visibility, low level winds and wind shear 04 p0543 A72-14692
- Automated meteorological telemetry and interrogation response system with terminal extensions for Paris airport 04 p0508 A72-14695
- Statistical characteristics of range-guard intrusions and airspace collision conflicts in terminal area 05 p0611 A72-16110
- Newark airport program, discussing land preparation, public facilities, terminal area, building design, support systems, organization and scheduling 05 p0644 A72-16696
- FAA air traffic control automation program, describing enroute and terminal ATC systems implementation 06 p0844 A72-17327
- Lounge planning model for airport terminal design simulation, taking into account scheduled arrivals and departures, aircraft types, passenger number, gate assignments, etc 06 p0780 A72-17979
- British regional airports development, discussing terminal facilities for scheduled and nonscheduled air carriers on domestic and international routes 10 p1459 A72-24170
- STOL aircraft systems development coordination, considering vehicle design, airport facilities and related ground environment, transportation modes interface and airspace management 11 p1574 A72-25255
- ATC system, discussing flight data and radar processing functions and terminal automation program 11 p1683 A72-25875
- Trends in civil ATC discussing plans to increase terminal capacity, surveillance system and use of multiple synchronous satellites for ocean travel efficiency improvement 12 p1842 A72-27103
- Hierarchical system of helicopter service terminals, calculating passenger lots for single and multiloop arrangements under given stochastic input conditions 15 p2337 A72-31498
- Airline maintenance program and facilities for Boeing 747 aircraft based on optimized service concept 15 p2181 A72-32430
- Terminal handling environment and air cargo requirements for noncontainerized freight 16 p2372 A72-33175
- Major civil airport development plan, discussing traffic forecasts, runways, noise, airspace capacity, access systems, freight installations, maintenance facilities, navigation aids, buildings, etc 16 p2373 A72-33328

Major civil airport passenger and cargo terminal complex design and layout planning, discussing various facilities and equipment requirements 16 p2373 A72-33329

STOL aircraft for civil transport applications, considering optimum design concepts, noise reduction and terminal facility requirements 16 p2348 A72-33331

Passenger transfer in airports with total separation between aircraft and permanent buildings for independent functioning, noting Dulles Airport mobile lounges 16 p2374 A72-34143

Airport planning requirements - An airline view. 17 p2535 A72-34224

Airport terminal design - The passenger's point of view. 17 p2535 A72-34225

STOL airports planning objectives, discussing ground and airspace congestion relief, terminal locations, flight safety and community acceptance 17 p2535 A72-34239

Kansas City International Airport facilities and features, discussing decentralized passenger processing system 17 p2535 A72-34242

Planning model for German air transport. 17 p2638 A72-34244

Atlanta airport redesign and expansion program including runway reconfiguration taxiway relocation and passenger and cargo terminal system improvement to relieve congestion 18 p2675 A72-36781

Boeing 747 aircraft impact on Chicago O'Hare airport design criteria, noting future terminal facilities planning 18 p2675 A72-36782

Application of optimization techniques to near terminal area sequencing and flow control. 19 p2832 A72-38255

An investigation of vehicle dependent aspects of terminal area ATC operation. 19 p2832 A72-38256

Airport medical design guide /with comment on certain operational matters/. 22 p3150 A72-42500

Critical assessment of air transport planning for German Federal Republic, advocating decentralized concept of major air terminals for intercontinental jumbo jet traffic 23 p3357 A72-43244

Air freight ground handling and distribution terminal facilities and methods, discussing future technical and organizational developments for efficient handling of increased traffic volume 23 p3358 A72-43246

Frankfurt/Main international airport central terminal facilities, describing efficiency oriented layout for large volume passenger and baggage handling and links to rail and road nets 23 p3278 A72-43247

Dala /Sweden/ regional airport, describing planning and financing, approach lighting, ILS system and facilities for tourist traffic and industrial development 23 p3278 A72-43248

Systems approach to airport passenger terminal planning. 24 p3387 A72-44585

International and regional scheduled air traffic terminals and general aviation airports characteristic objectives and operational aspects, discussing ATC, safety and noise problems [DGLR PAPER 72-033] 24 p3387 A72-44616

Airport power supply system to meet increased load terminal demands, describing main and emergency standby network layout and equipment 24 p3388 A72-45272

TERMINAL GUIDANCE

Terrain clearance during descent and approach of aircraft under radar control, discussing optimum profile, ATC, nav aids and rules 01 p0097 A72-10183

Trajectory optimization problems solution with terminal state constraints using combined parallel tangents/penalty function approach 02 p0280 A72-12264

Operational requirements of instrument landing systems, interferometers, correlation protected instruments, landing guidance systems and navigation aids 03 p0386 A72-13421

Terminal area air traffic guidance and control, discussing automation, all-weather precision approach and landing and failure detection 04 p0544 A72-14817

Optimal closed loop control of stochastic nonlinear systems by expanded cost function applied to reduced terminal error atmospheric entry problem 05 p0685 A72-16462

Optimal final value control systems in phase-variable canonical form, discussing feedback gain singularity structure for single and multiple input systems 06 p0793 A72-17954

Aircraft optimal terminal guidance nonlinear feedback control law, deriving maximum principle by digital computer program 07 p1033 A72-19287

Terminal guidance systems and techniques application to manned space flight rescue operations, discussing emergency location and rescue spacecraft communication and guidance 09 p1396 A72-23158

Hybrid area navigation and microwave instrument landing system, discussing approach control and terminal guidance 15 p2271 A72-32206

Discrete optimal terminal control, with application to missile guidance. 19 p2780 A72-38257

Reentry vehicle spiral descent terminal guidance, verifying control feasibility through hybrid man-in-loop simulators [AIAA PAPER 72-834] 20 p2950 A72-39093

An explicit automatic terminal energy management guidance technique for space shuttle. [AIAA PAPER 72-833] 20 p2950 A72-39094

Space shuttle terminal navigation with conventional navigation aids. [AIAA PAPER 72-832] 20 p2950 A72-39095

EOSS - A dynamic six degree-of-freedom environmental simulator for evaluation of electro-optical guidance systems. [AIAA PAPER 72-862] 20 p2911 A72-39135

Microwave landing system effect on the flight guidance and control system. [AIAA PAPER 72-755] 20 p2952 A72-40057

Characteristics and prospects for a new landing guidance system. 21 p3080 A72-40293

Terminal airspace navigation and aircraft ground handling control, discussing air traffic controllers and pilots functions in context of workload and automation 21 p3081 A72-40546

Automatic landing and microwave guidance system potential. 21 p3040 A72-41072

Stochastically optimal terminal control system synthesis for loss function dependence on finite phase coordinates of dynamic system, considering soft landing of flight vehicle 23 p3275 A72-43781

TERMINAL VELOCITY

Spacecraft soft orbital rendezvous guidance involving orbital transfer maneuver for velocity vector directional coincidence to reduce terminal relative velocity 05 p0729 A72-16757

Body center of mass position for stable fall in viscous fluid, determining terminal velocity as function of body geometry 10 p1470 A72-25067

Craters produced by high speed hardened spherical particles, investigating depth and diameter relationship to impact speed 11 p1738 A72-26919

Pontryagin maximum principle for optimal terminal velocity control of automatic space probe descent in Mars atmosphere 14 p2162 A72-30456

Spacecraft soft orbital rendezvous guidance involving orbital transfer maneuver for velocity vector directional coincidence to reduce terminal relative velocity 17 p2622 A72-35260

TERMINALS

Two way telephone communication to individual subscribers and thin route exchange terminals via satellites, discussing cost, performance and capacity [AIAA PAPER 72-541] 12 p1780 A72-27364

TERMINOLOGY

Proposed ASME procurement standards for gas turbines and generators, with compilation and definitions of specification terms [ASME PAPER 71-WA/GT-2] 05 p0703 A72-15895

Terminology definitions for redundant flight control systems [SAE ARP 1181] 11 p1684 A72-26031

TERNARY ALLOYS

Nb-Co-Sn and Nb-Ni-Sn ternary systems, investigating intermetallic compounds existence by X ray analysis 03 p0375 A72-13944

Y-Mn-Al ternary alloy solid solution phase diagram isothermal section construction from X ray structural data 03 p0376 A72-13945

Zincblende ternary and quaternary alloy systems, calculating charge distribution in space by pseudopotential approach 03 p0404 A72-14261

Mixed zincblende ternary and quaternary alloys, comparing empirical pseudopotential and dielectric model methods for energy gap calculation 03 p0404 A72-14262

Ti-Al-Mo-V alloy sustained load stress corrosion crack growth in salt and distilled water environments 04 p0534 A72-15570

Binary and ternary alloys of Cr and Fe with Ni, determining interaction coefficient and molar enthalpy for Cr at 1600 C by mass spectrometry 05 p0676 A72-17103

Ti-Zr-O ternary alloys radiocrystallographic analysis, relating microstructure to composition and thermal treatment 06 p0827 A72-17569

Hf-Co-Al system phase equilibria determination by partial microstructural and X ray analysis 07 p1017 A72-19991

Ni-Cr-Ti alloy hardening during intermetallic phases precipitation, discussing atom segregations, Guinier-Preston zones and fcc and hcp lattices 07 p1019 A72-20152

Critical temperature dependence of Nb-Al-Ge superconducting alloys on composition and heat treatment, discussing phase boundaries and electron state densities 07 p1049 A72-20154

Phase diagrams, superconducting properties and annealing critical temperature of Nb-Al-Ge alloys, establishing four phase peritectic equilibria 08 p1218 A72-21778

Nb-Al-Ge alloy superconductor deposits structure, transition temperature and critical current densities after preparation by triode sputtering and heat treatment 09 p1369 A72-22795

Magnetic susceptibility of ternary Al-Mn alloys with Ti, Va, Cr, Fe, Co, Ni, Cu and Zn, describing microstructure and aging experiments 10 p1494 A72-23832

Fe-Cr-Mn alloys structural changes during high temperature oxidation, noting subscale layer thickening and alpha phase detection after heat treatment 11 p1655 A72-25498

Neutron irradiation effects on GP zones and precipitates in ternary Al alloy, measuring X ray small angle scattering and electrical resistivity 11 p1655 A72-25514

Two phase and three phase composition of ternary alloys Nb-C-Re at 2000 C from X ray, metallographic and chemical analysis 13 p1973 A72-28567

Phase structure of Cr rich Cr-Ni, Cr-Fe, Cr-Co and Cr-Ni-Fe alloy particles produced by evaporation in Ar using X ray diffraction 13 p1974 A72-28660

Ordering in fcc lattice ternary alloys with allowance for atoms interchanges, noting phase transformation critical temperature and superlattices existence 13 p1976 A72-28691

Microstructural changes relationship to corrosion susceptibility in ternary Al alloy obtained from stress corrosion cracking tests and electron metallography, noting precipitate-free region 14 p2118 A72-30542

Phase composition of Nb-O-Hf and Nb-O-Zr ternary alloys, noting O solubility decrease 14 p2123 A72-30980

Interaction of W with transition metals in ternary and multicomponent alloy systems, noting phase diagrams 14 p2122 A72-30981

Mo-W-C system high temperature phase equilibria from X ray and microstructural analysis, noting decrease of C solid solubility with temperature 14 p2123 A72-30984

Nickel-trinickel alumide-trinickel niobumide system polythermal cross sections from X ray and microstructural analysis, noting electrical resistivity increase with Al content 14 p2123 A72-30988

Phase diagrams of Ru binary and ternary systems, noting admixtures interactions 14 p2123 A72-30992

Mn, Zr and Cr alloying effects on grain size and solid solution decomposition of cast Al-Zn-Mg alloy bars 14 p2125 A72-31039

Phase diagrams of rare earth ternary alloys with transition metals and Si, noting semiconductor properties 15 p2289 A72-31189

Thermodynamic interaction parameters of solid solution bcc V-Ti-Cr alloys by Knudsen effusion method combined with mass spectrometer 16 p2409 A72-33803

Ternary Ni-Cr-Al superalloys oxidation at 800-1300 C as function of composition, temperature, oxygen pressure and reaction time 16 p2410 A72-33811

Study of certain features of the electronic structure of the ternary alloys Ni3/Mn, Fe and Ni3/Mn, Co/Fe 17 p2568 A72-35518

Substitutional-interstitial interactions in bcc alloys. 18 p2699 A72-36396

The structure of the metastable precipitates formed during ageing of an Al-Mg-Si alloy. 18 p2702 A72-36743

Self-diffusion of cobalt in the ternary system Co-Ni-Fe 19 p2814 A72-37416

Internal stresses in a superplastic Mg alloy. 20 p2935 A72-39002

The mechanism of oxidation of Ni-Cr-Al alloys. 20 p2937 A72-39214

The internal oxidation of Ni-Cr-Al alloys. 20 p2937 A72-39215

Some results of an investigation of the tungsten-nickel-boron ternary system 21 p3066 A72-40393

Alpha stabilizing Al and Sn suppression effect on beta-omega transformation during Ti alloy hardening 22 p3189 A72-42278

The dynamic viscoelastic properties of some non-crystalline metals. 22 p3214 A72-42792

Physical properties and electronic structure of [V1-x Crx/3Si] ternary alloys 22 p3192 A72-43014

Constitution of the Ni-Cr-Fe system from 0 to 40 pct Fe including some effects of Ti, Al, Si, and Nb. 22 p3194 A72-43038

Enhanced strengthening of a spinodal Fe-Ni-Cu alloy by martensitic transformation. 22 p3194 A72-43040

Mechanical properties of titanium alloys with isomorphous beta-stabilizing elements 23 p3300 A72-43590

Three-phase equilibria of cast and annealed V-Zr-Cr alloy by X ray, metallographic and melting point analyses 24 p3414 A72-45384

TERNARY SYSTEMS

Equilibrium state and microhardness of phase diagrams in Mg-rich region of Mg-Nd-Zn system 03 p0370 A72-13185

X ray study of [Y-La-Ce]/[Al-Si]-B ternary systems structure at 500 C, noting binary compound presence 08 p2127 A72-21713

Ternary chalcopryrite semiconductors refractivity measurement over range of wavelengths and optical nonlinear coefficient for second harmonic generation from carbon dioxide laser 11 p1701 A72-26148

Thermodynamic description of metal rich side of Nb-Mo-N solid solution, determining equilibrium nitrogen solubility as function of pressure and temperature 11 p1664 A72-26842

Triple stellar system evolution and disintegration, discussing energy partitioning and initial velocity effects on stability 12 p1865 A72-27095

Annealed and quenched Fe-Mo-Co system, defining phase relationships in Fe-rich corner at 2200, 2000 and 1800 F 13 p1973 A72-28650

Ti-Mo-Ni system polythermal section microstructure, hardness, resistivity and thermal expansion characteristics 14 p2112 A72-30153

Equilibrium states difference of ternary metal-boron-nitrogen systems, taking into account chemical bond type and crystal structure of boride and nitride atoms 14 p2112 A72-30154

Thermoelectrical properties of ternary bismuth-antimony-tellurium alloy system obtained under Ar gas pressure in quartz and graphite crucibles 14 p2142 A72-30500

W-Nb-C system phase diagram from X ray and microstructural analyses, noting solid solubility, hardness and isothermal cross section 14 p2122 A72-30983

Co-Cr-C system carbon activity and solubility at 950-1200 C, deriving equation for temperature dependence and solid solution-carbide precipitation zone boundaries 16 p2407 A72-33441

Measurement of the electron work function in binary and ternary transition metal-nonmetal systems. 17 p2595 A72-34602

Microstructure and differential thermal analyses of ternary system Co-Mn-Al, presenting phase diagrams 19 p2818 A72-37852

Phase equilibria in the hafnium-niobium-boron and tantalum-chromium-boron systems 19 p2819 A72-38285

Unidirectionally oriented pseudobinary eutectic solidification in ternary systems, investigating crystallographic and mechanical characteristics of ZrCuSi fibers embedded in Cu matrix 20 p2940 A72-39441

Vitrification in ternary diamond-like semiconductors 21 p3096 A72-40380

Hydrogen in intermetallic phases, taking into account as an example the system titanium-nickel-hydrogen 21 p3070 A72-41647

TERNARY SYSTEMS [DIGITAL]

U DIGITAL SYSTEMS

TERRADYNAMICS

Elastic dislocation theory of Chandler wobble excitation by earthquakes 09 p1299 A72-22802

Internal structure dynamics of earth, moon and planets, showing density variation and bulk modulus

- as function of pressure with correction of Bullen hypothesis 16 p2461 A72-34176
- TERRAIN**
- Terrain clearance during descent and approach of aircraft under radar control, discussing optimum profile, ATC, nav aids and rules 01 p0097 A72-10183
- Energy cost /oxygen consumption/ prediction for treadmill and various levels terrain walking at two speeds under three different pack loads 14 p2080 A72-30706
- TERRAIN ANALYSIS**
- Silicate rocks mapping from aerial IR data, discussing method for discriminating emission from background radiation 02 p0208 A72-11877
- Phyto-ecological approach to remote sensing of man made ecosystems, comparing vegetation and landscapes in Old and New Worlds 02 p0210 A72-11797
- Interpretation model for aircraft and spacecraft remote sensing of tropical agricultural systems 02 p0210 A72-11798
- High altitude aircraft and Apollo 9 multispectral photography and simulated ERTS-A imagery evaluation, comparing with ground observations in Arizona 02 p0210 A72-11799
- Narrow beam millimeter wave radiometer with real-time TV display for terrain mapping, analyzing contours blurring caused by antenna pattern and output integration 02 p0191 A72-11821
- Earth surface feature recognition with IR imagery, evaluating Meteor satellite data 02 p0213 A72-11836
- Airborne sensors terrain classification, considering sample points clustering approach and signature analysis 02 p0227 A72-11844
- Land pattern mapping from monoisotropy analysis, using coordinate digitizer system with planimetric computer input 02 p0187 A72-11874
- Automatic geologic mapping with calibrated narrow band visible and near IR rock reflectivity data and computer processing 02 p0215 A72-11878
- Digital computer mapping of terrain by clustering techniques, using color IR film emulsion layers as three band spectrometer 02 p0215 A72-11879
- Multispectral photographic data preprocessing and computerized simulation of ERTS data channel to make terrain maps, testing classification accuracy improvement possibility 02 p0215 A72-11880
- Natural formation interpretation from spectrophotometric measurements of underlying earth surface from manned spacecraft Soyuz 7 and Soyuz 9 02 p0228 A72-11887
- Radar observation of Mars surface, noting rugged terrain and craters 04 p0579 A72-15360
- Acquisition probability equation for navigation systems terrain correlation devices, using two different correlation algorithms [AIAA PAPER 72-122] 05 p0688 A72-16974
- Computerized photogrammetric terrain analysis and representation in three dimensional coordinates, discussing construction of digital terrain model 06 p0813 A72-17429
- Block triangulation of arbitrary terrain without point transfer, using stereo comparator 06 p0806 A72-17755
- AS-11A stereoplotter computerized adaptation to stereo-modeling of SLAR terrain mapping 06 p0818 A72-18330
- Geostrophic drag coefficient for heterogeneous terrain as function of effective roughness length, considering surface friction effects in large scale atmospheric models 07 p0130 A72-19108
- Venus equatorial region surface height variations from interplanetary radar echo delay measurements, discussing resolution, repeatability and radius 07 p0173 A72-19352
- Aerial photographs inclination angles determination from stereocomparator measurements and terrain angles interrelationship 08 p1165 A72-21162
- Planetary and lunar surface relief reconstruction from photographic imagery, discussing statistical morphological characteristics determination from relief 08 p1238 A72-21833
- IR spectral emittance measurement with airborne spectrometer for geological mapping over Pisgah Crater /California/ 08 p1162 A72-22017
- Cosmos 243 microwave radiation analysis over cultivated terrain, showing radio brightness temperature dependence on soil temperature and humidity effect on emissivity 09 p1297 A72-22495

Multifactor landscape synthesis of aerial imagery for regional surveys 09 p1301 A72-23278

Aerial photointerpretation for landscape analysis with respect to agricultural land use, considering geomorphologic, hydrographic, soil and microclimatic conditions 09 p1301 A72-23280

Ecological study of damp wasteland according to seasons and with various photographic emulsions 09 p1303 A72-23293

Black and white vs color photography application to photogeological interpretation of West Greenland Precambrian terrain 09 p1303 A72-23294

Geomorphological and thermographic reconnaissance of Central Sahara, using orbital photographs 09 p1303 A72-23297

Terrain evaluation by aerial imagery, discussing various film types for conventional visible and IR black and white and color photography, thermal IR and/or radar 09 p1303 A72-23303

Terrain evaluation for engineering purposes through aerial photointerpretation in terms of physiography, geology, soil and vegetation 09 p1304 A72-23314

Crop classification by airborne multispectral observations, suggesting sample regions selection method for spectral signatures identification based on statistical similarities 11 p1628 A72-26985

Aerial photographs inclination angles determination from stereocomparator measurements and terrain angles interrelationship 17 p2552 A72-34453

Landscape site and vegetation /timber/ predictions from color and IR aerial imagery compared with ground data 18 p2686 A72-36318

Photomorphic units for regional analysis from hyperaltitude and spacecraft remote sensing data 18 p2690 A72-36321

Coherent optical terrain-relief determination using a matched filter 18 p2691 A72-36491

Learning strategy-based pattern recognition system for automatic classification of terrain type from aerial photography 18 p2691 A72-36494

Balloon nacelle for terrain photography from very high altitudes 24 p3403 A72-45229

Determination of the reflecting power of a hilly terrain, knowing the reflective power of a flat terrain of the same nature 24 p3381 A72-45769

TERRAIN FOLLOWING AIRCRAFT

Flight testing of Army helicopters terrain following and/or avoidance systems concepts for operational capability, performance and cost evaluation 05 p0686 A72-16658

Flight test evaluation of a forward looking radar system for search and rescue applications. [AHS PREPRINT 633] 17 p2490 A72-34499

Automatic structural mode control system with aerodynamic vanes for B-1 strategic bomber turbulence excitation during low altitude terrain following missions [AIAA PAPER 72-772] 19 p2751 A72-38132

TERRESTRIAL DUST BELT

Interplanetary and terrestrial dust detection, discussing zodiacal light photometric measurements by Helios space probe and light pressure, solar wind and Poynting-Robertson effect 01 p0126 A72-10201

Solar radiative constant and stratospheric volcanic dust effects on circulation and climate anomalies 06 p0840 A72-17623

Terrestrial dust belt particles origin, character and trapped time from observations of earth-moon system libration points 08 p1229 A72-20839

Earth capture of dust particles moving in ecliptic plane heliocentric orbits, using three gravitational bodies analysis 14 p2153 A72-30494

Earth capture of dust particles moving in ecliptic plane heliocentric orbits, using three gravitational bodies analysis 19 p2864 A72-38323

TERRESTRIAL MAGNETISM

U GEOMAGNETISM

TERRESTRIAL RADIATION

Earth surface thermal radio emission measurements by UHF radiometry onboard Cosmos 243 satellite, showing brightness profiles of water, ice and land areas 01 p0053 A72-10363

Earth radiation climatology, noting qualitative agreement between calculated and satellite measured outgoing radiation data with allowance for inaccuracies due to albedo levels overrating 01 p0095 A72-10958

Artificial satellites for earth resources and environmental contamination control, discussing remote sensing physical problems and earth surface radiative characteristics 02 p0207 A72-11778

Remote sensing of surface radiation temperature topographic variations by precision radiation thermometer equipped aircraft, calibrating for atmospheric attenuation 02 p0210 A72-11803

Terrestrial radiation emission mapping from imagery produced by scanning radiometer, discussing remote sensors used to study surface energy phenomena 02 p0210 A72-11804

Earth radiation flux spectral intensity measurements in winter, noting latitudinal distributions, day and night variations and oceanic and continental curves 05 p0656 A72-16234

Direct earth radiation, albedo and shadow effects on attitude dynamics of gravity orientated satellites 05 p0730 A72-16995

Earth upper atmosphere outgoing thermal radiation radiance calculation in near IR spectrum 06 p0808 A72-18041

Multispectral TV camera systems for satellite recording of earth surface electromagnetic radiation at separate wavelengths [DGLR PAPER 71-135] 06 p0817 A72-18232

Aircraft short wavelength measurements of cloud reflection and absorption properties for impact on earth radiation budgets 16 p2388 A72-34024

Studies on radiation balance at a tropical station. 18 p2722 A72-36759

Influence of the earth's outgoing radiation on the temperature of a rotating disk in space 19 p2856 A72-37496

Some results of measurements of short-wave and long-wave radiation fluxes from the Cosmos-320 satellite 22 p3168 A72-41875

TESSERAL HARMONICS

Skytel 1 synchronous satellite orbit determinations and longitude acceleration due to tesseral harmonics of earth gravity, using tracking station range data 15 p2321 A72-31949

Explorer 34 satellite orbit perturbation, noting earth gravitational tesseral harmonic effect on perigee passage time 24 p3399 A72-45557

TEST BEDS

U TEST EQUIPMENT

TEST CHAMBERS

NT ANECHOIC CHAMBERS
NT HYPERBARIC CHAMBERS
NT PRESSURE CHAMBERS
NT VACUUM CHAMBERS

Fatigue crack growth rate testing in gaseous environments at nonambient pressure and temperature in test chamber 05 p0643 A72-16186

Low temperature environmental chamber for F-111 proof load testing, describing components of cold air forced convection recirculation system with liquid nitrogen injection 15 p2214 A72-32612

Two chamber adiabatic test compression system design with controlled throttle for high temperature nitrogen and nitrous oxide-type gases with exothermal reactions 18 p2676 A72-37189

Application of an agar-agar chamber for the study of electromagnetic waves in an inhomogeneous medium. 21 p3015 A72-40359

TEST EQUIPMENT

Flammability tests for polymer materials used in computers and business machines, evaluating procedures in terms of reproducibility, difficulty and equipment requirements 01 p0145 A72-10287

Constant stress and compression creep testing in vacuum conditions, describing simple spring loaded apparatus characteristics and performance 01 p0071 A72-11171

Test equipment for glass and polymer fibers strength and lifetime in vacuum and inert bases under static loads 01 p0093 A72-11382

Refractory materials strength testing equipment and techniques at high temperatures, covering creep, hardness, fatigue, ultrasonic, energy dissipation and loading tests 02 p0291 A72-11636

Pulse amplitude modulated tester with shift register generated sequence and conventional data /PCM/ bit synchronizer and detector 02 p0192 A72-12148

Electrical and electronic measurement and test instrument - Conference, Ottawa, June 1971 02 p0200 A72-12476

Metal fatigue damage nondestructive detection, discussing inspection methods, equipment, advantages, limitations and test results
[AD-741977] 02 p0296 A72-12498

Passivation velocity apparatus for testing Al-Mg alloy sensitivity to corrosion under voltage
02 p0246 A72-12599

Hydraulic systems and components stationary operating conditions determination, discussing measuring apparatus, test equipment and interpretation methods
03 p0312 A72-13961

Ac and dc electric power transient test equipment satisfying MIL-STD-704A requirements
03 p0312 A72-14038

Surface active agent detection by device using ultrasonic vibrating mechanism to emulsify water with fuel, determining water retention or turbidity by photoelectric cell
04 p0564 A72-14419

Polymethyl methacrylate fatigue strength at elevated temperatures, discussing sample preparation, test equipment and procedures
04 p0537 A72-14750

German monograph on refractory materials elasticity modulus determination at elevated temperatures, describing device based on characteristic vibrations frequency relation to temperature
04 p0510 A72-15698

Arnold Engineering Development Center turbine engine testing facilities and techniques for flight conditions and environment simulation, air/fuel flow and thrust measurement, etc
[ASME PAPER 71-WA/GT-8] 05 p0642 A72-15901

Solid lubricant antifriction properties test methods and measuring apparatus design for wide temperature range
05 p0665 A72-16096

Computer controlled production test system for airborne phased array modules, describing various measurement capabilities
05 p0637 A72-16417

Split Hopkinson pressure bar for studying material plastic behavior under impact, discussing principles, equipment and test results
06 p0814 A72-17742

Combined tension-torsion creep testing of polymers, discussing equivalent stress and strain concept, testing apparatus and preliminary results for polythene
06 p0835 A72-17795

High temperature fatigue test assembly for symmetric tension compression cycles at 10 kHz with specimen heating in resistance furnace
06 p0797 A72-18568

High temperature testing assembly for reinforced plastics and binders in oxidizing and inert media under tension, compression, bending and cleavage loads
06 p0797 A72-18569

Explosive shock loading effect on materials mechanical properties, describing test equipment
06 p0797 A72-18659

Test equipment with variable deflection and twist for metal fatigue microcrack initiation and growth detection
07 p0987 A72-19849

Oscillatory shock pulse reproduction with specified spectrum for performing shock testing with electrodynamic or electrohydraulic shaker-amplifier-equalizer system
07 p0965 A72-20199

Lunar laser reflectors specifications and fabrication procedures, discussing lunar environment simulator and optical test equipment, techniques and results
07 p0947 A72-20261

Thermal shock transient test burner to test gas turbine ceramics under simulated operational environment conditions
08 p1147 A72-21434

Setup to determine sonic creep and acoustic fatigue in polymers under symmetrical and asymmetrical load cycles at sonic and ultrasonic oscillation frequencies
08 p1147 A72-21763

Test apparatus and measurement of sealing pressure and temperature in threads of concentric running screw viscosity seals in laminar flow
08 p1178 A72-21932

Epoxy resin tensile specimen fabrication and testing, discussing factors controlling data scatter
09 p1337 A72-22650

High pressure bulk modulus test rig for composite material specimen nondestructive test, discussing measurement method and errors
09 p1315 A72-23391

Shock testing machine based on free falling weight striking resilient block, describing design details and electrical circuitry
09 p1292 A72-23472

Hydraulic tank application to internal flow visualization in turbomachinery, describing test equipment and methods used for axial flow model
10 p1419 A72-24654

Test assembly for Brinell microhardness measurements of metal and alloy surfaces under tension during vacuum heating and in protective gas media
11 p1612 A72-25490

Test assembly design for microstructural studies of metal and alloy fatigue in vacuum during heating, describing electrical resistance measurement and stroboscopic illumination
11 p1612 A72-25492

Test facility design for aircraft crashworthiness evaluation and improvement, considering survivable accident surrounding conditions, equipment and testing methods
[SAE PAPER 720323] 11 p1576 A72-25586

Torsion testing machine for hot metal workability tests at constant strain rate
11 p1639 A72-25820

Test device for reinforced plastics mechanical properties under heating and pressure with allowance for gas permeability
11 p1613 A72-26813

Long term high temperature test machine to record structural changes of materials
12 p1795 A72-27464

Test method and apparatus to pressurize hermetically sealed components with Kr 85, comparing obtained leak rates with He mass spectrometric values
12 p1854 A72-27550

Test apparatus and technique for assessing Pellier thermoelectric cooling device operational characteristics
12 p1755 A72-27721

Electronic heating test arrangement for high temperature testing of metals and electrically conducting ceramics in vacuum, describing temperature control systems
12 p1796 A72-28249

Landolt ring radioactive plague night vision tester comparison with electretrography and Goldman-Weekers dark adaptometry apparatus from special tests of night blind patients
12 p1777 A72-28332

Operational evaluation for sun stabilized attitude control system in Aeros satellite, describing laboratory equipment and component static and dynamic tests
[DGLR PAPER 72-026] 13 p2052 A72-28967

High temperature strength of low ductile refractory metals, describing test equipment
13 p1978 A72-29446

High speed testing of materials mechanical behavior over range of loading rates
14 p2165 A72-30441

VFW 614 twin jet transport aircraft flight test program, detailing general task plan, test equipment installations and test schedule
14 p2072 A72-30679

Quantified design criteria for vibration and shock test fixtures to insure test repeatability, proposing chart inclusion in military test standards
15 p2215 A72-32619

Test equipment for high strain rates in shear with torsional split Hopkins pressure bar
16 p2373 A72-33196

Airborne external instrumentation pod containing IR scanner and associated test equipment for land and water surveys
16 p2393 A72-33635

Forces and strain rates measurement in elastic elements of dynamic systems under impact, discussing test equipment and strain gauge transducers
16 p2395 A72-33964

Cythere capsule for irradiation of experimental fuel elements under geometric and thermal conditions representative of thermionic converters
17 p2579 A72-34619

Scintillation telescopes for muon angular distribution, designing test device for photomultiplier tubes selection
17 p2556 A72-35437

Thermionic converters performance and life tests, discussing test equipment and diffusion effect on emitter stability
18 p2643 A72-36139

Loading rig in which axially compressed thin cylindrical shells buckle near theoretical values.
19 p2783 A72-37730

A method for the study of wear particles in lubricating oil.
19 p2803 A72-38376

Application of the optical transfer function to visual instruments.
20 p2922 A72-39043

Design analysis and performance characteristics of a circular test base.
[AIAA PAPER 72-845] 20 p2911 A72-39084

Stable microprecision test platforms construction and microseismic effects on motion sensing instrument calibration including gyroscopes and inertial navigation and guidance systems
[AIAA PAPER 72-893] 20 p2911 A72-39110

Potential measurement and stabilization of an isolated target using electron beams.
21 p3087 A72-40700

International Aerospace Instrumentation Symposium, 18th, Miami, Fla., May 15-17, 1972, Proceedings.
22 p3178 A72-42676

Plastic model shells design, construction and instrumentation for elastic stability studies in NDT, discussing deformation measurements for critical condition prediction
22 p3163 A72-42694

Automatic transmission and application of sky wave corrections with differential OMEGA navigation, discussing test equipment, procedures and results
22 p3203 A72-42948

Balancing aerospace bodies on industrial balancing machines.
[SAWE PAPER 929] 23 p3293 A72-43469

Test equipment for heat resistance determination of brittle refractory material, noting data processing procedure and formulas for temperature distribution and thermal stress
23 p3278 A72-43962

High-frequency fatigue testing facility, U-20P, with programmed control of the sample's vibration amplitude
23 p3278 A72-43970

Operational support of space shuttle transportation and payload systems with modular checkout and test equipment, noting service life and economy of operations
24 p3388 A72-45111

Bonded honeycomb structures. II - Bonded joints and non-destructive testing.
24 p3407 A72-45288

A bibliographical survey of acoustic emission.
24 p3408 A72-45293

TEST FACILITIES

NT ANECHOIC CHAMBERS
NT BALLISTIC RANGES
NT BLOWDOWN WIND TUNNELS
NT CASCADE WIND TUNNELS
NT COMBUSTION WIND TUNNELS
NT ENGINE TESTING LABORATORIES
NT ENVIRONMENTAL LABORATORIES
NT HOTSHOT WIND TUNNELS
NT HYPERVELOCITY WIND TUNNELS
NT LOW DENSITY WIND TUNNELS
NT LOW SPEED WIND TUNNELS
NT MISSILE RANGES
NT PLASMA JET WIND TUNNELS
NT RECTANGULAR WIND TUNNELS
NT ROCKET TEST FACILITIES
NT SHOCK TUNNELS
NT SLOTTED WIND TUNNELS
NT SUBSONIC WIND TUNNELS
NT SUPERSONIC WIND TUNNELS
NT TEST STANDS
NT TRANSONIC WIND TUNNELS
NT WIND TUNNELS

Depth-dose experiments with monodirectional 14 MeV neutrons in low scatter environment, describing test facility
[CERN-71-16] 02 p0162 A72-12068

Orthotropic glass fabric laminate creep under combined torsion and tension, describing test facility
02 p0250 A72-12677

Wind tunnel model instrumentation and captive trajectory facilities for aircraft stability, control and metric wing-pylon store tests for performance and structural predictions
03 p0339 A72-12921

High precision strain gage dynamometers design and testing at ONERA Modane test center, discussing accuracy limitation due to hysteresis and creep effects
[ONERA, TP NO. 995] 05 p0642 A72-15859

Automated jet engine development facility, discussing assembly and test area and computer controlled operation
[ASME PAPER 71-WA/GT-6] 05 p0642 A72-15899

USAF small gas turbine test complex, discussing machinery, equipment, simulated testing, altitude chambers and instrumentation
[ASME PAPER 71-WA/GT-7] 05 p0642 A72-15900

Arnold Engineering Development Center turbine engine testing facilities and techniques for flight conditions and environment simulation, air/fuel flow and thrust measurement, etc
[ASME PAPER 71-WA/GT-8] 05 p0642 A72-15901

Jet engine test facilities for JT9D experimental and production models
[ASME PAPER 71-WA/GT-12] 05 p0642 A72-15904

Dynamic test facility for Symphony satellite attitude control, discussing sun and earth sensors and analog computer for motion simulator
05 p0643 A72-16432

Dynamic test facility and methods for Europa 2 launch vehicle inertial guidance system
05 p0643 A72-16433

Spherical air bearing supported test facility for satellite attitude control system performance testing, discussing motion simulator and automatic balancing system
05 p0643 A72-16435

SLINGSHOT pilot aerodynamic test facility for very high acceleration, using encapsulated gas slug over fixed model
[AIAA PAPER 72-168] 05 p0645 A72-16962

Test facility for vibrations damping study of structural elements in water flow based on frequency and amplitude measurement at various flow conditions

06 p0796 A72-18364

Low temperature test facility for cryogenic and rocket materials under combined tension and torsion

06 p0797 A72-18648

Stress-strain diagrams of heat resistant alloys at high temperatures, describing test facility

06 p0834 A72-18684

Cascading turbomachine blades vibration measurement in subsonic and sonic high temperature gas flows, describing test facility

06 p0797 A72-18689

Multiple swept stroke flash technique to test lightning effects on aircraft

07 p0964 A72-18768

Lightning simulation laboratory for aircraft strike testing, using high energy generators

07 p0964 A72-18774

Test facility for studying temperature dependence of thermal diffusivity and true heat capacity of metals between minus 150 and plus 400 C

07 p0982 A72-18941

Test facility for thermal diffusivity measurements in solids by method of plane temperature waves using periodic optical heating at 1500 K

07 p0982 A72-18942

Experimental determination of torsional stresses in rod from moire patterns, describing facility and procedure

07 p1091 A72-19762

Mechanical properties and structural strength evaluation methods for metallic materials at low temperatures, describing hydraulic and pneumatic testing facilities

07 p1017 A72-20130

Test facility for graphites fracture under thermal stresses, considering stress-strain relations calculation method for annular samples

07 p1024 A72-20137

Test temperature effect on phase composition, mechanical properties and resistance to cavitation of unstable austenitic steels, describing test facility

07 p1018 A72-20140

High speed rotating test rig development for vibration testing of turbine blades, describing design layout

08 p1147 A72-22131

Dinitroxydiethyl nitramine burning, describing experimental facilities used to determine temperature profile of combustion front

09 p1411 A72-22884

Thermal behavior of explosively welded metals, describing test facility for temperature measurements of joints

09 p1319 A72-22891

Test facility for electric microthrusters, describing microbalance for thrust and propellant mass flow rate measurement

09 p1292 A72-23404

Analog and hybrid computers automated programming, setup and checking facilities for off and on-line program preparation and debugging

10 p1445 A72-24090

Test facility design for aircraft crashworthiness evaluation and improvement, considering survivable accident surrounding conditions, equipment and testing methods

[SAE PAPER 720323] 11 p1576 A72-25586

RF ion thruster flight prototype development, describing test facilities, design and performance

[AIAA PAPER 72-471] 11 p1709 A72-26202

Test facility for aircraft and spacecraft antennas radiation patterns and optimal installation determination

12 p1795 A72-27412

Rotating airfoil experimental test program for verification of Himmelskamp and Dwyer-McCroskey theoretical analysis, presenting graphs of lift coefficient vs angle of attack

12 p1752 A72-28124

Hydraulic test facility for dynamic characteristics of potentiometric pressure sensors with connecting lines of various geometries, shaping pressure pulse signal by electromagnetic valve

13 p1957 A72-29135

Design and operation of experimental facility for thermal fatigue testing of heat resistant materials

13 p1939 A72-29145

Tubular materials plane stress-strain test facility for combined axial load and internal pressure effects, describing principal components

14 p2092 A72-30442

Resonance type facility using dynamic hysteresis loop method to test metal fatigue and anelasticity in torsion at room and high temperatures

14 p2092 A72-30443

Inclined wind tunnel test section for free gliding investigation and aerodynamic design of flexible wing two body system

15 p2213 A72-31403

Organization and management requirements for environmental testing laboratory from viewpoint of test results, data handling, analysis and test reporting

15 p2340 A72-32617

Digital control and data processing system to replace analog instrumentation in vibration test laboratories, discussing signal generation, data acquisition, storage and analysis

15 p2215 A72-32618

Free flight follower support system with data reduction for V/STOL or helicopter models, recording flight path and attitude angles

16 p2372 A72-32886

Space environment simulation and testing techniques, considering vacuum systems, low temperature, solar radiation and motion simulation

18 p2676 A72-36833

Development of a hypervelocity wind tunnel.

18 p2676 A72-37095

Components analysis laboratory with curve tracers, third harmonic induct equipment, noise meters, TV X ray system and metallographic microscopes

18 p2676 A72-37132

Aircraft flight test facilities deficiencies and modernization impediments, recommending integrated facility research program establishment

19 p2783 A72-37676

Pneumatically isolated test platform local gravity vector active control to investigate seismic level disturbance effects on precision inertial components evaluation

[AIAA PAPER 72-843] 20 p2923 A72-39086

Advanced fighter controls flight simulator for all-systems compatibility testing.

[AIAA PAPER 72-837] 20 p2911 A72-39090

High speed accelerometers to determine test platform tilt and translational motion displacements, discussing instrument configurations without gyroscopes

[AIAA PAPER 72-818] 20 p2923 A72-39105

Dual spin spacecraft simulation on three axis air bearing ball in atmosphere testing propellant tank dissipation and spacecraft stability in autotrack mode

[AIAA PAPER 72-860] 20 p2911 A72-39108

Aerodynamic test facility data on swept wings, peaky airfoils, aircraft flutter and transonic flow, discussing shock tubes and wind tunnels development

20 p2912 A72-39846

Some results from tests in the NAE high Reynolds number two-dimensional test facility on 'shockless' and other airfoils.

[ICAS PAPER 72-33] 21 p2991 A72-41158

The design and operation of the Air Force Flight Dynamics Laboratory Ballistic Impact Test Facility.

[AIAA PAPER 72-998] 21 p3041 A72-41584

The design and operation of a large tube-vehicle aerodynamic testing facility.

[AIAA PAPER 72-1001] 21 p3041 A72-41586

National aerospace R and D facilities requirements, establishing priority order for V/STOL, aeropropulsion systems, high Reynolds number, large transonic and true-temperature hypersonic test facilities

[AIAA PAPER 72-1033] 21 p3043 A72-41608

High Reynolds number transonic wind tunnel facility /HIRT/ for improved aerodynamic testing of modern combat and commercial aircraft performance, maneuverability and handling qualities

[AIAA PAPER 72-1035] 21 p3043 A72-41609

Development of a digital control system for a spacecraft propulsion test facility.

22 p3163 A72-42685

Digital computer equipped facility for training simulators environmental simulation capability testing, describing electronics interface, control and display equipment

22 p3164 A72-42928

Experimental facility and diffusion technique for measuring turbulence characteristics during hydrocarbon fuels burning in air streams

23 p3287 A72-43658

Immiscible materials processing experiments in near weightlessness environments during Apollo 14 mission and on NASA short duration low gravity test facilities.

24 p3407 A72-45155

Test facilities for aeropropulsion systems, emphasizing utilization, cost and technical advantages, aircraft inlet-engine systems compatibility and test types

[AIAA PAPER 72-1034] 24 p3388 A72-45401

Wideband antenna test facility.

24 p3389 A72-45554

Mechanical properties and structural strength evaluation methods for metallic materials at low temperatures, describing hydraulic and pneumatic testing facilities

24 p3416 A72-45756

TEST PILOTS

External respiration gas metabolism and energy consumption measurements for test pilots during parabolic trajectory flights in weightlessness simulation experiments

02 p0163 A72-12347

Procedures followed by test pilot on first flight of new aircraft design

06 p0758 A72-18488

Aircraft launch envelope investigation for minimum catapult end airspeed determination at carrier bow, discussing optimum test pilot launch technique

06 p0759 A72-18498

Test pilots 1971 reports - Conference, Beverly Hills, California, September 1971

08 p1230 A72-21001

Test pilot role in attack aircraft avionics systems integration consisting of head-up display, projected map, digital computer, inertial platform, radar and Doppler systems, etc

08 p1165 A72-21012

Life support equipment and pressure suit operational requirements from viewpoint of flight crews and test pilots

12 p1771 A72-27516

TEST RANGES

NT BALLISTIC RANGES

NT MISSILE RANGES

TEST STANDS

Test stand for rolling wheel with pneumatic tire at variable drift angles, deriving kinematic parameters and elasticity coefficients from static and dynamic tests

09 p1351 A72-23177

Open-air jet engine test stand for flame stabilization, jet and compressor noise studies, noting provisions for rapid installation changes

12 p1795 A72-27416

Hypersonic missile trail conductivity measurement on ballistic test stand, calculating electron concentration decrease

14 p2069 A72-30312

A stand for quality control of the vibrational characteristics of 'ultraquiet' radial ball bearings

19 p2807 A72-37663

Electrohydraulic stand for vibration strength testing, discussing system design, specifications, frequency-amplitude characteristics and applications

23 p2278 A72-43760

Thrust stand for evaluation of thrust vectoring nozzle performance.

[AIAA PAPER 72-1029] 24 p3389 A72-45406

TEST VEHICLES

NT FLIGHT TEST VEHICLES

Unmanned systems flight testing by test bed vehicle conversion to man operated mode, discussing T-33A jet trainer conversion to drone operation

05 p0623 A72-16665

Tactical missile controlled test vehicle flight test analysis by six-degree-of-freedom digital simulation

07 p1086 A72-20351

Techniques for control of long-term reliability of complex integrated circuits. I - Reliability assurance by test vehicle qualification.

17 p2528 A72-34688

The design and operation of a large tube-vehicle aerodynamic testing facility.

[AIAA PAPER 72-1001] 21 p3041 A72-41586

TESTERS

U TEST EQUIPMENT

TESTES

Hazard rate of recurrence in germinal cell tumors of the testis.

22 p3150 A72-42498

TESTING MACHINES

U TEST EQUIPMENT

TESTING TIME

F-14A fighter accelerated flight test program with 18-month saving and 3600 flight time hours before 1973 operability

04 p0464 A72-14591

Automated telemetry system providing real time analytical capability and reduction of flight test time for F-14

04 p0486 A72-14592

Conditional probability and test time calculation for separable equipment truncated sequential life tests applying to A-7D/E aircraft reliability program

10 p1486 A72-23997

Temperature, oxygen pressure and exposure time effects on oxidation characteristics of molybdenum-zirconium oxide cermets

11 p1665 A72-26865

Gas turbine engine hot part equivalent tests duration determination by analytical method based on Larson-Miller parametric description of stress rupture strength

12 p1887 A72-28243

TESTS

NT SALT SPRAY TESTS

NT THERMAL VACUUM TESTS

TETHERED BALLOONS

A stability analysis for tethered aerodynamically shaped balloons.

23 p3250 A72-43332

TETHERING

Tethered flying rotor platform for reconnaissance, fire control and radio transmission assignments in naval missions, discussing system characteristics

04 p0465 A72-15652

Relative motion of two mass points linked by flexible weightless tether in orbit around planet

06 p0891 A72-18695

Small amplitude libration stability and damping; system for gravitationally stabilized tethered orbiting radio interferometer satellite system

16 p2462 A72-34020

TETHERLINES
Rotating cable of high slenderness ratio and small flexural rigidity with end masses, deriving transverse vibration mode shapes and natural frequencies from asymptotic solution
02 p0293 A72-12253
Tethered autostabilized rotor platform for military surveillance, target location and communication, discussing flight vehicle, tethering cable, ground station and guidance-control system
13 p1898 A72-30078

TETRAD THEORY
General relativistic generalized field equations for scalar dependent tetrad, noting identity with Brans-Dicke theory
04 p0549 A72-15021
Local Lorentz transformation in chronometric invariants, demonstrating appropriate operation for general covariant tensors from tetrad formalism
14 p2130 A72-30218
Lorentz-covariant reference-tetrad theories of gravitation
24 p3425 A72-44913

TETRAGONS
NT PARALLELOGRAMS
NT RECTANGLES
NT SQUARES [MATHEMATICS]
NT TRAPEZOIDS
Plasticity conditions of monocrystals of higher symmetry tetragonal system, using energy density and deformation relations
08 p1242 A72-20938

TETRAHEDRONS
Matrices and permutation rules for tetrahedral polynomial finite elements for Helmholtz equation, commenting on computer time and convergence rate
14 p2126 A72-30932
Linear and nonlinear dielectric properties of crystals with tetrahedral structure
24 p3412 A72-45772

TETRANITROTETRAZACYCLOCTANE
U HMX

TETRODES
Superposition method for potential distribution in plane tetrode field with unipotential and bipotential grids, noting electro-optical effect in cylindrical lenses
19 p2776 A72-38667

TETRYL
Leads and booster explosives replacements for tetryl, discussing military specifications and safety criteria of various newly developed compounds and mixtures
08 p1220 A72-20770

TEXAS
Structure of Sierra Madera, Texas, as a guide to central peaks of lunar craters.
21 p3049 A72-41114

TEXTBOOKS
Book on structural analysis covering statically indeterminate structures, force and displacement methods, flexibility and stiffness matrices, strain energy, virtual work, energy theorems, etc
15 p2325 A72-31517

TEXTILES
Deposition of finishes and dyes in materials dried using microwave heating.
22 p3183 A72-42480

TEXTS
Modified run-length encoding system for text and drawing documents to obtain higher data reduction ratio
13 p1922 A72-29349

TEXTURES
Magnesium alloys torsional vibration damping correlation with texture orientation resulting from fabrication method
03 p0375 A72-13930
Ti-Al-V alloy biaxial yield strength improvement by combined texture and age hardening, using hydroburst tests
07 p1011 A72-19482
Surface textures in rolled Al sheets, investigating friction and reduction
11 p1638 A72-25509
Deformation drawing textures of bcc metals, including W
11 p1644 A72-26838
X ray analysis of Ti-Al alloys for cold rolled texture diagrams at low and high deformation levels
14 p2112 A72-30159
Texture of Ti-Sn and Ti-Mn alloy specimens observed by X ray reflection technique after hot rolling, annealing and cold rolling
16 p2407 A72-33529
Cold rotatory forging and subsequent heating effects on microstructure, texture and mechanical properties of dispersion hardened Ni specimens obtained by hot extrusion
16 p2407 A72-33530
Texture synthesis by image processing equipment consisting of digital computer and input/output unit, noting image signatures of constant parameter areas
17 p2555 A72-35338

Influence of twinned growth crystals on the texture of nickel work hardened in tension
18 p2702 A72-36703
Changes in the structure of nickel-beryllium alloys during deformation, recrystallization, and aging
21 p3068 A72-40959
Metastable growth patterns in some terrestrial and lunar rocks.
23 p3339 A72-44133

TF-30 ENGINE
Gas generator performance shifts involving military trim level variations by TF-30 engines in high relative humidity environment caused by condensation in inlet duct
07 p1052 A72-18759

TH-55 HELICOPTER
Flight test investigation of the aerodynamic behavior of various-sized stabilizers on a small helicopter.
24 p3362 A72-45328

THALAMUS
Phase relations between alpha waves in EEG and automated rhythmic motoric activity as function of subject behavioral activity and thalamic pacemaker zones
07 p0916 A72-19109
Thalamus functional and organizational anatomy studies from improved neurophysiological research methods, emphasizing cytoarchitectural differentiation functional significance
07 p0922 A72-20274
Nembutal barbiturate effects on afferent signals transmission and thalamocortical level of somatosensory system
08 p1116 A72-21195
Functional organization and neurophysiological mechanisms of return corticothalamic system in anesthetized cats, showing axon terminal presynaptic depolarization
13 p1902 A72-28762
Morpho-physiological structures thalamic afferent switching mechanisms of visceral analysors in motor, premotor, frontal and limbic cerebral sections
21 p3000 A72-40753
Control, by the visual cortex, of the posterior lateral thalamic group in the cat
24 p3372 A72-45009

THALLIUM
NT THALLIUM COMPOUNDS
Crystal lattice disarrangement by melting In-Tl alloy, noting fcc and bcc metastable phases formation during rapid crystallization
16 p2441 A72-33536
Volt-ampere characteristics of Ba-Cs plasma thermionic converter with W emitter and Ta collector
18 p2646 A72-36199

THALLIUM COMPOUNDS
Scintillation TlCl/LiBe crystal response to 8 GeV ionizing negative pions, noting pulse shape and resolution characteristics
15 p2291 A72-31535
Electron spin resonance of divalent Mn ion doped in thallous azide single crystals, investigating temperature effects on spin Hamiltonian parameters
22 p3152 A72-42716

THAWING
U MELTING

THEODOLITES
NT CINETHEODOLITES
Digital theodolite for automatic angle measurement with photoelectric sensor and magnetic data recorder for computer use
16 p2394 A72-33800
Astro-azimuth comparative studies with Wild T3, Wild T4, and Kern DKM3 theodolites.
[AIAA PAPER 72-842]
20 p2923 A72-39087
An approximate method of determining the azimuth from observations of the passage of the solar disk across the horizontal thread of the instrument's telescope
24 p3437 A72-44755

THEOREM PROVING
Theorems derived for bulk semiconductor device static negative differential resistance exhibition
01 p0114 A72-10790
Fatou theorem at Martin boundary derived from Dynkin theory on excessive functions and exit space of Markov process
10 p1504 A72-24062

THEOREMS
NT BAYES THEOREM
NT BERNOULLI THEOREM
NT BINOMIAL THEOREM
NT CASTIGLIANO VARIATIONAL THEOREM
NT EXISTENCE THEOREMS
NT LEBESGUE THEOREM
NT POYNTING THEOREM
NT RECIPROCAL THEOREMS
NT SIMILARITY THEOREM
NT STOKES THEOREM [VECTOR CALCULUS]
NT UNIQUENESS THEOREM
Local theorem in strengthened form for independent integral-valued lattice random variables
04 p0539 A72-15256

Theorem proved for pattern classification system effectiveness for system reliability prediction
10 p1504 A72-23996

THEORETICAL PHYSICS
NT NEWTON THEORY
NT QUANTUM THEORY
Periodic integral convolution equations in elasticity theory and mathematical physics, demonstrating solution existence
05 p0739 A72-16589
Multidimensional Fourier transforms application to theoretical physics partial differential equations, using singular delta function for homogeneous equations general integral
07 p1027 A72-19436
Helmholtz equation numerical solution for potential field problems with arbitrary boundary conditions of wave propagation, diffusion and thermal conduction in mathematical physics
12 p1846 A72-27553
Russian book - Mathematical theory of friction
19 p2806 A72-37350
Conservative difference schemes for linear and nonlinear problems of mathematical physics, discussing gas dynamics and magnetogasdynamics problems requirements
19 p2833 A72-37383
Periodic integral convolution equations in elasticity theory and mathematical physics, demonstrating solution existence
19 p2872 A72-37561
Einstein theories of special and general relativity, taking into account physical concepts relation to mathematical formalism, equivalence principle, field equations and gravitational waves
20 p2954 A72-40002
Black hole physics compatibility with thermodynamics second law formulation based on black hole area as entropy measure
21 p3085 A72-41216
Hydrodynamic and Wiener-Siegel hidden parameter models incapability for quantum mechanics reduction to classical mechanics, obtaining proofs to von Neumann theorem
23 p3312 A72-43298
Inconsistency of gravitational constant variability in inverse proportion to time from viewpoint of stellar and solar system age, life development and physical three dimensional space
23 p3338 A72-44037
Theoretical framework for testing gravitation and general relativity theories, considering completeness, self consistency and agreement with Newtonian physics
23 p3314 A72-44262
Mathematical consequences of physical laws invariance hypothesis under space-time-dependent changes in unit length, discussing conformally covariant and cosmological theories interrelationship
24 p3447 A72-45626

THERAPY
NT CHEMOTHERAPY
NT PSYCHOTHERAPY
NT RADIATION THERAPY
Nonionizing electromagnetic radiation effects in biological systems, discussing microwave penetration, therapeutic warming, light scattering in tissues and medical instrument applications
16 p2359 A72-33754

THERMAL ABSORPTION
NT POLAR CAP ABSORPTION
Heat absorption and liberation by glass fabric laminates under uniaxial tension, determining thermal effects dependence on strain rate and test temperature by calorimetric measurements
08 p1195 A72-21853
Normal-mode expansion technique for unsteady radiative and conductive heat transfer in absorbing emitting isotropically scattering slab with reflective boundaries
16 p2478 A72-33438
A first initial boundary value problem for a semilinear heat equation.
17 p2573 A72-34339
Radiation with free convection in an absorbing, emitting and scattering medium.
17 p2637 A72-35046
Bubble and strip magnetic domains creation, annihilation and manipulation in epitaxial magnetic garnet films by laser beam thermal absorption induced local heating
22 p3185 A72-42612
On the validity of a generalized Kirchhoff's Law for a nonisothermal scattering and absorptive medium.
24 p3424 A72-44698

THERMAL ACCOMMODATION COEFFICIENTS
U ACCOMMODATION COEFFICIENT

THERMAL AGITATION
U THERMAL ENERGY

THERMAL BLOOMING
Thermal defocusing of high intensity continuous Ar laser radiation in absorbing medium with allowance for spherical aberrations
14 p2110 A72-30355

Turbulence and nonlinear thermal blooming effects as cause of refractive attenuation of laser beam intensities

15 p2249 A72-32160

Transverse wind self-induced thermal lens effects on target image quality in laser beam tracking systems

15 p2249 A72-32164

Dynamic thermo-optical distortions compensation in lamp pumped rhodamine 6G liquid laser by introducing auxiliary dish with dye into cavity

23 p3295 A72-43679

Change in the sign of the thermal lens of glass laser rods during variation of the thermo-optical constant of glass

23 p3296 A72-43926

THERMAL BOUNDARY LAYER

Electron thermal boundary layer effects on Langmuir probe measurements in subsonic cold plasma flow

01 p0071 A72-11191

Locally nonsimilar solutions for thermal boundary layer, presenting surface heat transfer and temperature distribution

[ASME PAPER 71-HT-L] 02 p0302 A72-12313

Radiative heat transfer within nonisothermal air plasma, presenting centerline temperature data for various boundary pressures and temperatures

[ASME PAPER 71-HT-G] 02 p0302 A72-12316

Two dimensional elasto-viscous incompressible fluid flow past porous wall with variable suction, analyzing temperature field of laminar thermal boundary layers

03 p0341 A72-13500

Thermal boundary layer of incompressible fluid under steady laminar flow, obtaining temperature field from energy equation for various wall temperature conditions

03 p0343 A72-14314

Holographic interferometer for heat transfer measurement, studying free convection thermal boundary layer on heated isothermal vertical flat plate

04 p0524 A72-15531

Thermal laminar boundary layer equations solution for power-law velocity distribution in external flow and arbitrary surface temperature distribution

05 p0742 A72-15844

Computerized calculations of turbulent shear layers with compressibility, heat transfer, three dimensionality or unsteady flow, using differential equation

[ASME PAPER 71-WA/FE-8] 05 p0646 A72-15934

Nonstationary oncoming flow temperature effect on heat transfer in thermal boundary layer at forward stagnation point

05 p0746 A72-16217

Thermal laminar three dimensional boundary layer on finite uniformly accelerated body in nonstationary regime, taking into account buoyancy effect

07 p1100 A72-19624

Laminar thermal boundary layer analysis, comparing heat transfer characteristics of continuous surface and semiinfinite plate

08 p1254 A72-21613

Thermal boundary layer interaction with distortions in shape or material of adjacent surface for space shuttle design

[AIAA PAPER 72-312] 11 p1614 A72-25246

Discrete random walk heat conduction equation for thin layer with stepwise temperature change, comparing with parabolic and hyperbolic solutions

11 p1744 A72-25266

Dynamic and thermal laminar compressible boundary layers on flat plate, noting interaction of two quasi-steady flows

[ONERA, TP NO. 1068] 12 p1797 A72-27167

Three dimensional hydrodynamic and thermal boundary layers and heat transfer for forced convection flow in rotating cylinder system

12 p1890 A72-28167

Isothermal vertical plate turbulent thermal boundary layer during free convection, noting temperature pulsations dispersion

13 p2066 A72-29899

Momentum transport in thermal incompressible turbulent boundary layers with constant wall temperature, using dimensional analysis and Stratford model

14 p2096 A72-31055

Forced convection and thermal boundary condition in parallel and tapered passages, discussing Nusselt numbers for exponentially decreasing wall heat fluxes

14 p2173 A72-31062

Thermal laminar boundary layer equations solution for power-law velocity distribution in external flow and arbitrary surface temperature distribution

15 p2334 A72-31263

Response of heat transfer from a moving flat plate in a parabolic flow

18 p2741 A72-36798

Calculation of thermal fluxes and temperatures on the surfaces of a plate in the presence of heat exchange between fluids incident on the surfaces

18 p2742 A72-37183

Heat transfer during uniform injection on a vertical surface under conditions of combined free and forced convection

20 p2982 A72-39225

A thermal boundary layer on a nonisothermal plate

20 p2987 A72-39917

Nonisothermal surface cooling for arbitrary temperature distribution and Prandtl number approaching zero, solving thermal boundary layer equations by series expansion

21 p3129 A72-41061

Variational formulation and computer solution for thermal boundary layer flow over flat plate in entrance region, assuming temperature dependent thermal conductivity and viscosity

22 p3156 A72-41959

Laser interferometer for studying boundary layers in liquids

22 p3178 A72-42473

THERMAL BUCKLING

Anisotropy and nonuniformity of bonded glass mat thermoelastic properties, investigating thermal buckling origin

09 p1337 A72-22703

Thermal buckling of parallelogram shaped plate under stationary temperature field and uniformly distributed forces, deriving critical load

09 p1402 A72-22733

Determination of the critical temperatures of cylindrical shells of variable thickness

22 p3243 A72-42053

THERMAL COMFORT

Optimal psychomotor performance in relation to thermal comfort conditions in man, using complex dual tests and subjective rating scales

01 p0016 A72-10117

Water cooled suits efficiency and effectiveness for heat removal, noting importance of head area

14 p2081 A72-31085

THERMAL CONDUCTIVITY

Thermal conductivity, electrical resistivity, Lorentz ratio and thermopower of Ti, Al and Ni alloys for aerospace structures over 4-300 K range

01 p0113 A72-10173

Multilayer insulation materials for reusable space vehicles thermal protection and radiation shielding, tabulating thermal conductivity values for various materials

01 p0092 A72-10780

Thermodynamic properties of gases at high temperatures, tabulating composition, enthalpy, entropy and thermal conductivity of combustion products with ion seeding

01 p0145 A72-11202

Controllable states insufficiency to characterize rigid heat conductors dependence on temperature fields in experimental materials measurements programs

01 p0146 A72-11389

Previous loading effect on contact area and prints number and size distribution and thermal conductance for two nominally flat surfaces in contact

[ASME PAPER 71-LUB-M] 02 p0234 A72-11528

Thermal conductivity and boundary conditions for unsteady thermal fields in thin anisotropic plates with heat emission

02 p0291 A72-11635

Wall conduction effect on heat transfer to laminar boundary layer, obtaining temperature distributions at plate surface by energy transport equation

02 p0202 A72-11670

Thermal conductivity measurement of dissociating nitrogen dioxide over 548-792 K and 1-30 atm

02 p0170 A72-12091

Fiberglass reinforced plastics heat conductivity as function of porosity, reinforcement factor and density

02 p0250 A72-12686

High temperature properties of composite contact stack composed of alternating thermal flux sensors and heaters, determining heat conductivity and energy dissipation

03 p0458 A72-14160

Unsteady thermal conductivity inverse problems, obtaining heated body surface temperature and heat flux from temperature measurement in interior

03 p0458 A72-14164

Se and Zn doped n and p type gallium arsenide point defects, considering thermal conductivity, relaxation time and phonon scattering cross section effects

03 p0404 A72-14239

High temperature thermal conductivity measurements of solids at 800-1500 C using heat pipe technique

04 p0547 A72-14544

ALSEP lunar heat flow experiment, describing instrument for temperature and thermal conductivity measurements in lunar subsurface

04 p0577 A72-15098

Thermal conductivity cell for dielectric materials powdered samples and thermal diffusivity and conductivity measurements, using line heat source principle

04 p0523 A72-15493

Zirconium carbide high temperature heat conductivity measurement by radial heat flux method combined with photographic technique

05 p0680 A72-15852

Nitrogen heat pipe axial temperature distribution and vapor pressure measurement, noting effective

thermal conductivity variation with power load and inclination angle

[ASME PAPER 71-WA/HT-28] 05 p0744 A72-15881

Two dimensional stationary temperature fields determination in ribs, cylinders and pipes with temperature independent heat conductivity

05 p0746 A72-16188

Electrical resistance and thermal joint conductance measurements at perfect contact interfaces from electroplating, soldering and explosive bonding

[AIAA PAPER 72-19] 05 p0666 A72-16859

Smooth curved metal surfaces thermal conductance at high vacuum, verifying contacting surfaces plastic deformation

[AIAA PAPER 72-20] 05 p0666 A72-16861

Partially insulated homogeneous cylinder temperature distribution from heat conductivity boundary value problem equations

05 p0751 A72-17142

Linear dispersion relation for pressure gradient driven drift waves instabilities from ion and electron thermal conductivity effects in collisional plasma

06 p0857 A72-17529

Refractory metallic and nonmetallic materials thermal conductivity above 1500 K, noting unreliable white oxides lattice conductivity results

06 p0828 A72-17612

Thermal conductivity, electrical resistivity, emissivity and specific heat of polycrystalline vanadium under electron bombardment heating at 1200 to 1800 K

06 p0828 A72-17613

Thermal conductivity of aluminum, beryllium and magnesium oxides lattices at high temperatures

06 p0828 A72-17615

Thermal behavior of electron and ion gases in ionosphere, analyzing heat gain, transfer, loss and conductivity terms of energy equation

06 p0809 A72-18278

Thin film materials and fabrication methods, discussing substrate requirements, surface properties, chemical stability, thermal conductivity and preparation of various resistors and capacitors

06 p0790 A72-18572

Electroconductivity, thermal conductivity and diffusivity, specific heat and emissivities of Ti at 1000-1700 K

07 p1010 A72-18935

Solar chromosphere radiative transfer and thermal conduction coupling, applying singular perturbation method to Frisch analysis

07 p1070 A72-19087

Thermal conductivities of gaseous binary mixtures of methyl nitrate with helium, neon, argon and nitrogen

07 p1051 A72-19365

Ti, Fe, Co, Ni, Pt and steels phase transformation and thermal defect effects on high temperature thermal conductivity

07 p1012 A72-19548

Thermal conductivity of stationary toroidal plasma in form of Pfirsch-Schluter diffusion factor, using ion heat balance equation

07 p1042 A72-19616

Thermal conductivity of argon, helium, hydrogen, nitrogen, carbon dioxide, methane and ethane gases at high temperature and pressure

07 p1099 A72-19620

Approximate solution to Elenbas-Geller equation of arc electric and radiation characteristics as function of thermal conductivity by Galerkin method

07 p1043 A72-19879

Lattice and photon components of thermal conductivity of cerium dioxide at high temperatures

07 p1044 A72-19881

Unsteady thermal conductivity and heat transfer in solid bodies heated by radiation, using cascade linearization method

07 p1100 A72-19884

Critique of paper on heat capacity and thermal conductivity of Apollo 11 lunar rocks at liquid helium temperatures, noting constraints imposed by Mossbauer data

07 p1084 A72-20521

Thermal conductivity measurements of liquid InSb and Ga at 250-550 C

07 p1036 A72-20566

Temperature dependence of electrical resistance and thermal conductivity in duralumin quenched at 77 K

07 p1022 A72-20663

Electrical resistance and thermal conductivity dependence on temperatures in duralumin quenched at 77 K

07 p1022 A72-20666

Heat transfer coefficient, maximum Nusselt number and particle thermal conductivity effect for gas fluidized beds, using surface renewal-penetration theory

[ASME PAPER 71-HT-Z] 08 p1251 A72-20879

Laser heating of plasma based on thermal conductivity mechanism, considering nuclear microfusion energy recovery

08 p1213 A72-21303

Thermal conductivity and thermal diffusion coefficients determination for plane plate heated unilaterally from above under fourth kind boundary conditions
08 p1252 A72-21313

Unsteady heat conductivity equation for finite dimensions parallelepiped, noting temperature dependence of specific heat and thermal conductivity
08 p1252 A72-21321

Heat transfer in shield-vacuum thermal insulation layers at various temperatures and pressures, noting conductivity anisotropy
08 p1253 A72-21451

Fiberglass heat transfer mathematical model, noting scattering effect and thermal conductivity
08 p1191 A72-21452

Under-lip temperatures and thermal conductivity in rotary shaft seals, using heat transfer analysis
08 p1178 A72-21934

Thermal diffusivity and conductivity and specific heat of hard electrode graphite intermediate medium in hydraulic hot extrusion of metals
08 p1181 A72-22072

Thermal conductivity measurement for gases and gas mixtures with water vapor, describing methods and results
09 p1413 A72-23689

Thermal conductivity, diffusivity and specific heat of lunar soil and basalt analogs, using Luna 16 samples
10 p1532 A72-23753

Thermal radiative cooling system characteristics determination, taking into account surface material thermal conductivity and blackness degree dependence on temperature
10 p1561 A72-23840

Bolted joint thermal conductance, considering interfacial pressure distribution and surface roughness effects
[AIAA PAPER 72-282] 11 p1741 A72-25222

Dimensionless thermal contact conductance parameter for determination of interstitial thermal control materials effectiveness for metallic junctions
[AIAA PAPER 72-284] 11 p1741 A72-25224

Thermal conductivity of two- and three phase solid mixtures of silicone rubber and Al, Pb, Ni and Bi powders, using line source method
11 p1744 A72-25264

Fiber reinforced plastics thermophysical properties, thermal conductivity and heat capacity, determining effects of reinforcement fiber type, resin amount and type
[AIAA PAPER 72-366] 11 p1669 A72-25391

Multilayer insulation apparent thermal conductivity measurement at low compressive loads, describing test calorimeter and experimental technique
[AIAA PAPER 72-367] 11 p1670 A72-25392

Charged particle thermodynamics in ionospheres, considering energy exchange due to collisions or thermal conductivity
11 p1621 A72-25837

Burnett theory of thermal transpiration in capillary with wall accommodation for polyatomic gases, using Chapman-Enskog constitutive relations
11 p1746 A72-26010

Hot wire cell measurement of specific heat in low pressure gases, determining thermal conductivity and accommodation coefficient
11 p1634 A72-26367

Electronic partition functions cut-off criteria effect on translational and reactive thermal conductivity and viscosity of thermal plasmas
11 p1698 A72-26602

Electrical and thermal conductivity, elastic properties and resistance to bending of porous tungsten in porosities region
11 p1665 A72-26868

Thermal conduction anomalies and electron phonon interaction in thin metallic sheet at low temperatures
12 p1888 A72-27182

Heat conductivity differential equation solution by hydraulic model system, facilitating temperature values conversion into electrical quantities for hybrid computer
12 p1888 A72-27301

ALSEP heat flow experiment design and calibration, presenting independent vertical temperature gradient and thermal conductivity measurements in regolith
12 p1869 A72-27331

Lunar granular materials thermophysical properties, emphasizing thermal conductivity data and heat transfer mechanisms
12 p1869 A72-27333

Apollo 11 and 12 lunar samples thermal properties, presenting diffusivity, conductivity and specific heat
12 p1869 A72-27334

Thermal conductivity measuring apparatus for small multispecimen thermoelectric materials
12 p1795 A72-27467

Phonon scattering and induced energy levels in electron irradiated Sb doped Ge in n to p-type conversion region, measuring thermal conductivity and Hall effect
12 p1857 A72-28057

Unsteady state of ideal quiescent heat conducting gas in half space, deriving asymptotic solutions to mass, temperature, pressure and density dynamic behavior expressions
13 p2064 A72-28678

Three dimensional steady temperature field calculation for solid bodies under concentrated heat source, using flow kinetic heat conduction method
13 p2065 A72-29151

Atomic hydrogen viscosity and thermal conductivity coefficients for 1-100,000 K, using quantum theory for low temperatures and classical mechanics for high temperatures
13 p2065 A72-29299

Electrothermal instability analysis for MHD generator, considering electron thermal conduction and wall boundaries effects for cases with current parallel or perpendicular to walls
13 p2014 A72-29366

One dimensional unsteady flow of dense magnetized plasma, investigating time evolution of temperature profile in wall layer and thermal conductivity
13 p2018 A72-29876

Cs vapors thermal conductivity at various temperatures and pressures, using low emissivity Ni cylinders
13 p2065 A72-29896

Ta thermal conductivity and electric resistance at various temperatures
13 p1981 A72-29897

High melting point transition metals carbides, nitrides, borides, silicides and oxides thermal conductivity as function of characteristic temperature
13 p1981 A72-29905

Apollo 12 fines thermal conductivity in vacuum at 200-400 K, using least squares technique for curve fit
14 p2154 A72-30509

Composite two-material circular sector two dimensional stationary temperature field determined for certain thermal conduction coefficient ratios
14 p2170 A72-30573

Experimental data gathering, processing and presentation for materials enthalpy, heat capacity, thermal conductivity, compressibility and volume over wide pressure and temperature ranges
14 p2130 A72-30599

Internal gravity waves and convective instability caused by liquid layer nonuniform vertical density distribution, noting error in thermal conductivity measurement near critical point
14 p2095 A72-31008

Orthogonal projection method for nonstationary heat conduction boundary value problem with thermal conductivity and specific heat as prescribed functions of position
14 p2126 A72-31049

Natural convection initiation in fluid confined above and below by rigid conducting surfaces and laterally by rigid insulating vertical walls
14 p2172 A72-31054

Free convection effect on vertical porous insulation layer thermal conductivity in high pressure gas environment
14 p2172 A72-31057

Dynamic spin disorder effect on electrical and thermal conductivity, noting low resonant frequency in metal atom magnon spectrum
15 p2290 A72-31388

Plasma containment in toroidal systems investigated on basis of fluid model containing inertia, momentum transfer, ionic collisions and thermal conductivity effects
15 p2285 A72-32273

High temperature lattice and radiative thermal conductivity measurements utilizing carbon dioxide laser and IR detector for diffusivity and mean extinction coefficient phase data
15 p2250 A72-32507

Optical measurement for simultaneous determination of transparent isotropic medium thermal diffusivity and conductivity
16 p2389 A72-32947

Sudden heating-induced deflection of rectangular plate fitted into equal sized excavation in elastic foundation with relatively very low thermal conductivity
16 p2475 A72-33148

Heat conductivity effect on structure and critical Mach number of shock wave propagation across magnetic field in cold rarefied plasma
16 p2435 A72-33152

Fillers effect on polytetrafluoroethylene friction properties, electroconductivity and thermal conductivity, noting friction coefficient reduction by laminar filler structures
16 p2413 A72-33269

Critical analysis of Senftleben modified hot-wire method for gas heat conductivity measurement
16 p2479 A72-33861

Temperature distribution and heat dissipation calculations for CW and pulsed laser optical elements
16 p2403 A72-33982

Thermal conductivity of W wire reinforced Cu as function of W content
16 p2411 A72-34017

Thermal analysis of high performance devices mounted on dielectric substrates.
17 p2527 A72-34677

Viscosity and thermal conductivity of moderately dense gas mixtures.
17 p2636 A72-34737

Simplified expressions for the calculation of the contribution of the heavy components to the transport coefficients of partially ionized gases.
17 p2589 A72-34896

Unsteady thermal conductivity and heat transfer in solid bodies heated by radiation, using cascade linearization method
17 p2637 A72-35132

Thermal conductivity and heat capacity measurement by temperature vs time curve shape by laser pulse absorption, using thermocouple
17 p2637 A72-35138

Upper and lower bounds of effective thermal conductivity for statistically homogeneous composite materials, using variational principles
17 p2638 A72-35285

Temperature dependence of electrical and thermal conductivity for transition metals at 20 to 1200 K, noting periodic variations associated with atomic structures periodicity
17 p2568 A72-35519

Heat conduction in a turbulent magnetic field, with application to solar-wind electrons.
17 p2601 A72-35584

Midlatitude red arc observations by satellite and ground station, suggesting thermal conduction theory of formation from ionospheric electron and ion temperatures and densities
18 p2685 A72-35989

The Apollo 15 lunar heat-flow measurement.
18 p2724 A72-36285

Temperature dependance of the electron thermal conductivity in rare gas plasmas.
18 p2716 A72-36958

Effect of structural parameters and temperature on the effective thermal conductivity of plasma-sputtered aluminum oxide
18 p2696 A72-37188

Transport coefficient of multi-layer film of semiconductors.
19 p2843 A72-37401

The thermal conductivity of a statistically isotropic heterogeneous medium.
19 p2880 A72-37462

Characteristics of temperature dependences for the thermal conductivity coefficients of niobium-zirconium solid solutions
19 p2817 A72-37739

Solution of boundary value problems in heat conduction by the method of the successive averaging of a desired function
19 p2881 A72-38042

Determination of the temperature dependence of the thermophysical characteristics of solid materials by the method of successive approximations
19 p2881 A72-38044

Thermal conductivity of compact samples of cubic BN
19 p2823 A72-38408

Effect of ionic viscosity on the stability of a finite-pressure plasma
19 p2842 A72-38529

Bulk viscosity coefficient and the second heat conduction coefficient near the critical condensation point
20 p2983 A72-39396

Temperature distribution control in n-dimensional space via quasi-inversion method with Fourier transformation for Cauchy problem solution of heat conductivity equation
20 p2983 A72-39466

Solution of mixed boundary value problems in heterogeneous media for multiply connected regions of complex shape by a structural method
20 p2946 A72-39469

The effect of thermal conductivity and base-temperature depression on fin effectiveness
20 p2983 A72-39489

The computation of dynamic equilibrium temperature distributions on substrates having a temperature-dependent thermal conductivity.
20 p2908 A72-39499

An investigation of a possible correlation between the laser output of a ruby rod and the chromous ion concentration.
20 p2934 A72-39643

Formulation of boundary conditions in the statement of thermal problems for bladed rotors of gas turbines
20 p2987 A72-39926

Analysis of the transport coefficients for simple dense fluids - Application of the modified Enskog theory.
21 p3084 A72-40723

Thermal conductivity measurements of nickel-cadmium aerospace cells. II - Component conductivities.
21 p2997 A72-40841

Wall temperature, thermal conductivity and acoustic vibration frequency as function of critical

- heat flux density for unstable water film boiling conditions
21 p3130 A72-41063
- Transition metals thermal conductivity periodic variations relation to free Fermi surfaces and valence electrons localization variations
21 p3070 A72-41646
- Pulsed GaAs injection laser heating application to thermal conductivity coefficient measurement in thin films, discussing lasing spectra kinetics
21 p3064 A72-41740
- Nonstationary method for measuring the heat conductivity of liquids and gases under high pressures
22 p3243 A72-41886
- Thermal conductivity of honeycomb sandwich panels for space applications.
22 p3244 A72-42650
- Comparative cut-bar thermal conductivity apparatus.
22 p3180 A72-42710
- Thermal properties of polymers below 4 K.
22 p3197 A72-42800
- Bi-Sb alloys for magneto-thermoelectric and thermomagnetic cooling.
22 p3215 A72-43089
- Thermal conductivity in the two-band model of superconducting transition metals containing nonmagnetic impurities.
23 p3323 A72-43274
- Thermal and electrical conductivities, thermal expansion and specific heat of commercial graphite obtained by precipitation of methane pyrolysis products on hot surface
23 p3306 A72-43689
- Parameters influencing the theoretical calculation of the thermal conductivity of a nitrogen plasma
23 p3321 A72-43692
- On the approximation of the thermal conductivity of rigid heat conductors as a Cauchy problem.
23 p3356 A72-43721
- Heat conduction with allowance for the temperature dependence of the coefficient of thermal conductivity. II - Correctness of the variational formalism
23 p3357 A72-44085
- Determination of the stationary temperature field in a plate with a crack in the presence of heat release from the lateral surfaces
23 p3357 A72-44086
- Thermal conductivity of superconducting layer in intermediate stage with Andreev electron excitation trajectories in magnetic field, using Green function and impurity distribution technique
23 p3325 A72-44486
- Determination of the radial heat conductivity of multilayer tubes for thermionic converters
24 p3461 A72-44875
- Study of dynamic and thermal processes during steady motion of a viscous gas
24 p3390 A72-44996
- Superhigh-frequency heating of a plasma and longitudinal electron heat conductivity in a magnetic field
24 p3429 A72-45492
- Methods for determining thermal properties of anisotropic systems.
24 p3465 A72-45633
- Thermal conductivity in dirty transition-metal superconductors near the upper critical field.
24 p3432 A72-45675
- THERMAL CONDUCTIVITY GAGES**
- Anemometer probe with thermistors for low velocities of liquids derived from pulsed thermal conductivity gage
10 p1479 A72-24066
- Russian monograph on heat measurement covering methods and instruments for heat flux determination, radiometers, thermal conductivity gages and electrical calorimeters
17 p2556 A72-35495
- THERMAL CONDUCTORS**
- Nonlinearly radiating semiinfinite heat conducting solid surface temperature, expressing heating rate as nonnegative integrable function of time
[AD-743353] 07 p1098 A72-18814
- One-dimensional shock waves in heat conducting materials with memory. I - Thermodynamics.
23 p3314 A72-44341
- THERMAL CONTROL COATINGS**
- Multilayer heat reflective coating optical thickness effect on temperature distributions, taking into account interlayer contact resistance and thermal radiation volume absorption
06 p0904 A72-18511
- Vehicle components oxidation in thermal control coatings, investigating resistance to oxidation by UV photoproduced ZnO electronic holes
[AIAA PAPER 72-264] 11 p1699 A72-25207
- Dimensionless thermal contact conductance parameter for determination of interstitial thermal control materials effectiveness for metallic junctions
[AIAA PAPER 72-284] 11 p1741 A72-25224
- Low conductivity insulating coating /graded thermal barrier/ to cool gas turbine engine with high pressure ratio and inlet temperature
[AIAA PAPER 72-361] 11 p1669 A72-25389
- Spacecraft thermal control coating damage by energetic Hg ion bombardment, using absorbance measurements
11 p1746 A72-26183
- Solar absorbance and thermal emittance of thermal control coatings contaminated by thruster exhaust in vacuum environment
[AIAA PAPER 72-263] 12 p1846 A72-27865
- Boron nitride coated boron fibers for metal matrix composite reinforcement, discussing surface nitriding process by heating
12 p1815 A72-28088
- Thin plates and coatings in thermal contact with standard, determining total emissivity by inverse methods of heat conduction
12 p1889 A72-28115
- SAS-A thermal control design and tests, considering solar cells, attitude control, command system, telemetry and data storage
15 p2320 A72-31805
- Spacecraft thermal control materials research, discussing surface selection, coatings, space simulation and environmental effects
15 p2260 A72-31806
- Recent development on thermal design of spacecraft.
21 p3115 A72-41125
- Approximate calculation of the temperature stresses in the thermal impact zone
22 p3232 A72-41871
- THERMAL CONVECTION**
- U FREE CONVECTION**
- THERMAL CURRENTS**
- U CONVECTIVE FLOW**
- THERMAL CYCLING TESTS**
- Silica based surface insulation material for space shuttle thermal protection system, discussing cyclic tests in simulated environment and fiber purity effects on crystallization
01 p0091 A72-10764
- Turbine blades adaptability limits to temperature variations, considering rectangular cross section plastic rod under programmed thermal and tensile load cycles
01 p0143 A72-11372
- Heat resistant alloys thermal microstresses effect on creep and fatigue life under thermal cycling conditions
02 p0242 A72-11633
- Supermagnetization and ac core loss temperature dependence under slow temperature cycling in vacuum, noting anomalous Barkhausen effect
04 p0564 A72-15718
- Elastoplastic creep analysis for cylindrical pressure vessel structural response during cyclic thermal shock, internal pressure and extended high temperature loading
[ASME PAPER 71-WA/PVP-12] 05 p0732 A72-15911
- Fatigue failure tests of soldered joint in solar cell interconnector designs under extended temperature cycling
05 p0615 A72-16552
- Fatigue life and creep tests of refractory materials under programmed thermal cycling for different stress levels
06 p0831 A72-18351
- Maximum temperature-holding time effects on plastic deformation and fracture of steel under thermal cyclic loads
06 p0831 A72-18359
- Gas turbine blades fatigue crack development and failure analysis under thermal cycling tests, considering chemical processes and thermal and mechanical stresses
06 p0898 A72-18550
- Gas turbine blades thermal fatigue test and analysis, investigating static tensile loading effects on heat resistance under thermal cycling
06 p0899 A72-18556
- Steel sheet creep, plastic deformation and service life under temperature and stress cycles
06 p0899 A72-18558
- Aircraft power plants sealing materials, emphasizing porous cermet seals heat resistance under thermal cyclic loads
06 p0797 A72-18658
- Gas turbine blades dynamics characteristics determination, investigating vibrational stresses, thermal cycles, alloy physicochemical properties and coatings effects
06 p0900 A72-18683
- Microwave temperature sensor for radiation environment use, discussing cavity resonator design and operation, thermal cycling tests and comparative radiometer technique
07 p0993 A72-20677
- Pipe joint flexible metal seal development and testing for Concorde Olympus 593 under thermal and pressure cycling
08 p1178 A72-21938
- Fatigue strength of heat resistant materials under thermal cyclic loads leading to sign variable plasticity and creep
09 p1402 A72-22732

- Power transistor thermal cycling ratings and fatigue testing under operating conditions
10 p1447 A72-24011
- Thermal shock and temperature cycling environmental testing, discussing military specifications, components thermal lag characteristics, environmental test chambers and various cooling methods
10 p1459 A72-24144
- Two dimensional elastoplastic finite element analysis of structural members under cyclic thermal-mechanical loadings
[ASME PAPER 72-GT-1] 11 p1734 A72-25604
- Creep tests for thermal preycling effect on time to failure and long term ductility of austenitic steel thin walled tubular samples
11 p1663 A72-26809
- Udimet 500 alloy dislocation substructure and fracture surface topography during deformation to failure in low cycle fatigue at high temperatures
11 p1667 A72-26938
- Long life leak-proof hermetic compression seals for alkaline batteries, describing design, fabrication and accelerated thermal cycle test method
[ECS PAPER 72] 13 p1899 A72-28434
- Heat resistance of corundum based ceramics with multiphase additions under thermal cycling tests
13 p1983 A72-28568
- High modulus yarn carbon-carbon three dimensional orthogonal composite material ablative and thermomechanical performance in nose tip ground tests
[AIAA PAPER 72-365] 13 p1983 A72-28956
- Aircraft engine components fatigue life assessment under small cycle temperature conditions, including temperature field and stress-strain determination in critical spot
14 p2145 A72-30279
- Cr-containing Fe-alloy and Ni steels, investigating thermal cycling effects on thermal resistance by factorial program
14 p2118 A72-30546
- Second order deformation theory for axially held strut during thermal cycling at creep relaxation temperature, using galerkin method with assumed sine wave
16 p2473 A72-34124
- Design and testing a high fuel volume fraction, externally finned, thermionic emitter.
17 p2495 A72-34586
- The effect of high vacuum on the low cycle fatigue law.
18 p2700 A72-36582
- The effects of environment on the elevated temperature fatigue behavior of nickel-base superalloy single crystals.
18 p2700 A72-36587
- Behavior of Fe-21.6 Ni, Fe-18.4 Ni-15.0 Co, Fe-16.8 Ni-5.0 Mo subjected to cumulative thermal cycling at 300 C/hr
18 p2701 A72-36701
- Comments on thermal cycles of silicon power transistors
18 p2667 A72-36794
- Comparison of experimental and theoretical thermal fatigue lives for five nickel-base alloys.
19 p2815 A72-37639
- Plasticity and rupture of heat-resistant materials subjected to a small number of cycles of simultaneous variation of temperature and load
19 p2818 A72-38006
- Refractory materials cyclic elastoplastic tests under shear with holding creep, showing relationship between creep rate and recurrent static deformation
19 p2876 A72-38007
- Multi-cycle plasma arc evaluation of oxidation inhibited carbon-carbon material for shuttle leading edges.
[ASME PAPER 72-ENAV-26] 20 p2894 A72-39151
- Fatigue damage of aluminum alloy at high temperature.
21 p3066 A72-40716
- Facility for studying the thermophysical properties of materials by quasi-stationary methods
22 p3176 A72-42289
- Aluminized thoria dispersed NiCr and Ni-20Cr alloys with protective alumina scales from pack diffusion, observing oxidation resistance by isothermal and cyclic oxidation tests
22 p3193 A72-43030
- Electron fractography of fatigue failure and macrocrack propagation in dual phase Ti alloy during cyclic loading at minus 140 to plus 150 C
23 p3303 A72-44097
- Heat treatment effects in multipass weldments of a high-strength steel.
23 p3304 A72-44310
- Thermal cycling tests for natural remanent magnetism of lunar soil samples, proposing magnetization mechanism of material buried in regolith
24 p3443 A72-45373
- Fatigue life and creep tests of refractory materials under programmed thermal cycling for different stress levels
24 p3416 A72-45738

Maximum temperature-holding time effects on plastic deformation and fracture of steel under thermal cyclic loads 24 p3416 A72-45746

THERMAL DECOMPOSITION
U PYROLYSIS
THERMAL DEFOCUSING
U THERMAL BLOOMING
THERMAL DEGRADATION
 Polyethylene and polypropylene combustion, investigating additives and surrounding gaseous composition effects on flammability and volatile products during thermal degradation 02 p0248 A72-11767

Boron-containing polymer heterogeneous combustion determination using hybrid regression rate with thermal degradation and surface temperature data 02 p0270 A72-12260

Repeated stretching effect on triacetic fibers thermal destruction in vacuum after hot air or steam thermosetting 08 p1194 A72-21759

Differential thermal analysis for electrical insulation thermal degradation and thermogram shape, combining equations for required life line 09 p1339 A72-23271

Laser induced degradation as rapid reproducible method for characterization of inorganic materials exhibiting low vapor pressures at usual temperatures 10 p1433 A72-23953

Metal matrix composites deformation and mechanical properties prediction from component phases information, examining interface role, residual stress effect and thermal degradation 10 p1553 A72-24176

Space shuttle orbiter thermal protection system metal interaction with chemical environment during reentry, emphasizing degradation in dissociated oxygen [AIAA PAPER 72-262] 11 p1590 A72-25206

CdTe thin film solar cell room temperature prolonged operation instability, thermal degradation and performance improvement by gas adsorption removal 12 p1756 A72-28017

Studies on flame-resistant epoxy resin - Pyrolysis of tetra-brominated epoxy resin and flame-resistant mechanism. 18 p2704 A72-36519

Experimental investigation of optical aberrations, due to temperature deformation and convective fluxes, by using a nonequal-arm interferometer with a coherent light source 19 p2801 A72-37920

Reversible changes in polyethylene coating adhesion due to thermo-oxidative destruction of polyethylene 21 p3072 A72-40082

Thermal decay of an infrared-laser-heated arc plasma. 21 p3090 A72-40341

THERMAL DIFFUSION
 Dimer formation effect on thermal diffusion factor at low temperatures for krypton-argon system 03 p0391 A72-13749

Diffusion saturation effects on thermal stress concentration in plate with circular hole under edge heating and lateral surface heat transfer 03 p0451 A72-14124

Temperature fluctuation structure in turbulent wake behind heated circular cylinder, investigating thermal convection, production and diffusion [AD-740540] 04 p0596 A72-15330

Gegenbauer /ultraspherical/ polynomials and Meijer G-functions for solution of heat production and diffusion in cylinder with internal sources leading to axisymmetric temperature distribution 05 p0747 A72-16791

Reactive solid or fuel combustion, deriving equations for movement and deformation of reaction front during oxidant diffusion through ash mantle 06 p0902 A72-18155

Temperature distribution in composite media with internal heat generation, solving diffusion equation via Voldicka type orthogonality relationship 07 p1100 A72-19626

Thermal conductivity and thermal diffusion coefficients determination for plane plate heated unilaterally from above under fourth kind boundary conditions 08 p1252 A72-21313

Uniform and crowded temperature distribution in large geometry power transistor, solving time dependent heat diffusion equation 08 p1141 A72-21419

Thermal diffusion in solids subject to deformation, using classical elasticity theory body force analogy for variational and reciprocal theorems 09 p1403 A72-22757

Reduced mass and asymmetry differences effects on elastic collision integrals and thermal diffusion factors for isotopic hydrogen molecules 10 p1515 A72-24340

Thermal release patterns and activation energies of spallogenic He, Ne and Ar from Carbo iron meteorite 12 p1866 A72-27116

Apollo 11 and 12 lunar samples thermal properties, presenting diffusivity, conductivity and specific heat 12 p1869 A72-27334

Tungsten-rhenium alloys and tungsten self diffusion coefficient temperature dependence investigation, noting Re addition effects 14 p2114 A72-30402

Carbon resistance thermometers time response and thermal diffusivity measurements in liquid helium temperature range 15 p2234 A72-31581

Nonspherical thermal wave propagation, considering two dimensional structure wave front radiative diffusion problem 15 p2336 A72-32513

Metal melting heat relationship to diffusion activation energy with vacancy mechanism equal numerically to crystal internal energy maximum change 15 p2259 A72-32691

Study of the diffusion of iron and cobalt along the grain boundaries of tungsten 17 p2569 A72-35522

Thermionic converters performance and life tests, discussing test equipment and diffusion effect on emitter stability 18 p2643 A72-36139

Steady state heat transfer in one dimensional flow involving simultaneous convective and diffusive transport via finite difference formulation 18 p2741 A72-37171

Analytical and low-speed experimental diffusion-thermo effects in turbulent binary boundary layers. [ASME PAPER 72-HT-56] 20 p2985 A72-39660

Russian book - Heat and mass transfer: A reference book. 21 p3128 A72-40350

Modal control theory for distributed parameter systems with multicigenvalue assignment implemented for one dimensional diffusion equation 21 p3037 A72-40642

Diffusion toward a particle in the case of shear flow of a viscous liquid - Approximation of the diffusion boundary layer 22 p3165 A72-41910

Grain size and temperature effects on Cr and Al diffusion coefficients and mobility in Ni-20Cr and thoriated dispersed NiCr alloys from measurement at 1038-1200 C 22 p3193 A72-43028

Effect of grain size on the thermal diffusion of copper in aluminum. 22 p3193 A72-43036

Thermal diffusion annealing improved Ni-B composite electrolytic coatings with uniform B distribution over bulk matrix 23 p3303 A72-44012

Thermal diffusion and convective stability. II - An analysis of the convected fluxes. 24 p3465 A72-45561

THERMAL DIFFUSIVITY
 Thermal conductivity cell for dielectric materials powdered samples and thermal diffusivity and conductivity measurements, using line heat source principle 04 p0523 A72-15493

Electroconductivity, thermal conductivity and diffusivity, specific heat and emissivities of Ti at 1000-1700 K 07 p1010 A72-18935

Test facility for studying temperature dependence of thermal diffusivity and true heat capacity of metals between minus 150 and plus 400 C 07 p0982 A72-18941

Test facility for thermal diffusivity measurements in solids by method of plane temperature waves using periodic optical heating at 1500 K 07 p0982 A72-18942

Thermal and momentum diffusivity measurements in turbulent stratified flow, obtaining velocity and temperature profiles [AIAA PAPER 72-80] 07 p0966 A72-18950

Two and three dimensional quasi-static coupled thermal diffusivity problem for deformable body, determining physicomechanical state of solid circular cylinder under cyclic loads 07 p1090 A72-19752

Thermal diffusivity and heat capacity measurement by temperature vs time curve shape by laser pulse absorption, using thermocouple 07 p1101 A72-19890

Heat exchange effects in thermal diffusivity measurements in dielectrics by plane temperature wave method, applying to rock and mineral studies 08 p1251 A72-21095

Thermal diffusivity and conductivity and specific heat of hard electrode graphite intermediate medium in hydraulic hot extrusion of metals 08 p1181 A72-22072

Material removal nature during focused laser radiation action on substances with different thermal diffusivity coefficients 13 p1968 A72-29508

Thermal diffusivity measurements by laser flash technique for liquid metals at high temperatures 13 p1971 A72-29756

Optical measurement for simultaneous determination of transparent isotropic medium thermal diffusivity and conductivity 16 p2389 A72-32947

Semiconductor thermal diffusivity and heat capacity measurements, using carbon bolometer and high sensitivity point microthermistor 16 p2442 A72-33855

Directional dependence of the high-temperature thermal diffusivity of crystal-oriented pyrolytic graphite 18 p2704 A72-37180

Measurement of the thermal diffusivity of semiconductors by the light pulse technique 21 p3095 A72-40133

A determination of thermal diffusivity under transient conditions 24 p3465 A72-45067

THERMAL DISSOCIATION
 Germanium nitride thermolysis, discussing allotropic alpha and beta phases stability and activation energies 01 p0023 A72-10191

Cold pressed powdered boron nitride, Mo, W, Nb disulfides and diselenides, investigating thermal dissociation in He by X ray analysis 03 p0380 A72-13551

Thermal decomposition kinetics of tetramethylene tetranitramine beta HMX from differential thermal analysis and activation energy calculation 08 p1219 A72-20755

Hydrogen and helium thermal dissociation and ionization at Jupiter and Saturn adiabatic atmospheric models conditions 08 p1211 A72-21127

Cubic SiC film growth rate on Si substrate by methylchlorosilane decomposition in hydrogen flow, noting dependence on mixture flow rate and temperature 12 p1860 A72-28114

IR internal reflection spectroscopy application to dynamic chemical changes study on ammonium perchlorate surface during thermal decomposition, observing crystal lattice transformation 15 p2296 A72-32313

Dissociative recombination at elevated temperatures. I - Experimental measurements in krypton afterglows. 23 p3316 A72-44346

THERMAL EFFECTS
U TEMPERATURE EFFECTS
THERMAL EFFICIENCY
U THERMODYNAMIC EFFICIENCY
THERMAL EMISSION
NT THERMIONIC EMISSION
 Quiet solar corona thermal emission flux at 169 MHz, showing constant brightness and electron temperatures during cycle 01 p0123 A72-10045

Apollo 12 lunar samples exoelectrons of thermally stimulated emission, noting concentration of traps for radiation history measurement 01 p0124 A72-10063

Earth surface thermal radio emission measurements by UHF radiometry onboard Cosmos 243 satellite, showing brightness profiles of water, ice and land areas 01 p0053 A72-10363

Microwave measurement and interpretation of oceanic thermal emission in terms of molecular temperature 02 p0214 A72-11866

Synchrotron and thermal H II region radio emission in Magellanic Clouds 03 p0425 A72-13259

Atmospheric vertical temperature profile inference from ground based measurement of microwave thermal emission spectrum from atmospheric oxygen 08 p1161 A72-21824

Cygnus Loop supernova remnant X ray emission structure from sounding rocket spectral data, showing thermal emission mechanism 09 p1378 A72-23699

Jupiter spectral observations, discussing presence of deuterated methane in atmosphere and comparison with solar spectra for telluric features identification 10 p1539 A72-24347

High resolution observation of stratospheric submillimeter thermal emission spectrum by helium-cooled InSb electron bolometer on board Comet 2E aircraft 10 p1476 A72-25023

Lower atmosphere vertical temperature profiles determination from clear air ground based measurements of microwave thermal emission by oxygen 11 p1591 A72-25764

Isolation and sintering techniques and thermoemission properties of lanthanum, yttrium and gadolinium borides 11 p1645 A72-26858

Apollo 11 EASEP nickel resistance thermometer lunar surface data, presenting unshadowed equivalent brightness temperature and thermal parameters and emission directional dependence 12 p1869 A72-27330

- Solar absorptance and thermal emittance of thermal control coatings contaminated by thruster exhaust in vacuum environment
[AIAA PAPER 72-263] 12 p1846 A72-27865
- Thin plates and coatings in thermal contact with standard, determining total emissivity by inverse methods of heat conduction 12 p1889 A72-28115
- Spatial-temporal coherent processing technique application to thermal radio emission random signal reception, deriving ambiguity function 13 p1920 A72-29282
- Calibrated thermal emission spectra under extreme temperature, surface reststrahlen and cloud conditions from Nimbus 4 IR spectroscopy 15 p2223 A72-31510
- Galaxy M87 X ray source origin, suggesting hot plasma thermal emission or ejected relativistic electrons interacting with intergalactic magnetic or radiation fields 16 p2452 A72-33135
- Normal-mode expansion technique for unsteady radiative and conductive heat transfer in absorbing emitting isotropically scattering slab with reflective boundaries 16 p2478 A72-33438
- Radiation with free convection in an absorbing, emitting and scattering medium. 17 p2637 A72-35046
- Solar thermal radio burst temperature and emission measure determination from flux spectrum, noting consistency with radio observation 17 p2608 A72-35090
- Observations of planetary nebulae at 1.65 to 3.4 microns. 19 p2854 A72-37233
- Heat emission from the lower faces of plane surfaces in the presence of a steady thermal flux under conditions of natural convection 20 p2982 A72-39322
- Thermal emissivity and directivity for V groove and rectangular cavities, optimizing geometry and surface properties for maximum focusing of emitted energy [ASME PAPER 72-HT-L] 20 p2984 A72-39651
- Thermal remote sensing of temperature distribution in semitransparent solids - A numerical experiment. [ASME PAPER 72-HT-5] 20 p2986 A72-39676
- Conceptual possibilities of studies of moisture content in the atmosphere from thermal radio emission in the submillimeter wavelength range 21 p3078 A72-41798
- Compton scattering by thermal electrons in X-ray sources. 23 p3328 A72-43230
- On the validity of a generalized Kirchhoff's Law for a nonisothermal scattering and absorptive medium. 24 p3424 A72-44698
- THERMAL ENERGY**
- Thermally excited E layer tidal winds based on UV radiation as thermal source, using isothermal atmosphere model 01 p0055 A72-10429
- Kink movement and cutting forest dislocation models of creep in thermally activated crystalline solids 01 p0140 A72-10857
- Rarefied gases thermal energy diffusion model, using radiative transfer electrical network analog [ASME PAPER 71-WA/HT-4] 05 p0743 A72-15865
- Welding thermal energy effect on residual ferrite of austenitic chrome-nickel steel deposits 07 p1010 A72-18971
- Mechanical energy consumption effects of thermal dissipation and cyclic straining methods during sample life tests 07 p1089 A72-19260
- Local and macroscopic thermal transport in turbulent air stream, discussing measurement from calorimeter instrumented sphere 10 p1417 A72-24148
- Shock response of two constituent composites /Eikonites/, predicting Hugoniot states with allowance for thermal energy transfer 10 p1556 A72-24259
- Thermal energy reaction rates determination for partial charge transfer chemical reactions, comparing with electron transfer efficiencies 10 p1514 A72-24336
- Absorbing sphere model for ion-ion recombination upper limit thermal energy reaction rate and total cross section energy dependence 10 p1515 A72-24342
- Atmospheric metal ion chemistry, tabulating thermal energy binary and three body reaction rate data 10 p1434 A72-25160
- Magnetic field effect on ruby laser generated plasma in solid target, measuring thermal ion energy increase 12 p1852 A72-27879
- Fusion welding of Ti-W and Ti-graphite composites, determining weldability and effect of weld thermal energy on fiber matrix reactions 13 p1966 A72-29423
- Stellar winds and breezes classification using energy flux and particles kinetic and thermal energies for criteria, noting coronal temperature effects 15 p2313 A72-32298
- Parabolic differential equations to define exponential spatial decay of heat equation solutions, replacing Edelman energy estimate by time-independent estimate 16 p2475 A72-33005
- Magnetic field effect on ruby laser generated plasma in solid target, measuring thermal ion energy increase 16 p2439 A72-33988
- Physics of strengthening mechanisms in crystalline solids. 19 p2843 A72-37444
- Low energy cosmic particle and soft X ray photon produced nonthermal electrons effect on interstellar gas ionization and thermal energy equilibrium 19 p2867 A72-38508
- Thermal energy dissipation in artificial antennas of large broadcasting transmitters studying cooling systems 23 p3278 A72-44311
- Physical limits of semiconductor devices miniaturization for electronic computers, considering thermal energy dissipation, electrical resistance and high current density induced electromigration effects 23 p3273 A72-44332
- THERMAL ENERGY STORAGE**
- U HEAT STORAGE**
- THERMAL ENVIRONMENTS**
- Thermal environment and fuel region simulation for nuclear light bulb engine, using rf induction heater and uranium and tungsten hexafluorides injection 01 p0113 A72-11355
- Fracture mechanical analysis for stability criteria and propagation behavior of thermal stress cracks in brittle ceramics in severe thermal environments 09 p1333 A72-22382
- Mathematical model of skin contact cooling tube device for human body thermoneutrality maintenance in various environments 09 p1270 A72-22821
- Environmental applications of airborne IR imagery, discussing detection, mapping and monitoring of water bodies thermal patterns and anomalous heat manifestations on land 09 p1312 A72-23301
- Thermal shock and temperature cycling environmental testing, discussing military specifications, components thermal lag characteristics, environmental test chambers and various cooling methods 10 p1459 A72-24144
- Underwater tests of instrument system for combined skin temperature and direct heat flow measurement in thermally stressful environments 12 p1768 A72-28334
- Optimal temperature control for microbial inactivation by composite environment of heat and gamma radiation, using quadratic technique 18 p2649 A72-36313
- The effect of a thermal and ultrahigh vacuum environment on the strength of precompressed granular materials. 22 p3173 A72-42528
- THERMAL EXPANSION**
- NT THERMAL BUCKLING**
- Internal electrostatic field effect on ion separation in expanding pulsed laser produced plasmas 01 p0105 A72-10021
- Zr and V linear thermal expansion coefficients explanation by alpha Zr hexagonal crystal lattice anisotropy 03 p0376 A72-13946
- Thermal deformation effects on metal bond fatigue failure modes in small signal transistors, micro and LSI circuits 03 p0365 A72-14291
- Pyroelectric IR detectors hf performance in direct and heterodyne modes, including thermal expansion effects 04 p0563 A72-15603
- Thermally expanding surface effects on aerodynamic roll torques on smoothly ablating spinning cones, comparing analytic study and hypersonic wind tunnel test results 05 p0608 A72-16923
- [AIAA PAPER 72-30] Electromagnetic wave propagation and thermal spread in uniform magnetoplasma at electron-cyclotron resonance frequencies, discussing kinetic and multifluid theory 06 p0854 A72-17489
- Stress fields around moving weld arc on Al sheet from isotherm map, calculating compressive and tensile stresses from heat induced material expansion 06 p0820 A72-17705
- Alloying additives effects on Ti and Zr resistivity, thermal expansion, crystal lattice parameters and polymorphous transformations temperatures 07 p1017 A72-19990
- Thermoelastic characteristics and crystal phase distribution effect on microstructural stresses and thermal expansion of polycrystalline refractory materials 07 p1018 A72-20133
- Al and Al-Si alloy thermal expansion at low temperatures, noting near-eutectic crystalline composition 07 p1019 A72-20156
- Graphite fiber reinforced composites with high mechanical strength and modulus at low weights, fatigue resistance, vibration damping and tailorable thermal expansion coefficient 08 p1193 A72-21689
- Reinforcing fiber frame incurvation influence on elasticity and thermal expansion coefficients of composite material 08 p1194 A72-21754
- Carbon-phenolic composite ablation and expansion in thermal environment during reentry shielding, using flight and simulation tests 11 p1669 A72-25390
- [AIAA PAPER 72-363] Thermal expansion measurements on graphite reinforced plastics, using Leitz dilatometer 11 p1670 A72-25460
- Liquid Rb and Cs density and thermal expansion measurements near fusion point, discussing temperature dependence and gamma ray irradiation method 11 p1746 A72-26237
- Ti-Mo-Ni system polythermal section microstructure, hardness, resistivity and thermal expansion characteristics 14 p2112 A72-30153
- Thermal expansion - Conference, Corning, New York, October 1971 15 p2259 A72-31254
- Ribbon glass effect on thermal expansion of reinforced thermoplastic composites, comparing with fiber reinforced materials 15 p2259 A72-31255
- Thermal expansion of carbon-carbon composites as function of temperature and fiber orientation by dilatometric measurements 15 p2260 A72-31256
- Thermal expansion in simple solids and structural composites due to anharmonic vibrations, using atomic density model 15 p2322 A72-31257
- Thermal expansion measurements of simulated volcanic and nonvolcanic lunar rocks as function of temperature 15 p2222 A72-31258
- Temperature effect on bonding strength between ceramic whiskers or fibers and metal matrices attributed to thermal expansion coefficients disparity 16 p2413 A72-33206
- Adhesion effects on tensile and thermal expansion properties of aluminum oxide particles filled epoxy-urethane polymer at ambient and liquid nitrogen temperatures 16 p2415 A72-33415
- Influence of cerium, lanthanum, neodymium, and boron on the critical points and the linear expansion coefficient of K17N2 steel 17 p2569 A72-35523
- Thermal expansion at elevated temperatures. III - A hemispherical laminar composite of pyrolytic graphite, silicon carbide and its constituents between 300 and 800 K. 19 p2822 A72-37463
- Correctness of boundary conditions in the method of measuring the heat exchange coefficient by the rate of the thermal deformation of samples 19 p2881 A72-38038
- Rational utilization of the strength capabilities of thermal-expansion compensators 21 p3127 A72-41702
- Thermal expansion coefficients of some fiberglass-reinforced plastics and their components under conditions of low and high temperatures 21 p3074 A72-41715
- Free oscillations of the sun and their possible stimulation by solar flares. 22 p3219 A72-42570
- Thermal and electrical conductivities, thermal expansion and specific heat of commercial graphite obtained by precipitation of methane pyrolysis products on hot surface 23 p3306 A72-43689
- Interferometric measurement of the elongation of a pulsed diode laser. 23 p3297 A72-44185
- Thermoelastic characteristics and crystal phase distribution effect on microstructural stresses and thermal expansion of polycrystalline refractory materials. 24 p3416 A72-45759
- THERMAL FATIGUE**
- Thermal shock fatigue tests on aircraft gas turbine engine inlet nozzles, showing cracks as function of material 01 p0143 A72-11373
- Automatic device for thermal and thermomechanical fatigue tests of steel specimens, noting crack nucleation and growth by hardening due to lattice defects 02 p0200 A72-11996
- Superalloys for gas turbine rotor and stator blades, testing long term heating effects on microstructure and mechanical and thermal fatigue properties 05 p0675 A72-16495

INCO 713C and IN 100 cast Ni base alloy gas turbine blades under thermal fatigue tests
05 p0675 A72-16497

Microstructure properties of heat resistant alloy for gas turbine blades as function of operational time
06 p0832 A72-18360

Gas turbine blades fatigue crack development and failure analysis under thermal cycling tests, considering chemical processes and thermal and mechanical stresses
06 p0898 A72-18550

Low cyclic failure resistance at elevated temperatures and static defects calculation based on fatigue and empirical endurance curves
06 p0898 A72-18555

Gas turbine blades thermal fatigue test and analysis, investigating static tensile loading effects on heat resistance under thermal cycling
06 p0899 A72-18556

Metal fatigue strength testing under programmed temperature regimes, using HF induction generator
12 p1796 A72-28247

Design and operation of experimental facility for thermal fatigue testing of heat resistant materials
13 p1939 A72-29145

Creep damage role in governing elevated temperature strain cycling fatigue lives of heat resistant stainless steel and cobalt alloy
19 p2817 A72-37712

Thermal fatigue resistance of KhN70VMiU boronized alloy
20 p2941 A72-39585

A study on the correlation between thermal fatigue and low-cycle fatigue at elevated temperatures.
21 p3119 A72-41008

Thermoplastics fatigue life dependence on stress with allowance for heating laws, noting heat accumulation effect on thermal failure
22 p3196 A72-42164

Investigation of the thermal fatigue of Kh18NiOT steel under complex stress-strain state conditions
23 p3301 A72-43956

Microstructure properties of heat resistant alloy for gas turbine blades as function of operational time
24 p3416 A72-45747

THERMAL INSTABILITY

Radiative cooling induced thermal instability mechanism for condensation in astrophysical plasma
07 p1040 A72-19348

Atmospheric free convection turbulence and diffusion, proposing statistical characteristics and formulas with horizontal thermal flux vertical and transverse velocity components
07 p1031 A72-20697

Three dimensional heat diffusion equation for multi-emitter power transistor, taking into account thermal instability due to geometry
08 p1141 A72-21418

LF self oscillation processes associated with burning powders, showing origin in thermal relaxation instability in heated condensed phase layer
09 p1411 A72-22883

Asymmetry and intermittency factors of temperature and velocity fluctuations in viscous substrate of hot plate turbulent boundary layer
10 p1464 A72-24064

Galactic formation initiation mechanism with thermal instability in expanding universe, noting Compton scattering energy exchange ensuring gravitational instability dominance
13 p2039 A72-29086

Thermal drift of floated spherical gyroscope calculation based on two dimensional free convection analysis of supporting fluid
15 p2235 A72-31727

Rayleigh-Brillouin light scattering in He-Xe gas mixtures, noting thermal fluctuations effect
16 p2422 A72-32943

Galactic magnetic field origin and large scale instability associated with Galactic field and cosmic rays, discussing thermal instability in interstellar gas
16 p2460 A72-33922

Atmospheric free convection turbulence and diffusion, proposing statistical formulas for components of horizontal thermal flux, vertical and transverse velocity and free diffusion tensor
20 p2948 A72-39012

Influence of thermal instability on the convective heat transfer coefficient for flows past slender bodies of arbitrary configuration
20 p2987 A72-39914

High strain rate and thermal instability torsional-impact machines for metal dynamic testing, using shear pin mode control
21 p3039 A72-40229

Study of the operation of a neodymium glass laser under nonsteady thermal conditions, with thermal insulation of the active element by air
22 p3185 A72-42172

Theory of thermal fluctuations in nonequilibrium systems
22 p3206 A72-42659

A nonacoustic wave instability of processes in a solid-fuel engine
22 p3217 A72-43182

Measurements of air motion in regions of clear air turbulence using high-power Doppler radar.
24 p3421 A72-44978

THERMAL INSULATION

High temperature insulation for radiative thermal protection system of space shuttle orbiter, evaluating survival chances under acoustic, vibration and thermal loads
01 p0091 A72-10760

Space shuttle reusable surface insulation thermal protection system, discussing thermal stress distribution, failure modes and mechanical properties
01 p0091 A72-10761

Reusable external thermal insulation multilayer for space shuttle vehicle, presenting conductivity, expansion coefficient, specific heat, stability, tensile strength and strain capability
01 p0091 A72-10762

Adhesive materials based on room temperature vulcanizing silicone elastomers for space shuttle vehicle reusable surface insulation bonding
01 p0075 A72-10763

Discretely oriented thread reinforced polyurethane cryogenic foam insulation systems for liquid hydrogen fuel tanks [MDAC-WD-1756]
01 p0092 A72-10981

One dimensional heat insulated structure under dynamic loads, showing thermoviscoelastic effects on spontaneous heating and stress-strain state
03 p0444 A72-13460

Heat conduction in vacuum insulated capillaries to prevent failure of level indicators and controllers based on condensation in evaporating cryogenic liquid
03 p0456 A72-13883

Thermal stress concentration at heat insulated holes in orthotropic plate, assuming external-load free contour
03 p0452 A72-14134

Nerve structures localized cooling device using vacuum insulated closed circuit controlled cryogenic probe with cooling range of plus/minus 20 C
04 p0481 A72-15252

Analytical model of thermal/structural optimization for long term storage cryogenic propellant systems [AIAA PAPER 72-142]
05 p0691 A72-16881

Partially insulated homogeneous cylinder temperature distribution from heat conductivity boundary value problem equations
05 p0751 A72-17142

Soviet book on superduty refractory porous ceramics covering preparation, structure and properties as thermal insulators, high temperature filters and catalyst carriers
06 p0836 A72-18520

Heat transfer in shield-vacuum thermal insulation layers at various temperatures and pressures, noting conductivity anisotropy
08 p1253 A72-21451

Performance characteristics and limitations of electrode and insulation materials for open and closed cycle MHD generators, noting ceramic compositions for channel
09 p1335 A72-22401

ELDO launch vehicle cryogenic tanks fabrication, discussing Al alloy selection and mechanical properties at low temperatures, manufacturing processes and thermal insulation
09 p1318 A72-22690

Thermal insulations in form of thin shells of revolution with rigid external and elastic internal layers resting on rigid core
09 p1400 A72-22713

Aircrews tolerance to cold water and life raft exposure, discussing prediction model based on thermal insulation effectiveness, assumed metabolism and body surface area and mass [AD-740276]
10 p1428 A72-23734

Venus probes thermal insulation materials development and testing under simulated Venus atmospheric conditions
11 p1744 A72-25393

Reusable external insulation materials for space shuttle thermal protection, evaluating local heat transfer at interface areas in plasma arc test facility [AIAA PAPER 72-388]
11 p1744 A72-25409

Space shuttle orbiter reentry heat shield materials, considering hot structures and hot radiative metallic, ceramic insulative and ablative heat shields
11 p1660 A72-26245

Structural design characteristics of low density fiber ceramic materials coated with refractory ceramics for space shuttle reusable surface insulation thermal protection systems
13 p2056 A72-28957

Heat losses due to spacecraft installation discontinuities on aluminized Mylar multilayer insulation, predicting blanket performance [AIAA PAPER 72-285]
14 p2171 A72-30829

Free convection effect on vertical porous insulation layer thermal conductivity in high pressure gas environment
14 p2172 A72-31057

Limiting ratio between ideal gas densities before and behind vertical shock wave in elastic thermal insulators
15 p2334 A72-31475

Statistical solution to unsteady heat conduction through flat multilayer insulating wall, using random walk method
16 p2477 A72-33407

Minimum weight passive insulation requirements for hypersonic cruise vehicles.
17 p2638 A72-35256

The manufacture of multilayer reusable surface insulation materials for space shuttle.
18 p2695 A72-36527

Zero-gravity thermal performance of the Apollo cryogenic gas storage system.
19 p2869 A72-38830

Structural thermal protection systems for Space Shuttle, noting reusable surface insulation with active cooling [ASME PAPER 72-ENAV-32]
20 p2976 A72-39145

The computation of dynamic equilibrium temperature distributions on substrates having a temperature-dependent thermal conductivity.
20 p2908 A72-39499

Mercury Hall ion engine principles and design, discussing plasma ion acceleration, mercury evaporation and ionization and acceleration channel electrical and thermal insulation
20 p2963 A72-39937

Heat transfer by radiation in a glass fiber insulator
22 p3243 A72-41891

Study of the operation of a neodymium glass laser under nonsteady thermal conditions, with thermal insulation of the active element by air
22 p3185 A72-42172

Facility for studying the thermophysical properties of materials by quasi-stationary methods
22 p3176 A72-42289

Aerospace vehicle passive thermal protection systems heat shield and bulk insulation estimation by weight prediction in conceptual phases of design [SAWE PAPER 934]
23 p3356 A72-43474

Despun conical flight vehicles eccentric insulation mass properties history, deriving preflight and in-flight equations for weight, center of gravity coordinates and moments and products of inertia
23 p3342 A72-43478

One dimensional heat insulated structure under dynamic loads, showing thermoviscoelastic effects on spontaneous heating and stress-strain state
24 p3458 A72-44935

THERMAL NEUTRONS

Epithermal neutrons energy spectra in atmospheric equilibrium layers at 57 geomagnetic N, noting agreement with experimental error limits
02 p0273 A72-11918

Epithermal neutron differential flux spectrum in equilibrium layers of atmosphere at 57 degrees north
07 p1066 A72-20652

Thermal neutron radiography industrial applications, describing nondestructive testing techniques
10 p1485 A72-23813

Thermal neutrons anomalous absorption by indium antimonide crystals, determining absorption coefficient by integral reflectivity measurements
10 p1527 A72-24980

Epithermal neutrons energy spectra in atmospheric equilibrium layers at 57 geomagnetic N, noting agreement with experimental error limits
13 p2030 A72-29230

The potential of a laser-induced fusion device as a thermal-neutron source.
17 p2591 A72-35353

Thermal neutron radiography as NDT technique for industrial inspection, noting advantages for low atomic number and radioactive materials
18 p2695 A72-36457

THERMAL NOISE

Synchronized multiple microwave oscillators power and noise characteristics at microwave and millimeter frequencies, discussing magic T configuration
01 p0037 A72-10648

Lf noise measurements of mercury telluride and Cd-Hg-Te semiconducting thin films using vacuum tube preamplifier and step-up transformer
02 p0268 A72-11523

Thermal zero signal instabilities and error reduction in devices using reluctance sensors
02 p0231 A72-12562

G-r noise in intrinsic photoconductors for Auger band-to-band radiative recombination
06 p0865 A72-17365

Noise effect in IMPATT and Gunn diode oscillators on phase/frequency fluctuation using series/parallel connected multiple active devices
06 p0783 A72-17483

Thermal noise and ion-acoustic waves excitation in Q machine two beam plasma with high temperature ratio in presence of inhomogeneous B-field, observing instability
06 p0856 A72-17517

Statistical model of signal amplitude distribution and thermoelectron noise of photoelectron multiplier
06 p0816 A72-17837

Motion dynamics of aircraft-autopilot closed loop system under influence of atmospheric turbulence and electric circuitry thermal noise
07 p0911 A72-18990

- Low frequency modulation noise generation due to conductance fluctuations in Gunn oscillators, measuring noise spectra temperature dependence
07 p0954 A72-19050
- FM mf equipment for 2700-channel Hertzian beam, considering thermal noise, intermodulation and equivalent distortion of amplifiers, discriminator, limiter, etc
07 p0954 A72-19190
- Reflected signal and receiver noise interference error in antenna temperature and calibration measurements by artificial moon method in centimeter and decimeter bands
08 p1142 A72-21726
- Transistor LF flicker background noise generation mechanism in terms of bulk effect due to temperature fluctuation or phonon electron interactions
09 p1286 A72-23107
- Background noise in FETs with junction gate, formulating hypothesis of warm carriers for transistor channel
09 p1287 A72-23110
- Excess, shot and channel thermal noises performance-limiting effects on junction FETs in high input impedance applications, considering minimization method
09 p1287 A72-23111
- HF thermal noise in single and double injection space charge limited solid state diodes
09 p1288 A72-23124
- IMPATT diode and transferred electron Gunn devices for systems applications, comparing thermal noise and physical properties
12 p1788 A72-27295
- Noise behavior of GaAs Schottky barrier FET with short gate length, showing channel thickness effect on intervalley scattering noise
12 p1790 A72-27439
- Thermal and shot noise and distortion in charge-coupled semiconductor devices used for imaging applications
12 p1791 A72-27673
- Correlation measurements of LF current noise and frequency fluctuations in Gunn oscillators, emphasizing generation-recombination noise component
14 p2088 A72-30916
- Distributed tunnel diode traveling wave amplifier load noise thermal and shot components, noting impedance boundaries
15 p2206 A72-31663
- Noise in bipolar junction transistors at low temperatures.
18 p2666 A72-36323
- FET noise at high temperatures.
18 p2666 A72-36324
- Thermal effects in JFET and MOSFET devices at cryogenic temperatures.
18 p2666 A72-36453
- Temperature dependence of low-frequency excess noise in junction-gate FET's.
18 p2666 A72-36454
- Thermal noise in double injection diodes operating in the insulator regime.
18 p2667 A72-36979
- French monograph - Ultrahigh-performance frequency generators
19 p2772 A72-37488
- A general analysis of noise in Gunn oscillators.
20 p2909 A72-39782
- Impulse noise in FM receivers in the presence of adjacent channel interference and thermal noise.
21 p3020 A72-40894
- Electrical fluctuations in ideal straight-staggered nondegenerate diodes
21 p3033 A72-40945
- SNR improvement by negative feedback and deterioration by positive feedback in amplifiers, discussing input circuit thermal noise
21 p3034 A72-41123
- Construction and operation of a Weber-type gravitational-wave detector and of a divided-bar prototype.
21 p3057 A72-41486
- THERMAL PLASMAS**
- Neutron production mechanism and energy spectrum in thermal plasma focus by time of flight spectrometry
01 p0109 A72-10243
- Electromagnetic wave propagation across external magnetic field in contraststreaming thermally anisotropic plasmas, investigating plasma stability
04 p0556 A72-14942
- Cylindrical positive probe behavior in high speed collisionless mesothermal plasma flow
[ONERA, TP NO. 1000]
05 p0660 A72-15860
- Dispersion relation for electrostatic plasma waves propagation at frequencies near electron cyclotron harmonics in warm magnetoplasma, determining refractive index curves
05 p0698 A72-17023
- Nighttime plasmopause and thermal ion plasma structures relationship to micropulsations, considering excitation in post storm recovery and diurnal plasma bulge regions
06 p0804 A72-17453
- Electrostatic wave propagation and damping in thermally ionized collisionless alkali plasma, determining electron and ion densities, electron temperature and ion distribution function
06 p0856 A72-17521
- Hard X ray emission by thermal plasma, applying relativistic corrections to photon bremsstrahlung Maxwell distribution and cross section
06 p0873 A72-18004
- Ground plane absorption coefficient effects on admittance of slot antenna radiating into warm lossy plasma
07 p0957 A72-19797
- Thermal plasma origin of solar X-ray emission and far UV flash observation during 28 August 1966 proton flare
07 p1060 A72-20013
- Electromagnetic wave propagation obliquely incident on thermal inhomogeneous plasma at frequencies near second electron cyclotron harmonic
09 p1365 A72-23521
- Electromagnetic wave propagation perpendicular to magnetic field in two-component warm plasma, obtaining dispersion relations for transverse waves
10 p1520 A72-24350
- Spectral measurements of temperature in low temperature plasma, describing line reversal method
10 p1485 A72-25110
- Electronic partition functions cut-off criteria effect on translational and reactive thermal conductivity and viscosity of thermal plasmas
11 p1698 A72-26602
- Electromagnetic wave absorption in warm homogeneous plasma under static magnetic field parallel to surface, taking into account plasma-vacuum boundary conditions
13 p2012 A72-29123
- Magnetosphere thermal plasma densities determination from hydromagnetic whistler digital sonograms and modified normalized dispersion curves
15 p2283 A72-31430
- The effect of ionization on heat transfer to wires immersed in a highly thermally-ionized plasma.
17 p2637 A72-34998
- Statistical model of chemical reactions in nonisothermal low pressure plasma.
18 p2715 A72-36567
- Electric dipole radiation at VLF in a uniform warm magneto-plasma.
19 p2840 A72-37833
- Kr I and II lines strength and relative transition probabilities, using thermal plasma behind reflected shock wave as spectroscopic light source
21 p3089 A72-40137
- Averaged equations of simultaneous hydrodynamic expansion and thermal heating of two-temperature plasma, taking the recovery of thermonuclear fusion into account. I - The plane problem. II - The spherical problem.
21 p3093 A72-41476
- Spatial and temporal variations of thermal plasma ion and electron densities as function of L at 3000-5700 km from polar orbiting OV 3-1 satellite observation
22 p3211 A72-42414
- Propagation of electromagnetic waves in a weakly ionized warm magnetoplasma.
22 p3155 A72-42991
- Self-ignited impulsive optical discharge in a laser erosion plasma
23 p3295 A72-43308
- THERMAL POLLUTION**
- Trajectory and flow properties of submerged heated effluents discharging into moving waterway
[AIAA PAPER 72-79]
05 p0659 A72-16912
- Heat transfer research review, discussing gas turbines, aeronautics, astronautics, nuclear power, thermal pollution and controlled fusion challenges
09 p1412 A72-23684
- Airborne remote sensing missions and instrumentation to investigate Penobscot River water ecology for thermal, chemical and solid pollutants
15 p2221 A72-31252
- Numerical climatic-change experiments - The effect of man's production of thermal energy.
20 p2947 A72-38962
- Detection of waste water effluents and of their surface spread in the English channel, the North sea and the Baltic sea, through determination of the surface temperature of the sea by means of infrared air pictures taken by satellites
24 p3398 A72-45223
- THERMAL POWER**
- U TURBOGENERATORS**
- THERMAL PROPERTIES**
- U THERMODYNAMIC PROPERTIES**
- THERMAL PROTECTION**
- Multiple reentry effects on space shuttle thermal protective superalloys mechanical properties, presenting cyclic simulation results for different temperatures, pressures and stresses
01 p0084 A72-10754
- Test program to evaluate metallic materials candidates for space shuttle booster thermal protection system
01 p0085 A72-10755
- Coated Nb alloys as radiative thermal protection system skin materials for space shuttle, investigating flaw growth
01 p0085 A72-10757
- Field repair of Nb alloy panels with protective coatings designed as part of space shuttle thermal protection system
01 p0091 A72-10758
- High temperature insulation for radiative thermal protection system of space shuttle orbiter, evaluating survival chances under acoustic, vibration and thermal loads
01 p0091 A72-10760
- Space shuttle reusable surface insulation thermal protection system, discussing thermal stress distribution, failure modes and mechanical properties
01 p0091 A72-10761
- Silica based surface insulation material for space shuttle thermal protection system, discussing cyclic tests in simulated environment and fiber purity effects on crystallization
01 p0091 A72-10764
- Space shuttle low density ablative thermal protection systems, emphasizing low cost refurbishment techniques
01 p0091 A72-10766
- Multilayer insulation materials for reusable space vehicles thermal protection and radiation shielding, tabulating thermal conductivity values for various materials
01 p0092 A72-10780
- Oxidation screening at 2200 F of Ni, Fe and Co wrought alloys for space shuttle thermal protection system, noting microstructural changes
01 p0085 A72-10781
- Space shuttle thermal protection system, discussing oxidation resistant coatings, refractory metals, heat shield technology, ballistic reentry programs, weight and cost
01 p0135 A72-10935
- Plasma arc testing of space shuttle Nb and Co alloys thermal protection materials, using IR radiometric and photographic techniques
01 p0048 A72-10977
- Arc jet simulation tests of thorium dispersed Ni and Co alloys for space shuttle Metallic Thermal Protection System, determining material degradation
01 p0086 A72-10978
- Nondestructive tests of Nb alloy radiative thermal protection heat shield design for space shuttle requirements
01 p0048 A72-10980
- Niobium alloy for reentry vehicle heat shields, describing slurry coating process reliability
01 p0077 A72-10982
- ALSEP structural/thermal/ design, outlining package hardware configuration, passive thermal protection and materials selection procedures
04 p0508 A72-15093
- Azur satellite temperature control system for protection against internal heat dissipation and external thermal loads due to earth radiation and albedo
04 p0582 A72-15651
- Thin wall airframe wire insulation relative thermal life and temperature rating evaluation procedure using Arrhenius plot
09 p1339 A72-23270
- High purity fine particle pigment materials preparation for spacecraft thermal control coatings, discussing hydrothermal, cryochemical and vapor phase processes
10 p1500 A72-24145
- Metallic materials for delta wing space shuttle configuration with metallic thermal protection system
10 p1498 A72-24876
- Space shuttle thermal protection refurbishment labor costs and techniques, noting motion studies results for maintenance tasks in terms of manpower and performance time
[AIAA PAPER 72-374]
11 p1726 A72-25398
- Space shuttle booster and orbiter thermal protection systems, examining heat sink, metallic radiative, reusable surface insulation and surface cooled designs
[AIAA PAPER 72-391]
11 p1726 A72-25412
- Manufacturing process for dispersion strengthened nickel-chromium-thorium dioxide alloys for space shuttle thermal protection system panels, discussing joining optimization and mechanical properties
11 p1659 A72-26035
- Analytical prediction of pressure-time relationship during evacuation of multilayer insulation thermal protection systems, taking into account outgassing effects
14 p2172 A72-30925
- Thermally protective life rafts and clothing evaluation for cold sea survival potential assessment and tolerance limit determination
14 p2081 A72-31088
- Thermal protection by liquid-gas laminar flow near critical point with coolant film liquid oxygen injection incident on blunt body
16 p2343 A72-33156
- Carbon-carbon composites for space shuttle reentry thermal protection.
17 p2572 A72-35667

- Structural thermal protection systems for Space Shuttle, noting reusable surface insulation with active cooling
[ASME PAPER 72-ENAV-32] 20 p2976 A72-39145
- Thermal control design for research applications module /RAM/ shuttle compatible payload carriers, using Freon 21-water system
[ASME PAPER 72-ENAV-31] 20 p2894 A72-39146
- Thermal control system incorporation into lunar roving vehicle /LRV/ for electronic component protection during translunar transportation and lunar surface operation
[ASME PAPER 72-ENAV-27] 20 p2894 A72-39150
- Panel-flutter analysis of a thermal protection shield concept for the space shuttle.
20 p2980 A72-39623
- The development of the Apollo entry thermal protection system.
21 p3115 A72-41124
- Aerospace vehicle passive thermal protection systems heat shield and bulk insulation estimation by weight prediction in conceptual phases of design
[SAWE PAPER 934] 23 p3356 A72-43474
- Space shuttle optimal entry trajectories for thermal protection system weight minimization, considering constant and variable angles of attack
[AIAA PAPER 72-977] 24 p3452 A72-45414
- THERMAL RADIATION**
- NT PHONON BEAMS**
- Tungsten heat capacity, electrical resistivity and thermal radiation measurement over 2000-3600 K range by pulse heating technique
01 p0082 A72-10174
- Atmospheric thermal sounding from meteorological satellites, reviewing measurement accuracy, equation kernel, spectral resolution, optimum measuring condition and interpretation techniques
01 p0070 A72-10959
- Differential thermal radiation scattering coefficients of submicron W refractory particles in hydrogen and nitrogen at temperatures to 1080 K
01 p0112 A72-11341
- Calorimetric and radiometric methods for thermal radiation properties of solids, considering reflectance, absorptance, transmittance and spectral emittance
02 p0223 A72-11499
- Thermal IR remote sensing of surface geothermal heat flow, presenting nighttime heat budget equation based on solar and geothermal energy
02 p0208 A72-11786
- Quantitative cloud information from satellite IR thermal imagery and vertical temperature profile data
02 p0211 A72-11808
- Thermal IR radiation attenuation by atmospheric particulates, comparing computer simulated brightness temperatures with airborne radiometer and Nimbus 3 observed data
02 p0213 A72-11863
- Thermal modeling for IR images geologic interpretation, discussing physical parameters role in materials natural environmental diurnal temperature behavior
02 p0214 A72-11877
- Earth surface remote sensing with thermal IR radiation, investigating uncovered soils with heat balance equations under various weather conditions and times of day
02 p0172 A72-12017
- Graphite, Mo, Ta and W thermal radiation total emittance measurement in 1200-2400 K range, evaluating recorded data by computer program
02 p0243 A72-12101
- Coupled thermoelasticity in infinite body with cavity, introducing Sommerfeld type scalar potential and temperature radiation conditions
02 p0259 A72-12236
- Hydrodynamics of matter-antimatter system embedded in thermal radiation, observing coalescence effect
03 p0416 A72-13013
- Solar energy exchange by thermal radiation, investigating monochromatic emission factors at 0.3-15 micron
04 p0596 A72-14702
- Human skin thermal radiation properties, presenting data on reflection, emission, transmission and complex refraction
[ASME PAPER 71-WA/HT-37] 05 p0620 A72-15888
- Radiation thermometry trends, considering photodetectors, optical pyrometers and filters
[ASME PAPER 71-WA/TEMP-3] 05 p0661 A72-15909
- Thermal signal propagation in flowing fluid, plane, line and point sources of varying heat, calculating temperature distribution with conduction and convection heat transfer equation
05 p0746 A72-16295
- Monochromatic radiation pulse transfer in absorbing plasma, deriving heat wave propagation velocity
05 p0696 A72-16680
- Wall thermal radiation influence on solid propellants burning rate in electrically heated tube furnace, noting correlation with laminar flame theory
[AIAA PAPER 72-35] 05 p0703 A72-16938
- Thermal IR imaging remote sensing device for aerial earth resource surveys, noting hydrogeology, volcanology, forest fire and geothermal region detection and ice sheet study applications
06 p0807 A72-17789
- Indirect reduction of vertical atmospheric water vapor profile from measured outgoing thermal radiation by regularization method
06 p0842 A72-18039
- Earth upper atmosphere outgoing thermal radiation radiance calculation in near IR spectrum
06 p0808 A72-18041
- Thermal emittance measuring methods for solids at temperatures above 1500 K, discussing emittance dependence on surface characteristics
06 p0818 A72-18253
- Nonlinearly radiating semiinfinite heat conducting solid surface temperature, expressing heating rate as nonnegative integrable function of time
[AD-743553] 07 p1098 A72-18814
- Radiative thermal flux model of Venus atmosphere, using Venera data and greenhouse effect
08 p1233 A72-21193
- Rock type discrimination from radioed airborne thermal IR scanner images of Pisgah Crater /California/
08 p1162 A72-22018
- Seyfert galactic nuclei structure, discussing thermal X rays indication of significant random motions and difficulty of energy source determination
09 p1386 A72-22686
- Environmental applications of airborne IR imagery, discussing detection, mapping and monitoring of water bodies thermal patterns and anomalous heat manifestations on land
09 p1312 A72-23301
- Thermal radiative cooling system characteristics determination, taking into account surface material thermal conductivity and blackness degree dependence on temperature
10 p1561 A72-23840
- Nonstationary radiative heat transfer between cylindrical body and ambient medium, determining regular heating condition region
10 p1561 A72-23842
- Thermal radiation effects on natural convection boundary layer adjacent to vertical flat surface with uniform heat flux input
10 p1562 A72-24466
- Sco X-1 simultaneous hard X ray and optical observations from balloon and ground correlating thermal X rays and optical emissions
10 p1530 A72-24949
- Energy transfer in thermally developing laminar gas flows with radiative interaction, using total band absorptance model
[AD-745475] 10 p1563 A72-25043
- Thermal diode heat pipe for advanced thermal control flight experiment, discussing engineering model analysis, design, fabrication and test
[AIAA PAPER 72-260] 11 p1739 A72-25205
- Thermal radiation shielding of porous surface on heated plate by absorbing gas transpiration, suggesting carbon dioxide, metal vapors and particulate mixture
[AIAA PAPER 72-277] 11 p1740 A72-25217
- Thermal emittance, reflectance, absorptance and transmittance of aerospace materials
[AIAA PAPER 72-307] 11 p1742 A72-25241
- Specular components of thermal reflectance as function of directional incident intensity variations
11 p1746 A72-25993
- High atomic energy levels population at low temperature, density and thermal radiation fields conditions in interstellar medium
11 p1720 A72-26111
- Thin Ta sheet spiral configuration for high efficiency high temperature vacuum heat shield
12 p1888 A72-27035
- Clear sky atmospheric thermal radiation from all-wave radiation and air temperature measurements, showing diurnal and desert condition induced deviations from empirical formula
12 p1840 A72-27706
- Atmospheric thermal radiation flux calculation, showing carbon dioxide concentration effects on summer and winter models
12 p1805 A72-27991
- Outgoing 15 micron carbon dioxide band radiation measurement optimization for atmospheric thermal sounding by satellite
14 p2099 A72-30243
- Nighttime lunar surface thermal properties from differential IR flux scans with earth based Cassegrain telescope, noting difference in brightness temperature gradients between highlands and maria
14 p2153 A72-30503
- Apollo 12 lunar fines spectral and thermal radiation properties as function of bulk density, presenting emittance as function of temperature and solar reflectance
14 p2154 A72-30513
- White dwarf background radiation and optical emission variations due to thermal bremsstrahlung from stellar coronae
14 p2147 A72-30554
- Atmospheric air pollution study by space techniques via thermal radiation spectral measurements and laser sounding, considering spaceborne photography
15 p2220 A72-31237
- Radiation measurements and thermal IR and photographic imaging techniques in meteorology and earth resources survey applications
15 p2221 A72-31241
- Fuor luminosity phenomena due to thermal coparcular radiation emitting energy sources
15 p2304 A72-31330
- Galactic background continuous radiation observation at 15 GHz, determining brightness temperature and thermal radiation component
15 p2313 A72-32348
- Thermal radiation effects on semiinfinite planar blunt leading edged body hypersonic flow field, using Lax and Rusanov artificial viscosity methods
15 p2337 A72-32593
- Monochromatic radiation pulse transfer in absorbing plasma, deriving heat wave propagation velocity
16 p2437 A72-33692
- Thermal X ray sources associated with rotating collapsed stars, discussing Scorpio X1 plasma shell heating mechanism
16 p2460 A72-33924
- Nomogram for heat detector size determination from thermal inertia index and Biot number
16 p2395 A72-33968
- Energy transfer of thermal coupled radiation with turbulent convection in electric arcs in atmospheric air plasma
[AIAA PAPER 72-685] 16 p2480 A72-34057
- Direct infrared measurements of thermal radiation from the nucleus of comet Bennett.
17 p2604 A72-34525
- Transient thermal waves in the general theory of heat conduction with finite wave speeds.
[ASME PAPER 72-APM-23] 17 p2636 A72-34794
- Analytical solutions for straight oblique shock waves in radiating gases.
17 p2542 A72-35616
- Predictions of solar induced response of thin-walled open-section booms for design.
18 p2733 A72-36364
- Moving periodic thermal wave induction of nonlinear motions in Boussinesq fluid layer, solving nonlinear two dimensional momentum and temperature equations
18 p2681 A72-36485
- New method for determining the integral radiative capacity of partially transparent materials at high temperatures
18 p2704 A72-37190
- Influence of the earth's outgoing radiation on the temperature of a rotating disk in space
19 p2856 A72-37496
- Influence of roughness on the thermal radiation emitted by opaque surfaces - Model test
19 p2881 A72-38393
- Spectral reflectance and emittance of Apollo 11 and 12 lunar material.
20 p2970 A72-39609
- The universal high temperature emissometer.
[ASME PAPER 72-HT-1] 20 p2926 A72-39675
- Influence of the structure on the emissivity of aluminum-chromium-phosphate coatings at high temperatures
21 p3072 A72-40383
- Neutron star detection based on nearby pulsar soft thermal X ray flux observations
21 p3107 A72-41218
- Infrared observations of the moon and their interpretation.
22 p3225 A72-42527
- Alternative description of laser plasma heating for spherical thermal wave, the fusion energy being taken into account.
22 p3211 A72-42629
- A transpiration radiometer for measurement of total thermal radiation from a flowing plasma.
22 p3179 A72-42691
- Atmospheric thermal IR radiation transmission function dependence on carbon dioxide concentration, calculating spectral and vertical distributions for standard, summer and winter model atmospheres
22 p3174 A72-43005
- Aircraft gas turbine engines environmental effects, considering thermal radiation, acoustic emissions and exhaust gases in relation to propulsion system design parameters
23 p3328 A72-44296
- Generalized integral equations of radiative heat exchange.
23 p3357 A72-44536
- Temperature calculation in a multilayered wall acted on by a thermal pulse.
23 p3357 A72-44537
- Study of the dependence of the spectral and integral radiation properties of bodies on the surface roughness.
23 p3357 A72-44538
- Remote sensing of earth resources by microwave radiometry.
24 p3402 A72-45107

THERMAL RADIO EMISSION

U RADIO EMISSION

U THERMAL EMISSION

THERMAL REACTORS

Transoceanic helium cooled thermal reactor powered air cushion freighter of gross weight 4500 metric tons, discussing design and performance characteristics

04 p0464 A72-14431

THERMAL RESISTANCE

Emitted light power of CW injection laser related to threshold current, electrical and thermal resistances and external quantum efficiency

01 p0079 A72-10325

Analog matrix, input data and procedure for Al frame and Cu-clad printed circuit board module thermal resistance analysis using ECAP program

01 p0035 A72-10380

Niobium anomalous oxidation below 600 C, noting suboxide formation between solid solutions and heat resistance reduction

02 p0243 A72-12214

Heat flow resistance measurement in avalanche diodes, noting junction temperature effect

04 p0498 A72-15133

Variable conductance heat pipe technology for overcoming thermal resistance barrier in electronic package design

04 p0596 A72-15227

Vacuum diffused Cr, Si, Ti and combined coatings effect on heat resistance of Nb and Nb alloys

04 p0534 A72-15660

Metal polymer interface synthesis based on linearly cyclic organoelementary high molecule compounds, analyzing heat and thermal oxidation resistances

05 p0680 A72-16202

Superplasticity relation to heat resistance in metal systems Ni-Cr, Ni-Cr-W-Ti-Al and Ti-Si

05 p0680 A72-17212

Heat resistance of magnesium, barium and calcium fluorides as solid lubricants in air, hydrogen and water vapor at 100-1100 C

06 p0836 A72-18433

Gas turbine blades thermal fatigue test and analysis, investigating static tensile loading effects on heat resistance under thermal cycling

06 p0899 A72-18556

Thermal resistance estimation for machine parts of heat resistant alloys under real working conditions

06 p0833 A72-18559

Aircraft power plants sealing materials, emphasizing porous cermet seals heat resistance under thermal cyclic loads

06 p0797 A72-18658

Heat resistant metals long time creep prediction at low stresses or temperatures

06 p0834 A72-18668

Thermal contact resistance measurement in double contact thermocouple specimens at 250-650 C in Ar and air-vacuum

07 p1098 A72-18987

IMPATT diode thermal resistance measurement from heat diffusion effect on small signal impedance of p-n junction

07 p0958 A72-20684

Gunn diode microwave oscillator thermal resistance reduction for increased output power and efficiency

07 p0958 A72-20685

Soviet book on temperature resistance of lubrication boundary layers and solid lubrication coatings during friction of metals and alloys

08 p1179 A72-22023

Fatigue strength of heat resistant materials under thermal cyclic loads leading to sign variable plasticity and creep

09 p1402 A72-22732

Thermal shielding and reduced resistance determination of flat thermoelectric battery in sandwich solar cell assembly

10 p1422 A72-24313

Rough surfaces thermal contact resistance in vacuum for normal height distribution, discussing bolted joint nonuniform stress distribution effect [AIAA PAPER 72-281]

11 p1741 A72-25221

Metallic foils effects on thermal joint resistance of interface between lathe turned and optically flat surfaces, noting optimal thickness

11 p1685 A72-25223

Superplasticity relation to heat resistance in metal systems Ni-Cr, Ni-Cr-W-Ti-Al and Ti-Si

11 p1727 A72-25338

Semiconductor laser thermal resistance and time constant evaluation, obtaining operating temperature range and maximum attainable pulse width

11 p1647 A72-25808

Multiphase Al alloys strengthening by dislocation substructures in repeated rolling and recovery cycles at elevated temperature

11 p1667 A72-26930

Synthetic diamond single crystals, investigating impurities and inclusions effects on ferromagnetic properties and heat resistance

12 p1833 A72-27768

Soft solder cracking and breaking alleviation in welding technique for solar cells, noting resistance to thermal cycles

12 p1814 A72-28039

Aromatic polyimide binder for compression moldable high performance composites preparation with thermal curing to obtain good thermal-oxidative stability and toughness

12 p1834 A72-28090

Laplace equation iterative solution for boundary value problems in structural hardening and heat resistance formulation, noting convergence

12 p1887 A72-28226

Stress rupture strength, short term strength, creep and heat resistance measurement arrangement for coated refractory materials at 1500-1700 C in air with radiative heating

12 p1796 A72-28248

Heat resistance of corundum based ceramics with multiphase additions under thermal cycling tests

13 p1983 A72-28568

Thermal shock produced edge effect, analyzing brittle material heat resistance and failure, using thermoelastic heated cylinder

14 p2165 A72-30437

Heat resistance of thermostable organic materials /amorphous glass and high polymers/, improving plastic stability by glass fibers addition, intermolecular arrangements modification and synthesis [ONERA, TP NO. 1107]

14 p2125 A72-30529

High temperature composite turbine blade materials, discussing service conditions and fiber/matrix selection, noting cast Ni and Mo based alloy fibers

14 p2125 A72-30533

Cr-containing Fe-alloy and Ni steels, investigating thermal cycling effects on thermal resistance by factorial program

14 p2118 A72-30546

Chemical interaction within crystals for generation of stacking fault vacancies and phenomena associated with solid solution microheterogeneity dislocations, discussing heat resistance

15 p2254 A72-31558

Heat resistance improvement by interface dislocation, dispersion hardening and reinforcement of Mo, Fe, Ni and Al metals and alloys

15 p2254 A72-31560

Refractory steels heat resistance improvement by surface saturation with Be and subsequent oxidation in air at 900-1000 C, comparing with aluminized steels

15 p2255 A72-31574

Mo and W simultaneous addition effects on Ni-Cr-Nb alloy properties, noting heat resistance increase and Nb solid solubility decrease

16 p2408 A72-33534

Heat resistant adhesives properties and selection, discussing thermosetting-thermoplastic resins and ceramic materials for temperatures to 4400 F

16 p2415 A72-33597

Thermal resistance of planar semiconductor structures.

17 p2594 A72-34296

Computer thermal analysis of hybrid microcircuits.

17 p2521 A72-34679

Multimesa versus annular construction for high average power in semiconductor devices.

18 p2666 A72-36455

Enhancement of heat resistance in Kh14G14N3T steel by microadditions of boron

20 p2941 A72-39579

Chromizing of steel sheet by diffusion

20 p2929 A72-39581

Oxidation of TD nickel at 1050 and 1200 C as compared to three grades of nickel of different purity.

21 p3067 A72-40915

Creep test diagrams plotted to estimate heat resistance for turbine blades design, predicting fatigue life with allowance for loading cycle form and duration

21 p3123 A72-41366

Thermal resistance of Gunn diodes - Analysis and measurement.

21 p3035 A72-41491

Weibull distribution government of dispersion of destructive temperature gradients characteristic of fireproof ceramic materials heat resistance

21 p3074 A72-41713

Approximate calculation of the temperature stresses in the thermal impact zone

22 p3232 A72-41871

Influence of a sinusoidal pressure variation on contact thermal resistances

22 p3244 A72-42644

Thermal design of hybrid modules and assemblies.

22 p3161 A72-43172

Production and properties of materials of the Si3N4-Cr2O3 system

23 p3298 A72-43283

Refractory materials heat resistance criteria, taking into account hollow cylinder thermal stress distribution

23 p3306 A72-43738

Test equipment for heat resistance determination of brittle refractory material, noting data processing

procedure and formulas for temperature distribution and thermal stress

23 p3278 A72-43962

Influence of the chemical composition of Kh25N16G7AR steel on its heat resistance

23 p3303 A72-44098

Thermoelastic characteristics and crystal phase distribution effect on microstructural stresses and thermal expansion of polycrystalline refractory materials

24 p3416 A72-45759

THERMAL SHIELDING

U HEAT SHIELDING

THERMAL SHOCK

Thermal shock fatigue tests on aircraft gas turbine engine inlet nozzles, showing cracks as function of material

01 p0143 A72-11373

Thermoelasticity equations for thermal shock effect on freely supported circular plate, describing deformation and temperature field interactions

05 p0741 A72-17147

Thermal shock transient test burner to test gas turbine ceramics under simulated operational environment conditions

08 p1147 A72-21434

Metallic four-lip seal performance, discussing force cycle, mechanical spring-back, reusability at room and higher temperatures and thermal shock behavior

08 p1179 A72-21939

Hot pressed baron nitride and composite oxidation tests in atmospheric arc jet, noting fabrication and composition effects on thermal shock and oxidation resistance

09 p1333 A72-22379

Thermal shock resistant composite materials with carbide or oxide matrices based on concept of crack propagation prevention, noting superiority from thermal simulation tests

09 p1334 A72-22384

Yttria stabilized hafnia based graphite and tungsten composites, investigating factors affecting thermal shock resistance

09 p1327 A72-22385

Silicon nitride ceramics resistance to thermal shock and stress in severe environments

09 p1334 A72-22386

Thermoelastic disturbance wave front propagation in elastic half space after thermal shock at surface

09 p1399 A72-22705

Thermoelastic coupling effect in thermal shock problem on surface of simply supported rectangular beam

09 p1401 A72-22719

Numerical solution of thermal shock equations for incompressible fluid with free convection and of motion equations in gravitational force field

09 p1410 A72-22882

Thermal shock and temperature cycling environmental testing, discussing military specifications, components thermal lag characteristics, environmental test chambers and various cooling methods

10 p1459 A72-24144

Diaphragmless electrothermal shock tube for collision in preheated Ar, using RF plasma heater

10 p1459 A72-24410

Mica glass ceramics mechanical properties and thermal shock behavior in terms of microstructural variables, discussing fracture propagation and secondary cracks formation

11 p1675 A72-26949

Hyperboloidal profile circular disk stress distribution induced by thermal pulse nonuniform temperature field

11 p1739 A72-26979

Rods resistance to thermal shock under coupled thermoelasticity conditions, calculating critical thermal flux during thermodynamic compression waves propagation

13 p2053 A72-28399

Low temperature shock effects on lunar glass spherules from two beam interferometry, discussing mechanical and thermal causes of fragmentation

14 p2149 A72-30266

Thermal shock produced edge effect, analyzing brittle material heat resistance and failure, using thermoelastic heated cylinder

14 p2165 A72-30437

Thermal shock induced thermoelastic vibrations of rectangular plate calculated by Ritz averaging method

15 p2333 A72-32689

Deformation and failure characteristics of joints in a Ni-Al system under the action of high thermal pulses

20 p2942 A72-39822

Application of variational methods to the solution of some thermal shock problems

21 p3128 A72-40978

Approximate calculation of the temperature stresses in the thermal impact zone

22 p3232 A72-41871

Prediction of thermal-shock resistance during heating at very high rates.

22 p3241 A72-43000

Stress function for thermal shock in plate with cylindrical heat source, noting thermal stress concentration in optical materials under electromagnetic radiation 23 p3348 A72-43792

THERMAL SIMULATION

Simulation of nuclear light bulb engine propellant radiative heating, using argon seeded with micronized carbon particles and 500 kw dc arc as radiant energy source

01 p0099 A72-11344

Induction plasma heating simulation of open cycle gas core nuclear rocket engine, describing plasma forming material feed, permeable walls and propellant seeding

01 p0112 A72-11346

Imperfect thermal modeling of spacecraft based on error states representation in multidimensional Euclidean space, evaluating approximate total error effect

03 p0441 A72-13635

Thermal simulator of flows with chemical wall reaction, plotting surface temperature variations with distance

03 p0456 A72-13793

Thermal modeling of space shuttle cryogenic turbopump, considering heat transfer for two-phase cryogen and gas impingement on turbine blades and rotating disks

[ASME PAPER 71-WA/HT-43] 05 p0664 A72-15890
Concorde airframe testing for thermal effects on structural strength and fatigue life, discussing facilities for flight conditions simulation

05 p0614 A72-17197

Digital simulation for steady state and transient thermal responses of LSI with metal within substrate, considering computer time cost

07 p0954 A72-19176

Thermal shock transient test burner to test gas turbine ceramics under simulated operational environmental conditions

08 p1147 A72-21434

Thermal shock resistant composite materials with carbide or oxide matrices based on concept of crack propagation prevention, noting superiority from thermal simulation tests

09 p1334 A72-22384

Simulated superposed coherent and chaotic thermal/radiation of arbitrary spectral shape, using laser beam modulation and photocount statistics

09 p1352 A72-23240

Thermal nodal analysis of spacecraft hull-canister model from space simulation test, using least squares estimation and regression analysis

09 p1412 A72-23497

Spacecraft cabin atmosphere thermal scale modeling based on radiative-convective-convective heat transfer, obtaining adequate thermal similitude through mass flux and heat transfer coefficient preservation

[AIAA PAPER 72-288] 11 p1741 A72-25226
Lunar regolith glassy particles formation processes modeling with molten soil samples, emphasizing liquid particles spattering with subsequent cooling during meteoritic impact

13 p2036 A72-28767

Artificial meteor ablation on iron oxides by arc heated air plasma stream for product and environment identification studies

14 p2150 A72-30319

Russian book on thermal simulation of spacecraft and space environment covering heat transfer, cosmic radiation, vacuum chambers, radiant flux simulators, etc

15 p2319 A72-31275

Thermal simulation tests for kinetic heating of aerospace structures and materials, describing facilities for supersonic flight and atmospheric reentry

16 p2475 A72-32897

Computer-aided thermal design of LSI packages.

17 p2527 A72-34681

A parametric study of the transient ablation of Teflon.

[ASME PAPER 72-HT-32] 20 p2986 A72-39671
A digital simulation system for heat transfer modelled by ordinary and partial differential equations.

[ASME PAPER 72-HT-25] 20 p2986 A72-39673
Lunar regolith glassy particles formation processes modeling with molten soil samples, emphasizing liquid particles spattering with subsequent cooling during meteoritic impact

21 p3102 A72-40268

Mechanical tests of laminated plastics in solar installations

22 p3197 A72-43192

THERMAL STABILITY

Germanium nitride thermolysis, discussing allotropic alpha and beta phases stability and activation energies

01 p0023 A72-10191

Flow characteristics, wave propagation and thermal stability of ferrofluids within uniform magnetic field

01 p0050 A72-10235

Planetary nebulae dynamic models, incorporating expanding shell thermal histories and thermal stability in terms of high temperature evolutionary phase

02 p0276 A72-11667

Thermally stable organic polymer fiber production methods and performance evaluation in high temperature environments, discussing structure types, flammability and tensile properties

02 p0248 A72-11771

Refractory metal oxides hot microhardness and thermal stability over wide temperature range, noting softening rate variation with temperature

02 p0244 A72-12350

Cavity resonator thermal stabilization, using gas pressure controlled membrane

02 p0196 A72-12698

Jet fuels hydrocarbon composition effect on thermal stability, considering nonaromatic components influence on aromatic hydrocarbons oxidation products coagulation

02 p0271 A72-12800

Materials stability testing in high temperature propane-butane combustion product flow, selecting compact silicon carbide for structural use in redox medium

02 p0251 A72-12866

Flame retardant mechanism in hydrocarbon polymer combustion, discussing halogen adverse effect on thermal stability

[PI PAPER 10] 03 p0380 A72-13244

Temperature dependence of X ray interference lines for Al-V alloy obtained at high cooling rate, noting metastable solid solution thermal stability

03 p0377 A72-14022

Corundum ceramics thermal stability, basing qualitative tests on thermal cycle number and quantitative tests on thermal gradient producing damage

05 p0680 A72-15755

Sprayed single component ceramic coating thermal stability enhancement techniques, noting limitations

05 p0680 A72-16093

Thermodynamics near steady state, considering stability criterion

05 p0746 A72-16159

Soviet book on nonmetallic material strength during nonuniform heating covering, load endurance, bending phenomena and thermal stability of fiberglass, pyroceramics and reinforced plastics

06 p0796 A72-18521

Graphite and molybdenum disulfide, investigating temperature effect, thermal stability and oxidation effect on weight by TGA and DTA

06 p0837 A72-18602

Low and high pass, bandpass and bandstop active filters, tabulating cut-off frequencies, thermal stability, impedance, power dissipation and voltage specifications

07 p0955 A72-19248

Inhomogeneous high-collision finite pressure plasma stability, finding thermal instability development under uniform temperature and arbitrary pressure

07 p1046 A72-20514

Fracture mechanical analysis for stability criteria and propagation behavior of thermal stress cracks in brittle ceramics in severe thermal environments

09 p1333 A72-22382

Blood serum proteins thermal stability in patients with vegetative vascular and neuroendocrine syndromes, discussing ATP effects

09 p1266 A72-22877

Niobium carbide resistors properties, investigating temperature dependence of electrical resistance and thermal stability

09 p1331 A72-23483

Thermally stable six stage transistorized amplifier with logarithmic relationship between input and output voltage

10 p1450 A72-24494

High temperature effects on stability, corrosion behavior, structure and protective effectiveness of Al coatings on Ni and Co alloys

11 p1664 A72-26852

Aircraft gas turbine engines synthetic lubricants thermal stability characteristics, describing coke deposition test apparatus and results

[ASLE PREPRINT 72AM 14] 13 p1983 A72-28971

Electrothermal instability analysis for MHD generator, considering electron thermal conduction and wall boundaries effects for cases with current parallel or perpendicular to walls

13 p2014 A72-29366

Truncated orthotropic conical shells thermostability at different temperature gradients, using Ritz method

14 p2163 A72-30193

Polyester bonded explosives mechanical and thermal properties, noting need for desensitizing against shock and friction effects

14 p2145 A72-30768

Steam-hydrogen treatment tests for high temperature stability of noble metal catalysts in hydrogen-oxygen reaction initiation

15 p2192 A72-32225

In and Gd substitution effect in calcium-vanadium garnets as potential microwave materials, discussing magnetic properties, resonance linewidth and temperature stability

15 p2293 A72-32243

Apiezone lubricants physicochemical properties comparison, noting aromatic hydrocarbons effect on thermo-oxidation stability and polyisoprene rubber type polymer additive effect on adhesiveness

16 p2413 A72-33171

Polymeric structural adhesives thermal stability evaluation, recommending thermogravimetric analysis and calorimetry to supplement thermogravimetric method

16 p2415 A72-33510

Thermal convective instability in semiinfinite constant temperature viscous fluid with lower boundary suddenly heated, calculating neutral stability curve and critical Rayleigh number

16 p2478 A72-33656

Thermal analysis of high performance devices mounted on dielectric substrates.

17 p2527 A72-34677

A study of the heat flow and thermal instabilities in high power hybrid integrated circuits.

17 p2527 A72-34678

Thermal and gravitational instability in universe, obtaining equation for growth rate of density contrast

17 p2618 A72-35910

Work function, thermal stability, and atomic structure of electropositive films adsorbed on single crystals of metals

18 p2656 A72-36132

The stability of structure of physical mechanical properties of molybdenum and tungsten after irradiation and thermal influence

18 p2698 A72-36153

Astrophysical theories of supernovae outbursts as stellar evolutionary nonstationary phase in terms of thermal instability of degenerated matter or stellar explosion

18 p2725 A72-36399

Stability and hot corrosion of aluminum coatings on the INCO 713C alloy and on cobalt alloys

18 p2701 A72-36595

High-stability capacitance strain gauge for use at extreme temperatures.

18 p2693 A72-37210

Steady combustion thermal stability of condensed explosives for burning rate limitation by condensed phase chemical reactions, noting surface temperature effects

19 p2879 A72-37356

Thermal stability of skewed plates

19 p2871 A72-37430

Gain and visualization of the modes of a thermally stabilized HCN laser.

19 p2810 A72-37455

The indirect determination of stability, heat and momentum fluxes in the atmospheric boundary layer from simple scalar variables during dry unstable conditions.

20 p2947 A72-38964

Microelectronic component system temperature distribution measurement by IR microscope and electrical technique to determine beam-lead IC thermal performance

20 p2908 A72-39498

Effect of wall conduction on the stability of a fluid in a rectangular region heated from below.

[ASME PAPER 72-HT-G] 20 p2985 A72-39655

Stability of convective heat transfer through horizontal air layer heated from below and constrained internally by thin walled honeycomb panels

[ASME PAPER 72-HT-60] 20 p2985 A72-39656

Intensity of turbulence within canopies with simple and complex roughness elements.

20 p2948 A72-39798

Contribution of the invar anomaly and the elinvar effect to the formation of the thermal stability of the modulus of elasticity of iron-nickel invars

21 p3068 A72-40952

Regime factor and stress concentration parameter for sudden heating of solid cylinders and disks, noting thermal stability criterion with allowance for statistical strength

21 p3123 A72-41361

An inverse problem in the momentlessness theory of shells of revolution situated in a temperature field

22 p3232 A72-41895

Thermal stability of lunar rock remanence, indicating magnetization components acquired after initial cooling

22 p3226 A72-42535

Thermal stability of sulphides of some metals in iron-base cermets

23 p3298 A72-43285

Problem of the spatial localization of thermal disturbances in nonlinear heat-conduction theory

23 p3356 A72-43529

Utilization of computers in mechanical strength studies

23 p3345 A72-43644

Influence of the nature of the particle distribution of the hardening phase in powders on the thermal stability of dispersion-strengthened nickel
23 p3302 A72-44011

Stability and oscillation characteristics of finite-element, finite-difference, and method of weighted residuals for transient two-dimensional heat conduction in structures.
24 p3461 A72-44608

THERMAL STRESSES

Beryllium microstructure and hexagonal close packed polycrystal material residual thermal stresses, calculating thermal expansion coefficients
01 p0087 A72-11028

Thermal radial stresses in axial compressor disk-to-drum transition areas of operating AM-3 aircraft engine
01 p0143 A72-11374

Thermal stresses, temperature distribution and displacement fields in elastic solid with spherical cavity and external crack
01 p0144 A72-11385

Fracture analysis of two dimensional thermal loaded solid propellant rocket grain models under cooldown [SESA PAPER 1927A]
02 p0270 A72-11513

Elastoplastic deformation in medium with initial dislocations and temperature field, expressing kinetic stress and distortion tensors by Hamiltonian derivatives
02 p0290 A72-11630

Temperature fields and stresses in thin elastic nonferromagnetic electrically conducting cylindrical shells heated by induction determined from heat source distribution and thin shell theory relations
02 p0290 A72-11631

Polycrystalline bodies thermoelastic behavior under random external forces, determining thermal microstress distribution parameters by statistical boundary value formulation
02 p0290 A72-11632

Heat resistant alloys thermal microstresses effect on creep and fatigue life under thermal cycling conditions
02 p0242 A72-11633

Aircraft gas turbine rotating disks thermal and mechanical stresses under variable thermal conditions, describing test assembly
02 p0199 A72-11637

Computer program for thermal stress and buckling analysis of nonuniformly heated segmented ring-stiffened cylindrical and conical shells
02 p0293 A72-12252

Isothermal analogy for thermal stress in cylindrical shells, presenting orthogonal coordinate boundary condition equations [ASME PAPER 71-PVP-18]
02 p0294 A72-12471

Optical interference measurement of various shaped elastic plates deflection and application to thermal stress problems
02 p0300 A72-12824

Nonstationary thermoelastic stress determination in hollow cylinder walls under convective heat transfer
03 p0443 A72-13459

Thermal stress concentration at circular heat-insulated hole in plate with elastoplastic strains, assuming temperature independent mechanical properties
03 p0445 A72-13575

Thermal stresses from inner surface temperature of micropolar hollow cylinder in static thermoelasticity problem with vanishing body loads
03 p0448 A72-13889

Temperature stresses near thermally insulated square holes in unbounded plane, determining temperature distribution
03 p0449 A72-13914

Elastic plate with two collinear thermally insulated cracks, calculating steady temperature field and stresses for uniform heat flux at infinity
03 p0450 A72-14112

Anisotropic plate with hole stiffened at edge by thin isotropic ring, calculating thermal stress distribution
03 p0450 A72-14113

Diffusion saturation effects on thermal stress concentration in plate with circular hole under edge heating and lateral surface heat transfer
03 p0451 A72-14124

Thermal stress concentration at heat insulated holes in orthotropic plate, assuming external-load free contour
03 p0452 A72-14134

Critical thermal loads during external and internal heating of annular channels, discussing curvature effect on density level in thermal flux during forced fluid motion
03 p0458 A72-14157

Metal-alumina-oxide-semiconductor capacitor flat band bias voltage measurement before and after thermal stressing, noting potential barrier in structure model
03 p0336 A72-14278

Optimal temperature field s and stress-strain state in orthotropic conical and cylindrical shells subject to local heating
04 p0588 A72-15051

Griffith fracture theory application to thermal crack propagation, computing stress-strain field and critical temperature [ASME PAPER 71-MET-N]
05 p0731 A72-15790

Thermal load effect on convective heat transfer in turbulent flow in circular duct
05 p0742 A72-15843

Linear two-temperature theory of thermoelasticity for investigating transient stresses arising from solid isotropic sphere aerodynamic heating [ASME PAPER 71-WA/APM-14]
05 p0733 A72-15966

Strength margin estimation in materials sustaining cumulative static and damage under cyclic thermal loads
05 p0735 A72-15994

Thermal stresses in thin symmetrically heated disk with time and temperature dependent mechanical properties, deriving integrodifferential equation defining stress function
05 p0740 A72-16624

Stress fields around moving weld arc on Al sheet from isotherm map, calculating compressive and tensile stresses from heat induced material expansion
06 p0820 A72-17705

Singular solutions for nonaxially symmetric shallow shells under concentrated normal or thermal loading
06 p0897 A72-18319

Failure analysis of plastic materials susceptible to cyclic strain hardening under thermal load, considering residual stress concentration
06 p0898 A72-18547

Approximate trigonometric solution to thermoelastic boundary value problem of plate with doubly periodic system of holes under unsteady temperature and thermal stress fields
06 p0899 A72-18563

Temperature stress distribution in infinite plate with time varying heat transfer coefficient
06 p0899 A72-18565

Two dimensional dynamic thermal stresses in Al plate, allowing for Newtonian surface heat transfer
06 p0899 A72-18642

Cylindrical shell under internal pressure, detailing axial thermal stresses relaxation
06 p0900 A72-18669

Moving heat source model of temperature profile and thermal stress propagation for laser drilled holes in alumina ceramic material
07 p0994 A72-19211

Generalized coupled thermoelasticity problem solution from wave equations for anisotropic plate in plane thermal stress state
07 p1094 A72-19987

Test facility for graphites fracture under thermal stresses, considering stress-strain relations calculation method for annular samples
07 p1024 A72-20137

Thermal stress measurement and thermoelastic behavior of carbon-carbon-materials for reentry nose cones, describing gage mounting, temperature compensation and data recording
08 p1164 A72-20921

Thermal stresses in anisotropic annular, circular and perforated plates with temperature dependent coefficients for lateral surfaces heat removal
08 p1245 A72-21505

Axisymmetric thermoelastic state of isotropic infinitely long circular cylinder with external annular cut, determining cut plane normal thermal stresses
08 p1245 A72-21668

Residual temperature stresses and deformations during thermal treatment of thick walled glass fiber reinforced plastic wound cylinders and rings
08 p1194 A72-21755

Heat stretching-induced changes effect on strength, sorption and structural properties of polyformaldehyde fibers, noting structural orientation enhancement and porosity growth
08 p1194 A72-21757

Nonlinear dynamic response of deformable solids under time and space dependent thermal and mechanical loads determined by finite element method
08 p1248 A72-21822

Residual shrinkage and thermal stresses in adhesion bond models of metal coatings and cemented seams
08 p1248 A72-21865

Thermocracking and thermal stresses in packing rings of face-type mechanical seals under dry friction
08 p1177 A72-21927

Fracture mechanical analysis for stability criteria and propagation behavior of thermal stress cracks in brittle ceramics in severe thermal environments
09 p1333 A72-22382

Silicon nitride ceramics resistance to thermal shock and stress in severe environments
09 p1334 A72-22386

Ceramic laser materials failure due to optically induced damage, estimating stresses and changes in refractive indices under thermal effects
09 p1336 A72-22403

Forbidden band thermal deformation effect on homogeneous steady state stability of semiconductor
09 p1367 A72-22492

X ray method characteristics in thermal interphase microstresses determination, considering spherical silicon inclusion surrounded by concentric Al matrix envelope
09 p1309 A72-22638

Stress-strain state produced by asymmetric physical and thermal loads in thin orthotropic viscoelastic shells of revolution
09 p1399 A72-22702

Temperature induced stresses and displacements in fiberglass reinforced plastic cylindrical shell
09 p1399 A72-22704

Temperature and thermal stress distribution in cylinder of finite length for mixed heating conditions
09 p1400 A72-22707

Linear uncoupled quasi-static thermoelasticity theory for thermal bending of nonuniformly heated parallelogram-shaped plates
09 p1400 A72-22710

Trapezoidal plate thermoelasticity problem for various thermal load distributions, solving Poisson equation for sectorial annular region
09 p1400 A72-22711

Thermal stress distribution in orthotropic cylindrical shell weakened by circular hole, obtaining general solution by small parameter method
09 p1400 A72-22715

Thermal stressed state determination for open thin walled cylindrical shells, using method of integral relations
09 p1400 A72-22716

Thermal stress-strain state analysis of nonlinear elastic medium by small parameter method
09 p1400 A72-22717

Solid cylinder stress-strain state under thermal and mechanical loads, obtaining analytical solutions via flow theory based on Von Mises yield condition
09 p1401 A72-22723

Finite difference analysis of dynamic deformation of thin elastoplastic shells of revolution under intense heating
09 p1401 A72-22728

Nonlinear creep characteristics of variably thick rotating disks under nonuniform heating conditions, determining critical rpm and temperature field and time to failure
09 p1402 A72-22731

Photothermoelasticity method for determining thermal stresses
09 p1402 A72-22737

Optical mirror method for bending strains study in welding cycles with applications to sheet metal thermal stress strain rates
09 p1318 A72-22738

Micropolar elasticity plane problem singular solution based on stress equations and elastic potentials methods, discussing thermal stress concentration
09 p1402 A72-22747

Axial thermal stresses in beams, investigating error in elementary calculations
09 p1405 A72-22999

Creep ratcheting deformation and rupture damage from thermal transient stress cycle and constant membrane force under high temperature metal creep conditions
09 p1406 A72-23197

Thermal stress analysis of laminated alternate ply cylindrical shells under internal pressure, using Donnell equations
10 p1556 A72-24257

Thermoelectric cooling battery performance of solar cell system, determining low temperature current requirements under various thermal loads
10 p1423 A72-24317

Heat conduction and thermoelasticity in solids, discussing thermomechanical coupling, structural analysis and thermal stresses and deformations [SMRT PAPER L 1/1]
10 p1556 A72-24394

Thin circular plate quasi-static thermal stresses induced by transient temperature distribution on upper face, obtaining series form solution in terms of Bessel functions
10 p1558 A72-24720

Classical boundary value problems in theory of thermal stresses in piecewise continuous anisotropic elastic bodies under coupling conditions
10 p1563 A72-24994

Thermal stresses and displacements in elastic medium containing parallel circular cracks, using perturbation technique
10 p1560 A72-25045

Precision temperature control system for spacecraft equipment thermal loads rejection by space radiator, using acetone variable conductance heat pipes [AIAA PAPER 72-270]
11 p1740 A72-25211

Dense silicon nitride and carbide ceramics for gas turbines, discussing critical properties for thermal stress calculation [ASME PAPER 72-GT-56]
11 p1674 A72-25647

Thermoelastic stress and displacement in thin finite rod due to distributed time dependent heat sources
11 p1736 A72-25991

Thermoelastic stresses in solid transparent isotropic homogeneous dielectric under self-focused laser beam
11 p1648 A72-26334

- Thermal stresses in cylindrical shell under moving hot spot with cooling effect of surrounding media
11 p1737 A72-26428
- Thermal stresses in homogeneous isotropic and composite curved beams for temperature distribution in polynomial form with coefficients representing functions of two remaining coordinates
11 p1737 A72-26665
- Plastic materials adaptability to solid and hollow turbine blades, deriving thermally and mechanically induced stresses
11 p1738 A72-26799
- Thermal stress distribution in orthotropic plates with variable heat transfer coefficient, using Fourier and Laplace transforms
12 p1878 A72-27084
- Chernikov approximation for general relativistic thermodynamics nonstationary equations of heat transfer, thermal and viscous stresses and entropy balance
12 p1844 A72-27188
- Linearized thermal viscoelasticity theory for stability, large strain and wave propagation problems, taking into account heat generating effects
12 p1880 A72-27233
- Rapid laser heating induced stress generation in carbon fiber-polyethyl methacrylate composite
12 p1833 A72-27286
- X ray determination of thermal microstresses in metal specimens surfaces
12 p1807 A72-27447
- Materials selection for models used in thermal stress studies by restrained shrinkage method with emphasis on polyurethanes
12 p1813 A72-27460
- Temperature gradient and thermoelastic stresses in Nd-YAG laser active elements under continuous pumping conditions, noting refractivity radial distribution
12 p1822 A72-27614
- Nonuniform heating effect on stability of eccentrically stiffened smooth cylindrical shells under combined loading
12 p1885 A72-27973
- Silicon solar cell interconnectors design for 5-10 years mission life, considering launch induced vibration stresses and thermal cycling stresses during mission
12 p1758 A72-28037
- Thermal stresses near pole of spherical reservoir during cooling, using thermoelastic equations of shell of revolution
12 p1887 A72-28242
- Russian book on hard alloys strength covering WC-Co and WC-TiC-Co alloys microstructure, thermal stresses and fracture mechanism
12 p1831 A72-28348
- Radial and circular thermal stresses in free and end-constrained orthotropic cylinders with axisymmetric temperature distributions, determining relation between temperature and thermoelastic coefficients
13 p2055 A72-28561
- Axisymmetric temperature problem with arbitrary load duration for disk-shaped crack fracture mechanics, using Fredholm equation with symmetrical kernel for temperature field determination
13 p2055 A72-28720
- Thermal stress distribution determination in isotropic plate with rigid circular insert, using small parameter technique
13 p2056 A72-28913
- Thermal stresses in elastic cylinder for variable linear expansion coefficient and temperature, noting welded seam between two constant temperature cylinders
13 p2059 A72-29492
- Quasi-static thermoviscoelasticity problem for infinite plate with circular hole, investigating plate surface heat transfer and material viscosity effect on temperature stresses
13 p2061 A72-29796
- Point heat source induced thermal stresses in elliptic plate with circular holes, determining stress-strain field by two dimensional elasticity theory
14 p2166 A72-30689
- Three dimensional photothermoelastic method of refrigeration with composite model to study transient thermal stresses in wing rib
14 p2168 A72-30907
- Concentration stress convection in slow gas mixture flow due to density gradients, noting similarity to thermal stress convection
14 p2096 A72-31015
- Thermal load effect on convective heat transfer in turbulent flow of viscous incompressible liquid in circular tube
15 p2334 A72-31262
- Elastic plates and shallow shells in finite deflection, obtaining iterative solution with good convergence for thermal stresses
15 p2324 A72-31488
- Large deflection vibrations of free circular plate of lenticular section with constant temperature gradient through thickness, noting thermal stresses effect
15 p2325 A72-31552
- Thermal stress and temperature distribution in rigidly bounded elastic half-space, taking into account coupling effects
15 p2325 A72-31637
- Thermal stresses in plane elasticity for doubly connected regions, considering temperature distribution, stress state problem formulation and nonconcentric annulus
15 p2329 A72-32287
- Thermoelastic stress bounds in fiber reinforced composite beams of arbitrary cross section, examining conditions for applicability of elementary beam theory
16 p2464 A72-32915
- Optimal composite structures of multilayer spherical vessels in terms of elastic deformation under critical loads in thermal field
16 p2467 A72-33158
- Quasi-static thermal stresses in circular disk due to rotating point heat source on surface
16 p2470 A72-33594
- Temperature dependent elastoplastic wing assemblies and continua analysis via matrix displacement method
16 p2471 A72-33791
- Low recession graphite nosetip design for ballistic reentry, considering blunt and sharp configurations in terms of thermally induced tensile strain survival [AIAA PAPER 72-705]
16 p2472 A72-34039
- Post irradiation examination of a UO₂-fueled thermionic diode with a revolver type emitter.
17 p2578 A72-34618
- Forbidden band thermal deformation effect on homogeneous steady state stability of semiconductor
17 p2595 A72-34656
- Stress analysis of axisymmetric solids with asymmetric properties.
17 p2632 A72-35227
- Programmable computation method based on matrix formulation for numerical solution of differential equations in heat conduction and thermal stress problems
17 p2635 A72-35898
- Predictions of solar induced response of thin-walled open-section booms for design.
18 p2733 A72-36364
- Reliability assurance of space equipment components, discussing drift and failure modes, computerized simulation and thermal maps
18 p2743 A72-37127
- Thermal displacements and stresses in cylindrical shells due to instantaneous line heat sources.
19 p2870 A72-37272
- Thermal circular and radial stresses in elastic orthotropic cylinders with anisotropic expansion coefficients
19 p2872 A72-37535
- Stress redistribution caused by creep in a thick walled circular cylinder under axial and thermal loading.
19 p2874 A72-37716
- Method for determining thermal strains in astronomical mirrors
19 p2801 A72-37968
- Thermal boundary equilibria in brittle bodies with heat conducting cracks under combined loads and temperature fields
19 p2877 A72-38198
- Thermal and athermal components of the flow stress in zone-refined titanium.
19 p2820 A72-38298
- Thermal stress induced flow around constant temperature solid sphere in rarefied gas with uniform temperature gradient, using asymptotic theory
19 p2788 A72-38433
- Computerized finite element three dimensional stress analysis, taking into account mechanical and thermal stresses
19 p2878 A72-38649
- Characteristics of the thermal and stressed states of cooled shell-type blades
20 p2963 A72-39911
- Experimental investigation of the stability of compressed heated three-layer plates beyond the proportional limit
20 p2981 A72-39920
- A flow induced by thermal stress in rarefied gas.
21 p2989 A72-40193
- The gamma-ray-irradiation method applied to three-dimensional thermal photoelasticity.
21 p3051 A72-40230
- Application of holography in high-temperature displacement measurements.
21 p3052 A72-40235
- Anatomy and thermal history of laser self-focusing damage tracks in glass.
21 p3062 A72-40245
- Stresses and strains in the plastic range in an annular disk due to steady-state radial temperature variation.
21 p3121 A72-41210
- Thermoelastic problems for multiply-connected plates with heat dissipation at both plane surfaces.
21 p3121 A72-41237
- Effect of the rate of pulsed heating of a bar on the magnitude of the thermoelastic stresses
21 p3126 A72-41548
- Rational utilization of the strength capabilities of thermal-expansion compensators
21 p3127 A72-41702
- Approximate calculation of the temperature stresses in the thermal impact zone
22 p3232 A72-41871
- Axisymmetric temperature problem with arbitrary load duration for disk-shaped crack fracture mechanics, using Fredholm equation with symmetrical kernel for temperature field determination
22 p3233 A72-42097
- Book - Thermal structural analysis programs: A survey and evaluation.
22 p3241 A72-43046
- German monograph - Heat stresses in circular plates subject to finite deflections.
22 p3241 A72-43058
- Strength of a cylindrical shell of variable thickness located in a temperature field
23 p3346 A72-43653
- Fibers-matrix force interaction effects in metal composites, analyzing stress-strain state of reinforced plate
23 p3306 A72-43728
- Refractory materials heat resistance criteria, taking into account hollow cylinder thermal stress distribution
23 p3306 A72-43738
- Thermal and mechanical stresses concentration near peripheral notches on ring-shaped graphite, noting notch sensitivity relationship to tip curvature and graphite grain size
23 p3306 A72-43755
- Stress function for thermal shock in plate with cylindrical heat source, noting thermal stress concentration in optical materials under electromagnetic radiation
23 p3348 A72-43792
- Change in the sign of the thermal lens of glass laser rods during variation of the thermo-optical constant of glass
23 p3296 A72-43926
- Effect of overheating on the creep resistance of metastable alloys
23 p3301 A72-43927
- Test equipment for heat resistance determination of brittle refractory material, noting data processing procedure and formulas for temperature distribution and thermal stress
23 p3278 A72-43962
- Photothermoelastic study of stress concentrations in a plate with internal heating.
23 p3349 A72-43986
- Thermoelastic contact problem of an elastic layer resting on an elastic foundation.
23 p3354 A72-44269
- Nonstationary thermoelastic stress determination in hollow cylinder walls under convective heat transfer
24 p3458 A72-44934
- Castigliano variational theorem for algebraic equation solution of thermal stresses determination in elastic parallelepiped, using Maxwell stress functions as cosine binomial series
24 p3459 A72-45267
- Solution of a boundary-value thermoelasticity problem for a turbine blade by the polymoment method
24 p3460 A72-45623
- Strength margin estimation in materials sustaining cumulative static and cyclic damage under thermocyclic loads
24 p3460 A72-45736
- Graphites fracture under thermal stresses, considering stress-strain relations calculation method for annular samples
24 p3418 A72-45762

THERMAL VACUUM TESTS

- High temperature gradients in pulsed heated Mo specimen under vacuum, using photomicrographic technique
11 p1629 A72-25267
- High temperature contact creep tests in vacuum and in metal melts, noting adsorption effect on surfaces plastic deformation
13 p1963 A72-28768
- Thermal vacuum tests of rhenium disulfide decomposition as function of temperature at 800-1200 C, using thermogravimetric method
13 p2023 A72-29649
- Mo addition effect on high temperature creep resistance and diffusion activation energy of Nb alloys tested in torsion and tension at 1100-1500 C in vacuum
14 p2116 A72-30436
- High temperature forging apparatus for refractory metals under vacuum or inert atmosphere
15 p2241 A72-32443
- Analysis of primary creep of molybdenum at high temperatures.
18 p2700 A72-36580
- The effect of high vacuum on the low cycle fatigue law.
18 p2700 A72-36582

- Investigation of the optical and pyrometric behavior of surface coatings for the Helios probe
19 p2880 A72-37493
- Interaction of titanium diboride with titanium disilicide and silicon at high temperatures
19 p2819 A72-38284
- Heat transfer by radiation in a glass fiber insulator
22 p3243 A72-41891
- Facility for studying the thermophysical properties of materials by quasi-stationary methods
22 p3176 A72-42289
- THERMALIZATION [ENERGY ABSORPTION]**
- Colliding ion streams thermalization beyond plasma pause via unstable ion waves excitation or Coulomb collisions
06 p0805 A72-17464
- Black radiation kinetics of photon thermalization in body cavity in static thermodynamic equilibrium
06 p0847 A72-17732
- Emission energy of positrons thermalized in moderators and coated with Au, suggesting Au negative work function existence
08 p1217 A72-21339
- Collisionless thermalization of ion beam by interaction with plasma, noting acoustic instability growth
10 p1524 A72-24921
- Black radiation kinetics of photon thermalization in body cavity in static thermodynamic equilibrium
11 p1685 A72-25336
- Thermalization lengths and mean numbers of scatterings for line photons.
20 p2956 A72-39759
- Impacting polar plasma thermalization during comet close approach to sun, considering solar wind-comet interaction role
24 p3445 A72-45470
- THERMIONIC CATHODES**
- Electron motion equations for threshold input signal of M type amplifiers with secondary emission cathode in interaction space
02 p0190 A72-11571
- Coaxial plasmatron with central electrode composed of cylindrical Cu and W thermionic cathodes, noting thermal efficiency
08 p1214 A72-21455
- Noise temperature and admittance of space charge limited double cathode tube with transit time effects at microwave frequencies
10 p1454 A72-25105
- Solid body model for electric arc acceleration in thermionic cathode rail accelerator, discussing plasma mass effects
11 p1706 A72-26162
- Rectifier tube cathode as colloid thruster electron gun type neutralizer, discussing efficiency and accelerated life tests
11 p1711 A72-26228
- Shot noise coefficient calculated from static I-V characteristics for modified thermionic diode with low potential virtual cathode
13 p1915 A72-28467
- Excess metal buildup kinetics and work function of oxide thermionic cathode activated by emission current, noting effect of metal and oxygen concentrations
21 p2997 A72-40789
- Fabrication and accelerated life tests of self sustained electron emission cathode with Cr film vapor deposition on Cu disk base
21 p2997 A72-40790
- Mechanical and thermophysical properties of heat resistant Nb alloys, noting application for thermionic cathodes
22 p3192 A72-42821
- THERMIONIC CONVERSION SYSTEMS**
- U THERMIONIC POWER GENERATION**
- THERMIONIC CONVERTERS**
- Dimensionless numbers system selection for generalizing I-V characteristics of thermionic heat converters
01 p0006 A72-10492
- German monograph on thermionic power supply equipment converter network reliability covering I-V characteristics and failure probability calculation
04 p0466 A72-15696
- German monograph on spectroscopic investigation of Cs plasma electron density and temperature and excited atom density in various operational states of thermionic converter
04 p0560 A72-15699
- Cesium plasma thermionic converters, discussing performance and efficiency improvement by governing electron transport in interelectrode space and cation generation
06 p0760 A72-18308
- Spectrographic measurement of electron temperature and ion density profiles in cesium plasma thermionic converter
06 p0862 A72-18309
- Thermionic converter electrode performance of electron emission current density in terms of Cs arrival rate and surface temperature
07 p0915 A72-20568

- Cesium oxide system stable phases as sources of Cs and oxygen vapors in thermionic energy converters, increasing power and reservoir operating temperature
09 p1263 A72-22959
- Thermionic converter model analysis for performance stability and inhomogeneities in Cs diode, considering emission current dependence on temperature
11 p1578 A72-26759
- Broadband correlation meter with multiplier using vacuum thermal converters for 1.5 KHz-15 MHz range and variable signal delay
13 p1961 A72-29920
- Dexter - A one-dimensional code for calculating thermionic performance of long converters.
17 p2521 A72-34587
- Reactor core length, externally configured thermionic converter.
17 p2495 A72-34589
- Development of a full-length external-fuel thermionic converter for in-pile testing.
17 p2495 A72-34590
- Implications of ceramic-insulator irradiation results for thermionic reactor design.
17 p2496 A72-34592
- Dielectric breakdown in electrical insulators used in thermionic converters.
17 p2496 A72-34593
- Oxygen adsorption effect in Cs-W thermionic converter system, comparing statistical-mechanical model analytical results with Alleau-Bacal experimental data
17 p2496 A72-34597
- Impurities and additives effects on electrode properties in Cs vapor thermionic converter, noting coadsorption model for Cs-W-O surface
17 p2496 A72-34598
- The formation of metal-oxygen compounds for additive thermionic converters.
17 p2595 A72-34600
- Output performance of a thermionic converter with an oriented tungsten /110/ emitter and a polycrystalline tungsten collector.
17 p2496 A72-34604
- Performance comparison of thermionic converters with several collector materials.
17 p2497 A72-34606
- Out-of-core evaluations of a nonfueled and a UO₂-fueled cylindrical thermionic converter.
17 p2497 A72-34608
- Evaluations of uranium-nitride fueled converters.
17 p2497 A72-34609
- Parametric optimization of a cylindrical converter with a molybdenum emitter and niobium collector.
17 p2497 A72-34610
- The influence of the electron temperature and other parameters on the electron density of a cesium plasma in a thermionic converter.
17 p2497 A72-34611
- Suppression of arc drop in thermionic converters.
17 p2497 A72-34612
- Computed performance data for a thermionic converter having a Cl-CVD-W emitter and a polycrystalline Nb collector.
17 p2521 A72-34613
- Applications of an improved formalism for the analysis of transport phenomena in gaseous mixtures and plasmas.
17 p2587 A72-34615
- Cythere capsule for irradiation of experimental fuel elements under geometric and thermal conditions representative of thermionic converters
17 p2579 A72-34619
- Effect of a transverse magnetic field on the operation of a thermionic converter under undercompensated Knudsen conditions.
17 p2497 A72-34862
- Cesium oxide system stable phases as sources of Cs and oxygen vapors in thermionic energy converters, increasing power and reservoir operating temperature
17 p2498 A72-35888
- Thermodynamic analysis of metal surfaces covered by electropositive adsorbates.
18 p2656 A72-36126
- W /100/ work function change during adsorption of oxygen, cesium, and oxygen-cesium co-adsorption
18 p2656 A72-36128
- Investigation of the properties of electrode materials made on the basis of high-melting-point compounds and alloys
18 p2698 A72-36136
- Vapor deposition of refractory metals applied to thermionic conversion - Performance of deposits obtained by reduction of fluorides at high temperature and low pressure
18 p2656 A72-36138
- Thermionic converters performance and life tests, discussing test equipment and diffusion effect on emitter stability
18 p2643 A72-36139
- Neutron irradiation effects on thermionic converter materials, performance and service life
18 p2707 A72-36140

- Thermionic converters fuel tests by uranium dioxide-Mo cermet irradiation, noting fission gas retention and metallic matrix deformation
18 p2708 A72-36144
- Studies of the influence of CVD tungsten depositing conditions on the formulation of pores resulting from interdiffusion in the emitters of thermionic converters
18 p2698 A72-36144
- Studies of physical-mechanical properties of monocrystal molybdenum and tungsten and electrical characteristics of TIC/thermionic converter/
18 p2698 A72-36158
- Ceramic-to-metal seal development for thermionic fuel elements.
18 p2695 A72-36161
- In-core thermionic converter emitters irradiation tests to determine fuel, fission gas venting system and emission layer performances
18 p2708 A72-36158
- Th 228 decay from short and long term simulation tests of thorium dioxide heat source in thermionic energy converter with W capsule
18 p2709 A72-36166
- Thermionic fuel cladding development, compatibility, stability and performance for uranium carbide-tungsten and uranium oxide-tungsten systems at high temperatures under irradiation
18 p2709 A72-36166
- Thermionic converter heated by gasoline flame or heat pipe, describing materials protection against corrosion and furnace design and operation
18 p2644 A72-36166
- State of development of an actinium fueled thermionic generator.
18 p2644 A72-36166
- Controlled dc to dc converter for a space-qualified thermionic reactor.
18 p2644 A72-36177
- Electronic temperature-flattening of thermionic reactors.
18 p2644 A72-36177
- Closed loop dynamics of in-core thermionic reactor systems.
18 p2644 A72-36177
- Possibility of an inhomogeneous charge distribution in an adsorbed layer
18 p2713 A72-36177
- Switch properties of thermionic diodes with cesium vapor.
18 p2645 A72-36177
- An out-of-core thermionic-converter system for nuclear space power.
18 p2645 A72-36177
- Diogenes development program to obtain information on converters mass production, selling price and service life under irradiation, noting application of thermoelectronic reactor construction
18 p2709 A72-36177
- Thermionic effect-based cesium plasma converter operation as caloelectric converter and cesium diodes
18 p2645 A72-36177
- Cylindrical Cs thermionic converter with unique emitter and five collectors, measuring I-V characteristics to determine emitter work function, ignition voltage and electric power
18 p2646 A72-36198
- Thermionic converters efficiency in commercial power generation applications, considering lifetime, reliability and cost
18 p2646 A72-36198
- Vapor pressure influence of Ba-Cs thermionic converter diodes on I-V characteristics and work functions in terms of anomalous Schottky effect
18 p2646 A72-36198
- The influence of magnetic pressure on the performance of a high-current discharge thermionic converter
18 p2646 A72-36198
- Emitter work function elevation in additive thermionic converters via tungsten oxides deposition on collector
18 p2646 A72-36198
- Sinusoidal potential distributions and volt-ampere characteristics of Knudsen-mode thermionic emission converters
18 p2646 A72-36198
- Volt-ampere characteristics of Ba-Cs plasma thermionic converter with W emitter and Ta collector
18 p2646 A72-36198
- Analytical description of thermionic converter phenomena, assuming position linearity of interelectrode electron energy distribution and local thermodynamic equilibrium in cesium plasma near collector
18 p2646 A72-36200
- High temperature cesium vapor sources based on cesium-graphite system for thermionic converters
18 p2646 A72-36200
- Investigation of physical processes and optimization of thermionic converters with a Cs-Ba filling
18 p2647 A72-36200
- Thermionic converter I-V performance improvement via oxygen addition, examining feasibility of cesium oxide-cesium solution as source
18 p2647 A72-36200

Nonlinear current oscillations in a plasma diode
18 p2714 A72-36205

Probe measurements of a cesium plasma in a simulated thermionic energy converter.
18 p2647 A72-36206

Nonequilibrium relaxation phenomena in the near-emitter region of the thermionic converter.
18 p2647 A72-36209

Short cesium plasma discharge diode as physical model for thermionic reactor, studying ionization, recombination and microwave radiation
18 p2714 A72-36212

Excitation and ionization processes in a low-voltage arc discharge
18 p2714 A72-36213

Investigation of transient pressures in the plasma of a thermionic emission converter
18 p2647 A72-36214

Arc mode thermionic converter at low cesium vapor pressures
18 p2647 A72-36216

On the discharge instability in thermionic converters with long electrodes
18 p2647 A72-36217

Polarization and interferometric investigations of discharge modes in thermionic energy converters
18 p2647 A72-36219

The influence of a nonequilibrium electron distribution function near the cathode and fractional coverage on the characteristics of a thermionic emission converter in the arc mode
18 p2647 A72-36220

Current instabilities and constriction in thermionic converters
18 p2647 A72-36221

Thermionic performance of fluoride CVD tungsten-niobium converter.
19 p2754 A72-37781

Developmental status of thermionic materials.
[GULF-GA-A12128] 19 p2833 A72-38575

Electric power generation by thermionic converters, discussing physical principles of operation and technology utilization in communications, meteorology, geophysics, oceanography and space exploration
20 p2890 A72-39940

Determination of the radial heat conductivity of multilayer tubes for thermionic converters
24 p3461 A72-44875

Thermionic reactor systems for space applications.
24 p3423 A72-45177

HERMIONIC DIODES

NT CESIUM DIODES

Shot noise coefficient calculated from static I-V characteristics for modified thermionic diode with low potential virtual cathode
13 p1915 A72-28467

Design of an external-fueled thermionic diode for in-pile testing.
17 p2495 A72-34585

Comparison of computer-acquired performance data from several fixed spaced planar diodes.
17 p2496 A72-34605

Cylindrical diode characteristics with sublimed electrode surfaces.
17 p2527 A72-34607

Post irradiation examination of a UO₂-fueled thermionic diode with a revolver type emitter.
17 p2578 A72-34618

Work function change of tungsten (110) planes as function of Mo coverage.
18 p2656 A72-36134

State of development of diodes for incore thermionic fuel elements.
18 p2708 A72-36159

Thermionic fuel element triple diode configuration, processing, assembly and performance during neutron irradiation testing in reactor
18 p2645 A72-36178

Switch properties of thermionic diodes with cesium vapor.
18 p2645 A72-36179

Neutronic studies for the French thermoelectronic program
18 p2645 A72-36179

Evaluation of sublimed molybdenum collector coatings for additive diode operation.
18 p2646 A72-36202

Model improvements for thermionic diode plasmas.
18 p2715 A72-36218

Thermionic performance of fluoride CVD tungsten-niobium converter.
19 p2754 A72-37781

Temperature dependence of thermionic emission current density of Pt additive powdered zirconium carbide deposit on diode cathode working surface
21 p2997 A72-40801

HERMIONIC EMISSION

Cs diode discharge current oscillations in Knudsen plasma containing electron and positive ion fluxes from thermionic emission and surface Cs ionization
09 p1361 A72-22960

Thermionic converter model analysis for performance stability and inhomogeneities in Cs diode, considering emission current dependence on temperature
11 p1578 A72-26759

Scandium substitution for lanthanum in lanthanum hexaboride crystal lattice, investigating effect on thermionic characteristics
12 p1854 A72-27309

Radiation damage to refractory metals as related to thermionic applications.
17 p2566 A72-34595

Electron currents injected through dielectrics
17 p2529 A72-34753

Cs diode discharge current oscillations in collisionless Knudsen plasma containing electron and positive ion fluxes from thermionic emission and surface Cs ionization
17 p2593 A72-35889

Local thermionic emission from bare and covered surfaces of cermetelectrodes.
18 p2646 A72-36193

Determination of the emission potential of cesium-coated surfaces at high temperatures with a plane-parallel cesium diode. I - Technology. II - Physical foundations and measurement results
19 p2754 A72-37779

Richardson and effective work functions measurements for thermionic emission from alkali and extended red-sensitive trialkali photocathodes, discussing error minimization
20 p2890 A72-39646

Excess metal buildup kinetics and work function of oxide thermionic cathode activated by emission current, noting effect of metal and oxygen concentrations
21 p2997 A72-40789

Temperature dependence of thermionic emission current density of Pt additive powdered zirconium carbide deposit on diode cathode working surface
21 p2997 A72-40801

Electric field intensity distribution function for thermoelectronic emission from hot cathodes in low temperature plasma, using Richardson formula
21 p3094 A72-41656

Physicochemical investigation of the thermionic emission properties of metals and alloys
22 p3191 A72-42811

THERMIONIC EMITTERS

Design and testing a high fuel volume fraction, externally finned, thermionic emitter.
17 p2495 A72-34586

Work functions of some emitting and collecting refractory metal single crystals.
17 p2595 A72-34601

Output performance of a thermionic converter with an oriented tungsten (110) emitter and a polycrystalline tungsten collector.
17 p2496 A72-34604

Performance comparison of thermionic converters with several collector materials.
17 p2497 A72-34606

Computed performance data for a thermionic converter having a Cl-CVD-W emitter and a polycrystalline Nb collector.
17 p2521 A72-34613

Post irradiation examination of a UO₂-fueled thermionic diode with a revolver type emitter.
17 p2578 A72-34618

Thermionic characteristics of carburized tungsten-rhenium alloys.
18 p2656 A72-36131

Inc core thermionic reactor cylindrical Mo emitter covered with two CVD W layers, discussing first layer adhesion and diffusion characteristics and work function stability
18 p2707 A72-36135

Crystal orientation effect on electron work function in chemical vapor deposited W layers on thermionic converter cylindrical emitters
18 p2717 A72-36142

State of development of diodes for incore thermionic fuel elements.
18 p2708 A72-36150

Room temperature ductility of different types of molybdenum after differing annealing
18 p2698 A72-36155

In-core thermionic converter emitters irradiation tests to determine fuel, fission gas venting system and emission layer performances
18 p2708 A72-36158

High-voltage thermionic reactor using double-sheath fuel elements.
18 p2644 A72-36171

Cylindrical Cs thermionic converter with unique emitter and five collectors, measuring I-V characteristics to determine emitter work function, ignition voltage and electric power
18 p2646 A72-36191

I-V-characteristics of a plane parallel cesium diode with tantalum and tungsten emitter.
18 p2646 A72-36196

Emitter work function elevation in additive thermionic converters via tungsten oxides deposition on collector
18 p2646 A72-36197

Volt-ampere characteristics of Ba-Cs plasma thermionic converter with W emitter and Ta collector
18 p2646 A72-36199

Nonequilibrium relaxation phenomena in the near-emitter region of the thermionic converter.
18 p2647 A72-36209

THERMIONIC POWER GENERATION

Split-core heat pipe reactor for out-of-core thermionic power systems, using center gap for fuel reactivity control
04 p0546 A72-14425

German monograph on thermionic power supply equipment converter network reliability covering I-V characteristics and failure probability calculation
04 p0466 A72-15696

Comet rendezvous and outer planet exploration mission operations by unmanned nuclear electric propulsion (NEP) system with incore thermionic reactors for electric power generation
11 p1722 A72-26173

Annual Thermionic Conversion Specialist Conference, 10th, San Diego, Calif., October 4-6, 1971, Conference Record.
17 p2494 A72-34576

Optimized 100 We multicell thermionic power supply design with high reliability, noting isomeric converter performance characteristics
17 p2495 A72-34583

Thermionic energy conversion with a Ba-Cs-diode.
17 p2496 A72-34603

Thermionic fuel element development status summary.
18 p2708 A72-36151

Multicell thermionic fuel element fabrication technology.
18 p2708 A72-36152

Reactor testing and performance of in-pile thermionic fuel elements, noting neutron radiographs
18 p2708 A72-36160

Breeder reactor testing of fast neutron irradiation effect on alumina and yttria cylinders for thermionic fuel rod designs
18 p2708 A72-36161

Inc core thermionic reactor application to meet European TV broadcasting satellite and submarine and underwater laboratory power requirements
18 p2644 A72-36166

Auxiliary power and electric propulsion applications of thermionic reactor power systems in manned and unmanned space missions
18 p2644 A72-36168

State of development of an actinium fueled thermionic generator.
18 p2644 A72-36169

Aspects on the modular lay-out of incore thermionic reactors.
18 p2645 A72-36175

Significance of the results of the ITR critical experiments for the calculation of an incore-thermionic reactor.
18 p2645 A72-36180

Measurements with thermionic fuel elements in the ITR critical facility.
18 p2645 A72-36181

Voltage-conversion for incore-thermionic-reactors.
18 p2645 A72-36182

A comparison of thermionic reactor designs employing a common thermionic fuel element.
18 p2645 A72-36183

Thermionic converters efficiency in commercial power generation applications, considering lifetime, reliability and cost
18 p2646 A72-36192

The ignited mode of cesium thermionic diode. II - The charge influence on the volt-ampere characteristics.
18 p2647 A72-36211

Thermionic reactor systems for space applications.
24 p3423 A72-45177

THERMIONIC REACTORS

U ION ENGINES

U NUCLEAR ROCKET ENGINES

THERMIONICS

Thermionic Cs arc theory applicability evaluation, considering collision dominated transport equations for plasma
17 p2587 A72-34616

Work function theory for Cs-/W/ and Cs-O-/W/.
18 p2656 A72-36133

THERMISTORS

Azur satellite flight data evaluation of thermal behavior, measuring temperature with thermistors
05 p0746 A72-16139

Atmospheric vapor pressure and temperature direct measurement, using copper-constantan thermocouples for wet-bulb temperature rapid fluctuations and thermistor for mean wet-bulb temperature
07 p0982 A72-19106

Temperature gradients and dynamics of transient heating and cooling processes in metallic thermistors connected in series to power supplies
08 p1252 A72-21307

Anemometer probe with thermistors for low velocities of liquids derived from pulsed thermal conductivity gage
10 p1479 A72-24066

Low cost radiation shield for thermistor deployment in atmospheric boundary layer, noting measurement accuracy relationship to data acquisition system
11 p1682 A72-26087

Atmospheric density variations from meteorological rocket soundings, discussing data reduction methods and error sources for bead thermistor and inflatable falling sphere instruments

11 p1626 A72-26473

Pneumatic thermistor transducer to measure steep ejection time interval between cardiac volume pulse upstroke start and maximum rise rate occurrence

11 p1588 A72-26633

Thermistor anemometers design and measurement of displacement or dispersion coefficients

11 p1636 A72-26699

Thermistor vacuum gage with interchangeable sensing heads, providing improved pressure response and direct interchanging without recalibration

11 p1636 A72-26776

Nose installed thermistor device for in-flight monitoring of pilot respiration and pulse rate

12 p1769 A72-27417

Junction field-effect transistor circuits for prescribed output functions.

18 p2665 A72-36307

Thermistor temperature observation and correction for errors due to refraction anomalies in latitude measurements

19 p2801 A72-37913

Dynamic characteristics of hot-wire anemometers with glass-coated thermistors

21 p3050 A72-40132

Investigation of nonstationary heating processes in thermal resistors fed from functional sources

21 p3129 A72-41060

Possibility of employing a transistorized self-excited oscillator with a thermistor as radio sensor of temperature

21 p3058 A72-41792

Radiation influences on a white-coated thermistor temperature sensor in a radiosonde.

24 p3401 A72-44620

THERMO-PHOTOVOLTAIC GENERATORS

U PHOTOELECTRIC GENERATORS

U THERMOELECTRIC GENERATORS

THERMOAEROELASTICITY

U AEROELASTICITY

U THERMOELASTICITY

THERMOCHEMICAL PROPERTIES

NT HEAT OF COMBUSTION

NT HEAT OF FORMATION

NT HEAT OF VAPORIZATION

Quasi-equilibrium analysis of the reaction of atomic and molecular fluorine with tungsten.

23 p3262 A72-44050

THERMOCHEMISTRY

NT AERTHERMOCHEMISTRY

Thermochemical methods for plasticized/stabilized cellulose nitrate kinetic constants determination for lifetime estimation, presenting isothermal decomposition curves

14 p2144 A72-30753

Thermochemical techniques application to corrosion protection of metallic powders, mechanical parts and tools, describing chromizing, chromaluminizing, tantalizing and niobiumizing processes

[ONERA, TP NO. 1049]

19 p2817 A72-37769

Development of the AEDC-VKF tunnel J - A real gas high density, true velocity, hypersonic, aerodynamic test facility.

[AIAA PAPER 72-993]

21 p3040 A72-41579

THERMOCINES

Internal waves in sheeted thermocline with finite discontinuities in density profile formulating eigenvalue problem as homogeneous Fredholm integral equation

16 p2386 A72-33573

THERMOCOMPRESSION

U COMPRESSING

U HEATING

THERMOCOUPLES

Thermocouple efficiency with respect to Thomson effect and electric resistivity temperature dependence

03 p0360 A72-13651

Refractory metal thermocouple research program, describing design and performance of ultrahigh vacuum high temperature furnace system

04 p0524 A72-15550

Turbine inlet temperature sensor for gas turbine engines, using noble metal thermoelements with high signal level

[SAE PAPER 720160]

06 p0812 A72-17322

Thermal contact resistance measurement in double contact thermocouple specimens at 250-650 C in Ar and air-vacuum

07 p1098 A72-18987

Atmospheric vapor pressure and temperature direct measurement, using copper-constantan thermocouples for wet-bulb temperature rapid fluctuations and thermistor for mean wet-bulb temperature

07 p0982 A72-19106

Small gage thermocouples calibration procedure, noting data correlation with thermoelectric theory

07 p0984 A72-19326

Assessment of regional myocardial temperature changes effect on blood flow measurements by heated cross-thermocouples in dogs

10 p1432 A72-25071

Resistance wires and wire thermocouple junctions temperature response in low pressure gases, taking into account wire mounting temperature effect

11 p1632 A72-26000

Digital precision measurement of thermocouple thermal emf at 200-1000 C, examining block diagram

11 p1634 A72-26457

Temperature control and measurement in electric wire annealing for standard Pu/Pt-10 Rh thermocouples

13 p1960 A72-29766

Temperature measuring instrument with thermocouple for differential thermal analysis equipment used in phase diagram construction

14 p2106 A72-30995

Fine wire thermocouple probe use for measurement of total temperature in shock tube lasers

15 p2241 A72-32524

Closed form solution for transient temperatures between two thermocouple readings, using Laplace transformation

15 p2336 A72-32583

Lateral heat exchange in a thermocouple

17 p2498 A72-35513

A thermal oscillator using the thermo-electric /Seebeck/ effect in silicon.

18 p2667 A72-36978

Study of reliability of Al-Au thermocompressions by measurement of resistance

18 p2668 A72-37105

Measurement of flow speed by the correlation method

21 p3056 A72-41252

Fine wire thermocouple probes for stagnation temperature measurements in hypersonic mixing layers [AIAA PAPER 72-1023]

21 p3057 A72-41601

THERMODYNAMIC COUPLING

Solar chromosphere radiative transfer and thermal conduction coupling, applying singular perturbation method to Frisch analysis

07 p1070 A72-19087

Sufficient conditions definition for existence of solution for heat conduction equation coupling to telegrapher equation

07 p1028 A72-19897

Thermodynamic coupling effects on temperature distribution, Nusselt number and cooling requirements in laminar nonisothermal pipe flow with coolant injection

11 p1745 A72-25734

Thermomechanical coupling effects in the longitudinal oscillations of a viscoelastic cylinder.

23 p3352 A72-44122

THERMODYNAMIC CYCLES

NT BRAYTON CYCLE

NT CARNOT CYCLE

NT OTTO CYCLE

NT RANKINE CYCLE

NT STIRLING CYCLE

Reversible thermodynamic cycle of chemical to electric energy conversion with electron gas as working body, discussing Gibbs-Helmholtz equations

16 p2350 A72-32994

Large-scale concentration and conversion of solar energy.

18 p2643 A72-36075

Cryopump cooling requirements, refrigeration, design and vacuum application, considering Brayton, Claude, Stirling cycles and Joule-Thomson and regenerative processes

18 p2696 A72-36838

Russian book - Optimization of thermal circuits of complex gas-turbine power plants

19 p2848 A72-37450

Thermodynamic cycle parameter effects on bypass turbofan jet engine fuel consumption and performance under various flight conditions and engine ratings

23 p3326 A72-44281

Metal vapor plasma as working medium in MHD generator, discussing hydrodynamic relations, power efficiency and thermodynamic cycle

24 p3428 A72-45169

THERMODYNAMIC EFFICIENCY

Analytical models for predicting mass transfer cooling effects on blade root efficiency of turbine airfoils [AIAA PAPER 72-11]

05 p0707 A72-16943

Heat transfer and hydraulic resistance of lamellar type heat exchangers with water/air working media, testing efficiency for various duct cross sections and Reynolds numbers

06 p0904 A72-18510

Basic thermodynamic efficiency relationships for irreversible processes under all system circumstances, introducing high grade energy concept

07 p1101 A72-20543

Coaxial plasmatron with central electrode composed of cylindrical Cu and W thermionic cathodes, noting thermal efficiency

08 p1214 A72-21455

Elements of the theory of gas-turbine-unit designs

21 p3100 A72-41700

THERMODYNAMIC EQUILIBRIUM

Two dimensional plasma under dc magnetic field, investigating thermal equilibrium with Liouville equation and BBGKY hierarchy

01 p0107 A72-10145

Book on thermodynamic theory of structure, flow stability and fluctuations covering equilibrium and nonequilibrium states, nonlinear situations and space-time behavior

02 p0261 A72-12624

Thermodynamic equilibrium variational theory for multiphase systems subject to nonhydrostatic stress considering diffusion and phase transformations

03 p0455 A72-12909

French papers on shock waves in fluids and solids covering gas flows in thermodynamic equilibrium and across conic shocks of revolution

03 p0341 A72-13683

Statistical thermodynamics models for determining vacancy concentration and atoms and vacancies arrangement in metals and alloys under thermodynamic equilibrium

03 p0378 A72-14255

Outer planets satellites physics and chemistry, discussing steady state thermal models based on energy equilibrium between internal radioactive decay and surface radiation

04 p0568 A72-14495

Equilibrium temperature formula derived for surface subjected to aerodynamic heating by gas from heat balance between convective and radiative heat flow

04 p0595 A72-14651

Energetic excitation of precursor compounds in gaseous phase for models of primordial atmospheres in thermodynamic equilibrium

04 p0552 A72-14759

Diffusion and thermal equilibrium models of stationary Tokamak, analyzing differences

04 p0558 A72-15173

Small sphere hydrodynamic drag in ionized gas at local thermodynamic equilibrium, taking into account nonlinear transport properties variations with temperature

[ASME PAPER 71-APM-CC]

04 p0558 A72-15176

Thermal nozzle combustion effects on supersonic flow of chemically reacting gas in thermodynamic equilibrium

05 p0599 A72-15846

Steady state operational characteristics of two component heat pipes, applying mass and energy conservation laws and thermodynamic phase equilibrium relations

[ASME PAPER 71-WA/HT-30]

05 p0745 A72-15853

Ni-Mo-N system alpha-solid solution thermodynamic analysis, deriving reaction enthalpies/entropies/free energy and interaction coefficients

05 p0676 A72-16795

Neutron star and white dwarf strong magnetic field generation mechanism involving thermodynamic equilibrium states of electron gas

05 p0723 A72-17163

Thermodynamic equilibrium relations in optical thin plasma models for hydrogen and argon systems

05 p0699 A72-17214

Thermodynamic equilibrium, transport and optical properties and quantum effects in nonideal plasmas using Monte Carlo method

05 p0700 A72-17223

Equilibrium temperatures of interstellar grains around early stars, discussing dependency on grain size and stellar distance

06 p0875 A72-17293

Black radiation kinetics of photon thermalization in body cavity in static thermodynamic equilibrium

06 p0847 A72-17733

Shielding of solid surface vaporizing under laser radiation effect in presence of thermal and ionization nonequilibrium, investigating absorption flare onset mechanism

06 p0825 A72-17909

Nonequilibrium thermodynamics description of rarified gas relaxation phenomena for very fast flow processes with translational temperatures

06 p0902 A72-18137

Nonequilibrium transitions for thermodynamic systems with generalized forces and flows by linear transformations, applying to nonelectrolyte solutions with concentration and temperature gradients

07 p1097 A72-18806

Thermal equilibrium fluctuations and Rayleigh light scattering in isotropic gyrotropic continuous medium with internal rotational degrees of freedom

07 p1034 A72-18909

Rate controlled partial thermodynamic equilibrium method for treating reacting gas mixtures, applying to freezing reactions in internal combustion engine

07 p1099 A72-19377

Thermodynamic models of gas-solid equilibria in cosmochemical systems containing H, O, Si, Mg, S, C, Cl and F

07 p1075 A72-19587

Hydrogen plasma ionization equilibrium and thermodynamic stability existence condition based on Saha equation

07 p1044 A72-19889

Non-LTE effects on mechanical heating in gray atmosphere applied to nonradiative energy input estimates for solar chromosphere from negative hydrogen ion emission

08 p1235 A72-21391

Non-LTE atmospheric model calculations for H, He I and II spectra of O stars, discussing He abundances 08 p239 A72-21949

Astrophysical abundances analysis, discussing assumptions of local thermodynamic equilibrium and microturbulence in stellar atmospheres 09 p1386 A72-22659

Thermodynamic formulation of noble gases equilibrium and transport properties at low and moderate densities, proposing corresponding states law 09 p1410 A72-22767

Radial temperature distribution in Ar plasma jet, assuming local thermodynamic equilibrium 09 p1364 A72-23387

Equilibrium thermodynamics of critical points, discussing phase transition theory and scaling hypothesis for single component systems 10 p1562 A72-24400

LTE solutions of relativistic Boltzmann equation in presence of external electromagnetic field 10 p1513 A72-24856

Black radiation kinetics of photon thermalization in body cavity in static thermodynamic equilibrium 11 p1685 A72-25336

Thermodynamic equilibrium theory for upper atmosphere /thermosphere/ temperature and density variations, noting Harris-Priester model 11 p1622 A72-25844

Thermal equilibrium coefficient of ionized plasma spatial diffusion transverse to strong uniform dc magnetic field, extending Taylor-McNamara calculation scheme to three dimensions 13 p2011 A72-29120

Thermal nozzle combustion effects on supersonic flow of chemically reacting gas in thermodynamic equilibrium 15 p2334 A72-31265

Formation mechanism of sodium sulfate from gas turbine fuel combustion, discussing thermodynamic equilibria and reaction kinetics 15 p2297 A72-31294

Solar photosphere and low chromosphere spectral lines non-LTE empirical analysis, relating coefficients of departure from LTE to elemental state temperatures 15 p2317 A72-32771

Mathematical model of atmospheric tides using Navier-Stokes equations for perfect gas in thermodynamic equilibrium 16 p2385 A72-33343

French book on thermodynamics of equilibrium and nonequilibrium composite systems covering entropy potentials for n degrees of freedom system 16 p2478 A72-33503

Radiant energy transfer in dispersive medium of low optical density under LTE and radiant equilibrium 16 p2427 A72-33859

Hydrogen plasma ionization equilibrium and thermodynamic stability existence condition based on Saha equation 17 p2590 A72-35137

Thermodynamic analysis of metal surfaces covered by electropositive adsorbates. 18 p2656 A72-36126

Analytical description of thermionic converter phenomena, assuming position linearity of interelectrode electron energy distribution and local thermodynamic equilibrium in cesium plasma near collector 18 p2646 A72-36200

Equilibria and degassing kinetics in the systems Mo-N, W-N, and Re-N 18 p2701 A72-36596

Thermodynamic description of the metal-rich part of the system niobium-molybdenum-nitrogen 18 p2701 A72-36597

Negative temperatures in two dimensional vortex motion. 18 p2681 A72-36669

The helium abundance in thirty-three main sequence B stars. 18 p2726 A72-36726

Negative index polytropic sphere gravitational collapse structure, noting application to interstellar gas clouds thermal equilibrium 19 p2857 A72-37794

Thermal boundary equilibria in brittle bodies with heat conducting cracks under combined loads and temperature fields 19 p2877 A72-38198

Thermohydrodynamic conditions at the peak flux of horizontal heaters in superfluid liquid helium II at zero net mass flow. 20 p2984 A72-39647

Application of the elementary-balance method to the calculation of the nonstationary temperature fields and aerodynamic characteristics of several versions of a surface-type heat exchanger 21 p3130 A72-41064

Ar plasma diagnostics from stabilized arc emission spectra, noting thermodynamic equilibrium in central zone of arc channel 22 p3209 A72-41880

Buildup of thermal equilibrium in a fluid near the critical point 22 p3242 A72-41882

Russian book - Radiation characteristics of gases at high temperatures. 22 p3243 A72-42075

Low abundance of solar photosphere iron from Fe I excitation and ionization computations, showing LTE departure effects on spectral lines 22 p3228 A72-42569

Dipole moment derivative of triatomic hydrogen ion electronic ground state, considering fundamental spectrum observation in hydrogen gas in local thermodynamic equilibrium 22 p3209 A72-42720

Nuclear reactions in a degenerate electron-nuclear plasma 22 p3209 A72-42964

Nonlinear hydrothermodynamic model of steady atmospheric motion in equatorial latitudes with energy influx approximation 23 p3284 A72-43533

Stability of Al₃Mg₂ particles against diffusive coagulation in aluminum-magnesium alloys 23 p3301 A72-43649

Thermal equilibrium calculations of the lower Venus atmosphere. 24 p3439 A72-44955

THERMODYNAMIC PROPERTIES

NT CRITICAL POINT

NT CRITICAL PRESSURE

NT CRITICAL TEMPERATURE

NT EMISSIVITY

NT ENTHALPY

NT ENTROPY

NT FREE ENERGY

NT GIBBS FREE ENERGY

NT HEAT OF COMBUSTION

NT HEAT OF FORMATION

NT HEAT OF SOLUTION

NT HEAT OF VAPORIZATION

NT MELTING POINTS

NT PYROELECTRICITY

NT SPECIFIC HEAT

NT SUPERCRITICAL PRESSURES

NT SURFACE ENERGY

NT THERMAL BUCKLING

NT THERMAL CONDUCTIVITY

NT THERMAL DIFFUSION

NT THERMAL DIFFUSIVITY

NT THERMAL EXPANSION

NT THERMAL INSTABILITY

NT THERMAL STABILITY

NT THERMOCHEMICAL PROPERTIES

NT THERMOPHYSICAL PROPERTIES

NT VAPOR PRESSURE

NT VOLATILITY

Aerospace adhesives applications, discussing thermal and mechanical properties, and cryogenic, epoxy, urethane silicone and fluorocarbon types 01 p0090 A72-10188

Carbon atoms thermodynamic properties in bcc and fcc Fe-Si-C solid solutions from equilibrium measurements with hydrogen-methane gas mixtures as function of temperature and carburizing gas composition 01 p0083 A72-10207

Solid materials inelastic constitutive relations, developing internal variable thermodynamic formalism for microstructural rearrangements 03 p0446 A72-13710

Vapor pressure and partial thermodynamic functions of Co-Ni alloys, observing negative deviations from Raoult law 03 p0374 A72-13928

Statistical mechanical calculation of thermodynamic properties of interstitial solid solutions involving second nearest neighbor solute atom mutual interactions based on Kirkwood expansions 03 p0459 A72-14252

High temperature thermal properties of solid and liquid metals and rocks and minerals, discussing earth heat balance and measurement methods for heat capacity and conductivity 04 p0596 A72-14653

Electromagnetic-thermal properties of lunar surface layers for radio communication around moon 04 p0577 A72-15121

Performance similarity of supersonic axial compressors with gas mixtures of different thermodynamic properties, verifying validity of critical Mach number of rotation [ONERA, TP NO. 966] 04 p0463 A72-15556

Bound states and Coulomb interaction effects on thermodynamic properties of cesium plasma calculated on computer for different pressures and temperatures 05 p0693 A72-15838

Model intermolecular interaction potentials constants determination for extrapolating thermodynamic properties of gases at high temperatures and pressures 05 p0692 A72-15842

Thermal and I-V characteristics of dc plasmatron with vortex stabilized arc, interelectrode insert and diverging arc channel for various nozzle diameters 05 p0694 A72-15854

Tantalum carbide specific heat and other thermodynamic properties over 0-3000 K range 05 p0672 A72-16097

Thermodynamic parameters correlation of planetary atmosphere with planetary probe parachute descent rate applied to Venera 5 and 6 data 05 p0721 A72-16769

Potential parameters determination from collision integrals in thermodynamic properties calculation for combustion products at moderate and low temperatures 05 p0751 A72-17067

Thermodynamic function error influence on rocket engine combustion product characteristics including combustion chamber temperature and specific pressure pulse 05 p0751 A72-17069

Aerodynamic and thermodynamic phenomena in Hartmann-Sprenger tube with converging walls and excited by subsonic or adapted supersonic jet 06 p0901 A72-17559

Viscoplasticity theory thermodynamic foundations, considering stress/strain states time and deformation path dependence 06 p0896 A72-17963

Dimensionless parameter for thermodynamic state prediction in atmospheric pressure plasma jets, using conservation equations 06 p0862 A72-18188

Lunar surface temperature-independent and dependent plane homogeneous models for thermal properties study, discussing surface roughness and localized thermal anomalies 06 p0887 A72-18227

Niobium carbide thermodynamic properties tabulated for 0-3000 K, deriving equation for heat capacity from low temperature experiments 06 p0832 A72-18430

Laplace equation internal Dirichlet and Neumann boundary value problems solution procedure for thermal potential of steady temperature field 07 p1098 A72-18988

Thermal and electrical characteristics of plasmatrons with interelectrode partition and distributed air supply, determining efficiency dependence on current 07 p1040 A72-18996

Nonstoichiometric compounds thermodynamic properties in terms of indistinguishability of ions /atoms/ in different valence states 07 p1048 A72-19544

Thermodynamic and electrical properties of tantalum nitride powders and thin films for semiconductors IC technology 07 p1049 A72-19935

Chemical composition, thermal properties and shock propagation in solar wind plasma 07 p1061 A72-20018

Lunar and terrestrial soil thermal and electrical properties measurement in vacuum and He atmospheres 08 p1232 A72-21150

Heisenberg ferromagnet thermodynamic properties in external magnetic field near Curie temperature, studying magnetization, susceptibility, entropy and magnetocaloric effect 08 p1217 A72-21520

Thermodynamic properties of atomic hydrogen-helium plasma for postulated conditions present in stagnation shock layer of spacecraft entering Jupiter atmosphere 08 p1254 A72-21598

Thermal and mechanical properties of randomly reinforced fiber/resin composites including boron/epoxy, Thorne/epoxy and S glass/epoxy materials 08 p1192 A72-21682

Spin excitation effects in superconductors, noting impurity concentration effects on transition temperature and thermodynamic properties 09 p1368 A72-22558

Thermal behavior of explosively welded metals, describing test facility for temperature measurements of joints 09 p1319 A72-22891

Thermodynamic properties of high temperature and density hydrogen, using Rowlinson equation of state 09 p1412 A72-23234

Nb-W equilibrium phase diagram estimation from known phase diagrams of Ni-Nb, Ni-W and Ni-Nb-W systems via Guggenheim quasi-chemical model application to Ni-Nb-W thermodynamic properties 10 p1496 A72-24233

Gruneisen tensor relationship to elastic and thermal properties of anisotropic quartz fiber-phenolic composite 10 p1500 A72-24251

Vanadium enthalpy and heat of fusion measurement with massive copper calorimeter 10 p1497 A72-24784

Russian book on radar studies of moon covering lunar motion, dimensions, mass, density and surface layer thermal and optical properties 11 p1720 A72-26047

Thermodynamic description of metal rich side of Nb-Mo-N solid solution, determining equilibrium

nitrogen solubility as function of pressure and temperature

11 p1664 A72-26842

Papers on thermal characteristics of moon covering earth based and in situ surface temperature measurements, radar mapping, heat flow experiments, etc

12 p1869 A72-27326

Apollo 11 and 12 lunar samples thermal properties, presenting diffusivity, conductivity and specific heat

12 p1869 A72-27334

Lunar surface roughness thermal characteristics, comparing IR data with three realistic models

12 p1870 A72-27335

Molecular structure and thermomechanical properties of polyimide and polyamide resins used for precision parts

12 p1833 A72-27406

Fiber reinforced Mod 3 carbon-carbon composites mechanical and thermal properties comparison with polycrystalline bulk graphite

12 p1834 A72-28087

Carbon-carbon composite material for high performance aircraft braking systems, noting weight savings and thermal characteristics improvements

12 p1835 A72-28093

Composite materials mechanical and thermal properties for ATS reflector supporting truss, noting graphite fiber reinforced epoxy plastic design, fabrication and tests

12 p1886 A72-28158

Statistical Coulomb potential and thermodynamic, kinetic and optical properties of nonideal dense plasma

12 p1853 A72-28173

Russian book on combustion products thermodynamic and thermophysical properties covering fuels and propellants characteristics, equilibrium fuel compositions, gas phase transfer and expansion processes, etc

12 p1890 A72-28336

Instrument to measure thermodynamic, electrical and optical properties of gases and liquids, describing thermostat for 83-923 K range

13 p1956 A72-28633

Thermodynamic limiting relations between physical measurement accuracy and measurement performance energy dissipation, considering equilibrium and nonequilibrium dynamic models

13 p2003 A72-28761

Combustion products thermodynamic parameters for natural gas burning in oxygen atmosphere, plotting gas temperature and flow rates against pressure and excess oxidant ratio

13 p2065 A72-29451

Air composition and thermodynamic properties at 12,000-25,000 K and 0.1-100 atm with allowance for Coulomb interaction effect on pressure and for ionization potential decrease

13 p2018 A72-29878

Shock wave and isentropic compression/expansion in plasma with anomalous thermodynamic properties due to strong particle interactions, discussing phase transitions types

13 p2019 A72-29904

Vanadium enthalpy and heat of fusion measurement using massive copper calorimeter with isothermal jacket

14 p2113 A72-30222

Non-Maxwellian inhomogeneous collisionless plasma equilibrium and stability, proposing statistical thermodynamic model

14 p2137 A72-30394

Alpha solid solution of nitrogen in Nb-Mo alloys, obtaining excess partial quantities and activity and interaction coefficients at high temperatures

14 p2121 A72-30773

Thermomechanical erosion prediction for ablative, composite material, reentry nosetip applications and model development for heating, pressure and shear forces

[AIAA PAPER 72-299]

14 p2171 A72-30827

Ferrite materials for microwave applications, discussing frequency and temperature limit extension, power level increase and loss reduction

14 p2088 A72-30833

Bound states and Coulomb interaction of continuum particles effects on thermodynamic properties of cesium plasma calculated on computer for different pressures and temperatures

15 p2283 A72-31259

Model intermolecular interaction potentials constants determination for extrapolating thermodynamic properties of gases at high temperatures and pressures

15 p2280 A72-31261

Thermal and I-V characteristics of dc plasmastron with vortex stabilized arc, interelectrode insert and diverging arc channel for various nozzle diameters

15 p2283 A72-31271

Monatomic ionized gas thermodynamic properties direct computation by numerical method without iteration or numerical differentiation

15 p2335 A72-31714

Thermodynamic freezing theory of small solution droplets containing insoluble particles, considering

ammonium sulfate concentration for ice formation in clouds

16 p2476 A72-33380

Thermodynamic properties of axisymmetric and planar stagnation flows of air with gas injection, taking into account mass transfer effects on heat transfer rate

16 p2477 A72-33428

Thermodynamic interaction parameters of solid solution bcc V-Ti-Cr alloys by Knudsen effusion method combined with mass spectrometer

16 p2409 A72-33803

Onsager irreversibility theory extension to nonlinear constitutive relations and with allowance for inclusion of all thermodynamic variables

16 p2479 A72-33826

Liquid metals thermodynamic properties tabulation, including high melting transition metals, based on levitation data and periodic table correlations

16 p2479 A72-34000

Thermodynamic properties of liquid Co and Pd metals by levitation calorimetry, including specific heat, heats of fusion and surface emissivities

16 p2480 A72-34025

Ionized gas-solid suspension thermal physical properties verification by micro-sized MgO dispersion in Ar plasma

16 p2439 A72-34054

Carbon fibre composites with ceramic and glass matrices. I - Discontinuous fibres.

17 p2570 A72-34668

Planetary atmosphere thermodynamic parameters correlation between spacecraft parachute descent rate and measured data, noting Venera spacecraft example

17 p2610 A72-35272

Influence of the transverse distribution of pumping on the energetics and the profile of thermo-optical distortions in a rhodamine 6G laser

17 p2563 A72-35302

Solid-gas phase equilibria and thermodynamic properties of cadmium selenide.

17 p2511 A72-35329

A computation method for the determination of thermodynamic values and performance data of rocket propellants, propellant charges for cannons, and ignition mixtures

17 p2596 A72-35418

Analytical investigation of normal shock waves in water near the thermodynamic critical point.

17 p2543 A72-35635

Thermodynamic properties of Cs-vapors.

18 p2713 A72-36210

Interdependence of the commutation and memorization effects and the thermal behavior in a series of chalcogenide glasses

18 p2718 A72-36344

Thermodynamics and phase relations in refractory metal solid solutions containing carbon, nitrogen, and oxygen.

18 p2699 A72-36576

Heterogeneously combusting binary gas mixture ignition time as function of initial state and thermokinetic properties, noting heat conduction equations for fuel and oxidizer

19 p2879 A72-37358

Thermal expansion at elevated temperatures. III - A hemispherical laminar composite of pyrolytic graphite, silicon carbide and its constituents between 300 and 800 K.

19 p2822 A72-37463

Thermodynamic properties and mathematical modeling of complex biological systems, considering energy and mass exchange in photosynthesizing organisms for exobiological life support

20 p2891 A72-38960

Mathematical models for radiative heat transfer prediction in real enclosures, noting directional characteristics of heat exchanging surfaces

[ASME PAPER 72-HT-K]

20 p2984 A72-39652

Finite difference calculus development of method to express thermodynamic limit of statistical-mechanical average as power series in number density, noting advantages and applicability

21 p3087 A72-40562

Problem of oscillation self-excitation due to the dependence of the normal velocity of a flame on the thermodynamic parameters of a gas

21 p3129 A72-40985

Thermodynamic parameters and reacting multicomponent mixture composition, using state equations and energy conservation equations for reaction kinetics

21 p3013 A72-40989

Internal energy and conductive and frictional dissipation, mass, momentum and energy production as functions of density, entropy and geometric state variables

21 p3130 A72-41228

High-temperature thermodynamic properties of the chromium carbides determined using the torsion-effusion technique.

22 p3193 A72-43029

Electron-beam flow visualization - Applications in the definition of configuration aerothermal characteristics.

[AIAA PAPER 72-1016]

24 p3404 A72-45405

Methods for determining thermal properties of anisotropic systems.

24 p3465 A72-45633

THERMODYNAMICS NT AEROTHERMODYNAMICS NT COMBUSTION PHYSICS

Elastic stability of body under conservative loads, deriving energy criterion with thermodynamic laws

02 p0292 A72-12003

Differential nonstationary heat equations numerical solution for bladed gas turbine air cooled disk, taking into account cascade vertical temperature variation and coolant heating

02 p0301 A72-12251

Book on thermodynamic theory of structure, flow stability and fluctuations covering equilibrium and nonequilibrium states, nonlinear situations and space time behavior

02 p0261 A72-12624

Gaseous general relativistic kinetic theory, detailing matter model, thermodynamics, cosmology and Einstein field equation completion with Liouville or Boltzmann equation

03 p0388 A72-13266

Thermodynamic theory of rheological materials with internal changes accounting for higher gradients of deformation and temperature

03 p0448 A72-13888

Thermal theory of criticality for spontaneous explosion of exothermic reactant mass in bodies of arbitrary shape

03 p0457 A72-13972

Thermodynamic and dissipative restrictions on isothermal stress relaxation functions in linear viscoelasticity

04 p0583 A72-14462

Electrochemical machining electrode processes thermodynamic and kinetic characteristics, discussing temperature, electrolyte viscosity and flow rate and current density effects on metal removal rate

04 p0526 A72-14475

Irreversible thermodynamics applications to physicochemical and biological stability, including allosteric activation model

04 p0482 A72-14754

Thermodynamic solids theory generalized for internal strains in perfect non-Bravais crystals, applying to trigonal Se and Te structure

04 p0562 A72-15470

Thermodynamics of holonomic media applied to perfect gases

05 p0648 A72-16123

Thermodynamics near steady state, considering stability criterion

05 p0746 A72-16159

Thermodynamic estimation of transition metal stacking fault energy, discussing relation to lattice stability and structural changes

05 p0679 A72-17149

French book on wave mechanics reinterpretation covering double solution theory, particle thermodynamics, guidance dynamics, etc

06 p0847 A72-17813

Green-Naghdi nonlinear thermodynamics of elastic-plastic deformation at finite strain, discussing relationship to nonisothermal theory

06 p0896 A72-17921

Thermodynamics of Mo silicidation reactions from gas phase in silicon chloride and hydrogen media, discussing glow discharge maximum yield

07 p0937 A72-20417

Unsteady heat conductivity equation for finite dimensions parallelepiped, noting temperature dependence of specific heat and thermal conductivity

08 p1252 A72-21321

Three dimensional heat diffusion equation for multiemitter power transistor, taking into account thermal instability due to geometry

08 p1141 A72-21418

Conductive heat transfer equation solved by finite difference scheme with uniform rapid convergence

08 p1253 A72-21458

Thermodynamics of ceramic oxide corrosion by sulphur and oxygen bearing atmospheres, considering formation products and furnace refractory materials choice

09 p1333 A72-22377

Averaging process in thermodynamic systems energy transformation description

09 p1410 A72-22635

Thermodynamic quantities expression in terms of S matrix to formulate questions pertaining to statistical mechanics-particle physics boundary, applying to cosmology

09 p1355 A72-22750

Mathematical thermodynamic theory for plastic deformation induced internal structure changes in rheological material, describing homogeneous response by temperature and deformation gradients

09 p1403 A72-22761

Equations of state for ultrahigh densities, obtaining relativistic statistical thermodynamics description of hadronic interactions

10 p1533 A72-23891

Generalized thermodynamic potentials and universal criteria for direction of evolution of irreversible processes from Gibbs function stability analysis
10 p1562 A72-24250

Monograph on fuel cells covering thermodynamics, electrode polarization principles, electrocatalysis, system requirements, operational principles and applications
10 p1423 A72-24700

Discrete random walk heat conduction equation for thin layer with stepwise temperature change, comparing with parabolic and hyperbolic solutions
11 p1744 A72-25266

Local and cosmological irreversibility and time anisotropy theories from thermodynamics, statistical mechanics, astrophysics and quantum-relativity viewpoints
11 p1716 A72-25775

Thermodynamics of human body metabolism, discussing energy conversion calorimetric measurements, body size, food intake, age, sex, endocrine and nervous effects
11 p1584 A72-26072

Heat equation for insulated uniform body, examining definition and continuity of mapping from linear manifold of assumed boundary values
11 p1747 A72-26555

Temperature anisotropy quasi-linear relaxation thermodynamics in collisionless plasma, analyzing system free energy
11 p1698 A72-26599

Thermodynamic analysis of heat of evaporation of sweat, considering ambient temperature and humidity effects, body heat storage and presence of solutes
11 p1586 A72-26610

Nonlocal elasticity theory from global equilibrium and second thermodynamics laws, deriving constitutive equations from Clausius-Duhem inequality and Gibbs thermodynamics
11 p1738 A72-26721

Chernikov approximation for general relativistic thermodynamics nonstationary equations of heat transfer, thermal and viscous stresses and entropy balance
12 p1844 A72-27188

Microstructure effects on thermomechanically processed dispersion strengthened Ni alloys yield strength at various temperatures
14 p2114 A72-30368

Constitutive equations for multipolar solid with memory, deriving boundary conditions and free energy equation from first and second thermodynamics laws respectively
15 p2273 A72-31363

Plasticity, elastic relaxation and stress-strain relation characterization for Schofield-Scott Blair media, using nonequilibrium thermodynamics method
15 p2331 A72-32482

Parabolic differential equations to define exponential spatial decay of heat equation solutions, replacing Edelman energy estimate by time-independent estimate
16 p2475 A72-33005

Numerical solution to Percus-Yevick equation and thermodynamic functions of dense gas in supercritical temperature range with Lenard-Jones potential
16 p2476 A72-33160

Heat equation kernel functions existence proof based on Harnack selection principle and inequality
16 p2476 A72-33187

Book on plasma production, diagnostics and thermodynamics for equilibrium and stationary ionization states covering magnetic confinement, toroidal and adiabatic traps, MHD flow, etc
16 p2435 A72-33450

French book on thermodynamics of equilibrium and nonequilibrium composite systems covering entropy potentials for n degrees of freedom system
16 p2478 A72-33503

Biological structures study, proposing generalized thermodynamics for dissipative structures role in living beings functions
16 p2354 A72-33519

Soviet book on continuum mechanics covering dynamic, thermodynamic and electrodynamic equations mechanic problems, three dimensional space, internal degrees of freedom, etc
16 p2425 A72-33578

Thermodynamic theory of materials with memory depending on temperature gradient summed history
16 p2425 A72-33587

Thermomechanical and thermogravimetric analyses of systematic series of polyimides
17 p2511 A72-34714

Thermodynamic basis for plasticity theory in case of small deformations, considering elastic region isotropic representation and linear relation as response to pure expansion
17 p2627 A72-34770

Thermodynamic infinitesimal theory of viscoplasticity
17 p2632 A72-35112

Thermodynamic analysis and parameter optimization of a solar thermoelectric power plant with heat removal by radiation
17 p2497 A72-35509

Nonequilibrium thermodynamics with rate equations as nonlinear solid mechanics foundation, noting viscoelastic, viscoplastic and plastic behavior
18 p2732 A72-36076

Book - Investigation of nonstationary heat and mass transfer processes by the net-point method
18 p2740 A72-36248

Caratheodory classical thermodynamics formulation presented in mathematically rigorous form by differential geometry and topology methods
18 p2741 A72-36508

Solution of some mixed boundary value problems of conducting medium thermodynamics by the method of variable separation
18 p2715 A72-36802

An improved method for the solution of the heat equation in Chebyshev series.
19 p2879 A72-37370

General solutions of the heat equation in finite regions.
19 p2880 A72-37411

Method of Lagrange multipliers for exploitation of the entropy principle.
19 p2825 A72-37842

Muller entropy principle-imposed restrictions on thermodynamic and thermodynamic constitutive relations for fluids in electromagnetic fields
19 p2834 A72-37843

Relativistic thermodynamics development based on invariant entropy concept, considering frictionless heat conduction and Carnot cycles
19 p2835 A72-37928

Economical difference schemes for solving the heat-conduction equation in polar, cylindrical, and spherical coordinates
19 p2883 A72-38847

Dynamic adjustment of initial model fields by using complete equations of hydrothermodynamics
20 p2949 A72-39943

Precipitation thermodynamics of unstable and metastable solid solutions, discussing interfaces, vacancies, spinodal decomposition, nucleation, reversion and microscopical diffusion
20 p2943 A72-40000

Digital simulation of the SEI-1 static electrointegrator for solving heat-type equations
21 p3127 A72-40160

Analog model for two dimensional heat conduction equation, noting electrical networks for one dimensional difference equations solution
21 p3127 A72-40179

Decomposition of multidimensional nonlinear equations of heat-conduction type and construction of nonlinear electrical integrators
21 p3128 A72-40181

Investigation of nonstationary heating processes in thermal resistors fed from functional sources
21 p3129 A72-41060

Black hole physics compatibility with thermodynamics second law formulation based on black hole area as entropy measure
21 p3085 A72-41216

Nonpolar thermodynamics of thermoelectric differential materials in terms of deformation gradient, temperature and Clausius-Duhem constraints
21 p3131 A72-41478

A non-equilibrium thermodynamic theory of simple materials based on a single-integral entropic functional.
21 p3124 A72-41505

Glassy materials rheological behavior description in terms of stress function, discussing molecular processes transformation range thermodynamics
22 p3196 A72-42791

Thermodynamic conditions for the development of convective clouds and a method of forecasting the quantity of rainfall
22 p3202 A72-42953

A determination of thermal diffusivity under transient conditions
24 p3465 A72-45067

Information theory and statistical mechanics applications to thermodynamics, discussing entropy and superiority of Georgian to Kelvin temperature scale
24 p3465 A72-45372

Some reflections on the nature of entropy, irreversibility and the second law of thermodynamics.
24 p3465 A72-45628

THERMOELASTICITY
NT AEROTHERMOELASTICITY

Temperature fields and stresses in thin elastic non-ferromagnetic electrically conducting cylindrical shells heated by induction determined from heat source distribution and thin shell theory relations
02 p0290 A72-11631

Polycrystalline bodies thermoelectric behavior under random external forces, determining thermal microstress distribution parameters by statistical boundary value formulation
02 p0290 A72-11632

Thermoelectricity quasi-static, dynamic and coupled problems in continuum mechanics, discussing formulation and variational principles methods for solution
02 p0290 A72-11634

Coupled thermoelectricity in infinite body with cavity, introducing Sommerfeld type scalar potential and temperature radiation conditions
02 p0259 A72-12236

General equations of thick shells for arbitrary material and large deflections, considering thermodynamic and velocity damping properties
02 p0293 A72-12344

Nonstationary thermoelectric stress determination in hollow cylinder walls under convective heat transfer
03 p0443 A72-13459

Thermal stresses from inner surface temperature of micropolar hollow cylinder in static thermoelectricity problem with vanishing body loads
03 p0448 A72-13889

Static thermoelectricity problems solutions using harmonic functions applied to contact problem of hot stamps
03 p0448 A72-13902

Edge temperature effects on contact stress concentration in anisotropic plate with elliptic hole under mixed boundary conditions of thermoelectricity
03 p0450 A72-14109

McNamee-Gibson displacement potential functions generalization to problems for compressible pore fluid in theory of consolidation or thermoelectricity
03 p0455 A72-14389

Thermoelectricity theory coupled linear equations for thin orthotropic shells, taking into account rotatory inertia and lateral shear
04 p0588 A72-15060

Linear two-temperature theory of thermoelectricity for investigating transient stresses arising from solid isotropic sphere aerodynamic heating [ASME PAPER 71-WA/APM-14]
05 p0733 A72-15966

Thermoelectric effect on flutter and vibration of built up delta wings with solid, stiffened and honeycomb/corrugated sandwich skins [AIAA PAPER 72-174]
05 p0740 A72-16834

Thermoelectricity equations for thermal shock effect on freely supported circular plate, describing deformation and temperature field interactions
05 p0741 A72-17147

Thin walled elastic isotropic shallow shell with thermal boundary conditions, obtaining thermoelectric solution in series form
06 p0899 A72-18657

Thermoelectric waves diffraction steady state problems in multiply connected cylindrical and spherical surfaces, deriving scalar wave equations
07 p1094 A72-19986

Generalized coupled thermoelectricity problem solution from wave equations for anisotropic plate in plane thermal stress state
07 p1094 A72-19987

Thermoelectric characteristics and crystal phase distribution effect on microstructural stresses and thermal expansion of polycrystalline refractory materials
07 p1018 A72-20133

Thermal stress measurement and thermoelectric behavior of carbon-carbon-materials for reentry nose cones, describing gage mounting, temperature compensation and data recording
08 p1164 A72-20921

Axissymmetric thermoelectric state of isotropic infinitely long circular cylinder with external annular cut, determining cut plane normal thermal stresses
08 p1245 A72-21668

Thermoelectricity theory for transversely isotropic shells, obtaining variational formulation of noncoupled quasi-static problem
08 p1247 A72-21811

Material properties nonuniformities effect on wound fiber glass reinforced plastic rings and cylinders thermoelectric residual stresses
08 p1196 A72-21858

Anisotropy and nonuniformity of bonded glass mat thermoelectric properties, investigating thermal buckling origin
09 p1337 A72-22703

Thermoelectric disturbance wave front propagation in elastic half space after thermal shock at surface
09 p1399 A72-22705

Heat conduction, stress-strain state and thermoelectricity of massive bodies of revolution under nonuniform heating
09 p1400 A72-22709

Linear uncoupled quasi-static thermoelectricity theory for thermal bending of nonuniformly heated parallelogram-shaped plates
09 p1400 A72-22710

Trapezoidal plate thermoelectricity problem for various thermal load distributions, solving Poisson equation for sectorial annular region
09 p1400 A72-22711

Thermoelectric problem of open orthotropic multilayer shell of revolution, obtaining one dimensional boundary value problem solutions by numerical orthogonalization method
09 p1400 A72-22712

Thin plates heated by heat sources, solving two dimensional problem in thermoelasticity via Fourier and Laplace transformations with allowance for heat propagation rate

09 p1400 A72-22718

Thermoelastic coupling effect in thermal shock problem on surface of simply supported rectangular beam

09 p1401 A72-22719

Homogeneous linear approximations in uncoupled problems of thermoradiative elasticity and plasticity of solid body under nonuniform heating and radioactive radiation

09 p1401 A72-22720

Two dimensional thermoelasticity problem with nonstationary temperature field and external boundary forces, using algorithm to evaluate stress-strain state of welded plates

09 p1401 A72-22725

Photothermoelasticity method for determining thermal stresses

09 p1402 A72-22737

Microplar thermoelasticity steady state axisymmetric problem solution from equilibrium equations, considering uniform surface temperature and surface heat doublet cases

09 p1403 A72-22749

Homogeneous isotropic elastic medium thermoelasticity equations based on variational principles noting definite integrals solutions by means of delayed potentials

09 p1406 A72-23070

Heat conduction and thermoelasticity in solids, discussing thermomechanical coupling, structural analysis and thermal stresses and deformations [SMRT PAPER L 1/1]

10 p1556 A72-24394

Classical boundary value problems in theory of thermal stresses in piecewise continuous anisotropic elastic bodies under coupling conditions

10 p1563 A72-24994

Photothermoelastic analysis of temperature and rupture stress in cryogenic tanker structures, using steel and plastic ship models

11 p1728 A72-25373

Thermoelastic waves propagation in homogeneous isotropic medium under external generic forces and with distributed heat sources

11 p1734 A72-25676

Thermoelastic stress and displacement in thin finite rod due to distributed time dependent heat sources

11 p1736 A72-25991

Thermoelastic stresses in solid transparent isotropic homogeneous dielectric under self-focused laser beam

11 p1648 A72-26334

Book on finite element method application to boundary value problems, nonlinear continuum thermodynamics and thermoviscoelasticity

12 p1882 A72-27325

Thermal stresses near pole of spherical reservoir during cooling, using thermoelastic equations of shell of revolution

12 p1887 A72-28242

Rods resistance to thermal shock under coupled thermoelasticity conditions, calculating critical thermal flux during thermodynamic compression waves propagation

13 p2053 A72-28399

Radial and circular thermal stresses in free and end-constrained orthotropic cylinders with axisymmetric temperature distributions, determining relation between temperature and thermoelastic coefficients

13 p2055 A72-28561

Dynamic thermo-magnetoelastic problems of long cylinder and infinite medium with hole under magnetic field, using variation method and Laplace transforms

13 p2056 A72-28882

Thermoelastic vibrations of simply supported rectangular plate produced by temperatures prescribed on faces, obtaining solution in trigonometric series form

13 p2056 A72-28888

Thermal stresses in elastic cylinder for variable linear expansion coefficient and temperature, noting welded seam between two constant temperature cylinders

13 p2059 A72-29492

Asymptotic solutions to dynamic problems of thermoelasticity estimation under homogeneous boundary conditions

13 p2062 A72-30067

Thermal shock produced edge effect, analyzing brittle material heat resistance and failure, using thermoelastic heated cylinder

14 p2165 A72-30437

Three dimensional photothermoelastic method of refrigeration with composite model to study transient thermal stresses in wing rib

14 p2168 A72-30907

Limiting ratio between ideal gas densities before and behind vertical shock wave in elastic thermal insulators

15 p2334 A72-31475

Exact nonlinear equation derived approximation for second order effects in thermoelasticity theory for

isotropic and transversely isotropic heat conducting elastic materials

15 p2329 A72-32282

Self excited increasing thermal wave generation models, using hyperbolic wave heat conduction and thermoelasticity equations

15 p2336 A72-32285

Mechanical models in thermoelasticity associated with boundary problems of classical physical fields with postulated laws of variation and periodicity

15 p2330 A72-32288

Nonlinear thermoelasticity theory in terms of continuum mechanics terminology, assessing strain gradients and couple stresses effects on stress distribution

15 p2330 A72-32293

Exact solutions for plane thermoelastic and magneto-thermoelastic wave frequency equations, determining specific loss extremum values

15 p2336 A72-32447

Thermoelastic stress analysis for hollow cylinder heated along helix, calculating stress function for given surface temperature distribution

15 p2333 A72-32687

Thermal shock induced thermoelastic vibrations of rectangular plate calculated by Ritz averaging method

15 p2333 A72-32689

Thermoelastic stress bounds in fiber reinforced composite beams of arbitrary cross section, examining conditions for applicability of elementary beam theory

16 p2464 A72-32915

Nonlinear thermoelasticity theory extension via entropy production inequality theorem, deriving expressions for stress tensor and heat conduction vector

16 p2465 A72-32980

Cosserat surface uniqueness theorem for non-homogeneous anisotropic thermoelastic shells small motions and temperature variations superposed on large deformation

16 p2465 A72-32981

Singular integral representations of displacement and rotation vectors for homogeneous isotropic centrosymmetric body, using Nowacki couple stress theory of thermoelasticity

16 p2465 A72-32984

First and second order shock discontinuity waves propagation in thermoelastic incompressible solids, deriving Piola-Kirchhoff stress tensor via Clausius-Duhem relation

16 p2423 A72-33109

Magnetothermoelastic temperature distribution effects due to linear heat source in infinite circular cylinder acted upon by magnetic field

16 p2425 A72-33595

Coupled thermoelastic theory for thin plates, using perturbation method to find free vibration frequencies of plates under various boundary conditions

16 p2471 A72-33785

Elementary plane waves in a Signorini-Cattaneo's thermoelastic solid.

18 p2735 A72-36512

Thermo-elastic interactions in an infinite elastic solid due to a concentrated transient heat source.

18 p2735 A72-36754

A study of thermoelastic waves by the method of characteristics.

18 p2737 A72-37068

On the numerical solution of a class of nonlinear problems in dynamic coupled thermoelasticity.

18 p2738 A72-37078

Wave propagation in generalized thermoelasticity.

19 p2870 A72-37412

A universal connexion for waves in anisotropic media.

19 p2875 A72-37840

Thermo-hypo-elasticity and derived fracture and yield conditions.

19 p2875 A72-37841

A plane contact problem of thermoelasticity for a composite rectangle

20 p2978 A72-39019

Thermoelasticity and magnetohydrodynamics equations and inequalities, covering Fourier law, stress relations, Bingham fluids, Ohms law, variational formulations and functional analysis

20 p2952 A72-39183

Proof of existence theorems for the principal dynamic problems of thermoelasticity

20 p2978 A72-39317

A multi-continuum theory for composite elastic materials.

21 p3072 A72-40676

Elastic isotropic material mechanical and thermal constitutive equations restrictions investigation to ensure local stability under perturbations of deformation gradient and temperature field

21 p3120 A72-41203

Thermoelastic problems for multiply-connected plates with heat dissipation at both plane surfaces.

21 p3121 A72-41237

Method of eigenfunctions in problems of thermoelasticity and electroelasticity

21 p3122 A72-41348

Nonpolar thermodynamics of thermoelastic differential materials in terms of deformation gradient, temperature and Clausius-Duhem constraints

21 p3131 A72-41478

Wave propagation in thermal rate dependent thermoelastic materials.

21 p3131 A72-41479

On the collision of a cold elastic plate with a hot elasto-plastic plate.

21 p3124 A72-41482

Heat exchange with external medium along boundary of region bounded by smooth contours with heat insulated lateral surfaces, noting thermoelastic confocal elliptic ring

21 p3126 A72-41544

Effect of the rate of pulsed heating of a bar on the magnitude of the thermoelastic stresses

21 p3126 A72-41548

Three dimensional thermoelastodynamic theory for elastic beams, deriving nonlinear motion equations by combined expansion and variational methods

22 p2325 A72-42523

Plane waves in a new theory of thermoelasticity.

22 p2329 A72-42856

Steady thermoelastic state in an infinite plate with a moving parabolic cut

23 p3345 A72-43586

Photothermoelastic study of stress concentrations in a plate with internal heating.

23 p3349 A72-43986

Thermoelastic contact problem of an elastic layer resting on an elastic foundation.

23 p3354 A72-44269

One-dimensional shock waves in heat conducting materials with memory. I - Thermodynamics.

23 p3314 A72-44341

Nonstationary thermoelastic stress determination in hollow cylinder walls under convective heat transfer

24 p3458 A72-44934

Plane thermoelastic one-dimensional waves in an inhomogeneous medium with allowance for connectedness

24 p3459 A72-45266

Thermoelastic waves propagation in homogeneous isotropic medium, considering potential functions

24 p3460 A72-45598

Solution of a boundary-value thermoelasticity problem for a turbine blade by the polymoment method

24 p3460 A72-45623

Thermoelastic characteristics and crystal phase distribution effect on microstructural stresses and thermal expansion of polycrystalline refractory materials

24 p3416 A72-45759

THERMOELECTRIC CONVERSION SYSTEMS

U THERMOELECTRIC POWER GENERATION

THERMOELECTRIC COOLING

Thermoelectric cooling battery performance of solar cell system, determining low temperature current requirements under various thermal loads

10 p1423 A72-24317

Test apparatus and technique for assessing Peltier thermoelectric cooling device operational characteristics

12 p1755 A72-27721

Thermoelectric cooling devices materials figure of merit upper limits above room temperature, using semiconductor parameters experimental values

12 p1755 A72-27722

Compound tellurides and their alloys for Peltier cooling - A review.

22 p3215 A72-43088

Bi-Sb alloys for magneto-thermoelectric and thermomagnetic cooling.

22 p3215 A72-43089

THERMOELECTRIC GENERATORS

Unitized bellow radioisotope thermoelectric generator concept for long term stability, using standardized design, fabrication and qualification

[ASME PAPER 71-WA/ENER-1]

05 p0615 A72-15940

Thermal shielding and reduced resistance determination of flat thermoelectric battery in sandwich solar cell assembly

10 p1422 A72-24313

Thermoelectric generators theory, design and performance characteristics, discussing Seebeck, Peltier and Thomson effects

15 p2182 A72-31375

Thermodynamic analysis and parameter optimization of a solar thermoelectric power plant with heat removal by radiation

17 p2497 A72-35509

The 20 kWe thermoelectronic reactor project

18 p2645 A72-36184

On-board nuclear power plants in space

24 p3423 A72-45119

United States Space Nuclear Electric Power Program.

24 p3424 A72-45179

THERMOELECTRIC MATERIALS

Thermally stimulated autophotocurrent emission from Cr-alloyed p-type GaAs electrode, determining spec-

tral distribution and light and electric field effects on current

08 p1216 A72-21071

Temperature controller with linear time variation for semiconductors thermally stimulated conductivity and thermoluminescence measurements at 90-300 K operating range

08 p1166 A72-21438

Measurement circuit for temperature dependence of thermal emf and electrical conductivity in thermoelectric materials

12 p1807 A72-27452

Thermal conductivity measuring apparatus for small multispecimen thermoelectric materials

12 p1795 A72-27467

Thermoelectric cooling devices materials figure of merit upper limits above room temperature, using semiconductors parameters experimental values

12 p1755 A72-27722

Thermoelectrical properties of ternary bismuth-antimony-tellurium alloy system obtained under Ar gas pressure in quartz and graphite crucibles

14 p2142 A72-30500

THERMOELECTRIC OUTER PLANET

SPACECRAFT

U TOPS [SPACECRAFT]

THERMOELECTRIC POWER GENERATION

Thermal conductivity, electrical resistivity, Lorentz ratio and thermopower of Ti, Al and Ni alloys for aerospace structures over 4-300 K range

01 p0113 A72-10173

Aerospace radioisotope power systems, discussing heat source technology, shielding, safety and thermoelectric integration

01 p0098 A72-10387

Screened impurity scattering determination in heavily doped covalent semiconductors from Hall mobility and thermoelectric power measurements

05 p0702 A72-17073

Resistivity, thermoelectric power and magnetoresistance of carbon fibers derived from heat treated polyacrylonitrile

07 p1024 A72-20550

Diogenes development program to obtain information on converters mass production, selling price and service life under irradiation, noting application to thermoelectric reactor construction

18 p2709 A72-36188

Absolute thermoelectric power of chromium-ruthenium alloys.

20 p2942 A72-39988

THERMOELECTRIC SPACECRAFT

U TOPS [SPACECRAFT]

THERMOELECTRICITY

Thermocouple efficiency with respect to Thomson effect and electric resistivity temperature dependence

03 p0360 A72-13651

Small gage thermocouples calibration procedure, noting data correlation with thermoelectric theory

07 p0984 A72-19326

Thermal and electric fields interaction in LF integrated circuits design, applying thermal feedback loops to bandpass filter, delay circuit and Schmidt-trigger oscillator

10 p1448 A72-24280

Thermoelectric generators theory, design and performance characteristics, discussing Seebeck, Peltier and Thomson effects

15 p2182 A72-31375

Metal specimens yield point in adiabatic tension determined by thermoelectric method from temperature-stress and stress-strain diagrams

15 p2259 A72-32690

Thermally stimulated current measurement application to Ag doped Si semiconductor for energy level and electron capture cross section determination

16 p2441 A72-32859

Five channel recording instrument for energy dissipation evaluation in electric machines from thermal emf measurements

16 p2392 A72-33284

Neutronic studies for the French thermoelectronic program

18 p2645 A72-36179

Thermionic effect-based cesium plasma converter operation as caloelectric converter and cesium diode

18 p2645 A72-36190

Electrical and thermoelectrical effects in GaAs-InAs solid solutions

19 p2844 A72-37752

Electroconductivity, thermal emf and Hall coefficient for single crystals of Bi-Sb alloys with Cd, In and Sn additions

19 p2847 A72-38683

An ultra-broadband probe for RF radiation measurements.

20 p2921 A72-38993

Optimization of the structural parameters of galvanic laminar heat-flux sensors

21 p3056 A72-41058

Thermoelectric properties of alloys of the gallium-nickel system under standard conditions

22 p3215 A72-43191

Isobar-isothermal potentials, entropy and formation heat of chromium silicides from thermoelectromotive force measurements of high temperature galvanic elements

23 p3298 A72-43286

THERMOGRAMS

U RECORDING INSTRUMENTS

U TEMPERATURE MEASURING INSTRUMENTS

THERMOGRAPHS

U RECORDING INSTRUMENTS

U TEMPERATURE MEASURING INSTRUMENTS

THERMOGRAVIMETRY

White thick layer anodic zirconium oxide water content determination by volumetric and thermogravimetric analysis of heated samples

05 p0667 A72-17051

High temperature testing of metals, discussing specimen preparation and oxidation behavior evaluation by gravimetric, volumetric and optical techniques

08 p1189 A72-22107

Thermogravimetric design, using electromagnetic microbalances and turbomolecular pump for automatic sorption isotherm measurements in surface area and pore size analyses

11 p1636 A72-26788

Polymeric structural adhesives thermal stability evaluation, recommending thermogravimetric analysis and calorimetry to supplement thermogravimetric method

16 p2415 A72-33510

Thermomechanical and thermogravimetric analyses of systematic series of polyimides.

17 p2511 A72-34714

THERMOLUMINESCENCE

Thermoluminescent phosphorus films irradiation by electrons with energies up to 15 keV in vacuum chamber

01 p0114 A72-10372

Impurity-related color centers and electron-hole traps in quartz by electron spin resonance and thermoluminescence observations

02 p0207 A72-11598

Heavy elements gamma heating, using LiF thermoluminescent dosimeters and computer programmed photon transport calculations

04 p0546 A72-14427

Temperature controller with linear time variation for semiconductors thermally stimulated conductivity and thermoluminescence measurements at 90-300 K operating range

08 p1166 A72-21438

Fossil track densities and thermoluminescence measurements of Luna 16 feldspar crystal samples compared to Apollo 12 samples

09 p1381 A72-22270

Thermoluminescent and luminescent properties of Apollo 12 lunar fines, core tube samples and rock chips

10 p1537 A72-24163

Thermoluminescence lunar samples - Measurement of temperature gradients in core material.

18 p2724 A72-36278

The role of Sm and Mn as activators in calcium sulphate and lithium tetraborate.

18 p2718 A72-36347

Ucera meteorite - Determination of differential atmospheric heating using its natural thermoluminescence.

19 p2858 A72-37859

Brief review of thermoluminescence studies in lunar samples.

20 p2970 A72-39402

Recombinational luminescence of NaI-Tl single crystals excited in the A-band of activation absorption

23 p3323 A72-43342

THERMOMAGNADYNAMICS

U THERMOMAGNETIC EFFECTS

THERMOMAGNETIC COOLING

Order-disorder transition cooling effects on V carbide superlattice domain structure, using electron and optical microscopy

03 p0370 A72-12997

Bi-Sb alloys for magneto-thermoelectric and thermomagnetic cooling.

22 p3215 A72-43089

THERMOMAGNETIC EFFECTS

Thermomagnetic slip produced by certain temperature gradient and magnetic field combinations in rarified polyatomic gas channel flow

07 p0973 A72-20399

Thermomagnetic effect in a plasma placed in a non-homogeneous magnetic field

17 p2588 A72-34838

Thermal stability of lunar rock remanence, indicating magnetization components acquired after initial cooling

22 p3226 A72-42535

Investigation of the structural state of the LuNDK40T7 high-coercivity alloy

23 p3300 A72-43594

THERMOMAGNETISM

U THERMOMAGNETIC EFFECTS

THERMOMECHANICS

U THERMODYNAMICS

THERMOMETERS

NT RESISTANCE THERMOMETERS

Electrical thermometer mounted on breathing mask for electropneumograms, measuring temperature change in respiration air flow

02 p0169 A72-12518

Air, wet bulb and soil temperature indications from automatic telemetering meteorological stations, comparing with Hg thermometer readings

10 p1483 A72-25012

THERMOMETRY

U TEMPERATURE MEASUREMENT

U THERMONUCLEAR ENERGY

U THERMONUCLEAR POWER GENERATION

THERMONUCLEAR EXPLOSIONS

Thermocuclear microbomb ignition with intense relativistic electron beams for rocket propulsion, discussing achievable exhaust velocities and system optimization

01 p0117 A72-11222

Natural oscillations of magnetosphere and trapped radiation transport by electromagnetic pulses as possible mechanism for disturbances from thermonuclear explosion reaction on particles in natural radiation belt

11 p1712 A72-25935

High altitude thermonuclear explosion fission fragments localization mechanism, considering magnetogravitational trap as potential well for heavy charged fragments

11 p1713 A72-25950

Thermonuclear detonation and reimplosion of dense stellar cores, studying beta-processes effect on post-detonation evolution

13 p2044 A72-29625

Thermonuclear microexplosion ignition by bombarding dense target with intense relativistic electron beam, noting energy requirement reduction by self magnetic beam field

16 p2433 A72-32814

Thermonuclear power generation

The potential of a laser-induced fusion device as a thermal-neutron source.

17 p2591 A72-35353

Pulsed power - A new technology for controlled thermonuclear fusion.

18 p2715 A72-36332

The possibility of producing plasma regions at thermonuclear fusion conditions in a supersonic flow by means of high power electron beam.

21 p3092 A72-41224

THERMONUCLEAR PROPULSION

U NUCLEAR PROPULSION

THERMONUCLEAR REACTIONS

NT CONTROLLED FUSION

NT NUCLEAR FUSION

Rotation and mass inclusion into study of energy barriers location effects on thermonuclear reaction dynamics

02 p0262 A72-11981

Massive star evolution, discussing stellar structure theory uncertainties, young clusters, helium burning and evolutionary tracks

03 p0425 A72-13262

Flow distribution behind shock wave with intense laser radiation absorption and laser-triggered thermonuclear reactions

04 p0559 A72-15351

[AD-736299] Soviet book on plasma physics and controlled thermonuclear synthesis covering plasma-electromagnetic interactions, magnetic traps and plasma cryogenic technology

09 p1361 A72-23201

Future interstellar ramjet concepts, considering interstellar hydrogen fuel use for thermonuclear reactor and problems of fuel energy losses, plasma containment and structural limitations

09 p1374 A72-23250

Spallation origin of anomalous He 3/He 4 ratio in 3 Centauri A, considering thermonuclear processes model

14 p2158 A72-30731

Electric and magnetic field effects on auroras formation, noting similarity with thermonuclear reactor plasma

16 p2456 A72-33518

Proton capture mean lifetimes in fast C-N cycle, presenting nitrogen/carbon abundance ratio variation with temperature

18 p2721 A72-36650

Laser-beam-scattering measurement of ion temperature in a theta-pinch plasma and evidence for thermonuclear reactions.

19 p2840 A72-37548

Hydrodynamic model of white dwarf envelope thermonuclear runaway evolution producing nova outburst, computed for various CNO nuclei initial abundances

20 p2966 A72-38908

Averaged equations of simultaneous hydrodynamic expansion and thermal healing of two-temperature plasma, taking the recovery of thermonuclear fusion into account. I - The plane problem. II - The spherical problem.

21 p3093 A72-41476

THERMOPHILES

Lactate dehydrogenase from an extremely thermophilic bacillus.

23 p3259 A72-44450

THERMOPHILIC PLANTS

NT BLUE GREEN ALGAE

THERMOPHYSICAL PROPERTIES

NT CRITICAL POINT

NT CRITICAL PRESSURE

NT CRITICAL TEMPERATURE

NT EMISSIVITY

NT HEAT OF SOLUTION

NT MELTING POINTS

NT PYROELECTRICITY

NT SPECIFIC HEAT

NT SUPERCRITICAL PRESSURES

NT THERMAL CONDUCTIVITY

NT THERMAL DIFFUSION

NT THERMAL DIFFUSIVITY

NT THERMAL STABILITY

NT VAPOR PRESSURE

NT VOLATILITY

Plane strain analysis of two bonded semiinfinite elastic media with different thermomechanical properties and cracks, calculating stress factors and maximum stress angles

01 p0140 A72-10990

High speed measurement techniques for thermophysical properties at temperatures above 2500 K, emphasizing subsecond duration methods for solid phase electrical conductors

02 p0223 A72-11500

Metals thermophysical characteristics temperature dependence determination by analog computer, using one dimensional temperature fields in thin infinite plates and cylindrical or spherical surfaces

03 p0458 A72-14165

Vacuum handling system for lunar materials thermophysical properties measurements under contamination preventive conditions

04 p0509 A72-15496

Metals, insulators, semiconductors and ceramics thermophysical parameters measurement during monotonic heating or cooling at 123-3273 K

06 p0904 A72-18514

Ultracure metals microimpurities determination from crystal lattice and atomic properties, comparing spectral analysis activation, mass spectrometric, thermophysical, recrystallization and kinetic methods

07 p1049 A72-20149

Thermomechanical and plastic deformation behavior of polycrystalline alumina at elevated temperatures

09 p1335 A72-22394

Book on heat and mass transfer analysis covering conduction, boundary layer and channel flow convection, thermal radiation, rarefied gas mechanics, thermophysical properties, etc

10 p1561 A72-23748

Fiber reinforced plastics thermophysical properties, thermal conductivity and heat capacity, determining effects of reinforcement fiber type, resin amount and type

11 p1669 A72-25391

Lunar granular materials thermophysical properties, emphasizing thermal conductivity data and heat transfer mechanisms

12 p1869 A72-27333

Russian book on combustion products thermodynamic and thermophysical properties covering fuels and propellants characteristics, equilibrium fuel compositions, gas phase transfer and expansion processes, etc

12 p1890 A72-28336

Hg fed hollow cathode ion thruster thermal and plasma heating characteristics, using Wiener-Kalman filtered temperature measurements

13 p2027 A72-28947

Stefan problem of metal evaporation duration after intense heat flux termination as function of thermophysical properties

15 p2334 A72-31504

Solar wind thermal properties from positive component energy distribution observation by ESRO Heos 1 satellite

15 p2298 A72-31518

Lunar surface diurnal temperature variations calculation based on Apollo 12 lunar fines thermophysical properties and surface layer core-tube sample density

16 p2454 A72-33432

Lattice dynamical model for Cs vibration frequency distribution, specific heat and electrical and thermal resistivity calculations

16 p2441 A72-33584

Simultaneous determination of the thermokinetic characteristics of solids by a variable regime method

17 p2638 A72-35749

An equipment for measuring thermophysical quantities by means of heat-pulse methods in the temperature region between 20-300 C.

17 p2557 A72-35758

Thermophysical properties of lunar material returned by Apollo missions.

18 p2725 A72-36290

Lunar and terrestrial soil thermal and electrical properties measurement in vacuum and He atmospheres

20 p2968 A72-39255

Differential equations for heat transfer in turbulent boundary layer flow of incompressible fluid with constant thermophysical characteristics

22 p3166 A72-42253

Facility for studying the thermophysical properties of materials by quasi-stationary methods

22 p3176 A72-42289

Mechanical and thermophysical properties of heat resistant Nb alloys, noting application for thermionic cathodes

22 p3192 A72-42821

Thermophysical properties of highly porous thermochemically treated metal-ceramic iron

23 p3299 A72-43295

Change in the sign of the thermal lens of glass laser rods during variation of the thermooptical constant of glass

23 p3296 A72-43926

Thermal anomalies in stressed Teflon.

24 p3417 A72-44766

THERMOPHYSICS

U THERMODYNAMICS

THERMOPLASTIC FILMS

U POLYMERIC FILMS

THERMOPLASTIC RESINS

Semiconductor-thermoplastic-dielectric hybrid ICs reliability, discussing interelement adhesive bonding properties and thermally induced strains effects

03 p0337 A72-14294

Carbon fiber reinforced thermoplastics tested for gears and bearings applications, including wear, static, dynamic, surface tension, stereoscan and microscopy effects

04 p0537 A72-14748

Glass variables effect on polypropylene, polystyrene and Nylon-6 glass filled thermoplastic composites mechanical properties, discussing silane coupling agents and injection moulding machine conditions

04 p0537 A72-15085

Chopped fiber glass reinforced high density thermoplastic polyethylene composite, determining critical fiber length, interfacial adhesion and fracture toughness

08 p1193 A72-21684

Wear resistance and friction coefficients in physiologic solution of thermoplastic materials for prosthetic application in hip joints

08 p1194 A72-21760

Fiberglass reinforced thermoplastics and thermosets for corrosive environments, noting composites performance increase by constituents change

12 p1833 A72-27404

Glass fiber reinforced thermoplastic resins chemical and hydrolytic resistance, noting composites and polymers long term performance prediction in aggressive environments

12 p1833 A72-27405

Continuous woven fabric or roving filament reinforced thermoplastics production, discussing polymer binder systems, coupling agents, impregnation technique, processing parameters and equipment

12 p1815 A72-28083

Ethylene-vinyl acetate-asphalt thermoplastic material properties, filler effects, application methods and commercial uses

12 p1835 A72-28094

Heat resistance of thermostable organic materials /amorphous glass and high polymers/, improving plastic stability by glass fibers addition, intermolecular arrangements modification and synthesis

14 p2125 A72-30529

Ribbon glass effect on thermal expansion of reinforced thermoplastic composites, comparing with fiber reinforced materials

15 p2259 A72-31255

Thermoplastic photoconductor media for holographic recording, discussing structure fabrication techniques and performance

15 p2239 A72-32359

Compressive strength and stiffness improvement for crystalline thermoplastic polymers via solid glass sphere reinforcement

16 p2414 A72-33370

Reinforced thermoplastics - Conference, El Segundo, California, March 1972

16 p2415 A72-33414

Thermosetting polybutadienes as co-curing plasticizers for thermoplastics reinforcement, noting oxidation resistance at room and moderately elevated temperatures

16 p2415 A72-33416

Design criteria for fiber reinforced thermoplastic resins performance optimization, discussing temperature, humidity and chemicals effects

16 p2415 A72-33417

Foam content effect on fiberglass reinforced thermoplastic foam tensile and impact strength, thermal distortion and mold shrinkage properties

16 p2415 A72-33418

Glass reinforced thermoplastic resins flammability resistance, discussing test methods and flame retardant additives

16 p2415 A72-33419

Flame retardant glass reinforced thermoplastic polyester Celanex processing and performance, considering flammability, and electrical/mechanical properties

16 p2415 A72-33420

Properties of internally lubricated glass-fortified thermoplastics for gears and bearings.

19 p2822 A72-37896

Joining plastic foils with the aid of high-frequency welding

20 p2930 A72-39942

Thermoplastics fatigue life dependence on stress with allowance for heating laws, noting heat accumulation effect on thermal failure

22 p3196 A72-42164

Design against fatigue failure in thermoplastics.

24 p3457 A72-44816

THERMOPLASTICITY

Thermoplasticity problems of materials with time dependent mechanical properties, obtaining approximate plastic deformation under cyclic loading

02 p0291 A72-11638

Rate dependent endochronic theory of thermoviscoplasticity without yield surface

03 p0444 A72-13503

Ductile plastics solid phase forming, discussing forging, extrusion deep drawing and rubber cushion forming techniques

04 p0538 A72-15451

Soviet monograph on thermoplastic hardening of high strength martensitic steels and Ti alloys by ordering dislocation structure

09 p1327 A72-22520

Fiber thermoplastics matrix breakdown and mechanical properties enhancement, examining lateral and longitudinal strain during uniaxial tensile creep and recovery

09 p1337 A72-22541

Homogeneous linear approximations in uncoupled problems of thermoradiative elasticity and plasticity of solid body under nonuniform heating and radioactive radiation

09 p1401 A72-22720

Computer algorithm for thermoplastic stress-strain state of thin shells of revolution based on plastic flow theory, taking into account loading history

09 p1401 A72-22724

Thermoplastic polypropylene sandwich molds stiffness variation with time, noting three point bending and creep tests

11 p1673 A72-25550

Thermoplastic materials casting procedures to mold high melting point metal compound powders

11 p1645 A72-26861

Surface charge density in thermoplastic recording, showing potential-relief modulation dependence on frequency, scanning rate and electron beam properties

13 p1954 A72-28402

Friction and molecular structure - The behaviour of some thermoplastics.

20 p2945 A72-39974

Some technological factors influencing the ductility of thermoplastic dross and the properties of niobium-carbide-based finished products

23 p3293 A72-44009

THERMORECEPTORS

Thermoregulatory hypothalamic and body sites for behavioral temperature regulation in squirrel monkey

03 p0314 A72-13072

Temperature sensitivity neurophysiological mechanism, discussing cold and heat sensitive receptors localized distribution in human skin and thermoregulatory function

22 p3146 A72-42779

THERMOREGULATION

Book on hibernation and hypothalamus covering central nervous system regulating mechanisms, biologic rhythmicity, migration, thermoregulation, torpor, human implications, etc

01 p0010 A72-10169

Ventilatory and metabolic responses of unanesthetized dogs exposed to various carbon dioxide concentrations at 2 and 18 C, discussing oxygen uptake relation to cold

02 p0159 A72-11954

Human short term thermoregulation feedback-forward control mechanism, using hypothalamic temperature as set point

02 p0168 A72-12036

Skin and hypothalamic temperature effects on human thermoregulatory responses, developing control mechanism for peripheral effects on skin sensors

02 p0160 A72-12041

Heat exposure effect on Sidman avoidance performance in rats, discussing organism thermoregulatory capacity disruption and shock and body temperature regulation

02 p0169 A72-12525

Central cooling and warming effects of preoptic-anterior hypothalamic region on thermoregulatory activity

ty of neuroendocrine, cardiovascular and neuromuscular systems

03 p0313 A72-13070

Thermoregulatory hypothalamic and body sites for behavioral temperature regulation in squirrel monkey

03 p0314 A72-13072

Biological tissue heat transport dimensionless parameters for steady state and transient analysis of homeotherm thermoregulation

04 p0472 A72-14864

Heat acclimatization, work habituation and exercise effects on body thermoregulation, measuring tympanic temperature, sweat rate and oxygen intake

04 p0472 A72-14896

Regulation of sweat secretion on skin surfaces overlying active and nonactive muscle tissue during skin or core temperature alterations

04 p0480 A72-15216

Active Na-K transport and passive permeability temperature adaptation in ground squirrel erythrocytes

04 p0475 A72-15546

Analytical model for living biological tissue transient heat transfer, taking into account conduction, storage, generation, convection and blood flow effects

[ASME PAPER 71-WA/HT-36] German monograph on analog model of thermoregulation in human body at rest and at work, describing heat transfer

05 p0621 A72-16047

Metabolic control of temperature compensation in circadian rhythm of *Euglena gracilis* strain

07 p0919 A72-19538

Thermal stability variations in blood serum protein after electrical stimulation of rabbit hypothalamic structures

07 p0920 A72-19649

Human temperature regulation during upright and supine exercise, showing nonlinear relationships between perspiration and skin and core temperatures

07 p0922 A72-20275

Battery powered dc integrated circuit for temperature regulation in small experimental animals, using thermistor probes and heating pads

08 p1114 A72-20895

Heat and cold acclimatization in hamsters, relating thermoregulatory response to helium-cold hypothermia induction

08 p1115 A72-21085

Peripheral thermoregulation in arctic canines, showing subzero bath-immersed foot temperature maintenance above tissue freezing point

08 p1120 A72-22019

Mathematical model of skin contact cooling tube device for human body thermoneutrality maintenance in various environments

09 p1270 A72-22821

Calorimetric measurements of human body temperature and of hot saline solution drinking effects on sweating rate

09 p1267 A72-23440

Oxygen consumption and body temperature in anesthetized, paralyzed and artificially ventilated dogs cooled in water bath at 34 C, measuring hypercapnia and beta-adrenergic blockade effects

10 p1424 A72-23735

Extravehicular life support systems for shuttle, space station, lunar base and Mars missions, considering thermal control, carbon dioxide control and oxygen supply subsystems

10 p1430 A72-24441

Bicycle ergometer measurements of thermoregulation input and output under wide range of work load and climatic conditions, deriving correlation equation

11 p1579 A72-25874

German papers on human body energy balance and temperature control covering energy conversion processes, chemical secretions, muscle activity, etc

11 p1584 A72-26071

Human body thermoregulatory processes under varying environmental conditions and metabolic rates, discussing role of blood circulation, sweating, nervous stimuli, hormones, etc

11 p1584 A72-26073

Thermoregulation in deeply hibernating rodents during separate chilling and steady hibernation temperature maintenance of skin and brain

12 p1762 A72-27827

Thermoregulation changes during simulated weightlessness of prolonged bed rest, noting lower sweating threshold and decreased vasodilation/autonomic dysfunction/

12 p1767 A72-28301

High temperature environment effects on rat organ and muscle tissue respiration, discussing temperature homeostasis maintenance

13 p1905 A72-29331

Human diaphoretic system physiology, discussing skin surface sweat excretion intensity relation to optimal balancing process in thermoregulation

14 p2076 A72-30672

Water loss replacement effect during rest and exercise in high temperature environment thermoregulation experiment

15 p2185 A72-31449

Two compartment analog model of thermoregulation during rest and exercise, considering temperature, heat conductance, sweat rate and oxygen uptake

15 p2185 A72-31450

Monograph on hot environments stress covering heat exchange at skin surface, clothing effect, body temperature regulation and sweating control

15 p2185 A72-31515

Hemodynamic thermoregulatory and sympathoadrenal responses to heat acclimatization in man during supine and upright position exercise

17 p2506 A72-35963

Skin temperatures in warm environments and the control of sweat evaporation.

17 p2506 A72-35969

Thermoregulation during positive and negative work at different environmental temperatures.

18 p2650 A72-36559

Effects of chloralose-urethane anesthesia on temperature regulation in dogs.

21 p2997 A72-40426

Russian book - Climatic conditions and the thermal state of man.

21 p3006 A72-40458

Thermal balance in man during 24 hours in a controlled environment

22 p3145 A72-42747

Temperature sensitivity neurophysiological mechanism, discussing cold and heat sensitive receptors localized distribution in human skin and thermoregulatory function

22 p3146 A72-42779

Role of the dorso-medial area of the posterior hypothalamus in thermal regulation and its functional relationships with the anterior hypothalamus

24 p3371 A72-44592

Analysis of changes in thermal regulation after destruction of the medial preoptic area of the hypothalamus

24 p3371 A72-44593

Pulse activity of neurons in the thermal regulation center of the anterior hypothalamus during chill shivering

24 p3371 A72-44594

THERMOSETTING RESINS

NT EPOXY RESINS

NT FURAN RESINS

NT NYLON (TRADEMARK)

NT PHENOLIC RESINS

NT POLYAMIDE RESINS

Polyarylates, polyimides and thermosetting polymers role in sliding friction of self lubricating plastics, noting temperature effects

06 p0837 A72-18599

Repeated stretching effect on triaxial fibers thermal destruction in vacuum after hot air or steam thermosetting

08 p1194 A72-21759

Short fiber reinforced thermoset composite materials for engineering construction, tabulating flexural properties and Charpy impact strengths

09 p1338 A72-23165

Dynamic properties of thermosetting plastic composites unidirectionally reinforced by high elastic moduli boron and carbon fiber for aircraft structural applications

12 p1882 A72-27343

Fiberglass reinforced thermoplastics and thermosets for corrosive environments, noting composites performance increase by constituents change

12 p1833 A72-27404

Aerothermochemical analysis of thermosetting hydrocarbon plastic ablation rate under heat transfer at reentry vehicle hypersonic stagnation point, describing pyrolysis by chemical kinetic equation

15 p2335 A72-32149

Thermosetting polybutadienes as co-curing plasticizers for thermoplastics reinforcement, noting oxidation resistance at room and moderately elevated temperatures

16 p2415 A72-33416

THERMOSPHERONS

Heat transfer characteristics of liquid metal filled closed thermospherons for hot wall boundary conditions of constant temperature and uniform heat flux

[ASME PAPER 72-GT-36]

11 p1745 A72-25631

Heat transfer performance of stationary two phase closed thermospherons with water and Freon as working fluids, discussing effects of operating pressure and heat flux

21 p3131 A72-41621

THERMOSPHERE

Meridional thermospheric wind effect on auroral atomic oxygen red line profile, noting inadequacy of diffusion hypothesis

01 p0052 A72-10079

Lower thermosphere temperature, air density and pressure models, using auroral zone midlatitude neutral thermal and molecular diffusion coefficient measurements

01 p0053 A72-10187

Seasonal variation in lower thermosphere atomic oxygen concentration deduced from static diffusion models, using incoherent scatter and orbital decay temperature measurements

01 p0062 A72-10907

F region neutral thermosphere temperature perturbation and circulation pattern due to global wind with anomalies of ionization calculated from two dimensional dynamic model

01 p0096 A72-11283

Mesosphere and lower thermosphere photochemical composition, allowing for molecular and eddy diffusion

03 p0345 A72-12980

Meridional model of oxygen and hydrogen compounds reactions in mesosphere and lower thermosphere, determining diurnal variations and vertical profiles

03 p0346 A72-13378

Energy conversions and mean vertical motions in high latitude summer mesosphere and lower thermosphere, observing reaction kinetics

03 p0346 A72-13380

Atmospheric tides wave dynamics in thermosphere, considering viscosity, thermal conduction, hydromagnetic forces and nonlinearity effects on transmission and excitation

04 p0514 A72-14722

Thermospheric neutral-air wind effects on ionospheric F 2 layer from atmospheric model

04 p0514 A72-14876

Aluminum oxide cloud formation for thermosphere temperature determinations, describing methane/oxygen payloads, spectrographs, photometers and atmospheric models

06 p0806 A72-17646

Electrodynamics of ionosphere and magnetosphere, discussing irregularities, red arc and auroral thermosphere density and temperature changes

06 p0809 A72-18279

Traveling ionospheric disturbance as diagnostic tool for thermospheric dynamics, monitoring wave polarization of ATS 3 signals

07 p0975 A72-19154

Laser radar observations of mesosphere and lower thermosphere optical scattering cross section variations due to tide-caused atmospheric density fluctuations

08 p1156 A72-21100

Thermospheric wind directional filtering of gravity waves traveling ionospheric disturbances over Australia

08 p1158 A72-21217

Wind measurements in lower thermosphere by meteor radar method, presenting models of prevailing circulation in meteor zone over Eurasia and Arctic

08 p1161 A72-21538

Planetary scale circulation systems effects on photochemistry and transport processes of minor neutral constituents in mesosphere and lower thermosphere

09 p1274 A72-22353

Model calculation for seasonal effects on minor neutral constituents distribution in mesosphere and lower thermosphere, suggesting large scale meridional circulation role

09 p1274 A72-22354

Frictioned force modification of lower thermosphere vertical neutral gas velocities with resulting atomic oxygen and molecular nitrogen density-height distribution deviation from barometric law

09 p1298 A72-22582

Thermospheric structure between 100 and 400 km from rocket soundings and ground observations, noting mass spectrometers chemical reactions influence on atmosphere model accuracy

09 p1300 A72-23015

Thermal stratification of mesosphere and lower thermosphere at low latitudes with allowance for turbulent mixing, showing molecular oxygen and ozone radiative heating prevalence

09 p1347 A72-23589

Mesospheric clouds composed of molecular complexes of extraterrestrial origin, considering chemical reactions, hydroxyl luminescence, thermospheric water vapor and auroras

09 p1347 A72-23590

Jupiter atmosphere thermospheric temperature profile from heat conduction equation, noting radiative and convective transfer

09 p1393 A72-23658

Papers on thermospheric circulation covering atmospheric dynamics, ionosphere, gravity waves, noctilucent clouds, meteor trail winds, radar observations, etc

10 p1473 A72-24701

Mesosphere and lower thermosphere heating and associated solar UV radiation absorption calculation based on diurnally varying photochemical diffusive model

10 p1475 A72-24943

Magnetic storm effects in atmospheric neutral composition, noting thermospheric wind circulation role due to Joule heating within auroral zone

10 p1476 A72-24957

Upper atmosphere /thermosphere/ physical variations, discussing diffusive equilibrium, energy absorption and heat transfer

11 p1621 A72-25842

Thermosphere and lower exosphere density and temperature variations from satellite decay

11 p1621 A72-25843

Thermodynamic equilibrium theory for upper atmosphere /thermosphere/ temperature and density variations, noting Harris-Priester model

11 p1622 A72-25844

Rocket-borne mass spectrometric studies of composition of lower thermosphere

11 p1622 A72-25847

Heat conduction and radiative transfer equations of IR cooling by atomic O in thermosphere

11 p1622 A72-25848

Rocket-borne mass spectrometer tested in high velocity molecular beam facility for thermospheric atomic oxygen density measurement

11 p1634 A72-26422

Semiannual variation in ionospheric drifts, zonal winds and vertical shear at thermosphere base

11 p1626 A72-26475

Thermosphere temperature measurement by high velocity probe, admitting atmospheric sample via free molecular flow inlet

12 p1806 A72-27044

Thermospheric ion, electron and neutral particle concentration, composition and temperature changes during 7 March 1970 solar eclipse from rocket measurements

12 p1778 A72-27152

Neutral atmospheric density profiles measurements in lower thermosphere by satellite-borne accelerometers, noting longitudinal variations at high latitudes

13 p1948 A72-28833

Polar thermospheric wind calculation from convection electric field measurements in polar cap ionosphere, using simple ionospheric model

13 p1950 A72-29385

Thermospheric density-temperature time lag, considering two dimensional time dependent model based on UV heat input dynamic excitation

13 p1951 A72-29388

Midlatitude sporadic E layer formation under wind shear action from artificial cloud data on lower thermosphere wind speed and direction

13 p1951 A72-29589

Gravity wave propagation in realistic thermospheric model, considering temperature, wind, Coriolis force, viscosity, thermal conduction and ion drag effects

13 p1951 A72-29652

Global ionospheric electron density variations and associated thermospheric winds during 15-21 June 1965 geomagnetic storm from ground based and satellite data

13 p1953 A72-29805

Thermospheric atomic hydrogen concentration diurnal variations from time dependent continuity and diffusion equations, using Jacchia background atmosphere thermal and density structure formulas

13 p1953 A72-29806

Polar zone thermospheric temperature variations due to atmospheric cooling, H component variations and discrete perturbation

14 p2097 A72-30133

Thermospheric parameters seasonal and latitudinal variations calculation based on atmospheric model with components ionization and molecular oxygen dissociation as main heat sources

14 p2128 A72-30463

Thermosphere kinetic temperature diurnal variation from heat conduction equation periodic solution, determining heat sources from solar radiation atmospheric absorption

14 p2101 A72-30640

Mesosphere and lower thermosphere temperature measurement by rocket-borne manometer, relating temperature variations to corpuscular flux intensity and sun generated geomagnetic excitations

15 p2225 A72-31910

Lower Arctic thermosphere neutral composition changes due to disturbances, considering atomic hydrogen, nitric oxide, hydroxyl, water vapor, nitrogen and oxygen

15 p2225 A72-31912

Nighttime molecular nitrogen and oxygen number density profiles at 130-220 km over Sardinia from ESRO mass spectrometer measurements

15 p2226 A72-31938

Lower thermospheric neutral gas density and composition rocket-borne mass spectrometric measurements with liquid He cooled ion source

15 p2236 A72-31942

Thermospheric composition global model for magnetically quiet conditions based onOGO-6 mass spectrometer measurements

15 p2227 A72-31954

Mesospheric and lower thermospheric composition from neutral atmospheric particles measurement by rocket-borne instrument consisting of RF quadrupole mass spectrometer

15 p2228 A72-31967

Thermospheric variations due to solar activity changes based on satellite drag data

15 p2228 A72-31979

Thermospheric density annual and semiannual variations due to solar heat input into ozone layer and Joule heating, discussing decomposition into Fourier terms

15 p2229 A72-32255

Thermospheric composition variations in south polar regions during magnetically quiet periods fromOGO-6 observations, considering atmospheric heating by electron precipitation cyclic variations

16 p2383 A72-32964

Lower thermosphere neutral composition from February 1969 rocket-borne mass spectrometer measurements over Fort Churchill, Canada

16 p2383 A72-32965

Summer upper mesosphere and lower thermosphere positive ion composition at high latitudes from Nike Cajun rocket soundings

16 p2383 A72-32966

Solar radiation induced molecular oxygen photodissociation rate as function of column density and temperature in mesosphere and lower thermosphere

16 p2383 A72-32967

Measurements of molecular oxygen in the thermosphere.

17 p2546 A72-34694

Thermospheric molecular oxygen from solar extreme-ultraviolet occultation measurements.

17 p2614 A72-35602

WKB approximation to suggest vertical phase velocity measurement at turning points of acoustic-gravity wave propagation in thermosphere

18 p2686 A72-36411

Nocturnal and semiannual variations of the intensity of 5577 A emission of atomic oxygen.

19 p2789 A72-37511

The variation of air density at 240 and 280 km from April to November 1967.

20 p2916 A72-39235

The influence of vertical motions on the diurnal variations of temperature and density in the thermosphere.

20 p2916 A72-39236

The problem of the boundary conditions in thermosphere dynamics.

22 p3201 A72-42510

Latitudinal variation of temperature in the lower thermosphere /80 to 100 km/

24 p3395 A72-44635

A thermospheric model from satellite orbital decay densities and incoherent scatter temperatures.

24 p3400 A72-45595

THERMOSTABILITY

U THERMAL STABILITY

THERMOSTATS

Instrument to measure thermodynamic, electrical and optical properties of gases and liquids, describing thermostat for 83-923 K range

13 p1956 A72-28633

Thermostat for electrical measurements of high resistance materials in air up to 1200 C

13 p1957 A72-29274

THERMOTROPISM

U ANISOTROPY

U TEMPERATURE EFFECTS

THERMOVISCOELASTICITY

One dimensional heat insulated structure under dynamic loads, showing thermoviscoelastic effects on spontaneous heating and stress-strain state

03 p0444 A72-13460

Nonlinear thermoviscoelasticity problem exact solution expressed as product of two functions, formulating conditions

03 p0445 A72-13576

Small parameter method solutions to linear viscoelasticity problems with nonhomogeneous temperature field applied to reinforced tube under internal pressure

03 p0454 A72-14217

Thermoviscoelastic stress analysis for hollow circular cylinder with reinforcing interlayer under pressure, axial tension and nonstationary temperature field

04 p0587 A72-15016

Nonlinear transient coupled thermoviscoelasticity problems solution by finite element method and iterative solution for integrodifferential equation

05 p0736 A72-16085

Linearized thermal viscoelasticity theory for stability, large strain and wave propagation problems, taking into account heat generating effects

12 p1880 A72-27233

Quasi-static thermoviscoelasticity problem for infinite plate with circular hole, investigating plate surface heat transfer and material viscosity effect on temperature stresses

13 p2061 A72-29796

Heat production effects in general linearized thermoviscoelasticity theory, deriving equations of motion, state and energy and boundary conditions for intensely strained objects

19 p2871 A72-37526

Thermoviscoelastic problem for semiinfinite plate, determining temperature field and stresses permitting heat propagation

23 p3347 A72-43749

One dimensional heat insulated structure under dynamic loads, showing thermoviscoelastic effects on spontaneous heating and stress-strain state

24 p3458 A72-44935

THETA PINCH

Line radiation from theta pinch with oscillatory ion and electron density applied to solar spectral studies

01 p0106 A72-10098

High speed streak cameras applicability to low density theta pinch studies, describing image converters design, operation and block diagrams

02 p0263 A72-11410

Time of flight mass spectrometers for plasmoids generated by theta pinch and discharge over organic glass, showing ion and electron currents oscillograms

02 p0223 A72-11420

Equilibrium state linear theta pinch plasma confinement dependence on nonuniform magnetic force lines curvature radius

03 p0396 A72-13655

Theta pinch plasma electron density with high time resolution by side-on interferometry at 10.6 microns

03 p0396 A72-13670

Plasma layer implosion in theta pinch, deriving modified snow plov equations from MHD equations

04 p0556 A72-14855

Argon ion spectra overlap with satellites to carbon and boron Lyman alpha lines, employing theta pinch

06 p0852 A72-17897

High-beta theta pinch plasma toroidal equilibrium by oscillating magnetic field superposition on main confining field

06 p0864 A72-18538

Pulsed IR carbon dioxide TEA laser for two dimensional interferometry of theta pinch plasma during discharge

07 p1005 A72-19416

Growth rate and boundary of drift dissipative instability in plasma under linear theta pinch conditions

07 p1045 A72-20477

Anisotropic equilibrium solution to Vlasov equation for high beta theta pinch plasma column

07 p1045 A72-20478

Plasma rotation during theta pinch collapse, determining ion azimuthal velocity from fields and pressure gradient measurements via Ohms law

08 p1213 A72-21255

Numerical solution of theta pinch in electron-hole plasma of Ge semiconductor under surface recombination as contactless method of current carrier injection

08 p1218 A72-22178

Pulsed carbon dioxide laser heating of theta pinch plasma by inverse bremsstrahlung and induced Compton processes

09 p1364 A72-23233

Theta pinch plasma heating by carbon dioxide laser transverse pulses, substantiating theoretical considerations by experimental observations

12 p1852 A72-27880

Plasma containment by superposed fields /sustained field/ technique application to theta pinch, studying hydrogen and helium discharge behavior

14 p2138 A72-30400

Cooperative enhanced scattering cross section of far IR laser radiation from nonthermal theta pinch plasmas in weak magnetic field

15 p2288 A72-32417

Turbulent heating and resistivity in cool electron theta pinches due to IF long wavelength modified two stream and drift instabilities

15 p2288 A72-32426

Dense helium theta pinch plasma heating by TEA carbon dioxide laser, studying temperature and density with high speed photography and spectroscopy

15 p2251 A72-32530

Theta pinch plasma heating by carbon dioxide laser transverse pulses, substantiating theoretical considerations by experimental observations

16 p2439 A72-33989

Experimental and two-dimensional computational study of end losses from a theta pinch.

17 p2592 A72-35628

The classification of transitions between levels of principal quantum numbers 3 and 4 in Fe IX to XVI and Mn VIII to XV.

17 p2586 A72-35834

Laser-beam-scattering measurement of ion temperature in a theta-pinch plasma and evidence for thermonuclear reactions.

19 p2840 A72-37548

The study of turbulence in theta-pinch plasma with azimuthal magnetic field.

21 p3091 A72-40571

Helical field experiments on a three-meter theta pinch.

21 p3094 A72-41636

New lines of neon ions in the range 50-200 A.

23 p3315 A72-43802

Vacuum ultraviolet absorption measurements on ionized species. 23 p3316 A72-44330

THICK FILMS

Ni-Cr thick films triode sputtering technique with temperature control by low-energy electron bombardment heating, presenting phase diagram 05 p0675 A72-16393

Switching behavior and attenuation of space division multiplex crosspoint circuit with end marking, discussing realization in thick film technology 11 p1604 A72-25908

Technological parameters effects on resistance values dispersion of thick film resistors, reviewing stability test performance 12 p1788 A72-27274

Screen printed large thick film multilayer interconnection board assemblies for electronic packaging, discussing fabrication and feasibility 16 p2368 A72-33194

An investigation of amorphous semiconductor memory devices utilizing thick film fabrication techniques. 17 p2527 A72-34682

Profile and depth of microcraters formed in glass. 18 p2736 A72-36972

Electrical properties of thick-film barium titanate dielectrics produced by flame spraying. 19 p2846 A72-38616

The relationship between the thick film conductor and substrate and its influence on conductor properties. 20 p2908 A72-39494

A comparison of manufacturing techniques for hybrid microwave circuits. 20 p2908 A72-39496

Fine line multilayer system packaging using hybrid thick film processing and materials 22 p3161 A72-43174

Accelerated life testing of thick film resistors. 24 p3384 A72-44668

THICK WALLS

Computer algorithm of initial functions for elastic thick finite hollow axisymmetric cylinders under static conditions 02 p0288 A72-11604

General equations of thick shells for arbitrary material and large deflections, considering thermodynamic and velocity damping properties 02 p0293 A72-12344

Radiation pattern and reflected field analysis for incident plane wave on phased arrays of thick wall rectangular waveguides 03 p0330 A72-13168

Thick walled rigid plastic cylinders under pressure, obtaining uniqueness and stability of finite deformation 03 p0446 A72-13706

Boundary conditions for unsteady flow fields bounded by incompressible elastic thick plane wall fixed to rigid surface 07 p0972 A72-20113

Fatigue strength and life estimation method for thick walled cylinders under pulsating internal pressure, using fracture mechanics crack propagation law [ASME PAPER 71-PVP-15] 08 p1244 A72-21482

Deformability and carrying capacity of glass fiber-polymer composite thick walled rings under internal or external pressure 08 p1195 A72-21764

Climatic load effects on carrying capacity of thick walled glass reinforced polymer rings with residual stresses 08 p1195 A72-21765

Plate and thin and thick walled shells treated as three dimensional solids, noting finite element method limitation 10 p1559 A72-24925

Stressed state induced in compound thick walled cylinder for testing residual tensile stresses effect on machine parts wear resistance 12 p1814 A72-27461

Heating rate effects on residual stresses in thick walled cylinders produced by winding heated binder impregnated fiberglass tape on cold spool 13 p1982 A72-28553

Internal pressure induced stresses, displacements and time-variable plasticity radii for thick walled fiber reinforced cylinder with hereditary elastic binder interlayers 13 p2055 A72-28557

Deformation limits in thin and thick walled metal blanks axisymmetric drawing process, determining stress-strain state based on prescribed velocity field 13 p1963 A72-28743

Turbine blade trailing edge wall thickness measurement by phase sensitive eddy current technique 16 p2397 A72-33201

Stable bifurcation mode prior to instability in thick walled cylindrical viscoplastic pressure vessel under internal hydrostatic pressure 16 p2474 A72-34129

Asymptotic singular perturbation solution to thick spherical shell with circular hole under axisymmetric external pressure 16 p2474 A72-34157

Thick shell and oriented surface theories. 19 p2873 A72-37694

Rotatory vibration of a thick spherical shell of isotropic non-homogeneous elastic material. 22 p3240 A72-42880

THICKENED LEADING EDGES

U LEADING EDGES

THICKENERS [MATERIALS]

Thickening properties of butoxyacrosil products of butyl alcohol vapor and silicon dioxide surface reactions for use as oil lubricant additives 09 p1336 A72-22500

THICKNESS

NT FILM THICKNESS

NT TARGET THICKNESS

Ultrasonic resonance thickness gage sensitivity and accuracy, noting damper, piezoelectric plate, protector and frequency band influence 03 p0361 A72-13986

Thickness function corresponding to constant velocity loading condition for orthotropic annular circular plate with uniform stress 04 p0591 A72-15279

Variable wall thickness influence on axisymmetric vibrations frequencies and reduced masses of cylindrical elastic shell filled with ideal incompressible fluid 08 p1247 A72-21815

Electrode vertex angle effect on fused weld bead geometry related to plate thickness in tungsten inert gas (TIG) welding 09 p1320 A72-23634

Optimum thickness variation in annular strip /curved beam/ under bending moment at constant stress based on Mises-Hencky yield criterion 10 p1558 A72-24847

Al alloy notch-bend and compact-tension specimens thickness and crack length effects on plane-strain fracture toughness test results 10 p1498 A72-24886

Vibration of simply supported rectangular plate with unidirectional linear thickness variation, using perturbation technique for eigenvalue problem derived by Galerkin method 11 p1735 A72-25739

Large deflection of variable thickness square plate under uniform load, using strain energy method 11 p1737 A72-26588

Nondestructive technique for continuous recording of thickness or contour profiles, using mechanical probes 13 p2000 A72-29760

Turbine blade trailing edge wall thickness measurement by phase sensitive eddy current technique 16 p2397 A72-33201

Metal barrier maximum puncturable thickness dependence on high velocity meteorite particle impact parameters 22 p3234 A72-42217

Electromagnetic thickness measurement on the AWACS radome. 24 p3384 A72-44901

THICKNESS RATIO

Hypersonic flow past final thickness delta wing, presenting conical flow equations with boundary value solution 06 p0757 A72-18128

Homogeneous differential equations of elastic rectangular plates with linear thickness variation, using Gran Olsson solution 16 p2471 A72-33682

Simple thickness modes for laminated composite materials. 22 p3235 A72-42465

Width/thickness ratio effect on steel, brass and molybdenum sheet specimens plasticity and deformation under tension at room temperature 23 p3301 A72-43758

THIN AIRFOILS

NT THIN WINGS

Thin airfoil and bridge deck flutter derivative from transient oscillatory states in test procedure 02 p0298 A72-12665

Three dimensional velocity field excitation by thin airfoil vibrations in supersonic flow, deriving function in semispace to satisfy boundary constrained wave equation 06 p0756 A72-18111

General solution for thin airfoil rectilinear motion in ideal incompressible gas, applying to rotor blade lift calculation 09 p1260 A72-22860

Integrodifferential equation for rigid tunnel walls effect on supercavitating flow past thin jet flapped airfoil, noting lift coefficient derivatives 10 p1469 A72-24562

Aerodynamic properties prediction procedure for thin jet flapped airfoil in incompressible inviscid flow bounded by different types of boundaries 15 p2179 A72-32147

The inviscid flowfield of an unsteady airfoil. [AIAA PAPER 72-681] 17 p2486 A72-35481

THIN FILMS

Calculation of an unsteady separation flow past a slender profile 18 p2642 A72-36900

Effects of transport velocity of vortex wake on aerofoil oscillations. 23 p3249 A72-44494

THIN BODIES

Maximum logarithmic decrement vs frequency of damped oscillation of elastic thin beam including internal and viscous resistance 01 p0144 A72-11384

Nonlinear development of instability wave in turbulent wake behind thin body based on integrals of mean flow momentum and kinetic energy equations 02 p0152 A72-12351

Orthotropicity orientation effect on supersonic flutter of infinite-length thin heterogeneous circular cylindrical structures in axisymmetric gas flow 04 p0584 A72-14520

Dynamic theory of thin elastic beams under large deflection, taking into account shear deformation and axial stress resultants [ASME PAPER 71-APM-EE] 04 p0590 A72-15183

Electromagnetic fields produced by quasi-stationary gravitational collapse of uniformly rotating current carrying relativistic thin disk 04 p0579 A72-15321

Thermal stresses in thin symmetrically heated disk with time and temperature dependent mechanical properties, deriving integrodifferential equation defining stress function 05 p0740 A72-16624

Lattice type structures as discrete elasticity problem, determining potential of thin rods connecting rigid nodes pairs from equations of motion and constitutive equations 08 p1244 A72-21302

Asymptotic method solution for boundary value problems for nonlinear differential equations describing transonic and slow supersonic flow past thin bodies 08 p1108 A72-21709

Thin viscoelastic beam free oscillations and material properties description by Volterra type nonlinear integral equation 08 p1249 A72-21869

Nonlinear plane bending of thin elastic rectilinear bar guide elements under concentrated force and torque 09 p1397 A72-22350

Perfectly conducting incompressible fluid motion past thin body in oblique field, discussing magnetic field influence on lift 09 p1365 A72-23559

Angular distribution of electrons at output of specimen observed by electron microscope, examining resolution problem for thin objects 11 p1635 A72-26483

Axisymmetric hypersonic motion around thin solid of revolution, taking into account boundary layer interaction with inviscid external flow 13 p1895 A72-29847

Numerical solution of algebraic equation encountered in aerodynamics of hypersonic boundary layer interacting with external flow on thin solids of revolution 13 p1895 A72-29848

Linear theory based analysis of compressible electroconductive fluid flow satisfying perfect gas equation in presence of thin profiles within quasi-aligned magnetic field 14 p2095 A72-30824

On the motion of a perfectly conducting fluid past a thin body. 17 p2485 A72-35055

On the finite deflections of thin beams. 17 p2634 A72-35404

Calculating the stability of centrally compressed thin-walled bars with various profiles 21 p3126 A72-41549

Velocity-dependent multiple scattering by two thin cylinders. 24 p3381 A72-45641

THIN FILMS

NT FERROMAGNETIC FILMS

Preparation and electrical properties of thin cadmium antimonide and arsenide layers, comparing to single crystal films 02 p0268 A72-12281

Fine scale surface oxide film roughness effects on metal substrate-oxide film system hemispherical emittance 02 p0303 A72-12319

Lateral surface heat transfer effect on thermophysical characteristics in thin layer coatings, discussing temperature gradients in corundum and zirconium oxide on copper 02 p0304 A72-12864

Au thin film effective optical constant calculation from measured reflection and transmission coefficients and thickness by approximate formulas 03 p0401 A72-13363

Superferromagnetism in thin polycrystalline Gd and Gd-Au films having Curie points near room temperature 03 p0401 A72-13583

Thin film optical waveguides using magneto-optic GdIG as substrate, discussing computerized design for propagation mode converter efficiency [IEEE PAPER 3,6] 03 p0332 A72-13755

Lubrication and friction problems regrouping in thin viscous fluid films mechanics 03 p0364 A72-14271

NbN thin film stabilization by metal overlays with reduction in ac losses, discussing superconducting reversibility to normal transition 04 p0560 A72-14542

RC network synthesis technique using grounded gyrator and summing amplifier, applying to thin film RC networks and IC operational amplifiers 04 p0504 A72-14570

Dry spot formation in nonboiling ethanol thin film on horizontal surface heated from below 04 p0595 A72-14597

Temperature dependence of quantizing thin films electroconductivity in case of scattering at neutral impurities 04 p0561 A72-15078

NbN film superconducting properties measured as function of thickness, discussing transition temperature, critical current and magnetic field 04 p0562 A72-15294

Refractory metal multilevel interconnection systems, comparing materials fabrication, yield and circuit performance with diffused Si planar runs and polycrystalline Si films 05 p0636 A72-16362

Thin sintered fluoride films bonding with monoaluminum phosphate, investigating friction and wear behavior 06 p0821 A72-17804

Vacuum chamber sputtering techniques for CsI/Tl and NaI/Tl thin films for soft proton scintillation detector 06 p0816 A72-17834

Nonlinear motion stability of finite amplitude wave solution in thin viscous incompressible liquid film 06 p0801 A72-18142

Microwave thin film microstrip IC tunnel diode amplifiers for broadband high performance receivers, discussing design, construction and performance 06 p0786 A72-18374

Papers on thin film and semiconductor IC and contact and connection technology 06 p0790 A72-18570

Thin film formation techniques including evaporation, sputtering, anodization, chemical vapor deposition, electrodeposition and sintering, discussing surface scattering, tunneling, Schottky emission and conduction mechanisms 06 p0790 A72-18571

Thin film materials and fabrication methods, discussing substrate requirements, surface properties, chemical stability, thermal conductivity and preparation of various resistors and capacitors 06 p0790 A72-18572

Thin film resistors and capacitors design, considering stability, power, size, film thickness, parasitic inductance capacitance and resistance and dielectric loss properties 06 p0790 A72-18573

Thin film conductors, distributed film resistors and capacitors design and associated IC layout to form functional arrays 06 p0790 A72-18574

Thin solid film lubricants for use with roller bearings at ambient and elevated temperatures, discussing surface treatment 06 p0823 A72-18585

Lubrication with thin molybdenum disulfide solid film under various temperatures and atmospheric pressures, examining friction and lifetime 06 p0823 A72-18587

Short time film stability followed by dry spot formation in thin heated draining liquid films on vertical walls, discussing minimum thickness 07 p1098 A72-18842

Thin film optical waveguide with crystal quartz as substrate, observing reversible TE to TM mode conversion due to anisotropy [AD-738761] 07 p0953 A72-18878

Multilayer thin film microcircuits and printed circuits partial capacitance and potential coefficient approximate calculation by matrix method 07 p0953 A72-19016

Integrated miniature guided wave optical transmission systems using crystals adapted to thin film nonlinear interaction and photolithographic technique 07 p1004 A72-19228

Wave propagation in thin film optical waveguides with gyrotropic and anisotropic substrates, deriving TE and TM mode conversion conditions [AD-739120] 07 p0940 A72-19230

MnBi thin films as potential storage media within holographic optical memory system having write-in reference beam for readout [CLEA PAPER 18,1] 07 p0950 A72-19399

Electrons and ionized impurities interaction in thin quantizing layers, discussing donor activation energy and kinetic characteristics 07 p1048 A72-19640

Love surface wave excitation in thin film layer by line source as function of propagation direction, frequency and film thickness 07 p1089 A72-19683

Detonation propagation through tubes coated with thin liquid fuel films, considering boundary layer displacement effect on propagation speed, pressure ratio and reaction zone length 07 p1100 A72-19728

Quartz crystal oscillator device for continuous monitoring and controlling thin film thickness in optical and electronic applications, noting temperature effects on crystal oscillating frequency 07 p0990 A72-20284

Thin films thickness control by piezoelectric quartz crystal, discussing electrically excited oscillations wavelength and damping characteristics 07 p0990 A72-20285

Thin films thickness and refraction index calculation from curves of specularly reflected X ray intensity vs grazing angle, obtaining surface roughness variance 07 p1050 A72-20405

Optical transmission, reflection and absorption of thin rubidium films for parallel and perpendicularly polarized monochromatic radiation, investigating volume and surface plasma oscillations 07 p1050 A72-20523

Band averaged optical constants and IR characteristics of thin plastic films with/without metal substrate, using transmittance measurements [ASME PAPER 70-WA/HT-15] 08 p1205 A72-20874

Two terminal semiconductor strain tensor based on evaporated piezoelectric layer for modulation of forward I-V characteristics of thin film diode 08 p1164 A72-20925

Lunar dust grain fossil coatings of ultrathin metamized amorphous layers resulting from solar wind ion implantation 08 p1230 A72-20982

Temperature distribution and zone melting in carbon thin films heated by electron beam, using Sn crystal indicators 08 p1253 A72-21446

Routine method for ultrathin carbon support film production for electron microscopy, noting mechanical stability and strength 08 p1172 A72-22020

Corrosion tests by ellipsometer, discussing apparatus design and bare metal surface and thin film properties 08 p1172 A72-22110

Light modulation by exciton electric absorption in thin high impedance recrystallized CdTe films within strong electric fields, showing spectral distribution curves 09 p1366 A72-22419

Electrical conductivity relationship to phase composition in thin CdTe films deposited on mica bases and annealed in Cd vapor 09 p1367 A72-22420

Recrystallization effects on thin ZnTe film structure, electrical and optical properties 09 p1367 A72-22421

Ferromagnetic thin film magnetometers operation and performance characteristics for magnetic field measurement 09 p1308 A72-22467

Transition metal superconducting thin films and rf cavity surface protective coverings, investigating properties by low energy electron diffraction and Auger spectroscopy 09 p1368 A72-22560

Josephson dc and ac effects in plane junctions with thin semiconducting film barrier of evaporated material between two superconductors 09 p1370 A72-22800

Reactivity evaporated titanium nitride resistors for thin film microcircuits, discussing nitrogen gas pressure and substrate temperature effects on electrical properties during evaporation 09 p1286 A72-22902

Diffusion coefficient and distribution of Ti atoms in thin Al film from electric current vs time curves for oxidation of solid solution 09 p1329 A72-23036

Thin organosilicon films for integrated optical circuits and devices, discussing transparency and loss characteristics and refractive index control 09 p1314 A72-23339

Thin GaP film composition and structure determination by laser Raman scattering 09 p1314 A72-23345

Laser damage resistance properties of thin film multilayer antireflection coatings for quartz optics 09 p1326 A72-23348

Capacitance depth gage for thin liquid films thickness measurement, noting application to interface waves amplitude and frequency measurements 09 p1316 A72-23410

Nonstabilized Ni-P thin films electrical conductivity at 50-280 C, using mass spectrographic, thermal differential, X ray diffraction and electron microdiffraction analyses 10 p1495 A72-24076

Magnetic domains in cobalt and cementite observed by electron microscopy, investigating thin film thickness effect on temperature 10 p1496 A72-24088

Gunn domain oscillations suppression by dielectric surface loading of transversely thin GaAs diodes 10 p1526 A72-24305

Thin film tunnel triode using p-type amorphous semiconductors to achieve injected current amplification 10 p1451 A72-24624

Monolithic, thin film and LSI technology development trends in microelectronics, noting heteroepitaxy, ion implantation and laser beam techniques 10 p1454 A72-25175

Colaminated boron-polyimide film effect on strength of graphite fiber-epoxy resin composite double lap bolted joints [AIAA PAPER 72-382] 11 p1730 A72-25405

Space charge limited current theory of thin film organic semiconductor systems, investigating energy spectrum of traps and free carrier capture kinetics 11 p1700 A72-25783

Charge carrier photoproduction and energy structure of trans-bis-indonylene (TBB) semiconductor thin films 11 p1700 A72-25784

Optimal flexible ferrite keeper for ferromagnetic thin film memories performance improvement, noting requirements for high permeability, low loss factor and dielectric constant, etc 11 p1601 A72-25899

Electrostatic rocket exhaust materials deposits effects on solar cells optical, thermal and electrical performance characteristics, using optical thin film theory [AIAA PAPER 72-447] 11 p1578 A72-26184

X ray diffusion by thin films under grazing incidence, using reciprocity theorem 11 p1689 A72-26484

Thin Se film for recording mode structure of 10.6 micron carbon dioxide laser emission, describing optical equipment 11 p1652 A72-26795

Vacuum technology - Conference, Boston, October 1971 12 p1805 A72-27034

Transition temperature and other superconducting properties of annealed Nb-Al-Ge thin films 12 p1853 A72-27044

Piezoelectric quartz crystal microbalance for material outgassing and optical element contamination film measurements 12 p1806 A72-27044

Low pressure hydrogen and titanium thin film reaction rate measurement, using flow technique 12 p1778 A72-27044

Vapor annealing effect on vacuum evaporator CdS thin films electroconductivity as function of pressure and temperature 12 p1854 A72-27244

Vacuum deposition process relation to thin metal film properties, discussing current conducting mechanism 12 p1854 A72-27274

Electron bombardment deposited polymer thin films electrical properties as function of formation current, noting increase in crosslinking and dangling bonds 12 p1788 A72-27277

Thin polymer film bleachable dye switches for switched laser to achieve high power single pulse radiation 12 p1822 A72-27614

Graphitization kinetics of amorphous thin carbon films under light impulses, discussing crystallite sizes, optical and electrical properties and two-stage character 12 p1833 A72-27855

French R and D programs on Si and various thin film photovoltaic solar cells, considering efficiency, reliability, and weight and cost reduction problems 12 p1756 A72-28000

British thin Si solar cells for large flexible lightweight arrays, considering radiation resistance, specific mass, area, contact material and antireflection coatings 12 p1756 A72-28000

Thin film Cu-CdS solar cell electrochemical plating: potential and solution composition effects on copper sulfide surface layer formation and cell efficiency 12 p1855 A72-28000

Postdip heat treatment effects on thin film copper sulfide-cadmium sulfide junction solar cells spectral response, diode parameters and resistance 12 p1855 A72-28010

CdS thin film conductivity reactions to grain boundary and stacking faults, correlating grain size to mobility 12 p1856 A72-28010

P-n thin film solar cell based on thermally and electrochemically stable II-IV semiconductors with graded energy gaps 12 p1756 A72-28010

Photovoltaic effects in CdS films evaporated onto barium titanate single crystal and ceramic ferroelectric substrates 12 p1856 A72-28014

Improved efficiency of cadmium sulfide-copper sulfide thin film solar cells, noting optimization of layer formation, grinding and encapsulation 12 p1756 A72-28016

CdTe thin film solar cell room temperature prolonged operation instability, thermal degradation and performance improvement by gas adsorption removal 12 p1756 A72-28017

Photoelectric properties of cadmium telluride thin film solar cells, discussing energy gap temperature dependence, work function and current variations anomalies 12 p1756 A72-28018

Heat treatment and electron irradiation tests for spatial reliability of CdS and CdTe thin film solar cells, noting photovoltaic properties 12 p1756 A72-28019

Radiovoltaic generator energy conversion by thin film solar cells, noting performance dependence on semiconductor band gap and radioisotope characteristics 12 p1757 A72-28021

Titanium dioxide thin film antireflection coating to minimize reflection losses in Si solar cells, discussing fabrication and optical and electrical characteristics 12 p1757 A72-28028

Cubic SiC film growth rate on Si substrate by methyltrichlorosilane decomposition in hydrogen flow, noting dependence on mixture flow rate and temperature 12 p1860 A72-28114

Oxide thin films effects on surface layers deformation and wear resistance of coated metals under friction, noting electrical resistance changes in annealing 12 p1818 A72-28189

Thin surface film lamination in anticorrosion carbon-graphite materials under critical specific pressure, discussing crystalline phase in wear products 12 p1818 A72-28192

Uniaxial elastic deformation pressure effects on electronic conduction in tetrahedrally bonded amorphous semiconducting thin films as function of temperature 13 p2021 A72-28574

Thin lubricant film angular inertia effect on externally pressurized MGD bearings load carrying capacity, solving nonlinear differential equation by Runge-Kutta method 13 p1963 A72-28747

Martensitic transformation in Cu-Al-Ni alloy thin film, investigating gamma-prime phase substructure formation and crystal growth pattern 13 p1976 A72-28907

Dc and RF sputter deposition in ionized inert gas of thin film coatings solid state microelectronics, solid lubricants and corrosion resistance applications [ASME PAPER 72-DE-37] 14 p2108 A72-30871

Thin film resistor manufacture and evaluation for stability and long-life characteristics 14 p2091 A72-31171

Electron work function for metallic sphere and thin film on dielectric substrate as function of radius, thickness and dielectric constant 15 p2290 A72-31222

Gallium aluminum arsenide light emitting diode thin structures grown on GaP substrates by liquid phase epitaxial method 15 p2290 A72-31381

Strain analysis of thin metallic films on low modulus structural substrate by light intensity measurement 15 p2325 A72-31526

Thin liquid films on rotating horizontal disk, measuring flow, thickness and stability with asymptotic-expansion solution 15 p2334 A72-31616

High electric field effects on I-V characteristics of Te-As-Ge-Si type chalcogenide thin film, noting Poole-Frenkel emission and electron tunneling roles 15 p2291 A72-31641

Low energy electron spectroscopy measurement of thin oxide layer growth on Al surface, noting oxidation uniformity dependence on residual gas water content 15 p2276 A72-31859

I-V characteristics of polarized and nonpolarized memory effects in GaAs thin films evaporated on tungsten substrates 15 p2292 A72-31869

Dynamic in situ thin film thickness monitoring during vacuum deposition by holographic interferometry, noting independence from high quality optical components 15 p2240 A72-32381

Tensor analysis for planar magnetoresistivity and Hall effect in Ni single crystal thin films, noting anisotropy effects in ferromagnetic crystals 15 p2294 A72-32386

Thin film superconductors conductivity evaluation above transition temperature through renormalization of impurity-scattering vertex by pair fluctuation effect inclusion 15 p2295 A72-32540

PTFE thin films interspersal with lumps and streaks from transfer to smooth surface during low speed sliding, discussing friction coefficient under various conditions 16 p2396 A72-32870

Turbulent flow of viscous incompressible liquid film falling down semiinfinite vertical plate under gravity influence 16 p2376 A72-33142

Structural and orientation study of sequentially evaporated MnBi thin films on glass substrates using electron diffraction and transmission microscopy 16 p2441 A72-33207

Flux quantization in superconductors demonstrated by magnetometer probe measurement of magnetic field trapped in thin In film holes 16 p2441 A72-33225

Holograms on bismuth and paraffin thin films with pulsed high power TEA carbon dioxide IR laser, discussing photosensitivity and capability for interferometric measurement 16 p2392 A72-33390

Fcc in thin films and bcc in thick vacuum condensates deposited from Nb molecular beams obtained by evaporation and condensation in mass spectrometer 16 p2407 A72-33528

Low field magnetization measurements at 4.2 K on bulk and thin film niobium nitride, discussing Pauli spin paramagnetism and spin-orbit scattering 16 p2442 A72-33843

Diffusion limitation avoidance at high current densities by fuel cell preparation via Pt thin film sputtering on porous vycor substrates 16 p2352 A72-33893

Study of transient phenomena by a TEA CO₂ laser associated with a liquid-crystal detector 17 p2562 A72-34285

Electron currents injected through dielectrics 17 p2529 A72-34753

An asymptotic solution for the laminar flow of a thin film on a rotating disk. [ASME PAPER 72-APM-38] 17 p2538 A72-34783

Contribution to the study of creep in thin permalloy films. 17 p2596 A72-35759

Book - Results of high-vacuum technology and the physics of thin films. Volume 2 18 p2712 A72-36826

Solid-body-surface and thin-layer analyses by the static method of secondary-ion mass spectroscopy 18 p2719 A72-36830

Thin films deposited by evaporation and sputtering - A comparative study 18 p2696 A72-36834

Ultra-high vacuum coater for thin film research 18 p2676 A72-36839

Changes of electrical and structural properties of Au thin films obtained by sputtering during the annealing process. 18 p2720 A72-36955

Reliability of nichrome film resistors deposited in vacuum by sublimation on a glass substrate 18 p2669 A72-37117

Organization of fabrication to obtain high-reliability hybrid circuits 18 p2669 A72-37118

Vapor grown solid state single crystal oxide thin films characteristics and synthesis by thermal vaporization, chemical vapor deposition and sputtering 19 p2843 A72-37443

One MeV electron irradiation of new technology silicon solar cells. 19 p2754 A72-37777

Evidence of crystal structure in some sputtered MoS₂ films. 19 p2823 A72-37897

Influence of heat treatment on the properties of Cr-SiO cermet thin films 19 p2844 A72-37948

Analysis of piezoelectric thin-film transducers for elastic surface waves. 19 p2804 A72-38607

Successive graphitization of amorphous carbon 19 p2823 A72-38676

Application of optimization techniques to the problem of determining optical constants of thin films. 20 p2959 A72-39052

Possible uses of plasma oscillations in thin metal films. 20 p2959 A72-39053

On the theory of electrical conductivity in semiconducting thin films under a high electric field. 20 p2959 A72-39216

Production of prototype hybrid micro-electronic modules using thin film substrates. 20 p2908 A72-39493

A comparison of manufacturing techniques for hybrid microwave circuits. 20 p2908 A72-39496

Energy absorption mechanisms of thin film optical waveguide surface in contact with low index dyes 21 p3050 A72-40147

Phenomena and interpretation of the transients caused by temperature change on capacitance of metal-oxide-metal systems. 21 p3097 A72-40690

Investigation of tantalum-compound films at the surface of acicular tungsten microcrystals 21 p3068 A72-40964

Pulsed GaAs injection laser heating application to thermal conductivity coefficient measurement in thin films, discussing lasing spectra kinetics 21 p3064 A72-41740

Arbitrary length thin liquid film cooling mass transfer data correlation, accounting for film roughness and entrainment effects 22 p3243 A72-41960

Influence of polycrystallinity on transconductance of thin-film transistor. 22 p3159 A72-42309

The switching behaviour of thin films of chalcogenide glass. 22 p3214 A72-42319

Current noise and conductance-temperature characteristics of thin discontinuous Pt films on glass substrate interpreted by quantum mechanical electron tunneling model 22 p3214 A72-42453

Fundamental transverse electric field /TE-sub 0/ mode selection for thin-film asymmetric light guides. 22 p3186 A72-42622

Masking techniques for thin film and semiconductor devices and ICs fabrication, discussing conventional and computerized optical and electron beam systems 22 p3159 A72-42634

Physical and electrical properties of thin-film barium titanate prepared by RF sputtering on silicon substrates. 22 p3215 A72-42999

German monograph - A contribution to the fabrication of thin-film transistors. 22 p3160 A72-43069

Niobium superconductive tunnel diode integrated circuit arrays. 22 p3161 A72-43090

Magnetic flux penetration into superconducting thin films. 23 p3323 A72-43271

Electrical resistivity changes in nichrome films sintering of various thickness with different heat treatment conditions, noting heat stability and thermal shock tests 23 p3292 A72-43280

Temperature and polarization dependence of arsenic sulfide single crystals and thin films intrinsic absorption edge, determining forbidden bandwidth and transitions types 23 p3324 A72-43688

Evanescent-field-pumped dye laser. 23 p3296 A72-43816

Full-range solution for the measurement of thin-film surface densities with proton-excited X rays. 24 p3431 A72-44715

Optical properties of thin cesium films over the wavelength range from 0.3 to 0.9 microns and their electrical resistance 24 p3426 A72-44801

Application of a field-emission microscope to the investigation of the work function of tungsten coated with a thin layer of silicon oxide and with tantalum 24 p3432 A72-44891

Field-emission microscopy of tungsten coated with a silicon oxide film 24 p3432 A72-44892

Reflection amplification in thin layers of n-GaAs. 24 p3385 A72-44971

Photochemistry of unsaturated polymers. 24 p3378 A72-45280

THIN LAYER CHROMATOGRAPHY

Thin layer chromatography technique for rapid quantification of bacterial cell adenosine triphosphate, using microscope ultraviolet photometer 06 p0763 A72-17872

German monograph on mass transport in thin fluid layers covering diffusion, convection, laminar flow rate distribution, flame ionization and gas chromatography measurements, etc 15 p2216 A72-31350

Qualitative determination of organometallic substances in solid propellants by thin layer chromatography 23 p3262 A72-43598

THIN PLATES

Thermal conductivity and boundary conditions for unsteady thermal fields in thin anisotropic plates with heat emission 02 p0291 A72-11635

Nonlinear deflections and radial surface stresses in thin elastic circular glass plates with coaxial rings 02 p0249 A72-12418

Finite element formulation for nonlinear large deflection elastic analysis of displacements and stresses in thin plate structures 02 p0298 A72-12657

Chordwise bending vibrations and flutter of thin isotropic rectangular plates, considering static and dynamic responses

03 p0443 A72-13404

Stresses due to initial elastic deformations in orthotropic thin plate strip, expressing Dirac function by Fourier series and integral

03 p0444 A72-13505

French book on thin elastic structures vibration, describing antivibrational devices and rotating machines balancing

03 p0445 A72-13682

Crack development in thin viscoelastic polymer plate, using two phase fracture model without Volterra principle

03 p0448 A72-13901

Doubly connected strain-hardened thin plate, calculating stress concentration and stress-strain state by variational principle of least additional potential energy

03 p0451 A72-14122

Dynamic stress concentration at circular hole generated by plane bending wave propagation in thin plate, analyzing dependence on vibration frequency

03 p0453 A72-14139

Generalized epicycloid properties application to fracture mechanics, considering stress fields of constrained plastic zones around cracks in thin elastic plate

03 p0455 A72-14388

Lens waveguides characteristics, analyzing Gaussian beams propagation through periodic system of thin plane-parallel nonlinear dielectric plates

04 p0489 A72-15389

Electrodynamical theory of artificial dielectrics based on rigorous solution for diffraction on system scattering elements consisting of periodical gratings formed by thin metallic strips

04 p0490 A72-15412

Turbulence intensities and shear stress measurements in wake of thin flat plate by rotating single hot-wire anemometer

04 p0524 A72-15498

Electron microscopic examination of molybdenum alloy thin plates aging at 700 C observing nucleation and precipitated phase

05 p0673 A72-16147

Thin circular flat plate simply supported at three points on circumference, obtaining vibration mode shapes and eigenvalues

05 p0738 A72-16532

Large deflection of rectangular thin elastic plates with unsupported edges, using finite difference technique based on dynamic relaxation methods

06 p0895 A72-17799

Temperature induced bending of thin freely supported rectangular plate, obtaining stress-strain state

06 p0899 A72-18564

Free vibration determination method for thin rectangular plate with arbitrary boundary conditions and thickness variations

07 p1092 A72-19857

Magnetoelastic vibrations of thin conducting plate in magnetic field, solving electrodynamic equations

07 p1095 A72-20315

Longitudinal plane harmonic elastic wave scattering and stress concentration at rough circular hole boundary in thin isotropic plate

08 p1243 A72-21230

Thin plates heated by heat sources, solving two dimensional problem in thermoelasticity via Fourier and Laplace transformations with allowance for heat propagation rate

09 p1400 A72-22718

Oblique magnetic fields effect on compressible conductive fluids motion in presence of thin foil, noting lift values in hyperbolic and double hyperbolic cases

09 p1365 A72-23560

Light beams diffraction patterns of thin plexiglass plate for load induced thickness variations, noting crack opening and edge sliding modes stress intensity factors

[ASME PAPER 71-APM-QQ] 10 p1553 A72-24178

Static deflections determination of thin rectangular plates with point clamped restraints, using Ritz method with Lagrange multipliers

10 p1555 A72-24193

Vibration of infinite thin plate coupled with acoustic field in surrounding fluid, using Fourier transformation

10 p1511 A72-24223

Thin circular plate quasi-static thermal stresses induced by transient temperature distribution on upper face, obtaining series form solution in terms of Bessel functions

10 p1558 A72-24720

Constrained zones and stress intensity factors in cracked thin elastic plates under combined tensile and shear loads

11 p1735 A72-25893

Bending of simply supported thin square plate clamped around central circular hole and under uniformly distributed transverse load

11 p1736 A72-25985

Proper vibration frequencies of thin imbedded plate obtained by layer potentials method

11 p1737 A72-26477

Cyclic loads frequency and environmental effects on fatigue crack propagation rate, comparing theoretical results with Al alloy thin plates experimental data

11 p1663 A72-26802

Electron microscope observed dislocation splitting in bent thin tantalum carbide sheet, analyzing results in terms of strain rate law and carbon diffusion model

11 p1669 A72-26948

Iterative solution existence for elastic equilibrium problem of thin plates and shells near boundary layer

12 p1886 A72-27997

Thin plates and coatings in thermal contact with standard, determining total emissivity by inverse methods of heat conduction

12 p1889 A72-28115

Thin circular plate free vibrations with mixed boundary conditions from differential equations for vibration modes of circular isotropic plate in dimensionless polar coordinates

13 p2053 A72-28395

Finite element method for calculating vibrations of thin rectangular plate with four degrees of freedom

13 p2000 A72-28466

Creep stability of bars and thin plates and shells for given loading force, considering instability criteria

13 p2054 A72-28481

Heat transfer dynamics during cooling of thin vertical plates, observing boundary layer formation and motion

13 p2065 A72-29454

Unsteady spherical shock wave effect on thin infinite elastic plate covering acoustic semispace, using integral transformation method

13 p1943 A72-29946

Finite element method application to dynamic stability of thin plates and shells, noting nuclear reactor structural analysis

14 p2166 A72-30723

Thin elastic plates finite displacement flexure behavior, using piecewise linear finite element incremental stiffness technique

14 p2168 A72-30933

Berger equation inconsistencies for large deflections of thin elastic plates with freely moveable edges

14 p2169 A72-31173

Finite element method application to thin plate bending problem to illustrate efficiency of sector elements for sectorial and annular plates

15 p2326 A72-31720

Poisson ratio changes effect on equilibrium problems solutions in thin plate theory via invariant imbedding technique, using Cauchy system formulation

15 p2330 A72-32444

Thin elastic isotropic plates and shells thickness variation for rigidity functional stationary value, reducing problem to stress-strain state equations simultaneous solution

15 p2333 A72-32688

Coupled thermoelastic theory for thin plates, using perturbation method to find free vibration frequencies of plates under various boundary conditions

16 p2471 A72-33785

Instantaneous and time dependent solutions for thin rectangular plates nonlinear creep bending within framework of Karman theory

16 p2473 A72-34126

Magnetoelastic buckling of beams and thin plates of magnetically soft material.

[ASME PAPER 72-APM-35] 17 p2624 A72-34311

Anisotropic laminated plates theories reliability comparison, noting applications to thin and sandwich plates

17 p2625 A72-34326

Bending of skew plates of variable rigidity.

17 p2626 A72-34329

Transient mode of a flow in the plane wake of a thin plate or cylinder

18 p2642 A72-36899

Plate vibrations and layer potentials

18 p2736 A72-37001

Vibration of an infinite thin plate coupled with a fluid

18 p2736 A72-37002

Contact interactions of smooth rigid punch impressing into thin laminar anisotropic reinforced plastic plate

19 p2872 A72-37541

Bubnov-Vlasov variational method for thin parallelogram plates bending under complex loads, calculating edge skew and side length effects

19 p2877 A72-38160

Computer solution of dynamic problems for bending of beams and thin plates beyond the elastic limit under alternating loads

19 p2877 A72-38194

Compressible laminar wake behind a thin flat plate.

19 p2747 A72-38798

Short-wave asymptotic representation of the solution to the problem of diffraction by a circular disk

19 p2769 A72-38849

Uniformly loaded thin elastic isotropic circular plate with partly clamped and simply supported edges, determining deflection via solution of biharmonic differential equation

20 p2979 A72-39331

Free vibrations of finite element plates subjected to complex middle-plane force systems.

21 p3116 A72-40330

Russian book - Plates strengthened by composite rings and elastic cover pieces.

21 p3116 A72-40385

Randomly coupled flexural and longitudinal vibrations of plates.

21 p3120 A72-41111

Stress-strain state of thin circular perforated Cu plate under uniform tensile load, showing applicability of small elastoplastic finite deformation theory

21 p3122 A72-41351

Electromagnetic waves interaction with transverse waves of thin piezoelectric plate in waveguide, noting transformation into acoustic waves

23 p3312 A72-43407

Nonlinear thin elastic plate deformation differential relations and static boundary conditions along contour, verifying theory by bending experiment on rectangular plate

23 p3348 A72-43791

Determination of the stationary temperature field in a plate with a crack in the presence of heat release from the lateral surfaces

23 p3357 A72-44086

Dynamic blast loads on preheated and prestressed thin plates.

24 p3454 A72-44607

Action of a moving load on a composite shell with elastic filler

24 p3459 A72-45262

Supersonic flutter of plane, rectangular, anisotropic, heterogeneous structures

24 p3459 A72-45440

THIN WALLED SHELLS

Initial interaction phase between thin shallow conical shell vibrating axisymmetrically and ideal incompressible fluid, determining hydrodynamic pressure effects

01 p0050 A72-10574

Torsional prestrain effects on 1100-F Al alloy thin walled tubes yield locus, calculating distortion degree by statistical characteristics

01 p0086 A72-11006

Thin walled sandwich cylindrical shells under internal pressure, calculating elastic-plastic zone propagation

01 p0141 A72-11001

Thin walled prismatic structural members under uneven axial moment distribution, formulating force deflection equations for torsional-flexural behavior

01 p0141 A72-11049

Wave propagation in thin elastic shells by similar formation of shell and nonlinear elasticity theories equations

01 p0142 A72-11197

Static loads effect on natural vibrations of thin truncated conical shells by shallow shell theory, determining resonant frequency spectrum due to prestressing

01 p0142 A72-11362

Thin shell creep and plasticity analyses reduced to linear programming problem by functionals and finite difference equations

02 p0290 A72-11622

Temperature fields and stresses in thin elastic nonferromagnetic electrically conducting cylindrical shells heated by induction determined from heat source distribution and thin shell theory relations

02 p0290 A72-11631

Vertical thin circular cylindrical shells partially or completely filled with stationary liquid, determining free vibration characteristics with finite element theory

02 p0293 A72-12371

Improved finite difference solutions for stress in thin cylindrical shells, using Donnell assumptions

[ASME PAPER 71-PVP-24] 02 p0295 A72-12475

Thin circular cylindrical shells under uniform axial compression loads, examining axially symmetrical creep buckling

02 p0296 A72-12531

Homogeneous isotropic thin elastic shells under forces along edge and with faces free of tractions, deriving refined interior equilibrium equations

03 p0447 A72-13882

Elastoplastic stress distribution in thin spherical metallic shells with cylindrical branch pipe under internal pressure

03 p0448 A72-13905

Curvilinear material anisotropy effects on temperature distributions of thin walled cylindrical shells of revolution

03 p0449 A72-13919

Ductility and fracture of metallic thin walled tubular samples under complex stress of internal pressure and axial tension

03 p0454 A72-14215

- Thin walled elastic axisymmetric fluid filled tanks under longitudinal vibrations, determining dynamic characteristics 04 p0586 A72-15011
- Iteration method error estimates for thin elastic shell basic stressed state and simple fringe effect relation to boundary stressed state 04 p0586 A72-15012
- Canonical form for boundary conditions of thin elastic shells with oscillating loads applied on edges 04 p0587 A72-15013
- Linearized equilibrium equations for thin spherical shell with internal pressure, obtaining free vibration modes 04 p0587 A72-15018
- Convergence of iterative schemes for calculating stress state of thin shells with allowance for nonlinear terms in the equilibrium equations 04 p0587 A72-15048
- Stress-strain state of thin ellipsoidal shell with central stiffened hole, using small elastoplastic deformation theory 04 p0588 A72-15050
- Thermoelasticity theory coupled linear equations for thin orthotropic shells, taking into account rotary inertia and lateral shear 04 p0588 A72-15060
- Stress and strain approximate analysis for thin elastic shells by rational derivation of two dimensional differential and constitutive equations [AD-745612] 04 p0592 A72-15506
- Thin cylindrical shell bending deformation from axisymmetrical temperature distribution generated by narrow heating element 05 p0736 A72-16113
- Thin elastic shell postbuckling behavior from asymptotic integration solution for differential equations, permitting dynamic effect modeling 05 p0738 A72-16425
- Meridional curvature effect on thin walled cylindrical shell buckling under external constant directional lateral pressure 05 p0739 A72-16546
- Triangular/KLI/ and quadrilateral/KQT/ thin shallow shell elements with 20 degrees of freedom, basing bending behavior on discrete Kirchhoff formulation 05 p0739 A72-16549
- Power parameter determination in rotary swaging of thin conical shells, discussing radial contact stresses 05 p0666 A72-16628
- Semiempirical stress analysis of cantilevered thin walled cylinder, obtaining local stresses via strain gages [SAE PAPER 720285] 06 p0893 A72-17324
- Flutter of thin elastic circular cylindrical fluid filled shells, presenting potential flow theory for coupled hydrodynamic forces 06 p0894 A72-17763
- Combined stress wave propagation in thin walled prestressed tube under longitudinal and torsional impact loading 06 p0898 A72-18321
- Plasticity of Al alloy thin walled tubular specimens under axial tension and internal pressure at 293, 173 and 93 K 06 p0833 A72-18561
- Thin walled elastic isotropic shallow shell with thermal boundary conditions, obtaining thermoelastic solution in series form 06 p0899 A72-18657
- Residual stresses and geometrical imperfections effects on compressive strength of thin walled welded box columns 07 p1088 A72-19114
- Stress-strain state of thin walled spherical shell in contact with internal rigid sphere, determining contact area size 07 p1091 A72-19756
- Equilibrium equations for thin walled shallow paraboloid shell of revolution, solving boundary value problem for edge fastened loaded circular planform region 07 p1091 A72-19757
- Elastoplastic stressed state of thin cylindrical shells with circular hole, using small strain theory 07 p1092 A72-19896
- Algorithm for solving boundary value problem of integrodifferential equations describing temperature field inside hollow thin walled rod within solar radiation field in vacuum 07 p1028 A72-20207
- Stress-strain state of unclamped thin elastic zero curvature shell under three component surface load and tangential boundary forces 07 p1095 A72-20313
- Asymptotic eigenvalue density estimates for edge-hinged thin elastic rectangular shell, determining shell stability linear equation solution conditions 07 p1095 A72-20324
- Trapped modes structure of rotating fluid in thin spherical shell, noting constitution of free oscillation periods 07 p0973 A72-20455
- Axially nonuniform thin cylindrical shells dynamic analysis, obtaining free flexural vibration characteristics by hybrid of finite element and classical shell theories 07 p1097 A72-20531
- Local stability of thin walled isotropic elastic cylinder, deriving characteristic equations for critical load calculation 08 p1244 A72-21290
- Elastic-plastic deformation of thin membrane shells 08 p1246 A72-21712
- Strength analysis of thin elastoplastic shell with allowance for compressibility, relating loads and moments to deformation of middle surface 08 p1247 A72-21810
- Elasticity theory method for nonlinear stress-strain relationships in thin anisotropic shells, discussing fiberglass reinforced cylindrical shell 08 p1248 A72-21821
- Thin shell theory analysis of thin walled cylindrical shell necking phenomenon as tensile deformation nonuniformity 08 p1249 A72-22096
- Secondary normal stresses in fixed flange zone of thin walled nonlinearly elastic pipe under bending moment and torsion 09 p1399 A72-22702
- Stress-strain state produced by asymmetric physical and thermal loads in thin orthotropic viscoelastic shells of revolution 09 p1400 A72-22713
- Thermal insulations in form of thin shells of revolution with rigid external and elastic internal layers resting on rigid core 09 p1400 A72-22716
- Thermal stressed state determination for open thin walled cylindrical shells, using method of integral relations 09 p1401 A72-22724
- Computer algorithm for thermoplastic stress-strain state of thin shells of revolution based on plastic flow theory, taking into account loading history 09 p1401 A72-22728
- Finite difference analysis of dynamic deformation of thin elastoplastic shells of revolution under intense heating 09 p1401 A72-22782
- Nonlinear vibrations of thin circular cylindrical shells under arbitrary boundary and loading conditions 09 p1407 A72-23456
- Axially homogeneous stress and strain in anisotropic thin walled cylindrical shells, considering pure bending, stretching and twisting [ASME PAPER 71-APMW-4] 10 p1554 A72-24181
- Dynamic response of pressurized thin walled circular cylindrical shell under initial biaxial stress and subjected to radial uniformly moving force, noting transient and steady state [ASME PAPER 71-APM-GGG] 10 p1554 A72-24186
- Natural axisymmetric vibration of thin elastic shell of revolution, deriving eigenvalues convergence to spectrum lower bound by asymptotic method 10 p1557 A72-24560
- Partial differential equation for thin walled circular cylindrical shells, deriving solutions for displacement and stresses in terms of surface coordinates low degree polynomials 10 p1557 A72-24630
- Stability loss in thin convex shells of revolution under axisymmetric stress, obtaining integrals for equilibrium equations 10 p1559 A72-24925
- Plate and thin and thick walled shells treated as three dimensional solids, noting finite element method limitation 10 p1729 A72-25383
- Finite element structural analysis for local buckling stresses in flat plates, panels and thin walled columns, deriving elastic and geometric stiffness matrices [ALAA PAPER 72-354] 11 p1731 A72-25457
- Elastic finite element analysis for stress distribution in gripped thin walled tubular anisotropic three dimensional composite specimens 11 p1735 A72-25877
- Von Mises yield criterion extended to thin walled circular cylinder plastic torsional straining, noting variations of anisotropic parameters and yield stresses with shear strain [ASME PAPER 71-MET-Y] 11 p1643 A72-26831
- Hot isostatic pressing techniques for thin wall Be tubes manufacture 11 p1739 A72-26920
- Viscoelasticity analysis of bending displacements in thin walled closed cylindrical shell loaded by moving moment 11 p1739 A72-26977
- Bubnov-Galerkin method for dynamic stability of closed thin walled orthotropic cylindrical shell loaded by variable external pressure 12 p1878 A72-27078
- Elastic truncated thin conical shell response to dynamically applied axial force from numerical solution of nonlinear equations 12 p1881 A72-27244
- Structural effects of meridian imperfections in symmetrically loaded elastic thin shell of revolution 12 p1881 A72-27255
- Closed thin circular cylindrical shells external pressure pulse and structural parameters effects on stability under dynamic loading 12 p1886 A72-28129
- Thin walled tubular carbon steel specimen deformation pattern under biaxial tension and internal pressure at normal and low temperatures 12 p1830 A72-28227
- Creep stability of bars and thin plates and shells for given loading force, considering instability criteria 13 p2054 A72-28481
- Optimal design of thin walled minimum weight aircraft shell structures, using linear programming 13 p2058 A72-29143
- Dynamic behavior of thin walled seminfinitesimal cylindrical shell with liquid under axial impact loads 13 p1943 A72-30008
- Thin wedge shaped shell bending under normal loads, discussing boundary value problems 13 p2062 A72-30066
- Stress-strain state of complex configured thin walled shell, deriving computer algorithm via tensor analysis and finite difference scheme 14 p1615 A72-30686
- Average stress and strain across thickness of liquid filled cylindrical elastic thin walled shell with rigid bottom under axial impact loads 14 p2166 A72-30698
- Finite element method application to dynamic stability of thin plates and shells, noting nuclear reactor structural analysis [SMRT PAPER M 2/1] 14 p2166 A72-30723
- Dynamic response of thin circular arches to in-plane forced excitation under cyclic symmetric and axisymmetric support movement 14 p2169 A72-31175
- Stability analysis of thin walled circular cylindrical shell under shearing force action to one end, calculating buckling modes 15 p2324 A72-31483
- Elastic deformation of thin walled spherical and cylindrical shells and associated rings under external loads for small displacements 15 p2325 A72-31604
- Zero moment stress effect on modal density spectrum of fluctuating thin cylindrical shells and cylindrical panels 15 p2327 A72-31737
- Adhesive bonding of L-1011 body shell panels for improved fatigue strength and corrosion resistance 15 p2245 A72-32429
- Thin walled elastic shells stability under finite deformations, deriving equilibrium conditions and constitutive equations 15 p2330 A72-32464
- Preloaded thin walled open section elastic column dynamic stability under free longitudinal vibrations, deriving criterion for flexural and torsional vibrations nonlinear coupling 15 p2332 A72-32560
- Natural frequency distribution theory of thin elastic shells under random vibrations in wideband field 15 p2332 A72-32677
- Thin elastic isotropic plates and shells thickness variation for rigidity functional stationary value, reducing problem to stress-strain state equations simultaneous solution 15 p2333 A72-32688
- Membrane and bending stress analysis for thin circular cylindrical shells with elliptic hole 16 p2464 A72-32918
- Vibrational frequency density analysis of thin spherical and cylindrical shells of revolution, using asymptotic integration method 16 p2464 A72-32935
- Constitutive and equilibrium equations for theory of thin shells with slowly varying curvature based on Novoshilov and Koiter assumptions 16 p2465 A72-33004
- Dynamic structural analysis of viscoplastic thin walled shells, noting time dependent profile of deflection 16 p2467 A72-33122
- Equilibrium equation for elastic deformation effect on free electricity redistribution in thin electroconductive shells 16 p2469 A72-33271
- Metal creep tests in thin walled ring shaped specimens for geometrical constancy under variable weights 16 p2472 A72-33850
- Small nonaxisymmetric initial shape deviations effect on creep buckling and critical time of thin walled circular cylindrical shell in axial compression 16 p2474 A72-34134

Matrix progression method analysis of free vibration problem for cantilever thin circular cylindrical elastic shells, using Flugge equations

16 p2475 A72-34173

Inflation pressure caused deformations of thin toroidal shells, discussing wrinkle development due to pressure reduction

[ASME PAPER 72-APM-32] 17 p2628 A72-34787

Longitudinal impact of cylindrical shells with discontinuous cross-sectional area.

[ASME PAPER 72-APM-24] 17 p2628 A72-34793

Governing equation derivation for coupled extension, flexure and torsion in pretwisted curved beams of thin walled open section, using three dimensional elasticity

[ASME PAPER 72-APM-5] 17 p2630 A72-34809

Elastic wave propagation in a joined cylindrical-conical-cylindrical shell.

[SESA PAPER 1983] 17 p2630 A72-34819

Thin spherical shells in equilibrium with displacement and stress fields, satisfying virtual work, kinematic and static requirements

17 p2633 A72-35351

On the flutter of thin cylindrical shells conveying fluid.

17 p2634 A72-35415

An approximate theoretical study of the dynamic plastic behavior of shells.

18 p2732 A72-36077

Predictions of solar induced response of thin-walled open-section booms for design.

18 p2733 A72-36364

Thermal displacements and stresses in cylindrical shells due to instantaneous line heat sources.

19 p2870 A72-37272

Longitudinal impact on a thin cylindrical shell

19 p2870 A72-37321

Further results on the stability of a finitely deformed thin cylindrical shell.

19 p2871 A72-37415

Loading rig in which axially compressed thin cylindrical shells buckle near theoretical values.

19 p2873 A72-37730

Creep buckling of slender or thin-walled structures, taking into account strain rate dependent time-hardening and elastic deformation effects

19 p2875 A72-37884

Vibrations of a concentrated mass on a ring coupled to a thin shell

20 p2981 A72-39908

Stresses in a circular cylindrical shell having two circular cutouts.

20 p2982 A72-40063

Plane acoustic pressure wave effect on motion of thin elastic truncated conical shell fastened in rigid screen, using Timoshenko theory

21 p3116 A72-40263

Transverse shear effect on thin shells collapse load, considering influence on Shapiro yield surfaces

21 p3121 A72-41213

Study on an incremental variational principle and its applications to finite element method and incremental thin shell theory.

21 p3121 A72-41240

Combined tension-torsion elastic-plastic waves as propagating singular surfaces.

21 p3121 A72-41244

An inverse problem in the momentless theory of shells of revolution situated in a temperature field

22 p3232 A72-41895

Steady-state creep of shells of revolution in the case of the Tresca criterion

22 p3233 A72-42051

Carrying capacity of thin-walled shells subjected to impulsive radial pressure loads

22 p3233 A72-42052

Determination of the critical temperatures of cylindrical shells of variable thickness

22 p3243 A72-42053

Equilibrium equation for unsteady creep of thin truncated conical shell under internal pressure, solving in successive time steps with Taylor series expansion

22 p3233 A72-42062

Cylindrical shells of optimal torsional stiffness

22 p3233 A72-42112

Symmetry transformations for thin elastic shells.

22 p3234 A72-42398

Wave propagation in a truncated conical shell.

22 p3235 A72-42524

On the formation of plastic adiabatic bands in a thin tube subjected to a dynamic torsion

22 p3236 A72-42638

Dynamic behavior of thin walled seminfinitesimal elastic cylindrical shell with compressible liquid under axial impact loads

22 p3167 A72-42736

Axissymmetric-multilobe creep buckling transition in thin walled circular cylindrical shells under uniformly distributed axial compressive load

22 p3239 A72-42844

Dynamic loading of a fluid-filled spherical shell.

22 p3240 A72-42891

Rigid-body motions and strain-displacement equations of curved shell finite elements.

22 p3240 A72-42892

Elastoplastic computation of thin cylindrical shells under cyclic loading

23 p3348 A72-43786

Limiting equilibrium of shallow conical shells of variable thickness

23 p3348 A72-43787

First order constraints in three dimensional continuous elastic fibrous media and thin shells, presenting equilibrium equations

23 p3349 A72-43825

Stress concentration of a cylindrical shell with one or two circular holes.

23 p3355 A72-44399

Parametric influences on the response of structural shells.

24 p3454 A72-44604

Free vibration frequencies and critical buckling loads for thin walled shells of revolution constructed out of layered or heterogeneous anisotropic materials

24 p3455 A72-44676

Triangular facet finite element application in thin cylindrical shell analysis by displacement method

24 p3456 A72-44792

Theory of thin elastic shells applied to pipe bends subjected to bending and internal pressure.

24 p3456 A72-44795

A finite element model for shells based on the discrete Kirchhoff hypothesis.

24 p3457 A72-44876

Multi-node elements model of isoparametric thin shell vibration for turbine blade application

24 p3457 A72-44881

Wave propagation in a thin hollow cone by a finite element method.

24 p3458 A72-44886

The transient electromagnetic response of a spherical shell of arbitrary thickness.

24 p3381 A72-45638

THIN WALLS

Local buckling and collapse of thin walled lipped channel beams under critical end moments

01 p0144 A72-11396

Strain anisotropy effect on thin walled tubular steel samples with combined bending and torsion, constructing matrix and stress vectors

03 p0445 A72-13578

Nonlinear theory of thin walled open elastic beams with deformations by large cross sectional rotation, using potential energy principle

07 p1096 A72-20430

Perturbation solution to nonlinear nonuniform torsion of thin walled open elastic beams with strain hardening dependent on torque-rotation behavior

07 p1096 A72-20431

Thin walled box beam optimal design, noting cross section areas and dimensions with permissible walls and flanges safety and stability

08 p1243 A72-21240

Thin walled Bourdon tube manometric spring deformation analysis by Ritz method in second approximation

09 p1397 A72-22349

Parametric dynamic stability equations and boundary conditions for thin walled open cross section beam under axial load, taking into account longitudinal deformation effect

[ASME PAPER 71-APM-LL] 10 p1554 A72-24184

Creep tests for thermal preycling effect on time to failure and long term ductility of austenitic steel thin walled tubular samples

11 p1663 A72-26809

Limiting load calculation for thin walled I-beam in oblique bending and torsion beyond elastic limit

13 p2055 A72-28734

Deformation limits in thin and thick walled metal blanks axisymmetric drawing process, determining stress-strain state based on prescribed velocity field

13 p1963 A72-28743

Resonant frequencies of two thin walled cylindrical panels connected by elastic filler, considering symmetric and asymmetric vibration modes

13 p2058 A72-29146

Plane stress solution for thin walled cantilever beam with end load extended for beam width effects in composite orthotropic beam bending

16 p2463 A72-32841

Thin walled elastic structures optimization by overall and local buckling coincidence, discussing compression column design

16 p2468 A72-33200

Torsion and flexure of curved, thin-walled beams or tubes.

19 p2874 A72-37696

Stability of convective heat transfer through horizontal air layer heated from below and constrained internally by thin walled honeycomb panels

[ASME PAPER 72-HT-60] 20 p2985 A72-39656

Calculating the stability of centrally compressed thin-walled bars with various profiles

21 p3126 A72-41549

Calculation of a thin-walled small-aspect-ratio wing beyond the limit of proportionality

23 p3346 A72-43654

Vibration of simply supported cylindrical shells with longitudinal stiffeners.

24 p3457 A72-44882

THIN WINGS

Circular jet discharging perpendicular to solid surface into transverse flow, discussing effects on infinitely thin circular wing aerodynamic characteristics

03 p0309 A72-13915

Heat transfer coefficients to both sides of finite one dimensional slab subject to phase-change coating technique boundary conditions, deriving thin wing correction factors

03 p0457 A72-13956

Symmetrically deformed delta wing in supersonic flow, considering leading edge flow separation induced vortices effects on downwash, pressure distribution and aerodynamic characteristics

04 p0463 A72-15741

Thin wing harmonic oscillation in subsonic flow developing analytical form of kernel function in generalized Possio integral equation

05 p0603 A72-16707

Supersonic flow around thin cruciform wing with antisymmetrical angle of attack distribution and horizontal plane with leading edge, considering flow separation at edges

10 p1420 A72-25118

Torsion problem of solid rod with wing profile shaped cross section solved by conformal mappings and gamma function derivative, calculating maximum stresses and rigidities

15 p2327 A72-31741

Iterative methods for the aerodynamic calculation of thin wings in a subsonic flow

24 p3363 A72-45378

THINNERS

U SOLVENTS

THIOPLASTICS

Epoxy-thiocol binder viscoelastic deformation under short and long term loads, noting stress-strain linearity limit

21 p3073 A72-41360

THOMAS-FERMI MODEL

Extended Thomas-Fermi isolated atom model for pulsar outermost crust magnetic field effects, using pressure-density equations of state

02 p0277 A72-11903

Free electrons in condensed matter under high pressure, calculating number with Thomas-Fermi statistical model

15 p2305 A72-31394

Equation of state of neutron-star matter at super nuclear densities.

22 p3228 A72-42564

THOMAS-FERMI THEORY

U THOMAS-FERMI MODEL

THOMSON EFFECT

U THERMOELECTRICITY

THOMSON SCATTERING

Energy-momentum tensor for radiation and radiative viscosity in optically thick matter having Thomson scattering with photon absorption and emission processes

01 p0129 A72-10794

Electron density measurements for traveling ionospheric disturbances by Thomson scatter technique using Faraday rotation

01 p0031 A72-10922

Spectral distribution of radiation arising from nonlinear Thomson scattering of strong electromagnetic wave by ultrarelativistic electrons

03 p0390 A72-13013

Stellar X ray emission polarization measurements using Thomson scattering polarimeter

[AD-736550] 03 p0353 A72-13044

Electron density and temperature temporal and radial profiles in megawatt MPD-arc thruster exhausts using Thomson scattering technique

[AIAA PAPER 72-209] 05 p0707 A72-16887

Thomson autooscillatory systems synchronization and small external sinusoidal emf effect with hard and soft bounding of amplitude deviations

08 p1142 A72-21769

Thomson scattering of electromagnetic wave in plasma and ionosphere for studying electron and ion temperatures

11 p1621 A72-25834

Ion velocity height profiles, ion temperature and electron density measurement with Thomson scattering facility during F region traveling ionospheric disturbance /gravity waves/

12 p1803 A72-27777

Variable circular polarization of X ray star SCO X-1 optical radiation due to Thomson scattering in magnetized plasma shell

15 p2304 A72-31322

Celestial Thomson-scattering X ray polarimeter design for OSO-1, optimizing sensitivity in 4-24 keV energy range by Monte Carlo simulation computer program

15 p2234 A72-31544

Effect of Thomson scattering on the emission spectrum of an optically semitransparent plasma

21 p3102 A72-41774

THOR AGENA LAUNCH VEHICLE

Delta and Thor/Agena satellite launch vehicles discussing costs, performance and mission planning

based on booster design flexibility, incorporating computer programmed strapdown inertial guidance
01 p0136 A72-10953

THOR LAUNCH VEHICLES
NT THOR AGENA LAUNCH VEHICLE
THORAD LAUNCH VEHICLES
NT THOR AGENA LAUNCH VEHICLE
THORAX
Lf subaudible chest wall vibration recordings, discussing external, epicardial surface and intraventricular pressure precordial displacement tracings
01 p0017 A72-10120
Nonsurgical ultrasonic technique to measure wall displacement and pulsatile changes in thoracic aorta [AD-739809]
07 p0930 A72-19447
Relative position of the rib within the chest and its determination on living subjects with the aid of a computer program.
24 p3372 A72-44957

THORIUM
NT THORIUM ISOTOPES
THORIUM ALLOYS
Tensile ductile-brittle transition temperature and slip mechanism of thoriated Cr, comparing with unalloyed Cr
05 p0678 A72-17117
Mg base alloys precipitation processes studied by electron microscopy, emphasizing Mn precipitation in Mg-Th alloy
16 p2405 A72-32998
Alloys of thorium with certain transition metals, VI-
The constitution of thorium-nickel alloys containing 50-96% nickel.
22 p3190 A72-42769

THORIUM COMPOUNDS
NT THORIUM OXIDES
Mutual interactions of thorium, lanthanides, and bismuth in Th-Ln-Bi solutions - Evidence for the formation of ThLnBi₃/y compounds.
20 p2942 A72-39986

THORIUM ISOTOPES
Lunar solar radiogenic U-Th-Pb analyses of Lunik 16 samples from Sea of Fertility
09 p1381 A72-22278
Th 228 decay from short and long term simulation tests of thorium dioxide heat source in thermionic energy converter with W capsule
18 p2709 A72-36162

THORIUM OXIDES
Arc jet simulation tests of thorium dispersed Ni and Co alloys for space shuttle Metallic Thermal Protection System, determining material degradation
01 p0086 A72-10978
Thoriated Ni-Cr alloys oxidation kinetics at high temperatures, discussing oxide formations as function of CR content
01 p0089 A72-11164
Thorium oxide dispersion strengthened Ni powder metallurgy alloys, noting thermomechanical processing effects on tensile strength
02 p0241 A72-11447
Mean free path and particle size distribution in dispersion hardened nickel-thoria alloys, obtaining interparticle spacing by Scheil method
02 p0245 A72-12549
Quenching effects on thorium-dispersed Ni sheet plastic stress relaxation and room temperature mechanical properties
02 p0247 A72-12822
Powder metallurgy Ni-Cr thorium cleaning by reduction with atmosphere of hydrogen plus HCl or HBr
10 p1488 A72-24697
Manufacturing process for dispersion strengthened nickel-chromium-thorium dioxide alloys for space shuttle thermal protection system panels, discussing joining optimization and mechanical properties
11 p1659 A72-26035
Dispersed phase nickel-thoria alloy production method based on organometallic compounds, avoiding high temperature and solvent elimination difficulties
11 p1664 A72-26849
Dispersion strengthened nickel-chromium-thoria alloy production methods, noting halogen gas phase diffusion process
11 p1645 A72-26850
High temperature creep properties of W-Re alloy under vacuum for thorium dispersion hardening from electron microscope and activation energy studies
11 p1665 A72-26863
High temperature constant load creep tests on pure powder metallurgy W and tungsten-thoria alloy, discussing stress dependence
13 p1975 A72-28665
Th 228 decay from short and long term simulation tests of thorium dioxide heat source in thermionic energy converter with W capsule
18 p2709 A72-36162
Pure and thoriated W compatibility with uranium carbide alloys at 1800 C, noting thermal gradient and thorium noneffects
18 p2699 A72-36163
Oxidation of TD nickel at 1050 and 1200 C as compared to three grades of different purity.
21 p3067 A72-40915

Grain size and temperature effects on Cr and Al diffusion coefficients and mobility in Ni-20Cr and thorium dispersed NiCr alloys from measurement at 1038-1200 C
22 p3193 A72-43028

Growth kinetics of dispersed thorium in Ni and Ni-Cr alloys.
24 p3415 A72-45480

THORIUM 228
U THORIUM ISOTOPES
THORIUM 230
U THORIUM ISOTOPES
THORIUM 234
U THORIUM ISOTOPES
THREADS
Concentric double and single screw seals in laminar Newtonian fluid flow operation, using mathematical methods for optimum thread geometry and maximum sealing coefficients
08 p1178 A72-21930

THREE BODY PROBLEM
Triangular points stability in restricted three body problem by computer program
01 p0122 A72-10004
Consecutive collision orbits characterized by particle ejection from mass along x axis in restricted three body problem
01 p0122 A72-10006
Particle escape within Newtonian gravitational system of three point masses, discussing necessary conditions
01 p0122 A72-10007
Stability of and motion about L4 in restricted three body problem with 3 to 1 commensurability between long and short periods of motion
01 p0122 A72-10010
Attitude motion at equilibrium libration points of axisymmetric smallest body in restricted three body problem
01 p0123 A72-10011
Periodic orbit families emanating from Lagrange triangular point L4 in restricted three body problem with mass ratio parameter equal to Routh critical mass ratio
01 p0123 A72-10013
Dynamical behavior classification for three bodies moving in plane under mutual gravitational influence
01 p0123 A72-10015
Zero relative velocity surfaces in bounded circular three body problem in presence of magnetic dipole, deriving Jacobi integral
01 p0127 A72-10358
Outer planet low thrust orbiter missions, comparing three body numerical results with two methods of patching together two body solutions
01 p0128 A72-10379
Three body ionic recombination as Markov process, deriving ion pairs quasi-equilibrium distribution equation identical to Bates-Flannery statistical theory
01 p0104 A72-10860
Jupiter outer satellite origin, considering capture orbit dimensions based on three body elliptical problem
02 p0275 A72-11594
Three dimensional angle dependent model for three body problem, considering exact quantum mechanical reactive scattering cross sections
02 p0262 A72-11911
Limited three body problem applied to planetary angular momentum increment due to accretion of particles in heliocentric orbits, discussing planet rotation laws
02 p0282 A72-12330
Book on celestial mechanics covering Hamiltonian systems and equations of motion for three body problem
02 p0285 A72-12857
Newton laws and solution existence of two and three body problems in remote universe
03 p0388 A72-13174
Liapunov stability of rigorous particular solutions /corresponding to libration points/ of three body problem, determining motions of satellite influenced by two spherical bodies
03 p0436 A72-13823
Mass changes in restricted quasi-circular variable mass three body problem with particle equations of motion having Jacobi integral
03 p0436 A72-13828
German monograph on Poincare orbit stability in restricted three body problem, using canonical mappings of annulus and perturbation method
05 p0689 A72-16044
Coupled equations for collision amplitudes in three body system involving particle redistribution
06 p0851 A72-17391
Elliptic restricted three body problem, using motion anomaly as independent variable
06 p0877 A72-17654
Generalized restricted three body problem with one point not exerting influence on others, discussing variational equations and Liapunov stability
06 p0877 A72-17662

Triangular points linear stability in elliptic restricted three body problem, determining exponents by convergent iteration method
06 p0878 A72-17664
Soviet book on qualitative methods in celestial mechanics covering differential equations of motion averaging schemes, Newton type convergence method, three body problems, etc
06 p0879 A72-17821
Quasi-periodic n-degrees of freedom solutions to Hamiltonian systems with 2n plus 2 variables, noting applicability to planar three body problem
06 p0839 A72-17882
Hamilton-Jacobi equation for bounded plane circular three body problem with construction of algebraic partial integrals and periodic orbits
06 p0850 A72-18709
Quantum gravitation theory and Mercury perihelion motion, calculating three body potentials from treatment of celestial bodies as nucleon assemblies
07 p1084 A72-20690
Bounded circular-space three body problem, obtaining Lagrangian solutions for triangular motion configuration stability
08 p1232 A72-21134
Sundman power series convergence enhancement in three body problem by Poincare transformation
09 p1350 A72-22482
Jacobi integrals in restricted three body problem of small bodies with massive sun and Jupiter in solar system
09 p1389 A72-23394
Rectilinear motions in three body problem with null live forces constant, using inequality deduced from virial theorem
09 p1392 A72-23542
Gravitational red shift due to three body effect as relativity test
10 p1532 A72-23850
First order asymptotic matching computational technique for calculation of perturbed moon-centered hyperbola parameters in earth-moon trajectory
11 p1720 A72-25996
Planar restricted three body problem periodic solutions with bridges connecting direct and retrograde circular orbits
11 p1721 A72-26153
Lunar motion as plane restricted three body problem in celestial mechanics
11 p1722 A72-26478
Triple stellar system evolution and disintegration, discussing energy partitioning and initial velocity effects on stability
12 p1865 A72-27095
Three body problem study of satellite capture by planets in elliptical orbits, deriving orbital elements in terms of mass ratio and planetary orbit eccentricity
12 p1865 A72-27096
Capture within restricted three body problem for close single encounters between massless particles and binary system lesser component
12 p1872 A72-27758
Limited three body problem applied to planetary angular momentum increment due to accretion of particles in heliocentric orbits, discussing planet rotation laws
13 p2039 A72-29214
Two body model for three body problem of uniformly distributed and isotropically expanding gravitational matter of Einstein-Sitter universe, noting metagalaxy cooling rate
14 p2149 A72-30211
Earth-moon system periodic orbits calculation by modified quasi-linearization combined with particular solutions method, using restricted three body model
14 p2149 A72-30232
Earth capture of dust particles moving in ecliptic plane heliocentric orbits, using three gravitational bodies analysis
14 p2153 A72-30494
Dynamic behavior of three masses moving under mutual gravitational attraction examined by numerical experiments for binary star formation via third star hyperbolic escape
14 p2160 A72-30877
Restricted three body problem in elliptical coordinate representation, solving Hamilton-Jacobi equation by separation of variables method
15 p2274 A72-31455
Direct periodic orbits in planar restricted barycentric three body problem, using Poincare variables and Hamiltonian function
15 p2307 A72-31763
Secular and long term periodic perturbation effects of third body upon particle motion in three body problem, discussing mass motion in Jovian gravitational field
15 p2312 A72-32120
Further periodic solutions of the three-dimensional restricted problem. II.
17 p2604 A72-34444
Numerical integration method with recurrent power series for motion and variational equations of elliptic restricted three body problem
19 p2862 A72-38019

Earth capture of dust particles moving in ecliptic plane heliocentric orbits, using three gravitational bodies analysis

19 p2864 A72-38323

Three body problem second kind periodic orbit existence proof based on Weinstein theorem

19 p2867 A72-38553

Regularized first order algorithm for ideal resonance problem in solar system, considering solution in terms of elliptic functions

20 p2968 A72-39199

Collision periodic orbits calculation in restricted three body problem

20 p2973 A72-39885

A two-parameter survey of periodic orbits in the restricted problem of three bodies.

21 p3106 A72-41049

Improved criteria for hyperbolic-elliptic motion in the general three-body problem.

21 p3109 A72-41333

Approximate analytic solution method for trajectory problem of planetary flyby or impact case of restricted three body problem

[AIAA PAPER 72-911] 21 p3111 A72-41558

Two body model for three body problem of uniformly distributed and isotropically expanding gravitational matter of Einstein-Sitter universe, noting metagalaxy cooling rate

23 p3334 A72-43241

The topology of the regularized integral surfaces of the 3-body problem.

23 p3309 A72-43982

Stability of motion at collinear libration centers in the restricted problem of three bodies with allowance for light pressure

24 p3437 A72-44762

Explicit series solutions for the frequencies of motion around the Lagrangean points in the restricted problem of three bodies.

24 p3440 A72-45136

Application of the restricted hyperbolic three-body problem to a star-sun-comet system.

24 p3442 A72-45234

Dynamic behavior of three point mass system with variable body mass ratios and constant total system mass, applying results to stellar systems

24 p3442 A72-45240

THREE DIMENSIONAL BOUNDARY LAYER

Increasing lift and Reynolds number effects on displacement and skin friction of three dimensional turbulent boundary layer on infinite swept wing

01 p0002 A72-11395

Iterative solutions for three dimensional turbulent boundary layers on rotating nose-body, using streamwise and cross flow momentum equations

01 p0002 A72-11397

Three dimensional boundary layer gas flow in large pressure gradient region, using two dimensional boundary layer equations

02 p0201 A72-11580

Self similar solutions for three dimensional laminar boundary layer equations under arbitrary surface conditions by quasi-linearization method

02 p0203 A72-11739

Laminar three dimensional boundary layer nonequilibrium effects at hypersonic wing swept leading edge with intensively cooled surface, considering sweep induced crossflow effect

[VPI-E-71-23] 02 p0152 A72-12422

Three dimensional laminar boundary layer about finite body nonuniformly moving along rectilinear trajectory

02 p0206 A72-12618

Two and three dimensional turbulent boundary layer development in incompressible and compressible flows, obtaining boundary layer equations similarity solutions via mixing length model

[DGLR PAPER 71-066] 02 p0206 A72-12719

Computerized calculations of turbulent shear layers with compressibility, heat transfer, three dimensionality or unsteady flow, using differential equation

[ASME PAPER 71-WA/FE-8] 05 p0646 A72-15934

Finite element algorithm derived for partial differential equation system governing laminar three dimensional boundary layer flow of multicomponent compressible fluid

[AIAA PAPER 72-108] 05 p0604 A72-16817

Three dimensional hypersonic turbulent boundary layer under normal and longitudinal pressure gradients and cross flow along windward symmetry plane of body of revolution

[AIAA PAPER 72-186] 05 p0605 A72-16841

Numerical solution method for laminar, time dependent and three dimensional boundary layer equations, applying to rotating flat plate in forward flight

[AIAA PAPER 72-109] 05 p0652 A72-16944

Thermal laminar three dimensional boundary layer on finite uniformly accelerated body in nonstationary regime, taking into account buoyancy effect

07 p1100 A72-19624

Monograph on three dimensional turbulent boundary layers in unsteady incompressible flow covering flow equations, eddy viscosity and mixing length models, etc

07 p0968 A72-19953

Near wall collateral layer with velocity vector magnitude changes existence in three dimensional turbulent boundary layer flow

08 p1150 A72-21615

Accuracy tests of Wang method for calculating three dimensional laminar compressible boundary layer flow equations

08 p1150 A72-21625

Yaw calibrations of Preston tubes for wall shear stress measurements in two and three dimensional turbulent boundary layers

08 p1254 A72-21627

Boundary layer transition effect on three dimensional shock interactions due to blunt protuberances and axial compression corner

[AD-743741] 08 p1150 A72-21629

Mixing length model for computing three dimensional turbulent boundary layers with small cross flow

[ONERA, TP NO. 985] 09 p1294 A72-22817

Equations of motion of steady viscous fluid flow in three dimensional boundary layer on walls of axial flow compressors and turbines, obtaining velocity field

10 p1420 A72-25120

Three dimensional laminar boundary layer on slender circular cone at angle of attack in supersonic flow, determining separated flow region via finite difference method

11 p1572 A72-25818

Three dimensional free convection boundary layer equations solution at two dimensional isothermal stagnation point with various Prandtl numbers

11 p1747 A72-26662

Three dimensional hydrodynamic and thermal boundary layers and heat transfer for forced convection flow in rotating cylinder system

12 p1890 A72-28167

Subsonic flow in separation zones of three dimensional turbulent boundary layer forming in front of cylindrical projections, rectangular parallelepipeds and shields

13 p1895 A72-29881

Three dimensional boundary layer instability, obtaining linearized perturbation equation on basis of Navier-Stokes equation

15 p2216 A72-31471

Three dimensional boundary layer separation on slender bodies, delta wings and propulsion intake systems, reviewing computing techniques for interfering inviscid flow fields

16 p2341 A72-32826

Three dimensional compressible turbulent boundary layer growth prediction, deriving entrainment equations from two dimensional incompressible flow relations

16 p2375 A72-32835

Velocity profiles for three dimensional turbulent boundary layer on end wall of axial flow compressor cascade passage under adverse pressure gradients

16 p2342 A72-32901

Iterative calculation of a three-dimensional boundary layer and comparison with experiment

17 p2543 A72-35748

Response of heat transfer from a moving flat plate in a parabolic flow.

18 p2741 A72-36798

Circular-elliptical transformation of jet propagating in homogeneous slipstream within unperturbed uniform transverse magnetic field, using linearized three dimensional boundary layer equations

18 p2716 A72-36815

Numerical analysis of three dimensional steady laminar free convection boundary layer due to heated ellipsoid, solving flow equations

19 p2881 A72-38394

Re-developing turbulent boundary layers behind yawed separation bubbles.

19 p2747 A72-38812

Stewartson transformation correlating three dimensional compressible boundary layer growth on impulsive moving body, assuming small cross flow

21 p3047 A72-41782

German monograph - Three-dimensional boundary layers at curved walls.

22 p3167 A72-43051

Influence of wall temperature on heat transfer in a compressible three-dimensional turbulent boundary layer

23 p3248 A72-43694

Series solution of the three-dimensional elasticity problem of a layer.

23 p3350 A72-44049

Incompressible continuous media three dimensional boundary problems solution by pure shear state analysis, discussing application to plasticity theory

23 p3314 A72-44222

The boundary layer of higher order at the stagnation line of a yawed cylinder in the case of strong suction or injection

23 p3249 A72-44297

A method of calculating meteorological elements for mesoscale processes

24 p3420 A72-44633

THREE DIMENSIONAL COMPOSITES

Strain gage tests on three dimensional composites for reentry vehicle structural design evaluation

02 p0287 A72-11506

Photoelastic measurement of stress concentration in three dimensional fiber reinforced brittle plastic matrix under uniaxial tension

[PI PAPER 1] 09 p1398 A72-22538

Macroscopic elastic constants of three dimensional multilaminar composites with anisotropic layers, assuming stress and displacement continuity

10 p1555 A72-24256

Elastic finite element analysis for stress distribution in gripped thin walled tubular anisotropic three dimensional composite specimens

11 p1731 A72-25441

Mechanical behavior of three dimensional reinforced ablative composites, including carbon-phenolic, quartz-phenolic and quartz-carbon materials

11 p1670 A72-25455

Fabrication, and physical, mechanical and ablation properties of three dimensional carbon-carbon cylinder composite materials

12 p1834 A72-28086

High modulus yarn carbon-carbon three dimensional orthogonal composite material ablative and thermomechanical performance in nose tip ground tests

[AIAA PAPER 72-365] 13 p1983 A72-28956

Carbon-carbon composites for space shuttle reentry thermal protection.

17 p2572 A72-35667

The development of high strength three dimensionally reinforced graphite composites.

17 p2573 A72-35670

THREE DIMENSIONAL FLOW

NT SECONDARY FLOW

Simplified Marker and Cell method extension for numerical solution of almost three dimensional incompressible flow and internal obstacle treatment

01 p0049 A72-10228

Alternating directional implicit numerical solution for three dimensional steady low density hypersonic flow over finite width flat plate

[AD-736572] 01 p0049 A72-10230

Steady sonic flow around three dimensional obstacles by pseudo-axisymmetrical flow approach, revealing singular perturbation of lift downstream at infinity

02 p0150 A72-12640

Rotation effects on three dimensional infinitesimal wave stability in Blasius boundary layer

02 p0205 A72-12340

Anisotropic and compressible work hardening materials three dimensional elastoplastic flow quasi-linear theory, deriving boundary integral equations

02 p0296 A72-12530

Navier-Stokes equation analysis of three dimensional steady radial expansion of viscous heat-conducting compressible fluid from spherical sonic source into vacuum

03 p0343 A72-14241

Nonlinear calculation of three dimensional flow over perfect incompressible fluid around wing of finite span with arbitrary form

04 p0463 A72-15558

Velocity profiles of turbulent three-dimensional incompressible air jet flow from rectangular orifice tangent to and along curved wall surface

[ASME PAPER 71-WA/FE-2] 05 p0647 A72-15938

Composite three-dimensional axisymmetric turbulent jet system, discussing jet interaction relation to boundary layer contact and resulting turbulent mixing

05 p0649 A72-16229

Difference equations and relaxation method for three dimensional transonic flow field about wings in terms of velocity potential

[AIAA PAPER 72-189] 05 p0605 A72-16844

Three dimensional supersonic flow about space shuttle, comparing method-of-characteristics and shock-capturing computations

[AIAA PAPER 72-191] 05 p0729 A72-16843

Characteristic schemes comparison for three dimensional steady isentropic supersonic flow

[AIAA PAPER 72-190] 05 p0605 A72-16844

Numerical analysis of three dimensional inviscid supersonic flow field about complex vehicle geometry, using finite difference technique and Rankine-Hugoniot relations

[AIAA PAPER 72-192] 05 p0606 A72-16845

Vector analysis of three dimensional nonequilibrium dissociative gas flow quantity variations along streamlines

05 p0652 A72-17001

Centrifugal impeller slip factor prediction from three dimensional flow influences, discussing fluid passage guidance, flow separation, eddy and viscous effects

05 p0610 A72-17241

Axial turbine three dimensional flow across blading compatible with velocity distribution, establishing mean surfaces of revolution equation

06 p0755 A72-17841

Asymptotic developments in transonic flows, considering three dimensional flows near shock and plane viscous and heat conducting flow

06 p0756 A72-18105

Three dimensional velocity field excitation by thin airfoil vibrations in supersonic flow, deriving function in semispase to satisfy boundary constrained wave equation

06 p0756 A72-18111

Subsonic three dimensional potential flow computational method lifting aerodynamic configurations analysis and design

[AIAA PAPER 72-188] 07 p0907 A72-18958

Axial flow turbomachines three dimensional flow theory, using orthogonal curved coordinate system

07 p0910 A72-20104

Digital simulation of two dimensional or marginally turbulent three dimensional flows by discretization and numerical integration, noting Galerkin method efficiency in avoiding errors

07 p0951 A72-20355

Numerical simulation of two dimensional and marginal three dimensional turbulent flows, discussing variable eddy viscosity model, discretization, numerical integration and Galerkin methods

08 p1200 A72-21492

Spatial plastic flow in arbitrary incompressible continuous medium with instantaneously inextensible family of planes, deriving velocity field formulas

09 p1403 A72-22758

Confined three dimensional boundary layers prediction, describing finite difference methods for flow equations solution

10 p1464 A72-23871

Turbulent boundary layer characteristics of rotating helical blade in annulus contained fluid, calculating boundary layer growth and streamline angles via momentum integral equations

10 p1466 A72-24296

Two and three dimensional turbulent boundary layers integral calculation method, presenting similarity solutions based on extended mixing length model

10 p1469 A72-24653

Suction or injection interaction with rotation in three dimensional MHD flow between two porous nonconducting disks under magnetic field

10 p1524 A72-25039

Method of characteristics for three dimensional supersonic flow of guiding center plasma, noting application to solar wind-moon interaction

11 p1573 A72-26601

Hot-wire probes to measure turbulent three dimensional flows with allowance for transducer directional sensitivity

11 p1636 A72-26698

Numerical simulation of three dimensional shape-preserving convective elements from buoyancy release in incompressible fluid, using Navier-Stokes equations

12 p1839 A72-27027

Streak photography for three dimensional structure of thermal convection in rotating fluid under horizontal temperature gradient, noting time variations of baroclinic waves

12 p1809 A72-27701

Steady three dimensional viscous vortex within circular cylinder with tangential fluid influx from jets on outer surface and efflux through sink on bottom

[AD-741352] 12 p1798 A72-27716

Predictor-corrector multiple iteration technique for three dimensional viscous flow problems applied to hypersonic leading edges and Burger equation

[PIBAL-72-19] 13 p1893 A72-28422

Stream surfaces of three dimensional sub and supersonic irrotational gas flows in variable cross section channels and nozzles

13 p1895 A72-30004

Three dimensional viscous flow near corner, constructing Stokes slow-flow solution

13 p1944 A72-30031

French monograph on flow near rotor blade tips, discussing three dimensional circulation and boundary layer effects, energy losses, velocity and pressure distributions, etc

14 p2069 A72-30950

Three dimensional structure of transverse uniform flow around motionless circular cylinder for Reynolds number 45,000, investigating correlations of velocities on parallels to generatrices

15 p2179 A72-31684

Optical, mechanical and electrical arrangements of laser Doppler velocimeter, presenting Doppler signals displays and three dimensional gas velocity profiles in vortex region

15 p2236 A72-32044

Three dimensional flow of steady neutral horizontally inhomogeneous planetary boundary layer, studying hodograph, velocity, vorticity, energetics and eddy coefficients

15 p2266 A72-32723

Three dimensional potential flow with lift about solid body calculated by distribution of sink, source and vortex type singularities satisfying Laplace equation

16 p2342 A72-32896

Inverse Laval problem of three dimensional subsonic and supersonic flows in nozzles and ducts of variable cross section in terms of asymptotic series

16 p2342 A72-32930

Three dimensional ideal incompressible fluid flows under small velocity perturbation, using linearized Euler equations with respect to steady flow

16 p2375 A72-32932

Three dimensional small perturbation effects on laminar and turbulent low and high speed boundary layer flows

[AIAA PAPER 72-713] 16 p2344 A72-34034

Three dimensional supersonic nozzle exhaust flow field numerical analysis based on reference plane characteristics, deriving difference equations for three coordinate systems

[AIAA PAPER 72-704] 16 p2344 A72-34040

Finite difference method computation of multishocked three dimensional wing-body supersonic flow fields with real gas effects, applying to delta winged space shuttle

[AIAA PAPER 72-702] 16 p2345 A72-34042

Small cross flow integral method for growth prediction of three dimensional compressible turbulent boundary layers on adiabatic walls

[AIAA PAPER 72-697] 16 p2345 A72-34046

Elliptic-hyperbolic relaxation algorithm for solution to three dimensional nonlinear transonic small disturbance potential equation for flow about swept wings

[AIAA PAPER 72-677] 16 p2346 A72-34063

Laser Doppler anemometer for three dimensional liquid and gas flow velocity measurements in water tunnels

16 p2396 A72-34158

Foreign gas injection into three-dimensional stagnation point flows.

17 p2483 A72-34205

Three-dimensional non-free vortex flow in axial fans.

17 p2487 A72-35896

Numerical simulations of three dimensional isotropic turbulence in incompressible fluid at low wind tunnel Reynolds numbers

18 p2671 A72-36007

A through-type counting method for two-dimensional and spatial supersonic flows. II

18 p2642 A72-36810

Calculation of spatial ideal gas flows without a symmetry plane

18 p2642 A72-36901

Two component reaction kinetics model for three dimensional analysis of combustion during two- and three dimensional supersonic steady flow of hydrogen-air fuel mixtures

19 p2880 A72-37389

Viscosity effect on hypersonic flow field near slender body, discussing eigenvalue solutions for two and three dimensional flow around triangular plate

19 p2745 A72-37393

Three dimensional flow field visualization, data acquisition and reduction via holography, noting applications in schlieren and interferometric techniques

19 p2798 A72-37620

Three-dimensional wall jet originating from a circular orifice.

19 p2747 A72-38811

A method of straight-through calculation for two-dimensional and three-dimensional supersonic flows. I

19 p2747 A72-38852

Three-dimensional structure and equivalence rule of transonic flows.

20 p2886 A72-39631

Supersonic and hypersonic combustion processes three dimensional characteristics, comparing wind tunnel test data with boundary layer equations numerical integration results

[ICAS PAPER 72-21] 21 p3130 A72-41146

Computation of three-dimensional non-equilibrium supersonic flows.

[ICAS PAPER 72-37] 21 p2992 A72-41162

Three-dimensional supersonic flows at large distances from a body of finite volume

21 p2994 A72-41661

A calculation procedure for heat, mass and momentum transfer in three-dimensional parabolic flows.

22 p3243 A72-41954

Numerical integration of three dimensional flow equations for supersonic jets of ideal gas exhausted from elliptical and rectangular nozzles

22 p3133 A72-42264

Stream surfaces of three dimensional sub and supersonic irrotational gas flows in variable cross section channels and nozzles

22 p3135 A72-42727

Evaluation of windward streamline effective cone boundary-layer analyses.

22 p3136 A72-42874

Turbulent interaction of air jets issuing from perforated surfaces into free space, determining three dimensional flow field via Reichardt free turbulence theory

23 p3248 A72-43625

Three dimensional supersonic flow past bodies with a smooth generatrix

23 p3248 A72-43651

The damping of precessing vortex cores by combustion in swirl generators.

24 p3464 A72-45060

Three dimensional shock wave configurations in front of cylindrical body on supersonic wing or of fluid jet injected into main supersonic flow, examining high pressure gradient regions

24 p3361 A72-45113

Explicit numerical solution of the three-dimensional incompressible turbulent boundary-layer equations.

24 p3395 A72-45781

THREE DIMENSIONAL MOTION

NT SECONDARY FLOW

NT THREE DIMENSIONAL FLOW

Three dimensional roll-controlled missile trajectory model for simple time-sharing digital or analog simulation, using wind-to-inertial axis transformation

01 p0130 A72-10964

Human body kinematics numerical analysis, obtaining space-time resolution by photogrammetric restitution and electronic data processing of photographic recordings

04 p0478 A72-14710

The measurement of three-dimensional body movements by the use of photogrammetry.

20 p2898 A72-39806

Optimal three dimensional maneuvering of a rocket powered hypervelocity vehicle.

24 p3450 A72-45151

THRESHOLD CURRENTS

Emitted light power of CW injection laser related to threshold current, electrical and thermal resistances and external quantum efficiency

01 p0079 A72-10325

Mode guiding improvement in p-n junction of symmetrical AlGaAs-GaAs heterojunction laser diode with narrow active region, obtaining low room temperature threshold current

01 p0080 A72-10788

Inhomogeneous plasmas parametric instabilities excitation, observing threshold electric field power requirement

02 p0266 A72-12370

Minimum threshold current density of double heterojunction injection lasers

03 p0367 A72-13412

Ions acceleration during current sharing through plasma, discussing maximum energies, threshold current and electron beam flux density

03 p0396 A72-13661

Radiative noise effect on threshold current, output power and quantum yield of injection laser, evaluating noise loss factor

04 p0531 A72-15077

Laser produced spark plasma, calculating threshold conditions for onset of stimulated scattering process and self focusing

04 p0559 A72-15346

Two mode lasers with photon intensity coupling near threshold treated by fluctuation theory detailing intensity, correlations and line widths

05 p0667 A72-16017

MOS components technology with low threshold voltage, noting wafer surface planarity and smallness of parasitic capacitances and layer resistivity

05 p0702 A72-16181

Injection laser threshold current density, radiation pattern and electric field distribution relation to layer thickness and dielectric constants, using waveguide theory

06 p0825 A72-17772

Sensitivity threshold of optical heterodyne receiver as function of laser radiation amplitude spectrum, using photodetector output noise

08 p1181 A72-20794

Normally off Si MESFET for simple dc coupled circuits, computing threshold voltage with two dimensional device model

08 p1141 A72-21426

Semiconductor laser threshold current dependence on doping degree and temperature based on optical transition model and energy band theory

11 p1647 A72-26327

Optimal active layer thickness in heterogeneous injection lasers, estimating minimal threshold currents

11 p1649 A72-26346

Low threshold current mesa-stripe-geometry double heterostructure injection lasers, eliminating current spreading by etching method

12 p1823 A72-27838

Pumping current pulse duration effect on lasing threshold of injection lasers with diffusion junctions and heterojunctions in GaAs-AlAs system

12 p1824 A72-27877

Room temperature GaAlAs single-heterojunction diode lasers structure, fabrication, threshold current density and quantum efficiency dependence on wavelength and temperature

15 p2247 A72-32032

Double heterostructure injection lasers with narrow active regions, discussing threshold current densities, emission polar diagrams and optical field penetration into boundary regions

15 p2249 A72-32327

- Pumping current pulse duration effect on lasing threshold of injection lasers with diffusion junctions and heterojunctions in GaAs-AlAs system
16 p2404 A72-33986
- Behavior of spontaneous emission across threshold in GaAs junction lasers.
19 p2811 A72-37865
- Reduction in the rate of increase of spontaneous emission from double-heterostructure injection lasers at threshold.
19 p2811 A72-37866
- Effect of pulsed voltages fed into the external modulating electrode on the threshold sensitivity of a photomultiplier
19 p2774 A72-38415
- Effect of uniaxial pressure on the threshold current of double-heterostructure GaAs lasers.
20 p2933 A72-39559
- Pulsed room temperature laser action of Si-doped double heterostructure GaAs p type diodes within 9100-9500 A wavelengths, discussing threshold current densities and wave efficiency
22 p3186 A72-42621
- THRESHOLD DETECTORS [DOSIMETERS]**
- Nuclear emulsion and solid track threshold dosimetry for ion spectrum division of heavy relativistic particles in primary cosmic rays [CERN-71-16]
02 p0162 A72-12065
- Radar IF voltage in-phase and quadrature components detection thresholds, evaluating square and octagonal approximations to circle for false alarm probabilities
10 p1438 A72-24693
- THRESHOLD GATES**
- Autonomous threshold elements diagnostic tests and verification control, noting cascade, pyramidal and branching schemes
06 p0785 A72-18303
- Autonomous threshold elements diagnostic tests and verification control, noting cascade, pyramidal and branching schemes
13 p1934 A72-30071
- Chalcogenide semiconductor monostable threshold and bistable memory switching devices, discussing fabrication and performance
13 p1934 A72-30090
- Threshold logic network synthesis with specific threshold-gate sensitivities.
17 p2533 A72-35364
- A threshold device for establishing the time of pulsed signals
21 p3035 A72-41727
- Shielded silicon gate complementary MOS integrated circuit.
24 p3385 A72-44972
- THRESHOLD LOGIC**
- Network synthesis of cascaded threshold logic elements to separate binary patterns into two classes by iterative computation of parameters
01 p0034 A72-10474
- Fluidic threshold logic application to fluidic control systems, comparing with AND-OR logic for number of elements and weight
[ASME PAPER 71-WA/FLCS-5]
05 p0615 A72-15918
- Complex sampling with cascaded triple input majority logic redundant systems, deriving failure probability
07 p0949 A72-19173
- Automatic digital detection of fluctuating Rice-distributed signals in presence of Gaussian noise, using M-out-of-N threshold detection criteria
07 p0947 A72-20194
- Multiplex electrohydraulic system for aircraft fly by wire actuators with majority voting and pressure logic, discussing frequency response and environmental tests
08 p1113 A72-22152
- Adaptive neural nets of threshold logic units as models of perception and memory in biological systems
09 p1273 A72-23580
- Reliability-maximizing digital computer synthesis based on multiple redundant network design, discussing majority structure distribution optimization technique
15 p2203 A72-32174
- Threshold logic network synthesis with specific threshold-gate sensitivities.
17 p2533 A72-35364
- Synthesis of threshold-logic networks using Karnaugh-mapping techniques.
21 p3037 A72-40636
- An iterative algorithm for solving the realization problem of a Boolean function by a single threshold element.
24 p3419 A72-45576
- THRESHOLD SHIFT**
- U THRESHOLDS**
- THRESHOLDS**
- Visual and automatic stereometric image analysis, citing minimum measurable contrast thresholds for various devices
10 p1478 A72-23826

- Electron energy threshold measurements in irradiated II-VI compounds interpreted in terms of damage on metal and chalcogenide sublatitudes
12 p1859 A72-28070
- THRESHOLDS [PERCEPTION]**
- Functional organization of visual cortex in monkeys, discussing monocular and binocular responses, trigger and stimulus abstraction
01 p0011 A72-10467
- Psychological threshold for successiveness, tabulating probabilities for correct guesses of stimuli order
01 p0013 A72-10713
- Threshold stimulus for visual motion discrimination as function of velocity and luminance
01 p0014 A72-10722
- Computer simulation of evoked cortical audio potentials in animals and humans, noting clinical application for hearing threshold measurements
01 p0016 A72-11324
- Directional hearing perception threshold in normal and auditory-defective patients, studying frontal and median planes for rising and falling noise frequencies
02 p0158 A72-11740
- Retinal annulus onset and offset thresholds, discussing neural signals delay characteristics
02 p0164 A72-12488
- Human centrifuge tests for semicircular canal gyroscopic stimulation during sensory deprivation, discussing angular acceleration detection thresholds
04 p0478 A72-14865
- Formant-coded voiced speech parameters smoothing and quantizing effects subjective evaluation, obtaining average quantization threshold levels
04 p0487 A72-15298
- Phenamine and amine effects on subthreshold sound perception and adrenoreactive excitability of unstable subjects under emotional stress
04 p0476 A72-15586
- Retinal cell adaptation as result of receptor membrane response range saturation, considering dark adaptation and increment threshold
06 p0761 A72-17604
- Pilot and nonpilot vestibular sensitivity to rotation, determining oculogyral illusion and rotation perception thresholds
06 p0767 A72-17867
- Human dark adaptometric visual threshold recovery and electroretinograms in response to double light flashes, using Fourier analysis of oscillatory potentials
07 p0916 A72-19024
- Flicker and flash threshold experiments, discussing flicker cut-off frequency and flash duration relations and visual sensitivity
07 p0926 A72-19028
- Moving target resolution threshold in retina, discussing visual acuity relation to target angular velocity during ocular pursuit
07 p0926 A72-19029
- Dark adaptation with logarithmically time decreasing background luminance, noting threshold time lag variation with rate of background change
07 p0930 A72-19827
- Achromatic and chromatic thresholds during dark adaptation against varying background luminances, noting trend change at transition from cone to rod function
07 p0930 A72-19828
- Noise level measurement scales, units datum points and mathematical formulas, suggesting method of quasi-peak level above masked threshold
07 p1035 A72-20164
- Spectral response and vision thresholds of human eye for light detection and color sensation
08 p1125 A72-21332
- Rod-cone interaction in human scotopic vision, presenting test flash threshold as function of conditioning flash interval
08 p1116 A72-21460
- Cat retina ganglion cell threshold and latent responses to separate stimulation of receptive field center and periphery
08 p1117 A72-21474
- Light variation threshold amounts for flicker and flickering pattern detection as function of variation frequency
09 p1269 A72-22615
- Average evoked potentials correlates of two flash perceptual discrimination in cats, discussing parallel changes as function of interflash intervals and peripheral level
10 p1427 A72-25178
- Olfactory receptor models sensitivity, discussing threshold dependence on adsorbed odoriferous agent amount and exposure time
11 p1585 A72-26453
- Geomagnetic field perturbation biological effects, studying geomagnetic storm field energy levels and magnetic flux variables relation to human sensitivity thresholds
12 p1773 A72-28210
- Semicircular canal function correlation to thresholds, aftereffects and power functions in pilot vestibular tests
12 p1764 A72-28259

- High threshold afferents role in dorsal surface potential formation in cat spinal cord
13 p1905 A72-29327
- Illumination intensity effects on circadian periodicity and behavioral thresholds in Rhesus monkey, demonstrating exception to Aschoff rule
13 p1906 A72-29844
- Microwave induced cutaneous heat and pain perception thresholds, noting usefulness as possible radiation hazard warning
15 p2188 A72-31506
- Lateral inhibition in auditory perception proved by psychophysical study of nervous activity stimuli patterns, noting erroneous measurement of pure tone masked threshold
16 p2357 A72-33971
- Peripheral contrast thresholds for moving images.
17 p2509 A72-35688
- An analytical description of the line element in the zone-fluctuation model of colour vision. I, II.
18 p2651 A72-36606
- Optokinetic thresholds in the normal monkey.
18 p2651 A72-36610
- Novelty, recency and frequency effects on visual recognition and pseudo-recognition thresholds.
18 p2651 A72-36909
- Visual Field Analyzer presentation of single and multiple stimuli for differential threshold levels investigation, discussing eccentricity, spatial orientation and supraliminal stimuli effects
19 p2756 A72-37831
- Calculating the perceived level of light and sound.
19 p2761 A72-38567
- Threshold excitation, temporal summation, and impulse response function in the retina of the cat - Temporal receptive fields of retinal ganglion cells
19 p2758 A72-38648
- Spatial interaction with different-diameter stimuli matched on the basis of threshold, luminance, or total luminous flux.
21 p3004 A72-40152
- Russian book - Neurophysiological background of tactile perception.
21 p2998 A72-40464
- Threshold detection model for foveal viewing by human observers using naked eye
21 p3007 A72-40733
- Discrimination sensitivity and black light density in the mesopic range
21 p3007 A72-40735
- The minimum brightness gain required in viewers using image intensifiers.
21 p3055 A72-40741
- The detectability of a brief gap in a pulse of light as a function of its temporal location within the pulse.
21 p3002 A72-41021
- On threshold mechanisms for achromatic and chromatic vision.
22 p3142 A72-42547
- Olfactory perception neurophysiological mechanism, discussing receptor cells sensory thresholds and time, temperature and humidity effects
22 p3146 A72-42787
- Taste organs neurophysiological structure and functioning, considering stimuli and excitation parameters effects on perception threshold
22 p3146 A72-42783
- Moving spot detection threshold measurement for varying exposures, noting product of stimulus duration and velocity for comparison with Bloch law
22 p3151 A72-42930
- Motion thresholds for fovea and peripheral retina with/without correction for peripheral refractive error
23 p3260 A72-43978
- Information aspects in visual perimetry, obtaining memory requirement for control computer in automated perimetry
23 p3261 A72-44378
- Line length detectors in the human visual system - Evidence from selective adaptation.
23 p3258 A72-44384
- Visual sensitivity measurement in retinal areas with stepwise change from one monochromatic light to another, discussing eye movements effects and perception thresholds
23 p3258 A72-44385
- THROATS**
- Effect of nozzle throat radius of curvature on gasdynamic laser gain.
17 p2561 A72-34210
- THROMBOCYTES**
- Monovalent K and Na and bivalent Ca and Mg plasma ion ratio effect on thrombocyte electrokinetic potential
13 p1901 A72-28635
- THROMBOPENIA**
- Interactions between gas bubbles and components of the blood - Implications in decompression sickness.
24 p3374 A72-45652
- THROMBOPLASTIN**
- Blood coagulation behavior in rats under fall induced intense trauma, attributing phenomenon to increase in extrinsic thromboplastin from damaged tissue
21 p3002 A72-41194

THROTTLING
Aerodynamic throttling effect due to air jet flow interaction in throat region of mainstream two dimensional nozzle flow 10 p1419 A72-24845
Military jet engines centrifugal fuel pumps power requirements for throttled operation, noting pressure stability improvement at low flow rates 18 p2694 A72-36041
Inlet throttle centrifugal fuel pumps for jet engine augmentation, discussing design features, performance, noise, life and reliability characteristics 18 p2694 A72-36044
Throttle characteristics and mixing chamber geometry effects on low pressure gas ejector operation, noting air flow and pressure rates in air ejectors 22 p3133 A72-41859
Constant coefficients for linearized flow rate equation of hydraulic throttle servodrive in closed circuit stability solution by Liapunov theorem 22 p3139 A72-41873
Development and evaluation of an energy-oriented guidance logic for air combat models. 22 p3137 A72-42354
Contribution to the determination of the characteristics of a gas turbine engine for a helicopter and to the choice of the throttling law 23 p3326 A72-44277

THRUST
NT JET THRUST
NT LOW THRUST
NT MICROTHRUST
NT ROCKET THRUST
NT STATIC THRUST
NT VARIABLE THRUST

THRUST BEARINGS
High speed radial thrust multipoint ball bearing design, discussing contact resistance, ball motion, ring deflection and centrifugal force effect on performance and service life 01 p0078 A72-11378
Pneumatic hammer /self oscillation/ in gas lubricated externally pressurized annular thrust bearing, presenting stability maps [ASME PAPER 71-LUB-U] 02 p0234 A72-11527
Series hybrid fluid film-rolling element bearing analytical and test evaluation for high speed thrust load turbine applications [ASME PAPER 71-LUB-15] 02 p0235 A72-11537
Static properties of circular hydrostatic thrust gas bearings with curved surfaces, comparing theory with measurements [ASME PAPER 71-LUB-22] 02 p0236 A72-11542
Unsteady gas flow in thrust bearing with spiral grooves, presenting Navier-Stokes and discontinuity equation 08 p1176 A72-21167
Rigidity calculation of double row radial thrust annular ball bearing loaded by axial and radial force and torque 11 p1646 A72-26978
Nonuniform gas pressure distribution near circular multipoint inlet of inherently compensated thrust bearing, considering inward-outward radial flow resistance differential 13 p1963 A72-28748
Optimization of self-acting step thrust bearings for load capacity and stiffness. 19 p2807 A72-37895

THRUST CHAMBERS
Aerospike rocket engine system for orbit-to-orbit space shuttle, discussing light-weight regeneratively cooled thrust chamber performance tests [SAE PAPER 710770] 01 p0116 A72-10264
TD nickel as construction material for rocket thrust chambers, discussing spin-forming, welding, machining, electric discharge machining and electroforming operations 01 p0075 A72-10753
Gas temperature variation effects on powder burning stability in rocket combustion chamber from unsteady powder burning theory 08 p1255 A72-21659

THRUST CONTROL
NT THRUST VECTOR CONTROL
Solid rocket on-off and acceleration control, discussing motor concepts, thrust modulation and potential technology applications [SAE PAPER 710767] 01 p0116 A72-10262
Optimal flight of material point in central field of forces subject to controlled small thrust 01 p0127 A72-10356
Optimal control for thrusting rocket guidance with controllable steering angle rate during insertion into circular orbit, using flat earth approximation 01 p0097 A72-10383
STOL aircraft integrated landing approach flight control system with elevator and thrust control coupling to angle of attack, altitude and other state variables 02 p0155 A72-12705
[DGLR PAPER 71-063]
Analytic solution for optimal control circular orbit escape with constant thrust rocket, using Euler-Lagrange equations and perturbation technique 03 p0437 A72-13839

Microaccelerometer for satellite drag measurement and compensating thrust control 06 p0892 A72-18260
Electric thruster for orbit and attitude control of nonspinning geostationary communications satellite [AIAA PAPER 72-436] 11 p1727 A72-26178
Prime 30 cm ion thruster power conditioning and control system development, integration and testing [AIAA PAPER 72-509] 12 p1860 A72-27424
Optimal thrust direction for planetary escape at residual speed, using approximate explicit closed loop guidance scheme 15 p2268 A72-31821
V/STOL weapon system VJ-101 design, discussing one axis rocking device, suspension structure and hovering flight thrust control 16 p2347 A72-33049
Russian book on solid propellant rocket engines covering combustion chamber and nozzle layouts, working cycle and thrust control 16 p2443 A72-33350
Guidance and navigation techniques for a solar electric Mercury orbiter [AIAA PAPER 72-917] 21 p3082 A72-41562
Conditions for impulsive thrust-coast-thrust minimum-time, fixed-fuel transfers between coplanar orbits. 24 p3440 A72-45149

THRUST FAULTS
U GEOLOGICAL FAULTS

THRUST LOADS
Tube flight vehicle system thrust and power requirements prediction by aerodynamic analysis with division of near and far flow fields 08 p1107 A72-21608

THRUST MEASUREMENT
Self magnetic coaxial plasma accelerator integral output data, presenting mass velocities and thrust measurement [DGLR PAPER 71-103] 02 p0266 A72-12736
Jet engine silencing plug nozzle suppressor configurations acoustic and thrust performance measurements [AIAA PAPER 72-160] 05 p0706 A72-16826
Test facility for electric microthrusters, describing microbalance for thrust and propellant mass flow rate measurement 09 p1292 A72-23404
Electron bombardment ion thruster ESKA 18-P thrust measurements by critically loaded columns suspension instrument and simultaneous beam diagnostics by electrostatic probes [AIAA PAPER 72-433] 11 p1707 A72-26176
The development of dynamic flight test techniques for the extraction of aircraft performance. [AIAA PAPER 72-785] 19 p2749 A72-38102

THRUST PROGRAMMING
Thrust profile shaping for spin stabilized vehicles, analyzing effect on wobble motion and pointing error 10 p1552 A72-24647
Electrostatic ion thruster ESKA 28 for interplanetary missions, calculating earth escape and optimal transfer orbits [AIAA PAPER 72-434] 11 p1707 A72-26177

THRUST REVERSAL
Optimal reversion coefficient determination for passenger aircraft engine thrust reversal 05 p0614 A72-17060
Optimal thrust reversing in pursuit evasion games between two aircraft in horizontal plane, considering cost functions and termination criteria 07 p0912 A72-19282
Noise generated by STOL core-jet thrust reversers. [AIAA PAPER 72-791] 19 p2849 A72-38108
A method for increasing thrust reverser utilization on STOL aircraft. [AIAA PAPER 72-782] 19 p2752 A72-38141

THRUST VECTOR CONTROL
Pintle-controlled rocket engine design with gimbaled supersonic splitline thrust vector control, featuring variable thrust, attitude controls and high propulsion efficiency [SAE PAPER 710763] 01 p0115 A72-10260
Air to air maneuverability of aircraft capable of in-flight thrust vectoring, indicating improved deceleration, normal acceleration g-force and turn rate 03 p0310 A72-13877
Interaction forces of gas jet injected into supersonic stream, examining data from thrust vector control gas injection tests 03 p0342 A72-13958
Rocket motion in general central force field, obtaining primer vector integration for optimal coasting arc during orbital transfer 06 p0890 A72-18386
Liquid fuel elastic rocket motion stability in supersonic flight, using vibration and thrust vector control equations for dynamic properties description 08 p1241 A72-21633
Vaporizer temperature effect on ion propulsion system thrust vector, presenting temperature control loop circuit diagram 10 p1528 A72-24652

Propulsion system/airframe matching in hybrid V/STOL airplanes, stressing thrust vector management, lift engine bypass ratio and power plant packaging design [ASME PAPER 72-GT-106] 11 p1576 A72-25671
ATS F ion thruster system for north-south station-keeping, discussing specific impulse, thrust vectoring, propellant system and power conditioning circuitry [AIAA PAPER 72-439] 11 p1707 A72-26180
Ion thruster development for Communications Technology Satellite, discussing synchronous orbit station-keeping requirements, thrust vector control and mounting positions [AIAA PAPER 72-491] 11 p1711 A72-26216
Solar electric propulsion subsystem performance tested on breadboard model, noting electrical power conversion, command, thrust vector control and propellant supply 11 p1711 A72-26227
Solid propellant rocket engine thrust vector control by four movable exhaust nozzles, nozzle exit cone secondary injection and flexible bearing nozzle 13 p2026 A72-28928
Steering algorithm for fail-safe guidance of continuously thrusting interplanetary spacecraft to maintain ballistic intercept target objective 15 p2271 A72-32195
STOL transport stability and control derivative prediction methods and accuracy requirements. [AIAA PAPER 72-780] 19 p2752 A72-38139
Harrier two seat aircraft design, performance, weapon systems, thrust vectoring and combat characteristics comparison with GR.1 23 p3252 A72-44391
Lateral flight path control during aircraft landing in gusty cross-winds by lateral thrust deflection, discussing design optimization 24 p3368 A72-45330
Thrust stand for evaluation of thrust vectoring nozzle performance. [AIAA PAPER 72-1029] 24 p3389 A72-45406

THRUST-WEIGHT RATIO
High turbine entry temperature effects on gas turbine engine specific power and fuel consumption, noting thrust/weight ratio increase in turbojet and turbofan engines 07 p1055 A72-20311
Thrust-weight ratio optimization for spacecraft orbit inclination change maneuver, deriving motion kinematics via point mass gravitational model 24 p3440 A72-45167

THRUSTORS
U ROCKET ENGINES

THUNDERSTORMS
VLF noise spectra in earth-ionosphere cavity due to thunderstorm discharges, noting resonance level splitting by geomagnetic field 01 p0028 A72-10598
Kennedy Space Center thunderstorm forecasting system, discussing data processing with conditional and exposure period probabilities and nonlinear predictors multiple regression equations 01 p0094 A72-10826
Air shower cores or relativistic monopoles as sources of straight lightning, considering thundercloud conditions over ocean and land areas 03 p0350 A72-14100
Remote meteorological elements sensing in terminal area, discussing radar, ceilings, thunderstorm warning, slant range visibility, low level winds and wind shear 04 p0543 A72-14692
Shock wave contributions from micrometeorites, meteors, meteorites and thunder to organic compounds formation in primeval atmosphere 04 p0572 A72-14760
Water vapor injection into stratosphere by thunderstorms from IR radiometric inference measurements on NASA jet laboratory 04 p0544 A72-15358
Synoptic and dynamic aspects of tornado-producing thunderstorms development from ATS 3 and aerological data, observing mesoscale convective disturbances 06 p0842 A72-18438
Thunderstorm flight testing for evaluation of rain, ice, lightning and turbulence effects on aircraft, engine and systems operating characteristics 06 p0760 A72-18500
Visual and radar echo location of organized updraft on thunderstorms and hailstorms 09 p1346 A72-22452
Ionospheric potential and thunderstorm activity annual variations during 1959-70 solar cycle from radiosonde measurements in free atmosphere 09 p1301 A72-23265
Thunderstorm detection and recording device with 200 km radius for weather prediction and air traffic information 09 p1312 A72-23269
Tropical thunderstorm precipitation current variations due to lightning produced atmospheric electric field changes, considering charged raindrops turbulent diffusion 12 p1839 A72-27502

Distant thunderstorm center location with VLF atmospheric, determining delay time difference of Fourier spectrum groups of 6 and 8 kHz

12 p1841 A72-27793

Worldwide thunderstorm activity model selection from Schumann resonance observations, using ELF noise measurements in lowest earth-ionosphere cavity modes

13 p1988 A72-28600

Kennedy Space Center area afternoon convective thunderstorm activity and associated weather phenomena prediction via multivariate regression analysis

13 p1989 A72-28803

Thunderstorm-associated aircraft mishaps relation to surrounding synoptic scale meteorological conditions, discussing storm interior condition contribution to flight stability upset

13 p1992 A72-28851

Thunderstorm penetration by F-100 aircraft to study turbulence hazard relation to updraft size and short period fluctuation-induced acceleration changes

13 p1992 A72-28852

Thunderstorm encounter probability at SST altitudes for selected cross country routes, using radar observation data

13 p1992 A72-28853

Thunderstorms physical mechanisms of charge generation and separation, considering correlation between lightning and precipitation

13 p1995 A72-29873

Single point thunderstorm ranging method based on two radio frequencies field intensity spectral components ratio

14 p2129 A72-30639

Hail size distribution and concentration in thunderstorm updraft regions from aircraft and S band radar observations

16 p2419 A72-33946

Gas dynamics and chemistry of lightning-produced shock waves /thunder/ in postulated primordial reducing atmosphere, noting amino acid production

18 p2650 A72-36443

A climatology of the potential vertical extent of giant cumulonimbus in some selected areas

18 p2707 A72-36700

Climatology of the occurrences of thundery weather over Gauhati Airport.

22 p3202 A72-42887

Worldwide thunderstorm activity model selection from Schumann resonance observations, using ELF noise measurements in lowest earth-ionosphere cavity modes

24 p3380 A72-45100

THYMIDINE

Prebiotic thymidine phosphorylation at 65 C by urea-phosphate mixtures in simulated desert conditions

15 p2185 A72-31629

THYRISTORS

NT SILICON CONTROLLED RECTIFIERS

Pulse modulator thyristor circuit design and optimum operating conditions for driving high peak power radar magnetron

02 p0195 A72-12694

Variable flux reset ferroresonator voltage regulator with adjustable terminal characteristics using magnetic and thyristor circuits

[IEEE PAPER 17.1]

03 p0311 A72-13770

Electronic system for electrodischarge machining, considering thyristor spark control and circuitry design for automatic feed down and short circuit clearance

04 p0502 A72-15530

Minimum charging resistance in relaxation generators for spark machining as function of supply voltage, using thyristor and voltage source circuit model

07 p0956 A72-19594

Energy level and V-I characteristics of solid state heterojunction devices, discussing diodes, transistors, thyristors and optoelectronic structures

08 p1139 A72-21054

Thyristors junction area current rise time extension, discussing emitter field regional delay times as function of p-n-p-n structural properties

08 p1140 A72-21266

Thyristor I-V characteristics, considering blocking and triggering

10 p1453 A72-24816

Output voltage characteristics of single phase thyristor inverter based on pulse duration modulation with direct shaping of control pulses, considering harmonic coefficients

11 p1603 A72-25277

Airport lights systems control with thyristors, discussing light intensity regulation, command board design and insulation test equipment

12 p1794 A72-27401

P-n-p-n junction thyristor turnoff process under reverse anode voltage at high injection level, examining current voltage curve and switching time constant

13 p1932 A72-29293

The relative merits of thyristors and power transistors for fast power-switching applications.

22 p3159 A72-42306

Thyristor I-V characteristics as function of voltage rise time, determining critical rate for given initial and final anode and cathode voltages

22 p3160 A72-43085

P-n-p and p-n-p-n transistors and thyristors with lateral structure geometry, discussing operational characteristics and effects of structural modification on semiconductor parameters

23 p3271 A72-43835

THYROID GLAND

Thyroid glands iodine concentrations, blood proteins and morphological changes in rats with acute hypoxic hypoxia and pulmonary edema

07 p0924 A72-20620

Lipid metabolism abnormality relation to hypothyroidism leading to atherosclerosis, noting thyroid parenchyma atrophy from autoimmune thyroiditis

08 p1117 A72-21544

Propranolol as adrenergic beta receptor inhibiting agent for hyperthyroidism symptom amelioration

08 p1118 A72-21550

Bed rest and centrifuging effects on human plasma thyroid hormone level, discussing total protein, albumin and thyroxine binding globulin concentrations

12 p1770 A72-27477

Neuroendocrine responses in microwave radiation exposed rats, correlating thyroid and thyrotropic activity

12 p1767 A72-28321

Epithelial follicle and mast cell role in peroxidase activity of thyroid gland during experimental burn development

13 p1905 A72-29330

Dog thyroid gland structural changes under repeated radial acceleration, noting atrophic process and autonomous reactions roles

13 p1905 A72-29334

Enzyme activity and ascorbic acid concentration as index of rat thyroid gland tissue functional activity during hyperthermia

14 p2077 A72-31098

Thyroidal influence on myocardial changes induced by simulated high altitude.

17 p2500 A72-34730

Protein synthesis in the cell-free system of the human thyroid gland

19 p2757 A72-38212

Thyroglobulin content and variations in the proteolytic activity of the thyroid gland tissue in animals under hypoxic conditions

20 p2893 A72-39727

Role of the thyrotropic region of the hypothalamus in the adaptation activity of the organism

22 p3141 A72-42167

Changes in blood serum proteins under the effect of hyperoxia in intact rats with thyroid gland dysfunction

22 p3142 A72-42283

Changes in the pituitary-thyroid and in the pituitary-gonad systems under conditions of functional loading and of physiological immobilization.

24 p3371 A72-44823

THYROXINE

Mitosis duration and mitotic activity diurnal rhythms in esophageal epithelium of rats given thyroxine

07 p0924 A72-20623

Inhibitive effect of immobilization on urinary catecholamine excretion and blood plasma thyroxine level in rats

09 p1265 A72-22648

TIBIA

Anatomy, pathology, etiology, diagnosis and therapy of posterior tibial nerve compression lesion, discussing tarsal tunnel syndrome

21 p3005 A72-40396

TID

U TRAVELING DISTURBANCES

IONOSPHERIC

TIDAL OSCILLATION

U TIDES

TIDAL WAVES

The problem of the boundary conditions in thermosphere dynamics.

22 p3201 A72-42510

Tidal waves of a two-layer liquid in a cylindrical basin of revolution rotating about its axis

24 p3392 A72-45073

A three-dimensional model of thermosphere dynamics. I - Heat input and eigenfunctions. II - Tidal waves. III - Planetary waves.

24 p3400 A72-45594

TIDES

NT ATMOSPHERIC TIDES

NT EARTH TIDES

NT LUNAR TIDES

Galactic rotation origin, discussing tidal, vortex and spinning core theories

01 p0127 A72-10290

Earth nutation tables, comparing precession-nutations and tidal potential

04 p0575 A72-15031

Galactic tidal field and multiple encounters role in stellar escape from star clusters, noting escape rates and kinetic energy involved

12 p1873 A72-27898

Deformation of the earth by surface loads.

20 p2916 A72-39335

Tidal perturbation of the non-radial oscillations of a star.

20 p2974 A72-39895

Earth geophysical effects due to tidal capture of moon from direct orbit, discussing volcanism, atmosphere and hydrosphere origins and biological evolution

22 p3226 A72-42539

To apparent equatorial radius, taking into account distortion due to Jupiter effects on rotation and tides

24 p3436 A72-44701

On the tidal effects in the motion of artificial satellites.

24 p3441 A72-45233

TIG WELDING

U GAS TUNGSTEN ARC WELDING

TIGHTNESS

NDT holographic interference pattern technique to determine Advanced Test Reactor fuel element swage joint tightness

01 p0078 A72-11110

TILT

U ATTITUDE [INCLINATION]

TILT ROTOR RESEARCH AIRCRAFT PROGRAM

Design studies and model tests of the stowed tilt-rotor concept.

[AIAA PAPER 72-804]

19 p2750 A72-38113

TILTED PROPELLERS

Tilt-propeller VTOL aircraft design evaluation, based on aerodynamic and aeroelastic model and full scale performance tests

[AIAA PAPER 72-803]

20 p2889 A72-40054

TILTING

U ATTITUDE [INCLINATION]

TILTING ROTORS

Tilt-propeller VTOL aircraft design evaluation, based on aerodynamic and aeroelastic model and full scale performance tests

[AIAA PAPER 72-803]

20 p2889 A72-40054

Helicopter development, discussing articulated, rigid, tilt and stowed rotors, compound helicopters, rotor drives, flight control and avionics systems

24 p3369 A72-45558

TIMBER IDENTIFICATION

Color aerial photographs interpretation for forest tree type composition determination, comparing to sensitive black and white films

09 p1302 A72-23240

Multiband photointerpretation of forested land units, using aerial black and white photographs and film-filter combinations

09 p1302 A72-23240

Landscape site and vegetation /timber/ predictions from color and IR aerial imagery compared with ground data

18 p2686 A72-36398

TIMBER INVENTORY

Earth resources information systems using satellite and aerial IR terrain photography and ground teams for international cooperation, emphasizing timber inventory

01 p0063 A72-10950

False color aerial photographs interpretation for cultivated wooded area inventory

09 p1302 A72-23240

Measurement accuracy and reliability of photogrammetric methods in stereoscopic height determinations of wooded areas

09 p1312 A72-23240

Multiband color aerial photography interpretation for forest appraisal in U.S.S.R.

09 p1302 A72-23240

United Nations FAO interest in remote sensing techniques application to agricultural, forestry and fisheries resources survey and management

15 p2220 A72-31222

TIMBER VIGOR

Visible and near IR reflectance spectra of some mineralized trees, using multispectral photographic filters

02 p0209 A72-11789

Ponderosa pine foliage visible and near IR spectral investigating soil copper contents effect on foliage spectral reflectance

02 p0209 A72-11790

Remote sensing of Indian resources, investigating Englemann Spruce beetle infestation, topographic features and potential mineral areas

02 p0213 A72-11844

Color aerial photograph evaluation for forest damage demarcation, using film-filter combinations

09 p1302 A72-23240

TIME

NT ACCESS TIME

NT BURNING TIME

NT CHRONAXY

NT DOWNTIME

NT EPHEMERIS TIME

NT FLIGHT TIME

NT MTBF

NT REACTION TIME

NT RELAXATION TIME

NT RESPONSE TIME [COMPUTERS]

- NT TESTING TIME
NT TRANSIT TIME
NT UNIVERSAL TIME
Time between noon and evening maxima in F 2 layer critical frequency compared with evening maximum period, showing dependence on noon solar zenith angle
01 p0059 A72-10615
- TIME CONSTANT**
NT PERCEPTUAL TIME CONSTANT
System distortion error characteristics for carrier gas type radiospirometers, considering relation to system time constant
01 p0017 A72-10399
- Ionospheric F region heating by hf transmitter, obtaining electron temperature maps and heating/cooling time constants
01 p0062 A72-10910
- Pulmonary RC network and multiple breath nitrogen washout time constants mathematical relationship for breathing mechanics measurement, discussing lung compliance and resistance
04 p0478 A72-14862
- Supersaturated semiconductor solid solutions decay kinetic equations and time constants, noting free current carriers effect
04 p0561 A72-15081
- Approximate model to reduce differential equation order for linear system of series connected elementary aperiodic components with different time constants
10 p1457 A72-24753
- Semiconductor laser thermal resistance and time constant evaluation, obtaining operating temperature range and maximum attainable pulse width
11 p1647 A72-25808
- Two stage magnetic operational amplifier transfer function, time constants and control stability conditions, using difference equation approach
11 p1605 A72-26466
- Time constant limited stability of numerical integration procedures for systems of kinetic equations, examining causes and effects of stiffness
13 p1985 A72-28419
- Time constant of aircraft gas turbine engines gas temperature regulating system, using two thermocouples with different rise times
13 p2028 A72-29138
- P-n-p-n junction thyristor turnoff process under reverse anode voltage at high injection level, examining current voltage curve and switching time constant
13 p1932 A72-29293
- Airborne thermal sensors time constants, giving temperature perturbation wavelength estimates
13 p1958 A72-29623
- Uniaxial gyrostabilizer dynamic control system based on degenerate equations neglecting small time constant terms
16 p2421 A72-33961
- Relaxation phenomena in the biological carbon cycle under conditions of variable atmospheric CO₂ content
17 p2500 A72-34897
- Dynamic errors of a metering system with successive correction of the sensor's time constant for certain types of aperiodic input
17 p2557 A72-35787
- Mathematical model for moving radiometer system for reflected solar radiation measurement, discussing instrument time constant effect on surface emittance variations reproduction
20 p2927 A72-39795
- TIME DEPENDENCE**
Autonomous Hamiltonian system with two degrees of freedom, investigating origin and periodic orbits stability with two time variable method
01 p0123 A72-10030
- Modified implicit continuous fluid Eulerian technique for numerical solution of time dependent fluid flow for Mach numbers from zero to infinity
01 p0049 A72-10226
- Vlf electromagnetic wave perturbations in transpolar propagation, noting time dependent behavior of polar cap absorption effects
01 p0056 A72-10441
- Fluid droplet collapse in two phase gas flows, noting time dependence
01 p0145 A72-10573
- Temporal behavior, intensity fluctuations and energy spectrum of pulsating X ray source Cygnus X-1 from Uhuru observations
01 p0121 A72-11092
- Satellite in eccentric Keplerian orbit transgressing Roche limit about rigid sphere, considering time dependent evolution problem with various centrifugal and tidal forces
01 p0134 A72-11145
- Nonlinear viscoelasticity theory, considering simplified stress-strain functional relationships with respect to time based on isotropy postulate
02 p0290 A72-11624
- Thermoplasticity problems of materials with time dependent mechanical properties, obtaining approximate plastic deformation under cyclic loading
02 p0291 A72-11638

Solar flares far UV radiation time structure correlation with hard X rays

02 p0272 A72-11773
Atmospheric pollutants time and spatial profiles monitoring by geosynchronous satellite remote sensors

02 p0211 A72-11806
Second decrease in Vela Pulsar period, noting time span between discontinuities and supernova remnant Vela X

02 p0277 A72-11904
Magnetosonic perturbations caused by ideally conducting sphere expansion in cold plasma, determining electric field and magnetic induction time dependences

02 p0217 A72-11939
Effective dose change after repeated radiation exposures as function of time intervals between fractions, evaluating space flight radiation hazards [CERN-71-16]
02 p0161 A72-12059

Two dimensional underexpanded jet plumes flow distribution determination using time dependent finite difference method
02 p0301 A72-12257

02 p0295 A72-12497
Metal fatigue time and cycle dependent deformation and fracture mechanisms in creep range from cumulative damage law standpoint for lifetime prediction

02 p0164 A72-12513
Extracardiac chronotropic effects on cardiac rhythm variations during fatigue, using variational pulsometry and autocorrelation and spectral analysis

02 p0206 A72-12620
Unsteady flow in laminar boundary layers along infinite porous flat plate with time dependent suction

02 p0283 A72-12630
Oblique rotator model for time dependent light polarization of red long period variables, considering dust particle alignment in outer atmospheric layers near magnetic poles

02 p0206 A72-12773
Time dependent unsteady flows visualization around circular cylinders and flat plates decelerated from steady speed

02 p0165 A72-12852
Reactions choice limiting cueing signals effect on reaction time, considering dependence on time interval between cueing and start signals

03 p0353 A72-13044
High energy solar and celestial X ray experiment with OSO 5, measuring spectrum as function of time, intensity and spatial distribution

03 p0424 A72-13220
Quiet sun radio emission observation, considering statistical minimum value and time varying structure

03 p0424 A72-13221
Solar decimeter and hectometer wavelength radio burst generation, examining dynamic spectra and source position as function of frequency and time

03 p0356 A72-13278
Solar magnetic fields time fluctuation determination using longitudinal, intensity and line of sight velocity measurements

03 p0428 A72-13303
Sunspot magnetic field evolution in time and space from four-camera spectral scanning method, obtaining magnetic flux and radial velocity field

03 p0429 A72-13314
Spectroheliogram movies of magnetic, velocity and intensity field in solar atmosphere, showing time resolution of line spectra

03 p0430 A72-13318
Solar magnetic fields time fluctuation determination using longitudinal, intensity and line of sight velocity measurements

03 p0430 A72-13327
Solar magnetic field variations in McMath Regions, using longitudinal magnetograms time sequences

03 p0431 A72-13344
Time evolution of large scale solar magnetic field, observing zonal harmonics

03 p0432 A72-13353
Solar polar and general magnetic field fine structure and statistical nature, discussing time fluctuations and interplanetary field

03 p0434 A72-13508
Lunar electrical conductivity model, determining vacuum transient response to time varying spatially uniform magnetic field

03 p0341 A72-13630
Two dimensional viscoelastic fluid flow past infinite plate with time dependent suction and constant and periodic free stream velocity

03 p0436 A72-13830
Time variation of mean values for magnetic field elements strength and size in solar polar regions, noting solar activity maximum effect

03 p0457 A72-13953
Liquid propellant rocket abort fireball model, specifying heat flux as function of time

03 p0317 A72-13989
Fast and slow human muscle fibers temporal response characteristics, using tensometric recording

Time and coordinate dependence of magnetic field for steady symmetric flows of compressible conducting fluid at large Reynolds numbers, investigating self excitation conditions
03 p0398 A72-14001

Time effects on stress concentration around circular and elliptical holes in infinite plate with nonlinear creep
03 p0451 A72-14126

03 p0458 A72-14155
Surface active materials adsorption on developing bubble surface, analyzing time dependence

04 p0583 A72-14447
Infinite elastic-plastic beam impact by semilinear elastic rod, computing strain-time profiles

04 p0566 A72-14723
Trapped particles induced by fluctuating magnetospheric electric and magnetic fields, calculating radial diffusion and energy distribution and time variations

04 p0464 A72-14843
Aircraft and other transient noise levels temporal characteristics effect on noise assessment

04 p0517 A72-14950
Hydromagnetic whistler traveling wave tube amplification in magnetosphere, deriving temporal growth rate dependence on plasma parameters

04 p0506 A72-15108
Time-varying systems with observer for feedback control, investigating stability

04 p0549 A72-15115
Time dependent hydromagnetic oscillations in contained rotating conducting fluid under magnetic field, using interior boundary layer expansion

04 p0512 A72-15263
Kinetic rate theory extended to time dependent flow behavior of viscoelastic materials/polymers/ under constant stress and shear

04 p0507 A72-15694
Multiple-input multiple-output linear time invariant feedback systems stability, investigating continuous-time case

04 p0514 A72-15704
Viscoelastic fluid flow past infinite plane porous wall with time dependent suction, investigating mean velocity profile and wall shear stress

05 p0708 A72-15767
Statistical investigations of solar burst time dependent fine structure, giving data for multichannel spectrograph and recording system design

05 p0616 A72-15946
Waspaloy sheet creep rupture time dependent sensitivity to sharp-edged notches at 1000-1400 deg F, optimizing smooth and notched specimen yield strengths [ASME PAPER 71-WA/MET-3]
05 p0670 A72-15906

05 p0616 A72-15946
Mechanical impedance and phase angle time variation in restrained primate during prolonged sinusoidal vibration

05 p0746 A72-15996
[ASME PAPER 71-WA/BHF-8]
Two dimensional time dependent nonlinear radiative transfer and nonequilibrium diffusion in arbitrary geometry by synthesis method

05 p0621 A72-16230
Light scattering time dependence, erythrocyte aggregation rates and hydrodynamic characteristics in ox, pig and horse blood stream

05 p0656 A72-16235
Ionospheric neutral composition variations as function of height, local time and solar activity

05 p0657 A72-16263
F 2 region electron density spatial and temporal distribution, investigating plasma vertical drift effects

05 p0657 A72-16269
Traveling ionospheric perturbations investigation by vertical sounding with interference method, presenting group path difference measurements as function of frequency and time

05 p0717 A72-16378
Spectral and time variations at radio frequencies of QSO and radio galaxies from Parkes catalog

05 p0709 A72-16518
Time behavior of temperature and emission measure in X ray flares observed from Vela 5 spacecraft

05 p0629 A72-16598
Amplitude, time and frequency domain analysis of random signals, measuring probability density, cross correlation and cross spectral density functions

05 p0622 A72-16638
Time shortage as stress factor affecting mental activity of operator in man-flying vehicle system, discussing control signal handling efficiency

05 p0669 A72-16691
Two-photon time distribution in mixture of light from He-Ne laser and Gaussian source of same central frequency

05 p0652 A72-16944
Numerical solution method for laminar, time dependent and three dimensional boundary layer equations, applying to rotating flat plate in forward flight [AIAA PAPER 72-109]

05 p0609 A72-16950
Multidimensional time dependent flow field analysis by split finite difference operator technique, using star mesh of quadrilateral cells [AIAA PAPER 72-154]

Upper atmosphere density fluctuations associated with solar activity and local time values, using Cosmos 14 satellite drag data

05 p0659 A72-17037

Linear time-varying control systems with one feedback nonlinearity, determining combined time-frequency condition for stability

05 p0642 A72-17090

Optimally sensitive closed loop control synthesis for systems containing uncertain time varying parameters, applying to stochastic systems

06 p0792 A72-17309

Time domain infinite matrices analysis methods for linear stationary and nonstationary multivariable systems, presenting recursion formulae

06 p0792 A72-17310

Linear time-varying control system synthesis for specific input and maximum admissible error, considering various weighting functions and constraints

06 p0792 A72-17311

Linear time-varying system under modulated signal excitation, obtaining quasi-stationary response by separable system approximation with parameter optimization

06 p0771 A72-17379

Solar wind speed variations, examining velocity structure recurrence at various rotations, time interval of steady state flow and temporal evolution effects

06 p0872 A72-17442

Solar wind stream-stream interactions, studying time profiles, velocity variations, corotating spiral, increased pressure due to radial compression and zonal flow directions

06 p0872 A72-17443

Pseudowaves and ion acoustic waves simulation, calculating time evolution of ion distribution for oscillating negative plasma potentials applied at grid

06 p0855 A72-17512

Electrons spatial and temporal response in collisionless plasma to externally applied voltage pulse

06 p0856 A72-17522

Four phase space density collisionless one dimensional stellar system evolution in time by following motion of boundary curves

06 p0876 A72-17577

Cosmic ray muon intensity in interplanetary magnetic field, revealing sidereal variation due to motion of solar system relative to local galactic rotation frame

06 p0873 A72-17648

Jacobian matrix partial derivatives for orbital motion representation by time step power series

06 p0877 A72-17651

Time independent or periodic Hamiltonian conservative differential equations, studying open, oscillating, limited and abnormal trajectories

06 p0877 A72-17661

Laser radiation intensity modulation by time varying magnetic field

06 p0825 A72-17685

Retinal ganglion cell spikes timing in mammalian retina, using electroretinography and computer analysis

06 p0762 A72-17721

Temporal characteristics of emission line broadening in lasers with dispersive resonators for Nd ion activated phosphate glasses and disordered crystals

06 p0826 A72-18011

Ionospheric electron density profiles and time variation of electron production rate for X-ray flare of 30 January 1968, observing decrease in effective recombination coefficient

06 p0874 A72-18088

Time characteristics preceding self-ignition of solid particle system suspended in gas, discussing quasi-steady state duration

06 p0903 A72-18202

Seasonal effects and propagation fluctuations in time-frequency comparison measurements with vlf waves, noting optimal RC filter

06 p0818 A72-18289

Complex bodies time dependent temperature distribution from temperature measurements at arbitrary points, using Duhamel integral

06 p0904 A72-18512

Turbulent layer generation in ideal two dimensional fluid flow, determining vortices time evolution from initial velocity discontinuity by numerical methods

06 p0802 A72-18525

Solid bodies crack development theory, emphasizing crack tip fine and hyperfine structures concepts and time dependent effects

06 p0898 A72-18554

Temperature stress distribution in infinite plate with time varying heat transfer coefficient

06 p0899 A72-18565

High time resolution of low latitude asymmetric disturbances in geomagnetic field by Fourier analysis for substorm activity studies

07 p0976 A72-19165

Time behavior of single axis gyro platforms, considering linear and nonlinear-suboptimal control

07 p0983 A72-19169

Time-variable multivariable systems reduction to completely controllable and observable systems by

subdivision and transformation procedures, using subsystems order matrices

07 p1026 A72-19271

Analog simulation of normal thermal explosions and cool flames, observing oscillations limits, time dependence of parameters and effect of changes in activation energy or initial temperature

07 p1098 A72-19366

Thermal blooming of laser beams in liquids and gases, investigating short and long time behavior under thermal conduction and viscosity effects

07 p1005 A72-19408

Wiener-Hermite random variable expansion technique with time dependent base for turbulence applied to Burger equation

07 p0967 A72-19502

Uniform asymptotic solution near wavefront of transient field propagation in inhomogeneous dispersive media

[AD-745077] 07 p0946 A72-19800

Dark adaptation with logarithmically time decreasing background luminance, noting threshold time lag variation with rate of background change

07 p0930 A72-19827

Diffusion kinetics in Nb-Al system for varying time and temperatures

07 p1015 A72-19930

Optimum exposure time for sintering in Ar flow of porous rolled product of Ti powders determined from physicochemical properties changes

07 p0996 A72-19964

Time independent incompressible micropolar fluid flow existence

07 p0970 A72-20082

Cross correlation identification of linear time varying processes based on pseudorandom sequences, presenting digital simulation results

07 p0948 A72-20390

Venusian atmospheric circulation experiments with time dependent two layer primitive equations model, discussing hot house and Goody-Robinson radiation transfer implications

07 p1083 A72-20452

High energy hadrons time structure in extensive air showers, considering production of nucleon-antinucleon pairs in particle interactions

07 p1067 A72-20687

Dynamic system time varying parameters on-line estimation using adaptive extended Kalman filter based on predicted error covariance matrix alteration

08 p1144 A72-20847

Maximum likelihood estimates of covariance parameters of time discrete nonstationary linear systems from residuals measurement of suboptimal sequential filter

08 p1145 A72-20865

Spatial-temporal temperature distribution on CW laser irradiated materials, noting application to water film

08 p1252 A72-21289

Automated mechanical system for solid propellant sheet stretch tests in two directions as function of time

08 p1147 A72-21331

Periodic and synchronously recurrent transient signal detectability in time-varying noisy environment

08 p1134 A72-21406

Time varying external pressure effect on creep collapse of long thin walled quasielliptic cylindrical shell, taking into account elastic deformation

08 p1245 A72-21612

Necessary conditions for burning rate stepwise variation with time of condensed systems

08 p1254 A72-21657

Time dependent progress of vibrational-rotational transitions in hydrogen-fluorine chemical laser investigated by oscillography with IKM-1 monochromator

08 p1183 A72-21715

Nd-glass laser time characteristics and radiation ordering from cavity lengthening

08 p1183 A72-21771

Nonlinear dynamic response of deformable solids under time and space dependent thermal and mechanical loads determined by finite element method

08 p1248 A72-21822

Brain structures role in fixation of temporal relationships in information memory function of central nervous system

08 p1118 A72-21836

GaAs semiconductor injection lasers, discussing time characteristics of current carriers, population inversion and resonator Q factor modulation

08 p1184 A72-22032

Reliability of recoverable information systems with temporal redundancy

08 p1180 A72-22058

Reliability of complex systems performing function with time dependent quantity

08 p1180 A72-22061

Hydrometeorological parameters spatial-temporal variations analysis and forecasting based on association functions and conditional probability distribution functions

08 p1202 A72-22116

Statistical characteristics of wind elements from vertical-temporal structure of wind field

08 p1202 A72-22118

Atmospheric boundary layer pressure field expansion into dual series of natural time dependent components to separate fluctuations within monthly period for weather forecasts

08 p1203 A72-22125

Barrier capacitance effect on transient characteristics of light diodes, obtaining time dependence of p-n junction volume charge voltage and recombination emission intensity

09 p1284 A72-22211

Probability density and distribution functions of first arrival time at boundary by steady normal random process

09 p1289 A72-22217

High temperature tests of graphite composites in air, determining material loss time dependence and correlation with observed strength data after oxidation

09 p1333 A72-22381

Nonlinear initial boundary value problem for time dependent convection-diffusion equation with ionization and recombination reactions

09 p1341 A72-22472

Time dependent phase modulation for high effective reference to object beam intensity ratio, noting linear recording of holograms

09 p1310 A72-22649

Solar general magnetic field nature, origin, fine structure and temporal variations, evaluating sunspots and active plage areas as field sources

09 p1387 A72-22752

Snow-plough model of plasma acceleration for determining time dependence, gas density distribution and energy transfer

09 p1359 A72-22819

Constitutive equations for materials with time dependent and time independent plasticity, applying to impact of identical bars

09 p1328 A72-22996

Single mode He-Ne laser output, predicting intensity correlation function form and decay time near threshold

[AD-742154] 09 p1324 A72-23081

Single picosecond light pulses from mode locked Nd-glass laser, discussing temporal structure, spectral energy distribution and pulse shape measurements

09 p1324 A72-23082

Weighted least squares stationary approximations to time varying linear systems, noting criterion for matrix choice

09 p1341 A72-23094

Linear time invariant multirate sampled data control systems characteristic equation simplification

09 p1290 A72-23099

Two spool gas turbine engine characteristics with speed reduction, determining time dependence of turbocompressor rpm, gas temperature and engine power

09 p1374 A72-23185

Time dependent parallel and cross polarized electromagnetic pulse propagation in magnetoionic medium for normal incidence

09 p1280 A72-23231

Early phase time development of far UV line radiation from plasma production by focusing Q switched ruby laser onto solid Mg target

09 p1325 A72-23232

Motion stability of linear discrete deterministic and random systems over finite time interval

09 p1291 A72-23428

Ionospheric electron concentrations and temperatures determined by time dependent continuity equations model during 11 September 1969 solar eclipse

09 p1390 A72-23518

Interferometric measurements of time dependent electron density in Xe pinched plasma laser, showing laser lines due to transitions in triply ionized species

09 p1366 A72-23700

Prediction method for computing maintenance technician reliability as probability of equipment repair completion within given time

10 p1486 A72-24000

Markovian characteristics of time dependent excursions and independent incursions processes provided with limits to left and continuous to right, noting Poisson punctual process and Borel sets

10 p1505 A72-24114

Ferrites electrical conductivity variations with time caused by cations distribution modification after cooling

10 p1525 A72-24121

Stability criteria for continuous dynamic system under parametric excitation derived by Liapunov direct method, using time dependent functionals and Rayleigh operators quotients

[ASME PAPER 71-APM-EEE] 10 p1510 A72-24187

Microwave amplitude modulation during propagation through RF plasma under perpendicular low intensity time dependent magnetic field

10 p1520 A72-24345

Self learning estimator for tracking, using heuristic technique for time-varying estimates sequence determination

10 p1457 A72-24500

- Oscillation development time in phantasticon oscillator, using linearization of nonlinear term
10 p1450 A72-24517
- Wind shear theory expectations tested by wind profiles and sporadic E layer observations, stressing time variations significance
10 p1477 A72-25155
- Temporal variations of sporadic E layer blanketing frequency, virtual height and occurrence rate, calculating electron density profiles and tidal wind influence
10 p1441 A72-25162
- Sampling theorem application to time varying systems, considering Hankel transform as example
11 p1675 A72-25293
- Stationary weighting pattern synthesis by linear time varying dynamic system, noting feedback system input-output mapping properly
11 p1608 A72-25321
- Thermoplastic polypropylene sandwich molds stiffness variation with time, noting three point bending and creep tests
11 p1673 A72-25550
- Time dependent viscous flow past impulsively started sphere using numerical solutions for governing equations based on Legendre series expansion of stream and vorticity functions
11 p1615 A72-25551
- Time dependent light emission from mesoplasmas in Si p-n junctions in pulse mode, showing carrier heating effect
11 p1700 A72-25780
- Time dependent solutions of Tokamak equilibrium equations for plasma diffusive processes
11 p1694 A72-25787
- Creep and low cycle fatigue dynamic behavior, noting stress concentration time dependence, strain hardening and local plastic deformations in dead annealed Al thin walled tubes
11 p1658 A72-25829
- Thermoelastic stress and displacement in thin finite rod due to distributed time dependent heat sources
11 p1736 A72-25991
- Sporadic E layer cyclic variations during solar activity cycle, noting time dependence of occurrence probability and critical frequency
11 p1623 A72-26281
- Semiautomatic analog to digital converter for pulse signals time dependent parameters, examining block diagrams and tunnel diode operation
11 p1605 A72-26456
- Heat transfer during film and transition boiling on vertical surfaces, taking into account time dependence
11 p1746 A72-26537
- Human performance dependence on time of day, discussing circadian and physiological rhythms relation and environmental change effects
11 p1580 A72-26677
- Time estimate criterion of lasing breakdown in photodissociative iodine-alkyl lasers with iodine molecule buildup
12 p1819 A72-27053
- High temperature dislocation rearrangement in lightly cold deformed Nb as function of time and temperature, using etch pit technique for evaluation
12 p1827 A72-27136
- Low temperature solid state phase transformations in 2H silicon carbide single crystals, noting time and temperature dependence
12 p1854 A72-27276
- Spatial and time dependence of electron velocity in short channel microwave FET, using Monte Carlo method
12 p1790 A72-27434
- Niobium diffusion into copper as function of time and temperature, obtaining rates by electrical resistance measurements
12 p1828 A72-27448
- Unsteady flow evolution at sphere and elliptical cylinder obtained by flow visualization techniques, showing streamline sequence dependence on angle of attack
12 p1797 A72-27469
- Computer analysis of helicopter pilots eye movement patterns dependence on visual task skill and performance time
12 p1770 A72-27475
- Stochastic time varying patterns classification by Kalman filter, discussing optimum dichotomizer with supervised learning
12 p1790 A72-27498
- Russian book on spectral, spatial and time characteristics of lasers covering luminescence and resonator theories, electromagnetic field structure and radiation dispersion
12 p1820 A72-27500
- Human motoneuron discharge time relations during isometric muscle contraction, measuring adjacent action potential and mean interspike intervals
12 p1761 A72-27653
- Time variable energy losses effects on cosmic ray nuclei composition, discussing fragmentation processes during heavy nuclei propagation through interstellar matter
12 p1864 A72-27692
- Streak photography for three dimensional structure of thermal convection in rotating fluid under horizontal temperature gradient, noting time variations of baroclinic waves
12 p1809 A72-27701
- Time structure of massive interacting particles with energies above 20 GeV near axes of cosmic ray showers of energy above 100 TeV
12 p1864 A72-27737
- Singly and doubly resonant pulsed optical parametric oscillators driven by time-dependent pump, deriving output power rise time by steady state analysis
12 p1792 A72-27751
- Equatorial spread F spatial and temporal distribution from short wave side reflection observations along Lindau-Tsumeb transequatorial HF radio transmission path
12 p1803 A72-27778
- Hybrid computer Monte Carlo solution algorithm for parabolic partial differential equations with time varying boundary conditions, applying to ferromagnetic rod magnetization problem
12 p1787 A72-28119
- Molecular-mechanical theory of external friction, taking into account surface roughness, time and temperature dependent mechanical properties and chemical processes
12 p1818 A72-28195
- Laplace transformation for mechanical response of piezoelectric composite transducer under action of thermal field and electric potential, noting time dependent modulus of elasticity
13 p1955 A72-28621
- Delaney case of Kovalevskaya gyroscopic motion, analyzing Euler equations time dependence
13 p1956 A72-28722
- Pulse plasma injector accelerating circuit resistance dependence on time and current amplitude calculated from current oscillograms
13 p2010 A72-28733
- Magnetosonic perturbations caused by ideally conducting sphere expansion in cold plasma, determining electric field and magnetic induction time dependences
13 p1949 A72-29251
- Time history model of transient ignition to self sustained propellant burning, taking into account pressure effects and igniter heat flux
13 p2065 A72-29305
- Time dependent and stationary two dimensional calculation of current and potential distributions in MHD generator preionizer and entrance region flow
13 p2013 A72-29358
- Low energy relativistic cosmic ray electrons temporal intensity variations from IMP satellite measurements, considering correlation with solar activity
13 p2030 A72-29376
- Rod antenna near field energy flow direction and intensity characterization by time independent and dependent components of Poynting vector
13 p1932 A72-29398
- Kinetic model and analysis of time characteristics of trifluoriodomethane photodissociation laser
13 p1968 A72-29428
- Carbon dioxide laser vibrational-rotational band small signal gain factor dependence on time elapsing after breakdown of equilibrium distribution
13 p2008 A72-29503
- Longitudinal vortices development in time-increasing boundary layers at concave walls, showing dependence on Reynolds number and boundary layer thickness
13 p1942 A72-29597
- Time evolution of chromosphere layer heated by energetic particle stream during solar flare, noting cooling by Lyman continuum radiation transfer
13 p2032 A72-29721
- Two fluid model application to microbridges between superconductors, investigating superconducting particles number time variation possibility
13 p2023 A72-29789
- Time varying magnetospheric electric field spatial distribution effect on plasmasphere temporal evolution, considering fine structure due to periodic gusts in convection electric field
13 p1953 A72-29804
- One dimensional unsteady flow of dense magnetized plasma, investigating time evolution of temperature profile in wall layer and thermal conductivity
13 p2018 A72-29876
- Semiconducting glass filter time dependent transition, absorption coefficient and luminescent spectral dependences, using monolayered ruby laser
13 p1971 A72-29909
- Spatial and temporal summation characteristics and relationship in human peripheral retina investigated for stimuli viewed at eccentricity against luminous background
13 p1907 A72-29970
- Time invariance violation in charge asymmetry experiment, showing K-meson decay rate difference reversal from world to antiworld with particle unchanged
14 p2130 A72-30265
- Eccentric geomagnetic dipole drift field as function of time dependent parameters, calculating potential components in spherical coordinates
14 p2103 A72-30667
- Analytical prediction of pressure-time relationship during evacuation of multilayer insulation thermal protection systems, taking into account outgassing effects
14 p2172 A72-30925
- Shock wave interaction with supersonic moving plate, calculating plate lift as function of time
14 p2071 A72-31024
- Time to failure under axial tension determined for gallium selenide single crystals at constant temperatures, noting tensile strength dependence
15 p2290 A72-31387
- Ionospheric plasma resonance time duration variation with latitude, altitude and ratio of electron plasma frequency to electron cyclotron frequency
15 p2223 A72-31429
- Elastic damping of spin stabilized space stations nutational oscillations induced by time-variant moments of inertia
15 p2319 A72-31458
- Nonlinear creep failure of imperfect sandwich structures under time variable loading, considering rod and cylindrical shell
15 p2324 A72-31490
- Time dependent orthogonal coordinate system rotation by unit vector along effective axis, obtaining angular velocity and effective angle interpretation
15 p2275 A72-31590
- Wave propagation in inhomogeneous anisotropic time varying moving media, discussing generalized dispersion equation
15 p2196 A72-31688
- Pioneer spacecraft intermittent solar wind streams data temporal variations analysis to account for anomalous type 3 bursts
15 p2299 A72-31964
- Time/frequency techniques in land, sea and air transportation environments, discussing characteristics and electronic traffic control systems applications
15 p2338 A72-32073
- MHD Couette flow of electrically conducting viscous incompressible fluid in transverse magnetic field with time dependent suction or injection
15 p2286 A72-32396
- Transversely excited pulsed carbon dioxide laser with and without hydrogen addition, observing gain spatial and temporal dependence
15 p2251 A72-32529
- Transverse electric discharge pulsed carbon dioxide laser, measuring refractivity time history by interferometry for comparison with prediction
15 p2251 A72-32537
- Time dependent finite difference /fluid-in-cell/ method for supersonic aerodynamic problems concerning inviscid compressible flow with contact surface and shock discontinuities
16 p2342 A72-32884
- Angular measurement error for group and repetition techniques as function of observation time, deriving formulas for comparison in terms of economy and efficiency
16 p2389 A72-33030
- Shock tube diaphragm rupture effect on density distribution in rarefaction wave as function of time, using mirror laser interferometer measurement
16 p2390 A72-33161
- Centaurus region hard X ray flux temporal variations from OSO-3 X ray telescope observations
16 p2446 A72-33458
- Time variable pulse front fluctuations effect on random error in digital pulse duration measurements
16 p2395 A72-33953
- Load cycle frequency and time characteristic effects on plastics fatigue behavior, considering relaxation, retardation and internal damping induced heating effects
16 p2416 A72-34145
- Velocity-pressure correlations in a homogeneous turbulence associated with a plane pure deformation
17 p2537 A72-34280
- Invariant imbedding in time-varying homogeneous nondispersive media
17 p2513 A72-34366
- State dependent state variable feedback method to control multiple input multiple output nonlinear and/or time varying systems
17 p2532 A72-34420
- Optical timing of the Crab pulsar, NP 0532.
17 p2605 A72-34535
- Time evolution of a rotating black hole immersed in a static scalar field.
17 p2605 A72-34536
- Absolute rate constant for the reaction $H + H_2CO$.
17 p2511 A72-34739
- Flow in an accelerated rocket nozzle - Effect of variation of total mass. II
17 p2621 A72-34918
- Fraunhofer lines emergent intensity fluctuation caused by temperature and pressure perturbation in solar atmosphere
17 p2608 A72-35080

ESRO 2 satellite observation of solar X-ray emission from active limb prominence, obtaining temperatures and emission measures as function of time

17 p2608 A72-35085

Temporal distribution of Cerenkov light from extensive air showers, discussing experimental setup and pulse shape

17 p2599 A72-35140

Monte Carlo calculation of radial and time dependence of isophote diagrams for Cerenkov light in 0.1 to 1 TeV extensive air shower

17 p2599 A72-35142

Spectral factorization in periodically time-varying systems and application to navigation problems.

17 p2578 A72-35492

Space and time variations of the solar Na D line profiles.

17 p2616 A72-35697

On the temporal distribution of type IV burst-active centres over the solar cycle / Research note.

17 p2602 A72-35715

Auroral proton energy time behavior estimation based on magnetic and ionospheric data from ground observations

17 p2550 A72-35855

Galactic spiral structure temporal decay based on density waves hypothesis

17 p2619 A72-35955

An investigation of the ionospheric D region at sunrise. I - Time variations of ozone, metastable molecular oxygen, and atomic oxygen. II - Estimation of some photodetachment rates. III - Time variations of negative-ion and electron densities.

18 p2656 A72-36295

The transient radiated field of a coaxial aperture antenna.

18 p2660 A72-36331

Pulsating modulations and peculiar absorptions of type IV emissions from the solar corona.

18 p2721 A72-36651

Time-resolved diagnostic method for hydrogen plasmas.

18 p2716 A72-36949

Time-dependent ionization equilibrium and line radiation under flarelike conditions.

19 p2849 A72-37241

Optimally sensitive adaptive control techniques for systems with unknown time-varying parameters, suggesting applicability to ATC

19 p2776 A72-37289

Motion stability of inertial navigation gyroscopic system with gyro horizon compass, noting constant and time dependent coefficients of motion equations

19 p2830 A72-37320

Models of neurons reacting to input signal alternation in space and time

19 p2759 A72-37424

Fourier-Bessel superposition and Laplace transformation methods for surface displacement produced by time dependent dipole in elastic half space, noting buried dipole case

19 p2876 A72-37887

Recent results concerning a graphical test for checking the stability of a linear time-invariant system.

19 p2826 A72-38251

Extended Kalman filter with fictitious noise input for adaptive tracking of time varying parameters applied to VTOL aircraft

19 p2781 A72-38265

Evolutionary clock - Nonconstancy of rate in different species.

19 p2758 A72-38551

Hybrid computer Monte Carlo solution algorithm for parabolic partial differential equations with time varying boundary conditions, applying to ferromagnetic rod magnetization problem

19 p2770 A72-38620

Hall field occurrence conditions in small semiconductor plates, discussing Hall generator design and layer temperature as function of time

19 p2776 A72-38725

Temporal relation of the second heart sound to aortic flow in various conditions.

19 p2759 A72-38818

Atmospheric transmittance measurements time and spatial representativeness optimization by allowing for fog element caused discontinuities

20 p2947 A72-38971

Creep-fatigue interaction interpretation for austenitic stainless steels from crack growth viewpoint, investigating time and cycle dependent failure at elevated temperature

20 p2937 A72-39213

Electrical conductivity of pressed cadmium antimonide

20 p2959 A72-39218

Laser action with coupled types of oscillations

20 p2931 A72-39319

Response of linear periodically time varying systems to random excitation.

20 p2946 A72-39636

Criteria for delayed fracture in solids and their experimental verification.

20 p2981 A72-39954

Noise and stimuli current time and spatial distribution effect on visual performance of eye with image intensifier

21 p3054 A72-40742

Optimal search in the presence of Poisson-distributed false targets.

21 p3075 A72-40837

Radiation of EM waves with Walsh-function time variation - Preliminary results.

21 p3020 A72-40902

Mathematical model for dielectrics with time dependent polarization, noting relaxation time distribution function

21 p3085 A72-41074

Time dependent deformation of isotropic viscoelastic materials, discussing rectilinear shear, circular cylinder torsion, spiral shear of layer and conical layer torsion

21 p3119 A72-41075

Broadband continua temporal behavior at type IV initial stages, recording by radio interferometers

21 p3101 A72-41296

Positive geomagnetic bays in evening high-latitudes and their possible connection with partial ring current.

21 p3049 A72-41387

On the plastic behaviour of time dependent materials - Theoretical and experimental investigation.

21 p3124 A72-41504

Theoretical and experimental investigation of the relationship between plastic and creep deformation of structures.

21 p3124 A72-41509

Second order optimality conditions for variable end time terminal control problems.

21 p3039 A72-41571

[AIAA PAPER 72-932]

Time scales and correlations in a turbulent boundary layer.

21 p3047 A72-41626

Stabilities and settling times of nonlinear and time-varying feedback systems.

22 p3161 A72-41937

Compatible controllers for time-varying linear plants.

22 p3161 A72-41939

Delaunay case of Kovalevskaya gyroscope motion, analyzing Euler equations time dependence

22 p3176 A72-42098

Aspect-sensitive reflections from ionization irregularities in the F-region.

22 p3154 A72-42364

Oxygen uptake kinetics for various intensities of constant-load work.

22 p3145 A72-42743

Physical characteristics of type I supernova envelopes during the initial expansion phase. II - Development of type I supernova spectra after maximum light.

23 p3333 A72-43228

Internal to total energy relation dependence on deformation time in impulsive loading of homogeneous free rod, noting energy conversion efficiency

23 p3344 A72-43338

Quantum impulse autocorrelation function of one dimensional harmonic crystal lattice, noting periodic time dependence at high and low temperatures

23 p3312 A72-43405

Temperature-time effects on fracture failure mode and strength of polymeric glasses in terms of Ludwig brittle-ductile transition hypothesis and Griffith theory

23 p3305 A72-43503

Optimisation of contraction-mapping algorithm for calculating optimal controls.

23 p3275 A72-43607

Decoupling and diagonalization conditions determination for nonlinear multivariable time-varying differential equations system by state feedback, giving illustrative examples

23 p3275 A72-43611

Optimally sensitive control for distributed parameter systems.

23 p3275 A72-43612

Optimal minimax regulation of a dynamic system.

23 p3276 A72-43860

Altitude limit as function of acclimatization time length for investigation of enhanced resistance to acute hypoxia in rats

23 p3255 A72-43908

Inconsistency of gravitational constant variability in inverse proportion to time from viewpoint of stellar and solar system age, life development and physical three dimensional space

23 p3338 A72-44037

Application of a time-dependent boundary-layer analysis to the problem of dynamic stall.

23 p3249 A72-44058

Explosive instability temporal development, noting linear damping role in nonlinear wave interaction under conservation laws of energy and momentum

23 p3282 A72-44318

Non-linear free vibration of a beam with time-dependent material properties.

23 p3355 A72-44374

Materials creep behavior and elevated temperature design.

24 p3453 A72-44553

Note on the experimental determination of photoconductive response characteristics of amorphous semiconductors.

24 p3431 A72-44716

The cosmic-ray spectral modulation above 2 GV. IV - The influence on the attenuation coefficient of the nucleonic component.

24 p3434 A72-44783

Use of characteristics for boundaries in time dependent finite difference analysis of multidimensional gas dynamics.

24 p3359 A72-44879

The damping of precessing vortex cores by combustion in swirl generators.

24 p3464 A72-45060

Equation of state relating time variations of stress and strain in elastoplastic material under tension

24 p3459 A72-45069

Maximum temperature-holding time effects on plastic deformation and fracture of steel under thermal cyclic loads

24 p3416 A72-45746

Microstructure properties of heat resistant alloy for gas turbine blades as function of operational time

24 p3416 A72-45747

TIME DISCRIMINATION

Satellite tracking radio interferometer with 1 deg sec directional accuracy, discussing low noise level and precise time allocation requirements [DGLR PAPER 71-125]

02 p0182 A72-12738

Time discrimination utilization in EMC, considering automatic position telemetering system using time division technique

03 p0325 A72-14047

Soviet book on astronaut activity psychological features covering space flight living conditions, space and time perception psychophysiological mechanism changes and weightlessness effects

03 p0317 A72-14246

Linear analysis and synthesis of three dimensional interference system stationary in space and time domains

09 p1278 A72-22573

High time resolution observations of photospheric velocity field, interpreting short period oscillations origin as result of combined image motion and Doppler velocity gradients

15 p2317 A72-32776

Non-monotonicity of temporal recognition of brief duration.

18 p2651 A72-36912

Psychometric test for auditory stimulus duration difference estimation, noting Weber fraction for temporal gaps marker condition

21 p3004 A72-40345

Linear analysis and synthesis of three dimensional interference system stationary in space and time domains

24 p3379 A72-44752

TIME DIVISION MULTIPLEXING

Microwave communication via satellites, discussing FDMA and TDMA transponders design

01 p0029 A72-10709

Time division multiple access systems for communication satellites, discussing performance and application in Intelsat network

01 p0033 A72-11301

Time division multiple access system with 100/50 M bit/s channel capacity for Symphonie and Intelsat satellite speech channels

01 p0033 A72-11302

Time division multiple access systems for satellite transmission, discussing burst transmission control problem associated with transmitting end synchronization

01 p0033 A72-11303

Time division multiple access systems transmitting and receiving end synchronization control criteria derivation, discussing code pattern selection for reliable detection

01 p0033 A72-11304

Switching operations in TDMA system, noting availability of signaling channels with broadcast mode

01 p0033 A72-11305

Twisted shielded pair /TSP/ time division multiplexed data bus with standard interfaces for use in aerospace applications

02 p0194 A72-12405

Communication satellites multiple access, using time division multiplex method

02 p0181 A72-12607

Time discrimination utilization in EMC, considering automatic position telemetering system using time division technique

03 p0325 A72-14047

Optical communication technique based on fiber optic light pipes and time, space or wavelength division multiplexing

03 p0325 A72-14050

Communication satellites performance improvement by time division multiple access techniques and use of frequencies above 10 GHz for localized coverage through highly directive beams

04 p0494 A72-15676

Time division multiple access /TDMA/ satellite communication system optimal design, discussing earth stations, satellites and transmission path characteristics 05 p0626 A72-16298

TDMA satellite communication system with convolutional encoding and Viterbi decoding, evaluating data buffering and control configurations 07 p0941 A72-19297

Multiple access to communication satellites in time division multiplex, discussing burst phase control and ground station receiving-transmitting systems 09 p1278 A72-22852

Spectral distribution of signal power in AM, FM and PM PCM systems with time division multiplexing 10 p1439 A72-24909

Time division multiplexing system for asynchronous high data rate telemetry, discussing design features 10 p1440 A72-25061

PAM time division multiplex crosspoint circuit with scanning filters, discussing applications to PBX, ground station and terminal exchanges with PCM transmission link 11 p1604 A72-25909

TDMA system for Intelsat 4 and subsequent satellites, discussing automatic synchronization acquisition, terrestrial network-satellite transmission channel modular interface, etc [AIAA PAPER 72-538] 12 p1780 A72-27361

Intelsat satellite time division multiple access system /TDMA/ using semiconductor technology with burst synchronization [AIAA PAPER 72-546] 12 p1781 A72-27369

Aerospace guidance multiprocessor with memory units attached to time-multiplexed data bus, predicting performance in terms of queueing theory, Markov process and simulation 12 p1786 A72-27433

Voice digital data rate reduction technique by exploiting zero and one bits imbalance in PCM TDM bit stream output encoding, discussing hardware implementation 12 p1785 A72-27845

Optical PCM communication system with megabits/sec information rate based on dye laser with combined frequency-time division multiplexing 15 p2198 A72-32060

Time division demultiplexing technique using two channel simulation of twenty-four channel digital optical PCM communication system 15 p2200 A72-32163

TDM and FDM digital communication systems performance comparison, noting equivalence in theoretical efficiency and generated waveforms 16 p2363 A72-33216

Aircraft FDM and TDM systems, considering signal processing, cable requirements and applications to aircraft weapon systems and telemetry [SAE AIR 1207] 18 p2692 A72-36529

Computer simulation of a digital satellite communications system utilizing TDMA and coherent quadriphase signalling. 21 p3020 A72-40895

A procedure for the design of asynchronous time division multiplexers. 21 p3021 A72-40909

Frame synchronization in time-multiplexed PCM telemetry with variable frame length. 23 p3265 A72-44182

Computer-aided binary code sequence selection for data acquisition system in PCM-TDMA satellite communication, evaluating performance and reliability 24 p3379 A72-44779

TIME FUNCTIONS

Parachute opening shock and filling time calculation based on aerodynamic drag, air mass and effective porosity time functions, using momentum and continuity equations 01 p0004 A72-10310

Discrete time systems unknown parameter identification, considering unified error function minimization approach 04 p0506 A72-15106

Weakly interacting waves Langevin equation in fluid, using characteristic functionals and time asymptotic methods 04 p0549 A72-15289

Kubo type time correlation formulas for incompressible heat conducting fluids turbulent transport coefficients, establishing relation to cascade and closure-of-hierarchy methods 06 p0801 A72-18173

Automatic zero suppression system for recording solar bursts time functions and data reduction without information loss 07 p0982 A72-19052

Generalized Navier-Stokes equations for incompressible turbulent flow time mean values, using nonlinear phenomenological theory 07 p0972 A72-20109

Mutually coupled continuous time orthogonal binary random processes, illustrating transition from discrete to exponential interval distribution 11 p1611 A72-26298

Nonlinear Boltzmann equation prediction of time correlation functions with long asymptotic time tails 15 p2278 A72-32307

Backward diffusion statistical properties in time for homogeneous unsheared stationary turbulent flow, using Eulerian velocity 15 p2218 A72-32402

Time domain analysis of long thin bar antenna response to gravitational signals, estimating sensitivity limit via noise background analysis 16 p2423 A72-33013

Time correlation functions for gases of linear molecules in a magnetic field. 17 p2589 A72-34894

Snap-off diodes for avalanche generators step pulse output rise time steepening, describing circuit diagram and time-volt-ampere characteristics 21 p3035 A72-41650

Time-periodic solutions of boundary layer equation systems 22 p3164 A72-41908

TIME LAG

Analog computer simulation of automatic control systems containing time delay element in feedback loop, evaluating errors 01 p0044 A72-10152

Decoder for delay-modulated digital data conversion to nonreturn to zero data, discussing time-phase ambiguity resolution capability in real time 01 p0025 A72-10331

Tropospheric effects on vhf satellite signal transmission noted from time lags between observed and calculated satellite rise time 01 p0027 A72-10409

Equatorial E region short wave oblique incidence propagation experiment showing transmitted impulse delay increase with frequency decrease 01 p0056 A72-10437

Smith method for radio wave propagation time lag calculation, assessing maximum error by comparing calculated with measured distance/frequency characteristics 01 p0028 A72-10617

High efficiency transferred electron microwave oscillators operated in short LSA mode, noting pulse-operated diode power appearance time delay behavior 01 p0036 A72-10634

Waveguide channel microwave bandpass filters for radio relay systems, discussing methods of improving group delay in passband and attenuation at harmonic frequencies 01 p0041 A72-10694

Semi-Markov process sojourn time within reducible subset of states, examining asymptotic behavior with algorithm developed for linear operators disturbances 01 p0094 A72-11265

Nonlinear systems absolute stability calculation, considering time lag, backlash type nonlinearity and process controller 02 p0196 A72-11674

Rigid plastic circular plate dynamic model with yield time delay, discussing residual deflection as function of load duration 02 p0293 A72-12426

Quenched and tempered high strength and maraging steels delayed failure properties from notched-tensile sustained-load tests in distilled water 02 p0246 A72-12560

Linear time optimal control system with retardations in controls, discussing controllability, existence and uniqueness, synthesis techniques and dynamic programming [AD-737927] 03 p0338 A72-13406

Loran C system time tick transmission delay during solar eclipse of 7 March 1970, discussing atmospheric electron density effects 03 p0322 A72-13533

Crab Nebula optical pulsar NP 0532 polarization minima delay mechanism, suggesting relativistic radiation from region orbiting relativistically around neutron star 03 p0434 A72-13553

Gas-liquid bipropellant rocket motor system instability boundaries under various operating and design conditions, interpreting experimental results via time lag model 03 p0406 A72-13632

Decoding technique for delay modulated digital data conversion to NRZ/c data, describing logic implementation and timing diagrams 04 p0486 A72-14490

Internal Q switching in CdS laser activated by exciton recombination, observing lag in emission onset after input pulses delivery 04 p0528 A72-14575

Shooting method and contraction mapping application to existence-uniqueness theorem derivation for numerical solution of second order delay differential equations boundary value problems 04 p0539 A72-15042

Linear feedback control systems with time lag, calculating integrated squared error by Liapunov function 04 p0506 A72-15110

Time delay effect on stability of viscoelastic cantilever column under retarded follower load 04 p0590 A72-15186

Variational theory for optimal relaxed control systems with time lag described by bounded uniformly continuous function defined on bounded closed sets 04 p0506 A72-15199

Stalled blade rows dynamic performance in terms of blade channel fluid inertia and surface boundary layer-caused time delay 05 p0602 A72-16487

Flash photolysis HF chemical laser pulse delay measurements, showing pressure, flash lamp intensity and optical cavity loss dependence 05 p0668 A72-16606

Additives effect on liquid hydrocarbon fuels ignition delay, testing peroxides, esters, polyethers and alcohols [AIAA PAPER 72-71] 05 p0703 A72-16958

Laser pulse induced stimulated Raman scattering /SRS/ in linearly dispersionless medium measuring delay between laser and Stokes pulse maxima by photon absorption fluorescence technique 05 p0693 A72-17170

Self induced transparency effect in ruby laser, investigating light transmission and pulse delay and broadening as function of input energy 05 p0670 A72-17171

Electric field rise times of first and subsequent lightning return strokes, discussing waveform oscillograms 06 p0841 A72-17822

Noise, delay and interruption caused communication degradation effects on feedback control system performance, considering air navigation and computer aided command and control on battlefield 06 p0794 A72-18242

Combined delay and loss common-control queueing system, obtaining stationary state loss and waiting probabilities and waiting time distribution function 06 p0794 A72-18243

Chemical reaction delayed effect on triple shock front confluence point trajectory in detonations, developing qualitative detonation cell model 06 p0904 A72-18530

Diffused failure model as basis for plotting delayed fracture curves in space of principal stresses 06 p0898 A72-18552

Stochastic optimal control for operations of plants with pure lag and two point estimate of performance index investigating systems stability 06 p0795 A72-18662

Phase lock loop receiving system digital simulation for estimating mean time to indicate lock and probability distribution function for wide SNR range 07 p0939 A72-19065

Steepened microwave bandpass filters with bypass and flattened reflection coefficient and delay, discussing design and implementation 07 p0954 A72-19175

First passage time boundary value problem for first order phase locked loop systems, determining probability density function of time to cycle-slip 07 p0959 A72-19273

Optimal control of lumped and distributed parameter systems with time lag, considering approach with extrapolator insertion and suboptimal solution based on system dynamic equation 07 p0962 A72-19718

Iteration procedure for approximate integration of nonlinear system of partial differential equations with time lag, presenting upper and lower estimates 07 p1028 A72-20209

Theorems for averaging of first order linear hyperbolic system with time lag, proving existence and uniqueness of solution to Cauchy problem 07 p1028 A72-20214

Cavity formation and drop transfer time correlation with welding current in powder covered /submerged/ arc welding, using high speed X ray photography 07 p0998 A72-20396

Kalman filter estimator for nonlinear human pilot model parameters including time delay 08 p1145 A72-20861

Iterative solution of Cauchy problem of partial differential equations nonlinear system with time lag, formulating uniqueness theorem 08 p1198 A72-20904

Krylov-Bogoliubov asymptotic method for oscillation analysis in time lag systems under pulse inputs 08 p1206 A72-20970

Self excited oscillations and transient responses of spacecraft stabilization relay system with delayed feedback, analyzing time delay effects in actuator circuit 08 p1241 A72-21170

Ignition time delay measurement between leading shock front and hydroxyl emission onset in two phase detonation of decane-oxygen 08 p1255 A72-22041

Fast IC signal delay time reduction by high packing density, discussing yield, power dissipation and cost problems 09 p1290 A72-22820

Stochastic approximation for identification of element with second order lag, noting convergence with optimum parameter

09 p1291 A72-23371

Aerodynamic lag effects on wing bending dynamic response at supersonic speeds, noting application to stress estimation under gust loads

11 p1572 A72-25922

Optimal control systems with time delays described by linear Volterra integral equations

11 p1677 A72-26090

Measuring information systems optimization, considering first order system with time lag

11 p1611 A72-26436

Self balanced microwave static calorimeter with substantial delay time, discussing system instability conditions

11 p1634 A72-26450

Ionospheric scattered wave propagation mode and weak echo delay explained by analysis-derived model

11 p1597 A72-26570

Geomagnetic activity index response time to fluctuations in interplanetary electric field azimuthal component, relating to magnetosphere average energy content

11 p1627 A72-26670

Wall effects on deflagration, combustion rate, and self and hot-point ignition temperature and delay

11 p1747 A72-26789

Electron density profiles calculation from ionograms, obtaining equivalent delay caused by ionization below minimum plasma frequency

12 p1802 A72-27307

Chebyshev phase and time delay approximations existence and characterization

12 p1836 A72-27572

Time delayed amplification effects in TEA carbon dioxide lasers, measuring gain decay times for various gas mixtures

12 p1823 A72-27753

Distant thunderstorm center location with VLF atmospherics, determining delay time difference of Fourier spectrum groups of 6 and 8 kHz

12 p1841 A72-27793

Shock heated methane-oxygen-argon mixtures ignition delay time from reaction kinetics calculations

12 p1778 A72-27852

Optoacoustic processing of large time-bandwidth signals, calculating insertion loss vs delay time

12 p1810 A72-27935

Second order systems time optimal control with delay, determining maximum number of switching points for control function

12 p1794 A72-28141

Solid propellants oscillatory burning with gas phase time lag, solving nonsteady governing differential equations by numerical integration

13 p2065 A72-29301

Thermospheric density-temperature time lag, considering two dimensional time dependent model based on UV heat input dynamic excitation

13 p1951 A72-29388

Target acquisition by systems with unlagged acceleration control or rate control with exponential time lag, discussing number of approach and control stick movements

13 p1911 A72-29819

TEA carbon dioxide laser time dependent gain and cavity losses analysis, using lasing onset delay with current pulse

14 p2109 A72-30184

Delay-lock discriminator to measure spatial delay time of noise-like signal received by two spaced antennas

14 p2088 A72-30336

Second order delay differential equations, investigating oscillatory behavior of stable and unstable equations solutions and nonoscillatory solution existence

15 p2264 A72-31765

Signal transmission through LSI logic circuit chains, discussing time delay measurement by step function testing

15 p2211 A72-31846

Whistlers nose frequency and minimum group time delay determined from model magnetosphere and from measurement, noting precision effect on electric field calculation accuracy

15 p2198 A72-31947

Time of delay signal information addition to OMEGA worldwide VLF navigation system by digital code applicable for clock resetting and timing for automatic data recording

15 p2199 A72-32077

Microwave propagation delay due to atmosphere in satellite-to-earth communication based on spherical smoothly varying model and geometrical optics techniques

15 p2200 A72-32102

Interplanetary magnetic field variations and auroral zone substorm activity observation, noting time delay between IMF southward turning and negative magnetic bay

16 p2451 A72-32974

Time delay measurements in the Athens /Greece/-Roma /Lesotho/ VHF trans-equatorial propagation circuit.

17 p2515 A72-34693

Onset of convection near a suddenly heated horizontal wire.

17 p2637 A72-35048

Controllability of linear continuous systems with a time-variable delay.

17 p2534 A72-35532

Optimal smoothing for continuous-time systems with multiple time delays.

17 p2534 A72-35536

Lyapunov functionals for a class of delay-differential systems.

18 p2709 A72-36052

Effective dimensional reduction in the computation of linear, discrete, time-delay problems.

18 p2672 A72-36302

On the apparent orbit of the Pulfrich pendulum.

18 p2653 A72-36608

Secondary ionization coefficients in a low-pressure discharge in mercury vapour.

19 p2836 A72-37459

Asymptotic series solution of optimal systems with small time-delay.

19 p2826 A72-38268

Automatically controlled delay in self-excited pulsating systems based on artificial muscles

19 p2761 A72-38464

Approximate integration of a nonlinear system of differential equations with time lag

19 p2827 A72-38468

Time characteristics of heterojunction injection lasers.

20 p2933 A72-39516

Best-fit estimate of relativistic effects in time-delay experiments.

20 p2972 A72-39871

Selection of an optimal control law for time-lag control systems subjected to random load disturbances

21 p3038 A72-40705

Atmospheric transmissivity in the 49- to 72-GHz band - Analysis and laboratory measurements.

21 p3021 A72-40906

Human or computer control role in teleoperator remote control mechanisms, discussing control modes, sensing and transmission time delay problems

21 p3011 A72-41416

Computerized supervisory control for interpretation of subgoal statements from human operator to permit teleoperator interaction with environment without long time delay

21 p3011 A72-41417

Extended Kalman filter application to delayed systems for state and time delay estimation, discussing two nonlinear estimators

[AIAA PAPER 72-902]

21 p3039 A72-41553

Type 4 decimetric, moving and quasi-stationary groups described in terms of onset time lags for different frequencies and components

21 p3101 A72-41763

A method of calculating the lag of the phase photoelectric installation of a time service

21 p3058 A72-41769

Optimal receivers for measuring time lags of pulse signals in the presence of fading

22 p3154 A72-42123

Optimal control of complex time lag systems with series connected lumped and distributed parameters described by linear differential equations

22 p3162 A72-42241

Flap-lag induced nonlinear oscillations in torsionally rigid helicopter blade, solving nonlinear equations of motion by multiple time scales asymptotic expansion [AIAA PAPER 72-956]

22 p3137 A72-42356

Uniform moving source radiated sound field from equivalent stationary source distribution via transformation based on retarded-time position and Doppler frequency shift

22 p3205 A72-42461

Linear multistep methods for a class of functional differential equations.

22 p3199 A72-42774

Optimal, on-line linear filtering with noisy, time-delayed observations.

23 p3276 A72-43855

Absolute accuracy of the pulse-echo overlap method and the pulse-superposition method for ultrasonic velocity.

23 p3313 A72-44114

Self ignition behaviour of some liquid fuels in an adiabatic compression machine.

23 p3325 A72-44252

Measurement of best time delay resolution obtainable along east-west and north-south ionospheric paths.

24 p3381 A72-45637

TIME LAPSE PHOTOGRAPHY

U CHRONOPHOTOGRAPHY

TIME MEASUREMENT

NT CLOCK PARADOX

Photoelectric and visual timings of occultations for lunar motions, comparing accuracy and systematic instrument errors

03 p0420 A72-13127

Temperature gradients measurements in transit-instrument pavilion and errors in time determination for two year period

03 p0361 A72-13822

Precision timekeeping, discussing atomic standards and Cs and Rb controlled molecular oscillators stability, cost and size

04 p0521 A72-14835

Hanle effect mean-life measurements on aligned Ar fast ion beam particles, comparing results with beam-foil measurement

04 p0552 A72-15151

Nitrogen to carbon dioxide vibrational energy transfer time measurement in gas dynamic laser

04 p0531 A72-15352

Scintillator crystal system with monitoring streak camera for flash X ray burst time measurements

04 p0523 A72-15482

Geophysical and gravimetric measurement time recording techniques, describing satellite tracking photochronograph and electronic printing chronographs

04 p0525 A72-15571

Transit instrument system year-to-year stability in astronomical time determination, considering seasonal wave causes and star coordinate errors

06 p0885 A72-18037

Noise contaminated pulse signal transit time measurement by receiver using digital filters

07 p0939 A72-19051

Uniform time systems relevance to precise astronomical observations and accurate determination of irregularities in earth rotation, outlining proposals for time signals

07 p1032 A72-19068

Coincidence model tests of photoperiodic time measurement relation to circadian system in moth *Pectinophora gossypiella*, using induction by skeleton photoperiods and light cycles

07 p0919 A72-19533

Unified time recording for aerial photographic surveys, using exact time synchronized control signal sequences in recording camera shutter release

07 p0988 A72-19893

Pulsar periods measurement with pulse arrival time calculation based on source position

07 p1080 A72-20052

Solar model inconsistencies, considering He and Fe abundances and solar age approximation

07 p1083 A72-20464

Gaussian noise quasi-optimal filtering in optical communication system, evaluating signal timing accuracy in detector-amplifier circuits

08 p1136 A72-21914

Eros and ATA /Air Transport Association/ time frequency collision avoidance systems, discussing synchronization methods, back-up mode operation, threat computation and displays

09 p1349 A72-22823

Time metrology achievements review, discussing time unit development, atomic and molecular frequency standards, atomic clocks, time scales and time signal broadcasting

10 p1481 A72-24399

Photographic observation of times of first and second contact and maximum phase for 15 February 1971 partial solar eclipse, discussing instruments and materials

11 p1717 A72-25903

Transit instrument system year-to-year stability in astronomical time determination, considering seasonal wave causes and star coordinate errors

11 p1719 A72-25973

Trajectory determination of supersessionally traveling object from shock arrival times observations at ground locations

11 p1617 A72-25994

Pneumatic thermistor transducer to measure steep ejection time interval between cardiac volume pulse upstroke start and maximum rise rate occurrence

11 p1588 A72-26633

Residence time of water vapor and aerosols in troposphere and lower stratosphere, noting application to air pollution buildup by aircraft

13 p1991 A72-28836

Earth-moon distance measurement by laser ranging methods, discussing retroreflectors, light collectors, time interval measuring devices and moon ranging stations

13 p2037 A72-28993

Solar eclipse timings by photoelectric, photographic and visual observation for comparison of Newcombe sun tables and improved lunar ephemeris reference systems

13 p2041 A72-29527

Electron beam excited P-15 phosphor 3900 A spectral component fast decay time measurement by delayed coincidence technique

13 p2000 A72-29762

GaAs doped Si light emitting diode as light source for optical timing system calibration, studying fast luminescent decay characteristics

13 p2000 A72-29763

Time data dissemination techniques, discussing astronomical and atomic time scales, frequency stan-

- dards, broadcasting and TV, navigation and satellite systems
14 p2085 A72-30364
- Laser radiation time characteristics measurement based on multiphoton processes in opposite light beams, estimating accuracy necessary for registration of ultrashort pulses
14 p2111 A72-30794
- Lunar laser ranging experiment single photon detection and nanosecond timing precision
15 p2233 A72-31530
- Signal transmission through LSI logic circuit chains, discussing time delay measurement by step function testing
15 p2211 A72-31846
- Time-frequency dissemination system design, discussing radio propagation, time signals, noise effects, synchronous satellite transponders and TV use, accuracy, geographical coverage and costs
15 p2198 A72-32065
- Precise time and frequency dissemination via Loran C navigation system, discussing user techniques, economics and radio propagation mode and terrain effects on accuracy
15 p2268 A72-32067
- VLF signal role in long range time dissemination, communication and navigation, comparing conventional and modern techniques with emphasis on OMEGA system accuracy
15 p2199 A72-32068
- Lunar radar measurement for remotely located clock time synchronization, discussing applications to deep space tracking, computer technique for time delay correction and accuracy
15 p2199 A72-32069
- Navy navigation satellite system, discussing time and frequency role, TIMATION satellite time standard and application for user equipment clock signal comparison
15 p2268 A72-32070
- Radio navigation satellite systems for ship and aircraft location determination, using time-frequency measurements
15 p2199 A72-32071
- Timing requirements in geodetic measurements with optical and electronic equipment, considering lunar laser ranging technique for high accuracy
15 p2229 A72-32075
- Time transfer measurement between two locations using nearly simultaneous reception times from optical pulsar signal transmission
15 p2199 A72-32076
- NASA global tracking network clock time synchronization to microseconds accuracy via GEOS-11 satellite
15 p2199 A72-32079
- ATS-3 C band dual transponders for geographically distant clocks time synchronization, using Cs clocks for accuracy verification
15 p2200 A72-32080
- Microwave diode switch operating at 35 GHz for spin lattice relaxation time measurement, discussing insertion loss, and rise and decay times characteristics
16 p2369 A72-33623
- Time delay measurements in the Athens/Greece/Roma/Lesotho/VHF trans-equatorial propagation circuit.
17 p2515 A72-34693
- Polymers ignition time measurement in cabinet with benzene flames and W filament lamps, noting black body radiation source absorptance and incident irradiance effects
17 p2636 A72-34719
- Measures of time in astronomy.
17 p2609 A72-35114
- Photographic observation of artificial earth satellites without the aid of time recording devices. II
17 p2517 A72-35384
- Monochromatic carbon dioxide TEA laser
17 p2564 A72-35424
- Around-the-world atomic clocks - Predicted relativistic time gains.
17 p2584 A72-35838
- Around-the-world atomic clocks - Observed relativistic time gains.
17 p2584 A72-35839
- Measurement of the characteristic times of detonation-wave formation in a tube filled with an acetylene-air mixture
18 p2676 A72-35999
- Dependence of the optical transfer function of a turbulent atmosphere on the averaging time
18 p2707 A72-36968
- Contact time determinations during 9 May 1970 Mercury passage across solar disk
19 p2864 A72-38327
- Determination of the time of hole formation in a metallic film under the action of single-pulse laser radiation
19 p2812 A72-38540
- Determination of systolic time intervals using the apex cardiogram and its first derivative.
19 p2759 A72-38817
- Operative memory mechanism as visual system neuron chain storage of stimuli from image recognition time measurements
20 p2891 A72-38936
- Harmonic frames of reference in Einstein's theory of gravitation
20 p2953 A72-39406
- Italian national time scale design and operation, discussing frequency standards, comparisons with national and international laboratories and time keeping
20 p2925 A72-39430
- Low cost design of linear pulse stretcher circuit for short duration pulse time measurement in nuclear instrumentation and computing counters
21 p3033 A72-40997
- A threshold device for establishing the time of pulsed signals
21 p3035 A72-41727
- Increasing the linearity of the time scale of a time-amplitude-code converter
21 p3035 A72-41728
- Analysis of the basic metrological characteristics of Vernier time-pulse converters
21 p3035 A72-41729
- An arrangement for studying the time characteristics of injection lasers
21 p3064 A72-41738
- A method of calculating the lag of the phase photoelectric installation of a time service
21 p3058 A72-41769
- Elimination of an ambiguity in the reading of digital computational devices
21 p3035 A72-41810
- Effect of fluorescence observation geometry on lifetime measurement, including the development of an approximation to the detector collection efficiency integral.
23 p3288 A72-43884
- Mathematical model for digit summation task search time distribution dependence on size of visual display with randomly arranged three digit numbers
24 p3374 A72-44558
- Observation error in time determination of solar limb contact with optical instrument hair, noting effect on accuracy of time and longitude measurement
24 p3438 A72-44859
- Nonlogarithmic calculation of chronometer corrections in azimuthal methods of determining time /Struve's method, Struve-Pavlov method, Dellen's method, and other methods/
24 p3438 A72-44864
- ## TIME MEASURING INSTRUMENTS
- NT ATOMIC CLOCKS
NT CHRONOMETERS
NT CLOCKS
NT TIMING DEVICES
- Delay-lock discriminator to measure spatial delay time of noise-like signal received by two spaced antennas
14 p2088 A72-30336
- Influence of instantaneous and prolonged pulses on the oscillations of timing-device oscillators
21 p3059 A72-41815
- ## TIME OF FLIGHT SPECTROMETERS
- Neutron production mechanism and energy spectrum in thermal plasma focus by time of flight spectrometry
01 p0109 A72-10243
- Time of flight mass spectrometers for plasmoids generated by theta pinch and discharge over organic glass, showing ion and electron currents oscillograms
02 p0223 A72-11420
- Microwave time of flight method for measuring electron drift velocity in GaAs semiconductors
12 p1855 A72-27667
- Time-of-flight measurements of molecular and atomic beams produced by cooled microwave discharge source, using hydrogen, helium, argon and nitrogen
16 p2430 A72-33061
- Aerodynamic coefficients determination from momentum and energy exchange between low velocity molecular jet and solid surfaces, describing time of flight measurement technique
16 p2390 A72-33069
- Particle trajectory and time of flight measurement in search for anti-alpha particles in primary cosmic radiation, using magnetic spectrometer with spark chambers
22 p3219 A72-42568
- ## TIME OPTIMAL CONTROL
- Time optimal phase locked AFC system synthesis based on Po ntryagin maximum principle, comparing computerized and experimental transient response
01 p0024 A72-10049
- Time optimal bang-bang response control of two pole single phase static inverter, giving output current transient response data
01 p0008 A72-11062
- Estimation and control relations separation for discrete time stochastic systems, considering assumptions on linearity, criteria, information pattern, constraints and noise distributions
01 p0047 A72-11306
- Self adjustment for time optimal nonstationary system control, developing algorithm for flutter
02 p0196 A72-11675
- Linear time optimal control system with retardations in controls, discussing controllability, existence and uniqueness, synthesis techniques and dynamic programming [AD-737927]
03 p0338 A72-13406
- Nonlinear programming iteration scheme for fuel-time optimization of satellite orbital rendezvous terminal phase
03 p0437 A72-13838
- Nuclear rocket time optimal start-up using distributed parameter system model with linear control and nonlinear state
04 p0547 A72-14672
- Hyperbolic and parabolic partial differential equations behavior comparison by studying point-to-point time optimal control for heat conduction and vibrating string motion
04 p0505 A72-14673
- Variational theory for optimal relaxed control systems with time lag described by bounded uniformly continuous function defined on bounded closed sets
04 p0506 A72-15199
- Minimal-time control of linear systems with energy constraints on input components, obtaining functional analysis solution by iterative method for nonlinear problem
05 p0639 A72-15802
- Optimal linear filtering for unmodeled time correlated driving disturbances of forcing function, applying to space navigation
05 p0685 A72-16461
- Time optimal control for pitch damping of gravity gradient stabilized satellite by mass distribution variation
05 p0727 A72-16465
- Time optimal and fuel optimal control of spin stabilized space vehicle for body-fixed and gimbaled jets, using maximum principle
05 p0728 A72-16476
- Optimal allocation and guidance for linear time varying interception and rendezvous problems of dynamic deterministic or stochastic systems
05 p0686 A72-16558
- Time optimal trajectory graphical construction procedure from energy state approximation as basis of computational algorithm for real time onboard flight optimization [AIAA PAPER 72-123]
05 p0688 A72-16968
- Time optimal control of system with distributed moments, deriving conditions for existence of fast response solution
05 p0683 A72-17134
- Optimal control synthesis for linear stochastic systems with random piecewise-continuous coefficients as function of time
05 p0683 A72-17139
- Nonlinear optimal control problems with undetermined final time, using conjugate-gradient method
06 p0792 A72-17312
- Game theory application to time optimal control strategy for independent operations set
06 p0794 A72-18168
- Multiplier method for discrete optimization problems with equality constraints, applying to time optimal control for V/STOL aircraft
06 p0794 A72-18387
- Resonant systems frequency characteristics measurement by sinusoidal input signal, determining optimal law of change in frequency scanning rate for minimal scan time
06 p0795 A72-18663
- Aircraft optimal control for case of continuous data flow on time variable flight conditions
07 p1032 A72-18979
- Linear plants time optimal control, deriving auxiliary equations system solution in accordance with Pontryagin maximum principle
07 p0959 A72-19127
- Singular surfaces for time optimal control in zero sum differential games between two aircraft in three dimensional space, assuming spherical acceleration vectorgram
07 p1027 A72-19279
- Quasi-time optimal nonlinear controller for steerable antennas or telescopes in target acquisition or slow mode, predicting performance by digital simulation
07 p0959 A72-19288
- Computer graphics system simulation of saccadic eye movement made for time optimal control behavior study, incorporating eye muscle characteristics
07 p0928 A72-19309
- Two-variable second order system for multivariable systems predictive control, deriving algorithm for near time optimal control
07 p0961 A72-19709
- Quasi-time optimal control synthesis of two-control variable system by equivalent switching signum function method
07 p0961 A72-19712

Algorithm for iterative computation of time and fuel optimal control functions for linear systems, presenting flow chart

07 p0962 A72-19714

Nonlinear multivariable system optimal control with respect to time and fuel consumption, discussing Gauss-Newton and Davidson methods and application to geostationary satellite

07 p0962 A72-19719

Nonlinear controls for single axis gyro platforms, using time optimal Luenberger observers

07 p0989 A72-20278

Time optimal self alignment of inertial platforms using gyros and accelerometers with Kalman-Bucy filter

07 p0989 A72-20279

Time optimal closed loop control system synthesis by phase space technique verifying results by state variable approach

07 p0964 A72-20595

Linear time optimal problem with analytical perturbations of initial conditions, determining optimal control switching points from convergent series representation

08 p1145 A72-21466

German monograph on optimal guidance of spin stabilized space bodies for combined attitude and angular velocity control and time optimal nutation damping

08 p1241 A72-21847

Mathematical models for hydraulic position servo, deriving time optimal controllers

08 p1113 A72-22156

Optimal estimates for nonlinear dynamic systems with time delay, using calculus of variations

10 p1454 A72-23784

Minimax feedback control of uncertain discrete time dynamic systems with set description, using dynamic programming

10 p1456 A72-23806

Time optimal control of distributed systems with random properties, considering n integral relations and flying wing vehicle torsional vibration problems

10 p1421 A72-24427

Terminal control solution in terms of finite dimensional minimization of convex function, applying to time optimal control and minimum energy problems

10 p1457 A72-24459

Time optimal control system for linear plant with transfer functions containing zeros

10 p1458 A72-24999

Regularization theorems for epsilon solutions to Bellman functions in optimal quick response problems

11 p1608 A72-25330

Minimum time thrust start-up of nuclear rocket as optimal control problem with integrodifferential constraints, using Pontryagin maximum principle and calculus of variations

11 p1685 A72-25870

Satellite circular orbit trajectory plane time optimal relocation, examining turn angle angular position and modulus of maximum lateral acceleration

11 p1718 A72-25928

Time optimal transfer trajectory in central Newtonian force field between two arbitrary points under jet acceleration

11 p1718 A72-25942

Optimal control systems with time delays described by linear Volterra integral equations

11 p1677 A72-26090

Second order systems time optimal control with delay, determining maximum number of switching points for control function

12 p1794 A72-28141

State space technique application to discrete linear control systems synthesis, discussing time-optimal and quadratic-cost problems, and pole assignment method

17 p2532 A72-34246

Maximum likelihood identification of time varying and random system parameters.

18 p2673 A72-36822

Switching curves and lobesweeping in origin seeking time optimal control for Duffing oscillator, using Pontryagin maximum principle

19 p2777 A72-37373

Optimality conditions for safe time in linear pursuit problems within n -dimensional Euclidean space

19 p2825 A72-37555

Isochronic corner generated difficulties avoidance in linear multivariable system minimum time controller, noting association with switchings

21 p3037 A72-40638

Unknown plant self organizing time optimal controller with variable switching surface and adaptation logic net, noting effectiveness by computer simulation

21 p3037 A72-40639

Perturbation guidance for minimum time flight paths of spacecraft.

[AIAA PAPER 72-915] 21 p3082 A72-41560

Second order optimality conditions for variable end time terminal control problems.

[AIAA PAPER 72-932] 21 p3039 A72-41571

Optimal control of the speed of a two-shaft helicopter turbine

23 p3326 A72-44278

Conditions for impulsive thrust-coast-thrust minimum-time, fixed-fuel transfers between coplanar orbits.

24 p3440 A72-45149

Modelled time optimal control process investigation for system with relay components, noting Hausdorff maximum principle application for optimal linear control

24 p3386 A72-45389

A near-time-optimal control circuit with a large number of relay elements

24 p3387 A72-45699

TIME RESPONSE

Random background noise effect on nonlinear self oscillation envelope passage time moments, discussing relationship between amplitude and frequency stabilities

01 p0035 A72-10032

Parachute inflation loads and times, presenting calculation method based on unsteady pressure distribution on decelerating inflating parabolic shell of revolution with unsteady starting vortex

01 p0004 A72-10311

Ribbon parachutes drop tests at Mach 0.57-1.70, measuring opening shock loads and functioning time sequence

01 p0004 A72-10312

Tropospheric effects on vhf satellite signal transmission noted from time lags between observed and calculated satellite rise time

01 p0027 A72-10409

Microwave oriented circuit analysis program /MODMAN/ to handle nonlinear, time-varying, lumped and distributed elements in time domain, using transmission line modeling algorithm

01 p0045 A72-10687

Radar backscatter time response waveforms for cube from If data and diffraction analysis

01 p0030 A72-10843

Burst and quasi-continuous forms atmospheric radio noise short term time characteristics above different thresholds, considering pulse duration and spacing

01 p0031 A72-10998

Laser pumped organic dye laser frequency-time characteristics, noting noncoincidence of amplification and photon density maxima

02 p0238 A72-12118

Time zone shift and p -chlorophenylalanine desynchronizing effects on sleep alteration and circadian rhythms in monkeys

03 p0318 A72-13071

Holographic optical techniques application to bulk magnetic storage for high information density and memory capacity and fast random access

03 p0361 A72-13776

Limiting approximation theorems for synthesis of linear circuits and signals in time-frequency domains

03 p0338 A72-13896

Pulsed injection laser current pulse height, width and rise time controls, comparing use of tube, transistor and SCR discharge circuits

04 p0528 A72-14420

Time domain analysis of wire antennas including straight, vee and zigzag dipoles

04 p0502 A72-15448

Three color optical pyrometer with microsecond resolution time based on three-wavelength double ratio method, displaying temperature/time relationship on cathode ray oscilloscope

04 p0522 A72-15476

Time optimal control of system with distributed moments, deriving conditions for existence of fast response solution

05 p0683 A72-17134

Gas jet control for spinning satellites attitude correction, deriving relations between satellite and control system parameters, response time and fuel consumption

05 p0731 A72-17196

Moderate power GaAs FET switching experiment, obtaining rise and fall times

07 p0952 A72-18826

Time behavior and spectra of relaxation oscillations in high gain IR xenon laser

07 p1001 A72-19199

Thin antenna hf time response from thin wire approximation and source gap model for integral equation solution

07 p0957 A72-19798

Conical foil radiation detectors sensitivity and time response, formulating time dependent thermal equations

08 p1166 A72-21433

Temperature controller with linear time variation for semiconductors thermally stimulated conductivity and thermoluminescence measurements at 90-300 K operating range

08 p1166 A72-21438

Temporal summation function form change during dark adaptation, noting relationship to change under other stimulus manipulations

09 p1269 A72-22616

Computer storage array of isolated electrodes imbedded between capacitor parallel plates, discussing

read-write cycle time, expected performance and experimental techniques

10 p1443 A72-23933

Response time and noise stability measurements of integrated circuit TTL /transistor-transistor logic/ and DTL /diode-transistor logic/ elements performing invert functions

10 p1449 A72-24286

Grid translation accelerator system for Kaufman ion thrusters beam deflection, noting response time and accelerated life tests

[AIAA PAPER 72-485] 11 p1710 A72-26211

Ideal low pass filter with fastest monotonic step response to permit no signal transmission outside prescribed frequency band

11 p1605 A72-26469

Continuous signal representations in time and frequency domains by Fourier series

12 p1783 A72-27628

Pressure effects on resonance fluorescence lifetimes in sulfur hexafluoride-air mixtures exposed to carbon dioxide laser radiation

12 p1826 A72-27929

Time response analysis for digital computer speed evaluation

13 p1925 A72-29270

Metal-dielectric-semiconductor junction transistor HF response analysis by digital computer, deriving switching time as function of impurity concentration and electrode voltage

13 p1932 A72-29294

Electron-optical parameters effect on GaP/Cs₃ dynode photomultiplier time response characteristics, describing computer simulation and pulse response measurement techniques

15 p2234 A72-31532

Carbon resistance thermometers time response and thermal diffusivity measurements in liquid helium temperature range

15 p2234 A72-31581

Nanosecond response magnetic probes to measure fast disturbances in oblique shock waves within collisionless plasma, describing experimental technique

15 p2235 A72-31646

Linear autonomous differential equations finite time stability theory, extending to systems driven by white noise

15 p2264 A72-31764

Limiting approximation theorems for synthesis of linear circuits and signals in time-frequency domains

15 p2212 A72-32707

Plasma electron density profile reflection coefficient frequency-dependent amplitude and phase determination by measuring time response to fast-rising voltage pulse

16 p2437 A72-33767

Hypoxia and peripheral visual stimulus position effects on response time during monitoring of centrally located stimulus light

16 p2357 A72-34095

Influence of carrier diffusion on the intrinsic response time of semiconductor avalanches.

18 p2717 A72-36083

Practical problems and solutions in modeling physical systems with time-domain input-output measurements or specifications.

18 p2663 A72-36327

Minority-carrier trapping and the luminescence time response of semiconductors.

19 p2844 A72-37946

Temperature-time characteristics of pulse-loaded temperature-measuring resistors

20 p2926 A72-39571

Response of linear periodically time varying systems to random excitation.

20 p2946 A72-39636

Isochronic corner generated difficulties avoidance in linear multivariable system minimum time controller, noting association with switchings

21 p3037 A72-40638

Synthesis of feedback systems with large plant ignorance for prescribed time-domain tolerances.

21 p3037 A72-40643

Frequency-sampling and transversal digital filter equalizers optimal design from specified unit impulse time response, using linear programming algorithm

21 p3033 A72-40900

Prediction displays based on the extrapolation method.

21 p3010 A72-41409

Thyristor I-V characteristics as function of voltage rise time, determining critical rate for given initial and final anode and cathode voltages

22 p3160 A72-43085

Computation of optimal parameter domains of components in the design of electronic circuits

23 p3268 A72-43440

TIME SERIES ANALYSIS

Digital computer techniques for randomly excited n -degrees of freedom structural system response by discrete time series with output covariance

06 p0895 A72-17857

Geomagnetic activity annual variations from daily international magnetic character figures analysis by

- time series numerical filter method, discussing sun-spot cycle effect
09 p1298 A72-22584
- Time series analysis of physiological and work study data in ATC tasks, using heart rate as strain indicator
09 p1271 A72-23137
- Running average method of data smoothing effect on persistence tendency change in meteorological time series
10 p1507 A72-25004
- Bandpass-filtered geophysical and meteorological time series data statistical evaluation by comparison with filtered test series with same variance and autocorrelation function
16 p2363 A72-33383
- Discrete frequencies search in time series via anharmonic frequency analysis, using integral transform
17 p2574 A72-34450
- Structure, analysis and synthesis of time series models, discussing kernel Hilbert space, spectral estimation, moving averages, identification, etc
18 p2678 A72-36023
- Upper atmospheric sodium and stratospheric warmings.
18 p2687 A72-36643
- Predictive filtering of multi-channel time series records with application to Doppler radar data.
19 p2781 A72-38272
- Time series analysis of meteoropathological disturbances of human regulation mechanisms, investigating annual variations of diurnal rhythms
22 p3147 A72-42977
- TIME SHARING**
- Symbol generation with black-and-white or color display devices and time shared computer for man-machine communication
01 p0034 A72-10484
- Time sharing three phase code transformation multitask effects on sustained performance
01 p0021 A72-11194
- Time shared performance test monitor function, operation and self repair of corporate fed array radars with computer control for long time internal reliability
03 p0321 A72-13165
- Hsu-Howe iterative hybrid method for partial differential equations solution by time sharing analog components, using dynamic scaling and incremental formulations for reduced sensitivity
04 p0495 A72-14418
- Time shared electronically patched hybrid computer for design automation, discussing remote terminal graphics capabilities and simulation language compiler
06 p0778 A72-17476
- Computer aided design in electronics, discussing interactive computing with time sharing teletype keyboards or CRT graphics and applications in IC, network analysis and optimization
06 p0780 A72-18236
- Time shared computer systems output maximization via degenerate exponential distribution function modeling, noting reducibility to Markov processes
11 p1601 A72-25900
- Time sharing radio communication system analysis with amplitude modulated carrier, noting power reduction, sideband content and multiplexing
15 p2201 A72-32566
- A time-sharing computer program for defining human thermal comfort conditions in any atmosphere. [ASME PAPER 72-ENAV-33]
20 p2905 A72-39142
- TIME SIGNALS**
- Frequency allocation for space research, radio astronomy, time signal and earth resources exploration, reviewing allowable power flux density and emitter power
02 p0177 A72-12386
- Wireless electronic time distributing system, investigating integrable digital receiver circuit and frequency bandwidths
02 p0197 A72-12696
- Loran C system time tick transmission delay during solar eclipse of 7 March 1970, discussing atmospheric electron density effects
03 p0322 A72-13533
- Uniform time systems relevance to precise astronomical observations and accurate determination of irregularities in earth rotation, outlining proposals for time signals
07 p1032 A72-19068
- Coordinated universal time system nature and consequences for international time signal users
07 p1032 A72-19069
- Unified time recording for aerial photographic surveys, using exact time synchronized control signal sequences in recording camera shutter release
07 p0988 A72-19893
- Time metrology achievements review, discussing time unit development, atomic and molecular frequency standards, atomic clocks, time scales and time signal broadcasting
10 p1481 A72-24399
- Photographic observation of satellites to sixth magnitude with K-24 aerial camera on Polaroid 3000 and
10,000 ASA film, recording time signals on magnetic tape
14 p2084 A72-30235
- Time data dissemination techniques, discussing astronomical and atomic time scales, frequency standards, broadcasting and TV, navigation and satellite systems
14 p2085 A72-30364
- Time-frequency dissemination system design, discussing radio propagation, time signals, noise effects, synchronous satellite transponders and TV use, accuracy, geographical coverage and costs
15 p2198 A72-32065
- VLF signal role in long range time dissemination, communication and navigation, comparing conventional and modern techniques with emphasis on OMEGA system accuracy
15 p2199 A72-32068
- Navy navigation satellite system, discussing time and frequency role, TIMATION satellite time standard and application for user equipment clock signal comparison
15 p2268 A72-32070
- Time of delay signal information addition to OMEGA worldwide VLF navigation system by digital code applicable for clock resetting and timing for automatic data recording
15 p2199 A72-32077
- Extractop model for time signal decoding for worldwide synchronization using Transit satellite system
15 p2199 A72-32078
- Discrete representation of continuous time signals and sequences by digital means, using frequency warping function
16 p2365 A72-33753
- Method and equipment for checking chronometers by one-second timing radio signals under field conditions
19 p2795 A72-37346
- Italian national time scale design and operation, discussing frequency standards, comparisons with national and international laboratories and time keeping
20 p2925 A72-39430
- The role of time/frequency in Navy navigation satellites.
22 p3202 A72-42749
- TIMERS**
- U TIMING DEVICES**
- TIMING**
- U TIME MEASUREMENT**
- TIMING DEVICES**
- Imperfect timing degradation of direct detection /noncoherent/ optical system using pulse position modulation bits
02 p0174 A72-12141
- Computerized bias optimization of telemetry timing accuracy applied to Minuteman system
02 p0174 A72-12144
- Aerodynamic compensation for ambient medium temperature effect on fluidic standard components and timing devices
04 p0466 A72-14993
- Satellite time-of-day code generator for data recording time identification, using ICs mounted on thick film multilayer printed ceramic substrates
07 p0944 A72-19605
- Unified time recording for aerial photographic surveys, using exact time synchronized control signal sequences in recording camera shutter release
07 p0988 A72-19893
- Gaussian noise quasi-optimal filtering in optical communication system, evaluating signal timing accuracy in detector-amplifier circuits
08 p1136 A72-21914
- Time resolution buffer for multichannel scaler, applying to digital signal averaging
11 p1632 A72-25701
- Narrow pulse optical communication digital systems with PPM and on-off keying, investigating timing error effects on bit error probabilities
11 p1592 A72-25885
- Earth stations synchronization to switched sequences of multiple access and cyclically interconnected multipot beam antennas satellite controlled by stable onboard clock
12 p1781 A72-27368
- Navy navigation satellite system, discussing time and frequency role, TIMATION satellite time standard and application for user equipment clock signal comparison
15 p2268 A72-32070
- Time/frequency technology application to reliable aircraft collision avoidance system, discussing precision time-ordered techniques, frequency control and synchronization and flying clocks
15 p2268 A72-32072
- Timing requirements in geodetic measurements with optical and electronic equipment, considering lunar laser ranging technique for high accuracy
15 p2229 A72-32075
- A method of realization of the functions of a program timer on a computer used in a spacecraft onboard equipment control system
17 p2522 A72-35028
- Book - Electromechanical system components.
20 p2890 A72-39811
- Symbol synchronization advances impact on PCM bit synchronizers design, discussing symbol detection and timing extraction circuits
22 p3155 A72-42706
- TIN**
- TIN ISOTOPES**
- Emitted phonon spectrum effects on detected signal response in superconducting Sn diodes, noting deviation from linearity
15 p2209 A72-32541
- Alpha stabilizing Al and Sn suppression effect on beta-omega transformation during Ti alloy hardening
22 p3189 A72-42278
- Influence of the properties of the materials on junction tunnelling characteristics.
22 p3214 A72-42454
- Magnetic flux penetration into superconducting thin films.
23 p3323 A72-43271
- Comparison of microwave-induced constant-voltage steps in Pb and Sn Josephson junctions.
23 p3323 A72-43272
- Changes in the grain-boundary free energy and the segregation of tin and antimony at grain boundaries in CrV steels
24 p3415 A72-45394
- TIN ALLOYS**
- Nb-Co-Sn and Nb-Ni-Sn ternary systems, investigating intermetallic compounds existence by X ray analysis
03 p0375 A72-13944
- Sn additions influence on Te structural characteristics relation to microhardness and current carrier mobility variations
09 p1322 A72-22204
- Calorimetric measurement of dissolution heat and partial enthalpy limit of Ga in Sn at 969 K
10 p1526 A72-24237
- Tensile strength, plastic properties and notch sensitivity from low temperature tests of binary Ti alloys, noting effects of Sn content and temperature
12 p1831 A72-28239
- Sn alloying effect on heat resistant Ni-Cr alloys plastic strain resistance and strength at room and high temperatures
14 p2114 A72-30274
- Phase equilibrium of Mg base solid solutions of Mg-Li-Sn system at 200-500 C, analyzing microstructure, microhardness and electrical resistivity
14 p2124 A72-31029
- Superlattice structure and electron correlation of Co-Sn system, using X ray and metallographic analyses
15 p2257 A72-32115
- Texture of Ti-Sn and Ti-Mn alloy specimens observed by X ray reflection technique after hot rolling, annealing and cold rolling
16 p2407 A72-33529
- Graphite content effect on vibration damping properties of Al-Sn and Al-Zn alloys
21 p3070 A72-41358
- Characteristics of superconducting niobium-tin alloys obtained by the vacuum evaporation method
22 p3192 A72-43013
- Effect of oxygen on the scale resistance of titanium-tin alloys
23 p3300 A72-43592
- Phase diagrams from X ray analysis of rapidly crystallized Ni-Sn alloys, noting crystal lattices and phase transformation
23 p3300 A72-43648
- TIN COMPOUNDS**
- NT NIOBIUM STANNIDES**
- NT TIN TELLURIDES**
- Influence of hydraulic extrusion on the composition and properties of the Nb3Sn compound
23 p3323 A72-43597
- TIN ISOTOPES**
- Neutron activation analysis of tin in geochemical and cosmochemical material, using 40 minute Sn-123.
20 p2900 A72-39843
- TIN TELLURIDES**
- Lead tin telluride photovoltaic p-n junction diode and lasers, discussing n-type layer fabrication by proton bombardment
10 p1450 A72-24552
- Tin lead telluride rock salt structure solid solutions phase stability at 356-500 C, using room temperature lattice parameter measurements
13 p1913 A72-29750
- Twinning faults in epitaxial films of germanium telluride and GeTe-SnTe alloys.
19 p2844 A72-37688
- Low capacitance high speed lead tin telluride photodiodes via liquid phase epitaxial growth, discussing frequency response to Nd:YAG and carbon dioxide lasers
22 p3159 A72-42620
- TIP DRIVEN ROTORS**
- Turboprop lift fan design developed for XV-5 VTOL research aircraft, reviewing changes for future commercial and research transport systems [ASME PAPER 72-GT-111]
11 p1576 A72-25674

TIP SPEED

High tip speed low loading transonic fan rotor design for weak oblique shocks with improved efficiency and stall margin
[AIAA PAPER 72-83] 07 p0907 A72-18951

TIP VORTICES

U TIP SPEED
U VORTICES

TIPS

NT BLADE TIPS
NT WING TIPS

Ultrasonic bonding tip design for densely wired electronic circuit boards, analyzing standing wave phenomena and resonant frequency
[SAE PAPER 710789] 01 p0074 A72-10279

TIRE AIRCRAFT TIRES

IR ray thermography, discussing application to tires testing and rubber manufacture 07 p0991 A72-20422

German monograph on tire rubber friction on dry and wet rough surfaces, taking into account loading, velocity and temperature effects 09 p1332 A72-22323

Drift angle effect on rolling wheel pneumatic tire lateral and angular deformation amplitudes, deriving formula for reaction forces 09 p1351 A72-23176

Test stand for rolling wheel with pneumatic tire at variable drift angles, deriving kinematic parameters and elasticity coefficients from static and dynamic tests 09 p1351 A72-23177

Two dimensional hydrodynamic flow analysis of pneumatic tire hydroplaning, taking into account tire deformation, viscous, inertial and turbulence effects 10 p1512 A72-24819

Mathematical two mass model for horizontal, angular and vertical vibrations of pneumatic wheel with allowance for inelastic tire resistance 13 p2003 A72-28918

Rolling radius of driven cylindrical wheel with solid rubber tire as function of normal load and tire dimensions 13 p2003 A72-28919

Rolling tire frequency response for angular oscillations about vertical axis through axle in wheel plane, using point contact theory 16 p2426 A72-33696

TIROS SATELLITES

Improved Tiros operational satellite visual and IR scanning radiometer data processing for polar and mercator map projection 02 p0173 A72-12127

Computer simulation prediction program for attitude disturbance torques for Tiros series spacecraft rotational motion control 07 p1086 A72-20361

Polar orbiting operational weather satellites. 24 p3451 A72-45197

TISSUES (BIOLOGY)

NT ENDOTHELIUM
NT EPICARDIUM
NT EPITHELIUM
NT NEUROGLIA

Bone tissue elastic behavior based on Voigt model of two phase composite material, using ultrasonically determined hydroxyapatite elastic moduli 01 p0136 A72-10112

Linear energy transfer distribution for negative pions beams in human tissue, calculating relative biological efficiency and oxygen enhancement ratio [CERN-71-16] 02 p0162 A72-12064

Epinephrine and norepinephrine effects on cerebral blood circulation volume and oxygen tension in tissues 02 p0165 A72-12517

Primary cosmic ray interaction with tissues, emphasizing biological effects and nuclear reactions induced radioactivity in astronaut body 03 p0313 A72-12911

Proliferative blood forming tissue activity under chronic gamma ray irradiation in guinea pigs by quantitative methods, showing myeloid and reticular disturbances of bone marrow 04 p0467 A72-14607

Neural tissues excitability relationship to precerebral organization, considering polyphosphate distribution in vertebrate tissues 04 p0470 A72-14789

Biological tissue heat transport dimensionless parameters for steady state and transient analysis of homeotherm thermoregulation 04 p0472 A72-14864

Immobilization hypercalciuria, discussing treatment by diet-induced extracellular volume depletion and possible pathophysiologic mechanism of intercompartmental fluid and electrolyte shift 04 p0479 A72-14871

Analytical model for living biological tissue transient heat transfer, taking into account conduction, storage, generation, convection and blood flow effects [ASME PAPER 71-WA/HT-36] 05 p0620 A72-15887

Rat tissue autolysis rate during hypokinesia, discussing relation to free amino acid background changes 05 p0619 A72-16648

Mathematical-physical model for laser pulsed radiation-induced pressure wave transmission through surface and internal biological tissues 06 p0768 A72-18150

Tobacco tissue cultures with Apollo 12 lunar material, determining endogenous sterols and fatty acids concentrations by gas chromatography and mass spectrometry 07 p0920 A72-19850

Uric acid to urea nitrogen ratio as assay test for identification of avian tissue in verifying bird ingestion or impact as aircraft accident cause [AD-737855] 07 p0922 A72-20184

Radial diffusion and convection capillary model for analysis of tissue protein concentration and colloidal osmotic pressure changes during transcapillary fluid movement 08 p1114 A72-20896

Virulike particles in salivary glands, muscles and nerves of normal and gamma irradiated *Drosophila melanogaster*, showing age dependent infection 08 p1116 A72-21198

Respiration control by extracellular pH in medullary tissue, studying chemoreceptor response to hydrogen ion concentration in cat cerebrospinal fluid 11 p1579 A72-26661

Liver and muscle type isozymes of DPN-linked glycerol-3-P dehydrogenase in chickens in terms of tissue distribution, ontogeny and avian evolution 12 p1759 A72-27161

Apollo 12 material effect on tobacco tissue cultures, noting pigment increase 12 p1761 A72-27626

Two stage description of middle germ layer chronic polyarthritis, noting heart muscle and vascular wall tissues necrosis 12 p1772 A72-27822

Cold adaptation effects on rat skeletal muscle tissue Vant-Hoff coefficient, considering phosphorylation and oxidation rate, P/O and mitochondrial ATP-ase activity 13 p1902 A72-28639

Radioprotectants/mexamine and cystamine/ effects on histo-hematic barrier permeability in rats under hypokinetic conditions 13 p1904 A72-29308

Six day bed rest effect on external respiration and subcutaneous tissue oxygen metabolism, noting oxygen consumption decline 13 p1905 A72-29324

High temperature environment effects on rat organ and muscle tissue respiration, discussing temperature homeostasis maintenance 13 p1905 A72-29331

Macaca nemestrina monkey organ tissue concentrations of lactic dehydrogenase (LDH), creatine phosphokinase and aldolase, with electrophoretic determination of LDH isozymes 13 p1906 A72-29861

Aluminum oxide chromatography for ethanol-amine acetyl derivatives detection and separation in animal tissue extracts, using water-butanol solution as solvent 14 p2077 A72-30972

Enzyme activity and ascorbic acid concentration as index of rat thyroid gland tissue functional activity during hyperthermia 14 p2077 A72-31098

Effect of Acetazolamide/Diamox at different dose levels on survival time of rats under acute hypoxia and on Na⁺/+K⁺/-ATP-ase activity of rat tissue microsomes. 17 p2499 A72-34546

Magnetic field effects in enzymes, tissue respiration and some metabolism characteristics of an intact organism 17 p2503 A72-35003

New data on physiological adaptations to arid zones 17 p2504 A72-35021

Fluid transfer between blood and tissues during exercise. 18 p2650 A72-36560

Dynamics of dissolution of gas bubbles or pockets in tissues. 18 p2655 A72-37027

Calcium metabolism conditions in calcified tissues of rats during a lasting hypodynamia and thyrocalcitonin administration 21 p2997 A72-40432

Cortico-visceral studies of spinal cord reticular formation stimulation and destruction effects on electroencephalogram, cardiac activity and interoceptive glycemic reflexes 21 p3000 A72-40757

Local necrosis, parenchyma incisions and vascularization of rabbit liver tissue under pulsed and continuous laser beams 21 p3002 A72-40991

Control of the circulating blood mass in the case of a functional detachment of various amounts of pulmonary tissue 21 p3012 A72-41825

Lysosomal enzymes of eye tissues during the action of hydrocortisone 22 p3141 A72-42275

Mechanism of adaptation to hypoxic hypoxia 23 p3255 A72-43907

The state of water in muscle tissue as determined by proton nuclear magnetic resonance. 24 p3371 A72-44774

TITAN

The bulk composition of Titan's atmosphere. 17 p2606 A72-34541

Titan and its atmosphere. 18 p2729 A72-36985

TITAN 3 LAUNCH VEHICLE

Hybrid computer simulation program used in development and software design validation of digital flight control system for Titan 3C space booster 02 p0186 A72-11655

Titan 3 family systems analysis for delivering multiple communication satellites to geostationary orbits [AIAA PAPER 72-570] 12 p1870 A72-27378

TITANATES

NT BARIUM TITANATES
NT ILMENITE

NT PEROVSKITES
NT STRONTIUM TITANATES

Inorganic single crystal titanate whisker fibers with high modulus strength for plastic reinforcement, noting mechanical, thermal and physical properties 08 p1193 A72-21685

TITANIUM

NT TITANIUM ISOTOPIES

Ti powder technology, discussing pressed and sintered parts, forging and extrusion preforms and composites 02 p0233 A72-11437

Allotropic transformations and recrystallization by precipitation hardening in pure Ti crystals, using field emission microscopy 02 p0242 A72-12007

Titanium melting, casting and molding techniques, discussing shapes, sizes and physical properties 03 p0370 A72-13104

Electrochemical crevice corrosion process of Ti in hot concentrated chloride solution, discussing temperature, set potential and surface treatment 03 p0374 A72-13714

Ultrasonic fatigue at small strain amplitudes in Ti developing solitary slip band microcracks 04 p0533 A72-14544

Ti anodic behavior in anhydrous liquid ammonia, noting oxidation by halogen intermediary 04 p0484 A72-14954

Ti leaching from granitic rocks by Penicillium, simplicissimum, discussing extraterrestrial life detection 05 p0616 A72-15805

Etch pit technique for titanium and zirconium crystal orientation determination, discussing etch pit locations and polycrystalline specimen goniometric observation 05 p0679 A72-17124

Temperature effects on anodic polarization of Ti open surface and corrosion crevices, discussing critical potential relation to pitting 06 p0829 A72-17944

Dynamic strain aging significance in titanium, observing reduction of temperature and strain rate effects on stress-strain curves shapes 06 p0830 A72-18054

Titanium powder metallurgy in ordnance applications, discussing hardware, weight economies and market development 06 p0822 A72-18074

Slip band formation and crack initiation in Ti as a function of cyclic loading frequency, considering plastic strain amplitude or distribution as causes [DFVLR-SONDDR-149] 06 p0832 A72-18424

Electroconductivity, thermal conductivity and diffusivity, specific heat and emissivities of Ti at 1000-1700 K 07 p1010 A72-18934

Alpha iron lattice dilation by titanium, measuring densities and lattice parameters 07 p1016 A72-19944

Optimum exposure time for sintering in Ar flow of porous rolled product of Ti powders determined from physicomaterial properties changes 07 p0996 A72-19964

Ti structures controlled path resistance welding, discussing welded joints metallographic and mechanical properties 07 p0996 A72-19994

Maximum allowable time between Ti metal surface preparation and agent application in adhesive bonding 07 p1024 A72-20254

Ti honeycomb brazing, discussing filler metals, furnace temperature and atmosphere control and use of protected graphite as furnace material 07 p0998 A72-20284

Alpha Ti plastic deformation behavior below 700 K determining activation area and enthalpy as function of stress and temperature 08 p1186 A72-21244

Ti crystallographic and topographical feature determination by hydrogen-ion microscopy, noting 08 p1186 A72-21244

- temperature effects on surface films and low index facets production 09 p1327 A72-22805
- Diffusion coefficient and distribution of Ti atoms in thin Al film from electric current vs time curves for oxidation of solid solution 09 p1329 A72-23036
- Interdiffusion of tight contact welded ring Ti-W pairs at high temperature, using X ray analysis and electron beam techniques 10 p1497 A72-24785
- Boron-epoxy reinforced Ti tubular truss for application to space shuttle booster thrust structure, evaluating performance [AIAA PAPER 72-393] 11 p1730 A72-25414
- Elastic r-value variation in Ti sheet from direct measurement of width and thickness strains 11 p1659 A72-25895
- Dislocation structure and strength of Ti at low and intermediate temperatures, investigating strain, grain size and interstitial solute hardening 11 p1666 A72-26927
- High temperature low pressure reaction kinetics of nitrogen sorption by titanium foil, using ultrahigh vacuum microbalance 12 p1777 A72-27045
- Low pressure hydrogen and titanium thin film reaction rate measurement, using flow technique 12 p1778 A72-27046
- Polycrystalline alpha Ti work hardening at low temperatures and different purities, discussing plastic strain effects 13 p1975 A72-28671
- Temperature dependent optical constants of Ti and W crystal surfaces cleaned by ion bombardment in ultrahigh vacuum 15 p2274 A72-31376
- Low energy X ray measurements with sealed Ti window proportional counter, applying to rocket observation of Sco X-1 15 p2240 A72-32438
- K line of X ray absorption spectra for pure Ti and compounds, discussing effects of valence, microstructure and electron configuration 15 p2259 A72-32700
- Stress-strain diagrams for constant strain rates in shear of Ti from torsion test machine, deriving constitutive equation for dynamic overstress 16 p2405 A72-33197
- Ti comparison with Al for effects on Fe alloy deformation and fracture, discussing intergranular failure suppression 16 p2411 A72-33823
- Cs adsorption on W and Ti observed by combination of ellipsometry, Auger spectroscopy and surface potential difference measurements, noting sticking coefficient and coverage 16 p2442 A72-33833
- Weibull life tests of Kemet solid tantalum chip capacitors at high accelerated voltages. 17 p2527 A72-34685
- Study of vacuum furnace atmospheres for brazing titanium honeycomb panels. 17 p2560 A72-34940
- Ways of reducing porosity in argon-arc welding of thin titanium sheets. 18 p2695 A72-36428
- Characterization of commercial titanium powders. 19 p2815 A72-37595
- Grain size distribution in recrystallized alpha-titanium. 19 p2820 A72-38297
- Thermal and athermal components of the flow stress in zone-refined titanium. 19 p2820 A72-38298
- Study of titanium and titanium oxide structures corresponding to different kinetics of oxidation obtained at 850 C 20 p2936 A72-39206
- Mechanical properties improvement of Al alloys for machine construction applications, suggesting Ti, Zr and Be additions optimal rate 20 p2941 A72-39577
- Effect of chloride on the anodic dissolution of titanium in methanolic solutions. 21 p3013 A72-40842
- Ti fabrication advances in forging, diffusion bonding, hot forming, chemical milling and laser cutting 21 p3061 A72-41335
- Mechanical properties of titanium strengthened by monodirectional molybdenum wires 21 p3069 A72-41354
- Nickel-titanium intermetallic phase effect on recrystallization of dispersion hardening high melting point steel during furnace and induction heating 21 p3071 A72-41789
- Modified Gilman equation relating dislocation velocity to applied effective stress shown in agreement with stress relaxation experiments on Ti 22 p3189 A72-42436
- Stress amplitude and hysteresis loop width changes in alpha Ti during cyclic work softening-work hardening with constant strain amplitude 22 p3189 A72-42438
- Recrystallization and grain growth in titanium. I - Characterization of the structure. 22 p3193 A72-43032
- Electron paramagnetic resonance hyperfine spectral observation of double quantum transitions of Ti positive ions in strontium chloride single cubic crystal host 24 p3378 A72-45311
- ### TITANIUM ALLOYS
- Thermal conductivity, electrical resistivity, Lorentz ratio and thermopower of Ti, Al and Ni alloys for aerospace structures over 4-300 K range 01 p0113 A72-10173
- Ti alloys omega phase transformations by cryogenic cooling of bcc beta phase, interpreting electron diffraction pattern change in terms of displacement type reactions 01 p0082 A72-10204
- Oxygen effect on dynamic elastic modulus of titanium-oxygen alloys by density and longitudinal ultrasonic wave velocity measurements 01 p0083 A72-10393
- Titanium alloys and superalloys selection for elevated temperature use on space shuttle 01 p0084 A72-10743
- Constant high tensile stress and rapid aerodynamic heating effect on maraging steels and Ti and Al alloys, evaluating test and simulation procedures for design data development 01 p0084 A72-10749
- Electrochemical potential microstructure and stress intensity factor effect on aqueous stress corrosion crack propagation rate in high strength Ti alloy 01 p0085 A72-10776
- Ti alloy honeycomb core sandwich panels fabricated by brazing or spot diffusion bonding, investigating elevated temperature effects on mechanical properties [ASM PAPER W 71-23.3] 01 p0086 A72-10875
- Continuous seam diffusion bonding application to Ti and superalloys lap, butt and T joints production [SME PAPER AD 71-264] 01 p0076 A72-10970
- Steel and Ti-Al-V alloy surface integrity during various machining methods, considering microstructures, residual stress profiles and fatigue characteristics [SME PAPER IQ 71-237] 01 p0076 A72-10972
- Ni, Fe and Ti alloys creep rupture characteristics in high temperature, high pressure gaseous hydrogen and helium 01 p0086 A72-10979
- Stress effects on TiNi compound martensitic transformation, investigating deformation as function of composition and heat treatment 01 p0087 A72-11023
- Hexagonal close packed Ti-Al alloys, determining stacking fault probability with X ray powder diffraction line profiles and Fourier analysis 01 p0087 A72-11029
- Ti-Al-V alloy under vacuum fatigue tests, examining temperature and chemical environment effects on fatigue crack growth 01 p0087 A72-11034
- Breakdown surfaces of thin Ti alloy specimens under tension as function of composition and heat treatment temperature 01 p0088 A72-11079
- Gas saturated surface layer deformation in rolled Ti alloys as function of specimen thickness reduction 01 p0077 A72-11080
- High strength Ti alloy development, composition modifications, physical and mechanical properties, ingot, heat treatment and fatigue crack evaluation 01 p0088 A72-11100
- Phase oriented precipitation patterns of Ti in Ti-C-O system, discussing composition independence and dislocation networks 01 p0089 A72-11184
- Ti-Al-V alloy powders electrically activated pressure sintering /spark sintering/, considering mechanical properties and economic factors 02 p0240 A72-11428
- Hot pressed Ti alloy powders, evaluating strength and toughness at cryogenic temperatures 02 p0240 A72-11439
- Atomic structural mechanism of solid solution decomposition by nucleation and equilibrium phase particles in Fe-Co-Ti alloy, using X ray analysis and transmission microscopy 02 p0242 A72-12008
- Ti-Nd and Ti-Nd-Al alloys heat treatment effects on tensile and bending strengths 02 p0244 A72-12245
- Ti-Al-Mo alloys thermomechanical treatment, investigating alloy composition effects on hardening 02 p0244 A72-12246
- VT22 high strength Ti alloy beta phase decomposition kinetics studies under heat treatment, noting omega and alpha phases role for low plasticity 02 p0244 A72-12247
- Heat treatment, quenching and aging caused metastable and stable alpha and beta structures effects on nitrogen diffusion rate in Ti alloy during nitriding 02 p0244 A72-12248
- VT3-1 Ti alloy with Al, Mo, Cr and Fe additives, investigating ductile type fracture after heat treatment by electron microscopy and tensile tests 02 p0244 A72-12249
- Hydrogen diffusivity and solubility in alpha-Ti alloys, considering absorption effect on stress corrosion cracking 02 p0244 A72-12481
- Ti-Cr alloys omega phase formation by measurements of hardness, Young modulus and internal friction 02 p0246 A72-12672
- Pressure induced b band deformation effect on magnetic susceptibility of Ti-V and V-Cr alloys 03 p0370 A72-13087
- Plane strain fracture toughness of notched high strength Al and Ti alloys at low temperatures 03 p0371 A72-13464
- Residual stress formation mechanism in two phase Ti alloys under cutting and plastic deformation, showing phase transformation composition and structure effects 03 p0363 A72-13467
- Beta structure effect on cyclic fatigue strength in Ti alloy under various heat treatments 03 p0372 A72-13595
- Scale factor and surface imbedded inserts effect on bending cyclic fatigue strength of nonhardened and roll hardened Al-Ti alloy 03 p0372 A72-13596
- Ti alloys for airframe shell construction based on room temperature strength, stiffness and densities comparison with Al alloys, stainless steel and Be data 03 p0372 A72-13615
- Ti alloys for aircraft structures, emphasizing weldability, tensile fatigue and residual strengths, shear-carrying qualities and fuselage shell design 03 p0373 A72-13616
- High strength Ti alloys for aircraft accessories structural materials, comparing room temperature physical properties of ultrahigh tensile steels and other alloys 03 p0373 A72-13617
- Ti effects on aircraft equipment design, considering use of Ni plated brake cylinder, wheel, engine control rams, tie bolts and rings 03 p0373 A72-13618
- Heat treated microstructures relation to equilibrium diagram in beta and alpha Ti alloys 03 p0374 A72-13715
- Silicide precipitation in Ti-Zr-Al-Si system, discussing microstructure correlation with mechanical properties 03 p0374 A72-13927
- Dilatometric investigation of martensitic transformation in TiNi compound, observing plastic memory effect 03 p0377 A72-14021
- Ti-Al-V room temperature creep, considering tensile and torsional loading, plastic deformation, stress relief and design limitations 03 p0377 A72-14171
- Forging techniques and applications for VF-12A aircraft Ti alloy bulkhead production, considering diffusion bonding and die shimming 04 p0527 A72-14914
- Nb-Ti alloy critical current density increase dependence on temperature, discussing evidence supporting rigidly pinned vortex lattice model 04 p0562 A72-15292
- Ti-Al-Mo-V alloy sustained load stress corrosion crack growth in salt and distilled water environments 04 p0534 A72-15570
- X ray spectral analysis of microchemical changes in surface films of titanium alloys during diffusive interaction with silicon carbide abrasive 04 p0534 A72-15654
- Titanium alloy microstructure effect on fatigue strength under symmetric bending load cycles in air and NaCl solution 04 p0535 A72-15663
- Stress corrosion crack tip electrochemical reactions simulation on Ti and alloy surfaces, using modified rotating disk apparatus with pH measurement 04 p0536 A72-15739
- Bend tests for minimum radius/thickness ratio of Ti and Be alloy sheets in pressurized fluid [ASME PAPER 71-WA/PT-8] 05 p0671 A72-15913
- Hardening of Fe-Mn-Ti ferritic and martensitic alloys, investigating microstructure and mechanical properties 05 p0672 A72-16144
- Transformations of Ti alloy in isothermal conditions, observing hardening and loss of ductility 05 p0673 A72-16149
- Ti alloys evaluation technique of arc melting, processing and testing of miniature ingots, discussing alloying and microstructural effects and correlation with plate properties 05 p0674 A72-16390
- Face-centered orthorhombic martensite in Ti-V alloy, determining axial ratios and lattice parameters by transmission electron microscopy and X ray diffraction 05 p0676 A72-17102

Hydrogen environment effects on fatigue crack growth rates in Ti-Al-V weldments over low ambient temperature range

05 p0678 A72-17116

Dynamic yielding of annealed and cold worked Fe-Ti alloy determined in shock compression tests

05 p0679 A72-17121

Critique of microstructure effect on strength, toughness and stress corrosion cracking susceptibility of metastable beta titanium alloy, discussing recrystallization conditions

05 p0679 A72-17122

Low temperature tensile strength and plasticity of Ti alloys containing zirconium

05 p0679 A72-17203

Superplasticity relation to heat resistance in metal systems Ni-Cr, Ni-Cr-W-Ti-Al and Ti-Si

05 p0680 A72-17212

Crystal structures and martensitic transformation mechanism of TiNi, using X ray diffraction and electrical resistivity measurements

06 p0827 A72-17421

Ti-Zr-O ternary alloys radiocrystallographic analysis, relating microstructure to composition and thermal treatment

06 p0827 A72-17569

Ti-Ni-Cu and Ti-Zr-Be alloys for brazing Ti heat exchangers, discussing flow characteristics and corrosion resistance

06 p0820 A72-17703

Al and Ti alloy fatigue after temperature reduction to 253, 77 and 4 K as function of surface purity after machining

06 p0831 A72-18356

Hydraulic sand blasting and annealing effects on Ti alloy sheet bending fatigue strength

06 p0831 A72-18357

V and Al addition effects on mechanical properties of oxygen rich Ti alloys

06 p0831 A72-18358

Hot pressing /extrusion/ of rods from metal-ceramic Ti, using pure and cermet powders with tungsten carbide

06 p0822 A72-18426

Titanium alloy durability under cyclic torsion in vacuum at various temperatures, investigating fatigue life and tensile strength

06 p0834 A72-18665

Unidirectionally and cross rolled Ti alloys elastic properties anisotropy during cooling, discussing Young modulus distribution

06 p0834 A72-18666

Sheet metal fatigue test method for transverse 100-1000 Hz bending at normal and high temperatures, applying to 1.5 mm Ti alloy sheet

06 p0900 A72-18671

Ti influence on ductility of normalized low alloy steel, considering crack initiation and propagation

06 p0834 A72-18687

Aging kinetics in Co-Ni-Ti alloys, noting three dimensional periodically modulated structure development

06 p0834 A72-18742

Hardening phases effect on plastic deformation resistance of Ti and Ti alloys

06 p0835 A72-18746

Monograph on diffusion couple technique for Ti-Al system interdiffusion phenomena, discussing layer growth, phase development, grain boundary diffusion mechanism, mass transport, etc.

07 p1011 A72-19267

Ti-Al-V alloy biaxial yield strength improvement by combined texture and age hardening, using hydroburst tests

07 p1011 A72-19482

Cu contents effect on Ti-Cu alloys physical and mechanical properties, discussing beta phase decomposition during annealing

07 p1012 A72-19574

Gas saturation of Ti alloy in air and vacuum at 750-1050 °C for 1-6 hr, discussing surface layer microstructure change after heat treatment

07 p1013 A72-19742

Phase and microstructure changes during nitriding process of Fe-Ti alloys, stressing Ti concentration effect

07 p1013 A72-19749

Cast and wrought Ti alloys Ar arc weldments microstructural and mechanical properties after different heat treatment sequences

07 p1013 A72-19750

High temperature strengthening of vacuum melted W-Ti alloys with Mo and Zr additions

07 p1014 A72-19843

Deformation rate and temperature effects on optimum strength and ductility of die forged and extruded Mo-Ti alloys

07 p1014 A72-19845

Environmental hydrogen embrittlement of Ti-Al alloy as function of test displacement rate and microstructure variation

07 p1016 A72-19933

Alloying additives effects on Ti and Zr resistivity, thermal expansion, crystal lattice parameters and polymorphous transformations temperatures

07 p1017 A72-19990

Gas quenching technique for vacuum brazing of Al, Ti and ferrous alloys, evaluating mechanical properties, surface contamination and He leak tightness

07 p0997 A72-19997

Al, Ti and ferrous alloys suitability for vacuum brazing-gas quenching processing for He leak-tight joints, using photomicrography

07 p0997 A72-19999

Solid solution yield strengthening and weakening of V-Ti alloys, investigating strain rate sensitivity temperature dependence as indication of two deformation mechanisms

07 p1021 A72-20434

Heat treatment, water quenching and aging effects on Ti-V alloys hardening and structural properties, discussing omega phase formation

07 p1023 A72-20667

Critical supercurrents in heat treated and cold worked Nb-Ti wires, proposing pinning model based on enhancement of Ginzburg-Landau parameter in cell walls

08 p1186 A72-21594

Composite processing, adhesive formulary, bonding processes and mechanical properties of low void content autoclave molded polyimide graphite composite stiffened titanium alloy structures

08 p1193 A72-21687

Mechanical surface strengthening effect on small cycle fatigue life of Ti alloy weakened by stress raiser

08 p1186 A72-21725

Ti-Co intermediate phase transformations discussing lattice formation, intermetallics melting points and stoichiometric composition

08 p1187 A72-21783

Ti-Ce-S alloys phase equilibria with isothermal cross section, discussing eutectic alloys anomalous structure and cerium monosulfide preparation method

08 p1187 A72-21784

Ti-alloyed SiC based material microstructure investigation by X ray metallography, optical and electron microscopy

08 p1188 A72-22099

Titanium-boron-epoxy composite materials selection and fracture mechanics criteria for B-1 bomber structural design

09 p1317 A72-22477

Soviet monograph on thermoplastic hardening of high strength martensitic steels and Ti alloys by ordering dislocation structure

09 p1327 A72-22520

Microstructural transformations in preaged Ti alloys with unstable beta phase under external tensile stresses

09 p1328 A72-23032

X ray spectral analysis of Ti-Cu alloys electronic structure

09 p1329 A72-23043

Wear resistance of steel and Ti alloys in free abrasive gas jet, noting surface microhardness increase effect

09 p1319 A72-23188

Parabolic oxidation kinetics of Ni-Ti alloy compound at elevated temperatures

09 p1330 A72-23358

Order-disorder transition in metastable splat cooled Ti rich Ti-Fe alloys from phase formation, constitution and crystal chemistry viewpoint

09 p1330 A72-23378

Beta-III Ti alloy mechanical properties dependence on heat treatment and elevated temperature exposure, illustrating associated microstructures

09 p1331 A72-23384

Ion and laser microprobes for concentration measurements of hot salt stress corrosion produced hydrogen on Ti alloy on microscopic scale

09 p1276 A72-23477

Al and oxygen effects on commercially pure Ti microhardness and microstructure, noting interstitial and substitutional atom inclusions effects on hexagonal cell dimensions

10 p1494 A72-23831

Authoradiographic study of stress intensity factor influence on hydrogen distribution at crack tips in Ti-Al-V alloy, using tritium doped salt water as corrosive medium

[ONERA, TP NO. 1052]

10 p1496 A72-24234

Electrochemical and stress corrosion tests of Ti-Ni alloys in acidic chloride solutions at ambient and elevated temperatures

[NACE PAPER 30]

10 p1497 A72-24321

Ti alloy sheets diffusion brazing, describing chemical cleaning, auxiliary metal cladding, heating and pressure augmented fusion processes involved in high quality joints production

10 p1497 A72-24658

Ti alloys fracture strength in air and sea water obtained by bending tests of notched specimens, noting stress corrosion resistance enhancement by Mo addition

10 p1499 A72-24891

Environmental sensitivity effect on crack propagation rates in steels and Al and Ti alloys, discussing corrosion fatigue

10 p1499 A72-24899

Chemical compositions, properties and heat treatment of Ti, Al alloys and steels used in aircraft industry

11 p1652 A72-25286

Superplasticity relation to heat resistance in metal systems Ni-Cr, Ni-Cr-W-Ti-Al and Ti-Si

11 p1729 A72-25338

Compressive strength of Ti alloy airframe skin stringer panels reinforced with B-Al composite by brazing

[AIAA PAPER 72-359]

11 p1729 A72-25387

Phase transformations and recrystallization study of Ti-steel bimetal with emission microscope, observing high temperature formation of titanium and vanadium carbides

11 p1654 A72-25491

Microsegregation in Ti-Mo, Ti-V and commercial Ti alloys, investigating cooling rate and alloying elements contents effects

11 p1655 A72-25500

Al microsegregation in Ti-Al and commercial Ti alloys, investigating effects of cooling rate from beta phase and of Al content

11 p1655 A72-25507

Titanium oxide, carbide and nitride fractional determination in Ni-Ti alloy, noting optimum extraction conditions

11 p1655 A72-25511

Al addition effect on thermal and mechanical stability, forgeability, cold workability, aging and oxidation resistance of Ti-Mo beta alloys

11 p1656 A72-25514

X ray diffraction by alpha Ti, calculating reflections relative intensity and position to identify peaks

11 p1658 A72-25826

Ti-Nb and Ti-Nb-Al alloys heat treatment effects on tensile and bending strengths

11 p1659 A72-26133

Ti-Al-Mo alloys thermomechanical treatment, investigating alloying effects on hardening

11 p1660 A72-26133

VT22 high strength Ti alloy beta phase decomposition kinetics under heat treatment, noting omega and alpha phases formation effect on ductility

11 p1660 A72-26133

Heat treatment produced metastable and stable alpha and beta structures effects on nitrogen diffusion rate in Ti alloy during nitriding

11 p1660 A72-26134

Ductile type fracture after heat treatment of VT3-1 Ti alloy with Al, Mo, Cr and Fe additives investigated by electron microscopy and tensile tests

11 p1660 A72-26135

Low temperature tensile strength and plasticity of Ti alloys with zirconium, investigating sensitivity to stress concentrations

11 p1660 A72-26135

Ti alloys processability by electrochemical methods, showing output rate and surface quality improvement from increased current density and electrolyte temperature

11 p1640 A72-26261

Nb-Ti alloy elasticity modulus temperature dependence, considering foreign atoms interactions with dislocations

11 p1662 A72-26773

Low temperature mechanical properties of Ti-based alloys, examining notched samples impact strength as function of temperature and notch depth

11 p1663 A72-26800

Ti alloys fatigue strength, stress concentration sensitivity and grain sizes effects at normal and high temperature under cyclic loads

11 p1663 A72-26882

Mechanical properties, microstructural characteristics and fracture behavior of beta Ti-V-Cr-Al alloys

11 p1667 A72-26933

Ti alloy metastable phases classification, including alpha-prime, secondary alpha, omega, beta and alpha phases

12 p1828 A72-27294

Tensile plastic deformation effect on structural evolution of Ti-Ni alloy under anisothermal heat treatment

12 p1830 A72-27733

Russian book on work hardening of surface components of heat resistant and Ti alloys for high temperature operation

12 p1816 A72-28156

Tensile strength, plastic properties and notch sensitivity from low temperature tests of binary Ti alloys, noting effects of Sn content and temperature

12 p1831 A72-28233

X ray spectral analysis of Ti-Mo system alloys, investigating K and L lines and electronic structure

13 p1972 A72-28499

Interdiffusion studies in bcc phase of Zr-Ti alloys, using geoscan electron microprobe

13 p1973 A72-28653

Pre-cracked Charpy specimens for fracture toughness impact and slow bend tests of Ti alloys using energy values

13 p1974 A72-28656

Mo addition effect on Al and Ti diffusion from intermetallic compounds into Ni matrix, noting increased high temperature stress rupture life

13 p1975 A72-28670

Leading angle effects on cutting force components, temperature and surface roughness in drawing of Ti alloys

13 p1963 A72-28746

Ti-V and Ti-Nb alloys mechanical strength and stress concentration resistance at low temperatures

13 p1977 A72-29018

Force distribution in refractory Ti alloy cutting with circular self turning blades, noting effects of feeding speed, cut area and cutter angle

13 p1966 A72-29467

Ti-Ni alloy strengthening by titanium nickelide intermetallic epsilon phase formation control via heat treatment

13 p1981 A72-29829

Chemical bond in Cu-Ti intermetallic phases, from X ray K absorption edges studies

13 p1981 A72-29914

Equiatomic ordered, bcc TiFe and TiNi electron density in outer energy band from X ray K emission spectra

13 p1981 A72-30006

Porous Ti alloys production with Mo, Cr and Pd, considering optimum sintering temperatures and hydrogenation

13 p1981 A72-30106

Pressed and sintered preforms of Ti and alloys for forge and extrusion operations, noting processing time reduction and smooth surface

13 p1982 A72-30120

Ti-Mo-Ni system polythermal section microstructure, hardness, resistivity and thermal expansion characteristics

14 p2112 A72-30153

Metal particle decomposition products composition in slags from smelted Cr, Ti, Ni and Zr alloys, using X ray microanalysis

14 p2112 A72-30157

Lower oxide mechanism in reduction-oxidation reactions during Ti steels electrosmelting with slag and gas phases

14 p2112 A72-30158

X ray analysis of Ti-Al alloys for cold rolled texture diagrams at low and high deformation levels

14 p2112 A72-30159

Phase precipitated helicoidal dislocations and vacancy-type stacking faults in aged austenite Fe-Ni-Ti alloy, using electron microscope diffraction contrast analysis

14 p2112 A72-30162

Optimal mechanical properties of Ti alloys with Cr, Mo, V, Nb and Ta additions, considering tensile strength, impact toughness, elongation and flattening

14 p2113 A72-30164

Al inhibitive of Ti oxidation at 800-1000 C due to interatomic bonds, lower oxygen solubility and diffusion rates

14 p2113 A72-30166

Ti alloy volume reduction during decomposition of metastable alpha-prime, alpha-two and beta phases after cooling from beta range

14 p2114 A72-30401

Flat Ti alloy sheet creep under variable loads at 300-400 C, comparing prediction with test data

14 p2116 A72-30434

Ti alloys hot salt stress corrosion cracking mechanism, discussing cold deformation and heat treatment effects, tensile tests, hydrogen analysis and microscope investigation

14 p2117 A72-30535

Uniformly distributed precipitates effect on hardness increase in aging of ferritic matrix Fe-Co-Ti and Fe-Co-Al alloys

14 p2119 A72-30605

Mill annealed Ti alloy fatigue at 600 F and room temperature, noting critical local stress for slip bands formation and cracking

14 p2120 A72-30611

Tensile properties from high temperature and room temperature tests of Ti alloys containing Ga correlated with creep resistance at 1000 F, noting activation energy

14 p2120 A72-30614

Si phase identification in super alpha Ti alloys, using electron transmission microscopy and diffraction analyses

14 p2120 A72-30616

Ti-Si system phase diagram and equilibrium states, noting crystal lattices and thermograms

14 p2123 A72-30986

Vacancy annealing effect on beta phase transformation during tempering of Ti alloy with Mo, showing strain hardening and contraction increase

14 p2124 A72-31032

Stress corrosion crack initiation and propagation for Ti alloy in sodium chloride solutions, noting anodic dissolution

15 p2253 A72-31295

Ti alloy initial H content effect on resistance to hot salt stress corrosion embrittlement and cracking, discussing annealing treatment influence

15 p2253 A72-31296

Ti-Al-V foil stress corrosion methanol cracking resistance improved by treatment with pentanedione, suggesting metal ions removal from protective film

15 p2253 A72-31297

Ti alloys hot salt stress corrosion during turbine engine operation, noting effects of alloy processing conditions, surface properties and cyclic exposures

15 p2297 A72-32136

Ti-Mo binary solid solution, investigating superconducting transition temperature, lattice instability and electron-to-atom ratio by calorimetric measurements

15 p2295 A72-32544

Premartensitic beta phase instability, lattice vibration and shape memory effect in noble metal base and Ti alloys

15 p2259 A72-32641

Plastic deformation and limiting strain curves of Ti alloys in plane stressed state, comparing with yield and rupture conditions

15 p2259 A72-32684

Heat capacity data analysis for solid solutions of superconducting Nb-Ti system, investigating electronic structure

15 p2296 A72-32692

K and L lines of X ray emission spectra of Ti in alloys with Nb, noting atomic structure change during alloy formation

15 p2259 A72-32701

Ti alloy fracture strength determination by crack propagation observation in specimen center, noting load-displacement curve construction from cyclic loading test

15 p2259 A72-32804

Temperature effect on fatigue crack growth in high strength annealed Ti-Al-V alloy in water, oxygen/hydrogen and vacuum environments

16 p2406 A72-33320

Texture of Ti-Sn and Ti-Mn alloy specimens observed by X ray reflection technique after hot rolling, annealing and cold rolling

16 p2407 A72-33529

Phase diagrams for W-Ta-Ti alloys at 1600 C from metallographic and X ray analysis

16 p2407 A72-33533

Quenching produced martensitic transformations from equilibrium beta phase region for Ti alloys with Ta

16 p2408 A72-33618

Precipitation reactions during tempering of Ti-Ta alloys, studying hcp and orthorhombic martensitic phases from electron microscope observations

16 p2408 A72-33619

Thermodynamic interaction parameters of solid solution bcc V-Ti-Cr alloys by Knudsen effusion method combined with mass spectrometer

16 p2409 A72-33803

Cd effect on alpha-beta transformation temperature and phase equilibrium in Ti rich end of Ti-Cd phase diagram, using metallographic and X ray techniques

16 p2409 A72-33806

Internal nitridation zones and growth kinetics for Cr and Cr-Ti alloys at 1000-1400 C, using Maak analysis

16 p2409 A72-33807

Liquidus temperatures and isotherms in Al corner of Al-Ti-B alloy phase diagram, using differential thermal analysis

16 p2409 A72-33808

Composition effect on strain-temperament and precipitation hardening of beta Ti alloys at 800-1100 F

16 p2410 A72-33813

As-quenched and aged form of omega phase in Ti-Nb alloys investigated by electron microscopy and X ray diffraction

16 p2410 A72-33818

Chemical diffusion in the titanium-aluminum system

17 p2510 A72-34275

Electron diffraction patterns of previously deformed Ti-Nb alloy containing unequal populations of omega phase variants, noting anisotropy

17 p2566 A72-34673

V-Ti alloys interstitial scavenging action dependence on titanium concentration via internal friction study

17 p2567 A72-34732

Critical species in the transgranular stress corrosion cracking of titanium alloys in aqueous solutions.

17 p2567 A72-34733

The structure and properties of thermomechanically treated beta-III titanium.

18 p2700 A72-36586

Effects of combined high and low temperature deformation processing of beta III titanium.

18 p2701 A72-36590

Composition dependence of density in NiTi and CoTi.

18 p2701 A72-36592

Inhomogeneity of high melting temperature elements in titanium alloys.

18 p2701 A72-36693

Effects of work hardening on the structural hardening of T-A6V6E2 titanium alloy

18 p2702 A72-36706

Zr and V alpha and beta stabilizing element effects on phase boundaries in arc fused Ti-Al alloy studied by diffusion layer method

19 p2817 A72-37754

Influence of the structure of VTZ-1 and VT-18 alloys on the fatigue strength for an asymmetrical loading cycle

19 p2819 A72-38017

Aging characteristics of Ti-Mo base beta alloys.

19 p2820 A72-38371

Optimization of thermo-mechanical deformation parameters for Ti-6Al-4V.

19 p2821 A72-38385

Super-alpha Ti alloy development, measuring physical and mechanical properties

20 p2936 A72-39205

Al-B and Al-Ti-B alloys fabrication, discussing quality control and grain refinement

20 p2936 A72-39207

Gaseous hydrogen-induced cracking of Ti-5Al-2.5Sn.

20 p2937 A72-39292

Mercury embrittlement of age-hardened Cu-1.9 wt pct cobalt and Cu-3.6 wt pct titanium.

20 p2938 A72-39296

Stress dependent cyclic creep rupture tests of Ti and Co-base alloys and stainless steel at 1300 F

20 p2938 A72-39305

Hydrogen gas effects on cleavage cracking in Ti-Al-Mo-V samples under static and cyclic loading

20 p2939 A72-39308

Decomposition, solubility and coherent phase stability of modulated structure Co-Ni-Ti system at high nucleation temperatures

20 p2939 A72-39312

Investigation of solid solution decay in cobalt-titanium, iron-cobalt-titanium-aluminum and iron-nickel-titanium-aluminum alloys

20 p2939 A72-39314

Fatigue tests at low cyclic loads of smooth and notched Ti alloy specimens, noting surface hardening effect on service life

20 p2941 A72-39580

The effect of Si, Zr, Al and Mo on the structure and strength of Ti martensite.

20 p2941 A72-39792

Mechanical properties of Ti-Mo alloys at low temperatures

20 p2942 A72-39824

Optimal planning of an experiment in a study of the properties of Ti-V-Al alloys

20 p2942 A72-39825

Crack arrest and crack initiation in a titanium alloy.

20 p2942 A72-39962

Beta to omega phase transformation and structure in Zr and Ti alloys bcc solid solutions by dark field electron microscopy, diffraction and ultrasonic technique

21 p3065 A72-40092

The nitriding behaviour of austenitic stainless steels containing titanium.

21 p3066 A72-40686

Stress-corrosion cracking of high strength steels and titanium alloys.

21 p3067 A72-40849

Phase precipitation structure of superconducting Nb-Ti alloys after cold working and low temperature annealing

21 p3067 A72-40951

The nature of solid solutions of the titanium-vanadium-oxygen and titanium-vanadium-aluminum-oxygen systems

21 p3068 A72-40962

Deformation microstructure of fine grained and plate-like structure two phase Ti alloys, noting plasticity decrease in beta phase presence

21 p3068 A72-40963

On the growth kinetics of Laves phase precipitates in Fe-Ti alloys at elevated temperatures.

21 p3069 A72-41011

Strain curves of VT-6C and VT-14 titanium alloys in the temperature range between 20 and 400 C

21 p3070 A72-41362

Comparison of the resistance to fracture of the K1c of the AK4-1Ti, V95Ti, and D16T aluminum alloys and VT8 and VT9 titanium alloys under static and cyclic loading

21 p3071 A72-41705

Ti based beta alloy strain hardening and failure characteristics, emphasizing initial deformation phase and microdefect onset and development

21 p3071 A72-41716

Investigation of the influence of multiple-pass welding on the mechanical properties of welded joints of VT6s and VT14 titanium alloys

22 p3182 A72-41861

Investigation of phase equilibria in alloys of silicon with molybdenum and titanium

22 p3188 A72-42150

Fine grained WC phase structure, physicochemical and cutting properties of Ti-Co alloy, using W

powder prepared by tungsten oxide reduction in single stage muffle furnace

22 p3188 A72-42192

Alpha stabilizing Al and Sn suppression effect on beta-omega transformation during Ti alloy hardening

22 p3189 A72-42278

Equiatomic ordered bcc TiFe and TiNi electron density in outer energy band from X ray K emission spectra

22 p3190 A72-42733

X-ray structural examination of phase transformations in the VT14 titanium alloy during heating

22 p3192 A72-43015

Thermomechanical manipulation of precipitate shape in a titanium-base alloy.

22 p3194 A72-43044

Influence of hydrogen on the fracture structure of OT4 titanium alloy

22 p3196 A72-43162

Surface layer grain boundary corrosion damage of Ti alloys during vacuum annealing, reducing rupture strength, vibration resistance and bending fatigue limit

23 p3293 A72-43589

Mechanical properties of titanium alloys with isomorphous beta-stabilizing elements

23 p3300 A72-43590

Martensitic transformation during deformation in titanium alloys with a metastable beta phase

23 p3300 A72-43591

Effect of oxygen on the scale resistance of titanium-titanium alloys

23 p3300 A72-43592

Tendency toward brittle failure of a simulated weld-seam region in Ti-Al-V system alloys

23 p3293 A72-43593

Investigation of the structural state of the InNDK4077 high-coercivity alloy

23 p3300 A72-43594

Standard Ti bars samples for spectral determination of H concentration and distribution in Ti alloys, using mathematical statistical method

23 p3287 A72-43676

Fatigue strength of two phase Ti alloys, considering work hardening, electrochemical finishing, electropolishing and protective media

23 p3301 A72-43757

Creep and fracture of OT-4 titanium alloy in the temperature range from 400 to 550 C

23 p3302 A72-43960

Energy dissipation in metals during high-frequency fatigue tests. II

23 p3302 A72-43964

Elastic stiffness of AT-2 and AT-3 titanium alloys and their welds at high and low temperatures

23 p3302 A72-43966

Electron fractography of fatigue failure and macrocrack propagation in dual phase Ti alloy during cyclic loading at minus 140 to plus 150 C

23 p3303 A72-44097

Fatigue behavior of a titanium 8Al-1Mo-1V alloy in a dry argon environment.

23 p3304 A72-44261

A study of cold-worked titanium-aluminum alloys by X-ray diffraction.

24 p3413 A72-44720

The application of Ti-6Al-4V titanium to helicopter fatigue loaded components.

24 p3366 A72-44732

Phase transformations in chromium-titanium compounds.

24 p3413 A72-44922

Plane strain fracture toughness of notched high strength Al and Ti alloys at low temperatures

24 p3413 A72-44939

Residual stress formation mechanism in two phase Ti alloys under cutting and plastic deformation, showing phase transformation composition and structure effects

24 p3407 A72-44942

Welding airframe structures in titanium using tensile loading to overcome distortion.

24 p3407 A72-45000

Influence of oxygen and hydrogen on the strength of titanium alloys

24 p3414 A72-45379

Relationship between the strength properties and the phase composition of annealed titanium alloys

24 p3414 A72-45383

Physicomechanical properties of titanium-tungsten solid alloys with deficiency of carbon in the carbide solid solution lattice

24 p3415 A72-45385

The mechanism of void formation, void growth, and tensile fracture in an alloy consisting of two ductile phases.

24 p3415 A72-45481

The mutual solubilities of titanium and boron in pure aluminum.

24 p3415 A72-45482

Al and Ti alloy fatigue after temperature reduction to 253, 77 and 4 K as function of surface purity after machining

24 p3416 A72-45743

Hydraulic sand blasting and annealing effects on Ti alloy sheet bending fatigue strength

24 p3416 A72-45744

V and Al addition effects on mechanical properties of oxygen rich Ti alloys

24 p3416 A72-45745

Reversible hydrogen brittleness development conditions in metals, deriving equations for hydrogen content effect on plasticity dip

24 p3416 A72-45758

TITANIUM BORIDES

Photocolorimetric determination of boron in nickel and titanium borides via Magnezone I in alkaline medium, determining solution pH, reaction time, light absorption, etc

18 p2655 A72-36099

Interaction of titanium diboride with titanium disilicide and silicon at high temperatures

19 p2819 A72-38284

TITANIUM CARBIDES

Titanium carbide based hard cermet alloys with Ni addition, testing wear resistance

03 p0372 A72-13549

Short range order and X ray diffused scattering in TiC-WC solid solution, using least squares method

06 p0834 A72-18741

Age hardening of Mo alloys with titanium and zirconium carbides at high temperatures after quenching

07 p1014 A72-19844

X ray analysis of cementite and titanium carbide precipitates in Cr-Mn-Mo-Ti steels weld zones

07 p1019 A72-20159

Reflection mode high energy electron diffraction study of titanium carbide single crystal surfaces in ultrahigh vacuum environment

07 p1019 A72-20408

Young modulus of TiC-Co and TiC-Ni hard composites as function of volumetric fraction, using bending tests

11 p1660 A72-26487

Plane titanium and niobium carbide precipitation in microalloyed steels during heat treatment above 1300 C, noting eutectic sulfide effect

12 p1827 A72-27102

Russian book on hard alloys strength covering WC-Co and WC-TiC-Co alloys microstructure, thermal stresses and fracture mechanism

12 p1831 A72-28348

Microfiber extrusion of plasticized mixtures based on titanium and silicon carbides, showing optimum extrusion rate dependent on deformation and strengthening

13 p1967 A72-30102

Shock wave reduction, microcracks and dislocation density of hot pressed titanium, zirconium and niobium carbide powders, using X ray crystal analysis

13 p1982 A72-30110

TiC high temperature oxidation and thermodynamic equilibria in air, using metallographic and X ray analyses

14 p2112 A72-30155

Octahedral TiC single crystals oxidation at high temperature in oxygen, carbon dioxide and mixtures, investigating oxygen partial pressure effects on kinetics

14 p2121 A72-30772

Effect of molybdenum on the properties of TiC-Ni cermet hard alloys

19 p2819 A72-38283

Relations between mechanical properties and microstructures in TiC-Mo2C-Ni alloy.

19 p2821 A72-38375

Structure of the energy bands of titanium, hafnium, and tantalum monocarbides

20 p2939 A72-39311

Structural and reaction kinetic characteristics of /W, Ti and Ta/C-Co systems, considering solubility, surface energy, diffusion, segregation and grain growth

21 p3071 A72-41849

Study of the hot pressing kinetics for niobium-cemented tungsten and titanium carbide alloys

22 p3182 A72-42191

Prospects of using carbonitrides as the hard component of cermet hard alloys

22 p3188 A72-42195

Rapid determination of total carbon content in titanium carbide

22 p3176 A72-42200

German monograph - Gas-phase precipitation and high-temperature oxidation of titanium carbide.

22 p3194 A72-43053

TITANIUM COMPOUNDS

NT ANATASE

NT BARIUM TITANATES

NT ILMENITE

NT PEROVSKITES

NT RUTILE

NT STRONTIUM TITANATES

NT TITANATES

NT TITANIUM BORIDES

NT TITANIUM CARBIDES

NT TITANIUM NITRIDES

NT TITANIUM OXIDES

Titanium disilicide oxidation mechanism at various temperatures, discussing surface quality effect, growth rate and protective mechanism

03 p0369 A72-12925

Titaniums sulfide initiation of pitting corrosion of Ti stabilized corrosion resistant Cr-Ni-Ti steels

03 p0379 A72-14367

Epitaxy and vacancy structure of TiSe with type B8 ordering

10 p1495 A72-24077

Electric discharge plasma generator consisting of concentric or parallel electrodes mounted on titanium hydride coated heat resistant ceramic disk

10 p1521 A72-24365

Titanium oxide, carbide and nitride fractional determination in Ni-Ti alloy, noting optimum extraction conditions

11 p1655 A72-25513

Phase diagram of Ti-Pd system, using metallographic, X ray and differential thermal analyses

13 p1982 A72-30116

K line of X ray absorption spectra for pure Ti and compounds, discussing effects of valence, microstructure and electron configuration

15 p2259 A72-32700

Electric discharge plasma generator consisting of concentric or parallel electrodes mounted on titanium hydride coated heat resistant ceramic disk

17 p2589 A72-34964

Some data on interatomic interaction in solid high-melting compounds of titanium, vanadium, and chromium with light metals

17 p2569 A72-35520

Niobium and molybdenum alloys containing borides and carbides of the IV-a group metals

22 p3191 A72-42814

TITANIUM DIOXIDE

U TITANIUM OXIDES

TITANIUM ISOTOPIES

Sunspot umbral TiO gamma system photoelectric spectra examination for less abundant stable Ti isotopes

15 p2314 A72-32372

TITANIUM NITRIDES

Maraging steel embrittlement by titanium carbonitrides lattices separation during cooling, suggesting rapid quenching and plastic deformation temperature reduction

07 p1012 A72-19677

Reactivity evaporated titanium nitride resistors for thin film microcircuits, discussing nitrogen gas pressure and substrate temperature effects on electrical properties during evaporation

09 p1286 A72-22902

Titanium nitride powder obtained by hydrogen reduction of titanium tetrachloride in nitrogen flow heated in microwave electrodeless discharge

13 p1967 A72-30111

X-ray spectra and electronic structure of titanium nitrides of limit composition and in the homogeneity range

19 p2821 A72-38406

Prospects of using carbonitrides as the hard component of cermet hard alloys

22 p3188 A72-42195

Titanium carbonitrides alloying with Ni in nitrogen atmosphere, noting N concentration effect on cermet wear resistance

23 p3298 A72-43281

Characteristics of the state of particles of titanium and vanadium mononitrides after nitriding and heat treatment

23 p3298 A72-43282

TITANIUM OXIDES

NT ANATASE

NT ILMENITE

NT RUTILE

Refractory titanium oxide deposition by hot front method of chemical reaction in vapor phase

02 p0170 A72-12166

Photochemical electron transfer evolution models, noting titanium and zinc oxides as photosensitizers

04 p0484 A72-14777

Ti surface oxide films ionic and electronic conductivity properties and correlation with crevice corrosion susceptibility in contact with polytetrafluoroethylene gaskets

04 p0535 A72-15732

Silicon solar cells antireflection coatings for performance loss minimization, obtaining improvement with titanium dioxide compared to silicon monoxide coatings

12 p1757 A72-28027

Titanium dioxide thin film antireflection coating to minimize reflection losses in Si solar cells, discussing fabrication and optical and electrical characteristics

12 p1757 A72-28028

Sunspot umbral TiO gamma system photoelectric spectra examination for less abundant stable Ti isotopes

15 p2314 A72-32372

Rutile titanium dioxide molecular orbital energy level diagram deduction from X ray emission and absorption band spectra, noting Ti and O states roles

15 p2295 A72-32539

- Strength of titania and aluminum silicate under combined stresses.
19 p2822 A72-37271
- Study of titanium and titanium oxide structures corresponding to different kinetics of oxidation obtained at 850 C
20 p2936 A72-39206
- Titanium oxide molecular spectrum band intensities measurement for vibrational temperature of M supergiant stars, noting atomic absorption effect on measurement accuracy
24 p3448 A72-45681
- TITRATION**
Continuous cotalimetric and thermocatalytic titration processes theory, deriving titration curves equations
12 p1755 A72-27444
- Adsorbed oxygen inhibition of reactions of hydrogen with tungsten.
23 p3298 A72-43270
- TNT [TRINITROTOLUENE]**
U TRINITROTOLUENE
- TOBACCO**
Tobacco tissue cultures with Apollo 12 lunar material, determining endogenous sterols and fatty acids concentrations by gas chromatography and mass spectrometry
07 p0920 A72-19850
- Apollo 12 material effect on tobacco tissue cultures, noting pigment increase
12 p1761 A72-27626
- TOCOPHEROL**
In vivo hemolysis due to hyperoxia - Role of H2O2 accumulation.
24 p3374 A72-45651
- TOLERANCES [MECHANICS]**
Informational reliability of automatic control system comparators, considering tolerance field contraction effect
10 p1456 A72-24081
- Tolerance intervals in multiple type acceptance sampling plans with attribute-based inspection
11 p1749 A72-26790
- Mathematical model of gas turbine parameters scatter and geometrical fabrication tolerances of flow through section
11 p1712 A72-26974
- Technical and economic processes representation of radioelectronic equipment synthesis optimization using elementary random magnitudes involving output parameters deterioration rates and fabrication tolerances
23 p3269 A72-43442
- TOLERANCES [PHYSIOLOGY]**
NT ACCELERATION TOLERANCE
NT ALTITUDE TOLERANCE
NT COLD TOLERANCE
NT HEAT TOLERANCE
NT HUMAN TOLERANCES
NT RADIATION TOLERANCE
- Acceleration force simulation for altered weight effect on animal tolerance to restraint, discussing body mass loss, reduced lymphocyte count and disorientation
04 p0472 A72-14866
- Chinchilla and guinea pig tolerances to hypoxia and hyperoxia in pressure chamber tests, suggesting relation to red blood cell size and number
09 p1265 A72-22647
- Organism response to extreme overload factors, discussing centrifuging and vibration stress effects on mean swimming time and post-irradiation survival time in mice
16 p2355 A72-33554
- Increased tolerance of leukemic mice to arabinosyl cytosine with schedule adjusted to circadian system.
17 p2505 A72-33597
- Altitude limit as function of acclimatization time length for investigation of enhanced resistance to acute hypoxia in rats
23 p3255 A72-43908
- TOLLMEIN-SCHLICHTING WAVES**
Boundary layers nonlinear resonant instability, investigating Tollmien-Schlichting wave triads interactions with energy transfer from primary shear flow to disturbance
03 p0340 A72-13160
- Wall curvature and flexibility effect on incompressible laminar boundary layer hydrodynamic stability, considering Tollmein-Schlichting transverse wave disturbances
06 p0801 A72-18134
- TOLUENE**
Alkyl substituent effects on gas phase acidities of toluene, p-xylene and acetylenes, using ion cyclotron resonance spectroscopy
07 p0936 A72-19494
- Optical Kerr constant measurement in liquid phosphoryl chloride and toluene and glasses, noting nonlinear refractivity
12 p1823 A72-27756
- TOPE**
U PITCH
- TONOMETRY**
U INTRAOCULAR PRESSURE
U PRESSURE MEASUREMENTS
- TONUS**
U MUSCULAR TONUS
- TOOLING**
Graphite filament reinforced plastics strength, performance properties, fabrication processes and tooling concepts
[SME PAPER EM 71-205] 01 p0076 A72-10968
- TOOLS**
NT BORING MACHINES
NT MACHINE TOOLS
NT SPACE TOOLS
NT WRENCHES
- TOOTH DISEASES**
Functional diagnostics of teeth condition as pilot health factor in stomatological aviation medicine, discussing caries, parodontosis and aerodontalgia
07 p0922 A72-20374
- TOPOGRAPHY**
NT LUNAR TOPOGRAPHY
NT TERRAIN
- Mars surface topographic characteristics relationship to earth features, using Mariner 6 and 7 photographs
04 p0569 A72-14501
- X ray topography of natural diamond, showing impurity platelet distribution, slip depth, temperature and stress conditions after plastic deformation
05 p0702 A72-16020
- Elevation-relief ratio, hypsometric integral and geomorphic area-altitude analysis, discussing calculation time
05 p0654 A72-16039
- Rotating homogeneous incompressible fluid flow over various bottom topographies, comparing numerical and analytical solutions with water tunnel experimental results
07 p0970 A72-20071
- Borrmann X ray topographic examination of dislocation structures, discussing geometric effects on linear defects image width
07 p0989 A72-20158
- Multiple projection assembly for topographic maps preparation by satellite photographs optical projection onto model surfaces, exemplifying by reverse lunar hemisphere
08 p1165 A72-21155
- Image scale selection for topographic map revision in orthophotograph production considering economics and suitability
09 p1311 A72-22968
- Multifactor landscape synthesis of aerial imagery for regional surveys
09 p1301 A72-23278
- Soil science and climatology use for archeological site detection on aerial photographs
09 p1303 A72-23296
- Topographical stereo map plotting apparatus with auxiliary device for orthophoto production, describing design for combined photointerpretation-cartographic applications
09 p1313 A72-23309
- Theoretical model of large scale topographical effects on wind generation through temperature advection, applying to Mars atmosphere general circulation
10 p1531 A72-23707
- Topography of swath around Venus equator from wavelength dependence of radar cross section
10 p1548 A72-24972
- Perturbation method study of governing differential equations for wave reflection by periodic two-dimensional topography
11 p1685 A72-25358
- Mercury topography and scattering characteristics from 3.8 cm radar observations, comparing to Mars and Venus
12 p1865 A72-27098
- Transstructural topographic and gravity profiles of three Mauritanian meteorite craters, showing residual negative gravity anomalies
13 p1947 A72-28756
- Topographic mapping from airborne radar geodetic measurements, evaluating photogrammetric accuracy
15 p2224 A72-31603
- High-orbital satellite global photographs and TV pictures, discussing planetary geographical and topographical data interpretation
15 p2225 A72-31807
- Mars topography variations from earth based surface height radar ranging and Mariner spectrophotometric observation of Mars atmosphere
15 p2313 A72-32346
- Holography application in photogrammetric contour mapping, discussing topographic data acquisition, storage, retrieval and display problems
19 p2797 A72-37609
- Multiple projection assembly for topographic maps preparation by satellite photographs optical projection onto model surfaces, exemplifying by reverse lunar hemisphere
20 p2924 A72-39260
- Mariner 7 ultraviolet spectrometer experiment - Topographic slopes of Mars' polar region.
21 p3110 A72-41457
- Computation and automatic drawing of the contour lines of functions of two independent variables
23 p3310 A72-44362
- Coordinates of features on the Mariner 6 and 7 pictures of Mars.
24 p3436 A72-44695
- TOPOLOGY**
NT FIXED POINTS [MATHEMATICS]
NT IMBEDDINGS [MATHEMATICS]
NT INVARIANT IMBEDDINGS
NT METRIC SPACE
- Topological structure of anharmonically coupled many body problem, describing generalized Bose operators formulation
02 p0262 A72-12049
- Mixtures, periods and factors of tau-regular probability laws in topological group or half group
05 p0682 A72-16121
- Topology of convergence precompact on locally convex space, defining p-infratunneled spaces by Banach-Dieudonne theorem
10 p1505 A72-21133
- Integrated circuits fabrication and design, describing internal physical processes, input and output signal values, functional operations and topological features
10 p1448 A72-24283
- Antagonistic pursuit games of prescribed duration in abstract topological space with defined distance function
11 p1676 A72-25326
- Measured and mean convergences in topological vector spaces, considering Banach space
12 p1836 A72-27176
- Bounded operators solution in locally convex topological vectorial spaces with meromorphic properties
13 p1987 A72-29778
- Magnetic field rapid dissipation induced by stochastic topology of lines of force, discussing implications for hydromagnetic turbulence, solar activity and cosmic ray diffusion
16 p2378 A72-33454
- Banach space order and compactness properties extension to general case of arbitrary regular space, discussing system topologies
18 p2704 A72-36461
- Caratheodory classical thermodynamics formulation presented in mathematically rigorous form by differential geometry and topology methods
18 p2741 A72-36508
- Energetic and topological effects in surface chemical reactions, considering intermolecular dispersion and dipole forces and chemisorption
18 p2657 A72-36828
- Topological analysis of the sensitivity of a digital system
21 p3036 A72-40222
- Equivariant integrality theorems for differentiable manifolds.
22 p3199 A72-42310
- The topology of the regularized integral surfaces of the 3-body problem.
23 p3309 A72-43982
- TOPS [SPACECRAFT]**
TWT amplifier converter design with semiconductors and magnetics to achieve voltage regulation and high power efficiency for TOPS spacecraft
08 p1111 A72-21412
- Spacecraft and missions for Jupiter exploration, discussing launch vehicle requirements, solar electric propulsion for midcourse correction, Pioneer flyby and orbiter missions, TOPS mission, etc
21 p3103 A72-40457
- TORCHES**
German monograph on plasma arc machining and cutting of metallic materials on lathe as function of electric power and torch performance
09 p1317 A72-22327
- Torch temperature measurements in vacuum by spectral radiative energy distribution method
16 p2476 A72-33258
- TORNADOES**
Tornado and funnel cloud comparison in seasonal and diurnal distributions, air mass instability, tropospheric vertical wind shear and geographical distribution
03 p0385 A72-14231
- Synoptic and dynamic aspects of tornado-producing thunderstorms development from ATS 3 and aerological data, observing mesoscale convective disturbances
06 p0842 A72-18438
- Tornado model from atmospheric thermodynamics nonlinear equations, examining air flow from lower boundary layer and ground friction
11 p1682 A72-26880
- A spheric arc azimuth-profile of the 1955 Blackwell, Oklahoma, tornado.
18 p2706 A72-36639
- Elementary considerations of the fluid mechanics of tornadoes and hurricanes.
24 p3421 A72-45021
- Boundary layer core flow model of concentrated columnar vortex interaction with plane solid nonrotating surface, applying to tornado interpretation
24 p3391 A72-45022
- TOROIDAL DISCHARGE**
NT RING DISCHARGE

- Experimental investigation of toroidal discharge electrostatic potential fluctuations in turbulently heated plasma, discussing correlation with effective conductivity 13 p2012 A72-29122
- Results of a computer simulation of an arc plasma in a curved discharge tube. 19 p2841 A72-38085
- TOROIDAL PLASMAS**
- Nonlocal theory of electrostatic trapped particle instability in collisionless toroidal plasma, estimating particle mode nonlinear diffusion coefficient 01 p0108 A72-10239
- German monograph on toroidal electric arc plasma with allowance for induced flow, covering tube wall heat transfer, electric field, MHD vortex development, mathematical model, etc 02 p0263 A72-11650
- MHD equilibrium equations for axially asymmetric finite beta toroidal plasma with diffuse boundaries 04 p0556 A72-14854
- Toroidal plasma column in Tokamak systems, discussing field inhomogeneity role in maintaining equilibrium with conducting casing, confirming magnetic field and transformer iron core 04 p0557 A72-15171
- Diffusion and thermal equilibrium models of stationary Tokamak, analyzing differences 04 p0558 A72-15173
- Equilibrium diffusion of rotating plasma in toroidal systems, deriving two fluid hydrodynamic equations with allowance for ion temperature perturbation 05 p0701 A72-17242
- Polarization electric field and depolarization current measurements in plasma flows along toroidal solenoid with diverter 06 p0853 A72-17387
- High-beta theta pinch plasma toroidal equilibrium by oscillating magnetic field superposition on main confining field 06 p0864 A72-18538
- Thermal conductivity of stationary toroidal plasma in form of Pfirsch-Schluter diffusion factor, using ion heat balance equation 07 p1042 A72-19616
- High frequency heating of dense toroidal plasma by nonaxisymmetric ion cyclotron waves resonant excitation in closed magnetic trap 07 p1043 A72-19636
- Stability conditions of dissipative trapped ion mode in axisymmetric toroidal confinement systems, investigating collisional damping rate 07 p1045 A72-20476
- Time dependent solutions of Tokamak equilibrium equations for plasma diffusive processes 11 p1694 A72-25787
- Ruby laser light scattering method for measuring magnetic field direction in Tokamak plasma, testing validity by numerical calculation of scattered spectrum 11 p1694 A72-25793
- Toroidal plasmas heating by neutral injection, discussing ion acceleration, charge exchange and fast ion trajectories 11 p1697 A72-26582
- Magnetic field direction measurement in Tokamak toroidal plasma by laser light scattering, using Fabry-Perot interferometer 11 p1697 A72-26583
- Holographic Fourier spectroscopy for microwave radiation spectra of toroidal plasma with turbulent heating 12 p1850 A72-27135
- Plasma containment in toroidal systems investigated on basis of fluid model containing inertia, momentum transfer, ionic collisions and thermal conductivity effects 15 p2285 A72-32273
- Quasi-linear diffusion theory for axisymmetric toroidal plasma, considering normal modes and energy conservation 15 p2287 A72-32413
- Magnetized plasma discharge steady state problem of finite cylinder positive column in magnetic field, detailing radial and axial solutions 15 p2288 A72-32508
- Azimuthal electric fields role in toroidal plasma transport properties based on kinetic theory for collision dominated regime 16 p2432 A72-32806
- Skin effect in large hot tokamaks predicted by computer studies based on empirical transport coefficients, discussing suppression by moving limiter 16 p2433 A72-32812
- Magnetic configuration for plasma confinement in torsatron with helical windings and no toroidal field coils 16 p2433 A72-32816
- Rotating plasmas steady MHD equilibria without PS factor enhancement, considering cases of vanishing and nonvanishing toroidal current 16 p2433 A72-32817

- Faraday ring currents induction by radial magnetic field in low pressure plasma supersonic ring channel flow driven by inductive hydrodynamic shock tube 16 p2437 A72-33749
- Particle and energy fluxes across magnetic field in axisymmetric toroidal magnetic traps and plasmas with weak collisions, calculating radial electric field 16 p2440 A72-34153
- Runaway electrons in toroidal plasma investigation by thick target bremsstrahlung measurement, noting energy distribution and runaway rate estimates 17 p2591 A72-35370
- Toroidal plasma spectroscopic investigation from current pulse start to afterglow, noting electron temperature and density radial distributions and energy balance 17 p2591 A72-35373
- Magnetic surface equation and collisional diffusion of finite beta tokamak plasma in low density regime 19 p2838 A72-37330
- Results of a computer simulation of an arc plasma in a curved discharge tube. 19 p2841 A72-38085
- The effect of asymmetry on toroidal hydromagnetic waves in a dipole field. 20 p2957 A72-39230
- Plasma equilibrium in configurations with a helical magnetic axis with allowance for toroidality. 20 p2957 A72-39353
- Low beta model of collision dominated plasma flow effect on toroidal confinement, simulating Stellarator, Levitron and Tokamak 20 p2957 A72-39356
- Resonant scattering of trapped particles by toroidal plasma modes. 21 p3092 A72-41217
- Spatial measurement of the magnetic field direction in plasma. 21 p3094 A72-41633
- High frequency heating of dense toroidal plasma by nonaxisymmetric cyclotron waves resonant excitation in closed magnetic trap 24 p3427 A72-44568
- Transformation of trapped charged particles to transit particles under the influence of a high-frequency electric field 24 p3429 A72-45494
- Rapid radial displacement of a toroidal plasma filament by a transverse magnetic field 24 p3429 A72-45506
- TOROIDAL SHELLS**
- Finite inflation of toroidal shell with edges bonded to rigid rim, using Runge-Kutta method to solve differential equations based on Mooney strain energy function [ASME PAPER 71-WA/APM-20] 05 p0733 A72-15960
- External pressure effects on stability of closed toroidal shell with circular cross section 07 p1087 A72-18993
- Stress and deflection distribution for circular and elliptical toroidal shells under internal pressure from first order differential equations solutions 07 p1088 A72-19118
- Green matrix computation algorithm extensible to spherical and toroidal closed shells of revolution for stress-strain state determination 08 p1246 A72-21672
- Inflation pressure caused deformations of thin toroidal shells, discussing wrinkle development due to pressure reduction [ASME PAPER 72-APM-32] 17 p2628 A72-34787
- TOROIDS**
- Mathematical model of gravitational wave zone for ring emanated smooth axisymmetric toroidal pulse 08 p1158 A72-21177
- Current distribution approximation for toroidal antennas of small cross section under incident electromagnetic excitation 10 p1453 A72-25104
- Stability theory for a star with a toroidal magnetic field 19 p2863 A72-38062
- Simplified theory for optimizing the design of a heat shield in an isochorically operated toroidal dewar. 19 p2805 A72-38843
- On the diffusion of the perturbing toroidal magnetic field from the core to the mantle. 21 p3048 A72-40501
- TORPEDO ENGINES**
- NT CONTROL ROCKETS**
- TORQUE**
- Orbiting space vehicle life extension by momentum management using gravity gradient torques 05 p0727 A72-16467
- Random vibrations and antitorque moments of rigid shaft with precision bearings, considering effects of geometrical fabrication defects and nonuniform film thickness 06 p0824 A72-18722
- Viscous fluid steady nonaxisymmetric flow past rotating sphere, obtaining antitorque moment expressions and resisting force projections 10 p1469 A72-24547

- Complete and simplified equations of motion for rate gyro installed in flight vehicle, taking into account bearing torques 11 p1635 A72-26580
- Rigidity calculation of double raw radial thrust annular ball bearing loaded by axial and radial force and torque 11 p1646 A72-26978
- Elastoplastic torsion of homogeneous and inhomogeneous torus segments of arbitrary cross section, noting plastic bands propagation with increasing torque 16 p2467 A72-33119
- Precessional torque of conducting fluid as source of geodynamo action, noting oblate spheroidal experiment 16 p2385 A72-33341
- Recommendations for selection and use of torque wrenches for aerospace propulsion systems applications [SAE AIR 1268] 18 p2648 A72-36531
- Nutational stability of a dual-spin satellite under the influence of applied reaction torques. 20 p2976 A72-39116
- Upper limit of the torque of the solar wind on the earth. 22 p3219 A72-42427
- Elastic and plastic deformations in torsional moment loaded rod, noting successive approximation for stress functions 23 p3348 A72-43794
- Residual drag torque on magnetically suspended rotating spheres. 23 p3315 A72-44540
- TORQUE MEASURING APPARATUS**
- U TORQUEMETERS**
- TORQUE MOTORS**
- Three-axis flight table with dc torque motors, discussing servo loops design and mechanical oscillations frequencies 02 p0257 A72-12541
- Hydraulic amplification of electric step motor torque, discussing system dynamic characteristics 09 p1263 A72-22689
- Electrostatic force for rotational torque production, applying to motor design 11 p1603 A72-25743
- TORQUEMETERS**
- Noncontact rotating shaft horsepower measurement, using phase displacement technique [ASME PAPER 72-GT-29] 11 p1630 A72-25627
- Variable torque determination in precision work technology, discussing electronic measurements of length, shaft deformation, torsion angle and force 14 p2104 A72-30485
- Electro-optical torque sensor based on slit aperture produced diffraction patterns [SESA PAPER 1925-II] 17 p2553 A72-34813
- A new instrument for the measurement of low dynamic torque. 18 p2692 A72-36826
- Electro-optical noncontracting torque sensor, using slit diffraction pattern technique 21 p3051 A72-40231
- The use of a torsion machine to measure the shear strength and modulus of unidirectional carbon fiber reinforced plastic composites. 23 p3306 A72-43562
- Viscous torque on sphere immersed in Newtonian and non-Newtonian fluids in rotating cylinder, comparing experimental results with Collins theory 23 p3280 A72-43714
- High accuracy contactless torque-measuring shaft with strain gage as sensor, describing circuit wiring 24 p3403 A72-45296
- TORSION**
- Torsion problem of inhomogeneous anisotropic viscoelastic rod transformation, using area variation coefficient for modeling 01 p0138 A72-10582
- Torsion of hollow beam consisting of two homogeneous isotropic rods with different elastic properties and simply connected cross sections, solving by conformal mapping 04 p0586 A72-14992
- Saint Venant problem for orthotropic almost cylindrical beams, investigating elongation, bending due to couple and transversal loads and torsion due to torque 04 p0594 A72-15747
- Stress state of variable thickness long elastic shallow shell in bending and torsion, applying equations to large turbine blades 05 p0735 A72-15986
- Torsion testing machine for hot metal workability tests at constant strain rate 11 p1639 A72-25820
- Testing machine for synthetic plastic cylindrical specimens cyclic cophasal compression-torsion load tests, describing mechanical and hydraulic subsystems and testing techniques 13 p1938 A72-28559

TORSIONAL STRESS

- Torsional stiffness /shear modulus/ of glass fiber reinforced plastic tubes as function of filament winding angle 01 p0141 A72-10999
- Torsional prestrain effects on 1100-F Al alloy thin walled tubes yield locus, calculating distortion degree by statistical characteristics 01 p0086 A72-11000
- Barrel shaped cylindrical shell stability and free vibrations under torque, evaluating distortion influence by small parameter method 01 p0142 A72-11364
- Finite plasticity incremental and total strain theories for nonproportionate loading of circular steel and Al alloy torsion-tension members assuming von Mises yield [SESA PAPER 1901] 02 p0288 A72-11519
- Temperature-time dependent torsional strength and fracture failure of Cr-Ni steel microalloyed with La and Ce as function of grain boundaries 02 p0243 A72-12010
- Lunar regolith powder weight density, compressibility and torsional strength determination at atmospheric pressure and He atmosphere 02 p0281 A72-12288
- Truncated conical shell buckling under combined torsion and internal pressure load, discussing prebuckling stress conditions 02 p0298 A72-12666
- Torsion and bending by transverse load for homogeneous orthotropic slightly curved bars 03 p0444 A72-13499
- Stressed state of reinforced physically nonlinear rods under torsion, using theory of functions of complex variables 03 p0447 A72-13731
- Plastic torsion of prismatic and anisotropic rods, emphasizing inhomogeneity problems numerical solution 03 p0447 A72-13853
- Tangential stress pulse effects on transversally isotropic half space surface wave motion under torsion 03 p0452 A72-14128
- Cylindrical shaft with circumferential groove, obtaining approximate solution for stress concentration at groove contour under torsion 03 p0452 A72-14130
- Dual integral equations method application to elastic bodies with plane circular cracks in torsion 03 p0452 A72-14135
- Stress-strain state of transverse isotropic plate with hole under bending and torsional moments 03 p0452 A72-14136
- Ti-Al-V room temperature creep, considering tensile and torsional loading, plastic deformation, stress relief and design limitations 03 p0377 A72-14171
- Elastic shaft bonded to dissimilar elastic disk, considering torsion problem 04 p0583 A72-14449
- Validity hypothesis for total creep rate potential in strain-hardenable materials, discussing carbon steel torsion and tensile tests 04 p0586 A72-15006
- Shear stress and stability of composite elastic double layer with plane circular crack under torsion 04 p0588 A72-15054
- Stress concentration around elliptic hole in infinitely long circular cylindrical shell under torsional loads 04 p0589 A72-15122
- Perturbation solution for stress concentration around elliptic hole in cylindrical shell under torsional loading 04 p0589 A72-15123
- Closed form equations for constrained torsion of turbine blades, estimating elastic twist and cross sectional deplanation on analog computer 04 p0589 A72-15166
- Creep surface in Al alloy under combined tension and torsion, obtaining strain rate vectors from probes 04 p0590 A72-15195
- Transient stress analysis for sudden twisting of penny-shaped crack in infinite elastic body under torsion, using integral transform [ASME PAPER 71-WA/APM-10] 05 p0734 A72-15969
- Fatigue test curves of notched Al alloys under bending with rotation 05 p0676 A72-17086
- Combined tension-torsion creep testing of polymers, discussing equivalent stress and strain concept, testing apparatus and preliminary results for polythene 06 p0835 A72-17795
- Resolved shear stress formula for shafts under simultaneous tangential bending and torsion acting at dangerous points of cross section 06 p0899 A72-18643
- Titanium alloy durability under cyclic torsion in vacuum at various temperatures, investigating fatigue life and tensile strength 06 p0834 A72-18665
- Fatigue testing machines for axial and torsional loadings at low temperatures in vacuum 06 p0797 A72-18667
- Collocation least square solutions of boundary value problems, applying to prismatic bar torsion and plate bending 07 p1025 A72-18790
- Steady state high temperature niobium creep in torsion under rarefied oxygen infiltration conditions, discussing surface interactions kinetics 07 p1012 A72-19679
- Experimental determination of torsional stresses in rod from moire patterns, describing facility and procedure 07 p1091 A72-19762
- Nonlinear theory of thin walled open elastic beams with deformations by large cross sectional rotation, using potential energy principle 07 p1096 A72-20430
- Perturbation solution to nonlinear nonuniform torsion of thin walled open elastic beams with strain hardening dependent on torque-rotation behavior 07 p1096 A72-20431
- Circular elastoplastic beam under combined torsion and tension via Mindlin elastic model for materials with microstructure, taking into account work hardening 07 p1097 A72-20534
- Bending and torsion of thin isotropic rod with identical principal rigidities in bending, writing elastic curve equation in cylindrical coordinate system 08 p1209 A72-21367
- Torsion test determination of interlayer and intralayer-plane shear moduli in annular specimens of glass fiber reinforced plastics 08 p1194 A72-21756
- Secondary normal stresses in fixed flange zone of thin walled nonlinearly elastic pipe under bending moment and torsion 08 p1249 A72-22096
- High strength Ni alloy hot working properties evaluation from extrusion simulation by torsion testing, considering stress-strain-time relations, microstructure, recrystallization and ductility 08 p1190 A72-22199
- German monograph on ring shaped continuous beams calculation, deriving optimum support under torsional stress 09 p1397 A72-22335
- Nonlinear plane bending of thin elastic rectilinear bar guide elements under concentrated force and torque 09 p1397 A72-22350
- Axisymmetric grid plate bending and torsion under normal forces and moment vectors loads, determining stress-strain state from finite difference equations 09 p1398 A72-22692
- Torsional behavior of twisted elastic orthotropic cylindrical shells after stability loss, using energy method 09 p1404 A72-22771
- Circumferential crack in cylindrical shell under torsion, presenting membrane and bending components of stress intensity factor ratio 09 p1404 A72-22918
- Damping coefficient increase in welded bodies under uniform stress and compression, torsion and bending vibration 09 p1406 A72-23076
- Lunar regolith powder weight density, compressibility and torsional strength determination at atmospheric pressure and He atmosphere 10 p1532 A72-23757
- Torsion of embedded infinite elastic circular cylindrical fiber with penny shaped crack, investigating breaking behavior from Fredholm integral equation iterative solution 10 p1553 A72-24094
- Torsional stress analysis of rectangular beam composed of two elastic materials, using complex variable and conformal mapping 11 p1733 A72-25544
- Prestressed circular ring snap-through under continuously distributed or discrete torsional loads, determining critical torque by asymptotic solution 11 p1734 A72-25721
- Von Mises yield criterion extended to thin walled circular cylinder plastic torsional straining, noting variations of anisotropic parameters and yield stresses with shear strain [ASME PAPER 71-MET-Y] 11 p1735 A72-25877
- Upper yield stress effect on elastoplastic behavior of mild steel in bending and torsion, noting relationship to strain rate 11 p1659 A72-25894
- Dynamical torsion theory of rods deduced from linear elasticity equations, using averaging technique 11 p1736 A72-25987
- Variable shear modulus circular isotropic plate torsion by rigid circular stamp, obtaining stresses and displacements by Fourier analysis 12 p1881 A72-27319
- Shearing stresses in rod under torsion, using Prandtl membrane analogy and moire interference fringes 13 p2053 A72-28397
- Limiting load calculation for thin walled I-beam in oblique bending and torsion beyond elastic limit 13 p2055 A72-28734
- Torsional behavior of prismatic rods with polygonal cross section, using method of summary representations 13 p2057 A72-29080
- Series solution for coaxial spherical cavity effect on torsional stress of finite length elastic circular cylinder 13 p2059 A72-29491
- Numerical calculation of stresses and displacements in variable radius bodies of revolution under axially symmetric torsional load, using Fredholm type integral equation 15 p2324 A72-31480
- Torsion problem of solid rod with wing profile shaped cross section solved by conformal mapping and gamma function derivative, calculating maximum stresses and rigidities 15 p2327 A72-31741
- Unsteady torsional creep of multiply connected cylindrical rod with arbitrary cross section, calculating elliptic rod relaxation 15 p2327 A72-31744
- Debonded laminar composite torsional stress intensification analysis near circular shaped imperfection based on Hankel transform and dual integral equations solution 15 p2261 A72-32247
- Torsion problem of bodies of revolution bounded by two intersecting spherical surfaces, obtaining solution by Mehler-Fock transform 15 p2330 A72-32294
- Variational principle for boundary value problem of elastic-plastic torsion of circular bars under quasi-static finite deformation 16 p2464 A72-32914
- Elastoplastic torsion of homogeneous and inhomogeneous torus segments of arbitrary cross section, noting plastic bands propagation with increasing torque 16 p2467 A72-33119
- Stress-strain diagrams for constant strain rates in shear of Ti from torsion test machine, deriving constitutive equation for dynamic overstress 16 p2405 A72-33197
- Bending and torsional mode deformations of two dimensional elastic wing under sinusoidal and random gust 16 p2469 A72-33229
- German monograph on rotating nonround shafts stability under torsion, obtaining equations of motion solution via convergent double series expansion 16 p2469 A72-33399
- Linear stability and critical stress formulas for isotropic cylindrical shells with stepwise variable wall thickness under torsion 16 p2470 A72-33411
- Transient elastic wave propagation in circular cylinder during sudden torsional shear stress application to end surface, noting surface particle velocity and stress 16 p2426 A72-33660
- Composite cylinder of helically wound fiber laminates, calculating torsional fracture strength with allowance for plastic deformation due to matrix distortion 16 p2472 A72-33949
- Permanent traction and torsion strains effect on ratio between pure compression and pure traction yield points of Al alloy 16 p2412 A72-34179
- An analysis of the split Hopkinson bar technique for strain-rate-dependent material behavior. [ASME PAPER 72-APM-26] 17 p2628 A72-34792
- The dynamic stress-strain behavior in torsion of 1100-O aluminum subjected to a sharp increase in strain rate. [ASME PAPER 72-APM-6] 17 p2629 A72-34808
- Governing equation derivation for coupled extension, flexure and torsion in pretwisted curved beams of thin walled open section, using three dimensional elasticity [ASME PAPER 72-APM-5] 17 p2630 A72-34809
- The evaluation of the stress intensity factors for cracks subjected to tension, torsion, and flexure by an efficient numerical technique. [ASME PAPER 72-MAT-B] 17 p2631 A72-34966
- Monograph - The elastic flexural-torsional buckling of beam-columns by discrete element techniques 17 p2634 A72-35548
- Fracture of cylindrical and spherical shells containing a crack. 17 p2634 A72-35645
- Torsion and flexure of curved, thin-walled beams or tubes. 19 p2874 A72-37696
- The comparison of torsion and tension creep data for a 0.18 per cent carbon steel. 19 p2816 A72-37709
- The influence of end plate and bulkhead on the shell of variable rectangular profile subjected to simultaneous torsion and bending at middle planes. 20 p2982 A72-40065

- High strain rate and thermal instability torsional-impact machines for metal dynamic testing, using shear pin mode control
21 p3039 A72-40229
- Stability of a twisted orthotropic cylindrical shell with a jump-wise variable wall rigidity
21 p3118 A72-40815
- Time dependent deformation of isotropic viscoelastic materials, discussing rectilinear shear, circular cylinder torsion, spiral shear of layer and conical layer torsion
21 p3119 A72-41075
- Comparison of experimental and numerical results concerning a hollow photoelastic bar with a slot subjected to torsion
21 p3122 A72-41337
- Certain class of solutions of the three-dimensional problem for a rigid perfectly plastic material with a family of momentarily inextensible planes
21 p3123 A72-41392
- Circular cracks in tension and torsion
21 p3123 A72-41395
- Investigation of fatigue-failure mechanisms and inelastic deformation of metals in torsion
21 p3071 A72-41703
- Cylindrical shells of optimal torsional stiffness
22 p3233 A72-42112
- On the formation of plastic adiabatic bands in a thin tube subjected to a dynamic torsion
22 p3236 A72-42638
- Torsional vibration of an orthotropic cylindrical shell
22 p3240 A72-42881
- Strength and deformation characteristics of fiberglass under torsional and compressive shear loads, investigating temperature effects on elastic modulus
23 p3306 A72-43730
- Stress state of arbitrary contour body of revolution under torsion using finite difference method
23 p3347 A72-43744
- Al alloy rupturing analysis in complex stress state, noting sublimation and self diffusion values of activation energy in torsional to tensile state transition
23 p3301 A72-43957
- The torsion of a circular cylinder containing a symmetric array of edge cracks
23 p3350 A72-44048
- Nonlinear elastic torsion analysis for aerospace materials
23 p3354 A72-44251
- A comparison of the axial and reversed-torsional strain cycling low-cycle fatigue strength of several structural materials
23 p3304 A72-44397
- Torsion analysis of prismatic bars of different cross sections based on dipolar stress theory, applying to anisotropic media
24 p3457 A72-44872
- Stress state of variable thickness long elastic shallow shell in bending and torsion, applying equations to large turbine blades
24 p3460 A72-45728
- TORSIONAL VIBRATION**
- Thin walled prismatic structural members under uneven axial moment distribution, formulating force deflection equations for torsional-flexural behavior
01 p0141 A72-11049
- Natural bending-torsional vibrations of turbine blades connected by ring junctions, using dynamic pliability principle
01 p0143 A72-11370
- Digital computer programmed numerical calculation based on admittance method for torsional forced vibration spectra of masses and stress distribution in transmission system
02 p0271 A72-12435
- Pretwisted tapered cantilever beam torsional vibration natural frequencies determination by Galerkin method for solution of differential equation of motion
02 p0297 A72-12533
- Viscous torsional vibrations inadequacy for interpreting solar activity cycles relative to magnetic field
03 p0436 A72-13811
- Magnesium alloys torsional vibration damping correlation with texture orientation resulting from fabrication method
03 p0375 A72-13930
- Natural torsional vibrations of curved shafts, discussing oscillating system with varying flywheels
04 p0584 A72-14470
- Torsional vibrations of shaft with multiple flywheels, presenting computer generated graphs for vibration modes
04 p0584 A72-14517
- Gravitational and inertial masses equivalence principle verification by pendulum torsional oscillation experiment with laser beam
04 p0519 A72-15070
- Axially symmetric torsional waves in elastic circular composite cylinders, plotting dispersion diagrams
04 p0590 A72-15185

- Cross section geometry and deformation effects on rods vibration damping, determining surface layer energy absorbing properties for longitudinal and torsional oscillations
05 p0735 A72-15988
- Torsional vibration induced by periodic circumferential shear force on composite circular cylinder with varying rigidity and density, obtaining solutions for various boundary conditions
05 p0740 A72-16727
- Flexural, longitudinal and torsional vibration damping of various size rods, taking into account surface layer energy loss
06 p0900 A72-18675
- Shallow elastic shell under periodic distributed torque loading, investigating static stability enhancement through nonlinear boundary value problem periodic solutions
06 p0900 A72-18697
- Torsional oscillation damping in circular rods coated with viscoelastic material as function of resonant frequency
07 p1087 A72-18924
- Torsional bending vibrations mode shapes of space frame with variable elastic and mass characteristics, determining eigenvalue error limits
08 p1205 A72-20957
- Transducers for piezoelectric detection of torsional waves for wire chambers
10 p1480 A72-24212
- Time optimal control of distributed systems with random properties, considering integral relations and flying wing vehicle torsional vibration problems
10 p1421 A72-24427
- Equations of motion for torsional vibrations in system with nonlinear elastic term and variable moments of inertia, noting analog computer simulation
11 p1739 A72-26982
- Frequency equation for torsional wave phase velocity in solid circular rod under initial tension, plotted for various propagation modes
13 p2002 A72-28620
- Torsional waves far-field structure in infinite elastic rod of elliptical cross section, using perturbation method
13 p2057 A72-29004
- Torsional vibration damping in circular rods coated with viscoelastic material, noting technique effectiveness at certain resonant frequencies
13 p2058 A72-29209
- Partial differential equations for longitudinal, torsional and transverse vibrations of bars with variable composition
13 p2006 A72-29885
- Unsteady laminar boundary layer on body of revolution with axial and torsional oscillations, calculating velocity distribution and shear stress variation
15 p2178 A72-31402
- Variable cross section rod free longitudinal and torsional vibration frequencies and mode shapes determined by slowly varying parameters approximation method
15 p2327 A72-31740
- Transient torsional vibration of asymmetric rotor with limited power supply near critical speed calculated by asymptotic method
16 p2463 A72-32874
- Collocation method for coupled bending-bending torsion vibrations of straight uniform cantilever beam with asymmetric airfoil cross section
16 p2464 A72-32908
- Stresses induced by torsional vibration in twisted composite cylindrical shell of cylindrically anisotropic materials for high and low frequencies
16 p2466 A72-33102
- Kinematic equations of motion for elastic shaft with circular plate under external forces and moments, noting transverse and torsional vibrations
16 p2469 A72-33250
- Perturbation theory for torsional earth oscillations - Second approximation
17 p2548 A72-35475
- Propagation of bending-torsional waves in a thin curved rod with allowance for the shear effect
19 p2877 A72-38189
- Application of the finite element method to torsional flutter analysis on an analog computer
20 p2980 A72-39907
- Simulation of torsional vibrations of rods without concentrated masses
21 p3116 A72-40167
- Inhomogeneous beam torsional vibration modes and frequencies calculation by initial parameters method, replacing beam by series connected oscillators
22 p3232 A72-41865
- Unsteady rotor aerodynamics at low inflow and its effect on flutter
22 p3135 A72-42349
- Longitudinal-torsional vibrations of a screw beam under axial excitation
22 p3240 A72-42954
- Blade torsional tuning to manage rotor stall flutter
24 p3369 A72-45412

- Cross section geometry and deformation effects on rods vibration damping, determining surface layer energy absorbing properties for longitudinal and torsional oscillations
24 p3460 A72-45730
- TORUSES**
- Free convection velocity fields measurements and stagnation point location around horizontal torus in air, using fine particle trajectories
[ASME PAPER 71-HT-X] 08 p1163 A72-20877
- Computer graphics for invariant torus behavior in four dimensional phase space, varying equation parameter over large intervals
15 p2263 A72-31758
- Elastoplastic torsion of homogeneous and inhomogeneous torus segments of arbitrary cross section, noting plastic bands propagation with increasing torque
16 p2467 A72-33119
- Singularity of noncircular cross section zero velocity torus circumscribing area with three dimensional orbit of stationary stellar system star
16 p2460 A72-34014
- TOUCH**
- NT TACTILE DISCRIMINATION**
- TOUCHDOWN**
- Pilot perception tests on estimating flight path inclination, ground image and touchdown time under poor visibility
05 p0684 A72-16180
- TOUGHNESS**
- NT NOTCH SENSITIVITY**
- Hot formed Cr-Ni-Mo and Ni-Mo prealloyed steel powders fatigue and toughness properties, determining hardness effects by varying draw temperature from 400 to 1000 F
02 p0240 A72-11435
- Hot pressed Ti alloy powders, evaluating strength and toughness at cryogenic temperatures
02 p0240 A72-11439
- Al alloys compressed strips, determining anisotropy of toughness and crack sensitivity by tests
02 p0244 A72-12244
- High strength low alloy type ferrite pearlite steel microstructural and compositional variations effect on work hardening, ductility and impact toughness
02 p0246 A72-12558
- Hot-rolled low-carbon Mn-Mo-Nb acicular ferrite steels with high strength, toughness and impact resistance
02 p0246 A72-12558
- Metals toughness under impact loading from explosive welding process, using optical metallographic techniques
06 p0822 A72-18214
- Impurities effect on Mo plastic properties and toughness, suggesting lower vacuum arc welding rates and increased electron beam zone refining runs
09 p1326 A72-22228
- Fiber toughening mechanisms in continuous filament unidirectionally reinforced composites with elastoplastic matrices, discussing tensile energy storage in debonded region
11 p1671 A72-25463
- TOWED BODIES**
- Equilibrium configuration of cable towed in circular path, presenting multivalued boundary value problem, mathematical analysis
[AD-73445] 01 p0102 A72-11132
- Parachuting and aerial towing physiological and force data FM telemetry for biomedical response assessment leading to human engineered equipment improvement and midair retrieval system development
02 p0168 A72-12138
- Towed cable flight vehicle system motion in uniform flow field, calculating equilibrium configuration during coordinated turn from two point boundary value problem numerical solution
08 p1110 A72-21604
- Two gyro three axis stabilizer with gyrocompass effect for gravimeter or magnetometer sensor stabilization in towed gondola
13 p1957 A72-29271
- Airborne towed cargo carrying bodies dynamic stability for single-point suspension system, using linearized small perturbation analysis
[AIAA PAPER 72-986] 22 p3136 A72-42328
- TOWED TARGETS**
- U TARGETS**
- U TOWED BODIES**
- TOWERING CUMULI**
- U CUMULUS CLOUDS**
- TOWING**
- Parachutist biomedical responses in aerial tow at 110-175 knots, determining heart and respiration rates and urinary catecholamines
12 p1774 A72-28272
- TOWNSEND AVALANCHE**
- Single collision beam experiments, swarms, Townsend current and capture processes in negative ions
05 p0693 A72-17219
- TOWNSEND DISCHARGE**
- NT GAS DISCHARGES**
- NT RING DISCHARGE**

NT TOROIDAL DISCHARGE
TOWNSEND SURFACES
U TOWNSEND AVALANCHE
TOXIC DISEASES
NT CARBON MONOXIDE POISONING
NT LEAD POISONING
TOXIC HAZARDS
Flammability smoke hazards and combustion product toxicity tests of plastics [PI PAPER 2] 03 p0379 A72-13243
CO contamination of cabin and hazard to pilots, discussing concentrations, avoidance, control and analysis 07 p0933 A72-20267
Toxicological evaluation of some synthetic materials designed for airtight space equipment 21 p2998 A72-40434
Toxicity of rocket fuels 24 p3433 A72-44781
TOXICITY
NT CARBON MONOXIDE POISONING
NT LEAD POISONING
Potassium cyanide effect on phospholipid exchange in rat brain and liver during histotoxic hypoxia as function of body temperature 05 p0618 A72-16357
Abdominal injected barbamyI somnificiant and toxic effect on mice subjected to hypokinesia and isolation 05 p0622 A72-16650
Synthetic carbohydrates toxicity effects on rat liver lysosomes application to astronaut potential food sources 14 p2074 A72-30381
TOXICITY AND SAFETY HAZARD
Russian book on powdered metals toxicity covering industrial dust, physiological effects, safety standards, electron configurations and crystalline structure 11 p1584 A72-26067
Intoxicating liquor and the general aviation pilot in 1971. 24 p3377 A72-45662
TOXICOLOGY
Toxicological control and chemical analysis of out-gassing products from nonmetallics in high temperature oxygen atmosphere, investigating use within LM crew compartment 01 p0019 A72-10771
Insecticide dichlorvos vapor toxicity in aircraft cabin atmosphere at 8000 ft, studying plasma cholinesterase activity, erythrocytes, dark adaptation and bronchiolar resistance 14 p2081 A72-31082
A note on the biological activity of the noble gas compound xenon trioxide. 18 p2652 A72-36444
TRACE CONTAMINANTS
Trace gas pollutant monitoring by microwave rotational absorption spectroscopy, discussing test results with Gunn diode cavity spectrometer [AIAA PAPER 71-1048] 01 p0023 A72-10524
Absorption cell heterodyne method for nondispersive IR detection of trace gases with molecular vibrational-rotational spectrum [AIAA PAPER 71-1064] 01 p0023 A72-10532
Remote sensing of atmospheric pollutants and trace contaminants, presenting high speed high resolution, Fourier interferometer breadboard model [AIAA PAPER 71-1109] 01 p0068 A72-10553
Miniaturized magnetic mass spectrometer for trace contaminants continuous monitoring and control, discussing applications to closed atmospheric systems in spacecraft and undersea environments [AIAA PAPER 71-1122] 01 p0068 A72-10558
Na and K trace amounts detection in Al based solid rocket propellants by neutron activation analysis, using gamma ray spectroscopy for nondestructive analysis 02 p0270 A72-11959
Spacecraft atmosphere trace contaminant sensor system using mass spectrometric analysis of contaminants concentrated on sorbents in monitor inlet system [ASME PAPER 72-ENAV-15] 20 p2896 A72-39162
Free energy changes and boundary segregation of tin and antimony in CrV steels. 21 p3070 A72-41648
TRACE ELEMENTS
Specific quantitative trace analysis technique for solids using spark source mass spectrometry 03 p0361 A72-13849
Major and trace element abundances in orogenic area volcanic rocks, considering geographic and stratigraphic relations and composition 05 p0658 A72-16721
Johnstown achondrite meteorite composition, presenting published and unpublished data on minor and trace elements 05 p0722 A72-17154
Trace element concentrations of Apollo 15 basalt and soil samples by atomic spectrophotometry, colorimetry and isotope dilution 06 p0888 A72-18269
Lunik 16 samples trace element concentration, suggesting feldspar excess and local regolith derivation 09 p1381 A72-22272

Rare earth and trace elements in Lunik 16 soil, comparing abundances with chondrites and Apollo samples 09 p1381 A72-22274
Lunik 16 soil samples trace elements composition suggesting meteoritic component presence and similarity to Apollo soils 09 p1381 A72-22276
Lunar anorthosites and parent liquids chemical composition from trace element analysis 10 p1537 A72-24158
Vacuum induction melting process for high temperature steels and superalloys fabrication, emphasizing control over temperature, pressure, beneficial trace elements and harmful impurities 13 p1964 A72-29100
Ti, B, Zr and Be trace additions effect on Al alloy grain refining from spectrochemical analysis 13 p1913 A72-29838
Ferric ion traces evidenced in lunar and meteoritic titanagites by charge transfer bands observations during heating, interpreting origin as caused by cosmic radiation 14 p2154 A72-30515
Dc arc plasma, investigating applied magnetic field, trace elements and gap spacing effects on spectral line intensity spatial distribution 14 p2139 A72-30783
Spectrochemical trace analyses in electric arc plasma, examining external magnetic field effects on spectral line intensity variation 14 p2139 A72-30784
Upper atmospheric trace constituents global mapping by laser radar probing from satellite, discussing feasibility and comparison with ground based system [AIAA PAPER 72-660] 16 p2365 A72-34074
Neutron activation and neutron-capture gamma ray analyses of igneous rock trace elements, discussing Tyrone Igneous Series granites 20 p2899 A72-39831
On the determination of trace elements in meteoritic phases by neutron activation analysis. 20 p2900 A72-39838
Minor constituents in planetary atmospheres - Ultraviolet spectroscopy from the Orbiting Astronomical Observatory. 21 p3111 A72-41459
Trace element geochemistry of Apollo 16 soil 68501. 23 p3337 A72-43939
TRACERS
Tracer particle motion behavior in laser anemometry for turbulent flow, comparing liquids with gases for accuracy 12 p1809 A72-27763
TRACING
The track method and its application in studies of atomized-fuel combustion kinetics 18 p2720 A72-36243
TRACKERS
U TRACKING [POSITION]
TRACKING [POSITION]
NT COMPENSATORY TRACKING
NT MISSILE TRACKING
NT OPTICAL TRACKING
NT PHOTOGRAPHIC TRACKING
NT PURSUIT TRACKING
NT RADAR TRACKING
NT RADIO TRACKING
NT RANGE AND RANGE RATE TRACKING
NT SATELLITE TRACKING
NT SPACE DETECTION AND TRACKING SYSTEM
NT SPACECRAFT TRACKING
NT STAR TRACKERS
NT WILDLIFE RADIOLOCATION
Simulated sonic boom effect on tracking performance and autonomic response, noting heart rates, skin conductance and startle reflex 06 p0767 A72-17868
Pilot glide slope and localizer tracking performance during successive in-flight simulated ILS approaches 12 p1773 A72-28260
External background and internal noise effects on automatic tracking systems accuracy, noting optimal operating point on transducer response curve 21 p3014 A72-40320
Evaluation of the mean time to tracking failure in a nonlinear pulsed servo with irregular signal input 21 p3038 A72-40708
Manual tracking control with continuously variable selective control gain in response to system state, noting intuitive optimization 21 p3011 A72-41425
Influence of stick efficiency on tracking error applying two slightly different control elements. 21 p3012 A72-41429
Velocity space maps and transforms of tracking observations, for orbital trajectory state analysis. 24 p3440 A72-45135
TRACKING ANTENNAS
U DIRECTIONAL ANTENNAS

TRACKING FILTERS
Phase stabilization of synchronized tracking oscillator with resonant frequency regulated by output voltage 03 p0333 A72-13895
Suboptimal decision algorithm to correlate sensor data with stored tracks in real time track-while-scan surveillance system 10 p1441 A72-23780
Optimal tracking filter for processing sensor data of imprecisely determined origin in surveillance system by minimizing effects of correlation uncertainties 10 p1455 A72-23787
Phase stabilization of synchronized tracking oscillator with resonant frequency regulated by output voltage 15 p2209 A72-32706
Target tracking based on the Kalman-Bucy filter 19 p2778 A72-37750
Reduced order observers design for optimal control of linear discrete time stochastic systems, considering velocity-aided tracking filter 23 p3276 A72-43856
TRACKING NETWORKS
NT DEEP SPACE NETWORK
NT GLOBAL TRACKING NETWORK
NT MANNED SPACE FLIGHT NETWORK
NT SPACE DETECTION AND TRACKING SYSTEM
International Satellite Geodesy Experiment based on laser telemetry technique, discussing ground stations network and tracking cameras 04 p0520 A72-15726
Phase locked loop bandwidth, acquisition time and SNR for Doppler tracking deep space communications for Venus and Jupiter probes 05 p0629 A72-16575
German monograph on models for automatic radar tracking methods covering error probabilities, reliability and false information reception 09 p1348 A72-23231
Global NASA communications network /NASCOM/ reliability, discussing design and performance goals 10 p1435 A72-23992
Digital command system second-order subcarrier tracking loop performance. 21 p3038 A72-40870
TRACKING RADAR
Angle tracking radar receiver signal analysis simplification by use of complex variables 10 p1437 A72-24684
Agile beam electronically scanned multitarget phased array tracking radar, dwell allocation strategy and trajectory extrapolation algorithm effects on target handling capacity 10 p1437 A72-24685
Tracking radar system rain clutter reduction by backscatter polarization technique for signal phase and magnitude adjustment 18 p2659 A72-36310
Parallel processing of ballistic missile defense radar data with PEPE. 24 p3383 A72-45667
TRACKING STATIONS
NT GLOBAL TRACKING NETWORK
NT SPACE DETECTION AND TRACKING SYSTEM
Sounding rocket radio tracking systems with real time trajectory plotting, developing computer program for exoatmospheric trajectory determination 07 p0939 A72-19089
Ground satellite control station network, including tracking stations for measuring Doppler effect with IRIS receivers [DGLR PAPER 72-009] 13 p1938 A72-28960
Space center trajectory and telemetry systems, including radar stations, interferometric equipment, optical methods and interlinked computers [DGLR PAPER 72-014] 13 p1938 A72-28961
Telemetry equipment of network tracking stations for CNES Symphonie satellites at 136-138 and 148 MHz [DGLR PAPER 72-015] 13 p1939 A72-28966
Low cost optimal earth resources technology satellite station for satellite tracking and image data reception and recording 15 p2213 A72-31246
Space tracking stations in Spain. I - The Madrid space station and its activities 17 p2536 A72-34945
Global network of ground based facilities /infrastructure/ including spacecraft launching, tracking, communication and readout sites for international space operations [AIAA PAPER 72-739] 18 p2742 A72-36545
Solution of the problem of cosmic triangulation by the generalized method of synchronous and quasi-synchronous straight lines 19 p2861 A72-37971
Comments on the figure of the moon from Apollo landmark tracking. 22 p3226 A72-42534
Optoelectronic flight path tracking systems 24 p3380 A72-45274

Potential of the navy navigation satellite system in predicting ionospheric characteristics.

24 p3447 A72-45555

TRACKING STUDIES

U TRACKING [POSITION]

TRACKS

A study of the vestigial records of cosmic rays in lunar rocks using a thick section technique.

23 p3341 A72-44459

TRACTION

Elastic stress field in hollow circular cylindrically anisotropic body under surface tractions expressed as Fourier series

[ASME PAPER 71-WA/APM-13]

05 p0734 A72-15967

Traction at interface between fiber and matrix in fiber reinforced composites, considering axially symmetric deformations and stress fields

09 p1339 A72-23173

Heteroplastic materials creep characteristics from constant strain rate isothermal traction tests, deriving deformation functions for material behavior beyond elastic range

16 p2412 A72-34120

Permanent traction and torsion strains effect on ratio between pure compression and pure traction yield points of Al alloy

16 p2412 A72-34179

On the solution of plane, orthotropic elasticity problems by an integral method.

[ASME PAPER 72-APM-BB]

23 p3350 A72-44056

TRADEOFFS

Power conditioning requirements and tradeoff considerations for space shuttle, warning against central power conversion use on orbiter and booster vehicles

01 p0007 A72-11052

Guided weapon systems design under cost restrictive conditions, discussing conceptual design planning and performance tradeoffs against cost and reliability

01 p0147 A72-11155

Hardware software firmware tradeoffs - IEEE Conference, Boston, September 1971

10 p1442 A72-23815

System tradeoffs for high performance pulsed MPD thruster in space mission application

[AIAA PAPER 72-457]

11 p1708 A72-26193

Production and test facilities availability effect on costs involved in obtaining item at required quality level, examining component rejects and defectives

18 p2670 A72-37133

TRADESCANTIA

Dynamics of secondary vacuole movement within cytoplasm of Tradescantia virginiana hair cells

15 p2186 A72-32350

Influence of temperature shocks on seed formation after irradiation of pollen from Tradescantia paludosa.

19 p2761 A72-38642

TRAFFIC

NT AIR TRAFFIC

TRAFFIC CONTROL

NT AIR TRAFFIC CONTROL

NT RADAR APPROACH CONTROL

Airfield surface radar detection equipment to control aircraft and ground vehicles under reduced visibility and darkness

02 p0173 A72-12105

Cellular electronic logic circuit planar array representing objects inertial motion, applying to traffic control, image processing and artificial intelligence

06 p0779 A72-17496

French space applications program for telecommunications, meteorology, natural resources survey and air/sea traffic control

08 p1256 A72-21201

Dioscours geostationary satellites project for Atlantic and Pacific ocean air and ship traffic safety based on radar tracking and multiplex numerical data transmission

09 p1396 A72-23400

Time/frequency techniques in land, sea and air transportation environments, discussing characteristics and electronic traffic control systems applications

15 p2338 A72-32073

Graphic color display adapted to traffic control for direct operator-computer dialogue, noting instruction repertoire, switching device and input devices

16 p2420 A72-32894

Solutions to transportation problems using time/frequency technology.

24 p3422 A72-44649

Safety design of space station against collision hazards with artificial orbiting bodies.

24 p3449 A72-45143

TRAINING EDGES

Axial and tangential velocity distributions within trailing line vortex to large distance downstreams of generating wing extended from available data

[AD-743599]

01 p0001 A72-11135

Drag and lift experimental determination for low aspect ratio rectangular wings with blunt trailing edges at Mach numbers 0.5-2.2

[DGLR PAPER 71-114]

02 p0152 A72-12712

Velocity and exit angle determination for flow behind turbine blade cascade with cooling air exhaust through blade trailing edges from continuity equations

05 p0707 A72-17063

Supersonic near wake flow around blunt and sharp cones with trailing edge turbulent boundary layer

06 p0757 A72-18141

Gas turbine nozzle guide vane trailing edge protection by air films cooling, measuring gas temperatures with chromel-alumel thermocouples

08 p1224 A72-21318

Base pressure drag reduction on rectangular wings with blunt trailing edges from low speed wind tunnel measurements

[DFVLR-SONDDR-219]

10 p1419 A72-24842

Slender body theory for flow calculation past low aspect ratio delta wing with straight trailing edge, noting lifting vortices distribution

10 p1420 A72-25131

Profile losses at turbine rotor blade in unsteady gas flow from experimental data analysis, noting effect of turbulence caused by trailing edge wakes

13 p1893 A72-28783

Turbine blade trailing edge wall thickness measurement by phase sensitive eddy current technique

16 p2397 A72-33201

Free jet reenergization efficiency, mixing distance and similarity analysis for boundary layer control at sharp trailing edges and cusps

[AIAA PAPER 72-700]

16 p2345 A72-34043

Rotary wings lift and efficiency increase by circulation control via tangential blowing about bluff trailing edge airfoils

[AHS PREPRINT 603]

17 p2489 A72-34492

Visualization study of flow near the trailing edge of an oscillating airfoil.

20 p2886 A72-40067

Conformal mapping procedure for numerical generation of airfoils with local curvature singularities, presenting test problem results for zero trailing edge angle

21 p2992 A72-41259

Theory of a boundary layer with abruptly varying boundary conditions

22 p3166 A72-42259

Pressure at the trailing edge and losses in turbine blades with air injection into the blade wake

23 p3248 A72-43661

Application of a time-dependent boundary-layer analysis to the problem of dynamic stall.

23 p3249 A72-44058

TRAINING-EDGE FLAPS

Wind tunnel investigation of unswept rectangular wing with externally blown single slotted flap, determining optimum slot width as function of momentum coefficient and flap deflection

04 p0462 A72-15461

Jet-STOL augmentor wing consisting of moderately thick airfoil with full span leading edge slat and double surface trailing edge flap

08 p1110 A72-21899

Three dimensional wind tunnel investigation of vortex augmented unswept wing with leading edge cusp flap and split upper and lower trailing edge flaps

[SAE PAPER 72-0321]

11 p1568 A72-25584

Rarefied hypersonic flow characteristics of delta wings and trailing edge spoilers.

17 p2485 A72-35229

Lift and control augmentation by spanwise blowing over trailing edge flaps and control surfaces.

[AIAA PAPER 72-781]

19 p2746 A72-38140

TRAILS

U TRACKS

TRAINEES

U STUDENTS

TRAINERS

U TRAINING DEVICES

TRAINING

U EDUCATION

TRAINING AIRCRAFT

NT JAGUAR AIRCRAFT

Trainer-combat turbojet or turboprop aircraft characteristics, comparing flight, weight, size, maintenance and development costs

05 p0611 A72-16178

Mitsubishi XT-2 jet trainer aircraft, presenting design, structural and performance data

10 p1421 A72-25107

Case report of rapid decompression in supersonic trainer aircraft pressurized cabin, discussing physical and blast effects, pressurization safety, decompression sickness and hypoxia

11 p1584 A72-26020

Cost effectiveness determination for different levels of reliability and maintainability of training aircraft, using computer simulation

13 p2067 A72-28355

HR 200 training and acrobatic two seater low wing metal aircraft series production, dimensions and maximum takeoff weight performances

13 p1898 A72-30039

Wind tunnel testing of Dassault-Breguet-Dornier Alpha Jet twin engine trainer, emphasizing tests for

wing-empennage flutter and jet induced interference effects

13 p1940 A72-30077

Canadian Armed Forces air navigation training program, noting emphasis on training flights

15 p2272 A72-32209

TRAINING DEVICES

NT TEACHING MACHINES

Educational and social applications of communication and meteorological satellite data dissemination, discussing learning and teaching model development

06 p0777 A72-18624

Training cockpit TL-29 mean time of failure-free operation from measurement data during development tests and two year guarantee, calculating avionics devices reliability

14 p2092 A72-30281

Digital computer controlled flight simulators for undergraduate pilot, electronic warfare, air-to-air combat and helicopter training

17 p2535 A72-34393

Simulated blind approach trainer for general aviation aircraft pilot training, discussing design concept and instrumentation with emphasis on components simplicity and economy

17 p2536 A72-35325

Physical training as a prophylactic measure against the hypodynamic syndrome

23 p3260 A72-43920

TRAINING SIMULATORS

NT COCKPIT SIMULATORS

NT FLIGHT SIMULATORS

Fighter pilots training by simulators, determining learning effectiveness by mathematical model based on renewal theory

[AIAA PAPER 72-161]

05 p0644 A72-16827

Aircraft safety enhancement by computer controlled flight simulator training of air crews, discussing Boeing 747 program

07 p0926 A72-18839

Night Carrier Landing Trainer flight and carrier environment simulator for A-7 aircraft pilot training, discussing performance predictions from computer data analysis

07 p0927 A72-19137

Star sky simulation in testing and training stands, using spherical mirror, collimator and imbedded spheres

09 p1310 A72-22949

Flight stress and performance of training in general aviation simulator compared with actual flight

12 p1774 A72-28261

Hypoxia effect on aircraft pilot performance, using Link GAT 1 trainer and controlled composition atmosphere under varied altitude conditions for simulated ILS landing approaches

12 p1776 A72-28310

Pressure chamber training effects on rats chain motor reflexes hypoxia adaptation, noting sinocarotid receptors importance in compensatory-adaptive reactions

13 p1902 A72-28641

Aircraft and other vehicle simulators for training crews, discussing evolution of needs, digital techniques, and visual and physiological experiences

14 p2092 A72-30844

ATC procedures training by digital radar simulators, taking into account geographic terrain, radar, wind and aircraft characteristics and flight plans

15 p2214 A72-32098

Computerized navigator training simulator for complete array of air navigation instruments, discussing design and human factors

15 p2214 A72-32208

Digital computer controlled flight simulators for undergraduate pilot, electronic warfare, air-to-air combat and helicopter training

17 p2535 A72-34393

Simulated blind approach trainer for general aviation aircraft pilot training, discussing design concept and instrumentation with emphasis on components simplicity and economy

17 p2536 A72-35325

Spatial simulator of tactical navigation

19 p2783 A72-37798

How United trains DC-10 pilots.

19 p2760 A72-37898

Studies in pilot training - The anatomy of transfer.

20 p2897 A72-39718

Visual simulation - A proven training method.

20 p2897 A72-39749

Use of fixed and moving base flight simulators for the aerodynamic design and development of the S-3A airplane.

[AIAA PAPER 72-764]

20 p2888 A72-40052

Problems arising in the transfer of training from simulated to real control systems.

21 p3010 A72-41412

Digital computer equipped facility for training simulators environmental simulation capability testing, describing electronics interface, control and display equipment

22 p3164 A72-42928

TRAJECTORIES

NT ASCENT TRAJECTORIES

NT BALLISTIC TRAJECTORIES
NT DESCENT TRAJECTORIES
NT EARTH-MARS TRAJECTORIES
NT EARTH-MOON TRAJECTORIES
NT EARTH-VENUS TRAJECTORIES
NT ELECTRON TRAJECTORIES
NT HYPERBOLIC TRAJECTORIES
NT INTERPLANETARY TRAJECTORIES
NT LUNAR TRAJECTORIES
NT MIDCOURSE TRAJECTORIES
NT MISSILE TRAJECTORIES
NT MOON-EARTH TRAJECTORIES
NT PARTICLE TRAJECTORIES
NT REENTRY TRAJECTORIES
NT RENDEZVOUS TRAJECTORIES
NT ROUND TRIP TRAJECTORIES
NT SPACECRAFT TRAJECTORIES

TRAJECTORY ANALYSIS
Consecutive collision orbits characterized by particle ejection from mass along x axis in restricted three body problem

Propagators in strong plasma turbulence, considering characteristic trajectories of Vlasov equation

Spacecraft flight trajectory parameters from unknown second moment matrix of navigation measurement errors

Three dimensional roll-controlled missile trajectory model for simple time-sharing digital or analog simulation, using wind-to-inertial axis transformation

Coriolis acceleration effects on flight of projectiles fired from earth surface, discussing horizontal and vertical velocities

I-V characteristics and bandwidth properties of distributed emission amplifier within magnetic field, analyzing averaged electron trajectories and hf potential distribution

Liquid and solid particle trajectory calculation in two phase Laval nozzle flows, determining density, velocity and temperature

Crater 9 meteorite /Argentina/ entry trajectory and orbital calculations, determining masses and velocities from dynamic conditions at impact

Soviet book on rocket dynamics covering history, variable mass point aerodynamics and ballistics, numerical and computer methods and trajectory analysis

Solar flare surges with hot spectrum and violent activity, analyzing trajectories

Computerized error function method of wreckage trajectory analysis in aircraft accident investigation, using fundamental equations of motion

Target trajectory detector optimization, using data and Markovian chain apparatus

Molecular collision model, comparing generalized phase shift approximation method with classical trajectory calculations for rotational inelasticity

Axissymmetric deflected turbulent jet flow, analyzing physical features and trajectories

Third order nonlinear van der Pol oscillating systems, discussing digital computer verification for existence of stable limit cycles in state space trajectory plots

Moving object trajectory determination by a posteriori Poisson signal transmission analysis with random parameters

Radio signal group trajectory in ionosphere expressed as series expansion in terms of increasing power of beam reflection height

Sign behavior of switching function defined for plane fuel-optimal flight on elliptical coast trajectories

Atmospheric rendezvous concept to increase space transportation system efficiency and flexibility, discussing structural weight savings

Trajectory and flow properties of submerged heated effluents discharging into moving waterway

Trajectory characteristics for multiple asteroid flyby missions to determine physical properties of minor planets

Mission analysis of Helios spacecraft swingby past Venus to acquire extraelectric trajectory

Center of mass motion of spacecraft in central gravitational field, analyzing programming of size and position of elements in mass geometry leading to arbitrarily large displacements

Electron and muon density fluctuations, trajectory distribution and azimuthal symmetry in cosmic ray air showers

Time independent or periodic Hamiltonian conservative differential equations, studying open, oscillating, limited and abnormal trajectories

Radio wave beam trajectories in laminar isotropic plasma layer, using dynamic systems theory

Two body problem trajectory equation method simplification, reducing entire solution to two integral evaluations

Mercury trajectory across solar disk plotted by telephoto lens cameras, for determining position angles, disk contact times and relative angular velocity

Nonlinear dynamic system mathematical model for unit mass particle escape trajectories from potential well, taking account of trapped motions and stable oscillations

Explicit analytic guidance technique for hyperbolic approach phases of lunar and interplanetary spacecraft trajectories from first order solution for perturbed planet centered trajectory

Two point boundary value solution for N-body trajectories, comparing asymptotic with numerical integration solutions for several lunar and interplanetary trajectories

Outer planets Grand Tour trajectory correction requirements, examining combined radio/onboard navigation system and delta V estimates

Sounding rocket radio tracking systems with real time trajectory plotting, developing computer program for exoatmospheric trajectory determination

Real time recursive algorithms for estimating coefficients of fixed knot spline approximation to trajectory

Recursive and nonrecursive real time spline methods for nonlinear estimation of independent trajectory parameters for vehicle entering earth atmosphere

Disturbing parameters effect on spacecraft trajectory X coordinate values estimation, including planetary masses and coordinates, astronomical unit and light speed

Trajectory properties of roots of characteristic equations with complex coefficients for two dimensional systems with feedforward and feedback cross couplings

Nonlinear closed loop system reduction of differential trajectory sensitivity to continuous variations or external disturbance

Differential geometry of reductive homogeneous spaces with invariant affine connections, identifying geodesic lines with subgroup trajectories of space motions

Trajectory dynamics for fluorine atoms reaction with H molecules, predicting total available energy from energy release on potential energy surface

Lift variation effect on rolling reentry vehicle trajectory, calculating deviation from zero-lift impact point

Radio wave beam trajectories in laminar isotropic plasma layer, using dynamic systems theory

Accuracy improvement of nonlinear systems phase trajectories graphic construction, noting second order ordinary differential equations solution

Interplanetary single impulse flight trajectories optimization and computation, determining geometrical and kinematic characteristics

Trajectory determination of supersonically traveling object from shock arrival times observations at ground locations

First order asymptotic matching computational technique for calculation of perturbed moon-centered hyperbola parameters in earth-moon trajectory

Wet and dry bent over plumes comparison, constructing plume paths for various atmospheric stability conditions

Cruise guidance, trajectory and navigation analysis for solar electric Mercury orbiter, considering engine performance, thrust and terminal errors

Proportional navigation with a maneuvering target

Trajectories behavior and finite time stability of differential equations system, using Liapunov techniques

Two step spacecraft reentry guidance involving skip trajectory at parabolic speeds, proposing algorithm for running coordinate and speed vector components values

Trajectory correction problem optimal measurement set, showing solution by linear programming simplex algorithm method

Runaway stars trajectories stability tested from clusters study, noting preservation of energy, velocity and position and reproducibility

Equations of motion and phase trajectory analysis for resonant oscillations of beam-pendulum system

Encounter trajectory design for solar electric propulsion rendezvous with low mass celestial bodies, noting target characteristics

Electrostatic field and electron trajectories calculation for focusing optoelectronic systems formed by interacting electrodes positioned on conducting surface

Absolute stability of nonlinear automatic control systems based on root locus trajectories and Popov line hodographs

One dimensional blast wave theory for trajectory analysis of shocks driven by solid explosives in linear shock tubes

Trajectory analysis for swingby technique using Jovian gravitational field for leaving ecliptic plane along heliocentric orbit and for solar flyby at specified distance

Comets formation from Jupiter satellite Io surface eruption using particle trajectory analysis and comet orbital elements calculation

Centers and foci composition of united trajectories of two autonomous scalar second order differential equations

Body of revolution motion in fixed center Newtonian field, investigating plane trajectories of center of inertia

Airborne electrostatic probe for cloud droplet size measurement, calculating flow distribution and particle trajectories

Russian book on flight dynamics covering horizontal flight, takeoff, climb and landing characteristics, meteorological conditions, helicopters, trajectory problems, stability and controllability analysis, etc

Spacecraft free fall trajectory calculation, using numerical optimization procedure based on Hamilton principle for two point boundary value problems

STOL aircraft minimum noise takeoff trajectories determination, taking into account engine thrust and listeners distance from noise source

Coriolis forces effect on bubbles trajectories in rotating containers, determining critical Reynolds number

Control function improvement method for flight dynamics variational problems solution, discussing dynamic programming, trajectories with uncontrolled elements and coordinate transformation

Entry of high-energy solar protons into the distant geomagnetic tail

Special control of spiral flight curves with the neutral and maneuver points as ultimate positions of the indifference points

Maximal contraction points of autonomous nonlinear system phase trajectories, using van der Pol differential equations

Two body problem trajectory equation method simplification, reducing entire solution to two integral evaluations

Mercury trajectory across solar disk plotted by telephoto lens cameras to determine position angles, disk contact times and relative angular velocity

Range correction computations for weapons dropped from aircraft

Proportional navigation with a maneuvering target

Trajectories behavior and finite time stability of differential equations system, using Liapunov techniques

Approximations and bifurcations in flight dynamic system, investigating singular point motion over trajectory during partition process

19 p2748 A72-37553

Reflectionless ionospheric propagation of non-guided VLF descending wave near low hybrid resonance maximum frequency, investigating energy trajectory

19 p2790 A72-37793

Variational method in the control system invariance problem

19 p2778 A72-37990

Monte Carlo trajectory calculations of the three-body recombination and dissociation of diatomic molecules.

19 p2838 A72-38805

Real time estimation of trajectory for lifting reentry vehicle of shuttle orbiter type, discussing iterated non-linear filter and adaptive filter

[AIAA PAPER 72-874] 20 p2966 A72-39126

An intermediate matching technique for solving two point boundary value problems using the perturbation method.

20 p2910 A72-39198

Disturbing parameters effect on spacecraft trajectory X coordinate values estimation, including planetary masses and coordinates, astronomical unit and light speed

20 p2969 A72-39256

Probability theory central limit theorem application to dynamic system generated by billiard scattering motion

20 p2945 A72-39403

Coincidence of the mapping point with the slip plane in the modified differential descent method

20 p2946 A72-39470

Best-fit estimate of relativistic effects in time-delay experiments.

20 p2972 A72-39871

A method of numerical integration for trajectories with variational equations.

[AIAA PAPER 72-910] 21 p3111 A72-41557

Approximate analytic solution method for trajectory problem of planetary flyby or impact case of restricted three body problem

[AIAA PAPER 72-911] 21 p3111 A72-41558

Mission design and navigation for a 1977-1978 Venus Swingby/Mercury Orbiter.

[AIAA PAPER 72-941] 21 p3113 A72-41577

Nonlinear problems of analyzing the observability of the trajectories of spacecraft motion on the basis of measured data

22 p3223 A72-42203

Low-drag artillery projectile aerodynamic characteristics and dynamic flight behavior from wind tunnel, spark range and instrumented flight tests, describing mathematical trajectory simulation

[AIAA PAPER 72-979] 22 p3134 A72-42334

Development and performance analysis of a trajectory estimator for an entry through the Martian atmosphere.

[AIAA PAPER 72-953] 22 p3224 A72-42352

Determination of characteristic magnitudes of toroidal electrostatic analyzers - Application to the optimization of analyzers used in space physics

22 p3180 A72-42935

A method for partitioning the phase space into regions with constant-sign increments of phase coordinates

23 p3275 A72-43780

Allowable region of approach height and desirable approach path of aircraft for safe landing, presenting optimal control trajectories

23 p3252 A72-44497

Search for trans-Plutonian planets with the aid of periodic comets

24 p3437 A72-44759

The concept of reference loci applied to four-body dynamics.

24 p3440 A72-45137

Spacecraft rendezvous trajectories and targeting maneuvers onboard sequential computation, taking into account maneuver constraints and state vector update information

24 p3450 A72-45172

Transportation of radioactive waste-materials into the sun.

24 p3450 A72-45184

Transport properties of a gas of diatomic molecules. VI - Classical trajectory calculations of the rotational relaxation time of the Ar-N₂ system.

24 p3427 A72-45308

SAM-D control test vehicle trajectory planning and flight test analysis.

24 p3451 A72-45338

Application of plane fixed equations of motion to reentry vehicle flight analysis.

24 p3452 A72-45345

Mariner 9 Mars orbital trajectory analysis from earth based radio data, considering gravity field, n-body perturbation and solar radiation pressure effects

[AIAA PAPER 72-928] 24 p3443 A72-45434

Mariner spacecraft Jupiter-Saturn 1977 gravity assisted flyby, discussing mission objectives and trajectory options

[AIAA PAPER 72-943] 24 p3444 A72-45438

Equations for the general motion of a rocket in a resistant medium

24 p3452 A72-45448

TRAJECTORY CONTROL

NT TRAJECTORY OPTIMIZATION

Spacecraft reentry trajectory parameter selection and optimal control algorithm under random atmospheric density variation

05 p0685 A72-16429

Missile trajectory stochastic optimal control systems with fuel constraint by mean path deviation optimization

05 p0725 A72-16452

KS-transformation based regularization technique modification for minimal fuel consumption rocket trajectory control during space maneuver

05 p0726 A72-16454

Optimization algorithms for jet transport aircraft in externally based flight trajectory control in turbulent atmosphere, comparing with ILS

05 p0685 A72-16472

Iterative process convergence in least squares and maximum likelihood methods of processing measurements in spacecraft trajectory control, space navigation and geodesy systems

05 p0633 A72-16761

Dynamic stability of controlled spacecraft with liquid propellant rocket engines, considering acceleration and braking sections of trajectory

05 p0730 A72-17027

Satellite launch vehicles guidance and control systems, discussing control parameters for minimum injection error

07 p1033 A72-20604

Mars and Venus probes entry into planetary atmospheres, discussing aerodynamics of trajectory control and soft landing

09 p1394 A72-23673

Spacecraft interplanetary guidance trajectory correction, deriving algorithm for optimal accuracy and minimum fuel expenditure

11 p1718 A72-25931

Two and three impulse trajectories for fixed time and angle rendezvous between vacant circular coplanar orbits, defining optimality domain

11 p1719 A72-25977

Point motion in random error region applied to synchronous satellite trajectory control by single impulse correction

11 p1684 A72-26902

Trajectory shaping advantages for outer planet orbiter solar electric propulsion, considering radiation belt constraints, dual launch and target orbit geometries

[AIAA PAPER 72-423] 13 p2036 A72-28938

Synthesis of a nonlinear law for spacecraft motion control in the earth's atmosphere

17 p2621 A72-35201

Iterative process convergence in least squares and maximum likelihood methods of processing measurements in spacecraft trajectory control, space navigation and geodesy systems

17 p2523 A72-35264

Nonlinear on-line rapid estimation scheme with application to trajectory maneuvering vehicles.

19 p2781 A72-38258

A versatile Kalman technique for aircraft or missile state estimation and error analysis using radar tracking data.

[AIAA PAPER 72-838] 20 p2950 A72-39089

A simulation technique used in the development of a flight control system for an aerodynamically controlled missile.

[AIAA PAPER 72-858] 20 p2976 A72-39136

Trajectory deviation conditions in second order linear differential escape game, using Pontryagin principle

22 p3204 A72-41903

A control algorithm for the orbital reentry of a space vehicle

22 p3223 A72-42206

Achievement of given motion by impulse correction under arbitrary disturbances /difference models/

23 p3313 A72-44044

Multistage rocket optimal control, deriving conditions for existence of minimum of performance index function of mass, position and velocity initial and final values

23 p3343 A72-44264

Energy management during the space shuttle transition.

24 p3452 A72-45347

TRAJECTORY MEASUREMENT

Telescopic meteors light curves, showing maximum point brightness distribution in visible trajectory with respect to stellar magnitudes

03 p0438 A72-13985

Two parameter trajectory measurement optimal planning reduced to quadratic programming based on linear programming generalization for continuous case

05 p0721 A72-16758

Algorithms for optimal planning of trajectory measurement times during sampling several parameters

05 p0641 A72-16759

Dynamic system observation accuracy in spacecraft trajectory measurement, deriving processing algorithm based on state-estimate error correlation matrix analysis with maximum likelihood procedure

05 p0721 A72-16760

Satellite motion state vector accuracy estimate algorithm based on angular measurements of stellar positions relative to satellite sent probe

05 p0687 A72-16762

Polynomial class random process realization based on statistical methods of processing spacecraft orbital measurement data, considering random and systematic errors

05 p0683 A72-16763

Methodical errors in spacecraft local vertical determination due to variability of physical effects, considering planet oblateness, atmospheric refraction, incident radiation fluctuations, etc

05 p0721 A72-16764

Geodetic satellite systems applications, describing trajectory beacons, telecontrol and telemetry stations and computing and operations center of French Geole system

06 p0809 A72-18258

Two parameter trajectory measurement optimal planning reduced to quadratic programming based on linear programming generalization for continuous case

17 p2610 A72-35261

Algorithms for optimal planning of trajectory measurement times during sampling several parameters

17 p2533 A72-35262

Dynamic system observation accuracy in spacecraft trajectory measurement, deriving processing algorithm based on state-estimate error correlation matrix analysis with maximum likelihood procedure

17 p2610 A72-35263

Satellite motion state vector accuracy estimate algorithm based on angular measurements of stellar positions relative to satellite launched probe

17 p2578 A72-35265

Polynomial class random process realization based on statistical methods of processing spacecraft orbital measurement data, considering random and systematic errors

17 p2576 A72-35266

Methodical errors in spacecraft local vertical determination due to variability of physical effects, considering planet oblateness, atmospheric refraction, incident radiation fluctuations, etc

17 p2610 A72-35267

Minimax technique in optimal control problems with incomplete information on phase vector, using dynamic programming and system position measurement refinements

20 p2911 A72-40027

Particle trajectory and time of flight measurement in search for anti-alpha particles in primary cosmic radiation, using magnetic spectrometer with spark chambers

22 p3219 A72-42568

TRAJECTORY OPTIMIZATION

Reentry glider approximate optimal atmospheric entry trajectories, maximizing function of terminal velocity, altitude, flight path and heading angles subject to three terminal nonlinear constraints

01 p0128 A72-10377

Minimum propellant impulsive optimal spacecraft guidance and trajectory problem, developing deterministic theory in discrete linear quadratic form with second order perturbation analysis

01 p0130 A72-10929

Trajectory optimization problems solution with terminal state constraints using combined parallel tangents/penalty function approach

02 p0280 A72-12264

Space shuttle optimal boost trajectories, showing payload increase by flying pitch profiles optimization

[AAS PAPER 71-325] 02 p0286 A72-12423

Aircraft trajectory optimization for maximum profit as decisional problem under risk conditions, determining probabilities by Monte Carlo method

02 p0257 A72-12747

Optimal trajectory in phase space, deriving differential motion equations with Euler-Lagrange method

02 p0199 A72-12880

Optimum instantaneous impulsive orbital injection for specified asymptotic velocity vector, noting results of radius and asymptotic vector angular separations

03 p0437 A72-13837

Nonlinear programming iteration scheme for fuel-time optimization of satellite orbital rendezvous terminal phase

03 p0437 A72-13838

Spacecraft trajectories optimization by gradient method combination with Euler equations in calculus of variations

04 p0571 A72-14631

Missile trajectory stochastic optimal control systems with fuel constraint by mean path deviation optimization

05 p0725 A72-16452

- KS-transformation based regularization technique modification for minimal fuel consumption rocket trajectory control during space maneuver
05 p0726 A72-16454
- Penalty function method validity for singular solutions to optimal trajectory control problems with state variable inequality constraints
05 p0641 A72-16531
- Reusable space tug mission profile for interplanetary spacecraft recovery, using branched trajectory, steepest descent optimization and propellant minimization
[AIAA PAPER 72-13] 05 p0730 A72-16949
- Time optimal trajectory graphical construction procedure from energy state approximation as basis of computational algorithm for real time onboard flight optimization
[AIAA PAPER 72-123] 05 p0688 A72-16968
- Conjugate gradient iterative method for optimal control problems with state variable constraint, noting optimal trajectory cases
06 p0793 A72-17953
- Shuttle ascent guidance and control, discussing self targeting, trajectory optimization problems and flight phases
06 p0892 A72-18178
- Rocket motion in general central force field, obtaining primer vector integration for optimal coasting arc during orbital transfer
[AD-741964] 06 p0890 A72-18386
- Approximating trajectory solution to state constrained optimal control problems, discussing convergence
07 p0959 A72-19289
- Optimal transfer trajectories between Earth and Mars presented as functions of idealized Hohmann transfer approximation
07 p1077 A72-19824
- Soviet book on optimal trajectory synthesis covering second order linear control systems analysis based on Pontryagin maximum principle and Boltyanski theory
08 p1197 A72-20750
- Combined signal detection and trajectory estimation functions optimization application to Monte Carlo simulation for trajectory moving across two dimensional grid
08 p1144 A72-20858
- German monograph on optimal planetary atmosphere effects for increasing hyperbolic velocity at flyby for Venus and Earth
09 p1383 A72-22322
- Singular control problems calculation in trajectory optimization using sufficient conditions for control values set form
09 p1291 A72-23432
- Discrete and continuous dynamic adaptation algorithms construction for extremal quality functional trajectory equations of adaptive control system
09 p1283 A72-23435
- Adjoint control transformations advantages in optimal trajectories determination by Pontryagin maximum principle
10 p1547 A72-24879
- Energy optimal single impulse transfer from hyperbolic trajectory to circular orbit
11 p1718 A72-25926
- Interplanetary single impulse flight trajectories optimization and computation, determining geometrical and kinematic characteristics
11 p1718 A72-25927
- Satellite circular orbit trajectory plane time optimal relocation, examining turn angle angular position and modulus of maximum lateral acceleration
11 p1718 A72-25928
- Spacecraft reentry into random medium atmosphere, determining optimal control procedure for prescribed arrival region and time with simulation equation
11 p1686 A72-25930
- Time optimal transfer trajectory in central Newtonian force field between two arbitrary points under jet acceleration
11 p1718 A72-25942
- Two and three impulse trajectories for fixed time and angle rendezvous between vacant circular coplanar orbits, defining optimality domain
11 p1719 A72-25977
- Trajectory optimization for low thrust mission and system analysis, exemplifying by Jupiter flyby and comet rendezvous missions
[AIAA PAPER 72-426] 11 p1721 A72-26171
- Trajectory correction problem optimal measurement set, showing solution by linear programming simplex algorithm method
11 p1684 A72-26901
- Gradient method and Euler equations application to low thrust earth-to-Mars spacecraft orbital transfer trajectory optimization
13 p2034 A72-28438
- Elliptical orbiting spacecraft minimum fuel consumption rendezvous maneuver, formulating variational extremum problem with constraints
14 p2150 A72-30329
- Spacecraft optimal control after transfer from hyperbolic trajectory to planetary satellite orbit by atmospheric drag, minimizing engine thrust
14 p2129 A72-30470
- Optimum elliptic orbit characteristics of planetary artificial satellite based on earth-planet-earth flight
14 p2151 A72-30472
- Orbit determination strategy, detailing optimization criterion correlation with measurement errors
15 p2307 A72-31817
- Orbital correction problems for vehicle around spherical planet, considering velocity, fuel consumption and trajectory optimization
15 p2308 A72-31819
- Iterative solution of boundary value problem in multiple burn rocket trajectory optimization
15 p2308 A72-31820
- Optimal thrust direction for planetary escape at residual speed, using approximate explicit closed loop guidance scheme
15 p2268 A72-31821
- Low thrust spacecraft navigation requirements for minimum propellant guidance, using neighboring extremal law
15 p2270 A72-32194
- Optimal deterministic guidance for bounded-thrust spacecrafts.
17 p2609 A72-35101
- Analytical guidance in the neighborhood of optimal multi-impulse trajectories.
17 p2609 A72-35102
- A method of solving the problem of choosing an optimal transfer orbit with the aid of an invariant nomographic scale
17 p2610 A72-35217
- Minimum norm and gradient projection constrained optimization techniques for iterative solution of trajectory optimization problems, presenting mathematical relations to prove equivalence
17 p2576 A72-35232
- Stochastic optimal path selection via N discrete points set, discussing probability distributions and computer requirements
18 p2672 A72-36055
- Optimal avoidance control to transfer dynamic system from initial to terminal state in maximum distance problem
[ASME PAPER 72-AUT-D] 19 p2778 A72-37724
- Singular control problems calculation in trajectory optimization using sufficient conditions for control values set form
19 p2782 A72-38515
- Discrete and continuous dynamic adaptation algorithms construction for extremal quality functional trajectory equations of adaptive control system
19 p2770 A72-38518
- Constrained payload-optimum extremal ascent trajectories for space shuttle vehicles.
[AIAA PAPER 72-829] 20 p2966 A72-39097
- Optimum aim point biasing in case of a planetary quarantine constraint.
20 p2968 A72-39196
- Real-time launch vehicle steering program selection.
[AIAA PAPER 72-830] 20 p2977 A72-40058
- Trajectory synthesis of optimal control
21 p3037 A72-40704
- The optimum configuration and the optimum reentry trajectory of space shuttle vehicles.
[ICAS PAPER 72-27] 21 p2991 A72-41152
- Shuttle flight opportunities between stations orbiting the earth and moon.
21 p3108 A72-41302
- Space shuttle ascent trajectory optimization by Davidson/Broyden crude search technique for matrix updating
[AIAA PAPER 72-907] 21 p3111 A72-41556
- Perturbation guidance for minimum time flight paths of spacecraft.
[AIAA PAPER 72-915] 21 p3082 A72-41560
- Computer simulation of retargeting procedure with closed form iterative solution and parameter optimization for nonlinear low thrust spacecraft guidance scheme
[AIAA PAPER 72-916] 21 p3082 A72-41561
- N-burn analytic solution for propellant-optimal transfer trajectories in vacuum, taking into account gravitational effects
[AIAA PAPER 72-929] 21 p3112 A72-41569
- Integrals of the motion for optimal trajectories in atmospheric flight.
[AIAA PAPER 72-931] 21 p3112 A72-41570
- Mariner spacecraft 1973 for flyby Venus and encounter Mercury, discussing launch and arrival conditions and aiming zones selection to maximize science return
[AIAA PAPER 72-942] 21 p3113 A72-41578
- Choice of parameters to be measured in determination of a spacecraft trajectory
22 p3223 A72-42201
- On application of Kalman filtering technique to on-line orbit estimation of a launching vehicle.
22 p3203 A72-43142
- Some numerical results using Kalaba's new approach to optimal control and filtering.
23 p3274 A72-43543
- Minimum energy trajectory and propellant consumption considerations for launch windows to Mars and Venus planets with Grand Tour mission possibilities
23 p3336 A72-43553
- Optimal guidance for the space shuttle transition.
24 p3422 A72-45186
- Low thrust constant acceleration trajectories for a Mercury orbit.
24 p3441 A72-45208
- Rendezvous at specified destinations through optimum transfer paths
24 p3442 A72-45281
- Space shuttle optimal entry trajectories for thermal protection system weight minimization, considering constant and variable angles of attack
[AIAA PAPER 72-977] 24 p3452 A72-45414
- Lifting entry optimization equations for fixed angle of attack with path control for roll modulation of lift, considering space shuttle orbiter configuration
[AIAA PAPER 72-933] 24 p3443 A72-45435
- Analysis of the Radio Astronomy Explorer lunar orbit mission.
[AIAA PAPER 72-940] 24 p3444 A72-45437
- TRANQUILIZERS**
Tranquilizers effect on pilot in-flight performance, discussing flight safety, alcohol potentiating effect, student pilot stress reactions and airsickness treatment
06 p0768 A72-18158
- Chlorpromazine tranquilizer influence on squirrel monkeys in electric shock tests, shifting postevent aggressivity to pre event anticipation
07 p0916 A72-18975
- The effect of chloridazepoxide on visual field, extraocular muscle balance, colour matching ability and hand-eye co-ordination in man.
17 p2505 A72-35915
- Effect of psychotropic substances on human resistance to acceleration
21 p3006 A72-40443
- The simultaneous action of stimulants and tranquilizers on the efficiency of a human operator
23 p3260 A72-43923
- TRANSCIEVERS**
U TRANSMITTER RECEIVERS
TRANSCENDENTAL FUNCTIONS
NT EXPONENTIAL FUNCTIONS
NT LOGARITHMS
NT PERIODIC FUNCTIONS
NT TANGENTS
NT TRIGONOMETRIC FUNCTIONS
Engineering curves and surfaces representation by spline functions, discussing computerized approximation methods for algebraic, transcendental and transfer functions
07 p1024 A72-17777
- Transcendence of baryon number conservation law, discussing static black hole properties as final massive star collapse state
07 p1076 A72-19667
- Integral operators functions approximation for elasticity and materials aging equations, noting transcendental functions in solutions
08 p1243 A72-21239
- Stress distribution near corner point in interface section of body with two prismatic components, noting state singularity investigation reduction to transcendental equation solution
08 p1249 A72-21944
- Table of indefinite and definite integrals of products of error functions with transcendental and special functions
15 p2262 A72-31589
- Approximate representation of a type of transcendental polynomials describing wave systems with fractional rational functions
19 p2834 A72-37751
- Solution of the equations of consumption in gasdynamic problems
20 p2914 A72-39927
- Transcendental equations solution for satellite Kepler orbit determination from coordinates, velocity and time components, using Lambert-Euler relation
22 p3223 A72-42204
- Longitudinal rib reinforced cylindrical shell under axial compression loads, determining equilibrium stability with approximation of transcendental equations
23 p3347 A72-43748
- TRANSDUCERS**
NT BOURDON TUBES
NT DIGITAL TRANSDUCERS
NT ELECTROACOUSTIC TRANSDUCERS
NT ELECTRONIC TRANSDUCERS
NT IMAGE TRANSDUCERS
NT MAGNETIC TRANSDUCERS
NT MICROPHONES
NT MODE TRANSFORMERS
NT PIEZOELECTRIC GAGES
NT PIEZOELECTRIC TRANSDUCERS
NT PIEZORESISTIVE TRANSDUCERS
NT PRESSURE SENSORS
NT QUARTZ TRANSDUCERS
NT SOUND TRANSDUCERS
NT ULTRASONIC WAVE TRANSDUCERS

- Double frequency stroboscopic method for absolute calibration of vibration transducers, analyzing errors 06 p0815 A72-17766
- Strain biased transparent ferroelectric electro-optic ceramics for coherent transducers /page composers/ for holographic memories and optical data processing [CLEA PAPER 18,6] 07 p0950 A72-19401
- Elastic wave fields reconstruction from measurements over transducer array, stressing ultrasonic imaging system development 07 p0986 A72-19647
- Two electrical transducer techniques for dilatometer study of quenched-in point defects 07 p0993 A72-20589
- Mathematical model of capacitive transducer for displacement measurement in open mesh grid structures 08 p1163 A72-20918
- Semiconductor IC transducers for electrical readout of optical radiation, mechanical stress and magnetic field strength 10 p1448 A72-24282
- Cotton wick probe-transducer assembly for pneumograph recording of rabbit respiratory rate 11 p1587 A72-26619
- Data processing in isolated crab biological strain receptor formed by muscle, transducer and encoder, noting pulse frequency modulation in encoding process 12 p1771 A72-27577
- Fluid amplification principles, discussing bistable and proportional amplification, signal transmission and transduction to and from fluid signals [ASME PAPER 72-DE-20] 14 p2073 A72-30864
- Presupposition, aim and methods for teaching transducer technology to users and designers, reviewing transducer static and dynamic performance characteristics and classifications 16 p2393 A72-33632
- Dynamic characteristics of electrical measuring instruments and transducers, discussing static calibration curve, dynamic tests and parameters determination 17 p2557 A72-35757
- Systematic approach to study energy and information flow through measuring system in experimental mechanics, using transducer model 18 p2690 A72-36356
- German monograph - A theoretical and experimental contribution to the equivalent circuits of electrofluidic transducers operating on the nozzle/deflecting plate principle 19 p2754 A72-37653
- Electromechanical measurement systems using analog transducers with ohmic resistance, electric and magnetic fields and digital/frequency and stochastic outputs 19 p2800 A72-37755
- Measurement transducers in industrial process control, discussing requirements for dynamic properties, stability, linearity and computer applications 19 p2803 A72-38315
- Transducing techniques for displacements in picometer-mm range into electrical signals 21 p3051 A72-40202
- A ten-inch extensometer measuring small low-frequency strains. 21 p3052 A72-40234
- External background and internal noise effects on automatic tracking systems accuracy, noting optimal operating point on transducer response curve 21 p3014 A72-40320
- Use of a linear air bearing sled for dynamic calibration of velocity transducers. 22 p3179 A72-42693
- Variable impedance transducer measuring instruments for in-flight aircraft performance tests under environmental thermal effects 22 p3180 A72-42711
- Instrumentation systems design for extended bandwidth data acquisition, discussing problem areas in transducers, amplifiers and signal conditioning, data recording and playback 22 p3157 A72-42712
- Operational dynamics of inductive and capacitive differential circuits of small-displacement transducers 24 p3403 A72-45314
- TRANSEQUATORIAL PROPAGATION**
- Spread F effects on transequatorial ionospheric short wave oblique incidence path great circle deviations 01 p0056 A72-10438
- Supermode F range spreading and evening type transequatorial propagation, considering single scattering in east-west plane 03 p0321 A72-12994
- Equatorial spread F spatial and temporal distribution from short wave side reflection observations along Lindau-Tsueb transequatorial HF radio transmission path 12 p1803 A72-27778
- Transequatorial off-path propagation outside of great circle at decametric waves associated with forward scattering by field aligned irregularities in equatorial ionosphere 14 p2084 A72-30129
- Time delay measurements in the Athens /Greece/ - Roma /Lesotho/ VHF trans-equatorial propagation circuit. 17 p2515 A72-34693
- On an anomaly in long-range short-wave propagation from the equatorial region to central Europe. 18 p2657 A72-36232
- TRANSFER FUNCTIONS**
- Collisionless motion of solar wind ions in helical magnetic field, giving transfer function of charged particles 01 p0118 A72-10360
- Closed linear systems optimal stabilization determining transfer function from Wiener Hopf equation 01 p0045 A72-10572
- Transfer function compensation technique for processing sampled imagery data prior to recording on hard copy to remove degrading effect for quality improvement 01 p0046 A72-10873
- Frequency contrast characteristics derivation method with devices for determining transfer functions of objectives and film, using electron-optical bench 02 p0229 A72-12171
- Affined RC or RL networks, investigating real and equal or imaginary, conjugate and inverse voltage and current transmittances 02 p0197 A72-12240
- Active all-pass circuits transfer function and synthesis, including delay lines, phase correctors and wide-band phase shifter applications 03 p0338 A72-13169
- Atmospheric turbulence induced laser beam spread estimation from spherical wave modulation transfer function 03 p0367 A72-13442
- Energy transfer rate from photoelectrons to thermal electrons, presenting function of three independent variables 03 p0413 A72-13532
- Fading medium transfer function estimation via homomorphic and Kalman filtering, considering multiplicative noise 03 p0326 A72-14195
- Soviet book on linear automatic control systems with variable parameters covering pulse transfer function determination algorithms, signal transmission characteristics and systems stability 03 p0339 A72-14245
- Numerical method and computerized design for feedback controller pulse transfer function in overall error criterion minimization, comparing results with sampled error method 03 p0329 A72-14355
- Optimization programs for linear control systems with nonconvex constraints on phase coordinates applied to material point transfer 04 p0504 A72-14624
- Nonstationary hydroacoustic wave diffraction at curvilinear rigid surface, deriving transfer function and radiation pressure 04 p0589 A72-15062
- Single scan TV-radiography system for providing A-D converter analog signal for digital data acquisition, obtaining transfer functions 04 p0522 A72-15226
- Multiple-input multiple-output linear time invariant feedback systems stability, investigating continuous-time case 04 p0507 A72-15694
- Optical image recording, transformation, readout, transmission and data processing techniques and instruments, discussing transfer function, cut-off frequency and information quantity concepts and holography 04 p0525 A72-15700
- Temperature, flow, end conditions and branching on small signal sinusoidal amplitude frequency response of pneumatic lines, investigating transfer functions [ASME PAPER 71-WA/AUT-5 (FLCS)] 05 p0615 A72-15958
- Aircraft steering dynamics model with translational and rotational equations, considering zero sideslip and acceleration and lift bank angle transfer functions 05 p0611 A72-16112
- Precipitation effects on optical transfer function of turbulent atmosphere at 1.2 km, comparing to clear, overcast and cloudy skies 05 p0656 A72-16176
- Parameter adjustment algorithm for simplified sensitivity model in adaptive nonsearching control system of linear plant with polynomial transfer function 05 p0641 A72-16318
- Holographic measurement for optical transfer function of lenses, considering negative black and white photographic indicator emulsion effect 05 p0663 A72-16728
- Plane symmetrical exothermic reaction center dynamic behavior, deriving system nonlinear transfer

- function-pressure pulse and unit mass heat release relationships [AIAA PAPER 72-67] 05 p0750 A72-16934
- Electromagnetic wave scattering from curved rough surfaces and transmission through turbulent medium, obtaining solution by spatial Fourier transform of three transfer functions product 06 p0771 A72-17340
- Wide angle lenses off-axis modulation transfer function measurement, explaining extrapolation method with MTF and conversion diagrams 06 p0813 A72-17439
- Higher harmonics in lunar transfer functions for surface magnetic field tangential components, discussing lunar electrical conductivity models 06 p0875 A72-17448
- Engineering curves and surfaces representation by spline functions, discussing computerized approximation methods for algebraic, transcendental and transfer functions 07 p1024 A72-18777
- Complex systems calibration based on computer derived transfer function, discussing theory, Fortran calibration program, error analysis and applications 07 p0949 A72-18818
- Optical image transfer functions characteristics and modulation in isolated retinas and retinal receptors, noting similarity to optical fiber bundles 07 p0916 A72-19027
- Frequency response design for interactive multivariable feedback control systems, using characteristic transfer functions 07 p0960 A72-19704
- Microdensitometer system analysis by partial coherence theory, determining optical transfer function for linear operation 07 p0987 A72-19830
- Nonlinear difference schemes for quasi-linear transfer equation in gas dynamics and shock wave computations 07 p0971 A72-20085
- Interactive graphics technique for design of single input linear feedback systems described by state equations or cascaded transfer functions 07 p0963 A72-20391
- Optimal pulse height analyzer with quadratic transfer function for gamma ray spectrometer on OSO-H 08 p1167 A72-21516
- Closed and open loop transfer function coefficients relationship for steady state linear system with proportional elements in feedback and parallel paths 10 p1457 A72-24724
- Transfer function sensitivity characteristics comparison of doubly terminated LC filters with active cascade and inductance simulation schemes 10 p1452 A72-24800
- Time optimal control system for linear plant with transfer functions containing zeros 10 p1458 A72-24999
- Parameter adjustment algorithm for simplified sensitivity model in adaptive nonsearching control system of linear plant with polynomial transfer function 10 p1458 A72-25072
- Methods of moments, rational transform approximation, Taylor series expansion and modulating functions used for process identification model, determining system transfer functions 11 p1607 A72-25282
- Pulse amplitude system with finite data recording time, deriving transfer function for signal shaper 11 p1609 A72-25444
- Absolute stability conditions of zero solution for PAM automatic control systems equations in terms of transfer function 11 p1609 A72-25446
- Pulsed perturbation and Q coupled extremal control systems with noise distortion, obtaining optimal transfer functions with Kolmogoroff-Wiener method 11 p1610 A72-25448
- Transfer functions algebraic determination for stationary object from random processes realizations, proposing algorithm 11 p1610 A72-25451
- Lumped-distributed active network function sensitivity formulas in terms of admittance parameters 11 p1610 A72-25747
- Weather stations data analysis with unequally spaced observations, considering errors and variances transfer functions 11 p1680 A72-26076
- Computerized filter design, discussing frequency analysis and synthesis programs for quadrupole eigenmodes and transfer function 11 p1604 A72-26089
- Two stage magnetic operational amplifier transfer function, time constants and control stability conditions, using difference equation approach 11 p1605 A72-26466
- Lens evaluation procedure based on optical transfer function data, discussing computer displays and merit parameters 12 p1810 A72-27936

- Lens MTF calculation in presence of diffraction patterns via image mathematical model construction yielding Fourier transform 12 p1810 A72-27937
 - Spectroscopy by synthesis of two or more fixed or moving diffraction gratings, obtaining transfer functions for total information increase 12 p1811 A72-27943
 - Active transistorized low pass RC filter providing fourth-order transfer function and uniform frequency response 13 p1927 A72-28381
 - Analytical expression for digital element transfer function derived with Laplace transforms 13 p1927 A72-28413
 - Statistical physics multiple wave scattering-phenomenological radiation transfer equation relations, using Green function 13 p2002 A72-28512
 - Radiation transfer equations solved in isotropic light scattering approximation, relating transfer function to motion picture film optical properties 13 p1955 A72-28519
 - Transfer matrices determination for two terminal pair network derived from four terminal pair network, considering bandpass filters 13 p1931 A72-29060
 - Transfer function of polynomial discrete linear pulse systems for differential equation solution 13 p1936 A72-29269
 - Vibration stability and interference transfer function of onboard transponder with phase lock AFC used in Doppler system for measuring spacecraft trajectory parameters 13 p1958 A72-29456
 - Modulation transfer functions of optical system producing image of distant object in turbulent boundary layer of atmosphere, determining refractive index fluctuation intensities 14 p2130 A72-30241
 - Precipitation effects on optical transfer function of turbulent atmosphere at 1.2 km, comparing to clear, overcast and cloudy skies 14 p2099 A72-30245
 - Hydraulic servosystem performance analysis, determining transfer function for time variant input-output relationship, gain levels and stability assurance 14 p2073 A72-30420
 - Lunar core-crust conductivity models compatibility with lunar surface field/interplanetary magnetic field transfer function from Apollo 12 magnetometer data 12 p2153 A72-30502
 - Pilot trainer transfer function identification for man-machine and on-line adaptive control system using analog/hybrid computer 14 p2091 A72-30721
 - Lumped approximation to distributed RC notch networks for linear IC, deriving open circuit voltage transfer functions and root locus graphs 14 p2092 A72-31170
 - Multimode millimeter waveguides and optical fibers, deriving signal transmission distortion from transfer function and corresponding impulse response statistics 15 p2193 A72-31351
 - Signal distortion minimization for random waveguides with frequency-dependent optimum coupling based on transfer function covariance and impulse response time domain statistics 15 p2194 A72-31352
 - Distributed lumped active network configuration and design chart for realizing all-pass voltage transfer function 15 p2210 A72-31508
 - Sine, square and triangular wave targets for optical transfer function measurements, comparing modulations in partial coherent light under different illumination conditions 15 p2246 A72-31613
 - Open circuit voltage transfer function synthesis to realize arbitrary real rational function in complex variable, using generalized positive impedance converter 15 p2211 A72-31847
 - Transfer function estimates in random vibration test control, using digital techniques for rapid reduction of statistical errors 15 p2215 A72-32626
 - Random vibration optimal control by transfer function estimation, using relative phase information in cross spectral density functions to sort out self noise 15 p2215 A72-32629
 - Earth atmosphere water vapor mixing ratio profiles from relaxation method for full radiative transfer equation inverse solution 15 p2266 A72-32724
 - Optical system production acceptance test based on modulation transfer function, discussing instrument design and test philosophy 16 p2389 A72-32847
 - Experiments on the phase contrast transfer functions of a superconducting lens 17 p2594 A72-34284
 - Sampled imagery transfer function compensation by inverse function, noting truncation effects on processing array SNR performance 17 p2521 A72-34412
 - The influence of the modulation transfer function of the dioptric apparatus on the acuity and contrast of the retinal image in Rana esculenta. 17 p2508 A72-34883
 - On structures for nonrecursive digital filters. 17 p2516 A72-35221
 - The radiative transfer equation and environmental effects in the upper atmosphere. [AIAA PAPER 72-663] 17 p2583 A72-35485
 - Rotating body linear dynamic control by complex transfer function approach with application to stability conditions for controlled gyro and homing missiles 17 p2583 A72-35528
 - Stability of linear time-invariant distributed parameter single-loop feedback systems. 17 p2534 A72-35535
 - Modulation measurement applied to the focusing of aerial cameras. 17 p2558 A72-35948
 - Mathematical modeling assumptions and procedures in experimental mechanics, considering transfer function, impedance and human factor roles 18 p2709 A72-36353
 - Optimal control of plants whose transfer functions contain zeros. 18 p2673 A72-36724
 - Dependence of the optical transfer function of a turbulent atmosphere on the averaging time 18 p2707 A72-36968
 - Elastically supported dry two degrees of freedom tuned gyroscopes, analyzing open-loop transfer function for characteristic errors 19 p2794 A72-37280
 - Errors due to gimbaling system asymmetries and rotor angular offsets effects in multigimbal elastically supported tuned gyroscope, deriving gyro translational transfer function 19 p2794 A72-37281
 - Determination of linear circuit sensitivity to circuit parameter changes in the equations of state variables 19 p2777 A72-37312
 - Uniqueness of the solution for identification of linear systems by the modulating function method 19 p2779 A72-38086
 - Oscillations, statics and transfer matrices of composite shells of revolution contacting elastic bases, using initial parameters method 19 p2876 A72-38156
 - Transfer-characterization and the unique realization of linear time-invariant multivariable systems. 19 p2780 A72-38238
 - Transfer function concept extension to analytical representation of linear time-invariant plants and controllers with multiple inputs and outputs 19 p2780 A72-38242
 - Precise transfer function of a clamper for a commutation switch with a finite closing time 19 p2782 A72-38463
 - Application of the optical transfer function to visual instruments. 20 p2922 A72-39043
 - Significance of OTF methods in assessing lenses to be used with partially coherent illumination. 20 p2931 A72-39049
 - Electronic circuit for linearizing the transfer function of a photographic plate used in mass-spectrometry. 20 p2925 A72-39428
 - Topological analysis of the sensitivity of a digital system 21 p3036 A72-40222
 - Photographic material characteristics for adequate diffraction efficiency and contrast and noise levels and acceptable nonlinear distortions of holograms, noting optical transfer function optimization 21 p3052 A72-40389
 - Communication receivers interference modeling - Nonlinear transfer functions from circuit analysis - Mild excitations. 21 p3019 A72-40890
 - Some contributions to the theory of linear models describing the control behaviour of the human operation. 21 p3011 A72-41419
 - The influence of a prediction display on the human transfer characteristics. 21 p3012 A72-41432
 - Optimum spatial filter for an anisotropic background-noise. 21 p3036 A72-41839
 - Modulation transfer function for solar telescopes and atmospheric turbulence. 22 p3175 A72-42047
 - Multidimensional asynchronous FM sampled data systems stability, considering continuous linear part transfer matrix poles located on imaginary axis 22 p3162 A72-42080
 - Determination of optical transfer functions by Fourier transformation in spatially incoherent light 22 p3205 A72-42296
 - Voltage generalized-impedance converter synthesis with RC circuits for obtaining current transfer function proportional to square of s with application to filter design 22 p3140 A72-42303
 - Spectrally shaped transient forcing functions for frequency response testing. 22 p3206 A72-42463
 - Analog and digital automatic control systems for aerospace and process applications, discussing transfer function and state variable methods 22 p3162 A72-42714
 - Limitations on the synthesis of control systems in the case of incompletely accessible state variables 22 p3162 A72-42739
 - Biological system transfer-function extraction using swept-frequency and correlation techniques. 22 p3151 A72-42773
 - Design of controllers for open-loop unstable multivariable system using inverse Nyquist array. 23 p3275 A72-43609
 - Digital filter realizations using a special-purpose stored-program computer. 23 p3267 A72-43815
 - An approach for generation of second order RC-active filters. 23 p3276 A72-43863
 - Transfer matrix approach for determining stresses and displacements in elastostatics of laminated composites [ASCE PREPRINT 1674] 23 p3351 A72-44105
 - Determination of the operational transfer functions of a gas turbine engine on a digital computer 23 p3327 A72-44292
 - Theory of magnetically tunable band-pass filters 23 p3273 A72-44360
 - Measurements of the modulation transfer functions of focusing screens. 24 p3425 A72-44770
 - Hydraulic duct transfer function determination for prediction of liquid-fuel engine space launcher LF vibrations, investigating incompressible flow rate modulation by deformable walls 24 p3392 A72-45117
 - Measurement of the optical transfer function of an onboard objective in the space environment 24 p3403 A72-45225
 - Parametric optimization of the equivalent transfer function of a system with the aid of the error integral 24 p3387 A72-45700
 - Allowable regions for stability multiplier characteristics. 24 p3420 A72-45787
- ### TRANSFER OF TRAINING
- Skill acquisition in performance of three phase code transformation task 01 p0021 A72-11193
 - Earth Resources Survey /ERS/ program personnel training and education, discussing trainee selection, knowledge categories and training methods for remote sensing 02 p0304 A72-11855
 - Training effect on oxygen consumption in negative muscular work, considering connective tissue strengthening and muscle viscosity changes 03 p0315 A72-13676
 - Physical training effect on subjective rating of perceived exertion, investigating correlation with heart rate and blood lactate concentration 03 p0319 A72-13678
 - Mental rehearsal and physical practice relation to learning rate for rotary pursuit tracking skill acquisition 07 p0925 A72-18801
 - Apollo manned mission real time ground support computer simulation for NASA flight controller training to maximize flight crew safety 07 p0933 A72-20329
 - Component duration and relative response rates in multiple schedules of pigeon training 08 p1128 A72-22175
 - Exercise capacity in a population of domestic fowl - Effects of selection and training. 17 p2499 A72-34726
 - Rotary pursuit task practice effects on transfer of motor skill from slower to faster speeds 18 p2654 A72-36915
 - Studies in pilot training - The anatomy of transfer. 20 p2897 A72-39718
 - Problems arising in the transfer of training from simulated to real control systems. 21 p3010 A72-41412
- ### TRANSFER ORBITS
- #### NT INTERPLANETARY TRANSFER ORBITS
- Aerospike rocket engine system for orbit-to-orbit space shuttle, discussing light-weight regeneratively cooled thrust chamber performance tests [SAE PAPER 710770] 01 p0116 A72-10264
 - Transfer from high elliptical to circular orbit, using successive spacecraft braking maneuvers in planetary atmosphere with incomplete information 01 p0130 A72-10927

Satellite low orbit transfer to stationary orbit, emphasizing stage and payload recovery effects on performance

01 p0130 A72-10936

Satellite orbit determination accuracy from radio interferometer tracking data containing systematic errors, using digital computer techniques on Symphonie transfer orbit

[DFVLR-SONDDR-212] 02 p0182 A72-12744

Minimum velocity change noncoplanar two and three impulse orbital transfer from regressing oblate earth assembly parking ellipse into flyby trans-Martian asymptotic velocity vector

03 p0434 A72-13634

Optimum instantaneous impulsive orbital injection for specified asymptotic velocity vector, noting results of radius and asymptotic vector angular separations

03 p0437 A72-13637

Extremum of satellite orbit perigee or apogee height in Hohmann transfer

05 p0713 A72-16006

Iterative method for approximate determination of local minima in fuel optimal finite thrust orbit transfer

05 p0719 A72-16541

Rocket motion in general central force field, obtaining primer vector integration for optimal coasting arc during orbital transfer

[AD-741964] 06 p0890 A72-18386

Nonoptimality of Lawden spiral for minimum fuel transfer orbits in space navigation

07 p1033 A72-20246

Minimum fuel continuous low thrust orbit transfer problem of optimal control, solving boundary value problem with Multiple Substitution Polynomials and Marquardt method

10 p1552 A72-24486

Energy optimal single impulse transfer from hyperbolic trajectory to circular orbit

11 p1718 A72-25926

Satellite circular orbit trajectory plane time optimal relocation, examining turn angle angular position and modulus of maximum lateral acceleration

11 p1718 A72-25928

Time optimal transfer trajectory in central Newtonian force field between two arbitrary points under jet acceleration

11 p1718 A72-25942

Two and three impulse trajectories for fixed time and angle rendezvous between vacant circular coplanar orbits, defining optimality domain

11 p1719 A72-25977

Attitude determination during transfer orbit operation of SKYNET and NATO synchronous communications satellites

[ALAA PAPER 72-544] 12 p1876 A72-27367

Solar electric propulsion for satellite transport into geostationary orbit, discussing launchers, energy supply, electrostatic ion thruster and mass/power ratio

[ALAA PAPER 72-505] 12 p1860 A72-27422

Interplanetary spacecraft transfer maneuver for hyperbolic trajectory change into eccentric orbit, using aerodynamic drag to obtain nearly circular orbit

14 p2151 A72-30471

Orbital correction problems for vehicle around spherical planet, considering velocity, fuel consumption and trajectory optimization

15 p2308 A72-31819

Algorithm for minimax parameter optimization by linear and quadratic programming with application to earth orbiting satellite orbital transfer

16 p2366 A72-33191

Shuttle flight opportunities between stations orbiting the earth and moon.

21 p3108 A72-41302

Perturbation guidance for minimum time flight paths of spacecraft.

[ALAA PAPER 72-915] 21 p3082 A72-41560

N-burn analytic solution for propellant-optimal transfer trajectories in vacuum, taking into account gravitational effects

[ALAA PAPER 72-929] 21 p3112 A72-41569

Cometary parent bodies transfer to short period orbits by Jupiter caused gravitational disturbances, noting qualitative analysis of orbits evolution

22 p3219 A72-41913

Conditions for impulsive thrust-coast-thrust minimum-time, fixed-fuel transfers between coplanar orbits.

24 p3440 A72-45149

Thrust-weight ratio optimization for spacecraft orbit inclination change maneuver, deriving motion kinematics via point mass gravitational model

24 p3440 A72-45167

On required guidance for transfer from hyperbolic trajectory to the planetary satellite orbit by aerodynamic drag in atmosphere.

24 p3450 A72-45176

The Agena orbit transfer stage as an interim space tug.

24 p3451 A72-45195

Rendezvous at specified destinations through optimum transfer paths

24 p3442 A72-45281

Analysis of the Radio Astronomy Explorer lunar orbit mission.

[ALAA PAPER 72-940] 24 p3444 A72-45437

TRANSFORM INTEGRALS

U INTEGRAL TRANSFORMATIONS

TRANSFORMATION TENSORS

U TENSORS

TRANSFORMATIONS

Torsion problem of inhomogeneous anisotropic viscoelastic rod transformation, using area variation coefficient for modeling

01 p0138 A72-10582

TRANSFORMATIONS [MATHEMATICS]

NT COORDINATE TRANSFORMATIONS

NT FOURIER-BESSEL TRANSFORMATIONS

NT INTEGRAL TRANSFORMATIONS

NT LAPLACE TRANSFORMATION

Invariant imbedding technique application to linear partial differential equations boundary value problems conversion to Cauchy problem via generalized Riccati transformations

01 p0093 A72-11116

Digital fast transform methods application to satellite image processing, comparing with nontransform algorithms

02 p0227 A72-18483

Power law bodies lift and drag coefficients interrelationship under Newtonian nonaffine similarity laws, presenting rules for equivalent transformations identification

02 p0151 A72-12273

Spatial transformation in geodesy, considering point in space as position function for orthogonal and curvilinear coordinates

03 p0351 A72-14329

Transformation of differential equations describing interaction between electric arc and gas flow by taking temperature as independent variable, considering Laval nozzle example

03 p0344 A72-14392

Generalized transformation of plane compressible and axisymmetric equation for self similar solutions of dissipative boundary layer for bodies with variable surface

04 p0510 A72-14468

Computer aided Foldy-Wouthuysen canonical transformation on Dirac Hamiltonian with electromagnetic potentials included

04 p0496 A72-15627

Book on similarity laws and modeling covering dimensional analysis, transformations, differential equations, gas flows and nonequilibrium processes

04 p0513 A72-15675

Stability conditions and effective bandwidths of first and second degree pulsed phase locked AFC systems with proportionately integrating filter, using Z transform method

05 p0625 A72-15825

General MHD duct flow problems solution using machine transformation and finite difference technique supplemented by successive overrelaxation [ASME PAPER 71-WA/APM-15]

05 p0694 A72-15965

KS-transformation based regularization technique modification for minimal fuel consumption rocket trajectory control during space maneuver

05 p0726 A72-16454

Flight mechanics derivative transformations by matrix methods for changing coordinate or independent variable systems

[DFVLR-SONDDR-175] 05 p0612 A72-16706

Controlled motion dynamics of spacecraft performing maneuvers, applying point transformation to third-order nonlinear system moving about center of mass in lateral motion

05 p0730 A72-17029

Hough transformation for detection of lines and curves in pictures, using angle radius instead of slope intercept parameters for efficient computation

05 p0664 A72-17164

Higher order nonlinear autonomous oscillation system limit cycle and stability determination by numerical solution based on Andronov point transformation and Liapunov theory

06 p0838 A72-17377

Fourier, Hadamard and Karhunen-Loeve transformations for digital speech processing, comparing bit rate requirements

06 p0772 A72-17405

Amplitude and phase modulated radar pulse train representation by complex number sequences, discussing generation, processing, and Z transform application to combination codes

06 p0773 A72-17495

Electromagnetic radiation in uniformly moving homogeneous medium obtained by transformation and four dimensional Green function method

06 p0847 A72-17712

Time-variable multivariable systems reduction to completely controllable and observable systems by subdivision and transformation procedures, using subsystems order matrices

07 p1026 A72-19271

Mathematical model for dissipative dual-spin satellite analysis, making use of high speed rotor symmetry to permit quasi-holonomic transformation

07 p1085 A72-19280

Bounds estimation for thermal explosion critical parameters for exothermic reaction, using geometric transformation

07 p1098 A72-19364

Lens antennas for amplitude and phase transformations, examining existence of solutions and bounds in terms of parameters

07 p0985 A72-19404

Linear multivariable systems feedback invariant structure of controllable matrix pair under rich transformation group including regular linear coordinate and state-feedback transformations

07 p0960 A72-19700

Elastic body dynamics partial differential equations transformation into boundary value problem for Monge-Ampere equation

07 p1095 A72-20218

Input binary sequence transformation in chain of series connected on-off neuron models, applying to n-stage linear filter analysis

08 p1138 A72-20870

Transformation of integrodifferential equation of motion of heavy solid body about fixed point

08 p1207 A72-21341

Einstein and Einstein-Maxwell equations solutions by zero coupling transformations

09 p1349 A72-22201

Learning systems mathematical scheme to identify classes invariant with respect to transformation groups, realizing functionals with coherent and incoherent optics

09 p1282 A72-22218

Sundman power series convergence enhancement in three body problem by Poincare transformation

09 p1350 A72-22482

Algorithm for transformation of generalized companion forms for multivariable linear systems into Jordan canonical form

09 p1341 A72-23071

Applied nonlinear mechanics problems solutions by variable scale method, choosing transformations for linearization of differential equations

09 p1343 A72-23602

Dimensional analysis pi-theorem local generalization by Lie transformation group investigation, constructing local canonical coordinate systems to obtain factoring properties of certain functions

10 p1503 A72-23921

Differential equations similarity analysis, using Lie infinitesimal contact transformation group as search method for other possible transformation groups

10 p1503 A72-23922

Third order nonlinear differential equation invariants to obtain integrable forms

10 p1504 A72-24053

Linear processes coupling and cylindrical probability imaging through nonlinear mappings, noting relationship to Ito theory of stochastic integrals

10 p1505 A72-24073

Lie transformations for perturbed canonical systems of differential equations solution, proposing parameter square root series development for resonances problems of celestial mechanics

10 p1536 A72-24151

Clebsch transformation in relativistic MHD, considering Maxwell equations in vacuum and electromagnetic perfect fluid in isentropic flow

10 p1519 A72-24129

Feature selection from pattern recognition of Gaussian distributed classes by mapping of vector samples from n dimensional space to m dimensional space via transformation matrix

10 p1445 A72-24465

Transient calculation method for electric drive units described by first and second order differential equations, using special transformation for integral curve curvature determination

10 p1423 A72-24754

Darlington method in dissipative systems studies representing R-functions as fractionally linear transforms with coefficients matrix function

10 p1512 A72-24786

Nonlinear transformation for improper integral calculation, noting faster convergence than linear methods

10 p1506 A72-24995

Methods of moments, rational transform approximation, Taylor series expansion and modulating functions used for process identification model, determining system transfer functions

11 p1607 A72-25283

Optimality conditions for dynamic control systems considering multidimensional singular controls and state space transformations

11 p1608 A72-25322

Eigenfunction transform investigation of wedge diffraction of scalar pulse wave in three space dimensions, analyzing Green function

11 p1591 A72-25355

- Nonlinear resistive network analysis by piecewise linear mappings, studying Lipschitz condition and global homomorphism 11 p1608 A72-25360
- Stiffly stable implicit linear multistep algorithm for deriving stability properties from extended complex plane transformation 11 p1677 A72-25860
- Numerical stability in linear algebraic equations, considering mapping from input data to desired output information 11 p1677 A72-25861
- Boundary value problems to initial value problems transformation method extended by physical parameters invariant properties, noting fluid mechanics nonlinear equations 11 p1616 A72-25878
- Hypersonic polytropic transformation of ideal fluid under mechanical or geometrical conditions 11 p1572 A72-26092
- Heat equation for insulated uniform body, examining definition and continuity of mapping from linear manifold of assumed boundary values 11 p1747 A72-26555
- Linear difference equations solved by indefinite Z transformations technique using Cramer rule for simultaneous algebraic equations 11 p1678 A72-26664
- Nonlinear algebraic transformation to determine straight line and second order curve intersection point in aircraft lofting problem 13 p1986 A72-28742
- Initial value method for Ambarzumian integral equation by transformation to Cauchy system 14 p2126 A72-30889
- Nonlinear variable transformation method to determine locking band and transition processes in automatic phase and frequency control systems 14 p2087 A72-31132
- Relations between Haar and Walsh/Hadamard transforms to wield orthogonal transforms with common fast algorithm 15 p2264 A72-32081
- Torsion problem of bodies of revolution bounded by two intersecting spherical surfaces, obtaining solution by Mehler-Fock transform 15 p2330 A72-32294
- Pseudo-one dimensional dissociative nonequilibrium nozzle flow, presenting governing equations transformation via similarity parameter for oxygen 16 p2375 A72-32906
- Damping perturbation of high order nonlinear autonomous Liapunov system, reducing system equations integration to quadratures via transformation to lower order quasi-linear nonautonomous system 16 p2422 A72-32938
- Inverse transformations in mathematical models of elasticity and plasticity problems reducible to biharmonic equation 16 p2468 A72-33163
- Performance criteria for transform data coding schemes evaluation under computational constraints, presenting numerical examples for Fourier, Walsh, Haar and Karhunen-Loeve transforms 16 p2366 A72-33214
- On the Gaussian elimination method for inverting sparse matrices. 17 p2573 A72-34237
- Transformations of the compressible boundary layer equations. 17 p2538 A72-34341
- Pattern recognition computer programs for input data preprocessing with characterization and transformation through layered recognition cone 17 p2570 A72-34405
- Application of a limit theorem to solutions of a stochastic differential equation. 17 p2575 A72-34866
- Independent variable transformations for stepwise solution of differential equations of motion power series expansions, considering convergence radius 17 p2609 A72-35105
- Freedoms retention determination eigenvalue analysis of complex structures large dynamic matrices deriving transformation vectors based on maximum swept volume deformation modes 17 p2576 A72-35253
- Experimental study of image coding by complex Haar and Hadamard transformations 17 p2518 A72-35673
- Formal extension of the possibilities of the method of integral transforms in the study of linear distributed systems with constant parameters 19 p2834 A72-37432
- Direct and inverse transformations between phase variable and canonical forms. 19 p2826 A72-38230
- Coincidence of the mapping point with the slip plane in the modified differential descent method 20 p2946 A72-39470
- Group properties of ordinary linear second-order differential equations 20 p2946 A72-39471
- A long line as a limit of an infinite quadrupole chain 20 p2904 A72-39592
- Invariance problems in terms of Lagrangian domain of definition and Euler-Lagrange mapping intrinsic geometric characterization, reviewing theory of fiber bundles 20 p2954 A72-40006
- Measurement and transformation of two-port S parameters in terms of three-port parameters for a more general characterization of transistors - Errors 21 p3025 A72-40224
- Lorentz contraction and transformation of equilibrium forces and moments in inertial reference systems transition, discussing special relativity theory 21 p3084 A72-40938
- Irreducible sparse matrix transformation to upper triangular form by row-column permutation formulated as linear integer programming problem 21 p3075 A72-41312
- Man machine system input via human controller output transformation, illustrating with spacecraft lateral position manual control problem 21 p3010 A72-41411
- Satellite vibration-rotation motions studied via canonical transformations. 21 p3115 A72-41564
- [AIAA PAPER 72-919] Symmetry transformations for thin elastic shells. 21 p3234 A72-42398
- The construction of invariant transformations in plane rotational gasdynamics. 22 p3199 A72-42399
- Uniform moving source radiated sound field from equivalent stationary source distribution via transformation based on retarded-time position and Doppler frequency shift 22 p3205 A72-42461
- Integral equations and transformations in application to problems of elasticity theory 22 p3236 A72-42625
- Berner simulation method /BERSIM/ based on lumping recurring combinations of operations into component subsystems representing specified transformations of input into output variables 23 p3267 A72-44143
- Non-Abelian gauge fields with two masses 23 p3314 A72-44155
- Ray optics applications to electromagnetics and other disciplines, discussing matrix representation for wavefront curvature and field computation simplification via transformations 23 p3314 A72-44331
- Equivalence conditions for classes of linear and non-linear distributed parameter systems. 23 p3277 A72-44369
- Mechanical systems generalization using multilinear transformations and multiple index system flow formalism 24 p3424 A72-44624
- Stokes series for perturbing potential determination from gravity anomalies expressed as sum of two convergent series 24 p3418 A72-44858
- On an augmentation of the error made by numerical treatment of second-order conservative point transformations 24 p3419 A72-45071
- A 'length and area principle' type inequality for images in which certain integral functionals remain bounded in an n-dimensional space 24 p3419 A72-45261
- Invariant transformation of the control laws in ergatic systems 24 p3376 A72-45510
- TRANSFORMERS**
NT INSTRUMENT TRANSFORMERS
NT MODE TRANSFORMERS
 Dc feedback controlled constant voltage transformer, comparing with ferroresonant regulator [IEEE PAPER 17,2] 03 p0311 A72-13771
 Sequential faults examination on three-phase distribution transformer, suggesting protection scheme modifications 03 p0313 A72-14186
 Regulated dc-to-dc converter for voltage step-up or step-down with input-output isolation, using bistable comparator output voltage control through encoder 04 p0465 A72-14488
 Ring loaded corrugated waveguide for improved frequency broadbanding and transformer matching in horn antenna systems for satellite communication ground stations 04 p0498 A72-14721
 Kilowatt rotary dc-dc power transformer in modular sections for spacecraft applications, discussing electrical and mechanical designs and characteristics 08 p1112 A72-21414
 Low resistance thermometry with transformer coupled potentiometer circuit to obtain size reduction and ability for direct exposure to fluid 10 p1482 A72-24806
 Conditions derived for reactive two-terminal-pair matching transformer networks operation at maximum power transfer efficiency 14 p2087 A72-30334
 Characterization of a bilateral DC converter as a DC transformer. 17 p2497 A72-34705
- Bilateral tunnel-diode amplifiers using ferrite transformers. 18 p2665 A72-36306
- Losses in high-voltage transformers encapsulated by epoxy resins. 18 p2669 A72-37113
- Mobile X ray apparatus for radiographic flaw detection, describing tuned transformer high voltage source as power supply to sealed sectionalized X ray tube 19 p2805 A72-38766
- TRANSFORMS**
U TRANSFORMATIONS [MATHEMATICS]
TRANSFUSION
 Simulation of the human cardiovascular system - A model with normal responses to change of posture, blood loss, transfusion, and autonomic blockade. 17 p2507 A72-34445
- TRANSRORIZON RADIO PROPAGATION**
 Vhf waves transhorizonal propagation and day types correlation with sporadic E ionospheric layers in temperate zone, discussing wind shear theories 05 p0659 A72-16782
- Experimental investigation of the parameters of a statistical Gaussian field model for centimeter waves beyond the radio horizon 17 p2515 A72-34834
- TRANSIENT HEATING**
NT PULSE HEATING
NT SHOCK HEATING
 Thin circular plate quasi-static thermal stresses induced by transient temperature distribution on upper face, obtaining series form solution in terms of Bessel functions 10 p1558 A72-24720
- Thermal stresses in cylindrical shell under moving hot spot with cooling effect of surrounding media 11 p1737 A72-26428
- Three dimensional photothermoelastic method of refrigeration with composite model to study transient thermal stresses in wing rib 14 p2168 A72-30907
- Thermo-elastic interactions in an infinite elastic solid due to a concentrated transient heat source. 18 p2735 A72-36754
- Gas-core reactor power transient analysis. 19 p2833 A72-37632
- Transient radiative heat transfer in a non-gray medium. 19 p2880 A72-37835
- A technique for determining the transient heat flux at a solid interface using the measured transient interfacial temperature. 20 p2987 A72-39687
- [ASME PAPER 72-HT-18] Investigation of nonstationary heating processes in thermal resistors fed from functional sources 21 p3129 A72-41060
- On free vibrations at temperature-dependent material properties and transient temperature fields. [ASME PAPER 72-APM-J] 23 p3350 A72-44053
- Stability and oscillation characteristics of finite-element, finite-difference, and method of weighted residuals for transient two-dimensional heat conduction in structures. 24 p3461 A72-44608
- TRANSIENT LOADS**
NT BLAST LOADS
NT GUST LOADS
NT IMPACT LOADS
NT LANDING LOADS
NT SHOCK LOADS
 Electromagnetic plane stress wave generation by capacitor bank for transient loading of photoelastic models along straight and curved boundaries [SESA PAPER 1907A] 02 p0199 A72-11503
- Transient stress pulses propagation in obliquely laminated composites, comparing analytically predicted waveforms with experimental results 13 p2060 A72-29693
- Effect of electrical generator parameters on transient suppressors. 19 p2753 A72-37291
- Dynamic snap-buckling of shallow arches under inclined loads. 20 p2980 A72-39617
- TRANSIENT OSCILLATIONS**
 Oscillation transient in molecular Q switched ammonia beam maser following Stark voltage pulse in resonant cavity 01 p0081 A72-11186
- Energy-phase time transformations of damped Liapunov system applied to nonlinear spring pendulum and betatron transient oscillations 01 p0103 A72-11387
- Thin airfoil and bridge deck flutter derivative from transient oscillatory states in test procedure 02 p0298 A72-12665
- Mechanical oscillator model for experimental investigation of multistage electrical frequency multipliers subharmonic transient oscillations, considering energy flow under constant and/or phase modulated excitation 14 p2131 A72-30719

Axisymmetric flight vehicles motion stability and transient behavior via Liapunov method, taking into account nonlinear characteristics

15 p2318 A72-31203

High time resolution observations of photospheric velocity field, interpreting short period oscillations origin as result of combined image motion and Doppler velocity gradients

15 p2317 A72-32776

Theoretical model for computer calculation of transients in oscillator consisting of nonlinear amplifier with feedback through sequence of matched LC circuits

16 p2371 A72-33280

Transient and steady state vorticity generated by horizontal temperature gradients.

20 p2987 A72-40016

Energy transfer in vibration damping of pendulum with elastic suspension, noting periodic regimes and transient oscillations

21 p3086 A72-41547

TRANSIENT PRESSURES

The use of an expansion tube with cold gas to determine rocket engine starting transient pressures during silo launch.

[AIAA PAPER 72-997]

21 p3040 A72-41583

The transient processes in hybrid solid propellant combustion chamber throttled by supersonic nozzle.

24 p3434 A72-45198

TRANSIENT RESPONSE

Transient shock produced plasma flow interactions with transverse magnetic field

01 p0105 A72-10020

Large-signal IC equivalent circuit model for DC, linear and nonlinear transient time circuit analysis of lateral p-n-p transistors, including isolation junction interactions

01 p0044 A72-10126

Finite element method for determining transient response of box-type structure to traveling sonic pressure wave

01 p0136 A72-10219

Phase locked IMPATT diode microwave oscillator transients for reflection amplifier or pulse modulated source applications

01 p0037 A72-10646

Time optimal bang-bang response control of two pole single phase static inverter, giving output current transient response data

01 p0008 A72-11062

Transient electromagnetic plane wave ionospheric transmission and reflection, considering impulsive and step modulated sine wave excitations

01 p0031 A72-11102

Transient response of Al cylindrical shells to longitudinal impact, indicating wave front propagation at plate velocity

[SESA PAPER 1885]

02 p0287 A72-11505

Transient characteristics of phase lock automatic frequency control system with integrating filter, using nonlinear phase-plane method

02 p0176 A72-12224

Optimal stabilization law for ensuring gyroscope equilibrium position asymptotic stability in rms error, aperiodicity and system transient response time

02 p0230 A72-12338

MOS transistor frequency and transient response characteristics for equivalent circuit synthesis, using Bessel functions in differential equation solution

02 p0196 A72-12761

Transient response of negatively biased Langmuir probes for planar and cylindrical plasma sheaths under large amplitude pulsed potentials

[AD-739787]

03 p0361 A72-13924

Ac and dc electric power transient test equipment satisfying MIL-STD-704A requirements

03 p0312 A72-14038

Transient radiation effects on silicon diodes in avalanche breakdown, considering voltage regulating diode response and temperature compensating junction effects

03 p0334 A72-14090

Premixed combustible system in laminar axisymmetric stagnation flow, considering steady state and transient response of state variables, blow off extinction, ignition and heat flux

[AD-743387]

03 p0458 A72-14222

Pulsed current changes in positive column of He and Ne discharges, observing gradient and electron concentration transient behavior

03 p0399 A72-14348

Transient response of solid state YIG crystal dispersion filter, noting application to main radar bang generation with intrapulse frequency modulation

03 p0337 A72-14379

Current density nonlinear transient response and energy absorption of weakly ionized plasma under pulsed electric field

04 p0555 A72-14532

Control system synthesis from transient process estimates via Liapunov functions, proposing optimality criteria based on Gaussian minimum constraint principle extension

04 p0505 A72-14997

Transient signal propagation in unbounded time-spatial dispersive hot plasmas, using convolution integral equations

04 p0490 A72-15402

Analytical model for living biological tissue transient heat transfer, taking into account conduction, storage, generation, convection and blood flow effects

[ASME PAPER 71-WA/HT-36] 05 p0620 A72-15887

Contacting-both-wall switching transients of bistable fluidic amplifiers with low setbacks, including unsteady effects in jet and attachment zone

[ASME PAPER 71-WA/FLCS-6]

05 p0615 A72-15917

Semifinite circular fluid transmission line transient response to step function

[ASME PAPER 71-WA/FE-10] 05 p0646 A72-15932

Modeling techniques for fluid line transients, considering heat transfer and viscous dissipation

[ASME PAPER 71-WA/FE-9] 05 p0646 A72-15933

Linear two-temperature theory of thermoelasticity for investigating transient stresses arising from solid isotropic sphere aerodynamic heating

[ASME PAPER 71-WA/APM-14]

05 p0733 A72-15966

Transient stress analysis for sudden twisting of penny-shaped crack in infinite elastic body under torsion, using integral transform

[ASME PAPER 71-WA/APM-10]

05 p0734 A72-15969

Single- and many degree of freedom nonlinear structural systems transient dynamic response by presentation of equations of motion, damping and restoring force functions

05 p0736 A72-16082

Nonlinear transient coupled thermoviscoelasticity problems solution by finite element method and iterative solution for integrodifferential equation

05 p0736 A72-16085

Transient effect in electron-photon shower on readings of ionization chamber and scintillation counter

06 p0871 A72-17291

Peak parametric envelope calculation for hf pulse transients

06 p0773 A72-17571

Phase-plane analysis of transient response of on-off control system relative to sinusoidal inputs

06 p0795 A72-18714

Transient plane wave reflection and scattering by periodic grating of thin conducting cylinders

06 p0777 A72-18736

Transient gain measurements on laser dyes of flashlamp pumped rhodamine 6G-ethanol solutions with air and nitrogen

07 p1002 A72-19208

Thermal blooming of laser beams in liquids and gases, investigating short and long time behavior under thermal conduction and viscosity effects

07 p1005 A72-19408

Transient effects due to electromagnetic cascades in Pb during Cu wall passage in ionization calorimeter

07 p0988 A72-19871

Heat transfer steady state and transient response problems nodal formulation and numerical solution on digital computer

07 p1101 A72-19918

Linear first order differential equation transient response computer simulation using transition matrix method

07 p1028 A72-20340

Transients determined for Cs vapor discharge phases, observing current fluctuations between steady states in negative resistance zone above 0.2 torr

07 p1046 A72-20517

Zero velocity lag servomechanism transient response sensitivity from intuitive approach to convolution problem, noting feedback compensation advantages in sensitivity reduction

07 p0964 A72-20593

Oscillographic transient analysis of electric spark machining processes with electrode natural or forced vibrations

08 p1174 A72-21037

Self excited oscillations and transient responses of spacecraft stabilization relay system with delayed feedback, analyzing time delay effects in actuator circuit

08 p1241 A72-21170

Temperature gradients and dynamics of transient heating and cooling processes in metallic thermistors connected in series to power supplies

08 p1252 A72-21307

Periodic and synchronously recurrent transient signal detectability in time-varying noisy environment

08 p1134 A72-21406

Optimal stabilization law for ensuring gyroscope equilibrium position asymptotic stability in rms error, aperiodicity and system transient response time

08 p1168 A72-21553

Building structures response to transient pressures caused by sonic booms, discussing three dimensional loading effects, air cavity coupling and nonlinearities influence

08 p1249 A72-21908

Horizontally polarized impulsive plane electromagnetic wave reflection from perturbed linear ionosphere model, obtaining transient response as inverse Fourier transform

08 p1136 A72-21979

Barrier capacitance effect on transient characteristics of light diodes, obtaining time dependence of p-n junction volume charge voltage and recombination emission intensity

09 p1284 A72-22211

Transient processes in heat exchanger, allowing for coolant variable density

09 p1410 A72-22413

Transient characteristics and steady state off-design operation of mixed and unmixed type turbofan engines, noting peculiarities in control characteristics

09 p1374 A72-22626

Transient strain in axially impacted hollow non-homogeneous cone with axially varying modulus of elasticity and density

10 p1555 A72-24195

MOS transistor logic circuits pulse noise stability dependence on transient response, emphasizing supply voltage effect

10 p1449 A72-24290

Liquid rocket LF unsteady transient behavior calculation from droplet evaporation and combustion parameters

10 p1528 A72-24644

Transient calculation method for electric drive units described by first and second order differential equations, using special transformation for integral curve curvature determination

10 p1423 A72-24754

Longitudinal and transverse vibrations and transient response of elastically coupled nonlinear mechanical system

11 p1732 A72-25534

Mechano-acoustical network model for room-hallway-window system response to sonic booms or other transient loads, determining damping ratios

11 p1686 A72-25729

Phase noise and transient times for binary quantized digital phase locked loops in white Gaussian noise

11 p1592 A72-25886

Fe-Mo solid solutions transient creep behavior as function of applied stress, noting temperature effect

11 p1662 A72-26656

Fourier transform approximate inversion solution for transient pulse propagation from spherical cavity with surface under impulsive pressure in viscoelastic medium

12 p1844 A72-27196

Transient current density in plasma subjected to pulsed electric field derived from Boltzmann transfer equation

12 p1850 A72-27278

Plasma ion temperature determination by measuring transient current to cylindrical Langmuir probe under collision free conditions

12 p1851 A72-27399

Bandpass filter harmonic signal phase shift distortion effect on transient response in PSK of multichannel transmission

12 p1783 A72-27630

Holographic interferometry for impact loaded object transient impulse response recording with double-pulse Q switched laser

12 p1809 A72-27761

Frequency modulation and transient effects in resonant propagation of coherent light pulses

12 p1826 A72-27939

Mathematical model of reactive fluid flows during postignition transients in hybrid propellant rocket system

13 p2025 A72-28416

Fourier transforms for linear systems transient time and frequency characteristics, using discrete functional values for initial information

13 p1985 A72-28675

Turboprop engines dynamic parameters experimental determination by rpm transient response to instantaneous fuel supply changes

13 p2027 A72-29137

Second order phase lock AFC system transient response duration calculation for rectangular and sawtooth characteristics of phase detector, using averaging method

13 p1921 A72-29284

Transients analysis for nonlinear branched dynamic systems by integral manifold and small parameter method

13 p2007 A72-29997

Observational bias source in lunar transient events correlation with perigee and tidal stresses, using statistical analysis for 1947-1967 period

14 p2150 A72-30324

Nonlinear variable transformation method to determine locking band and transition processes in automatic phase and frequency control systems

14 p2087 A72-31132

Nonlinear processes in oscillatory systems with semiconductor diodes, calculating amplitude and phase characteristics in steady state and transient conditions

14 p2090 A72-31133

- Nodal equations derivation for lumped circuit representation of Gunn diode with steadily propagating domain under steady state and transient conditions 15 p2205 A72-31317
- Tapered elastic rod transient behavior under end impact due to mass striking, computing fixed end stress, struck end velocity and impact time duration 15 p2323 A72-31404
- Magnetic dipole or small current loop over homogeneous flat earth, calculating transient electromagnetic field for airborne remote sensing 15 p2224 A72-31672
- Transient phase object high sensitivity measurement by He-Ne laser beam transmission through differential interferometer and signal detection with p-i-n photodiode 15 p2235 A72-31784
- Jointly optimal filters for fixed range radar filter-sampler-filter system, determining impulse response function forms 15 p2207 A72-31793
- Integral Laplace-Fourier transform stability during transient response functions reconstruction from frequency characteristics in linear circuits 15 p2264 A72-31879
- MOS junction transistor turn-off behavior calculation based on model with carrier source and drain for channel formation 15 p2207 A72-31891
- Precession theory for transient response of gyroscope to rotation by Hook sphere using supplementary rotor 15 p2235 A72-31897
- Steepest descent path of integral describing transient plane wave propagation in anisotropic cold plasma, relating to evanescent wave arrival 15 p2285 A72-32109
- Transient flow induced in convergent-divergent nozzles by shock front impingement, investigating nozzle shape and Mach number effects on formation process of reflected shock 15 p2179 A72-32143
- Transient flow induced by shock front impingement on Laval nozzles observed by schlieren method, noting time variations of temperature and pressure 15 p2179 A72-32144
- Closed form solution for transient temperatures between two thermocouple readings, using Laplace transformation 15 p2336 A72-32583
- Transient torsional vibration of asymmetric rotor with limited power supply near critical speed calculated by asymptotic method 16 p2463 A72-32874
- Dynamic analysis of transient impact response of finite crack opened by in-plane shear tractions 16 p2464 A72-32920
- Unsteady Falkner-Skan flow solution by finite difference method for pressure gradient effect on transient response of laminar boundary layer 16 p2376 A72-33015
- Aircraft instrumentation system accuracy relation to aerodynamic derivatives evaluated from flight data, proposing input and transient response measurement system 16 p2394 A72-33640
- Transient elastic wave propagation in circular cylinder during sudden torsional shear stress application to end surface, noting surface particle velocity and stress 16 p2426 A72-33660
- Amplitude-controlled harmonic oscillator transient response time reduction by sampling techniques in control loop without introducing distortion 16 p2369 A72-33763
- Electromagnetic transient coupling between ungrounded loops for two layer conducting half space approximation of earth 16 p2388 A72-34007
- Correlation technique for transient response of a hysteretically-damped dynamic system to stationary random excitation. 17 p2579 A72-34231
- Study of transient phenomena by a TEA CO₂ laser associated with a liquid-crystal detector 17 p2562 A72-34285
- Experimental evidences for a transient ion layer formation in connection with sudden ionospheric disturbances in the height range 20-50 km. 17 p2545 A72-34630
- Initial value techniques in free-surface hydrodynamics. 17 p2538 A72-34644
- Free vibrations analysis of linear aerodynamic conservative structures in elastic range by finite element method, applying to transient or random forced responses calculation 17 p2626 A72-34742
- Longitudinal impact of cylindrical shells with discontinuous cross-sectional area. 17 p2628 A72-34793
- [ASME PAPER 72-APM-24] Evidence for the role of the transient neural 'off-response' in perception of light decrement - A psychophysical test derived from neuronal data in the cat. 17 p2500 A72-34884
- The effect of axial boundary motion on pressure surge generation. [ASME PAPER 71-WA/FE-15] 17 p2539 A72-34969
- Onset of convection near a suddenly heated horizontal wire. 17 p2637 A72-35048
- Stability and transient behavior of composite nonlinear systems. 17 p2534 A72-35530
- Transient turbulent free convection in a closed container with heating at the sides only. 17 p2638 A72-35642
- Binomial electronic filter design for nonnegative impulse transient response to obtain fast rise times via in-line pole-zero configuration 18 p2672 A72-36053
- Investigation of transient pressures in the plasma of a thermionic emission converter 18 p2647 A72-36214
- The transient radiated field of a coaxial aperture antenna. 18 p2660 A72-36331
- Relations between the experimental parameters describing the steady-state and transient creep. 18 p2732 A72-36343
- Current and capacitance transient responses of MOS capacitor. I - General theory and applications to initially depleted surface without surface states. 18 p2718 A72-36346
- Transient behaviour of laser generated carrier mobility in n-Ge. 18 p2697 A72-36351
- Mechanical component acceleration-induced stress and transient phenomena analysis by dynamic photoelastometry and interferometry, applying to elastic birefringent and other materials 18 p2734 A72-36373
- Transient acoustic point source disturbance transmission in two dimensional idealized jet, noting velocity profile effects on noise radiated to far field 18 p2679 A72-36406
- Sonic boom duration effects on thin circular elastic plate transient axisymmetric vibration via Hankel and Laplace transforms 18 p2734 A72-36409
- On the dynamic response of an infinite Bernoulli-Euler beam. 18 p2735 A72-36758
- On the transient response of a closed spherical shell to a local radial impulse. 18 p2739 A72-37089
- Transient characteristics of lumped-parameter delay lines 18 p2674 A72-37216
- Gas-core reactor power transient analysis. 19 p2833 A72-37632
- MOS transistor frequency and transient response characteristics for equivalent circuit synthesis, using Bessel functions in differential equation solution 20 p2907 A72-39067
- Unsteady heat transfer and temperature for Stokesian flow about a sphere. [ASME PAPER 72-HT-C] 20 p2983 A72-39482
- Time characteristics of heterojunction injection lasers. 20 p2933 A72-39516
- Transient laminar free convection in closed spherical containers. [ASME PAPER 72-HT-37] 20 p2986 A72-39669
- On the hydrographic response to transient meteorological disturbances. 21 p3077 A72-40465
- Resonant growing standing internal gravity waves, considering transient behavior, numerical results, break due to local gravitational instability, maximum amplitude and secondary flow generation 21 p3048 A72-40648
- Phenomena and interpretation of the transients caused by temperature change on capacitance of metal-oxide-metal systems. 21 p3097 A72-40690
- Effect of single-bit digitization in adaptive array control loops. 21 p3034 A72-41085
- Observation of transient behavior of picosecond laser pulses. 21 p3064 A72-41380
- Three-phase heat transfer - Transient condensing and freezing from a pure vapor onto a cold horizontal plate - Analysis and experiment. 22 p3243 A72-41957
- Optimizing functional for combined control of dynamic control plant, synthesizing stabilization system for maximal transient damping 22 p3162 A72-42091
- Pulse time positioning under background noise in radar and radio navigation range finders, noting root-mean-square errors and transient response 22 p3153 A72-42117
- Transient response of threshold lowering circuit with frequency converter for single contour IF amplifier with resonant frequency equal to carrier frequency 22 p3153 A72-42121
- Precipitation rate characteristics in age hardenable quenched alloys explained by transient analysis of vacancy annealing kinetics 22 p3189 A72-42441
- Spectrally shaped transient forcing functions for frequency response testing. 22 p3206 A72-42463
- Finite difference and extended Newton methods application to transient and steady state creep deformation in shells of revolution under high temperature and high stress 22 p3235 A72-42482
- Transient test techniques for modal survey testing. 22 p3163 A72-42698
- Analysis of the transient response of shell structures by numerical methods. 22 p3237 A72-42762
- Calculation of transient processes in a capacitance parametron by the phase approximation method 23 p3312 A72-43351
- The dynamics and control of Eulerian turbomachines. [ASME PAPER 72-AUT-S] 23 p3279 A72-43633
- Efficient method to multiply successively functions of the companion matrix and applying the method to evaluate transient response. 23 p3309 A72-43862
- Dynamic response of viscoelastic shallow spherical shells. 23 p3349 A72-43972
- On the determination of minority carrier lifetime and surface recombination velocity from the transient response of MOS capacitors. 23 p3324 A72-44071
- Metal-oxide varistor - A new way to suppress transients. 23 p3272 A72-44100
- Equivalent linear solution for transient free vibration of beams with strain dependent, frequency independent stress-strain hysteresis loop with sharp corners 23 p3352 A72-44120
- Response of shallow spherical shells to pulse pressure loads. 24 p3454 A72-44605
- Metallic solid material transient displacement field measurement by moire fringe photographic recording technique with computer program for data analysis 24 p3401 A72-44611
- Theory of pulsed internal optical parametric oscillators. 24 p3409 A72-44714
- Smoked foil observation technique for transient behavior produced by perturbing equilibrium configuration detonation waves 24 p3462 A72-45033
- A determination of thermal diffusivity under transient conditions 24 p3465 A72-45067
- A method for synthesizing feasible correcting devices with a minimum number of constraints on the optimized transient pulse response function 24 p3386 A72-45318
- Pulse transient response function for gyroscopic course indicator with gyrocompass error filtered out and nondistorted directional gyroscope error 24 p3405 A72-45320
- The transient electromagnetic response of a spherical shell of arbitrary thickness. 24 p3381 A72-45638
- TRANSIENTS [SURGES]**
- U SURGES**
- TRANSISTOR AMPLIFIERS**
- Transistorized pulse amplifier stage, showing gain as function of resistor parameters in collector circuit 01 p0035 A72-10200
- S band transistor power amplifier design and performance, noting application for 960 telephone channel radio relay system 01 p0038 A72-10657
- Computer program for microwave circuit scattering matrix sensitivity, applying to stripline elliptic low pass filters and thin-film negative resistance transistor amplifier 01 p0034 A72-10688
- Large signal nonlinear modeling and digital simulation of microwave transistor power amplifier and GaAs Gunn relaxation oscillator 01 p0041 A72-10691
- Broadband uhf power amplifier for AM signals output power of 100 W, using eight parallel transistors 06 p0774 A72-17750
- High power L-band microminiaturized hybrid type integrated transistor amplifier design and realization by computer 06 p0785 A72-18314
- Transistor power amplifier for 2.5 GHz range directional transmitters, noting cooling problems elimination 08 p1140 A72-21306
- Junction and MOS FETs noise sources interaction with small signal model parameters and signal source admittance parameters, investigating amplifier IF performance 08 p1141 A72-21428

Secondary breakdown effects on hf power transistor amplifier electrical characteristics, describing operation limits

09 p1288 A72-23364

Thermally stable six stage transistorized amplifier with logarithmic relationship between input and output voltage

10 p1450 A72-24494

Multistage broadband microwave amplifier design based on bipolar transistors cascade coupling, using scattering parameters

10 p1451 A72-24572

Transistorized microwave amplifier/limiter for upper part of decimeter wave range, suggesting limitation in automatic gain control transistors

10 p1451 A72-24588

MOSFET for input impedance measuring amplifier, discussing input stage temperature drift and protection from overvoltage

10 p1482 A72-24599

VHF and UHF radio transmitters with strip transmission lines, discussing transistor power amplifier design

10 p1441 A72-25116

Wide dynamic range analog multiplier with variable transconductance divider in operational transistor amplifier feedback path

11 p1603 A72-25742

Transistorized measuring amplifiers optimal initial regimes calculation with generalized junction voltage method, noting circuits analysis and internal feedback loops

11 p1605 A72-26467

Transistorized amplifier input elements design for biopotentials recording, providing minimum noise at high input impedance

11 p1585 A72-26468

Design analysis of emitter- and collector-base gain stabilized junction transistor amplifier at elevated temperatures using passive elements

11 p1606 A72-26569

Wideband push-pull transistorized power amplifier free of nonlinear distortions due to scattering inductance of load transformer

13 p1926 A72-28378

Single circuit amplifier design characterized by cascade connections of transistors to resonance network

13 p1929 A72-28900

Large signal four-pole parameters and optimum conditions determination for RF high gain amplifiers with class C operated transistors

13 p1921 A72-29344

Cascade section parameters calculation for multisection amplifiers with composite transistors and correction elements

13 p1934 A72-29978

Transistorized pulse amplifier stage, showing gain as function of resistor parameters in collector circuit

15 p2206 A72-31624

Transistorized microwave amplifiers with dissipative equalizing networks, describing transistor equivalent circuit

15 p2206 A72-31659

Monopole antenna height reduction by transistor amplifier incorporation in antenna structure

15 p2208 A72-32391

Circuits for electromagnetic interference reduction in broadband solid state radio transmitters, discussing balanced transistor amplifier

15 p2209 A72-32564

Ac voltage squaring with semiconductor power amplifier based on electronic servo principle and feedback circuit

16 p2370 A72-33958

The fabrication and evaluation of a micropower transistor and hybrid RF amplifier.

17 p2528 A72-34688

Design and analysis of transistorized, selective HF amplifiers with allowance for sensitivity properties

17 p2532 A72-35978

Optimal number of parallel transistor connections in feedback amplifier to improve SNR

18 p2665 A72-36108

The theoretical amplification limit of modulation amplifiers with correlation detection

18 p2668 A72-37035

Design considerations of a 3.1-3.5 GHz GaAs FET feedback amplifier.

19 p2771 A72-37269

Single and dual gate GaAs FET integrated amplifiers in C band.

19 p2771 A72-37270

Allowance for transistor parameter dispersion in transistor IF amplifier designs with staggered-cascade pairs

20 p2906 A72-38895

Microwave low noise amplifiers for use in radar systems.

20 p2907 A72-39220

Certain features of the use of controllable-gain transistors

21 p3033 A72-40944

Amplification cascade designs for harmonic and pulsed signals with a high frequency emitter correction

21 p3033 A72-40946

Optimization of planar transistor operation modes in cascades with inductive correction

21 p3034 A72-41121

Push-pull transistor amplifier fed from two different voltage power supplies, noting power efficiency improvement

22 p3158 A72-42115

A preamplifier with high input impedance for use with piezoelectric sensors

22 p3160 A72-42923

Cross-modulation dynamic range of amplifiers used in the input stages of receiver equipment

23 p3271 A72-43839

TRANSISTOR CIRCUITS

Bipolar transistor model for device and circuit performance prediction, determining parameter from charge distribution by regional approximation technique

01 p0042 A72-10786

Efficiency/reliability design requirements of driven transistor synchronous rectifiers in low output voltage applications

01 p0042 A72-11053

Pulse width modulated transistor series inverter with inductor transformer in low power applications, noting short circuit and no-load protection

01 p0007 A72-11060

Equivalent circuits and characteristics of multiwire and small active transistorized antennas including unipoles, loops, Franklin arrays and mast antennas

02 p0191 A72-11685

Dual-gate MOS transistor structure, operational principles and electrical characteristics, noting suitable properties for use in low noise microwave amplifier

03 p0330 A72-12969

P-channel MOS/silicon-on-sapphire transistor logic circuits for aerospace systems, investigating radiation hardness and performance potential

03 p0334 A72-14086

Gamma and neutron radiation effects on bipolar transistor current gain response predicted from multiple linear regression analysis

03 p0335 A72-14091

Frequency response of passive dipole antennas fed by transistor circuit, investigating power gain, bandwidth and voltage SWR

04 p0503 A72-15670

Frequency characteristics effect to determine voltage and current smoothing coefficients and resistances of transistor ripple filter with emitter circuit load

05 p0634 A72-16168

Book on transistors in pulse circuits covering switching diodes and circuits, multivibrators, blocking oscillators, etc

05 p0640 A72-16288

One dimensional bipolar junction transistor, comparing charge control and regional mathematical models for suitability in device and circuit computerized analysis and design

05 p0636 A72-16359

Plastic encapsulated transistors and IC moisture resistance tests for reliability under laboratory and field conditions

06 p0782 A72-17363

Transistorized automatic feedback power level control for centimeter band reflex klystron oscillator for electron paramagnetic resonance studies

06 p0784 A72-18166

Microwave IC oscillators design for broadband high performance receivers, exemplifying thin film Gunn effect, step- and varactor-tuned transistor oscillators

06 p0786 A72-18373

System potential of microwave solid state generation and amplification, comparing IMPATT, TRAPATT, Gunn, LSA, transistor and transistor-multiplier devices

06 p0787 A72-18456

Microwave receiver double diffused MOS transistor /D-MOST/ device advantages over bipolar device

06 p0790 A72-18485

Power generation and low noise amplification devices development during past decade, considering avalanche diodes, transferred electron and acoustoelectric devices and microwave transistors

07 p0952 A72-18825

Frequency and power characteristics of transistorized generators of harmonic oscillations

07 p0956 A72-19569

I-V characteristics of junction transistors with avalanche breakdown mechanism

07 p0958 A72-19895

Magnetic-transistor master oscillator with digital analog converter as programmer for needed output voltage frequency shifts

07 p0946 A72-19959

YIG-tuned microwave transistor oscillator design and performance, considering resonance phenomena and magnetic circuit effects on applications

08 p1139 A72-20985

Transistorized static pulse generators for spark erosion machining, discussing operating principle, design, applications, automatic control system and maintenance procedures

08 p1146 A72-21038

Transistor damage by electrostatic discharges, noting charge stored by humans and protection techniques

08 p1140 A72-21064

MOS IC reliability based on p-channel enhancement mode transistors, discussing failure modes and mechanisms

08 p1142 A72-21588

German monograph on frequency noise of microwave transistor power oscillators covering generation mechanism and spectral density determination

09 p1285 A72-22340

Six channel integrated MOS switch, discussing MOS transistor operation and circuits structure

09 p1288 A72-23363

Power transistor thermal cycling ratings and fatigue testing under operating conditions

10 p1447 A72-24011

MOS transistor logic circuits pulse noise stability dependence on transient response, emphasizing supply voltage effect

10 p1449 A72-24290

Pulse width modulated regulating dc-to-dc converter with small number of transistors to improve circuit reliability

10 p1452 A72-24680

Radio electronic equipment IC and microelectronics development trends, considering bipolar and MOS transistors applications in digital and analog computers and telemetry

10 p1454 A72-25176

Complementary monolithic IC n-p-n and p-n-p transistor circuit structure with high sheet and low saturation resistance

11 p1606 A72-26567

Active transistorized low pass RC filter providing fourth-order transfer function and uniform frequency response

13 p1927 A72-28381

Transistorized electronic equipment with delay line for optimal filtration of PSK signals

13 p1930 A72-29047

Distributed base resistance effect on stripline geometry transistor input characteristic, using equivalent circuit with pseudo-junction having high saturation current

13 p1930 A72-29059

Destabilizing factors effect on parameters of transistorized single circuit phase modulator with varicap control

13 p1932 A72-29451

Base resistance coupled transistorized multivibrator design characterized by superior frequency stability regardless of wide voltage fluctuation

13 p1934 A72-30017

Transistorized oscillators for variable-frequency generators designed to feed synchronous motor drives of equatorial telescopes

14 p2073 A72-30685

Nonlinear electronic /transistor/ system mapping-on by matrix dynamic transform algorithms, comparing with Newton-Raphson method

15 p2210 A72-31491

Passive and active electric circuit analysis by structural numbers method with computer time and space advantages, noting application to transistor circuits

16 p2370 A72-32851

A study of the heat flow and thermal instabilities in high power hybrid integrated circuits.

17 p2527 A72-34678

Contact-type level gauge with a transistorized decimal code converter

17 p2529 A72-34764

Magnetic and transistorized magnetic digital-to-analog converters

17 p2529 A72-34768

NAND gate logic transistor circuit design, layout, fabrication and electrical parameters, noting base and resistors diffusion welding

17 p2530 A72-35069

Junction field-effect transistor circuits for prescribed output functions.

18 p2665 A72-36307

Comments on thermal cycles of silicon power transistors

18 p2667 A72-36794

Quality assurance of transistor chips for the user

18 p2669 A72-37120

Quality and reliability evaluation method for integrated circuits using MOS transistors - Option: Circuits on request

18 p2671 A72-37141

Low noise high power bipolar and field effect transistors monolithic integration potentials for microwave applications

19 p2771 A72-37261

French monograph - Contribution to the study of the behavior of bipolar transistors during high frequency dynamic operation

19 p2772 A72-37485

Calculation of the transmission factor of a parametric microwave transistor multiplier

19 p2774 A72-38423

Some problems of microwave electromagnetic oscillation phase control by using an inductance transistor
19 p2776 A72-38670

Multivibrator with p-n-p and n-p-n transistors, noting circuit diagram, operation and power dissipation
20 p2906 A72-38898

Self excited LC and RC oscillator networks based on FETs, discussing frequency tuning and FM methods
20 p2906 A72-38899

New active all-pass network with linear group delay.
20 p2910 A72-39431

A fast, high repetition rate avalanche transistors pulser for capacitive loads.
20 p2907 A72-39435

Mathematical model for MOS transistor circuit analysis, noting parameters measurement and environmental effects representation
20 p2909 A72-39783

Analysis of the characteristics of an MOS transistor as a switching element
21 p3025 A72-40163

A method of calculating the parameters of a linearized transistor model
21 p3027 A72-40475

Broad-band transistorized receiving antennas in the frequency range between 10 kHz and 10 MHz
21 p3030 A72-40526

Avalanche transistor circuit with controlled S shaped I-V characteristics, discussing equivalent circuits and operating points stability
21 p3034 A72-41119

Possibility of employing a transistorized self-excited oscillator with a thermistor as radio sensor of temperature
21 p3058 A72-41792

Parameters and properties of special avalanche transistors
21 p3035 A72-41809

Frequency and power characteristics of transistorized generators of harmonic oscillations
22 p3158 A72-42087

Final stages of transistorized sweep generators
22 p3158 A72-42114

Computation of the maximum oscillation frequency of bipolar transistors
23 p3269 A72-43448

Linearization of relaxation-time control in a transistorized multivibrator
23 p3270 A72-43765

MOS logic circuit design simplification by replacing series and parallel transistor networks by equivalent single transistor inverter circuit
23 p3271 A72-43843

An approach for generation of second order RC-active filters.
23 p3276 A72-43863

Parametric preamplifiers for transistorized nuclear-emission detectors and their capabilities
24 p3402 A72-44894

Circuit analysis and operation of analog multipliers with MOSFET, applying to industrial automatic control systems and measuring instruments
24 p3384 A72-44896

TRANSISTOR LOGIC

Optimization algorithm for minimum margin efficiency of electronic circuits, applying to IC TTL gate and transistorized bistable multivibrator /flip-flop/
07 p0944 A72-19568

Response time and noise stability measurements of integrated circuit TTL /transistor-transistor logic/ and DTL /diode-transistor logic/ elements performing invert functions
10 p1449 A72-24286

Bipolar insulated gate FET IC buffer driver, discussing input and output interface capacitance and impedance characteristics and application to transistor-transistor logic
11 p1603 A72-25269

Micropower IC approach based on complementary transistor-transistor logic
11 p1606 A72-26566

Aluminum-silicon Schottky diode clamped transistor-transistor logic circuits parameters optimization for high switching speed and IC applications
11 p1606 A72-26568

Low power TTL IC in plastic and hermetic packages tested for reliability via critical dc parameters measurement in initial and post-stress states
14 p2091 A72-31168

Univac 1616 computer design featuring uses of 16-bit word technology, medium and large scale integration, and transistor-transistor logic
16 p2366 A72-33243

Optimization algorithm for minimum margin efficiency of electronic circuits, applying to IC TTL gate and transistorized bistable multivibrator /flip-flop/
22 p3158 A72-42086

TRANSISTORS

- NT FIELD EFFECT TRANSISTORS
- NT JUNCTION TRANSISTORS
- NT PHOTOTRANSISTORS
- NT SILICON TRANSISTORS

Bipolar transistor model for device and circuit performance prediction, determining parameter from charge distribution by regional approximation technique
01 p0042 A72-10786

Optical regulation of I-V characteristics in avalanche transistor
02 p0195 A72-12584

MOS transistor frequency and transient response characteristics for equivalent circuit synthesis, using Bessel functions in differential equation solution
02 p0196 A72-12761

Thermal deformation effects on metal bond fatigue failure modes in small signal transistors, micro and LSI circuits
03 p0365 A72-14291

Burst noise in bulk materials and transistors attributed to crystallographic defects, investigating gold addition effects
04 p0498 A72-15131

Minority carrier diffusion effect on current gain in miniature bipolar transistors
04 p0498 A72-15132

Pinch-in effect due to emitter current distribution instability in transistors with emitter-stripe geometry
04 p0499 A72-15209

Three layer bipolar transistor structure with negative resistance region in I-V characteristics
04 p0503 A72-15668

Coordinated characterization and mathematical modeling for device, circuit and system designs and computer analysis, applying to bipolar transistor
06 p0778 A72-17477

Laser triggered avalanche transistor voltage generator for picosecond streak camera used in laser pulse diagnostics
07 p0999 A72-18881

Hf and shf power transistor gain, efficiency and electrical characteristics for wideband linear amplifiers
08 p1139 A72-21051

Operational and equivalent circuit characteristics of low noise hf and shf transistors in wideband amplifiers
08 p1139 A72-21052

Energy level and V-I characteristics of solid state heterojunction devices, discussing diodes, transistors, thyristors and optoelectronic structures
08 p1139 A72-21054

Physical parameters of transistor, discussing carrier transfer, space charge and potential drop as function of current and voltage changes
08 p1139 A72-21058

One dimensional model for drift transistor at low injection level with minority carrier mobility dependence on impurity concentration
08 p1140 A72-21063

Three dimensional heat diffusion equation for multiemitter power transistor, taking into account thermal instability due to geometry
08 p1141 A72-21418

Uniform and crowded temperature distribution in large geometry power transistor, solving time dependent heat diffusion equation
08 p1141 A72-21419

Small signal microwave transistors design with arsenic and phosphorus diffused emitters, comparing performance in terms of power gain-bandwidth product, maximum frequency and noise figure
08 p1142 A72-21743

Microwave transistor noise factor measurement for various geometries and parameter values correlation with predictions
09 p1286 A72-23104

Transistor LF flicker background noise generation mechanism in terms of bulk effect due to temperature fluctuation or phonon electron interactions
09 p1286 A72-23107

MOS transistor low level background flicker noise equivalent voltage relationship to gate voltage and input capacitance and interface state density
09 p1286 A72-23108

P-channel MOS transistor LF background noise components analysis for different dependencies on gate bias and temperature
09 p1286 A72-23109

Cost effective nonstatistical procurement of VHF power transistors with high degree of confidence in reliability
10 p1447 A72-24014

MOS transistor current fluctuation relation to capture centers surface density, energy position and gate potential, determining spectral amplitude distribution
10 p1449 A72-24284

Microwave power transistors and active two terminal devices performance, describing representative applications
11 p1607 A72-26983

Active loop dipole aerials with height reduction properties at resonance, investigating transistor configurations in loop monopole aerial
12 p1792 A72-27699

Spurious oscillations in external excitation oscillators due to internal feedback in transistor, investigat-

ing frequency dependence of stability coefficient in cascade with common emitter
13 p1929 A72-28896

Correlation between internal noise sources of microwave transistors at low collector currents
14 p2088 A72-30917

MOS transistor injection level dependent theory, calculating drain region saturation conductance by iterative procedure
15 p2205 A72-31318

Calculations showing the reduction in the frequency dependence of a two-element array antenna fed by microwave transistors.
17 p2514 A72-34369

Thermal analysis of high performance devices mounted on dielectric substrates.
17 p2527 A72-34677

Monoplastic solid encapsulant for n-p-n and p-n-p silicon planar passivated signal transistors
17 p2528 A72-34715

Properties of a composite transistor
17 p2530 A72-35066

French monograph - Experimental characterization and analysis of the effect of ionizing radiation on the electrical properties of MOS transistors
17 p2531 A72-35650

Stability of the dynamic parameters of a transistor in a small signal mode superimposed on a static injection mode
17 p2596 A72-35801

Charge injection into the gate dielectric of MOS transistors during junction avalanche.
18 p2668 A72-37104

Correlation between the reliability of silicon bipolar transistors and their excess background noise
18 p2669 A72-37110

Physical parameters and structure of microwave power transistors, noting scanning electron microscope analysis of fine structure
18 p2671 A72-37144

A measuring method for MOST transconductance and its variation.
19 p2773 A72-37901

An elegant method for measuring MOST drain-source conductance in the saturated current region.
19 p2773 A72-37902

Allowance for transistor parameter dispersion in transistor IF amplifier designs with staggered-cascade pairs
20 p2906 A72-38895

MOS transistor frequency and transient response characteristics for equivalent circuit synthesis, using Bessel functions in differential equation solution
20 p2907 A72-39067

A precise method for measuring low-frequency small-signal conductance parameters of an MOS transistor.
20 p2907 A72-39273

Measurement and transformation of two-port S parameters in terms of three-port parameters for a more general characterization of transistors - Errors
21 p3025 A72-40224

The distribution of gate-channel capacitance between source and drain in the equivalent circuit of a MOS transistor
21 p3035 A72-41490

Forward and reverse characteristics of self-aligned double-diffused M.O.S. transistors.
22 p3160 A72-42754

German monograph - A contribution to the fabrication of thin-film transistors.
22 p3160 A72-43069

Dependence of MOS transistor parameters on carrier mobility
23 p3272 A72-44139

TRANSIST SATELLITES

High order harmonic equations in gravitational potential from Transit 1B orbit inclination, comparing with Ariel 3
08 p1158 A72-21216

Extractop model for time signal decoding for worldwide synchronization using Transit satellite system
15 p2199 A72-32078

TRANSIT TIME

Doping profile effects on reflection-type IMPATT diode microwave amplifiers, presenting power-gain vs frequency curves
01 p0037 A72-10643

High stability and power IMPATT oscillator design for line-of-sight communication links, avoiding spurious resonances and mode jumping
01 p0037 A72-10645

Voltage and current waveforms monitoring on sampling oscilloscope for TRAPATT microwave oscillator performance optimization
01 p0038 A72-10653

Hybrid IC at 30 GHz, considering IMPATT oscillators, circulators, frequency multipliers and filters configuration and performance
01 p0046 A72-10699

Punch-through transit time negative resistance semiconductor device utilizing injection from Schottky barrier, deriving small signal theory for microwave impedance
01 p0042 A72-10787

Solid state components for millimeter wave systems, including IMPATT diode power sources and amplifiers, P-I-N diode modulators and switches and Schottky barrier mixers

02 p0192 A72-12183

Heavier-than-helium cosmic ray nuclei composition inferring galactic confinement of particles, path lengths and transit times

03 p0409 A72-13137

Hadrons in extensive air showers, predicting arrival time spectra from fireball and isobar-p ionization models for high energy interactions

03 p0409 A72-13147

Ion transit time effects on plasma sheath RF admittance, using equivalent circuits for representation in low and high frequency ranges

03 p0394 A72-13150

Numerical integration of element T /transit time through perihelion/ in perturbations of near parabolic comet orbits

03 p0436 A72-13829

Mercury isophotometric measurements in white and H alpha light during transit across sun on 9 May 1970

04 p0573 A72-14904

Si p-n-p and Cr-n-p junction transit time diode oscillators microwave and dc characteristics comparison, noting similarity

04 p0499 A72-15206

Avalanche transit time diodes noise mechanisms and performance in microwave amplifier, oscillator and mixer applications

04 p0500 A72-15302

Ion transit time in ion cyclotron resonance spectrometer, using combination of pulsed ion formation and time dependent trapping conditions

04 p0523 A72-15484

Transit time and LSA oscillations at millimeter and submillimeter wavelengths in n-type GaAs

04 p0563 A72-15593

Venus transit, across solar face, detailing black drop effect on computation of exact ingress moment

04 p0581 A72-15620

Large signal IMPATT diode microwave oscillator lumped model, considering steady state oscillation

04 p0503 A72-15672

Interplanetary magnetic field effect on flare-generated weak shock wave propagation speed and transit time

06 p0875 A72-17461

Noise effect in IMPATT and Gunn diode oscillators on phase/frequency fluctuation using series/parallel connected multiple active devices

06 p0783 A72-17483

Meteor passage time determination by optical shutter with wedge-shaped blades for light flux periodic intersection and production of two discontinuous lines for identification

06 p0816 A72-17930

Low noise IMPATT diode design for arbitrary signal levels, using Read model

06 p0787 A72-18382

High efficiency microwave avalanche diode oscillators circuit design in TRAPATT mode

06 p0787 A72-18455

System potential of microwave solid state generation and amplification, comparing IMPATT, TRAPATT, Gunn, LSA, transistor and transistor-multiplier devices

06 p0787 A72-18456

Computer simulation data on pulsed IMPATT microwave oscillator performance improvement via double-drift diodes and second harmonic tuning

06 p0788 A72-18463

GaAs IMPATT diodes technology and performance at C, X and K band frequencies

06 p0788 A72-18466

Transit effects in grid plate gap of triode for generating microwave oscillations in regime similar to IMPATT diode

07 p0953 A72-19015

Noise contaminated pulse signal transit time measurement by receiver using digital filters

07 p0939 A72-19051

Gigahertz reflection amplifiers with low cost avalanche transit time diodes, measuring characteristics of amplification by synchronization at center frequency

07 p0955 A72-19191

IMPATT diode thermal resistance measurement from heat diffusion effect on small signal impedance of p-n junction

07 p0958 A72-20684

IMPATT diode microwave oscillator stabilized by two external resonant circuits, investigating self oscillation characteristics

08 p1138 A72-20745

Optimal output power of avalanche transit time diode oscillator in millimeter band as function of electric field and diode geometry

08 p1141 A72-21378

Coupled line microstrip circuit for high power and efficiency L and S band TRAPATT diode oscillators

10 p1450 A72-24307

Travel time effects on electron motion in HF electromagnetic fields, reviewing phase focusing and achromatic electron lens development

10 p1513 A72-24976

Noise temperature and admittance of space charge limited double cathode tube with transit time effects at microwave frequencies

10 p1454 A72-25105

Si Pd-n-p/plus/ transit time diode microwave oscillator, discussing fabrication, FM noise spectrum and bias current fluctuation

11 p1604 A72-25748

Computer aided circuit design by TRAPATT diode model consisting of nonlinear capacitance shunted by voltage- and current-controlled switch

12 p1791 A72-27672

Room temperature time of flight electron and hole mobility and trapping time measurements in zinc selenides as function of electric field

12 p1855 A72-27835

Nonequilibrium carrier distribution in drift junction transistor, considering base region hindering field effect on transit time, current gain cut-off and frequency response

13 p1926 A72-28371

Transit time, retarded domain and suppressed domain mode simulation of Gunn oscillator, using LF analog

13 p1927 A72-28405

Stable mirror plasma machine, determining particle distribution near loss cone by asymptotic analysis based on transit to mean collision times ratio

16 p2432 A72-32808

BARITT, IMPATT, TRAPATT and Gunn diodes, discussing power, noise and thermal dissipation problems

17 p2526 A72-34465

Avalanche diode oscillators.

17 p2526 A72-34563

Meteor passage time determination by optical shutter with wedge-shaped blades for light flux periodic intersection and production of two discontinuous lines for identification

18 p2693 A72-37155

K-band high power single-tuned IMPATT oscillator stabilized by hybrid-coupled cavities.

19 p2771 A72-37263

Intermodulation characteristics of X-band IMPATT amplifiers.

19 p2771 A72-37265

A 22 percent C.W. efficiency solid state microwave oscillator.

19 p2771 A72-37266

IMPATT diode circuits operation as microwave amplifiers, presenting data on intermodulation distortion, amplitude to pulse modulation conversion and reliability

20 p2910 A72-39851

Transit time heating in stochastic electromagnetic fields.

21 p3092 A72-41222

Effects of tunneling on an IMPATT oscillator.

21 p3034 A72-41382

Resonances in the collisionless heating of a plasma by transit time magnetic pumping.

21 p3094 A72-41631

Linear theory of a microwave distributed amplifier based on an avalanche transit-time diode

23 p3271 A72-43776

Negative resistance, transit time and limited space charge accumulation modes of semiconductor devices operation with electron transitions

23 p3272 A72-44138

Microwave phase shifting with gain using IMPATT diodes.

24 p3385 A72-44963

TRANSITION

Uniform progressing wave expansion solution to wave equation for transition region boundary value problems

03 p3388 A72-12988

Saturated absorption spectroscopy of ammonia, considering Stark effect on IR transition

10 p1491 A72-24122

TRANSITION FLOW

Incompressible nonsimilar turbulent and transitional flows numerical analysis in wakes, jets and boundary layers, using turbulent viscosity equations

02 p2022 A72-11587

Transition on plane plate in presence of vortices detached from cylinder in free flow

03 p0342 A72-13788

Laminar turbulent transition Reynolds number increase at finite perturbations in longitudinal magnetic field

03 p0398 A72-14003

Numerical solutions of integral equation for transition and turbulent flows through pipes and channels, discussing computer simulations

04 p0510 A72-14469

Bearing operating characteristics within transition range between laminar and fully developed turbulent flow, accounting for film thickness variation and pressure gradients

04 p0528 A72-15701

Mass addition distribution and gas injectant effects on heat transfer rates, transition locations and surface pressures of sharp cone

[AIAA PAPER 72-183] 05 p0748 A72-16838

Hartmann number for velocity pulsation free transition from turbulent MHD flow to laminar, noting difference relative to linear stability theory

06 p0860 A72-17679

Laminar to turbulent flow transition spectral evolution and catastrophic transition, discussing visual experiments and analytical methods

06 p0800 A72-18121

Nonequilibrium transitions for thermodynamic systems with generalized forces and flows by linear transformations, applying to nonelectrolyte solutions with concentration and temperature gradients

07 p1506 A72-18800

High altitude rocket plume rarefaction effects, predicting inviscid, merged, transition, first collision and free molecular flow regimes

08 p1128 A72-21610

Convective motions in rotating laterally heated annulus with contacting rigid lid, determining radial temperature difference for transition to vortex regime

10 p1506 A72-24420

Diffuser performance and idling characteristics in shock tube at Mach 8, discussing pressure recovery factor laminar and transition flows in boundary layer

10 p1419 A72-24545

Computerized numerical model of mixed subsonic and supersonic gas flow with sonic transition in turbine curvilinear channel

11 p1574 A72-26967

Kinetic freezing effects of supersonic gas flow with solid particles into vacuum, analyzing continuous to collisionless transition flow for Maxwell molecules

14 p2094 A72-30295

Sharp flat plate laminar, transitional and turbulent skin friction via finite difference integration of compressible boundary layer equations

15 p2180 A72-32596

Curved surface laminar flow turbulence from expansion rates measurement at high Reynolds number on experimental setup, considering centrifugal forces

16 p2379 A72-33792

Inviscid surface streamlines and laminar, transitional and turbulent heating of blunt nose shuttle configurations in hypersonic flow

16 p2345 A72-34041

Development of transition in the wake of a cylinder perpendicular to a supersonic flow

17 p2484 A72-34769

Fluid transition through critical value, considering self oscillation onset mode frequency

18 p2681 A72-36663

Transition to a turbulent flow mode in the boundary layer of a plane plate with various turbulence scales in the incident flow

18 p2682 A72-36888

Transient mode of a flow in the plane wake of a thin plate or cylinder

18 p2642 A72-36899

Perturbations development in laminar flow and transition to turbulent flow based on nonlinear theory of hydrodynamic stability

19 p2785 A72-37468

Laminar to turbulent transition in axisymmetrical submerged jets and slipstream flows of air and He, discussing Reynolds number effect

22 p3166 A72-42270

Velocity profile of near-wall turbulent boundary layer with adverse pressure gradient, noting skin friction

24 p3393 A72-45351

Rarefied gas flow through a slit.

24 p3395 A72-45572

TRANSITION LAYERS

Solar chromosphere-corona transition region models based on UV resonance emission lines intensity, deriving temperature gradient from radio data

03 p0424 A72-13222

Dispersion equations and resonant absorption of plane and cylindrical surface waves in transition layers between plasmas, noting Langmuir oscillations

15 p2286 A72-323851

Structure and properties of transition layers formed in the epitaxy process.

18 p2718 A72-36340

Transition in compressible free shear layers.

21 p2993 A72-41310

The derivation of temperature gradient and electron density maps from EUV spectroheliograms.

22 p3222 A72-42036

TRANSITION METALS

NT CADMIUM
NT CHROMIUM
NT COBALT
NT GOLD
NT HAFNIUM
NT IRIIDIUM
NT IRON
NT MANGANESE
NT MANGANESE ISOTOPES
NT MOLYBDENUM
NT NICKEL
NT NIOBIUM

NT PALLADIUM
NT PLATINUM
NT REFRACTORY METALS
NT RHENIUM
NT RHODIUM
NT SCANDIUM
NT SILVER
NT TANTALUM
NT TITANIUM
NT TUNGSTEN
NT VANADIUM
NT YTTRIUM
NT ZINC
NT ZIRCONIUM

Electron microscopy and diffraction analysis of lattice imperfections of layered superconducting transition metal dichalcogenide intercalation complexes
01 p0113 A72-10019

Physical properties of transition metal nitrides, carbonitrides and nitride-based cemented hard alloys, discussing carbides stability in presence of high pressure nitrogen
02 p0241 A72-11450

Positive and negative deviations of linear electrical resistance of d-transition metals at high temperatures as function of Debye temperature and Fermi level
02 p0242 A72-12006

Transition metal oxides hot extrusion sintering, discussing temperature and pressure effects on compacting density
02 p0244 A72-12349

Fe group transition metal impurities in semiconductors, calculating ground state wave functions and photoionization cross section dependence on wavelength
04 p0563 A72-15473

Thermodynamic estimation of transition metal stacking fault energy, discussing relation to lattice stability and structural changes
05 p0679 A72-17149

Electrical resistance, Hall coefficient and magnetic susceptibility of transition metal nitrides at low and room temperatures
06 p0827 A72-17386

Transition metals distribution of IV-VI and VIII a groups in metastable refractory nickel alloys gamma and gamma-prime phases
07 p1012 A72-19678

Transition metals addition effect on Al-Cu alloys strength and aging characteristics, determining lattice constant increase by X ray microstructural analysis
07 p1014 A72-19841

Transition metal borides chemical bonding mechanism from Nb and Cr boride phases thermal emf and expansion, resistivity, Hall coefficient and carrier mobility
07 p1017 A72-19992

Cold brittleness of transition metal alloys with bcc lattices, discussing elastic characteristics, packing defects energy, plastic deformation and rhenium admixture
07 p1018 A72-20143

Transition metals and alloys electron structure and packing defect energy theory, discussing crystal atomic interactions and brittle breakdown
07 p1049 A72-20148

Superconductivity in d- and f-band transition metals - Conference, University of Rochester, New York, October 1971
09 p1367 A72-22551

Transition metal superconductors transition temperatures survey, considering d-band solid solution alloys and intermetallics and ferromagnetic element compounds
09 p1367 A72-22552

Electron phonon coupling in tight-binding approximation for phonon frequency renormalization and transition metal superconductivity coupling constant computation
09 p1368 A72-22555

BCS theory for transition metals and alloys superconductivity, discussing electron phonon coupling, transition temperatures and Cooper pair fluctuations
09 p1368 A72-22556

Transition metal superconducting thin films and rf cavity surface protective coverings, investigating properties by low energy electron diffraction and Auger spectroscopy
09 p1368 A72-22560

Phonon dispersion curves from inelastic neutron scattering for actinide and transition metals carbides, noting superconducting properties
09 p1369 A72-22564

Electron phonon coupling and IR optical constants relationship to superconductivity in transition metals
09 p1369 A72-22566

Transition metals IR spectral absorptivity evaluation at room and liquid He temperatures from reflectivity measurement relative to vapor deposited Au mirror
09 p1309 A72-22604

Phonon dispersion curves of bcc transition metals for normal lattice vibration modes
09 p1369 A72-22680

X ray emission bands related to K line intensity for iron group transition metals, using orthogonalized plane wave method
09 p1370 A72-22840

X ray emission spectroscopy of electronic structure of transition metals and alloys, obtaining electron energy spectrum
09 p1370 A72-22841

Electron spectroscopy for chemical analysis /ESCA/ application to band structure measurements in transition metals, discussing photoexcitation, energy loss and escape depth
09 p1371 A72-22843

Ultrasoft X ray region photoionization absorption spectra features of inert gases, solids, rare earth elements and transition metals
09 p1357 A72-22845

Ti, Zr and Hf hcp-bcc phase transformation isochromat spectroscopic investigation, noting fine structures to confirm electron state density
09 p1371 A72-22849

German monograph on transition elements Cr, Mn and Zr influence on Al-Zn-Mg alloys stress corrosion covering electron microscope studies and loop-bending tests
10 p1493 A72-23769

Hubbard mathematical model for metal-insulator transition due to electrons correlations, noting schematic phase diagram and transition metal oxides
10 p1527 A72-24939

Transition series oxides metal-insulator phase transition based on electron phonon interaction model
11 p1701 A72-26024

Magnetic phenomena effects on superconductivity in simple and transition metals and dilute rare earth alloys
11 p1701 A72-26025

Russian book on transition metals and alloys electron structure and electronic properties covering paramagnetism, positron annihilation, magnetic transformations and electron heat capacity
11 p1659 A72-26069

Electronic configuration effect on wetting characteristics of hard material mixed crystals, investigating transition metals carbides, nitrides and oxides
11 p1665 A72-26873

Transition metals silicides additions effect on sintering and oxidation resistance at high temperatures of Ti and Zr diborides
11 p1665 A72-26874

Relative valence effect of transition metal additions on alpha-gamma phase equilibrium in Fe-Cr-Mn system
12 p1827 A72-27099

Metallic chromium band structure determination by Green functions method, explaining transition metals X ray emission lines by single electron approach
13 p1972 A72-28489

Electron structure of Al atoms in alloys with transition metals obtained from emission spectra
13 p1973 A72-28492

High melting point transition metals carbides, nitrides, borides, silicides and oxides thermal conductivity as function of characteristic temperature
13 p1981 A72-29905

Interaction of W with transition metals in ternary and multicomponent alloy systems, noting phase diagrams
14 p2122 A72-30981

Phase diagrams of rare earth ternary alloys with transition metals and Si, noting semiconductor properties
15 p2289 A72-31189

Chalcogenide semiconductor compounds of b-subgroup transition elements, discussing binary system diagrams, stoichiometric composition and electrical properties
15 p2290 A72-31193

Interstitial phases, crystal structure and chemical bonds of titanium, vanadium and niobium carbohydrides, comparing with transition metal carbides
15 p2252 A72-31195

Electronic structure of binary phase diagrams of group III-VI transition metals, using valence separation and condensed state model
15 p2252 A72-31198

Dynamic elastic moduli of diffusion saturated high melting point nitrides, carbides and borides of Ti, Zr, Nb, W, Mo and Ta
15 p2252 A72-31199

Vacuum vaporization of niobium, tantalum, zirconium and hafnium carbide phases, using Langmuir method
15 p2253 A72-31200

Transition metals additives effect on binary Mo alloys softening, noting influence of temperature and electron concentration change
15 p2258 A72-32135

Transition metal doped lithium niobate for holographic storage, measuring recording sensitivity, maximum diffraction efficiency and erase behavior
15 p2339 A72-32354

Tight binding model for binding energy determination in transition atoms adsorption on same series

TRANSITION POINTS

transition metal substrate, using moments expansion technique
15 p2281 A72-32379

Current noise spectra in single crystals and polycrystals of transition metal compounds, discussing flicker noise origin
15 p2293 A72-32384

Two band model explanation of Hall effect in dirty type-II transition metal superconductors near upper critical field, noting interband impurity scattering role
15 p2295 A72-32542

German book on welding of special metals covering Ti, Zr, Mo, Ta, W, Va, Nb and Be welding techniques
16 p2398 A72-33372

Liquid metals thermodynamic properties tabulation, including high melting transition metals, based on levitation data and periodic table correlations
16 p2479 A72-34000

Measurement of the electron work function in binary and ternary transition metal-nonmetal systems.
17 p2595 A72-34602

Temperature dependence of electrical and thermal conductivity for transition metals at 20 to 1200 C, noting periodic variations associated with atomic structures periodicity
17 p2568 A72-35519

Transition element distribution in stony meteorites and in terrestrial and lunar rocks.
17 p2619 A72-35936

Investigation of the properties of electrode materials made on the basis of high-melting-point compounds and alloys
18 p2698 A72-36136

Use of X-ray photoelectron spectroscopy to study bonding in Cr, Mn, Fe, and Co compounds.
18 p2657 A72-36568

Transition metals physical and mechanical properties, production, refining and vacuum processing techniques
18 p2696 A72-36840

Hot pressing of transition metal nitrides and their properties
19 p2808 A72-38281

Phase equilibria in the hafnium-niobium-boron and tantalum-chromium-boron systems
19 p2819 A72-38285

Systems of niobium monocarbide with transition metals.
20 p2942 A72-39985

Russian book on electron configuration model of condensed matter based on Hubbard model covering physicochemical properties of transition metals, alloys and compounds
21 p3066 A72-40348

Interaction of nonmetallic refractory compounds with transition metals and ferroalloys
21 p3066 A72-40394

Correlation between the work function of transition metal carbides and the surface recombination of hydrogen atoms in the region of homogeneity
21 p3070 A72-41372

Transition metals thermal conductivity periodic variations relation to free Fermi surfaces and valence electrons localization variations
21 p3070 A72-41646

Relation between the work function and adsorption and catalytic properties of transition metal borides in the reaction of recombination of hydrogen and nitrogen atoms
22 p3187 A72-41926

Prospects of using carbonitrides as the hard component of cermet hard alloys
22 p3188 A72-42195

Dependence of the properties of monocarbides of group IV-V transition metals on carbon content
22 p3189 A72-42198

Alloys of thorium with certain transition metals. VI - The constitution of thorium-nickel alloys containing 50-96% nickel.
22 p3190 A72-42769

Binary and multicomponent Re alloys with W, Mo, Ni, Co and Cr, noting elastic and strength properties for torsional suspension structures
22 p3191 A72-42805

Thermal conductivity in the two-band model of superconducting transition metals containing nonmagnetic impurities.
23 p3323 A72-43274

High temperature creep activation energies relationship to diffusion in TiC, ZrC and UC
24 p3413 A72-44936

Thermal conductivity in dirty transition-metal superconductors near the upper critical field.
24 p3432 A72-45675

TRANSITION POINTS

Stratospheric aerosol boiling point measurement with photoelectric particle counter, observing sulfate radical as major constituent
01 p0059 A72-10833

Ferritic steel nil-ductility transition temperature data analysis correlating irradiation results with activation fluences and temperature
04 p0547 A72-14430

- Free radicals formation during elastomers mechanical degradation by grinding below and above glass transition point at liquid nitrogen and room temperatures 04 p0484 A72-15264
- Microscopic-macroscopic transition in heterogeneous metal polycrystals and multiphase composites at finite strain 06 p0897 A72-18068
- Upper atmosphere minor component distribution rearrangement, investigating transition time to diffusion equilibrium 08 p1155 A72-20803
- Solar chromosphere-corona transition region theoretical and empirical models, studying acoustic flux generated above convective zone 11 p1717 A72-25906
- Creep deformation transition theory in spherical shells, using generalized strain measure for asymptotic solution 14 p2169 A72-30999
- Position of the transition point through the sonic velocity behind the detonation front 21 p3045 A72-40987
- Slow electromagnetic waves in antiferromagnetics near the point of transition to the ferromagnetic phase 21 p3098 A72-41685
- TRANSITION PROBABILITIES**
- Phosphorus absolute transition probabilities determination from P I and P II lines strength measurement, using gas-driven shock tube 01 p0104 A72-11111
- Solar corona transition probabilities in intermediate coupling between Fe XVII configurations, including full configuration mixing 03 p0416 A72-13006
- Atomic data for UV and X ray astronomy, considering atomic wave functions and energy levels, radiative transition probabilities and electron-ion collision cross sections 03 p0420 A72-13125
- Carbon monoxide oxidation by hydroxyl radicals at high and low temperatures from transition state theory, confirming flame and shock tube results [WSCI PAPER 71-36] 04 p0482 A72-14584
- Collision induced vibration-rotation transition probabilities for molecular motions, using state averaged potentials 06 p0851 A72-17299
- Radiative transition probabilities and recombination coefficients of ion C IV 09 p1354 A72-22664
- Transition probabilities of ionized Ar spectral lines for excitation temperature measurements 09 p1355 A72-22672
- Molecular X ray emission spectra interpretation based on singly ionized states observation by photoelectron spectroscopy and transition probability calculation 09 p1357 A72-22838
- Vacuum UV excitation cross sections measurement by electron impact on nitric oxide, tabulating threshold energies and transition probabilities 09 p1357 A72-22857
- Attractive well potential effects on vibrational transition probability during atom-diatom molecule collinear collision 10 p1514 A72-24335
- Transition probabilities and line shapes and widths of unimolecular problem computed using numerical methods for scattering processes 10 p1514 A72-24337
- Hydroxyl vibration levels excitation rates calculation from transition probabilities and band sequence nightglow intensity measurements 13 p1954 A72-29816
- Corrections to collision induced vibration transition probability calculated from three dimensional semiclassical model 13 p2009 A72-30062
- Hydrogen molecule highly excited electronic levels, developing transition probabilities estimation method 14 p2135 A72-30888
- Microscopic theory of weakly ionized plasma conductivity, showing particle diffusion function or transition probability description by linear Boltzmann equation 15 p2287 A72-32412
- Vibrational energy transfer probabilities for inelastic collisions between diatomic molecules, considering system represented by harmonic oscillators coupled by time dependent interaction potential 16 p2431 A72-33582
- Excitation of molecular vibration on collision - Simultaneous vibrational and rotational transitions in hydrogen + argon at high collision velocities. 17 p2585 A72-35467
- Two quantum induced photon-plasmon transition probability for hydrogen atom in processes of nebulae and stellar chromospheres 19 p2837 A72-38058
- Evaluation of rotational temperature at high vibrational temperature in electron beam fluorescence technique. 19 p2803 A72-38434

Transition probabilities and collision-induced transitions in excited levels of neon. 21 p3061 A72-40136

Kr I and II lines strength and relative transition probabilities, using thermal plasma behind reflected shock wave as spectroscopic light source 21 p3089 A72-40137

On the ergodic coefficients concerning generalized random systems with complete bonds 22 p3199 A72-42637

TRANSITION TEMPERATURE

High transition temperature alloys, layered intermetallic and organic superconductors development and properties 01 p0113 A72-10163

Thermomechanical conditions of plasticity-to-brittleness transition temperature for optimal rolling of cermet W strips 01 p0078 A72-11088

Strong coupling superconductors transition temperature derivation from Coulomb pseudopotential and Einstein-type phonon spectrum 03 p0402 A72-13672

Physicomechanical properties of metals at crystallization temperatures, considering density, viscosity, strength, hardness, elasticity and creep 03 p0378 A72-14219

Uniaxial stress effect on monocrystalline niobium stannide superconducting transition temperature, considering crystal structure 04 p0562 A72-15293

NbN film superconducting properties measured as function of thickness, discussing transition temperature, critical current and magnetic field 04 p0562 A72-15294

Fe-Cr-Al and Fe-Cr-Si type ferritic steels, investigating additives effects on ductile-brittle transition temperature 05 p0672 A72-16012

Tensile ductile-brittle transition temperature and slip mechanism of thoriated Cr, comparing with unalloyed Cr 05 p0678 A72-17117

Oxygen isotopic temperatures and mineral compositions of equilibrated ordinary chondrites 07 p1076 A72-19588

Rare earth metals effects on chromium brittle transition temperature, showing maximum plasticity with lanthanum addition 07 p1019 A72-20151

Cr-Ti-V-B alloys rod specimens grain size and brittleness-viscosity transition temperature after heat treatment, cooling and bending tests 07 p1023 A72-20668

Transition metal superconductors transition temperatures survey, considering d-band solid solution alloys and intermetallics and ferromagnetic element compounds 09 p1367 A72-22552

Maximum superconducting transition temperature estimation, discussing optimum resonant frequency for attractive interaction, umklapp electron scattering and lattice instabilities 09 p1367 A72-22553

BCS theory for transition metals and alloys superconductivity, discussing electron phonon coupling, transition temperatures and Cooper pair fluctuations 09 p1368 A72-22556

Spin excitation effects in superconductors, noting impurity concentration effects on transition temperature and thermodynamic properties 09 p1368 A72-22558

Superconductivity observation in Na, K and Rb intercalates of molybdenum disulfide comparing transition temperatures 09 p1368 A72-22561

Pressure effects on transition temperature and electronic structure of narrow band superconductors 09 p1368 A72-22562

Transition temperature pressure dependence determination for d- and f-band superconductor metals, alloys and compounds 09 p1368 A72-22563

NbN family high transition temperature values application to phonon spectrum prediction based on superconductivity microscopic theory 09 p1369 A72-22565

Nb-Al-Ge alloy superconductor deposits structure, transition temperature and critical current densities after preparation by triode sputtering and heat treatment 09 p1369 A72-22795

Enthalpy measurements of allotropic transformation of Co alloys during hcp-fcc transition with additive elements 10 p1498 A72-24850

Vibration viscometer measurement of viscosity of alkali metals Rb, Cs, Na and K near solidification temperature, studying oxygen effects on metal surface 11 p1746 A72-26236

Liquid Rb and Cs density and thermal expansion measurements near fusion point, discussing temperature dependence and gamma ray irradiation method 11 p1746 A72-26237

Heat transfer during film and transition boiling on vertical surfaces, taking into account time dependence 11 p1746 A72-26537

Transition temperature and other superconducting properties of annealed Nb-Al-Ge thin films 12 p1853 A72-27038

High refractory gadolinium oxide-strontium oxide system phase diagram and transition temperature by X ray and differential thermal analyses 13 p1984 A72-30109

Metallurgical and superconducting properties of beta-tungsten structure niobium aluminide with high critical temperature 14 p2119 A72-30607

German monograph on superconductors transition temperature calculation by iteration method using phonon spectrum approximation 14 p2143 A72-30947

Multifilamentary superconducting Nb-Sn composite wires in ductile metal matrix, determining transition temperature and critical current density 15 p2294 A72-32534

Thin film superconductors conductivity evaluation above transition temperature through renormalization of impurity-scattering vertex by pair fluctuation effect inclusion 15 p2295 A72-32540

Ti-Mo binary solid solution, investigating superconducting transition temperature, lattice instability and electron-to-atom ratio by calorimetric measurements 15 p2295 A72-32544

Charpy impact tests of neutron irradiated nuclear reactor component steels to determine ductile/brittle transition temperature, describing setup and gas heating and cooling procedures 16 p2373 A72-33222

Notch toughness criteria of metals with S shape transition temperature curve, considering experimental design and impact test model 16 p2406 A72-33322

Cd effect on alpha-beta transformation temperature and phase equilibrium in Ti rich end of Ti-Cd phase diagram, using metallographic and X ray techniques 16 p2409 A72-33806

Precipitation hardening effects on yield strength, toughness and ductile to brittle transition temperature of low alloy steels containing Nb 16 p2409 A72-33809

Superconductivity. 17 p2594 A72-34565

Properties of high-purity chromium 17 p2569 A72-35525

Anisotropy and strong-coupling effects on the critical-magnetic-field curve of elemental superconductors. 18 p2719 A72-36710

Superconducting energy gaps and transition temperatures of disordered cadmium and zinc films. 19 p2844 A72-37690

The grain-size-dependences of the failure mode and ductility transition temperatures of melted chromium and tungsten. 20 p2935 A72-39139

Correlation of irradiation data using activation fluences and irradiation temperature. 21 p3083 A72-40763

Crystal structures and transition temperatures of polymorphous metals, discussing mechanical properties, thermal conditions for deformation and metal working by pressure 22 p3190 A72-42803

Alloying and impurity effects on mechanical and recrystallization properties of Ta obtained by arc, electron beam and zone melting 22 p3191 A72-42809

Superconducting transition temperature increase in Nb-Al-Si alloys as function of composition under tetragonal lattice crystallization 22 p3192 A72-43020

TRANSITS NT CINETHEODOLITES NT THEODOLITES

TRANSLATING NT MACHINE TRANSLATION

TRANSLATIONAL MOTION NT SECONDARY FLOW NT THREE DIMENSIONAL FLOW NT THREE DIMENSIONAL MOTION

Low density monatomic gas supersonic spherical source flow, presenting departure from translational equilibrium 02 p0205 A72-12359

Hydrogen shock waves density profiles measurement, noting uncoupled translational and rotational relaxation processes 02 p0263 A72-12360

Gyrostal translational rotational motion equations in canonical form without trigonometric expressions in Hamiltonian 05 p0724 A72-16164

Spinning drag-free satellite trapping control phenomenon due to proof mass effect on translation controller design 05 p0725 A72-16445

Post-threshold translational energy dependence of endoergic cross sections for vibrational excitation and reactive scattering of diatomic molecules by atomic or molecular impact
09 p1357 A72-22858

Dynamic and kinematic equations of attitude and translational motions of symmetric rigid body under body fixed force
09 p1351 A72-22991

Relativistic Zeeman-Stark effect on molecular jet due to molecular translational motion in continuous magnetic field
10 p1514 A72-24135

Combined translational and internal relaxation theory of sound propagation in polyatomic gases, using I7 moment approximation
11 p1687 A72-26054

Vertical gravitational gradiometer capable of separating in space gravitational field elements and mechanical motion translational acceleration
11 p1635 A72-26463

Hollow elastic momentless spherical shell translatory displacements in compressible fluid under nonstationary spherical wave
12 p1880 A72-27234

Plane monochromatic electromagnetic wave scattering by rotating metallic cylinder, noting frequency shift dependence on cylinder translational motion velocity
13 p1914 A72-28370

Superposed forced oscillations of liquid and of elastically mounted bulkhead with translational harmonic displacements of cavity, noting damping increase
13 p1942 A72-29498

High speed accelerometers to determine test platform tilt and translational motion displacements, discussing instrument configurations without gyroscopes
[AIAA PAPER 72-818]
20 p2923 A72-39105

A form of the translational dynamical equations for relative motion in systems of many non-rigid bodies.
22 p3205 A72-42113

Control simulation models of three dimensional joint angle motions, including circle, ellipse and straight line trajectories and orientations in space
22 p3162 A72-42187

Conjugate and disjunctive optokinetic eye movements in the rabbit, evoked by rotatory and translatory motion.
23 p3257 A72-44243

About the first integrals of the generalized problem of translatory-rotary motion of rigid bodies.
24 p3442 A72-45235

Investigation of the dependence of the smoothness of rectilinear motion in precision-equipment mechanisms on the form of the microrief of contacting surfaces
24 p3403 A72-45325

TRANSLATORS
Process computation systems, discussing translator programs for conversion of user programs into machine language
21 p3024 A72-41002

TRANSLUCENCE
Near field characteristics of solid state laser frequency converters emission, determining medium transphosence during single pulse excitation of organic phosphors
10 p1490 A72-24052

Thermoprobe - An instrument for determining the temperature of opaque, translucent, and transparent surfaces in the incandescent temperature range.
19 p2795 A72-37513

TRANSLUNAR SPACE
U INTERPLANETARY SPACE

TRANSMISSION
NT AERODYNAMIC HEAT TRANSFER
NT CONDUCTIVE HEAT TRANSFER
NT CONVECTIVE HEAT TRANSFER
NT DATA TRANSMISSION
NT DIFFRACTION PROPAGATION
NT DOUBLE SIDEBAND TRANSMISSION
NT ELECTRIC POWER TRANSMISSION
NT ELECTROMAGNETIC WAVE TRANSMISSION
NT GROUND WAVE PROPAGATION
NT HEAT TRANSFER
NT HEAT TRANSMISSION
NT HYPERSONIC HEAT TRANSFER
NT IONOSPHERIC F-SCATTER PROPAGATION
NT IONOSPHERIC PROPAGATION
NT LAMINAR HEAT TRANSFER
NT LIGHT SCATTERING
NT LIGHT TRANSMISSION
NT MICROWAVE ATTENUATION
NT MICROWAVE TRANSMISSION
NT MULTIPATH TRANSMISSION
NT MULTIPLEXING
NT RADAR TRANSMISSION
NT RADIATIVE HEAT TRANSFER
NT RADIO TRANSMISSION
NT SATELLITE TRANSMISSION
NT SCATTER PROPAGATION

NT SELF PROPAGATION
NT SHOCK WAVE PROPAGATION
NT SHORT WAVE RADIO TRANSMISSION
NT SIGNAL TRANSMISSION
NT SINGLE SIDEBAND TRANSMISSION
NT SOUND TRANSMISSION
NT STRESS PROPAGATION
NT SUPERSONIC HEAT TRANSFER
NT TELEPHONY
NT TELEVISION TRANSMISSION
NT TIME DIVISION MULTIPLEXING
NT TRANSEQUATORIAL PROPAGATION
NT TURBULENT HEAT TRANSFER
NT WAVE PROPAGATION

TRANSMISSION EFFICIENCY
Radio communication accuracy characteristics in calculation of maximum frequency, skip distance and emission angle by transmission curves for midlatitude ionosphere
01 p0028 A72-10600

Microwave TRAPATT oscillator efficiency, using avalanche diode in coaxial cavity, slug and tapered sleeve
01 p0038 A72-10654

Adaptive variable length coding for efficient compression of spacecraft TV data of Grand Tour missions
06 p0771 A72-17401

Transmission locked differentials and variable ratio drive improvement effect on engine driven machine high speed performance and stability
08 p1113 A72-22097

Probability distribution density of amplitude difference of target signal and correlated noise sum for radar efficiency estimation
11 p1596 A72-26309

Target position information for radar energy potential calculation and detection quality, describing transmitter power reduction for normal range distribution density
11 p1596 A72-26313

Transmission and reflection coefficients of ULF waves incident on lower ionosphere layer with exponential electron density profile
11 p1597 A72-26707

Microwave two port waveguide transmission efficiency determination by reflection coefficient measurements
11 p1599 A72-26997

RC network synthesis for accurate realization of complex transmission zeros without capacitor adjustment
12 p1794 A72-27696

Conditions derived for reactive two-terminal-pair matching transformer networks operation at maximum power transfer efficiency
14 p2087 A72-30334

TDM and FDM digital communication systems performance comparison, noting equivalence in theoretical efficiency and generated waveforms
16 p2363 A72-33216

Efficiency of holographic gratings in nonpolarized light under vacuum in the ultraviolet
19 p2799 A72-37670

Transmission efficiency of gas chromatography algorithmic data compression and coding for spacecraft atmosphere studies
21 p3053 A72-40549

Television transmission performance of an experimental small aperture earth station.
21 p3018 A72-40878

Progress in the efficiency of free-space microwave power transmission.
22 p3140 A72-42481

Asymptotic methods of calculating the effectiveness of one variant procedure of selecting operational subchannels in an adaptive multichannel communications system
23 p3266 A72-44207

TRANSMISSION FLUIDS
Laboratory evaluation of engine oils, transmission lubricants and hydraulic fluids utilization in hydraulic power transmission systems
08 p1192 A72-21635

TRANSMISSION LINES
NT BEAM WAVEGUIDES
NT COAXIAL CABLES
NT COMMUNICATION CABLES
NT FLUID TRANSMISSION LINES
NT PLASMA GUIDES
NT STRIP TRANSMISSION LINES
NT WAVEGUIDES

Microwave oriented circuit analysis program /MODMAN/ to handle nonlinear, time-varying, lumped and distributed elements in time domain, using transmission line modeling algorithm
01 p0045 A72-10687

Microwave propagation on nonlinear transmission lines by examination of energy dissipation in shock front, considering distributed and lumped-parameter models
01 p0029 A72-10692

Resonance rail line scattering range using flat parallel conductor transmission line for radar cross section measurement
01 p0032 A72-11251

TWT small parameters measurement for gain calculation, using equivalent transmission line model
02 p0193 A72-12229

Optimization methods in digital data transmission systems, discussing equalization circuits for base band channel using metallic lines
02 p0182 A72-12691

Microwave precision coaxial connectors in terms of dimensional specifications, material properties, surface characteristics and other parameters for transmission standards effects
03 p0330 A72-13230

High power reflection-type pulsed microwave amplifier using high efficiency antiparallel avalanche diode pair connected at transmission line ends
04 p0497 A72-14714

Small arbitrary shape antennas with inner transmission line loading, showing efficiency without external matching circuit
04 p0501 A72-15432

Bulk storage applications in Illiac 4 system, discussing Univac 690 mass memory for Advanced Research Projects Agency network of telephone lines and interface message processors
[IEEE PAPER 23.4]
04 p0496 A72-15714

Frequency characteristics theory for two-stage electron tube microwave amplifiers coupled by transmission line on order of wavelength
05 p0634 A72-15827

Refractory metal multilevel interconnection systems, comparing materials fabrication, yield and circuit performance with diffused Si planar runs and polycrystalline Si films
05 p0636 A72-16362

Microwave lumped element impedance measurements from 1 to 12 GHz by resonant transmission line frequency and Q perturbation technique
05 p0637 A72-16419

LSA oscillators performance and control optimization, discussing multiaxis radial microwave cavity effectiveness in oscillation starting and coupling to coaxial transmission line
06 p0789 A72-18481

One- and two-conductor transmission lines electromagnetically coupled to rocket, deriving current bounds in load impedances under incident plane monochromatic wave
07 p0956 A72-19556

Fast rise high current constant trigger circuit for electroexplosive devices, using flat two-conductor transmission line to minimize inherent inductance
08 p1219 A72-20761

Digital frequency shift keying modulation of Gunn microwave oscillator by cavity placed between output and transmission line
08 p1141 A72-21432

Solid state microwave power amplifier with unidirectional transmission line loaded by negative resistance diode series, calculating large signal characteristics
08 p1142 A72-21558

Microelectronic IC functional logic systems design with S-type semiconductor devices, describing procedures for logic functions, shift register and directional transmission line
10 p1448 A72-24278

Hybrid neuristor transmission lines with planar p-n-p-n semiconductor structures, discussing development, testing and electrical parameters
10 p1448 A72-24281

Stationary waves properties dependence on weak skin effect in distributed tunnel diode type of nonlinear active transmission lines
10 p1453 A72-24902

Ignition energy measurement by nanosecond electric sparks produced by transmission line method, recording voltage pulses onto spark gap
10 p1563 A72-25138

Coaxial integrated pulse generator and gas laser with double transmission line for energy storage, noting design parameters selection
12 p1823 A72-27700

Reflectometer based on quasi-optical transmission line using conversion of incident and reflected waves into opposed circularly polarized components
13 p1954 A72-28375

Transmission lines with nonlinear capacitance semiconductor diodes, investigating electromagnetic traveling and standing waves instabilities and self amplitude modulation
14 p2086 A72-30795

Beam trajectory distortions due to turbulent air refractive index fluctuations in optical transmission line
15 p2197 A72-31885

Thin wire parallel to interface between two homogeneous half spaces, deriving transmission current wave propagation constant from boundary value problem solution
15 p2200 A72-32108

Generator for data transmission lines stochastic noise bursts simulation with statistically independent burst durations and intervals
15 p2201 A72-32475

Quasi-optical transmission line stability improvement, investigating pulsating light beam concept
15 p2202 A72-32663

Transmission line with feedback, deriving Nyquist stability from Michailov criterion with application to liquid fuel rocket model
17 p2621 A72-35100

Ceramic waveguide microwave integrated circuits.
17 p2534 A72-35570

Composite quasi-optical-broad waveguide transmission lines for millimeter and submillimeter waves with spectrum phase correction
18 p2664 A72-36106

End line matching for high gain traveling wave amplifier constructed from heterogeneous transmission line sections with negative resistance
18 p2665 A72-36110

Model random medium with two kinds of dielectric layers stacked in arbitrary proportions, calculating electromagnetic wave propagation characteristics by transmission line analogy
19 p2767 A72-38613

Electromagnetic compatibility problem of RF oscillators and switching operations in power network as interference source, discussing transmission line shielding and coupling impedance
20 p2901 A72-38988

The effects of transmitter source and load impedance on harmonic output spectrum - A new measurement method.
20 p2921 A72-38996

High speed logic circuit interconnecting transmission line matching by nonlinear resistance, recommending use of Schottky diodes
20 p2909 A72-39737

Analysis and design of TEM-line antennas.
21 p3026 A72-40353

Microwave filter of interdigital or comb construction, calculating attenuation coefficient relationship to impedance of slabline with cylindrical inner conductor
21 p3032 A72-40628

Application of the transmission-line-matrix method to homogeneous waveguides of arbitrary cross-section.
21 p3032 A72-40629

Signal quality monitoring of computer data transmission.
[ASME PAPER 72-AERO-1] 22 p3156 A72-43146

Frequency characteristics theory for two-stage electron tube microwave amplifiers coupled by transmission line on order of wavelength
23 p3268 A72-43435

TRANSMISSION LOSS

Temperature compensated high dielectric constant material, discussing low loss at microwave frequencies, reproducibility and mechanical properties
01 p0044 A72-11308

Low loss reactive wall rectangular and circular waveguides with periodic dielectric structures for millimeter wave and high power applications
02 p0190 A72-11678

Low loss wideband characteristics of groove and H guides for efficient signal transmission
02 p0190 A72-11679

Low loss wideband circular wave guide bend characteristics and branching filters for millimeter wave large capacity digital transmission
02 p0190 A72-11682

High resolution atmospheric transmission measurement of wavelength dependence of absorption losses in carbon dioxide of solid state Er laser radiation
02 p0238 A72-12201

Acoustic pulse generation and transmission loss characteristics measurement by single pulse method with simple shape to facilitate Fourier analysis
03 p0388 A72-12955

Tropospheric forward electromagnetic scatter propagation path loss prediction by modified Yeh method with empirically derived correction function
03 p0323 A72-14031

Analytical optimization of point to point communication above spherical ground, obtaining frequency minimizing transmission losses
03 p0325 A72-14193

Dissipative loss effects on frequency response and miniaturization limits for minimum loss conditions in microwave filters with Chebyshev characteristics
05 p0638 A72-17188

Small samples acoustic transmission loss measurement with constant energy flow in small duct
08 p1206 A72-21296

Diffraction losses and corrections for lower order transverse modes and resonance conditions in optical resonators with cylindrical mirrors
08 p1133 A72-21371

Microwave transmission loss prediction formula for obliquely incident plane wave leakage through perforated flat metal plate
08 p1135 A72-21559

Sound transmission loss through double leaf walls, noting correction for LF calculations
11 p1687 A72-26038

Conversion losses as function of signal power and circuit impedance in narrow band triode frequency converter under large amplitude operating conditions
11 p1598 A72-26733

Microstrip propagation and loss filling factor design formulas for magnetic substrates
11 p1599 A72-26991

Microwave radio link transmission loss Rayleigh-like long term distribution explained by two-path propagation model
12 p1784 A72-27796

Radar range reduction by snowfall, considering path attenuation and clutter power backscattered from near target precipitation
13 p1917 A72-28699

Sound transmission loss and diffraction measurements by combined correlation and Fourier techniques
13 p2006 A72-29768

Reflection and transmission coefficients of long lossy single mode waveguide line with random inhomogeneities
15 p2195 A72-31654

Dissipative loss effects on frequency response and miniaturization limits for minimum loss conditions in microwave filters with Chebyshev characteristics
19 p2775 A72-38624

Multimode dielectric waveguide with random coupling, discussing pulse dispersion improvement and loss penalty from power spectrum derivation
20 p2901 A72-38923

Wave scattering at a step in a circular multiwave waveguide
21 p3016 A72-40781

A high-frequency transmitted power meter using a laser signal
21 p3064 A72-41730

Experimental procedure for determining the strength losses in the individual elements of wave-type toothed gears
22 p3182 A72-41866

Optimal parallel-type varactor frequency multiplier calculation for reverse-biased conditions in terms of nonlinear conductance loss and diffusion capacitance Q factor
23 p3270 A72-43774

Transmission losses in glass and plastic single mode and liquid core optic fibers for long distance data links and image transmission
24 p3380 A72-45252

Determination of pressure losses in turbomachines.
24 p3393 A72-45353

Permittivity measurement of nonmagnetic materials samples in waveguide systems with an unknown movable reflecting load
24 p3404 A72-45504

TRANSMISSIVITY

Fabry-Perot interferometers as narrow band optical filters, discussing transmission and construction for various wavelengths
03 p0355 A72-13059

Optical losses, reflectivity and transmissivity measurements of He-Ne laser Fabry-Perot resonator elements, using laser output power dependence on element losses
07 p1006 A72-19905

Fabry-Perot spectrometer/premonochromator assembly integral transmissivity as function of spectral tuning noting selectivity by amplitude modulation
08 p1172 A72-22035

Epitaxial film system parameters determination based on variational technique of computing electromagnetic waves reflectance and transmissivity in semiconductor structures
14 p2142 A72-30811

Two beam optical recording instrument for atmospheric IR transmissivity, discussing spectrophotometers with changeable NaCl, KBr and LiF prisms
16 p2392 A72-33294

Resultant modulation transmission function of projection photometry photographic materials, discussing techniques for resolution and sharpness
16 p2392 A72-33364

Optical properties of transmission echelette high-pass filters.
21 p3055 A72-40823

TRANSMISSOMETERS

Double-ended, folded-path and double-reflecting transmissometers operation principles, and measurement error sources consideration for relative merits and disadvantages
20 p2923 A72-39054

TRANSMITTANCE

Vlf propagation across discontinuous daytime-nighttime transitions in anisotropic terrestrial waveguide, developing dominant mode approximations of transmission and reflection coefficients
01 p0032 A72-11239

Gain and bandwidth properties of microwave and optical devices with isotropic active medium, investigating transmission coefficient
02 p0189 A72-11566

Plant leaves light reflectance, transmittance and absorptance characteristics relationship to leaf

mesophyll arrangement, considering interpretation of aircraft/spacecraft remotely sensed data
02 p0213 A72-11856

Green and blue-green algae reflectance and transmittance characteristics, selecting spectral bands for multispectrum scanning of algal suspensions in water bodies
02 p0213 A72-11857

Reflection and transmission coefficients for radio waves incident upon thin highly ionized layers, comparing with sporadic E reflections
03 p0344 A72-12976

Au thin film effective optical constant calculation from measured reflection and transmission coefficients and thickness by approximate formulas
03 p0401 A72-13363

Normal diathermancy coefficient determination from quartz and distilled water spectral transmittance data, applying to diathermic cooling system design
05 p0751 A72-17071

Electromagnetic plane wave diffraction by infinite slit in screen with surface impedance, deriving field and transmission coefficient by asymptotic numerical solution
06 p0771 A72-17352

Longitudinal and transverse nonresonant slots on waveguide, calculating susceptance, conductance, reflectance and transmittance as function of wavenumber
07 p0952 A72-18843

Complex transmission coefficient of waveguide with two arbitrarily spaced infinitely thin plane parallel inhomogeneities, using Galerkin method for single-parameter approximation of electrodynamic problem
07 p0938 A72-19002

Modal matching method evaluating planar surface waveguide junction transmission and reflection coefficients, comparing to integral equation method
07 p0955 A72-19253

Angular transmittance model of visible light scattering through overcast cloud layer
07 p1030 A72-19411

Spherical scatterers extinction efficiency effect on photometer optical systems transmittances, using Mie equation and numerical methods
07 p0987 A72-19831

Anomalous refraction maxima in bidirectional plane polarized radiant flux transmittances of roughened dielectric surfaces
[AIAA PAPER 72-302] 11 p1742 A72-25236

Transmittance and Faraday effect characteristics of Te doped InSb samples with free carriers measured at 10.6 microns
11 p1648 A72-26338

Single layer overcast clouds visible light angular transmittance profiles, noting correlation with hemispheric and narrow-angle pyrheliometric transmittances
13 p1995 A72-29621

Regional observation of atmospheric spectral transmittance by Bouguer and high/low star methods
13 p2044 A72-29650

Sky spectral brightness, transmittance and indicatrix measurements at near IR wavelengths
15 p2222 A72-31398

Spectral transmittance enhancement in Fabry-Perot narrow band light filter by wavelength shifted dielectric mirror technique
15 p2233 A72-31414

Reflection and transmission coefficients of long lossy single mode waveguide line with random inhomogeneities
15 p2195 A72-31654

Elastic wave scattering by moving slab, calculating reflection and transmission coefficients for various incidence angles, frequencies and motion velocities
15 p2219 A72-32476

Atmospheric transmittance calculation from 0.76-micron oxygen band fine structure parameters
16 p2417 A72-33289

Quantization and other nonlinear distortions of the hologram transmittance.
17 p2553 A72-34724

Atmospheric transmittance measurements time and spatial representativeness optimization by allowing for fog element caused discontinuities
20 p2947 A72-38971

Measurement of the vertical atmosphere transmittance in the IR spectral region with the aid of an artificial source
21 p3079 A72-41800

TRANSMITTER RECEIVERS

Polarization distortion of partially polarized wave emission and reception by two channel horn antennas, noting radio astronomy, radar and optics applications
08 p1138 A72-20788

Multiple access to communication satellites in time division multiplex, discussing burst phase control and ground station receiving-transmitting systems
09 p1278 A72-22852

An all solid-state MIC transmit-receive module.
19 p2771 A72-37268

Radiation of EM waves with Walsh-function time variation - Preliminary results.
21 p3020 A72-40902

Delay-lock repeater tracking system utilizing super-regenerative interrogator. 21 p3082 A72-41084

TRANSMITTERS

NT INSTRUMENT TRANSMITTERS

NT IONOSONDES

NT RADAR TRANSMITTERS

NT RADIO BEACONS

NT RADIO TRANSMITTERS

NT RADIOSONDES

NT RADIOTELEPHONES

NT RAWINSONDES

NT REPEATERS

NT TRANSMITTER RECEIVERS

Technical characteristics of vhf/AM receiving transmitter, noting MTBF improvement 02 p0182 A72-12651

Minimum frequency separation between avionics receivers and transmitters for acceptable interference level 08 p1131 A72-20929

Common collector micropower monolithic transmitter for single or multichannel biomedical telemetry 11 p1586 A72-26563

TE mode propagation properties in circular waveguide, determining communication link transmitting and receiving equipment requirements 12 p1784 A72-27795

Theoretical analyses on Apollo lunar surface electrical properties experiment transmitter antenna. 17 p2515 A72-34423

A 5-kw peak transmitter for the 7-m wavelength 17 p2519 A72-35960

Experimental effects of finite transmitter-apertures on scintillations. 20 p2932 A72-39500

Detection of whistler mode signals from VLF transmitter in Australia. 21 p3023 A72-41386

Book - EMI prediction and analysis techniques. 22 p3156 A72-43198

TRANSOCEANIC COMMUNICATION

Airline air/ground radio communications and data link service implementation for San Francisco-Hawaii center 06 p0770 A72-17337

TRANSOCEANIC SYSTEMS

NT TRANSOCEANIC COMMUNICATION

Synchronous satellite surveillance system for transoceanic ATC, using suboptimal/modified Kalman/ filter for aircraft position and velocity computation 08 p1204 A72-21091

OMEGA navigation system operation aboard NOAA ship Discoverer in conjunction with satellite system, noting Trans-Atlantic tracklines 13 p1998 A72-29194

TRANSONIC AIRCRAFT

U SUPERSONIC AIRCRAFT

TRANSONIC COMPRESSORS

Transonic compressor design for minimum number of stages and hub/tip ratio and maximum inlet axial velocity, assuming axisymmetric flow 05 p0601 A72-16482

TRANSONIC FLIGHT

Unsolved aerodynamic problems in sub- and transonic civil and military aircraft design, considering flow problems during transonic flight, takeoff and landing [DGLR PAPER 71-105] 02 p0153 A72-12745

Transonic air transport design, discussing wind tunnel tests, supercritical flow technology, sonic beam avoidance, cruising speed, operating costs and transport family development 03 p0310 A72-13487

Ground focus line location of sonic bang propagating in stratified atmosphere with wind for transonically accelerating aircraft 07 p0912 A72-19645

TRANSONIC FLOW

Velocity field of sonic flow about aircraft wing profile, solving mixed Cauchy problem 01 p0001 A72-11178

Sonic line neighborhood of uniform axisymmetric supersonic air jet impinging on perpendicular flat plate, measuring shock shapes and surface pressures 01 p0002 A72-11398

Mathematical analogy between nonequilibrium and viscous inert transonic flows for reacting mixtures with relaxation and freezing 02 p0150 A72-11736

Steady sonic flow around three dimensional obstacles by pseudo-axisymmetrical flow approach, revealing singular perturbation of lift downstream at infinity 02 p0150 A72-12096

Compressible gas subsonic or transonic flow in front of obstacle, determining stagnation pressure with thermal relaxation time by numerical and wind tunnel methods 02 p0151 A72-12097

Noise generation from turbulent supersonic shear layers, including low supersonic and transonic ranges for jet noise applications 04 p0463 A72-15566

Pressure source model of sound radiated by sonic jet, deriving frequency spectra ratio and jet pressure 05 p0600 A72-16105

Flow calculations for subsonic and transonic portions of ring nozzles and plane curvilinear channels 05 p0601 A72-16226

Difference equations and relaxation method for three dimensional transonic flow field about wings in terms of velocity potential [AIAA PAPER 72-189] 05 p0605 A72-16843

Axisymmetric bodies with discontinuous curvature in transonic flow, calculating surface pressure distribution [AIAA PAPER 72-137] 05 p0606 A72-16891

Subsonic and transonic compressible potential flow over nonlifting hovering helicopter rotor blades, calculating flow field by three-dimensional nonlinear relaxation scheme [AIAA PAPER 72-39] 05 p0607 A72-16901

Finite difference method for transonic airfoil design for wide range of angles of attack and Mach numbers 06 p0755 A72-17629

Increased Reynolds number simulation with roughness set on aircraft model in transonic flow, investigating flow separation by parietal visualization technique 06 p0758 A72-17846

Two dimensional transonic and hypersonic shock structures, discussing flow equations, mathematical properties and similarity rules [AD-742561] 06 p0799 A72-17960

Asymptotic developments in transonic flows, considering three dimensional flows near shock and plane viscous and heat conducting flow 06 p0756 A72-18105

Lax finite difference scheme application to transonic two dimensional Laval nozzle and supersonic blunt body flow with detached shock wave, considering inviscid thermally nonconducting 06 p0756 A72-18126

Irrational two dimensional transonic flow past symmetric profile with and without shock 07 p0909 A72-20068

Transonic flow past wing airfoils, obtaining numerical solution by fitting mixed initial boundary conditions 07 p0909 A72-20079

Asymptotic method solution for boundary value problems for nonlinear differential equations describing transonic and slow supersonic flow past thin bodies 08 p1108 A72-21709

Steady inviscid irrotational transonic flow in two dimensional symmetric and axially symmetric nozzle throats 10 p1417 A72-23875

Plane transonic gas flows through Laval nozzle and symmetrical wedge-shaped profile, solving boundary value problem by reduction to singular integral equation 10 p1418 A72-24433

Axisymmetric plane transonic flow past convex corner point, obtaining characteristics by mapping into hodograph plane 10 p1468 A72-24435

Two dimensional transonic turbine blade cascade downstream flow losses determination [ASME PAPER 72-GT-43] 11 p1570 A72-25637

Constant density solutions for flow fields behind concave shock waves, noting approximation for transonic free stream Mach numbers 11 p1572 A72-25919

Perturbation analysis of perfect gas unsteady transonic irrotational inviscid flow in two dimensional channel, presenting numerical computation of flow structure temporal change 11 p1618 A72-26635

Numerical calculation of sonic flow around wing section with rounded leading edges, obtaining Mach number distribution, boundary characteristic shape and velocity field 12 p1751 A72-27181

Harmonically oscillating rectangular wing in unsteady transonic flow, obtaining two part boundary value problem for linear potential equation 12 p1751 A72-27545

Aileron vibration pressure measurement in plane-parallel transonic flow, evaluating damping characteristics with allowance for shock motion caused non-linear effects 14 p2071 A72-31026

Axisymmetric convergent cone profile synthesis to transform parallel flow at inlet to uniform sonic flow at outlet, examining solution convergence 15 p2177 A72-31206

Local subsonic flow region in transonic free flow past airfoil profile, transforming flow differential equations into linear Beltrami equations system via Chaplygin transformation 15 p2178 A72-31473

Deflection and energy dissipation of thin cascade profiles in transonic flow for given pressure distribution, noting boundary layers and separated flow 15 p2178 A72-31501

German monograph on plane steady isentropic flow past obtuse apex angle wedge at zero angle of attack and free stream sonic velocity 16 p2343 A72-33400

Transonic plane flow past wavy wall during choked wind tunnel operation, calculating flow velocity from Mach-Zehnder interferometer measured density distribution 16 p2378 A72-33508

Transonic airfoil section design to given surface pressure distribution, applying finite difference procedures to transonic small disturbance equations [AIAA PAPER 72-679] 16 p2346 A72-34062

Elliptic-hyperbolic relaxation algorithm for solution to three dimensional nonlinear transonic small disturbance potential equation for flow about swept wings [AIAA PAPER 72-677] 16 p2346 A72-34063

Aerodynamic normal shock noise measurements on nose cylinder bodies in transonic flow [AIAA PAPER 72-669] 16 p2346 A72-34068

Computation of transonic flow about finite lifting wings. 17 p2486 A72-32528

Transonic viscous flow around lifting two-dimensional airfoils. [AIAA PAPER 72-678] 17 p2486 A72-35479

Analysis of a transonic flow in elliptic nozzles 18 p2642 A72-36898

Intrinsically transonic /almost equal frozen and equilibrium sound velocities/ flows of chemically active gas mixture, developing nonlinear perturbation theory 19 p2745 A72-37390

Three-dimensional structure and equivalence rule of transonic flows. 20 p2886 A72-39631

Aerodynamic test facility data on swept wings, peaky airfoils, aircraft flutter and transonic flow, discussing shock tubes and wind tunnels development 20 p2912 A72-39846

New results concerning the numerical calculation of the sonic flow around a given airfoil section 22 p3135 A72-42639

Modified Newton-Kantorovich variational method for calculating flows in subsonic and transonic portions of circular nozzles, noting savings in computer time 23 p3248 A72-43659

Transonic flow past a wavy wall with compression shocks 24 p3360 A72-44999

Extension of the Prandtl-Glauert similarity rule to loss including cascade flow. 24 p3363 A72-45352

TRANSONIC FLUTTER

Dynamically similar wind tunnel models for transonic aeroelastic studies of aircraft failures or structural damage and flutter margins [ONERA, TP NO. 1082] 13 p1939 A72-29672

TRANSONIC INLETS

U SUPERSONIC INLETS

TRANSONIC NOZZLES

Subsonic, transonic, and supersonic nozzle flow by the inverse technique. 17 p2483 A72-34206

TRANSONIC SPEED

Dynamic stability, control and structural response of transonic jet transport to atmospheric turbulence 05 p0611 A72-16348

Turbulent boundary layer development for airfoil at high transonic speeds, discussing viscous-inviscid flow interaction [AIAA PAPER 72-5] 05 p0606 A72-16863

Photoelastic studies of plane stress fields in plate induced by moving loads at subsonic, transonic and supersonic speeds 10 p1553 A72-23746

Study of circular arc airfoils with asymptotic critical Mach number. I 17 p2484 A72-34744

Variable sweep wings aerodynamic characteristics in subsonic, transonic and supersonic flight, considering lift, drag, stability and control 18 p2643 A72-36976

Book - A theory of supercritical wing sections, with computer programs and examples. 21 p2993 A72-41534

Full-scale inlet/engine testing at high maneuvering angles at transonic velocities. [AIAA PAPER 72-1026] 21 p3042 A72-41604

Characteristics of gas flows in diffusers at transonic velocities 21 p2994 A72-41698

TRANSONIC TURBINES

U SUPERSONIC TURBINES

TRANSONIC WIND TUNNELS

Transonic air transport design, discussing wind tunnel tests, supercritical flow technology, sonic beam avoidance, cruising speed, operating costs and transport family development 03 p0310 A72-13487

Two dimensional airfoil pressure distribution measurements at high subsonic speeds, comparing normal

- force coefficients corrected for wind tunnel interference effects with theoretical calculations
[DFVLR-SONDDR-168] 03 p0308 A72-13609
- Correction factors for Aerodynamic Research Institute Goettingen transonic wind tunnel, comparing calculated values with AGARD calibration models test results
[DFVLR-SONDDR-167] 03 p0308 A72-13610
- Two dimensional transonic airfoil section testing at ONERA S3MA wind tunnel, comparing results with helicopter rotor blades test data
[ONERA, TP NO. 1028] 03 p0308 A72-13642
- Transonic plane flow past wavy wall during choked wind tunnel operation, calculating flow velocity from Mach-Zehnder interferometer measured density distribution
16 p2378 A72-33508
- Flow quality improvements in a blowdown wind tunnel using a multiple shock entrance diffuser.
[AIAA PAPER 72-1002] 21 p3041 A72-41587
- Evaluation of transonic and supersonic wind-tunnel background noise and effects of surface pressure fluctuation measurements.
[AIAA PAPER 72-1004] 21 p3041 A72-41588
- Application of wall corrections to transonic wind tunnel data.
[AIAA PAPER 72-1009] 21 p3041 A72-41591
- High Reynolds number transonic wind tunnel facility /HIRT/ for improved aerodynamic testing of, maneuver combat and commercial aircraft performance, maneuverability and handling qualities
[AIAA PAPER 72-1035] 21 p3043 A72-41609
- Computation of wall effects in ventilated transonic wind tunnels.
[AIAA PAPER 72-1007] 24 p3388 A72-45403
- Transonic wall interference effects on bodies of revolution.
[AIAA PAPER 72-1008] 24 p3389 A72-45404
- An initial two-dimensional wall interference investigation in a transonic wind tunnel with variable porosity test section walls.
[AIAA PAPER 72-1011] 24 p3389 A72-45409
- ### TRANSONICS
- #### U TRANSONIC FLOW
- ### TRANSPARENCE
- High performance aerospace vehicles transparent materials, discussing glasses, plastics and optical coatings, solar properties, refractive index, UV transmittance and radiation damage susceptibility
01 p0091 A72-10765
- Transparent fused silica wall irradiation induced optical absorption and heat deposition in nuclear light bulb engine
01 p0103 A72-11356
- Holographic measurements of dioptric powers and glass defects in thin transparent sheet under vertical or oblique parallel and divergent light
05 p0662 A72-16190
- Self induced transparency effect in ruby laser, investigating light transmission and pulse delay and broadening as function of input energy
05 p0670 A72-17171
- Heating dynamics of transparent dielectrics exposed to pulsed laser beam operating in free laser mode
06 p0825 A72-17697
- High intensity pulsed laser beam heating of solid transparent materials
07 p1002 A72-19212
- Laser flare luminosity front displacements and atom density at surfaces of transparent dielectrics as function of pulse intensities
07 p1007 A72-20123
- Low temperature Si photoconverters transparent in IR solar spectrum tested on Cosmos satellites
07 p0915 A72-20616
- Transparent and opaque materials fracture mechanism analogies under laser beam action, determining dislocation structure
08 p1185 A72-22093
- Transparence and polarization characteristics of three four-component Industrar-52 lenses with 1.5 aperture ratio and 50 cm focal length
09 p1309 A72-22516
- Recording holographic networks in polycrystalline transparent ferroelectric ceramics of lead and lanthanum titanate-zirconate system
10 p1480 A72-24111
- Heat transfer process in boundary layer of transparent gas flowing past plane emitting plate with prescribed surface heat flux
10 p1418 A72-24540
- Optical transparencies - Conference, London, June 1971
12 p1752 A72-27001
- Structural design and optical problems of external vision and cockpit transparencies in military aircraft
12 p1753 A72-27002
- Optical quality requirements for aircraft transparencies, considering resolution, haze, halation, light transmission, distortion, binocular deviation, double images, scratches and inclusions
12 p1832 A72-27003
- Aircraft transparencies from civil operator viewpoint, considering replacement cost of flight deck and cabin windows
12 p1753 A72-27005
- Acrylics and polycarbonates properties in aircraft transparencies design, emphasizing cost and optical, mechanical, thermal and chemical properties
12 p1832 A72-27009
- Polycarbonates applications in aircraft transparencies, discussing chemical, heat, impact and abrasion resistance, toughness and weathering
12 p1832 A72-27010
- Transparent aircraft polycarbonate glazing systems shielding properties for projectile and bird impacts
12 p1832 A72-27015
- High power light pulse generation with steep leading edges in Nd-glass laser, noting duration change based on transparency increase under light transmission
12 p1820 A72-27583
- Transparent dielectric surface photoelectric emission current under laser pulse illumination, noting correlation to surface treatment and damage threshold
12 p1822 A72-27613
- Resonant interaction and self transparency effect of coherent ultrashort light pulse passing through semiconductor
12 p1824 A72-27868
- Transparent materials study by interferometric methods, emphasizing holographic bench advantages for stress analysis and aerodynamic flows observation
[ONERA, TP NO. 1037] 12 p1812 A72-28048
- Digital computer synthesis of transparent object holograms, noting image discretization, two dimension Fourier transformations spectrum and digital data correlation with optical parameters
13 p1958 A72-29617
- Blackness degree calculation for semitransparent film on nontransparent substrate with layer temperature gradients, allowing for polarization emission and multiple reflections
14 p2130 A72-30296
- Off-axis phase holograms of photographic transparencies recording, comparing Fresnel, Fraunhofer and lensless Fourier transform holograms
15 p2239 A72-32358
- Resonant interaction and self transparency effect of coherent ultrashort light pulse passing through semiconductor
16 p2403 A72-33977
- Transparent and opaque crystal surface fracture mechanism analogies under laser beam action, determining dislocation structure
17 p2562 A72-34664
- Facility and procedure for measuring the spectral transmittance of the atmosphere in the range from 0.48 to 12 microns with moderate resolution
18 p2692 A72-36965
- New method for determining the integral radiative capacity of partially transparent materials at high temperatures
18 p2704 A72-37190
- Thermoprobe - An instrument for determining the temperature of opaque, translucent, and transparent surfaces in the incandescent temperature range.
19 p2795 A72-37513
- Measurement of three-dimensional refractive-index fields by holographic interferometry.
19 p2798 A72-37621
- An analysis of the spectral scanning technique for determining the temperature distribution in a semi-transparent medium.
[ASME PAPER 72-HT-6] 20 p2986 A72-39677
- Influence of hygroscopic substances on the transparency of aerosols from combustion products of condensed systems
20 p2987 A72-40043
- Atmospheric window at 10-12 micron wavelength, investigating absorption coefficient of clear atmosphere water vapor
21 p3048 A72-40398
- Digital computer synthesis of Fourier holograms of transparencies, noting significance to digital filtering method development for optical signal processing
21 p3054 A72-40670
- Radiant conduction heat transfer in semitransparent solid materials
22 p3243 A72-41955
- ### TRANSPARENT MATERIALS
- #### U TRANSPARENCE
- ### TRANSPARATION
- Turbulent boundary layer fluid dynamic behavior under transpiration and acceleration effects, presenting mean velocity profile data, skin friction and mixing length model
[ASME PAPER 71-HT-F] 02 p0205 A72-12315
- Heat transfer characteristics of transpired and accelerated turbulent boundary layer on porous plate, comparing with prediction techniques
[ASME PAPER 71-HT-BB] 08 p1251 A72-20880
- Thermal radiation shielding of porous surface on heated plate by absorbing gas transpiration, suggesting carbon dioxide, metal vapors and particulate mixture
[AIAA PAPER 72-277] 11 p1740 A72-25217
- Burnett theory of thermal transpiration in capillary with wall accommodation for polyatomic gases, using Chapman-Enskog constitutive relations
11 p1746 A72-26010
- Rayleigh problem in presence of magnetic field, discussing transpiration effects on MHD flow near oscillating flat plate
11 p1696 A72-26542
- Gas side, coolant side and interstitial heat transfer in gas turbines transpiration air cooling
12 p1860 A72-27350
- Blowing and suction effects on heat transfer and friction coefficients of transpired turbulent boundary layer, presenting theoretical models and experimental results
16 p2378 A72-33431
- Kinetic theory of a modified Knudsen's absolute manometer.
22 p3175 A72-41941
- A transpiration radiometer for measurement of total thermal radiation from a flowing plasma.
22 p3179 A72-42691
- ### TRANSPARATION COOLING
- #### U SWEAT COOLING
- ### TRANSPANTATION
- Influence of X-ray irradiation in 25- and 250-r doses on the transplant immunity in mice differing by weak and strong histoincompatibility systems
23 p3255 A72-43910
- ### TRANSPONDERS
- Integrated receiver module for satellite transponders, including tunnel diode amplifier, Schottky barrier mixer, Gunn oscillator and low pass filter
01 p0041 A72-10701
- Microwave communication via satellites, discussing FDMA and TDMA transponders design
01 p0029 A72-10709
- Pulse coded processing system EMC performance measurement, considering CW and pulsed interference effects and application to ATC radar beacon system transponders
03 p0324 A72-14033
- ATC radar beacon system developments, considering diversity transponders, interrogator environment control, electronic scan cylindrical array antenna design and discrete address mode
04 p0508 A72-14832
- Orthogonal mode waveguide cavities bandpass filters for communication satellite transponders, comparing with Chebyshev design
07 p0958 A72-20489
- Weak signal turnaround transponder design for pseudonoise coded ranging systems, discussing band width optimization and performance comparison between various receiver configurations
10 p1452 A72-24688
- Digital solid state altitude encoder for ATC transponder reporting, covering Gray and Gillham codes
[SAE PAPER 720314] 11 p1630 A72-25578
- Dynamic range errors and noise bands for phase comparison radar range finders with mutual automatic frequency control in interrogator and transponder
11 p1596 A72-26302
- Aircraft distance measuring equipment with VOR radio receivers and ground station transponder for pulse interrogation
12 p1842 A72-27105
- Intelsat 4 satellite communication transponder design for broadband multicarrier operation, using frequency and pulse modulation techniques
[AIAA PAPER 72-535] 12 p1780 A72-27358
- Flight prototype satellite communications repeater with two transponder channels and dual beam antenna, discussing design parameters and advanced systems application
[AIAA PAPER 72-579] 12 p1789 A72-27381
- Vibration stability and interference transfer function of onboard transponder with phase lock AFC used in Doppler system for measuring spacecraft trajectory parameters
13 p1958 A72-29456
- ATS-3 C band dual transponders for geographically distant clocks time synchronization, using Cs clocks for accuracy verification
15 p2200 A72-32080
- Apollo 15 gravity analysis from the S-band transponder experiment.
18 p2724 A72-36286
- Design of a 14/12 GHz transponder for the Communications Technology Satellite.
[AIAA PAPER 72-734] 18 p2660 A72-36540
- ATC IC transponder used with secondary surveillance radar, discussing design features
18 p2662 A72-37048
- A solid-state transponder source using high-efficiency silicon avalanche oscillators.
19 p2774 A72-38400
- Satellite adjacent-channel interference due to multicarrier transponder operation.
21 p3020 A72-40892
- The Symphonic transponder in the integration phase
24 p3380 A72-45273
- ### TRANSPORT AIRCRAFT
- #### NT CARGO AIRCRAFT
- #### NT CONCORDE AIRCRAFT

NT ELECTRA AIRCRAFT
NT SHORT HAUL AIRCRAFT
Future aircraft design trends for transcontinental and short haul operation, considering traffic forecasts, current transport aircraft and potential derivatives and technology
[SAE PAPER 710749] 01 p0002 A72-10248
Commercial transport market and technology forecasting, considering all-cargo, STOL, SST and CTOL aircraft
[SAE PAPER 710750] 01 p0002 A72-10249
STOL transport aircraft technology assessment, analyzing airports growth problems
[SAE PAPER 710751] 01 p0003 A72-10250
Industry assisted state of art assessment of high lift turbofan configurations for USAF STOL tactical transport technology program
[SAE PAPER 710758] 01 p0003 A72-10255
Mach 0.80 quiet intercity STOL transport design comparison for turbofan, prop-fan and turboprop systems
[SAE PAPER 710759] 01 p0003 A72-10256
Propulsion system optimization for commercial transport aircraft design under Advanced Transport Technology study, considering impact on aircraft gross weight
[SAE PAPER 710760] 01 p0115 A72-10257
Advanced technology air transports propulsion system requirements, considering design, engine performance and reliability, maintenance, airline problems, noise and pollution control
[SAE PAPER 710761] 01 p0115 A72-10258
Propulsion system optimization in transonic transport aircraft design, considering nacelle integration, engine choice, noise attenuation and technology utilization
[SAE PAPER 710762] 01 p0115 A72-10259
Flight test procedures for subsonic transport aircraft pilot static pressure system, recommending trailing cone calibration method
[SAE ARP 921] 01 p0064 A72-10389
Externally blown flaps for STOL characteristics in medium and heavy jet transport aircraft, demonstrating aerodynamic and flight mechanical feasibility
02 p0155 A72-12502
U.S.S.R. high-subsonic freight transport jet aircraft IL-76 for arctic areas, Siberia and Far East, noting independence of large airports availability
03 p0310 A72-13471
Transonic air transport design, discussing wind tunnel tests, supercritical flow technology, sonic boom avoidance, cruising speed, operating costs and transport family development
03 p0310 A72-13487
Le Bourget Exposition data for displayed civil transport aircraft
03 p0310 A72-13638
VFW-614 short range twin jet passenger transport aircraft, analyzing service performance and economic efficiency requirements influence on design characteristics
03 p0310 A72-13643
American civil aviation future development, discussing passenger and freight markets growth, aircraft types and FAA role
04 p0464 A72-14811
Air transport maintenance regulation as part of National Aviation System program, discussing airworthiness, safety and reliability in relation to design requirements
04 p0526 A72-14814
Civil aircraft technological constraints and requirements, discussing noise, congestion and performance characteristics of rotorcraft, STOL, VTOL, hypersonic and supersonic transports
05 p0611 A72-15774
VTOL transport aircraft use in densely populated urban areas, discussing travel time, airport requirements, noise and design problems
05 p0612 A72-16733
Soviet air traffic service productivity increase and manpower saving by introduction of new airliner types
05 p0612 A72-16779
Low wing loading STOL transport with ride smoothing automatic control system, noting thrust-weight ratio
[AIAA PAPER 72-64] 05 p0613 A72-16942
French civil aircraft displayed at 1971 Le Bourget Air Show, discussing design and performance characteristics of Airbus, Concorde, Caravelle, Corvette, Falcon, Fregate, STOL-A-904 and Mercure
05 p0614 A72-17193
STOL transport passenger market demand model selection based on estimation of traffic patterns between two population centers and service frequency and fare considerations
06 p0905 A72-17586
Federal Air Regulations procedures for civil transport aircraft flight testing under natural and/or simulated icing conditions
06 p0760 A72-18501
Cockpit instrumentation for jet transport aircraft flight path management, emphasizing dependability, safety and economy
08 p1168 A72-21524

Physiological evaluation of modified jet transport passenger oxygen mask from altitude chamber experiments
08 p1126 A72-21571
Future civil air transport trends, considering passenger and cargo growth, travel frequency per capita income and STOL market
08 p1257 A72-22150
Technology forecasting and risk assessment in V/STOL transport area, examining mission issues and selection criteria
09 p1261 A72-22473
Aerodynamic efficiency of plane slotted blade cascades of adjustable nozzle diaphragms in transport aircraft axial flow gas turbine engines
09 p1374 A72-23186
STOL and V/STOL transport aircraft design requirements consideration based on common propulsion and lift engine types use, noting fan lift solution superiority
10 p1421 A72-24865
Transport aircraft fuselage computerized design, determining optimal structural distribution for strength and displacement constraints
[AIAA PAPER 72-330] 11 p1727 A72-25366
Convective cooling system design for Mach 6 hypersonic transport Al alloy airframe, using water glycol loop network
[AIAA PAPER 72-334] 11 p1574 A72-25369
NASA aerodynamic technology program, emphasizing airframe and engine development for next generation subsonic CTOL jet transport requirements
[SAE PAPER 720319] 11 p1575 A72-25582
Integral and remote powered lift fan engines design for large civilian VTOL transports
[ASME PAPER 72-GT-65] 11 p1704 A72-25654
NASA quiet engine program, discussing noise reduction technology for subsonic civil transport aircraft propulsion system
[ASME PAPER 72-GT-96] 11 p1705 A72-25667
LOX supply systems installation for civil transport aircraft crew and/or passenger breathing oxygen
[SAE AIR 1223] 11 p1584 A72-26030
Near ground pressure differentials caused by large transport aircraft induced wake vortices, comparing measured data with Bernoulli formula theoretical values
12 p1752 A72-28122
Russian book on An-12 turboprop transport aircraft structural and aerodynamic characteristics covering engine operation, piloting, stability, controllability, etc
12 p1755 A72-28343
High cruise altitude operational advantages for commercial transport aircraft utilizing technological innovations in structures, propulsion, controls, avionics and aerodynamics
13 p1996 A72-28875
Long range transport aircraft structures and composite materials technology for airframe and engine systems
[AIAA PAPER 72-362] 13 p1897 A72-28955
Acoustic measurements for STOL turboprop transport aircraft propeller configurations under static, taxi and flyover conditions, discussing quiet propeller noise signature
13 p1897 A72-29571
Small transport aircraft horizontal tail surfaces flow characteristics determination for stress calculation during flight in turbulent atmosphere
14 p2071 A72-30284
VFW 614 twin jet transport aircraft flight test program, detailing general task plan, test equipment installations and test schedule
14 p2072 A72-30679
Twin-turboprop transport aircraft, helicopter and all-terrain ground vehicle simulators, discussing control load, visual attachment, cabin motion and sound subsystems
14 p2092 A72-30845
Fokker V170L transport aircraft designs, considering payload, range, runway conditions, noise, military capabilities and operational costs
16 p2347 A72-33048
Commercial transport aircraft engine technology contribution to world air transportation, considering social and ecological compatibility with community
16 p2348 A72-33314
Military transport helicopter optimum secondary power system, considering onboard auxiliary power unit, electric or hydraulic engine start system, environmental control, etc
[AHS PREPRINT 664] 17 p2494 A72-34480
New VTOL transport aircraft designs by VFW Fokker II
17 p2492 A72-35477
Internal engine generator application to commercial transport aircraft
17 p2498 A72-35566
Computer control of aircraft landing
17 p2578 A72-35950
V/STOL - Selection and problems of the new medium
18 p2643 A72-37215

Advanced subsonic transport technology.
19 p2748 A72-37677
Graphite-epoxy composites application to commercial transports for weight and cost reduction
19 p2873 A72-37680
Investigation of the commonality in development of military and commercial STOL transports.
[AIAA PAPER 72-808] 19 p2750 A72-38114
Advanced technology transport (ATT) aircraft configurations design parameters analysis, considering cruise speed, passenger capacities, ranges, noise level and economics
[AIAA PAPER 72-757] 19 p2751 A72-38127
Economic impact of applying advanced technologies to transport airplanes.
[AIAA PAPER 72-758] 19 p2751 A72-38128
Advanced technology applications to present and future transport aircraft.
[AIAA PAPER 72-759] 20 p2888 A72-40051
STOL performance criteria for military transport aircraft.
[AIAA PAPER 72-806] 20 p2889 A72-40055
High subsonic transport aircraft design development based on supercritical aerodynamic configuration and advanced structural, flight control and propulsion system technologies
[AIAA PAPER 72-756] 20 p2889 A72-40056
An exploratory study of flying qualities of very large subsonic transport aircraft in landing approach.
[ICAS PAPER 72-07] 21 p2995 A72-41132
Hypersonic transports commercial applications, examining economic and noise and air pollution aspects
[ICAS PAPER 72-32] 21 p2995 A72-41157
Reliability analysis in the estimation of transport-type aircraft fatigue performance.
22 p3241 A72-42971
Empty weight and cruise performance of very large subsonic jet transports.
[SAWE PAPER 919] 23 p3251 A72-43466
Observations on designing to combat fatigue and its effects on the economics of civil transport aircraft.
24 p3368 A72-44745

TRANSPORT COEFFICIENTS
U COEFFICIENTS
U TRANSPORT PROPERTIES
TRANSPORT EQUATION
U BOLTZMANN TRANSPORT EQUATION

TRANSPORT PROPERTIES
NT ATMOSPHERIC CONDUCTIVITY
NT CARRIER MOBILITY
NT DIFFUSION COEFFICIENT
NT EDDY VISCOSITY
NT ELECTRICAL RESISTIVITY
NT ELECTRON MOBILITY
NT GAS VISCOSITY
NT GASEOUS DIFFUSION
NT HOLE MOBILITY
NT IONIC MOBILITY
NT IONOSPHERIC CONDUCTIVITY
NT MAGNETORESISTIVITY
NT PHOTOCONDUCTIVITY
NT PLASMA CONDUCTIVITY
NT SUPERCONDUCTIVITY
NT THERMAL CONDUCTIVITY
NT THERMAL DIFFUSIVITY
NT VISCOSITY
Thermal conductivity, electrical conductivity, viscosity and diffusivity of ionized gas-solid suspension in electric field, using transport equations and particle interaction potentials
01 p0111 A72-1332
Transport coefficients of relativistic gas by method of moments, assuming constant differential cross section of particle interactions in center of mass system
04 p0547 A72-14630
Small sphere hydrodynamic drag in ionized gas at local thermodynamic equilibrium, taking into account nonlinear transport properties variations with temperature
[ASME PAPER 71-APM-CC] 04 p0558 A72-15176
Resonant transport properties of polyatomic gases in collinear static and oscillating magnetic fields, using microscopic kinetic equation
04 p0553 A72-15633
Radiation transport mechanism and transport coefficients in high pressure Ar cascade arc, measuring electric field strength, radiated power and radial temperature distribution
05 p0695 A72-16157
Transfer equation system solution for nonscattering medium with stationary homogeneous magnetic field, considering boundary value problem in Fraunhofer line theory
05 p0690 A72-16513
Hypoxia, hypercapnia and hyperoxia effects on active glucose transport in rat small intestines
05 p0618 A72-16633
Transport coefficients of electron gas in electromagnetic field, using Grad thirteen moment method
05 p0697 A72-17005
Thermodynamic equilibrium, transport and optical properties and quantum effects in nonequilibrium plasmas, using Monte Carlo method
05 p0700 A72-17223

Potential around moving test particle in quiescent plasma, discussing energy loss, transport properties and gravitational analog

06 p0859 A72-17549

Macroscopic boundary conditions of gas-solid interface interaction as function of gas temperature and transport coefficients variation in shock reflection problems

06 p0902 A72-18107

Kubo type time correlation formulas for incompressible heat conducting fluids turbulent transport coefficients, establishing relation to cascade and closure-of-hierarchy methods

06 p0801 A72-18173

German monograph on lattice and solid metal surface transport processes, discussing atom migration, activation energies, impurity atom diffusion, Kossel-Stranski model, etc

08 p1212 A72-22173

Temperature effects on electrical conductivity and transport mechanisms in sapphire from measurements under protection against surface and gas phase conduction

09 p1335 A72-22400

Thermodynamic formulation of noble gases equilibrium and transport properties at low and moderate densities, proposing corresponding states law

09 p1410 A72-22767

Optimum pressure and field conditions for intense relativistic electron beam transport in longitudinal magnetic field

09 p1360 A72-22870

Current carrier flow parameter fluctuations associated with steady state transport noise in semiconductor devices, considering generation-recombination processes, drift, diffusion and dielectric relaxation

09 p1288 A72-23125

Low transverse energy, high nu/gamma electron beam propagation characteristics, reviewing transport, compression and combination beam-handling concepts

10 p1518 A72-23959

Spectral line formation in atmosphere with plane parallel layers and frequency independent source function, using matrix approach for transfer equation solution

10 p1535 A72-24058

Transport coefficients calculation in gas kinetic theory by relativistic generalization of Enskog-Chapman method

10 p1510 A72-24106

Local and macroscopic thermal transport in turbulent air stream, discussing measurement from calorimeter instrumented sphere

10 p1417 A72-24148

Book on binary metal oxides covering non-stoichiometry, electrical conductivity, diffusion theory, point defects, high temperature creep and electrochemical transport properties

10 p1527 A72-25075

Regular tidal winds and irregular gravity waves domination of E region transport processes

10 p1477 A72-25161

High mass transfer rate effect of foreign gas on transport coefficients in fully developed turbulent flow [AIAA PAPER 72-293]

11 p1614 A72-25231

Non-Maxwellian collisionless transport properties of neutral gas constituents in planetary exospheres, discussing ballistic particle and heat transport and escape fluxes

11 p1716 A72-25846

Third order constitutive equations for transport coefficients in rarefied gases, using Chapman-Enskog theory

11 p1617 A72-26009

Electron bombardment effects on transport properties and carrier lifetime degradation of Li doped Si solar cells

12 p1856 A72-28024

Equatorial F region photoionization and chemical loss rates for electrons from simultaneous observations of vertical drift velocity and electron concentration, deriving plasma transport

13 p1949 A72-29336

German monograph on mass transport in thin fluid layers covering diffusion, convection, laminar flow rate distribution, flame ionization and gas chromatography measurements, etc

15 p2216 A72-31350

Amorphous semiconductors theories, discussing electron states and transport properties in terms of Cohen, Mott and Gubanov models

15 p2293 A72-32234

Landau-Placzek autocorrelation functions analysis method application to fluids transport coefficients LF characteristics

15 p2279 A72-32648

Fluctuation renormalized transport coefficients in corrected nonlinear transport equations derivation from generalized Fokker-Planck equation

15 p2337 A72-32653

Azimuthal electric fields role in toroidal plasma transport properties based on kinetic theory for collision dominated regime

16 p2432 A72-32806

Skin effect in large hot tokamaks predicted by computer studies based on empirical transport coefficients, discussing suppression by moving limiter

16 p2433 A72-32812

Generalized phase shift effect on classical limit of rotational excitation collision cross sections related to transport properties of diatomic gas molecules

16 p2428 A72-32925

Radiative transfer equation application to ionospheric photoelectrons transport, predicting photoelectrons angular distribution and escape flux

16 p2444 A72-32963

Be doped p-type Si piezoresistance and hole transport properties dependence on temperature, crystal orientation and doping concentration

16 p2442 A72-33834

MHD fluid model for collisionless shock waves in turbulent plasma with enhanced transport coefficients, noting laboratory experiments and satellite and radio observations

16 p2439 A72-33932

Foreign gas injection into three-dimensional stagnation point flows.

17 p2483 A72-34205

Simplified expressions for the calculation of the contribution of the heavy components to the transport coefficients of partially ionized gases.

17 p2589 A72-34896

Transport of cosmic rays in the solar corona.

17 p2599 A72-35094

Self-consistent kinetic equations.

17 p2581 A72-35152

Triple collision effects in the transport properties for a gas of hard spheres.

17 p2585 A72-35157

Charge carriers interaction with metal ions studied from electrical transport of Fe and Co in Fe-Cr alloy

17 p2569 A72-35521

Nonequilibrium transport equations for chemically reacting inhomogeneous gas mixtures, using Hermite tensor polynomials of molecular velocities

18 p2713 A72-36895

On the role of density gradients in the continuum theory of mixtures.

18 p2712 A72-37076

Transport coefficient of multi-layer film of semiconductors.

19 p2843 A72-37401

Experimental technique for oxygen negative ions destruction by associative detachment reaction with hydrogen in oxygen-hydrogen mixtures, calculating transport and ionization coefficients

19 p2836 A72-37458

Results of a preliminary experimental investigation of a vapor transport fuel pin.

19 p2832 A72-37631

Thickness dependence of the electrical transport properties of germanium films.

19 p2844 A72-37685

A study of the liquid-vapor phase change of mercury based on irreversible thermodynamics.

20 p2983 A72-39481

Effects of magnetic field on electron transport properties in gallium arsenide.

20 p2960 A72-39704

Flux vortices and transport currents in type II superconductors.

20 p2961 A72-39809

Characteristics of turbulent transfer in jets of variable density

20 p2914 A72-39910

One dimensional stationary gas flow across normal shock wave, taking into account nonequilibrium factors and momentum, mass and energy transport

20 p2914 A72-39970

The relativistic Boltzmann equation.

20 p2955 A72-40012

Computer simulations of transport processes.

21 p3024 A72-40247

Solar wind models of energy transport mechanisms and nonthermal heating requirements, comparing predictions with spacecraft observation

21 p3100 A72-40484

Higher harmonics and transport coefficients of plasmas in circularly polarized magnetic fields and additional electromagnet fields.

21 p3091 A72-40489

Carrier transport and storage effects in Au ion implanted SiO₂ structures.

21 p3097 A72-40699

Analysis of the transport coefficients for simple dense fluids - Application of the modified Enskog theory.

21 p3084 A72-40723

Unsteady state description of living corneal mass transport modes, elucidating cornea thickness control mechanism

21 p3001 A72-40912

German monograph - The transfer behavior of premixed flames.

22 p3244 A72-43076

Manifestation of the effect of adsorptive reduction in strength under conditions of selective transport during boundary friction

22 p3183 A72-43138

Spacecraft functional properties degradation due to surface contamination with outgassing vapors, discussing contaminant materials transport and sorption characteristics

23 p3254 A72-43619

Calculation of transport coefficients of a non-Lorentzian plasma

23 p3321 A72-43821

Effects of transport velocity of wake vortex on aerofoil oscillations.

23 p3249 A72-44494

Transport properties of a gas of diatomic molecules. V - GPS calculation of the rotational relaxation time of the Ar-N₂ system.

24 p3427 A72-45307

TRANSPORT THEORY

NT CHAPMAN-ENSKOG THEORY

NT MIXING LENGTH FLOW THEORY

Plastic flow material transport during sintering, considering dislocation nucleation mechanism

02 p0232 A72-11429

Isotropic turbulence energy transport approximation by local differential equation analogous to Fokker-Planck equation, noting Kolmogoroff distribution for infinite Reynolds number

02 p0205 A72-12449

Large-scale solar magnetic field dynamics, considering joint transport action by regular velocity field, diffusion, sinking and sources of origin and destruction

03 p0433 A72-13358

Plasmoid transport in quadrupole and octupole magnetic fields, measuring plasma amounts in axial region charged particle densities and flux densities at vacuum chamber wall

03 p0395 A72-13568

Heavy elements gamma heating, using LIF thermoluminescent dosimeters and computer programmed photon transport calculations

04 p0546 A72-14427

Macroscopic integrodifferential transport equations for gas mixture with internal degrees of freedom and chemical reactions from model kinetic equation

04 p0552 A72-14633

Transport processes in electrolytic solutions, considering current and potential distributions in localized corrosion

04 p0536 A72-15737

Radiative transfer in gray medium with prescribed spatial temperature distribution in rectangular enclosures with nonisothermal walls, deriving exact solutions by radiation transport theory [AIAA PAPER 72-21]

05 p0748 A72-16869

Transport processes theory in mixtures of chemically active gases using Boltzmann equation and Sonin polynomials expansion

06 p0852 A72-17989

Diffusion model applicability to lateral transport in terrestrial and lunar exospheres, using kinetic theory

07 p1056 A72-18902

Vorticity transport and definition of equations for axisymmetric incompressible viscous vortex ring, solving coupled system numerically [AIAA PAPER 72-151]

07 p0907 A72-18956

Transport phenomena theory for semiconductors in strong electric fields, examining negative differential conductivity and nonmonotonic current behavior

07 p1048 A72-19637

Ultrarelativistic cosmic plasma analysis of high density electron beams transport across strong magnetic fields with application to pulsar NP 0532 spectrum

07 p1064 A72-20634

Quantum mechanical transport equation for radiation interactions with molecules subject to perturber atom collisions, describing macroscopic density matrix evolution [AD-739082]

07 p1039 A72-20683

Planetary scale circulation systems effects on photochemistry and transport processes of minor neutral constituents in mesosphere and lower thermosphere

09 p1274 A72-22353

Numerical algorithm for matrix case extension of transport problem in periodic media

09 p1342 A72-23368

High temperature sintering induced dislocations in refractory materials, studying material and diffusion transport processes

10 p1496 A72-24244

Transport theory Boltzmann equation and Monte Carlo methods applied to semiconductor negative differential mobility calculation

10 p1526 A72-24398

Temperature dependence of gas flow coefficients at low pressures, determining isothermal permeability and heats of transport of He, Ne and Ar capillary flow

10 p1469 A72-24600

Intermolecular collisions distribution on centerline of freely expanding axisymmetrical jet, using ellipsoidal statistical model and simplified transport equations

11 p1615 A72-25557

Plasmoid transport in quadrupole and octupole magnetic fields, measuring axial charged particle and flux densities at vacuum chamber wall 11 p1699 A72-26755

Metal silicide phase formation for Nb, Ta, Mo and W, examining Si diffusion and transport processes 11 p1664 A72-26859

Asymptotic and exact methods for light scattering problems in radiative transport theory, discussing finitely thick plane layer luminescence 13 p2001 A72-28503

Monte Carlo method for radiative transport theory problems, considering mathematical models of light scattering media and photon trajectory random elements 13 p2001 A72-28505

Transport processes theory in chemically active gases mixtures using Boltzmann equation and Sonin polynomials expansion 14 p2133 A72-30216

General purpose simulation system /GPSS/ to program discrete time dependent mathematical models related to transport and queueing processes 17 p2521 A72-34471

Applications of an improved formalism for the analysis of transport phenomena in gaseous mixtures and plasmas. 17 p2587 A72-34615

General theory of spherically symmetric boundary-value problems of the linear transport theory. 17 p2583 A72-35825

Perturbation method in inelastic interaction model for transport processes in reacting gases described by Boltzmann kinetic equation 18 p2713 A72-36807

Steady state heat transfer in one dimensional flow involving simultaneous convective and diffusive transport via finite difference formulation 18 p2741 A72-37171

Transport phenomena in an electron-phonon system in strong magnetic fields at low temperatures 20 p2953 A72-39310

Lower planetary boundary layer mesoscale flow patterns and transport climatology, using hourly averaged wind data from wind tower station network 21 p3077 A72-40252

Application of Tolubinskii's integral method to the solution of boundary value problems of nonstationary convective diffusion 21 p3129 A72-41056

General transport theory of noise in pn junction-like devices. I Three-dimensional Green's function formulation. 22 p3160 A72-43083

General transport theory of noise in pn junction-like devices. II - Carrier correlations and fluctuations for high injection. 22 p3160 A72-43083

Transfer equations for stellar systems 23 p3338 A72-44035

Transport phenomena theory for semiconductors in strong electric fields, examining negative differential conductivity and nonmonotonic current behavior 24 p3427 A72-44569

TRANSPORT VEHICLES
Air transport vs other travel, discussing time, costs, popularity and technology 03 p0459 A72-13485

TRANSPORTATION
NT AIR TRANSPORTATION
NT RAIL TRANSPORTATION
NT RAPID TRANSIT SYSTEMS
NT SPACE TRANSPORTATION
NT URBAN TRANSPORTATION
Transportation noises - Conference, University of Washington, Seattle, March 1969 07 p0931 A72-20162

Design criteria for transportation system noise regulation, considering ambient noise, hearing damage, speech interference and subjective reactions 07 p0932 A72-20173

Real time computer simulation of command and control in transportation systems, detailing models, and programming technique and ATC controller effectiveness evaluation 07 p0952 A72-20363

Physical principles, design and operation of air cushion vehicles for passenger transportation over water 07 p0913 A72-20371

Technological forecasting and long range planning in transportation, considering roles of expert opinion, trend extrapolation, normative models and social impact 11 p1748 A72-26285

Time/frequency techniques in land, sea and air transportation environments, discussing characteristics and electronic traffic control systems applications 15 p2338 A72-32073

Total weight estimates of electric power supply system for transport vehicles involving power generators and primary electrical network with distribution system 16 p2350 A72-32997

Transportation - Conference, Washington, D.C., May-June 1972 16 p2347 A72-33180

The application of operational research to transport problems; Proceedings of the Conference, Sandefjord, Norway, August 14-18, 1972. 24 p3466 A72-44576

Solutions to transportation problems using time/frequency technology. 24 p3422 A72-44649

TRANSURANIUM ELEMENTS
NT PLUTONIUM ISOTOPES
Transuranium elements in HD 25354. 22 p3224 A72-42381

TRANSVERSE ACCELERATION
Histological examination of transverse acceleration stress effect on inner ear development of gestating rat embryos 07 p0923 A72-20446

Rat adrenal cortex morphology after 24 hour transverse acceleration stress, studying changes in lipid, ascorbic acid and RNA content and acid phosphatase activity 13 p1904 A72-29310

Single-cycle electron acceleration in focused laser fields. 20 p2934 A72-39720

TRANSVERSE FAULTS
U GEOLOGICAL FAULTS
TRANSVERSE OSCILLATION
NT H WAVES
Gas slip flow and transverse oscillations boundary value problems solution, using Wiener Hopf integral equation 02 p0205 A72-12355

Forced and free transverse vibrations of flat rectangular plates with attached concentrated masses 04 p0584 A72-14521

Transverse vibrations stability of launching rocket body, allowing for propellant sloshing and body elastic deformation 05 p0731 A72-17187

Forced transverse vibration damping of end loaded elastic cantilever beam, determining hysteresis loop contour from resonance curves 06 p0900 A72-18673

Librational transverse oscillations boundary value problems of heavy thread on orbiting satellite, determining equilibrium and eigenfunctions 08 p1240 A72-21142

Small turbulences growth in two dimensional incompressible wake, noting transverse oscillations of mean velocity profile [AD-742006] 10 p1467 A72-24367

Longitudinal and transverse vibrations and transient response of elastically coupled nonlinear mechanical system 11 p1732 A72-25534

Static loading and monoharmonic excitation influence on transverse vibrations of eccentrically prestressed metallic beam 11 p1732 A72-25535

Nonlinear traveling string transverse oscillations frequency, using Panavko direct linearization method 11 p1688 A72-26324

Cantilever beam transverse vibrations induced by time varying linear displacements of clamped end under external loads, taking into account internal energy dissipation 11 p1738 A72-26797

Natural and associated transverse vibrations of elastic beam under uniformly distributed moving load 12 p1879 A72-27092

Finite element method application to variable thickness circular and annular plates free transverse vibration 12 p1879 A72-27191

Nonlinear transverse forced resonant oscillations in isotropic elastic body and ideally conducting compressible fluid flowing in external magnetic field 13 p2010 A72-28719

HF transverse resonant vibrations of annular Al plates with polychlorovinyl and polyamide base coatings, noting damping and strain relationship to energy dissipation 14 p2164 A72-30427

Nonlinear analysis of helicopter rotor blade free transverse vibration under air and centrifugal loadings during forward flight, using matrix method 15 p2323 A72-31407

Flow induction by cylinder performing transverse periodic vibrations in viscous fluid, noting jet flow with large streaming Reynolds number 15 p2217 A72-31617

Cantilever beam tapered linearly in horizontal and vertical planes, obtaining computer solution for free transverse vibration fundamental frequency and harmonics 15 p2328 A72-32022

Transversely excited high pressure carbon dioxide laser cavity dumping with reproducible time delay between current excitation and gain-switched laser pulses 16 p2403 A72-33844

Free vibrations of elastic plate with random properties - The eigenvalue problem. 17 p2623 A72-34228

Transverse vibration of a viscoelastic beam carrying an arbitrary number of mass bodies. 17 p2631 A72-35053

Application of the Bubnov-Galerkin method to the approximate integration of a Timoshenko-type equation 19 p2877 A72-38188

Librational transverse oscillations boundary value problems of heavy thread on orbiting satellite, determining equilibrium and eigenfunctions 20 p2977 A72-39247

Single longitudinal mode operation of a transversely excited CO2 laser. 21 p3062 A72-40243

Nonlinear transverse forced resonant oscillations in isotropic elastic body and ideally conducting compressible fluid flowing in external magnetic field 22 p3210 A72-42096

Transverse oscillations of a jet in a jet-splitter system. [ASME PAPER 72-FLCS-1] 23 p3281 A72-44065

Free-transverse vibrations of an axially moving mass. 23 p3355 A72-44457

TRANSVERSE VALLEYS
U VALLEYS
TRANSVERSE VIBRATION
U TRANSVERSE WAVES
TRANSVERSE WAVES
NT H WAVES
Rankine vortex conducting gas rotating about cylinder axis, investigating magnetic field effects on transverse waves 01 p1016 A72-10132

Linear theory of transverse electromagnetic waves and instabilities in uniform plasma during propagation along magnetic field, considering multifold and kinetic description 01 p1018 A72-10189

Fast cyclotron and synchrotron transverse waves noise measurement in electron flux, using resonator with homogeneous electric field 02 p0190 A72-11573

Signal modification of microwaves propagating transversely in underdense turbulent plasma jet 02 p0265 A72-12365

He-Ne laser active medium excitation and resonator geometry effects on TEM wave field 02 p0239 A72-12520

Finite element discrete model for large aspect ratio wing transverse vibrations, using inhomogeneous elements with various stiffness-length relations 03 p0442 A72-13189

Transverse shock waves fine structure and saturation of ion-acoustic turbulence in collisionless plasma, using magnetic field probe and MHD equations 03 p0399 A72-14068

Longitudinal and transverse wave diffraction on cavities, investigating field pattern by dynamic photoelasticity method with flat models 03 p0452 A72-14131

Three dimensional transverse wave structure effect on detonation wave and Chapman-Jouguet gross properties, using planar model 04 p0510 A72-14410

Nonrelativistic charged particle resonating with circularly polarized transverse electromagnetic wave in nonuniform magnetic field, showing Fresnel diffraction pattern-like motion 04 p0557 A72-14951

Collision resonance effects on transverse wave propagation direction in collisionless plasma for upper ionospheric sounding 04 p0490 A72-15403

Electromagnetic wave propagation in plane and spherical waveguide channels with conducting lower wall, investigating transverse wave spectrum dependence on curvature and boundary conditions 04 p0492 A72-15441

Spontaneous oscillations generation on transverse surface wave, discussing experimental realization with semiconducting CdS single crystals 05 p0626 A72-16282

Transverse acoustoelectric surface wave domain in piezo-semiconducting body, obtaining gain coefficient and generation threshold criterion 05 p0702 A72-16283

Transverse ultrasonic wave propagation in low viscosity liquids, investigating fine structure of Rayleigh line wing 05 p0690 A72-16682

Coupled longitudinal and transverse plasma waves propagating normal to applied magnetic field, using three fluid model 05 p0700 A72-17230

Cracks interactions with transversal and surface elastic waves, relating crack propagation threshold conditions to critical pulse duration 06 p0893 A72-17419

Surface roughness effect on TEM mode propagation, discussing perturbation and Bessel series methods 06 p0774 A72-17738

Nonlinear self excited oscillations in uniformly distributed oscillators interacting with traveling transverse or surface waves of elastic body 06 p0849 A72-18698

Thin film optical waveguide with crystal quartz as substrate, observing reversible TE to TM mode conversion due to anisotropy [AD-738761] 07 p0953 A72-18878

Radially conducting cone wave spectrum calculation for nonconformal excitation, noting circularly polarized TEM and elliptically polarized TM wave amplitudes 07 p0938 A72-19003

Transverse electromagnetic instabilities in anisotropic plasmas, confirming by computer simulation energy constants derived from nonlinear Vlasov-Maxwell equations 07 p1041 A72-19509

Rf excitation of external terminated longitudinal conductor axially parallel to rocket skin by transverse electromagnetic field, deriving currents in cable-connecting impedances 07 p0956 A72-19555

Energy dissipation associated with transverse vibrations of sandwich metallic samples with damping coatings 07 p1094 A72-20135

Transverse hydromagnetic plane waves existence in uniformly heated electrically conducting fluid under temperature gradient and magnetic field 07 p1045 A72-20442

Cylindrically guided hybrid TE and TM electromagnetic wave reflection and transmission from Maxwell equations and boundary value problems solution 09 p1278 A72-22605

Rayleigh type transverse surface wave existence in continuous elastic body with nonlocal interaction 09 p1403 A72-22748

Alternative TEM and waveguide type equivalent circuits for rectangular resonator loaded by lumped capacitance 09 p1289 A72-23365

Electromagnetic wave propagation perpendicular to magnetic field in two-component warm plasma, obtaining dispersion relations for transverse waves 10 p1520 A72-24350

Stationary HF Rayleigh waves in surface waveguide, considering transverse and longitudinal wave velocities in half space with elastic medium 11 p1685 A72-26378

Elasticity theory dynamic equations solutions concentrated near longitudinal or transverse wave beams propagating in inhomogeneous isotropic space 11 p1689 A72-26383

Magnetospheric equatorial compressional wave propagation to ground observed as transverse wave, noting plane of polarization 11 p1625 A72-26413

Growth rates of unstable electromagnetic waves propagating perpendicularly to symmetric counterstreaming finite temperature plasmas 13 p2012 A72-29129

Frequency converter dynamics, considering transverse vibrations of mechanical system composed of string with centrally lumped mass 13 p1932 A72-29457

Approximate analytical method for diffraction losses and corrections to lower transverse modes and resonance condition in symmetrical stable cavities with round spherical mirrors 13 p1970 A72-29679

Partial differential equations for longitudinal, torsional and transverse vibrations of bars with variable composition 13 p2006 A72-29885

Quasi-hydrodynamic equations for transverse waves in inhomogeneous plasma, using geometric optics approximation 13 p2019 A72-29986

Ionosphere heating effects produced by transverse electric field, discussing strong nighttime source 14 p2100 A72-30631

Plane and circular dielectric waveguides with thermal losses, considering transverse wave numbers behavior behind cut-off value and dispersion equations solution 14 p2086 A72-30797

Ideally conducting and dielectric coaxial solids of revolution, investigating joint excitation by TM wave 15 p2209 A72-32658

Magnetoactive plasma transverse waves propagation near electron gyrofrequency harmonics, taking into account electron collisions and relativistic effects 15 p2289 A72-32734

Longitudinal, transverse and bending waves propagation in elastic shells, using Hadamard method within linear shell theory 16 p2465 A72-32982

Longitudinal and transverse waves propagation and decay in elastic membranes with allowance for coupling effects, using Hadamard method 16 p2465 A72-32983

Growth of an acceleration wave in an elastoplastic isotropic medium undergoing finite deformation 17 p2580 A72-34277

Transverse vibration frequencies and mode shapes of clamped or supported orthotropic plates by energy method, using Rayleigh-Ritz technique 17 p2626 A72-34327

Transverse vibrations of bars with concentrated additional masses 17 p2627 A72-34772

Nonlinear vibrations of a hinged beam including nonlinear inertia effects. [ASME PAPER 72-APM-51] 17 p2627 A72-34779

Determination of the unloading boundary in transverse impact of an elastic-plastic string. [ASME PAPER 72-APM-12] 17 p2629 A72-38404

D region electron density profile determination based on LF link operating on one-hop ionospheric propagation of ordinary and quasi-transverse wave 18 p2689 A72-37163

Theory for transverse vibrations of beams during elastoplastic deformations 19 p2877 A72-38179

Electromagnetic self induced vibrations in homogeneous unbounded electron beam moving with time dependent velocity, noting longitudinal and transverse wave generation 19 p2842 A72-38527

Optimum generation conditions for a neon-helium laser operating in the axial TEM/sub 00/ mode 19 p2814 A72-38784

Identification of transverse Kelvin-Helmholtz turbulence in a magnetoplasma column. 21 p3091 A72-40768

Application of a method using slowly changing parameters for the approximate calculation of transverse vibrations of rods 21 p3126 A72-41550

Plasma-electromagnetic interaction with surface wave propagation along boundary, obtaining boundary conditions for longitudinal and transverse wave amplitudes with allowance for particles interaction 22 p3213 A72-43117

The coupled transverse vibrations of a spinning membrane disk with a central hub. 23 p3355 A72-44367

Energy dissipation associated with transverse vibrations of sandwich metallic samples with damping coatings 24 p3461 A72-45760

TRAPEZOIDAL TAIL SURFACES

Vibration of trapezoidal cantilever plates with partial root chord support. 21 p3121 A72-41225

TRAPEZOIDS

Natural frequencies and vibration mode shapes of simply supported symmetric trapezoidal plates 04 p0592 A72-15564

Vibration characteristics of simply supported unsymmetric trapezoidal plates 07 p1089 A72-19644

TRAPPED MAGNETIC FIELDS

Neutral current sheets in slow moving plasma with frozen-in magnetic field with null force line 03 p0438 A72-14070

Trap magnetic system with coil generated field increasing towards periphery, showing radial dependence and acting ponderomotive forces 09 p1363 A72-23215

Flux quantization in superconductors demonstrated by magnetometer probe measurement of magnetic field trapped in thin film holes 16 p2441 A72-33225

TRAPPED PARTICLES

NT ARTIFICIAL RADIATION BELTS
NT INNER RADIATION BELT
NT MAGNETICALLY TRAPPED PARTICLES
NT OUTER RADIATION BELT
NT PROTON BELTS
NT RADIATION BELTS

Electrostatic wave-particle interactions in inhomogeneous collisionless plasma, calculating resonant distribution function, charge densities and trapping periods 01 p0107 A72-10136

Nonlocal theory of electrostatic trapped particle instability in collisionless toroidal plasma, estimating particle mode nonlinear diffusion coefficient 01 p0108 A72-10239

Trapped protons low energy differential spectra from polar orbiting Injun 5 satellite measurements, suggesting radiation belts impulsive acceleration mechanism 01 p0120 A72-10891

Electric field induced splitting of drift shells composed of trapped particles, taking into account non-dipole field components to lowest order 01 p0062 A72-10905

Impurity-related color centers and electron-hole traps in quartz by electron spin resonance and thermoluminescence observations 02 p0207 A72-11598

Galactic cosmic ray self trapping, discussing hydromagnetic wave velocity of ray propagation from sources 02 p0274 A72-12190

Trapped particles induced by fluctuating magnetospheric electric and magnetic fields, calculating radial diffusion and energy distribution and time variations 04 p0566 A72-14723

Trapping probability in gas-surface interactions from empirical accommodation coefficients, using simple model based on assumed attractive square well and impulsive-repulsive potential 05 p0624 A72-16399

Interplanetary magnetic field fluctuations correlation with trapped particles redistribution, deriving magnetospheric electric field properties 06 p0875 A72-17468

Langmuir wave-caused electron plasma distribution function deformation, discussing particle trapping effects 06 p0858 A72-17542

Electrostatic hf wave propagation in one dimensional collisionless plasma, describing electron trapping and oscillations and resonance-produced sidebands 06 p0858 A72-17544

Trapped ion instability in collisionless plasma ion acoustic waves, discussing sideband waves frequency spectrum and growth rate 06 p0859 A72-17545

Trapped particle motion response to collapsing dipole moment in secularly varying geomagnetic field 07 p1058 A72-19158

Magnetospheric trapped particle diffusion coefficients and acceleration in earth radiation belts 07 p1062 A72-20035

Magnetosphere If electric fields influence on trapped radiation region particle behavior, considering magnetic drift rates 07 p1062 A72-20036

Stability conditions of dissipative trapped ion modes in axisymmetric toroidal confinement systems, investigating collisional damping rate 07 p1045 A72-20476

Terrestrial dust belt particles origin, character and trapped time from observations of earth-moon system libration points 08 p1229 A72-20838

Optical absorption in UV and IR of proton bombarded potassium chloride at liquid nitrogen temperature attributed to trapped protons 08 p1211 A72-21208

Trapped He, Ne and Ar isotopic variations present in meteorites due to rare gas ions implantation by solar wind and flares 09 p1385 A72-22599

Trapped particle induced frequency shift on response of electrostatic wave to adiabatic and sudden excitations, obtaining distribution functions and nonlinear dispersion relation [AD-741547] 11 p1693 A72-25566

One dimensional time independent solution to Vlasov-Poisson system of nonlinear electrostatic plasma waves, noting Maxwell distributions for free and trapped particles 11 p1697 A72-26599

Nature and requirements of electrostatic inertia plasma confinement, deriving potential and particle densities as function of radius, grid voltage and current 12 p1850 A72-27288

Electron wave sideband frequencies and wave trapped electron oscillations as cause of plasma instability 12 p1851 A72-27436

Theory of magnetotail elongation based on magnetospheric neutral layer drift motion due to electric current from trapped charge carriers inside surrounding plasma sheath 12 p1802 A72-27770

Negative photoconductivity in CdSe single crystal, due to free carrier mobility decrease after surface treatment in gas discharge, noting neutron traps role 13 p2024 A72-30044

ESRO IA satellite observations of trapped and precipitated proton energy spectrum as function of invariant latitude on 8 March 1970 14 p2146 A72-30144

One dimensional Maxwellian electron plasma simulation by electron bunches, describing Landau damping of wave initially excited in medium and nonlinear effects of trapping 15 p2284 A72-31677

Positron annihilation lifetimes and trapping probabilities for vacancies and dislocations in Al single crystal 15 p2258 A72-32222

Electron trapping data in neutron irradiated high purity Si, using space charge limited current measurements 15 p2294 A72-32511

- High latitude trapping boundary for 20 KeV electrons and 100 KeV protons during intense geomagnetic storms, observing field-line motion
16 p2444 A72-32958
- BARRITT, IMPATT, TRAPATT and Gunn diodes, discussing power, noise and thermal dissipation problems
17 p2526 A72-34465
- High latitude observation of precipitating electron spikes by polar orbiter OGO 4 satellite, noting population dependence on local trapping limit
17 p2601 A72-35591
- Geomagnetically trapped alpha particles. I - Off-equator particles in the outer zone.
17 p2548 A72-35595
- Photon trapping in photosystem II of photosynthesis - The fluorescence rise curve in the presence of 3-[3,4-dichlorophenyl]-1,1-dimethylurea.
17 p2505 A72-35761
- Minority-carrier trapping and the luminescence time response of semiconductors.
19 p2844 A72-37946
- Several observations of low-energy solar-proton spectra and possible interpretations.
19 p2852 A72-38727
- VLF emission artificial triggering by whistler morse pulses in magnetosphere, explained in terms of resonant trapped particle current and wave field behavior
20 p2903 A72-39549
- Thermally-stimulated current from the gold acceptor trapping level in silicon.
21 p3097 A72-40996
- Resonant scattering of trapped particles by toroidal plasma modes.
21 p3092 A72-41217
- Experimental determination of ion density trapped by electron beam.
21 p3034 A72-41463
- Sideband waves excitation by large amplitude ion-acoustic waves in collisionless plasma, noting frequency spectrum and growth rate agreement with trapped particles theory
21 p3094 A72-41629
- Limits to energetic proton fluxes trapped in Jupiter's magnetosphere.
22 p3221 A72-42021
- Effects of radiation trapping on mode competition and dispersion in the ring laser.
23 p3296 A72-43878
- Electron impact ionization of ions trapped in a hollow electron beam.
23 p3316 A72-44343
- Electron polar cap and the boundary of open geomagnetic field lines.
23 p3286 A72-44522
- TRAPPED RADIATION**
U RADIATION BELTS
U TRAPPED PARTICLES
TRAPPING
Model for large signal losses prediction in charge coupled devices due to fast interface state trapping
10 p1526 A72-24625
- TRAPS**
NT ION TRAPS (INSTRUMENTATION)
Quasi-continuous charge carrier traps in molecular single crystals associated with polarization energy dissipation
11 p1700 A72-25782
- Frequency dependent deep level trap admittance and field effect transparency of p-n junctions calculated by truncated space charge approximation
22 p3161 A72-43086
- TRAVELING CHARGE**
Oxygen and oxygen-nitrogen mixtures dc and hf discharges, evaluating traveling low field domains in positive column
03 p0400 A72-14350
- Coherent synchrotron radiation from model with charge distribution moving on ring, applying to pulsars
04 p0566 A72-14555
- TRAVELING IONOSPHERIC DISTURBANCES**
Backscatter hf radar signature analysis in relation to medium scale traveling ionospheric disturbances, using computer ray tracing technique
01 p0030 A72-10837
- Electron density measurements for traveling ionospheric disturbances by Thomson scatter technique using Faraday rotation
01 p0031 A72-10922
- Traveling ionospheric perturbations in investigation by vertical sounding with interference method, presenting group path difference measurements as function of frequency and time
05 p0657 A72-16269
- Traveling ionospheric disturbance as diagnostic tool for thermospheric dynamics, monitoring wave polarization of ATS 3 signals
07 p0975 A72-19154
- Thermospheric wind directional filtering of gravity waves traveling ionospheric disturbances over Australia
08 p1158 A72-21217
- Traveling ionospheric disturbances observations during March 1970 solar eclipse from ATS 3 total electron content measurements
12 p1801 A72-27156
- Ionospheric HF Doppler dispersion during 7 March 1970 solar eclipse, noting traveling ionospheric disturbance
12 p1801 A72-27157
- Traveling ionospheric disturbances radio sounding during 7 March 1970 solar eclipse time, noting wave front orientation
12 p1801 A72-27158
- Ion velocity height profiles, ion temperature and electron density measurement with Thomson scatter facility during F region traveling ionospheric disturbance /gravity waves/
12 p1803 A72-27777
- Amplitude probability distribution of radio waves reflected from traveling ionospheric disturbances superimposed on small scale irregularities
13 p1921 A72-29338
- Analytic ray trajectory model of radio wave lateral incidence on traveling large scale ionospheric inhomogeneities as function of location and azimuthal angle departure
23 p3263 A72-43377
- TRAVELING WAVE AMPLIFIERS**
Transferred electron microwave oscillators /three-level and LSA relaxation types/ and amplifiers /reflection and traveling wave types/ fabrication, technology and performance capabilities
01 p0035 A72-10627
- Resonant traveling wave IMPATT oscillators wave propagation and power output characteristics, taking into account metal conductor and semiconductor substrate losses
01 p0038 A72-10651
- Transverse fields effects on electron dynamics and energy conversion in O-type linear beam devices of traveling wave amplifiers
03 p0330 A72-13231
- Traveling wave Ar laser with only fundamental TEM modes, examining mode self locking and composition and intensity as functions of frequency misalignment
03 p0366 A72-13366
- TWT amplifier converter design with semiconductors and magnetics to achieve voltage regulation and high power efficiency for TOPS spacecraft
08 p1111 A72-21412
- German monograph on luminous intensity amplification by means of solid state lasers covering experiments with GaAs and ruby lasers and traveling wave amplifiers
09 p1322 A72-22331
- TWT amplifiers electronic reflections and gain ripple
12 p1790 A72-27435
- Single frequency generation stability of one dimensional model of traveling wave laser using inhomogeneously broadened active material
13 p1967 A72-28470
- Carrier wave behavior in n-type GaAs slab under crossed dc electric and magnetic fields, investigating traveling space charge amplifier magnetic control
14 p2143 A72-30941
- Carrier wave propagation at semiconductor surface with electron drift, discussing solid state traveling wave amplifier design
15 p2290 A72-31288
- Three-frequency parametric traveling wave amplifier gain and conversion factors calculation by numerical method with allowance for fast and slow space charge wave effects
15 p2206 A72-31661
- Distributed tunnel diode traveling wave amplifier load noise thermal and shot components, noting impedance boundaries
15 p2206 A72-31663
- TWT off-transmission band area exponentially fading wave effects on electron beam modulation and amplification
15 p2209 A72-32670
- Active medium spontaneous radiation level effect on traveling wave amplifier gain factor, supporting theoretical results by experiments with superluminescent Ne-He active medium
16 p2400 A72-33277
- Russian book on microwave electronics covering linear-beam and cross-field backward and traveling wave amplifiers and oscillators, klystrons, masers, plasma devices, etc
17 p2532 A72-34650
- End line matching for high gain traveling wave amplifier constructed from heterogeneous transmission line sections with negative resistance
18 p2665 A72-36110
- TOP 1369 traveling wave amplifier tube
18 p2671 A72-37147
- Frequency-variable semiconductor-oscillator in the microwave region.
23 p3272 A72-43948
- Reflection amplification in thin layers of n-GaAs.
24 p3385 A72-44971
- TRAVELING WAVE MASERS**
Optimal location of nonreciprocal disk shaped YIG element traveling wave quantum ruby paramagnetic amplifier for weak magnetic levels
08 p1138 A72-20795
- TRAVELING WAVE MODULATION**
Intracavity modulation of high-gain gas laser with traveling light waves nonuniform amplitude distribution, presenting results for lithium niobate crystal resonator equipped He-Ne laser
02 p0183 A72-12762
- Polarization modes of anisotropic optical traveling wave resonator using half wave plate and Faraday rotation cell
12 p1824 A72-27870
- TWT off-transmission band area exponentially fading wave effects on electron beam modulation and amplification
15 p2209 A72-32670
- Polarization modes and phase shifts of normal oscillation modes in anisotropic optical traveling wave resonator with Brewster winders half wave plate and Faraday rotation cell
16 p2403 A72-33979
- Intracavity modulation of high-gain gas laser with traveling light waves nonuniform amplitude distribution, considering lithium niobate crystal resonator equipped He-Ne laser
20 p2931 A72-39068
- Unidirectional single frequency traveling wave CW pumped Nd-YAG ring laser, noting spatial hole burning elimination
22 p3185 A72-42614
- TRAVELING WAVE TUBES**
MHD boundary waves properties, noting application to traveling wave nonreciprocal devices and planar structures based on microwave integrated circuits
01 p0029 A72-10703
- Design and performance of Intelsat III dual TWT power supply, noting space, weight and cost savings
01 p0007 A72-11056
- Complete suppression of one signal in dual frequency mode of TWT operation, showing electron beam current and accelerating potential dependence on signal amplitude
02 p0189 A72-11565
- TWT small parameters measurement for gain calculation, using equivalent transmission line model
02 p0193 A72-12229
- Soviet monograph on electron flux nonlinear interaction with slow electromagnetic waves in TWT, discussing output power and efficiency increase
03 p0333 A72-13949
- Narrow band medium power X, Ku and C band solid state amplifiers, demonstrating TWT replacement with GaAs and avalanche diodes
03 p0334 A72-14072
- Hydromagnetic whistler traveling wave tube amplification in magnetosphere, deriving temporal growth rate dependence on plasma parameters
04 p0517 A72-14950
- TWT amplifier converter design with semiconductors and magnetics to achieve voltage regulation and high power efficiency for TOPS spacecraft
08 p1111 A72-21412
- Vacuum tube developments for radar, TV and communication applications, discussing microwave, traveling wave, cathode ray, memory and vidicon tubes, magnetrons, klystrons and tetrodes
11 p1606 A72-26544
- Maximum transmission delay in microwave TWT delay lines as function of electron beam size, current, shape and velocity distribution
12 p1782 A72-27436
- Voltage variable TWT delay line design, discussing electron beam velocity dispersion causes
12 p1782 A72-27437
- Semiconductor devices with extended slow wave-carrier interaction region for vacuum traveling wave tube replacement
13 p1927 A72-28401
- One dimensional periodic slow wave structure interaction with charged particles beam, considering system operation as TWT and backward wave tube
13 p1931 A72-29288
- High reliability long life grid pulsed L band traveling wave tube with integral solenoid focusing for high power radar use
14 p2089 A72-31046
- TWT off-transmission band area exponentially fading wave effects on electron beam modulation and amplification
15 p2209 A72-32670
- Parametric amplification and frequency conversion in a dual section TWT
19 p2774 A72-38411
- A design method for the electron beams of TWT's.
19 p2775 A72-38610
- A numerical evaluation and experimental study of the intermodulation noise spectra of traveling wave tubes.
21 p3033 A72-40880
- Large-signal analysis of efficiency and nonlinear phase distortion in a phase velocity tapered traveling-wave tube.
24 p3385 A72-45283

- Frequency multiplication with a traveling-wave tube. I - Computation of the current harmonics in a traveling-wave tube by the large-signal theory. 24 p3386 A72-45284
- Frequency multiplication with a traveling-wave tube. II - Numerical analysis of a traveling-wave frequency multiplier by the large-signal theory. 24 p3386 A72-45285
- TRAVELING WAVES**
- Finite element method for determining transient response of box-type structure to traveling sonic pressure wave 01 p0136 A72-10219
- Tubular traveling wave antenna array for radar applications and microwave television transmitters, describing computer program for design 01 p0039 A72-10668
- Traveling wave antenna for exciting ion cyclotron waves in cylindrical anisotropic magnetoplasma 02 p0188 A72-11468
- Electromagnetic traveling plane wave diffraction from arbitrary angled dielectric wedge, investigating surface currents on walls 04 p0491 A72-15420
- Nonlinear self excited oscillations in uniformly distributed oscillators interacting with traveling transverse or surface waves of elastic body 06 p0849 A72-18698
- High specific impulse-medium thrust propulsion device based on gas acceleration by traveling conduction waves 07 p1054 A72-19694
- Acoustic and gravity waves nonlinear propagation and structural deformation in isothermal and incompressible atmospheres with traveling wave induction 07 p0981 A72-20696
- Passive optical shutter implementation for unidirectional emission from traveling wave ruby laser, using diffraction grating 08 p1184 A72-22037
- Multimode ring laser gyro phase modulation theory based on oppositely directed traveling waves 09 p1324 A72-23084
- Nonlinear dispersive medium characteristics determination from higher harmonic oscillations and beats analysis based on traveling waves concept 09 p1353 A72-23486
- Frequency characteristics of traveling wave deflection system for wideband CRT deflector, improving sensitivity by low beam accelerating voltage 10 p1446 A72-23939
- Traveling wave mode ring laser operation, obtaining active medium polarization changes through longitudinal magnetic field excitation by capacitor discharge through spiral pump lamps 10 p1492 A72-24363
- Wideband microwave device with diode and single component correction circuits Q factors measurement from frequency dependence of input traveling wave coefficients 10 p1453 A72-24918
- Shear stress and traveling wave response of plate bonded to randomly vibrating viscoelastic half space for soil vibration studies 11 p1688 A72-26062
- Nonlinear traveling string transverse oscillations frequency, using Panavko direct linearization method 11 p1688 A72-26324
- Moving striations in tapered gaseous discharge tube, noting frequency dependence on tube radius 11 p1698 A72-26644
- Gas laser with strong absorption saturation to obtain high peak power and frequency self stabilization by generation of quasi-traveling wave in resonator 12 p1820 A72-27585
- Pulse excitation of traveling wave antenna array, describing spectral method of solving high resolution side-looking radar limitation 13 p1915 A72-28526
- O-type synchronous electron beam waves interaction with electrodynamic structured traveling wave, noting linear gain dependence on beam current and magnetic field 13 p1931 A72-29291
- Transmission lines with nonlinear capacitance semiconductor diodes, investigating electromagnetic traveling and standing waves instabilities and self amplitude modulation 14 p2086 A72-30795
- N-dimensional traveling waves in nonviscous polytropic gas with prescribed flow variable boundary conditions on arbitrarily shaped hypersurface, discussing application to radial flow 15 p2216 A72-31310
- Kinematic equations derivation for traveling displacements field in Cosserat continuum by Lagrange formalism, noting analogy with Maxwell equations 15 p2274 A72-31474
- Light signal modulation by traveling wave in circular waveguide with coaxial KDP crystal 15 p2207 A72-31881
- Variable amplitude and phase velocity electromagnetic traveling wave field distribution in diverging

- MHD induction machine channel with liquid metal flow 16 p2435 A72-33282
- Some comments on the generation of electromagnetic traveling and standing waves for inductive acceleration of plasmas [DFVLR-SONDDR-209] 17 p2589 A72-34895
- Traveling wave mode ring laser operation, obtaining active medium polarization changes through longitudinal magnetic field excitation by capacitor discharge through spiral pump lamps 17 p2563 A72-34962
- Acoustic and gravity waves nonlinear propagation and structural deformation in isothermal and incompressible atmospheres with traveling wave induction 20 p2915 A72-39011
- Evaluation of the reliability of diversity reception by antennas of different polarizations 23 p3271 A72-43777
- Effects of radiation trapping on mode competition and dispersion in the ring laser. 23 p3296 A72-43878
- The active field in an irregular slow-wave structure in the presence of a dynamic relative slip between the wave and the particle clusters 23 p3316 A72-44161
- Analysis of the polarization properties of TW laser emission 24 p3411 A72-45497
- Resonator polarization parameters effect on backwave attenuation in three and four mirror TW ring laser, noting colliding waves intensity dependence on polarization angle 24 p3411 A72-45505
- TREADMILLS**
- Maximum oxygen intake during exercise on treadmill compared with bicycle ergometer, analyzing circulatory dynamic factors and cardiac output relation to oxygen transport capacity 07 p0922 A72-20251
- Physical work capacity comparison during bicycle ergometry and treadmill walking tests, measuring oxygen uptake, ventilatory parameters and excess carbon dioxide production 11 p1579 A72-26095
- Maximal oxygen uptake and heart rate during ladder climbing, inclined treadmill running and cycling ergometer tests 11 p1586 A72-26612
- Energy cost /oxygen consumption/ prediction for treadmill and various levels terrain walking at two speeds under three different pack loads 14 p2080 A72-30706
- TREES [MATHEMATICS]**
- Combinational tree networks of AND and OR gates without internal fan-out, proposing test generation strategy for maximizing detected multifault sets size 05 p0640 A72-16163
- Complex system represented by fault-free with independent components, calculating confidence interval for failure probability by moment method 10 p1444 A72-24018
- Algorithm for optimal binary search tree construction with minimum weighted and restricted maximum path lengths 11 p1676 A72-25354
- Digital computer hierarchical structure based on tree model using request/service resources as nodes, examining parallel multiple-stream organizations effectiveness 20 p2906 A72-39735
- Parallelized algorithms for computer solution of spanning tree, distance and path problems on cellular array of identical modules containing memory and combinational logic 22 p3157 A72-43023
- TREES [PLANTS]**
- Visible and near IR reflectance spectra of soil mineralized trees, using multispectral photographic filters 02 p0209 A72-11789
- Ponderosa pine foliage visible and near IR spectra, investigating soil copper contents effect on foliage spectral reflectance 02 p0209 A72-11790
- TREMORS**
- Hand steadiness during unrestricted linear arm movements and eye-hand coordination tasks, showing tremor occurrence in up-down plane 10 p1432 A72-25113
- Hand tremor measurement methods, discussing pickup system selection for given tasks 21 p3012 A72-41521
- TRENCHES**
- U GEOLOGICAL FAULTS**
- TRENDS**
- Technological forecasting method evaluation for R and D planning, fitting trend curves to sets of technological data 07 p1105 A72-20268
- Rotary wing head weight estimation for helicopter preliminary design and parametric studies, deriving semiempirical trend formula [SAWE PAPER 914] 23 p3344 A72-43461

- TRESCA FLOW**
- Effective plastic strain for Tresca and von Mises materials, investigating hot rolled mild steel specimens 04 p0590 A72-15187
- Large deflection calculation of circular and annular strain hardenable rigid plastic plates under axisymmetric load, using Kirchhoff-Love hypothesis and Tresca flow condition 14 p2165 A72-30440
- Viscoplastic flow of inhomogeneous shells of revolution obeying Tresca condition, noting plastic deformation velocity relation to stresses 15 p2325 A72-31605
- Yielding of fiber reinforced Tresca material. 19 p2873 A72-37695
- Steady-state creep of shells of revolution in the case of the Tresca criterion 22 p3233 A72-42051
- TRIACETIN**
- Repeated stretching effect on triacetic fibers thermal destruction in vacuum after hot air or steam thermosetting 08 p1194 A72-21759
- TRIANGLES**
- Triangular points linear stability in elliptic restricted three body problem, determining exponents by convergent iteration method 06 p0878 A72-17664
- Properties of a nonisosceles triangular grid planar phased array. 17 p2524 A72-34352
- TRIANGULAR WINGS**
- U DELTA WINGS**
- TRIANGULATION**
- Aerial triangulation for optimum photogrammetric project parameters, discussing flight altitude, bridging distance and control points for computerized optimization 01 p0066 A72-10462
- Ritz approximation to two dimensional strain elasticity and heat flow boundary value problems, considering piecewise linear and cubic functions for complete triangulation 03 p0381 A72-13620
- Europe-Africa geodetic link in spatial triangulation of passive Pigeos satellite, discussing laser telemetry operation 04 p0520 A72-15725
- Block triangulation of arbitrary terrain without point transfer, using stereo comparator 06 p0806 A72-17755
- Lateral refraction dependence on earth rotation and correction formula for angle measurement errors in class I triangulation 09 p1299 A72-22946
- Cloud height measurements and instrumentation discussing rotating and fixed beam triangulation and French lidar and ruby laser ranging ceilometers 10 p1484 A72-25094
- Apollo mapping camera system synchronized laser altimetry utilization in astro-photogrammetric triangulation 12 p1872 A72-27814
- Ground station-observed balloon-borne radio beacon method for Finnish stellar triangulation network measurement 15 p2226 A72-31929
- Error analysis of East European triangulation network photographic observations of Echo and Pigeos satellites from ground stations 16 p2387 A72-33798
- Stellar oriented Apollo metric mapping camera system for photo geodesy, discussing planned coverage triangulation methods, control network and gravity model improvements 16 p2396 A72-34105
- Landmark navigation rule, a new navigation device. 19 p2830 A72-37296
- Solution of the problem of cosmic triangulation by the generalized method of synchronous and quasi-synchronous straight lines 19 p2861 A72-37971
- Aerotriangulation by simultaneous adjustment of photogrammetric and geodetic observations /SAGO/ incorporating geodetic distances, horizontal angles, Laplace azimuths, longitudes, latitudes and elevation differences 20 p2927 A72-39738
- Navigation satellite system based on triangulation distance measurement between two satellites and aircraft, noting simplification of air- and satellite-borne equipment requirements 21 p3080 A72-40285
- Stochastic models for block triangulation by bundle approach, comparing theoretical accuracies obtained from different block adjustment methods 23 p3284 A72-43631
- Investigations regarding the condition of normal equations in the case of block triangulation according to the bundle method. I 23 p3284 A72-43632
- Determination of the mutual position of points on the earth's surface from synchronous laser observations of artificial earth satellites 24 p3397 A72-44860

Numerical analysis of global satellite triangulation grid projects 24 p3397 A72-44868

TRIATOMIC MOLECULES
Molecular orbital calculation of the isotropic hyperfine interactions in triatomic nitrogen radicals. 21 p3013 A72-40564

TRIAxIAL STRESSES
Earth triaxiality from satellite data, obtaining non-zero values for harmonic coefficients 03 p0351 A72-14327
Stress-strain curve correction for triaxial stress state and strain rate at arbitrary temperatures, describing instrument for continuous test specimen profile measurement 16 p2469 A72-33232

TRIAxIALITY
U TRIAXIAL STRESSES

TRICHLORIDES
U CHLORIDES

TRIGATRONS
Unipolar pulsed plasma accelerator, describing trigatron circuit design for generation of 100 kA unipolar current pulses of 35 microsec duration 07 p1040 A72-19316

TRIGGER CIRCUITS
Avalanche pulse generator with pretrigger output for reflection coefficient and step function response measurements 02 p0195 A72-12605
Fast rise high current constant trigger circuit for electroexplosive devices, using flat two-conductor transmission line to minimize inherent inductance 08 p1219 A72-20761
Sequential machine realization with trigger or flip-flop elements and Boolean function feedback 10 p1445 A72-24401
SCR trigger circuits design generating short control pulses for converters based on SCR elements, presenting circuit diagrams 11 p1603 A72-25280
Engine ignition electronic system for triggering detonators in Aeros aeronomy satellite blastoff and release devices, discussing prototypes acceptance tests 11 p1610 A72-25803
Dc X ray timing pulse generator for light gas gun triggering based on projectile interruption technique 15 p2241 A72-32441
High voltage nanosecond pulse generator triggered by laser radiation from transmission stripline discharger for multichannel synchronous operation 16 p2400 A72-33083
Bistable trigger stages composed of digital multiplexer with IC logic modulus replacing NAND or NOR circuits 23 p3267 A72-43990

TRIGONOMETRIC FUNCTIONS
NT TANGENTS
Mixed boundary value problem of Laplace equation solution by dual trigonometric series equations approach, applying to microstrip transmission line capacitance determination 01 p0093 A72-10508
Trigonometric series solution of Tricomi problem for Chaplygin-type equation in half plane 04 p0461 A72-14628
Radio direction finding techniques using amplitude-trigonometric interpolation between signals received at circular antenna array 05 p0628 A72-16555
Approximate trigonometric solution to thermoelastic boundary value problem of plate with doubly periodic system of holes under unsteady temperature and thermal stress fields 06 p0899 A72-18563
Freely supported rectangular plate flexure under arbitrarily distributed load, obtaining differential equations solution in trigonometric polynomials 10 p1559 A72-24996
Evaluation of the norm of a function in terms of its Fourier coefficients, convenient in problems of approximation theory 24 p3419 A72-45549
Approximation of analytic functions by trigonometric polynomials over an interval smaller than the period 24 p3419 A72-45550

TRIM [BALANCE]
U AERODYNAMIC BALANCE

TRIMETHYL COMPOUNDS
Trimethylphosphite interaction with acetyl- and benzoyl-p-quinone in dry nitrogen atmosphere, noting phosphate formation through intermediate bipolar ion 06 p0770 A72-17986
Electron impact induced fragmentations of o-, m- and p-hydroxyalkylphenones and trimethylsilyl/TMS/ether derivatives, using high resolution mass spectrometry, metastable defocusing and deuterium labeling 07 p0936 A72-19499

TRINITROTOLUENE
Method of measuring the fine structure of detonation fronts in solid explosives. 24 p3463 A72-45039

TRINITROTRIAZOCYCLOHEXANE
U RDX

TRIODES
Grid controlled 100 W microwave transmitter power triode for space applications, noting high reliability and stability through use of metal dispenser cathode 01 p0009 A72-11223
Low pressure glow cathode triodes gas discharges, determining electron energy distribution function in double layer by probe measurements 03 p0400 A72-14349
Optimal hf triode oscillation tripler with allowance for power limitation by thermal losses on plate and grid electrodes 05 p0638 A72-17184
Transit effects in grid plate gap of triode for generating microwave oscillations in regime similar to IMPATT diode 07 p0953 A72-19015
Twin triodes type parameters stability in microwave region as function of cathode service life and temperature 09 p1284 A72-22243
Thin film tunnel triode using p-type amorphous semiconductors to achieve injected current amplification 10 p1451 A72-24624
Triode electron gun design for narrow electron beam under highly convergent lens action, using field emission source 19 p2775 A72-38611

TRIPLE AXIS SPECTROMETERS
U NEUTRON SPECTROMETERS

TRIPLET EXCITATION
U ATOMIC ENERGY LEVELS

TRIPLET STATE
U ATOMIC ENERGY LEVELS

TRIPROPELLANTS
U LIQUID ROCKET PROPELLANTS

TRITIUM
Cumulation-laser heating of D-T plasma for cylindrical wave, investigating pulse energy increase for critical temperature attainment from average value mathematical model 05 p0695 A72-16279
Nuclear microfusion energy recovery threshold increase during laser pulse heating process of D-T plasma 05 p0695 A72-16280
Laser heating and fusion energy recovery of D-T plasma by mechanical-magnetic cumulation, considering cylindrical wave system 09 p1365 A72-23553
RF discharge gap in cascaded plasma limiters, using tritium igniter as reliable electron priming source 18 p2715 A72-36451
Deuterium-tritium heating to thermonuclear temperatures by means of ion-ion collisions in the presence of intense laser radiation. 21 p3094 A72-41632

TROCHOIDS
U PIVOTS

TROILITE
Instrumental neutron-activation analysis of the troilite of the Sikhote-Alin meteorite 22 p3225 A72-42472

TROJAN ORBITS
Trojan deep space communications systems, maintaining powerful relay satellites in equilibrium at Lagrangian points of earth, Mars and Venus orbits 10 p1548 A72-24975

TROPICAL METEOROLOGY
Mesometeorological processes in tropic and subtropic zone based on cloud photographs obtained from aircraft and satellites 02 p0255 A72-12792
Tropical east-west atmospheric circulation geometrical, thermal and intensity characteristics during northern summer 03 p0384 A72-14143
Short period height and longer period kinetic energy oscillations in 10-level primitive equation model for circulation prediction in tropical region 03 p0385 A72-14232
Variance spectral techniques in detecting wave modes of synoptic scale tropospheric wind in midlatitudes and tropics 06 p0841 A72-17634
Tropical disturbances effect on general atmospheric circulation, considering Hadley cell rising branch and cumulonimbus clouds heat release 07 p1029 A72-19096
Mass and energy exchange in tropical convective cloud systems from ATS cloud photographs 09 p1344 A72-22430
Asian subtropics western disturbances movement prediction by primitive equation barotropic model with east-west cyclic boundary conditions, presenting forecast charts and error statistics 11 p1681 A72-26077
Tropical depression analysis based on radar data, observing large divergence in maximum vorticity areas 11 p1681 A72-26079

Morning glory, showing squall formation by atmospheric hydraulic jump favored by slack pressure gradients, cloudless skies and low latitudes 11 p1681 A72-26080

Tropical hurricane model describing initial whirlwind and self exciting wind velocity development and dependence on ocean surface temperature 11 p1682 A72-26879

Time-spectral characteristics and geographic variations of large scale cloud activity in tropical Pacific 12 p1837 A72-27018

Test flights into weather at midlatitudes and tropical systems with airborne OMEGA navigation system, discussing E field and H field antennas 13 p1999 A72-29203

Scale analysis of large scale tropical disturbances in conditionally unstable atmosphere, estimating geopotential height dependence on stream function via heat balance equation 14 p2128 A72-30345

Balloon flight tracking by Nimbus D satellite to sound tropical stratosphere air motions, noting northward drift maximum in Northern Hemisphere winter 14 p2128 A72-30350

Tropical sporadic E reflections and vertical plasma instabilities as function of equatorial electrojet and electron drift ratio based on ionogram observations 16 p2382 A72-32867

Barbados Oceanographic and Meteorological Experiment to compare synoptic scale-measured vertical vapor fluxes over tropical ocean 16 p2417 A72-33169

Studies on radiation balance at a tropical station. 18 p2722 A72-36759

Features of zonal circulation in the stratosphere and lower mesosphere of the equatorial region during the period of increasing solar activity /1967-1968/ 19 p2790 A72-37999

Response of the tropical atmosphere to local, steady forcing. 21 p3077 A72-40248

Direct observation of a complete unit of meridian circulation from the equatorial belt up to the polar front - Synthesis of concepts of the pseudofront, of the equatorial mesosystem, and of the subsidence well 21 p3078 A72-41344

Air motions in the tropical stratosphere deduced from satellite tracking of horizontally floating balloons. 21 p3078 A72-41612

An updated theory for the quasi-biennial cycle of the tropical stratosphere. 22 p3201 A72-42503

Nonlinear hydrothermodynamic model of steady atmospheric motion in equatorial latitudes with energy influx approximation 23 p3284 A72-43533

Annual height and temperature distribution charts of polar and tropical tropopause over Northern Hemisphere 23 p3310 A72-43534

Scale analysis of atmospheric large-scale motions in low latitudes. 23 p3311 A72-44241

Mass and heat budget estimates of the Atlantic SE trade wind flow at the equator. 24 p3420 A72-44756

TROPICAL REGIONS
Mt. Agung volcanic eruption dust effects on monthly-mean lower stratospheric temperatures for tropical stations 01 p0096 A72-11284
Martian equatorial zone brightness distribution formula, noting agreement with observations near zero phase and 6-45 deg phase angles 02 p0282 A72-12328
Manual reduction of Faraday rotation observations of ionospheric electron density at low latitudes, comparing with computer ray trace analysis 02 p0221 A72-12462
Cosmic noise ionospheric absorption measurements with riometers, showing mid and low latitudinal variation 02 p0221 A72-12464
Positive ion composition in equatorial D region, investigating reaction kinetics 03 p0412 A72-13522
Geomagnetic control over latitude variation of total electron content in equatorial ionosphere 04 p0515 A72-14931
Statistical analysis of low latitude F 2 layer disturbances associated with sudden commencement type geomagnetic storms, investigating critical frequencies 04 p0516 A72-14937
Low latitude low dispersion whistlers, discussing origin as vlf waves radiated from return stroke of lightning discharge 04 p0517 A72-14949
Thumba night time equatorial E region electron density profiles from rocket-borne Langmuir probe experiments 04 p0517 A72-14957

Proton measurements in ring current by OGO-3 satellite compared with geomagnetic field data at low and high latitudes

05 p0711 A72-17034

Electron content measurement for low latitude station obtained at sunspot maximum by Syncom 3, observing seasonal variation and winter anomaly effect

06 p0874 A72-18089

Tropical upper tropospheric motion field during Northern Hemisphere summer, computing energy exchange between zonal flow and eddies

06 p0842 A72-18437

F 2 ionization distribution diurnal variations from airborne ionosonde measurements during June-July 1966 over Tamanrasset meridien, correlating magnetic activity with wind variations

06 p0810 A72-18731

Low latitude surface horizontal magnetic field intensity depression due to quiet time ring current in magnetosphere as function of solar wind velocity

07 p1055 A72-18884

High time resolution of low latitude asymmetric disturbances in geomagnetic field by Fourier analysis for substorm activity studies

07 p0976 A72-19165

Latitude dependent discrepancy between low latitude satellite drag deduced densities at high latitudes and Jacchia model

07 p0976 A72-19167

Venus equatorial region surface height variations from interplanetary radar echo delay measurements, discussing resolution, repeatability and radius

07 p1073 A72-19352

Midlatitude and equatorial geomagnetic micropulsations during 13-14 January 1967 world-wide magnetic storm from ground and satellite observations

08 p1157 A72-21107

North-south ionospheric movements at low latitude station, investigating diurnal and seasonal velocity variations from cross correlation and similar fades time delays measurements

08 p1136 A72-21981

Thermal stratification of mesosphere and lower thermosphere at low latitudes with allowance for turbulent mixing, showing molecular oxygen and ozone radiative heating prevalence

09 p1347 A72-23589

Airborne IR radiometric measurements of upward vertical radiance from tropical sea surface at 10-12 microns, noting absorption coefficient dependence on water vapor

10 p1474 A72-24747

Whistler dispersion and occurrence rate characteristics at low latitudes during solar cycle, noting annual variations and magnetospheric electron density

11 p1623 A72-26105

Low latitude geomagnetic field diurnal variations caused by solar wind associated component, noting evening side depression

11 p1713 A72-26109

Electrostatic resonances associated with maximum frequencies of cyclotron-harmonic waves at high and low latitudes, presenting dispersion curves and ray paths

11 p1624 A72-26400

Martian equatorial zone brightness distribution formula, noting agreement with observations near zero phase and 6-45 deg phase angles

13 p2039 A72-29212

F 2 region maximum electron density level height and molecular temperature diurnal variations at equatorial latitudes from Ibadan station data

13 p1949 A72-29253

Daily variations in E region horizontal drift at Thumba/India, showing daytime westward and nighttime eastward drifts

13 p1949 A72-29275

Monthly mean pattern variations for equatorial stratospheric easterly and westerly winds, noting continuity of low latitude regimes

14 p2129 A72-30806

Equatorial ionospheric vertical electron density profiles measurement by rocket-borne phase measuring swept RF probe with dc biased sensor, comparing data with ionograms

15 p2226 A72-31940

Ionospheric electron content semiannual and seasonal variations as function of solar and geomagnetic activity from low and mid-northern latitude observations

16 p2385 A72-33378

Ion concentration inhomogeneities in the ionosphere at an altitude of 600 km

17 p2547 A72-35207

Atomic oxygen green line emission in nightglow from OGO-F photometer observations, calculating tropical F region electron density spatial distribution

17 p2549 A72-35604

Equatorial anomaly changes caused by ionospheric disturbances, noting diurnal variations of magnetic storm effect

17 p2551 A72-35868

Atmospheric model synthesis of observed electron temperatures and concentrations in tropical ionosphere during 8 March 1970 magnetic storm, noting F 2 region features

18 p2686 A72-36296

Equatorial tropospheric waves induced by diabatic heat sources.

18 p2687 A72-36628

Low latitude equatorial electrojet analysis based on three dimensional electric field equation for ionosphere and magnetosphere

18 p2687 A72-36854

Place of tropical pathology in medical assessment of aircrew

19 p2757 A72-37882

Equatorial ionosphere irregularities vertical drift velocity calculation, showing agreement with incoherent scatter results

22 p3170 A72-42370

Theoretical calculations of the F-region tropical ultraviolet airglow intensity.

22 p3171 A72-42418

Description of global-scale circulation cells in the tropics with a 40-50 day period.

22 p3201 A72-42506

A diagnostic study of the vorticity balance at 200 mb in the tropics during the Northern summer.

22 p3201 A72-42507

Synchronous observations of lower-ionospheric wind conditions in Dushanbe and at the equator

23 p3285 A72-44166

Compilation of azimuth tables for the North star /for the tropical zone/

24 p3438 A72-44866

TROPICAL STORMS

NT HURRICANES

Tropical hurricanes and storm outflow layer wind analyses from ATS 3 satellite data, noting cyclonic eddy asymmetric structure

03 p0384 A72-14144

Tropical storms generated midlatitudinal cloud bands relation to autumnal large scale circulation, analyzing heat and moisture injection effects

09 p1344 A72-22429

Tropical thunderstorm precipitation current variations due to lightning produced atmospheric electric field changes, considering charged raindrops turbulent diffusion

12 p1839 A72-27502

TROPICS

U TROPICAL REGIONS

TROPISM

NT AEOLOTROPISM

NT GEOTROPISM

NT GYROTROPISM

NT NEUROTROPISM

TROPOPAUSE

Venusian polar tropopause and cloud layer from IR spectral recording in carbon dioxide band near inferior conjunction for crescent regions

03 p0436 A72-13814

Annual height and temperature distribution charts of polar and tropical tropopause over Northern Hemisphere

23 p3310 A72-43534

TROPOSPHERE

Tropospheric wind estimation from ATS 1 satellite cloud motions over equatorial Pacific

01 p0060 A72-10856

Tropospheric layer structures effect on long range vhf radio communication, calculating wave modes attenuation rate and electric field patterns

01 p0032 A72-11238

Approximate height formula for radio ray propagating through spherically stratified smoothly varying troposphere, evaluating exponential model atmosphere

01 p0032 A72-11253

Report on U.S. telecommunications telemetry information theory in period 1966-1969, discussing ionospheric and tropospheric data transmission

02 p0171 A72-11687

Tropospheric processes effects on Northern Hemisphere stratospheric meridional transformations in geopotential field and air circulation

02 p0253 A72-11732

Ageostrophic flow relations in tropospheric high wind fields, discussing Scheibe equation and vector calculation

02 p0255 A72-12788

Satellite measurements of tropospheric and earth surface state parameters for long term numerical weather forecasting, discussing data fluctuations

02 p0255 A72-12789

Air exchange between stratosphere and troposphere from cosmic ray produced radionuclides and fallout comparison with weather development

03 p0351 A72-14359

French monograph on atmospheric ozone utilization as tracer for troposphere-stratosphere exchanges covering investigations at various locations

05 p0654 A72-15799

Variance spectral techniques in detecting wave modes of synoptic scale tropospheric wind in midlatitudes and tropics

06 p0841 A72-17634

Tropical upper tropospheric motion field during Northern Hemisphere summer, computing energy exchange between zonal flow and eddies

06 p0842 A72-18437

Vertical macroturbulence diffusion coefficient and Na 22 and Be 7 flux from stratosphere to troposphere estimated using ground level measurements and two layer model

09 p1376 A72-22416

Three parameter prognosis model for geopotential vertical profile in troposphere and stratosphere, describing vortex and heat influx in quasi-geostrophic and adiabatic approximations

09 p1297 A72-22549

Elevation angle and range error correction equations for satellite tracking data processing with assumed spherical tropospheric refractivity

09 p1281 A72-23510

Optical path calculation in ionosphere and troposphere, determining term due to astronomical refraction with respect to frequency

10 p1475 A72-24859

Calibration technique for meteorological superpressure balloon hygrometers designed for horizontal sounding of troposphere and stratosphere

10 p1484 A72-25087

Atmospheric temperature measurement up to 2 km height, reviewing sounding equipment and techniques

10 p1508 A72-25091

Ionosphere electron content annual mean difference from semiannual amplitude as seasonal fluctuation indication for tropospheric circulation

12 p1803 A72-27774

Quasi-steady and sporadic corpuscular fluxes as basic solar activity effect on troposphere, showing magnetosphere interaction time relation to meridional atmospheric circulation changes

12 p1842 A72-28208

Upper troposphere-lower stratosphere geostrophic wind deviation from rawinsonde and pressure-height data in El Paso-White Sands area, using finite difference method

13 p1988 A72-28447

Density function for lower troposphere vertical turbulence diffusion coefficient derived from atmosphere radiometric probe data

13 p2029 A72-28456

Near horizon anomalies in astronomical refraction due to ground air layer effects on tropospheric processes

13 p1945 A72-28495

Solar activity effects on atmospheric electricity during favorable weather conditions, discussing troposphere potential gradient and earth air current

13 p2029 A72-28622

Diffraction antenna use in visual range to study troposphere modulated laser radiation propagation in turbulent atmosphere, presenting light intensity distribution

13 p1917 A72-28690

Residence time of water vapor and aerosols in troposphere and lower stratosphere, noting application to air pollution buildup by aircraft

13 p1991 A72-28836

Hydrodynamic theory of atmospheric action center formation due to pressure migration for Northern troposphere two level meteorological forecasting

14 p2127 A72-30261

SHF signal propagation through troposphere at low elevation angles, comparing fading measurements in winter and summer

15 p2194 A72-31550

Physical interpretation of electromagnetic waves at attenuation function HF singularity during diffraction over spherical surface, applying to short wave diffraction in tropospheric model

15 p2195 A72-31651

Tropospheric meridional ozone profiles between Europe and South Africa from measurements aboard commercial airliners, noting seasonal variations

16 p2382 A72-32889

Photochemistry of the lower troposphere.

17 p2511 A72-34635

Fluctuations of water vapour content in the troposphere as derived from interferometric observations of celestial radio sources.

17 p2545 A72-34690

Meteorological applications of the Nimbus 4 temperature-humidity infrared radiometer, 6.7 micron channel data.

18 p2707 A72-36718

Computer program for numerical analysis of atmospheric fronts in lower troposphere based on models for spatial distribution of hydrothermal characteristic in air mass

19 p2829 A72-38771

Balloon measurements of tropospheric turbulence vertical profiles, obtaining temperature and refractive index structure coefficients

21 p3077 A72-40144

Fine structure of temperature stratification in the troposphere and stratosphere

21 p3079 A72-41799

Sea level tropospheric pressure distribution persistence correlation to solar corpuscular radiation measured by planetary scale geomagnetic disturbance
22 p3219 A72-42517

Variation of tropospheric slant-path attenuation in the UK at 11.75 and 17 GHz.
22 p3155 A72-42751

TROPOSPHERIC SCATTERING

Forward error correction code performance on hf troposcatter and satellite channels, considering adaptive and nonadaptive convolutional and cyclic coding
01 p0026 A72-10338

Tropospheric transhorizon meter, decimeter and centimeter wave propagation mechanisms, suggesting model for scattering and partial reflection effects
01 p0054 A72-10402

Analog FM multiplex signal intermodulation formula based on time-variable electromagnetic waves tropospheric scatter propagation
01 p0027 A72-10411

Tropospheric forward electromagnetic scatter propagation path loss prediction by modified Yeh method with empirically derived correction function
03 p0323 A72-14031

Turbulent tropospheric temperature fluctuations effects on optical waves propagation with random scattering, considering amplitude, phase, angle-of-arrival and polarization
04 p0548 A72-14736

Tropospheric scatter path characteristics as communication channel with random fluctuations, deriving signal autocorrelation function from mean power pulse response
08 p1132 A72-21329

Secondary scattered light component of tropospheric twilight from electrophotometric observations, comparing with upper atmospheric scattering
13 p1954 A72-30070

Frequency sharing between broadcast satellites and tropospheric scatter systems.
20 p2901 A72-38978

TROPOSPHERIC WAVES

Tropospheric transhorizon meter, decimeter and centimeter wave propagation mechanisms, suggesting model for scattering and partial reflection effects
01 p0054 A72-10402

Tropospheric effects on vhf satellite signal transmission noted from time lags between observed and calculated satellite rise time
01 p0027 A72-10409

Lee waves characteristics relationship to air flow and temperature layers in troposphere based on satellite pictures
02 p0255 A72-12791

Book on radio wave propagation covering ground, tropospheric and ionospheric waves, atmospheric and cosmic noise, reflection, attenuation, signal distortion, space communication, etc
04 p0487 A72-15269

High resolution measurement of microwave refraction including arrival and fire angles on short line-of-sight tropospheric paths
07 p0946 A72-19790

Energy and momentum removal from troposphere and lower atmosphere by mountain lee wave breaking, discussing effects on atmospheric circulation evolution and maintenance
08 p1203 A72-22167

Noctiluculent cloud wave structure, discussing motions in high atmosphere, ice crystal formation, energy sources and observations
10 p1474 A72-24707

Receiving and transmitting antennas directional gain effect on microwave long distance tropospheric propagation
12 p1783 A72-27632

Equatorial tropospheric waves induced by diabatic heat sources.
18 p2687 A72-36628

Non-Boussinesq effects and further development in a model of upper tropospheric frontogenesis.
19 p2829 A72-38558

Tropospheric wave motions with baroclinic basic flow in equatorial latitudes.
24 p3399 A72-45485

TROUBLESHOOTING

U MAINTENANCE

TRUNCATION [MATHEMATICS]

U APPROXIMATION

TRUNCATION ERRORS

Iterative truncation error estimates in solution for plane wave diffraction by grating
02 p0171 A72-11738

Fourier series terms number effect on sandwich plate critical shear stress calculation accuracy
02 p0294 A72-12438

Truncation error bounds for continued fractions, considering application to Gauss hypergeometric functions
04 p0538 A72-14728

[AD-738403] Truncation error correction based on Richardson extrapolation in finite difference approximation of nonlinear partial differential operators
07 p1101 A72-20328

Computational mean square error due to roundoff in digital filters implemented on fixed point computers
07 p1033 A72-20346

Power series solutions to transition and matrix covariance differential equations, obtaining truncation error bounds and polynomial approximations
09 p1341 A72-23093

Increased accuracy cubic spline approximation to two-point boundary value problems for differential equation, noting truncation error
10 p1502 A72-23722

Fifth order modified Runge-Kutta integration algorithm, presenting truncation error estimation method and computation procedure flow chart
10 p1505 A72-24091

Short period terms in earth rotation rate and polar motion, considering data truncation effects on periodograms
10 p1475 A72-24872

Moore-Penrose pseudoinverse matrix computation, using single and multiple modulus arithmetic method for reduced roundoff error
11 p1676 A72-25505

Sampling theorem with small truncation error for band limited signals, discussing applications to pulse transmission filter design
13 p1922 A72-29397

Shift register implemented binary transversal filter type digital pulse waveform generators truncation and approximation error spectrum analysis via inverse Fourier transform
16 p2362 A72-32854

A study of the upward continuation of gravity data from a plane surface.
17 p2544 A72-34271

Sampled imagery transfer function compensation by inverse function, noting truncation effects on processing array SNR performance
17 p2521 A72-34412

Finite word length effects on digital filter implementation.
18 p2663 A72-36303

Numerical solution of Volterra integral equation.
18 p2705 A72-36601

A-stable, accurate averaging of multistep methods for stiff differential equations.
18 p2705 A72-37019

Nonlinear time evolution of firehose unstable MHD waves, noting quasi-linear theory truncation error for low wave numbers relaxation time and energy growth
19 p2839 A72-37334

A note on a comparison of confidence interval techniques in truncated life tests.
21 p3075 A72-40828

Variable-step truncation error estimates for Runge-Kutta methods of order 4 or less.
22 p3199 A72-42746

On the efficient reduction of truncation error in numerical weather prediction models.
23 p3311 A72-43675

TRUNKS [LINES]

U TRANSMISSION LINES

TRUNNIONS

U SHAFTS [MACHINE ELEMENTS]

TRUSSES

Boron-epoxy tubular struts for one third scale space shuttle booster thrust truss structure, discussing design, analysis, fabrication, weight, test and quality control
01 p0138 A72-10735

Book on matrix structural analysis covering matrix algebra concepts, direct stiffness matrix methods, lifting surface, nonlinear truss and structural partitioning analysis, etc
07 p1092 A72-19908

Boron-epoxy reinforced Ti tubular truss for application to space shuttle booster thrust structure, evaluating performance
11 p1730 A72-25414

[AIAA PAPER 72-393] Control theory application to nonlinear elastic analysis of trusses, partitioning structure into statically determinate stages
11 p1736 A72-25989

Minimum weight hinged and unhinged cantilever truss design as variational problem, using dynamic programming method
14 p2166 A72-30690

Equations of motion and free vibration for trusswork structures under nonperiodic dynamic loads, calculating longitudinal and transverse end forces
15 p2322 A72-31360

Optimal plane elastic trusses under alternative loads, designing for smallest total volume of bars with upper stress bound
16 p2466 A72-33017

Optimal design of indeterminate truss using geometric programming.
23 p3354 A72-44256

TRYPTAMINES

NT SEROTONIN

Protein biosynthesis inhibitors retardation of noradrenaline and serotonin induced hyperpolarization of neuron membranes in cortical sensorimotor region of rabbits
08 p1122 A72-22192

TRYPTOPHAN

Insulin injection or carbohydrate consumption effects on serotonin and tryptophan concentrations in rat brains
02 p0165 A72-12845

Serotonin precursor 5-oxytryptophan effects on hypothalamic-hypophyseal-adrenal complex under complete deafferentation of medial-basal hypothalamus
13 p1907 A72-30016

Human tryptophan and tyrosine metabolism - Effects of acute exposure to cold stress.
21 p2997 A72-40417

TU-104 AIRCRAFT

Tu-104 turboprop aircraft flight noise measurements and spectral changes at different distances from landing strip, evaluating public nuisance and resident reactions
14 p2072 A72-30446

Tu-104 turboprop aircraft flight noise measurements and spectral changes at different distances from landing strip, evaluating annoyance factors and resident reactions
21 p3009 A72-41110

TU-144 AIRCRAFT

Supersonic Tu 144 aircraft design, discussing engine and aerodynamic characteristics, stabilization and control, propulsion, wing structure, landing gear and operation
03 p0310 A72-13473

TU-154 AIRCRAFT

Tu-154 aerodynamic design, discussing arrow wing and propulsion unit characteristics
12 p1753 A72-27268

TUBE ANODES

Multichannel photomultiplier matrix anode design for various tube types fabrication
11 p1631 A72-25687

TUBE CATHODES

NT COLD CATHODE TUBES

NT COLD CATHODES

NT HOT CATHODES

NT PHOTOCATHODES

NT PHOTOMULTIPLIER TUBES

NT THERMIONIC CATHODES

Ultrasonic device with magnetostriction vibrator for suspension coating oxide cathodes, noting superiority to spray coating by compressed air
16 p2374 A72-33969

TUBE GRIDS

Transit effects in grid plate gap of triode for generating microwave oscillations in regime similar to IMPATT diode
07 p0953 A72-19015

Superposition method for potential distribution in plane tetrede field with unipotential and bipotential grids, noting electro-optical effect in cylindrical lenses
19 p2776 A72-38667

TUBE HEAT EXCHANGERS

Construction of a high-performance resistojet for satellite propulsion.
23 p3328 A72-44324

TUBERCULOSIS

Isoniazid tuberculosis chemoprophylaxis safety in aviation personnel, discussing renal function, serum transaminase activity, hematology, electrocardiograms and neurological examinations
04 p0479 A72-14872

TUBES

Hot isostatic pressing techniques for thin wall Be tubes manufacture
11 p1643 A72-26831

Tubular materials plane stress-strain test facility for combined axial load and internal pressure effects, describing principal components
14 p2092 A72-30442

Temperature distribution in a helically heated tube
20 p2984 A72-39648

Bursting strength and toughness of wire reinforced composite tubes under uniaxial/hoop stress.
21 p3120 A72-41208

Bursting of wire reinforced composite tubes under biaxial tension stresses.
21 p3121 A72-41209

TUBING

U PIPES [TUBES]

TUMBLING MOTION

Determination of the parameters of motion of a container and its load with allowance for their interaction during internal vibrational finishing operations
19 p2824 A72-37426

Despinning and detumbling satellites in rescue operations.
24 p3450 A72-45160

TUMORS

NT CANCER

NT LEUKEMIAS

Effect of a magnetic field on experimental tumors /direct and via nervous system/
17 p2503 A72-35011

Brain tumors in irradiated monkeys.
17 p2505 A72-35647

TUNERS

NT WAVEGUIDE TUNERS

- Ferrite microwave devices design, covering non-reciprocal circuit and electrical tuner
01 p0041 A72-10696
- Cross-modulation in tuning circuits with nonlinear capacitances.
21 p3039 A72-41830
- Wavelength tuning of an intracavity pumped CW mode-locked dye laser.
22 p3184 A72-41989
- TUNGSTATES**
- Rare earth tungstate refractory ceramics, determining mechanical properties, crystalline structure and electrical/chemical parameters
05 p0675 A72-16700
- Melting points and phase diagrams for various tungsten oxide systems, noting alkaline earth and transition and trivalent metal tungstates
10 p1497 A72-24731
- Spectroscopic and stimulated emission properties of neodymium ions in potassium yttrium tungstate crystals at 77 and 300 K
11 p1701 A72-26362
- TUNGSTEN**
- Tungsten heat capacity, electrical resistivity and thermal radiation measurement over 2000-3600 K range by pulse heating technique
01 p0082 A72-10174
- Porosity and W inclusions effects on Al alloy weld strength, presenting radiographic and tensile test data
01 p0074 A72-10282
- Line profile shape analysis of X ray diffraction broadening from deformed W, showing close approximation to Voigt distribution
01 p0088 A72-11046
- Interstitial impurities and grain size effects on cold brittleness in W melts in deformed and recrystallized states
01 p0088 A72-11082
- Recrystallization and rolling temperature effects on W strength and plasticity
01 p0088 A72-11083
- Deformation and compression characteristics of W wire rolled from flattened vacuum melts
01 p0077 A72-11084
- Plastic deformation, heat treatment and grinding of set blank W casts for strip and foil production
01 p0088 A72-11085
- Thermomechanical conditions of plasticity-to-brittleness transition temperature for optimal rolling of cermet W strips
01 p0078 A72-11088
- Hydrogen condensation on tungsten as function of temperature, coverage and population of binding states, noting initial sticking coefficients variations
01 p0089 A72-11113
- Uranium and tungsten plasmas emission and absorption properties at shock tube generated pressures of 3-48 atm and temperatures of 7,000-12,000 K
01 p0112 A72-11339
- Differential thermal radiation scattering coefficients of submicron W refractory particles in hydrogen and nitrogen at temperatures to 1080 K
01 p0112 A72-11341
- Argon-hydrogen plasma seeded with submicron tungsten particles, measuring composition, temperature, radiant heat output and opacity
01 p0112 A72-11343
- Chloride process produced tungsten powder for tungsten carbides production, discussing impurities, particle shape and size distribution, carburization behavior and applications
02 p0239 A72-11427
- High purity W ion irradiated in situ under ultrahigh vacuum at high temperature, examining depleted zone defect structure by field ion microscope
02 p0242 A72-11909
- Powder metallurgical tungsten fine wire creep behavior at 2100-3000 C, determining activation energy and stress dependence
03 p0370 A72-12996
- Rolling workability of pure W single crystals grown by electron beam zone melting technique, discussing crack occurrence
03 p0374 A72-13718
- Tungsten wire deformation structure from swaging or rolling and drawing processes, noting cylindrical texture superimposed on fiber texture
03 p0375 A72-13933
- NDT for detecting density variation, local anomalies regions and completeness of copper-infiltrated W powder rocket nozzle inserts
03 p0364 A72-14025
- Intermittent ion emission enhancement from tungsten surface in He-W field-ion microscope upon Ne addition to imaging gas
04 p0552 A72-14547
- Trimethylchlorosilane film boiling for silicon carbide deposit on vertical heated tungsten filaments, investigating mass transport rate
04 p0595 A72-14600
- Internal friction in annealed and deformed tungsten at room temperature to 950 C, examining carbon contents, dislocations and temperature effects on carbon Snoek peak
06 p0830 A72-18295

- Tensile strength of tungsten reinforced nickel, determining temperature effect on fibers deformation after vacuum rolling simultaneously with plastic matrix
06 p0832 A72-18362
- Compressive strength of Cu-W fiber metal matrix composite as function of temperature, comparing to cermet
06 p0832 A72-18363
- Nichrome matrix composites with W and Mo reinforcing fibers
07 p1013 A72-19744
- Tungsten dispersion strengthening by hafnium nitride covapor deposition, discussing effects of matrix microstructure and dispersoids number, size and spacing variations
07 p1019 A72-20366
- Photographic observations of W particle clusters high velocity impact against polystyrene, paraffin and W targets for energy dissipation in meteorite impact simulations
08 p1232 A72-21152
- Coaxial plasmatron with central electrode composed of cylindrical Cu and W thermionic cathodes, noting thermal efficiency
08 p1214 A72-21455
- Yttria stabilized hafnia based graphite and tungsten composites, investigating factors affecting thermal shock resistance
09 p1327 A72-22385
- Two mechanism model for anomalous field ion microscope images in W, noting end form difference in high and low evaporation rates
09 p1370 A72-22803
- Electron reflection mechanism and gas adsorption effect at W /001/ surface in energy range 1-10 eV
09 p1370 A72-22804
- Nitrogen adsorption kinetics on bulk W targets investigated by ultrahigh vacuum, molecular beam, reflexion detector method
09 p1276 A72-22806
- Methane, hydrogen and oxygen adsorption and displacement on crystal surface of W investigated by thermal desorption and work function changes
09 p1276 A72-22807
- Ta and W X ray spectra fine structure measurement, providing electron states density in unoccupied regions of energy bands of solids
09 p1370 A72-22842
- Dislocation loops in thin W foil due to ion irradiation, using electron microscopic analysis
09 p1331 A72-23505
- Radiation damage in bcc metal Mo and W foils under energetic Au ion irradiation, noting vacancy dislocation loops
09 p1331 A72-23506
- Pulsed arc TIG welding with modulation of current from standard power source, comparing performance with steady dc method
09 p1320 A72-23632
- Interdiffusion of tight contact welded ring Ti-W pairs at high temperature, using X ray analysis and electron beam techniques
10 p1497 A72-24785
- Pendulum impact resistance of tungsten fiber-metal matrix composites, noting heat treatment and test temperature effects
11 p1653 A72-25473
- Critical aspect ratio of W fiber in copper matrix for stress rupture applications
11 p1654 A72-25482
- Porous-tungsten mercury vaporizers design and tests for flow rate, liquid intrusion pressure level and mechanical strength
[AIAA PAPER 72-484]
11 p1710 A72-26210
- Specific heat temperature coefficient measurement of W at 2000 to 3600 K for defect and phase transition studies
11 p1661 A72-26625
- Explosive compaction of metal powders by direct method with emphasis on W
11 p1643 A72-26833
- Chemical vapor deposition of W and Mo by hydrogen reduction of hexafluorides, noting crystal structure and microporosity
11 p1644 A72-26837
- Deformation drawing textures of bcc metals, including W
11 p1644 A72-26838
- Electrical and thermal conductivity, elastic properties and resistance to bending of porous tungsten in porosities region
11 p1665 A72-26868
- Carbon and other inclusions effects on cast W strength at elevated temperatures from microscopic observation
11 p1666 A72-26877
- Ordered growth and etching of uranium and zirconium oxide-tungsten fiber refractory composites, using X ray diffraction and scanning electron microscopy
11 p1668 A72-26943
- Statistical adsorption kinetics model with electron desorption of oxygen on polycrystalline W, noting sticking coefficients
13 p1912 A72-28523

- High temperature microporosity in W wire at 3000-3350 C, using electron microscopy and fractography
13 p1973 A72-28651
- High temperature constant load creep tests on pure powder metallurgy W and tungsten-thoria alloy, discussing stress dependence
13 p1975 A72-28665
- Current breaks due to capacitor discharges in W and Mo wires, noting duration proportional to wire mass
13 p2007 A72-29980
- Modified geometrical model for sintering Ni-doped W, including surface tension effect at Ni-vapor interface
14 p2121 A72-30770
- Temperature dependent optical constants of Ti and W crystal surfaces cleaned by ion bombardment in ultrahigh vacuum
15 p2274 A72-31376
- Vacuum UV reflectance dependence of Re and W vapor-deposited films on substrate temperature during deposition, film thickness and aging in air
15 p2274 A72-31377
- Total energy distributions of field emitted electrons from tungsten as function of coverage by hydrogen and deuterium, observing elastic and inelastic spectrum
15 p2275 A72-31851
- Surface damage induced by ion bombardment of monocrystalline W and Mo, determining degradation rate dependence on collisional energy transfer
15 p2276 A72-31853
- I-V characteristics of polarized and nonpolarized memory effects in GaAs thin films evaporated on tungsten substrates
15 p2292 A72-31869
- Micropores pinning effect on grain boundaries mobility during drawn tungsten wire recrystallization, determining pores induced repulsive force
15 p2257 A72-32116
- Chemically vapor deposited W heat pipe fabrication and evaluation for application to high temperature nuclear reactors
15 p2244 A72-32126
- Mo and W simultaneous addition effects on Ni-Cr-Nb alloy properties, noting heat resistance increase and Nb solid solubility decrease
16 p2408 A72-33534
- Fracture-surface energy model for Cu-W fiber metal matrix composites, using plastic flow analysis
16 p2470 A72-33613
- Cs adsorption on W and Ti observed by combination of ellipsometry, Auger spectroscopy and surface potential difference measurements, noting sticking coefficient and coverage
16 p2442 A72-33833
- Thermal conductivity of W wire reinforced Cu as function of W content
16 p2411 A72-34017
- Fabrication and testing of tungsten heat pipes for heat pipe cooled reactors.
17 p2636 A72-34596
- Output performance of a thermionic converter with an oriented tungsten /110/ emitter and a polycrystalline tungsten collector.
17 p2496 A72-34604
- Performance comparison of thermionic converters with several collector materials.
17 p2497 A72-34606
- Computed performance data for a thermionic converter having a Cl-CVD-W emitter and a polycrystalline Nb collector.
17 p2521 A72-34613
- Metal working and testing of nuclear rocket engine components with Mo as structural material and uranium dioxide as fuel, discussing Mo-W interdiffusion
17 p2559 A72-34617
- Compatibility of buffered uranium carbides with tungsten.
17 p2579 A72-34620
- Study of the diffusion of iron and cobalt along the grain boundaries of tungsten
17 p2569 A72-35522
- W /100/ work function change during adsorption of oxygen, cesium, and oxygen-cesium co-adsorption
18 p2656 A72-36128
- Work function dependence on crystal orientation for W with special emphasis to the variation near the /110/ orientation.
18 p2656 A72-36130
- Work function theory for Cs-/W/ and Cs-O-/W/.
18 p2656 A72-36133
- Work function change of tungsten /110/ planes as function of Mo coverage.
18 p2656 A72-36134
- Incore thermionic reactor cylindrical Mo emitter covered with two CVD W layers, discussing first layer adhesion and diffusion characteristics and work function stability
18 p2707 A72-36135
- Crystal orientation effect on electron work function in chemical vapor deposited W layers on thermionic converter cylindrical emitters
18 p2717 A72-36142

Studies of the influence of CVD tungsten depositing conditions on the formulation of pores resulting from interdiffusion in the emitters of thermionic converters. 18 p2698 A72-36145

The vapor deposition of high work function materials in a gas discharge. 18 p2656 A72-36149

The stability of structure of physical mechanical properties of molybdenum and tungsten after irradiation and thermal influence 18 p2698 A72-36153

Studies of physical-mechanical properties of monocrystal molybdenum and tungsten and electrical characteristics of TIC/thermionic converter/ 18 p2698 A72-36154

Th 228 decay from short and long term simulation tests of thorium dioxide heat source in thermionic energy converter with W capsule 18 p2709 A72-36162

Pure and thoriated W compatibility with uranium carbide alloys at 1800 C, noting thermal gradient and thoria noneffects 18 p2699 A72-36163

Volt-ampere characteristics of Ba-Cs plasma thermionic converter with W emitter and Ta collector 18 p2646 A72-36199

Kinetics and annealing and mechanical properties of W chemical vapor deposition, discussing high temperature tests 18 p2656 A72-36398

Surface energy and cleavage plane observation of brittle fracture for W single crystal in tension as function of orientation and temperature 18 p2702 A72-36750

Flash desorption spectrum and LEED studies of CO adsorption on W single crystal planes, measuring work function increase as function of coverage 18 p2657 A72-37040

Study of tungsten and molybdenum coatings obtained by arc discharge in a vacuum 19 p2808 A72-38186

The grain-size-dependences of the failure mode and ductility transition temperatures of melted chromium and tungsten. 20 p2935 A72-39139

A LEED investigation of the chemisorption of nitrous oxide on a tungsten /100/ surface. 20 p2898 A72-39188

Measurement of melting point and electrical resistivity /above 3600 K/ of tungsten by a pulse heating method. 20 p2941 A72-39722

Vapor deposition effects on high density Mo, W and Nb obtained by carbonyls pyrolysis or chlorides and fluorides reduction 20 p2941 A72-39821

Investigation by the mass transfer method of the diffusion of nickel at a /110/ surface of tungsten single crystals 21 p3068 A72-40955

Investigation of tantalum-compound films at the surface of acicular tungsten microcrystals 21 p3068 A72-40964

Chemisorption of CO on tungsten /100/ - Combined flash desorption and electron stimulated desorption study. I. 22 p3152 A72-42297

Photoelectron energy distributions from clean polycrystalline W, observing surface state 22 p3190 A72-42477

Photoemission from surface states on tungsten. 22 p3190 A72-42478

Adsorbed oxygen inhibition of reactions of hydrogen with tungsten. 23 p3298 A72-43270

Heat resistant Ni-base composite stiffened with W wires, investigating interaction between alloy and fibers from metallographic and X ray diffraction microscopy data 23 p3301 A72-43740

Pores visualization in porous materials by liquid filling and subsequent solidification and basic material removal, observing porous samples of sintered W and nichrome powders 23 p3290 A72-44016

Quasi-equilibrium analysis of the reaction of atomic and molecular fluorine with tungsten. 23 p3262 A72-44050

Electric resistance and enthalpy of molybdenum and tungsten 23 p3272 A72-44167

Field-ion microscopic study of the interstitial plasticity of tungsten single crystals 23 p3304 A72-44484

Application of a field-emission microscope to the investigation of the work function of tungsten coated with a thin layer of silicon oxide and with tantalum 24 p3432 A72-44891

Field-emission microscopy of tungsten coated with a silicon oxide film 24 p3432 A72-44892

The effect of annealing temperature on certain properties of molybdenum and tungsten fibers 24 p3415 A72-45396

Energy spectra of Cs+ ions scattered by the surface of a tungsten single crystal 24 p3429 A72-45501

Compressive strength of Cu-W fiber metal matrix composite as function of temperature, comparing to cermets 24 p3416 A72-45750

TUNGSTEN ALLOYS

Ta and Nb addition effects on W solid solution strengthening, determining W-Nb-Ta alloys phase diagram and melting point 03 p0375 A72-13943

C 14 diffusion coefficients in W and W-Re alloys single crystals at 1500-1800 C, discussing tracer activation energy and frequency factor 05 p0676 A72-16731

Electron beam welding of W-base alloy to W-base alloy, avoiding Re induced embrittlement by pure Mo transition piece 06 p0821 A72-17710

High temperature tests of creep rupture strength of W composite cast with heat resistant alloy coatings 06 p0829 A72-17947

Phase composition and electrical and mechanical properties of compacted zirconium diboride/tungsten alloys after sintering in argon, carbonaceous medium and vacuum 06 p0832 A72-18428

Phase equilibria of Mo-Mn-C and W-Mn-C systems by X ray analysis, showing eutectoid decomposition involving rhombic modification 06 p0833 A72-18432

High temperature tests of short time strength, hardness and moduli of elasticity of W-MO alloys subject to plastic deformation and annealing 06 p0833 A72-18633

Carbon effects on strength, ductility, brittle transition and plastic strains of tungsten at high temperatures 06 p0833 A72-18634

Tungsten alloy filaments as reinforcing agent of heat resistant composite chromium alloy, investigating long term high temperature effects 07 p1013 A72-19745

High temperature strengthening of vacuum melted W-Ti alloys with Mo and Zr additions 07 p1014 A72-19843

Bcc solid solutions formation in Cr-W binary alloys, investigating interface reaction and two phase grain boundary diffusion by X ray diffraction and microscopy 08 p1185 A72-21246

Nb-W equilibrium phase diagram estimation from known phase diagrams of Ni-Nb, Ni-W and Ni-Nb-W systems via Guggenheim quasi-chemical model application to Ni-Nb-W thermodynamic properties 10 p1496 A72-24233

Tungsten alloy wires strength, creep properties and fatigue limit, investigating fracture characteristics 11 p1663 A72-26807

High temperature creep properties of W-Re alloy under vacuum for thoria dispersion hardening from electron microscope and activation energy studies 11 p1665 A72-26863

W-Ni-Mo alloys obtained by powdered metals sintering, investigating mechanical properties, phase distribution and composition 11 p1666 A72-26876

Fracture micromechanism in liquid-phase sintered W-Fe-Ni powder composites, using scanning electron microscopy 11 p1668 A72-26942

W addition effect on Co-Nb alloys, noting phase structure transformation from cubic to hexagonal due to mean electron density increase 12 p1829 A72-27642

Electron shell structure in annealed and plastically deformed W-Re alloys from positron annihilation angular distributions 13 p1981 A72-29908

Tungsten and carbon combined solubility in solid niobium at 2000, 1700 and 1100 C 14 p2113 A72-30165

Ni-Mo-W alloys hardness rating and corrosion resistance to sulfuric and hydrochloric acids, discussing dispersion hardening, quenching and aging treatments 14 p2114 A72-30272

Tungsten-rhenium alloys and tungsten self diffusion coefficient temperature dependence investigation, noting Re addition effects 14 p2114 A72-30402

Sintering and melting preparation effects on mechanical properties of refractory W-Re alloys, considering sigma phase in solid alpha solution 14 p2114 A72-30530

Work functions of dilute W alloys from vacuum emission vehicle and thermionic microscope measurements, noting additives effect 14 p2120 A72-30613

Disilicide coated Ta-W alloy system oxidation behavior at 927-1482 C, using thermogravimetric, X ray diffraction and electron microprobe analyses 14 p2121 A72-30771

TUNGSTEN CARBIDES

Interaction of W with transition metals in ternary and multicomponent alloy systems, noting phase diagrams 14 p2122 A72-30981

Phase diagram of quaternary W-Mo-Nb-Ta alloy system, noting dependence of hardness on composition and temperature 14 p2122 A72-30982

Phase diagrams for W-Ta-Ti alloys at 1600 C from metallographic and X ray analysis 16 p2407 A72-33533

C diffusion mobility and coefficients in W-Mo steels gamma and alpha phases, discussing ionization effect on activation energy increase 16 p2408 A72-33538

Gravimetric and polarographic determination of W in binary W-Mo alloys, noting methods accuracy 18 p2655 A72-36098

Thermionic characteristics of carburized tungsten-rhenium alloys. 18 p2656 A72-36131

Effect of low-pressure oxygen on the creep properties of W-25 pct Re. 18 p2700 A72-36581

Emissivity and electrical resistivity of tungsten-yttrium oxide cermets as function of composition at 1200-3200 K 19 p2819 A72-38286

Some results of an investigation of the tungsten-nickel-boron ternary system 21 p3066 A72-40393

Strengthening of tungsten by powder metallurgical internal oxidation. 21 p3067 A72-40833

Phase compositions, impurity effects, crystallization and production of plastic W and Mo alloys and heat resistant W-based alloys 22 p3192 A72-42815

Antifriction and electrical properties of WSe₂-NbSe₂ quasi-binary alloys 23 p3299 A72-43292

Solid powder metallurgy tungsten alloys, determining scale factor effect on bending strength and fatigue limit 23 p3301 A72-43751

High temperature interaction between W and ZrC constructing isothermal structure 23 p3303 A72-44151

Physicomechanical properties of titanium-tungsten solid alloys with deficiency of carbon in the carbide solid solution lattice 24 p3415 A72-45385

TUNGSTEN CARBIDES

Chloride process produced tungsten powder for tungsten carbides production, discussing impurities, particle shape and size distribution, carburization behavior and applications 02 p0239 A72-11427

Composition, microstructure and mechanical properties of binder metal in cobalt bonded tungsten carbide 02 p0241 A72-11451

Carbon content effect on phase relationships and mechanical properties of sintered Fe-WC alloys, noting high strength 02 p0241 A72-11452

Tungsten carbide dislocation structures analysis by transmission electron microscopy, deriving Burger vectors from energy considerations and electron micrographs contrast 03 p0370 A72-12995

Short range order and X ray diffused scattering in TiC-WC solid solution, using least squares method 06 p0834 A72-18741

WC powder milling and sintering, investigating strain and dislocation density effects on behavior by scanning electron microscope 08 p1176 A72-21440

Ball milling effects on alumina and tungsten carbide powder sinterability due to particle comminution and microstrains 11 p1642 A72-26827

Russian book on hard alloys strength covering WC-Co and WC-TiC-Co alloys microstructure, thermal stresses and fracture mechanism 12 p1831 A72-28348

Combined thermal, vibrational and dimensional treatments effect on WC-Co alloy physical and mechanical properties, noting tensile and impact strength increase 13 p1979 A72-29480

Electron microscopic investigation of slip processes during plastic deformation of WC-Co based cermets, observing WC grain boundary sliding and Co phase crystal lattice transformations 15 p2257 A72-32117

Sintered WC effects on fuel cell electrochemical oxidation in acid electrolytes, analyzing hydrogen, hydrazine, formaldehyde, acetaldehyde, formic acid and carbon monoxide fuels 16 p2351 A72-33882

Method of investigating the wear of hard tungsten carbide cobalt alloys in a liquid nitrogen medium. 20 p2941 A72-39715

Structural and reaction kinetic characteristics of W, Ti and Ta/C-Co systems, considering solubility, surface energy, diffusion, segregation and grain growth

21 p3071 A72-1849

The effect of mixed milling on the sintering of WC-Co hardmetals.

22 p3188 A72-41975

Study of the hot pressing kinetics for niobium-cemented tungsten and titanium carbide alloys

22 p3182 A72-42191

Fine grained WC phase structure, physicochemical and cutting properties of Ti-Co alloy, using W powder prepared by tungsten oxide reduction in single stage muffle furnace

22 p3188 A72-42192

Fracture of WC-Co from a continuum viewpoint.

24 p3413 A72-44815

TUNGSTEN COMPOUNDS

NT SCHEELITE

NT TUNGSTATES

NT TUNGSTEN CARBIDES

NT TUNGSTEN FLUORIDES

NT TUNGSTEN OXIDES

Tungsten, molybdenum and tantalum disulfides oxidation rate determination by fluidized bed technique, calculating kinetic and diffusive processes activation energy

03 p0370 A72-13184

TUNGSTEN FLUORIDES

Thermal environment and fuel region simulation for nuclear light bulb engine, using rf induction heater and uranium and tungsten hexafluorides injection

01 p0113 A72-11355

Thermionic performance of fluoride CVD tungsten-niobium converter.

19 p2754 A72-37781

TUNGSTEN HALIDES

NT TUNGSTEN FLUORIDES

TUNGSTEN INERT GAS WELDING

U GAS TUNGSTEN ARC WELDING

TUNGSTEN OXIDES

NT SCHEELITE

Plasma sprayed tungsten and zirconium dioxide coatings porosity on chromium bronze, Ti and Al alloys and steel

03 p0363 A72-13550

Mass spectroscopic rate constants for reactions of negative ions of rhenium and tungsten oxides with chlorine and nitrogen dioxide

04 p0484 A72-15639

Tantalum and tungsten vanadium trioxide oxides crystallographic order ratio from diffraction spectrum intensities and overstructure lines disappearance

05 p0675 A72-16699

Tungsten and rhenium oxides negative ions source, presenting mass analysis table

07 p1037 A72-19323

Cold shortness of W and related refractory metals, noting oxide phases and impurities effects on mechanical properties temperature dependence

09 p1326 A72-22226

Melting points and phase diagrams for various tungsten oxide systems, noting alkaline earth and transition and trivalent metal tungstates

10 p1497 A72-24731

Ni additive effects on tungsten trioxide reduction with hydrogen and W powder sinterability

11 p1643 A72-26835

Emitter work function elevation in additive thermionic converters via tungsten oxides deposition on collector

18 p2646 A72-36197

Low-temperature reduction of molybdenum and tungsten oxides

20 p2941 A72-39820

Electrical conductivity of tungsten trioxide (WO₃).

21 p3096 A72-40198

Oxidation of W(110). I - LEED study of the oxide formation at 1000 K.

24 p3378 A72-44952

TUNGSK METEORITE

Silicate microspheres distribution anomaly in peats of Tunguska meteorite fall area

02 p0281 A72-12293

Tunguska explosion of 30 June 1908, determining air waves propagation velocity

03 p0438 A72-13981

Tunguska meteorite explosion energy values for various altitudes from investigation of shock wave propagation in variable density atmosphere

14 p2152 A72-30492

Tunguska meteorite explosion energy values for various altitudes from investigation of shock wave propagation in variable density atmosphere

19 p2864 A72-38321

Gas dynamics of the flight and explosion of meteorites.

24 p3439 A72-45020

TUNING

NT SCHULER TUNING

Electronic tuning of transverse Gunn effect microwave oscillators by varying voltage on third electrode incorporated between cathode and anode

01 p0036 A72-10637

Electrically excited tunable IR molecular gas lasers with rotational lines overlapping due to high pressure broadening

03 p0366 A72-12965

Narrow band electrically controlled interferential polarization filter with fine tuning capability for solar physical research, discussing design and operation

03 p0357 A72-13369

Tunable multiple wavelength organic dye laser using optical feedback through partially transparent mirrors

03 p0367 A72-13443

Fluctuation theory for single mode laser detuning effect on photon intensity and spectral line width

03 p0368 A72-13671

Three terminal voltage-tunable Gunn effect microwave oscillator, discussing depletion depth and electric field control modes for frequency

04 p0496 A72-14479

Dye laser monochromatic coherent light wavelength tuning with minimized optical cavity degradation and without external optics

04 p0531 A72-15502

Tunable optical and IR radiation source by rotating lithium niobate crystal in front of Q switched ruby laser

04 p0550 A72-15599

Tunable semiconductor and spin-flip Raman lasers for IR applications

[AD-738713] 05 p0667 A72-15788

Multicircuit hf filters tuning drive with mechanical synchronization correction

06 p0774 A72-17749

High power tunable IR gas lasers based on anharmonic molecules vibrational-rotational transitions excitation at gas pressures of 10 atm

06 p0825 A72-17786

Varactor tuned high performance Gunn oscillators, emphasizing specifications for level power output with frequency, tuning linearity and rate

06 p0789 A72-18479

Optical sweep generator using single frequency He-Ne lasers with Michelson interferometer for mode selection to provide smooth tuning throughout Doppler width

07 p1000 A72-19010

Tunable lasers using improved Littrow-mounted diffraction grating technique with mirror for spectral characteristics control

07 p1000 A72-19037

Wavelength tunable dye laser pumped by dual pulse lamps with Fabry-Perot interferometer in resonator

07 p1009 A72-20614

YIG-tuned microwave transistor oscillator design and performance, considering resonance phenomena and magnetic circuit effects on applications

08 p1139 A72-20985

Encapsulation influence on Gunn effect devices from circuit analysis of wideband tunable transferred electron microwave oscillators

12 p1790 A72-27440

Wide tuning range organic dye laser design, using nitrogen laser line as transverse pumping source

13 p1971 A72-29869

Narrow band retuned dc pumped amplifier-filter design based on diffractor, considering electron beam interaction

14 p2088 A72-30798

CW dye laser output tuning by mirror-grating combination with interspersed output coupling element, noting orders of magnitude reduction of fluorescence background intensity

16 p2401 A72-33388

Tunable output dye and semiconductor lasers application to absorption spectroscopy and air pollution monitoring

17 p2564 A72-35381

Wavelength tunable UV dye laser pumped by the fourth harmonic of Nd:YAG laser.

19 p2810 A72-37407

Some tuning characteristics and oscillation conditions of a waveguide-mounted transferred-electron diode oscillator.

19 p2772 A72-37569

German monograph - Multiple tuning of cooled parametric amplifiers

19 p2772 A72-37651

Bandwidth and threshold calculations for angle-tuned parametric oscillators.

19 p2813 A72-38689

High-resolution spectroscopy using magnetic-field-tuned semiconductor lasers.

20 p2933 A72-39561

Self-tuning and self-programming antenna matching devices for the frequency range 1.5-30 MHz and their application

21 p3031 A72-40538

Nonpeaked emission of a ruby laser with frequency tuning and selection

22 p3184 A72-42103

A single-tuned oscillator circuit for Gunn diode characterizations.

23 p3272 A72-44194

Theory of magnetically tunable band-pass filters

23 p3273 A72-44360

The efficient generation of coherent radiation continuously tunable from 2500 A to 3250 A.

24 p3409 A72-44803

TUNNEL DIODES

Tunnel diode microwave oscillator design by circle diagrams of operational and load characteristics

01 p0035 A72-10048

Integrated receiver module for satellite transponders, including tunnel diode amplifier, Schottky barrier mixer, Gunn oscillator and low pass filter

01 p0041 A72-10701

Tunnel diode quartz oscillator frequency stability improvement and dc power requirement reduction using nonlinear feed circuits

03 p0331 A72-13555

Book on microwave semiconductor devices, considering point contact crystal, varactor, Schottky-barrier, tunnel, backward and p-i-n diodes, transistors, Gunn effect devices and integrated circuits

03 p0333 A72-13845

Solid state tunnel diode amplifier-rectifier expander for microwave pulse regenerators

03 p0335 A72-14184

Wideband tunnel diode amplifier design, discussing circulator off-band impedance characteristics improvement through voltage standing wave ratio suppression network

05 p0638 A72-16594

Tunnel diode amplifier stability under parameter variation due to fabrication tolerances, aging, heating, etc

05 p0638 A72-17189

Wideband tunnel diode microwave amplifier design with coaxial line, considering band-edge stability and impedance matching

06 p0785 A72-18310

Microwave thin film microstrip IC tunnel diode amplifiers for broadband high performance receivers, discussing design, construction and performance

06 p0786 A72-18374

Microwave frequency mixer using two inverted tunnel diodes in series connection

10 p1450 A72-24519

Stationary waves properties dependence on weak skin effect in distributed tunnel diode type of nonlinear active transmission lines

10 p1453 A72-24902

Stabilization bandwidth reduction in microwave parallel tuned tunnel diode amplifier circuits synthesis

10 p1453 A72-24910

Semiautomatic analog to digital converter for pulse signals time dependent parameters, examining block diagrams and tunnel diode operation

11 p1605 A72-26456

Linear approximations and grapho-analytical method for neuristor line analysis, noting conditions for tunnel diode parameters

12 p1789 A72-27397

Tunnel diode amplifier for 8 GHz band, considering gain, bandwidth, noise factor and stability characteristics

12 p1790 A72-27533

Receptor membrane pulse generation electronic model with tunnel diode negative resistance circuit

12 p1771 A72-27578

Computerized synthesis of wideband series stabilized tunnel diode amplifier based on distributed constant elements

13 p1931 A72-29286

Distributed tunnel diode traveling wave amplifier load noise thermal and shot components, noting impedance boundaries

15 p2206 A72-31663

Tunnel diode harmonic relaxation frequency divider, obtaining large division factors and wide synchronization bands with sinusoidal output signal

15 p2206 A72-31666

German monograph on microwave broadband tunnel diode mixers theory and design, taking into account parasitic elements as part of filter networks

16 p2368 A72-33507

Set of steady states of a system composed of two delay lines and tunnel diodes

17 p2529 A72-34759

Digital pulse counter with delay line and tunnel diodes

17 p2529 A72-34760

Series stabilization reflection type tunnel diode microwave amplifier synthesis with allowance for real circulator reactance

18 p2665 A72-36107

Bilateral tunnel-diode amplifiers using ferrite transformers.

18 p2665 A72-36306

Amplitude and harmonic oscillation characteristics of quaternary RC parametron using tunnel diodes

19 p2773 A72-38211

Tunnel diode amplifier stability under parameter variation due to fabrication tolerances, aging, heating, etc

19 p2775 A72-38625

Effect of a junction capacitance nonlinearity on the spectral characteristics of a tunnel diode current

20 p2906 A72-38897

- Binary information storage with bipolar transistors, tunnel diodes, MIS and glass semiconductors, considering Gunn effect devices application
20 p2905 A72-39425
- Conductance associated with interface states in MOS tunnel structures.
21 p3032 A72-40701
- A regenerative high multiplicity tunnel-diode frequency multiplier
21 p3034 A72-41122
- Effects of tunneling on an IMPATT oscillator.
21 p3034 A72-41382
- Calculation of the electronic readjustment of a tunnel-diode oscillator by a varactor
22 p3159 A72-42246
- Niobium superconductive tunnel diode integrated circuit arrays.
22 p3161 A72-43090
- Influence of fluctuations on the electromagnetic properties of Josephson tunneling contacts
22 p3208 A72-43124
- RC, RL and RLC networks associated tunnel diode circuits normalized graphs, design method and stability consideration
23 p3272 A72-43988
- Self-excitation of oscillations in a system consisting of a delay line, inductance, and tunnel diodes
24 p3384 A72-44895
- TUNNEL RESISTORS**
U ELECTRON TUNNELING
U RESISTORS
TUNNELS
Integrodifferential equation for rigid tunnel walls effect on supercavitating flow past thin jet flapped airfoil, noting lift coefficient derivatives
10 p1469 A72-24562
- TUPOLEV AIRCRAFT**
TU-154 lift and drag augmenting devices for takeoff and landing characteristics improvement
03 p0310 A72-13472
- Instruments installation effect on soviet passenger aircraft pilot performance, discussing Tupolev aircraft control systems
21 p2994 A72-40173
- TURBIDITY**
Water quality monitoring by radiative transport equation for reflectance measurements of laser light scattered from turbid water polluted with absorber and scatterer particles
[AIAA PAPER 71-1098] 01 p0058 A72-10547
- Soyuz manned spacecraft meteorological observations, dealing cloud cover in various climatic zones, atmospheric turbidity and snow cover in mountain areas
02 p0253 A72-11731
- Polarization and atmospheric inhomogeneity effects on solar radiative transfer in turbid atmospheres, using diffused reflection and transmission matrices
02 p0222 A72-12836
- Short narrow light pulse reflection from thick turbid medium with strong anisotropic scattering, obtaining backscattering signal power from unsteady transport equation solution
05 p0690 A72-16292
- SNR expressions for image transmission through turbid medium, showing quality dependence on energy transfer, contrast frequency and sensor phonon illumination level
06 p0774 A72-17936
- Narrow light beam attenuation and scattering characteristics in turbid medium as function of distance from source from transport equation solution
06 p0774 A72-17938
- Global radiation flux and energy sum calculation from turbidity factor and cloud cover parameters, comparing with measurements in tropics and polar region
08 p1201 A72-21797
- Seasonal and diurnal variations of earth albedo from turbidity measurements, showing lower atmosphere moisture effect
08 p1237 A72-21799
- Radiative transfer equation for solar irradiance penetration of turbid atmosphere and plant canopy, using four point quadrature method
09 p1297 A72-22442
- Multiple laser light scattering from turbid medium, relating reflectance to polluted water parameters for aerial photographic surveillance
12 p1826 A72-27948
- Light propagation from unsteady source through homogeneous turbid light scattering media, using analytic and numerical methods for unsteady radiative transport equation solution
13 p2001 A72-28507
- SNR expressions for image transmission through turbid medium, showing quality dependence on energy transfer, contrast frequency and sensor phonon illumination level
16 p2426 A72-33777
- Narrow light beam attenuation and scattering characteristics in turbid medium as function of distance from source from transport equation solution
16 p2426 A72-33779
- Light attenuation coefficient measurement in water of various turbidity with AR and Kr lasers, interpreting results by Mie scattering theory
20 p2931 A72-39270
- TURBINE BLADES**
Graphite fiber composite fan blade design for subsonic turbofan engines, discussing weight and fatigue sensitivity reductions and performance test results
[SAE PAPER 710771] 01 p0116 A72-10265
- Clearance, friction and load effects on turbine blade root fastening stress distribution, comparing finite element method with photoelastic experimental results
01 p0141 A72-11048
- Nonuniform flow along axial turbomachine blades, presenting pressure loss evaluation method under boundary layer effect on external walls
01 p0002 A72-11271
- Natural bending-torsional vibrations of turbine blades connected by ring junctions, using dynamic pliability principle
01 p0143 A72-11370
- Turbine blades adaptability limits to temperature variations, considering rectangular cross section plastic rod under programmed thermal and tensile load cycles
01 p0143 A72-11372
- One dimensional unsteady flow in turbine engines rotating and static vane cascades, discussing vibrations propagation
02 p0202 A72-11584
- Differential nonstationary heat equations numerical solution for bladed gas turbine air cooled disk, taking into account cascade vertical temperature variation and coolant heating
02 p0301 A72-12251
- Heat transfer from gas to air-cooled turbine blade, obtaining solution by brute force technique
04 p0595 A72-14649
- Closed form equations for constrained torsion of turbine blades, estimating elastic twist and cross sectional deformation on analog computer
04 p0589 A72-15166
- Environmental effects on superalloy high temperature corrosion in gas turbines, noting blade surface temperature as critical factor
[ASME PAPER 71-WA/CD-1] 05 p0704 A72-15945
- Stress state of variable thickness long elastic shallow shell in bending and torsion, applying equations to large turbine blades
05 p0735 A72-15986
- Al and Al-Zr coating effects on heat resistant alloy turbine blades high temperature fatigue resistance under bending-torsion cyclic loads
05 p0671 A72-15990
- Through flow analysis of low speed axial flow compressor, deriving blades deviations and losses
05 p0600 A72-16114
- Radial inflow gas turbine rotating blades aerodynamic characteristics, noting exducer shape effect on turbine performance
05 p0601 A72-16484
- Superalloys for gas turbine rotor and stator blades, testing long term heating effects on microstructure and mechanical and thermal fatigue properties
05 p0675 A72-16495
- INCO 713C and IN 100 cast Ni base alloy gas turbine blades under thermal fatigue tests
05 p0675 A72-16497
- Turbine blade local heat transfer coefficient calculation with digital computer program and naphthalene blade mass transfer in cascade flow
05 p0747 A72-16498
- Turbine blade row coolant flow velocity, injection location and temperature effects on kinetic energy output
[AIAA PAPER 72-12] 05 p0707 A72-16866
- Film cooled turbine vanes external heat transfer distribution in turbulent gas stream, measuring heat transfer coefficients with and without blowing
[AIAA PAPER 72-9] 05 p0707 A72-16877
- Analytical models for predicting mass transfer cooling effects on blade row efficiency of turbine airfoils
[AIAA PAPER 72-11] 05 p0707 A72-16943
- Gas turbine blade cooling channel hydraulic resistance calculation based on energy and continuity equations
05 p0707 A72-17061
- Velocity and exit angle determination for flow behind turbine blade cascade with cooling air exhaust through blade trailing edges from continuity equations
05 p0707 A72-17063
- Gas turbine blade temperature measurement by radiation pyrometer, discussing thermal radiation sensing and fiber optics transmission, signal processing and real time temperature characteristic display
[SAE PAPER 720159] 06 p0812 A72-17321
- Velocity field induced by blade row in axial flow turbine
06 p0755 A72-17844
- Axial turbine three dimensional flow across blading compatible with velocity distribution, establishing mean surfaces of revolution equation
06 p0755 A72-17849
- Microstructure properties of heat resistant alloy for gas turbine blades as function of operational time
06 p0832 A72-18360
- Gas turbine blades fatigue crack development and failure analysis under thermal cycling tests, considering chemical processes and thermal and mechanical stresses
06 p0898 A72-18550
- Gas turbine blades thermal fatigue test and analysis, investigating static tensile loading effects on heat resistance under thermal cycling
06 p0899 A72-18556
- Stress and temperature fields in cooled gas turbine blades with allowance for elasticity, plasticity and creep
06 p0899 A72-18628
- Cyclic bending stress distribution in fir tree turbine blade root for arbitrary loading phase
06 p0899 A72-18629
- Stress distribution during plastic deformation of steel turbine disk from hardness measurements
06 p0900 A72-18670
- Gas turbine blades dynamics characteristics determination, investigating vibrational stresses, thermal cycles, alloy physicomechanical properties and coatings effects
06 p0900 A72-18683
- JP-5 fuel sulfur content effect on aircraft engine turbine blades hot corrosion under marine environmental conditions
07 p1010 A72-18752
- Economical performance of single rim supersonic turbine stage with repeated low level admission of working body
07 p0908 A72-18986
- Cavitation phenomena role in liquid drop impact erosion of steam turbine blades leading edges
07 p0967 A72-19262
- Boundary conditions in heat conduction for nozzle blades with shrouds exposed to cooling air on one side
08 p1222 A72-20945
- Gas flow analysis of heat transfer coefficient in turbine blade cascades of active and reactive profiles
08 p1222 A72-20946
- Steady heat conduction of cooled gas turbine hollow nozzle blades with gas temperature variation along cascade
08 p1223 A72-20948
- Steady heat conduction solution for gas turbine shrouded blade and disk of hyperbolic profile with central hole
08 p1223 A72-20949
- Numerical integration of unsteady heat conduction equations for gas turbine rotor with shrouded blades, using grid method
08 p1223 A72-20950
- Steady heat conduction solution for intensified cooling of turbine rotor blade leading edge with holes and air channel
08 p1223 A72-20951
- Ritz-Galerkin process applied to coupled differential equations of motion of pretwisted tapered cantilever turbine blade vibrating in flexure
08 p1244 A72-21483
- High speed rotating test rig development for vibration testing of turbine blades, describing design layout
08 p1147 A72-22131
- Vibration modes of bladed turbine wheel, formulating mathematical model
08 p1224 A72-22132
- Turbine blade root attachment service life determination from fatigue tests with T shaped models
09 p1373 A72-22300
- Ceramic fiber reinforced Ni base alloy for gas turbine blades, improving creep resistance at high temperatures
09 p1335 A72-22396
- Creep properties in turbine disks of heat resistant alloy under plastic deformation due to nonstationary thermal conditions
09 p1401 A72-22730
- Aerodynamic efficiency of plane slotted blade cascades of adjustable nozzle diaphragms in transport aircraft axial flow gas turbine engines
09 p1374 A72-23186
- Reynolds number and mainstream turbulence effects on laminar separation bubbles behavior in boundary layers on turbine blades in cascade
10 p1416 A72-23873
- Axial flow compressor and turbine loss coefficients, correlating blade rows geometric and aerodynamic variables effects
[ASME PAPER 72-GT-18] 11 p1703 A72-25617
- Four stage gas turbine, measuring blade surface roughness and profile changes effects on flow characteristics and efficiency
[ASME PAPER 72-GT-34] 11 p1704 A72-25630
- Small radial inflow turbines for space applications, considering blade-shroud clearance, blade loading and exit diffuser design
[ASME PAPER 72-GT-42] 11 p1704 A72-25636
- Two dimensional transonic turbine blade cascade downstream flow losses determination
[ASME PAPER 72-GT-43] 11 p1570 A72-25637

Two dimensional flow losses of turbine blade cascade with incompressible boundary layer injection [ASME PAPER 72-GT-46] 11 p1570 A72-25638

Supersonic turbine cascade flow properties and pressure distributions on blades, comparing calculated results with experimental data [ASME PAPER 72-GT-47] 11 p1570 A72-25639

High temperature metal fiber reinforced ceramic matrix composites for turbine vanes, showing strength toughness and crack depths dependence on interfacial bond [ASME PAPER 72-GT-51] 11 p1704 A72-25643

Local heat transfer coefficient distribution in multiple air jet cooled cavity, noting application to gas turbine blade leading edge cooling [ASME PAPER 72-GT-59] 11 p1745 A72-25650

Turbine blade alloys vibrational fatigue and creep properties under high and low frequency axisymmetric loads at room and elevated temperatures 11 p1662 A72-26798

Plastic materials adaptability to solid and hollow turbine blades, deriving thermally and mechanically induced stresses 11 p1738 A72-26799

Cooling efficiency and load endurance of aircraft turbine engine blades as function of ambient temperature and air flow rates 11 p1712 A72-26892

Ordered crystallization casting of Ni superalloys for turbine blades, using power down and high rate solidification processes 11 p1646 A72-26894

Turbine nozzle vanes edge losses dependence on profile edge thickness, allowing flow velocity variation 12 p1861 A72-28135

Energy dissipation for turbulent flow in turbine blades guide vanes calculated with allowance for effects of Reynolds number and turbulence intensity 12 p1752 A72-28137

Simulation model test for effects of cooling air exhaust into gas flow area on turbine blading efficiency, obtaining dimensionless expression for experimental data generalization 12 p1862 A72-28148

Semiempirical determination of local thermal fluxes and heat transfer coefficients for turbine blades based on thin film thermocouples 13 p2025 A72-28730

Computer program in ALGOL 60 language for calculation of long blades twist in axial flow turbines and compressors 13 p1893 A72-28782

Unsteady loading effects in high temperature fatigue tests of refractory alloys for turbine blades, noting steady and programmed notch tests 13 p1980 A72-29494

High temperature composite turbine blade materials, discussing service conditions and fiber/matrix selection, noting cast Ni and Mo based alloy fibers 14 p2125 A72-30533

Alloying characteristics of heat resistant Ni base Ni-Cr-Al-Ti-Nb-Mo disk alloy 15 p2255 A72-31566

Dispersion hardening Ni base alloys for gas turbine blades, considering composition, structure, gamma phase and embrittlement avoidance 15 p2255 A72-31568

Blade tip losses in bandaged axial turbines, noting effects of Mach number, initial flow turbulence and geometry 15 p2179 A72-31701

Mechanical properties of high temperature steels and alloys for gas turbine rotors, disks and blades 15 p2256 A72-31703

Boundary conditions for resonant frequencies calculation of turbine blades with Z-shaped and combined coupling sections 15 p2326 A72-31704

Turbine blade trailing edge wall thickness measurement by phase sensitive eddy current technique 16 p2397 A72-33201

Ceramic coatings measure the complex stresses in gas-turbine blades. 19 p2875 A72-37732

Stress calculations for lifetime prediction in turbine blades. [ONERA, TP NO. 1097] 19 p2875 A72-37770

Turbine engine sensors for high temperature applications. 19 p2802 A72-38048

Effect of the slope and curvature of meridional current lines on the long-blade twist in axial turbomachines 20 p2979 A72-39588

Heat transfer in a channel with a porous wall for turbine cooling application. [ASME PAPER 72-HT-39] 20 p2986 A72-39667

Characteristics of the thermal and stressed states of cooled shell-type blades 20 p2963 A72-39911

Aircraft engine lifetime and turbine blade reliability 20 p2963 A72-39916

Influence of cooling-air exhaust into the air-gas flow area on the flow-rate characteristics of cooled profiles 20 p2963 A72-39923

Influence of baffle geometry on heat transfer in the cooling channel of air-cooled blades 21 p3099 A72-41062

Creep test diagrams plotted to estimate heat resistance for turbine blades design, predicting fatigue life with allowance for loading cycle form and duration 21 p3123 A72-41366

Influence of deviations in the shape of the base surface on the precision of turbine blade machining operations 22 p3182 A72-41863

Nonstationary processes in the intervane apertures of turbomachines 22 p3133 A72-42247

Causes for the formation of internal discontinuities of the metal in forged blanks of turbine blades prepared from EI893 alloy 22 p3216 A72-42249

Precision forged turbine and compressor blades. 22 p3183 A72-42518

Pressure at the trailing edge and losses in turbine bladings with air injection into the blade wake 23 p3248 A72-43661

Gasdynamic investigation of a turbine with evaporative air cooling of the nozzle guide vanes 23 p3325 A72-43662

Three dimensional temperature distribution of internally cooled hollow airfoil section turbine blades, deriving heat transfer equations for digital computation 23 p3325 A72-43667

Gas turbine blades of cast ZhS6K heat resistant alloy, investigating structural strength from fatigue test data 23 p3347 A72-43734

Gas turbine blade models of heat resistant ZhS6K alloy under operational temperature variations, observing fatigue strength 23 p3347 A72-43735

Application of the method of hydrodynamic singularities to the calculation of the velocity distribution in doubly-periodic infinite blade cascade systems 24 p3390 A72-44874

Multi-node elements model of isoparametric thin shell vibration for turbine blade application 24 p3457 A72-44881

Determination of pressure losses in turbomachines. 24 p3393 A72-45353

Suction side velocity distribution parameter characteristic relationship to profile geometrical parameters in turbine blade cascade system 24 p3394 A72-45366

Frictionless core flow and friction layers at turbomachine walls and blades for real two dimensional cascade flow modeling 24 p3394 A72-45370

Aerodynamic characteristics of turbine blade cascades in unsteady incompressible and compressible fluid flow, considering axial flow turbine blades vibration 24 p3364 A72-45524

Solution of a boundary-value thermoelasticity problem for a turbine blade by the polymoment method 24 p3460 A72-45623

Heat release and resistance of the cylindrical heat exchangers of blades with a dual flow cooling system 24 p3434 A72-45625

Stress state of variable thickness long elastic shallow shell in bending and torsion, applying equations to large turbine blades 24 p3460 A72-45728

Al and Al-Zr coating effects on heat resistant alloy turbine blades high temperature fatigue resistance under bending-torsion cyclic loads 24 p3415 A72-45732

Microstructure properties of heat resistant alloy for gas turbine blades as function of operational time 24 p3416 A72-45747

TURBINE ENGINES

NT GAS TURBINE ENGINES

NT JET ENGINES

NT PULSEJET ENGINES

NT RAMJET ENGINES

NT SUPERSONIC COMBUSTION RAMJET ENGINES

NT TURBOFAN ENGINES

NT TURBOJET ENGINES

NT TURBOPROP ENGINES

Arnold Engineering Development Center turbine engine testing facilities and techniques for flight conditions and environment simulation, air/fuel flow and thrust measurement, etc [ASME PAPER 71-WA/GT-8] 05 p0642 A72-15901

Dusty inlet air filtering in aircraft turbine engines, discussing engine operation, dust and filter characteristics 05 p0704 A72-16179

Aircraft engines high pressure turbine guide vanes air cooling by internal insert, analyzing thermal stresses [AIAA PAPER 72-7] 05 p0707 A72-16864

Onboard and ground based hydraulic starter systems design, construction and operation for aircraft turbine engines 08 p1224 A72-21484

Accelerated full scale aircraft turbine engine corrosion tests in controlled environment, simulating salt, high temperature and humidity conditions [NACE PAPER 76] 10 p1528 A72-24320

Aircraft scheduled maintenance, discussing turbine engine and component reliability protection, controlled overhaul, test and repair 10 p1565 A72-24867

Hydraulic starter systems for aircraft turbine engines, examining operation loads and fluid supply and pressure requirements 11 p1702 A72-25284

Crash safe turbine fuel to reduce fire probability and severity during aircraft ground crash, investigating physical and chemical properties [ASME PAPER 72-GT-28] 11 p1702 A72-25624

Small radial inflow turbines for space applications, considering blade-shroud clearance, blade loading and exit diffuser design [ASME PAPER 72-GT-42] 11 p1704 A72-25636

Turbine aerodynamics research trends, covering engine cooling, high work factor turbines, pneumatic variable geometry and computer analysis 11 p1572 A72-26036

Inward radial flow turbines under unsteady flow conditions with full and partial admission, predicting performance by method of characteristics 12 p1751 A72-27349

Hodographic equations solution containing critical point for compressible fluid two dimensional flow, noting calculation of wing profiles and turbine engine cascades [ONERA, TP NO. 1048] 14 p2095 A72-30841

Turbulent flow between rotating disk and turbine engine body calculated from equations of axisymmetric viscous incompressible fluid flow 15 p2217 A72-31702

Ti alloys hot salt stress corrosion during turbine engine operation, noting effects of alloy processing conditions, surface properties and cyclic exposures 15 p2297 A72-32136

Russian book on aircraft turbine and spacecraft rocket engine assembly covering process schedules, work organization, precision, joints and couplings, quality control, etc 16 p2399 A72-33373

Procedure for the continuous sampling and measurement of gaseous emissions from aircraft turbine engines. [SAE ARP 1256] 18 p2721 A72-36532

TURBINE EXHAUST NOZZLES

Aladin 2 noiseless STOL jet aircraft project, describing exhaust nozzle configuration, design and economics 02 p0155 A72-12503

Two dimensional cascade test of air-cooled turbine nozzle, describing aerodynamic characteristics and heat transfer properties 05 p0602 A72-16489

Cascade nozzle gas particle flow properties, discussing flow pressure experiments and theory at different streamlines 05 p0602 A72-16490

Gas turbine nozzle guide vane trailing edge protection by air films cooled, measuring gas temperatures with chromel-alumel thermocouples 08 p1224 A72-21318

TURBINE INSTRUMENTS

Capacitive electret pressure sensors calibration for interior measurements in turbine engines, jets and exhaust nozzles [ONERA, TP NO. 982] 09 p1310 A72-22815

Compressor blade vibration indicator measurement by positioning one inductive sensor by rotor blades and another by toothed gear on rotor shaft 13 p1956 A72-28784

Optimal invariant conversion of information from a turbine flow meter and a capacitive fuel gauge 21 p3058 A72-41801

Pressure transmitter for flow parameter measurements of aerodynamic nozzles and static pressure taps rotating on turbine rotor blades 22 p3176 A72-42250

Study of a turbine type flowmeter with helical blades. 24 p3404 A72-45354

TURBINE PUMPS

Slit element flow in shear flow turbopump rotors, presenting solutions for laminar and turbulent flow between two parallel disks rotating with same angular velocity 02 p0204 A72-12227

Thermal modeling of space shuttle cryogenic turbopump, considering heat transfer for two-phase cryogen and gas impingement on turbine blades and rotating disks [ASME PAPER 71-WA/HT-43] 05 p0664 A72-15890

Turbopump rotating assembly bearing parameters and inertia products estimation and identification by extended Kalman filtering 08 p1173 A72-20844

Flexural vibrations of nonrotating turbopump rotor due to kinematic excitation of casing, deriving integral equation yielding stress-strain state and fatigue strength 12 p1886 A72-28150

Gas turbine pumps; Proceedings of the Joint Conference, San Francisco, Calif., March 26, 27, 1972. 18 p2693 A72-36040

Flow phenomena in turbomolecular pumps 18 p2696 A72-36837

Optimal arrangement of conical nozzles in a segment of a partial supersonic turbine stage 20 p2963 A72-39913

Determination of the probability for passage of molecules through the working rotor of a turbomolecular vacuum pump with nonparallel walls of the channel between vanes 22 p3139 A72-41862

A study of loss of radial equilibrium solution in axial-flow blade row design calculations. 24 p3393 A72-45358

TURBINE WHEELS

Dynamic characteristics of turborotor simulator supported on gas lubricated foil bearings of reduced length with starting and stopping unaided by external pressurization [ASME PAPER 71-LUB-16] 02 p0235 A72-11538

Stress concentration at eccentric holes and effect on strength of full size rotating turbine disks 03 p0450 A72-14108

Gas turbine wheel design analysis, presenting procedures for estimating revolution rates, blade numbers and component configurations effects on wheel weight for prescribed stresses 05 p0735 A72-15995

Materials research for investment cast turbine wheel, investigating Fe base specimens 05 p0666 A72-16496

Turbine rotating disk hyperbolic thickness critical profile by radial displacement solution 06 p0894 A72-17794

Dynamic properties of turbine wheels under bending vibrations, classifying resonant frequencies on basis of vibration modes 06 p0899 A72-18644

Dimensionless functions for heat transfer coefficients on blade cascade rotor surfaces of axial flow gas turbine for arbitrary ambient air temperature 08 p1223 A72-20947

Steady heat conduction solution for gas turbine shrouded blade and disk of hyperbolic profile with central hole 08 p1223 A72-20949

Profile thickness effect on air cooling of gas turbine disks in central and peripheral sections 08 p1223 A72-20952

Temperature measurements of axial gas turbine rotor for start-up heating and cooling tests 08 p1223 A72-20953

Vibration modes of bladed turbine wheel, formulating mathematical model 08 p1224 A72-22132

Rotor blades setting angle and twist influence on steam turbine wheels vibrational modes and frequency spectra 11 p1732 A72-25537

Linear maximization of turbine disk natural vibration frequencies combination, solving optimal control problem via Pontryagin maximum principle 11 p1734 A72-25727

Heat transfer to casing in axial clearance space between nozzle diaphragm and turbine wheel 12 p1861 A72-28134

Flexural vibrations of nonrotating turbopump rotor due to kinematic excitation of casing, deriving integral equation yielding stress-strain state and fatigue strength 12 p1886 A72-28150

Cyclic nonisothermal plastic deformation of ductile disk, verifying experimentally with turbine disk of heat resistant alloys 13 p2053 A72-28398

Temperature effects on nonelastic behavior of turbine rotor disk for steady and cyclic loading, noting creep solutions, transient stress and plastic strain 14 p2167 A72-30906

Mechanical properties of high temperature steels and alloys for gas turbine rotors, disks and blades 15 p2256 A72-31703

Balancing procedure for statically determinate turbine rotors with multiple supports 16 p2443 A72-33241

Evaluation of the tendency to brittle fracture of turbine rotors made from steels of medium strength 19 p2876 A72-38001

Influence of the structural format on the range of critical rotational speeds of rotors in aircraft engines 20 p2963 A72-39801

Formulation of boundary conditions in the statement of thermal problems for bladed rotors of gas turbines 20 p2987 A72-39926

Experimental investigation of the elastic characteristics of composite bearings in turbine machinery

for the purpose of increasing their efficiency and reliability during nonlinear vibrations of the rotor 22 p3181 A72-41860

Postoperative states of turbine disk alloys at 280-500 and 550-630 C, noting lower durability values 23 p3347 A72-43737

Investigation of the state of the structure of turbine-disk materials after operation 23 p3302 A72-43965

Optimal modes of operation of a centripetal-compressor wheel with preswirling of the flow 24 p3364 A72-45622

Gas turbine wheel design analysis, presenting procedures for estimating revolution rates, blade numbers and component configurations effects on wheel weight for prescribed stresses 24 p3460 A72-45737

TURBINES

NT AXIAL FLOW TURBINES

NT GAS TURBINES

NT SHROUDED TURBINES

NT STEAM TURBINES

NT SUPERSONIC TURBINES

Circular network analysis by conformal mapping method, evaluating physical and geometric magnitudes in turbine driven machinery 04 p0461 A72-14514

Soviet book on hydraulics, hydraulic machines and hydraulic drives covering fluid dynamics, pipe flows, jet pumps, turbines, bladed transmissions, etc 04 p0466 A72-15247

Turbine casing components stresses in presence of creep, demonstrating calculation method validity for thick-walled structures by elastoplastic analogy 05 p0734 A72-15985

Determination of the efficiency and range of application of turbines with velocity stages with the aid of the complex power coefficient 23 p3325 A72-43666

Turbine casing components stresses in presence of creep, demonstrating calculation method validity for thick-walled structures by elastoplastic analogy 24 p3460 A72-45727

TURBOALTERNATORS

U AC GENERATORS

U TURBOGENERATORS

TURBOCHARGERS

U TURBOCOMPRESSORS

TURBOCOMPRESSORS

Jet aircraft turbofan engine fan compressor noise reduction by acoustic linings, giving R and D results [BAS PAPER 71 SA6] 01 p0115 A72-10223

Thermal radial stresses in axial compressor disk-drum transition areas of operating AM-3 aircraft engine 01 p0143 A72-11374

Axial compressors lengthwise compaction and compression ratio increase per unit length by blade chords and clearances reduction and blades number proportional increase 02 p0271 A72-12740

[DGLR PAPER 71-098]

Chaplygin compressibility law in calculation of flow characteristics around compressor blading of axial turbomachines 03 p0308 A72-13544

Periodic pressure fluctuations measurements on fixed blades of high power axial compressor, describing calibration and data acquisition methods [ONERA, TP NO. 967] 04 p0463 A72-15555

Performance similarity of supersonic axial compressors with gas mixtures of different thermodynamic properties, verifying validity of critical Mach number of rotation [ONERA, TP NO. 966] 04 p0463 A72-15556

Through flow analysis of low speed axial flow compressor, deriving blades deviations and losses 05 p0600 A72-16114

Supersonic axial flow shock-in-rotor type compressor performance tests, discussing factors responsible for low efficiency 05 p0601 A72-16481

Transonic compressor design for minimum number of stages and hub/tip ratio and maximum inlet axial velocity, assuming axisymmetric flow 05 p0601 A72-16482

Axial flow multistage compressor design, discussing high speed flow measurements and Reynolds number and blade airfoil shape effect on aerodynamic performance 05 p0601 A72-16483

Two dimensional cascade performance data correction for rotating blade row stream surface inclination in axial flow turbines 05 p0602 A72-16486

Stalled blade rows dynamic performance in terms of blade channel fluid inertia and surface boundary layer-caused time delay 05 p0602 A72-16487

Bleed air type gas turbine compressor development, presenting reliability improvement program 05 p0705 A72-16500

Multistage axial flow compressor adjustment by flow geometrical dimension changes obtaining in-

fluence coefficient from linearized mathematical model 05 p0708 A72-17064

Cascade wind tunnel and water table determination for trajectories and velocities of suspended particles in fluid flow through axial compressor stage 07 p0907 A72-18756

Circumferential inlet pressure distortion index derivation for high hub-tip ratio multistage axial flow compressor from one dimensional isentropic flow expressions 07 p1053 A72-18762

Turbojet engine compressor efficiency relationship to cascade characteristics diagram, using influence coefficients 07 p1054 A72-18995

Compressibility effects on straight through labyrinth seal performance in regenerative turbomachine 08 p1178 A72-21935

Partial load computation for axial flow compressor stages, describing computer method limitations 09 p1374 A72-22632

Secondary flow types and measurement in axial flow compressor cascades, discussing energy losses 09 p1260 A72-22633

Secondary losses reduction procedure in axial flow turbine stages, using boundary layer fences on blades profile suction side 09 p1374 A72-22634

Two spool gas turbine engine characteristics with speed reduction, determining time dependence of turbocompressor rpm, gas temperature and engine power 09 p1374 A72-23185

Equations of motion of steady viscous fluid flow in three dimensional boundary layer on walls of axial flow compressors and turbines, obtaining velocity field 10 p1420 A72-25120

Three component flow calculation at inlet of axial flow compressor stage, linearizing hydrodynamic equations of ideal incompressible fluid with velocity perturbations 10 p1420 A72-25132

Finite difference method application to axial flow compressors rotating stall nonlinear analysis, taking into account blade row characteristics [ASME PAPER 72-GT-3] 11 p1568 A72-25606

Noise reduction effects of wake interaction between rotor blade rows in axial flow compressor, cancelling velocity defect at stator position [ASME PAPER 72-GT-15] 11 p1569 A72-25614

Axial flow compressor and turbine loss coefficients, correlating blade rows geometric and aerodynamic variables effects 11 p1703 A72-25617

[ASME PAPER 72-GT-18]

Shocked flow and pressure loss computation for axial flow compressor cascades, using time dependent finite difference technique [ASME PAPER 72-GT-31] 11 p1569 A72-25627

Turbocompressor deceleration cascades blades surface roughness effects on boundary layer, noting pressure and velocity distributions [ASME PAPER 72-GT-48] 11 p1570 A72-25640

Flow measurement instrumentation for turbomachine rotors, noting telemetry type data transmission system with strain gauge pressure transducers for turbocompressor [ASME PAPER 72-GT-55] 11 p1630 A72-25646

Flow data reduction validity for supersonic axial compressors, presenting experimental results for rotating supersonic cascade [ASME PAPER 72-GT-100] 11 p1571 A72-25669

Steady state radial inlet pressure distortion index for axial flow compressor, examining radial velocity, continuity equation and mathematical model [ASME PAPER 72-GT-109] 11 p1571 A72-25673

Measurement of spatially coherent and incoherent structure of axial compressor-generated noise modes propagating in duct [ONERA, TP NO. 1045] 12 p1861 A72-28049

Computer program in ALGOL 60 language for calculation of long blades twist in axial flow turbines and compressors 13 p1893 A72-28782

Subsonic and supersonic heavily loaded axial flow rotors noise, discussing helicopter blade slap effect and compressor rotor-stator interaction 13 p1897 A72-29570

Fan engine compressor noise measurement by spinning mode synthesizer for use in duct liner optimization 13 p2028 A72-29574

Noise generated by free flow turbulence incident on rotor or stator in axial flow fans and compressors, noting sound spectrum dependence 13 p2028 A72-29575

Linear mathematical model for twin shaft gas turbine with isolated turbocompressor, calculating dynamic constants as function of operational modes 14 p2146 A72-30581

Stage removal and addition effect on multistage axial compressor for application in engine design 15 p2179 A72-31706

Velocity profiles for three dimensional turbulent boundary layer on end wall of axial flow compressor cascade passage under adverse pressure gradients

16 p2342 A72-32901

Influence of the angle of attack on the performance of high-deflection stator blades

17 p2484 A72-34889

Pressurized air assisted gas turbine fuel system, describing single stage centrifugal turbocompressor and rotary-lobe compressor designs and performance characteristics

18 p2694 A72-36043

Behavior of boundary layers on rough compressor blades

18 p2641 A72-36420

Interaction effects between blade rows in turbomachines.

19 p2745 A72-37275

German monograph - Computational and experimental investigations regarding the operational characteristics of a three-stage axial-flow compressor with high performance per stage

19 p2745 A72-37490

Effect of the slope and curvature of meridional current lines on the long-blade twist in axial turbomachines

20 p2979 A72-39588

Iterative solution to aerodynamic design of axial flow compressors used in turbojet engines, calculating meridional velocity distribution

21 p3099 A72-40930

Engine inlet total pressure distortion effects on multistage axial compressor and turbojet/turbofan engine performance and stability, considering inlet-engine compatibility

21 p2991 A72-41144

The development of inlet flow distortions in multistage axial compressors of high hub-tip ratio.

21 p3099 A72-41145

Digital computer controlled testing equipment for separately driven coaxial gas turbine low and high pressure compressors, emphasizing reliability and flexibility in system design

22 p3157 A72-42682

Measurement, in a duct, of the space-structure of the discrete-frequency noise generated by an axial compressor.

22 p3216 A72-42913

Analysis by hydraulic analogy of rotating separation in compressors

22 p3167 A72-43091

Effect of the ratio of the axial-flow velocities in front of and behind the cascade on the aerodynamic coefficients of a plane compressor cascade

24 p3360 A72-44995

A study of loss of radial equilibrium solution in axial-flow blade row design calculations.

24 p3393 A72-45358

Flow analysis in the axial-flow compressor impeller with meridional stream acceleration.

24 p3394 A72-45371

Optimal modes of operation of a centripetal-compressor wheel with preswirling of the flow

24 p3364 A72-45622

TURBOCONVERTERS

U TURBOGENERATORS

TURBOELECTRIC CONVERSION

U TURBOGENERATORS

TURBOFAN AIRCRAFT

NT CONCORDE AIRCRAFT

Industry assisted state of art assessment of high lift turbofan configurations for USAF STOL tactical transport technology program

[SAE PAPER 710758] 01 p0003 A72-10255

Mach 0.80 quiet intercity STOL transport design comparison for turbofan, prop-fan and turboprop systems

[SAE PAPER 710759] 01 p0003 A72-10256

Trainer-combat turbojet or turbofan aircraft characteristics, comparing flight, weight, size, maintenance and development costs

05 p0611 A72-16178

Eight-place turbofan powered business jet aircraft design, discussing structure, fuel system, engines crew station and safety features

08 p1109 A72-21572

Application of advanced methods to the determination of design loads of the Lockheed L-1011 TriStar.

[AIAA PAPER 72-775] 19 p2752 A72-38134

Fan jet Falcon design and certification tests.

24 p3366 A72-44731

TURBOFAN ENGINES

Jet aircraft turbofan engine fan compressor noise reduction by acoustic linings, giving R and D results

[BAS PAPER 71 SA6] 01 p0115 A72-10223

Graphite fiber composite fan blade design for subsonic turbofan engines, discussing weight and fatigue sensitivity reductions and performance test results

[SAE PAPER 710771] 01 p0116 A72-10265

Small three spool, reverse and mixed flow turbofan engine for business jets, discussing fuel consumption reduction, thermodynamic performance, efficiency and maintainability

[SAE PAPER 710776] 01 p0116 A72-10268

CF6 high bypass ratio turbofan engine design improvements for fuel consumption, thrust/weight ratio, starting, noise level, smoke emission, maintenance, monitoring and accessory replacement

[SAE PAPER 710779] 01 p0117 A72-10271

GE CF6-50 high-bypass two-spool engine development, discussing configuration, installation, endurance tests and various failures

03 p0406 A72-13681

National Aviation System technology, discussing wide body jets, smokeless turbofans, all-weather operational capability, collision avoidance and noise reduction

04 p0597 A72-14824

Aerodynamic characteristics of STOL aircraft with externally blown jet augmented flaps, predicting interference between lifting surfaces and turbofan engines

[AIAA PAPER 72-63] 05 p0609 A72-16953

F-14 Tomcat test program for hydraulic systems, spinning, low speed performance, stalling, afterburning turbofan engines, in-flight refueling and automatic telemetry equipment

06 p0758 A72-17582

Fighter/attack aircraft turbojet and turbofan engines testing with/without afterburners

06 p0868 A72-18495

Catapult steam ingestion test of turbofan engines in A-7 aircraft, correlating compressor stall occurrences with temperature increase rate in distorted region

07 p1052 A72-18760

Inlet duct and turbofan engine compatibility without stalling and surge conditions obtained by design optimization and wind tunnel testing

07 p1052 A72-18761

JT15D turbofan engine antiicing system development, discussing icing test program and results

07 p1053 A72-18765

Astafan turbofan engine with variable pitch fan rotor blades for thrust variation, discussing gearbox and core engine design

07 p1055 A72-20459

Commercially available aircraft turbofan engines specifications, describing design features and performance characteristics

07 p1055 A72-20625

Transient characteristics and steady state off-design operation of mixed and unmixed type turbofan engines, noting peculiarities in control characteristics

09 p1374 A72-22626

Dynamic model of high bypass ratio turbofan engines for L-1011 wind tunnel flutter test program

[AIAA PAPER 72-376] 11 p1703 A72-25400

Two spool geared fan jet engine design and development for general aviation, discussing performance, reliability and ecological aspects

[SAE PAPER 720351] 11 p1703 A72-25602

High bypass ratio JT15D-1 turbofan engine design and development testing

[SAE PAPER 720352] 11 p1703 A72-25603

Variable pitch ultrahigh bypass ratio ducted fan engine design for STOL transport aircraft

[ASME PAPER 72-GT-61] 11 p1704 A72-25652

Turbofan engine trends for short haul conventional and STOL aircraft, considering variable pitch fans, reduction gears, thrust reversal and noise and environmental pollution

[ASME PAPER 72-GT-86] 11 p1705 A72-25661

Turbomeca Astafan geared fan engine with axial centrifugal compressor design, specifications and performance

12 p1861 A72-27748

Composite turbofan blades for high temperature applications, discussing weight reduction and design procedure

12 p1816 A72-28102

Low noise aircraft-engine configuration feasibility, discussing turbofan engine noise reduction

15 p2181 A72-32322

RB 211 three-shaft turbofan engine for L-1011 airliner, describing design for noise reduction

15 p2298 A72-32428

F-100 and F-401 turbofan engine design and development for F-15 and F-14, discussing impingement cooling, Ti alloys, powder metallurgy and metal composites, etc

17 p2597 A72-34390

Specific fuel consumption and specific thrust optimization methods in turbofan cycles, noting optimum fan pressure ratio increase with turbine inlet temperature

19 p2848 A72-37746

Thermodynamic cycle parameter effects on bypass turbofan jet engine fuel consumption and performance under various flight conditions and engine ratings

23 p3326 A72-44281

TURBOFANS

NASA Quiet Engine experimental program for jet aircraft noise reduction, discussing aerodynamic and acoustic evaluation and tests of three fans

03 p0406 A72-13679

Multiple pure tone noise generation from turbofan blade to blade nonuniformities in rotor geometry, using two dimensional inviscid flow model

04 p0565 A72-15568

Turbofan multiple pure tone noise analysis, discussing rotor geometry, relative Mach number and incidence angle effect on sound emission

[AIAA PAPER 72-127] 05 p0706 A72-16824

Stator blade design to shield turbofan from pressure disturbances arising in downstream subsonic duct

[AIAA PAPER 72-84] 05 p0707 A72-16883

High tip speed low loading transonic fan rotor design for weak oblique shocks with improved efficiency and stall margin

[AIAA PAPER 72-83] 07 p0907 A72-18951

Variable pitch fans for STOL aircraft thrust/shaft engine, noting short field capability and quietness

09 p1374 A72-23447

Jet turbine engine front fans with and without snubbers, estimating flow field by streamline curvature technique

[ASME PAPER 72-GT-4] 11 p1568 A72-25607

Low pressure ratio Q-FAN propulsor noise reduction tests on wind tunnel model, discussing source components and design configurations

[ASME PAPER 72-GT-40] 11 p1569 A72-25634

Turboprop lift fan design developed for XV-5 VTOL research aircraft, reviewing changes for future commercial and research transport systems

[ASME PAPER 72-GT-111] 11 p1576 A72-25674

Interaction effects between blade rows in turbomachines.

19 p2745 A72-37275

NASA program for low cost turbojet and turbofan engine fabrication for missile and light aircraft propulsion

19 p2848 A72-37637

Installation caused flow distortion and its effect on noise from a fan designed for turbofan engines.

[AIAA PAPER 72-1006] 21 p2993 A72-41590

Tone noise from rotor/stator interactions in high speed fans.

24 p3433 A72-44917

TURBOGENERATORS

Aircraft turboalternator governing theory for frequency error detection, comparing performance of mechanical- and electro-hydraulic governors

06 p0868 A72-18249

Onboard turbogenerator igniter operating conditions determination from fuel-air ratio obtained from nomogram

12 p1861 A72-28145

Digital computer studies of control loop parameters and configurations effects on performance of synchronous turbogenerator with two field windings

15 p2183 A72-32793

TURBOJET AIRCRAFT

U JET AIRCRAFT

TURBOJET ENGINE CONTROL

Spectrometric oil analysis program /SOAP/ method for turbojet and helicopter transmissions damage monitoring and flight safety

09 p1319 A72-22933

Aircraft jet-engine control; Conference, Velešín, Czechoslovakia, June 12-16, 1972, Proceedings

23 p3326 A72-44276

Determination of the operational transfer functions of a gas turbine engine on a digital computer

23 p3327 A72-44292

TURBOJET ENGINES

NT TURBOFAN ENGINES

NT TURBOPROP ENGINES

Turbojet aircraft engine overhauling planning and execution, discussing dismantling, washing, galvanic treatments, acceptance checks and quality controls

05 p0643 A72-16014

Jet noise simple-source theory experimental verification, determining relation of measured sound power and jet pressure levels of turbojet engine

06 p0867 A72-17856

Fighter/attack aircraft turbojet and turbofan engines testing with/without afterburners

06 p0868 A72-18495

Simulated testing of turbojet engine ingestion of missile exhaust, determining design criteria for aircraft engine inlets from altitude chamber test data

07 p1052 A72-18758

Turbojet engine compressor efficiency relationship to cascade characteristics diagram, using influence coefficients

07 p1054 A72-18995

Steady axisymmetrical twisted gas flow parameters in channels with geometries similar to turbojet engine units

08 p1149 A72-21310

Runway fog dispersal system based on underground installed flight-discarded turbojet engines, discussing system efficiency and economics

09 p1292 A72-22910

Turbojet engine oil circuit contamination rate determination by spectrometric analysis, obtaining mathematical theory for data interpretation

[SAE PAPER 720303] 11 p1703 A72-25567

Turbojet simulator for supersonic wind tunnel models, simulating inlet mass flow ratio and exhaust nozzle pressure ratio

[ASME PAPER 72-GT-89] 11 p1705 A72-25664

- Air bleeding location to cool turbojet engine turbine of supersonic aircraft, presenting graphs
12 p1862 A72-28147
- NASA program for low cost turbojet and turbofan engine fabrication for missile and light aircraft propulsion
19 p2848 A72-37637
- Aircraft engine lifetime and turbine blade reliability
20 p2963 A72-39916
- Fluid flow across balance surface moving at constant velocity relative to coordinate system, calculating energy balance of turbojet engine
21 p3099 A72-40814
- Iterative solution to aerodynamic design of axial flow compressors used in turbojet engines, calculating meridional velocity distribution
21 p3099 A72-40930
- TURBOMACHINE BLADES**
NT COMPRESSOR BLADES
NT ROTOR BLADES [TURBOMACHINERY]
NT STATOR BLADES
NT TURBINE BLADES
- Turbomachine blade frequency disalignment effects on resonant vibrations and stress distribution, using wheel model and computer solution
01 p0143 A72-11367
- Resonant vibration and stresses of dynamically nonuniform annular cascade under aerodynamic interaction of alternating different blades
01 p0143 A72-11368
- Natural vibrations and resonant stresses of turbomachine blade rings and elastic bodies with cyclic symmetry, noting paradoxical frequency decrease
01 p0143 A72-11369
- Blade cascades pressure distribution for plane incompressible flow with boundary layer separation near trailing edges, replacing blade profiles by vortex fields
[DGLR PAPER 71-097] 02 p0153 A72-12728
- Two dimensional unsteady flow of incompressible fluid around passing turbomachine blades, determining instantaneous pressure, forces and moments as function of time
04 p0463 A72-15559
- Circular arc blades two dimensional cascade performance test data for various cambers comparison with potential theory data
05 p0602 A72-16485
- Two dimensional cascade performance data correction for rotating blade row stream surface inclination in axial flow turbines
05 p0602 A72-16486
- Finite pitch airfoil theory relations for turbomachine moving blade rows interference effect on cascade flutter
05 p0738 A72-16488
- Viscous flow through movable and immovable cascades of blades, determining velocity field by airfoil center line vortex distribution
06 p0757 A72-18131
- Cascading turbomachine blades vibration measurement in subsonic and sonic high temperature gas flows, describing test facility
06 p0797 A72-18689
- Unsteady lift on airfoils in moving cascades with inlet axial flow disturbances, estimating lift on reference blade between blade channels
[ASME PAPER 72-GT-5] 11 p1568 A72-25608
- Aerodynamic damping of turbomachine blade vibrations under varied conditions of stagger angle, pressure ratio and relative velocity, using pure bending mode excitation
[ASME PAPER 72-GT-8] 11 p1568 A72-25611
- Hodograph method involving conformal mapping for turbomachine blade subsonic flow profile calculation
[ASME PAPER 72-GT-41] 11 p1570 A72-25635
- Fatigue testing of blade materials at high temperatures with periodic spray moistening by liquid corrosive medium
12 p1829 A72-27459
- Interaction effects between blade rows in turbomachines.
19 p2745 A72-37275
- Dispersion hardening fabrication of hollow cooled blades of thin cermet layer and embedded plastic metal core, using aluminum oxynitrate in water-alcohol solution
19 p2809 A72-38282
- Dynamic strength of tangentially wound toothed blade roots
20 p2979 A72-39586
- Some problems in the mathematical simulation of blade vibrations in turbomachines
21 p3116 A72-40169
- Unsteady aerodynamic and aeroelastic effects in turbomachine blade cascades supersonic flow, discussing trends in fan and compressor technology
21 p3118 A72-40969
- Study of a turbine type flowmeter with helical blades.
24 p3404 A72-45354
- TURBOMACHINERY**
NT AXIAL FLOW TURBINES
NT CENTRIFUGAL COMPRESSORS
- NT CENTRIFUGAL PUMPS
NT GAS TURBINES
NT SHROUDED TURBINES
NT STEAM TURBINES
NT SUPERSONIC TURBINES
NT TURBINE PUMPS
NT TURBINES
NT TURBOCOMPRESSORS
NT TURBOFANS
NT TURBOGENERATORS
- Uniqueness of turbomachinery flow calculations using streamline curvature and matrix through-flow methods
03 p0308 A72-13648
- Aircraft turbo-alternator speed control for constant frequency power supply, presenting theoretical relationships for electrohydraulic or mechohydraulic control loops
04 p0466 A72-15462
- Navier-Stokes equations solution for unsteady viscous flow around oscillating elliptic airfoil in turbomachinery flutter analysis, obtaining pressure and shear stress distributions
05 p0600 A72-16002
- Axial flow turbomachines three dimensional flow theory, using orthogonal curved coordinate system
07 p0910 A72-20104
- Contactless induction multipoint current sensor design and operation principles for turbomachine rotating component temperature measurement
09 p1310 A72-22740
- Centrifugal turboengine diffuser with high enlargement area compared with logarithmic spiral types, discussing boundary layers, secondary flow, shapes and aerodynamic parameters
10 p1463 A72-23747
- Hydraulic tank application to internal flow visualization in turbomachinery, describing test equipment and methods used for axial flow model
10 p1419 A72-24654
- Computer method of optimal turbomachine disk design, using local search techniques to determine disk minimum weight
15 p2328 A72-31746
- Laser Doppler velocimetry system design for optical measurement of intrablade flow velocity in turbomachinery
15 p2237 A72-32045
- The acoustics of axial flow machines.
18 p2685 A72-37204
- Experimental investigation of the elastic characteristics of composite bearings in turbine machinery for the purpose of increasing their efficiency and reliability during nonlinear vibrations of the rotor
22 p3181 A72-41860
- The dynamics and control of Eulerian turbomachines.
[ASME PAPER 72-AUT-S] 23 p3279 A72-43633
- Determination of pressure losses in turbomachines.
24 p3393 A72-45353
- A method for estimation of axial turbomachinery stage characteristics on the basis of experimentally obtained data with a runner tested in a free blow-out aerodynamical scheme.
24 p3363 A72-45364
- Study of a viscous flow in rotating centrifugal impellers.
24 p3363 A72-45368
- Investigation of a partial admission double-vane-ring stage with bypass of the second ring
24 p3364 A72-45621
- TURBOPROP AIRCRAFT**
NT ELECTRA AIRCRAFT
- Mach 0.80 quiet intercity STOL transport design comparison for turbofan, prop-fan and turboprop systems
[SAE PAPER 710759] 01 p0003 A72-10256
- Russian book on An-12 turboprop transport aircraft structural and aerodynamic characteristics covering engine operation, piloting, stability, controllability, etc
12 p1755 A72-28343
- Acoustic measurements for STOL turboprop transport aircraft propeller configurations under static, taxi and flyover conditions, discussing quiet propeller noise signature
13 p1897 A72-29571
- Twin-turboprop transport aircraft, helicopter and all-terrain ground vehicle simulators, discussing control load, visual attachment, cabin motion and sound subsystems
14 p2092 A72-30845
- The DHC-7, first generation transport category STOL - Particular design challenges.
[ALAA PAPER 72-809] 19 p2750 A72-38115
- TURBOPROP ENGINES**
- Altitude-velocity dependence of turboprop engine equivalent horse power, propeller output and specific fuel consumption, discussing performance characteristics relation to ambient air temperature
05 p0708 A72-17100
- Turboprop electric igniter climatic test problems and equipment for assessing quality control
07 p0954 A72-19112
- T63/250 engine program current status, covering turboshaft helicopter engine and fixed wing aircraft powerplant models and applications
[SAE PAPER 720350] 11 p1703 A72-25601
- Turbine inlet gas temperature limiting systems design and operation in turboprop engines, describing blocking mechanism, delaying element and altitude compensation
12 p1861 A72-27863
- Turboprop engines dynamic parameters experimental determination by rpm transient response to instantaneous fuel supply changes
13 p2027 A72-29137
- Mathematical model for dynamics simulation of aircraft turboprop engines, using digital, analog and hybrid computers
23 p3327 A72-44288
- TURBOPUMPS**
U TURBINE PUMPS
- TURBOROTORS**
U TURBINE WHEELS
- TURBOshafts**
- T63/250 engine program current status, covering turboshaft helicopter engine and fixed wing aircraft powerplant models and applications
[SAE PAPER 720350] 11 p1703 A72-25601
- Air lubricated bearings for high performance aircraft gas turbines, studying design and performance in turboshaft engine
[ASME PAPER 72-GT-38] 11 p1638 A72-25632
- Linear mathematical model for twin shaft gas turbine with isolated turbocompressor, calculating dynamic constants as function of operational modes
14 p2146 A72-30581
- Lynx helicopter RS 360 turboshaft engine, describing modular design for maintainability
17 p2597 A72-34927
- TURBOSUPERCHARGERS**
U TURBOCOMPRESSORS
- TURBULENCE**
NT ATMOSPHERIC TURBULENCE
NT CLEAR AIR TURBULENCE
NT GUSTS
NT HOMOGENEOUS TURBULENCE
NT ISOTROPIC TURBULENCE
NT LOW LEVEL TURBULENCE
NT LOW TURBULENCE
NT MAGNETOHYDRODYNAMIC TURBULENCE
NT PLASMA TURBULENCE
- Book on random functions and turbulence covering probability theory, random processes and fields, statistical correlation and spectral methods, numerical weather forecasting, etc
05 p0649 A72-16397
- Wiener-Hermite random variable expansion technique with time dependent base for turbulence applied to Burger equation
07 p0967 A72-19502
- Antisymmetric turbulence linear stability in incompressible plane Poiseuille flow between flexible walls solved by variational boundary value problem formulation
10 p1468 A72-24372
- Goldberg and Unno method application to microturbulent velocity determination in stellar atmosphere with convection
13 p2047 A72-29732
- Relaxation oscillations in dynamic systems describing turbulence in fluid, rigid body and particle motions
15 p2263 A72-31755
- Heat conduction in infinite incompressible fluid with turbulent velocity field, deriving physically impossible growth in time of long-wavelength modes of average temperature
16 p2424 A72-33127
- Laser velocimeter measurement of Reynolds stress and turbulence in dilute polymer solutions.
17 p2541 A72-35252
- Statistical models and turbulence; Proceedings of the Symposium, University of California, La Jolla, Calif., July 15-21, 1971.
18 p2676 A72-36001
- Two fluid model for qualitative interpretation of turbulent intermittency, noting governing equations analogy to Landau equations for superfluidity
19 p2787 A72-38428
- TURBULENCE EFFECTS**
- Air flow and acoustic characteristics of speech sounds produced with turbulence noise at glottal constriction, using flow equations
[AD-744389] 01 p0101 A72-10162
- Asymptotic intensity fluctuations of plane light wave propagating in turbulent medium, using parabolic equation and Markov model
01 p0050 A72-10348
- Isothermally contracting turbulent gas sphere for stellar formation from extension of Chandrasekhar work on Jeans criterion for static turbulent medium
01 p0129 A72-10799
- Sonic boom pressure signatures during F-104 overflights at Mach 1.3 and 30,000 ft, explaining variations by atmospheric turbulence
01 p0006 A72-11158

Far field diffraction due to annular apertures of plane wave light rendered partially coherent by atmospheric turbulence

01 p0103 A72-11166

Multiple scattering of incident coherent light wave propagating in turbulent medium, considering irradiance intensity fluctuations and spectral and correlation characteristics

01 p0103 A72-11167

Narrow groove theory for spiral groove viscous pump gas bearings generalized to include rarefied gas and turbulence effects

[ASME PAPER 71-LUB-1] Aircraft ride comfort problem in turbulent air, comparing free and fixed wing aircraft responses

02 p0234 A72-11531

Turbulence intensity effects on mass transfer from cylinders in cross flow at various Reynolds numbers

[ASME PAPER 70-WA/HT-3] Turbulence degree effects on aerodynamic properties of planar decelerating cascades at Reynolds numbers 50,000-250,000, discussing blade boundary layer characteristics

[DGLR PAPER 71-096] Steady state turbulent solar magnetic fields dynamic evolution, considering weak random magnetic excitation in electrically conducting fluid under varying kinematic conditions

02 p0153 A72-12716

Atmospheric turbulence induced laser beam spread estimation from spherical wave modulation transfer function

03 p0430 A72-13336

Image blurring effects due to atmospheric boundary layer refractivity turbulent fluctuations during remote optical radiation source observations

03 p0367 A72-13442

Solar magnetic field generation by gyrotropic turbulence, noting inadequacy of Steenbeck explanation for quantitative estimates of solar cycle parameters

03 p0359 A72-13482

Two dimensional meridional ozone model for seasonal ozone concentration behavior at 15-45 km, taking into account advective and turbulent effects

03 p0436 A72-13825

CAT inducing atmospheric conditions effects on SST flight, discussing turbulence in convective clouds and kinetic energy spectra of atmospheric motions

03 p0351 A72-14360

Small amplitude velocity waves turbulent distribution in infinite medium, demonstrating kinematic dynamo regeneration

04 p0543 A72-14693

Laser light beam attenuation, considering turbulent pulsation effects in closed channel fluid flow axial region

04 p0573 A72-14906

Amplitude fluctuations of laser beam with Gaussian amplitude distribution on short line-of-sight path propagation through artificial turbulent atmosphere

04 p0530 A72-14989

Optical wave front transmission through turbulent atmosphere, predicting saturation phenomenon accompanying sea level turbulence

04 p0488 A72-15383

Angular momentum and Li diffusive transport induced by mild thermally driven turbulence associated with Goldreich-Schubert-Fricke instability, discussing solar rotation slowdown

[AD-735988] Mean velocity and turbulent fluctuation distributions for sub- and supersonic jets in convergent nozzles, obtaining sound power spectra

05 p0690 A72-16675

Atmospheric turbulence effects on aircraft flight and design, covering accidents and costs, turbulence generation, prediction, measurements and load alleviation devices

[AIAA PAPER 72-157] Atmospheric turbulence induced scintillations of Intelsat geostationary satellite signals at 4 and 6 GHz

[AIAA PAPER 72-179] Electromagnetic wave scattering from curved rough surfaces and transmission through turbulent medium, obtaining solution by spatial Fourier transform of three transfer functions product

05 p0651 A72-16872

Atmospheric contrast degradation and turbulence effects on photography from space with computerized optimization of ground resolution

05 p0684 A72-16885

Statistical equations for turbulent fluctuations of energy, concentration and rotation in compressible flows

05 p0631 A72-16966

Cardiac murmur level dependence on blood stream Reynolds number, tracing cardiac noise origin to blood turbulence

05 p0631 A72-16966

Turbulence effects in stratified shearing flow, determining relationship between measured mass flux and overall Richardson number

06 p0771 A72-17340

Pressure gradient effects on hypersonic turbulent skin friction and boundary layer temperature, velocity and Mach number distributions and shape factors

06 p0799 A72-17923

Cyclonic turbulence generation of large scale magnetic field of Galaxy, using Steenbeck differential rotation mechanism

06 p0883 A72-18017

Thunderstorm flight testing for evaluation of rain, ice, lightning and turbulence effects on aircraft, engine and systems operating characteristics

06 p0760 A72-18500

Droplets coalescence in clouds, considering microturbulence effects due to laminar shear flow

07 p1030 A72-19102

Dynamic model of galactic clusters in terms of cosmological turbulence, estimating velocity dispersion and rotation and chaotic velocity contributions to kinetic energy

07 p1076 A72-19805

Similarity theory for turbulently stratified fluid with horizontal and vertical dimensionalities analysis, discussing Karman constant dependence

07 p1031 A72-20698

Wind shear, turbulence, precipitation, temperature, visibility and ceiling effects on airport capacity, suggesting weather data integration into ATC system for pilots information

08 p1147 A72-21521

Solar magnetic fields forced latitudinal drift rate due to differential rotation, taking into account turbulent friction and pressure forces

09 p1382 A72-22286

Turbulent LF electric field fluctuations relationship with disturbed F region, spread F and scintillations of radio stars and satellites

09 p1300 A72-23025

Nonlinear longitudinal aerodynamic characteristics effect on rigid aircraft response to normal acceleration due to atmospheric turbulence, using power spectral technique

09 p1263 A72-23461

Conical diffuser response to velocity distribution and turbulence intensity at inlet

10 p1416 A72-23858

Reynolds number and mainstream turbulence effects on laminar separation bubbles behavior in boundary layers on turbine blades in cascade

10 p1416 A72-23873

Kinematic and thermal turbulent fluctuations isolation by means of hot-wire anemometric probe

10 p1479 A72-24055

Nonlinear hydrodynamic effects in dynamic motions of metagalactic turbulence in pre-Friedmann universe

10 p1536 A72-24141

Turbulence generated sound due to interaction with sound absorbent liners, investigating dynamic process via rigid boundary model with homogeneous array of circular orifices or pistons

10 p1511 A72-24424

Turbulence theory 2/3 law applicability to optical spherical wave propagation through turbulent atmosphere, comparing to von Karman model

11 p1686 A72-25772

Cyclonic turbulence generation of large scale magnetic field of Galaxy, using Steenbeck differential rotation mechanism

11 p1718 A72-25953

Image blurring effects due to atmospheric boundary layer refractivity turbulent fluctuations during remote optical radiation source observations

11 p1633 A72-26252

High intensity free stream turbulence effects on flow past circular cylinder at subcritical Reynolds numbers, measuring unsteady lift and drag

11 p1573 A72-26640

Correlation function of depolarized finite collimated Gaussian laser beam in atmospheric turbulent medium

11 p1599 A72-26748

Telescope performance reciprocity in laser transmitter or optical heterodyne receiver functionings, considering atmospheric turbulence effects

11 p1636 A72-26750

Small transport aircraft horizontal tail surfaces flow characteristics determination for stress calculation during flight in turbulent atmosphere

14 p2071 A72-30284

Atmospheric turbulence induced wave front distortion effects on fast-tracking laser antenna performance, considering infinite plane wave random complex phase modulation

14 p2110 A72-30550

Low-altitude flight imposed psychophysiological stresses due to air turbulence discomfort, instrument dial vibration and ground-based navigational objects recognition difficulty

14 p2080 A72-30747

Free stream turbulence effect on mass transfer from circular cylinder in cross flow as function of Schmidt and Reynolds numbers, using electrochemical measurement method

14 p2096 A72-31061

Turbulence effects on electron, ion, aerosol, water vapor and ozone concentration in atmospheric layers

15 p2222 A72-31395

Turbulence and nonlinear thermal blooming effects as cause of refractive attenuation of laser beam intensities

15 p2249 A72-32160

Extended Huygens-Fresnel principle for mutual coherence /cross correlation/ function of finite optical beam propagation in turbulent medium

15 p2249 A72-32161

Low cost flight simulator for general aviation pilot training, containing IFB instrumentation and turbulence injection device

15 p2214 A72-32211

Optical measurements of electric fields turbulence level in gun plasma, noting compatibility with spatial Landau damping

15 p2287 A72-32409

Single degree of freedom system displacement response exceedance of given level under nonstationary random excitation, considering aircraft flight through turbulent region with variable intensity

15 p2279 A72-32592

Focused light beam intensity fluctuations measurements during passage through turbulent atmosphere, discussing random walks effects on dispersion

16 p2364 A72-33494

Infinite cross section electron beam interaction with infinite turbulent plasma slab with finite thickness

16 p2438 A72-33831

Turbulence induced sound pressure level measurement for noise generated by grill in air flow, using streamlined probe microphone

16 p2344 A72-34001

Energy balance equation of free turbulent boundary layer in incompressible fluid, deriving semiempirical formulas for turbulent viscosity coefficient

16 p2380 A72-34022

Atmospheric surface layer temperature, humidity and vertical wind velocity variances dependence on turbulent fluctuation inputs

16 p2419 A72-34148

Gaussian electromagnetic radiation beam propagation in turbulent medium, calculating broadening dependence on outer scale by modified Karman spectrum characterization

17 p2580 A72-34291

On galaxy formation from primeval universal turbulence. The effect of atmospheric turbulence on the error of an optoelectronic angle sensor.

17 p2606 A72-34574

Combustion product plasma electrical conductivity dependence on neutral component density fluctuation

17 p2554 A72-34941

Heat conduction in a turbulent magnetic field, with application to solar-wind electrons.

17 p2590 A72-35136

Vortex model of galactic clusters evolution, estimating velocity dispersion and rotation and chaotic velocity contributions to kinetic energy

17 p2601 A72-35584

Book - The earth's atmosphere

17 p2617 A72-35729

Combustion noise generation by burning fuel-air mixtures induced pressure fluctuations as result of time variable heat release rate due to turbulence

17 p2550 A72-35797

Atmospheric turbulence and the ATC system.

18 p2741 A72-36505

Automatic structural mode control system with aerodynamic vanes for B-1 strategic bomber turbulence excitation during low altitude terrain following missions

18 p2663 A72-37049

An experimental study of the sensitivity to free-stream turbulence of heat transfer in wakes of cylinders in crossflow.

19 p2751 A72-38132

Secondary flows in ducts of square cross-section.

19 p2787 A72-38396

19 p2879 A72-38795

- Similarity theory for turbulence in stratified fluid from horizontal and vertical dimensional analysis approach, discussing Karman constant dependence 20 p2948 A72-39013
- Electrostatic, reticular vorticity, turbulence effects and equivalences with tensional and spectral elastic fields. 20 p2953 A72-39419
- An advanced stochastic model for threshold crossing studies of rotor blade vibrations. 20 p2885 A72-39622
- Improving diffuser performance by artificial means. 20 p2885 A72-39624
- Propagation of weak shock waves through turbulence. 21 p3044 A72-40114
- Resonant growing standing internal gravity waves, considering transient behavior, numerical results, break due to local gravitational instability, maximum amplitude and secondary flow generation 21 p3048 A72-40648
- Low frequency electrostatic waves in a turbulent plasma. 21 p3092 A72-41221
- Physical model of the onset of turbulent burning of compacted systems in a half-closed volume 21 p3131 A72-41699
- Effect of external turbulence on the boundary layer of a flow 22 p3166 A72-42258
- Analytical method for combining the interaction of inlet distortion and turbulence. 23 p3247 A72-43330
- Turbulent mixing of three plane isothermal jets with various velocity ratios, showing jet initial length shortening due to initial turbulence increase 23 p3279 A72-43657
- Study of target edge response viewed through atmospheric turbulence over water. 23 p3289 A72-43896
- Ultrasonic holography in large phase disturbance. 23 p3290 A72-43950
- Forward scattering of laser coherent light by acoustic or turbulent wave pressure variations, noting phase fluctuation spectrum 23 p3313 A72-44113
- Parasitic pitch angle diffusion of radiation belt particles by ion cyclotron waves. 23 p3333 A72-44527
- Book - The effects of the turbulent atmosphere on wave propagation. 24 p3379 A72-44650
- Dynamic simulation of an aircraft under the effect of vortex wake turbulence. 24 p3368 A72-45346
- TURBULENCE METERS**
- Optical acoustic field recordings application to turbulent characteristics measurement for transparent media 05 p0660 A72-15848
- Dynamic calibration of inclined and crossed hot-wire flowmeters for absolute turbulence intensity measurements, using known sinusoidal oscillations in steady flow 11 p1636 A72-26637
- Hot-wire probes to measure turbulent three dimensional flows with allowance for transducer directional sensitivity 11 p1636 A72-26698
- Laser Doppler-type remote sensor for wind velocity and atmospheric turbulence measurements 13 p1956 A72-28859
- Optical acoustic field recordings application to turbulent characteristics measurement for transparent media of fluid flows 15 p2232 A72-31267
- Experimental facility and diffusion technique for measuring turbulence characteristics during hydrocarbon fuels burning in air streams 23 p3287 A72-43658
- TURBULENT AIR CURRENTS**
- U AIR CURRENTS**
- U TURBULENT FLOW**
- TURBULENT BOUNDARY LAYER**
- Acoustic power radiated by jet aircraft fuselage structure exposed to turbulent boundary layer pressure field, evaluating noise reduction treatments 01 p0002 A72-10216
- Unsteady flow about two dimensional airfoils, determining surface pressure fluctuations induced by turbulent boundary layers 01 p0001 A72-10217
- Increasing lift and Reynolds number effects on displacement and skin friction of three dimensional turbulent boundary layer on infinite swept wing 01 p0002 A72-11395
- Iterative solutions for three dimensional turbulent boundary layers on rotating nose-body, using streamwise and cross flow momentum equations 01 p0002 A72-11397
- Turbulent boundary layer flow past surface with arbitrary temperature distribution, presenting approximate heat transfer solution with allowance for pressure gradient and Reynolds number 02 p0201 A72-11582
- Velocity profiles of turbulent boundary layers with injection or suction through porous walls as function of momentum thickness by Truckenbrodt method 02 p0202 A72-11663
- Flat plate incompressible smooth surface boundary layer examination emphasizing turbulence production near wall, using hydrogen-bubble and hot-wire measurements with dye visualization 02 p0203 A72-11975
- Turbulent boundary layer fluid dynamic behavior under transpiration and acceleration effects, presenting mean velocity profile data, skin friction and mixing length model [ASME PAPER 71-HT-F] 02 p0205 A72-12315
- Two and three dimensional turbulent boundary layer development in incompressible and compressible flows, obtaining boundary layer equations similarity solutions via mixing length model [DGLR PAPER 71-066] 02 p0206 A72-12719
- Compressible turbulent boundary layer equations for flow on B wall of MHD accelerator, including electron thermal nonequilibrium and finite rate ionization 03 p0397 A72-13923
- Diffusion rate of diluted drag reducing polymers in turbulent boundary layer 03 p0343 A72-14319
- Suppressed turbulent diffusion of drag reducing polymer solution in turbulent boundary layer, measuring concentration with laser-phototransistor unit [AD-737467] 03 p0343 A72-14321
- Flexible surface effects on shear stress fluctuations beneath turbulent boundary layer, using fiber optic displacement probe 03 p0343 A72-14324
- Asymptotic theory of heat transfer in two dimensional turbulent boundary layers of incompressible fluid at large Reynolds numbers 03 p0459 A72-14390
- Geometrical and aerodynamic characteristics of circular cross section diffuser channels from turbulent boundary layer calculation at preseparation flow stage 04 p0461 A72-14647
- Pressure field calculations for random vibrations in wide class of elastic shells containing acoustic medium, discussing turbulent boundary layer-caused pulsations 04 p0586 A72-15010
- Spatial structure coherence in sublayer of turbulent boundary layer, using spanwise flow hot-wire anemometer measurements 04 p0462 A72-15116
- Noise generation from turbulent supersonic shear layers, including low supersonic and transonic ranges for jet noise applications 04 p0463 A72-15566
- Longitudinal curvature effects on laminar and turbulent boundary layer flows predicted from Navier-Stokes equations, noting mixing length assumption validity [ASME PAPER 71-WA/FE-37] 05 p0645 A72-15920
- Integral methods application to turbulent corner flow problem, obtaining mean velocity profile first approximation for turbulent boundary layer with streamwise pressure gradient [ASME PAPER 71-WA/FE-36] 05 p0646 A72-15921
- Flow separation of turbulent boundary layer ahead of inward-projecting normal step predicted by rotational flow analysis via iterative solution [ASME PAPER 71-WA/FE-32] 05 p0599 A72-15924
- Computerized calculations of turbulent shear layers with compressibility, heat transfer, three dimensionality or unsteady flow, using differential equation [ASME PAPER 71-WA/FE-8] 05 p0646 A72-15934
- Integral computation for nonequilibrium compressible turbulent boundary layers using moment, momentum and skin friction equations [ASME PAPER 71-WA/APM-12] 05 p0647 A72-15968
- Frequency-contrast characteristics of optical system producing image of distant object in turbulent boundary layer of atmosphere, determining refractive index fluctuation intensities 05 p0689 A72-16172
- Heat flux calculation in laminar turbulent boundary layer transition zone using Schlichting model of turbulent spot formation 05 p0649 A72-16222
- Heat transfer in kinetic burning in turbulent boundary layer on porous surface for carbon dioxide blown in air stream with dissociated oxygen 05 p0746 A72-16223
- Compressible turbulent boundary layer properties on porous cone at Mach 8, examining Crocco theory for flows with mass addition 05 p0602 A72-16536
- Jet interaction induced supersonic turbulent boundary layer separation, obtaining flat plate pressure measurements and jet plume shadowgraphs 05 p0602 A72-16537
- Velocity profile shapes computation in supersonic compressible turbulent boundary layers with adverse pressure gradients, discussing data and theory discrepancy, curvature, and three dimensional effects 05 p0649 A72-16544
- Turbulent boundary layer on yawed flat plate, measuring velocity profiles and flow directions [DFVLR-SONDDR-177] 05 p0603 A72-16703
- High resolution mean flow and turbulence measurements in turbulent boundary layer on cooled hypersonic wind tunnel side wall at Mach 9.37 [AIAA PAPER 72-73] 05 p0650 A72-16802
- Finite periodic beam response to turbulent boundary layer pressure field fluctuation, using transfer matrix technique [AIAA PAPER 72-171] 05 p0650 A72-16832
- Turbulence generation in hypersonic boundary layer from hot-wire correlation and disturbance convection velocity measurements on cone-ogive-cylinder in Mach 7.2 flow [AIAA PAPER 72-182] 05 p0650 A72-16837
- Mass transfer effects on hypersonic turbulent boundary layer properties from profile measurements on porous cone [AIAA PAPER 72-184] 05 p0650 A72-16839
- Three dimensional hypersonic turbulent boundary layer under normal and longitudinal pressure gradients and cross flow along windward symmetry plane of body of revolution [AIAA PAPER 72-186] 05 p0605 A72-16841
- Finite difference integration based on theoretical model analysis of three dimensional turbulent boundary layer on sharp cone at angle of attack in supersonic flow [AIAA PAPER 72-187] 05 p0650 A72-16842
- Flexible elastic plate nonlinear vibration response and noise transmission from turbulent boundary layer by Monte Carlo technique, discussing subsonic and supersonic flow regions [AIAA PAPER 72-199] 05 p0651 A72-16850
- Pressure gradient effect on mixing length for equilibrium turbulent boundary layers, calculating eddy viscosity [AIAA PAPER 72-213] 05 p0651 A72-16855
- Turbulent boundary layer development for airfoil at high transonic speeds, discussing viscous-inviscid flow interaction [AIAA PAPER 72-5] 05 p0606 A72-16863
- Supersonic turbulent boundary layer interaction with compression corner, noting static pressure distributions, flow visualization and schlieren photographs [AIAA PAPER 72-114] 05 p0610 A72-16976
- Two dimensional turbulent boundary layer before rectangular step, investigating heat exchange in separation regions 05 p0751 A72-17048
- Low turbulence wind tunnel with closed circuit design and pressure gradient adjustment capability for turbulent boundary layer studies 06 p0795 A72-17713
- Similitude solutions for turbulent boundary layers in compressible flow with pressure gradient and heat transfer at wall, obtaining velocity and enthalpy profiles 06 p0798 A72-17845
- Asymptotic theory of turbulent boundary layer in incompressible liquid with positive pressure gradient and injection 06 p0799 A72-17910
- Supersonic near wake flow around blunt and sharp cones with trailing edge turbulent boundary layer 06 p0737 A72-18141
- Turbulent layer generation in ideal two dimensional fluid flow, determining vortices time evolution from initial velocity discontinuity by numerical methods 06 p0802 A72-18525
- Turbulence model for near-wall boundary layer flows, solving differential equations for kinetic energy and length scale 06 p0802 A72-18527
- Wall blowing discontinuity effect on two dimensional incompressible turbulent boundary layers, discussing flow relaxation length separation by penetration point trajectory 07 p0966 A72-18841
- Attached and separated turbulent viscous regions resulting from shock wave-boundary layer interactions in hypersonic flow [AIAA PAPER 72-74] 07 p0966 A72-18949
- Continuum plasma turbulent boundary layer structure in shear flow, showing electron to ion saturation currents ratio decrease from laminar case [AIAA PAPER 72-107] 07 p1040 A72-18953
- Monograph on three dimensional turbulent boundary layers in unsteady incompressible flow covering flow equations, eddy viscosity and mixing length models, etc 07 p0968 A72-19953
- Two dimensional compressible boundary layer turbulent velocity profile on adiabatic and isothermally cooled walls with zero pressure gradient 07 p0970 A72-20080
- Turbulent boundary layer model with eddy viscosity representation of inner wall region for cases with suction or injection, presenting wall shear calculation method 07 p0973 A72-20248

Heat transfer characteristics of transpired and accelerated turbulent boundary layer on porous plate, comparing with prediction techniques [ASME PAPER 71-HT-BB] 08 p1251 A72-20880

Laminar and turbulent wall boundary layer and shock attenuation effects on flow uniformity in shock tubes 08 p1149 A72-21018

Air injection from wall slot into turbulent boundary layer of high temperature gas channel flow, calculating film cooling effectiveness in flat plate 08 p1252 A72-21316

Near wall collateral layer with velocity vector magnitude changes existence in three dimensional turbulent boundary layer flow 08 p1150 A72-21615

Flat plate boundary layer transition equations for supersonic wind tunnels, taking into account free stream turbulence 08 p1150 A72-21616

Modified mixing length velocity distribution predictions for turbulent boundary layers with uniform mass transfer for low and high Reynolds numbers 08 p1150 A72-21622

Yaw calibrations of Preston tubes for wall shear stress measurements in two and three dimensional turbulent boundary layers 08 p1254 A72-21627

Initial dynamic length effects on heat transfer in turbulent boundary layer with blowing demonstrated by subsonic wind tunnel tests 08 p1151 A72-21665

Earth location effect in Fresnel diffraction zone on comparator performance, measuring phase difference fluctuations in turbulent atmospheric boundary layer radio waves 09 p1284 A72-22232

Boundary layer stability and turbulence observation by flow visualization using dense Al flake suspension 09 p1292 A72-22304

Mixing length model for computing three dimensional turbulent boundary layers with small cross flow [ONERA, TP NO. 985] 09 p1294 A72-22817

Mixing length model for turbulent boundary layer in incompressible flow with fluid injection at wall, extending solution to compressible case [ONERA, TP NO. 986] 09 p1294 A72-22818

Pressure recovery calculation for subsonic adiabatic air flow through diffusers with tail pipes, assuming turbulent inlet boundary layer 10 p1415 A72-23855

Turbulent boundary layer growth measurement on annular diffuser containing free vortex swirl 10 p1416 A72-23857

Rotational, centrifugal and Coriolis force effects on turbulent boundary layer development, discussing changes in structure and shear stress distribution 10 p1464 A72-23870

Asymmetry and intermittency factors of temperature and velocity fluctuations in viscous substrate of hot plate turbulent boundary layer 10 p1464 A72-24064

Wall law for axisymmetric turbulent boundary layers in zero pressure gradient fluid flow through circular cylinders, noting negative and positive wake regions [ASME PAPER 71-APM-VV] 10 p1465 A72-24177

Turbulent boundary layer characteristics of rotating helical blade in annulus contained fluid, calculating boundary layer growth and streamline angles via momentum integral equations 10 p1466 A72-24296

Wind tunnel investigation of adiabatic compressible turbulent boundary layer in adverse and favorable pressure gradients at supersonic speed 10 p1468 A72-24421

Laminar and turbulent boundary layer flow stability with forward separation areas 10 p1418 A72-24535

Two and three dimensional turbulent boundary layers integral calculation method, presenting similarity solutions based on extended mixing length model 10 p1469 A72-24653

Fluctuating turbulent stresses effects on flow over wavy boundary, comparing calculated with measured pressure distributions [AD-742545] 10 p1470 A72-25066

Adverse pressure gradients effect on two dimensional supersonic turbulent boundary layer, measuring axial distribution of pressure, temperature, mass flow, turbulence intensity and wall shear [AIAA PAPER 72-311] 11 p1614 A72-25245

Hydrodynamics of turbulent free convection boundary layer on vertical flat plate and ethyl alcohol film 11 p1743 A72-25258

Heat transfer and laminarization prediction by two equation turbulence model for accelerated boundary layer flows at low Reynolds number 11 p1743 A72-25260

Rectangular skin panel vibration modes aerodynamic damping dependence on Mach number, dynamic pressure, mode shape and turbulent boundary layer thickness [AIAA PAPER 72-402] 11 p1568 A72-25243

Compressible turbulent boundary layer with arbitrary pressure gradients on solid or permeable surfaces, using extended mixing length theory 11 p1616 A72-25917

Supersonic axisymmetric turbulent boundary layer characteristics over circular cone, predicting blowing effect on separation 11 p1617 A72-25995

Transverse outflow effects on flow field characteristics of hypersonic finite span separated flows with turbulent boundary layer 11 p1572 A72-26004

Impact probe displacement effects in supersonic turbulent boundary layer in terms of Mach number profiles 11 p1572 A72-26005

Turbulent separating and reattaching supersonic boundary layer flows in two dimensional compression corner, noting Reynolds number effect on separated shear layer length 11 p1618 A72-26634

Surface roughness effects on air flow in turbulent atmospheric boundary layer, using finite difference method 12 p1838 A72-27026

Primary velocities distribution in two dimensional turbulent boundary layer inside dihedral 12 p1797 A72-27179

Ekman boundary layer in two level quasi-geostrophic general circulation numerical model, representing physical characteristics of boundary layer turbulence increase with height 12 p1840 A72-27708

Turbulent gas flow mass transfer coefficient derived from Lapin relation between vertical velocity and concentration distributions in turbulent boundary layer near semipermeable surface 12 p1889 A72-28136

Numerical methods for inverse solution to turbulent swirling boundary layer combustion flow problem 13 p2063 A72-28420

Wind shear third and fourth moments and distribution function in atmospheric boundary layer, emphasizing longitudinal turbulent velocity vertical variations 13 p1993 A72-28860

Surface temperature distribution for porous plate in supersonic flow with gas injection into turbulent boundary layer 13 p1893 A72-28917

Acoustic dipole radiation by wall pressure fluctuations in turbulent boundary layer flow over rigid and plane surface at low Mach number 13 p1894 A72-29583

Subsonic flow in separation zones of three dimensional turbulent boundary layer forming in front of cylindrical projections, rectangular parallelepipeds and shields 13 p1895 A72-29881

Isothermal vertical plate turbulent thermal boundary layer during free convection, noting temperature pulsations dispersion 13 p2066 A72-29899

Hypersonic turbulent boundary layer flow parameters and heat exchange during blowing of coolant air and He through slot 13 p1895 A72-29901

Large scale motion of turbulent boundary layer during relaminarization under strong pressure gradient, obtaining fluctuating velocity components and tangential Reynolds stress 13 p1944 A72-30028

Modulation transfer functions of optical system producing image of distant object in turbulent boundary layer of atmosphere, determining refractive index fluctuation intensities 14 p2130 A72-30241

Viscosity, velocity gradient and wall effects on pitot tube measurement of gas flow velocity measurement in turbulent boundary sublayer 14 p2094 A72-30294

Turbulent Ekman boundary layer characteristics in laboratory rotating apparatus compared with atmospheric field observation data and theories, noting similarity relation validity 14 p2094 A72-30418

Air injection as neutral atmospheric boundary layer thickening simulation, presenting mean velocity and turbulence intensity profiles 14 p2093 A72-30849

Reichardt mixing model for turbulent boundary layer calculation in wall flow, noting supersonic and nonisothermal jet flow 14 p2095 A72-31002

Recovery factors on porous surface within gas screen region in supersonic turbulent boundary layer for various air injection rates 14 p2070 A72-31017

Turbulent boundary layer separation zone subsonic flow before two dimensional rectangular step, examining flow pattern and static pressure distribution 14 p2096 A72-31020

Air and carbon dioxide intensive injection effects on turbulent boundary layer of subsonic channel air flow 14 p2097 A72-31159

Shear stress distribution and local heat flux at surface of axisymmetric bodies for laminar and turbulent boundary layer flows 14 p2071 A72-31163

Wind tunnel measurement of intermittency in turbulent boundary layer on porous plate for alternating laminar and turbulent air flow 15 p2217 A72-31610

Two dimensional incompressible turbulent boundary layer in arbitrary pressure gradient, obtaining mathematical model for solution by implicit finite difference method 15 p2217 A72-31718

Higher moments of Reynolds stress fluctuations and velocity components in turbulent boundary layer, obtaining probability density distributions 15 p2218 A72-32401

Subsonic and supersonic steady two dimensional compressible turbulent boundary layer flow past wavy wall, presenting wall pressure and temperature distributions 16 p2341 A72-32828

Three dimensional compressible turbulent boundary layer growth prediction, deriving entrainment equations from two dimensional incompressible flow relations 16 p2375 A72-32835

Velocity profiles for three dimensional turbulent boundary layer on end wall of axial flow compressor cascade passage under adverse pressure gradients 16 p2342 A72-32901

Pressure, shear stress and yaw angle measurements in flow through aircraft intake S-shaped ducts with turbulent boundary layer at entry, noting vortex generation 16 p2377 A72-33403

Blowing and suction effects on heat transfer and friction coefficients of transpired turbulent boundary layer, presenting theoretical models and experimental results 16 p2378 A72-33431

Incompressible flow drag caused by slot suction provided in bodies of revolution for preventing laminar boundary layer transition into turbulent state 16 p2344 A72-33678

Energy balance equation of free turbulent boundary layer in incompressible fluid, deriving semiempirical formulas for turbulent viscosity coefficient 16 p2380 A72-34022

Shock wave interactions with nozzle wall turbulent boundary layer, discussing shock strength variation to produce unseparated, incipient and fully separated flow fields [AIAA PAPER 72-715] 16 p2380 A72-34030

Three dimensional small perturbation effects on laminar and turbulent low and high speed boundary layer flows [AIAA PAPER 72-713] 16 p2344 A72-34034

Numerical finite difference prediction of inert turbulent boundary layer swirling jet flow, using nonisotropic energy-length model [AIAA PAPER 72-699] 16 p2380 A72-34044

Small cross flow integral method for growth prediction of three dimensional compressible turbulent boundary layers on adiabatic walls [AIAA PAPER 72-697] 16 p2345 A72-34046

Asymptotic character of turbulent boundary layer longitudinal velocity distribution along flat plate at low Reynolds number, using Hirsch theory for potential flow 17 p2539 A72-34900

On the structure of hypersonic turbulent boundary layers 17 p2540 A72-35188

The response of a turbulent boundary layer to a step change in surface roughness. II - Rough-to-smooth. 17 p2540 A72-35199

Nonlinear panel response from a turbulent boundary layer 17 p2632 A72-35222

Calculations of the turbulent boundary layer in supersonic nozzles. 17 p2485 A72-35237

Hypersonic wake aerodynamics at high Reynolds numbers. [AIAA PAPER 72-701] 17 p2486 A72-35484

Turbulent boundary layer with discontinuity in wall temperature and concentration 17 p2638 A72-35744

Shear stresses distribution in isothermal incompressible turbulent boundary layer with positive pressure gradient by diffusers in open jet wind tunnel 17 p2544 A72-35930

On the extension of particular solutions of the energy equation of compressible turbulent boundary layers. 17 p2544 A72-35955

Statistical self-similarity and inertial subrange turbulence. 18 p2678 A72-36022

Stress state and velocity fluctuations in a perturbed boundary layer 18 p2680 A72-36464

- Calculation of the development of a turbulent boundary layer in the presence of an equally turbulent external field - Experimental verification 18 p2680 A72-36469
- Experimental study of the structure of a turbulent boundary layer on a plate with helium injection 18 p2682 A72-36888
- Transition to a turbulent flow mode in the boundary layer of a plane plate with various turbulence scales in the incident flow 18 p2682 A72-36889
- Velocity profile measurements in a turbulent boundary layer on a permeable plate 18 p2642 A72-37184
- Flow equations for flat plate turbulent boundary layer with Reynolds, continuity and energy components, deriving semiempirical differential equation for turbulence scale 19 p2785 A72-37471
- Statistical characteristics of surface pressure pulsations in turbulent boundary layer of incompressible fluid, discussing effects near smooth flat wall 19 p2785 A72-37472
- Solution of the equations of the compressible boundary layer /laminar, transition, turbulent/ by an implicit finite difference technique. 19 p2785 A72-37521
- German monograph - A photometric method for measuring the concentration distribution in turbulent boundary layers 19 p2799 A72-37652
- Integral and correlation methods for separation and reattachment phenomena in aerodynamics, applying to turbulent boundary layer [ONERA, TP NO. 1072] 19 p2786 A72-37762
- Boundary layer closure in the conical shock tube. 19 p2788 A72-38431
- Similarity predictions for shear stress and heat flux cospectral behavior in atmospheric turbulent boundary layer 19 p2829 A72-38560
- Re-developing turbulent boundary layers behind yawed separation bubbles. 19 p2747 A72-38812
- Viscous sublayer pulsations elongation in longitudinal direction, noting decay of turbulent friction near wall as third power of distance from wall 20 p2912 A72-39360
- Pressure pulsations relationship to fixed boundary of turbulent flow with kinematic structure, considering phase transitions effect 20 p2912 A72-39361
- Pressure pulsation measurements at nose of well-streamlined body of revolution at high Reynolds numbers, noting turbulent pressure field intensity growth and decay 20 p2912 A72-39362
- Turbulent boundary layer static pressure and heat exchange dependence on gas injection through porous surface 20 p2912 A72-39363
- Turbulent boundary layer calculation, investigating surface roughness, pressure gradient and surface temperature effects 20 p2912 A72-39365
- Cooled supersonic turbulent boundary layer separated by a forward facing step. 20 p2886 A72-39632
- The prediction of compressible turbulent boundary-layer flows with mass addition. [ASME PAPER 72-HT-58] 20 p2914 A72-39658
- Analytical and low-speed experimental diffusion-thermo effects in turbulent binary boundary layers. [ASME PAPER 72-HT-56] 20 p2985 A72-39660
- Film cooling effect on surface heat transfer in laminarizing mainstream turbulent boundary layer for injection through flush angled two dimensional slots [ASME PAPER 72-HT-11] 20 p2986 A72-39682
- A two-equation model of turbulence applied to the prediction of heat and mass transfer in wall boundary layers. [ASME PAPER 72-HT-15] 20 p2986 A72-39685
- Prediction of turbulent boundary layer heat transfer with pressure gradient and mass transfer. [ASME PAPER 72-HT-16] 20 p2987 A72-39686
- Some features of instantaneous point source diffusion within a turbulent boundary layer. 21 p3078 A72-40467
- Laminar and turbulent boundary-layer studies at hypersonic speeds. [ICAS PAPER 72-09] 21 p2990 A72-41134
- Theoretical and experimental study of the pressure and heat-flux distributions on a control surface in the presence of a thick hypersonic turbulent boundary layer [ICAS PAPER 72-23] 21 p2991 A72-41148
- Perturbation analysis of aerodynamic test flow in Ludwig tubes, investigating nonsteady coupling effects on nozzle turbulent boundary layer [AIAA PAPER 72-994] 21 p2993 A72-41580
- Time scales and correlations in a turbulent boundary layer. 21 p3047 A72-41626
- Measurements of Reynolds shear stress fluctuations in a turbulent boundary layer. 21 p3047 A72-41638
- Fundamental studies of turbulent boundary layers with injection or suction through porous wall. III - Investigations on the separation of turbulent boundary layers in strong adverse pressure gradients with injection through porous flat plate. 22 p3165 A72-41945
- Flat compressible turbulent boundary layers of air, predicting foreign gas injection effects on mass and heat transfer Stanton numbers and skin friction 22 p3165 A72-41958
- Differential equations for heat transfer in turbulent boundary layer flow of incompressible fluid with constant thermophysical characteristics 22 p3166 A72-42253
- Velocity distribution in turbulent air flow over perforated plates with gas injection in turbulent boundary layer 22 p3166 A72-42256
- Effect of external turbulence on the boundary layer of a flow 22 p3166 A72-42258
- Wind tunnel measurement for demonstrating similarity of atmospheric turbulent boundary layer mean velocity and shear stress at high Reynolds number 22 p3201 A72-42598
- Analysis of the structure of the flow downstream of a sudden widening 22 p3167 A72-42643
- Vibration measurements of an airplane fuselage structure. I - Turbulent boundary layer excitation. II - Jet noise excitation. 22 p3139 A72-42912
- German monograph - Contribution to the experimental investigation of the heat transfer in a turbulent wall boundary layer in the region of a strong pressure rise. 22 p3167 A72-43064
- Calculation of separation points in incompressible turbulent flows. 23 p3279 A72-43328
- Influence of wall temperature on heat transfer in a compressible three-dimensional turbulent boundary layer 23 p3248 A72-43694
- Influence of wall injection on the turbulent tensions in the exterior regions of a boundary layer 23 p3279 A72-43698
- A simple theory for the two-dimensional compressible turbulent boundary layer. [ASME PAPER 72-FE-15] 23 p3280 A72-44062
- Interferograms of turbulent boundary layer separation in critical blowing of gas through porous plate, noting velocity and concentration profiles of blowing parameters 23 p3281 A72-44082
- Velocity distribution in the turbulent boundary layer of a supersonic gas flow 23 p3249 A72-44084
- Unsteady flow field near wall and Reynolds stress measurement in turbulent boundary layer, using conditional sampling technique with digital computer 23 p3282 A72-44304
- Pressure fluctuations resulting from the interaction between a shock wave and a turbulent boundary layer. 24 p3359 A72-44682
- Rectangular wind tunnel study of suction effect on velocity profiles and characteristics of turbulent boundary layer 24 p3390 A72-45005
- Water tunnel study of turbulent boundary layers structure in incompressible fluid with longitudinal pressure gradient at inlet section of converging and diverging nozzles 24 p3390 A72-45006
- Turbulent boundary layer calculation behind surface cusp, taking into account external flow turbulence and thermal stratification 24 p3390 A72-45008
- Turbulent supersonic boundary layer flow in the neighborhood of a 90 deg corner. 24 p3361 A72-45204
- The large Reynolds number - Asymptotic theory of turbulent boundary layers. 24 p3392 A72-45248
- Velocity profile of near-wall turbulent boundary layer with adverse pressure gradient, noting skin friction 24 p3393 A72-45357
- Prediction of velocity profiles for turbulent boundary layers on the blading of radial impellers. 24 p3393 A72-45360
- Explicit numerical solution of the three-dimensional incompressible turbulent boundary-layer equations. 24 p3395 A72-45781
- Nonsimilar solution for laminar and turbulent boundary-layer flows over ablating surfaces. 24 p3364 A72-45782
- TURBULENT DIFFUSION**
- Concentration distribution in turbulent flow as function of velocity field, deriving differential equations from characteristic functionals to describe diffusion process 01 p0049 A72-10190
- Turbulent flow development in concentric annuli from modified Reichart integral equation model for eddy diffusivity of momentum 02 p2023 A72-12103
- Passive scalar field diffusion in homogeneous turbulence, solving Fourier transformed flow equations by iterative procedure 02 p2024 A72-12174
- Diffusion flames turbulence measurements by microphones, hot wire probes, Pitot tubes and photodiodes, evaluating density fluctuations by indirect methods 02 p3033 A72-12854
- Mesosphere and lower thermosphere photochemical composition, allowing for molecular and eddy diffusion 03 p0345 A72-12980
- Magnetic field and turbulence in sunspots, studying local variations of saturation and Doppler broadening 03 p0428 A72-13297
- Fluctuations and diffusion correlation analysis in linear octupole magnetic confinement, determining dispersion relation for interchange instability 03 p0396 A72-13660
- Suppressed turbulent diffusion of drag reducing polymer solution in turbulent boundary layer, measuring concentration with laser-phototransistor unit [AD-737467] 03 p0343 A72-14321
- Turbulent shear flow mean velocity profiles, calculating eddy diffusivity for momentum and Reynolds stress 03 p0343 A72-14323
- Turbulent particle diffusion statistical mechanical model, using random walk 03 p0344 A72-14331
- Geometrical and aerodynamic characteristics of circular cross section diffuser channels from turbulent boundary layer calculation at preseparation flow stage 04 p0461 A72-14647
- Planetary boundary layer mixing length flow hypothesis with dependence on Reynolds tangential stress permitting turbulent diffusion coefficient maximum values computation 04 p0519 A72-15458
- Turbulent diffusion flame model in Couette flow, including wall effect [AIAA PAPER 72-214] 05 p0748 A72-16856
- Nonuniform potential and dissipation flow structure of turbulent diffusion flame front at high Reynolds numbers 06 p0902 A72-18104
- Kubo type time correlation formulas for incompressible heat conducting fluids turbulent transport coefficients, establishing relation to cascade and closure-of-hierarchy methods 06 p0801 A72-18173
- Horizontal transport in upper atmosphere by large scale circulation, presenting altitude variation of atmospheric constituents concentration for various eddy diffusion coefficient values 07 p0978 A72-20040
- Atmospheric free convection turbulence and diffusion, proposing statistical characteristics and formulas with horizontal thermal flux vertical and transverse velocity components 07 p1031 A72-20697
- Energy transfer from radiative heat source near summer pole to radiative heat sink near winter pole, investigating large scale eddies and gravity waves 08 p1161 A72-21536
- One dimensional atmospheric turbulent diffusion model and semiempirical equation, considering jumplike changes in particle velocity 08 p1201 A72-21999
- Plasma turbulent diffusion effects on particle trajectories in phase space as Weiner process 09 p3358 A72-22294
- Vertical macroturbulence diffusion coefficient and Na 22 and Be 7 flux from stratosphere to troposphere estimated using ground level measurements and two layer model 09 p1376 A72-22416
- Meteors radio echo duration dependence on electron attachment, photodetachment and turbulent and ambipolar diffusion deionization processes 09 p1383 A72-22502
- Meteor method for determining errors in rate measurement of electron attachment to neutral air particles based on nonexistent recombination, turbulent diffusion and photodetachment 09 p1383 A72-22503
- Photometric parameters of Leonid meteor ionized trail and turbulent diffusion in M zone, determining electron attachment rate 09 p1384 A72-22510
- Electron attachment, photodetachment and turbulent diffusion deionization effects on duration distribution of Geminid meteor radio echoes 09 p1384 A72-22512

Asymmetric flow in plane channel characterized by diffusional transport of turbulent shear stress and kinetic energy from rough to smooth wall regions
10 p1467 A72-24368

Turbulent diffusion of scalar contaminant passively advected by homogeneous stationary flow, expanding velocity and scalar fields in stochastic Wiener-Hermite functionals
10 p1469 A72-24606

Flow phenomena, mixing and stability of high speed enclosed multijet turbulent diffusion flames fed by propane and air
10 p1563 A72-25139

Molecular and eddy diffusion transport velocities for helium and hydrogen distributions in upper atmosphere
11 p1622 A72-25845

Viscous effects on turbulent diffusion shear flow past semiinfinite flat plate, using Wiener-Hopf equations [DFVLR-SONDDR-171]
11 p1617 A72-26370

Relative atmospheric dispersion in enstrophy/half squared vorticity/- cascading inertial range of homogeneous two dimensional turbulence
12 p1839 A72-27031

Enhanced turbulent diffusion of nitrous oxide in parallel wall duct with obstructions for high Reynolds numbers
12 p1797 A72-27536

Turbulence microcharacteristics of rarefied suspension gas flow, using Topler schlieren-diffusion technique
12 p1752 A72-28172

Tangential and radial eddy diffusivity effects on nonsymmetric turbulent diffusion in plain impervious tube as function of Schmidt number
14 p2096 A72-31069

Turbulent diffusion limiting flux variation with angular rotation velocity of rough rotating disk
15 p2217 A72-31676

Backward diffusion statistical properties in time for homogeneous unsharped stationary turbulent flow, using Eulerian velocity
15 p2218 A72-32402

Quantum mechanics variational methods reformulation for turbulent diffusion of marked particles
16 p2379 A72-33570

Dynamo instability and feedback in a stochastically driven system.
18 p2678 A72-36013

Some observed properties of atmospheric turbulence.
18 p2705 A72-36019

Observations of the variability of dissipation rates of turbulent velocity and temperature fields.
18 p2678 A72-36022

The turbulence diffusion in free jets and flames
18 p2740 A72-36245

Eddies memory in turbulent shear flow from experiments on plane turbulent wakes undergoing equilibrium transition under impulsive pressure gradient effect
18 p2680 A72-36476

Atmospheric free convection turbulence and diffusion, proposing statistical formulas for components of horizontal thermal flux, vertical and transverse velocity and free diffusion tensor
20 p2948 A72-39012

Estimation of the turbulent diffusion coefficient and of the vertical wind velocity component from the distribution of natural radioactivity
20 p2964 A72-39320

Turbulent diffusion in Laval nozzle, studying mixing of weakly heated jet coaxial with main flow in subsonic flow region
20 p2913 A72-39368

An experimental study of turbulent diffusion of helium jets issued upwards into the air at rest.
23 p3281 A72-44273

Developing turbulent flow and heat transfer in concentric annuli.
[CSME PAPER 71-39]
24 p3465 A72-45253

Resonant diffusion in the presence of strong plasma turbulence.
24 p3430 A72-45567

TURBULENT FLOW

NT CAVITATION FLOW

NT SUPERCAVITATING FLOW

Pt coated W hot-wire anemometers sensitivities in supersonic turbulent flow at low Reynolds numbers
[ONERA, TP NO. 1024]
01 p0064 A72-10037

Space-time correlations of convection turbulent velocities in smooth circular duct with longitudinal separations
01 p0049 A72-10038

Concentration distribution in turbulent flow as function of velocity field, deriving differential equations from characteristic functionals to describe diffusion process
01 p0049 A72-10190

Sound radiation from axial flow fans running in turbulent flow, evaluating fluctuating lift on rotor blades due to incident gusts
01 p0002 A72-10220

Flow in turbulent trailing vortex, considering circulation profiles and Reynolds stress distribution [AD-740436]
01 p0049 A72-10232

Heat transfer in turbulent flow of equilibrium dissociating nitrogen tetroxide within round tube, considering pressure, temperature and mass flow rate effects
01 p0145 A72-10490

Ultrasonic rotameter for wind velocity circulation measurement, using cylindrical electroacoustic capacitor converter with solid dielectric for radiators and receivers
01 p0094 A72-10560

Laser anemometer system for instantaneous velocity measurement in turbulent pipe flow, determining two point velocity correlation coefficients
01 p0071 A72-11169

Equilibrium shear flow of stratified brine in cyclically continuous rectangular tank, discussing stable density region erosion by turbulent layers, Richardson numbers, transition layer and entrainment
01 p0051 A72-11228

Turbulent flow velocity measurement pulsed wire technique
01 p0072 A72-11229

Energy spectrum equations for steady state turbulent convection model based on Heisenberg statistical theory, noting application to convection in planetary and stellar atmospheres
01 p0146 A72-11311

Conical hydrostatic bearing optimization for minimum friction in laminar and turbulent flows, developing flow rate, load capacity and friction torque equations [ASME PAPER 71-LUB-19]
02 p0235 A72-11539

Incompressible nonself similar turbulent and transitional flows numerical analysis in wakes, jets and boundary layers, using turbulent viscosity equations
02 p0202 A72-11587

Laminar free jets characteristics, investigating transition to turbulence
02 p0150 A72-11730

Turbulent flow development in concentric annuli from modified Reichart integral equation model for eddy diffusivity of momentum
02 p0203 A72-12103

Slit element flow in shear flow turbopump rotors, presenting solutions for laminar and turbulent flow between two parallel disks rotating with same angular velocity
02 p0204 A72-12227

Incompressible two dimensional laminar/turbulent wall jet characteristics, obtaining Prandtl mixing theory from apparent kinematic viscosity
02 p0206 A72-12619

Turbulent supersonic separated flow field analysis and pressure measurements for two dimensional and axisymmetric internal and external flow models [DGLR PAPER 71-076]
02 p0152 A72-12710

Acoustic attenuation calculation for turbulent flow in rigid tubes, determining critical flow velocity dependence on wall roughness and sound wave frequency
03 p0340 A72-12954

Turbulent flow internal intermittency and fine structure distribution as function of Reynolds number, using hot-wire anemometer for velocity field measurements
03 p0340 A72-13156

Acoustic, turbulent and thermal fluctuating motions interdependence in gas flow, considering application to aerodynamic noise theory
03 p0341 A72-13405

Residence time of foreign gas introduced within wake recirculation region behind slender body in axisymmetric supersonic laminar/turbulent flow [AD-733525]
03 p0308 A72-13633

Closure problem in statistical theory of isotropic turbulent velocity field
03 p0342 A72-13900

Two dimensional MHD turbulent flow generation in strong magnetic field
03 p0398 A72-14004

Flat plate in turbulent shear flow polymer solution, predicting maximum drag reduction with interactive layer concept
03 p0343 A72-14322

Turbulent shear flow mean velocity profiles, calculating eddy diffusivity for momentum and Reynolds stress
03 p0343 A72-14323

Ekman boundary layer shear stress due to laminar and turbulent flow over hills
03 p0386 A72-14336

Photomultiplier signal for water axial velocity in glass pipe, providing turbulent liquid flow information and laser Doppler velocimeter evaluation
04 p0520 A72-14438

Numerical solutions of integral equation for transition and turbulent flows through pipes and channels, discussing computer simulations
04 p0510 A72-14469

Supercritical pressure turbulent forced fluid heat transfer mechanism hypothesis, explaining anomalous transfer improvements and deteriorations
04 p0511 A72-14641

Weakly ionized turbulent gas flow in pipe, comparing neutral and plasma fluctuations with laser beam scintillations
04 p0558 A72-15331

Turbulent flow from rotating disk, calculating mean velocities, turbulent intensities and Reynolds stress component
04 p0513 A72-15332

Turbulence intensities and shear stress measurements in wake of thin flat plate by rotating single hot-wire anemometer
04 p0524 A72-15498

Bearing operating characteristics within transition range between laminar and fully developed turbulent flow, accounting for film thickness variation and pressure gradients
04 p0528 A72-15701

Initial boundary layer effect on turbulent free shear layer velocity profiles, deriving procedure applicable at any streamwise station
05 p0645 A72-15795

Thermal load effect on convective heat transfer in turbulent flow in circular duct
05 p0742 A72-15843

Stochastic aerodynamic heating of shallow shell in supersonic turbulent flow by Monte Carlo method
05 p0599 A72-15845

Integral methods application to turbulent corner flow problem, obtaining mean velocity profile first approximation for turbulent boundary layer with streamwise pressure gradient [ASME PAPER 71-WA/FE-36]
05 p0646 A72-15921

Turbulent flow in smooth and rough pipes at Reynolds numbers 30,000-480,000, presenting velocity mean and fluctuating components rms and cross correlation values [ASME PAPER 71-WA/FE-7]
05 p0647 A72-15935

White noise mean square sound pressure in turbulent flow in cylindrical duct, using cross correlation technique [ASME PAPER 71-WA/FE-5]
05 p0647 A72-15936

Incompressible turbulent flow in parallel-plate channel with one porous bounding wall, using velocity slip model [ASME PAPER 71-WA/FE-1]
05 p0647 A72-15939

Turbulent flow and heat transfer characteristics of non-Newtonian fluids on flat plate, measuring velocity and temperature distributions
05 p0648 A72-16005

Statistical description of Brownian particle motion in turbulent flow, using theory of canonical correlations
05 p0648 A72-16171

German book on turbulent flow theory and applications covering isotropic and homogeneous nonisotropic fields, shear flows, pipe flows, free turbulence, boundary layers, etc
05 p0649 A72-16286

Velocity field time history of interacting shear waves in infinite homogeneous chemically reacting fluid for turbulent combustion studies
05 p0747 A72-16367

Two dimensional turbulence stationary states from statistical equilibria for Navier-Stokes equation
05 p0649 A72-16686

Noncoagulating polydisperse aerosol deposition from two dimensional turbulent boundary layer and fully developed turbulent pipe flows [AIAA PAPER 72-81]
05 p0650 A72-16806

High speed boundary layer flow three dimensional disturbances interaction with thermal and ablative response in adjacent surface material, considering laminar and turbulent compressible flows [AIAA PAPER 72-93]
05 p0748 A72-16811

Film cooled turbine vanes external heat transfer distribution in turbulent gas stream, measuring heat transfer coefficients with and without blowing [AIAA PAPER 72-9]
05 p0707 A72-16877

Explicit finite difference procedure to solve time averaged equations of motion for unstalled turbulent duct flows in coordinate system approximating real flow streamlines [AIAA PAPER 72-43]
05 p0651 A72-16878

Fluctuating flow in idealized model of turbulent shear layer composed of many discrete two dimensional vortices, analyzing noise generation [AIAA PAPER 72-155]
05 p0609 A72-16955

Homogeneous compressible turbulence field with large amplitude and density fluctuations generated in subsonic wind tunnel by rapid mixing of hot and cold air streams [AIAA PAPER 72-119]
05 p0652 A72-16980

Turbulent flow field velocity fluctuations errors by hot-wire anemometer filaments vibrations from fluctuating aerodynamic loads in Karman vortex street
05 p0664 A72-17013

Polarographic method for simultaneous measurement of wall gradients of velocity and of concentration in unsteady laminar or steady turbulent flow
06 p0797 A72-17558

Turbulent velocity field calculation for rectilinear duct with noncircular cross section, using integral transformation and dimensionless velocity ratio
06 p0800 A72-18110

Incompressible fluid turbulent flow variational principles, discussing Malkus principle for maximum dissipation rate and minimum entropy production principle for convective and dissipative systems 06 p0800 A72-18116

Laminar to turbulent flow transition spectral evolution and catastrophic transition, discussing visual experiments and analytical methods 06 p0800 A72-18121

Surface pressure fluctuations near axisymmetric stagnation point in flow over simple impinged body, showing fluid strain suppression of turbulence 06 p0757 A72-18133

Equilibrium turbulent flow of incompressible fluid in plane diffusers, taking into account channel cross section including viscous sublayer 06 p0801 A72-18144

Blading, flow and characteristic line calculations for machine with axial turbulent flow, using plane cascade measurements 06 p0757 A72-18690

Fluctuating and steady model for turbulent reactive and nonreactive flow, solving for turbulent kinetic energy and density by averaging procedure [AIAA PAPER 72-68] 07 p0966 A72-18948

Thermal and momentum diffusivity measurements in turbulent stratified flow, obtaining velocity and temperature profiles [AIAA PAPER 72-80] 07 p0966 A72-18950

Heat transfer in thermal entrance region with turbulent flow between parallel plates, solving energy equation by difference methods 07 p1099 A72-19622

Temperature pulsation spectra of turbulent mercury flow in horizontal pipe at various Reynolds numbers, showing dependence on magnetic field 07 p1100 A72-19882

Two dimensional subsonic flow behind symmetrical blade cascade, taking into account initial flow turbulence 07 p0909 A72-20078

Computerized simulation of two dimensional turbulent flow in Fourier space with random initial conditions on coefficients, discussing velocity, pressure and vorticity fields 07 p0971 A72-20084

Wave mechanics theory of turbulence based on Schroedinger equation, discussing resonance and flutter aspects 07 p0971 A72-20095

Sound generation in shear flow turbulence, discussing dependence on mean flow velocity and temperature 07 p0909 A72-20097

Generalized Navier-Stokes equations for incompressible turbulent flow time mean values, using nonlinear phenomenological theory 07 p0972 A72-20109

Turbulence velocity field analysis by repeated cascade theory via partial Fourier transform, predicting Kolmogoroff law in line with experimental results 07 p0972 A72-20112

Incompressible fluid near equilibrium turbulent flow velocity distribution through plane diffuser, taking into account upstream conditions 07 p0972 A72-20115

Intermittency and scale similarity in turbulent flow structure, analyzing eddies distribution inhomogeneity 07 p0973 A72-20319

Digital simulation of two dimensional or marginally turbulent three dimensional flows by discretization and numerical integration, noting Galerkin method efficiency in avoiding errors 07 p0951 A72-20355

Atmospheric kinetic and temperature energy spectral balances in thermally stratified turbulent flow without shear 07 p0980 A72-20454

Rotor components vibration destabilizing effects on dual spin spacecraft dynamics, considering turbulent liquid sloshing in Intelsat 4 propellant tank 07 p0973 A72-20488

Air flow turbulent behavior and dynamic characteristics dependence on underlying surface roughness variations 07 p1031 A72-20695

Flow field model of convective heat transfer along reattachment surface in planar supersonic turbulent flow [ASME PAPER 71-HT-W] 08 p1251 A72-20876

Heat transfer in laminar and turbulent Newtonian fluid flow in narrow channels with allowance for temperature dependence of viscosity and energy dissipation 08 p1148 A72-20955

Identification method applicability to Prandtl number determination in turbulent flow 08 p1149 A72-21312

Descriptive geometric method for distribution of axes of uniform rotation of body containing ideal homogeneous incompressible fluid in uniform turbulent motion 08 p1209 A72-21364

Numerical simulation of two dimensional and marginal three dimensional turbulent flows, discussing variable eddy viscosity model, discretization, numerical integration and Galerkin methods 08 p1200 A72-21492

Turbulent friction coefficients and velocity distribution in channel and pipe flow, using eddy viscosity model 08 p1150 A72-21623

Unsteady uniform turbulent flow of incompressible liquid in circular pipe, verifying mathematical model with velocity distribution calculations 08 p1151 A72-21666

Turbulent flow model based on two equations for kinetic energy distribution and vorticity fluctuations, comparing flow and heat transfer prediction with experimental data 08 p1152 A72-22169

Turbulence measurements in liquids - Conference, Rolla, Missouri, September 1969 09 p1292 A72-22301

Two dimensional laser Doppler forward and backscatter velocimetry in turbulent flows, applying to four inch pipe 09 p1305 A72-22303

Electrochemical techniques for time averaged turbulent velocity gradient and components of fluctuating velocity gradient at solid surface 09 p1306 A72-22305

Turbulence measurements in shear flow systems including pipe, tank and multijet reactor configurations 09 p1292 A72-22306

Turbulence generated by moving obstacle in tank of stably stratified fluid, measuring velocity and concentration fluctuations with hot-film and electrode conductivity probes 09 p1293 A72-22308

Frequency response of hot-film wedge probe in turbulent flow of viscoelastic fluid 09 p1293 A72-22309

Visual observations of wall in turbulent pipe flow, using suspending solid MgO particles 09 p1306 A72-22310

Boundary condition for plane or axisymmetric stagnation point flow of micropolar fluid over flat plate, giving numerical solutions for turbulent characteristics 09 p1293 A72-22621

Turbulent gas flow induced by laser heating, emphasizing Rayleigh number as stability criterion 09 p1295 A72-23492

Steady turbulent flow and heat transfer downstream of circular pipe sudden enlargement, computing streamline and temperature profiles and wall fluxes 09 p1412 A72-23687

Aerodynamic noise generation in turbulent fluid at low Mach number due to source near half plane by applying Kutta-Joukowski condition 10 p1415 A72-23724

German monograph on gas dynamic properties of turbulent subsonic compressible flow of ideal gas at insulator walls in MHD generator 10 p1517 A72-23771

Turbulence models application to internal flow prediction, using two-, three- and five-equation models and shear stress hypothesis 10 p1463 A72-23854

Turbulent shear stress and kinetic energy characteristics of subsonic air flow in straight conical diffuser, using hot-wire anemometry measurements 10 p1416 A72-23862

Secondary flows effect on turbulent longitudinal velocity distribution in square ducts, using Navier-Stokes and continuity equations 10 p1463 A72-23864

Turbulent shear stress calculation from mean velocity data for complex flows with inappropriate boundary layer approximations, using method of characteristics 10 p1463 A72-23866

Stress and thermal relaxation effects in viscoelastic behavior of turbulent flows of liquids and gases 10 p1464 A72-23867

Numerical prediction of inert and reacting steady in ternal two dimensional recirculating flows by finite difference method, including turbulence and combustion models 10 p1561 A72-23868

Numerical solution of turbulent recirculating flow, using energy equation to estimate eddy viscosity distribution 10 p1464 A72-23869

Spanwise velocity distribution effect on drag measurement of short struts in two dimensional turbulent airstreams 10 p1417 A72-23881

Forced convection heat transfer for turbulent flow over flat surface with attached protrusion for varying Reynolds number and boundary layer thickness 10 p1561 A72-23882

Statistical solution of steady natural turbulent convection at large Grashof numbers 10 p1465 A72-24103

Turbulent flow velocity and pressure fluctuations mean square values measurement by electrokinetic probe based on electrical properties of double metal-fluid interface layer 10 p1480 A72-24204

Entrainment interface evolution in turbulent flow, examining surface slope discontinuities and curvature and overall speed of advance 10 p1467 A72-24332

Turbulent shear layer flow in reattachment region downstream of backward facing step and non-monotonic return to ordinary boundary layer state, noting eddy length scale decrease 10 p1468 A72-24467

Fully developed turbulence spectrum of incompressible viscoelastic fluids 10 p1469 A72-24534

Ohmic law generalization in electrodynamics for electrically conductive fluid medium in turbulent motion, taking into account Hall effect 10 p1524 A72-24931

Laminar boundary layer velocity profiles in convergent nozzle incompressible swirling flow, considering boundary layer growth effects on free stream axial and tangential velocities 10 p1471 A72-25068

Friction drag coefficient determination for cylindrical bodies in laminar and turbulent incompressible fluid flow 10 p1420 A72-25135

Two phase axisymmetrical air jet turbulence intensity determination from heat distribution parameters in wake of wire heated by electric current 10 p1471 A72-25172

Helical turbulent flow through concentric annulus with rotating inner cylinder, examining axial and tangential velocity distribution and shear stresses 10 p1471 A72-25190

High mass transfer rate effect of foreign gas on transport coefficients in fully developed turbulent flow [AIAA PAPER 72-293] 11 p1614 A72-25231

Flow and heat transfer model for turbulent cylindrical wall jets based on Prandtl mixing length theory 11 p1744 A72-25268

Real time hologram-moire interferometry for visualization of turbulence phenomena in liquid flow through cylindrical pipe 11 p1629 A72-25317

Equilibrium state dynamics of Burger turbulence model with two velocity components, using Fourier amplitude representation 11 p1615 A72-25553

Non-Newtonian pipe flow turbulence measurements by laser anemometer, describing optical system and signal processing instrumentation [AD-742872] 11 p1646 A72-25554

Magnetic field generation in presence of turbulent velocity distribution, considering gyrotropy parameter equation and nonlinearity 11 p1686 A72-25716

Turbulent flow time averaged description by Navier-Stokes equations, determining Reynolds number dependent stress tensor coefficients 11 p1615 A72-25722

Book on turbulence covering Reynolds stresses, kinetic theory of gases, vorticity dynamics and mixing length models 11 p1616 A72-25925

Turbulent free shear flow intermittency factor determination by electronic circuit, discussing calibration and errors 11 p1617 A72-25997

Boundary layer turbulence development by gas flow interaction with arc plasma in supersonic nozzle, causing light emission fluctuations [AIAA PAPER 72-415] 11 p1617 A72-26165

Noncoincidence of maximum velocity and zero shear stress due to asymmetric turbulent velocity profiles, considering effect on momentum, heat and mass transfer in noncircular channels 11 p1618 A72-26534

Laminar transition and turbulent natural convection mass transfer measurements on inclined and vertical surfaces by electromechanical method 11 p1635 A72-26536

Smoke generator for fluid flow visualization, presenting photographs of turbulent rotating air flow in cylindrical enclosure [AD-746416] 11 p1613 A72-26540

Laminar and turbulent compressible wall jet characteristics, obtaining density variation as function of velocity and Mach number at exit 11 p1618 A72-26593

Turbulent pipe flow laminarization by fluid injection, measuring axial turbulence intensity field and streamwise velocity distribution by hot-film anemometer 11 p1619 A72-26636

Ergodic boundary in initial conditions space for turbulent two dimensional flow, explaining phenomenon in terms of negative temperatures for point vortex model 12 p1797 A72-27183

Atmospheric models for critical flux Richardson number prediction for turbulence maintenance in stratified flows

12 p1840 A72-27702

Tracer particle motion behavior in laser anemometry for turbulent flow, comparing liquids with gases for accuracy

12 p1809 A72-27763

Turbulence model based on transport equations for Reynolds stress tensor and energy dissipation rate, deriving simplified version for boundary layer flows

12 p1798 A72-27830

Frequency modulation demodulation technique for turbulence velocity measurements by laser Doppler velocimeter

[AD-744534]

12 p1809 A72-27836

Viscous incompressible gas turbulent flow in axisymmetric channel under preliminary twist conditions at inlet, using computer numerical solution

12 p1752 A72-28126

Flow velocity fluctuation intensity relationship to turbulent energy dissipation based on Kolmogoroff similarity hypothesis

12 p1799 A72-28133

Turbulent gas flow mass transfer coefficient derived from Lapin relation between vertical velocity and concentration distributions in turbulent boundary layer near semipermeable surface

12 p1889 A72-28136

Energy dissipation for turbulent flow in turbine blades guide vanes calculated with allowance for effects of Reynolds number and turbulence intensity

12 p1752 A72-28137

Turbulent mixing length velocity, temperature pulsations and viscous sublayer thickness in steady incompressible fluid flow past infinite plate

12 p1799 A72-28179

Heat transfer to surfaces in turbulent incompressible gas flows with various boundary conditions

13 p2063 A72-28627

Statistical theory of nonuniform turbulent incompressible fluid flow, presenting approximate formulas of nonisotropic two point correlation tensors

13 p1941 A72-28629

Effect of magnetic field superimposed on turbulent shear flow of electrically conducting fluid, discussing turbulent friction in plane flow

13 p2010 A72-28764

Swirling flow in round pipe with sudden expansion, discussing separation and reversal characteristics

13 p1942 A72-29640

Asymptotic theory of turbulent flows established with bubbles, showing limiting relations existence at increasing liquid discharge rates

13 p1943 A72-29785

Carbon dioxide turbulent flow heat exchange in single phase near critical region under forced and free convection

13 p2066 A72-29900

Scaling invariance hypothesis for local structure of turbulence, using quantum field theory methods

13 p1943 A72-29994

Von Karman constant in low Reynolds number turbulent flows, observing shear stress gradients effects on viscous sublayer

13 p1944 A72-30027

Hypersonic blowdown tunnel investigation of turbulent shock-boundary layer interactions at two dimensional wedge compression corner

13 p1944 A72-30030

Statistical description of Brownian particle velocity in turbulent flow, using theory of canonical correlations

14 p2093 A72-30240

Differential turbulent shear flow equation reduction to deduce similarity criteria for velocity pulsations, using Karman transformation

14 p2094 A72-30292

Turbulent hot gas stream self ignition in oxidizer flow for hydrogen-air and gasoline-air mixtures

14 p2170 A72-30293

Passive scalar dispersion in turbulent incompressible flow characterized by inhomogeneous and nonstationary statistics, expanding velocity and scalar concentration fields in Wiener-Hermite functions

14 p2128 A72-30348

French monograph on hot-wire anemometry techniques covering support aerodynamic perturbations, crossed wire probes and turbulent flow free boundary

14 p2106 A72-30946

French monograph on turbulent free flow boundaries covering two dimensional plane jet mixing zone characteristics from thermal signal measurements

14 p2095 A72-30948

Lighthill method for ohmic dissipation pulsation effect on sound field generated by turbulent flow of conducting fluid

14 p2141 A72-31001

Turbulent friction relation to averaged velocity profile of liquid flow in pipes and channels

14 p2096 A72-31019

Temperature distribution and heat transfer coefficients in turbulent separated flow region downstream

of rearward step in subsonic wind tunnel, using Mach-Zehnder interferometer

15 p2333 A72-31204

Thermal load effect on convective heat transfer in turbulent flow of viscous incompressible liquid in circular tube

15 p2334 A72-31262

Stochastic aerodynamic heating of shallow shell in supersonic turbulent flow by Monte Carlo method

15 p2178 A72-31264

Turbulent viscous flow near wall, deriving characteristics from equations of motion for comparison with hot wire anemometer measurement

15 p2216 A72-31469

Kinematic eddy viscosity for incompressible two dimensional turbulent flow, obtaining Navier-Stokes equations and conditions for equilibrium and nonequilibrium boundary layers

15 p2216 A72-31470

Wind tunnel measurement of intermittency in turbulent boundary layer on porous plate for alternating laminar and turbulent air flow

15 p2217 A72-31610

Microscale static pressure fluctuation measurements in lower atmospheric boundary layer turbulent flow using Eulerian measurements

15 p2265 A72-31618

Turbulent flow between rotating disk and turbine engine body calculated from equations of axisymmetric viscous incompressible fluid flow

15 p2217 A72-31702

Backward diffusion statistical properties in time for homogeneous unseparated stationary turbulent flow, using Eulerian velocity

15 p2218 A72-32402

Heated thin film gages calibration for skin friction measurements in laminar and turbulent flows, discussing wall temperature distribution and turbulence effects

15 p2241 A72-32577

Sharp flat plate laminar, transitional and turbulent skin friction via finite difference integration of compressible boundary layer equations

15 p2180 A72-32596

Nonrotating Hadley cells turbulence from steady one dimensional flow instabilities in thin nonrotating differentially heated atmosphere or ocean

15 p2219 A72-32722

Fully developed turbulent air flow through concentric annuli, measuring inner wall shear stress distribution by zero-shear position location and sliding sleeve technique

16 p2375 A72-32875

Turbulent flow of viscous incompressible liquid film falling down semiinfinite vertical plate under gravity influence

16 p2376 A72-33142

Generalized continuum mechanics application to turbulent flows developing from unstable vortex wakes

16 p2377 A72-33143

German monograph on surface roughness effects on pressure loss and heat transfer in high temperature turbulent flow, deriving universal laws

16 p2478 A72-33506

Heat transfer and friction coefficients for turbulent flow in rough tubes as function of Reynolds and Prandtl number, using von Karman method

16 p2478 A72-33513

Grid-generated turbulence distortion approaching two dimensional bluff body stagnation region

16 p2344 A72-33569

Drag reducing polymers influence on velocity gradients at wall for turbulent pipe flow, observing viscous sublayer thickening

16 p2379 A72-33574

Curved surface laminar flow turbulence front expansion rates measurement at high Reynolds number on experimental setup, considering centrifugal forces

16 p2379 A72-33792

Negative pressure gradients effects on turbulent viscosity profiles for gas flow through tubes, comparing dependence on transverse coordinates to incompressible flow case

16 p2380 A72-33860

Microphotometric chemiluminescence measurement for analysis of turbulent flame fine structure for homogeneous air-fuel mixtures at high Reynolds numbers

16 p2479 A72-34005

Reattachment heat transfer for laminar or turbulent separated shear layers, comparing predictions with measurements for cavities, ramps, spiked-nose bodies and forward facing step

[AIAA PAPER 72-717]

16 p2344 A72-34031

Turbulent solutions of certain linear and nonlinear partial differential equations

17 p2537 A72-34194

A method of solving partial differential equations for boundary layers

17 p2537 A72-34195

Atmospheric turbulence statistical theory, discussing random flow field characterization by property expressed in ergodic theorem

17 p2537 A72-34273

Supplement to the asymptotic theory of steady turbulent flows with bubbles

17 p2537 A72-34278

Velocity-pressure correlations in a homogeneous turbulence associated with a plane pure deformation

17 p2537 A72-34280

Prediction of the flow and heat transfer in a rectangular wall cavity with turbulent flow.

[ASME PAPER 72-APM-Q]

17 p2636 A72-34305

Micromorphic description of turbulent channel flow.

17 p2538 A72-34868

Memories of longitudinal fluctuations of velocity in a smooth circular duct

17 p2539 A72-34907

Compressible swirling flow through convergent-divergent nozzles.

17 p2485 A72-34999

A laser velocimeter for Reynolds stress and other turbulence measurements.

17 p2555 A72-35235

Mass spectrometer sampling system for measuring effluent concentrations downwind of stacks at various positions in turbulent flow within atmospheric simulation facility

17 p2536 A72-35478

Effect of a distributed sand roughness on the spectrum of wall pressure pulsations in a turbulent flow in a tube

17 p2541 A72-35542

Some specific characteristics of turbulent wall pressure fluctuations in a flow in a tube

17 p2541 A72-35545

Further comparison of theory and experiment for decay of homogeneous turbulence.

17 p2542 A72-35629

Turbulence model equations for calculation of supersonic and hypersonic flows, representing Reynolds stresses and turbulent heat flux vector in terms of eddy viscosity

17 p2543 A72-35639

Numerical simulation studies of two-dimensional turbulence. I - Models of statistically steady turbulence.

17 p2543 A72-35765

Integral scales existence as necessary condition for asymptotical independence of stationary process, showing relationship of conditions for central limit and related theorems

18 p2677 A72-36001

General closed form solutions to Burger equation with forcing terms in Navier-Stokes equation for turbulence studies

18 p2677 A72-36001

Three point distribution function related to lower order functions for closure of hierarchy of equations for turbulent probability distribution functions

18 p2677 A72-36001

The bounding theory of turbulence and its physical significance in the case of turbulent Couette flow.

18 p2677 A72-36006

Low order model and error rates for two dimensional turbulent motion prediction in atmosphere spectrum

18 p2677 A72-36009

Cameron-Martin-Wiener /C-M-W/ representations of nonlinear random process tested on Burger turbulence for real fluid problem

18 p2677 A72-36010

Nonlinear functional homogeneous chaos expansions for stationary stochastic processes in turbulence theory

18 p2678 A72-36011

Non-analytic character of the shear-tensor distribution function in incompressible turbulence.

18 p2678 A72-36012

Mathematical solution to equations of turbulent motion in viscous fluids asymptotic to strange attractors

18 p2678 A72-36015

Random geometric problems suggested by turbulence.

18 p2678 A72-36016

Possible refinement of the lognormal hypothesis concerning the distribution of energy dissipation in intermittent turbulence.

18 p2678 A72-36018

Some measurements of the fine structure of large Reynolds number turbulence.

18 p2678 A72-36020

Reynolds stress development in wall region of turbulent shear flow of oil investigated by hot film measurement technique and anemometer signal analysis

18 p2680 A72-36478

Mean period of fluctuations near the wall in turbulent flows.

18 p2682 A72-36721

Turbulence characteristics of flows with large velocity gradients in rectangular MHD channel with copper walls

18 p2715 A72-36813

Flow phenomena in turbomolecular pumps

18 p2696 A72-36837

Transition to a turbulent flow mode in the boundary layer of a plane plate with various turbulence scales in the incident flow

18 p2682 A72-36889

- Two dimensional channel contraction induced flow acceleration effect on turbulence structure
18 p2683 A72-36995
- Application of boundary layer concepts to turbulent lubrication theory of bearings and seals.
18 p2696 A72-37052
- Experimental study of conditions for heat transfer deterioration in a turbulent carbon dioxide flow under supercritical pressure
18 p2742 A72-37185
- An automatic data processing system for laser anemometers.
19 p2795 A72-37287
- Solid rocket propellant erosion burning in turbulent gas flow, discussing burning velocity dependence on Pobedonostsev criterion
19 p2878 A72-37351
- Luminance profiles photometry for axisymmetrical propagation in propane-air turbulent flow combustion with turbulence level control in jet core
19 p2879 A72-37366
- General solutions of the heat equation in finite regions.
19 p2880 A72-37411
- Perturbations development in laminar flow and transition to turbulent flow based on nonlinear theory of hydrodynamic stability
19 p2785 A72-37468
- Wyld diagram method extended to turbulence decay, considering operators expressed as integrals with kernels
19 p2785 A72-37469
- Stokes fluids nonlinearity effects on turbulent flow with lateral shear in terms of stress and deformation tensors
19 p2785 A72-37470
- Closed system of differential equations derived for kinematic characteristics of nonstationary turbulent flow in pressurized smooth pipe
19 p2785 A72-37473
- Development of a hot-wire anemometer for hypersonic turbulent flows.
19 p2795 A72-37517
- Simple proof of fluid line growth in stationary homogeneous turbulence.
19 p2787 A72-38427
- The mechanics of an organized wave in turbulent shear flow. II - Experimental results.
19 p2789 A72-38793
- The mechanics of an organized wave in turbulent shear flow. III - Theoretical models and comparisons with experiments.
19 p2789 A72-38794
- Turbulence theory generalization for flow near wall with various surface roughness modes, presenting velocity profiles
20 p2912 A72-39359
- Viscous sublayer pulsations elongation in longitudinal direction, noting decay of turbulent friction near wall as third power of distance from wall
20 p2912 A72-39360
- Pressure pulsations relationship to fixed boundary of turbulent flow with kinematic structure, considering phase transitions effect
20 p2912 A72-39361
- Thermoanemometer measurements of turbulence degree in wake behind square mesh grids in water flow within low speed wind tunnel
20 p2912 A72-39364
- An analysis of heat transfer in turbulent pipe flow with variable properties.
[ASME PAPER 72-HT-59] 20 p2985 A72-39657
- Saturated liquid film boiling on vertical surface, calculating local heat transfer rates as function of height and superheat from turbulent vapor flow model
[ASME PAPER 72-HT-38] 20 p2986 A72-39668
- The calculation of low-Reynolds-number phenomena with a two-equation model of turbulence.
[ASME PAPER 72-HT-20] 20 p2914 A72-39688
- One dimensional migratory dynamo model for alpha effect turbulence controlled by increasing magnetic field, considering oscillatory antisymmetric solutions relation to solar cycle
20 p2972 A72-39877
- Characteristics of turbulent transfer in jets of variable density
20 p2914 A72-39910
- High Reynolds number turbulence and vortices in journal bearings, discussing validity of flow field models based on mixing length and pipe flow theory
20 p2930 A72-39972
- Pulsation rates of continuous and discrete components of dispersed flow
20 p2915 A72-40047
- Bounds for heat transport in a porous layer.
21 p3127 A72-40119
- Determination of the characteristics of the averaged motion of the carrier medium in turbulent gas flow with suspended particles
21 p3044 A72-40126
- Intensification of heat transfer in channels with turbulent gas flows
21 p3127 A72-40127
- Hot wire data corrections in low and in high turbulence intensity flows.
21 p3051 A72-40220
- Magnetic field effects on turbulent shear flow of electrically conducting fluid, discussing turbulence level, friction stress and heat exchange
21 p3089 A72-40260
- Reagent concentration and temperature fluctuation effects on turbulent burning rate, noting temperature pulsations influence on energy balance
21 p3128 A72-40976
- Critical description of combustion stability in a turbulent flow of a homogeneous mixture
21 p3129 A72-40980
- Statistical continuous random process theory of homogeneous and isotropic turbulence in terms of energy transfer in wave number space based on Kolmogoroff hypothesis
21 p3045 A72-41025
- Microstructure of turbulent flow in the stabilized flow region in a channel
21 p3045 A72-41054
- Experimental friction factors for turbulent flow with suction in a porous tube.
21 p3047 A72-41618
- Burgers model equation for shear flow turbulence with complex physical processes and nonlinearities in governing equations
21 p3047 A72-41637
- Turbulent flow experimental and theoretical investigation, discussing Reynolds stress transport equations, shear layers and turbulence models in context of digital prediction methods
21 p3047 A72-41639
- Thermal state of selectively absorbing plane gas layer blown from porous plate into stabilized turbulent high temperature gas flow, considering radiative and convective heat transfer
21 p3131 A72-41672
- Heat transfer, adiabatic enthalpy /temperature/ of the wall, and hydrodynamic resistance in the presence of turbulent and laminar flow of a compressible fluid in a round tube
22 p3164 A72-41883
- Velocity distribution in turbulent air flow over perforated plates with gas injection in turbulent boundary layer
22 p3166 A72-42256
- A time-interval amplitude analyzer for turbulent flow processes and its application for the control of a chronophotographic measurement installation
22 p3177 A72-42393
- Prediction error growth computation by test-field model for inertial range atmospheric turbulent flows in three and two dimensions
22 p3167 A72-42501
- Turbulent interaction of air jets issuing from perforated surfaces into free space, determining three dimensional flow field via Reichardt free turbulence theory
23 p3248 A72-43625
- Length of the separation region behind a bluff body in a bounded flow
23 p3248 A72-43685
- Descriptive model of the turbulent motion of an isovolumetric fluid
23 p3279 A72-43699
- Experimental study of the plane deformation of a homogeneous turbulence
23 p3280 A72-43822
- An investigation of confined vortex flow phenomena.
[ASME PAPER 72-FLCS-3] 23 p3281 A72-44067
- Drag spectra of simple structures in turbulence.
23 p3281 A72-44102
- The intermittent small-scale structure of turbulence - Data-processing hazards.
23 p3282 A72-44305
- Experimental determination of the turbulent exchange coefficient in the case of homogeneous isotropic turbulence
23 p3282 A72-44489
- Modification of the Rankine-Hugoniot relations for shocks in space.
23 p3341 A72-44510
- Double hierarchy in repeated cascade theory of turbulence.
24 p3390 A72-44997
- The structure of turbulent flows adjacent to walls.
24 p3390 A72-45001
- Velocity profiles of plane turbulent flow of incompressible fluid on porous surface in presence of suction
24 p3390 A72-45007
- Turbulent boundary layer calculation behind surface cusp, taking into account external flow turbulence and thermal stratification
24 p3390 A72-45008
- Reacting and nonreacting swirl recirculation bubble gasdynamic structure in fuel combustion systems, noting anisotropic turbulence from hot-wire anemometer measurements
24 p3461 A72-45024
- Developing laminar and turbulent duct flow with chemical reaction.
24 p3378 A72-45061
- Statistical analysis of the turbulence near a wall by conditional sampling
24 p3392 A72-45066
- Developing turbulent flow and heat transfer in concentric annuli.
[CSME PAPER 71-39] 24 p3465 A72-45253
- Turbulent flow of drag reducing fluids between concentric rotating cylinders.
[CSME PAPER 71-52] 24 p3393 A72-45254
- Investigation of the characteristics of turbulent air flow in a channel with elastic walls
24 p3393 A72-45257
- A means of measuring the rms value of velocity fluctuations in unsteady turbulent flow
24 p3403 A72-45259
- Contributions to the study of turbulent flow in the vicinity of a flat wall
24 p3394 A72-45443
- Kinetic theory of turbulent flow.
24 p3394 A72-45563
- Diffusion flame in homologous turbulent shear flows.
24 p3395 A72-45564
- TURBULENT HEAT TRANSFER**
- Turbulent boundary layer flow past surface with arbitrary temperature distribution, presenting approximate heat transfer solution with allowance for pressure gradient and Reynolds number
02 p2021 A72-11582
- Asymptotic theory of heat transfer in two dimensional turbulent boundary layers of incompressible fluid at large Reynolds numbers
03 p0459 A72-14390
- Heat flux calculation in laminar turbulent boundary layer transition zone using Schlichting model of turbulent spot formation
05 p0649 A72-16222
- Radiative heat transfer damping rates of turbulent temperature pulsations in upper planetary atmospheres, assuming Kirchhoff radiation law validity
06 p0882 A72-17935
- Reynolds analogy based correlation method for Stanton number prediction for turbulent heat and mass transfer in smooth tubes
06 p0903 A72-18186
- Plasma turbulent heating effectiveness by longitudinal ion current in mirror machine, determining hot ion lifetime and energy distribution function
07 p1039 A72-18913
- Transitional and turbulent heat transfer measurements on yawed blunt cone nosetip in supersonic air flow at various angles of attack
07 p0964 A72-18960
- Initial dynamic length effects on heat transfer in turbulent boundary layer with blowing demonstrated by subsonic wind tunnel tests
08 p1151 A72-21665
- Turbulent flow model based on two equations for kinetic energy distribution and vorticity fluctuations, comparing flow and heat transfer prediction with experimental data
08 p1152 A72-22169
- Free turbulent jet heat and mass exchange and axial flow characteristics
09 p1292 A72-22235
- German monograph on heat transfer in chemically reacting gases covering laminar and turbulent tube flows for dissociated dinitrogen tetroxide
09 p1274 A72-22339
- Short laser pulses for plasma heating, considering turbulent heating mechanisms, neutron yield and electromagnetic radiation
09 p1364 A72-23444
- Laminar and turbulent convective heating distributions on delta wing space shuttle boosters with interference effects
[AIAA PAPER 72-315] 11 p1567 A72-25249
- Nucleate pool boiling three component heat flux theory, taking into account latent heat transport, molecular heat conduction and turbulent convection
11 p1746 A72-26539
- Atmospheric surface layer turbulent transfer mechanisms, studying direct measurements of momentum, heat and moisture turbulent fluxes
12 p1840 A72-27705
- Boundary layer theory for convective heat transfer of two dimensional film cooling systems in turbulent regime, noting momentum, enthalpy and concentration equations
13 p2063 A72-28630
- Convective clouds effect on air temperature gradient and turbulent heat fluxes in near-surface layers
13 p1995 A72-25993
- Dense isothermal plasma heating due to electron and ion scattering on turbulent pulsations of electric field oscillations
13 p2019 A72-29916
- Radiative heat transfer damping rates of turbulent temperature pulsations in upper planetary atmospheres, assuming Kirchhoff radiation law validity
16 p2459 A72-33776
- Energy transfer of thermal coupled radiation with turbulent convection in electric arcs in atmospheric air plasma
[AIAA PAPER 72-685] 16 p2480 A72-34057
- Prediction of the flow and heat transfer in a rectangular wall cavity with turbulent flow.
[ASME PAPER 72-APM-Q] 17 p2636 A72-34305

- Ion heating via turbulent ion acoustic waves.
17 p2588 A72-34873
- Transient turbulent free convection in a closed container with heating at the sides only.
17 p2638 A72-35642
- Turbulent boundary layer with discontinuity in wall temperature and concentration
17 p2638 A72-35746
- Plasma turbulent heating effectiveness by longitudinal ion current in mirror machine, determining hot ion lifetime and energy distribution function
20 p2957 A72-39379
- Experimental study of heat transfer in a subsonic jet impinging normally on a plane baffle.
21 p3128 A72-40949
- Propagation rate and the existence range of turbulent flame
21 p3131 A72-41660
- Possible mechanisms of turbulent heating of a plasma by ultrashort laser emission pulses
21 p3095 A72-41823
- Current induced drift rate of plasma electrons in electric and magnetic fields, noting electron velocities in turbulent heating of plasma
24 p3429 A72-45507

TURBULENT JETS

- Velocity and temperature effects on momentum and temperature equalization in coaxial turbulent jet mixing in pipe inlet section
[DFVLR-SONDDR-183] 01 p0051 A72-11257
- Integral method for predicting streamwise development of plane turbulent jets and wall jets in uniform streaming flow
01 p0051 A72-11393
- Near pressure field within subsonic circular turbulent cold jet potential cone, noting peak in power spectra
02 p0150 A72-11974
- Differential equations solution for turbulent two dimensional jet flows bounded by parallel planes
02 p0156 A72-12000
- Plane mixing boundary layer flow of high temperature turbulent gas jet in longitudinal magnetic field
03 p0397 A72-13998
- Axisymmetric deflected turbulent jet flow, analyzing physical features and trajectories
[ASME PAPER 71-APM-SS] 04 p0462 A72-15177
- Velocity profiles of turbulent three-dimensional incompressible air jet flow from rectangular orifice tangent to and along curved wall surface
[ASME PAPER 71-WA/FE-2] 05 p0647 A72-15938
- Theoretical and experimental heat transfer at plate in longitudinal jet flow with strong transverse inhomogeneity
05 p0649 A72-16228
- Composite three-dimensional axisymmetric turbulent jet system, discussing jet interaction relation to boundary layer contact and resulting turbulent mixing
05 p0649 A72-16229
- Interaction produced by diametrically opposed plane turbulent wall jet collision in still air, discussing resultant free jet
[AIAA PAPER 72-211] 05 p0606 A72-16854
- Turbulent jets interaction with cross flow, presenting longitudinal and transverse velocity, temperature and turbulence distributions
[AIAA PAPER 72-149] 05 p0651 A72-16870
- Directionality and far field structure of combustion generated noise, using premixed turbulent flame models
[AIAA PAPER 72-198] 05 p0748 A72-16875
- Turbulent shear stress, intensity and velocity field in coflowing axisymmetric jets, using eddy viscosity model
[AIAA PAPER 72-47] 05 p0652 A72-16926
- Cross correlation analysis of turbulent jet flow noise with pressure fluctuation as acoustic source
[ASA PAPER H 12] 08 p1150 A72-21488
- Free turbulent jet heat and mass exchange and axial flow characteristics
09 p1292 A72-22235
- Monostable three output fluid amplifier models with curved walls in turbulent jet flow, comparing wall design in dynamic and static tests
09 p1263 A72-22931
- Supersonic axisymmetric turbulent jet density fluctuations measurement by single beam schlieren system, using preheater to reduce jet static/ambient temperature difference
10 p1466 A72-24292
- Axisymmetric turbulent jets local entrainment rate as function of axial distance from nozzle exit, using Ricou-Spalding porous wall technique
10 p1481 A72-24425
- IR measurement of hot jets turbulence intensity axial and transverse profiles, noting application to sound sources detection
10 p1563 A72-24656
- Turbulent jets effectiveness in protection of aircraft surfaces from rain, describing wind tunnel simulation of takeoff and landing
10 p1463 A72-25137
- Flow and heat transfer model for turbulent cylindrical wall jets based on Prandtl mixing length theory
11 p1744 A72-25268

Blowing and suction effects on pulsations of isothermal turbulent jets propagating along porous cylinder
12 p1752 A72-28169

Vorticity and energy transfer equations for subsonic jet impingement on flat plate, noting turbulent jet effect on friction factor
12 p1799 A72-28171

Calculation procedure for reaction thrust of semibounded turbulent jet in boundary layer blowing and blow type antiicing systems
13 p1897 A72-28728

Holographic interferometry of Mach wave field generation by supersonic turbulent jet, noting visible conical wave front from core edge
13 p1898 A72-29580

Supersonic jet exhaust noise radiation from turbulent shear layer instability waves, noting acoustic energy flux dependence on streamwise distance
13 p2028 A72-29581

Unstable discharge regime of nonisothermal axisymmetric subsonic turbulent jet in acoustic field with local perturbations
13 p1943 A72-29883

Jet turbulence interaction and velocity effects on noise level of proportional fluid amplifiers
16 p2350 A72-33177

Pressure recovery and control characteristics of turbulence amplifiers with jet of rectangular section, using large scale water model
16 p2350 A72-33178

Statistical correlation of X-band microwave scattering by overdense intermittently turbulent ionized Ar jet with flux fluctuations from electrostatic probe observations
[AIAA PAPER 72-674] 16 p2440 A72-34065

Direct correlation measurement of turbulent jet noise and flow by cross correlating narrow filtered input turbulence and output acoustic signals
[AIAA PAPER 72-640] 16 p2381 A72-34092

High temperature turbulent jet facility for studying ionic species produced by high temperature air and ablation products interaction with cool ambient air
[AIAA PAPER 72-676] 17 p2536 A72-35480

Free hot jet turbulence space-time correlation function measurement based on IR detection
18 p2680 A72-36468

Measurement of pressure fluctuations within subsonic turbulent jets.
18 p2681 A72-36575

Structure of turbulent underexpanded jets expelled into a submerged space and into a slipstream
18 p2642 A72-36884

Calculation of axisymmetric swirling and non-swirling turbulent jets
18 p2682 A72-36890

An expansion scheme for the noise from circular jets.
[DFVLR-SONDDR-217] 18 p2683 A72-36941

The intrinsic structure of turbulent jets.
18 p2684 A72-37201

Three-dimensional wall jet originating from a circular orifice.
19 p2747 A72-38811

Turbulent gas jets formed in cryogenic substance discharge into gas at supercritical pressure and gas into gas of different molecular weight and temperature
20 p2912 A72-39366

Space correlations of the fluctuating pressure in subsonic turbulent jets.
20 p2913 A72-39555

Characteristics of turbulent transfer in jets of variable density
20 p2914 A72-39910

Propagation of viscous fluid jets in a medium with a density discontinuity
21 p3047 A72-41666

Laminar to turbulent transition in axisymmetrical submerged jets and slipstream flows of air and He, discussing Reynolds number effect
22 p3166 A72-42270

German monograph - Turbulence behavior and degree of nonmixing of jets and jet flames.
22 p3245 A72-43077

Experimental investigation of the structure of turbulent jets expelled from a rectangular nozzle and nozzles with a limited head
23 p3280 A72-44020

TURBULENT MIXING

Turbulent mixing length formulation and velocity profiles for non-Newtonian power law fluids, determining friction factor for pipe flow at high Reynolds numbers
03 p0343 A72-14318

Theoretical model for turbulent mixing of confined jet, including wall boundary layer
[ASME PAPER 71-WA/FE-31] 05 p0646 A72-15925

Composite three-dimensional axisymmetric turbulent jet system, discussing jet interaction relation to boundary layer contact and resulting turbulent mixing
05 p0649 A72-16229

Contact surface turbulent mixing instability in free piston high enthalpy shock tunnel waves with test air and argon gases
05 p0644 A72-16548

Turbulent boundary layer analog mathematical model for turbulent mixing and buoyancy effects on aircraft trailing vortex wake motion and persistence
[AIAA PAPER 72-42] 05 p0607 A72-16903

Spectral measurements of jet turbulence noise in core and annular mixing region, using subsonic test experiments
[AIAA PAPER 72-158] 07 p0966 A72-18957

Compressible axisymmetric coaxial jets turbulent mixing in constant area duct, considering axial and radial pressure distributions
07 p0967 A72-19094

Turbulent mixing of high temperature Ar jet injected into ring slipstream of air in dc plasmatron with coaxial nozzle and fixed arc
09 p1410 A72-22671

Parallel air and hydrogen flows confluence numerical examination to determine self ignition conditions in turbulent mixing layer, noting reaction zone
[ONERA, TP NO. 981] 09 p1410 A72-22814

Thermal stratification of mesosphere and lower thermosphere at low latitudes with allowance for turbulent mixing, showing molecular oxygen and ozone radiative heating prevalence
09 p1347 A72-23589

Linear initial value problem of partially mixed cylindrical wake in uniformly stratified fluid, obtaining exact solutions for density and velocity distributions
10 p1466 A72-24299

Turbulent mixing length velocity, temperature pulsations and viscous sublayer thickness in steady incompressible fluid flow past infinite plate
12 p1799 A72-28179

Russian book on combustion and turbulent mixing processes in jet engines covering temperature and velocity profiles, combustion chamber design and fuel injection characteristics
12 p1862 A72-28340

Electromagnetic waves scattering by underdense plasmas, examining intermittency phenomenon due to mixing between turbulent inner and outer inviscid wake
13 p1922 A72-29474

Round air jet turbulent mixing with incompressible transverse flow, examining interaction behavior as function of relative momentum
13 p1943 A72-29641

Subauroral red arcs formation mechanism involving magnetosphere-ionosphere energy conduction at lower atmosphere neutral composition changes due to turbulent mixing
13 p1952 A72-29813

Turbulent mixing layers analytical and experimental mean velocity profiles, discussing Goetel eddy viscosity theory
16 p2374 A72-32813

Water vapor condensation in jet turbulent mixing zone of confluent high velocity high temperature gas streams for finite axisymmetric nozzle
16 p2377 A72-33216

Rotating flow introduction effects on jet noise levels, combustion and turbulent mixing processes and flame stability
[AIAA PAPER 72-645] 16 p2480 A72-34087

Circulating toroidal vortex pattern in initial region of turbulent coaxial jet stream mixing obtained with hot wire anemometer, static pressure probes and shadowgraphy
[ASME PAPER 72-APM-30] 17 p2538 A72-34789

Heat mass and momentum transport in free turbulent mixing.
17 p2543 A72-35638

Chemical reactions in inhomogeneous mixtures. The effect of the scale of turbulent mixing.
17 p2543 A72-35644

Central probability limit theorems and asymptotic normality in fluid mechanics for random stationary processes with uniform ergodicity and strong mixing.
18 p2677 A72-36007

Computer aided study of nondiffusive plane convection mixing of scalar field by isotropic turbulence of single velocity modes
18 p2678 A72-36011

Atmospheric boundary layer turbulence modeling considering terrain roughness effects, vertical mixing high frequency spectra, energy dissipation rate and vertical component variance
19 p2828 A72-38557

A Monte Carlo model of turbulent mixing for the prediction of NO production in steady-flow combustors.
[WSCI PAPER 72-8] 20 p2982 A72-38977

Free gas jets turbulent mixing flow, considering development of submerged air jet with action of mechanical turbulence generator ahead of nozzle
20 p2913 A72-39366

Turbulent mixing of fluids of different density moving in a tube
21 p3044 A72-40121

Velocity distribution in turbulent mixing of compressible reacting gases, noting flame length measurement of submerged H jet
21 p3129 A72-40988

Optical method for measuring the concentrations of axisymmetric gas jets
21 p3055 A72-40999

German monograph - Turbulence behavior and degree of nonmixing of jets and jet flames. 22 p3245 A72-43077

Turbulent mixing of three plane isothermal jets with various velocity ratios, showing jet initial length shortening due to initial turbulence increase 23 p3279 A72-43657

Kinetic equations solution approximation for two species isothermal reactions in homogeneous turbulent mixing 24 p3392 A72-45059

TURBULENCE WAKES

NT PROPELLER SLIPSTREAMS
NT SLIPSTREAMS

Nonlinear development of instability wave in turbulent wake behind thin body based on integrals of mean flow momentum and kinetic energy equations 02 p0152 A72-12351

Temperature fluctuation structure in turbulent wake behind heated circular cylinder, investigating thermal convection, production and diffusion [AD-740540] 04 p0596 A72-15330

Turbulent wake calculations with eddy viscosity model, predicting velocity profiles and displacement thicknesses 05 p0603 A72-16538

Hot-wire anemometers signals resolution into velocity-temperature fluctuations correlations in compressible flow with shear turbulence wakes [AIAA PAPER 72-117] 05 p0664 A72-16822

Turbulent boundary layer analogy mathematical model for turbulent mixing and buoyancy effects on aircraft trailing vortex wake motion and persistence [AIAA PAPER 72-42] 05 p0607 A72-16903

Wind tunnel measurements for near flow field velocity distribution in rectangular wing wake turbulence, comparing with flight measurements [AIAA PAPER 72-41] 05 p0609 A72-16948

Wake instabilities and vortices spacing, position and strength behind slender cylindrical bodies at large incidence with subcritical cross flow Reynolds numbers 05 p0610 A72-17010

Turbulent wake of slender cone at Mach 12.5, measuring density and temperature fluctuations simultaneously [AIAA PAPER 72-118] 10 p1479 A72-24080

Small turbulences growth in two dimensional incompressible wake, noting transverse oscillations of mean velocity profile [AD-742006] 10 p1467 A72-24367

Dynamic pressure distribution and propulsive contours of trailing vortex wake downwind of external flow jet flap, using five-hole probe measurements 10 p1420 A72-25070

Hydrodynamic forces in sinusoidal vibrations of air in water channel with toroidal vorticity wake pattern, applying results to flapping wing mechanics 10 p1471 A72-25129

Mean velocity distribution and Reynolds stresses in turbulent wake behind flat plate in uniform incompressible flow 12 p1798 A72-27718

Turbulent intensity induced by wakes near secondary air jet inlet to gas turbine engine flame tube 12 p1861 A72-28131

Profile losses at turbine rotor blade in unsteady gas flow from experimental data analysis, noting effect of turbulence caused by trailing edge wakes 13 p1893 A72-28783

Electromagnetic waves scattering by underdense plasmas, examining intermittency phenomenon due to mixing between turbulent inner and outer inviscid wake 13 p1922 A72-29473

Electron density fluctuation measurements in hypervelocity projectile hypersonic turbulent wakes, showing power spectra 15 p2242 A72-32584

Generalized continuum mechanics application to turbulent flows developing from unstable vortex wakes 16 p2377 A72-33143

Crocco-Lee theory extension to flow behavior prediction for two dimensional supersonic turbulent near wake behind bluff body during recompression 16 p2343 A72-33402

Three dimensional electron density fluctuations scattering spectra in Mach 16 spherical projectile turbulent wakes from fine wire electron collection probe measurements [AIAA PAPER 72-673] 16 p2432 A72-34066

Vortex growth in two-dimensional coalescing jets. 17 p2539 A72-34970

An experimental investigation of an asymmetrical turbulent wake. 17 p2485 A72-35187

Eddies memory in turbulent shear flow from experiments on plane turbulent wakes undergoing equilibrium transition under impulsive pressure gradient effect 18 p2680 A72-36476

Theoretical model for plane turbulent wakes subject to adverse, favorable and mixed pressure gradients based on Reynolds stress equation, describing experimental verification 18 p2680 A72-36477

Transient mode of a flow in the plane wake of a thin plate or cylinder 18 p2642 A72-36899

Influence of a trailing vortex on friction pulsations in the near-wall region of the leading stagnation point of a cylinder in transverse flow 19 p2786 A72-38041

Decay of isotropic turbulence generated by a mechanically agitated grid. 19 p2787 A72-38426

Large-scale instabilities of turbulent wakes. 21 p3044 A72-40116

Turbulent base heating on a slender re-entry vehicle. 21 p2992 A72-41308

Machine code for finite difference solution of wake vortex governing equations and far flow field prediction in trailing vortices, developing turbulent energy model [AIAA PAPER 72-989] 22 p3134 A72-42326

Flight test studies of the formation of trailing vortices and a method to accelerate vortex dissipation. [AIAA PAPER 72-988] 22 p3134 A72-42327

Velocity, enthalpy and turbulent energy distributions calculation for plane wake behind flat body by asymptotic solution based on turbulence theory 23 p3249 A72-44083

The structure of blunt base wakes in swirling flow. 24 p3391 A72-45023

TURING MACHINES

Computer programming for minimization of time required for retranslation with compilers, discussing finite state machine modeling with circulating page loose system 24 p3383 A72-45670

TURNING FLIGHT

Aircraft steering dynamics model with translational and rotational equations, considering zero sideslip and acceleration and lift bank angle transfer functions 05 p0611 A72-16112

Spacecraft banking control during reentry, deriving dynamic equations of angular motion 05 p0730 A72-17026

Towed cable flight vehicle system motion in uniform flow field, calculating equilibrium configuration during coordinated turn from two point boundary value problem numerical solution 08 p1110 A72-21604

The flight mechanics of STOL aircraft. 17 p2488 A72-34241

Special control of spiral flight curves with the neutral and maneuver points as ultimate positions of the indifference points 18 p2643 A72-36942

Optimum turns to a specified track for a supersonic aircraft. 19 p2753 A72-38277

Game theoretical modeling of fighter aircraft turning tactics competition in pursuit combat, using minimax technique [AIAA PAPER 72-950] 22 p3138 A72-42359

Supersonic aircraft focused sonic boom suppression by slowing down during turning flight, obtaining conditions for focus cut-off at ground by atmospheric refraction 23 p3251 A72-44125

Supersonic aircraft energy turns. 23 p3252 A72-44196

TURNSTILE ANTENNAS

Turnstile antennas polydirectional emission and polarization characteristics, discussing relationship formulation by Scott-Soo Hoo theorem 21 p3030 A72-40531

Polar orbiting Aeros aeronomy satellite turnstile antenna system with nearly spherical radiation pattern, discussing design modifications for optimization 21 p3030 A72-40533

TVC [CONTROL]

U THRUST VECTOR CONTROL

TWENTY-FOUR HOUR ORBITS

TV-radio satellite receiver equipment, considering power requirements, antenna, energy supply and placing into 24-hour orbit 23 p3262 A72-43300

TWENTY-SEVEN DAY VARIATION

Rotating solar magnetic dipole with 26 7/8 day period from polar geomagnetic and spacecraft interplanetary field observations 02 p0277 A72-11899

Cosmic ray intensity long term modulation and 27 day recurrence relationship to solar activity 03 p0407 A72-12945

Solar magnetic field large scale patterns and apparent regularities, noting active longitude 27-day rotation periods and polarity differences 03 p0432 A72-13354

Active region sources of solar proton streams, discussing 27-day recurrence, acceleration and confinement in interplanetary space 07 p1060 A72-20010

Autocorrelation analysis of Mariner 2 data for solar wind velocity, noting 27 day recurrences 16 p2444 A72-32954

TWISTING

Solar cosmic ray anisotropy 27-day variations during IGY from global network stations neutron component data 18 p2722 A72-36876

Energy and mass content of high-speed solar-wind streams. 23 p3332 A72-44508

TWILIGHT

U TWILIGHT GLOW

TWILIGHT GLOW

Quadrantid meteoritic shower upper atmosphere contamination effects on twilight and night sky brightness 02 p0283 A72-12467

Late twilight airflow vacuum UV spectra from sounding rocket observation, noting conjugate-point electron excitation role in O I emissions 03 p0350 A72-13525

Upper atmosphere twilight optical inhomogeneities relation to noctilucent clouds, using electrophotometry methods 06 p0807 A72-17933

Twilight atmospheric sounding in oxygen absorption bands to reduce noise level in secondary light scattering 06 p0807 A72-17943

Earth horizons nighttime, twilight and daytime visual observations from manned Soyuz spacecraft, discussing upper atmosphere emission layer structure and aureole development 08 p1158 A72-21148

Atmospheric Na, Li and K layers height, width, abundance and thickness from twilightglow measurements, using birefringent filter type photometers 08 p1159 A72-21224

Mesospheric ozone measurement for altitude profiles, comparing rocket and ground based observations of 1.27 micron emission band at twilight 09 p1296 A72-22355

Twilight and nighttime ionospheric temperatures from oxygen 6300 and 5577 A spectral line profiles obtained with Fabry-Perot interferometers 11 p1625 A72-26406

Secondary scattered light component of tropospheric twilight from electrophotometric observations, comparing with upper atmospheric scattering 13 p1954 A72-30070

Upper atmospheric Na abundance from daytime spectroscopic absorption measurement compared with twilight glow observation 16 p2383 A72-32970

Twilight atmospheric sounding in oxygen absorption bands to reduce noise level in secondary light scattering 16 p2386 A72-33784

Upper atmospheric sodium and stratospheric warnings. 18 p2687 A72-36643

Earth horizons nighttime, twilight and daytime visual observations from manned Soyuz spacecraft, discussing upper atmosphere emission layer structure and aureole development 20 p2916 A72-39253

A comparison of the observed twilight with the vertical scatter distribution. 22 p3170 A72-42373

TWINNING

NT MECHANICAL TWINNING

Twinning in alloys cubic superlattices, discussing crystal structure criteria 02 p0247 A72-12815

CdTe condensed films hexagonal modification and twinning boundaries birefringence reflection, using electron microscope and diffraction analysis 07 p1047 A72-18856

Electron diffraction study of transformation twin rotations in Fe-Ni martensites, showing foil plane uncertainty effect with respect to image plane 13 p1975 A72-28666

Gamma-prime phase crystal structure in Cu-Al-Ni alloy from electron microscopic study, noting twinning and substructure during formation 14 p2115 A72-30406

Nucleation and growth of deformation twins in Mo-35 at. % Re alloy. 18 p2702 A72-36748

Twinning faults in epitaxial films of germanium telluride and GeTe-SnTe alloys. 19 p2844 A72-37688

Effect of twins produced by annealing on high-temperature failure of chromium-nickel-molybdenum steel 20 p2939 A72-39316

TWISTED WINGS

Wing load distribution and induced drag control by warping, summarizing linear theory and wind tunnel test results 10 p1417 A72-24218

TWISTING

Matrix method calculation for aerodynamic loads, transverse forces, bending moments, torques and twist of hinged main rotor blades in helicopter during forward flight 02 p0294 A72-12440

- Pretwisted tapered cantilever beam torsional vibration natural frequencies determination by Galerkin method for solution of differential equation of motion
02 p0297 A72-12533
- Transient stress analysis for sudden twisting of penny-shaped crack in infinite elastic body under torsion, using integral transform
[ASME PAPER 71-WA/APM-10]
05 p0734 A72-15969
- Tapered I-beams elastic twisting and flexural-torsional buckling, considering critical loads as function of taper ratio
08 p1249 A72-21924
- Computer program in ALGOL 60 language for calculation of long blades twist in axial flow turbines and compressors
13 p1893 A72-28782
- Singularities of cylindrical shell under concentrated twisting couple, investigating axial and circumferential deformations and shear stress distribution
15 p2329 A72-32139
- Governing equation derivation for coupled extension, flexure and torsion in pretwisted curved beams of thin walled open section, using three dimensional elasticity
[ASME PAPER 72-APM-5]
17 p2630 A72-34809
- A note on the twisting deformation of a non-homogeneous shaft containing a circular crack.
23 p3346 A72-43708
- Equilibrium and stress resultant displacement equations of thin rings based on virtual work principle, stressing warping and twisting moments
23 p3351 A72-44101
- Reissner-Sagoci problem for semiinfinite elastic solid stress and displacement determination, discussing generalization to nonhomogeneous media with circular part under axisymmetric twisting.
23 p3314 A72-44266
- TWITCHING**
Cat middle ear muscles motor units twitch tension and contraction time in response to motor neuron threshold stimulation
08 p1116 A72-21137
- TWO BODY ORBITS**
U TWO BODY PROBLEM
TWO BODY PROBLEM
Outer planet low thrust orbiter missions, comparing three body numerical results with two methods of patching together two body solutions
01 p0128 A72-10379
- Newton laws and solution existence of two and three body problems in remote universe
03 p0388 A72-13174
- Spatial motion of two thread-coupled bodies along satellite circular orbit, discussing system equilibrium position stability and phase trajectories
04 p0582 A72-15003
- Soviet book on geometrical space geodesy covering satellite observation, Keplerian laws, two body problem and orbit element determination
06 p0879 A72-17817
- Two body problem trajectory equation method simplification, reducing entire solution to two integral evaluations
06 p0881 A72-17931
- Restricted two body problem anomalistic and sidereal orbital periods in coordinate and proper time, noting cosmological constant
06 p0884 A72-18035
- Multiparticle time regularization technique based on kinetic energy potential, noting application to two body encounters
06 p0885 A72-18073
- Autonomous two body system described by nonlinear differential equations of motion, obtaining free relative vibration solution in terms of elliptic functions
06 p0849 A72-18694
- Relative motion of two mass points linked by flexible weightless tether in orbit around planet
06 p0891 A72-18695
- Orbital elements evolution for two body problem with decreasing mass according to Jeans mode
08 p1236 A72-21638
- Forced vibrations of two-mass system with damping through inelastic collisions, determining periodic motions stability regions with allowance for elastic coupling and friction
09 p1352 A72-23179
- Restricted two body problem anomalistic and sidereal orbital periods in general relativistic coordinate and proper time, noting cosmological constant
11 p1719 A72-25971
- Fourth order polynomial method and computational algorithm for direct integration of n body systems, discussing two body encounters and binary systems
12 p1875 A72-27917
- Two body model for three body problem of uniformly distributed and isotropically expanding gravitational matter of Einstein-Sitter universe, noting metagalaxy cooling rate
14 p2149 A72-30211
- Invariant mechanics principles for two body system dynamic properties, analyzing mass center motion, system energy and gravitational theory role
14 p2152 A72-30481

- Equinoctial orbit elements position and velocity vectors partial derivatives matrices for two body problem, discussing application to general and special perturbations
17 p2609 A72-35104
- Two body problem trajectory equation method simplification, reducing entire solution to two integral evaluations
18 p2730 A72-37156
- Undisturbed eccentric anomaly difference as the independent variable in the perturbation differential equations.
19 p2856 A72-37520
- Numerical stabilization of the differential equations of Keplerian motion.
21 p3106 A72-41050
- Stationary motions of a triaxial body and their stabilities.
21 p3109 A72-41334
- Equinoctial orbit elements - Application to artificial satellite orbits.
21 p3112 A72-41575
- [AIAA PAPER 72-937]
Two body model for three body problem of uniformly distributed and isotropically expanding gravitational matter of Einstein-Sitter universe, noting metagalaxy cooling rate
23 p3334 A72-43241
- Differential equations of motion of two mutually perturbing bodies, noting series expansion of perturbation function for close commensurability of mean motions
24 p3437 A72-44761
- Hyperbolic two body problem in celestial mechanics, discussing E , r , α , β , summability procedure for analytic continuation
24 p3442 A72-45236

TWO DIMENSIONAL BODIES

- Two dimensional and axisymmetric body viscous drag in incompressible flows, using implicit finite difference boundary layer method
[AIAA PAPER 72-1]
05 p0606 A72-16860
- Two dimensional airfoil unsteady stall in incompressible flow, comparing calculated loading during transient and sinusoidal pitching motions with measured values
[AIAA PAPER 72-37]
05 p0607 A72-16899
- Dynamics of two dimensional body with cavity containing viscous incompressible fluid, noting obstacle interaction and free surface motion problems
06 p0801 A72-18139
- Wake analysis of asymmetric hypersonic flow past two dimensional profiles at small angles of attack, using perturbation techniques
06 p0757 A72-18143
- Unsteady incompressible laminar boundary layer theory on two dimensional body motion through fluid at rest at infinity, considering skin friction
08 p1151 A72-21794
- Incompressible laminar subcritical flow with separated wake past symmetric two dimensional bluff body, calculating upstream pressure distribution and separation point
12 p1751 A72-27172
- Uniqueness and existence theorems for nonideal thermal contact between three dimensional solid parts in heat conduction theory, noting case of two dimensional body
12 p1889 A72-27996
- Numerical calculation of electromagnetic scattering properties of two dimensional bodies with arbitrary cross section, considering TM polarization of excitation and fields mode matching
13 p1916 A72-28534
- Monte Carlo simulation method for flow field around two dimensional or axisymmetric body immersed in hypersonic rarefied gas flow
16 p2342 A72-32882
- Grid-generated turbulence distortion approaching two dimensional bluff body stagnation region
16 p2344 A72-33569
- Wave-front singularities for two-dimensional anisotropic elastic waves.
18 p2739 A72-37175
- Periodic wave of oscillating and stationary two dimensional bodies immersed in uniform incompressible stream, investigating semiinfinite vortex trails relationship to oscillating airfoils
21 p2989 A72-40651
- Karman vortex street in a uniform shear flow.
21 p2992 A72-41247
- Finite difference theory for Lamé equations of elastic waves propagation in two dimensional body under mixed boundary conditions
22 p3234 A72-42144
- TWO DIMENSIONAL FLOW**
NT COUETTE FLOW
Two dimensional plasma under dc magnetic field, investigating thermal equilibrium with Liouville equation and BBGKY hierarchy
01 p0107 A72-10145
- Distributed impedance controller synthesis for stabilization of plane fluid flows, investigating Rayleigh-Taylor instability
01 p0050 A72-10504

- Two dimensional scanning electron beam pumped laser, describing production of coherent emission
01 p0079 A72-10522
- Discrete ionospheric model of supersonic two dimensional low density plasma flow past large bodies, using quasi-neutrality condition
01 p0001 A72-10588
- Two dimensional transient inviscid flow field from secondary injection in missile control, describing distribution with artificial viscosity finite difference method
01 p0097 A72-10940
- Two dimensional unsteady incompressible boundary layer near forward stagnation point of infinite plane wall with uniform suction or injection, obtaining iterative solution
01 p0050 A72-11106
- Nozzle boundary layers effect on reattachment position of two dimensional jet to adjacent flat plate, noting Reynolds number influence
02 p0150 A72-11729
- Nonlinearity effects on two dimensional steady supersonic dissipative flow governed by Navier-Stokes equations, obtaining expressions for flows past thin airfoil and wedge
02 p0203 A72-11976
- Two dimensional diffusers flow patterns with laminar boundary layer entry, investigating wall shape and vanes effects with water table test facility
02 p0204 A72-12231
- Least squares and point matching techniques compared for solution of two dimensional steady state heat conduction problems with irregularly shaped boundaries
[ASME PAPER 71-HT-P]
02 p0302 A72-12318
- Plane cavity flow past symmetric ogival obstacles, applying variational principle to fixed point theorem
02 p0206 A72-12625
- Blade cascades pressure distribution for plane incompressible flow with boundary layer separation near trailing edges, replacing blade profiles by vortex fields
[DGLR PAPER 71-097]
02 p0153 A72-12728
- Two dimensional MHD channel flow of inviscid fluid in circular nonuniform magnetic field
02 p0267 A72-12771
- Velocity and temperature distributions for unsteady plane Poiseuille flow of viscous incompressible fluid between two parallel plates
03 p0340 A72-13000
- Wall jet flow displacement on curved surface, deriving two dimensional solution for second-order boundary layer equations
03 p0307 A72-13159
- Two dimensional elasto-viscous incompressible fluid flow past porous wall with variable suction, analyzing temperature field of laminar thermal boundary layers
03 p0341 A72-13500
- Two dimensional viscoelastic fluid flow past infinite plate with time dependent suction and constant and periodic free stream velocity
03 p0341 A72-13630
- Two dimensional transonic airfoil section testing at ONERA S3MA wind tunnel, comparing results with helicopter rotor blades test data
[ONERA, TP NO. 1028]
03 p0308 A72-13642
- Two dimensional MHD turbulent flow generation in strong magnetic field
03 p0398 A72-14004
- Asymptotic theory of heat transfer in two dimensional turbulent boundary layers of incompressible fluid at large Reynolds numbers
03 p0459 A72-14390
- Steady two dimensional cavity flow past infinite number of airfoils using linearized theory
04 p0461 A72-14460
- Generalized transformation of plane compressible and axisymmetric equation for self similar solutions of dissipative boundary layer for bodies with variable surface
04 p0510 A72-14468
- Plane steady flow of two viscous fluids in contact, presenting normal and tangential pressure
04 p0510 A72-14513
- Maxwell boundary conditions method application in kinetic theory of gases, investigating linearized plane Couette flow
04 p0510 A72-14594
- Linear stability of nearly parallel steady plane viscous flows, using method of multiple scales
[ONERA, TP NO. 1044]
04 p0511 A72-14969
- German monograph on two dimensional unsteady boundary layer calculation with unstable effects, using Navier-Stokes equations
04 p0512 A72-15245
- Incompressible power law pseudo-plastic material plane flow in converging channel and axially symmetric converging flow in circular cone
04 p0513 A72-15287
- Two dimensional unsteady flow of incompressible fluid around passing turbomachine blades, determining instantaneous pressure, forces and moments as function of time
04 p0463 A72-15559

Circular arc blades two dimensional cascade performance test data for various cambers comparison with potential theory data 05 p0602 A72-16485

Two dimensional cascade performance data correction for rotating blade row stream surface inclination in axial flow turbines 05 p0602 A72-16486

Two dimensional cascade test of air-cooled turbine nozzle, describing aerodynamic characteristics and heat transfer properties 05 p0602 A72-16489

Finite difference calculations for two dimensional unsteady inviscid expanding flow of perfect gas through nozzle, obtaining flow field patterns 05 p0603 A72-16539

Two dimensional turbulence stationary states from statistical equilibria for Navier-Stokes equation 05 p0649 A72-16686

Interaction produced by diametrically opposed plane turbulent wall jet collision in still air, discussing resultant free jet [AIAA PAPER 72-211] 05 p0606 A72-16854

Atmospheric turbulence incompressible two dimensional model, comparing Navier-Stokes equations numerical integration results with finite difference simulation [AIAA PAPER 72-152] 05 p0651 A72-16871

Two dimensional lift characteristics of multielement airfoils, using potential flow method based on surface source distribution and finite difference boundary layer method [AIAA PAPER 72-3] 05 p0608 A72-16935

Finite difference model application to supersonic planar viscous near wake determining parameter range by physical and numerical restraints [AIAA PAPER 72-115] 05 p0609 A72-16971

Plane Poiseuille flow stability from Orr-Sommerfeld equation solution by Chebyshev polynomials expansion and QR matrix eigenvalue algorithm 05 p0653 A72-17009

Steady two dimensional symmetric viscous flow past parabolic cylinder in uniform stream, correlating calculated nose skin friction with boundary layer theory 05 p0610 A72-17012

Two dimensional turbulent boundary layer before rectangular separation, investigating heat exchange in separation regions 05 p0751 A72-17048

Plane two dimensional wall jet, investigating flow dynamic structure 06 p0901 A72-17562

Two-dimensional asymptotic solutions to Navier-Stokes equations for weak vortex discontinuity flow with vanishing viscosity 06 p0798 A72-17680

Two dimensional flow attachment to flat plates, investigating Coanda effect 06 p0798 A72-17776

Two dimensional flow of gas jet around dihedral obstacle, investigating screen proximity and fluid compressibility effects 06 p0799 A72-17912

Two dimensional transonic and hypersonic shock structures, discussing flow equations, mathematical properties and similarity rules [AD-742561] 06 p0799 A72-17960

Asymptotic developments in transonic flows, considering three dimensional flows near shock and plane viscous and heat conducting flow 06 p0756 A72-18105

Steady two dimensional magnetodynamic flow past nonconducting wedge with perpendicular magnetic field at different shock attachment angles 06 p0861 A72-18113

Small parameter method solution of two dimensional incompressible flow Navier-Stokes equations, exemplifying application to viscous incompressible flow past semiinfinite plate 06 p0801 A72-18127

Marginally unstable plane parallel flow nonlinear response to two dimensional disturbance, noting localized burst relationship to Landau constant 06 p0801 A72-18163

Plane two dimensional flow in channel of rocket engine with solid propellant combustion, obtaining burning rates 06 p0867 A72-18207

Turbulent layer generation in ideal two dimensional fluid flow, determining vortices time evolution from initial velocity discontinuity by numerical methods 06 p0802 A72-18525

Finite element solution for Boussinesq approximation of two dimensional viscous fluid dynamic problems, using variational principle 07 p0965 A72-18794

Plane stationary flow of ideal incompressible fluid past large camber profiles of arbitrary shape and thickness, using computerized Fourier expansion 07 p0908 A72-18976

Difference method for numerical integration of Navier-Stokes equations for two dimensional incompressible steady flow along flat thin plate 07 p0908 A72-19170

Monograph on boundary layer generation, presenting two dimensional singular perturbation method 07 p0967 A72-19265

Two dimensional and axisymmetric flow with heat addition, deriving flow field by inverse methods 07 p0909 A72-20062

Irrotational two dimensional transonic flow past symmetric profile with and without shock 07 p0909 A72-20068

Two dimensional subsonic flow behind symmetrical blade cascade, taking into account initial flow turbulence 07 p0909 A72-20078

Two dimensional compressible boundary layer turbulent velocity profile on adiabatic and isothermally cooled walls with zero pressure gradient 07 p0970 A72-20080

Computerized simulation of two dimensional turbulent flow in Fourier space with random initial conditions on coefficients, discussing velocity, pressure and vorticity fields 07 p0971 A72-20084

Dirichlet and Volterra problem with prescribed singularities for plane with rectilinear boundary slits, applying to fluid mechanics 07 p0971 A72-20092

Perfect fluid two dimensional steady flow equation solution for viscous flow with specified boundary conditions, considering vortex flow 07 p0971 A72-20099

Interference induced unsteady aerodynamic forces on tandem airfoils in subsonic flow, using two dimensional model 07 p0910 A72-20101

Plane irrotational flow of fluid with arbitrary thermodynamic properties in throat of Laval nozzle, solving flow equations 07 p0972 A72-20111

Digital simulation of two dimensional or marginally turbulent three dimensional flows by discretization and numerical integration, noting Galerkin method efficiency in avoiding errors 07 p0951 A72-20355

Flow field model of convective heat transfer along reattachment surface in planar supersonic turbulent flow [ASME PAPER 71-HT-W] 08 p1251 A72-20876

Parabolic differential equation system for boundary layer behavior of steady plane gas flow 08 p1107 A72-20911

Stream functions for steady two dimensional flow field of viscous liquid near circular whirl 08 p1148 A72-20937

Numerical simulation of two dimensional and marginal three dimensional turbulent flows, discussing variable eddy viscosity model, discretization, numerical integration and Galerkin methods 08 p1200 A72-21492

Critical Reynolds numbers estimation for flows having velocity profile with point of inflection, discussing plane parallel flows stability energetic analysis 08 p1151 A72-21660

Two dimensional laser Doppler forward and backscatter velocimetry in turbulent flows, applying to four inch pipe 09 p1305 A72-22303

Equilibrium statistics of randomly forced two dimensional viscous flow three mode representation constructed by numerical integration of nonlinear equations system 09 p1293 A72-22459

Two dimensional MHD conducting fluid flow past insulating cylinder in presence of arbitrarily oriented magnetic field, determining lift and drag coefficients for small Hartmann numbers 09 p1359 A72-22533

Boundary condition for plane or axisymmetric stagnation point flow of micropolar fluid over flat plate, giving numerical solutions for turbulent characteristics 09 p1293 A72-22621

Potential equations and singularities methods comparison for two dimensional flow field cascades and stress distribution elasticity theories 09 p1260 A72-22627

Energy spectrum and decay of random two dimensional vorticity distributions at large Reynolds number [AD-740486] 09 p1294 A72-22943

Two dimensional creeping flow in fiber reinforced composite under uniform tension, discussing matrix shear stress and fiber direct stress distributions 09 p1338 A72-23168

Numerical prediction of inert and reacting steady internal two dimensional recirculating flows by finite difference method, including turbulence and combustion models 10 p1561 A72-23868

Steady inviscid irrotational transonic flow in two dimensional symmetric and axially symmetric nozzle throats 10 p1417 A72-23875

Instantaneous velocity vector determination in two dimensional flow by hot-wire anemometer and on-line digital computer technique 10 p1478 A72-23877

Spanwise velocity distribution effect on drag measurement of short struts in two dimensional turbulent airstreams 10 p1417 A72-23881

Small turbulences growth in two dimensional incompressible wake, noting transverse oscillations of mean velocity profile [AD-742006] 10 p1467 A72-24367

Two dimensional low Mach number sound field from line vortex passage around rigid half plane edge, calculating space-time variation by perturbation methods 10 p1468 A72-24370

Antisymmetric turbulences linear stability in incompressible plane Poiseuille flow between flexible walls solved by variational boundary value problem formulation 10 p1468 A72-24372

Finite amplitude disturbances effect on plane Poiseuille flow hydrodynamic stability, presenting numerical method for solving parabolic partial differential equations derived from Navier-Stokes equation 10 p1468 A72-24422

Infinitesimal centered disturbance effect on plane Poiseuille flow at supercritical Reynolds number, determining modulated wave as function of position and time 10 p1562 A72-24423

Plane transonic gas flows through Laval nozzle and symmetrical wedge-shaped profile, solving boundary value problem by reduction to singular integral equation 10 p1418 A72-24433

Axisymmetric plane transonic flow past convex corner point, obtaining characteristics by mapping into hodograph plane 10 p1468 A72-24435

Steady two dimensional flow of monatomic rarefied gas past semiinfinite beam 10 p1418 A72-24543

Two and three dimensional turbulent boundary layers integral calculation method, presenting similarity solutions based on extended mixing length model 10 p1469 A72-24653

Two dimensional hydrodynamic flow analysis of pneumatic tire hydroplaning, taking into account tire deformation, viscous, inertial and turbulence effects 10 p1512 A72-24819

Rectangular and D-shaped cylinders pressure distribution and aerodynamic force measurements in two dimensional flow as function of cross sectional height/width ratio 10 p1419 A72-24840

Aerodynamic throttling effect due to air jet flow interaction in throat region of mainstream two dimensional nozzle flow 10 p1419 A72-24845

Plane irrotational motion of ideal incompressible fluid perturbed by profile movement and deformation, obtaining aerodynamic forces power 10 p1420 A72-24853

Two dimensional unsteady stagnation point flow against plane wall with impulsive motion 10 p1470 A72-25040

Plane laminar semibounded incompressible fluid jet propagation into slipstream along moving plate, solving boundary layer equations 10 p1471 A72-25136

Adverse pressure gradients effect on two dimensional supersonic turbulent boundary layer, measuring axial distribution of pressure, temperature, mass flow, turbulence intensity and wall shear [AIAA PAPER 72-311] 11 p1614 A72-25245

Two dimensional transonic turbine blade cascade downstream flow losses determination [ASME PAPER 72-GT-43] 11 p1570 A72-25637

Two dimensional flow losses of turbine blade cascade with incompressible boundary layer injection [ASME PAPER 72-GT-46] 11 p1570 A72-25638

Two dimensional cascades supersonic exit flow field, using Oswatitsch method of characteristics and conservation laws [ASME PAPER 72-GT-49] 11 p1570 A72-25641

Perturbation analysis of perfect gas unsteady transonic irrotational inviscid flow in two dimensional channel, presenting numerical computation of flow structure temporal change 11 p1618 A72-26635

Relative atmospheric dispersion in estuary / half squared vorticity / - cascading inertial range of homogeneous two dimensional turbulence 12 p1839 A72-27031

Unbounded wall effect on complex potential of two dimensional flow produced by arbitrary displacement of body within ideal incompressible fluid 12 p1797 A72-27119

Limiting form of equations for perfect gas steady two dimensional flow under gravity effects [ONERA, TP NO. 1087] 12 p1797 A72-27177

Primary velocities distribution in two dimensional turbulent boundary layer inside dihedral 12 p1797 A72-27179

Plane Poiseuille flow Orr-Sommerfeld problem numerical solutions comparison and computer program implementation

12 p1797 A72-27192

Asymptotic behavior of velocity profiles in laminar boundary layers of steady incompressible fluid two dimensional flow past rigid wall

12 p1798 A72-27713

Two dimensional Prandtl-Meyer flow anisotropy of ideal gas expanding into vacuum, using free path probe-molecule technique

12 p1799 A72-28178

Plane potential flow stability with respect to bounded and free hollow vortices, using conformal mapping method

13 p1941 A72-28716

Plane unsteady potential isentropic gas flow equations solution interpreted as shallow water motion over horizontal bottom

13 p1893 A72-28717

Effect of magnetic field superimposed on turbulent shear flow of electrically conducting fluid, discussing turbulent friction in plane flow

13 p2010 A72-28764

Uniform suction effect at stationary plate on longitudinal and transverse velocities of plane Couette flow between parallel plates

13 p1941 A72-28884

Orr-Sommerfeld equation solution by variable mesh finite difference method, applying to plane Poiseuille flow

13 p1986 A72-29112

Two dimensional laminar compressible flow of electrically conducting gas at thermodynamic equilibrium and perpendicular to magnetic field lines

13 p2013 A72-29362

Hypersonic blowdown tunnel investigation of turbulent shock-boundary layer interactions at two dimensional wedge compression corner

13 p1944 A72-30030

Inviscid plane Couette flow infinitesimal instability as initial value problem, using distribution-theoretic approach

14 p2126 A72-30230

Localized point centered initial disturbances effects on marginally unstable plane parallel flow, presenting differential equations solution for nonlinear response

14 p2094 A72-30366

Third order extension of perturbation method to solve Oseen equations for two dimensional steady viscous flow past cylindrical body at low Reynolds number

14 p2095 A72-30722

Hodographic equations solution containing critical point for compressible fluid two dimensional flow, noting calculation of wing profiles and turbine engine cascades

[ONERA, TP NO. 1048]

14 p2095 A72-30841

Plane nonlinear wave propagation in transonic region of two dimensional and axisymmetric steady flows, considering disturbance at arbitrary point

14 p2095 A72-31000

Ideal liquid theory application for unsteady separated flow calculation around arbitrary shape bodies, noting numerical solution for plane flow around circular cylinder

14 p2070 A72-31010

Two dimensional two phase steady supersonic wedge flow patterns analysis based on equations for flow between wedge surface and shock wave

14 p2070 A72-31011

Velocity and temperature profiles of plane Poiseuille flow with finite amplitude convection and longitudinal vortices, investigating uniform axial temperature gradient effect

14 p2173 A72-31063

Plane unsteady convective motion of viscous incompressible liquid in infinite horizontal vessel of rectangular cross section due to wall temperature fluctuations

14 p2174 A72-31157

Two dimensional viscous flow past semiinfinite flat plate and smooth obstacle, using Navier-Stokes equations for lift force relationship investigation

15 p2216 A72-31312

Kinematic eddy viscosity for incompressible two dimensional turbulent flow, obtaining Navier-Stokes equations and conditions for equilibrium and nonequilibrium boundary layers

15 p2216 A72-31470

Two dimensional incompressible turbulent boundary layer in arbitrary pressure gradient, obtaining mathematical model for solution by implicit finite difference method

15 p2217 A72-31718

Laminar boundary layer separation point in steady two dimensional constant density flow past solid surface, deriving pressure-vorticity gradient relationship

15 p2218 A72-32467

Nonlinear stability theory for plane Poiseuille flow under finite amplitude perturbations, solving Orr-Sommerfeld boundary value problem via finite difference method

15 p2218 A72-32469

Heat transfer to two dimensional laminar flow, calculating axial conduction and fluid preheating effects on adiabatic forced convection at low Peclet number

15 p2336 A72-32478

Subsonic and supersonic steady two dimensional compressible turbulent boundary layer flow past wavy wall, presenting wall pressure and temperature distributions

16 p2341 A72-32828

Nonlinear instability of two dimensional unbounded incompressible viscous fluid flows under periodic small perturbation

16 p2376 A72-32933

German monograph on plane steady isentropic flow past obtuse apex angle wedge at zero angle of attack and free stream sonic velocity

16 p2343 A72-33400

Time behavior of two dimensional laminar free convection flow between heated vertical parallel plates, calculating temperature and velocity distributions as function of Grashof number

16 p2477 A72-33426

Transonic plane flow past wavy wall during choked wind tunnel operation, calculating flow velocity from Mach-Zehnder interferometer measured density distribution

16 p2378 A72-33508

Plane Poiseuille flow stability of incompressible second order fluids, noting destabilizing influence of viscoelasticity

16 p2379 A72-33829

Shear stress and dimensionless velocity profiles of plane incompressible fluid wall jet propagation along curved surface

16 p2380 A72-33856

Prediction of the flow and heat transfer in a rectangular wall cavity with turbulent flow.

[ASME PAPER 72-APM-Q]

17 p2636 A72-34305

Solution of the two-dimensional, unsteady, compressible Navier-Stokes equations using a second-order accurate numerical scheme.

17 p2538 A72-34646

Theorem for instability of rectilinear vortices in two dimensional steady flow of ideal liquid with or without submerged obstacle

17 p2539 A72-34910

Vortex growth in two-dimensional coalescing jets.

17 p2539 A72-34970

An experimental investigation of an asymmetrical turbulent wake.

17 p2485 A72-35187

Numerical simulation studies of two-dimensional turbulence. I - Models of statistically steady turbulence.

17 p2543 A72-35765

Cavitation zone structure behind circular cylinder model in plane flow investigated by high speed motion picture photography and with short exposure time flash

17 p2544 A72-35897

Low order model and error rates for two dimensional turbulent motion prediction in atmosphere spectrum

18 p2677 A72-36009

Eddies memory in turbulent shear flow from experiments on plane turbulent wakes undergoing equilibrium transition under impulsive pressure gradient effect

18 p2680 A72-36476

A through-type counting method for two-dimensional and spatial supersonic flows. II

18 p2642 A72-36810

Two dimensional channel contraction induced flow acceleration effect on turbulence structure

18 p2683 A72-36995

Slow motion in a two-dimensional semi-infinite channel with moving walls.

18 p2683 A72-37044

A comparison of the solutions of Prandtl's and Navier-Stokes equations in a superposed fluctuating flow.

18 p2684 A72-37084

Two component reaction kinetics model for numerical analysis of combustion during two- and three dimensional supersonic steady flow of hydrogen-air fuel mixtures

19 p2880 A72-37389

Viscosity effect on hypersonic flow field near slender body, discussing eigenvalue solutions for two and three dimensional flow around triangular plate

19 p2745 A72-37393

Finite amplitude neutrally stable two dimensional disturbances in parallel flows for large Reynolds numbers, investigating phase shift across critical layer

19 p2786 A72-37572

Rotor and grid motions associated with holomorphic two dimensional fluid velocity, obtaining aerodynamic forces

19 p2746 A72-37787

On a method of computing the plane steady flow around a profile situated between straight parallel lines.

19 p2786 A72-38098

Analysis of the interaction of jets and airfoils in two dimensions.

[AIAA PAPER 72-777]

19 p2746 A72-38136

Calculation of the plane potential flow past rotating radial blade cascades

19 p2746 A72-38547

A method of straight-through calculation for two-dimensional and three-dimensional supersonic flows. I

19 p2747 A72-38852

Study of the flow of a heavy fluid with free surface from a symmetrical tank

20 p2913 A72-39417

Kramer and Couette flows using the Bhatnagar-Gross-Krook model.

20 p2913 A72-39418

Decay of a diamond shock pattern.

20 p2913 A72-39606

Motion of particles injected from the surface into stagnation-point flow.

20 p2913 A72-39611

Theory of heat transfer in a two-dimensional porous cooled medium and application to an eccentric annular region.

[ASME PAPER 72-HT-47]

20 p2985 A72-39663

Interaction between the droplets of a polydispersed condensate in a nozzle flow

20 p2915 A72-40046

Steady capillary-gravitational waves of finite amplitude generated by pressure periodically distributed along the flow surface of a fluid of finite depth.

21 p3044 A72-40261

Axial velocity distribution and streamline boundary selection to derive two dimensional infinite duct shapes for inviscid irrotational compressible flows

[ICAS PAPER 72-08]

21 p2990 A72-41133

Two-dimensional subsonic linearized theory of the unsteady flow through a blade-row with small steady pitch and camber angle.

[ICAS PAPER 72-12]

21 p2990 A72-41137

Heat transfer in separated regions in supersonic and hypersonic flows.

[ICAS PAPER 72-14]

21 p2991 A72-41139

Some results from tests in the NAE high Reynolds number two-dimensional test facility on 'shockless' and other airfoils.

[ICAS PAPER 72-33]

21 p2991 A72-41158

Two-dimensional stationary problem with a free boundary for the Navier-Stokes equations

21 p3047 A72-41663

Two dimensional MHD fluctuating flow of incompressible electrically conducting rarefied gas past infinite porous wall for slip-flow regime with variable suction

21 p3095 A72-41784

Quasi-two dimensional turbulence model of energy spectra and potential entropy transfer in synoptic large scale quasi-horizontal atmospheric motions

21 p3049 A72-41793

Researches on the two-dimensional retarded cascade. I, II.

22 p3133 A72-41944

Conformal mapping for interaction of two dimensional flow of ideal fluid and injected counterflow with jet formation, calculating cavitation void dimensions

22 p3165 A72-42065

Plane potential flow stability with respect to small perturbation flow of bounded and free hollow vortices, using conformal mapping method

22 p3165 A72-42093

Plane unsteady potential isentropic gas flow equations solution interpreted as shallow water motion over horizontal bottom

22 p3165 A72-42094

A simple quadrature method for computing laminar boundary layers.

22 p3165 A72-42110

Particle collisions integral in Boltzmann equation for arbitrary distribution function, with particular attention to two dimensional flows

22 p3205 A72-42266

Equations of plane potential electrohydrodynamic flow, noting jet and quasi-one dimensional flows of charged particles in curvilinear electrostatic field

22 p3210 A72-42269

Calculation of two-dimensional flows in hydrodynamics and the heat-transfer of a viscous fluid

22 p3166 A72-42287

Two-dimensional model for thermal compression.

22 p3136 A72-42868

Pressure effect at arbitrary Knudsen numbers

23 p3279 A72-43216

An improved solution of the two-dimensional jet-flapped airfoil problem.

23 p3247 A72-43329

Turbulent mixing of three plane isothermal jets with various velocity ratios, showing jet initial length shortening due to initial turbulence increase

23 p3279 A72-43657

A simple theory for the two-dimensional compressible turbulent boundary layer.

[ASME PAPER 72-FE-15]

23 p3280 A72-44062

Falkner-Skan flows with slip.

23 p3281 A72-44068

Steady two-dimensional viscous flow in a jet.

23 p3282 A72-44303

A numerical experiment on two-dimensional turbulent separation.

24 p3389 A72-44687

- Periodic solutions of a nonlinear mixed problem for the Navier-Stokes equations 24 p3418 A72-44780
 - Two-dimensional supersonic flow with flame sheets. 24 p3360 A72-44988
 - Plane stationary flow of ideal incompressible fluid past large camber profiles of arbitrary shape and thickness, using computerized Fourier expansion 24 p3360 A72-45002
 - Velocity profiles of plane turbulent flow of incompressible fluid on porous surface in presence of suction 24 p3390 A72-45007
 - Axisymmetric and two-dimensional flow with attached shock waves. 24 p3361 A72-45161
 - The large Reynolds number - Asymptotic theory of turbulent boundary layers. 24 p3392 A72-45248
 - Frictionless core flow and friction layers at turbomachine walls and blades for real two dimensional cascade flow modeling 24 p3394 A72-45370
 - Mach reflection from overexpanded nozzle flows. 24 p3365 A72-45794
- TWO DIMENSIONAL JETS**
- Integral method for predicting streamwise development of plane turbulent jets and wall jets in uniform streaming flow 01 p0051 A72-11393
 - Differential equations solution for turbulent two dimensional jet flows bounded by parallel planes 02 p0156 A72-12000
 - Two dimensional underexpanded jet plumes flow distribution determination using time dependent finite difference method 02 p0301 A72-12257
 - Incompressible two dimensional plane jet spatial stability analysis, presenting disturbance vorticity, Reynolds stress and energetics distribution in cross stream direction [AD-741988] 02 p0152 A72-12352
 - Incompressible two dimensional laminar/turbulent wall jet characteristics, obtaining Prandtl mixing theory from apparent kinematic viscosity 02 p0206 A72-12619
 - Plane air jet ejection into dead ended rectangular and parabolic channels, discussing effects of geometry, length and pressure 03 p0309 A72-14156
 - Jet mixing flow from slotted source into longitudinal cross flow shown analogous to heat expansion in plane jets 05 p0648 A72-16220
 - Two dimensional transverse subsonic hot-air jet interaction with freestream flow at various jet/freestream velocity ratios, measuring jet velocity and temperature distributions [AIAA PAPER 72-292] 11 p1567 A72-25230
 - Uniform and parallel magnetic field effects on hydromagnetic instability of two dimensional jet at small magnetic Reynolds numbers 11 p1693 A72-25521
 - French monograph on turbulent free flow boundaries covering two dimensional plane jet mixing zone characteristics from thermal signal measurements 14 p2095 A72-30948
 - Describing equations derivation by implicit finite difference scheme for chemically nonreactive two dimensional symmetric and axisymmetric jet and wake problem 16 p2381 A72-34170
 - Transient acoustic point source disturbance transmission in two dimensional idealized jet, noting velocity profile effects on noise radiated to far field 18 p2679 A72-36406
 - Topler schlieren study of diffusion flame structure of plane laminar hydrogen-air jets in rectangular channel with vortex generators 19 p2879 A72-37365
 - Two dimensional underexpanded free jet flow into static medium, presenting wind tunnel nozzle experimental data and graphic solutions from method of characteristics 20 p2885 A72-39619
 - Experimental and design investigation of a supersonic wall jet in a supersonic slipstream 22 p3133 A72-42254
- TWO FLUID MODELS**
- MHD instabilities of plasma with current, using two fluid model in crossed magnetic-electric fields 01 p0109 A72-10486
 - Solar wind two component model with protons collisionless beyond ten solar radii, discussing effects of variable electron temperature 01 p0119 A72-10879
 - Gas dynamic lasers theory based on two fluid model of optically active medium, investigating medium velocity effect on lasing mechanism 01 p0081 A72-11210
 - He film two fluid model consistency with equilibrium between film and vapor 03 p0390 A72-14375
 - Current source generated electromagnetic and electroacoustic wave propagation through homogeneous, isotropic compressible electron-ion plasma, using two fluid continuum theory 04 p0554 A72-14510
 - Collisionless solar wind in spiral interplanetary magnetic field, using two fluid model with hydrodynamically treated electrons 06 p0872 A72-17441
 - Two fluid plasma longitudinal ion and electron waves nonlinear interactions excitation of type 2 bursts, considering radiation flux density 06 p0862 A72-18175
 - Two fluid MHD model to study cylindrical plasma condenser resonance properties in axial magnetic and alternating electric fields 09 p1360 A72-22952
 - Two fluid MHD model for flat plasma condenser in crossed magnetic and alternating electric fields, calculating impedance and disturbed plasma parameters 09 p1360 A72-22953
 - Isochoric heat capacity peaks of water and argon near boundary in two phase region at critical state 11 p1747 A72-26964
 - Temperature oscillations associated with surface gravity waves at two fluid model compressible vapor-incompressible superfluid interface 12 p1845 A72-27386
 - Collisional plasma shock waves structure in electromagnetic shock tube with strong transverse bias magnetic field, using two fluid Navier-Stokes equations 13 p2011 A72-29119
 - Two fluid model application to microbridges between superconductors, investigating superconducting particles number time variation possibility 13 p2023 A72-29789
 - Electron temperature radial dependence in two fluid models of solar wind, noting unrealistic assumption of heat conduction dominated electron gas energy equation 13 p2034 A72-29961
 - Flat homogeneous isotropic relativistic cosmological two fluid model, using Robertson-Walker metric 15 p2307 A72-31795
 - Two fluid cosmological model in conformal and conformally flat forms, deriving solutions in elementary functions 15 p2307 A72-31796
 - A two-fluid solar wind model with anisotropic proton temperature. 17 p2599 A72-35097
 - Two fluid MHD model to study cylindrical plasma condenser resonance properties in crossed axial magnetic and alternating electric fields 17 p2593 A72-35881
 - Two fluid MHD model for flat plasma condenser in crossed magnetic and alternating electric fields, calculating impedance and disturbed plasma parameters 17 p2593 A72-35882
 - Two fluid model for qualitative interpretation of turbulent intermittency, noting governing equations analogy to Landau equations for superfluidity 19 p2787 A72-38428
 - Non-Boussinesq effects and further development in a model of upper tropospheric frontogenesis. 19 p2829 A72-38558
 - One dimensional variable slip and homogeneous model predictions of momentum flux in two phase two component low quality flow 21 p3130 A72-41179
 - Eigenvalue numerical solution for dispersion relation and propagation characteristics of nonlocal drift waves in cylindrical plasma based on two fluid model 21 p3093 A72-41495
 - Effects of parallel wavelength on the collisional drift instability. 21 p3093 A72-41627
 - Thermal diffusion and convective stability. II - An analysis of the convected fluxes. 24 p3465 A72-45561
 - Stability of coaxial rotating jet and vortex of different densities. 24 p3394 A72-45562
- TWO PHASE FLOW**
- Fluid droplet collapse in two phase gas flows, noting time dependence 01 p0145 A72-10573
 - Two phase flow equations model application to fluidized beds and foams, predicting bed stability to small perturbations for comparison with experiment 01 p0093 A72-11272
 - Liquid containment in gas driven vortex with air-water mixture densities above 100 times gas flow, discussing applicability to colloidal core nuclear reactor performance estimation 01 p0100 A72-11360
 - Liquid and solid particle trajectory calculation in two phase Laval nozzle flows, determining density, velocity and temperature 02 p0149 A72-11588
 - Shock wave damping and droplet atomization function of relaxation zone in noncombustible two phase gas-liquid mixtures 02 p0202 A72-11592
 - Kinetic energy losses due to liquid-to-solid phase transformation in heated two-component flow ascending in tube 03 p0342 A72-14161
 - Thermal modeling of space shuttle cryogenic turbopump, considering heat transfer for two-phase cryogen and gas impingement on turbine blades and rotating disks [ASME PAPER 71-WA/HT-43] 05 p0664 A72-15890
 - Fluid motion model with gas bubbles, noting energy dependence on temperature and density 05 p0649 A72-16224
 - Boundary layer of gas-particle flows with pressure gradient, numerically integrating momentum equation for cascade particulate flow [AIAA PAPER 72-87] 05 p0604 A72-16808
 - Heat pipe temperature gradient initial conditions for ideal gas model, introducing two phase Mach number for choking phenomena analysis [AIAA PAPER 72-22] 05 p0749 A72-16913
 - One dimensional two phase flow transpiration cooling through porous metals [AIAA PAPER 72-24] 05 p0749 A72-16915
 - Two phase heat transfer in porous metal transpiration cooling system, comparing measured with calculated temperature distribution [AIAA PAPER 72-25] 05 p0749 A72-16916
 - Two phase flow model of water droplets velocity in air stream, using Fresnel biprism and laser differential scheme 07 p1000 A72-18940
 - Two phase boundary layer flow for laminar two dimensional steady forced film condensation with pressure gradients for fluids of small Prandtl numbers [ASME PAPER 71-HT-Y] 08 p1251 A72-20878
 - Hydrodynamics of dispersed annular two phase flow in cylindrical channels characterized by concurrent motion of flow core and liquid film at wall 08 p1151 A72-21667
 - Two phase axisymmetrical air jet turbulence intensity determination from heat distribution parameters in wake of wire heated by electric current 10 p1471 A72-25172
 - Noncondensable gas and forced convection effects on laminar film condensation for two phase flows 11 p1743 A72-25261
 - Critical discharge regimes of two phase steam/water mixture flow from nozzles, using counterpressure effect 11 p1619 A72-26674
 - Inhomogeneous two phase flow past sphere comparing structural and hydrodynamic characteristics on basis of X ray photographs 13 p2066 A72-30003
 - Velocity calculation from pitot tube pressure measurements in compressible two phase flow, taking into account droplet momentum loss 14 p2104 A72-30252
 - Two phase propellant flow rate through simulated rotating liquid core nuclear rocket fuel bed under high centrifugal acceleration 14 p2129 A72-30923
 - Two dimensional two phase steady supersonic wedge flow patterns analysis based on equations for flow between wedge surface and shock wave 14 p2070 A72-31011
 - Thermal protection by liquid-gas laminar flow near critical point with coolant film liquid oxygen injection incident on blunt body 16 p2343 A72-33156
 - Steam-condensate mixture transpiration layer flow along curved body surface with arbitrary pressure gradient at low Mach number and constant physical properties 16 p2378 A72-33437
 - Optical method for measuring the velocity of particles entrained in a flow 17 p2554 A72-34892
 - Measurement of the parameters and the structure of a wet vapor flow with interphase heat and mass transfer in the relaxation zone behind the front of a shock wave. 17 p2637 A72-35130
 - Particle motion behind oblique shock wave in two phase supersonic wedge flow, deriving expressions for particle trajectories and velocity equalization time 17 p2487 A72-35926
 - Fluid jets and droplets deformation in transverse supersonic two phase gas flow 17 p2544 A72-35932
 - Stability of the Couette rotatory motion of two-phase media 19 p2787 A72-38209
 - A theoretical solution of the Lockhart and Martinelli flow model for calculating two-phase flow pressure drop and hold-up. 19 p2787 A72-38392
 - The enhancement of heat transfer by waves in stratified gas-liquid flow. 19 p2787 A72-38398
 - Mechanism and characteristics of condensed system ignition by a dispersed flow 19 p2882 A72-38451
 - Techniques for determining average density and related parameters in two-phase cryogenic flow systems. 19 p2805 A72-38835

- Generalized relations for determining specific impulse losses in nonequilibrium two-phase nozzle flows
20 p2914 A72-39909
- Two phase flow types defined as flow problems of two-phase matter mixtures /solid, liquid, gas or plasma/ and interface interaction
20 p2915 A72-39971
- Detonation shock wave study of liquid fuel droplets in gaseous oxidizing agent flow, using schlieren and scanning photography
20 p2962 A72-40044
- Interaction between the droplets of a polydispersed condensate in a nozzle flow
20 p2915 A72-40046
- Pulsation rates of continuous and discrete components of dispersed flow
20 p2915 A72-40047
- One dimensional variable slip and homogeneous model predictions of momentum flux in two phase two component low quality flow
21 p3130 A72-41179
- Heat transfer performance of stationary two phase closed thermosiphon with water and Freon as working fluids, discussing effects of operating pressure and heat flux
21 p3131 A72-41621
- Inhomogeneous two phase flow past sphere, comparing structural and hydrodynamic characteristics on basis of X ray photographs
22 p3167 A72-42726
- Theoretical analysis of a rotating two-phase detonation in liquid rocket motors.
24 p3433 A72-45053
- Gas dynamics and shock wave physics of supersonic flow in two phase media, noting evaporation, condensation and phase transformations
24 p3364 A72-45525
- Fraunhofer single beam holography application to gas/liquid mixture high velocity flow cross section determination, observing liquid component effects on droplet dispersion composition
24 p3405 A72-45624
- TWO PHASE SYSTEMS**
U BINARY SYSTEMS [MATERIALS]
TWO REFLECTOR ANTENNAS
- Geometric optics method applied in design of dual-mirror antenna illumination system, noting diffraction effects and near field influence
04 p0499 A72-15242
- Phase errors and main lobe orientation changes during beam scanning of two reflector Cassegrain antennas
08 p1139 A72-20934
- Two reflector Cassegrain antenna secondary reflector random fluctuations effects on drift in main lobe direction
08 p1143 A72-21846
- Microwave two reflector rectangular backfire antenna with dielectric surface wave structure as waveguide prolongation, obtaining far field radiation pattern
11 p1604 A72-25749
- Pyramidal-horn primary element axial position effect on dual mirror Cassegrain microwave antenna main lobe pattern, obtaining optimal position
13 p1929 A72-29040
- Reflector antennas for satellite communication, discussing hybrid mode, dielguide and lens feeds, spherical and stepped reflectors, and high efficiency paraboloid antennas
21 p3028 A72-40513
- A 3-meter Cassegrain antenna for the frequency range from 2.1 to 2.3 GHz
21 p3029 A72-40521
- Radar double beam dielectric radiator antenna design for ATC in 1250-1350 MHz range
21 p3030 A72-40530
- Radiation patterns and structural design of two mirror millimeter wave Cassegrain antennas with horn radiator
23 p3271 A72-43778
- TYCHO CRATER**
- Lunar igneous activity and differentiation, discussing volcanic flows near Tycho, flow patterns in maria, sinuous rilles and crust lineaments
03 p0418 A72-13107
- TYPE 2 BURSTS**
- Two fluid plasma longitudinal ion and electron waves nonlinear interactions excitation of type 2 bursts, considering radiation flux density
06 p0862 A72-18175
- Solar wind kinetic energy from flare associated solar wind disturbances relation to types 2 and 4 radio bursts, using satellite observations
09 p1378 A72-23399
- Theory for plasma radiation from collisionless MHD shock waves applied to Type 2 solar radio bursts, comparing to type 4 bursts
16 p2446 A72-33461
- Shock wave propagation in the solar corona as the cause of type II radio bursts
19 p2851 A72-38064
- Homologous complex radio bursts of type IV-II in the solar atmosphere
19 p2852 A72-38498

- The heating of the solar plasma due to microwave phenomena correlated with type II meter bursts.
22 p3222 A72-42041
- TYPE 3 BURSTS**
- Type 3 and 3/5 solar radio bursts coupling with microwave bursts, considering connection with H alpha flares and X ray emission
01 p0118 A72-10414
- Solar outer corona steamer density and temperature data from type 3 solar radio burst observation by space radio astronomy
03 p0424 A72-13223
- Solar type 3 bursts from high resolution radio spectrographs, deriving coronal temperatures from decay times
06 p0876 A72-17576
- Type 3 bursts mean polarization level at 20-200 MHz, considering vertical spacing of radio waves emission levels
07 p1077 A72-19813
- Plasma interpretation of solar type 3 and spike bursts associations from high time resolution radiospectrographic observations
09 p1392 A72-23540
- Predicting electron density for type 3 solar burst excitation by LF satellite radio observations
13 p2032 A72-29723
- Nonlinear coupling of wave modes in cold magnetized plasma, applying to electrostatic wave transformation in connection with solar type 3 radiation
15 p2283 A72-31431
- Pioneer spacecraft intermittent solar wind streams data temporal variations analysis to account for anomalous type 3 bursts
15 p2299 A72-31964
- Coronal scattering effects on type 3 solar bursts, using radio sources scintillation model and Monte Carlo ray tracing technique
15 p2316 A72-32752
- HF radiation in type 3 burst sources, discussing amplification by proton and electron streams
15 p2316 A72-32753
- Heliograph and interferometer observations of type 3 bursts, plotting relative positions of fundamental and second harmonic radiation sources
16 p2445 A72-33044
- Near earth interplanetary electron source detection related to coronal site type 3 bursts, using 80 MHz radioheliograph observations
16 p2445 A72-33044
- Charged particle stream neutralization and stabilization in solar corona, noting plasma wave and relation to type 3 radio bursts
17 p2608 A72-35093
- Type 3 bursts mean polarization level at 20-200 MHz, considering vertical spacing of radio waves emission levels
17 p2618 A72-35738
- Type 3 solar burst spectral characteristics relationship to flare class and magnetic field configuration in spot group
17 p2618 A72-35739
- Correlation of polarization in type III solar radio bursts at frequencies of 23.5 and 30 MHz
19 p2851 A72-38065
- The type IIb burst - A precursor of decameter type III radio-burst.
20 p2965 A72-39882
- Relativistic quasi-linear equations solution in dynamic theory of type III solar radio bursts under initial conditions of local explosion
21 p3101 A72-41295
- Type 3 solar burst distinction from auroral type high pass noise via spectrum analysis
22 p3222 A72-42043
- TYPE 4 BURSTS**
- Narrow-band type 4 bursts behavior comparison with synchrotron radiation in media with refractive index less/equal unity, determining magnetic field and electron energy
01 p0118 A72-10415
- Type 4 solar radio burst multiple magnetic loop structure and polarization observation by 80 MHz heliograph
02 p0272 A72-11648
- Spectral and polarization characteristics of type 4 bursts with respect to energetic particle emission and solar-terrestrial phenomena
03 p0407 A72-12938
- Solar moving type 4 bursts and coronal magnetic fields evidence from 80 MHz radioheliograph data
03 p0411 A72-13347
- Type 4 solar radio bursts peak flux spectra center to limb variation association with proton flares
05 p0709 A72-16073
- Moving type 4 radio burst observation with radioheliograph, suggesting isolated self contained synchrotron emitting plasmoid and relation to coronal magnetic field
05 p0710 A72-16521
- Type 4 solar burst spectral characteristics relationship to flare class and magnetic field configuration in spot group
07 p1077 A72-19814

- Solar wind kinetic energy from flare associated solar wind disturbances relation to types 2 and 4 radio bursts, using satellite observations
09 p1378 A72-23399
- Quantitative evolution model for time variable flux densities and polarization characteristics of isolated moving type 4 events
16 p2444 A72-33041
- Solar stationary type 4 radio bursts caused by gyromagnetic radiation of bunched electrons
16 p2449 A72-33920
- Radio spectrographic measurements of type 4 solar radio bursts harmonic and pulsation structures
16 p2459 A72-33921
- On the temporal distribution of type IV burst-active centres over the solar cycle /Research note/.
17 p2602 A72-35715
- Homologous complex radio bursts of type IV-II in the solar atmosphere
19 p2852 A72-38498
- Broadband continua temporal behavior at type IV initial stages, recording by radio interferometers
21 p3101 A72-41296
- Type 4 decimetric, moving and quasi-stationary groups described in terms of onset time lags for different frequencies and components
21 p3101 A72-41763
- Solar flare associated relativistic electron acceleration relationship to cosmic ray and type 4 radio burst production
22 p3217 A72-42010
- Peculiar absorption and emission microstructures in the type IV solar radio outburst of March 2, 1970.
22 p3217 A72-42044
- Some characteristics of microwave type IV radio bursts and the acceleration of solar cosmic rays.
23 p3328 A72-43616
- TYPE 5 BURSTS**
- Type 3 and 3/5 solar radio bursts coupling with microwave bursts, considering connection with H alpha flares and X ray emission
01 p0118 A72-10414
- TYPEWRITERS**
- Optimum performance typewriter keyboard design, discussing biomechanical improvements in finger positioning facilitation, operator postural muscular strain reduction, etc
10 p1433 A72-25114
- U**
- U BENDS**
- Steady compressible fluid flow and plane shock wave propagation in pipe bends, discussing parameter effects and boundary conditions
10 p1464 A72-23878
- Stress concentration in symmetrical U-notched plates, comparing data with Baratta, Neal, Neuber and Heywood formulas
14 p2167 A72-30904
- U TUBES**
U MANOMETERS
U.S.S.R. SPACE PROGRAM
- Soviet-France Project Omega for near space disturbance studies, using ground and balloon measurements at conjugate points
01 p0063 A72-11075
- Soviet manned space flight history and characteristics, discussing Vostok, Voskhod and Soyuz vehicles
03 p0440 A72-13475
- Soviet space program review from Sputnik 1 launch discussing launch sites and vehicles, lunar, planetary and manned missions, civil and military programs and future goals
05 p0722 A72-17091
- Skylink project as prospective joint American-Soviet space mission, combining Skylab and Soyuz spacecraft
05 p0731 A72-17092
- Soviet book on space exploration in U.S.S.R. covering Elektron, Proton and Cosmos research satellites, communication and meteorological satellites, lunar and manned spacecraft, etc
06 p0879 A72-17815
- Soviet interplanetary spacecraft Mars 2 and 3, describing design, mission objectives, onboard systems and instrumentation
09 p1395 A72-22974
- Soviet unmanned Luna 20 mission, describing launch, lunar trajectory injection, midcourse correction, lunar orbit and landing, surface soil sampling and return to earth
14 p2163 A72-30680
- U.S.-U.S.S.R. space cooperation, considering Eisenhower and Kennedy initiatives, NASA-Soviet Academy negotiations and current situation
14 p2176 A72-31145
- Report to COSPAR on 1971 Soviet space programs, discussing moon, planets, cosmic radiation, interplanetary medium, magnetosphere, upper at-

mosphere, meteorological, orbital station and biomedical studies

15 p2337 A72-32002

UBV SPECTRA

UBV photometric studies of eclipsing variable R Canis Majoris confirming primary component as F1V star, discussing ordinary semidetached system possibility

01 p0129 A72-10793

Calibrations consistency of UVBY beta and GNMK photometries of binary stars with G or K giants and A or F main sequence components

01 p0132 A72-11014

B and Be type stars intrinsic polarization, considering UVB spectra and effects on observed polarization

02 p0283 A72-12628

Single channel photometer measurement possibility in UVB magnitudes of variable stars

03 p0359 A72-13497

Interstellar absorption in Perseus OB 2 association direction from UVBY-beta photometry of early type stars in four fields

03 p0438 A72-13875

Extrasolar planets UVB color indices calculation, noting relative reflectivity and primary star color

04 p0570 A72-14507

Markarian galaxies photometric observations, presenting emission line intensities and UVB magnitudes

04 p0578 A72-15309

UBV magnitude measurement for stars in open clusters NGC 6613 and 6716, determining spectral classes, absorption and distances

05 p0712 A72-15768

Beta Cephei type variable stars, determining KP Persei times of maximum light, mean UVB magnitudes and light ranges

06 p0882 A72-18006

Observed light curve amplitude phase relations in Ap magnetic star UVB system, using oblique rotator model

06 p0882 A72-18008

UBV photometry for stars near quasars and N and Seyfert galaxies, noting suitability as secondary photoelectric standards or photographic sequences for monitoring programs

07 p1071 A72-19336

Photometric UVB and polarimetric observations of rotation period, polarization curves and phase coefficients of asteroid Flora, comparing with moon

10 p1531 A72-23709

UBVr colors of supergiants as function of radiation pressure, sphericity, microturbulence and effective temperatures

10 p1542 A72-24609

OB star distribution in Puppis from UVB and H beta photometry, noting correlation with hydrogen concentration

10 p1542 A72-24615

Photoelectric UVB photometry for galactic cluster NGC 7039 region stars, discussing MK spectral classifications and peculiar A stars

10 p1545 A72-24827

Short period RR Lyrae variables, presenting light curves in UVB system

10 p1550 A72-25198

Computed and observed color indices of intermediate band UPXYZVS and wideband UVB photometric systems, evaluating response curve validity for parameter determination

11 p1715 A72-25295

UBV photometric properties and probability of discovery in blue light of detached close binaries models

12 p1867 A72-27214

Quasar color indices and redshift correlation, using catalog data on U, B and V colors

14 p2150 A72-30371

Stellar photometric observations in Magellanic Clouds, presenting photoelectric sequences in UVB system, interstellar reddening and extinction data

14 p2159 A72-30737

Discoveries on southern objective-prism plates. III- Three new hydrogen-deficient stars and a bright B-type subdwarf.

17 p2609 A72-35116

The type II supernova 1969 I in NGC 1058.

18 p2728 A72-36763

The colour-magnitude diagram of the globular cluster NGC 6981.

19 p2855 A72-37342

The colour-magnitude diagram of the globular cluster NGC 7099.

19 p2855 A72-37343

Absolute magnitudes of E and S0 galaxies in the Virgo and Coma clusters as a function of U-B color.

20 p2965 A72-38902

A study of the interstellar extinction in the Carina-Centaurus region.

20 p2973 A72-39881

A spectroscopic and photometric study of the pulsating R Coronae Borealis type variable, RY Sagittarii.

23 p3334 A72-43255

Stellar and Uranus photometric measurements for solar /B-V/ and /U-B/ color indices determination, using K and H delta lines and G band filters

23 p3337 A72-43615

Spectral classification of stars with respect to non-broadened low-dispersion spectra. III - Classification method and criteria

24 p3447 A72-45678

UDIMET ALLOYS

Cast high temperature Ni base alloy Udimet 500 low cycle fatigue, determining total stress and strain range vs fatigue life at elevated temperatures

01 p0087 A72-11030

Hydropressed sintered U-700 superalloy powder, noting weakened particle grain boundary conditions from mechanical properties and fracture studies

02 p0240 A72-11444

Diffusion welding of cast and wrought Udimet 700 superalloy gas turbine engine components, discussing interfacial grain boundary migration and microstructural homogeneity effects on weld joint quality

07 p0997 A72-19998

Udimet 500 alloy dislocation substructure and fracture surface topography during deformation to failure in low cycle fatigue at high temperatures

11 p1667 A72-26938

UFO

U UNIDENTIFIED FLYING OBJECTS

UH-1 HELICOPTER

Hydrofluidic three-axis stability augmentation system to improve UH-1B helicopter damping and handling qualities during high speed gunfiring missions

16 p2350 A72-33650

UHTREX [NUCLEAR REACTORS]

U HIGH TEMPERATURE NUCLEAR REACTORS

UHURU SATELLITE

X ray observatory with gas filled proportional counters, discussing pulse height analyzer, command system, calibration and power distribution

08 p1167 A72-21512

Uhuru satellite development history and preliminary X ray observation, analysis of radiation source emission characteristics, locations and identifications

10 p1533 A72-23892

Uhuru satellite observation of transient X ray source in constellation Lupus, discussing five month period intensity variation

14 p2157 A72-30572

NASA X ray satellite UHURU and HEAO-C instruments and observational data on supernova remnants, pulsars, extars quasars, radio galaxies and galactic clusters

24 p3446 A72-45539

ULM [LIGHT MODULATION]

U ULTRASONIC LIGHT MODULATION

ULNA

Human arm muscle motor neuron reflex response to rectangular pulse excitation of ulnar nerve

04 p0476 A72-15587

ULTRA SHORT WAVE RADIO EQUIPMENT

U VERY HIGH FREQUENCY RADIO EQUIPMENT

ULTRAHIGH FREQUENCIES

Broadband high efficiency mode /HEM/ TRAPATT amplifiers for S band, discussing bandpass and input-output characteristics with Ichebycheff filter

01 p0038 A72-10652

Prototype compact ruggedized crystal-controlled L-band artillery telemetry transmitter design and performance

02 p0192 A72-12156

Uhf aeronautical satellite system, presenting ATC trends, international aspects, available flight levels, weather conditions and long haul conflicts

02 p0257 A72-12383

Uhf varactors reliability, establishing rejection criterion by statistical analysis

02 p0194 A72-12444

Solid state oscillator phase and frequency synchronization by injection of stable sinusoidal uhf signal modulated by 0-180 deg phase jump

02 p0194 A72-12569

L band in satellite system for aerial navigation aid, discussing position accuracy, data transmission and voice communication and modulation methods

02 p0257 A72-12642

Satellite navigational aid system technical and operational characteristics, emphasizing voice communications links in L band

03 p0386 A72-12972

High latitude scintillation effects on vhf and S band polar orbiting satellite transmissions, examining ionospheric irregularities

04 p0487 A72-14952

FSK transmission experiments on uhf satellite link, noting threshold convolutional decoding contribution to SNR

06 p0773 A72-17599

Narrow band frequency drifts of polarized Jovian I bursts from simultaneous radio observations

10 p1532 A72-23713

Diurnal variability of atmospheric refraction index at UHF in boundary layer for various weather types during summer-fall season

13 p1995 A72-29590

Extensive air showers at zenith, measuring associated UHF radio pulses with optical Cerenkov emission receiver as trigger source

14 p2147 A72-30858

Minimum amplitude and phase distortion selective bandpass filters/equalizers for satellite communications, noting realizability in UHF and microwave bands

14 p2089 A72-31048

L band optimum monopulse high power feed using dominate and higher order waveguide modes to develop sum and difference patterns

17 p2526 A72-34421

Plastics in very-high and ultrahigh frequency applications

17 p2571 A72-35068

Bremsstrahlung as a possible source of UHF emissions from lightning.

19 p2828 A72-37894

Electromagnetic compatibility and interference problems of radar altimeters, collision avoidance systems and air and marine mobile satellite communication equipment in 1600 MHz region

20 p2901 A72-38977

Utilization of frequency bands allocated to satellite broadcasting for regional or domestic systems.

21 p3018 A72-40875

High resolution observations of 3C390.3 at 2.7 and 5 GHz.

21 p3111 A72-41471

ULTRAHIGH VACUUM

High purity W ion irradiated in situ under ultrahigh vacuum at high temperature, examining depleted zone defect structure by field ion microscope

02 p0242 A72-11909

Windowless ultrahigh vacuum photoelectron spectrometer for high resolution studies of gas-metal surface reactions, measuring electron energy levels

04 p0523 A72-15489

Hydrogen evacuation with He condensation pump in ultrahigh vacuum region

06 p0795 A72-17698

Prepumped systems with ion sorption and titanium sublimation vacuum pumps for ultrahigh vacuum production

07 p0914 A72-19906

Ultrahigh vacuum measurement by Bayard-Alpert hot cathode ionization gages, showing ion current component influence on lower pressure limit

07 p0914 A72-19907

Sliding friction and normal force adhesion under ultrahigh vacuum environment, describing test apparatus for real time analysis via contact resistance measurement

08 p1176 A72-21436

Sulfur dioxide and carbon dioxide interaction with clean silver surface at ultrahigh vacuum, using Auger electron spectroscopy and work function measurement

13 p1912 A72-28684

Microcalorimetric investigation of energy transfer from atomic and molecular hydrogen beams to various surfaces at liquid helium temperatures and ultrahigh vacuum conditions

15 p2281 A72-31863

Gauges for ultrahigh vacuum.

19 p2803 A72-38390

High and ultrahigh vacuum equipment and components selection, discussing gas-surface interactions, contamination and cleaning problems

19 p2835 A72-38391

Installation for the simultaneous measurement of the functional properties of sliding contacts

20 p2928 A72-39936

Electron beam evaporator with multiple source suitable for use in ultrahigh vacuum, noting control of evaporation rate

21 p3051 A72-40205

A versatile ultrahigh vacuum scanning electron microscope.

21 p3051 A72-40217

The effect of a thermal and ultrahigh vacuum environment on the strength of precompressed granular materials.

22 p3173 A72-42528

ULTRALOW FREQUENCIES

U EXTREMELY LOW RADIO FREQUENCIES

ULTRAPURE METALS

Annealed pure Al polycrystals fatigue behavior data under elevated temperatures, using transmission electron microscopy

02 p0242 A72-11525

Boundary segregate concentration during grain growth annealing of ultrapure Al as function of migration rate and distance

03 p0379 A72-14259

Zone melting high vacuum facility with cryogenic pumping and residual gas carbon-containing components exclusion for ultrapure metals production

06 p0796 A72-17992

- Ultrature metals microimpurities determination from crystal lattice and atomic properties, comparing spectral analysis activation, mass spectrometric, thermophysical, recrystallization and kinetic methods 07 p1049 A72-20149
- High purity Al single crystal orientation explained by Rowland transformation model, observing recrystallization grains 12 p1828 A72-27300
- Zone melting high-vacuum system with cryogenic pumping for zone refining Zr 14 p2092 A72-30220
- Heat treatment hardening effect on stress corrosion resistance of ultrature maraging and stainless steels, emphasizing hydrogen embrittlement 14 p2117 A72-30540
- Properties of high-purity chromium 17 p2569 A72-35525
- Recrystallization and polygonization conditions in high purity metals, noting critical temperature and additives effect 21 p3065 A72-40093
- Ultrasonic treatment of the MA2-1 alloy during recrystallization 23 p3303 A72-44096
- ULTRASONIC AGITATION**
- Ultrasonic cavitation effects on martensitic specimens, observing plastic deformation, softening, phase transformations and decay 03 p0370 A72-13187
- Ultrasonic oscillations effects on alloy castings grain size and heat resistance, suggesting waveguide direction for oriented solidification 11 p1642 A72-26822
- A method of improving the physicochemical properties of filled epoxy compounds by treatment in an ultrasonic field 19 p2823 A72-38184
- Ultrasonic treatment of the MA2-1 alloy during recrystallization 23 p3303 A72-44096
- ULTRASONIC GRINDING MACHINES**
- U ULTRASONIC MACHINING**
- ULTRASONIC INSPECTION**
- U ULTRASONIC TESTS**
- ULTRASONIC LIGHT MODULATION**
- Ultrasonic diffraction grating for noninterference sampling of high power carbon dioxide laser beam, discussing diffraction profiles obtained from lasers operating in Gaussian and donut modes 05 p0669 A72-16608
- Quartz crystals ultrasonic vibrations produced by laser beam, noting light modulation depth dependence on effective cross section and amplitude 09 p1322 A72-22415
- Ruby laser radiation modulation by mirror ultrasonic vibrations, discussing mechanism 09 p1326 A72-23681
- Far field diffraction of Gaussian light beam passing through ultrasonic cylindrical standing waves 11 p1687 A72-26052
- Liquid optoacoustical modulator for laser radiation control operating on pulse amplitude modulated ultrasonic traveling waves with membrane partitions 16 p2400 A72-33081
- Ultrasonic imaging system based on side-looking synthetic aperture radar principles, using B-scan technique 19 p2798 A72-37624
- Mode locked carbon dioxide with transverse pulse pumping, using Ge ultrasonic diffraction cell as active loss modulator 20 p2934 A72-39965
- Holographic techniques in high intensity acoustic fields analysis, applying to chemistry, medicine and engineering 23 p3287 A72-43549
- ULTRASONIC MACHINING**
- Metal powder hot compacting under vacuum and ultrasound action, considering porous body three dimensional viscous flow 05 p0665 A72-16091
- Machine parts surface hardening and smoothing by vibrating hard alloy sphere impact at ultrasonic frequency 08 p1176 A72-21050
- ULTRASONIC RADIATION**
- Oxygen effect on dynamic elastic modulus of titanium-oxygen alloys by density and longitudinal ultrasonic wave velocity measurements 01 p0083 A72-10393
- Ultrasonic fatigue at small strain amplitudes in Ti, developing solitary slip band microcracks 04 p0533 A72-14539
- Longitudinal ultrasonic sound attenuation in superconducting Mo-Re alloys as function of temperature, magnetic field and frequency, using evaporated thin film CdS transducers 04 p0562 A72-15295
- Ultrasonically produced cavitation events correlation to amoeba cells number decrease under 1 MHz irradiation 04 p0475 A72-15299

- Transverse ultrasonic wave propagation in low viscosity liquids, investigating fine structure of Rayleigh line wing 05 p0690 A72-16682
- Light intensity distribution from ultrasonic surface waves reflection to probe surface acoustic propagation characteristics [AD-739047] 06 p0848 A72-17851
- Sound velocity and attenuation variations with magnetic field from ultrasonic continuous wave spectrometry 07 p0984 A72-19321
- IF amplifier automatic gain control /AGC/ for ultrasonic pulse echo measurements 11 p1633 A72-26055
- Impurity centers formation and development in AgBr/I/ photographic emulsion under ultrasonic irradiation 11 p1636 A72-26794
- Ultrasonic signal propagation with distance along steel sphere surface compared with lunar seismic signal, discussing surface dent and lunar crater effects 13 p2035 A72-28619
- Ultrasound reflection from molten core during spot welding of steel alloys as function of geometrical dimensions and configuration and transition zone dimensions 13 p1965 A72-29152
- Hydraulic flows fluid measurement in pipes by ultrasonic waves convection method, discussing transducers performance and mounting [ONERA, TP NO. 1078] 13 p1959 A72-29668
- Single pulses and random samplings signal spectrum analysis on real time scale by ultrasonic dispersion waveguide 13 p1934 A72-30018
- Ultrasonic wave excitation in potassium seeded flame, showing amplitude proportional to harmonic perturbation frequency imposed on plasma 14 p2170 A72-30417
- Ultrasound damping in Mg and Al alloys by structural grains and dislocation oscillations during work hardening, recrystallization and oversaturated solid solution decay 14 p2122 A72-30957
- Crystal lattice and dislocation anharmonicities interdependence and stress-strain correlation in presence of interaction between ultrasonic waves of different frequencies 14 p2169 A72-30959
- Ultrasonic wave propagation in single crystals, discussing linear elastic wave attenuation, anisotropic interactions, particle displacement polarization and energy flux deviation 15 p2292 A72-31834
- Theoretical model for HF mechanical waves interaction with crystal lattices based on measurements of high amplitude ultrasonic waves attenuation in metal crystals 15 p2292 A72-31835
- High amplitude ultrasonic stress waves effect on metals elastic and plastic deformation characteristics, verifying model for sound waves-lattice structure interactions 15 p2328 A72-31842
- HF electric field effect on ultrasound wave propagation in semiconductor, noting amplification factor dependence on electron heating 15 p2279 A72-32739
- Ultrasonic wave propagation in metal-matrix composites. 17 p2560 A72-35287
- Space-modulated lateral emission of an ultrasonic beam in a solid 17 p2583 A72-35546
- Experimental determination of ultrasonic wave velocities in plastics, elastomers, and syntactic foam as a function of temperature. 18 p2703 A72-36415
- Observation and analysis of simulated ultrasonic acoustic emission waves in plates and complex structures. 20 p2925 A72-39284
- Response of the average pressure acting on the surface of an emitting circular transducer due to different reflecting objects. 21 p3055 A72-40948
- Magnesium alloys containing rare-earth metals as materials with special physical properties 22 p3192 A72-42817
- Absolute accuracy of the pulse-echo overlap method and the pulse-superposition method for ultrasonic velocity. 23 p3313 A72-44114
- Ultrasonic diffraction loss and phase change for broad-band pulses. 23 p3313 A72-44115
- Ultrasonic attenuation and velocity in hot specimens by the momentary contact method with pressure coupling, and some results on steel to 1200 C. 23 p3294 A72-44116
- Energy measurement of primary particles from shower formation in solids, discussing ultrasonic

- waves generation in metal plates and electromagnetic waves excitation in ferrites 23 p3291 A72-44437
- Time dependence of the divergence of the radiation emitted by a rhodamine laser pumped by a pinched discharge. 24 p3411 A72-45612
- ULTRASONIC SPEEDS**
- U SUPERSONIC SPEEDS**
- ULTRASONIC TESTS**
- Coextruded Be fiber-Ti alloy matrix composite sheets for light weight structures, describing ultrasonic inspection and mechanical properties 01 p0084 A72-10734
- Flat hole model for defect size definition from ultrasonic inspection as function of echo amplitude and depth 01 p0076 A72-10809
- Multielectrode piezoelectric chip ultrasonic transducer, sampling and readout techniques for radioisotope encapsulation testing 01 p0069 A72-10810
- Clad-to-core bond testing in radioisotope irradiation strips by pulsed laser ultrasonic schlieren system 01 p0080 A72-10811
- Portable self contained ultrasonic field inspection equipment for nondestructive crack detection in T53 gas turbine compressor disks 01 p0076 A72-10814
- DGS diagrams for defect size determination in ultrasonic NDT 01 p0070 A72-11016
- Ultrasonic scatter effect on attenuation for macrostructure measurement, noting application to emulsions and metal grain boundaries 01 p0070 A72-11017
- Ultrasonic excitation induced vibration measurement for detecting incipient electrical breakdown in transducers, using laser-Michelson interferometer 01 p0081 A72-11018
- Macroscopic metal crystal plastic deformation applications to aircraft and spacecraft materials production, considering internal friction and energy conversion into strain energy and heat 01 p0071 A72-11020
- Automatic ultrasonic testing equipment for NDT tests of helicopter rotor blades 01 p0071 A72-11021
- Schlieren photography for visualizing ultrasonic pulse propagation and reflection in solids and liquids, applying to crack detection in steel tubes 01 p0071 A72-11022
- Bats auditory cortex electrical responses to ultrasonic stimuli, determining maximum sensitivity frequency range 02 p0159 A72-11769
- Ultrasonic measurement of orthotropic laminated composites elastic moduli, describing stress-strain response [AD-736007] 02 p0249 A72-11994
- Resistive force on moving dislocations at low temperature in solids and crystal defect studies by ultrasonic methods, determining temperature dependence of mechanical properties 03 p0362 A72-13224
- Ultrasonic resonance thickness gage sensitivity and accuracy, noting damper, piezoelectric plate, protector and frequency band influence 03 p0361 A72-13986
- Ultrasonic flaw detector pulse transducers operation using electrodynamic and capacitance receivers 03 p0361 A72-13987
- Ultrasonic defectoscope sensitivity, discussing statistical character of random signal level distribution and test conditions 03 p0364 A72-13988
- Nondestructive examination of steel plate weld specimen, comparing ultrasonic and X ray techniques 04 p0527 A72-14840
- Ultrasonic acoustic holography for real time non-destructive testing of cracks, voids, nonbonds and other defects in metals, ceramics and plastics [SAE PAPER 720173] 06 p0811 A72-17319
- X ray, ultrasonic and eddy current nondestructive testing of aircraft structure for maintenance and special problems 07 p0994 A72-18840
- Aircraft light alloy integral construction for stress concentration and fatigue failure avoidance, describing continuous casting process, stress relieving and ultrasonic flaw testing procedures 07 p0995 A72-19725
- Plane harmonic waves propagation in stressed polycrystalline bodies with slight orthotropy in unstressed state, substantiating theory for initial stress determination by ultrasonic technique 07 p1090 A72-19753
- Al wrought alloys dynamic elasticity modulus and Poisson ratio dependence on temperature, using ultrasonic measurement method 07 p1019 A72-20239
- Optimal selection of flawless nose cones from graphite billets, obtaining mathematical model based on ultrasonic reflection test data 07 p1086 A72-20350

- Nondestructive ultrasonic determination of defects in structural steel blanks 07 p0991 A72-20423
- Propagating crack properties characterization during fatigue cycling, using ultrasonic flaw detection and acoustic emission 09 p1310 A72-22922
- Diffusion bonded joints tensile strength determination from ultrasonic pulse echo and attenuation measurements, discussing contamination and SNR effects 10 p1485 A72-23814
- Delayed pulse echo and through-transmission ultrasonic techniques for nondestructive inspection and quality control of braze bonds in high current electric contact assemblies 10 p1487 A72-24173
- Ultrasonic Doppler flowmeter for instantaneous measurement of blood vessel flow velocity by averaging frequency shift over received signal power density spectrum 10 p1430 A72-24373
- Be elastic constants at 25-300 C, using ultrasonic pulse technique 11 p1657 A72-25774
- Multifrequency ultrasonic pulse echo interference effect applying to flaw detection in metals 11 p1687 A72-26051
- High power ultrasonics in metal fatigue studies, considering crack propagation and slip patterns for high and low frequencies 11 p1639 A72-26053
- Instantaneous and continuous blood flow velocity measurement by Doppler ultrasonic flowmeter using transcutaneous and implanted probes 11 p1589 A72-26778
- Rolled polycrystalline metal samples principal anisotropy direction determination by acoustic measurements at ultrasonic frequencies 12 p1806 A72-27086
- Optimal level of recording defects in ultrasonic flaw detection, taking into account inspection conditions and defect size probability distribution 13 p1956 A72-28924
- Ultrasonic inspection effectiveness and equipment errors relationship to a priori acceptability of products 13 p1963 A72-28925
- Aluminum aircraft wheels ultrasonic inspection, noting reliability, simplicity and time economy as compared to eddy current or fluorescent penetrant methods 13 p1966 A72-30037
- Reliability of nondestructive ultrasonic testing methods of quality control, discussing defect size distribution and detectability coefficient 14 p2106 A72-30149
- Lamb acoustic surface wave method for rapid nondestructive evaluation of rolling texture in arbitrarily thick metal sheets and plates 14 p2107 A72-30615
- Carbon fiber reinforced plastics nondestructive testing by ultrasonic compressional and shear wave resonance 14 p2107 A72-30856
- Space Shuttle Orbiter onboard ultrasonic system for structural integrity tests and assessment, noting limitation factors due to configuration and vehicle launch noise effects 15 p2256 A72-31698
- Structure-borne acoustic nondestructive testing for readiness assessment, fault isolation and automatic checkout of space vehicle mechanical devices 15 p2214 A72-31699
- Fcc metal defect structure due to ultrasonic fatigue observation via transmission electron microscopy for dislocations 15 p2256 A72-31836
- Microcrack initiation and propagation in ductile metals at low cycle and ultrasonic frequencies, investigating fatigue fracture mechanism by scanning electron microscope 15 p2256 A72-31838
- Metal fatigue tests at various frequencies to observe surface structure, dislocations in crack vicinity, plastic deformation and ultrasonic resonance techniques 15 p2257 A72-31839
- Carbon and graphite fiber reinforced composites elastic constants derived from ultrasonic immersion technique 15 p2261 A72-32503
- Ultrasonic flaw detector data analysis, discussing digital computer interface and encoders 16 p2397 A72-33202
- Reliable nondestructive microstructure testing via surface ultrasonic waves 16 p2399 A72-33822
- Nondestructive ultrasonic inspection of braze bonds in high current electrical contact assemblies 18 p2695 A72-36116
- Ultrasonic tests for incipient fatigue, hardness and elastic constants-tensile strength relationship in metals 18 p2690 A72-36125
- Ultrasonic velocity measurement of elastic constants of Al-Al3Ni unidirectionally solidified eutectic. 18 p2701 A72-36591
- Changes of the mitral echocardiogram with ageing and the influence of atherosclerotic risk factors. 18 p2652 A72-37031
- Nondestructive testing of advanced composites. 19 p2799 A72-37669
- Crack depth measurement with surface waves. 19 p2809 A72-38569
- Young and shear moduli of binary Fe base alloys as functions of composition and temperature by ultrasonic pulse echo technique 20 p2937 A72-39287
- Bilateral version of an ultrasonic velocimetric method of defectoscopy. 21 p3057 A72-41721
- Ultrasonic evidence against multiple energy gaps in superconducting niobium. 22 p3190 A72-42476
- Ultrasonic detection of fatigue damage. 24 p3457 A72-44820
- Electromagneto-acoustic non-destructive testing in the Soviet Union. 24 p3408 A72-45291
- NDT techniques selection, economics and organization for aircraft industry, considering ultrasonic holographic and adhesion tests 24 p3408 A72-45292
- A bibliographical survey of acoustic emission. 24 p3408 A72-45293
- Ultrasonic defect detection and evaluation techniques, stressing limitations for defect geometry, size and nature 24 p3408 A72-45294
- ULTRASONIC WAVE TRANSDUCERS**
- Multi-electrode piezoelectric chip ultrasonic transducer, sampling and readout techniques for radioisotope encapsulation testing 01 p0069 A72-10810
- Ultrasonic excitation induced vibration measurement for detecting incipient electrical breakdown in transducers, using laser-Michelson interferometer 01 p0081 A72-11018
- Motional feedback systems comparison for ultrasonic transducers operated as resonant emitters, describing circuitry for self excitation 01 p0070 A72-11019
- Pohlman cell for ultrasonic hologram production, describing construction, resolution and real time reconstruction 02 p0225 A72-11751
- Ultrasonic delay lines design and construction for 100-2000 MHz using evaporated CdS on sapphire and quartz and sputtered ZnO transducers 05 p0626 A72-16010
- Ultrasonic transducer monitoring of decompression-caused gas bubbles in rat thigh muscle tissue for decompression sickness time course development studies 07 p0921 A72-20183
- Flexural vibrating free edge plate transducer with stepped thickness for high directional ultrasonic radiation generation in fluids 11 p1687 A72-26060
- Hydraulic fluids flow measurement in pipes by ultrasonic waves convection method, discussing transducers performance and mounting [ONERA, TP NO. 1078] 13 p1959 A72-29668
- High-frequency ultrasonic devices. 17 p2526 A72-34564
- One path ultrasonic flowmeter using electroacoustic feedback. 17 p2556 A72-35427
- Ultrasonic wave generation in solids using transducer composed of high rigidity dielectric /polypropylene/ between two electrodes 18 p2691 A72-36402
- Technique for varying the conversion loss against frequency of a surface-wave transducer without apodisation. 18 p2667 A72-36692
- Methods for measuring the HF oscillation frequency in ultrasound pulses of equipment for diagnostic ultrasonography. 19 p2759 A72-37399
- Precordial monitoring for pulmonary gas embolism and decompression bubbles. 19 p2762 A72-38710
- On diffraction and focusing in anisotropic crystals. 20 p2961 A72-39779
- Spherical focusing transducers with Gaussian surface velocity distribution. 21 p3057 A72-41477
- Electronic devices with Rayleigh ultrasonic acoustic surface wave excitation for storage, recognition and separation of electrical signals usually requiring computerized operation 23 p3314 A72-44148
- ULTRASONIC WAVES**
- U ULTRASONIC RADIATION**
- ULTRASONIC WELDING**
- Ultrasonic bonding tip design for densely wired electronic circuit boards, analyzing standing wave phenomena and resonant frequency [SAE PAPER 710789] 01 p0074 A72-10279
- Ultrasonic bond formation between soft fcc metals, observing dislocation processes 04 p0526 A72-14837
- German monograph - Contribution to the ultrasonic seam welding of metals 19 p2807 A72-37655
- ULTRASONICS**
- Ultrasonics - Conference, London, September 1971 01 p0070 A72-11015
- Mo single crystal internal dislocational friction and ultrasound damping dependence on oscillation amplitude, exposure time and annealing temperature 08 p1185 A72-21073
- Telecommunications ultrasonic resonators, electromechanical and piezoelectric filters and microacoustic surface elastic wave devices 09 p1281 A72-23468
- Metal rolling speed effect on force and friction reduction by ultrasonic vibrations imposed on rollers, noting coefficient of friction dependence on deformation 12 p1814 A72-27645
- Ultrasonic imaging technique based on optical pulse compression, noting image forming and range discriminating capability 12 p1808 A72-27677
- Medical monitoring system for enclosed men, using ultrasonic Doppler-cardiography for heart rate determination 14 p2078 A72-30384
- High power ultrasonics - Conference, Graz, Austria, September 1970 15 p2256 A72-31831
- Ultrasonic sound influence on metal physical and mechanical characteristics, utilizing in testing and manufacturing procedures 15 p2275 A72-31832
- Ultrasonic metal fatigue, discussing crack initiation and growth and frequency effects 15 p2256 A72-31837
- Ultrasonic device with magnetostriction vibrator for suspension coating oxide cathodes, noting superiority to spray coating by compressed air 16 p2374 A72-33969
- Ultrasonic range finder 17 p2553 A72-34763
- Measurements of ultrasonic velocities using a digital averaging technique. 18 p2691 A72-36401
- Ultrasonic velocity measurement by small power He-Ne laser visualization of standing waves in Fresnel diffraction region 18 p2697 A72-36416
- Analysis of left ventricular wall motion by reflected ultrasound - Application to assessment of myocardial function. 19 p2755 A72-37497
- Evaluation of left ventricular function by echocardiography. 19 p2755 A72-37498
- Echocardiography in the diagnosis of congenital mitral stenosis and in evaluation of the results of mitral valvotomy. 19 p2755 A72-37499
- Echocardiographic determination of left ventricular dimensions, volumes and performance. 19 p2762 A72-38819
- Low-temperature part of a spectrometer for gigahertz-ultrasonics and ultrasonic paramagnetic resonance. 21 p3051 A72-40215
- Ultrasonic sound beam measurement of flow circulation variations in circular cylinder wake, evaluating probability distribution of beam phase fluctuations 21 p2990 A72-40947
- Echocardiographic investigation of heart rate, sex and normal aging effects on mitral valve leaflet movement in healthy subjects 22 p3148 A72-43021
- Ultrasonic holography in large phase disturbance. 23 p3290 A72-43950
- ULTRAVIOLET ABSORPTION**
- Continuum UV radiation absorption by vibrationally excited molecular oxygen in Schumann-Runge system 02 p0221 A72-12457
- UV absorption levels in different areas of Jupiter disk from spectrophotometric studies at 3300-4800 A, noting temporal variations in reflectance 08 p1237 A72-21828
- UV absorption measurements across Saturn disk at 3300-4800 A, considering rings and distribution in short wave region 08 p1238 A72-21829
- Extreme UV absorption cross sections ratios for atomic oxygen in upper atmosphere, observing solar radiation attenuation with satellite instruments 09 p1297 A72-22578
- Molecular gases absorption coefficients measurement in extreme UV, analyzing photoionization curves in energy range far beyond threshold 09 p1356 A72-22829

Absorption by Nd laser generated ionized Al plasma of extreme UV radiation due to inverse bremsstrahlung and photoionization 09 p1360 A72-22831

Ultraviolet absorption lines in the spectrum of Vega. 23 p3337 A72-43826

A rocket measurement of the vertical distribution of atmospheric ozone. 23 p3285 A72-44242

Vacuum ultraviolet absorption measurements on ionized species. 23 p3316 A72-44330

ULTRAVIOLET FILTERS

Properties of metal interference filters for 1200-3000 Å, of dichroic mirrors for 1700-3000 Å and of multielectric narrow passband interference filters for 2000-3000 Å 20 p2923 A72-39051

ULTRAVIOLET LIGHT

U ULTRAVIOLET RADIATION

ULTRAVIOLET PHOTOGRAPHY

Large aperture ratio wide field VCN-UV camera exploration of night sky, presenting isophotes of zodiacal light and Milky Way 04 p0525 A72-15685

Far UV view of Orion from Aerobee rocket-borne electronic camera photographs of Orion-Monoceros-Canis Major region 08 p1164 A72-20994

Spectrophotographic recording of UV auroral emissions during rocket probe flight, noting excitation by electron impact on molecular nitrogen 08 p1159 A72-21225

Anastigmatic optical systems with two high aperture ratio mirrors for UV image tubes 08 p1169 A72-21952

Extreme UV solar images televised in flight with rocket-borne SEC vidicon system, noting pictures reconstruction enhancement 12 p1810 A72-27930

Lunar color boundaries and their relationship to topographic features - A preliminary survey. 18 p2724 A72-36281

Venus observation experiment with the aid of a television system 19 p2858 A72-37820

Apollo 16 far-ultraviolet camera/spectrograph - Earth observations. 21 p3105 A72-40600

ULTRAVIOLET PHOTOMETRY

Photometric calibration of long wavelength vacuum UV standards by synchrotron and plasma black body radiation 01 p0073 A72-11399

Space vehicles guidance with UV optical systems, describing photometric celestial images with various receptors and different wavelength bandwidth selection 03 p0354 A72-13054

NGC 3031 spiral galaxy photometry and large scale structure determination by UBVRI integral equidensity curves method 08 p1234 A72-21280

Camera tube used in Faust program of spatial and astronomical UV photometry and spectrophotometry. 08 p1169 A72-21953

Space astronomy experiments with UV scanning, discussing data from Celestcope catalog of UV observations and photometric and astrometric accuracy 08 p1170 A72-21957

Image dissector application to D2B astronomical satellite position field plotting in solar and stellar UV photometry 08 p1172 A72-21976

Mesosphere ozone number densities from rocket photometric measurement of lunar UV radiation absorption 09 p1385 A72-22583

Geocoronal hydrogen Lyman alpha glow intensity and zenith angle dependence from observations by rocket-borne extreme UV photometers 09 p1298 A72-22593

Solar UV radiation and Lyman alpha flux observation during 7 March 1970 solar eclipse with Nike-Apache rocket photometer soundings 12 p1862 A72-27145

Error corrections for UV photometric measurements with light filters involving Bouguer formula 15 p2233 A72-31400

Rocket-borne Cassegrain optic stellar electrophotometer for early star observations in 1300-2000 Å region 19 p2796 A72-37585

Auroral EUV flux observation by Javelin sounding rocket photometers, comparing with visible and X ray emissions 22 p3171 A72-42417

ULTRAVIOLET RADIATION

NT FAR ULTRAVIOLET RADIATION

NT LYMAN ALPHA RADIATION

NT LYMAN BETA RADIATION

NT NEAR ULTRAVIOLET RADIATION

UV airglow in 1304 Å line of oxygen from Cosmos 215 satellite 01 p0053 A72-10362

Thermally excited E layer tidal winds based on UV radiation as thermal source, using isothermal atmosphere model 01 p0055 A72-10429

Cosmic soft X ray and UV radiation sources, discussing transition radiation emission in interstellar space 01 p0121 A72-11121

Gas flow visualization technique using fluorescent plate with UV irradiated ozone tracer, noting application to wall attachment fluidic elements 01 p0072 A72-11198

Total ozone estimation by interpolation from Nimbus 4 satellite data on backscattered UV earth radiance attenuation 01 p0096 A72-11285

Materials remote active sensing from ground, air and space by UV and visible laser induced luminescence, using excitation and emission spectral specificity for species identification 02 p0225 A72-11822

Space environment simulator with ultrahigh vacuum chamber and UV and corpuscular radiation for material samples physical properties in-situ measurement 02 p0201 A72-12701

Solar UV flux measurements by balloon-borne grating monochromator, using FM-FM analog and PCM telemetry systems for computerized data analysis 03 p0409 A72-13051

Absolute UV calibration of rocket photometers used to update OAO calibration for determining energy distribution of reference stars 03 p0355 A72-13065

Solar UV and X radiation, considering chromospheric temperature and density profiles and coronal electron densities 03 p0409 A72-13123

Atomic data for UV and X ray astronomy, considering atomic wave functions and energy levels, radiative transition probabilities and electron-ion collision cross sections 03 p0420 A72-13125

Solar UV radiation role in mesosphere, investigating absorption cross sections of ozone and molecular oxygen 03 p0411 A72-13385

Photochemical reactions in pyrimidine base of DNA after UV irradiation, relating mutagenic and lethal effect to dimerization 04 p0467 A72-14608

UV astronomy techniques and devices, discussing hot stars, stellar chemical composition and interstellar medium 04 p0582 A72-15686

UV sensitive fire detector in manned space vehicle, discussing simulation in aircraft flying zero gravity parabolas 06 p0814 A72-17584

Gas breakdown in front of metal targets laser flare from UV radiation ionizing action, using pulsed holographic technique 06 p0818 A72-18412

Photon counting system for low level radiation measurement in UV visible region, discussing simplifications 07 p0983 A72-19133

High power UV light pulse generation using Nd-YAG laser with frequency doubling 07 p1002 A72-19202

Methanol and formaldehyde photoionization by UV irradiation, determining ion yields as function of wavelength by mass spectrometric analysis 07 p1038 A72-20498

ESRO program in imaging detector development for UV and soft X ray space missions, presenting image storage target details 08 p1171 A72-21971

UV radiation effects on pyrolytic boron nitride lattice imperfections, using space environment simulator 09 p1336 A72-22404

High energy UV solar radiation transfer by stratospheric aerosols to biosphere, considering radiation injury to human lung 09 p1298 A72-22662

Simple and multiple electronic processes in X and XUV region - Conference, Paris, September 1970 09 p1356 A72-22826

Rare earth elements outer electrons X ray and UV photoemission spectra interpretation by multiplet splitting of final state 09 p1371 A72-22844

Hydrogen cloud structure of interstellar medium, assuming UV star Stromgren sphere radiation effects 09 p1390 A72-23526

Ribonuclease molecule damage and enzyme activity under UV irradiation and repeated freezing and thawing 09 p1274 A72-23594

UV radiation intensity altitude dependence and absorption by ozone, considering diurnal and annual variations and biological effects 09 p1268 A72-23625

Cygnus X-1 model with hard X rays from inverse Compton scattering of B star UV photons and IR synchrotron radiation from other component 10 p1530 A72-24944

Optical mirrors contamination by condensation of outgassed spacecraft materials in vacuum under UV irradiation, describing test apparatus and results with various materials 11 p1637 A72-25208

[AIAA PAPER 72-267] Carbon monoxide quantum yield measurements of carbon dioxide photolysis by radiation at 1470 and 1500-1670 Å 11 p1590 A72-26423

UV light production of free radicals in proteins and model compounds in vacuum and low temperatures, using EPR techniques 12 p1778 A72-27223

Life on Mars, investigating ground based and probe observations of atmospheric composition and pressure, surface temperature and features and UV radiation 12 p1761 A72-27624

Nd-glass amplifier gain saturation by 1.06 micron light pulses determined by two laser states lifetimes and degeneracies and thermalization rates 12 p1792 A72-27752

Upper atmospheric measurement of incident solar UV radiation penetration to lower levels, discussing measuring instruments 13 p0300 A72-28826

Thermospheric density-temperature time lag, considering two dimensional time dependent model based on UV heat input dynamic excitation 13 p1951 A72-29388

Ozone photochemical reactions measurements for quantum yield of UV photolysis in strong Hartley band with water vapor chain decomposition effects 14 p2083 A72-30134

RKR Franck-Condon factors for blue and UV transitions of metal oxides, hydrides and halides, discussing interstellar abundances 14 p2160 A72-30898

Stellar UV radiation spectral energy distribution investigation of stellar composition and atmosphere and interstellar gas, discussing observation restriction by earth atmosphere absorption 15 p2302 A72-31284

List of galaxies with UV continuum, noting emission lines, Seyferts, quasars and spectral energy distribution 15 p2304 A72-31326

Model for hot stars mass outflow due to gas acceleration by radiation absorption in UV resonance lines 15 p2305 A72-31341

Flashlamp pumped cryptocyanine Q switched high peak power ruby lasers, noting UV radiation responsible for methanolic solution photochemical decomposition 15 p2249 A72-32156

Simulated Nimbus orbital electron, proton and UV radiation effects on wide bandpass glass and narrow bandpass thin film interference filters and fused silica 15 p2277 A72-32157

Visible and UV stimulated emission in plasma of direct pinch discharge on Ar II and III ions, discussing application possibility to plasma diagnostics 16 p2400 A72-33297

Blue green algae Anacystis nidulans UV light-sensitive mutants photorecovery capacity following irradiation 16 p2356 A72-33673

Onboard radiometric measurement of bow shock generated UV radiation during atmospheric reentry of experimental sphere [AIAA PAPER 72-692] 16 p2462 A72-34050

Photoionization models for the emission-line regions of quasi-stellar and related objects. 17 p2605 A72-34527

Gas breakdown in front of metal targets laser flare from UV radiation ionizing action, using pulsed holographic technique 17 p2554 A72-34860

Atmospheric ozone and the history of life. 18 p2686 A72-36626

Wavelength tunable UV dye laser pumped by the fourth harmonic of Nd:YAG laser. 19 p2810 A72-37407

French monograph - Determination of the absolute value of the absorption in the bands of the Schumann-Runge system of molecular oxygen 19 p2836 A72-37476

Efficiency of holographic gratings in nonpolarized light under vacuum in the ultraviolet 19 p2799 A72-37670

Lipid peroxidation on the human skin surface following erythrogenic UV irradiation 19 p2757 A72-38087

Observation of ultraviolet radiation from a rocket exhaust plume at high altitudes. 20 p2984 A72-39641

Mathematical models from UV, IR and radio observations of chromosphere and transition region to corona, noting temperature effects of shock wave dissipation 22 p3229 A72-42903

Equatorial UV airglow azimuthal variations from spinning rocket measurements, attributing origin to 22 p3229 A72-42903

- electron collision excited atomic hydrogen Lyman alpha emission
23 p3282 A72-43263
- Development of phosphorescence during ruby irradiation
23 p3323 A72-43412
- Calculation of middle ultraviolet radiation detector response to solar radiation as a function of altitude.
23 p3289 A72-43897
- The efficient generation of coherent radiation continuously tunable from 2500 Å to 3250 Å.
24 p3409 A72-44803
- Photochemistry of unsaturated polymers
24 p3378 A72-45280

ULTRAVIOLET REFLECTION

- Vacuum UV reflectance dependence of Re and W vapor-deposited films on substrate temperature during deposition, film thickness and aging in air
15 p2274 A72-31377
- Cerenkov counter for astronomical observatory high energy cosmic ray experiments, discussing UV-reflecting paint, radiator and photomultiplier positioning improvements
15 p2234 A72-31536

ULTRAVIOLET SPECTRA

- Quantitative interpretation of correlation mask remote sensors UV, visible and IR spectral data, discussing beam transmittance attenuation by absorption, scattering and emission
[AIAA PAPER 71-1061]
01 p0066 A72-10530
- High speed photographs of plasma emission spectra in UV and soft X radiation spectrum regions, discussing theory, design and operation of facilities
02 p0223 A72-11408
- Solc-type tunable birefringent filter for near UV spectrum, discussing optical design and transmission characteristics
03 p0355 A72-13058
- Solar UV line spectrum identification and intensity analysis, emphasizing electron spectra in soft X ray region and forbidden transitions
03 p0420 A72-13124
- Solar corona research, discussing radio and radar astronomy and UV spectrum observations
03 p0422 A72-13202
- Late twilight airglow vacuum UV spectra from sounding rocket observation, noting conjugate-point electron excitation role in O I emissions
03 p0350 A72-13525
- Gum Nebula size, emission features and expansion dynamics, discussing Zeta Puppis UV spectrum and Vela X radio emission
03 p0440 A72-14364
- Missing solar UV opacity from band adsorption coefficient comparison between photospheric diatomic molecules and metals and hydrogen
04 p0579 A72-15327
- Extreme UV observations of flare surge at solar limb
05 p0710 A72-16520
- Interstellar extinction curves for stellar far UV radiation, discussing required multicomponent interstellar dust model
05 p0720 A72-16717
- UV spectrophotometry of late-type giant star [Arcurus]/from Aerobee rocket, identifying Mg II doublet resonance line for stellar chromosphere
06 p0881 A72-17893
- Neutral B I vacuum UV spectra from hollow cathode light source, remeasuring electron transitions to higher accuracy
06 p0852 A72-17896
- Mariner 9 UV spectrometry observations of Mars airglow spectrum containing CO Cameron band and atomic oxygen and hydrogen lines
06 p0890 A72-18344
- Early type stars photoelectric spectra obtained with Mariner 9 UV spectrometer, obtaining resonant line features and spectral energy distribution
06 p0890 A72-18347
- Electron beam induced dissociative excitation of vacuum UV emission from atomic nitrogen multiplets, using normal incidence monochromator and pulse counting techniques
07 p1036 A72-18925
- Zeta Orionis spectra at 922-1453 Å from rocket spectroscopy, matching lines with stellar atmosphere models
07 p1072 A72-19346
- Unstable binary RW Aur spectrophotometric study with stellar evolution and outer atmosphere implications, relating Balmer continuum to UV excess
08 p1233 A72-21277
- Stellar atmosphere UV spectral line broadening by electron collision, radiative and classical damping
08 p1237 A72-21750
- Spaceborne Uvicor/Telescope astronomical observatory for stellar UV TV pictures, discussing system design requirements
08 p1170 A72-21958
- Venus, Mars, Jupiter and Saturn UV spectra from OAO-2 objective grating spectrophotometry, obtaining planetary albedos from G-type stars observations
09 p1382 A72-22288

Multiple charge Al and C ions X-UV spectra use for studying laser produced plasmas build up and expansion regions
09 p1359 A72-22830

Quantum yield of ruby crystals luminescence for excitation in UV region, noting Cr concentration effect
10 p1490 A72-24043

Absorption spectrum of molecular nitrogen in 730-980 Å band, investigating absorption cross sections and optical oscillator strengths
12 p1848 A72-27853

Solar spectrum measurements at 2100-3200 Å by Aerobee rocket mounted Ebert-Fastie spectrometer with LiF diffusion plates
13 p2040 A72-29408

Electron transfer frequencies and triplet-triplet transition spectra of polyphenyl compound molecule scintillators for UV lasers, using chaotic phase method
13 p1968 A72-29509

UV solar spectrum recorded by rocket-borne spectrograph with diffraction grating echelle in Czerny-Turner arrangement
13 p2044 A72-29703

Solar transition zone and corona EUV lines formation heights measurement from OSO-4 spectroheliograms
13 p2050 A72-29939

Auroral spectra recorded at 2000-3000 Å with fast Ebert Fastie scanning spectrometer aboard ESRO rockets
14 p2098 A72-30139

High resolution observations of UV stellar spectra by ESRO-borne spectrophotometer, emphasizing Mg II lines
14 p2150 A72-30370

UV stellar spectra observation with orbiting stellar spectrophotometer aboard ESRO TD1A satellite, noting Mg II lines
15 p2308 A72-31927

Solar O VI, Ne VIII and Mg X spectral lines intensity ratios from XUV rocket measurements, comparing data with Jordan-Allen-Dupree ionization equilibrium calculations
[AD-745811]
15 p2318 A72-32783

Mercuric chloride, bromide and iodide gas phase UV absorption spectra, discussing correlation with intermolecular charge transfer transitions
16 p2360 A72-32926

Studies of extremely young clusters. VI - Spectroscopic observations of the ultraviolet-excess stars in the Orion Nebula cluster and NGC 2264.
17 p2605 A72-34530

Orbiting astronomical observatory - Review of scientific results.
18 p2731 A72-36555

Early data from the ultraviolet sky-scan telescope in the TDI satellite.
19 p2857 A72-37524

Interstellar lines in the ultraviolet spectrum of zeta Ophiuchi.
21 p3105 A72-41035

OSO-4 observations of coronal EUV hole, considering association with regions of diverging magnetic fields
21 p3106 A72-41042

Mariner 7 ultraviolet spectrometer experiment - Topographic slopes of Mars' polar region.
21 p3110 A72-41457

Distribution of total ozone content in the atmosphere according to spacecraft observations
21 p3050 A72-41797

The derivation of temperature gradient and electron density maps from EUV spectroheliograms.
22 p3222 A72-42036

Polarimeter for recording of magnetooptical rotation dispersion and Kerr equatorial effect in visible, near UV and near IR spectral ranges
22 p3176 A72-42108

New lines of neon ions in the range 50-200 Å.
23 p3315 A72-43802

Stimulated emission in vacuum far ultraviolet during rapid heating of the plasma electrons by ultrashort light pulses
23 p3322 A72-44466

Photoionization and photoabsorption cross sections of CO₂ at 584 Å.
23 p3317 A72-44519

The influence of ultraviolet line blanketing on the neutral helium triplet lines in B-type stars.
24 p3438 A72-44834

UV and IR observations of galactic and intergalactic matter from space stations, noting spatial resolution increase
24 p3446 A72-45532

ULTRAVIOLET SPECTROGRAPHS

U ULTRAVIOLET SPECTROMETERS

ULTRAVIOLET SPECTROMETERS

- High spectral resolution UV space astronomy spectrographs with echelle gratings
03 p0354 A72-13052
- High spectral resolution balloon-borne spectrograph for near UV solar Mg II resonance lines
05 p0354 A72-13053

Rocket-borne spectrometers calibration for observing absolute intensity and center-to-limb variations of sun in vacuum UV region
03 p0355 A72-13066

Double beam scanning vacuum UV spectrometer and logarithmic radiometer for reflectivity and transmission measurements on solids, liquids and gases
[AD-745497]
09 p1313 A72-23329

Mars nonpolar region photometric and topographic characteristics from Mariner 6 and 7 UV spectrometer observations
15 p2311 A72-32084

ULTRAVIOLET SPECTROPHOTOMETERS

Gimbale telescope/UV spectrophotometer combination with star tracking facilities for use on ESRO TD-1 A satellite
03 p0355 A72-13061

Mars south polar cap surface roughness and photometric function from Mariner 7 UV spectrometric experiment
10 p1531 A72-23708

Calibration model for UV stellar photometer using secondary electron conduction (SEC) vidicon
11 p1631 A72-25684

Solar UV Lyman alpha radiation intensity measurements, using Vertikal-1 rocket-borne photometer and photoelectron analyzer
14 p2128 A72-30465

Balloon-borne UV spectrophotometer observation of Mg II resonance doublet at 2795 and 2802 Å in stellar spectra, comparing to Ca II line widths
20 p2965 A72-38907

ULTRAVIOLET SPECTROSCOPY

Stabilized hydrogen plasma arc spectral radiation as light source for vacuum UV radiometry, comparing output with W strip and carbon sources
01 p0073 A72-11400

High resolution UV stellar spectroscopy in star stabilized Skylark rocket vehicle, using Cassegrain echelle optics and image intensification
03 p0354 A72-13056

Spacecraft-borne UV spectroheliograph with spherical mirror, considering moving part weight reduction
03 p0355 A72-13057

Solar spectral radiation intensity calibration methods in 10-4000 Å range, including black body source, tungsten lamp, carbon arc, detectors, synchrotron radiation, etc
03 p0355 A72-13064

Vacuum UV spectra of free plasma column in microwave field at high pressures for discharge in helium-deuterium mixture
03 p0394 A72-13084

Ozone photolysis in UV region, determining primary products from oxygen optical emission detection using time-resolved flow system
03 p0320 A72-13394

Emission spectra of exploding copper wires in air and vacuum in IR, UV, visible and vacuum UV regions
05 p0691 A72-16991

SAS-D borne TV type UV sensitive detector with camera tubes for high resolution astronomical spectroscopy
08 p1169 A72-21954

TD-1A satellite functional description for stellar UV spectroscopy and solar and cosmic ray experiments, emphasizing attitude control subsystem
09 p1396 A72-23263

Emission spectra of exploding copper wires in air and vacuum in IR, UV, visible and vacuum UV regions
12 p1843 A72-27134

Vacuum UV spectra of free plasma column in microwave high pressure discharge in helium-deuterium mixture
13 p2015 A72-29434

EUV observations of solar quiet region with OSO 6 spectroheliometer, noting chromospheric network structure
17 p2616 A72-35703

Martian atmosphere atomic oxygen concentration estimation from Mariner 6 and 7 O I 1304 and 1356 Å data analysis
19 p2868 A72-38734

Minor constituents in planetary atmospheres - Ultraviolet spectroscopy from the Orbiting Astronomical Observatory.
21 p3111 A72-41459

Energy degradation calculation for electron interaction with carbon dioxide molecules, discussing relationship with Mariner UV data
22 p3171 A72-42421

Vacuum ultraviolet absorption measurements on ionized species.
23 p3316 A72-44330

Orbiting telescopes improved angular resolution and access to UV spectra as advantages in determining stellar composition, mass, luminosity and distance
24 p3446 A72-45531

UMBILICAL CONNECTORS

Space shuttle umbilical systems for mating, connection and checkout of carrier assemblies and couplings

- for cryogenic, electrical, pneumatic and hydraulic services
15 p2213 A72-31695
- UMBRA [SHADOWS]**
U SHADOWS
UMKEHR EFFECT
Atmospheric ozone photochemistry, discussing pure oxygen and moist atmospheres, NO mechanism, tracer applications, stratospheric dynamics and Umkehr observations
07 p0979 A72-20228
Vertical ozone distribution observed by Umkehr and IR methods
08 p1159 A72-21226
- UMKLAPP PROCESS**
Maximum superconducting transition temperature estimation, discussing optimum resonant frequency for attractive interaction, umklapp electron scattering and lattice instabilities
09 p1367 A72-22553
- UNCAMBERED WINGS**
NT RING WINGS
UNCERTAINTY
U PROBABILITY THEORY
UNCONSCIOUSNESS
NT BLACKOUT [PHYSIOLOGY]
NT BLACKOUT PREVENTION
NT NARCOSIS
UNCOUPLED MODES
Coordinate transformation for decoupling equations for tangential electric and magnetic field propagation through series of uniform cylindrical layers with arbitrary properties
07 p0946 A72-19799
Thermomechanical interactions between elastic waves and nonstationary temperature fields in solid continua, considering coupled and uncoupled theories
13 p2064 A72-29093
- UNDAMPED OSCILLATIONS**
HP-115 slender wing research aircraft linear motion and undamped Dutch roll oscillations at high angles of attack
[AIAA PAPER 72-62]
05 p0613 A72-16932
Mathematical model for multiple bearing supported isotropic undamped rotors with arbitrary stiffness and mass distribution, taking into account horizontal/vertical motion coupling
07 p1096 A72-20529
Optimal nomographic determination of surface gyrocompass parameters ensuring minimum period of undamped precession oscillations
09 p1307 A72-22346
Nonaxisymmetric vibrations of arbitrarily thick circular cylindrical shells
23 p3345 A72-43624
- UNDERCARRIAGES**
Deterministic optimization of aircraft undercarriage suspension characteristics for taxiing induced vibration minimization, discussing damping and stiffness functions and hybrid computer solution
09 p1407 A72-23458
Undercarriage loadings of three aircraft - Porter PC-6, Venom DH-112 and Mirage IIIS.
24 p3367 A72-44738
- UNDERGROUND COMMUNICATION**
Subsurface electromagnetic fields of current carrying cable line source on flat earth conducting half space, considering mine rescue operations
01 p0060 A72-10840
Conducting half space electric dipole model of radio propagation through earth at 1-10 MHz
01 p0033 A72-11254
- UNDERGROUND EXPLOSIONS**
International Colloquium on Gasdynamics of Explosions and Reactive Systems, 3rd, Marseille, France, September 12-17, 1971, Proceedings.
24 p3461 A72-45016
- UNDERGROUND NUCLEAR EXPLOSIONS**
U NUCLEAR EXPLOSIONS
U UNDERGROUND EXPLOSIONS
UNDERWATER ACOUSTICS
Seismic and underwater effects of sonic booms, comparing theory with experiments
08 p1162 A72-21907
Environmental, medical and acoustic investigations with underwater laboratory, discussing cabin atmosphere control, depressurization, health conditions and sonar operation
20 p2898 A72-39938
- UNDERGROUND COMMUNICATION**
Biotelemetry system for EEG monitoring of free swimming diver at 15 meter depth, discussing power requirements, antenna design and signal attenuation
12 p1770 A72-27478
- UNDERWATER ENGINEERING**
The 20 kWe thermoelectronic reactor project
18 p2645 A72-36184
Filament wound cylindrical pressure vessel design and development for operation under cyclic-loaded high hydraulic pressure in underwater environment
19 p2877 A72-38166

- UNDERWATER OPTICS**
Scattering media visibility improvement analysis, using theoretical evaluations and experimental electro-optical measurement techniques in fog and underwater
02 p0253 A72-12644
- UNDERWATER PROPULSION**
Incore thermionic reactor application to meet European TV broadcasting satellite and submarine and underwater laboratory power requirements
18 p2644 A72-36166
- UNDERWATER SOUND**
U UNDERWATER ACOUSTICS
UNDERWATER TESTS
Underwater tests of instrument system for combined skin temperature and direct heat flow measurement in thermally stressful environments
12 p1768 A72-28334
Environmental, medical and acoustic investigations with underwater laboratory, discussing cabin atmosphere control, depressurization, health conditions and sonar operation
20 p2898 A72-39938
- UNDERWATER VEHICLES**
NT SUBMARINES
Environmental, medical and acoustic investigations with underwater laboratory, discussing cabin atmosphere control, depressurization, health conditions and sonar operation
20 p2898 A72-39938
- UNIAXIAL STRAIN**
U AXIAL STRAIN
UNIDENTIFIED FLYING OBJECTS
UFO sighting case history and analysis, discussing bright light approaching on collision course during night instrument flight rules
09 p1269 A72-22646
- UNIFORM FLOW**
NT BLASIUS FLOW
Integral method for predicting streamwise development of plane turbulent jets and wall jets in uniform streaming flow
01 p0051 A72-11393
Confined laminar jet mixing of two uniform streams flowing in parallel plate channel, obtaining velocity field from linearized governing equation
[ASME PAPER 71-WA/APM-2]
05 p0647 A72-15973
Poloidal Hall current calculation in hydrodynamic approximation for stationary weakly interacting and conducting cylindrical plasma flow with uniform transverse flow parameter distribution
05 p0701 A72-17240
Descriptive geometric method for distribution of axes of uniform rotation of body containing ideal homogeneous incompressible fluid in uniform turbulent motion
08 p1209 A72-21364
Uniform flow past semiinfinite flat plate for large Reynolds numbers and strong blowing, noting injected fluid region separation from free stream by shear boundary layer
10 p1467 A72-24369
Columnar disturbance strengths upstream of obstacle in uniformly stratified or rotating flows relative to validity of Long hypothesis
10 p1470 A72-25063
Wind tunnel tests for flutter characteristics of rectangular block model oscillating freely in uniform flow, discussing galloping and vortex excitation
11 p1572 A72-26373
Conjugate unsteady problem of convective heat transfer for uniform flow over solid body with matching boundary conditions at interface
13 p2064 A72-28889
Three dimensional structure of transverse uniform flow around motionless circular cylinder for Reynolds number 45,000, investigating correlations of velocities on parallels to generatrices
15 p2179 A72-31684
Sound attenuation in acoustically lined circular ducts in the presence of uniform flow and shear flow.
17 p2582 A72-35411
Flexible cable in uniform flow field, calculating coupling between longitudinal and transverse modes to obtain centripetal acceleration effects on tension
18 p2734 A72-36418
Drag of a finite flat plate set parallel to a uniform flow.
18 p2683 A72-37045
Steady flow past body fixed in uniform flow of dusty gas, obtaining velocity distribution
21 p2989 A72-40195
Karman vortex street in a uniform shear flow.
21 p2992 A72-41247
A note on the laminar mixing of two uniform parallel semi-infinite streams.
23 p3281 A72-44301
- UNIMOLECULAR STRUCTURES**
Transition probabilities and line shapes and widths of unimolecular problem computed using numerical methods for scattering processes
10 p1514 A72-24337
- UNIPOLAR TRANSISTORS**
U FIELD EFFECT TRANSISTORS

- UNIQUENESS**
Regularity of nonunique solutions of degenerate elliptic-parabolic partial differential equations systems without compactness requirement for associated differential quadratic form
06 p0839 A72-17627
One dimensional conductive and radiative heat transfer through gray medium bounded by two diffuse surfaces, noting solutions existence and uniqueness
09 p1412 A72-23586
- UNIQUENESS THEOREM**
Book on uniqueness theorems in linear elasticity covering three and two dimensional elastostatics, whole and half spaces, mixed boundary value problems, elastodynamics, etc
01 p0136 A72-10000
Soviet book on theory of differential equations with deviating argument covering step methods, existence and uniqueness theorems, solutions stability, approximations, etc
02 p0252 A72-12124
Stress and velocity distributions in homogeneous viscoelastic rigid body, deriving uniqueness theorems and minimum principles for limits problem
02 p0297 A72-12596
Uniqueness of turbomachinery flow calculations using streamline curvature and matrix through-flow methods
03 p0308 A72-13648
Thick walled rigid plastic cylinders under pressure, obtaining uniqueness and stability of finite deformation
03 p0446 A72-13706
Linear elastic Cosserat continuum mixed boundary-initial value problem uniqueness theorem, using Kirchhoff proof in classical elastostatics
03 p0382 A72-14363
Mass service process differential equations with losses, annihilation and multiplication processes, demonstrating unique solution existence
04 p0538 A72-14627
Shooting method and contraction mapping application to existence-uniqueness theorem derivation for numerical solution of second order delay differential equations boundary value problems
04 p0539 A72-15042
Self consistent theory of waves in fluctuating plasma, discussing Klimontovich-Maxwell electromagnetic field equations uniqueness solution and kinetic equation
04 p0493 A72-15449
Implicit equations in nonlinear network analysis deriving conditions for existence of unique solutions
04 p0540 A72-15698
Theorems for averaging of first order linear hyperbolic system with time lag, proving existence and uniqueness of solution to Cauchy problem
07 p1028 A72-20214
Radial gas bearing air lubrication theory, proving existence and uniqueness theorems for Reynolds equation periodic solution
07 p0998 A72-20473
Iterative solution of Cauchy problem of partial differential equations nonlinear system with time lag, formulating uniqueness theorem
08 p1198 A72-20904
Uniqueness theorems for linearized Boltzmann equation with Maxwell boundary conditions, using Gauss theorem and Schwartz inequality
08 p1149 A72-21252
Solutions existence and uniqueness for linear invariant relation to gyrostat motion under nonholonomic constraint
08 p1208 A72-21362
Uniqueness theorem for dynamic infinitesimal invariant theory of hereditary elasticity, defining conditions of continuity and positive determinability
08 p1246 A72-21708
Solution uniqueness in physically nonlinear viscoelasticity dynamic theory
08 p1195 A72-21761
Asymptotic motion stability for part of periodic and continuous systems variables, deriving solution uniqueness sufficient conditions
09 p1350 A72-22206
Existence and uniqueness theorem for weak solution of clamped elastic plate equilibrium problem, using micropolar flat plate bending theory
10 p1555 A72-24202
Kinetic equations solution for homogeneous multiatomic gas relaxation, proving solution existence and uniqueness
10 p1516 A72-24629
Dynamic logic control systems theory based on axiomatic concepts of models, deriving conditions for existence and uniqueness of solution for differential logic equations
10 p1457 A72-24636
Function space linear bounded phase coordinate control problems under regularity and normality conditions discussing solution existence and uniqueness conditions
11 p1608 A72-25322

Sufficient conditions for existence, uniqueness and finite-dimensional approximation of solution to first order infinite-dimensional vector differential equation 11 p1676 A72-25357

Existence and uniqueness of general solutions of initial value problem for nonlinear Maxwell-Boltzmann equation with finite time interval 12 p1836 A72-27122

Two heat conducting phases free boundary problem with temperature distribution within phases, proving existence and uniqueness theorems 12 p1836 A72-27124

Uniqueness of solutions to displacement problem for unbounded bodies in linear elastodynamics 12 p1884 A72-27564

Uniqueness theorem for solution to boundary value problem in anisotropic viscoelasticity, considering stress-strain relation in nonlinear Volterra equation form 12 p1886 A72-27983

Uniqueness and existence theorems for nonideal thermal contact between three dimensional solid parts in heat conduction theory, noting case of two dimensional body 12 p1889 A72-27996

Boundary value problem solution uniqueness relation to existence for nonlinear differential equations of arbitrary order satisfying solution compactness condition 15 p2263 A72-31753

Cosserat surface uniqueness theorem for non-homogeneous anisotropic thermoelastic shells small motions and temperature variations superposed on large deformation 16 p2465 A72-32981

Uniqueness principle application to construction of gravitational field generated by complex of elastic bodies for mass tensor 16 p2424 A72-33366

Existence and uniqueness theorems for Cauchy problem solution for linear singular integrodifferential operator equation 16 p2417 A72-34010

Criterion for unique periodic solution of perturbed Liénard equation for small amplitude periodic perturbation 17 p2574 A72-34400

Conditions for the uniqueness of the solution to the Cauchy problem for special systems of equations with variable coefficients 17 p2575 A72-34775

Investigation of the solution of a two-dimensional nonlinear Volterra integral equation 19 p2825 A72-38203

Approximate integration of a nonlinear system of differential equations with time lag 19 p2827 A72-38468

Local Vogt-Russell theorem confirmation by linear approximation for stellar structure nonlinear differential equations, discussing equilibrium model local uniqueness and stellar stability 20 p2973 A72-39888

Classes of uniqueness of solutions to the Cauchy problem 21 p3074 A72-40255

Classes of uniqueness of solutions to a boundary value problem in an infinite layer for systems of linear difference-differential equations 21 p3074 A72-40257

Navier-Stokes evolution inequality bounded solution existence and uniqueness theorems for two dimensional space 22 p3200 A72-43201

Existence and uniqueness theorems of elliptic equations with eigenfunction exponential decrease at infinity and 2m order self adjoint differential operator in n-dimensional Euclidean space 23 p3307 A72-43223

UNITED NATIONS

United Nations international space law development, discussing concepts of state jurisdiction, territorial sovereignty, damage liability, etc 06 p0905 A72-17814

United Nations activities in space law, discussing creation of Committee on Peaceful Uses of Outer Space 07 p1102 A72-19453

United Nations role as center of international cooperation in space law norms elaboration 07 p1102 A72-19454

Structure and organization of UN bodies concerned with space activities, discussing legal contribution 07 p1102 A72-19455

Liability for damage caused by space objects, noting UN resolution 07 p1103 A72-19460

UN registry of space vehicles, reviewing historical development of registration procedures in U.S. and U.S.S.R. 07 p1103 A72-19463

UN agencies role in communication satellites technology exploitation, discussing international cooperation in outer space peaceful use and exploration and development of space law 07 p1074 A72-19468

Satellite broadcasting for direct individual and community reception as mass communication means, discussing UN role and international juridical problems 07 p1104 A72-19472

Conventions on international responsibility for damage caused by space objects, studying UN juridical subcommittee resolution 08 p1255 A72-21076

United Nations activity in international space program for earth resources and environmental pollution surveillance by satellites 15 p2220 A72-31227

United Nations FAO interest in remote sensing techniques application to agricultural, forestry and fisheries resources survey and management 15 p2220 A72-31228

The role of the United Nations in earth resources satellites. 24 p3468 A72-45185

UNITED STATES OF AMERICA

NT ALASKA

NT CALIFORNIA

NT FLORIDA

NT HAWAII

NT TEXAS

NT WASHINGTON

UNITS OF MEASUREMENT

Aircraft noise measurement units and methods, discussing engine design for noise reduction 05 p0611 A72-16026

Aerodynamic noise measurement, discussing physical units, spectral analysis, conversion and correction formulas 05 p0614 A72-17195

Noise level measurement scales, units datum points and mathematical formulas, suggesting method of quasi-peak level above masked threshold 07 p1035 A72-20164

German book on principles and applications of similarity theory in physical-technical research covering coherent dimensional units and invariance principle, physical dimensions, etc 15 p2218 A72-31900

UNIVAC COMPUTERS

Univac 1616 computer design featuring uses of 16-bit word technology, medium and large scale integration, and transistor-transistor logic 16 p2366 A72-33243

Univac 1832 multiprocessor avionics computer for airborne ASW, discussing input/output controllers and interfaces and IC design features 16 p2367 A72-33245

UNIVERSAL TIME

Nighttime laser ranging of French reflector for Soviet Lunokhod, discussing universal-ephemeris time difference determination 05 p0721 A72-16771

Coordinated universal time system nature and consequences for international time signal users 07 p1032 A72-19069

Prime geocentric meridian longitudes and UT, discussing position in terrestrial rectangular coordinates in relation to earth pole motion 07 p0976 A72-19816

Eastern and western polar electrojets intensity diurnal variations with respect to universal time 08 p1154 A72-20740

Radio echo observation of Quadrantid meteor showers right ascension and declination, observing mean range and influx rate as function of universal time 10 p1545 A72-24808

Nighttime laser ranging of French reflector for Soviet Lunokhod, discussing universal-ephemeris time difference determination 17 p2611 A72-35274

Prime geocentric meridian longitudes and UT, discussing position in terrestrial rectangular coordinates in relation to earth pole motion 17 p2549 A72-35741

Easterly and westerly polar electrojets intensity diurnal variations with respect to universal time and geo- and heliophysical phenomena 19 p2791 A72-38368

UNIVERSE

Radio source counts, cosmology and evolution in uniform model universes 01 p0127 A72-10323

Diffuse gravitational background radiation in universe, assuming gravitational field fluctuations macroscopic nature and Einstein equations applicability 03 p0417 A72-13095

Galactic superclusters and matter distribution in universe, considering systematic catalog errors and uncertainty of statistical tests 03 p0421 A72-13172

Expanding rotating shearing Bianchi type IX universe, investigating rotation effects on singularity 04 p0549 A72-15290

Universe cluster expansion model, showing velocity dispersion increases from center to turnover radius 04 p0578 A72-15308

UNIVERSE

Black hole prediction in gravitational collapse of star and universe in terms of quantum principle, chemical mechanics and superspace dynamics 05 p0690 A72-16528

CP-noninvariance model of baryon interaction and charge asymmetry of universe, postulating kappa particle/neutral massive fermion/ 06 p0875 A72-17275

Parametric solution of Brans-Dicke cosmological equations for flat Friedmann type expanding universe for time, density, expansion parameter and scalar field 07 p1074 A72-19525

Chronology of universe - Conference, Padua, Italy, November 1970 07 p1083 A72-20463

Local deviation limits of universe from homogeneous isotropic model, considering velocity field perturbations and galaxy counts 08 p1234 A72-21381

Book on physical cosmology development covering universe expansion, steady state, isotropy, Hubble constant, cosmic time scale, mass density, etc 08 p1236 A72-21480

Cosmological implications of radioactive decays study by Rutherford, suggesting evolving nonstatic universe 09 p1386 A72-22688

Book on astronomy and cosmology covering big bang, steady state and oscillating universe theories, radio sources, galaxies, interstellar meteor relativity and extraterrestrial life 09 p1389 A72-23248

Nonlinear hydrodynamic effects in dynamic motions of metagalactic turbulence in pre-Friedmann universe 10 p1536 A72-24141

Friedmann cosmological models in terms of conformally invariant gravitation theory, noting two physically connected universe halves 10 p1541 A72-24474

Rapid perturbation growth conditions for expanding universe, discussing background density decrease with time 10 p1543 A72-24661

Nonlinear theory of gravitational instability in expanding universe, discussing density and velocity perturbations amplification at intermediate stage 11 p1715 A72-25527

Diffuse gravitational background radiation in universe, assuming gravitational field fluctuations macroscopic nature and Einstein equations applicability 11 p1716 A72-25703

X ray observation inconsistency with matter creation in steady state universe due to inner bremsstrahlung from neutron decay 11 p1713 A72-26125

Expanding hot universe evolution from astrophysical cosmology point of view, emphasizing galaxy formation relation to state of matter and radiation in early universe 13 p2038 A72-29084

Expanding universe postulate vs tired light effect for cosmological red shift explanation, discussing possible tests 14 p2155 A72-30551

Universe evolution, discussing constituents, matter and antimatter, quasars and radio stars in various galaxies 14 p2157 A72-30623

Energy release mechanism during early universe expansion leading to distortion of relic black body spectrum, noting Comptonization effects 16 p2461 A72-34151

Galactic and metagalactic background radiation 18 p2722 A72-36723

Many-body forces and the effect of the matter distribution in the universe to the gravitational constant. 18 p2728 A72-36800

German book - Relativistic astrophysics 19 p2868 A72-38721

Hamiltonian approach to the dynamics of expanding homogeneous universes in the Brans-Dicke cosmology. 19 p2869 A72-38807

Weinberg model application to hot universe of weakly interacting particles at nonzero temperature, noting long range character 21 p3084 A72-40726

On the cosmological equations in a universe with small scale condensations. 22 p3220 A72-41998

Universe evolution study from contemporary chemical composition of cosmic matter, noting concentration changes of protons, neutrons and He 4 22 p3222 A72-42140

Exact expressions for the properties of the zero-pressure Friedmann models. 22 p3229 A72-42890

On irrotational Bianchi-type universes in the Brans-Dicke cosmology. 23 p3314 A72-44314

UNIVERSITY PROGRAM

Earth Resources Survey /ERS/ program personnel training and education, discussing trainee selection, knowledge categories and training methods for remote sensing

02 p0304 A72-11855

UNKNOWN

U PROBLEM SOLVING

UNLOADING

Unloading wave propagation in semiinfinite elastoplastic cylindrical rod for concave stress-strain diagram with no initial linear segment

13 p2053 A72-28388

UNMANNED SPACECRAFT

NT BEACON SATELLITES
NT GEODETIC SATELLITES
NT JUPITER PROBES
NT LUNAR PROBES
NT LUNIK LUNAR PROBES
NT MARINER SPACE PROBES
NT MARINER SPACECRAFT
NT MARS PROBES
NT NAVIGATION SATELLITES
NT NAVSTAR SATELLITES
NT OSO
NT OSO-E
NT OSO-G
NT OSO-H
NT PAGEOS SATELLITE
NT PASSIVE SATELLITES
NT PIONEER SPACE PROBES
NT RANGER LUNAR PROBES
NT SOLAR OBSERVATORIES
NT SOLAR PROBES
NT SPACE PROBES
NT SURVEYOR LUNAR PROBES
NT TRANSIT SATELLITES
NT VENERA SATELLITES
NT VENUS PROBES
NT ZOND SPACE PROBES

Solar electric low thrust unmanned Mercury orbiter missions, considering spacecraft subsystems and ballistic and swingby trajectories

[AIAA PAPER 72-425] 11 p1721 A72-26170

Spacecraft nuclear electric propulsion system multimission performance evaluation, discussing launch mode and vehicle capability factors in system size selection

[AIAA PAPER 72-503] 11 p1685 A72-26226

Soviet unmanned Luna 20 mission, describing launch, lunar trajectory injection, midcourse correction, lunar orbit and landing, surface soil sampling and return to earth

14 p2163 A72-30680

Mission operations for unmanned nuclear electric propulsion outer planet exploration with a thermionic reactor spacecraft.

17 p2606 A72-34578

A teleoperator system for space application.

24 p3407 A72-45174

Comparative merits of manned and unmanned /automated/ space exploration, considering lunar observatories, earth orbiting space stations and interplanetary missions

24 p3441 A72-45220

Unmanned OAO spacecraft series and experiment packages, discussing space astronomy scientific achievements, mission plans and space shuttle role

24 p3453 A72-45535

Manned and unmanned space-based astronomical observatory systems pros and cons, discussing experiment management complexity and cost reduction

24 p3447 A72-45546

UNSTABLE BURNING

U COMBUSTION STABILITY

UNSTEADY FLOW

NT OSCILLATING FLOW

Unsteady flow about two dimensional airfoils, determining surface pressure fluctuations induced by turbulent boundary layers

01 p0001 A72-10217

Two dimensional transient inviscid flow field from secondary injection in missile control, describing distribution with artificial viscosity finite difference method

01 p0097 A72-10940

Two dimensional unsteady incompressible boundary layer near forward stagnation point of infinite plane wall with uniform suction or injection, obtaining iterative solution

01 p0050 A72-11106

Unsteady compressible free convection near infinite vertical flat plate with temperature and velocity variations in boundary layer

01 p0146 A72-11392

One dimensional unsteady flow in turbine engines rotating and static vane cascades, discussing vibrations propagation

02 p0202 A72-11584

Multicellular viscous vortex core embedded in unsteady outer potential swirling flow, obtaining numerical solution

02 p0253 A72-11971

Nonstationary temperature field determination in steam turbine casing-connector nozzle by difference method based on heat balances, comparing results with electric analog studies

02 p0303 A72-12534

Unsteady boundary layer flow of viscous incompressible fluid between two rotating coaxial parallel disks

02 p0205 A72-12538

Unsteady flow in laminar boundary layers along infinite porous flat plate with time dependent suction

02 p0206 A72-12620

Time dependent unsteady flows visualization around circular cylinders and flat plates decelerated from steady speed

02 p0206 A72-12773

Velocity and temperature distributions for unsteady plane Poiseuille flow of viscous incompressible fluid between two parallel plates

03 p0340 A72-13000

Unsteady flow theory for radial gas lubricated bearing, deriving velocity and pressure distribution expressions

03 p0363 A72-13577

Self similar solutions for unsteady shear flows of conducting Newtonian fluids with rheological power law under transverse magnetic field

03 p0397 A72-13997

Nonsteady molecular beam approximation for strong shock structure problem, considering Boltzmann equation

03 p0399 A72-14053

Thermal boundary layer of incompressible fluid unsteady laminar flow, obtaining temperature field from energy equation for various wall temperature conditions

03 p0343 A72-14314

Generalized equation for incompressible unsteady laminar boundary layer in external flow with arbitrary time dependent velocity distribution, discussing expanding cylindrical body

03 p0343 A72-14315

Obukhov contribution to turbulence in atmosphere with nonuniform temperature, discussing dynamic scale length and asymptotic states of boundary layer in unstable flows

03 p0385 A72-14333

Linearized constant temperature hot-wire anemometer calibration for shock tube unsteady flow velocity measurements with low strength wave propagation

04 p0521 A72-14920

Unsteady radial flow between fixed and oscillating walls, obtaining flow equations and air bearings stability conditions

04 p0511 A72-14970

Unsteady approach to nonisothermal flow theory for Couette flow, making general assumptions concerning rheological law and temperature dependence of fluidity

04 p0512 A72-14985

Unsteady nonisothermal gas flow through semiinfinite porous medium, using linearized flow equations for small pressure variation

04 p0512 A72-15200

German monograph on two dimensional unsteady boundary layer calculation with unstable effects, using Navier-Stokes equations

04 p0512 A72-15245

Two dimensional unsteady flow of incompressible fluid around passing turbomachine blades, determining instantaneous pressure, forces and moments as function of time

04 p0463 A72-15559

Similar unsteady one dimensional motion of viscous heat conducting gas due to sudden energy release at surface

[ASME PAPER 71-WA/HT-3] 05 p0743 A72-15864

High velocity unsteady flow calculations in metal pipes by numerical methods for boundary conditions, including turbomachinery, column separation and gas accumulator

[ASME PAPER 71-WA/FE-13] 05 p0646 A72-15931

Conservation equations for blast waves one dimensional nonsteady flow field, considering Eulerian space and time profiles

[ASME PAPER 71-WA/APM-1] 05 p0745 A72-15974

Navier-Stokes equations solution for unsteady viscous flow around oscillating elliptic airfoil in turbomachinery flutter analysis, obtaining pressure and shear stress distributions

05 p0600 A72-16002

Nonlinear unsteady potential flow of incompressible fluid past slender wing, using linearized vortex distribution method

05 p0600 A72-16214

Nonstationary oncoming flow temperature effect on heat transfer in thermal boundary layer at forward stagnation point

05 p0746 A72-16217

Finite difference calculations for two dimensional unsteady inviscid expanding flow of perfect gas through nozzle, obtaining flow field patterns

05 p0603 A72-16539

Fluctuating flow in idealized model of turbulent shear layer composed of many discrete two dimensional vortices, analyzing noise generation

[AIAA PAPER 72-155] 05 p0609 A72-16955

One dimensional continuous electrode shock tube driven MHD accelerator, analyzing unsteady flow behind ionizing shock wave by method of characteristics

[AIAA PAPER 72-102] 05 p0697 A72-16973

Unsteady boundary layer on hemisphere embedded on infinite plane during normal liquid impingement, using inner and outer expansions method to study separation time

05 p0653 A72-17003

Unsteady axisymmetric incompressible pipe flow stability near piston, using Navier-Stokes equations solution with finite difference forms

05 p0653 A72-17006

Convergent power series solution in powers of time for unsteady viscous flow near stagnation after impulsive motion of bluff body from vorticity distribution viewpoint

06 p0757 A72-18135

Marginally unstable plane parallel flow nonlinear response to two dimensional disturbance, noting localized burst relationship to Landau constant

06 p0801 A72-18163

Unsteady thermal conductivity and heat transfer in solid bodies heated by radiation, using cascade linearization method

07 p1100 A72-19884

Contact discontinuity motion past slender body of revolution in shock tube, solving unsteady supersonic flow problem by method of integral transformation

07 p0909 A72-20072

Fluid mechanics of blood pulsatile flow in microcirculation, considering plasma layer nature and transcapillary mass transfer

07 p0931 A72-20087

Interference induced unsteady aerodynamic forces on tandem airfoils in subsonic flow, using two dimensional model

07 p0910 A72-20101

Boundary conditions for unsteady flow fields bounded by incompressible elastic thick plane wall fixed to rigid surface

07 p0972 A72-20113

Unsteady laminar viscous incompressible electrically conducting flow between nonconducting parallel flat plates with applied constant magnetic field

07 p1044 A72-20242

MHD dynamo model for incompressible real electrically conducting fluid unsteady flow

07 p1044 A72-20304

Unsteady flow of viscous incompressible electrically conducting fluid past infinite nonconducting plate within uniform transverse magnetic field

08 p1212 A72-21079

Unsteady gas flow in thrust bearing with spiral grooves, presenting Navier-Stokes and discontinuity equation

08 p1176 A72-21167

Unsteady uniform turbulent flow of incompressible liquid in circular pipe, verifying mathematical model with velocity distribution calculations

08 p1151 A72-21666

Unsteady incompressible laminar boundary layer theory on two dimensional body motion through fluid at rest at infinity, considering skin friction

08 p1151 A72-21794

Three phase bidirectional pulsating flow hydraulic control system, discussing design, performance and applications

08 p1114 A72-22162

Pulsed plasma flow interaction with spatially periodic magnetic field generated by coaxial coils with alternating currents, noting MHD stability

09 p1362 A72-23207

Newton cooling law applicability to unsteady heat and mass transfer approximate calculation for ion exchange process

09 p1412 A72-23685

Rectilinear impulsive motion of compressible boundary layer on infinite plate, deriving integration method for differential equations of motion under energy dissipation neglect

10 p1465 A72-24203

Wind tunnel inlet effect on pulsed flow, relating velocity and pressure pulses

10 p1417 A72-24216

Unsteady laminar boundary layer on semiinfinite flat plate induced by small free stream velocity fluctuations, showing far downstream double layer structure via asymptotic and numerical solutions

[AD-745486] 10 p1467 A72-24334

Subsonic unsteady aerodynamic pressures on blades of compressor wheel rotating freely in air stream

[ONERA, TP NO. 1077] 10 p1420 A72-24854

Two dimensional unsteady stagnation point flow against plane wall with impulsive motion

10 p1470 A72-25040

Computerization of panel flutter boundary calculations with aerodynamic forces derived from linear three dimensional unsteady potential flow theory

[AIAA PAPER 72-403] 11 p1731 A72-25424

- Time dependent viscous flow past impulsively started sphere using numerical solutions for governing equations based on Legendre series expansion of stream and vorticity functions
11 p1615 A72-25551
- Unsteady laminar wall boundary layers formation within finite expansion or compression waves in tube with gas at rest
11 p1616 A72-25981
- Simple waves in one dimensional unsteady nonequilibrium dissociative gas dynamics, discussing internal, chemical bond and dissociation energies
11 p1616 A72-25982
- Dynamic response of MHD flow under impulsive pressure gradient, obtaining approximate analytic solutions for conduits of arbitrary cross sections by complex variable approach
11 p1695 A72-26039
- Fluid compressibility effect on nonstationary laminar flow within infinite cylindrical pipe
11 p1618 A72-26502
- Perturbation analysis of perfect gas unsteady transonic irrotational inviscid flow in two dimensional channel, presenting numerical computation of flow structure temporal change
11 p1618 A72-26635
- Hot-wire measurement of vector velocity modulus and sign in one dimensional unsteady gas flow
12 p1806 A72-27178
- Unsteady viscous incompressible electrically conducting fluid flow generated by porous disk rotation, investigating transverse magnetic field effect
12 p1851 A72-27305
- Inward radial flow turbines under unsteady flow conditions with full and partial admission, predicting performance by method of characteristics
12 p1751 A72-27349
- Unsteady flow evolution at sphere and elliptical cylinder obtained by flow visualization techniques, showing streamline sequence dependence on angle of attack
12 p1797 A72-27469
- Harmonically oscillating rectangular wing in unsteady transonic flow, obtaining two part boundary value problem for linear potential equation
12 p1751 A72-27545
- Copper resistance thermocouple measurement for channel unsteady air flow rate measurement, discussing design, operation principles and maximum error
12 p1812 A72-28146
- Nonstationary interaction flow field between subsonic and composite jet on flat plate with vortex formation and reverse currents, using finite difference technique
12 p1799 A72-28168
- Blowing and suction effects on pulsations of isothermal turbulent jets propagating along porous cylinder
12 p1752 A72-28169
- Parametric approximation of unsteady laminar boundary layer in incompressible fluid in terms of flow velocity and friction characteristics
12 p1799 A72-28177
- Plane unsteady potential isentropic gas flow equations solution interpreted as shallow water motion over horizontal bottom
13 p1893 A72-28717
- Profile losses at turbine rotor blade in unsteady gas flow from experimental data analysis, noting effect of turbulence caused by trailing edge wakes
13 p1893 A72-28783
- Skin friction response to angle and perturbation in flow past axisymmetric body with unsteady main stream
13 p1941 A72-28887
- Conjugate unsteady problem of convective heat transfer for uniform flow over solid body with matching boundary conditions at interface
13 p2064 A72-28889
- Electrical analog simulation of internal combustion engines intake and exhaust systems nonstationary gas flow, considering cylinder, turbine and supercharger operation
13 p2027 A72-29136
- Hall currents effect on unsteady MHD flow of electrically conducting fluid past flat plate imbedded in uniform external transverse magnetic field
13 p2012 A72-29225
- Nonstationary laminar zero-discharge MHD Couette flow produced by sudden movement of highly conductive plate in closed volume filled with conducting liquid
13 p2016 A72-29607
- One dimensional unsteady flow of dense magnetized plasma, investigating time evolution of temperature profile in wall layer and thermal conductivity
13 p2018 A72-29876
- Passive scalar dispersion in turbulent incompressible flow characterized by inhomogeneous and nonstationary statistics, expanding velocity and scalar concentration fields in Wiener-Hermite functions
14 p2128 A72-30348
- Ideal liquid theory application for unsteady separated flow calculation around arbitrary shape bodies, noting numerical solution for plane flow around circular cylinder
14 p2070 A72-31010
- Plane unsteady convective motion of viscous incompressible liquid in infinite horizontal vessel of rectangular cross section due to wall temperature fluctuations
14 p2174 A72-31157
- Unsteady laminar boundary layer on body of revolution with axial and torsional oscillations, calculating velocity distribution and shear stress variation
15 p2178 A72-31402
- Navier-Stokes equation for unsteady asymptotic suction flow over flat plate, plotting velocity distribution profiles
15 p2178 A72-31406
- Perfect gas unsteady compressible homentropic flow with zero spatial pressure gradient, deriving characteristic equations
15 p2218 A72-32324
- Unsteady viscous flow effects on aerodynamic forces exerted on oscillating elliptic airfoil for various Reynolds numbers, angles of attack and frequencies
15 p2180 A72-32344
- Velocity and temperature distribution for viscous incompressible fluid unsteady flow between two parallel plates with pressure gradient linearly varying with time
15 p2219 A72-32599
- Power law fluids impulsively started flow over plate, presenting analytical expressions for velocity distribution, shear stress and boundary layer thickness
16 p2375 A72-32833
- Unsteady boundary layer flow equations for arbitrarily smooth bodies moving relatively slowly through rotating liquid [DFVLR-SONDDR-211]
16 p2376 A72-33007
- Unsteady Falkner-Skan flow solution by finite difference method for pressure gradient effect on transient response of laminar boundary layer
16 p2376 A72-33015
- Solution of the two-dimensional, unsteady, compressible Navier-Stokes equations using a second-order accurate numerical scheme.
17 p2538 A72-34646
- Unsteady flow at the junction of a branched duct.
17 p2539 A72-34971
- Unsteady thermal conductivity and heat transfer in solid bodies heated by radiation, using cascade linearization method
17 p2637 A72-35132
- Kinetic and kinematic equations for inviscid unsteady gas flow, noting pseudostationary vortex geometry
17 p2541 A72-35436
- Determination of the parameters associated with a singular pressure loss permitting the calculation of acoustic resonance phenomena and the role of these parameters
18 p2680 A72-36465
- Convective cells formation in fluid unsteady flow between two horizontal rigid boundaries with time periodic temperature distribution
18 p2681 A72-36483
- Unsteady motion of a compressible viscous fluid in a spherical layer
18 p2682 A72-36882
- Self-similar unsteady magnetogasdynamic flows of a radiating gas produced by the motion of a piston
18 p2716 A72-36897
- Calculation of an unsteady separation flow past a slender profile
18 p2642 A72-36900
- The unsteady boundary layer flow in a convergent channel.
18 p2683 A72-36930
- Time dependent solution to motion and energy equations for unsteady laminar spherical Couette flow of incompressible constant viscosity fluid
18 p2684 A72-37055
- A comparison of the solutions of Prandtl's and Navier-Stokes equations in a superposed fluctuating flow.
18 p2684 A72-37084
- Experimental investigation of nonstationary heat exchange for flow around a flat plate
19 p2880 A72-37665
- Hypersonic unsteady compressible boundary layer dependence on Prandtl number.
19 p2787 A72-38429
- Pressure propagation rate relation to local sound speed in unsteady anisotropic gas flow with particle-varying specific entropy
19 p2788 A72-38564
- Solution of the problem of the unsteady motion of a mixture in a flat duct using a quasi-homogeneous model with allowance for deposition on the walls
19 p2788 A72-38589
- The friction drag factor for an unsteady motion in tubes
20 p2913 A72-39392
- Unsteady axisymmetric flows of a liquid draining from a circular tank.
20 p2913 A72-39605
- Pulsation rates of continuous and discrete components of dispersed flow
20 p2915 A72-40047
- Nonstationary laminar zero-discharge MHD Couette flow produced by sudden movement of highly conductive plate in closed volume filled with conducting liquid
21 p3091 A72-40661
- Unsteady aerodynamic and aeroelastic effects in turbomachine blade cascades supersonic flow, discussing trends in fan and compressor technology
21 p3118 A72-40969
- Synthesis of Tolubinskii's integral method and the perturbation method in nonstationary transport problems with nonlinear boundary conditions
21 p3129 A72-41053
- Two-dimensional subsonic linearized theory of the unsteady flow through a blade-row with small steady pitch and camber angle.
21 p2990 A72-41137
- [ICAS PAPER 72-12]
Hydrodynamic test tunnel for unsteady pressure and force measurements and hydrogen bubble flow visualization data acquisition
21 p3041 A72-41585
- [AIAA PAPER 72-999]
Two dimensional MHD fluctuating flow of incompressible electrically conducting rarefied gas past infinite porous wall for slip-flow regime with variable suction
21 p3095 A72-41784
- Transverse magnetic field effect on unsteady incompressible laminar MHD boundary layer flow, noting cylindrical body oscillations in fluid
21 p3095 A72-41786
- Unsteady laminar flow in a tube with arbitrary variation of the flow rate in time
21 p3164 A72-41892
- Plane unsteady potential isentropic gas flow equations solution interpreted as shallow water motion over horizontal bottom
22 p3165 A72-42094
- Nonstationary processes in the intervane apertures of turbomachines
22 p3133 A72-42247
- Effect of external turbulence on the boundary layer of a flow
22 p3166 A72-42258
- Entropy and simple waves in multidimensional gas flow.
22 p3166 A72-42314
- Unsteady rotor aerodynamics at low inflow and its effect on flutter.
22 p3135 A72-42349
- [AIAA PAPER 72-959]
Unsteady wake effects on progressing/regressing forced rotor flapping modes.
22 p3137 A72-42350
- [AIAA PAPER 72-957]
Variational solution of a nonlinear boundary value problem for unsteady flow of gas.
22 p3199 A72-42854
- Analysis by hydraulic analogy of rotating separation in compressors
22 p3167 A72-43091
- Flutter analysis and unsteady pressure fields induced by pitching motions of wall mounted sweptback wing, verifying experimentally lifting surface theory in high subsonic range
22 p3241 A72-43094
- Unsteady convective heat transfer in the initial section of a pipe with a smooth inlet
23 p3356 A72-43670
- The effects of magnetic field oscillations on the boundary layer flow past a magnetized plate.
23 p3321 A72-43725
- Pulsatile flow of linear viscoelastic fluids in elastico-viscous tubes.
23 p3280 A72-43823
- Unsteady flow field near wall and Reynolds stress measurement in turbulent boundary layer, using conditional sampling technique with digital computer
23 p3282 A72-44304
- Analysis of a nuclear magnetic resonance blood flowmeter for pulsatile flow.
24 p3401 A72-44574
- Use of characteristics for boundaries in time dependent finite difference analysis of multidimensional gas dynamics.
24 p3359 A72-44879
- Radiation properties of the semi-infinite vortex sheet.
24 p3359 A72-44918
- High order terms diffusion equation derivation for strong fluctuating flows by random walk method, discussing phenomenological analogy with equations of motion
24 p3390 A72-44994
- A means of measuring the rms value of velocity fluctuations in unsteady turbulent flow
24 p3403 A72-45259
- Contributions to the study of turbulent flow in the vicinity of a flat wall
24 p3394 A72-45443
- Aerodynamic characteristics of turbine blade cascades in unsteady incompressible and compressible fluid flow, considering axial flow turbine blades vibration
24 p3364 A72-45524

Effects of upstream unsteadiness on hypersonic flow past a wedge. 24 p3364 A72-45565

On the unsteady magnetohydrodynamic flow over yawed infinite cylinder. 24 p3395 A72-45599

UNSTEADY STATE

Heat and mass transfer equations for unsteady transpiration cooling, taking into account temperature gradient between coolant and surface 03 p0457 A72-14154

Differential equations describing dynamic behavior of unsteady plane exothermic reaction front in gaseous system 06 p0903 A72-18204

Porous cooling unsteady state problem approximation based on elementary thermal balance concept, solving differential equations by computerized Euler method 06 p0904 A72-18513

Solar activity effects on biospheric processes for biological and physicochemical systems in unsteady state, considering maximum effects on man at certain electromagnetic wave frequencies 12 p1773 A72-28211

Unsteady state propagation of weak nonlinear plasma waves in magnetic field, discussing shock wave formation and compression pulse evolution 13 p2012 A72-29124

Instrument to determine steady and unsteady stress state of elastic fluids in viscometric flow, noting rheological measurements in solved polymers 14 p2094 A72-30421

Normal-mode expansion technique for unsteady radiative and conductive heat transfer in absorbing emitting isotropically scattering slab with reflective boundaries 16 p2478 A72-33438

Book - Investigation of nonstationary heat and mass transfer processes by the net-point method 18 p2740 A72-36248

Study of unsteady processes in the ionosphere and outer space by using quantum frequency stabilizers 18 p2687 A72-36853

Fourier transformation relating autocorrelation to spectral density of power bounded and energy bounded functions, discussing unsteady stochastic processes 20 p2953 A72-39552

Qualitative analysis of the linearization of quasi-linear problems of nonstationary heat conduction 21 p3129 A72-41055

Application of Tolubinskii's integral method to the solution of boundary value problems of nonstationary convective diffusion 21 p3129 A72-41056

Investigation of nonstationary heating processes in thermal resistors fed from functional sources 21 p3129 A72-41060

Analytical calculation of unsteady heat fields in planar devices 22 p3158 A72-42116

Study of the operation of a neodymium glass laser under nonsteady thermal conditions, with thermal insulation of the active element by air 22 p3185 A72-42172

A method for calculating canonic realizations for linear, unsteady, discrete systems 23 p3277 A72-43989

UNSWEPT WINGS

NT RECTANGULAR WINGS

NT RING WINGS

Wind tunnel investigation of unswept rectangular wing with externally blown single slotted flap, determining optimum slot width as function of momentum coefficient and flap deflection 04 p0462 A72-15461

Three dimensional wind tunnel investigation of vortex augmented unswept wing with leading edge cusp flap and split upper and lower trailing edge flaps [SAE PAPER 720321] 11 p1568 A72-25584

UPCONVERTERS

U PARAMETRIC FREQUENCY CONVERTERS

UPDRAFTS

U VERTICAL AIR CURRENTS

UPPER AIR

U UPPER ATMOSPHERE

UPPER ATMOSPHERE

NT D REGION

NT E REGION

NT EXOSPHERE

NT F REGION

NT IONOSPHERE

NT LOWER IONOSPHERE

NT MAGNETOPAUSE

NT MAGNETOSPHERE

NT MESOPAUSE

NT MESOSPHERE

NT SPORADIC E LAYER

NT THERMOSPHERE

NT UPPER IONOSPHERE

Altitude dependent superrotation of earth upper atmosphere, using nonlinear continuity, momentum conservation and state equations of gas dynamics 01 p0052 A72-10076

Neutral H concentration in upper atmosphere during solar minimum, using ion thermal energies from rocket and satellite mass spectrometric, radio and proton whistler measurements 01 p0053 A72-10361

Latitude dependence of upper atmosphere corpuscular radiation intensity, analyzing sounding data from Indian Ocean area 01 p0118 A72-10369

Upper atmosphere neutral oxygen density diurnal variations from incoherent scatter and satellite drag data, noting deviations from Jacchia static diffusion model predictions 01 p0062 A72-10911

Atomic oxygen layer height and peak concentration in earth upper atmosphere, considering solar dissociative radiation and turbulent diffusion for equinox conditions 02 p0217 A72-19244

Quadrantid meteoritic shower upper atmosphere contamination effects on twilight and night sky brightness 02 p0283 A72-12467

Upper atmosphere ozone, aerosol and neutral constituent density profiles estimation by recursive filtering algorithm for satellite observation data 02 p0222 A72-12811

Internal gravity waves and tidal oscillations excitation mechanism in upper atmosphere 03 p0346 A72-13383

Quenching rate of vibrationally excited hydroxyl with molecular oxygen in fast flows for airglow studies in upper atmosphere 03 p0321 A72-13899

Soviet book on calms and storms in upper atmosphere covering energy variations, auroras, geomagnetic storms, weather forecasting, etc 03 p0350 A72-13967

Upper atmosphere He, Ne, Na and K atoms collisions with molecular oxygen, determining ejected electron energy during fast Na, K, Rb and Cs ionization for meteor phenomena modeling 03 p0438 A72-13980

Upper atmospheric turbulence correlation to supersonic aircraft dynamics, noting Concorde contribution 04 p0542 A72-14681

Upper atmosphere and ionosphere magnetic storm phenomena, showing atomic to molecular concentration ratio decrease 04 p0516 A72-14938

Upper atmospheric density measurements accuracy from triaxial accelerometer instrumented inflated falling sphere 04 p0519 A72-15156

Collisionless shock wave interaction with particle stream in upper solar corona from decimeter radio observation 05 p0708 A72-15764

Internal gravity wave interaction with median wind in upper atmosphere from solution of system of linearized hydrothermodynamic equations 05 p0656 A72-16175

Upper atmosphere supplementary electron flux data relationship to geomagnetic disturbance obtained from high altitude balloon experiments 05 p0709 A72-16236

Vibrationally excited oxygen molecules formation and decomposition in upper atmosphere, calculating day and night equilibrium concentrations 05 p0657 A72-16252

Electron flux and energy spectra measurements at 200-600 km altitude by Cerenkov counters onboard Proton 1 and 2 05 p0709 A72-16254

Additional high energy electrons flux detection in upper atmosphere after magnetic perturbations 05 p0710 A72-16525

Pressure modulated carbon dioxide radiometer for remote temperature sounding in upper atmosphere 05 p0663 A72-16692

Temperature variation with latitude in upper solar photosphere from photoelectric meridional and equatorial limb-darkening scans [AD-744409] 05 p0719 A72-16710

Upper atmosphere atomic hydrogen H alpha emission, correlating intensity and hydroxyl vibration temperature 05 p0659 A72-17036

Upper atmosphere density fluctuations associated with solar activity and local time values, using Cosmos 14 satellite drag data 05 p0659 A72-17037

Upper atmosphere density and heating near auroral zones, using satellite Molniya 1K data 06 p0805 A72-17637

Upper atmosphere Na abundance compared to radio meteor rate after diurnal effects elimination 06 p0876 A72-17645

Upper atmosphere analytical model expressing density as function of exospheric temperature and altitude 06 p0806 A72-17658

Optical observation program for upper atmosphere and interplanetary space investigations, discussing

zodiacal light, earth atmosphere composition and stratification, interplanetary dust clouds, etc 06 p0881 A72-17927

Upper atmosphere twilight optical inhomogeneities relation to noctilucent clouds, using electrophotometry methods 06 p0807 A72-17933

Radiative heat transfer damping rates of turbulent temperature pulsations in upper planetary atmospheres, assuming Kirchhoff radiation law validity 06 p0882 A72-17935

Earth upper atmosphere outgoing thermal radiation radiance calculation in near IR spectrum 06 p0808 A72-18044

Sounding rocket programs and balloon implementation upper atmosphere research in Australia 07 p1070 A72-19088

Horizontal transport in upper atmosphere by large scale circulation, presenting altitude variation of atmospheric constituents concentration for various eddy diffusion coefficient values 07 p0978 A72-20040

High energy electrons and gamma quantum flux in upper atmospheric layers from high altitude balloon measurements 07 p1065 A72-20639

Upper atmosphere temperature measurement by homodyne detection of excited atoms and molecules radiation, using photodiode beat frequencies produced by spectral line emission 08 p1154 A72-20739

Upper atmosphere minor component distribution rearrangement, investigating transition time to diffusion equilibrium 08 p1155 A72-20803

Earth horizons nighttime, twilight and daytime visual observations from manned Soyuz spacecraft, discussing upper atmosphere emission layer structure and aureole development 08 p1158 A72-21148

Jeans escape rate prediction validity for hydrogen atoms in upper atmosphere and error sources in physical models 08 p1159 A72-21401

Radio meteor observations of upper atmosphere long period wind variations, determining oscillation spectra peaks by harmonic analysis 08 p1161 A72-21537

Air masses circulation in atmospheric upper layer during IQSY from meteor trail drifts observation by radar tracking method 08 p1161 A72-21584

Diurnal and seasonal variation of ambipolar diffusion coefficient in meteor trail zone within upper atmosphere 08 p1238 A72-21884

Upper atmospheric oxygen red line diurnal variations and midnight minimum, noting emission relation to kinetic temperature in magnetic storm 09 p1296 A72-22234

Radar equipment complex in Dushanbe for upper atmosphere wind measurements in meteor physics studies 09 p1308 A72-22504

Leonid meteor trail drift measurements in upper atmosphere, comparing radar system with precision photometric capabilities to photographic methods 09 p1383 A72-22504

Electron attachment rate relation to altitude in radar observation of meteor trails 09 p1384 A72-22513

Geomagnetic field effects on initially spherically symmetric ion cloud diffusive motion in earth upper atmosphere 09 p1297 A72-22577

Extreme UV absorption cross sections ratios for atomic oxygen in upper atmosphere, observing solar radiation attenuation with satellite instruments 09 p1297 A72-22578

Diurnal phase anomaly in upper atmospheric density and temperature inferred from satellite drag and incoherent scattering observations 09 p1298 A72-22590

Radio transmitter characteristics for radar sounding of upper atmosphere and meteor trails 09 p1278 A72-22874

Differential photoelectron fluxes at 560 km altitude observed by OVI-18 satellite on 22 March 1969, noting latitudinal variation 09 p1378 A72-23013

Microbaroms produced by ocean waves radiated in infrasound, noting dependence on upper atmosphere temperature and winds 09 p1348 A72-23656

Upper atmospheric dynamics and electrodynamic processes for evaluation of meteor trail radar observations in synoptic meteorology 10 p1473 A72-24702

Noctilucent cloud wave structure, discussing motions in high atmosphere, ice crystal formation, energy sources and observations 10 p1474 A72-24707

Photochemical models to simulate composition and reactions of upper atmosphere, noting transport importance 10 p1474 A72-24713

Airglow intensities and upper atmosphere physical processes relationship, discussing spectral features, emission brightness and excitation sources 10 p1474 A72-24714

Meteor trail radar data processing for upper atmosphere research, proposing dissemination for dynamosphere synoptic exploration 10 p1438 A72-24716

Loran-Omega course and track equipment /LO-CATE/ of integrated upper air meteorological sounding systems, describing radiosonde navigational aids 10 p1484 A72-25086

Radiosonde balloon tracking errors in upper atmosphere wind measurement with Loran C, Omega and radar transmitters 10 p1441 A72-25092

Upper atmosphere physics - Conference, Erice, Italy, June 1970, Volume 2 11 p1621 A72-25834

Upper atmosphere /thermosphere/ physical variations, discussing diffusive equilibrium, energy absorption and heat transfer 11 p1621 A72-25842

Thermodynamic equilibrium theory for upper atmosphere /thermosphere/ temperature and density variations, noting Harris-Priester model 11 p1622 A72-25844

Molecular and eddy diffusion transport velocities for helium and hydrogen distributions in upper atmosphere 11 p1622 A72-25845

Upper atmospheric satellite and rocket soundings reliability and utility, covering ionospheric radio propagation, numerical weather prediction and gravity waves 11 p1623 A72-26390

Luminous emissions of upper atmosphere, discussing relation to airglow and auroral phenomena 11 p1626 A72-26431

Upper atmosphere neutral particle pressure, temperature and density profiles during 7 March 1970 solar eclipse from pitot tube soundings 12 p1800 A72-27144

Electron precipitation in upper atmosphere at midlatitudes from positive ionized nitrogen molecules electrophoretic observation and night airglow and geomagnetic field measurements 12 p1802 A72-27302

Upper atmosphere density measurement techniques used by Sputnik 3 and San Marco 1 and 2 satellites 12 p1802 A72-27683

Upper atmosphere particle flux density determined from nocturnal electromagnetic absorption caused by geomagnetic storms, noting ionization process time lag in lower ionosphere 13 p1945 A72-28580

Upper atmosphere atomic oxygen distribution calculated for D and E region aeronomy problems solution 13 p1947 A72-28604

Upper atmosphere observatory, noting application to long distance radio communication, long range weather prediction and international cooperation in research and education 13 p1947 A72-28613

Upper wind measurement by balloon-borne targets or radiosondes tracking by primary and secondary radars and radio theodolites 13 p1917 A72-28697

Upper atmospheric measurement of incident solar UV radiation penetration to lower levels, discussing measuring instruments 13 p2030 A72-28826

Upper atmosphere water vapor sources and sinks, discussing Hadley cell circulation, convective storm, stratospheric-tropospheric interchange, methane oxidation and volcanic activity 13 p1948 A72-28835

Atomic oxygen layer height and peak concentration in earth upper atmosphere, considering solar dissociative radiation and turbulent diffusion for equinox conditions 13 p1948 A72-29236

Upper atmosphere mm emission spectrum from aircraft observation, comparing with rocket and ground based data 13 p1923 A72-29963

Upper atmosphere research rockets missions, payloads and measurements, describing various international aeronomy research projects 13 p2052 A72-30081

Internal gravity wave interaction with median wind in upper atmosphere from solution of system of linearized hydrothermodynamic equations 14 p2099 A72-30244

Midlatitude upper atmosphere wind, tide and turbulence measurements, using radar observations of meteor trails 14 p2099 A72-30248

Vertical propagation of large scale disturbances in long wave radiation field into upper atmosphere, using linearized hydrothermodynamic equations 14 p2127 A72-30262

Upper atmosphere horizontal wind velocity from meteor trails radio echoes, noting structural function anisotropy 14 p2127 A72-30263

Wind profiles, turbulence, and temperature and density distribution of neutral upper atmosphere obtained via sounding with Skylark rockets carrying chemical seeding payloads 15 p2223 A72-31435

Upper atmosphere temperature and wind variations over Antarctic from meteorological rocket sounding, noting winter cyclonic vortex level 15 p2225 A72-31906

Upper atmosphere density from orbital drag on Cannon Ball II and Musket Ball satellites 15 p2227 A72-31963

Aerodynamic drag at high latitudes observed from Molniya satellites orbit analysis, suggesting upper atmosphere density change 15 p2229 A72-31989

Supernovae produced fluorescence pulses search in upper atmosphere by automatic coincident light receivers 15 p2313 A72-32233

Rocket released artificial Cs plasma clouds in upper atmosphere, measuring electron density by HF radar observation 15 p2231 A72-32330

Rocket-borne laser radar for aerosol observation in upper atmosphere, noting light scattering layer relation to noctilucent cloud appearance 15 p2231 A72-32331

Stationary plasma flow interaction with dipole magnetic field to study geophysical phenomena in upper atmosphere 15 p2286 A72-32343

Upper atmospheric Na abundance from daytime spectroscopic absorption measurement compared with twilight glow observation 16 p2383 A72-32970

Floating forces contribution to heat flux during turbulent mixing of upper atmosphere 16 p2417 A72-33292

Dust influx into upper atmosphere above 30 km determined from laser radar measurement 16 p2386 A72-33610

Radiative heat transfer damping rates of turbulent temperature pulsations in upper planetary atmospheres, assuming Kirchhoff radiation law validity 16 p2459 A72-33776

Venus comet-like interaction with solar wind explained via He outer atmosphere with preferential heating by wind 16 p2459 A72-33915

Atomic, molecular and ionic species detection in upper atmosphere by measurement of resonance fluorescence radiation excited by tunable laser radiation [AIAA PAPER 72-661] 16 p2388 A72-34073

Upper atmospheric trace constituents global mapping by laser radar probing from satellite, discussing feasibility and comparison with ground based system [AIAA PAPER 72-660] 16 p2365 A72-34074

Atmospheric properties effect on satellite aerodynamic characteristics, noting gas composition and upper atmospheric winds [AIAA PAPER 72-659] 16 p2347 A72-34075

Upper atmosphere zonal winds speed vs local time from data based on Cosmos 316 orbit analysis 17 p2547 A72-35075

Prediction of upper atmosphere density over the lifetime of a satellite 17 p2547 A72-35215

The radiative transfer equation and environmental effects in the upper atmosphere. [AIAA PAPER 72-663] 17 p2583 A72-35485

Electron temperature in the Martian ionosphere. 17 p2613 A72-35499

A 5-kW peak transmitter for the 7-m wavelength 17 p2519 A72-35960

On the boundary conditions in theoretical model calculations of the distributions of minor neutral constituents in the upper atmosphere. 18 p2659 A72-36294

Space and upper atmosphere environmental effects on spacecraft and instrument surfaces, considering high energy particle radiation, interstellar and lunar dust effects, etc 18 p2712 A72-36832

Determination of upper atmosphere parameters by measuring the ambipolar diffusion coefficient by the method of meteor trail radar observations 18 p2688 A72-36862

Study of the motion of ionized artificial clouds in the upper atmosphere 18 p2688 A72-36864

Vibrationally excited nitrogen in upper atmosphere 18 p2688 A72-36865

UPPER IONOSPHERE

Optical observation program for upper atmosphere and interplanetary space investigations, discussing zodiacal light, earth atmosphere composition and stratification, interplanetary dust clouds, etc. 18 p2730 A72-37152

An atomic oxygen beam system for the investigation of mass spectrometer response in the upper atmosphere. 19 p2795 A72-37515

Upper atmosphere temperature measurement by homodyne detection of excited atoms and molecules radiation, using photodiode beat frequencies produced by spectral line emission 19 p2791 A72-38367

Metastable atomic oxygen deactivation in upper atmosphere by inelastic collisions and by spontaneous irradiation, noting airglow intensity dependence on red lines irradiation 19 p2792 A72-38633

Earth horizons nighttime, twilight and daytime visual observations from manned Soyuz spacecraft, discussing upper atmosphere emission layer structure and aureole development 20 p2916 A72-39253

Superrotation of the upper atmosphere. 20 p2916 A72-39336

Simulation in plasma wind tunnels of the environmental conditions for sounding rocket experiments 20 p2912 A72-39928

Structure and circulation of the upper atmosphere over East Antarctica in 1969 and 1970 20 p2949 A72-39949

Altitudinal dependence of upper atmosphere winds according to radar and ionosphere data 20 p2920 A72-40074

The observation of chemical releases in the upper atmosphere. 22 p3152 A72-42022

Uranus methane brightening at limb and south pole explained by Rayleigh scattering and haze in upper atmosphere 22 p3228 A72-42573

The occultation of beta Sco by Jupiter. 24 p3436 A72-44699

Rocket-borne GaAs laser radar system with scatter light detector and data processor for upper atmosphere aerosol and pollution measurements 24 p3409 A72-44778

Energy releases in the upper atmosphere during geomagnetic disturbances. 24 p3396 A72-44847

Flashlamp-pumped dye lasers for investigations of the upper atmosphere. 24 p3409 A72-44948

Upper atmosphere particle flux density determined from nocturnal electromagnetic absorption caused by geomagnetic storms, noting ionization process time lag in lower ionosphere 24 p3397 A72-45080

Upper atmosphere atomic oxygen distribution calculated for D and E region aeronomy problems solution 24 p3398 A72-45104

Distribution of hydrogen and helium in the upper atmosphere. 24 p3400 A72-45593

UPPER IONOSPHERE NT F REGION

Night sky upper ionospheric electron concentration perturbations during magnetic storm, noting latitudinal distribution 02 p0217 A72-11940

Autocorrelation functions of topside incoherent scatter data, using computerized least square gradient search 02 p0220 A72-12454

Hydrogen density and proton flux in topside ionosphere over Arecibo from incoherent scatter observations 02 p0274 A72-12455

Plasma resonances due to satellite antenna from ionospheric topside sounder observations 02 p0222 A72-12838

Meteorological elements, upper ionospheric data and solar radio emission intensities during winter stratomesospheric temperature rises 03 p0383 A72-13477

Plasma models of topside ionosphere, investigating electrostatic wave propagation 05 p0698 A72-17022

Supersonic hydrogen plasma flow in collapsing postsunset upper ionosphere, noting nonvanishing temperature gradient effect on critical point location 07 p0974 A72-18899

Plasmasphere structure as outermost ionospheric region from direct measurements by particle traps, ion mass spectrometers and Langmuir probes on satellites 07 p0978 A72-20044

Large scale structure of plasmopause in equatorial plane based on whistler and upper ionosphere sounding data 07 p0978 A72-20045

Topside ionosphere characteristics, discussing particle mean free path and geomagnetic field effects on

- conductivity, plasma anisotropies and latitudinal variations
10 p1473 A72-24704
- Meteorological elements, upper ionospheric data and solar radio emission intensities during winter stratomesospheric temperature rises
11 p1682 A72-26247
- Atmospheric neutral density measurement near 400 km during daytime by microphone density gage on OGO 6
11 p1625 A72-26407
- Daytime and nighttime electron temperatures from topside resonances, using oblique echo theory
11 p1625 A72-26409
- Neutral upper ionosphere temperature measurement with manometer device onboard Cosmos 320 satellite, noting equatorial fluctuations at 250 km
13 p1955 A72-28586
- Latitudinal and diurnal development of seasonal anomaly in upper ionosphere from Alouette 1 data, discussing vertical electron density profiles
13 p1946 A72-28594
- Night sky upper ionospheric electron concentration perturbations during magnetic storm, noting latitudinal distribution
13 p1949 A72-29252
- Review of symposium on D region, upper polar ionosphere, magnetosphere and wave-particle interactions
15 p2229 A72-32251
- Models for F region and topside ionospheric storms morphology, discussing electric current disturbance at polar region
18 p2685 A72-35994
- Polar upper ionosphere morphology above E layer, discussing effects of winds, field aligned currents and electron precipitation
20 p2918 A72-39534
- Neutral upper ionosphere temperature measurement with manometer device onboard Cosmos 320 satellite, noting equatorial fluctuations at 250 km
24 p3402 A72-45086
- Latitudinal and diurnal development of seasonal anomaly in upper ionosphere from Alouette 1 data, discussing vertical electron density profiles
24 p3398 A72-45094
- O-plus/ H-plus/ and He-plus/ ion distributions in a new polar wind model.
24 p3400 A72-45587
- URANIUM**
NT URANIUM ISOTOPES
NT URANIUM PLASMAS
- Apollo 12 lunar rock 12013, examining uranium distribution in apatite, whitlockite, zircon and beta phases
01 p0124 A72-10062
- Sphene U-Pb age resistance to thermal metamorphism, discussing zircon U-Pb and biotite and hornblende K-Ar ages within thermal aureole
01 p0052 A72-10069
- High temperature gaseous U fission plasma core reactor engine concepts for space propulsion
01 p0099 A72-11327
- Unstable sound waves in uranium plasma, taking into account fission power density, radiation diffusion and ionization variations
01 p0112 A72-11336
- Uranium arc plasma visible and near UV emission coefficients as function of U partial pressure and corresponding temperatures
01 p0112 A72-11337
- High temperature U plasma generation at near gas core reactor conditions by sliding spark discharge into capillary channel lined with sintered uranium dioxide
01 p0112 A72-11338
- Uranium and tungsten plasmas emission and absorption properties at shock tube generated pressures of 3-48 atm and temperatures of 7,000-12,000 K
01 p0112 A72-11339
- Lunar thermal history and radioactivity upper limits determination consistent with proposed temperature distribution and Apollo chondrite data, implying low uranium content
04 p0581 A72-15579
- Density and flux measurements by Langmuir probes in uranium plasma produced in single ended Q device, noting application to isotope separation
06 p0855 A72-17506
- Cr and U contents effect on high strength Cr-Mo-Va alloy steel sheet hot cracking susceptibility, using Huxley test method
06 p0820 A72-17704
- Uranium content and radiogenic ages by fission track analysis in hypersthene, bronzite, amphibolite and carbonaceous chondrites
06 p0878 A72-17791
- Uranium distribution in basalt fragments of five lunar samples.
23 p3261 A72-43399
- URANIUM ALLOYS**
U-Zr-Nb and U-Nb-Mo alloys gamma solid solution phase isothermal transformation kinetics at 500-600 C from dilatometric, microstructural and X ray analyses, noting decomposition
14 p2114 A72-30403

The low strain tensile behavior of U-7.5 wt pct Nb-2.5 wt pct Zr.
20 p2938 A72-39303

URANIUM CARBIDES

Stress corrosion of uranium carbide ceramics in atmospheric environments containing water
09 p1335 A72-22399

Compatibility of buffered uranium carbides with tungsten.
17 p2579 A72-34620

Pure and thoriated W compatibility with uranium carbide alloys at 1800 C, noting thermal gradient and thoria noneffects
18 p2699 A72-36163

Thermionic fuel cladding development, compatibility, stability and performance for uranium carbide-tungsten and uranium oxide-tungsten systems at high temperatures under irradiation
18 p2709 A72-36164

URANIUM COMPOUNDS

NT URANIUM CARBIDES
NT URANIUM FLUORIDES
NT URANIUM OXIDES

Uranium mononitride as nuclear reactor fuel for space vehicle power supply applications, discussing fabrication techniques and irradiation behavior
09 p1349 A72-22406

U bearing phase zirkelite in Apollo 12 and 14 lunar rocks, using electron microprobe
15 p2303 A72-31303

Evaluations of uranium-nitride fueled converters.
17 p2497 A72-34609

Uranyl fluoride crystals luminescence spectrum study, calculating anion normal vibration frequencies
20 p2960 A72-39413

URANIUM FLUORIDES

Ballistic piston fissioning plasma production involving compression of uranium hexafluoride
01 p0111 A72-11333

Electrical properties of subsonic argon plasma stream seeded with uranium hexafluoride, using electrostatic probe
01 p0111 A72-11334

Thermal environment and fuel region simulation for nuclear light bulb engine, using rf induction heater and uranium and tungsten hexafluorides injection
01 p0113 A72-11355

Uranium hexafluoride pulsed plasma core reactor with artificial neutron source for spark plug and enclosed by cylinder and piston analogous to internal combustion engine
01 p0100 A72-11361

Critical spherical symmetry benchmark experiment on gas core nuclear reactor using uranium hexafluoride
05 p0688 A72-16387

URANIUM ISOTOPES

Lunar soil radiogenic U-Th-Pb analyses of Lunik 16 samples from Sea of Fertility
09 p1381 A72-22278

URANIUM OXIDES

Molybdenum-uranium dioxide cermet fuel pins fission heating at 1145 K in forced convection He cooled reactor, measuring dimensional changes and U 235 burnup
04 p0546 A72-14424

Out-of-core evaluations of a nonfueled and a UO₂-fueled cylindrical thermionic converter.
17 p2497 A72-34608

Metal working and testing of nuclear rocket engine components with Mo as structural material and uranium dioxide as fuel, discussing Mo-W interdiffusion
17 p2559 A72-34617

Post irradiation examination of a UO₂-fueled thermionic diode with a revolver type emitter.
17 p2578 A72-34618

Thermionic converters fuel tests by uranium dioxide-Mo cermets irradiation, noting fission gas retention and metallic matrix deformation
18 p2708 A72-36141

Behavior of tungsten-clad Mo-UO₂ fuel under neutron irradiation at high temperature.
18 p2708 A72-36143

Thermionic fuel cladding development, compatibility, stability and performance for uranium carbide-tungsten and uranium oxide-tungsten systems at high temperatures under irradiation
18 p2709 A72-36164

URANIUM PLASMAS

Uranium plasmas - Conference, Atlanta, November 1971
01 p0099 A72-11326

URANIUM 238

Pu 244/U 238 fission track retention age of whitlockite crystal in lunar breccia 14321 from Fra Mauro formation
15 p2307 A72-31722

URANUS (PLANET)

Outer planets mass determination noting anomalous latitude residuals of Uranus
04 p0575 A72-15033

Uranus IR spectral albedo, discussing methane absorption
04 p0580 A72-15365

Microwave absorption in high pressure hydrogen based on radio astronomical measurements of Uranus brightness temperature
08 p1239 A72-22088

Methane contribution to thermal opacity in Uranus and Neptune atmospheres for atmospheric model synthesis
09 p1383 A72-22293

Jupiter, Saturn, Uranus, Neptune and Pluto state of knowledge, noting angular momentum fraction, red spot, albedos, densities, atmospheric compositions, natural satellites, etc
12 p1870 A72-27345

Monochromatic brightness coefficient measurements for Jupiter and Saturn disk centers and Uranus geometric albedo
14 p2152 A72-30491

Uranus, Neptune and Pluto disk temperature observations via National Radio Astronomy Observatory interferometer
16 p2455 A72-33464

Microwave absorption in high pressure hydrogen based on radio astronomical measurements of Uranus brightness temperature
17 p2606 A72-34651

Secular variations of the first order of elements for the four major planets - Comparison with Le Verrier and Gaillot
18 p2727 A72-36734

Exact positions of Uranus for 1919 through 1969 according to photographic observations at Pulkovo and Tashkent
19 p2859 A72-37915

Monochromatic brightness coefficient measurements for Jupiter and Saturn disk centers and Uranus geometric albedo
19 p2864 A72-38320

The masses, densities and moments of inertia of Uranus and Neptune.
20 p2967 A72-39184

New observations on the Kuiper bands of Uranus.
21 p3106 A72-41043

Uranus methane brightening at limb and south pole explained by Rayleigh scattering and haze in upper atmosphere
22 p3228 A72-42573

Stellar and Uranus photometric measurements for solar B-V/ and U-B/ color indices determination, using K and H delta lines and G band filters
23 p3337 A72-43615

URBAN AREAS**U CITIES****URBAN DEVELOPMENT**

Southeast Florida 13 year urban and agricultural development recorded by high altitude color and color-IR photographs, demonstrating capability for detail and macroscale patterns
02 p0230 A72-12199

METROMEX field project to investigate inadvertent weather modification by urban-industrial effects and man-made precipitation changes
03 p0384 A72-13636

Potential effects of air cushion vehicle (ACV) multihousand ton freighter on city development
05 p0752 A72-15776

Air transport planning in coordination with urban and country development in West Germany
05 p0644 A72-16697

Urban geography of U.S. cities on vertical aerial photography, considering site, location, street orientation, expansion, business districts and transportation networks
09 p1301 A72-23281

Dallas/Fort Worth airport planning and construction economics impact on community economy and life style
16 p2373 A72-33307

Airport economic and social impact on environs in terms of community development
16 p2373 A72-33309

URBAN PLANNING

New York-New Jersey megalopolis offshore jetport feasibility, considering noise, air-water pollution, land conservation, cost, etc
13 p1938 A72-28792

URBAN RESEARCH

Urban geographic spatial-pattern determination with aerial photographic interpretation
02 p0229 A72-12019

Urban area aerial photography survey for large scale photomaps, discussing building feature examination and universal stereophotogrammetric instruments utilization
03 p0362 A72-14311

Remote sensing of urban 'heat islands' from an environmental satellite.
20 p2919 A72-39717

URBAN TRANSPORTATION**NT RAIL TRANSPORTATION**

Mach 0.80 quiet intercity STOL transport design comparison for turbofan, prop-fan and turboprop systems
01 p0003 A72-10256

Airport terminal flow and interface transportation systems, discussing access, passenger traffic and cargo handling and government controls
03 p0339 A72-13414

VTOL transport aircraft use in densely populated urban areas, discussing travel time, airport requirements, noise and design problems
05 p0612 A72-16733

Rotorcraft based on VTOL concept for aircraft noise reduction in urban transportation
06 p0758 A72-18248

Ultrashort haul common carrier air transportation system based on VTOL aircraft for suburban-to-city center trips, comparing with land based transport
16 p2480 A72-33113

Helicopters and turbotrains as space conserving alternatives for automobile urban transportation, emphasizing comfort and convenience
17 p2639 A72-35505

Short haul intercity air transportation systems requirements for successful competition with lower cost ground modes
[ICAS PAPER 72-16] 21 p2995 A72-41141

Prototype interurban IFR STOL transportation system demonstration project, considering area navigation, scanning beam microwave landing systems and STOLport planning
[ICAS PAPER 72-41] 21 p3040 A72-41166

The design and operation of a large tube-vehicle aerodynamic testing facility.
[AIAA PAPER 72-1001] 21 p3041 A72-41586

UREAS

Uric acid to urea nitrogen ratio as assay test for identification of avian tissue in verifying bird ingestion or impact as aircraft accident cause
[AD-737855] 07 p0922 A72-20184

Solute rejection in hyperfiltration of sodium chloride and urea with porous glass ion exchange membrane as function of pressure, temperature and concentration
07 p0937 A72-20601

Urea determination in urine and water wastes for recycling process, using N-dimethylaminobenzaldehyde colorimetric method
13 p1910 A72-29325

Urease-active colloidal organo-complex extraction from Dublin clay loam soil, describing filtration procedure
13 p1913 A72-29399

Prebiotic thymidine phosphorylation at 65 C by urea-phosphate mixtures in simulated desert conditions
15 p2185 A72-31629

Polyphosphate and trimetaphosphate formation under potentially prebiotic conditions.
23 p3261 A72-43566

Formation of urea and guanidine by irradiation of ammonium cyanide.
23 p3262 A72-43569

URETHANES

Mechanical characteristics of natural and synthetic rubber, noting features of cork filled urethane
10 p1502 A72-24861

URIC ACID

Uric acid to urea nitrogen ratio as assay test for identification of avian tissue in verifying bird ingestion or impact as aircraft accident cause
[AD-737855] 07 p0922 A72-20184

Hyperuricemia, gout and lithiasis among operating air crews, discussing diagnosis and relation to arteriosclerosis
08 p1125 A72-21271

URINALYSIS

Confinement, physical deconditioning and hypercappnia effects on human musculoskeletal protein by chromatographic method for quantifying urinary peptides and free amino acids
[AD-736665] 06 p0767 A72-17869

Inhibitive effect of immobilization on urinary catecholamine excretion and blood plasma thyroxine level in rats
09 p1265 A72-22648

Food deprivation stress effects on urinary excretion values in unrestrained chimpanzees
10 p1426 A72-28422

Parachutist biomedical responses in aerial tow at 110-175 knots, determining heart and respiration rates and urinary catecholamines
12 p1774 A72-28272

Heat, noise and vibration stress combined effects on skin and rectal temperature, heart rate, weight loss and biochemical urinalysis
[AD-746083] 17 p2508 A72-34551

URINATION

Isolation stress effect on micturition circadian rhythm and diuresis occurrence in unrestrained chimpanzee under entrained and free running conditions
[AD-739468] 07 p0921 A72-20180

Interrelation of interoceptors and exteroceptors in the process of urination and defecation reflex act maturation in ontogeny
17 p2504 A72-35022

URINE

Ground and flying activity endurance training effect on urinary excretion of noradrenaline and adrenaline
04 p0478 A72-14868

Immobilization hypercalciuria, discussing treatment by diet-induced extracellular volume depletion and possible pathophysiological mechanism of intercompartmental fluid and electrolyte shift
04 p0479 A72-14871

Human urine regenerated water in various dilutions effect on fish and rat erythropoiesis
05 p0622 A72-16651

Urine and plasma protein and creatinine measurements in acclimatized and unacclimatized men before, during and after high altitude ascent
10 p1426 A72-24482

Sleep deprivation effect on circadian rhythms in human performance, psychological fatigue ratings, catecholamine excretion and urine flow
11 p1581 A72-26692

Urea determination in urine and water wastes for recycling process, using N-dimethylaminobenzaldehyde colorimetric method
13 p1910 A72-29325

Hyperbaric environment decompression effects on human blood and urine chemistry and hemostatic system, showing physiological parameter alteration in presence and absence of bends symptoms
14 p2081 A72-31087

Nitrogen excretion as a measure of protein metabolism in man under different conditions of renal function.
21 p3003 A72-41523

Unconjugated urinary corticosterone excretion in laboratory rats exposed to high pressure helium-oxygen environments.
24 p3374 A72-45656

UROLITHIASIS

Hyperuricemia, gout and lithiasis among operating air crews, discussing diagnosis and relation to arteriosclerosis
08 p1125 A72-21271

UROLOGY

Space medical urological problems from experience with Biosatellite 3 monkey, discussing closed catheter conduit system, urinary calcium changes in immobilized animals and urinary diuresis
10 p1424 A72-23728

UTILITY AIRCRAFT

Marchetti SV-20-A twin engine winged commercial/utility helicopter, describing design details, on-board systems and payload accommodations
09 p1262 A72-22907

Fixed wing agricultural aircraft, comparing different designs in terms of performance, safety, handling and economic efficiency
09 p1262 A72-22940

German Bo 105 five/six seat light utility helicopter with rigid glass-fiber reinforced plastic rotor blades, presenting design and performance
14 p2072 A72-30678

Flying crane helicopters utilization in construction industry for materials transport and structural erection work, discussing technical and economic aspects
23 p3251 A72-43637

Agricultural aircraft flight loads - Typical spectra and some observations on airworthiness.
24 p3366 A72-44734

UTILITY AIRCRAFT
NT PIPER AIRCRAFT
UTILIZATION
NT WASTE UTILIZATION

V

V BAND
U EXTREMELY HIGH FREQUENCIES

V GROOVES

Rough surfaces with orthogonal parallel V grooves, studying shadowing, interreflection and masking effects on bidirectional reflectance from He-Ne laser illumination
[AIAA PAPER 72-55] 06 p0848 A72-17924

High temperature tensile tests of Mo with helical and circular V grooves, discussing stress concentration sensitivity relations for grooved and smooth samples
07 p1018 A72-20141

Thermal emissivity and directivity for V groove and rectangular cavities, optimizing geometry and surface properties for maximum focusing of emitted energy
[ASME PAPER 72-HT-L] 20 p2984 A72-39651

Plane elastostatic analysis of V grooved rectangular plates notch angle and specimen geometry effects on stress intensity factors and fracture toughness measurements
23 p3346 A72-43703

High temperature tensile tests of Mo with helical and circular V grooves, discussing stress concentration sensitivity relations for grooved and smooth samples
24 p3417 A72-45766

V/STOL AIRCRAFT
NT COMPOUND HELICOPTERS
NT FLYING PLATFORMS
NT HELICOPTERS
NT MILITARY HELICOPTERS
NT RIGID ROTOR HELICOPTERS
NT ROTARY WING AIRCRAFT
NT SHORT TAKEOFF AIRCRAFT
NT VERTICAL TAKEOFF AIRCRAFT

Free flight simulation tests for V/STOL aircraft nonlinear attitude control system adaptation to helicopter pitch and roll control
[DGLR PAPER 71-060] 02 p0155 A72-12714

Disk shaped lift engine providing additional thrust during takeoff and transition phases of V/STOL aircraft, returning to ground by jet after task accomplishment
02 p0272 A72-12900

Navy hovering vehicle versatile automatic control system for V/STOL flight test program, using airborne digital computer for navigation/guidance computations
05 p0687 A72-16661

Multiplier method for discrete optimization problems with equality constraints, applying to time optimal control for V/STOL aircraft
06 p0794 A72-18387

VAK 191 B V/STOL reconnaissance fighter prototype test program, describing simulations, bench, ground, static, hovering and flight tests
07 p0912 A72-19249

VJ-101A and B V/STOL weapon system design, describing various propulsion system configurations
07 p0912 A72-19250

V/STOL weapon system VJ-101, describing He-231 design development from tailsitter concept to canard configuration with tilting wing-tip engines
07 p0912 A72-19251

V/STOL development for short haul air transportation, discussing requirements for quiet pollution-free operation, ATC systems, navigation and landing aids
08 p1108 A72-21010

Technology forecasting and risk assessment in V/STOL transport area, examining mission issues and selection criteria
09 p1261 A72-22473

Anthropotechnical aspects of V/STOL aircraft control, discussing instrument and control systems concepts based on development and flight tests of experimental Do-31 VTOL aircraft
09 p1270 A72-22784

STOL and V/STOL transport aircraft design requirements consideration based on common propulsion and lift engine types use, noting fan lift solution superiority
10 p1421 A72-24865

Flight airworthiness requirements development for supersonic transports, V/STOL and transport and general aviation aircraft, exploring critical control and stability parameters
11 p1575 A72-25570

Business V/STOL aircraft economic viability based on cost benefit analysis and comparison with turbine powered aircraft
[SAE PAPER 720306] 11 p1576 A72-25594

SAE PAPER 720334 11 p1576 A72-25594

Propulsion control systems design for military and commercial V/STOL aircraft, considering power management performance with minimum weight and maximum reliability and maintainability
[ASME PAPER 72-GT-79] 11 p1705 A72-25659

Propulsion system flexibility in V/STOL aircraft with one lift-cruise engine, discussing takeoff thrust requirements and cruise fuel consumption efficiency
[ASME PAPER 72-GT-105] 11 p1576 A72-25670

Propulsion system/airframe matching in hybrid V/STOL airplanes, stressing thrust vector management, lift engine bypass ratio and power plant packaging design
[ASME PAPER 72-GT-106] 11 p1576 A72-25671

German VAK 191B V/STOL fighter aircraft design, development and flight tests, noting redundant control systems
12 p1753 A72-27166

STOL, VTOL and V/STOL air transportation systems development, characteristics and requirements, presenting economic forecast
12 p1754 A72-27661

Meteorological information requirements for V/STOL aircraft design, airport location, runway orientation, aircraft operations and ATC simulation
13 p1994 A72-28869

V/STOL aircraft potential for short haul civil air traffic, discussing present technology and investment costs in comparison with advanced ground transportation systems
13 p1898 A72-30076

Free flight follower support system with data reduction for V/STOL or helicopter models, recording flight path and attitude angles
16 p2372 A72-32886

Aerodynamic noise and structural fatigue failure research and test facility, concerning supersonic jet and V/STOL aircraft
16 p2342 A72-32900

- V/STOL weapon system VJ-101 design, discussing one axis rocking device, suspension structure and hovering flight thrust control 16 p2347 A72-33049
- V/STOL flight control - Trend and requirements. 17 p2487 A72-34240
- Critical review of Mil-F-83300 V/STOL flying qualities specifications as applied to helicopter design and missions, suggesting inappropriateness for Navy helicopters [AHS PREPRINT 643] 17 p2490 A72-34503
- Design of V/STOL ports. 18 p2675 A72-36783
- V/STOL developments in Hawker Siddeley Aviation Limited. 18 p2643 A72-37096
- V/STOL - Selection and problems of the new medium 18 p2643 A72-37215
- VJ-101 V/STOL aircraft design, development and flight testing, discussing takeoff and landing, hovering and transition flight and associated control problems 19 p2749 A72-38032
- Development of STOLAND, a versatile navigation, guidance and control system. [AIAA PAPER 72-789] 19 p2831 A72-38106
- Quiet engine design for V/STOL and reduced takeoff and landing /RTOL/ aircraft, discussing various engine noise sources, countermeasures and tolerance levels 20 p2963 A72-39819
- V/STOL aircraft configurations with lifting counter-rotating disks, presenting aerodynamic coefficients from rotating water tank experiments 21 p2990 A72-41070
- Noise radiation from V/STOL aircraft. [ICAA PAPER 72-22] 21 p2995 A72-41147
- Experience with the NRC 10 ft. x 20 ft. V/STOL propulsion tunnel - Some practical aspects of V/STOL engine model testing. 23 p3278 A72-44247
- VACANCIES [CRYSTAL DEFECTS]**
- NT FRENKEL DEFECTS**
- Polycrystalline materials wedge crack growth enhancement by vacancy diffusion under creep failure conditions, considering grain boundary sliding mechanism 03 p0442 A72-12998
- Different pair potentials for simulating vacancy in Al, discussing program planning for relaxations calculation around vacancy to effect computing time reduction 03 p0378 A72-14253
- Statistical thermodynamics models for determining vacancy concentration and atoms and vacancies arrangement in metals and alloys under thermal equilibrium 03 p0378 A72-14255
- High resolution electron microscope observation of voids in amorphous Ge films, noting density dependence on substrate temperature 04 p0562 A72-15152
- Microfibrillar superlattice with vacancy defect and point dislocation in microcrack formation and propagation in nylon 6 fibers 05 p0681 A72-16308
- Ni-Al alloy, investigating Y addition effect on vacancy agglomeration suppression during oxidation 06 p0829 A72-17787
- Vacancy effects on residual electrical resistance of binary ordering fcc lattice alloys as function of composition and annealing temperature 06 p0832 A72-18422
- Vacancy supersaturation effect on enhanced precipitation by high flux electron irradiation in stainless steel 07 p1033 A72-20410
- Three and four layer vacancy defects annealing in quenched Al for stacking fault removal 07 p1020 A72-20412
- Guinier-Preston zone nucleation and growth as function of vacancies in Al-Cu alloy 08 p1190 A72-22166
- Piezoresistance magnitude and temperature dependence changes of electron irradiated n-type silicon due to oxygen vacancy complex /A center/ 09 p1372 A72-23239
- Epitaxy and vacancy structure of TiSe with type B8 ordering 10 p1495 A72-24077
- Inhomogeneous sink distribution effect on vacancy annealing kinetics and activation energy in metals 10 p1499 A72-24983
- Abrikosov vortex lattice in superconductors, calculating resonance linewidth and vacancy formation energy 11 p1699 A72-25718
- Impurity atoms effects on grain boundary motion velocity, considering interactions with metal lattice vacancies 11 p1662 A72-26655
- Phase precipitated helicoidal dislocations and vacancy-type stacking faults in aged austenite Fe-Ni-

Ti alloy, using electron microscope diffraction contrast analysis 14 p2112 A72-30162

Vacancy annealing effect on beta phase transformation during tempering of Ti alloy with Mo, showing strain hardening and contraction increase 14 p2124 A72-31032

Chemical interaction within crystals for generation of stacking fault vacancies and phenomena associated with solid solution microheterogeneity dislocations, discussing heat resistance 15 p2254 A72-31558

Positron annihilation lifetimes and trapping probabilities for vacancies and dislocations in Al single crystal 15 p2258 A72-32228

Metal melting heat relationship to diffusion activation energy with vacancy mechanism equal numerically to crystal internal energy maximum change 15 p2259 A72-32691

The mechanisms of diffusion in metals and alloys. 20 p2962 A72-39999

Precipitation thermodynamics of unstable and metastable solid solutions, discussing interfaces, vacancies, spinodal decomposition, nucleation, reversion and macroscopic diffusion 20 p2943 A72-40000

Recombination and annihilation rates of interstitial atoms and vacancies in crystal lattices, taking account of diffusion 21 p3088 A72-41690

Effect of voids on angular correlation of positron annihilation photons in molybdenum. 22 p3187 A72-41967

Precipitation rate characteristics in age hardenable quenched alloys explained by transient analysis of vacancy annealing kinetics 22 p3189 A72-42441

VACUUM

NT HIGH VACUUM
NT ULTRAHIGH VACUUM

Source gas expansion flow into vacuum, solving spherical coordinates representation of BGK kinetic equation by numerical method 13 p1942 A72-29116

VACUUM APPARATUS

NT BAYARD-ALPERT IONIZATION GAGES
NT CONDENSATION PUMPS
NT ION PUMPS
NT IONIZATION GAGES
NT KNUDSEN GAGES
NT MOLECULAR PUMPS
NT PENNING GAGES
NT VACUUM CHAMBERS
NT VACUUM FURNACES
NT VACUUM GAGES
NT VACUUM PUMPS

Vacuum handling system for lunar materials thermophysical properties measurements under contamination preventive conditions 04 p0509 A72-15496

Computer controlled vacuum optical calibration bench for astronomical satellites, describing pumping system 05 p0644 A72-16755

Zone melting high vacuum facility with cryogenic pumping and residual gas carbon-containing components exclusion for ultrapure metals production 06 p0796 A72-17992

Lunar soil electric properties, density, microhardness, abrasive properties and frictional and shear resistance determinations by Tor I operating in high vacuum 07 p1075 A72-19562

Vacuum welding by electron beam bombardment, discussing electron gun arrangements with plane-radial, plane-linear and linear electron beams 08 p1176 A72-21049

Sliding friction and normal force adhesion under ultrahigh vacuum environment, describing test apparatus for real time analysis via contact resistance measurement 08 p1176 A72-21436

Vacuum and inert gas TOR-I device for studying physical properties of lunar soil and terrestrial analogs 10 p1478 A72-23754

Vacuum technology - Conference, Boston, October 1971 12 p1805 A72-27034

Thin Ta sheet spiral configuration for high efficiency high temperature vacuum heat shield 12 p1888 A72-27035

High temperature low pressure reaction kinetics of nitrogen sorption by titanium foil, using ultrahigh vacuum microbalance 12 p1777 A72-27045

In-line high vacuum conductance valve with attached diffusion pump for shock tube evacuation 13 p1959 A72-29758

Zone melting high-vacuum system with cryogenic pumping for zone refining Zr 14 p2092 A72-30220

Soft and out-of-vacuum electron beam welding system for high productivity, describing characteristics 16 p2397 A72-33224

High vacuum and rarefied atmosphere creep apparatus. 17 p2536 A72-35846

Ultra-high vacuum coater for thin film research 18 p2676 A72-36839

Investigation of the operation of a vane anemometer in vacuum with the aid of an optical transducer for the rotational frequency 21 p3059 A72-41820

VACUUM CHAMBERS

Thermoluminescent phosphorus films irradiation by electrons with energies up to 15 keV in vacuum chamber 01 p0114 A72-10372

Space environment simulator with ultrahigh vacuum chamber and UV and corpuscular radiation for material samples physical properties in-situ measurement 02 p0201 A72-12701

Vacuum chamber and instrumentation for friction and wear tests at temperatures to 1800 C in vacuum and inert media 04 p0510 A72-15659

Vacuum chamber simulation of solar radiation effects on space satellites and components at 300-400 miles, using short arc xenon lamps 05 p0643 A72-16386

Nb-Zr alloy vacuum chamber tests for oxygen reaction rates, showing oxide surface film relation to sticking probability 05 p0674 A72-16391

Cartridge system for substrate heating to 500 C in vacuum chamber during metals or semiconductor vapor deposition, describing carbon block-high intensity quartz lamp assembly 07 p0984 A72-19325

Solar absorptance and thermal emittance of thermal control coatings contaminated by thruster exhaust in vacuum environment [AIAA PAPER 72-263] 12 p1846 A72-27865

Low pressure chamber as aerospace medical diagnostics tool for flying personnel examinations regarding oxygen deficiency, low air pressure and air pressure fluctuations tolerance 14 p2080 A72-30819

Russian book on thermal simulation of spacecraft and space environment covering heat transfer, cosmic radiation, vacuum chambers, radiant flux simulators, etc 15 p2319 A72-31275

Core axial density distribution in gas jets freely expanding into vacuum from double concentric orifices, using electron beam fluorescence technique 15 p2218 A72-32150

Molecular flux distribution in cylindrical vacuum chambers with various inlet and pumping configurations under assumption of Knudsen law validity, describing computer program 15 p2183 A72-32382

VACUUM DEPOSITION

Semiconductor film compound decomposition, chemical composition and metastable modifications presence during condensation in vacuum, discussing defect formation in crystal structure 05 p0701 A72-15752

Vacuum chamber sputtering techniques for CsI/Tl and NaI/Tl thin films for soft proton scintillation detector 06 p0816 A72-17834

Al, Ti and ferrous alloys suitability for vacuum brazing gas quenching processing for He leak-tight joints, using photomicrography 07 p0997 A72-19999

Filler metal compositions and procedures for Al alloys vacuum brazing, describing experimental vacuum furnace apparatus 07 p0997 A72-20000

Electrostatic rocket exhaust materials deposits effects on solar cells optical, thermal and electrical performance characteristics, using optical thin film theory [AIAA PAPER 72-447] 11 p1578 A72-26184

Vapor annealing effect on vacuum evaporator CdSe thin films electroconductivity as function of pressure and temperature 12 p1854 A72-27249

Vacuum deposition process relation to thin metal film properties, discussing current conducting mechanism 12 p1854 A72-27275

Dynamic in situ thin film thickness monitoring during vacuum deposition by holographic interferometry, noting independence from high quality optical components 15 p2240 A72-32381

Developments in vacuum braze coating of aero-engine nozzle guide vanes. 17 p2559 A72-34937

Thin films deposited by evaporation and sputtering - A comparative study 18 p2696 A72-36834

Reliability of nichrome film resistors deposited in vacuum by sublimation on a glass substrate
18 p2669 A72-37117

Study of tungsten and molybdenum coatings obtained by arc discharge in a vacuum
19 p2808 A72-38186

Vapor deposition in vacuum under conditions of constant vapor flow with the aid of electron emission current control
20 p2954 A72-39694

Deposition of dielectric films on the electrodes of an electrostatic gyroscope
21 p3059 A72-41814

Composite materials obtained by depositing boron layers under vacuum on aluminum sheets
22 p3190 A72-42646

Characteristics of superconducting niobium-tin alloys obtained by the vacuum evaporation method
22 p3192 A72-43013

Strain gage resistor with BiTeSb compound semiconductor film vacuum deposited on dielectric substrate, noting high sensitivity and operation without amplifiers
23 p3287 A72-43348

VACUUM EFFECTS

HF capacitive discharge plasma resonance under weak transverse magnetic field in vacuum
01 p0106 A72-10041

Bare and coated Nb alloy in high temperature vacuum conditions, discussing tensile and bend tests and mechanical properties
01 p0084 A72-10747

Ti-Al-V alloy under vacuum fatigue tests, examining temperature and chemical environment effects on fatigue crack growth
01 p0087 A72-11034

Constant stress and compression creep testing in vacuum conditions, describing simple spring loaded apparatus characteristics and performance
01 p0071 A72-11171

Optimal radiative capacity of star shaped radiator with mirror reflecting surfaces for vacuum cooling of elongated finned bodies
02 p0304 A72-12867

Lunar electrical conductivity model, determining vacuum transient response to time varying spatially uniform magnetic field
03 p0434 A72-13508

Metal powder hot compacting under vacuum and ultrasound action, considering porous body three dimensional viscous flow
05 p0665 A72-16091

Ta-W-Hf alloy ultrahigh vacuum high temperature creep tests, showing deoxidation effect on creep behavior and early test stage oxygen-associated dynamic strain aging
05 p0674 A72-16392

Surface oxide film effects on hydrogen liberation rate from Al and alloys in high vacuum at 20-450 C
05 p0675 A72-16627

Lunar mineral resources from analyses of moon samples, discussing solar cell and vacuum process manufacturing
05 p0722 A72-17099

Nonheat treated extruded Mo alloy under tension and vacuum conditions at various temperatures, investigating cylindrical samples size effects on mechanical properties
06 p0833 A72-18635

Titanium alloy durability under cyclic torsion in vacuum at various temperatures, investigating fatigue life and tensile strength
06 p0834 A72-18665

Steel/teflon sliding friction in high vacuum at stepwise controlled oscillation frequencies, sliding rates and loads
07 p0964 A72-18863

Alumoborosilicate glass fibers vacuum tensile strength tests, noting fiber strength increase with vacuum and exposure time
07 p1023 A72-19778

Reflection mode high energy electron diffraction study of titanium carbide single crystal surfaces in ultrahigh vacuum environment
07 p1019 A72-20408

Gas density distributions in argon and carbon dioxide supersonic jets with low angular divergence in vacuum, using Laval supersonic nozzle
07 p0973 A72-20512

Temperature effects on microorganism survival in deep space vacuum, using molecular sink test
09 p1265 A72-22641

Vacuum arc stationary cathode mechanism theoretical analysis, determining cathodic temperature and current density
10 p1524 A72-24930

Rough surfaces thermal contact resistance in vacuum for normal height distribution, discussing bolted joint nonuniform stress distribution effect
11 p1741 A72-25221

Test assembly for Brinell microhardness measurements of metal and alloy surfaces under tension during vacuum heating and in protective gas media
11 p1612 A72-25490

Test assembly design for microstructural studies of metal and alloy fatigue in vacuum during heating, describing electrical resistance measurement and stroboscopic illumination
11 p1612 A72-25492

Ni fatigue crack propagation under low cyclic loads at high temperature in vacuum after annealing and mechanical treatment
11 p1655 A72-25497

High temperature creep properties of W-Re alloy under vacuum for thorium dispersion hardening from electron microscope and activation energy studies
11 p1665 A72-26863

Rolling operations in vacuum for protection of metallic materials underprocessing
11 p1645 A72-26867

Lunar surface neutral gas pressure measurement by Apollo 14 cold cathode ionization gage, determining day and night temperature effects on vacuum quality
12 p1805 A72-27041

Low pressure hydrogen and titanium thin film reaction rate measurement, using flow technique
12 p1778 A72-27046

UV light production of free radicals in proteins and model compounds in vacuum and low temperatures, using EPR techniques
12 p1778 A72-27223

Living organisms defense and preservation via refrigeration and vacuum combined use in lyophilization technique
12 p1769 A72-27293

Clean metallic surfaces adhesion coefficients in vacuum at 77-293 K as function of load, loading time and contact cycles
12 p1818 A72-28193

Vacuum gap discharge conditions as function of electron beam parameters and metal vapor pressure
13 p2017 A72-29611

Kinetic freezing effects of supersonic gas flow with solid particles into vacuum, analyzing continuous to collisionless transition flow for Maxwell molecules
14 p2094 A72-30295

Vacuum vaporization of niobium, tantalum, zirconium and hafnium carbide phases, using Langmuir method
15 p2253 A72-31200

Spherical source jet flow expansion of single monatomic gas into vacuum on basis of BGK kinetic equation
16 p2375 A72-32887

Vapor pressure and velocity distributions in rarefied gas flows through narrow slits under vacuum conditions with ice sublimation
16 p2380 A72-33854

Laplace equation to generate stationary electromagnetic vacuum fields, generalizing from Papapetrou-Majumdar class of static fields
17 p2580 A72-34425

Studies of the influence of CVD tungsten depositing conditions on the formulation of pores resulting from interdiffusion in the emitters of thermionic converters.
18 p2698 A72-36145

High temperature and vacuum solar furnace processing of refractory metals in space or on moon
19 p2857 A72-37675

Hydrogen and nitrogen desorption phenomena associated with a stainless steel 304 low energy electron diffraction /LEED/ and molecular beam assembly.
19 p2762 A72-38023

Kinetics of carbothermal reduction of quartz under vacuum.
21 p3073 A72-40934

Effects of simulated space vacuum on bacterial cells.
23 p3254 A72-43395

Surface layer grain boundary corrosion damage of Ti alloys during vacuum annealing, reducing rupture strength, vibration resistance and bending fatigue limit
23 p3293 A72-43589

Ion acceleration during expansion of a rarefied plasma
23 p3322 A72-44482

Response to daily lower body negative pressure /LBNP/ exposure /-70mm Hg/, with emphasis on plasma renin activity, sodium and potassium excretion.
24 p3377 A72-45658

VACUUM FURNACES

Book on vacuum brazing covering dissimilar metals joining, stress cracking, corrosion resistance, joint design, heat treatment and production engineering problems
01 p0073 A72-10165

Aluminum vacuum furnace fluxless brazing process, eliminating flux entrapment, postbrazing cleaning and water pollution
01 p0074 A72-10281

Miniature vacuum furnace for Mossbauer spectroscopic samples heating to 1000 C, discussing temperature control, use of inert atmospheres, etc
04 p0523 A72-15481

Refractory metal thermocouple research program, describing design and performance of ultrahigh vacuum high temperature furnace system
04 p0524 A72-15550

Gas quenching technique for vacuum brazing of Al, Ti and ferrous alloys, evaluating mechanical properties, surface contamination and He leak tightness
07 p0997 A72-19997

Ti honeycomb brazing, discussing filler metals, furnace temperature and atmosphere control and use of protected graphite as furnace material
07 p0998 A72-20288

Refractory metals vacuum melting for ingot production and purification in arc and electron bombardment furnaces
14 p2107 A72-30531

Study of vacuum furnace atmospheres for brazing titanium honeycomb panels.
17 p2560 A72-34940

Brazing furnaces and heat treatment under vacuum
22 p3163 A72-42635

Technological aspects concerning the structural elements in the development of resistance furnaces under vacuum
22 p3163 A72-42636

VACUUM GAGES

NT BAYARD-ALPERT IONIZATION GAGES

NT IONIZATION GAGES

NT KNUDSEN GAGES

NT PENNING GAGES

Bayard-Albert ionization vacuum meter use as primary standard, investigating ion orbiting and collecting processes
03 p0361 A72-13880

Pressure measuring method with piston manometers for absolute vacuum gage calibration
04 p0507 A72-14440

Transit tube manometric system with fast particle beam ionization of residual gas molecules for vacuum measurements
09 p1364 A72-23226

Temperature effects on low pressure calibration in vacuum gage metrology
09 p1312 A72-23249

Thermistor vacuum gage with interchangeable sensing heads, providing improved pressure response and direct interchanging without recalibration
11 p1636 A72-26776

Vacuum gage calibration standardization by piston manometer method of pressure determination from direct force-area measurement
12 p1805 A72-27037

Gauges for ultrahigh vacuum.
19 p2803 A72-38390

VACUUM MELTING

Oxygen determination in cemented carbides, metal powders and presintered and finished sintered products by vacuum fusion method, comparing with neutron activation method
02 p0245 A72-12548

Nb-Ti-B ternary system melts hardened in vacuum, determining solidus temperature and surface from phase diagram
03 p0370 A72-13186

Mechanical and microstructural properties of Be-base alloys consolidated by vacuum arc melting, reporting results of tensile tests, hardness measurements and microprobe analysis
05 p0674 A72-16389

Oxygen effect on structure and mechanical, technological and corrosive properties of stainless steel melted in open and vacuum furnaces
07 p1013 A72-19739

Mechanical properties anisotropy in heat resistant Ni alloys due to strengthening phase nonmetallic inclusions distribution, suggesting purification by vacuum melting
09 p1327 A72-22231

Arc cast vacuum melted Mo base alloy properties, production and applications to heat pipes, aerospace structures and pressure vessels
11 p1644 A72-26844

High melting point alloy and metal powder production by vacuum atomization, using rotary vane and electron beam melting techniques
11 p1645 A72-26860

Electroslag and vacuum remelted maraging steel rolling contact, investigating fatigue life as function of lubricant film thickness/surface roughness ratio
12 p1816 A72-28109

Vacuum induction melting process for high temperature steels and superalloys fabrication, emphasizing control over temperature, pressure, beneficial trace elements and harmful impurities
13 p1964 A72-29100

Refractory metals vacuum melting for ingot production and purification in arc and electron bombardment furnaces
14 p2107 A72-30531

Inhomogeneity of high melting temperature elements in titanium alloys.
18 p2701 A72-36693

Transition metals physical and mechanical properties, production, refining and vacuum processing techniques
18 p2696 A72-36840

Desulfurization of cobalt, nickel, and their eutectic carbon alloys during noncrucible zone melting in vacuum
23 p3300 A72-43647

Laser spin melting experiments for glass production in space from high melting metal and rare earth oxide ceramics
24 p3417 A72-45156

VACUUM PUMPS

NT CONDENSATION PUMPS

NT ION PUMPS

NT MOLECULAR PUMPS

Prepumped systems with ion sorption and titanium sublimation vacuum pumps for ultrahigh vacuum production
07 p0914 A72-19906

Target jet density variations effect on vacuum in neutral atom beam ionization region of fast neutral particle magnetic trap
09 p1363 A72-23223

Cryogenic techniques for high vacuum differential pump with low conductivity cooled channels and supersonic jet target
09 p1364 A72-23225

Flow phenomena in turbomolecular pumps
18 p2696 A72-36837

Cryopump cooling requirements, refrigeration, design and vacuum application, considering Brayton, Claude, Stirling cycles and Joule-Thomson and regenerative processes
18 p2696 A72-36838

VACUUM SPECTROSCOPY

Windowless ultrahigh vacuum photoelectron spectrometer for high resolution studies of gas-metal surface reactions, measuring electron energy levels
04 p0523 A72-15489

Emission spectra of exploding copper wires in air and vacuum in IR, UV, visible and vacuum UV regions
05 p0691 A72-16991

Electron beam induced dissociative excitation of vacuum UV emission from atomic nitrogen multiplets, using normal incidence monochromator and pulse counting techniques
07 p1036 A72-18925

Vertically oriented double crystal attachment to vacuum X ray spectrograph for enhanced resolution of ionic solids and solutions molecular spectra
07 p0983 A72-19317

Aspiration condenser spectrometry of small ion mobility as function of height and atmospheric conditions
09 p1346 A72-23267

Emission spectra of exploding copper wires in air and vacuum in IR, UV, visible and vacuum UV regions
12 p1843 A72-27134

High vacuum mass spectroscopic analysis of volatile products released under friction from solid synthetic resin lubricants with molybdenum disulfide as antifriction filler
12 p1835 A72-28199

Mo and stainless Ni-Cr steel surfaces chemical composition determination by Auger electron spectroscopy during heating in high vacuum
16 p2406 A72-33251

Torch temperature measurements in vacuum by spectral radiative energy distribution method
16 p2476 A72-33258

Single crystal disk substrate design with electron bombardment heating for LEED and Auger electron spectroscopy studies in ultrahigh vacuum
17 p2553 A72-34642

Attachment for studying optical properties of highly cooled crystals in the vacuum ultraviolet region
17 p2555 A72-35309

VACUUM SYSTEMS

Equipment and techniques for He sorption by condensed gas layers at 0.1 picotorr
09 p1364 A72-23227

Electronic heating test arrangement for high temperature testing of metals and electrically conducting ceramics in vacuum, describing temperature control systems
12 p1796 A72-28249

Probe gas flow modulation in leak search device tested in vacuum system
13 p2007 A72-29921

Work functions of dilute W alloys from vacuum emission vehicle and thermionic microscope measurements, noting additives effect
14 p2120 A72-30613

Thermoemission ion gage stability and design aspects, discussing application as secondary standard for vacuum measurements
16 p2394 A72-33871

German book on vacuum technology covering theory, measurement techniques and applications in nuclear physics research facilities, electronic tubes, space environment simulation, mass transfer, etc
18 p2709 A72-36250

Space environment simulation and testing techniques, considering vacuum systems, low temperature, solar radiation and motion simulation
18 p2676 A72-36833

Measuring instruments for gas pressure determination in vacuum systems, noting application of thermal conductivity or ionization characteristics of gas molecules
18 p2692 A72-36835

The measurement of partial pressure in vacuum technology and vacuum physics
18 p2692 A72-36836

High and ultrahigh vacuum equipment and components selection, discussing gas-surface interactions, contamination and cleaning problems
19 p2835 A72-38391

Vacuum thermal decompositions of the nitrate salts of hydrazine.
19 p2848 A72-38876

Determination of the magnetic field B in vacuum for general two-dimensional MHD-equilibria.
20 p2957 A72-39352

A versatile ultrahigh vacuum scanning electron microscope.
21 p3051 A72-40217

VACUUM TUBE OSCILLATORS

NT BACKWARD WAVE TUBES

NT CATHODE RAY TUBES

NT CELESTROSCOPES

NT COLD CATHODE TUBES

NT GAS DISCHARGE TUBES

NT IMAGE ORTHICONS

NT IMAGE TUBES

NT KLYSTRONS

NT MAGNETRONS

NT MICROWAVE OSCILLATORS

NT MICROWAVE TUBES

NT PHOTOMULTIPLIER TUBES

NT PLANOTRONS

NT THERMIONIC DIODES

NT TRAVELING WAVE TUBES

NT VIDICONS

Optimal hf triode oscillation tripler with allowance for power limitation by thermal losses on plate and grid electrodes
05 p0638 A72-17184

Electrostatic focusing field inhomogeneity /gradients/ effects on high frequency electron-wave interaction processes in linear beam backward wave oscillator tube
07 p0952 A72-18845

Frequency distortions of signals in frequency-modulated self-excited oscillators
21 p3032 A72-40782

Influence of fluctuations on the synchronization of frequency-modulated oscillators
22 p3159 A72-42658

VACUUM TUBES

NT BACKWARD WAVE TUBES

NT CATHODE RAY TUBES

NT CELESTROSCOPES

NT COLD CATHODE TUBES

NT GAS DISCHARGE TUBES

NT IMAGE ORTHICONS

NT IMAGE TUBES

NT KLYSTRONS

NT MAGNETRONS

NT MICROWAVE OSCILLATORS

NT MICROWAVE TUBES

NT ORTHICONS

NT PHOTOMULTIPLIER TUBES

NT PICTURE TUBES

NT PLANOTRONS

NT THERMIONIC DIODES

NT TRAVELING WAVE TUBES

NT VACUUM TUBE OSCILLATORS

NT VIDICONS

Vacuum tube developments for radar, TV and communication applications, discussing microwave, traveling wave, cathode ray, memory and vidicon tubes, magnetrons, klystrons and tetrodes
11 p1606 A72-26544

Semiconductor devices with extended slow wave-carrier interaction region for vacuum traveling wave tube replacement
13 p1927 A72-28401

Fetron high voltage hybrid junction field effect /J-FET/ devices for direct replacement of vacuum tubes in unchanged circuits
13 p1928 A72-28431

Circuit of two parallel connected vacuum pentodes with different reactances to provide exact voltage division of ac signals by another
13 p1930 A72-29045

Frequency characteristics theory for two-stage electron tube microwave amplifiers coupled by transmission line on order of wavelength
23 p3268 A72-43435

VACUUM ULTRAVIOLET RADIATION

U FAR ULTRAVIOLET RADIATION

VALENCE

Impurity diffusion of Ag, Cd, In, Sn and Sb in magnesium single crystals, observing valence effect on activation energy
03 p0378 A72-14254

Electron states in glassy amorphous semiconductors, constructing trial wave functions for valence band
06 p0866 A72-18180

Nonstoichiometric compounds thermodynamic properties in terms of indistinguishability of ions /atoms/ in different valence states
07 p1048 A72-19544

Nonstoichiometric solid solutions based on ZrC and NbC, investigating microhardness variation due to differing valences of atoms in metal sublattices
08 p1188 A72-22100

Energy operator diagonalization of interacting valence electrons in semiconductor and metal models
09 p1352 A72-23356

Relative valence effect of transition metal additions on alpha-gamma phase equilibrium in Fe-Cr-Mn system
12 p1827 A72-27099

X ray photoelectron spectroscopic measurements of Fe and Cu valence states produced by ion sputtering reduction, applying to multiplet splitting and isoelectronic shifts
16 p2389 A72-33026

VALIDITY

Validity hypothesis for total creep rate potential in strain-hardenable materials, discussing carbon steel torsion and tensile tests
04 p0586 A72-15006

Fluid dynamics layer-type singular perturbation problems, constructing inner and outer asymptotic approximations with overlapping domains of validity
11 p1615 A72-25502

VALLEYS

Rille Rima Goclenius II formation, describing fractures mechanisms
04 p0571 A72-14563

Lunar sinuous rills location and origin, discussing Orbiter photographic maps, predominance in maria and similarity to terrestrial lava tubes
06 p0887 A72-18219

Terrestrial volcanic lava conduits origin and development association with lunar maria channels and sinuous rills
13 p2037 A72-28992

VALSALVA EXERCISE

Valsalva and M-1 maneuvers acceleration tolerance protective effects during high-g centrifuging with and without anti-g suits
12 p1767 A72-28318

Vascular headache of acute mountain sickness.
22 p3150 A72-42491

Induction of hemodynamic deterioration by the hypogravic state - An evaluation of mechanisms and prevention.
24 p3373 A72-45199

VALSALVA MANEUVER

U VALSALVA EXERCISE

VALUE

NT Q VALUES

VALUE ENGINEERING

Value engineering based cost data application to design of aircraft in production
06 p0906 A72-18435

VALVES

NT ARTIFICIAL HEART VALVES

NT CONTROL VALVES

NT GAS VALVES

NT HEART VALVES

NT PRESSURE REGULATORS

NT SOLENOID VALVES

Poppet valve design with flow force compensation for high pressure oil hydraulic systems, discussing dynamic stabilization
03 p0312 A72-13964

Hydraulic actuator servomechanism performance dependence on asymmetrical spool valve lap and closed loop system stability
08 p1113 A72-22153

Nonsymmetrical cylinders and valves under nonsymmetrical loading
08 p1113 A72-22157

Pneumatic fluid power valve flow rate derivation in terms of flow passage effective area and critical pressure ratio
08 p1113 A72-22158

Hydraulic ball valve elements and logic gates for applications requiring short switching times under large flow and high pressure conditions
08 p1114 A72-22159

Ball, globe, gate, butterfly, Y-type and safety-and-relief valves assessed for cryogenic applications
11 p1642 A72-26777

High pressure cryogenic hydraulically actuated valve for repeated sealing of liquid He-containing cell
15 p2183 A72-32436

The mitral apparatus - Functional anatomy of mitral regurgitation.
20 p2892 A72-39460

VAN ALLEN RADIATION BELTS

U RADIATION BELTS

VAN DE GRAAFF ACCELERATORS

Laboratory irradiation tests with van de Graaff generator for simulation of spacecraft components radiation damage due to high energy space protons and electrons
12 p1863 A72-27552

VAN DER WAAL FORCES

Van der Waal broadening of shock excited emission lines at 5000 K for astrophysical applications
06 p0852 A72-18053

Lattice expansion of metal chalcogenide superconducting organometallic structures with aromatic or aliphatic Lewis bases sandwiched into van der Waal gap
08 p1216 A72-21214

Stellar spectra differential analysis from solar curve of growth for Fe I with revised gf-scale, noting van der Waals broadening and microturbulence
10 p1547 A72-24868

Investigation of the 0.63-micron line shift in an He-Ne/20/ laser with an absorbing cell
19 p2814 A72-38787

Broadening and shift of magnesium lines by van der Waals interaction with argon atoms and by microfields.
22 p3208 A72-42388

VANADIUM
Fe XI to XV emission lines from transitions and isoelectronic spectra in manganese, chromium and vanadium
03 p0391 A72-13750

Zr and V linear thermal expansion coefficients explanation by alpha Zr hexagonal crystal lattice anisotropy
03 p0376 A72-13946

Thermal conductivity, electrical resistivity, emissivity and specific heat of polycrystalline vanadium under electron bombardment heating at 1200 to 1800 K
06 p0828 A72-17613

V, Nb and Ta deoxidizing capability in liquid Fe from oxide phase formation identification by electronographic and X ray analyses
07 p1011 A72-19545

Va crystal lattice interatomic bonds and elastic and inelastic X ray scattering intensity calculation
09 p1329 A72-23042

Vanadium enthalpy and heat of fusion measurement with massive copper calorimeter
10 p1497 A72-24784

Vanadium enthalpy and heat of fusion measurement using massive copper calorimeter with isothermal jacket
14 p2113 A72-30222

Relation between hydrogen embrittlement and the formation of hydride in the group V transition metals.
18 p2700 A72-36578

Interaction between vanadium in gas turbine fuels and sulfidation attack.
19 p2817 A72-37766

The effect of pre-strain on the yield behavior of vanadium.
24 p3413 A72-44721

VANADIUM ALLOYS
Pressure induced δ band deformation effect on magnetic susceptibility of Ti-V and V-Cr alloys
03 p0370 A72-13087

Temperature dependence of X ray interference lines for Al-V alloy obtained at high cooling rate, noting metastable solid solution thermal stability
03 p0377 A72-14022

Order-disorder reaction in Ni-V, Ni-V-Nb and Ni-V-Ta alloys, estimating critical temperature
05 p0671 A72-15999

Face-centered orthorhombic martensite in Ti-V alloy, determining axial ratios and lattice parameters by transmission electron microscopy and X ray diffraction
05 p0676 A72-17102

V and Al addition effects on mechanical properties of oxygen rich Ti alloys
06 p0831 A72-18358

Structure, hardness, density and electrical resistance of binary alloys V-Ti, V-Cr, V-Al and V-Sn
07 p1013 A72-19741

Long-time isothermal temper embrittlement in Ni-Cr-Mo-V steels, noting tensile ductility decrease and intergranular fracture
07 p1015 A72-19932

Solid solution yield strengthening and weakening of V-Ti alloys, investigating strain rate sensitivity temperature dependence as indication of two deformation mechanisms
07 p1021 A72-20434

Heat treatment, water quenching and aging effects on Ti-V alloys hardening and structural properties, discussing omega phase formation
07 p1023 A72-20667

Microsegregation in Ti-Mo, Ti-V and commercial Ti alloys, investigating cooling rate and alloying elements contents effects
11 p1655 A72-25506

Ti-V and Ti-Nb alloys mechanical strength and stress concentration resistance at low temperatures
13 p1977 A72-29018

Rare earth metals interactions with V, Nb and Mo alloys, describing procedures for interstitial impurities removal
15 p2252 A72-31190

Thermodynamic interaction parameters of solid solution bcc V-Ti-Cr alloys by Knudsen effusion method combined with mass spectrometer
16 p2409 A72-33803

V-Ti alloys interstitial scavenging action dependence on titanium concentration via internal friction study
17 p2567 A72-34732

Carbide hardening of chromium-molybdenum-vanadium steel
20 p2941 A72-39578

Optimal planning of an experiment in a study of the properties of Ti-V-Al alloys
20 p2942 A72-39825

The nature of solid solutions of the titanium-vanadium-oxygen and titanium-vanadium-aluminum-oxygen systems
21 p3068 A72-40962

Free energy changes and boundary segregation of tin and antimony in CrV steels.
21 p3070 A72-41648

Superconducting alloys of niobium and vanadium
22 p3191 A72-42808

Physical properties and electronic structure of V1-x Crx/3Si ternary alloys
22 p3192 A72-43014

Tendency toward brittle failure of a simulated weld-seam region in Ti-Al-V system alloys
23 p3293 A72-43593

Increasing the boundary strength of electron-beam-melted cast molybdenum by vanadium microadditions
23 p3302 A72-43967

Co-V solid solution decomposition by equilibrium phase precipitation at aging temperatures, using electron microscopic and X ray analysis
24 p3414 A72-45382

Three-phase equilibria of cast and annealed V-Zr-Cr alloy by X ray, metallographic and melting point analyses
24 p3414 A72-45384

Changes in the grain-boundary free energy and the segregation of tin and antimony at grain boundaries in CrV steels
24 p3415 A72-45394

V and Al addition effects on mechanical properties of oxygen rich Ti alloys
24 p3416 A72-45745

VANADIUM CARBIDES
Order-disorder transition cooling effects on V carbide superlattice domain structure, using electron and optical microscopy
03 p0370 A72-12997

Vanadium carbide diffraction spectrum reflection intensity under Mo and CuK-alpha irradiation, showing crystalline structure and interatomic ionic interaction
04 p0533 A72-14618

An electron microscopy study of carbide precipitation in vanadium.
18 p2699 A72-36577

VANADIUM COMPOUNDS
NT VANADIUM CARBIDES
NT VANADIUM OXIDES
NT VANADYL COMPOUNDS
Vanadium emission spectra studies of energy band structure in vanadium silicides, showing p-subzone splitting
13 p1980 A72-29798

Some data on interatomic interaction in solid high-melting compounds of titanium, vanadium, and chromium with light metals
17 p2569 A72-35520

Characteristics of the state of particles of titanium and vanadium mononitrides after nitriding and heat treatment
23 p3298 A72-43282

VANADIUM OXIDES
Nonstoichiometric vacancy order in vanadium monoxide from electron microscopy and diffraction patterns, proposing partial phase diagram
03 p0401 A72-13584

Tantalum and tungsten vanadium trioxide oxides crystallographic order ratio from diffraction spectrum intensities and overstructure lines disappearance
05 p0675 A72-16699

VANADYL COMPOUNDS
Electron paramagnetic resonance spectrum of vanadyl acetylacetonate dissolved in liquid crystal or isotropic solvent
21 p3013 A72-41177

VANELESS DIFFUSERS
Vaneless diffuser air flow calculation based on helical flow model with back currents in boundary layer
09 p1259 A72-22299

Compressible flow measurement and loss prediction in radial vaneless diffuser in centrifugal compressor, using hot-wire anemometers
10 p1416 A72-23861

Hub and shroud boundary layer growth in centrifugal compressor vaneless diffusers, comparing predicted and measured performance at high pressure ratio per stage
11 p1570 A72-25645

[ASME PAPER 72-GT-54]

VANES
NT GUIDE VANES
NT JET VANES
NT WIND VANES

VAPOR DEPOSITION
Stroboscopic measurement of elastic untwisting angles of axial compressor rotor vanes under centrifugal and aerodynamic forces
01 p0143 A72-11371

Wide angle conical diffuser performance improvement by conical splitter vanes, considering static pressure recovery
10 p1416 A72-23860

Cascade technology for centrifugal compressor vane diffuser design, comparing performance results with conventional diffuser data
11 p1569 A72-25633

[ASME PAPER 72-GT-39]

Reynolds analogy for twisted liquid flow in tube with swirl vanes
11 p1619 A72-26968

Turbine nozzle vanes edge losses dependence on profile edge thickness, allowing flow velocity variation
12 p1861 A72-28135

Hydrodynamic pivoting-pad vane tips for high-speed vane pumps.
18 p2694 A72-36046

VAPOR DEPOSITION
NT VACUUM DEPOSITION
Refractory titanium oxide deposition by hot front method of chemical reaction in vapor phase
02 p0170 A72-12166

Thin film formation techniques including evaporation, sputtering, anodization, chemical vapor deposition, electrodeposition and sintering, discussing surface scattering, tunneling, Schottky emission and conduction mechanisms
06 p0790 A72-18571

Cartridge system for substrate heating to 500 C in vacuum chamber during metals or semiconductor vapor deposition, describing carbon block-high intensity quartz lamp assembly
07 p0984 A72-19325

Optical high precision surfaces correction method for laser based reflectors on vacuum vapor differential deposition
07 p1007 A72-20262

Tungsten dispersion strengthening by hafnium nitride covapor deposition, discussing effects of matrix microstructure and dispersoids number, size and spacing variations
07 p1019 A72-20366

Reactivity evaporated titanium nitride resistors for thin film microcircuits, discussing nitrogen gas pressure and substrate temperature effects on electrical properties during evaporation
09 p1286 A72-22902

Chemical vapor deposition of W and Mo by hydrogen reduction of hexafluorides, noting crystal structure and microporosity
11 p1644 A72-26837

Chemical vapor deposition of boron on carbon monofilament substrate to eliminate fracture and boron damage and achieve good strength
12 p1834 A72-28085

Phase composition and lattice constants of carbide films from vaporized Zr interaction on graphite surface at 1700 C
13 p1912 A72-28566

Minimum ion source temperatures for glow discharge ion flux deposition of films and coatings on metallic and nonmetallic substrates
15 p2244 A72-31573

Chemically vapor deposited W heat pipe fabrication and evaluation for application to high temperature nuclear reactors
15 p2244 A72-32126

Structural and orientation study of sequentially evaporated MnBi thin films on glass substrates using electron diffraction and transmission microscopy
16 p2441 A72-33207

High strength-high modulus boron vapor deposited on a carbon monofilament substrate.
17 p2572 A72-35657

Atmospheric organic vapor effects on electric contact erosion, deriving showering arc duration, gap breakdown, arc number and energy
18 p2665 A72-36118

Vapor deposition of refractory metals applied to thermionic conversion - Performance of deposits obtained by reduction of fluorides at high temperature and low pressure
18 p2656 A72-36138

The vapor deposition of high work function materials in a gas discharge.
18 p2656 A72-36149

Kinetics and annealing and mechanical properties of W chemical vapor deposition, discussing high temperature tests
18 p2656 A72-36398

Ultra-high vacuum coater for thin film research
18 p2676 A72-36839

Vapor grown solid state single crystal oxide thin films characteristics and synthesis by thermal vaporization, chemical vapor deposition and sputtering
19 p2843 A72-37443

Vapor deposition in vacuum under conditions of constant vapor flow with the aid of electron emission current control

20 p2954 A72-39694

Vapor deposition effects on high density Mo, W and Nb obtained by carbonyls pyrolysis or chlorides and fluorides reduction

20 p2941 A72-39821

Fabrication and accelerated life tests of self sustained electron emission cathode with Cr film vapor deposition on Cu disk base

21 p2997 A72-40790

Theory of laminar film condensation of flowing vapor.

21 p3128 A72-40950

Fabricating aluminum matrix composites. I - A survey of aluminum matrix composites.

22 p3182 A72-41996

VAPOR GENERATORS

U VAPORIZERS

VAPOR LIQUID EQUILIBRIUM

U LIQUID-VAPOR EQUILIBRIUM

VAPOR PHASES

Sodium heat pipes sonic limit, describing vapor dissociation-recombination and homogeneous vapor condensation phenomena

[ASME PAPER 71-WA/HT-11] 05 p0743 A72-15871
Gas phase basicities of aliphatic amines by ion cyclotron resonance spectroscopy

07 p0936 A72-19493

Alkyl substituent effects on gas phase acidities of toluene, p-xylene and acetylenes, using ion cyclotron resonance spectroscopy

07 p0936 A72-19494

Thermodynamics of Mo silicidation reactions from gas phase in silicon chloride and hydrogen media, discussing glow discharge maximum yield

07 p0937 A72-20417

Flow characteristics of liquid layers adjacent to vapor bubble, visualizing flow via particle motion

08 p1151 A72-21670

Vertical distribution of nitric acid vapor concentration in lower stratosphere from balloon sounding

11 p1622 A72-26086

Solid propellants oscillatory burning with gas phase time lag, solving nonsteady governing differential equations by numerical integration

13 p2065 A72-29301

Computerized determination of cryogenic gas behavior near vapor region, obtaining state equation coefficients from curve fitting program

15 p2334 A72-31580

Mercuric chloride, bromide and iodide gas phase UV absorption spectra, discussing correlation with intermolecular charge transfer transitions

16 p2360 A72-32926

Gas phase photodetachment of electron from selenide ion, determining affinity and spin-orbit coupling constant for SeH negative ion

16 p2360 A72-33580

Solid-gas phase equilibria and thermodynamic properties of cadmium selenide.

17 p2511 A72-35329

Vibrational analysis of electronic absorption spectra of 3-methyldiazirine and 3-methyl-4,3-diazirine in vapor phase

18 p2657 A72-36566

Aluminum oxide and silicon carbide whiskers fabrication by homogeneous gas reaction process, discussing gas composition, temperature and substrate effects on production yield

20 p2940 A72-39440

Coriolis constants for prolate symmetric top molecules from gas phase Raman band contours observation, noting comparison with IR spectroscopy

22 p3209 A72-42719

German monograph - Gas-phase precipitation and high-temperature oxidation of titanium carbide.

22 p3194 A72-43053

German monograph - Heat transfer at a vapor bubble growing on a heated wall during boiling.

22 p3244 A72-43059

Evidence for vapor fractionation in the origin of chondrules.

23 p3339 A72-44134

VAPOR PRESSURE

Vapor pressure and partial thermodynamic functions of Co-Ni alloys, observing negative deviations from Raoult law

03 p0374 A72-13928

Nitrogen heat pipe axial temperature distribution and vapor pressure measurement, noting effective thermal conductivity variation with power load and inclination angle

[ASME PAPER 71-WA/HT-28] 05 p0744 A72-15881

Atmospheric vapor pressure and temperature direct measurement, using copper-constantan thermocouples for wet-bulb temperature rapid fluctuations and thermistor for mean wet-bulb temperature

07 p0982 A72-19106

Vapor pressure and composition in As-I system, investigating entropy and enthalpy changes and temperature dependence of equilibrium constant

09 p1373 A72-23481

Effective atmospheric emissivity for clear skies, showing dependence on surface vapor pressure [AD-742882]

11 p1681 A72-26084

Passive Q factor modulation in carbon dioxide laser by resonance absorption saturation in osmium tetroxide vapors, noting vapor pressure effects

11 p1650 A72-26355

Vapor annealing effect on vacuum evaporator CdSe thin films electroconductivity as function of pressure and temperature

12 p1854 A72-27249

Atmospheric nitric acid vapor radiation absorption measurements at various partial pressures

12 p1805 A72-27993

Gaseous buffering for oxygen fugacity control in high temperature gas systems at one atmosphere

12 p1778 A72-28104

High pressure oxygen control for synthesis and vapor phase equilibria, discussing tensiometric measurements and cold seal pressure vessel techniques

12 p1778 A72-28105

Cryogenic liquids cavitation erosion of plastic and cold-short metals at 77 K, determining vapor pressure effect

13 p1979 A72-29479

Vacuum gap discharge conditions as function of electron beam parameters and metal vapor pressure

13 p2017 A72-29611

Passive Q factor modulation in carbon dioxide laser by resonance absorption saturation in osmium tetroxide vapors, noting vapor pressure effects

16 p2402 A72-33708

Vapor pressure and velocity distributions in rarefied gas flows through narrow slits under vacuum conditions with ice sublimation

16 p2380 A72-33854

Vapor pressure influence of Ba-Cs thermionic converter diodes on I-V characteristics and work functions in terms of anomalous Schottky effect

18 p2646 A72-36194

Arc mode thermionic converter at low cesium vapor pressures

18 p2647 A72-36216

Study of cesium vapor pressure by the boiling point method

18 p2713 A72-37179

Vapor pressure decrease rate during cooling agent introduction in semiclosed volume, determining pressure drop from energy and mass conservation equations

19 p2879 A72-37355

Atmospheric nitric acid vapor radiation absorption measurements at various partial pressures

22 p3174 A72-43007

Investigation of the parachute inflation aid utilizing liquid vapor pressure.

22 p3139 A72-43141

VAPOR TRAILS

U CONTRAILS

VAPORIZATION HEAT

U HEAT OF VAPORIZATION

VAPORIZERS

NT EVAPORATORS

Fuel vaporizer for gas turbine engine, investigating heat transfer coefficient

05 p0747 A72-16492

Vaporizer temperature effect on ion propulsion system thrust vector, presenting temperature control loop circuit diagram

10 p1528 A72-24652

Porous-tungsten mercury vaporizers design and tests for flow rate, liquid intrusion pressure level and mechanical strength

[AIAA PAPER 72-484]

11 p1710 A72-26210

Design and performance characteristics of ion thruster feed system components including high voltage isolator, liquid Hg flowmeter and W vaporizer

[AIAA PAPER 72-487]

11 p1710 A72-26213

VAPORIZING

NT BOILING

NT EVAPORATION

NT FILM BOILING

NT LEIDENFROST PHENOMENON

NT NUCLEATE BOILING

NT PROPELLANT EVAPORATION

NT SUBLIMATION

NT TRANSPIRATION

Motion picture technique for studying vapor bubbles formation, determining temperature fluctuations on heated surface below active region

03 p0457 A72-14153

Apollo 14 basaltic evidence for selective volatilization on lunar surface, using electron probe analysis

03 p0439 A72-14273

Combusting polymers gasification effective heat values determination from correlation of surface regression rate and oxygen impingement rate data

[AIAA PAPER 72-34]

05 p0749 A72-16898

High intensity laser beams for solid surface material removal by vaporization and explosion, noting surface and subsurface temperature relations

07 p1002 A72-19210

Gas content determination in metals by melting and vaporizing measured microvolumes using laser microprobe and magnetic mass spectrometer

07 p1006 A72-19549

Temperature and concentration fields of liquid solution droplets during unsteady vaporization process in high temperature gas media

08 p1252 A72-21308

Maximum volatile solute vaporization escape prior to droplet solidification during metal vapor chemical release process

08 p1128 A72-21618

Equation of state data of solids from shock vaporization, using spectroscopic technique

09 p1351 A72-28556

Quenched specimen anisotropic surface heating effect in liquid vaporization characteristics determination

10 p1561 A72-24207

Cooling system based on vaporization of solar cell preheated solution drawn through chamber with atomizing injector

10 p1422 A72-24314

Vaporization characteristics of carbon heat shields under radiative heating, presenting estimates of vaporization heat from energy balance

[AIAA PAPER 72-296]

11 p1741 A72-25234

Vaporization and condensation effects on Apollo 11 glass spherules from microbreccia samples, suggesting concentration gradients as result of impact event

11 p1723 A72-26522

Lithium diffusion into silicon by evaporation and homogenization technique, discussing dislocations and oxygen effects from aging in Ar at 150 C

12 p1757 A72-28025

High vacuum mass spectroscopic analysis of volatile products released under friction from solid synthetic resin lubricants with molybdenum disulfide as antifriction filler

12 p1835 A72-28199

Shock induction melting and vaporization in metals, investigating initial porosity effect

14 p2113 A72-30185

Vacuum vaporization of niobium, tantalum, zirconium and hafnium carbide phases, using Langmuir method

15 p2253 A72-31200

Results of a preliminary experimental investigation of a vapor transport fuel pin.

19 p2832 A72-37631

Experimental evidence against the role of selective volatilization on the lunar surface.

21 p3013 A72-40452

Vapor phase formation during high temperature oxidation.

21 p3066 A72-40551

Diffusive and radiative effects on vaporization times of drops in film boiling.

21 p3130 A72-41185

VAPORS

NT CESIUM VAPOR

NT MERCURY VAPOR

NT METAL VAPORS

NT SODIUM VAPOR

NT WATER VAPOR

VARACTOR DIODE CIRCUITS

Quasi-optical 30-60 GHz varactor doubler circuit filters, waveguide tuners and mounts for frequency multipliers

04 p0507 A72-15617

Regenerative nonlinear RC amplifier oscillations due to series opposed varicap diode capacitance

18 p2665 A72-36109

Parallel-type varactor frequency multipliers. I - Spectral analysis of the voltage at a partially forward-biased varactor

23 p3270 A72-43764

Optimal parallel-type varactor frequency multiplier calculation for reverse-biased conditions in terms of nonlinear conductance loss and diffusion capacitance Q factor

23 p3270 A72-43774

VARACTOR DIODES

Varactor diode microwave parametric amplifiers for radio astronomy interferometer, discussing system design features for gain and phase stabilities

02 p0192 A72-12043

Uhf varactors reliability, establishing rejection criterion by statistical analysis

02 p0194 A72-12444

Book on microwave semiconductor devices, considering point contact crystal, varactor, Schottky-barrier, tunnel, backward and p-i-n diodes, transistors, Gunn effect devices and integrated circuits

03 p0333 A72-13845

Microwave IC oscillators design for broadband high performance receivers, exemplifying thin film Gunn effect, step- and varactor-tuned transistor oscillators

06 p0786 A72-18373

FM/CW varactor Gunn diode oscillator powered subminiature IC radar altimeter design on homodyne principle for ultralight reliable minimum chance detection

06 p0819 A72-18473

- Varactor tuned high performance Gunn oscillators, emphasizing specifications for level power output with frequency, tuning linearity and rate
06 p0789 A72-18479
- Millimeter wave pumped X band balanced diode type parametric amplifier using GaAs Schottky barrier varactors for operation at room temperature
09 p1289 A72-23417
- German book on HF semiconductor electronics covering planar and field effect transistors, varactors, n-p, p-i-n, avalanche and Schottky barrier diodes, Gunn devices, etc
10 p1452 A72-24699
- High quality GaAs varactor diodes for double diode low noise wideband parametric amplifiers at idler frequencies up to 43 GHz without refrigeration
12 p1788 A72-27174
- Varactor broken voltage-capacitance curve due to uncompensated impurities concentration change at p-n junction
13 p1926 A72-28379
- GaAs varactor diode design optimization based on calculation of cut-off frequency vs carrier concentration with consideration of skin effect
14 p2088 A72-30588
- Microwave varactors for communications satellites
18 p2670 A72-37122
- Microwave and optoelectronic devices performance and component reliability, considering varactors, p-i-n, avalanche and Gunn diodes, ICs, FETs, light emitters and liquid crystals
18 p2720 A72-37137
- Gallium arsenide varactors
18 p2671 A72-37145
- Improved injection locking of microwave FM-oscillators.
19 p2771 A72-37262
- Nonlinear double T-shaped RC filter
19 p2774 A72-38417
- Calculation of the electronic readjustment of a tunnel-diode oscillator by a varactor
22 p3159 A72-42246
- VARIABLES**
U VARACTOR DIODES
VARIABLE AREA WINGS
U TRAILING-EDGE FLAPS
VARIABLE GEOMETRY STRUCTURES
Graphite reinforced epoxy stiffeners for variable geometry fuel tank to meet light weight requirement, discussing billet fabrication, assembly and installation
08 p1176 A72-21688
- Turbine aerodynamics research trends, covering engine cooling, high work factor turbines, pneumatic variable geometry and computer analysis
11 p1572 A72-26036
- Extendible variable profile nozzle for various flow regimes operation, developing numerical design algorithm
18 p2641 A72-36661
- Configuration analysis as applied to aerospace vehicle design synthesis.
[SAWE PAPER 911]
23 p3342 A72-43458
- VARIABLE LIFT**
U LIFT
VARIABLE MASS SYSTEMS
Soviet book on rocket dynamics covering history, variable mass point aerodynamics and ballistics, numerical and computer methods and trajectory analysis
02 p0286 A72-12123
- Mass changes in restricted quasi-circular variable mass three body problem with particle equations of motion having Jacobi integral
03 p0436 A72-13828
- Oscillation periods of single degree of freedom variable mass point, using stiffening hypothesis
03 p0390 A72-14220
- Center of mass motion of spacecraft in central gravitational field, analyzing programming of size and position of elements in mass geometry leading to arbitrarily large displacements
05 p0731 A72-17032
- Orbital elements evolution for two body problem with decreasing mass according to Jeans mode
08 p1236 A72-21638
- Differential equations solutions stability for physical discrete systems with delayed argument, impact excitation, variable mass or structure, disturbances or weak couplings
09 p1343 A72-23601
- One degree of freedom mechanical system with jump-like variable mass, determining displacement and velocity statistical characteristics under random excitation and mass addition
09 p1353 A72-23608
- Impulse and kinetic momentum equations for dynamics of variable mass solid using mechanical model
12 p1846 A72-27543
- Quadrature solution for variable mass point motion under perturbing force in trajectory plane normal to velocity vector
13 p2003 A72-28725
- Certain problems in continuum mechanics for a deformed body of variable mass
19 p2835 A72-38471
- A bivariate normal theory maximum-likelihood technique when certain variances are known.
21 p3075 A72-40826
- Equations of motion for the variable mass flow-variable exhaust velocity rocket.
[AIAA PAPER 72-912]
21 p3112 A72-41559
- Ascent acceleration maximization of variable mass particle, calculating optimal parameters of multistage rocket
22 p3204 A72-42066
- Quadrature solution for trajectory mass point motion under perturbing force in trajectory plane normal to velocity vector
22 p3205 A72-42101
- Relativistic test particle escape from circular orbit around central mass due to mass loss, considering orbiting body corrections due to general relativity
23 p3355 A72-43265
- Equations of motion of nonlinear nonholonomic mechanical systems of variable mass with impulsive constraint factors
23 p3313 A72-43848
- Dynamic behavior of three point mass system with variable body mass ratios and constant total system mass, applying results to stellar systems
24 p3442 A72-45240
- VARIABLE PITCH PROPELLERS**
Astafan turbofan engine with variable pitch fan rotor blades for thrust variation, discussing gearbox and core engine design
07 p1055 A72-20459
- Variable pitch fans for STOL aircraft thrust/shaft engine, noting short field capability and quietness
09 p1374 A72-23447
- Variable pitch ultrahigh bypass ratio ducted fan engine design for STOL transport aircraft
[ASME PAPER 72-GT-61]
11 p1704 A72-25652
- Variable pitch fans - Successors to the aircraft propeller.
22 p3216 A72-42927
- VARIABLE STARS**
NT CEPHEID VARIABLES
NT NOVAE
NT SUPERNOVAE
NT T TAURI STARS
Spectral analyses of Mira-type variable stars near light maximum, discussing empirical curve of growth, Doppler velocity, damping constant and electron pressures
01 p0129 A72-10792
- Radio variable sources PKS 0727-11 and 1514-24 observation at 2295 MHz, presenting flux measurements and drift curves
01 p0134 A72-11161
- Rapidly varying radio source VRO 42.22.01 /BL Lac/ observations, presenting flux density and linear polarization variations
02 p0277 A72-11774
- Soviet monograph on variable stars observation covering photographic photometry, photoelectric observation, image processing devices and computer techniques
02 p0279 A72-12122
- Periodicities from power spectrum analysis of light curve of RR Tauri variable
[AD-739638]
02 p0281 A72-12302
- Oblique rotator model for time dependent light polarization of red long period variables, considering dust particle alignment in outer atmospheric layers near magnetic poles
02 p0283 A72-12630
- He abundances in universe, discussing stellar structure and evolution, He production, variable stars and globular clusters H-R diagrams shape
03 p0418 A72-13112
- Eclipsing variable star EQ Taurus photoelectric brightness variation observations in B and V light
03 p0433 A72-13488
- Single channel photometer measurement possibility in UVB magnitudes of variable stars
03 p0359 A72-13497
- Soviet book on long period variable stars covering spectral data photometric characteristics, spatial and kinematic properties, absorption effect and evolution
03 p0439 A72-14224
- Eclipsing variable system AW Peg spectrophotometric data, examining spectral line geometries and intensities and atmospheric conditions
03 p0439 A72-14244
- Photoelectric observations in different colors of eclipsing variable TX Cancri, presenting tables
05 p0723 A72-17199
- VV Pup binary light variations correlation with primary component variable disk dimensions, considering nova-like processes
06 p0882 A72-18003
- MHz IR/OH sources, discussing M type Mira variables or M supergiants photospheric temperature and dust shell structure
07 p1069 A72-19075
- Type R Corona Borealis variable stars luminosity variations attributed to formation of carbon layer from He nuclear transformation process at stellar core-envelope boundary
08 p1231 A72-21086
- Pleiades flare stars with slow cyclical variations from 1969-1970 observations
08 p1233 A72-21276
- Semiregular variable CH Cygni observations from 1967 to 1969 with continuous spectrum variations comparison to monochromatic brightness changes
08 p1233 A72-21278
- Stellar brightness variations of T Cep during January 1969-November 1971, considering visual estimates and period length observations
10 p1542 A72-24571
- Statistical equilibrium analysis of fluorescent Fe I emission in long period variables
10 p1542 A72-24610
- Binary stars convective zones reaction to periodic gravitational fluctuations due to stellar revolutions asynchronism, using incompressible fluid plane layer model
10 p1543 A72-24631
- Visual observations of eclipsing period elements of nova-like variable V Sagittae for estimate of total magnitude of unclipped binary
10 p1545 A72-24829
- Light curve of TW Delphini from visual observations, noting relationship to RV Tauri-type stars
10 p1546 A72-24830
- R Coronae Borealis type variable stars spectral, IR and polarimetric studies, outlining common features and hypotheses for phenomenon explanation
10 p1549 A72-25055
- Blue white dwarf HL Tau-76 rapid variations, suggesting underlying driving mechanism from high speed three color photometric observations
10 p1549 A72-25193
- Omega Velorum revelation as beta Canis Majoris type variable stars from photoelectric and spectrographic observations
12 p1867 A72-27207
- Ap stars with variable periods from magnetic and photometric data analysis
12 p1868 A72-27221
- Variable white dwarf radial pulsation periods explained by nonradial oscillations and gravity modes, considering atmospheric mixing with degenerate core
12 p1868 A72-27260
- Stellar population in Galactic nuclear bulge, considering interstellar reddening and variable stars
13 p2038 A72-29011
- Eclipsing binary WZ Sge observation for light curves with 3-sec time resolution, noting amplitude variation similarity to other cataclysmic variables
15 p2314 A72-32368
- Photoelectric photometry of binary VV Pup with 3-sec time resolution, suggesting qualitative model from eclipses identification
15 p2314 A72-32369
- Helium stars linear and nonlinear pulsation and evolutionary computations, establishing instability strip with two solar mass models
16 p2458 A72-33720
- Photometric observations of Haro-Chavira IR stars, noting variable nature predominance
17 p2604 A72-34443
- Minimum-light spectra of nine M-type variable stars.
17 p2610 A72-35118
- New measurements of circular polarization and an ephemeris for the variable white dwarf G195-19.
17 p2611 A72-35298
- Radio detection of Cygnus X-3.
17 p2612 A72-35366
- Radio observations of Cygnus X-3.
17 p2612 A72-35367
- Narrow-band photoelectric photometry of the peculiar Wolf-Rayet eclipsing binary CV Serpentis.
17 p2617 A72-35732
- Near-infrared photometry of Mira variables.
18 p2729 A72-37018
- Least squares method for Y Cyg spectroscopic elements improvement based on radial velocity measurements, noting nonexistence of gamma velocity variability
19 p2858 A72-37809
- Spectrophotometric study of eclipsing-variable system components. I
19 p2858 A72-37811
- Study of the spectrally variable silicon Ap star 56 Ari
19 p2862 A72-38055
- Photometric and power spectrum observation of peculiar blue variable star, showing low amplitude high frequency luminosity oscillations, hydrogen deficiency and degeneracy
20 p2966 A72-38921
- Far-infrared and uvby photometry of V 1057 Cygni.
20 p2973 A72-39887
- Variation of the spectrophotometric temperature from the center of the disk to the limb of stars of the spectral classes B and A
21 p3102 A72-40094
- Pulsating variables in the Pleiades cluster.
21 p3105 A72-41032
- The kinematics of semi-regular red variables in the solar neighbourhood.
21 p3111 A72-41473

Bright red giants of the globular clusters M 3, M 5, and M 13 21 p3113 A72-41756

Red variables in globular clusters, in the galactic centre and in the solar neighbourhood. 22 p3222 A72-42135

A spectroscopic and photometric study of the pulsating R Coronae Borealis type variable, RY Sagittarii. 23 p3334 A72-43255

Investigation of the variable stars WR-96, GR-29, and WR-96 [2] 24 p3448 A72-45682

Photographic observations of variable stars in the proximity of NGC 6830 24 p3448 A72-45683

Proper motions of 122 eclipsing variables 24 p3448 A72-45688

VARIABLE SWEEP WINGS

B-1 strategic supersonic bomber design, emphasizing variable sweep wing, landing gear, control and instrumentation 02 p0154 A72-12226

Low subsonic region unsteady interference effects on harmonically oscillating wing-tailplane model with variable sweep wing [DGLR PAPER 71-081] 02 p0152 A72-12709

Variable sweep wings aerodynamic characteristics in subsonic, transonic and supersonic flight, considering lift, drag, stability and control 18 p2643 A72-36976

VARIABLE THRUST

Astafan turbofan engine with variable pitch fan rotor blades for thrust variation, discussing gearbox and core engine design 07 p1055 A72-20459

Overall characteristics of optimal quasi-steady plasma thruster system, discussing mass, burning time and thrust variations as function of power supply and pulse duration [AIAA PAPER 72-456] 11 p1708 A72-26192

Equations of motion for the variable mass flow-variable exhaust velocity rocket. 21 p3112 A72-41559

Experimental performance of coaxial injectors in thrust-variable LO₂/GH₂-rocket engines. 24 p3434 A72-45181

VARIANCE [STATISTICS]

NT ANALYSIS OF VARIANCE

NT MULTIVARIATE STATISTICAL ANALYSIS

Vertical wind velocity variances and spectra above atmospheric surface layer for flat and mountain terrains 03 p0386 A72-14335

Bias and variance prediction efficiency in two stage sampling designs 03 p0383 A72-14368

Upper and lower bounds for expected value and variance of minimum material weight necessary for random resistance structure able to support assigned loads 04 p0593 A72-15648

Variance estimate of second order moment by nonlinear correlator in presence of additive amplitude and phase modulation and normal noise 07 p0939 A72-19021

Computer simulation of empirical confidence limits for variance spectra, applying to Gaussian random noise data stochastic model 07 p0951 A72-20360

Significance criteria for comparing strength parameter against expectation from random group of vectors in variance matrix applications 09 p1341 A72-23023

Safety factor distribution function for plastic collapse of structure with random resistance members, discussing variance-expected value ratio 09 p1406 A72-23075

Band limited background noise variance measurements by analog and digital techniques 09 p1280 A72-23103

Weather stations data analysis with unequally spaced observations, considering errors and variance transfer functions 11 p1680 A72-26076

Algorithms for photogrammetric model coordinates variance and covariance estimation, considering convergence properties 16 p2384 A72-33029

Satellite measurement of ground-based CW Ar laser source scintillation, deriving log amplitude variance, probability distribution and power spectral density from telemetered data 17 p2513 A72-34289

The observability of unforced physical systems by linear non-sequential estimators in the validation of linear error analysis. [AIAA PAPER 72-876] 20 p2910 A72-39123

Performance improvement of amplitude-constrained minimum-variance controller by minimising sum of variance. 20 p2911 A72-39772

Variation analysis and design of experiments as an aid to design quality assurance. 20 p2930 A72-39856

In-flight alignment and calibration of inertial measurement units. I - General formulation. II - Experimental results. 21 p3081 A72-41079

Independent cascaded multicomponent random variable system gain statistics relationship to individual component based on moment derivation, obtaining curves from variance equation 21 p3022 A72-41087

Variance reduction in Monte Carlo analysis of rarefied gas diffusion. 21 p3046 A72-41183

On the calculation of variances of solutions to linear simultaneous equation. 21 p3075 A72-41233

Diffusion from a continuous source in relation to the Eulerian properties of turbulence. 21 p3046 A72-41248

The application of Monte Carlo methods to the nonlinear filtering problem. 23 p3274 A72-43541

Reliability estimation in life testing in the presence of an outlier observation. 23 p3309 A72-43807

Optimal, on-line linear filtering with noisy, time-delayed observations. 23 p3276 A72-43855

VARIATION METHOD U CALCULUS OF VARIATIONS VARIATIONAL PRINCIPLES

Thermoelectricity quasi-static, dynamic and coupled problems in continuum mechanics, discussing formulation and variational principles methods for solution 02 p0290 A72-11634

Plane cavity flow past symmetric oval obstacles, applying variational principle to fixed point theorem 02 p0206 A72-12625

Bogoliubov-Mitropolski-Hale integral manifold theorem for perturbed nonlinear differential equations, using generalized variation of parameters formula 03 p0381 A72-12907

Thermodynamic equilibrium variational theory for multiphase systems subject to nonhydrostatic stress, considering diffusion and phase transformations 03 p0455 A72-12908

Rotating star global axisymmetric dynamic stability, deriving local criteria by variational principle 03 p0417 A72-13021

Continuous solid medium electroelastic equations of state, obtaining solution by variational principles application 03 p0390 A72-13916

Doubly connected strain-hardened thin plate, calculating stress concentration and stress-strain state by variational principle of least additional potential energy 03 p0451 A72-14122

Computer solution to vector variational formulation of electromagnetic Maxwell equations for dielectrically loaded rectangular waveguide 03 p0335 A72-14249

Dual variational principles application to distributed parameter system suboptimal control strategy evaluation, considering control variable and feedback gain as piecewise function of time 04 p0505 A72-14665

Elastic strip stresses and displacements, using eigenfunctions with coefficients determined by variational principles [ASME PAPER 71-APMW-24] 04 p0589 A72-15181

Variational theory for optimal relaxed control systems with time lag described by bounded uniformly continuous function defined on bounded closed sets 04 p0506 A72-15199

Polytropic masses oscillations under rapid uniform rotation, using variational principle 04 p0579 A72-15320

Variational principles for elasticity theory problem of three dimensional linearly elastic incompressible anisotropic body with highly elastic deformations 05 p0741 A72-17143

Variational principles in general relativity, deriving Einstein field equations and equations of motion for charged and uncharged self gravitating fluids 06 p0847 A72-17254

Generalized restricted three body problem with one point not exerting influence on others, discussing variational equations and Liapunov stability 06 p0877 A72-17662

Plane Couette flow of incompressible non-Newtonian viscous fluid between parallel plates, using minimum entropy production variational principle 06 p0798 A72-17779

Steady heat conduction boundary value problems from complementary variational principles 06 p0902 A72-17780

Incompressible fluid turbulent flow variational principles, discussing Malkus principle for maximum dissipation rate and minimum entropy production principle for convective and dissipative systems 06 p0800 A72-18116

Single species one dimensional Vlasov plasma linearized analysis as initial value problem with

periodic boundary conditions, using Hamilton variational principle 06 p0864 A72-18537

Large elastic deformation problems analysis by incremental finite element technique, using variational principles 07 p1087 A72-18782

Variational principle of Hamiltonian type for classical field theory, noting application to nonlinear heat transfer and fluid flow in Eulerian description 08 p1252 A72-21287

Biot variational principle for phase change problem with constant heat flux boundary condition and without melt removal, noting linear temperature profile choice 08 p1254 A72-21611

Elastic stability of nonlinearly elastic anisotropic body analyzed via variational principles in three dimensional theory 08 p1246 A72-21707

Thermal diffusion in solids subject to deformation, using classical elasticity theory body force analogy for variational and reciprocal theorems 09 p1403 A72-22757

Homogeneous isotropic elastic medium thermomechanical equations based on variational principles noting definite integrals solutions by means of delayed potentials 09 p1406 A72-23070

Automatic classification algorithms using heuristic, partitioning and variational techniques 09 p1283 A72-23429

Shock wave profile equation derivation based on minimal entropy rate variational principle for stationary irreversible processes, using local potential for Boltzmann type equation 09 p1295 A72-23473

Asymmetric Einstein equations with impulse-energy tensor in canonical form derived from variational principle, defining space-time continuum as pseudo-Riemann manifold 10 p1510 A72-24120

Structural design systematology of statics and dynamics numerical approximate procedures based on variational principles and differential equations [SMRT PAPER M 7/4] 10 p1505 A72-24397

Nonlinear elasticity theory variational principles modification for finite deformation of elastic body 10 p1557 A72-24420

Variational minimum principle for two elastic bodies frictionless contact, discussing Hertzian and non-Hertzian normal half space problems 11 p1690 A72-26667

Variational and statistical methods for adiabatic electron plasma with self consistent field interaction in terms of Lagrange, Hamilton and Liouville formalization 12 p1850 A72-27185

Asymptotic expansion method for nonsinusoidal wave processes described by Lagrange-type partial differential equations, using averaged form of generalized Hamiltonian variational principle 13 p2003 A72-28718

Nonlinearity effect on electron plasma wave dispersion relation, using numerical simulation and theoretical analysis by perturbation expansion and Hamilton variational principle 13 p2011 A72-29121

Variational principles for linearized dynamic and static problems of elastic incompressible bodies for highly elastic initial deformations 13 p2059 A72-29499

Harmonic elastic wave propagation in composites with periodic structures by variational methods developed from crystal lattice studies 13 p2060 A72-29696

Natural oscillation frequencies of cavity-contained liquid in weak gravitational field, using variational principles 13 p1943 A72-29791

Variational principle for boundary value problem of elastic-plastic torsion of circular bars under quasi-static finite deformation 16 p2464 A72-32914

Variational principles application to nonlinear heat transfer problems, using Euler-Lagrange equation 16 p2478 A72-33435

Nonlocal linear theory of gravitation without zero divergence assumption, deriving field equations by variational means 16 p2426 A72-33622

Variational principle by imposing time-independent spatial variation on hypothetical system governed by differential equation 16 p2416 A72-33664

Book - The method of weighted residuals and variational principles: With application in fluid mechanics, heat and mass transfer 17 p2573 A72-34250

Variational methods for dispersion relations and elastic properties of composite materials. [ASME PAPER 71-APMW-21] 17 p2623 A72-34302

Elastic-plastic medium with doubly periodic square array of circular cylindrical voids, obtaining finite ele-

ment solution for uniaxial deformation by variational principle
[ASME PAPER 72-APM-36] 17 p2628 A72-34784
Upper and lower bounds of effective thermal conductivity for statistically homogeneous composite materials, using variational principles 17 p2638 A72-35285
Variational principles in nonlinear viscoelasticity. 17 p2633 A72-35402
Flow problems solutions estimation by variational principles application, exemplifying by plane Couette and Poiseuille and axisymmetric pipe flow 18 p2679 A72-36391
Variational principle of linear differential equations. 18 p2705 A72-36717
German monograph - Finite elements according to a theory of the second order on the basis of an extended variational principle with an application to the stability and stress computation of simple symmetrical I-beams under consideration of the deformation of the cross-section 19 p2871 A72-37479
Variational principles of the nonlinear theory of elasticity - Case of superposition of a small deformation on a finite deformation. 19 p2872 A72-37559
Lagrangian approach to kinematic-dynamo equations for astrophysical bodies, obtaining variational principle for eigenvalue computation 20 p2966 A72-38911
Kramer and Couette flows using the Bhatnagar-Gross-Krook model. 20 p2913 A72-39418
On the choice of a reference state in the application of Hamilton's principle in elastodynamics. 20 p2979 A72-39420
Geometrical non-linear analysis of structures by finite elements. 21 p3120 A72-41204
Study on an incremental variational principle and its applications to finite element method and incremental thin shell theory. 21 p3121 A72-41240
Application of the variational principle to the solution of problems of crack theory in viscoelastic media 21 p3126 A72-41539
Asymptotic expansion method for nonsinusoidal wave processes described by Lagrange-type partial differential equations, using averaged form of generalized Hamiltonian variational principle 22 p3204 A72-42095
Variational method for invariance problem solution for optimal finite state of nonlinear dynamic systems under external disturbances 22 p3162 A72-42240
Variational solution of a nonlinear boundary value problem for unsteady flow of gas. 22 p3199 A72-42854
A new variational principle for finite elastic displacements. 23 p3350 A72-44047
Necessary conditions for steady state in radiation-Matter interaction and the role of entropy. 24 p3461 A72-44806
Dual extremum variational principles relevant to nonlinear heat transfer, applying to temperature distribution on thin walled spherical spacecraft surface 24 p3465 A72-45474
VARIATIONS
NT ANNUAL VARIATIONS
NT DIURNAL VARIATIONS
NT GEOMAGNETIC MICROPULSATIONS
NT GEOMAGNETIC PULSATIONS
NT MAGNETIC VARIATIONS
NT NOCTURNAL VARIATIONS
NT PERIODIC VARIATIONS
NT TWENTY-SEVEN DAY VARIATION
NT WIND VARIATIONS
VARIOMETERS
Geomagnetic field measurement, discussing variometers and magnetographs theory 06 p0812 A72-17370
Magnetovariometers design, operation and applications, discussing ferromagnetic materials properties effect on performance characteristics 12 p1792 A72-27739
Variometer system for sailplanes sinking or climbing rates direct readout, describing pressure difference measuring concept based on reservoir-capillary system 21 p3051 A72-40225
Variometer system for sailplanes sinking or climbing rates direct readout, describing pressure difference measuring concept based on reservoir-capillary system 23 p3292 A72-44451
VARISTORS
Metal-oxide varistor - A new way to suppress transients. 23 p3272 A72-44100
VASCULAR SYSTEM
NT AORTA
NT ARTERIES
NT BLOOD VESSELS
NT CAPILLARIES (ANATOMY)

NT GLOMERULUS
NT VEINS

Coronary blood flow measurement in various hemodynamic conditions by argon technique, determining oxygen consumption and coronary vascular resistance 03 p0315 A72-13183
Cerebral vascular disorder biochemical analysis, noting retinal vascular change relation to coronary arteriosclerosis and anoxia and flight stress effect on serum lipid and cholesterol 07 p0923 A72-20448
Splanchnic vascular bed role in human blood pressure regulation from lower body negative pressure tests, measuring blood flow from hepatic dye removal rates 08 p1123 A72-20889
Two stage description of middle germ layer chronic polyarthritis, noting heart muscle and vascular wall tissues necrosis 12 p1772 A72-27822
Respiratory and vasculomotor autonomic centers functional state relation to vestibular system from labyrinth electrical stimulation and shaking experiments 14 p2075 A72-30387
Vasopressin /antidiuretic hormone/ role in central vascular volume and fluid balance maintenance during continuous positive pressure breathing in dogs 17 p2505 A72-35917
Venous responses to stimulation of carotid chemoreceptors by hypoxia and hypercapnia. 18 p2648 A72-36025
Role of the autonomic nervous system in the hypoxic response of the pulmonary vascular bed. 18 p2650 A72-36572
Intravascular injection and histology studies of human embryonic and fetal choroidal vasculature development 19 p2755 A72-37398
Optimal vascular pressure measurements with transducers located outside body with rigid and elastic tube couplings 19 p2760 A72-37757
Vascular headache of acute mountain sickness. 22 p3150 A72-42491
Carotid rete role in brain protection against extreme elevations of systemic blood pressure, presenting goat cerebral blood flow measurement procedure 22 p3144 A72-42671
VASOCONSTRICTION
Antinatriuretic effect of acute thoracic and abdominal inferior vena cava constriction on arterial pressure, renal hemodynamics and electrolyte excretion 02 p0157 A72-11660
Cardiac output and autonomic nervous system role in antinatriuretic response to acute thoracic superior vena cava constriction 02 p0157 A72-11661
Spinal mesenteric vascular reflexes of vasoconstriction effect of pressure drop in coeliac artery relation to Rein nutritional hepatic reflex 04 p0473 A72-15125
Splanchnic vasoconstriction in hyperthermic man independent of falling blood pressure 04 p0480 A72-15217
Carbon monoxide induced hypoxia inhibition of reflex vasoconstriction in man in presence of normal arterial oxygen tension 07 p0929 A72-19438
Stretch activation of myogenic oscillation of isolated contractile structures of heart muscle in ATP salt solution 07 p0923 A72-20427
Sympathetic responses in human skin nerves with accompanying vasomotor reactions induced by emotional, thermal and respiratory stimuli 10 p1424 A72-24241
Acceleration stress effects on splanchnic blood flow due to organ displacement and neurogenic vasoconstriction in vascular beds 12 p1765 A72-28285
Vasomotor reflex locking level 17 p2504 A72-35025
Vasomotor reflexes and the principle of descending control 21 p2999 A72-40597
Unresponsiveness of pial precapillary vessels to catecholamines and sympathetic nerve stimulation 22 p3140 A72-41934
VASOCONSTRICTOR DRUGS
NT SEROTONIN
Autonomic blockade effects on reflex bradycardia due to phenylephrine induced arterial pressure in man during rest and supine exercise 07 p0925 A72-20688
VASODILATION
Distensibility and stress relaxation characteristics of capacitance and resistance vessels of isolated rabbit ear as function of vasa tone 04 p0473 A72-15124
Intravascular pressure and extravascular structure effects on radial and longitudinal distensibility of arterial microvessels in dog mesentery 07 p0922 A72-20426

VECTOR SPACES

Sudden pilot incapacitation and death due to subarachnoid hemorrhage secondary to ruptured intracranial aneurysm 10 p1429 A72-23742
Thermoregulation changes during simulated weightlessness of prolonged bed rest, noting lower sweating threshold and decreased vasodilation /autonomic dysfunction/ 12 p1767 A72-28301
Vasomotor reflex locking level 17 p2504 A72-35025
Studies of the influence of the theophylline on the vasodilating action of different medications on the cerebral and coronary circulation of man 18 p2651 A72-36799
VASOMOTOR NERVOUS SYSTEM
U NERVOUS SYSTEM
VECTOR ANALYSIS
NT COLLINEARITY
NT VORTICITY
Stochastic differential equations vector solution by two-time method, applying to random harmonic oscillators and wave propagation in random media [AD-733125] 01 p0093 A72-10510
Creep theory by rheonomic body interpretation as controlled system with unknown vectors at input and output, obtaining stress-strain curves for experimental verification 02 p0289 A72-11620
Optimum instantaneous impulsive orbital injection for specified asymptotic velocity vector, noting results of radius and asymptotic vector angular separations 03 p0437 A72-13837
Computer solution to vector variational formulation of electromagnetic Maxwell equations for dielectrically loaded rectangular waveguide 03 p0335 A72-14249
N-port resistive network synthesis involving use of vectors, cones, bilinear inequalities and matrices 05 p0639 A72-15801
Vector analysis of three dimensional nonequilibrium dissociative gas flow quantity variations along stream lines 05 p0652 A72-17001
Boundary value problems in micropolar theory of elasticity, obtaining displacement and rotation vectors from singular integral equations 09 p1402 A72-22745
Book on tensor analysis and continuum mechanics covering strain, permutation and stress tensors, vector and tensor comparison, application to elasticity and shell theory, etc 09 p1406 A72-23000
Matrix notation for replacing vector analysis in control theory by introduction of differential operators similar to Hamiltonian operator 09 p1352 A72-23369
Jet stream types derived from vector conditions for surface with maximum geostrophic wind velocity 10 p1507 A72-25002
Sufficient conditions for existence, uniqueness and finite-dimensional approximation of solution to first order infinite-dimensional vector differential equation 11 p1676 A72-25357
Gosiewski vorticity tensor formula generalization from moving unit vector associated with material point to vector field relative to moving continuum 16 p2423 A72-33112
Vortex concept and related vector analysis in fluid dynamics, crystal dislocations, superconductors and superfluid He 18 p2711 A72-36489
Vector wave solution of light beam propagating along lenslike medium. 20 p2903 A72-39266
VECTOR CALCULUS
U VECTOR SPACES
VECTOR CONTROL
U DIRECTIONAL CONTROL
VECTOR DOMINANCE MODEL
Pion exchange and the cosmic-ray nucleon cascade. 19 p2851 A72-37923
VECTOR SPACES
NT ADJOINTS
NT BANACH SPACE
NT CANONICAL FORMS
NT EIGENVALUES
NT EIGENVECTORS
NT HILBERT SPACE
NT JORDAN FORM
NT MATRICES [MATHEMATICS]
NT STATE VECTORS
NT STOKES THEOREM [VECTOR CALCULUS]
NT VECTORS [MATHEMATICS]
NT VORTICITY
Stability relative to part of variables of n-dimensional vector equation, considering applications to solid bodies with fluid filled cavities and gyrostat satellite optimal stabilization 02 p0251 A72-11494
Chebyshev polynomials best approximation with respect to linear space spanned by odd degree polynomials, obtaining extreme point sets 04 p0539 A72-14729

Minimax optimal control problems with incomplete information, using dynamic programming and phase space location measurements

07 p0963 A72-19970

Significance criteria for comparing strength parameter against expectation from random group of vectors in variance matrix applications

09 p1341 A72-23023

Measured and mean convergences in topological vector spaces, considering Banach space

12 p1836 A72-27176

Ubiquitous convex groups of real vectorial space of infinite dimension, obtaining characterization via decomposition family concept

13 p1987 A72-29777

Bounded operators solution in locally convex topological vectorial spaces with meromorphic properties

13 p1987 A72-29778

Dense convexes class characterization in real seminormalized space on basis of decomposition family concept

13 p1987 A72-29779

Vectorial differential equations in potential theory, discussing Fredholm alternative in normalized spaces, generalized harmonic vector fields, Poisson equation and Robins-Praeger problem

15 p2261 A72-31452

Electromagnetic wave propagation and wave-vector diagram in space-time periodic media

17 p2514 A72-34381

Maximal contraction points of autonomous nonlinear system phase trajectories, using van der Pol differential equations

18 p2674 A72-37149

Existence theorems for dynamical systems admissible controls for avoidance of given set of state spaces, considering control process governed by ordinary differential equations

[ASME PAPER 72-AUT-C] 19 p2778 A72-37723

Minimax technique in optimal control problems with incomplete information on phase vector, using dynamic programming and system position measurement refinements

20 p2911 A72-40027

Six dimensional vector space of stresses in elastic piecewise linear material divided into separate regions having different linear stress-strain relation

21 p3122 A72-41345

Differential equation solution existence in complete locally convex topological Hausdorff vector space defined by saturated seminorms

21 p3076 A72-41783

Computer-aided vector Taylor series approximation of fundamental matrix of ordinary first order differential equations with variable coefficients

21 p3076 A72-41785

A priori estimates and Harnack's inequality for general solutions of second-order degenerate quasi-linear parabolic equations

22 p3198 A72-42159

Mathematical formulation of linear programming problem, reducing vector value optimal management plan determination to quadratic programming problem

22 p3198 A72-42179

The branch and boundary method as a regular method of solving irregular problems of mathematical programming. I

22 p3198 A72-42188

Linear vector formulation of pursuit problems with pursuer discrimination, using Mishchenko-Pontryagin curvature conditions

23 p3307 A72-43220

Representation of solenoidal vector fields in bounded domains by poloidal and toroidal scalar potentials, discussing applications in fluid mechanics, elastic vibrations and electromagnetic theory

23 p3313 A72-43716

VECTORCARDIOGRAPHY

Clinical electrocardiography diagnostic capability, discussing phase plane cardiogram sensitivity to aberrations in QRS contours

01 p0017 A72-10148

QRS amplitude relation to frontal QRS axis and heart-electrode distance, using 12-lead ECG

03 p0320 A72-13881

Electrophysiological responses to maximum exercise in healthy humans from polarcardiographic display of heart vector changes

07 p0916 A72-18891

Coronary artery disease and vessel involvement severity predictions from electrocardiographic and vectorcardiographic patterns of anterior wall myocardial infarction

07 p0931 A72-19994

ECG and VCG in diagnosis of myocardial infarction and QRS changes

07 p0920 A72-20174

Diurnal and beat-to-beat variation factors in vectorcardiograms, noting respiratory movements, electrode location shift, skin-electrode impedance and heart electrical center mobility

08 p1127 A72-21849

Vectorcardiographic and ECG diagnosis of left anterior hemiblock combined with complete right bundle branch block, discussing coexisting myocardial infarction influence

08 p1127 A72-21850

Gabor-Nelson myocardium electrical activity model for mathematical construction of vectorcardiograph from ECG for comparison of various lead systems

11 p1588 A72-26629

Stress vectorcardiography quantitative analysis of ECG response to treadmill exercise test to establish diagnosis criteria for coronary heart disease

12 p1775 A72-28282

Computerized measurement and analysis of day-to-day variations of corrected orthogonal ECG and vectorcardiogram in normal subjects, using results as assessment standards

14 p2077 A72-30967

Vectorcardiographic and electrocardiographic differentiation between cor pulmonale and anterior wall myocardial infarction.

21 p3001 A72-40769

The Macruz index and its clinical evaluation in electrocardiography with regard to the selection and control of air crews

21 p3009 A72-41193

Comparison of the vectors of the ventricular depolarization and repolarization of man during immersion in a standing position

24 p3372 A72-44924

VECTORS [MATHEMATICS]

NT EIGENVECTORS

NT STATE VECTORS

NT VORTICITY

Programmed minimax target acquisition in rendezvous game between conflictingly controlled motion and given set of vectors

07 p1028 A72-19969

Moving and inertial trihedron orientation determination from absolute angular velocity vector, solving Poisson equations system

08 p1205 A72-21802

Scalar and vector partitions of forecasts probability score in two state situation

11 p1681 A72-26078

Singular integral representations of displacement and rotation vectors for homogeneous isotropic centrosymmetric body, using Nowacki couple stress theory of thermoelasticity

16 p2465 A72-32984

Programmed minimax target acquisition in rendezvous game between conflict controlled motion and given set of vectors

20 p2947 A72-40026

Accuracy of alpha-analog simulation of linear algebraic equations in the case of a nonzero discrepancy vector

21 p3074 A72-40170

VEGARD-KAPLAN BANDS

Deactivation of A-state nitrogen molecules in auroras, reinterpreting rocket observations of nitrogen Vegard-Kaplan system in terms of atmospheric model based on mass spectrometer measurements

[AD-737434] 05 p0655 A72-16072

VEGETATION

Agriculture and natural vegetation remote sensing programs, discussing dichotomous keys for side-looking airborne radar imagery analysis

01 p0056 A72-10457

Phyto-ecological approach to remote sensing of man made ecosystems, comparing vegetation and landscapes in Old and New Worlds

02 p0210 A72-11797

Forest vegetation distributional and statistical parameters ecological analysis by multiband remote sensing in areas devoid of ground control

02 p0212 A72-11815

Spectral reflectance of various soils and vegetation, measuring solar energy reflection as function of sun elevation in UV, visible and near IR regions

06 p0810 A72-18446

Multiband aerial photography application to vegetal cover determination, evaluating film types, seasons and scales

09 p1302 A72-23287

Spectral brightness coefficient and photodensity measurements for remote vegetation productivity sensing in visible band

15 p2222 A72-31396

Intensity of turbulence within canopies with simple and complex roughness elements.

20 p2948 A72-39798

VEGETATION GROWTH

NT CROP GROWTH

VEHICLE WHEELS

NT NOSE WHEELS

Aircraft landing gear wheel damage and antiskid mechanisms under operational conditions

08 p1109 A72-21485

Drift angle effect on rolling wheel pneumatic tire lateral and angular deformation amplitudes, deriving formula for reaction forces

09 p1351 A72-23176

Test stand for rolling wheel with pneumatic tire at variable drift angles, deriving kinematic parameters and elasticity coefficients from static and dynamic tests

09 p1351 A72-23177

Aircraft wheel mechanics, discussing freely turning and braked wheels, tire drift and antiskid braking systems for landing gear

11 p1574 A72-25287

Runway motion stability of aircraft with three wheel landing gear, assuming elastic response to moment induced drift

12 p1753 A72-27235

Mathematical two mass model for horizontal, angular and vertical vibrations of pneumatic wheel with allowance for inelastic tire resistance

13 p2003 A72-28918

Rolling radius of driven cylindrical wheel with solid rubber tire as function of normal load and tire dimensions

13 p2003 A72-28919

Rolling tire frequency response for angular oscillations about vertical axis through axle in wheel plane, using point contact theory

16 p2426 A72-33696

VEHICLES

Minimal energy stochastic controller design for electrically driven vehicles, using dynamic programming

06 p0795 A72-17304

VEINS

Antinatriuretic effect of acute thoracic and abdominal inferior vena cava constriction on arterial pressure, renal hemodynamics and electrolyte excretion

02 p0157 A72-11660

Blood viscosity and distributed external constraints and viscoelastic properties of vessels effects on wave dispersion and dissipation in arteries and veins, using membrane model

04 p0481 A72-15466

Dog mesentery terminal venous microvessel distensibility characteristics from response to arterial and venous pressure changes

06 p0765 A72-18196

Combined photoelectric-photographic and plethysmographic technique for continuous measurement of rabbit ear vein diameter and tissue volume changes

09 p1273 A72-23444

Rat vena porta muscle cells spontaneous activity intensified by direct current depolarization and inhibited by hyperpolarization, noting effects of calcium and sodium ions

13 p1902 A72-28649

Prolonged bed rest induced muscular activity restriction effect on arterial and venous tone in different body areas

14 p2074 A72-30385

Dependence of muscle efficiency on oxygen concentration in the venous blood

22 p3141 A72-42157

Cardiovascular system venous part responsiveness to central nervous and humoral influences

22 p3148 A72-43167

VELOCITY

NT ACOUSTIC VELOCITY

NT AIRSPEED

NT ANGULAR VELOCITY

NT CRITICAL VELOCITY

NT ESCAPE VELOCITY

NT EXHAUST VELOCITY

NT FLOW VELOCITY

NT GROUP VELOCITY

NT HIGH SPEED

NT HYPERSONIC SPEED

NT LIGHT SPEED

NT ORBITAL VELOCITY

NT PHASE VELOCITY

NT PROPAGATION VELOCITY

NT RADIAL VELOCITY

NT RELATIVISTIC VELOCITY

NT ROTOR SPEED

NT SOLAR VELOCITY

NT SUBSONIC SPEED

NT SUPERSONIC SPEEDS

NT TERMINAL VELOCITY

NT TIP SPEED

NT TRANSONIC SPEED

NT WIND VELOCITY

Velocity (viscous) slip coefficient and diffusion slip velocity in multicomponent gas mixtures by linearized Boltzmann equation

04 p0513 A72-15334

VELOCITY DISTRIBUTION

Concentration distribution in turbulent flow as function of velocity field, deriving differential equations from characteristic functionals to describe diffusion process

01 p0049 A72-10190

Fluid immersed body velocity fluctuations due to irregular molecular impacts

01 p0001 A72-10234

Quiet time solar wind temperature profile calculation from energy equation using observed velocity profile data at earth orbit
[AD-742176] 01 p0120 A72-10881

Axial and tangential velocity distributions within trailing line vortex to large distance downstreams of generating wing extended from available data
[AD-743599] 01 p0001 A72-11135

Subsonic linearized theory for symmetrical cranked wings at zero incidence, presenting corrected formulas for streamwise and spanwise perturbation velocity components due to wing thickness
01 p0001 A72-11154

Velocity field of sonic flow about aircraft wing profile, solving mixed Cauchy problem
01 p0001 A72-11178

Nonhomogeneous fluid geostrophic flow, establishing relationship between velocity and density fields
01 p0051 A72-11230

Kinetic energy velocity and acceleration formulas of penny shaped crack propagation in brittle body under triaxial tensile stress
01 p0144 A72-11391

Velocity profiles of turbulent boundary layers with injection or suction through porous walls as function of momentum thickness by Truelsenbrodt method
02 p0202 A72-11663

Lower bound deformation theorem for rigid plastic continua under impulsive loads, emphasizing kinematically admissible velocity field
02 p0259 A72-12237

Wake blockage paradox in two dimensional perforated wall wind tunnel, investigating interference velocity distribution
02 p0151 A72-12271

MHD flow development in parallel plate channel entrance region, obtaining numerical solution for velocity distribution, pressure drop and length at different Hartmann numbers
02 p0266 A72-12493

Stress and velocity distributions in homogeneous viscoelastic rigid body, deriving uniqueness theorems and minimum principles for limits problem
02 p0297 A72-12596

MHD flow due to impulsive rotation of infinite disk, observing magnetic field strength effects on velocity components and boundary layer displacement thickness
02 p0267 A72-12772

Velocity and temperature distributions for unsteady plane Poiseuille flow of viscous incompressible fluid between two parallel plates
03 p0340 A72-13000

Laminar two dimensional hypersonic flow over stepwise accelerated flat plate at zero angle of attack, obtaining time dependent velocity and temperature profiles by linearized flow equations
03 p0442 A72-13236

Magellanic Clouds neutral hydrogen distribution, concentrations and velocity structure, noting H II correlation with supergiant stars
03 p0425 A72-13256

Magnetic and velocity fields and brightness in solar atmosphere, using double magnetograph
03 p0429 A72-13309

Supergranule velocity and magnetic fields concentrations in solar atmosphere
03 p0429 A72-13311

Solar hydrodynamic dynamo theories concerning convective zone large scale velocity fields and magnetic activity cycle
03 p0433 A72-13360

Unsteady flow theory for radial gas lubricated bearing, deriving velocity and pressure distribution expressions
03 p0363 A72-13577

Current lines and temperature fields in square cavity with one movable wall and viscous flow and heat transfer, solving equations numerically
03 p0456 A72-13629

Plate under projectile impact, calculating motion response due to random initial velocity distribution over surface by stochastic model
03 p0447 A72-13852

Closure problem in statistical theory of isotropic turbulent velocity field
03 p0342 A72-13900

Generalized equation for incompressible unsteady laminar boundary layer in external flow with arbitrary time dependent velocity distribution, discussing expanding cylindrical body
03 p0343 A72-14315

Turbulent mixing length formulation and velocity profiles for non-Newtonian power law fluids, determining friction factor for pipe flow at high Reynolds numbers
03 p0343 A72-14318

Turbulent shear flow mean velocity profiles, calculating eddy diffusivity for momentum and Reynolds stress
03 p0343 A72-14323

Linearized continuous baroclinic atmospheric model, discussing stability for planetary vorticity gradient
04 p0541 A72-14452

Small amplitude velocity waves turbulent distribution in infinite medium, demonstrating kinematic dynamo regeneration
04 p0573 A72-14906

Electron heating by oscillating electric field in presence of steady magnetic field, solving Boltzmann transport equation for electron velocity distribution in plasma
04 p0556 A72-14947

Intensity-height profiles for molecular oxygen first and second negative bands in F region, using equilibrium velocity distribution of photoelectrons
04 p0518 A72-14963

Carrier mobility field dependence effects on validity of gradual channel approximation in insulated-gate field effect transistors, discussing velocity field relationship
04 p0498 A72-15135

Rectangular and triangular duct entrance region laminar flow pressure losses from velocity profiles and integral energy equation
04 p0512 A72-15194

Universe cluster expansion model, showing velocity dispersion increases from center to turnover radius
04 p0578 A72-15308

Flutelike microinstabilities in mirror-confined homogeneous magnetized one-species plasma with broad perpendicular velocity distribution
04 p0559 A72-15354

Viscoelastic fluid flow past infinite plane porous wall with time dependent suction, investigating mean velocity profile and wall shear stress
04 p0514 A72-15704

Initial boundary layer effect on turbulent free shear layer velocity profiles, deriving procedure applicable at any streamwise station
05 p0645 A72-15795

Thermal laminar boundary layer equations solution for power-law velocity distribution in external flow and arbitrary surface temperature distribution
05 p0742 A72-15844

Integral methods application to turbulent corner flow problem, obtaining mean velocity profile first approximation for turbulent boundary layer with streamwise pressure gradient
05 p0646 A72-15921

[ASME PAPER 71-WA/FE-36] Velocity profiles of turbulent three-dimensional incompressible air jet flow from rectangular orifice tangent to and along curved wall surface
05 p0647 A72-15938

Confined laminar jet mixing of two uniform streams flowing in parallel plate channel, obtaining velocity field from linearized governing equation
05 p0647 A72-15973

Turbulent flow and heat transfer characteristics of non-Newtonian fluids on flat plate, measuring velocity and temperature distributions
05 p0648 A72-16003

Velocity field time history of interacting shear waves in infinite homogeneous chemically reacting fluid for turbulent combustion studies
05 p0747 A72-16367

Fracture theory application to rotating cylinder velocity field determination, equilibrium and flow behavior
05 p0738 A72-16424

Geometric displacements and space-time derivatives determining velocity and strain fields in solids under deformation
05 p0738 A72-16529

Turbulent wake calculations with eddy viscosity model, predicting velocity profiles and displacement thicknesses
05 p0603 A72-16538

Velocity profile shapes computation in supersonic compressible turbulent boundary layers with adverse pressure gradients, discussing data and theory discrepancy, curvature, and three dimensional effects
05 p0649 A72-16544

Centrifugal compressor diagonal type impeller profiling through ruled surfaces delineated by rectilinear generatrices, calculating velocity field of rotating cascade
05 p0603 A72-16626

Turbulent boundary layer on yawed flat plate, measuring velocity profiles and flow directions
05 p0603 A72-16703

[DFVLR-SONDDR-177] Internal axisymmetrical steady inviscid rotational flow velocity profiles simulation by means of shaped wire gauze screens
05 p0650 A72-16830

[AIAA PAPER 72-165] Difference equations and relaxation method for three dimensional transonic flow field about wings in terms of velocity potential
05 p0605 A72-16843

[AIAA PAPER 72-189] Turbulent jets interaction with cross flow, presenting longitudinal and transverse velocity, temperature and turbulence distributions
05 p0651 A72-16870

[AIAA PAPER 72-149] Mean velocity and turbulent fluctuation distributions for sub- and supersonic jets in convergent nozzles, obtaining sound power spectra
05 p0651 A72-16872

[AIAA PAPER 72-157] Helicopter rotor boundary layer, comparing analytical shear stress and velocity distributions obtained by momentum integral techniques with hot wire probe experimental data
05 p0607 A72-16900

[AIAA PAPER 72-38] Turbulent shear stress, intensity and velocity field in coflowing axisymmetric jets, using eddy viscosity model
05 p0652 A72-16926

[AIAA PAPER 72-47] Wind tunnel measurements for near flow field velocity distribution in rectangular wing wake turbulence, comparing with flight measurements
05 p0609 A72-16948

[AIAA PAPER 72-41] Whistler instability of electron plasmas with non-Maxwellian velocity distribution function
05 p0698 A72-17015

Velocity distribution in mixing layer between fluid at rest and in uniform stream by solving Blasius equation with boundary points
05 p0653 A72-17078

Laminar flow airfoils for gliders, optimizing profiles for favorable velocity and pressure distribution
05 p0610 A72-17194

Solar wind speed variations, examining velocity structure recurrence at various rotations, time interval of steady state flow and temporal evolution effects
06 p0872 A72-17442

Solar wind stream-stream interactions, studying time profiles, velocity variations, corotating spiral, increased pressure due to radial compression and zonal flow directions
06 p0872 A72-17443

Solar wind structure from long lived inhomogeneities in corona, allowing for velocity, density and temperature perturbations
06 p0872 A72-17444

Wave exciting grid-plasma interaction in single ended Q device, determining ion velocity distribution function
06 p0855 A72-17510

Perturbed density and ion velocity distribution functions of grid-excited ion acoustic waves in collisionless plasma in single ended Q device
06 p0855 A72-17511

Plasma microinstabilities due to ion acoustic waves propagation with double-humped ion velocity distribution function in Q machine
06 p0855 A72-17516

Electrostatic energy analyzer for local ion velocity distribution function measurement in double ended Q machine plasma column
06 p0814 A72-17551

Cyclotron resonance interaction between electromagnetic waves and nonthermal plasmas for Cauchy velocity distributions yielding algebraic dispersion equations
06 p0860 A72-17745

Exact linear dielectric operator for stratified plasma streams with velocity gradients for diagnostics with electromagnetic waves
06 p0861 A72-17748

Velocity field induced by blade row in axial flow turbine
06 p0755 A72-17844

Axial turbine three dimensional flow across blading compatible with velocity distribution, establishing mean surfaces of revolution equation
06 p0755 A72-17849

Cumulus clouds vertical motion velocity spectra curves, turbulence dissipation rates and energy determination from aircraft measurements
06 p0842 A72-17941

Stellar velocity distribution functions in nonrotating clusters, considering encounter multiplicity effects and dissipation increase from masses dispersion
06 p0883 A72-18024

Solar wind model of electrons, protons and alpha particles velocity and temperature differences dependence on distance from sun
06 p0873 A72-18025

Velocity and temperature pulsations as function of stratification parameter in atmospheric boundary layer
06 p0842 A72-18044

Turbulent velocity field calculation for rectilinear duct with noncircular cross section, using integral transformation and dimensionless velocity ratio
06 p0800 A72-18110

Three dimensional velocity field excitation by thin airfoil vibrations in supersonic flow, deriving function in semispice to satisfy boundary constrained wave equation
06 p0756 A72-18111

Steady subsonic potential gas flow in multiply connected regions, determining velocity field via boundary value problem solution for quasi-linear elliptic equations set
06 p0801 A72-18123

Viscous flow through movable and immovable cascades of blades, determining velocity field by airfoil center line vortex distribution
06 p0757 A72-18131

Boltzmann equation solution analysis for Maxwell-Lorentz gas in electric field, discussing conditions for electron velocity distribution isotropic part evolution towards Maxwellian distribution
06 p0861 A72-18162

Cascade wind tunnel and water table determination for trajectories and velocities of suspended particles in fluid flow through axial compressor stage

07 p0907 A72-18756

Numerical analysis of computing velocity distribution in vortex row cascade profiles by method of singularities

07 p0965 A72-18787

Thermal and momentum diffusivity measurements in turbulent stratified flow, obtaining velocity and temperature profiles

[AIAA PAPER 72-80]

07 p0966 A72-18950

Magnetized solar wind velocities and fields obtained by three dimensional model using perturbation technique with spherically symmetric boundary conditions

07 p1057 A72-19142

Bilaterally symmetric vortex rings dynamic behavior, computing pointwise induced velocity via Biot-Savart law for hydrodynamic and Rankine vortex models

[AD-739139]

07 p0967 A72-19501

Two dimensional compressible boundary layer turbulent velocity profile on adiabatic and isothermally cooled walls with zero pressure gradient

07 p0970 A72-20080

Computerized simulation of two dimensional turbulent flow in Fourier space with random initial conditions on coefficients, discussing velocity, pressure and vorticity fields

07 p0971 A72-20084

Turbulence velocity field analysis by repeated cascade theory via partial Fourier transform, predicting Kolmogoroff law in line with experimental results

07 p0972 A72-20112

Incompressible fluid near equilibrium turbulent flow velocity distribution through plane diffuser, taking into account upstream conditions

07 p0972 A72-20115

Atmospheric free convection turbulence and diffusion, proposing statistical characteristics and formulas with horizontal thermal flux vertical and transverse velocity components

07 p1031 A72-20697

Velocity space instability in hot electron plasma created by adiabatic compression in pulsed magnetic mirror, observing radiation bursts below electron cyclotron frequency during compression

[AD-740408]

08 p1213 A72-21257

Parameter calculation for laminar incompressible fluid jet expanding in gradient slipstream along moving surface, determining velocity distribution in jet axis

08 p1149 A72-21309

Surface friction coefficient dependence on Mach number and velocity gradients in adiabatic compressible laminar gas flow

08 p1107 A72-21311

Conjugate solution for Poisson equation of heat transfer in laminar flow with developed velocity profile in flat channel with internal constant heat sources

08 p1252 A72-21314

Local deviation limits of universe from homogeneous isotropic model, considering velocity field perturbations and galaxy counts

08 p1234 A72-21381

Modified mixing length velocity distribution predictions for turbulent boundary layers with uniform mass transfer for low and high Reynolds numbers

08 p1150 A72-21622

Turbulent friction coefficients and velocity distribution in channel and pipe flow, using eddy viscosity model

08 p1150 A72-21623

Laminar MHD boundary layer lateral velocity component profile for conducting fluid injection at oblique incidence, considering drag force and pressure gradient effects

08 p1214 A72-21647

Critical Reynolds numbers estimation for flows having velocity profile with point of inflection, discussing plane parallel flows stability energetic analysis

08 p1151 A72-21660

Unsteady uniform turbulent flow of incompressible liquid in circular pipe, verifying mathematical model with velocity distribution calculations

08 p1151 A72-21666

Laser plasma density and velocity distributions and mass flow from surface and plasma pressure in target heating process based on interferometric measurements

08 p1215 A72-21719

Numerical forecasting model with precipitation as function of vertical velocity and humidity distribution, noting orographic influence and atmosphere static stability

08 p1200 A72-21796

Impact interaction between free two body system with elastic spring coupling and fixed plane, considering mass ratio and velocity restitution coefficient

08 p1209 A72-21803

Electrochemical techniques for time averaged turbulent velocity gradient and components of fluctuating velocity gradient at solid surface

09 p1306 A72-22305

Initially stationary axisymmetric disk of stars evolution calculated by gravitational potential solver for various values of velocity dispersion

09 p1383 A72-22460

Spatial plastic flow in arbitrary incompressible continuous medium with instantaneously inextensible family of planes, deriving velocity field formulas

09 p1403 A72-22758

Molecular beam velocity distribution measurement from integral quantity, obtaining precise results in noisy environment and probability density function by numerical deconvolution

09 p1356 A72-22793

Radial velocity distribution at supersonic compressor inlet from duct-cowl and wall pressure measurements

[ONERA, TP NO. 975]

09 p1260 A72-22812

Earth bow shock laminar profile at low Mach number by crossing satellites on 12 February 1969, determining mean velocity along normal

09 p1387 A72-23004

Wave propagation effects on irregularities observation in equatorial electrojet, presenting velocity profile and typical ray path

09 p1300 A72-23024

Markov processes in stellar dynamics, discussing relaxation and evaporation times and star velocity distribution for galactic cluster models

09 p1390 A72-23504

Flat plate Langmuir probe measurement of electron temperature in plasma with elliptically anisotropic velocity distribution, discussing probe orientation effects

09 p1366 A72-23578

Wind velocity distribution structural laws in vertical and horizontal planes for large mesospheric and atmospheric processes

09 p1347 A72-23591

Conical diffuser response to velocity distribution and turbulence intensity at inlet

10 p1416 A72-23858

Adiabatic velocity profiles and pressure variations of developing laminar flow in circular tube, using finite difference computation in FORTRAN IV

10 p1463 A72-23863

Secondary flows effect on turbulent longitudinal velocity distribution in square ducts, using Navier-Stokes and continuity equations

10 p1463 A72-23864

Turbulent shear stress calculation from mean velocity data for complex flows with inappropriate boundary layer approximations, using method of characteristics

10 p1463 A72-23866

Spanwise velocity distribution effect on drag measurement of short struts in two dimensional turbulent airstreams

10 p1417 A72-23881

Velocity dispersions and discrepant red shifts in groups of galaxies, using virial theorem for galaxy mass calculations

10 p1534 A72-23903

Kinematic and thermal turbulent fluctuations isolation by means of hot-wire anemometric probe

10 p1479 A72-24055

Asymmetry and intermittency factors of temperature and velocity fluctuations in viscous substrate of hot plate turbulent boundary layer

10 p1464 A72-24064

Schwarzschild solution to Vlasov equation for velocity distribution function of self gravitating stellar system

10 p1535 A72-24112

Argon plasma jet mean flow velocity radial distribution measurement method

10 p1520 A72-24205

Nonlinear analysis of gravitational stability perturbation based on Maxwellian velocity distribution

10 p1538 A72-24214

Linear initial value problem of partially mixed cylindrical wake in uniformly stratified fluid, obtaining exact solutions for density and velocity distributions

10 p1466 A72-24299

Unsteady laminar boundary layer on semiinfinite flat plate induced by small free stream velocity fluctuations, showing far downstream double layer structure via asymptotic and numerical solutions

10 p1467 A72-24334

Small turbulences growth in two dimensional incompressible wake, noting transverse oscillations of mean velocity profile

10 p1467 A72-24367

Arterial velocity profiles measurement in dogs thoracic aorta by hot-film probe, relating flow disturbances and turbulence to Reynolds number

10 p1431 A72-24468

Turbulent diffusion of scalar contaminant passively advected by homogeneous stationary flow, expanding velocity and scalar fields in stochastic Wiener-Hermite functionals

10 p1469 A72-24606

Velocity slip effect on squeeze film between porous rectangular plates, calculating pressure, load carrying capacity, film thickness and response time

10 p1488 A72-24820

Radial velocities of galaxies derived from spectrograms, describing reduction procedure

10 p1548 A72-24965

Interior and exterior hydrodynamics of spherical droplet submerged in unbounded arbitrary velocity field, including effects of surface active agents

10 p1470 A72-25042

Laminar boundary layer velocity profiles in convergent nozzle incompressible swirling flow, considering boundary layer growth effects on free stream axial and tangential velocities

10 p1471 A72-25068

Equations of motion of steady viscous fluid flow in three dimensional boundary layer on walls of axial flow compressors and turbines, obtaining velocity field

10 p1420 A72-25120

Helical turbulent flow through concentric annulus with rotating inner cylinder, examining axial and tangential velocity distribution and shear stresses

10 p1471 A72-25190

Two dimensional transverse subsonic hot-air jet interaction with freestream flow at various jet/freestream velocity ratios, measuring jet velocity and temperature distributions

[AIAA PAPER 72-292]

11 p1567 A72-25230

Ionized plasma electron velocity distribution function relaxation numerical calculation to validate local Maxwellian form during transport process

11 p1693 A72-25523

Turbocompressor deceleration cascades blades surface roughness effects on boundary layer, noting pressure and velocity distributions

[ASME PAPER 72-GT-48]

11 p1570 A72-25640

Radial turbine flow analysis, comparing calculated shroud static pressure distribution and outlet velocity profile with measured data

[ASME PAPER 72-GT-50]

11 p1570 A72-25642

Axial flow turbines aerodynamic loading increase via control of velocity distribution and boundary layer evolution around airfoil profiles

[ASME PAPER 72-GT-78]

11 p1571 A72-25658

Magnetic field generation in presence of turbulent velocity distribution, considering gyrotropy parameter equation and nonlinearity

11 p1686 A72-25716

Stellar velocity distribution functions in nonrotating clusters, considering encounter multiplicity effects and dissipation increase from masses dispersion

11 p1719 A72-25960

Solar wind model of electrons, protons and alpha particles velocity and temperature differences dependence on distance from sun

11 p1713 A72-25961

Cosmic spherical rotating bodies angular velocity zonal distribution determination, noting application to Jupiter and Saturn

11 p1723 A72-26481

Noncoincidence of maximum velocity and zero shear stress due to asymmetric turbulent velocity profiles, considering effect on momentum, heat and mass transfer in noncircular channels

11 p1618 A72-26534

Perturbation velocity corrections for eccentric model position and different air flow ducting in rectangular wind tunnels

[DFVLR-SONDDR-191]

11 p1573 A72-26581

Turbulent pipe flow laminarization by fluid injection, measuring axial turbulence intensity field and streamwise velocity distribution by hot-film anemometer

11 p1619 A72-26636

Neutral gas velocity distribution, transverse drift velocity, particle and energy densities in column under free fall conditions, considering wastage by ionization processes

11 p1698 A72-26645

Atmospheric vertical motions velocities prediction based on satellite cloud data

11 p1683 A72-26887

Wind velocities field in vortices leeward of islands derived from Navier-Stokes equation for isolated axisymmetric viscous vortex

12 p1839 A72-27032

Nonlinear interactions between synthesized plasma positive and negative ion beams, discussing effect on individual velocity distribution functions

12 p1849 A72-27058

Primary velocities distribution in two dimensional turbulent boundary layer inside dihedral

12 p1797 A72-27179

Numerical calculation of sonic flow around wing section with rounded leading edges, obtaining Mach number distribution, boundary characteristic shape and velocity field

12 p1751 A72-27181

Electron beam velocity distribution function fine structure for plasma-beam discharge in hydrogen within longitudinal magnetic field

12 p1850 A72-27261

Spatial and time dependence of electron velocity in short channel microwave FET, using Monte Carlo method

12 p1790 A72-27434

- Voltage variable TWT delay line design, discussing electron beam velocity dispersion causes
12 p1782 A72-27437
- Asymptotic behavior of velocity profiles in laminar boundary layers of steady incompressible fluid two dimensional flow past rigid wall
12 p1798 A72-27713
- Mean velocity distribution and Reynolds stresses in turbulent wake behind flat plate in uniform incompressible flow
12 p1798 A72-27718
- Boundary curves for collective relaxation in one dimensional collisionless two phase space density self gravitating stellar system evolution, noting velocity dispersions dependence
12 p1875 A72-27913
- Viscoplastic media flow rate in noncircular tube from Newtonian fluid velocity profile, using Green formula
12 p1799 A72-27981
- Mean linear velocity of rotation on solar equator to improve Hart rotatory velocity fluctuation values, giving expressions for statistical reestimation of mean square errors
13 p2035 A72-28441
- Strong field electromagnetic wave interactions with anisotropic plasmas, considering electron velocity distribution function
13 p2009 A72-28449
- Optical anemometers for mean and fluctuating velocities in premixed flame of town gas-air combustion system, noting velocity probability density distribution
13 p1955 A72-28546
- Hydrodynamic approximation for solar wind nonuniformity in ecliptic plane, noting linear disturbances caused by nonuniform velocity of plasma flow from corona
13 p2029 A72-28577
- Multilayer plasma model for MHD pulse propagation in ionospheric waveguide, noting approximation of Alfvén velocity distribution by plasma layers
13 p1946 A72-28585
- Nonuniform inlet velocity profile effect on laminar flow development between parallel plates, solving equations by finite difference method
13 p1941 A72-28706
- Additional deformation work for splines forming in splined circular profiles pressing, deriving characteristic displacement velocity distribution equations
13 p1963 A72-28744
- Small scale atmospheric turbulent motions sensing by FPS-16 Radar-Jimsphere meteorological balloon system, analyzing wind velocity data from dual radar measurements
13 p1990 A72-28818
- Wind shear third and fourth moments and distribution function in atmospheric boundary layer, emphasizing longitudinal turbulent velocity vertical variations
13 p1993 A72-28860
- Radar observation of meteor geocentric velocity dependence on radiant elongation angle
13 p2038 A72-29035
- Atmospheric turbulence anisotropy from meteor trails radar observations statistics, presenting plots of velocity field transverse structure
13 p2038 A72-29036
- Number density, particle, momentum and energy fluxes in model ion-exosphere with open magnetic field and asymmetric Maxwellian velocity distribution
13 p1948 A72-29115
- Velocity field at strain center during steel channel rolling, deriving relations for center contour calculation
13 p1964 A72-29149
- Velocity field measurements from M82/NGC 3034/galaxy H alpha, forbidden N II and S II emission lines, suggesting expanding ejecta cloud rotating about axis normal to galactic plane
13 p2040 A72-29401
- Incompressible boundary layer velocity profile on swept wings, comparing critical Reynolds number to straight wing value
13 p1894 A72-29639
- Soviet wind tunnel for power plant-environment interactions studies, discussing working sections velocity distributions calibration
13 p1939 A72-29644
- Lower solar chromosphere two dimensional models, noting effects of macroscopic velocity fields
13 p2045 A72-29709
- Goldberg and Unno method application to microturbulent velocity determination in stellar atmosphere with convection
13 p2047 A72-29732
- Solar photosphere velocity field photoelectric measurements, emphasizing long periods and low spatial wave numbers in deep layers
13 p2048 A72-29927
- Gas dynamics of steady rotating azimuthally dependent solar wind under magnetic field influence, calculating azimuthal distribution of radial velocity near earth orbit
13 p2034 A72-29960
- Large scale motion of turbulent boundary layer during relaminarization under strong pressure gradient, obtaining fluctuating velocity components and tangential Reynolds stress
13 p1944 A72-30028
- Slow viscous incompressible conducting fluid MHD flow between two nonparallel walls, obtaining velocity profile solution in power series for small Reynolds numbers
13 p2020 A72-30047
- Velocity distribution downstream of nonuniform single and multiple smoothing screens, presenting theory based on energy losses and flow direction changes
13 p1940 A72-30100
- Gravitational wave diffraction by liquid on surface of vertical circular cylindrical shells, determining velocity potentials
14 p2093 A72-30192
- Quasi-stationary spherical system structure model for stars of different masses with isotropic velocity distribution
14 p2149 A72-30212
- Atmospheric turbulent characteristics and velocity longitudinal component intensity profiles, applying to dynamic wind loads computation
14 p2127 A72-30264
- Differential turbulent shear flow equation reduction to deduce similarity criteria for velocity pulsations, using Karman transformation
14 p2094 A72-30292
- Hypervelocity impact parameters calculated from shock wave equations of motion, discussing viscosity effect on velocity and stress distributions
14 p2164 A72-30297
- Passive scalar dispersion in turbulent incompressible flow characterized by inhomogeneous and nonstationary statistics, expanding velocity and scalar concentration fields in Wiener-Hermite functions
14 p2128 A72-30348
- Initial dihedral wing-body interaction for supersonic leading edges, determining expansion of velocity potential on root chord
14 p2069 A72-30365
- Air injection as neutral atmospheric boundary layer thickening simulation, presenting mean velocity and turbulence intensity profiles
14 p2093 A72-30849
- French monograph on velocity profile in laminar boundary layer on semiinfinite flat plate in harmonic oscillation of uniform incompressible flow
14 p2095 A72-30949
- French monograph on flow near rotor blade tips, discussing three dimensional circulation and boundary layer effects, energy losses, velocity and pressure distributions, etc
14 p2069 A72-30950
- Asymptotic solution for velocity distribution in viscous liquid axisymmetric flow in conical diffusers
14 p2070 A72-31006
- Laminar mixing zone calculated for two homogeneous compressible gas flows with pressure gradient, noting coincidence of velocity distribution for identical gas dynamic parameters
14 p2070 A72-31009
- Acoustic wave diffraction at fixed plate boundary, determining velocity field by inverting Volterra-type integral equations
14 p2070 A72-31016
- Turbulent friction relation to averaged velocity profile of liquid flow in pipes and channels
14 p2096 A72-31019
- Velocity and temperature profiles of plane Poiseuille flow with finite amplitude convection and longitudinal vortices, investigating uniform axial temperature gradient effect
14 p2173 A72-31063
- Heat and mass transfer in steady viscous flow through curved circular tubes, investigating velocity and temperature profiles
14 p2173 A72-31064
- Thermal laminar boundary layer equations solution for power-law velocity distribution in external flow and arbitrary surface temperature distribution
15 p2334 A72-31263
- Massive stars velocity distribution function in clusters, determining escape rate and energy dissipation
15 p2305 A72-31339
- Iterative numerical solution of linear differential equations system for wind vertical velocity and local pressure variation along vertical line
15 p2265 A72-31344
- Unsteady laminar boundary layer on body of revolution with axial and torsional oscillations, calculating velocity distribution and shear stress variation
15 p2178 A72-31402
- Navier-Stokes equation for unsteady asymptotic suction flow over flat plate, plotting velocity distribution profiles
15 p2178 A72-31406
- Velocity distributions for slow steady rotational motion of non-Newtonian inelastic viscous fluid contained between two concentric spheres, using successive approximations
15 p2217 A72-31689
- Out-of-plane density distribution and in-plane velocity distribution measurements for low energy helium scattering inelastically from 550 K silver
15 p2276 A72-31861
- Eole satellite observed meteorological balloon data analysis, obtaining mean zonal velocity, meridional velocity and temperature vs latitude from statistical estimates
15 p2266 A72-31980
- Higher moments of Reynolds stress fluctuations and velocity components in turbulent boundary layer, obtaining probability density distributions
15 p2218 A72-32401
- Singularity method treatment of vortex distribution induced velocity perturbations on flat plate at angle of attack, noting results similarity to lifting surface theory
15 p2180 A72-32466
- Streaming MHD flow past semiinfinite flat plate in presence of perpendicular uniform magnetic field, obtaining velocity field at large distances
15 p2288 A72-32480
- Hypersonic transition boundary layers, obtaining disturbance convection velocities as function of fluctuation scale and wall distance
15 p2219 A72-32581
- Velocity and temperature distribution for viscous incompressible fluid unsteady flow between two parallel plates with pressure gradient linearly varying with time
15 p2219 A72-32599
- Nonequilibrium relativistic plasma fluctuations with direct movement of particles, considering isotropic velocity distribution of particles
15 p2289 A72-32695
- Alpha effect solar dynamo model magnetic field and velocity expansion in spherical harmonics, solving mean field induction equation
15 p2316 A72-32755
- High time resolution observations of photospheric velocity field, interpreting short period oscillations origin as result of combined image motion and Doppler velocity gradients
15 p2317 A72-32776
- Macroscopic velocity fields in solar prominence based on solar spectra and monochromatic photographs, proposing helical model
15 p2318 A72-32779
- Turbulent mixing layers analytical and experimental mean velocity profiles, discussing Goetler eddy viscosity theory
16 p2374 A72-32832
- Power law fluids impulsively started flow over plate, presenting analytical expressions for velocity distribution, shear stress and boundary layer thickness
16 p2375 A72-32833
- Hypersonic boundary layer profiles upstream of transition point on cone surface from pitot surveys, heat transfer and wall pressure measurements and spark schlieren photographs
16 p2341 A72-32837
- Shock wave propagation in gas with discrete velocity distribution, comparing solutions based on Euler, exact and Navier-Stokes equations respectively
16 p2375 A72-32861
- Velocity profiles for three dimensional turbulent boundary layer on end wall of axial flow compressor cascade passage under adverse pressure gradients
16 p2342 A72-32901
- Three dimensional ideal incompressible fluid flows under small velocity perturbation, using linearized Euler equations with respect to steady flow
16 p2375 A72-32932
- Hypersonic sound attenuation and velocity dispersion in sulfur fluoride near critical point determined by light scattering measurement
16 p2422 A72-32946
- Velocity distributions of molecular beams evaporating into vacuum from polycrystalline hexachlorobenzene and sulfur surfaces
16 p2429 A72-33058
- Spatial flow velocity fields of incompressible continuous media with family of instantaneously inextensible planes, applying plastic flow theory
16 p2423 A72-33107
- Flow equations for corner boundary layer with favorable pressure gradients, indicating separation type main velocity profile
16 p2378 A72-33406
- Heat transfer through laminar boundary layer with allowance for streamwise pressure gradient effect on velocity field, using Lighthill method
16 p2477 A72-33427
- Stellar velocity dispersion in elliptical galaxy NGC 7332 from coude spectrum obtained by SEC vidicon TV camera and telescope
16 p2454 A72-33453
- German monograph on pressure loss and heat transfer in heat exchangers, taking into account hydrodynamic and thermal inflow velocity and temperature distribution
16 p2478 A72-33504
- Cumulus clouds vertical motion velocity spectra curves, turbulence dissipation rates and energy determination from aircraft measurements
16 p2418 A72-33782

Vapor pressure and velocity distributions in rarefied gas flows through narrow slits under vacuum conditions with ice sublimation

16 p2380 A72-33854

Shear stress and dimensionless velocity profiles of plane incompressible fluid wall jet propagation along curved surface

16 p2380 A72-33856

Supersonic vortex boundary layer flow velocity profiles behind flat plate indentation for Mach numbers 1.7-3.0 and Reynolds numbers to 40,000,000

16 p2380 A72-33857

Solar wind heat flux measurements comparison with collision dominated heat transfer theory in ionized medium, noting deviations from Maxwellian velocity distribution

16 p2449 A72-33908

Velocity-pressure correlations in a homogeneous turbulence associated with a plane pure deformation

17 p2537 A72-34280

Boundary layer velocity profiles on a helicopter rotor blade in hovering and forward flight. [AHS PREPRINT 622]

17 p2484 A72-34482

Random gravitational encounters and the evolution of spherical systems. IV - Isolated systems of identical stars.

17 p2605 A72-34528

On the kinematic distribution of galactic neutral hydrogen.

17 p2606 A72-34572

Micromorphic description of turbulent channel flow.

17 p2538 A72-34868

Memories of longitudinal fluctuations of velocity in a smooth circular duct

17 p2539 A72-34907

Asymptotic character of turbulent boundary layer longitudinal velocity distribution along flat plate at low Reynolds number, using Hirsch theory for potential flow

17 p2539 A72-34908

Effect of rotation on laminar compressible fluid flow in a vertical cylinder.

17 p2539 A72-34972

Master equations for finite systems.

17 p2576 A72-35153

An experimental investigation of an asymmetrical turbulent wake.

17 p2485 A72-35187

Calculations of the turbulent boundary layer in supersonic nozzles.

17 p2485 A72-35237

Computation of transonic flow about finite lifting wings.

17 p2486 A72-35258

Velocity distribution and Mach number in a supersonic molecular beam of plane symmetry

17 p2486 A72-35423

Whistler side-band growth due to nonlinear wave-particle interaction.

17 p2517 A72-35601

Approximations yielding closed equations for isotropic turbulence compared to laboratory and computer experiments, emphasizing Langevin type model equation for velocity

18 p2677 A72-36008

Observations of the variability of dissipation rates of turbulent velocity and temperature fields.

18 p2678 A72-36022

MHD inlet flow into channel, obtaining velocity profile numerical solution in Prandtl approximation with modified boundary conditions

18 p2714 A72-36121

Flat plate withdrawal at high speed from quiescent liquid baths, calculating velocity profile via boundary condition transformation and eigenfunction expansion method

18 p2678 A72-36122

Velocity structure and properties of the lunar crust.

18 p2725 A72-36292

Experiments using the birefringence of fluids in motion

18 p2679 A72-36367

Transient acoustic point source disturbance transmission in two dimensional idealized jet, noting velocity profile effects on noise radiated to far field

18 p2679 A72-36406

Spheroids with surface vibration at specified normal velocity distributions, calculating acoustic radiation by Green function approach

18 p2710 A72-36412

Stress state and velocity fluctuations in a perturbed boundary layer

18 p2680 A72-36464

Calculation of the development of a turbulent boundary layer in the presence of an equally turbulent external field - Experimental verification

18 p2680 A72-36469

Polarization and velocity field in the galaxy M 82.

18 p2727 A72-36729

Turbulence characteristics of flows with large velocity gradients in rectangular MHD channel with copper walls

18 p2715 A72-36813

The unsteady boundary layer flow in a convergent channel.

18 p2683 A72-36930

On the steady flow between a rotating and a stationary disk with a uniform suction at the stationary disk.

18 p2683 A72-36994

Velocity profile measurements in a turbulent boundary layer on a permeable plate

18 p2642 A72-37184

Numerical tests of resolution of detached flows on thick bodies

18 p2684 A72-37198

Radial velocities and brightness distribution in active and quiet solar atmosphere from magnetograph measurements, discussing motion directions in photosphere and chromosphere

19 p2858 A72-37818

Plasma electron velocity distributions determined from the polarization of free-free bremsstrahlung.

19 p2841 A72-38439

Magnetohydrodynamic channel flow with an arbitrary inlet velocity profile.

19 p2842 A72-38446

Atmospheric free convection turbulence and diffusion, proposing statistical formulas for components of horizontal thermal flux, vertical and transverse velocity and free diffusion tensor

20 p2948 A72-39012

Turbulence theory generalization for flow near wall with various surface roughness modes, presenting velocity profiles

20 p2912 A72-39359

Turbulent gas jets formed in cryogenic substance discharge into gas at supercritical pressure and gas into gas of different molecular weight and temperature

20 p2912 A72-39366

Improving diffuser performance by artificial means.

20 p2885 A72-39624

Direct measurement of the velocity gradient in a fluid flow.

20 p2926 A72-39633

Measurements of plasma velocity distributions in free-burning dc arcs up to 2160 A.

20 p2958 A72-39644

An application of the shooting method to the stability problem for a stratified, rotating boundary layer.

21 p3043 A72-40106

Determination of the characteristics of the averaged motion of the carrier medium in turbulent gas flow with suspended particles

21 p3044 A72-40126

Flow of a non-Newtonian fluid in a tube with sinusoidal deformation.

21 p3044 A72-40192

Some features of instantaneous point source diffusion within a turbulent boundary layer.

21 p3078 A72-40467

The solution of sharp-cone boundary-layer equations in the plane of symmetry.

21 p2989 A72-40650

Speed-dependent collisional width and shift parameters in spectral profiles.

21 p3088 A72-40820

Iterative solution to aerodynamic design of axial flow compressors used in turbojet engines, calculating meridional velocity distribution

21 p3099 A72-40930

Velocity distribution in turbulent mixing of compressible reacting gases, noting flame length measurement of submerged H jet

21 p3129 A72-40981

Axial velocity distribution and streamline boundary selection to derive two dimensional infinite duct shapes for inviscid irrotational compressible flows [ICAS PAPER 72-08]

21 p2990 A72-41133

Spherical focusing transducers with Gaussian surface velocity distribution.

21 p3057 A72-41477

Transverse mass flow past a sphere at small Reynolds numbers

21 p3047 A72-41664

Determination of the velocity field of the wake of a hypersonic sphere with the aid of ion probe arrays

21 p3057 A72-41725

Digital-computer analysis of electron guns for cathode-ray tubes by taking into account initial thermal velocities.

21 p3088 A72-41834

Velocity distribution of quasi-steady and steady flow of ideal incompressible fluids with congruent streamlines, investigating conditions for vortex and irrotational flow

22 p3164 A72-41906

Micro- and macroturbulent motions and the velocity spectrum of the solar photosphere.

22 p3221 A72-42030

Observations of the horizontal velocity field surrounding sunspots.

22 p3221 A72-42033

Fluidic flow-mode amplifiers physical dimensions and operating pressures restrictions, presenting design and performance evaluation theory and velocity profiles

22 p3139 A72-42048

Three-dimensional disturbances in the boundary layer along a concave wall

22 p3165 A72-42111

Velocity distribution in turbulent air flow over perforated plates with gas injection in turbulent boundary layer

22 p3166 A72-42256

Interpolation formulae for the electron impact excitation of ions in the H-, He-, Li-, and Ne-sequences.

22 p3224 A72-42379

Incompressible free shear layers instability, considering Reynolds number, velocity profile, disturbances and compressibility effects

22 p3167 A72-42579

New results concerning the numerical calculation of the sonic flow around a given airfoil section

22 p3135 A72-42639

A problem of electromagnetic wave propagation in a moving plane stratified medium

22 p3155 A72-42653

Initial electron velocity and emitter surface roughness effects on oscillatory velocities dispersion in helical electron beams used in cyclotron resonance masers

22 p3208 A72-42664

Low flying aircraft wake vortices tracking, describing sensing techniques based on acoustic pulse deflection and velocity field measurements

22 p3179 A72-42709

Iterative method for calculating the deformations of an induced flow

22 p3136 A72-42919

Calculation of a profile or of a cascade of profiles for a velocity distribution given as a function of potential

22 p3136 A72-43096

Physical characteristics of type I supernova envelopes during the initial expansion phase. II - Development of type I supernova spectra after maximum light.

23 p3333 A72-43228

Quasi-stationary spherical system structure model for stars of different masses with isotropic velocity distribution

23 p3334 A72-43242

The velocity distribution of electrons in beams formed by high-perveance three-electrode guns

23 p3319 A72-43401

Investigation of the applicability of different laws of extremal-value statistics to the approximation of empirical distributions of maximum wind velocities

23 p3310 A72-43531

Probability distribution of velocities and temperatures near a wall

23 p3279 A72-43696

Influence of wall injection on the turbulent tensions in the exterior regions of a boundary layer

23 p3279 A72-43696

Boundary layer flow on a circular cylinder moving in a fluid at rest.

23 p3248 A72-43715

Influence of tangential fluid injection on the performance of two-dimensional diffusers.

23 p3280 A72-44064

Interferograms of turbulent boundary layer separation in critical blowing of gas through porous plate, noting velocity and concentration profiles of blowing parameters

23 p3281 A72-44082

Velocity, enthalpy and turbulent energy distributions calculation for plane wake behind flat body by asymptotic solution based on turbulence theory

23 p3249 A72-44083

Velocity distribution in the turbulent boundary layer of a supersonic gas flow

23 p3249 A72-44084

The intermittent small-scale structure of turbulence - Data-processing hazards.

23 p3282 A72-44305

Magnetohydrodynamic flow between parallel rotating disks. I - Influence of finite wall-conductance.

23 p3322 A72-44400

Annual variation of the interplanetary He+ velocity distribution at 1 AU.

23 p3332 A72-44505

Application of the method of hydrodynamic singularities to the calculation of the velocity distribution in doubly-periodic infinite blade cascade systems

24 p3390 A72-44874

The effect of a harmonic-oscillator velocity distribution on an ideal solid-state laser.

24 p3409 A72-44953

Velocity distribution function and balance parameters of electrons in a nonisothermal argon plasma at degrees of ionization from 0.00000001 to 0.01

24 p3428 A72-44968

Diffraction of an acoustic wave by a stationary plate

24 p3360 A72-44987

High order terms diffusion equation derivation for strong fluctuating flows by random walk method, discussing phenomenological analogy with equations of motion

24 p3390 A72-44990

Rectangular wind tunnel study of suction effect on velocity profiles and characteristics of turbulent boundary layer
24 p3390 A72-45005

Velocity profiles of plane turbulent flow of incompressible fluid on porous surface in presence of suction
24 p3390 A72-45007

Measurement of thermal relaxation time of vibration of polyatomic molecules by the impact tube method
24 p3402 A72-45045

Measurement of the velocity distribution in the boundary layer over a flat plate with a diffusion flame.
24 p3464 A72-45062

Intermittent character of the viscous sublayer and interpretation of probability density measurements
24 p3392 A72-45072

Hydrodynamic approximation for solar wind nonuniformity in ecliptic plane, noting linear disturbances caused by nonuniform velocity of plasma flow from corona
24 p3435 A72-45077

Multilayer plasma model for MHD pulse propagation in ionospheric waveguide, noting approximation of Alfvén velocity distribution by plasma layers
24 p3397 A72-45085

Turbulent flow of drag reducing fluids between concentric rotating cylinders.
[CSME PAPER 71-52] 24 p3393 A72-45254

Velocity profile of near-wall turbulent boundary layer with adverse pressure gradient, noting skin friction
24 p3393 A72-45357

Prediction of velocity profiles for turbulent boundary layers on the blading of radial impellers.
24 p3393 A72-45360

The determination of a general relation between the aerodynamic properties of a single airfoil and those of the same airfoil arranged in an arbitrary cascade.
24 p3363 A72-45363

Suction side velocity distribution parameter characteristic relationship to profile geometrical parameters in turbine blade cascade system
24 p3394 A72-45366

Nonlinear interactions between synthesized plasma positive and negative ion beams, discussing effect on individual velocity distribution functions
24 p3431 A72-45711

VELOCITY ERRORS
Algorithms for object apparent velocity calculation from linear acceleration and angular velocity integrators readings, estimating errors
01 p0135 A72-10507

Linearization errors and calibration functions for hot-wire anemometry taking into account higher order velocity fluctuations
01 p0071 A72-11170

Sensitivity algorithms for finite memory batch processing smoother /Kalman filter/, applying to ship inertial velocity error estimation
05 p0686 A72-16572

Turbulent flow field velocity fluctuations errors by hot-wire anemometer filaments vibrations from fluctuating aerodynamic loads in Karman vortex street
05 p0664 A72-17013

Coordinate and speed error dependence on instrumental errors of inertial navigation system using gyrohorizoncompass
16 p2420 A72-33960

Integrated navigation systems and Kalman filtering - A perspective.
24 p3386 A72-44642

VELOCITY FIELDS
U VELOCITY DISTRIBUTION
VELOCITY MEASUREMENT
NT WIND VELOCITY MEASUREMENT
Wall friction effect on current sheet speed of magnetically driven shock tube, establishing steady state existence
01 p0105 A72-10027

Fluidic device for measuring angular velocities based on pressure output proportional to shaft revolutions per unit time, discussing equivalent circuit
01 p0064 A72-10171

Laser optical anemometry system, describing fringe, Doppler and reference beam operation modes
01 p0081 A72-11168

Laser anemometer system for instantaneous velocity measurement in turbulent pipe flow, determining two point velocity correlation coefficients
01 p0071 A72-11169

Cooled miniature pneumatic probes for high temperature gases dynamic or stagnation pressure and velocity measurement
01 p0072 A72-11213

Turbulent flow velocity measurement pulsed wire technique
01 p0072 A72-11229

Crater 9 meteorite /Argentina/ entry trajectory and orbital calculations, determining masses and velocities from dynamic conditions at impact
02 p0275 A72-11599

Split-film anemometer probe determination of convective heat transfer coefficient azimuthal dependence in low Reynolds number flow over cylinders, discussing axial heat losses
02 p0224 A72-11725

Laser flow anemometer technology, discussing velocity and spatial resolution, chromatic and temporal coherence, signal processing, frequency discrimination, spectrum analyzer and tracking filter.
02 p0224 A72-11743

He-Ne traversing laser velocimeter for instantaneous axial fluid velocity measurement, describing signal analyzing system, construction and calibration
02 p0224 A72-11744

He-Ne laser velocimeter for roller bearing elements rotational speed measurements, discussing instrument construction and spatial resolution
02 p0224 A72-11745

Fluidic sensors methods for position, angular velocity, fluid level, flow rate and temperature measurement
02 p0155 A72-11998

Spectral broadening in laser Doppler velocimeter, showing identity of wave vectors spread for incident and detected fields and scattering center finite volumetric stay
02 p0229 A72-12094

Turbulent flow internal intermittency and fine structure distribution as function of Reynolds number, using hot-wire anemometer for velocity field measurements
03 p0340 A72-13156

Solar magnetic fields time fluctuation determination using longitudinal, intensity and line of sight velocity measurements
03 p0356 A72-13278

Solar magnetic fields time fluctuation determination using longitudinal, intensity and line of sight velocity measurements
03 p0430 A72-13318

Cold plasma flow rate determination from emission inhomogeneities, using time of flight method and high speed streak photography for instantaneous velocity measurements
03 p0396 A72-13663

Functional speed measurements of propagating devices based on cylindrical domains in orthoferrites and garnets, noting storage capability
[IEEE PAPER 28,2] 03 p0333 A72-13783

Velocity measurement of glass particles emerging from plasma flame by high speed cine-streak photography
03 p0361 A72-13992

Linearized constant temperature hot-wire anemometer calibration for shock tube unsteady flow velocity measurements with low strength wave propagation
04 p0521 A72-14920

Earth mantle shear velocity model derived from S waves travel time gradient direct measurement, disregarding deep depth lateral homogeneity assumption
04 p0519 A72-15578

Velocity dependence of ionization cross section of Ar, Kr and Xe during thermal energy metastable neon atoms impact, obtaining secondary electron ejection efficiency
04 p0553 A72-15640

Pulse and Doppler microwave radars comparison with respect to accuracy of moving targets velocity measurements and power characteristics
05 p0661 A72-16034

Display device for engine rotational speed nonuniformity parameters indication on oscilloscope without supplementary computation
05 p0662 A72-16125

Doppler ultrasonic probe phonocardiography for human cardiovascular velocity measurement, showing normal tracings and aging effects
05 p0617 A72-16154

Doppler cardiometry determination of human cardiovascular velocities in patients with heart diseases, discussing impaired left ventricular function detection
05 p0617 A72-16155

Altitude dependent vertical drift velocity of small scale ionospheric inhomogeneities, using correlation of signal time lag scanning in frequency domain
05 p0657 A72-16270

Goldberg-Unno method accuracy for solar photospheric microturbulent velocities, discussing correction for damping effect and LTE deviation
05 p0718 A72-16503

Horizontally averaged nonthermal velocities determination in lower solar chromosphere, observing Doppler widths of weak rare earth emission lines in H and K wings
05 p0718 A72-16504

Wind tunnel measurements for near flow field velocity distribution in rectangular wing wake turbulence, comparing with flight measurements
[AIAA PAPER 72-41] 05 p0609 A72-16948

Polarographic method for simultaneous measurement of wall gradients of velocity and of concentration in unsteady laminar or steady turbulent flow
06 p0797 A72-17558

Two phase flow model of water droplets velocity in air stream, using Fresnel biprism and laser differential scheme
07 p1000 A72-18940

Atmospheric turbulence measurements over sea from 30 m to 1 km, examining rms vertical velocity variations with altitude
07 p1030 A72-19104

Micron sized particle velocity relaxation measurement in shock wave, using laser Doppler methods
[CLEA PAPER 11,3] 07 p1005 A72-19389

Two channel high resolution spectrometric measurements of plasma velocity from intrinsic radiation in optical range by Doppler effect
07 p1044 A72-19885

Laser Doppler velocimeter signals statistical properties, examining bandwidth, counting time and input SNR effects on zero crossing counter output fluctuations rms value
07 p0990 A72-20370

Overheat resistance calibration of constant temperature hot-wire anemometers at low velocities in water with variable temperature
[ASME PAPER 71-HT-9] 08 p1163 A72-20873

Free convection velocity fields measurements and stagnation point location around horizontal torus in air, using fine particle trajectories
[ASME PAPER 71-HT-X] 08 p1163 A72-20877

Sectorial radio measurement of meteor trail drifts with IF radar signals, determining Doppler shift sign and period
08 p1238 A72-21887

North-south ionospheric movements at low latitude station, investigating diurnal and seasonal velocity variations from cross correlation and similar fades time delays measurements
08 p1136 A72-21981

Burning velocity measurement techniques for methane-air mixtures
08 p1255 A72-22047

Velocity measurement by Doppler light scattering due to particle finite residence time, estimating ambiguity and noise effects on turbulent spectra of frequency fluctuation
09 p1305 A72-22302

Two dimensional laser Doppler forward and backscatter velocimetry in turbulent flows, applying to four inch pipe
09 p1305 A72-22303

Electrochemical techniques for time averaged turbulent velocity gradient and components of fluctuating velocity gradient at solid surface
09 p1306 A72-22305

Turbulence generated by moving obstacle in tank of stably stratified fluid, measuring velocity and concentration fluctuations with hot-film and electrode conductivity probes
09 p1293 A72-22308

Optical measurement of point velocity on surface of moving solid, applying to Mylar foil accelerated by plasma gun
09 p1310 A72-22773

Instantaneous velocity vector determination in two dimensional flow by hot-wire anemometer and on-line digital computer technique
10 p1478 A72-23877

Turbulent flow velocity and pressure fluctuations mean square values measurement by electrokinetic probe based on electrical properties of double metal-fluid interface layer
10 p1480 A72-24204

Coherent and noncoherent modes of optical beating in laser Doppler velocity measurement using light scattered from single and multiple particles
10 p1481 A72-24412

Arterial velocity profiles measurement in dogs thoracic aorta by hot-film probe, relating flow disturbances and turbulence to Reynolds number
10 p1431 A72-24468

Flight vehicle angular velocity measurement by accelerometers, deriving equations of motion
10 p1481 A72-24497

Response equation for hot-wire anemometry over wide velocity range using modified King law
11 p1629 A72-25265

Coordinate transformation equations derivation to determine third orthogonal velocity component from measurements at common point by two rotationally displaced laser Doppler velocimeter systems
11 p1629 A72-25308

T-tube plasma flow velocity measurement via shock wave attenuation recording technique
11 p1693 A72-25561

Instantaneous and continuous blood flow velocity measurement by Doppler ultrasonic flowmeter using transcutaneous and implanted probes
11 p1589 A72-26778

Hot-wire measurement of vector velocity modulus and sign in one dimensional unsteady gas flow
12 p1806 A72-27178

Tracer particle motion behavior in laser anemometry for turbulent flow, comparing liquids with gases for accuracy
12 p1809 A72-27763

Frequency modulation demodulation technique for turbulence velocity measurements by laser Doppler velocimeter
[AD-744534] 12 p1809 A72-27836

Copper resistance thermoanemometer for channel unsteady air flow rate measurement, discussing design, operation principles and maximum error
12 p1812 A72-28146

Velocimeter design for MHD boundary layer flow velocity measurement, using Doppler frequency shift of laser light scattered from added macroscopic particles
13 p1957 A72-29360

Doppler laser velocimeter and hot-wire anemometer readings in cylinder wake compared, describing instrument caused spectrum broadening effects neutralization method
13 p1960 A72-29889

High resolution angular velocity measurement by high speed digital transducer feeding photosensor pick-up pulses into pulse shaping circuit
14 p2103 A72-30199

Viscosity, velocity gradient and wall effects on pitot tube measurement of gas flow velocity measurement in turbulent boundary sublayer
14 p2094 A72-30294

Earth velocity through microwave background, discussing absolute and relative motion, inertial frame and distant matter distribution and Mach principle
14 p2157 A72-30624

Galactic spiral arm hypothesis for positive velocity neutral hydrogen clouds above galactic plane, surveying distribution
14 p2158 A72-30732

H II regions radial velocities in Carina arms from Fabry-Perot interferometric H α measurements, determining early stars distances from spectroscopic and photoelectric observations
14 p2159 A72-30740

Multiply charged ions motion velocity measurement for pulsed discharge plasma in nitrogen, krypton and xenon
14 p2139 A72-30777

Composition dependence of ultrasonic velocity in binary Mg base alloys measured by pulse method
14 p2143 A72-31030

Optical, mechanical and electrical arrangements of laser Doppler velocimeter, presenting Doppler signals displays and three dimensional gas velocity profiles in vortex region
15 p2236 A72-32044

Laser Doppler velocimetry system design for optical measurement of intrablade flow velocity in turbomachinery
15 p2237 A72-32045

Laser Doppler velocimeter designs for atmospheric applications, discussing illuminating techniques, SNR, performance comparison and system selection
15 p2237 A72-32051

Momentary velocity measurement of human walking in forward movement by frequency response of signal on magnetic tape
15 p2190 A72-32200

Doppler navigation system suitability for area navigation, discussing routes versatility, accuracy and continuous velocity vector sensor
15 p2271 A72-32203

Shock wave propagation velocity increase in combustion shock tubes through intermediate pressure chamber, using streak camera and microwave Doppler technique for velocity measurements
16 p2375 A72-32839

Gaussian beam laser Doppler velocimeter system under high scattering center concentrations and steady flow conditions, deriving noise spectral densities and SNR
16 p2390 A72-33210

Monitor and regulator for automatic speed control and flow velocity measurement in wind tunnel
16 p2392 A72-33609

Instantaneous velocity nonuniformity measurement of mechanism motion using phaseometers with magnetic data recording
16 p2395 A72-33963

Operation and calibration of three blade rotating vane anemometer for rarefied gas flow velocity measurement
16 p2395 A72-33966

Laser Doppler anemometer for three dimensional liquid and gas flow velocity measurements in water tunnels
16 p2396 A72-34158

Boundary layer velocity profiles on a helicopter rotor blade in hovering and forward flight.
[AHS PREPRINT 622] 17 p2484 A72-34482

Optical method for measuring the velocity of particles entrained in a flow
17 p2554 A72-34892

Two channel high resolution spectrometric measurements of plasma velocity from intrinsic radiation in optical range by Doppler effect
17 p2590 A72-35133

A laser velocimeter for Reynolds stress and other turbulence measurements.
17 p2555 A72-35235

Laser velocimeter measurement of Reynolds stress and turbulence in dilute polymer solutions.
17 p2541 A72-35252

Hydrogen and helium velocities in the solar wind.
17 p2602 A72-35716

Simple two-dimensional laser velocimeter optics.
17 p2558 A72-35845

A relative performance analysis of atmospheric laser Doppler velocimeter methods.
17 p2558 A72-35949

Laboratory studies on seismic and electrical properties of the moon.
18 p2724 A72-36282

Measurements of ultrasonic velocities using a digital averaging technique.
18 p2691 A72-36401

WKB approximation to suggest vertical phase velocity measurement at turning points of acoustic-gravity wave propagation in thermosphere
18 p2686 A72-36411

Ultrasonic velocity measurement by small power He-Ne laser visualization of standing waves in Fresnel diffraction region
18 p2697 A72-36416

Ultrasonic velocity measurement of elastic constants of Al-Al3Ni unidirectionally solidified eutectic.
18 p2701 A72-36591

Velocity profile measurements in a turbulent boundary layer on a permeable plate
18 p2642 A72-37184

Rotational velocities of Ap stars.
19 p2855 A72-37237

A historical survey of the application of the Doppler principle for radio navigation.
19 p2830 A72-37276

An automatic data processing system for laser anemometers.
19 p2795 A72-37287

Double system HD 175514. III - Analysis of 1968 observations
19 p2858 A72-37810

The effect of wire length and separation on X-array hot-wire anemometer measurements.
19 p2801 A72-37903

Measurements of burning velocity in a flat flame front.
19 p2883 A72-38872

Thermoanemometer measurements of turbulence degree in wake behind square mesh grids in water flow within low speed wind tunnel
20 p2912 A72-39364

A unified analysis on laser Doppler velocimeters.
21 p3061 A72-40211

Measurement of flow speed by the correlation method
21 p3056 A72-41252

Bilateral version of an ultrasonic velocimetric method of defectoscopy.
21 p3057 A72-41721

Determination of radio-meteor velocity with a minimum rms error
22 p3220 A72-41918

Hot wire anemometer calibration for measurements of small gas velocities.
22 p3175 A72-41953

Reverse flow sensing hot wire anemometer.
22 p3177 A72-42392

Noise-cancelling signal difference method for optical velocity measurements.
22 p3177 A72-42394

Self-aligning comparison beam methods for one-, two- and three-dimensional optical velocity measurements.
22 p3177 A72-42395

Measurements of the local velocity of shock and detonation waves by schlieren interferometry of Doppler-shifted laser light.
22 p3178 A72-42455

Analysis of the structure of the flow downstream of a sudden widening
22 p3167 A72-42643

Laser Doppler velocimeter operating in forward- and back-scatter modes for supplementing wind tunnel flow field measurements in subsonic, transonic and supersonic regimes
23 p3179 A72-42678

Use of a linear air bearing sled for dynamic calibration of velocity transducers.
23 p3179 A72-42693

Low flying aircraft wake vortices tracking, describing sensing techniques based on acoustic pulse deflection and velocity field measurements
23 p3179 A72-42709

Ultrasonic attenuation and velocity in hot specimens by the momentary contact method with pressure coupling, and some results on steel to 1200 C.
23 p3294 A72-44116

A differential laser Doppler velocity meter employing a Fabry-Perot interferometer
23 p3292 A72-44472

Solar wind velocity determination from radio sources interplanetary scintillation observations, noting magnitude and direction variations with time
23 p3333 A72-44529

Simultaneous measurements of temperature and velocity in heated flows.
23 p3292 A72-44541

Condensed liquid explosive detonation pressure from free surface velocity measurement, noting pressure curve dependence on charge diameter and wall thickness
24 p3463 A72-45036

A means of measuring the rms value of velocity fluctuations in unsteady turbulent flow
24 p3403 A72-45259

VELOCITY MODULATION

Subsonic wind tunnel for pulsed flows with speed modulation as periodic function of time
16 p2372 A72-32898

Three-dimensional pattern of instability development during the interaction between a modulated electron beam and a plasma
21 p3092 A72-40800

Suppression of oscillations in a plasma-beam system by modulation of low frequency signals
21 p3095 A72-41681

Development of nonlinear oscillations in the interaction between a modulated electron beam and a plasma
22 p3211 A72-42651

VELOCITY POTENTIALS

U FLOW DISTRIBUTION

U VELOCITY DISTRIBUTION

VELOCITY PROBES

U PITOT TUBES

U SPEED INDICATORS

VELOCITY PROFILES

U VELOCITY DISTRIBUTION

VENERA SATELLITES

Venus atmospheric investigation by Venera 4, 5 and 6 probes, discussing satellite components and instrumentation, and atmospheric composition, depth, density, pressure, temperature and model
01 p0130 A72-10931

Thermodynamic parameters correlations of planetary atmosphere with planetary probe parachute descent rate applied to Venera 5 and 6 data
05 p0721 A72-16769

Digital computer investigation of radio signals transmitted by Vener 7 during Venus soft landing, describing spectral analysis and telemetric data detection methods
05 p0630 A72-16770

Earth-moon system gravitational effect on Venera automatic interplanetary stations motion away from earth
08 p1239 A72-22086

Venera 7 satellite data during descent through Venus atmosphere and activity after soft landing on 25 December 1970, noting temperature and pressure measurements
11 p1718 A72-25937

Radio wave propagation characteristics in Venusian atmosphere and interplanetary plasma from Venera 7 probe data
11 p1599 A72-26907

Venera satellite parachute probe method for Doppler measurement of Venus atmosphere wind velocity and turbulence
14 p2151 A72-30466

Subcloud Venus atmospheric wind velocity and turbulence from Venera Doppler measurements
15 p2308 A72-31905

Earth-moon system gravitational effect on Venera automatic interplanetary stations motion away from earth
17 p2606 A72-34655

Planetary atmosphere thermodynamic parameters correlation between spacecraft parachute descent rate and measured data, noting Venera spacecraft example
17 p2610 A72-35272

Digital computer investigation of radio signals transmitted by Venera 7 during Venus soft landing, describing spectral analysis and telemetric data detection methods
17 p2516 A72-35273

VENERA 6 SATELLITE

Determination of shock wave velocity in the interplanetary medium
18 p2728 A72-36875

VENERA 7 SATELLITE

Wind velocity and some Venusian surface characteristics monitored by the 'Venera-7' automatic interplanetary station
17 p2610 A72-35210

Results of cosmic ray intensity measurements on the Venus-7 automatic station
22 p3218 A72-42213

VENEZIANO MODEL

Duality concept in elementary particle physics, discussing pion-nucleon scattering, amplitude exchange degeneracy, Regge poles and Veneziano models
05 p0692 A72-17077

VENTILATION

Physiological effects of localized ventilation, noting human comfort improvement association with reductions in average skin temperature and sweat rate
02 p0159 A72-11955

Nonlinear theory of pulmonary ventilation distribution in two compartment model of human lungs
16 p2358 A72-33025
Computation of wall effects in ventilated transonic wind tunnels.
[AIAA PAPER 72-1007] 24 p3388 A72-45403

VENTILATION FANS
Three-dimensional non-free vortex flow in axial fans.
17 p2487 A72-35896
Comparison of two types of blade profile for axial-flow fans
18 p2720 A72-36000

VENTING
Flow area computerized prediction for multicompartment series-parallel spacecraft venting satisfying pressure differential requirements
[AIAA PAPER 72-707] 16 p2462 A72-34038
A comparison of sealed and vented Ni/Cd battery characteristics.
17 p2498 A72-35567

VENTURI TUBES
Flow rate metering by multiple Venturi systems, discussing internal fluid mechanics for design optimization
[ASME PAPER 71-WA/FE-27] 05 p0661 A72-15926
Approximate determination of the change in the aerosol distribution spectrum in a Venturi coagulator tube
20 p2928 A72-40039
Heat and mass transfer in Venturi tubes
20 p2928 A72-40048

VENUS [PLANET]
Review of papers on planetology given at Brighton symposium, covering moon, Venus, Mars and Jupiter
01 p0132 A72-11071
Venus transit, across solar face, detailing black drop effect on computation of exact ingress moment
04 p0581 A72-15620
Venus, M17 and M82 observation on ground through 345 micron atmospheric window, discussing IR fluxes
05 p0710 A72-16709
Mission analysis of Helios spacecraft swingby past Venus to acquire extraecliptic trajectory
[AIAA PAPER 72-50] 05 p0721 A72-16951
Venus 8.2 mm radio emission dependence on sun-light phase angle, considering implications regarding day/night atmospheric temperature variations
06 p0884 A72-18031
Venus equatorial region surface height variations from interplanetary radar echo delay measurements, discussing resolution, repeatability and radius
07 p1073 A72-19352
Telescopic requirements posed by Venus near sun, discussing sky brightness in image plane, atmospheric dust and Rayleigh scattering
08 p1230 A72-20993
Venus, Mars, Jupiter and Saturn UV spectra from OAO-2 objective grating spectrophotometry, obtaining planetary albedos from G-type stars observations
09 p1382 A72-22288
Venus and Mars visible geocentric declinations from daytime observations with Wanschaff vertical circle compared to nighttime results
09 p1388 A72-23065
Topography of swath around Venus equator from wavelength dependence of radar cross section
10 p1548 A72-24972
Venus 8.2 mm radio emission dependence on sun-light phase angle, considering implications for day/night atmospheric temperature variations
11 p1719 A72-25967
Venus spectrum carbon dioxide absorption lines model with double cloud system and adiabatic atmosphere
11 p1721 A72-26120
Mars and Venus instrumented spacecraft flight results, describing planetary topographies, atmospheres and magnetic fields
12 p1877 A72-27650
Planetary distance and velocity measurement with radar signal frequency modulation, describing Venus observations
14 p2148 A72-30209
Mars and Venus automatic station data transmission systems for surface and atmosphere studies, discussing relay and direct transmission modes
15 p2203 A72-31823
Venus brightness temperature and phase dependence at 2.7 cm wavelength during 1968-1970
15 p2311 A72-32088
Wind velocity and some Venusian surface characteristics monitored by the 'Venera-7' automatic interplanetary station
17 p2610 A72-35210
Precision interferometric observations of Venus at 11.1-centimeter wavelength.
17 p2611 A72-35322
Right ascensions of the sun, Mercury, and Venus observed with the transit instrument at Nikolaev during 1966-1967
19 p2861 A72-37982

Declinations of the sun, Mercury, and Venus in the FK4 system as deduced from observations with the vertical circle of the Nikolaev Observatory during 1966-1967
19 p2861 A72-37983
Attempt at determining the exact positions of Venus from photographic observations on the short-focus double astrophotograph and the 26-in. refractor of the Pulko Observatory
19 p2861 A72-37984
Mathematical model for Venus phase anomaly, noting upper limit of reflecting layer for refraction effect
20 p2972 A72-39874
Planetary distance and velocity measurement with radar signal frequency modulation, describing Venus observations
23 p3333 A72-43239
New optical measurements of planetary diameters. II - Planet Venus.
24 p3436 A72-44694

VENUS ATMOSPHERE
Venusian atmosphere heat transfer processes, calculating radiant fluxes and convective motion model
01 p0127 A72-10364
Venus subcloud layer, investigating radiant heat transfer in convective lower atmosphere
01 p0128 A72-10370
Radiative heat transfer equilibrium in Earth, Venus and Mars atmospheres, taking into account interaction with ground
01 p0058 A72-10561
Venus lower atmosphere from Venera 4, 5 and 6 and Mariner 5 data, evaluating greenhouse effect by microwave absorption and by nonray radiative model
01 p0129 A72-10795
Venus atmospheric investigation by Venera 4, 5 and 6 probes, discussing satellite components and instrumentation, and atmospheric composition, depth, density, pressure, temperature and model
01 p0130 A72-10931
Venus cloud reflected radiation flux and polarization by Monte Carlo technique, using models with different particle size distributions
02 p0280 A72-12193
Venusian ionosphere thermal proton destruction, discussing helium and oxygen replacement candidates for principal ion components
03 p0434 A72-13537
Venusian polar tropopause and cloud layer from IR spectral recording in carbon dioxide band near inferior conjunction for crescent regions
03 p0436 A72-13814
Venus cloudy atmosphere IR absorption line spectra interpretation, suggesting HCl and HF formations dependence on condensation phases
03 p0439 A72-14149
Jupiter and Venus cloudy atmosphere reflected sunlight circular polarization measurement, noting sense variations with phase angle and location on disk
03 p0439 A72-14150
Mars and Venus explorations, discussing Mariner probes, Mars craters, volcanism, polar areas, surface temperature and atmosphere and Venus radar astronomy and atmospheric model
03 p0440 A72-14305
Extraterrestrial life on Mars and Venus and Jupiter atmospheres, discussing abiogenesis failures on life-supportable planets
04 p0471 A72-14805
Reduced collision integrals for components of Venus and Mars type carbon dioxide atmospheres at 1000-11,000 K, using intermolecular interaction potentials
05 p0712 A72-15851
Radio absorption spectra sounding for planetary atmospheric impurities calculating water vapor content in Venus cloud level
05 p0715 A72-16169
Venus cloud top chemical composition from spectroscopic data, discussing cloud refractive index and reflectivity
05 p0719 A72-16711
Venus daytime ionosphere at 100-500 km, discussing ion clustering processes below 100 km forming UV haze layer and atmospheric composition
05 p0723 A72-17163
Spectral composition of emitted radiation, emissivity and absorptivity of Venus atmosphere at high temperatures
07 p1068 A72-18933
Mars, Venus and Jupiter atmosphere composition and structure from spectral analysis, discussing equilibrium temperature, radiative heat transfer, integrated density and adiabatic temperature gradient
07 p1073 A72-19353
Venusian atmospheric circulation experiments with time dependent two layer primitive equations model, discussing hot house and Goody-Robinson radiation transfer implications
07 p1083 A72-20452
Venus clouds composition from spectral and polarization data, considering hydrochloric acid particles model
08 p1230 A72-20980

Numerical modeling of Venus atmospheric circulation, taking into account short wave radiation absorption, boundary layer, mesoscale convection and horizontal friction
08 p1233 A72-21191
Radiative thermal flux model of Venus atmosphere, using Venera data and greenhouse effect
08 p1233 A72-21193
Venus atmosphere chemical composition, temperature and pressure, discussing model cloud layer, circulation and upper atmospheric structure
08 p1236 A72-21400
Venus upper clouds composition from Mariner 5 occultation data analysis concerning temperature and pressure profiles, abundances, polarization characteristics, reflection and emission spectra
08 p1236 A72-21496
Planetary atmospheres composition diversity, discussing evolution of Mars, Venus, earth and Jupiter from primitive solar nebula
08 p1119 A72-22012
Spectral line formation in cloudy planetary atmospheres, applying to Venus
09 p1386 A72-22669
Spectroscopic evidence for spectral line structure of visible Venus cloud layers
09 p1386 A72-22670
Carbon dioxide atmospheric models for Mars and Venus, discussing aeronomy, Mariner probes, gas dissociation by solar radiation, and electron density inconsistency
09 p1386 A72-22685
Steady state model for Venus atmosphere water vapor loss, noting hydrogen and oxygen escape due to dynamic outflow of constituents from upper region
09 p1393 A72-23657
Spectrophotometric observations of Venus, showing unreliability of evidence for dihydrated ferrous chloride in upper cloud layers
10 p1532 A72-23715
Venusian atmosphere RF refractive attenuation height dependence, field strength measurements comparison, inversion layer influence and surface echoes effects
10 p1541 A72-24501
Venus probes thermal insulation materials development and testing under simulated Venus atmospheric conditions
[AIAA PAPER 72-368] 11 p1744 A72-25393
Venera 7 satellite data during descent through Venus atmosphere and activity after soft landing on 25 December 1970, noting temperature and pressure measurements
11 p1718 A72-25937
Venus spectrum carbon dioxide absorption lines model with double cloud system and adiabatic atmosphere
11 p1721 A72-26120
Venus lower atmosphere enhanced microwave attenuation explained by water vapor and droplet layer, calculating mass density distributions
11 p1724 A72-26762
Radio wave propagation characteristics in Venusian atmosphere and interplanetary plasma from Venera 7 probe data
11 p1599 A72-26907
Venus atmosphere IR synthetic spectra of carbon dioxide band and water line formation for isotropic scattering, comparing with terrestrial clouds
13 p2040 A72-29410
Comet-like interaction of Venus atmosphere with solar wind from Venus probe data, noting absence of bow shock wave and ionospheric tail
13 p2050 A72-29956
Radio absorption spectra sounding for planetary atmospheric impurities calculating water vapor content in Venus cloud level
14 p2149 A72-30238
Venera satellite parachute probe method for Doppler measurement of Venus atmosphere wind velocity and turbulence
14 p2151 A72-30466
Venus atmospheric parameters below critical refraction and surface refractive index from signal amplitude measurement by radio holographic occultation techniques
14 p2151 A72-30467
Venus and earth atmospheres dissimilarity from radio astronomy and space probes observations
14 p2158 A72-30695
Radiative transfer in Mars and above-cloud Venus carbon dioxide atmospheres, studying diurnal variations in temperature profile
14 p2160 A72-30897
Reduced collision integrals for components of Venus and Mars type carbon dioxide atmospheres at 1000-11,000 K, using intermolecular interaction potentials
15 p2302 A72-31270
Venus long wave radiation spectral composition, angular distribution and carbon dioxide transmission from thermal, structure and vertical radiation absorption profile
15 p2305 A72-31394

- Subcloud Venus atmospheric wind velocity and turbulence from Venera Doppler measurements
15 p2308 A72-31905
- Carbon dioxide abundance variations from Venus high resolution spectra, discussing HCl and hydrogen fluoride line formation
15 p2310 A72-31994
- Photometric search for Venus halo effect during 1970 inferior conjunction in relation to brightness maximum and ice in cloud tops
15 p2312 A72-32089
- Venus comet-like interaction with solar wind explained via He outer atmosphere with preferential heating by wind
16 p2459 A72-33915
- Spectral observations of Venus in the frequency interval 18.5-24.0 GHz - 1964 and 1967-68.
17 p2610 A72-35120
- Some optical properties of the Venusian atmosphere and possible interpretations of photometric and polarization measurements
17 p2610 A72-35211
- How to measure surface and atmospheric conditions on Venus by microwave interferometry.
17 p2611 A72-35321
- Existence, structure and thermodynamic and kinetic stability of ClOO radical in Venus atmosphere, using quantum statistics methods for unimolecular decomposition rate
18 p2726 A72-36647
- Upward and downward motions of Venus atmosphere in terms of continuous cloud cover effects, considering solid cloud cover hypothesis
18 p2729 A72-36984
- Venus observation experiment with the aid of a television system
19 p2858 A72-37820
- Temperature range estimation method for planetary atmospheric component generating spectral lines, applying to Venus observations at 7820 A carbon dioxide band
21 p3106 A72-41045
- Venus atmosphere constituent abundances and temperature and pressure profiles from Venera probe data
21 p3110 A72-41451
- Determination of the characteristics of scattering particles in the Venusian atmosphere on the basis of photometric measurements
22 p3223 A72-42215
- Venus high albedo, discussing compound reflecting layer and liquid Hg cloud models
24 p3436 A72-44692
- Thermal equilibrium calculations of the lower Venus atmosphere.
24 p3439 A72-44955

VENUS PROBES

- NT VENERA SATELLITES
- Mariner Venus/Mercury 1973 flyby mission imaging experiment, discussing mission constraints, objectives and use of real time transmission vidicon camera and high resolution UV photography
04 p0568 A72-14494
- Mars and Venus probes entry into planetary atmospheres, discussing aerodynamics of trajectory control and soft landing
09 p1394 A72-23673
- Venus probes thermal insulation materials development and testing under simulated Venus atmospheric conditions
[AIAA PAPER 72-368]
11 p1744 A72-25393
- Comet-like interaction of Venus atmosphere with solar wind from Venus probe data, noting absence of bow shock wave and ionospheric tail
13 p2050 A72-29956
- Venus and earth atmospheres dissimilarity from radio astronomy and space probes observations
14 p2158 A72-30695
- Multiple probe targeting from spacecraft for 1977 Venus mission, considering trajectory, spin, release, attack angle, location and navigation and control accuracy effects
15 p2312 A72-32193
- Mission design and navigation for a 1977-1978 Venus Swingby/Mercury Orbiter.
[AIAA PAPER 72-941]
21 p3113 A72-41577
- VENUS RADAR ECHOES
- Moon and Venus relief from backscattering diagrams based on radar echoes, calculating root-mean-square angles of surface inclination
14 p2151 A72-30468
- Specific effective scattering area of the lunar, Martian, and Venusian surfaces in the radio range
22 p3223 A72-42214

VERBAL COMMUNICATION

- Bisensory performance in simultaneous auditory and visual verbal information recognition, demonstrating integrative action between hearing and vision
06 p0768 A72-17949
- Noise rating methods for speech communication effectiveness evaluation, presenting charts and tables for intelligibility limits with various communication techniques and equipment
07 p0932 A72-20167

Group composition and n-dominance personality trait effects on decision and communication task efficiency in laboratory triads
08 p1125 A72-21200

Air traffic control messages syllabic and word prominence patterns, discussing impact on continuous speech recognition by machine
09 p1274 A72-23581

VERNIER ENGINES

NT CONTROL ROCKETS

VERTEBRAL COLUMN

Human spine elastic deformation due to bending stresses, presenting statistical data on caudocephalad acceleration effects in vertebral column injuries
01 p0016 A72-10111

VERTEBRATES

NT BATS
NT BIRDS
NT CATS
NT CHIMPANZEES
NT FISHES
NT FROGS
NT GROUND SQUIRRELS
NT HOMOTHERMS
NT HUMAN BEINGS
NT MAMMALS
NT MICE
NT MONKEYS
NT PIGEONS
NT PRIMATES
NT RABBITS
NT SNAKES
NT SWINE

Vertebrates visual processes - Conference, University of Chile, Santiago, November-December, 1970
06 p0762 A72-17718

Synaptic contacts in vertebrate retinas, reviewing bipolar terminals, ganglion cells and amacrine responses from electron microscopy
06 p0762 A72-17719

VERTICAL AIR CURRENTS

Ionospheric horizontal drifts during large vertical convection of mid dip-latitude postmidnight F region, using spaced antenna measurements
01 p0052 A72-10087

Hall effect and magnetic field characteristics in lower ionosphere by vertical magnetospheric currents, using gyrotopic model
01 p0059 A72-10590

Small scale turbulence time-space variability in atmospheric boundary layer in presence of unstable stratification from vertical air flow measurements
03 p0383 A72-13481

Tornado and funnel cloud comparison in seasonal and diurnal distributions, air mass instability, tropospheric vertical wind shear and geographical distribution
03 p0385 A72-14231

Vertical wind velocity variances and spectra above atmospheric surface layer for flat and mountain terrains
03 p0386 A72-14335

Northern Hemisphere mean zonal flow across arbitrary horizontal surfaces, evaluating vertical transports of kinetic energy
04 p0541 A72-14454

High speed helicopter elastic rotor blade suboptimal motion controller decreasing flapping motion and bending loads despite small control angles and vertical gusts
04 p0465 A72-15504

Wind velocity vertical component determination through meteor trail drift observation, presenting mean diurnal measurements data
05 p0657 A72-16272

Vertical motions in stratified cloudy atmosphere as function of plane divergence distribution and heat influx
06 p0840 A72-17621

Mathematical two dimensional model of vertical wind shear near convective cloud in free atmosphere
06 p0840 A72-17622

Cumulus clouds vertical motion velocity spectra curves, turbulence dissipation rates and energy determination from aircraft measurements
06 p0842 A72-17941

Rain amount forecasting based on five level atmosphere model and hydrothermodynamics equations, calculating vertical currents under uniform atmospheric boundary layer stratification conditions
07 p1029 A72-18859

Vertical air motion three dimensional field measurement near mobile fronts by high precision tracking of air-dropped radar reflectors, noting quantitative rainfall prediction
07 p1029 A72-19098

Atmospheric turbulence measurements over sea from 30 m to 1 km, examining rms vertical velocity variations with altitude
07 p1030 A72-19104

Visual and radar echo location of organized updraft on thunderstorms and hailstorms
09 p1346 A72-22452

Atmospheric vertical shear at visible cloud level in Jupiter equatorial zone from blue and red wavelength photographs
10 p1531 A72-23712

Small scale turbulence time-space variability in atmospheric boundary layer in presence of unstable stratification from vertical air flow measurements
11 p1682 A72-26251

Conditional instability of second kind /CISK/ model of surface cyclonic vorticity dependence on vertical distribution of latent heat release
12 p1838 A72-27019

Thunderstorm penetration by F-100 aircraft to study turbulence hazard relation to updraft size and short period fluctuation-induced acceleration changes
13 p1992 A72-28852

Aircraft atmospheric flow measurements of horizontal and vertical motions on mesoscales, using inertial reference system
14 p2127 A72-30300

Wind direction rotation with altitude and time dependent downward phase propagation observed by vapor trail experiments, suggesting upward propagation of atmospheric waves
16 p2383 A72-32969

Cumulus clouds vertical motion velocity spectra curves, turbulence dissipation rates and energy determination from aircraft measurements
16 p2418 A72-33782

Hail size distribution and concentration in thunderstorm updraft regions from aircraft and S band radar observations
16 p2419 A72-33946

Atmospheric surface layer temperature, humidity and vertical wind velocity variances dependence on turbulent fluctuation inputs
16 p2419 A72-34148

Studies of vertical motions in cloud systems by using a coherent pulse radar in the decimeter wavelength range
19 p2829 A72-38773

Further study of the severe storm with a rotating updraft configuration.
21 p3077 A72-40466

Atmospheric boundary layer definition by height of maximum vertical kinetic energy flux, considering stable and unstable stratifications
24 p3421 A72-44954

Tropospheric wave motions with baroclinic basic flow in equatorial latitudes.
24 p3399 A72-45485

VERTICAL DISTRIBUTION

NT STAR DISTRIBUTION

Electromagnetic wave propagation anomalies over sea, comparing calculated and measured field strengths based on simultaneous refractivity vertical distribution measurement
01 p0026 A72-10405

Ionospheric neutral gas wind and altitude effects on Spanish short wave absorption winter anomaly
01 p0055 A72-10435

Remote sensing of regional vertical air column pollutants, discussing sulfur dioxide and nitrogen dioxide measurements by correlation spectrometer
[AIAA PAPER 71-1060]
01 p0057 A72-10529

Global satellite horizon-scanning monitoring technique permitting scattered solar radiation horizon profile conversion into aerosol vertical distribution
[AIAA PAPER 71-1111]
01 p0058 A72-10555

Wind profile determinations at 90-100 km from meteor trail drift and ionosphere inhomogeneity radar data, noting semidiurnal harmonics in wind components
01 p0058 A72-10563

Atmospheric water vapor vertical distribution from satellite IR spectrometer measurements, noting effects, absorption coefficients and temperature profiles errors
01 p0095 A72-10831

Vertical ozone distribution model using four variable parameters for stratospheric studies, climatology, scattering or radiometric measurements from ground or satellite
01 p0059 A72-10834

Nighttime sodium layer observation by tuned laser beam resonance scattering technique, measuring seasonal variation in Na abundance and height distribution
01 p0063 A72-10915

Nimbus 4 vertical atmospheric sounding techniques, obtaining temperature, water vapor and ozone profiles with Michelson IR interferometer
01 p0095 A72-10957

Steady state convection in solar atmosphere outer layers, plotting physical parameters as functions of geometrical depth
02 p0276 A72-11645

Ground based passive remote sensing of low altitude vertical temperature profiles by microwave radiometry
02 p0211 A72-11807

Quantitative cloud information from satellite IR thermal imagery and vertical temperature profile data
02 p0211 A72-11808

- Absorbed doses at various depths in water target exposed to charged pions, muons and electron beams, using Monte Carlo program
[CERN-71-16] 02 p0162 A72-12063
- Depth-dose experiments with monodirectional 14 MeV neutrons in low scatter environment, describing test facility
[CERN-71-16] 02 p0162 A72-12068
- Vertical distribution of ionospheric and magnetospheric electric fields, estimating Joule heating
02 p0220 A72-12324
- Ageostrophic vertical wind field determination from satellite cloudiness data, including geopotential pressure equations
02 p0253 A72-12537
- Wind altitude and maximal velocity computation for jet stream structure and turbulence
02 p0255 A72-12786
- Relief effects on atmospheric natural radioactivity vertical distribution
02 p0275 A72-12879
- Altitude, photon wavelength and solar activity effects on photoionization yield of ionospheric monatomic and diatomic oxygen and nitrogen via Monte Carlo simulation
03 p0345 A72-12983
- Ground based atmospheric vertical temperature profiles measurement by Raman backscatter from molecular nitrogen
03 p0348 A72-13430
- Midday oval, cusp region and polar cap auroral electron precipitation at low magnetic activity, presenting intensity vs altitude profiles for nitrogen ion line emissions
03 p0350 A72-13531
- Earth limb radiance measurements inversion, yielding temperature distribution as function of altitude in real atmospheres
03 p0384 A72-14146
- Short period height and longer period kinetic energy oscillations in 10-level primitive equation model for circulation prediction in tropical region
03 p0385 A72-14232
- Forbidden O I and molecular nitrogen ions emission lines ratio variation with height in aurora
03 p0352 A72-14382
- Stratospheric circulation and air temperature horizontal and vertical distribution, discussing CAT at supersonic transport heights
04 p0541 A72-14676
- Magnetospheric heat flux effect on height variation of electron and ion temperatures and ion composition in topside ionosphere
04 p0515 A72-14929
- Electronic collision frequency relationship with radio frequency in F region, investigating height, diurnal and seasonal variations
04 p0516 A72-14933
- Lower ionosphere 5777 and 5893 Å and hydroxyl band emissions interrelationships, observing atomic O and vertical eddy transport effects
04 p0518 A72-14961
- Height profiles for volume emission rate and intensity of second positive band of nitrogen molecule excited by photoelectron impact, noting solar activity effects
04 p0518 A72-14962
- Intensity-height profiles for molecular oxygen first and second negative bands in F region, using equilibrium velocity distribution of photoelectrons
04 p0518 A72-14963
- Free atmosphere vertical temperature structure at mesoscale, using continuous recording sonde
[AD-739147] 04 p0519 A72-15158
- Ionospheric neutral composition variations as function of height, local time and solar activity
05 p0656 A72-16235
- F 2 region electron density spatial and temporal distribution, investigating plasma vertical drift effects
05 p0657 A72-16263
- Altitude dependent vertical drift velocity of small scale ionospheric inhomogeneities, using correlation of signal time lag scanning in frequency domain
05 p0657 A72-16270
- Atmospheric short wave radiation angular and vertical distribution relation to aerosol scattering parameters, using transport equation
05 p0658 A72-16291
- N/h/ electron concentration profile in ionospheric D layer by exponent of frequency dependence of radio wave absorption
05 p0627 A72-16401
- Diffusion equations of ion components of plane stratified plasma /ionosphere/, taking into account wind effect and vertical temperature distribution
05 p0658 A72-16402
- Oxygen ions vertical flux altitude distribution in F layer from incoherent scatter radar measurements, noting existence in protonosphere during daytime
[AD-737929] 05 p0629 A72-16616
- Vertical extensive air showers at aircraft heights, constructing integral spectrum based on particle number
06 p0870 A72-17280
- Energy spectrum of muon formed electromagnetic cascades in vertical cosmic radiation flux
06 p0871 A72-17287
- Rocket-borne vector magnetometer measurements of midlatitude ionospheric currents near sporadic E, noting nearly uniform vertical distribution
06 p0804 A72-17459
- Indirect reduction of vertical atmospheric water vapor profile from measured outgoing thermal radiation by regularization method
06 p0842 A72-18039
- Rising/falling spherical wind sensors responses to atmospheric wind perturbations on vertical wind profile, using Fourier transform techniques
06 p0843 A72-18445
- Meteorological elements vertical profiles under cloud cover condition by solving heat and humidity transfer equations based on satellite data
07 p01029 A72-18860
- Ozone content and vertical distribution variations as causes of winter stratospheric warmings in Northern Hemisphere
07 p0973 A72-18861
- Electroconductivities and electrostatic field structure within equatorial electrojet, observing vertical distribution
07 p1056 A72-18896
- Radionuclides formation rate as function of depth in moon for bombardments by galactic cosmic ray particles and by solar protons
07 p1057 A72-19140
- Vertical density gradients as source of two stream instability irregularities in radio aurora theory
07 p0976 A72-19164
- Exact and approximate expressions derived for energy content of vertical air column extending from earth surface to stratosphere
07 p0977 A72-19856
- Horizontal transport in upper atmosphere by large scale circulation, presenting altitude variation of atmospheric constituents concentration for various eddy diffusion coefficient values
07 p0978 A72-20040
- Exosphere geocoronal hydrogen density, vertical structure and diurnal variability from Lyman spectra observational data, discussing polar wind origins
07 p0978 A72-20041
- Electroconductivity distribution and vertical gradients in photospheric layers of solar active region, using approximate model
07 p1082 A72-20293
- Radio meteors observability and wave reflection from trails, discussing velocities, deceleration and vertical distribution
08 p1130 A72-20712
- Sudden ionospheric perturbation effect on D region vertical distribution profiles, finding sixfold electron concentration increase at 75-80 km
08 p1154 A72-20729
- Altitude dependence of vlf field of vertical electric dipole in spherical waveguide of radially inhomogeneous ionosphere and earth, using Sommerfeld integral representations
08 p1130 A72-20736
- F 2 region magnetic disturbances conjugacy mechanisms, considering vertical ionization profiles
08 p1155 A72-20801
- Vertical distribution of electron density seasonal anomaly and storm effects in daytime midlatitudes topside ionosphere from Alouette 1 data
08 p1155 A72-20814
- Quarter thickness variation and particle temperature dependence on height and frequency in summer daytime F region
08 p1155 A72-20815
- Radio absorption in lower ionosphere obtained from vertical distribution of electron density and production rates from solar protons energy spectrum
08 p1226 A72-20816
- Magnetic field components of vertical currents at magnetosphere boundary and earth surface, using computerized Gaussian method
08 p1156 A72-20822
- Ionogram electron density-height distributions for analysis of multiple cusp structure near E region critical frequency
08 p1156 A72-21101
- Atmospheric vertical humidity profile from ground measurements of radio wave absorption at 1.35 cm water vapor line
08 p1158 A72-21192
- Vertical ozone distribution observed by Umkehr and IR methods
08 p1159 A72-21226
- Fading method measurement of normal and sporadic E region drift, reviewing height gradient data
08 p1161 A72-21539
- Atmospheric vertical temperature profile inference from ground based measurement of microwave thermal emission spectrum from atmospheric oxygen
08 p1161 A72-21824
- Statistical characteristics of wind elements from vertical-temporal structure of wind field
08 p1202 A72-22118
- Mesospheric ozone measurement for altitude profiles, comparing rocket and ground based observations of 1.27 micron emission band at twilight
09 p1296 A72-22355
- Atmospheric temperature vertical profiles by laser Raman backscatter measurements
09 p1307 A72-22439
- Cloud and Aitken nuclei vertical distribution upwind and downwind of urban pollution sources from simultaneous airborne observations
09 p1345 A72-22443
- Three parameter prognosis model for geopotential vertical profile in troposphere and stratosphere, describing vortex and heat influx in quasi-geostrophic and adiabatic approximations
09 p1297 A72-22549
- Frictioned force modification of lower thermosphere vertical neutral gas velocities with resulting atomic oxygen and molecular nitrogen density-height distribution deviation from barometric law
09 p1298 A72-22582
- Aspiration condenser spectrometry of small ion mobility as function of height and atmospheric conditions
09 p1346 A72-23267
- Continuous scan diffraction spectrometer for thermal sounding experiment on Meteor satellite, presenting vertical temperature and humidity profiles
09 p1347 A72-23588
- Wind velocity distribution structural laws in vertical and horizontal planes for large mesospheric and atmospheric processes
09 p1347 A72-23591
- UV radiation intensity altitude dependence and absorption by ozone, considering diurnal and annual variations and biological effects
09 p1268 A72-23625
- Meteor trail photoobservations for atmospheric small scale turbulences vertical profile, determining eddy minima velocities and turbulent energy dissipation in M zone
09 p1393 A72-23650
- Nucleonic cascade model analysis of underground vertical muon curve for primary cosmic ray nucleon spectrum below 40 TeV
10 p1529 A72-24417
- Atmospheric models of vertical structure of semi-diurnal atmospheric gravitational tides, taking into account Coriolis force and vertical acceleration components
10 p1473 A72-24530
- Magnetospheric electrons precipitation into ionosphere due to conjugate conductivity asymmetry caused by wind induced ions vertical redistribution, using atmospheric model
10 p1530 A72-24791
- Frequency distribution of ionospheric horizontal winds vertical shear, noting altitude independence, turbulence and viscous energy dissipation
10 p1477 A72-25157
- Atmospheric humidity vertical profile determination by measuring microwave radiation from satellite
11 p1620 A72-25274
- Ground based radiometric measurements of vertical temperature profiles in planetary boundary layer, describing data reduction technique
11 p1681 A72-26083
- Vertical distribution of nitric acid vapor concentration in lower stratosphere from balloon sounding
11 p1622 A72-26086
- SID coincident with solar photon burst, showing vertical variations of electron concentration
11 p1713 A72-26269
- Geometric parameters variations of ionospheric N/h/ profiles and characteristics during magnetic storm, discussing prognosis procedures from solar activity, latitude and season
11 p1594 A72-26273
- F region N/h/ profiles and parameters deviations during ionospheric and magnetic storms, discussing perturbation index
11 p1594 A72-26275
- Angles of arrival and skip distances prediction of radio waves near MUF, using monthly forecasts of quiet and perturbed ionospheric parameters and N/h/ profiles
11 p1594 A72-26276
- Noontime N/h/ profiles forecasts and annual variation in F region, relating solar activity levels to vertical distribution of electron concentration
11 p1594 A72-26277
- Statistical approach to atmospheric optics inverse problems solution, considering application to vertical temperature and humidity profiles determination
11 p1683 A72-26888
- Mass spectrometer measurements of hydrogen, helium, nitrogen, oxygen and nitrogen oxide ion concentrations vertical profiles in ionosphere at midlatitudes
11 p1628 A72-26906
- Vertical electron concentration and temperature profiles at 80-170 km measured by rocket launched on 10 July 1969 at Volgograd
11 p1628 A72-26917

Simultaneous measurements of ionospheric electrons number vertical distribution by incoherent ground radio wave scattering and coherent signals from Intercosmos 2 and Cosmos 321 satellites

11 p1628 A72-26918

ATS observed ionospheric columnar electron content variation during March 1970 solar eclipse, discussing neutral winds effects

12 p1801 A72-27155

Point discharge current and precipitation effect on atmospheric potential gradient vertical profile

12 p1839 A72-27501

Ekman boundary layer in two level quasi-geostrophic general circulation numerical model, representing physical characteristics of boundary layer turbulence increase with height

12 p1840 A72-27708

Sea level absolute vertical cosmic ray muon intensity from range spectrometer measurements within tropic zone

12 p1864 A72-28225

Exponential functions model for D region vertical distribution of electron density profiles, taking into account solar X- and cosmic rays

13 p1945 A72-28581

Total precipitable water in atmosphere vertical column relate to surface humidity from measurements at desert, coastal and maritime sites

13 p1989 A72-28812

Satellite aerodynamics effect on atmospheric density determination, discussing drag coefficient dependence on altitude

13 p1990 A72-28821

Mesosphere and stratosphere density and temperature variability with seasons and altitude

13 p1947 A72-28830

Wind shear third and fourth moments and distribution function in atmospheric boundary layer, emphasizing longitudinal turbulent velocity vertical variations

13 p1993 A72-28860

Vertical concentration profile and diurnal variations of N and NO vs solar activity from satellite horizon airglow experiment

13 p1948 A72-29237

Vertical distribution of atomic nitrogen ions in F-region produced by dissociative photoionization and charge transfer, suggesting undiscovered source at 300 km altitude

13 p1954 A72-29815

Solar chromosphere model based on Lyman spectra observations, calculating temperature, gas and electron pressure and particle densities as function of height

13 p2049 A72-29932

E region electron collision frequency vertical distribution by ground measurement of radio wave absorption, using electron concentration data obtained by rocket-borne interferometer

14 p2100 A72-30462

Internal gravity waves and convective instability caused by liquid layer nonuniform vertical density distribution, noting error in thermal conductivity measurement near critical point

14 p2095 A72-31008

Iterative numerical solution of linear differential equations system for wind vertical velocity and local pressure variation along vertical line

15 p2265 A72-31344

Ionospheric plasma resonance time duration variation with latitude, altitude and ratio of electron plasma frequency to electron cyclotron frequency

15 p2223 A72-31429

Atmospheric desorbed water molecules and ions number density vertical distribution in lower ionosphere and thermosphere

15 p2225 A72-31913

Equatorial ionospheric vertical electron density profiles measurement by rocket-borne phase measuring swept RF probe with dc biased sensor, comparing data with ionograms

15 p2226 A72-31940

Atmospheric density and temperature measurements by rocket-borne spheres during 1972 winter, observing variability with altitude

15 p2227 A72-31959

Aladdin experiment atmospheric composition, total neutral density, temperature and ion density vertical profiles

15 p2228 A72-31969

Selective chopper radiometer (SCR) radiances comparison to rocketsonde data, showing vertical resolution of stratosphere and mesosphere temperature changes during midwinter disturbance

15 p2228 A72-31976

Nighttime F region vertical velocity estimation, using electron density profiles vs true height

15 p2231 A72-32267

Geocorona and interplanetary He glow EUV emission altitude distribution measured by exospheric sounding rocket-borne thin film photon counters

15 p2231 A72-32327

Near IR airglow observation by sound rocket to determine layer height diurnal variation and rocket axis zenith angle

15 p2231 A72-32328

Sounding rocket observation for emission height of night airglow continuum near 6050 Å, using photoelectric photometers

15 p2231 A72-32329

Solar radiation absorption measurements in 2150 Å region as function of altitude to obtain oxygen and ozone densities

16 p2384 A72-32975

Barbados Oceanographic and Meteorological Experiment to compare synoptic scale-measured vertical vapor fluxes over tropical ocean

16 p2417 A72-33169

Dawn and dusk ionospheric conductivity gradients effects on equatorial electrojet, deriving vertical currents existence

16 p2385 A72-33377

Local vertical porosity and heat transfer coefficient relation to diluted fluidized bed relative height

16 p2479 A72-33851

Relative vorticity and balanced height distributions from cloud velocities associated with cloud structure of extratropical cyclone over continental U.S.

16 p2419 A72-33945

On the boundary conditions in theoretical model calculations of the distributions of minor neutral constituents in the upper atmosphere

18 p2659 A72-36294

Photodetachment of electrons from major negative ions in the lower D region

18 p2686 A72-36622

Water vapor flux periodic and spatial variations from airborne measurements, confirming height variation of maximum spectral density wavelength for crosswind runs

18 p2706 A72-36632

A climatology of the potential vertical extent of giant cumulonimbus in some selected areas

18 p2707 A72-36700

Lower ionosphere N/H⁺ profile calculation from ionograms with incomplete layer information

18 p2689 A72-36880

D region electron density profile determination based on LF link operating on one-hop ionospheric propagation of ordinary and quasi-transverse wave

18 p2689 A72-37163

High level atmospheric refraction of electromagnetic waves as function of elevation and meteorological element vertical stratification

19 p2764 A72-37349

Height-frequency characteristic forecasting for E layer at arbitrary time and point location, using solar zenith angle relationship

19 p2790 A72-38336

Radio meteors observability and wave reflection from trails, discussing velocities, deceleration and vertical distribution

19 p2765 A72-38340

Sudden ionospheric disturbance effect on D region vertical distribution profiles, finding sixfold electron concentration increase at 75-80 km

19 p2791 A72-38357

Altitude dependence of VLF field of vertical electric dipole in spherical waveguide of radially inhomogeneous ionosphere and earth, using Sommerfeld integral representations

19 p2766 A72-38364

The possible use of Laguerre polynomials for representing the vertical structure of numerical models of the atmosphere

19 p2829 A72-38562

The determination of the vertical structure of the atmosphere from satellite measurements

19 p2792 A72-38700

Effect of vertical flow structures on the cloud cover in the intratropical convergence zone

20 p2949 A72-39950

Balloon measurements of tropospheric turbulence vertical profiles, obtaining temperature and refractive index structure coefficients

21 p3077 A72-40144

Measurement of the vertical atmosphere transmittance in the IR spectral region with the aid of an artificial source

21 p3079 A72-41800

Rocket radiometers measurement of oxygen IR atmospheric system altitude profile at night, noting auroral enhancement possibility

22 p3170 A72-42365

Electron and positive ion density altitude distributions in the equatorial D-region

22 p3170 A72-42366

A comparison of the observed twilight with the vertical scatter distribution

22 p3170 A72-42373

Rocket measurement after sunset for altitude distribution of 1.27 micron band nightglow emission from diatomic oxygen molecules

22 p3172 A72-42435

A method for determining the electron density distribution about the F2 peak of the ionosphere

22 p3174 A72-42992

Variations of the planetary values of the F2 layer thickness and the parameters of the neutral atmosphere

23 p3284 A72-43375

Theoretical estimate of the effective recombination coefficient in the D region

23 p3284 A72-43818

Calculation of middle ultraviolet radiation detector response to solar radiation as a function of altitude

23 p3289 A72-43897

Variation with electron velocity powers of electron collision frequency and energy transport coefficients in weakly ionized plasmas - Earth's lower ionosphere

23 p3285 A72-43994

Probability distribution of vertical longitudinal shear fluctuations

23 p3281 A72-44146

A rocket measurement of the vertical distribution of atmospheric ozone

23 p3285 A72-44242

Experimental determination of the vertical gradient of the gravity force from a known geopotential

24 p3397 A72-44862

Exponential functions model for D region vertical distribution of electron density profiles, taking into account solar X- and cosmic rays

24 p3397 A72-45081

Distribution of hydrogen and helium in the upper atmosphere

24 p3400 A72-45593

VERTICAL FINIS

U FINIS

VERTICAL FLIGHT

Vertical flight direction determination by gyrostabilizers with integral compensation, noting variable platform orientation and vibration damping correction

21 p3059 A72-41812

VERTICAL MOTION

Kinematic vertical motions computation from radiosonde wind observations, correlating with synoptic features

01 p0095 A72-10855

Thermal advection statistical relation to vertical motion, discussing conventional synoptic meteorological empirical facts utilization in numerical models for long term weather forecasting

02 p0254 A72-12779

Quasi-geotropic wind field vertical motions in ground friction layer from continuity equation

02 p0254 A72-12780

Energy conversions and mean vertical motions in high latitude summer mesosphere and lower thermosphere, observing reaction kinetics

03 p0346 A72-13380

Vertical motions of midlatitude F2 layer during magnetospheric substorms, investigating electric field distribution

03 p0349 A72-13519

Lower F2 region positive oxygen ion distribution with allowance for vertical motions, production and recombination processes, using atmospheric models

08 p1152 A72-20708

Algorithm to compute inertial navigation system altitude and vertical velocity by closed feedback loop with accelerometer output mixed with pressure altitude reference

08 p1204 A72-21411

Electron density maxima position relationship to wind profiles in sporadic E layer with electric fields and vertical ion motion

10 p1530 A72-25165

Internal gravity waves effects on energy budgets and vertical angular momentum transport over mountainous terrain in southwestern U.S. from handheld camera pictures on Apollo 9

11 p1682 A72-26472

Slow drop of heavy rigid spheres through vertical tube filled with viscous liquid, noting minimization of errors due to temperature and trajectory path

11 p1617 A72-26501

Atmospheric vertical motions velocities prediction based on satellite cloud data

11 p1683 A72-26887

Kinematic estimate of large scale atmospheric vertical motion field patterns, using polynomial approximation of wind profiles

12 p1840 A72-27707

Vertical propagation of large scale disturbances in long wave radiation field into upper atmosphere, using linearized hydrothermodynamic equations

14 p2127 A72-30262

Time behavior of two dimensional laminar free convection flow between heated vertical parallel plates, calculating temperature and velocity distributions as function of Grashof number

16 p2477 A72-33426

Blowing and suction effects on free convection boundary layer on seminfinitesimal vertical flat plate, taking into account temperature difference between plate and fluid

16 p2477 A72-33429

Filtering polynomial technique to estimate wind, divergence and vertical motion profiles, suppressing random error effects

16 p2418 A72-33667

Doppler shift of solar photospheric spectral lines related to downward motions over plagues
17 p2617 A72-35705

Upward and downward motions of Venus atmosphere in terms of continuous cloud cover effects, considering solid cloud cover hypothesis
18 p2729 A72-36984

Lower F 2 region positive oxygen ion distribution with allowance for vertical motions, production and recombination processes, using atmospheric models
19 p2790 A72-38333

The influence of vertical motions on the diurnal variations of temperature and density in the thermosphere.
20 p2916 A72-39236

Convective instability of a fluid in hydrodynamically connected vertical channels
22 p3166 A72-42260

Equatorial ionosphere irregularities vertical drift velocity calculation, showing agreement with incoherent scatter results
22 p3170 A72-42370

VERTICAL PERCEPTION

Sjoberg hypothesis for zero gravity produced inversion illusion mechanism in aircraft parabolic flight, noting otolith membrane deflection result of force on maculae
02 p0167 A72-11710

Rotating disk background and speed effects on perception of verticality motion in clockwise or counterclockwise direction
08 p1124 A72-20987

Neck proprioception effects and otolith organ activity in perceived visual target elevation under centrifuging stress
12 p1776 A72-28305

Airline pilot rotation perception during angular acceleration tests, noting power law description of subjective motion for three major body axes
16 p2358 A72-33649

Division and orientation in the vertical-horizontal illusion.
18 p2651 A72-36913

Vertical posture control mechanisms in man
19 p2757 A72-37992

VERTICAL STABILIZERS
U STABILIZERS (FLUID DYNAMICS)

VERTICAL TAILS
U STABILIZERS (FLUID DYNAMICS)

VERTICAL TAKEOFF

VTOL short haul transportation applications discussing concept evolution and economic factors
16 p2480 A72-33181

Buoyancy systems and parawings application in short haul passenger transportation, discussing VTOL and STOL operations
16 p2348 A72-33183

Main results of nonlinear rotor theory
23 p3247 A72-43419

VERTICAL TAKEOFF AIRCRAFT
NT FLYING PLATFORMS

STOL and VTOL aircraft performance and efficiency, discussing landing and takeoff distances reduction
01 p0006 A72-11258

VTOL transport aircraft use in densely populated urban areas, discussing travel time, airport requirements, noise and design problems
05 p0612 A72-16733

All-weather landing aids for civil VTOL aircraft and helicopters, discussing Doppler and inertial navigations, instrument landing systems and ground visibility improvement
05 p0688 A72-16780

Model following variable stability system for X-14B VTOL aircraft, discussing hardware design and flight evaluation
[AIAA PAPER 72-96] 05 p0613 A72-16978

Rotorcraft based on VTOL concept for aircraft noise reduction in urban transportation
06 p0758 A72-18248

Integral and remote powered lift fan engines design for large civilian VTOL transports
[ASME PAPER 72-GT-65] 11 p1704 A72-25654

Propulsion system design for military VTOL aircraft, emphasizing subsonic cruise to maximum thrust ratio and exhaust downwash characteristics
[ASME PAPER 72-GT-73] 11 p1704 A72-25655

STOL, VTOL and V/STOL air transportation systems development, characteristics and requirements, presenting economic forecast
12 p1754 A72-27661

Aircraft tires design and performance characteristics, considering VTOL and Concorde operating conditions
13 p1901 A72-30098

Rotary wing and VTOL aircraft induced downwash effects on ground personnel, considering injuries, body heat loss, work capability impairment and sound pressure effects
14 p2072 A72-30425

Optimum low noise engine selection for transport and combat aircraft relative to range or payload performance, considering CTOL, VTOL, SST and fighter aircraft
15 p2297 A72-32127

Jet lift VTOL flight path optimization for minimum landing transition distance, evaluating deceleration as function of incidence and thrust vector angles
15 p2272 A72-32323

Fokker VTOL transport aircraft designs, considering payload, range, runway conditions, noise, military capabilities and operational costs
16 p2347 A72-33048

Ultrashort haul common carrier air transportation system based on VTOL aircraft for suburban-to-city center trips, comparing with land based transport
16 p2480 A72-33113

Axissymmetric jet impact on ground board for different nozzle configurations and heights in VTOL aircraft aerodynamic studies
16 p2377 A72-33404

A pilot's opinion - VTOL control design requirements for the instrument approach task.
[AHS PREPRINT 644] 17 p2490 A72-34504

New VTOL transport aircraft designs by VFW Fokker. II
17 p2492 A72-35477

The VAK 191 B VTOL fighter and reconnaissance aircraft
19 p2748 A72-37825

Extended Kalman filter with fictitious noise input for adaptive tracking of time varying parameters applied to VTOL aircraft
19 p2781 A72-38265

Tilt-propotor VTOL aircraft design evaluation based on aerodynamic and aeroelastic model and full scale performance tests
[AIAA PAPER 72-803] 20 p2889 A72-40054

VTOL aircraft noise reduction through design methods and flight path management in terminal area, evaluating acoustical annoyance to surrounding community
[ICAS PAPER 72-34] 21 p2995 A72-41159

Calculation of the recirculation flow of VTOL lift engines.
[ICAS PAPER 72-42] 21 p3099 A72-41167

German monograph - Model-analytical investigation of short-haul air traffic with VTOL aircraft in the Federal Republic of Germany.
22 p3245 A72-43068

Jet impingement under VTOL aircraft.
24 p3364 A72-45779

VERTICAL TAKEOFF AND LANDING
U VERTICAL TAKEOFF

VERTIGO

Obedience to rotation-indicating visual displays as a function of confidence in the displays.
17 p2510 A72-35943

VERTOL MILITARY HELICOPTERS
U BOEING AIRCRAFT

VERY HIGH FREQUENCIES

Composite incidental man-made radio noise data correlation to envelope statistic transformation hypothesis based on vlf airborne measurements of metropolitan area noise
03 p0324 A72-14041

Cost effective nonstatistical procurement of VHF power transistors with high degree of confidence in reliability
10 p1447 A72-24014

Coronal randomly distributed anisotropic density inhomogeneities induced refraction and scattering effects on solar radio sources at 80 MHz
16 p2452 A72-33042

Plastics in very-high and ultrahigh frequency applications
17 p2571 A72-35068

Results of observation of spectra and polarization of meter solar radio emission with high time resolution - May-June, 1969.
17 p2602 A72-35714

Radar auroral echo VHF power spectrum analysis of ionospheric irregularities, using range-time-intensity film strips
22 p3171 A72-42415

VERY HIGH FREQUENCY RADIO EQUIPMENT

German vhf ground telemetry satellite tracking system radio interferometer, discussing specifications and performance
[DGLR PAPER 71-124] 02 p0182 A72-12732

VHF remote control anemometer network with digital receiving station for wind measurement and gale warning system
10 p1463 A72-25013

VHF and UHF radio transmitters with strip transmission lines, discussing transistor power amplifier design
10 p1441 A72-25116

VERY LOW FREQUENCIES

Atmospheric waveforms in relation to source location, source vicinity electric field properties, VLF radio wave propagation, frequency spectra and lightning discharges
01 p0024 A72-10124

Vlf electromagnetic wave perturbations in transpolar propagation, noting time dependent behavior of polar cap absorption effects
01 p0056 A72-10441

VERY LOW FREQUENCIES

Lower ionosphere continuous electron density measurements with ground vlf transmitter, determining limiting altitude ceiling for diurnal and seasonal data
01 p0027 A72-10442

VLF noise spectra in earth-ionosphere cavity due to thunderstorm discharges, noting resonance level splitting by geomagnetic field
01 p0028 A72-10598

Ionospheric propagation, reflection and absorption of vlf hiss in aurora from rocket observation during quiet and substorm conditions
02 p0221 A72-12458

Nonducted vlf wave propagation near plasmapause during whistlers based on diffusive equilibrium and collisionless models for magnetospheric electron density distribution
02 p0222 A72-12873

Periodic micropulsations in amplitude and bandwidth observed in long duration vlf whistler mode signals from ground stations, considering explanations
03 p0322 A72-13530

Bremsstrahlung X rays from electron precipitation associated with discrete vlf emissions, recording wave-particle experiment near plasmapause with balloon-borne counters in Antarctica
03 p0413 A72-13536

Vlf phase regressions at sunrise related to variations of reflection coefficient in D region, using IENGf data
04 p0485 A72-14465

X ray stars atmospheric ionization effects by vlf phase tracking relative to Omega navigation accuracy, diurnal shift variations and astrophysical data
04 p0486 A72-14877

Low latitude low dispersion whistlers, discussing origin as vlf waves radiated from return stroke of lightning discharge
04 p0517 A72-14949

Complex eigenvalues computation for vlf wave propagation in spherical earth-ionosphere waveguide
04 p0492 A72-15442

Nonlinear propagation effects of monochromatic circularly polarized vlf waves /whistlers, heli cons/ along field lines in magnetosphere
05 p0658 A72-16603

Vlf propagation and D region aeronomy model for vlf phase behavior predictions and observations during two solar eclipses
05 p0630 A72-16618

Vlf phenomena of magnetospheric origin, presenting whistlers classification table
06 p0803 A72-17375

Phase velocity of first order mode of vlf waves propagating in earth ionosphere
06 p0773 A72-17598

Electron irradiation effects on MOS structures at vlf, considering inversion layer cut-off frequency and surface state density
06 p0865 A72-17610

Seasonal effects and propagation fluctuations in time-frequency comparison measurements with vlf waves, noting optimal RC filter
06 p0818 A72-18289

Slip effect in diurnal phase and amplitude cycles of vlf signals in lower ionosphere due to wave interference at transmitting point
08 p1130 A72-20710

Altitude dependence of vlf field of vertical electric dipole in spherical waveguide of radially inhomogeneous ionosphere and earth, using Sommerfeld integral representations
08 p1130 A72-20736

Vlf hiss with lower hybrid resonance cut-off recorded by Alouette 1, emphasizing midlatitude events and electromagnetic energy transportation by multion duct in topside ionosphere
09 p1279 A72-23007

Laboratory simulation of VLF/ELF radio waves transpolar ionospheric propagation, taking into account polar cap absorption
09 p1279 A72-23016

Mode theory of long distance VLF propagation, deriving equation for flat earth-ionosphere waveguides
09 p1282 A72-23570

Regular and irregular classes of amplitude fluctuations within artificially stimulated VLF emissions by low power pulses from ground transmitter
10 p1440 A72-24950

Global ground stations for lower VLF atmospherics arrival directions and spectral parameters observation
12 p1804 A72-27792

Distant thunderstorm center location with VLF atmospherics, determining delay time difference of Fourier spectrum groups of 6 and 8 kHz
12 p1841 A72-27793

Quasi-static and full wave calculation of VLF/ELF input impedance of arbitrarily oriented loop antenna in cold collisionless multicomponent magnetoplasma
13 p2009 A72-28542

Operational advantages of low cost VLF/OMEGA digital navigation system for various aircraft types
13 p1998 A72-29196

ELF and VLF waves propagation, deriving ionospheric field stable solutions by modified matrix multiplication technique for vertical geomagnetic field and large local refractivity

13 p1921 A72-29337

VLF long distance radio propagation in earth-ionosphere waveguide, considering earth magnetic field effects in mode conversion and refraction error calculation

13 p1922 A72-29655

VLF and LF electromagnetic waves amplitude and phase velocity in spherical earth-ionosphere waveguide, discussing wave hop method

13 p1923 A72-29661

Midlatitude VLF emissions intensity relationship to daytime auroral particle precipitation flux

15 p2194 A72-31437

Whistler mode VLF signal transmission in ground transmitter and magnetically conjugate zones, observing spectrum broadening and AM in magnetosphere

15 p2197 A72-31919

VLF signal role in long range time dissemination, communication and navigation, comparing conventional and modern techniques with emphasis on OMEGA system accuracy

15 p2199 A72-32068

Antarctic ice sheet complex permittivity in VLF band from reduction of measurement data with buried dipole antenna under snow surface

15 p2200 A72-32104

Antarctic D region reflection heights from relative phase measurements on VLF transmissions at several phase locked frequencies, interpreting results by waveguide mode theory

15 p2200 A72-32105

VLF wave normal direction measurement during propagation through ionosphere by Doppler technique, using rocket-borne receivers

15 p2201 A72-32332

First mode calculations for VLF atmospheric parameters of group delay time and spectral amplitude ratio based on Wait-Walters model

16 p2362 A72-32890

Association between quasi-periodic VLF emission and micropulsation.

17 p2516 A72-35065

Observation of very-low-frequency whistler-mode waves in the region of the radiation-belt slot.

17 p2517 A72-35598

Collisional losses in a very-low-frequency duct associated with the lower-hybrid-resonance frequency.

17 p2517 A72-35608

VLF hiss intensity, polarization, incidence angle and arriving direction observation at Antarctica station during magnetic disturbances

18 p2660 A72-36431

Observations of D-region modifications at low and very low frequencies.

18 p2662 A72-37009

Slip effect in diurnal phase and amplitude cycles of VLF signals in lower ionosphere due to wave interference at transmitting point

19 p2765 A72-38338

Altitude dependence of VLF field of vertical electric dipole in spherical waveguide of radially inhomogeneous ionosphere and earth, using Sommerfeld integral representations

19 p2766 A72-38364

The propagation of very low-frequency waves in ducts in the magnetosphere. II.

20 p2916 A72-39192

Polar ionosphere ELF/VLF noise distribution from Alouette 2 electric dipole observations

20 p2903 A72-39538

VLF emission artificial triggering by whistler mode pulses in magnetosphere, explained in terms of resonant trapped particle current and wave field behavior

20 p2903 A72-39549

Whistler propagation through magnetosphere.

21 p3049 A72-40975

VLF electromagnetic radiation frequency observation for pulsar pulsation or rotation period

21 p3111 A72-41485

Geomagnetic tail magnetic and electric fields ULF, VLF and ELF fluctuations, considering relationship to substorm processes

24 p3397 A72-44857

VESSELS

Glass silvered Dewar for liquid helium without auxiliary shielding cryogenics, using surrounding annular space for radiation shielding

15 p2214 A72-32431

VESTA ASTEROID

Pallada, Vesta, Irida and Harmony asteroids positions computed from observations with 400 mm photographic telescope

09 p1389 A72-23066

VESTIBULAR TESTS

Vestibular system tests using optokinetic, caloric, positional and rotational stimuli

01 p0022 A72-11292

Vestibular nuclei bulbar complex evoked potentials under visceral and somatic nerves electric stimulation in anesthetized cats

02 p0164 A72-12512

Human vestibulo-ocular responses to oscillatory rotational stimulation during various sleep and arousal stages, discussing Sugie-Jones reflex system mathematical model

04 p0474 A72-15249

Visceral afferentation role in vestibular system activity from experiments on rabbit stomach and rectum mechanoreceptor stimulation effects on vestibulo-oculomotor reflexes

05 p0618 A72-16630

Human vestibular stability under frontal and sagittal head tilts in rotating chairs, discussing motion sickness onset

05 p0622 A72-16640

Formulas derived for forces on receptor formation of vestibular apparatus from mathematical analysis of natural human head movements, discussing otoliths and semicircular canals

05 p0622 A72-16641

Auto- and cross correlation functions for neuron reactions in vasomotor center to adequate stimulation of cats vestibular apparatus

05 p0762 A72-17673

Pilot and nonpilot vestibular sensitivity to rotation, determining oculogyral illusion and rotation perception thresholds

06 p0767 A72-17867

Vestibulometric swing to obtain measured doses of receptor stimulation in otolith apparatus and semicircular labyrinth ducts with simultaneous physiological data recording

06 p0769 A72-18200

Galvanic skin response techniques for palmar and dorsal sweat detection during motion sickness by vestibular stimulation, comparing arousal and thermal sweat response

07 p0933 A72-20185

Field and intracellular potentials in cat trochlear nucleus following vestibular nerve and nuclei stimulation for synaptic organization study of vestibulo-ocular reflex

07 p0923 A72-20501

Nystagmus and illusory phenomena in man under simultaneous rotation in two perpendicular planes as function of vestibular excitation

09 p1267 A72-23593

Efferent vestibular activity in response to horizontal plane rotary stimulation in frog, showing efferent relations between both ears

10 p1426 A72-25099

Tandem walking on floor with eyes closed as ataxia test for vestibular function assessment

12 p1770 A72-27476

Vestibular, auditory, acceleration and altitude decompression testing of pilot following endolymphatic shunt surgery for Menieres disease

12 p1771 A72-27485

Brief vestibular disorientation test technique for assessment of potential nonpilot airborne specialists or naval flight officers

12 p1773 A72-28256

Motion sickness experience correlations to vestibular tests in pilots and nonpilots

12 p1764 A72-28257

Vision influence on acute motion sickness elicitation in slow rotation room, comparing with vestibular factors

12 p1764 A72-28258

Semicircular canal function correlation to thresholds, aftereffects and power functions in pilot vestibular tests

12 p1764 A72-28259

Nystagmus eye movements relationship to oculogyral illusion from test involving vestibular stimulation and visual stimuli velocity estimates

12 p1776 A72-28304

Quantitative model to describe vestibular detection of body sway motion in postural response mode

13 p1905 A72-29374

Respiratory and vasculomotor autonomic centers functional state relation to vestibular system from labyrinth electrical stimulation and shaking experiments

14 p2075 A72-30387

Human leg muscle reflex excitability changes during angular acceleration, suggesting vestibular apparatus as coordination means in quasi-static and dynamic movement control

14 p2075 A72-30388

Alcohol ingestion effect on vestibular responses to angular acceleration and Coriolis stimulation, discussing nystagmus and subjective responses

14 p2082 A72-31090

Prophylactic otolaryngological investigation of vestibular analyzer function in aviation medicine

15 p2186 A72-31769

Vestibular behavior of fish during diminished g-force and weightlessness.

17 p2499 A72-34549

Effects of different alcohol dosages and display illumination on tracking performance during vestibular stimulation.

17 p2508 A72-34554

Parallel swing with affixed luminous disks test for induced vestibular stimulation effects on moon illusion, noting eye movement factors

20 p2893 A72-38900

Vestibular labyrinth reactions and nystagmus thresholds in dogs during negative angular accelerations and simulated chronic galactic radiation from Co 60 gamma source

21 p2998 A72-40439

Vestibular and optical stimuli interaction in human orientation, testing via Barany chair on rotating platform surrounded by optokinetic drum

21 p3007 A72-40751

Influence of vision on susceptibility to acute motion sickness studied under quantifiable stimulus-response conditions.

24 p3377 A72-45659

VESTIBULES

Case history of student aviator with psychosomatic Lymphogranuloma venereum related to vestibular apparatus

02 p0167 A72-11712

Soviet book on gravitation receptor covering evolution of structural, cytochemical and functional organization in invertebrates /statocyst/ and vertebrates /vestibular apparatus/

03 p0316 A72-13850

Electrical stimulation of vestibular nuclei - Effects on light-evoked activity of lateral geniculate nucleus neurons.

19 p2758 A72-38220

The vestibular apparatus. I - The physics and physiology of the otoliths and the semicircular canals

22 p3146 A72-42787

Vestibular system functional relationship to postural reflex mechanism involving labyrinth and gravireceptors responses

22 p3147 A72-42788

VFR (RULES)

U VISUAL FLIGHT RULES

VHF OMNIRANGE NAVIGATION

Statistical analysis of track keeping Strumble VOR data for lateral navigation separation standards and collision risk in continental environment

01 p0097 A72-10179

VOR, Direct Measuring Equipment and TACAN polar coordinate radio navigation systems history, improvements and future development

02 p0257 A72-12646

Omega system in short range navigation supplementing VORTAC for coverage at low altitudes in mountain areas

06 p0844 A72-17334

Operational requirements for VORTAC system improvements, including precision VOR, navigation broadcast, DME capacity and CAS signals synchronization

06 p0845 A72-17336

Double parasitic loop counterpoise antenna radiation properties comparison to VOR systems, noting siting error reduction

06 p0782 A72-17357

Combined inertial/radio navigation systems for cost reduction, noting superior accuracy of VOR and DME

06 p0846 A72-18286

Area navigation systems, discussing VOR/DME, Doppler and inertial systems, CRT displays, data links, etc

08 p1204 A72-21523

Airborne VHF omnirange /VOR/ systems minimum operational standards for navigation and communication in air traffic control

10 p1509 A72-24725

VOR and Doppler VOR ground station equipment based on reliable solid state radio transmitters and signal generating devices for aircraft navigation

12 p1779 A72-27104

Aircraft distance measuring equipment with VOR radio receivers and ground station transponder for pulse interrogation

12 p1842 A72-27105

Integrated inertial-VOR-DME or inertial-TACAN navigation system, presenting slant range and bearing adjustment procedure via least squares method

16 p2421 A72-34136

Updating inertial navigation systems with VOR/DME information.

20 p2950 A72-39083

Antenna with printed elements for a VOR-S navigation installation

21 p3031 A72-40536

VIABILITY

The effects of various cure cycles upon the viability of *Bacillus subtilis* var. niger spores within solid propellant.

18 p2652 A72-36437

VIBRATION

NT BENDING VIBRATION
NT BREATHING VIBRATION
NT COMBUSTION VIBRATION
NT FLUTTER
NT FORCED VIBRATION
NT FREE VIBRATION
NT LATTICE VIBRATIONS
NT LINEAR VIBRATION

- NT MISSILE VIBRATION
NT PANEL FLUTTER
NT POGO EFFECTS
NT RANDOM VIBRATION
NT RESONANT VIBRATION
NT SELF INDUCED VIBRATION
NT STRUCTURAL VIBRATION
NT SUBSONIC FLUTTER
NT SUPERSONIC FLUTTER
NT TORSIONAL VIBRATION
NT TRANSONIC FLUTTER
- Hyperbolic and parabolic partial differential equations between comparison by studying point-to-point time optimal control for heat conduction and vibrating string motion 04 p0505 A72-14673
- Vibration theory calculations using parametric matrix function method and associated operators 04 p0550 A72-15543
- Stability-instability zones of solutions of Whittaker equation in vibration theory 05 p0690 A72-16353
- Layer potentials continuity in theory of vibrations of elastic medium 06 p0894 A72-17556
- Porous materials fabrication from chromium carbide powders, considering compaction procedures involving sinusoidal and pulsating vibrations 07 p1017 A72-19968
- Black hole vibrations explained as gravitational waves in spiral orbits 09 p1383 A72-22291
- Stability-instability zones of solutions of Whittaker equation in vibration theory 11 p1685 A72-25334
- Noise and vibration control engineering - Conference, Purdue University, Indiana, July 1971 13 p2005 A72-29553
- Instability regions of vibratory system with two degrees of freedom under random parametric effect, calculating bounds by numerical and analytical methods 15 p2275 A72-31608
- Flow distribution, vibration, wear and rupturing of rods in vertical pipe for various inlet flows investigated with high speed cameras, photography and transducers 16 p2376 A72-32996
- Spatial spark jitter measurements of highly charged nuclei for optical spark chambers 21 p3055 A72-41003
- VIBRATION DAMPERS**
U VIBRATION ISOLATORS
VIBRATION DAMPING
- Flutter equation approximate true damping or rate-of-decay solution by determinant iteration 01 p0142 A72-11133
- Maximum logarithmic decrement vs frequency of damped oscillation of elastic thin beam including internal and viscous resistance 01 p0144 A72-11384
- Stress waves propagation in woven-fabric composites, obtaining dynamic moduli and vibration damping coefficients by resonance technique [AD-736006] 02 p0291 A72-11984
- Control axes misalignment effects on spinning satellite wobble damping and requirements for active momentum exchange controllers 02 p0286 A72-12267
- Impact dampers with spring connection of masses, analyzing periodic motion 02 p0298 A72-12617
- Additive type composite oscillations in nonlinear damped vibratory system with two degrees of freedom, presenting modified Galerkin method 03 p0382 A72-13628
- French book on thin elastic structures vibration, describing antivibrational devices and rotating machines balancing 03 p0445 A72-13682
- Magnesium alloys torsional vibration damping correlation with texture orientation resulting from fabrication method 03 p0375 A72-13930
- Elastoplastic body random vibration analysis by statistical linearization, obtaining free elastic vibration mode shapes and damping constants 04 p0586 A72-15005
- Alloying, thermal and mechanical treatment effects on Mg alloys damping properties under elastic vibrations, showing test results consistency with materials microdeformation theory 05 p0671 A72-15987
- Cross section geometry and deformation effects on rods vibration damping, determining surface layer energy absorbing properties for longitudinal and torsional oscillations 05 p0735 A72-15988
- Magnetic damping comparison with internal viscous damping effect on circulatory elastic system equilibrium stability 05 p0689 A72-16061
- Infinitely long Euler-Bernoulli damped periodic aluminum beam with elastic springs, determining distance for steady state sinusoidal response to spatial decay 05 p0736 A72-16111
- Forced vibration and mechanical impedance of damped circular and annular membranes under central mass loads 05 p0739 A72-16615
- Earth satellite plane periodic oscillations damping with respect to center of mass in orbital plane during motion on elliptical Kepler orbit 05 p0730 A72-17030
- Damping of lateral oscillatory processes by end terminal displacement compensation, noting spring energy 05 p0691 A72-17132
- Damping effect in discrete one dimensional nonlinear lattice model leading to weakly dissipative Korteweg-de Vries equation 06 p0838 A72-17301
- Test facility for vibrations damping study of structural elements in water flow based on frequency and amplitude measurement at various flow conditions 06 p0796 A72-18364
- Damping characteristics of Ni base heat resistant alloys at high temperatures, showing increase with cyclic strain amplitude 06 p0833 A72-18630
- Forced transverse vibration damping of end loaded elastic cantilever beam, determining hysteresis loop contour from resonance curves 06 p0900 A72-18673
- Flexural, longitudinal and torsional vibration damping of various size rods, taking into account surface layer energy loss 06 p0900 A72-18675
- Energy dissipation of vibrating structures in complex stress state, using generalized stresses and strains as coordinates 06 p0900 A72-18677
- Forced vibrations and stability of one degree of freedom system with damping proportional to velocity, determining amplitude and phase resonance curves 06 p0901 A72-18710
- Weakly damped harmonic oscillator, using perturbation methods for approximate solution to boundary value problem differential equation 07 p1034 A72-18816
- Torsional oscillation damping in circular rods coated with viscoelastic material as function of resonant frequency 07 p1087 A72-18924
- Random vibrational stress and displacement spectra for linear complex mechanical dissipative systems with strong resistance and finite degrees of freedom 07 p1091 A72-19763
- Energy dissipation associated with transverse vibrations of sandwich metallic samples with damping coatings 07 p1094 A72-20135
- Asymptotic approximation method for damping force as function of velocity from successive oscillations amplitudes measurement 07 p1096 A72-20474
- Dynamic characteristics of strongly damped pendulum, assessing vibrations effects on vertical determination accuracy 08 p1206 A72-20974
- Soviet handbook on vibration absorbing properties of construction materials under cyclic straining, covering energy dissipation and dynamic strength 08 p1185 A72-20975
- Mo single crystal internal dislocational friction and ultrasound damping dependence on oscillation amplitude, exposure time and annealing temperature 08 p1185 A72-21073
- Particle mass spatial distribution effect on particulate damping of combustion acoustic vibrations in solid rocket propellants 08 p1224 A72-21617
- Graphite fiber reinforced composites with high mechanical strength and modulus at low weights, fatigue resistance, vibration damping and tailorable thermal expansion coefficient 08 p1193 A72-21689
- Frictional stick-slip autooscillations suppression by resonance effect during forced vibration in normal direction 08 p1181 A72-22181
- Two independent damping systems impact vibration analysis from solution of equations of motion by Laplace transformation 09 p1399 A72-22695
- Earth Love waves and toroidal oscillations attenuation, presenting frequency dependent model of internal friction 09 p1299 A72-22801
- Correlation functions for angular vibrations of operating aerial camera during working cycle 09 p1310 A72-22947
- Damping coefficient increase in welded bodies under uniform stress and compression, torsion and bending vibration 09 p1406 A72-23076
- Forced vibrations of two-mass system with damping through inelastic collisions, determining periodic motions stability regions with allowance for elastic coupling and friction 09 p1352 A72-23179
- Pressure distribution around circular cylinder with shrouds of various geometry for suppressing flow induced vibrations at subcritical and transition Reynolds number 09 p1261 A72-23315
- Deterministic optimization of aircraft undercarriage suspension characteristics for taxiing induced vibration minimization, discussing damping and stiffness functions and hybrid computer solution 09 p1407 A72-23458
- Random vibration of linearly elastic lumped mass systems containing, nonlinear damping to ideal stationary Gaussian white noise excitation 09 p1408 A72-23460
- Slip contact joint frictional damping of vibration of beam on elastic support 09 p1408 A72-23464
- Raman spectra of azoanisole and anizaldazine in liquid crystal states excited by Ar laser, revealing lattice vibrations attenuation near transition point 10 p1490 A72-24042
- Damping measurements of hydrodynamic vibrations of cylinder excited by random pressure field of liquid flow 10 p1465 A72-24073
- Maximum dynamic to static deflection ratio for thermally induced vibrations of elastic beams and plates, considering damping and axial load effects [ASME PAPER 71-APM-UU] 10 p1554 A72-24185
- Circular plates free flexural vibrations with and without damping, calculating resonant frequencies from corresponding Bessel functions 10 p1555 A72-24194
- Rectangular skin panel vibration modes aerodynamic damping dependence on Mach number, dynamic pressure, mode shape and turbulent boundary layer thickness [AIAA PAPER 72-402] 11 p1568 A72-25423
- Vibration characteristics of unidirectional filamentary boron-epoxy composite panels, obtaining nodal patterns, natural frequencies and damping coefficients 11 p1732 A72-25477
- Optimal parameters selection for natural vibrations maximum damping rate, applying method to two mass electromechanical system 11 p1686 A72-25533
- Aerodynamic damping of turbomachine blade vibrations under varied conditions of stagger angle, pressure ratio and relative velocity, using pure bending mode excitation [ASME PAPER 72-GT-8] 11 p1568 A72-25611
- Mechano-acoustical network model for room-hallway-window system response to sonic booms or other transient loads, determining damping ratios 11 p1686 A72-25729
- Damping additions for plates using constrained thin viscoelastic sheets and metallic layers 11 p1688 A72-26063
- Dynamic relaxation critical damping estimation in terms of mass dependent load vector concept involving vibration and Rayleigh principle 12 p1844 A72-27197
- Periodic solutions of forced oscillatory system with hysteresis damping 12 p1844 A72-27246
- Structural energy loss mechanisms, considering hysteresis, edge damping of panels, acoustic losses, dry friction, multilayer sandwich damping, etc 12 p1882 A72-27342
- Resonant contact vibrations of sliding element in direction normal to friction surface, noting lubrication damping effect 12 p1818 A72-28188
- Linear oscillatory system, investigating effects of pulsed dynamic damper with mass vibrations bounded by limiters 12 p1887 A72-28235
- Vibratory effects of disturbances transmitted from vehicle to viscoelastic vibroprotective damping coating in presence and absence of resonance 13 p2055 A72-28558
- Silicone based elastomers acoustic excitation damping properties at 213-423 K, discussing testing technique and results at 200-1000 Hz 13 p1957 A72-29090
- Torsional vibration damping in circular rods coated with viscoelastic material, noting technique effectiveness at certain resonant frequencies 13 p2058 A72-29209
- Superposed forced oscillations of liquid and of elastically mounted bulkhead with translational harmonic displacements of cavity, noting damping increase 13 p1942 A72-29498
- Vibrational relaxation mechanism in supersonic flows of chemically reacting carbon dioxide-nitrogen mixture, using numerical integration 13 p1913 A72-29502
- Undesirable mechanical vibration control concepts for acoustic noise reduction, considering environment characteristics, attenuation degrees and passive and active control mechanisms 13 p2005 A72-29555

Noise and vibration control in industrial and aerospace environments, discussing materials and techniques for structural vibration damping

13 p2059 A72-29557

HF transverse resonant vibrations of annular Al plates with polychlorovinyl and polyamide base coatings, noting damping and strain relationship to energy dissipation

14 p2164 A72-30427

Parameter resonances influenced by nonlinear damping amplitude-limiting due to vibrating systems nonlinearities with periodic coefficients

14 p2131 A72-30712

Aileron vibration pressure measurement in plane-parallel transonic flow, evaluating damping characteristics with allowance for shock motion caused nonlinear effects

14 p2071 A72-31026

Nonlinear oscillation systems mathematical model, determining periodic mode parameters, self excitation and damping mechanisms by point mapping method

14 p2133 A72-31126

Three stage linear damping of satellite roll and yaw oscillations, using slip motion procedure

15 p2319 A72-31492

Orthogonal vibration damping matrix numerical evaluation, comparing Caughey series and direct approaches

15 p2326 A72-31711

Low speed wind tunnel investigation of vortex formation effect on angle section columns galloping response, varying stiffness and damping characteristics

15 p2332 A72-32594

Anelastic damping of cold worked Nb sheet as function of vibration frequency, temperature, rolling rate and oxygen content

15 p2258 A72-32638

Equations of motion for damped vibrating system excited by periodic impulsive forces, calculating minimum residual vibration amplitude and force transmitted to foundation

16 p2423 A72-33121

Kinematically forced vibration damping in mechanical systems, discussing amplitude reduction by inertial compensation

16 p2424 A72-33149

Hybrid computer simulation of cochlea mathematical model, noting nonlinear damping

16 p2359 A72-33971

Combustion instability oscillations damping in rocket motors by short nozzles, calculating acoustic losses

17 p2635 A72-34233

Investigation of the damping features of a pressure regulator

17 p2559 A72-34916

Exact solution for dynamic oscillations of re-entry bodies.

17 p2622 A72-35231

Damping coefficient measurement for sound waves inside cylindrical tube closed at one end and excited at other end by loudspeaker

17 p2582 A72-35426

Local potential concept based variational method for eigenvalue problems of disturbance damping or amplification in stability analysis

17 p2583 A72-35641

Equipment vibration isolation principles, discussing damping, viscoelastic materials and shock absorbers

18 p2731 A72-35992

The effects of damping on a non-linear system with two degrees of freedom.

18 p2709 A72-36080

Frictional stick-slip autooscillations suppression by resonance effect during forced vibration in normal direction

18 p2695 A72-36238

LSA diode relaxation oscillator loading effect on oscillation damping, calculating optimum loading as function of conductance

18 p2667 A72-36690

Determination of the motion of a model, possessing a mass and a viscoelastic element, for a given harmonic law of motion of the vibrating support

19 p2871 A72-37427

Measurement of the damping capacity and dynamic modulus of high-damping metals under direct cyclic stresses.

19 p2795 A72-37460

Stability characteristics of floating bush bearings. [ASME PAPER 71-LUB-9]

19 p2807 A72-37698

Experimental investigation of flexural vibration damping in supported square plates with coatings

19 p2876 A72-38004

Effect of stress amplitude and number of vibration cycles on the damping decrement in metals

19 p2878 A72-38217

Low-frequency vibrations in a rarefied bounded plasma

19 p2842 A72-38530

Equivalent-damping and generalized-stagger distributions in single-circuit stagger-stage IF amplifiers at critical staggering

20 p2906 A72-38894

Weight saving, vibration proofing and heat dissipating techniques in avionics packaging, considering B-1 bomber electronic multiplexing system example

20 p2909 A72-39768

Determination of flexural-vibration deflections of structural elements with allowance for internal friction damping

20 p2981 A72-39921

Bending vibration test of glass-textolites, noting temperature effect on vibration damping properties

21 p3073 A72-41357

Graphite content effect on vibration damping properties of Al-Sn and Al-Zn alloys

21 p3070 A72-41358

On the destabilizing effect in a non-conservative system with slight internal and external damping.

21 p3124 A72-41483

Energy transfer in vibration damping of pendulum with elastic suspension, noting periodic regimes and transient oscillations

21 p3086 A72-41547

Solar pressure control of a spinning satellite with a stabilized platform.

[AIAA PAPER 72-918]

21 p3115 A72-41563

Comparison of three oscillatory techniques for cones at incidence.

[AIAA PAPER 72-1015]

21 p3042 A72-41595

A new method for the evaluation of slotted wind tunnel interference parameters applicable to subsonic oscillatory tests.

21 p3043 A72-41642

Suppression of oscillations in a plasma-beam system by modulation of low frequency signals

21 p3095 A72-41681

Vertical flight direction determination by gyro-stabilizers with integral compensation, noting variable platform orientation and vibration damping correction

21 p3059 A72-41812

Optimum damping for accelerometers.

22 p3175 A72-41930

Machine vibration diagnostics and damping, emphasizing filter lattice foundation structures, probability analysis and Bayes formula application

22 p3182 A72-42127

Small oscillations of gravity gradient satellite in circular near-equatorial orbit, discussing operational efficiency of magnetic damping systems

22 p3230 A72-42223

Thermoelastic martensite caused elastic vibration damping in Cu-Al-Ni alloy, observing shape memory effect

22 p3190 A72-42442

Linear system proper frequencies and vibration dampings obtained by mathematical smoothing of mechanical admittance measurements

22 p3241 A72-43093

Method of measuring modal characteristics of a structure subjected to a random excitation

22 p3242 A72-43095

Relationship between the dissipative properties of a vibrational system and its amplitude-phase-frequency characteristics

23 p3313 A72-43785

Equivalent linear solution for transient free vibration of beams with strain dependent, frequency independent stress-strain hysteresis loop with sharp corners

23 p3352 A72-44120

Explosive instability temporal development, noting linear damping role in nonlinear wave interaction under conservation laws of energy and momentum

23 p3282 A72-44318

Technique for measuring damping properties of thin viscoelastic layers.

24 p3402 A72-44885

Electronically-damped pendulum acceleration measuring device with analog restoring mechanism. I

24 p3403 A72-45271

Cross section geometry and deformation effects on rods vibration damping, determining surface layer energy absorbing properties for longitudinal and torsional oscillations

24 p3460 A72-45730

Energy dissipation associated with transverse vibrations of sandwich metallic samples with damping coatings

24 p3461 A72-45760

VIBRATION EFFECTS

NT POGO EFFECTS

Human and monkey muscle tonic vibration reflex response to vibratory stimulation dependent on frequency range, electromyograph discharge interval length, etc

02 p0163 A72-12250

Self oscillations and drift motion of gyroscopic integrator of linear accelerations under hf vibrations, assuming ideal relay gimbal compensation

02 p0231 A72-12567

Thin walled elastic axisymmetric fluid filled tanks under longitudinal vibrations, determining dynamic characteristics

04 p0586 A72-15011

Frog and rabbit sciatic nerve afferent impulse recordings during prolonged sinusoidal vibration of foot

04 p0474 A72-15235

Vibrations effect on corrosion rate by experimental method, comparing reaction kinetics on two specimens with and without alternating stresses

04 p0591 A72-15237

Mechanical impedance and phase angle time variation in restrained primate during prolonged sinusoidal vibration

[ASME PAPER 71-WA/BHF-8]

05 p0616 A72-15946

Small elastoplastic cyclic strain effects on internal friction and energy dissipation in metals during vibrations

06 p0834 A72-18679

Thermostable and heat resistant steels and alloys vibration loading frequency effects on fatigue at high temperatures

06 p0834 A72-18688

Harmful influence of random vibrations on human organism, discussing Fokker-Planck analysis and amplitude and frequency variation effects

06 p0770 A72-18720

Angular and linear vibrations effect on dynamic errors of two stage gyrocompass, obtaining nonlinear equations of motion approximate solutions

07 p0981 A72-18928

Boundary value problems in supporting surfaces vibrations theory, constructing Green function from part of differential operator

07 p1093 A72-19984

Subharmonic oscillations excited by horizontal vibrations of mathematical pendulum suspension

07 p1036 A72-20323

Rotor components vibration stabilizing effects on dual spin spacecraft dynamics, considering turbulent liquid sloshing in Intelsat 4 propellant tank

07 p0973 A72-20488

Dynamic characteristics of strongly damped pendulum, assessing vibrations effects on vertical determination accuracy

08 p1206 A72-20974

Optimization for maximum productivity of electric spark machining with vibrating electrode, noting erosion product removal difficulties

08 p1174 A72-21033

Oscillographic transient analysis of electric spark machining processes with electrode natural or forced vibrations

08 p1174 A72-21037

Machine parts surface hardening and smoothing by vibrating hard alloy sphere impact at ultrasonic frequency

08 p1176 A72-21050

Slow adiabatic motions of vibratory suspended bodies and determination of carrying body parameters and orientation from oscillations monitoring

08 p1206 A72-21229

Two reflector Cassegrain antenna secondary reflector random fluctuations effects on drift in main lobe direction

08 p1143 A72-21846

Concorde sonic boom measurement, discussing structural vibrational response

08 p1111 A72-21911

Vibrating membrane generated acoustic pressure wave propagation in rarefied gas, applying to solid surface-gas interaction models

09 p1294 A72-22762

Liapunov theory solutions stability for oscillations along galactic axis of symmetry

09 p1390 A72-23396

Ruby laser radiation modulation by mirror ultrasonic vibrations, discussing mechanism

09 p1326 A72-23681

Cardiovascular changes produced by whole body vibration of dogs and pigs, obtaining resonant frequencies of organ systems

10 p1426 A72-24484

Human biodynamic and behavioral response to whole body vibration, discussing subjective judgment of vibration intensity and effects on performance

10 p1431 A72-24797

Aircraft pilot seating protection from dynamic environment by active vibration isolation, discussing human frequency response characteristics

11 p1585 A72-26391

Helicopter rotor blade spars shot peening in centrifugal vibrator, optimizing Cr-Mo-Ni steel surfaces work hardening

11 p1642 A72-26820

Variable white dwarf radial pulsation periods explained by nonradial oscillations and gravity modes, considering atmospheric mixing with degenerate core

12 p1868 A72-27260

Biothermal response of increased core temperature in rhesus monkey to mechanical vibration, noting implications for pilot performance during prolonged buffeting

12 p1774 A72-28268

Angular oscillation in yaw effect of pilot visual performance, showing vestibulo-ocular compensation and frequency response

12 p1774 A72-28269

Supine human body mechanical impedance under combined stress of vibration and sustained acceleration

12 p1765 A72-28270

- Vibratory effects of disturbances transmitted from vehicle to viscoelastic vibroprotective damping coating in presence and absence of resonance
13 p2055 A72-28558
- Vibration stability and interference transfer function of onboard transponder with phase lock AFC used in Doppler system for measuring spacecraft trajectory parameters
13 p1958 A72-29456
- Combined thermal, vibrational and dimensional treatments effect on WC-Co alloy physical and mechanical properties, noting tensile and impact strength increase
13 p1979 A72-29480
- Human hand-arm system vibration characteristics, describing mechanical impedance measurements for mathematical modeling
13 p1910 A72-29559
- Mechanical vibration induced physiological changes in rats, determining plasma Ca, Mg and inorganic phosphate concentration and xanthine oxidase activity response to frequency and g-levels
13 p1910 A72-29560
- Dynamic contact problems of stamps bands oscillation on elastic layer surface or cylinder, analyzing vibrationally induced elastic waves
14 p2163 A72-30223
- Modified Al-Si eutectic solidification behavior and microstructure, investigating LF mechanical vibration effects
14 p2120 A72-30617
- Quantum mechanical calculation of interaction potential energy surface role in vibrational excitation of diatomic molecules
14 p2134 A72-30750
- French monograph on velocity profile in laminar boundary layer on semiinfinite flat plate in harmonic oscillation of uniform incompressible flow
14 p2095 A72-30949
- Vigilance effects for noise or vibration stimuli duration judgment task performed with or without simultaneous mental arithmetic task
14 p2080 A72-30964
- Noise and vibration stress combined effects on human mental performance as function of time of day, taking into account circadian rhythm factor
14 p2081 A72-31083
- Plastic deformation in metals and highly crystalline polymers as function of shear strain, strain rate, frequency and vibrational amplitude
15 p2328 A72-31840
- Mechanical vibrations effect on flow stress and strain rate from tensile and creep tests as function of amplitude
15 p2257 A72-31841
- Diatomic molecular vibrational excitation and dissociation effects on imploding shock waves, comparing shock tube data to prediction
15 p2192 A72-32148
- Diatomic gas flow behind blast wave, discussing vibrational nonequilibrium effects and solution of governing equations via characteristics method
16 p2378 A72-33440
- Organism response to extreme overload factors, discussing centrifuging and vibration stress effects on mean swimming time and post-irradiation survival time in mice
16 p2355 A72-33554
- Equations of motion for small vibrations superposed on time depending deformation of elastic body, discussing acoustic wave propagation
16 p2425 A72-33590
- LF whole body vibration effects on rat escape conditioning in terms of frequency, amplitude and controls for noise and activation
16 p2357 A72-33868
- Calculation procedure involving wave function for vibrational correction to electron scattering cross section of hydrogen molecule in Born approximation
17 p2585 A72-34261
- Independent moving vibrational /acoustic/ source-induced wave losses during friction of two elastic bodies
18 p2696 A72-36966
- The resonance mechanism of the biological action of vibration
20 p2897 A72-39409
- Equal comfort contours for whole body vertical, pulsed sinusoidal vibration.
20 p2897 A72-39551
- Comparison of irregular vibrations of a limited frequency range with sinusoidal vibrations in regard to their effect on man
20 p2897 A72-39804
- The study of vibration patterns using real-time hologram interferometry.
20 p2927 A72-39848
- Incorporation of methionine-S 35 in the proteins of the digestive organs of rabbits under the action of radiation and vibration
21 p2998 A72-40440
- Flying personnel auditory defects caused by environmental conditions, discussing aircraft noise, vibrations and atmospheric pressure effects
21 p3002 A72-40924
- Body orientation under vertical sinusoidal vibration.
21 p3008 A72-41019
- Finite radial oscillations of uniformly rotating gravitating magnetized fluid cylinder model of star formation dynamics
21 p3109 A72-41331
- Applied research into the effects of vibration upon displays.
21 p3011 A72-41424
- Behavioral features of a composite hydrostatic suspension of a gyrocompass under conditions of vibration
21 p3058 A72-41807
- Experimental investigation of the elastic characteristics of composite bearings in turbine machinery for the purpose of increasing their efficiency and reliability during nonlinear vibrations of the rotor
22 p3181 A72-41860
- Effect of vibration on the permeability of the blood-brain barrier
22 p3149 A72-42070
- Russian book - Dynamics and acoustics of machines.
22 p3182 A72-42126
- Viscoelastic and active vibration isolators for foundation isolation of polyharmonic vibrational effects of operating machines
22 p3182 A72-42131
- Influence of a sinusoidal pressure variation on contact thermal resistances
22 p3244 A72-42644
- Image motion in the Culgoora solar magnetograph - The role of vibration.
23 p3278 A72-43617
- The vortex street in the wake of a vibrating cylinder.
23 p3281 A72-44302
- Errors caused by hot-wire filament vibration.
24 p3402 A72-44949
- Evaluation of the danger of damage to mechanical systems exposed to random vibrations
24 p3459 A72-45449
- The influence of static stresses on the dissipation of energy due to forced oscillations.
24 p3461 A72-45767
- VIBRATION ISOLATORS**
Shock isolator model, using passive elements and variable Coulomb friction force to minimize transmitted shock and relative displacement
01 p0047 A72-10218
- Squeeze-film bearings nonlinear vibration performance in aircraft gas turbine engines, emphasizing lubricant viscosity importance
07 p0999 A72-20532
- Speckle reference beam holography for object motion compensation with reduced vibration isolation requirements, discussing CW and pulsed laser use
09 p1314 A72-23338
- Aircraft pilot seating protection from dynamic environment by active vibration isolation, discussing human frequency response characteristics
11 p1585 A72-26391
- Undesirable mechanical vibration control concepts for acoustic noise reduction, considering environment characteristics, attenuation degrees and passive and active control mechanisms
13 p2005 A72-29555
- Pilots seating active and passive isolation from LF vibrations in helicopters and jet aircrafts, discussing human factors and dynamic environment
13 p1910 A72-29558
- Nonlinear vibration damper system subject to forced vibrations considered as stochastic processes in form of white noise and stationary and ergodic processes
16 p2467 A72-33144
- Synthesis of a resin-metal damper whose characteristic shows minimum deviation from a constant-frequency response
19 p2806 A72-37429
- Calculation of the nonlinear viscoelastic oscillations of a vibronic protective layer
19 p2872 A72-37537
- Isolator elastomers properties, discussing spring isolators, combination springs and pneumatic systems
19 p2806 A72-37550
- A stand for quality control of the vibrational characteristics of 'ultraquiet' radial ball bearings
19 p2807 A72-37663
- Mathematical model of seismic isolation block and pneumatic suspension for inertial guidance component tests to describe design factors effects on vibration behavior
20 p2950 A72-39085
- [AIAA PAPER 72-844]
Pneumatically isolated test platform local gravity vector active control to investigate seismic level disturbance effects on precision inertial components evaluation
20 p2923 A72-39086
- [AIAA PAPER 72-843]
Comparison of design procedures of vibration absorbers for systems with random excitations.
21 p3121 A72-41230
- Design of vibration absorbers minimizing human discomfort.
21 p3009 A72-41231
- Viscoelastic and active vibration isolators for foundation isolation of polyharmonic vibrational effects of operating machines
22 p3182 A72-42131
- VIBRATION MEASUREMENT**
Ultrasonic excitation induced vibration measurement for detecting incipient electrical breakdown in transducers, using laser-Michelson interferometer
01 p0081 A72-11018
- Gas turbine rotor disk and blade vibrations piezoelectric measurement, describing capacitive transmitter system devoid of rotor mounted power supplies
02 p0232 A72-12735
- Noncoherent moire contour-sum contour-difference and vibration analysis of three dimensional objects using grid projection and offset camera
03 p0358 A72-13438
- Natural torsional vibrations of curved shafts, discussing oscillating system with varying flywheels
04 p0584 A72-14470
- Test facility for vibrations damping study of structural elements in water flow based on frequency and amplitude measurement at various flow conditions
06 p0796 A72-18364
- Cascading turbomachine blades vibration measurement in subsonic and sonic high temperature gas flows, describing test facility
06 p0797 A72-18689
- German monograph on vibration amplitudes interferometric measurement, discussing methods for resolution improvement and phase measurements, distortion and sonic field effects, etc
07 p0983 A72-19264
- Accelerometer sensitivity calibration by laser interferometer for vibration measurement, discussing frequency range, accuracy and advantage over spectral lamp
07 p0984 A72-19350
- Vibrational amplitude measurement of diffuse surface by modulation of projected fringes in optical field
07 p0985 A72-19407
- Vibration measurements of gyromotors with aerodynamic spherical and ball bearings
09 p1263 A72-22347
- Vibration measurement based on moire pattern fringes motion due to line gratings respective displacement, noting high accuracy and resolution
09 p1315 A72-23388
- Holographic method for investigating piston type vibrations with phase modulated reference light beam
09 p1317 A72-23682
- Mechanical and electrical methods of measuring vibration rates, displacements, accelerations and time derivatives, examining magnetoelectric and piezoelectric sensors characteristics
11 p1635 A72-26462
- Compressor blade vibration indicator measurement by positioning one inductive sensor by rotor blades and another by toothed gear on rotor shaft
13 p1956 A72-28784
- Eddy current sensor for mechanical vibration measurements, describing circuit design for stable and reliable operation at 30 MHz
13 p1930 A72-29051
- Glass and carbon fiber reinforced plastic beam specimens dynamic moduli and loss factors determination from vibration frequency and decay rate measurements
13 p1984 A72-29095
- TV speckle pattern recording for coherent laser light measurement of mechanical vibrations in micrometer range
13 p1961 A72-30026
- Aileron vibration pressure measurement in plane-parallel transonic flow, evaluating damping characteristics with allowance for shock motion caused nonlinear effects
14 p2071 A72-31026
- Calibrated LF acceleration vibrocardiography to examine hemodynamics indices relation to main wave amplitudes
15 p2188 A72-31313
- Time-average holography with thin phase recording materials, obtaining characteristic function solution for sinusoidal vibration and constant velocity motion
15 p2235 A72-31614
- Coherent light signal optoelectronic processing techniques application to engineering components displacement measurement and vibration amplitude real time imaging
15 p2238 A72-32168
- Speckle pattern method of laser holography for structural vibration and surface strain study, noting real time operation
16 p2388 A72-32821
- Laser interferometric calibration for vibration measurement, discussing operation principle and detector error
16 p2391 A72-33248
- A diffraction transducer for vibration analysis.
17 p2626 A72-34722
- Contactless parameter measurements of a vibrating bar.
17 p2554 A72-35148

Real-time vibration analysis of rib-stiffened plates by holographic interferometry.

18 p2690 A72-36361

Flat beam linear vibration analysis from mode measurement and moiré technique, applying to prototype turbine compressor blade

18 p2734 A72-36375

The non-stroboscopic visualisation of vibrational patterns by real-time/time averaged hologram interferometry.

19 p2873 A72-37618

Use of a projected-ruling moiré method for vibration and deflection measurements of three-dimensional structures.

19 p2799 A72-37629

Inertial plasma effect in a glow discharge - A new principle of oscillation measurement

19 p2800 A72-37756

Surface tilt and vibration measurements by laser speckle pattern photography, comparing with moiré fringes in strain analysis

20 p2930 A72-39032

Vibration measurements of temperature dependent dynamic moduli of Al/resin/Al sandwich bars with cyanocrylate adhesives

21 p3118 A72-40720

Book - Vibration and acoustic measurement handbook.

21 p3086 A72-41533

New methods of measuring the parameters of multidimensional vibrations of linear mechanical systems

22 p3176 A72-42130

Vibration measurements of an airplane fuselage structure. I - Turbulent boundary layer excitation. II - Jet noise excitation.

22 p3139 A72-42912

A preamplifier with high input impedance for use with piezoelectric sensors

22 p3160 A72-42923

Measurement of small strain amplitudes in internal friction experiments by means of a laser interferometer.

24 p3402 A72-44947

VIBRATION METERS

NT LUNAR SEISMOGRAPHS

NT SEISMOGRAPHS

Double frequency stroboscopic method for absolute calibration of vibration transducers, analyzing errors

06 p0815 A72-17766

Miniaturized piezoelectric transducer electronics versus charge amplifiers - A comparison of the two systems in vibration and pressure applications.

22 p3159 A72-42702

VIBRATION MODE

NT UNCOUPLED MODES

Statistical variance of eigenvalues and eigenvectors in random structure dynamic analysis by component mode synthesis

01 p0137 A72-10277

Algorithms for mass and stiffness matrices synthesis from experimental vibration modes applied to cantilever beam

01 p0137 A72-10278

Lateral vibration of thin conical bar with clamped base and free tip, calculating characteristic modes and frequencies

01 p0138 A72-10509

Bulk InP three level transferred electron microwave oscillators, observing current-controlled instabilities and operation modes

01 p0036 A72-10632

Moving load effect on circular cylindrical shell in acoustic medium, discussing free axisymmetric vibration mode, shape and frequencies

02 p0290 A72-11627

Unpredicted structural vibration in Comet and Electra aircraft, Graf Zeppelin dirigible, missile antennas, etc

02 p0292 A72-12002

Rotating cable of high slenderness ratio and small flexural rigidity with end masses, deriving transverse vibration mode shapes and natural frequencies from asymptotic solution

02 p0293 A72-12253

Unstiffened cylinders natural frequency equations, determining modal density distribution and acoustic radiation efficiency

02 p0293 A72-12373

Flutter problem wing-air flow energy exchange at instability limit, obtaining vibration mode shapes from homogeneous boundary value problem analog model

03 p0442 A72-13191

Regenerative system reliability, examining oscillation mode selector

03 p0333 A72-13833

Multimass multiply branched multistage elastic systems natural frequencies and oscillation modes, presenting algorithm and iterative calculation procedure

03 p0449 A72-13913

Torsional vibrations of shaft with multiple flywheels, presenting computer generated graphs for vibration modes

04 p0584 A72-14517

Elastoplastic body random vibration analysis by statistical linearization, obtaining free elastic vibration mode shapes and damping constants

04 p0586 A72-15005

Linearized equilibrium equations for thin spherical shell with internal pressure, obtaining free vibration modes

04 p0587 A72-15018

Optimal design of solid and three layer rods with prescribed natural frequencies for longitudinal and transverse vibrations, using minimum mass criterion

04 p0587 A72-15047

Step-by-step perturbation method for calculating vibration modes of aerospace structure

[ONERA, TP NO. 968] 04 p0592 A72-15552

Natural frequencies and vibration mode shapes of simply supported symmetric trapezoidal plates

04 p0592 A72-15564

Dispersion equation derived for acoustic-gravity type natural modes in solar atmosphere

05 p0712 A72-15769

Hybrid representation for structural component by vibration modes with free or fixed connection points and boundary conditions selection to optimize accuracy

05 p0736 A72-16084

Vibration mode shapes and frequencies determination by finite element method using consistent and lumped masses formulations in differential equation solution, considering convergence rate

[AD-739820] 05 p0736 A72-16086

Conical cavity resonator design for submillimeter wave electron beam devices, investigating mode and resonant frequency dependence on cavity size

05 p0636 A72-16364

Thin circular flat plate simply supported at three points on circumference, obtaining vibration mode shapes and eigenvalues

05 p0738 A72-16532

Algorithm for selective computation of large structural modifications effect on eigenmodes of linear structure

06 p0895 A72-17848

Localized vibration modes of light impurities in gallium phosphide crystals from absorption spectrum analysis

06 p0866 A72-18182

Transferred electron microwave oscillators design for various peak and average power levels, considering tradeoff between operating mode and device configuration

06 p0789 A72-18475

Dynamic properties of turbine wheels under bending vibrations, classifying resonant frequencies on basis of vibration modes

06 p0899 A72-18644

Free solid body kinetic moment vector effects on long period motion in resonant state during transition from rotational to somersaulting mode

06 p0849 A72-18699

Nonlinear elastic systems with distributed parameters, obtaining single frequency mode random oscillations solution of boundary value problem by asymptotic method and Markov process

06 p0850 A72-18700

Mechanical systems with nonlinear position functions, elastic elements or self damping, investigating oscillation mode onset and stability conditions

06 p0850 A72-18701

Numerical approximation of Pochhammer-Chree longitudinal vibration modes in elastic cylinders by quadratic spline functions

07 p1087 A72-18797

Natural frequencies and vibration modes of simply supported tapered skew rhombic plates, considering thickness and skew angle effects

07 p1088 A72-19116

Shallow spherical shell equations solution for vibration mode and natural frequencies from analogous vibrating plate solution

07 p1089 A72-19489

Vibration characteristics of simply supported unsymmetric trapezoidal plates

07 p1089 A72-19644

Equivoluminal vibration modes of multipolar elastic plate with traction free faces

07 p1089 A72-19646

Vibration modes and stability of nonequilibrium low density He-Cs plasma in magnetic field

07 p1043 A72-19876

Trapped modes structure of rotating fluid in thin spherical shell, noting constitution of free oscillation periods

07 p0973 A72-20455

Symmetrically loaded uniform thin circular ring natural vibration frequencies in radial and axial flexural modes, comparing experimental data with values predicted by group theory

07 p1096 A72-20499

Pinned-free beam response to transient support excitation, using pinned-pinned beam modal parameters

07 p1096 A72-20526

Torsional bending vibrations mode shapes of space frame with variable elastic and mass characteristics, determining eigenvalue error limits

08 p1205 A72-20957

Free oscillations frequencies and mode shapes determination of two parallel elastically coupled rods of variable cross section, applying Bubnov-Galerkin iterative method

08 p1243 A72-21231

Orthotropic circular cylindrical elastic shell vibration mode shape analysis by Vlasov equations, using asymptotic method

08 p1247 A72-21813

Resonant frequencies of rectangular plate with two sides subject to mixed boundary conditions, expressing vibration modes in terms of Fourier series

08 p1249 A72-21946

Soviet book on longitudinal vibrations of rocket with liquid propellant engine covering rocket element dynamic characteristics and free vibration mode shape and frequency calculations

08 p1241 A72-22025

Vibrational characteristics dependence on structural flexibility in gimbal bearings and supporting structure of two axis free gyroscopes and single axis rate gyroscopes

08 p1173 A72-22129

Vibration modes of bladed turbine wheel, formulating mathematical model

08 p1224 A72-22132

Nonlinear programming analysis of free vibration of simply supported beam

08 p1249 A72-22136

Nonlinear mode coupling in equations of motion for thin panel vibration as function of membrane stretching-bending energy ratio

09 p1408 A72-23465

Vibration frequencies of slender beams and circular plates with boundary stiffness and damping

[ASA PAPER E 5] 09 p1408 A72-23525

Oscillation modes and stability region of harmonic oscillators with homogeneous nonlinear rheological differential equations of motion

10 p1513 A72-24998

Free in-plane vibrations of hinged and fixed uniform circular arches, discussing natural frequencies and flexural and extensional vibration modes

10 p1560 A72-25186

Rotor blades setting angle and twist influence on steam turbine wheels vibrational modes and frequency spectra

11 p1732 A72-25537

Radiation resistance of baffled beam modes from far field acoustic power intensity

11 p1687 A72-26058

Sound radiation impedance of vibrating prolate spheroids as function of nearfield variation

11 p1688 A72-26064

Mode chart and unloaded quality factor of elliptic microstrip resonator operating in inverse or radial TM modes

11 p1607 A72-26996

Natural vibration modes of coupled spring-mass nonlinear system with two degrees of freedom from stability analysis

12 p1844 A72-27245

Approximate theory for high frequency elastic plate vibrations in terms of thickness mode expansion

12 p1881 A72-27251

Ring stiffened truncated cone shells vibration mode tests, describing air and electrodynamic shakers and mobile noncontacting displacement sensitive sensor system

12 p1882 A72-27340

Resonant frequency and vibration modes of variable cross section bar in elastic medium under transversal force, noting dynamic programming combined with optimization principle

12 p1845 A72-27538

Nonresonant mode and nutation damping of rotational-vibrational motion of free solid body with elastic elements

12 p1846 A72-27968

Fourth order normal modes and resonances of nonlinear vibrations, applying to gyro horizon compass sensitive element gimbal motion

13 p2000 A72-28382

Thin circular plate free vibrations with mixed boundary conditions from differential equations for vibration modes of circular isotropic plate in dimensionless polar coordinates

13 p2053 A72-28395

Mathematical two mass model for horizontal, angular and vertical vibrations of pneumatic wheel with allowance for inelastic tire resistance

13 p2003 A72-28918

Resonant frequencies of two thin walled cylindrical panels connected by elastic filler, considering symmetric and asymmetric vibration modes

13 p2058 A72-29146

Free and forced vibrations of circular plates with associated rigidities and masses, obtaining orthogonality condition for natural vibration modes

13 p2059 A72-29501

- Random vibration of two multimodal mechanical systems with point coupling, obtaining power flow spectral density by statistical energy analysis
13 p2005 A72-29563
- Sound generation by finite rectangular plate vibrations, deriving radiated power as function of aspect ratio and vibration pattern
13 p2005 A72-29564
- Second order moments of system with parametric excitation by filtered white noise calculated with Fokker-Planck equation, giving condition for mean-square-stability
14 p2131 A72-30711
- Nonlinear oscillation systems mathematical model, determining periodic mode parameters, self excitation and damping mechanisms by point mapping method
14 p2133 A72-31126
- Honeycomb sandwich beams dynamic analysis by finite element method with three degrees of freedom per discrete element, obtaining flexural, in-plane and shearing modes
14 p2169 A72-31146
- Open terminations of cylindrical waveguide periodically loaded by metallic irises, investigating cavity resonator size effects on resonant frequency, mode and quality factor
15 p2194 A72-31547
- High efficiency X band pulse operation of transferred electron oscillator in hybrid mode, noting high material quality and optimum impedance match
15 p2206 A72-31548
- Nonlinear systems normal mode vibrations analysis by group theory using symmetry properties
15 p2275 A72-31732
- Zero moment stress effect on modal density spectrum of fluctuating thin cylindrical shells and cylindrical panels
15 p2327 A72-31737
- Variable cross section rod free longitudinal and torsional vibration frequencies and mode shapes determined by slowly varying parameters approximation method
15 p2327 A72-31740
- Frequency shift and mode shapes for equatorial vibrations of flexible boom on spin stabilized satellite, applying to thermal flutter resonance and nutational stability
15 p2320 A72-31803
- Elastic shell initial stress effects on dynamic response in all free vibration modes, considering transverse shear and normal strains
15 p2328 A72-32021
- Quantitative measure for sensitivities of natural frequencies to perturbations leaving modes invariant
15 p2278 A72-32279
- Complex structures dynamic analysis by component mode technique, treating modal characteristics as random variables
15 p2331 A72-32555
- Azomethane and azomethane-d6 IR and Raman spectra, discussing fundamental modes vibrational assignment based on band contours, isotopic shift ratios and group frequency correlations
16 p2360 A72-32923
- Free small steady oscillations of liquid in solid tanks, considering HF modes
16 p2375 A72-32931
- Singular perturbation methods for deflections, frequencies and eigenmodes of statically loaded or freely vibrating circular or annular membrane
16 p2467 A72-33106
- Natural frequencies and vibration modes of free glider, using symmetrical matrix to replace three dimensional structure by approximate model
16 p2348 A72-33409
- Instantaneous and averaged spiking emission spectra of injection laser under spontaneous pulsation as function of oscillation mode and photon distribution
16 p2404 A72-33984
- Transverse vibration frequencies and mode shapes of clamped or supported orthotropic plates by energy method, using Rayleigh-Ritz technique
17 p2626 A72-34327
- Rocket body longitudinal autooscillation modes, taking into account pipeline fluid discontinuous cavitation oscillations
17 p2620 A72-34469
- An energy technique for use in the vibration testing of complex structures.
17 p2626 A72-34720
- Vibration modes and stability of nonequilibrium low density He-Cs plasma in magnetic field
17 p2589 A72-35126
- Finite element analysis of the axisymmetric vibrations of cylinders.
17 p2634 A72-35409
- Structural mode vibration control system design for B-1 aircraft to improve ride during atmospheric turbulence and terrain following
17 p2493 A72-35563
- Balancing of a flexible rotor by means of mode separation.
18 p2732 A72-36072
- Free vibration mode shapes mapping of spherical and paraboloidal plastic shells under acoustic excitation via noncontact fiber optics instrumentation
18 p2690 A72-36372
- Flat beam linear vibration analysis from mode measurement and moire technique, applying to prototype turbine compressor blade
18 p2734 A72-36375
- Vibrational relaxation of the bending mode of shock-heated CO₂ by laser-absorption measurements.
18 p2697 A72-36562
- Fluid transition through critical value, considering self oscillation onset mode frequency
18 p2681 A72-36663
- Composite sphere and cylinder vibrations, considering radial and rotatory/torsional vibrations
18 p2735 A72-36756
- Higher vibration modes by matrix iteration.
18 p2736 A72-36772
- The behaviour of a Gunn oscillator in the domain-delayed mode.
18 p2667 A72-36945
- Longitudinal impact on a thin cylindrical shell
19 p2870 A72-37321
- Determination of the natural frequencies and modes of oscillation of a spherical resinous shell
19 p2873 A72-37662
- Slowly rotating relativistic stars. VI - Stability of the quasi-radial modes.
20 p2966 A72-38909
- The non-stroboscopic visualisation of vibration patterns by the real time-time averaged hologram interferometry.
20 p2921 A72-39028
- Dynamic characteristics of composite laminates.
20 p2979 A72-39558
- Stability of nonradial vibrational modes of relativistic neutron stars.
20 p2972 A72-39869
- Randomly coupled flexural and longitudinal vibrations of plates.
21 p3120 A72-41111
- Vibration of trapezoidal cantilever plates with partial root chord support.
21 p3121 A72-41225
- Hydrodynamic forces acting on rigid disk and circular membrane vibrating in ideal incompressible fluid, noting dependence on phase shift between vibration modes
21 p3126 A72-41552
- Electromechanical filter with attenuation poles consisting of multi-mode vibrators.
21 p3036 A72-41828
- Inhomogeneous beam torsional vibration modes and frequencies calculation by initial parameters method, replacing beam by series connected oscillators
22 p3232 A72-41865
- Analysis of static deflections by holographically recorded vibration modes.
22 p3177 A72-42397
- The use of simple three-dimensional acoustic finite elements for determining the natural modes and frequencies of complex shaped enclosures.
22 p3206 A72-42464
- Simple thickness modes for laminated composite materials.
22 p3235 A72-42465
- On the stability of axisymmetric systems to axisymmetric perturbations in general relativity. II - A criterion for the onset of instability in uniformly rotating configurations and the frequency of the fundamental mode in case of slow rotation.
22 p3206 A72-42566
- Method of measuring modal characteristics of a structure subjected to a random excitation
22 p3242 A72-43095
- Free vibrations of an arbitrary structure in terms of component modes.
23 p3350 A72-44054
- [ASME PAPER 72-APM-T] Free flexural vibrations of an elliptical plate with simply supported edge.
23 p3352 A72-44121
- The coupled transverse vibrations of a spinning membrane disk with a central hub.
23 p3355 A72-44367
- Free-transverse vibrations of an axially moving mass.
23 p3355 A72-44457
- Vibration frequencies and modes determination for clamped rectangular plates of orthotropic material, using weighted residual technique and polynomial approximation
24 p3455 A72-44683
- Fiber optics development and physical foundations, discussing reflection, optical waveguides, vibrational modes during light transmission and fabrication from inhomogeneous glass and mixed monomers
24 p3425 A72-44782
- Self-excitation of oscillations in a system consisting of a delay line, inductance, and tunnel diodes
24 p3384 A72-44895
- The damping properties of elastically supported sandwich plates.
24 p3458 A72-44915
- High speed mixing of nitrogen vibrationally excited with carbon dioxide
24 p3464 A72-45065
- VIBRATION PICKUPS**
U TRANSDUCERS
U VIBRATION METERS
VIBRATION PROTECTION
U VIBRATION ISOLATORS
VIBRATION SIMULATORS
Vibration simulation of elastohysterical systems on analog computers using photocurrent-voltage relationship of polycrystalline photoresistors
06 p0900 A72-18674
- Simulation of flexural vibrations of rods without concentrated masses
21 p3116 A72-40168
- VIBRATION TESTING MACHINES**
U VIBRATION SIMULATORS
VIBRATION TESTS
NT DAMPING TESTS
Vibration space analysis for human voice characteristics change during unintended speech under experimental psychological stresses and actual emergency situations
01 p0017 A72-10213
- Al-Mg-Si alloy fatigue, vibration creep and creep strength tests at room temperature, determining mean stress effects on fatigue strength and cumulative damage
02 p0297 A72-12536
- Thin airfoil and bridge deck flutter derivative from transient oscillatory states in test procedure
02 p0298 A72-12665
- Flight vibration testing methods for ascertaining flutter stability of high speed aircraft
[DGLR PAPER 71-083] 02 p0155 A72-12725
- Alloying, thermal and mechanical treatment effects on Mg alloys damping properties under elastic vibrations, showing test results consistency with materials microdeformation theory
05 p0671 A72-15987
- Electrodynamic vibration exciters with interchangeable heads for environmental vibration testing
05 p0644 A72-16596
- Aerospace structures harmonic vibration tests, discussing structures natural frequency spectrum, mode isolation, eigenmodes and inertial characteristics
06 p0896 A72-17948
- System parameters random step changes effect on nonlinear system steady vibration stability
07 p1088 A72-19172
- Olympus engine flight testing for relighting and anti-icing, engine control and noise and vibration assessments in support of Concorde aircraft development
08 p1224 A72-21898
- High speed rotating test rig development for vibration testing of turbine blades, describing design layout
08 p1147 A72-22131
- Helicopter noise and vibration testing and cabin soundproofing for improved comfort
08 p1128 A72-22141
- Spacecraft structural dynamics, design and testing, using Fourier transform and analog vibration simulation
[AIAA PAPER 72-349] 11 p1728 A72-25378
- Digital control and data processing system to replace analog instrumentation in vibration test laboratories, discussing signal generation, data acquisition, storage and analysis
15 p2215 A72-32618
- Quantified design criteria for vibration and shock test fixtures to insure test repeatability, proposing chart inclusion in military test standards
15 p2215 A72-32619
- Dynamic input to cargo in turbojet aircraft studied during C141 and C5A flights, discussing instrumentation, test procedures, data reduction processes and results
15 p2181 A72-32625
- Transfer function estimates in random vibration test control, using digital techniques for rapid reduction of statistical errors
15 p2215 A72-32626
- Nondestructive vibration analysis of mechanical structures, using digital computer technique for sound wave spectrum analysis
16 p2397 A72-33220
- Nondestructive vibration tests of fatigue crack damage in composite structures, investigating glass reinforced epoxy and polyester laminates
16 p2414 A72-33318
- Vibrational diagnostics of operational conditions of machines for wear, design faults and efficiency evaluation
16 p2425 A72-33408
- An energy technique for use in the vibration testing of complex structures.
17 p2626 A72-34720
- Device for fatigue testing of fiberglass-reinforced plastic samples in a symmetrical tension-compression regime at acoustic oscillation frequencies
20 p2920 A72-38944

- Bending vibration test of glass-textolites, noting temperature effect on vibration damping properties
21 p3073 A72-41357
- Spectrally shaped transient forcing functions for frequency response testing.
22 p3206 A72-42463
- Procedures for simple resonance testing of sailplanes
22 p3139 A72-42920
- Electrohydraulic stand for vibration strength testing, discussing system design, specifications, frequency-amplitude characteristics and applications
23 p3278 A72-43760
- Aeroacoustic, vibration and shock environments for the space shuttle orbiter.
24 p3448 A72-44679
- VIBRATIONAL FREEZING**
Rapid expansion nozzles for gas dynamic laser working gas vibrational energy freezing to obtain population inversion, considering size and shape effects on performance
[AIAA PAPER 72-148] 05 p0669 A72-16965
- VIBRATIONAL FREQUENCIES**
U VIBRATIONAL SPECTRA
VIBRATIONAL RELAXATION
U MOLECULAR RELAXATION
VIBRATIONAL SPECTRA
Error fluctuation component spectral density determination in closed automatic nonlinear system for controlling random vibration spectrum
01 p0045 A72-10505
- High precision rotational constants and transition frequencies in ground state interstellar molecule cyanoacetylene
01 p0023 A72-11147
- Digital computer programmed numerical calculation based on admittance method for torsional forced vibration spectra of masses and stress distribution in transmission system
02 p0271 A72-12435
- Non-Boltzmann molecular nitrogen vibrational distribution in aurora during electron bombardment as function of altitude
02 p0221 A72-12456
- Resonance electron spectrometry experiments on electron collisions involving vibrational excitation, deactivation and attachment in molecular oxygen
03 p0347 A72-13391
- Vibrational population of molecular nitrogen electronic states in normal auroras, examining electron impact and cascade contributions
03 p0349 A72-13524
- CW longitudinal flow carbon monoxide chemical laser system analysis, discussing vibrational levels, population densities, excitation and relaxation processes and dynamic model
03 p0368 A72-13858
- Vibrational IR and Raman spectra of dimethylaminodichlorophosphine, determining molecular structure symmetry in liquid and solid phases
04 p0481 A72-14444
- Fluorescence polarization and intensities of nitric oxide vibrational bands from Cd line and continuum excitation for spectrometer calibration
04 p0552 A72-14893
- Extremal problems of natural vibration spectrum optimal control in mechanical systems with constraints, using mathematical programming methods
04 p0586 A72-15004
- Carbon dioxide gas dynamic laser mixture at high pressure, investigating gain and vibrational kinetics
04 p0531 A72-15336
- Carbon dioxide-nitrogen-water or He mixtures expansion through supersonic nozzles, showing population inversion of vibrational energy levels
04 p0513 A72-15337
- Nitrogen to carbon dioxide vibrational energy transfer time measurement in gas dynamic laser
04 p0531 A72-15352
- Vibration-rotation double resonance transitions in symmetrical top molecules in millimeter range under chopped laser radiation
04 p0532 A72-15615
- Artificial barium oxide clouds band spectrum analysis, calculating rotational and vibrational temperatures in total wavelength region
05 p0655 A72-16069
- Giant M stars atmospheres absorption coefficient calculation from vibrational and pure rotational bands of H₂O, CO and OH
05 p0715 A72-16167
- Collision induced vibration-rotation transition probabilities for molecular motions, using state averaged potentials
06 p0851 A72-17299
- Spectral properties of differential displacement equations system describing natural vibrations of shell of revolution with m waves along parallel
06 p0897 A72-17990
- Vibrationally excited nitrogen photoionization spectrum obtained with quadrupole mass spectrometer in flowing nitrogen at terglow
07 p1037 A72-19434

- Ferroelectrics with strong hydrogen bonds, deriving self consistent optical phonon frequency and coupled proton-phonon vibration spectrum
09 p1366 A72-22221
- Post-threshold translational energy dependence of endoergic cross sections for vibrational excitation and reactive scattering of diatomic molecules by atomic or molecular impact
09 p1357 A72-22858
- Vibrational laser Raman scattering from flame gases for nitrogen, oxygen and water vapor
09 p1276 A72-22978
- Initially axially stressed Timoshenko beam equations of motion derived from three dimensional theories, discussing buckling loads and vibration frequencies
10 p1555 A72-24191
- Attractive well potential effects on vibrational transition probability during atom-diatom molecule collinear collision
10 p1514 A72-24335
- Steady state operation of automatic control system to stabilize random vibration spectra, noting maximum control accuracy at optimum loop gain
10 p1457 A72-24635
- Isotope effect calculation hydrogen and deuterium solubility in fcc metals, analyzing elastic vibrational spectrum of crystal with impurity atom in intermode
10 p1498 A72-24873
- Rotor blades setting angle and twist influence on steam turbine wheels vibrational modes and frequency spectra
11 p1732 A72-25537
- Chemical laser dynamics review, discussing population inversion, molecular vibrational relaxation and reactions initiation methods
12 p1822 A72-27605
- Carbon dioxide laser vibrational-rotational band small signal gain factor dependence on time elapsing after breakdown of equilibrium distribution
13 p2008 A72-29503
- Hydroxyl vibration levels excitation rates calculation from transition probabilities and band sequence nightglow intensity measurements
13 p1954 A72-29816
- Spontaneous radiative dissociation in molecular hydrogen vibrational levels as function of emission wavelength, discussing fluorescent spectra, radiation lifetimes and centrifugal distortion
13 p2008 A72-30058
- Hydroxyl emission bands intensity, and vibrational and rotational temperatures sporadic and harmonic components in seasonal and diurnal variations
14 p2098 A72-30142
- Spectral properties of differential displacement equations system describing natural vibrations of shell of revolution with m waves along parallel
14 p2163 A72-30217
- CW tunable semiconductor laser measurement of CO laser amplifier gain line shape for several vibration-rotation lines
15 p2245 A72-31382
- Spectral intensity distribution of vibrational electron interaction with strong coupling during polymerization of monomer cyanine dye and dimer molecules
15 p2280 A72-31410
- CO overtone band and vibrational transitions in CW carbon disulfide-oxygen chemical laser, discussing pressure effects
15 p2250 A72-32525
- Random vibration optimal control by transfer function estimation, using relative phase information in cross spectral density functions to sort out self noise
15 p2215 A72-32629
- Electron beam-plasma system oscillation spectrum control through modulation by external HF signal, discussing theory and experimental verification
15 p2289 A72-32671
- Vibrational frequency density analysis of thin spherical and cylindrical shells of revolution, using asymptotic integration method
16 p2464 A72-32935
- Natural vibration frequency spectra of circular cylindrical and spherical shells of revolution, using Bessel function
16 p2465 A72-32936
- Laser apparatus for natural resonant frequencies and oscillation amplitudes measurement of semiconductor devices structural elements
16 p2402 A72-33701
- HF vibrational relaxation measurements using the combined shock tube-laser-induced fluorescence technique.
17 p2511 A72-34735
- Excitation of molecular vibration on collision - Simultaneous vibrational and rotational transitions in hydrogen + argon at high collision velocities.
17 p2585 A72-35467
- Tunable Raman excitation and vibrational relaxation in diatomic molecules.
17 p2586 A72-35802
- Experimental analysis of the vibrational-rotational line content of a Q-switched CO₂ laser.
18 p2697 A72-36501

- Vibrational analysis of electronic absorption spectra of 3-methyldiazirine and 3-methyl-d3-diazirine in vapor phase
18 p2657 A72-36566
- Vibrationally excited nitrogen in upper atmosphere
18 p2688 A72-36865
- Strict allowance for the variation of the system of normal coordinates in the theory for the vibronic spectra of polyatomic molecules
19 p2838 A72-38777
- Intramolecular interactions and vibronic spectra of polyatomic molecules. IV - Electronic relaxations: Configurational and relaxational spectra - The four-level arrangement
19 p2838 A72-38778
- Rate constant determination for reaction product molecule in vibrational and rotational quantum states, obtaining spectral energy distribution
19 p2763 A72-38803
- Uranyl fluoride crystals luminescence spectrum study, calculating anion normal vibration frequencies
20 p2960 A72-39413
- Vibration spectra of the isomorphous proustite-pyrargyrite series.
20 p2932 A72-39506
- Temperature effects on modulation sensitivity and vibrational spectra in Gunn diode oscillators, suggesting frequency stability improvement method
21 p3032 A72-40792
- Various ground configuration level intervals from gaseous nebulae and solar coronal forbidden transitions observations and laboratory investigations of resonance lines
21 p3108 A72-41286
- Free vibrations of a system with a generalized piecewise-continuous characteristic
21 p3122 A72-41349
- Inhomogeneous beam torsional vibration modes and frequencies calculation by initial parameters method, replacing beam by series connected oscillators
22 p2322 A72-41865
- Study of the variation of the intensity of vibration-rotation spectra of hydrogen halide molecules under the action of compressed foreign gases
22 p3209 A72-43047
- Interaction between a plasma and an electron-beam modulated by low-frequency oscillations
23 p3318 A72-43309
- Computation of the maximum oscillation frequency of bipolar transistors
23 p3269 A72-43448
- Microwave generation with high energy electrons in magnetic undulator with transverse electromagnetic field, calculating frequency distribution of undulator radiation
23 p3265 A72-44158
- Bounds to bending frequencies of a rotating beam.
23 p3354 A72-44249
- Investigation of EAS characteristics at sea level with the aid of the classical method and by the method of recording radio emission
23 p3330 A72-44423
- VIBRATIONAL STRESS**
Short term response of insulin, glucose, growth hormone and corticosterone to acute vibration stress in rats
01 p0015 A72-11289
- Resonant vibration and stresses of dynamically nonuniform annular cascade under aerodynamic interaction of alternating different blades
01 p0143 A72-11368
- Natural vibrations and resonant stresses of turbomachine blade rings and elastic bodies with cyclic symmetry, noting paradoxical frequency decrease
01 p0143 A72-11369
- Rectangular plates nonlinear vibrations under combined static and vibrational loads, using Bubnov-Galerkin method on Karman type nonlinear differential equations
04 p0588 A72-15061
- Two-mirror optical system to study energy dissipation in elastic systems subjected to cyclic straining and vibrations
06 p0819 A72-18649
- Energy dissipation of vibrating structures in complex stress state, using generalized stresses and strains as coordinates
06 p0900 A72-18677
- Gas turbine blades dynamics characteristics determination, investigating vibrational stresses, thermal cycles, alloy physicochemical properties and coatings effects
06 p0900 A72-18683
- Dynamic response and functional state of human operator subjected to harmonic and random vibrational excitations, discussing biodynamic nonlinear oscillatory system model construction
06 p0770 A72-18728
- Random vibrational stress and displacement spectra for linear complex mechanical dissipative systems with strong resistance and finite degrees of freedom
07 p1091 A72-19763
- Additional vibrational loading effect on thin tubular glass fabric reinforced plastic samples creep under shear in reinforced plane at 20-50 C
08 p1195 A72-21854

Acoustically generated vibration stresses in rigidly clamped Al alloy circular plate, noting stress amplitude distribution dependence on loading frequency bandwidth

11 p1738 A72-26805

Silicon solar cell interconnectors design for 5-10 years mission life, considering launch induced vibration stresses and thermal cycling stresses during mission

12 p1758 A72-28037

Forced axisymmetric response of fluid filled spherical shells.

18 p2684 A72-37063

Dynamic strength of tangentially wound toothed blade roots

20 p2979 A72-39586

VIBRATORS

U ELECTRIC CHOPPERS

VIBRATORY LOADS

Endurance tests of D16AMO alloy sheets under high intensity acoustic, harmonic and electrodynamic vibrator loading

03 p0371 A72-13470

Acoustically generated vibration stresses in rigidly clamped Al alloy circular plate, noting stress amplitude distribution dependence on loading frequency bandwidth

11 p1738 A72-26805

Fatigue testing machine for material behavior under elastoplastic bending loads with constant or smoothly varying programmed vibration frequency and amplitude

12 p1795 A72-27463

Mathematical model for hydraulic fatigue testing machine, analyzing nonlinear control stability of vibratory loading process

12 p1796 A72-27978

Computerized optimal design by nonlinear programming for minimum weight elastic plates crossed with rigid ribs for vibrational loading to meet natural frequencies condition

14 p2165 A72-30576

Testing machine for creep resistance of foam plastics under simultaneous static and vibration loads

14 p2092 A72-30591

Atmospheric humidity, temperature, vibrational and static loads effects on composite and double base rocket propellants strength and safety characteristics

14 p2145 A72-30764

Control design for dynamic (vibratory) loading of high speed rotating machinery, discussing rotor, bearing span and support stiffness and coupling centering. [ASME PAPER 72-DE-39]

14 p2167 A72-30872

Equations of motion for damped vibrating system excited by periodic impulsive forces, calculating minimum residual vibration amplitude and force transmitted to foundation

16 p2423 A72-33121

Crack propagation in Al-Cu-Mg alloy sheet under vibratory bending loads, noting crack length to loading cycles number relationship

16 p2408 A72-33677

The effect of an elastic edge restraint on the forced vibration of a rectangular plate.

18 p2737 A72-37066

Resonant frequency, fatigue and energy dissipation relations for endurance limit determination in Al alloy specimens under vibrational loads

21 p3070 A72-41368

Effect of inertial loading on the compression of powdered materials by a vibration process

21 p3061 A72-41369

Asymptotic analysis of the behavior of an elastic rod under aperiodic intense loading

21 p3127 A72-41670

Endurance tests of D16AMO alloy sheets under high intensity acoustic, harmonic and electrodynamic vibrator loading

24 p3414 A72-44945

Alloying, thermal and mechanical treatment effects on Mg alloys damping properties under elastic vibrations, showing test results consistency with materials microdeformation theory

24 p3415 A72-45729

VIBRATORY POLISHING

Determination of the parameters of motion of a container and its load with allowance for their interaction during internal vibrational finishing operations

19 p2824 A72-37426

IBROCARDIOGRAPHY

U PHONOCARDIOGRAPHY

IBROMETERS

U VIBRATION METERS

VIDEO COMMUNICATION

Rate distortion theory model for visual communication fidelity assessment via weighted noise measurement and K rating

18 p2657 A72-36251

Intraframe coding for picture transmission.

18 p2657 A72-36252

Video data transmission minimum channel capacity requirement calculation from rate distortion function of source with known probability distribution

18 p2657 A72-36253

Receiver terminals for satellite television systems.

18 p2662 A72-36849

An optical communication system using envelope modulation.

19 p2766 A72-38604

VIDEO DATA

Multichannel multispectral airborne IR imaging system and video data processing for U.S. geological survey

02 p0227 A72-11851

Real time programmable video data compression system for microwave transmission of ATS satellite pictures between acquisition station and central computer processing

02 p0173 A72-12128

ERTS multispectral scanner data telemetry demodulator/processor capable of demodulating five spectral bands of digital video data

02 p0175 A72-12162

Visual film, TV and optical data systems unified classification for performance criteria based on equation similar to ideal imaging system description by Rose

03 p0329 A72-14188

Alphanumeric data representation by TV receivers, describing coding device and gate system for video signal generation

05 p0634 A72-15813

Image data coding by adaptive block classification and quantization of source output symbols, evaluating performance

06 p0772 A72-17402

Run length encoding for removing redundancy from video signals, determining upper bound on compression ratio based on first order Markov model

06 p0773 A72-17488

Channel coding/decoding schemes compatibility with TV data compressor for planetary missions in real time transmission

07 p0941 A72-19274

Video information transmission over planar and rectangular multimode waveguides under excitation by coherent light, calculating field distribution by geometrical optics approximation

11 p1633 A72-26330

Left ventricular volume time course from computer processing of video angiocardiac data based on X ray densitometry measurements

11 p1587 A72-26627

The image-processing system for the Earth Resources Technology Satellite.

18 p2674 A72-36496

Video signals generation from binary data and mixing with analog information from cameras or tape recorders for simultaneous display on cathode ray tubes

19 p2769 A72-37936

Comparison of information takeoff from a shadow-indication instrument by television and photographic techniques

20 p2928 A72-40049

Data link design for planetary video data transmission back to earth based on rate distortion theory generalization of information theory

21 p3019 A72-40891

Effect of the video signal shaping mechanism in a photosensitive scanistor sensor on the optical data processing accuracy

21 p3058 A72-41735

VIDEO EQUIPMENT

Computer aided biplane roentgen videometry system for dynamic circulatory structure studies including blood flow and heart volume determination

01 p0020 A72-11040

Moving window displays for IR scanner signals, producing images on magnetic video tape

02 p0228 A72-11852

High density digital tape recorder with combined phase encoded digital electronics and helical scan video transport

02 p0229 A72-12152

Splash detection radar digital signal processing by off-line computer using wideband video recorder

02 p0178 A72-12399

Digital videomagnetograph providing real time display of line of sight component of solar magnetic fields

03 p0356 A72-13281

Real time analog video magnetogram, describing differential photometer for electronic subtraction technique

03 p0357 A72-13286

Book on logarithmic video amplifiers covering design, analysis, performance and applications

10 p1452 A72-24698

Weighting factor and transmission time optimization in video MTI radar.

21 p3022 A72-41082

VIDICONS

NT RETURN BEAM VIDICONS

ERTS satellite return beam vidicon TV system and multispectral scanner images, describing photogrammetric and cartographic evaluations

01 p0065 A72-10449

Digitized SEC vidicon detector for OSO-H satellite coronagraph, describing optics

08 p1170 A72-21959

Low light level small intensifier/vidicon camera tube using bombardment induced conductivity target, and planar photocathode, detailing design and performance

08 p1171 A72-21969

Si diode array vidicon for ground based and spaceborne planetary and stellar imaging, noting integration time, storage and slow scan capabilities extension through cooling

08 p1171 A72-21970

High resolution vidicons, image orthicons, esicons and ebicons design for space missions

08 p1171 A72-21972

Image dissector, silicon photodiode and vidicon behavior comparison for medium resolution star mappers design for three axis stabilized vehicles

08 p1172 A72-21975

Integrating two dimensional silicon diode array vidicon astronomical photometer for telescope use

09 p1313 A72-23330

Viking Mars Orbiter imaging experiment with high resolution contiguous coverage by vidicon cameras for landing sites selection and surface study

10 p1539 A72-24377

Calibration model for UV stellar photometer using secondary electron conduction (SEC) vidicon

11 p1631 A72-25684

Integrating silicon target vidicon photometer for two dimensional photometric images of planets and stars

11 p1631 A72-25686

Extreme UV solar images televised in flight with rocket-borne SEC vidicon system, noting pictures reconstruction enhancement

12 p1810 A72-27930

Spectroscopy of pulsed HF chemical lasers using an infrared vidicon camera tube.

17 p2562 A72-34641

VIKING LANDER SPACECRAFT

Viking Mars Orbiter and Lander radio and radar science experiments, noting surface tracking, dual frequency S and X band data and communications system

10 p1539 A72-24380

Viking Lander imaging experiments with stereoscopic camera system to study Martian surface and atmospheric morphology, composition and evolution

10 p1540 A72-24382

Viking Lander mass spectroscopic analysis of organic compounds, water and volatile constituents of Martian atmosphere and surface

10 p1540 A72-24383

Biological experiments of Viking Mars lander 1975 mission regarding Oparin-Haldane evolution hypothesis

10 p1430 A72-24384

Viking Lander carbon 14 assimilation experiment for life detection in Martian soils

10 p1540 A72-24385

Viking Lander detection of metabolically produced radioactive labeled gas in Mars surface samples

10 p1540 A72-24386

Viking Lander light scattering experiment to detect microbial growth from aqueous turbidity changes in contact with Martian soil

10 p1430 A72-24387

Viking Lander meteorology experiments to measure Martian atmosphere pressure, temperature, wind speed and direction and water vapor content

10 p1540 A72-24388

Viking Lander seismic investigations for Martian tectonic activity, internal structure and composition, core size and conditions of formation

10 p1540 A72-24389

Viking Lander physical properties experiments for Martian soil, studying bearing strength, cohesion, adhesion, grain size, porosity, thermal properties and internal friction

10 p1540 A72-24390

Viking Lander magnetic properties investigation of Martian surface with implications for planetary composition and differentiation and atmospheric interaction

10 p1541 A72-24391

Viking conical aeroshell structural prototype design, analysis and testing, comparing buckling failure data with theoretical predictions

11 p1725 A72-25395

Viking orbiter/lander spacecraft instrumentation for Mars soil biological life experiments, discussing pyrolytic and labeled release, light scattering and gas exchange techniques

13 p1956 A72-29024

Biological instrumentation for the Viking 1975 mission to Mars.

23 p3259 A72-43396

Viking Mars exploration project, discussing orbiter and lander design and operational features and scientific experiments relevant to existence of life

24 p3440 A72-45123

VIKING MARS PROGRAM

Viking Mars 1975 mission with spacecraft orbiters and landers, describing experiments with emphasis on life detection

10 p1539 A72-24376

Martian atmosphere water vapor detection and mapping during Viking missions, discussing experimental approach and spectrometer choice
10 p1539 A72-24378

Mars atmospheric entry experiments for Viking 1975 mission, discussing onboard neutral gas mass spectrometer and retarding potential analyzer
10 p1540 A72-24381

Biological experiments of Viking Mars lander 1975 mission regarding Oparin-Haldane evolution hypothesis
10 p1430 A72-24384

Viking mission gas exchange experiment for life detection in Martian soil, covering design of experiment
14 p2084 A72-30876

Navigational aspects of two impulse transfer initiated rendezvous with Deimos using modified Viking Monte Carlo error analysis program
15 p2269 A72-32177

Orbital trim by velocity factoring for Viking Mars mission terminal rendezvous and intermediate timing constraints involving orbital operations
15 p2269 A72-32179

Mars Viking 1975 mission objectives and navigation activities from trans-Mars injection through post-landing stationkeeping phase, considering trajectory dispersions
15 p2269 A72-32180

Biological instrumentation for the Viking 1975 mission to Mars.
23 p3259 A72-43396

Viking Mars exploration project, discussing orbiter and lander design and operational features and scientific experiments relevant to existence of life
24 p3440 A72-45123

VIKING ORBITER SPACECRAFT

Viking Mars Orbiter imaging experiment with high resolution contiguous coverage by vidicon cameras for landing sites selection and surface study
10 p1539 A72-24377

Viking Mars Orbiter IR thermal mapper /IRTM/ to study surface kinetic temperature, thermal balance, anomalous cooling regions, ground frosts and water vapor
10 p1539 A72-24379

Viking Mars Orbiter and Lander radio and radar science experiments, noting surface tracking, dual frequency S and X band data and communications system
10 p1539 A72-24380

Parameters influencing dynamic stability characteristics of Viking-type entry configurations at Mach 1.76.
17 p2622 A72-35494

Viking Mars exploration project, discussing orbiter and lander design and operational features and scientific experiments relevant to existence of life
24 p3440 A72-45123

VIKING ORBITER 1975

Mars 1975 Viking mission profile, describing soft landing/orbiter probes and life detection experiments
12 p1877 A72-27687

Viking orbiter/lander spacecraft instrumentation for Mars soil biological life experiments, discussing pyrolytic and labeled release, light scattering and gas exchange techniques
13 p1956 A72-29024

VIKING ROCKET VEHICLE

Viking 2 rocket engines for Europa 3 first stage propulsion, describing engine components design and functions and performance test results
22 p3216 A72-42649

VIKING 75 ENTRY VEHICLE

Viking configuration pitch damping derivatives as influenced by support interference and test technique at transonic and supersonic speeds.
[AIAA PAPER 72-1012]
21 p3041 A72-41593

VINYL COPOLYMERS

Ethylene-vinyl acetate-asphalt thermoplastic material properties, filler effects, application methods and commercial uses
12 p1835 A72-28094

VINYL CYANIDE

U ACRYLONITRILES

VINYL POLYMERS

Ignition conditions for pyroxylin and polyvinyl-nitrate in air flow containing spherical aluminosilicate and aluminum oxide particles
06 p0903 A72-18211

VIRGO STAR CLUSTER

Statistical investigation of 1500 galaxies in MCG catalog with weak surface brightness, noting sculpture type spheroidal galaxies in Virgo cluster
03 p0435 A72-13807

Galactic center region, Virgo and Crab Nebula gamma ray observations, measuring intensity and energy spectra
04 p0578 A72-15312

VIRIAL THEOREM

Galaxy clusters stability, obtaining mass distribution function from combined virial theorem and mass to light ratios
01 p0131 A72-11003

Second virial coefficient, temperature derivatives and additive components for /12-7/ potential of charged particle interaction in gas
05 p0692 A72-15841

Statistical group theory of two component associated gas mixtures, noting erroneous virial coefficient
05 p0692 A72-16356

Inherent uncertainties in virial mass determinations of bound and unstable groups of galaxies, computing evolution tracks for different mass loss mechanisms and rates
07 p1072 A72-19341

Nonspherical and nonadditive interactions contribution to third virial coefficient of polyatomic gas, discussing anisotropy, shape factor, and intermolecular forces
08 p1211 A72-21292

Rectilinear motions in three body problem with null live forces constant, using inequality deduced from virial theorem
09 p1392 A72-23542

Velocity dispersions and discrepant red shifts in groups of galaxies, using virial theorem for galaxy mass calculations
10 p1534 A72-23903

Second virial coefficient, temperature derivatives and additive components for /12-7/ potential of charged particle interaction in gas
15 p2280 A72-31260

The gravitational acceleration perpendicular to the galactic plane.
17 p2603 A72-34441

Numerical calculation of third virial coefficient in equation of state of real gases eliminating errors associated with substitution of integration infinite integral
19 p2838 A72-38462

A generalized virial equation of state and its application to vapor-liquid equilibria at low temperatures.
19 p2883 A72-38838

The estimation of masses of individual galaxies in clusters of galaxies.
22 p3227 A72-42551

VIRTUAL PROPERTIES

EEG discharges virtual dipolar sources computation, using mathematical model with homogeneous spherical conductive medium to simulate human head
06 p0769 A72-18201

Galerkin method application to nonconservative nonself-adjoint aeroelasticity problems based on interpretation as mathematical formulation of virtual work principle
07 p1025 A72-18788

Virtual displacement application to nonholonomic systems with arbitrary constraints to derive Lagrange and Appell equations of motion
10 p1513 A72-24995

VIRTUAL WORK

U EQUILIBRIUM

VIRUSES

NT BACTERIOPHAGES

Viruslike particles in salivary glands, muscles and nerves of normal and gamma irradiated *Drosophila melanogaster*, showing age dependent infection
08 p1116 A72-21198

VISCERA

NT ADRENAL GLAND

NT BLADDER

NT ENDOCRINE GLANDS

NT GONADS

NT INTESTINES

NT KIDNEYS

NT LIVER

NT LUNGS

NT ORGANS

NT PANCREAS

NT PARATHYROID GLAND

NT PITUITARY GLAND

NT SPLEEN

NT TESTES

NT THYROID GLAND

Vestibular nuclei bulbar complex evoked potentials

under visceral and somatic nerves electric stimulation in anesthetized cats
02 p0164 A72-12512

Visceral afferentation role in vestibular system activity from experiments on rabbit stomach and rectum mechanoreceptor stimulation effects on vestibular-oculomotor reflexes
05 p0618 A72-16630

Acceleration stress effects on splanchnic blood flow due to organ displacement and neurogenic vasoconstriction in vascular beds
12 p1765 A72-28285

Hippocampus morphology and physiology in relationship to emotion and memory mechanisms, time links, visceral activity and motivations and endocrine control
16 p2353 A72-33099

Russian book - Cortico-visceral interrelations in physiology, biology and medicine.
21 p3000 A72-40752

Morpho-physiological structures thalamic afferent switching mechanisms of visceral analysors in motor, premotor, frontal and limbic cerebral sections
21 p3000 A72-40753

Polysynaptic sympatho-reticular and somatic afferent visceral links between internal organs and cerebrum in interoceptive reflex fields
21 p3000 A72-40755

Pathology of the cardiovascular system in terms of the theory of cortico-visceral interrelations
21 p3000 A72-40756

Cortico-visceral studies of spinal cord reticular formation stimulation and destruction effects on electroencephalogram, cardiac activity and interoceptive glycemic reflexes
21 p3000 A72-40755

Behavior concept formulation for visceral systems, considering digestive system data and extension from motor function concepts
24 p3370 A72-44586

VISCOELASTIC CYLINDERS

Torsion problem of inhomogeneous anisotropic viscoelastic rod transformation, using area variation coefficient for modeling
01 p0138 A72-10582

Numerical method for wave propagation and dynamic stresses in viscoelastic cylinders under internal and external loads
01 p0144 A72-11375

Dynamic behavior of stiffened hollow viscoelastic cylinder and elastic shell-contained sphere, taking into account compressibility and internal pressure
07 p1090 A72-19751

Impact-produced deformations in nonlinear viscoelastic rod of finite length, studying pulse propagation as nonlinear boundary value problem
11 p1685 A72-25353

Rheological stress-strain relations in nonlinear viscoelasticity theory, calculating relaxation parameters for isotropic viscoelastic circular cylinder
13 p0259 A72-29493

Heat generation in oscillating torsional spring modeled by viscoelastic hollow cylinder subjected to sinusoidal shear stresses, calculating stress and temperature distribution and displacement
17 p2635 A72-34232

Thermomechanical coupling effects in the longitudinal oscillations of a viscoelastic cylinder.
23 p3352 A72-44122

VISCOELASTIC DAMPING

U ELASTIC DAMPING

U VISCOUS DAMPING

VISCOELASTIC FLOW

U VISCOELASTICITY

VISCOELASTICITY

NT PHOTOVISCOELASTICITY

NT THERMOVISCOELASTICITY

Rate-type viscoelastic materials, deriving weak shock structure by wave front, ray and singular surface theories and asymptotic expansions
01 p0101 A72-10033

Small dilatation and short time approximate constitutive equations for compressible nonlinear viscoelastic materials, using multiple integrals and kernel functions
01 p0137 A72-10319

Correspondence principle application to numerical solution for plane boundary value problem of linear viscoelasticity theory based on Kelvin point force solution to field equations
01 p0138 A72-10512

Viscoelastic parameters calculation for orthotropic composite materials reinforced by unidirectional fibers, giving time dependence of relaxation functions
01 p0142 A72-11177

Affine similarity in static problems with mixed boundary conditions for inhomogeneous anisotropic linearly and nonlinearly elastic and viscoelastic and elastoplastic bodies
02 p0288 A72-11607

Contact problem of rigid sphere intrusion into viscoelastic half space, obtaining solution by Green's function construction and integral-operator equation formulation
02 p0289 A72-11615

Isothermal uniaxial stress analysis of material consistent with linear law of heredity theory, determining viscoelastic relaxation function
02 p0290 A72-11621

Stress-strain characteristics of stochastically reinforced materials of high rigidity orthotropic elastic layers alternating with isotropic elastic or viscoelastic layers
02 p0248 A72-11623

Nonlinear viscoelasticity theory, considering simplified stress-strain functional relationships with respect to time based on isotropy postulate
02 p0290 A72-11624

Flexible viscoelastic orthotropic plates and shells obeying linear heredity relations, solving stability and bending problems by Laplace transform
02 p0290 A72-11625

Viscoelastic fluids continuum mechanical theory, discussing constitutive equation and tensor analysis
[AD-736009]
02 p0203 A72-12004

- Linear viscoelasticity theory dynamic functions, deriving delay and relaxation times distribution functions in polymers 02 p0293 A72-12211
- Anelastic solid energy dissipation linear memory models based on viscoelasticity theory, applied to earth and metals experimental data and dynamic loading problems 02 p0294 A72-12447
- Stress and velocity distributions in homogeneous viscoelastic rigid body, deriving uniqueness theorems and minimum principles for limits problem 02 p0297 A72-12596
- Rigid mass impact against viscoelastic bear of finite length, investigating longitudinal waves propagation and interaction 02 p0298 A72-12682
- Elastic-viscous incompressible fluid laminar boundary layer flow past infinite plane porous wall, deriving velocity and temperature distributions by two-sided Laplace transform technique 03 p0340 A72-13024
- Two dimensional elasto-viscous incompressible fluid flow past porous wall with variable suction, analyzing temperature field of laminar thermal boundary layers 03 p0341 A72-13500
- Two dimensional viscoelastic fluid flow past infinite plate with time dependent suction and constant and periodic free stream velocity 03 p0341 A72-13630
- Linear viscoelastic solid defined by constitutive equations replacing bounded domain in time interval on real axis, deriving theorem regarding solution of second problem of limits 03 p0447 A72-13787
- Crack development in thin viscoelastic polymer plate, using two phase fracture model without Volterra principle 03 p0448 A72-13901
- Closed quasi-linear cubic theory of viscoelasticity for bodies with force and moment physical nonlinearity 03 p0454 A72-14218
- Thermodynamic and dissipative restrictions on isothermal stress relaxation functions in linear viscoelasticity 04 p0583 A72-14462
- Three dimensional analysis for free vibrations of simply supported viscoelastic rectangular plates 04 p0585 A72-14841
- Time delay effect on stability of viscoelastic cantilever column under retarded follower load 04 p0590 A72-15186
- Stochastic signal method for measuring dynamic viscoelastic properties of isometric frog sartorius muscle at rest and contraction, using white noise vibrations 04 p0480 A72-15221
- Kinetic rate theory extended to time dependent flow behavior of viscoelastic materials /polymers/ under constant stress and shear 04 p0512 A72-15263
- Shock response of simply supported sandwich beam with viscoelastic core, using four element model for dynamic shear properties 04 p0591 A72-15274
- Magnetic field effect on heat transfer in steady plane laminar conducting incompressible viscoelastic liquid flow in channel with nonconducting walls 04 p0560 A72-15580
- Viscoelastic fluid flow past infinite plane porous wall with time dependent suction, investigating mean velocity profile and wall shear stress 04 p0514 A72-15704
- Rectangular channel flow of two immiscible viscoelastic Maxwell fluids with transient pressure gradient, deriving interface velocity, flow rate and wall resistance components 04 p0514 A72-15705
- Disturbances in infinite plate of viscoelastic material due to impulsive radial forces and twist on inner surface of circular hole, using Laplace transformation 04 p0594 A72-15709
- Subcritical crack extension in elastoplastic or viscoelastic-plastic matrix, showing similar mathematical representations for fatigue crack propagation and creep rupture under sustained loads 05 p0737 A72-16302
- Homogeneous viscoelastic boundary value problem, demonstrating Volterra principle validity 05 p0739 A72-16590
- Viscoelastic effect on cylindrical liquid jets capillary breakup after ejection into inviscid atmosphere 05 p0654 A72-17246
- Linearized hydrodynamic stability of viscoelastic fluid Couette flow in gravity field 06 p0798 A72-17778
- Polymers mechanical losses temperature-frequency dependence, using nonlinear viscoelastic theory 06 p0838 A72-18678
- Mixed boundary value problem of partial differential equations describing nonlinear viscoelastic vibration of clamped rods, examining asymptotic solution stability 06 p0901 A72-18716
- Critical stability and supercritical equilibrium behavior of compressed viscoelastic rod 07 p1091 A72-19761
- Sphere unsteady motion in viscoelastic liquids, noting falling-ball technique use for elastic parameters determination 07 p0973 A72-20549
- Stress concentration near elliptic and square orifices in plates with nonlinear viscoelastic hereditary creep properties 08 p1244 A72-21242
- Laminar free convective flow of viscoelastic fluid past infinite porous plate 08 p1151 A72-21748
- Nonlinear viscoelastic body model for stress relaxation of amorphous linear polymers below vitrification temperature for various deformations, temperatures and deformation speeds 08 p1194 A72-21751
- Solution uniqueness in physically nonlinear viscoelasticity dynamic theory 08 p1195 A72-21761
- Perforated flexible polymer plates stressed state problem with boundary conditions and viscoelastic and creep properties effects 08 p1248 A72-21861
- Thin viscoelastic beam free oscillations and material properties description by Volterra type nonlinear integral equation 08 p1249 A72-21869
- Frequency response of hot-film wedge probe in turbulent flow of viscoelastic fluid 09 p1293 A72-22309
- Polymers viscoelastic behavior during crosslinking reactions, deriving equations for creep response to step increase in crosslink density 09 p1336 A72-22521
- Temperature fields produced in viscoelastic cylindrical, conical and spherical shells by cyclic loads, calculating displacements from zero moment stress theory formulas 09 p1399 A72-22701
- Stress-strain state produced by asymmetric physical and thermal loads in thin orthotropic viscoelastic shells of revolution 09 p1399 A72-22702
- Energy methods for nonlinear viscoelastic bodies based on constitutive relations affecting critical state in advanced creep 09 p1403 A72-22764
- Three dimensional dynamic analysis of multilayered orthotropic viscoelastic plates, taking into account skin effect [AD-739806] 09 p1405 A72-22995
- Stress and thermal relaxation effects in viscoelastic behavior of turbulent flows of liquids and gases 10 p1464 A72-23867
- Fully developed turbulence spectrum of incompressible viscoelastic fluids 10 p1469 A72-24534
- Mathematical model for arterial system pressure, blood flow and dimensional changes, examining cardiac ejection dynamics and vasculature mechanical properties and viscoelasticity 10 p1432 A72-24812
- Direct numerical integration scheme for viscoelastoplastic response of isotropic axisymmetric shells under impulsive loads 11 p1731 A72-25421
- Linear viscoelasticity theory dynamic functions, deriving delay and relaxation times distribution functions in polymers 11 p1734 A72-25709
- Shear stress and traveling wave response of plate bonded to randomly vibrating viscoelastic half space for soil vibration studies 11 p1688 A72-26062
- Viscoelasticity analysis of bending displacements in thin walled closed cylindrical shell loaded by moving moment 11 p1739 A72-26920
- Two dimensional approximation for viscoelastic inhomogeneous material with hereditary properties varying in radial direction, deriving integrodifferential equations 12 p1878 A72-27088
- Incompressible viscoelastic isotropic fluid stability in Couette flow, discussing physical parameters effect on critical Reynolds number and cells shape of secondary flow 12 p1797 A72-27169
- Fourier transform approximate inversion solution for transient pulse propagation from spherical cavity with surface under impulsive pressure in viscoelastic medium 12 p1844 A72-27196
- Book on finite element method application to boundary value problems, nonlinear continuum thermodynamics and thermoviscoelasticity 12 p1882 A72-27325
- Energy method for boundary conditions of beam vibrations under linear viscoelastic stress-strain law, deriving uniqueness, boundedness and stability theorems 12 p1885 A72-27848
- Uniqueness theorem for solution to boundary value problem in anisotropic viscoelasticity, considering stress-strain relation in nonlinear Volterra equation form 12 p1886 A72-27983
- Averaging technique for nonlinear viscoelastic dynamic problems, considering forced oscillations of oscillator with weakly nonlinear hereditary elastic characteristics 13 p2054 A72-28551
- Iterative method for continuous one dimensional linear systems with space-time invariant properties, applying to dynamic mixed problem of linear viscoelasticity 13 p2006 A72-29783
- Inhomogeneous viscoelastic shell stability, determining correlation functions for first approximations of sag, stress functions and critical time alterations 13 p2062 A72-29886
- Boussinesq problem for homogeneous viscoelastic half space governed by deformation law of typical body under concentrated or sinusoidal loads 13 p2062 A72-30092
- Stress distribution variations and wave propagation in viscoelastic rod of finite length under impact 14 p2163 A72-30191
- Orthogonality condition application to continuum mechanics systems with zero free energy, viscoelastic materials and chemical problems 14 p2130 A72-30419
- Stress analysis of thick walled hollow viscoelastic circular cylinder enclosed in elastic shell and subjected to nonlinear creep conditions, noting temperature effects 14 p2165 A72-30439
- Finite element method for nonlinear analysis of nuclear reactor structures, noting elasticity, viscoelasticity and elastoplasticity problems [SMRT PAPER M 2/2] 14 p2166 A72-30724
- Higher order differential equations solutions for viscoelastic stress-strain functional relationships, recommending Runge-Kutta integration technique 14 p2168 A72-30929
- Turbulent friction values diminished by reading errors in pitot tube flow measurement of solid particles suspensions and polymer solutions caused by viscoelastic associations 14 p2106 A72-31007
- Viscoelastic model for constitutive nonlinear creep law with combined strain and time hardening assumptions, evaluating material parameters for Al alloys 15 p2254 A72-31554
- Nonlinear creep, viscoelasticity and elastoplasticity boundary value problems, discussing matrix constitutive differential equation formulation and higher order numerical methods 15 p2326 A72-31712
- Constitutive equations of linear viscoelastic dielectrics, assuming small displacements, velocities and temperature independent memory functions 15 p2208 A72-32289
- Probst-Gold viscoelastic model of superionic flow induced surface cross-hatching assessment against Dowell studies on plates and shells flutter 16 p2463 A72-32838
- Reversible instantaneous deformations and internal energy in viscoelastic incompressible fluids, using Oldroyd and De Witt hydrodynamic models 16 p2376 A72-32937
- Depolarized light scattering spectra splitting in nonassociated liquids, noting viscoelastic theory with allowance for antisymmetric part of microscopic stress tensor 16 p2428 A72-32950
- Upper and lower bounds for complex elastic moduli of composite materials with isotropic linear viscoelastic phases behaving as homogeneous isotropic materials 16 p2468 A72-33199
- Nonlinear viscoelastic behavior of isotropic unoriented crystalline polyethylene terephthalate at 70-100 C, using creep, recovery and load tests 16 p2416 A72-33614
- Plane Poiseuille flow stability of incompressible second order fluids, noting destabilizing influence of viscoelasticity 16 p2379 A72-33829
- Book on mathematical methods for viscoelasticity problems covering shear stress, viscometric flow, stress analysis, Fourier and Laplace transforms, momentum, equilibrium and constitutive equations, etc 16 p2427 A72-33975
- Three dimensional elastoviscoplastic theory for complex structures static-dynamic creep deformation under time varying stress and temperature fields, generalizing Odqvist-Hoff law 16 p2473 A72-34121
- Temperature and stress fields generated by pulsating internal pressure in viscoelastic hollow sphere with temperature dependent material properties, using iterative numerical procedure 16 p2473 A72-34122
- Wave propagation in a viscoelastic fiber subjected to transverse impact. [ASME PAPER 72-APM-27] 17 p2570 A72-34791

Transverse vibration of a viscoelastic beam carrying an arbitrary number of mass bodies.

17 p2631 A72-35053

Theory of nonlinear viscoelasticity and its applications

17 p2631 A72-35109

Constitutive equations to characterize rubberlike nonlinear viscoelastic materials under finite deformation stress, obtaining numerical solutions via finite difference technique

17 p2633 A72-35401

Variational principles in nonlinear viscoelasticity.

17 p2633 A72-35402

Nonequilibrium thermodynamics with rate equations as nonlinear solid mechanics foundation, noting viscoelastic, viscoplastic and plastic behavior

18 p2732 A72-36076

Griffith crack propagation through viscoelastic solid at under subcritical stresses, measuring growth rate for comparison with theory

18 p2733 A72-36366

Mathematical model and simulation for contact problems involving elastic half spaces and viscoelastic and friction effects

18 p2734 A72-36371

On disturbances in a viscoelastic rod of variable cross-section/ of Reiss type placed in a magnetic field.

18 p2711 A72-36752

A method of analysis for compressible viscoelastic solids.

18 p2736 A72-36936

Propagation and attenuation of harmonic waves in a viscoelastic circular cylinder.

18 p2738 A72-37070

Viscoelastic fluid lines dynamic behavior, considering viscosity, stress-strain relaxation times and compressibility effects in transfer functions derivation for pressure-velocity relations

18 p2684 A72-37077

Viscoelastic analysis of graphite under neutron irradiation and temperature distribution.

18 p2704 A72-37088

Experimental determination of viscoelastic characteristics

18 p2740 A72-37211

Determination of the motion of a model, possessing a mass and a viscoelastic element, for a given harmonic law of motion of the vibrating support

19 p2871 A72-37427

A model of a nonlinear viscoelastic medium allowing for the effects of cumulative damage

19 p2871 A72-37528

Calculation of the nonlinear viscoelastic oscillations of a vibronic protective layer

19 p2872 A72-37537

Homogeneous viscoelastic boundary value problem, demonstrating Volterra principle validity

19 p2872 A72-37562

Combined stress creep of non-linear viscoelastic material.

19 p2822 A72-37714

A universal connexion for waves in anisotropic media.

19 p2875 A72-37840

Coriolis force influence on convective stability in viscoelastic fluid layer heated from below, contrasting with rotation effects on ordinary viscous fluid

20 p2982 A72-39326

Criteria for delayed fracture in solids and their experimental verification.

20 p2981 A72-39954

Forced motion of isotropic and transversely isotropic viscoelastic Timoshenko beams using measured material.

21 p3116 A72-40331

Time dependent deformation of isotropic viscoelastic materials, discussing rectilinear shear, circular cylinder torsion, spiral shear of layer and conical layer torsion

21 p3119 A72-41075

Theoretical and experimental features and methods of creep.

[ICAS PAPER 72-45] 21 p3069 A72-41170

Behavior of viscoelastic shallow spherical shells subjected to dynamic pressure.

21 p3122 A72-41245

Epoxy-thiocol binder viscoelastic deformation under short and long term loads, noting stress-strain linearity limit

21 p3073 A72-41360

Multilayer shell theories with allowance for transverse shear and transverse normal deformation of layers, noting viscoelastic material and anisotropic shallow shells

21 p3125 A72-41537

Application of the variational principle to the solution of problems of crack theory in viscoelastic media

21 p3126 A72-41539

Viscoelastic and active vibration isolators for foundation isolation of polyharmonic vibrational effects of operating machines

22 p3182 A72-42131

The dynamic viscoelastic properties of some non-crystalline metals.

22 p3214 A72-42792

Technological utilization of Weissenberg viscoelastic effect for sliding bearings centripetal pressure lubrication, noting analogy with human and animal skeletal joints lubrication

22 p3183 A72-42875

Propagation of Rayleigh waves on visco-elastic cylindrical surfaces placed in a magnetic field.

22 p3207 A72-42876

Computer simulation of fracture spreading in a visco-elastic solid.

23 p3267 A72-43702

Pulsatile flow of linear viscoelastic fluids in elastico-viscous tubes.

23 p3280 A72-43823

Dynamic response of viscoelastic shallow spherical shells.

23 p3349 A72-43972

Useful range of a mechanical impedance technique for measurement of dynamic properties of materials.

23 p3294 A72-44126

Forced vibration analysis of sandwich beams with viscoelastic core.

23 p3354 A72-44253

Technique for measuring damping properties of thin viscoelastic layers.

24 p3402 A72-44885

Equations of motion of a viscous fluid with relaxation properties

24 p3393 A72-45256

Dispersion relations of scalar hereditary theory of nonlinear viscoelasticity, representing integral operators as orthonormalized function series in Fourier space

24 p3459 A72-45264

Unsteady longitudinal viscoelastic vibrations of a rod of variable thickness at small values of time

24 p3459 A72-45265

A comparison of single-integral non-linear viscoelasticity theories.

24 p3460 A72-45695

A power-law model for the multiple-integral theory of non-linear viscoelasticity.

24 p3460 A72-45696

VISCOMETERS

Oscillating torus shaped crucible viscometer, discussing oscillating viscous liquid fluid dynamic problem

04 p0522 A72-15480

Nonvertical alignment effect on performance of falling cylinder Newtonian fluid filled viscometer

07 p0992 A72-20552

Vibration viscometer measurement of viscosity of alkali metals Rb, Cs, Na and K near solidification temperature, studying oxygen effects on metal surface

11 p1746 A72-26236

VISCOMETRY

Kinetic energy correction in capillary viscometry, observing pressure drops and mass flow rates

02 p0202 A72-11724

Viscosity measurement error estimates for Newtonian incompressible fluid flow through deformed capillary tube

07 p0991 A72-20535

Torsional crystal measurements of viscosity for He 4 and He 3-He 4 mixture at lambda points

12 p1888 A72-27388

Instrument to determine steady and unsteady stress state of elastic fluids in viscometric flow, noting rheological measurements in solved polymers

14 p2094 A72-30421

Book on mathematical methods for viscoelasticity problems covering shear stress, viscometric flow, stress analysis, Fourier and Laplace transforms, momentum, equilibrium and constitutive equations, etc

16 p2427 A72-33975

A new instrument for the measurement of low dynamic torque.

18 p2692 A72-36820

Viscous torque on sphere immersed in Newtonian and non-Newtonian fluids in rotating cylinder, comparing experimental results with Collins theory

23 p3280 A72-43714

VISCOPLASTIC FLOW U VISCOPLASTICITY VISCOPLASTICITY

One dimensional elastoplastic wave propagation symposia review emphasizing elastoviscoplastic media, jet penetration into half space and polymer tests by transverse impact

02 p0290 A72-11628

Viscous friction effects on phonon-electron interactions and dislocation velocity by deformation measurement of metallic crystals under pulsating magnetic fields

02 p0243 A72-12169

Rate dependent endochronic theory of thermoviscoplasticity without yield surface

03 p0444 A72-13503

Mechanical response of Al and Cu under complex strain histories conditions, using endochronic theory of viscoplasticity without yield surface

03 p0444 A72-13504

Viscoplasticity theory thermodynamic foundations, considering stress/strain states time and deformation path dependence

06 p0896 A72-17963

Load bearing capacity of shells of revolution, applying viscoplastic strain hardenable material model

06 p0899 A72-18656

Similarity solution for nonlinear viscoplastic semi-infinite rod under constant velocity impact

07 p1088 A72-19115

Wave propagation in hollow elastic/viscoplastic sphere under impact load, assuming Mises condition, isotropic hardening and incompressibility

07 p1096 A72-20429

Rotationally symmetrical cylindrical shell loaded by uniform pressure distribution along length, calculating quasi-steady viscoplastic flow under Huber-Mises condition

09 p1399 A72-22696

Viscoplastic media flow rate in noncircular tube from Newtonian fluid velocity profile, using Green formula

12 p1799 A72-27981

Viscoplastic flow of inhomogeneous shells of revolution obeying Tresca condition, noting plastic deformation velocity relation to stresses

15 p2325 A72-31605

Elastic-viscoplastic solution for deformation of impulsively loaded strain rate sensitive steel rings

16 p2464 A72-32916

Dynamic structural analysis of viscoplastic thin walled shells, noting time dependent profile of deflection

16 p2467 A72-33122

Multiple plastic and viscoplastic potentials for single crystal and polycrystal with mean densities and mean lengths of dislocations as internal variables

16 p2470 A72-33615

Stable bifurcation mode prior to instability in thick walled cylindrical viscoplastic pressure vessel under internal hydrostatic pressure

16 p2474 A72-34129

Dynamically loaded elastic, viscous, plastic and rigid, viscoplastic structures instantaneous mode responses definitions and characterization by variational criteria with isometric constraints [ASME PAPER 72-APM-17]

17 p2628 A72-34799

Thermodynamic infinitesimal theory of viscoplasticity

17 p2632 A72-35112

Effects of disorientation of grains on the viscoplastic behavior of fcc polycrystals

17 p2634 A72-35407

Nonequilibrium thermodynamics with rate equations as nonlinear solid mechanics foundation, noting viscoelastic, viscoplastic and plastic behavior

18 p2732 A72-36076

Viscoplasticity of face-centered-cubic metals

18 p2703 A72-37017

A new morphological element on the viscous break down microsurface of hypoeutectoid steels

19 p2817 A72-37737

Elasto-visco-plastic constitutive equations for quasi-static structures calculations.

[ONERA, TP NO. 1089] 19 p2875 A72-37763

Propagation of two-dimensional strong discontinuity waves in an elastic-viscoplastic medium.

21 p3124 A72-41503

A study of the effect of grain orientation misfit on the viscoplastic behavior of polycrystalline metals /fcc system/

24 p3414 A72-45251

VISCOPUMPS

Narrow groove theory for spiral groove viscous pump gas bearings generalized to include rarefied gas and turbulence effects

[ASME PAPER 71-LUB-1] 02 p0234 A72-11531

VISCOSITY

NT EDDY VISCOSITY

NT GAS VISCOSITY

Viscosity and additive effects on jet engine fuel antiwear properties improvement

02 p0270 A72-11968

Coulomb logarithm for hot plasma viscosity coefficient in magnetic field by quantum mechanical unified theory

02 p0267 A72-12770

Electrochemical machining electrode processes thermodynamic and kinetic characteristics, discussing temperature, electrolyte viscosity and flow rate and current density effects on metal removal rate

04 p0526 A72-14475

Blood viscosity and distributed external constraints and viscoplastic properties of vessels effects on wave dispersion and dissipation in arteries and veins, using membrane model

04 p0481 A72-15466

Viscosity and constraints effects on wave dispersion and dissipation in blood vessels, comparing theory with experiments on dogs

04 p0481 A72-15467

Hydraulic fluids behavior under extreme temperature, pressure and filtration conditions, considering viscosity, wear and corrosion resistance

05 p0681 A72-17084

Viscosity calculation of earth core at inner and outer boundary, using Andrade formula
06 p0807 A72-17760

Isothermal elasto-hydrodynamic theory for full range of pressure-viscosity coefficient, considering film thickness effect
06 p0821 A72-17805

Hydrodynamic lubricating films with viscosity variations perpendicular to direction of motion, evaluating friction coefficient changes for constant film thickness and load carrying capacity [ASME PAPER 72-LUB-E]
06 p0821 A72-17806

Flow in gas lubricated conical bearings, considering analytical and numerical solutions for axisymmetric flow model with temperature dependent viscosity and dissipation coefficients
06 p0801 A72-18124

Al alloy melts with Fe, Cr, Co and Ni, measuring kinematic viscosity by oscillatory-rotary method using logarithmic damping decrement
07 p1012 A72-19550

Isotropic turbulence spectrum based on Heisenberg theory of viscosity limiting effect on fluid motion degrees of freedom, taking into account nonlinear inertial transfer term
07 p0968 A72-19671

Viscosity measurement error estimates for Newtonian incompressible fluid flow through deformed capillary tube
07 p0991 A72-20535

Heat transfer effect on Poiseuille flow in channel, using modified Orr-Sommerfeld equation with additional viscosity gradient terms
08 p1252 A72-21253

Frequency distribution of ionospheric horizontal winds vertical shear, noting altitude independence, turbulence and viscous energy dissipation
10 p1477 A72-25157

Vibration viscometer measurement of viscosity of alkali metals Rb, Cs, Na and K near solidification temperature, studying oxygen effects on metal surface
11 p1746 A72-26236

Electronic partition functions cut-off criteria effect on translational and reactive thermal conductivity and viscosity of thermal plasmas
11 p1698 A72-26602

Hydraulic vortex amplifiers with and without diffusers, discussing supply pressure and liquid viscosity effects on system performance
11 p1578 A72-26980

Shock wave solutions of nonlinear hyperbolic system of conservation laws, considering case of zero viscosity
13 p1940 A72-28616

Hypervelocity impact parameters calculated from shock wave equations of motion, discussing viscosity effect on velocity and stress distributions
14 p2164 A72-30297

Ion viscosity tensor and ion thermal flux derived for microinstabilities of inhomogeneous collisional high pressure plasma, noting second derivatives of temperature
14 p2137 A72-30395

Complex Ca lubricants strength, colloidal and mechanical stability and thermal hardening relationship to dispersion medium viscosity
16 p2413 A72-33172

Energy balance equation of free turbulent boundary layer in incompressible fluid, deriving semiempirical formulas for turbulent viscosity coefficient
16 p2380 A72-34022

Elastic-plastic-viscous model for creep analysis of rheo-mobile materials, taking into account cracks and other defects
16 p2412 A72-34116

Viscosity and thermal conductivity of moderately dense gas mixtures.
17 p2636 A72-34737

Simplified expressions for the calculation of the contribution of the heavy components to the transport coefficients of partially ionized gases.
17 p2589 A72-34896

Stress wave propagation observation in rigid high modulus epoxy polymer by slow motion photography, noting photoelastic properties and viscosity effect
18 p2734 A72-36380

Stress state and velocity fluctuations in a perturbed boundary layer
18 p2680 A72-36464

Effect of ionic viscosity on the stability of a finite-pressure plasma
19 p2842 A72-38529

Investigation of the viscosity and density of solution melts intended for growing yttrium-iron garnet (YIG)/single crystals
19 p2847 A72-38684

Bulk viscosity coefficient and the second heat conduction coefficient near the critical condensation point
20 p2983 A72-39396

Hydrodynamic instability of a plasma boundary with a magnetic field, taking viscosity into account
22 p2310 A72-42277

Elastomers fracture strength and failure modes under tension, tearing, ozone cracking, fatigue and abrasive wear associated with viscous resistance energy losses
23 p3305 A72-43506

Some technological factors influencing the ductility of thermoplastic dross and the properties of niobium-carbide-based finished products
23 p3293 A72-44009

VISCOUS DAMPING
Dynamic stabilization of Rayleigh-Taylor instability at interface between two heavy fluids by viscosity and interfacial tension
01 p0108 A72-10231

Maximum logarithmic decrement vs frequency of damped oscillation of elastic thin beam including internal and viscous resistance
01 p0144 A72-11384

Incompressible fluid unsteady kinetic energy equation periodic solution for harmonic oscillation viscous dissipation influence on temperature field, considering Couette steady flow solution
05 p0750 A72-17007

Torsional oscillation damping in circular rods coated with viscoelastic material as function of resonant frequency
07 p1087 A72-18924

Modal damping matrix off diagonal terms measurement in viscous damping exploration for dynamic analysis of linear structures
11 p1736 A72-25988

Damping additions for plates using constrained thin viscoelastic sheets and metallic layers
11 p1688 A72-26063

Vibratory effects of disturbances transmitted from vehicle to viscoelastic vibroprotective damping coating in presence and absence of resonance
13 p2055 A72-28558

Torsional vibration damping in circular rods coated with viscoelastic material, noting technique effectiveness at certain resonant frequencies
13 p2058 A72-29209

Correlation technique for transient response of a hysterically-damped dynamic system to stationary random excitation.
17 p2579 A72-34231

Equipment vibration isolation principles, discussing damping, viscoelastic materials and shock absorbers
18 p2731 A72-35992

Damping characteristics of a liquid squeeze film.
18 p2683 A72-37053

Some properties pertaining to the stability of circulatory systems.
18 p2737 A72-37060

Simply supported column dynamic stability under axial periodic load, discussing external viscous damping effect
21 p3121 A72-41242

Viscously damped miniature piezoresistive biaxial accelerometer for operation in single cavity to 250 F
22 p3179 A72-42701

Relationship between the dissipative properties of a vibrational system and its amplitude-phase-frequency characteristics
23 p3313 A72-43785

VISCOUS DRAG
Computer model of dislocation motion acted on by viscous drag through point obstacle array for tensile stress and shock deformation tests
04 p0584 A72-14528

Viscous fluid flow at small Reynolds numbers past porous permeable sphere, obtaining drag formula
04 p0511 A72-14858

Plane physical pendulum motion stability under randomly oscillating suspension point with allowance for viscous friction
04 p0549 A72-15055

Two dimensional and axisymmetric body viscous drag in incompressible flows, using implicit finite difference boundary layer method [AIAA PAPER 72-1]
05 p0606 A72-16860

Drag reducing polymers influence on velocity gradients at wall for turbulent pipe flow, observing viscous sublayer thickening
16 p2379 A72-33574

Effect of gas slipping on drag in a system of parallel cylinders at low Reynolds numbers
22 p3133 A72-42268

VISCOUS FLOW
NT BOUNDARY LAYER FLOW
NT BOUNDARY LAYER SEPARATION
NT COUETTE FLOW
NT REATTACHED FLOW
NT SECONDARY FLOW
NT SEPARATED FLOW
NT STOKES FLOW
Pressure drop relation to entropy production in viscous low velocity adiabatic pipe flow, showing analogy with Oswatitch theorem
01 p0051 A72-11255

Equivalence laws and approximate equations for incompressible and compressible viscous flows in pipes with variable cross sections
01 p0051 A72-11256

Slow viscous flow shear stress and velocity field analysis, using photoviscosity and bubble technique [SESA PAPER 1902]
02 p0201 A72-11508

Mathematical analogy between nonequilibrium and viscous inert transonic flows for reacting mixtures with relaxation and freezing
02 p0150 A72-11736

Multicellular viscous vortex core embedded in unsteady outer potential swirling flow, obtaining numerical solution
02 p0253 A72-11971

Compressible viscous flow between concentric fixed and rotating disks, comparing analog computer calculation with experiment on radial flow
02 p0203 A72-12099

Current lines and temperature fields in square cavity with one movable wall and viscous flow and heat transfer, solving equations numerically
03 p0456 A72-13629

Two dimensional viscoelastic fluid flow past infinite plate with time dependent suction and constant and periodic free stream velocity
03 p0341 A72-13630

Steady laminar viscous conducting fluid flow in infinite rectangular channel in crossed electric and magnetic fields, deriving flow rate and potential distribution
03 p0398 A72-14008

Steady flow of viscous incompressible conducting fluid in rectangular channel with sectional walls under longitudinal external magnetic field, deriving velocity distribution
03 p0398 A72-14009

Viscous fluid flow at small Reynolds numbers past porous permeable sphere, obtaining drag formula
04 p0511 A72-14858

Laminar viscous flow past finite flat plate at high Reynolds numbers, solving Navier-Stokes equations
04 p0511 A72-14859

Linear stability of nearly parallel steady plane viscous flows, using method of multiple scales [ONERA, TP NO. 1044]
04 p0511 A72-14969

Initial viscous heat conducting gas dynamic state one dimensional decay problem solution, using kinetic theory with Boltzmann equation
04 p0512 A72-14982

Navier-Stokes equations numerical solution by computerized simulation for viscous channel flow with diaphragm orifice reducing cross section
04 p0513 A72-15644

Hydrodynamic resistance reduction for bodies moving under water, analyzing dynamic equations of viscous incompressible fluid
04 p0514 A72-15703

Navier-Stokes equations solution for unsteady viscous flow around oscillating elliptic airfoil in turbomachinery flutter analysis, obtaining pressure and shear stress distributions
05 p0600 A72-16002

Viscous incompressible flow past longitudinally cambered small aspect ratio slender wing near solid interface
05 p0600 A72-16215

High Reynolds number flow between two infinite rotating disks, investigating viscosity effects on flow velocity distribution type from analytic approximation
05 p0649 A72-16611

Circle moving under fluid dynamic and gravitational forces in viscous incompressible flow, describing dynamic interaction by numerical method [AIAA PAPER 72-111]
05 p0604 A72-16819

Numerical solution to Navier-Stokes equations for viscous annular flow between rotating long eccentric cylinders
05 p0605 A72-16821

Computerized analytical model of two dimensional multicomponent air flow in viscous subsonic flow [AIAA PAPER 72-2]
05 p0606 A72-16861

Turbulent boundary layer development for airfoil at high transonic speeds, discussing viscous-inviscid flow interaction [AIAA PAPER 72-5]
05 p0606 A72-16863

Finite difference model application to supersonic planar viscous near wake, determining parameter range by physical and numerical restraints [AIAA PAPER 72-115]
05 p0609 A72-16971

Combined viscous-inviscid analytical procedure for predicting boundary layer effects on supersonic inlet flow field [AIAA PAPER 72-44]
05 p0609 A72-16975

Viscous incompressible flow in straight duct, relating duct wall drag, axial pressure gradient, flux rate and cross sectional area
05 p0653 A72-17002

Steady two dimensional symmetric viscous flow past parabolic cylinder in uniform stream, correlating calculated nose skin friction with boundary layer theory
05 p0610 A72-17012

MHD flow of viscous fluid between two oscillating flat plates, observing velocity damping by magnetic field
05 p0699 A72-17179

Relativistic hydrodynamics, considering Cauchy problem in fluid evolution, ideal isentropic fluids, electromagnetic field effect and viscous/heat conducting thermodynamic flow models
06 p0846 A72-17252

Magneto-viscous interactions in combustion plasma, measuring velocity distributions for ordinary hydrodynamic and MHD flow with transverse magnetic field

06 p0859 A72-17618

Two-dimensional asymptotic solutions to Navier-Stokes equations for weak vortex discontinuity flow with vanishing viscosity

06 p0798 A72-17680

Cylindrically symmetrical low viscosity fluid distortion and homogeneous spiral flow stability under rotational self excitation

06 p0799 A72-17981

Viscous incompressible flow past circular cylinder at Reynolds numbers 20-100 by finite difference methods, taking into account wake region behind body

06 p0756 A72-18125

Viscous flow through movable and immovable cascades of blades, determining velocity field by airfoil center line vortex distribution

06 p0757 A72-18131

Convergent power series solution in powers of time for unsteady viscous flow near stagnation after impulsive motion of bluff body from vorticity distribution viewpoint

06 p0757 A72-18135

Attached and separated turbulent viscous regions resulting from shock wave-boundary layer interactions in hypersonic flow

[AIAA PAPER 72-74] 07 p0966 A72-18949

Vorticity transport and definition of equations for axisymmetric incompressible viscous vortex ring, solving coupled system numerically

[AIAA PAPER 72-151] 07 p0907 A72-18956

Perfect fluid two dimensional steady flow equation solution for viscous flow with specified boundary conditions, considering vortex flow

07 p0971 A72-20099

Viscous interaction effects on pressure distributions and heat transfer rate on two dimensional surface under high altitude hypersonic flight conditions

07 p0910 A72-20110

Temperature fields and mass and heat transfer at surface of solid spherical particle in laminar viscous fluid flow

07 p0973 A72-20318

Stream functions for steady two dimensional flow field of viscous liquid near circular whirl

08 p1148 A72-20937

Unsteady flow of viscous incompressible electrically conducting fluid past infinite nonconducting plate within uniform transverse magnetic field

08 p1212 A72-21079

Viscous incompressible flow past circular cylinder at Reynolds numbers 100-1000, obtaining oscillatory drag, lift and torque by governing equations numerical solution

08 p1107 A72-21251

Sealing pressure and optimal groove form for concentric running screw viscosity seals in laminar flow

08 p1178 A72-21931

Test apparatus and measurement of sealing pressure and temperature in threads of concentric running screw viscosity seals in laminar flow

08 p1178 A72-21932

Pressure gradient relations for viscous fluid flow in clearance seals at high pressures

08 p1178 A72-21937

Equilibrium statistics of randomly forced two dimensional viscous flow three mode representation constructed by numerical integration of nonlinear equations system

09 p1293 A72-22459

Numerical integration of viscous and inviscid fluid flow equations, comparing various methods with exact solution

09 p1293 A72-22463

Viscous boundary layer equations for MHD flow near rear stagnation point at small Reynolds number

09 p1296 A72-23674

Initial disturbance level effects on laminar viscous jet stability from calculation of maximum amplification rate as function of physical parameters

10 p1465 A72-24149

Laminar viscous flow past semiinfinite flat plate at zero incidence, using Oseen approximation in matching leading edge and potential flow regions

11 p1615 A72-25522

Time dependent viscous flow past impulsively started sphere using numerical solutions for governing equations based on Legendre series expansion of stream and vorticity functions

11 p1615 A72-25551

Computer program for biowaste resistojet nozzle performance prediction, taking into account viscous effect at low Reynolds number

[AIAA PAPER 72-450] 11 p1708 A72-26187

Viscous effects on turbulent diffusion shear flow past semiinfinite flat plate, using Wiener-Hopf equations

[DFVLR-SONDDR-171] 11 p1617 A72-26370

Wind velocities field in vortices leeward of islands derived from Navier-Stokes equation for isolated axisymmetric viscous vortex

12 p1839 A72-27032

Laplace-Carson transform solution for integrodifferential equation of motion for droplet suspended in viscous gas slipstream

12 p1796 A72-27093

Unsteady viscous incompressible electrically conducting fluid flow generated by porous disk rotation, investigating transverse magnetic field effect

12 p1851 A72-27305

Steady three dimensional viscous vortex within circular cylinder with tangential fluid influx from jets on outer surface and efflux through sink on bottom

[AD-741352] 12 p1798 A72-27716

Viscous flow stability between two rotating nonconcentric cylinders, obtaining approximate solution to eigenvalue problem by perturbation method

12 p1799 A72-27846

Viscous incompressible gas turbulent flow in axisymmetric channel under preliminary twist conditions at inlet, using computer numerical solution

12 p1752 A72-28126

Predictor-corrector multiple iteration technique for three dimensional viscous flow problems applied to hypersonic leading edges and Burger equation

[PIBAL-72-19] 13 p1893 A72-28422

Viscous incompressible flow between two coaxial rotating circular cylinders with small uniform injection at inner cylinder, obtaining solution of Navier-Stokes equations

13 p1941 A72-28883

Slow viscous incompressible conducting fluid MHD flow between two nonparallel walls, obtaining velocity profile solution in power series for small Reynolds numbers

13 p2020 A72-30047

Computation method for rotating and nonrotating viscous flows boundary vorticity iteration parameters for use with time centered or alternating direction implicit time differencing approximation

14 p2093 A72-30228

Viscosity, velocity gradient and wall effects on pitot tube measurement of gas flow velocity measurement in turbulent boundary sublayer

14 p2094 A72-30294

Steady nonrotating axisymmetric viscous incompressible flows with zero and negative ring circulation flux, studying solutions in three dimensional phase space

14 p2094 A72-30708

Temperature difference between steadily flowing fluid and solid sphere due to viscous dissipation determined for simultaneous conduction and radiation

[DFVLR-SONDDR-220] 14 p2105 A72-30710

Third order extension of perturbation method to solve Oseen equations for two dimensional steady viscous flow past cylindrical body at low Reynolds number

14 p2095 A72-30722

Heat and mass transfer in steady viscous flow through curved circular tubes, investigating velocity and temperature profiles

14 p2173 A72-31064

Two dimensional viscous flow past semiinfinite flat plate and smooth obstacle, using Navier-Stokes equations for lift force relationship investigation

15 p2216 A72-31312

Turbulent viscous flow near wall, deriving characteristics from equations of motion for comparison with hot wire anemometer measurement

15 p2216 A72-31469

Unsteady viscous flow effects on aerodynamic forces exerted on oscillating elliptic airfoil for various Reynolds numbers, angles of attack and frequencies

15 p2180 A72-32344

Perturbation theory for equations of motion of electrically and thermally conducting viscous compressible flow in homogeneous magnetic field, calculating fluctuation modes

16 p2435 A72-33008

Perturbation methods for density stratified viscous flow past flat plate, using boundary layer and low Reynolds number approximations

[AIAA PAPER 72-646] 16 p2381 A72-34086

Viscous dissipation effects on unsteady free convective flow past an infinite, vertical porous plate with constant suction.

17 p2637 A72-35047

Stability of spiral flow and of the flow in a curved channel.

17 p2540 A72-35051

Flow near an accelerated porous flat plate.

17 p2540 A72-35054

Transonic viscous flow around lifting two-dimensional airfoils.

[AIAA PAPER 72-678] 17 p2486 A72-35479

Viscous hypersonic flow over a flat plate at angle of attack with leeside boundary layer separation.

[AD-744593] 17 p2486 A72-35634

Flow of a viscous liquid round a cylinder for Reynolds numbers 60 and 80.

18 p2679 A72-36233

On motions with a history of constant deformation

18 p2680 A72-36463

Mean period of fluctuations near the wall in turbulent flows.

18 p2682 A72-36721

Laminar flow in an annulus with porous outer wall.

18 p2683 A72-37054

Numerical studies of flow between rotating coaxial disks.

19 p2784 A72-37374

Viscosity effect on hypersonic flow field near slender body, discussing eigenvalue solutions for two and three dimensional flow around triangular plate

19 p2745 A72-37393

Flow between eccentric rotating cylinders.

[ASME PAPER 72-LUB-J] 19 p2786 A72-37699

Motion of particles injected from the surface into stagnation-point flow.

20 p2913 A72-39611

Hypersonic viscous, slip flow over insulated wedges.

20 p2885 A72-39612

Instability of hypersonic viscous shock layer with finite rate chemistry.

20 p2886 A72-39635

Viscous non-adiabatic laminar flow through a supersonic nozzle - Experimental results and numerical calculations.

[ASME PAPER 72-HT-49] 20 p2985 A72-39662

Note on the symmetries of certain material tensors for a particle in Stokes flow.

21 p3044 A72-40113

A similarity solution for viscous internal waves.

21 p3044 A72-40118

Influence of blowing on the resistance of a sphere in laminar viscous fluid flow

21 p3047 A72-41665

Blowing of a foreign gas in a hypersonic viscous shock layer

22 p3133 A72-42265

Fluid dynamic forces exerted by Newtonian fluid axisymmetric creeping flow on accelerating body of arbitrary shape, calculating pressure gradient via Navier-Stokes equation

23 p3347 A72-43726

Steady two-dimensional viscous flow in a jet.

23 p3282 A72-44302

Viscous interaction over concave and convex surfaces at hypersonic speeds.

23 p3249 A72-44308

Intermittent character of the viscous sublayer and interpretation of probability density measurements

24 p3392 A72-45077

Equations of motion of a viscous fluid with relaxation properties

24 p3393 A72-45256

Study of a viscous flow in rotating centrifugal impellers.

24 p3363 A72-45368

Rarefied gas flow through a slit.

24 p3395 A72-45572

VISCOUS FLUIDS

Unsteady boundary layer flow of viscous incompressible fluid between two rotating coaxial parallel disks

02 p0205 A72-12538

Book on mathematical fluid dynamics covering viscous and ideal fluid motion, boundary theory, constitutive equations, hydrodynamics and kinematics

02 p0206 A72-12623

Viscous electroconducting liquid two unidimensional Hartmann flows electromagnet coupling under transverse magnetic field induction

03 p0396 A72-13790

Navier-Stokes equation analysis of three dimensional steady radial expansion of viscous heat-conducting compressible fluid from spherical sonic source into vacuum

03 p0343 A72-14247

Start-up flow of viscous incompressible fluid under constant head in entrance region of circular tube

03 p0344 A72-14343

Plane steady flow of two viscous fluids in contact, presenting normal and tangential pressure

04 p0510 A72-14513

Stationary viscous incompressible conducting fluid in conical flow, investigating diverging and converging electric current effects

[AD-740536] 04 p0558 A72-15342

Book on fluid dynamics covering theories of perfect, viscous and compressible fluids, infinite and finite span wings, boundary layer flow, etc

04 p0462 A72-15357

Oscillating torus shaped crucible viscometer, discussing oscillating viscous liquid fluid dynamic problem

04 p0522 A72-15480

Similar unsteady one dimensional motion of viscous heat conducting gas due to sudden energy release at surface

[ASME PAPER 71-WA/HT-3] 05 p0743 A72-15864

Concentration profile equations for finite length flat vertical plate moving in viscous incompressible fluid

05 p0650 A72-16783

Coriolis force effect on axially symmetric body oscillating slowly along axis in rotating viscous fluid

05 p0610 A72-17081

- MHD convection in rotating electrically conducting viscous fluid layer within magnetic field, investigating linear stability 06 p0861 A72-18069
- Unsolved fluid dynamic problems, considering viscous fluids, epihydrodynamics, magnetohydrodynamics, relativistic field dynamics and interstellar gas dynamics 06 p0800 A72-18112
- Nonlinear motion stability of finite amplitude wave solution in thin viscous incompressible liquid film 06 p0801 A72-18142
- Navier-Stokes equations numerical solution for viscous incompressible fluid in circular cylinder with rotating top disk, computing secondary flow at Reynolds numbers to 400 06 p0802 A72-18526
- Finite element solution for Boussinesq approximation of two dimensional viscous fluid dynamic problems, using variational principle 07 p0965 A72-18794
- Flow field induced by electric current jet in incompressible viscous conducting fluid, solving nonlinear momentum equation by series expansion procedure 07 p0967 A72-19504
- Flow stability of viscous fluid in annular space between rotating inner and axially oscillating coaxial outer cylinder, using perturbation method 07 p0971 A72-20089
- Nonlinear stability theory for laminar flow of viscous incompressible liquids, noting application to Couette-Taylor flow between two concentric rotating cylinders 07 p0971 A72-20091
- Steady viscous incompressible fluid flow in circular disk with prescribed velocity components at low Reynolds numbers, considering computer tested numerical method 07 p0972 A72-20102
- Unsteady laminar viscous incompressible electrically conducting flow between nonconducting parallel flat plates with applied constant magnetic field 07 p1044 A72-20245
- Sphere unsteady motion in viscoelastic liquids, noting falling-ball technique use for elastic parameters determination 07 p0973 A72-20549
- Corrugated cylinder steady rotation in incompressible viscous fluid based on linear or Stokes approximation 09 p1293 A72-22411
- Hydrodynamic stability of electrically conducting hot viscous fluid surrounded by perfectly conducting rigid boundary in presence of magnetic field 09 p1359 A72-22825
- Motion equations approximate solution for viscous fluid Couette flow instability caused by spiral symmetry vortices 09 p1295 A72-23073
- Resonant frequencies of viscous liquid in rectangular tank calculated from stream functions, assuming two dimensional oscillations and laminar flow 09 p1295 A72-23074
- Perturbed motion of rotating solid body with viscous fluid filled cavity, linearizing motion and Navier-Stokes equations 09 p1295 A72-23487
- Electrically conducting viscous incompressible fluid rotating with oscillating disk in magnetic field 09 p1366 A72-23575
- Asymmetry and intermittency factors of temperature and velocity fluctuations in viscous substrate of hot plate turbulent boundary layer 10 p1464 A72-24064
- Electromagnetic coupling between one dimensional laminar flows of viscous conducting fluid in presence of magnetic field, noting static and dynamic efficiencies dependence on Hartmann number 10 p1519 A72-24065
- Prolate and oblate spheroids flow field generated by axial translatory oscillations in still incompressible viscous fluid from Stokes linearized equations, deriving formulas for drag 10 p1418 A72-24462
- Gas flow effect on undulating flow of viscous fluid film down vertical wall, using Fourier series 10 p1469 A72-24532
- Fully developed turbulence spectrum of incompressible viscoelastic fluids 10 p1469 A72-24534
- Interacting viscous conducting media flow in inclined channel in presence of transverse magnetic field, using Moiseev asymptotic method for steady flows with wavy interface 10 p1522 A72-24546
- Viscous fluid steady nonaxisymmetric flow past rotating sphere, obtaining antitorque moment expressions and resisting force projections 10 p1469 A72-24547
- MHD sheet pinch model time dependent nonequilibrium stability determined by equations of incompressible viscous resistive magnetofluid [AD-739661] 10 p1523 A72-24751
- Parallel viscous modification of resistive tearing instability in Cartesian model of hard core pinch plasma confinement 10 p1523 A72-24795
- Hydrodynamic field generated by sphere motion along viscous fluid filled cylinder axis beyond Stokes regime 10 p1470 A72-24852
- Body center of mass position for stable fall in viscous fluid, determining terminal velocity as function of body geometry 10 p1470 A72-25067
- Equations of motion of steady viscous fluid flow in three dimensional boundary layer on walls of axial flow compressors and turbines, obtaining velocity field 10 p1420 A72-25120
- Axisymmetric three component flow of viscous incompressible fluid, finding exact solutions to second problem of dynamics 10 p1471 A72-25133
- Navier-Stokes equations system integration for axisymmetric vortex flow of viscous incompressible three component fluid 10 p1471 A72-25134
- Temperature distributions in constant viscosity incompressible Couette flow with additional pressure gradients 11 p1743 A72-25262
- Viscous liquid impulsive flow past semiinfinite plate, showing leading edge effects and boundary layer singularity existence 11 p1614 A72-25351
- Slow drop of heavy rigid spheres through vertical tube filled with viscous liquid, noting minimization of errors due to temperature and trajectory path 11 p1617 A72-26501
- Tacky adhesive tearing between two flexible strips, solving Newtonian viscous fluid slow flow problem by iterative numerical scheme 12 p1798 A72-27831
- Axial impact effect on thin elliptical layer of viscous/ideal fluid with allowance for inertial forces, analyzing spreading process stability 13 p1943 A72-29880
- Equations of motion for incompressible viscous fluid thin layer on cylinder outer side under gravity, calculating wave number, phase velocity and film thickness 14 p2094 A72-30699
- Asymptotic solution for velocity distribution in viscous liquid axisymmetric flow in conical diffusers 14 p2070 A72-31006
- Plane unsteady convective motion of viscous incompressible liquid in infinite horizontal vessel of rectangular cross section due to wall temperature fluctuations 14 p2174 A72-31157
- Finite difference solution to Navier-Stokes equations for axisymmetric flow of incompressible viscous fluid 15 p2216 A72-31446
- Velocity distributions for slow steady rotational motion of non-Newtonian inelastic viscous fluid contained between two concentric spheres, using successive approximations 15 p2217 A72-31689
- Turbulent flow between rotating disk and turbine engine body calculated from equations of axisymmetric viscous incompressible fluid flow 15 p2217 A72-31702
- Steady laminar MHD flow of viscous incompressible electrically conducting fluid between long concentric rotating porous cylinders under radial magnetic field 15 p2287 A72-32397
- Incompressible elastico-viscous liquid steady state laminar source flow between stationary infinite porous disks, noting Reynolds number effects 15 p2219 A72-32512
- Velocity and temperature distribution for viscous incompressible fluid unsteady flow between two parallel plates with pressure gradient linearly varying with time 15 p2219 A72-32599
- Spherical particle accelerated motion in stationary viscous fluid, using numerical integration technique for velocity and displacement computations 16 p2375 A72-32907
- Nonlinear instability of two dimensional unbounded incompressible viscous fluid flows under periodic small perturbation 16 p2376 A72-32933
- Turbulent flow of viscous incompressible liquid film falling down semiinfinite vertical plate under gravity influence 16 p2376 A72-33142
- Thermal convective instability in semiinfinite constant temperature viscous fluid with lower boundary suddenly heated, calculating neutral stability curve and critical Rayleigh number 16 p2478 A72-33656
- Plane-strain compression of rigid plastic material between flat platens, approximating frictional boundary conditions by entrapped viscous fluid lubricant 16 p2428 A72-34171
- Micromorphic description of turbulent channel flow 17 p2538 A72-34868
- Numerical calculation of the supersonic flow of a viscous fluid about a parabolic obstacle 17 p2484 A72-34887
- Motion of a gyrostat with respect to its center of mass in a central field 17 p2622 A72-35804
- Mathematical solution to equations of turbulent motion in viscous fluids asymptotic to strange attractors 18 p2678 A72-36015
- Rotation of a cylinder about an eccentric parallel axis in a viscous fluid 18 p2680 A72-36479
- Numerical study of a viscous gas flow in the wake of a plane body 18 p2642 A72-36804
- Unsteady motion of a compressible viscous fluid in a spherical layer 18 p2682 A72-36882
- Self-similar motions of a viscous heat conducting gas during an abrupt energy release 18 p2683 A72-36894
- Heat transfer from a slowly rotating sphere 18 p2741 A72-36934
- Slow motion in a two-dimensional semi-infinite channel with moving walls 18 p2683 A72-37044
- Time dependent solution to motion and energy equations for unsteady laminar spherical Couette flow of incompressible constant viscosity fluid 18 p2684 A72-37055
- Oscillatory flow of a viscous fluid in a flexible walled two dimensional channel 18 p2684 A72-37064
- Viscoelastic fluid lines dynamic behavior, considering viscosity, stress-strain relaxation times and compressibility effects in transfer functions derivation for pressure-velocity relations 18 p2684 A72-37077
- Boundary value problem approximate solution for Stokes flow of unbounded viscous Newtonian fluid past single body, applying algorithm to spheroidal shapes 19 p2784 A72-37369
- Numerical solution of the problem of the motion of a circular cylinder in a viscous fluid flow 19 p2784 A72-37395
- Small forced oscillations produced by infinite plate vibrations in stratified and rotating viscous fluids, investigating resonance effects on propagation 20 p2912 A72-39330
- Viscous sublayer pulsations elongation in longitudinal direction, noting decay of turbulent friction near wall as third power of distance from wall 20 p2912 A72-39360
- An asymptotic solution for steady flow above an infinite rotating disc with suction 20 p2886 A72-40015
- Free and forced trapped oscillation properties in inviscid rotating fluid, considering modifications for viscosity 21 p3049 A72-40654
- Draining of a fluid from a rotating cylindrical tank 21 p3046 A72-41307
- The motion of a viscous fluid past an impulsively started semi-infinite flat plate 21 p3046 A72-41316
- Two-dimensional stationary problem with a free boundary for the Navier-Stokes equations 21 p3047 A72-41663
- Propagation of viscous fluid jets in a medium with a density discontinuity 21 p3047 A72-41666
- A system of linear equations with partial derivatives 21 p3077 A72-41822
- Diffusion toward a particle in the case of shear flow of a viscous liquid - Approximation of the diffusion boundary layer 22 p3165 A72-41910
- Calculation of two-dimensional flows in hydrodynamics and the heat-transfer of a viscous fluid 22 p3166 A72-42287
- Boundary value problems of viscous fluid dynamic system generated by Navier-Stokes equations, using Hopf theory 22 p3208 A72-43137
- Polish book - Fluid mechanics. Volume 2 - Gasdynamics. 22 p3168 A72-43199
- Pulsatile flow of linear viscoelastic fluids in elastico-viscous tubes 23 p3280 A72-43823
- Noncoaxial rotations of a disk and a fluid at infinity 23 p3248 A72-43824
- Periodic solutions of a nonlinear mixed problem for the Navier-Stokes equations 24 p3418 A72-44780

Study of dynamic and thermal processes during steady motion of a viscous gas

24 p3390 A72-44996

Similarity problems of a non-isothermal boundary layer of an incompressible non-linear viscous medium with regard for dissipation.

24 p3395 A72-45634

VISIBILITY

NT LOW VISIBILITY

Visibility relationships to atmospheric liquid water content in fog derived from fog drop size distribution model

01 p0096 A72-11281

Scattering media visibility improvement analysis, using theoretical evaluations and experimental electro-optical measurement techniques in fog and underwater

02 p0253 A72-12644

Moving display visibility effect on pilot tracking performance, discussing dependence on illumination intensity and color

04 p0477 A72-14445

Aircraft engine exhaust geometry effects on smoke plume visibility, describing carbon particles light absorption characteristics by Beer-Lambert law [ASME PAPER 71-WA/GT-10]

05 p0704 A72-15903

Book on information theory of atmospheric visibility covering vision threshold conditions, eye as radiation detector and short waves field near ground

11 p1691 A72-26697

Clear line-of-sight probabilities for atmosphere from whole sky photos, visual cloud cover, sunshine recorder traces, satellite and in-flight observations

13 p1989 A72-28809

FAA airport fog dispersal program, discussing techniques effectiveness evaluation vs defined goals

13 p1992 A72-28843

Human and instrumental observations of aviation visibility, discussing measurements of extinction coefficient and light scatter and sensors testing

13 p1992 A72-28845

Sensor measurements correlation to human visibility via sensor equivalent visibility /SEV/ concept, discussing data processing scheme

13 p1992 A72-28846

Slant range visibility measurements by lidar for aircraft landing operations under low clouds and fog at coastal region

13 p1992 A72-28847

Random variations in interferometer complex visibility function magnitude and phase, refractive index and source angular size

14 p2156 A72-30561

Airport lighting for pilot guidance during approach and landing under category I-III visibility conditions, discussing runway layouts and power requirements

14 p2092 A72-30621

U.S.S.R. civil aviation regulations on takeoff and landing minimum conditions for cloud ceilings and visibility range for various aircraft characteristics and equipment

14 p2129 A72-30820

Flight experiments to determine horizontal visual restriction effects on T-33 aircraft front cockpit during approaches and landings

15 p2180 A72-31697

Effects of different alcohol dosages and display illumination on tracking performance during vestibular stimulation.

17 p2508 A72-34554

Determining the detectability range of camouflaged targets.

17 p2510 A72-35690

Luminous intensity, visibility duration, condensation nuclei and mass balance of noctilucent clouds

18 p2686 A72-36504

Head-up display performance in Falcon fan-jet aircraft during taxiing, takeoff, cruise, descent and landing approach, noting low-visibility hazards reduction during landing phase

20 p2952 A72-39744

The visibility range when observing an aircraft with and without field-glasses.

21 p3007 A72-40750

Visibility variations at Schiphol-Airport, Amsterdam.

22 p3202 A72-42886

VISIBLE RADIATION

U LIGHT [VISIBLE RADIATION]

VISIBLE SPECTRUM

U LIGHT [VISIBLE RADIATION]

VISION

NT BINOCULAR VISION

NT COLOR VISION

NT MONOCULAR VISION

NT NIGHT VISION

NT STEREOSCOPIC VISION

Vertebrates visual processes - Conference, University of Chile, Santiago, November-December, 1970

06 p0762 A72-17718

Book on information theory of atmospheric visibility covering vision threshold conditions, eye as radiation detector and short waves field near ground

11 p1691 A72-26697

Sight impairment-caused flight personnel disqualification analysis, establishing eye disease structure, sight damage preconditions and ophthalmological practice inadequacies

14 p2080 A72-30748

Visible and invisible nonionizing radiation produced human injuries, considering visual and retinal effects and induced thermal stresses

17 p2499 A72-34300

Light induced alterations in growth pattern of the avian eye.

17 p2500 A72-34880

Continuous objective measurement of the accommodation of the human eye

21 p3007 A72-40730

Preprocessing of nerve pulse sequences for analysis by digital computer

23 p3261 A72-44349

Influence of vision on susceptibility to acute motion sickness studied under quantifiable stimulus-response conditions.

24 p3377 A72-45659

Human physiological responses to high magnitude short duration positive accelerations, considering peripheral vision loss as function of time

24 p3377 A72-45660

VISIOPLASTICITY

U FLOW VISUALIZATION

U PLASTIC FLOW

VISORS

Glass-vinyl retractable windshield visor development for Concorde aircraft, considering rain, hail and icing effects, strength and stiffness under aerodynamic loading and heating

09 p1261 A72-22900

VISUAL ACCOMMODATION

Pupil size spontaneous oscillation /Hippus/, discussing development by repeated light step and accommodation and disappearance due to mental activity

02 p0164 A72-12490

Head movement adaptation to horizontal and vertical field displacements, discussing eye movement direction learning

06 p0765 A72-17410

Oculomotor accommodation and convergence as distance perception cues, showing size perception change relation to glasses adaptation

06 p0765 A72-17411

Human visual system frequency specific color adaptation, considering neural channels sensitivity to color and frequency input

06 p0761 A72-17412

Oculomotor cue-based distance perception, discussing glasses adaptation-caused accommodation and convergence changes in stereoscopic depth perception

06 p0765 A72-17414

Visual adaptation to light and dark in humans and animals, discussing cellular mechanisms

06 p0762 A72-17720

Computerized simulation from model of human pupillary motor behavioral response to light, accommodation and fusional inputs

07 p0928 A72-19310

Counteradaptation and cue discrepancy as perceptual adaptation basis, considering changes in registered and apparent distance of luminous object moving in dark

08 p1115 A72-20988

Adjustment to subjective horizontal, vertical and 45 deg tilt in dark as function of age in 3-20 year old subjects

08 p1124 A72-20989

Auditory flutter fusion frequency changes in humans during prolonged visual deprivation

12 p1769 A72-27418

Circadian rhythms of visual accommodation responses and physiological correlations during target tracking, recording monocular focus state by IR optometer

12 p1767 A72-28306

Human visual accommodation biorhythm and reactions under hard physical work and visual stress

13 p1909 A72-28749

Differential effects of refractive errors and receptive field organization of central and peripheral ganglion cells.

19 p2756 A72-37826

Hering's law of equal innervation and the position of the binoculars.

19 p2756 A72-37828

Continuous objective measurement of the accommodation of the human eye

21 p3007 A72-40730

Apparent movement and change in perceived location of a stimulus produced by a change in accommodative vergence.

21 p3002 A72-41024

VISUAL ACUITY

Human visual system multiple channels sensitivity to patterns at low luminance or high drift rates, noting retinal ganglion cells selective sensitivity

06 p0761 A72-17602

Moving target resolution threshold in retina, discussing visual acuity relation to target angular velocity during ocular pursuit

07 p0926 A72-19029

Dynamic visual acuity and eye movement data for moving targets, deriving retinal target image position and velocity errors during ocular pursuit

07 p0926 A72-19030

Aging effect on visual acuity variations relation to refraction variations in flight deck personnel, noting eye functional value diminution

07 p0927 A72-19244

Visual acuity measurement methods, comparing angular acuity by Beysse optometer and morphoscopic acuity by Mercier optometric scale

07 p0927 A72-19246

Dazzle glare effects and acuity recuperation among aircrew, noting civil and military aircraft accidents during daytime and nighttime flights

08 p1125 A72-21272

Stereoscopic acuity for photometrically matched background wavelengths at scotopic and photopic levels, plotting variable depth error as function of retinal illuminance

10 p1425 A72-24269

Visual evoked cortical responses in objective refraction related to retinal image clarity for clinical applications

11 p1582 A72-25349

Retina visual acuity testing by zero and first order moire fringes, using square-wave amplitude gratings

12 p1772 A72-27953

Angular oscillation in yaw effect of pilot visual performance, showing vestibulo-ocular compensation and frequency response

12 p1774 A72-28269

Visual acuity measurement by dynamic and static tests as function of target velocity and exposure time

13 p1911 A72-30042

Eye movements and dynamic visual acuity as function of tracking velocity, analyzing pursuit and saccadic component by electrooculography

13 p1912 A72-30043

Eagle eye retinal image quality determination by ophthalmoscopic method, comparing to human visual acuity

15 p2186 A72-31724

The effect of target contrast variation on dynamic visual acuity and eye movements.

17 p2508 A72-34876

The influence of the modulation transfer function of the dioptric apparatus on the acuity and contrast of the retinal image in Rana esculenta.

17 p2508 A72-34883

Fixation eye movements and the processing of visual information.

21 p3007 A72-40740

Analysis and synthesis of visual phenomena in microscopic vision - with particular reference to visual acuity.

21 p3084 A72-40748

Visual acuity restoration improvement after flash blindness by monocular shielding and ingestion of vitamin complexes containing ATP with pyridoxal, considering twilight vision

21 p3012 A72-41748

Ophthalmoscopic, photocalorimetric and ophthalmodynamometric examinations of test subjects visual acuity during bed rest in hypokinetic antiorthostatic position

23 p3255 A72-43916

Signal detection analysis of meridional variations to vertical and horizontal gratings.

23 p3259 A72-44389

VISUAL AIDS

Airport lighting for pilot guidance during approach and landing under category I-III visibility conditions, discussing runway layouts and power requirements

14 p2092 A72-30621

Visual aid-to-eye direct coupling, evaluating partial coherence effects on imagery optical performance by computer program

20 p2931 A72-39050

VISUAL CONTROL

Automatic instrumental measurement of runway visual range at airport

04 p0508 A72-14679

Tracker recovery strategy during temporary target obscuration in pursuit tracking task, analyzing control stick movements

13 p1911 A72-29820

VISUAL CUES

U CUES

U VISUAL PERCEPTION

VISUAL DISCRIMINATION

Intervening discrete elements effects on filled duration illusion in auditory, tactual and visual presentation

01 p0014 A72-10720

Threshold stimulus for visual motion discrimination as function of velocity and luminance

01 p0014 A72-10722

Temporal characteristics of wavelength and luminance modulated light perception, discussing visual system dynamics of color discrimination
02 p0164 A72-12487

Color defective vision performance predictions during day and night tests of aviation color signal light discrimination
06 p0767 A72-17871

Visual discrimination task-trained monkeys performance and physiology after pulsed mixed gamma-neutron irradiation, noting blood pressure and respiratory and heart rate changes
06 p0763 A72-17873

Objects visual detection probability distribution as function of angular size, contrast and search time, comparing binocular and monocular searches effectiveness
07 p0931 A72-19919

Natural visual capture result of vision and touch conflict in bilateral comparisons of object length
10 p1430 A72-24270

Neural effects on human visual resolution of horizontal and vertical gratings resulting from early abnormal visual inputs due to astigmatism
10 p1430 A72-24348

Vigilance performance prediction for difficulty-matched auditory and loosely and closely coupled visual intensity discrimination tasks
10 p1433 A72-25127

Average evoked potentials correlates of two flash perceptual discrimination in cats, discussing parallel changes as function of interflash intervals and peripheral level
10 p1427 A72-25178

Extrageniculostriate vision in monkey, discussing circle vs triangle and red vs green discrimination
11 p1582 A72-26772

Interhemispheric effects on choice reaction times to single and multiple letter displays, analyzing cerebral dominance and visual information transmission compared with verbal response
12 p1768 A72-27075

Color discrimination threshold determination for spectral sensitivity in subjects with congenital color vision disorders
13 p1903 A72-28763

Opponent color responses of monkey optic tract fibers to monochromatic lights, using chromatic adaptation and microelectrode recording
15 p2184 A72-31369

Experimental testing of theory of signal detectability derived psychophysical models application to two-pulse visual stimuli temporal discrimination
15 p2184 A72-31379

Visual-tactile senses conflict experimental examination, discussing vision as dominant modality
17 p2507 A72-34249

Effect of target-background luminance contrast on binocular depth discrimination at photopic levels of illumination
17 p2508 A72-34879

An analytical description of the line element in the zone-fluctuation model of colour vision, I, II
18 p2651 A72-36606

Theoretical models for speed-accuracy tradeoff during difficult visual discrimination tasks under time pressure
18 p2655 A72-37220

Psychological tests for diurnal variations of human visual discrimination threshold by varying test object illumination level
20 p2891 A72-38931

Discrimination sensitivity and black light density in the mesopic range
21 p3007 A72-40735

Perceptual differentiation of sequential visual patterns
21 p3008 A72-41021

Interactions of signal and background variables in visual processing
22 p3152 A72-42931

Simultaneous detection and recognition of chromatic flashes
22 p3152 A72-42933

VISUAL DISPLAYS
U DISPLAY DEVICES
VISUAL FIELDS

Visual response to monocularly and dichoptically presented flashed patterns, discussing physiological mechanism based on cortical visual field concept
02 p0164 A72-12485

Contrast vision enhancement in Hermann grid with variable figure-ground ratio, using Baumgartner receptive field hypothesis
03 p0315 A72-13624

Successive visual motion illusion during perception of rotating kymograph drum by human eye
04 p0476 A72-15588

Head movement adaptation to horizontal and vertical field displacements, discussing eye movement direction learning
06 p0765 A72-17410

Cerebral cortex striate area relation to visual field in various animals
06 p0763 A72-17722

Visual space geometry and perception experiments, demonstrating size-distance relations for various visual cues
07 p0926 A72-19031

Moving visual stimuli apparatus with independent control over size, shape, background intensity, orientation and velocity of motion, describing cat neuronal sensitivity studies
07 p0926 A72-19032

Human vision light adaptation effects on dichromatic color matches for bipartite centrally fixated circular matching field
07 p0927 A72-19033

Afterimage apparent motion preceding smooth eye movement association with target tracking, noting unequal impairment occurrence over entire visual field
07 p0927 A72-19034

Uniform visual field influence on electroencephalographic alpha rhythm in man, discussing ocular fixation, visual attention and vigilance change effects
07 p0916 A72-19040

Optic disk drusen and Marcus Gunn pupillary phenomenon relation to visual field defects, discussing need for calibrated perimetry and binocular field testing
07 p0933 A72-20190

Cat retina ganglion cell threshold and latent responses to separate stimulation of receptive field center and periphery
08 p1117 A72-21474

Single lateral geniculate neuron recording during receptive field-centered flashing spot variations for intensity response function comparison with optic neurons in cats
10 p1427 A72-25177

Structural design and optical problems of external vision and cockpit transparencies in military aircraft
12 p1753 A72-27002

Optical qualities of aircraft windshields and direct vision windows, considering color, light transmission, faults, heating, distortion, inside reflections and double images
12 p1832 A72-27004

Cortico-subcortical connections transaction effect on cat lateral geniculate body and visual cortex neurons spontaneous activity
12 p1761 A72-27652

Cat visual cortex receptive field responses to light bands of variable widths and intervals
14 p2074 A72-30256

Voluntary saccade length dependence on visual foveal nontarget stimuli number, locus and distance from target
14 p2077 A72-30966

Disparity-associated depth sensation masking, suggesting visual signal processing inhibitory mechanisms for crossed and uncrossed stimuli
15 p2184 A72-31366

Monkey retinal ganglion and lateral geniculate nucleus cell maintained discharge rate indication of receptive field organization for various light stimulus intensities
15 p2184 A72-31370

IR and visible parametric laser image upconversion experiments, demonstrating wavelength dependence on view field by black body radiometric measurements
15 p2249 A72-32152

The relative importance of contrast and motion in visual detection
17 p2509 A72-35689

The effect of chlorthalidoxepine on visual field, extraocular muscle balance, colour matching ability and hand-eye co-ordination in man
17 p2505 A72-35915

Visual half-field differences in the recognition of bilaterally presented single letters and vertically spelled words
18 p2653 A72-36908

Considerations in the design of an automatic visual field tester
18 p2654 A72-37013

Discontinuity of seen motion reduces the visual motion aftereffect
19 p2760 A72-37600

Differential effects of refractive errors and receptive field organization of central and peripheral ganglion cells
19 p2756 A72-37826

Visual Field Analyzer presentation of single and multiple stimuli for differential threshold level investigation, discussing eccentricity, spatial orientation and supraliminal stimuli effects
19 p2756 A72-37831

Receptive fields of units in the visual cortex of the cat in the presence and absence of bodily tilt
19 p2758 A72-38646

Investigations concerning the problem of virtual contours in visual perception
19 p2759 A72-38719

An electronic model of visual receptive fields
20 p2897 A72-39271

Parametric adjustment to a shifting target alternating with saccades to a stationary reference point
21 p3009 A72-41250

VISUAL OBSERVATION

Interactions between spatial and kinetic dimensions in movement aftereffect
21 p3003 A72-41254

Temporal and spatial characteristics of selective encoding from visual displays
21 p3009 A72-41255

Analysis of the activity evoked in the cerebellar cortex by stimulation of the visual pathways
21 p3003 A72-41460

Visual experience as a determinant of the response characteristics of cortical receptive fields in cats
21 p3003 A72-41461

Visual angle and apparent size of objects in peripheral vision
22 p3152 A72-42932

Motion thresholds for fovea and peripheral retina with/without correction for peripheral refractive error
23 p3260 A72-43978

Information aspects in visual perimetry, obtaining memory requirement for control computer in automated perimetry
23 p3261 A72-44378

Photopic and scotopic contributions to the human visually evoked cortical potential
23 p3261 A72-44380

Line length detectors in the human visual system - Evidence from selective adaptation
23 p3258 A72-44384

Techniques for analysing differences in VERs: Colored and patterned stimuli
23 p3258 A72-44387

Small field tritanopia of central fovea in terms of dichromatic area color response mechanism and adaptation speed
23 p3259 A72-44390

Visual stimuli distance estimation with head stationary or moving, discussing performance after monocular motion parallax training
24 p3374 A72-44557

Optical directionality of retinal receptors and corresponding points. I - Nasal-temporal asymmetry of retinal spatial values and orientation of receptors: Are the corresponding points cones. II - Variation of form of the experimental horoptera, and possibility of reorganization of the retinal correspondence according to the orientation of the eyes
24 p3371 A72-44907

Functional organization of the periphery effect in retinal ganglion cells
24 p3371 A72-44908

The effects of simultaneous and successive contrast on perceived brightness
24 p3372 A72-44910

Control, by the visual cortex, of the posterior lateral thalamic group in the cat
24 p3372 A72-45009

VISUAL FLIGHT RULES

Aircraft collision near misses under IFR and VFR conditions, discussing ATC coordination, equipment failure and personal and planning problems
09 p1349 A72-22972

VISUAL OBSERVATION

Photoelectric and visual timings of occultations for lunar motions, comparing accuracy and systematic instrument errors
03 p0420 A72-13127

Meteor showers of March 1969, noting delta L yrids, gamma Cygnids and beta Ursae Minorids observations
03 p0438 A72-13984

Meteor count by naked eye and binocular visual observation in Crimea, obtaining luminosity functions
06 p0881 A72-17932

Optical observation of southern radio sources with 60 inch telescope at Cerro Tololo /Chile/, measuring red shifts for radio galaxies
07 p1072 A72-19342

Pulsars optical counterpart observation, noting Crab Nebula pulsar visual magnitude
07 p1080 A72-20050

Telescopic requirements posed by Venus near sun, discussing sky brightness in image plane, atmospheric dust and Rayleigh scattering
08 p1230 A72-20993

Binocular observation of astronomical objects, discussing binocular design of astronomical telescopes
08 p1165 A72-21087

Earth horizons nighttime, twilight and daytime visual observations from manned Soyuz spacecraft, discussing upper atmosphere emission layer structure and aureole development
08 p1158 A72-21148

Visual observations of wall in turbulent pipe flow, using suspending solid MgO particles
09 p1306 A72-22310

Visual and radar echo location of organized updraft on thunderstorms and hailstorms
09 p1346 A72-22452

Geodetic azimuth determination by multiple observations of bright stars near meridian
09 p1297 A72-22485

Disk diameter errors due to wire thickness in reduction of visual planetary observations
09 p1311 A72-23062

Venus and Mars visible geocentric declinations from daytime observations with Wanschaff vertical circle compared to nighttime results

09 p1388 A72-23065

Visual and automatic stereometric image analysis, citing minimum measurable contrast thresholds for various devices

10 p1478 A72-23826

Jupiter polar caps, Red Spot and equatorial belts visual observations during 1970 opposition

10 p1542 A72-24570

Stellar brightness variations of T Cep during January 1969-November 1971, considering visual estimates and period length observations

10 p1542 A72-24571

Southern Hemisphere interstellar clouds radial velocities from optical and radio observations

10 p1542 A72-24612

Visual observations of eclipsing period elements of nova-like variable V Sagittae for estimate of total magnitude of uneclipsed binary

10 p1545 A72-24829

Light curve of TW Delphini from visual observations, noting relationship to RV Tauri-type stars

10 p1546 A72-24830

Automatic telemetering meteorological stations and visual observation data processor control

10 p1507 A72-25020

IR and optical observations of cluster surrounding Herbig Be type star BD plus 40.4124, noting extreme youth of group

11 p1721 A72-26122

Crab pulsar period speedup observed by optical timing on 26 October 1971, noting similarity to September 1969 event

11 p1724 A72-26573

Flash symmetry observed during fading and brightening of beta Scorpii A in occultation by Jupiter

12 p1868 A72-27297

Detection range, color, brightness and flash subjective response tests to evaluate light signals for nighttime sea navigation and visual collision avoidance

12 p1777 A72-28326

Clear line-of-sight probabilities for atmosphere from whole sky photos, visual cloud cover, sunshine recorder traces, satellite and in-flight observations

13 p1989 A72-28809

Human and instrumental observations of aviation visibility, discussing measurements of extinction coefficient and light scatter and sensors testing

13 p1992 A72-28845

Fourier transformations for convolution integral calculation in image distortion correction by ground visual observations of solar intensity distribution, noting successive approximations method

13 p2046 A72-29726

Aircraft and other vehicle simulators for training crews, discussing evolution of needs, digital techniques, and visual and physiological experiences

14 p2092 A72-30844

Visual observation of continuous hydrocyanic acid laser modes and beam energy distribution, using cholesteric liquid crystal image converter

14 p2111 A72-30851

White background noise intensity effects on human visual target detection performance considering display difficulty levels, target location, detection time and error

14 p2083 A72-31156

Human vision sensitivity to covert IR illuminators for image intensification during night observation

15 p2189 A72-32046

Lunar transient phenomena during 1540-1970, tabulating observation reports

15 p2312 A72-32093

Visual evaluation of concave diffraction gratings with high ruling frequency, noting Foucault knife edge test limitations due to image faults

15 p2238 A72-32155

Optical observations of the supernova in NGC 5253.

18 p2726 A72-36648

Physical observations of comets. XVII

18 p2726 A72-36722

Meteor count by naked eye and binocular visual observation in Crimea, obtaining luminosity functions

18 p2730 A72-37157

The non-stroboscopic visualisation of vibrational patterns by real-time/time averaged hologram interferometry.

19 p2873 A72-37618

Limiting magnitudes of stars in visual telescopic observations/Ground and extraatmospheric locations of instrument and observer/

19 p2859 A72-37907

Minimum perceivable stellar magnitudes in visual observations by naked eye and telescope, discussing image contrast and angular scale

19 p2860 A72-37961

Perseid shower radiants observation in August 1969, indicating presence of one secondary and two main radiants

19 p2864 A72-38328

Visual optical system evaluation from viewpoint of human operator target detection under field conditions

in terms of resolution, transfer functions, aberration and eye movements

20 p2893 A72-39041

Earth horizons nighttime, twilight and daytime visual observations from manned Soyuz spacecraft, discussing upper atmosphere emission layer structure and aureole development

20 p2916 A72-39253

Effect of a temporal shift in the min II of eclipsing binaries

20 p2975 A72-40072

The visibility range when observing an aircraft with and without field-glasses.

21 p3007 A72-40750

Ground observation for outer planets natural satellites ephemeris, using astrometric telescopes, photographic and plate reduction techniques [AIAA PAPER 72-904]

24 p3443 A72-45426

VISUAL PERCEPTION

NT AUTOKINESIS

NT CRITICAL FLICKER FUSION

NT SPACE PERCEPTION

NT VISUAL DISCRIMINATION

Neuron responses in cat visual system /retina, geniculate body, primary, secondary and tertiary visual cortex/to simple visual stimulus pattern

01 p0011 A72-10466

Functional organization of visual cortex in monkeys, discussing monocular and binocular responses, trigger and stimulus abstraction

01 p0011 A72-10467

Sensory psychological invariance formation for perceptual functions in human visual system

01 p0011 A72-10468

Psychology of visual form perception in relation to neurophysiological principles of lateral interaction and organization, considering retinal images, aftereffects, binocular vision, etc

01 p0011 A72-10469

Neural substrates of sensory tactile vision substitution for information mediation in blind subjects, using TV camera

01 p0011 A72-10470

Electronic analog models of human retina and visual system, discussing optical character recognition, signal processing, photoreceptor stimulation, visual cortex excitation and further model development

01 p0017 A72-10471

Sensorimotor preconditions of single image impression in human binocular vision

01 p0018 A72-10477

Psychophysical perceived orientation experiments on Poggendorff illusion /transversal interrupted by parallel lines/

01 p0013 A72-10717

Position constancy and motion perception tests of head movement feedback calibration of perceived direction of optical motions

01 p0013 A72-10719

Human pattern analysis by stabilized retinal image fragmentation as function of fade frequencies for angle and line stimuli in different orientations

01 p0014 A72-10721

Lateral spatial interactions of sensory receptors, discussing mathematical theory for monocular visual inputs described by real valued functions on continuum

01 p0021 A72-11196

Inert gas narcosis under hyperbaric conditions relationship to mental performance and auditory and visual evoked responses in man

[AD-736736]

02 p0166 A72-11705

Eye-hand coordination modifiable parameters under optical distortion conditions, deriving quadratic equation for hand response adaptation

02 p0167 A72-11897

Visual response to monocularly and dichoptically presented flashed patterns, discussing physiological mechanism based on cortical visual field concept

02 p0164 A72-12485

Temporal characteristics of wavelength and luminance modulated light perception, discussing visual system dynamics of color discrimination

02 p0164 A72-12487

Lateral inhibition effect on disappearance mode of visual perceptual units /lines and angles/

02 p0164 A72-12489

Optic nerve axon diameters in central and peripheral cat retina related to conduction velocity groups

03 p0315 A72-13622

Concurrent and terminal display exposure effects on perceptual adaptation for localizing movements with displacing prism

03 p0319 A72-13788

Visual guidance of locomotion, discussing expansion information and target drift theories

03 p0319 A72-13879

Moving display visibility effect on pilot tracking performance, discussing dependence on illumination intensity and color

04 p0477 A72-14445

Successive visual motion illusion during perception of rotating kymograph drum by human eye

04 p0476 A72-15588

Visual persistence and perceptual moment hypotheses for time-dependent visual illusion from viewing moving stroboscopically illuminated object

05 p0621 A72-16150

Involuntary eye movements effects on visual images, emphasizing drift and tremor effects on spatial frequency distortion

05 p0623 A72-16674

Head movement adaptation to horizontal and vertical field displacements, discussing eye movement direction learning

06 p0765 A72-17410

Human visual system frequency specific color adaptation, considering neural channels sensitivity to color and frequency input

06 p0761 A72-17412

Human visual system selective adaptability to speed, size and orientation, suggesting motion analysis by visual cortex neural subsystems

06 p0761 A72-17603

Darkness enhancement measurement in intermittent light as function of flicker frequency, describing experimental assembly

06 p0762 A72-17605

Occipital and vertex visual evoked response relation to sensory information, perception and stimulation

06 p0763 A72-17723

Phylo-ontogenetic maturation of corticopetal projections of visual cortex, using evoked potential measurements in rabbits

06 p0763 A72-17736

Bisensory performance in simultaneous auditory and visual verbal information recognition, demonstrating integrative action between hearing and vision

06 p0768 A72-17949

Dynamic manned vehicle cockpit simulator for visual and aural effects and acceleration changes, discussing STOL and VTOL characteristics

06 p0796 A72-18246

Suppression of visual evoked responses to low intensity light flashes and shifting stripe patterns during saccadic eye movements

07 p0926 A72-19025

Flicker and flash threshold experiments, discussing flicker cut-off frequency and flash duration relations and visual sensitivity

07 p0926 A72-19028

Visual space geometry and perception experiments, demonstrating size-distance relations for various visual cues

07 p0926 A72-19031

Moving visual stimuli apparatus with independent control over size, shape, background intensity, orientation and velocity of motion, describing cat neuronal sensitivity studies

07 p0926 A72-19032

Optic disk drusen and Marcus Gunn pupillary phenomenon relation to visual field defects, discussing need for calibrated perimetry and binocular field testing [AD-737860]

07 p0933 A72-20190

Reaction time to visual orientation change, obtaining aftereffects as function of orientation specific adaptation duration and separation angle between inspection and test lines

08 p1124 A72-20986

Rotating disk background and speed effects on perception of verticality motion in clockwise or counterclockwise direction

08 p1124 A72-20987

Three color response of human vision, noting relationships to color matching function and brightness

09 p1269 A72-22617

Psychological aspects in aerial photointerpretation, discussing importance of perception of image contrast, contours and areal distribution

09 p1272 A72-23299

Visual search model from perceptual theory, animal studies and search data, discussing selection, inspection and naming single cued letters in visual array

09 p1274 A72-23647

Stochastic model for eye movements during fixation on stationary target

10 p1429 A72-23795

Visual and haptic perception in angle reproduction matching task, noting performance differences relation to nature of form discrimination and task

10 p1433 A72-25126

Spatial frequency specificity of edge contour color aftereffects

10 p1427 A72-25182

Vascular-capillary study of age related angioarchitectonic features of human brain optic lobe

11 p1580 A72-26675

Bed rest and positive radial acceleration effect on peripheral visual response time, considering blackout or grayout prediction possibilities

12 p1766 A72-28297

Neck proprioception effects and otolith organ activity in perceived visual target elevation under centrifuging stress

12 p1776 A72-28305

Sensor measurements correlation to human visibility via sensor equivalent visibility /SEV/ concept, discussing data processing scheme
13 p1992 A72-28846

Relationship of visibility fluctuations in set of luminous circles to verbal response learned for each circle, showing word association influence on stimuli perception
13 p1911 A72-29851

Visual latencies measurement as function of stimulus luminance and adaptation state by stereoscopic null method, characterizing relationship by inverse power function
13 p1911 A72-29968

Matched luminance chromatic stimuli wavelength effects on human visual latency
14 p2074 A72-30267

Pupil reflex loss /pupillonia/ diagnosis in pilots, testing sensitivity to methacholine chloride [AD-744368]
14 p2082 A72-31096

Human eye relative luminous efficiency for near IR and UV coherent light, using ruby laser pumped tunable dye laser primary and second harmonic outputs
15 p2184 A72-31380

Visual and acoustic image processing rates during letter sequencing tasks, suggesting implicit verbal control involvement
15 p2188 A72-32764

Stabilized retinal image techniques to examine functional relationships between nonstabilized grating pattern orientation adaptation and stabilized line stimuli fading rates
16 p2358 A72-33646

Occipital EEG activity during fluctuations of perception under stabilized image and simplified stimulus conditions.
17 p2506 A72-34247

Visual depth perception response functions for sine and square wave modulated binocular parallax
17 p2498 A72-34293

Evidence for the role of the transient neural 'off-response' in perception of light decrement - A psychophysical test derived from neuronal data in the cat.
17 p2500 A72-34884

Quantitative decision criteria for identification of visual evoked responses obtained during binocular rivalry.
18 p2652 A72-36312

On the apparent orbit of the Pulfrich pendulum.
18 p2653 A72-36608

Novelty, recency and frequency effects on visual recognition and pseudo-recognition thresholds.
18 p2653 A72-36909

Assessment of life span age difference relations in visual perceptual tasks, taking into account maturational and generational differences
18 p2653 A72-36910

Effects of visual cues on the standing body sway of males and females.
18 p2654 A72-36918

Manipulation of projected afterimages by means of the physiological theory imposed on the observer.
18 p2654 A72-36920

Minimum perceivable stellar magnitudes in visual observations by naked eye and telescope, discussing image contrast and angular scale
19 p2860 A72-37961

Calculating the perceived level of light and sound.
19 p2761 A72-38567

Investigations concerning the problem of virtual contours in visual perception
19 p2759 A72-38719

An electronic model of visual receptive fields.
20 p2897 A72-39271

General principles and detail similarities in visual pattern analysis by single neuron operation, computer programs and psychological perception
20 p2891 A72-39275

Visual performance when using optical instruments; Symposium, Munich, West Germany, July 21-23, 1971, Technical Papers.
21 p3054 A72-40727

Age dependence of changes in pupil diameter in the dark.
21 p3007 A72-40732

Threshold detection model for foveal viewing by human observers using naked eye
21 p3007 A72-40733

Liminal stimuli binoptic detection variation with ratio of left eye to right eye detection probabilities
21 p3007 A72-40734

Night vision performance measure based on object recognition experiments with optical instruments, noting improvement with image intensifier
21 p3007 A72-40741

Noise and stimuli current time and spatial distribution effect on visual performance of eye with image intensifier
21 p3054 A72-40742

The minimum brightness gain required in viewers using image intensifiers.
21 p3055 A72-40744

Some structural and functional characteristics of a retina projection onto the visual cortex of cats
21 p3001 A72-40808

Parametric adjustment to a shifting target alternating with saccades to a stationary reference point.
21 p3009 A72-41250

The effect of size, retinal locus, and orientation on the visibility of a single afterimage.
21 p3003 A72-41253

Temporal and spatial characteristics of selective encoding from visual displays.
21 p3009 A72-41255

Display device design and human operator training based on visual and auditory sensation and perception principles, emphasizing fitting between man and information
21 p3010 A72-41407

The airborne visual simulation as an electronic display.
21 p3010 A72-41410

Visual information space-time dependent filtering by retinal and geniculate body neural nets
22 p3142 A72-42299

1971 Rayleigh Gold Medal Address - Calculating the perceived level of light and sound.
22 p3205 A72-42462

On threshold mechanisms for achromatic and chromatic vision.
22 p3142 A72-42547

Visibility variations at Schiphol-Airport, Amsterdam.
22 p3202 A72-42886

Visual perception of accelerated nitrogen nuclei interacting with the human retina.
23 p3256 A72-43940

Complete assimilation of briefly presented lines.
23 p3261 A72-44150

Information aspects in visual perimetry, obtaining memory requirement for control computer in automated perimetry
23 p3261 A72-44378

Visual sensitivity measurement in retinal areas with stepwise change from one monochromatic light to another, discussing eye movements effects and perception thresholds
23 p3258 A72-44385

Perceptual latency as a function of stimulus onset and offset and retinal location.
23 p3258 A72-44386

The suppression-recovery effect in relation to stimulus repetition and rapid light adaptation.
24 p3372 A72-44909

The effects of simultaneous and successive contrast on perceived brightness.
24 p3372 A72-44910

Perception smear suppression during saccadic eye movements in terms of metacontrast determined by post-saccadic accumulated luminance relation to stimuli masking
24 p3373 A72-45377

VISUAL PHOTOMETRY
Light distribution photometry in Japan, discussing photometers, luminous flux integration and source distribution and positioning errors
03 p0358 A72-13426

NGC 3031 spiral galaxy photometry and large scale structure determination by UBYR integral equidensity curves method
08 p1234 A72-21280

Nocturnal low intensity auroral red arcs observations by meridian scanning photometer, comparing with green emission
14 p2097 A72-30136

Spectral brightness coefficient and photodensity measurements for remote vegetation productivity sensing in visible band
15 p2222 A72-31396

Colorimetric photometric matching tests, showing subject differences in parafoveal spectral sensitivity indicated by photopic curve peaks
17 p2508 A72-34882

VISUAL SIGNALS
Optimal flash rate and duty cycle for flashing visual indicators, testing observer ability to determine indicator state
01 p0018 A72-10565

Alerting light and audio signals for aircraft pilots, considering implications for aircraft design
01 p0021 A72-11291

Color defective vision performance predictions during day and night tests of aviation color signal light discrimination
06 p0767 A72-17871

Vibrotactile warning device effectiveness under auditory and visual loadings, investigating reaction time and errors number
08 p1126 A72-21569

Russian book on visual sensor signal dynamics covering nerve signal transformation, light stimuli responses, afferent flow, bionics, neurocybernetics and communication theory
11 p1584 A72-26049

VISUAL STIMULI
Detection range, color, brightness and flash subjective response tests to evaluate light signals for nighttime sea navigation and visual collision avoidance
12 p1777 A72-28326

Detection and recognition of colored signal lights.
17 p2510 A72-35691

Rate distortion theory model for visual communication fidelity assessment via weighted noise measurement and K rating
18 p2657 A72-36251

Image processing in the context of a visual model.
18 p2658 A72-36256

Visual information electronic display systems from human factors engineering viewpoint, discussing intelligibility optimization in terms of human vision physiological characteristics
19 p2803 A72-38309

The detectability of a brief gap in a pulse of light as a function of its temporal location within the pulse.
21 p3002 A72-41023

Interactions of signal and background variables in visual processing.
22 p3152 A72-42931

Simultaneous detection and recognition of chromatic flashes.
22 p3152 A72-42933

Semaphore channel signaling reliability, presenting error protection and correction system
24 p3381 A72-45770

VISUAL STIMULI
Physiological response to affective visual stimuli, observing signal value change effect on forehead pulse amplitude and galvanic skin response
01 p0014 A72-10854

Spatio-temporal scalp mapping localization of human visual evoked responses to full field light adapted stimulation, comparing to half-field situation
01 p0015 A72-11185

Body cooling effect on human vigilance in hot environments, testing reaction time to visual stimuli and auditory signal detection rate
01 p0021 A72-11290

Visual masking effect due to light offset, investigating human identification response to tachistoscopic test stimuli on lighted background with simultaneous shut-off
02 p0166 A72-11550

Visual cortex neuron responses to light flashes under hypothalamic and reticular electric stimulation in rats
02 p0158 A72-11758

Visual response to monocularly and dichoptically presented flashed patterns, discussing physiological mechanism based on cortical visual field concept
02 p0164 A72-12485

Lateral inhibition effect on disappearance mode of visual perceptual units /lines and angles/
02 p0164 A72-12489

Fragmentation and closure in afterimages of bright flash stimuli
03 p0317 A72-13938

Cortical responses to visually displayed word and nonsense syllable stimuli, using EEG and computer techniques
04 p0474 A72-15248

Human trace responses generation and storage under light stimulus reinforcement of sound conditioning from galvanic skin reactions observation
04 p0475 A72-15581

Perceived common rotary motion of ambiguous stimuli as criterion of perceptual grouping
06 p0765 A72-17413

Occipital and vertex visual evoked response relation to sensory information, perception and stimulation
06 p0763 A72-17723

Retina, tectum opticum and Rostral brain structures role in analysis and processing of visual sensory stimuli in toad distinguishing between prey and enemies
07 p0915 A72-18775

Suppression of visual evoked responses to low intensity light flashes and shifting stripe patterns during saccadic eye movements
07 p0926 A72-19025

Moving target resolution threshold in retina, discussing visual acuity relation to target angular velocity during ocular pursuit
07 p0926 A72-19029

Dynamic visual acuity and eye movement data for moving targets, deriving retinal target image position and velocity errors during ocular pursuit
07 p0926 A72-19030

Moving visual stimuli apparatus with independent control over size, shape, background intensity, orientation and velocity of motion, describing cat neuronal sensitivity studies
07 p0926 A72-19032

Occipital electroencephalographic response to slowly repeated aperiodic light flashes, discussing alpha wave and rhythmic afteractivity amplitude changes
07 p0916 A72-19041

Evoked cortical potentials changes from emotional visual word stimuli stress under amytil anticholinesterase drug influence
08 p1116 A72-21194

Hypothalamic single neuron unit discharge pattern response to acoustic, light and somatosensory stimulation in cats

08 p1116 A72-21471

Cat retina ganglion cell threshold and latent responses to separate stimulation of receptive field center and periphery

08 p1117 A72-21474

Light variation threshold amounts for flicker and flickering pattern detection as function of variation frequency

09 p1269 A72-22615

Photically induced and spontaneously discharged neuron impulse propagation through direct pathways from superior colliculus to dorsal and ventral lateral geniculate nuclei in cats

09 p1265 A72-22863

Isolated specific color dependent waveforms of visual evoked response to strong colored lights relating luminance and wave amplitude changes

09 p1267 A72-23500

Photostimulated potentials of human visual cortex, determining retinal macular area involvement

10 p1426 A72-24786

Single lateral geniculate neuron recording during receptive field-centered flashing spot variations for intensity response function comparison with optic neurons in cats

10 p1427 A72-25177

Stimulus complexity effect on amplitude of human cyclofusional response, evaluating relative roles of compensatory eye movements and central responses

10 p1427 A72-25180

Anisotropic responses to dot and line visual stimuli, obtaining judgments on apparent straightness for various visual field locations and dot densities

10 p1427 A72-25183

Visual evoked cortical responses in objective refraction related to retinal image clarity for clinical applications

11 p1582 A72-25349

Lenticular conditioning-shock stimulation effect on cat visual cortex response to light stimuli, noting lateral gyrus photically evoked potential amplitude increase

11 p1578 A72-25801

Orienting response indication by EEG alpha rhythm desynchronization in relation to visual stimulation intensity

11 p1585 A72-26238

Intraelectroretinographic analysis of light signal spatial summation at different retinal nerve levels in frogs

11 p1585 A72-26454

Response latencies and correlation in single units and visual evoked potentials in cat striate cortex following monocular and binocular stimulations

11 p1582 A72-26771

Image visual recognition during voluntary saccadic eye movements, noting stimuli visible luminance change effect

12 p1760 A72-27310

Visual cortex neuronal background activity in unanesthetized rabbits under stimulation and depression of lateral geniculate body and mesencephalic reticular formation, considering synaptic organization

12 p1761 A72-27646

Spatial characteristics of equal energy visual stimuli in metacontrast design for targets and masks of constant separation and varying width, deriving weighting functions

12 p1762 A72-27680

Vision influence on acute motion sickness elicitation in slow rotation room, comparing with vestibular factors

12 p1764 A72-28258

Nystagmus eye movements relationship to oculogyral illusion from test involving vestibular stimulation and visual stimuli velocity estimates

12 p1776 A72-28304

Frequency-specific color aftereffects as result of alternate exposure of subject to inspection gratings of different spatial frequencies

13 p1901 A72-28615

Conditioned stimuli presentation role in successive differentiation and inhibition limits in monkeys

13 p1902 A72-28644

Illumination code efficiency in impulse activity of neurons of outer geniculate body of cat visual system, emphasizing pulse per group technique

13 p1903 A72-28780

Visual cortex neuron reactions to antidromic stimulation of cat pyramidal tract, noting axon activation increased discrimination in analyzer

13 p1903 A72-28781

Human flexible processing accomplishment in speeded recognition task with visual stimulus dimension relevancy contingent upon other dimension stimuli values

13 p1911 A72-29832

Relationship of visibility fluctuations in set of luminous circles to verbal response learned for each circle, showing word association influence on stimuli perception

13 p1911 A72-29851

Spatial and temporal summation characteristics and relationship in human peripheral retina investigated for stimuli viewed at eccentricity against luminous background

13 p1907 A72-29970

Cat visual cortex receptive field responses to light bands of variable widths and intervals

14 p2074 A72-30256

Matched luminance chromatic stimuli wavelength effects on human visual latency

14 p2074 A72-30267

Visual cortex repetitive stimulation effect on primary response habituation in young normal rabbits and adults with septum pellucidum lesion

14 p2076 A72-30596

Voluntary saccade length dependence on visual field nontarget stimuli number, locus and distance from target

14 p2077 A72-30966

Compensatory tracking task performance with continuous error information feedback via visual, auditory or electrocutaneous displays

14 p2083 A72-31152

Target and surrounding nontarget stimuli size differences effect on visual search time for displays with large fields

14 p2083 A72-31153

Heat chamber treadmill work-induced thermal stress effects on reaction time to foveally and peripherally presented visual stimuli

14 p2078 A72-31154

Human retinal rod rhodopsin bleaching and regeneration measurements, tracing dark adaptation curves

15 p2184 A72-31364

Dark adaptation studies of bleach-induced visual threshold rise and subsequent return to rhodopsin level

15 p2184 A72-31365

Disparity-associated depth sensation masking, suggesting visual signal processing inhibitory mechanisms for crossed and uncrossed stimuli

15 p2184 A72-31366

Linear systems theory for mathematical model of retinal image and ganglion cell excitation, calculating receptor layer luminance distributions for several stimulus patterns

15 p2184 A72-31367

Visual stimulus orientation effect on movement perception, relating physiological and psychological factors

15 p2184 A72-31368

Monkey retinal ganglion and lateral geniculate nucleus cell maintained discharge rate indication of receptive field organization for various light stimulus intensities

15 p2184 A72-31370

Experimental testing of theory of signal detectability derived psychophysical models application to two-pulse visual stimuli temporal discrimination

15 p2184 A72-31379

Foveal light pulse duration effects on reaction time, showing stimulus intensity-time reciprocity

15 p2188 A72-31509

Size scaling rate from retinal image size comparison judgment time during observation of briefly presented concentric rectangles of varying size and orientation

15 p2187 A72-32762

Stabilized retinal image techniques to examine functional relationships between nonstabilized grating pattern orientation adaptation and stabilized line stimuli fading rates

16 p2358 A72-33646

Hypoxia and peripheral visual stimulus position effects on response time during monitoring of centrally located stimulus light

16 p2357 A72-34095

Occipital EEG activity during fluctuations of perception under stabilized image and simplified stimulus conditions.

17 p2506 A72-34247

Stimulus complexity and the EEG - Differential effects of the number and the variety of display elements.

17 p2507 A72-34248

Electroretinographic evidence for a photopic system in the rat.

17 p2500 A72-34878

Peripheral contrast thresholds for moving images.

17 p2509 A72-35688

Effect of selective adaptation on detection of simple and compound parafoveal stimuli.

18 p2651 A72-36607

Optokinetic thresholds in the normal monkey.

18 p2651 A72-36610

Model to account for visual responses to light flashes of dark adapted eye, discussing perceived brightness variation with intensity

18 p2651 A72-36611

Vergence eye movements to pairs of disparity stimuli with shape selection cues.

18 p2651 A72-36612

Hue shifts accompany phase induced modulation enhancement of sinusoidally flickering lights.

18 p2651 A72-36613

Visual half-field differences in the recognition of bilaterally presented single letters and vertically spelled words.

18 p2653 A72-36908

Non-monotonicity of temporal recognition of brief duration.

18 p2651 A72-36912

Division and orientation in the vertical-horizontal illusion.

18 p2651 A72-36913

Perception of tachistoscopic binary patterns, examining reproduction accuracy with respect to pattern length and fixation and end-segregation reference points

18 p2653 A72-36914

Repression-sensitization and duration of visual attention.

18 p2654 A72-36917

Effect of set size, age, and mode of stimulus presentation on information-processing speed.

18 p2654 A72-36922

Contour-contingent color aftereffects - Retinal area specificity.

19 p2755 A72-37273

Mach band measurement by psychological compensation technique, causing band disappearance by changes in stimulus pattern luminance and brightness distribution relations

19 p2760 A72-37827

Psychophysical procedures to investigate selective visual adaptation to light of different wavelengths from test gratings with various orientations and spatial frequencies

19 p2756 A72-37829

Visual Field Analyzer presentation of single and multiple stimuli for differential threshold levels investigation, discussing eccentricity, spatial orientation and supraliminal stimuli effects

19 p2756 A72-37831

Electrical stimulation of vestibular nuclei - Effects on light-evoked activity of lateral geniculate nucleus neurones.

19 p2758 A72-38220

Parallel swing with affixed luminous disks test for induced vestibular stimulation effects on moon illusion, noting eye movement factors

20 p2893 A72-38900

Influence of rhythmical photostimulation on lower-order monkeys with hyperkinesia of post-encephalitic origin

20 p2890 A72-38936

Operative memory mechanism as visual system neuron chain storage of stimuli from image recognition time measurements

20 p2891 A72-38936

Spatial interaction with different-diameter stimuli matched on the basis of threshold, luminance, or total luminous flux.

21 p3004 A72-40152

Liminal stimuli binoptic detection variation with ratio of left eye to right eye detection probabilities

21 p3007 A72-40734

Noise and stimuli current time and spatial distribution effect on visual performance of eye with image intensifier

21 p3054 A72-40742

Vestibular and optical stimuli interaction in human orientation, testing via Barany chair on rotating platform surrounded by optokinetic drum

21 p3007 A72-40751

Characteristics of certain parameters of memory for visual signals in lower monkeys

21 p3001 A72-40804

Perceptual differentiation of sequential visual patterns.

21 p3008 A72-41021

Target distance and adaptation in distance perception in the constancy of visual direction.

21 p3008 A72-41022

Apparent movement and change in perceived location of a stimulus produced by a change in accommodative vergence.

21 p3002 A72-41024

The effect of size, retinal locus, and orientation on the visibility of a single afterimage.

21 p3003 A72-41253

Temporal and spatial characteristics of selective encoding from visual displays.

21 p3009 A72-41255

Book - Aspects of motion perception.

21 p3012 A72-41531

Moving spot detection threshold measurement for varying exposures, noting product of stimulus duration and velocity for comparison with Bloch law

22 p3151 A72-42930

Visual angle and apparent size of objects in peripheral vision.

22 p3152 A72-42932

Simultaneous detection and recognition of chromatic flashes.

22 p3152 A72-42933

Development of a defensive conditioned reflex to a light stimulus after previous visual deprivation

23 p3257 A72-44078

- Synaptic events during specific and nonspecific inhibition of visual cortex neurons 23 p3257 A72-44088
- Neuronal and focal reactions of the parietal associative cortex to various peripheral stimuli 23 p3257 A72-44089
- Responses of anterior suprasylvian gyrus neurons to peripheral stimuli of different modalities 23 p3257 A72-44090
- Photopic and scotopic contributions to the human visually evoked cortical potential. 23 p3261 A72-44380
- Sensitivity of the human ERG and VEP to sinusoidally modulated light. 23 p3258 A72-44383
- Perceptual latency as a function of stimulus onset and offset and retinal location. 23 p3258 A72-44386
- Techniques for analysing differences in VERs: Colored and patterned stimuli. 23 p3258 A72-44387
- Signal detection analysis of meridional variations to vertical and horizontal gratings. 23 p3259 A72-44389
- Visual stimuli distance estimation with head stationary or moving, discussing performance after monocular motion parallax training 24 p3374 A72-44557
- Ensemble characteristics of the human visual evoked response - Periodic and random stimulation. 24 p3374 A72-44575
- Functional organization of the periphery effect in retinal ganglion cells. 24 p3371 A72-44908
- The suppression-recovery effect in relation to stimulus repetition and rapid light adaptation. 24 p3374 A72-44909
- The effects of simultaneous and successive contrast on perceived brightness. 24 p3372 A72-44910
- Perception smear suppression during saccadic eye movements in terms of metacontrast determined by post-saccadic accumulated luminance relation to stimuli masking 24 p3373 A72-45377
- VISUAL TASKS**
- Methodological problems in unidimensional information transmission involving circular light identification tasks 01 p0013 A72-10718
- Selective attention and short term memory encoding, using tachistoscopic visual display arrangements of capital letters 02 p0166 A72-11549
- Perspective effects on direction of rotation judgments, using figures with rectangular and trapezoidal contours 02 p0167 A72-11898
- Head mounted monkey eye orientation measuring system for performance of brightness discrimination tasks 03 p0318 A72-13073
- Ishihara charts readings in artificial daylight at low color temperatures, low light intensity and limited exposure time by normal and color defective subjects 03 p0317 A72-13939
- Horizontal and vertical eye motions temporal relations in tracking light spot, discussing saccadic system orthogonal interaction mechanism 06 p0761 A72-17601
- Human vision light adaptation effects on dichromatic color matches for bipartite centrally fixated circular matching field 07 p0927 A72-19033
- Uniform visual field influence on electroencephalographic alpha rhythm in man, discussing ocular fixation, visual attention and vigilance change effects 07 p0916 A72-19040
- Visual search model from perceptual theory, animal studies and search data, discussing selection, inspection and naming single cued letters in visual array 09 p1274 A72-23647
- Stochastic models of human performance effectiveness functions reliability and correctability from error data generated by tracking and vigilance tasks 10 p1429 A72-24001
- Hand steadiness during unrestricted linear arm movements and eye-hand coordination tasks, showing tremor occurrence in up-down plane 10 p1432 A72-25113
- Multichannel information processing task complexity relation to operator performance for rapidly increasing input conditions 10 p1433 A72-25115
- Vigilance performance prediction for difficulty-matched auditory and loosely and closely coupled visual intensity discrimination tasks 10 p1433 A72-25127
- Anisotropic responses to dot and line visual stimuli, obtaining judgments on apparent straightness for various visual field locations and dot densities 10 p1427 A72-25183
- Short sleep period and oxygen breathing effects on arousal level of air traffic controller during detection task performance 11 p1588 A72-26686
- Work-rest scheduling and sleep loss effect on operator performance in watchkeeping and active multiple visual tasks 11 p1589 A72-26689
- Cumulative sleep deficit, preceding sleep or wakefulness period duration and body temperature effects on reaction time in multiple choice visual task 11 p1581 A72-26690
- Project Pegasus vigilance tasks for mental performance aspects of time zone change effects on human circadian rhythms 11 p1589 A72-26695
- Character recognition experiments to determine attention control and temporal-spatial capacity limitation during visual information processing 12 p1768 A72-27074
- Interhemispheric effects on choice reaction times to single and multiple letter displays, analyzing cerebral dominance and visual information transmission compared with verbal response 12 p1768 A72-27075
- Computer analysis of helicopter pilots eye movement patterns dependence on visual task skill and performance time 12 p1770 A72-27475
- Human visual accommodation biorhythm and reactions under hard physical work and visual stress 13 p1909 A72-28749
- Individual differences in motion-in-depth detection from Lissajous pattern test for judgment of object approach, receding and movement rate 14 p2081 A72-30965
- Target and surrounding nontarget stimuli size differences effect on visual search time for displays with large fields 14 p2083 A72-31153
- Predictive model for human operator performance in short term visual information processing based on psychological research to obtain decision accuracy and response time 16 p2359 A72-33865
- Hypoxia and peripheral visual stimulus position effects on response time during monitoring of centrally located stimulus light 16 p2357 A72-34095
- The effect of target contrast variation on dynamic visual acuity and eye movements. 17 p2508 A72-34876
- Colorimetric photometric matching tests, showing subject differences in parafoveal spectral sensitivity indicated by photopic curve peaks 17 p2508 A72-34882
- Eye movement pattern monitoring to investigate retinal afterimage role in release of pursuit movements 17 p2508 A72-34886
- Experimental tests of Voth-Mayman hypothesis of autokinesia mediation by attention distribution mechanism 18 p2653 A72-36904
- Assessment of life span age difference relations in visual perceptual tasks, taking into account maturational and generational differences 18 p2653 A72-36910
- Theoretical models for speed-accuracy tradeoff during difficult visual discrimination tasks under time pressure 18 p2655 A72-37220
- Night vision performance measure based on object recognition experiments with optical instruments, noting improvement with image intensifier 21 p3007 A72-40741
- Team size and decision rule in the performance of simulated monitoring teams. 21 p3008 A72-41016
- Proximity and direction of arrangement in numeric displays. 21 p3008 A72-41017
- Error search reading tasks to investigate practical applicability of blinking display coding techniques, noting reading speed reduction compared to steady display 21 p3008 A72-41018
- Body orientation under vertical sinusoidal vibration. 21 p3008 A72-41019
- A psychologist's laboratory approach to a human factors problem. 21 p3012 A72-41430
- Human operator dynamics for aural compensatory tracking. 22 p3149 A72-41950
- Intermittent movement control theory for prediction of visual correction applied to target aiming during illumination loss 22 p3142 A72-42546
- Visually directed pointing as a function of target distance, direction, and available cues. 22 p3151 A72-42929
- Moving spot detection threshold measurement for varying exposures, noting product of stimulus duration and velocity for comparison with Bloch law 22 p3151 A72-42930
- Role of eye movements in the perception of apparent motion. 23 p3259 A72-43804
- Mathematical model for digit summation task search time distribution dependence on size of visual display with randomly arranged three digit numbers 24 p3374 A72-44558
- VISUAL TRACKING**
- U OPTICAL TRACKING
- VISUALIZATION OF FLOW**
- U FLOW VISUALIZATION
- VITAMIN B 06**
- U PYRIDOXINE
- VITAMIN C**
- U ASCORBIC ACID
- VITAMIN E**
- U TOCOPHEROL
- VITAMINS**
- NT ASCORBIC ACID
- NT NICOTINIC ACID
- NT PYRIDOXINE
- NT TOCOPHEROL
- Visual acuity restoration improvement after flash blindness by monocular shielding and ingestion of vitamin complexes containing ATP with pyridoxal, considering twilight vision 21 p3012 A72-41748
- A special vitamin complex for prophylaxis of atherosclerosis in aviation personnel 23 p3261 A72-44153
- VITREOUS MATERIALS**
- Lithic and vitreous particles in Lunik 16 core tube samples from Mare Fecunditatis, discussing particle type proportions and petrological and mineralogical aspects 09 p1379 A72-22256
- Refractory glass formulation principles, compositions and properties, discussing vitreous silica production 10 p1501 A72-24727
- Lunar crater region ray systems origin and brightness variation mechanism from surface vitreous spherules examination 11 p1715 A72-25300
- VJ-101 AIRCRAFT**
- VJ-101 V/STOL aircraft design, development and flight testing, discussing takeoff and landing, hovering and transition flight and associated control problems 19 p2749 A72-38032
- VLASOV EQUATIONS**
- Propagators in strong plasma turbulence, considering characteristic trajectories of Vlasov equation 01 p0109 A72-10244
- Higher moment Vlasov equations of collisionless fully ionized plasma for studying solar wind proton thermal anisotropy, heat flux and distribution function 01 p0119 A72-10880
- Plasma physics computer simulation of double stream and beam instabilities, wavelength nonlinearities and velocity distribution, using superparticle and Vlasov equation models 02 p0263 A72-11691
- Vlasov equation phase space boundary integration for evolution of one dimensional self gravitating collisionless stellar systems with constant density 05 p0714 A72-16056
- Vlasov equation stability properties of collisionless plasma and stellar gas, removing energy variation difficulties with multiple water bag model 05 p0694 A72-16060
- Single-ended Q machine grid-excited density perturbation and ion wave propagation properties from linearized Vlasov equations 06 p0855 A72-17514
- Single species one dimensional Vlasov plasma linearized analysis as initial value problem with periodic boundary conditions, using Hamilton variational principle 06 p0864 A72-18537
- Infinite uniform Vlasov plasma response to steady state transverse excitation, considering spatial electron cyclotron damping 06 p0864 A72-18539
- Plasma Dory-Guest-Harris type instability nonlinear evolution from numerical integration of Vlasov equation, using particle simulation and Fourier-Hermite transform methods 06 p0865 A72-18542
- Statistical hypothesis of Van Allen radiation belts, using Vlasov equations for self consistent plasma fields 07 p1055 A72-18805
- Book on unmagnetized plasma theory covering Vlasov and Klimontovich models, electrostatic solutions, plasma oscillations, nonlinear phenomena, statistical descriptions, BBGKY correlations, etc 07 p1041 A72-19449
- Nonlinear Landau damping of longitudinal plasma waves in dc magnetic field, obtaining wave-particle interactions from Vlasov equation by perturbation theory and method of characteristics 07 p1041 A72-19505
- Magnetospheric instabilities theory based on Vlasov equation and Landau damping 07 p0978 A72-20033

Anisotropic equilibrium solution to Vlasov equation for high beta theta pinch plasma column

07 p1045 A72-20478

Schwarzschild solution to Vlasov equation for velocity distribution function of self gravitating stellar system

10 p1535 A72-24112

Intermediate length open noncircular cylindrical shells analysis based on Vlasov semimembrane theory

10 p1559 A72-24992

Vlasov perturbation theory of nonlinear plasma wave with Landau damping based on Korteweg-de Vries equation

11 p1692 A72-25517

One dimensional time independent solution to Vlasov-Poisson system of nonlinear electrostatic plasma waves, noting Maxwell distributions for free and trapped particles

11 p1697 A72-26596

Nonlinear waves in nonuniform plasma, extending Butler and Gribbon formulation for Vlasov-Poisson equations

11 p1697 A72-26598

Statistical mechanics of one dimensional model for many body self gravitating system with canonical and microcanonical ensembles, noting isothermal solution of Vlasov equation

12 p1846 A72-27907

One and two boundary curves systems for Vlasov equation of one dimensional collisionless self gravitating stellar systems evolution with constant phase space density

12 p1874 A72-27912

Stability properties for collisionless plasma and encounterless self gravitational stellar gas described by Vlasov equations

12 p1875 A72-27916

Covariant statistical mechanics equations system for distribution function of relativistic particles in steady external gravitational field, noting Vlasov equation as limiting case

13 p2035 A72-28465

Waves and particles interaction in weakly turbulent collision-free Vlasov plasma under pure Coulomb interaction and zero magnetic field

14 p2140 A72-30937

Difference scheme for initial value problem of one dimensional Vlasov equation for collisionless electron plasma with homogeneous ion background

16 p2434 A72-33006

Kinetic equations with radiation effects.

17 p2590 A72-35155

The self-consistent test particle approach to relativistic kinetic theory.

17 p2590 A72-35156

Constants of the linearized motion of Vlasov-plasmas.

17 p2590 A72-35158

Superposition principle in test particle method for reducing plasma cloud kinetic theory to determination of conditional probability function involving Vlasov equation

17 p2591 A72-35163

Vlasov and Maxwell equations solution for surface waves dispersion in semiinfinite hot plasma

18 p2716 A72-36925

Electromagnetic and space charge disturbance transmission and reflection at plasma boundary and oblique incidence, discussing isotropic Vlasov plasma

19 p2839 A72-37336

Bubnov-Vlasov variational method for thin parallelogram plates bending under complex loads, calculating edge skew and side length effects

19 p2877 A72-38160

Continuum eigenmodes of an inhomogeneous plasma.

20 p2956 A72-39015

Reductive perturbation method application to Vlasov equation governing one dimensional motion of collisionless plasmas, investigating nonlinear modulation of plasma waves

21 p3089 A72-40188

An asymptotic method for the Vlasov equation. III - Transition from amplitude oscillation to linear Landau damping.

21 p3089 A72-40190

Characteristics and constants of motion method for collisional kinetic equations.

24 p3426 A72-44984

Self-consistent electromagnetic waves in relativistic Vlasov plasmas.

24 p3430 A72-45569

VLF EMISSION RECORDERS

VLF atmospherics count comparability in broad- and narrow-band operation, presenting amplitude frequency response

09 p1301 A72-23268

VLF recorder for measurement of incident direction, polarization, phase and amplitude of 16 and 60 kHz transmitter signals

12 p1796 A72-27791

The generation and propagation of VLF emissions.

20 p2904 A72-39984

Midlatitude VLF emissions in magnetosphere due to plasma resonance instability near plasmapause, using ground, rocket and satellite observations, estimating electron energy

23 p3263 A72-43515

VOICE

Vibration space analysis for human voice characteristics change during unintended speech under experimental psychological stresses and actual emergency situations

01 p0017 A72-10213

Human vocal apparatus anatomical and neural structure, considering linguistic sounds composition

22 p3147 A72-42789

VOICE COMMUNICATION

NT TELEPHONY

NT VOICE DATA PROCESSING

Voice quality improvement in He atmospheres by on-line segment dilation

01 p0101 A72-10158

AFC for suppressed-carrier SSB voice signal reception, using phase locking procedure or comparative zero-crossing-rate measurement

01 p0025 A72-10333

Time division multiple access system with 100/50 M bit/s channel capacity for Symphonic and Intelsat satellite speech channels

01 p0033 A72-11302

Satellite navigational aid system technical and operational characteristics, emphasizing voice communications links in L band

03 p0386 A72-12972

Single-channel-per-voice-carrier transmission system application to data communication and small earth station operation, discussing modular design and performance

07 p0948 A72-20494

Skylab communications system, discussing voice, data, TV and command mission requirements and microwave instrumentation [ALAA PAPER 72-543]

12 p1781 A72-27366

Voice digital data rate reduction technique by exploiting zero and one bits imbalance in PCM TDM bit stream output encoding, discussing hardware implementation

12 p1785 A72-27845

PCM speech transmission systems, comparing pseudorandomly dithered quantization with fixed level method by intelligibility and subjective appreciation tests and statistical analysis

14 p2087 A72-30942

ATC operational systems, discussing global surveillance and voice and data communication between aircraft and earth station

14 p2129 A72-31141

A comparison of voice communication techniques for aeronautical and marine applications.

17 p2512 A72-34267

Radar EMI to voice communication receivers.

20 p2902 A72-38991

Geostationary satellite system for air navigation via voice and data communication, discussing ground facilities and avionics

21 p3080 A72-40284

Bandwidth economy for multiplexed digital signals.

21 p3020 A72-40897

Suppressed clock pulse duration modulation for noisy voice communication channels with hard limiting satellite repeaters, discussing system design and test data

21 p3020 A72-40898

VOICE DATA PROCESSING

Digital adaptive echo cancellation mathematical technique for voice circuits derived from satellite transmission

12 p1780 A72-27362

VOID RATIO

The mechanism of void formation, void growth, and tensile fracture in an alloy consisting of two ductile phases.

24 p3415 A72-45481

VOIDS

Anisotropic electrical properties and void structure of amorphous Ge, discussing low- and high-field resistivity measurement in planar and transverse directions

09 p1371 A72-22873

Elastic-plastic medium with doubly periodic square array of circular cylindrical voids, obtaining finite element solution for uniaxial deformation by variational principle

17 p2628 A72-34784

Interaction energy and force between screw dislocation and spherical inhomogeneity, discussing voids growth in irradiated materials

18 p2718 A72-36510

Formation of voids and dislocation loops in near-stoichiometric NiAl by aging at 700 to 900 C, and some effects on alloy properties.

20 p2937 A72-39288

Void lattice model for Mo physical properties and equilibrium lattice spacing determination, calculating defect Green function

21 p3066 A72-40623

VOIGT EFFECT

Line profile shape analysis of X ray diffraction broadening from deformed W, showing close approximation to Voigt distribution

01 p0088 A72-11046

VOLATILITY

Early catastrophic degassing of earth, considering mechanisms and times from volatiles abundances and distribution in atmosphere, hydrosphere and crust

03 p0350 A72-13744

Distillation experiments showing volatility-caused amino acid contamination of commercially available aqueous hydrochloric acid

05 p0624 A72-16079

Vapor-liquid equilibrium analysis of water soluble volatile organic compounds in closed airtight systems by gas chromatography

13 p1910 A72-29326

Effect of evaporation of the volatile component on the electrical properties of CdSb

19 p2845 A72-38402

VOLATILIZATION

U VAPORIZING

VOLCANICS

U VOLCANOLOGY

VOLCANOLOGY

Continental growth by island arc volcanism, observing Si, K, Rb, Ba, Sr and light rare earth element abundances

01 p0052 A72-10068

Mt. Agung volcanic eruption dust effects on monthly-mean lower stratospheric temperatures for tropical stations

01 p0096 A72-11284

Lunar igneous activity and differentiation, discussing volcanic flows near Tycho, flow patterns in maria, sinuous rilles and crust lineaments

03 p0418 A72-13107

Ecogenesis of volcanic island of Surtsey after 1967 lava eruption, discussing terrestrial and marine littoral and sublittoral biomes

04 p0473 A72-14916

Northeast Bank, Southern California Borderland volcanic petrology and geologic history, investigating basaltic rocks, hyaloclastites and fossil fragments

04 p0520 A72-15589

Lunar volcanology, discussing domes, crater chains, halos, sinuous rills, mare wrinkle ridges, dark smooth level material and ring dike-like structures

04 p0581 A72-15619

Major and trace element abundances in orogenic area volcanic rocks, considering geographic and stratigraphic relations and composition

05 p0658 A72-16721

Volcanic basalt geochemistry in Afar Triple Junction, suggesting relation to crustal thinning and melting zone shallowing under rift

05 p0658 A72-16722

Recent moon exploration, discussing Ranger and Lunar Orbiter photographs for crater and volcano studies and landing site mapping and Apollo program rock studies

06 p0887 A72-18217

Lunar Mare Ibrum lava flow geology and nature, mascon origins and explosive, collapse and impact mechanisms for small crater origin

06 p0887 A72-18218

Lunar sinuous rills location and origin, discussing Orbiter photographic maps, predominance in maria and similarity to terrestrial lava tubes

06 p0887 A72-18219

Lunar maria material igneous origin, relating surface features to various volcanic eruption types

06 p0887 A72-18220

Tycho, Aristarchas and neighboring small craters volcanic origin, discussing inner and outer rim lava flows and impact crater resemblance

06 p0887 A72-18221

Lunar crater origin mechanisms, considering single and multiple meteor impact and volcanic explosions, low velocity excavation, collapse and material emission

06 p0887 A72-18223

Lava tube formation in pahoehoe basalt and flow activity in vent near Alae Crater, Hawaii

07 p0980 A72-20462

Gaseous or solid particle Hg from fumaroles, suggesting natural and industrial sources of Hawaiian air pollution

09 p1305 A72-23648

Model for volcanic origin of Descartes Formation high albedo region, suggesting young age and endogenic nature of bright surface deposit

09 p1394 A72-23666

Terrestrial volcanic lava conduits origin and development association with lunar maria channels and sinuous rills

13 p2037 A72-28992

Regional stratigraphy and fabric distribution of volcanic ash flow sheets in northwestern Mogollon Plateau by flow direction technique

15 p2223 A72-31578

Thermal history and early magmatism for lunar models, considering high near-surface temperatures and radionuclides upward transport during melting 15 p2311 A72-32082

Lunar surface breccias origin, using exploration data to reappraise ballistic theory of giant craters and maria formation in favor of volcanic concepts 16 p2461 A72-34180

Morphology and petrography of volcanic ashes. 18 p2685 A72-36222

Planetary volcanic activity and matter disintegration as source of development in solar system, using density and rotational energy data 18 p2725 A72-36521

Savonoski crater, Alaska - A possible meteorite impact structure. 19 p2790 A72-37861

Lunar volcanic gas release rate estimation from orbiting Apollo spacecraft-borne mass spectrometer detection, noting atmospheric perturbation 19 p2868 A72-38736

Magnetic anomalies in New Guinea-New Zealand region from geomagnetic measurements with proton magnetometer, noting effects of andesite-basalt volcanic processes and nuclear precession signal 23 p3284 A72-43380

VOLT-AMPERE CHARACTERISTICS

Nonisothermal theory of electrostatic probe in weakly ionized plasma, giving I-V characteristics 01 p0108 A72-10238

Fluorinated ethylene propylene encapsulated N/P Si solar cells, investigating simulated micrometeoroid exposure effects on I-V performance in shock tube 01 p0006 A72-10381

Dimensionless numbers system selection for generalizing I-V characteristics of thermionic heat converters 01 p0006 A72-10492

Lateral photoelectric effect in junction FET under homogeneous illumination, detailing current-voltage characteristics 01 p0114 A72-10859

Dc and ac Josephson effects in bulk granular superconductor, presenting junction I-V characteristics 02 p0268 A72-11472

Static I-V characteristics and gain properties of lateral p-n-p transistors, using multijunction analysis 02 p0189 A72-11522

I-V characteristics and bandwidth properties of distributed emission amplifier within magnetic field, analyzing averaged electron trajectories and hf potential distribution 02 p0189 A72-11568

High efficiency GaAs transferred electron device operation and microwave oscillator design by simple static I-V characteristics description for time domain computer simulation 02 p0193 A72-12230

Optical regulation of I-V characteristics in avalanche transistor 02 p0195 A72-12584

Oscillographically measured semiconductor element I-V characteristics plotting optimization by considering measuring instrument and sampling signal shape and frequency effects on hysteresis 03 p0330 A72-12968

Transverse photoconductivity and dark I-V characteristics of n-GaAs compensated with Cr in high electric field at room temperature 03 p0401 A72-13586

Low energy electron beam irradiation of aluminum-silicon nitride-silicon structures for elimination of bias polarization effects on I-V characteristics 03 p0402 A72-13865

Two dimensional solar cell model with partial differential equation relating arbitrary point potential to cell parameters for I-V characteristics prediction 04 p0465 A72-14480

Gunn diode microwave oscillator with moving reflector as self-excited mixer and load variation detector, analyzing performance by I-V characteristics model 04 p0497 A72-14713

Frequency response and I-V characteristics of metal/chalcogenide glass/metal diode structures 04 p0498 A72-15079

Current transport and I-V characteristics of metal-semiconductor-metal structures with back-to-back contact interfaces 04 p0562 A72-15128

Carrier mobility field dependence effects on validity of gradual channel approximation in insulated-gate field effect transistors, discussing velocity field relationship 04 p0498 A72-15135

Electrical measurements on capillary-fed colloid thruster with Zener diode-like I-V characteristic and constant propellant mass flow rate 04 p0565 A72-15204

Closed solution to Gunn effect field domain formation and propagation, using approximate I-V curve and method of characteristics 04 p0563 A72-15503

Josephson junction as 100 GHz oscillator-mixer for heterodyne frequency conversion in millimeter and submillimeter regions, observing I-V characteristics 04 p0503 A72-15604

Three layer bipolar transistor structure with negative resistance region in I-V characteristics 04 p0503 A72-15668

German monograph on thermionic power supply equipment converter network reliability covering I-V characteristics and failure probability calculation 04 p0466 A72-15696

Thermal and I-V characteristics of dc plasmatron with vortex stabilized arc, interelectrode insert and diverging arc channel for various nozzle diameters 05 p0694 A72-15854

N-channel MOS FET, measuring X ray irradiation effects on drain current and transfer characteristics at room temperature 05 p0634 A72-16033

Frequency characteristics effect to determine voltage and current smoothing coefficients and resistances of transistor ripple filter with emitter circuit load 05 p0634 A72-16168

Hysteresis loops during breakdown in reverse bias segment of p-PbS point contact diodes I-V curves 05 p0638 A72-17177

Static high pressure spherical plasma probe theories verification, showing saturation currents and I-V characteristics agreement with calculated values [AD-740015] 06 p0853 A72-17416

Hydrostatic pressure effects on I-V characteristics of amorphous semiconductor germanium telluride sulfide arsenide 06 p0865 A72-17493

High temperature GaAs bipolar transistor n-p-n junction fabrication by vapor phase growth technique, considering I-V characteristics dependence on procedure 06 p0783 A72-17607

Semiconductor device physical behavior, discussing energy levels, impurity conduction, p-n junction capacitance and bipolar and unipolar transistor I-V characteristics 06 p0790 A72-18575

Electrical contacts conduction principles, considering circuit voltage, current, variable resistance and resistive, mechanical, heating and adhesive properties 06 p0791 A72-18578

Vibration simulation of elastohysteretic systems on analog computers using photocurrent-voltage relationship of polycrystalline photoresistors 06 p0900 A72-18674

State density singularities elimination in inhomogeneous superconductors by electron interactions nonuniformities, resulting in tunnel junction current-voltage characteristic fluctuation 07 p1047 A72-18919

Amplitrion stability in optimal frequency regime, relating cut-off voltage and plate current as function of magnetic field, input power and geometrical parameters 07 p0953 A72-19014

I-V characteristics of junction transistors with avalanche breakdown mechanism 07 p0958 A72-19895

Pulse rate and pumping power effects on emission spectra and I-V characteristics of multielement GaAs injection lasers 08 p1181 A72-20796

Two terminal semiconductor strain tensor based on evaporated piezoelectric layer for modulation of forward I-V characteristics of thin film diode 08 p1164 A72-20925

Energy level and V-I characteristics of solid state heterojunction devices, discussing diodes, transistors, thyristors and optoelectronic structures 08 p1139 A72-21054

Physical parameters of transistor, discussing carrier transfer, space charge and potential drop as function of current and voltage changes 08 p1139 A72-21058

Low level current operation in insulated gate FET, obtaining analytical expression for voltage 08 p1142 A72-21744

Single and double probe measurements of electron temperatures in flames, discussing difficulties in obtaining reliable I-V characteristics 08 p1129 A72-22043

German monograph on Ranvier node steady state I-V characteristics transition range and control by altered external solutions and morphological effects on nerve fiber 09 p1264 A72-22336

Xenon plasma produced in cascaded arcs, investigating spectral line widths, temperature and electron density profiles, transition probabilities and I-V characteristics 09 p1364 A72-23392

Diode junction parameters and inverse saturation current measurements as function of current density and temperature 09 p1289 A72-23418

Avalanche carrier multiplication influence on semiconductor device p-n junction quality, discussing

current distribution and I-V characteristics during avalanche breakdown 10 p1446 A72-23849

Validity range of applied voltage relationship to majority carrier current in Schottky diodes, assessing minority carrier current importance 10 p1448 A72-24108

Thyristor I-V characteristics, considering blocking and triggering 10 p1453 A72-24816

High efficiency CW performance of InP transferred electron microwave oscillator with anomalous I-V characteristics temperature dependence 11 p1604 A72-25750

Capillary fed annular colloid thruster operating characteristics, considering I-V relationship, thrust and exhaust velocities and propulsive efficiency [AIAA PAPER 72-490] 11 p1710 A72-26215

Epitaxial InP diode for high efficiency circuit controlled microwave oscillator, discussing solution growth technique, layers electrical properties and I-V performance 12 p1854 A72-27162

P-n junction diodes fabricated by ion implantation doping, calculating I-V characteristics for comparison with measured breakdown voltages 12 p1789 A72-27312

Static and impedance characteristics and equivalent circuit of p-n-p-n inductance diode, using ambipolar diffusion length 12 p1790 A72-27499

Pulsed Si p-n junction mesoplasma dynamic I-V characteristics explained by mechanism based on hot carrier annihilation 12 p1853 A72-28113

Shot noise coefficient calculated from static I-V characteristics for modified thermionic diode with low potential virtual cathode 13 p1915 A72-28467

I-V characteristics of metal-semiconductor-metal structures based on oxide glasses, noting temperature dependence and current limitation 13 p2021 A72-28688

P-n-p-n junction thyristor turnoff process under reverse anode voltage at high injection level, examining current voltage curve and switching time constant 13 p1932 A72-29293

HF follower currents effect on dc arc I-V characteristics, indicating use of HF follower arc for quasi-steady arc power control 13 p2017 A72-29645

Negative photoconductivity effect in high resistance n-type indium phosphide single crystals, noting photocurrent spectral distribution and I-V characteristics 13 p2022 A72-29647

Conversion efficiency and polarization behavior of Gunn diodes in resonant cavities, using I-V characteristics 13 p1937 A72-29866

Electro-optical regenerative assembly with p-n-p structure, emphasizing positive feedback and I-V characteristics 13 p1933 A72-29976

Energy absorption inelastic surface mechanisms effect on I-V characteristics profile for bounded semiconductors with negative differential conductivity 13 p2023 A72-29991

Solar photosensitive elements prepared p-type GaAs liquid epitaxy on n-type GaAs substrate, measuring dark and light I-V characteristics and spectral response 14 p2142 A72-30225

Proton beam effect on carbon dioxide laser discharge I-V characteristics and emission power 14 p2109 A72-30352

S-type negative resistance segment formation on rectilinear branch of I-V characteristics of p-n-n structure 14 p2089 A72-30969

Polyphase ac power systems I-V characteristics determination via application of symmetrical sequence components principle, examining system protection and reliability aspects 15 p2204 A72-31216

Thermal and I-V characteristics of dc plasmatron with vortex stabilized arc, interelectrode insert and diverging arc channel for various nozzle diameters 15 p2283 A72-31271

High electric field effects on I-V characteristics of Te-As-Ge-Si type chalcogenide thin film, noting Poole-Frenkel emission and electron tunneling roles 15 p2291 A72-31641

Automatically controlled plasma arc welding for uniform cross section weld seams production under fluctuating electric current conditions, describing electronic control system 15 p2244 A72-31773

I-V characteristics of polarized and nonpolarized memory effects in GaAs thin films evaporated on tungsten substrates 15 p2292 A72-31869

Transverse magnetic field effects on n-type GaAs Gunn diodes microwave power, coherence and dynamic I-V characteristics [ONERA, TP NO. 1051] 15 p2207 A72-31884

Silicon dislocation density relationship to solar cell current loss at low temperature, presenting temperature-diffusion length and I-V characteristics 15 p2183 A72-32132

Negative resistance devices, stability under open and short circuits from dc I-V characteristic shape 16 p2368 A72-32857

Harmonic oscillators with negative resistance elements, discussing simplified mathematical calculation for I-V characteristics nonlinearity and applications to various diodes and transistors 16 p2368 A72-32858

Langmuir probe dc and second harmonic characteristics measuring system, describing switching circuitry 16 p2392 A72-33608

Current-voltage and specific power-energy relationships for high temperature electrochemical cells with alkali metal anodes and chalcogen or halogen cathodes 16 p2352 A72-33900

Metal-insulator-metal tunnel junctions, investigating effect of nonparabolic band structure energy-momentum relation on I-V characteristics 16 p2370 A72-34101

Performance comparison of thermionic converters with several collector materials. 17 p2497 A72-34606

Parametric optimization of a cylindrical converter with a molybdenum emitter and niobium collector. 17 p2497 A72-34610

Suppression of arc drop in thermionic converters. 17 p2497 A72-34612

Computed performance data for a thermionic converter having a Cl-CVD-W emitter and a polycrystalline Nb collector. 17 p2521 A72-34613

Applications of an improved formalism for the analysis of transport phenomena in gaseous mixtures and plasmas. 17 p2587 A72-34615

Effect of a transverse magnetic field on the operation of a thermionic converter under undercompensated Knudsen conditions. 17 p2497 A72-34862

Characteristics of Gunn elements CGY 11 to 14 and their application as microwave oscillators. II 17 p2530 A72-35150

Transverse magnetic field effects on cylindrical hollow cathode discharge voltage-current characteristics, noting sustaining potential and recombination probability changes 17 p2593 A72-35886

Cylindrical Cs thermionic converter with unique emitter and five collectors, measuring I-V characteristics to determine emitter work function, ignition voltage and electric power 18 p2646 A72-36191

Vapor pressure influence of Ba-Cs thermionic converter diodes on I-V characteristics and work functions in terms of anomalous Schottky effect 18 p2646 A72-36194

I-V-characteristics of a plane parallel cesium diode with tantalum and tungsten emitter. 18 p2646 A72-36196

Sinusoidal potential distributions and volt-ampere characteristics of Knudsen-mode thermionic emission converters 18 p2646 A72-36198

Volt-ampere characteristics of Ba-Cs plasma thermionic converter with W emitter and Ta collector 18 p2646 A72-36199

Thermionic converter I-V performance improvement via oxygen addition, examining feasibility of cesium oxide-cesium solution as source 18 p2647 A72-36204

Arc discharge transition from diffusion to arc mode, presenting theory on I-V characteristics negative resistance section and on hysteresis causes 18 p2714 A72-36207

The ignited mode of cesium thermionic diode. II - The charge influence on the volt-ampere characteristics. 18 p2647 A72-36211

Arc mode thermionic converter at low cesium vapor pressures 18 p2647 A72-36216

Current instabilities and constriction in thermionic converters 18 p2647 A72-36221

Electrical characteristics of bulk n-InP oscillators. 18 p2666 A72-36456

Transition from sheath-convection to saturation-current behaviour of a Langmuir probe in a flowing plasma. 18 p2715 A72-36688

The behaviour of a Gunn oscillator in the domain-delayed mode. 18 p2667 A72-36945

Behavior of epitaxial bipolar transistors in the strong injection regime 18 p2668 A72-37103

I-V characteristics of electric noise generated by flame between double probe electrodes during coke particle burning in air flow 19 p2882 A72-38458

The static current-voltage characteristic of four-layer structures in two-collector operation at a low injection level 19 p2846 A72-38573

Effect of the filling of the capture levels with increasing current on the formation of negative resistance under double injection conditions 19 p2846 A72-38574

Fixed-bias floating double-probe technique with simple Langmuir-probe characteristics. 19 p2804 A72-38592

Stabilization of relaxation oscillators with components having an S-shaped current-voltage characteristic 20 p2906 A72-38891

Relation between diffusion and defect formation rates in silicon detectors exposed to gamma radiation 20 p2959 A72-38956

Four-terminal Si controlled switches, discussing negative resistance and linear amplification I-V characteristics and applications in oscillators and modulators 20 p2907 A72-39274

Infrared testing of solar cell arrays. 20 p2890 A72-39339

State density singularities elimination in inhomogeneous superconductors by electron interactions nonuniformities, resulting in tunnel junction I-V characteristic fluctuation 20 p2960 A72-39385

Metal-insulator-semiconductor-insulator-metal structure light pulse amplification investigating power gain and photocurrent dependences on applied voltage and applicability as radiation detector 20 p2960 A72-39517

Some results of testing M.O.S. transistors at elevated temperatures. 20 p2909 A72-39774

Pulsed metallic-plasma generators. 20 p2958 A72-39781

Relaxation oscillations induced in semi-insulating CdS with helium neon laser irradiation. 20 p2934 A72-39817

Fast-neutron-compensated n-germanium as a model of amorphous semiconductors. 20 p2961 A72-39853

A technique for recording Langmuir probe characteristics in afterglow plasmas. 21 p3051 A72-40212

Carrier transport and storage effects in Au ion implanted SiO₂ structures. 21 p3097 A72-40699

Conductance associated with interface states in MOS tunnel structures. 21 p3032 A72-40701

Observation on phenomena associated with a slowly varying surface barrier at niobium oxide and aluminum interface. 21 p3097 A72-40702

The aluminum electrode in AlCl₃-alkali-halide melts. 21 p3013 A72-40844

An apparatus to investigate plasmas at very high pressure. 21 p3056 A72-41004

Avalanche transistor circuit with controlled S shaped I-V characteristics, discussing equivalent circuits and operating points stability 21 p3034 A72-41119

I-V, spectral and temperature characteristics of autophotocathode emission in p-type silicon cathodes with varying acceptor concentrations 21 p3098 A72-41692

Approximate calculation of a laminar arc discharge in a cylindrical channel 22 p3210 A72-42285

A CW Gunn diode bistable switching element. 22 p3159 A72-42610

Thyristor I-V characteristics as function of voltage rise time, determining critical rate for given initial and final anode and cathode voltages 22 p3160 A72-43085

Pulse discharge plasma in Ar with gas ionization level near unity, noting plasma cylinder parameters, electron temperature and I-V characteristics 22 p3212 A72-43103

Effect of an alternating current on the steady characteristics of Josephson point contacts 22 p3208 A72-43109

Comparison of microwave-induced constant-voltage steps in Pb and Sn Josephson junctions. 23 p3323 A72-43272

Static and dynamic characteristics of double-injection currents in p'-n-n' diode structures with deep impurities and nonideally injecting junctions 23 p3268 A72-43346

Metal-oxide varistor - A new way to suppress transients. 23 p3272 A72-44100

The field-effect modified transistor - A high-responsivity photosensor. 23 p3273 A72-44455

VOLTAGE

U ELECTRIC POTENTIAL
VOLTAGE AMPLIFIERS

Feedback and feedforward circuits to double operational amplifier output voltage swing with increased slew rate 11 p1604 A72-25746

Ac voltage squaring with semiconductor power amplifier based on electronic servo principle and feedback circuit 16 p2370 A72-33958

Feedback circuitry for dc amplifiers voltage drift compensation, discussing performance criteria in terms of residual offset voltage, system stability, correction and measurement time 18 p2671 A72-37150

Use of selective RC amplifiers in the radio-frequency amplifier stages of superheterodyne radio receivers 23 p3271 A72-43775

VOLTAGE BREAKDOWN

U ELECTRICAL FAULTS
VOLTAGE GENERATORS
NT PHOTOVOLTAIC CELLS

Laser triggered avalanche transistor voltage generator for picosecond streak camera used in laser pulse diagnostics 07 p0999 A72-18881

Minimum charging resistance in relaxation generators for spark machining as function of supply voltage, using thyristor and voltage source circuit model 07 p0956 A72-19594

Low induction 500-kV 1-microsecond 5-kJ pulsed voltage generator, discussing design features 07 p0946 A72-19958

Sawtooth voltage generator with switching circuit to achieve small retrace time via blocking generator 11 p1605 A72-26320

Fall time calculation and junction capacitance effect in diodes with nonuniform base doping switched off by voltage and current generators 11 p1607 A72-26963

A generator with a pulse-width modulator, producing arbitrarily shaped high voltage 21 p3058 A72-41734

VOLTAGE MEASUREMENT

U ELECTRICAL MEASUREMENT
VOLTAGE REGULATORS

Lunar Roving Vehicle navigation subsystem power converter design, discussing circuits, performance and voltage regulators and preregulators 01 p0009 A72-11069

Variable flux reset ferroresonant voltage regulator with adjustable terminal characteristics using magnetic and thyristor circuits 03 p0311 A72-13770

[IEEE PAPER 17,1] 03 p0311 A72-13770

Dc feedback controlled constant voltage transformer, comparing with ferroresonant regulator [IEEE PAPER 17,2] 03 p0311 A72-13771

Double shunt feedback controlled ferroresonant voltage regulator using magnetic component with simulated core saturation [IEEE PAPER 17,3] 03 p0311 A72-13772

EMC improvement with least sacrifice of power efficiency in designing dc/dc converters and switching voltage regulators 03 p0312 A72-14049

Regulated dc-to-dc converter for voltage step-up or step-down with input-output isolation, using bistable comparator output voltage control through encoder 04 p0465 A72-14488

Ac and dc power regulation by switched capacitor, analyzing voltage spectrum for resistive load 07 p0958 A72-20389

TWT amplifier converter design with semiconductor and magnetics to achieve voltage regulation and high power efficiency for TOPS spacecraft 08 p1111 A72-21412

High power series voltage regulators, discussing power hybrid microelectronic design techniques 08 p1112 A72-21415

Background noise at 200 Hz-1 MHz of avalanche effect voltage regulating diodes 09 p1288 A72-23120

Circuitry and operational characteristics of variable output voltage regulator with low temperature coefficient, noting suitability for monolithic integration 12 p1792 A72-27740

Voltage controlled low power current sources characteristics, discussing circuits, transistor and emitter resistance and operational amplifiers 13 p1900 A72-30052

Servomechanism and reduction gear ratio selection for arc welding voltage regulator, taking into account welded joints properties 15 p2244 A72-31611

Linear analog to pulsewidth converter insertion into control loop in dc/dc regulators for space applications to permit high sampling frequencies 21 p2997 A72-41081

VOLTAGE VARIATION INDICATORS

U VOLTMETERS

VOLTERRA EQUATIONS

Step-by-step algorithmic numerical solution for nonlinear Volterra integro-differential equation, considering convergence 01 p0093 A72-11105

Uniformly and asymptotically stable solutions to linear Volterra integrodifferential equation system, discussing Liapunov stability 02 p0252 A72-11997

Nonlinear stochastic systems stability conditions description by Volterra integral equation, applying to distributed parameter feedback control system with nonlinear amplifier of random gain 04 p0504 A72-14663

Nonsteady high-rate heat transfer control in boundary layer by conjugate problem treatment and reduction to Volterra equation, considering limiting-regime and stability 04 p0596 A72-14666

Homogeneous viscoelastic boundary value problem, demonstrating Volterra principle validity 05 p0739 A72-16590

Nonlinear stochastic systems analysis by extended Volterra-functional method for first and higher order linear plants with constant or time varying parameters 06 p0838 A72-17376

Quasi-linearized solution to nonlinear Volterra equations in design of structures under creep deformations 06 p0897 A72-18318

Dirichlet and Volterra problem with prescribed singularities for plane with rectilinear boundary slits, applying to fluid mechanics 07 p0971 A72-20092

Thin viscoelastic beam free oscillations and material properties description by Volterra type nonlinear integral equation 08 p1249 A72-21869

Antisymmetric pseudorandom signal performance in measurement of second order kernels in Volterra series representation of nonlinear system by cross correlation 10 p1439 A72-24805

Optimal control problems characterized by nonlinear Volterra equations system, obtaining necessary conditions for extremality in maximum principle integral form 11 p1675 A72-25319

Optimal control systems with time delays described by linear Volterra integral equations 11 p1677 A72-26090

Random Fredholm and Volterra integral equations applied to stochastic systems, investigating absolute stability concept 11 p1679 A72-26780

Uniqueness theorem for solution to boundary value problem in anisotropic viscoelasticity, considering stress-strain relation in nonlinear Volterra equation form 12 p1886 A72-27983

Numerical solution of Volterra integral equation. 18 p2705 A72-36601

Homogeneous viscoelastic boundary value problem, demonstrating Volterra principle validity 19 p2872 A72-37562

Solution of nonlinear integro-differential Volterra equations and their systems with the aid of power series 19 p2825 A72-38196

Investigation of the solution of a two-dimensional nonlinear Volterra integral equation 19 p2825 A72-38203

VOLTMETERS
Diode half wave rectifier for ac-to-dc signal conversion in electronic voltmeter 09 p1306 A72-22343

Additive noise effect on accuracy of integrating digital voltmeters using pulse frequency and pulse time converters 16 p2370 A72-33955

Integrating digital voltmeter - Operating principles and accuracy. 24 p3403 A72-45275

VOLUME
NT BODY VOLUME [BIOLOGY]
Increased volume fraction effect on transverse rupture strength and fracture toughness of hot pressed and annealed composites of polycrystalline magnesium oxide 13 p1980 A72-29828

VOLUMETRIC ANALYSIS
Volumetric analysis of blood oxygen and CO, showing combination with hemoglobin without significant molecular volume increase 05 p0619 A72-16786

White thick layer anodic zirconium oxide water content determination by volumetric and thermogravimetric analysis of heated samples 05 p0667 A72-17051

Continuous volume-temperature dilatometer measurement of small liquid samples in biological application 13 p1959 A72-29752

Ti alloy volume reduction during decomposition of metastable alpha-prime, alpha-two and beta phases after cooling from beta range 14 p2114 A72-30401

Volumetric analysis of Th, Zr and Li hydrides precipitation in Mg alloys, determining rate equation and activation energy 15 p2257 A72-32118

Effect of beta-adrenergic blockade on plasma volume in human subjects. 19 p2757 A72-38029

Echocardiographic determination of left ventricular dimensions, volumes and performance. 19 p2762 A72-38819

A method for spiropographic display of functional residual capacity and other lung volumes. 21 p3005 A72-40427

Electrically sensed changes in chest and abdomen diameter for tidal volume, respiratory frequency and minute ventilation measurements 21 p3006 A72-40428

Evaluation of the pulse-contour method of determining stroke volume in man. 23 p3256 A72-43934

Surface tension, density, and volume change on melting of Al₂O₃ systems, Cr₂O₃, and Sm₂O₃. 24 p3417 A72-44925

VOLUMETRIC STRAIN
Transverse strains in solid body due to volumetric stresses counteraction to external load stresses 06 p0899 A72-18566

Compression strength theory for monodirectional reinforced homogeneous anisotropic and piecewise homogeneous composite materials using microvolume stability loss failure mechanism. 06 p0838 A72-18655

Dilatometric studies of volume compression effect during aging of nimonic alloy showing linear dependence of matrix lattice constant on gamma prime phase 21 p3068 A72-40957

VOMITING
Neuroinhibition in the regulation of emesis. 18 p2650 A72-36449

VON KARMAN EQUATION
Von Karman constant in low Reynolds number turbulent flows, observing shear stress gradients effects on viscous sublayer 13 p1944 A72-30027

VON MISES THEORY
U STRESS FUNCTIONS
VON ZEIPPEL METHOD
Hori perturbation theory equivalence to von Zeipel theory established to third order approximations in perturbed elliptic motions 01 p0129 A72-10796

Hamiltonian algorithms based on Lie transforms and von Zeipel method, discussing application to non-Hamiltonian system perturbation solution 06 p0839 A72-17660

VOR SYSTEMS
U VHF OMNIRANGE NAVIGATION
VORTEX BREAKDOWN
Towing tank for flow visualization studies of trailing vortices formation and breakdown 07 p0909 A72-20088

Effect of air injection on the torque produced by a trailing vortex. 23 p3247 A72-43333

Effect of several wing tip modifications on a trailing vortex. 23 p3247 A72-43334

The structure of blunt base wakes in swirling flow. 24 p3391 A72-45023

The dissipation of tip vortices by mass injection with application to rotor systems. 24 p3362 A72-45329

VORTEX COLUMNS
U VORTICES
VORTEX DISTURBANCES
U VORTICES
VORTEX FLOW
U VORTICES
VORTEX GENERATION
U VORTEX GENERATORS
VORTEX GENERATORS
Aerodynamics of vortex chambers with symmetrical air injection, discussing core and end boundary layer flows interaction and momentum loss from end surfaces friction 09 p1260 A72-22676

Shock wave propagation in ducts with abrupt area expansion, discussing vortices generation and wave diffraction and reflection effects on ducted flow. 10 p1464 A72-23880

Pressure, shear stress and yaw angle measurements in flow through aircraft intake S-shaped ducts with turbulent boundary layer at entry, noting vortex generation 16 p2377 A72-33403

Transient and steady state vorticity generated by horizontal temperature gradients. 20 p2987 A72-40016

Investigation of the stability of the tip vortex generated by hovering propellers and rotors. 24 p3361 A72-45327

VORTEX INJECTORS
Discharge coefficients of centrifugal screw-type swirl injector with helical channel, calculating drag and surface geometry effects 11 p1712 A72-26970

The dissipation of tip vortices by mass injection with application to rotor systems. 24 p3362 A72-45329

VORTEX RINGS

Vorticity transport and definition of equations for axisymmetric incompressible viscous vortex ring, solving coupled system numerically [AIAA PAPER 72-151] 07 p0907 A72-18956

Bilaterally symmetric vortex rings dynamic behavior, computing pointwise induced velocity via Biot-Savart law for hydrodynamic and Rankine vortex models [AD-739139] 07 p0967 A72-19501

Experimentally produced vortex ring structure and stability, using dye and hydrogen bubble techniques for flow field, ring velocity and growth rate observations 10 p1466 A72-24327

Small cross section steady vortex rings existence in inviscid uniformly dense ideal fluid, deriving asymptotic formulas for rings shape and properties 10 p1467 A72-24333

Solar flare induced vortex ring formation, describing photographic observations by Okayama Astrophysical Observatory solar telescope on 30 October 1970 13 p2048 A72-29741

Analytical prediction of vortex-ring boundaries for helicopters in steep descents. 20 p2886 A72-38949

A steady vortex ring close to Hill's spherical vortex. 22 p3166 A72-42312

Flight test studies of the formation of trailing vortices and a method to accelerate vortex dissipation. [AIAA PAPER 72-988] 22 p3134 A72-42327

VORTEX SHEETS
Multivortex model of vortex sheet development on slender axisymmetric bodies at angle of attack 03 p0307 A72-12919

Wing tip shape effects on vortex sheet rolling calculation by Belotserkovskii method 06 p0755 A72-17850

Trailing vortex core decay with axial injection as function of momentum flux parameter 09 p1261 A72-23673

Dynamic pressure distribution and propulsive contours of trailing vortex wake downwind of external flow jet flap, using five-hole probe measurements 10 p1420 A72-25070

Incompressible potential flow model of porous parachute canopy flow field, using Stokes stream function for axisymmetric vortex sheet in uniform steady stream 12 p1755 A72-28123

Vortex sheet simulation method for slender wing-canard surface nonlinear interaction investigation 16 p2458 A72-33695

Plane vortex sheet in incompressible inviscid and finitely conducting fluids, investigating discontinuity in density and conductivity on hydromagnetic stability 16 p2438 A72-33842

Vortical flow of incompressible fluid in finite region bounded by potential flow and with Bernoulli constant jump at boundary 19 p2785 A72-37552

Radiation properties of the semi-infinite vortex sheet. 24 p3359 A72-44918

VORTEX STREETS
NT KARMAN VORTEX STREET
Lin parameter and eddy viscosity of atmospheric vortex streets, using TIROS and Gemini data 08 p1200 A72-21621

Vortex growth in two-dimensional coalescing jets. 17 p2539 A72-34970

Periodic vortex formation and shedding in flows past bluff bodies, considering cylinder forced and self excited vibrations and interaction with wake 18 p2679 A72-36389

Periodic wave of oscillating and stationary two dimensional bodies immersed in uniform incompressible stream, investigating semiinfinite vortex trails relationship to oscillating airfoils 21 p2989 A72-40651

On the vortex street behind a circular cylinder in non-Newtonian flows. 21 p2992 A72-41227

VORTEX TUBES
U VORTICES
VORTICES
Flow in turbulent trailing vortex, considering circulation profiles and Reynolds stress distribution [AD-740436] 01 p0049 A72-10232

Axial and tangential velocity distributions within trailing line vortex to large distance downstream of generating wing extended from available data [AD-743599] 01 p0001 A72-11135

Liquid containment in gas driven vortex with air-water mixture densities above 100 times gas flow, discussing applicability to colloidal core nuclear reactor performance estimation 01 p0100 A72-11360

Multicellular viscous vortex core embedded in unsteady outer potential swirling flow, obtaining numerical solution 02 p0253 A72-11971

Axial flow effect on vortex filaments stability by slender body analysis of force balance between Kutta-Joukowski lift and momentum flux inside filament [AD-740965] 03 p0307 A72-13157

Photospheric vortex motions effect on flare productive magnetic patterns in solar active regions 03 p0411 A72-13330

Vortex flow structure in axial gas turbines near inlet and outlet of blade row 03 p0307 A72-13538

Transition on plane plate in presence of vortices detached from cylinder in free flow 03 p0342 A72-13788

Decelerating MHD effect on rotational funnel flow excited by vortex line or radial converging currents 03 p0397 A72-13994

Symmetrically deformed delta wing in supersonic flow, considering leading edge flow separation induced vortices effects on downwash, pressure distribution and aerodynamic characteristics 04 p0463 A72-15741

Complex perturbation potential of constant vortex shear flows around airfoil activated by motion in presence of rectilinear wall 05 p0600 A72-16122

Elliptic wing-vortex interaction for various aspect ratios 05 p0603 A72-16542

Vortical flow of incompressible fluid in finite region bounded by potential flow and with Bernoulli constant jump at boundary 05 p0649 A72-16581

Steady inviscid diabatic complex lamellar gas flow geometric properties, correlating stream and vortex lines via Beltrami surfaces in Euclidean space 05 p0747 A72-16667

Sound effect on diffusion flames, presenting vortex model 05 p0747 A72-16701

Periodic aspects of nonphenomenal Euroatlantic blocking systems persistence, noting dominant role played by cyclonic vortices 05 p0684 A72-16794

Vortex production of intense localized heating to leeward regions of bodies in hypersonic flows, proposing flow field models [AIAA PAPER 72-77] 05 p0604 A72-16804

Internal axisymmetrical steady inviscid rotational flow velocity profiles simulation by means of shaped wire gauze screens [AIAA PAPER 72-165] 05 p0650 A72-16830

Subsonic wind tunnel investigation of aircraft wake far field structure, measuring trailing vortex decay by yawhead pressure probe [AIAA PAPER 72-40] 05 p0607 A72-16902

Turbulent boundary layer analogy mathematical model for turbulent mixing and buoyancy effects on aircraft trailing vortex wake motion and persistence [AIAA PAPER 72-42] 05 p0607 A72-16903

Fluctuating flow in idealized model of turbulent shear layer composed of many discrete two dimensional vortices, analyzing noise generation [AIAA PAPER 72-155] 05 p0609 A72-16955

Wake instabilities and vortices spacing, position and strength behind slender cylindrical bodies at large incidence with subcritical cross flow Reynolds numbers 05 p0610 A72-17010

Two-dimensional asymptotic solutions to Navier-Stokes equations for weak vortex discontinuity flow with vanishing viscosity 06 p0798 A72-17680

Circular vortex rings with nonsimilar vorticity distributions submerged in inviscid stream, considering motion and decay by inner and outer asymptotic expansions matching [AD-741267] 06 p0798 A72-17781

Viscous flow through movable and immovable cascades of blades, determining velocity field by airfoil center line vortex distribution 06 p0757 A72-18131

Turbulent layer generation in ideal two dimensional fluid flow, determining vortices time evolution from initial velocity discontinuity by numerical methods 06 p0802 A72-18525

Numerical analysis of computing velocity distribution in vortex row cascade profiles by method of singularities 07 p0965 A72-18787

Rotational flow computation, using iteration methods for irrotational and solenoidal vector field components 07 p0966 A72-18811

Atmospheric eddy flux spatial variations in constant flux layer, noting heat and momentum flux variability of less than 10 percent 07 p1030 A72-19107

Perfect fluid two dimensional steady flow equation solution for viscous flow with specified boundary conditions, considering vortex flow 07 p0971 A72-20099

Intermittency and scale similarity in turbulent flow structure, analyzing eddies distribution inhomogeneity 07 p0973 A72-20319

Durando model overprediction of deflected jet vortex strength in subsonic cross flow 08 p1151 A72-21631

Pinning force of vortex lines and microstructural inhomogeneities in superconductors, using magnetization and critical current measurements 09 p1369 A72-22796

Motion equations approximate solution for viscous fluid Couette flow instability caused by spiral symmetry vortices 09 p1295 A72-23073

Meteor trail photoobservations for atmospheric small scale turbulences vertical profile, determining eddy minima velocities and turbulent energy dissipation in M zone 09 p1393 A72-23650

Turbulent boundary layer growth measurement on annular diffuser containing free vortex swirl 10 p1416 A72-23857

Aerodynamic forces calculation for constant vortex shear flows around airfoil fixed between rectilinear walls, noting resultant perpendicularity to Ox axis 10 p1465 A72-24115

Reduction of governing equation for thin nonstretching vortex filament in incompressible inviscid fluid to nonlinear Schroedinger equation describing helical motion propagation 10 p1466 A72-24293

Two dimensional low Mach number sound field from line vortex passage around rigid half plane edge, calculating space-time variation by perturbation methods 10 p1468 A72-24370

Numerical solution of nonlinear integrodifferential equation governing finite amplitude wave propagation on concentrated vortices 10 p1468 A72-24419

Convective motions in rotating laterally heated annulus with contacting rigid lid, determining radial temperature difference for transition to vortex regime 10 p1506 A72-24420

Nonuniform vortex flow of compressible gas past cascade of plates, noting monochromatic pressure waves at harmonics of plate vibration frequency 10 p1418 A72-24538

Laminar boundary layer instability to longitudinal vortices onset due to homogeneous suction from slightly concave permeable wall, determining Goertler parameter and wavenumber critical values 10 p1470 A72-25064

Navier-Stokes equations system integration for axisymmetric vortex flow of viscous incompressible three component fluid 10 p1471 A72-25134

Three dimensional wind tunnel investigation of vortex augmented swept wing with leading edge cusp flap and split upper and lower trailing edge flaps [SAE PAPER 720321] 11 p1568 A72-25584

Single spiral vortex cavity termination model for second order solution of flat plate hydrofoil cavitation flow 11 p1616 A72-25879

Book on turbulence covering Reynolds stresses, kinetic theory of gases, vorticity dynamics and mixing length models 11 p1616 A72-25925

Wind tunnel tests for flutter characteristics of rectangular block model oscillating freely in uniform flow, discussing galloping and vortex excitation 11 p1572 A72-26373

Experimental data on twin vortices formed behind impulsively started or uniformly accelerated circular cylinders 11 p1572 A72-26375

Hydraulic vortex amplifiers with and without diffusers, discussing supply pressure and liquid viscosity effects on system performance 11 p1578 A72-26980

Wind velocities field in vortices leeward of islands derived from Navier-Stokes equation for isolated axisymmetric viscous vortex 12 p1839 A72-27032

Streamlines and fluid diffusion determination for axisymmetric irrotational and rotational flows in ducted propellers, noting conformal mapping of arbitrarily shaped domain onto rectangle 12 p1751 A72-27168

Ergodic boundary in initial conditions space for turbulent two dimensional flow, explaining phenomenon in terms of negative temperatures for point vortex model 12 p1797 A72-27183

Steady three dimensional viscous vortex within circular cylinder with tangential fluid influx from jets on outer surface and efflux through sink on bottom [AD-741352] 12 p1798 A72-27716

Steady laminar boundary layer generated by vortex over fixed coaxial disk, solving governing equations by numerical integration 12 p1798 A72-27833

Near ground pressure differentials caused by large transport aircraft induced wake vortices, comparing measured data with Bernoulli formula theoretical values 12 p1752 A72-28122

Nonstationary interaction flow field between subsonic and composite jet on flat plate with vortex formation and reverse currents, using finite difference technique 12 p1799 A72-28168

Plane potential flow stability with respect to bounded and free hollow vortices, using conformal mapping method 13 p1941 A72-28716

Longitudinal vortices development in time-increasing boundary layers at concave walls, showing dependence on Reynolds number and boundary layer thickness 13 p1942 A72-29597

Swirling flow in round pipe with sudden expansion discussing separation and reversal characteristics 13 p1942 A72-29644

Wind tunnel investigation of wake pressure and vortex shedding characteristics of flow past spheres as function of Reynolds number 13 p1896 A72-30099

Velocity and temperature profiles of plane Poiseuille flow with finite amplitude convection and longitudinal vortices, investigating uniform axial temperature gradient effect 14 p2173 A72-31063

Vortex-lattice method for subsonic aircraft aerodynamic coefficients calculation, verifying results with airbus lifting surface wind tunnel test data 15 p2178 A72-31401

Contracting or diverging stream flow mean velocity change effects on airfoil pressure distribution, circulation and lift, deriving vortex distribution expression 15 p2179 A72-32023

Electrical pumping discharge confined by liquid wall of vortex channel in dye laser solution 15 p2251 A72-32528

Nonfriction vortices generation by jet flow in stationary fluid, using conservation of momentum principle 15 p2219 A72-32554

Low speed wind tunnel investigation of vortex formation effect on angle section columns galloping response, varying stiffness and damping characteristics 15 p2332 A72-32594

Generalized continuum mechanics application to turbulent flows developing from unstable vortex wakes 16 p2377 A72-33143

Spanwise correlation measurement of vortex shedding behind circular cylinder in subcritical Reynolds number region 16 p2379 A72-33651

Supersonic vortex boundary layer flow velocity profiles behind flat plate indentation for Mach numbers 1.7-3.0 and Reynolds numbers to 40,000,000 16 p2380 A72-33857

Airfoil vortex shedding noise in low-turbulence flow at helicopter blade Reynolds numbers, obtaining correlation coefficients for far field noise and surface pressure fluctuations [AIAA PAPER 72-656] 16 p2347 A72-34078

Rotating flow introduction effects on jet noise levels, combustion and turbulent mixing processes and flame stability [AIAA PAPER 72-645] 16 p2480 A72-34087

Wind tunnel simulation of full scale vortices. [AHS PREPRINT 623] 17 p2483 A72-34477

Linear air mass flow injection at helicopter rotor blade tips, considering effects on trailing vortex circulation strength [AHS PREPRINT 624] 17 p2484 A72-34498

Circulating toroidal vortex pattern in initial region of turbulent coaxial jet stream mixing obtained with hot-wire anemometer, static pressure probes and shadowgraphy [ASME PAPER 72-APM-30] 17 p2538 A72-34789

Discrete vortex model numerical simulation of Onsager negative temperature instability for interacting line vortices two dimensional motions 17 p2538 A72-34871

Theorem for instability of rectilinear vortices in two dimensional steady flow of ideal liquid with or without submerged obstacle 17 p2539 A72-34910

Vortex induced wing loads. 17 p2486 A72-35257

Kinetic and kinematic equations for inviscid unsteady gas flow, noting pseudostationary vortex geometry 17 p2541 A72-35346

Three-dimensional non-free vortex flow in axial fans. 17 p2487 A72-35896

Flow of a viscous liquid round a cylinder for Reynolds numbers 60 and 80. 18 p2679 A72-36233

Swirling flows vortex breakdown in nozzles, diffusers and combustion chambers, considering analogy to boundary layer separation 18 p2641 A72-36385

Acoustic ray deflection by aircraft wake vortices with viscous core, observing maximum deflection angles during large aircraft landing 18 p2641 A72-36417

Vortex concept and related vector analysis in fluid dynamics, crystal dislocations, superconductors and superfluid He 18 p2711 A72-36489

Negative temperatures in two dimensional vortex motion. 18 p2681 A72-36669

Rotational theory of laminar boundary layer separation of incompressible fluid from smooth surface under pressure gradients 18 p2682 A72-36887

Calculation of axisymmetric swirling and non-swirling turbulent jets 18 p2682 A72-36890

Ultimate configuration of the self-similar separated flow of an ideal fluid 19 p2785 A72-37396

The motion of a vortex pair in a stratified atmosphere. 19 p2785 A72-37571

The motion of a vortex filament with axial flow. 19 p2786 A72-37598

Complex vortex core fine structure around propeller tip observed via smoke and stroboscopic lighting, presenting photographs 19 p2786 A72-37747

Propulsive performance of a 30 kW arc-jet thruster stabilized by vortex and magnetic forces. 19 p2848 A72-37925

Influence of a trailing vortex on friction pulsations in the near-wall region of the leading stagnation point of a cylinder in transverse flow 19 p2786 A72-38041

Decay of pregalactic vortex motions 19 p2862 A72-38057

Spectral theory of Taylor vortices. I - Structure of unstable modes. 19 p2788 A72-38550

Surface vorticity theory for axisymmetric potential flow past annular aerofoils and bodies of revolution with application to ducted propellers and cowls. 19 p2747 A72-38554

High energy particle and photon orbital and vortical motions in Kerr metric outside equatorial plane in gravitational field 20 p2953 A72-39341

Effect of ground wind shear on aircraft trailing vortices. 20 p2886 A72-39630

Flux vortices and transport currents in type II superconductors. 20 p2961 A72-39809

High Reynolds number turbulence and vortices in journal bearings, discussing validity of flow field models based on mixing length and pipe flow theory 20 p2930 A72-39972

Electrodynamics analysis of superconducting vortices interaction with cylindrical cavities /pinning/, calculating critical currents in type II superconductors in external magnetic field 21 p3096 A72-40416

Finite core infinite extent helical vortex filament stability to small sinusoidal displacements of centerline 21 p3045 A72-40649

An experimental investigation of the formation of vortices behind the isosceles triangular cross-sectional obstacles protruding from the plane wall. 21 p2992 A72-41246

Velocity distribution of quasi-steady and steady flow of ideal incompressible fluids with congruent streamlines, investigating conditions for vortex and irrotational flow 22 p3164 A72-41906

Plane potential flow stability with respect to small perturbation flow of bounded and free hollow vortices, using conformal mapping method 22 p3165 A72-42093

Vortex and source lattices in a variable layer of an incompressible fluid 22 p3133 A72-42248

Machine code for finite difference solution of wake vortex governing equations and far field prediction in trailing vortices, developing turbulent energy model [AIAA PAPER 72-989] 22 p3134 A72-42326

The construction of invariant transformations in plane rotational gasdynamics. 22 p3199 A72-42399

Singular points in conical flow streamline patterns, considering rotational and irrotational flows 22 p3135 A72-42580

Low flying aircraft wake vortices tracking, describing sensing techniques based on acoustic pulse deflection and velocity field measurements 22 p3179 A72-42709

Coning motion, autorotation, and vortex systems of slender flight vehicles 22 p3231 A72-42904

Stationary spherical vortices in a perfect fluid. 22 p3167 A72-42980

Equilibrium equations for vortex lines with allowance for interaction with boundary of ideal superconductor, calculating extremum values of magnetic field 23 p3312 A72-43316

Effect of several wing tip modifications on a trailing vortex. 23 p3247 A72-43334

Main results of nonlinear rotor theory 23 p3247 A72-43419

An investigation of confined vortex flow phenomena. [ASME PAPER 72-FLCS-3] 23 p3281 A72-44067

Satellite-observed Southern Hemisphere cloud vortices in relation to conventional observations. 23 p3285 A72-44145

Effects of transport velocity of wake vortex on aerofoil oscillations. 23 p3249 A72-44494

Investigation of propeller vortex noise including the effects of boundary layer control. 24 p3359 A72-44680

Boundary layer core flow model of concentrated columnar vortex interaction with plane solid nonrotating surface, applying to tornado interpretation 24 p3391 A72-45022

The damping of precessing vortex cores by combustion in swirl generators. 24 p3464 A72-45060

Investigation of the stability of the tip vortex generated by hovering propellers and rotors. 24 p3361 A72-45327

Trailing vortex effects on wing pressure distribution from low speed wind tunnel tests, discussing effect of wing-vortex distance 24 p3362 A72-45331

Vortex control on an inclined body of revolution. 24 p3362 A72-45335

Dynamic simulation of an aircraft under the effect of vortex wake turbulence. 24 p3368 A72-45346

Stability of coaxial rotating jet and vortex of different densities. 24 p3394 A72-45562

VORTICITY

Stator-rotor induced annular incompressible rotating flow, allowing for blade loading generated vorticity within actuator disk theory [ASME PAPER 71-WA/FE-18] 05 p0599 A72-15929

Convergent power series solution in powers of time for unsteady viscous flow near stagnation after impulsive motion of bluff body from vorticity distribution viewpoint 06 p0757 A72-18135

Navier-Stokes equation numerical solution methods, expressing boundary conditions by separate equations for vorticity and stream function 07 p0970 A72-20077

Energy spectrum and decay of random two-dimensional vorticity distributions at large Reynolds number [AD-740486] 09 p1294 A72-22943

Frontogenesis models based on horizontal deformation field, noting uniform and nonuniform potential vorticity 09 p1347 A72-23652

Numerical solution for super-Alfvénic supersonic aligned MGD flow over cone with attached shock wave, obtaining surface pressure coefficients, current and vorticity distributions 10 p1418 A72-24463

Smoke trail motions in winds with constant shear, considering potential, vorticity and stratified flows [AD-742738] 10 p1475 A72-24748

Tropical depression analysis based on radar data, observing large divergence in maximum vorticity areas 11 p1681 A72-26079

Conditional instability of second kind /CISK/ model of surface cyclonic vorticity dependence on vertical distribution of latent heat release 12 p1838 A72-27019

Relative atmospheric dispersion in enstrophy /half squared vorticity/ - cascading inertial range of homogeneous two dimensional turbulence 12 p1839 A72-27031

Computation method for rotating and nonrotating viscous flows boundary vorticity iteration parameters for use with time centered or alternating direction implicit time differencing approximation 14 p2093 A72-30228

Singularity method treatment of vortex distribution induced velocity perturbations on flat plate at angle of attack, noting results similarity to lifting surface theory 15 p2180 A72-32466

Vorticity jump across stationary MHD discontinuity generalization from gas dynamics problem, noting results validity for shock and detonation waves 16 p2435 A72-33011

Relative vorticity and balanced height distributions from cloud velocities associated with cloud structure of extratropical cyclone over continental U.S. 16 p2419 A72-33945

Effects of vorticity, displacement speed and curvature on heat transfer with dissipation. 17 p2638 A72-35747

Motion of a sphere in an electrically conducting rotating fluid. 18 p2714 A72-36123

A vortex model for the study of the flow at the rotor blade of a helicopter 18 p2642 A72-36975

Electrostatic, reticular vorticity, turbulence effects and equivalences with tensional and spectral elastic fields. 20 p2953 A72-39419

A diagnostic study of the vorticity balance at 200 mb in the tropics during the Northern summer. 22 p3201 A72-42507

Scale analysis of atmospheric large-scale motions in low latitudes. 23 p3311 A72-44241

VORTICITY EQUATIONS

Turbulent flow model based on two equations for kinetic energy distribution and vorticity fluctuations, comparing flow and heat transfer prediction with experimental data 08 p1152 A72-22169

Barotropic instability and vorticity equation of zonal flow with superposed Rossby waves limiting predictability of real atmosphere 12 p1838 A72-27021

Vorticity and energy transfer equations for subsonic jet impingement on flat plate, noting turbulent jet effect on friction factor 12 p1799 A72-28171

Gosiewski vorticity tensor formula generalization from moving unit vector associated with material point to vector field relative to moving continuum 16 p2423 A72-33112

Numerical simulation studies of two-dimensional turbulence. I - Models of statistically steady turbulence. 17 p2543 A72-35765

VORTICITY TRANSPORT HYPOTHESIS

Planetary wave description by linear difference equation for vorticity transport on hemisphere, considering Laplace operator error 14 p2099 A72-30260

VOSKHOD MANNED SPACECRAFT

Soviet manned space flight history and characteristics, discussing Vostok, Voskhod and Soyuz vehicles 03 p0440 A72-13475

VOSTOK SPACECRAFT

Soviet manned space flight history and characteristics, discussing Vostok, Voskhod and Soyuz vehicles 03 p0440 A72-13475

Design features of Soyuz life support and launch escape systems and Vostok rocket booster stage 23 p3343 A72-44335

VTO FIGHTER AIRCRAFT

U FIGHTER AIRCRAFT

U VERTICAL TAKEOFF AIRCRAFT

VTOL

U VERTICAL TAKEOFF

VTOL AIRCRAFT

U VERTICAL TAKEOFF AIRCRAFT

VULNERABILITY

Unique features of the B-1 flight control systems. [AIAA PAPER 72-872] 20 p2889 A72-40062

W

W WINGS

U VARIABLE SWEEP WINGS

WAFERS

Ion implantation doping of MOSFET and IC for wafer production, using automatic vacuum pumpdown and cycle control 10 p1447 A72-23950

Surface piezoelectric effects of mechanical bending of noncentrosymmetric CdS semiconductor wafers 13 p2020 A72-28524

Surface defects evaluation on GaAs and Si wafers by metallographic and electrochemical techniques 15 p2296 A72-32758

A means of reducing custom LSI interconnection requirements. 23 p3273 A72-44454

WAKEFULNESS

Wake-sleep cycle importance in military service, considering drugs effects on wakefulness 07 p0922 A72-20383

Neurophysiological mechanisms of sleep, studying sleep and wakefulness state evoked potentials relation to cortex and subcortical activity levels 09 p1264 A72-22224

Sleep-wakefulness cycle variations effect on reaction time and spontaneous tempo during time isolation experiment, showing tendency toward circadian rhythm 11 p1581 A72-26687

Nocturnal primate Aotus trivirgatus wakefulness-sleep cycles during dark/light periods expressed in REM/non-REM percentages 13 p1903 A72-29300

Weightlessness effects on animal voluntary motor activity and wakefulness from brain and muscle area electrical activity recordings during ballistic flight 16 p2355 A72-33548

Cerebral blood flow and metabolic changes during wakefulness, sleep, coma and epileptic seizures in terms of homeostatic mechanisms 16 p2356 A72-33558

Biotelemetry and computer analysis techniques for steep states and wakefulness studies during aerospace flight

16 p2356 A72-33560

Dynamics of the electrical activity of various regions of the neocortex during the sleep-wakefulness cycle

22 p3147 A72-42955

WAKES

NT AIRCRAFT WAKES
NT HELICOPTER WAKES
NT HYPERSONIC WAKES
NT LAMINAR WAKES
NT NEAR WAKES
NT PROPELLER SLIPSTREAMS
NT SLIPSTREAMS
NT SUPERSONIC WAKES
NT TURBULENCE WAKES

Wake blockage paradox in two dimensional perforated wall wind tunnel, investigating interference velocity distribution

02 p0151 A72-12271

Wake outflow concept application to flow separation phenomena, enabling determination of base pressure for drag calculations

[DFVLR-SÖNDDR-176] 05 p0603 A72-16702

Telemetry system on board beryllium sphere reentry vehicle for hypersonic gas dynamics and wake chemistry experiments, using flush mounted antennas with isotropic radiation pattern

[AIAA PAPER 72-176] 05 p0631 A72-16836

Wake behind body moving in plasma parallel to magnetic field, observing coupling with parallel ion acoustic waves and with perpendicular Bernstein modes

06 p0875 A72-17525

Wake behind obstacle immersed in plasma flow of single ended Q-machine, using experiment as diagnostic of ion distribution function

06 p0856 A72-17526

Thermally induced convection flow characteristics in separated or wake formation regions over heated cylindrical surface submerged in water

07 p1100 A72-19630

Reynolds number and cylindrical spacing effect on Karman vortex street formation from smoke visualizations of single and tandem cylinder wakes

09 p1261 A72-22939

Interplanetary magnetic field perturbations by solar wind and moon, noting lunar wake anomalies positive correlation with plasma beta value

09 p1387 A72-23003

Wall law for axisymmetric turbulent boundary layers in zero pressure gradient fluid flow through circular cylinders, noting negative and positive wake regions

[ASME PAPER 71-APM-VV] 10 p1465 A72-24177

Linear initial value problem of partially mixed cylindrical wake in uniformly stratified fluid, obtaining exact solutions for density and velocity distributions

10 p1466 A72-24299

Noise reduction effects of wake interaction between rotor blade rows in axial flow compressor, cancelling velocity defect at stator position

[ASME PAPER 72-GT-15] 11 p1569 A72-25614

Atmospheric temperature measurement by neutral particle wake method, using satellite-borne mass spectrometer

11 p1634 A72-26408

Incompressible laminar subcritical flow with separated wake past symmetric two dimensional bluff body, calculating upstream pressure distribution and separation point

12 p1751 A72-27172

Near ground pressure differentials caused by large transport aircraft induced wake vortices, comparing measured data with Bernoulli formula theoretical values

12 p1752 A72-28122

Doppler laser velocimeter and hot-wire anemometer readings in cylinder wake compared, describing instrument caused spectrum broadening effects neutralization method

13 p1960 A72-29889

Wind tunnel investigation of wake pressure and vortex shedding characteristics of flow past spheres as function of Reynolds number

13 p1896 A72-30099

Electron pressure effect on lunar wake shape and size, calculating electric field created by charge separation

15 p2308 A72-31925

Photographic flow visualization of steady recirculating wakes behind sphere and oblate spheroids for low Reynolds numbers

15 p2180 A72-32419

Describing equations derivation by implicit finite difference scheme for chemically nonreactive two dimensional symmetric and axisymmetric jet and wake problem

16 p2381 A72-34170

Inert and reactive gas injection in near wake behind blunt bodies in supersonic flow, considering influence on base pressure and temperature

17 p2487 A72-35930

Theoretical models for cavity and wake flows, outlining numerical methods for solving functional equations

18 p2679 A72-36387

Periodic vortex formation and shedding in flows past bluff bodies, considering cylinder forced and self excited vibrations and interaction with wake

18 p2679 A72-36389

Numerical study of a viscous gas flow in the wake of a plane body

18 p2642 A72-36804

Ultrasonic sound beam measurement of flow circulation variations in circular cylinder wake, evaluating probability distribution of beam phase fluctuations

21 p2990 A72-40947

Flow parameters and geometric factors effect on wake structure behind nozzle cascades with cooling air ejection through blade trailing edges, evaluating energy losses due to flow mixing process

23 p3248 A72-43665

The vortex street in the wake of a vibrating cylinder.

23 p3281 A72-44302

Effects of transport velocity of wake vortex on aerofoil oscillations.

23 p3249 A72-44494

Resistance in potential flows with no wakes and with steady closed wake, calculating normal and tangential thrusts contributions for sphere and circular cylinder

24 p3390 A72-44986

The breakup of liquid droplet columns by shock waves.

24 p3391 A72-45048

WALKING

Tandem walking on floor with eyes closed as ataxia test for vestibular function assessment

12 p1770 A72-27476

Energy cost /oxygen consumption/ prediction for treadmill and various levels terrain walking at two speeds under three different peak loads

14 p2080 A72-30706

Momentary velocity measurement of human walking in forward movement by frequency response of signal on magnetic tape

15 p2190 A72-32200

Metabolic energy requirements for pushing loaded handcarts, measuring expenditure during treadmill and outdoor asphalt circuit walking

21 p3005 A72-40419

WALKING MACHINES

Artificial biped locomotion dynamic equilibrium, representing mathematical model by two nonlinear differential equations with variable coefficients

06 p0769 A72-18703

Digital-computer simulation of the motion of a walking machine

23 p3278 A72-44002

WALL FLOW

Inertia effects in fully developed axisymmetric laminar flow between two parallel rotating walls, solving Navier-Stokes equation in nonlinear form

[ASME PAPER 71-LUB-J] 02 p0234 A72-11529

Wall conduction effect on heat transfer to laminar boundary layer, obtaining temperature distributions at plate surface by energy transport equation

02 p0202 A72-11670

Flat plate incompressible smooth surface boundary layer examination emphasizing turbulence production near wall, using hydrogen-bubble and hot-wire measurements with dye visualization

02 p0203 A72-11975

Wall jet flow displacement on curved surface, deriving two dimensional solution for second-order boundary layer equations

03 p0307 A72-13159

Thermal simulator of flows with chemical wall reaction, plotting surface temperature variations with distance

03 p0456 A72-13793

Rigid and compliant walls longitudinal curvature and compliance effects on incompressible laminar boundary layer hydrodynamic stability

03 p0342 A72-13854

Heat transfer from burning gas mixture flow to receiver wall, taking into account exothermal reactions due to catalytic effects

03 p0458 A72-14166

Nozzle and cavity wall cooling limitations on uranium plasma nuclear rocket specific impulse, discussing wall heat flux and transpirational cooling by propellant flow

03 p0387 A72-14383

Freezing of hot fluid flowing onto flat cold wall, solving nonlinear integrodifferential equation for temperature distribution by iteration method

04 p0595 A72-14650

Unsteady radial flow between fixed and oscillating walls, obtaining flow equations and air bearings stability conditions

04 p0511 A72-14970

Newtonian fluid laminar free convection over curved wall with arbitrary temperature variation, investigating similarity solutions existence by method of free parameters

04 p0596 A72-15193

Theoretical model for turbulent mixing of confined jet, including wall boundary layer

[ASME PAPER 71-WA/FE-31] 05 p0646 A72-15925

Complex perturbation potential of constant vortex shear flows around airfoil activated by motion in presence of rectilinear wall

05 p0600 A72-16122

Free convection flow along infinite vertical flat plate under periodically varying suction and with fluctuating plate temperature, analyzing mean velocity and temperature profiles

05 p0747 A72-16668

High resolution mean flow and turbulence measurements in turbulent boundary layer on cooled hypersonic wind tunnel side wall at Mach 9.37

[AIAA PAPER 72-73] 05 p0650 A72-16802

Polarographic method for simultaneous measurement of wall gradients of velocity and of concentration in unsteady laminar or steady turbulent flow

06 p0797 A72-17558

Similitude solutions for turbulent boundary layers in compressible flow with pressure gradient and heat transfer at wall, obtaining velocity and enthalpy profiles

06 p0798 A72-17845

Wall curvature and flexibility effect on incompressible laminar boundary layer hydrodynamic stability, considering Tollmein-Schlichting transverse wave disturbances

06 p0801 A72-18134

Turbulence model for near-wall boundary layer flows, solving differential equations for kinetic energy and length scale

06 p0802 A72-18527

Wall blowing discontinuity effect on two dimensional incompressible turbulent boundary layers, discussing flow relaxation length separation by penetration point trajectory

07 p0966 A72-18841

Short time film stability followed by dry spot formation in thin heated draining liquid films on vertical walls, discussing minimum thickness

07 p1098 A72-18842

Two dimensional compressible boundary layer turbulent velocity profile on adiabatic and isothermally cooled walls with zero pressure gradient

07 p0970 A72-20080

Shape and structure of shock wave moving along plane wall in gas, comparing experimental results with De Boer theory

07 p0971 A72-20096

Boundary conditions for unsteady flow fields bounded by incompressible elastic thick plane wall fixed to rigid surface

07 p0972 A72-20113

Compressible boundary layer flow past swept wavy wall with heat transfer and ablation, measuring pressure and temperature disturbances

07 p1101 A72-20247

Turbulent boundary layer model with eddy viscosity representation of inner wall region for cases with suction or injection, presenting wall shear calculation method

07 p0973 A72-20248

Laminar and turbulent wall boundary layer and shock attenuation effects on flow uniformity in shock tubes

08 p1149 A72-21018

Near wall collateral layer with velocity vector magnitude changes existence in three dimensional turbulent boundary layer flow

08 p1150 A72-21615

German monograph on steady flow past sphere and cylinder near wall, discussing drag, lift and flow visualization

08 p1108 A72-21950

Visual observations of wall in turbulent pipe flow, using suspending solid MgO particles

09 p1306 A72-22310

Monostable three output fluid amplifier models with curved walls in turbulent jet flow, comparing wall design in dynamic and static tests

09 p1263 A72-22931

Equations of motion for discrete structure fluid, discussing equilibrium pressure and fluid-wall interaction effects

09 p1296 A72-23691

Wall law for axisymmetric turbulent boundary layers in zero pressure gradient fluid flow through circular cylinders, noting negative and positive wake regions

[ASME PAPER 71-APM-VV] 10 p1465 A72-24177

Asymmetric flow in plane channel characterized by diffusional transport of turbulent shear stress and kinetic energy from rough to smooth wall regions

10 p1467 A72-24368

Antisymmetric turbulences linear stability in incompressible plane Poiseuille flow between flexible walls solved by variational boundary value problem formulation

10 p1468 A72-24372

Gas flow effect on undulating flow of viscous fluid film down vertical wall, using Fourier series

10 p1469 A72-24532

Integrodifferential equation for rigid tunnel walls effect on supercavitating flow past thin jet flapped airfoil, noting lift coefficient derivatives

10 p1469 A72-24562

Two dimensional unsteady stagnation point flow against plane wall with impulsive motion

10 p1470 A72-25040

Flow fields and inviscid core of two dimensional diffuser with fluid extraction on diverging walls, describing streamline patterns, stagnation region and stall conditions

[ASME PAPER 72-GT-2] 11 p1568 A72-25605

Unsteady laminar wall boundary layers formation within finite expansion or compression waves in tube with gas at rest

11 p1616 A72-25981

Unbounded wall effect on complex potential of two dimensional flow produced by arbitrary displacement of body within ideal incompressible fluid

12 p1797 A72-27119

Enhanced turbulent diffusion of nitrous oxide in parallel wall duct with obstructions for high Reynolds numbers

12 p1797 A72-27536

Asymptotic behavior of velocity profiles in laminar boundary layers of steady incompressible fluid two dimensional flow past rigid wall

12 p1798 A72-27713

Longitudinal vortices development in time-increasing boundary layers at concave walls, showing dependence on Reynolds number and boundary layer thickness

13 p1942 A72-29597

Reichardt mixing model for turbulent boundary layer calculation in wall flow, noting supersonic and nonisothermal jet flow

14 p2095 A72-31002

Frictionless, Helmholtz and flat jet incompressible flows from slot in thick plane wall, comparing characteristics with free jet vicinity

15 p2216 A72-31464

Turbulent viscous flow near wall, deriving characteristics from equations of motion for comparison with hot wire anemometer measurement

15 p2216 A72-31469

Velocity gradient induced by local wall deformation, investigating effect on unstable natural frequency amplification in laminar boundary layer

15 p2217 A72-31683

Transonic plane flow past wavy wall during choked wind tunnel operation, calculating flow velocity from Mach-Zehnder interferometer measured density distribution

16 p2378 A72-33508

Small cross flow integral method for growth prediction of three dimensional compressible turbulent boundary layers on adiabatic walls

[AIAA PAPER 72-697] 16 p2345 A72-34046

Prediction of the flow and heat transfer in a rectangular wall cavity with turbulent flow

[ASME PAPER 72-APM-Q] 17 p2636 A72-34305

Magnetohydrodynamic flow in the region of a conductivity discontinuity at the wall

17 p2587 A72-34460

Reynolds stress development in wall region of turbulent shear flow of oil investigated by hot film measurement technique and anemometer signal analysis

18 p2680 A72-36478

Mean period of fluctuations near the wall in turbulent flows

18 p2682 A72-36721

Motion of a fluid and gas bubbles with allowance for their relative displacement

18 p2682 A72-36891

Slow motion in a two-dimensional semi-infinite channel with moving walls

18 p2683 A72-37044

Oscillatory flow of a viscous fluid in a flexible walled two dimensional channel

18 p2684 A72-37064

On the use of the Preston tube in elliptical ducts

18 p2676 A72-37094

Solution of the problem of the unsteady motion of a mixture in a flat duct using a quasi-homogeneous model with allowance for deposition on the walls

19 p2788 A72-38589

MHD instability of two dimensional laminar boundary layer in incompressible electrically conducting fluid along concave wall with periodic three dimensional disturbances

20 p2957 A72-39328

Turbulence theory generalization for flow near wall with various surface roughness modes, presenting velocity profiles

20 p2912 A72-39359

Viscous sublayer pulsations elongation in longitudinal direction, noting decay of turbulent friction near wall as third power of distance from wall

20 p2912 A72-39360

Heat transfer in a channel with a porous wall for turbine cooling application

[ASME PAPER 72-HT-39] 20 p2986 A72-39667

Stability of laminar boundary layers on concave walls in presence of magnetic field

20 p2958 A72-40066

An inverse problem in boundary-layer flows - Numerical determination of pressure gradient for a given wall shear

21 p3043 A72-40108

Optimization of acoustic linings in presence of wall shear layers

21 p3083 A72-40334

Experimental study of heat transfer in a subsonic jet impinging normally on a plane baffle

21 p3128 A72-40949

Two dimensional MHD fluctuating flow of incompressible electrically conducting rarefied gas past infinite porous wall for slip-flow regime with variable suction

21 p3095 A72-41784

Three-dimensional disturbances in the boundary layer along a concave wall

22 p3165 A72-42111

Laminar boundary layer at critical point of blunt body in molecular oxygen flow, noting wall influence on condensation

22 p3243 A72-42257

The characteristics of a cylindrical probe at high subsonic speeds. I - The case of zero inclination angle

22 p3135 A72-42484

Influence of the intermodal exchange on the wall heat flow in a gas possessing internal energy

22 p3244 A72-42641

German monograph - Three-dimensional boundary layers at curved walls

22 p3167 A72-43051

Probability distribution of velocities and temperatures near a wall

23 p3279 A72-43696

Influence of wall injection on the turbulent tensions in the exterior regions of a boundary layer

23 p3279 A72-43698

Unsteady flow field near wall and Reynolds stress measurement in turbulent boundary layer, using conditional sampling technique with digital computer

23 p3282 A72-44304

MHD Couette flow between conducting walls with heat transfer

24 p3428 A72-44970

Transonic flow past a wavy wall with compression shocks

24 p3360 A72-44999

The structure of turbulent flows adjacent to walls

24 p3390 A72-45001

Statistical analysis of the turbulence near a wall by conditional sampling

24 p3392 A72-45066

Velocity profile of near-wall turbulent boundary layer with adverse pressure gradient, noting skin friction

24 p3393 A72-45357

Computation of wall effects in ventilated transonic wind tunnels

[AIAA PAPER 72-1007] 24 p3388 A72-45403

Transonic wall interference effects on bodies of revolution

[AIAA PAPER 72-1008] 24 p3389 A72-45404

Contributions to the study of turbulent flow in the vicinity of a flat wall

24 p3394 A72-45443

Integrodifferential equations for curved walls effect on laminar boundary layer characteristics, noting wall friction, layer thickness and transverse pressure

24 p3394 A72-45447

WALL JETS

Integral method for predicting streamwise development of plane turbulent jets and wall jets in uniform streaming flow

01 p0051 A72-11393

Incompressible two dimensional laminar/turbulent wall jet characteristics, obtaining Prandtl mixing theory from apparent kinematic viscosity

02 p0206 A72-12619

Velocity profiles of turbulent three-dimensional incompressible air jet flow from rectangular orifice tangent to and along curved wall surface

[ASME PAPER 71-WA/FE-2] 05 p0647 A72-15938

Interaction produced by diametrically opposed plane turbulent wall jet collision in still air, discussing resultant free jet

[AIAA PAPER 72-211] 05 p0606 A72-16854

Plane two dimensional wall jet, investigating flow dynamic structure

06 p0901 A72-17562

Flow and heat transfer model for turbulent cylindrical wall jets based on Prandtl mixing length theory

11 p1744 A72-25268

Flow separation reduction by transverse jet blowing, illustrating flow patterns by water tunnel visualization on cylinders, perpendicular flat plates, contoured walls, steps, wings, etc

[ONERA, TP NO. 1070] 11 p1572 A72-25814

Laminar and turbulent compressible wall jet characteristics, obtaining density variation as function of velocity and Mach number at exit

11 p1618 A72-26593

Shear stress and dimensionless velocity profiles of plane incompressible fluid wall jet propagation along curved surface

16 p2380 A72-33856

Three-dimensional wall jet originating from a circular orifice

19 p2747 A72-38811

Experimental and design investigation of a supersonic wall jet in a supersonic slipstream

22 p3133 A72-42254

Influence of tangential fluid injection on the performance of two-dimensional diffusers

[ASME PAPER 72-FE-16] 23 p3280 A72-44064

WALL PRESSURE

Supersonic and subsonic jet flows coexistence in constant section duct, analyzing pressure on walls and in fluid and schlieren visualization

[ONERA, TP NO. 976] 09 p1294 A72-22813

Acoustic dipole radiation by wall pressure fluctuations in turbulent boundary layer flow over rigid and plane surface at low Mach number

13 p1894 A72-29583

Some specific characteristics of turbulent wall pressure fluctuations in a flow in a tube

17 p2541 A72-35545

Stresses around one hole or two holes subjected to internal pressures in semi-infinite or infinite medium

21 p3118 A72-40717

Integrodifferential equations for curved walls effect on laminar boundary layer characteristics, noting wall friction, layer thickness and transverse pressure

24 p3394 A72-45447

WALL TEMPERATURE

Wall double layer temperature and plasma oscillations effect on electron energy distribution in low discharge plasma column

03 p0394 A72-13192

Nonstationary thermoelastic stress determination in hollow cylinder walls under convective heat transfer

03 p0443 A72-13459

Tube wall temperature and acoustic noise spectra dependence on thermal flux density in bubble coalescence

03 p0458 A72-14162

Laminar boundary layers on heated plane wall behind shock wave in dissociating oxygen for thermodynamic and frozen flow

03 p0344 A72-14342

Forced convective heat transfer of laminar flow in curved channel with square cross section at constant wall heat flux

04 p0510 A72-14595

Heat transfer from nitrogen plasma jet mixed with cold gas to cooled reactor channel walls at various channel expansion degree values

04 p0555 A72-14645

Uniform normal magnetic field effect upon MHD free convection from vertical wall with instantaneous heat source, considering shear stress

04 p0556 A72-14856

Asymptotic integration method solution of heat transfer equation with constant wall temperature for low speed slip flow regime

[ASME PAPER 71-WA/HT-5] 05 p0599 A72-15866

Heat and mass transfer along axially conducting gas controlled heat pipes, discussing wall temperature profiles and condenser characteristics

[ASME PAPER 71-WA/HT-29] 05 p0745 A72-15882

Free convection flow along infinite vertical flat plate under periodically varying suction and with fluctuating plate temperature, analyzing mean velocity and temperature profiles

05 p0747 A72-16668

Film and convection cooling interaction and effect on wall cooling efficiency for gas turbine applications

[AIAA PAPER 72-8] 05 p0748 A72-16873

Kinetic theory of wall temperature jump and near-wall temperature distribution in polyatomic gases, solving simultaneous singular linear integral equations by numerical methods

06 p0904 A72-18528

Calorimetric gage for convective and radiative wall heat flux measurements in Ar arc plasma

08 p1254 A72-21628

Heat transfer characteristics of liquid metal filled closed thermophons for hot wall boundary conditions of constant temperature and uniform heat flux

[ASME PAPER 72-GT-36] 11 p1745 A72-25631

Mass transfer effect on adiabatic wall enthalpy and recovery factors in laminar boundary layer flow at high injection rates, using self similar solutions

11 p1746 A72-26535

Heat transfer during gas injection through mesh packet porous wall, using gradient method

11 p1748 A72-26972

Momentum transport in thermal incompressible turbulent boundary layers with constant wall temperature, using dimensional analysis and Stratford model

14 p2096 A72-31055

Plane unsteady convective motion of viscous incompressible liquid in infinite horizontal vessel of rectangular cross section due to wall temperature fluctuations

14 p2174 A72-31157

Stationary heat conduction between stagnant binary gas mixture and two constant temperature plane parallel walls for arbitrary Knudsen numbers

15 p2334 A72-31462

Temperature and pressure requirements for producing superfluid liquid molecular hydrogen, noting use of solid deuterium or Ne walls to prevent hydrogen solidification 16 p2422 A72-32911

Statistical solution to unsteady heat conduction through flat multilayer insulating wall, using random walk method 16 p2477 A72-33407

Steady state temperature field and heat flux at wall for metallic coolant flow in thin walled axisymmetric pipe with nonhomogeneous Neumann boundary condition 16 p2477 A72-33413

Wall and ambient temperature distribution effects on free convection heat transfer from nonisothermal vertical flat plate in temperature stratified medium for Prandtl number range 16 p2477 A72-33434

Turbulent boundary layer with discontinuity in wall temperature and concentration 17 p2638 A72-35746

Incident thermal flux parameters and wall temperature effects on flow characteristics in preseparation zone of laminar boundary layer and separation point location 17 p2487 A72-35927

Solution of heat transfer problems with the aid of Laplace transforms. I - Development of analytical solutions for two specific boundary value problems 18 p2740 A72-36422

Experimental study of conditions for heat transfer deterioration in a turbulent carbon dioxide flow under supercritical pressure 18 p2742 A72-37185

Cooled supersonic turbulent boundary layer separated by a forward facing step. 20 p2886 A72-39632

Temperature distribution in a helically heated tube 20 p2984 A72-39648

Effect of wall conduction on the stability of a fluid in a rectangular region heated from below. [ASME PAPER 72-HT-G] 20 p2985 A72-39655

An analytical solution of wall-temperature distribution for transpiration and local mass injection over a flat plate. [ASME PAPER 72-HT-57] 20 p2985 A72-39659

Wall temperature, thermal conductivity and acoustic vibration frequency as function of critical heat flux density for unstable water film boiling conditions 21 p3130 A72-41063

A method of computing skin friction and adiabatic wall temperature in a laminar boundary-layer without pressure gradient. 21 p3046 A72-41202

Heat transfer, adiabatic enthalpy /temperature/ of the wall, and hydrodynamic resistance in the presence of turbulent and laminar flow of a compressible fluid in a round tube 22 p3164 A72-41883

Three-phase heat transfer - Transient condensing and freezing from a pure vapor onto a cold horizontal plate - Analysis and experiment. 22 p3243 A72-41957

German monograph - Heat transfer at a vapor bubble growing on a heated wall during boiling. 22 p3244 A72-43059

Influence of wall temperature on heat transfer in a compressible three-dimensional turbulent boundary layer 23 p3248 A72-43694

An experimental study of heat transfer downstream of a rearward-facing step with small coolant injection. 23 p3357 A72-44271

Nonstationary thermoelastic stress determination in hollow cylinder walls under convective heat transfer 24 p3458 A72-44934

Pressure and temperature change on the wall surface in strong shock wave diffraction. 24 p3391 A72-45047

Factors affecting phase-change paint heat-transfer data reduction with emphasis on wall temperatures approaching adiabatic conditions. [AIAA PAPER 72-1030] 24 p3389 A72-45407

WALL TEMPERATURE DISTRIBUTION

U TEMPERATURE DISTRIBUTION

U WALL TEMPERATURE

WALLS

NT BULKHEADS

NT NOZZLE WALLS

NT POROUS WALLS

NT THICK WALLS

NT THIN WALLS

NT WIND TUNNEL WALLS

Resonant and nonresonant sound transmission through cylinder walls, using statistical analysis 02 p0260 A72-12374

Wall effects on deflagration, combustion rate, and self and hot-point ignition temperature and delay 11 p1747 A72-26789

Wall contour effect on shock wave shape, comparing Whitham theory with schlieren photographs from shock tube tests 15 p2219 A72-32595

Plastic composite container cylindrical wall fabrication by two stage procedure combining radial and cross winding of glass fiber rovings 16 p2398 A72-33305

WALSH FUNCTION

Walsh functions, sequence and Gray codes computations on finite binary n-tuple domain 03 p0326 A72-14248

Spectral analysis with sinusoids and Walsh functions, using Rademacher function 05 p0628 A72-16564

Relations between Haar and Walsh/Hadamard transforms to yield orthogonal transforms with common fast algorithm 15 p2264 A72-32081

Performance criteria for transform data coding schemes evaluation under computational constraints, presenting numerical examples for Fourier, Walsh, Haar and Karhunen-Loeve transforms 16 p2366 A72-33214

Methods using Walsh functions for multiplexing and transmitting signals 19 p2765 A72-37942

Dyadic correlation function method for structured radar signal sidelobe suppression during reception, noting Walsh function role 21 p3020 A72-40901

Radiation of EM waves with Walsh-function time variation - Preliminary results. 21 p3020 A72-40902

WARFARE

NT ANTISUBMARINE WARFARE

NT CHEMICAL WARFARE

NT COMBAT

Remotely manned vehicles /RMV/ application in aerial warfare, considering antiaircraft defenses lethality increase, equipment costs and role of man during combat mission 13 p1896 A72-28451

WARMING

U HEATING

WARNING DEVICES

U WARNING SYSTEMS

WARNING SIGNALS

U WARNING SYSTEMS

WARNING SYSTEMS

Microwave oscillator detector Gunn diode as inexpensive alarm device for Doppler radar application 01 p0028 A72-10642

Pilot collision warning indicator performance in terminal area traffic, using computer fast-time simulation for traffic model 01 p0098 A72-11134

Alerting light and audio signals for aircraft pilots, considering implications for aircraft design 01 p0021 A72-11291

FAA activity in collision avoidance system and pilot warning instrument areas 02 p0256 A72-12379

Flight display systems current state and future developments, discussing dual attitude indicators and automatic chart systems CRTs, engine displays and malfunction warning systems 03 p0357 A72-13423

Collision avoidance systems and pilot warning instruments, minimizing cost by pilot detection, evaluation and avoidance execution 04 p0545 A72-14823

Incipient wing stall detection by unsteady pressure monitoring via flush-mounted microphones, discussing flow patterns on models 07 p0908 A72-19093

Aircraft midair collision prevention in dense air traffic environments, suggesting problem solution based on proximity warning system 08 p1204 A72-21090

Aircraft hazard detection and warning system selection criteria 08 p1109 A72-21561

Vibrotactile warning device effectiveness under auditory and visual loadings, investigating reaction time and errors number 08 p1126 A72-21569

Automation in planning and execution of flights, considering navigation, communication, flight instruments monitoring, control/stabilization and warning systems 09 p1269 A72-22780

Collision avoidance systems requirements and criteria, evaluating Eros time frequency and Secant interrogation-and-reply systems 09 p1349 A72-22822

Eros and ATA /Air Transport Association/ time-frequency collision avoidance systems, discussing synchronization methods, back-up mode operation, threat computation and displays 09 p1349 A72-22823

C-band pulse beacon ranging system for collision avoidance, detailing interrogation, response and system test modes 09 p1349 A72-22908

Pilot warning systems for visual midair collision avoidance, noting reaction to imminent threats, scanning patterns and display sector size effects [SAE PAPER 720312] 11 p1583 A72-25576

Stall warning system for general aviation aircraft, using signal discriminator for rough or gusting air [SAE PAPER 720331] 11 p1630 A72-25592

Pulse operated multichannel annunciator system for pilot warning of aircraft systems malfunctions, describing circuit design [SAE PAPER 720333] 11 p1630 A72-25593

Altitude information warning devices and systems, discussing requirements and performance and qualification tests [SAE ARP 1061] 11 p1632 A72-26032

Head-up omnidirectional two dimensional auditory display device for visual detection facilitation in aircraft collision avoidance systems 12 p1777 A72-28327

Probability functional formulas for quasi-determinate signal on unsteady normal noise background for use in false alarm and correct detection 15 p2195 A72-31664

Worldwide distress alarm, identification and position location system for downed aircraft, discussing GRAN feasibility tests 15 p2272 A72-32214

SECANT collision avoidance system, describing operational principles and flight test results 16 p2421 A72-34137

Altimeters development history from Wright brothers to Boeing 747, discussing altitude alert systems providing aural and visual warnings to pilot 20 p2952 A72-39747

Midair collision prevention independent of ATC, discussing aircraft lighting, collision avoidance systems and proximity warning indicator 21 p3081 A72-40297

Boeing aircraft altitude alerting systems development and design to meet FAR 91-51 requirements, discussing retrofit programs and altimeter encoding 22 p3179 A72-42689

Detection of hazards associated with aerospace operations. 23 p3287 A72-43424

Midair collision prevention for Army aircraft. 24 p3422 A72-44645

SECANT midair collision avoidance system based on nonsynchronous microsec pulse transmission and receiving via randomly selected frequency, describing modular components and operating principles 24 p3422 A72-44647

Satellite relay and Omega navigation system for distress signal transmission and reception in global rescue alarm network serving ships, aircraft and spacecraft 24 p3467 A72-45134

WARPAGE

Warpage control of large Al alloy forgings machining of jumbo jet components, using packing and storage methods [SAE PAPER 710801] 01 p0074 A72-10280

Wing load distribution and induced drag control by warping, summarizing linear theory and wind tunnel test results 10 p1417 A72-24218

Equilibrium and stress resultant displacement equations of thin rings based on virtual work principle, stressing warping and twisting moments 23 p3351 A72-44101

WASHERS [CLEANERS]

Freon 30 bidistillate as washing liquid for flight vehicle hydraulic systems, discussing industrial methylene chloride purification 11 p1675 A72-26818

WASHINGTON

Lava tubes of the Cave Basalt, Mount St. Helens, Washington. 19 p2790 A72-38296

WASPALOY

Waspaloy sheet creep rupture time dependent sensitivity to sharp-edged notches at 1000-1400 deg F, optimizing smooth and notched specimen yield strengths [ASME PAPER 71-WA/MET-3] 05 p0670 A72-15906

WASTE DISPOSAL

Food ration effect on metabolite elimination rate in humans wearing isolation garment at rest or performing physical labor 05 p0622 A72-16644

Catalytic oxidation of gaseous products formed during thermal treatment of human wastes, considering hopcalite, Cu-Cr, Cu-Co, Pt and Pd 05 p0622 A72-16646

Aerospace waste and water management technologies for community and household applications 06 p0769 A72-18617

Space and atmosphere contamination by industrial wastes, aircraft and spacecraft exhaust and radioactive waste disposal, considering legal safeguards 07 p1104 A72-19466

Reliability design for airborne ecological system for jumbo jets, discussing toilet flushing and multiple server queueing model 10 p1429 A72-23999

Human waste management system evaluation in zero gravity flight tests, presenting design concept for collection by air flow technique 15 p2189 A72-31825

Space shuttle waste collection system development, discussing human-interface requirements, zero gravity effects and operational considerations [ASME PAPER 72-ENAV-13] 20 p2896 A72-39164

Development of a spacecraft wet oxidation waste processing system. [ASME PAPER 72-ENAV-3] 20 p2896 A72-39174

Dry incineration of wastes for aerospace waste management systems. [ASME PAPER 72-ENAV-2] 20 p2896 A72-39175

Some transport techniques for liquid human wastes and wash water under space flight conditions 21 p3006 A72-40436

Transportation of radioactive waste-materials into the sun. 24 p3450 A72-45184

Detection of waste water effluents and of their surface spread in the English channel, the North sea and the Baltic sea, through determination of the surface temperature of the sea by means of infrared air pictures taken by satellites 24 p3398 A72-45223

WASTE UTILIZATION

Ten mlb concentric tubes biowaste resistojet thrust performance for hydrogen, water, methane, carbon dioxide and biopropellant mixtures, discussing vibration, shock and acceleration tests [SAE PAPER 710769] 01 p0116 A72-10263

Biowaste resistojet propulsion system development program, discussing design, propellant management and control subsystems [AIAA PAPER 72-448] 11 p1707 A72-26185

Computer program for biowaste resistojet nozzle performance prediction, taking into account viscous effect at low Reynolds number [AIAA PAPER 72-450] 11 p1708 A72-26187

High temperature biowaste resistojets with electrically conducting ceramic heaters, discussing lifetime and space station power systems adaptability [AIAA PAPER 72-454] 11 p1708 A72-26190

Water and waste management subsystem design for a space station prototype. [ASME PAPER 72-ENAV-8] 20 p2896 A72-39169

Compression distillation unit design and development for integrated water and waste management system onboard spacecraft, describing reliability and performance tests [ASME PAPER 72-ENAV-1] 20 p2897 A72-39176

System design of a near-self-supporting lunar colony. 24 p3388 A72-45192

Spacecraft food synthesis, using carbon dioxide and water from chemically regenerated human metabolic and waste products 24 p3376 A72-45277

WASTES

NT HUMAN WASTES

NT METABOLIC WASTES

NT RADIOACTIVE WASTES

NT SEWAGE

NT URINE

WATERS

U CLOCKS

WATER

NT COLD WATER

NT GROUND WATER

NT HEAVY WATER

NT SEA WATER

D region positive and negative ion chemistry review, noting dominant roles of water ion clusters, NO cation and hydrates 02 p0219 A72-11979

Water absorber lateral scattering effect on absorbed dose from 400 MeV neutron and proton beams [CERN-71-16] 02 p0162 A72-12062

Absorbed doses at various depths in water target exposed to charged pions, muons and electron beams, using Monte Carlo program [CERN-71-16] 02 p0162 A72-12063

Acoustic wave excitation in water droplet with giant pulse radiation from Q switched laser, noting diffraction effects on laser power density requirement 03 p0367 A72-13372

Wind velocity spatial derivative determination by radar observation of signal reflection from atmospheric water particles 03 p0383 A72-13483

Water radiolysis within sealed Al capsules in nuclear reactor, calculating pressure rise due to water decomposition via predictive models derived by multiple regression analysis 04 p0546 A72-14429

Spore survival in dry heat sterilization as function of water activity, indicating entropy-molecular stability relationship 04 p0475 A72-15259

Water molecules absorption lines in sunspots umbral near IR spectrum, noting improved spectrometric apparatus 05 p0719 A72-16515

Normal diathermancy coefficient determination from quartz and distilled water spectral transmittance data, applying to diathermic cooling system design 05 p0751 A72-17071

Hydrodynamic characteristics of freely falling water droplets in air, establishing relationships among Reynolds, Laplace and Bond criteria 07 p1030 A72-19854

Water effect at epoxy resin-steel interface on adhesive bond strength as function of vitrification temperature 08 p1196 A72-21863

Supercooled water drops freezing by contact nucleation with AgI and silicate particles, determining effective temperature in updraft wind tunnel experiments 09 p1345 A72-22445

Thin liquid surface water film cooling tests for mass loss under simulated reentry heating and shear conditions 10 p1563 A72-24648

Ion dipole capture cross sections at low ion and rotational energies compared with reaction cross sections for ammonia and water parent-ion collisions 11 p1692 A72-26014

Wind velocity spatial derivative determination by radar observation of signal reflection from atmospheric water particles 11 p1682 A72-26253

Isochoric heat capacity peaks of water and argon near boundary in two phase region at critical state 11 p1747 A72-26964

Venus atmosphere IR synthetic spectra of carbon dioxide band and water line formation for isotropic scattering, comparing with terrestrial clouds 13 p2040 A72-29410

Russian book - Water in the universe 19 p2789 A72-37743

Six-month test program of two water electrolysis systems for spacecraft cabin oxygen generation. [ASME PAPER 72-ENAV-5] 20 p2896 A72-39172

Light attenuation coefficient measurement in water of various turbidity with AR and Kr lasers, interpreting results by Mie scattering theory 20 p2931 A72-39270

Temperature effects on water refractive index from normal incidence IR spectral reflectance measurements 21 p3012 A72-40150

Cloud liquid water content measurement via digital radar system, presenting two dimensional display of storm system characteristics 21 p3077 A72-40250

Cross polarizing effects of a water film on a paraboloid reflector at microwave frequencies. 21 p3027 A72-40375

Hydroxyl and water radio sources scale and geometry constraints placed by interstellar maser gain saturation relation to emission solid angle 21 p3062 A72-40565

The state of water in muscle tissue as determined by proton nuclear magnetic resonance. 24 p3371 A72-44774

Classical calculations of H2O rotational excitation in energetic atom-molecule collisions. 24 p3427 A72-45309

WATER BALANCE

Prolonged jet flight effect on passenger interstitial and intracellular fluid volumes from plasma, extracellular and total body water measurements, noting dehydration and foot swelling 06 p0767 A72-17866

Water loss replacement effect during rest and exercise in high temperature environment thermoregulation experiment 15 p2185 A72-31449

Gas induced osmosis as factor in pulmonary homeostasis, showing differential water retention in lungs ventilated with normoxic nitrous oxide compared with air 17 p2506 A72-35970

Relationship of sodium deprivation to +Gz acceleration tolerance. 24 p3377 A72-45653

WATER CONSUMPTION

Posthypoxic thirst and relative dehydration of rats after return from hypoxia to normoxia, measuring body weight and water intake 02 p0165 A72-12835

Influence of thermal, osmotic, and chemical stimulations on food and water intake 17 p2504 A72-35016

WATER CONTENT

U MOISTURE CONTENT

WATER COOLED REACTORS

Reactor core length, externally configured thermionic converter. 17 p2495 A72-34589

WATER CURRENTS

NT OCEAN CURRENTS

WATER FLOW

Disk pump driven fluid layer device for density stratified water channel flow measurements, using hydrogen bubble technique 04 p0509 A72-15118

Test facility for vibrations damping study of structural elements in water flow based on frequency and amplitude measurement at various flow conditions 06 p0796 A72-18364

Hydrodynamic flow parameters in laminar incompressible water boundary layer on heated plate, noting plate surface heating effect on velocity profile 07 p0968 A72-19766

Critical discharge regimes of two phase steam/water mixture flow from nozzles, using counterpressure effect 11 p1619 A72-26674

Plane unsteady potential isentropic gas flow equations solution interpreted as shallow water motion over horizontal bottom 13 p1893 A72-28717

The physically defined flame and its representation in the water model 18 p2656 A72-36242

Forced convection heat transfer from cylinders to water in cross flow, quantifying method of accounting for fluid property variation 19 p2881 A72-38397

Numerical gas dynamic calculations by difference method with two moving curve families, noting water mass impact on plane solid wall 19 p2789 A72-38851

The friction drag factor for an unsteady motion in tubes 20 p2913 A72-39392

Water film formation and breakdown during motion over solid surfaces, predicting flow rate difference due to contact angle hysteresis 21 p3085 A72-41178

Plane unsteady potential isentropic gas flow equations solution interpreted as shallow water motion over horizontal bottom 22 p3165 A72-42094

A gradient method of expanding a group data handling method to new plants not studied by experiments 22 p3162 A72-42242

Waterways outfall detection from color and IR color aerial photography, describing photointerpretation technique 22 p3181 A72-43197

Streamflow forecasting project to assess feasibility of air and spaceborne remote sensed data acquisition application to watershed hydrological behavior prediction 24 p3398 A72-45215

WATER INJECTION

Aircraft gas turbine engine emission reduction, showing nitrogen oxide control with water injection [ASME PAPER 71-WA/GT-9] 05 p0704 A72-15902

Heat transfer in water droplets and its role in the calculation of highly stressed injection coolers [DFVLR-SONDDR-196] 20 p2911 A72-39075

WATER INTAKES

Spinal cord heating and cooling effects on body temperature, respiratory and heart rates and arterial blood pressure, investigating feeding and drinking behaviors 22 p3150 A72-42672

WATER JETS

U HYDRAULIC JETS

WATER LANDING

Splash detection radar digital signal processing by off-line computer using wideband video recorder 02 p0178 A72-12399

Parachute systems and flotation gear used to recover sounding rocket payloads and components after water landings 15 p2320 A72-31691

WATER LOSS

Heat transfer for water at pressures near atmospheric in wicks formed of stainless steel screen layers, obtaining steady and maximum evaporation rates [ASME PAPER 71-WA/HT-12] 05 p0744 A72-15872

Weight loss due to respiratory tract evaporative water loss during exercise, from humidity change, ventilatory exchange and oxygen uptake data 11 p1586 A72-26613

Water loss replacement effect during rest and exercise in high temperature environment thermoregulation experiment 15 p2185 A72-31449

Tectonic dewatering and strain in the Michigamme Slate, Michigan. 18 p2686 A72-36223

Effect of activity and temperature on metabolism and water loss in snakes. 22 p3144 A72-42669

WATER MANAGEMENT

Environmental analysis of Lake Tahoe Basin from small scale multispectral aerial imagery, discussing color enhancement usefulness for interpretation and management of natural resources 02 p0210 A72-11800

Aerospace waste and water management technologies for community and household applications 06 p0769 A72-18617

Water and waste management subsystem design for a space station prototype. [ASME PAPER 72-ENAV-8] 20 p2896 A72-39169

WATER POLLUTION

Aluminum vacuum furnace fluxless brazing process, eliminating flux entrapment, postbrazing cleaning and water pollution 01 p0074 A72-10281

Microwave emission characteristics of oil slicks, showing dependence on oil type, film thickness and sea state

[AIAA PAPER 71-1071] 01 p0057 A72-10533

Synthetic aperture radar application to oil spill detection and monitoring for ocean surface, demonstrating feasibility

[AIAA PAPER 71-1072] 01 p0057 A72-10534

Remote airborne sensors for sea water oil pollution surveillance in near UV, thermal IR and microwave regions

[AIAA PAPER 71-1073] 01 p0057 A72-10535

Sky light polarization, cloudiness and view angle effects on oil remote detection over water surface, describing passive radiometric techniques

[AIAA PAPER 71-1075] 01 p0057 A72-10536

Aerial multispectral scanners and ground data stations for water quality measurements and pollution abatement

[AIAA PAPER 71-1096] 01 p0067 A72-10545

Rapid water pollution assessment by airborne chlorophyll measurement using differential, correlation and IR radiometers

[AIAA PAPER 71-1097] 01 p0058 A72-10546

Water quality monitoring by radiative transport equation for reflectance measurements of laser light scattered from turbid water polluted with absorber and scatterer particles

[AIAA PAPER 71-1098] 01 p0058 A72-10547

Laser fluorosensor for remote environmental probing, considering applications to oil slick mapping, locating lignin sulphate pollution sources and hydrologic monitoring of tracer dye dispersal

[AIAA PAPER 71-1121] 01 p0080 A72-10559

Water depth attenuation coefficients and bottom reflectance characteristics from large area multispectral scanner measurements for discharge and concentrations monitoring

02 p0211 A72-11812

Oil slicks aerial photographic and multispectral scanner investigation, discussing detection effectiveness of UV, blue, green and IR imagery

02 p0226 A72-11829

Oil spills remote detection by multispectral photography, IR scanner imagery and microwave radiometry

02 p0226 A72-11830

Microwave and IR radiometer surveillance of oil spills, discussing sources tracking, sea surface oil volume and flow rate determination and terminal location prediction

05 p0658 A72-16599

Buffalo photographic aircraft for oil slick remote sensing, using aerial cameras and thermal IR scanner

05 p0658 A72-16600

Airborne optical detection of oil on water based on reflected sunlight, investigating contrast and absorption bands

05 p0658 A72-16689

Remote sensing of oil pollution on water by laser induced fluorescence, using airborne spectroscopy

[AIAA PAPER 71-1076] 07 p0981 A72-18822

Multiple laser light scattering from turbid medium, relating reflectance to polluted water parameters for aerial photographic surveillance

12 p1826 A72-27948

New York-New Jersey megalopolis offshore jetport feasibility, considering noise, air-water pollution, land conservation, cost, etc

13 p1938 A72-28792

Airborne remote sensing missions and instrumentation to investigate Penobscot River water ecology for thermal, chemical and solid pollutants

15 p2221 A72-31252

Oil spills remote sensing in marine environment, using laser excited fluorescence for detection, identification and quantification

15 p2251 A72-32623

Remote sensing system for oil pollution spectral signature properties, analyzing UV, IR, visible light, radar and microwave data

15 p2242 A72-32624

Detection of waste water effluents and of their surface spread in the English channel, the North sea and the Baltic sea, through determination of the surface temperature of the sea by means of infrared air pictures taken by satellites

24 p3398 A72-45223

WATER PRESSURE

Sonic boom induced pressure wave propagation and attenuation in water, comparing ballistic range measurements with theoretical predictions

[AIAA PAPER 72-654] 16 p2349 A72-34080

Filament wound cylindrical pressure vessel design and development for operation under cyclic-loaded high hydraulic pressure in underwater environment

19 p2877 A72-38166

WATER PURIFICATION

U WATER TREATMENT

WATER RECLAMATION

Water disinfection by Ag coated filters obtained by silver nitrate reduction with ascorbic acid, hydroquinone, formaldehyde and sodium tartrate activated carbon and ion exchange resin surfaces

05 p0622 A72-16637

Human urine regenerated water in various dilutions effect on fish and rat erythropoiesis

05 p0622 A72-16651

Closed loop life support systems, discussing manned ninety day test in space station simulator, Soviet experiments and water and oxygen regeneration

10 p1432 A72-24973

Reclaimed surface, ground and sewage water oxidizability measurement, studying oxidation kinetics of potassium bichromate distilled urine condensate admixtures

13 p1910 A72-29313

Urea determination in urine and water wastes for recycling process, using N-dimethylaminobenzaldehyde colorimetric method

13 p1910 A72-29325

Man, chlorella and wheat plant in life-supporting biological system, showing compatibility relative to gas and water exchange

15 p2189 A72-31826

An automated instrument for monitoring the quality of recovered water.

[ASME PAPER 72-ENAV-16] 20 p2895 A72-39161

Development of a spacecraft wet oxidation waste processing system.

[ASME PAPER 72-ENAV-3] 20 p2896 A72-39174

Compression distillation unit design and development for integrated water and waste management system onboard spacecraft, describing reliability and performance tests

[ASME PAPER 72-ENAV-1] 20 p2897 A72-39176

Sanitary-hygienic evaluation of the extraction method for water recycling in atmospheric moisture condensates

21 p3006 A72-40435

The problem of decontaminating and preserving drinking water in spacecraft water supply systems

24 p3375 A72-45121

WATER RECOVERY

U WATER RECLAMATION

WATER TEMPERATURE

Overheat resistance calibration of constant temperature hot-wire anemometers at low velocities in water with variable temperature

[ASME PAPER 71-HT-9] 08 p1163 A72-20873

Gulf Stream surface front structure, temperature and salinity observation from ship, aircraft and satellite

11 p1620 A72-25348

Detection of waste water effluents and of their surface spread in the English channel, the North sea and the Baltic sea, through determination of the surface temperature of the sea by means of infrared air pictures taken by satellites

24 p3398 A72-45223

WATER TREATMENT

Vapor-liquid equilibrium analysis of water soluble volatile organic compounds in closed airtight systems by gas chromatography

13 p1910 A72-29326

Some transport techniques for liquid human wastes and wash water under space flight conditions

21 p3006 A72-40436

The problem of decontaminating and preserving drinking water in spacecraft water supply systems

24 p3375 A72-45121

WATER TUNNELS

U HYDRAULIC TEST TUNNELS

WATER VAPOR

Raman scattering from water vapor for Ar laser wavelengths in remote atmospheric humidity measurements

[AIAA PAPER 71-1085] 01 p0104 A72-10542

Atmospheric water vapor vertical distribution from satellite IR spectrometer measurements, noting effects, absorption coefficients and temperature profiles errors

01 p0095 A72-10831

Interstellar OH and water maser regions, deriving density, diameter and temperature

01 p0133 A72-11142

Micrometer particle formation by water vapor photolysis at 1500-1700 Å, noting particle production rate and implications to planetary atmosphere physics

02 p0220 A72-12207

Electrically charged low mobility droplet production by water vapor condensation on to gaseous ions from aircraft static discharger

02 p0231 A72-12556

Vapor bubble growth on heated surface with random temperature distribution and liquid microfilm for water and boiling potassium

02 p0303 A72-12862

Dissociative recombination coefficients of water vapor and nitric oxide in determining D region electron densities

03 p0347 A72-13389

Absorption effects of dimers of water molecule in atmosphere, using spectroscopic and maser measurements

03 p0348 A72-13400

Stratospheric water vapor concentration annual variability from regression analysis of monthly measurements initiated as IQSY program

03 p0385 A72-14148

Mars atmospheric water vapor observations, examining spectroscopic plates water line strengths at 8200 Å

04 p0569 A72-14497

Water vapor laser pumping by upper lasing level excitation through direct electron impact, explaining mechanism by model

[AD-735585] 04 p0529 A72-14587

Pressure broadened water vapor line shape resonance dispersion at 22 GHz, deriving expression for instrument induced deviation from Lorentzian behavior

04 p0552 A72-14891

Water vapor injection into stratosphere by thunderstorms from IR radiometric inference measurements on NASA jet laboratory

04 p0544 A72-15358

Water heat pipes transient thermal impedance, monitoring evaporator, vapor space and condenser temperature

[ASME PAPER 71-WA/HT-9] 05 p0743 A72-15869

Oxygen and hydrogen stable isotopes utilization for studying water vapor in precipitations, constructing meteorological model

05 p0684 A72-16793

Airborne or satellite-mounted millimeter wave radiometer for atmospheric water vapor determination noting accuracy advantage over IR measurement

06 p0814 A72-17589

Water vapor condensation in centered rarefaction wave arising in supersonic flow around apex of obtuse angle

06 p0799 A72-17911

Indirect reduction of vertical atmospheric water vapor profile from measured outgoing thermal radiation by regularization method

06 p0842 A72-18039

Surface layer humidity correlation to height of atmosphere emitting in IR spectral region, determining water vapor content by recording earth radiation angular distribution

06 p0808 A72-18046

Total atmospheric water vapor content from solar radiation absorption observation at millimeter wavelengths

06 p0817 A72-18091

Balloon-borne radiometer-sonde measurement of stratospheric downward emission in absorption spectral region of water vapor rotational band

07 p0982 A72-19105

CW gas laser operating in far IR, discussing water vapor excitation by dc discharges

07 p0946 A72-19961

Ground based Raman laser backscatter measurement of stratospheric water vapor content, noting 1 ppm accuracy

08 p1161 A72-21825

Stratospheric ozone photochemistry through nitrogen oxides and hydrogen compounds reactions, noting controlling effect of water vapor

09 p1298 A72-22674

Pressure effect on combustion rate of Mg particles in water vapors

09 p1411 A72-22887

Steady state model for Venus atmosphere water vapor loss, noting hydrogen and oxygen escape due to dynamic outflow of constituents from upper region

09 p1393 A72-23657

Radiational cooling and heating rates for ice and water clouds based on radiative divergence measurements with allowance for latent load

09 p1348 A72-23660

Thermal conductivity measurement for gases and gas mixtures with water vapor, describing methods and results

09 p1413 A72-23689

Atmospheric water vapor submillimeter absorption lines in high resolution radiation transmission measurements with Froome type plasma metal junction device

10 p1472 A72-24175

Martian atmosphere water vapor detection and mapping during Viking missions, discussing experimental approach and spectrometer choice

10 p1539 A72-24378

Viking Mars Orbiter IR thermal mapper (IRTM) to study surface kinetic temperature, thermal balance, anomalous cooling regions, ground frosts and water vapor

10 p1539 A72-24379

Neutral atmosphere effects on lower ionosphere, considering D region atomic oxygen, nitric oxide and water vapor and electron density distributions

10 p1474 A72-24712

Airborne IR radiometric measurements of upward vertical radiance from tropical sea surface at 10-12 microns, noting absorption coefficient dependence on water vapor

10 p1474 A72-24747

Time resolved gain in water and water-gas mixtures as function of composition and excitation current, considering relaxation rate in pulsed water vapor laser 11 p1691 A72-25302

Atmospheric water vapor measurements by Raman backscatter from pulsed laser radar, comparing with meteorological tower data 11 p1680 A72-25347

Venus lower atmosphere enhanced microwave attenuation explained by water vapor and droplet layer, calculating mass density distributions 11 p1724 A72-26762

Overlap emissivity of atmospheric carbon dioxide and water vapor for computer simulated earth surface temperature calculations 11 p1628 A72-26986

Intracavity gas cell for carbon monoxide laser oscillations restriction to lines coincident with atmosphere transmission bands, noting absorption by atmospheric water vapor 12 p1823 A72-27837

Radial temperature and water vapor concentration profiles of radiating combustion source from optical method, using IR band model 12 p1811 A72-27945

Upper atmosphere water vapor sources and sinks, discussing Hadley cell circulation, convective storm, stratospheric-tropospheric interchange, methane oxidation and volcanic activity 13 p1948 A72-28835

Residence time of water vapor and aerosols in troposphere and lower stratosphere, noting application to air pollution buildup by aircraft 13 p1991 A72-28836

Stratospheric subsonic and supersonic aircraft emission estimation for water vapor and nitrogen oxides 13 p1991 A72-28838

Turbulence effects on electron, ion, aerosol, water vapor and ozone concentration in atmospheric layers 15 p2222 A72-31395

Earth atmosphere water vapor mixing ratio profiles from relaxation method for full radiative transfer equation inverse solution 15 p2266 A72-32724

Barbados Oceanographic and Meteorological Experiment to compare synoptic scale-measured vertical vapor fluxes over tropical ocean 16 p2417 A72-33169

Water vapor condensation in jet turbulent mixing zone of confluent high velocity high temperature gas streams for finite axisymmetric nozzle 16 p2377 A72-33260

Apparent-actual size relation in astronomical masers for internal physical conditions of homogeneous spherical and tubular OH or water maser clouds 16 p2455 A72-33456

Fluctuations of water vapour content in the troposphere as derived from interferometric observations of celestial radio sources. 17 p2545 A72-34690

Spectral observations of Venus in the frequency interval 18.5-24.0 GHz - 1964 and 1967-68. 17 p2610 A72-35120

Stratospheric pollution by SST exhaust gases, discussing water vapor and nitrogen oxides effects on ozone concentration 17 p2597 A72-35327

Water vapor, CO2 and particulate effects on the atmospheric temperature profile. 17 p2549 A72-35636

Water vapor flux periodic and spatial variations from airborne measurements, confirming height variation of maximum spectral density wavelength for crosswind runs 18 p2706 A72-36632

Microwave celestial water-vapor sources. 18 p2729 A72-36990

Mars polar caps formation at aerographic latitudes, assuming water vapor condensation on ground and water presence in carbon dioxide snow 19 p2863 A72-38072

Influence of water vapor on the normal flame velocity of a methane-air mixture at high pressures 19 p2882 A72-38459

Environmental acceleration of fatigue-crack growth in a high-strength steel. 20 p2935 A72-39140

Development of a desiccant CO2 adsorbent tailored for shuttle application. [ASME PAPER 72-ENAV-11] 20 p2896 A72-39166

Integrated water vapor electrolysis oxygen generator and hydrogen depolarized carbon dioxide concentrator development. [ASME PAPER 72-ENAV-7] 20 p2896 A72-39170

Seasonal and latitudinal relation between Mars white clouds occurrence frequency and global water distribution, suggesting cloud composition as water vapor 20 p2968 A72-39241

Atmospheric window at 10-12 micron wavelength, investigating absorption coefficient of clear atmosphere water vapor 21 p3048 A72-40398

Calculation of the radiation of two plane isothermal layers of carbon dioxide and/or water vapor 22 p3242 A72-41884

Radiation absorption calculation for nonisothermal gas containing combustion products, noting approximation for water vapor radiation 22 p3243 A72-41885

Electron deposition in water vapor, with atmospheric applications. 22 p3171 A72-42420

WATER VEHICLES

NT AIRCRAFT CARRIERS

NT LIFEBOATS

NT SHIPS

NT SUBMARINES

NT TANKER SHIPS

NT UNDERWATER VEHICLES

Physical principles, design and operation of air cushion vehicles for passenger transportation over water 07 p0913 A72-20371

Aircraft and water vehicles mobile communications via stationary satellite, discussing optimum multiple access and repeater configuration [AIAA PAPER 72-565] 12 p1781 A72-27376

WATER WAVES

NT TIDAL WAVES

Sea waves energy spectra from optical Fourier analysis of ocean photographs under particular skylight irradiance 02 p0211 A72-11809

Microbaroms produced by ocean waves radiated in frasonic, noting dependence on upper atmosphere temperature and winds 09 p1348 A72-23656

Hovercraft heaving response to regular head or following seas, determining dependency on craft natural frequency and damping, wave frequency and cushion platform 14 p2071 A72-30254

Satellite anemometry for ocean waves and weather forecasting, discussing Skylab microwave radiometer-scatterometer potential design 15 p2221 A72-31239

Sea surface wind-caused waves spectral component phase velocity measurement method based on statistical treatment of synchronous continuous records of surface elevation 16 p2417 A72-33291

Internal waves in sheeted thermocline with finite discontinuities in density profile formulating eigenvalue problem as homogeneous Fredholm integral equation 16 p2386 A72-33573

Analytical investigation of normal shock waves in water near the thermodynamic critical point. 17 p2543 A72-35635

WATERPROOFING

Water damage in glass fiber-polyester resin composites, discussing fiber debonding, crack propagation and water resistance 11 p1675 A72-26950

WATERSHEDS

Streamflow forecasting project to assess feasibility of air and spaceborne remote sensed data acquisition application to watershed hydrological behavior prediction 24 p3398 A72-45215

WATTMETERS

Portable electronic wattmeter for nonsinusoidal waveform low power factor circuit measurement, discussing design, calibration and applications [IEEE PAPER 8,2] 03 p0332 A72-13757

WAVE AMPLIFICATION

Second order nongeostrophic effects on exponential amplification of two layer baroclinic wave system in uniform zonal current 14 p2127 A72-30342

Amplification of cylindrical electromagnetic waves reflected from a rotating body 23 p3262 A72-43307

WAVE ATTENUATION

NT ACOUSTIC ATTENUATION

NT RADAR ATTENUATION

NT RADIO ATTENUATION

NT SHOCK WAVE ATTENUATION

Modified Born approximation for electromagnetic backscattering cross section from turbulent plasmas, noting attenuation leading to saturation and cross-polarization 01 p0031 A72-10846

Nonlinear skin effects in gas discharge and semiconductor plasmas during electromagnetic wave propagation and dissipation, obtaining wave amplitude and carrier temperature dependence on reflection parameters 01 p0102 A72-10974

Tropospheric layer structures effect on long range vhf radio communication, calculating wave modes attenuation rate and electric field patterns 01 p0032 A72-11238

Gyroresonance plasma wave absorption in corona, investigating solar radio bursts fine structure 03 p0415 A72-12935

Propagation modes attenuation and phase shift of electromagnetic plane wave in superconducting coaxial cylindrical waveguide 03 p0321 A72-13170

Weak dissipation and damping of nonlinear long waves propagating in rotating fluids by Korteweg-deVries equation 04 p0513 A72-15329

Short waves damping or increasing in bounded thick waveguide with real or complex refraction index 04 p0492 A72-15446

Microwave spectrometer crystal current leveler for broadband video detector and rotary wave attenuator control 04 p0524 A72-15541

Attenuation characteristics of corrugated rectangular waveguides propagating dominant hybrid mode 05 p0638 A72-17076

Ion sound waves decay instability induced by large amplitude Bernstein mode in plasma 06 p0859 A72-17546

Wave propagation in single node clad glass fiber light waveguide, discussing fiber core minimum diameter and various loss mechanisms 06 p0825 A72-17773

Comb type slow wave structures properties outside passband, obtaining dispersion and field distribution expressions by electrodynamic analysis 08 p1135 A72-21738

Electron wave attenuation technique for current transit determination through semiconducting films with various crystal structures 09 p1284 A72-22209

Clear air turbulence association with rapid temperature change over Bahrain, suggesting convectionally induced internal wave dissipation in inversion layer as turbulence mechanism 09 p1346 A72-23424

Wide rectangular low loss metal waveguide with dielectric layer on opposite walls, noting attenuation based on eigenwaves 10 p1451 A72-24585

Initially sharp cylindrical pressure pulse propagation and stress wave attenuation in linear elastic fiber reinforced composites [AIAA PAPER 72-394] 11 p1730 A72-25415

Slow wave structures attenuation effect on dispersion characteristics from equivalent circuit representation as two terminal pair networks 13 p1926 A72-28376

Computerized simulation of single large amplitude whistler wave propagation in plasma, noting collisionless damping, oscillations and equilibrium 13 p2012 A72-29128

Surface waves generation and absorption by interdigital transducer with uniform finger spacing, discussing parallel equivalent circuit derived in weak coupling approximation 13 p1960 A72-29769

Enhanced damping of electrostatic wave primary mode due to combination scattering from plasma electron density oscillations 13 p2018 A72-29854

Nonlinear damping of potential monochromatic waves in inhomogeneous plasma, obtaining resonance particle distribution function 13 p1923 A72-29984

Design data of guided wave structures for electrooptical modulation, evaluating propagation wave numbers, attenuation rate, phase modulation rate and dispersion characteristic 15 p2246 A72-31667

Ultrasonic wave propagation in single crystals, discussing linear elastic wave attenuation, anisotropic interactions, particle displacement polarization and energy flux deviation 15 p2292 A72-31834

Turbulence and nonlinear thermal blooming effects as cause of refractive attenuation of laser beam intensities 15 p2249 A72-32160

Electromagnetic waves attenuation and phase velocity correction in polycrystals with anisotropic crystal distribution 16 p2365 A72-34013

Sonic boom induced pressure wave propagation and attenuation in water, comparing ballistic range measurements with theoretical predictions [AIAA PAPER 72-654] 16 p2349 A72-34080

One-dimensional wave pulses in steel-epoxy composites. [SESA PAPER 1945] 17 p2631 A72-34823

Stress pulse attenuation in cloth-laminate quartz phenolic. 17 p2571 A72-35284

Independent moving vibrational/acoustic/ source-induced wave losses during friction of two elastic bodies 18 p2696 A72-36966

Propagation and attenuation of harmonic waves in a viscoelastic circular cylinder. 18 p2738 A72-37070

- Longitudinal electric waves absorption in interstellar space due to electron-heavy particle collisions, considering photon rest mass 20 p2969 A72-39348
- Fresnel-like interference on an ion-wave decay in a plasma. 21 p3089 A72-40200
- Nonexistence of ion acoustic waves and Landau damping driven electrostatically in an ideal Q machine. 21 p3090 A72-40340
- Partial reflections from a thin parabolic layer in the lower D-region. 22 p3170 A72-42374
- Long wave oscillations attenuation by charged particle collisions in one- and two-component hot and cold Boltzmann plasma, using kinetic and polarization vector equations 23 p3318 A72-43325
- Wave attenuation during plasma propagation, discussing particle collisions, absorption effect on geometric optics and linear mode coupling in cold magnetized plasma 23 p3320 A72-43519
- Resonator polarization parameters effect on backwave attenuation in three and four mirror TW ring laser, noting colliding waves intensity dependence on polarization angle 24 p3411 A72-45505
- ### WAVE DIFFRACTION
- Diffraction theory of microwave holography, presenting computer aided imaging approach for alleviating optically reconstructed image distortion 01 p0068 A72-10707
- Radar backscatter time response waveforms for cube from If data and diffraction analysis 01 p0030 A72-10843
- Far field diffraction due to annular apertures of plane wave light rendered partially coherent by atmospheric turbulence 01 p0103 A72-11166
- Soviet book on electromagnetic fields and waves covering propagation in anisotropic media, waveguides and cavity resonators, diffraction interactions, etc 01 p0031 A72-11200
- Monochromatic electromagnetic field diffraction problems in homogeneous medium, presenting computer aided numerical analysis 02 p0171 A72-11690
- Iterative truncation error estimates in solution for plane wave diffraction by grating 02 p0171 A72-11738
- Gaussian electromagnetic wave beam diffraction and scattering problems solutions by optics formula application to beam transformation through optical systems 02 p0261 A72-12603
- Diffraction of plane electromagnetic waves of arbitrary orientation and incidence on triangular grid of cylindrical conductors 02 p0183 A72-12753
- Plane electromagnetic wave diffraction on magnetoactive plasma cylinder, using energy method and particle scattering model 02 p0183 A72-12754
- Time harmonic electromagnetic wave diffraction by thin conducting circular disk at different media plane interface, calculating induced surface current density and scattering cross section 03 p0322 A72-13237
- Longitudinal and transverse wave diffraction on cavities, investigating field pattern by dynamic photoelasticity method with flat models 03 p0452 A72-14131
- Stress intensity and plane dilatational wave diffraction in elastic material with finite crack 04 p0583 A72-14459
- Thin amplitude dynamic holograms diffraction efficiency, showing dependence on interference pattern, modulation depth, radiation intensity and material properties 04 p0521 A72-14659
- Kirchhoff diffraction theory of scalar and electromagnetic waves application to elastic media, discussing Huygens principle, elastic waves tensor potential and Fresnel and Fraunhofer diffraction 04 p0548 A72-14740
- Forced vibrations of elastic plate with infinite series of identical circular holes, discussing elastic wave diffraction and stresses at/near holes 04 p0587 A72-15017
- Nonstationary hydroacoustic wave diffraction at curvilinear rigid surface, deriving transfer function and radiation pressure 04 p0589 A72-15062
- Book on holographic technology covering fundamentals of holography and classical optics, diffraction theory, Huygens principle, lasers, illumination sources, holographic interferometry, etc 04 p0522 A72-15271
- Zwischenmedium concept application to electromagnetic diffraction problems in waveguides with one or more interfaces and continuity condition met by orthogonal expansion 04 p0488 A72-15378
- Asymptotic theory of diffraction at waveguide open end, using generalization by ray and parabolic equation methods 04 p0489 A72-15385
- Short wave asymptotic formulas for shadow zone of plane diffraction, discussing asymptotic solutions for field from point source 04 p0489 A72-15386
- Hf electromagnetic wave scattering and diffraction by smooth dielectric cylinder and sphere based on Lorentz excitation theory 04 p0490 A72-15397
- Conformal transformations applications to plane electromagnetic wave diffraction by infinitely conducting network, discussing energy distribution 04 p0490 A72-15410
- Plane wave diffraction by infinite strip grating, providing closed form solution by boundary value problem reduction to singular integral equation 04 p0490 A72-15411
- Electrodynamical theory of artificial dielectrics based on rigorous solution for diffraction on system scattering elements consisting of periodical gratings formed by thin metallic strips 04 p0490 A72-15412
- Plane electromagnetic wave diffraction on two cylinders with different radii, assuming infinite length and ideal conductivity 04 p0491 A72-15413
- Plane electromagnetic wave diffraction by periodic lattice of long finite conductivity cylinders with arbitrary electric radius 04 p0491 A72-15414
- Electromagnetic wave scattering and diffraction on lattice of dipole vibrators 04 p0491 A72-15415
- Numerical solution for diffraction on conducting finite and infinite lattice of cylinders with circumferential cross section 04 p0491 A72-15416
- Electromagnetic wave diffraction on infinite lattice of perfectly conducting arbitrary flat elements from numerical method, determining secondary field and strips current distribution 04 p0491 A72-15417
- Diffraction anomaly from infinitely extended strip grating solution by successive approximation technique combination with singular integral equation 04 p0491 A72-15418
- Electromagnetic traveling plane wave diffraction from arbitrary angled dielectric wedge, investigating surface currents on walls 04 p0491 A72-15420
- Plane harmonic electromagnetic wave diffraction by conducting parallel half planes in uniaxially anisotropic media 04 p0492 A72-15447
- Flow field due to diffraction of shock wave at wedge moving at supersonic speed 05 p0600 A72-16212
- Plane electromagnetic wave diffraction by infinite cylinder with unsteady impedance boundary conditions 05 p0627 A72-16409
- Asymptotic solution to short wave diffraction by convex cylinder, constituting geometrical optic expansion and caustic curves for illuminated and shadow region 05 p0628 A72-16411
- Ultrasonic diffraction grating for noninterference sampling of high power carbon dioxide laser beam, discussing diffraction profiles obtained from lasers operating in Gaussian and donut modes 05 p0669 A72-16608
- Amplitude holograms diffraction effectiveness increase by conversion to phase holograms through photoemulsion bleaching, evaluating various bleaching agents effectiveness 05 p0663 A72-16614
- Scintillation effects on synchronous satellite communications systems at 250 MHz in equatorial region, discussing diversity techniques and composite diffraction refraction theory 05 p0631 A72-16906
- [ALAA PAPER 72-178] Electromagnetic plane wave diffraction by infinite slit in screen with surface impedance, deriving field and transmission coefficient by asymptotic numerical solution 06 p0771 A72-17352
- Dual integral equations solutions to electromagnetic wave diffraction at plane conducting slotted screen 06 p0773 A72-17689
- Diffraction theory relevance to aerodynamic noise theory, considering If and hf behavior 06 p0847 A72-17767
- Thermoelastic waves diffraction steady state problems in multiply connected cylindrical and spherical surfaces, deriving scalar wave equations 07 p0194 A72-19986
- Plane oblique shock wave diffraction on wedge moving in homogeneous gas flow at supersonic speed, reducing boundary value problem to Hilbert problem 07 p0910 A72-20317
- Geomagnetic variations propagation theory for If electromagnetic and Alfvén waves diffraction at stratified earth in thin gyrotopical ionosphere 08 p1130 A72-20711
- Electromagnetic wave diffraction on arbitrary spheres, calculating scattering cross sections and attenuation by four water droplets 08 p1131 A72-20789
- Kirchhoff method application to asymptotic solution of plane wave diffraction on dielectric conical shells, calculating electromagnetic field vector 08 p1131 A72-20931
- Diffraction losses and corrections for lower order transverse modes and resonance conditions in optical resonators with cylindrical mirrors 08 p1133 A72-21371
- Strong shock wave diffraction from wedge reduced to Hilbert problem, noting nonregular refraction theory nonexistence 08 p1151 A72-21662
- Spherical wave functions in analysis of infinite systems of algebraic equations describing elastic wave diffraction in sequence of spherical cavities 08 p1246 A72-21706
- Mossbauer gamma radiation diffraction by Y-Fe garnet crystals with Mossbauer nuclei in magnetic and electric field nodes 08 p1217 A72-21767
- Soviet book on Riemann-Hilbert problem method in electromagnetic waves theory, covering wave diffraction, scattering and propagation, waveguides and open resonators 08 p1137 A72-22021
- Hologram diffraction efficiency for bleached high resolution photoemulsions for blue line of He-Cd laser 09 p1311 A72-22964
- Interferometry in volume holograms with recording of wave fronts by double exposure technique and reconstruction by diffraction 09 p1315 A72-23350
- Radiation pattern of spacecraft dipole antenna mounted on conducting finite length cone calculated by superposition of radiated and diffracted waves 09 p1282 A72-23524
- Shock wave propagation in ducts with abrupt area expansion, discussing vortices generation and wave diffraction and reflection effects on ducted flow 10 p1464 A72-23880
- Frequency splitting by diffraction at resonator mirrors of gas ring laser, deriving opposed waves lasing equations 10 p1490 A72-24045
- Nonlinear diffraction of weak shock waves near rigid wall with sharp bend, obtaining approximate solution by matched asymptotic expansion method 10 p1468 A72-24432
- Plane electromagnetic wave diffraction on ideally conducting convex body of large electrical dimensions, obtaining Maxwell equations asymptotic solution 10 p1436 A72-24577
- Electromagnetic wave diffraction by dielectric steps in waveguides, calculating microwave scattered field by modified residue calculus technique 10 p1451 A72-24593
- Eigenfunction transform investigation of wedge diffraction of scalar pulse wave in three space dimensions, analyzing Green function 11 p1591 A72-25359
- Far field diffraction of Gaussian light beam passing through ultrasonic cylindrical standing waves 11 p1687 A72-26052
- Superhigh frequency electromagnetic waves diffraction by conducting screen circular aperture with phase change by dielectric disk and multiple internal reflections, noting patterns and backscattering apparatus 11 p1597 A72-26371
- Russian papers on mathematical problems of wave propagation and diffraction theory, covering elastic and short waves and point sources 11 p1688 A72-26377
- Cylindrical elastic wave diffraction on semiinfinite screen, describing motion with displacement vector consistent with Lamé equation 11 p1688 A72-26380
- Point source wave field diffraction on nontransparent circular cone, using steepest descent method and integral transformations 11 p1597 A72-26385
- Electromagnetic cylindrical wave diffraction by linear emitter in parabolic cylinder with slots 13 p1917 A72-28709
- Orthogonalization method application to problems of diffraction on several bodies through reduction to integral equations 13 p1920 A72-29278
- Electromagnetic wave diffraction on ideally conducting homogeneous bodies of revolution with arbitrary complex permittivity and permeability, using variables separation method 13 p1920 A72-29279

- Opposing wave generation in gas ring laser with allowance for diffraction by finite apertures of cavity mirrors
13 p1970 A72-29678
- Sound transmission loss and diffraction measurements by combined correlation and Fourier techniques
13 p2006 A72-29768
- Acoustic shock wave diffraction at moving or static plate immersed in ideal gas
13 p1943 A72-30011
- Gravitational wave diffraction by liquid on surface of vertical circular cylindrical shells, determining velocity potentials
14 p2093 A72-30192
- Acoustic wave diffraction at fixed plate boundary, determining velocity field by inverting Volterra-type integral equations
14 p2070 A72-31016
- Physical interpretation of electromagnetic waves attenuation function HF singularity during diffraction over spherical surface, applying to short wave diffraction in tropospheric model
15 p2195 A72-31651
- Longitudinal shear crack propagation after stability loss in infinite elastic medium, discussing wave diffraction at edges
15 p2327 A72-31734
- Visual evaluation of concave diffraction gratings with high ruling frequency, noting Foucault knife edge test limitations due to image faults
15 p2238 A72-32155
- Elastic wave diffraction on multiconnected cylindrical or spherical regions in nonsymmetric elasticity theory, determining constants of series solution
15 p2330 A72-32290
- Plane electromagnetic wave diffraction on periodic arbitrary profile array, presenting near and far field asymptotic characteristics
15 p2202 A72-32660
- Antiplane shear wave diffraction by two coplanar Griffith cracks in infinite isotropic homogeneous elastic medium
16 p2464 A72-32919
- Elastic wave diffraction by rigid ellipsoid, deriving scattering cross section for incident P wave from integral equation solution
16 p2426 A72-33659
- Book on basic acoustics covering mathematical methods, diffraction phenomena, statistical theory of signal processing, wave acoustics, membrane sound radiation, music, source array theory, etc
16 p2427 A72-33973
- The behavior of electromagnetic fields at edges.
17 p2513 A72-34357
- Diffraction of electromagnetic waves by a two-dimensional aperture with arbitrary cross-sectional shape.
17 p2514 A72-34385
- Diffraction of a plane electromagnetic wave on an anisotropic half-plane in free space and in a plane waveguide
17 p2515 A72-34828
- Averaged boundary conditions for a grid consisting of nonparallel and nonrectilinear conductors positioned on a nonplanar surface
17 p2529 A72-34830
- Application of the impedance treatment to diffraction problems for a rectangular waveguide
17 p2529 A72-34848
- Solution to a boundary value problem in the theory of diffraction of electromagnetic waves at a circular hole in a plane screen between two media
17 p2518 A72-35724
- Two sided error estimates for electrodynamic impedance, admittance and scattering matrices in diffraction theory
18 p2657 A72-36104
- Simplified method of calculating microwave diffraction loss over spherical earth.
18 p2660 A72-36517
- Diffraction by an aperture between two wedges.
18 p2712 A72-36938
- Diffraction and potentials of multilayers
18 p2736 A72-37003
- Bending waves diffraction and scattering by mass impedance loadings of infinite plane plate, considering point load and semiinfinite rib arrays
18 p2739 A72-37203
- Use of amplitude filter to improve the partially space coherent diffraction of a defocused circular aperture.
19 p2833 A72-37402
- A note on the low frequency diffraction of elastic waves by a Griffith crack.
19 p2870 A72-37414
- Geomagnetic variations propagation theory for LF electromagnetic and Alfvén waves diffraction at stratified earth in thin gyrotropic ionosphere
19 p2765 A72-38339
- Application of dual integral equations to the problem of electromagnetic wave diffraction by a thin conducting ribbon
19 p2766 A72-38256
- Paraxial electromagnetic wave packets diffraction on thin conducting periodic structures and dielectric plate, noting packet width and phase front curvature changes
19 p2767 A72-38653
- Plane and cylindrical electromagnetic waves diffraction on infinitely long cylindrical bodies, calculating induced currents, diffraction patterns and near fields
19 p2767 A72-38654
- Plane wave diffraction in a plane waveguide array with protruding dielectric plates
19 p2768 A72-38655
- Plane TE polarized electromagnetic wave diffraction on infinite conducting cylinder in nonhomogeneous medium, calculating far field diffraction patterns
19 p2768 A72-38656
- Short-wave asymptotic representation of the solution to the problem of diffraction by a circular disk
19 p2769 A72-38849
- Method of characteristics for nonlinear equations of perturbed motion of fluid near contact point between shock and diffraction waves
20 p2912 A72-39023
- Plane electromagnetic waves diffraction at arbitrary orientation and incidence on triangular grid of cylindrical conductors
20 p2902 A72-39059
- Plane electromagnetic wave diffraction on magnetoactive plasma cylinder, using energy method and particle scattering model
20 p2902 A72-39060
- Unstable resonator theory with geometrical optics and diffraction approximation, applying to laser mode selection and beam divergence reduction
20 p2932 A72-39501
- Diffraction of a laser beam by domains in yttrium iron garnet.
20 p2933 A72-39521
- On diffraction and focusing in anisotropic crystals.
20 p2961 A72-39779
- Radiometry error analysis for diffraction at radiation beam limiting screens, calculating corrections for circular source and detector
21 p3050 A72-40149
- Main-reflector-rim diffraction in back direction.
21 p3032 A72-40632
- Crack tip vicinity stress generated by plane transient tension-stress wave diffraction, examining ductility effects on fracture modes
21 p3117 A72-40672
- Diffraction of plane waves by a strip - Exact and asymptotic solutions.
21 p3016 A72-40839
- Partial differential equation solution for plane electromagnetic wave diffraction by infinite dielectric cylinder of arbitrary cross section
21 p3085 A72-41199
- Diffraction of electromagnetic plane waves by infinite slit perforated in a conducting screen with finite thickness.
21 p3022 A72-41267
- Correction of diffraction errors in acoustic-surface-wave pulse-compression filters.
21 p3034 A72-41464
- Diffraction of an elastic wave at a disk
21 p3127 A72-41669
- Diffraction of an electromagnetic wave by a noninfinitely conductive cylindrical object of arbitrary cross section
22 p3153 A72-41991
- Diffraction by an infinite corner reflector transversely loaded by concentric dielectric slabs.
22 p3159 A72-42301
- Power-law wavenumber spectrum deduced from ionospheric scintillation observations.
22 p3171 A72-42416
- Diffraction of plane electromagnetic wave at a corrugated dielectric surface
22 p3155 A72-42662
- Acoustic shock wave diffraction at moving or stationary flat plate immersed in ideal gas
22 p3206 A72-42732
- The diffraction of light by progressive supersonic waves: Oblique incidence of light. I - Approximate solution of the Raman-Nath equations.
22 p3207 A72-42852
- Investigation of stepped irregularities in coaxial lines with allowance for higher-order modes
23 p3263 A72-43447
- Diffraction of a plane wave by a ribbon grating in the case of short wavelengths
23 p3264 A72-43527
- Diffraction of an acoustic wave by a stationary plate
24 p3360 A72-44987
- Pressure and temperature change on the wall surface in strong shock wave diffraction.
24 p3391 A72-45047
- High resolution imagery with the large space telescope.
24 p3404 A72-45537
- Axial-radar cross section of finite cones by the equivalent-current concept with higher-order diffraction.
24 p3381 A72-45640
- Electromagnetic propagation from flanged waveguide, studying diffraction, radiation patterns and reflection/modal coefficients
24 p3381 A72-45642
- WAVE DISPERSION
- Periodic inhomogeneous plasma electrostatic waves, considering dispersion relation and longitudinal oscillations
01 p0107 A72-10141
- Real gas effects in atmosphere to make sonic bang shock wave full dispersion and thickness wide variations
02 p0154 A72-11972
- Electromagnetic wave propagation perpendicular to applied uniform magnetic field in relativistic plasma, deriving dispersion relation for stability criterion
02 p0264 A72-12024
- Plane wave intensity fluctuations behind random phase screen, discussing phase structural function relation to field statistical properties and fluctuation dispersion
02 p0181 A72-12590
- Spatial dispersion effects in crystal optics, obtaining dispersion law for normal waves in crystals via electromagnetic field tensor equations
04 p0548 A72-14739
- Pressure broadened water vapor line shape resonance dispersion at 22 GHz, deriving expression for instrument induced deviation from Lorentzian behavior
04 p0552 A72-14891
- Dispersion relation for MHD wave propagation through partially ionized magnetoplasma, discussing collision frequencies effects
04 p0556 A72-14943
- Magnetic latitude effect on wave dispersion in drifts and random movements of ionization irregularities in E region, suggesting charged particle precipitation role
04 p0518 A72-14964
- Electron beam interaction with bounded solid state plasma, deriving slow wave dispersion relations
04 p0561 A72-15080
- Cylindrical grid-like antenna in anisotropic compressible homogeneous plasma, obtaining magnetic field effects on wave dispersion by numerical solution
04 p0488 A72-15306
- Electromagnetic wave transformation at moving boundary discontinuity with reactive parameters in dispersive medium by Lagrangian field equations
04 p0489 A72-15388
- Boundary effects on light incoherent scattering by dispersing molecules, using quantum statistics
04 p0490 A72-15398
- Network formulations of electromagnetic fields in moving dispersive plasma media by equivalent parameter representation
04 p0490 A72-15400
- Blood viscosity and distributed external constraints and viscoelastic properties of vessels effects on wave dispersion and dissipation in arteries and veins, using membrane model
04 p0481 A72-15466
- Viscosity and constraints effects on wave dispersion and dissipation in blood vessels, comparing theory with experiments on dogs
04 p0481 A72-15467
- Dispersion equation derived for acoustic-gravity type natural modes in solar atmosphere
05 p0712 A72-15769
- Dispersion and energy characteristics of azimuthally asymmetrical waves in microwave logarithmic or arithmetical spiral antenna deposited on isotropic magnetodielectric layer
05 p0636 A72-16338
- Dispersion characteristics of laminated cylindrical dielectric waveguide in millimeter band, noting application to permittivity measurement
05 p0627 A72-16341
- Dispersion properties of drift waves in low-beta weakly collisional plasma in presence of ion acoustic or Langmuir waves parallel to magnetic lines
05 p0698 A72-17019
- Dispersion relations for frequencies near first two harmonics of perpendicular magnetosonic waves in relativistic anisotropic plasmas
05 p0698 A72-17020
- Dispersion relation for electrostatic plasma waves propagation at frequencies near electron cyclotron harmonics in warm magnetoplasma, determining refractive index curves
05 p0698 A72-17023
- Hall fields effect on interaction of MHD waves in inhomogeneous plasma, considering MHD wave dispersion
05 p0701 A72-17237
- Damping effect in discrete one dimensional nonlinear lattice model leading to weakly dissipative Korteweg-de Vries equation
06 p0838 A72-17301
- Linear dispersion relation for pressure gradient driven drift waves instabilities from ion and electron thermal conductivity effects in collisional plasma
06 p0857 A72-17529

- Plasma wave growth from large diameter electron beam interaction with quiet collisionless unmagnetized discharge plasma, measuring linear dispersion properties 06 p0858 A72-17539
- Resonant frequency, phase velocities and dispersion curves for wave propagation in isotropic elastic cylinders 06 p0895 A72-17854
- Microwave dispersive line structures with nonlinear phase characteristics, considering use of empty waveguide segment near cut-off 06 p0785 A72-18312
- Metal clad dielectric slab waveguide for integrated optics, obtaining dispersion equation solution and propagation modes from simplified model 07 p0940 A72-19229
- Pulsar rotation and dispersion from polarization and pulse arrival time observations, calculating magnetic field components in path to pulsars 07 p1072 A72-19343
- Dispersion relation for uhf drift waves in nonuniform plasma with cold electrons drift through stationary ions, deriving plasma stability conditions 07 p1042 A72-19612
- Uniform asymptotic solution near wavefront of transient field propagation in inhomogeneous dispersive media [AD-745077] 07 p0946 A72-19800
- Electrostatic ion wave stability in electrogydynamic channel flow from approximate numerical solution of dispersion equations 08 p1211 A72-21305
- Comb type slow wave structures properties outside passband, obtaining dispersion and field distribution expressions by electrodynamic analysis 08 p1135 A72-21738
- Electromagnetic wave propagation along open rectangular dielectric waveguide, deriving dispersion equations for surface waves propagation constants 08 p1136 A72-21739
- Electrostatic plasma wave conversion into electromagnetic waves, calculating dispersion relation at all wavelengths for perpendicular propagation mode 08 p1137 A72-21989
- Spiral density waves in galactic model with differentially rotating interstellar gas and stars, deriving dispersion equation by frequency to wave numbers relation 09 p1384 A72-22517
- Phonon dispersion curves of bcc transition metals for normal lattice vibration modes 09 p1369 A72-22680
- Single- and multiphase theories of slowly varying nonlinear dispersive waves, noting stability solutions to large scale variations and shocks 09 p1351 A72-22942
- Modulated electromagnetic wave transmission in dispersive medium with cubic nonlinearity, discussing solitary wave and instabilities in two-wave interaction 09 p1352 A72-23475
- Plane stratified earth crust parameters determination from dispersion curve of Rayleigh surface waves fundamental tone 09 p1304 A72-23488
- Electromagnetic wave propagation perpendicular to magnetic field in two-component warm plasma, obtaining dispersion relations for transverse waves 10 p1520 A72-24350
- Periodic axisymmetric waveguide with complex structure, obtaining slow wave dispersion equation solutions 10 p1439 A72-24901
- Linear wave dispersion in homogeneous beam plasma system, considering pressure anisotropies generated by external magnetic field 10 p1524 A72-24927
- Trapped particle induced frequency shift in response of electrostatic wave to adiabatic and sudden excitations, obtaining distribution functions and nonlinear dispersion relation [AD-741547] 11 p1693 A72-25566
- Electrostatic resonances associated with maximum frequencies of cyclotron-harmonic waves at high and low latitudes, presenting dispersion curves and ray paths 11 p1624 A72-26400
- Bounded systems dispersion relations interpretation for plasma waves and instabilities on finite cylinders, with emphasis on end plate damping and axial current effects on Q machines 11 p1697 A72-26597
- Electromagnetic wave field effects on cold magnetoactive plasma potential oscillations, solving dispersion equation for sub-ion gyroscopic frequencies 12 p1849 A72-27066
- Ionospheric HF Doppler dispersion during 7 March 1970 solar eclipse, noting traveling ionospheric disturbance 12 p1801 A72-27157
- Multiple scale asymptotic method for nonlinear theory of dispersive periodic waves with slowly varying parameters, noting equations for irrotational motion of perfect relativistic fluid 12 p1843 A72-27170
- Cylindrical waveguide proper modes instability regions boundary calculation, determining dispersion characteristics and waves phase and group velocities 12 p1791 A72-27537
- Slow wave structures attenuation effect on dispersion characteristics from equivalent circuit representation as two terminal pair networks 13 p1926 A72-28376
- Dispersion properties of complex waves in shielded circular two layer waveguide 13 p1928 A72-28472
- Averaging variational Euler-Lagrange equation for nonlinear waves with dispersion in nonconservative system 13 p2003 A72-28774
- Nonlinearity effect on electron plasma wave dispersion relation, using numerical simulation and theoretical analysis by perturbation expansion and Hamilton variational principle 13 p2011 A72-29121
- Computerized calculation of wave dispersion curves for hot Maxwellian electron magnetoplasma, applying to upper hybrid and cyclotron frequencies 13 p2013 A72-29340
- Mathematical model for ionized plasma response to sinusoidal perturbations, calculating dispersive waves in MHD generators with working fluid of potassium seeded argon 13 p2014 A72-29372
- Dispersion equations for electron and ion cyclotron waves propagating perpendicularly to magnetic field in plasma 13 p2016 A72-29602
- Dispersion characteristics of ion-acoustic waves in positive gas discharge plasma column 13 p2019 A72-29912
- Dispersion equation derivation for HF electromagnetic waves in weakly ionized plasma in crossed fields, noting oscillation spectrum 13 p2020 A72-30048
- Nonlinear dispersive wave propagation problems singly and multiply periodic solutions, using perturbation and numerical approximation methods 14 p2130 A72-30227
- Closed form solutions for one dimensional nonlinear waves in strain rate-sensitive elastoplastic material, describing dispersed wave motion behind propagating shock front 14 p2164 A72-30298
- Waldman-Snyder equation application to sound absorption and dispersion in dilute polyatomic gases, presenting truncation procedure for perturbation function expansion in irreducible Cartesian tensors 14 p2131 A72-30673
- Pulsars distance computation, considering period-luminosity relationship and uncertainties inherent in dispersion measure (DM) method 14 p2159 A72-30738
- Nova Delphini evolution from metallic absorption lines observations before December 1967 maximum, obtaining dispersion variation with wavelength 14 p2159 A72-30741
- Plane and circular dielectric waveguides with thermal losses, considering transverse wave numbers behavior behind cut-off value and dispersion equations solution 14 p2086 A72-30797
- Multimode optical fiber waveguide theoretical model to predict pulse propagation dispersion for comparison with measurements 15 p2194 A72-31546
- Dispersion equation determining periodic structures natural modes propagation constants, using induced electromotive and magnetomotive forces method 15 p2195 A72-31655
- German monograph on wave expansion in gases with thermodynamic relaxation covering steady dispersed compression wave development in piston barrel for two component mixtures [DFVLR-SONDERR-184] 15 p2218 A72-31768
- Kinetic energy and momentum of longitudinal waves in plasmas, deriving Landau dispersion equation from conservation laws 15 p2285 A72-32272
- Plane wave dispersion and nonlocal elasticity equations linearization, demonstrating continuum treatment of lattice dynamics 15 p2330 A72-32445
- Lamb wave technique for bond strength testing of laminated or clad metal sheets, calculating displacement and stress dispersion and amplitude distribution for different modes 16 p2391 A72-33230
- Variational methods for dispersion relations and elastic properties of composite materials. [ASME PAPER 71-APMW-21] 17 p2623 A72-34302
- Alouette 2 plasma resonances observation near ionospheric electron cyclotron frequency harmonics, interpreting frequency shift as wave dispersion effects 17 p2546 A72-34692
- One-dimensional wave pulses in steel-epoxy composites. [SESA PAPER 1945] 17 p2631 A72-34822
- Dispersion equation of a corrugated elliptical waveguide 17 p2515 A72-34844
- Analysis of the dispersion equation of a dual-layer elliptic waveguide for critical conditions 17 p2529 A72-34844
- A modified Navier-Stokes equation, and its consequences on sound dispersion. 17 p2540 A72-35144
- Numerical calculation of energy storage, wave dispersion and propagation in waveguides of periodic resonator chains at high frequencies 18 p2657 A72-36100
- A photon rest mass and the dispersion of longitudinal electric waves in interstellar space. 18 p2728 A72-36922
- Growth rate and frequency dispersion characteristics of drift waves in an RF collisional plasma. 18 p2716 A72-36922
- Vlasov and Maxwell equations solution for surface waves dispersion in semiinfinite hot plasma 18 p2716 A72-36922
- Nature of sound dispersion in a plasma 18 p2717 A72-37177
- Wave propagation and dispersion in space-time periodic media. 18 p2663 A72-37200
- Dispersion curves of mixing mode between electrostatic and electromagnetic waves propagating perpendicularly to ambient magnetic field for hydrogen plasma with Maxwellian velocity profile 19 p2839 A72-37333
- Analysis of multiple hologram optical elements with low dispersion and low aberrations. 19 p2796 A72-37577
- Infrared dispersion of second-order electric susceptibilities in semiconducting compounds. 19 p2844 A72-37944
- Design of a system for automatic compensation of atmospheric dispersion 19 p2801 A72-37960
- Computer aided analysis of hologram optical elements for aberration and dispersion reduction and recording on thick media 20 p2922 A72-39033
- Electromagnetic wave dispersion in ionized cosmological medium for spatially flat Brans-Dicke cosmology 20 p2969 A72-39260
- Dispersion of flexural waves in circular cylindrical shells. 20 p2982 A72-39977
- Boundary conditions in the exciton absorption region. 21 p3096 A72-40177
- Magnetospheric propagation of auroral hiss with whistler mode dispersive properties, suggesting burst source locations and mechanisms 21 p3048 A72-40394
- Partial derivatives of dispersion curves for high modes of Love waves in a single-layered medium. 21 p3084 A72-40404
- Dispersion equations solved for electron and ion cyclotron waves propagating perpendicularly to magnetic field in plasma 21 p3091 A72-40631
- Linear and Alfvén waves propagation in incompressible beam-plasma systems, deriving dispersion law 21 p3092 A72-40949
- Dispersive waves in a slightly ionized nonequilibrium plasma. 21 p3092 A72-41233
- Eigenvalue numerical solution for dispersion relation and propagation characteristics of nonlocal drift waves in cylindrical plasma based on two fluid model. 21 p3093 A72-41499
- On the energy and momentum conservation laws for linearized electromagnetic fields in a dispersive medium. 21 p3085 A72-41499
- The effect of an interferometer selector on the spectrum of the characteristic frequencies of a dispersive resonator 22 p3176 A72-42244
- Asymptotic method for nonlinear wave systems of periodic structure 22 p3155 A72-42655
- Determination of the refractive index of air by a dispersion method based on the use of radio waves. 22 p3155 A72-42727
- Wave propagation in plasma modulated by external electric field, noting dispersion equation for coupled waves and instability conditions 22 p3212 A72-43110
- Use of the simulation method for the solution of dispersion problem for the propagation of symmetric magnetic waves in a rectangular waveguide filled with a nonhomogeneous plasma 23 p3263 A72-43434
- Effects of radiation trapping on mode competition and dispersion in the ring laser. 23 p3296 A72-43877

IR spectroscopy techniques based on Pfund triple-pass absorption cell, image slicer and achromatic doublet lenses, presenting graphs for prism dispersion design parameters

23 p3289 A72-43895

Circular waveguide in an anisotropic medium

23 p3264 A72-44156

Results of a numerical solution of a complex dispersion equation for the HE-sub 11 wave in a two-layer circular waveguide

23 p3273 A72-44214

Theory of dispersion in relation to light shifts.

24 p3409 A72-44921

Multicomponent plasmas with static magnetic field, deriving dielectric tensor and dispersion relation for wave propagation by linearization technique

24 p3428 A72-44967

Electromagnetic wave field effects on cold magnetoactive plasma potential oscillations, solving dispersion equation for sub-ion gyroscopic frequencies

24 p3431 A72-45719

WAVE DRAG

NT INTERFERENCE DRAG

Wave drag reduction by antisymmetric wing and body arrangement, discussing application to transport aircraft at supersonic speeds

05 p0602 A72-16534

WAVE EQUATIONS

NT DIRAC EQUATION

NT EIKONAL EQUATION

NT KLEIN-GORDON EQUATION

NT LAME WAVE EQUATIONS

NT SCHROEDINGER EQUATION

Uniform progressing wave expansion solution to wave equation for transition region boundary value problems

03 p0388 A72-12988

Detonation waves in gas mixtures, liquids and solids, presenting wave equations for real gases

03 p0456 A72-13687

Nonlinear ionization wave equation, calculating nonlinear response of unstable positive plasma column to weak pulse disturbance

03 p0399 A72-14346

Closed form solution of wave equation for sound wave scattering by rotating cylinders and spheres

04 p0550 A72-15567

One dimensional nonhomogeneous wave equations solution for linear and hyperbolic moving boundary conditions applied to resonator fields

05 p0627 A72-16407

Thermoelastic waves diffraction steady state problems in multiply connected cylindrical and spherical surfaces, deriving scalar wave equations

07 p1094 A72-19986

Generalized coupled thermoelasticity problem solution from wave equations for anisotropic plate in plane thermal stress state

07 p1094 A72-19987

Post bifurcation finite amplitude baroclinic instability, emphasizing wave vectors configuration with quadratic nonlinear interactions

09 p1347 A72-23654

Probabilistic derivation of quantum mechanics wave equations for Brownian motion and spatial-temporal diffusion

10 p1505 A72-24071

Wave equation derivation for electromagnetic and gravitational radiations in Schwarzschild field, obtaining third order corrections for scalar waves

10 p1514 A72-25168

Perturbation method for asymptotic solutions of initial value problems for hyperbolic wave equations with small nonlinearities

11 p1676 A72-25355

Perturbation method study of governing differential equations for wave reflection by periodic two-dimensional topography

11 p1685 A72-25358

Elastic body transverse impact against vibrating rectangular plate with allowance for rotatory inertia and shearing forces, using wave equation

11 p1732 A72-25532

Characteristic finite difference method for solution of two dimensional wave equation represented by one parameter differential systems

11 p1677 A72-25863

Wave equation for sound velocity propagation in suspensions based on mass and momentum balances

11 p1687 A72-26056

Waveguide point source field, analyzing short wave asymptotic properties of Helmholtz equation Green function in inhomogeneous medium

11 p1689 A72-26382

Surface waves propagation in inhomogeneous elastic body, deriving wave equations asymptotic solutions

11 p1689 A72-26384

Decoupled formulation of vector wave equation in orthogonal curvilinear coordinates, applying to ferrite-filled and curved waveguide of general cross section

11 p1607 A72-26995

Multiple scale asymptotic method for nonlinear theory of dispersive periodic waves with slowly vary-

ing parameters, noting equations for irrotational motion of perfect relativistic fluid

12 p1843 A72-27170

Antisymmetry principle for solving equation of elastic surface wave caused by waveguide

12 p1845 A72-27392

Colliding plane gravitational waves equations for linear polarization

12 p1845 A72-27409

Wave equations for electromagnetic wave propagation in electron-ion-neutral particle magnetoplasma, using macroscopic approach

12 p1852 A72-27850

Liapunov direct stability method extension to partial differential equations, using functional analysis and wave equation example

13 p1985 A72-28483

Wave equations and photon absorption cross section of relativistic electron in magnetic field, taking into account relativistic energies

13 p2002 A72-28647

Averaging variational Euler-Lagrange equation for nonlinear waves with dispersion in nonconservative system

13 p2003 A72-28774

Planetary wave description by linear difference equation for vorticity transport on hemisphere, considering Laplace operator error

14 p2099 A72-30260

Laser amplifier nonlinear properties by simplification of partial differential equations of amplitude and phase behavior, considering signal pulse deformation

14 p2111 A72-31113

One dimensional wave equation for stress wave propagating at variable velocity for case of monotone decreasing rate

15 p2327 A72-31738

Plane wave dispersion and nonlocal elasticity equations linearization, demonstrating continuum treatment of lattice dynamics

15 p2330 A72-32445

Exact solutions for plane thermoelastic and magnetothermoelastic wave frequency equations, determining specific loss extremum values

15 p2336 A72-32447

Spatial diffusion dynamics, spin, and the Pauli equation

17 p2573 A72-34193

Asymptotic solutions of inhomogeneous initial boundary value problems for weakly nonlinear partial differential equations.

17 p2574 A72-34342

The effect of axial boundary motion on pressure surge generation.

[ASME PAPER 71-WA/FE-15]

17 p2539 A72-34969

Wave-wave interactions due to scattering by electrons.

17 p2591 A72-35162

The mechanics of an organized wave in turbulent shear flow. II - Experimental results.

19 p2789 A72-38793

The mechanics of an organized wave in turbulent shear flow. III - Theoretical models and comparisons with experiments.

19 p2789 A72-38794

Large-scale instabilities of turbulent wakes.

21 p3044 A72-40116

Steady solutions of generalized Korteweg-de Vries equation for oscillatory solitary waves in dispersive media

21 p3089 A72-40197

Wave equation for infinitely long slotted screen in elliptic cylindrical coordinates, noting radiation pattern for phased antenna array of metallized hyperbolic striplines

21 p3028 A72-40507

Asymptotic solution of the wave equation with variable velocity and boundary conditions.

21 p3075 A72-40838

Electron processes in nonrelativistic electron streams against stationary ion background as wave packet envelope deformation in space and time

21 p3094 A72-41652

Time evaluation of discontinuity occurrence in solutions of boundary problems for second-order hyperbolic quasi-linear systems

22 p3198 A72-41912

Propagation of electromagnetic waves in a weakly ionized warm magnetoplasma.

22 p3155 A72-42991

Field components of coupled electromagnetic and electron acoustic waves in warm stratified plasmas, using first order wave equations and Heading embedded form

23 p3322 A72-44319

Asymptotic behavior of the solutions of the third external boundary value problem for a wave equation with two space variables

23 p3310 A72-44488

Rotating black holes - Separable wave equations for gravitational and electromagnetic perturbations.

24 p3439 A72-45014

Wave and polarization equations for short coherent light pulses transmission in linear amplifying and absorbing media, noting single pulse formation in lasers

24 p3410 A72-45420

WAVE EXCITATION

NT ACOUSTIC EXCITATION

NT HARMONIC EXCITATION

Transient electromagnetic plane wave ionospheric transmission and reflection, considering impulsive and step modulated sine wave excitations

01 p0031 A72-11102

Traveling wave antenna for exciting ion cyclotron waves in cylindrical anisotropic magnetoplasma

02 p0188 A72-11468

He-Ne laser active medium excitation and resonator geometry effects on TEM wave field

02 p0239 A72-12520

Rain type periodic solar radio bursts interpreted on basis of stream instability pulsating regime, considering plasma waves excitation

03 p0406 A72-12936

Diffuse cosmic background radiation measurements, emphasizing microwave and X ray spectra and excitation mechanism

03 p0409 A72-13138

Internal gravity waves and tidal oscillations excitation mechanism in upper atmosphere

03 p0346 A72-13383

Book on metallic and dielectric antennas covering planar, cylindrical and plasma types for symmetrical, dipole and ring excitations

04 p0497 A72-14612

Atmospheric tides wave dynamics in thermosphere, considering viscosity, thermal conduction, hydromagnetic forces and nonlinearity effects on transmission and excitation

04 p0514 A72-14722

Linearly polarized wave excitation with specified phase shift and predetermined amplitude ratio by waveguide slots, giving slot configuration design formulas

04 p0487 A72-15243

Linear antenna input admittance calculation, computing excitation integral by field expansion in Legendre functions

04 p0501 A72-15431

Longitudinal wave interaction and excitation by plasma instability in equatorial electrojet, considering energy transfer mechanism

05 p0656 A72-16242

Filter configuration for detecting pulse excitation smaller than kT, noting SNR and resolving time

05 p0631 A72-17075

Hot plasma transverse and longitudinal wave parametric excitation by intense laser light near plasma frequency, noting instability role in resonant coupling mechanism

05 p0699 A72-17172

Linear time-varying system under modulated signal excitation, obtaining quasi-stationary response by separable system approximation with parameter optimization

06 p0771 A72-17379

Vlf wave excitation during sudden storm commencement, causing magnetosphere trapped energetic electrons to diffuse and precipitate into lower ionosphere

06 p0803 A72-17451

Wave exciting grid-plasma interaction in single ended Q device, determining ion velocity distribution function

06 p0855 A72-17510

Parametric excitation of ion-acoustic waves in Q machine plasma, controlling electron temperature by amplitude modulated rf heating

06 p0855 A72-17513

Thermal noise and ion-acoustic waves excitation in Q machine two beam plasma with high temperature ratio in presence of inhomogeneous B-field, observing instability

06 p0856 A72-17517

Ion acoustic wave excitation in plasma by modulated energetic electron beam, compared with grid excitation

06 p0856 A72-17519

Coherence function and phase shift dependence of free ocean surface on angular energy distribution in two dimensional wind induced wave spectrum

06 p0841 A72-17625

Ion acoustic and cyclotron harmonic plasma waves parametric excitation by hf electric field, measuring thresholds and growth rates agreeable with theory

06 p0861 A72-17827

Fast electron-cyclotron wave excitation with infinite phase velocity along magnetic field in nonequilibrium electron plasma

06 p0862 A72-18402

Radially conducting cone wave spectrum calculation for noncircular excitation, noting circularly polarized TEM and elliptically polarized TM wave amplitudes

07 p0938 A72-19003

Rf excitation of external terminated longitudinal conductor axially parallel to rocket skin by transverse

electromagnetic field, deriving currents in cable-connecting impedances

07 p0956 A72-19555

High frequency heating of dense toroidal plasma by nonaxisymmetric ion cyclotron waves resonant excitation in closed magnetic trap

07 p1043 A72-19636

Love surface wave excitation in thin film layer by line source as function of propagation direction, frequency and film thickness

07 p1089 A72-19683

Reactive mechanism of nonlinear mixing in resonant excitation of ion plasma waves by vlf and whistler waves

07 p1046 A72-20540

Quasi-stationary three dimensional array excitation by large phase shift calculated for circular conducting elements

08 p1140 A72-21262

Electromagnetic field radiation from linearly and sinusoidally variable thickness layered structures under plane wave and concentrated source excitations

08 p1137 A72-21986

Sonic boom effects on structures, discussing ground motion, direct excitation by shock waves and damages

09 p1304 A72-23318

Fluctuating turbulent stresses effects on flow over wavy boundary, comparing calculated with measured pressure distributions

[AD-742545] 10 p1470 A72-25066

Trapped particle induced frequency shift in response of electrostatic wave to adiabatic and sudden excitations, obtaining distribution functions and nonlinear dispersion relation

[AD-741547] 11 p1693 A72-25566

Plasma parametric instabilities excitation by radio waves in ionosphere, noting LF ionic and HF electrostatic wave growth

11 p1628 A72-26767

Longitudinal electromagnetic wave excitation in restricted plasma by relativistic electron beam injection, determining increments, frequency distribution and width of spectra

12 p1849 A72-27064

Compressible anisotropic magnetoplasma filled cylindrical waveguide excitation by electric dipole, plotting electric field patterns as function of electron temperature and density

12 p1782 A72-27489

Reflection and transmission of plane E wave incident on moving conducting medium, discussing growing wave excitation

12 p1782 A72-27490

Parametric instability of magnetoactive plasma relative to nonpotential oscillations excitation, deriving threshold value of HF field strength

13 p2016 A72-29601

Experimental investigation of electrostatic cyclotron harmonic waves excited in inhomogeneous plasma column with axial magnetic field by RF capacitor field

14 p2138 A72-30398

Hydromagnetic waves excited by transverse magnetic dipole in finite-conductivity plasma

14 p2102 A72-30662

Properties of natural waves excited in Fabry-Perot resonator by external laser beams, noting stability dependence on wave type

15 p2245 A72-31420

One dimensional Maxwellian electron plasma simulation by electron bunches, describing Landau damping of wave initially excited in medium and nonlinear effects of trapping

15 p2284 A72-31678

Broadband arrays and multimode fed antenna excitation pattern mathematical synthesis in terms of optimization in Hilbert space

15 p2197 A72-31892

Monochromatic plasma wave excitation by cold electron beam, obtaining instability maximum amplitude and oscillation period

15 p2285 A72-32270

Ion acoustic and guided electron plasma waves excitation by grid antenna produced LF signals in cylindrical plasma column

15 p2289 A72-32650

Ideally conducting and dielectric coaxial solids of revolution, investigating joint excitation by TM wave

15 p2209 A72-32658

Plasma wave excitation by monoenergetic relativistic electron beam, investigating beam-plasma wave synchronism during instability development

16 p2434 A72-32912

Theory for the excitation of SHF elastic waves by multiple-film transducers / Allowance for the influence of metallic and dielectric layers /

17 p2529 A72-34843

Fast electron cyclotron wave excitation with infinite phase velocity along magnetic field in nonequilibrium electron plasma

17 p2588 A72-34853

Alfven waves development and high pressure plasma hydrodynamic and kinetic instabilities dependence on magnetic field to temperature gradients ratio

17 p2593 A72-35883

Excitation of nanosecond waves on positive columns.

19 p2838 A72-37328

Parametric excitation of electromagnetic waves.

19 p2834 A72-37718

Parametric excitation of Bernstein waves in inhomogeneous magneto-plasmas.

21 p3089 A72-40187

Coaxial exciter for parabolic antennas with high area efficiency and small halation

21 p3029 A72-40514

Double-dipole exciter for the primary focus of the 100-m radio telescope Effelsberg

21 p3029 A72-40518

Focus field and horn exciter regarding parabolic antennas with small f/D-relation

21 p3029 A72-40523

Parametric instability of magnetoactive plasma relative to nonpotential oscillations excitation, deriving threshold value of HF field strength

21 p3091 A72-40655

Excitation of electromagnetic waves in a plasma by a relativistic electron beam

21 p3092 A72-40787

Excitation of volume ion-acoustic oscillations in an inhomogeneous dense plasma by the field of an electromagnetic wave.

21 p3092 A72-40836

Sideband waves excitation by large amplitude ion-acoustic waves in collisionless plasma, noting frequency spectrum and growth rate agreement with trapped particles theory

21 p3094 A72-41629

Wave excitation during inclined charged-particle flight through a waveguide

21 p3089 A72-41841

Nonlinearity and inhomogeneity effects on plasma wave excitation by beating two laser beams, taking into account Lorentz force modulation by large amplitude plasma wave

22 p3185 A72-42475

Equatorial stratospheric waves induced by diabatic heat sources.

22 p3201 A72-42508

German monograph - Electromagnetic wave propagation inside a paraboloid of revolution subjected to different types of excitation.

22 p3156 A72-43070

Surface wave parametric excitation by weak HF electric field in semibounded plasma, calculating near threshold instability by dispersion equation

23 p3318 A72-43322

Ray tracing in ionosphere and magnetoionic theory application to coupling in cold plasma waves, considering linear waves, electrodes, particles and echoes as exciters

23 p3319 A72-43516

Energy measurement of primary particles from shower formation in solids, discussing ultrasonic waves generation in metal plates and electromagnetic waves excitation in ferrites

23 p3291 A72-44437

High frequency heating of dense toroidal plasma by nonaxisymmetric cyclotron waves resonant excitation in closed magnetic trap

24 p3427 A72-44568

Longitudinal electromagnetic wave excitation in restricted plasma by relativistic electron beam injection, determining increments frequency distribution and width of spectra

24 p3431 A72-45717

WAVE FRONT DEFORMATION

Isoplanatic instrument wave aberration determination, using longitudinal defocusing

03 p0360 A72-13563

Apodized interdigital transducers acoustic surface wave front distortion, describing perturbation and compensation method

03 p0360 A72-13602

Measuring device for holographic virtual image reconstruction deformations due to relative orientation errors between reference beam and holographic plate

06 p0818 A72-18329

Acoustic and gravity waves nonlinear propagation and structural deformation in isothermal and incompressible atmospheres with traveling wave induction

07 p0981 A72-20696

Atmospheric turbulence induced wave front distortion effects on fast-tracking laser antenna performance, considering infinite plane wave random complex phase modulation

14 p2110 A72-30550

The steepening of the wavefront due to nonlinearities / An electric model test regarding the origin of shock waves /

17 p2582 A72-35428

Non-Boussinesq effects and further development in a model of upper tropospheric frontogenesis.

19 p2829 A72-38558

Acoustic and gravity waves nonlinear propagation and structural deformation in isothermal and incompressible atmospheres with traveling wave induction

20 p2915 A72-39011

Optical measurement of wave front lens or mirror surface contours by laser unequal path interferometry combined with computer data reduction

20 p2922 A72-39020

WAVE FRONT RECONSTRUCTION

Diffraction theory of microwave holography presenting computer aided imaging approach for alleviating optically reconstructed image distortion

01 p0068 A72-10700

Microwave holographic interferometry with optical wave front reconstruction for visual mapping of large objects deformation

01 p0072 A72-11222

Crimped films for object reconstruction and image storage, comparing performance to holographic films

01 p0073 A72-11313

Focused image holographic interferometer with reduced blur in deep object image reconstruction with white light source

02 p0224 A72-11700

Double reference beam holograms, evaluating interference effects of misalignment on image reconstruction

02 p0225 A72-11700

Pohlman cell for ultrasonic hologram production describing construction, resolution and real time reconstruction

02 p0225 A72-11700

Diffusely illuminated objects holographic reconstruction with suppressed granularity by incoherent superposition of reconstruction waves longitudinal modes, describing experimental setup

02 p0229 A72-12111

Wave front sampling points in spatial filtering of nonequidistant discrete holograms of flat objects

02 p0232 A72-12700

Focused image holography in multimode He-Ne laser radiation, using diffusely scattered reference wave and lens for high quality reconstruction

03 p0357 A72-13322

Computer based analysis of holography using ray tracing and wave front matching aberrations

03 p0358 A72-13433

Three dimensional hologram synthesis from two dimensional pictures with parallax preservation [AD-736057]

03 p0359 A72-13440

Book on holography applications covering wave front reconstruction, wave sources, propagation, interference and coherence, single and split beam, color and polarization holography, etc

04 p0525 A72-15000

White light shadowgram production during holographically recorded distorted wavefront reconstruction, discussing illuminating slit performance, image producing diaphragm, lenses and collimator

06 p0815 A72-17700

Complete measurement in holography using complex coefficients of conversion matrix of interaction between coherent beam and recorded object

06 p0817 A72-18000

Measuring device for holographic virtual image reconstruction deformations due to relative orientation errors between reference beam and holographic plate

06 p0818 A72-18329

Acoustic /ultrasonic/ holography techniques for acoustic field recording and image reconstruction of coherent light, including applications

07 p0981 A72-18970

Elastic wave fields reconstruction from measurements over transducer array, stressing ultrasonic imaging system development

07 p0986 A72-19600

Plateholder for on site wet processing of holograms in real time holographic interferometry, obtaining undistorted reconstructed image by liquid gate immersion

07 p0992 A72-20580

Constant period discrete holograms features, investigating laser visualization, recording, reconstruction and image focusing

08 p1163 A72-20700

Limiting resolution of reconstructed image of focused hologram in electron microscopes as function of aberration and spatial coherence

08 p1166 A72-21318

Three dimensional hologram recording and reconstruction, discussing image geometry, reference beam intensity, size finiteness, transition limits and photosensitive materials

08 p1166 A72-21318

Holographic image reconstruction for individual transverse laser modes radiation intensity distributions

08 p1169 A72-21911

Interferometry in volume holograms with recording of wave fronts by double exposure technique and reconstruction by diffraction

09 p1315 A72-23355

Holograms image formation characteristics with extended reference beam source, presenting reconstructed image and noise field calculations

11 p1633 A72-26350

Laser irradiance modulation effect on high error fringes brightness in time average hologram reconstruction, noting exposure time increase

12 p1809 A72-27682

Holograms with high diffraction efficiency, describing bleaching experiments and SNR measurements in reconstructed image

12 p1810 A72-27887

Dispersive optical imaging systems for chromatic aberration correction, considering broadband holographic reconstruction and generation, optical information processing and diffraction pattern achromatization

12 p1811 A72-27950

Holograph generation, electric signal conversion and transmission and remote location simultaneous Lumatron reconstruction

12 p1811 A72-27951

Acoustic /ultrasonic/ holography techniques for acoustic field recording and image reconstruction in coherent light, including applications

13 p1957 A72-29206

Quantization background noise during hologram approximation by step function, discussing effect on diffraction field forming reconstructed image

13 p1959 A72-29684

Radiation pattern reconstruction of radio telescope parabolic Cassegrain reflector antennas from Fresnel zone emission source, using holography and optical processing

14 p2103 A72-30221

In-line holography, determining effects of limited information on reconstructed image characteristics

15 p2237 A72-32057

Computer printing device for improved image recording of binary and half tone synthesized amplitude holograms

16 p2390 A72-33084

Holograms image formation characteristics with extended reference beam source, presenting reconstructed image and noise field calculations

16 p2394 A72-33705

Holographic developments during 1948-1971, discussing three dimensional object imaging, phase, diffused and three-color holograms, Sorot lens, electron microscopy and interferometry, etc

16 p2394 A72-33751

Zeiss /Jena/ stereoplanigraph design and operation to obtain purely optical projection for object reconstruction, discussing human operator replacement by objective electro-optical system

16 p2394 A72-33870

Holograms with high diffraction efficiency, describing bleaching experiments and SNR measurements in reconstructed image

16 p2395 A72-33996

Holographic image reconstruction using He-Ne laser as coherent light source and black-white and color photographic emulsions

17 p2554 A72-34930

A theoretical calculation of edge smear in far-field holography.

19 p2797 A72-37610

Single pulse holographic flow visualization.

19 p2798 A72-37622

Historical review of holographic interferometry development, giving attention to contouring technique and image reconstruction

19 p2800 A72-37775

Wave front sampling points in spatial filtering of nonequidistant discrete holograms of flat objects

20 p2923 A72-39057

Phase holograms wave front formation as replacement of optical elements with aspherical surfaces and multilens objectives

20 p2926 A72-39519

A unitized and portable holographic interferometer. [ASME PAPER 72-HT-10]

20 p2927 A72-39681

Photoemissive method of recording Mertz shadowgrams and vibrating electrode technique for reading out images in reconstruction of X ray sources original distribution

21 p3051 A72-40219

Possibilities of optical elements design using phase holograms.

21 p3054 A72-40613

Modeling a holographic process on a computer

23 p3287 A72-43531

Characteristics and measurements of an aperture-limited in-line hologram image.

23 p3288 A72-43886

Studying hologram imagery by a ray-tracing method.

24 p3401 A72-44773

A new method for linear recording in holography retaining the reconstruction efficiency.

24 p3401 A72-44775

WAVE FRONTS

NT SHOCK FRONTS

Rate-type viscoelastic materials, deriving weak shock structure by wave front, ray and singular surface theories and asymptotic expansions

01 p0101 A72-10033

Pseudowave front spreading at leading edge of plasma slab during injection at high velocity into denser background plasma

02 p0265 A72-12364

Plane wave intensity fluctuations behind random phase screen, discussing phase structural function relation to field statistical properties and fluctuation dispersion

02 p0181 A72-12590

Vertically polarized logarithmically periodic monopole antenna for incoming wave front reception with low elevation angles in 1.5 to 30 MHz frequency range

02 p0195 A72-12697

Uniform progressing wave expansion solution to wave equation for transition region boundary value problems

03 p0388 A72-12988

Inhomogeneous nonstationary medium caused electromagnetic wavefront phase disturbance reduction in holography by averaging

04 p0522 A72-15381

Wave front division interferometry for small scale solar features study at visible wavelengths

07 p1076 A72-19598

Uniform asymptotic solution near wavefront of transient field propagation in inhomogeneous dispersive media

[AD-745077] 07 p0946 A72-19800

Fluid motion near wave front junction point, expanding unknown functions and independent variables into series of parameters characterizing shock wave and angular distances

08 p1152 A72-21945

Schlieren visualization of radiated wave fronts for Al plates illuminated with short acoustical pulses in water, comparing with Lamb theory

11 p1687 A72-26057

Traveling ionospheric disturbances radio sounding during 7 March 1970 solar eclipse time, noting wave front orientation

12 p1801 A72-27158

Holographic interferometry of Mach wave field generation by supersonic turbulent jet, noting visible conical wave front from core edge

13 p1898 A72-29580

Numerical analysis of steady one dimensional quasi-shock waves in collisionless plasma within longitudinal uniform magnetic field, noting oscillations behind wave front

15 p2284 A72-31584

Nonspherical thermal wave propagation, considering two dimensional structure wave front radiative diffusion problem

15 p2336 A72-32513

Strain rate history effects on stress incremental wave front propagation in elastic bars, considering Taylor-Karman-Rakhmatulin theory

16 p2466 A72-33103

Wave-front singularities for two-dimensional anisotropic elastic waves.

18 p2739 A72-37175

Twyman-Green interferometer to test large aperture optical systems.

19 p2811 A72-37590

Position of the transition point through the sonic velocity behind the detonation front

21 p3045 A72-40987

Holographic interferometry with variable sensitivity

21 p3058 A72-41745

Problem of the spatial localization of thermal disturbances in nonlinear heat-conduction theory

23 p3356 A72-43529

Multimoded components wavefront arrival angle from measurements of signal induced in linear array, discussing numerical calculation from linear equation solution and polynomial roots

23 p3264 A72-43601

Ray optics applications to electromagnetics and other disciplines, discussing matrix representation for wavefront curvature and field computation simplification via transformations

23 p3314 A72-44331

WAVE FUNCTIONS

NT MOLECULAR ORBITALS

Integrals for atomic wave functions of Slater orbitals, obviating numerical snags by Euler transformation

02 p0262 A72-11980

Atomic data for UV and X ray astronomy, considering atomic wave functions and energy levels, radiative transition probabilities and electron-ion collision cross sections

03 p0420 A72-13125

Hydrogen molecular ion g tensor calculation, determining approximate ground state wave functions

03 p0391 A72-13152

Fe group transition metal impurities in semiconductors, calculating ground state wave functions and photoionization cross section dependence on wavelength

04 p0563 A72-15473

Energy dependence of solar proton-proton reaction, generating p-p wave function from Schroedinger equation

05 p0718 A72-16501

French book on wave mechanics reinterpretation covering double solution theory, particle thermodynamics, guidance dynamics, etc

06 p0847 A72-17813

Electron states in glassy amorphous semiconductors, constructing trial wave functions for valence band

06 p0866 A72-18180

Discrete wave packets observed in solar wind, discussing mechanism similar to echo phenomenon in plasma physics

07 p1057 A72-19143

Source distribution estimate in radar mapping, comparing prolate spherical wave functions inverse versus truncated Fourier transform methods

07 p0946 A72-19792

Perturbation theory oscillatory wave function for second order correction to oxygen 16 nucleus bonding energy

08 p1211 A72-21067

Spherical wave functions in analysis of infinite systems of algebraic equations describing elastic wave diffraction in sequence of spherical cavities

08 p1246 A72-21706

Atomic variational scattering calculation by method of models, using modified Hamiltonian form to avoid difficulties due to inexact target wave functions

09 p1355 A72-22787

Preresonance Raman scattering tensor in Born-Oppenheimer approximation of molecular wave functions

10 p1491 A72-24110

Finite range Fredholm integral equations with band limited displacement kernels in terms of prolate spheroidal wave functions

10 p1506 A72-24460

Expansion formulas for Kampe de Fériet and radial wave functions application to heat conduction and quantum mechanics problems

15 p2336 A72-32398

Hamiltonian for first order wave function in charge exchange perturbation theory

17 p2584 A72-34259

Calculation procedure involving wave function for vibrational correction to electron scattering cross section of hydrogen molecule in Born approximation

17 p2585 A72-34261

Wave function and resonance parameters for autoionization and ground states of helium and hydrogen

17 p2586 A72-35774

A simple, radially correlated ground state wavefunction for two electron atoms.

17 p2586 A72-35828

Semiempirical method for determining electron wave-function parameters in solids

20 p2959 A72-38955

WAVE GENERATION

NT HARMONIC GENERATIONS

Bond zone wave formation in explosion cladding, predicting critical collision velocity and angle with fluid flow model

01 p0077 A72-11031

Microwaves and optical generation and amplification - Conference, Amsterdam, September 1970, covering microwave tubes, solid state devices and quantum electronics

01 p0044 A72-11278

Electromagnetic plane stress wave generation by capacitor bank for transient loading of photoelastic models along straight and curved boundaries

[SESA PAPER 1907A] 02 p0199 A72-11503

Mm and sub mm wave generation by semiconductor devices, showing power vs frequency plots for IMPATT, Gunn and LSA oscillator diodes

02 p0268 A72-11694

Digital telemetry data transmitter featuring triangular wave generator and signal mixer for reducing sensitivity to transmission path characteristics variations

02 p0179 A72-12415

Detection of atmospheric gravity waves produced by focusing of shock front generated by supersonic aircraft, calculating flight trajectories

03 p0345 A72-12984

Flare associated waves suggested by optically observed phenomena, using time lapse photography of solar chromosphere

03 p0423 A72-13212

Digital sine wave generator, discussing advantages over conventional RC and LC oscillators due to superior phase constancy

05 p0634 A72-15814

Spontaneous oscillations generation on transverse surface wave, discussing experimental realization with semiconducting CdS single crystals

05 p0626 A72-16282

Transverse acoustoelectric surface wave domain in piezo-semiconducting body, obtaining gain coefficient and generation threshold criterion

05 p0702 A72-16283

Acoustic waves generation in afterglow of weakly ionized low pressure He plasma, using electrostatic probe

05 p0699 A72-17083

Cylindrically symmetric blast wave generated by infinitely long line explosion in cold and homogeneous gas rotating rigidly within self gravitational field

07 p1070 A72-19134

Firing characteristics of insensitive electroexplosive devices under impulsive waveforms, discussing theory, design and application of waveform generators

08 p1220 A72-20763

Whistling atmospherics generation mechanism, showing ionic sound excitation by hydromagnetic wave propagation through magnetospheric rapid plasma concentration change regions

08 p1155 A72-20807

Cyclotron magnetoacoustic wave generation by planets and binary stars in circular orbits, deriving interstellar gas density variations

08 p1231 A72-21122

Vibrating membrane generated acoustic pressure wave propagation in rarefied gas, applying to solid surface-gas interaction models

09 p1294 A72-22762

Large amplitude electrostatic ion acoustic shock production by superposing pulsed photoionized plasma slab on dc background

09 p1360 A72-22871

German monograph on pulsed laser induced spherical unsteady blast waves in stationary and flowing gases

09 p1325 A72-23161

Sonic booms generation and propagation, discussing effects on animate and inanimate objects

09 p1262 A72-23316

Long wave trains of gravitational waves from vibrating black hole, stressing hole dynamical entity

09 p1394 A72-23697

Supersonic auroral motions relationship to infrasonic waves generation, showing acoustic pulse within electrojet arcs due to collisions with neutral gas of positive ions

11 p1624 A72-26403

Bibliography on infrasonic sound wave generation, propagation and detection at ground level and ionospheric heights

11 p1690 A72-26520

Slow and fast plane magnetoacoustic waves mutual transformation and reflection at plasma and magnetic field inhomogeneities

11 p1698 A72-26643

Submillimeter plane waves formation by quasi-optical line and diverging lens with phase front adjustment

11 p1598 A72-26719

Holograph generation, electric signal conversion and transmission and remote location simultaneous Lumatron reconstruction

12 p1811 A72-27951

Local perturbation generated waves in homogeneous plasma at rest subjected to uniform magnetic field

13 p2010 A72-28680

Opposing wave generation in gas ring laser with allowance for diffraction by finite apertures of cavity mirrors

13 p1970 A72-29678

Surface waves generation and absorption by interdigital transducer with uniform finger spacing, discussing parallel equivalent circuit derived in weak coupling approximation

13 p1960 A72-29769

Clear air turbulence nonlinear generation mechanism based on finite amplitude periodic waves in stratified shear flow critical layers, considering buoyancy, viscosity and heat conduction effects

14 p2127 A72-30226

Isolated finite amplitude electrostatic oscillations production in thin plasma layer between two parallel metallic surfaces in magnetic field

14 p2136 A72-30302

Detonation wave generation in gas discharge plasma by pulsed electrical discharge

14 p2137 A72-30313

Laminar Ekman boundary layer instability for incompressible fluid over rigid boundary with fixed vertical temperature gradient, investigating internal gravity waves generation

14 p2100 A72-30347

Plasma radiation from collisionless MHD shock waves, discussing waves generation and angular distribution

14 p2138 A72-30555

Electromagnetic and gravitational waves emission by suprlight sources in vacuum, considering multiparticle and form factor cut-off effect

14 p2130 A72-30625

Gravity waves parametric generation on liquid surface, presenting threshold values for space distribution of amplitudes and phases

14 p2097 A72-31111

Difference-frequency mixing of pulsed carbon dioxide lasers with non-phase-matched GaAs for submillimeter wave generation

15 p2290 A72-31384

Self excited increasing thermal wave generation models, using hyperbolic wave heat conduction and thermoelasticity equations

15 p2336 A72-32285

MHD wave propagation and generation during spin-up of rotating viscous incompressible electrically conducting fluid

16 p2436 A72-33572

Some comments on the generation of electromagnetic traveling and standing waves for inductive acceleration of plasmas

[DFVLR-SONDDR-209] 17 p2589 A72-34895

Nonlinear collisional excitation of plasma waves.

17 p2591 A72-35372

Determination of the locking range from the reactive power balance of the oscillator.

17 p2530 A72-35430

Measurement of the characteristic times of detonation-wave formation in a tube filled with an acetylene-air mixture

18 p2676 A72-35999

Ultrasonic wave generation in solids using transducer composed of high rigidity dielectric /polypropylene/ between two electrodes

18 p2691 A72-36402

Electromagnetic self induced vibrations in homogeneous unbounded electron beam moving with time dependent velocity, noting longitudinal and transverse wave generation

19 p2842 A72-38527

Nonlinear theory of particle motion in monochromatic Alfvén wave field application to Pc-1 geomagnetic pulsations evolution

20 p2917 A72-39408

Use of stress wave emission for nondestructive testing of materials and articles.

21 p3061 A72-41720

The problem of the boundary conditions in thermosphere dynamics.

22 p3201 A72-42510

Isolated finite amplitude electrostatic oscillations production in thin plasma layer between two parallel metallic surfaces in magnetic field

23 p3317 A72-43204

Detonation wave generation in gas discharge plasma by pulsed electrical discharge

23 p3318 A72-43215

Microwave generation with high energy electrons in magnetic undulator with transverse electromagnetic field, calculating frequency distribution of undulator radiation

23 p3265 A72-44158

Waves generated in the configuration of a magnetically confined and field-permeated axisymmetric jet.

23 p3322 A72-44307

Tidal waves of a two-layer liquid in a cylindrical basin of revolution rotating about its axis

24 p3392 A72-45073

WAVE INTERACTION

NT SHOCK WAVE INTERACTION

MHD waves nonlinear interaction in magnetosphere, calculating transverse Alfvén and magnetosonic and longitudinal acoustic wave decay instabilities

01 p0109 A72-10618

Rotation effects on three dimensional infinitesimal wave stability in Blasius boundary layer

02 p0205 A72-12354

Asymptotic method for investigating multiwave interaction processes in one dimensional weakly nonlinear distributed systems with slowly changing parameters

02 p0261 A72-12585

Yield relationship to coupling of plastic waves, obtaining stress-strain diagrams

02 p0297 A72-12613

Rigid mass impact against viscoelastic bar of finite length, investigating longitudinal waves propagation and interaction

02 p0298 A72-12682

Boundary layers nonlinear resonant instability, investigating Tollmien-Schlichting wave triads interactions with energy transfer from primary shear flow to disturbance

03 p0340 A72-13160

Simple wave interaction solutions for nonlinear plane k-waves of nonelliptic quasi-linear differential equations using Riemann invariants

03 p0389 A72-13885

Soviet monograph on electron flux nonlinear interaction with slow electromagnetic waves in TWT, discussing output power and efficiency increase

03 p0333 A72-13949

Ionospheric hydromagnetic and acoustic gravity wave interactions, examining stratified nonisothermal atmospheric model

04 p0516 A72-14934

Large amplitude whistler mode wave packet multiparticle emissions model including wave-particle interactions

04 p0517 A72-14948

Weakly interacting waves Langevin equation in fluid, using characteristic functionals and time asymptotic methods

04 p0549 A72-15289

Electromagnetic wave transformation at moving boundary discontinuity with reactive parameters in dispersive medium by Lagrangian field equations

04 p0489 A72-15388

Monograph on head-on collision of combustion wave with shock wave and rarefaction wave covering gas dynamics, interactions, reflection process, etc

05 p0746 A72-16046

Collisionless stellar dynamics, considering Lin wave interactions for orbital theory

05 p0713 A72-16053

Internal gravity wave interaction with median wind in upper atmosphere from solution of system of linearized hydrothermodynamic equations

05 p0656 A72-16175

Velocity field time history of interacting shear waves in infinite homogeneous chemically reacting fluid for turbulent combustion studies

05 p0747 A72-16367

Natural fluctuations effect on beat frequency dependence of opposed waves in ring laser on rotation velocity

05 p0668 A72-16405

Dispersion properties of drift waves in low-beta weakly collisional plasma in presence of ion acoustic or Langmuir waves parallel to magnetic lines

05 p0698 A72-17019

Nonlinear wave coupling, scattering and radiation in plasmas for diagnostics application

05 p0699 A72-17221

Hall fields effect on interaction of MHD waves in inhomogeneous plasma, considering MHD wave dispersion

05 p0701 A72-17237

Piezoelectric interaction between Lamb waves and charge carriers in piezoelectric plate inserted into semiconductor

06 p0865 A72-17388

Lamb waves interaction with conduction electrons in piezosemiconductor, deriving dispersion equation for CdS wafers

06 p0865 A72-17393

Langmuir wave-caused electron plasma distribution function deformation, discussing particle trapping effects

06 p0858 A72-17542

Longitudinal electron plasma waves interaction with electron distribution, investigating energy transfer

06 p0858 A72-17543

Two fluid plasma longitudinal ion and electron waves nonlinear interactions excitation of type 2 bursts, considering radiation flux density

06 p0862 A72-18175

Magnetospheric plasma sources, discussing wave-particle interactions and acceleration mechanisms

06 p0810 A72-18281

Electrostatic focusing field inhomogeneity /gradients/ effects on high frequency electron-wave interaction processes in linear beam backward wave oscillator tube

07 p0952 A72-18845

Ion-acoustic solitary waves formation and interaction in collisionless warm plasma, using Vlasov equation for ions and Boltzmann distribution for electrons

07 p1041 A72-19507

Quasi-linear theory of magnetosphere gyroresonant wave-particle interactions, discussing particle distribution function anisotropy, wave packet effects, whistler mode, energy and pitch angle distributions, etc

07 p0978 A72-20034

Gas dynamics K-wave interaction in nonlinear media described by nonlinear partial differential equations

07 p0972 A72-20103

Quantum coherent spin wave interactions in ferromagnetics, showing retained emission field

07 p1007 A72-20125

Mathematical model of gravitational wave zone for ring emanated smooth axisymmetric toroidal pulse

08 p1158 A72-21177

Differential equation solution for plane self focusing and one dimensional self modulation of waves interacting in nonlinear media

08 p1209 A72-21718

Meteorological synoptic analysis of stratospheric planetary wave interaction with lower ionosphere in terms of wind, temperature and ionospheric electron density profiles

09 p1297 A72-22375

Modulated electromagnetic wave transmission in dispersive medium with cubic nonlinearity, discussing solitary wave and instabilities in two-wave interaction

09 p1352 A72-23475

Post bifurcation finite amplitude baroclinic instability, emphasizing wave vectors configuration with quadratic nonlinear interactions

09 p1347 A72-23654

Wave particle interaction around lower hybrid resonance frequency, deriving whistler mode wave growth rate during propagation in magnetoactive plasma penetrated by nonthermal particles

10 p1476 A72-24959

Critique of Rees theory of primordial gravitational radiation concerning galaxy clusters interaction with very long wavelength universal gravitational waves
10 p1550 A72-25200

Resonant three wave interaction in magnetized spatially uniform plasma under constant magnetic field
11 p1698 A72-26603

Nonlinear wave interaction in plasma with random inhomogeneities, using quasi-hydrodynamic approximation
12 p1849 A72-27062

Hydromagnetic wave scattering of high energy cosmic rays in highly ionized interstellar gas to confine cosmic rays to Milky Way
12 p1864 A72-27745

Gas and solid state lasers amplitude and phase fluctuations calculated from Langevin equations, noting spectral line width and collision waves
12 p1826 A72-28050

Semiconductor devices with extended slow wave-carrier interaction region for vacuum traveling wave tube replacement
13 p1927 A72-28401

Infinite plane plates sound radiation due to bending waves interactions with density and stiffness fluctuations in material
13 p2004 A72-29094

O-type synchronous electron beam waves interaction with electrodynamicallly structured traveling wave, noting linear gain dependence on beam current and magnetic field
13 p1931 A72-29291

Standing wave and colliding wave lasing and synchronization region in ring laser using active gas isotopic mixture
13 p1968 A72-29511

Quasi-monochromatic wave interaction with second harmonic in weakly nonlinear medium, obtaining exact nonstationary solutions
13 p1971 A72-29911

Electron beam-helicons interaction in semiconductor plasma, determining instabilities onset conditions for unbounded system
14 p2141 A72-30172

Internal gravity wave interaction with median wind in upper atmosphere from solution of system of linearized hydrothermodynamic equations
14 p2099 A72-30244

Dispersion of polyhelical nonrelativistic electron flow interacting with slow waves of magnetized cold plasma, observing instability in presence of Doppler effects
14 p2136 A72-30304

Nonlinear interaction between oscillations produced by monoenergetic particles beam passing through plasma
14 p2136 A72-30306

Free electron waves interaction with coherent laser light in crystalline medium, discussing quantum mechanical treatment and path integral approach
14 p2110 A72-30725

Kinetic equations for turbulent magnetized plasma, considering wave-wave interactions and wave energy in terms of second order Markov differential equation
14 p2141 A72-30940

Crystal lattice and dislocation anharmonicities interdependence and stress-strain correlation in presence of interaction between ultrasonic waves of different frequencies
14 p2169 A72-30959

Small parameter method for analysis of encounter waves nonlinear self oscillations in ring gas laser, noting periodic energy transfer
14 p2111 A72-31104

Nonlinear coupling of wave modes in cold magnetized plasma, applying to electrostatic wave transformation in connection with solar type 3 radiation
15 p2283 A72-31431

Electro-optical media for initial light radiation frequency shift maximum, analyzing circular light/modulating wave interactions
15 p2197 A72-31880

Review of symposium on D region, upper polar ionosphere, magnetosphere and wave-particle interactions
15 p2229 A72-32251

Sounding rocket experiment on nonlinear interaction between two electron plasma waves and ion acoustic wave in ionosphere to investigate artificial realization feasibility
15 p2231 A72-32333

Weak homogeneous turbulence analysis by Bogolubov statistical mechanics theory, deriving kinetic equations for nonlinear wave interaction
15 p2278 A72-32383

Microwaves interaction with ultrashort laser pulse generated traveling refractive index changes in liquids with orientational Kerr effect
15 p2252 A72-32652

Ideal fluids isentropic flow equations solution via Riemann invariants method, describing nonlinear waves linear interactions
16 p2376 A72-33110

Nonlinear wave interaction in anisotropic plasmas, discussing helicon decay with acoustic wave emission and quasi-longitudinal waves with magnetoacoustic wave emission
16 p2436 A72-33478

Nonlinear electromagnetic wave interaction in rarefied plasma cylinder subject to constant magnetic field in hydrodynamic approximation
16 p2363 A72-33479

Planetary wave interaction in two level baroclinic atmosphere, using quasi-geostrophic equations
16 p2418 A72-33602

Langmuir wave coupling in inhomogeneous plasma due to combined density gradient and external HF electric field
16 p2436 A72-33654

Coupled mode equations derivation for wave interactions in plasmas, considering oscillations production and cold magnetized plasma
17 p2589 A72-34923

Kinetic theory of waves in hot, low density plasma.
17 p2591 A72-35161

Wave-wave interactions due to scattering by electrons.
17 p2591 A72-35162

VLF wave propagation and its interaction with the magnetoplasma.
17 p2516 A72-35357

Nonlinear collisional excitation of plasma waves.
17 p2591 A72-35372

Whistler side-band growth due to nonlinear wave-particle interaction.
17 p2517 A72-35601

Normal mode formulation of spin wave-helicon wave interactions in ferromagnetic semiconductors.
18 p2718 A72-36452

Dual amplitude construction possibility from general field theory couplings and propagators, considering factorization on multiperipheral configuration in translational and rotational modes
18 p2713 A72-36516

Nonlinear equations for explosive instabilities of three plasma waves interaction with mutually different linear damping
19 p2838 A72-37326

Dispersion curves of mixing mode between electrostatic and electromagnetic waves propagating perpendicularly to ambient magnetic field for hydrogen plasma with Maxwellian velocity profile
19 p2839 A72-37335

The enhancement of heat transfer by waves in stratified gas-liquid flow.
19 p2787 A72-38398

Method of characteristics for nonlinear equations of perturbed motion of fluid near contact point between shock and diffraction waves
20 p2912 A72-39023

Polarization effect of attenuation of opposed-wave competition in ring lasers
20 p2932 A72-39412

Interaction between weak gravitational waves and a gas
21 p3084 A72-40402

Nonlinear interaction of p and s ionization waves in neon.
21 p3090 A72-40487

Rarefaction wave generation by solar wind shock wave interaction with magnetosphere, noting geomagnetic field weakening during magnetic storm
22 p3217 A72-41894

Dispersion of polyhelical nonrelativistic electron flow interacting with slow waves of magnetized cold plasma, observing instability in presence of Doppler effects
23 p3317 A72-43206

Nonlinear interaction between oscillations produced by monoenergetic particles beam passing through plasma
23 p3317 A72-43208

Particle distribution function evolution effect on turbulent plasma heating by wave interaction, considering stochastic heating of ions
23 p3318 A72-43314

Electromagnetic waves interaction with transverse waves of thin piezoelectric plate in waveguide, noting transformation into acoustic waves
23 p3312 A72-43407

Symposium on Waves and Resonances in Plasmas, St. John's, Newfoundland, Canada, July 5-9, 1971, Proceedings.
23 p3319 A72-43511

Forward scattering of laser coherent light by acoustic or turbulent wave pressure variations, noting phase fluctuation spectrum
23 p3313 A72-44113

Explosive instability temporal development, noting linear damping role in nonlinear wave interaction under conservation laws of energy and momentum
23 p3282 A72-44318

Investigation wave transformation and absorption by a plasma in the upper hybrid frequency range
24 p3429 A72-45491

Nonlinear wave interaction in plasma with random inhomogeneities, using quasi-hydrodynamic approximation
24 p3431 A72-45715

WAVE OSCILLATORS
U OSCILLATORS

WAVE PROPAGATION

NT DIFFRACTION PROPAGATION
NT GROUND WAVE PROPAGATION
NT IONOSPHERIC F-SCATTER PROPAGATION
NT IONOSPHERIC PROPAGATION
NT LIGHT SCATTERING
NT MICROWAVE TRANSMISSION
NT MULTIPATH TRANSMISSION
NT SCATTER PROPAGATION
NT SHOCK WAVE PROPAGATION
NT TRANSEQUATORIAL PROPAGATION

LF large scale oblique Alfvén wave propagation in turbulent ion acoustic plasma, investigating dispersion relation, Landau damping and interactions
01 p0107 A72-10137

Monochromatic waves propagating in uniform magnetoplasma, considering resonant interaction with electrostatic approximation
01 p0107 A72-10138

Flow characteristics, wave propagation and thermal stability of ferrofluids within uniform magnetic field
01 p0050 A72-10235

Stochastic differential equations vector solution by two-time method, applying to random harmonic oscillators and wave propagation in random media
01 p0093 A72-10510

Initial strains effect on propagation rate of elastic waves, applying finite deformation theory
01 p0138 A72-10581

Magnetosphere transmittance for fast magnetosonic waves, considering refraction, reflection and earth surface intersection
01 p0058 A72-10587

Resonant traveling wave IMPATT oscillators wave propagation and power output characteristics, taking into account metal conductor and semiconductor substrate losses
01 p0038 A72-10651

Characteristic equation of surface wave propagation on two dimensional corrugated structures for phased array applications
01 p0030 A72-10845

Electromagnetic instability of linearly polarized mode propagation perpendicular to magnetic field in two colliding plasma streams
01 p0110 A72-11112

Wave propagation in thin elastic shells by similar formation of shell and nonlinear elasticity theories equations
01 p0142 A72-11197

Large amplitude linearly or elliptically polarized Alfvén wave propagation parallel to magnetic field, calculating nonlinear Landau damping rate
01 p0111 A72-11227

Propagating waves characteristics measurement on Yagi-Uda array, obtaining k-beta diagrams and phase velocities
01 p0043 A72-11244

Book on microwave techniques covering Maxwell equations, electromagnetic wave propagation in conducting media, complex notation, plane polarized waves transmission and reflection, wave equations, etc
01 p0043 A72-11275

Numerical method for wave propagation and dynamic stresses in viscoelastic cylinders under internal and external loads
01 p0144 A72-11375

Shf electromagnetic radiation interaction with solid body plasma, explaining wave propagation in solid state plasma waveguides
02 p0170 A72-11561

Wave propagation in nonlocal isotropic elastic medium of ordinary kinematic structure with energy density as functional of displacement gradient field
02 p0288 A72-11609

One dimensional elastoplastic wave propagation symposia review emphasizing elastoviscoplastic media, jet penetration into half space and polymer tests by transverse impact
02 p0290 A72-11628

Orbiting lunar spacecraft Endeavor radio transmission postocclusion reception, considering surface wave propagation and mountain formation prismatic refraction
02 p0171 A72-11753

Stress waves propagation in woven-fabric composites, obtaining dynamic moduli and vibration damping coefficients by resonance technique
02 p0291 A72-11984

ATF-S satellite short and long term data processing, detailing millimeter wave propagation experiment
02 p0177 A72-12384

Human pulse wave propagation velocity measurement, using biotelemetry system of photoresistance sensors and endoscopic bulbs connected to electrocardiograph
02 p0169 A72-12519

Rigid mass impact against viscoelastic bear of finite length, investigating longitudinal waves propagation and interaction

02 p0298 A72-12682

Magnetospheric hydromagnetic waves propagation characteristics, discussing isotropic/poloidal and guided/toroidal modes coupling in conjunction with hydromagnetic wedge model

02 p0268 A72-12870

Short periodical pulsations in solar atmosphere related to magnetosound propagation in area of temperature minimum with directed perpendicular magnetic field

03 p0436 A72-13813

Tunguska explosion of 30 June 1908, determining air waves propagation velocity

03 p0438 A72-13981

Tangential stress pulse effects on transversely isotropic half space surface wave motion under torsion

03 p0452 A72-14128

Compression wave propagation from cylindrical cavity in weakly conducting magnetoelastic medium under unperturbed magnetic field

03 p0452 A72-14129

Dynamic stress concentration at circular hole generated by plane bending wave propagation in thin plate, analyzing dependence on vibration frequency

03 p0453 A72-14139

Cylindrical blast wave propagation in MGD, deriving closed-form solutions for line explosion in medium with constant pressure, density and axial magnetic field

03 p0400 A72-14391

Finite amplitude stress wave propagation behind shock in unidirectionally reinforced fiber matrix composites under impact loads

04 p0585 A72-14534

Cauchy-Poisson problem of infinitely deep fluid wave motion resulting from initial particle velocities and horizontal equilibrium surface change

04 p0511 A72-14648

Storm effects on SST operations, discussing wave initiation at storm top and tropospheric propagation

04 p0542 A72-14683

Long wave propagation in curved ducts and pipes, considering plane wave transition and distortion

04 p0548 A72-14698

Atmospheric tides wave dynamics in thermosphere, considering viscosity, thermal conduction, hydromagnetic forces and nonlinearity effects on transmission and excitation

04 p0514 A72-14722

Density waves propagation and amplification in p-InSb electron-hole plasmas, investigating dependence on frequency and injection level

04 p0561 A72-14851

Small amplitude velocity waves turbulent distribution in infinite medium, demonstrating kinematic dynamo regeneration

04 p0573 A72-14906

Rectangular pulse propagation through inhomogeneous medium as plasma diagnostics, investigating electron collisions effect on signal distortion

04 p0556 A72-14946

Low latitude low dispersion whistlers, discussing origin as vlf waves radiated from return stroke of lightning discharge

04 p0517 A72-14949

Weak dissipation and damping of nonlinear long waves propagating in rotating fluids by Korteweg-de Vries equation

04 p0513 A72-15329

Nonlinear surface wave propagation on pinched cylindrical plasma, developing asymptotic approach from I. undquist equations

04 p0559 A72-15348

High beta plasma If wave parallel propagation to equilibrium magnetic field, deriving large scale length perturbations from coupled nonlinear partial differential equations

04 p0559 A72-15349

Collision resonance effects on transverse wave propagation direction in collisionless plasma for upper ionospheric sounding

04 p0490 A72-15403

Electromagnetic surface field propagation on dielectric wedge excited by line source, using steepest descent method

04 p0491 A72-15419

Waveguide structures partially filled with bulk negative differential conductivity media, describing wave propagation characteristics and power distributions

04 p0501 A72-15427

Infinitely long rectangular waveguide discontinuity problem, calculating reflection and transmission coefficients of wave propagation

04 p0491 A72-15428

Discrete variable approach for stress wave propagation in axisymmetric layered elastic-plastic solids

04 p0593 A72-15626

Two dimensional axisymmetric surface waves motion in inviscid incompressible homogeneous electrically conducting fluid under uniform magnetic and electric fields, considering surface tension effects

04 p0560 A72-15744

Error bounds on elastic-plastic strain wave measurements, considering one dimensional wave propagation in semifinite bar

[ASME PAPER 71-MET-W] 05 p0731 A72-15789

Weakly divergent beam propagation of electromagnetic waves in statistically inhomogeneous nonlinear medium with dielectric constant dependence, using small perturbation method

05 p0625 A72-15818

First and second order moduli of elasticity for finitely deformed elastic materials, deriving acceleration waves propagation condition and growth equation

05 p0735 A72-16028

Tensor calculus theorem application to elastic isotropic materials finite deformation, considering acceleration waves propagation and moduli of elasticity

05 p0735 A72-16029

Stability characteristics of finite difference schemes based on lumped-parameter model and numerical integrator for wave propagation in continuous media

05 p0735 A72-16081

Nonlinear propagation effects of monochromatically circularly polarized vlf waves /whistlers, heli cons/ along field lines in magnetosphere

05 p0658 A72-16603

Monochromatic radiation pulse transfer in absorbing plasma, deriving heat wave propagation velocity

05 p0696 A72-16680

Transverse ultrasonic wave propagation in low viscosity liquids, investigating fine structure of Rayleigh line wing

05 p0690 A72-16682

Large deflection microstructure continuum model for composite beam flexural wave propagation and free vibration, deriving equations of motion

[AIAA PAPER 72-140] 05 p0741 A72-16937

Anisotropic plasma stability to magnetosonic wave near ion cyclotron frequency propagating almost perpendicular to magnetic field

05 p0698 A72-17017

Two dimensional space charge wave propagation in semiconductors with anisotropic small signal mobility, investigating stability

05 p0632 A72-17097

Coupled longitudinal and transverse plasma waves propagating normal to applied magnetic field, using three fluid model

05 p0700 A72-17230

Circularly polarized hydromagnetic wave propagation upstream in solar wind, noting Doppler shifted whistler and slow electron cyclotron modes

06 p0872 A72-17449

Single-ended Q machine grid-excited density perturbation and ion wave propagation properties from linearized Vlasov equations

06 p0855 A72-17514

Plasma microinstabilities due to ion acoustic waves propagation with double-humped ion velocity distribution function in Q machine

06 p0855 A72-17516

Electrostatic wave propagation and damping in thermally ionized collisionless alkali plasma, determining electron and ion densities, electron temperature and ion distribution function

06 p0856 A72-17521

Electrostatic hf wave propagation in one dimensional collisionless plasma, describing electron trapping and oscillations and resonance-produced sidebands

06 p0858 A72-17544

Stratified anisotropic multilayer plasma wave propagation from transverse field equations, using Green function and Fourier transform method

06 p0773 A72-17597

Papers on microwave engineering covering surface finish importance for waveguide propagation, parametric amplifiers and voltage breakdown of microwave antennas

06 p0783 A72-17737

Free flexural wave propagation in doubly periodic structures, obtaining natural frequencies

06 p0894 A72-17764

Wave propagation in single node clad glass fiber light waveguide, discussing fiber core minimum diameter and various loss mechanisms

06 p0825 A72-17773

Resonant frequency, phase velocities and dispersion curves for wave propagation in isotropic elastic cylinders

06 p0895 A72-17854

Blood flow mathematical formulation, considering tissues constitutive equations, geometrical configurations, arterial wave propagation, etc

06 p0768 A72-17959

Seasonal effects and propagation fluctuations in time-frequency comparison measurements with vlf waves, noting optimal RC filter

06 p0818 A72-18289

Low frequency drift instability in local electron cyclotron resonance produced plasma, discussing oscillation fundamental frequency characteristics, wave propagation, density and potential waves, etc

07 p1039 A72-18799

Ring-plane type slow wave structure hot tested near 3 cm for scale modeling in mm range

07 p0938 A72-18854

Nonlinear monochromatic Alfvén wave propagation parallel to magnetic field in anisotropic plasma with long wavelength beam instability

07 p1039 A72-18915

Ionization wave propagation in inert gas due to microwave resonance quanta diffusion, explaining plasmaguide phenomena

07 p1040 A72-18916

Carrier wave growth during propagation through negative differential mobility n-type GaAs under nonuniform dc bias conditions

07 p1047 A72-19044

Wave propagation in thin film optical waveguides with gyrotropic and anisotropic substrates, deriving TE and TM mode conversion conditions

[AD-739120] 07 p0940 A72-19230

Composite elastic beams equations under initial stress, investigating flexural wave propagation and structural stability

07 p1090 A72-19733

Plane harmonic waves propagation in stressed polycrystalline bodies with slight orthotropy in unstressed state, substantiating theory for initial stress determination by ultrasonic technique

07 p1090 A72-19753

Uniform asymptotic solution near wavefront of transient field propagation in inhomogeneous dispersive media

[AD-745077] 07 p0946 A72-19800

Wave diffusion related to phenomena governed by linear hyperbolic partial differential equations of second order, presenting Cauchy problem solution

07 p1035 A72-20090

Wave propagation in hollow elastic/viscoplastic sphere under impact load, assuming Mises condition, isotropic hardening and incompressibility

07 p1096 A72-20429

Drift waves propagation in ionized plasma, considering drift rate, ion sound phase velocity and effect of impurities

07 p1045 A72-20444

One dimensional nonlinear waves propagation in dissipative gas, obtaining exact solutions by method of separation of variables

07 p0973 A72-20500

Acoustic and gravity waves nonlinear propagation and structural deformation in isothermal and incompressible atmospheres with traveling wave induction

07 p0981 A72-20696

Geomagnetic field fluctuations during storms, considering Alfvén waves generation and propagation in solar wind and magnetosphere

08 p1153 A72-20717

Hf potential effect on high amplitude waves propagation in magnetoactive plasma plane layer, noting particle density distribution

08 p1212 A72-21211

Nonisentropic flow behavior behind propagating self similar blast wave

[AD-745485] 08 p1252 A72-21260

Longitudinal elastic wave propagation along composite bar with conical sections and interface discontinuities in material properties, solving multiple reflection by finite difference method

08 p1245 A72-21606

Steady nonlinear waves propagation along ring electron beam axis analogous to ionospheric E layer

08 p1215 A72-21723

Plane wave propagation in laminated reinforced elastic plates with difference-differential equations analysis

08 p1247 A72-21809

Landau instability effect on density waves propagation in self gravitating disk of differentially rotating and nonrotating stars populations, noting radial flow of matter

09 p1384 A72-22518

Galactic spiral density waves instability effects, noting local centroid radial motion and apex deviation

09 p1384 A72-22519

Physical optics approximation study of gravitational waves effect on electromagnetic propagation, noting unobservability of local scintillation effect

09 p1351 A72-22683

Thermoelastic disturbance wave front propagation in elastic half space after thermal shock at surface

09 p1399 A72-22705

Wave propagation effects on irregularities observation in equatorial electrojet, presenting velocity profile and typical ray path

09 p1300 A72-23024

Stress wave reflection and transmission at interfaces between homogeneous isotropic linear elastic materials

09 p1353 A72-23501

Linear theory of elasticity application to wave propagation in homogeneous isotropic material with deformable microstructure, presenting approximate solution method

09 p1353 A72-23552

Wave propagation in bonded discretely inhomogeneous elastic cylindrical rods, including longitudinal and radial motions

09 p1409 A72-23563

Post bifurcation finite amplitude baroclinic instability, emphasizing wave vectors configuration with quadratic nonlinear interactions 09 p1347 A72-23654

VLF waves propagation dependence on ionospheric horizontal electron density gradients associated with midlatitude depression from FR-1 satellite observation 10 p1472 A72-24060

Input impedance of plane antenna immersed in plasma within magnetic field and propagating sheath waves 10 p1520 A72-24132

Numerical solution of nonlinear integrodifferential equation governing finite amplitude wave propagation on concentrated vortices 10 p1468 A72-24419

Internal Alfvén gravity waves propagation in rotating Boussinesq inviscid adiabatic conducting fluid shear flow within transverse magnetic field, considering electromagnetic and Coriolis forces effects 10 p1511 A72-24476

Stability of superluminous and subluminal waves propagating transversely to external uniform magnetic field in streaming relativistic plasmas 10 p1522 A72-24608

Book on continuous transitions in open waveguides covering plane directive surface, single wire transmission line and layered waveguide surface wave propagation modes 10 p1436 A72-24675

Closed form solution for spherical and cylindrical wave propagation in laser conductively heated plasma, considering account of nuclear fusion energy recovery 10 p1522 A72-24721

Phase velocity and Landau damping of ion acoustic waves propagating through plasma boundary layer at conducting sphere or cylinder based on two fluid model 10 p1523 A72-24746

Electromagnetic wave propagation in weakly nonstationary plasma, determining variations of wave amplitudes and polarization characteristics 10 p1523 A72-24782

Electromagnetic wave propagation and absorption in weakly inhomogeneous plasma layer, calculating conditions for transformation into plasma wave 10 p1523 A72-24799

Electron-neutral collisions effects on wavelength and damping of electrostatic waves propagation in Ar and He plasmas 10 p1525 A72-25143

Impact-produced deformations in nonlinear viscoelastic rod of finite length, studying pulse propagation as nonlinear boundary value problem 11 p1685 A72-25353

Grid produced LF electrostatic perturbations propagation and damping in near isothermal plasma, discussing ion ballistic contributions to ion acoustic waves 11 p1692 A72-25520

Thermoelastic waves propagation in homogeneous isotropic medium under external generic forces and with distributed heat sources 11 p1734 A72-25676

Acoustic and elastic HF waves propagation in nonuniform cylindrical waveguides, deriving asymptotic approximate solutions 11 p1686 A72-25726

Pump and unloading valve hydraulic system model with waves processes allowance in connecting pipe, discussing liquid mass and leakage effects on stability 11 p1578 A72-25770

Turbulence theory 2/3 law applicability to optical spherical wave propagation through turbulent atmosphere, comparing to von Karman model 11 p1686 A72-25772

Magnetoacoustic wave propagation and reflection in equilibrium inhomogeneous plasma under nonuniform magnetic field 11 p1695 A72-26094

Russian papers on mathematical problems of wave propagation and diffraction theory, covering elastic and short waves and point sources 11 p1688 A72-26377

Elasticity theory dynamic equations solutions concentrated near longitudinal or transverse wave beams propagating in inhomogeneous isotropic space 11 p1689 A72-26383

Surface waves propagation in inhomogeneous elastic body, deriving wave equations asymptotic solutions 11 p1689 A72-26384

Magnetospheric equatorial compressional wave propagation to ground observed as transverse wave, noting plane of polarization 11 p1625 A72-26413

Hydromagnetic waves propagation and horizontal group velocity westward from dawn terminator to dark hemisphere, inferring magnetosphere properties 11 p1625 A72-26414

Radiation propagation in optically thin anisotropic noncrystalline media, obtaining explicit formulas for Stokes parameters of transmitted and scattered radiation 12 p1865 A72-27052

Resultant material and spatial energy propagation vectors for waves of small amplitude superposed on large static deformation in elastic materials 12 p1879 A72-27123

Elastic wave propagation and energy scattering in materials reinforced by inextensible fibers 12 p1881 A72-27252

Longitudinal elastic impact wave propagation along branched thin rods, using Timoshenko theory 12 p1881 A72-27256

Reflection and transmission of plane E wave incident on moving conducting medium, discussing growing wave excitation 12 p1782 A72-27490

Two dimensional wave motion generated in prestressed body by crack extension, noting consistency with fracture criterion related to cohesive traction zones near crack tip 12 p1883 A72-27560

Wave packet group velocity concept interpretation and application, considering propagation in dissipative media 12 p1783 A72-27719

Acceleration waves propagation in elastic-plastic strain hardening rate independent solids, obtaining solution for discontinuity change in strength in homogeneously prestressed medium 12 p1846 A72-27729

Experimental earth station for wave propagation studies in satellite communications using frequency range above 10 GHz 12 p1785 A72-27801

Wave equations for electromagnetic wave propagation in electron-ion-neutral particle magnetoplasma, using macroscopic approach 12 p1852 A72-27850

Velocity behavior of shear waves propagating in uniaxially prestressed isotropic elastic body 12 p1886 A72-27982

Unloading wave propagation in semiinfinite elastoplastic cylindrical rod for concave stress-strain diagram with no initial linear segment 13 p2053 A72-28388

Transient planetary Rossby waves dynamics in winter stratosphere forced from below, using quasigeostrophic midlatitude beta plane approximations 13 p1988 A72-28550

Ultrasonic signal propagation with distance along steel sphere surface compared with lunar seismic signal, discussing surface dent and lunar crater effects 13 p2035 A72-28619

Frequency equation for torsional wave phase velocity in solid circular rod under initial tension, plotted for various propagation modes 13 p2002 A72-28620

Asymptotic expansion method for nonsinusoidal wave processes described by Lagrange-type partial differential equations, using averaged form of generalized Hamiltonian variational principle 13 p2003 A72-28718

Unsteady state propagation of weak nonlinear plasma waves in magnetic field, discussing shock wave formation and compression pulse evolution 13 p2012 A72-29124

Computerized simulation of single large amplitude whistler wave propagation in plasma, noting collisionless damping, oscillations and equilibrium 13 p2012 A72-29128

Acoustically scaled simulation of sonic boom N-wave energy penetration into ocean for flat air-water interface 13 p1951 A72-29587

Gravity wave propagation in realistic thermospheric model, considering temperature, wind, Coriolis force, viscosity, thermal conduction and ion drag effects 13 p1951 A72-29652

Harmonic elastic wave propagation in composites with periodic structures by variational methods developed from crystal lattice studies 13 p2060 A72-29696

Elastic waves propagation in randomly inhomogeneous fiber reinforced or layered composites from perturbation methodology for electron and vibrational waves in disordered media 13 p2061 A72-29697

Stationary nonlinear ion acoustic oscillations in dense weakly ionized current carrying plasma, considering wave propagation velocity and instability process 13 p2019 A72-29988

Negative ions and collision frequency effects on circularly polarized F.L.F and V.L.F wave propagation in ionosphere 14 p2084 A72-30128

Quasi-longitudinal and quasi-transverse plane wave propagation in anisotropic elastic-plastic solids, approximating Be single crystal behavior 14 p2163 A72-30176

Harmonic waves propagation in infinite transversely isotropic cylinder with elliptic cross section, obtaining solution in terms of Mathieu functions 14 p2163 A72-30190

Stress distribution variations and wave propagation in viscoelastic rod of finite length under impact 14 p2163 A72-30191

Electromagnetic wave propagation in weakly nonstationary plasma, determining variation with time and polarization plane rotation 14 p2136 A72-30219

Nonlinear dispersive wave propagation problems singly and multiply periodic solutions, using perturbation and numerical approximation methods 14 p2130 A72-30227

Closed form solutions for one dimensional nonlinear waves in strain rate-sensitive elastoplastic material, describing dispersed wave motion behind propagating shock front 14 p2164 A72-30298

Electrostatic cyclotron harmonic waves propagation in inhomogeneous electron plasma slab, deriving RF electric field 14 p2138 A72-30397

Plane nonlinear wave propagation in transonic region of two dimensional and axisymmetric steady flows, considering disturbance at arbitrary point 14 p2095 A72-31000

Rietz-Kantorovich method reduction of scalar problem for wave propagation along direction surface to boundary value problem, discussing parametric resonance and periodic waveguides 14 p2132 A72-31118

Carrier wave propagation at semiconductor surface with electron drift, discussing solid state traveling wave amplifier design 15 p2290 A72-31288

German monograph on theory of simple waves and application in continuum mechanics covering phase curves for quasi-linear autonomous system 15 p2275 A72-31505

One dimensional wave pulse propagation, attenuation and dispersion in uniaxially reinforced steel-epoxy resin composites 15 p2325 A72-31528

Submillimeter plane monochromatic waves propagation in ground layer of turbulent atmosphere, deriving received signals levels fluctuations 15 p2195 A72-31653

Wave propagation in inhomogeneous anisotropic time varying moving media, discussing generalized dispersion equation 15 p2196 A72-31688

One dimensional wave equation for stress wave propagating at variable velocity for case of monotone decreasing rate 15 p2327 A72-31738

Ultrasonic wave propagation in single crystals, discussing linear elastic wave attenuation, anisotropic interactions, particle displacement polarization and energy flux deviation 15 p2292 A72-31834

Steepest descent path of integral describing transient plane wave propagation in anisotropic cold plasma, relating to evanescent wave arrival 15 p2285 A72-32109

VLF wave normal direction measurement during propagation through ionosphere by Doppler technique, using rocket-borne receivers 15 p2201 A72-32332

Nonlinear anisotropic elastic constitutive equations for micromorphic and micropolar mixtures, investigating plane wave propagation via field equations with restricted coupling 15 p2278 A72-32446

Nonspherical thermal wave propagation, considering two dimensional structure wave front radiative diffusion problem 15 p2336 A72-32513

Wave packet theory application to multimode laser cavity electromagnetic/optical/field analysis 15 p2251 A72-32649

Ferrite and dielectric element waveguide phase shifters with rectangular hysteresis loop, deriving differential phase and attenuation constants for wave propagation 15 p2202 A72-32662

Magnetoactive plasma transverse waves propagation near electron gyrofrequency harmonics, taking into account electron collisions and relativistic effects 15 p2289 A72-32734

HF electric field effect on ultrasound wave propagation in semiconductor, noting amplification factor dependence on electron heating 15 p2279 A72-32739

Wind direction rotation with altitude and time dependent downward phase propagation observed by vapor trail experiments, suggesting upward propagation of atmospheric waves 16 p2383 A72-32969

Longitudinal, transverse and bending waves propagation in elastic shells, using Hadamard method within linear shell theory 16 p2465 A72-32982

Longitudinal and transverse waves propagation and decay in elastic membranes with allowance for coupling effects, using Hadamard method 16 p2465 A72-32983

Strain rate history effects on stress incremental wave front propagation in elastic bars, considering Taylor-Karman-Rakhmatulin theory 16 p2466 A72-33103

First and second order shock discontinuity waves propagation in thermoelastic incompressible solids, deriving Piola-Kirchhoff stress tensor via Clausius-Duhem relation 16 p2423 A72-33109

Plane hydromagnetic wave propagation in rotating fluid permeated by variable magnitude and direction magnetic field, observing wave-associated critical level 16 p2436 A72-33567

MHD wave propagation and generation during spin-up of rotating viscous incompressible electrically conducting fluid 16 p2436 A72-33572

Transient elastic wave propagation in circular cylinder during sudden torsional shear stress application to end surface, noting surface particle velocity and stress 16 p2426 A72-33660

Russian monograph on ionospheric measurements covering plasma parameters, wave propagation, absorption sounding methods and radio communication applications 16 p2387 A72-33875

Alfven wave propagation in interplanetary medium for solar wind microscale fluctuations, using stationary spherically symmetrical model 16 p2449 A72-33912

Sonic boom induced pressure wave propagation and attenuation in water, comparing ballistic range measurements with theoretical predictions 16 p2349 A72-34080 [ALAA PAPER 72-654]

Growth of an acceleration wave in an elastoplastic isotropic medium undergoing finite deformation 17 p2580 A72-34277

First and second moment of an optical wave propagating in a random medium - Equivalence of the solution of the Dyson and Bethe-Salpeter equation to that obtained by the Huygens-Fresnel principle. 17 p2580 A72-34290

Analysis of wave propagation in elastic cylindrical shells by the perturbation method. 17 p2623 A72-34307

The hodograph transformation in plastic waves with discontinuous loading conditions. [ASME PAPER 71-APMW-12] 17 p2624 A72-34308

Constitutive equations for plane harmonic waves propagation in composite fiber reinforced elastic material 17 p2625 A72-34321

Electromagnetic wave propagation and wave-vector diagram in space-time periodic media. 17 p2514 A72-34381

A lattice model for stress wave propagation in composite materials. [ASME PAPER 72-APM-52] 17 p2627 A72-34778

Wave propagation in a viscoelastic fiber subjected to transverse impact. [ASME PAPER 72-APM-27] 17 p2570 A72-34791

On natural vibrations and waves in laminated orthotropic plates. [ASME PAPER 72-APM-14] 17 p2581 A72-34803

Longitudinal pulses propagation in straight hollow circular elastic tubes, presenting strain-time records [ASME PAPER 72-APM-10] 17 p2629 A72-34806

WKB large frequency expansion solution for elastic waves propagating into inhomogeneous elastic medium with harmonic periodicity, using perturbation method [ASME PAPER 72-APM-3] 17 p2630 A72-34810

Elastic wave propagation in a joined cylindrical-conical-cylindrical shell. [SESA PAPER 1983] 17 p2630 A72-34819

One-dimensional wave pulses in steel-epoxy composites. [SESA PAPER 1945] 17 p2631 A72-34823

Propagation of spherical waves in a weak static gravitational field 17 p2581 A72-35170

Ultrasonic wave propagation in metal-matrix composites. 17 p2560 A72-35287

The propagation of non-axisymmetric Alfven waves in an argon plasma. 17 p2591 A72-35371

Rayleigh wave propagation on a piezoelectric-semiconductor boundary 17 p2596 A72-35541

On the stability of obliquely propagating whistlers. 17 p2517 A72-35600

Propagation and instability characteristics of small signal electro-fluid-mechanical space charge and polarization waves in nonhomogeneous fluids 17 p2542 A72-35612

Calculations of electron-profile disturbances in the F region during the passage of a neutral wave 17 p2551 A72-35861

Theoretical explanation of the solar limb effect. 17 p2618 A72-35895

Numerical calculation of energy storage, wave dispersion and propagation in waveguides of periodic resonator chains at high frequencies 18 p2657 A72-36105

German monograph - Wave propagation in glass-fiber light waveguides 18 p2697 A72-36249

Propagation mechanism of tensor wave in solid elastic body due to impact. 18 p2734 A72-36377

Theory of elastic wave propagation in composite materials. 18 p2703 A72-36395

Moving periodic thermal wave induction of non-linear motions in Boussinesq fluid layer, solving non-linear two dimensional momentum and temperature equations 18 p2681 A72-36485

Elementary plane waves in a Signorini-Cattaneo's thermoelastic solid. 18 p2735 A72-36512

Dual amplitude construction possibility from general field theory couplings and propagators, considering factorization on multiperipheral configuration in translational and rotational modes 18 p2713 A72-36516

Equatorial tropospheric waves induced by diabatic heat sources. 18 p2687 A72-36628

Strong intensity fluctuations of a spherical wave propagating in a randomly refractive medium 18 p2661 A72-36659

Weak waves, characteristics, and the problem of flows past slender profiles in electrohydrodynamics 18 p2716 A72-36896

Fourth moment of a wave propagating in a random medium. 18 p2712 A72-37025

Digital computer simulation of human systemic arterial pulse wave transmission - A nonlinear model. 18 p2655 A72-37028

Wave propagation in half plane consisting of two joined elastic quarter planes under in-plane disturbances normal to free surface, obtaining stresses at interface 18 p2738 A72-37069

Propagation and attenuation of harmonic waves in a viscoelastic circular cylinder. 18 p2738 A72-37070

Wave propagation and dispersion in space-time periodic media. 18 p2663 A72-37208

Sideband growth in nonlinear Landau wave-particle interaction. 19 p2838 A72-37327

Wave propagation in generalized thermoelasticity. 19 p2870 A72-37412

Determination, by X-ray photometry, of the frequencies of thermal oscillations which propagate themselves, following the axes of symmetry in a potassium chloride single crystal, at temperatures of 295, 80, and 5 K 19 p2844 A72-37791

Reflectionless ionospheric propagation of non-guided VLF descending wave near low hybrid resonance maximum frequency, investigating energy trajectory 19 p2790 A72-37793

A universal connexion for waves in anisotropic media. 19 p2875 A72-37840

Asymptotic method application to wave propagation in nonlinearly elastic rods, describing displacement field by perturbation series 19 p2875 A72-37885

Wave reflection and transmission characteristics of angled rectangular waveguide, deriving scattering matrix 19 p2764 A72-37938

Propagation of bending-torsional waves in a thin curved rod with allowance for the shear effect 19 p2872 A72-38189

Geomagnetic field fluctuations during storms, considering Alfven waves generation and propagation in solar wind and magnetosphere 19 p2791 A72-38345

Solitary waves properties and propagation at right angles to magnetic field in two ion beam magnetized plasma 19 p2841 A72-38441

Wave propagation in plasmas with fluctuations. 19 p2842 A72-38525

Unsteady weakly nonlinear waves in a multicomponent plasma with allowance for weak dissipation 19 p2842 A72-38528

Propagation of surface waves along a plane boundary between two magnetoactive plasmas 19 p2842 A72-38532

Energy propagation in a Cauchy elastic material. 19 p2878 A72-38718

Propagation of Alfven-gravitational waves in a stratified perfectly conducting flow with transverse magnetic field. 19 p2843 A72-38791

Constitutive equations and wave propagation of anisotropic perfectly plastic materials. 19 p2878 A72-38800

Acoustic and gravity waves nonlinear propagation and structural deformation in isothermal and incompressible atmospheres with traveling wave induction 20 p2915 A72-39011

Elastic wave propagation in a rod of finite length with a variable cross section 20 p2978 A72-39321

Small forced oscillations produced by infinite plate vibrations in stratified and rotating viscous fluids, investigating resonance effects on propagation 20 p2912 A72-39330

Nonlinear monochromatic Alfven wave propagation along magnetic field in anisotropic rarefied plasma with firehose instability 20 p2957 A72-39381

Propagation of ionization wave in rarefied noble gases due to microwave resonance quanta diffusion, explaining plasmaguide phenomena 20 p2957 A72-39382

A long line as a limit of an infinite quadrupole chain 20 p2904 A72-39592

A similarity solution for viscous internal waves. 21 p3044 A72-40118

Quasi-one-dimensional analysis of gaseous free detonations. 21 p3044 A72-40194

Fresnel-like interference on an ion-wave decay in a plasma. 21 p3089 A72-40200

Microwave scattering from a radially propagating ion acoustic wave in a positive column. 21 p3089 A72-40201

Nonexistence of ion acoustic waves and Landau damping driven electrostatically in an ideal Q machine. 21 p3090 A72-40340

Nonlinear theory of the monochromatic circularly polarized VLF and ULF waves in the magnetosphere. 21 p3015 A72-40480

Spin wave theory and sublattice magnetization of Cr obtaining wave velocity 21 p3097 A72-40626

Propagation of horizontally polarized VLF waves - Systems implications. 21 p3021 A72-40905

Linear and Alfven waves propagation in incompressible beam-plasma systems, deriving dispersion law 21 p3092 A72-40994

Variational theorems for harmonic waves in elastic composites with periodic structures, considering wave propagation in layered and in fiber reinforced composites 21 p3119 A72-41101

Linear equilibrium stability relationship to wave propagation through elastic medium, considering Hadamard theorem proofs 21 p3085 A72-41102

Combined tension-torsion elastic-plastic waves as propagating singular surfaces. 21 p3121 A72-41244

Wave propagation in thermal rate dependent thermoelastic materials. 21 p3131 A72-41479

Propagation of two-dimensional strong discontinuity waves in an elastic-viscoplastic medium. 21 p3124 A72-41503

Holographic system resolving capacity increase by oblique illumination of object, analyzing plane monochromatic wave transmission through one dimensional semitransparent body 21 p3058 A72-41791

Numerical analysis of wave processes in a three-layer strip with rigid filler 22 p3232 A72-41872

Evanescent and internal gravity wave propagation effects on atmospheric dynamics, considering momentum transfer, energy dissipation and turbulence 22 p3168 A72-41964

Asymptotic expansion method for nonsinusoidal wave processes described by Lagrange-type partial differential equations, using averaged form of generalized Hamiltonian variational principle 22 p3204 A72-42095

Bending waves propagation through flat plate forming rigid sound bridge between two parallel plates, calculating energy transfer at LF oscillations 22 p3234 A72-42128

Finite difference theory for Lamé equations of elastic waves propagation in two dimensional body under mixed boundary conditions 22 p3234 A72-42144

Multiple scattering of bending waves by random inhomogeneities. 22 p3235 A72-42460

The problem of the boundary conditions in thermosphere dynamics. 22 p3201 A72-42510

Wave propagation in a truncated conical shell. 22 p3235 A72-42524

Atmospheric waves observed in the planetary boundary layer using an acoustic sounder and a microbarograph array. 22 p3202 A72-42599

Asymptotic method for nonlinear wave systems of periodic structure 22 p3155 A72-42657

- Dynamic photoelasticity application to periodic/vibrating and pulse/stress wave fields, considering loading rate effect on material fringe value
22 p3237 A72-42767
- Some recent experimental investigations in stress-wave propagation and fracture.
22 p3237 A72-42768
- Plane waves in a new theory of thermoelasticity.
22 p3239 A72-42856
- Propagation of Rayleigh waves on visco-elastic cylindrical surfaces placed in a magnetic field.
22 p3207 A72-42876
- On the propagation of Love type waves in an infinite cylinder with rigidity and density varying linearly with the radial distance.
22 p3207 A72-42878
- Wave propagation in plasma modulated by external electric field, noting dispersion equation for coupled waves and instability conditions
22 p3212 A72-43101
- Nonlinear evolution of a quasi-monochromatic packet of spiral waves in a plasma
23 p3318 A72-43324
- Plasma frequency, hybrid frequency and harmonic gyrofrequency electron resonances due to electrostatic waves in ionosphere observed with topside sounders aboard rockets and satellites
23 p3263 A72-43513
- Wave attenuation during plasma propagation, discussing particle collisions, absorption effect on geometric optics and linear mode coupling in cold magnetized plasma
23 p3320 A72-43519
- Apparent constant wavelength oscillations in a bounded plasma.
23 p3320 A72-43577
- Parabolic approximation of spatially bounded square and Lorentz two dimensional light pulse propagation in homogeneous isotropic linear medium without dispersion
23 p3313 A72-43682
- Modified Hellinger-Reissner variational method applicable to harmonic waves moving normal to fiber reinforced layered elastic composite, tabulating eigenfrequencies
23 p3351 A72-44061
- Integration scheme for two-dimensional impulsive waves in a linear acoustic medium.
23 p3314 A72-44250
- Acceleration waves in orthotropic elastic materials.
23 p3354 A72-44342
- Acoustic transmission and reflection by a shear discontinuity separating hot and cold regions.
23 p3315 A72-44373
- Book - The effects of the turbulent atmosphere on wave propagation.
24 p3379 A72-44650
- Wave propagation in a thin hollow cone by a finite element method.
24 p3458 A72-44886
- Method of characteristic application to curved beam motion under pulse type loading, investigating photoelastic fringe patterns and pulse propagation
24 p3458 A72-44888
- A new concept for correcting the attenuation effects in a shock tube.
24 p3388 A72-44985
- Divergent cylindrical detonation of nitromethane
24 p3463 A72-45037
- Unsteady longitudinal viscoelastic vibrations of a rod of variable thickness at small values of time
24 p3459 A72-45265
- Tropospheric wave motions with baroclinic basic flow in equatorial latitudes.
24 p3399 A72-45485
- Thermoelastic waves propagation in homogeneous isotropic medium, considering potential functions
24 p3460 A72-45598
- Radiation propagation in optically thin anisotropic noncrystalline media, obtaining explicit formulas for Stokes parameters of transmitted and scattered radiation
24 p3425 A72-45705
- WAVE RADIATION**
U ELECTROMAGNETIC RADIATION
WAVE REFLECTION
- Small harmonic oscillations of isothermal atmosphere due to acoustic-gravity wave downward reflection caused by kinematic viscosity increase with altitude
01 p0102 A72-10229
- Electromagnetic wave line-of-sight propagation based on geometrical optics for different refractivity profiles above sea, noting earth surface reflection role
01 p0026 A72-10404
- Sporadic E layer reflection behavior measurements from two closely located stations, deriving drift direction and critical frequencies daily variation
01 p0055 A72-10431
- Earth surface roughness effects on vertical Hertz dipole electromagnetic field reflection
01 p0027 A72-10447
- Magnetoinic component with fluctuating elliptical polarization during wave reflection from F 2 layer, discussing suppression mechanism
01 p0028 A72-10593
- Electron concentration profiles in D region from radio wave partial reflection coefficients
01 p0028 A72-10614
- Nonlinear skin effects in gas discharge and semiconductor plasmas during electromagnetic wave propagation and dissipation, obtaining wave amplitude and carrier temperature dependence on reflection parameters
01 p0102 A72-10974
- Transient electromagnetic plane wave ionospheric transmission and reflection, considering impulsive and step modulated sine wave excitations
01 p0031 A72-11102
- Ionospheric reflection height calculation according to oblique electromagnetic backscatter sounding data at two frequencies
02 p0172 A72-11943
- Nighttime ionospheric radio wave propagation, determining geomagnetic latitude variations effects on absorption and reflection
02 p0218 A72-11944
- Acoustic absorption materials weak shock wave reflection and attenuation determination by shadowgraph-schlieren photography and pressure transducers
02 p0259 A72-12177
- Electromagnetic wave reflection and transmission by stratified multilayered parallel moving plasma media, using propagation matrices
02 p0182 A72-12652
- Diffuse reflection of point source/flare/light emission for cold dwarf star semiinfinite plane parallel atmosphere, calculating polarization
02 p0285 A72-12831
- Sound reflection by dense doubly periodic grating parallel to rigid baffle, describing asymptotic characteristics by double lattice virtual mass including mirror image
03 p0387 A72-12914
- Plane electromagnetic wave reflection and transmission at moving boundary between two dielectric media
03 p0321 A72-13091
- Rayleigh distance for reflection from curved surfaces in Cassegrain subreflector geometrical optics design
04 p0499 A72-15207
- Electromagnetic wave reflection from region with variable drift velocity and polarization of waves propagating in nonuniformly moving medium, applying to isotropic plasma
04 p0491 A72-15421
- Fock reflecting formulae expansion to moving interfaces from Fresnel laws, interpreting solution in terms of geometrical optics
04 p0491 A72-15422
- Reflection from aperture of long E-plane sectoral horn antenna, determining electrical impedance by asymptotic diffraction theory
04 p0501 A72-15424
- Infinitely long rectangular waveguide discontinuity problem, calculating reflection and transmission coefficients of wave propagation
04 p0491 A72-15428
- Long E-plane sectoral horn, deriving complex reflection coefficient from aperture by geometrical diffraction theory
06 p0781 A72-17346
- Light intensity distribution from ultrasonic surface waves reflection to probe surface acoustic propagation characteristics
[AD-739047]
06 p0848 A72-17851
- Acoustic waves refraction, reflection and transmission from moving medium layer with space-dependent velocity, considering Poiseuille flow three sublayer approximation
06 p0848 A72-17852
- Radiation intensity angular distribution from optically thick plane cloud layer reflection, relating photon survival probability and scattering functions
06 p0807 A72-17939
- Pulse reflection of polarized plane electromagnetic wave from cold plasma ionosphere model with vertical magnetic field
06 p0777 A72-18729
- Transient plane wave reflection and scattering by periodic grating of thin conducting cylinders
06 p0777 A72-18736
- Pattern recognition through atmospheric turbulence by reflected coherent light power spectrum recording technique, using Wiener-Khinchin theorem
07 p0982 A72-19054
- Pulsed radiography of X ray absorption by plasma behind incident shock wave in Cs vapors, noting mirror behind shock front and wave reflection
07 p1044 A72-19887
- Radio meteors observability and wave reflection from trails, discussing velocities, deceleration and vertical distribution
08 p1130 A72-20712
- Multicomponent meteoritic composition effects on meteor trails radio wave reflections, obtaining ionospheric electron concentration distribution
08 p1131 A72-20805
- Horizontally polarized impulsive plane electromagnetic wave reflection from perturbed linear ionosphere model, obtaining transient response as inverse Fourier transform
08 p1136 A72-21979
- Electromagnetic impulse wave impingement on semiinfinite isotropic plasma slabs with arbitrary incidence angle and polarization, calculating signal reflection in terms of Bessel functions
08 p1137 A72-21990
- Cylindrically guided hybrid TE and TM electromagnetic wave reflection and transmission from Maxwell equations and boundary value problems solution
09 p1278 A72-22605
- Layer-like atmosphere discontinuities effects on earth-space communications, noting electromagnetic waves alteration and reflection by grazing incidence
09 p1279 A72-22898
- Electromagnetic and plasma wave reflection at interface between moving dielectric medium and compressible plasma
09 p1364 A72-23243
- Backscattering by turbulent irregularities derived in context of single scattering corresponding to weak microwave reflections observed in atmospheric sounding
09 p1280 A72-23412
- Stress wave reflection and transmission at interfaces between homogeneous isotropic linear elastic materials
09 p1353 A72-23501
- Two dimensional shock wave interaction with bends in rectangular duct, showing far wall Mach reflection
10 p1464 A72-23879
- Rough surface effects on EM reflection for electromagnetic probing in geophysics, using Rayleigh and Kirchhoff methods
10 p1512 A72-24738
- Reflected light beam transverse shift calculated by energy flux conservation argument, noting circular polarization and quasi-limit total reflection
10 p1513 A72-24932
- Perturbation method study of governing differential equations for wave reflection by periodic two-dimensional topography
11 p1685 A72-25358
- Inhomogeneous rarefied plasma, investigating non-local, linear and nonlinear effects on electromagnetic wave reflection and transmission
11 p1694 A72-25717
- X ray diffraction by alpha Ti, calculating reflections relative intensity and position to identify peaks
11 p1658 A72-25826
- Magnetoacoustic wave propagation and reflection in equilibrium inhomogeneous plasma under nonuniform magnetic field
11 p1695 A72-26094
- Angles of arrival and skip distances prediction of radio waves near MUF, using monthly forecasts of quiet and perturbed ionospheric parameters and N(h) profiles
11 p1594 A72-26276
- Superhigh frequency electromagnetic waves diffraction by conducting screen circular aperture with phase change by dielectric disk and multiple internal reflections, noting patterns and backscattering apparatus
11 p1597 A72-26371
- Slow and fast plane magnetoacoustic waves mutual transformation and reflection at plasma and magnetic field inhomogeneities
11 p1698 A72-26643
- Microwave two port waveguide transmission efficiency determination by reflection coefficient measurements
11 p1599 A72-26997
- Boundary reflection and transmission of N-shaped acoustic shock wave radiated from circular pipe into free air space
12 p1844 A72-27262
- High angular resolution optical system to measure light reflection from rough surfaces
13 p2002 A72-28513
- Obliquely incident electromagnetic waves reflection and transmission by moving compressible plasma slab, applying field and wave-four vectors Lorentz transformations to wave equations
13 p2010 A72-28543
- Plane longitudinal displacement wave reflection from fixed surface in micropolar elastic half space, presenting reflection laws and amplitude ratios for specific cases
13 p2056 A72-29001
- Ultrasound reflection from molten core during spot welding of steel alloys as function of geometrical dimensions and configuration and transition zone dimensions
13 p1965 A72-29152

Ionospheric reflection height calculation according to oblique electromagnetic backscatter sounding data at two frequencies

13 p1920 A72-29255

Nighttime ionospheric radio wave propagation, determining geomagnetic latitude variations effects on absorption and reflection

13 p1949 A72-29256

Oblique radio wave propagation through horizontally stratified ionosphere, considering electron collisions effects, reflection behavior and coupling levels

13 p1923 A72-29657

E region drift velocity estimates from amplitude and phase measurements of pulsed radio waves reflected from lower ionosphere

13 p1923 A72-29664

Ionospheric attenuation of 3-100 MHz radio waves, interpreting scatter mode propagation mechanism as total reflection from lower ionizational irregularities

14 p2086 A72-30658

Partial reflection method to obtain D region electron density profiles and collision number

14 p2086 A72-30791

Ionic collision effects on spatial ion wave echoes in single-ended Q machine plasma, noting echo peak amplitude damping

15 p2288 A72-32423

Plane acoustic-gravity wave reflection, refraction and amplification at interface separating two fluids in relative motion, noting shear flow speed effect

16 p2383 A72-32968

Mathematical models for radio attenuation in ice by electromagnetic absorption and reflection from interfaces, noting radar tracking

16 p2363 A72-33290

Longitudinal and transverse electromagnetic wave penetration into semiinfinite collisional plasma with fractionally accommodating boundary, obtaining reflection coefficient and surface impedance

16 p2435 A72-33449

Monochromatic electromagnetic wave reflection and transmission at oblique incidence on sharp plasma boundary of moving ionization source

16 p2363 A72-33481

Nonlinearity effects on finite amplitude, plane uniform oblique shock wave reflection, using inviscid gas analogous solution techniques

16 p2426 A72-33661

Radiation intensity angular distribution from optically thick plane cloud layer reflection, relating photon survival probability and scattering functions

16 p2426 A72-33780

Aircraft short wavelength measurements of cloud reflection and absorption properties for impact on earth radiation budgets

16 p2388 A72-34024

Wave propagation in a stratified turbulent magnetized plasma. I.

17 p2587 A72-34516

Pulsed radiography of X ray absorption by plasma behind incident shock wave in Cs vapors, noting mirror behind shock front and wave reflection

17 p2590 A72-35135

Reflection of weak shock waves from permeable materials.

17 p2581 A72-35250

Wave interference effect in whistler mode reflection coefficients for model lower ionospheres.

17 p2548 A72-35465

Reflection of microwave through laboratory plasma.

18 p2716 A72-36947

Reflection and refraction of elastic waves in edge-impacted rectangular plates.

18 p2737 A72-37065

Wave reflection and transmission characteristics of angled rectangular waveguide, deriving scattering matrix

19 p2764 A72-37938

Radio meteors observability and wave reflection from trails, discussing velocities, deceleration and vertical distribution

19 p2765 A72-38340

Scattering resonances of electromagnetic wave by an infinite plane grating with reflector.

19 p2767 A72-38612

An Irtran-1 reflection filter for the 20-micron atmospheric window.

20 p2928 A72-39897

Book - Terrestrial propagation of long electromagnetic waves.

21 p3023 A72-41532

A problem of electromagnetic wave propagation in a moving plane stratified medium

22 p3155 A72-42653

Reflection and transformation of sound waves in a superfluid liquid at a solid boundary

22 p3207 A72-42956

Acoustic transmission and reflection by a shear discontinuity separating hot and cold regions.

23 p3315 A72-44373

Reflection amplification in thin layers of n-GaAs.

24 p3385 A72-44971

Permittivity measurement of nonmagnetic materials samples in waveguide systems with an unknown movable reflecting load

24 p3404 A72-45504

Reflection and transmission of electromagnetic waves by a moving inhomogeneous medium.

24 p3381 A72-45644

WAVE RESISTANCE

Waveguide model for calculating microstrip discontinuities and T-junctions wave impedances, using orthogonal series procedure

15 p2201 A72-32470

Experimental research on the wave resistance of a thin spindle with an annular shield in a superconic axial flow

24 p3364 A72-45393

WAVE SCATTERING

NT ACOUSTIC SCATTERING

NT ATMOSPHERIC SCATTERING

NT ELECTROMAGNETIC SCATTERING

NT HALOS

NT IONOSPHERIC F-SCATTER PROPAGATION

NT LIGHT SCATTERING

NT MICROWAVE SCATTERING

NT MIE SCATTERING

NT RAMAN SPECTRA

NT RAYLEIGH SCATTERING

NT TROPOSPHERIC SCATTERING

NT X RAY SCATTERING

Numerical-integral equation approach to plane wave scattering from nonplanar conducting surface with sinusoidal height profile for magnetic field parallel to surface ridges

[AD-735574] 01 p0032 A72-11237

Hf wave scattering in inhomogeneous medium, examining asymptotic methods

03 p0390 A72-13973

Parallel polarized electromagnetic waves scattering by radially inhomogeneous isotropic dielectric cylinders, computing scattered field coefficients by Fourier least squares fit technique

04 p0485 A72-14413

Spontaneous and induced Compton scattering of high frequency waves by relativistic electrons in synchrotron sources

04 p0487 A72-14902

Laser produced spark plasma, calculating threshold conditions for onset of stimulated scattering process and self focusing

04 p0559 A72-15346

Light diffuse transmission and reflection by semiinfinite atmosphere with four term scattering indicatrix

06 p0884 A72-18029

Transient plane wave reflection and scattering by periodic grating of thin conducting cylinders

06 p0777 A72-18736

Longitudinal plane harmonic elastic wave scattering and stress concentration at rough circular hole boundary in thin isotropic plate

08 p1243 A72-21230

Plane harmonic compression waves scattering by circular holes in thin elastic plate, calculating dynamic stresses concentration

10 p1554 A72-24179

Dynamic stress concentration around elliptical discontinuities in elastic medium, considering rigid and empty cavity scatterers for compression and vertically polarized shear incident waves

[ASME PAPER 72-APM-D] 10 p1554 A72-24180

Light diffuse transmission and reflection by semiinfinite atmosphere with four term scattering indicatrix

11 p1719 A72-25965

Statistical physics multiple wave scattering-phenomenological radiation transfer equation relations, using Green function

13 p2002 A72-28512

Plane sound wave scattering by acoustically soft sphere at constant subsonic velocity

13 p2003 A72-28797

Enhanced damping of electrostatic wave primary mode due to combination scattering from plasma electron density oscillations

13 p2018 A72-29854

Nonequilibrium plasma wave scattering cross section dependence on energy bands shape and field orientation in semiconductors

13 p2023 A72-29992

Lunar seismogram characteristics interpretation in terms of Gold-Soter powder layer theory, taking into account elastic wave scattering by surface undulations

14 p2154 A72-30506

Diffraction of plane waves scattered by impedance structures in anisotropic medium, noting wedge shaped region with cold plasma under external magnetic field

14 p2086 A72-30809

Langmuir waves scattering by denser plasma ions as dominant turbulent process momentum exchange between dynamic plasmas, applying to galaxies expansion into intergalactic media

15 p2285 A72-32269

Elastic wave scattering by moving slab, calculating reflection and transmission coefficients for various incidence angles, frequencies and motion velocities

15 p2219 A72-32476

Radiation with free convection in an absorbing, emitting and scattering medium.

17 p2637 A72-35046

Propagation mode and scattering loss of a two-dimensional dielectric waveguide with gradual distribution of refractive index.

17 p2530 A72-35469

A model for drift pair and hook burst emission from the solar corona.

17 p2617 A72-35712

Scattering of elastic waves by moving objects.

18 p2709 A72-36403

Bending waves diffraction and scattering by mass impedance loadings of infinite plane plate, considering point load and semiinfinite rib arrays

18 p2739 A72-37203

Scattering of Langmuir waves produced by a beam with finite transverse dimensions.

19 p2839 A72-37337

Source function for radiative fields produced by uniform parallel irradiation of scattering absorbing medium of finite optical thickness, using radiative transfer linearity

19 p2834 A72-37837

A multiple-scattering model of the diffuse component of lunar radar echoes.

20 p2903 A72-39473

Stability of nonradial vibrational modes of relativistic neutron stars.

20 p2972 A72-39869

Wave scattering at a step in a circular multiwave waveguide

21 p3016 A72-40781

Scattering of a spherical wave at a spherical discontinuity with an arbitrary radial distribution of the refractive index

21 p3016 A72-40793

Randomly coupled flexural and longitudinal vibrations of plates.

21 p3120 A72-41111

Applicability bounds for the equation describing the mean field in a discrete scattering medium with allowance for the correlation of the scatterers

22 p3155 A72-42660

WAVE SUPERHEATERS

U HYPERVELOCITY WIND TUNNELS

U SHOCK TUBES

WAVEFORMS

NT PULSE AMPLITUDE

NT PULSE DURATION

NT SAWTOOTH WAVEFORMS

NT SQUARE WAVES

Atmospheric waveforms in relation to source location, source vicinity electric field properties, VLF radio wave propagation, frequency spectra and lightning discharges

01 p0024 A72-10124

Voltage and current waveforms monitoring on sampling oscilloscope for TRAPATT microwave oscillator performance optimization

01 p0038 A72-10653

Radar backscatter time response waveforms for cube from If data and diffraction analysis

01 p0030 A72-10843

Signal waveform ensuring maximum reception stability on correlated noise background with peak limiting

02 p0183 A72-12760

Power spectrum analysis of multilevel digital signals phased modulated by arbitrary pulse shapes, giving examples for rectangular and raised-cosine pulses

02 p0183 A72-12797

Acoustic pulse generation and transmission loss characteristics measurement by single pulse method with simple shape to facilitate Fourier analysis

03 p0388 A72-12955

Galactic spiral arm structure theory, discussing density wave pattern and material objects concepts

03 p0418 A72-13105

Laser pumping pulse shape effects on second harmonic emission waveform during nonlinear crystal excitation by ultrashort light pulse

03 p0366 A72-13368

Single mode solid state laser periodic Q switching effects on spike pulse shape and synchronization by harmonic analysis with convergent series

03 p0366 A72-13371

Portable electronic wattmeter for nonsinusoidal waveform low power factor circuit measurement, discussing design, calibration and applications [IEEE PAPER 8,2]

03 p0332 A72-13757

Computerized simulation for AM radio receiver waveform performance degradation under pulsed interference

03 p0324 A72-14035

N-wave dynamic magnification factors for sonic bangs response on complicated structures

04 p0464 A72-14849

- Electric field rise times of first and subsequent lightning return strokes, discussing waveform oscillograms
06 p0841 A72-17822
- Shf resonator small resonant frequency shift and Q factor changes measurement based on FM signal envelope shape analysis
07 p1046 A72-20508
- Firing characteristics of insensitive electroexplosive devices under impulsive waveforms, discussing theory, design and application of waveform generators
08 p1220 A72-20763
- Optimal synthesis of four radar waveform classes with distinct resolution properties based on target environment analysis
08 p1133 A72-21403
- Single picosecond light pulses from mode locked Nd-glass laser, discussing temporal structure, spectral energy distribution and pulse shape measurements
09 p1324 A72-23082
- Pulsed carbon dioxide laser output monitor with Ge cylinder using photon drag effect to measure radiation pulse profile
09 p1326 A72-23389
- Noctilucous cloud wave structure, discussing motions in high atmosphere, ice crystal formation, energy sources and observations
10 p1474 A72-24707
- Output voltage characteristics of single phase thyristor inverter based on pulse duration modulation with direct shaping of control pulses, considering harmonic coefficients
11 p1603 A72-25277
- Laser pulse form effect on confined plasma heating, taking into account inverse electron-ion bremsstrahlung and stimulated Compton scattering
11 p1651 A72-26672
- ELF wideband noise receiver for atmospheric waveshape magnetic tape recording, computer processing and system simulation
12 p1791 A72-27637
- Transient stress pulses propagation in obliquely laminated composites, comparing analytically predicted waveforms with experimental results
13 p2060 A72-29693
- Noiselike FM signals shaping by numerical periodic sequences, analyzing FSK signals
14 p2085 A72-30337
- Crab pulsar LF radiation polarization parameters and pulse shapes, showing highly polarized precursor component
14 p2156 A72-30567
- Steady state laser mode locking with saturable absorber, describing pulse shape and amplitude as function of quantity of absorbing medium
14 p2111 A72-30793
- Short signal pulse shaping based on phase and amplitude selective properties of distributed parametric amplifiers operating under nonlinear conditions
14 p2090 A72-31112
- Laser interference fringe jitter due to wavelength instability, suggesting pulse shape blurring intensity variation control by flat or large-angle wedge beam splitter
15 p2249 A72-32166
- Nonspatial thermal wave propagation, considering two dimensional structure wave front radiative diffusion problem
15 p2336 A72-32513
- Shift register implemented binary transversal filter type digital pulse waveform generators truncation and approximation error spectrum analysis via inverse Fourier transform
16 p2362 A72-32854
- TDM and FDM digital communication systems performance comparison, noting equivalence in theoretical efficiency and generated waveforms
16 p2363 A72-33216
- The steepening of the wavefront due to nonlinearities /An electric model test regarding the origin of shock waves/
17 p2582 A72-35428
- Performance of a modified Askania iris photometer.
18 p2692 A72-36768
- Complex detection - A waveform preserving technique for single-sideband demodulation.
18 p2661 A72-36844
- Gage-length errors in the resolution of dispersive stress waves.
19 p2800 A72-37729
- Design of band-limited signal with no intersymbol interference - An extension of sampling function.
19 p2767 A72-38606
- Signal waveform ensuring maximum reception stability on correlated noise background with peak limiting
20 p2903 A72-39066
- Current and voltage waveform measurements with sampling oscilloscope and capacitive voltage-divide probe to verify TRAPATT diode oscillator theoretical model
21 p3032 A72-40635
- Complex detection - A waveform preserving technique for single-sideband demodulation.
21 p3017 A72-40862
- Signal voltage density, pulse shape and noise power spectrum analysis of matched filter configurations in IR scanning system model
21 p3033 A72-41078
- Signal voltage density, pulse shape and noise power spectrum analysis of running integrator output in IR scanner model
21 p3056 A72-41086
- Plane waves in a new theory of thermoelasticity.
22 p3239 A72-42856
- Experimental investigation of finite-amplitude acoustic oscillations in a closed tube.
23 p3314 A72-44124
- ### WAVEGUIDE ANTENNAS
- #### NT HORN ANTENNAS
- Broadband beam scanned linear waveguide antenna array design with FMCW short range high resolution radar for airport navigational aid in fog
01 p0039 A72-10669
- Boundary value problem solution for multiple interleaved phased arrays of waveguide radiators operating at different frequencies, investigating transmission characteristics
01 p0042 A72-11234
- Passive electric microwave probe with balancing capacitance for studying waveguide fields at high microwave power levels in radiative plasma accelerators
02 p0223 A72-11418
- Parallel longitudinal resonant slots in rectangular waveguide broad wall, determining mutual impedance from magnetic field reaction
02 p0173 A72-12109
- Dielectric loaded cavity or waveguide slot antennas for telemetry applications, describing design and fabrication
02 p0192 A72-12157
- Arbitrarily located inclined resonant slot in waveguide antenna, obtaining condition for circularly polarized radiation from scattering parameters analysis
04 p0499 A72-15205
- Waveguide radiators linear phased array impedance matching during E-plane wide angle scanning improved by reflection coefficient variation compensation
04 p0499 A72-15239
- Ground plane curvature effect on aperture admittance of waveguide fed axial slot on teflon coated metal cylinder for underdense plasma
06 p0771 A72-17354
- Single slotted waveguide linear arrays, discussing microwave antenna design and feeding and cross polarization suppression
06 p0784 A72-17740
- Circular and rectangular waveguide excited dielectric spheres as antenna feed, noting gain and polarization linearity
07 p0957 A72-19796
- Microwave two reflector rectangular backfire antenna with dielectric surface wave structure as waveguide prolongation, obtaining far field radiation pattern
11 p1604 A72-25749
- Scattering matrix derivation for parallel plate waveguide array terminated in infinite plane, determining neighboring guides TEM modes mutual coupling
13 p1921 A72-29345
- Electromagnetic boundary value problem of two rectangular waveguides coupled by aperture radiating into free space, solving integral equation by moments method
15 p2205 A72-31357
- A broad-band wide-angle scan matching technique for large environmentally restricted phased arrays.
17 p2513 A72-34353
- Computer aided impedance matching of an interleaved waveguide phased array.
17 p2525 A72-34373
- Frequency-scanned X-band waveguide array.
17 p2525 A72-34374
- Book - Theory and analysis of phased array antennas
17 p2515 A72-34621
- Surface waves in the corrugated conical horn.
17 p2517 A72-35387
- Airborne waveguide element reliable advanced solid state radar /RASSR/ phased array radiation patterns and design
17 p2531 A72-35571
- Plane wave diffraction in a plane waveguide array with protruding dielectric plates
19 p2768 A72-38655
- The determination of active array impedance with multielement waveguide simulators.
21 p3026 A72-40357
- A metallized channel guide antenna for use over a cylindrical ground screen.
21 p3027 A72-40372
- Ground-based Doppler navigation waveguide slot antenna design for optimal directional multilobe reception from aircraft
21 p3028 A72-40509
- Plexiglas spheres and cubes effect on circular and rectangular waveguide aperture antennas directive radiation patterns and sidelobe reduction
21 p3021 A72-40904
- Wideband limitations of waveguide arrays.
23 p3270 A72-43573
- Beam port coupled waveguide antenna radiation patterns for uniform and cosine plus pedestal radiating aperture distribution, using coupled mode theory
23 p3264 A72-43602
- Simple small primary feed for large opening angles and high aperture efficiency.
24 p3385 A72-44961
- ### WAVEGUIDE FILTERS
- Low loss wideband circular wave guide bend characteristics and branching filters for millimeter wave large capacity digital transmission
02 p0190 A72-11682
- Characteristic impedance formulas for rectangular waveguides with dielectric slab, discussing interference filter design application
05 p0627 A72-16343
- Narrow bandpass waveguide filters synthesis, using orthogonal mode cavities to realize negative coupling elements
10 p1451 A72-24591
- Susceptance inductive loaded evanescent mode waveguide filters with reduced length, using quartz tuned elements
12 p1792 A72-27697
- Two-variable resonant ladder network synthesis for prescribed amplitude response with closed-form solution, illustrating with waveguide bandstop filter
14 p2091 A72-30945
- ### WAVEGUIDE TUNERS
- Quasi-optical 30-60 GHz varactor doubler circuit filters, waveguide tuners and mounts for frequency multipliers
04 p0507 A72-15617
- Method to obtain optimal efficiency gyroamplifier circuits with short waveguide selector by prior grouping of electronic oscillators
13 p1928 A72-28799
- ### WAVEGUIDE WINDOWS
- Rectangular slot antennas radiation through inhomogeneous plasma layer with dielectric window, obtaining input admittances by fields modal expansion
04 p0554 A72-14412
- ### WAVEGUIDES
- #### NT BEAM WAVEGUIDES
- #### NT OPTICAL WAVEGUIDES
- #### NT PLASMA GUIDES
- Atmospheric water vapor role in waveguide effects above sea on millimeter and centimeter propagation along transhorizon and beyond horizon paths
01 p0026 A72-10403
- Atmospheric wave propagation mode parameters frequency dependence analysis from duct model, calculating received signal time behavior by waveguide transfer function
01 p0027 A72-10408
- Gunn diode microwave oscillator postcoupling to waveguide, deriving theory based on equivalent circuit for load impedance assessment
01 p0037 A72-10640
- Self admittance and radiation conductance characteristics of stripline feed slots in waveguide walls
01 p0029 A72-10683
- Waveguide channel microwave bandpass filters for radio relay systems, discussing methods of improving group delay in passband and attenuation at harmonic frequencies
01 p0041 A72-10694
- Ferrite-loaded waveguide Y-junction field mode identification by eigenvalue phase-frequency characteristics measurement, applying to millimeter wave circulator synthesis
01 p0041 A72-10697
- Vlf propagation across discontinuous daytime-nighttime transitions in anisotropic terrestrial waveguide, developing dominant mode approximations of transmission and reflection coefficients
01 p0032 A72-11239
- Nonreciprocal guiding devices for electromagnetic surface waves, noting large bandwidth and nonrectilinear polarization of alternating magnetic field
01 p0044 A72-11323
- Shf electromagnetic radiation interaction with solid body plasma, explaining wave propagation in solid state plasma waveguides
02 p0170 A72-11561
- Nonaxisymmetric tubular spiral electron beam interaction with fast waves in cylindrical waveguide within longitudinal magnetic field
02 p0170 A72-11563
- Low loss high power hf coaxial, twin wire and surface waveguides for long distance transmission
02 p0190 A72-11677
- Low loss reactive wall rectangular and circular waveguides with periodic dielectric structures for millimeter wave and high power applications
02 p0190 A72-11678
- Low loss wideband characteristics of groove and H guides for efficient signal transmission
02 p0190 A72-11679

Dielectric surface waveguides for millimeter and optical wavelength applications, discussing technologies, materials, fabrication and measurement

02 p0191 A72-11683

Hollow waveguide problem considering numerical solution with scalar field approximation, Green function and conformal transformation

02 p0191 A72-11692

Critical frequency computation for partially filled elliptical waveguide with dielectric rod

02 p0183 A72-12752

Electromagnetic wave scattering by electron charge density fluctuations in plane waveguide with magnetoactive plasma, showing cross section spectrum function of plasma properties

02 p0183 A72-12766

Propagation modes attenuation and phase shift of electromagnetic plane wave in superconducting coaxial cylindrical waveguide

03 p0321 A72-13170

Radiation pattern from open ended parallel plate waveguide with arbitrary electric or magnetic aperture field distribution, using Wiener Hopf technique

03 p0331 A72-13409

Mie scattering by spherical particles in low loss glasses for fiber optic waveguides, discussing angular dependence

03 p0359 A72-13445

Electric and magnetic field scattering on ellipsoidal inhomogeneities in circular waveguides from integrodifferential equation derived expressions

03 p0322 A72-13735

Thin film optical waveguides using magneto-optic GdIG as substrate, discussing computerized design for propagation mode converter efficiency

03 p0332 A72-13755

Computer solution to vector variational formulation of electromagnetic Maxwell equations for dielectrically loaded rectangular waveguide

03 p0335 A72-14249

Ring loaded corrugated waveguide for improved frequency broadbanding and transformer matching in horn antenna systems for satellite communication ground stations

04 p0498 A72-14721

Guided gravitational wave possibility from analogy to Maxwell electromagnetic equations

04 p0574 A72-14979

Linearly polarized wave excitation with specified phase shift and predetermined amplitude ratio by waveguide slots, giving slot configuration design formulas

04 p0487 A72-15243

Bandwidth widening of waveguide H-plane Y-circulator with cylindrical ferrite post coated by dielectric sleeve

04 p0499 A72-15244

Zwischenmedium concept application to electromagnetic diffraction problems in waveguides with one or more interfaces and continuity condition met by orthogonal expansion

04 p0488 A72-15378

Wave harmonics method application to problems of free oscillations in longitudinally regular screened waveguides partially filled with homogeneous isotropic media

04 p0488 A72-15379

Asymptotic theory of diffraction at waveguide open end, using generalization by ray and parabolic equation methods

04 p0489 A72-15385

Lens waveguides characteristics, analyzing Gaussian beams propagation through periodic system of thin plane-parallel nonlinear dielectric plates

04 p0489 A72-15389

Electromagnetic fields and energy flow lines in waveguide bifurcations with arbitrary passive terminations

04 p0489 A72-15392

Field modification for integrodifferential equation solution for voltage on exponentially narrow waveguide slit, discussing further changes in method

04 p0501 A72-15409

Air-filled elliptical waveguide with nonmagnetic metal wall, determining dominant TE mode attenuation by perturbation method with Bessel function

04 p0491 A72-15426

Waveguide structures partially filled with bulk negative differential conductivity media, describing wave propagation characteristics and power distributions

04 p0501 A72-15427

Infinitely long rectangular waveguide discontinuity problem, calculating reflection and transmission coefficients of wave propagation

04 p0491 A72-15428

Electromagnetic wave propagation in plane and spherical waveguide channels with conducting lower wall, investigating transverse wave spectrum dependence on curvature and boundary conditions

04 p0492 A72-15441

Complex eigenvalues computation for vlf wave propagation in spherical earth-ionosphere waveguide

04 p0492 A72-15442

Short waves damping or increasing in bounded thick waveguide with real or complex refraction index

04 p0492 A72-15446

Cut-off frequencies of degenerate LSE and LSM modes in rectangular waveguides containing dielectric layers in H plane

04 p0502 A72-15526

Waveguide with slanted aperture, determining propagation mode and wave amplitude from radiation level at Brillouin angle

05 p0625 A72-15828

Electric field distribution in waveguide-slot radiator, describing measurement technique

05 p0635 A72-16333

Dispersion characteristics of laminated cylindrical dielectric waveguide in millimeter band, noting application to permittivity measurement

05 p0627 A72-16341

Ray-optical calculation of modes scattered by obstacle in two dimensional waveguide or duct with weakly inhomogeneous medium and nonvanishing surface impedance walls

05 p0630 A72-16622

Papers on microwave engineering covering surface finish importance for waveguide propagation, parametric amplifiers and voltage breakdown of microwave antennas

06 p0783 A72-17377

Hollow waveguide performance numerical solution review covering finite difference and element methods, polynomial approximation, point matching, integral equations and conformal transformation

06 p0784 A72-18237

L- and X-band Y junction waveguide circulators for medium and peak high powers in radar applications, discussing operation principle and design

06 p0785 A72-18311

Microwave dispersive line structures with nonlinear phase characteristics, considering use of empty waveguide segment near cut-off

06 p0785 A72-18312

Dissipative magnetic parameters measurement in ferrite and insertion loss measurement in waveguide Y-circulators below microwave resonance

06 p0786 A72-18367

Waveguide integral equation numerical solution by moment method, suggesting algorithm for detecting and alleviating relative convergence behavior

[AD-745595] 06 p0775 A72-18368

Visual/graphical recording microwave reflectometer for measuring reflection coefficient along waveguide component, based on Fourier transform evaluation by real time analog method

06 p0786 A72-18369

Longitudinally magnetized fully filled square waveguide reciprocal ferrite phase shifter, predicting frequency characteristics by rotational error analysis

06 p0786 A72-18370

Computer aided renormalized perturbation method for inhomogeneously loaded waveguide performance calculation

06 p0786 A72-18377

Top wall and multiple branch hybrid junction waveguide couplers for millimeter wavelengths, measuring insertion loss performance

06 p0787 A72-18378

Deschamps graphical method application to multiport waveguide junction scattering coefficient measurement with averaging and least square fitting for error reduction

06 p0787 A72-18379

Parallel plate waveguide radiation into dielectric or plasma layer, using Hübner formulation

06 p0791 A72-18734

Hollow and dielectric loaded waveguide modes solution, comparing finite element and finite difference methods based on coefficient matrices and computing time considerations

07 p0952 A72-18793

Longitudinal and transverse nonresonant slots on waveguide, calculating susceptance, conductance, reflectance and transmittance as function of wavenumber

07 p0952 A72-18843

Rectangular and orthogonal circular waveguides hybrid junction with magnetized ferrite resonators along axes, discussing design and applications

07 p0952 A72-18844

Dielectric substrate layer surface wave parasitic resonance effects on microstripline waveguide conductor

07 p0958 A72-18855

Equilibrium hf gas discharge theory for waveguides and gas flow without restrictions on penetration depth and skin effect magnitude of field

07 p1040 A72-18917

Complex transmission coefficient of waveguide with two arbitrarily spaced infinitely thin plane parallel inhomogeneities, using Galerkin method for single-parameter approximation of electrodynamic problem

07 p0938 A72-19002

Wave propagation in thin film optical waveguides with gyrotropic and anisotropic substrates, deriving TE and TM mode conversion conditions

07 p0940 A72-19230

Modal matching method evaluating planar surface waveguide junction transmission and reflection coefficients, comparing to integral equation method

07 p0955 A72-19253

Direct coupled waveguide cavity resonator equalizer networks, determining reflection coefficient, phase, amplitude and time delay characteristics by scattering matrix theory

07 p0955 A72-19327

Scattering properties of conducting cylindrical obstacle in rectangular waveguide, deriving scattered field integral representation via Green function

07 p0944 A72-19593

Open ended parallel plate waveguide, calculating radiation pattern variation with diaphragm dimension

07 p0945 A72-19663

Anomalous wave nulls and relation to endfire surface wave radiation on phased arrays of TEM waveguides with metallic fences perpendicular to ground plane

07 p0945 A72-19788

Orthogonal mode waveguide cavities bandpass filters for communication satellite transponders, comparing with Chebyshev design

07 p0958 A72-20489

Long distance atmospheric propagation in earth-ionosphere waveguide, obtaining phase velocities and damping factors

08 p1131 A72-20802

Phased directional surface wave splitters and microwave and integrated optics elements based on single mode, dielectric and rectangular waveguides

08 p1131 A72-20935

Integral relations derivation for stationary and nonstationary potential motions in cases of zero and infinite conductivity, applying to wave expansion in cylindrical waveguide

08 p1212 A72-20966

Electromagnetic wave propagation along open rectangular dielectric waveguide, deriving dispersion equations for surface waves propagation constants

08 p1136 A72-21739

Soviet book on Riemann-Hilbert problem method in electromagnetic waves theory, covering wave diffraction, scattering and propagation, waveguides and open resonators

08 p1137 A72-22021

Resonator dielectric waveguide structure in electron beam pumped semiconductor laser, noting reduction of diffraction losses and of laser action threshold

08 p1184 A72-22089

Long distance communications multimode waveguides and probability distributions on symplectic group in extension of mathematical model with random inhomogeneities

09 p1277 A72-22474

Cylindrically guided hybrid TE and TM electromagnetic wave reflection and transmission from Maxwell equations and boundary value problems solution

09 p1278 A72-22605

Monograph on slotted circular waveguide analysis: covering boundary value problem solution by Wiener-Hopf and Galerkin procedures and application to far field determination

09 p1279 A72-22925

Alternative TEM and waveguide type equivalent circuits for rectangular resonator loaded by lumped capacitance

09 p1289 A72-23365

Orthogonality conditions for VLF height gains in vertically inhomogeneous anisotropic earth ionosphere waveguide

09 p1282 A72-23517

Mode theory of long distance VLF propagation, deriving equation for flat earth-ionosphere waveguides

09 p1282 A72-23570

German monograph on radiation characteristics of planar systems in aperture plane of parallel plate waveguide, obtaining relationship between electric and magnetic fields

10 p1434 A72-23775

Electromagnetic wave diffraction by dielectric steps in waveguides, calculating microwave scattered field by modified residue calculus technique

10 p1451 A72-24593

Microwave attenuation factor of TE and TM modes in hollow conducting elliptical waveguides, using first order perturbation formula for calculation

10 p1451 A72-24594

Book on continuous transitions in open waveguides covering plane directive surface, single wire transmission line and layered waveguide surface wave propagation modes

10 p1436 A72-24675

Microwaves propagation through circular waveguide partially filled with lossless cold electron plasma dielectric, presenting computed dispersion curves for waveguide and plasmaguide modes

10 p1522 A72-24677

Periodic axisymmetric waveguide with complex structure, obtaining slow wave dispersion equation solutions

10 p1439 A72-24901

Dyadic Green functions for cylindrical circular or rectangular waveguides with moving isotropic homogeneous media

10 p1440 A72-25046

Multimode dielectric slab waveguide power coupling due to core-cladding interface irregularities, obtaining power distribution and radiation losses 11 p1603 A72-25270

Acoustic and elastic HF waves propagation in nonuniform cylindrical waveguides, deriving asymptotic approximate solutions 11 p1686 A72-25726

Video information transmission over planar and rectangular multimode waveguides under excitation by coherent light, calculating field distribution by geometrical optics approximation 11 p1633 A72-26330

Stationary HF Rayleigh waves in surface waveguide, considering transverse and longitudinal wave velocities in half space with elastic medium 11 p1688 A72-26378

Waveguide point source field, analyzing short wave asymptotic properties of Helmholtz equation Green function in inhomogeneous medium 11 p1689 A72-26382

Ultrasonic oscillations effects on alloy castings grain size and heat resistance, suggesting waveguide direction for oriented solidification 11 p1642 A72-26822

Eigenfunctions, eigenvalues and microwave attenuation constants in square and rectangular waveguides with rounded corners 11 p1607 A72-26994

Decoupled formulation of vector wave equation in orthogonal curvilinear coordinates, applying to ferrite-filled and curved waveguide of general cross section 11 p1607 A72-26995

Microwave two port waveguide transmission efficiency determination by reflection coefficient measurements 11 p1599 A72-26997

Antisymmetry principle for solving equation of elastic surface wave caused by waveguide 12 p1845 A72-27392

Compressible anisotropic magnetoplasma filled cylindrical waveguide excitation by electric dipole, plotting electric field patterns as function of electron temperature and density 12 p1782 A72-27489

Ferrite loaded X band waveguide Y junctions eigenvalue frequency dependence measurement to identify modal resonance and arrange displacement for circulator operation 12 p1790 A72-27508

Cylindrical waveguide proper modes instability regions boundary calculation, determining dispersion characteristics and waves phase and group velocities 12 p1791 A72-27537

ELF wave propagation velocities in earth-ionosphere waveguide, studying fast and slow modes 12 p1784 A72-27789

TE mode propagation properties in circular waveguide, determining communication link transmitting and receiving equipment requirements 12 p1784 A72-27795

Waveguides for primary and hybrid mode horns for secondary feeders of deep paraboloid reflector radio telescope in Effelsberg, West Germany 12 p1793 A72-27811

Space-time correlation of field amplitude and phase in plane waveguide with statistically irregular boundary, using Born approximation and perturbation theory method 13 p1928 A72-28471

Dispersion properties of complex waves in shielded circular two layer waveguide 13 p1928 A72-28472

Numerical description of electromagnetic radiation from open-ended flanged waveguides, giving truncation corrected expressions for field behavior in aperture perimeter vicinity 13 p1915 A72-28520

Relations between normal mode radio propagation parameters and properties of earth-lower ionosphere isotropic waveguide, allowing for geomagnetic field 13 p1945 A72-28583

Magnetosonic waves interactions with energy particles in plasmasphere, demonstrating magnetosonic waveguide channel existence around earth below plasmasphere 13 p1947 A72-28605

Design of parabolic reflector antenna with pyramidal horn radiator closed by quadratic waveguide, calculating radiation pattern 13 p1929 A72-29039

Mechanical fabrication of rectangular to cylindrical waveguide transitions for X band 13 p1932 A72-29475

Single pulses and random samplings signal spectrum analysis on real time scale by ultrasonic dispersion waveguide 13 p1934 A72-30018

Plane and circular dielectric waveguides with thermal losses, considering transverse wave numbers behavior behind cut-off value and dispersion equations solution 14 p2086 A72-30797

Hollow elliptical waveguide numerical analysis by polygon approximation with computer program to obtain cutoff wavelength without Mathieu functions 14 p2087 A72-30943

Dielectric waveguide X band telemetry system for remote power and multiplexing applications in noisy electromagnetic pulse environment 14 p2087 A72-31047

Rietz-Kantorovich method reduction of scalar problem for wave propagation along direction surface to boundary value problem, discussing parametric resonance and periodic waveguides 14 p2132 A72-31118

Equivalent circuit characterization of waveguide-mounted IMPATT diode oscillators and associated circuit parasitics at millimeter wave frequencies 15 p2205 A72-31315

Multimode millimeter waveguides and optical fibers, deriving signal transmission distortion from transfer function and corresponding impulse response statistics 15 p2193 A72-31351

Signal distortion minimization for random waveguides with frequency-dependent optimum coupling based on transfer function covariance and impulse response time domain statistics 15 p2194 A72-31352

Simplified equivalent circuit analysis for Gunn diode coupling to rectangular waveguide by inductive post, using perturbation approximation 15 p2205 A72-31353

Rectangular, elliptical and parabolic waveguides TM and TE modes relation and cutoff wavelength analysis by finite element method, suggesting mode classifying system 15 p2205 A72-31354

Multiple port waveguide circulators bandwidth performance calculation to include higher order cylindrical and evanescent modes 15 p2205 A72-31356

Low storage numerical solution of waveguide problem based on impulse analysis, using random walk technique to eliminate large matrix processing 15 p2194 A72-31542

Open terminations of cylindrical waveguide periodically loaded by metallic irises, investigating cavity resonator size effects on resonant frequency, mode and quality factor 15 p2194 A72-31547

Wall-impedance waveguide propagation constant determination from Rayleigh-Schrodinger power expansion of perturbed eigenvalues 15 p2194 A72-31549

Reflection and transmission coefficients of long lossy single mode waveguide line with random inhomogeneities 15 p2195 A72-31654

Microwave waveguide semiconductor modulator with p-n-n diode as control element, taking into account semiconductor control element conductivity change along waveguide wall 15 p2206 A72-31662

Microwave measurements on high permittivity materials with slotted waveguides excited in E mode 15 p2207 A72-31894

Attenuation rate of electromagnetic waves for dominant ELF and VLF modes of earth crust waveguide 15 p2200 A72-32110

Three resonant mode waveguide circulator adjustment with eigenvalues associated to resonant field patterns 15 p2208 A72-32388

Waveguide model for calculating microstrip discontinuities and T-junctions wave impedances, using orthogonal series procedure 15 p2201 A72-32470

Nondispersive guidance structure for acoustic surface waves due to velocity reduction of thin conducting strip on piezoelectric substrate 15 p2278 A72-32506

Ferrite and dielectric element waveguide phase shifters with rectangular hysteresis loop, deriving differential phase and attenuation constants for wave propagation 15 p2202 A72-32662

Relativistic electron ring oscillations in circular waveguide with allowance for walls finite conductivity, noting radiative instability at subcritical frequencies 15 p2210 A72-32738

Earth crust waveguide three layer model for electromagnetic wave propagation, showing mode relation to absorption conditions 16 p2362 A72-33074

Acoustic tunnel effect in elastic waveguide, noting penetration coefficient and quantum mechanics potential barrier 16 p2364 A72-33588

Piezosemiconductor crystal acoustoelectric surface domain waveguide effects for classical and transverse surface waves 16 p2441 A72-33596

Piezoelectric waveguide generalized treatment via field representation by sum of normal mode waves, using modified orthogonality relation 16 p2369 A72-33761

Love wave tapping in isotropic microacoustic surface waveguide by partial transduction into bulk wave at discontinuity 16 p2428 A72-34178

Resonator dielectric waveguide structure in electron beam pumped semiconductor laser, noting reduction of diffraction losses and of laser action threshold 17 p2562 A72-34660

Diffraction of a plane electromagnetic wave on an anisotropic half-plane in free space and in a plane waveguide 17 p2515 A72-34828

Possible field expansions in open waveguides and resonators 17 p2515 A72-34829

Dispersion equation of a corrugated elliptic waveguide 17 p2515 A72-34845

Calculation of the critical frequencies of higher-order modes in a hollow elliptic waveguide 17 p2516 A72-34846

Analysis of the dispersion equation of a dual-layer elliptic waveguide for critical conditions 17 p2529 A72-34847

Application of the impedance treatment to diffraction problems for a rectangular waveguide 17 p2529 A72-34848

Parametric emission of relativistic electron clusters in a waveguide with a layered dielectric filling 17 p2529 A72-34850

Hollow dielectric waveguide for distributed feedback lasers. 17 p2564 A72-35346

Circular waveguides lined with artificial anisotropic dielectrics. 17 p2530 A72-35468

Propagation mode and scattering loss of a two-dimensional dielectric waveguide with gradual distribution of refractive index. 17 p2530 A72-35469

Ceramic waveguide microwave integrated circuits. 17 p2534 A72-35570

Numerical calculation of energy storage, wave dispersion and propagation in waveguides of periodic resonator chains at high frequencies 18 p2657 A72-36105

Composite quasi-optical-broad waveguide transmission lines for millimeter and submillimeter waves with spectrum phase correction 18 p2664 A72-36106

German monograph - Wave propagation in glass-fiber light waveguides 18 p2697 A72-36249

Scattering characteristics of a cross-junction of oversized waveguides. 18 p2660 A72-36486

Some tuning characteristics and oscillation conditions of a waveguide-mounted transferred-electron diode oscillator. 19 p2772 A72-37569

Wave reflection and transmission characteristics of angled rectangular waveguide, deriving scattering matrix 19 p2764 A72-37938

An analytical equivalent circuit representation for waveguide-mounted Gunn oscillators. 19 p2773 A72-38291

Waveguides of arbitrary cross section by solution of a nonlinear integral eigenvalue equation. 19 p2773 A72-38292

Inductive post influence in perfectly conducting waveguides, calculating shunt impedance with allowance for spatial harmonics effect 19 p2766 A72-38413

High power microwave nanosecond pulse generator with waveguide standing wave resonator, noting power gain and pulse shape 19 p2776 A72-38672

The Helmholtz equation in a waveguide /Factorization of the boundary condition from infinity/ 19 p2768 A72-38848

Multimode dielectric waveguide with random coupling, discussing pulse dispersion improvement and loss penalty from power spectrum derivation 20 p2901 A72-38923

Critical frequency computation for partially filled elliptical waveguide with dielectric rod 20 p2902 A72-39058

Electromagnetic wave scattering by electron charge density fluctuations in plane waveguide with magnetoactive plasma, showing cross section spectrum function of plasma properties 20 p2903 A72-39072

The propagation of very low-frequency waves in ducts in the magnetosphere. II. 20 p2916 A72-39192

A quasi-optical directional coupler. 20 p2907 A72-39222

Equilibrium HF gas discharge theory for waveguides and gas flow without restrictions on penetration depth and skin effect magnitude of field
20 p2957 A72-39383

A variation-iteration technique for the design of wall-impedance waveguides.
20 p2903 A72-39429

Energy absorption mechanisms of thin film optical waveguide surface in contact with low index dyes
21 p3050 A72-40147

Stationary expressions for scattering coefficients of rectangular waveguides with dielectric plugs constituting a finite planar array.
21 p3027 A72-40371

Application of the transmission-line-matrix method to homogeneous waveguides of arbitrary cross-section.
21 p3032 A72-40629

Electromagnetic-wave propagation along a horizontal wire above ground.
21 p3015 A72-40633

Wave scattering at a step in a circular multiwave waveguide
21 p3016 A72-40781

Experimental investigation of the propagation of electromagnetic waves in a rectangular waveguide partially filled with n-InSb in the presence of a transverse magnetic field
21 p3016 A72-40796

Ground, satellite, terrestrial glass fiber channel and waveguide radiation systems for laser communications
21 p3023 A72-41398

Book - Terrestrial propagation of long electromagnetic waves.
21 p3023 A72-41532

Design and frequency characteristics of cylindrical waveguide diode for microwave range, noting semiconductor junction effect on device efficiency
21 p3036 A72-41837

Wave excitation during inclined charged-particle flight through a waveguide
21 p3089 A72-41841

Radiation of electron bunches passing through a dielectric plate in a waveguide
21 p3036 A72-41842

Design equations for comb type bandpass filter formed by cascade connection of symmetrical networks containing coupled waveguides and coaxial lines
22 p3158 A72-42125

Coupling by slots in rectangular waveguides with arbitrary wall thickness.
22 p3159 A72-42752

Waveguide with slanted aperture, determining propagation mode and wave amplitude from radiation level at Brillouin angle
23 p3263 A72-43436

Investigation of stepped irregularities in coaxial lines with allowance for higher-order modes
23 p3263 A72-43447

Ferrite component for waveguide commutator used as microwave switching element and modulator, noting application in navigation instruments and avionics
23 p3270 A72-43768

Analysis of the electric field distribution in a rectangular waveguide with a flat transverse inhomogeneity
23 p3272 A72-44141

Circular waveguide in an anisotropic medium
23 p3264 A72-44156

Cylindrical waveguide with density modulated electron beam pumped by external electromagnetic field, considering Doppler effect conditions in beam radiation spectrum
23 p3265 A72-44157

The active field in an irregular slow-wave structure in the presence of a dynamic relative slip between the wave and the particle clusters
23 p3316 A72-44161

A wide-band Gunn-effect CW waveguide amplifier.
23 p3272 A72-44193

Results of a numerical solution of a complex dispersion equation for the HE-sub 11 wave in a two-layer circular waveguide
23 p3273 A72-44214

Relations between normal mode radio propagation parameters and properties of earth-low ionosphere isotropic waveguides, taking into account geomagnetic field
24 p3397 A72-45083

Magnetosonic waves interactions with energy particles in plasmasphere, demonstrating magnetosonic waveguide channel existence around earth below plasmasphere
24 p3398 A72-45105

Permittivity measurement of nonmagnetic materials samples in waveguide systems with an unknown movable reflecting load
24 p3404 A72-45504

Electromagnetic propagation from flanged waveguide, studying diffraction, radiation patterns and reflection/modal coefficients
24 p3381 A72-45642

Radiation from an open-ended waveguide with extended dielectric loading.
24 p3381 A72-45643

WAVELENGTHS

Calorimeter for measuring energy pulses and wavelengths from frequency doubled neodymium to carbon dioxide lasers
02 p0224 A72-11748

High resolution atmospheric transmission measurement of wavelength dependence of absorption losses in carbon dioxide of solid state Er laser radiation
02 p0238 A72-12201

Fabry-Perot interferometers as narrow band optical filters, discussing transmission and construction for various wavelengths
03 p0355 A72-13059

Three frequency radar spectral measurements of two stream and gradient plasma instabilities in equatorial electrojet as function of wavelength
03 p0349 A72-13521

Wavelength tuning effect on lasing threshold in electron beam pumped GaAs lasers as function of current density and voltage
04 p0528 A72-14545

Gas lasers application to precise length measurements via absorbing medium resonance determined wavelength
04 p0530 A72-14734

Visual display IR spectrometer for pulsed transversely excited carbon dioxide laser, tabulating observed wavelengths
04 p0524 A72-15540

Collisional drift instability dependence on parallel wavelength in potassium Q device plasma
06 p0857 A72-17528

Electronic cameras to record and measure weak stars 1000-11000 A, noting atmospheric turbulence suppression and night sky brightness reduction
08 p1170 A72-21962

Double beam single detector wavelength modulation spectrometer for background elimination from observed spectra, noting application to semiconductors band structure determination
09 p1315 A72-23402

Electron-neutral collisions effects on wavelength and damping of electrostatic waves propagation in Ar and He plasmas
10 p1525 A72-25143

Ambiguity of radar phase measurement above sea within radio horizon, noting optimal relation between wavelength and optical paths difference of direct and reflected ray
12 p1784 A72-27799

Wavelength choice for ground based operational weather radar systems as function of reflectivity dependence on scattering hydrometeors /raindrops, hailstones/
13 p1917 A72-28694

Solar corona spectral line width and wavelength measurements during 7 March 1970 total eclipse, using Fabry-Perot photographic interferometer
13 p2043 A72-29548

He-Cd laser emission wavelength determination at Lamb dip center for development of interferometer operation in violet spectral region
13 p1970 A72-29688

Isoelectronic wavelength calculations for Ar line spectra, presenting table with identifications and interpolations
13 p2045 A72-29704

IR and visible parametric laser image upconversion experiments, demonstrating wavelength dependence on view field by black body radiometric measurements
15 p2249 A72-32152

Fraunhofer holograms wavelength dependent distortion reduction by system parameters optimization, applying to color holotape
15 p2239 A72-32357

Radiation patterns of dielectric antenna of size comparable to radiator wavelength in air, discussing narrow band and broadband configurations
21 p3030 A72-40528

Effects of parallel wavelength on the collisional drift instability.
21 p3093 A72-41627

Wavelength tuning of an intracavity pumped CW mode-locked dye laser.
22 p3184 A72-41989

Type II supernova spectral intensity minima due to blueshifted absorption lines of hydrogen and Fe II based on observed and synthetic spectra wavelength comparison
23 p3334 A72-43257

The influence of the atmosphere on the wavelength of the He-Ne laser and the solution of corrections of the laser interferometer.
24 p3409 A72-44771

WAXES

Simple composite propellant modelled by ammonium perchlorate-wax mixtures, noting stoichiometric composition effects on explosive properties
09 p1373 A72-23142

WEAPON SYSTEM MANAGEMENT

Polaris submarine-weapon system autonomous organization and management technique based on team combining Navy and civilian contractors in close working relationship
23 p3358 A72-44358

WEAPON SYSTEMS

NT GROUND OPERATIONAL SUPPORT SYSTEM

NT MISSILE SYSTEMS

Variable speed constant frequency power generation equipment influence weapon system effectiveness, considering weight and cost
01 p0008 A72-11067

Guided weapon systems design under cost restrictive conditions, discussing conceptual design planning and performance tradeoffs against cost and reliability
01 p0147 A72-11155

Joint venture and international collaboration in guided weapon systems design, development and production, discussing cost sharing coordination between governments and contractors
01 p0147 A72-11156

French missile and rocket weapon systems based on solid propellants, describing various ground-to-ground, short and medium range, antitank and other missile types
03 p0441 A72-13644

A-7 D/E navigation/weapon delivery system flight testing, using photogrammetric technique
05 p0663 A72-16656

Weapon firing and external store separation tests by flight test methods for determining safe weapon release envelope
06 p0759 A72-18499

VJ-101A and B V/STOL weapon system design, describing various propulsion system configurations
07 p0912 A72-19250

V/STOL weapon system VJ-101, describing He-231 design development from tail-sitter concept to canard configuration with tilting wing-tip engines
07 p0912 A72-19251

Technological advances and program risks assessment by operations research and systems analysis techniques, applying to cost overruns and schedule slippages in weapon systems
07 p1106 A72-20270

Fighter aircraft maneuverability, range and armament requirements, discussing canard vs delta configurations
11 p1577 A72-26657

Man computer weapons effectiveness and system test environment /WESTE/ instrumentation system with Decca navigation for simulated combat environmental flight tests
12 p1754 A72-27515

Pilot-aircraft system model for relationship between weapons delivery accuracy and manual flight control system design, noting display, computation and control aids to pilot
12 p1773 A72-28121

Reliability requirements and optimization for complex systems, discussing method to improve component reliability of aircraft weapon system
13 p1961 A72-28353

Weapon systems reliability assessment based on limited prototype flight test results
13 p1962 A72-28359

Weapon system reliability improvement through integrated maintenance data collection and evaluation system, considering maintenance organization and operation
13 p2067 A72-28368

Time parameter in military air operations, discussing weapon systems R and D, all-weather capability, communications, reliability and maintainability, manpower training, etc
15 p2339 A72-32453

Electronic displays with weapon aiming sensors in aircraft navigator-attack systems
15 p2273 A72-32634

V/STOL weapon system VJ-101 design, discussing one axis rocking device, suspension structure and hovering flight thrust control
16 p2347 A72-33049

Fighter bomber Loran-inertial data processing with digital computer to combine navigation, guidance and weapon delivery into fully integrated system
16 p2420 A72-33246

Military system and equipment Level of Repair optimization for minimum life cycle costs, considering weapon systems deployment, operation level and mobility requirements
16 p2482 A72-33793

Multimode flight control for precision weapon delivery.
17 p2493 A72-35561

Range correction computations for weapons dropped from aircraft.
19 p2747 A72-37286

Tactical aircraft weapon system development, describing navigation, target acquisition, release point guidance and delivery modes
20 p2951 A72-39107

Defense systems development based on balance between theoretical studies and hardware prototyping for uncertainty reduction in performance and cost
21 p3132 A72-40971

The INAS device of Ferranti as integrated weapon system for the HS Harrier
21 p3083 A72-41846

Harrier two seat aircraft design, performance, weapon systems, thrust vectoring and combat characteristics comparison with GR.1
23 p3252 A72-44391

WEAPONS

NT ARTILLERY

WEAPONS DEVELOPMENT

F-14A fighter accelerated flight test program with 18-month saving and 3600 flight time hours before 1973 operability
04 p0464 A72-14591

Time parameter in military air operations, discussing weapon systems R and D, all-weather capability, communications, reliability and maintainability, manpower training, etc
15 p2339 A72-32453

Competitive prototype strategy to reduce weapon system development risks and uncertainties with emphasis on simplified management and procurement
18 p2742 A72-36074

VJ-101 V/STOL aircraft design, development and flight testing, discussing takeoff and landing, hovering and transition flight and associated control problems
19 p2749 A72-38032

Tactical aircraft weapon system development, describing navigation, target acquisition, release point guidance and delivery modes
[AIAA PAPER 72-896] 20 p2951 A72-39107

Defense systems development based on balance between theoretical studies and hardware prototyping for uncertainty reduction in performance and cost
21 p3132 A72-40971

Successful engineering design teams characteristics in development of complex defense systems, discussing organization size, experience, documentation and procurement practices
21 p3132 A72-40972

USAF aerospace medical research on human capabilities as limiting factor in defense systems development, discussing environmental simulators and human test facilities
21 p3008 A72-40973

WEAR

Statistical calculation of wear rate in friction pair with linear contact, analyzing errors
04 p0528 A72-15711

Metal wear mechanism during electromechanical processing explained by configurational localization model
05 p0665 A72-16094

Surface reaction mechanisms analysis in adhesion, friction, wear and lubrication, using electron diffraction, Auger spectroscopy and ellipsometry techniques
12 p1813 A72-27036

Statistical methods for friction and wear processes, noting Rayleigh distribution of wear particles, surface dispersion velocity, energy dissipation and friction force
12 p1818 A72-28186

Adhesive and abrasive wear technology assessment, considering design equations use for prediction
[ASME PAPER 72-DE-2] 14 p2108 A72-30859

Friction and adhesive and abrasive wear of ceramics, discussing effect of environmental water and hydrocarbons
15 p2260 A72-32129

Friction and wear properties of carbon fiber reinforced polymers sliding against metals in pure and sea water and aqueous solutions
16 p2396 A72-33123

Tribological properties of gold for electric contacts.
18 p2693 A72-35980

A method for the study of wear particles in lubricating oil.
19 p2803 A72-38376

Adhesive wear theoretical model based on asperity interactions number, area and volume, considering implications for friction and surface temperature analysis
19 p2809 A72-38377

WEAR INHIBITORS

Organophosphorus antiwear additives in neopentyl polyol ester lubricants on 440C stainless steel surfaces, using four ball wear test machine
[AD-740055] 02 p0250 A72-12849

Oxidation resistant solid lubricants for high temperature air and gaseous environments applications, considering oxide and fluoride coatings with silicate additives for wear life improvement
06 p0837 A72-18600

Fuel lubricity effects on aircraft engine fuel pump wear, discussing remedial use of corrosion inhibitors and change to noncorroding pump construction materials
08 p1222 A72-21450

Antiwear properties of mixed anhydrides of alkyl xanthogene and phosphorus containing acids for use as oil lubricant additives
09 p1336 A72-22499

Antioxidative and antiwear action of S-containing and S-free phosphoric acid ester additives in lubricating oils
12 p1835 A72-28201

Coating materials for metal surface wear inhibition by adhesive and abrasive interactions minimization, discussing laminar solids, plastics, ceramics and soft metals
[ASME PAPER 72-DE-48] 14 p2108 A72-30874

Effect of molybdenum on the properties of TiC-Ni cermet hard alloys
19 p2819 A72-38283

Electrolytic and nonelectrolytic diffusion methods for protective coatings production from gas, liquid or solid phase, discussing wear resistance enhancement in bonded steels
20 p2929 A72-39449

WEAR TESTS

Viscosity and additive effects on jet engine fuel antiwear properties improvement
02 p0270 A72-11968

Steels gas-powder facing with boron carbide, testing microhardness and wear resistance
03 p0363 A72-13547

Steel coatings produced by plasma jets on experimental machine parts, determining friction wear resistance by successive tests
03 p0363 A72-13548

Titanium carbide based hard cermet alloys with Ni addition, testing wear resistance
03 p0372 A72-13549

Sliding friction and wear behavior of carbon fiber reinforced composites with thermosetting resins, thermoplastic polymers and metal base materials
04 p0537 A72-14747

Strain hardened layers effect on wear resistance of 50Kh steel
04 p0534 A72-15653

Vacuum chamber and instrumentation for friction and wear tests at temperatures to 1800 C in vacuum and inert media
04 p0510 A72-15659

Wear, bending and corrosion resistance of stainless steels with Cr thermal vacuum diffused coating
04 p0535 A72-15661

Erosion of materials under drip impact loads, determining wear rate dependence on drop size, impact velocity and material properties
05 p0734 A72-15981

Martensite and solid Cr-containing inclusion effects on wear resistance of cermet steel during dry friction with R18 steel
05 p0665 A72-16095

Hydraulic fluids behavior under extreme temperature, pressure and filtration conditions, considering viscosity, wear and corrosion resistance
05 p0681 A72-17084

Thin sintered fluoride films bonding with monoaluminum phosphate, investigating friction and wear behavior
06 p0821 A72-17804

Nimonic 75 sliding pin and rotating disk frictional force, wear rate and surface temperature
06 p0830 A72-18156

Friction and wear characteristics at high temperature of plain bearing embedded with pellets of graphite, sodium fluoride and tungsten disulfide lubricating mixture
06 p0823 A72-18584

Molybdenum disulfide lubricating film and wear-in study by scanning electron microscopy and testing machine
06 p0836 A72-18586

Wear behavior of molybdenum disulfide and antimony trioxide bonded solid film lubricant with air curing silicone resin, noting temperature and pretreatment effects
06 p0823 A72-18593

Filler particles orientation effects on plastic bearing materials friction and wear properties, discussing experimental testing methods
06 p0836 A72-18595

Graphite fluoride as solid lubricant, investigating friction coefficient and wear resistance
06 p0837 A72-18598

Friction coefficient, standard wear and surface layer temperature of seal for dry friction pairs in jet engines, investigating crystal lattice parameters
07 p0996 A72-19768

Electromechanical machining metal removal mechanism based on configurational localization model, relating wear processes to electron exchange and free energy margin decrease
07 p0996 A72-19989

Wear resistance and friction coefficients in physiologic solution of thermoplastic materials for prosthetic application in hip joints
08 p1194 A72-21760

Electron microscopy application to dynamic wear studies of Ni on Ni surface and subsurface topography and microstructure in nitrogen atmosphere
08 p1179 A72-21943

Wear resistance of steel and Ti alloys in free abrasive gas jet, noting surface microhardness increase effect
09 p1319 A72-23188

Self lubricating materials for maintenance-free clocks antifriction bearings, discussing friction and wear behavior
09 p1319 A72-23562

Wear mechanism of lead-bronze dry sliding in air on hardened steel ring
11 p1638 A72-25510

Carbon and low alloy steels resistance to abrasive wear as function of hardness, heat treatment and composition
12 p1829 A72-27455

Stressed state induced in compound thick walled cylinder for testing residual tensile stresses effect on machine parts wear resistance
12 p1814 A72-27461

Wear resistance of artificial and natural diamond grindstones in ruby cutting, noting tests for grain geometry and fabrication technique effects
12 p1814 A72-27765

Oxide thin films effects on surface layers deformation and wear resistance of coated metals under friction, noting electrical resistance changes in annealing
12 p1818 A72-28189

Wear micromechanism in hard and brittle chromium steels under cyclic slide friction loads
12 p1818 A72-28194

Molybdenum disulfide-tantalum compact solid lubricant wear rate as function of load and sliding velocity, presenting test data statistical interpretation
[ASLE PREPRINT 72AM 15] 13 p1964 A72-28972

Cr and V additions effects on Mn steels mechanical properties and wear resistance, noting strength limit increase
13 p1977 A72-29021

Jet fuel hydrocarbon group chemical composition effects on antiwear characteristics in sliding friction and rolling simulation experiments
13 p2024 A72-29073

Machine oil wear degree and Fe content determination by placing sample into induction coil and measuring coil Q at RF
13 p1957 A72-29142

Steels shafts fatigue failure under cyclic loading and fretting corrosion, indicating fatigue strength increase through surface layer wear resistance augmentation
13 p1979 A72-29476

Metallic, ceramic, polymeric, composite and solid film lubricant friction and wear properties and testing
[ASME PAPER 72-DE-28] 14 p2108 A72-30869

Carbon fibers reinforced polymer wear rate decrease in organic fluids associated with films development on steel counterface, noting application in lubricated systems
16 p2397 A72-33124

Supramolecular scale microscopic dynamic model for solid body macroscopic friction and wear effects
16 p2398 A72-33367

Negative slip reversal effect formation mechanism during friction, discussing elimination via oleic acid as lubricant additive
17 p2559 A72-34663

Friction and wear of electroplated hard gold deposits for connectors
18 p2693 A72-35981

Friction, wear and noise of slip ring and brush contacts for synchronous satellite use.
18 p2693 A72-35982

Evaluation of gold electrodeposits for use in dry circuit applications.
18 p2664 A72-35983

The dry wear behaviour of porous cobalt.
18 p2696 A72-36795

Vacuum-friction temperature resistance and durability of a molybdenum-disulfide coating deposited on steel by the detonation method
19 p2809 A72-38290

Method of investigating the wear of hard tungsten carbide cobalt alloys in a liquid nitrogen medium.
20 p2941 A72-39715

Changes in the wear resistance of polymer surface layers in aggressive and biologically active media
21 p3072 A72-40081

Industrial pyroceramic materials usable under friction without lubrication
21 p3061 A72-41374

The limiting strength of worn metal surfaces.
22 p3194 A72-43039

Influence of the degree of strain-hardening and roughness of friction surfaces on wear rate and carrying capacity
22 p3183 A72-43157

Investigation of the wear resistance carbonized chromium coatings on various brands of steel
22 p3195 A72-43159

- Erosion of materials under drip impact loads, determining wear rate dependence on drop size, impact velocity and material properties 24 p3460 A72-45723
- WEATHER**
NT COLD WEATHER
 Aircraft accidents during nonprecision approaches under adverse weather conditions, discussing landing aids use for corporate jet aircraft 20 p2952 A72-39745
- WEATHER CHARTS**
U METEOROLOGICAL CHARTS
WEATHER CONDITIONS
U WEATHER
WEATHER CONTROL
U WEATHER MODIFICATION
WEATHER DATA RECORDERS
 Aircraft and airports weather instrumentation for all-weather landing and takeoff, discussing application of laser technology and digital presentation 08 p1168 A72-21522
 Eole satellite relay system for weather balloon location and data collection and transmission to ground stations 09 p1394 A72-22600
 Thunderstorm detection and recording device with 200 km radius for weather prediction and air traffic information 09 p1312 A72-23269
 Automatic remote transmitting meteorological station, discussing development, working principle, technological features and sensors 10 p1462 A72-25010
 Sensors measurement accuracy for rainfall amount and duration determination by automatic remote transmitting meteorological station 10 p1483 A72-25017
 Mean wind direction determining circuit for meteorological data collecting system 10 p1484 A72-25018
- WEATHER FORECASTING**
NT LONG RANGE WEATHER FORECASTING
NT NUMERICAL WEATHER FORECASTING
NT STATISTICAL WEATHER FORECASTING
 Terminal aerodrome forecasts usefulness and accuracy assessment 01 p0095 A72-10864
 Associative array digital processors application to numerical solution of partial differential equations, illustrating methodology on weather forecasting equations 02 p0186 A72-11658
 World Weather Watch and Global Atmospheric Research Program remote sensing applications, considering weather prediction and modification, atmosphere pollution monitoring and global atmosphere mathematical modeling and simulation 02 p0208 A72-11784
 Remote sensing applications to operational weather forecasting including ground optical measurement of cloud base height and radar observation of precipitation 02 p0253 A72-11825
 Weather prediction - Conference, Ostseebad Kuhlungsborn, East Germany, October 1969 02 p0253 A72-12776
 Temperature advection mesostructure from wind measurements for precise short term forecasts 02 p0254 A72-12778
 Wind velocity and direction vertical changes for weather dynamics, emphasizing jet streams 02 p0255 A72-12785
 Nonmeteorological scientists and engineers views on meteorology and weather forecasting, discussing uses, problem areas and knowledgeability 03 p0384 A72-13637
 Italian monograph on ionospheric radio propagation, covering weather forecasts and radio communications 03 p0323 A72-13844
 Soviet book on calms and storms in upper atmosphere covering energy variations, auroras, geomagnetic storms, weather forecasting, etc 03 p0350 A72-13967
 Environmental research with instrumented aircraft, discussing application to operational forecasting and weather modification experiments in hurricanes and tropical convective clouds 04 p0542 A72-14682
 Gliding flight atmospheric energy utilization through aerology, discussing value of weather forecasts to glider pilots 04 p0542 A72-14684
 Computerized synoptic weather map forecasting of heavy snowfall in Colorado 04 p0542 A72-14685
 Storm forecasts by meteorological satellites, describing TV monitoring of cyclones and hurricanes 05 p0683 A72-15978
 Combined radar-acoustic system for lower atmosphere temperature sounding, considering use in air pollution studies and short range weather forecasting [AD-739790] 05 p0663 A72-16690

- Meteorological satellites TV, visual and IR cloud imaging and atmospheric sounding techniques for short and long range weather forecasting 06 p0892 A72-18066
 Meteorological satellites data gathering equipment including TV cameras, temperature humidity, ozone and radiation measuring devices, discussing data processing and evaluation for weather forecasting [DGLR PAPER 71-131] 06 p0892 A72-18231
 Aviation weather forecasting improvements due to radar, computer, satellites and high speed communications contributions 07 p1029 A72-18838
 Rain amount forecasting based on five level atmosphere model and hydrothermodynamics equations, calculating vertical currents under uniform atmospheric boundary layer stratification conditions 07 p1029 A72-18859
 Prediction of weather induced airline operating delays, discussing fog, snow, freezing rain, thunderstorms, crosswind, headwinds, CAT, wind shear, wet runways and tail winds 07 p1030 A72-19597
 Weather forecasting techniques improvement by synoptic meteorology analysis 07 p1031 A72-20449
 Satellite system and data processing center feasibility for carrying out meteorological surveys in Mediterranean area 07 p0993 A72-20605
 Atmospheric humidity forecasts from field evolution and transfer and specific humidity deficit description with equations system 07 p1031 A72-20699
 Weather analysis for mountainous terrain from potential temperature surface maps and vertical cross sections 09 p1344 A72-22431
 Atmospheric temperature profiles real time retrieval from Nimbus 4 satellite IR spectrometric observation, describing method used in dynamical weather forecasting 09 p1345 A72-22440
 Visual and radar echo location of organized updraft on thunderstorms and hailstorms 09 p1346 A72-22452
 Thunderstorm detection and recording device with 200 km radius for weather prediction and air traffic information 09 p1312 A72-23269
 VHF remote control anemometer network with digital receiving station for wind measurement and gale warning system 10 p1463 A72-25013
 Real time pilot reports via digital ground-air-ground data link, discussing encoding and processing equipment, meteorological codes and automatic real time weather forecasts 10 p1440 A72-25079
 Military weather forecasting requirements by 1980, discussing decision making, data processing, satellite data, mission and terminal forecasts, display and computer flight planning 10 p1508 A72-25096
 Asian subtropics western disturbances movement prediction by primitive equation barotropic model with east-west cyclic boundary conditions, presenting forecast charts and error statistics 11 p1681 A72-26077
 Scalar and vector partitions of forecasts probability score in two state situation 11 p1681 A72-26078
 Snow accumulation determination from snow intensity based on visibility estimates, noting application to forecasting 11 p1682 A72-26085
 Monthly weather forecasting synoptic method development prospects, noting macroprocesses phasing and global experiment program realization impact 11 p1683 A72-26885
 Baroclinic primitive equation prediction model for non-tropical part of Northern Hemisphere with allowance for moisture exchange, radiative heat influx and cloud formation processes 11 p1683 A72-26886
 Atmospheric vertical motions velocities prediction based on satellite cloud data 11 p1683 A72-26887
 Weather satellite data use to obtain forecasts for aircraft and ships in Southern Hemisphere and for Antarctic research stations 11 p1683 A72-26890
 Space techniques application to meteorological prediction, noting Meteosat and Eole satellites capabilities 12 p1840 A72-27506
 Radio wave propagation control by superrefraction layers, investigating daily weather forecast technology improvement 12 p1784 A72-27797
 Interdiction bombing mission effectiveness model for bad and good weather aircraft type selection depending on weather conditions at target site 13 p1896 A72-28400

- Kennedy Space Center area afternoon convective thunderstorm activity and associated weather phenomena prediction via multivariate regression analysis 13 p1989 A72-28803
 Computer and meteorological satellite effects on weather support for manned space missions, discussing Gemini 5 and Apollo 11 landing weather predictions and cloud climatology 13 p1989 A72-28804
 Weather forecasting support of NASA programs involving earth oriented viewing and sensing experiments from aircraft and spacecraft 13 p1990 A72-28816
 Hybrid forecast model for hydrometeors short range prediction based on meteorological satellites cloud pattern observations and quasi-Lagrangian advection analog 13 p1993 A72-28858
 CAT forecasting based on fluid mechanics experimental studies of stratified shear flows stability and meteorological analyses of aircraft CAT encounters 13 p1994 A72-28866
 Aeronautical requirements for meteorological reporting and instruments at aerodromes, discussing surface wind, visibility, runway range, weather, temperature and pressure observations 13 p1938 A72-28868
 Cost effectiveness model for evaluating general aviation weather dissemination techniques, stressing design variables and time periods 13 p1994 A72-28871
 Air Force Global Weather Central computer simulation of specific aircraft flight plans, using update weather information for specified route profile 13 p1924 A72-28873
 Shower precipitation amounts forecasting by layer method, showing inadequacy from viewpoint of physical principles 13 p1995 A72-29594
 Hydrodynamic theory of atmospheric action formation due to pressure migration for Northern troposphere two level meteorological forecasting 14 p2127 A72-30261
 Satellite anemometry for ocean waves and weather forecasting, discussing Skylab microwave radiometer-scatterometer potential design 15 p2221 A72-31239
 Local climatic forecasts via influence equations based on past meteorological data as initial conditions, obtaining solution by operational analysis methods 16 p2418 A72-33379
 Worldwide weather data system as important factor for search and rescue operations implementation 17 p2488 A72-34432
 Information-prediction value of the tidal solar-lunar rhythmicity of certain meteorological processes 17 p2577 A72-35779
 Dynamic adjustment of initial model fields by using complete equations of hydrothermodynamics 20 p2949 A72-39943
 Russian book - Aviation meteorology. 22 p3200 A72-42024
- WEATHER FRONTS**
U FRONTS [METEOROLOGY]
WEATHER MAPS
U METEOROLOGICAL CHARTS
WEATHER MODIFICATION
NT CLOUD SEEDING
 Channel clearing through clouds by laser beam, considering cross section expansion dynamics, channel growth rate, cloud motion and blurring 01 p0078 A72-10155
 World Weather Watch and Global Atmospheric Research Program remote sensing applications, considering weather prediction and modification, atmosphere pollution monitoring and global atmosphere mathematical modeling and simulation 02 p0208 A72-11784
 METROMEX field project to investigate inadvertent weather modification by urban-industrial effects and man-made precipitation changes 03 p0384 A72-13636
 Environmental research with instrumented aircraft, discussing application to operational forecasting and weather modification experiments in hurricanes and tropical convective clouds 04 p0542 A72-14682
 Airport cold fog attenuation by propane atomization technique, discussing application at Orly 04 p0508 A72-14686
 Warm fog dissipation by helicopter downwash mixing, heat, hygroscopic particle and polyelectrolytes seeding 04 p0543 A72-14694
 Fog modification at all temperatures with physicochemical techniques, discussing blowing hygroscopic salts and use of alginates of sodium and marine algae extracts 04 p0543 A72-14696
 Weather modification as example of government managed and funded technological innovation, discussing various evolutionary R and D and operational phases 07 p1102 A72-18974

Airport fog dispersion methods review, noting seeding and hot air injection techniques
08 p1201 A72-21920

One dimensional model for climatological evaluation of ice phase seeding for isolated cumulus cloud modification
09 p1345 A72-22448

Developing cumulus clouds annihilation, considering ascending and descending spontaneous convective streams initiated by explosions
12 p1841 A72-27989

FAA airport fog dispersal program, discussing techniques effectiveness evaluation vs defined goals
13 p1992 A72-28843

Mathematical model for numerical simulation of warm fog modification by seeding hygroscopic particles, taking into account turbulent diffusion and horizontal wind advection
13 p1992 A72-28844

Triggered lightning and some unsuspected lightning hazards.
22 p3170 A72-42375

Developing cumulus clouds annihilation, considering ascending and descending spontaneous convective streams initiated by explosions
22 p3202 A72-43003

WEATHER RADAR

U METEOROLOGICAL RADAR

WEATHER STATIONS

Radar meteorology, discussing equipment design, radar observation station net need, aeronautical applications and laser devices utilization
02 p0254 A72-12783

Snow lines determination from ESSA-APT weather satellite pictures, comparing with ground data
09 p1303 A72-23295

Automatic meteorological stations - Conference, Potsdam, East Germany, March 1970
10 p1507 A72-25007

Automatic meteorological stations development in populated areas, foreseeing data gathering by sensors with satellite and radar efficiency taken into account
10 p1507 A72-25008

Standardized automatic telemetering hydrometeorological station, discussing structure, operation, working principles and sensors
10 p1462 A72-25009

Automatic remote transmitting meteorological station, discussing development, working principle, technological features and sensors
10 p1462 A72-25010

Reliability, operational safety and system concept interrelationship in automatic meteorological stations
10 p1463 A72-25011

Air, wet bulb and soil temperature indications from automatic telemetering meteorological stations, comparing with Hg thermometer readings
10 p1483 A72-25012

Automatic hydrometeorological stations standardized sensors, describing data converters for atmospheric pressure, precipitation, humidity and wind and water and soil temperature measurements
10 p1483 A72-25014

Air hygrometer with heated electrolytic sensor for atmospheric humidity determination by automatic meteorological stations
10 p1483 A72-25016

Automatic meteorological station MME-1 data storage and interrogation device for transmission to central station
10 p1445 A72-25019

Automatic telemetering meteorological stations and visual observation data processor control
10 p1507 A72-25020

Classification of automatic meteorological ground stations networks in populated areas, discussing required equipment, data transmission, real time operation and costs
10 p1507 A72-25021

Probability density distributions for distance from arbitrary point to randomly distributed weather stations
11 p1592 A72-25767

Weather stations data analysis with unequally spaced observations, considering errors and variance transfer functions
11 p1680 A72-26076

Cost analysis of high altitude meteorological network data with respect to research effectiveness and data reduction
13 p1990 A72-28820

Lower planetary boundary layer mesoscale flow patterns and transport climatology, using hourly averaged wind data from wind tower station network
21 p3077 A72-40252

WEATHERING

Corrosion effects evaluation from electrode potentials, noting copper pitting and weathering
08 p1189 A72-22108

WEAVING

Experimental weave pattern for three dimensional continuously woven fiber glass reinforced composite fabric impregnated with epoxy resin
[SAE PAPER 720340]
11 p1673 A72-25597

Tridimensional textiles for composites.
17 p2571 A72-34935

WEBS

Webbing joints stitching strain, considering nylon and flax yarns stretching properties and various stitching patterns strengths
01 p0005 A72-10315

WEBS [MEMBRANES]

U MEMBRANES

WEBS [SUPPORTS]

Tensile load elastostatic transfer from rectangular cross section web to two infinite parallel sheets, deriving Cauchy type integral equation for adhesive bond force density
07 p1095 A72-20241

Stiffness, stress and deformation analysis of discretely attached corrugated shear webs, using minimum potential energy and calculus of variations methods
11 p1728 A72-25380

Boron-epoxy reinforced composite metal shear web design for space shuttle orbiter main engine thrust beam structure
[AIAA PAPER 72-395]
11 p1726 A72-25416

WEDGE FLOW

Hypersonic source flow past wedges and cones, calculating flow nonuniformities effects on shock shape, velocity, pressure and density by perturbation analysis
01 p0033 A72-11394

Laminar shear flow over impulsively started wedges, describing flow field by Goldstein-Rosenhead method of approximate series expansion
04 p0590 A72-15190

Flow field due to diffraction of shock wave at wedge moving at supersonic speed
05 p0600 A72-16212

Supersonic interaction in streamline corner of intersecting wedges, including pitot traverse, surface pressure and oil flow visualization measurements
[AIAA PAPER 72-6]
05 p0606 A72-16862

Steady two dimensional magnetodynamic flow past nonconducting wedge with perpendicular magnetic field at different shock attachment angles
06 p0861 A72-18113

Plane transonic gas flows through Laval nozzle and symmetrical wedge-shaped profile, solving boundary value problem by reduction to singular integral equation
10 p1418 A72-24433

Eigenfunction transform investigation of wedge diffraction of scalar pulse wave in three space dimensions, analyzing Green function
11 p1591 A72-25359

Wedge reflected shock profiles, comparing results for various Mach numbers and incidence angles with predictions based on Whitham theory
11 p1616 A72-25918

Hypersonic blowdown tunnel investigation of turbulent shock-boundary layer interactions at two dimensional wedge compression corner
13 p1944 A72-30030

Two dimensional two phase steady supersonic wedge flow patterns analysis based on equations for flow between wedge surface and shock wave
14 p2070 A72-31011

Supersonic interaction effects on boundary layer flow structure in intersecting wedge corner at high Reynolds numbers from surface pressure measurements and oil flow visualization
16 p2341 A72-32830

German monograph on plane steady isentropic flow past obtuse apex angle wedge at zero angle of attack and free stream sonic velocity
16 p2343 A72-33400

Flow over infinite wedge with mass transfer by boundary suction or injection, solving nonlinear boundary layer equations by parametric differentiation method
17 p2485 A72-35230

Pressure distribution on a yawed wedge interacted by an oblique shock.
17 p2485 A72-35239

Inviscid perfect gas supersonic steady irrotational flow past wedge, investigating analytical solution validity in downstream region behind shock
17 p2544 A72-35900

Particle motion behind oblique shock wave in two phase supersonic wedge flow, deriving expressions for particle trajectories and velocity equalization time
17 p2487 A72-35926

Hypersonic viscous, slip flow over insulated wedges.
20 p2885 A72-39612

German monograph - Pressure variation along a plane slender wedge and along a slender cone of revolution at decelerated flight in the supersonic range near sonic velocity.
22 p3136 A72-43074

Effects of upstream unsteadiness on hypersonic flow past a wedge.
24 p3364 A72-45565

Hypersonic leading edge problem - Wedges and cones.
24 p3364 A72-45778

WEDGES

Electromagnetic surface field propagation on dielectric wedge excited by line source, using steepest descent method
04 p0491 A72-15419

Inverse scattering by ray optics for conducting wedge, considering TE and TM edge diffracted fields
04 p0551 A72-15671

Plane theory of elasticity for infinite triangular wedge with notched apex, reducing problem to non-homogeneous Hilbert problem
05 p0737 A72-16301

Elastic equilibrium of infinite wedge with apical asymmetric notch, reducing to Hilbert problem fo; holomorphic vectors
07 p1093 A72-19976

Plane oblique shock wave diffraction on wedge moving in homogeneous gas flow at supersonic speed, reducing boundary value problem to Hilbert problem
07 p0910 A72-20317

Mellin transforms application to two dimensional elasticity problem for anisotropic wedge with continuous mechanical characteristics under concentrated force
08 p1243 A72-21238

Strong shock wave diffraction from wedge reduced to Hilbert problem, noting nonregular refraction theory nonexistence
08 p1151 A72-21662

Stress intensity factor of Griffith crack in elastic solid opened by thin symmetric wedge, using triple integral equations
12 p1883 A72-27558

Stress boundary value problems for infinite wedges in linear elasticity theory solved by Mellin transforms
12 p1883 A72-27561

Algebraic equations for displacement and stress vectors at faces and interfaces of elastic multilayered cylinders and infinite wedges, using matrix method
12 p1884 A72-27565

Wiener Hopf integral equation for problem of smooth stamp impression into elastic wedge face, solving by gamma and hypergeometric functions
13 p2059 A72-29500

Thin wedge shaped shell bending under normal loads, discussing boundary value problems
13 p2062 A72-30066

Nearly incompressible elastic solid compressibility effects theory, applying to annular wedge straightening, stretching and shearing and cylindrical tube telescopic shear problems
15 p2330 A72-32477

The plane solution for anisotropic elastic wedges under normal and shear loading.
[ASME PAPER 72-APM-13]
17 p2629 A72-34802

Diffraction by an aperture between two wedges.
18 p2712 A72-36938

Scattering of electromagnetic pulse waves by conducting wedge in an uniaxially anisotropic medium.
20 p2903 A72-39269

Singular stress concentration at sharp edge of wedge in contact with half plane in elastostatics
21 p3119 A72-41104

Two-dimensional problem of elasticity theory for an anisotropic inhomogeneous wedge
24 p3459 A72-45263

The wedge probe - A review.
24 p3404 A72-45355

Aerodynamic characteristics of two-dimensional waverider configurations.
24 p3365 A72-45793

WEIBULL DENSITY FUNCTIONS

Field and test data analysis with time share computer, using Weibull probability plotting, hazard rates and least squares regression
02 p0185 A72-11555

Point estimate calculation of underlying distribution function for probability plot, developing confidence coefficient for Weibull model
02 p0252 A72-11557

Maximum likelihood estimation for Weibull distribution parameters from multicensored samples by Monte Carlo simulation
08 p1200 A72-21589

Stress rupture data from S glass composite matrix effectiveness tests, noting skewed lifetime distribution in statistical patterns
08 p1192 A72-21683

Lower confidence bound for reliability and specifications for nonnominally distributed stress corrosion test data, using Weibull statistical distribution
08 p1189 A72-22102

Bayes analysis application to Weibull distribution parameters estimation, using entropy concept for figure of merit to assess reliability analysis
10 p1444 A72-23987

Statistical inferences on two parameter Weibull reliability function from classical, Bayesian and structural probability viewpoint
15 p2264 A72-31800

Random scale parameter of Weibull distribution with known shape parameter obtained via empirical Bayes estimation
16 p2398 A72-33346

Joint maximum likelihood estimation of three parameters of Weibull distribution, obtaining modified quasi-linearization algorithm for nonlinear equations iterative solution

16 p2416 A72-33348

Weibull distribution parameters estimation for general device class from limited failure data through regression models, using least squares method

16 p2398 A72-33349

Weibull life tests of Kemet solid tantalum chip capacitors at high accelerated voltages.

17 p2527 A72-34685

Weibull distribution government of dispersion of destructive temperature gradients characteristic of fireproof ceramic materials heat resistance

21 p3074 A72-41713

Bayesian decision analysis of the hazard rate for a two-parameter Weibull process.

22 p3198 A72-41981

Best linear invariant estimation of Weibull parameters - Samples censored by time and truncated distributions.

22 p3199 A72-42969

Mean square invariant forecasters for the Weibull distribution.

24 p3418 A72-44664

WEIERSTRASS FUNCTIONS

Discontinuity problems in optimal control of systems describable by ordinary differential equations, deriving Weierstrass optimality conditions

16 p2371 A72-32939

WEIGHT [MASS]

NT ATOMIC WEIGHTS

NT BODY WEIGHT

NT ORGAN WEIGHT

NT STRUCTURAL WEIGHT

Natural inertia moment effect of balance weight at wing tip on critical flutter rate

08 p1242 A72-21092

WEIGHT ANALYSIS

Variable speed constant frequency power generation equipment influence weapon system effectiveness, considering weight and cost

01 p0008 A72-11067

Minimum weight panel designs subject to supersonic flutter constraint, approximating governing differential equations by difference equations

[AIAA PAPER 72-170]

05 p0741 A72-16908

Computerized design and weight estimation of high voltage power conditioner for communication spacecraft

08 p1112 A72-21417

Automated minimum weight design of ring and stringer stiffened conical shells, using membrane theory for prebuckling analysis

08 p1245 A72-21599

Wing structural weight estimation for civil aircraft preliminary deriving generalized formula based on wing root bending moment for specified flight condition

09 p1262 A72-22909

Pavel stony meteorite microspectral analysis to obtain metallic elements weight percentages in chondrules, matrix and core, using laser source for local vaporization and excitation

14 p2159 A72-30785

Total weight estimates of electric power supply system for transport vehicles involving power generators and primary electrical network with distribution system

16 p2350 A72-32997

Minimum weight passive insulation requirements for hypersonic cruise vehicles.

17 p2638 A72-35256

Weight estimation methods.

19 p2871 A72-37451

Fast method for aircraft rebalance.

19 p2748 A72-37453

Aircraft structures weight reduction through fiber-matrix composite materials, discussing anisotropic elastic and failure behavior of composite light shell structures

[ICAS PAPER 72-38]

21 p3120 A72-41163

Minimum weight design of circular plates with limited thickness.

21 p3125 A72-41515

Weight minimization for elastic circular plates of variable thickness under uniformly distributed load with given stress function conditions

22 p3232 A72-41896

Russian book - Design principles in aircraft construction.

22 p3136 A72-42074

S-3A aircraft weight control program organization and methods, considering cost and schedule performance

[SAWE PAPER 906]

23 p3250 A72-43453

The weight module - A keystone in the aircraft synthesis program.

[SAWE PAPER 912]

23 p3250 A72-43459

Computerized airframe manufacturing cost and weight analysis, using technique for detailed parts list generation from configuration concept as input

[SAWE PAPER 913]

23 p3293 A72-43460

Rotary wing head weight estimation for helicopter preliminary design and parametric studies, deriving semiempirical trend formula

[SAWE PAPER 914]

23 p3344 A72-43461

Helicopter design figure of merit weight ratios definition in terms of rotor thrust coefficient, substituting pure airframe structure weight for conventionally used empty weight

[SAWE PAPER 916]

23 p3250 A72-43463

Moment sampling method as selfvalidating aircraft weight and balance accounting procedure

[SAWE PAPER 920]

23 p3251 A72-43467

L-1011 computerized weight reporting system present and future capabilities.

[SAWE PAPER 932]

23 p3251 A72-43472

Computerized weight data storage, recording and information system to aid in aerospace vehicle design

[SAWE PAPER 933]

23 p3266 A72-43473

Aircraft hydraulic secondary power system weight estimation, presenting components loads and weights breakdown in tables and charts

[SAWE PAPER 935]

23 p3252 A72-43475

Aircraft design structural weight estimation based on post-design analysis of production aircraft, discussing weight factors application to new designs

[SAWE PAPER 936]

23 p3251 A72-43476

Aerospace vehicles preliminary design computer program to include cost, reliability, maintainability and safety parameters in addition to weight as performance determining factors

[SAWE PAPER 940]

23 p3342 A72-43480

Space shuttle optimal entry trajectories for thermal protection system weight minimization, considering constant and variable angles of attack

[AIAA PAPER 72-977]

24 p3452 A72-45414

WEIGHT FACTORS

U WEIGHT [MASS]

WEIGHT INDICATORS

NT MICROBALANCES

Indian low speed wind tunnel, describing design, six component balance and calibration

04 p0509 A72-15277

Wind tunnel six component magnetic balance system, describing ferromagnetic body forces and moments relationship to applied magnet fields and gradients

[AIAA PAPER 72-164]

05 p0645 A72-16829

Superconducting magnetic suspension and balance facility of supersonic wind tunnel for dynamic stability studies

10 p1460 A72-24757

Superconducting coil design for magnetic suspension of supersonic wind tunnel balance

10 p1460 A72-24759

Aerodynamic force and moment measurements on model in magnetic wind tunnel balance system, using field equations

10 p1461 A72-24765

WEIGHT MEASUREMENT

Quasar mass determination, attributing absorption line red shift to radially moving gas clouds

05 p0723 A72-17157

Inherent uncertainties in virial mass determinations of bound and unstable groups of galaxies, computing evolution tracks for different mass loss mechanisms and rates

07 p1072 A72-19341

Airline operational weighing and balancing of 747 aircraft, discussing accuracy and calibration procedures for electronic load cells, mobile platform scales and onboard aircraft weighing systems

[SAWE PAPER 917]

23 p3251 A72-43464

WEIGHTING FUNCTIONS

Linear antenna array optimal power pattern synthesis by best approximation, using weighting function in man-machine iteration

01 p0029 A72-10665

Compressible boundary layer flow problems, using weighted residuals method with exponentials in velocity and enthalpy approximations

02 p0204 A72-12258

Meteorological fields matching by Sasaki method combined with optimum interpolation, using weighting functions

05 p0683 A72-16724

Optimal linear multivariable control systems design with prescribed eigenvalues, presenting method for corresponding weighting matrix elements

06 p0792 A72-17315

Weighting matrices effect on optimal regulator for linear time invariant multivariable systems

07 p0961 A72-19713

Meteorological measurements representativeness and analog discrete filters synthesis with optimal data processing and weighting function averaging procedures

08 p1203 A72-22123

Weighted least squares stationary approximations to time varying linear systems, noting criterion for matrix choice

09 p1341 A72-23094

Stationary weighting pattern synthesis by linear time varying dynamic system, noting feedback system input-output mapping properly

11 p1608 A72-25321

Weighting patterns application to linear finite dimensional systems analysis and synthesis, presenting discrete time realizability condition

11 p1677 A72-26154

Spatial characteristics of equal energy visual stimuli in metaccontrast design for targets and masks of constant separation and varying width, deriving weighting functions

12 p1762 A72-27680

Aircraft applications of composite signal OMEGA configuration with phase data combined at separate carrier with weighting coefficients, discussing advantages over uncompensated navigation systems

13 p1998 A72-29192

Elastic crack tip stress fields, considering weight function

15 p2322 A72-31347

Message circuit noise evaluation in commercial telephone system, discussing noise measurements and weighting curves

15 p2202 A72-32575

Book - The method of weighted residuals and variational principles: With application in fluid mechanics, heat and mass transfer

17 p2573 A72-34250

Functional relationships between the conventional steady-state error characteristics and the weighting matrices in the quadratic performance index.

18 p2672 A72-36058

Finite word length effects on digital filter implementation.

18 p2663 A72-36303

Combined finite element-weighted residuals method for linearized BGK Boltzmann kinetic theory equation, considering cylindrical Couette flow

18 p2684 A72-37168

Homogeneous linear partial differential equation for optimal control with boundary condition formed by terminal component, noting weighting functions for linear plant

19 p2778 A72-37989

Structural-matrix methods for discrete automatic control system designs

19 p2779 A72-38185

Weighting factor and transmission time optimization in video MTI radar.

21 p3022 A72-41082

Use of rotated electrodes for amplitude weighting in interdigital surface-wave transducers.

22 p3178 A72-42619

Functional method investigations of imbedding theorems for random weight spaces of high order irregular elliptic equations with uniform boundary conditions

23 p3307 A72-43222

Man machine control system synthesis, noting quality criteria and estimates for weighting function coefficients of optimization potential

24 p3376 A72-45508

Whittaker method for astronomical observational data smoothing, noting correlation function for latitude weighting functions determination

24 p3447 A72-45677

WEIGHTLESS FLUIDS

Navier-Stokes equations asymptotic solution for compressible weightless conducting fluid flow in plane channel with intense blowing from walls

05 p0648 A72-16219

WEIGHTLESSNESS

Sjoberg hypothesis for zero gravity produced inversion illusion mechanism in aircraft parabolic flight, noting otolithic membrane deflection result of force on maculae

02 p0167 A72-11710

Industrial and biological processing possibilities under weightless condition, considering crystal growth, metal processing, vaccine production and electrophoresis in space manufacturing

02 p0278 A72-11961

Astronaut zero gravity adaptive responses in performance, locomotion, orientation, sleep and physiological and functional characteristics

03 p0319 A72-13867

Soviet book on astronaut activity psychological features covering space flight living conditions, space and time perception psychophysiological mechanism changes and weightlessness effects

03 p0317 A72-14246

Dielectrophoresis force measurements and wedge shaped capacitor separation properties in satellite zero gravity conditions

04 p0549 A72-14988

Space environment weightlessness and radiation effects on leeches biorhythm, metabolism, reproduction and growth from rocket biological experiments

04 p0481 A72-15729

Soviet book on gravitational effects on animal evolution covering land and aqueous conditions adaptation and weightlessness in space

06 p0763 A72-17818

NASA materials science and manufacturing in space program involving space shuttle reusable equipment and weightlessness applications experiments

06 p0797 A72-18621

Capillary forces effects on free surface liquid behavior in partial or total weightlessness, reviewing sloshing problem mathematical treatments
06 p0802 A72-18717

Calcium metabolism perturbations in astronauts under weightlessness conditions and in immobilized test subjects, noting bone tissue renewal cycle modification, calciuria variations and bone calcification
07 p0927 A72-19245

Medicobiological investigations of prolonged weightlessness effects on astronaut physiological system based on Soyuz flight program
10 p1425 A72-24409

Sounding rocket heat pipe experiment in zero gravity, testing spiral and pedestal arteries and plain groove designs
[AIAA PAPER 72-259] 11 p1739 A72-25204

Weightlessness effects on human organism, discussing physiological changes, artificial gravity by spacecraft rotation and exercise to counter adverse reactions
11 p1589 A72-26891

Apollo 14 experiments to demonstrate flow patterns of convection and heat transfer in gases and liquids under weightlessness
13 p2035 A72-28614

Prevention of weightlessness effects on blood hydrostatic pressure, musculoskeletal system and sensorimotor performance, discussing space flight training and space environment simulation tests
13 p1909 A72-28787

Zero gravity earth orbital cloud physics facility requirements and design concepts, noting experiments feasibility relative to astronaut performance
13 p1990 A72-28815

Human organism readaptation after prolonged hypokinesia and weightlessness, discussing coordination disturbances, vegetative and vascular system instabilities, reduced orthostatic stability and asthenia
14 p2076 A72-30745

Human waste management system evaluation in zero gravity flight tests, presenting design concept for collection by air flow technique
15 p2189 A72-31825

Medical investigations during Salut space station flight, discussing weightlessness effects and efficiency evaluation of preventive measures for crewmembers high performance in space flight
15 p2189 A72-31918

Long term weightlessness-induced physiological response normalization by muscle bioelectrostimulation, muscular tissue energy load increase and mineral metabolism stabilization
16 p2354 A72-33543

Technology R and D program to qualify man for long term weightlessness, assessing space flight stress effects on physiology and psychology
16 p2358 A72-33544

Prolonged weightlessness effects on cardiovascular, digestive, musculoskeletal and nervous systems, blood and metabolism, noting compensatory reactions
16 p2354 A72-33546

Physiological effects on prolonged weightlessness in dogs aboard Cosmos 110 biosatellite, emphasizing body weight loss and enzyme activity and bone tissue mineral concentration changes
16 p2354 A72-33547

Weightlessness effects on animal voluntary motor activity and wakefulness from brain and muscle area electrical activity recordings during ballistic flight
16 p2355 A72-33548

Space environment weightlessness induced perceptual deprivation, considering hand-eye coordination, visual judgments and motion and time perception
16 p2355 A72-33549

Long term space flight weightlessness and hypodynamic effects on orthostatic and vestibular tolerances, infection susceptibility and drug reactivity
16 p2355 A72-33550

Weightlessness effects on calcium and electrolyte metabolism from measurements during Gemini 7 flight, using dietary control and excreta collection techniques
16 p2355 A72-33552

Sleep factors and limitations during prolonged space flights, considering weightlessness, hypokinesia, nervous tension, cabin confinement, rhythm, environment and noise effects
16 p2356 A72-33561

Vestibular behavior of fish during diminished g-force and weightlessness.
17 p2499 A72-34549

Russian book - Intracranial blood circulation under conditions of accelerations and weightlessness
17 p2509 A72-35460

Zero-gravity thermal performance of the Apollo cryogenic gas storage system.
19 p2869 A72-38830

Space shuttle waste collection system development, discussing human-interface requirements, zero gravity effects and operational considerations
20 p2896 A72-39164

[ASME PAPER 72-ENAV-13] 20 p2896 A72-39164

Determination of the optimal parameters of high-pressure cryogenic fluid storage systems.
20 p2962 A72-39358

Free oscillations of a liquid rotating in a cylindrical vessel under conditions of weightlessness
22 p3165 A72-42251

Effects of weightlessness on astronauts - A summary.
23 p3253 A72-43385

Effects of an 18-day flight on the human body.
23 p3253 A72-43386

Functional insufficiency of the neuromuscular system caused by weightlessness and hypokinesia.
23 p3253 A72-43387

Studies on weightlessness in a primate in the Biosatellite 3 experiment.
23 p3253 A72-43388

Calcium metabolism under stress and in repose.
23 p3254 A72-43389

OFO A orbital flight recording of bullfrog vestibular gravity sensor nerve fiber pulses for assessing necessity of artificial gravity during prolonged weightlessness
23 p3254 A72-43391

Economic materials processing in orbiting spacecraft under zero gravity conditions, emphasizing single crystal electronic materials and high purity biologicals
24 p3407 A72-45157

WEIGHTLESSNESS SIMULATION

External respiration gas metabolism and energy consumption measurements for test pilots during parabolic trajectory flights in weightlessness simulation experiments
02 p0163 A72-12347

UV sensitive fire detector in manned space vehicle, discussing simulation in aircraft flying zero gravity parabolas
06 p0814 A72-17584

Interface stability of floating liquid zones of water/ethanol solutions in simulated zero gravity
07 p1036 A72-20561

Modular microbiology laboratory design considerations and zero gravity experiments to investigate microbial culture systems behavior
12 p1765 A72-28280

Thermoregulation changes during simulated weightlessness of prolonged bed rest, noting lower sweating threshold and decreased vasodilation /autonomic dysfunction/
12 p1767 A72-28301

Water immersion tests to study body fluid balance disturbances during weightlessness, observing diuretic reflex control of blood volume
16 p2355 A72-33551

Effects of combined O-G simulation and hypergravity on eggs of the nematode, *Ascaris suum*.
[DFVLR-SÖNDR-225] 17 p2499 A72-34547

Acceleration tolerance of man after a lasting exposure to conditions of simulated weightlessness
21 p3006 A72-40442

Thirty day experiment for assessment of weightlessness simulation test methods and evaluation of applicable prophylactics
23 p3259 A72-43912

Lower-body negative pressure as a method of preventing shifts associated with changes in the hydrostatic pressure of blood
23 p3256 A72-43919

Induction of hemodynamic deterioration by the hypogravic state - An evaluation of mechanisms and prevention.
24 p3373 A72-45199

WEIGHTS (COEFFICIENTS)

U COEFFICIENTS

WELD STRENGTH

Porosity and W inclusions effects on Al alloy weld strength, presenting radiographic and tensile test data
01 p0074 A72-10282

Heat input, interpass temperature and panel width effects on butt welds strength in Al alloy plate
04 p0526 A72-14838

Boron/aluminum composite sheet quality evaluation by radiography, ultrasonic C-scanning and micro-ohm resistance measurement, correlating with resistance weld strength
04 p0526 A72-14839

Axisymmetric stress analysis in various weld configurations of stub end high pressure pipe connections, using finite element method
06 p0820 A72-17709

Cast and wrought Ti alloys Ar arc weldments microstructural and mechanical properties after different heat treatment sequences
07 p1013 A72-19750

Ti structures controlled path resistance welding, discussing welded joints metallographic and mechanical properties
07 p0996 A72-19996

Residual stresses effect on technical cohesive strength of welded cylindrical shell with surface defects, presenting plane strain fracture toughness determination method
07 p0997 A72-20131

Al alloys welding with Pb sheathed linear ribbon RDX explosives by parallel plate process, achieving high weld strength
08 p1173 A72-20779

Metal inert gas /MIG/ spot welding process effects on weld dimensions, shape and strength
09 p1320 A72-23630

Diffusion bonding compared to other processes, discussing mechanical properties, metallurgical condition, fatigue, pressure, temperature and production problems
09 p1320 A72-23633

Diffusion bonded joints tensile strength determination from ultrasonic pulse echo and attenuation measurements, discussing contamination and SNR effects
10 p1485 A72-23814

Continuous drive friction welding of mild steel, noting burn-off rate relationship to tensile strength
11 p1641 A72-26492

Sintered Mo diffusion weld strength dependence on contact surface flatness and smoothness
11 p1644 A72-26847

Weld solidification synthesis with crystalline organic materials, investigating substructure size, growth rate and thermal gradients
13 p1966 A72-29424

Automatically controlled plasma arc welding for uniform cross section weld seams production under fluctuating electric current conditions, describing electronic control system
15 p2244 A72-31773

Mechanical properties and residual stresses in and adjacent to interface of explosively welded Al-Zn-Mg alloy with steel, noting microcracks effect on weld strength
15 p2257 A72-32111

German monograph - Contribution to the ultrasonic seam welding of metals
19 p2807 A72-37655

Distortion and residual stresses in welded aluminum structures.
20 p2928 A72-39204

Technical cohesive strength of welded joints at various temperatures and loading rates
23 p3293 A72-43961

Residual stresses effect on technical cohesive strength of welded cylindrical shell with surface defects, presenting plane strain fracture toughness determination method
24 p3408 A72-45757

WELD TESTS

Mathematical model of porosity gas transport test for automated fusion welding operation using mass spectrometer
01 p0076 A72-10815

Nondestructive tests of welded joint heterogeneities and corrosion cavities by densitometric photometric differentiation of radiographs
07 p0995 A72-19674

Pulsed laser beam effect on residual stresses behavior in transverse weld on cylindrical shell
07 p0996 A72-19776

Tensile and fatigue tests of dissimilar metal joints made by friction pressure welding
09 p1321 A72-23640

Microstructure and mechanical properties of heat treated friction welds at high temperatures
11 p1641 A72-26489

Underbead hardness determination in carbon and low alloy steels, noting weld tests/theory correlation
11 p1641 A72-26493

Ferritic stainless weld metal ductility, investigating yield and fracture stresses after heat treatment
11 p1661 A72-26494

Ta alloys fusion weld ductility, discussing welding parameters, alloy components, interstitial impurities and weldment microstructure effects
15 p2244 A72-31775

Nondestructive test for measuring the state of heat treatment in closure welds.
18 p2695 A72-36672

Factors governing radiographic crack detectability in steel weld specimens.
18 p2695 A72-36673

Selection of characteristics for automatic classification of welding defects in radiographic testing.
19 p2805 A72-38763

Use of acoustic emission for the detection of weld and stress corrosion cracking.
20 p2925 A72-39283

A radiographic technique using an electron beam welder.
20 p2929 A72-39340

Ni alloys weld testing for hot cracking resistance, describing varesstraint test method
21 p3060 A72-40848

German monograph - Influence of programmed welding cycle temperatures on the microstructure formation and corrosion behavior of austenitic corrosion-resistant steels.
22 p3195 A72-43075

Elastic stiffness of AT-2 and AT-3 titanium alloys and their welds at high and low temperatures
23 p3302 A72-43966

WELDABILITY

High chromium ferritic stainless steels weldability and mechanical properties, showing C, N, Ti and

residuals effects on recrystallization, toughness, tensile behavior and corrosion resistance

01 p0083 A72-10283

Refractory alloy weldability and brazing, discussing manual and automatic tungsten arc and electron beam processes and fillers

01 p0075 A72-10752

Ti alloys for aircraft structures, emphasizing weldability, tensile fatigue and residual strengths, shear-carrying qualities and fuselage shell design

03 p0373 A72-13616

Alloy additions and heat treatment effects on mechanical properties and weldability of quenched and aged high strength Ni steels

03 p0378 A72-14173

Heat resistant weldable precipitation hardened Ni base alloy, discussing intermetallic phase hardening

07 p1014 A72-19842

Low temperature resistant stainless steels mechanical properties, microstructure and weldability, discussing compositions and heat treatments

10 p1498 A72-24838

Al alloy-graphite composites brazing and welding feasibility, tabulating spot welding parameters

11 p1641 A72-26491

Cu surface contamination effect on hot crack susceptibility and weldability of Co based superalloys

13 p1965 A72-29419

Fusion welding of Ti-W and Ti-graphite composites, determining weldability and effect of weld thermal energy on fiber matrix reactions

13 p1966 A72-29423

Aluminum alloys electron beam weldability, considering precleaning, welding speed, voltage, pre- and post-weld heat treatments effects

17 p2561 A72-35799

Filler wire composition effects on solidification cracking resistance in weldable Al-Zn-Mg alloy

18 p2699 A72-36426

German monograph - Significance of the manganese-carbon ratio in the brittle-fracture behavior and weldability of high-strength fine-grained structural steels

19 p2816 A72-37661

WELDED JOINTS

NT SPOT WELDS

Brazed joints shear strength and ductility tests, discussing deformation, hardness, corrosion, irradiation, structure and microanalysis

01 p0074 A72-10285

Dye penetrant surface defect indications on 2014-T6 Al gas metal arc weldments heat affected zone, considering minimization by arc stabilization and caustic etch time reduction

02 p0236 A72-12775

Pulsed Nd laser drilling and welding of metal, metal-semiconductor and semiconductor elements, discussing bond penetration and character, mechanical strength and I-V characteristics

03 p0363 A72-13860

Nondestructive examination of steel plate weld specimen, comparing ultrasonic and X ray techniques

04 p0527 A72-14840

Hydrogen environment effects on fatigue crack growth rates in Ti-Al-V weldments over low ambient temperature range

05 p0678 A72-17116

Beryllium joining by resistance welding, electron beam welding, dip brazing and braze welding

06 p0820 A72-17701

Static and fatigue strength in tension of welded joints composed of low carbon and austenitic steel

07 p0996 A72-19767

Ti structures controlled path resistance welding, discussing welded joints metallographic and mechanical properties

07 p0996 A72-19996

Vacuum hot press diffusion welding of nickel-chromium-thorium dioxide sheet, describing specimen preparation, welding procedure and welded joints photomicrographic microstructure

07 p0997 A72-20002

X ray analysis of cementite and titanium carbide precipitates in Cr-Mn-Mo-Ti steels weld zones

07 p1019 A72-20159

Metal welded joints formation as diffusion intensification from atom jumps stimulation by phonons from atomic thermal vibrations or crystal defects generation

09 p1319 A72-22867

Welded high strength maraging steels fatigue performance, stressing nondestructive testing technique

09 p1332 A72-23617

Cumulative fatigue damage in Al-Zn-Mg alloy fillet welded joints, analyzing constant amplitude and programmed load fatigue test results

09 p1332 A72-23618

Data scatter reduction in Al-Zu-Mg welded specimens cumulative fatigue damage testing, noting fatigue life improvement by shot peening and static or dynamic prestressing

09 p1332 A72-23619

Electrode vertex angle effect on fused weld bead geometry related to plate thickness in tungsten inert gas (TIG) welding

09 p1320 A72-23634

Acoustic emission monitoring of postweld heat treatment cracking in Rene 41 weldments, correlating relative crack susceptibility of different microstructures

11 p1653 A72-25345

Crystallization discontinuity and layer thickness in welded joints as function of overcooling and isotherm shape

13 p1963 A72-28922

Thermal effects on phase structure of welded joints of Al alloy with Cu addition

13 p1978 A72-29022

Literature survey of fatigue behavior of Al alloy welded joints, discussing testing and analysis methods

14 p2113 A72-30250

Servomechanism and reduction gear ratio selection for arc welding voltage regulator, taking into account welded joints properties

15 p2244 A72-31611

Al alloy welded seams corrosion fatigue strength increase by epoxy polymer coatings under cyclic tensile stresses

16 p2397 A72-33268

Welded Al joints fatigue resistance from iterative nonlinear regression analysis with multiparameter endurance curves

16 p2412 A72-34141

Thermal effects in the seam area during impact welding

19 p2809 A72-38461

Fatigue strength of welded aluminum-connections - Investigation with the aid of multiparameter life length lines

20 p2930 A72-39941

Load tests in air to evaluate maraging steels weldments for rocket motor case applications

20 p2942 A72-39955

Strength of welded joints of high-strength stainless steels at cryogenic temperatures

21 p3061 A72-41365

Investigation of the influence of multiple-pass welding on the mechanical properties of welded joints of VT6s and VT14 titanium alloys

22 p3182 A72-41861

German monograph - The causes of hot crack formation in welded joints of austenitic steel with 16 percent chromium and 16 percent nickel

22 p3195 A72-43079

Tendency toward brittle failure of a simulated weld-seam region in Ti-Al-V system alloys

23 p3293 A72-43593

Technical cohesive strength of welded joints at various temperatures and loading rates

23 p3293 A72-43961

Determination of the stressed state in a welded joint in plastic deformation

23 p3293 A72-44019

Fatigue crack propagation in A514 base plate and welded joints

23 p3354 A72-44309

Heat treatment effects in multipass weldments of a high-strength steel

23 p3304 A72-44310

WELDED STRUCTURES

NT STEEL STRUCTURES

Residual stresses and geometrical imperfections effects on compressive strength of thin welded box columns

07 p1088 A72-19114

Two dimensional thermoelasticity problem with nonstationary temperature field and external boundary forces, using algorithm to evaluate stress-strain state of welded plates

09 p1401 A72-22725

Damping coefficient increase in welded bodies under uniform stress and compression, torsion and bending vibration

09 p1406 A72-23076

Welded structures fatigue, - Conference, Abington, England, July 1970

09 p1332 A72-23615

Fracture mechanics application to welded structures fatigue, using crack propagation law

09 p1409 A72-23616

Fatigue indicators with analytic or visual notched and cracked coupons techniques and strain multipliers for welded structures

09 p1316 A72-23620

Design information for machinery to incorporate welding positions and joints, fatigue mechanisms, loads, combined stresses and plate and cast materials properties

09 p1409 A72-23621

Statistical evaluation of welded airframe component fatigue damage increment during cyclic loading with constant force amplitude

10 p1559 A72-24922

Welded steel airframe residual fatigue life tests by nonstationary random loading, applying to jet trainer aircraft landing gear

14 p2107 A72-30277

Welded machine component service history effects on residual fatigue life from statistical evaluation of factor experiment

14 p2107 A72-30278

Welded Al alloys at temperatures above 100 C, discussing traditional and powder metallurgy and mechanical properties dependence on time, temperature and creep

14 p2116 A72-30528

Fatigue crack initiation and propagation in welded structures, considering low and high cyclic stresses, microstructure and environment effects

17 p2635 A72-35919

Distortion and residual stresses in welded aluminum structures

20 p2928 A72-39204

WELDING

NT ARC WELDING

NT BRAZING

NT DIFFUSION WELDING

NT ELECTRIC WELDING

NT ELECTRON BEAM WELDING

NT EXPLOSIVE WELDING

NT FLASH WELDING

NT FUSION WELDING

NT GAS TUNGSTEN ARC WELDING

NT GAS WELDING

NT PLASMA ARC WELDING

NT PRESSURE WELDING

NT ULTRASONIC WELDING

Jet engine component overhaul procedures for fatigue damage repair, detailing distressed metal removal, replacement and welding techniques

02 p0271 A72-12499

Inconel 718 welding techniques, investigating microfissuring, impact strength, penetration and ductility

02 p0246 A72-12774

Solid phase friction welding, discussing metallurgy and engineering applications

03 p0362 A72-12990

Pulsed Nd laser drilling and welding of metal, metal-semiconductor and semiconductor elements, discussing bond penetration and character, mechanical strength and I-V characteristics

03 p0363 A72-13860

Al sheet weld cracking, discussing hold-down, localized heating, welding speed and gap effects

06 p0820 A72-17702

Welding thermal energy effect on residual ferrite of austenitic chrome-nickel steel deposits

07 p1010 A72-18971

High power carbon dioxide laser beam applications to deep penetration metal welding, including cutting tests

07 p0994 A72-19214

Laser applications in industrial machining and welding, describing theory and operation of optically pumped ruby, glass-Nd, YAG-Nd, Ar and carbon dioxide lasers

07 p1007 A72-20224

Laser beam welding operational and economic aspects, discussing comparative merits vs conventional welding techniques in terms of quality, speed, depth and power limitations

07 p0998 A72-20397

Pulsed carbon dioxide laser welding of miniature explosive detonators

08 p1221 A72-20778

Optical mirror method for bending strains study in welding cycles with applications to sheet metal thermal stress strain rates

09 p1318 A72-22738

Advances in welding processes - Conference, Abington, Cambridge, England, April 1970

09 p1319 A72-23626

Laser welding theory and applications to microelectronics, nuclear and aerospace fields

10 p1485 A72-23968

Solidification mode of weld metal in Inconel 718, using optical and electron transmission microscopy, etch-pit technique and electron-microprobe analysis

11 p1653 A72-25344

Microwelding and microsoldering equipment control systems, discussing ac phase cut-off, dual pulse, dc and intermediate frequency units

11 p1639 A72-25810

High strength quenched steel with high ductility at cryogenic temperatures and negligible cooling rate effects on plasticity during welding

11 p1660 A72-26136

Safe welding procedures for carbon manganese steels, noting hydrogen cracking association with hardening of heat affected zone

11 p1641 A72-26490

Commercially available laser systems applications to welding, drilling, scribing and other machining operations

11 p1652 A72-26984

Soft solder cracking and breaking alleviation in welding technique for solar cells, noting resistance to thermal cycles

12 p1814 A72-28039

Inertia welded bimetallic fasteners for aerospace industrial applications, noting cost advantages

12 p1817 A72-28166

Deep penetration welding and cutting with high power CW carbon dioxide lasers, describing experimental setup 13 p1965 A72-29422

Nd glass laser drilling and welding applications and tests on materials to evaluate feasibility and operational advantages, identifying optimal pulse energies and durations 15 p2244 A72-32028

German book on welding of special metals covering Ti, Zr, Mo, Ta, W, Va, Nb and Be welding techniques 16 p2398 A72-33372

Laser beam welding of small components 17 p2559 A72-34925

Brazed-welded lightweight high pressure aerospace tube-fittings. 17 p2560 A72-34939

Chromium-based powdered alloys used in highly alloyed steel welding 19 p2809 A72-38289

WELDING MACHINES

Mathematical model of porosity gas transport test for automated fusion welding operation using mass spectrometer 01 p0076 A72-10815

Vacuum welding by electron beam bombardment, discussing electron gun arrangements with plane-radial, plane-linear and linear electron beams 08 p1176 A72-21049

Pneumatic machine for microfriction stud welding of dissimilar metals 09 p1320 A72-23631

Pulse shaping, arc plasma jets and torch movement indexing for high precision pulsed tungsten inert gas (TIG) welding 09 p1321 A72-23635

Prototype fine wire feed unit and microplasma welding torch and equipment for butt welding of Ni maraging steel, testing welds mechanically 09 p1321 A72-23636

Automatic electron beam welding machine for small components, discussing design, performance and inspection methods 09 p1321 A72-23637

Electron beam welding, discussing problem areas, equipment trends and industrial needs 10 p1485 A72-23966

German monograph - Improvement of the ductility characteristics of flash butt welding joints involving carbon steels by pulse normal annealing and hot heading in the welding machine 19 p2807 A72-37659

The versatility of resistance welding machines for joining boron/aluminum composites. 21 p3060 A72-40847

Welding airframe structures in titanium using tensile loading to overcome distortion. 24 p3407 A72-45000

Investigation of the possibility of using radiant solar energy for welding and soldering of materials 24 p3407 A72-45126

WENTZEL-KRAMER-BRILLUIN METHOD

WKB type solution for electromagnetic wave propagation in circularly cylindrical coordinate system with rho-dependent refractivity, using Bessel function 04 p0488 A72-15384

WKB large frequency expansion solution for elastic waves propagating into inhomogeneous elastic medium with harmonic periodicity, using perturbation method [ASME PAPER 72-APM-3] 17 p2630 A72-34810

WKB approximation and oscillatory behaviour of null geodesics in general relativity. 17 p2583 A72-35795

WKB approximation to suggest vertical phase velocity measurement at turning points of acoustic-gravity wave propagation in thermosphere 18 p2686 A72-36411

WEST GERMANY

U GERMANY

WESTLAND AIRCRAFT

Lynx helicopter RS 360 turboshaft engine, describing modular design for maintainability 17 p2597 A72-34927

WETNESS

U MOISTURE CONTENT

WETTABILITY

Carbon fiber reinforced material porosity source, applying equilibrium configurations of liquid films on parallel uniform cylindrical rod hexagonal and cubic arrays 04 p0537 A72-15087

Coating of fibers and the fabrication of fiber-reinforced composite materials 20 p2929 A72-39443

WETTING

Electronic configuration effect on wetting characteristics of hard material mixed crystals, investigating transition metals carbides, nitrides and oxides 11 p1665 A72-26873

Graphite wetting with liquid V, Nb and Mo as function of metal melting point and sample temperature 15 p2243 A72-31223

Hexagonal and cubic boron nitride surface wetting by liquid metals as function of contact interaction and chemical affinity 15 p2253 A72-31224

C concentration and temperature dependence of graphite wetting by liquid Ni and Co and melts of Ni-C and Co-C alloys, noting nonequilibrium effect 16 p2415 A72-33537

WHEEL BRAKES

Carbon/epoxy composite reinforced plastic materials feasibility for application to aircraft landing gear wheel fabrication 08 p1193 A72-21686

Aircraft wheel mechanics, discussing freely turning and braked wheels, tire drift and antiskid braking systems for landing gear 11 p1574 A72-25287

WHEELS

NT FLYWHEELS

NT NOSE WHEELS

NT REACTION WHEELS

NT TURBINE WHEELS

NT VEHICLE WHEELS

Aluminum aircraft wheels ultrasonic inspection, noting reliability, simplicity and time economy as compared to eddy current or fluorescent penetrant methods 13 p1966 A72-30037

Wheel balancing by static and dynamic trial method, using Churchill Mark 3 apparatus 15 p2213 A72-31635

WHIRL INSTABILITY

U ROTARY STABILITY

WHIRLING

U ROTATION

WHIRLING TESTS

U SPIN TESTS

WHISKER COMPOSITES

Temperature effect on bonding strength between ceramic whiskers or fibers and metal matrices attributed to thermal expansion coefficients disparity 16 p2413 A72-33206

Composites technology, costs and performance review covering metal matrix composites, ceramic reinforced plastics and whisker composites 17 p2571 A72-35652

Magnesium aluminate spinel reinforced with sapphire whiskers, investigating whisker content, temperature and deflection rate effects on yield strength 17 p2572 A72-35661

WHISKERS [SINGLE CRYSTALS]

Ceramic whisker and fiber reinforcement of metals, discussing manufacturing and testing problems 04 p0533 A72-15088

Inorganic single crystal titanate whisker fibers with high modulus strength for plastic reinforcement, noting mechanical, thermal and physical properties 08 p1193 A72-21685

Antimony compounds single crystal whiskers permittivity determination at microwave frequencies from power reflection and transmission coefficients 09 p1366 A72-22417

Bloch walls and Landau domain configurations in iron whiskers from DC to 200 kHz by direct magnetization measurements 11 p1659 A72-25912

Effective separation technique for small diameter whiskers. 17 p2572 A72-35662

Alpha aluminum oxide whiskers growth in presence of lead by vapor/liquid/solid phase mechanism in moist hydrogen at 1200-1400 C 19 p2823 A72-38279

Aluminum oxide and silicon carbide whiskers fabrication by homogeneous gas reaction process, discussing gas composition, temperature and substrate effects on production yield 20 p2940 A72-39440

Alpha aluminum whiskers growth in mullite ceramic composition following vapor-liquid-solid phase 23 p3303 A72-44152

WHISTLER RECORDERS

Intercoms 3 satellite vlf radiation and natural signals recording with circular antenna, whistler recorders, sonograms and spectroanalyzers 08 p1157 A72-21146

Intercoms 3 satellite VLF radiation and natural signals recording with circular antenna, whistler recorders, sonograms and spectroanalyzers 20 p2903 A72-39251

WHISTLERS

Io modulation of Jupiter decametric emissions, using cyclotron magnetosphere model and coupling by whistler mode electromagnetic waves 01 p0125 A72-10084

Tweaks contribution to atmospheric radio noise background, discussing nighttime ionospheric source information 01 p0056 A72-10444

Outer zone energetic electron precipitation, elf whistler and plasmopause location measurements by polar satellite OV-3-3 instruments 01 p0120 A72-10890

Nonducted vlf wave propagation near plasmopause during whistlers based on diffusive equilibrium and collisionless models for magnetospheric electron density distribution 02 p0222 A72-12873

Periodic micropulsations in amplitude and bandwidth observed in long duration vlf whistler mode signals from ground stations, considering explanations 03 p0322 A72-13530

Large amplitude whistler mode wave packet multiple emissions model including wave-particle interactions 04 p0517 A72-14948

Low latitude low dispersion whistlers, discussing origin as vlf waves radiated from return stroke of lightning discharge 04 p0517 A72-14949

Hydromagnetic whistler traveling wave tube amplification in magnetosphere, deriving temporal growth rate dependence on plasma parameters 04 p0517 A72-14950

Whistler instability of electron plasmas with non-Maxwellian velocity distribution function 05 p0698 A72-17015

Relativistic electron pitch-angle diffusion driven by oblique lf whistler-mode turbulence in collisionless plasma immersed in static magnetic field 05 p0699 A72-17024

Vlf phenomena of magnetospheric origin, presenting whistlers classification table 06 p0803 A72-17375

Interference above ionosphere of lf radio waves emitted by multiple lightning discharges concluded from spectrographic observation of whistler received onboard Injun 5 satellite 06 p0773 A72-17567

Magnetoguided whistler propagation, observing longitudinal current in ionospheric plasma 06 p0808 A72-18064

Geoelectric field strengths deduction from mid-frequency slopes on diurnal incidence plot of pc 1 hydromagnetic whistlers 07 p0974 A72-18904

Ogo 6 ionospheric measurement of proton whistlers wave-normal vector, investigating propagation modes 07 p1057 A72-19148

Hf instability on whistler branch of finite pressure plasma with nonmonotonic ion distribution function under Landau damping effect 07 p1042 A72-19615

Large scale structure of plasmopause in equatorial plane based on whistler and upper ionosphere sounding data 07 p0978 A72-20045

Duskside magnetic activity relationship with bulge detection by whistler method, investigating plasmopause deformation 07 p0979 A72-20381

Reactive mechanism of nonlinear mixing in resonant excitation of ion plasma waves by vlf and whistler waves 07 p1046 A72-20540

Whistling atmospherics generation mechanism, showing ionic sound excitation by hydromagnetic wave propagation through magnetospheric rapid plasma concentration change regions 08 p1155 A72-20807

Magnetic fluctuations in elf and vlf waves in space, discussing whistler phenomena and applications to magnetospheric probes 08 p1158 A72-21189

Stability of steady large amplitude whistler wave supported by weak electrostatic waves in collisionless magnetoplasma, constructing distribution function via Vlasov equation solution 08 p1213 A72-21258

Polarization characteristics measurement for PC 1 geomagnetic micropulsations propagated through ionospheric ducts, noting hydromagnetic emissions and whistlers relation to high latitude source region 09 p1299 A72-22989

Digital lightning goniometry for flash locations at great distances by atmospherics and whistlers analysis 09 p1304 A72-23471

Whistler damping factor dependence on magnetic field strength in geometrical optics approximation, emphasizing nonlinear effects at low frequencies in ionospheric propagation 09 p1282 A72-23516

Wave particle interaction around lower hybrid resonance frequency, deriving whistler mode wave growth rate during propagation in magnetoactive plasma penetrated by nonthermal particles 10 p1476 A72-24959

Whistler dispersion and occurrence rate characteristics at low latitudes during solar cycle, noting annual variations and magnetospheric electron density 11 p1623 A72-26105

Ogo-5 observation of lower hybrid resonance noise, bursts, VLF hiss and whistlers near plasmopause during large magnetic storm 11 p1624 A72-26399

Magnetospheric equator plane electron density profiles determination from plasmopause whistlers observed in UK

11 p1626 A72-26421

Computerized simulation of single large amplitude whistler wave propagation in plasma, noting collisionless damping, oscillations and equilibrium

13 p2012 A72-29128

Whistler mode signals observation in conjugate region of 200 kHz broadcast station by satellite-borne narrow band receiver, considering field-aligned ducted and nonducted propagation

13 p1950 A72-29384

Helicon /whistler/ turbulence spectra in collisionless plasma due to ion scattering, considering self trapping and stability along magnetic field with Landau absorption decay

14 p2137 A72-30357

Nonlinear AM and FM due to bonded nature of quasi-monochromatic whistler packets in magnetosphere

14 p2085 A72-30448

Whistler waves amplification in magnetosphere, obtaining particles pitch angle and energy diffusion coefficients and one dimensional Fokker-Planck equation

15 p2194 A72-31427

Magnetosphere thermal plasma densities determination from hydromagnetic whistler digital sonograms and modified normalized dispersion curves

15 p2283 A72-31430

Whistler propagation in magnetosphere disturbed by ring current, explaining electron density decrease

15 p2194 A72-31433

Whistler mode VLF signal transmission in ground transmitter and magnetically conjugate zones, observing spectrum broadening and AM in magnetosphere

15 p2197 A72-31919

Whistlers noise frequency and minimum group time delay determined from model magnetosphere and from measurement, noting precision effect on electric field calculation accuracy

15 p2198 A72-31947

Rocket-observed energetic electron flux association with ground recorded plasmasphere whistler in terms of gyroresonant wave-particle interaction

15 p2198 A72-31948

Nightside magnetosphere convection electric field from motions of whistler ducts within plasmasphere, considering interplanetary magnetic field theta component

16 p2382 A72-32960

Model for VLF emissions triggered by whistlers and man-made radio signals, noting effects of wave packet and second order resonance

16 p2365 A72-33905

Investigation of energetic charged particles and VLF emissions on the 'Interkosmos-3' satellite

17 p2600 A72-35209

Ring current effect on magnetospheric electron density profiles derived from plasmopause whistlers.

17 p2600 A72-35368

Wave interference effect in whistler mode reflection coefficients for model lower ionospheres.

17 p2548 A72-35465

Observation of very-low-frequency whistler-mode waves in the region of the radiation-belt slot.

17 p2517 A72-35598

On the stability of obliquely propagating whistlers.

17 p2517 A72-35600

Whistler side-band growth due to nonlinear wave-particle interaction.

17 p2517 A72-35601

Nonequilibrium energy constants associated with large-amplitude electron whistlers.

17 p2517 A72-35620

Whistler activity in central Europe during the period of increasing solar activity from 1964 to 1968.

18 p2657 A72-36230

On the reflection of whistler mode waves from model lower ionospheres.

18 p2660 A72-36430

Parametric excitation of electromagnetic waves.

19 p2834 A72-37718

Electric dipole radiation at VLF in a uniform warm magneto-plasma.

19 p2840 A72-37833

The propagation of very low-frequency waves in ducts in the magnetosphere. II.

20 p2916 A72-39192

Radiation belt electron lifetimes and removal through pitch angle diffusion by plasmaspheric whistler waves in cyclotron harmonics

20 p2918 A72-39532

VLF emission artificial triggering by whistler Morse pulses in magnetosphere, explained in terms of resonant trapped particle current and wave field behavior

20 p2903 A72-39549

Magnetospheric propagation of auroral hiss with whistler mode dispersive properties, suggesting burst source locations and mechanisms

21 p3048 A72-40399

Whistler propagation through magnetosphere.

21 p3049 A72-40975

Detection of whistler mode signals from VLF transmitter in Australia.

21 p3023 A72-41386

Ionospheric refractivity and attenuation surface deformation relationship to ion cyclotron whistlers near cross-over level between zero and critical coupling angles

22 p3168 A72-42006

Pc 1 hydromagnetic whistlers and emissions polarization characteristics measured in plane of earth surface

22 p3169 A72-42019

Use of the three-dimensional covariance matrix in analyzing the polarization properties of plane waves.

23 p3315 A72-44518

Instability of the whistler structure of oblique hydromagnetic shocks.

24 p3428 A72-45013

WHITE BLOOD CELLS

Mathematical model for blood leucocyte population changes after radiation exposure within Blair model leucocytes hemopoietic to cardiovascular systems transport

05 p0618 A72-16635

Picoscale blood diagnostic device for red and white cell count, noting piston principle electronic operation

09 p1272 A72-23257

WHITE DWARF STARS

Gravitational waves proposed origin, considering black holes, star collapse, white dwarf and neutron star formation and galaxy center neutron star clustering

04 p0576 A72-15074

Circular polarization change with wavelength in white dwarf Grw plus 70 deg 8247

04 p0580 A72-15367

White dwarf Grw plus 70 deg 8247 circular polarization spectral structure with molecular absorption bands coincident with Minkowski bands

04 p0580 A72-15368

Neutron star and white dwarf strong magnetic field generation mechanism involving thermodynamic equilibrium states of electron gas

05 p0723 A72-17162

White dwarf magnetic fields decay time scale for dipolar and toroidal configurations

06 p0876 A72-17581

High speed photometry of nova variables with white dwarf and late-type binary star flickering, using Cassegrain focus

06 p0889 A72-18332

White dwarfs rotation parameters relation to angular velocity within general relativity compared to analogous calculations in Newtonian theory

08 p1234 A72-21284

Cen X-3 model with X ray emission from atmosphere heated by shock waves generated by surface pulsations of white dwarf

10 p1544 A72-24668

Main sequence, red giant and white dwarf stars convective envelopes evolution, discussing mixing length theory inadequacy

10 p1545 A72-24826

Blue white dwarf HL Tau-76 rapid variations, suggesting underlying driving mechanism from high speed three color photometric observations

10 p1549 A72-25193

Cold static superdense model for white dwarf and neutron stars, using relativity theory and variational principles for stellar structure in hydrostatic equilibrium

11 p1715 A72-25528

Pulsar rotational models, considering white dwarves, neutron stars, oblique rotators, etc

11 p1718 A72-25907

Variable white dwarf radial pulsation periods explained by nonradial oscillations and gravity modes, considering atmospheric mixing with degenerate core

12 p1868 A72-27260

White dwarf background radiation and optical emission variations due to thermal bremsstrahlung from stellar coronae

14 p2147 A72-30554

Degenerate electron gas magnetic properties implications for metals, white dwarfs and neutron stars, discussing nonmagnetic state for thermal equilibrium

14 p2158 A72-30728

Rotating white dwarfs and neutron stars quasi-radial pulsations frequencies, discussing central densities critical values

15 p2304 A72-31336

Pulsating X ray sources with 1 sec periods as stars with central densities between neutron stars and white dwarfs

17 p2599 A72-35074

New measurements of circular polarization and an ephemeris for the variable white dwarf G195-19.

17 p2611 A72-35298

Landau orbital ferromagnetism appearance likelihood in white dwarf stars, noting temperature requirements of noninteracting electron gas

19 p2859 A72-37891

Nuclear energy sources in overdense celestial bodies

19 p2862 A72-38061

Hydrodynamic model of white dwarf envelope thermonuclear runaway evolution producing nova outbursts, computed for various CNO nuclei initial abundances

20 p2966 A72-38908

Line spectra and continuum polarization in magnetic white dwarfs.

20 p2971 A72-39760

Nuclear reactions in a degenerate electron-nuclear plasma

22 p3209 A72-42964

WHITE NOISE

NT THERMAL NOISE

High speed decision sequential decoder design and tests for digital errors, white noise and real channels

01 p0026 A72-10341

Fluctuating white and narrow band noise and interference pulse effects on monopulse goniometer

02 p0176 A72-12220

Kalman type optimal filter for linear distributed-parameter systems under white Gaussian and boundary noise, obtaining Wiener-Hopf equation by calculus of variations

04 p0505 A72-14668

Nonlinear plant and observation models with white Gaussian noise and continuous data, obtaining state vector a posteriori probability density for optimal prediction

04 p0506 A72-15112

Radio signal parameters with unknown envelope approximated by orthonormal function series during white noise background reception

05 p0625 A72-15823

White noise mean square sound pressure in turbulent flow in cylindrical duct, using cross correlation technique

05 p0647 A72-15936

Optimal control synthesis for linear systems with quadratic functional under random white noise

05 p0641 A72-16314

Range resolution effect on distributed radar target detection in white noise and clutter, using square law envelope detector with linear integrator

05 p0628 A72-16567

Coupled detection-estimation of Gauss-Markov processes in white Gaussian noise, deriving Bayes optimal recursive rules

06 p0775 A72-18388

Frequency response of spectral noise amplitude in chalcogenide glass switches

09 p1366 A72-22215

Potential noise stability of wideband communications systems during discrete signal reception on combined background of quasi-white noise and spectrally lumped interference

09 p1277 A72-22569

Random vibration of linearly elastic lumped mass systems containing, nonlinear damping to ideal stationary Gaussian white noise excitation

09 p1408 A72-23460

Quadratic cost, nonlinear optimal adaptive stochastic control of linear plant and measurement models excited by white Gaussian noise and with unknown parameters

10 p1455 A72-23792

Recursive minimum variance linear filter and controller for systems with white state-dependent noise

10 p1455 A72-23800

Optimal detection of rectangular radio signal pulse envelope distortions by multiplex fluctuations over white noise background

10 p1436 A72-24516

Linear least mean square estimate of additive white noise-corrupted signal considered as purely nondeterministic process of multiplicity one

11 p1591 A72-25352

Optimal control synthesis for linear systems with quadratic functional under random white noise

11 p1610 A72-25797

Periodic, continuous and aperiodic white noise effects on human serial decoding performance, relating subjective and autonomic responses

12 p1775 A72-28289

Optimal reception system synthesized for FM signal with phase fluctuation masked by narrow band AM and white noise

13 p1914 A72-28414

White background noise intensity effects on human visual target detection performance considering display difficulty levels, target location, detection time and error

14 p2083 A72-31156

Lf white noise voltage theory of avalanche diode extended to small multiplication M values and unequal hole and electron avalanche ionization coefficients

15 p2206 A72-31642

Linear autonomous differential equations finite time stability theory, extending to systems driven by white noise

15 p2264 A72-31764

Excess white noise source in photomultiplier as function of temperature from voltage, intensity and ion pulse measurements, noting effect on photon counting statistics

15 p2207 A72-32238

Nonlinear vibration damper system subject to forced vibrations considered as stochastic processes in form of white noise and stationary and ergodic processes 16 p2467 A72-33144

Earplugs effectiveness for narrow band white noise real-ear attenuation and wearability 16 p2358 A72-33325

Design requirements for a quiet helicopter. [AHS PREPRINT 604] 17 p2488 A72-34484

Optimal signal design for digital center of gravity feedback communications over white noise channels, using energy ratio functions 18 p2659 A72-36316

Optimal filtering in linear distributed-parameter systems. 18 p2673 A72-36823

Some problems concerning stability in the presence of small random disturbances 19 p2833 A72-37324

Optimal decentralized control of two coupled linear stochastic systems, introducing fake plant white noise for weak coupling effects compensation 19 p2779 A72-38236

Woodward ambiguity function extension to random signals, noting Gaussian signal in white noise with given autocorrelation function 19 p2766 A72-38418

Effectiveness of error-correcting codes during reception on the whole in the presence of additive normal white noise 21 p3014 A72-40310

Phase noise types in digital satellite communication links, discussing continuous binary phase shift keyed modulation systems with coherent detection 21 p3020 A72-40896

Parametric method of statistical synthesis with incomplete initial information on signal and noise distribution, discussing signal detection in white noise with unknown spectral density 22 p3154 A72-42230

Radio signal parameters with unknown envelope approximated by orthonormal function series during white noise background reception 23 p3263 A72-43431

Optimal, on-line linear filtering with noisy, time-delayed observations. 23 p3276 A72-43855

Potential noise stability of wideband communications systems during discrete signal reception on combined background of quasi-white noise and spectrally lumped interference 24 p3379 A72-44748

WHITHAM RULE

Self similar solutions for piston driven shock wave motion, examining Whitham approximation rule validity 07 p0970 A72-20075

Wedge reflected shock profiles, comparing results for various Mach numbers and incidence angles with predictions based on Whitham theory 11 p1616 A72-25918

Wall contour effect on shock wave shape, comparing Whitham theory with schlieren photographs from shock tube tests 15 p2219 A72-32595

WHITTAKER FUNCTIONS

Stability-instability zones of solutions of Whittaker equation in vibration theory 05 p0690 A72-16353

Stability-instability zones of solutions of Whittaker equation in vibration theory 11 p1685 A72-25334

WICKS

Heat transfer for water at pressures near atmospheric in wicks formed of stainless steel screen layers, obtaining steady and maximum evaporation rates [ASME PAPER 71-WA/HT-12] 05 p0744 A72-15872

Pressure drop of homogeneous and annular wick heat pipes using hydrogen, nitrogen and oxygen working fluids, discussing heat transfer capacity [ASME PAPER 71-WA/HT-13] 05 p0744 A72-15873

High thermal power density ammonia heat pipe with porous grooved wick concept [ASME PAPER 71-WA/HT-20] 05 p0744 A72-15879

Vaporization heat transfer characteristics for heat pipe wick samples of felted metal and sintered metal powder [AIAA PAPER 72-256] 11 p1739 A72-25201

Tunnel wick heat pipe artery with priming in gravity environment by temperature induced pressure differences, using ammonia as working fluid [AIAA PAPER 72-273] 11 p1740 A72-25213

Cotton wick probe-transducer assembly for pneumograph recording of rabbit respiratory rate 11 p1587 A72-26619

Optimization of heat pipe with wick and annulus liquid flow, investigating effect of pressure loss and recovery in vapor passage [ASME PAPER 71-HT-V] 15 p2335 A72-31767

WIDE ANGLE LENSES

Wide angle lenses off-axis modulation transfer function measurement, explaining extrapolation method with MTF and conversion diagrams 06 p0813 A72-17439

Central band-type wide angle camera shutter design, noting stress examination in machine parts by optical method 21 p3052 A72-40306

WIDEBAND

U BROADBAND

WIDEBAND COMMUNICATION

Wideband data transmission on group-band communication channels, using dual single-sideband modulation with basic transmission rate of 48 kbit/sec 01 p0024 A72-10113

Wideband FSK receiver for space telemetry, calculating error probability in multipath signal fading due to planetary surface reflections 01 p0025 A72-10329

FM radio link superposed parabolic antenna systems adjustment for space diversity reception for scatter propagation and broadband multichannel transmission in 1.9 GHz range 01 p0027 A72-10410

Broadband dipole antenna design based on method of moments, noting VSWR and current distribution 01 p0043 A72-11241

Circuit design techniques used for wideband signal processing systems, considering 1000 MB/S microwave communication link 02 p0176 A72-12163

Wideband spectrum utilization above 10 GHz for high speed digital communications and ecological monitoring 02 p0176 A72-12182

Wideband high power radars alignment and testing, including range sidelobe reduction 02 p0178 A72-12392

Tactical optical ground communication systems, discussing use of GaAs and carbon dioxide lasers and ultrawideband data links 04 p0485 A72-14482

He-Ne laser controlled frequency shift in wideband optical heterodyne communications systems with Currie low reflection mirror 05 p0668 A72-16346

Wideband electro-optic FM of laser light for optical communication, discussing modulator design, construction and testing [AIAA PAPER 72-177] 05 p0631 A72-16961

Automatic measurements of wideband antenna radiation characteristics, using microwave generators linked with analyzers 06 p0775 A72-18194

Microwave IC oscillators design for broadband high performance receivers, exemplifying thin film Gunn effect, step- and varactor-tuned transistor oscillators 06 p0786 A72-18373

Nonorthogonality noise at matched radio filter output between stations operating simultaneously in same frequency band in discrete address wideband communication system, defining minimum SNR conditions 07 p0937 A72-18849

Wideband laser communication for space applications, comparing carbon dioxide and Nd-YAG systems on basis of SNR 07 p0941 A72-19239

Digital system for wideband and Gaussian noise generation using simultaneously generated PN-sequence with analog summation of independent binary waveforms 07 p0941 A72-19284

Potential noise stability of wideband communications systems during discrete signal reception on combined background of quasi-white noise and spectrally lumped interference 09 p1277 A72-22569

Estimate of effectiveness of utilization of composite signals to combat external interference with available a priori data 10 p1436 A72-24580

Intelsat 4 satellite communication transponder design for broadband multicarrier operation, using frequency and pulse modulation techniques [AIAA PAPER 72-535] 12 p1780 A72-27358

Communication satellites microwave circular array antenna for wideband circularly polarized isotropic radiation [AIAA PAPER 72-529] 12 p1789 A72-27419

Intelsat 3 global multichannel wideband multiple access communication system, describing technological advancements in communication performance, attitude control and testing procedures [AIAA PAPER 72-534] 13 p1918 A72-28982

Pulse signal transmission through bandpass error free wideband PCM communications systems 13 p1919 A72-29055

Surface wave devices signal processing for space communication, developing fast lock up spread spectrum communication link broadband 13 p1920 A72-29106

A wideband antenna array 17 p2531 A72-35766

An optical communication system using envelope modulation. 19 p2766 A72-38604

The 20 and 30 GHz communications system for the ATS-F millimeter wave experiment. 21 p3019 A72-40882

Wideband limitations of waveguide arrays. 23 p3270 A72-43573

Wideband pulsed-RF phase measurement. 23 p3270 A72-43575

Broad-band information transfer with the aid of laser-beam coupling fields 23 p3266 A72-44359

Potential noise stability of wideband communications systems during discrete signal reception on combined background of quasi-white noise and spectrally lumped interference 24 p3379 A72-44748

Wideband antenna test facility. 24 p3389 A72-45554

WIDMANSTATTEN STRUCTURE

Iron River meteorite, discussing history, physical characteristics, element distribution and Widmanstatten structure 01 p0126 A72-10105

Phosphorus effect on Widmanstatten pattern in iron meteorites, using Fe-Ni-P phase diagram and cooling experiments 06 p0878 A72-17792

Isothermal profiles for Nb-Zr-C and Nb-Ti-C alloys from microstructural and X ray analyses, noting Widmanstatten structure, and second phase formation 12 p1829 A72-27643

Parent-body models for the formation of iron meteorites. 17 p2615 A72-35687

Thermomechanical manipulation of precipitate shape in a titanium-base alloy. 22 p3194 A72-43044

WIENER FILTERING

Discrete-time adaptive Kalman filter based on learning process and parameter estimate updating in operational cycle, comparing with simple Kalman and Wiener filters 05 p0639 A72-15758

Optimum bounding filter design based on error covariance for Kalman-Bucy and Wiener filters with inexactly known parameters, obtaining performance figure of merit 10 p1454 A72-23785

Optimal filter for narrow band stochastic signal processing, using Wiener theory 10 p1441 A72-25103

Optimal matched Wiener discrete filters investigated with operator-matrix concepts 13 p1918 A72-28894

Fast computational techniques for generalized two dimensional Wiener filtering. 17 p2532 A72-34402

Wiener filter design for optimal processing of AM signals distorted during transmission through randomly dispersive medium 19 p2763 A72-37288

Infinite systems of stochastic differential equations arising in optimal nonlinear filtering theory 19 p2824 A72-37323

WIENER HOPF EQUATIONS

Closed linear systems optimal stabilization determining transfer function from Wiener Hopf equation 01 p0045 A72-10572

Gas slip flow and transverse oscillations boundary value problems solution, using Wiener Hopf integral equation 02 p0205 A72-12355

Kalman type optimal filter for linear distributed-parameter systems under white Gaussian and boundary noise, obtaining Wiener-Hopf equation by calculus of variations 04 p0505 A72-14668

Wiener Hopf integral equation for problem of smooth stamp impression into elastic wedge face, solving by gamma and hypergeometric functions 13 p2059 A72-29500

Temperature-slip problem in rarefied gases, obtaining exact solution by generalized BGK scattering model and Wiener Hopf technique 14 p2095 A72-30882

Optimal filtering in linear distributed-parameter systems. 18 p2673 A72-36823

Approximate solution, in generalized functions, to integral and integrodifferential equations with difference kernels 22 p3198 A72-42145

Radiation from an open-ended waveguide with extended dielectric loading. 24 p3381 A72-45643

WIGHTMAN THEORY

U FIELD THEORY (PHYSICS)

U QUANTUM THEORY

U RELATIVISTIC THEORY

WIGNER COEFFICIENT

Random matrix spectra of eigenvalues in terms of Wigner set for statistical description of heavy nuclei energy levels

15 p2282 A72-32449

WILDLIFE

NT BATS
NT BIRDS
NT CHIMPANZEES

WILDLIFE RADIOLOCATION

Telemetric instrumentation for remote physiological and behavioral observations of free roaming animals

07 p0930 A72-19912

Satellite system for telemetering environmental and physiological data from winter den of hibernating black bear, discussing instrumentation and equipment performance

07 p0931 A72-19913

Biomedical telemetry instrumentation for radio sensing and transmitting biological information from animals and man, including location by satellite-borne receivers

07 p0931 A72-19915

WIND [METEOROLOGY]

NT GEOSTROPHIC WIND
NT GROUND WIND
NT GUSTS
NT JET STREAMS [METEOROLOGY]
NT SQUALLS
NT WINDS ALOFT

Internal gravity wave interaction with median wind in upper atmosphere from solution of system of linearized hydrothermodynamic equations

05 p0656 A72-16175

Variance spectral techniques in detecting wave modes of synoptic scale tropospheric wind in midlatitudes and tropics

06 p0841 A72-17634

D and E region winds over Europe - Conference, London, April 1971

08 p1159 A72-21526

Wind vector field computation by forced dynamical adjustment to observed height field data, using Mintz-Arakawa two level atmospheric circulation model

09 p1344 A72-22433

Wind and temperature fields periodic updating, considering error reduction as function of time intervals between updates

09 p1348 A72-23659

Meteorological reference level location without wind information for use in numerical weather prediction

12 p1838 A72-27024

Polar thermospheric wind calculation from convection electric field measurements in polar cap ionosphere, using simple ionospheric model

13 p1950 A72-29385

Internal gravity wave interaction with median wind in upper atmosphere from solution of system of linearized hydrothermodynamic equations

14 p2099 A72-30244

Elementary considerations of the fluid mechanics of tornadoes and hurricanes.

24 p3421 A72-45021

O/plus/ H/plus/ and He/plus/ ion distributions in a new polar wind model.

24 p3400 A72-45587

WIND CIRCULATION

U ATMOSPHERIC CIRCULATION

WIND DIRECTION

Book on pressure probe methods for wind speed and direction covering incompressible and subsonic compressible flow pressures, temperature, etc

01 p0072 A72-11273

Wind velocity and direction vertical changes for weather dynamics, emphasizing jet streams

02 p0255 A72-12785

Ageostrophic flow relations in tropospheric high wind fields, discussing Scheibe equation and vector calculation

02 p0255 A72-12788

Winds velocity, direction and diffusion coefficients over Heiss Island from artificial luminous clouds observations

08 p1160 A72-21534

Paired Gill propeller anemometer response function in generalized wind vector sensor application, proposing algorithm for magnitude and direction errors reduction in output analyses

09 p1307 A72-22434

Air pollutants lateral dispersion coefficient determination from turbulence intensity, presenting formula for wind direction frequency distribution function

09 p1344 A72-22436

Sporadic E layer critical frequency relationship to ionospheric wind direction for midlatitudes in summer period

10 p1472 A72-24079

Mean wind direction determining circuit for meteorological data collecting system

10 p1484 A72-25018

Surface pressure and vector wind fields computerized analysis from satellite radar radiometer simulation and conventional data

13 p1995 A72-29619

Wind direction rotation with altitude and time dependent downward phase propagation observed by vapor trail experiments, suggesting upward propagation of atmospheric waves

16 p2383 A72-32969

Sea level wind and pressure data adjustment to governing dynamical equations by numerical variational analysis, using Sasaki matching technique

16 p2419 A72-33941

On the possibility of a simultaneous measurement of wind speed, wind direction, air density and air temperatures at heights which correspond to the upper D-region /max. 95 km/ with chaff cloud sensors.

17 p2545 A72-34631

WIND EFFECTS

Meridional thermospheric wind effect on auroral atomic oxygen red line profile, noting inadequacy of diffusion hypothesis

01 p0052 A72-10079

Ion and electron temperature increases by friction heating between neutral gas winds and plasma in ionosphere

01 p0054 A72-10424

Neutral gas wind effect on Doppler shifts in frequency spectrum of atmospheric gravity waves in F region with resultant phase altitude dependence alteration

01 p0054 A72-10426

Ionospheric neutral gas wind and altitude effects on Spanish short wave absorption winter anomaly

01 p0055 A72-10435

F region neutral thermosphere temperature perturbation and circulation pattern due to global wind with anomalies of ionization calculated from two dimensional dynamic model

01 p0096 A72-11283

Sporadic E layer motion and spreading under constant horizontal wind action, estimating lifetime

02 p0218 A72-11942

Thermospheric neutral-air wind effects on ionospheric F2 layer from atmospheric model

04 p0514 A72-14876

Diffusion equations of ion components of plane stratified plasma (ionosphere), taking into account wind effect and vertical temperature distribution

05 p0658 A72-16402

Direct side force control by rudder deflection and asymmetrical drag utilization to cancel yawing moment, discussing variable stability T-33 flight tests

05 p0613 A72-16946

Coherence function and phase shift dependence of free ocean surface on angular energy distribution in two dimensional wind induced wave spectrum

06 p0841 A72-17625

Crosswind landing under adverse runway conditions, illustrating technique with sketches

07 p0911 A72-18833

Midlatitude F region wavelike disturbances detection by hf radio echo techniques, discussing correlation with jet stream associated tropopause wind patterns

07 p0974 A72-18885

Laser beam diffraction effects on self induced thermal distortion in crosswind, noting dependence on Fresnel number

07 p0942 A72-19379

Neutral wind influence on lower ionosphere nighttime electron and NO ion density profiles

08 p1157 A72-21112

Thermospheric wind directional filtering of gravity waves traveling ionospheric disturbances over Australia

08 p1158 A72-21217

Wind shear, turbulence, precipitation, temperature, visibility and ceiling effects on airport capacity, suggesting weather data integration into ATC system for pilots information

08 p1147 A72-21521

Laser beam induced thermal blooming in absorbing gases from combined fluid dynamics and eikonal geometric optics theory, considering wind effects

09 p1352 A72-23333

Plane wave solutions to atmospheric gravity waves, including effects of nonlinearity, instability, molecular dissipation, temperature, wind and diurnal tides

10 p1473 A72-24705

Magnetospheric electrons precipitation into ionosphere due to conjugate conductivity asymmetry caused by wind induced ions vertical redistribution, using atmospheric model

10 p1530 A72-24791

Magnetic storm effects in atmospheric neutral composition, noting thermospheric wind circulation role due to Joule heating within auroral zone

10 p1476 A72-24957

Temporal variations of sporadic E layer blanketing frequency, virtual height and occurrence rate, calculating electron density profiles and tidal wind influence

10 p1441 A72-25162

Time dependent power spectral density function for first passage probabilities in nonstationary random processes in civil engineering involving earthquakes and wind

10 p1514 A72-25188

Nonregular oceanic level fluctuations dependence on atmospheric pressure and tangential wind stress, deriving fluctuation spectrum from linear hydrodynamic model

11 p1682 A72-26882

ATS observed ionospheric columnar electron content variation during March 1970 solar eclipse, discussing neutral winds effects

12 p1801 A72-27155

Millimeter to meter waves propagation conditions prediction in horizontally inhomogeneous coastal foreground by meteorological parameters, considering wind effects on refractivity

12 p1784 A72-27798

Earth atmosphere boundary layer nonstationary problems, considering diurnal changes of meteorological fields and nonperiodic evolution of elements from wind variations

12 p1841 A72-27988

Mars surface particulate matter eroded by atmospheric winds, noting erosive and settling velocities and yellow clouds distribution

13 p2036 A72-28794

Sporadic E layer motion and spreading under constant horizontal wind action, estimating lifetime

13 p1949 A72-29254

Midlatitude sporadic E layer formation under wind shear action from artificial cloud data on lower thermosphere wind speed and direction

13 p1951 A72-29589

Gravity waves on leeward side of Continental Divide in Colorado, noting generation by winds and storms

14 p2128 A72-30343

Transverse wind self-induced thermal lens effects on target image quality in laser beam tracking systems

15 p2249 A72-32164

Sea surface wind-caused waves spectral component phase velocity measurement method based on statistical treatment of synchronous continuous records of surface elevation

16 p2417 A72-33291

Atmospheric properties effect on satellite aerodynamic characteristics, noting gas composition and upper atmospheric winds

16 p2347 A72-34075

Behavior of spherical balloons in wind shear layers. [AIAA PAPER 72-659]

18 p2643 A72-36963

A method for increasing thrust reverser utilization on STOL aircraft.

19 p2752 A72-38141

Diurnally varying neutral wind effects on lower F region ionization distribution, noting Appleton anomaly disappearance time

19 p2794 A72-38865

Sand deposition due to wind action in Martian craters, comparing to terrestrial analogs

20 p2969 A72-39389

Polar upper ionosphere morphology above E layer, discussing effects of winds, field aligned currents and electron precipitation

20 p2918 A72-39534

Nonperiodic oceanic level fluctuations dependence on atmospheric pressure and tangential wind stress, deriving fluctuation spectrum from linear hydrodynamic model

20 p2948 A72-39569

Earth surface and background wind effects on mesoscale and large scale meteorological processes in free stably stratified atmosphere

21 p3078 A72-41794

Earth atmosphere boundary layer nonstationary problems, considering diurnal changes of meteorological fields and nonperiodic evolution of elements from wind variations

22 p3202 A72-43002

Lateral flight path control during aircraft landing in gusty cross-winds by lateral thrust deflection, discussing design optimization

24 p3368 A72-45330

WIND EROSION

Effects of aeolian erosion on microbial release from solids.

23 p3253 A72-43384

WIND MEASUREMENT

NT WIND VELOCITY MEASUREMENT

Kinematic vertical motions computation from radiosonde wind observations, correlating with synoptic features

01 p0095 A72-10855

Tropospheric wind estimation from ATS 1 satellite cloud motions over equatorial Pacific

01 p0060 A72-10856

Ageostrophic vertical wind field determination from satellite cloudiness data, including geopotential pressure equations

02 p0253 A72-12537

Temperature advection mesostructure from wind measurements for precise short term forecasts

02 p0254 A72-12778

Solar streamline flow patterns analysis test on terrestrial wind data

03 p0414 A72-12928

Tropical hurricanes and storm outflow layer wind analyses from ATS 3 satellite data, noting cyclonic eddy asymmetric structure

03 p0384 A72-14144

Jimsonde high resolution temperature "nsor for FPS-16 Radar/Jimsphere wind system, analyzing rms errors

04 p0522 A72-15157

Mountain stations wind measurement usefulness for small aircraft traffic guidance

04 p0544 A72-15625

Wind velocity vertical component determination through meteor trail drift observation, presenting mean diurnal measurements data

05 p0657 A72-16272

Altitude dependent turbulence characteristics in atmospheric boundary layer over wavy ocean surface from wind pulsation measurements

06 p0841 A72-17624

Rising/falling spherical wind sensors responses to atmospheric wind perturbations on vertical wind profile, using Fourier transform techniques

06 p0843 A72-18445

Vanes for sensing incidence angles of airstream with respect to aircraft, noting correlation coefficient

06 p0796 A72-18450

Scintillation measurement of transverse component of wind blowing across laser beam, using correlation method

07 p0942 A72-19378

Wind and density measurements by small sounding rockets, comparing results with ground observed radio wave absorption diurnal variations

08 p1160 A72-21531

Wind measurements in lower troposphere by meteor radar method, presenting models of prevailing circulation in meteor zone over Eurasia and Arctic

08 p1161 A72-21538

Mean monthly statistical characteristics of wind regime from meteor trail drifts observations

08 p1162 A72-21885

Optimal variant of meteor wind patrol radar station for atmospheric circulation study

08 p1147 A72-21886

Radar equipment complex in Dushanbe for upper atmosphere wind measurements in meteor physics studies

09 p1308 A72-22506

Meteor trail winds over Europe, discussing continuous wave radar observations and measurement errors with respect to height and time

10 p1474 A72-24708

Radio meteor winds determination in Southern Hemisphere from vertically emitted continuous wave radiation, considering diurnal variations and wind and turbulence effects

10 p1474 A72-24709

Meteor trail wind radar measurements over Illinois, discussing scattering properties and monostatic vs multistatic coherent systems

10 p1474 A72-24710

Stanford pulse Doppler radar and digital data acquisition system for meteor trail wind measurements

10 p1438 A72-24711

Smoke trail motions in winds with constant shear, considering potential, vorticity and stratified flows

10 p1475 A72-24748

Atmospheric isotropic turbulence kinetic energy dissipation and wind spectra estimation from Doppler spectra of precipitation particle velocities

10 p1507 A72-25001

VHF remote control anemometer network with digital receiving station for wind measurement and gale warning system

10 p1463 A72-25013

Mean wind direction determining circuit for meteorological data collecting system

10 p1484 A72-25018

GMD-1 tracking system for mesoscale wind data, minimizing elevation angle errors in jet stream CAT program by upwind release of rawinsonde

10 p1508 A72-25080

Fluidic wind sensor measurements from low threshold to high velocities, noting wind angle resolution from output differential pressure signal

10 p1484 A72-25083

Wind profile measurements to 200 meters by acoustic echo sounder and Doppler shift, describing signal emission and data reduction

10 p1508 A72-25084

Radiosonde balloon tracking errors in upper atmosphere wind measurement with Loran C, Omega and radar transmitters

10 p1441 A72-25092

Regular tidal winds and irregular gravity waves domination of E region transport processes

10 p1477 A72-25161

French-U.S. Fole meteorological satellite project to map Southern Hemisphere winds, describing system based on pressurized balloons for data acquisition

11 p1680 A72-25813

East African low level cross equatorial air current exploration, using light aircraft-borne Doppler radar wind finding equipment

12 p1840 A72-27703

Upper wind measurement by balloon-borne targets or radiosondes tracking by primary and secondary radars and radio theodolites

13 p1917 A72-28697

Ballistic density and wind determination from radiances observed by satellite IR spectrometer /SIRS/ onboard Nimbus 3

13 p1991 A72-28825

Roughened and smooth spherical wind sensors lift and drag, calculating aerodynamic coefficient spectra from velocity

13 p1894 A72-29620

Midlatitude upper atmosphere wind, tide and turbulence measurements, using radar observations of meteor trails

14 p2099 A72-30248

Meteor trail drifts at 95 km over Turkmenistan from November 1969-August 1970 radar observations, comparing to Frunze, Dushanbe and Kharkov wind data

15 p2305 A72-31372

Rocket and radar-meteor wind observations of zonal flow, noting annual and semiannual components for northern latitudes at 60-130 km

15 p2229 A72-31985

Wind direction rotation with altitude and time dependent downward phase propagation observed by vapor trail experiments, suggesting upward propagation of atmospheric waves

16 p2383 A72-32969

Determination of the predominant wind vector from meteor radar observations

19 p2857 A72-37740

Cup anemometer response to fluctuating wind speeds.

20 p2920 A72-38966

Wind profiles from velocity measurements at 20-160 meters, noting atmospheric stratification effect

21 p3078 A72-40766

Experimental determination of fall rate of 'NS' chaff on the heights 50-90 km.

21 p3049 A72-41498

Stratospheric winds over Leba rocket sounding station in spring and autumn, 1970.

21 p3049 A72-41500

Results of a comparison between radar meteor wind measurements and simultaneous lower ionosphere drift measurements in the same area.

22 p3154 A72-42361

An improved pressure-sphere anemometer.

22 p3178 A72-42596

Smoke-trail method for obtaining wind profiles.

22 p3202 A72-43144

Probability distribution of vertical longitudinal shear fluctuations.

23 p3281 A72-44146

Synchronous observations of lower-ionospheric wind conditions in Dushanbe and at the equator

23 p3285 A72-44166

Mass and heat budget estimations of the Atlantic SE trade wind flow at the equator.

24 p3420 A72-44756

Measurements of air motion in regions of clear air turbulence using high-power Doppler radar.

24 p3421 A72-44978

WIND PRESSURE

Atmospheric turbulent characteristics and velocity longitudinal component intensity profiles, applying to dynamic wind loads computation

14 p2127 A72-30264

Wind tunnel investigation of shapes for balloon shelters.

20 p2885 A72-38967

Description of global-scale circulation cells in the tropics with a 40-50 day period.

22 p3201 A72-42506

WIND PROFILES

Wind profile determinations at 90-100 km from meteor trail drift and ionosphere inhomogeneity radar data, noting semidiurnal harmonics in wind components

01 p0058 A72-10563

Quasi-geotriptic wind field vertical motions in ground friction layer from continuity equation

02 p0254 A72-12780

Disturbance evolution on zonal flow background in baroclinic atmosphere with given wind profile, determining average-time energy distribution

03 p0383 A72-13479

Vertical wind velocity variances and spectra above atmospheric surface layer for flat and mountain terrains

03 p0386 A72-14335

Radar observed apparent land breeze front off Wallops Island, giving temperature and wind profiles

06 p0843 A72-18441

Geopotential and longitudinal and transverse wind components correlation coefficients in nonhomogeneous nonisotropic atmosphere

06 p0843 A72-18444

Rising/falling spherical wind sensors responses to atmospheric wind perturbations on vertical wind profile, using Fourier transform techniques

06 p0843 A72-18445

Extrapolation procedure for determining small-scale wind shear definition from Rawinsonde vertical wind profiles statistical data for aerospace vehicle design

07 p1085 A72-19687

Mesospheric temperature and wind profiles during stratospheric warming from rocket grenade experiments

08 p1160 A72-21533

Wind shear theory of midlatitude sporadic E formation, using wind profiles from artificial luminous cloud observations

08 p1161 A72-21540

Statistical characteristics of wind elements from vertical-temporal structure of wind field

08 p1202 A72-22118

Theoretical model of large scale topographical effects on wind generation through temperature advection, applying to Mars atmosphere general circulation

10 p1531 A72-23707

Wind profile measurements to 200 meters by acoustic echo sounder and Doppler shift, describing signal emission and data reduction

10 p1508 A72-25084

Wind shear theory expectations tested by wind profiles and sporadic E layer observations, stressing time variations significance

10 p1477 A72-25155

Electron density maxima position relationship to wind profiles in sporadic E layer with electric fields and vertical ion motion

10 p1530 A72-25165

Disturbance evolution on zonal flow background in baroclinic atmosphere with given wind profile, determining average-time energy distribution

11 p1682 A72-26249

Kinematic estimate of large scale atmospheric vertical motion field patterns, using polynomial approximation of wind profiles

12 p1840 A72-27707

High level Canberra flight for three dimensional picture of wind and temperature fields, showing CAT, gravity waves and smooth flight characteristics

12 p1841 A72-27709

Near-ground daytime temperature and humidity fine structure relation to heat flux, net radiation and temperature and wind gradients

12 p1841 A72-27711

Smoothed wind fields generated from ATS 3 cloud motions measurements observed on computer display system

13 p1991 A72-28827

Wind profiles determination by Locate System in connection with OMEGA navigation system as sensing device

13 p1997 A72-29183

Air injection as neutral atmospheric boundary layer thickening simulation, presenting mean velocity and turbulence intensity profiles

14 p2093 A72-30849

Numerical wind profiles calculation over Mediterranean based on satellite photograph sequences of clouds

15 p2220 A72-31235

Wind profiles, turbulence, and temperature and density distribution of neutral upper atmosphere obtained via sounding with Skylark rockets carrying chemical seeding payloads

15 p2223 A72-31435

Mixing length theory derivation of barotropic planetary boundary layer profiles for geostrophic wind deviations, Reynolds stress, eddy viscosity and turbulent kinetic energy dissipation

15 p2224 A72-31675

Atmospheric stratification, wind profiles and vertical density distribution of ions and neutral particles determined by rocket sounding

15 p2228 A72-31968

Filtering polynomial technique to estimate wind, divergence and vertical motion profiles, suppressing random error effects

16 p2418 A72-33667

Upper atmosphere zonal winds speed vs local time from data based on Cosmos 316 orbit analysis

17 p2547 A72-35075

A spheric rate azimuth-profile of the 1955 Blackwell, Oklahoma, tornado.

18 p2706 A72-36639

A theoretical study of the diurnal wind variations in the planetary boundary layer.

18 p2706 A72-36645

Wind patterns at meteor altitudes /75-105 kilometers/ above College, Alaska, associated with mid-winter stratospheric warmings.

18 p2689 A72-36962

Altitudinal dependence of upper atmosphere winds according to radar and ionosphere data

20 p2920 A72-40074

Lower planetary boundary layer mesoscale flow patterns and transport climatology, using hourly averaged wind data from wind tower station network

21 p3077 A72-40252

- Wind profiles from velocity measurements at 20-160 meters, noting atmospheric stratification effect
21 p3078 A72-40766
- Stratospheric winds over Leba rocket sounding station in spring and autumn, 1970.
21 p3049 A72-41500
- Russian book - Calculated wind velocities at heights of the lower atmospheric layer.
22 p3200 A72-42077
- Wind profile development above a locally adjusted sea surface.
22 p3202 A72-42600
- Smoke-trail method for obtaining wind profiles.
22 p3202 A72-43144
- A method for balancing geopotential and wind fields
24 p3420 A72-44765
- WIND SHEAR**
- Tornado and funnel cloud comparison in seasonal and diurnal distributions, air mass instability, tropospheric vertical wind shear and geographical distribution
03 p0385 A72-14231
- Remote meteorological elements sensing in terminal area, discussing radar, ceilings, thunderstorm warning, slant range visibility, low level winds and wind shear
04 p0543 A72-14692
- Mathematical two dimensional model of vertical wind shear near convective cloud in free atmosphere
06 p0840 A72-17622
- Vertical two-point longitudinal velocity differences or wind shear in atmospheric boundary layer, obtaining standard deviation from turbulence measurements
06 p0841 A72-17666
- Extrapolation procedure for determining small-scale wind shear definition from Rawinsonde vertical wind profiles statistical data for aerospace vehicle design
07 p1085 A72-19687
- Wind shear, turbulence, precipitation, temperature, visibility and ceiling effects on airport capacity, suggesting weather data integration into ATC system for pilots information
08 p1147 A72-21521
- Wind shear theory of midlatitude sporadic E formation, using wind profiles from artificial luminous cloud observations
08 p1161 A72-21540
- Smoke trail motions in winds with constant shear, considering potential, vorticity and stratified flows [AD-742738]
10 p1475 A72-24748
- Small scale wind shear effects on overdense and underdense radio meteor echoes, noting premature decay and scatter in decay time
10 p1440 A72-24952
- Simultaneous rocket observation of wind shear and electron density profile in lower ionosphere, noting sporadic E layer formation
10 p1477 A72-25154
- Wind shear theory expectations tested by wind profiles and sporadic E layer observations, stressing time variations significance
10 p1477 A72-25155
- Frequency distribution of ionospheric horizontal winds vertical shear, noting altitude independence, turbulence and viscous energy dissipation
10 p1477 A72-25157
- Wind shear and midlatitude sporadic E layer theories, discussing metal ions production and loss
10 p1477 A72-25158
- Metal ion sheaths in midlatitude sporadic E layer caused by vertical redistribution of neutral ionization, discussing wind shear discontinuities
10 p1477 A72-25159
- Sporadic E layer altitude and density variations caused by lunar influences, using model for electrostatic field and wind shear effects
10 p1478 A72-25163
- Semiannual variation in ionospheric drifts, zonal winds and vertical shear at thermosphere base
11 p1626 A72-26475
- Wind shear third and fourth moments and distribution function in atmospheric boundary layer, emphasizing longitudinal turbulent velocity vertical variations
13 p1993 A72-28860
- Low level vertical wind shear effect on aircraft control, considering runway selection with respect to surface wind conditions
13 p1993 A72-28862
- Midlatitude sporadic E layer formation under wind shear action from artificial cloud data on lower thermosphere wind speed and direction
13 p1951 A72-29589
- Persistent intense CAT in upper level frontal zone, discussing synoptic features, vertical wind shears, radar echoes and turbulence intensity
13 p1995 A72-29622
- Midlatitude nighttime sporadic E layer relationship to geomagnetic field, considering wind shear theory
15 p2224 A72-31798
- The effect of wind shear gradients on underdense radio meteor decay times.
17 p2517 A72-35398
- Observations of Helmholtz waves in the lower atmosphere with an acoustic sounder.
18 p2687 A72-36635
- Behavior of spherical balloons in wind shear layers.
18 p2643 A72-36963
- Effect of ground wind shear on aircraft trailing vortices.
20 p2886 A72-39630
- Probability distribution of vertical longitudinal shear fluctuations.
23 p3281 A72-44146
- WIND TUNNEL APPARATUS**
- NT WIND TUNNEL DRIVES
NT WIND TUNNEL NOZZLES
- Wind tunnels measuring equipment and procedures and data acquisition and processing systems electronics, describing computerized real time data processing system
02 p0201 A72-12898
- Indian low speed wind tunnel, describing design, six component balance and calibration
04 p0509 A72-15277
- Wind tunnel six component magnetic balance system, describing ferromagnetic body forces and moments relationship to applied magnet fields and gradients
05 p0645 A72-16829
- [AIAA PAPER 72-164]
Electrofluid-dynamic wind tunnel velocity augmentation by enthalpy addition during expansion at constant static pressure and temperature for aerospace vehicles flight conditions simulation
05 p0645 A72-16831
- [AIAA PAPER 72-166]
German monograph on shaft and wall effect in aerodynamic measurements with three orifice pressure probes in wind tunnels
09 p1259 A72-22320
- Wind tunnel diffuser design for separated region spread reduction based on egg box principle
10 p1416 A72-23859
- Superconducting magnetic suspension and balance facility of supersonic wind tunnel for dynamic stability studies
10 p1460 A72-24757
- Superconducting coil design for magnetic suspension of supersonic wind tunnel balance
10 p1460 A72-24759
- Aerodynamic force and moment measurements on model in magnetic wind tunnel balance system, using field equations
10 p1461 A72-24765
- Oscillating flapped vane system for large amplitude uniform sinusoidal lateral gust generation in semiopen jet wind tunnel
16 p2374 A72-33699
- Status of hotshot wind tunnels for hypersonic aerodynamic studies.
24 p3388 A72-45203
- WIND TUNNEL BALANCES**
- U WEIGHT INDICATORS
U WIND TUNNEL APPARATUS
- WIND TUNNEL CALIBRATION**
- Correction factors for Aerodynamic Research Institute Goettingen transonic wind tunnel, comparing calculated values with AGARD calibration models test results
03 p0308 A72-13610
- [DFVLR-SONDDR-167]
Indian low speed wind tunnel, describing design, six component balance and calibration
04 p0509 A72-15277
- Perturbation velocity corrections for eccentric model position and different air flow ducting in rectangular wind tunnels
11 p1573 A72-26581
- [DFVLR-SONDDR-191]
Soviet wind tunnel for power plant-environment interactions studies, discussing working sections velocity distributions calibration
13 p1939 A72-29644
- Wind tunnel data correction for interference due to flow boundary constraints /wall effects/, acoustic and model support effects
21 p3043 A72-41640
- An initial two-dimensional wall interference investigation in a transonic wind tunnel with variable porosity test section walls.
24 p3389 A72-45409
- [AIAA PAPER 72-1011]
WIND TUNNEL DRIVES
- Refinements in high-Reynolds-number shock-tunnel technology.
21 p3040 A72-41582
- [AIAA PAPER 72-996]
WIND TUNNEL MODELS
- Nonporous rigid parachute models three component measurements, using low speed wind tunnel for testing skirt length effects on aerodynamic characteristics
01 p0003 A72-10303
- Wind tunnel and rocket sled results with ribbon parachutes for supersonic release, discussing aerodynamic, structural flutter and inflation time characteristics.
01 p0004 A72-10308
- Wing-fuselage combination aerodynamic coefficients, comparing experimental data with subsonic linear and nonlinear theoretical results
02 p0153 A72-12723
- [DGLR PAPER 71-115]
Wind tunnel model instrumentation and captive trajectory facilities for aircraft stability, control and metric wing-pylon store tests for performance and structural predictions
03 p0339 A72-12921
- Correction factors for Aerodynamic Research Institute Goettingen transonic wind tunnel, comparing calculated values with AGARD calibration models test results
03 p0308 A72-13610
- [DFVLR-SONDDR-167]
Flat plate wing autorotation experiments about spanwise axis in low speed wind tunnel
04 p0462 A72-15117
- Wind tunnel investigation of unswept rectangular wing with externally blown single slotted flap, determining optimum slot width as function of momentum coefficient and flap deflection
04 p0462 A72-15461
- Inlet duct and turbofan engine compatibility without stalling and surge conditions obtained by design optimization and wind tunnel testing
07 p1052 A72-18761
- Miniature three-position pressure valve for on-board calibration of pressure transducers in wind tunnel models, noting time lag reduction
08 p1164 A72-20923
- Wind tunnel investigation of adiabatic compressible turbulent boundary layer in adverse and favorable pressure gradients at supersonic speed
10 p1468 A72-24421
- Wind tunnel investigation of Reynolds number effects on boundary layer separation incidence and maximum lift coefficient of high-lift device equipped aircraft model
10 p1419 A72-24657
- Electromagnetic remote model positioning sensing system for wind tunnels with magnetic suspension, using differential transformer action
10 p1461 A72-24762
- Wind tunnel model magnetic suspension system with remote position sensor based on optical contrasts scanning analysis
10 p1461 A72-24763
- Optical TV scanning for wind tunnel model position detection in magnetic suspension system for sphere low density drag measurements
10 p1461 A72-24764
- [ONERA, TP NO. 988]
Aerodynamic force and moment measurements on model in magnetic wind tunnel balance system, using field equations
10 p1461 A72-24765
- Data acquisition and reduction for model aerodynamics in superconducting magnetic suspension and balance of supersonic wind tunnel facility
10 p1461 A72-24766
- Wind tunnel model remote position sensing and control systems, discussing drift reduction in magnetic suspension
10 p1461 A72-24768
- Static aerodynamic characteristics of bulbous based cone models and slender wings at subsonic speed, using magnetic suspension and balance system
10 p1461 A72-24769
- Aerodynamic data acquisition with magnetic balance on wind tunnel model delta and AGARD G wing planforms and body of revolution
10 p1462 A72-24770
- Spheres drag coefficient measurements in laminar flow as function of Reynolds number, using wind tunnel model magnetic suspension system
10 p1419 A72-24772
- Magnetic simulation of gravity for wind tunnel investigations of aircraft jetison processes, considering Froude number and relationships between model and full scale aircraft
10 p1462 A72-24775
- Iron rotational hysteresis effect in cold magnetic balance wind tunnel system for spinning aircraft configurations and subsonic flow regimes
10 p1462 A72-24776
- Dynamic model of high bypass ratio turbofan engines for L-1011 wind tunnel flutter test program [AIAA PAPER 72-376]
11 p1703 A72-25400
- Subsonic powered nacelle wind tunnel model for investigation of geometric variables effect on pressure drag
11 p1568 A72-25613
- [ASME PAPER 72-GT-14]
Low pressure ratio Q-FAN propulsor noise reduction tests on wind tunnel model, discussing source components and design configurations
11 p1569 A72-25634
- [ASME PAPER 72-GT-40]
Turbojet simulator for supersonic wind tunnel models, simulating inlet mass flow ratio and exhaust nozzle pressure ratio
11 p1705 A72-25664
- [ASME PAPER 72-GT-89]
Wind tunnel tests for flutter characteristics of rectangular block model oscillating freely in uniform flow, discussing galloping and vortex excitation
11 p1572 A72-26373
- Perturbation velocity corrections for eccentric model position and different air flow ducting in rectangular wind tunnels
11 p1573 A72-26581
- [DFVLR-SONDDR-191]
Dynamically similar wind tunnel models for transonic aeroelastic studies of aircraft failures or structural damage and flutter margins
13 p1939 A72-29672
- [ONERA, TP NO. 1082]

Aeroelastic model response comparison to amplitudes of sectional and linear wind tunnel models, indicating incorrectness of direct scaling
16 p2342 A72-32904
[AHS PREPRINT 623]
Wind tunnel simulation of full scale vortices,
17 p2483 A72-34477
Wind tunnel experiments on aerodynamic superstall, describing stability tests and models
17 p2492 A72-35374
Design studies and model tests of the stowed tilt-rotor concept.
[AIAA PAPER 72-804]
19 p2750 A72-38113
Dynamic pressure, downwash and pressure gradient corrections of wind tunnel model measurements, discussing displacement limit for adequate accuracy
[DFVLR-SONDDR-214]
19 p2747 A72-38687
Use of an infrared-imaging camera to obtain convective heating distributions.
20 p2926 A72-39640
A wind-tunnel experiment concerning atmospheric vortex streets.
20 p2948 A72-39796
Augmentor wing design for Buffalo STOL aircraft, discussing operational principle and wind tunnel test results
21 p2994 A72-40684
Potential flow calculations to support two-dimensional wind tunnel tests on high-lift devices.
[ICAS PAPER 72-13]
21 p2991 A72-41138
Application of wall corrections to transonic wind tunnel data.
[AIAA PAPER 72-1009]
21 p3041 A72-41591
Comparison of three oscillatory techniques for cones at incidence.
[AIAA PAPER 72-1015]
21 p3042 A72-41595
Characteristics of an ejector-type engine simulator for STOL model testing.
[AIAA PAPER 72-1028]
21 p3042 A72-41607
Aerodynamic characteristics of bodies of revolution with large fineness ratios at Mach numbers ranging from 0.2 to 6.0
22 p3134 A72-42286
Flow distortion and performance measurements on a 12-inch fan-in-wing model for a range of forward speeds and angle of attack settings.
22 p3134 A72-42323
Ablative nose shape change effects on re-entry vehicle aerodynamic performance.
[AIAA PAPER 72-974]
22 p3230 A72-42337
Trailing vortex effects on wing pressure distribution from low speed wind tunnel tests, discussing effect of wing-vortex distance
24 p3362 A72-45331

WIND TUNNEL NOZZLES
Two dimensional underexpanded free jet flow into static medium, presenting wind tunnel nozzle experimental data and graphic solutions from method of characteristics
20 p2885 A72-39619
Refinements in high-Reynolds-number shock-tunnel technology.
[AIAA PAPER 72-996]
21 p3040 A72-41582

WIND TUNNEL STABILITY TESTS
Wind tunnel model instrumentation and captive trajectory facilities for aircraft stability, control and metric wing-pylon store tests for performance and structural predictions
03 p0339 A72-12921
Wind tunnel stability tests of aerodynamic pitch damping of aircraft model oscillating in two degrees of freedom
03 p0307 A72-13539
Wind tunnel study of space shuttle longitudinal dynamic stability at supersonic speeds, discussing damping-in-pitch
[AIAA PAPER 72-135]
05 p0730 A72-16890
Three degrees of freedom motions of slender cones with slight compounded asymmetries in hypersonic flight wind tunnel stability tests
[AIAA PAPER 72-28]
05 p0608 A72-16939
Dynamic model of high bypass ratio turbofan engines for L-1011 wind tunnel flutter test program
[AIAA PAPER 72-376]
11 p1703 A72-25400
Wind tunnel tests for flutter characteristics of rectangular block model oscillating freely in uniform flow, discussing galloping and vortex excitation
11 p1572 A72-26373
LB 21 and space shuttle orbiter aerodynamic testing, discussing computer program supplementing reentry vehicle free flight aerodynamic testing
13 p1894 A72-28934
Wind tunnel testing of Dassault-Breguet-Dornier Alpha Jet twin engine trainer, emphasizing tests for wing-empennage flutter and jet induced interference effects
13 p1940 A72-30077
Results of preliminary studies of a bearingless helicopter rotor concept.
[AHS PREPRINT 600]
17 p2489 A72-34490
Wind-tunnel Magnus testing of a canted fin or self-rotating configuration.
17 p2486 A72-35254
Wind tunnel experiments on aerodynamic superstall, describing stability tests and models
17 p2492 A72-35374

Parameters influencing dynamic stability characteristics of Viking-type entry configurations at Mach 1.76.
17 p2622 A72-35494
F-111A inlet nozzle dynamic distortion diagnostics for airframe-propulsion integration based on flight and transonic wind tunnel tests
[ICAS PAPER 72-18]
21 p2991 A72-41143
Aerodynamic characteristics of the slotted fin.
21 p2992 A72-41262
Forced vibration solution and wind tunnel investigation of shallow cylindrical shells under moving pulsating pressure discontinuities, noting compression shock effects
21 p3122 A72-41352
Experimental determination of asymmetry-induced trim angles of attack.
[AIAA PAPER 72-1032]
21 p2993 A72-41605
A new method for the evaluation of slotted wind tunnel interference parameters applicable to subsonic oscillatory tests.
21 p3043 A72-41642
Bi-planar wind tunnel free flight test and instrumentation for difference between nonplanar and planar dynamic stability of blunt and sharp half cones, providing angular documentation
[AIAA PAPER 72-983]
22 p3163 A72-42331

WIND TUNNEL WALLS
Wind tunnel wall blockage and lift interference reduction by streamwise porosity distribution
11 p1613 A72-26001
Localized magnetic field for wind tunnel wall-plasma heat transfer minimization, preserving flow characteristics
12 p1852 A72-27684
Application of wall corrections to transonic wind tunnel data.
[AIAA PAPER 72-1009]
21 p3041 A72-41591
Wall interference effects on cone-cylinder pressure distribution in variable porosity transonic wind tunnel as function of model blockage and Mach number
[AIAA PAPER 72-1010]
21 p3041 A72-41592
Researches on the two-dimensional retarded cascade. I, II.
22 p3133 A72-41944

WIND TUNNELS
NT BLOWDOWN WIND TUNNELS
NT CASCADE WIND TUNNELS
NT COMBUSTION WIND TUNNELS
NT HOTSHOT WIND TUNNELS
NT HYPERVELOCITY WIND TUNNELS
NT LOW DENSITY WIND TUNNELS
NT LOW SPEED WIND TUNNELS
NT PLASMA JET WIND TUNNELS
NT RECTANGULAR WIND TUNNELS
NT SHOCK TUNNELS
NT SLOTTED WIND TUNNELS
NT SUBSONIC WIND TUNNELS
NT SUPERSONIC WIND TUNNELS
NT TRANSONIC WIND TUNNELS
Wake blockage paradox in two dimensional perforated wall wind tunnel, investigating interference velocity distribution
02 p0151 A72-12271
Hypersonic boundary layer transition in presence of wind tunnel noise, indicating rms sound pressure relationship to transition Reynolds number
02 p0151 A72-12278
Shock interference heating in hypersonic flows, measuring pressure and heat transfer in wind tunnels
[AIAA PAPER 72-78]
05 p0604 A72-16805
Wind tunnel disturbances effects on hypersonic boundary layer transition on sharp cones, comparing hot-wire anemometer and surface pressure measurements
[AIAA PAPER 72-181]
05 p0605 A72-16825
Wind tunnel measurements for near flow field velocity distribution in rectangular wing wake turbulence, comparing with flight measurements
[AIAA PAPER 72-41]
05 p0609 A72-16948
Low turbulence wind tunnel with closed circuit design and pressure gradient adjustment capability for turbulent boundary layer studies
06 p0795 A72-17713
Stationary high beta plasma shock waves generated in plasma wind tunnel by impinging on magnetic field, comparing with earth bow shock
07 p1042 A72-19617
Laughing gull metabolism dependence on flight speed and angle during wind tunnel tests from oxygen consumption, carbon dioxide production and aerodynamic forces analyses
08 p1115 A72-21080
Sonic boom simulation devices and techniques, including wind tunnels, ballistic ranges, spark discharges and shock tubes
08 p1147 A72-21906
Wind tunnel inlet effect on pulsed flow, relating velocity and pressure pulses
10 p1417 A72-24216
Electromagnetic position sensor for magnetically supported model in wind tunnel, discussing design, operation principles and performance
10 p1462 A72-24773

Stability of free shear layer in wind tunnel two layered temperature differentiated air flow against small periodic disturbances, noting critical Richardson number
11 p1619 A72-26638
Tone burst pulse measurements of acoustic absorption coefficients in noisy environments for electronic simulation of wind tunnel noise
13 p2006 A72-29584
Wind tunnel investigation of supersonic air flow behavior on rotatable right dihedral formed by two plane plates with sharp edges
13 p1894 A72-29636
Wind tunnel investigation of pressure perturbations on plane surface due to gas jet injected from surface into subsonic air drift flow
13 p1894 A72-29637
Soviet wind tunnel for power plant-environment interactions studies, discussing working sections velocity distributions calibration
13 p1939 A72-29644
Photon correlation spectrometer for laboratory wind tunnel measurement of laser Doppler signals backscattered from dust particles
14 p2111 A72-30854
Inclined wind tunnel test section for free gliding investigation and aerodynamic design of flexible wing two body system
15 p2213 A72-31403
Wind tunnel measurement of intermittency in turbulent boundary layer on porous plate for alternating laminar and turbulent air flow
15 p2217 A72-31610
Wind tunnel ventilation duct aerodynamic stability analysis for incompressible and slightly compressible flow
16 p2378 A72-33439
Monitor and regulator for automatic speed control and flow velocity measurement in wind tunnel
16 p2392 A72-33609
Atmospheric boundary layer and diffusion over three dimensional mountainous terrain by laboratory simulation with meteorological wind tunnel and scale model
[AIAA PAPER 72-648]
16 p2419 A72-34085
Influence of the angle of attack on the performance of high-deflection stator blades
17 p2484 A72-34889
Single pulse holographic flow visualization.
19 p2798 A72-37622
Design and development of the United Aircraft Research Laboratories acoustic research tunnel.
[AIAA PAPER 72-1005]
21 p3041 A72-41589
Total enthalpy measurement from blunt body gas cap emission in arc-heated wind tunnels - Results and application.
[AIAA PAPER 72-1021]
21 p2993 A72-41599
Laser Doppler velocimeter operating in forward- and back-scatter modes for supplementing wind tunnel flow field measurements in subsonic, transonic and supersonic regimes
22 p3179 A72-42678
A near real time data acquisition/reduction facility for the Boeing wind tunnels.
22 p3164 A72-42699
Experience with the NRC 10 ft. x 20 ft. V/STOL propulsion tunnel - Some practical aspects of V/STOL engine model testing.
23 p3278 A72-44247

WIND VANES
Electronic computing wind vane for meteorological support during atmospheric diffusion studies
06 p0843 A72-18449
Vanes for sensing incidence angles of airstream with respect to aircraft, noting correlation coefficient
06 p0796 A72-18450

WIND VARIATIONS
Lidar measurements of atmospheric aerosol distributions over large areas including urban haze, scattering layers, trade wind inversion and Sahara dust stream in Caribbean
[AIAA PAPER 71-1055]
01 p0057 A72-10526
Wind resonance in ionosphere under pressure fluctuations, noting turbulent friction factor above 110 km
01 p0058 A72-10589
Ocean winds velocity, temperature and humidity fluctuations second and third order structure functions, deriving Kolmogoroff constants
03 p0383 A72-13154
Vertical wind velocity variances and spectra above atmospheric surface layer for flat and mountain terrains
03 p0386 A72-14335
Steady state geostrophic wind vector variation hodographs in planetary baroclinic boundary layer, considering thermal influence linear superposition on internal friction effects
06 p0841 A72-17667
Wind, pressure and temperature diurnal and semidiurnal variations to 30 km altitude over tropical western Pacific, considering atmospheric model based on linearized equations of motion
07 p1029 A72-19099

Horizontal neutral winds meridional component from incoherent scatter measurements of F region ionization drifts, noting diurnal variations

08 p1156 A72-21098

Semiannual latitude dependent mesospheric wind patterns from meteor trail observations, suggesting heat inputs from solar radiation and magnetic storm related auroral heating

08 p1159 A72-21227

Tidal and seasonal wind variations from ionospheric drift If range measurements, comparing with radar-meteor data

08 p1160 A72-21528

Radio meteor observations of upper atmosphere long period wind variations, determining oscillation spectra peaks by harmonic analysis

08 p1161 A72-21537

Inferred perturbation effects of Arecibo large nighttime gravity wave on neutral atmosphere velocity and temperature

09 p1300 A72-23021

Semiannual variation in ionospheric drifts, zonal winds and vertical shear at thermosphere base

11 p1626 A72-26475

Meteorological rising balloon systems accuracy limitation, noting response to wind field changes, aerodynamic self oscillations and radar tracking errors

13 p1990 A72-28817

Daily difference analysis of magnitude, vertical and latitudinal structure of irregular mesospheric wind variations due to gravity waves

13 p1948 A72-28832

Semiannual equatorial wind oscillations in upper stratosphere and lower mesosphere dependence on temperature variations in high and middle latitudes

14 p2099 A72-30259

Monthly mean pattern variations for equatorial stratospheric easterly and westerly winds, noting continuity of low latitude regimes

14 p2129 A72-30806

Upper atmosphere temperature and wind variations over Antarctic from meteorological rocket sounding, noting winter cyclonic vortex level

15 p2225 A72-31906

Russian book on atmosphere studies covering determination of periodic variations in meteorological elements to assess sea level pressure, temperature and wind variations

17 p2546 A72-34975

Features of zonal circulation in the stratosphere and lower mesosphere of the equatorial region during the period of increasing solar activity (1967-1968)

19 p2790 A72-37999

Diurnally varying neutral wind effects on lower F region ionization distribution, noting Appleton anomaly disappearance time

19 p2794 A72-38865

A method for simulating wind conditions during atmospheric stagnation periods.

20 p2947 A72-38965

The anomaly of the neutral wind at a height of approximately 200 km at high latitudes.

20 p2918 A72-39536

Stratospheric winds over Leba rocket sounding station in spring and autumn, 1970.

21 p3049 A72-41500

An updated theory for the quasi-biennial cycle of the tropical stratosphere.

22 p3201 A72-42503

Probability distribution of vertical longitudinal shear fluctuations.

23 p3281 A72-44146

WIND VELOCITY

Remote passive microwave sensing of ocean surface wind fields, discussing sea microwave brightness temperature dependence on wind speed

02 p0214 A72-11864

Composite scattering theory mathematical model for radar backscattering cross section relation to ocean surface conditions and wind velocity

02 p0172 A72-11868

Wind velocity and direction vertical changes for weather dynamics, emphasizing jet streams

02 p0255 A72-12785

Wind altitude and maximal velocity computation for jet stream structure and turbulence

02 p0255 A72-12786

Ocean winds velocity, temperature and humidity fluctuations second and third order structure functions, deriving Kolmogoroff constants

03 p0383 A72-13154

Vertical wind velocity variances and spectra above atmospheric surface layer for flat and mountain terrains

03 p0386 A72-14335

Mars topographic map study of high velocity relief winds, showing seasonal and secular changes

04 p0569 A72-14502

Wind velocity vertical component determination through meteor trail drift observation, presenting mean diurnal measurements data

05 p0657 A72-16272

Comet Bennett tail and coma surface brightness distribution, estimating solar wind velocity

05 p0717 A72-16426

Synoptic velocity fluctuations from empirical structural functions of wind fields, proposing spectral kinetic energy distribution model for atmospheric turbulence

07 p1031 A72-20694

Winds velocity, direction and diffusion coefficients over Heiss Island from artificial luminous clouds observations

08 p1160 A72-21534

Auroral zone neutral wind velocity and atmospheric temperature correlations with geomagnetic activity, considering ion-neutral particle drag as accelerating mechanism during magnetic storms

08 p1161 A72-21535

Radio meteor measurements of ionospheric drifts by two separated stations, obtaining wind velocities mean hourly values correlation coefficient

08 p1238 A72-21883

Wind velocity distribution structural laws in vertical and horizontal planes for large mesospheric and atmospheric processes

09 p1347 A72-23591

Jet stream types derived from vector conditions for surface with maximum geostrophic wind velocity

10 p1507 A72-25002

Atmospheric wind velocity time variations at 80-100 km altitudes from ionospheric drift data, finding planetary oscillation periodicities relationship to solar activity cycle

11 p1620 A72-25273

Tropical hurricane model describing initial whirlwind and self exciting wind velocity development and dependence on ocean surface temperature

11 p1682 A72-26879

Wind velocities field in vortices leeward of islands derived from Navier-Stokes equation for isolated axisymmetric viscous vortex

12 p1839 A72-27032

Mars surface particulate matter eroded by atmospheric winds, noting erosive and settling velocities and yellow clouds distribution

13 p2036 A72-28794

Small scale atmospheric turbulent motions sensing by FPS-16 Radar-Jimsphere meteorological balloon system, analyzing wind velocity data from dual radar measurements

13 p1990 A72-28818

Horizontal and vertical scales of atmospheric boundary layer turbulence for various temperature stratifications, noting space and time correlations for longitudinal wind velocity component

13 p1995 A72-29592

Venera satellite parachute probe method for Doppler measurement of Venus atmosphere wind velocity and turbulence

14 p2151 A72-30466

Iterative numerical solution of linear differential equations system for wind vertical velocity and local pressure variation along vertical line

15 p2265 A72-31344

Meteor trail drifts at 95 km over Turkmenistan from November 1969-August 1970 radar observations, comparing to Frunze, Dushanbe and Kharkov wind data

15 p2305 A72-31372

Sea level wind and pressure data adjustment to governing dynamical equations by numerical variational analysis, using Sasaki matching technique

16 p2419 A72-33941

Atmospheric surface layer temperature, humidity and vertical wind velocity variances dependence on turbulent fluctuation inputs

16 p2419 A72-34148

Wind velocity and some Venusian surface characteristics monitored by the 'Venera-7' automatic interplanetary station

17 p2610 A72-35210

Saltation threshold velocity simulation by dynamic model with terrestrial and Martian surface applications, using particle trajectory equations for near ground-atmosphere interface

17 p2614 A72-35637

A theoretical study of the diurnal wind variations in the planetary boundary layer.

18 p2706 A72-36645

Cup anemometer response to fluctuating wind speeds.

20 p2920 A72-38966

Synoptic velocity fluctuations from empirical structural functions of wind fields, proposing spectral kinetic energy distribution model for atmospheric turbulence

20 p2948 A72-39009

Estimation of the turbulent diffusion coefficient and of the vertical wind velocity component from the distribution of natural radioactivity

20 p2964 A72-39320

Ground humidity and wind velocity effects on terrestrial scintillation, considering adiabatic temperature stratification factor

21 p3007 A72-40738

Russian book - Calculated wind velocities at heights of the lower atmospheric layer.

22 p3200 A72-42077

Wind tunnel measurement for demonstrating similarity of atmospheric turbulent boundary layer

mean velocity and shear stress at high Reynolds number

22 p3201 A72-42598

Wind velocity components determination in Cartesian coordinates based on rectilinear uniform air particle motion, noting difference with respect to geostrophic approximation

23 p3310 A72-43532

Investigation of the applicability of different laws of extremal-value statistics to the approximation of empirical distributions of maximum wind velocities

23 p3310 A72-43535

WIND VELOCITY MEASUREMENT

Ultrasonic rotameter for wind velocity circulation measurement, using cylindrical electroacoustic capacitor converter with solid dielectric for radiators and receivers

01 p0094 A72-10560

Book on pressure probe methods for wind speed and direction covering incompressible and subsonic compressible flow pressures, temperature, etc

01 p0072 A72-11273

Wind velocity spatial derivative determination by radar observation of signal reflection from atmospheric water particles

03 p0383 A72-13483

Antenna azimuthal radiation patterns and meteor radiant distribution effects on wind velocity measurement by radar observation of meteor trains

05 p0715 A72-16251

Stationary-nonstationary temporal sampling for synoptic meteorological networks, illustrating oceanic wind speed measurements

06 p0842 A72-18436

Atmospheric turbulence, wind velocity, temperature and density measurements at 90-250 km, using explosive contaminants release from Skylark rockets

07 p0979 A72-20265

Airborne radar measurement of 2.25 cm backscatter from sea surface, obtaining wind speed by computerized clustering data analysis techniques

09 p1296 A72-22312

Paired Gill propeller anemometer response function in generalized wind vector sensor application, proposing algorithm for magnitude and direction errors reduction in output analyses

09 p1307 A72-22434

CW carbon dioxide laser Doppler radar for remote measurement of atmospheric wind velocity and turbulence, obtaining Doppler signal via homodyned radiation scattered by airborne particles

09 p1315 A72-23407

Momentum anemometer for wind velocity and vorticity measurement, discussing design principle and performance advantages

10 p1484 A72-25089

Wind velocity spatial derivative determination by radar observation of signal reflection from atmospheric water particles

11 p1682 A72-26253

Laser Doppler-type remote sensor for wind velocity and atmospheric turbulence measurements

13 p1956 A72-28859

Optical measurement of crosswind from effects produced by atmospheric turbulence and wind velocity relationships

13 p1994 A72-28870

Upper atmosphere horizontal wind velocity from meteor trails radio echoes, noting structural function anisotropy

14 p2127 A72-30263

Subcloud Venus atmospheric wind velocity and turbulence from Venera Doppler measurements

15 p2308 A72-31905

On the possibility of a simultaneous measurement of wind speed, wind direction, air density and air temperatures at heights which correspond to the upper D-region /max. 95 km/ with chaff cloud sensors.

17 p2545 A72-34631

Measurement of aerosol motion and wind velocity in the lower troposphere by Doppler optical radar.

18 p2706 A72-36638

Spectral characteristics of surface-layer turbulence.

19 p2829 A72-38559

WINDING

NT FILAMENT WINDING

NT HELICAL WINDINGS

NT WIRE WINDING

Winding fiber reinforced plastics, investigating fiber curvature effects on elastic constants and tensile strength optimization

02 p0248 A72-11626

WINDMILLING

U AUTOROTATION

WINDOWS

Fabry-Perot interferometer application as filter with transmission windows at regular intervals in wave numbers to detect Raman scattered radiation from atmospheric gases

01 p0067 A72-10537

Mechano-acoustical network model for room-hallway-window system response to sonic booms or other transient loads, determining damping ratios

11 p1686 A72-25729

Window response to sonic booms, establishing upper bounds by mechano-acoustical network modeling of one and two degree of freedom dynamic systems 13 p2057 A72-29091

An Irtran-1 reflection filter for the 20-micron atmospheric window. 20 p2928 A72-39897

Atmospheric window at 10-12 micron wavelength, investigating absorption coefficient of clear atmosphere water vapor 21 p3048 A72-40398

WINDOWS [APERTURES]

Signal injection through laser transmitting window, showing effects on resonant frequency and locking mode [AD-738988] 07 p1009 A72-20680

Optical qualities of aircraft windshields and direct vision windows, considering color, light transmission, faults, heating, distortion, inside reflections and double images 12 p1832 A72-27004

Aircraft transparencies from civil operator viewpoint, considering replacement cost of flight deck and cabin windows 12 p1753 A72-27005

Aircraft fuselage acrylic glazing design, covering passenger cabin window, cockpit windscreen and various surface coatings 12 p1753 A72-27008

Concorde aircraft optical transparency components design characteristics and reliability tests, noting visor, pilot forward windshield, flight deck side windows and cabin windows 12 p1753 A72-27012

Mathematical model for thermal lensing of IR laser window, discussing aberrations effect on diffraction-limited far field focus time 12 p1819 A72-27284

Solar and geocoronal hydrogen Lyman alpha radiation detector, discussing ion chamber with magnesium difluoride window and nitric oxide gas 15 p2239 A72-32336

Low energy X ray measurements with sealed Ti window proportional counter, applying to rocket observation of Sco X-1 15 p2240 A72-32438

Supersonic flow aerodynamic window for high power laser beam extraction through nonabsorbing gas medium while supporting pressure difference between cavity and ambient atmosphere [AIAA PAPER 72-710] 16 p2404 A72-34036

An estimate of sonic boom damage to large windows. 17 p2623 A72-34234

Photogrammetric method for determining the deflection of light beams by spacecraft windows during flight 21 p3052 A72-40305

Effect of environmental changes on the ghosting of distant objects in twin-glazed windows. 21 p3084 A72-40616

Light transmission, reflection and environment problems of hydrophilic coatings for fog and frost protection in aviation instrument window design 22 p3196 A72-42519

WINDOWS [INTERVALS]

NT LAUNCH WINDOWS

WINDS ALOFT

NT GEOSTROPHIC WIND

NT JET STREAMS [METEOROLOGY]

Thermally excited E layer tidal winds based on UV radiation as thermal source, using isothermal atmosphere model 01 p0055 A72-10429

D region neutral gas winds, density changes and short wave radio absorption correlation, determining air mass flow rates from chaff fall rate measurements 08 p1160 A72-21532

Auroral zone neutral wind velocity and atmospheric temperature correlations with geomagnetic activity, considering ion-neutral particle drag as accelerating mechanism during magnetic storms 08 p1161 A72-21535

Radio meteor observations of upper atmosphere long period wind variations, determining oscillation spectra peaks by harmonic analysis 08 p1161 A72-21537

D region neutral gas winds, density variations and short wave absorption, determining correlation from ultrahigh chaff and absorption measurements at 2.83 MHz. 09 p1277 A72-22374

Winds aloft forecast use to predict southwestern mountain lee wave behavior for general aviation cross country flights 13 p1993 A72-28863

Global ionospheric electron density variations and associated thermospheric winds during 15-21 June 1965 geomagnetic storm from ground based and satellite data 13 p1953 A72-29805

Meteor trail drifts at 95 km over Turkmenistan from November 1969-August 1970 radar observations, comparing to Frunze, Dushanbe and Kharkov wind data 15 p2305 A72-31372

Stratospheric winds and winter warmings in the Southern Hemisphere. 20 p2948 A72-39862

Height structure of tidal winds as inferred from incoherent scatter observations. 22 p3169 A72-42014

WINDSCREENS

U WINDSHIELDS

WINDSHIELDS

Glass-vinyl retractable windshield visor development for Concorde aircraft, considering rain, hail and icing effects, strength and stiffness under aerodynamic loading and heating 09 p1261 A72-22900

Optical qualities of aircraft windshields and direct vision windows, considering color, light transmission, faults, heating, distortion, inside reflections and double images 12 p1832 A72-27004

Aircraft windscreen design, discussing high impact strength glass, electroconductive film, transparency service life and weight reduction 12 p1753 A72-27006

Aircraft fuselage acrylic glazing design, covering passenger cabin window, cockpit windscreen and various surface coatings 12 p1753 A72-27008

Aircraft windscreen reliability, discussing delamination, interface shear stress effects and analogy to metal fatigue 12 p1812 A72-27011

Concorde aircraft optical transparency components design characteristics and reliability tests, noting visor, pilot forward windshield, flight deck side windows and cabin windows 12 p1753 A72-27012

Concord aircraft windshield panels bird impact resistance, noting effects of edge clamping width, ply thickness, composition and temperature 12 p1812 A72-27013

Aircraft windshield bird impact resistance, noting weight, speed, angle and window geometry effects 12 p1813 A72-27014

High light transmission electrically conducting Hyviz and gold film laminates for aircraft windshields and window heating applications 13 p1898 A72-30038

WINDWARD

U WIND [METEOROLOGY]

WING CAMBER

Viscous incompressible flow past longitudinally cambered small aspect ratio slender wing near solid interface 05 p0600 A72-16215

Airfoil contour design as envelope of family of circles with centers lying on mean camber line 09 p1259 A72-22298

Hughes 500 and OH-6 helicopter tail rotor cambered blades, comparing thrust and stall characteristics with symmetrical blades 14 p2072 A72-30290

WING FLAPS

NT LEADING EDGE SLATS

NT TRAILING-EDGE FLAPS

Externally blown flap noise tests at various nozzle exhaust velocities for STOL aircraft noise reduction [AIAA PAPER 72-129] 07 p0908 A72-18962

Externally blown flap impingement noise. [AIAA PAPER 72-664] 17 p2487 A72-35961

WING FLOW METHOD TESTS

Aerodynamic forces and pressure distribution measurement on wing-body combination model, investigating boundary layer on wing upper surface 02 p0151 A72-12228

Wind tunnel simulation of full scale vortices. [AHS PREPRINT 623] 17 p2483 A72-34477

Conical caret wings supersonic characteristics, examining flow transition from weak to strong attached shock waves 24 p3361 A72-45114

WING LOADING

Increasing lift and Reynolds number effects on displacement and skin friction of three dimensional turbulent boundary layer on infinite swept wing 01 p0002 A72-11395

Thin shock layer theory of lifting properties of reentry caret and flat delta wings and waveriders at high incidence angles and Mach number 02 p0152 A72-12345

Flutter problem wing-air flow energy exchange at instability limit, obtaining vibration mode shapes from homogeneous boundary value problem analog model 03 p0442 A72-13191

Lifting surface linearized potential theory for unsteady aerodynamic forces on wing and horizontal tail surfaces, using computer program 03 p0308 A72-13541

Low wing loading STOL transport with ride smoothing automatic control system, noting thrust-weight ratio [AIAA PAPER 72-64] 05 p0613 A72-16942

Wing load distribution and induced drag control by warping, summarizing linear theory and wind tunnel test results 10 p1417 A72-24218

Aircraft wing structure fatigue life estimates based on flight load time histories from counter accelerometer [SAE PAPER 720305] 11 p1733 A72-25569

Transport aircraft aerodynamic design technology application to general aviation propeller driven twin engine aircraft, discussing wing loading and aspect ratio optimization 11 p1576 A72-25595

Aerodynamic lag effects on wing bending dynamic response at supersonic speeds, noting application to stress estimation under gust loads 11 p1572 A72-25922

Three dimensional photothermoelastic method of refrigeration with composite model to study transient thermal stresses in wing rib 14 p2168 A72-30907

Bending and torsional mode deformations of two dimensional elastic wing under sinusoidal and random gust 16 p2469 A72-33229

Vortex induced wing loads. 17 p2486 A72-35257

Downwash distribution at surface of rectangular planform wings with prescribed subsonic aerodynamic loading for various aspect ratios 19 p2747 A72-38809

Evaluation of the downwash integral for rectangular planforms by the BAC subsonic lifting-surface method. 19 p2747 A72-38810

Augmentor wing design for Buffalo STOL aircraft, discussing operational principle and wind tunnel test results 21 p2994 A72-40684

Trailing vortex effects on wing pressure distribution from low speed wind tunnel tests, discussing effect of wing-vortex distance 24 p3362 A72-45331

An experimental investigation of a jet issuing from a wing in crossflow. 24 p3362 A72-45332

WING OSCILLATIONS

Thin wing harmonic oscillation in subsonic flow, developing analytical form of kernel function in generalized Possio integral equation 05 p0603 A72-16707

Subsonic oscillating surface theory for wings with partial span controls, noting computer program rapidity [AIAA PAPER 72-61] 05 p0608 A72-16931

Inverse integral Fourier transforms to solve steady periodic motions of wing close to solid surface, deriving equations of lift and principal moment 08 p1108 A72-21701

Approximate method for nonlinear differential equations of motion solution in flight dynamics, applying to control surface buzz and slender wing oscillations 09 p1262 A72-23453

Hydrodynamic forces in sinusoidal vibrations of disk in water channel with toroidal vorticity wake pattern, applying results to flapping wing mechanics 10 p1471 A72-25129

Hingeless blades flap-lag oscillations linear stability characteristics in hovering flight, examining precone, elastic and pitch-lag coupling and induced inflow aerodynamic effects 14 p2072 A72-30289

Application of the finite element method to torsional flutter analysis on an analog computer 20 p2980 A72-39907

Flap-lag induced nonlinear oscillations in torsionally rigid helicopter blade, solving nonlinear equations of motion by multiple time scales asymptotic expansion [AIAA PAPER 72-956] 22 p3137 A72-42356

Investigation of the interaction between a circular wing and a flow of ideal liquid 23 p3348 A72-43796

WING PANELS

Prediction of the stalling of a wing section in incompressible flow [ONERA, TP NO. 1088] 19 p2746 A72-37760

Transport aircraft wing compression panel failure in bending test due to stringer interruptions, analyzing structural deficiency via column and beam bending theories 22 p3183 A72-42827

A crack stopper concept for filamentary composite laminates. 23 p3305 A72-43498

WING PLANFORMS

NT ARROW WINGS

NT DELTA WINGS

NT SWEEPBACK WINGS

NT VARIABLE SWEEP WINGS

Wave drag reduction by antisymmetric wing and body arrangement, discussing application to transport aircraft at supersonic speeds 05 p0602 A72-16534

- Concorde aerodynamic configuration R and D, discussing wing layout in terms of drag, stability, control and weight distribution characteristics
07 p0911 A72-19057
- Aerodynamic data acquisition with magnetic balance on wind tunnel model delta and AGARD G wing planforms and body of revolution
10 p1462 A72-24770
- Supersonic aerodynamic influence coefficients matrices calculation for wings of arbitrary planform, constructing computer program
12 p1752 A72-28142
- Vortex induced wing loads.
17 p2486 A72-35257
- Computation of transonic flow about finite lifting wings.
17 p2486 A72-35258
- Triangular and conical wings in hypersonic flow with Mach reflection of shock waves from leading edge with optimal L/D ratio
18 p2642 A72-36893
- Downwash distribution at surface of rectangular planform wings with prescribed subsonic aerodynamic loading for various aspect ratios
19 p2747 A72-38809
- Investigation of the interaction between a circular wing and a flow of ideal liquid
23 p3348 A72-43796
- WING PROFILES**
NT WING SPAN
Velocity field of sonic flow about aircraft wing profile, solving mixed Cauchy problem
01 p0001 A72-11178
- Elliptic wing-vortex interaction for various aspect ratios
05 p0603 A72-16542
- Laminar/turbulent boundary layer transition on parabolic wing profile in supersonic wind tunnel, noting critical Reynolds number increase with leading edge thickness
09 p1259 A72-22407
- Supercritical thick wing for structural weight reduction and increased cruise speeds flight tested on Navy T2-C aircraft
[SAE PAPER 720320]
11 p1576 A72-25583
- Numerical calculation of sonic flow around wing section with rounded leading edges, obtaining Mach number distribution, boundary characteristic shape and velocity field
12 p1751 A72-27181
- Book of aircraft design illustrations covering three view and perspective form low drag airfoil, aspect ratio, plain split, slotted and multiple flaps
14 p2167 A72-30776
- Hodographic equations solution containing critical point for compressible fluid two dimensional flow, noting calculation of wing profiles and turbine engine cascades
[ONERA, TP NO. 1048]
14 p2095 A72-30841
- Torsion problem of solid rod with wing profile shaped cross section solved by conformal mapping and gamma function derivative, calculating maximum stresses and rigidities
15 p2327 A72-31741
- Asymptotic solution for inviscid conducting fluid flow past arbitrary wing profile in magnetic field
16 p2434 A72-32929
- Coordinate perturbation and multiple scale techniques application to supersonic flow field around two dimensional wing and oscillations in closed tube
16 p2379 A72-33576
- Vortex sheet simulation method for slender wing-canard surface nonlinear interaction investigation
16 p2458 A72-33695
- Unified area rule for hypersonic and supersonic wing-bodies.
17 p2485 A72-35251
- Calculation of an unsteady separation flow past a slender profile
18 p2642 A72-36900
- Three-dimensional wings in hypersonic flow.
19 p2747 A72-38797
- Supersonic aircraft wing form influence on sonic boom, discussing supersonic wind tunnel tests for noise reduction
20 p2888 A72-39931
- WING ROOTS**
Initial dihedral wing-body interaction for supersonic leading edges, determining expansion of velocity potential on root chord
14 p2069 A72-30365
- WING SLATS**
U LEADING EDGE SLATS
WING SLOTS
Wind tunnel investigation of unswept rectangular wing with externally blown single slotted flap, determining optimum slot width as function of momentum coefficient and flap deflection
04 p0462 A72-15461
- WING SPAN**
Flat plate wing autorotation experiments about spanwise axis in low speed wind tunnel
04 p0462 A72-15117

- Nonlinear calculation of three dimensional flow of perfect incompressible fluid around wing of finite span with arbitrary form
04 p0463 A72-15558
- Lift and induced drag characteristics of jet flapped finite span wings in close proximity to ground, using method of matched asymptotic expansions
16 p2341 A72-32827
- Evaluation of Reissner's correction for finite span aerodynamic effects.
18 p2736 A72-36774
- Optimization of the wing parameters of a glider hovercraft
20 p2888 A72-39902
- WING STALL**
U BOUNDARY LAYER SEPARATION
WING TANKS
Utilization of wing and empennage volume for aircraft fuel tankage, presenting equations and charts for quick determination of available volume
11 p1576 A72-25811
- WING TIPS**
Tip clearance effect on compressor blade aerodynamic characteristics, applying Bolyan analysis to low aspect ratio rectangular wing
02 p0153 A72-12825
- Wing tip shape effects on vortex sheet rolling calculation by Belotserkovskii method
06 p0755 A72-17850
- Natural inertia moment effect of balance weight at wing tip on critical flutter rate
08 p1242 A72-21092
- Blade characteristics of axial flow fan with orifice fan guide investigation by theoretical model with flat plate parallel to wing tip surface
15 p2179 A72-32142
- Effect of several wing tip modifications on a trailing vortex.
23 p3247 A72-43334
- WING-FUSELAGE STORES**
Wind tunnel model instrumentation and captive trajectory facilities for aircraft stability, control and metric wing-pylon store tests for performance and structural predictions
03 p0339 A72-12921
- WINGED ROCKET BOOSTERS**
U LAUNCH VEHICLES
U WINGED VEHICLES
WINGED VEHICLES
Time optimal control of distributed systems with random properties, considering n integral relations and flying wing vehicle torsional vibration problems
10 p1421 A72-24427
- Ground effect wing vehicles stability in forward motion, deriving characteristic equations by linear analysis
10 p1421 A72-24844
- WINGS**
NT ARROW WINGS
NT CARET WINGS
NT CRUCIFORM WINGS
NT DELTA WINGS
NT FIXED WINGS
NT FLEXIBLE WINGS
NT LIFTING ROTORS
NT LOW ASPECT RATIO WINGS
NT PARAWINGS
NT RECTANGULAR WINGS
NT RIGID ROTORS
NT RING WINGS
NT ROTARY WINGS
NT SLENDER WINGS
NT SUPERCRITICAL WINGS
NT SWEPT WINGS
NT SWEPTBACK WINGS
NT THIN WINGS
NT TILTING ROTORS
NT TIP DRIVEN ROTORS
NT TWISTED WINGS
NT UNSWEPT WINGS
NT VARIABLE SWEEP WINGS
Difference equations and relaxation method for three dimensional transonic flow field about wings in terms of velocity potential
[AIAA PAPER 72-189]
05 p0605 A72-16843
- Incipient wing stall detection by unsteady pressure monitoring via flush-mounted microphones, discussing flow patterns on models
07 p0908 A72-19093
- Jet-STOL augmentor wing consisting of moderately thick airfoil with full span leading edge slat and double surface trailing edge flap
08 p1110 A72-21899
- Wing structural weight estimation for civil aircraft preliminary deriving generalized formula based on wing root bending moment for specified flight condition
09 p1262 A72-22909
- Automated optimization for preliminary design of supersonic aircraft wings, noting flutter, stresses and resonant frequency as dynamic constraints
[AIAA PAPER 72-333]
11 p1727 A72-25368

- Unsteady aerodynamic loadings of flexible aircraft with nonplanar wings and wing-tail surfaces in supersonic flow
[AIAA PAPER 72-378]
11 p1574 A72-25402
- Hot versus shielded aerodynamic surfaces trade study for space shuttle booster wings and fins design, considering materials, structural weight and cost estimates
[AIAA PAPER 72-390]
11 p1726 A72-25411
- Shot peen contouring of Boeing 747 wing skins combined with incremental chip forming, noting principles and manufacturing process
[ASM PAPER W 72-31.4]
12 p1817 A72-28160
- DC 10 aircraft wing stringers fabrication and processing, discussing stress relieving and stretch form contouring techniques, aging and tempering processes and flaw detection
[ASM PAPER W 72-31.3]
12 p1817 A72-28161
- Airframe and wing fatigue life testing, discussing results recomputation for changed operating conditions
14 p2092 A72-30276
- Temperature dependent elastoplastic wing assemblies and continua analysis via matrix displacement method
16 p2471 A72-33791
- Influence of wing deformations measured during flight tests upon the flight performance of a glider made of synthetic materials. I
23 p3252 A72-44452
- WINTER**
Spanish winter anomalous ionospheric short wave absorption observed by high precision ground based measurements
01 p0055 A72-10434
- Ionospheric neutral gas wind and altitude effects on Spanish short wave absorption winter anomaly
01 p0055 A72-10435
- Meteorological elements, upper ionospheric data and solar radio emission intensities during winter stratospheric temperature rises
03 p0383 A72-13477
- Anomalous changes in ionospheric radio absorption during winter at midlatitudes, investigating diurnal and seasonal variations and stratospheric warming
04 p0518 A72-14967
- Earth radiation flux spectral intensity measurements in winter, noting latitudinal distributions, day and night variations and oceanic and continental curves
05 p0656 A72-16234
- Ozone content and vertical distribution variations as causes of winter stratospheric warmings in Northern Hemisphere
07 p0973 A72-18861
- D region positive ion and electron conductivities and densities measurement by parachute borne blunt probes during 1970-1971 winter anomaly
09 p1376 A72-22373
- Primitive equation multilayer model for winter precipitation prediction in U.S. northeast coastal region, noting correlation with observational data
09 p1344 A72-22428
- Mars biology likelihood from long winter model, suggesting north polar cap summer remnant vaporization as atmosphere, liquid water and greenhouse effect source
10 p1424 A72-23717
- Temperature indetermination and large scale weather patterns in winter from 70 year temperature records
10 p1507 A72-25003
- Meteorological elements, upper ionospheric data and solar radio emission intensities during winter stratospheric temperature rises
11 p1682 A72-26247
- Transient planetary Rossby waves dynamics in winter stratosphere forced from below, using quasi-geostrophic midlatitude beta plane approximations
13 p1988 A72-28550
- Auroral sporadic E layer diurnal distribution correlation to charged particle integral flux diurnal variations observed by satellite in winter, noting Kp index effect
14 p2102 A72-30655
- Ionospheric radio waves absorption and stratosphere temperature variations with respect to season and sunspot cycles, examining 1963-5 winter anomaly
15 p2195 A72-31555
- Atmospheric density and temperature measurements by rocket-borne spheres during 1972 winter, observing variability with altitude
15 p2227 A72-31959
- Wind patterns at meteor altitudes /75-105 kilometers/ above College, Alaska, associated with mid-winter stratospheric warmings.
18 p2689 A72-36962
- Stratosphere circulation variation in autumns preceding cold winters
20 p2949 A72-39947

- WIRE**
NT ELECTRIC WIRE
NT EXPLODING WIRES

Aerospace wire and cables testing methods standards for evaluating mechanical, electrical and chemical properties, coating thicknesses, continuity flaws, flammability, geometrical characteristics, etc [SAE AS 1198] 01 p0006 A72-10384

Deformation and compression characteristics of W wire rolled from flattened vacuum melts

01 p0077 A72-11084

Powder metallurgical tungsten fine wire creep behavior at 2100-3000 C, determining activation energy and stress dependence

03 p0370 A72-12996

Evaluation of Collis-Williams and Davies-Fisher heat transfer formulas for flow past fine wires based on Nusselt vs Reynolds number relationship

10 p1562 A72-24294

Superconductive behavior of cold-worked sintered Nb wires, examining effects of aluminum oxide addition on residual resistivity, magnetization behavior and critical current density

11 p1662 A72-26742

Tungsten alloy wires strength, creep properties and fatigue limit, investigating fracture characteristics

11 p1663 A72-26807

High temperature microporosity in W wire at 3000-3350 C, using electron microscopy and fractography

13 p1973 A72-28651

Micropores pinning effect on grain boundaries mobility during drawn tungsten wire recrystallization, determining pores induced repulsive force

15 p2257 A72-32116

Storage characteristics of plated magnetic wire for nondestructive read and write

16 p2369 A72-33672

The effect of ionization on heat transfer to wires immersed in a highly thermally-ionized plasma

17 p2637 A72-34998

WIRE GRID LENSES

Reflectivity dependence of triple polarization grid on elements spacing and wires orientation, noting bandwidth of ray guide matching transformer

23 p3269 A72-43446

WIRE WINDING

Mechanical properties of titanium strengthened by monodirectional molybdenum wires

21 p3069 A72-41354

Critical superconductivity currents measurement in niobium based U shaped and coiled wires within steady magnetic field

22 p3190 A72-42735

WIRING

Algebraic scheme describing electric element and subnetwork interconnection into networks by wiring operators having conversation capability with computer

06 p0778 A72-17475

A means of reducing custom LSI interconnection requirements

23 p3273 A72-44454

WIRING SYSTEMS

U WIRING

WKB APPROXIMATION

U WENTZEL-KRAMER-BRILLOUIN METHOD

WOOD AIRCRAFT CONSTRUCTION

U AIRCRAFT STRUCTURES

WORDS [LANGUAGE]

NT MESSAGES

NT SYLLABLES

Cortical responses to visually displayed word and nonsense syllable stimuli, using EEG and computer techniques

04 p0474 A72-15248

Relationship of visibility fluctuations in set of luminous circles to verbal response learned for each circle, showing word association influence on stimuli perception

13 p1911 A72-29851

Language and speech capacity of the right hemisphere

19 p2757 A72-38150

WORK

NT PHYSICAL WORK

Operator, task level and workload effects on operative strategy, showing controllers methods modification in ATC center

09 p1270 A72-23130

Frankfurt Airport air traffic controller opinion survey of attitudes toward work and working environment

09 p1271 A72-23138

Additional deformation work for splines forming in splined circular profiles pressing, deriving characteristic displacement velocity distribution equations

13 p1963 A72-28744

WORK CAPACITY

Human exercise capacity assessment from maximal oxygen intake estimates and Harvard step test

01 p0016 A72-10116

Optimum muscle work conditions experiments with rabbits, correlating total work performance and power output with muscle temperature variations

02 p0160 A72-12013

Control technique and flight quality for crew workload reduction to improve military and civil aircraft flight safety

03 p0310 A72-13640

Human mental working capacity estimation relation to functional state, discussing brain performance tests

03 p0316 A72-13721

General aviation type light airplanes pilot workload during steep landing approach, comparing flight tested control response parameters with handling qualities criteria

[AIAA PAPER 72-125] 05 p0613 A72-16941

CO hypoxia effect on oxygen transport during exercise, discussing changes in cardiac and respiratory functions and work capacity

08 p1114 A72-20893

Ground based ATC information processing systems analysis, considering controllers work load

09 p1348 A72-22778

ATC tasks work load assessment - Conference, Darmstadt University of Technology, June 1971

09 p1270 A72-23126

Operator mental processes during ATC task performance, discussing work load effect, mental representation and operator algorithm definition

09 p1270 A72-23129

Pilot and ATC radar controller workload variations relation, discussing distraction stress effects

09 p1271 A72-23132

ATC task analysis by subjective rating of work load, discussing information processing measures, scoring method and observer rating procedure

09 p1271 A72-23135

Time series analysis of physiological and work study data in ATC tasks, using heart rate as strain indicator

09 p1271 A72-23137

Acceptable load standards in ATC tasks, defining moments of conscious brain control as mental load measure

09 p1271 A72-23139

Ergonomic simulators for testing individual mental working capacity, using stress-strain and fatigue relation

09 p1272 A72-23140

Aerobic work capacity indices of gas exchange pulse rate, pulmonary ventilation and acid base balance in runners, determining maximum oxygen utilization

09 p1268 A72-23596

Prolonged water immersion effects on renal function and plasma volume in trained and untrained subjects, noting deleterious effect on orthostatic tolerance and work capacity

10 p1428 A72-23738

Physical work capacity comparison during bicycle ergometry and treadmill walking tests, measuring oxygen uptake, ventilatory parameters and excess carbon dioxide production

11 p1579 A72-26095

Maximal oxygen uptake and heart rate during ladder climbing, inclined treadmill running and cycling ergometer tests

11 p1586 A72-26612

Sleep deprivation effects relation to work duration, time of day, circadian rhythm, memory function, task performance, environmental factors, drug use and age

11 p1580 A72-26678

Work capacity evaluation from fatigue, biological rhythm, tissue respiration and oxygen consumption studies, discussing pharmacological stimulation effects

14 p2078 A72-30376

Annual clinical and physiological evaluation of test pilots physical performance over ten year period from body composition, pulmonary function and work capacity measurements

14 p2082 A72-31093

Work capacity and physiological responses to maximum exercise in 54 year old men in relation to heart disease and cardiovascular hazard studies

17 p2505 A72-35822

Area navigation systems integration into existing ATC and man/machine relationship problems, considering cockpit workload coordination

21 p3079 A72-40280

An area navigation system for a long range airplane

21 p3079 A72-40281

Muscle metabolism of ATP, CP, glycogen and lactates at rest and during submaximal and maximal exercise

21 p3005 A72-40421

Mental and physical workload measure and differentiation in man machine systems

21 p3012 A72-41427

Changes in certain hemodynamic indices during muscular strain in people with differing capacity to perform work

24 p3370 A72-44591

Pilot workload assessment technique during transport aircraft approach and landing, correlating with aircraft serviceability, crew efficiency, navigation aids, meteorological conditions and control procedure factors

24 p3377 A72-45657

Stressed state of radial bearings hollow rollers under loads concentrated along generatrix, evaluating test results by statistical analysis

24 p3408 A72-45726

WORK DECREMENT

U WORK CAPACITY

WORK FUNCTIONS

Punch-through transit time negative resistance semiconductor device utilizing injection from Schottky barrier, deriving small signal theory for microwave impedance

01 p0042 A72-10787

Polycrystalline Mo work function calculation from electron emission microscopy, determining crystallographic grain orientation effects

01 p0071 A72-11027

Electron work function and electrode physicochemical properties and surface temperature on boundary layer formation and thickness at electrodes in MKD channel

01 p0009 A72-11206

Solid state components for millimeter wave systems, including IMPATT diode power sources and amplifiers, P-I-N diode modulators and switches and Schottky barrier mixers

02 p0192 A72-12183

GaAs Schottky barrier and germanium backward diodes in microwave integrated circuit applications, describing design and performance as frequency changers and low level detectors

03 p0334 A72-14073

Power Schottky diode design and advantages, comparing with junction diode

04 p0498 A72-15130

GaAs Schottky barrier diodes design, manufacture and characteristics, discussing radar receiver and communication equipment applications

05 p0638 A72-16595

Mo-Nb alloys single crystals work function, obtaining thermionic emission pattern

06 p0832 A72-18414

GaAs and Si millimeter wave Schottky barrier mixer diodes fabrication, noting low noise broadband mixer/preamp

06 p0790 A72-18486

Low noise GaAs Schottky barrier FET for X and Ku bands applications

07 p0955 A72-19257

Schottky barrier and n-n heterojunction diodes hf noise, considering ideality factor effect

07 p0955 A72-19358

Schottky barrier semiconductor devices characteristics, fabrication and application to pulse microwave diodes and IC elements

08 p1139 A72-21053

Emission energy of positrons thermalized in moderators and coated with Au, suggesting Au negative work function existence

08 p1217 A72-21339

LF excess flicker noise in metal semiconductor Schottky barrier diodes due to barrier height fluctuation

09 p1287 A72-23114

Validity range of applied voltage relationship to majority carrier current in Schottky diodes, assessing minority carrier current importance

10 p1448 A72-24108

Schottky barrier crystal microwave video diodes design and fabrication to maximize burnout resistance and dynamic range for given detection sensitivity

10 p1450 A72-24553

Schottky barrier gate FET design, device packaging and low noise characteristics

12 p1788 A72-27294

Noise behavior of GaAs Schottky barrier FET with short gate length, showing channel thickness effect on intervalley scattering noise

12 p1790 A72-27439

C and X band CW GaAs Schottky barrier IMPATT oscillators with nichrome as barrier metal, noting high power efficiency and low noise performance

12 p1793 A72-27966

Photoelectric properties of cadmium telluride thin film solar cells, discussing energy gap temperature dependence, work function and current variations anomalies

12 p1756 A72-28018

Epitaxial GaAs carrier concentration profile, deep traps detection and properties determination, using Schottky barrier on semiconductors

13 p0204 A72-30035

Schottky diode microwave down-converter conversion loss calculation as function of image terminal with consideration of barrier capacitance, series resistance and voltage drop

14 p2088 A72-30586

Work functions of dilute W alloys from vacuum emission vehicle and thermionic microscope measurements, noting additives effect

14 p2120 A72-30613

Electron work function for metallic sphere and thin film on dielectric substrate as function of radius, thickness and dielectric constant

15 p2290 A72-31222

Transient 10 MeV electron radiation effects on RF power and recovery time of GaAs Schottky barrier IMPATT diodes

16 p2370 A72-33766

Work functions of some emitting and collecting refractory metal single crystals.

17 p2595 A72-34601

Measurement of the electron work function in binary and ternary transition metal-nonmetal systems.

17 p2595 A72-34602

Performance comparison of thermionic converters with several collector materials.

17 p2497 A72-34606

Mo-Nb alloys single crystals work function, obtaining thermionic emission pattern

17 p2567 A72-34863

Thermodynamic analysis of metal surfaces covered by electropositive adsorbates.

18 p2656 A72-36126

Plasma immersion probe measurements of electron work function.

18 p2690 A72-36127

W /100/ work function change during adsorption of oxygen, cesium, and oxygen-cesium co-adsorption

18 p2656 A72-36128

Electron work function change of interstitial compounds of the 4a and 5a metals in dependence on the nonmetal content.

18 p2656 A72-36129

Work function dependence on crystal orientation for W with special emphasis to the variation near the /110/ orientation.

18 p2656 A72-36130

Thermionic characteristics of carburized tungsten-rhenium alloys.

18 p2656 A72-36131

Work function, thermal stability, and atomic structure of electropositive films adsorbed on single crystals of metals

18 p2656 A72-36132

Work function theory for Cs-/W/ and Cs-/O-/W/

18 p2656 A72-36133

Work function change of tungsten /110/ planes as function of Mo coverage.

18 p2656 A72-36134

Incore thermionic reactor cylindrical Mo emitter covered with two CVD W layers, discussing first layer adhesion and diffusion characteristics and work function stability

18 p2707 A72-36135

Crystal orientation effect on electron work function in chemical vapor deposited W layers on thermionic converter cylindrical emitters

18 p2717 A72-36142

The vapor deposition of high work function materials in a gas discharge.

18 p2656 A72-36149

Cylindrical Cs thermionic converter with unique emitter and five collectors, measuring I-V characteristics to determine emitter work function, ignition voltage and electric power

18 p2646 A72-36191

Vapor pressure influence of Ba-Cs thermionic converter diodes on I-V characteristics and work functions in terms of anomalous Schottky effect

18 p2646 A72-36194

Emitter work function elevation in additive thermionic converters via tungsten oxides deposition on collector

18 p2646 A72-36197

Dependence of emission on work function variation in metals under tension

18 p2699 A72-36350

An investigation of impurities segregation to the /001/ nickel surface during thermal treatment - Work function changes and Auger electron spectroscopy using the LEED camera.

18 p2720 A72-37022

Flash desorption spectrum and LEED studies of CO adsorption on W single crystal planes, measuring work function increase as function of coverage

18 p2657 A72-37040

Richardson and effective work functions measurements for thermionic emission from bialkali and extended red-sensitive trialkali photocathodes, discussing error minimization

20 p2890 A72-39646

Excess metal buildup kinetics and work function of oxide thermionic cathode activated by emission current, noting effect of metal and oxygen concentrations

21 p2997 A72-40789

Correlation between the work function of transition metal carbides and the surface recombination of hydrogen atoms in the region of homogeneity

21 p3070 A72-41372

Relation between the work function and adsorption and catalytic properties of transition metal borides in the reaction of recombination of hydrogen and nitrogen atoms

22 p3187 A72-41926

Physicochemical investigation of the thermionic emission properties of metals and alloys

22 p3191 A72-42811

Application of a field-emission microscope to the investigation of the work function of tungsten coated with a thin layer of silicon oxide and with tantalum

24 p3432 A72-44891

WORK HARDENING

NT STRAIN HARDENING

Analytic yield surface in work hardening including stress in transition range after load change /Bauschinger effect/

01 p0144 A72-11388

Anisotropic and compressible work hardening materials three dimensional elastoplastic flow quasi-linear theory, deriving boundary integral equations

02 p0296 A72-12530

High strength low alloy type ferrite pearlite steel microstructural and compositional variations effect on work hardening, ductility and impact toughness

02 p0246 A72-12558

Fibrous structure of precipitates produced at bottom of trace due to friction in work hardened Al-Cu alloy solid solution

03 p0376 A72-13970

Cu single crystal fatigue life explanation by work hardening using statistical theory of slip

03 p0379 A72-14258

Dislocation creep model for work hardening and recovery, deriving mechanical equation of states for various magnitudes and directions

04 p0589 A72-15160

Substitutional dynamic strain aging effects on Fe-Nb alloys mechanical properties, attributing ductility reduction to work hardening and strain rate effects

04 p0534 A72-15576

Mn additions effects on austenitic stainless steels yield strength, work hardening characteristics, corrosion resistance and machinability

07 p1011 A72-19478

Deformable thermally work hardenable Al-Mg-Li alloy, detailing phase composition changes during aging

07 p1014 A72-19838

Cold working effects on plasticity of hardened Al at 20-400 C

07 p1015 A72-19902

Shock wave propagation and structure in elastoplastic material with translational work hardening, obtaining closed system of discontinuity equations

07 p1093 A72-19977

Numerical analysis of passing screw dislocation arrays under stress for computerized work hardening model

07 p1097 A72-20556

Work hardening after ausforming and heat treatment effects on mechanical properties of metastable austenitic Ni-Cr steel

08 p1190 A72-22165

Dislocations distribution in Al single crystals observed by X ray topography, noting effects of critical work hardening with annealing and secondary recrystallization

10 p1495 A72-24068

Impurities effects on stress corrosion and work hardening induced dislocation structures in stainless steels, considering stacking fault energy relationship

10 p1496 A72-24231

Alpha Zr tensile properties tests noting strain aging effects on strain rate, work hardening and ductility anomalies

11 p1661 A72-26595

Ga alloying effect on Al single crystals work hardening, noting Portevin-Chatelier effect at higher Ga contents

11 p1662 A72-26739

Diamond burnishing effect on surface quality and fatigue strength of steel, noting work hardening increase and compressive residual stresses buildup in surface layer

11 p1642 A72-26811

Helicopter rotor blade spars shot peening in centrifugal vibrator, optimizing Cr-Mo-Ni steel surfaces work hardening

11 p1642 A72-26820

Work hardening and recrystallization grain structure of sintered and electron bombardment melted Ta after annealing

11 p1644 A72-26839

Russian book on work hardening of surface components of heat resistant and Ti alloys for high temperature operation

12 p1816 A72-28156

Polycrystalline alpha Ti work hardening at low temperatures and different purities, discussing plastic strain effects

13 p1975 A72-28671

Work hardening-recovery model of dislocation creep, deriving multiaxial mechanical equation of states for strain/time relationship under arbitrary temperature-stress sequences

13 p2061 A72-29872

Plastic deformation in bcc metal single crystals, discussing glide and work hardening, dislocations, core structure and atomic calculations

13 p2061 A72-29874

Internal friction and relaxation mechanisms in substructure hardened fcc alloys and bcc metals, presenting dislocation parameters for annealed and cold worked Fe alloys

14 p2122 A72-30960

Recovery-work hardening model of steady state creep for Al, assuming equal internal and applied stress

15 p2259 A72-32642

Work hardening and anisotropy coefficients effects on deep drawing limit curves for extramild steel, noting rupture strain and deformation trajectories

16 p2396 A72-32873

Tensile deformation of Co single crystal in high temperature fcc phase, noting dislocations effect on work hardening

16 p2410 A72-33819

Influence of twinned growth crystals on the texture of nickel work hardened in tension

18 p2702 A72-36703

Secondary recrystallization of nickel 270 work-hardened by tension

18 p2702 A72-36704

Effects of work hardening on the structural hardening of T-A6V6E2 titanium alloy

18 p2702 A72-36706

Tensile and compressive flow strength and work hardening behavior in maraging steels, attributing strength differential to nonlinear elastic interactions between interstitials and dislocations

20 p2939 A72-39306

On the plastic behaviour of time dependent materials - Theoretical and experimental investigation.

21 p3124 A72-41504

Dislocation pile-ups in periodic internal stresses.

22 p3214 A72-42316

Stress amplitude and hysteresis loop width changes in alpha Ti during cyclic work softening-work hardening with constant strain amplitude

22 p3189 A72-42438

Pure Co single crystals allotropic transformation effects on deformation behavior, noting flow stress and work hardening rate relationship to history

22 p3193 A72-43034

Fatigue strength of two phase Ti alloys, considering work hardening, electrochemical finishing, electropolishing and protective media

23 p3301 A72-43757

WORK-REST CYCLE

Human cardiocirculatory responses to submaximal physiologically paced bicycle ergometry, recording prejection period, isovolumic contraction, left ventricular ejection and pulse transmission time

01 p0010 A72-10147

Sleep pattern relation to duty hours of aircrew operating worldwide east-west routes

07 p0932 A72-20178

Wake-sleep cycle importance in military service, considering drugs effects on wakefulness

07 p0922 A72-20383

Various work-rest cycles and environmental temperature effects on body temperature, determining external auditory canal and core temperature relationship

08 p1123 A72-20886

Circadian adrenal periodicity of plasma corticosteroid levels in man under random living schedule

09 p1265 A72-22643

Rest and activity patterns effect on space crews well-being and operational effectiveness during prolonged extraterrestrial missions, noting work load effect on long-haul transport aircrews

10 p1427 A72-23727

Day/night workers sleep patterns in terms of intrasleep REM-NREM ultradian cycle, noting sleep temporal instability for night workers

10 p1428 A72-23730

Work-rest schedules endocrine and metabolic effects on aircrews during 50 hour flight missions in C-141 aircraft, using urinary test techniques [AD-740992]

10 p1428 A72-23737

Fatigue factors in aircrew related to shift working and technological advances, considering implications for industry and work-rest cycles

10 p1432 A72-24988

Bicycle ergometer measurements of thermoregulation input and output under wide range of work load and climatic conditions, deriving correlation equation

11 p1579 A72-25874

Sleep loss and work-rest cycle effects on combat efficiency, considering psychomotor reactivity, vigilance and decision making capacity

11 p1588 A72-26688

Work-rest scheduling and sleep loss effect on operator performance in watchkeeping and active multiple visual tasks

11 p1589 A72-26689

Adaptation period to inverted work-rest cycle observed with encephalograph, noting effect of brain bioelectric activity circadian rhythms stability

13 p1904 A72-29315

Pulse rate studies of human adaptation to 16 hour work-rest cycle, showing persistence of 24 hour cycle

13 p1904 A72-29316

Heart rate change regularities during inverted work-rest cycle of isolated man, noting relation to circadian rhythm

13 p1904 A72-29317

Diurnal changes in gas exchange and metabolic rate under normal and inverted day-night schedule conditions, studying human adaptation to shifted schedule

13 p1904 A72-29318

EEG diurnal rhythms during 72 hour insomnia, considering adaptation to altered work-rest cycle in subjects with stable and unstable brain activity rhythms

13 p1904 A72-29319

Human respiratory rate diurnal rhythm adjustments during inverted work-rest cycles in isolation chamber with controlled comfortable atmospheres

14 p2075 A72-30390

Heart rate diurnal rhythm adaptation to work-rest cycle change, using recumbent and sitting position data parameters

14 p2075 A72-30391

Cardiac stroke volume measurements during supine bicycle exercise and recovery period, using indicator-dilution technique

14 p2079 A72-30701

Water loss replacement effect during rest and exercise in high temperature environment thermoregulation experiment

15 p2185 A72-31449

Two compartment analog model of thermoregulation during rest and exercise, considering temperature, heat conductance, sweat rate and oxygen uptake

15 p2185 A72-31450

Cardiac cycle length /RR interval/ and QT interval mathematical relationship from ECG obtained during exercise and recovery periods

15 p2187 A72-32747

Possibilities and dangers during long working periods in space rescue.

17 p2507 A72-34436

Self-paced ergometer performance - Effects of pedal resistance, motivational contingency and inspired oxygen concentration.

18 p2653 A72-36911

WORKING FLUIDS

Pressure drop of homogeneous and annular wick heat pipes using hydrogen, nitrogen and oxygen working fluids, discussing heat transfer capacity

[ASME PAPER 71-WA/HT-13] 05 p0744 A72-15873

Heat pipe radiator with 50 kW heat rejection capability for potassium working fluid of Rankine cycle space power system, discussing design, fabrication and testing

[ASME PAPER 71-WA/HT-16] 05 p0744 A72-15875

High thermal power density ammonia heat pipe with porous grooved wick concept

[ASME PAPER 71-WA/HT-20] 05 p0744 A72-15879

Electrostatic surface and bulk ionization ion thrusters current densities for propulsive and working fluid utilization efficiency

05 p0705 A72-16772

Ultrahigh enthalpy gas generation by steady multicomponent flow process with kinetic energy transfer from low molecular weight gas to higher weight working medium

[AIAA PAPER 72-167] 05 p0750 A72-16979

Heat transfer and hydraulic resistance of lamellar type heat exchangers with water/air working media, testing efficiency for various duct cross sections and Reynolds numbers

06 p0904 A72-18510

Dielectric sulfur activated liquids for high productivity electroerosion machining of steels and metallic carbides, comparing with petroleum

08 p1174 A72-21034

Capillary evaporation cooling system with water as working medium, measuring effectiveness in terms of heat flux density vs water consumption

[DFVLR-SONDDR-112] 10 p1561 A72-24023

Self priming high capacity spiral artery heat pipe with ammonia as working fluid for flight on OAO 3, discussing development models analysis, design and testing

[AIAA PAPER 72-258] 11 p1725 A72-25203

Tunnel wick heat pipe artery with priming in gravity environment by temperature induced pressure differences, using ammonia as working fluid

[AIAA PAPER 72-273] 11 p1740 A72-25213

Mathematical model for ionized plasma response to sinusoidal perturbations, calculating dispersive waves in MHD generators with working fluid of potassium seeded argon

13 p2014 A72-29372

Boundary conditions influence on heat and mass transfer in low temperature heat pipes with freon as working fluid

16 p2479 A72-33853

A study of film-cooling effectiveness of some gas-turbine stator surfaces.

17 p2597 A72-34468

Heat transfer performance of stationary two phase closed thermosiphon with water and Freon as working fluids, discussing effects of operating pressure and heat flux

21 p3131 A72-41621

Investigation of the stability of a hydraulic servo motor with rigid feedback

22 p3139 A72-41858

Metal vapor plasma as working medium in MHD generator, discussing hydrodynamic relations, power efficiency and thermodynamic cycle

24 p3428 A72-45169

WORLD

U EARTH (PLANET)

WORLD DATA CENTERS

World Weather Watch and Global Atmospheric Research Program remote sensing applications, considering weather prediction and modification, atmosphere pollution monitoring and global atmosphere mathematical modeling and simulation

02 p0208 A72-11784

WORMS

Space environment weightlessness and radiation effects on leeches biorhythm, metabolism, reproduction and growth from rocket biological experiments

04 p0481 A72-15729

WRAP

Plywrap process for low cost automated fabrication of fiber reinforced plastic composites, noting applications from missile interstages to modular housing

12 p1815 A72-28081

WRECKAGE

Computerized error function method of wreckage trajectory analysis in aircraft accident investigation, using fundamental equations of motion

03 p0309 A72-13250

WRENCHES

Recommendations for selection and use of torque wrenches for aerospace propulsion systems applications.

[SAE AIR 1268] 18 p2648 A72-36531

WRINKLING

Symmetrical and antisymmetrical wrinkling of sandwich panels.

18 p2736 A72-37056

WROUGHT ALLOYS

Oxidation screening at 2200 F of Ni, Fe and Co wrought alloys for space shuttle thermal protection system, noting microstructural changes

01 p0085 A72-10781

Wrought superalloys microstructure and mechanical properties control by precipitating phases

02 p0245 A72-12506

Recrystallized and unrecrystallized deformed semifinished wrought Al alloy under cyclic and static loads, investigating macrofracture kinetics

07 p1014 A72-19840

Diffusion welding of cast and wrought Udimet 700 superalloy gas turbine engine components, discussing interfacial grain boundary migration and microstructural homogeneity effects on weld joint quality

07 p0997 A72-19998

Al wrought alloys dynamic elasticity modulus and Poisson ratio dependence on temperature, using ultrasonic measurement method

07 p1019 A72-20239

Deformable wrought stainless steels phase diagram for structural state estimation from chemical composition, considering various austenite, martensite and ferrite combinations

11 p1659 A72-26127

Quenched powder metallurgy of high strength-high conductivity wrought Cu-Zr and Cu-Zr-Cr alloys, using nitrogen atomization

13 p1974 A72-28659

Phase structure and solution kinetics of cast and wrought Al alloys after plastic deformation by rolling

18 p2700 A72-36585

WURTZITE

Photoemission studies of wurtzite zinc oxide.

24 p3432 A72-45387

X

X BAND

U SUPERHIGH FREQUENCIES

X RAY ABSORPTION

High energy gamma ray telescope based on absorption induced Cerenkov radiation in low density gas, using parabolic mirror for focusing on photomultiplier tubes

03 p0352 A72-13033

Pulsed radiography of X ray absorption by plasma behind incident shock wave in Cs vapors, noting mirror behind shock front and wave reflection

07 p1044 A72-19887

Pionic X ray fields and transitions in Li 6, Be 9, C 12 and O 16, obtaining 2p level absorption broadening

10 p1515 A72-24418

Pulsed laser plasma temperature determination by radiation measurements in X ray and visible spectral regions using foil method

13 p2018 A72-29887

Chemical bond in Cu-Ti intermetallic phases, from X ray K absorption edges studies

13 p1981 A72-29914

Interstellar absorption of Crab Nebula soft X ray from Aerobee rocket photographic scan, estimating average volume densities for H, O, Ne, Si and Mg

16 p2445 A72-33129

Pulsed radiography of X ray absorption by plasma behind incident shock wave in Cs vapors, noting mirror behind shock front and wave reflection

17 p2590 A72-35135

Experimental indications of plasma instabilities induced by laser heating.

19 p2840 A72-37549

X RAY ANALYSIS

Ta-Ra-B ternary alloy, investigating phase equilibria and isothermal cross sections with X ray analysis

03 p0374 A72-13739

Ta-Co system phase diagram from differential thermal, X ray, and microstructural analyses, determining composition, temperature, structural type and lattice constant

03 p0374 A72-13740

Y-Mn-Al ternary alloy solid solution phase diagram isothermal section construction from X ray structural data

03 p0376 A72-13945

Erichmanite /natural osmium disulfide/ chemical analysis and X ray data, noting osmium abundance

03 p0351 A72-14369

Basal dislocations determination in sapphire single crystals, using X ray transmission topography

05 p0701 A72-16018

X ray topography of natural diamond, showing impurity platelet distribution, slip depth, temperature and stress conditions after plastic deformation

05 p0702 A72-16020

X ray study of structural changes in Ni single crystals during recrystallization process after uniaxial deformation under compression loads with high loading rates

06 p0834 A72-18744

X ray, ultrasonic and eddy current nondestructive testing of aircraft structure for maintenance and special problems

07 p0994 A72-18840

Y-Fe-Al alloys ternary system X ray structural analysis after arc furnace preparation, annealing and quench hardening

07 p1048 A72-19681

Hf-Co-Al system phase equilibria determination by partial microstructural and X ray analysis

07 p1017 A72-19991

X ray analysis of cementite and titanium carbide precipitates in Cr-Mn-Mo-Ti steels weld zones

07 p1019 A72-20159

Nb-Ga system equilibrium phase diagram determination by differential thermal, tempering microstructural and X ray analysis techniques, discussing various compounds formation temperatures and characteristics

07 p1050 A72-20161

X ray study of [Y-La-Ce]/-Al-Si-B ternary systems structure at 500 C, noting binary compound presence

08 p1217 A72-21713

X ray study of martensite fine structure produced by plastic deformation in Fe-Ni alloy

08 p1188 A72-21788

Helium cryostat for X ray studies of phase transformations and structural changes in single metal crystals

08 p1169 A72-21792

X ray method characteristics in thermal interphase microstresses determination, considering spherical silicon inclusion surrounded by concentric Al matrix envelope

09 p1309 A72-22638

X ray determination of thermal microstresses in metal specimens surfaces

12 p1807 A72-27447

Isothermal profiles for Nb-Zr-C and Nb-Ti-C alloys from microstructural and X ray analyses, noting Widmanstätten structure, and second phase formation

12 p1829 A72-27643

X ray and Mossbauer spectral analyses of thermomagnetically treated nickel ferrite samples containing Co, investigating ordering mechanism

13 p2020 A72-28490

X ray spectral analysis of Ti-Mo system alloys, investigating K and L lines and electronic structure

13 p1972 A72-28491

X ray analysis of Ti-Al alloys for cold rolled texture diagrams at low and high deformation levels

14 p2112 A72-30159

Mossbauer and X ray structural analysis of nickel ferrite-chromite magnetic moments, comparing with theoretical data

14 p2141 A72-30171

Russian papers on phase diagrams of metallic systems covering thermodynamic, X ray and metallographic alloys analysis

14 p2122 A72-30976

Nb-Ti-Zr-Hf system phase diagram from X ray analysis, observing beta solid solution below solid curve

14 p2122 A72-30977

W-Nb-C system phase diagram from X ray and microstructural analyses, noting solid solubility, hardness and isothermal cross section

14 p2122 A72-30983

Mo-W-C system high temperature phase equilibria from X ray and microstructural analysis, noting decrease of C solid solubility with temperature
14 p2123 A72-30984

Mo-Ni-Al system phase equilibria at 600 C from X ray and microstructural analysis, noting hardness dependence on composition
14 p2123 A72-30985

Cr-N alloy phase diagram from thermal and X ray analysis, metallographic observation and hardness tests, noting melts crystallization
14 p2123 A72-30987

Nickel-trinickel alumide-trinickel niobiumide system polythermal cross sections from X ray and microstructural analysis, noting electrical resistivity increase with Al content
14 p2123 A72-30988

Ni-Al-Nb-Mo system phase diagram from X ray and microstructural analysis, noting solid solubility and dependence of hardness and electrical resistivity on components
14 p2123 A72-30989

Ce-N alloys phase diagram from durometric, X ray, metallographic and differential thermal analyses
14 p2123 A72-30991

Stratospheric particles analysis by X ray detector on scanning electron microscope, comparing results with data on volcanic particles and cosmic dust
15 p2227 A72-31958

Bremsstrahlung photon emission rate from Maxwellian plasma, determining soft X ray diagnostic techniques applicability for laser produced plasmas
15 p2285 A72-32271

Low energy X ray measurements with sealed Ti window proportional counter, applying to rocket observation of Sco X-1
15 p2240 A72-32438

Texture of Ti-Sn and Ti-Mn alloy specimens observed by X ray reflection technique after hot rolling, annealing and cold rolling
16 p2407 A72-33529

Phase diagrams for W-Ta-Ti alloys at 1600 C from metallographic and X ray analysis
16 p2407 A72-33533

Application of the moving-slit X-ray automono-chromatization method in structural studies of planar diodes and an attempt to correlate electrical properties with lattice defects.
17 p2595 A72-34749

X-ray analysis of iron-chrome solid solutions
19 p2821 A72-38572

Radiographic examination of rhenium-aluminum-boron and rhenium-silicon-boron ternary systems
19 p2822 A72-38679

Roentgenologic studies of the effects of rapid decompression and hypoxia on the gall bladder in cats.
19 p2758 A72-38705

Anomalous increase in the total X-ray background at balloon altitude.
19 p2853 A72-38755

Determination of the elastic modulus of the left-ventricle myocardium with the aid of X-ray kymography
20 p2893 A72-38940

X-ray structural examination of phase transformations in the VT14 titanium alloy during heating
22 p3192 A72-43015

Influence of alloying elements on ordering in alloys of the nickel-molybdenum system
22 p3192 A72-43016

X ray and differential thermal analysis for phase diagrams of binary alloys of samarium oxides and gadolinium oxides with calcium oxides, noting solid solutions formation
23 p3304 A72-43250

Determination of mosaic-block disorientations in the creep of aluminum by the method of low-angle X-ray scattering
23 p3299 A72-43341

X ray, microstructural and differential thermal analysis for binary Zr alloys, noting formation of ternary phases and solid solutions
23 p3300 A72-43588

Phase diagrams from X ray analysis of rapidly crystallized Ni-Sn alloys, noting crystal lattices and phase transformation
23 p3300 A72-43648

Determination of Ni, Ga, and Ge in iron meteorites by X-ray fluorescence analysis.
23 p3262 A72-44128

Full-range solution for the measurement of thin-film surface densities with proton-excited X rays.
24 p3431 A72-44715

X RAY APPARATUS

Multilayer X ray chamber for gamma quanta energy spectrum determination by primary photon impact and absorber calorimetric methods
06 p0869 A72-17266

High dose rate electron beam irradiation using telescoping drift tube for flash X ray machine
10 p1509 A72-23935

X ray milliprobe apparatus adaptation for examining single crystals from lunar samples
13 p1960 A72-29839

Radiographic measurement of gas turbine components during response to thrust changes, using linear accelerator for X ray generation
14 p2092 A72-30620

Portable X ray calorimeter for simultaneous fluence and front surface dose measurement in Ta from pulsed electron accelerations
15 p2241 A72-32440

Dc X ray timing pulse generator for light gas gun triggering based on projectile interruption technique
15 p2241 A72-32441

Experimental evidence of an X-ray laser /Coherent radiation/copper/III/ gel target/neodymium-glass pump/.
19 p2811 A72-37774

Mobile X ray apparatus for radiographic flaw detection, describing tuned transformer high voltage source as power supply to sealed sectionalized X ray tube
19 p2805 A72-38766

A sealed, sectionalized million-V X-ray tube.
19 p2776 A72-38767

X RAY ASTRONOMY

Temporal behavior, intensity fluctuations and energy spectrum of pulsating X ray source Cygnus X-1 from Uhuru observations
01 p0121 A72-11092

Cygnus X-6 soft X ray source location, presenting polycarbonate pulse-height spectrum and counter response to different model source energy spectra
01 p0121 A72-11096

Cosmic soft X ray and UV radiation sources, discussing transition radiation emission in interstellar space
01 p0121 A72-11121

Pulsar NP 0532 pulsed hard X ray energy spectrum measurement, using balloon sounding data
01 p0134 A72-11160

Magellanic Clouds X ray sources from Uhuru satellite observations, discussing time variability
02 p0280 A72-12195

X ray rocket observations of time variation of SCO X-1 energy spectrum and optical luminosity at 2-20 keV
02 p0281 A72-12307

Galactic disk component of diffuse X radiation from unresolved red dwarf flare stars
03 p0408 A72-12993

Supernovae remnants intrinsic luminosity-diameter correlations from soft X ray emission data, taking into account interstellar medium
03 p0408 A72-13008

Gamma ray astronomy, discussing energy spectrum, diffuse background flux, extragalactic origin and Crab Nebula emission
03 p0408 A72-13027

X ray astronomy observations, discussing Sco X-1 and Tau X-1 sources
03 p0408 A72-13036

X ray astronomy techniques survey, covering image forming telescopes, detectors, nondispersive spectrometers and polarimeters
03 p0353 A72-13037

Bragg crystal spectrometer for Sco X-1 spectrum scanning, using Aerobee 170 rocket
03 p0353 A72-13039

Long wavelength focusing collector for X ray astronomy with effective bandpass of 100-280 eV determined by low energy transmitting counter windows and paraboloid mirror reflectivity
03 p0353 A72-13040

Stellar X ray emission polarization measurement using Thomson scattering polarimeter
03 p0353 A72-13041

Cosmic X ray sources polarization, spectra and locations measurement, describing Skylark experiments and UK-5 satellite-borne instruments
03 p0409 A72-13042

Balloon-borne galactic X ray detection unit, obtaining high directivity with honeycomb collimator and angular resolution with solar sensor
03 p0353 A72-13043

High energy solar and celestial X ray experiment with OSO 5, measuring spectrum as function of time, intensity and spatial distribution
03 p0353 A72-13044

Astronomical Netherlands Satellite automatic stabilized detection system for soft celestial X rays measurement, describing various modes of operation
03 p0354 A72-13048

Atomic data for UV and X ray astronomy, considering atomic wave functions and energy levels, radiative transition probabilities and electron-ion collision cross sections
03 p0420 A72-13125

Astrophysical cosmology, discussing universe expansion, Robertson-Walker models, radio sources, quasars, cosmic X ray background, intergalactic media, etc
03 p0426 A72-13268

Nucleosynthesis model for gamma ray astronomy, covering explosive events
03 p0413 A72-14275

Small astronomy satellite program for X ray experiments and mapping, discussing structure design, systems, testing and launching
03 p0441 A72-14395

Universal steady X ray background theory, examining superposition of radiation from pulsars in various galaxies
04 p0566 A72-14909

Cyg X-1 type X ray sources evolution, discussing white dwarf and supernovae stages, parent mass and angular momentum
04 p0568 A72-15508

X ray and gamma astronomy, discussing old and blue stars, supernova remnants, radio galaxies, quasars and pulsars
04 p0582 A72-15687

TD-1, HEOS-B and COS-B satellite-borne experiments, discussing X ray and gamma astronomy
04 p0582 A72-15690

X ray and gamma astronomy, discussing satellite-borne experiments for electromagnetic and nuclear reaction rates and antimatter existence in cosmic radiation
04 p0582 A72-15692

High energy X ray and gamma ray astronomy for galactic and extragalactic observations, noting SAS satellite and HEAO program
05 p0712 A72-15773

X ray pulsations mechanism in Cyg X-1 related to high magnetic fields produced by flare-like events
06 p0873 A72-17636

Variable circular polarization in optical emission of X ray source Sco X-1, noting oscillations amplitude
06 p0878 A72-17785

Soft X ray survey of galactic plane from Sagittarius to Vela by proportional counter, observing radiation sources
06 p0873 A72-17890

Short lived X ray burst precursor of X ray nova Centaurus XR-4, investigating event intensity
06 p0881 A72-17899

Cosmological red shift and galactic evolution effects on line features in X ray background due to young pulsars in supernova remnants
06 p0891 A72-18509

Loop structure of Monoceros supernova remnant, predicting thermal soft X ray point source as cooling neutron star
07 p1073 A72-19421

Rocket astronomy development, reviewing V-2, Aerobee rocket and balloon-rocket flights for solar X rays and flares and galactic and extragalactic experiments
07 p1076 A72-19675

X ray spectrum analysis of Sco XR-1 sources, showing plasma sheath with high electron temperature
07 p1076 A72-19804

X ray power density spectrum observation of pulsars, detecting Crab Nebulae pulsar radiation
07 p1080 A72-20051

Interferometer detection of variable radio emission associated with X ray source GX9 plus 1, observing also GX349 plus 2 and GX350 plus 0
08 p1232 A72-21176

Upper soft X ray limits to Virgo sources from Aerobee 170 rocket sounding
08 p1227 A72-21394

Balloon observations of low energy Scorpius X-1 gamma ray spectrum
08 p1227 A72-21395

North Polar Spur soft X rays observed by Aerobee 150 rocket launched from Woomera for enhanced emission
08 p1227 A72-21398

X ray observatory with gas filled proportional counters, discussing pulse height analyzer, command system, calibration and power distribution
08 p1167 A72-21512

ESRO program in imaging detector development for UV and soft X ray space missions, presenting image storage target details
08 p1171 A72-21971

Black body X ray sources creation due to neutron stars rotational energy dissipation by strain hysteresis in crust
09 p1382 A72-22284

Periodic intensity and period variations of X ray pulsating source Cen X-3 caused by occulting binary system from Uhuru satellite observation
09 p1382 A72-22289

Hard X radiation source in Vela X supernova remnant direction detected during balloon flight on 25 November 1970
09 p1383 A72-22290

Seyfert galactic nuclei structure, discussing thermal X rays indication of significant random motions and difficulty of energy source determination
09 p1386 A72-22686

Weak extragalactic X ray sources radio identification, suggesting production by inverse Compton losses of electrons from radio galaxies
09 p1377 A72-22988

Cygnus Loop supernova remnant X ray emission structure from sounding rocket spectral data, showing thermal emission mechanism

09 p1378 A72-23699

Uhuru satellite development history and preliminary X ray observation, analysis of radiation source emission characteristics, locations and identifications

10 p1533 A72-23892

X ray background radiation from discrete sources, considering inverse Compton mechanism in galaxies and intergalactic space and soft component origin

10 p1529 A72-23913

Spectrum studies of extragalactic diffuse background radiation fields consisting of X ray and thermal or microwave background

10 p1529 A72-23914

Skylark 904 sounding rocket cosmic X ray experiment, discussing detector and counter operation and data retrieval technique

10 p1529 A72-24198

Coma galaxy cluster X ray and radio source region magnetic field origin as primordial metagalactic flux or strong radio source remnant

10 p1542 A72-24617

Extragalactic supernovae X ray luminosity upper limits from OSO 3 data, estimating total energies

10 p1544 A72-24667

Cygnus X-1 model with hard X rays from inverse Compton scattering of B star UV photons and IR synchrotron radiation from other component

10 p1530 A72-24944

Coma constellation hard X ray intensity sky map at 20-150 keV from balloon observations

10 p1530 A72-24948

Sco X-1 simultaneous hard X ray and optical observations from balloon and ground correlating thermal X rays and optical emissions

10 p1530 A72-24949

Magnetometers for balloon-borne X ray astronomy payload azimuth determination, noting misorientation, earth and spurious magnetic fields effects on measurement effectiveness

10 p1530 A72-24954

X and gamma ray astronomy with multiple pinhole cameras and a posteriori image synthesis, obtaining SNR gain

11 p1629 A72-25313

Programmed electro-optical systems of multichannel solar spectrometer for ground observations of X ray and EUV emission regions

11 p1630 A72-25680

High sensitivity search for X rays from supernova remnants in Aquila

11 p1713 A72-26121

X ray observation inconsistency with matter creation in steady state universe due to inner bremsstrahlung from neutron decay

11 p1713 A72-26125

Ionospheric detection of cosmic X rays by VLF links using nova sources

11 p1714 A72-26417

Soft X ray emission from supernova remnants, considering maximum linear diameter dependence on remnant distance from galactic plane

12 p1863 A72-27222

Sco X-1 2-14 keV X ray flux variations from Skylark 901 and S55 observations

12 p1864 A72-27694

High X ray luminosity associated with richest galaxy clusters, noting inverse Compton effect by relativistic electrons and bremsstrahlung from hot gas

13 p2040 A72-29412

Crab Nebula X ray emission synchrotron model confirmation by sounding rocket polarimeter polarization detection data

14 p2156 A72-30565

X ray source Cygnus X-1 pulsation periodicity analysis, showing random shot noise characteristics

14 p2156 A72-30571

Uhuru satellite observation of transient X ray source in constellation Lupus, discussing five month period intensity variation

14 p2157 A72-30572

Low energy X ray astronomical observation, considering hot plasma existence in old supernova remnants

14 p2157 A72-30676

Celestial Thomson-scattering X ray polarimeter design for OSO-1, optimizing sensitivity in 4-24 keV energy range by Monte Carlo simulation computer program

15 p2234 A72-31540

Variable cosmic X ray source location determination, noting Crab pulsar as radio, optical, X ray and gamma source

15 p2298 A72-31599

Report to COSPAR on Australian space program covering earth atmosphere, cosmic and synchrotron radiation, X ray astronomy, weather satellites, deep space and sounding rockets

15 p2338 A72-32007

Galactic X and gamma ray astronomical observations from balloons, rockets and satellites, discussing radiation counters

16 p2445 A72-33075

Galaxy M87 X ray source origin, suggesting hot plasma thermal emission or ejected relativistic electrons interacting with intergalactic magnetic or radiation fields

16 p2452 A72-33135

Diffuse X ray emission from galaxy interarm region, suggesting population of unresolvable low luminosity sources as emission model

16 p2445 A72-33138

Uhuru observed galactic X ray sources related to binary systems or supernova remnants, noting galaxy clusters

16 p2454 A72-33362

Galactic X ray sources from June 1969 rocket flight in Brazil, comparing spectra to bremsstrahlung, black body and power law models

16 p2446 A72-33457

Centaurus region hard X ray flux temporal variations from OSO-3 X ray telescope observations

16 p2446 A72-33458

Uhuru satellite data on periodic pulsating X ray source in Hercules, interpreting intensity variations as occulting binary star system effect

16 p2446 A72-33475

Cen X-3 system X ray flux amplitude periodic variations, proposing model composed of source orbiting around massive body with ionized gas cloud in between

16 p2446 A72-33611

Stellar X ray emission flux calculation for UV Ceti flares, using similarities between solar and stellar flares

16 p2450 A72-34161

X ray flux anomalous minima observations in Cen X-3 with rocket-borne argon-methane proportional counter

16 p2461 A72-34162

Decametric radio identification of an extragalactic X-ray source.

17 p2604 A72-34520

Binary nature of the B supergiant in the error box of the Vela X-ray source.

17 p2604 A72-34521

Galactic ridge of discrete diffuse X ray sources, calculating intensity in terms of scale height and radial gradient

17 p2598 A72-34523

A graphite crystal polarimeter for stellar X-ray astronomy.

17 p2553 A72-34637

X ray sources associated with galactic clusters resulting from relativistic electrons Compton scattering on microwave background radiation

17 p2599 A72-35072

Radio detection of Cygnus X-3.

17 p2612 A72-35366

Radio observations of Cygnus X-3.

17 p2612 A72-35367

X ray astronomy observational procedures, discussing source location and models, X ray detectors, satellite-borne equipment, correlation maps and diffuse X ray background studies

17 p2612 A72-35377

X ray spectrum analysis of Sco X-1 type sources, showing plasma sheath with high electron temperature

17 p2617 A72-35727

Observation of a hard X-ray flare in Cyg X-1.

18 p2729 A72-37006

X ray observation inadequacy in detection of background radiation surface brightness fluctuations due to irregular distribution within galactic cluster sources

18 p2729 A72-37006

Soft X-ray emission from intergalactic gas in the neighbourhood of the Galaxy.

19 p2855 A72-37345

Relationship between X-ray luminosity and velocity dispersion in clusters of galaxies.

19 p2856 A72-37501

Extragalactic origin of the transient X-ray sources.

19 p2856 A72-37502

The association of X-ray sources with bright stars.

19 p2856 A72-37507

Eclipsing and spectroscopic binary beta Persei radio star, suggesting X ray source nature

19 p2851 A72-37889

Interferometer detection of radio sources near pulsing extar Hercules X-1 during low X ray luminosity period

20 p2963 A72-38918

X-ray emission from intergalactic gas in the neighbourhood of galaxies.

20 p2964 A72-39240

Statistical analysis for best fit of compact X ray object spectra to black body, bremsstrahlung and power law models

20 p2969 A72-39387

A variable spacing modulation collimator for X-ray astronomy.

20 p2928 A72-39891

Photoemissive method of recording Mertz shadowgrams and vibrating electrode technique for reading out images in reconstruction of X ray sources original distribution

21 p3051 A72-40219

Search for high frequency optical variability in X-ray sources.

21 p3100 A72-40685

On a galactic origin for the soft X-ray background.

21 p3100 A72-41029

Neutron star detection based on nearby pulsar soft thermal X ray flux observations

21 p3107 A72-41218

Balloon techniques in X ray astronomy, considering emission mechanisms of discrete cosmic sources

21 p2996 A72-41616

The interaction of Sco X-1 with its environment.

22 p3218 A72-42387

Observation of several X-ray sources in 1970 September.

22 p3219 A72-42554

Compton scattering by thermal electrons in X-ray sources.

23 p3328 A72-43230

Accretion disc models for compact X-ray sources.

24 p3435 A72-44828

A further high-resolution search for Fe XXV line emission from Scorpius X-1.

24 p3438 A72-44838

Low energy X-ray survey from the Crab Nebula to Cygnus.

24 p3435 A72-44842

Precision X-ray telescopes on HEAO-C.

24 p3403 A72-45202

Radiation pressure supported stars, degenerate dwarfs, neutron stars and black holes high energy observations from space platforms

24 p3446 A72-45536

NASA X ray satellite UHURU and HEAO-C instruments and observational data on supernova remnants, pulsars, extars quasars, radio galaxies and galactic clusters

24 p3446 A72-45539

X RAY DENSITY MEASUREMENT

Isotope radiometric density measurement errors for thin material sections, presenting mathematical analysis for measurement procedures optimization

07 p0995 A72-19651

Comparative study of two direct methods of bone mineral measurement.

17 p2508 A72-34552

Surface tension, density, and volume change on melting of Al₂O₃ systems, Cr₂O₃, and Sm₂O₃.

24 p3417 A72-44925

X RAY DIFFRACTION

Line profile shape analysis of X ray diffraction broadening from deformed W, showing close approximation to Voigt distribution

01 p0088 A72-11046

X ray diffraction analysis of dilute Nb-C alloys epsilon phase, discussing Bravais lattice and unit cell dimensions

03 p0375 A72-13932

Centroid shift of diffraction line due to X ray diffractometer geometry in stress measurement

04 p0547 A72-14527

Stress measurement at surface of polycrystalline bodies by nondestructive X ray diffractometry method

04 p0525 A72-15553

Stable austenite formation during maraging steel aging at 300-750 C determined by X ray diffraction

07 p1022 A72-20525

Low power X ray diffractometer with multiwire proportional counter detector array for remote mineralogical analysis of lunar, planetary or asteroid soils detector array

08 p1167 A72-21507

Corrosion products X ray analysis using Powder Diffraction File, noting manual and computer searches

08 p1129 A72-22109

Optical petrographic, electron microprobe and single crystal X ray diffraction analysis of basaltic and monomineralic soil fragments of Lunik 16 core sample from Sea of Fertility

09 p1379 A72-22257

X ray diffraction and chemical phase analysis of Nb alloys in cast and heat treated state, considering hardening mechanism

09 p1327 A72-22636

X ray diffraction study of molten Mg-Cd alloy atomic structure, demonstrating existence of Mg-Cd compounds

10 p1497 A72-24678

Lattice source interference method for detection of X ray diffraction in Al-Zn solid solutions, taking into account precipitation effects

10 p1499 A72-24981

X ray diffraction by alpha Ti, calculating reflections relative intensity and position to identify peaks

11 p1658 A72-25826

X ray diffraction patterns of aging nimonin alloys, noting effects of atomic volume difference between precipitation phase and matrix

13 p1976 A72-28766

X ray diffraction discovery of borides with yttrium chromium boride type orthorhombic structure

13 p1984 A72-29799

- Coarse grain transformation in TD-nickel bar subjected to deformation and annealing, noting abnormal growth caused by thermomechanical effects
14 p2119 A72-30602
- Solid surface inspection by X ray diffraction, electron microscopy and chemical techniques
14 p2131 A72-30693
- As-quenched and aged form of omega phase in Ti-Nb alloys investigated by electron microscopy and X ray diffraction
16 p2410 A72-33818
- Two-phase crystal structure microdeformation measurement by combined holographic interferometry and X ray diffraction
18 p2690 A72-36358
- X ray diffraction study of crystal structure of metastable phase in rapidly solidified Al-Zr alloys
20 p2939 A72-39307
- Anomalous line broadening in the low temperature X-ray diffraction pattern of niobium.
20 p2942 A72-39989
- Crystal structure and shear strength of solids and imperfections in metals in framework of X ray diffraction and dislocation theory
20 p2942 A72-39998
- On Maxwell's equations in three-dimensional anisotropic periodic media - Tensor formulation of the problem and the N-beam approximation.
20 p2962 A72-40019
- X ray diffraction patterns of aging nimonin alloys, noting effects of atomic volume difference between precipitation phase and matrix
21 p3065 A72-40267
- X-ray diffraction studies on liquids at very high pressures along the melting curve. I, II.
21 p3084 A72-40558
- Two-dimensional lattice orientation and three-dimensional crystallinity in carbon fibres.
21 p3073 A72-40687
- Determination of the refractive index by the X-ray interferometry method
23 p3287 A72-43414
- Phase extraction and analysis in superalloys - Summary of investigations by ASTM Committee E-4 Task Group 1.
23 p3304 A72-44257
- The effects of irradiation with protons on the crystallographic order of the compound Bi₂Te₂Se.
24 p3432 A72-45200
- X RAY FLUORESCENCE**
Apollo 15 geochemical X ray fluorescence experiment, noting differential lunar highland crust existence
06 p0889 A72-18273
- Fluorescent X ray spectroscopy for K and L emission band structures of Mg, Al and V and metal compounds
09 p1370 A72-22839
- X ray fluorescence spectrometric analysis of carbonaceous chondrites for chemical subgroups
11 p1723 A72-26525
- X RAY FLUORESCENCE ANALYSIS**
U X RAY ANALYSIS
U X RAY FLUORESCENCE
- X RAY INSPECTION**
Nondestructive examination of steel plate weld specimen, comparing ultrasonic and X ray techniques
04 p0527 A72-14840
- FET devices stacking faults induced leakage currents, pinpointing critical processing steps by diagnostic X ray charts
06 p0782 A72-17364
- Borrmann X ray topographic examination of dislocation structures, discussing geometric effects on linear defects image width
07 p0989 A72-20158
- Radiographic measurement of gas turbine components during response to thrust changes, using linear accelerator for X ray generation
14 p2092 A72-30620
- Operation and performance characteristics of flying spot scanning X ray imaging systems for rapid film safe parcel inspection
18 p2692 A72-36671
- Factors governing radiographic crack detectability in steel weld specimens.
18 p2695 A72-36673
- X-ray inspection of the AWACS radome attachment locations.
24 p3406 A72-44902
- X RAY IRRADIATION**
Cosmic and X ray irradiated quartz particles as contributor to interstellar extinction, discussing grain radiation damage measurements and absorption spectra in wavelengths of approximately 1600 Å to 20 micrometers
01 p0134 A72-11163
- Sublethal X radiation effects on rat erythropoietic system during altitude hypoxia acclimatization
04 p0476 A72-15721
- N-channel MOS FET, measuring X ray irradiation effects on drain current and transfer characteristics at room temperature
05 p0634 A72-16033

- Relative biological effectiveness of high X ray doses given to radish seeds, studying irradiation rate effect on germination probability
09 p1265 A72-22524
- Microwave, X ray and corpuscular emission by gas discharges in coaxial plasma gun, measuring pressure and current distribution
09 p1362 A72-23212
- Dose response curves for pink somatic mutations in Tradescantia after neutron and X ray irradiation
15 p2186 A72-31723
- Brain tumors in irradiated monkeys.
17 p2505 A72-35647
- Neuropathological evaluation of monkeys exposed to body-alone X-radiation.
18 p2649 A72-36439
- The use of a scintillation counter to measure diagnostic X-ray tube kilovoltage, radiation exposure rates and contamination by low energy gamma emitters.
18 p2655 A72-37197
- Ionisation equilibrium and line intensities for an X-ray heated H₁ gas.
19 p2852 A72-38509
- The effects of X-ray irradiation on MAS diodes.
21 p3032 A72-40695
- Changes produced in the nerve structures of the stellate ganglion by total X-ray irradiation
22 p3140 A72-41925
- Summary of latent effects in long term survivors of whole body irradiations in primates.
23 p3254 A72-43393
- Influence of X-ray irradiation in 25- and 250-r doses on the transplant immunity in mice differing by weak and strong histoincompatibility systems
23 p3255 A72-43910
- Photoionization of N₂, O₂, NO, CO, and CO₂ by soft X rays.
24 p3426 A72-45302

- X RAY PHOTOGRAPHY**
U PHOTOGRAPHY
U RADIOGRAPHY
- X RAY SCATTERING**
Short range order and X ray diffused scattering in TiC-WC solid solution, using least squares method
06 p0834 A72-18741
- X ray diffuse scattering from Al crystal at 100-500 V, considering phonon modes effects on anharmonicity and atomic deformation
08 p1186 A72-21591
- Va crystal lattice interatomic bonds and elastic and inelastic X ray scattering intensity calculation
09 p1329 A72-23042
- X ray diffusion by thin films under grazing incidence, using reciprocity theorem
11 p1689 A72-26484
- Co-Cu alloy phase formation and separation morphology changes with temperature and anomalous diffusive X ray scattering in solid solutions
13 p1976 A72-28905
- Al crystal block structure and size changes during creep evaluated by small-angle X ray scattering technique
13 p1977 A72-28909
- X ray Brillouin scattering investigation of phonon phenomena for small momentum transfers with Bragg condition nearly satisfied
15 p2250 A72-32308

- X RAY SPECTRA**
Sounding rocket observations of quasar 3C 273 X ray spectrum for upper limits to absolute abundance of He in intergalactic medium
16 p2446 A72-33451
- Thick target processes during hard X ray emission, noting electron bombardment during solar flare impulsive phase and white light flare optical continuum production
21 p3100 A72-41292
- High-intensity X-ray spectra and stimulated emission from laser plasmas.
22 p3210 A72-41990
- The decay characteristics of models of solar hard X-ray bursts.
22 p3217 A72-42040
- The solar X-ray spectrum deduced from a proportional counter experiment and the resultant production of ionization in the mesosphere.
22 p3170 A72-42368
- Compton scattering by thermal electrons in X-ray sources.
23 p3328 A72-43230
- Signal-to-energy conversion function in the photometry of solar soft X-radiation with broad-band detectors.
23 p3329 A72-44238
- A study of cold-worked titanium-aluminum alloys by X-ray diffraction.
24 p3413 A72-44720
- Transfer effects on X-ray lines in optically thick celestial sources.
24 p3435 A72-44843

- X RAY SPECTROGRAPHY**
U X RAY SPECTROSCOPY
X RAY SPECTROMETRY
U X RAY SPECTROSCOPY

X RAY SPECTROSCOPY

- Nondestructive identification of alloy elements by nondispersive X ray fluorescence spectroscopy using Si/Li⁺ detectors and radioisotope sources for mobile applications
01 p0069 A72-10805
- High speed photographs of plasma emission spectra in UV and soft X radiation spectrum regions, discussing theory, design and operation of facilities
02 p0223 A72-11408
- Stilbene scintillator detector for gamma ray spectrometry in energy range 0.5-5 MeV, separating gamma rays from neutrons by pulse shape discrimination technique
03 p0408 A72-13031
- Cosmic X ray sources polarization, spectra and locations measurement, describing Skylark experiments and UK-5 satellite-borne instruments
03 p0409 A72-13042
- Diffuse cosmic background radiation measurements, emphasizing microwave and X ray spectra and excitation mechanism
03 p0409 A72-13138
- Solar active regions and flares X ray spectroscopic data, observing ionized silicon emission lines
03 p0423 A72-13217
- NGC 5128 X ray spectrum from sounding rocket and balloon observations, presenting inverse Compton models
04 p0568 A72-15372
- X ray pulse spectra measurement from Z-pinch plasma focus devices, describing Ross filter system with silicon diode detector capable of nanosecond time resolution
04 p0524 A72-15537
- Vertically oriented double crystal attachment to vacuum X ray spectrograph for enhanced resolution of ionic solids and solutions molecular spectra
07 p0983 A72-19317
- High resolution rocket-borne X ray spectrometer with cooled lithium drifted semiconductor detectors for measuring differential X ray energy spectrum of SCO XR-1
08 p1168 A72-21518
- Ionic and atomic temperature measurement in low pressure Ar plasma by X ray absorption spectroscopy
09 p1360 A72-22832
- Molecular X ray emission spectra interpretation based on singly ionized states observation by photoelectron spectroscopy and transition probability calculation
09 p1357 A72-22838
- Fluorescent X ray spectroscopy for K and L emission band structures of Mg, Al and V and metal compounds
09 p1370 A72-22839
- X ray emission spectroscopy of electronic structure of transition metals and alloys, obtaining electron energy spectrum
09 p1370 A72-22841
- Ta and W X ray spectra fine structure measurement, providing electron states density in unoccupied regions of energy bands of solids
09 p1370 A72-22842
- Ultrasoft X ray region photoionization absorption spectra features of inert gases, solids, rare earth elements and transition metals
09 p1357 A72-22845
- X ray K absorption edges in binary solid solutions of Co, Fe and Ni with localized hole increases
09 p1371 A72-22846
- X ray spectral analysis of Ti-Cu alloys electronic structure
09 p1329 A72-23043
- Electron cyclotron resonance in Penning ion source, measuring electron temperature from X ray emission spectra
10 p1516 A72-25029
- X ray fluorescence spectrometric analysis of carbonaceous chondrites for chemical subgroups
11 p1723 A72-26525
- He-like lines in solar X-ray spectrum observed by Bragg crystal spectrometer, noting absolute wavelengths determination with shaft encoder for angle readout
11 p1714 A72-26572
- X ray spectroscopy - Conference, Ivano-Frankovsk, Ukrainian SSR, February 1971
13 p1972 A72-28488
- Multiplicative factors for energy scale corrections of OSO-3 ion chamber for solar X-ray monitoring
13 p1033 A72-29748
- Equiatomic ordered, bcc TiFe and TiNi electron density in outer energy band from X ray K emission spectra
13 p1981 A72-30006
- Soft X ray appearance potential spectrometer construction and operation for metal film diffusion detection in microcircuit technology
15 p2241 A72-32442
- Stainless steel surface alloy composition characterization as function of vacuum annealing temperature, using proton-induced X rays
15 p2258 A72-32527

Rutile titanium dioxide molecular orbital energy level diagram deduction from X ray emission and absorption band spectra, noting Ti and O states roles 15 p2255 A72-32539

K line of X ray absorption spectra for pure Ti and compounds, discussing effects of valence, microstructure and electron configuration 15 p2259 A72-32700

K and L lines of X ray emission spectra of Ti in alloys with Nb, noting atomic structure change during alloy formation 15 p2259 A72-32701

Mossbauer spectroscopy theory and application to steel technology, discussing spectral characteristics of various iron phases and corrosion and stress effects 16 p2405 A72-32824

X ray photoelectron spectroscopic measurements of Fe and Cu valence states produced by ion sputtering reduction, applying to multiplet splitting and isoelectronic shifts 16 p2389 A72-33026

Semiconductor low-energy X-ray spectrometry 17 p2552 A72-34335

Stratospheric model for bremsstrahlung X ray relation emission to auroral electron flux, considering photon energy release in scintillation counters 17 p2551 A72-35872

Use of X-ray photoelectron spectroscopy to study bonding in Cr, Mn, Fe, and Co compounds. 18 p2657 A72-36568

X-ray spectra and electronic structure of titanium nitrides of limit composition and in the homogeneity range 19 p2821 A72-38406

Recrystallized Al monocrystals applications to optics and X ray spectroscopy, describing preparation methods 21 p3065 A72-40085

Equiatomic ordered bcc TiFe and TiNi electron density in outer energy band from X ray K emission spectra 22 p3190 A72-42733

Interpretation of X-ray emission bands of AlIII-BV compounds 24 p3432 A72-44914

X RAY STRESS ANALYSIS

X ray analysis of internal friction strains in nickel molybdenide during ordering process at 650-700 C, using torsional pendulum method for friction measurements 11 p1662 A72-26654

X RAY STRESS MEASUREMENT

Centroid shift of diffraction line due to X ray diffractometer geometry in stress measurement 04 p0547 A72-14527

Preferred orientation effects on X ray stress measurement of Young modulus and Poisson ratio of Al alloy 06 p0829 A72-17793

X ray and resistance strain gage techniques for bar and metal plate simultaneous residual stress determination 07 p0993 A72-20606

X RAY TELESCOPES

High energy gamma ray telescope based on absorption induced Cerenkov radiation in low density gas, using parabolic mirror for focusing on photomultiplier tubes 03 p0352 A72-13033

Proton bombarded CsI crystal spallation-caused radioactive decay products contribution to background rate in satellite X ray telescope detector 06 p0853 A72-18084

Optical properties of paraboloid-hyperboloid mirror X ray telescopes evaluated by ray tracing method, noting resolution and focal plane curvature approximation 07 p0985 A72-19405

Large grazing incidence X ray telescope mirrors for HEAO-C mission observations, noting single stars resolution in clusters and galaxies study 11 p1630 A72-25682

Solar long term X-ray emitting regions from grazing incidence X ray telescope onboard OSO-4 13 p1033 A72-29744

Extra-atmospheric astronomical studies and instruments, discussing spaceborne, X ray and heavy orbiting telescopes and ground-space radio interferometer designs 16 p2462 A72-33516

Observation of a hard X-ray flare in Cyg X-1. 18 p2721 A72-36649

Galactic X rays investigation with X ray telescope on Lunokhod 1, noting observed singularities connection with statistical distribution of quasars and radio galaxies 19 p2802 A72-38090

An albedo horizon sensor using hybrid circuitry. 21 p3050 A72-40122

Particle, plasma and field detectors for rocket investigations in and above atmosphere, considering PCM telemetry system and balloon-borne X ray telescope system 21 p3057 A72-41617

Precision X-ray telescopes on HEAO-C.

24 p3403 A72-45202

X RAY TESTING

U X RAY INSPECTION

X RAYS

NT SOLAR X-RAYS

Rocket-borne apparatus for X ray measurement in 25 to 200 keV range, noting primary diffuse component and earth albedo spectral analyses 02 p0231 A72-12448

Digital computer automated test equipment and procedures for remote sensors and electronics for scanning celestial sphere for X rays prior to spacecraft launch 02 p0200 A72-12479

Bremsstrahlung X rays from electron precipitation associated with discrete vlf emissions, recording wave-particle experiment near plasmapause with balloon-borne counters in Antarctica 03 p0413 A72-13536

Holographic analysis of periodic microobjects at X ray wavelengths, obtaining high contrast 03 p0360 A72-13669

X ray background model based on photons bremsstrahlung emission by subcosmic metagalactic electrons or protons 03 p0413 A72-13804

Temperature dependence of X ray interference lines for Al-V alloy obtained at high cooling rate, noting metastable solid solution thermal stability 03 p0377 A72-14022

Scintillator crystal system with monitoring streak camera for flash X ray burst time measurements 04 p0523 A72-15482

Background phonon X ray and gamma quanta intensities dependence on solar activity from Geiger counter recordings in deep space 05 p0711 A72-17046

X ray detection on Jupiter with actively collimated balloonborne scintillation counter, noting decametric emission due to electron precipitation 06 p0872 A72-17445

Biological damage inflicted to rats by protons, X rays and gamma rays 06 p0762 A72-17675

Hard X ray emission by thermal plasma, applying relativistic corrections to photon bremsstrahlung Maxwell distribution and cross section 06 p0873 A72-18004

Auroral zone electron precipitation events before and at negative magnetic bays onset, presenting balloon recordings of bremsstrahlung X-rays intensity 06 p0808 A72-18092

Nighttime ionospheric dynamo current modulation due to galactic X ray ionization, observing diurnal sidereal time variation in geomagnetic field 07 p1056 A72-18898

Crab Nebula pulsed X radiation from balloon flights, extracting pulsar profile 07 p1056 A72-19135

Simultaneous auroral X ray, bremsstrahlung and visible bursts observations from balloons. 07 p1058 A72-19166

X ray spectrum and D-D neutrons emission from high temperature plasma produced by two pulsed Nd-glass laser systems 07 p1041 A72-19394

[CLEA PAPER 12.3] Thin films thickness and refraction index calculation from curves of specularly reflected X ray intensity vs grazing angle, obtaining surface roughness variance 07 p1050 A72-20405

Auroral X ray radiation measurements in midnight sector during solar storm of 8 March 1970 08 p1155 A72-20806

High energy electron precipitation events in auroral zone X rays, showing exponential daytime and flat nighttime energy spectra 08 p1226 A72-21110

UK-5 satellite all sky X ray monitor consisting of pinhole camera, position sensitive proportional counter and data processing electronics 08 p1228 A72-21513

Models of galactic diffuse sources of soft cosmic X rays, estimating spectrum and intensity 08 p1228 A72-21650

Nighttime D region ionization production by cosmic X rays from various celestial sources and galactic background 09 p1375 A72-22359

Simple and multiple electronic processes in X and XUV region - Conference, Paris, September 1970 09 p1356 A72-22826

Ultraviolet X ray absorption spectra features of inner atomic shell photoionization in molecules 09 p1356 A72-22827

Optical and inner shell X ray transitions in highly ionized Cu, Fe and Ti observed from point plasma source generated in linear vacuum discharge 09 p1360 A72-22833

X ray emission bands related to K line intensity for iron group transition metals, using orthogonalized plane wave method 09 p1370 A72-22840

Rare earth elements outer electrons X ray and UV photoemission spectra interpretation by multiplet splitting of final state 09 p1371 A72-22844

Al alloys solid binary solution soft X ray emission spectra interpretation by rigid band and virtual band state models 09 p1371 A72-22847

Soft X ray emission spectra from Al-Nb and Al-Pd alloys, deducing electron state density near Al ions 09 p1371 A72-22848

X ray effect from Scorpio XR-1 on lower ionosphere long wave transmissions, considering transit times and field intensity variations 09 p1305 A72-23572

Optical and X ray pulsars, discussing Crab pulsar, emission behavior, pulse intensity, periodicity, polarization properties and antenna emission, plasma maser and Chiu models 10 p1547 A72-24919

Spacecraft-based observations of gamma and X radiation resulting from planetary surface and atmosphere processes to obtain source medium chemical composition 10 p1530 A72-25060

Metallic chromium band structure determination by Green functions method, explaining transition metals X ray emission lines by single electron approach 13 p1972 A72-28489

Cosmic X ray background intensity and spectrum interpretation in terms of metagalactic origin within evolutionary cosmology framework 13 p2030 A72-29087

Circular polarization disputed for Seyfert galaxy NGC 1068, quasar 3C 273 and X ray source Sco X-1 13 p2041 A72-29414

Crab Nebula pulsar X ray radiation pulses at 100-400 keV searched for via balloon flights with NaI detector 13 p2034 A72-29965

X ray flux associated with gravitational radiation pulses, determining upper limit with balloon-borne apparatus 13 p2007 A72-30121

Soft X ray emission for plasma temperature determination in laser induced gas breakdown for air and He 14 p2139 A72-30805

Semiconductor devices application to gamma ray, X ray and nuclear radiations detection and analysis 15 p2235 A72-31644

Background spallation source errors in satellite measurements of diffuse cosmic X ray spectrum with crystal scintillators 15 p2300 A72-31986

Relativistic charged particles produced transition radiation as diffuse cosmic X rays source, discussing validity based on interstellar space energy density consideration 15 p2301 A72-32716

Primary cosmic rays extragalactic origin, considering high energy electrons, background X and gamma rays and cosmic protons 16 p2445 A72-33126

Thermal X ray sources associated with rotating collapsed stars, discussing Scorpio X1 plasma shell heating mechanism 16 p2460 A72-33924

Pulsars radiation mechanism relationship to magnetospheric conditions, considering optical, X ray and gamma radiation 16 p2460 A72-33928

Origin of the low energy diffuse cosmic X-ray flux. 17 p2599 A72-35071

On the contribution of transition radiation from dust grains to the diffuse X-ray background. 17 p2600 A72-35314

X-ray bremsstrahlung in the stratosphere and the auroral activity of January 21 and February 3, 1969 18 p2722 A72-36863

Attenuation of X rays in interstellar space. 19 p2852 A72-38600

Observational evidence against supernovae being the source of the universal X-ray background. 20 p2965 A72-38906

Auroral EUV flux observation by Javelin sounding rocket photometers, comparing with visible and X ray emissions 22 p3171 A72-42417

Sharp focused short pulse X ray source with laser flash synchronization for radiographic plasma diagnostics 24 p3429 A72-45495

X-Y PLOTTERS

Legibility criterion of records from X-Y recorders, applying to Lissajous figures of stationary signals and phase trajectories 06 p0817 A72-18165

Investigation of the UIM-21 coordinate-measuring machine 19 p2802 A72-37988

Computation and automatic drawing of the contour lines of functions of two independent variables 23 p3310 A72-44362

X-14 AIRCRAFT

Model following variable stability system for X-14B VTOL aircraft, discussing hardware design and flight evaluation
[AIAA PAPER 72-96] 05 p0613 A72-16978

X-22 AIRCRAFT

Integrated airborne-ground based instrumentation system for variable stability X-22A aircraft flying qualities research, discussing telemetry, mobile van, landing aids and airplane design 16 p2348 A72-33628

An integrated system of airborne and ground-based instrumentation for flying qualities research with the X-22A airplane.
[AHS PREPRINT 654] 17 p2536 A72-34486

An experimental investigation of STOL longitudinal flying qualities in the landing approach using the variable stability X-22A aircraft.
[AHS PREPRINT 642] 17 p2490 A72-34502

XANTHINES

NT GUANINES

NT URIC ACID

Mechanical vibration induced physiological changes in rats, determining plasma Ca, Mg and inorganic phosphate concentration and xanthine oxidase activity response to frequency and g-levels 13 p1910 A72-29560

Studies of the influence of theophylline on the vasodilating action of different medications on the cerebral and coronary circulation of man 18 p2651 A72-36799

XENON

NT XENON ISOTOPES

Hibonite /Ca-Al-Ti rich xenoliths/ from Leoville and Allende polymict brecciated HL group chondritic meteorites 01 p0125 A72-10067

Continuously burning optical discharge in Ar and Xe at atmospheric pressures, evaluating laser beam energy absorption, electron density and plasma temperature 05 p0669 A72-16679

Time behavior and spectra of relaxation oscillations in high gain IR xenon laser 07 p1001 A72-19199

High gain xenon laser spectral narrowing dependence on line-broadening mechanism including saturation and distributed loss effects 07 p1001 A72-19201

High repetition rate pulsed IR xenon laser using transversely excited discharge 07 p1003 A72-19221

Schlieren cinematographic and holographic diagnostic of giant pulse ruby laser produced plasma in Xe [CLEA PAPER 12,2] 07 p1040 A72-19393

Transverse mode effects on gain and dispersion focusing in high gain Xe laser [AD-739448] 07 p1005 A72-19409

Third harmonic radiation generation in phase matched mixture of Rb vapor and Xe, observing non-linear susceptibility [AD-739764] 08 p1211 A72-21197

Xenon plasma produced in cascaded arcs, investigating spectral line widths, temperature and electron density profiles, transition probabilities and I-V characteristics 09 p1364 A72-23392

Radiation efficiency of electric power-energy conversion during pulsed discharge in Xe tube 11 p1651 A72-26364

Stimulated laser emission in vacuum UV by liquid Xe excitation with electron beam, determining threshold current density, radiation divergence and line half width 12 p1820 A72-27582

Xenon filled coaxial pulse tube for pumping organic dye solutions, obtaining intensive light flashes 13 p1971 A72-29923

Radioisotope camera based on electron avalanche in liquid Xe, noting spatial and energy resolution advantages over existing gamma ray cameras 15 p2234 A72-31537

Electrical conductivity of shock wave produced Xe plasma measured by probe, noting dependence on Mach number 15 p2284 A72-31583

High gain CW He-Xe laser transitions due to Xe 5d level long-lived decaying emission 15 p2250 A72-32301

Continuously burning optical discharge in Ar and Xe at atmospheric pressures, evaluating laser beam energy absorption, electron density and plasma temperature 16 p2402 A72-33691

Radiation efficiency of electric power-energy conversion during pulsed discharge in Xe tube 16 p2403 A72-33716

Laser action on unclassified xenon transitions in a highly ionized plasma. 21 p3089 A72-40242

XENON COMPOUNDS

A note on the biological activity of the noble gas compound xenon trioxide. 18 p2652 A72-36444

XENON ISOTOPES

Pu-244 fission Xe isotopic composition parameters in achondrite meteorites, using lunar spallation systematics 01 p0124 A72-10058

Apollo 12 lunar igneous rocks 12004, 12040, 12051 and 12053, obtaining Kr 78/Kr 83 and Xe 131/Xe 126 spallation component ratios correlation line 01 p0124 A72-10065

Excess Xe 131 in lunar Ba feldspar rocks, discussing results of reactor irradiation experiments with fast and epithermal neutrons 03 p0414 A72-12901

Xe and Kr abundance and isotopic composition in silicate inclusions of iron meteorites 03 p0435 A72-13690

Xe and Kr mass fractionation and isotopic anomalies in ordinary chondrites, analyzing meteorite samples by mass spectrometry 07 p1084 A72-20497

Anomalous high concentration of lunar rock Xe-131 relation to Ba-130 nonthermal neutron-capture cross section in resonance energy region 20 p2967 A72-39180

Xenon isotope fission component due to extinct Pu-244 in lunar breccia, noting storage details in terms of crustal material dating 20 p2967 A72-39182

XENON LAMPS

Integration sphere facility with water cooled long arc xenon sources for pyranometer calibration, discussing operation theory and system design 22 p3163 A72-42692

XENON 133

Myocardial blood flow measurement value in ischemic heart disease assessment, discussing Xenon 133 injection into coronary arteries 03 p0315 A72-13179

Xenon 133 method for coronary blood flow measurement during exercise, noting unsuitability for patients with coronary disease 03 p0319 A72-13180

Xenon 133 myocardial clearance method accuracy and reliability in determining high and low left coronary artery blood flow under different hemodynamic conditions 03 p0319 A72-13181

Myocardial blood flow measurement by Xe 133 clearance method after direct application of isotope into subendocardial and subepicardial layers of left ventricle 03 p0315 A72-13182

Blood flow stratification effect on alveolar gas exchange in liquid filled lungs in dogs from Xe 133 concentration measurements 10 p1425 A72-24481

Coronary flow determination in experimental conditions with the use of radioactive xenon. 19 p2755 A72-37475

XV-5 AIRCRAFT

Turbolift lift fan design developed for XV-5 VTOL research aircraft, reviewing changes for future commercial and research transport systems [ASME PAPER 72-GT-111] 11 p1576 A72-25674

XYLENE

Morphology of poly-p-xylylene crystallized during polymerization from X ray measurements, electron and optical microscopy and differential thermal analysis 02 p0247 A72-11465

Crystal structure of alpha poly-p-xylylene films from electron microscopy and diffraction and X ray scattering 02 p0248 A72-11466

Alkyl substituent effects on gas phase acidities of toluene, p-xylene and acetylenes, using ion cyclotron resonance spectroscopy 07 p0936 A72-19494

Y

Y AXIS

U COORDINATES

YAG [GARNET]

U YTTRIUM-ALUMINUM GARNET

YAG LASERS

Welding with a CW YAG laser beam 17 p2563 A72-35181

Q switched Nd-YAG laser with lithium niobate crystal cut at Brewster angle for reproducible and controllable giant pulse generation 20 p2933 A72-39562

Unidirectional single frequency traveling wave CW pumped Nd-YAG ring laser, noting spatial hole burning elimination 22 p3185 A72-42614

Fluorescent organic dyes solutions for Nd:YAG laser output performance improvement 23 p3297 A72-44191

Theory of pulsed internal optical parametric oscillators. 24 p3409 A72-44714

A new method of optical coupling of two laser cavities which permits stable generation of ultrashort optical pulses 24 p3410 A72-45075

Angular spectra and frequency characteristics of quasi-continuous monomode and two mode Nd-YAG lasers with spherical resonator 24 p3412 A72-45707

YAGI ANTENNAS

Propagating waves characteristics measurement on Yagi-Uda array, obtaining k-beta diagrams and phase velocities 01 p0043 A72-11244

Dipole theory application to directional characteristics of Yagi antenna systems, assuming harmonic current distribution along radiating elements 02 p0193 A72-12221

Yagi antenna radiation pattern parameters optimization for maximum directional gain, minimum sidelobe and optimal slope curvature 07 p0952 A72-18852

Yagi-Uda helical antenna array with moderate gain and compact mechanical design, determining electrical characteristics 19 p2773 A72-37941

Bubnov-Galerkin solutions to wire-antenna problems. 21 p3032 A72-40631

YARNS

Webbing joints stitching strain, considering nylon and flax yarns stretching properties and various stitching patterns strengths 01 p0005 A72-10315

YAW

Aircraft pitching and yawing cross couplings compensation at high speed 01 p0005 A72-10506

Yaw calibrations of Preston tubes for wall shear stress measurements in two and three dimensional turbulent boundary layers 08 p1254 A72-21627

Airplane sideslip and yaw rate perturbations by continuous random vertical and side gusts, using low pass filtered white noise representation for mathematical modeling 12 p1755 A72-28125

Angular oscillation in yaw effect of pilot visual performance, showing vestibulo-ocular compensation and frequency response 12 p1774 A72-28269

Three stage linear damping of satellite roll and yaw oscillations, using slip motion procedure 15 p2319 A72-31492

Congruent and spurious motion in the learning and performance of a compensatory tracking task. 17 p2510 A72-35692

Full-scale inlet/engine testing at high maneuvering angles at transonic velocities. 21 p3042 A72-41604

The characteristics of a cylindrical probe at high subsonic speeds. I - The case of zero inclination angle. 22 p3135 A72-42484

The wedge probe - A review. 24 p3404 A72-45355

YAWING MOMENTS

Direct side force control by rudder deflection and asymmetrical drag utilization to cancel yawing moment, discussing variable stability T-33 flight tests [AIAA PAPER 72-94] 05 p0613 A72-16946

Hovercraft internal and external aerodynamic forces, discussing control, suspension, yawing moments, directional and roll stability and random surface performances 09 p1260 A72-22824

Occurrence and inhibition of large yawing moments during high-incidence flight of slender missile configurations. [AIAA PAPER 72-968] 24 p3364 A72-45411

YAWMETERS

U ATTITUDE INDICATORS

U YAW

YEAST

Yeast glycolytic pathway oscillations relation to concentration of diphosphopyridine nucleotide and other metabolites, noting analogy to biochemical and physiological rhythms 07 p0920 A72-19541

Influence of Cosmos 368 space flight conditions on radiation effects in yeasts, hydrogen bacteria and seeds of lettuce and pea. 23 p3254 A72-43390

YIELD

Generalized quantum yield for sensitivity of photoelectric devices, considering multistage image converter and photomultiplier 02 p0223 A72-11411

Computational technique for crack growth prediction in metal subjected to variable amplitude cyclic loading, taking into account yield zone ahead of crack tip [ASME PAPER 71-MET-X] 11 p1735 A72-25876

Bauschinger effect analysis based on yield theory, noting effects of stress relaxation and isotropic dehardening 16 p2471 A72-33786

YIELD POINT

Torsional prestrain effects on 1100-F Al alloy thin walled tubes yield locus, calculating distortion degree by statistical characteristics

Polycarbonate yield locus from strain rate, creep, isotropy, isoclinic and reloading tests on perforated plates
[SESA PAPER 1819]

Rigid plastic circular plate dynamic model with yield time delay, discussing residual deflection as function of load duration

Yield relationship to coupling of plastic waves, obtaining stress-strain diagrams

Empirical power law application to secondary creep, steady state hot working and high temperature tensile or compressive yielding, discussing activation parameters interrelations

Tubular and rod extruded age hardenable Al alloys, determining mechanical anisotropic properties from yield loci and r values

Yield stress effects at high strain rate on finite crack unsteady motion

Grain size effect on age hardened Mg-Zn alloy yield and flow stress, using tensile test and electron and optical microscopy at various temperatures

Yield stress of solid solution iron and Fe-Ge alloys with bcc structure, obtaining interaction energy between solute atoms and screw dislocation

Yield point elongated and strain hardened rectangular plates, calculating plastic coefficients in geometrically nonlinear bending problem

Foundry Al alloys elasticity limit estimation via regression formulas, discussing application to quality control

Safe stressing of high strength and locally nonbrittle solid bodies, testing hard polymers at room temperature

Metastable Fe-Cr-Ni austenitic stainless steels, demonstrating test phenomenon at elastic limit

Plastic deformation fatigue theory extended to tests at stresses below elastic limit, explaining cyclic loading frequency effect on fatigue life

Interaction surfaces for structural members under combined axial, shear force and bending moment, investigating shear effect on yielding of arches

Moment stresses and deflections of rigidly clamped hinged and simply supported square elastic plates beyond elastic limit, deriving equilibrium and strain compatibility equations

Elastic rods and rings stability under compression beyond elasticity limit, determining equilibrium branching characteristics near bifurcation point

Strain rate effects on strain hardening of duralumin, copper and lead, noting yield stress sensitivity to deformation induced temperature changes

Metals cold working mechanics about stress state and yield points, proposing theoretical model for mechanism and applications in extrusion molding, drawing and hollow forging

Biaxial tension and combined tension-torsion induced initial yield surfaces and plastic deformation onset, using localized strain theory

Anisotropic plate theory for perfectly plastic flow, expressing yield condition in terms of mixed stress-anisotropy tensors

Loading path effect on yield surfaces of pure Al at elevated temperatures under tension

Anomalous structural dependence of elastic limit in Mo, determining mechanisms responsible for deviations from Petch law

Plastic compression of short cylinders prepared from incompressible rigid-plastic material with variable vertical yield point distribution, deriving variational equation of plastic flow

Polycrystalline Mo fatigue behavior under cyclic stresses, discussing grain size effect on fatigue life and relationship between cycle dependent yield and French damage line

Stepwise compression loading effect on yield stress of carbon and alloy steels in cylindrical samples with end plane cylindrical notches filled with solid lubricant

Mathematical model for dynamic yield point dependence in strain rate based on similarity and dimensionality theories and Weierstrass theorem

Fatigue crack growth rate in precracked steel samples observed at 100 C by etching technique, noting flow stress and yield in plastic zone

Carrying capacity of rigidly hinged shell of revolution with concentric reinforcing rib, applying to shallow spherical shell under uniform external pressure

CdTe single crystals photoplastic characteristics, detailing illumination effect on yield stress and resistivity

Metal specimens yield point in adiabatic tension determined by thermoelectric method from temperature-stress and stress-strain diagrams

Elastic-plastic medium yield zone spread from penny shaped crack determined from continuous distribution of dislocations, noting system energy change

Error analysis of dynamic yield point measurements based on residual deformation from impact tests of Al alloy and steel specimens

Permanent traction and torsion strains effect on ratio between pure compression and pure traction yield points of Al alloy

Effects of yielding and size upon fracture of plates and pressure cylinders.

Differences in the creep characteristics at room temperature of steels with and without distinct yield point

Plastic buckling theory, presenting yield surfaces in tension-torsion stress space for pure aluminum

Creep delay in low-carbon steel at room temperature

The influence of the surface orientation on yield in Mo single crystals.

Anisotropy and hydrostatic stress effects on yield criteria of nonwork-hardening plastic material under plane strain conditions

An experimental investigation of yield surfaces at elevated temperatures.

Constant strength shells theory generalization from axially symmetric to nonsymmetric case, using Von Mises yield condition

Transverse shear effect on thin shells collapse load, considering influence on Shapiro yield surfaces

On basic principles of the slip theory of plasticity.

Equilibrium equations for given stress concentration in circular and annular plates under tensile loads with different yield points in tension and compression

Analysis of the mechanisms of yield-stress variation during compacting of metal-ceramic materials by rolling

The effect of pre-strain on the yield behavior of vanadium.

YIELD STRENGTH

Yield-fracture criterion for angle ply laminate cylinders wound with filament in biaxial tension

Analytic yield surface in work hardening including stress in transition range after load change /Bauschinger effect/

Mg-Zn alloys precipitation hardening mechanism at various aging stages, considering yield strength increase due to interface dislocations

Waspaloy sheet creep rupture time dependent sensitivity to sharp-edged notches at 1000-1400 deg F, optimizing smooth and notched specimen yield strengths [ASME PAPER 71-WA/MET-3]

Oxygen and/or nitrogen interstitial solute pick-up effects on yield stress during Nb annealing, discussing Hall-Petch plot parameter values

Dynamic yielding of annealed and cold worked Fe-Ti alloy determined in shock compression tests

Mn additions effects on austenitic stainless steels yield strength, work hardening characteristics, corrosion resistance and machinability

High pressure hydrogen effects on austenitic stainless steel embrittlement, determining yield, tensile and fracture strength

Ti-Al-V alloy biaxial yield strength improvement by combined texture and age hardening, using hydroburst tests

Austenitic stainless steel with improved corrosion resistance, yield strength and hot workability

Jerky flow /serrated yielding/ in Co-Ni-Cr-C fcc alloys during tensile testing, noting no correlation to dislocation-precipitate interactions

Solid solution yield strengthening and weakening of V-Ti alloys, investigating strain rate sensitivity temperature dependence as indication of two deformation mechanisms

Strength and strain theory statistical analysis for perfectly brittle and plastic materials, assuming ultimate or elastic limit strain as governing factor

Polycarbonate yield dependence on temperature in uniaxial compression and tensile tests described by modification of Eyring theory of non-Newtonian viscosity

Von Mises yield criterion extended to thin walled circular cylinder plastic torsional straining, noting variations of anisotropic parameters and yield stresses with shear strain
[ASME PAPER 71-MFT-Y]

Upper yield stress effect on elastoplastic behavior of mild steel in bending and torsion, noting relationship to strain rate

Fatigue properties of Ni-Al-W alloy with gamma-prime matrix, noting high endurance limit/yield strength ratio at room temperature

High temperature Ni base alloys microstructure via transmission electron microscopy and electron diffraction contrast theory, predicting yield and creep strength

Microstructure effects on thermomechanically processed dispersion strengthened Ni alloys yield strength at various temperatures

Prestraining effect on metal fatigue strength, showing increase relation to yield strength and ultimate strength

Yield conditions formulation restrictions for large elastoplastic deformations, discussing isotropic and anisotropic hardening

Aircraft gas turbine engine Ni base alloy disks and shafts thermomechanical treatment, considering yield strength and high and low cycle fatigue resistance

Plane strain fracture toughness tests of compact thick maraging steel specimens at various yield strength levels as function of aging

Precipitation hardening effects on yield strength, toughness and ductile to brittle transition temperature of low alloy steels containing Nb

Plastic flow, yield strength and fracture of unidirectional Al-B fiber composite sheet under biaxial tension

Initial yield surface of a unidirectionally reinforced composite.

Magnesium aluminate spinel reinforced with sapphire whiskers, investigating whisker content, temperature and deflection rate effects on yield strength

Yielding of fiber reinforced Trecsa material.

Thermo-hypo-elasticity and derived fracture and yield conditions.

The influence of interstitial nitrogen on the asymmetry of the yield stress of tantalum.

Tensile and compressive stress coarsening effects on coherent gamma prime precipitate yield strength of Ni-base superalloy single crystals

Yielding and fracture of D16T alloy at low temperatures under conditions of complex stress-strain state

Limit analysis and plastic design of structural elements of complex shape.

Effects of hydrostatic stress on the yielding of cold rolled metals and fiber-reinforced composites.

Heat treatment effects in multipass weldments of a high-strength steel.

YIG [GARNET]
Y YTTRIUM-IRON GARNET
YOUNG MODULUS
U MODULUS OF ELASTICITY

YTTERBIUM

Yb and Er cations dominant sites examination in zinc selenide from fluorescence emission spectra
03 p0404 A72-14265

YTTERBIUM COMPOUNDS

Phase diagrams of yttrium, erbium and ytterbium oxides at 1500-2400 C, using annealing and quenching method with differential thermal analysis
07 p1047 A72-18858

YTTRIUM

Ni-Al alloy, investigating Y addition effect on vacancy agglomeration suppression during oxidation
06 p0829 A72-17787

Isolation and sintering techniques and thermoelectric properties of lanthanum, yttrium and gadolinium borides
11 p1645 A72-26858

Co-Cr alloy high temperature oxidation kinetics reduction by Y addition, presenting metallographic study
14 p2118 A72-30543

Y and La action on oxidation rates of Cr and Mo at high temperature in air
15 p2252 A72-31191

Oxygen monolayer amounts adsorption on yttrium films and molybdenum foil investigated by Auger electron spectroscopy, observing growth of shifted peaks
15 p2292 A72-31860

Exploratory investigation of Y, La, and Hf coatings for nitridation protection of chromium alloys.
20 p2944 A72-39290

A differential spectrophotometric extraction method of determining yttrium-subgroup rare-earth elements (REE) in complex objects
23 p3324 A72-44164

YTTRIUM ALLOYS

Y-Mn-Al ternary alloy solid solution phase diagram isothermal section construction from X ray structural data
03 p0376 A72-13945

Y-Fe-Al alloys ternary system X ray structural analysis after arc furnace preparation, annealing and quench hardening
07 p1048 A72-19681

Thermal and microstructural analysis of phase interactions in Mg alloys of Mg-Nd-Y system
14 p2124 A72-31028

Yttrium alloys isoperiodic lines, solidus isotherms, equal hardness lines and resistivity presented diagrammatically
15 p2289 A72-31185

Deformable magnesium alloys with scandium and yttrium
22 p3192 A72-42820

Stress-strain diagrams from high and low temperature tests of Y alloy rods, noting temperature effects on plastic deformation
24 p3413 A72-44724

YTTRIUM COMPOUNDS

NT YTTRIUM OXIDES

NT YTTRIUM-ALUMINUM GARNET

NT YTTRIUM-IRON GARNET

Cooperative and sequential sensitization effect on He emissive states population in polycrystalline barium and yttrium fluorides with trivalent Yb
10 p1525 A72-24044

Spectroscopic and stimulated emissive properties of neodymium ions in potassium yttrium tungstate crystals at 77 and 300 K
11 p1701 A72-26362

X ray diffraction discovery of borides with yttrium chromium boride type orthorhombic structure
13 p1984 A72-29799

Lasing properties of yttrium orthoaluminate doped with rare-earth metals
22 p3187 A72-42943

YTTRIUM OXIDES

Phase diagrams of yttrium, erbium and ytterbium oxides at 1500-2400 C, using annealing and quenching method with differential thermal analysis
07 p1047 A72-18858

Yttria stabilized hafnia based graphite and tungsten composites, investigating factors affecting thermal shock resistance
09 p1327 A72-22385

Emissivity and electrical resistivity of tungsten-yttrium oxide cermets as function of composition at 1200-3200 K
19 p2819 A72-38286

YTTRIUM-ALUMINUM GARNET

Pinched vortex tube high current arc discharges for continuous pumping of ion crystal YAG-Nd lasers
06 p0825 A72-17839

Ho doped YLF and YAG laser threshold and slope characteristics at room temperature, considering Q-switched operation lifetime
07 p1004 A72-19233

Continuous TEM power from single longitudinal mode Nd-YAG laser pumped with tungsten-iodine lamp
07 p1004 A72-19235

Pumping conditions relationship to tube filling in Nd-YAG pulsed laser
11 p1649 A72-26344

Angular spectra and frequency characteristics of quasi-continuous monomode and two mode Nd-YAG lasers with spherical resonator
12 p1819 A72-27054

Nd-YAG laser bibliography covering oscillation, dynamics, engineering, materials and harmonic generation
12 p1826 A72-27957

High power CW Nd-YAG laser efficiency improvement by optical pump wavelength, power coupling and balance factors, noting krypton arc lamp contribution
15 p2247 A72-32029

Spiking response of luminescent diode pumped CW Nd-YAG laser to sinusoidal modulation, showing agreement with relaxation oscillation resonance prediction
15 p2250 A72-32526

Output fluctuations of CW-pumped Nd-YAG lasers.
17 p2564 A72-35345

Radio luminescence of an yttrium-aluminum garnet activated by rare-earth elements
19 p2845 A72-38181

Harmonic mode locking of the Nd:YAG laser.
19 p2813 A72-38688

Influence of gas pressure in arc lamps on the pumping efficiency of CW garnet lasers.
20 p2933 A72-39513

YTTRIUM-IRON GARNET

Transient response of solid state YIG crystal dispersion filter, noting application to main radar bang generation with intrapulse frequency modulation
03 p0337 A72-14379

YIG tuning of X band Gunn effect stripline oscillator circuit, noting application to microwave ICs
07 p0955 A72-19357

Optimal location of nonreciprocal disk shaped YIG element traveling wave quantum ruby paramagnetic amplifier for weak magnetic levels
08 p1138 A72-20795

YIG-tuned microwave transistor oscillator design and performance, considering resonance phenomena and magnetic circuit effects on applications
08 p1139 A72-20985

Mossbauer gamma radiation diffraction by Y-Fe garnet crystals with Mossbauer nuclei in magnetic and electric field nodes
08 p1217 A72-21767

Bulk effect diodes combination with YIG elements to provide oscillator operation up to 18 GHz, discussing design, circuit diagrams and performance
10 p1448 A72-24037

YIG tuned Gunn oscillator phase locking and shifting over 3 GHz range in X band, using feedback control
10 p1451 A72-24596

Investigation method for shock wave induced demagnetization in YIG, noting impact study of magnetic properties
13 p1959 A72-29757

Microwave pulse frequency shift and frequency modulation in YIG bar magnetostatic delay line with adiabatically varying parameters
13 p1923 A72-30095

Epitaxial YIG film separated from conductive plane by thin dielectric layer, considering magnetostatic propagation dispersion and insertion loss
15 p2294 A72-32502

YIG filter banks for ECM and communications.
19 p2772 A72-37523

Investigation of the viscosity and density of solution melts intended for growing yttrium-iron garnet /YIG/ single crystals
19 p2847 A72-38684

Diffraction of a laser beam by domains in yttrium iron garnet.
20 p2933 A72-39521

Parallel pumping of spin waves in yttrium garnet single crystals
21 p3096 A72-40413

Measurement of internal magnetic field distribution in axially magnetized YIG rods based on magnetoelastic resonance absorption.
21 p3097 A72-40692

Z

Z AXIS

U COORDINATES

Z TRANSFORM

U LAPLACE TRANSFORMATION

ZEEMAN EFFECT

Prominent Zeeman multiplets in photosphere, penumbra, umbra and sunspot spectra, presenting ratios for temperature sensitivity measurements
03 p0415 A72-12933

Pressure scanning Fabry-Perot magnetometer using KDP crystal and Glan-Thompson prism with echelle interferometer spectrograph for polarized Zeeman components
03 p0356 A72-13283

Sacramento Peak magnetograph, discussing modified Doppler-Zeeman analyzer for separate measurements of circularly polarized line displacement
03 p0356 A72-13284

Telescopic phase retardation effect on Zeeman triplet Fe of polar sunspot umbrae in Stokes parameter measurements
03 p0357 A72-13288

Coherence properties of polarized radiation in weak magnetic fields, considering scattering redistribution for normal Zeeman triplet
03 p0427 A72-13292

Magnetographic observations of magnetic fields in quiescent solar prominences, using Zeeman effect on H, He, and metal lines
03 p0428 A72-13298

Zeeman spectroheliograms of photospheric magnetic fields in Ca I 6102.7 Å line
03 p0430 A72-13317

Microwave-range optical heterodyne system with magnetically tuned /Zeeman effect/ laser emissions mixing and AFC
05 p0668 A72-16345

Zeeman patterns and energy level Lande g factors from spectrograms of As ion electrodeless discharge tubes in presence of 24,025 G magnetic field
07 p0987 A72-19832

Magnetic field effect on gain saturation in CW Ar laser associated with Zeeman splitting
08 p1184 A72-22036

Light polarization in anisotropic Zeeman laser under axial magnetic field
10 p1491 A72-24134

Relativistic Zeeman-Stark effect on molecular jet due to molecular translational motion in continuous magnetic field
10 p1514 A72-24135

Zeeman effects in hyperfine structure of atomic iodine photodissociation laser emission, noting magnetic fields effect on time behavior
11 p1692 A72-26558

Zeeman triplet with unsplit upper level formation in isothermal atmosphere under magnetic field, considering Doppler and Lorentz frequency profiles of transitions
15 p2304 A72-31332

Magnetic dipole matrix elements for atomic transitions between Zeeman levels at microwave frequencies
17 p2585 A72-35769

Theoretical study of the Zeeman spectrum and of the magnetic resonance in the evanescent wave of Fresnel - Case of the magnetic transverse mode
19 p2834 A72-37790

Magneto-optic effects in Fraunhofer lines with Zeeman splitting
19 p2835 A72-38495

The treatment of the Stokes parameters and measurement of magnetic field.
20 p2970 A72-39755

Line spectra and continuum polarization in magnetic white dwarfs.
20 p2971 A72-39760

Investigations on spectroscopy by nonlinear Zeeman-resonances of a multimode laser.
20 p2934 A72-39845

Magnetic-field variations in 78 Virginis, beta Coronae Borealis, and 73 Draconis.
21 p3106 A72-41036

Coexisting weak and strong opposite-polarity magnetic field regions as cause of sunspot umbra Zeeman spectra pi-component splitting
21 p3108 A72-41283

ZENER DIODES

U AVALANCHE DIODES

ZENER EFFECT

Zener diode surface and bulk breakdown mechanisms by scanning electron microscopy, discussing microplasma noise
03 p0336 A72-14289

Electrical measurements on capillary-fed colloid thruster with Zener diode-like I-V characteristic and constant propellant mass flow rate
04 p0565 A72-15204

Electrical breakdown in reverse biased semiconductor p-n junctions involving Zener effect and avalanche mechanisms
07 p1048 A72-19821

Installation of a production line for high-reliability silicon diodes - Results obtained: Application of the underlying principles to more complex components
18 p2670 A72-37121

ZENITH

Geocoronal hydrogen Lyman alpha glow intensity and zenith angle dependence from observations by rocket-borne extreme UV photometers
09 p1298 A72-22593

Extensive air showers at zenith, measuring associated UHF radio pulses with optical Cerenkov emission receiver as trigger source
14 p2147 A72-30858

Circumzenithal instrument for latitude and longitude determination and star transits observation through almcantar
15 p2238 A72-32122

- Investigation of the Talcott levels of zenith telescopes and determination of their division value
19 p2802 A72-37980
- ZERO ANGLE OF ATTACK**
Laminar two dimensional hypersonic flow over stepwise accelerated flat plate at zero angle of attack, obtaining time dependent velocity and temperature profiles by linearized flow equations
03 p0442 A72-13236
Navier-Stokes equations numerical solution for laminar incompressible flow past paraboloid of revolution at zero angle of attack
[AIAA PAPER 72-110] 05 p0604 A72-16818
Laminar viscous flow past semiinfinite flat plate at zero incidence, using Oseen approximation in matching leading edge and potential flow regions
11 p1615 A72-25522
German monograph on plane steady isentropic flow past obtuse apex angle wedge at zero angle of attack and free stream sonic velocity
16 p2343 A72-33400
Closed form solution to conical inviscid hypersonic flow over circular cone at zero angle of attack
17 p2486 A72-35433
The characteristics of a cylindrical probe at high subsonic speeds. I - The case of zero inclination angle.
22 p3135 A72-42484
Spin response of symmetric ablating vehicle at zero angle of attack, noting spin-up by ablation-induced grooving and spin-down by crosshatching effects
24 p3362 A72-45339
- ZERO CROSSINGS**
U ROOTS OF EQUATIONS
- ZERO GRAVITY**
U WEIGHTLESSNESS
- ZERO LIFT**
Experimental results regarding drag in supersonic flow without lift in the case of flight bodies with three in front pointed bodies
[DFVLR-SONDDR-215] 19 p2747 A72-38686
- ZERO-ZERO WEATHER**
U CEILINGS [METEOROLOGY]
U WEATHER
- ZINC**
Copper, zinc and aluminum mechanical properties comparison by cyclic and steady state compressive load tests, noting stress-strain curve relationship to strain rate
08 p1188 A72-21921
Elastoplastic deformation of Zn single crystals under uniaxial tensile loads, noting critical stresses relationship to current pulses
10 p1553 A72-23766
Electric current pulses effect on Zn monocrystals plastic deformation before brittle rupture, noting critical normal stresses increase
14 p2115 A72-30411
Zn concentration in chromatoid bodies of ribosome crystals in Entamoeba invadens, using absorption spectroscopy, electron microprobe and dithizone staining techniques
15 p2186 A72-31725
Boltzmann-Matano analysis of substitutional interstitial diffusion profiles of Zn in GaAs by radio tracer techniques
16 p2441 A72-33209
Superconducting energy gaps and transition temperatures of disordered cadmium and zinc films.
19 p2844 A72-37690
L-S coupling interpretation of high-resolution LMM Auger spectra of Cu and Zn.
19 p2846 A72-38597
Condensed zinc particle size determined by a time discrete sampling apparatus.
20 p2913 A72-39608
GaP /Zn-O/ diodes light emission efficiency increase by forward bias, relating to precipitation in n and p layers
22 p3159 A72-42613
Deformation mechanism of aluminum and zinc single crystals during low-temperature cavitation
22 p3192 A72-43019
Simultaneous neutron-activation analyses of scandium, cobalt, iron, and zinc in biological objects with the aid of a total-absorption gamma spectrometer
23 p3259 A72-43347
- ZINC ALLOYS**
German monograph on Zn and Zn-Cu-Ti-Al alloy creep resistance under high loads covering grain boundary precipitation, rotation-shear hole and annealing
04 p0535 A72-15697
German monograph on transition elements Cr, Mn and Zr influence on Al-Zn-Mg alloys stress corrosion covering electron microscope studies and loop-bending tests
10 p1493 A72-23769
Stress corrosion crack paths in Al-Zn-Mg alloys, showing normal coincidence with grain boundaries
11 p1652 A72-25289
Zn, Ge and P based semiconductor alloy specimens chemical composition determination via ac polarograms
12 p1854 A72-27443

- Electron microprobe analysis of solute segregation near grain boundaries in Al-Zn-Mg alloy after quenching and aging heat treatment
13 p1973 A72-28652
Crystal lattice defects induced by cyclic straining in quenched Al-Zn alloy, noting fatigue effects on dislocations accumulation and grain boundary migration
14 p2120 A72-30610
Al-Zn-Mg-Cu forgings fracture toughness increase with Fe content reduction, discussing overload fracture following grain and stringers
16 p2405 A72-33000
Discontinuous precipitation and site nucleation in quenched and aged Al based Zn alloys as function of temperature
16 p2410 A72-33812
Hydrogen solubility in Zr-Nb-H systems as function of composition, temperature and hydrogen equilibrium pressure
16 p2410 A72-33816
New observations of preprecipitation phenomena in Al-Mg and Al-Mg-Zn alloys
17 p2566 A72-34286
Graphite content effect on vibration damping properties of Al-Sn and Al-Zn alloys
21 p3070 A72-41358
Cyclic hardening of Al-Zn single crystals at constant plastic strain amplitude, observing similarity between fatigue hardening and work hardening
22 p3189 A72-42439
- ZINC COATINGS**
High speed photographic analysis of spot welding galvanized steel, observing three stage process
13 p1958 A72-29421
- ZINC COMPOUNDS**
NT WURTZITE
NT ZINC OXIDES
NT ZINC SELENIDES
NT ZINC SULFIDES
NT ZINC TELLURIDES
NT ZINCBLLENDE
Zinc dithiophosphate and bisphenol effects on surface activation of additive compositions with succinimide base in lubricant applications
07 p1023 A72-19903
Solid lubricant additives effects in oils and fats, discussing molybdenum disulfide and zinc pyrophosphate solid film formation on metal surfaces under contact friction conditions
07 p1024 A72-20395
Comparative evaluation of zinc borate 2:3:3.5 with antimony oxide using various fire testing methods.
20 p2898 A72-39699
- ZINC OXIDES**
Zinc oxide longitudinal acoustic microwave transducer, measuring untuned insertion loss and electroacoustic coupling constant
01 p0042 A72-10705
Radiation damage in MgO, ZnO and magnesium difluoride, considering energy dependence and roles of radiolysis and elastic collisions
03 p0404 A72-14088
Photochemical electron transfer evolution models, noting titanium and zinc oxides as photosensitizers
04 p0484 A72-14777
Ultrasonic delay lines design and construction for 100-2000 MHz using evaporated CdS on sapphire and quartz and sputtered ZnO transducers
05 p0626 A72-16010
Photoelectrically excited electrons diffusion and dc effect in ZnO single crystals, calculating drift mobility and lifetime product
05 p0667 A72-16158
Zinc oxide as refractory material, discussing optical, elastic and electro- and photoconductivity properties
10 p1501 A72-24732
Vehicle components oxidation in thermal control coatings, investigating resistance to oxidation by UV photoproduced ZnO electronic holes
[AIAA PAPER 72-264] 11 p1699 A72-25207
Zinc oxide effect on alumina dispersion, energy of formation, nucleation and particle size reduction, calculating critical nucleus radii
16 p2476 A72-33255
Photoemission studies of wurtzite zinc oxide.
24 p3432 A72-45387
- ZINC SELENIDES**
Yb and Er cations dominant sites examination in zinc selenide from fluorescence emission spectra
03 p0404 A72-14265
Heterojunction p-GaAs-n-ZnSe diodes electrical and photovoltaic properties, showing space charge limited current effects
11 p1606 A72-26624
Room temperature time of flight electron and hole mobility and trapping time measurements in zinc selenides as function of electric field
12 p1855 A72-27835
- ZINC SULFIDES**
NT WURTZITE
NT ZINCBLLENDE
Optical quenching of the Gudden-Pohl effect in zinc sulfide lumiphors and IR photography
21 p3057 A72-41680

ZINC TELLURIDES

- Recrystallization effects on thin ZnTe film structure, electrical and optical properties
09 p1367 A72-22421
Investigation of resistance strain gauges based on zinc telluride and cadmium telluride semiconductor films
19 p2845 A72-38206

ZINC-OXYGEN BATTERIES

- Metal-air fuel cell systems characteristics, noting electrochemical processes in zinc-air systems
16 p2352 A72-33897

ZINCBLLENDE

- Zincblende ternary and quaternary alloy systems, calculating charge distribution in space by pseudopotential approach
03 p0404 A72-14261
Mixed zincblende ternary and quaternary alloys, comparing empirical pseudopotential and dielectric model methods for energy gap calculation
03 p0404 A72-14262
Semiconductors with diamond and zincblende structures, calculating dielectric function by empirical pseudopotential method
03 p0405 A72-14270

ZIRCALOY 2 [TRADEMARK]

- Magnetic-explosive welding /magneweld/ process using capacitor discharge through wire coil, noting sintered Al powder and Zircaloy 2 applications
09 p1321 A72-23638
Cold rolled Zircaloy 2 sheet microstructure, microstrains and hardness by X ray diffraction and electron microscopy
11 p1657 A72-25757

ZIRCALOYS [TRADEMARK]

- Zircaloy plastic properties and fatigue fracture modes under strain controlled push-pull cyclic loads, noting plastic anisotropy changes for warm cross rolled and recrystallized materials
05 p0678 A72-17120

ZIRCONATES

NT STRONTIUM ZIRCONATES

ZIRCONIUM

- Partial molar enthalpy measurement of oxygen mixture in substoichiometric Zr at 1300 C, using Tian-Calvet microcalorimeter
02 p0170 A72-12167
Stress induced oxygen diffusion in alpha Zr, attributing temperature dependent internal friction peak to oxygen-titanium interactions
02 p0247 A72-12818
Zr and V linear thermal expansion coefficients explanation by alpha Zr hexagonal crystal lattice anisotropy
03 p0376 A72-13946
Etch pit technique for titanium and zirconium crystal orientation determination, discussing etch pit locations and polycrystalline specimen goniomicroscopic observation
05 p0679 A72-17124
Superheating in Zr-oxygen combustion system during autoignition period
08 p1128 A72-21219
Electron microscopic investigation of niobium-oxygen alloys with Zr and Hf additions, measuring oxygen solubility
08 p1187 A72-21787
Electrical resistivity restoration in Van Arke type Zr deformed by lamination at 78 K attributed to point defects elimination
10 p1495 A72-24085
Zirconium rich metal oxides mineral group in Apollo 14 and 15 lunar rocks from feldspar-phyric basalt and pyroxene ferrobasalt, noting optical and chemical properties
11 p1717 A72-25868
Solid solutions of stabilized Zr in cubic form prepared from zirconium and yttrium oxide mixture by ammonia precipitation and heat treatment
11 p1660 A72-26486
Alpha Zr tensile properties tests noting strain aging effects on strain rate, work hardening and ductility anomalies
11 p1661 A72-26595
Dislocations with Burgers vector during Zr single crystals deformation at different temperatures, examining shear plane foils by electron microscope
13 p1978 A72-29223
Zone melting high-vacuum system with cryogenic pumping for zone refining Zr
14 p2092 A72-30220
Zr-Cu-Mo system phase diagram from microscopy, X ray analysis and mechanical tests, noting beta solid solution transformation into alpha, omega and beta phase mixtures
14 p2122 A72-30978
Al and Zr single thin strands burning rates at various total oxygen pressures, comparing photographic observation to computations
16 p2479 A72-34003
Oxygen diffusion coefficient variation with temperature observed during dissolution in alpha-zirconium, noting oxygen content effect on oxygen atom elementary jump length
19 p2817 A72-37795

Mechanical properties improvement of Al alloys for machine construction applications, suggesting Ti, Zr and Be additions optimal rate 20 p2941 A72-39577

ZIRCONIUM ALLOYS

NT ZIRCALOYS [TRADEMARK]

Silicide precipitation in Ti-Zr-Al-Si system, discussing microstructure correlation with mechanical properties 03 p0374 A72-13927

Zr alloys hydride distribution after oxidation in steam at 550 C, discussing hydrogen uptake 04 p0534 A72-15362

Quaternary Mo-Zr-Cr-C system, investigating fcc phase ligation from phase diagram by chemical, metallographic and X ray analyses 05 p0666 A72-16099

Nb-Zr alloy vacuum chamber tests for oxygen reaction rates, showing oxide surface film relation to sticking probability 05 p0674 A72-16391

Zr and Zr-Cr alloys corrosion behavior in steam, noting parabolic rate law breakaway point to linear rate 05 p0676 A72-16797

Low temperature tensile strength and plasticity of Ti alloys containing zirconium 05 p0679 A72-17203

Ti-Zr-O ternary alloys radiocrystallographic analysis, relating microstructure to composition and thermal treatment 06 p0827 A72-17569

Phase composition and electrical and mechanical properties of compacted zirconium diboride/tungsten alloys after sintering in argon, carbonaceous medium and vacuum 06 p0832 A72-18428

High temperature strengthening of vacuum melted W-Ti alloys with Mo and Zr additions 07 p1014 A72-19843

Alloying additives effects on Ti and Zr resistivity, thermal expansion, crystal lattice parameters and polymorphous transformations temperatures 07 p1017 A72-19990

Mo-Zr solid solutions internal boriding, discussing diffusion controlled process and hardness dependence on Zr 10 p1494 A72-23833

Low temperature tensile strength and plasticity of Ti alloys with zirconium, investigating sensitivity to stress concentrations 11 p1660 A72-26138

Interdiffusion studies in bcc phase of Zr-Ti alloy, using geoscan electron microprobe 13 p1973 A72-28653

Quenched powder metallurgy of high strength-high conductivity wrought Cu-Zr and Cu-Zr-Cr alloys, using nitrogen atomization 13 p1974 A72-28659

Metal particle decomposition products composition in slags from smelted Cr, Ti, Ni and Zr alloys, using X ray microanalysis 14 p2112 A72-30157

Mutual solid solubilities of rare earth metals with Zr extended by splat quenching, noting metastable low temperature allotropic forms of solid solutions 14 p2119 A72-30609

Ru-Nb-Zr alloys phase diagrams from physicochemical analysis, noting components interaction 14 p2123 A72-30993

Dispersion hardening of Nb-Zr-O and Nb-Hf-O alloys, discussing composition and heat treatment effects on aging, recrystallization temperature and grain growth 15 p2255 A72-31567

Amorphous structure analysis of splat quenched Cu-Zr noncrystalline phase, using electron microscopy 16 p2410 A72-33814

Nitrogen interactions in Nb-Zr alloys, investigating interior friction spectra peaks 18 p2702 A72-36707

Characteristics of temperature dependences for the thermal conductivity coefficients of niobium-zirconium solid solutions 19 p2817 A72-37739

The low strain tensile behavior of U-7.5 wt pct Nb-2.5 wt pct Zr. 20 p2938 A72-39303

X ray diffraction study of crystal structure of metastable phase in rapidly solidified Al-Zr alloys 20 p2939 A72-39307

Beta to omega phase transformation and structure in Zr and Ti alloys bcc solid solutions by dark field electron microscopy, diffraction and ultrasonic technique 21 p3065 A72-40092

X ray, microstructural and differential thermal analysis for binary Zr alloys, noting formation of ternary phases and solid solutions 23 p3300 A72-43588

Structure of the 01420 alloy with zirconium 23 p3303 A72-44094

Three-phase equilibria of cast and annealed V-Zr-Cr alloy by X ray, metallographic and melting point analyses 24 p3414 A72-45384

ZIRCONIUM CARBIDES

Physical properties of monocarbides of Zr, Nb and alloys in homogeneity range, explaining electronic structure relationship to composition changes 02 p0241 A72-11453

High temperature creep activation energies relationship to diffusion in TiC, ZrC and UC 03 p0371 A72-13461

Zirconium carbide high temperature heat conductivity measurement by radial heat flux method combined with photographic technique 05 p0680 A72-15852

Cast electron-beam remelted Mo, investigating carbon and zirconium carbide additions effects on cold shortness and low temperature plasticity 06 p0833 A72-18645

Age hardening of Mo alloys with titanium and zirconium carbides at high temperatures after quenching 07 p1014 A72-19844

Nonstoichiometric solid solutions based on ZrC and NbC, investigating microhardness variation due to differing valences of atoms in metal sublatitudes 08 p1188 A72-22100

Phase composition and lattice constants of carbide films from vaporized Zr interaction on graphite surface at 1700 C 13 p1912 A72-28566

Zirconium oxycarbide formation, solubility and one phase properties by X ray diffraction, chemical and metallographic analyses 13 p1982 A72-30107

Shock wave reduction, microcracks and dislocation density of hot pressed titanium, zirconium and niobium carbide powders, using X ray crystal analysis 13 p1982 A72-30110

Zirconium carbide creep characteristics and limit at 2450-2810 K, examining test conditions effects on parameters 14 p2116 A72-30435

Temperature dependence of thermionic emission current density of Pt additive powdered zirconium carbide deposit on diode cathode working surface 21 p2997 A72-40801

Physicomechanical properties of fiber carbides 23 p3299 A72-43291

Some strength characteristics of graphite/zirconium carbide composites 23 p3307 A72-44013

Influence of the sintering medium on the quality of metalceramic hard alloys containing zirconium and hafnium carbides 23 p3303 A72-44017

High temperature interaction between W and ZrC constructing isothermal structure 23 p3303 A72-44151

High temperature creep activation energies relationship to diffusion in TiC, ZrC and UC 24 p3413 A72-44936

ZIRCONIUM COMPOUNDS

NT STRONTIUM ZIRCONATES

NT ZIRCONIUM CARBIDES

NT ZIRCONIUM HYDRIDES

NT ZIRCONIUM NITRIDES

NT ZIRCONIUM OXIDES

Zirconium diboride-silicon carbon-graphite composition for lifting entry vehicle hot leading edges, investigating mechanical behavior by tension and flexural tests 01 p0091 A72-10767

Oxide scale formation on zirconium diboride materials, observing microstructural features as function of temperature and reaction time 09 p1333 A72-22380

Crystal structure of iron-zirconium disulfide and cobalt-zirconium disulfide systems 10 p1496 A72-24089

Electrical discharge machining of zirconium diboride, considering operations and tooling requirements 11 p1637 A72-25365

Optimum dispersion time and size particle determination for zirconium diboride powder grinding in vibrating mill, using gas flow ratio method 13 p1967 A72-30101

Zirconium diboride oxidation processes at temperatures above 520 C, noting zirconium oxide formation 14 p2121 A72-30850

U bearing phase zirkelite in Apollo 12 and 14 lunar rocks, using electron microprobe 15 p2303 A72-31303

Solid phase reaction kinetics in zirconium beryllide alloys with Ta and Nb at 900-1400 C, noting Be diffusion effect 16 p2408 A72-33535

Niobium and molybdenum alloys containing borides and carbides of the IV-a group metals 22 p3191 A72-42814

ZIRCONIUM HYDRIDES

Zr alloys hydride distribution after oxidation in steam at 550 C, discussing hydrogen uptake 04 p0534 A72-15362

ZIRCONIUM NITRIDES

HfB2 and ZrN alloys

19 p2845 A72-38409

ZIRCONIUM OXIDES

Molybdenum-zirconium oxide cermets oxidation behavior, noting change of Mo oxidation characteristic from linear to parabolic time law above molybdenum oxide melting point 02 p0246 A72-12550

Plasma sprayed tungsten and zirconium dioxide coatings porosity on chromium bronze, Ti and Al alloys and steel 03 p0363 A72-13550

Soviet papers on anodic oxidation of metals covering aluminum and zirconium oxides, oxide films, anion sorption capacity, chemical composition, structure and physicochemical properties 05 p0667 A72-17050

White thick layer anodic zirconium oxide water content determination by volumetric and thermogravimetric analysis of heated samples 05 p0667 A72-17051

High temperature and ZrO2 ceramic electrolyte effects on ionic partial conductivity and fuel cells longevity 06 p0760 A72-18337

Zirconium dioxide white pigment coatings for spacecraft thermal control, discussing impurities effects on optical absorption properties 07 p1023 A72-19692

Differential thermal and X ray analyses of ignition and preignition solid-solid reactions in Zr-Mo trioxide delay system over 440-475 C 08 p1219 A72-20756

Zirconia ceramics for high performance storage heaters, discussing operating conditions, optimal properties for heater design, engineering evaluation tests and in-service performance 09 p1333 A72-22383

Fusion cast zirconia-alumina-silica refractories manufacturing process, phase diagrams, chemical and physical properties and industrial applications 10 p1502 A72-24734

Temperature, oxygen pressure and exposure time effects on oxidation characteristics of molybdenum-zirconium oxide cermets 11 p1665 A72-26865

Zirconium oxycarbide formation, solubility and one phase properties by X ray diffraction, chemical and metallographic analyses 13 p1982 A72-30107

Zr oxidation kinetics at 440-850 C for 3 min maximum exposure time, observing type oxide change relationship to activation energy 14 p2113 A72-30247

Zirconium diboride oxidation processes at temperatures above 520 C, noting zirconium oxide formation 14 p2121 A72-30850

Time-temperature correlated phase transformations in zirconia nucleated magnesium-aluminum-silicon oxide glass ceramics for isothermal heat treatment 16 p2413 A72-33205

Cubic stabilized zirconia utilization as solid electrolyte in high temperature fuel cell system for efficient and economical energy conversion 16 p2352 A72-33894

Destabilization and aging mechanisms for ionic conductivity decrease in stabilized zirconia type electrolytes, discussing yttria stabilization 16 p2361 A72-33895

Investigation of the influence of the gas medium on the phase composition and certain properties of refractory materials containing zirconium 23 p3306 A72-43690

Contribution to the study of some HfO2-MO systems 23 p3302 A72-43999

Contribution to the study of phenomena of ordering of defects in single crystals of alumina- or zirconia-base refractory materials 23 p3302 A72-44000

ZODIACAL LIGHT

Interplanetary and terrestrial dust detection, discussing zodiacal light photometric measurements by Helios space probe and light pressure, solar wind and Poynting-Robertson effect 01 p0126 A72-10201

Large aperture ratio wide field VCN-UV camera exploration of night sky, presenting isophotes of zodiacal light and Milky Way 04 p0525 A72-15685

D-2B satellite mission, describing attitude, orbit and experiments on zodiacal light, stellar radiation and antistar data 04 p0583 A72-15689

Satellite photometric observation of diffuse celestial sources such as Milky Way, zodiacal light and gegenschein 10 p1546 A72-24863

Helios solar probe-borne zodiacal light photometer for diffuse light measurements in interplanetary space 11 p1632 A72-25805

Daytime zodiacal light intensity and polarization measurement at elongation angles between 15-30 degrees from Skylark rocket photometric observations 15 p2227 A72-31951

SUBJECT INDEX

- Zodiacal light brightness and polarization measurement from OSO-5 with photometers at 4180 and 6820 Å
16 p2385 A72-33467
- Mie scattering models of zodiacal light based on spherical particles, commenting on inadequacy for nonspherical particles at elongations above 120 deg
19 p2792 A72-38506
- Circular polarisation measurements of the zodiacal light.
20 p2920 A72-39899
- Zodiacal light, airglow and lightning monitoring by wide field broad bandpass OSO-5 experiment, obtaining height profile, cell size and intensity variations of nightglow
21 p3054 A72-40619
- ZONAL HARMONICS**
Time evolution of large scale solar magnetic field, observing zonal harmonics
03 p0431 A72-13344
- Secular perturbations of artificial earth satellites Keplerian orbital elements from arbitrary-order zonal harmonics in geopotential series expansion
07 p1078 A72-19982
- Long-term prediction of artificial satellite motion along almost circular orbits allowing for a random number of zonal harmonics
17 p2607 A72-35033
- The determination of zonal harmonic coefficients of the terrestrial potential
19 p2790 A72-38173
- ZOND SPACE PROBES**

- Cosmic proton and neutron produced recoil proton energy spectra measurements along earth-moon-earth trajectory with nuclear emulsions aboard Zond 5 and 7 [CERN-71-16]
02 p0273 A72-12074
- Space flight effects on chlorella cell survival and mutability in Zond automatic stations
05 p0623 A72-16775
- Proton recording equipment onboard automatic interplanetary stations Zond 4 and 5 at 1.5-50 MeV using silicon drift counters
06 p0814 A72-17699
- Low energy solar cosmic ray measurements in interplanetary space with Zond space probes, comparing to galactic cosmic rays
07 p1061 A72-20022
- Biological experiments on plants, animals and bacteria aboard Zond 5, 6 and 7 space probes, noting flight conditions effect on physiological functions and hereditary structures
11 p1579 A72-25941
- Space flight effects on chlorella cell survival and mutability in Zond automatic stations
17 p2504 A72-35278
- ZOND 5 SPACE PROBE**
Cytological, genetic and physiological analyses of space flight factors effects on seeds and plants aboard Zond 5 probe
15 p2186 A72-31828
- ZONE MELTING**
Rolling workability of pure W single crystals grown by electron beam zone melting technique, discussing

ZONE REFINING

- crack occurrence
03 p0374 A72-13718
- Binary Al alloys with variable melting volume and liquid zone velocities, investigating crystallization during zone melting
07 p1022 A72-20572
- Temperature distribution and zone melting in carbon thin films heated by electron beam, using Sn crystal indicators
08 p1253 A72-21446
- Guinier-Preston zone nucleation and growth as function of vacancies in Al-Cu alloy
08 p1190 A72-22166
- Impurities effect on Mo plastic properties and toughness, suggesting lower vacuum arc welding rates and increased electron beam zone refining runs
09 p1326 A72-22228
- Thermal and athermal components of the flow stress in zone-refined titanium.
19 p2820 A72-38298
- Electrical properties and fabrication details of integral diode matrices with controllable avalanche breakdown produced from zone melted silicon under temperature gradient
19 p2774 A72-38416
- Desulfurization of cobalt, nickel, and their eutectic carbon alloys during noncrucible zone melting in vacuum
23 p3300 A72-43647
- ZONE REFINING**
U ZONE MELTING



AIAA TECHNICAL INFORMATION SERVICE

750 THIRD AVENUE

NEW YORK, N. Y. 10017